A publication of the
American Pharmaceutical Association—
the National Professional Society
of Pharmacists

JOURNAL OF PHARMACEUTICAL SCIENCES

INDEX TO AUTHORS
INDEX TO SUBJECTS

VOLUME 71
JANUARY TO DECEMBER, 1982

Published monthly under the supervision of the Board of Trustees

Involving IRBs In The Drug Approval Process

Everyone knows that the Food and Drug Administration is slow, bureaucratic, inflexible, and unimaginative. After all, haven't we all heard and read such allegations on numerous occasions? Moreover, many of us in the pharmaceutical field have had some personal experiences that have confirmed—or at least seem to have supported—just such conclusions regarding that federal agency.

Consequently, it strikes us as strange that there is little notice or interest when the FDA advances a proposal that would be expected to (a) speed up drug approval, (b) reduce government involvement, (c) provide a major departure from current drug approval processing, and (d) represent innovative thinking on the entire regulation of early drug testing.

We refer to FDA's proposals to expand the role, function, and responsibility of Institutional Review Boards (IRBs). These are the local review committees which are now set up and operating in many private and public institutions, and which serve as a sort of peer review group to examine and pass upon the suitability of proposed research involving human subjects or patients prior to the start of such studies.

Evidently, the general track record to date of these IRBs has been quite satisfactory. Experience seems to have shown that they are effective and that they work rather well in accomplishing their objective of protecting human subjects from undue risks.

The FDA has taken note of this performance and has advanced the thought that IRBs might provide an excellent vehicle to expedite Phase I testing in the consideration of Investigational New Drugs (INDs). Phase I is the initial testing in humans that involves short-term studies in a small number of normal subjects or patients to test the properties of the drug and levels of toxicity, metabolism, and pharmacologic effects.

After basic information about the drug is obtained in these preliminary studies, and assuming the results are favorable and encouraging, the effectiveness and relative safety of the drug are then studied by larger and more detailed investigations in patients; this is referred to as Phase II. Finally, at Phase III, more extensive testing is performed on patients to systematically assess the drug's safety and effectiveness.

For various reasons, many compounds tested never get beyond Phase I. Moreover, this is a time-consuming process that requires practically the same degree of scientific review resources to evaluate as the subsequent phases which involve many more human subjects. Consequently, Phase I drains off a considerable, and perhaps disproportionate, fraction of FDA's available resources for conducting medical reviews.

And at the same time, a parallel process is being conducted by the IRBs. If not identical, the process is very similar and the ultimate objectives are comparable. Furthermore, it has been argued that due to local familiarity, the IRB is able to assess the situation far better than any agency hundreds of miles away with only a batch of papers on which to make its judgments and render a decision.

Consequently, certain officials within the FDA—along with a few outside clinical investigators—have raised the question of whether it might eliminate duplication, expedite drug approval processing, lower research costs, and conserve scarce resources if the FDA were to reduce its review functions during the Phase I/early-Phase II period of the IND, conditioned upon a willingness of the IRBs to accept increased responsibilities in this area. Such a transfer would not change the standards of human subject protection and, hence, would not put patients at any greater risk than under the present arrangement.

The FDA informally has been "floating" this idea for at least a year. And, in the *Federal Register* of September 11, FDA formally described its interest in pursuing such a possible arrangement by publishing a summary of the issue and inviting comments from all interested parties. The *FR* item asks for views on five specific points as well as inviting responses to the general proposition.

The FDA appears to be genuinely interested in achieving some positive result in this matter. FDA Commissioner Arthur Hull Hayes, Jr., has supplemented the *FR* notice with a personal mailing to a broad spectrum of individuals and groups to call their attention to this issue and to invite the widest possible response.

On the surface, this concept (of using local IRBs to a greater extent as a trade-off for reducing most FDA oversight during Phase I and early-Phase II drug studies) makes a good deal of sense to us. But, as noted above, for some strange reason the idea seems to have generated little interest or publicity among any of the usually vocal and active groups on the drug scene: the lay press, broadcast media, consumer advocates, pharmaceutical trade organizations, Congress, or special interest groups.

It would be most regrettable—indeed, even tragic—if one of the few real potential solutions to reducing government "red tape" and the so-called "drug lag" were allowed to die simply because of apathy and neglect on the part of all concerned.

—EDWARD G. FELDMANN
American Pharmaceutical Association
Washington, D.C.

0022-3549/82/0100-0001$01.00/0

JOURNAL OF PHARMACEUTICAL SCIENCES

JANUARY 1982
VOLUME 71 NUMBER 1

RESEARCH ARTICLES

Quantitative Evaluation of Pharmaceutical Effervescent Systems I: Design of Testing Apparatus

NEIL R. ANDERSON ˣ, GILBERT S. BANKER, and GARNET E. PECK

Received February 4, 1981, from the *School of Pharmacy and Pharmacal Sciences, Purdue University, West Lafayette, IN 47907.* Accepted for publication May 13, 1981.

Abstract □ Two new devices were developed to monitor the reactivity of pharmaceutical effervescent systems. The first method monitored carbon dioxide pressure generation during the effervescent reaction in a plastic pressure vessel fitted with a pressure gauge. The second method monitored weight loss, attributed to carbon dioxide loss to the atmosphere, by means of a double cantilever beam and an electromagnetic proximity transducer. In the pressure device, the quantification of an effervescent reaction was accomplished by measuring the dissolution time of the effervescent system and the pressure generated. Quantification of an effervescent reaction using the beam device utilized the total carbon dioxide weight loss, the rate of weight loss, and the effervescent reaction lag time.

Keyphrases □ Effervescent pharmaceuticals—quantitative evaluation, design of testing apparatus □ Reactivity—quantitative evaluation of effervescent pharmaceuticals, design of testing apparatus □ Instrumentation—design of testing apparatus to quantitate reactivity of effervescent pharmaceuticals

Acid–base reactions between alkali metal carbonates or bicarbonates and citric or tartaric acid have been used for many years to produce effervescent pharmaceutical preparations on the addition of water. The greatest problem with effervescent products is the loss of reactivity with time due to their premature reaction on exposure to moisture. Even exposure to atmospheric moisture when opening and closing a multiple-dose container can rapidly destroy reactivity.

BACKGROUND

Studies to design improved effervescent tablet systems have suffered from the absence of methodology to quantitate effervescent reactions. To study the rate of an effervescent reaction such as between sodium bicarbonate and citric acid in excess water, producing carbon dioxide, water, and sodium citrate, one can theoretically measure the increase in one reaction product or the decrease in one reactant. The obvious element to measure continuously would be the carbon dioxide generated. This procedure would permit measurement of the amount of carbon dioxide generated by a particular system as well as the rate of the reaction.

Chemical analysis of carbon dioxide, following total evolution of the gas, can be accomplished by several means. However, none of the methods permits the direct kinetic determination of carbon dioxide evolution during various time points in the process of a rapidly reacting system. Carbon dioxide can be measured by a volumetric method using the Chittick apparatus (1), by a combination of gas measurement and gas absorption, or by a weight loss method (2). Carbon dioxide is also determined by absorption on liquid or solid media, measuring the amount of gas evolved by weighing (3). The use of the absorption method has been modified many times by using different detection methods to determine the amount of gas absorbed (4–6). None of these methods is satisfactory for quantitating an effervescent reaction that is completed in <30–60 sec.

One possible method of continuously monitoring carbon dioxide evolution is to monitor the pressure generated in a closed system. However, this approach may not simulate the normal effervescent tablet reaction occurring in an open container of water at constant atmospheric pressure.

A simple, continuous, immediate response weight loss procedure was thought to offer the most direct and applicable technique to determine the total amount of carbon dioxide evolved, the reaction rate, and other characteristics of the reaction process. Development of such a system requires the development of an adequately sensitive weighing system, providing immediate response and continuous recording. The response characteristics must be rapid to quantitate totally a reaction that is completed in 30 sec or less and sensitive enough to measure accurately weight losses <1 g from an initial mass of ~100 g.

Transducers capable of responding quickly to applied forces have been used in the pharmaceutical industry for more than 20 years. Strain-gauge transducers have been shown (7, 8) to be widely and successfully used in instrumenting tableting machines in research, development, and production capacities. A device was developed (9) for the continuous recording of the flow of powders or granular material from various hoppers with strain gauges. Later, an instrument was developed (10) to determine granule strength using strain gauges in a beam apparatus similar to the flow device. Taylor (11) developed a flowing measure instrument with strain gauges and a specially designed double-cantilever beam, and the same equipment was adapted to quantify suspension pourability (12). While the newer strain-gauge devices permit continuous recording of applied loads, such systems are not adequately sensitive to monitor carbon dioxide loss during an effervescent reaction.

This report describes a new balance system utilizing an electromagnetic proximity transducer and a specifically designed double-cantilever beam that is sensitive enough for the continuous gravimetric measurement of carbon dioxide loss during an effervescent reaction. Utilizing the proximitor balance system as well as pressure generation measurements, effervescent systems and reactions were quantitated as to their reaction

0022-3549/82/0100-0003$01.00/0

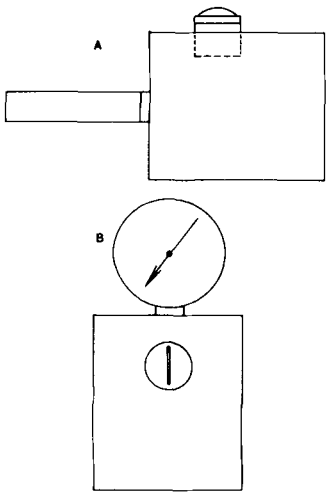

Figure 1—*Pressure monitoring device in the filling position (A) and in the testing position (B).*

rates, carbon dioxide losses, dissolution times, and lag times to initiation of reaction. A reactivity index was developed, and a correlation between the two new methods of examining effervescent reactions was found.

EXPERIMENTAL

Instrumentation—Reactivity testing based on monitoring pressure generation of effervescent tablet systems was done in a cylindrical plastic pressure vessel especially designed for effervescent tablets. The pressure generated during the effervescent reaction in the vessel was measured by a 0–60 psi pressure gauge[1] mounted on the pressure vessel. The volume of the pressure vessel was ~250 ml. Attached to the side of the vessel was the sample tablet holder(Figs. 1A and 1B). The tablet holder was cylindrical in design and built perpendicularly into the side of the pressure vessel. The end opening to the interior of the vessel consisted of two perpendicular crosspieces, which held the sample tablet out of the interior of the vessel in the filling position (Fig. 1A), but allowed the water in the vessel to flow into the sample holder to cover the tablet when placed in the vertical test position (Fig.1B). A pressure-tight, clear plastic screw cap sealed the system at the exterior end of the cylindrical sample holder.

The new balance system for the continuous recording of carbon dioxide weight loss utilized a double-cantilever beam with a proximity transducer to monitor beam deflection. The proximity transducer consisted of a probe and a proximitor. The actual transducer consisted of a flat coil of wire located in the ceramic tip of the probe. This probe then became a gap-to-voltage transducer used to measure distances and change in distances to any electrically conductive material. The probe was driven by a radio frequency (RF) voltage developed by the proximitor. The output signal from the proximitor to a chart recorder was at a voltage proportional to the distance between the probe and the conductive surface.

Basically, the proximitor takes the voltage supplied to it from a power supply and converts it to an RF signal. This signal is then applied to the probe and the probe coil, which radiates this signal into the surrounding area as a magnetic field. If there is no conductive surface to interfere with the magnetic field there is no RF signal loss. However, as a conductive surface approaches the probe and interferes with the magnetic field, eddy currents are generated on the surface of the material, the RF signal is lost, and power is consumed. As the surface moves closer to the probe, more and more power is absorbed and the RF signal decreases. The proximitor measures the RF signal voltages and sends out an output voltage equal to the negative RF signal peaks (13). The output voltages can then be directly measured on a volumeter or used to drive a chart recorder.

The new beam/proximitor (b/p) balance system (Fig. 2) consisted of a double-cantilever beam specifically designed for a maximum load of 100 g to be placed on the 5.1-cm sample pan. The proximity transducer probe[2] was mounted directly below the electrically conductive surface needed for the proximity measurement. The proximitor[2] itself was housed

[1] Ashcroft, Dresser Valve and Instrument Division, Dresser Industries, Stratford, Conn.
[2] Bently Nevada Co., Minden, Nev.

Table I—Theoretical and Observed Recorder Span Responses of the Beam/Proximitor Balance to Various Weights Applied to a 99-g Load

Weight Applied, g	Theoretical Span Response, division	Actual Span Response, division
1.00	90.0	90.0
0.75	67.5	67.5
0.50	45.0	45.0
0.25	22.5	22.5
0.10	9.0	9.0
0.05	4.5	4.5
0.02	1.8	1.75
0.01	0.9	1.0

Table II—Beam/Proximitor Balance Recorder Span Precision and Reproducibility [a]

Trial	Number of Tests Run	Average Span Response ± SD, division
1	30	90.09 ± 0.154
2	35	89.98 ± 0.195
3	31	90.00 ± 0.144

[a] One gram produces a 90-division span response.

with an 18-v power supply. A line filter[3] was needed to filter out electrical noise, and a voltage divider was needed to reduce the input voltage to the recorder to match the 100-mv span on the recorder[4]. The b/p balance was housed during tests in a plexiglass hood to reduce the possibilities of air currents affecting the balance.

The double-cantilever beam system of the balance was designed and constructed to provide a linear response in beam deflections to various load weights. The b/p balance was then designed to measure weight loss by monitoring beam deflections with the proximitor and probe. Using this design, the b/p balance could monitor up to a 1-g weight loss from an initial load of up to 100 g.

Pressure Vessel Test Method—With the pressure vessel placed in the horizontal filling position (Fig. 1A), the cap of the tablet holder was removed and 150 ml of deionized, distilled water (20°) was quickly transferred into the pressure device through the tablet holder. Any water adhering to the tablet holder was removed to prevent premature reaction. The tablet to be tested was placed in the tablet holder, and the cap was replaced and secured. The pressure vessel was then lifted to the vertical test position (Fig. 1B), causing the water to contact the tablet in the tablet holder and produce the effervescent reaction. At 5-sec intervals, the pressure was read from the pressure gauge and recorded. The dissolution time of the effervescent tablet, as observed through the transparent cap of the tablet holder, was recorded, as well as the pressure that developed at the dissolution time. Finally, the entire device was shaken for a few seconds and the final pressure was recorded.

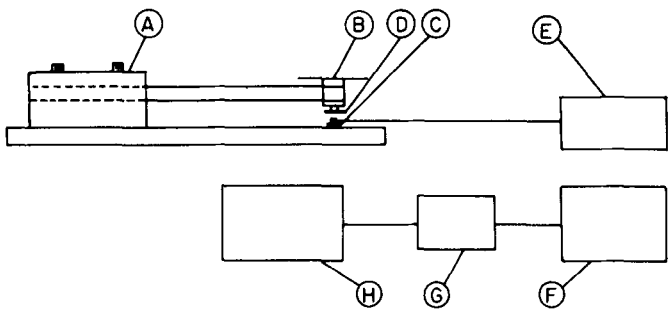

Figure 2—*The balance system utilizing a double-cantilever beam and proximity transducer. Key: A, double-cantilever beam assembly; B, sample pan; C, proximity probe; D, electrically conductive surface; E, power supply; F, electrical line filter; G, voltage divider; and H, recorder.*

[3] Model 3321 filter, Krohn-Hite Corp., Cambridge, Mass.
[4] Model SRG, Sargent-Welch Scientific Co., Skokie, Ill.

Table III—Carbon Dioxide Weight Loss [a] After 2 Min from Effervescent Tablets

Trial	Number of Tablets	Commercial Analytical Balance: Average Tablet Weight, g	Commercial Analytical Balance: Average Carbon Dioxide, mg	Commercial Analytical Balance: Loss, % (w/w)	Beam/Proximitor Balance: Average Tablet Weight, g	Beam/Proximitor Balance: Average Carbon Dioxide, mg	Beam/Proximitor Balance: Loss, % (w/w)
1	4	3.5006	553.3	15.81	3.5413	606.4	17.12
2	3	3.4345	560.5	16.32	3.4605	574.4	16.60
3	5	3.4987	581.5	16.62	3.4870	584.4	16.76

[a] As measured by an analytical balance and the beam/proximitor balance.

Balance Test Method—Polypropylene beakers (100-ml) were used as the effervesecent tablet reaction vessels. Because the effervescent reaction was violent enough to cause a loss of water as well as carbon dioxide from the beaker, a circular beaker cover (7.0 cm in diameter) was made from high density polyethylene material. This cover had a rectangular slot, 2.9 × 0.6 cm, cut in the center through which the effervescent tablets were dropped into the beaker.

After prestressing the balance beam with a 100-g load for 30–40 min to stabilize the base (0% span) and top lines (90% span) on the recorder, ~80 ml of deionized, distilled water at 20° was measured into the reaction beaker and the total weight of the beaker, cover, water, and tablet was adjusted to 100 g or 90% of full recorder span with 20° water. With the recorder on "standby" and the chart speed set at 12.7 cm/min, the tablet was set on its edge at the edge of the slot in the cover. After initial beam vibration had subsided, the tablet was gently dropped through the slot into the beaker. Immediately after the tablet entered the water, the recorder was turned to "record," and the effervescent reaction was monitored for at least 2 min. The tablet dissolution time was determined visually and indicated on the recording.

Calibration of Balance—After prestressing the beam with a 99-g load, the b/p balance was calibrated by placing various known loads, 10 mg–1 g, on the balance. The recorder span was set at 90%. The actual recorder response to the various loads was in very close agreement to the theoretical response. Only slight deviations occurred at even the 20- and 10-mg loads (Table I).

The recorder span (90%) reproducibility was measured by repeatedly adding and removing a 1-g weight from the b/p balance loaded with 99 g. Table II shows the precision and reproducibility resulting from the three trials performed.

Tests were run to compare reacting effervescent tablet carbon dioxide weight loss values obtained with the b/p balance to values obtained with a commercial balance. Effervescent tablets[5] were reacted in a beaker of water, and the weight loss was noted after 2 min of reaction time on a commercial analytical balance[6] and compared to the weight loss of tablets run on the experimental balance. The data in Table III show close agreement in the total weight loss after 2 min between the b/p balance and the commercial analytical balance, which further verified the accuracy of the b/p unit.

Materials—Several different experimental effervescent tablets were made for effervescent reactivity testing with the pressure vessel and b/p balance methods. Each tablet system was a 3-g tablet containing a stoichiometric ratio of acid and base (Table IV). A standard 3-g tablet was made of citric acid–sodium bicarbonate (1.3:1.7). All materials were either USP, NF, or pharmaceutical grade.

The materials were first passed through a 30-mesh screen and then through an 80-mesh screen, mixed, and compressed on a hydraulic press[7] between 25.4-mm, flat-faced, beveled-edge tooling. The compression force generated for each tablet was 897 kg/cm^2 and was held for a 5-sec dwell time. All operations were conducted at 23–25° and a relative humidity of ≤30%.

RESULTS AND DISCUSSION

The standard tablets were run in the pressure device first. Table V shows the pressure and dissolution time results of the 28 standard formulation tablets run. The standard tablets were then run on the b/p balance to measure carbon dioxide loss (Table VI).

The experimental effervescent tablets were then run in the pressure device and on the b/p balance. The resultant carbon dioxide weight loss values and gas pressure values were divided by the corresponding values obtained from the standard tablets to generate relative pressure values and relative weight loss values listed in Table VII. Figure 3 shows the relationship between the relative values obtained from the two test methods. The calculated correlation coefficient for the graph was 0.937.

Table IV—Experimental Effervescent Tablets Run in The Pressure Monitoring Device and the Beam/Proximitor Balance

Composition	Composition Ratio, g:g
Citric acid–sodium bicarbonate (standard)	1.3:1.7
Malic acid–potassium bicarbonate	1.72:1.28
Glutaric acid–potassium bicarbonate	1.19:1.81
Maleic acid–potassium bicarbonate	1.10:1.90
Glutaric acid–sodium bicarbonate	1.32:1.68
Malic acid–sodium bicarbonate	1.85:1.15
Maleic acid–sodium bicarbonate	1.22:1.77

Table V—Average Pressure Generation and Dissolution Time of Sodium Bicarbonate–Citric Acid Run [a] in the Pressure Monitoring Device

	Pressure Developed, psi	Dissolution Time, sec
Average	26.75	28.89
Variance	0.435	5.65
SD	0.669	2.38
SEM	0.125	0.45

[a] Twenty-eight samples were run.

Table VI—Average Carbon Dioxide Weight Loss of the Standard 3-g Tablets of Sodium Bicarbonate–Citric Acid Run on the Beam/Proximitor Balance

	Amount
Tablet weight	
Number of tablets tested	30
Average weight, g	2.9914
Variance, g	0.0004
SD, g	0.0062
SEM, g	0.0011
Calculated carbon dioxide weight loss (W_F)	
Number of tablets tested	30
Average loss, g	0.5419
Variance, g	0.0003
SD, g	0.0177
SEM, g	0.0032

Table VII—Relative [a] Pressure Values and Carbon Dioxide Weight Loss Values of the Experimental Effervescent Tablets Run in the Pressure Monitoring Device and the Beam/Proximitor Balance

Tablet Composition	Relative Pressure (psig) Values	Relative Weight Loss Values
Citric acid–sodium bicarbonate (standard)	1.00	1.00
Malic acid–potassium bicarbonate	0.93	0.95
Glutaric acid–potassium bicarbonate	1.02	0.98
Maleic acid–potassium bicarbonate	0.98	1.02
Glutaric acid–sodium bicarbonate	1.01	1.00
Malic acid–sodium bicarbonate	0.84	0.84
Maleic acid–sodium bicarbonate	0.86	0.83

[a] Experimental tablet values for pressure and weight loss were divided by the standard tablet values of 26.75-psi pressure and 0.5419-g weight loss to calculate the relative values.

[5] Alka-Seltzer tablets, Miles Laboratories, Elkhart, Ind.
[6] Model H-10 Mettler Instrument Corp., Princeton, N.J.
[7] Carver laboratory press model C, Fred S. Carver and Co., Summit, N.J.

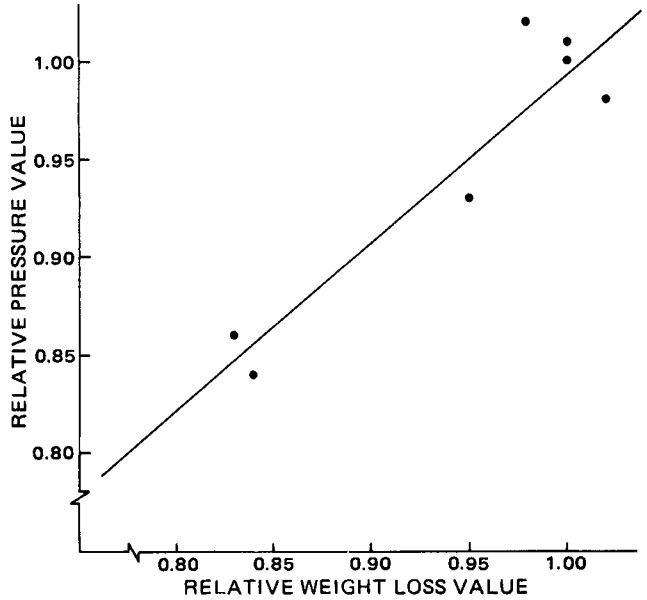

Figure 3—*Relationship between the relative pressure values from the pressure monitoring device and the relative weight loss values from the beam/proximitor balance (Table IV).*

The correlation was judged to be good considering that the sensitivity of the pressure gauge on the pressure device was 2 psi/division and the sensitivity of the b/p balance was 0.0111 g/division.

The milligrams of carbon dioxide lost at any time (t) during an effervescent reaction were designated W_t and could be calculated from the chart recording (Fig. 4) by multiplying the number of divisions corresponding to the weight loss at time t by 11.1 mg/division. The final weight loss measured 2 min after the reaction was started was designated W_F. Plotting log ($W_F - W_t$) *versus* time produced a graph like the one in Fig. 5. The graph can be divided into three segments corresponding to the three events observed during the effervescent reactions. Period A of Fig. 5, the distance between the y-axis and the time at which the graph first approaches linearity, represents an induction period or lag time during which the tablet is wetted by the water and the effervescent reaction is initiated. Period C represents the period after the effervescent reaction has ceased and when carbon dioxide is slowly coming out of solution. Period B represents the actual time of the effervescent reaction of the tablet. In this section of the graph, a straight line can be drawn, the slope determined by linear regression, and an observed first-order rate constant (k) can be calculated for the reaction.

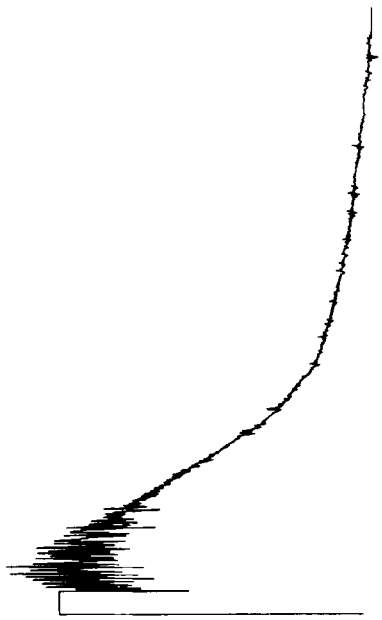

Figure 4—*Typical chart recording from a beam/proximitor balance effervescent tablet run.*

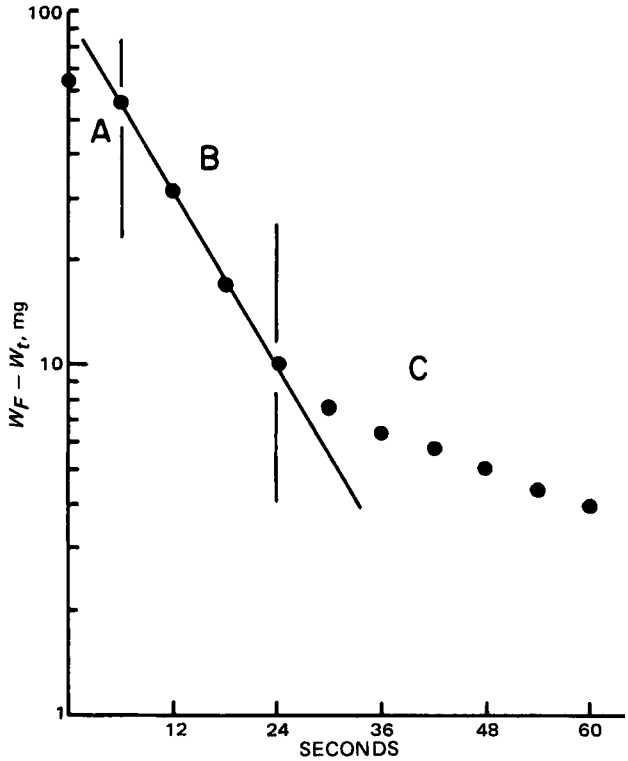

Figure 5—*Example plot of beam/proximitor balance data treatment using log* ($W_F - W_T$) versus *time relationship.*

In a statistical evaluation of reactivity, a single measurement of both the reaction rate and the total carbon dioxide evolved is required since differing effervescent systems could conceivably have a fast reaction rate and yet produce little carbon dioxide (and vice versa). Therefore, Eq. 1 can be used to quantitate each effervescent tablet system for both k and W_F in a single indicator, the index of reactivity (I_R):

$$I_R = kW_F \qquad \text{(Eq. 1)}$$

SUMMARY

While the described pressure monitoring device did not lend itself to effervescent reaction characterization or rate determinations, the results obtained did correlate with weight loss data obtained from the balance device. The pressure monitoring device could be used as an effective, quick screening device for experimental effervescent system reactivity or as a possible quality control instrument.

REFERENCES

(1) "Official Methods of Analysis of the Association of Official Analytical Chemists," 11th ed., W. Horwitz, Ed., Association of Official Analytical Chemists, Washington, D.C., 1970, p. 139.

(2) "Standard Methods of Chemical Analysis," 6th ed., N. Furman, Ed., Van Nostrand, Princeton, N.J., 1962, pp. 298–307.

(3) M. Earnshaw, *Ind. Chem. Chem. Manf.*, **33**, 253 (1957).

(4) E. Bruins, *Anal. Chem.*, **35**, 1935 (1963).

(5) H. Pobiner, *ibid.*, **34**, 878 (1962).

(6) J. Thomas, Jr., and G. Hieftje, *ibid.*, **38**, 500 (1966).

(7) P. Wray, *Ind. Drug Cosmet. Ind.*, **105** (9), 58 (1969).

(8) H. Rahm, *Pharm. Acta Helv.*, **46**, 65 (1971).

(9) G. Gold, R. Duvall, and B. Palermo, *J. Pharm. Sci.*, **55**, 1133 (1966).

(10) G. Gold, R. Duvall, B. Palermo, and R. Hurtle, *ibid.*, **60**, 922 (1971).

(11) G. Taylor, Master's thesis, Purdue University, West Lafayette, Ind., 1972.

(12) D. Hagman, Ph.D. thesis, Purdue University, West Lafayette, Ind., 1972.

(13) "Theory of Operation," Bently Nevada Probe and Proximitor Installation Manual, Bently Nevada Co., Minden, Nev.

ACKNOWLEDGMENTS

Supported by a grant from Miles Laboratories, Elkhart, IN 46514.

Quantitative Evaluation of Pharmaceutical Effervescent Systems II: Stability Monitoring by Reactivity and Porosity Measurements

NEIL R. ANDERSON ˣ, GILBERT S. BANKER, and GARNET E. PECK

Received February 4, 1981, from the *School of Pharmacy and Pharmaceutical Sciences, Purdue University, West Lafayette, IN 47907.* Accepted for publication May 13, 1981.

Abstract □ The stability of selected effervescent tablet systems was monitored by means of mercury intrusion porosimetry and by a cantilever beam/proximity transducer balance. The porosity measurements proved to be useful in elucidating tablet pore structure changes over time. The measured parameter, percent pores greater than the experimental range, was a useful measure of porosity for statistical evaluations. The study showed that compression pressure and manufacturing conditions are not significant factors in the stability of an effervescent tablet system when nonhygroscopic materials are used.

Keyphrases □ Effervescent pharmaceuticals—quantitative evaluation, monitoring of stability by reactivity and porosity measurements □ Stability—of effervescent pharmaceuticals, monitoring by reactivity and porosity measurements □ Tablets—effervescent, measurement of stability by reactivity and porosity measurements

Accelerated stability tests are used in the systematic design of solid dosage forms to examine the changes in physical characteristics brought about by environmental stress conditions. To use any stability test successfully, the characteristics being monitored must be quantitatively measured.

The greatest problem with effervescent tablet products is their loss of reactivity with time, particularly from contact with moisture. Methods of quantitatively characterizing effervescent tablet systems are limited and do not lend themselves to direct measurement. However, a balance device utilizing a double-cantilever beam with a proximity transducer was recently developed to allow continuous recording of carbon dioxide weight loss from rapidly reacting effervescent systems (1). That study also described treatment of the data obtained, including calculation of an index of reactivity (I_R) to quantify the effervescent reactions.

A previous study (2) investigated the stability of a hydrolizable drug, aspirin, in relation to the porosity characteristics of the dosage form by means of mercury intrusion porosity measurements. Since effervescent tablets based on citric acid and sodium bicarbonate react prematurely, with carbon dioxide being generated and liberated, the porosity characteristics of such a tablet might be expected to change as the premature reaction proceeds. Therefore, mercury intrusion porosity data might provide useful information on the physical changes in effervescent systems with aging or decomposition, as well as data that might be correlated with other tablet reactivity measurements, resulting in a more quantitative method of stability assessment.

The present studies were undertaken to determine the stability of several experimental effervescent tablets. An index of reactivity (1) was developed as a stability indicator. The mercury intrusion measurement of the porosity of the effervescent tablets, used to monitor structural changes in the effervescent tablets with time under the influence of water vapor and high temperature, was also developed as a stability indicator.

EXPERIMENTAL

Materials—The compositions of the effervescent tablets used are listed in Table I. All materials were passed through a number 30 screen and then through a number 80 screen, mixed, and compressed at room temperature with a relative humidity (RH) of either 20 or 60%. The effervescent tablets contained a stoichiometric ratio of acid to base, with the tablets containing a base other than sodium bicarbonate equivalent to 1.9 g of sodium bicarbonate. Because of the large amount of sodium glycine carbonate and sodium dihydrogen citrate required in such formulations, the total weight of these tablets (Table I) was reduced by 63.5 and 25%, respectively. Corrections were later made so that the carbon dioxide loss data were reported as equivalent to a 1.9-g sodium bicarbonate formula.

Experimental Design—The stability study was designed as a factorial experiment to investigate the effects of the tablet manufacturing conditions (I), tablet formulations (J), tablet compression pressures (K), storage conditions (L), and storage times (M). The dependent variables measured were the index of reactivity, I_R, and a measure of the tablet porosity.

Large 25.4-mm, flat-faced, beveled-edge tablets were compressed at two different compression pressures, 897 or 1077 kg/cm^2, using a motorized hydraulic press[1]. Similar 12.7-mm tablets were also compressed to densities equal to the 25.4-mm tablets. The densities were measured on a commercial air comparison pycnometer[2] (Table II). The 12.7-mm tablets were required to accommodate the porosity measuring device used in the study. Prior to compression, the raw materials were oven dried at 120° for 24 hr, weighed out, mixed, and exposed to the manufacturing environment for 1 hr. The effervescent tablets were either compressed at an ambient relative humidity of ≤20% or at 60% RH. The relative humidity was monitored by means of a sling psychrometer[3].

During the high humidity stability test, the tablets were stored in glass bottles[4] without caps in a sealed rigid plastic case, equipped with a small fan for air circulation, containing a saturated salt solution of sodium chloride to produce 75% RH at 25°. The humidity was monitored by a hygrometer[5] placed inside the case. The second storage condition of the stability test was 50°, achieved in an oven[6]; tablets were stored in the oven in capped glass bottles[4].

The tablets were stored in the glass bottles in an alternating stack of 25.4- and 12.7-mm tablets with a polystyrene plastic disk[7] as filler on the top and bottom of each stack. Enough tablets were placed in a bottle to complete the necessary samplings at 0, 2, and 4 weeks of storage at each condition. For each bottle of sample tablets, a backup bottle containing one tablet of each size, along with the disks, was stored.

The general procedure for setting up and running the stability test started with the establishment of the 20 or 60% RH manufacturing conditions. The compression equipment was then moved to the location providing that condition. The five different effervescent tablet formulations to be compressed at two different compression pressures were coded and assigned an order of compression using a random number table. The raw materials for each of the 10 combinations (five formula-

[1] Motorized conver press, Fred S. Carver, Menomonee Falls, Wis.
[2] Model 930, Beckman Instruments, Fullerton, Calif.
[3] Taylor Instrument Co., Rochester, N.Y.
[4] Glass bottles for Alka-Seltzer 8's, Miles Laboratories, Elkhart, Ind.
[5] Model R560, Abrax Instrument Corp., Jamaica, N.Y.
[6] Thelco model 18, Precision Scientific Co., Chicago, Ill.
[7] Styrofoam filler plugs for Alka-Seltzer bottles, Miles Laboratories, Elkhart, Ind.

0022-3549/82/0100-0007$01.00/0

Table I—Effervescent Tablet Formulations Used in the Effervescent Tablet Stability Study

Ingredient	Tablet Formulations, g				
	A	B	C	D	E
Citric acid anhydrous	1.45	1.08	—	—	—
Sodium dihydrogen citrate	—	—	1.82	—	—
Glutaric acid	—	—	—	1.49	—
Sodium bicarbonate	1.90	—	1.43	—	—
Sodium glycine carbonate	—	2.02	—	1.90	—
Total tablet weight	3.35	3.10	3.25	3.39	3.696[a]

[a] Experimental effervescent tablet. Granulation supplied by project sponsor.

Table II—Densities of Effervescent Tablets Compressed at Pressures[a] to Produce Equivalent Densities

Tablet Composition	Tablet Size, mm	Applied Compression Pressure, kg	Density
Citric acid–sodium bicarbonate	25.4	5455	1.912
	12.7	909	1.946
Citric acid–sodium glycine carbonate	25.4	5455	1.784
	12.7	909	1.790
Sodium dihydrogen citrate–sodium bicarbonate	25.4	5455	1.912
	12.7	909	1.910
Glutaric acid–sodium bicarbonate	25.4	5455	1.782
	12.7	909	1.726

[a] Pressure calculated by geometric and force transmission considerations for 12.7 mm tablets.

tions × two pressures) were then weighed out, and enough of both of the 25.4- and 12.7-mm tablets were compressed to meet the sampling and backup requirements of the stability test.

The tablets were then randomly placed in the glass bottles, labeled, and placed in the appropriate storage condition. Initial values of the reactivity and porosity measurements were taken. This procedure was repeated until all 20 combinations (five formulations × two pressures × two manufacturing conditions) were compressed and stored and initial values were taken.

At the appropriate times, the top 25.4- and 12.7-mm tablets in each sample bottle were removed from storage and their reactivities and porosities were determined. The tablets were sampled and measured in the same order as they were made, using one tablet per measurement.

The total stability study was replicated a second time in the described manner. The second replication was needed to provide some measure of the error between test measurements and between the manufacture of the tablets to make statistical tests on the major factors after the study.

The data collected in the study was analyzed statistically by analysis of variance. The experimental design contained three inherent restrictions on randomization, which were accounted for in the design of the statistical analysis model (3–5). The first restriction occurred when all tablet compression work was done under one manufacturing condition prior to the second condition. Second, each tablet formulation was compressed in turn at the high or low compression pressure prior to the other pressure being used. Third, the tablets were assigned storage conditions and had to be sampled at the specified storage times in the same order that they were made. With these errors accounted for in the model, property tests could be run on the dependent variables after the study was concluded.

The analysis of variance for the study design is shown in Table III. This design was used for the analysis of each dependent variable of reactivity and porosity measured at both storage conditions for 0, 2, and 4 weeks of storage. Analysis of variance was done by computer using a statistical library program[8].

Pooling of the error terms was performed to determine the mean square error (MS_{error}) to facilitate F testing by having a single MS_{error} with greater degrees of freedom (6). Pooling was performed as indicated in Table III.

[8] Purdue University, Computer Center, West Lafayette, Ind.

Table III—Analysis of Variance for One Dependent Variable in Two Storage Conditions[a]

Source	Degrees of Freedom	E.M.S.[c]
I	1	$\sigma_\epsilon^2 + \sigma_\eta^2 + \sigma_\omega^2 + \sigma_\delta^2 + 60\sigma_{N(I)}^2 + 120\sigma_I^2$
$N(I)$	2	$\underline{\sigma_\epsilon^2 + \sigma_\eta^2 + \sigma_\omega^2 + \sigma_\delta^2 + 60\sigma_{N(I)}^2}$
δ[d]	0	$\sigma_\epsilon^2 + \sigma_\eta^2 + \sigma_\omega^2 + \sigma_\delta^2$
J	4	$\sigma_\epsilon^2 + \sigma_\eta^2 + \sigma_\omega^2 + 12\sigma_{N(I)J}^2 + 48\sigma_J^2$
IJ	4	$\sigma_\epsilon^2 + \sigma_\eta^2 + \sigma_\omega^2 + 12\sigma_{N(I)J}^2 + 24\sigma_{IJ}^2$
$N(I)J$	8	$\underline{\sigma_\epsilon^2 + \sigma_\eta^2 + \sigma_\omega^2 + 12\sigma_{N(I)J}^2}$
K	1	$\sigma_\epsilon^2 + \sigma_\eta^2 + \sigma_\omega^2 + 30\sigma_{N(I)K}^2 + 120\sigma_K^2$
IK	1	$\sigma_\epsilon^2 + \sigma_\eta^2 + \sigma_\omega^2 + 30\sigma_{N(I)K}^2 + 60\sigma_{IK}^2$
$N(I)K$	2	$\underline{\sigma_\epsilon^2 + \sigma_\eta^2 + \sigma_\omega^2 + 30\sigma_{N(I)K}^2}$
JK	4	$\sigma_\epsilon^2 + \sigma_\eta^2 + \sigma_\omega^2 + 6\sigma_{N(I)JK}^2 + 24\sigma_{JK}^2$
IJK	4	$\sigma_\epsilon^2 + \sigma_\eta^2 + \sigma_\omega^2 + 6\sigma_{N(I)JK}^2 + 12\sigma_{IJK}^2$
$N(I)JK$	8	$\underline{\sigma_\epsilon^2 + \sigma_\eta^2 + \sigma_\omega^2 + 6\sigma_{N(I)JK}^2}$
ω[e]	0	$\sigma_\epsilon^2 + \sigma_\eta^2 + \sigma_\omega^2$
L	1	$\sigma_\epsilon^2 + \sigma_\eta^2 + 30\sigma_{N(I)L}^2 + 120\sigma_L^2$
IL	1	$\sigma_\epsilon^2 + \sigma_\eta^2 + 30\sigma_{N(I)L}^2 + 60\sigma_{IL}^2$
$N(I)L$	2	$\underline{\sigma_\epsilon^2 + \sigma_\eta^2 + 30\sigma_{N(I)L}^2}$
JL	4	$\sigma_\epsilon^2 + \sigma_\eta^2 + 60_{N(I)JL} + 24\sigma_{IL}^2$
IJL	4	$\sigma_\epsilon^2 + \sigma_\eta^2 + 60_{N(I)JL} + 12\sigma_{IJL}^2$
$N(I)JL$	8	$\underline{\sigma_\epsilon^2 + \sigma_\eta^2 + 60_{N(I)JL}}$
KL	1	$\sigma_\epsilon^2 + \sigma_\eta^2 + 15\sigma_{N(I)KL}^2 + 60\sigma_{KL}^2$
IKL	1	$\sigma_\epsilon^2 + \sigma_\eta^2 + 15\sigma_{N(I)KL}^2 + 30\sigma_{IKL}^2$
$N(I)KL$	2	$\underline{\sigma_\epsilon^2 + \sigma_\eta^2 + 15\sigma_{N(I)KL}^2}$
JKL	4	$\sigma_\epsilon^2 + \sigma_\eta^2 + 3\sigma_{N(I)JKL}^2 + 12\sigma_{JKL}^2$
$IJKL$	4	$\sigma_\epsilon^2 + \sigma_\eta^2 + 3\sigma_{N(I)JKL}^2 + 6\sigma_{IJKL}^2$
$N(I)JKL$	8	$\underline{\sigma_\epsilon^2 + \sigma_\eta^2 + 3\sigma_{N(I)JKL}^2}$
η[f]	0	$\sigma_\epsilon^2 + \sigma_\eta^2$
M	2	$\sigma_\epsilon^2 + 20\sigma_{N(I)M}^2 + 80\sigma_M^2$
IM	2	$\sigma_\epsilon^2 + 20\sigma_{N(I)M}^2 + 40\sigma_{IM}^2$
$N(I)M$	4	$\underline{\sigma_\epsilon^2 + 20\sigma_{N(I)M}^2}$
JM	8	$\sigma_\epsilon^2 + 4\sigma_{N(I)JM}^2 + 16\sigma_{JM}^2$
IJM	8	$\sigma_\epsilon^2 4\sigma_{N(I)JM}^2 + 8\sigma_{IJM}^2$
$N(I)JM$	16	$\underline{\sigma_\epsilon^2 + 4\sigma_{N(I)JM}^2}$
KM	2	$\sigma_\epsilon^2 + 10\sigma_{N(I)KM}^2 + 40\sigma_{KM}^2$
IKM	2	$\sigma_\epsilon^2 + 10\sigma_{N(I)KM}^2 + 20\sigma_{IKM}^2$
$N(I)KM$	4	$\underline{\sigma_\epsilon^2 + 10\sigma_{N(I)KM}^2}$
JKM	8	$\sigma_\epsilon^2 + 2\sigma_{N(I)JKM}^2 + 8\sigma_{JKM}^2$
$IJKM$	8	$\sigma^2 + 2\sigma_{N(I)JKM}^2 + 4\sigma_{IJKM}^2$
$N(I)JKM$	16	$\underline{\sigma_\epsilon^2 + 2\sigma_{N(I)JKM}^2}$
LM	2	$\sigma_\epsilon^2 + 10\sigma_{N(I)LM}^2 + 40\sigma_{LM}^2$
ILM	2	$\sigma_\epsilon^2 + 10\sigma_{N(I)LM}^2 + 20\sigma_{ILM}^2$
$N(I)LM$	4	$\underline{\sigma_\epsilon^2 + 10\sigma_{N(I)LM}^2}$
JLM	8	$\sigma_\epsilon^2 + 2\sigma_{N(I)JLM}^2 + 8\sigma_{JLM}^2$
$IJLM$	8	$\sigma_\epsilon^2 + 2\sigma_{N(I)JLM}^2 + 4\sigma_{IJLM}^2$
$N(I)JLM$	16	$\underline{\sigma_\epsilon^2 + 2\sigma_{N(I)JLM}^2}$
KLM	2	$\sigma_\epsilon^2 + 5\sigma_{N(I)KLM}^2 + 20\sigma_{KLM}^2$
$IKLM$	2	$\sigma_\epsilon^2 + 5\sigma_{N(I)KLM}^2 + 10\sigma_{IKLM}^2$
$N(I)KLM$	4	$\underline{\sigma_\epsilon^2 + 5\sigma_{N(I)KLM}^2}$
$JKLM$	8	$\sigma_\epsilon^2 + \sigma_{N(I)JKLM}^2 + 4\sigma_{JKLM}^2$
$IJKLM$	8	$\sigma_\epsilon^2 + \sigma_{N(I)JKLM}^2 + 2\sigma_{IJKLM}^2$
$N(I)JKLM$	16	$\underline{\sigma_\epsilon^2 + \sigma_{N(I)JKLM}^2}$
ϵ	0	σ_ϵ^2

[a] Measured at 0, 2, and 4 weeks. [b] Key: I, manufacturing condition; N, replicate; J, tablet formulation; K, tablet compression pressure; L, storage condition; and M, storage time. [c] The error terms were pooled within the various sections as indicated by underlining. The pooled errors were then used to test the significance of those factors and interactions within the respective sections. [d] First restriction of randomization error. [e] Second restriction of randomization error. [f] Third restriction of randomization error.

In the case of significant two-way interactions from analysis of variance of a dependent variable, a Newman–Keuls sequential range test (6) was performed on the means involved to determine significant differences.

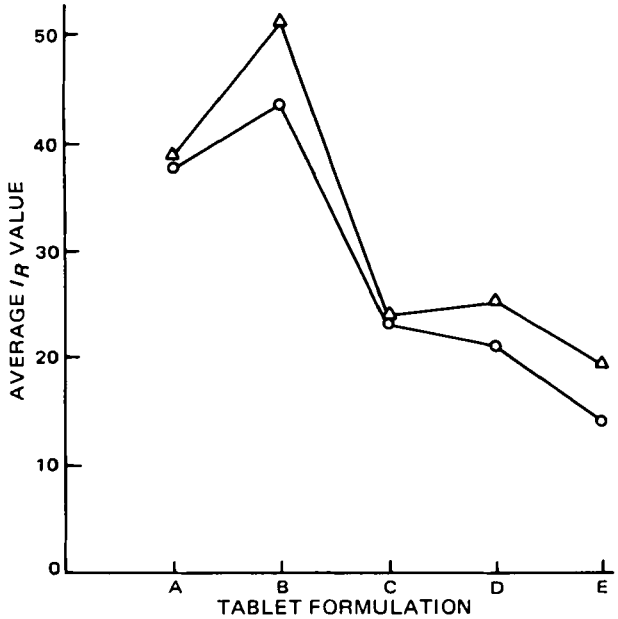

Figure 1—*Index of reactivity (I_R) analysis for J × I interaction. Key: △, 20% RH manufacture; ○, 60% RH manufacture; A, citric acid–sodium bicarbonate; B, sodium glycine carbonate–citric acid; C, sodium dihydrogen citrate–sodium bicarbonate; D, glutaric acid–sodium bicarbonate; and E, Tablet E.*

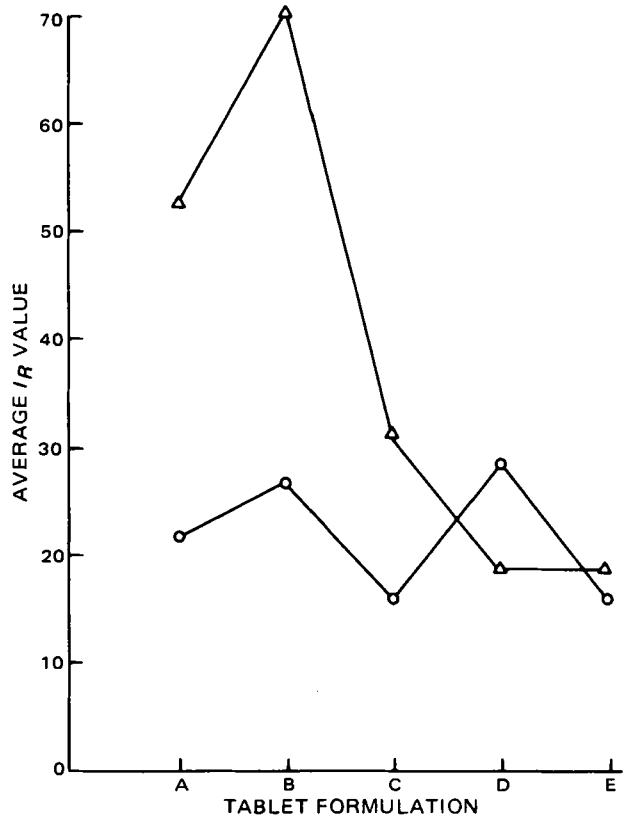

Figure 2—*Index of reactivity analysis for J × L interaction. Key: △, 50° storage condition; ○, 75% RH storage condition; A, citric acid–sodium bicarbonate; B, sodium glycine carbonate–citric acid; C, sodium dihydrogen citrate–sodium bicarbonate; D, glutaric acid–sodium bicarbonate; and E, Tablet E.*

The effervescent tablet porosity measurements were performed on a commercial mercury intrusion porosimeter using a method described previously (2, 7). In this procedure, several characteristics of a tablet's pore structure were calculated and could be used to express tablet porosity. However, statistical evaluation requires that a single dependent variable value be used. In this study, the calculated value of the percent pores greater than the experimental range (PPGTER) was used as the dependent variable value for porosity. The selection of the PPGTER values was based on the fact that moisture can interfere with mercury intrusion in pore-size distribution determinations within the experimental range (8, 9). Even though each tablet was pretreated by drying at room temperature under vacuum[9] for 15 hr as part of the mercury intrusion determinations, the effervescent reaction, however slow it may be, would not have ceased; therefore, water would still have been produced and been available to interfere with the measurements. The PPGTER value is not significantly influenced by moisture.

The true densities of the tablets required for the porosity calculations were determined by an air comparison technique using a commercial pycnometer[3]. Room air was used as the gas. Before each determination, a zero measurement check was made to correct for possible zero offset. Measurements were carried out by starting at an initial pressure of 1 atm and compressing the gas to 2 atm.

The reactivity of the 25.4-mm effervescent tablets at the selected storage times was determined by means of the beam/proximitor (b/p) balance previously described (1).

RESULTS AND DISCUSSION

As already mentioned, tablets containing sodium glycine carbonate and sodium dihydrogen citrate required weight reductions of 63.5 and 25%, respectively, and did not contain base equivalent to the 1.9 g of sodium bicarbonate in the standard tablet. From the standpoint of density and porosity, the weight reduction was not a factor. However, in trying to relate the reduced weight tablets to the standard tablet by means of the index of reactivity, I_R, the weight reduction is very crucial because:

$$I_R = kW_F \qquad \text{(Eq. 1)}$$

where W_F is the final weight loss of carbon dioxide from the effervescent solution and k is the rate constant of the effervescent reaction (1). Therefore, the data collected for the reduced tablets were multiplied by a correction factor. This factor was determined by measuring W_F on the b/p balance from tablets containing the full 1.9 g of sodium bicarbonate equivalent and from the reduced tablets. Dividing W_F for the full-base tablets by W_F for the reduced-base tablets gave a factor by which each data point generated on the b/p balance by the reduced tablets could be multiplied to yield data representative of tablets containing base equivalent to 1.9 g of sodium bicarbonate.

Analysis of variance of the adjusted I_R means revealed, at the 0.01 level, significant differences in I_R values with the following factors:

J = tablet formulation
L = storage condition
M = storage time
$J \times I$ = interaction
$J \times L$ = interaction
$J \times M$ = interaction
$L \times M$ = interaction
$I \times J \times M$ = interaction
$I \times K \times M$ = interaction
$J \times K \times M$ = interaction
$J \times L \times M$ = interaction
$I \times J \times K \times M$ = interaction

The individual factors of compression pressure (K) and manufacturing conditions (I) were not significant.

Analysis of variance showed that I_R appears to be a function not only of J but also of L and M. The single effects are supported by examination of the four significant two-way interactions involving the factors. Newman–Keuls (NK) tests were run, and the means were plotted for each interaction (Figs. 1–4).

Figure 1 shows the I_R means plotted for the interaction of tablet formulation and manufacturing conditions ($J \times I$). Figure 1 clearly shows the difference in I_R values according to the different formulas and supports the analysis of variance finding that manufacturing conditions did not have any significant effect on I_R values in that only the citric acid–sodium glycine carbonate tablet showed any significant difference, 0.01 level, between the two manufacturing conditions. With only this one difference, the total interaction is of doubtful significance.

[9] Thelco model 19 vacuum oven, Precision Scientific Co., Chicago, Ill.

Table IV—General Physical Observations

Tablet	Storage	Observations
A	75% RH	Some swelling, surface rough
A	50°	No change
B	75% RH	Surface rough, some swelling
B	50°	No change
C	75% RH/50°	No change
D	75% RH	Some swelling
D	50°	Very enlarged and porous ("sponge")
E	75% RH	Enlarged
E	50°	Very enlarged and porous ("sponge")

Investigation of the $J \times L$ interaction (Fig. 2) shows significant differences in the I_R means caused by storage conditions, with the citric acid–sodium bicarbonate and citric acid–sodium glycine carbonate tablets recording the largest I_R losses. The I_R values of the glutaric acid–sodium bicarbonate tablet support the observation (Table IV) that this composition was better, or was more stable, at 75% RH storage than at 50° storage in that its I_R value was greater after the former. Tablet E appeared to be equally low in I_R value in either storage condition.

A study of the $J \times M$ interaction in Fig. 3 shows that the I_R definitely decreased with storage time for all tablets. Moreover, there were no significant differences between the 2- and 4-week values of I_R for each tablet. The loss of stability appeared to take place during the first 2 weeks of storage.

The obvious relationship between L and M is supported by the interaction in Fig. 4. There was a significant loss of I_R at 50° between 0, 2, and 4 weeks. There was also a significant loss of I_R between 0, 2, and 4 weeks at 75% RH storage. The losses at 50° were significantly less than the losses at 75% RH storage. This result can be explained by the fact that only the glutaric acid–sodium bicarbonate and Tablet E lost a significant amount of reactivity at 50° storage whereas all tablets lost reactivity at the 75% RH storage condition.

The three-way and four-way interactions, calculated by analysis of variance to be statistically significant, were ignored since the significance

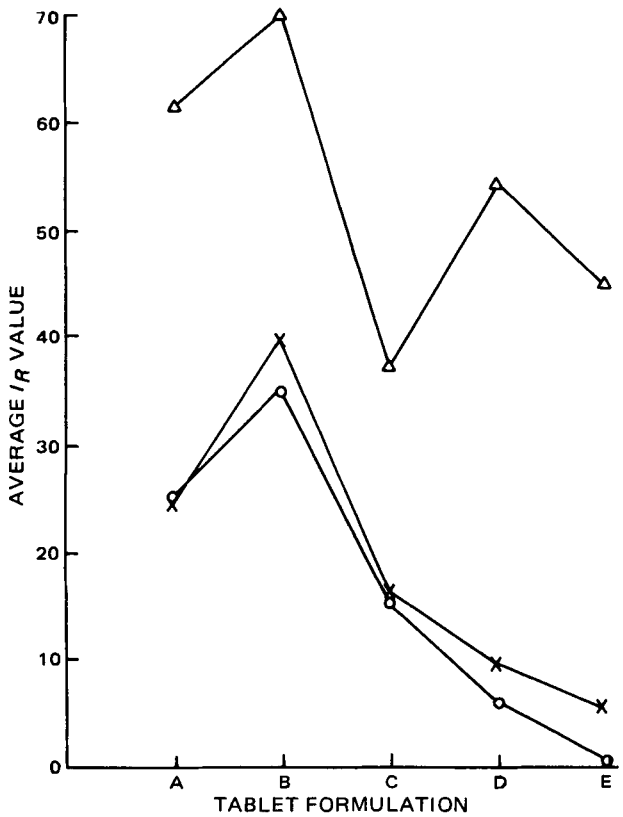

Figure 3—*Index of reactivity analysis for* J × M *interaction. Key:* △, *initial (0 week);* ×, *2 weeks of storage;* ○, *4 weeks of storage; A, citric acid–sodium bicarbonate; B, sodium glycine carbonate–citric acid; C, sodium dihydrogen citrate–sodium bicarbonate; D, glutaric acid–sodium bicarbonate; and E, Tablet E.*

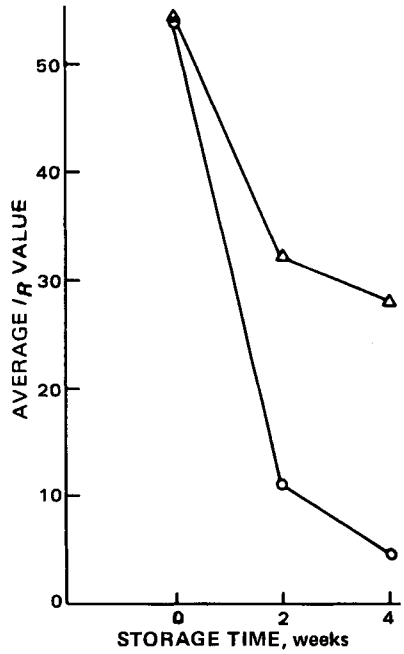

Figure 4—*Index of reactivity analysis for* L × M *interaction. Key:* ○, *75% RH storage condition; and* △, *50° storage condition.*

in the higher order interactions was probably caused by the strong common factor of storage time (M).

Analsis of Tablet Porosity Using PPGTER—Analysis of variance shows four significant differences in PPGTER values, at the 0.01 level, caused by the factors of J, M, $J \times M$, and $J \times L$. None of the other factors and interactions were significant. In a plot of both interactions (Figs. 5 and 6), the sodium dihydrogen citrate–sodium bicarbonate tablet values of PPGTER remain approximately constant.

Analysis of $J \times L$ by NK testing and plotting (Fig. 5) shows significant differences within tablets at the two storage conditions with the exception of the sodium dihydrogen citrate–sodium bicarbonate tablet formulation. The citric acid–sodium bicarbonate and citric acid–sodium glycine carbonate tablets appeared to have low PPGTER values at 50° and high values at 75% RH. The reverse was true for glutaric acid–sodium bicarbonate and Tablet E where the PPGTER values at 75% RH storage were lower than those at 50° storage. This interchange of values, causing the differences to perhaps cancel each other, probably eliminated the significance of L from the analysis of variance. Analysis of the $J \times M$ interaction (Fig. 6) shows that there was no significant difference between the citric acid–sodium bicarbonate and citric acid–sodium glycine carbonate tablets. The sodium dihydrogen citrate–sodium bicarbonate

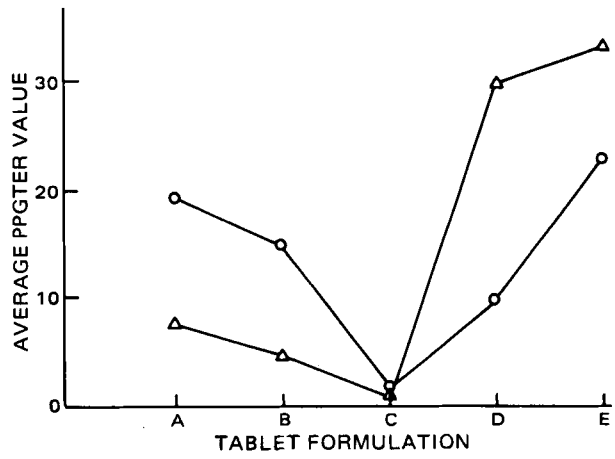

Figure 5—*Percent pores greater than experimental range (PPGTER) analysis for* J × L *interaction. Key:* ○, *75% RH storage condition;* △, *50° storage condition; A, citric acid–sodium bicarbonate; B, sodium glycine carbonate–citric acid; C, sodium dihydrogen citrate–sodium bicarbonate; D, glutaric acid–sodium bicarbonate; and E, Tablet E.*

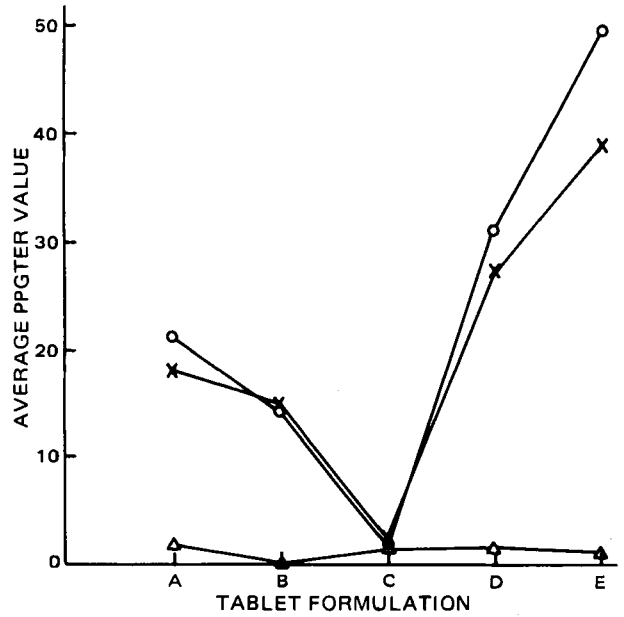

Figure 6—*PPGTER analysis for J × M interaction. Key: △, initial (0 week); ×, 2 weeks of storage; ○, 4 weeks of storage; A, citric acid–sodium bicarbonate; B, sodium glycine carbonate–citric acid; C, sodium dihydrogen citrate–sodium bicarbonate; D, glutaric acid–sodium bicarbonate; and E, Tablet E.*

tablets appeared to be lower in value and remained unchanged. As already shown, most of the significance came from the glutaric acid–sodium bicarbonate and Tablet E alone being greatly different from their initial values compared with the other tablets. The values at 2 and 4 weeks showed no significant differences, indicating that the loss in PPGTER stability occurred within the first 2 weeks of storage.

Analysis of variance of I_R values shows the sodium glycine carbonate–citric acid tablet to be good in comparison with the standard tablet (citric acid–sodium bicarbonate). There is also an indication that while

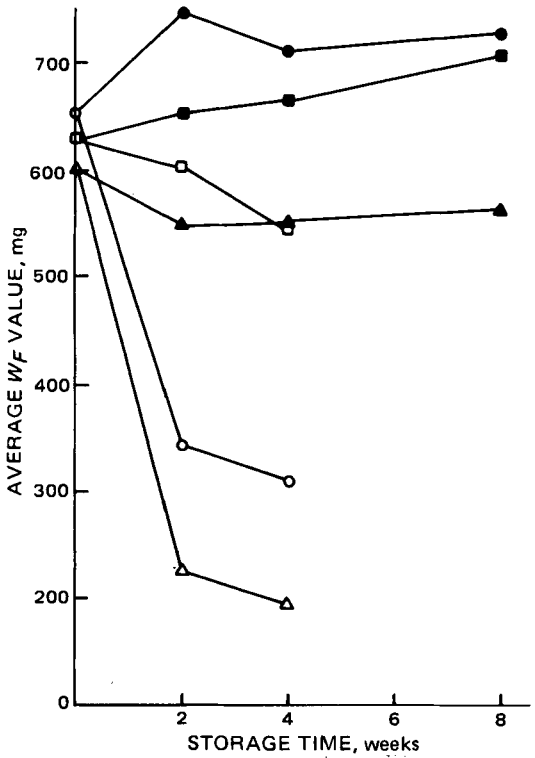

Figure 7—*Average final weight loss of carbon dioxide (W_F) at each storage condition and time for Tablets A (△), B (○), and C (□). Open figures represent the 75% RH storage condition; closed figures represent the 50° storage condition.*

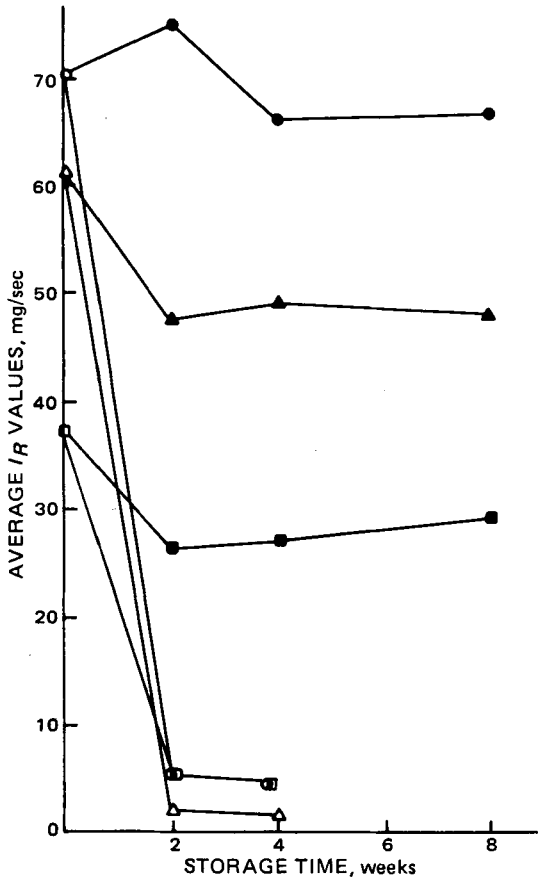

Figure 8—*Average index of reactivity (I_R) at each storage condition and time for Tablets A (△), B (○), and C (□). Open figures represent the 75% RH storage condition; closed figures represent the 50° storage condition.*

low in its I_R value, the sodium dihydrogen citrate–sodium bicarbonate tablet is quite stable. When restricting the discussion to these three formulations, analysis of variance of PPGTER shows that the sodium

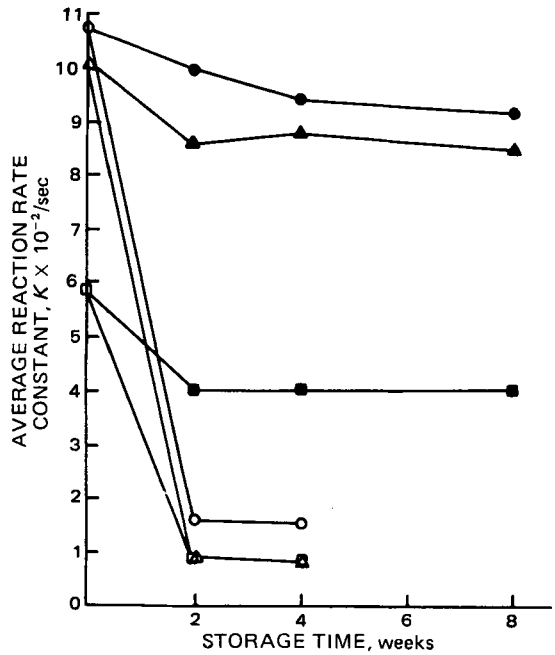

Figure 9—*Average reaction rate constant (k) at each storage condition and time for Tablets A (△), B (○), and C (□). Open figures represent the 75% RH storage condition; closed figures represent the 50° storage condition.*

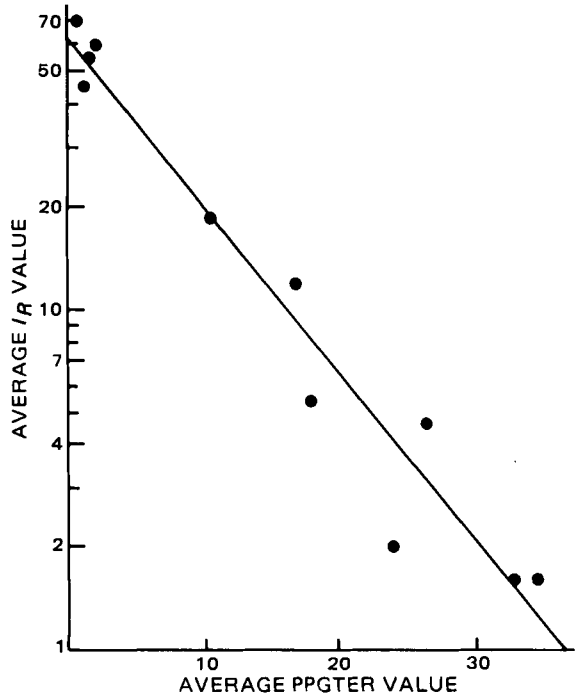

Figure 10—*Relationship between* I_R *and PPGTER.*

dihydrogen citrate composition underwent the least amount of internal structural changes, with the sodium glycine carbonate composition being second best. In addition, plots of the different reactivity data parameters (k, W_F, and I_R) in Figs. 7–9 show that the sodium glycine carbonate–citric acid tablet and the standard tablet were quite similar in initial reaction rate (Fig. 9); but on storage at 75% RH, the standard tablet lost ~67% of its carbon dioxide-producing capacity (W_F) compared with a 50% loss for the sodium glycine carbonate composition tablet (Fig. 7). The sodium dihydrogen citrate–sodium bicarbonate tablet retained its carbon dioxide-producing capacity at both storage conditions (Fig. 7); therefore, the low I_R values of the tablet (Fig. 8) were caused by low reaction rates (k) alone and not a combination of both W_F and k losses over time as would be indicated by Eq. 1.

It was shown that both the I_R PPGTER values are significantly affected by storage time. It appears that a correlation should exist between PPGTER and I_R. If it is assumed that the loss of reactivity is caused by the slow premature reaction of the tablets, then the loss of the reacting compounds to form the escaping carbon dioxide could alter the pore structure of the tablet by causing new pores to be formed and old pores to become larger.

A correlation does exist between PPGTER and I_R and is shown when the average PPGTER values for 0, 2, and 4 weeks in 75% RH storage are plotted against the log of the average I_R values at 0, 2, and 4 weeks of storage at 75% RH for the standard tablet, citric acid–sodium glycine carbonate, glutaric acid–sodium bicarbonate, and Tablet E (Fig. 10). For those tablets whose stability decreases in the 75% storage condition, the log of I_R decreases as the PPGTER increases.

Thus far, porosity has been limited to a discussion of PPGTER only.

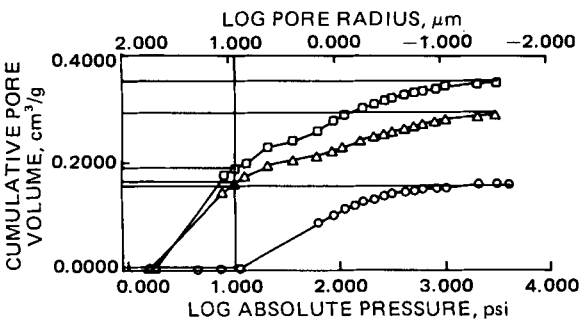

Figure 11—*Cumulative pore volume of the citric acid–sodium bicarbonate tablet in the 75% RH, 25° storage condition. Key: ○, initial (0 week); △, 2 weeks of storage; and □, 4 weeks of storage.*

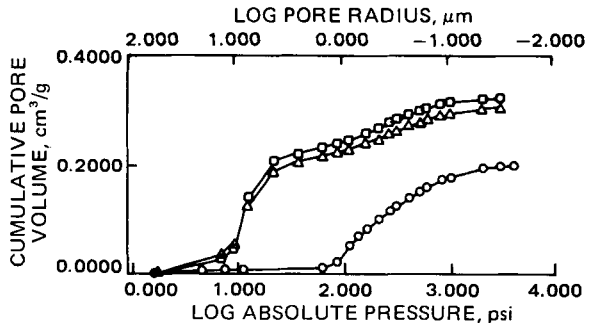

Figure 12—*Cumulative pore volume of the sodium glycine carbonate–citric acid tablet in the 75% RH 25° storage condition. Key: ○, initial (0 week); △, 2 weeks of storage; and □, 4 weeks of storage.*

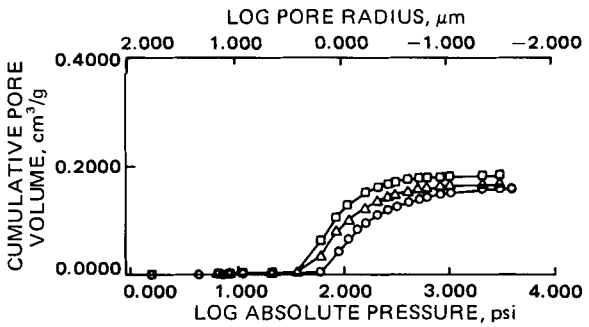

Figure 13—*Cumulative pore volume of the sodium dihydrogen citrate–sodium bicarbonate tablet in the 75%, RH, 25° storage condition. Key: ○, initial (0 week); △, 2 weeks of storage; and □, 4 weeks of storage.*

Mercury intrusion measurements can be presented graphically to illustrate the changes that occur in the tablet pore structure.

Examination of the mercury intrusion data[10] for the standard tablet stored in the 75% RH condition (Fig. 11) shows that at 10 psi, the smallest pore intruded by mercury was ~9 μm in radius. In the initial porosity determination, a negligible amount of mercury was intruded at pressures of <10 psi when compared to the total amount intruded. However, at the 2- and 4-week determinations, the amount of mercury intruded into pores ~≥9 μm in radius amounted to ~50% of the total mercury intrusion. In addition, the 2- and 4-week determinations revealed a greater total amount of mercury intruded compared to the initial determination. This finding indicates that as the tablet is exposed to the relative humidity of the storage condition, the pore structure of the tablet increases in total

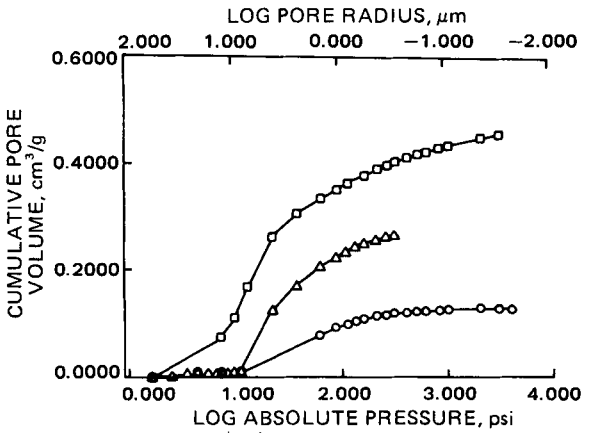

Figure 14—*Cumulative pore volume of the glutaric acid–sodium bicarbonate tablet in the 75% RH, 25° storage condition. Key: ○, initial (0 week); △, 2 weeks of storage; and □, 4 weeks of storage.*

[10] Although mercury intrusion measurements were made up through 15,000 psi, there was no significant intrusion beyond 4000 psi, and the mercury intrusion data plots are therefore not plotted beyond 4000 psi.

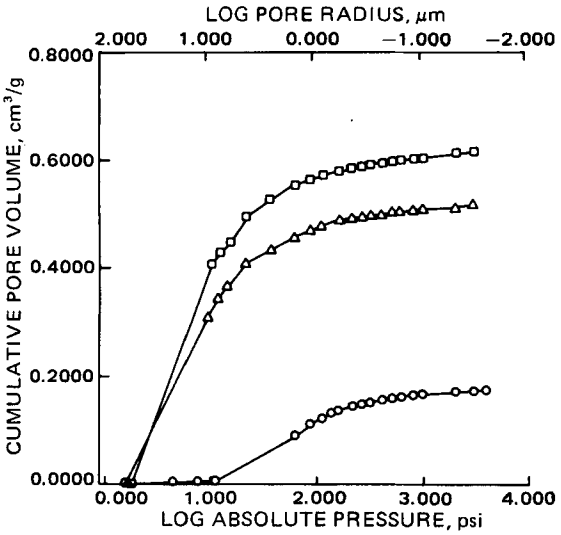

Figure 15—*Cumulative pore volume of Tablet E in the 75% RH, 25° storage condition. Key:* ○, *initial (0 week);* △, *2 weeks of storage; and* □, *4 weeks of storage.*

volume and the larger pores become a larger part of the pore-size distribution.

The use of the PPGTER values as a porosity indicator is supported by the distribution plots (Figs. 11–15). Tablets with storage time and storage condition combinations that produced large PPGTER values show up in the plots as having increased total mercury intrusion, with the distribution shifted toward the large pore sizes. For example, the $J \times M$ interaction in the PPGTER analysis in Fig. 6 shows that the glutaric acid–sodium bicarbonate and Tablet E had very high PPGTER values after 2 and 4 weeks. Figures 14 and 15 dramatically show the shift to larger pore sizes and the increased total mercury intrusion volume.

With the mercury intrusion plots, the differences in tablet pore structure caused by the different storage conditions for the standard, sodium glycine carbonate, glutaric acid, and sponsor composition tablets can be visualized as well as the stability of the sodium dihydrogen citrate composition tablet. Some resistance to higher humidity storage can be seen in the glutaric acid tablet (Fig. 14), supporting the earlier I_R data, in that a dramatic shift in pore distribution to large pore sizes occurred at the 4-week point and not at the 2-week point, as was seen with some other formulations (Figs. 11, 12, and 15).

SUMMARY

1. Mercury intrusion porosimetry was shown to be a useful tool in helping to elucidate pore structure changes in effervescent tablets.

2. The use of the index of reactivity (I_R) proved to be a successful indicator of effervescent tablet reactivity, combining both the amount of carbon dioxide generation and the reaction rate of the effervescent reaction.

3. The stability study of the selected experimental effervescent systems appeared to show that the manufacturing condition factor had little effect on the stability of the effervescent tablets studied, including the standard tablet of citric acid–sodium bicarbonate, which is well known as being sensitive to manufacturing conditions. This lack of effect on the standard tablet could be due to the materials used to make the tablets not having been exposed to the different manufacturing conditions long enough to influence stability significantly.

4. Statistical analysis did not demonstrate a statistically significant compression pressure factor (K). The stability of effervescent tablets apparently was not affected by the pressure at which the tablets were manufactured.

5. The study of effervescent systems showed that the stability of the effervescent tablet was dependent on the tablet formulation, storage conditions, and length of time the tablet was stored.

6. The citric acid–sodium glycine carbonate tablet appears to have better reaction properties and reaction property stability than does the standard citric acid–sodium bicarbonate tablet. The sodium dihydrogen citrate–sodium bicarbonate tablet appears to be inferior in reaction properties and reaction property stability to the standard tablet. However, the sodium dihydrogen citrate composition tablet was the only system to retain high W_F values in the 75% RH storage condition (Fig. 8), although its reaction rate (K) was lower than the other tablets and did decrease with time (Fig. 10).

REFERENCES

(1) N. R. Anderson, G. S. Banker, and G. E. Peck, *J. Pharm. Sci.*, **70,** 0000 (1981).

(2) H. Gucluyildiz, G. S. Banker, and G. E. Peck, *ibid.*, **66,** 407 (1977).

(3) V. L. Anderson, *Biometrics*, **26,** 25 (1970).

(4) V. L. Anderson and R. A. McLean, *Am. Stat.*, **28,** 145 (1974).

(5) N. R. Anderson, V. L. Anderson, and G. E. Peck, *Drug Dev. Ind. Pharm.*, **7(4),** 371 (1981).

(6) V. L. Anderson and R. A. McLean, "Design of Experiments: A Realistic Approach," Dekker, New York, N.Y., 1974, pp. 40–78, 181–189.

(7) H. Gucluyildiz, G. E. Peck, and G. S. Banker, *J. Chem. Educ.*, **49,** 440 (1972).

(8) S. Diamond, *Clay Miner.*, **8,** 7 (1970).

(9) D. Winslow and S. Diamond, *J. Mater.*, **5,** 564 (1970).

ACKNOWLEDGMENTS

Supported by a grant from Miles Laboratories, Elkhart, IN 46514.

Prediction of Stability in Pharmaceutical Preparations XIX: Stability Evaluation and Bioanalysis of Clofibric Acid Esters by High-Pressure Liquid Chromatography

EDWARD R. GARRETT [x] **and MICHAEL R. GARDNER**

Received February 9, 1981, from *The Beehive, College of Pharmacy, J. Hillis Miller Health Center, University of Florida, Gainesville, FL 32610.* Accepted for publication April 9, 1981.

Abstract □ Specific, sensitive, reversed-phase high-pressure liquid chromatographic assays of clofibric acid esters, clofibrate and etofibrate, and their hydrolysis products, clofibric acid and its monoglycolate and nicotinic acid and its monoglycolate, have been developed in aqueous solution and in biological fluids. Sensitivities of 100 ng/ml of injected mobile phase, a 10-fold increase over existing methods, are reported. Plasma concentrations as low as 200 ng/ml can be analyzed easily in the miscible phase after acetonitrile denaturation. The compounds and their products can be extracted with haloalkane solvents. The extracts were evaporated, reconstituted, and assayed in minimal amounts of mobile phase, resulting in sensitivities of 10 ng/ml of plasma. Conditions are presented that minimize interferences with plasma components. The assay was used to determine the stability of the clofibric acid esters in aqueous solutions, to establish log k–pH profiles at various temperatures, and to evaluate Arrhenius parameters. Hydrolysis was by specific acid–base catalysis. The initial product of etofibrate solvolysis at pH > 6 is the monoglycol ester of clofibric acid; at pH < 3, it is the monoglycol ester of nicotinic acid. Clofibric acid esters are highly unstable to mild alkali (1–3 hr at pH 10 and 30°); even in the estimated pH range of maximum stability, they have half-lives of 100–200 days at 30°. They have half-lives of 4–7 min at 37.5° in fresh dog plasma, and data presented indicate that clofibric acid monoglycolate is an inital product of etofibrate solvolysis.

Keyphrases □ Clofibric acid—esters, stability evaluation and bioanalysis by high-pressure liquid chromatography □ High-pressure liquid chromatography—stability evaluation and bioanalysis of clofibric acid esters □ Stability—prediction and bioanalysis using high-pressure liquid chromatography, clofibric acid esters

The pharmacokinetics of clofibrate, the ethyl ester of clofibric acid, a drug that decreases cholesterol and triglyceride levels (1–4), has not been reported. Only the derived clofibric acid (Scheme I), presumably the only observable material in plasma from clofibrate administration, has been monitored in plasma and urine.

BACKGROUND

Thorp (1) stated that clofibrate was rapidly hydrolyzed by tissue and serum to clofibric acid. His assay was of low sensitivity and was based on spectrophotometric determination in dilute alkali of p-chlorophenol. Subsequent authors (5–7) stated that clofibrate was rapidly hydrolyzed during or after absorption.

GLC assays of clofibric acid have shown sensitivities of 1 μg/ml of plasma (8–10). Recently, a GLC method was proposed (11) for the simultaneous assay of clofibric acid and clofibrate with a sensitivity limit of 10 μg/ml. It was proposed that sensitivity could be increased to 1 μg/ml by evaporation and reconstitution in less solvent.

An evaluation of potential toxicity of the clofibric acid product of clofibrate led to temporary withdrawal of clofibrate from the market in 1979 (12). This fact renewed interest in other clofibric acid esters such as etofibrate (Scheme II), a glycol diester of clofibric acid and nicotinic acid, another hypolipidemic agent. It was postulated that efficacy could be effected through the intact molecule or the monoglycolate esters rather than through the biohydrolytic release of clofibric acid, the presumed source of the adverse reaction (12, 13).

Differences in hypolipidemic effects between clofibrate and etofibrate and possible differences in their rates of clofibric acid release *in vivo* had been discerned (12). The monoester products of microsomal transformations (Scheme II) and their etofibrate precursor were characterized by TLC, GLC, and mass spectroscopy (12), and studies were conducted on their stabilities to GI and blood esterases (13).

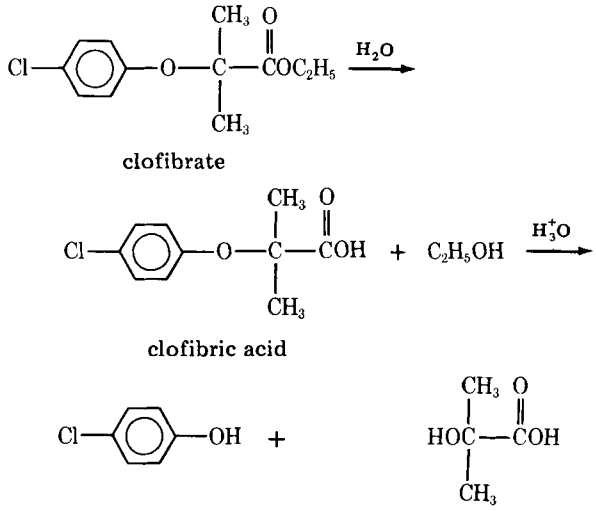

Scheme I—Hydrolysis of clofibrate.

This paper presents specific and simultaneous assays of clofibrate, clofibric acid, and etofibrate and its monoesters (Schemes I and II). The high-pressure liquid chromatographic (HPLC) and extracting techniques developed resulted in sensitivities of 10 ng/ml of plasma, a 100-fold increase over existing methods. The determination of the partitioning of these compounds into organic solvents as a function of pH permitted optimal extraction conditions. The methods were applied to the determination of the log k–pH stability profiles of the clofibric acid esters and their stabilities in plasma. Optimum conditions were established for their assays in biological fluids where transformations during storage and analysis did not occur.

EXPERIMENTAL

Materials—The following analytical grade materials were used: di-[1] and monobasic sodium[2] and potassium[3] phosphates, anhydrous sodium acetate[2], acetic acid[2], volume concentrates of sodium hydroxide and hydrochloric acid[4], boric acid[1], ACS methylene chloride[5], and GLC, TLC, and UV grade chloroform and acetonitrilie[6]. Pure (GLC and TLC) clofibrate, etofibrate, clofibric acid, nicotinic acid, and clofibric acid monoglycolate reference standards[7] were used as received. The nicotinic acid monoglycolate[7] contained 5% glycol dinicotinate by TLC and GLC since further purification by distillation was not possible. The monoester

[1] Baker analyzed reagent, J. T. Baker Chemical Co., Phillipsburg, N.J.
[2] Mallinckrodt Chemical Works, St. Louis, MO 63160.
[3] Fisher Scientific Co., Chemical Manufacturing Division, Fair Lawn, N.J.
[4] Harleco, Philadelphia, PA 19143.
[5] Mallinckrodt, Paris, KY 40361.
[6] Burdick & Jackson Laboratories, Muskegon, MI 49442.
[7] Clofibrate, batch 12976, analysis 1349; clofibrate, batch 12479, analysis 3579; clofibric acid, batch 1517, analysis F 1341; nicotinic acid, batch 22179, analysis F5951; clofibric acid monoglycolate, batch VR 27679; and nicotinic acid monoglycolate, batch 27679 Merz and Co., Chemische Fabrik, Eckenheimer Landstrasse 100, 6000 Frankfurt (Main), West Germany.

0022-3549/82/0100-0014$01.00/0

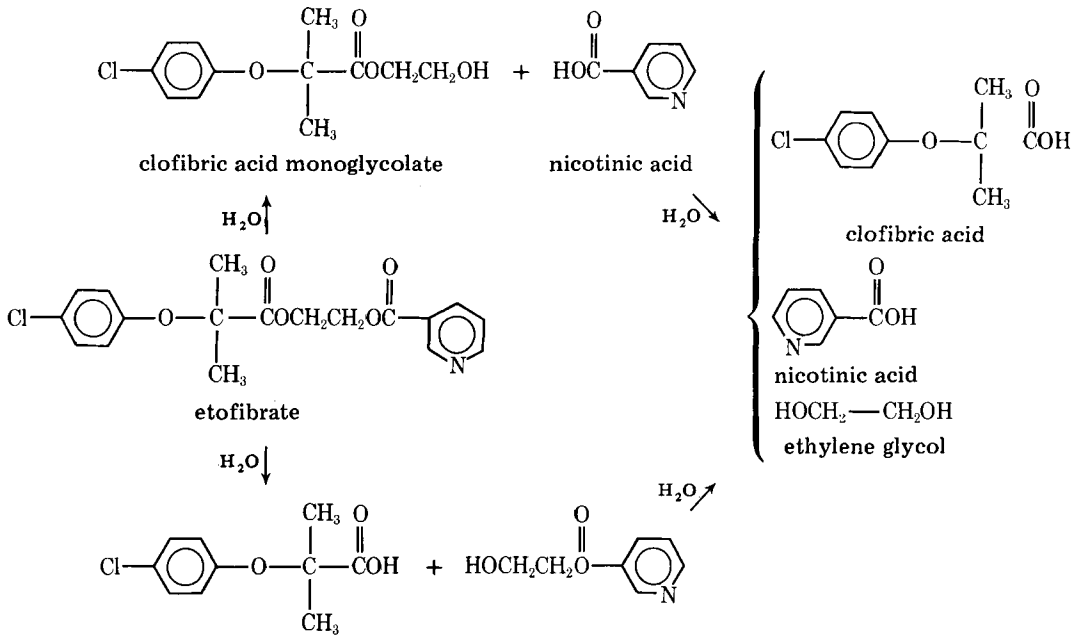

Scheme II—Pathways of etofibrate hydrolysis.

is thermolabile, and considerable transesterification takes place at distillation temperatures.

Apparatus—A high-pressure liquid chromatograph[8] equipped with a variable wavelength UV detector[8] was used with a reversed-phase alkylphenyl column[9] and a radial compression C_{18} reversed-phase column[10]. A guard column[11] was used. Areas under the chromatogram peaks were measured by an integrator[12].

HPLC Procedures—Prepared buffer solutions of sodium acetate of known molarity were adjusted to a measured pH with acetic acid and filtered through a 0.45-μm filter. Solutions were generally 0.10 or 0.05 *M* and were adjusted to pH 3.74 or 3.5, respectively. The mobile phases were mixtures of this buffer and acetonitrile or methanol. Their composition and the HPLC conditions and retention times of various substances are given in Table I. The mixed mobile phase was degassed under vacuum with simultaneous ultrasonication for 1 min.

The variable-wavelength detector was adjusted to 225 nm for the simultaneous analysis of clofibrate and clofibric acid or of etofibrate, clofibric acid monoglycolate, and clofibric acid. The maximum absorbance of clofibrate and clofibric acid was 223.5 nm with a weak absorbance maximum at 277 nm and a negligible absorbance at 254 nm in water. The detector was set in the 263–268-nm range for the simultaneous analysis of nicotinic acid and nicotinic acid monoglycolate where the solvent peaks had less interference than at 225 nm. Both nicotinic acid and its monoglycolate had maximum absorbances at 263 and 225 (or less) nm in mobile phase III with a minimal absorbance at 238 nm.

Solubilities of Clofibric Acid Esters—Plots of the spectrophotometric absorbance of clofibrate in water at its λ_{max} of 223.5 nm against molecular concentration at room temperature showed an initial straight line through the origin of slope 1138, the molar absorptivity. Absorbance at higher concentrations was characterized by a line of slope 67.4 and an intercept of 0.42 absorbance. These two straight line segments intersected at a clofibrate concentration of 4.0×10^{-4} *M*, which was the solubility of clofibrate in water at room temperature. A previously reported (13) solubility was 0.004% (1.65×10^{-4} *M*) at 22° in pH 7.4 phosphate buffer.

Etofibrate (1 mg) was added to 10 ml of various solutions in the pH 1–11 range (theoretically 2.75×10^{-4} *M*). The solutions were vortexed and filtered in a 0.45-μm syringe system. An aliquot (1.00 ml) of the filtrate was diluted to 3.00 ml with acetonitrile that was 1.69×10^{-4} *M* in the internal standard, thymol. A 25-μl aliquot was injected onto HPLC System III (Table I), and the etofibrate concentration was determined from a prepared calibration curve, concentration *versus* peak height ratio, of etofibrate to thymol.

At room temperature, the solubility of etofibrate, pKa 6.41 (12), at pH values ≥ 4 was 2.0×10^{-5} *M* with solubilities of 3.8×10^{-5} *M* at pH 3, 1.99×10^{-4} at pH 2, and $> 2.5 \times 10^{-4}$ *M* at pH 1. A previously reported (13) solubility was 0.002% (5.5×10^{-5} *M*) at 22° in pH 7.4 phosphate buffer. Thus, the best procedure in alkaline stability studies at 20–30° was to add pH 2 solutions of etofibrate to the reaction solutions at the higher pH values so that the final concentration was $\sim 10^{-5}$ *M* in etofibrate.

The solubility of clofibric acid monoglycolate was reported previously (13) as 0.4% (0.0155 *M*) in pH 7.4 phosphate buffer.

Hydrolysis Kinetics—Weighted amounts of clofibrate, sufficient to give $1.4–3.8 \times 10^{-4}$ *M* clofibrate solvents in 10 ml of solvent or $2.9–3.3 \times 10^{-4}$ *M* etofibrate in 20 ml of hydrochloric acid, were dissolved with vortexing in buffer thermally preequilibrated at the reaction temperature. Aliquots (50 and 200 μl for clofibrate and etofibrate acid solvolysis, respectively) were taken at timed intervals and mixed with reaction-quenching solution (50 and 400 μl for clofibrate and etofibrate acid solvolysis studies, respectively), which contained the internal standard, morphine sulfate for clofibrate studies and thymol for etofibrate. The quenching solution had sufficient hydrochloric acid or sodium hydroxide and acetate buffer solution to adjust the final pH of the quenched solution to the 4–5 range of high stability.

Either a 25% methanol concentration in, or mobile phase composition of, the quenched solution of the clofibrate solvolysis studies gave a finer separation of the solvent front from clofibric acid in the chromatogram of System I (Table I). The quenched solution for all etofibrate studies in acid solution always had the same composition as the mobile phase and was injected onto System III. In these clofibrate studies, the total concentrations of clofibric acid and clofibrate in the assayed quenched solutions were $0.7–2.0 \times 10^{-4}$ and $2–5 \times 10^{-5}$ *M* in morphine, respectively. The total concentration of etofibrate and its acid solvolysis products was 1×10^{-4} *M* in the assayed quenched solution and 1.75×10^{-4} *M* in thymol.

The samples were tightly capped and kept refrigerated until inserted in the automatic injector to inject 25 μl. Some fast reaction studies in the alkaline range were effected by vigorous mixing, for a few seconds, 5 ml of thermally preequilibrated stock solutions of clofibrate with 5 ml of thermally equilibrated sodium hydroxide of twice the concentration desired in the final reacting mixture to be maintained in the constant-temperature bath.

System II (Table I) was used for the clofibrate solvolysis studies in borate buffer (pH 9–10 at 60°) and in 0.01, 0.03, and 0.06 *N* NaOH at 30° and for all other solvolysis studies for etofibrate that were not done in acid. The quenching solutions were prepared from concentrated buffer solutions and acetonitrile so that the solvent compositions of the quenched solutions to be injected approached those of the mobile phases.

[8] Model 6000A solvent delivery system and U6K injector equipped with a variable-wavelength UV detector, model 450, and a WISP automatic injector system, Waters Associates, Milford, MA 01757.

[9] μBondapak alkylphenyl, Waters Associates, Milford, MA 01757.

[10] Radial compression RCM 100 with C_{18}, Waters Associates, Milford, MA 01757.

[11] Bondapak Phenyl/Corasil, Waters Associates, Milford, MA 01757.

[12] Hewlett-Packard model 3380A integrator, Avondale, Pa.

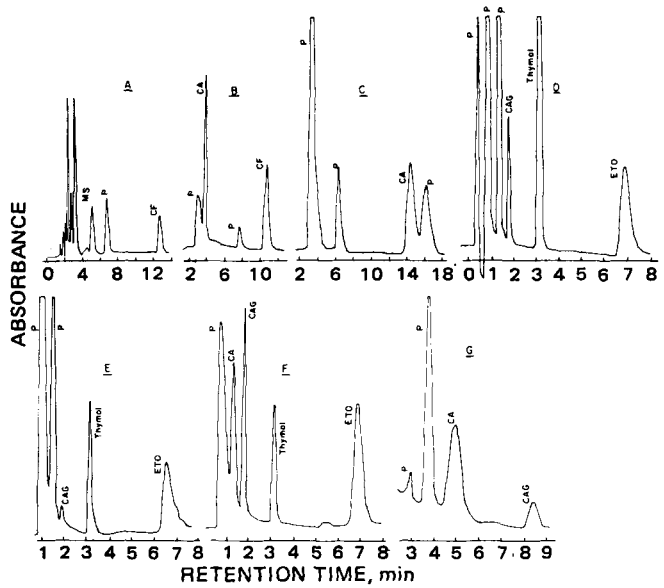

Figure 1—*Reversed-phase chromatograms at 225-nm UV detection for plasma assays of clofibrate (CF), etofibrate (ETO), clofibric acid (CA), clofibric acid monoglycolate (CAG), and the internal standard, thymol or morphine sulfate (MS). The HPLC systems and their mobile phases are given in Table I. Key: A, CF, and CA (6.25 × 10^{-6} M in 1 ml of plasma at pH 2.5, extracted with 4 ml of chloroform of which 2 ml was evaporated and reconstituted in 100 μl of mobile phase that was 3.13 × 10^{-5} M in MS) on System I; B, CF and CA (5 × 10^{-5} M in plasma mixed 1:1 with acetonitrile) on System III; C, CA (2 × 10^{-5} M in 1 ml of plasma at pH 2.5, extracted with 4 ml of chloroform of which 3 ml was evaporated and reconstituted in mobile phase) on System IV; D, assay of ETO degrading for 7.0 min in fresh dog plasma at 37.5° (initially 5.89 × 10^{-5} M in plasma, 0.5 ml adjusted to pH 2.5, extracted with 3 ml of methylene chloride, of which 1 ml was evaporated and reconstituted in 0.75 ml of acetonitrile that was 1.625 × 10^{-5} M in thymol) on System VI; E, assay of ETO degrading for 5.3 min in fresh dog plasma at 37.5° (initially 3.5 × 10^{-5} M in plasma, mixed 1:3 with acetonitrile) on System VI; F, ETO, CA, and CAG (5 × 10^{-5} M in outdated human plasma) and mixed 1:2 with acetonitrile that was 1.625 × 10^{-5} M in thymol) on System VI; and G, assay of ETO degrading for 12 min in fresh dog plasma (initially 5 × 10^{-5} M in plasma, mixed 1:3 with acetonitrile) on System VII.*

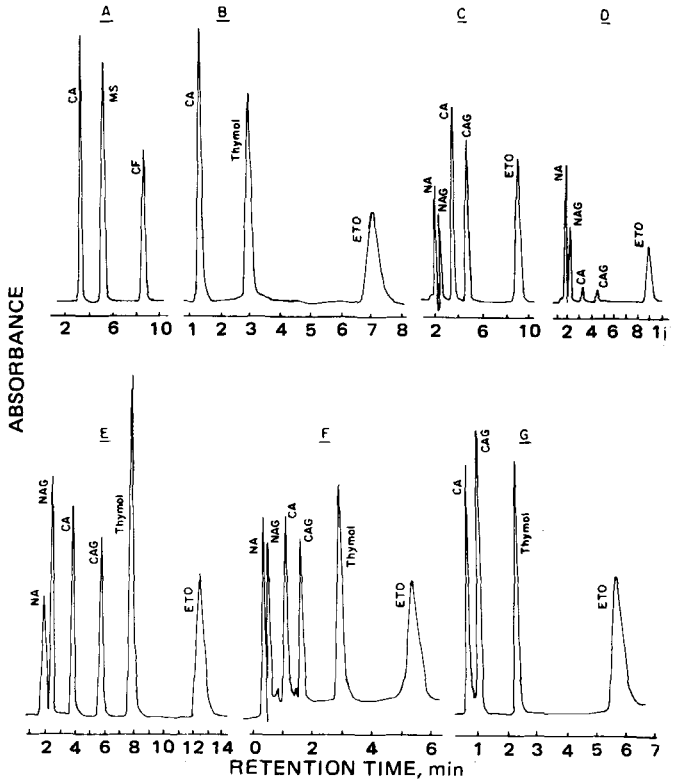

Figure 2—*Reversed-phase chromatograms at 225-nm UV detection (unless stated otherwise) of clofibrate (CF), etofibrate (ETO), clofibric acid (CA), clofibric acid monoglycolate (CAG), nicotinic acid monoglycolate (NAG), nicotinic acid (NA), and the internal standards, morphine sulfate (MS) and thymol, injected into the mobile phase. The HPLC systems and their mobile phases are given in Table I. Key: A, CF and CA (2.5 × 10^{-5} M) and MS (2.94 × 10^{-5} M) on System I; B, CF and CA (7.5 × 10^{-6} M) and thymol (1.63 × 10^{-5} M) on System II; C and D, NA, NAG, CA, CAG, and ETO (2.5 × 10^{-4} M) on System I (225 and 263 nm, respectively); E, NA, NAG, CA, CAG, and ETO (5 × 10^{-5} M) and thymol (1.75 × 10^{-4} M) on System III; F, NA, NAG, CA, CAG, and ETO (5 × 10^{-6} M) and thymol (1.625 × 10^{-5} M) on System II; and G, ETO, CA, and CAG (7.5 × 10^{-6} M) and thymol (1.625 × 10^{-5} M) in System VI.*

Table I—Composition, Conditions, and Retention Times of Clofibrate (CF), Clofibric Acid [a] (CA), Morphine Sulfate (MS), Thymol, Etofibrate (ETO), Clofibric Acid Monoglycolate (CAG), Nicotinic Acid Monoglycolate [b] (NAG), and Nicotinic Acid [b] (NA) in Various HPLC Systems [c]

HPLC [d] System	Mobile Phase	Flow Rate, ml/min	Pressure psi	Column	Typical Retention Times, min: CF	ETO	CA	CAG	NAG	NA	MS	Thymol	Plasma Interferences
I	50:50 acetonitrile–0.1 *N* acetate, pH 3.75	1.5	700	Akylphenyl	10.7	—	3.37	—	—	—	4.68	—	<3.75
II	50:50 acetonitrile–0.05 *N* acetate, pH 3.5	6.0	900	RCM 100 C_{18} (8-mm i.d.)	9.2	5.4	1.20	1.65	0.51	0.35	—	3.10	<3.0
III	45:55 acetonitrile–0.1 *N* acetate, pH 3.75	1.5	750	Alkylphenyl	10.6	12.05	3.92	5.83	2.43	1.93	4.71	7.78	<2.65, 7.55
IV	35:65 methanol–0.1 *N* acetate, pH 3.75	1.5	1600	Alkylphenyl	>40	—	14.4	—	—	—	6.51	—	<4.2 6.30, 16.23
V	50:50 methanol–0.05 *N* acetate, pH 3.50	3.0	1500	RCM 100 C_{18} (5-mm i.d.)	—	>40	5.4	—	<0.3	<0.3	—	—	0–2, 7–8
VI	50:50 acetonitrile–0.05 *N* acetate, pH 3.50	3.0	1000	RCM 100 C_{18} (5-mm i.d.)	—	5.8	0.6	1.35	—	—	—	2.5	0–1
VII	30:70 acetonitrile–0.5 *N* acetate, pH 3.50	3.0	600	RCM 100 C_{18} (5-mm i.d.)	—	—	5.1	8.6	—	—	—	—	0–1.5, 3.8

[a] Additional studies were performed for clofibric acid using the alkylphenyl column. The systems all had plasma interferences with clofibric acid and were, with (parenthetical) retention times (minutes) of clofibric acid: 50:50 acetonitrile–0.1 *N* acetate, pH 7 (1.8); 40:60 acetonitrile–0.1 *N* acetate, pH 3.75 (4.21); 50:50 methanol–0.1 *N* acetate, pH 3.75 (5.62); and 50:50 methanol–0.1 *N* acetate, pH 7.0 (3.36), with plasma interferences at 2.49, 3.47, 4.03, and 7.08 min. Some separation was effected with 40:60 methanol–0.1 *N* acetate, pH 3.75 (8.97) with plasma peaks at 4.81, 5.83, and 7.56 min. System IV gave the best separation of clofibric acid and plasma peaks that interfered with the peak for morphine. [b] Nicotinic acid and nicotinic acid monoglycolate were better separated on the RCM 100 C_{18} column with 35:65 acetonitrile–0.05 *N* acetate, pH 3.5, with retention times of 0.60 (NA), 1.00 (NAG), 2.50 (CA), and 3.25 min (CAG) where ETO and thymol hung up on the column. [c] All peaks were detected spectrophotometrically at 225 nm, except that NAG and NA were detected at 266 nm. [d] Fifty microliters were injected into Systems II and V–VII; 25 μl was used in the other systems.

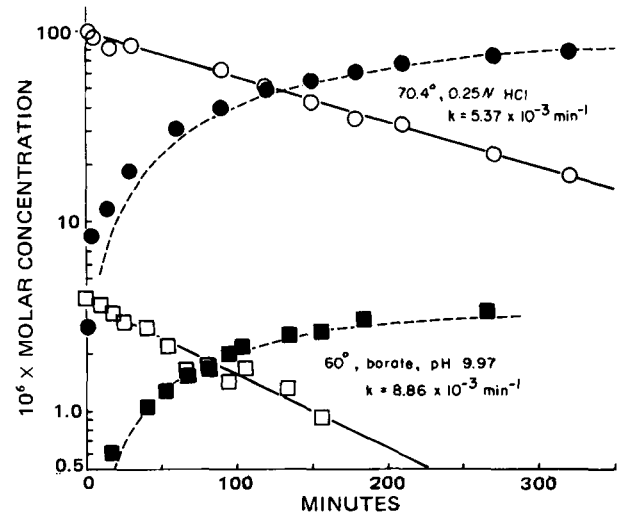

Figure 3—*Semilogarithmic plots of clofibrate (solid line) and clofibric acid (dashed line) concentrations* versus *time for solvolyses in the acidic (System I) and buffered regions (System II). The samples were injected in pH 4–5 mobile phase. The clofibric acid concentrations were fitted to [clofibric acid] = C_∞ (1 − e^{-kt}), where C_∞ is the clofibric acid concentration formed at infinite time and* k *(Table III) is the apparent first-order rate constant for the first-order degradation of clofibrate.*

This procedure minimized negative injection peaks.

In these clofibrate studies, the total concentrations of clofibrate and clofibric acid in the degrading and quenched solutions were 6.91 and 3.46 × 10^{-4} *M*, respectively. The maximum concentrations of etofibrate and its solvolysis products in the degrading solutions at higher temperature and in the quenched solution were 4 and 1 × 10^{-5} *M*, respectively. Etofibrate was maintained in solution under these conditions.

Calibration curves, usually at 1.0–40 × 10^{-5} *M* clofibrate (Systems I and III) or 0.1–1.25 × 10^{-5} *M* clofibrate (System II), were constructed with appropriate amounts of concentrated stock solutions of clofibrate, clofibric acid, etofibrate, clofibric acid monoglycolate, nicotinic acid monoglycolate in acetonitrile, nicotinic acid in pH 5 acetate buffer, and either thymol (acetonitrile) or morphine sulfate (aqueous as internal standards in 2 ml of mobile phase. Either 25 or 50 μl was injected onto the HPLC systems (Table II).

Buffer Solutions for Solvolyses Studies—Phosphate buffers were prepared by mixing 0.10 *N* (for clofibrate solvolyses) and 0.05 *N* (for etofibrate solvolyses) mono- and dibasic potassium phosphate to obtain the desired pH. Borate buffers were prepared by mixing 0.10 or 0.05 *N* boric acid and sodium borate, or by mixing 0.025 *N* boric acid with concentrated sodium hydroxide to an appropriate pH. Appropriate amounts of sodium chloride were added to maintain 0.1 ionic strengths.

The pH meter was standardized at the reaction temperature with two standard buffers with known pH values at that temperature that straddled the pH of the desired reaction solution. The pH values of the prepared buffered solutions were read at the reaction temperature.

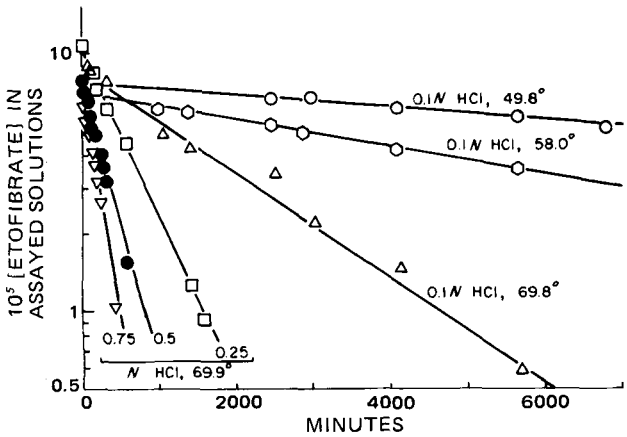

Figure 4—*First-order plots of etofibrate concentrations in hydrochloric acid* versus *time. The reacting solutions before dilution for injection on System III and pH 4–5 mobile phase were 2.9–3.3* × 10^{-4} M.

Partition Studies as Functions of pH—Solutions of 1.25 × 10^{-5} *M* clofibric acid and clofibrate, separate and in combination, were prepared in 0.1 and 0.01 *N* HCl, in 0.1 *N* acetate buffer adjusted to pH 3.0, 4.0, and 5.0, and in 0.1 *N* phosphate buffer adjusted to pH 6.0 and 7.0. Aliquots (2 ml) were extracted with 2 ml of methylene chloride with 5 min of mild shaking. After centrifugation for 5 min, the aqueous layer was removed by aspiration. Then 1 ml of the organic layer was evaporated under nitrogen in a reaction vial and reconstituted in 100 μl of acetonitrile–water containing morphine sulfate (3.13 × 10^{-5} *M*) as an internal standard; 25 μl was injected onto the HPLC system with mobile phase I (Table I).

The quantity extracted was determined from a calibration curve (Table II). Clofibric acid was extracted 102 ± 5% at pH 1–4, 60% at pH 5, 16% at pH 6, and 0 and 0.3% at pH 7.0 when alone and admixed with clofibrate. Clofibrate was extracted 85 ± 3% over this pH range with no significant effects when alone; but when combined with clofibric acid, it showed only 20% extraction.

When 1.00 ml of pH 2.5 aqueous solution containing 1.25 × 10^{-5} *M* clofibric acid and clofibrate was extracted with 4 ml of methylene chloride, analysis revealed that 104 ± 4% of the clofibric acid and 57 ± 2% of the clofibrate were extracted. When 1.00 ml of plasma adjusted to pH 2.5 was used, there was an interference of the plasma with the clofibric acid peak, but the recovery of clofibrate was similar.

When the same procedure was used on spiked pH 2.5 aqueous solution with chloroform as the extracting solvent, 78 ± 3% of the clofibrate and 95 ± 2% of the clofibric acid were extracted. From pH 2.5 plasma, 89% of the clofibrate was extracted, whereas the plasma impurity interfered with the clofibric acid assay.

Similar studies were made on 2 ml of buffer solutions that were 5.56 × 10^{-6} *M* each in etofibrate and clofibric acid and its monoglycolate at unit pH intervals of 1–10. Each buffer solution was extracted with 3 ml of methylene chloride by shaking for 10 min, aspirating off the aqueous phase, and evaporating under nitrogen 2 ml of the methylene chloride layer. The residue was reconstituted in 500 μl of mobile phase that was 1.50 × 10^{-5} *M* in the compounds and 1.63 × 10^{-5} *M* in thymol. A 50-μl aliquot was injected using System II. All of the etofibrate and clofibric acid monoglycolate was extracted at pH 2–10, with 77% of the etofibrate extracted at pH 1.0. The clofibric acid extraction was 97–100% at pH 1–4, 69.5% at pH 5, 20.3% at pH 6, and negligible at pH ≥7.

Assays of Clofibrate and Clofibric Acid in Plasma—*Procedure A: Acetonitrile Deproteinization of Plasma*—Acetonitrile (0.5 or 1.0 ml) was added to an equal volume of human or dog plasma. The mixture was vortexed and centrifuged for 10 min at 3000 rpm; the internal standard morphine sulfate was added to the supernate, and 25 μl was injected in System I (Fig. 1A) or III (Table I). The latter system adequately, but not completely, separated the peak of a plasma impurity and clofibric acid in this procedure (Fig. 1B) but gave a good calibration curve for both (Study F, Table II) at plasma concentrations of 5.0–40 × 10^{-5} *M*. When such acetonitrile-denatured plasma was stored overnight and reassayed,

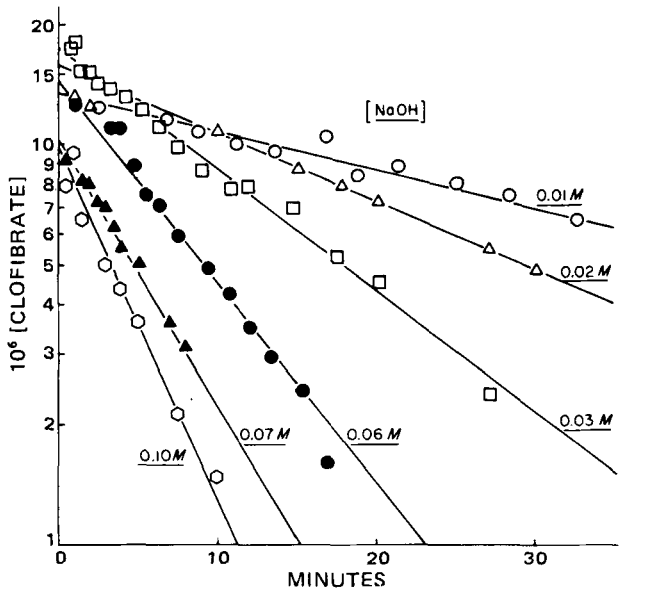

Figure 5—*First-order plots of clofibrate concentrations* versus *time at 30° in various concentrations of sodium hydroxide (System I at 0.02, 0.07, and 0.10* M *NaOH and System II at 0.01, 0.03, and 0.06* M *NaOH).*

Table II—Typical Statistics[a] of HPLC Assays of Clofibrate (CF), Clofibric Acid (CA), Clofibric Acid Monoglycolate (CAG), Etofibrate (ETO), Nicotinic Acid Monoglycolate (NAG), and Nicotinic Acid (NA) in Accordance with $10^5\ C \pm s_{10^5 c.x} = (m \pm s_m)X + b \pm s_b$

Study	HPLC System	$10^5\ M$ Range	Compound	Clofibrate Study X^b	$s_{10^5 c.x}$	m	s_m	b	s_b	n	xxx in $r^2 = 0.99xxx$
A	I	2.5–25	CF	PHR	0.64	7.00	0.26	−1.16	0.54	4	735
		2.5–40	CA		0.51	4.62	0.08	−1.41	0.37	5	992
		2.5–40	CF	10^{-3}PA	0.63	0.01096	0.00022	−0.76	0.44	5	882
			CA		0.37	0.00987	0.00012	−2.09	0.27	4	970
		2.5–40	CF	PAR	0.10	6.44	0.21	−0.44	0.07	5	997
			CA		0.28	5.71	0.05	−1.78	0.21	4	982
B	I	1.0–20	CF	PHR	0.09	6.17	0.03	−0.17	0.06	6	988
			CA		0.16	3.41	0.03	−0.13	0.11	6	965
C	II	0.1–1.0	CF	PH	0.007	0.1929	0.0019	−0.010	0.006	5	972
		0.1–1.25	CA		0.017	0.0627	0.0012	−0.0003	0.017	5	897
		0.1–1.0	CF	PHR	0.007	1.696	0.017	−0.019	0.006	5	971
		0.1–0.75	CA		0.0096	0.585	0.011	−0.028	0.010	4	926
D	II	0.1–1.25	ETO	PH	0.021	0.116	0.003	0.02	0.02	6	813
				PHR	0.039	0.982	0.039	0.04	0.03	6	387
		0.1–1.25	CAG	PH	0.008	0.0725	0.0006	−0.003	0.006	6	977
				PHR	0.011	0.628	0.007	0.0009	0.009	6	947
		0.1–1.25	CA	PH	0.016	0.0643	0.0011	−0.006	0.013	6	892
				PHR	0.017	0.557	0.009	0.005	0.013	6	887
		0.1–1.25	NAG	PH	0.020	0.123	0.003	−0.010	0.016	6	833
				PHR	0.027	0.372	0.010	−0.03	0.01	6	709
		0.1–1.25	NA	PH	0.048	0.109	0.005	−0.04	0.04	6	058
				PHR	0.030	0.335	0.010	−0.07	0.03	6	628
E	III	1–10	ETO	PH	0.35	0.91	0.03	−0.13	0.27	5	503
		1–12.5	ETO	PHR	0.34	12.96	0.44	−0.08	0.26	6	535
				10^{-3}PA	1.25	0.0308	0.0040	1.11	0.86	6	600[c]
				PAR	0.27	7.81	0.22	−0.04	0.21	6	697
		1–12.5	CAG	PH	0.29	0.72	0.02	−0.23	0.23	6	666
				PHR	0.90	11.13	0.93	−1.16	0.70	6	289[d]
				10^{-3}PA	0.29	0.0566	0.0017	−0.23	0.23	6	649
				PAR	0.33	12.82	0.43	−0.17	0.25	6	560
		1–12.5	CA	PH	0.26	0.61	0.02	0.05	0.20	6	725
				PHR	0.24	8.70	0.21	0.09	0.18	6	759
				10^{-3}PA	0.24	0.0506	0.0012	0.03	0.18	6	765
				PAR	0.20	11.48	0.23	0.09	0.15	6	838
		1–12.5	NAG	PH	0.40	1.34	0.05	−0.25	0.32	6	346
				PHR	0.33	4.76	0.16	−0.09	0.25	6	562
				10^{-3}PA	0.25	0.208	0.005	−1.09	0.21	6	752
				PAR	0.28	10.84	0.31	−0.20	0.22	6	671
		1–12.5	NA	PH	0.26	1.28	0.03	−0.14	0.21	6	713
				PHR	0.19	4.53	0.09	0.03	0.15	6	847
				10^{-3}PA	0.42	0.163	0.009	0.05	0.44	5	151
				PAR	0.08	9.74	0.08	−0.44	0.07	6	972
F	III	5.0–40[e]	CF	PH	1.09	2.72	0.10	−1.84	1.00	5	568
			CA		0.59	1.55	0.03	−2.93	0.56	5	876
			CF	PHR	1.44	11.5	0.58	−1.55	1.3	5	247
			CA		1.00	6.55	0.23	−2.68	0.94	5	637
G	IV	0.25–2.0[f,g]	CA	PH	0.063	0.45	0.02	−0.13	0.06	5	413
				10^{-3}PA	0.068	0.0016	0.0001	−0.05	0.06	5	315
H	VI	0.4–5.0[h]	ETO	PH	0.21	0.365	0.020	−0.001	0.165	6	831[i]
				PHR	0.26	4.78	0.31	0.11	0.19	6	302[i]
			CAG	PH	0.081	0.2289	0.0047	−0.26	0.07	6	832
				PHR	0.106	3.00	0.08	−0.14	0.08	6	711
			CA	PH	0.160	0.341	0.025	−0.02	0.27	5	973[i]
				PHR	0.101	4.30	0.19	0.26	0.15	5	593
I	VI	0.5–5.0[j]	ETO	PH	0.042	0.465	0.005	−0.07	0.03	6	954
			CAG	PH	0.046	0.305	0.004	−0.05	0.04	6	944
J	VII	0.5–5.0[j]	CAG	PH	0.032	0.357	0.003	−0.26	0.03	6	973
			CA	PH	0.163	0.524	0.022	0.22	0.12	6	303

[a] The concentrations, C, of clofibrate and clofibric acid are the molarities injected into the mobile phase except for Studies F and G. Regressions were performed on $10^5 \times C$. The constants m and b are the slope and intercept, respectively, where $s_{10^5 c.x}$, s_m, and s_b are the standard errors of estimate (14) of $10^5 \times$ concentration on the measured parameter of the slope and intercept, respectively. The dependent variables, X, are the parameters of measurement, *i.e.*, peak height (PH), $10^{-3} \times$ peak area (PA), peak height ratio to that of the internal standard (PHR), and peak area ratio to that of the internal standard (PAR). The values of n and r^2 are the numbers of data pairs and the square of the correlation coefficient, respectively. [b] The internal standard was $5.9 \times 10^{-5}\ M$ morphine sulfate in the injected solutions of Studies A, B, and F; $1.625 \times 10^{-5}\ M$ thymol in Studies C, D, and H; and $1.75 \times 10^{-4}\ M$ thymol in Study E. [c] For $0.93xxx$. [d] For $0.97xxx$. [e] Concentration in original plasma diluted 1:1 with acetonitrile and supernate injected. [f] Concentration in original plasma that was extracted and evaporated, with the residue reconstituted in 100 μl of mobile phase before injection. [g] Plasma components interfered with the peak of morphine. [h] Concentration in original plasma (outdated human) that was diluted 1:2 with acetonitrile and the supernate injected. [i] For $0.98xxx$. [j] Concentration in original dog plasma diluted 1:3 with acetonitrile and the supernate injected. Both Studies I and J were effected on same spiked plasma studies.

the peak height ratios to the internal standard did not change significantly, although the clofibric acid–plasma peak interference was more pronounced.

Clofibric acid concentrations were best determined by injecting another aliquot into System IV (Table I and Fig. 1C), although plasma components did interfere with the morphine sulfate peak.

Procedure B: Chloroform Extraction of Plasma—Plasma (0.5 or 1.0 ml) was extracted with 4 ml of chloroform with mild shaking for 10 min and was centrifuged for 10 min at 3000 rpm. The aqueous layer was aspirated, and 2 or 3 ml of chloroform was evaporated to dryness and reconstituted in 100 μl of mobile phase containing morphine sulfate as the internal standard. This procedure is more sensitive than Procedure A. Aliquots can be injected into Systems I–III for clofibrate assay (Fig. 1A) and into System IV, where plasma interferences are minimized, for clofibric acid assay (Fig. 1C and Study G, Table II).

Assays of Etofibrate and Its Solvolytic Products in Plasma—*Procedure C: Acetonitrile Deproteinization of Plasma*—Acetonitrile, with or without internal standard thymol, was added to 0.5, 1, or 2 ml of

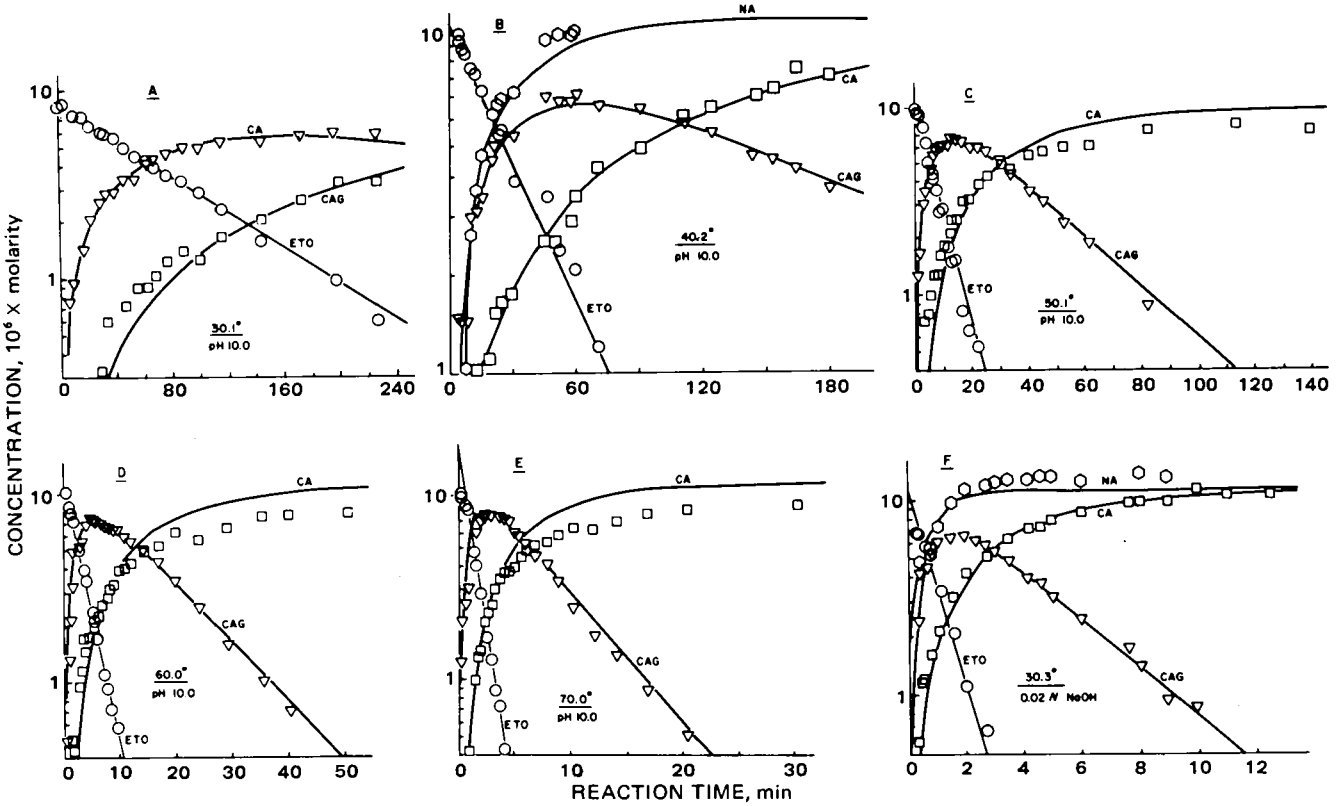

Figure 6—*Semilogarithmic plots of assayed concentrations of etofibrate (ETO), clofibric acid monoglycolate (CAG), clofibric acid (CA), and nicotinic acid (NA)* versus *time for etofibrate degradation in borate buffers and sodium hydroxide. The lines through the CAG, CA, and NA values were calculated from the kinetic parameters given in Table IV.*

human or dog plasma in 1:1, 2:1, 3:2, or 3:1 ratios. The mixture was vortexted and centrifuged for 10 min at 3000 rpm, and an aliquot was injected into Systems II, V, or VI (Table I). At 1:1 and 1:2 mixture ratios, Systems II and VI gave minimal or negligible plasma peak interferences with etofibrate, clofibric acid monoglycolate, and thymol (Fig. 1E) but significant interferences with clofibric acid in fresh dog plasma (Fig. 1E and Study I, Table II). Good calibration curves were established for clofibric acid in outdated human plasma (Fig. 1F and Study H, Table II) at plasma concentrations of $0.4–5.0 \times 10^{-5}$ *M*. Plasma constituents had retention times similar to those of nicotinic acid and nicotinic acid monoglycolate in these systems and thus interfered with their assay.

Clofibric acid in plasma was best assayed separately in System IV (Fig. 1C), V, or VII (Fig. 1G and Study J, Table II) where it was well separated from plasma interferences, although etofibrate was held on the column. The last system could also assay for clofibric acid monoglycolate. Etofibrate-spiked plasma ($1.28 \times 10^{-}$ *M*) diluted 1:2 with acetonitrile showed no change in the etofibrate peak for more than 24 hr.

Procedure D: Methylene Chloride Extraction of Plasma—Plasma (1.0 ml) was adjusted to pH 2.5 with 125 μl of 1 *N* HCl with vortexing, extracted with 3 ml of methylene chloride, shaken at low speed for 10 min, and centrifuged for 10 min at 3000 rpm. The aqueous protein phase was aspirated and discarded. An aliquot of the methylene chloride layer (1.00 ml) was evaporated under nitrogen at room temperature and reconstituted in mobile phase that was 1.625×10^{-5} *M* in thymol, and an aliquot was injected onto System VI. This system assayed for etofibrate and clofibric acid monoglycolate (Fig. 1D) but had plasma peak interferences with the other solvolytic products of etofibrate. Clofibric acid could be assayed by injection of an aliquot into System IV (Fig. 1C), V, and possibly VII (Fig. 1G) where plasma interferences with clofibric acid peaks were minimal.

Clofibric acid could be assayed to 5×10^{-6} *M* concentrations in plasmas by reextracting 1 ml of methylene chloride into 1.00 ml of pH aqueous buffer with System VI.

RESULTS AND DISCUSSION

Reversed-Phase HPLC Assays of Clofibric Acid Esters and Their Products for Degradation Studies—HPLC Systems I–III were used for clofibric acid esters and their degradation products. Typical chromatograms (Studies A–C and F of Table II) are given in Figs. 2A–2G. The aliquots of degrading solutions taken with time were neutralized to the relatively stable region of pH 4–5. The quenched solution had the same composition as the mobile phase used. Morphine sulfate or thymol, added in the quenching solution, were internal standards.

Calibration curves of concentration against peak height, peak areas, and their ratios to the respective parameters of the internal standard showed excellent linear regressions (Table II). In general, it could not be concluded that one measured parameter was significantly better than another.

The standard errors of estimation (14) of clofibrate and clofibric acid concentrations were $\sim 0.6 \times 10^{-5}$ *M* (1.46 μg/ml) and 0.3×10^{-5} *M* (0.64 μg/ml), respectively, for calibration curves prepared with System I (Study A of Table III) in the $2.5–40 \times 10^{-5}$ *M* range (5–100 μg/ml) and indicated analytical sensitivities of 1–3 μg/ml. The standard errors of estimation of concentration of etofibrate and its degradation products were $\sim 0.30 \times 10^{-5}$ *M* (1.0 μg/ml) for calibration curves prepared with System III (Study E of Table II) in the $1–12.5 \times 10^{-5}$ *M* range (3.6–45 μg/ml of etofibrate) and indicated analytical sensitivities of 2.0 μg/ml.

The radial compression systems gave sharper peaks, lessened retention time, and heightened sensitivities for clofibrate, etofibrate, and their degradation products in Systems II and V–VII (Table I) when injected in the mobile phase. The standard errors of estimation of concentrations were $1–2 \times 10^{-7}$ *M* for clofibrate (24–48 ng/ml), etofibrate (36–72 ng/ml), and clofibric acid (21–52 ng/ml) and its monoglycolate (26–52 ng/ml) (Studies C and D of Table II with System II and 225 nm detection) for calibration curves in the $1–12.5 \times 10^{-6}$ *M* range (200–2500 ng/ml). Thus, analytical sensitivities of 100 ng/ml were indicated. System VI gave similar results (Fig. 2G). Solvent front interferences with nicotinic acid and nicotinic acid monoglycolate on these systems at 225-nm detection were minimized at 263-nm detection, but sensitivities were 200–400 ng/ml (Study D of Table II and Figs. 1B and 1F).

Decreased acetonitrile and methanol content in the mobile phase with acetate buffer increased the retention times of all components and permitted separation of clofibric acid from plasma components (Table I). The use of methanol in the mobile phase gave higher retention times than acetonitrile and well-separated plasma components and clofibric acid peaks (Fig. 1C).

Reversed-Phase HPLC Assays of Clofibric Acid Esters and Their Solvolytic Products in Plasma—Partition studies showed that clofibrate, etofibrate, and clofibric acid monoglycolate could be well extracted

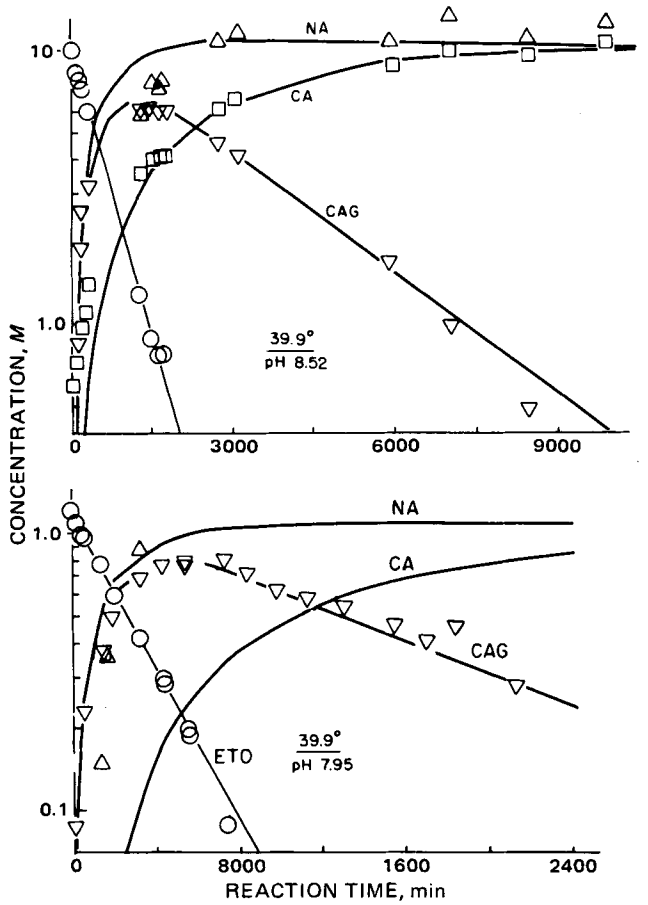

Figure 7—*Semilogarithmic plots of assayed concentrations of etofibrate (ETO), clofibric acid monoglycolate (CAG), clofibric acid (CA), and nicotinic acid (NA)* versus *time for etofibrate degradation in phosphate buffers. The lines through the CAG, CA, and NA values were calculated from the kinetic parameters given in Table IV.*

at a pH > 2 with chloroform or methylene chloride (Procedures B and D). Clofibric acid was completely extracted at pH < 4 and negligible at pH > 7. The haloform extracts could be evaporated to dryness and reconstituted in 100 μl of mobile phase for injection. Assays of clofibrate,

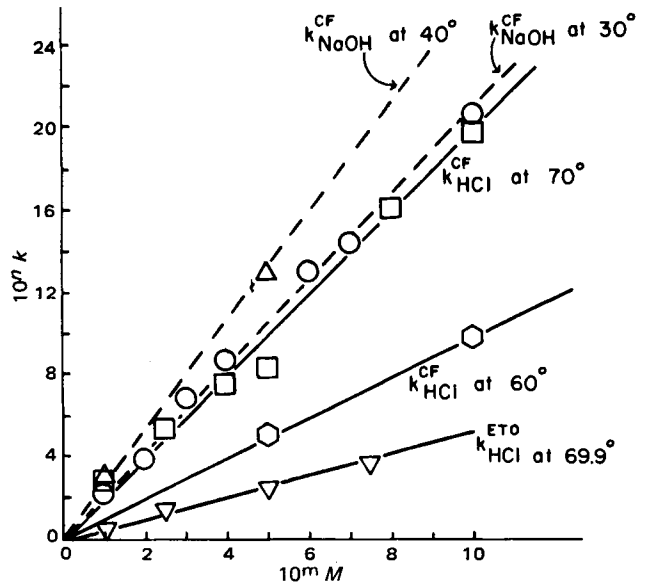

Figure 8—*Plots of first-order rate constants of clofibrate (k^{CF}) and etofibrate (k^{ETO}) hydrolysis* versus *molarities of sodium hydroxide (dashed line, n = 2, m = 2) and hydrochloric acid (solid line, n = 3, m = 1) at several temperatures.*

Table III—First-Order Rate Constants (k, min^{-1}) for the Hydrolysis of Clofibrate

Temperature	Sodium Hydroxide Concentration	10^3k	pH[a]
30.2°	0.010	22.2	11.76
30.5°	0.020	38.9	12.05
30.1°	0.030	69.0	12.23
30.3°	0.040	86.3	12.35
30.1°	0.060	130.5	12.52
29.9°	0.070	144.5	12.58
29.5°	0.100	206	12.73
40.0°	0.010	30.8	11.46
40.0°	0.050	129	12.14
	Hydrochloric Acid Concentration		
61°	0.500	5.0	0.39
60.1°	1.000	9.7	0.12
70.8°	0.100	3.03	1.05
70.4°	0.250	5.37	0.74
70.5°	0.400	7.55	0.54
70.4°	0.500	8.23	0.45
70.4°	0.800	16.1	0.24
70.4°	1.00	19.6	0.13
	Buffer		
60.0°	Phosphate	0.043	6.00
60.0°	Phosphate	0.043	7.00
61.0°	Phosphate	0.349	8.00
60.8°	Borate	1.55	9.01
60.0°	Borate	8.66	9.97
70.0°	Phosphate	0.072	6.00
70.0°	Phosphate	0.110, 0.087	7.00

[a] The pH values for sodium hydroxide and hydrochloric acid solutions were calculated from $pH = pK_w + \log f_{NaOH}[NaOH]$ and $pH = -\log f_{HCl}[HCl]$, respectively, from the pK_w values and activity coefficients, f_{NaOH} and f_{HCl}, available in the literature (15) for the designated temperatures. The pK_w values at respective temperatures were: 13.83, 30°; 13.52, 40°; 13.26, 50°; 13.02, 60°; and 12.78, 70°

etofibrate, and clofibric acid monoglycolate could be effected in Systems I (Fig. 1A), II, III, and VI (Fig. 1D and Table I). While the clofibric acid peaks had retention times similar to plasma components in this system, no such interferences occurred with Systems IV (Fig. 1C), V, and VII (Table I). These extraction procedures with reconstitution with System II and V–VII provided assays sensitive to 10 ng/ml of plasma from 1 ml of plasma.

A more facile, but less sensitive assay used acetonitrile deproteinization of plasma (Procedures A and C). The supernate, after addition of acetonitrile to plasma in 1:1, 2:1, 3:2, or 3:1 ratios, was injected directly into the system. The standard error of estimation of clofibrate and clofibric acid concentrations was 1–1.5 × 10^{-5} M (2–3 μg/ml) for calibration curves prepared with System III (Fig. 1B and Study F of Table II) for plasma concentrations of 5–40 × 10^{-5} M (10–100 μg/ml). Analytical sensitivities of 5–6 μg/ml were indicated.

The use of the radial compression systems increased plasma assay sensitivities *via* acetonitrile denaturation (Figs. 1E–1G). The standard errors of estimation of plasma concentrations of etofibrate and clofibric acid and its monoglycolate were 0.5–2 × 10^{-6} M (100–400 ng/ml) for calibration curves prepared with System VI or VII (Studies H–J of Table II) for plasma concentrations in the 4–50 × 10^{-6} M range (0.8–10 μg/ml). Thus, analytical sensitivities of 0.2–0.8 μg/ml were indicated.

Kinetics of Solvolyses—At constant pH, clofibrate and etofibrate degrade by apparent first-order processes. Representative semilogarithmic plots of concentrations *versus* time are given for hydrochloric acid solutions (Figs. 3 and 4), sodium hydroxide solutions (Figs. 5 and 6), borate buffers (Figs. 3 and 6 and Tables III and IV), and phosphate buffers (Fig. 7), where the apparent first-order rate constant, k, was obtained from the slopes in accordance with:

$$\log C = -\frac{kt}{2.303}t + \log C_0 \qquad \text{(Eq. 1)}$$

where C and C_0 are the concentrations at time t and time zero, respectively.

The pH values of the degrading buffer solutions were experimentally determined at the study temperature. The pH values for hydrochloric acid were calculated from

$$pH = -\log \gamma[HCl] \qquad \text{(Eq. 2)}$$

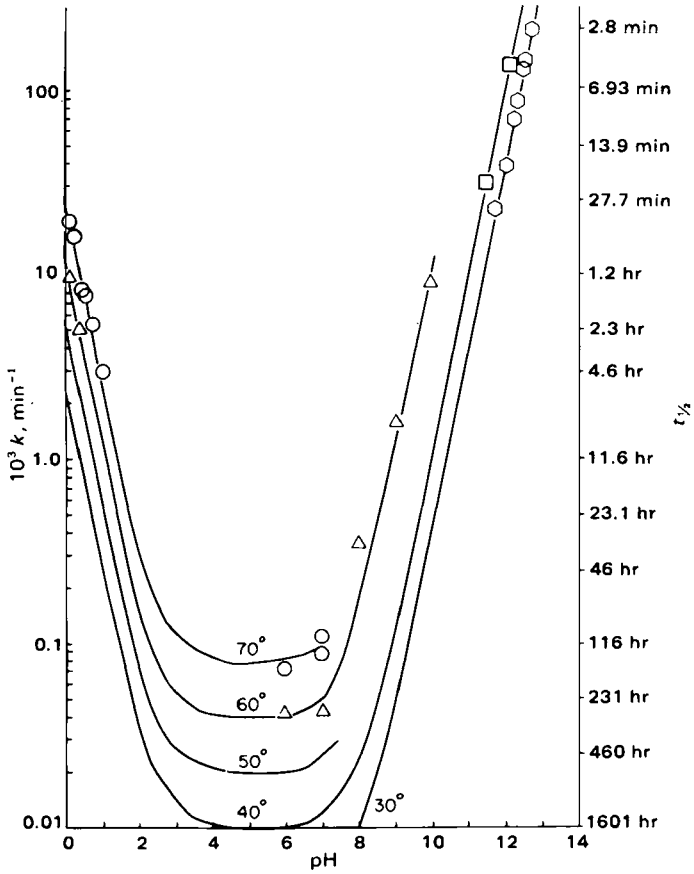

Figure 9—*Fitted log* k–*pH profiles for the hydrolyses of clofibrate at various temperatures. Corresponding half-lives are given on the right.*

where γ is the mean activity coefficient for the hydrochloric acid solution. For sodium hydroxide:

$$pH = pK_w - pOH = pK_w + \log \gamma[NaOH] \qquad \text{(Eq. 3)}$$

where γ is the mean activity coefficient for the sodium hydroxide (15). Values of $pK_w = -\log K_w$ are given in Footnote *f* of Table I; K_w is the hydrolysis constant for water.

The aparent first-order rate constants for clofibrate, etofibrate, or clofibric acid monoglycolate hydrolysis can be characterized in terms of actual concentrations of strong acid or alkali as:

$$k = k_{HCl}[HCl] \qquad \text{(Eq. 4)}$$

and:

$$k = k_{NaOH}[NaOH] \qquad \text{(Eq. 5)}$$

The bimolecular rate constants, k_{HCl} and k_{NaOH}, at various temperatures were obtained from the slopes of plots of k *versus* these concentrations (Table V).

Log *k*–pH Profiles (16) and Solvolysis Routes–When activities of hydrogen, a_H, and hydroxide, a_{OH}, ions are considered as catalytic species:

$$a_H = 10^{-pH} \qquad \text{(Eq. 6)}$$

$$a_{OH} = 10^{-pOH} = 10^{-(pK_w - pH)} \qquad \text{(Eq. 7)}$$

the acid and alkaline branches of the log k–pH profiles (Figs. 9–11) that characterize the attack of hydrogen- and hydroxyl-ion activities, respectively, conform to:

$$\log k = \log k_H - pH \qquad \text{(Eq. 8)}$$

and:

$$\log k = \log k_{OH} + pH - pK_w \qquad \text{(Eq. 9)}$$

The profiles at the temperatures where no studies were made were constructed so as to be consistent with the Arrhenius parameters, ΔH_a and ln P, calculated or determined from the slopes and intercepts of the Arrhenius plots (Fig. 12).

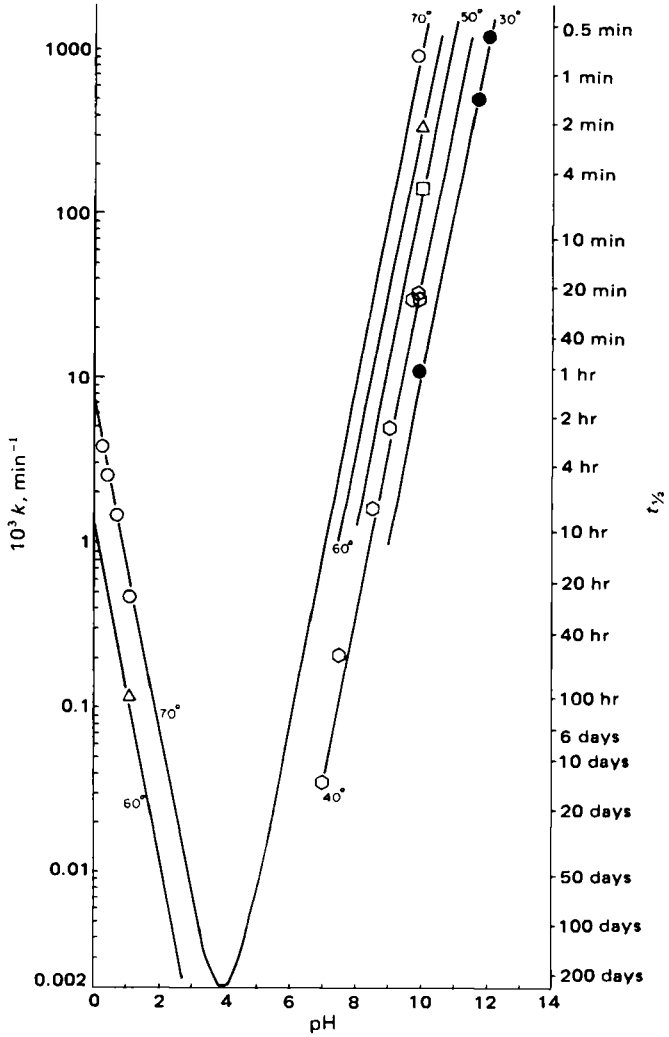

Figure 10—*Fitted log* k–*pH profiles for the hydrolyses of etofibrate at various temperatures. Corresponding half-lives are given on the right.*

The constants are given in Table V and can be used to calculate the apparent first-order rate constant for hydrolysis at any pH and temperature using:

$$k = k_H a_H + k_{OH} a_H + k_0 \qquad \text{(Eq. 10)}$$

when Eqs. 6 and 7 and the Arrhenius equation:

$$\ln k_H \text{ or } \ln k_{OH} = \ln P - \Delta H_a/1.987(1/T) \qquad \text{(Eq. 11)}$$

where T is degrees plus 273° and ΔH_a is in calories per mole, are considered.

A pH-independent component, k_0^{CF}, had to be considered in the case of clofibrate solvolysis (Fig. 9 and Table V) to account for first-order rate constants between pH 6 and 7 that were higher than those predicted from the sum of the extrapolation of the acid and alkaline branches of the clofibrate log k–pH profile.

The predicted minimum in the log k–pH profile for etofibrate (Fig. 10) is probably not exact but should be displaced a few 10ths of a pH unit to the right since etofibrate is protonated in the region of acid solvolysis. In addition, hydrogen-ion attack on a nonprotonated compound would be faster.

Pharmaceutical Significances of Stability Studies—The high solvolytic instability of clofibric acid esters, even in mildly alkaline solutions, requires that the microscopic environment be kept as acidic as possible (pH 4) in the formulation of liquid and solid dosage forms. Alkaline lubricants and excipients should not be used, and granulations should be kept as free of water as possible. Even at 30° and pH 4–6, the half-lives of clofibrate and etofibrate in aqueous solutions are predicted (Figs. 9 and 10) to be 120 and 240–2000 days, respectively; at pH 7, they

Table IV—First-Order Rate Constants (k_1, min^{-1}) for the Hydrolysis of Etofibrate and the Glycol Esters of Clofibric Acid (k',min^{-1}) and Nicotinic Acid (k'', min^{-1})

Temperature	Hydrochloric Acid Concentration	(k'',min^{-1}) 10^3k	$10^3k''$[a]	pH[b]	f[c]
49.8°	0.100	0.055	—	1.11	0.00
58.0°	0.100	0.188	—	1.08	0.00
69.8°	0.100	0.474	—	1.11	0.00
69.9°	0.250	1.46	—	0.74	0.16
69.9°	0.500	2.58	0.75	0.45	0.00
69.9°	0.750	3.76	1.0	0.27	0.05
	Sodium hydroxide concentration		$10^3k'$		
29.5°	0.010	497	175	11.77	1.00
30.3°	0.020	1187	285	12.97	0.90
	Buffer				
30.1°	Borate	10.9	3.0	9.98	0.94
40.2°		32.6	6.37	9.96	0.83
40.2°		30.3	5.70	9.95	0.85
40.2°		29.7	5.00	9.85	0.75
39.9°		4.94	0.962	9.02	1.00
39.9°		1.58	0.290	8.52	0.82
40.0°	Phosphate	0.314	0.0724	7.95	0.95
39.9°		0.206	0.032	7.53	1.00
39.9°		0.035	—	6.94	1.00
50.1°	Borate	138	31	9.98	1.00
59.95°		339	72	10.03	1.00
70.0°		898	160	9.91	1.00

[a] Estimates are crude for the hydrolysis of the glycol ester of nicotinic acid since studies were not carried out long enough. [b] The pH values for sodium hydroxide and hydrochloric acid solutions were calculated from $pH = pK_w + \log f_{NaOH}[NaOH]$ and $pH = -\log f_{HCl}[HCl]$, respectively, from the pK_w values and activity coefficients, f_{NaOH} and f_{HCl}, available in the literature (15) for the designated temperatures. [c] Estimated fraction of clofibrate hydrolyzed to the monoglycol ester of clofibric acid where 1 − f is the estimated fraction hydrolyzed to clofibric acid and the monoglycol ester of nicotinic acid.

would be 160 and 20 days, respectively. Thus, these compounds must be assayed immediately and not stored in samples of biological tissues and fluids. Extraction from plasma into haloalkane solvents or mixing plasma with equivalent volumes of acetonitrile can maintain the integrity of the esters for several days prior to assay.

Routes of Solvolyses—The primary product of clofibrate solvolysis is clofibric acid at all pH values (Fig. 3), although *p*-chlorophenol can be generated in strong acidic solutions (Scheme I).

The routes of etofibrate solvolysis differ for the acidic and alkaline regions. The initial products of acid hydrolysis were nicotinic acid monoglycolate and clofibric acid (Scheme II), and no clofibric acid monoglycolate was observed (Fig. 13). The initial products of solvolyses at pH > 7 were nicotinic acid and clofibric acid monoglycolate, and the latter subsequently hydrolyzed to clofibric acid and ethylene glycol (Figs. 6 and 7). No nicotinic acid monoglycolate was observed within the level of analytical sensitivities.

If the products of etofibrate (ETO) solvolyses in the alkaline region are only clofibric acid monoglycolate (CAG) and nicotinic acid (NA) and if no glycol ester of nicotinic acid (NAG) (Scheme II) is generated, then the concentration of clofibric acid monoglycolate may be calculated from the expression (17):

$$[CAG]' = [ETO]_0 \frac{k}{k' - k}(e^{-kt} - e^{-k't}) \qquad \text{(Eq. 12)}$$

where $[ETO]_0$ is the initial etofibrate concentration and $[CAG]'$ is clofibric acid monoglycolate concentration on the presumption that the sole route of hydrolysis is as shown in Scheme III, where k and k' are the apparent first-order rate constants for the sequential hydrolyses.

$$ETO \xrightarrow{k} CAG + NA \xrightarrow{k'} CA + glycol + NA$$

Scheme III

If nicotinic acid monoglycolate is generated but is so low in concentration that it cannot be observed, Scheme IV could be postulated.

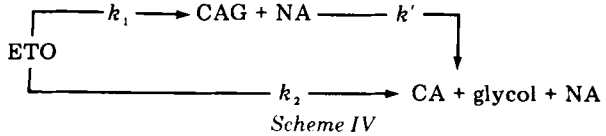

Scheme IV

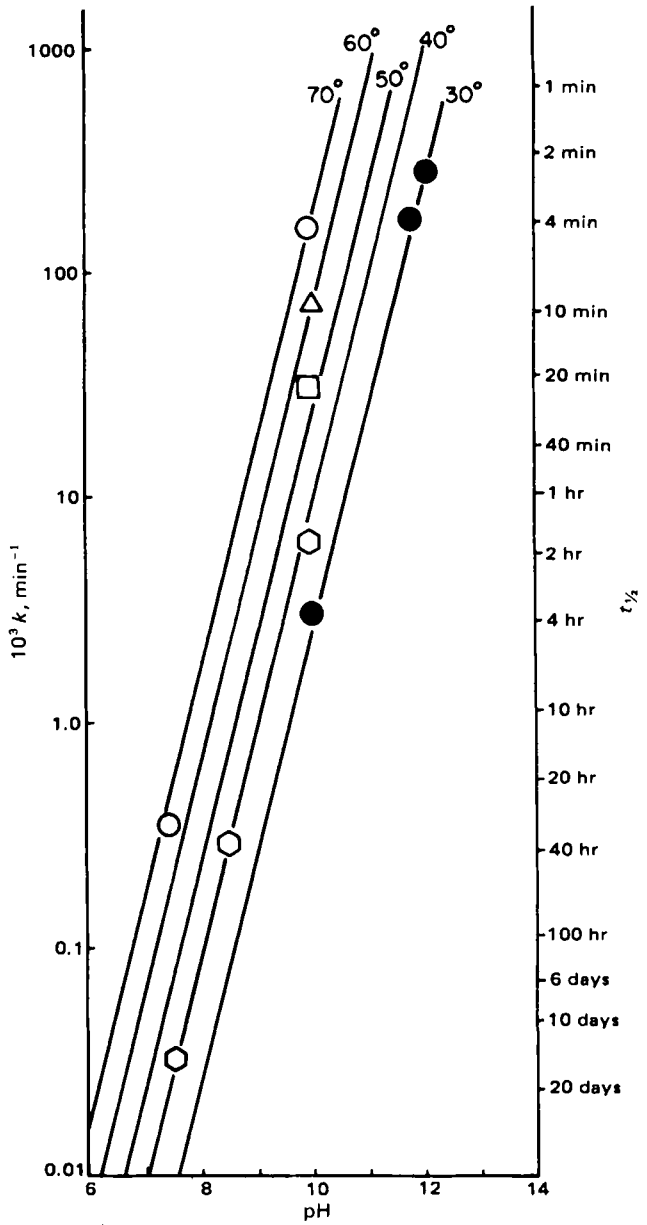

Figure 11—*Fitted log k-pH profiles for the hydrolyses of clofibric acid monoglycolate at various temperatures. Corresponding half-lives are given on the right.*

There is no storage in this form due to its extremely rapid hydrolysis, and $k = k_1 + k_2$ and (18):

$$[CAG] = [ETO]_0 \frac{k_1}{k' - k}(e^{-kt} - e^{-k't})$$

$$= f[ETO]_0 \frac{k}{k' - k}(e^{-kt} - e^{-k't}) \qquad \text{(Eq. 13)}$$

where:

$$f = [CAG]/[CAG'] = k_1/k \qquad \text{(Eq. 14)}$$

This signifies that the ratio, f, of the experimental concentration of clofibric acid monoglycolate to the theoretical concentration, calculated on the premise of no nicotinic acid monoglycolate intermediate, is constant at all specified times.

The apparent first-order rate constant, k', for the solvolysis of clofibric acid monoglycolate could be obtained from the terminal slope of the plots of its generation with time (Figs. 6 and 7) from etofibrate. It was also obtained by the apropriate adjustment of the f and k' values of Eq. 13 that gave the best fit to the time course of generated clofibric acid monoglycolate in Figs. 6 and 7. These values are listed in Table IV and demonstrate that negligible etofibrate is solvolyzed through a nicotinic acid monoglycolate intermediate above a pH of 7. Separate studies of

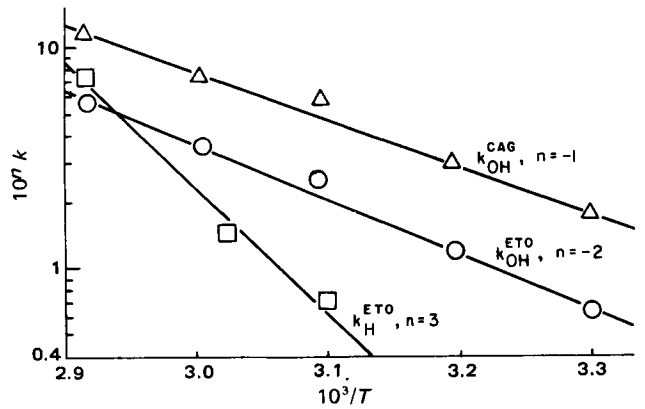

Figure 12—*Arrhenius plots of bimolecular rate constants for the alkaline solvolyses of etofibrate (ETO) and clofibric acid monoglycolate (CAG) and the acid solvolysis of etofibrate (ETO).*

clofibric acid monoglycolate solvolyses at these pH values confirmed the k' values estimated by this procedure. The lines through the concentrations of nicotinic and clofibric acids in Figs. 6 and 7 were drawn in accordance with:

$$[NA] = [ETO]_0 (1 - e^{-k_1 t}) \quad \text{(Eq. 15)}$$

$$[CA] = [ETO]_0 - [ETO] - [CAG] \quad \text{(Eq. 16)}$$

where [CAG] was calculated from Eq. 13.

A similar approach was used to estimate k'', the apparent first-order rate constant at a given pH for the acidic hydrolysis of nicotinic acid monoglycolate (Fig. 13). However, the k'' values given in Table IV are crude estimates since these kinetic studies were not conducted for adequate lengths of time.

Stabilities of Clofibric Acid Esters in Plasma—Clofibrate stability was monitored by HPLC assay in fresh dog plasma. The apparent half-lives of $1–2 \times 10^{-5}$ *M* clofibrate in plasma were 9.75 min at 24° and 4.57 min at 37.6° using Procedure B (Fig. 14). When Procedure A was used for assay of degrading 1.83×10^{-4} *M* clofibrate in fresh plasma at 24.6°, degradation was apparent zero order (7.0×10^{-7} mole/liter/min) and an apparent time for half-degradation was 130 min (curve A of Fig. 15). A similar study by Procedure A, conducted at room temperature, showed a half-degradation time of 125 min for 5.8×10^{-3} *M* clofibrate in fresh plasma. The fact that apparent first-order degradation of clofibrate with an apparent half-life of 10 min at 24° occurs at low concentrations (curve B of Figs. 14 and 15) indicates that the plasma enzymes responsible for clofibrate solvolysis are readily saturated and give slower degradation rates at higher plasma concentrations.

The stability of etofibrate in fresh dog plasma assayed by Procedure C gave apparent half-lives of 4.4 min for 3.6×10^{-5} *M* etofibrate in two separate studies (Fig. 16).

The apparent half-life for an initial plasma concentration of etofibrate ($[ETO]_0 = 5.9 \times 10^{-5}$ *M*), assayed by Procedure D, was 6.9 min ($k = 0.100$ min^{-1}) with an apparent terminal half-life of 11.2 min for clofibric acid monoglycolate solvolyses ($k' = 0.0619$ min^{-1}) (Fig. 16). The maximum peak height ratio of 0.37 for this compound at 10 min corresponded to an approximate concentration of 2.85×10^{-5} *M* clofibric acid monoglycolate. On the assumption that the degradation pathway is solely through clofibric acid monoglycolate (Scheme III), the maximum concentration, $[CAG]_{max}$, can be estimated (17) from:

$$[CAG]_{max} = [ETO]_0 (1/k')(k/k')^{k'/(k'-k)} = 2.7 \times 10^{-5} M \quad \text{(Eq. 17)}$$

The coincidence of this calculated maximum and that experimentally determined provides strong evidence that clofibric acid monogycolate is the primary product of etofibrate solvolysis in plasma.

With Procedure C at 37.5°, 1.19×10^{-4} *M* etofibrate in plasma showed a half-life of 5.7 min ($k = 0.121$ min^{-1}) by the solvolysis route through clofibric acid monoglycolate. The latter had a half-life of 5.8 min (0.119 min^{-1}) when the data were fit as described by Eqs. 13, 14, and 16; $f = 1$ (Fig. 17). Solubility in plasma is expected to be much greater than in buffer due to high protein binding (13). Using Procedure C, clofibric acid monoglycolate, 4.25×10^{-5} *M* in plasma, showed a half-life of 11.5 min (Fig. 17).

Table V—Estimated Kinetic Parameters (16) for the Hydrolyses of Clofibrate (k^{CF}), Etofibrate (k^{ETO}), and the Glycol Esters of Clofibric Acid (k^{CAG}) and Nicotinic Acid (k^{NAG})

Microscopic Rate Constant	30°	40°	50°	60°	70°	ΔH_a	ln P^a
k_{OH}^{CF}[b], liters/mole/min	2.7	3.3	—	—	—	3.8[c]	7.3
k_{NaOH}^{CF}[d]	2.11	2.71	—	—	—	4.8[c]	8.7
$10^3 k_H^{CF}$[b]	—	—	—	12	25	16.2[c]	20
$10^3 k_{HCl}^{CF}$[d]	—	—	—	9.8	20	16.6[c]	20.4
$10^3 k_0^{CF}$[d], min^{-1}	—	—	—	0.04	0.08	16[c]	13.6
k_{OH}^{ETO}[b], liters/mole/min	63.5	119	251	351[f]	554	11.4[a]	23.1
$10 k_H^{ETO}$[b]	—	—	0.70	1.4	7.1	26.4[a]	33.8
k_{OH}^{CAG}[b]	17.9	29.5	59.2	75.3	111.5	9.8[a]	19.1
$10^3 k_H^{NAG}$[b]	—	—	—	—	2.2	—	—
$10^3 k_{HCl}^{NAG}$[d]	—	—	—	—	5.2	—	—

[a] These heats of activation (kilocalories per mole) and ln *P* values were obtained from Fig. 12 in accordance with the Arrhenius function $\ln k = \ln P - (\Delta H_a/R)(1/T)$, where $R = 1.987$ cal/degree and ΔH_a is in calories per mole. The values of k_{OH}^{ETO} obtained from the best linear fit of this function were used in the log *k*–pH profile at 50 and 70° and were 210 and 590, respectively. Similarly, the values of k_{OH}^{CAG} at 50° was 47.5. [b] Bimolecular rate constants in liters/mole/min for hydrogen- and hydroxide-ion catalysis obtained from intercepts of the alkaline and acid branches, respectively, of the log k *versus* pH profile (Fig. 9 for clofibrate, Fig. 10 for etofibrate, and Fig. 11 for the monoglycol ester of clofibric acid) where the logarithm of the apparent first-order rate constant for solvolysis is $\log k = \log k_{OH} + pH - pK_w$, where pH is calculated from $pH = pK_w + \log f_{NaOH}[NaOH]$ in the former case, and $\log k = \log k_{aH} - pH$, where $pH = -\log f_{HCl}[HCl]$ in the latter. The pK_w values and activity coefficients, f_{NaOH} and f_{HCl}, were obtained from the literature (15). [c] Estimates of heats of activation (kilocalories per mole) of these rate processes were calculated from $\Delta H_a = 1.987 \times (\ln k_{T_1} - \ln k_{T_2})/[(1/T_2) - (1/T_1)]$, where T_1 and T_2 are the respective temperatures in degrees Kelvin (°C + 273) for the two studies. [d] Bimolecular rate constants for sodium hydroxide- and hydrochloric acid-catalyzed solvolysis obtained from slopes of plots of the apparent first-order rate constants against sodium hydroxide and hydrochloric acid, respectively (Fig. 8). [e] Apparent first-order rate constants for pH-independent solvolysis of clofibrate. [f] Actually 58.0°.

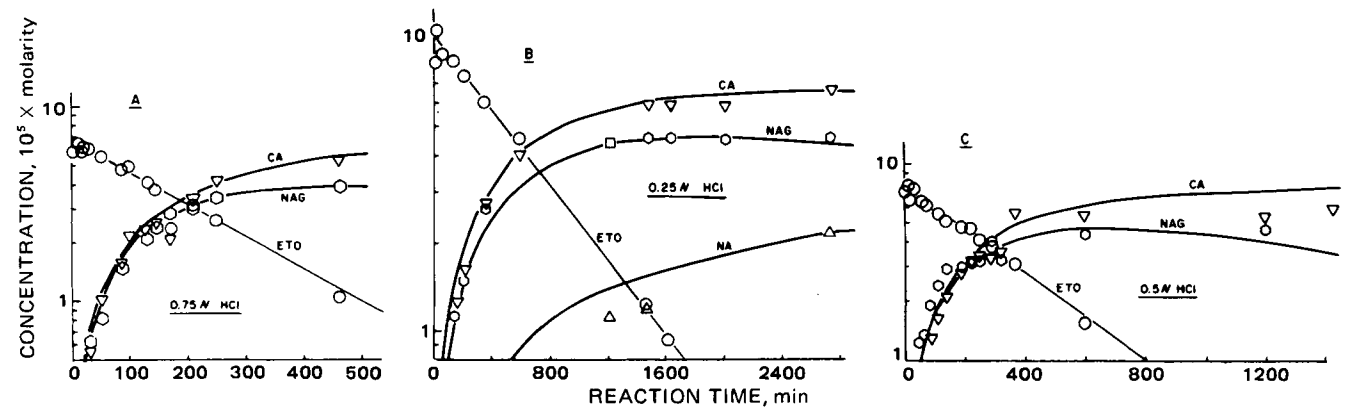

Figure 13—*Semilogarithmic plots of assayed concentrations of etofibrate (ETO) and solvolysis products, nicotinic acid monoglycolate (NAG), clofibric acid (CA), and nicotinic acid (NA), degrading at 69.9° in hydrochloric acid with an original concentration of 3×10^{-4} M etofibrate.*

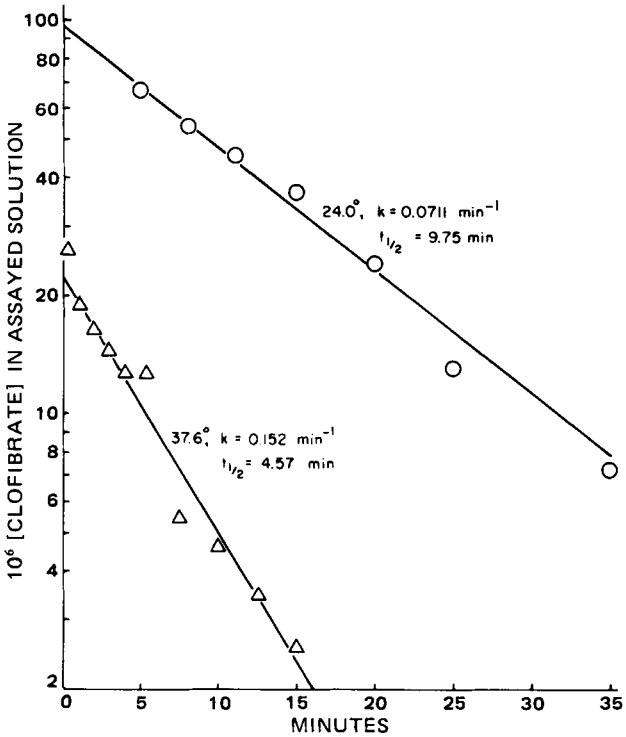

Figure 14—*Semilogarithmic plots of clofibrate concentrations with time in fresh dog plasma where blood was withdrawn 2–4 hr before by Procedure B. Aliquots (3.00 and 2.00 ml) of the 4-ml chloroform extracts of 1.00 ml of plasma were evaporated and reconstituted in 100 μl of mobile phase for injection in the 24 and 37.6° studies, respectively. The respective initial clofibrate concentrations were 1.00 and 1.77 × 10^{-5} M.*

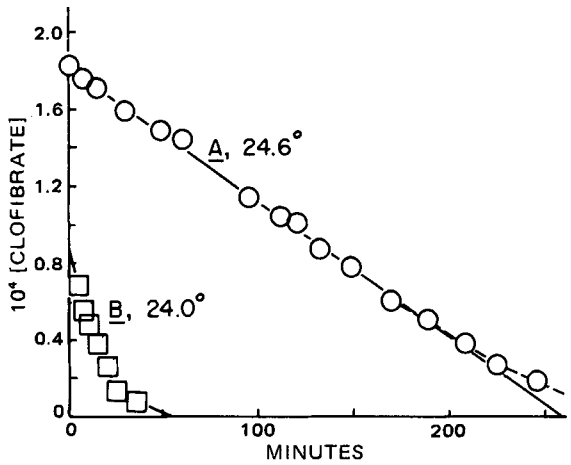

Figure 15—*Linear plots of clofibrate concentration with time at 24.5° in fresh dog plasma, 1.5 hr after withdrawal, as assayed by Procedure A for curve A with an initial plasma concentration of 1.83 × 10^{-4} M and as assayed by Procedure B for curve B with an initial plasma concentration of 1 × 10^{-5} M. The ordinate is for assayed concentrations (curve B) and plasma concentrations (curve A).*

In summary, etofibrate was readily hydrolyzed at 37.5° in fresh dog plasma with apparent half-lives of 4.4–6.9 min. The major product of this solvolysis was the glycol monoester of clofibric acid with a half-life of 5.8–11.5 min. Although the 4–5-min half-life of etofibrate determined previously (13) in diluted human blood (2.5% blood in isotonic pH 7.4 phosphate buffer) agreed with the present values, the half-lives of clofibrate (24 min) and clofibric acid monoglycolate (48 min) in diluted blood (15% blood in isotonic pH 7.4 phosphate buffer) were much greater than the present 5.8–11.5 min in whole dog plasma.

It was claimed (13) that the major route of etofibrate solvolysis in diluted blood is at the clofibric acid ester linkage, in contrast to the present findings in undiluted dog plasma that the major route is by the splitting

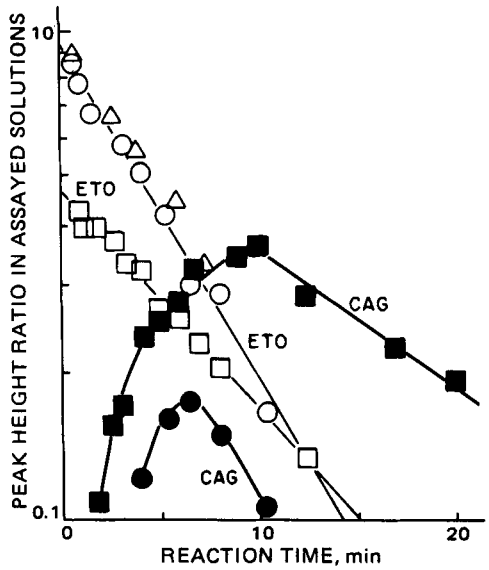

Figure 16—*Semilogarithmic plots of assayed etofibrate (open symbols) and clofibric acid monoglycolate (solid symbols) concentrations with time at 37.5° in fresh dog plasma. Procedure C was used for assay of degrading 3.6 × 10^{-5} M etofibrate in original plasma (○, ●, ▲). Procedure D was used for the assay of degrading 5.9 × 10^{-5} M etofibrate in original plasma (□, ■).*

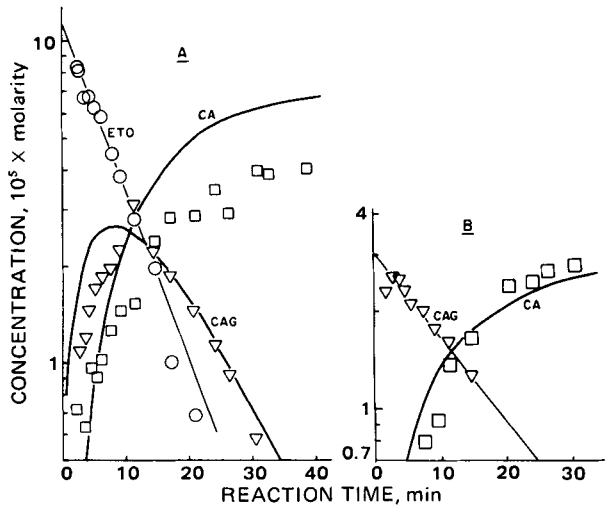

Figure 17—*Semilogarithmic plots of assayed (Procedure C) concentrations of etofibrate (ETO), clofibric acid monoglycolate (CAG), and etofibric acid (CA) for degradation of 1.19 × 10^{-4} M etofibrate (A) and 4.23 × 10^{-5} M clofibric acid monoglycolate (B) by Procedure C in fresh dog plasma. The lines through the CAG and CA values in A were calculated in accordance with Eqs. 13 and 16 for f = 1 (Eq. 14). The line through the CA values in B was calculated in accordance with [CA] = $[CAG]_0(1 - e^{-k_2 t})$.*

of the nicotinic acid ester linkage. The differences in results could be due to the fact that the present study used fresh dog plasma and the earlier study used diluted human blood with etofibrate concentrations in great excess of its solubility. The solvolyses of etofibrate and the half esters in highly diluted blood were not first order in the previous study as they were in the present study. The previous first-order semilogarithmic plots of diluted blood concentrations *versus* time showed a diminishing slope indicating decreasing esterase activity with time, which is contrary to what would be expected for saturable enzyme kinetics.

These discrepancies need clarification by further studies.

REFERENCES

(1) J. M. Thorp, *Lancet*, **1962**, 1323.

(2) A. M. Barrett and J. M. Thorp, *Br. J. Pharmacol. Chemother.*, **32**, 381 (1968).

(3) S. M. Grundy, E. H. Ahrens, Jr., G. Salen, P. H. Schreibman, and P. J. Nestel, *J. Lipid Res.*, **13**, 531 (1972).
(4) R. Pichardo, L. Boulet, and J. Davignon, *Atherosclerosis*, **26**, 573 (1977).
(5) R. Gugler, D. W. Shoeman, D. H. Huffman, J. B. Cohlman, and D. L. Azarnoff, *J. Clin. Invest.*, **55**, 1182 (1975).
(6) A. Sedaghat and E. H. Ahrens, Jr., *Eur. J. Clin. Invest.*, **5**, 177 (1975).
(7) R. Gugler and J. Hartlapp, *Clin. Pharmacol. Ther.*, **24**, 432 (1978).
(8) G. Houin, J. J. Thebault, Ph. D'Athis, J. P. Tillement, and J. L. Beaumont, *Eur. J. Clin. Pharmacol.*, **8**, 433 (1975).
(9) A. Sedaghat, H. Nahamura, and E. H. Ahrens, Jr., *J. Lipid Res.*, **15**, 352 (1974).
(10) R. Gugler and C. Jensen, *J. Chromatogr.*, **117**, 175 (1976).
(11) M. S. Wolf and J. J. Zimmerman, *J. Pharm. Sci.*, **69**, 92 (1980).
(12) M. Kummer, W. Schatton, H. Linde, and H. Oelschläger, *Pharm. Ztg.*, **124**, 1312 (1979).
(13) H. Oelschläger, D. Rothley, M. Ewert, and P. Nachev, *Arzneim.-Forsch.*, **30**, 984 (1980).
(14) Stat-1-22A "Linear Regression" HP-65 Stat-Pac 1, Hewlett-Packard, Cupertino, Calif., pp 49–51.
(15) H. S. Harned and B. B. Owen, "The Physical Chemistry of Electrolytic Solutions," 3rd ed., Reinhold, New York, N.Y., 1958.
(16) E. R. Garrett, in "Advances in Pharmaceutical Sciences," vol. II, H. S. Bean, A. H. Beckett, and J. E. Carless, Eds., Academic, New York, N.Y., 1967, pp 1–94.
(17) S. Glasstone, "Textbook of Physical Chemistry," 2nd ed., Van Nostrand, New York, N.Y., 1946, p. 1075.
(18) E. R. Garrett, *J. Am. Chem. Soc.*, **86**, 4549 (1958).

ACKNOWLEDGMENTS

Supported in part by a grant from Merz and Co., Frankfurt (Main) West Germany.

The research assistance of Peter Scherm in the determination of solubilities is gratefully acknowledged.

Effect of 4-Dimethylaminomethyl-1-(3-hydroxyphenyl)-1-nonen-3-one Hydrochloride and Related Compounds on Respiration in Rat Liver Mitochondria

N. W. HAMON ˣ, D. L. KIRKPATRICK, E. W. K. CHOW, and J. R. DIMMOCK

Received February 5, 1981, from the *College of Pharmacy, University of Saskatchewan, Saskatoon, Saskatchewan, S7N 0W0, Canada.* Accepted for publication May 14, 1981.

Abstract □ 4-Dimethylaminomethyl-1-(3-hydroxyphenyl)-1-nonen 3-one hydrochloride (II) was shown to stimulate respiration in rat liver mitochondria at levels of 2.5 μmoles or less; but at levels higher than 5.0 μmoles, respiration was inhibited when succinate and 3-hydroxybutyrate were the substrates. Compound II caused inhibition of respiration in the presence of glutamate over the dose range studied. The stimulating effect of II was attributed to its functioning as an uncoupling agent. Its inhibiting properties were considered to be due to its behaving like antimycin A in blocking transport of electrons between cytochromes b and c_1. The effect of II on respiration in mitochondria varied with the pH of the medium. A conjugated styryl ketone, which contained a nuclear hydroxy function and was structurally related to II, also stimulated respiration at low doses while inhibiting respiration at higher concentrations. Etherification of the hydroxy group led to compounds in which only stimulation of respiration was noted.

Keyphrases □ Respiration, mitochondria—effect of 4-dimethylaminomethyl-1-(3-hydroxyphenyl)-1-nonen-3-one hydrochloride and styryl ketone derivatives □ Mannich bases—prepared from styryl ketones, effect on respiration in mitochondria □ Styryl ketones—preparation of Mannich bases

A number of Mannich bases (I) derived from styryl ketones containing chlorine or hydrogen atoms in the aromatic ring have been shown to inhibit the electron transport chain in mitochondria of both rat liver cells and yeast (1, 2). These compounds were considered to exert their effect by competition with coenzyme Q_{10} (1). Recently, 4-dimethylaminomethyl-1-(3-hydroxyphenyl)-1-nonen-3-one hydrochloride (II), which is a Mannich base with a nuclear hydroxy group, was synthesized (3). Although it had little action against murine P-388 lymphocytic leukemia in contrast to some dichlorinated derivatives of I (4), it displayed anti-inflammatory analgesic properties as well as antifungal activity (3).

Therefore, the questions were asked whether II would affect mitochondrial function and, if so, whether its site of action would differ from that in series I. In addition, if II affected the electron transport chain, which is found in the inner membrane of the mitochondria, it could be a carrier group to which other molecular entities may be attached *via* the hydroxyl group. Furthermore, two related α,β-unsaturated ketones, III*a* and III*d*, differed in their activity towards P-388 lymphocytic leukemia (3), which could be due to a variation in effect on mitochondria. Thus, it was of interest to examine the effects of II, III*a*, III*d*, and the related compounds III*b* and III*c* on the electron transport chain in rat liver mitochondria.

DISCUSSION

Table I indicates the effect of II on respiration in rat liver mitochondria using three different substrates. In the case of succinate and 3-hydroxybutyrate, respiration was stimulated at low concentrations; at higher doses of II, inhibition of respiration was noted. When glutamate was the substrate, no stimulation of respiration was noted and only inhibition of respiration was found over the dose range studied.

The inhibiting effect of II at 5 μmoles with succinate as the substrate was considered. The related compounds I*a* and I*b* caused inhibition of respiration by competition with coenzyme Q_{10}, which could be reversed by addition of coenzyme Q_{10} (1). Therefore, a possible site for the respiration-inhibiting action of II might be similar. However, addition of coenzyme Q_{10} to mitochondria whose respiration had been inhibited by II did not alter the percentage of respiration inhibition, so the mode of action of II appears to differ from that of I.

A number of compounds inhibit respiration by blocking the transport

0022-3549/82/0100-0025$01.00/0

(3) S. M. Grundy, E. H. Ahrens, Jr., G. Salen, P. H. Schreibman, and P. J. Nestel, *J. Lipid Res.*, **13**, 531 (1972).
(4) R. Pichardo, L. Boulet, and J. Davignon, *Atherosclerosis*, **26**, 573 (1977).
(5) R. Gugler, D. W. Shoeman, D. H. Huffman, J. B. Cohlman, and D. L. Azarnoff, *J. Clin. Invest.*, **55**, 1182 (1975).
(6) A. Sedaghat and E. H. Ahrens, Jr., *Eur. J. Clin. Invest.*, **5**, 177 (1975).
(7) R. Gugler and J. Hartlapp, *Clin. Pharmacol. Ther.*, **24**, 432 (1978).
(8) G. Houin, J. J. Thebault, Ph. D'Athis, J. P. Tillement, and J. L. Beaumont, *Eur. J. Clin. Pharmacol.*, **8**, 433 (1975).
(9) A. Sedaghat, H. Nahamura, and E. H. Ahrens, Jr., *J. Lipid Res.*, **15**, 352 (1974).
(10) R. Gugler and C. Jensen, *J. Chromatogr.*, **117**, 175 (1976).
(11) M. S. Wolf and J. J. Zimmerman, *J. Pharm. Sci.*, **69**, 92 (1980).
(12) M. Kummer, W. Schatton, H. Linde, and H. Oelschläger, *Pharm. Ztg.*, **124**, 1312 (1979).
(13) H. Oelschläger, D. Rothley, M. Ewert, and P. Nachev, *Arzneim.-Forsch.*, **30**, 984 (1980).
(14) Stat-1-22A "Linear Regression" HP-65 Stat-Pac 1, Hewlett-Packard, Cupertino, Calif., pp 49–51.
(15) H. S. Harned and B. B. Owen, "The Physical Chemistry of Electrolytic Solutions," 3rd ed., Reinhold, New York, N.Y., 1958.
(16) E. R. Garrett, in "Advances in Pharmaceutical Sciences," vol. II, H. S. Bean, A. H. Beckett, and J. E. Carless, Eds., Academic, New York, N.Y., 1967, pp 1–94.
(17) S. Glasstone, "Textbook of Physical Chemistry," 2nd ed., Van Nostrand, New York, N.Y., 1946, p. 1075.
(18) E. R. Garrett, *J. Am. Chem. Soc.*, **86**, 4549 (1958).

ACKNOWLEDGMENTS

Supported in part by a grant from Merz and Co., Frankfurt (Main) West Germany.

The research assistance of Peter Scherm in the determination of solubilities is gratefully acknowledged.

Effect of 4-Dimethylaminomethyl-1-(3-hydroxyphenyl)-1-nonen-3-one Hydrochloride and Related Compounds on Respiration in Rat Liver Mitochondria

N. W. HAMON ˣ, D. L. KIRKPATRICK, E. W. K. CHOW, and J. R. DIMMOCK

Received February 5, 1981, from the *College of Pharmacy, University of Saskatchewan, Saskatoon, Saskatchewan, S7N 0W0, Canada.* Accepted for publication May 14, 1981.

Abstract □ 4-Dimethylaminomethyl-1-(3-hydroxyphenyl)-1-nonen 3-one hydrochloride (II) was shown to stimulate respiration in rat liver mitochondria at levels of 2.5 μmoles or less; but at levels higher than 5.0 μmoles, respiration was inhibited when succinate and 3-hydroxybutyrate were the substrates. Compound II caused inhibition of respiration in the presence of glutamate over the dose range studied. The stimulating effect of II was attributed to its functioning as an uncoupling agent. Its inhibiting properties were considered to be due to its behaving like antimycin A in blocking transport of electrons between cytochromes b and c_1. The effect of II on respiration in mitochondria varied with the pH of the medium. A conjugated styryl ketone, which contained a nuclear hydroxy function and was structurally related to II, also stimulated respiration at low doses while inhibiting respiration at higher concentrations. Etherification of the hydroxy group led to compounds in which only stimulation of respiration was noted.

Keyphrases □ Respiration, mitochondria—effect of 4-dimethylaminomethyl-1-(3-hydroxyphenyl)-1-nonen-3-one hydrochloride and styryl ketone derivatives □ Mannich bases—prepared from styryl ketones, effect on respiration in mitochondria □ Styryl ketones—preparation of Mannich bases

A number of Mannich bases (I) derived from styryl ketones containing chlorine or hydrogen atoms in the aromatic ring have been shown to inhibit the electron transport chain in mitochondria of both rat liver cells and yeast (1, 2). These compounds were considered to exert their effect by competition with coenzyme Q_{10} (1). Recently, 4-dimethylaminomethyl-1-(3-hydroxyphenyl)-1-nonen-3-one hydrochloride (II), which is a Mannich base with a nuclear hydroxy group, was synthesized (3). Although it had little action against murine P-388 lymphocytic leukemia in contrast to some dichlorinated derivatives of I (4), it displayed anti-inflammatory analgesic properties as well as antifungal activity (3).

Therefore, the questions were asked whether II would affect mitochondrial function and, if so, whether its site of action would differ from that in series I. In addition, if II affected the electron transport chain, which is found in the inner membrane of the mitochondria, it could be a carrier group to which other molecular entities may be attached *via* the hydroxyl group. Furthermore, two related α,β-unsaturated ketones, III*a* and III*d*, differed in their activity towards P-388 lymphocytic leukemia (3), which could be due to a variation in effect on mitochondria. Thus, it was of interest to examine the effects of II, III*a*, III*d*, and the related compounds III*b* and III*c* on the electron transport chain in rat liver mitochondria.

DISCUSSION

Table I indicates the effect of II on respiration in rat liver mitochondria using three different substrates. In the case of succinate and 3-hydroxybutyrate, respiration was stimulated at low concentrations; at higher doses of II, inhibition of respiration was noted. When glutamate was the substrate, no stimulation of respiration was noted and only inhibition of respiration was found over the dose range studied.

The inhibiting effect of II at 5 μmoles with succinate as the substrate was considered. The related compounds I*a* and I*b* caused inhibition of respiration by competition with coenzyme Q_{10}, which could be reversed by addition of coenzyme Q_{10} (1). Therefore, a possible site for the respiration-inhibiting action of II might be similar. However, addition of coenzyme Q_{10} to mitochondria whose respiration had been inhibited by II did not alter the percentage of respiration inhibition, so the mode of action of II appears to differ from that of I.

A number of compounds inhibit respiration by blocking the transport

0022-3549/82/0100-0025$01.00/0

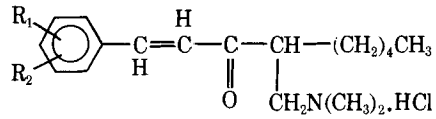

I: $R^1 = R^2 = H, Cl$

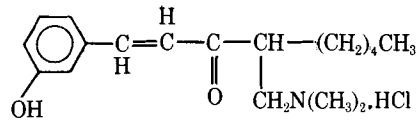

II

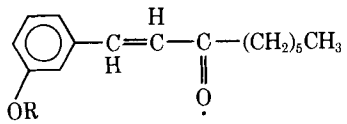

IIIa: R = $CH_2OC_2H_5$
IIIb: R = CH_2OCH_3
IIIc: R = CH_3
IIId: R = H

of electrons along the cytochromes. On occasion, this blockade and cytochromes may be discerned by examining the difference in the visible spectra of cytochromes in both the oxidized and reduced states (5). During respiration, electrons are transported along the cytochromes from coenzyme Q_{10} to oxygen (Scheme I), and the cytochromes become reduced during this process. After a blockade has occurred, the cytochromes prior to the block become reduced and the cytochromes after the block become more oxidized due to the pseudoreversibility of the respiration chain.

Examination of the visible spectra of II showed the presence of cytochrome b with its Soret band at 430 nm and its α band at 563 nm, suggesting a block between cytochromes b and c_1. The visible spectra of antimycin A was identical to that obtained for II. Since antimycin A is known to block between cytochromes b and c_1 (6), a similar mode of action for II was suggested. To confirm the site of action, respiration was examined in the presence of an inhibiting concentration of II, and then tetramethyl-*p*-phenylenediamine was added, which caused respiration to return to 95% of the rate prior to the addition of II. This result suggests that the block by II occurs between cytochromes b and c_1. Antimycin A was shown to act in a similar manner. After respiration was inhibited by this compound, tetramethyl-*p*-phenylenediamine caused the respiration rate to return to normal.

The reason for stimulation of respiration by II at low doses was also investigated with succinate as the substrate. Since II and coenzyme Q_{10} are α,β-unsaturated ketones, both compounds possibly might act as recipients of electrons from various flavoproteins (Scheme I), and these electrons are subsequently transferred to the cytochromes. Coenzyme Q_{10} was removed from the mitochondria; in the presence of succinate, neither succinoxidase nor succinate cytochrome c reductase was active, but activity was partially restored by the addition of coenzyme Q_{10}. Substitution of II for coenzyme Q_{10} did not permit respiration to occur, and it seems unlikely, therefore, that II acts in a capacity similar to this coenzyme. This finding substantiates the observation of earlier workers that a number of electron acceptors related to coenzyme Q_{10} failed to stimulate its action (7) and that mitochondria may have a specific requirement for this coenzyme.

Table I—Effect of II on Respiration in Rat Liver Mitochondria Using Succinate, Glutamate, and 3-Hydroxybutyrate as the Substrates[a]

Concentration, μmoles	Substrate: Succinate[b] Inhibition, % ± *SE*	Glutamate[c] Inhibition, % ± *SE*	3-Hydroxybutyrate[d] Inhibition, % ± *SE*
0.05	−18.80 ± 3.18	1.70 ± 1.70	−15.45 ± 3.20
0.1	−28.64 ± 7.52	0.00 ± 0.00	−21.16 ± 1.85
0.25	−47.90 ± 0.62	6.65 ± 1.60	−48.03 ± 4.01
0.5	−59.53 ± 11.38	17.80 ± 4.22	−48.10 ± 2.64
1.0	−75.34 ± 11.85	49.26 ± 6.24	−57.88 ± 10.77
1.25	−77.68 ± 6.17	51.28 ± 9.87	−41.93 ± 1.65
2.5	−36.06 ± 3.20	62.08 ± 0.95	83.10 ± 1.42
5	73.43 ± 1.72	66.17 ± 2.28	98.04 ± 1.11
10	97.43 ± 0.72	81.52 ± 2.51	—

[a] Figures prefaced by a negative sign indicate stimulation of respiration. [b] At a concentration of 0.125 μmole, stimulation of respiration was 29.78% (*SE* = 8.09). At concentrations of 3.75, 4.25, 7.5, and 12.5 μmoles, the percentage inhibition of respiration was 8.34 (*SE* = 3.74), 49.52 (*SE* = 5.30), 58.87 (*SE* = 1.65), 92.79 (*SE* = 1.92), and 99.70 (*SE* = 0.30), respectively. [c] At concentrations of 0.75, 15, 20 and 25 μmoles, the percentage inhibition was 13.70 (*SE* = 6.35), 81.13 (*SE* = 3.61), 85.50 (*SE* = 1.80), and 86.87 (*SE* = 1.13), respectively. [d] At a concentration of 0.75 μmole, stimulation of respiration was 58.88% (*SE* = 5.50).

Increased respiration in mitochondria could occur by II acting as an uncoupling agent, especially since II is a phenolic compound and some substituted phenols (such as 2,4-dinitrophenol) are known to be uncoupling agents. In the case of 2,4-dinitrophenol, respiration is stimulated at low concentrations and inhibited at higher concentrations (8, 9), which is a situation similar to that found with II. Uncouplers do not interfere with the transport of electrons from the flavoproteins to oxygen, but adenosine triphosphate (ATP) is not formed during this process, *i.e.*, oxidation and phosphorylation no longer function in unison. Uncouplers may be identified by their effect on the P:O ratio, that is, the number of moles of adenosine diphosphate (ADP) phosphorylated to produce adenosine triphosphate per gram atoms of oxygen consumed (10). In tightly coupled mitochrondria with succinate as the substrate, such a ratio should be 2 (Scheme I).

The effect of II on the P:O ratio was examined, and it was found that utilization of inorganic phosphate decreased while oxygen consumption was unchanged from that of the control. This result caused the P:O ratio to fall to 25% of the value obtained in the absence of II. As well as uncoupling of oxidative phosphorylation (11), 2,4-dinitrophenol and some related phenols also stimulate latent adenosine triphosphatase activity of normal mitochondria (12, 13). If II acted in the same manner as 2,4-dinitrophenol, one would expect to see stimulation of adenosine triphosphatase along with the uncoupling effects, *i.e.*, a decreased P:O ratio. It was found that low concentrations of II (0.20–2.00 μmoles) caused stimulation of adenosine triphosphatase activity and a subsequent increase in hydrolysis of adenosine triphosphate to adenosine diphosphate. Higher concentrations of II (3 μmoles or greater) caused inhibition of this enzyme.

In a study of a series of uncoupling agents, 2,4-dinitrophenol caused stimulation and subsequent inhibition of respiration in the presence of both succinate and glutamate. However, in the case of the uncoupler 3-nitrophenol, stimulation of mitochondrial respiration occurred in the presence of succinate but not glutamate, a situation identical to that found with II (8). With both 3-nitrophenol and II, electron-attracting groups are present in the *meta* position to the phenolic function, which may reflect similar structural requirements for the mode of action of these two compounds.

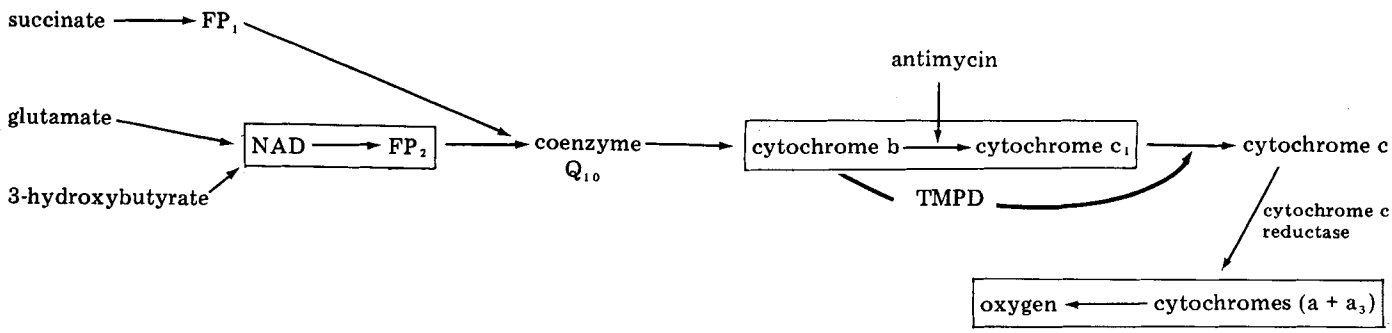

Scheme I—The rectangles indicate the sites where ADP is converted into ATP. Flavoproteins are represented as FP_1 and FP_2.

Table II—Effect of II on Respiration in Rat Liver Mitochondria Using Succinate as the Substrate at pH Levels of 6.4, 6.9, and 7.4 [a]

Concentration, μmoles	pH 6.4[b] Inhibition, % ± SE	pH 6.9[c] Inhibition, % ± SE	pH 7.4[d] Inhibition, % ± SE	Levels of Significance (p) between pH Values of 6.4 and 6.9	6.9 and 7.4	6.4 and 7.4
0.25	−32.07 ± 10.79	−42.51 ± 2.74	−47.90 ± 0.62	0.50	0.05	0.10
0.50	−43.06 ± 1.13	−55.67 ± 0.01	−59.53 ± 11.38	0.02	>0.50	0.50
1.00	−33.31 ± 1.07	−94.06 ± 1.51	−75.34 ± 11.85	0.001	0.50	0.10
1.25	−72.72 ± 8.97	−61.64 ± 12.79	−77.68 ± 6.17	0.50	0.50	>0.05
2.50	−56.33 ± 13.10	−55.14 ± 3.91	−36.06 ± 3.20	>0.50	0.10	0.10
4.25	+4.81 ± 9.86	+81.63 ± 7.26	+49.52 ± 5.30	0.01	0.05	0.01
4.50	+11.97 ± 3.25	+84.45 ± 4.34	+58.87 ± 1.65	0.01	<0.001	<0.001
5.00	+52.85 ± 6.35	+92.55 ± 1.63	+73.43 ± 1.72	0.01	<0.001	0.01
7.50	+98.25 ± 1.76	+97.62 ± 2.38	+92.79 ± 1.92	>0.50	0.50	0.10
10.00	+99.08 ± 0.93	+99.38 ± 0.62	+97.43 ± 0.72	>0.50	0.50	0.50

[a] Figures prefaced by a negative sign indicate stimulation of respiration. [b] At a concentration of 0.75 μmole, stimulation of 28.13% (SE = 0.85) occurred. At a concentration of 6.00 μmoles, inhibition of 65.80% (SE = 6.92) occurred. [c] At a concentration of 0.75 μmole, stimulation of 60.22% (SE = 0.95) occurred. At a concentration of 3.50 μmoles, inhibition of 37.27% (SE = 12.71) occurred. [d] At concentrations of 0.05, 0.10, and 0.125 μmoles, stimulation of respiration was 18.80% (SE = 3.18), 28.64% (SE = 7.52), and 29.78% (SE = 8.09), respectively. At concentrations of 3.75 and 12.50 μmoles, the percentage inhibition of respiration was 8.34 (SE = 3.74) and 99.70 (SE = 0.30), respectively.

A recent study revealed that the amount of I inhibiting respiration in mitochondria obtained from both normal rat liver and from a Morris hepatoma varied according to the pH of the medium (14). In general, the compounds had increased respiration-inhibiting properties as the pH was lowered. The three pH values chosen were 7.4, that of normal physiological conditions; 6.9, which is claimed to be the pH of certain tumors (15, 16); and 6.4, which has been reported to be the pH of some tumors after administration of glucose while normal tissue was unaffected (15, 16). Thus, the question was raised as to whether the effect of II would vary markedly with such pH changes. If respiration was inhibited, preferentially at lower pH levels, some selectivity towards tumors may be possible under certain conditions.

Table II shows that at the lower stimulating concentrations of II, the percentage increase in respiration generally fell as the pH of the medium was lowered. This respiration-stimulatory effect became less pronounced as inhibiting concentrations of II were approached. When inhibition of respiration occurred at concentrations greater than 2.50 μmoles, there was mainly an optimal inhibition of respiration at pH 6.9 but less inhibition at pH 6.4 than at pH 7.4. Hence, these results of inhibition differ from those reported for series I (14).

Finally, the conjugated styryl ketones (III), which are related to II, were evaluated for their effect on respiration in rat liver mitochondria (Table III). At the optimal dose levels, II and III*a*–III*d* increased the survival time in mice with P-388 lymphocytic leukemia by 6, 25, 13, 5, and 4%, respectively; little correlation between effect on respiration and anticancer activity was seen. The ethers III*a*–III*c* caused moderate stimulation of respiration over the dose range studied, and no inhibition of respiration was noted. However, at concentrations of >1.0 μmole, for example, inhibition of respiration may occur at the same time as stimulation but the latter effect predominates. The phenolic compound III*d* behaves in a similar manner to the corresponding Mannich base II, and hence the observed inhibition of respiration appears to be associated with the presence of a phenolic group.

This study has shown that a Mannich base derived from a nuclear hydroxy conjugated styryl ketone (II) has uncoupling action at low concentrations while at higher doses it acts like antimycin A in blocking electron transport between cytochromes b and c_1. The effect on mitochondria varies depending on the pH of the medium. While III*d* showed a similar biphasic response as II, etherification of the hydroxy group of III*d* produced derivatives III*a*–III*c*, which showed only slight stimulating effects on respiration.

EXPERIMENTAL[1]

Syntheses of Compounds—Compounds II, III*a*, and III*b* were prepared according to literature methodology (3). (*E*)-1-(*m*-Methoxymethyloxyphenyl)-1-nonen-3-one (III*b*), prepared by the same scheme as III*a* in a 58% yield, was a yellow oil, bp 187°/0.3 mm [lit. (17) bp 177°/0.16 mm].

Anal.—Calc. for $C_{17}H_{24}O_3$: C, 73.88; H, 8.75. Found: C, 73.42; H, 8.70.

(*E*)-1-(*m*-Methoxyphenyl)-1-nonen-3-one (III*c*) was prepared as follows. A mixture of 2-octanone (5.13 g, 0.04 mole), *m*-methoxybenzaldehyde (4.42 g, 0.0325 mole), and sodium hydroxide (0.68 g, 0.017 mole) in water (20 ml) was heated under reflux for 24 hr with mechanical stirring. On cooling, the aqueous layer was extracted three times with benzene (20 ml), and the combined organic phases were washed twice with water (20 ml) and dried with anhydrous magnesium sulfate. Removal of benzene by a water aspirator afforded a yellow oil, which was purified by distillation to give III*c* as a colorless oil, bp 144–146°/0.35 mm, in a 52% yield.

Anal.—Calc. for $C_{16}H_{22}O_2$: C, 78.01; H, 9.00. Found: C, 77.94; H, 8.98.

Effect of II and III*a*–III*d* on Mitochondria Isolated from Rat Livers—Pellets of mitochondria obtained from the livers of male Wistar rats were isolated by the literature methodology (1) and suspended in 3.4 m*M* tromethamine hydrochloride[2] buffer (pH 7.40) containing 0.25 m*M* sucrose and 1 m*M* ethylene glycol bis(aminomethyl)tetraacetate at 0°. The protein content was 4 mg/ml as determined by a modification (18) of a previously reported procedure (19). The medium for the determination of mitochondrial respiration was that described previously (1) and will be referred to subsequently as the respiration media. Compounds III*c* and III*d* were dissolved in absolute ethanol and II in 10 m*M* tromethamine hydrochloride buffer (pH 7.40), while the oils III*a* and III*b* were added directly to the mitochondrial suspension. The media and methodology required for generating the data recorded in Tables I and II were those employed previously (1) using an oxygen monitor[3]. At least four determinations per compound were obtained at each dose level.

Effect of II and Antimycin A on Visible Spectra of Cytochromes—A mitochondrial suspension (0.5 ml containing 4 mg protein/ml) was placed in two 1-cm cells containing the respiration media (pH 7.40, 2.5 ml). Solutions of disodium succinate (15 μmoles) in 7.5 μl of 10 m*M* tromethamine hydrochloride buffer (pH 7.4) and adenosine diphosphate (1 μmole) in 1 μl of 10 m*M* tromethamine hydrochloride were placed in each cell. One cell was aerated by agitation while toluene was added to the other one. The visible spectra[4] of oxidized and reduced cytochromes were then recorded between 390 and 590 nm.

The two cells containing mitochondria, disodium succinate, and adenosine diphosphate in the respiration media (pH 7.4) were aerated by agitation. Compound II (5.0 μmoles in 10 m*M* tromethamine hydrochloride buffer, pH 7.4) was added to one cell and allowed to stand at room temperature for 3 min. Just before the spectrum was recorded, II was added to the reference cell. This addition eliminated the interference caused by II with the difference spectrum. The spectrum was then recorded between 590 and 490 nm. A fresh reference cell was prepared and aerated, II was added, and the spectrum recorded between 490 and 390 nm. All determinations were carried out at room temperature.

Mitochondria, disodium succinate, and adenosine diphosphate in the respiration media were added to the cells in the quantities indicated above. Antimycin A[2] (0.009 μmoles in 2 μl of 10 m*M* tromethamine hydrochloride buffer, pH 7.4) was added to one cell; after both were aerated, the difference spectra were recorded.

Effect of II and Antimycin A on Tetramethylphenylenediamine Bypass—Mitochondria (0.5 ml containing 4 mg protein/ml) were added to the respiration media (2.5 ml) in the cell of an oxygen monitor at 37°, and uptake of oxygen started with the addition of disodium succinate

[1] Elemental analyses were carried out by Mr. R. E. Teed, Department of Chemistry and Chemical Engineering, University of Saskatchewan. Boiling points are uncorrected.

[2] Sigma Chemical Co., St. Louis, MO 63178.

[3] Model 53, Yellow Springs Instrument Co., Yellow Springs, OH 45387.

[4] Cary 15M spectrometer, Varian Instrument Division, Monrovia, CA 91016.

Table III—Effect of IIIa–IIId on Respiration in Rat Liver Mitochondria Using Succinate as the Substrate [a]

Concentration, μmoles	IIIa Stimulation, % ± *SE*	IIIb [b] Stimulation, % ± *SE*	IIIc Stimulation, % ± *SE*	IIId [c] Stimulation, % ± *SE*
0.01	7.93 ± 6.32	7.23 ± 2.87	12.09 ± 4.77	26.43 ± 6.46
0.1	25.75 ± 1.30	14.99 ± 5.10	20.74 ± 4.26	86.07 ± 13.64
1.0	27.98 ± 8.35	22.74 ± 8.89	25.45 ± 16.09	−47.23 ± 7.31
2.5	27.38 ± 10.70	13.45 ± 5.29	5.59 ± 2.52	−87.56 ± 4.63
5.0	20.18 ± 6.00	8.19 ± 3.30	14.63 ± 5.92	—
50.0	5.72 ± 3.66	16.25 ± 1.95	23.74 ± 5.37	—

[a] Figures prefaced by a negative sign indicate inhibition of respiration. [b] At a concentration of 10 μmoles, stimulation of 11.39% (*SE* = 1.13) occurred. [c] At a concentration of 5.0 μmoles or greater, 100% inhibition occurred.

(15 μmoles in 7.5 μl of 10 m*M* tromethamine hydrochloride buffer, pH 7.4). Respiration was inhibited by either antimycin A (0.009 μmole) or II (5.0 μmole), and then tetramethyl-*p*-phenylenediamine (0.013 μmole) in 10 m*M* tromethamine hydrochloride buffer, pH 7.4 (25 μl), was added. The change in the rate of oxygen uptake was recorded.

Effect of II on Succinoxidase and Succinate–Cytochrome c Reductase Reactions—Acetone-treated particles were prepared from rat liver mitochondria by the literature method (20), and 0.5 ml of a suspension of these particles (3 mg protein/ml) was placed in the cell of an oxygen monitor containing monobasic potassium phosphate (100 μmoles), disodium succinate (150 μmoles), cytochrome c[5] (0.2 mg), and sufficient sucrose solution to produce 3 ml of a 0.2 *M* solution with a pH of 7.4. After 9-min incubation at 37°, various quantities of coenzyme Q_{10}[2] solutions (4 mg in 2 ml of ethanol, 95% w/v) and II (1.25 μmoles in 2.5 μl of 10 m*M* tromethamine hydrochloride buffer, pH 7.4) were added, and the effect on oxygen uptake was recorded. This experiment was carried out four times.

A mixture of the acetone-treated particles (10 μl, 3 mg protein/ml), monobasic potassium phosphate (180 μmoles), and cytochrome c (15 mg), with or without II and coenzyme Q_{10} (20 μg) in a total volume of 3 ml of water, was placed in the cell of an oxygen monitor. After incubation at 30° for 10 min, 0.1 ml of a solution containing disodium succinate (135 μmoles) and potassium cyanide (3 μmoles) in water was added, and the reaction was monitored at 550 nm[6] for 30 min. This determination was carried out in duplicate.

Effect of II on P:O Ratio—The P:O ratio of aerobic phosphorylation of mitochondria in the presence of II (1.25 μmole) was carried out at 30° using the literature methodology (21). The quantity of inorganic phosphate was determined by the method described previously (22). In an experiment involving three separate determinations, 1.43 (±0.38 *SE*) μmoles of inorganic phosphate were taken up, and 1.05 (±0.03 *SE*) μatoms of oxygen was consumed in the absence of II, indicating a P:O ratio of 1.36. In the presence of II, 0.26 (±0.14 *SE*) μmole of inorganic phosphate and 1.03 (±0.11 *SE*) μatoms of oxygen were utilized, indicating a P:O ratio of 0.25, *i.e.*, 18% of the P:O ratio of the control value.

In a second experiment involving three separate determinations, 1.33 (±0.30 *SE*) μmoles of inorganic phosphate and 0.685 (±0.003 *SE*) μatom of oxygen were consumed in the absence of II, producing a P:O ratio of 1.94. In the presence of II, 0.41 (±0.04 *SE*) μmole of inorganic phosphate and 0.66 (±0.03 *SE*) μatom of oxygen were used, producing a P:O ratio of 0.61, *i.e.*, 31% of the control values.

Effect of II and 2,4-Dinitrophenol on Adenosine Triphosphatase Activity—The adenosine triphosphatase activity of mitochondria was determined by the literature method (23). Compound II was dissolved in 10 m*M* tromethamine hydrochloride buffer (100 μmoles/ml), and 2,4-dinitrophenol was dissolved in absolute ethanol (200 μmoles/ml). The media (1.5 ml), as described in the literature (23), were added to a number of centrifuge tubes (15 ml), and varying concentrations of II or 2,4-dinitrophenol were added to each tube. The reaction was commenced by the addition of a suspension of mitochondria in 3.4 m*M* tromethamine hydrochloride buffer (pH 7.4) (0.5 ml containing 2 mg protein/ml), and the combined reaction mixture was incubated at 37° for 15 min. After quenching with ice-cold trichloroacetic aid (2 ml, 10% w/v), the reaction mixture was centrifuged at 35,000 rpm (average radius of 8.5 cm) for 5 min to remove protein. The liberated inorganic phosphate in the supernate was determined using a modification (22) of a literature method (24) involving measurement[7] of the absorbance at 700 nm.

The amounts of inorganic phosphate liberated at varying concentrations of II, given in parentheses, were as follows. All figures indicate micromole quantities, and those prefaced by a negative sign indicate that the inorganic phosphate concentration was less than the control values, *i.e.*, inhibition of latent adenosine triphosphatase activity occurred: −0.0243 (0.20), 0.0845 (0.40), 0.1874 (0.60), 0.3256 (0.80), 0.3462 (1.00), 0.5086 (1.20), 0.3844 (1.40), 0.4535 (1.60), 0.4322 (1.80), 0.2412 (2.00), 0.0074 (2.50), −0.0784 (3.00), −0.1874 (4.00), and −0.2058 (5.00). The amounts of inorganic phosphate liberated when 2,4-dinitrophenol was used in place of II were as follows: 0.7754 (0.20), 0.5604 (1.00), 0.5898 (2.00), 0.5990 (3.00), −0.3675 (10.00), and −0.4116 (20.00). The figures obtained were the average values of six determinations.

Screening of Compounds—Details of the anticancer screening of II, IIIa, and IIId were described earlier (3). Compounds IIIb and IIIc were evaluated by the Drug Research and Development Division of the National Cancer Institute, Bethesda, Md., using their protocols (25), and were administered as a suspension in saline with polysorbate 80[8] by the intraperitoneal route on 9 successive days using male CD_2F_1 mice and male $B_6D_2F_1$ mice, respectively. The maximum increases in median survival times were 13% (100 mg/kg) for IIIb and 5% (100 mg/kg) for IIIc. There were five out of six survivors on Day 5 when IIIc was administered at 200 mg/kg and six out of six survivors on Day 5 at a dose of 100 mg/kg. No mortalities for IIIb were noted at a dose of 200 mg/kg.

REFERENCES

(1) N. W. Hamon, D. L. Bassendowski, D. E. Wright, J. R. Dimmock, and L. M. Noble, *J. Pharm. Sci.*, **67**, 1539 (1978).

(2) J. R. Dimmock, N. W. Hamon, K. W. Hindmarsh, D. G. Mills, L. E. Negrave, G. H. Rank, and A. J. Robertson, *ibid.*, **65**, 482 (1976).

(3) J. R. Dimmock, C. B. Nyathi, and P. J. Smith, *ibid.*, **68**, 1216 (1979).

(4) J. R. Dimmock and W. G. Taylor, *ibid.*, **64**, 241 (1975).

(5) B. Chance and G. R. Williams, *J. Biol. Chem.*, **217**, 395 (1955).

(6) C. S. Rossi and E. Carafoli, in "Fundamentals of Biochemical Pharmacology," Z. M. Bacq, Ed., Pergamon, Toronto, Canada, 1971, p. 157.

(7) R. L. Lester and S. Fleischer, *Biochim. Biophys. Acta*, **47**, 358 (1961).

(8) V. P. Skulachev, L. S. Yagushinski, A. A. Jasaitis, E. A. Liberman, V. P. Topali, and L. A. Zofina, in "The Energy Level and Metabolic Control in Mitochondria," S. Papa, J. M. Tager, E. Quagliariello, and E. C. Slater, Eds., Adriatica Editrice, Bari, Italy, 1969, p. 283.

(9) H. C. Hemker, *Biochim. Biophys. Acta*, **81**, 1 (1964).

(10) P. A Whittaker and S. M. Danks, "Mitochondria: Structure, Function and Assembly," Longman, New York, N.Y., 1978, p. 70.

(11) W. F. Loomis and F. Lipmann, *J. Biol. Chem.*, **179**, 503 (1949).

(12) H. A. Lardy and H. Wellman, *ibid.*, **201**, 357 (1953).

(13) V. R. Potter, P. Seikevitz, and H. C. Simonson, *ibid.*, **205**, 893 (1953).

(14) J. R. Dimmock, N. W. Hamon, E. W. K. Chow, D. L. Kirkpatrick, L. M. Smith, and M. G. Prior, *Can. J. Pharm. Sci.*, **15**, 84 (1980).

(15) M. Eden, B. Haines, and H. Kahler, *J. Natl. Cancer Inst.*, **16**, 541 (1955).

(16) H. Kahler and W. B. Robertson, *ibid.*, **3**, 495 (1943).

(17) C. B. Nyathi, Ph.D. thesis, University of Saskatchewan, Saskatoon, Canada, 1978.

(18) G. L. Miller, *Anal. Chem.*, **31**, 964 (1959).

(19) O. H. Lowry, N. J. Rosebrough, L. Fair, and R. J. Randall, *J. Biol.*

[5] Sigma type 3, Sigma Chemical Co., St. Louis, MO 63178.

[6] Pye Unicam SP1700 uv spectrophotometer.

[7] Model 250 spectrophotometer with a rapid sampler (model 2443-A), Gilford Instrument Laboratories Inc., Oberlin, OH 44074.

[8] Tween 80, Atlas Chemical Industries.

Chem., **193**, 265 (1951).
(20) R. L. Lester, "Methods in Enzymology," vol. 10, R. W. Estabrook and M. E. Pullman, Eds., Academic, New York, N.Y., 1967, p. 264.
(21) H. Lees, *Biochim. Biophys. Acta*, **105**, 184 (1965).
(22) J. B. Sumner, *Science*, **100**, 413 (1944).
(23) D. K. Myers and E. C. Slater, *Biochem. J.*, **67**, 558 (1957).
(24) C. H. Fiske and Y. Subbarow, *J. Biol. Chem.*, **66**, 375 (1925).
(25) R. I. Geran, N. H. Greenberg, M. M. MacDonald, A. M. Schumacher, and B. J. Abbott, *Cancer Chemother. Rep. Part 3*, **1972**, 3.

ACKNOWLEDGMENTS

The authors thank the Medical Research Council of Canada for the award of an operating grant (MA-5538) to J. R. Dimmock and a Summer Undergraduate Research Scholarship to E. W. K. Chow. Acknowledgment is made with gratitude to the University of Saskatchewan who provided a Graduate Scholarship to D. L. Kirkpatrick and also the University of Saskatchewan Alumni Association who awarded D. L. Kirkpatrick the John and Mary Spinks Scholarship.

Pharmacokinetic Interactions of Tolazamide and Oxyphenbutazone in Dogs

S. E. ABIDI *, A. H. KIBBE ˣ, R. W. CLEARY, A. B. JONES, and E. C. HARLAND

Received October 14, 1980, from the *Department of Pharmaceutics University of Mississippi, University, MS 38677.* Accepted for publication May 13, 1981. * Present address: School of Pharmacy, West Virginia University, Morgantown, WV 26506.

Abstract □ The described pharmacokinetic analysis involved two separate studies on nine dogs randomly assigned to three groups of three dogs each. In the first study, the effect of varying the dosage of tolazamide was examined. The second study concerned the effect of varying the dosage of oxyphenbutazone on tolazamide. A 3 × 3 Latin square was used to study both effects. Each group received each treatment, with a minimum of 1 week separating each session. The pharmacokinetics of tolazamide followed a two-compartment open model. The hybrid rate constants, α and β, were not significantly different at the three dosages when measured by a three-way analysis of variance. The only significant difference at the three dosage levels of tolazamide was in the apparent volume of distribution. In the pharmacokinetic interaction associated with intravenous administration of one dose of tolazamide and three doses of oxyphenbutazone, the apparent volume of distribution and the hybrid rate constant α did not change significantly while the hybrid rate constant for tolazamide, β, seemed to decrease with increasing oxyphenbutazone.

Keyphrases □ Pharmacokinetics—tolazamide and oxyphenbutazone interactions, dogs □ Tolazamide—pharmacokinetic interactions with oxyphenbutazone, dogs □ Oxyphenbutazone—pharmacokinetic interactions with tolazamide, dogs

Enhanced hypoglycemic effects have been reported when patients, stabilized on a sulfonylurea (tolbutamide or tolazamide), have had phenylbutazone and/or its analog, oxyphenbutazone, added to the treatment regimen (1). Hussar (2) suggested that phenylbutazone/oxyphenbutazone enhanced the hypoglycemic effects of tolbutamide or tolazamide.

Other investigators (3) found significant prolongation of the half-life of tolbutamide when phenylbutazone was administered at the same time. However, there have been few studies on this pharmacokinetic interaction and its clinical significance. None of the studies dealt with the pharmacokinetic parameters involved in the interaction of oxyphenbutazone and tolazamide when administered simultaneously.

There are three possible mechanisms for a pharmacokinetic interaction that enhances the hypoglycemic effects of tolazamide and other sulfonlyureas in the presence of phenylbutazone or oxyphenbutazone:

1. Inhibition of drug metabolism, *i.e.*, a decrease in metabolism of tolazamide/sulfonylurea, which could be caused by the presence of oxyphenbutazone or phenylbutazone.
2. Displacement of tolazamide/sulfonylurea from protein binding sites, which could result in increased blood concentrations of unbound, pharmacologically active tolazamide/sulfonylurea or its metabolites and could also produce high urinary concentrations of unchanged drug and its metabolites.
3. Inhibition of the excretion of tolazamide/sulfonylurea by a direct effect on the kidney.

The purpose of this study was to determine if a measurable pharmacokinetic interaction existed between tolazamide and oxyphenbutazone and which mechanism might explain it.

EXPERIMENTAL

Experimental Design—A 3 × 3 Latin square was used to study the effect of varying dosage on tolazamide pharmacokinetics. A similar Latin square design was used for the tolazamide–oxyphenbutazone interaction study, in which the dose of tolazamide was kept constant and the doses of oxyphenbutazone were varied.

Nine dogs were randomly assigned to three groups of three dogs each. Each group received each treatment, with a minimum of 1 week of rest separating each session.

The study was conducted over 3 months, with the sequence of treatments in accordance with a Latin square design (Table I). In the first study, Treatments A, B, and C were 5, 20, and 35 mg of tolazamide/kg, respectively. In the second study, Treatments A, B, and C were 10, 15, and 20 mg of oxyphenbutazone/kg, respectively, all with 20 mg of tolazamide/kg.

Typical Sampling Times—Zero time for tolazamide sampling was taken to be the midpoint of the tolazamide injection. Sampling times were 2, 5, 10, and 30 min and 1, 2, 4, 6, 8, 12, and 24 hr after the tolazamide injection.

Animals—Nine mongrel dogs, 9.0–16.5 kg, were obtained from the local animal shelter. These animals were vaccinated and given appropriate treatment for parasites; after acclimation, they were certified as healthy.

A catheter was surgically placed in the jugular vein so that the tip was

Table I—Latin Square Design for the Study of Tolazamide Pharmacokinetics

Group	Dog Identification Number	Week 1	2	3
1	1, 2, 3	A	B	C
2	4, 5, 6	B	C	A
3	7, 8, 9	C	A	B

0022-3549/82/0100-0029$01.00/0

Chem., **193**, 265 (1951).
(20) R. L. Lester, "Methods in Enzymology," vol. 10, R. W. Estabrook and M. E. Pullman, Eds., Academic, New York, N.Y., 1967, p. 264.
(21) H. Lees, *Biochim. Biophys. Acta*, **105**, 184 (1965).
(22) J. B. Sumner, *Science*, **100**, 413 (1944).
(23) D. K. Myers and E. C. Slater, *Biochem. J.*, **67**, 558 (1957).
(24) C. H. Fiske and Y. Subbarow, *J. Biol. Chem.*, **66**, 375 (1925).
(25) R. I. Geran, N. H. Greenberg, M. M. MacDonald, A. M. Schumacher, and B. J. Abbott, *Cancer Chemother. Rep. Part 3*, **1972**, 3.

ACKNOWLEDGMENTS

The authors thank the Medical Research Council of Canada for the award of an operating grant (MA-5538) to J. R. Dimmock and a Summer Undergraduate Research Scholarship to E. W. K. Chow. Acknowledgment is made with gratitude to the University of Saskatchewan who provided a Graduate Scholarship to D. L. Kirkpatrick and also the University of Saskatchewan Alumni Association who awarded D. L. Kirkpatrick the John and Mary Spinks Scholarship.

Pharmacokinetic Interactions of Tolazamide and Oxyphenbutazone in Dogs

S. E. ABIDI *, A. H. KIBBE ˣ, R. W. CLEARY, A. B. JONES, and E. C. HARLAND

Received October 14, 1980, from the *Department of Pharmaceutics University of Mississippi, University, MS 38677.* Accepted for publication May 13, 1981. * Present address: School of Pharmacy, West Virginia University, Morgantown, WV 26506.

Abstract □ The described pharmacokinetic analysis involved two separate studies on nine dogs randomly assigned to three groups of three dogs each. In the first study, the effect of varying the dosage of tolazamide was examined. The second study concerned the effect of varying the dosage of oxyphenbutazone on tolazamide. A 3 × 3 Latin square was used to study both effects. Each group received each treatment, with a minimum of 1 week separating each session. The pharmacokinetics of tolazamide followed a two-compartment open model. The hybrid rate constants, α and β, were not significantly different at the three dosages when measured by a three-way analysis of variance. The only significant difference at the three dosage levels of tolazamide was in the apparent volume of distribution. In the pharmacokinetic interaction associated with intravenous administration of one dose of tolazamide and three doses of oxyphenbutazone, the apparent volume of distribution and the hybrid rate constant α did not change significantly while the hybrid rate constant for tolazamide, β, seemed to decrease with increasing oxyphenbutazone.

Keyphrases □ Pharmacokinetics—tolazamide and oxyphenbutazone interactions, dogs □ Tolazamide—pharmacokinetic interactions with oxyphenbutazone, dogs □ Oxyphenbutazone—pharmacokinetic interactions with tolazamide, dogs

Enhanced hypoglycemic effects have been reported when patients, stabilized on a sulfonylurea (tolbutamide or tolazamide), have had phenylbutazone and/or its analog, oxyphenbutazone, added to the treatment regimen (1). Hussar (2) suggested that phenylbutazone/oxyphenbutazone enhanced the hypoglycemic effects of tolbutamide or tolazamide.

Other investigators (3) found significant prolongation of the half-life of tolbutamide when phenylbutazone was administered at the same time. However, there have been few studies on this pharmacokinetic interaction and its clinical significance. None of the studies dealt with the pharmacokinetic parameters involved in the interaction of oxyphenbutazone and tolazamide when administered simultaneously.

There are three possible mechanisms for a pharmacokinetic interaction that enhances the hypoglycemic effects of tolazamide and other sulfonlyureas in the presence of phenylbutazone or oxyphenbutazone:

1. Inhibition of drug metabolism, *i.e.*, a decrease in metabolism of tolazamide/sulfonylurea, which could be caused by the presence of oxyphenbutazone or phenylbutazone.
2. Displacement of tolazamide/sulfonylurea from protein binding sites, which could result in increased blood concentrations of unbound, pharmacologically active tolazamide/sulfonylurea or its metabolites and could also produce high urinary concentrations of unchanged drug and its metabolites.
3. Inhibition of the excretion of tolazamide/sulfonylurea by a direct effect on the kidney.

The purpose of this study was to determine if a measurable pharmacokinetic interaction existed between tolazamide and oxyphenbutazone and which mechanism might explain it.

EXPERIMENTAL

Experimental Design—A 3 × 3 Latin square was used to study the effect of varying dosage on tolazamide pharmacokinetics. A similar Latin square design was used for the tolazamide–oxyphenbutazone interaction study, in which the dose of tolazamide was kept constant and the doses of oxyphenbutazone were varied.

Nine dogs were randomly assigned to three groups of three dogs each. Each group received each treatment, with a minimum of 1 week of rest separating each session.

The study was conducted over 3 months, with the sequence of treatments in accordance with a Latin square design (Table I). In the first study, Treatments A, B, and C were 5, 20, and 35 mg of tolazamide/kg, respectively. In the second study, Treatments A, B, and C were 10, 15, and 20 mg of oxyphenbutazone/kg, respectively, all with 20 mg of tolazamide/kg.

Typical Sampling Times—Zero time for tolazamide sampling was taken to be the midpoint of the tolazamide injection. Sampling times were 2, 5, 10, and 30 min and 1, 2, 4, 6, 8, 12, and 24 hr after the tolazamide injection.

Animals—Nine mongrel dogs, 9.0–16.5 kg, were obtained from the local animal shelter. These animals were vaccinated and given appropriate treatment for parasites; after acclimation, they were certified as healthy.

A catheter was surgically placed in the jugular vein so that the tip was

Table I—Latin Square Design for the Study of Tolazamide Pharmacokinetics

Group	Dog Identification Number	Week 1	2	3
1	1, 2, 3	A	B	C
2	4, 5, 6	B	C	A
3	7, 8, 9	C	A	B

0022-3549/82/0100-0029$01.00/0

Table II—Pharmacokinetic Parameters (Mean ± *SD*) Calculated from Tolazamide Plasma Concentrations Obtained after Intravenous Administration of Three Dosages

Parameter	Treatment[a] A	B	C
A, μg/ml	21.51 (4.15)	69.14 (35.36)	124.07 (53.38)
B, μg/ml	21.17 (8.69)	114.49 (37.91)	234.71 (42.24)
α, hr^{-1}	5.69 (2.40)	5.84 (4.63)	7.04 (3.37)
β, hr^{-1}	0.11 (0.01)	0.11 (0.02)	0.11 (0.02)
C_p^0, μg/ml	43.40 (11.43)	179.90 (61.82)	362.27 (64.91)
k_{21}, hr^{-1}	2.94 (1.44)	3.38 (1.99)	4.48 (2.50)
k_e, hr^{-1}	0.23 (0.04)	0.18 (0.08)	0.17 (0.04)
k_{12}, hr^{-1}	2.83 (2.07)	2.30 (2.16)	2.44 (1.68)
k_{12}/k_{12}	0.91 (0.38)	0.59 (0.47)	0.53 (0.28)
$V_d$ext liters	3.02 (0.80)	2.40 (0.96)	1.91 (0.50)

[a] A is 5, B is 20, and C is 35 mg of tolazamide/kg of body weight.

in the anterior vena cava. The catheter was directed subcutaneously from the jugular vein to a 2.0-cm incision in the back between the scapulae. It was attached to a 18-gauge needle with an infusion cap to allow for ease of sample removal.

Preparation of Material—The dogs were weighed the afternoon prior to treatment. The amount of the drug to be administered was determined according to the corresponding dose for that treatment session and the weight of the animal. Tolazamide and oxyphenbutazone solutions for intravenous injection were prepared and filtered through a 0.22-μm filter to ensure sterility.

Treatment—Food, but not water, was withdrawn from the dogs 12 hr prior to administration. Food was allowed *ad libitum* after the collection of the 4-hr sample. Dogs 1–9 received 5, 20, or 35 mg of tolazamide/kg of body weight iv in the first phase of the study.

In the second phase, Dogs 1–9 received intravenous injections of 20 mg of tolazamide/kg of body weight, immediately followed by 10, 15 or 20 mg of oxyphenbutazone/kg of body weight iv. Intravenous administration was selected to avoid any problem with drug absorption that would prevent determination of the volume of distribution.

The dose of tolazamide was selected to obtain measurable blood concentrations of the drug for at least three to five biological half-lives. This procedure allowed reproducible measurement of the magnitude of peak concentrations as well as accurate measurement of the lower values at the end of the experiment. Blood samples were withdrawn through a catheter or by venous puncture. A 3.0-ml blood sample was mixed with heparin and centrifuged immediately after mixing. The plasma was separated, transferred into a screw-capped culture tube (7 mm), and frozen at −20° until assayed.

Preparation and Extraction of Plasma Standards—A standard solution of tolazamide was prepared by dissolving 100 mg of tolazamide in 5 ml of 0.1 *N* NaOH in a 100-ml volumetric flask and brought to volume with distilled water.

Aliquots of the standard solution of tolazamide containing 5, 10, 20, 30, 40, 50, and 60 μg were placed in 50-ml screw-capped centrifuge tubes. To each centrifuge tube, 0.5 ml of dog plasma was added and mixed well. An aliquot (0.2-ml) of the internal standard solution containing 20 μg of trihexyphenidyl was then added to each centrifuge tube. To these samples, 1 ml of buffer solution (0.5 *M* KH_2PO_4,Na_2HPO_4) of pH 6 was added. Then 20 ml of chloroform was added to each centrifuge tube. The centrifuge tubes were shaken for 20 min on a table shaker and centrifuged for 5 min at 100 × *g* to break the emulsion. The aqueous phase was removed by aspiration, and 10 ml of the organic phase was transferred to a 10-ml sample vial. Samples were evaporated at room temperature in a hood overnight. The residue was dissolved in 20 μl of chloroform and analyzed by gas chromatography (GC).

Plasma Specimens—Aliquots (0.5 ml) of the plasma samples were placed in 50-ml centrifuge tubes, and the samples were processed in the same manner as the plasma standards. Duplicate aliquots from each sample were analyzed. Analysis was carried out on a gas chromatograph[1] equipped with a flame-ionization detector and a glass column (U-shaped, 183 cm length × 2-mm i.d.) packed with 3% OV-17 on 100–200 mesh Gas Chrom Q. Nitrogen was the carrier gas at a flow rate of 65 ml/min, and the rates for air and hydrogen were 250 and 45 ml/min, respectively. The column oven was operated isothermally at 180°, the flash heater was at 230, and the detector was at 280°. Under these conditions, tolazamide and trihexyphenidyl had retention times of 4 and 20 min, respectively.

[1] Beckman GC-45.

Table III—Statistical Analysis of $V_d$ext for Tolazamide at Three Dosages

Source of Variation	*df*	*SS*	*MS*	*F*
Total	26	19.86	—	—
Subject	8	8.71	1.09	2.86[b]
Group	2	0.78	0.39	1.03[a]
Subject/group	6	7.93	1.32	3.47[b]
Week	2	0.28	0.14	0.37[a]
Treatment	2	0.28	0.14	0.37[a]
Residual	14	5.36	0.36	—

[a] Not significant.
[b] Significant at the 1% level.

When using peak height ratios of tolazamide to internal standard, the calibration data (over concentration ratios of 0.25–3.00 and peak height ratios of 0.10–1.25) were linear with a correlation coefficient of 0.994.

Assay Specificity—To ensure assay specificity, a standard solution (1 mg/ml) of tolazamide was prepared in chloroform. Similarly, a standard solution of the internal standard (1 mg/ml) was prepared.

Five microliters of the standard solution of tolazamide were placed in a sample vial, and 2 μl were analyzed by GC. Retention times under the described conditions were 4 min for tolazamide and 20 min for trihexphenidyl.

As a further check on specificity, the following experiment was performed on one dog's plasma extract. Plasma extract (20 μl) was chromatographed on precoated TLC plates of silica gel F-254 of 250-μm thickness. A reference sample containing 20 μg of pure tolazamide was utilized. The plate was developed in a solvent system of chloroform–methanol–formic acid (59:4:1). The zones of tolazamide were located by examination of the chromatogram using a UV lamp (254 nm).

The R_f value (0.59) of tolazamide from all plasma extracts was identical to that of the pure tolazamide sample. The zones were removed separately and extracted with chloroform (3 × 2 ml). To each extract was added 0.1 ml of internal standard, and the total was evaporated to dryness. The residue was reconstituted in 15 μl of chloroform and analyzed. The chromatogram showed identical retention times for the TLC extract of pure tolazamide and for the samples obtained from separately extracted spots from dog plasma extracts.

Data Analysis—Results obtained from analysis of the plasma samples were corrected to reflect the plasma tolazamide concentration. These plasma concentrations and their corresponding times were utilized to calculate the pharmacokinetic parameters for each animal using AUTOAN (4).

Analysis of variance was performed to determine the significance of the differences between pharmacokinetic parameters due to treatment effect, variation among subjects and time period, and overall residual effect.

RESULTS AND DISCUSSION

The pharmacokinetic analysis involved two separate studies on an equal number of dogs. In the first study, the effect of varying the tola-

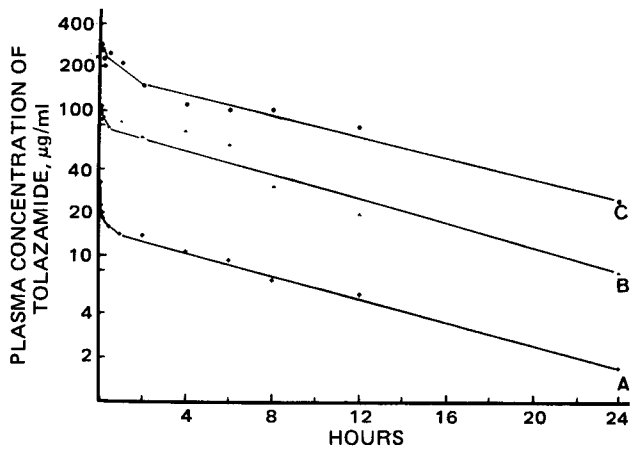

Figure 1—*Plasma concentration* versus *time curves of tolazamide for Dog 9. Key: curve A (+);5 mg of tolazamide/kg of body weight; curve B (△), 20 mg of tolazamide/kg of body weight; and curve C (●), 35 mg of tolazamide/kg of body weight.*

Table IV—Pharmacokinetic Parameters (Mean ± *SD*) Calculated from Tolazamide Plasma Concentrations Obtained after Intravenous Administration of Three Dosages of Oxyphenbutazone

Parameter	Treatment[a] TA	TB	TC
A, μg/ml	57.67 (23.29)	78.17 (35.71)	61.49 (42.18)
B, μg/ml	106.85 (20.47)	109.36 (17.68)	120.30 (36.74)
α, hr^{-1}	9.31 (7.18)	8.02 (5.64)	8.47 (6.07)
β, hr^{-1}	0.14 (0.02)	0.11 (0.02)	0.09 (0.02)
C_p^0, μg/ml	165.50 (31.69)	181.58 (32.63)	178.07 (41.92)
k_{21}, hr^{-1}	4.54 (3.71)	5.83 (4.87)	4.42 (2.96)
k_e, hr^{-1}	0.03 (0.16)	0.18 (0.05)	0.15 (0.04)
k_{12}, hr^{-1}	4.36 (3.89)	4.20 (4.56)	3.15 (1.84)
k_{12}/k_{12}	1.07 (1.09)	0.64 (0.25)	0.63 (0.35)
$V_d$ext, liters	2.31 (0.73)	2.21 (0.56)	2.23 (1.01)

[a] T is 20 mg of tolazamide/kg of body weight, and A is 10, B is 15, and C is 20 mg of oxyphenbutazone/kg of body weight.

zamide dose was examined. In the second study, the effect of varying the oxyphenbutazone doses on tolazamide was analyzed.

The data were analyzed by a two-compartment open model. In the statistical analysis, only three major parameters, α, β, and V_d extrapolated ($V_d$ext), were utilized because they are key factors in explaining a two-compartment open model. Other parameters change with changes in α and β.

Dose-Related Pharmacokinetics of Tolazamide—The pharmacokinetics of tolazamide were studied after intravenous administration of three different doses in each of nine dogs to determine if any dose-dependent changes in tolazamide kinetics were apparent (Table I). The plasma concentration data obtained at each dosage was biphasic (Fig. 1). Therefore, the data were analyzed by a two-compartment open model.

The hybrid rate constants, α and β, and the apparent volume of distribution, $V_d$ext, after intravenous administration of three different dosages of tolazamide in nine dogs are reported in Table II. The hybrid rate constant, α, which represents the rapid distribution of the drug in the body, did not change significantly. Similarly, β, which represents the loss of the drug from the body, did not change significantly with the change in the dosage levels of tolazamide.

A possible explanation for the lack of a significant difference in subject, group, and subject/group could be that mongrel dogs were used and these animals do not represent a genetically controlled breed. The only significant difference observed was in the apparent volume of distribution $V_d$ext at the three dose levels of tolazamide (Table III). It is entirely feasible that $V_d$ext might change without changing α or β as dose increases. Wagner and Pernarowski (5) suggested that the $V_d$ext will vary as a function of dose if the drug has the property of changing its diffusivity or permeability. The pharmacokinetics of tolazamide associated with intravenous administration was dose independent as measured by α and β.

Tolazamide Pharmacokinetics in Presence of Three Oxyphenbutazone Dosages—Results from the pharmacokinetic analysis of the

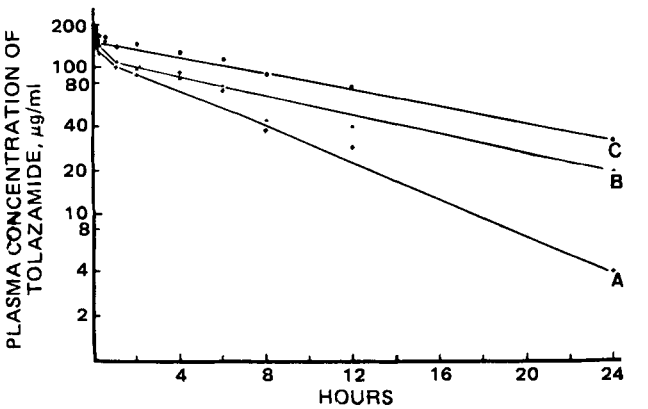

Figure 2—*Plasma concentration* versus *time curves of tolazamide (20 mg/kg of body weight) in presence of oxyphenbutazone for Dog 9. Key: curve A (+), 10 mg of oxyphenbutazone/kg of body weight; curve B (▲), 15 mg of oxyphenbutazone/kg of body weight; curve C (●), 20 mg of oxyphenbutazone/kg of body weight.*

Table V—Statistical Analysis of $V_\beta$ext for Tolazamide at Three Dosages of Oxyphenbutazone

Source of Variation	*df*	*SS*	*MS*	*F*
Total	26	0.0199	—	—
Subject	8	0.0095	0.00119	7.93[a]
Group	2	0.0023	0.00115	7.67[a]
Subject/group	6	0.0072	0.00120	8.00[a]
Week	2	0.0008	0.00040	2.67[b]
Treatment	2	0.0075	0.00375	25.00[a]
Residual	14	0.0021	0.00015	—

[a] Significant at the 1% level. [b] Not significant.

blood concentration data obtained from a dog that received 20.0 mg of tolazamide/kg iv followed by 10.0, 15.0, or 20.0 mg of oxyphenbutazone/kg are depicted in Fig. 2, which shows a biphasic trend. Therefore, blood concentration data were analyzed by a two-compartment open model. Tables IV and V contain the estimated pharmacokinetic parameters and statistical analysis data for these animals.

The parameters α, β, and $V_d$ext obtained from nine dogs after intravenous administration of 20.0 mg of tolazamide/kg followed by one of the three dosages of oxyphenbutazone were analyzed by a three-way analysis of variance. For tolazamide, α and $V_d$ext did not change significantly in the presence of the three oxyphenbutazone doses. However, β was significantly different for tolazamide in the presence of these three oxyphenbutazone doses.

Thus, it can be concluded that oxyphenbutazone only affects the β hybrid rate constant of tolazamide. This effect of oxyphenbutazone appears to be more pronounced as its dose increases. From the data reported here, only a trend can be seen, as depicted graphically in Fig. 3. The decrease in β with increasing dose of oxyphenbutazone represents a decrease in the overall elimination rate of tolazamide from the body. The value for β that was calculated from the first experiment in which the dogs received tolazamide alone cannot statistically be included in the analysis of the second experiment, but it was of the same order of magnitude.

These changes can be explained on the basis of three possible mechanisms of interaction of tolazamide and oxyphenbutazone.

The first possible mechanism involves inhibition of the tolazamide metabolism caused by the presence of oxyphenbutazone. A possible explanation could be that oxyphenbutazone may promote the synthesis of a form of cytochrome P-450 that has a lower metabolic capacity for tolazamide. Induction of this hepatic microsomal monooxygenase system is well established in animals (6). Some inducing agents can also decrease the microsomal oxidative capacity for a substrate (7). Any one or a combination of several of these changes could be the reason for the significant differences in β.

The second possible mechanism involves the displacement of tolazamide from protein binding sites. The values of α and $V_d$ext for tolazamide were not significantly different at the three oxyphenbutazone doses. This finding suggests that there might be little or no competitive displacement of tolazamide from protein binding sites in the presence of oxyphenbutazone.

The third possible mechanism could be inhibition of tolazamide excretion. Many acidic drugs and their metabolites are actively secreted

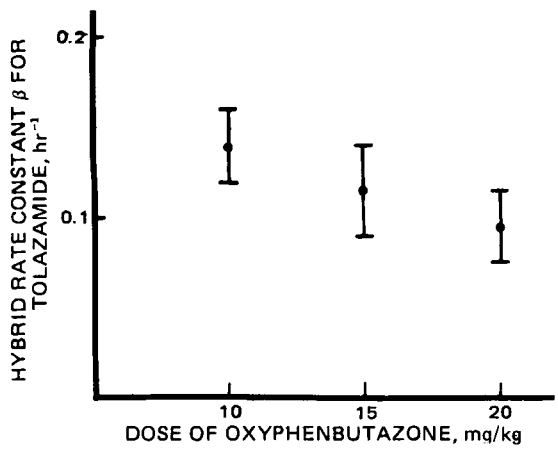

Figure 3—*Mean hybrid rate constant β obtained from nine dogs for tolazamide* versus *dose of oxyphenbutazone.*

by the proximal tubular active transport mechanism, and drug–drug interactions may result from competition with this system. Since tolazamide and oxyphenbutazone are weakly acidic drugs, they might compete for active secretion by the proximal tubular active transport mechanism. The hypoglycemic action of acetohexamide is enhanced by the simultaneous administration of phenylbutazone by the same mechanics (8). Similarly, the hypoglycemic action of tolbutamide is enhanced by the presence of phenylbutazone (9). The value of β for tolazamide seems to decrease with increasing oxyphenbutazone, which could result in an enhanced hypoglycemic effect of tolazamide.

REFERENCES

(1) M. Rowland and S. B. Martin, *J. Pharmacokinet. Biopharm.*, **1**, 553 (1973).

(2) D. A. Hussar, *J. Am. Pharm. Assoc.*, **NS10**, 619 (1970).

(3) L. K. Christensen, J. M. Hansen, and M. Kristensen, *Lancet*, **2**, 1298 (1963).

(4) A. Sedman, and J. G. Wagner, "Manual for Autoan, A Decision-Making Pharmacokinetic Program," Publication Distribution Service, University of Michigan, Ann Arbor, Mich., 1974.

(5) J. G. Wagner, and M. Pernarowski, "Biopharmaceutics and Relevant Pharmacokinetics," Drug Intelligence, Hamilton, Ill., 1971, p. 257.

(6) L. F. Prescott, P. Roscoe, and J. A. H. Forrest, in "Biological Effects of Drugs in Relation to Their Plasma Concentrations," D. S. Davies and B. H. C. Prichard, Eds., University Park Press, London, England, 1973, p. 51.

(7) S. M. Pond, D. J. Birkett, and D. N. Wade, *Clin. Pharmacol. Ther.*, **22**, 573 (1977).

(8) J. G. Field, M. Ohta, C. Boyle, and A. Remer, *N. Engl. J. Med.*, **277**, 889 (1967).

(9) K. F. Ober, *Eur. Clin. Pharmacol.*, **7**, 291 (1974).

ACKNOWLEDGMENTS

Supported by the Research Institute of Pharmaceutical Sciences.

Influence of Food and Fluid Volume on Chlorothiazide Bioavailability: Comparison of Plasma and Urinary Excretion Methods

PETER G. WELLING ˣ and RASHMI H. BARBHAIYA *

Received February 23, 1981, from the *School of Pharmacy, University of Wisconsin, Madison, WI 53706.* Accepted for publication May 13, 1981.

* Present address: Department of Drug Metabolism and Pharmacokinetics, Bristol Laboratories, Syracuse, NY 13201.

Abstract □ The bioavailability of chlorothiazide from oral tablets was examined under fasting and nonfasting conditions in healthy male volunteers. Bioavailability was determined from urinary excretion data and plasma chlorothiazide concentrations. Two fasting treatments and one nonfasting treatment yielded similar plasma chlorothiazide profiles, characterized by sharply ascending and descending segments until 12–13 hr postdosing, followed by a prolonged period with variable and erratic chlorothiazide levels. A triexponential function that adequately described mean data from each treatment could not be applied to individual plasma curves because of their variable nature. Chlorothiazide absorption was not influenced by different accompanying water volumes in fasted individuals but was doubled when tablets were administered immediately after a standard meal. Urinary excretion of chlorothiazide correlated well with plasma drug concentrations; 48-hr urinary recovery accounted for 24.7% of a 500-mg dose in nonfasted subjects compared to 12.3 and 14.9% in fasted subjects receiving the drug with 20 and 250 ml of water, respectively. Observed relationships between chlorothiazide dosage and absorption efficiency are consistent with previous suggestions that chlorothiazide absorption from the GI tract is saturable and site specific.

Keyphrases □ Chlorothiazide—effect of food and fluid volume on bioavailability, plasma and urinary excretion methods compared □ Bioavailability—chlorothiazide, effect of food and fluid volume, plasma and urinary excretion methods compared □ Diuretics—chlorothiazide, influence of food and fluid volume on bioavailability, plasma and urinary excretion methods compared

Chlorothiazide is poorly absorbed after oral doses. Less than 25% of orally administered compound is recovered in urine, compared to >90% following intravenous injection (1–4). Inefficient GI absorption of chlorothiazide may be partly due to its low aqueous solubility but also may be related to saturable and site-specific absorption (5, 6).

The presence of food and the variation in fluid volumes with which a drug is administered can markedly influence drug bioavailability (7–9) with possible clinical consequences (10). The poor and possibly site-specific absorption characteristics of chlorothiazide make it conducive to a bioavailability study under varying dosage conditions.

This report describes chlorothiazide bioavailability following oral doses of commercial tablets to healthy male volunteers in fasting and nonfasting states and with small and large accompanying water volumes. Plasma concentrations and urinary excretion of chlorothiazide were compared using recently described high-pressure liquid chromatographic (HPLC) procedures (11).

EXPERIMENTAL

Subjects—Nine healthy male volunteers[1], 22–33 years of age (mean 27) and weighing 62–88 kg (mean 74), participated in the study after giving informed consent. No subject had histories of drug allergy.

Protocols—Subjects were instructed to take no drugs for 1 week before the study and no drugs other than chlorothiazide during the study. No caffeine-containing beverages were permitted for 1 day before or during the plasma and urine sampling periods following each chlorothiazide dose.

Chlorothiazide[2] was administered as three oral treatments: Treatment A, two 250-mg tablets with 250 ml of water following an overnight fast; Treatment B, two 250-mg tablets with 20 ml of water following an overnight fast; and Treatment C, two 250-mg tablets with 250 ml of water given immediately after a standard breakfast (cornflakes with milk, 150 ml (5 oz) orange juice, two poached eggs, two slices of toast, and one cup of caffeine-free coffee).

Subjects were randomly divided into three groups of three, and the treatments were administered according to a 3 × 3 Latin square design at 1-week intervals. Each treatment was given after an overnight fast; no food, apart from the standard breakfast for those receiving Treatment

[1] Technical staff and graduate students.

[2] Chlorothiazide tablets USP (250 mg), lot 559-197, Lederle Laboratories, American Cyanamid Co., Pearl River, NY 10965.

0022-3549/82/0100-0032$01.00/0

by the proximal tubular active transport mechanism, and drug–drug interactions may result from competition with this system. Since tolazamide and oxyphenbutazone are weakly acidic drugs, they might compete for active secretion by the proximal tubular active transport mechanism. The hypoglycemic action of acetohexamide is enhanced by the simultaneous administration of phenylbutazone by the same mechanics (8). Similarly, the hypoglycemic action of tolbutamide is enhanced by the presence of phenylbutazone (9). The value of β for tolazamide seems to decrease with increasing oxyphenbutazone, which could result in an enhanced hypoglycemic effect of tolazamide.

REFERENCES

(1) M. Rowland and S. B. Martin, *J. Pharmacokinet. Biopharm.*, **1**, 553 (1973).

(2) D. A. Hussar, *J. Am. Pharm. Assoc.*, **NS10**, 619 (1970).

(3) L. K. Christensen, J. M. Hansen, and M. Kristensen, *Lancet*, **2**, 1298 (1963).

(4) A. Sedman, and J. G. Wagner, "Manual for Autoan, A Decision-Making Pharmacokinetic Program," Publication Distribution Service, University of Michigan, Ann Arbor, Mich., 1974.

(5) J. G. Wagner, and M. Pernarowski, "Biopharmaceutics and Relevant Pharmacokinetics," Drug Intelligence, Hamilton, Ill., 1971, p. 257.

(6) L. F. Prescott, P. Roscoe, and J. A. H. Forrest, in "Biological Effects of Drugs in Relation to Their Plasma Concentrations," D. S. Davies and B. H. C. Prichard, Eds., University Park Press, London, England, 1973, p. 51.

(7) S. M. Pond, D. J. Birkett, and D. N. Wade, *Clin. Pharmacol. Ther.*, **22**, 573 (1977).

(8) J. G. Field, M. Ohta, C. Boyle, and A. Remer, *N. Engl. J. Med.*, **277**, 889 (1967).

(9) K. F. Ober, *Eur. Clin. Pharmacol.*, **7**, 291 (1974).

ACKNOWLEDGMENTS

Supported by the Research Institute of Pharmaceutical Sciences.

Influence of Food and Fluid Volume on Chlorothiazide Bioavailability: Comparison of Plasma and Urinary Excretion Methods

PETER G. WELLING ˣ and RASHMI H. BARBHAIYA *

Received February 23, 1981, from the *School of Pharmacy, University of Wisconsin, Madison, WI 53706.* Accepted for publication May 13, 1981.

* Present address: Department of Drug Metabolism and Pharmacokinetics, Bristol Laboratories, Syracuse, NY 13201.

Abstract □ The bioavailability of chlorothiazide from oral tablets was examined under fasting and nonfasting conditions in healthy male volunteers. Bioavailability was determined from urinary excretion data and plasma chlorothiazide concentrations. Two fasting treatments and one nonfasting treatment yielded similar plasma chlorothiazide profiles, characterized by sharply ascending and descending segments until 12–13 hr postdosing, followed by a prolonged period with variable and erratic chlorothiazide levels. A triexponential function that adequately described mean data from each treatment could not be applied to individual plasma curves because of their variable nature. Chlorothiazide absorption was not influenced by different accompanying water volumes in fasted individuals but was doubled when tablets were administered immediately after a standard meal. Urinary excretion of chlorothiazide correlated well with plasma drug concentrations; 48-hr urinary recovery accounted for 24.7% of a 500-mg dose in nonfasted subjects compared to 12.3 and 14.9% in fasted subjects receiving the drug with 20 and 250 ml of water, respectively. Observed relationships between chlorothiazide dosage and absorption efficiency are consistent with previous suggestions that chlorothiazide absorption from the GI tract is saturable and site specific.

Keyphrases □ Chlorothiazide—effect of food and fluid volume on bioavailability, plasma and urinary excretion methods compared □ Bioavailability—chlorothiazide, effect of food and fluid volume, plasma and urinary excretion methods compared □ Diuretics—chlorothiazide, influence of food and fluid volume on bioavailability, plasma and urinary excretion methods compared

Chlorothiazide is poorly absorbed after oral doses. Less than 25% of orally administered compound is recovered in urine, compared to >90% following intravenous injection (1–4). Inefficient GI absorption of chlorothiazide may be partly due to its low aqueous solubility but also may be related to saturable and site-specific absorption (5, 6).

The presence of food and the variation in fluid volumes with which a drug is administered can markedly influence drug bioavailability (7–9) with possible clinical consequences (10). The poor and possibly site-specific absorption characteristics of chlorothiazide make it conducive to a bioavailability study under varying dosage conditions.

This report describes chlorothiazide bioavailability following oral doses of commercial tablets to healthy male volunteers in fasting and nonfasting states and with small and large accompanying water volumes. Plasma concentrations and urinary excretion of chlorothiazide were compared using recently described high-pressure liquid chromatographic (HPLC) procedures (11).

EXPERIMENTAL

Subjects—Nine healthy male volunteers[1], 22–33 years of age (mean 27) and weighing 62–88 kg (mean 74), participated in the study after giving informed consent. No subject had histories of drug allergy.

Protocols—Subjects were instructed to take no drugs for 1 week before the study and no drugs other than chlorothiazide during the study. No caffeine-containing beverages were permitted for 1 day before or during the plasma and urine sampling periods following each chlorothiazide dose.

Chlorothiazide[2] was administered as three oral treatments: Treatment A, two 250-mg tablets with 250 ml of water following an overnight fast; Treatment B, two 250-mg tablets with 20 ml of water following an overnight fast; and Treatment C, two 250-mg tablets with 250 ml of water given immediately after a standard breakfast (cornflakes with milk, 150 ml (5 oz) orange juice, two poached eggs, two slices of toast, and one cup of caffeine-free coffee).

Subjects were randomly divided into three groups of three, and the treatments were administered according to a 3 × 3 Latin square design at 1-week intervals. Each treatment was given after an overnight fast; no food, apart from the standard breakfast for those receiving Treatment

[1] Technical staff and graduate students.

[2] Chlorothiazide tablets USP (250 mg), lot 559-197, Lederle Laboratories, American Cyanamid Co., Pearl River, NY 10965.

0022-3549/82/0100-0032$01.00/0

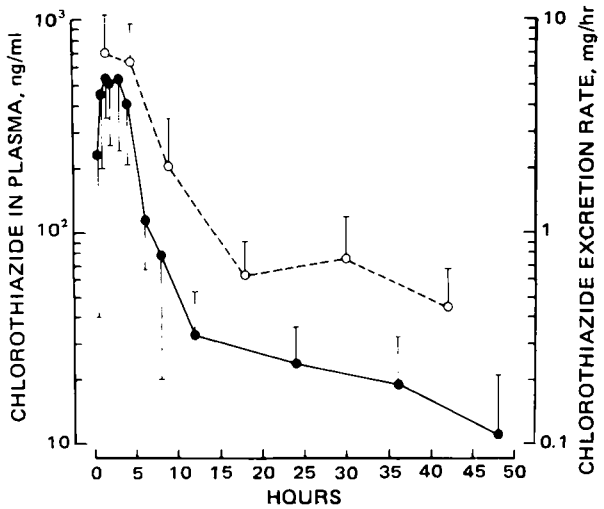

Figure 1—*Mean plasma concentrations (●) and urinary excretion rates (○) of chlorothiazide following Treatment A. Error bars indicate one standard deviation.*

C, was permitted until 4 hr after each chlorothiazide dose, after which time normal eating and drinking were permitted.

On the morning of each treatment, 250 ml of water was ingested on rising, at least 1 hr before dosing. Chlorothiazide was administered at 8 am. Tablets were swallowed whole, without chewing.

Blood samples (10 ml) were taken from a forearm vein into vacuum tubes[3] containing heparin as anticoagulant immediately before and then serially to 48 hr after dosing. Urine was collected immediately before and then quantitatively at intervals up to 48 hr after dosing. Plasma was separated by centrifugation, and plasma and urine samples were stored at −20° until assayed, generally within 2 weeks.

Analytical—Concentrations of chlorothiazide in plasma and in urine were determined by the HPLC methods described previously (11). The methods, both involving extraction steps prior to chromatography, are linearly sensitive to chlorothiazide concentrations of 2–100 μg/ml in urine and 10–750 ng/ml in plasma with coefficients of variation of <10% within these concentration ranges. The occasional plasma samples that contained chlorothiazide concentrations of >750 ng/ml were appropriately diluted with water and reassayed. Dilution with water had no effect on the extraction efficiency of chlorothiazide or the internal standard.

Data Analysis—The irregular nature of plasma chlorothiazide curves in individual subjects precluded data description in terms of a general mathematical function. However, the means of plasma curves obtained from each treatment were fitted to a triexponential function using

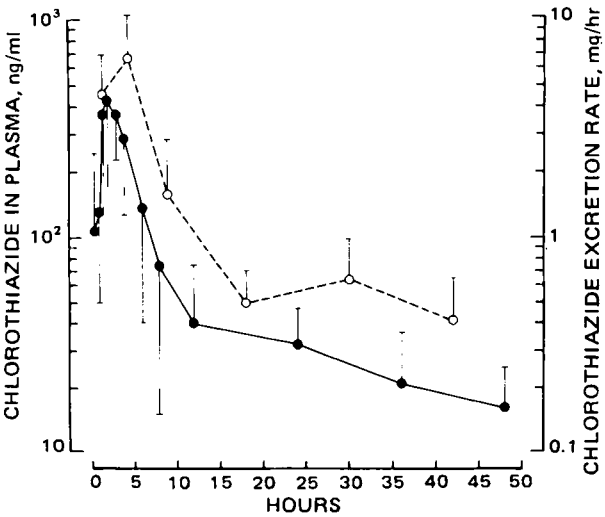

Figure 2—*Mean plasma concentrations (●) and urinary excretion rates (○) of chlorothiazide following Treatment B.*

[3] Vacutainer.

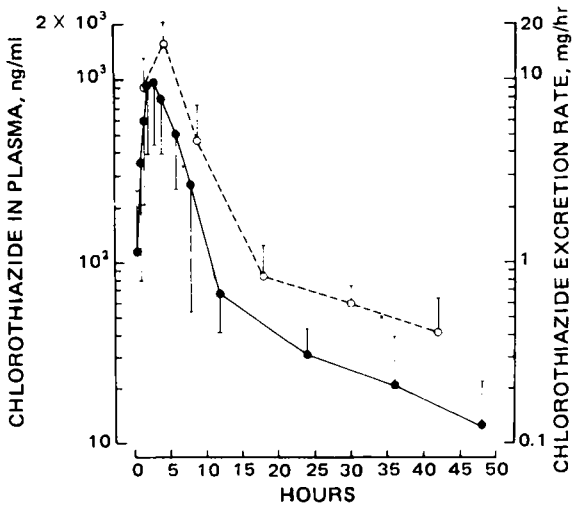

Figure 3—*Mean plasma concentrations (●) and urinary excretion rates (○) of chlorothiazide following Treatment C.*

standard graphical procedures. Improved parameter estimates, together with statistical analysis, were obtained using the computer program NREG (12) on a digital computer[4].

Plasma and urine data from the three treatments were compared by analysis of variance for a crossover design. Differences between individual treatments were examined by Tukey's test (13).

Reagents—Human plasma for assay standardization was purchased[5]. Human drug-free urine was obtained from male donors as required. Chlorothiazide[6], hydrochlorothiazide[6], and hydroflumethiazide[7] of reference standard quality for chromatography and methanol[8], acetonitrile[8], acetic acid[9], sodium perchlorate[10], and perchloric acid[11] of analytical grade quality were used as received.

RESULTS

Plasma Chlorothiazide Levels—The mean plasma chlorothiazide levels resulting from each treatment are shown in Figs. 1–3. For comparison, the mean plasma curves are combined in Fig.4.

The overall characteristics of the chlorothiazide plasma curves were similar for all treatments. Levels reached peak values at 2–3 hr and then

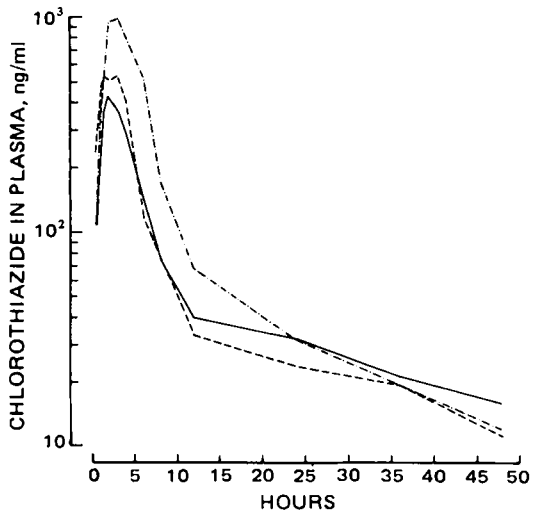

Figure 4—*Mean plasma concentrations of chlorothiazide following Treatments A (- -), B (—), and C (-•-•-).*

[4] Univac model 1110, Madison Academic Computer Center, Madison, Wis.
[5] American Red Cross, Madison, Wis.
[6] Merck Sharp and Dohme, West Point, Pa.
[7] Bristol Laboratories, Syracuse, N.Y.
[8] Burdick & Jackson, Muskegon, Mich.
[9] Allied Chemical Corp., Morristown, N.J.
[10] Fisher Scientific Co., Fair Lawn, N.J.
[11] J. T. Baker Chemical Co., Phillipsburg, N.J.

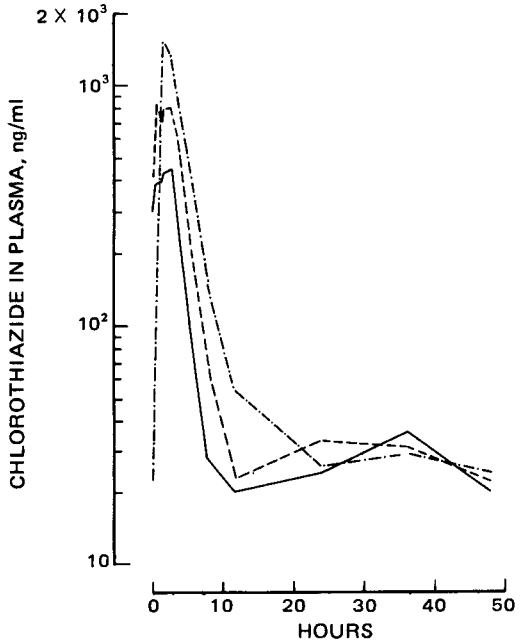

Figure 5—*Plasma concentrations of chlorothiazide in one subject following Treatments A (- -), B (—), and C (- • - •).*

declined rapidly until 12–13 hr. At later sampling times, mean chlorothiazide levels declined more slowly.

Despite the similarity in the plasma chlorothiazide profiles from the treatments, significant differences existed between treatments in the absolute values obtained. Chlorothiazide concentrations at each sampling time were statistically indistinguishable between the two fasting treatments, A and B. However, Treatment C gave rise to drug concentrations that were significantly higher compared to both fasting treatments at 2, 3, 4, 6, and 8 hr and significantly higher than Treatment A alone at 1.5 hr and then Treatment B alone at 12 hr. The mean peak chlorothiazide level from Treatment C (1107 ± 577 ng/ml) was approximately twofold higher than the levels from Treatments A (513 ± 205 ng/ml) and B (681 ± 214 ng/ml); the mean trapezoidal area under the plasma level *versus* time curve from 0 to 48 hr for Treatment C (6.4 ± 2.5 μg/hr/ml) was also twofold larger than the areas for Treatments A (3.0 ± 1.0 μg/hr/ml) and B (3.4 ± 1.1 μg/hr/ml). The mean time of peak levels from Treatment C (3.7 ± 2.1 hr) was significantly longer than those from Treatments A (2.0 ± 0.8 hr) and B (2.1 ± 1.0 hr).

Analysis of the mean chlorothiazide profiles in Figs. 1–4 in terms of a simple, triexponential function yielded the values in Eqs. 1–3 for Treatments A–C, respectively:

$$C' = -1627e^{-0.70t} + 1526e^{-0.38t} + 56.6e^{-0.026t} \quad \text{(Eq. 1)}$$

$$C' = -2626e^{-0.73t} + 2547e^{-0.43t} + 48.7e^{-0.029t} \quad \text{(Eq. 2)}$$

$$C' = -2914e^{-0.58t} + 2658e^{-0.26t} + 108e^{-0.046t} \quad \text{(Eq. 3)}$$

In the equations, C' is the plasma chlorothiazide concentration at time t. The coefficients of determination between mean plasma levels and those predicted from the respective equations were 0.97, 0.98, and 0.95.

The high coefficients of determination imply that chlorothiazide plasma levels may be adequately described by such a function following oral doses and that the mean terminal phase plasma half-life varied from 15 to 27 hr. Examination of individual chlorothiazide curves, however, shows that the apparent slow terminal elimination phase was largely artifactual, resulting from the averaging of individual data. Typical drug level curves for one subject are shown in Fig. 5. The steeply ascending and descending segments are well defined for all treatments, but drug levels during the post 12-hr period are erratic, exhibiting a "saw-tooth" effect. Thus, it was not possible to describe this section of the curve mathematically.

If the sharply descending portion of the chlorothiazide concentration curve is considered separately, the mean half-lives obtained from this segment are 2.2 ± 0.7, 2.2 ± 1.0, and 2.5 ± 0.8 hr from Treatments A, B, and C, respectively.

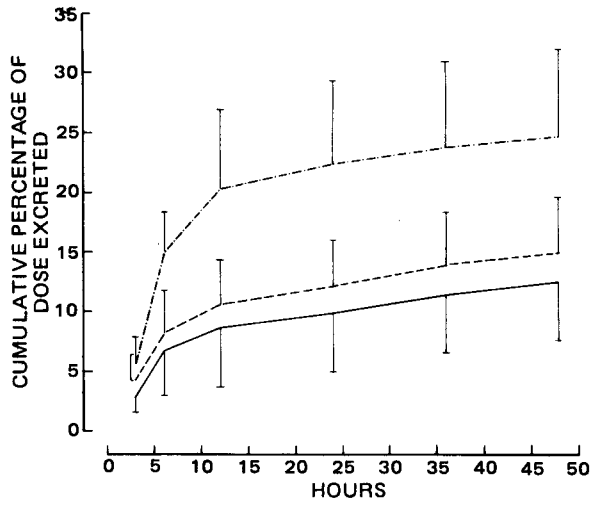

Figure 6—*Mean cumulative percentage of chlorothiazide dose excreted in urine following Treatments A (- -), B (—), and C (- • - •). Error bars indicate one standard deviation.*

Urinary Excretion of Chlorothiazide—The mean cumulative excretion of chlorothiazide during the 48-hr postdosing period is shown in Fig. 6. Following Treatment A, 8.6% of the administered dose was recovered at 12 hr, 9.8% at 24 hr, and 12.3% at 48 hr. Following Treatment B, recoveries at these times were 10.5, 12.1, and 14.9%, respectively. In contrast, the recoveries from Treatment C were 20.3, 22.3, and 24.7% at 12, 24, and 48 hr, respectively. The recovery values from Treatment C were significantly higher than those from both fasted treatments at all urine sampling intervals. The urinary recovery of chlorothiazide from the fasting treatments was similar to values reported previously (3, 4).

The renal clearances of chlorothiazide, calculated by dividing the quantity of drug recovered in 48-hr urine by the area under the chlorothiazide plasma curve during the same time period, were 3.56 ± 1.07, 37.3 ± 1.06, and 3.46 ± 11.0 ml/min from Treatments A, B, and C, respectively. The high renal clearance of chlorothiazide indicate that it is eliminated by both renal filtration and secretion.

DISCUSSION

Until recently, the low circulating levels of chlorothiazide following therapeutic doses prevented accurate description of its pharmacokinetics; bioavailability determinations were based on urinary excretion data (3). The recent development of a sensitive assay for chlorothiazide in plasma (6) has made it possible to examine the pharmacokinetics of chlorothiazide in plasma and to compare quantitatively the plasma profiles and urinary excretion rates resulting from oral chlorothiazide doses.

The plasma profiles obtained in the present study were similar to those reported by Shah et al. (3). In their study, peak chlorothiazide plasma levels of 245 and 500 ng/ml were obtained in two subjects 3 hr after a 500-mg tablet dose. Plasma levels during the 12–48-hr sampling period also exhibited a variable, saw-tooth effect.

The cause of the variable chlorothiazide plasma levels during later sampling times is not clear but may be related to drug release from extravascular storage depots or to an enterohepatic cycling effect. It is a consistent phenomenon and occurred in every subject.

The close similarity of plasma profiles and urinary excretion rates of chlorothiazide following the Treatments A and B indicates that, unlike some therapeutic agents (14–16), chlorothiazide absorption is not influenced by the accompanying fluid volume when taken on an empty stomach. However, chlorothiazide absorption efficiency is doubled when taken immediately following a meal.

The increased but delayed absorption of chlorothiazide in nonfasting individuals can possibly be explained in terms of an altered stomach emptying rate and saturable, site-specific absorption. Solid food delays stomach emptying (7) and is likely to reduce the rate at which chlorothiazide passes the absorption site and the drug concentration at the absorption surface. These combined effects give rise to more efficient but somewhat slower drug absorption into the systemic circulation. Propantheline bromide, a potent inhibitor of stomach emptying and intestinal motility, has been shown to increase GI absorption of chlorothiazide in dogs (5). Increased systemic availability in the presence of food, due

to nonsaturation of specific absorption sites, was demonstrated previously for riboflavin (17).

Increasing the accompanying water volume in fasted subjects might be expected to increase the dissolution rate of chlorothiazide and to accelerate the stomach emptying rate (7). However, neither factor should markedly alter the absorption efficiency of chlorothiazide. Faster stomach emptying would increase the rate at which drug passes the active absorption site and, hence, reduce its bioavailability. Faster dissolution should have little effect since chlorothiazide has been shown to be only 25% bioavailable when dosed as an oral solution (6).

It is instructive to compare chlorothiazide plasma levels and urinary excretion as indicators of chlorothiazide bioavailability. The mean urinary recoveries of chlorothiazide from Treatments A, B, and C were 12.3, 14.9, and 24.7% of the dose, respectively, while the respective areas under the plasma curves to 48 hr were 3.0, 3.4, and 6.4 μg hr/ml, indicating excellent agreement between plasma and urine data. The overall correlation between the percentage of dose excreted and the areas under the plasma level curves was 0.726 ($p < 0.001$), while the correlation between peak drug levels in plasma and percent excretion was somewhat lower at 0.480.

Similarly, the mean ratios of the percentage of dose excreted between Treatments A and B, A and C, and B and C were 0.87, 0.51, and 0.63; the equivalent ratios of areas under the plasma curves between these treatments were 0.92, 0.47, and 0.57.

To compare the kinetics of chlorothiazide recovery in urine with those of drug loss from plasma, the urinary excretion rates following the three treatments were calculated at the midpoint of each urine collection interval and the mean values were plotted along with the plasma levels in Figs. 1–3. Comparison of the curves indicates close similarity between the urinary excretion rates and plasma chlorothiazide levels throughout the entire sampling period.

Chlorothiazide absorption, which is normally poor, is doubled by the presence of food. This fact, together with the insensitivity of chlorothiazide absorption to varying fluid volumes, supports the view that chlorothiazide absorption is saturable and occurs at a particular site in the GI intestinal tract (5, 6). For optimal absorption, chlorothiazide tablets should be taken with or immediately after meals.

REFERENCES

(1) R. E. Kauffman and D. L. Azarnoff, *Clin. Pharmacol. Ther.*, **14**, 886 (1973).

(2) M. C. Meyer and A. B. Straughn, *Curr. Ther. Res.*, **22**, 573 (1977).

(3) V. P. Shah, V. K. Prasad, B. E. Cabana, and P. Sojka, *ibid.*, **24**, 366 (1978).

(4) A. B. Straughn, A. P. Melikian, and M. C. Meyer, *J. Pharm. Sci.*, **68**, 1009 (1979).

(5) D. E. Resetarits and T. E. Bates, *J. Pharmacokinet. Biopharm.*, **7**, 463 (1979).

(6) P. G. Welling, D. M. Walter, R. B. Patel, R. H. Barbhaiya, W. A. Porter, G. L. Amidon, T. S. Foster, V. P. Shah, J. P. Hunt, and V. K. Prasad, *Curr. Ther. Res.*, **29**, 815 (1981).

(7) P. G. Welling, *J. Pharmacokinet. Biopharm.*, **5**, 291 (1977).

(8) A. Melander, *Clin. Pharmacokinet.*, **3**, 337 (1978).

(9) R. D. Toothaker and P. G. Welling, *Ann. Rev. Pharmacol. Toxicol.*, **20**, 173 (1980).

(10) P. G. Welling, *Prog. Drug Metab.*, **4**, 131 (1980).

(11) R. H. Barbhaiya, T. A. Phillips, and P. G. Welling, *J. Pharm. Sci.*, **70**, 291 (1981).

(12) "MACC Nonlinear Regression Routines," Academic Computer Center, University of Wisconsin, Madison, Wis.

(13) J. Neter and W. Wasserman, "Applied Linear Statistical Models," Richard D. Irwin, Inc., Homewood, Ill., 1974, p. 475.

(14) P. A. Koch, C. A. Schultz, R. J. Wills, S. L. Hallquist, and P. G. Welling, *J. Pharm. Sci.*, **67**, 1533 (1978).

(15) P. G. Welling, L. L. Lyons, W. A. Craig, and G. A. Trochta, *Clin. Pharm. Ther.*, **17**, 475 (1975).

(16) P. G. Welling, H. Huang, P. A. Koch, W. A. Craig, and P. O. Madsen, *J. Pharm. Sci.*, **66**, 549 (1977).

(17) G. Levy and W. J. Jusko, *ibid.*, **55**, 285 (1966).

ACKNOWLEDGMENTS

Funds for this study were provided by National Institutes of Health Grant GM 20327.

Tray Drying of Pharmaceutical Wet Granulations

J. T. CARSTENSEN* [x] **and M. A. ZOGLIO**[‡]

Received August 5, 1980, from the *School of Pharmacy, University of Wisconsin, Madison, WI 53706 and [‡]Merrell-National Laboratories, Cincinnati, OH 45201. Accepted for publication May 15, 1981.

Abstract □ It is shown that in tray drying wet granulated materials, the expected log–linear plots give slopes that are inversely proportional to the bed depth, rather than to the depth squared. A model is proposed for this giving diffusion coefficents of the order of magnitude expected for liquid-water diffusion. The temperature dependence also suggests that this is the rate-limiting process rather than vapor diffusion.

Keyphrases □ Tray drying—wet granulated materials, mathematical models □ Models, mathematical—tray drying of wet granulated materials □ Granulations—tray drying, mathematical models

The drying of granulations is an important pharmaceutical operation and tray drying is a frequently used method of water removal. The way in which drying takes place from a tray (1–3) can be visualized in several ways. The drying could be a function of the individual granule rather than of the mass of granules, *i.e.*, the bed. In that case, the bed thickness would not be a factor (in fluid bed drying it is not of great importance). However, bed thickness is important, and the drying is a function of the properties of the bed. In this case there are two possibilities: (*a*) either the movement through the void space between the granules is important (*i.e.*, the vapor diffusion is rate determining), or (*b*) the drying is primarily from the *bed* surface, and liquid movement up through the bed maintains a water concentration profile in the bed.

BACKGROUND

In the following discussion, the nomenclature outlined in Fig. 1 will be used. The bed is l-cm deep, has a porosity of ϵ (*i.e.*, a solids fraction of $(1 - \epsilon)$). It has a cross-sectional area of A cm^2. The density of an anhydrous granule is ρ gm/cm^3. The wet granulation before drying contains C^* g of moisture per g of anhydrous solid, and after drying contains c g of moisture per g of anhydrous solid. If c is the equilibrium concentration, then $C^* - c = C_0$ is the initially removable moisture concentration, and $C' - c = C$ is the moisture concentration which is removable at time t. The latter is the quantity which will be dealt with in the following discussion. Granules containing c g of moisture/g of anhydrous weight will be denoted dry. If x is a distance coordinate measured from the top of the bed (Fig. 1), then the diffusional equation governing the situation is Fick's law, *i.e.*, at time t:

$$\partial C/\partial t = D\partial^2 C/\partial x^2 \qquad \text{(Eq. 1)}$$

where D is the diffusion coefficient of water. Crank (4) solved this equation using the following boundary conditions: $C = 0$ at $x = 0$, for t

to nonsaturation of specific absorption sites, was demonstrated previously for riboflavin (17).

Increasing the accompanying water volume in fasted subjects might be expected to increase the dissolution rate of chlorothiazide and to accelerate the stomach emptying rate (7). However, neither factor should markedly alter the absorption efficiency of chlorothiazide. Faster stomach emptying would increase the rate at which drug passes the active absorption site and, hence, reduce its bioavailability. Faster dissolution should have little effect since chlorothiazide has been shown to be only 25% bioavailable when dosed as an oral solution (6).

It is instructive to compare chlorothiazide plasma levels and urinary excretion as indicators of chlorothiazide bioavailability. The mean urinary recoveries of chlorothiazide from Treatments A, B, and C were 12.3, 14.9, and 24.7% of the dose, respectively, while the respective areas under the plasma curves to 48 hr were 3.0, 3.4, and 6.4 μg hr/ml, indicating excellent agreement between plasma and urine data. The overall correlation between the percentage of dose excreted and the areas under the plasma level curves was 0.726 ($p < 0.001$), while the correlation between peak drug levels in plasma and percent excretion was somewhat lower at 0.480.

Similarly, the mean ratios of the percentage of dose excreted between Treatments A and B, A and C, and B and C were 0.87, 0.51, and 0.63; the equivalent ratios of areas under the plasma curves between these treatments were 0.92, 0.47, and 0.57.

To compare the kinetics of chlorothiazide recovery in urine with those of drug loss from plasma, the urinary excretion rates following the three treatments were calculated at the midpoint of each urine collection interval and the mean values were plotted along with the plasma levels in Figs. 1–3. Comparison of the curves indicates close similarity between the urinary excretion rates and plasma chlorothiazide levels throughout the entire sampling period.

Chlorothiazide absorption, which is normally poor, is doubled by the presence of food. This fact, together with the insensitivity of chlorothiazide absorption to varying fluid volumes, supports the view that chlorothiazide absorption is saturable and occurs at a particular site in the GI intestinal tract (5, 6). For optimal absorption, chlorothiazide tablets should be taken with or immediately after meals.

REFERENCES

(1) R. E. Kauffman and D. L. Azarnoff, *Clin. Pharmacol. Ther.*, **14**, 886 (1973).

(2) M. C. Meyer and A. B. Straughn, *Curr. Ther. Res.*, **22**, 573 (1977).

(3) V. P. Shah, V. K. Prasad, B. E. Cabana, and P. Sojka, *ibid.*, **24**, 366 (1978).

(4) A. B. Straughn, A. P. Melikian, and M. C. Meyer, *J. Pharm. Sci.*, **68**, 1009 (1979).

(5) D. E. Resetarits and T. E. Bates, *J. Pharmacokinet. Biopharm.*, **7**, 463 (1979).

(6) P. G. Welling, D. M. Walter, R. B. Patel, R. H. Barbhaiya, W. A. Porter, G. L. Amidon, T. S. Foster, V. P. Shah, J. P. Hunt, and V. K. Prasad, *Curr. Ther. Res.*, **29**, 815 (1981).

(7) P. G. Welling, *J. Pharmacokinet. Biopharm.*, **5**, 291 (1977).

(8) A. Melander, *Clin. Pharmacokinet.*, **3**, 337 (1978).

(9) R. D. Toothaker and P. G. Welling, *Ann. Rev. Pharmacol. Toxicol.*, **20**, 173 (1980).

(10) P. G. Welling, *Prog. Drug Metab.*, **4**, 131 (1980).

(11) R. H. Barbhaiya, T. A. Phillips, and P. G. Welling, *J. Pharm. Sci.*, **70**, 291 (1981).

(12) "MACC Nonlinear Regression Routines," Academic Computer Center, University of Wisconsin, Madison, Wis.

(13) J. Neter and W. Wasserman, "Applied Linear Statistical Models," Richard D. Irwin, Inc., Homewood, Ill., 1974, p. 475.

(14) P. A. Koch, C. A. Schultz, R. J. Wills, S. L. Hallquist, and P. G. Welling, *J. Pharm. Sci.*, **67**, 1533 (1978).

(15) P. G. Welling, L. L. Lyons, W. A. Craig, and G. A. Trochta, *Clin. Pharm. Ther.*, **17**, 475 (1975).

(16) P. G. Welling, H. Huang, P. A. Koch, W. A. Craig, and P. O. Madsen, *J. Pharm. Sci.*, **66**, 549 (1977).

(17) G. Levy and W. J. Jusko, *ibid.*, **55**, 285 (1966).

ACKNOWLEDGMENTS

Funds for this study were provided by National Institutes of Health Grant GM 20327.

Tray Drying of Pharmaceutical Wet Granulations

J. T. CARSTENSEN* [x] **and M. A. ZOGLIO**[‡]

Received August 5, 1980, from the *School of Pharmacy, University of Wisconsin, Madison, WI 53706 and [‡]Merrell-National Laboratories, Cincinnati, OH 45201. Accepted for publication May 15, 1981.

Abstract □ It is shown that in tray drying wet granulated materials, the expected log–linear plots give slopes that are inversely proportional to the bed depth, rather than to the depth squared. A model is proposed for this giving diffusion coefficents of the order of magnitude expected for liquid-water diffusion. The temperature dependence also suggests that this is the rate-limiting process rather than vapor diffusion.

Keyphrases □ Tray drying—wet granulated materials, mathematical models □ Models, mathematical—tray drying of wet granulated materials □ Granulations—tray drying, mathematical models

The drying of granulations is an important pharmaceutical operation and tray drying is a frequently used method of water removal. The way in which drying takes place from a tray (1–3) can be visualized in several ways. The drying could be a function of the individual granule rather than of the mass of granules, *i.e.*, the bed. In that case, the bed thickness would not be a factor (in fluid bed drying it is not of great importance). However, bed thickness is important, and the drying is a function of the properties of the bed. In this case there are two possibilities: (*a*) either the movement through the void space between the granules is important (*i.e.*, the vapor diffusion is rate determining), or (*b*) the drying is primarily from the *bed* surface, and liquid movement up through the bed maintains a water concentration profile in the bed.

BACKGROUND

In the following discussion, the nomenclature outlined in Fig. 1 will be used. The bed is l-cm deep, has a porosity of ϵ (*i.e.*, a solids fraction of $(1 - \epsilon)$). It has a cross-sectional area of A cm^2. The density of an anhydrous granule is ρ gm/cm^3. The wet granulation before drying contains C^* g of moisture per g of anhydrous solid, and after drying contains c g of moisture per g of anhydrous solid. If c is the equilibrium concentration, then $C^* - c = C_0$ is the initially removable moisture concentration, and $C' - c = C$ is the moisture concentration which is removable at time t. The latter is the quantity which will be dealt with in the following discussion. Granules containing c g of moisture/g of anhydrous weight will be denoted dry. If x is a distance coordinate measured from the top of the bed (Fig. 1), then the diffusional equation governing the situation is Fick's law, *i.e.*, at time t:

$$\partial C/\partial t = D\partial^2 C/\partial x^2 \qquad \text{(Eq. 1)}$$

where D is the diffusion coefficient of water. Crank (4) solved this equation using the following boundary conditions: $C = 0$ at $x = 0$, for t

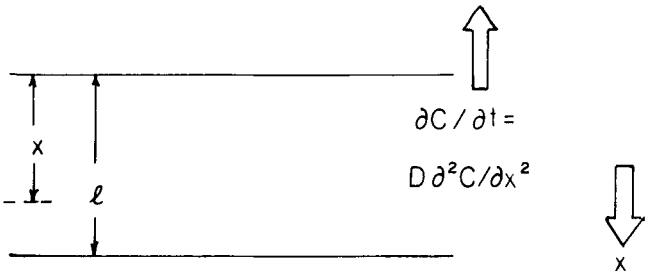

Figure 1—*Schematic of drying from a bed.*

> 0 (no moisture on the surface); $C = C_0$ for $0 < x < l$ at $t = 0$ (the same amount of moisture exists at each point throughout the interior at time zero); and $\partial C/\partial x$ at $x = 0$ equals zero for $t > 0$. Under these conditions it can be shown that Eq. 1 leads to the equation:

$$\ln(M/M_0) = -\{\pi^2 D/(4l^2)\}t + \ln(8/\pi^2) = -kt - 0.2 \quad \text{(Eq. 2)}$$

where M is the amount of removable water or the volume multiplied by $(C' - c)$. The equation is valid after a short lag time, and is based on the stated boundary conditions. For tray drying of granulations, the condition that the surface moisture for $t > 0$ is zero, is questionable. In Eq. 2, k is a drying rate constant given by:

$$k = -\pi^2 D/(4l^2) \quad \text{(Eq. 3)}$$

This equation predicts that the drying data (after a short lag time) should be log-linear when the amount of removable moisture is plotted *versus* time. This drying profile is encountered frequently (*e.g.*, in the so-called falling-rate period). The drying rate constant should have the same temperature dependence as D, the diffusion coefficient for liquid water. Furthermore, k should be inversely proportional to the second power of the bed thickness.

If vapor diffusion through the bed is the rate-limiting step (3–9), it is the movement through the void space of the bed which is rate-limiting. The change from constant to falling rate was postulated (10) to be the change from a process where there is capillary action within the granule to one where there is moisture movement within the void space of the bed. Beyond this some authors (11–13) considered the drying as a receding front down through the bed. This was shown to be feasible (14), and for a fine powder the diffusion coefficient is equal to that of water vapor diffusion.

In this type of drying there will be a dry part containing c g of moisture/g of anhydrous solid (x cm in Fig. 1) and a wet part containing C_0 g of moisture/g of dry solid [the lower $(l - x)$ cm in Fig. 1]. Drying occurs by vapor diffusion over a thickness of x cm through a free cross-section of $A\epsilon$ cm^2. Fick's law now takes the form:

$$-(1/|A\epsilon|)\, dM/dt = \Pi P/x \quad \text{(Eq. 4)}$$

for a steady state where Π is a permeability constant, and P is the water vapor pressure. This is assumed equal to zero in the air stream. There is C_0 g of moisture/g of dry solid in the lower $(l - x)$ cm of the bed and it is apparent that P is a function of C_0.

Figure 1 shows that in drying a section of thickness dx, the amount of water removed is:

$$-dM = C_0\rho(1 - \epsilon)A\, dx \quad \text{(Eq. 5)}$$

Introducing Eq. 5 into Eq. 4 then gives:

$$[C_0\rho\{(1 - \epsilon)/\epsilon\}]dx/dt = P\Pi/x \quad \text{(Eq. 6)}$$

which can be integrated, taking initial conditions into account, to give:

$$x = F \cdot \sqrt{t} \quad \text{(Eq. 7)}$$

where:

$$F^2 = 2P\Pi\epsilon/\{C_0(1 - \epsilon)\rho\} \quad \text{(Eq. 8)}$$

The removable moisture content in the bed at time t (neglecting the amount in the vapor phase) is $M = C_0(l - x)A(1 - \epsilon)\rho$, and that at time zero it is $M_0 = C_0 lA(1 - \epsilon)\rho$ (Fig. 1), so that:

$$M/M_0 = 1 - (x/l) = 1 - (F/l) \cdot \sqrt{t} \quad \text{(Eq. 9)}$$

Equation 9 predicts a drying rate which is a square root of time dependence and where the rate constant is K, given by:

$$K = F/l \quad \text{(Eq. 10)}$$

i.e., inversely proportional to bed depth.

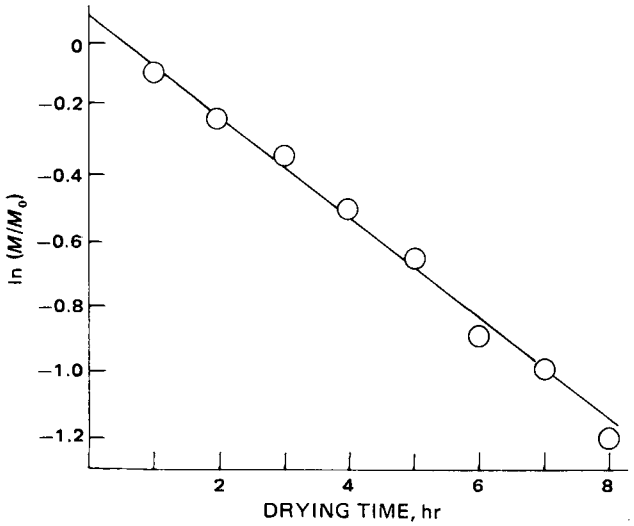

Figure 2—*Typical drying profile in tray drying.* T = *50°*, l = *1.91 cm (3/4 in.).*

The above hypotheses (Eq. 2 and Eq. 9) are *a priori* possible for tray drying. The model leading to Eq. 9 would seem more logical in the drying of wet granulations. Several reports (15–18) have reported this type of drying. Some investigators (17, 18) have shown that the equilibrium granule is primarily a fairly coarse and porous body. In tray drying the bed is loosely spread and fairly shallow (19–21), and movement in the highly porous space is probably not rate limiting. Nevertheless, the present report will show that some inconsistencies exist relating to Eq. 9, and the purpose of the present report is to probe which of the two situations (if any) actually exists. If neither applies an alternate model consistent with the data presented will be suggested.

EXPERIMENTAL

Granulations were made in the following manner: 5.75 kg of lactose USP and 0.8 kg of cornstarch USP were mixed in a sigma-type blender[1], 2 liters of cornstarch paste containing 10% cornstarch were added, and the mass kneaded for 15 min. It was passed through a No. 4 hand screen and spread onto a drying tray, which was placed in a tray drying oven[2]. The tray was removed at given intervals and weighed *in toto* on a balance[3]. The temperature was recorded on a digital readout thermometer[4]. Weights were usually monitored every hour for the complete drying period. Experiments were carried out at five bed depths and four different temperatures, as shown in Table I.

DISCUSSION

It should first be stated that the drying curves in this study were all semilogarithmic in time (Fig. 2). Hence, Eq. 9 is not obeyed in the strictest sense. Equation 2, however, is not strictly obeyed either. The drying curves have intercepts close to zero[5] (or slightly above), certainly not close to −0.2. The least-squares fit values for the slopes and intercepts are shown in Table I. Adherence to the semilogarithmic relation $\ln(M/M_0) = -k^*t$ seems excellent under all conditions.

The conventional diffusion model leading to Eq. 2 requires that the rate constants, k, be inversely proportional to the second power of the bed depth. A plot of $\ln k$ *versus* $\ln l$ is shown in Fig. 3. This plot has a slope of ~−1.0 and hence k appears to be inversely proportional to l and not inversely proportional to l^2. The model leading to Eq. 2 fails on two points. Equation 9 would appear to fail based on the time dependence, but the bed thickness effect, on the surface, would be of the correct dependence. The following presents a probe of whether Eq. 9 could indeed be the correct model. This is in spite of the time dependence failure. This may

[1] Z-bar blender, J. H. Day Co., Cincinnati, Ohio.
[2] Stokes model 38A dryer. Tray is 71.1 cm × 88.9 cm (28 in. × 35 in.) Oven is 91.4 cm (36 in.) wide and 144.8 cm (57 in.) high with pilot tube. It is 82.55 cm (32.5 in.) deep and has a 16-tray capacity. The air velocity is 8.93 m^3/min (280 ft^3/min).
[3] Mettler, P.S. 30.
[4] Mensor Co. platinum probe thermometer with digital readout.
[5] It should be pointed out that the models presented do not account for thermal effects. The time required for initial thermal equilibrium, experimentally, could account for the zero or slightly positive intercepts.

Table I—Least-Squares Parameters for the Drying Data (Eq. 2)

Temperature	Thickness l, cm	Thickness $\ln l$	Intercept	Negative of Slope, k hr	Correlation Coefficient, r^2	$1000/T$, °K^{-1}	$\ln k$	$\ln k$ (adjusted to 12.5°)[a]
60°	2.54	0.93	0.1073	0.1595	0.997	3.002	−1.836	−3.828
60°	2.54	0.93	0.1110	0.1472	0.995	3.002	−1.916	−3.908
55°	2.54	0.93	0.0480	0.119	0.999	3.047	−2.129	−3.941
50°	5.08	1.63	0.0086	0.0481	0.999	3.104	−3.034	−4.618
50°	2.54	0.93	0.034	0.1045	0.999	3.095	−2.259	−3.879
50°	2.54	0.93	0.040	0.0992	0.999	3.095	−2.311	−3.931
50°	1.91	0.65	0.0877	0.1544	0.997	3.104	−1.868	−3.452
40°	1.27	0.24	0.059	0.116	0.998	3.193	−2.154	−3.096
40°	1.91	0.65	0.0311	0.1028	0.999	3.193	−2.275	−3.382
40°	1.91	0.65	0.110	0.1093	0.984	3.193	−2.214	−3.503
40°	2.54	0.93	0.019	0.0697	0.999	3.193	−2.663	−3.442

[a] It is shown at a later point that the activation energy for k is 8,000 cal/mole. The adjustment to 12.5° ($1/T = 0.0035$) has hence been made by the formula: $\ln k(12.5°) = \ln k - 4000(0.0035 - 1/T) = \ln k - 14 + 4(1000/T)$ where $\ln k$ is the value listed in the next to the last column. The average value of $\ln k$ at a 2.54-cm depth (six values) is −3.822 with a standard error of the mean of 0.078 and the average vaue of $\ln k$ at a bed depth of 1.91 cm (three values) is −3.446 with a standard error of the mean of 0.035. The means and 95% confidence limits are shown in Fig. 3. The least squares fit of $\ln k(25°)$ regressed on $\ln l$ for all the values (11 points) is: $\ln k(25°) = -1.14 \ln l - 2.754$ (correlation coefficient: −0.938).

not be serious since it has been shown (23) that in limited ranges, square root relations may have the appearance of semilogarithmic plots.

To evaluate this, theoretical values of M/M_0 have been calculated for various drying times, t, according to Eq. 9 (Table II). The total drying time, θ, for situations given by Eq. 9 are the points in time where M reaches zero at $x = l$, *i.e.*, where $(F/l) \cdot \sqrt{\theta} = 1$. If, for example, this were 9 hr, then $(F/l) = 1/3$. Values for θ are shown in the headings of Table II for four chosen values of (F/l). Once (F/l) is fixed one can calculate M for various times; four time values (t = 1, 2, 3, and 4 hr) are chosen here and are shown in Table II. The value of $\ln(M/M_0)$ calculated for each value of t is shown in the table. For each value of (F/l) there are hence four values of t and $\ln(M/M_0)$. The least-squares fit of:

$$\ln(M/M_0) = -k''t + b \qquad \text{(Eq. 11)}$$

has been calculated and the least-squares fit parameters for slope ($-k''$) and intercept (b) shown (Table II). The correlation coefficients are good, showing that the square root data are well approximated by a log–linear equation (Eq. 2) for the four chosen values of (F/l). The intercepts are close to zero. An explanation for the approximation is given in *Appendix I*.

It is seen from the last two lines in Table II that there is a connection between the calculated values of k'' and the chosen values of (F/l). This is presented graphically in Fig. 4, and good linearity seems to exist demonstrated by the fact that the least-squares fit:

$$\ln k'' = 2.24 \ln(F/l) + 1.055 \qquad \text{(Eq. 12)}$$

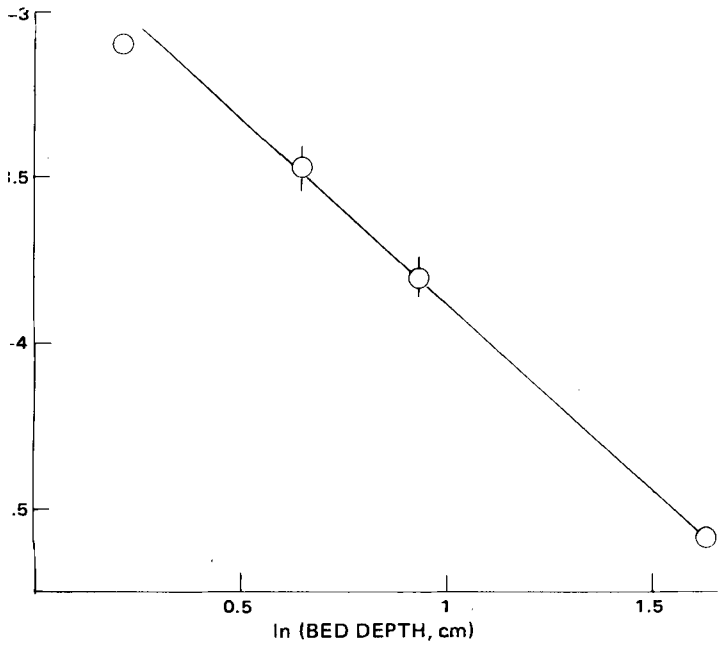

Figure 3—*Drying rate constants (adjusted to standard temperature) as a function of bed depth. Detailed data are shown in Table I. Least-squares fit is ln k = −1.14, ln l −2.754.*

has a correlation coefficient of 0.997. Hence k'' is approximately inversely proportional to the bed depth squared. Equations 2 and 9 are therefore experimentally indistinguishable. When the amount of removable moisture is plotted logarithmically *versus* time, approximately straight lines will occur in both cases. According to either model, however, the drying rate constants should be inversely proportional to the bed depth squared (or raised to a power higher than 2). Over a longer period of drying time the approximation leading to Eq. 11 is less precise and the treatment, so far, would favor some model based on the general principles leading to Eq. 2.

The original boundary conditions leading to Eq. 5 are that $C = 0$ at the surface, that C equals a non-zero value at the interior, and that dC/dx is equal to zero at $t > 0$ right at the surface of the bed. Other reasonable concentration profiles can be visualized in the interior as shown in Fig. 5. In this figure it is assumed that the moisture content increases steadily (although not linearly) down through the bed; it attains its largest value at the bottom ($x = l$) and is smallest at the surface ($x = 0$). The profile will change with time; both $C(l)$ and $C(0)$ will decrease. If it is assumed that $C(l)$ is proportionally larger than $C(0)$ at all times, so that:

$$C(l) = \gamma C(0) \qquad \text{(Eq. 13)}$$

at all times (where γ is a time-independent constant), then it is possible to find a trigonometric function such that Eqs. 1 and 13 are both satisfied and that the drying rate constant k will be inversely proportional to the bed depth, l. The function:

$$C(x,t) = (\beta \sin \lambda x + \cos \lambda x) \cdot \exp(-\lambda^2 Dt) \qquad \text{(Eq. 14)}$$

is a solution to Eq. 1 (β and λ are constants discussed later). It will obey Eq. 13 provided that:

$$\gamma = \beta \sin \lambda l + \cos \lambda l \qquad \text{(Eq. 15)}$$

which is simply a numerical requirement implying time independence.

For k ($= \lambda^2 D$) to be proportional to l^{-1}, it is necessary that λ^6 be proportional to $l^{-1/2}$, or:

$$\lambda = \alpha \cdot l^{-1/2} \qquad \text{(Eq. 16)}$$

For the function to be monotonically increasing in the interval (*i.e.*, having no maximum, which would occur if the trigonometric argument

Table II—Data Adhering to Eq. 9 Treated According to Eq. 11

Parameter	$\ln(M/M_0)$ at Time t[a] 6	9	12	15
1	−0.52	−0.41	−0.34	−0.30
2	−0.86	−0.64	−0.52	−0.45
3	−1.23	−0.86	−0.69	−0.59
4	−1.70	−1.10	−0.86	−0.73
(F/l)	0.408	0.333	0.289	0.258
Correlation coefficient, $\ln(M/M_0)$ *versus* t	−0.997	−0.9999	−0.9999	−0.9999
k''	−0.391	−0.229	−0.173	−0.143
Intercept	−0.1	−0.18	−0.17	−0.16
$\ln(F/l)$	−0.90	−1.11	−1.24	−1.35
$\ln k''$	−0.94	−1.47	−1.75	−1.94

[a] Total drying time = θ.

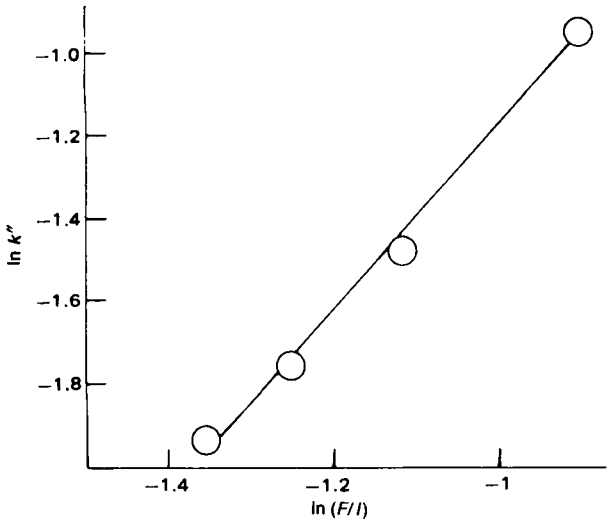

Figure 4—*Data from Table II (9 hr drying time); ln* M/M_0 *plotted as a function of time according to Eq. 9 for data adhering to Eq. 17.*

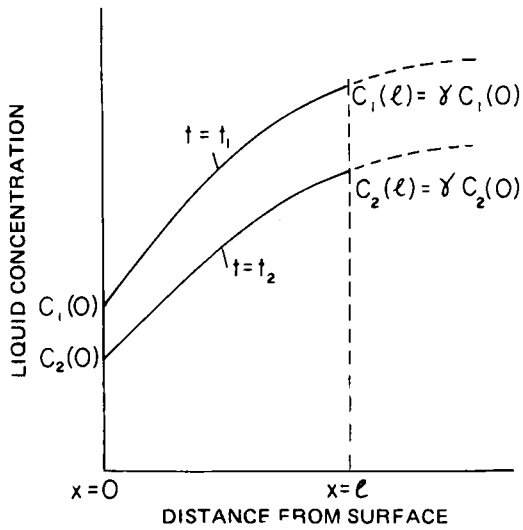

Figure 5—*Anticipated moisture concentration profiles in a tray (bed) at two different times,* t_1 *and* t_2. *Curves are according to Eq. 14, and boundary conditions are according to Eq. 13.*

could have the value $\pi/2$, *Appendix II*), it is necessary that:

$$\lambda l < \pi/4 \qquad \text{(Eq. 17)}$$

Inserting this in Eq. 16 gives:

$$\alpha l^{1/2} < \pi/4 \quad \text{so} \quad \alpha \leq \pi/(4\sqrt{l}) \qquad \text{(Eq. 18)}$$

The amount of moisture in the bed at time t is now given by:

$$M = A(1-\epsilon)\rho e^{-\lambda^2 Dt}\int_0^l (\beta \sin \lambda x + \cos \lambda x)dx =$$

$$A(1-\epsilon)\rho e^{-\lambda^2 Dt}(1/\lambda)(\sin \lambda l - \beta \cos \lambda l + \beta) \qquad \text{(Eq. 19)}$$

and at time zero it is:

$$M_0 = A(1-\epsilon)\rho(1/\lambda)(\sin \lambda l - \beta \cos \gamma l + \beta) \qquad \text{(Eq. 20)}$$

Combining Eqs. 19 and 20:

$$\ln(M/M_0) = -k^* t \qquad \text{(Eq. 21)}$$

where:

$$k^* = (\alpha^2 D/l) \qquad \text{(Eq. 22)}$$

This has the correct dependence on l (as opposed to Eqs. 3 and 12). The treatment developed produced three models, two of them conventional (denoted A and B below) and one proposed (denoted C below), the latter based on a trigonometric concentration profile with boundary conditions different from A. The drying curves predicted by the three models are:

model A; $\ln(M/M_0) = -kt - 0.2$ (see Eq. 2)

where $k = -\pi^2 D/(4l^2)$ (see Eq. 3)

model B; $\ln(M/M_0) = -k''t + b$ (see Eq. 11)

where k'' is approximately proportional to $l^{-2.5}$ (see Eq. 12)

model C; $\ln(M/M_0) = -k^*t$ (see Eq. 21)

where $k^* = (\alpha^2 D/l)$ (see Eq. 22)

Models A and B fail on two counts: (*a*) the experimental drying curves are log-linear with zero or slightly positive intercepts (Table I), and (*b*) the drying rate constants are experimentally proportional to l^{-1}, not l^{-2}. This prevents calculation of D, the diffusion coefficient, by these models. Model C, on the other hand, predicts zero intercepts and proportionality of drying rate constants to l^{-1} when the fraction of removable moisture is plotted log-linearly in time. This is in accord with experimental results, and permits order of magnitude calculation of D. A test for the reasonability of the model is therefore such a calculation, which should result in values of D in the range expected for a diffusion coefficient, and having a predictable temperature dependence.

It is seen from the inequalities in Eq. 18 that at the limit, α is equal to $\pi/(4\sqrt{l})$, which when inserted in Eq. 22 gives an upper limit for k of $D\pi^2/(16l^2)$. The upper limit for D is then:

$$D = 16kl^2/\pi^2 \qquad \text{(Eq. 23)}$$

At 50°, for instance (Table I), l = 2.54 cm, and k = 0.1 hr^{-1}, so that:

$$D = (16)\,(0.1)\,(2.54)^2/(3600)\,(3.14)^2 = 28 \times 10^{-5}\ cm^2/sec, \qquad \text{(Eq. 24)}$$

which is a reasonable upper limit. Wilburn, *et al.* (23) quote a value of 2×10^{-5} cm^2/sec at 30° for the liquid diffusion coefficient of water. On the other hand, the D-value in Eq. 24 is not in line with the vapor diffusion coefficient for water [which at 8° is 0.25 cm^2/sec, (24)].

The value for D determined in Eq. 24 is an upper limit.

A second criterion is the temperature dependence. It is seen from Eq. 22 that k^* should have the same temperature dependence as D:

$$\ln k^* = \ln D + \ln(\alpha^2/l) = -E_d/RT + N \qquad \text{(Eq. 25)}$$

where N is a constant, and E_d is the activation energy for the diffusion coefficient of water. The data in Table I (2.54-cm bed depth) have been plotted in this fashion in Fig. 6. The least-squares fit line is

$$\ln k^* = -(4015/T) + 1.021\ (r^2 = 0.99) \qquad \text{(Eq. 26)}$$

where r^2 is the correlation coefficient. Although the value for E_d (8030 cal/mol) is somewhat higher than that for the self-diffusion of water (E_d = 4000 cal/mole) (24), it is orders of magnitude different from the value of E_d for water vapor.

The model C, where the positional dependence of moisture concentration is a single argument trigonometric term, and where the

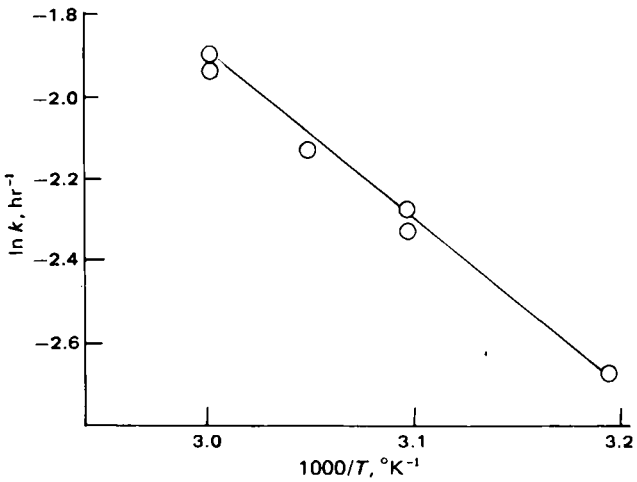

Figure 6—*Arrhenius plot of drying rate constants, 2.54-cm bed.*

boundary restriction is that the moisture concentration on the bottom of the tray (during steady state) is a constant (*i.e.*, time-dependent) factor times that on the surface, predicts a behavior in agreement with experimental data. The drying data are log–linear with a zero intercept. The drying constant is inversely proportional to bed depth and the drying rate constant is logarithmically linear with inverse temperature. The absolute magnitude of calculated diffusion coefficients and their temperature dependence are in fair agreement with that expected for liquid-water diffusion.

APPENDIX I

If the approximation:

$$y = 1 - (F/l) \cdot \sqrt{t} \simeq Ae^{-kt}, (A \simeq 1) \qquad \text{(Eq. A1)}$$

holds, then:

$$(1 - y)^2 = (F/l)^2 \cdot t \simeq (1 - Ae^{-kt})^2$$
$$\simeq (1 - 2A + A^2) + t[2Ak(1 - A)] + t^2[Ak^2(2A - 1)] \qquad \text{(Eq. A2)}$$

where the exponential expansion $e^x \simeq 1 + x + x^2/2$ has been truncated for third and higher power terms. The requirements for the approximation in Eq. A2 is that like power terms have equal coefficients, *i.e.*:

$$1 - 2A + A^2 \simeq 1 \qquad \text{(Eq. A3)}$$

$$(F/l)^2 = 2Ak(1 - A) \qquad \text{(Eq. A4)}$$

$$t^2Ak^2(2A - 1) \simeq t2Ak(1 - A) \qquad \text{(Eq. A5)}$$

The last requirement is that $t^2Ak^2(2A - 1)$ be zero or negligible, and this is equivalent to it being significantly smaller than the t term.

The requirement in Eq. A3 is fulfilled when $A \simeq 1$ or $A \simeq 2$. Table II shows that $A \simeq \exp(-0.2) = 0.8$, *i.e.*, that $A \simeq 1$. The second requirement is that $(F/l)^2 = 2Ak(1 - A) \simeq 0.32k$, which in logarithmic form becomes:

$$\ln k = 2 \ln(F/l) - 1.14 \qquad \text{(Eq. A6)}$$

which compares favorably with Eq. 12, and predicts that k should be proportional to l^{-2} as stated in the text.

The times for which the approximation can hold are deduced from Eq. A5 which can be rearranged to:

$$t < 2(1 - A)/k \qquad \text{(Eq. A7)}$$

where k is the range 0.1–0.4 in Table II (or 0.1–0.2 in Table I), and A is ~0.8, so that:

$$t < (2 \cdot 0.8/0.1) \text{ to } (2 \cdot 0.8/0.4) = 4\text{–}16 \qquad \text{(Eq. A8)}$$

as upper limits. The t values in Table II correspond to this. The k, (F/l), and t ranges used in Table II are within the bounds of the approximation.

APPENDIX II

The function:

$$y = \beta \sin \lambda x + \cos \lambda x \qquad \text{(Eq. A9)}$$

has the derivative:

$$\partial y/\partial x = \beta\lambda \cos \lambda x - \lambda \sin \lambda x \qquad \text{(Eq. A10)}$$

This equals zero when:

$$\tan \lambda x = \beta \qquad \text{(Eq. A11)}$$

β is at least 1 (since C is higher at the bottom of the tray than at the surface), so since $\tan(\pi/4) = 1$, it is necessary that in this limit:

$$\lambda l < \pi/4 \qquad \text{(Eq. A12)}$$

REFERENCES

(1) W. K. Lewis, *Ind. Eng. Chem.*, **13,** 427 (1921).
(2) T. K. Sherwood, *Trans. Am. Inst. Chem. Eng.*, **27,** 190 (1931).
(3) N. F. H. Ho and T. J. Roseman, *J. Pharm. Sci.*, **68,** 1170 (1979).
(4) J. Crank, "The Mathematics of Diffusion," Oxford at the Clarendon Press, 5th ed., Oxford University Press, London WL, England, 1970, pp. 46–49.
(5) T. Higuchi, *J. Pharm. Sci.*, **52,** 1145 (1963).
(6) T. R. Oliver and D. M. Newitt, *Trans. Inst. Chem. Eng.*, **27,** 1 (1949).
(7) J. F. Pearse, T. R. Oliver, and D. M. Newitt, *ibid.*, **27,** 9 (1949).
(8) J. R. Bell and A. H. Nissan, *Am. Inst. Chem. Eng. J.*, **5,** 344 (1959).
(9) A. H. Nissan, W. G. Kaye, and A. R. Bell, *ibid.*, **5,** 103 (1959).
(10) A. H. Nissan, H. H. George, and A. R. Bell, *ibid.*, **6,** 406 (1960).
(11) E. F. Adams, Ph.D. thesis, Rensselaer Polytechnical Institute, Troy, N.Y., 1962.
(12) A. V. Luikov, *Int. J. Heat Mass Transf.*, **6,** 559 (1963).
(13) R. P. Morgan and S. Yerazunis, *Am. Inst. Chem. Eng. J.*, **13,** 136 (1967).
(14) K. Ridgway and J. A. B. Callow, *J. Pharm. Pharmacol.*, **19,** 155S (1967).
(15) B. R. Bhutani and V. N. Bhatia, *J. Pharm. Sci.*, **64,** 135 (1975).
(16) P. M. Hill, *ibid.*, **65,** 313 (1976).
(17) M. A. Zoglio, H. E. Huber, G. Koehne, P. L. Chan, and J. T. Carstensen, *ibid.*, **65,** 1205 (1976).
(18) J. T. Carstensen, T. Lai, D. W. Flickner, H. E. Huber, and M. A. Zoglio, *ibid.*, **65,** 992 (1976).
(19) J. T. Carstensen and P. C. Chan, *ibid.*, **66,** 1235 (1977).
(20) W. Schicketanz, *Powder Technol.*, **9,** 49 (1974).
(21) M. C. Coelho and N. Harnby, *ibid.*, **20,** 197 (1978).
(22) J. T. Carstensen, *J. Pharm. Sci.*, **63,** 1 (1974).
(23) D. J. Wilburn, T. DeFries, and J. Jonas, *J. Chem. Phys.*, **65,** 1783 (1976).
(24) "Handbook of Chemistry and Physics," 48th ed., R. C. Weast and S. M. Selby, Eds., Chemical Rubber Co., Cleveland, OH, 1967/68, p. F-45.

ACKNOWLEDGMENTS

Presented at the 27th Academy of Pharmaceutical Sciences National Meeting, Kansas City, Mo., Nov. 11–15, 1979.

Quantitation of Methadone Enantiomers in Humans Using Stable Isotope-Labeled [$^2H_3$]-, [$^2H_5$]-, and [$^2H_8$]Methadone

K. NAKAMURA *, D. L. HACHEY *§x, M. J. KREEK ‡, C. S. IRVING *, and P. D. KLEIN *

Received September 8, 1980, from the * *Division of Biological and Medical Research, Argonne National Laboratory, Argonne, IL 60439,* and the ‡ *Rockefeller University, New York, NY 10021.* Accepted for publication March 25, 1981. § Present address: Children's Nutrition Research Center, Department of Pediatrics, Baylor College of Medicine, Houston, TX 77030.

Abstract □ A new technique for simultaneous stereoselective kinetic studies of methadone enantiomers was developed using three deuterium-labeled forms of methadone and GLC–chemical-ionization mass spectrometry. A racemic mixture (1:1) of (*R*)-(−)-[$^2H_5$]methadone (*l*-form) and (*S*)-(+)-[$^2H_3$]methadone (*d*-form) was administered orally in place of a single daily dose of unlabeled (±)-[$^2H_0$]methadone in long-term maintenance patients. Racemic (±)-[$^2H_8$]methadone was used as an internal standard for the simultaneous quantitation of [$^2H_0$]-, [$^2H_3$]-, and [$^2H_5$]methadone in plasma and urine. A newly developed extraction procedure, using a short, disposable C_{18} reversed-phase cartridge and improved chemical-ionization procedures employing ammonia gas, resulted in significant reduction of the background impurities contributing to the ions used for isotopic abundance measurements. These improvements enabled the measurement of labeled plasma methadone levels for 120 hr following a single dose. This methodology was applied to the study of methadone kinetics in two patients; in both patients, the analgesically active *l*-enantiomer of the drug had a longer plasma elimination half-life and a smaller area under the plasma disappearance curve than did the inactive *d*-form.

Keyphrases □ Methadone—enantiomers, quantitation in humans using stable isotope labeling □ Enantiomers—of methadone, quantitation in humans using stable isotope labeling □ Narcotics—methadone, quantitation of enantiomers in humans using stable isotope labeling

Racemic methadone is used in maintenance therapy of heroin addicts (1, 2). The (*R*)-(−)-enantiomer (*l*-form) is the more pharmacologically active isomer in experimental animals and humans (3, 4). In addition, small amounts of the (*S*)-(+)-enantiomer (*d*-form) may be converted to an active enantiomer of dimepheptanol by hepatic microsomal drug-metabolizing enzymes (5). It has been shown that the binding of methadone and other narcotics to specific opiate receptors is stereospecific (6–12). It was also shown that several aspects of narcotic disposition, including metabolism, may be stereoselective (13, 14).

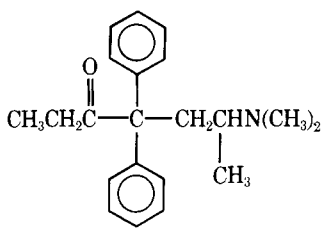

(±)-methadone

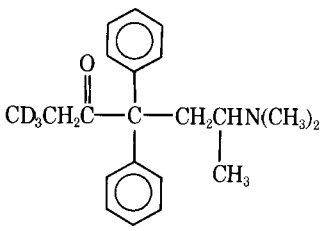

(*S*)-(+)-[$^2H_3$]methadone

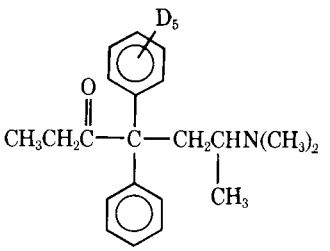

(*R*)-(−)-[$^2H_5$]methadone

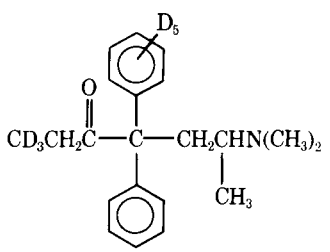

(±)-[$^2H_8$]methadone internal standard

BACKGROUND

Little work has been devoted to clarifying the disposition and pharmacokinetic differences between active and inactive enantiomers of methadone (4, 13). Such studies have been hindered by rapid and extensive drug distribution into tissues, with resultant low plasma levels, and by ethical constraints on the use of large amounts of radioisotopes in research patients.

Stable isotope-labeled compounds are now used often as tracers for the quantitation of drugs and drug metabolites in biological fluids (15, 16). Racemic [$^2H_3$]methadone (17) and [$^2H_5$]methadone (18) have been used as internal standards or tracers in the determination of methadone in plasma by GLC–chemical-ionization mass spectrometry. The pharmacokinetics of (*R*)-(−)- and (*S*)-(+)-methadone in maintenance patients using the separate enantiomers of [$^2H_5$]methadone as tracers were reported (13). In that study, kinetic differences were found between the two enantiomers in three clinically well-stabilized methadone maintenance patients; in each case, (*R*)-(−)-methadone had a significantly longer elimination half-life than the inactive enantiomer.

Exploration of these differences in normal patients as well as in patients whose drug disposition may be altered by liver disease, alcoholism, multiple drug abuse, or anticonvulsant therapy, etc., requires the performance of three sequential studies in each patient. Multiple studies are more difficult and expensive; the status of the patient may also change. Ideally, one would like to quantitate and trace both enantiomers simultaneously in the same patient using stable isotope tracers.

Three forms of deuterium-labeled methadone were synthesized: the two enantiomers, (*R*)-(−)-[$^2H_5$]methadone and (*S*)-(+)-[$^2H_3$]methadone, and racemic (±)-[$^2H_8$]methadone. Technology for the simultaneous measurement of all three labeled forms as well as unlabeled racemic (±)-methadone was developed using GLC–chemical-ionization mass spectrometry. In addition, clinical studies were carried out using these stable isotopic tracers; significant differences in the disposition and pharmacokinetics of the two enantiomers were observed in each patient.

EXPERIMENTAL

Synthesis—(*S*)-(+)-[$^2H_3$]Methadone was prepared from ethyl-2,2,2-[$^2H_3$]magnesium bromide and (*S*)-(+)-4-dimethylamino-2,2-diphenyl-valeronitrile according to known procedures (17). (*R*)-(−)-[$^2H_5$]Methadone was prepared from ethyl bromide and (*R*)-(−)-4-dimethylamino-2-phenyl-2-[$^2H_5$]phenyl-valeronitrile (18). Racemic (±)-[$^2H_8$]methadone was prepared by coupling ethyl-2,2,2-[$^2H_3$]magnesium bromide with racemic 4-dimethylamino-2-phenyl-2-[$^2H_5$]phenyl-valeronitrile by analogy to known procedures (18). Hydrochloride salts were prepared by dissolving the free bases in 25 ml of anhydrous ethanol and passing dry hydrogen chloride gas into the ice-cold solution. The ethanolic hydrogen chloride solution was then treated with 100 ml of ether and chilled at −10° until crystallization was complete. The salts were recrystallized twice from ethanol–ether (1:10).

Standard Solutions—Aqueous stock solutions, 1 mg/ml of (±)-[$^2H_0$]methadone, (*S*)-(+)-[$^2H_3$]methadone, (*R*)-(−)-[$^2H_5$]methadone, and (±)-[$^2H_8$]methadone hydrochloride, were prepared separately. Aliquots of these standard solutions were added to methadone-free plasma and urine obtained from healthy adult donors to establish standard curves. The plasma solution of combined enantiomers of unlabeled methadone and [$^2H_3$]- and [$^2H_5$]methadone was prepared gravimetrically. Concentrations ranged from 25 to 800 ng/g of plasma for methadone and

0022-3549/82/0100-0040$01.00/0

Table I—Fractional Ion Abundances of the Deuterated Methadone Isotopic Species

Number of ^2H Atoms	$[^2H_0]$	$[^2H_3]$	$[^3H_5]$	$[^2H_8]$
0	78.98	0.12	0.12	
1	18.49	0.20		
2	2.32	2.04	0.58	
3	0.18	77.32	2.93	
4		17.94	13.39	
5		2.21	56.37	0.07
6		0.17	16.58	0.40
7			5.80	6.04
8			3.96	74.55
9				16.92
10				2.00

from 5 to 200 ng/g of plasma for $[^2H_3]$- and $[^2H_5]$methadone. Urine concentrations ranged from 0.1 to 10 μg/ml of urine for each methadone species.

Sample Preparation—*Plasma Analysis*—Plasma (1 g) was mixed with 1 ml of the internal standard, $[^2H_8]$methadone (200 ng/ml), and allowed to equilibrate at room temperature for 45 min. The sample solution was poured into a 10-ml syringe barrel fitted with a C_{18} silica gel cartridge[1]. Prior to use, the cartridge was conditioned by washing with 2 ml of methanol followed by 4 ml of water. The sample solution was forced through the cartridge with the syringe plunger and was followed by 2 ml of water and 3 ml of 0.01 *M* NH_4OH. The methadone was eluted with 6 ml of ethyl acetate and an additional 3 ml of 0.01 *M* NH_4OH (19).

The aqueous layer was discarded, and the organic phase was evaporated under nitrogen. The residue was dissolved in 3 ml of 0.3 *N* HCl and was shaken with 4 ml of *n*-heptane to remove residual lipids. After two extractions with *n*-heptane, the methadone-containing aqueous layer was separated and adjusted to pH 9–10 with 3 ml of 0.6 *M* NH_4OH. The aqueous layer was then extracted with 6 ml of ethyl acetate, and the organic layer was washed with an additional 3 ml of 0.6 *M* NH_4OH and evaporated under nitrogen. The residue was reconstituted with 10 μl of methanol, and the entire sample was analyzed. Recovery of methadone by this procedure was 40–70%.

Urine Analysis—Urine (1 ml) was mixed with 1 ml of internal standard (10 μg/ml). The sample was adjusted to pH 9–10 with 3 ml of 0.6 *M* NH_4OH, and the solution was extracted with 6 ml of ethyl acetate. The aqueous layer was discarded, and the organic phase was evaporated under nitrogen. The residue was reconstituted with 50 μl of methanol. A 2–3-μl aliquot was used for analysis. Recovery was 85–90%.

Mass Spectrometric Analysis—Analyses were performed using a quadrupole mass spectrometer[2] operating at an ion source temperature of 160° with a 0.5-torr ion source pressure of ammonia reagent gas (20). Samples were introduced through the GLC inlet system and were analyzed on a 1.8-m × 1.0- mm i.d. glass column packed with 10% OV-17 on Chromosorb W-HP (100–120 mesh) at a column temperature of 250° and a helium flow rate of 9 ml/min. Under these conditions, the retention time of methadone was 3.5 min. Isotopic ratios were measured by monitoring the intensity of the protonated molecular ions at *m/z* 310, 313, 315, and 318 for $[^2H_0]$-, $[^2H_3]$-, $[^2H_5]$-, and $[^2H_8]$methadone, respectively, using a microprocessor-based data system[3].

Standard isotope dilution curves were prepared for each methadone series in plasma and urine by plotting the observed, corrected isotopic ratio against the mole ratio of $[^2H_0]$methadone/$[^2H_8]$methadone, $[^2H_3]$methadone/$[^2H_8]$methadone, and $[^2H_5]$methadone/$[^2H_8]$methadone. In all cases, plasma and urine blank values were determined daily with each set of samples. The isotopic ratio data were mathematically treated to correct the values for the small cross-contributions to the ion intensities by the individual deuterated methadone species using the following methods.

Patients and Clinical Procedures—*Patient 1*—Patient 1, a 24-year-old male, began to use alcohol at age 11 and heroin at age 13. He began methadone maintenance treatment at age 18 with no subsequent problems with illicit narcotics or other drug abuse. He had a history of chronic alcoholism since age 21 but was detoxified and remained alcohol free for 9 months prior to the present study. He was stabilized on 80 mg of methadone/day and received no other medications. Physical examination revealed no significant abnormalities. Laboratory findings included: Hgb 15.0, Hct 44, WBC 6.2 with normal differential, normal urinalysis, hepatitis B antigen negative, SGOT 15, alkaline phosphatase 59, bilirubin 0.3, 5′-nucleotidase 6, total protein 6.7, albumin 4.0, and BUN 16, all within normal limits.

Patient 2—Patient 2, a 37-year-old male, began to use illicit narcotics at age 17. He entered a methadone maintenance treatment program at age 30 and subsequently remained free of heroin abuse. Over the past 10 years, he consumed no alcohol nor used other drugs. At age 33, he was told of abnormal liver function test results and subsequently had a liver biopsy, which showed chronic active hepatitis. At the time of these studies, he was receiving 100 mg of methadone/day with no other medications. Positive findings on physical examination revealed spider angiomata on the face and thorax and enlarged firm, nontender liver but an otherwise normal physical examination. Laboratory results included: Hgb 16.6, Hct 49.3, WBC 6.7 with normal differential, normal urinalysis, and hepatitis B antigen negative. His SGOT was 67 (upper normal 25), alkaline phosphatase was 127 (upper normal 82), bilirubin was 0.5, 5′-nucleotidase was 18 (upper normal 14), total protein was 7.4, and BUN was 18.

Both patients were admitted[4] for metabolic studies, and oral and written informed consent was obtained. The oral daily dose of methadone was substituted by a single dose of the same amount of stable isotopic methadone (containing equal amounts of *d*-$[^2H_3]$- and *l*-$[^2H_5]$methadone) for each patient on 1 study day. On the following day, oral dosing with unlabeled methadone was resumed. Multiple blood specimens were obtained on the study day and once daily thereafter. On several days following the initial study day, multiple blood samples also were obtained and analyzed for protocols unrelated to the results reported here. Six-hour urine collections were made on the 1st study day, and 24-hr collections were made daily thereafter.

Table II—Summary of Plasma Disappearance Half-Life and Area under the Curve (*AUC*)

Patient	Enantiomer	$T_{1/2\beta}$, hr	$(AUC)_0^{119}$, ng hr	Plasma Compartment, %
1	(*S*)-(+)-	28.1 ± 0.7	5296	1.58
	(*R*)-(−)-	37.9 ± 4.4	4002	1.19
2	(*S*)-(+)-	34.8 ± 2.4	4795	1.14
	(*R*)-(−)-	58.9 ± 4.8	2596	0.62

Data Analysis—Each isotopic species of methadone contributes a known, but variable, fraction to the ion intensity measured at a given mass. The ion intensity at a given mass (I_x), can be described as the sum of the individual fractional ion intensities according to:

$$I_x = A_1X_1 + A_2X_2 + \ldots A_nX_n \qquad \text{(Eq. 1)}$$

where *A* is the fractional ion abundance listed in Table I, X_n is the unknown fractional contribution to be determined, and I_x is the measured ion intensity at a given mass. The set of four linear equations, which consists of one equation for each ion measured, can be solved by linear least-squares techniques described previously (21, 22). The corrected ion intensity ($I_{x'}$) was normalized to the corrected ion intensity ($I_{318'}$) of the internal standard to give a set of three corrected isotope ratio values (R_{310}, R_{313}, and R_{315}) for each sample. The actual mole ratio for each component in a sample was obtained from linear calibration curves as described[5].

Plasma drug concentration *versus* time data were fitted to a three-exponential decay function using the SAAM 27 computer program (23). Areas under the curves were calculated using computer routines that employ the trapezoidal rule to perform the integration. The kinetic data for both patients are summarized in Table II.

RESULTS AND DISCUSSION

The isotopic composition of the various deuterated methadone species was determined by ammonia GLC–chemical-ionization mass spectrometry. The data, expressed as the fractional ion abundances of the various species, are listed in Table I. Multiple isotopic tracer studies employed in the present work were complicated by isotopic overlap of the various deuterated compounds. The problem was minimized, but not

[1] Sep-Pak cartridge, Waters Associates, Milford, Mass. Different lots of cartridges had different abilities to remove undesired compounds from plasma samples.

[2] Biospect quadrupole mass spectrometer, Chemetron Medical Products, St. Louis, Mo.

[3] Spectral analysis microprocessor, Chemetron Medical Products, St. Louis, Mo.

[4] Rockefeller University Hospital Clinical Research Center.

[5] A general purpose computer program written in the SPEAKEZ language to perform the calculations for any number of isotopic species is available from the authors

Table III—Contributions of Plasma and Urine to the Ion Species Used to Quantitate [$^2H_0$]-, [$^2H_3$]-, and [$^2H_5$]Methadone Using [$^2H_8$]-Methadone as an Internal Standard

Sample	Extraction Method	Chemical-Ionization gas	n	Isotope Ratio, % m/z 310/318	m/z 313/318	m/z 315/318
Buffer[a]	—	Isobutane	3	0.13 ± 0.10	0.46 ± 0.08	0.90 ± 0.29
Plasma[b]	Solvent[c]	Isobutane	3	4.66 ± 3.04	8.18 ± 4.04	22.14 ± 6.74
Plasma	Cartridge[d]	Isobutane	12	1.06 ± 0.32	6.27 ± 1.17	3.32 ± 0.94
Buffer	—	Ammonia	9	0.16 ± 0.14	0.18 ± 0.14	0.21 ± 0.13
Plasma	Cartridge	Ammonia	17	1.65 ± 0.95	1.24 ± 0.49	0.65 ± 0.47
Urine	Solvent[e]	Ammonia	4	0.16 ± 0.14	0.14 ± 0.14	0.10 ± 0.06

[a] Internal standard solution in buffer ([$^2H_8$]methadone, 100 ng/μl), 2 μl/injection. [b] Control plasma, 1 g + internal standard ([$^2H_8$]methadone, 200 ng/ml), 1 ml. [c] Solvent extraction including back-extraction procedure. [d] Sep-Pak C_{18} cartridge cleanup. [e] Solvent extraction alone.

eliminated completely, by using isotopic tracers separated by two or more mass units. The worst case of isotopic overlap occurred between [$^2H_3$]-methadone and [$^2H_5$]methadone, where the latter contributed 5.19% of its relative ion intensity to the ion intensity of [$^2H_3$]methadone measured at m/z 313.

The problem can be viewed as a special case of mixture analysis, where each component of the mixture contributes a small portion to the measured abundance of the other components. Mathematically, ion intensity can be expressed as a set of simultaneous linear equations describing all isotopic contributions to the ions being measured. These equations can be solved by simple matrix algebraic techniques (21, 22, 24). The ratio of (*S*)-(+)-[$^2H_3$]methadone to (*R*)-(−)-[$^2H_5$]methadone in plasma varies only between 2:1 and 1:2, even though the actual total drug concentration in plasma may range over a 40-fold span during a single clinical study. The relative isotopic cross-contribution of one enantiomer to the other is <10% between the two isotopic species. Both [$^2H_0$]methadone and [$^2H_8$]methadone are present in relatively constant amounts (200 ng/g) in plasma; consequently, there is very little interference (typically 0.1–0.2%) between the latter two species and the two *in vivo* kinetic tracers.

In plasma studies, the intensity of the background spectrum, often referred to as "matrix interference," depends strongly on the isolation procedure used to recover methadone from biological samples and on the reagent gas used for chemical-ionization mass spectrometry. It is imperative in these studies to minimize matrix interference to quantitate the low levels of isotopically labeled methadone expected in plasma.

Data presented in Table III show that simple solvent extraction of buffered control plasma containing only [$^2H_8$]methadone had an ion intensity ~20–30 times that of the background level obtained with the pure standard determined with isobutane as the reagent gas. This interference effectively precludes measurement of drug levels below 45 ng/g. Using a short C_{18} silica gel cartridge to recover methadone reduces ion contamination, especially for (*R*)-(−)-[$^2H_5$]methadone, so that detection limits fall to 6–12 ng/g. However, use of the highly selective ammonia reagent gas further decreases the background for masses m/z 313 and 315 so that the detection limits fall to 3–5 ng/g (20).

A simple solvent extraction is sufficient to recover methadone from urine and gives results identical to those of the pure standard obtained using ammonia reagent gas. The lower detection limit in the calibration curve and in the individual patient studies is usually ~1–5 ng/g for [$^2H_3$]- and [$^2H_5$]methadone or approximately twice the blank plasma background level. Two advantages from using the C_{18} silica gel cartridges for extracting methadone from plasma are that the GLC column lifetime is improved markedly and analysis time is shortened to ~5 min/sample since no interfering peaks elute from the column after methadone.

The present data illustrate the practicality of using multiple stable isotopic tracers in a clinical research protocol. Previous studies, using only a single isotopic tracer, required three separate stable isotopic tracer experiments to explore the behavior of the separate enantiomers. Such studies were exceedingly tedious, both with respect to performance of the clinical study and the time required for the analyses. During such lengthy studies, the patient's status is subject to change. Thus, the multiple, simultaneous stable isotopic tracer technique described here offers significant advantages in studying complex drug systems such as methadone in a steady-state, multiple-dose protocol.

Data from Patient 1 (Table II and Fig. 1) reconfirm earlier observations that (*R*)-(−)-methadone is metabolized ~1.35 times slower than (*S*)-(+)-methadone (13). Plasma drug level data *versus* time were fitted to a three-exponential decay function, where the half-life is that of the terminal exponential component. In both cases, (*S*)-(+) methadone reaches and maintains a higher peak plasma level over the first 48 hr of the study than does the (*R*)-(−)-methadone. Thereafter, the (*R*)-(−)-methadone curve crosses the (*S*)-(+)-methadone concentration curve and remains higher for the rest of the study. The area under the plasma disappearance curve was integrated over the first 119 hr. These data indicate that (*S*)-(+)-methadone has a higher plasma level and, therefore, higher relative bioavailability following an oral dose than does (*R*)-(−)-methadone. The total plasma compartment for methadone (both enantiomers) accounts for only 1.8–2.8% of the administered dose.

The second patient (Fig. 2) displays similar pharmacokinetic behavior but with two differences: (*a*) the plasma disappearance half-life of *R*-(−)-methadone is 1.69 times as long as that of the (*S*)-(+)-enantiomer, compared with the more normal 1.35-fold difference observed in the first patient; and (*b*) the integrated area under the plasma disappearance curves of *S*-(+)-methadone is 1.85 times greater than that of the (*R*)-(−)-enantiomer. The significance of these observations is not yet clear; Patient 1 had a history of chronic alcohol misuse, and Patient 2 had a history of chronic acute hepatitis.

The described methodology for plasma drug level measurements can also be applied to measure urinary excretion of unmetabolized methadone

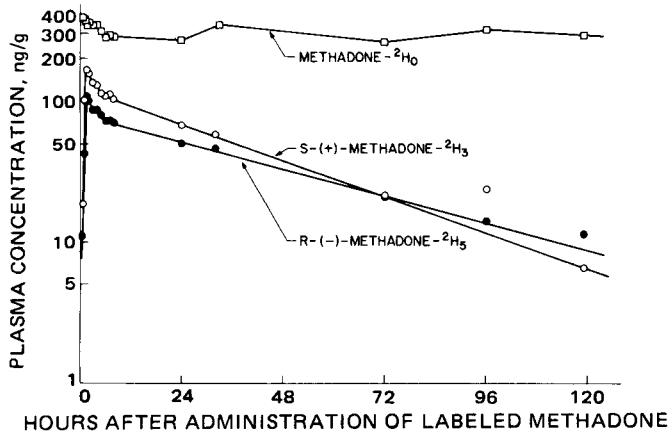

Figure 1—*Plasma methadone disappearance curves for methadone, (R)-(−)-[$^2H_5$]methadone, and (S)-(+)-[$^2H_3$]methadone determined in Patient 1.*

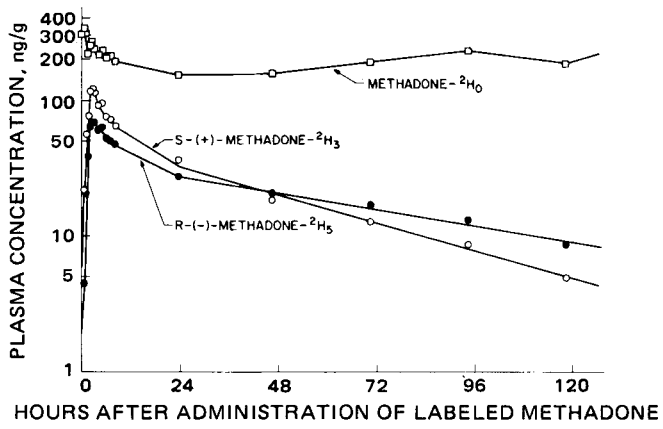

Figure 2—*Plasma methadone disappearance curves for methadone, (R)-(−)-[$^2H_5$]methadone, and (S)-(+)-[$^2H_3$]methadone determined in Patient 2.*

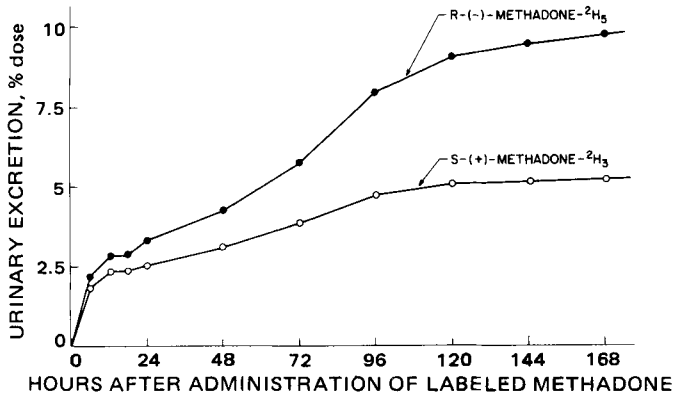

Figure 3—*Cumulative urinary excretion of (R)-(−)-[$^2H_5$]methadone and (S)-(+)-[$^2H_3$]methadone determined in Patient 1.*

enantiomers. Data presented in Fig. 3 illustrate the cumulative urinary excretion of the two methadone enantiomers in Patient 1. (*S*)-(+)-methadone reaches a cumulative excretion plateau value of 5.2% by 120 hr. In contrast, the (*R*)-(−)-methadone continues to be excreted throughout the study; by 168 hr, 9.8% of the dose was excreted as the unmetabolized drug. The urinary data, together with the plasma drug level data, suggest a differential renal clearance mechanism for the excretion of the unchanged methadone enantiomers. Full assessment of each step of the disposition of the separate enantiomers of methadone and its metabolites, including hepatic uptake metabolism, biliary excretion, fecal excretion, and urinary clearance, is needed before the mechanisms underlying the observed differences in overall disposition can be evaluated (25).

REFERENCES

(1) V. P. Dole, M. E. Nyswander, and M. J. Kreek, *Arch. Intern. Med.*, **118**, 304 (1966).

(2) M. J. Kreek, "Heroin Dependency: Medical, Economic and Social Aspects," Stratton Intercontinental Medical Book Corp., New York, N.Y., 1975, p. 232.

(3) B. A. Judson, W. H. Horns, and A. Goldstein, *Clin. Pharmacol. Ther.*, **20**, 445 (1976).

(4) G. D. Olsen, H. A. Wendel, J. D. Livermore, R. M. Leger, R. K. Lynn, and N. Gerber, *ibid.*, **21**, 147 (1977).

(5) H. R. Sullivan, S. E. Smits, S. L. Due, R. E. Booher, and R. E. McMahon, *Life Sci.*, **11**, 1093 (1972).

(6) N. A. Ingoglia and V. P. Dole, *J. Pharmacol. Exp. Ther.*, **175**, 84 (1970).

(7) A. Goldstein, L. I. Lowney, and B. K. Pal, *Proc. Natl. Acad. Sci. USA*, **68**, 1742 (1971).

(8) A. L. Misra and S. J. Mulé, *Nature*, **241**, 281 (1973).

(9) S. E. Smits and M. D. Myer, *Res. Commun. Chem. Pathol.*, **7**, 651 (1974).

(10) H. R. Sullivan, S. L. Due, and R. E. McMahon, *J. Pharm. Pharmacol.*, **27**, 728 (1975).

(11) C. B. Pert and S. H. Snyder, *Science*, **170**, 1011 (1973).

(12) E. J. Simon, J. M. Miller, and I. Edelman, *Proc. Natl. Acad. Sci. USA*, **70**, 1947 (1973).

(13) M. J. Kreek, D. L. Hachey, and P. D. Klein, *Life Sci.*, **24**, 925 (1979).

(14) A. Pohland, H. E. Boaz, and H. R. Sullivan, *J. Med. Chem.*, **14**, 194 (1971).

(15) E. R. Klein and P. D. Klein, *Biomed. Mass Spectrom.*, **5**, 91 (1978).

(16) *Ibid.*, **5**, 321 (1978).

(17) H. R. Sullivan, F. J. Marshall, R. E. McMahon, E. Anggaard, L. M. Gunne, and J. H. Holmstrand, *Biomed. Mass Spectrum.*, **2**, 197 (1975).

(18) D. L. Hachey, M. J. Kreek, and D. H. Mattson, *J. Pharm. Sci.*, **66**, 1579, (1977).

(19) M. J. Kreek, C. L. Gutjahr, J. W. Garfield, D. V. Bowen, and F. H. Field, *Ann. N.Y. Acad. Sci.*, **281**, 350 (1976).

(20) D. A. Knowlton, A. F. Fentiman, and R. J. Foltz, "Research Report to the National Institute on Drug Abuse," Battelle Columbus Laboratories, Columbus, Ohio, Dec. 1, 1978.

(21) J. I. Brauman, *Anal. Chem.*, **38**, 607 (1966).

(22) D. L. Hachey, J. C. Blais, and P. D. Klein, *ibid.*, **52**, 1131 (1980).

(23) M. Berman and M. F. Weiss, "SAAM 27 Users Manual," Department of Health, Education and Welfare Publication Number (NIH) 78-180, U.S. Government Printing Office, Washington, DC 20402.

(24) D. J. Jenden, M. Roch, and R. A. Booth, *Anal. Biochem.*, **55**, 438 (1973).

(25) H. R. Sullivan and S. L. Due, *J. Med. Chem.*, **16**, 909 (1973).

ACKNOWLEDGMENTS

Supported by the U.S. Department of Energy through Contract W-31-109-ENG-38, National Institute on Drug Abuse Grant DA-01138, and National Institutes of Health General Clinical Research Center Grant RR-00102. Publication of this manuscript was supported in part by the Children's Nutrition Research Center, SEA, USDA, the Department of Pediatrics, Baylor College of Medicine, and Texas Children's Hospital.

M. J. Kreek was the recipient of a Research Scientist Award (DA-00049) from the NIDA.

The authors acknowledge the support of D. K. Murayama, Director of Central Research Laboratories, Sankyo Co., Tokyo, Japan, given to K. Nakamura during his stay at Argonne National Laboratory.

Effect of Surface Charge and Particle Size on Gel Structure of Aluminum Hydroxycarbonate Gel

JOSEPH R. FELDKAMP *, JOE L. WHITE *, and STANLEY L. HEM ‡x

Received March 6, 1981, from the **Department of Agronomy and the* ‡*Department of Industrial and Physical Pharmacy, Purdue University, West Lafayette, IN 47907.* Accepted for publication May 14, 1981.

Abstract □ The effect of surface charge and particle size on the gel structure of aluminum hydroxycarbonate gel was studied through the use of a specially designed tension cell. Surface charge has a major effect on the coefficient of bulk compressibility. The charged state is more compressible at lower tensions while the neutral gel is more compressible at higher tensions. In addition, physical properties of gels having a small particle size are more profoundly influenced by interparticle forces than are gels consisting of larger particles. The effect of surface charge and particle size on gel structure is applied to physical properties such as viscosity and dewatering.

Keyphrases □ Aluminum hydroxycarbonate gel—gel structure, effect of surface charge and particle size □ Gels—aluminum hydroxycarbonate, effect of surface charge and particle size on structure □ Physicochemistry—effect of surface charge and particle size on gel structure of aluminum hydroxycarbonate gel

Investigation of the structure of aluminum hydroxide gel at an atomic level has led to improved understanding of the arrangement of atoms and the types of bonds present in the various materials collectively known as aluminum hydroxide (1–4). An equally important type of structure, gel structure, which deals with the manner in

0022-3549/82/0100-0043$01.00/0

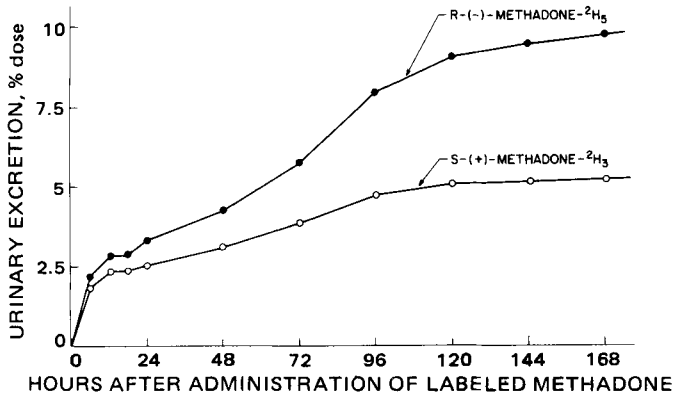

Figure 3—*Cumulative urinary excretion of (R)-(−)-[$^2H_5$]methadone and (S)-(+)-[$^2H_3$]methadone determined in Patient 1.*

enantiomers. Data presented in Fig. 3 illustrate the cumulative urinary excretion of the two methadone enantiomers in Patient 1. (*S*)-(+)-methadone reaches a cumulative excretion plateau value of 5.2% by 120 hr. In contrast, the (*R*)-(−)-methadone continues to be excreted throughout the study; by 168 hr, 9.8% of the dose was excreted as the unmetabolized drug. The urinary data, together with the plasma drug level data, suggest a differential renal clearance mechanism for the excretion of the unchanged methadone enantiomers. Full assessment of each step of the disposition of the separate enantiomers of methadone and its metabolites, including hepatic uptake metabolism, biliary excretion, fecal excretion, and urinary clearance, is needed before the mechanisms underlying the observed differences in overall disposition can be evaluated (25).

REFERENCES

(1) V. P. Dole, M. E. Nyswander, and M. J. Kreek, *Arch. Intern. Med.*, **118**, 304 (1966).

(2) M. J. Kreek, "Heroin Dependency: Medical, Economic and Social Aspects," Stratton Intercontinental Medical Book Corp., New York, N.Y., 1975, p. 232.

(3) B. A. Judson, W. H. Horns, and A. Goldstein, *Clin. Pharmacol. Ther.*, **20**, 445 (1976).

(4) G. D. Olsen, H. A. Wendel, J. D. Livermore, R. M. Leger, R. K. Lynn, and N. Gerber, *ibid.*, **21**, 147 (1977).

(5) H. R. Sullivan, S. E. Smits, S. L. Due, R. E. Booher, and R. E. McMahon, *Life Sci.*, **11**, 1093 (1972).

(6) N. A. Ingoglia and V. P. Dole, *J. Pharmacol. Exp. Ther.*, **175**, 84 (1970).

(7) A. Goldstein, L. I. Lowney, and B. K. Pal, *Proc. Natl. Acad. Sci. USA*, **68**, 1742 (1971).

(8) A. L. Misra and S. J. Mulé, *Nature*, **241**, 281 (1973).

(9) S. E. Smits and M. D. Myer, *Res. Commun. Chem. Pathol.*, **7**, 651 (1974).

(10) H. R. Sullivan, S. L. Due, and R. E. McMahon, *J. Pharm. Pharmacol.*, **27**, 728 (1975).

(11) C. B. Pert and S. H. Snyder, *Science*, **170**, 1011 (1973).

(12) E. J. Simon, J. M. Miller, and I. Edelman, *Proc. Natl. Acad. Sci. USA*, **70**, 1947 (1973).

(13) M. J. Kreek, D. L. Hachey, and P. D. Klein, *Life Sci.*, **24**, 925 (1979).

(14) A. Pohland, H. E. Boaz, and H. R. Sullivan, *J. Med. Chem.*, **14**, 194 (1971).

(15) E. R. Klein and P. D. Klein, *Biomed. Mass Spectrom.*, **5**, 91 (1978).

(16) *Ibid.*, **5**, 321 (1978).

(17) H. R. Sullivan, F. J. Marshall, R. E. McMahon, E. Anggaard, L. M. Gunne, and J. H. Holmstrand, *Biomed. Mass Spectrum.*, **2**, 197 (1975).

(18) D. L. Hachey, M. J. Kreek, and D. H. Mattson, *J. Pharm. Sci.*, **66**, 1579, (1977).

(19) M. J. Kreek, C. L. Gutjahr, J. W. Garfield, D. V. Bowen, and F. H. Field, *Ann. N.Y. Acad. Sci.*, **281**, 350 (1976).

(20) D. A. Knowlton, A. F. Fentiman, and R. J. Foltz, "Research Report to the National Institute on Drug Abuse," Battelle Columbus Laboratories, Columbus, Ohio, Dec. 1, 1978.

(21) J. I. Brauman, *Anal. Chem.*, **38**, 607 (1966).

(22) D. L. Hachey, J. C. Blais, and P. D. Klein, *ibid.*, **52**, 1131 (1980).

(23) M. Berman and M. F. Weiss, "SAAM 27 Users Manual," Department of Health, Education and Welfare Publication Number (NIH) 78-180, U.S. Government Printing Office, Washington, DC 20402.

(24) D. J. Jenden, M. Roch, and R. A. Booth, *Anal. Biochem.*, **55**, 438 (1973).

(25) H. R. Sullivan and S. L. Due, *J. Med. Chem.*, **16**, 909 (1973).

ACKNOWLEDGMENTS

Supported by the U.S. Department of Energy through Contract W-31-109-ENG-38, National Institute on Drug Abuse Grant DA-01138, and National Institutes of Health General Clinical Research Center Grant RR-00102. Publication of this manuscript was supported in part by the Children's Nutrition Research Center, SEA, USDA, the Department of Pediatrics, Baylor College of Medicine, and Texas Children's Hospital.

M. J. Kreek was the recipient of a Research Scientist Award (DA-00049) from the NIDA.

The authors acknowledge the support of D. K. Murayama, Director of Central Research Laboratories, Sankyo Co., Tokyo, Japan, given to K. Nakamura during his stay at Argonne National Laboratory.

Effect of Surface Charge and Particle Size on Gel Structure of Aluminum Hydroxycarbonate Gel

JOSEPH R. FELDKAMP *, JOE L. WHITE *, and STANLEY L. HEM ‡x

Received March 6, 1981, from the **Department of Agronomy and the* ‡*Department of Industrial and Physical Pharmacy, Purdue University, West Lafayette, IN 47907.* Accepted for publication May 14, 1981.

Abstract □ The effect of surface charge and particle size on the gel structure of aluminum hydroxycarbonate gel was studied through the use of a specially designed tension cell. Surface charge has a major effect on the coefficient of bulk compressibility. The charged state is more compressible at lower tensions while the neutral gel is more compressible at higher tensions. In addition, physical properties of gels having a small particle size are more profoundly influenced by interparticle forces than are gels consisting of larger particles. The effect of surface charge and particle size on gel structure is applied to physical properties such as viscosity and dewatering.

Keyphrases □ Aluminum hydroxycarbonate gel—gel structure, effect of surface charge and particle size □ Gels—aluminum hydroxycarbonate, effect of surface charge and particle size on structure □ Physicochemistry—effect of surface charge and particle size on gel structure of aluminum hydroxycarbonate gel

Investigation of the structure of aluminum hydroxide gel at an atomic level has led to improved understanding of the arrangement of atoms and the types of bonds present in the various materials collectively known as aluminum hydroxide (1–4). An equally important type of structure, gel structure, which deals with the manner in

0022-3549/82/0100-0043$01.00/0

which the aluminum hydroxide particles are arranged in space, has not been as extensively studied. For this reason, a series of studies was initiated utilizing a specially designed tension cell to elucidate various relationships between gel structure and physical properties. The role of surface charge and particle size in determining the gel structure of aluminum hydroxycarbonate gel was examined in this study.

BACKGROUND

The tension cell was designed for the study of the gel structure of aluminum hydroxide (5) and was developed from experimental methods used to study clays and related porous materials (6). The tension cell was used to measure the coefficient of bulk compressibility for two aluminum hydroxycarbonate gels having a pH-dependent surface charge and a substantially different particle size.

The coefficient of bulk compressibility, α, is used by soil physicists to describe the degree of consolidation of a solid particle or colloidal matrix on the application of an external load or stress and is typically defined as (7, 8):

$$\alpha = -\frac{1}{V}\frac{dV}{d\sigma} \qquad \text{(Eq. 1)}$$

where σ represents an applied stress and V is the volume of the system, including both the particle volume and the pore volume. When the tension cell is used, the stress is supplied by applying a small negative pressure or tension, τ. Since the cross-sectional area of the tension cell chamber is constant, the coefficient of bulk compressibility may be expressed in terms of L, the length of the column of gel in the tension cell, and the applied tension:

$$\alpha = -\frac{1}{L}\frac{dL}{d\tau} \qquad \text{(Eq. 2)}$$

The coefficient of bulk compressibility may be readily calculated if an empirical relationship between the applied tension and the corresponding length of the column at equilibrium can be established. Such a relationship may be obtained through trial and error testing of various mathematical relationships. A particularly successful equation is:

$$L = A(e^{-\beta\tau} + B) \qquad \text{(Eq. 3)}$$

where A, B, and β are constants adjusted to best fit the (τ, L) data pairs. Upon determining the proper empirical form, the coefficient of bulk compressibility is calculated by substituting Eq. 3 into Eq. 2.

EXPERIMENTAL

Two aluminum hydroxycarbonate gels were obtained commercially, and the coefficient of bulk compressibility was determined with the tension cell following dilution to 9.3% equivalent aluminum oxide.

The zero point of charge (ZPC), the pH at which the net surface charge is zero, is an important property of colloidal systems that possess a pH-dependent surface charge. At this pH, the densities of the positive and negative charges are equal (9). The zero point of charge of aluminum hydroxycarbonate gels 1 and 2 was determined to be 6.34 and 7.60, respectively, by a titration procedure (10). The desired surface charge was obtained through adjustment of the pH relative to the zero point of charge by the addition of small quantities of hydrochloric acid or sodium hydroxide to produce a positive, neutral, or negative surface charge. Aluminum hydroxycarbonate gel 1 was adjusted to pH 5.70, 6.34, and 7.40; gel 2 was adjusted to pH 5.50 and 7.00.

The rate of acid neutralization was determined by pH-stat titration at pH 3 and 25° (11).

The relative particle size of the two aluminum hydroxycarbonate gels was determined by measuring the rate of sedimentation of 100 ml of a 1% (w/v) dilution of each gel in a 100-ml graduated cylinder following pH adjustment to equal the zero point of charge. The sedimentation rate is expressed as t_{50}, the time required to settle halfway from the initial height in the 100-ml cylinder to the equilibrium sediment height.

The previously described tension cell procedure (5) was used to determine the equilibrium water outflow as a result of applied tensions up to 15 cm of water. Two modifications were made in the tension cell apparatus to provide more convenient and precise measurements. Since the gel undergoes a decrease in volume due to the outflow of water, the applied tension will decrease during the experiment. This undesirable effect was previously minimized through the manual readjustment of the height of the tension cell chamber by 0.05 cm for every 1.5 ml of water outflow so that the applied tension remained essentially constant.

This procedure was replaced with a digital motor-drive system, which readjusted the tension on sensing a downward movement of the upper gel surface. The motor triggering mechanism consisted of a pair of platinum electrodes sealed in glass tubing, which were positioned to contact the gel surface. As long as the electrodes contacted the surface, a very small dc current (<0.1 μamp) moved through the completed circuit. As outflow of water from the gel proceeded, the gel surface dropped below the electrodes, interrupting the current and activating the digital motor-drive system. The sample chamber was raised to reestablish contact between the electrodes and the gel surface. This apparatus maintained the applied tension within 0.03 cm. A vernier system was attached to the digital motor drive so the accumulated height changes of the tension cell chamber could be measured. At each tension level setting, the overall displacement of the tension cell was equal to the length change of the gel column.

A second modification was made to record automatically the water outflow as a function of time. Water flowed dropwise from the outlet tube and entered a small volumetric flask, which was fitted with a cover having a capillary opening. The flask rested on a weighing pan, which was displaced linearly according to the amount of water in the flask. The downward movement of the weighing pan was monitored with a linear variable differential transformer whose output was continuously recorded. Thus, the equilibrium outflow of water at a particular tension could be easily determined. Equilibrium times ranged from 8 to 48 hr. In every case, the equilibrium outflow of water was equal to the volume change of the gel.

RESULTS AND DISCUSSION

The applied tension is related to the amount of work required, per mole of water, $\Delta\overline{G}_{H_2O}$, to remove water from the system (12):

$$\Delta\overline{G}_{H_2O} = -\rho g \overline{V}\tau \qquad \text{(Eq. 4)}$$

where ρ is the density of water, $\overline{V}$ is the molar volume of water, and g is the acceleration due to gravity. To remove dn_{H_2O} moles of water from the system requires that an amount of work equal to δW be done on the system:

$$\delta W = \Delta\overline{G}_{H_2O}\, dn_{H_2O} \qquad \text{(Eq. 5)}$$

Equation 5 may be rewritten with the aid of Eq. 4 to give:

$$\delta W = -\rho g \tau A\, dL \qquad \text{(Eq. 6)}$$

where A is the area of the tension cell chamber and dL represents a small displacement of the length of the gel column. The work of compression, δW, is expended against the efforts of the gel to retain its original particle arrangement or gel structure. A large work of compression implies either that cohesive forces (van der Waals) are present, tending to prevent the distortion of the particles into a smaller space, or that interparticle repulsive forces (coulombic) are present, which resist a closer approach of particle surfaces.

Although the work of compression is a macroscopic concept, it is ultimately tied to phenomena occurring on a microscopic scale. As illustrated in Fig. 1, each particle may be viewed as residing in a potential well, the depth and width of which are controlled by interparticle force fields. Movement of any particle along some trajectory from one well to another requires that the particle attain sufficient energy to pass over the interposed barrier. If thermal energy is insufficient, there is no appreciable translational motion and the system gels. In such cases, the necessary energy may be provided by applying an external stress such as shear or, in this case, a pressure gradient (tension). The extent to which particles are free to move under an applied external stress is directly dependent on the nature of adjacent energy barriers.

The work of compression is further illustrated in Fig. 2 (A and B) by the shaded regions that are proportional to the work of compression required to displace the gel from a length of 4.5–4.0 cm. The work required to compress the neutral aluminum hydroxycarbonate gel over this range is approximately twice that required to compress the charged aluminum hydroxycarbonate gel, indicating that cohesive forces present in the neutral gel tend to prevent the movement of the particles to a greater extent than the repulsive forces present in the positively charged system.

It is clear that Eq. 3 is a suitable mathematical expression to describe the tension *versus* gel column length relationship since the solid lines

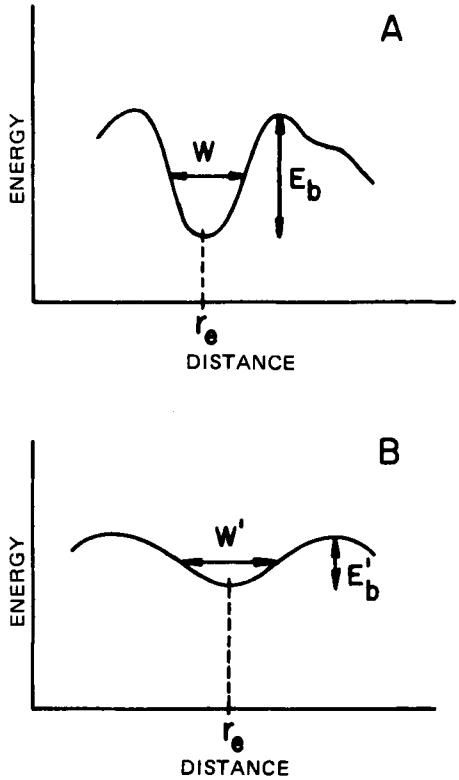

Figure 1—*Energy–distance profiles. Key: A, high particle density gel; B, low particle density gel; E_b, depth of the potential well; W, characteristic width of the potential well; and r_e, equilibrium position of the particle.*

representing the fitted equation coincide with the data points. Thus, the data in Fig. 2 were used to calculate the compressibility curves shown in Fig. 3.

The coefficient of bulk compressibility of aluminum hydroxycarbonate gel 1 is clearly affected by the presence of surface charge (Fig. 3, A and B). At tension levels less than ~9 cm, the positively charged system was considerably more compressible than the neutral gel. This result is similar to the previously observed effect of surface charge on the viscosity of aluminum hydroxycarbonate gel in which the maximum viscosity occurred when the pH equaled the zero point of charge (10).

The underlying mechanism explaining both phenomena is that when

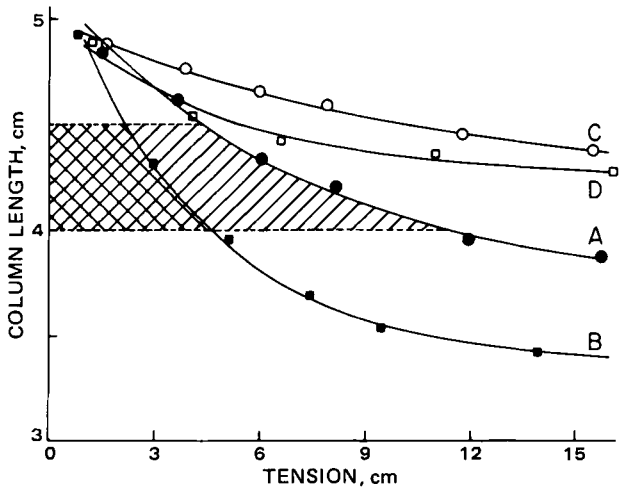

Figure 2—*Change in the column length as a result of applied tension. Shaded areas indicate the relative work of compression required to displace aluminum hydroxycarbonate gels 1 and 2 from a length of 4.5 to 4.0 cm. Key: A, gel 1 at pH 6.34 (ZPC = 6.34); B, gel 1 at pH 5.7; C, gel 2 at pH 7.0 (ZPC = 7.60); D, gel 2 at pH 5.5; data points are from tension cell experiments and the solid lines were obtained by fitting Eq. 3 to the data points.*

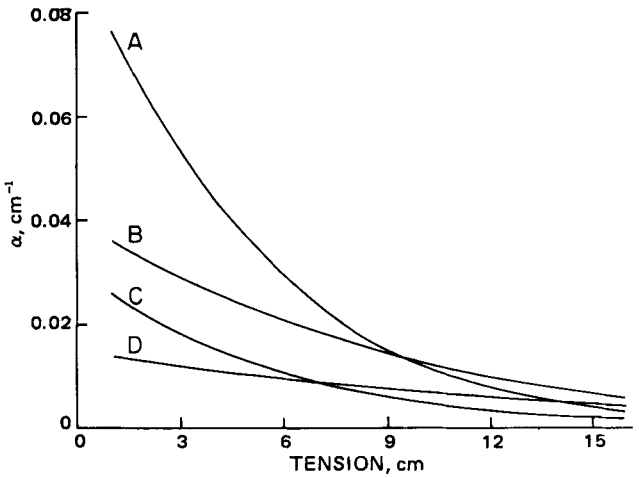

Figure 3—*Effect of tension on the coefficient of bulk compressibility, α. Key: A, gel 1 at pH 6.34 (ZPC = 6.34); B, gel 1 at pH 5.7; C, gel 2 at pH 7.0 (ZPC = 7.60); and D, gel 2 at pH 5.5.*

sufficient coulombic repulsion is developed to overcome van der Waals attractive forces, the particles are free to move in a less restricted manner. Particles are considered to be more free or mobile under the influence of repulsion than attraction since repelling particles tend to utilize the entire space of the system, whereas attractive forces usually produce structures that confine the particles to rigid, linear chains so that considerable unused space exists (13). Since the charged particles are not so severely confined in space, consolidation of the colloidal matrix in response to water removal may readily take place, leading to a more compressed system. In addition, the absence of attractive forces tending to lock the particles into position permits shear rather easily. At the zero point of charge, however, substantial cohesive forces (van der Waals) resist distortion of the gel structure to form some new structural arrangement.

However, as seen in Fig. 3 (A and B) the charged gel was less compressible than the neutral gel when the applied tension exceeded 9 cm of water. This is a consequence of the initial freedom of movement of the charged particles during consolidation and leads to a more efficiently packed collection of particles. This dense collection of particles is able to resist further compaction more effectively than the neutral gel due to the substantially increased level of coulombic repulsion. In addition, when the aluminum hydroxycarbonate gel is at the zero point of charge, the initial randomness or disorder of the gel structure is locked into place by van der Waals cohesive forces, preventing the formation of an efficiently packed particle network. Consequently, the compressibility of the neutral gel is greater than that of the charged gel at high tensions.

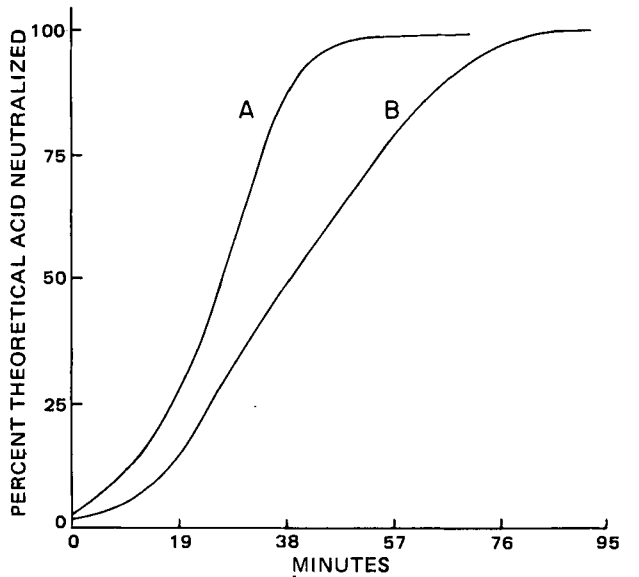

Figure 4—*Rate of acid neutralization at pH 3.0 and 25°. Key: A, gel 1; and B, gel 2.*

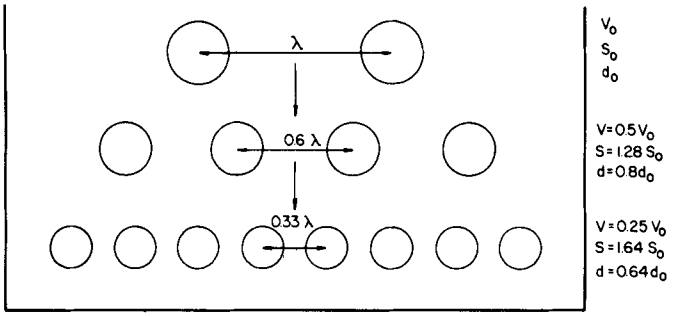

Figure 5—*Effect of particle density on interparticle distance. Key: λ, interparticle distance; V, volume of each particle; S, total surface area; and d, diameter of each particle. The volume of each particle is reduced by 50% in each step while the total volume of the particles is constant.*

A practical consequence of this behavior is that the charged state permits more convenient water removal, but only when the water content is below that corresponding to a tension of 9 cm of water. Above 9-cm water tension, the neutral state is more desirable for operations involving water removal.

The zero point of charge of gel 2 was 7.6. This gel is believed to have a smaller particle size and, therefore, a greater surface area than gel 1 since this gel became too viscous to mix as the pH was brought to the zero point of charge. It was not possible to adjust the pH to 7.6 where the maximum viscosity occurs because of the high viscosity. This behavior is in contrast to that of gel 1, which became more viscous as the pH was adjusted to its zero point of charge but still remained fluid at the zero point of charge.

The smaller particle size of gel 2 was confirmed by comparing the rate of settling of 1% equivalent aluminum oxide dilutions of gels 1 and 2. The t_{50} value for the sedimentation of gel 1 was 1.8 hr while gel 2 required 4.3 hr for an equivalent degree of sedimentation. The more rapid rate of acid neutralization by gel 2 at pH 3 (where both aluminum hydroxycarbonate gels will be highly charged) also reflects its smaller particle size (Fig. 4).

It was not possible to repeat exactly the tension cell experiment for gel 2 since the viscosity was too great at the zero point of charge. However, the effect of charge on the gel 2 structure was similar to that observed for gel 1 (Fig. 2, C and D). Gel 2 was more compressible when in a highly charged state, *i.e.*, at pH 5.5, up to a tension of ~7 cm of water (Fig. 3, C and D). The less charged state, *i.e.*, at pH 7.0, was more compressible at higher tension levels. The point at which the charged gel became more compressible than the neutral gel (7 cm of water) occurred at a lower tension than was observed for gel 1 due to the much greater charge on gel 2.

The most striking difference between gels 1 and 2 was that gel 2 was less compressible regardless of its charge. Since the same types of forces are present in both gels and each gel has the same equivalent aluminum oxide content, the factor responsible for the difference in behavior must be the smaller particle size and, consequently, the greater surface area of 2. Reducing the particle size while maintaining a constant solids concentration will cause gel 2 to have a higher particle density.

The effect of particle density may be illustrated by the example provided in Fig. 5 in which individual particle volume is sequentially halved in a one-dimensional arrangement of particles. Such a system is especially relevant since linear chains are frequently formed under the influence of van der Waals attractive forces (13). Although surface area does not increase substantially upon two subdivisions, the average interparticle distance decreases signficantly. Consequently, a gel having a smaller particle size is much more likely to form an extended chain-like network when cohesive interparticle forces exist.

The effect of particle density for the general case of three-dimensional particle arrays with either attractive or repulsive interparticle forces present may be further clarified through the microscopic energy–distance profiles of Fig. 1 (A and B). As was shown, a higher particle density leads to a smaller average interparticle separation distance. Since forces depend inversely on separation distance, the net restoring force exerted on a given particle by all others during a small displacement of the particle from its equilibrium position is greater (as in Fig. 1A). A low particle density yields the opposite effects (as in Fig. 1B) so that particles are less influenced by one another and are not held as tightly in place. This conclusion follows for coulombic-type forces as well as van der Waals forces so that gel 2 is predicted to be less compressible than gel 1 in both its charged and discharged states. The experimental results observed in Fig. 3 support this conclusion.

REFERENCES

(1) S. L. Nail, J. L. White, and S. L. Hem, *J. Pharm. Sci.*, **65**, 1188 (1976).

(2) J. L. White and S. L. Hem, *ibid.*, **64**, 468 (1975).

(3) C. J. Serna, J. L. White, and S. L. Hem, *Soil Sci. Soc. Am. Proc.*, **41**, 1009 (1977).

(4) C. J. Serna, J. L. White, and S. L. Hem, *J. Pharm. Sci.*, **67**, 1144 (1978).

(5) E. A. Lipka, J. R. Feldkamp, J. L. White, and S. L. Hem, *J. Pharm. Sci.*, in press.

(6) D. Swartzendruber, in "The Flow of Water in Unsaturated Solids," R. J. M. DeWeist, Ed., Academic, New York, N.Y., 1969, chap. 6.

(7) J. Bear, "Dynamics of Fluids in Porous Media," American Elsevier, New York, N.Y., 1972, pp. 52–56.

(8) E. H. Davis and G. P. Raymond, *Geotechnique*, **15**, 161 (1965).

(9) R. G. Gast, in "Minerals in Soil Environments," J. B. Dixon and S. B. Weed, Eds., Soil Science Society of America, Madison, Wis., 1977, pp. 27–73.

(10) J. R. Feldkamp, D. N. Shah, S. L. Meyer, J. L. White, and S. L. Hem, *J. Pharm. Sci.*, **70**, 638 (1981).

(11) N. J. Kerkhof, R. K. Vanderlaan, J. L. White, and S. L. Hem, *ibid.*, **66**, 1528 (1977).

(12) P. F. Low, *Soil Sci.*, **93**, 6 (1962).

(13) J. Mahanty and B. W. Ninham, "Dispersion Forces," Academic, New York, N.Y., 1976, pp. 21, 22.

ACKNOWLEDGMENTS

Supported in part by William H. Rorer, Inc.

This report is Journal Paper 8456, Purdue University Agricultural Experiment Station, West Lafayette, IN 47907.

Comparison of Effects of Cyanide and Acetylcholine on Renal Hemodynamics and Sodium Excretion

RONALD L. WILLIAMS *[x], JAMES E. PEARSON [‡], and FRANCISCO M. GONZALEZ [‡]

Received March 18, 1981, from the *Department of Pharmacology and the [‡]Department of Medicine, Louisiana State University Medical Center, New Orleans, LA 70112. Accepted for publication May 14, 1981.

Abstract □ The present study compared the effects of acetylcholine to cyanide under the same experimental conditions of renal clearance in anesthetized dogs. Since cyanide is one of the few drugs for which the mechanism of action is known (cytotoxic hypoxia), some insight may be gained into the renal effects of acetylcholine since both produce direct natriuresis and diuresis. Infusion of 0.2 μg/kg/min of acetylcholine and 12.0 μg/kg/min of sodium cyanide into the left renal artery resulted in similar effects, *i.e.*, increased fractional excretion of sodium, potassium, calcium, and magnesium. These effects were immediate and ipsilateral. Both agents increased the renal plasma flow to the same extent. In addition, regression plots of the relation between changes in sodium excretion and changes in renal plasma flow were similar for both agents. The pattern of similar renal functional changes suggested that acetylcholine is not a mere renal vasodilator but that its action is also mediated through alterations on direct tubular transport of ions.

Keyphrases □ Hemodynamics, renal—effects of cyanide and acetylcholine compared □ Cyanide—effects on renal hemodynamics and sodium secretion, comparison with acetylcholine □ Acetylcholine—effects on renal hemodynamics and sodium secretion, comparison with cyanide

May and Carter (1) showed that something other than simple vasodilation is responsible for the saluretic action of cholinergic drugs. When they infused cholinergic drugs into the renal portal system of chickens, there was an ipsilateral saluresis; however, noncholinergic drugs (isoproterenol, papaverine, and dopamine) produced no saluresis despite similar renal vasodilation.

BACKGROUND

The prevalent conclusion has been that vasodilating agents induce changes in sodium excretion mainly by altering renal blood flow (2, 3). Using autoperfused kidneys, no correlation was found between changes in renal perfusion pressure and changes in sodium excretion for either acetylcholine or isoproterenol (4). Itskovitz and Campbell (5) infused seven different vasodilators into isolated blood-perfused canine kidneys at constant pressure. Despite similar hemodynamic effects on renal blood flow, perfusion pressure, and intrarenal distribution of blood flow, their effects on glomerular filtration rate (*GFR*), sodium excretion, and urine flow were dissimilar. Acetylcholine was by far the most natriuretic. Eledoisin, one of the vasodilators examined, actually decreased sodium excretion.

Stein *et al.*, (6) showed that acetylcholine (in micropuncture studies) decreased fractional and absolute sodium reabsorption in the proximal tubule. During this depression of proximal tubular reabsorption of sodium, there was no redistribution of glomerular filtration to outer cortical nephrons. Hayslett *et al.* (7), using a split-droplet method of micropuncture, infused acetylcholine into the abdominal aorta of rats and obtained a natriuresis despite a 50% reduction of glomerular filtration and renal blood flow. However, they interpreted the natriuresis to be due to intrarenal hydrostatic pressure and extraepithelial physical factors.

This study investigated renal vasodilation and the relation between hemodynamic and natriuretic changes by comparing intrarenal infusion of cyanide to that of acetylcholine.

EXPERIMENTAL

Materials and Methods—Five mongrel dogs were anesthetized with pentobarbital sodium, 30 mg/kg iv. Both ureters were cannulated through an abdominal midline incision, and the cannulas were positioned ~2 cm below the ureteral pelvic junction. A femoral vein and artery were cannulated, and the arterial cannula was connected to a transducer with a three-way stopcock for recording blood pressure with a polygraph. Arterial blood samples were obtained through the three-way stopcock.

Solutions containing creatinine, *p*-aminohippurate, and normal saline were infused at a rate of 5 ml/min through the venous system using a dual-syringe constant-flow infusion pump. A 27-gauge hypodermic needle, attached to a number 10 polyethylene tube, was placed in the left renal artery in the direction of blood flow. Through this renal arterial system, a solution of isotonic sodium chloride was continuously infused at a rate of 0.1 ml/min.

Solutions of drugs were also infused through the system at the same rate by changing the renal arterial infusate to one containing test drugs dissolved in normal saline. Both acetylcholine and sodium cyanide were infused into the same animal under the same experimental conditions. One to two hours was allowed for equilibration, and then collections of 10-min urine samples from each kidney were begun. Blood samples, drawn every 20 min from the femoral artery, were heparinized and centrifuged, and the plasma was immediately removed. At least three control urine samples were collected before these agents were infused into the kidney. The order of drug infusion was altered in some experiments.

Analysis—Chloride concentrations in urine and plasma were determined using a titrametric chloridometer; sodium and potassium concentrations in urine and in plasma were determined using a flame photometer with an internal lithium standard; a modification of a previous method (8) was used in the creatinine determinations. *p*-Aminohippurate determinations were made using a reported method (9). Tubular maximal secretion rates of *p*-aminohippurate were obtained by infusing high concentrations intravenously and then subtracting the amount filtered from the total excreted (10). The osmolalities were determined by freezing-point depression.

In addition to the electrolyte excretion rates, the glomerular filtration rates, the effective renal plasma flow, and the tubular rejection fraction of sodium were calculated. Calcium and magnesium were measured by atomic absorption spectrophotometry. Statistical methods for regression lines and significance of mean differences were taken from Snedecor (11).

Table I—Comparison of Intrarenal Infusion of Acetylcholine to that of Sodium Cyanide[a]

Parameter	Acetylcholine, 0.88 nmole/kg/min Δ[b]	*SE*	Sodium Cyanide, 0.25 μmole/kg/min Δ	*SE*
V, ml/min	1.03	±0.22	2.89	±0.72
C_{osm}, ml/min	0.99	±0.24	2.48	±0.57
GFR, ml/min	1.3	±1.8	3.0	±1.0
C_{PAH}, ml/min	11	±5.0	11	±3.8
$U_{Na^+}V$, μEq/min	145	±32	359	±109
$U_K V$, μEq/min	9	±4	28	±18
$U_{Ca^{2+}}V$, μEq/min	14	±6	15	±7
$U_{mg^{2+}}V$, μEq/min	4.0	±2	3.8	±1.2

[a] All drugs were infused into the left renal artery. [b] Each value is the mean change from five dogs obtained by subtracting the changes in the right, control kidneys from changes in the left, infused kidneys; Δ = (left kidney: drug period − control period) − (right kidney: drug period − control).

0022-3549/82/0100-0047$01.00/0

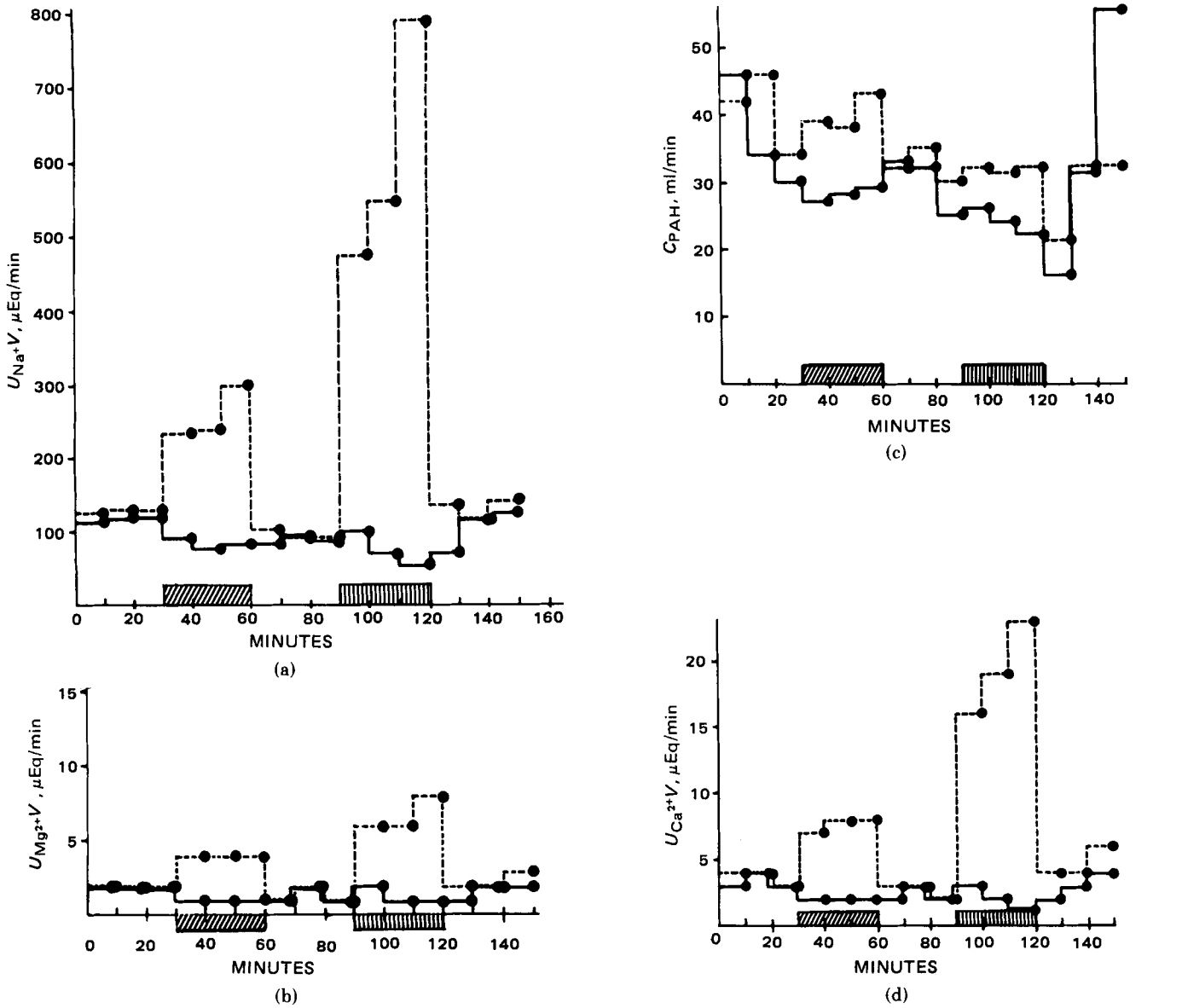

Figure 1—*Comparison of renal effects of cyanide and acetylcholine during infusion into the left renal artery. Key: - - -, left; —, right;* ▨, *acetylcholine bromide (0.2 μg/kg/min); and* ▥, *sodium cyanide (12.0 μg/kg/min).*

RESULTS

The effects of acetylcholine and local hypoxia on renal function were compared during the infusion of 0.2 μg/kg/min of acetylcholine bromide and 12.0 μg/kg/min of sodium cyanide into the left renal artery of the same animal at different times (Figs. 1*a* and 1*b*). (Converted to a molar basis, the infusion rate would be 0.88 nmole of acetylcholine bromide and 0.25 μmole of sodium cyanide/kg/min, respectively.) During the infusion of each drug, there were immediate ipsilateral increases in sodium, potassium, and calcium excretion, in osmolar clearance, creatinine clearance, *p*-aminohippurate (PAH) clearance, and urine flow. When either drug infusion was stopped, there was an immediate return to control values, even for cyanide.

Both acetylcholine and cyanide actually increased *p*-aminohippurate secretion from the tubules (Fig. 2).

The relationship between changes in sodium excretion ($U_{Na^+}V$) and changes in renal plasma flow (*RPF*) are shown in Figs. 3 and 4. The regression line for acetylcholine (Fig. 3) was $U_{Na^+}V = 8.71\ (RPF) + 29$ with a correlation coefficient of 0.83 ($p < 0.05$); the regression line for cyanide (Fig. 4) was $U_{Na^+}V = 11.5\ (RPF) + 44$ with a correlation coefficient of 0.89 ($p < 0.05$). Therefore, with the assumption of a linear relationship, cyanide produced the same effect as acetylcholine on sodium excretion and renal blood flow.

To exclude systemic influences from direct renal effects during acetylcholine or cyanide infusion into the left renal artery, the data were arranged in Table I in the following manner: (*a*) mean changes in the excretion of fluid and electrolytes were calculated along with their respective standard errors; and (*b*) each change was obtained by subtracting the changes in right, noninfused kidneys from the changes in left, experimental kidneys. Both acetylcholine and sodium cyanide produced increased excretion of each electrolyte.

DISCUSSION

Both agents increased renal blood flow and increased tubular secretion of *p*-aminohippurate. The natriuretic effects of cholinergic drugs are of the muscarinic type inhibited by atropine (12, 13). Intrarenal infusion of the muscarinic agent bethanechol (12) produced natriuresis, which was unrelated to washout of the medullary concentration gradient. No correlation was shown (14) between sodium excretion and medullary blood flow when acetylcholine was infused into a renal artery. It was postulated (13) that cholinergic drugs produce saluresis by direct action on the renal tubule, but the influence of vasodilation could not be eliminated. Cyanide, which is known to depress the energy from the electron transport system for active sodium reabsorption, also produces vasodilation. Vasodilation does not explain the natriuresis of cyanide and, therefore, may not explain the natriuresis of acetylcholine. Although a correlation between two variables does not prove a cause and effect relationship, this comparison of acetylcholine with cyanide does add indirect evidence that acetylcholine acts directly on renal tubular sodium transport in some way.

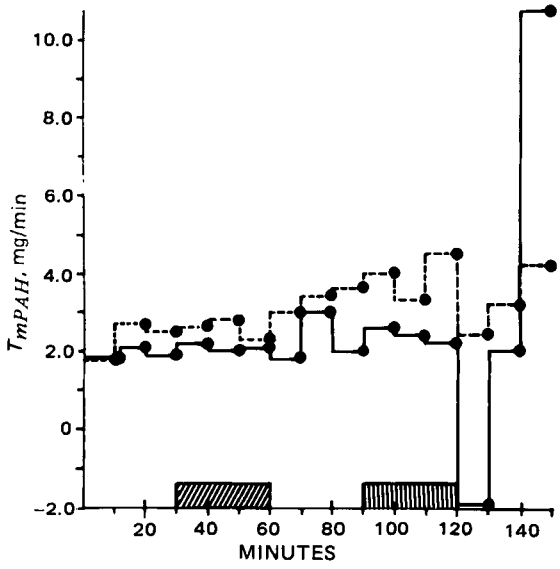

Figure 2—*Effects of intrarenal acetylcholine bromide and cyanide on tubular secretion of* p-*aminohippurate* (T_{mPAH}) *Key: - - -, left; — right;* ▨, *acetylcholine bromide (0.2 μg/kg/min); and* ▥, *sodium cyanide (12.0 μg/kg/min).*

The direct natriuretic effect of cholinergic agents was shown in chicken (12, 15) and dog (13, 16–18) kidneys. Some workers concluded direct tubular effects from micropuncture studies (6, 19); others interpreted the saluretic effect to be a result of intrarenal physical alterations due to hemodynamic changes from vasodilation (2, 3, 7). However, papaverine, a noncholinergic vasodilator, was found to be natriuretic in anesthetized sheep but not in conscious sheep (20). In conscious sheep, there was an inverse relationship between sodium excretion and changes in renal blood flow. In fact, there was a reduction in sodium excretion from the conscious animals despite an increase in renal blood flow. Cholinergic agents were shown (1) to be natriuretic in chickens, but noncholinergic vasodilators were not natriuretic even though blood flow was increased. The natriuretic action of acetylcholine cannot be explained by a redistribution of blood flow to shorter cortical nephrons (6).

The physiological importance of acetylcholine is an interesting question

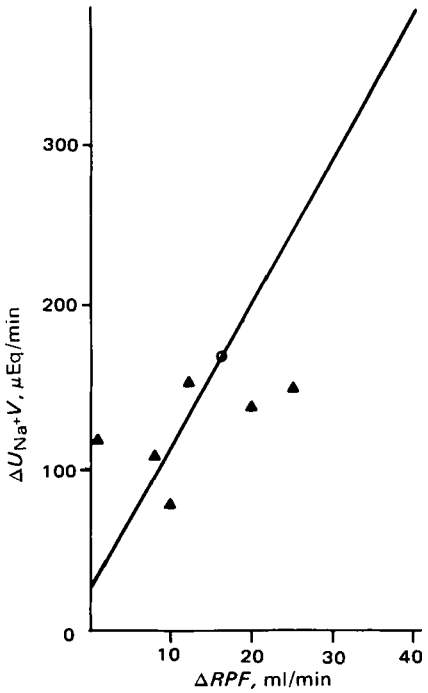

Figure 3—*Linear regression for changes in sodium excretion* ($U_{Na^+}V$) *and changes in renal plasma flow* (RPF) *during infusion of acetylcholine bromide into the left renal artery* ($y = bx + c$, $\Delta U_{Na^+}V = 8.71$ (ΔRPF) + 29, $\bar{y} = 172 \pm 47$, $\bar{x} = 16 \pm 4$, $r = 0.83$, *and* $p < 0.05$).

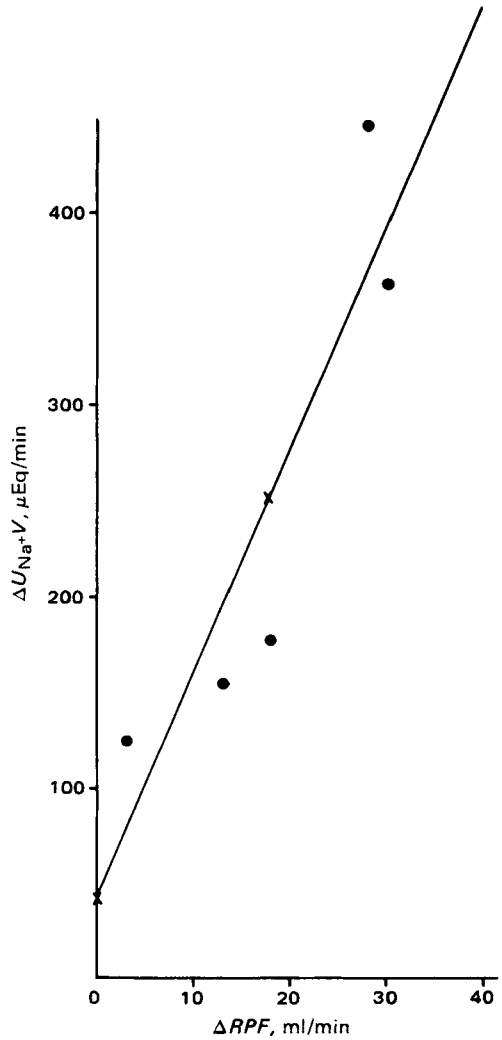

Figure 4—*Linear regression for changes in sodium excretion and changes in renal plasma flow* (RPF) *during infusion of sodium cyanide into the left renal artery* ($y = bx + c$, $\Delta U_{Na^+}U = 11.5$ (ΔRPF) + 44, $\bar{y} = 254 \pm 14$, $\bar{x} = 18 \pm 11$, $r = 0.89$, *and* $p < 0.05$).

since renal tubules were shown (21) to be directly innervated by autonomic nerves. In addition, the renal effects of acetylcholine are similar to cyanide, which inhibits aerobic metabolism equally in the renal cortex and outer medulla (10, 22, 23), resulting in natriuresis. Cyanide-induced natriuresis was one of the first observations relating sodium transport in the kidney to oxidative metabolism (24). Surprisingly, cyanide does not inhibit *p*-aminohippurate secretion (25); therefore, its clearance can be used to measure effective renal plasma flow. Cyanide also increases renal blood flow (23, 26).

In this study, the slopes of the lines for the function $U_{Na^+}V = b(RPF) + c$, where b is the slope of the line and c is the y intercept for a line ($y = bx + c$), for acetylcholine and cyanide were not significantly different (Figs. 3 and 4), assuming linear regression. The pattern of electrolyte excretion was apparently the same for each drug, including that of sodium, potassium, calcium, and magnesium. Just as cyanide acts on both the proximal and more distal portions of the nephron (23), so does acetylcholine according to micropuncture work (6). Therefore, *in vivo* comparison of acetylcholine and cyanide under identical clearance conditions in dogs substantiates that acetylcholine is not merely a vasodilator but either acts directly on tubular transport or increases the permeability and back-leak of sodium, causing a net increase in sodium excretion. There were increases in volume of urine flow, osmolar clearance, and excretion of potassium, calcium, and magnesium. Both acetylcholine and cyanide increased effective renal plasma flow.

REFERENCES

(1) D. G. May and M. K. Carter, *Am. J. Physiol.*, **218**, 417 (1970).
(2) J. A. Martino and L. E. Earley, *Circ. Res.*, **23**, 371 (1968).

(3) L. R. Willis, J. H. Ludens, J. B. Hook, and J. E. Williamson, *Am. J. Physiol.*, **217,** 1 (1969).
(4) R. L. Williams, J. E. Maines, and J. E. Pearson, *Arch. Int. Pharmacodyn. Ther.*, **196,** 393 (1972).
(5) H. D. Itskovitz and W. B. Campbell, *Proc. Soc. Exp. Biol. Med.*, **153,** 161 (1976).
(6) J. H. Stein, J. H. Reineck, R. W. Osgood, and T. F. Ferris, *Am. J. Physiol.*, **220,** 227 (1971).
(7) J. P. Hayslett, D. T. Domoto, M. Kashgarian, and F. H. Epstein, *Am. J. Physiol.*, **218,** 880 (1970).
(8) R. W. Bonsnes and H. H. Taussky, *J. Biol. Chem.*, **158,** 581 (1945).
(9) A. C. Bratton and E. K. Marshall, Jr., *J. Biol. Chem.*, **128,** 537 (1939).
(10) R. L. Weiner and T. W. Skulan, *Am. J. Physiol.*, **221,** 86 (1971).
(11) G. W. Snedecor, "Statistical Methods," 5th ed., Iowa State University, Iowa, 1956.
(12) B. Avrunin and M. K. Carter, *Proc. Soc. Exp. Biol. Chem.*, **133,** 901 (1970).
(13) R. L. Williams, J. E. Pearson, and M. K. Carter, *J. Pharmacol. Exp. Ther.*, **147,** 32 (1965).
(14) K. Aukland and E. W. Loyning, *Acta Physiol. Scand.*, **79,** 95 (1970).
(15) D. G. May and M. K. Carter, *Am. J. Physiol.*, **212,** 1351 (1967).
(16) A. J. Vander, *Am. J. Physiol.*, **206,** 117 (1963).
(17) A. R. Lavender, I. Aho, and T. N. Pullman, *Proc. Soc. Exp. Biol. Med.*, **119,** 887 (1965).
(18) J. E. Pearson and R. L. Williams, *Br. J. Pharmacol.*, **33,** 223 (1968).
(19) G. R. Marchand, C. E. Ott, F. C. Long, R. F. Greger, and F. G. Knox, *Am. J. Physiol.*, **232,** F 147 (1977).
(20) E. H. Blaine, *Proc. Soc. Exp. Biol. Med.*, **158,** 250 (1978).
(21) J. Muller and L. J. Barajas, *Ultrastruct. Res.*, **41,** 533 (1972).
(22) M. Fujimoto, F. D. Nash, and R. H. Kessler, *Am. J. Physiol.*, **260,** 1237 (1964).
(23) N. Martinez-Maldonado, G. Eknoyan, and W. N. Suki, *Am. J. Physiol.*, **217,** (1964).
(24) E. H. Starling and E. B. Verney, *Proc. R. Soc. London Ser. B.*, **97,** 321 (1925).
(25) J.C. Strickler and R. H. Kessler, *Am. J. Physiol.*, **205,** 117 (1963).
(26) J. Johannesen, M. Lie, and F. Kiil, *ibid.*, **233,** F 207 (1977).

ACKNOWLEDGMENTS

Presented in part at the 62nd annual meeting of the Federation of American Societies for Experimental Biology, Atlantic City, N.J., 1978.

Kinetics of Chlorambucil Hydrolysis Using High-Pressure Liquid Chromatography

DULAL C. CHATTERJI ˣ, RUSSELL L. YEAGER, and JOSEPH F. GALLELLI

Received October 23, 1980, from the *Pharmaceutical Development Service, Pharmacy Department, Clinical Center, National Institutes of Health, Bethesda, MD 20205.* Accepted for publication May 12, 1981.

Abstract □ A stability-specific high-pressure liquid chromatographic (HPLC) method was developed to assay intact chlorambucil (I) in the presence of its hydrolytic decomposition products. The HPLC method was used to follow the degradation kinetics of I over pH 1.0–10.0 in the presence of various buffers with and without added chloride ion. In the absence of chloride ion, the hydrolysis of I followed first-order kinetics and the pH rate profile showed a sharp inflection around pH 2.5 attributable to the ionization of the nitrogen mustard and a shallower inflection around pH 5.0 attributable to the ionization of the carboxylic group. The rate was pH independent over pH 6.0–10.0 and independent of buffer species in the absence of chloride ion. In the presence of chloride ion, the kinetics of I hydrolysis was still first order. However, the degradation half-life at a particular pH and buffer concentration increased linearly with chloride concentration. Kinetic evidence is presented to show that the mechanism of chloride stabilization involves the attack of chloride ion on the unstable cyclic ethyleneimmonium intermediate to give back I. Implications of the kinetic data obtained on the fate of orally administered I are discussed.

Keyphrases □ Chlorambucil—kinetics of hydrolysis, high-pressure liquid chromatography □ Hydrolysis—chlorambucil, analysis of kinetics using high-pressure liquid chromatography □ High-pressure liquid chromatography—analysis of chlorambucil hydrolysis kinetics □ Kinetics—chlorambucil hydrolysis, high-pressure liquid chromatography

Nitrogen mustards were one of the first classes of cancer chemotherapeutic agents systematically studied, and they still are used clinically (1). Although the general mechanisms of hydrolysis and alkylation for nitrogen mustards are well known (1–6), little detailed kinetic data are available on their hydrolysis. One reason for the lack of comprehensive kinetic work on the mustards has been the lack of suitable stability-specific analytical methods.

BACKGROUND

Most early work on the kinetics of mustards was performed by estimating the amount of free chloride ion liberated. However, this indirect method of determining intact nitrogen mustards and subsequent kinetic analysis can lead to incorrect stability estimates (3). Furthermore, the stabilizing effect of chloride on mustard hydrolysis cannot be quantitatively evaluated with this method. More recent reports (4, 5) on the hydrolysis of melphalan using stability-specific high-pressure liquid chromatography (HPLC) produced some useful information on the kinetics of melphalen hydrolysis and on the effect of chloride ion on its stability.

Chlorambucil (I), an aromatic nitrogen mustard, is considered stable enough to be administered primarily as an oral dosage form. However, there are no reported data on the stability of I over the GI pH range at 37°. It was recently shown (3), using a stability-specific HPLC method for I, that the half-life of I degradation was only 25 min at pH 3.0 and 37°. Since pH 3.0 is not unrealistic for the stomach, these data showed potential stability problems for orally administered I. Thus, a kinetic study of I hydrolysis over the pH range of the GI system seemed warranted.

EXPERIMENTAL

Materials—Chlorambucil USP reference standard was used for all kinetic studies. Water was double distilled in an all-glass apparatus, and glass-distilled solvents[1] were used for HPLC. All other chemicals were reagent grade.

Buffers—Citrate buffers (pH 2.0–7.0), acetate buffers (pH 3.5–5.5), phosphate buffers (pH 6.0–9.0), and borate buffers (pH 8.5–10.0) were prepared from the 0.25 *M* stock solutions of citric acid, acetic acid, monobasic sodium phosphate, and boric acid, respectively, by the addition of sodium hydroxide solution to the desired pH. Addition of chloride ion was avoided except when specified. Ionic strength was maintained con-

[1] Burdick & Jackson Laboratories, Muskegon, Mich.

0022-3549/82/0100-0050$01.00/0

(3) L. R. Willis, J. H. Ludens, J. B. Hook, and J. E. Williamson, *Am. J. Physiol.*, **217,** 1 (1969).
(4) R. L. Williams, J. E. Maines, and J. E. Pearson, *Arch. Int. Pharmacodyn. Ther.*, **196,** 393 (1972).
(5) H. D. Itskovitz and W. B. Campbell, *Proc. Soc. Exp. Biol. Med.*, **153,** 161 (1976).
(6) J. H. Stein, J. H. Reineck, R. W. Osgood, and T. F. Ferris, *Am. J. Physiol.*, **220,** 227 (1971).
(7) J. P. Hayslett, D. T. Domoto, M. Kashgarian, and F. H. Epstein, *Am. J. Physiol.*, **218,** 880 (1970).
(8) R. W. Bonsnes and H. H. Taussky, *J. Biol. Chem.*, **158,** 581 (1945).
(9) A. C. Bratton and E. K. Marshall, Jr., *J. Biol. Chem.*, **128,** 537 (1939).
(10) R. L. Weiner and T. W. Skulan, *Am. J. Physiol.*, **221,** 86 (1971).
(11) G. W. Snedecor, "Statistical Methods," 5th ed., Iowa State University, Iowa, 1956.
(12) B. Avrunin and M. K. Carter, *Proc. Soc. Exp. Biol. Chem.*, **133,** 901 (1970).
(13) R. L. Williams, J. E. Pearson, and M. K. Carter, *J. Pharmacol. Exp. Ther.*, **147,** 32 (1965).
(14) K. Aukland and E. W. Loyning, *Acta Physiol. Scand.*, **79,** 95 (1970).
(15) D. G. May and M. K. Carter, *Am. J. Physiol.*, **212,** 1351 (1967).
(16) A. J. Vander, *Am. J. Physiol.*, **206,** 117 (1963).
(17) A. R. Lavender, I. Aho, and T. N. Pullman, *Proc. Soc. Exp. Biol. Med.*, **119,** 887 (1965).
(18) J. E. Pearson and R. L. Williams, *Br. J. Pharmacol.*, **33,** 223 (1968).
(19) G. R. Marchand, C. E. Ott, F. C. Long, R. F. Greger, and F. G. Knox, *Am. J. Physiol.*, **232,** F 147 (1977).
(20) E. H. Blaine, *Proc. Soc. Exp. Biol. Med.*, **158,** 250 (1978).
(21) J. Muller and L. J. Barajas, *Ultrastruct. Res.*, **41,** 533 (1972).
(22) M. Fujimoto, F. D. Nash, and R. H. Kessler, *Am. J. Physiol.*, **260,** 1237 (1964).
(23) N. Martinez-Maldonado, G. Eknoyan, and W. N. Suki, *Am. J. Physiol.*, **217,** (1964).
(24) E. H. Starling and E. B. Verney, *Proc. R. Soc. London Ser. B.*, **97,** 321 (1925).
(25) J.C. Strickler and R. H. Kessler, *Am. J. Physiol.*, **205,** 117 (1963).
(26) J. Johannesen, M. Lie, and F. Kiil, *ibid.*, **233,** F 207 (1977).

ACKNOWLEDGMENTS

Presented in part at the 62nd annual meeting of the Federation of American Societies for Experimental Biology, Atlantic City, N.J., 1978.

Kinetics of Chlorambucil Hydrolysis Using High-Pressure Liquid Chromatography

DULAL C. CHATTERJI ˣ, RUSSELL L. YEAGER, and JOSEPH F. GALLELLI

Received October 23, 1980, from the *Pharmaceutical Development Service, Pharmacy Department, Clinical Center, National Institutes of Health, Bethesda, MD 20205.* Accepted for publication May 12, 1981.

Abstract □ A stability-specific high-pressure liquid chromatographic (HPLC) method was developed to assay intact chlorambucil (I) in the presence of its hydrolytic decomposition products. The HPLC method was used to follow the degradation kinetics of I over pH 1.0–10.0 in the presence of various buffers with and without added chloride ion. In the absence of chloride ion, the hydrolysis of I followed first-order kinetics and the pH rate profile showed a sharp inflection around pH 2.5 attributable to the ionization of the nitrogen mustard and a shallower inflection around pH 5.0 attributable to the ionization of the carboxylic group. The rate was pH independent over pH 6.0–10.0 and independent of buffer species in the absence of chloride ion. In the presence of chloride ion, the kinetics of I hydrolysis was still first order. However, the degradation half-life at a particular pH and buffer concentration increased linearly with chloride concentration. Kinetic evidence is presented to show that the mechanism of chloride stabilization involves the attack of chloride ion on the unstable cyclic ethyleneimmonium intermediate to give back I. Implications of the kinetic data obtained on the fate of orally administered I are discussed.

Keyphrases □ Chlorambucil—kinetics of hydrolysis, high-pressure liquid chromatography □ Hydrolysis—chlorambucil, analysis of kinetics using high-pressure liquid chromatography □ High-pressure liquid chromatography—analysis of chlorambucil hydrolysis kinetics □ Kinetics—chlorambucil hydrolysis, high-pressure liquid chromatography

Nitrogen mustards were one of the first classes of cancer chemotherapeutic agents systematically studied, and they still are used clinically (1). Although the general mechanisms of hydrolysis and alkylation for nitrogen mustards are well known (1–6), little detailed kinetic data are available on their hydrolysis. One reason for the lack of comprehensive kinetic work on the mustards has been the lack of suitable stability-specific analytical methods.

BACKGROUND

Most early work on the kinetics of mustards was performed by estimating the amount of free chloride ion liberated. However, this indirect method of determining intact nitrogen mustards and subsequent kinetic analysis can lead to incorrect stability estimates (3). Furthermore, the stabilizing effect of chloride on mustard hydrolysis cannot be quantitatively evaluated with this method. More recent reports (4, 5) on the hydrolysis of melphalan using stability-specific high-pressure liquid chromatography (HPLC) produced some useful information on the kinetics of melphalen hydrolysis and on the effect of chloride ion on its stability.

Chlorambucil (I), an aromatic nitrogen mustard, is considered stable enough to be administered primarily as an oral dosage form. However, there are no reported data on the stability of I over the GI pH range at 37°. It was recently shown (3), using a stability-specific HPLC method for I, that the half-life of I degradation was only 25 min at pH 3.0 and 37°. Since pH 3.0 is not unrealistic for the stomach, these data showed potential stability problems for orally administered I. Thus, a kinetic study of I hydrolysis over the pH range of the GI system seemed warranted.

EXPERIMENTAL

Materials—Chlorambucil USP reference standard was used for all kinetic studies. Water was double distilled in an all-glass apparatus, and glass-distilled solvents[1] were used for HPLC. All other chemicals were reagent grade.

Buffers—Citrate buffers (pH 2.0–7.0), acetate buffers (pH 3.5–5.5), phosphate buffers (pH 6.0–9.0), and borate buffers (pH 8.5–10.0) were prepared from the 0.25 *M* stock solutions of citric acid, acetic acid, monobasic sodium phosphate, and boric acid, respectively, by the addition of sodium hydroxide solution to the desired pH. Addition of chloride ion was avoided except when specified. Ionic strength was maintained con-

[1] Burdick & Jackson Laboratories, Muskegon, Mich.

0022-3549/82/0100-0050$01.00/0

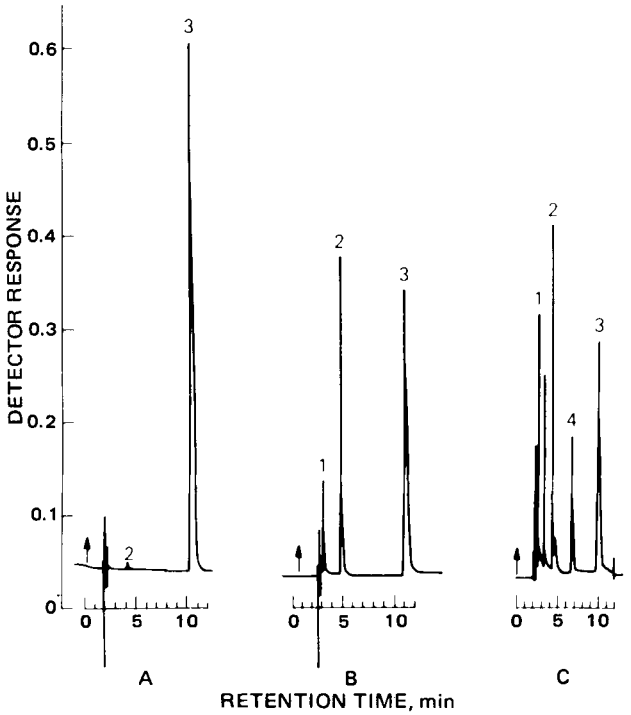

Figure 1—*Chromatogram obtained by the described HPLC method. Key: A, freshly prepared solution of I in water, 200 μg/ml; B, solution of I degraded ~50% in water; and C, solution of I degraded ~50% in 0.05* M *acetate buffer, pH 3.5.*

stant where noted with potassium nitrate. Other ingredients, when added, were weighed into the buffers before adjustment of pH.

Equipment—The high-pressure liquid chromatograph[2] was equipped with a fixed-volume loop injector[3] and a fixed-wavelength detector[4]. A 250- × 4.6-mm i.d. reversed-phase column[5] was used. All pH measurements[6] were taken at room temperature. All kinetic runs were carried out in a constant-temperature water bath[7] capable of maintaining the temperature within ±0.1°. Chloride-ion determinations were made with an automatic chloride titrator[8].

Kinetic Studies—Solutions of I were prepared by adding stock solution of I in acetone to 25.0 ml of buffer preequilibrated at the desired temperature for at least 30 min. The concentration of I in the final solution was ~0.04 mg/ml, and acetone concentration in the final reaction mixture was <1%. The solutions were kept in the constant-temperature water bath and were assayed for intact I at various time intervals. In several cases, the solutions were also assayed for chloride-ion production as described previously (3).

HPLC Assay Method—Separation was performed on a reversed-phase column[5] and methanol–acetonitrile–0.01 *M* acetate buffer, pH 4.5 (65:5:30), at a flow rate of 1.6 ml/min was used as the mobile phase. A 10-μl full loop volume was quantitatively injected, and the recorder was set at 0.32 aufs (254-nm detector). The peak due to I had a retention time of ~10.6 min and was the last to elute in the chromatogram. The peak height of I was used to calculate the amount of intact I present in the sample.

RESULTS AND DISCUSSION

Chromatography—The reversed-phase liquid chromatography permitted the analysis of intact I in the presence of its major hydrolytic degradation products in various buffer systems. Figure 1A shows the chromatogram of a freshly prepared solution of I in water. Peak 3, with a retention time of 10.6 min, was due to I; the small peak (peak 2), with a retention time of 4.0 min, was attributed to the monohydroxy product (II). When completely degraded solutions of I, both in water alone and in various buffer systems, were chromatographed, no peak corresponding to the retention time of I was observed. Therefore, none of the final degradation products interfered with the assay for intact I. During the degradation of I in water, peak 2 was the first to appear and increased through approximately one half-life of I, after which time it began decreasing.

Peak 1, which eluted close to the solvent front, increased steadily throughout the degradation; Fig. 1B shows a typical chromatogram when ~50% of I had degraded in water. Based on the mechanism of I hydrolysis, peak 2 was attributed to II and peak 1 was attributed to the dihydroxy product (III). This is also consistent with the order of elution of these peaks, where the dihydroxy compound, III, eluted faster than the monohydroxy compound, II, which, in turn, eluted faster than the relatively nonpolar I. The order of elution was similar to that reported for the reversed-phase HPLC of melphalan (4). Therefore, major intermediate degradation products in water alone do not interfere with the assay.

When I degrades in the presence of various buffers, other peaks, in addition to those due to II and III, also appear. Thus, Fig. 1C shows the chromatogram of a solution of I degraded in 0.05 *M* acetate buffer, pH 3.0. The peaks, in addition to those due to I–III, were probably due to the degradation products resulting from the attack of nucleophilic buffer species on reactive cyclic ethyleneimmonium intermediates. Thus, based on the time course of appearance and disappearance and also the retention time of peaks, peak 4 in Fig. 1C was tentatively attributed to the

Table I—Effect of pH and Buffer Concentration on Rate and Half-Life of I Hydrolysis at 37°

pH	Buffer[a]	$t_{1/2}$, min	K_{obs} (±*SD*)[b] × 10^2 min^{-1}
1.20	0.1 *M* nitric acid	378.0	0.18
2.00	0.01 *M* nitric acid	95.1	0.73
2.50	0.01 *M* citrate, 0.1 *M* ionic strength	34.9	1.99 (±0.06)
2.50	0.05 *M* citrate	38.4	1.81
3.00	0.01 *M* citrate, 0.1 *M* ionic strength	26.0	2.67 (±0.08)
3.00	0.05 *M* citrate	27.6	2.51
3.50	0.01 *M* citrate	21.4	3.24 (±0.11)
3.50	0.05 *M* citrate	21.7	3.19
3.60	0.01 *M* citrate, 0.1 *M* ionic strength	21.4	3.23 (±0.18)
3.85	0.01 *M* citrate, 0.1 *M* ionic strength	21.3	3.26 (±0.17)
4.00	0.01 *M* acetate	19.6	3.54
4.00	0.05 *M* citrate	19.6	3.54
4.10	0.01 *M* citrate, 0.1 *M* ionic strength	21.0	3.32 (±0.40)
4.35	0.01 *M* citrate, 0.1 *M* ionic strength	18.5	3.74 (±0.25)
4.50	0.05 *M* citrate	19.4	3.58
4.60	0.01 *M* citrate, 0.1 *M* ionic strength	19.2	3.61(±0.07)
4.85	0.01 *M* citrate, 0.1 *M* ionic strength	18.7	3.70 (±0.15)
5.00	0.01 *M* acetate	16.8	4.14
5.00	0.05 *M* acetate	16.9	4.13
5.00	0.05 *M* citrate	18.3	3.79
5.10	0.01 *M* citrate, 0.1 *M* ionic strength	16.8	4.13 (±0.06)
5.35	0.01 *M* citrate, 0.1 *M* ionic strength	16.5	4.20 (±0.06)
5.60	0.01 *M* citrate, 0.1 *M* ionic strength	16.4	4.23 (±0.14)
5.85	0.01 *M* citrate, 0.1 *M* ionic strength	16.4	4.23 (±0.03)
6.00	0.05 *M* citrate	15.4	4.51
6.10	0.01 *M* citrate, 0.1 *M* ionic strength	15.6	4.44 (±0.27)
6.50	0.01 *M* citrate, 0.1 *M* ionic strength	15.7	4.43 (±0.25)
7.00	0.01 *M* citrate, 0.1 *M* ionic strength	15.7	4.42 (±0.02)
7.00	0.02 *M* phosphate	16.1	4.31
7.00	0.05 *M* phosphate	16.1	4.32
8.00	0.05 *M* phosphate	16.3	4.26
9.00	0.05 *M* phosphate	15.5	4.47
10.00	0.05 *M* borate	15.4	4.50

[a] Buffers contained no chloride ion, and ionic strength was maintained only where noted. [b] Standard deviations, where noted in parentheses, are for three runs.

[2] Model 3500B, Spectra-Physics, Santa Clara, Calif.
[3] Velco-type valve, Spectra-Physics, Santa Clara, Calif.
[4] Model 225, Spectra-Physics, Santa Clara, Calif.
[5] Zorbax C-8 column, 6 μm average particle size, Dupont Instruments, Wilmington, Del.
[6] Expandomatic SS-2 pH meter, Beckman Instruments, Fullerton, Calif.
[7] Electronic relay system, Precision Scientific Co., Chicago, Ill.
[8] Model 4-4433, American Instrument Co., Silver Spring, Md.

Table II—Effect of Chloride Ion and Other Buffers on the Rate and Half-Life of I Hydrolysis in 0.02 *M* Phosphate Buffer, pH 7.0, at 37°

Run	Additive	Chloride-Ion Concentration, moles/liter	$t_{1/2}$, min	$K_{obs} \times 10^2$ min^{-1}
1	—	—	16.6	4.18
2	0.08 *M* potassium chloride	0.08	27.9	2.48
3	0.10 *M* potassium chloride	0.10	29.2	2.38
4	0.20 *M* potassium chloride	0.20	41.6	1.66
5	0.24 *M* potassium chloride	0.24	50.3	1.38
6	0.40 *M* potassium chloride	0.40	67.8	1.19
7	0.08 *M* potassium nitrate	—	16.0	4.34
8	0.24 *M* potassium nitrate	—	15.0	4.63
9	0.40 *M* potassium nitrate	—	15.2	4.56
10	0.08 *M* imidazole	—	18.8	3.69
11	0.40 *M* potassium nitrate + 0.08 *M* imidazole	—	15.8	4.38
12	0.08 *M* potassium chloride + 0.08 *M* imidazole	0.08	21.8	3.18
13	0.10 *M* potassium chloride + 0.30 *M* imidazole	0.10	19.1	3.63
14	0.40 *M* potassium chloride + 0.08 *M* imidazole	0.40	34.1	2.04

monoacetyl derivative of I. Similarly, when the solvents contained substantial amounts of methanol or ethanol, other peaks that probably were due to the methoxy- or ethoxy-substituted compounds appeared. No further attempts were made to isolate and identify these peaks, and the major concern was to make sure that these peaks did not interfere with the assay of intact I.

The peak height due to I was linearly related with its concentration over 10–200 μg/ml. Therefore, peak heights were used to calculate the amount of intact I present in the sample. Acetone was used as the solvent for the stock solution, because I degrades slowly in hydroxylic solvents such as methanol or ethanol.

Kinetic Studies—Hydrolysis of I followed first-order kinetics over pH 1.0–10.0 as determined from linear semilogarithmic plots of the amount of intact I remaining *versus* time. Table I summarizes the rates of I hydrolysis in various buffers and pH values in the absence of added chloride ion. Table II shows the rates in the presence of added chloride ion. The rate of I hydrolysis was relatively independent of buffer species and concentration but was strongly influenced by pH and chloride-ion concentration. Therefore, the effects of pH and chloride-ion concentration are discussed separately.

Effect of pH—Figure 2 shows the pH rate profile for I hydrolysis at 37° in buffered solutions with 0.1 *M* ionic strength where no chloride ion was added. The profile shows a sharp inflection around pH 2.5 and a shallower one around pH 5.0, followed by a plateau region at pH 6.0–10.0

The pH-independent rate of I hydrolysis at pH 6.0–10.0 excludes the possibility of a significant hydroxide-ion catalysis for I hydrolysis over pH 1.0–10.0. In addition, the decreasing rate of I hydrolysis as the pH was lowered suggests that hydrogen-ion catalysis is also not important in this range. Thus, change in the rate of I hydrolysis with pH in this range must be attributable to the ionization of reactive functional groups in I.

The sharp inflection around pH 2.5 is attributable to the ionization of the nitrogen mustard of I. The mechanism of nitrogen mustard hydrolysis is known to involve the attack of unprotonated nitrogen mustard to expel chloride, forming an unstable cyclic ethyleneimmonium intermediate. This is followed by the attack of water and other nucleophiles to give subsequent products (1–6). The availability of a free electron pair on the nitrogen mustard is essential for its reactivity (1), and protonation of this nitrogen makes the compound much less reactive. The pKa of the nitrogen mustard of I was reported (2) to be on the order of 2.5. Therefore, as pH increases from 1.0 to 4.0, more of I would be in the unprotonated form and the rate of I hydrolysis should increase. The sharp inflection (Fig. 2) near the pKa of I strongly supports the mechanism that the unprotonated nitrogen mustard is the reactive species.

This mechanism alone, however, does not explain the shallow inflection around pH 5.0. If the ionization of the nitrogen mustard was the only determinant in the rate of I hydrolysis, a plateau above pH 4.5 (*i.e.*, 2 pH units above the pKa) would be expected. However, the difference in rate constants in the final plateau region (pH >6.0) and that of the plateau range of pH 4.0–4.5 is real. Experiments in this pH region (pH 3.0–5.5) were done at very frequent pH intervals (Fig. 2 and Table I), often repeated three times each, and ionic strength was strictly maintained, thus leaving little doubt that there is an inflection between pH 4.5 and 6.0.

Since the rate of I hydrolysis in the pH 4–6-range is totally independent of hydrogen ion, hydroxide ion, or buffer catalysis (acetate, citrate, and phosphate buffer concentration had no effect on the rate, Table I), the increase in rate with increasing pH in this range must be attributed to ionization of another group in I that would affect the rate of I hydrolysis. The only ionizable group in I (except the nitrogen mustard) is the carboxylic group, and thus the inflection must be attributed to this group. The inflection region around pH 5.0 is also consistent with the ionization constant of an aliphatic carboxylic group.

A slightly higher rate of hydrolysis of I^- over I is also not unreasonable. The ionization of the carboxylic group and resultant formal negative charge on the alkyl substituent is expected to have some long-range electron-donating inductive effect on the nitrogen mustard, making it slightly more reactive than I where the carboxylic group is unionized. Therefore it is suggested that the second inflection point is due to the ionization of the carboxylic group and that the plateau area, in the 6.0–10.0-range, is the limiting rate of ionized I^- (Scheme I).

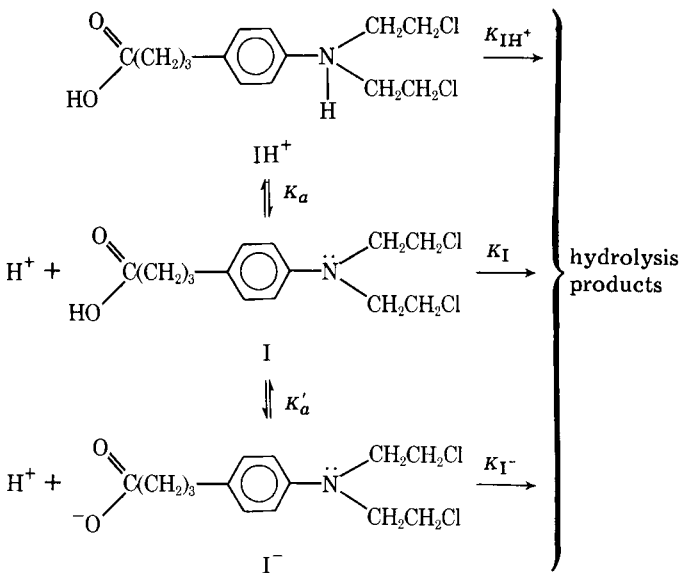

Scheme I

This mechanism is supported by calculation of rate at any particular pH. Thus, for the reaction shown in Scheme I, it can be shown that:

$$K_{obs} = (K_{IH^+}[H^+]^2 + K_I[H^+]K_a + K_{I^-}K_aK'_a)\frac{I_t}{D} \quad \text{(Eq. 1)}$$

where K_{obs} is the observed rate constant; K_a and K'_a are the ionization constants of the species IH^+ and I, respectively; and:

$$I_t = [IH^+] + [I] + [I^-] \quad \text{(Eq. 2)}$$

$$D = [H^+]^2 + K_a[H^+] + K_aK'_a \quad \text{(Eq. 3)}$$

The value of K_{IH^+} can be estimated from pH 1 data and thus shown to be negligible. The value of K_{I^-} can be obtained from the limiting rate at pH >6, which was experimentally found to be 0.0440 min^{-1} (Table I). The pKa value was reported (2) to be on the order of 2.5; that of pKa′, the ionization constant of an aliphatic carboxylic group, should be on the order of 5.0. The value of K_I should be close to the rate between pH 3.5 and 4.0, which was experimentally found to be between 0.032 and 0.035 min^{-1}. The solid line in Fig. 2, obtained using Eq. 1 and $K_{IH^+} = 0.0$ min^{-1}, $K_I = 0.0335$ min^{-1}, $K_{I^-} = 0.0440$ min^{-1}, pKa = 2.4, and pKa′ = 4.9 (all realistic values), represented the best fit of the theoretical line to the

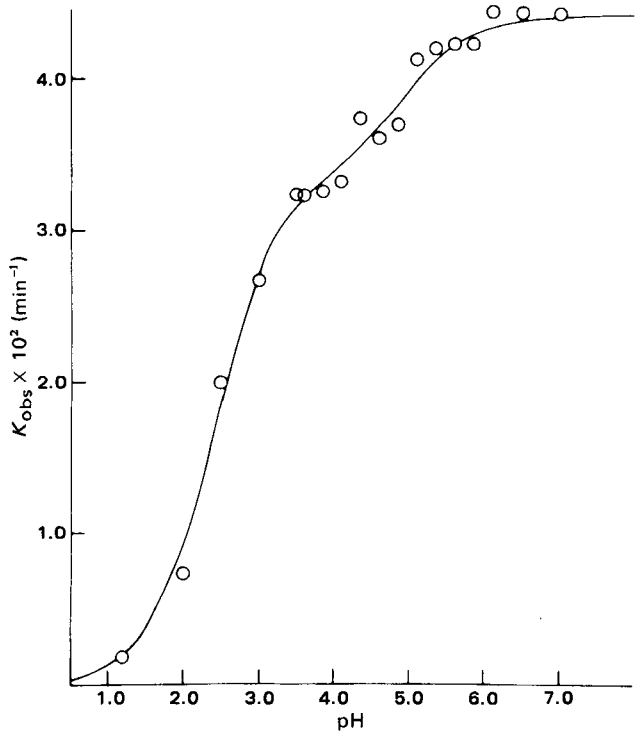

Figure 2—*The pH rate profile for degradation of I in the absence of added chloride ion at 37°. The solid line is the best fit theoretical line using Eq. 1 and values mentioned in the text. Circles are experimental points. All points above pH 2.0 were determined in 0.01* M *citrate buffer, 0.1* M *ionic strength.*

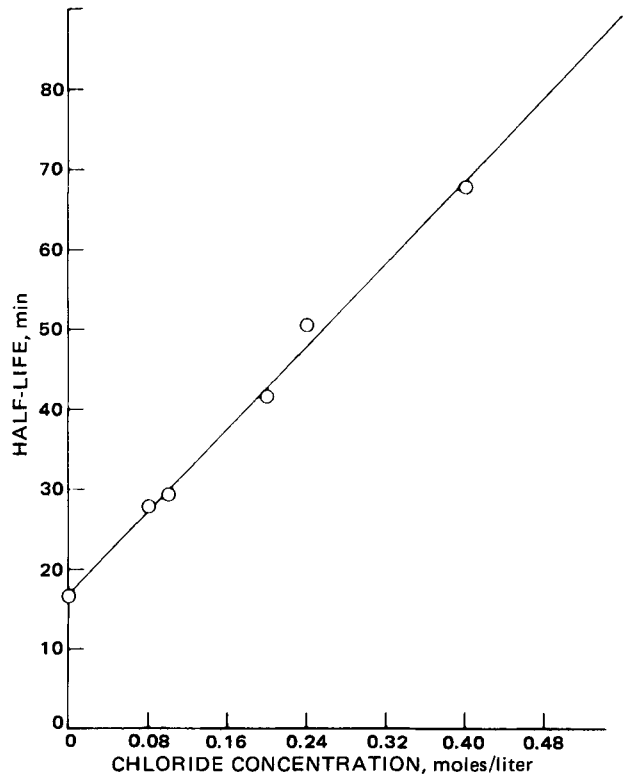

Figure 3—*Plot of adjusted half-life (see text) for I hydrolysis* versus *the concentration of added chloride ion.*

experimental points. This result supports the proposed kinetic analysis (Scheme I) for the hydrolysis of I.

Effect of Chloride Ion—Hydrolysis of I followed first-order kinetics in the presence of excess chloride ion. However, at a particular pH and fixed buffer concentration, the rate of I hydrolysis decreased in the presence of added chloride ion. As seen in Table II, the half-life of I hydrolysis increased with increasing chloride concentration. Although the rate of I hydrolysis was relatively independent of buffer concentrations in the absence of added chloride ion, it was strongly influenced by buffer concentration when excess chloride ion was present.

The absence of significant effects of other ions, buffer species, and specific hydrogen-ion or hydroxyl-ion catalysis (except for the pH effect on the ionization of I and consequent effects on the rate) strongly suggest that the stabilizing effect of chloride ion in I hydrolysis is a specific one. Based on these observations, the mechanism of chloride stabilization probably involves the reverse attack of chloride ion on the cyclic ethyleneimmonium intermediate (I^+) to give back parent I (Scheme II). The same mechanism was recently suggested (5) for the chloride-ion stabilization of melphalan hydrolysis.

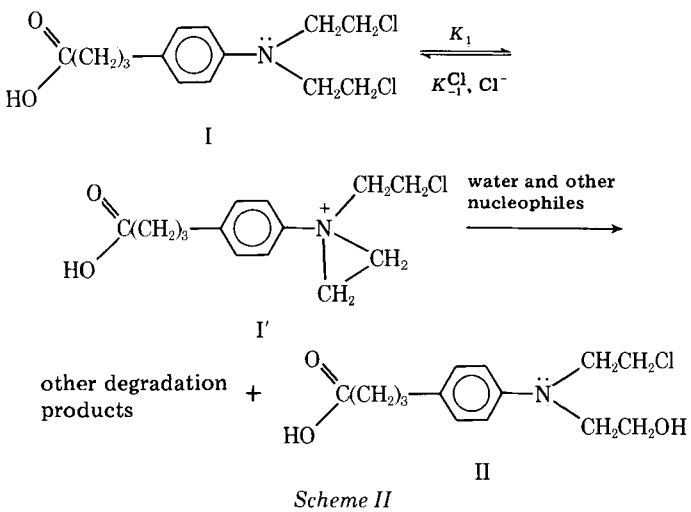

Scheme II

The cyclic intermediate, I′, is susceptible to attack by water and other nucleophiles present in the reaction mixture. It is reasonable, therefore, to suggest that chloride ion competes with water and other nucleophiles to attack I′. The attack of water and all other nucleophiles except chloride ion yields irreversible degradation products, while the attack of chloride ion yields I. It follows that stabilization would increase as the ratio of chloride ion to other nucleophiles (including water) is increased. This relation qualitatively explains why the half-life of I hydrolysis increases with increasing concentration of added chloride ion.

The rate of I hydrolysis increases when the concentration of nucleophilic buffer species (*i.e.*, imidazole) increases in the presence of a constant excess concentration of chloride ion (compare values of Runs 2, 3, and 6 with those of Runs 12–14 in Table II). However, except for a minor ionic strength effect, buffers and other ions had no significant effect on rate when no chloride ion was added (Table I). This result can be explained by Scheme II, where increasing the concentration of other species competing to attack I′ results in a smaller share of I′ available for chloride attack and, hence, reduces stabilization. Without chloride ion, attack of I by all species leads to irreversible degradation products. Therefore, increasing the buffer concentration only changes the ratio of degradation products without affecting the rate of I hydrolysis.

This mechanism of chloride-ion stabilization is also substantiated by the kinetic analysis of the results in the presence of added chloride ion. If it is assumed that the concentration of the reactive intermediate, I′, reaches steady state, then applying classical steady-state kinetics dictates (Appendix) that, in the presence of constant excess chloride ion, the loss of I is first order with respect to I and that the half-life of I hydrolysis is related linearly to the chloride-ion concentration if all other conditions remain constant.

To check these criteria, experiments were designed to study the kinetics of I hydrolysis at a fixed pH and buffer concentration in the presence of various amounts of sodium chloride concentration. Since ionic strength would influence the rate by affecting the pKa if the pH was in the inflection region of the pH rate profile for I hydrolysis, these experiments were performed in 0.02 *M* phosphate buffer (pH 7.0), which was well within the plateau region (Fig. 2). At this pH, small changes in K_a and K'_a of I would have a minimal effect on the rate. To account for the ionic strength effect of added chloride ion on the rates, rate constants for I hydrolysis were also determined in 0.02 *M* phosphate buffers (pH 7.0) in the presence of various concentrations of potassium nitrate. The adjusted rate constants at any chloride-ion concentration were calculated by:

$$K_{adj} = K_{obs}\frac{K_0}{K'} \quad \text{(Eq. 4)}$$

where K_{adj} is the adjusted rate constant, K_{obs} is the observed rate constant at a specified sodium chloride concentration, K' is the rate constant in the absence of added chloride ion but in the presence of the same molar concentration of potassium nitrate as the concentration of sodium chloride added to determine K_{obs}, K_0 is the rate constant in the absence of any other added ion except the 0.02 M phosphate buffer (pH 7.0), and $(t_{1/2})_{adj} = 0.693/K_{adj}$.

Plotting the concentrations of I remaining against time gave first-order plots, and Fig. 3 shows the plot of adjusted half-lives against sodium chloride concentrations. The good linear plot in Fig. 3 lends strong support to Scheme II.

Physiological Implications—The preceding kinetic data suggest that I is reasonably stable at 37° to 0.1 N HCl (half-life ~12 hr). However, the stomach pH varies from 1.5 to 5.0 (7); if the pH is ~3.0, a 25-min half-life at 37° (Table I) would mean that ~10% drug would degrade in 4 min. Even in the presence of a substantial chloride-ion concentration in the stomach (*e.g.*, 0.1 M), the half-life of I would be ~50 min at pH 3.0 and 37° (still a very fast rate for an orally administered drug). Therefore, the amount of drug available for absorption apparently would be a function of stomach pH at a particular time. Thus, there is a serious potential for inconsistency in the availability of orally administered I.

The hydrolysis rate of I in human plasma at 37° was ~10–20 times slower than in the buffer of pH 7.4. This stabilization was attributed to the binding of I with plasma proteins as suggested previously (8, 9). The similar favorable effect of the proteins in the GI tract on the stability of orally administered I was not investigated in this study.

APPENDIX: EFFECT OF CHLORIDE ION ON KINETICS OF I HYDROLYSIS

For the reaction shown in Scheme II:

$$I \underset{K_{-1}^{Cl}}{\overset{K_1}{\rightleftharpoons}} I' + Cl^- \xrightarrow[H_2O,\ \text{other nucleophiles}]{K_x} \text{II + other products}$$

Scheme AI

where K_1 is the first-order rate constant of initial cyclization of I, K_{-1}^{Cl} is second-order rate constant for chloride-ion attack on I′ to yield I, and K_x is the pseudo-first-order rate constant for breakdown of I′ by all nucleophiles (including water), except chloride ion, to yield II and other degradation products:

$$-dI/dt = K_1[I] - K_{-1}^{Cl}[Cl^-][I'] \quad \text{(Eq. A1)}$$

$$dI'/dt = K_1[I] - K_{-1}^{Cl}[Cl^-][I'] - K_x[I'] \quad \text{(Eq. A2)}$$

If I′ is assumed to be very unstable and its concentration reaches steady state, then at steady state:

$$dI'/dt = 0 \quad \text{(Eq. A3)}$$

and

$$K_1[I] - K_{-1}^{Cl}[Cl^-][I'] - K_x[I'] = 0 \quad \text{(Eq. A4)}$$

Collecting terms and simplifying (Eq. A4) gives:

$$I' = \frac{K_1}{K_{-1}^{Cl}[Cl^-] + K_x}[I] \quad \text{(Eq. A5)}$$

Substituting Eq. A5 into Eq. A1 gives:

$$\frac{-dI}{dt} = K_1[I] - \frac{K_{-1}^{Cl}K_1[Cl^-]}{K_{-1}^{Cl}[Cl^-] + K_x}[I] \quad \text{(Eq. A6)}$$

Simplifying Eq. A6 gives:

$$\frac{-dI}{dt} = \frac{K_1K_x}{K_{-1}^{Cl}[Cl^-] + K_x}[I] \quad \text{(Eq. A7)}$$

If chloride ion is in excess, its concentration does not change significantly by the chloride ion liberated during the hydrolysis of I. Therefore, the term $K_1K_x/(K_{-1}^{Cl}[Cl^-] + K_x)$ in Eq. A7 is constant and designated as K_{obs}:

$$K_{obs} = \frac{K_1K_x}{K_{-1}^{Cl}[Cl^-] + K_x} \quad \text{(Eq. A8)}$$

and:

$$-dI/dt = K_{obs}[I] \quad \text{(Eq. A9)}$$

Equation A9 shows that loss of I in the presence of a fixed excess concentration of chloride ion should be the first order with respect to I with the rate constant K_{obs}. Inverting Eq. A8 yields:

$$\frac{1}{K_{obs}} = \frac{K_{-1}^{Cl}[Cl^-]}{K_1K_x} + \frac{K_x}{K_1K_x} \quad \text{(Eq. A10)}$$

Cancelling terms and multiplying Eq. A10 with 0.693 gives:

$$\frac{0.693}{K_{obs}} = \frac{0.693\,K_1^{Cl}}{K_1K_x}[Cl-] + \frac{0.693}{K_1} \quad \text{(Eq. A11)}$$

Equation A11 shows that the plot of the observed half-life ($0.693/K_{obs}$) versus the chloride-ion concentration should be a straight line, with the intercept representing the half-life when no chloride ion is present.

REFERENCES

(1) "The Pharmacological Basis of Therapeutics," L. S. Goodman and A. Gilman, Eds., 5th ed., Macmillan, New York, N.Y., 1975, pp. 1254–1265.

(2) W. R. Owen and P. J. Stewart, *J. Pharm. Sci.*, **68**, 992 (1979).

(3) D. C. Chatterji, *ibid.*, **69**, 859 (1980).

(4) K. P. Flora, S. L. Smith, and J. C. Cradock, *J. Chromatogr.*, **177**, 91 (1979).

(5) S. Y. Chang, T. L. Evans, and D. S. Alberta, *J. Pharm. Pharmacol.*, **31**, 853 (1979).

(6) W. J. Ross, "Biological Alkylating Agents," Butterworth, London, England, 1962, pp. 13–31.

(7) M. Gibaldi, in "The Theory and Practice of Industrial Pharmacy," L. Lachman, H. A. Lieberman, and J. L. Kanig, Eds., Lea & Febiger, Philadelphia, Pa., 1970, p. 238.

(8) W. J. Hopwood and J. A. Stock, *Chem.-Biol. Interactions*, **4**, 31 (1971/72).

(9) S. Y. Chang, D. S. Alberts, D. Farquhar, L. R. Melnick, P. D. Walson, and S. E. Salmon, *J. Pharm. Sci.*, **67**, 682 (1978).

Stability of Intravenous Nitroglycerin Solutions

ANDREA H. SCHEIFE ˣ, JOSEPH A. GRISAFE, and LEON SHARGEL

Received September 24, 1980, from the *College of Pharmacy and Allied Health Professions, Northeastern University, Boston, MA 02115.* Accepted for publication May 15, 1981.

Abstract □ The stability of intravenous nitroglycerin solutions prepared from either sublingual tablets or a 10% nitroglycerin–lactose adsorbate (powder) was examined under various conditions. Nitroglycerin concentration was measured by high-pressure liquid chromatography. Nitroglycerin stock solutions (0.8–1.0 mg/ml) prepared from tablets or powder in 0.9% saline were stored upright in refrigerated multidose vials for 6 months without a significant decrease in concentration. Storage of the solutions at room temperature resulted in a 20% loss after 3 months. Intravenous nitroglycerin solutions (0.2 mg/ml) prepared from tablets or powder in either 0.9% saline or 5% dextrose in water were stored in glass intravenous bottles at temperatures between 6 and 38° for 24 hr with a maximum loss of 18%. Stability was not affected by light. Solutions in contact with rubber stoppers, plastic intravenous bags, or plastic administration sets exhibited decreased nitroglycerin concentration characteristic of sorption. Nitroglycerin concentrations decreased to a greater extent when the administration sets were equipped with plastic burets. Brief contact of nitroglycerin solutions with a plastic syringe did not result in decreased concentration. The stability of intravenous nitroglycerin solutions packaged in glass was not dependent on light, the vehicle, or the source of nitroglycerin. Contact with rubber or plastic surfaces should be minimized.

Keyphrases □ Nitroglycerin—intravenous solutions, stability, effect of temperature, light, source, and packaging □ Stability—effect of temperature, light, source, and packaging on intravenous nitroglycerin solutions □ Vasodilators—nitroglycerin, stability of intravenous solutions

Intravenous nitroglycerin is used clinically in various cardiovascular conditions (1–5). At present, only an investigational nitroglycerin formulation is commercially available for intravenous infusions. Consequently, many pharmacists prepare intravenous nitroglycerin solutions from sublingual nitroglycerin tablets (6, 7) or from a nitroglycerin–lactose adsorbate (8, 9). The stablity of nitroglycerin tablets was defined after the advent of single-tablet assays, particularly automated single-tablet assays (10–15). However, initial stability data on nitroglycerin in intravenous solutions were anecdotal (16) or conflicting (17, 18). Recently, the results of several investigations were reported (19–24).

This investigation examined the stability of nitroglycerin parenteral solutions under various conditions of temperature, exposure to light, packaging materials, nitroglycerin source, vehicle, administration set, and time.

EXPERIMENTAL

Assay—Nitroglycerin was measured by a modified high-pressure liquid chromatographic (HPLC) method (25). A high-pressure liquid chromatograph[1] equipped with a universal liquid chromatographic injector[2], UV absorbance detector[3] (254 nm), and a strip-chart recorder[4] was used for all analyses. Samples (25 μl) were chromatographed at room temperature on a microparticulate, reversed-phase, 30 cm × 4-mm i.d. column[5] with an eluting mobile phase of 60% methanol in water at a flow rate of 2 ml/min. The inlet pressure varied from 2400 to 3000 psi and was noted on a daily basis. The retention time of nitroglycerin was ~4 min, and samples could be injected every 5 min.

The technique was sensitive to injections of >100 ng of nitroglycerin. Precision was 1.0% over a solution range of 190–300 μg of nitroglycerin/ml. Standard solutions were prepared from 0.4-mg sublingual nitroglycerin tablets[6] and 10% (w/w) nitroglycerin–lactose adsorbate[7] (powder). Standard curves were linear ($r \geq 0.99$) over the concentration range used.

Stability Study—The stability of nitroglycerin solutions with initial concentrations of 0.8 or 1.0 mg/ml (stock) and 0.2 mg/ml (intravenous) was tested.

Stock Solutions—Nitroglycerin stock solutions were pipetted into 5-ml multidose vials[8] for stability testing. Rubber stoppers[9] (20 mm) were fitted to the vials with a metal tear-off seal[10].

Vials containing 5 ml of nitroglycerin solution (1.0 mg/ml) prepared from tablets in 0.9% saline were stored in groups of three under conditions of varied temperature, light, and contact with the rubber stopper (Solutions VRT, VU, VF, VO, and VR, Table I).

In addition, five vials containing 5 ml of nitroglycerin solution (0.8 mg/ml) prepared from tablets in 0.9% saline (Solution VT) and five vials containing 5 ml of nitroglycerin solution (0.8 mg/ml) prepared from powder in 0.9% saline (Solution VP) were stored under fluorescent light at 22–30° in an upright position.

Intravenous Solutions—Intravenous nitroglycerin solutions (0.2 mg/ml) were prepared in 250-ml plastic bags of 0.9% saline[11] or in 250-ml glass bottles of 0.9% saline[12] or 5% dextrose in water[13]. Initially, 50 ml of the saline or 5% dextrose solution was removed from the container; a glass syringe was then used to add 50 ml of freshly prepared nitroglycerin stock solution. Containers were inverted throughout the stability study. A tubing clamp attached to the bags and a glass rod inserted into the bottles sealed the administration ports.

Intravenous nitroglycerin solutions were first prepared in saline from a tablet nitroglycerin stock solution. Five bags and five bottles containing the nitroglycerin solutions were stored under each condition of light and temperature (Solutions PRT, PF, PR, PO, GRT, GF, GR, and GO, Table II).

Five solutions of tablet nitroglycerin in bottles of saline (Solution GT) were compared to five solutions of tablet nitroglycerin in bottles of 5% dextrose solution (Solution GD) and to five solutions of powder nitroglycerin in bottles of saline (Solution GP). These solutions were stored between 26 and 28° under fluorescent light. At the same time, solutions of tablet nitroglycerin were prepared in 10 bottles and five bags of saline. Administration tubing[14] (1.8 m) was connected to each bag (Solution PTu) and five bottles (Solution GTu). The tubing was immediately filled with solution and then continually perfused at 0.5 ml/min by gravity.

Administration tubing (2.1 m) with a buret[15] was connected to the remaining five bottles (Solution GBu) and was similarly filled and perfused. One hundred milliliters of solution remained within the buret chamber throughout the perfusion. Solutions PTu, GTu, and GBu were sampled simultaneously from the container and the terminal end of the administration set. All containers and tubing were stored between 26 and 28° under fluorescent light.

Two-tailed t tests (26) were used to compare the sample means. When

[1] Model ALC/GLC 204, Waters Associates, Milford, MA 01757.
[2] M-6000A, SDS-4126, Waters Associates.
[3] M-440, S-440-00634, Waters Associates.
[4] Recordal series 5000, Fisher Scientific, Pittsburgh, PA 15219.
[5] μBondapak C_{18}, P/N 27324, S/N 067552, Waters Associates.
[6] No. 161, lot 2AE55B, exp. Mar. 1, 1980, Eli Lilly and Co., Indianapolis, IN 46206.
[7] SDM No. 17, lot J17-H12, drum no. 2, ICI Americas, Inc., Specialty Chemicals Division, Wilmington, DE 19897.
[8] Serum bottle S-104E, No. 223738, Wheaton Industries, Millville, NJ 08332.
[9] No. 224124, Wheaton Industries.
[10] No. 224193, Wheaton Industries.
[11] No. 2B1322, lot CP412XO, exp. Mar., 1980, Travenol Laboratories, Deerfield, IL 60015.
[12] No. 2A1322, lot G431L2, exp. Nov., 1979, Travenol Laboratories.
[13] No. 2A0062, lot G454R6A, exp. Mar., 1980, Travenol Laboratories.
[14] Solution administration set, minidrip 60 drops/ml, no. 2C0002, lot H259W1, Travenol Laboratories.
[15] Buret solution administration set with ball valve, minidrip 60 drops/ml, No. 2C0132, lot U18X3, Travenol Laboratories.

0022-3549/82/0100-0055$01.00/0

Table I—Nitroglycerin Stock Solutions [a]

Symbol	Initial Nitroglycerin Concentration, mg/ml	Nitroglycerin Source[b]	Storage		
			Position	Light Exposure	Temperature
VRT	1.0[c]	Tablets	Upright	Fluorescent	22–30°
VU	1.0[c]	Tablets	Inverted	Fluorescent	22–30°
VF	1.0[c]	Tablets	Upright	Dark (foil-wrapped)	22–30°
VO	1.0[c]	Tablets	Upright	Dark	38°
VR	1.0[c]	Tablets	Upright	Dark	6°
VT	0.8[d]	Tablets	Upright	Fluorescent	22–30°
VP	0.8[d]	Powder	Upright	Fluorescent	22–30°

[a] Containers were multidose vials (5 ml) with rubber stoppers, and the vehicle was (1.0 mg/ml) saline. [b] Tablets were 0.4-mg sublingual tablets, and powder was 10% (w/w) nitroglycerin–lactose adsorbate. [c] Vials were prepared from the same nitroglycerin solution. [d] The stability of nitroglycerin solutions (0.8 and 1.0 mg/ml) was measured at the same time.

Table II—Nitroglycerin Intravenous Solutions (Initial Concentration, 0.2 mg/ml)

Symbol[a]	Container[b]	Administration Set	Perfusion Rate, ml/min	Nitroglycerin Source[c]	Vehicle[d]	Storage	
						Light Exposure	Temperature
GRT	Bottle	—	—	Tablet	Saline	Fluorescent	28–30°
GF	Bottle	—	—	Tablets	Saline	Dark (foil-wrapped)	28–30°
GO	Bottle	—	—	Tablets	Saline	Dark	38°
GR	Bottle	—	—	Tablets	Saline	Dark	6°
PRT	Bag	—	—	Tablet	Saline	Fluorescent	28–30°
PF	Bag	—	—	Tablets	Saline	Dark (foil-wrapped)	28–30°
PO	Bag	—	—	Tablets	Saline	Dark	38°
PR	Bag	—	—	Tablets	Saline	Dark	6°
GT	Bottle	—	—	Tablets	Saline	Fluorescent	
GP	Bottle	—	—	Powder	Saline	Fluorescent	26–28°
GD	Bottle	—	—	Tablets	5% dextrose in water	Fluorescent	
GTu	Bottle	Tubing (1.8 m)	0.5	Tablets	Saline	Fluorescent	
PTu	Bag	Tubing (1.8 m)	0.5	Tablets	Saline	Fluorescent	26–28°
GBu	Bottle	Tubing (2.1 m) with buret	0.5	Tablets	Saline	Fluorescent	

[a] Stability of solutions GRT through PR was measured separately from that of solutions GT through GBu. [b] Bottle was inverted glass infusion bottle, 250 ml; bag was plastic infusion bag, 250 ml. [c] Tablets were 0.4-mg sublingual tablets; powder was 10% (w/w) nitroglycerin-lactose adsorbate. [d] Saline was 0.9% saline.

the data could be fitted to the equation of a straight line, slopes were statistically tested (27) for difference.

RESULTS

To assess the uniformity of the nitroglycerin source, solutions were prepared from different samples of tablets or powder (five tablets or ~20 mg of powder/sample). The HPLC peak height responses were 34.4 ± 1.5 cm/mg of tablet and 296 ± 14 cm/mg of powder.

Although a glass syringe was used in this study to transfer nitroglycerin solutions, hospital personnel often use plastic, disposable syringes. The concentration in 50 ml of a nitroglyerin solution (1.0 mg/ml) was measured before and after two successive 1-min exposures to a 50-ml plastic syringe. Concentration did not change significantly after contact with the syringe.

USP XX (28) specifications allow the average potency of sublingual nitroglycerin tablets to vary 20% from the labeled strength. The concentration of nitroglycerin stock solutions (1.0 mg/ml) prepared from tablets in saline and stored upright in multidose vials under fluorescent light at 22–30° decreased 20% after 87 days and 35% after 6 months (Solution VRT, Table III). When the vials were stored at 38° (VO), nitroglycerin concentration decreased 20% after 50 days and 67% after 6 months. Solutions that were protected from light (VF) showed decreases of 20% after 98 days and 31% after 6 months. When vials were stored inverted (VU), the concentration decreased 20 and 58% after 2 days and 6 months, respectively. In nitroglycerin solutions stored upright at 6° (VR), no change in concentration was observed over 6 months. Nitroglycerin stock solutions prepared from tablets at 0.8 mg/ml (VT) declined in concentration by 20% in 87 days and by 41% in 6 months. Similar solutions prepared from powder (VP) had concentration decreases of 20 and 43% after 82 days and 6 months, respectively.

The observed concentration changes were linear with time during the study for all solutions except those stored inverted (VU). The rate of concentration change in solutions stored at 22–30° under fluorescent light differed from that in solutions stored at 6 or 38° ($p < 0.001$, Fig. 1) but did not significantly differ from that in solutions protected from light. The rate of concentration change was independent of the initial concentration (0.8 or 1.0 mg/ml) and the source of the nitroglycerin (powder or tablet). The concentration of solutions stored inverted differed significantly from that in solutions stored upright after 1 month ($p < 0.001$, Fig. 2).

The concentration of intravenous nitroglycerin solutions (0.2 mg/ml) stored in plastic bags differed from the initial concentration after 1.3 hr, regardless of storage temperature or exposure to light ($p < 0.05$). After 8 hr, the concentration of solutions stored under fluorescent light at 28–30° (Solution PRT) in the dark at 28–30° (PF), 38° (PO), or 6° (PR)

Table III—Stability of Nitroglycerin Stock Solutions

Variables[a]	Predicted[b] Time for Nitroglycerin Concentration to Decrease 20%, days	Decrease in Nitroglycerin Concentration, %		
		1 Month	3 Months	6 Months
Tablet solutions, 1.0 mg/ml				
6°, dark, upright (VR)	—	−11	−5	−8
38°, dark, upright (VO)	50	23[c]	51[c]	67[c]
22–30°, light, inverted (VU)	2	39[c]	58[c]	58[c]
22–30°, dark upright (VF)	98	2	26[c]	31[c]
22–30°, light, upright (VRT)	87	5	29[c]	35[c]
0.8 mg/ml solutions				
22–30°, light, upright				
Tablets (VT)	87	5[c]	18[c]	41[c]
Powder (VP)	82	13[c]	28[c]	43[c]

[a] Nitroglycerin solutions were prepared in 0.9% saline and packaged in multidose vials. Variables included initial concentration; nitroglycerin source, and storage conditions. [b] Values were predicted by least-squares method except VU, which was estimated graphically. [c] Significantly different from initial ($p < 0.05$).

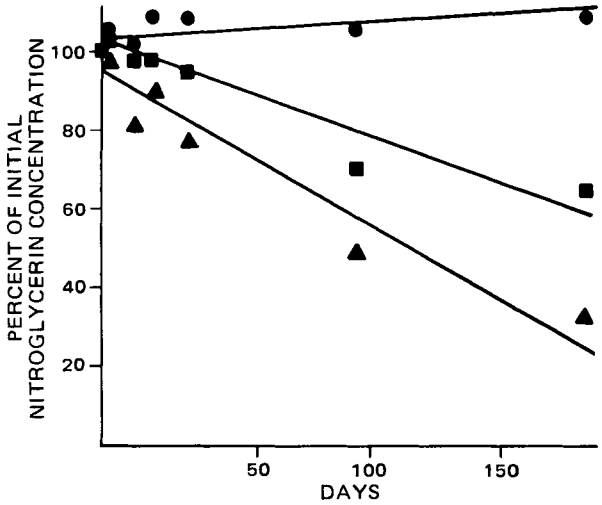

Figure 1—*Effect of temperature on nitroglycerin stock solutions, (p < 0.001). Solutions (1.0 mg/ml) were prepared from tablets in saline, packaged in multidose vials and stored upright. Key: ●, 6°, Solution VR; ■, 22–30°, Solution VRT; and ▲, 38°, Solution VO.*

decreased 44, 38, 46, and 14%, respectively. The concentration decrease of solutions stored at 28–30° under fluorescent light differed from that of solutions stored at 6° ($p < 0.001$) but did not differ from that of solutions protected from light for 52 hr. After 27 hr, the concentration decrease of solutions stored at 38° (68%) differed significantly ($p < 0.001$) from that of solutions stored at 28–30° (61%).

The concentration of intravenous nitroglycerin solutions (0.2 mg/ml) stored in glass bottles under fluorescent light at 28–30° (Solution GRT) or in the dark at 28–30° (GF), 38° (GO), or 6° (GR) did not differ significantly from the initial value after 52 hr. The rate of concentration change did not differ among these solutions. In a separate comparison, the concentration of nitroglycerin solutions stored in glass bottles decreased <18% after 24 hr at 26–28° under fluorescent light when solutions were prepared from powder in saline (GP), tablets in 5% dextrose solution (GD), or tablets in saline (GT). The rate of concentration change was independent of the vehicle (5% dextrose solution or saline) and of the source of nitroglycerin (tablet or powder).

At 1.3 hr, the nitroglycerin concentrations (expressed as a percentage of the initial value) in solutions stored in plastic bags were as follows:

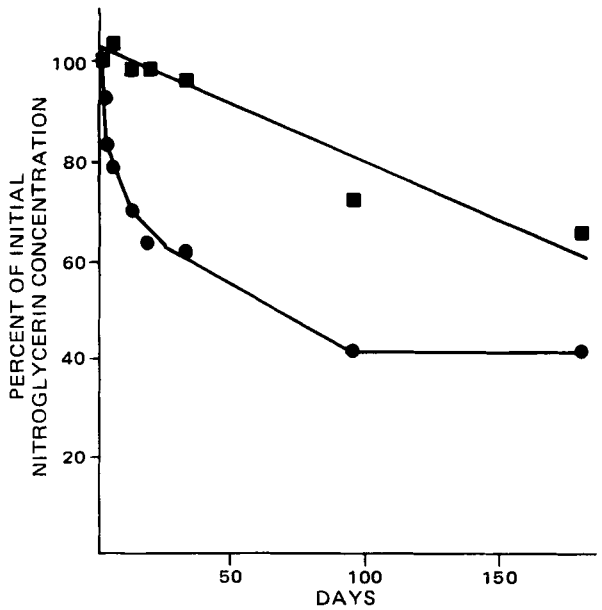

Figure 2—*Effect of contact with the rubber stopper of multidose vials on nitroglycerin concentration (p < 0.001). Solutions (1.0 mg/ml) were prepared from tablets in saline and stored at 22–30° under fluorescent light. Key: ●, stored inverted, Solution VU; and ■, stored upright, Solution VRT.*

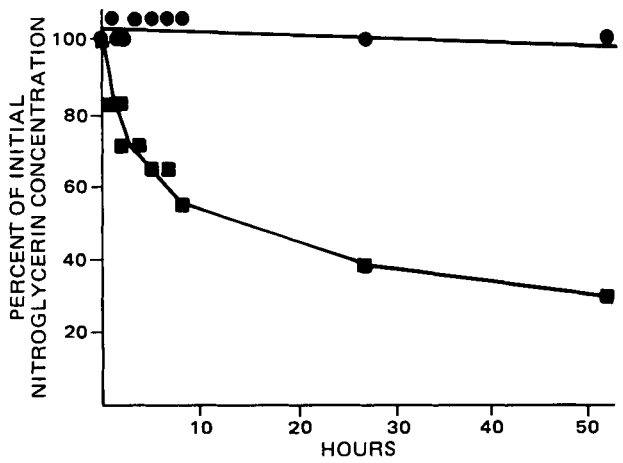

Figure 3—*Effect of glass and plastic intravenous containers on nitroglycerin concentration (p < 0.01). Solutions (0.2 mg/ml) were prepared from tablets in saline and stored at 28–30° under fluorescent light. Key: ●, glass bottles, Solution GRT; and ■, plastic bags, Solution PRT.*

under fluorescent light at 28–30°, 85%; in the dark at 28–30°, 87%; at 6°, 90%; and at 38°, 79%. Similarly, after 1.3 hr, solutions stored in glass bottles under identical conditions had concentrations that were 100, 103, 108, and 105% of the initial value, respectively. The values for solutions stored in plastic bags were different in all instances from the values for solutions stored in glass bottles ($p < 0.01$, Fig. 3).

When intravenous nitroglycerin solutions were packaged in glass (G) or plastic (P) containers and perfused through administration sets, concentration decreases occurred in the bulk solution remaining in the container and the solution perfusing the administration set. Concentration changes in the bulk solution were not significantly different from those in similar solutions without an administration set. However, concentration changes following perfusion of the administration sets were significant in all solutions ($p < 0.001$).

The mean concentration decrease of the solution perfusing administration tubing for 8 hr from a glass container (GTu) was 37% of nitroglycerin concentration in the container and differed ($p < 0.02$) from that of the solution perfusing tubing with a buret (50%, GBu). The mean decrease after perfusion of tubing from a glass container also differed from that of identical tubing attached to a plastic bag (27%, PTu, $p < 0.02$, Table IV). The largest decrease in nitroglycerin concentration occurred during the 1st hr of perfusion. After 4 hr, concentrations no longer changed with time and decreases in concentration remained as follows: tubing from glass bottle, 35%; tubing with buret from glass bottle, 55%; and tubing from plastic bag, 20% (Fig. 4).

Following an 8-hr perfusion, the mean decrease from the initial nitroglycerin concentration for the total administration system (container

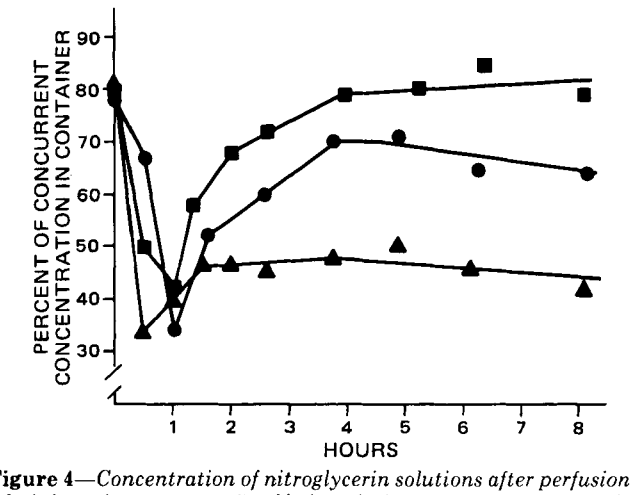

Figure 4—*Concentration of nitroglycerin solutions after perfusion of administration sets at 0.5 ml/min relative to concurrent container concentration (p < 0.001). Key: ■, plastic intravenous bag, tubing without buret, solution PTu; ●, glass intravenous bottle, tubing without buret, Solution GTu; and ▲, glass intravenous bottle, tubing with buret, Solution GBu.*

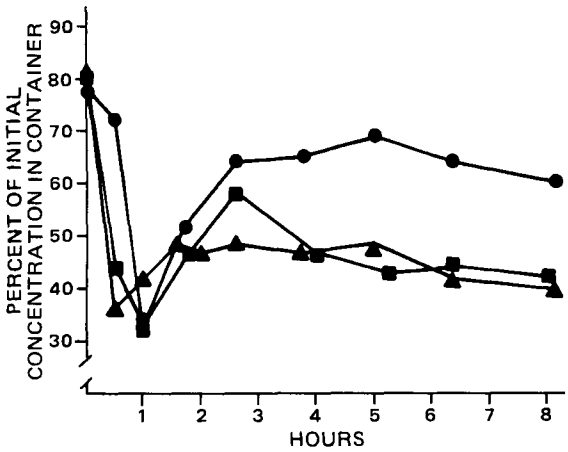

Figure 5—*Decrease from initial nitroglycerin concentration in container after perfusion of sets at 0.5 ml/min ($p < 0.001$). Key: ■, plastic intravenous bag, tubing without buret, Solution PTu; ●, glass intravenous bottle, tubing without buret, Solution GTu; and ▲, glass intravenous bottle, tubing with buret, Solution GBu.*

plus administration set) was 38% for tubing with a glass bottle (GTu), 51% for tubing with buret and a glass bottle (GBu), and 50% for tubing with a plastic bag (PTu). The decrease that occurred when tubing was used with a plastic bag differed ($p < 0.01$) from that of the system of tubing and a glass bottle but did not differ from that of the system of tubing with buret and a glass bottle (Table IV, Fig. 5).

DISCUSSION

The stability of nitroglycerin stock solutions (0.8–1.0 mg/ml) did not depend on exposure to light or the nitroglycerin source. However, nitroglycerin concentration significantly decreased with time in solutions stored at elevated temperatures or in contact with rubber stoppers (Figs. 1 and 2). Nitroglycerin stock solutions in upright multidose vials were refrigerated for ~6 months without a significant decrease in concentration. Storage of the vials at room temperature resulted in a 20% decrease in nitroglycerin concentration after ~3 months (Table III). The marked decrease in nitroglycerin concentration following contact of solutions with rubber stoppers suggests that any vial found inverted or on its side should be discarded or that an all-glass packaging system (*e.g.*, ampul) should be used.

The stability of intravenous nitroglycerin solutions (0.2 mg/ml) was not dependent on the vehicle, nitroglycerin source, or exposure to light. Storage in glass bottles for 24 hr at 6–38° resulted in a maximum loss of 18%. However, during storage in plastic infusion bags or during perfusion of plastic administration sets, nitroglycerin concentration decreased significantly with time (Figs. 3–5). Administration tubing with a buret removed more nitroglycerin from solution than did tubing without a buret. The increased stability realized by packaging nitroglycerin solutions in glass rather than plastic was negated when administration tubing with a buret was used instead of tubing without a buret (Table IV and Fig. 5).

Other studies have similarly reported minimal concentration changes in nitroglycerin solutions refrigerated in multidose vials for up to 6 months (19, 20). Autoclaving nitroglycerin solutions (400 μg/ml) at 121° for 20 min resulted in a 5% decrease in concentration (19). However, storage of nitroglycerin solutions in inverted multidose vials for 1 month resulted in a 45% decrease in nitroglycerin concentration (18).

Similar losses of nitroglycerin from solutions stored in plastic bags have been reported, but reports on the stability of nitroglycerin solutions stored in glass bottles were conflicting (17, 18, 20–23). However, stability in glass bottles was greater than that in plastic bags (18, 21–23). Contact of solutions with plastic administration sets resulted in 15–75% decreases in nitroglycerin content (21, 23, 24).

Nitroglycerin formulations may exhibit instability by degradation, volatilization (29, 30), intertablet migration (11, 30), and sorption by packaging materials (13, 15, 30, 32). Nitroglycerin degrades by hydrolysis to mono- or dinitroglycerin (15) and, at elevated temperatures, to nitric acid and glycerol (33). Microbial degradation also has been reported (34). Sorption of nitroglycerin by rubber surfaces was reported for aqueous solutions (18) and propylene glycol–ethanol solutions (35) of nitroglycerin. Nitroglycerin was recovered by methanolic extraction from plastic bags (22) and was reported to leave an oily residue on glass (36).

Table IV—Effect of the Administration Set or System on the Stability of Nitroglycerin Solutions

Administration System[a]	Mean Decrease in Nitroglycerin Concentration, %[b]	
	Administration Set Alone	Administration System
Glass bottle, tubing with buret (GBu)	50[c]	51[d]
Glass bottle, tubing without buret (GTu)	37	38
Plastic bag, tubing without buret (PTu)	27[c]	50[d]

[a] Container and administration set. [b] Percent decrease in the nitroglycerin concentration of solutions perfused through administration sets (0.5 ml/min). [c] Significantly different from GTu ($p < 0.02$). [d] Significantly different from GTu ($p < 0.01$).

The sorption of nitroglycerin during perfusion of the plastic administration sets in this study may have occurred by two processes. Nitroglycerin may have first adsorbed onto the tubing in a concentrated layer and then absorbed into the plastic matrix while nitroglycerin from the solution replenished the concentrated layer. Until the surface layer was saturated, adsorption was rapid with respect to the perfusion rate, and nitroglycerin was largely removed from solution. As saturation of the concentrated layer occurred, the extraction ratio of nitroglycerin declined; nitroglycerin concentration in the solution emerging from the tubing rose to a constant fraction of that in the container (Fig. 4). While adsorption may have accounted for the initially rapid clearance of nitroglycerin by the tubing, a greater quantity of nitroglycerin probably was removed by absorption (37).

Adsorption and absorption were capacitance (surface area) and perfusion rate limited. The nitroglycerin concentration decreased faster and remained lower when the surface area perfused by the solution was increased by the use of administration tubing with a buret rather than tubing without one (Fig. 4). Similarly, concentration decreases were more rapid and extensive at slower perfusion rates (24) as a result of the increased contact time between the solution and the surface of the administration set.

The reversible nature of nitroglycerin sorption to plastic could account for the observation that the tubing attached to bags removed a smaller percentage of nitroglycerin than did identical tubing attached to bottles (Table IV). Adsorption of the concentrated layer may have reached equilibrium during the first 1 or 2 hr of perfusion when the nitroglycerin concentration in the bag was relatively high. As the nitroglycerin level decreased in the bag, the solution perfusing the tubing was too dilute relative to the concentrated layer, and nitroglycerin desorbed into the solution. Consequently, the effect of the tubing on the nitroglycerin concentration was lessened.

The short contact of nitroglycerin solutions with a plastic syringe, unlike the longer contact with administration sets, was not associated with a decrease in nitroglycerin concentration. Plastic syringes may be used for the transfer of nitroglycerin solutions, but prolonged storage of nitroglycerin solutions in plastic syringes may result in a decreased concentration.

REFERENCES

(1) J. P. Derrida, R. Sal, and P. Chiche, *N. Engl. J. Med.*, **297**, 336 (1977).

(2) R. C. Leinbach and H. K. Gold, *Circulation (Suppl.)*, **55–56**, III-194 (1977).

(3) J. A. Kaplan, R. W. Dunbar, and E. L. Jones, *Anesthesiology*, **45**, 14 (1976).

(4) E. B. Stinson, E. L. Holloway, G. Derby, P. E. Oyer, J. Hollingsworth, R. B. Griepp, and D. C. Harrison, *Circulation (Suppl.)*, **51–52**, I-26 (1975).

(5) N. R. Fahmy, *Anesthesiology*, **49**, 17 (1978).

(6) P. W. Armstrong, D. C. Walker, J. R. Burton, and J. O. Parker, *Circulation*, **52**, 1118 (1975).

(7) J. T. Flaherty, P. R. Reid, D. T. Kelly, D. R. Taylor, M. L. Weisfeldt, and B. Pitt, *ibid.*, **51**, 132 (1975).

(8) H. L. Fung and C. T. Rhodes, *Am. J. Hosp. Pharm.*, **32**, 139 (1975).

(9) J. W. Ward, A. I. Sandler, and S. V. Tucker, *Drug Intell. Clin. Pharm.*, **13**, 14 (1979).
(10) F. K. Bell, *J. Pharm. Sci.*, **53**, 752 (1964).
(11) S. A. Fusari, *ibid.*, **62**, 122 (1973).
(12) *Ibid.*, **62**, 2012 (1973).
(13) B. Dorsch and R. F. Shangraw, *Am. J. Hosp. Pharm.*, **32**, 795 (1975).
(14) S. K. Yap, C. T. Rhodes, and H. L. Fung, *ibid.*, **32**, 1039 (1975).
(15) M. J. Pikal, D. A. Bibler, and B. Rutherford, *J. Pharm. Sci.*, **66**, 1293 (1977).
(16) P. E. Stach, *Am. J. Hosp. Pharm.*, **30**, 579 (1973).
(17) D. J. Ludwig and C. T. Ueda, *ibid.*, **35**, 541 (1978).
(18) J. K. Sturek, T. D. Sokoloski, W. T. Winsley, and P. E. Stach, *ibid.*, **35**, 537 (1978).
(19) T. W. Dean and D. C. Baun, *ibid.*, **32**, 1036 (1975).
(20) L. G. Cacace, A. Harralson, and T. Clougherty, *Am. Heart J.*, **97**, 816 (1979).
(21) J. C. Boylan, R. L. Robison, and P. M. Terrill, *Am. J. Hosp. Pharm.*, **35**, 1031 (1978).
(22) B. L. McNiff, E. F. McNiff, and H. L. Fung, *ibid.*, **36**, 173 (1979).
(23) W. G. Crouthamel, B. Dorsch, and R. F. Shangraw, *N. Engl. J. Med.*, **299**, 262 (1978).
(24) P. A. Cossum, A. J. Galbraith, M. S. Roberts, and G. W. Boyd, *Lancet*, **2**, 349 (1978).
(25) W. G. Crouthamel and B. Dorsch, *J. Pharm. Sci.*, **68**, 237 (1979).
(26) T. Colton, "Statistics in Medicine," Little, Brown, Boston, Mass., 1974.
(27) R. G. D. Steel and J. H. Torrie, "Principles and Procedures of Statistics," McGraw-Hill, New York, N.Y., 1960.
(28) "The United States Pharmacopeia," 20th rev., Mack Publishing Co., Easton, Pa., 1979, p. 552.
(29) M. D. Richman, C. D. Fox, and R. F. Shangraw, *J. Pharm. Sci.*, **54**, 447 (1965).
(30) R. F. Shangraw and A. M. Contractor, *J. Am. Pharm. Assoc.*, **NS12**, 633 (1972).
(31) D. Banes, *J. Pharm. Sci.*, **57**, 893 (1968).
(32) B. A. Edelman, A. M. Contractor, and R. F. Shangraw, *J. Am. Pharm. Assoc.*, **NS11**, 30 (1971).
(33) C. E. Waring and G. Krastins, *J. Phys. Chem.*, **74**, 999 (1970).
(34) T. M. Wendt, J. H. Cornell, and A. M. Kaplan, *Appl. Environ. Microbiol.*, **36**, 693 (1978).
(35) A. M. Contractor, J. M. Snyder, H. P. Fletcher, and R. F. Shangraw, *J. Pharm. Sci.*, **63**, 907 (1974).
(36) E. M. Johnson, in "Organic Nitrates," P. Needleman, Ed., Springer-Verlag, New York, N.Y., 1975, p. 22.
(37) P. H. Yuen, S. L. Denman, T. D. Sokoloski, and A. M. Burkman, *J. Pharm. Sci.*, **68**, 1163 (1979).

ACKNOWLEDGMENTS

Presented at the American Society of Hospital Pharmacists Midyear Clinical Meeting, Las Vegas, December 1979.

Abstracted in part from a thesis submitted by A. H. Scheife to Northeastern University in partial fulfillment of the Master of Science degree requirements.

Contribution of drugs and supplies by the Department of Pharmacy, Beth Israel Hospital, is gratefully acknowledged.

Preparation and Screening of Some New Thioacetals, Sulfones, and Derivatives of 4-Dichloromethylbenzoyl and 4-Trichloromethylbenzoyl Chloride as Potential Antimalarials

EVA H. MØRKVED *x **and MARSHALL W. CRONYN** *‡

Received October 22, 1980, from the *Organic Chemistry Laboratories, Norwegian Institute of Technology, University of Trondheim, N-7034 Trondheim-NTH, Norway and the ‡ Department of Chemistry, Reed College, Portland, OR 97202. Accepted for publication May 15, 1981.

Abstract □ The preparation and screening of some potential antimalarials are reported. The new compounds which are inactive as antimalarials are several benzene-, benzyl-, and fluorene thioacetals, β-disulfones derived from these thioacetals, α-chlorobenzyl sulfones, amides, and thioesters derived from 4-dichloromethylbenzoyl chloride and 4-trichloromethylbenzoyl chloride. The known compounds bis(4-aminophenyl)sulfone and 4′-aminophenyl-4-aminobenzene thiolsulfonate also were prepared and showed some antimalarial activity.

Keyphrases □ Antimalarials—preparation of new thioacetals, sulfones, and 4-dichloromethylbenzoyl and 4-trichloromethylbenzoyl chloride derivatives □ Thioacetals—preparation of potential antimalarials □ Sulfones—preparation of potential antimalarials □ Derivatives—of 4-dichloromethylbenzoyl and 4-trichloromethylbenzoyl chloride, preparation of potential antimalarials

Malaria is still an important health problem in tropical areas. Various factors contribute to this situation including the development of malaria strains resistant to known antimalarials. This development has led to at least one recent antimalarial program (1). The purpose of the present work was to prepare potential antimalarials based on two model systems of known antimalarials, 1,4-bis(trichloromethyl)benzene which has been known as an active antimalarial for many years (2), and derivatives of bis(4-aminophenyl)sulfone which are more useful as suppressives than as therapeutic agents (3).

The synthesized compounds (Scheme I) share similarities with known antimalarials (2, 3). The trichloromethylaryl derivatives had no antimalarial activity, but the α-disulfone VIII*b* and the thiolsulfonate IX*b* showed some antimalarial activity.

RESULTS AND DISCUSSION

Thioacetals may be prepared by various methods (4–6) among which the reaction of *gem*-dihalides with sodium thiolates is a convenient one. Compound I*a* (Table I) was prepared from benzal chloride and a triethylammonium thiophenolate whereas VII*a* was formed easily from the *gem*-dihalide and a thiophenol. Acid-catalyzed reactions between 4-(trichloromethyl)benzaldehyde and various thiophenols gave the thioacetals I*c*, I*d*, and III*a*.

Two methods considered for the preparation of β-disulfones were a reaction of triethylammonium sulfinates with *gem*-dihalides or an oxi-

0022-3549/82/0100-0059$01.00/0

(9) J. W. Ward, A. I. Sandler, and S. V. Tucker, *Drug Intell. Clin. Pharm.*, **13**, 14 (1979).
(10) F. K. Bell, *J. Pharm. Sci.*, **53**, 752 (1964).
(11) S. A. Fusari, *ibid.*, **62**, 122 (1973).
(12) *Ibid.*, **62**, 2012 (1973).
(13) B. Dorsch and R. F. Shangraw, *Am. J. Hosp. Pharm.*, **32**, 795 (1975).
(14) S. K. Yap, C. T. Rhodes, and H. L. Fung, *ibid.*, **32**, 1039 (1975).
(15) M. J. Pikal, D. A. Bibler, and B. Rutherford, *J. Pharm. Sci.*, **66**, 1293 (1977).
(16) P. E. Stach, *Am. J. Hosp. Pharm.*, **30**, 579 (1973).
(17) D. J. Ludwig and C. T. Ueda, *ibid.*, **35**, 541 (1978).
(18) J. K. Sturek, T. D. Sokoloski, W. T. Winsley, and P. E. Stach, *ibid.*, **35**, 537 (1978).
(19) T. W. Dean and D. C. Baun, *ibid.*, **32**, 1036 (1975).
(20) L. G. Cacace, A. Harralson, and T. Clougherty, *Am. Heart J.*, **97**, 816 (1979).
(21) J. C. Boylan, R. L. Robison, and P. M. Terrill, *Am. J. Hosp. Pharm.*, **35**, 1031 (1978).
(22) B. L. McNiff, E. F. McNiff, and H. L. Fung, *ibid.*, **36**, 173 (1979).
(23) W. G. Crouthamel, B. Dorsch, and R. F. Shangraw, *N. Engl. J. Med.*, **299**, 262 (1978).
(24) P. A. Cossum, A. J. Galbraith, M. S. Roberts, and G. W. Boyd, *Lancet*, **2**, 349 (1978).
(25) W. G. Crouthamel and B. Dorsch, *J. Pharm. Sci.*, **68**, 237 (1979).
(26) T. Colton, "Statistics in Medicine," Little, Brown, Boston, Mass., 1974.
(27) R. G. D. Steel and J. H. Torrie, "Principles and Procedures of Statistics," McGraw-Hill, New York, N.Y., 1960.
(28) "The United States Pharmacopeia," 20th rev., Mack Publishing Co., Easton, Pa., 1979, p. 552.
(29) M. D. Richman, C. D. Fox, and R. F. Shangraw, *J. Pharm. Sci.*, **54**, 447 (1965).
(30) R. F. Shangraw and A. M. Contractor, *J. Am. Pharm. Assoc.*, **NS12**, 633 (1972).
(31) D. Banes, *J. Pharm. Sci.*, **57**, 893 (1968).
(32) B. A. Edelman, A. M. Contractor, and R. F. Shangraw, *J. Am. Pharm. Assoc.*, **NS11**, 30 (1971).
(33) C. E. Waring and G. Krastins, *J. Phys. Chem.*, **74**, 999 (1970).
(34) T. M. Wendt, J. H. Cornell, and A. M. Kaplan, *Appl. Environ. Microbiol.*, **36**, 693 (1978).
(35) A. M. Contractor, J. M. Snyder, H. P. Fletcher, and R. F. Shangraw, *J. Pharm. Sci.*, **63**, 907 (1974).
(36) E. M. Johnson, in "Organic Nitrates," P. Needleman, Ed., Springer-Verlag, New York, N.Y., 1975, p. 22.
(37) P. H. Yuen, S. L. Denman, T. D. Sokoloski, and A. M. Burkman, *J. Pharm. Sci.*, **68**, 1163 (1979).

ACKNOWLEDGMENTS

Presented at the American Society of Hospital Pharmacists Midyear Clinical Meeting, Las Vegas, December 1979.

Abstracted in part from a thesis submitted by A. H. Scheife to Northeastern University in partial fulfillment of the Master of Science degree requirements.

Contribution of drugs and supplies by the Department of Pharmacy, Beth Israel Hospital, is gratefully acknowledged.

Preparation and Screening of Some New Thioacetals, Sulfones, and Derivatives of 4-Dichloromethylbenzoyl and 4-Trichloromethylbenzoyl Chloride as Potential Antimalarials

EVA H. MØRKVED *x **and MARSHALL W. CRONYN** *‡

Received October 22, 1980, from the *Organic Chemistry Laboratories, Norwegian Institute of Technology, University of Trondheim, N-7034 Trondheim-NTH, Norway and the ‡ Department of Chemistry, Reed College, Portland, OR 97202. Accepted for publication May 15, 1981.

Abstract □ The preparation and screening of some potential antimalarials are reported. The new compounds which are inactive as antimalarials are several benzene-, benzyl-, and fluorene thioacetals, β-disulfones derived from these thioacetals, α-chlorobenzyl sulfones, amides, and thioesters derived from 4-dichloromethylbenzoyl chloride and 4-trichloromethylbenzoyl chloride. The known compounds bis(4-aminophenyl)sulfone and 4′-aminophenyl-4-aminobenzene thiolsulfonate also were prepared and showed some antimalarial activity.

Keyphrases □ Antimalarials—preparation of new thioacetals, sulfones, and 4-dichloromethylbenzoyl and 4-trichloromethylbenzoyl chloride derivatives □ Thioacetals—preparation of potential antimalarials □ Sulfones—preparation of potential antimalarials □ Derivatives—of 4-dichloromethylbenzoyl and 4-trichloromethylbenzoyl chloride, preparation of potential antimalarials

Malaria is still an important health problem in tropical areas. Various factors contribute to this situation including the development of malaria strains resistant to known antimalarials. This development has led to at least one recent antimalarial program (1). The purpose of the present work was to prepare potential antimalarials based on two model systems of known antimalarials, 1,4-bis(trichloromethyl)benzene which has been known as an active antimalarial for many years (2), and derivatives of bis(4-aminophenyl)sulfone which are more useful as suppressives than as therapeutic agents (3).

The synthesized compounds (Scheme I) share similarities with known antimalarials (2, 3). The trichloromethylaryl derivatives had no antimalarial activity, but the α-disulfone VIII*b* and the thiolsulfonate IX*b* showed some antimalarial activity.

RESULTS AND DISCUSSION

Thioacetals may be prepared by various methods (4–6) among which the reaction of *gem*-dihalides with sodium thiolates is a convenient one. Compound I*a* (Table I) was prepared from benzal chloride and a triethylammonium thiophenolate whereas VII*a* was formed easily from the *gem*-dihalide and a thiophenol. Acid-catalyzed reactions between 4-(trichloromethyl)benzaldehyde and various thiophenols gave the thioacetals I*c*, I*d*, and III*a*.

Two methods considered for the preparation of β-disulfones were a reaction of triethylammonium sulfinates with *gem*-dihalides or an oxi-

0022-3549/82/0100-0059$01.00/0

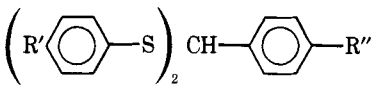

Ia: R′ = CH_3CONH, R″ = H
Ib: R′ = NH_3Cl, R″ = H
Ic: R′ = H, R″ = Cl_3C
Id: R′ = CH_3CONH, R″ = Cl_3C
Ie: R′ = NH_3Cl, R″ = CH_3OOC

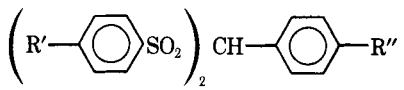

IIa: R′ = CH_3CONH, R″ = H
IIb: R′ = H_2N, R″ = H
IIc: R′ = H, R″ = Cl_3C
IId: R′ = CH_3CONH, R″ = Cl_3C
IIe: R′ = H_2N, R″ = Cl_3C
IIf: R′ = H, R″ = HOOC

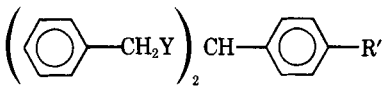

IIIa: Y = S, R′ = Cl_3C
IIIb: Y = SO_2, R′ = Cl_3C
IIIc: Y = SO_2, R′ = HOOC

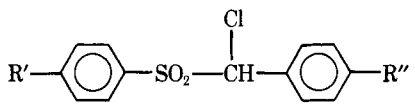

IVa: R′ = CH_3CONH, R″ = H
IVb: R′ = H_2N, R″ = H
IVc: R′ = H, R″ = Cl_3C

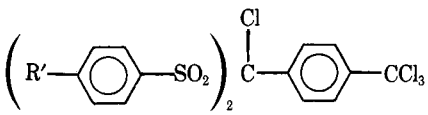

Va: R′ = H
Vb: R′ = CH_3CONH

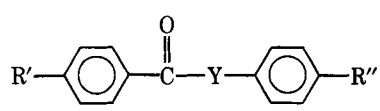

VIa: R′ = Cl_2HC, Y = NH, R″ = H
VIb: R′ = Cl_2HC, Y = NH, R″ = HOOC
VIc: R′ = Cl_2HC, Y = S, R″ = CH_3CONH
VId: R′ = Cl_3C, Y = NH, R″ = H
VIe: R′ = Cl_3C, Y = NH, R″ = NO_2
VIf: R′ = Cl_3C, Y = S, R″ = H
VIg: R′ = Cl_3C, Y = S, R″ = CH_3CONH

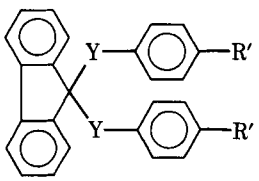

VIIa: Y = S, R′ = CH_3CONH
VIIb: Y = SO_2, R′ = CH_3CONH
VIIc: Y = SO_2, R′ = H_2N

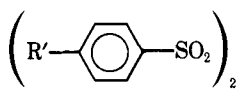

VIIIa: R′ = CH_3CONH
VIIIb: R′ = H_2N

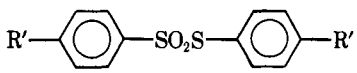

IXa: R′ = CH_3CONH
IXb: R′ = H_2N

Scheme I

dation of the thioacetals I, IIIa, and VIIa. However, only one of the halide atoms of benzal chloride was replaced by an aryl sulfinate and IVa was obtained, but only 9-fluorenone and water-soluble products were formed from 9,9-dichlorofluorene and the same aryl sulfinate. Oxidations of thioacetals with a solution of peracetic acid in dry methylene chloride yielded the corresponding β-disulfones in excellent yields, provided a large excess (12 molar equivalents) of the peracid was used. Reactions of the thioacetal Ia with the usual oxidation mixture, peracetic acid in acetic acid, yielded benzaldehyde and the known thiol sulfonate IXa. The formation of IXa most likely occurs *via* the *O*-protonated thioacetal *S*-oxide (7, 8). Such compounds are known to be extremely sensitive to acids and decompose to a resonance-stabilized sulfoxonium ion and a sulfenic acid. A nucleophilic attack by the sulfenic acid on the sulfoxonium ion will give a sulfenic ester which spontaneously fragments to form benzaldehyde and a disulfide (9), the latter being oxidized to the thiolsulfonate IXa. Alternatively, an attack by water on the sulfoxonium ion would give benzaldehyde and a thiophenol, which will lead to the thiolsulfonate *via* a sulfinic acid under these reaction conditions (10, 11).

Recently IXa was prepared (12) by the fragmentation of a benzenesulfonohydrazide by hydrochloric acid in acetic acid, with the arylsulfinic acid postulated as an intermediate.

Reactions of the β-disulfones IIc and IId with sodium hypochlorite gave chlorination of the α-methylene group and Va and Vb were formed, respectively. An attempt to prepare Va from the thioacetal Ic by chlorination using sulfuryl chloride, and subsequent oxidation of the crude product using peracetic acid in dry methylene chloride, resulted in loss of one sulfhydryl group, and compound IVc was obtained in good yield. Reactions of sulfides with sulfuryl chloride give various products depending on the reaction conditions; α-chlorination usually occurs (13), but recently thioacetals have been found to undergo *S*-oxidation by sulfuryl chloride in the presence of wet silica gel (14). Therefore, if the thioacetal Ic undergoes both *S*-oxidation and α-chlorination by sulfuryl chloride, the product IVc may be accounted for by a mechanism involving the formation of a sulfoxonium ion and simultaneous loss of a sulfenic acid.

Side-chain chlorinations of 4-methylbenzoyl chloride and 1,4-dimethylbenzene are to a large extent dealt with in the patent literature; a common problem to these reactions are mixtures of polychlorinated products which are not easily separated. However, 4-dichloromethylbenzoyl chloride was prepared in satisfactory yield by a peroxide-catalyzed chlorination of 4-methylbenzoyl chloride in carbon tetrachloride. The 4-trichloromethylbenzyl derivatives required the preparation of either pentachlorinated 1,4-dimethylbenzene or 4-trichlormethylbenzoyl chloride which could be reduced to the aldehyde. The radical chlorination methods reported previously (15–19) were unsatisfactory for the preparation of large quantities of these compounds. A zinc chloride-catalyzed chlorination of 1,3-benzenedicarboxylic acid by 1,4-bis(trichloromethyl)benzene[1] gave good yields of 4-trichloromethylbenzoyl chloride. Similar reactions were reported recently (20–24) but the objectives were to prepare various benzenedicarbonyl chlorides instead of 4-trichloromethylbenzoyl chloride.

1,4-Bis(trichloromethyl)benzene is an active antimalarial and various derivatives of this compound were prepared earlier (25). The prepared derivatives were tested[2] for activity in suppression of *Plasmodium gallinaceum* in the mosquito *Aedes aegypti*. The antimalarial test results showed that the chlorinated compounds were inactive but the previously known α-disulfone VIIIb suppressed the sporozoites completely in the mosquito salivary glands when administered in a 0.01% concentration of the mosquito feed. The only other compound which showed some antimalarial activity was the thiolsulfonate IXb. However, 4-trichloromethylbenzaldehyde showed activity earlier[3].

EXPERIMENTAL[4]

4-Methylbenzoyl Chloride—This was prepared from 4-methylbenzoic acid and thionyl chloride, bp_{36} 124–127° [lit. (26), bp_{36} 125°].

[1] Dr. R. F. Horvath, Research Department, Diamond Alkali Co., personal communication.

[2] Tests by Walter Reed Army Medical Center, Washington DC.

[3] National Institutes of Health, Cancer Research Department, Bethesda Md.

[4] IR spectra were recorded on a Perkin-Elmer 254 grating spectrometer. All melting points are uncorrected and were obtained on a Büchi "Tottoli" melting-point apparatus. Elemental analyses were carried out at Galbraith Laboratories. Peracetic acid (40%) was obtained from Becco. Raney nickel No. 28 was obtained from W. R. Grace & Co., and lithium tri-*tert*-butoxyaluminum hydride was obtained from Ventron Corp.

Table I—Thioacetals and β-Disulfones

Compound	Yield, %	Melting Point (Recrystallization Solvent)	Formula (mol. wt.)		Analysis, % C	H	Cl	N	S
Ia	81	189–190° (ethanol)	$C_{23}H_{22}N_2O_2S_2$ (422.58)	Calc.	65.37	5.25		6.63	15.18
				Found	65.40	5.09		6.70	15.29
Ib	85	224–225° dec. (acetonitrile–acetone)	$C_{19}H_{20}Cl_2N_2S_2$ (411.45)	Calc.	55.46	4.90	17.24	6.81	15.59
				Found	56.51	4.71	16.72	6.81	15.23
Ic	73	88–89° (heptane)	$C_{20}H_{15}Cl_3S_2$ (425.86)	Calc.	56.41	3.55	24.98		15.06
				Found	56.47	3.58	25.05		14.91
Id	45	169–170° dec. (acetonitrile)	$C_{24}H_{21}Cl_3N_2O_2S_2$ (539.97)	Calc.	53.38	3.92	19.70	5.19	11.88
				Found	53.51	4.09	19.78	5.30	11.85
Ie	90	218–219° dec. (ethanol)	$C_{21}H_{22}Cl_2N_2O_2S_2$ (469.50)	Calc.	53.73	4.72	15.10	5.97	13.66
				Found	53.66	4.65	15.09	5.82	13.35
IIa	95	259–260° dec. (*N,N*-dimethylformamide–water)	$C_{23}H_{22}N_2O_6S_2$ (486.58)	Calc.	56.78	4.56		5.76	13.18
				Found	57.03	4.72		5.80	13.65
IIb	53	205–207° dec. (acetone)	$C_{19}H_{18}N_2O_4S_2$ (402.51)	Calc.	56.70	4.51		6.96	15.93
				Found	57.03	4.95		6.63	15.42
IIc	88	222–223° (chloroform–benzene)	$C_{20}H_{15}Cl_3O_4S_2$ (489.86)	Calc.	49.04	3.09	21.72		13.09
				Found	49.18	3.19	21.90		12.87
IId	96	171° dec. (acetonitrile)	$C_{24}H_{21}Cl_3N_2O_6S_2$ (603.97)	Calc.	47.72	3.51	17.61	4.64	10.62
				Found	48.09	3.42	18.00	5.73	10.12
IIe	94	>300° (chloroform–tetrahydrofuran)	$C_{20}H_{17}Cl_3N_2O_4S_2$ (519.90)	Calc.	46.20	3.30	20.46	5.39	12.34
				Found	46.19	3.56	20.37	5.13	12.42
IIf	81	271–276° dec. (chloroform)	$C_{20}H_{16}O_6S_2$ (416.49)	Calc.	57.68	3.87			15.40
				Found	58.16	3.94			14.60
IIIa	65	89–90° (cyclohexane)	$C_{22}H_{19}Cl_3S_2$ (453.91)	Calc.	58.21	4.22	23.43		14.14
				Found	58.22	4.65	23.56		14.08
IIIb	92	250–251° dec. (chloroform)	$C_{22}H_{19}Cl_3O_4S_2$ (517.91)	Calc.	51.01	3.70	20.54		12.39
				Found	50.75	3.61	20.77		12.63
IIIc	41	247–249° (methanol)	$C_{22}H_{20}O_6S_2$ (444.54)	Calc.	59.44	4.53			14.43
				Found	59.68	4.47			14.68
Va	64	193–196° (carbon tetrachloride–cyclohexane)	$C_{20}H_{14}Cl_4O_4S_2$ (524.31)	Calc.	45.81	2.69	27.05		12.24
				Found	45.58	2.74	27.36		12.35
Vb	47	220° dec. (acetonitrile)	$C_{24}H_{20}Cl_4N_2O_6S_2$ (638.42)	Calc.	45.14	3.16			10.06
				Found	45.60	3.32			10.08
VIIa	89	209–210° dec. (acetonitrile)	$C_{29}H_{24}N_2O_2S_2$ (496.66)	Calc.	70.14	4.87		5.64	12.91
				Found	69.55	4.92		5.75	12.95
VIIb	83	272–273° dec. (tetrahydrofuran)	$C_{29}H_{24}N_2O_6S_2$ (560.66)	Calc.	62.13	4.31		5.00	11.44
				Found	62.11	4.49		5.03	11.52
VIIc	66	>290° (acetone–acetonitrile)	$C_{25}H_{20}N_2O_4S_2$ (476.59)	Calc.	63.00	4.23		5.88	13.46
				Found	63.22	4.30		5.94	13.03

4-Dichloromethylbenzoyl Chloride (X)—A carbon tetrachloride solution of 4-methylbenzoyl chloride was heated under reflux and chlorinated for 6 hr in the presence of catalytic amounts of benzoyl peroxide to give X (86%), $bp_{0.12-0.2}$ 88–93°, mp 43–59°; recrystallized from carbon tetrachloride, mp 45–47° [lit. (18) bp_{745} 285–286°, mp 44–45°].

4-Trichloromethylbenzoyl Chloride (XI)—A mixture of 1,4-bis(trichloromethyl)benzene (15.7 g, 50 mmoles), 1,3-benzenedicarboxylic acid (4.15 g, 25 mmoles), and zinc chloride (~200 mg) was protected from moisture. The mixture was heated at 185° for 4.5 hr until 95% of the 5% aqueous sodium hydroxide (40 ml, 50 mmoles) connected to the reaction flask was neutralized by the hydrogen chloride formed. The dark liquid reaction mixture was distilled under reduced pressure to give 14.2 g of a clear liquid, $bp_{0.4-0.45}$ 93–100°. This mixture of XI and 1,3-benzenedicarbonyl chloride was redistilled under reduced pressure on a polytef spinning band column and gave 1,3-benzenedicarbonyl chloride as the lower boiling fraction and 7.2 g (56%) of XI, mp 27.5–28.5°, $bp_{0.2-0.15}$ 88–91°; index of refraction, n_D^{25} = 1.5822, [lit. (18) bp_{756} 296°].

4-Trichloromethyl Benzaldehyde (27)—A stirred solution of XI (12.9 g, 50 mmoles) in 75 ml of dry tetrahydrofuran was cooled to −70°. A solution of lithium tri-*tert*-butoxyaluminum hydride (15.3 g, 60 mmoles) in 80 ml of dry tetrahydrofuran was added over 1.5 hr through a pressure-equalizing dropping funnel fitted with a polyethylene jacket filled with 2-ethoxyethanol and carbon dioxide. The reaction mixture was kept at −65° for 1 hr after all the reducing agent had been added, and for 15 min after ethanol (2 ml) had been added. The solution was poured onto a vigorously stirred mixture of 300 g of ice, 100 ml of 5% aqueous hydrochloric acid, and 100 ml of methylene chloride. The aqueous phase was extracted with another 100 ml of methylene chloride and the combined methylene chloride extracts were washed with 5% aqueous hydrochloric acid, aqueous sodium bicarbonate, and water, and were dried over magnesium sulfate. The residue, after filtration and removal of the solvent gave 11.1 g (99%) of 4-trichloromethyl benzaldehyde; IR (film): 1710 cm^{-1}.

An attempt to prepare 4-trichloromethyl benzaldehyde from VI*f* and Raney nickel (28) gave a mixture of VI*f* and 4-trichloromethyl benzaldehyde.

Peracetic Acid in Methylene Chloride—Solutions were prepared by extraction of 40% peracetic acid in acetic acid with four volumes of methylene chloride. The aqueous phase was removed and the organic phase was dried over magnesium sulfate. The strength of the peracid solution was determined by titration with 0.1 *M* sodium thiosulfate (29).

Thioacetals—*Bis(4-acetamidothiophenyl)phenylmethane* (*Ia*)—Triethylamine (12.1 g, 120 mmoles) was added to a solution of 4-acetamidothiophenol (20 g, 120 mmoles) and benzal chloride (9.65 g, 60 mmoles) in 120 ml of dry benzene. A second layer formed, and the two-phase solution was heated under reflux for 55 hr. The lower phase crystallized slowly. The crystalline material was filtered after cooling, stirred with water, and was recrystallized three times from ethanol to give I*a*; IR (mineral oil) 3300 and 1660 cm^{-1}.

Bis(4-aminothiophenyl)phenylmethane Dihydrochloride (*Ib*)—This was obtained by acid hydrolysis of I*a* in boiling methanol and hydrochloric acid.

Bis(thiophenyl)-4-trichloromethylphenyl Methane (*Ic*)—A solution of *p*-toluenesulfonic acid (~100 mg) in 80 ml of benzene was dried by heating to reflux under a Dean-Stark trap. The solution was cooled, the trap was drained, and 4-trichloromethyl benzaldehyde (50 mmoles, crude) was transferred into the reaction flask. Thiophenol (11 g, 100 mmoles) was added, and the reaction mixture was heated to reflux under a Dean-Stark trap for 3 hr. Approximately 500 mg (55.5%) of water was formed. The benzene solution was cooled and was extracted with two 50-ml portions of 2% aqueous sodium hydroxide, and two 50-ml portions of water and dried over magnesium sulfate. Compound I*c* was obtained from the benzene extract.

Bis(4-acetamidothiophenyl)-4-trichloromethylphenyl Methane (*Id*)—4-Acetamidothiophenol and 4-trichloromethyl benzaldehyde were used in the same procedure as described for I*c* except that chloroform was used as a solvent. Compound I*d* was recrystallized from acetonitrile; IR (mineral oil): 3300–3250, and 1680 cm^{-1}.

Bis(4-aminothiophenyl)-4-carbomethoxyphenyl Methane Dihydrochloride (*Ie*)—Compound I*d* was treated with boiling methanol and hydrochloric acid for 1.5 hr; IR (mineral oil): 1700 cm^{-1}.

Bis(thiobenzyl)-4-trichloromethylphenyl Methane (*IIIa*)—The method described for I*c* was used to prepare III*a* from thiobenzyl alcohol and 4-trichloromethyl benzaldehyde.

9,9-Bis(4-acetamidothiophenyl)fluorene (*VIIa*)—A solution of

Table II—α-Chlorobenzyl Sulfones and Benzoyl Derivatives

Compound	Yield, %	Melting Point (Recrystallization Solvent)	Formula (mol. wt.)		Analysis, % C	H	Cl	N	S
IV*a*	84	211–212° (tetrahydrofuran–ether)	$C_{15}H_{14}ClNO_3S$ (323.42)	Calc.	55.71	4.36	10.96	4.33	9.91
				Found	55.54	4.21	11.20	4.38	9.80
IV*b*	84	277–279° dec. (2-butanone)	$C_{13}H_{12}ClNO_2S$ (281.78)	Calc.	55.42	4.29	12.58	4.97	11.38
				Found	55.67	4.34	12.80	5.00	11.20
IV*c*	67	175–176° (cyclohexane)	$C_{14}H_{10}Cl_4O_2S$ (384.14)	Calc.	43.77	2.62	36.93		8.35
				Found	43.91	2.65	37.10		8.59
VI*a*	89	196–197° (tetrahydrofuran)	$C_{14}H_{11}Cl_2NO$ (280.17)	Calc.	60.02	3.96	25.31	5.00	
				Found	59.64	4.02	25.65	5.22	
VI*b*	88	>280° (acetone)	$C_{15}H_{11}Cl_2NO_3$ (324.19)	Calc.	55.58	3.42	21.88	4.32	
				Found	54.87	3.52	23.41	4.22	
VI*c*	90	216–217° (ethanol)	$C_{16}H_{13}Cl_2NO_2S$ (354.29)	Calc.	54.24	3.70	20.02	3.96	9.05
				Found	54.07	3.43	20.17	4.07	8.74
VI*d*	91	188–189° (acetone)	$C_{14}H_{10}Cl_3NO$ (314.62)	Calc.	53.44	3.20	33.82	4.45	
				Found	54.02	3.35	33.96	4.46	
VI*e*	72	210–212° (methanol)	$C_{14}H_9Cl_3N_2O_3$ (359.62)	Calc.	46.76	2.52	29.58	7.79	
				Found	46.96	2.64	29.46	7.73	
VI*f*	86	109–110° (cyclohexane)	$C_{14}H_9Cl_3OS$ (331.67)	Calc.	50.70	2.74	32.07	9.67	
				Found	50.66	2.82	32.31	9.71	
VI*g*	92	239–240° dec. (tetrahydrofuran)	$C_{16}H_{12}Cl_3NO_2S$ (388.74)	Calc.	49.44	3.11	27.36	3.61	8.25
				Found	49.67	3.24	26.75	3.62	7.82

9,9-dichlorofluorene (2.35 g, 10 mmoles) and 4-acetamidothiophenol (3.34 g, 20 mmoles) in 50 ml of dry acetonitrile was heated under reflux for 18 hr. Compound VII*a* was obtained after removal of the solvent and recrystallization; IR (mineral oil): 3310–3250, and 1660 cm^{-1}.

β - Disulfones—*Bis(4-acetamidophenylsulfonyl)phenylmethane* (*II*a)—A 3.7 *M* solution of peracetic acid in methylene chloride (16.2 ml, 60 mmoles) was added to a suspension of I*a* (2.11 g, 5 mmoles) in 170 ml of dry methylene chloride over 15 min and the reaction mixture was stirred for 114 hr. The crystalline material removed by filtration gave II*a* after recrystallization; IR (mineral oil): 3350, 3310, 3280, 1670, 1315, and 1150 cm^{-1}.

Bis(4-aminophenylsulfonyl)phenylmethane (*II*b)—This compound was obtained by heating a suspension of II*a* in methanol and hydrochloric acid for 3 hr. When II*b* was recrystallized from methanol, the compound crystallized with solvent molecules, whereas using acetone as solvent would give pure II*b*; IR (mineral oil): 3460, 3360, 1320, and 1130 cm^{-1}.

Bis(phenylsulfonyl)-4-trichloromethylphenyl Methane (*II*c)—This compound was prepared by oxidation of I*c* by the method described for II*a*; IR (mineral oil): 1330, 1161, and 1150 cm^{-1}.

Bis(4-acetamidophenylsulfonyl)-4-trichloromethylphenyl Methane (*II*d)—This compound was prepared from I*d* by the method described for II*a*; IR (mineral oil): 3400, 1690, 1330, and 1150 cm^{-1}.

Bis(4-aminophenylsulfonyl)-4-trichloromethylphenyl Methane (*II*e)—Compound II*d* was acid hydrolyzed in hot ethanol and hydrochloric acid to give II*e* which was recrystallized; IR (mineral oil): 3460, 3390, 1310–1320, and 1135–1145 cm^{-1}.

4-Bis(phenylsulfonyl)methylbenzoic Acid (*III*f)—A 0.054 *M* aqueous solution of sodium hydroxide (74.5 ml, 4 mmoles) was added to a solution of II*c* (490 mg, 1 mmole) in 40 ml of tetrahydrofuran. The reaction mixture was stirred for 22 hr at ambient temperature. The tetrahydrofuran was removed under reduced pressure and the aqueous solution was extracted with two 30-ml portions of chloroform. The aqueous solution was acidified with 5% aqueous hydrochloric acid and extracted with two 30-ml portions of chloroform. The combined chloroform extracts were washed with water, dried over magnesium sulfate, and gave II*f* which was stirred with benzene; IR (mineral oil): 1690 cm^{-1}. Two recrystallizations of II*f* from acetonitrile gave a compound with mp 264–265°; IR (mineral oil): 3400 and 1730 cm^{-1}.

Anal.—Calc. for $C_{20}H_{16}O_7S_2$—C, 55.54; H, 3.73; S, 14.83. Found: C, 56.59, 56.35; H, 4.08, 3.87; S, 14.32.

Bis(benzylsulfonyl)-4-trichloromethylphenyl Methane (*III*b)—This was prepared from III*a* by the method described for II*a*; IR (mineral oil): 1320, 1150, and 1125 cm^{-1}.

4-Bis(benzylsulfonyl)methylbenzoic Acid (*III*c)—A 0.6 *M* aqueous solution of sodium hydroxide (20 ml, 12 mmoles) was added to a solution of III*b* (1.55 g, 3 mmoles) in 180 ml of tetrahydrofuran. The reaction mixture was stirred for 17 hr at ambient temperature. The organic solvent was removed under reduced pressure and the solution was acidified with 5% aqueous hydrochloric acid. Compound III*c* was extracted from the aqueous phase with chloroform and recrystallized.

Bis(phenylsulfonyl)-4-trichloromethylphenyl Chloromethane (*V*a)—A 5.25% aqueous solution of sodium hypochlorite (10 ml, 7 mmoles) was added to a solution of II*c* (490 mg, 1 mmole) in 25 ml of tetrahydrofuran. The solution was stirred at ambient temperature for 5 min and the organic layer yielded V*a* which was recrystallized; IR (mineral oil): 1350, 1330, 1320, and 1150 cm^{-1}.

Bis(4-acetamidophenylsulfonyl)-4-trichloromethylphenyl Chloromethane (*V*b)—This compound was prepared from II*d* and sodium hypochlorite by the method described for V*a*; IR (mineral oil): 3310, 3270, and 1670 cm^{-1}.

9,9-Bis(4-acetamidophenylsulfonyl)fluorene (*VII*b)—Oxidation of VII*a* by the method described for II*a* gave VII*b*; IR (mineral oil): 3310, 3280, 1670, 1350, and 1162 cm^{-1}. An attempt to prepare VII*b* from 9,9-dichlorofluorene and two molar equivalents of triethylammonium-4-acetamidophenyl sulfinate in acetonitrile yielded 90% of 9-fluorenone and 12% of IX*a* after heating the reaction mixture under reflux for 39 hr.

9,9-Bis(4-Aminophenylsulfonyl)fluorene (*VII*c)—This compound was prepared from VII*b* by acid hydrolysis in hot methanol and hydrochloric acid; IR (mineral oil): 3440, 3350, 1315, and 1150 cm^{-1}.

α-Chlorobenzyl Sulfones—*4-Acetamidophenyl-α-chlorobenzyl sulfone* (*IV*a)—A solution of triethylammonium-4-acetamidophenyl sulfinate (15 g, 50 mmoles), and benzal chloride (4.03 g, 25 mmoles) in 30 ml of *N,N*-dimethylformamide was heated at 100–105° for 46 hr. The reaction mixture was poured into 400 ml of water and the oily precipitate that formed hardened slowly. The IV*a* crystals were filtered after 24 hr, washed with water, and air dried; IR (mineral oil): 3360, 1700, 1325, and 1145 cm^{-1}.

4-Aminophenyl-α-chlorobenzyl Sulfone (*IV*b)—This compound was prepared from IV*a* by acid hydrolysis with 11.6 *M* aqueous hydrochloric acid at 100° for 17 hr; IR (mineral oil): 3400, 3450, 1295, and 1140 cm^{-1}.

4-Trichloromethylphenyl Phenylsulfonyl Chloromethane (*IV*c)—A solution of sulfuryl chloride (0.92 ml, 11.3 mmoles) in 60 ml of *n*-pentane was added to a boiling solution of Ic (3.44 g, 8.09 mmoles) in 100 ml of *n*-pentane during 1 hr (13). The reaction mixture was heated under reflux for an additional 2 hr. The *n*-pentane was removed under reduced pressure. The residue was dissolved in 200 ml of methylene chloride and a 1.59 *M* solution of peracetic acid in methylene chloride (61 ml, 97 mmoles) was added with stirring over 30 min. The reaction mixture was stirred at ambient temperature for 144 hr. The solution was concentrated under reduced pressure to 20 ml and white crystals precipitated upon addition of 5 ml of cyclohexane. The crystals were separated by filtration and washed with cyclohexane to give IV*c* which was recrystallized; IR (mineral oil): 1320 and 1150 cm^{-1}.

Derivatives of 4-Dichloromethylbenzoyl Chloride (X)—*4-Dichloromethylbenzanilide* (*VI*a)—This compound was prepared from a solution of X and aniline in benzene; IR (mineral oil): 3330 and 1640 cm^{-1}.

4'-Carboxy-4-dichloromethylbenzanilide (*VI*b)—This compound was prepared from a solution of X, 4-aminobenzoic acid, and pyridine in tetrahydrofuran; IR (mineral oil): 3310 and 1690–1640 cm^{-1}.

4-Acetamidophenyl-4-dichloromethyl Thiolbenzoate (*VI*c)—This compound was prepared from a solution of X, 4-acetamidothiophenol, and pyridine in tetrahydrofuran, IR (mineral oil): 3300 and 1660 cm^{-1}.

Derivatives of 4-Trichloromethylbenzoyl Chloride (XI)—*4-Trichloromethylbenzanilide* (*VI*d)—A solution of XI and aniline in tetrahydrofuran gave VI*d*; IR (mineral oil): 3310 and 1650 cm^{-1}.

4'-Nitro-4-trichloromethylbenzanilide (*VI*e)—A solution of XI, 4-nitroaniline, and triethylamine in acetonitrile gave VI*e*; IR (mineral oil): 3390 and 1670 cm^{-1}.

S-(Phenyl)-4-trichloromethyl Thiolbenzoate (*VI*f)—A solution of XI, thiophenol, and triethylamine in tetrahydrofuran gave VI*f*; IR (mineral oil): 1660 cm^{-1}.

S-(4-Acetamidophenyl)-4-trichloromethyl Thiolbenzoate (*VI*g)—A solution of XI, 4-acetamidothiophenol, and triethylamine in tetrahydrofuran gave VI*g*; IR (mineral oil): 3250 and 1660 cm^{-1}.

α-Disulfones and Thiolsulfonates—*Bis(4-acetylaminophenyl Sulfone)* (*VIII*a)—This was prepared (30) from 4-acetamidophenyl sulfinic acid and potassium permanganate, mp 245° [lit. (30) mp 245–250° dec.].

Bis(4-aminophenyl Sulfone) (*VIII*b)—Acid hydrolysis of VIII*a* in hydrochloric acid, methanol, and *N*-methyl-2-pyrrolidone at 100° for 2 hr gave VII*b*. Compound VIII*b* was recrystallized from a mixture of *N*-methyl-2-pyrrolidone and water, mp 215° dec. (31); IR (mineral oil): 3490, 3400, 1320, and 1125 cm^{-1}.

Anal.—Calc. for $C_{12}H_{12}N_2O_4S_2$; C, 46.14; H, 3.88; N, 8.97; S, 20.53. Found: C, 48.87; H, 4.10; N, 8.89; S, 20.39.

4'-Acetamidophenyl-4-acetamidobenzene Thiolsulfonate (*IX*a)—Compound I*a* (6.35 g, 15 mmoles) was suspended in 55 ml of acetic acid, and 30% hydrogen peroxide (8.55 g, 75 mmoles) was added during 30 min. The temperature of the reaction mixture was kept below 35° with occasional ice cooling during the addition of hydrogen peroxide. Stirring was continued for 37 hr. The suspension was poured into 450 ml of water and the undissolved material was filtered, and washed with water giving 4.34 g (81.5%) of IX*a*, mp 219–221° dec. Recrystallization from a mixture of *N,N*-dimethylformamide and water gave 3.22 g (59%) of IX*a*, mp 223–224° dec. [lit. (30) mp 236–237° dec.].

4'-Aminophenyl-4-aminobenzene Thiolsulfonate (*IX*b)—This compound was prepared by acid hydrolysis of IX*a* in hydrochloric acid and methanol, mp 185–186° dec. [lit. (30) mp 183°].

REFERENCES

(1) C. S. Genther and C. C. Smith, *J. Med. Chem.*, **20,** 237 (1977).

(2) P. E. Thompson and L. M. Werbel, in "Medicinal Chemistry," vol. 12, G. deStevens, Ed., Academic, New York, N.Y. 1972, pp. 314, 315.

(3) D. F. Clyde, *J. Trop. Med. Hyg.*, **72,** 81 (1969).

(4) W. Tagaki, in "Organic Chemistry of Sulfur," S. Oae, Ed., Plenum, New York, N.Y., 1977, p. 244.

(5) H. Alper and G. Wall, *J. Chem. Soc. Chem. Commun.*, **1976,** 263.

(6) A. W. Herriott, *Synthesis*, 1975, 447.

(7) R. Kuhn and F. A. Neugebauer, *Chem. Ber.*, **94,** 2629 (1961).

(8) R. Kuhn, W. Baschang-Bister, and W. Dafeldecker, *Ann.*, **641,** 160 (1961).

(9) G. E. Veenstra and B. Zwanenburg, *Tetrahedron*, **34,** 1585 (1978).

(10) J. L. Kice and K. W. Bowers, *J. Am. Chem. Soc.*, **84,** 605 (1962).

(11) J. L. Kice, G. Guaraldi, and C. G. Venier, *J. Org. Chem.*, **31,** 3561 (1966).

(12) D. K. Jung, T. P. Forrest, A. R. Manzer, and M. L. Gilroy, *J. Pharm. Sci.*, **66,** 1009 (1977).

(13) F. G. Bordwell and B. M. Pitt, *J. Am. Chem. Soc.*, **77,** 572 (1955).

(14) M. Hojo and R. Masuda, *Synthesis*, **1976,** 678.

(15) D. D. Wheeler, D. C. Young, and D. S. Erley, *J. Org. Chem.*, **22,** 547 (1957).

(16) A. E. Kretov and A. D. Syrovatko, *J. Gen. Chem. USSR*, **30,** 2993 (1960); through *Chem. Abstr.*, **55,** 16455d (1961).

(17) D. H. Hey and J. Peters, *J. Chem. Soc.*, **1960,** 79.

(18) W. Davies and W. Perkin, *ibid.*, **121,** 2202 (1922).

(19) N. K. Beresneva, E. N. Barantsevich, T. S. Saburova, and L. S. Bresler, *J. Appl. Chem. USSR*, **50,** 601 (1977); through *Chem. Abstr.*, **87,** 134337v (1977).

(20) B. F. Malichenko, *ibid.*, **40,** 1330 (1967); through *Chem. Abstr.*, **68,** 12648j (1968).

(21) I. N. Uspenskaya, G. V. Motsarev, and V. M. Korosteleva, *Sov. Chem. Ind.*, **6:2,** 92 (1974); through *Chem. Abstr.*, **80,** 120468g (1974).

(22) C. S. Rondestvedt, Jr., *J. Org. Chem.*, **41,** 3574 (1976).

(23) T. Nakano, K. Ohkawa, H. Matsumoto, and Y. Nagai, *J. Chem. Soc. Chem. Commun.*, **1977,** 808.

(24) F. Englaender, H. Fünten, P. Riegger, K.-D. Steffen, G. Weisgerber, and G. Zoche, *Chem. Zgt.*, **103,** 9 (1979).

(25) E. T. McBee and T. Hodgins, *US Gov. Res. Dev. Rep.*, Inform. AD 1969 AD-688174.

(26) G. T. Morgan and E. A. Coulson, *J. Chem Soc.*, **1929,** 2203.

(27) H. C. Brown and R. F. Farlin, *J. Am. Chem. Soc.*, **80,** 5372 (1958).

(28) G. B. Spero, A. V. McIntosh, and R. H. Levin, *ibid.*, **70,** 1907 (1948).

(29) N. P. Neureiter, *J. Org. Chem.*, **30,** 1313 (1965).

(30) R. Child and S. Smiles, *J. Chem. Soc.*, **1926,** 2699.

(31) E. Riez, O. I. Bayo, and W. Wolf, *Conger. Int. Biochim., Résumés Commun.*, *2*, 1952, p. 449; through *Chem. Abstr.*, **48,** 8874h (1954).

ACKNOWLEDGMENTS

Supported by Grant DA-MD-49-193-66-G9214 from the US Army Medical Research & Development Command, Washington, DC.

GLC Analysis of Trifluoperazine in Human Plasma

J. I. JAVAID *x, H. DEKIRMENJIAN ‡, and J. M. DAVIS *

Received March 6, 1981, from the **Illinois State Psychiatric Institute, Chicago, IL 60612*, and the ‡*National Psychopharmacology Laboratory, Knoxville, TN 37923.* Accepted for publication May 21, 1981.

Abstract □ This report describes a sensitive gas chromatographic procedure for the measurement of trifluoperazine in human plasma. Trifluoperazine was extracted into heptane–2-propanol by a two-step procedure and analyzed directly without derivatization. Prochlorperazine was employed as an internal standard because its structural and extraction characteristics were similar to trifluoperazine. The use of a nitrogen detection system reduced the number of interfering peaks. The within-day coefficient of variation in the method, over a 0.2–20-ng/ml concentration range was 9.4%.

Keyphrases □ Trifluoperazine—gas chromatographic measurement in human plasma □ Gas chromatography—measurement of trifluoperazine in human plasma □ Tranquilizers—trifluoperazine, gas chromatographic measurement in human plasma

The relationship between plasma concentrations of various psychoactive drugs and their clinical effects was recently discussed (1, 2). It was shown that drug concentrations can vary widely among patients receiving identical doses (3–6). Based on such interindividual variations in plasma levels of psychoactive drugs, it was suggested that

0022-3549/82/0100-0063$01.00/0

Derivatives of 4-Trichloromethylbenzoyl Chloride (XI)—*4-Trichloromethylbenzanilide* (*VI*d)—A solution of XI and aniline in tetrahydrofuran gave VI*d*; IR (mineral oil): 3310 and 1650 cm^{-1}.

4'-Nitro-4-trichloromethylbenzanilide (*VI*e)—A solution of XI, 4-nitroaniline, and triethylamine in acetonitrile gave VI*e*; IR (mineral oil): 3390 and 1670 cm^{-1}.

S-(Phenyl)-4-trichloromethyl Thiolbenzoate (*VI*f)—A solution of XI, thiophenol, and triethylamine in tetrahydrofuran gave VI*f*; IR (mineral oil): 1660 cm^{-1}.

S-(4-Acetamidophenyl)-4-trichloromethyl Thiolbenzoate (*VI*g)—A solution of XI, 4-acetamidothiophenol, and triethylamine in tetrahydrofuran gave VI*g*; IR (mineral oil): 3250 and 1660 cm^{-1}.

α-Disulfones and Thiolsulfonates—*Bis(4-acetylaminophenyl Sulfone)* (*VIII*a)—This was prepared (30) from 4-acetamidophenyl sulfinic acid and potassium permanganate, mp 245° [lit. (30) mp 245–250° dec.].

Bis(4-aminophenyl Sulfone) (*VIII*b)—Acid hydrolysis of VIII*a* in hydrochloric acid, methanol, and *N*-methyl-2-pyrrolidone at 100° for 2 hr gave VII*b*. Compound VIII*b* was recrystallized from a mixture of *N*-methyl-2-pyrrolidone and water, mp 215° dec. (31); IR (mineral oil): 3490, 3400, 1320, and 1125 cm^{-1}.

Anal.—Calc. for $C_{12}H_{12}N_2O_4S_2$; C, 46.14; H, 3.88; N, 8.97; S, 20.53. Found: C, 48.87; H, 4.10; N, 8.89; S, 20.39.

4'-Acetamidophenyl-4-acetamidobenzene Thiolsulfonate (*IX*a)—Compound I*a* (6.35 g, 15 mmoles) was suspended in 55 ml of acetic acid, and 30% hydrogen peroxide (8.55 g, 75 mmoles) was added during 30 min. The temperature of the reaction mixture was kept below 35° with occasional ice cooling during the addition of hydrogen peroxide. Stirring was continued for 37 hr. The suspension was poured into 450 ml of water and the undissolved material was filtered, and washed with water giving 4.34 g (81.5%) of IX*a*, mp 219–221° dec. Recrystallization from a mixture of *N,N*-dimethylformamide and water gave 3.22 g (59%) of IX*a*, mp 223–224° dec. [lit. (30) mp 236–237° dec.].

4'-Aminophenyl-4-aminobenzene Thiolsulfonate (*IX*b)—This compound was prepared by acid hydrolysis of IX*a* in hydrochloric acid and methanol, mp 185–186° dec. [lit. (30) mp 183°].

REFERENCES

(1) C. S. Genther and C. C. Smith, *J. Med. Chem.*, **20,** 237 (1977).

(2) P. E. Thompson and L. M. Werbel, in "Medicinal Chemistry," vol. 12, G. deStevens, Ed., Academic, New York, N.Y. 1972, pp. 314, 315.

(3) D. F. Clyde, *J. Trop. Med. Hyg.*, **72,** 81 (1969).

(4) W. Tagaki, in "Organic Chemistry of Sulfur," S. Oae, Ed., Plenum, New York, N.Y., 1977, p. 244.

(5) H. Alper and G. Wall, *J. Chem. Soc. Chem. Commun.*, **1976,** 263.

(6) A. W. Herriott, *Synthesis*, 1975, 447.

(7) R. Kuhn and F. A. Neugebauer, *Chem. Ber.*, **94,** 2629 (1961).

(8) R. Kuhn, W. Baschang-Bister, and W. Dafeldecker, *Ann.*, **641,** 160 (1961).

(9) G. E. Veenstra and B. Zwanenburg, *Tetrahedron*, **34,** 1585 (1978).

(10) J. L. Kice and K. W. Bowers, *J. Am. Chem. Soc.*, **84,** 605 (1962).

(11) J. L. Kice, G. Guaraldi, and C. G. Venier, *J. Org. Chem.*, **31,** 3561 (1966).

(12) D. K. Jung, T. P. Forrest, A. R. Manzer, and M. L. Gilroy, *J. Pharm. Sci.*, **66,** 1009 (1977).

(13) F. G. Bordwell and B. M. Pitt, *J. Am. Chem. Soc.*, **77,** 572 (1955).

(14) M. Hojo and R. Masuda, *Synthesis*, **1976,** 678.

(15) D. D. Wheeler, D. C. Young, and D. S. Erley, *J. Org. Chem.*, **22,** 547 (1957).

(16) A. E. Kretov and A. D. Syrovatko, *J. Gen. Chem. USSR*, **30,** 2993 (1960); through *Chem. Abstr.*, **55,** 16455d (1961).

(17) D. H. Hey and J. Peters, *J. Chem. Soc.*, **1960,** 79.

(18) W. Davies and W. Perkin, *ibid.*, **121,** 2202 (1922).

(19) N. K. Beresneva, E. N. Barantsevich, T. S. Saburova, and L. S. Bresler, *J. Appl. Chem. USSR*, **50,** 601 (1977); through *Chem. Abstr.*, **87,** 134337v (1977).

(20) B. F. Malichenko, *ibid.*, **40,** 1330 (1967); through *Chem. Abstr.*, **68,** 12648j (1968).

(21) I. N. Uspenskaya, G. V. Motsarev, and V. M. Korosteleva, *Sov. Chem. Ind.*, **6:2,** 92 (1974); through *Chem. Abstr.*, **80,** 120468g (1974).

(22) C. S. Rondestvedt, Jr., *J. Org. Chem.*, **41,** 3574 (1976).

(23) T. Nakano, K. Ohkawa, H. Matsumoto, and Y. Nagai, *J. Chem. Soc. Chem. Commun.*, **1977,** 808.

(24) F. Englaender, H. Fünten, P. Riegger, K.-D. Steffen, G. Weisgerber, and G. Zoche, *Chem. Zgt.*, **103,** 9 (1979).

(25) E. T. McBee and T. Hodgins, *US Gov. Res. Dev. Rep.*, Inform. AD 1969 AD-688174.

(26) G. T. Morgan and E. A. Coulson, *J. Chem Soc.*, **1929,** 2203.

(27) H. C. Brown and R. F. Farlin, *J. Am. Chem. Soc.*, **80,** 5372 (1958).

(28) G. B. Spero, A. V. McIntosh, and R. H. Levin, *ibid.*, **70,** 1907 (1948).

(29) N. P. Neureiter, *J. Org. Chem.*, **30,** 1313 (1965).

(30) R. Child and S. Smiles, *J. Chem. Soc.*, **1926,** 2699.

(31) E. Riez, O. I. Bayo, and W. Wolf, *Conger. Int. Biochim., Résumés Commun.*, *2*, 1952, p. 449; through *Chem. Abstr.*, **48,** 8874h (1954).

ACKNOWLEDGMENTS

Supported by Grant DA-MD-49-193-66-G9214 from the US Army Medical Research & Development Command, Washington, DC.

GLC Analysis of Trifluoperazine in Human Plasma

J. I. JAVAID *x, H. DEKIRMENJIAN ‡, and J. M. DAVIS *

Received March 6, 1981, from the **Illinois State Psychiatric Institute, Chicago, IL 60612*, and the ‡*National Psychopharmacology Laboratory, Knoxville, TN 37923.* Accepted for publication May 21, 1981.

Abstract □ This report describes a sensitive gas chromatographic procedure for the measurement of trifluoperazine in human plasma. Trifluoperazine was extracted into heptane–2-propanol by a two-step procedure and analyzed directly without derivatization. Prochlorperazine was employed as an internal standard because its structural and extraction characteristics were similar to trifluoperazine. The use of a nitrogen detection system reduced the number of interfering peaks. The within-day coefficient of variation in the method, over a 0.2–20-ng/ml concentration range was 9.4%.

Keyphrases □ Trifluoperazine—gas chromatographic measurement in human plasma □ Gas chromatography—measurement of trifluoperazine in human plasma □ Tranquilizers—trifluoperazine, gas chromatographic measurement in human plasma

The relationship between plasma concentrations of various psychoactive drugs and their clinical effects was recently discussed (1, 2). It was shown that drug concentrations can vary widely among patients receiving identical doses (3–6). Based on such interindividual variations in plasma levels of psychoactive drugs, it was suggested that

0022-3549/82/0100-0063$01.00/0

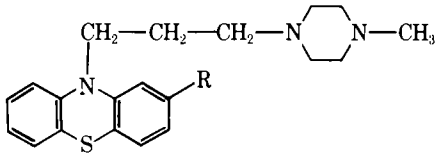

I: R = CF_3
II: R = Cl

an effective treatment regimen for the individual patient may be approached by monitoring the blood levels of the drug and relating them to clinical outcome. Therefore, specific and sensitive methods for measuring neuroleptic drug levels in schizophrenic patients (7, 8) are needed.

Trifluoperazine (I), a phenothiazine neuroleptic, is commonly used for the treatment of schizophrenia. Although a TLC method for the measurement of trifluoperazine and its metabolites in rat tissues was reported (9), the method was not sensitive enough to measure the low therapeutic levels in humans. The present report describes a specific and sensitive method for measuring trifluoperazine in biological fluids. Prochlorperazine (II) was the internal standard. The method was applied to measure plasma trifluoperazine concentrations in schizophrenic patients treated with the drug.

EXPERIMENTAL

Materials—Trifluoperazine hydrochloride[1] and prochlorperazine maleate[1] were used. Heptane[2] and 2-propanol[2] were glass distilled. All other reagents were analytical grade.

The gas chromatograph[3] was equipped with a nitrogen–phosphorus detector; 3% OV-101 on 80–100-mesh support[4] was used as packing material. The highest purity[5] air, helium, and hydrogen available were used.

Procedures—Blood was drawn into tubes[6] containing ethylenediaminetetraacetate (1 mg/ml of blood) from patients receiving trifluoperazine. Rubber[6] stoppers were avoided since it was reported (10) that contact with the stopper may alter the distribution of drugs between plasma and red blood cells. The plasma and red blood cells were separated by centrifugation and stored at −16° until analysis. For determining recoveries and preparing standard curves, outdated plasma was used since there were no differences in recoveries with fresh and outdated blood.

Extraction from Plasma—Five-milliliter plasma samples, (unknown, drug-free, and plasma standards containing known amounts of the drug) were transferred to 15-ml test tubes, and prochlorperazine (as the internal standard) was added to unknown samples and plasma standards. To each tube, 1.0 ml of 2 *N* NaOH was added, and the mixture extracted with 5 ml of heptane–2-propanol (9:1, v/v). After shaking for 20 min, the tubes were centrifuged to separate the organic and aqueous layers.

The upper organic layer was transferred to another 15-ml tube containing 1 ml of 0.1 *N* HCl. The mixture was shaken for 15 min, and the organic layer was discarded by aspiration after centrifugation. The acid layer was transferred to a 5-ml centrifuge tube containing 0.1 ml of 5 *N* NaOH, and the mixture was extracted with 0.3 ml of heptane–2-propanol after shaking for 5 min and centrifuging as described. The organic layer (3–5 μl) was then injected into the gas chromatograph.

Chromatographic Conditions—The instrument was set according to the instruction manual provided by the manufacturer, except that the off-set current applied to the detector was increased until an optimum signal-to-noise ratio was obtained to maximize sensitivity. Generally, the detector voltage was set to give a 20% deflection of the recorder chart at the range setting of 1 and an attenuation of 32 at a 190° oven temperature.

When a 0.9 m glass column (2-mm i.d.), packed with 3% OV-101 was used, the chromatographic conditions were as follows: isothermal column temperature, 250°; injection port temperature, 300°; detector temperature, 300°; carrier gas (helium) flow, 30 ml/min; air flow, 50 ml/min; hydrogen flow, 3 ml/min; range, 1; and attenuation, 2–32.

Calculations—A standard curve was prepared with every analysis by plotting the ratio of peak heights for trifluoperazine and prochlorperazine against various concentrations of trifluoperazine added to the drug-free plasma samples. The inverse of the slope of the line thus obtained was used to calculate the trifluoperazine concentration in unknown samples.

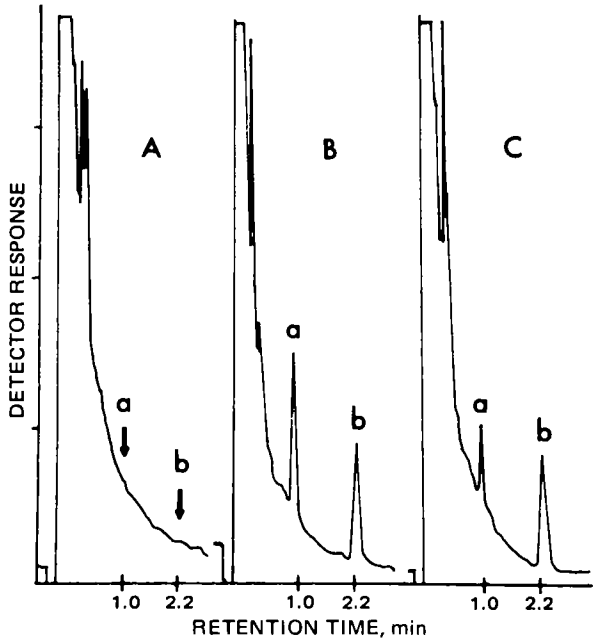

Figure 1—*Typical chromatogram of drug-free plasma carried through the procedure (A), drug-free plasma to which trifluoperazine (a) and prochlorperazine (b) were added (B), and plasma from a patient receiving trifluoperazine (C). Prochlorperazine was added as an internal standard.*

RESULTS

Figure 1 shows a typical chromatogram obtained for the analysis of trifluoperazine with the internal standard, using a 0.9 m column packed with 3% OV-101 at 250°. There were no interfering peaks at the retention times for trifluoperazine and prochlorperazine (Fig 1A). The peaks for trifluoperazine and prochlorperazine were symmetrical, and relationship was linear between the peak height and concentration of each drug injected into the chromatograph. There was also a linear relationship when the ratios of the peak height of trifluoperazine to the peak height of prochlorperazine were plotted against the various concentrations of trifluoperazine ($y = 0.055 + 0.126x$, $r = 0.996$).

Recovery of Extraction Procedure—The recoveries of trifluoperazine and prochlorperazine were determined by adding varying concentrations of the standard solution to drug-free plasma. These samples were then extracted and analyzed by the described procedure. The recoveries were calculated by comparing the extracted samples with the standard curves obtained by directly injecting the methanolic solutions of the drugs without extraction.

Trifluoperazine recovery from plasma averaged 79% and was constant over a wide concentration range (0.2–100 ng/ml). The average recovery of prochlorperazine from plasma was 72%.

Table I—Accuracy of Trifluoperazine Determination in Human Plasma [a]

Added, ng/ml	Determined, ng/ml	*SD*	Number of Determinations
20.0	20.77	1.1	9
2.0	2.17	0.13	10
0.2	0.23	0.02	10
0.1	0.16	0.07	6

[a] Different concentrations of trifluoperazine were added to drug-free plasma, and samples were then analyzed by the described procedure.

[1] Smith Kline and French Laboratories, Philadelphia, Pa.
[2] Burdick & Jackson Laboratories, Muskegon, Mich.
[3] Model 5730-A, Hewlett-Packard, Avondale, Pa.
[4] Supelco, Bellefonte, Pa.
[5] Liquid Carbonic, LaGrange, Ill.
[6] Vacutainer, Becton-Dickinson, Rutherford, N.J.

Table II—Reproducibility of Trifluoperazine Determination over Time [a]

Amount Added, ng/ml	Amount Determined over Time, ng/ml: 1 Day	3 Days	4 Days	6 Days	8 Days	33 Days	Average ± *SD*
1.0	0.93	1.03	0.83	0.83	0.82	1.1	0.92 ± 0.11
2.0	1.9	1.70	1.70	1.60	2.0	2.4	1.88 ± 0.27
4.0	4.3	3.7	3.6	4.4	3.3	3.8	3.85 ± 0.39
8.0	8.0	7.7	7.6	7.5	7.7	7.8	7.72 ± 0.16

[a] Different concentration of trifluoperazine were added to drug-free plasma and kept frozen in aliquots. Each aliquot was thawed on the day of analysis.

Accuracy and Reproducibility—The accuracy of the method was determined by adding different concentrations of trifluoperazine and analyzing six to 10 samples for each concentration according to the described procedure. These results are summarized in Table I. The within-day coefficient of variation over the concentration range of 0.2–20 ng/ml plasma was calculated as 6.7%.

To determine the day-to-day reproducibility, four different trifluoperazine concentrations were added to drug-free plasma and the samples were analyzed over the next several days. The average day-to-day coefficient of variation over the 1.0–8.0-ng/ml concentration range was calculated as 9.4%. These results (Table II) also indicate that the trifluoperazine in plasma samples was stable for at least 1 month when kept frozen.

Specificity and Sensitivity—Evidence for the specificity of the method was provided by characteristic retention times of trifluoperazine and prochlorperazine and the lack of interfering peaks in drug-free plasma when the samples were analyzed by the described procedure. Ten commonly used psychoactive drugs and three metabolites of trifluoperazine were also screened for interference in the assay by directly injecting their methanolic solutions under the described chromatographic conditions. The retention times of these drugs relative to trifluoperazine were as follows: butaperazine, 5.92; clomipramine, 0.50; desipramine, 0.33; desmethyltrifluoperazine, 0.83; diazepam, 0.58; fluphenazine, 2.50; haloperidol, 2.00; 7-hydroxytrifluoperazine, 2.42; imipramine, 0.25; mesoridazine, 5.83; piperacetazine, 10.00; prochlorperazine, 2.18; thioridazine, 2.75; 2-trifluomethylphenothiazine, 0.17; and trifluoperazine, 1.00. None of the drugs tested interfered with the assay of trifluoperazine or prochlorperazine.

Although 0.1 ng of trifluoperazine/ml could be measured by the described procedure, the coefficient of variation was too large (43.8%, Table I) for quantitative purposes. Hence, the actual sensitivity of the method to quantitate trifluoperazine in plasma was 0.2 ng/ml (coefficient of variation of 8.7%, Table I) when 5 ml of plasma sample was used.

Trifluoperazine Levels in Clinical Samples—The described method was used for measuring plasma concentrations of trifluoperazine in patients who received therapeutic doses for schizophrenia. The steady-state plasma levels in 21 patients receiving different doses of trifluoperazine are shown in Fig. 2. Although there were large interindividual differences in steady-state plasma concentrations in patients receiving identical doses of trifluoperazine, there was good correlation between drug concentation in plasma and dose administered ($r = 0.93$). However, some patients received other medication along with trifluoperazine. These data are given to show the applicability of the method in patients treated with trifluoperazine.

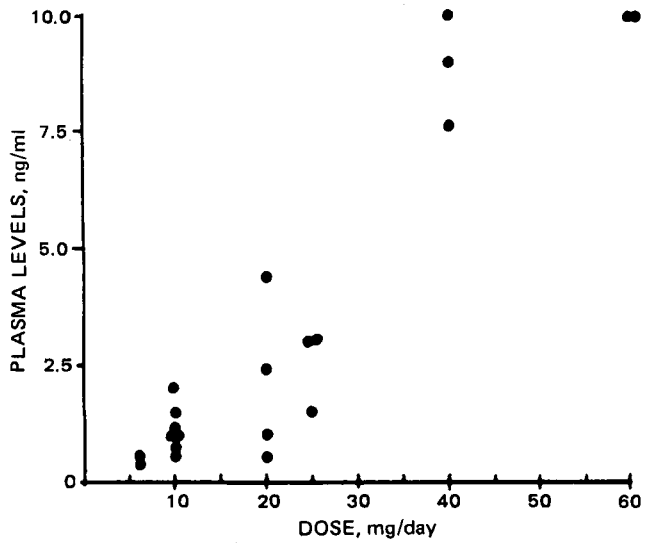

Figure 2—*Trifluoperazine concentrations in plasma from patients receiving different doses of the drug.*

DISCUSSION

The described procedure is sensitive enough to measure low therapeutic levels, is specific, and is reproducible for trifluoperazine. Detector response for trifluoperazine and prochlorperazine was linear over a wide concentration range, and retention times were similar.

In one experiment where trifluoperazine was added to drug-free plasma without any preservative and the sample was analyzed over the next 33 days, the sample was stable when kept frozen. However, during more than 1 year of analysis of plasma samples from patients, samples were found to be more prone to losses without any preservative.

Although there are no systematic studies on the stabilities of neuroleptics, it was reported (11) that amitriptyline hydrochloride in aqueous solutions is broken down by heavy metal contaminants. If this is also the case for neuroleptics, all the glassware should be acid washed and rinsed thoroughly with distilled water. This procedure minimizes occasional problems with the assay. Furthermore, 0.5 mg of sodium metabisulfite or ascorbic acid/ml of plasma should be added to samples to avoid loss by oxidation. In addition, all standard solutions should be stored in dark bottles or covered with aluminum foil. Although trifluoperazine standard solutions were stable for up to 3 weeks when kept at −16° in the dark, the prochlorperazine standard was stable for only 1 week.

The steady-state plasma concentrations of trifluoperazine showed interindividual variability in patients receiving identical doses. Such interindividual variabilities are characteristic of most of the drugs and represent the differences in absorption, distribution, metabolism, and excretion due to genetic, physiological, and environmental differences. Steady-state plasma concentrations were similar to those reported for another high potency neuroleptic, fluphenazine (12, 13), but were much lower than with chlorpromazine (14) or butaperazine (7). In one patient, the pharmacokinetics of trifluoperazine after a single dose were also studied using the described procedure. Highest concentrations were obtained in 4 hr after oral drug administration and then decreased over the next 24 hr.

Although radioreceptor assay was recently introduced (15) for measuring total neuroleptic concentrations, this assay did not differentiate between the parent compound and active metabolites. Furthermore, the lower limit of sensitivity of the radioreceptor assay for trifluoperazine is 2.2 ng/ml (15) because <200 μl of plasma or serum must be used in the assay system; at higher protein concentrations, the nonspecific inhibition in the binding system becomes significant. On the other hand, the lower limit of sensitivity of the described method is 0.2 ng/ml, because 5 ml of the plasma can be used for extraction.

GLC with nitrogen detection is becoming increasingly popular for measuring low drug levels in therapeutic conditions. The nitrogen detector is 10–100-fold more sensitive than the conventional flame-ionization detector and is as sensitive as the electron-capture detector for nitrogen-containing compounds. The selectivity of the nitrogen detector reduces the number of interfering peaks and decreases the time for sample analysis. The method described here for trifluoperazine determination does not require any derivatization and takes only 3 min for each sample analysis after extraction.

REFERENCES

(1) J. M. Davis, S. Ericksen, and H. Dekirmenjian, in "Psychopharmacology: A Generation of Progress," M. A. Lipton, A. DiMascio, and K. F. Killam, Eds., Raven, New York, N.Y., 1978, pp. 905–915.

(2) A. H. Glassman and J. M. Perel, *ibid.*, pp. 917–922.

(3) W. Hammer and F. Sjoqvist, *Life Sci.*, **6**, 1895 (1967).

(4) B. Alexanderson, *Eur. J. Clin. Pharmacol.*, **4**, 82 (1972).
(5) A. Forsman, G. Folsch, M. Larsson, and R. Ohmann, *Curr Ther. Res.*, **21**, 606 (1977).
(6) D. L. Garver, H. Dekirmenjian, J. M. Davis, R. Casper, and S. Ericksen, *Am. J. Psychiatry*, **134**, 304 (1977).
(7) J. I. Javaid, H. Dekirmenjian, U. Liskevych, and J. M. Davis, *J. Chromatogr. Sci.*, **17**, 666 (1979).
(8) J. I. Javaid, H. Dekirmenjian, M. Dysken, and J. M. Davis, *Adv. Biochem. Psychopharmacol.* **24**, 585 (1980).
(9) U. Breyer and G. Schmalzing, *Drug Metab. Dispos.*, **5**, 97 (1977).
(10) E. Cochran, J. Carl, I. Hanin, S. Koslow, and E. Robins, *Commun. Psychopharmacol.*, **2**, 491 (1978).
(11) R. P. Enever, A. Li Wan Po, and E. Shotton, *J. Pharm Sci.*, **66**, 1087 (1977).
(12) M. Franklin, D. H. Wiles, and D. J. Harvey, *Clin. Chem.*, **24**, 41 (1978).
(13) J. I. Javaid, H. Dekirmenjian, U. Liskevych, R.-L. Lin, and J. M. Davis, *J. Chromatogr. Sci.*, in press.
(14) G. W. Christoph, D. E. Schmidt, J. M. Davis, and D. Janowsky, *Clin. Chim. Acta*, **38**, 265 (1972).
(15) I. Creese and S. H. Snyder, *Nature*, **270**, 180 (1977).

ACKNOWLEDGMENTS

The authors thank Smith Kline and French Laboratories for their generous gift of the drugs. The excellent technical assistance of Ms. J. Balcer and Ms. U. Liskevych is greatly appreciated.

Contribution of Lungs to Total Body Clearance: Linear and Nonlinear Effects

JERRY M. COLLINS ˣ and ROBERT L. DEDRICK

Received October 29, 1980, from the *Biomedical Engineering and Instrumentation Branch, Division of Research Services, National Institutes of Health, Bethesda, MD 20205.* Accepted for publication May 13, 1981.

Abstract □ The contribution of the lungs to the total body clearance of drugs is examined in a framework that emphasizes their anatomical position. For intravenous administration, the lung is the only organ other than blood that can account for a total body clearance in excess of the cardiac output. Systemic arterial drug concentration and tissue drug exposure are inversely proportional to total body clearance. Although the role of the lung has been overshadowed by that of the liver, several examples are presented to demonstrate that a relatively small amount of pulmonary activity can produce a large reduction in systemic arterial drug concentration. For oral administration, first-pass elimination by the liver and lungs in series results in a synergistic increase in total body clearance. Nonlinear effects caused by saturation of elimination pathways are also examined. Increased emphasis on experimental investigation of the pulmonary contribution is warranted, especially for drugs with high apparent clearance.

Keyphrases □ Lungs—role in total body clearance, linear and nonlinear effects □ Pharmacokinetics—role of lungs in total body clearance, linear and nonlinear effects □ Pulmonary metabolism—role in total body clearance, linear and nonlinear effects

Application of the techniques used to study hepatic drug metabolism to the lung has led to a growing literature on pulmonary metabolism. Although smaller in weight than the liver (600 *versus* 1500 g for humans), the processing of the entire cardiac output (*versus* 25% for the liver) places the lungs in a unique position for drug metabolism.

This report describes the contribution of the lungs to drug metabolism, including interaction with other drug-eliminating organs. Both saturating and nonsaturating conditions were examined.

BACKGROUND

Of the three types of clearance mechanisms (metabolism, excretion, and irreversible binding), this report concentrates on metabolic clearance. Transport, including excretion, of volatile substances is a primary function of the lungs; however, this topic was previously detailed (1). Uptake and/or binding of substances by the lung was documented by Junod (2). He suggested that the lungs can function as a capacitor that dampens out large variations in plasma concentration by rapid uptake and slow release processes. While such a role could have major importance for the pharmacodynamics of drug effect, reversible uptake or binding makes no net contribution to apparent clearance. Only irreversible binding decreases the total amount of drug delivered to the systemic circulation.

The demonstration of drug metabolism at the cellular (3) and subcellular level (4, 5) was a first step in the stimulation of more interest in pulmonary metabolism. Although some metabolic activity was shown in subcellular preparations from the lungs, recent work (6) raised the possibility that pulmonary activity has been substantially underestimated due to undetermined methodological factors. The isolated perfused lung preparation was shown to possess 10 times more drug clearance capability than was projected on the basis of experiments using subcellular preparations.

The isolated perfused lung has had a major role in demonstrating the importance of pulmonary metabolism. An earlier report (7) detailed the capability of this preparation to extract certain endogenous substances, especially the prostaglandins (8), serotonin (9), and other hormones. Metabolic clearance by the isolated perfused lung has now been demonstrated for many exogenous substances including drugs such as mescaline (10), isoproterenol hydrochloride (11), and the tetrahydrocannabinols (12) and chemicals such as *N*-methylaniline (13), aldrin (14), and trichloroethylene (15).

Direct comparisons of lung and liver elimination capacity were made by Roth and coworkers for three substances. In all cases, the effect of blood flow limitation increased the relative role of the lungs *versus* the liver when organ clearance was compared with organ enzyme capacity. Using literature values (16, 17) for benzpyrene in rats with induced enzymes, Roth and Wiersma (18) calculated nearly equal organ clearances for the liver and lungs, despite the fact that the liver contained 64 times more total enzyme capacity than the lungs. Similar calculations were reported (10) for data on mescaline metabolism in homogenates of rabbit lungs and liver. Approximately equal organ clearances were predicted, despite five times more enzyme capacity in the liver. For serotonin, Wiersma and Roth (6) found 17 times as much activity in the liver as in the lungs and predicted five times more clearance in the liver than the lungs. Their predictions for the perfused liver agreed well with their experimental results, but they underpredicted perfused lung clearance by a factor of 10. This discrepancy may be attributed to either suboptimal lung homogenate experiments or strong binding of serotonin by lung tissue.

The demonstration of *in vivo* pulmonary metabolism fully established the key role of the lungs in the overall process of drug elimination from the body. Two studies (19, 20) demonstrated a pulmonary extraction for phenol of ~60% in the rat by comparing the area under the plasma concentration–time curve following intravenous and intra-aortic administration.

0022-3549/82/0100-0066$01.00/0

(4) B. Alexanderson, *Eur. J. Clin. Pharmacol.*, **4**, 82 (1972).
(5) A. Forsman, G. Folsch, M. Larsson, and R. Ohmann, *Curr Ther. Res.*, **21**, 606 (1977).
(6) D. L. Garver, H. Dekirmenjian, J. M. Davis, R. Casper, and S. Ericksen, *Am. J. Psychiatry*, **134**, 304 (1977).
(7) J. I. Javaid, H. Dekirmenjian, U. Liskevych, and J. M. Davis, *J. Chromatogr. Sci.*, **17**, 666 (1979).
(8) J. I. Javaid, H. Dekirmenjian, M. Dysken, and J. M. Davis, *Adv. Biochem. Psychopharmacol.* **24**, 585 (1980).
(9) U. Breyer and G. Schmalzing, *Drug Metab. Dispos.*, **5**, 97 (1977).
(10) E. Cochran, J. Carl, I. Hanin, S. Koslow, and E. Robins, *Commun. Psychopharmacol.*, **2**, 491 (1978).
(11) R. P. Enever, A. Li Wan Po, and E. Shotton, *J. Pharm Sci.*, **66**, 1087 (1977).
(12) M. Franklin, D. H. Wiles, and D. J. Harvey, *Clin. Chem.*, **24**, 41 (1978).
(13) J. I. Javaid, H. Dekirmenjian, U. Liskevych, R.-L. Lin, and J. M. Davis, *J. Chromatogr. Sci.*, in press.
(14) G. W. Christoph, D. E. Schmidt, J. M. Davis, and D. Janowsky, *Clin. Chim. Acta*, **38**, 265 (1972).
(15) I. Creese and S. H. Snyder, *Nature*, **270**, 180 (1977).

ACKNOWLEDGMENTS

The authors thank Smith Kline and French Laboratories for their generous gift of the drugs. The excellent technical assistance of Ms. J. Balcer and Ms. U. Liskevych is greatly appreciated.

Contribution of Lungs to Total Body Clearance: Linear and Nonlinear Effects

JERRY M. COLLINS ˣ and ROBERT L. DEDRICK

Received October 29, 1980, from the *Biomedical Engineering and Instrumentation Branch, Division of Research Services, National Institutes of Health, Bethesda, MD 20205.* Accepted for publication May 13, 1981.

Abstract □ The contribution of the lungs to the total body clearance of drugs is examined in a framework that emphasizes their anatomical position. For intravenous administration, the lung is the only organ other than blood that can account for a total body clearance in excess of the cardiac output. Systemic arterial drug concentration and tissue drug exposure are inversely proportional to total body clearance. Although the role of the lung has been overshadowed by that of the liver, several examples are presented to demonstrate that a relatively small amount of pulmonary activity can produce a large reduction in systemic arterial drug concentration. For oral administration, first-pass elimination by the liver and lungs in series results in a synergistic increase in total body clearance. Nonlinear effects caused by saturation of elimination pathways are also examined. Increased emphasis on experimental investigation of the pulmonary contribution is warranted, especially for drugs with high apparent clearance.

Keyphrases □ Lungs—role in total body clearance, linear and nonlinear effects □ Pharmacokinetics—role of lungs in total body clearance, linear and nonlinear effects □ Pulmonary metabolism—role in total body clearance, linear and nonlinear effects

Application of the techniques used to study hepatic drug metabolism to the lung has led to a growing literature on pulmonary metabolism. Although smaller in weight than the liver (600 *versus* 1500 g for humans), the processing of the entire cardiac output (*versus* 25% for the liver) places the lungs in a unique position for drug metabolism.

This report describes the contribution of the lungs to drug metabolism, including interaction with other drug-eliminating organs. Both saturating and nonsaturating conditions were examined.

BACKGROUND

Of the three types of clearance mechanisms (metabolism, excretion, and irreversible binding), this report concentrates on metabolic clearance. Transport, including excretion, of volatile substances is a primary function of the lungs; however, this topic was previously detailed (1). Uptake and/or binding of substances by the lung was documented by Junod (2). He suggested that the lungs can function as a capacitor that dampens out large variations in plasma concentration by rapid uptake and slow release processes. While such a role could have major importance for the pharmacodynamics of drug effect, reversible uptake or binding makes no net contribution to apparent clearance. Only irreversible binding decreases the total amount of drug delivered to the systemic circulation.

The demonstration of drug metabolism at the cellular (3) and subcellular level (4, 5) was a first step in the stimulation of more interest in pulmonary metabolism. Although some metabolic activity was shown in subcellular preparations from the lungs, recent work (6) raised the possibility that pulmonary activity has been substantially underestimated due to undetermined methodological factors. The isolated perfused lung preparation was shown to possess 10 times more drug clearance capability than was projected on the basis of experiments using subcellular preparations.

The isolated perfused lung has had a major role in demonstrating the importance of pulmonary metabolism. An earlier report (7) detailed the capability of this preparation to extract certain endogenous substances, especially the prostaglandins (8), serotonin (9), and other hormones. Metabolic clearance by the isolated perfused lung has now been demonstrated for many exogenous substances including drugs such as mescaline (10), isoproterenol hydrochloride (11), and the tetrahydrocannabinols (12) and chemicals such as *N*-methylaniline (13), aldrin (14), and trichloroethylene (15).

Direct comparisons of lung and liver elimination capacity were made by Roth and coworkers for three substances. In all cases, the effect of blood flow limitation increased the relative role of the lungs *versus* the liver when organ clearance was compared with organ enzyme capacity. Using literature values (16, 17) for benzpyrene in rats with induced enzymes, Roth and Wiersma (18) calculated nearly equal organ clearances for the liver and lungs, despite the fact that the liver contained 64 times more total enzyme capacity than the lungs. Similar calculations were reported (10) for data on mescaline metabolism in homogenates of rabbit lungs and liver. Approximately equal organ clearances were predicted, despite five times more enzyme capacity in the liver. For serotonin, Wiersma and Roth (6) found 17 times as much activity in the liver as in the lungs and predicted five times more clearance in the liver than the lungs. Their predictions for the perfused liver agreed well with their experimental results, but they underpredicted perfused lung clearance by a factor of 10. This discrepancy may be attributed to either suboptimal lung homogenate experiments or strong binding of serotonin by lung tissue.

The demonstration of *in vivo* pulmonary metabolism fully established the key role of the lungs in the overall process of drug elimination from the body. Two studies (19, 20) demonstrated a pulmonary extraction for phenol of ~60% in the rat by comparing the area under the plasma concentration–time curve following intravenous and intra-aortic administration.

0022-3549/82/0100-0066$01.00/0

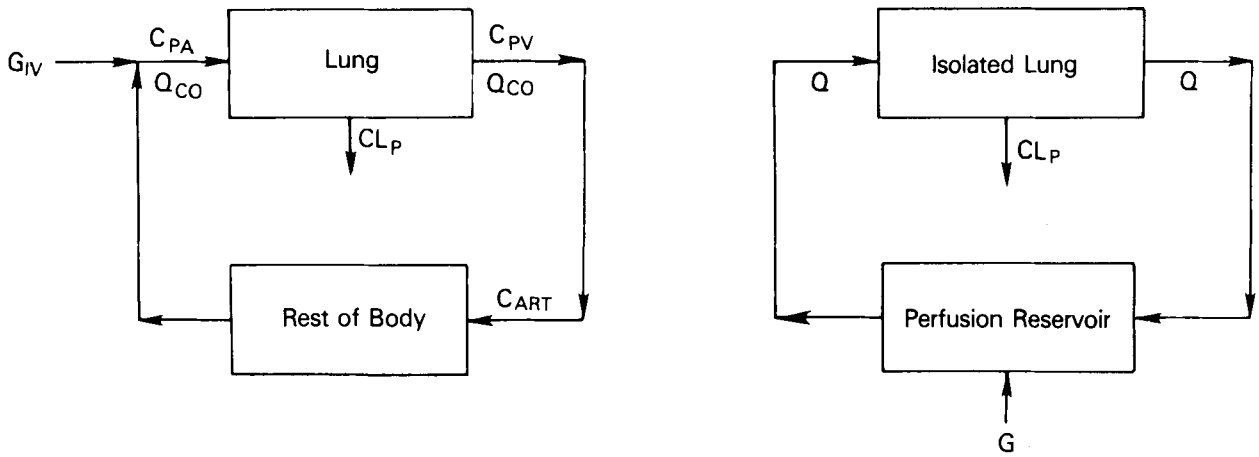

Scheme I—Pulmonary clearance in vivo *(left) and in isolated perfused lung (right).*

Pulmonary clearance should be examined for drugs that exhibit an apparent clearance in excess of liver blood flow. The lungs and blood are the only organs capable of generating an apparent clearance greater than the cardiac output. Elsewhere, a major role was suggested for pulmonary clearance of fluorouracil (21) and thymidine on the basis of high apparent clearance (5 and 25 liters/min, respectively) and the apparent lack of substantial clearance by the blood; however, direct confirmation of the lung's role has not been made. An apparent clearance of 14 liters/min for nitroglycerin was reported (20).

When indicated for patient care, placement of a pulmonary artery catheter in combination with any peripheral arterial drug measurement effectively isolates the lungs *in vivo* for determination of pulmonary extraction. The high apparent clearance of lorcainide, 1.7 liters/min, suggests a possible pulmonary role, but Jahnchen *et al.* (23) was unable to measure any concentration differences in samples obtained from catheters in the pulmonary artery and the aorta.

Kates and Leier (24) determined an apparent clearance of 4.4 liters/min for dobutamine based on mixed venous blood obtained *via* a pulmonary artery catheter as the reference concentration. Unfortunately, no peripheral measurements were reported. With more widespread appreciation of the potential role for pulmonary metabolism, especially in cases in which apparent clearance exceeds liver blood flow, it is anticipated that more investigators will directly determine pulmonary clearance. However, the clearance contribution of the lung *in vivo* will be difficult to determine for drugs with an apparent clearance of ≤500 ml/min. If the apparent clearance is 500 ml/min and only the lung eliminates the drug, pulmonary extraction is ~10%, which may be difficult to measure. On the other hand, if the liver were the exclusive organ of elimination, an easily measured difference of ~30–50% would be expected.

KINETIC ANALYSIS

The basic equations needed for kinetic analysis of pulmonary clearance are presented. Most examples in this section can be conceptualized in terms of a steady-state analysis, in which the rate of drug elimination equals a constant rate of drug input to the body. Variables are defined in the *Appendix*.

Exclusive Pulmonary Clearance–Scheme I (left) illustrates the role of the lung *in vivo* for the case in which the lungs eliminate a drug administered by intravenous infusion. Apparent clearance is G_{iv}/C_{art} or G_{iv}/C_{pv} (21):

$$Cl_{app} = Q_{co}E_p/(1 - E_p) \quad \text{(Eq. 1)}$$

Equation 1 illustrates a key principle of pulmonary elimination, namely that the apparent clearance will exceed organ blood flow and cardiac output whenever E_p is greater than 50%. This result is a direct consequence of first-pass elimination since only $(1 - E_p)$ of the delivered dose is actually available to systemic tissues (*i.e.*, tissues that obtain their drug supply *via* the arterial system).

Clearance by the perfused lung (Scheme I, right) is usually calculated from the decline in concentration observed in samples taken from the reservoir. When appropriately calculated, this method yields identical results to those obtained when steady state is achieved during single-pass operation and clearance is calculated from pulmonary extraction:

$$Cl_{organ} = Q_{co}E_p \quad \text{(Eq. 2)}$$

This quantity is always less than the clearance suggested by Eq. 1 for *in vivo* elimination. The key difference is that organ clearance is referred to reservoir concentration, which is equivalent to C_{PA}, while *in vivo* clearance is referred to C_{PV} (or C_{art}). To compare perfused lung experiments with the *in vivo* situation, E_p should be measured (or calculated as $E_p = Cl_{organ}/Q_{co}$) and used to evaluate Eq. 1. Perfused lung experiments are often operated at flow rates below cardiac output, which requires correction of the observed pulmonary extraction before substitution into Eq. 1.

Pulmonary extraction may be expressed in terms of intrinsic pulmonary clearance, Cl_p, and blood flow:

$$E_p = Cl_p/(Cl_p + Q_{co}) \quad \text{(Eq. 3)}$$

It will be assumed that the clearance process follows Michaelis–Menten kinetics:

$$Cl_p = V_{max,p}/(K_M + C_{PV}) \quad \text{(Eq. 4)}$$

Substitution of Cl_p from Eq. 4 into Eq. 3 yields:

$$E_p = V_{max,p}/(Q_{co}K_M + Q_{co}C_{PV} + V_{max,p}) \quad \text{(Eq. 5)}$$

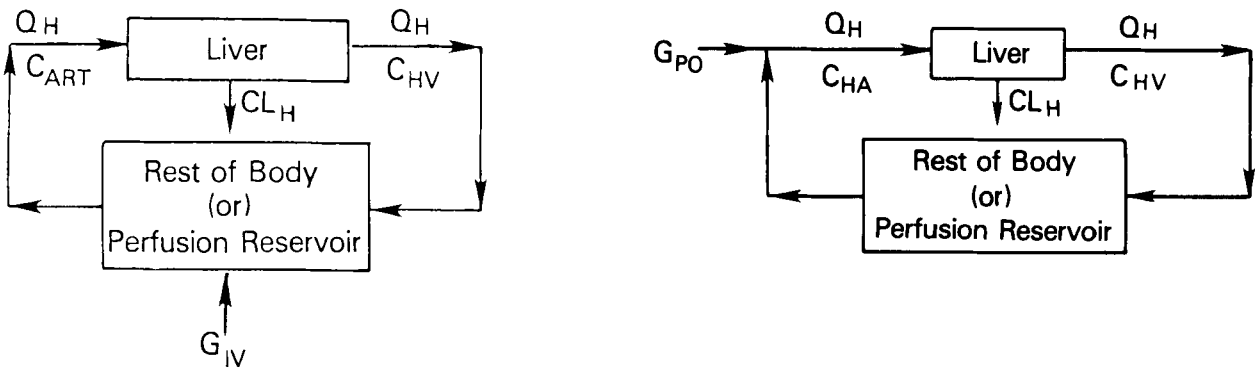

Scheme II—Hepatic clearance for in vivo *intravenous infusion or in an isolated perfusion circuit (left) and for oral (or portal vein or hepatic artery) infusion (right). For simplicity, the hepatic artery and portal vein are combined into a single input.*

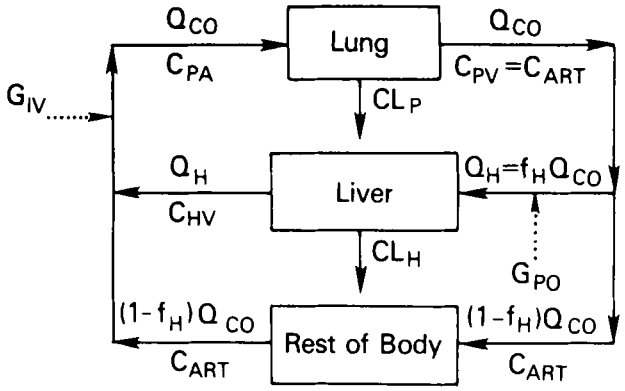

Scheme III—Simultaneous pulmonary and hepatic clearance. For simplicity, the hepatic artery and portal vein are combined into a single input.

If Eqs. 1 and 5 are combined and simplified:

$$Cl_{app} = V_{max,p}/(K_M + C_{PV}) = Cl_p \qquad \text{(Eq. 6)}$$

Equation 6 shows that the apparent clearance of the lungs (calculated on the basis of peripheral arterial blood concentration) during intravenous infusion is equal to intrinsic clearance.

Exclusive Hepatic Clearance—Scheme II (left) depicts clearance by the liver during *in vivo* intravenous infusion or in an isolated perfusion circuit. Apparent clearance for the liver is based on a reference concentration in arterial blood (or reservoir blood), while the elimination mechanisms operate at the liver concentration, which may be approximated by C_{HV}. Therefore, flow limitation is expressed as:

$$Cl_{app} = Q_H E_H = Q_H Cl_H/(Q_H + Cl_H)$$
$$= Q_H V_{max,H}/(Q_H K_M + Q_H C_{HV} + V_{max,H}) \qquad \text{(Eq. 7)}$$

The role of the liver following oral administration or hepatic artery or portal vein infusion is analogous to the role of the lungs during intravenous or other systemic administration. As shown in Scheme II (right), the liver receives the full drug input before it reaches the measurement location. Since the liver is the sole organ of elimination in this example, $C_{art} = C_{HV}$:

$$Cl_{app} = Cl_H = V_{max,H}/(K_M + C_{art}) \qquad \text{(Eq. 8)}$$

Thus, there is no flow limitation, and the intrinsic clearance of the liver is fully expressed.

Simultaneous Pulmonary and Hepatic Clearance—When the lungs and liver both eliminate a drug, the relative contribution of each organ to apparent clearance should be determined. Scheme III illustrates both the lungs and liver as eliminating organs *in vivo*. For intravenous administration, apparent clearance (G_{iv}/C_{art}) is the sum of the individual clearances:

$$Cl_{app} = Cl_P + Q_H Cl_H/(Q_H + Cl_H) = Cl_P + Q_H E_H \qquad \text{(Eq. 9)}$$

From this formula, the relative clearance contributions of the lungs and liver are:

$$\left(\frac{\text{lung}}{\text{liver}}\right) = \left(\frac{Cl_P}{Q_H E_H}\right) \qquad \text{(Eq. 10)}$$

Equation 10 is applicable to both linear and nonlinear kinetic regions. For nonlinear kinetics, Cl_P and E_H are not constants but are functions of C_{art} and C_{HV}. For linear kinetics ($C \ll K_M$), the expression for the Cl_P (Eq. 4) reduces to:

$$Cl_P = V_{max,P}/K_M \qquad \text{(Eq. 11)}$$

The expression for $Q_H E_H$ (Eq. 7), reduces to:

$$Q_H E_H = \frac{Q_H V_{max,H}}{Q_H V_{max,H}/(Q_H K_M + V_{max,H})} \qquad \text{(Eq. 12)}$$

Thus, the relative clearance contributions of the lungs and liver are:

$$\left(\frac{\text{lung}}{\text{liver}}\right) = \left(\frac{V_{max,P}/K_M}{Q_H V_{max,H}/(Q_H K_M + V_{max,H})}\right) \qquad \text{(Eq. 13)}$$

For oral administration, the apparent clearance (G_{po}/C_{art}) can be viewed as a modification of the expression for intravenous administration (Eq. 9). Due to the elimination by the liver of a certain fraction, E_H, of the administered dose, only the remainder is available for elimination by the lungs. Once this remainder, $1 - E_H$, leaves the liver, it is immaterial to the lungs whether the drug was given intravenously or orally. Hence, the right side of Eq. 9 can be divided by the available dose, $1 - E_H$, to yield an expression for apparent clearance for oral administration:

$$Cl_{app} = Cl_P/(1 - E_H) + Q_H E_H/(1 - E_H) = Cl_P/(1 - E_H) + Cl_H \qquad \text{(Eq. 14)}$$

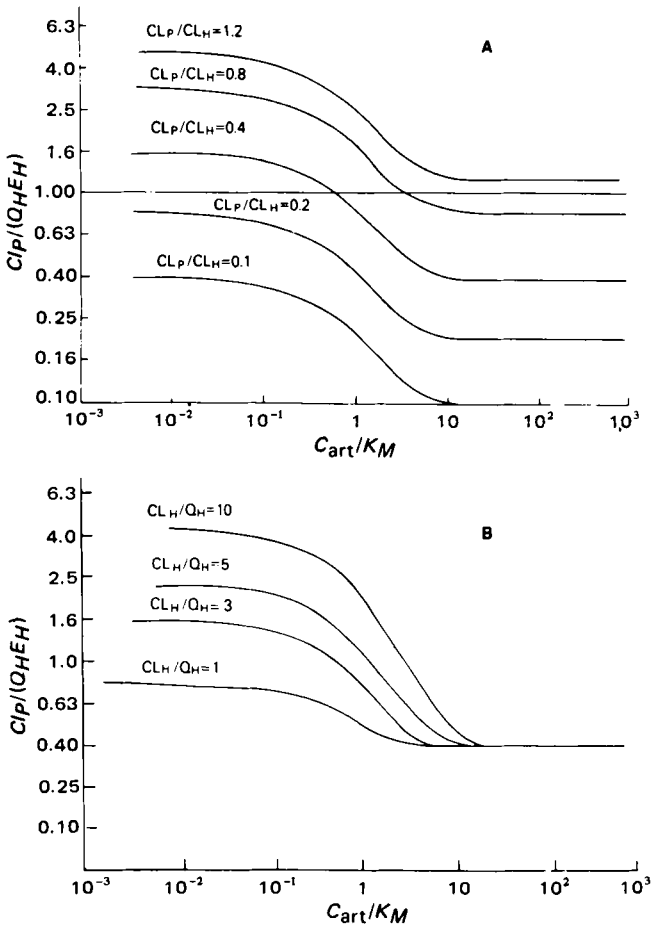

Figure 1—*Ratio of pulmonary clearance to hepatic clearance for intravenous infusion (Eq. 10) A:* Cl_H *fixed at three times* Q_H, *with* Cl_p/Cl_H *variable. B:* Cl_p/Cl_H *fixed at 0.4, with* Cl_H/Q_H *variable.*

It can be seen from Eq. 14 that the contributions of the lungs and liver to apparent clearance are interconnected. The contribution of pulmonary clearance is magnified by hepatic first-pass elimination, $1 - E_H$. Thus, there is no simple relationship similar to Eq. 10 that can be used to evaluate the relative clearance of the two organs.

RESULTS

The importance of pulmonary clearance for the determination of drug concentration is clearcut whenever the elimination capacity of the lungs is greater than that of any other organ (such as the liver). Even when the pulmonary elimination capacity is less than that of the liver, pulmonary clearance can dominate nonpulmonary clearance, or at least have a substantial impact on apparent clearance. For intravenous administration, hepatic clearance may not be fully expressed due to flow limitation so the relative impact of the lungs is enhanced. For oral administration, the coupling of pulmonary and hepatic clearances can accentuate the pulmonary impact.

Figures 1A and 1B demonstrate the relative contribution of the lungs and liver to overall drug elimination during intravenous infusion (Eq. 10). It is assumed that K_M is identical for liver and lung tissue. When $C_{art} \ll K_M$, elimination processes in both the lungs and liver are linear. At these low concentrations, the lung–liver elimination ratio is maximal since hepatic elimination is flow limited but pulmonary elimination is not. As the arterial concentration increases, the lung–liver elimination ratio

decreases since elimination processes are beginning to saturate, organ extraction is decreasing, and flow limitation is less pronounced. Finally, at $C_{art} \gg K_M$, the elimination ratio is simply the ratio of enzyme capacity, $V_{max,P}/V_{max,H}$.

As shown in Figs. 1A and 1B, for some parameter combinations the dominant role for elimination can be held by either organ or can shift from the lungs to the liver as C_{art} increases. For the lungs to dominate in the linear region, the following relationship must be satisfied, based on Eq. 13:

$$\left(\frac{V_{max,P}}{K_M}\right) > \left(\frac{Q_H V_{max,H}}{Q_H K_M + V_{max,H}}\right) \quad (15)$$

The liver always dominates in the zero-order region as long as $V_{max,H} > V_{max,P}$. As a reference point, the weight ratio of the lungs to the liver in humans is ~0.6 kg/1.5 kg or 0.4 (25). Since the clearances of both the lungs and liver are referred to the same arterial concentration, the mass elimination ratio (organ extraction times mass input to organ) is identical to the clearance ratio.

As already discussed, the contribution of the lungs to apparent clearance for oral administration is difficult to separate from the contribution of the liver. Figure 2 presents one possible interpretation of the lung's importance. Only the linear kinetic region is considered; Cl_{app} was calculated from Eq. (14) for various combinations of pulmonary and hepatic intrinsic clearance. The ability of the lungs to increase apparent clearance is rather substantial. As one example, a pulmonary elimination capacity that is 40% of hepatic capacity (*i.e.*, equivalent capacity per unit of weight multiplied by the organ weight ratio) produces a 133% increase in apparent clearance when the hepatic intrinsic clearance is three times the hepatic blood flow (75% extraction).

As a second example, a pulmonary elimination capacity of only 5% of hepatic capacity (*i.e.*, one-eighth the capacity per unit of weight multiplied by the organ weight ratio) increases Cl_{app} by 55% when hepatic clearance is 10 times the hepatic blood flow (91% extraction).

Since arterial concentration and systemic tissue exposure are inversely related to Cl_{app}, a relatively small amount of pulmonary activity can have a large impact. The mass elimination ratio does not provide the same perspective. The lungs account for 18% of mass elimination in the first example and only 3% in the second. These lower rates of mass elimination (as well as lower total elimination capacities) may lead one to ignore their role, while consideration of changes in Cl_{app} or systemic arterial concentration underscores the potential importance of pulmonary elimination.

DISCUSSION

Except for regionalized delivery such as topical, intraarterial, or intrathecal, the anatomical position of the lung presents it with the opportunity to modify the amount of drug available to the target tissues. Previous pharmacokinetic analyses focused primarily on the role of hepatic metabolism while essentially ignoring the lungs. In an earlier study that focused on the role of drug binding and GI or hepatic metabolism, Gillette and Pang (26) commented on the lack of flow limitation for the lung and the interactions of the liver with other organs for oral administration.

The role of the liver overshadowed that of the lungs in previous analyses for three major reasons:

1. The larger size of the liver may permit a greater total enzyme capacity. The actual magnitude of this difference is less for humans (1.5–2.5 times) than for other mammalian species: seven to 10 times for rats, eight times for rabbits, five times for monkeys, and three to four times for cats and dogs.

2. The well-known role of the liver in controlling the entry of exogenous substances into the body makes it a likely organ for drug elimination. Since the lungs play a major role in the regulation of endogenous substances, they might be expected to regulate exogenous substances also.

3. Lower specific enzyme activity (units per gram) has often been found in lung tissue compared with liver tissue. It was noted earlier that this apparently lower specific enzyme activity may be the result of suboptimal experimental conditions. In addition, interorgan differences in enzyme affinity for a drug (K_M) may offset a lower enzyme amount. Other studies (27) isolated an enzyme with a 10-fold lower K_M value in lung than liver tissue. Since intrinsic clearance under nonsaturating conditions is the ratio of enzyme capacity (V_{max}) to K_M, the lung can possess a larger intrinsic clearance than the liver, despite lower enzyme levels. On the other hand, studies by Gram (5) showed similar K_M values for other enzymes in the liver and lung. Finally, flow limitation can prevent expression of intrinsic clearance of the liver but not the lungs; thus, the lung can dominate even if it has lower intrinsic clearance.

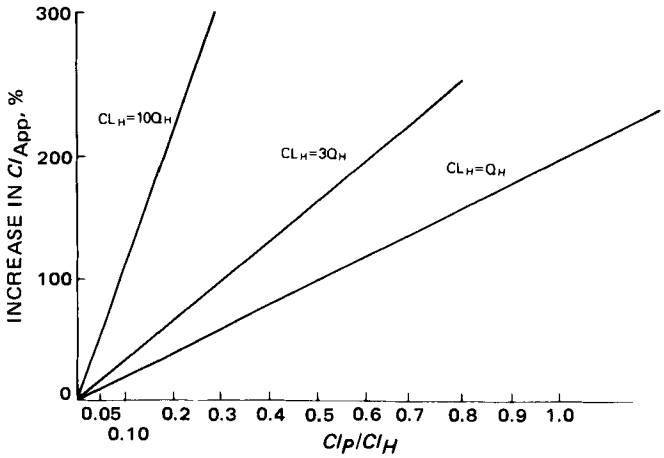

Figure 2—*Increase in apparent clearance for oral administration at various levels of pulmonary intrinsic clearance added to existing hepatic intrinsic clearance. Only the linear kinetic region is considered.*

Although it is suspected that the liver is a more important organ than the lungs for most drugs, the reasons for its dominance probably have been overstressed. Additional investigations are warranted to establish the actual pulmonary contribution, especially for drugs with high apparent clearance.

The concept of apparent clearance is especially relevant for a description of the lung's role in pharmacokinetics since it is simply a ratio of dose rate to arterial drug exposure. The related concept of organ clearance can be misleading when applied to the role of the lungs since it fails to account for first-pass effects. It is especially important that this difference is realized when the results from isolated perfused lung experiments are interpreted.

The synergism between the lung and liver for oral (or hepatic artery or portal vein) administration is especially noteworthy. The anatomical relationship of these organs results in a powerful filter, which can either protect systemic tissues from undesired exogenous chemicals or prevent achievement of therapeutic drug levels. For these two organs, neither the ratio of mass eliminated nor the ratio of elimination capacities is always a useful indicator of the control of tissue drug exposure. Although the liver may be responsible for the elimination of most of the drug mass eliminated from the body, the lung can still have a substantial impact on arterial drug concentration.

APPENDIX

Cl_p = intrinsic pulmonary clearance, $V_{max,P}/(K_M + C_{art})$
Cl_H = intrinsic hepatic clearance, $V_{max,H}/(K_M + C_{HV})$
Cl_{app} = apparent clearance, G/C_{art}
E_P = pulmonary extraction, (in–out)/in
E_H = hepatic extraction, (in–out)/in
G = drug input rate
Q = blood flow
C_{art} = arterial blood concentration
C_{PV} = pulmonary vein blood concentration
C_{PA} = pulmonary artery blood concentration
C_{HV} = hepatic vein blood concentration
K_M = half-saturating concentration (Michaelis constant)
V_{max} = maximal drug elimination capacity of whole organ
f = fraction of cardiac output which perfuses liver
co = cardiac output
P = pulmonary
H = hepatic
ia = intraarterial
iv = intravenous
po = oral

REFERENCES

(1) L. E. Farhi, *Resp. Physiol.*, **3**, 1 (1967).

(2) A. F. Junod, in "Lung Metabolism," A. F. Junod and R. de Heller, Eds., Academic, New York, N.Y., 1975, p. 219.

(3) T. R. Devereux, G. E. R. Hook, and J. R. Fouts, *Drug Metab. Disp.*, **7**, 70 (1979).
(4) G. E. R. Hook and J. R. Bend, *Life Sci.*, **18**, 279, (1976).
(5) T. E. Gram, *Drug Metab. Rev.*, **2**, 1 (1973).
(6) D. A. Wiersma and R. A. Roth, *J. Pharmacol. Exp. Ther.*, **212**, 97 (1980).
(7) Y. S. Bakhle and J. R. Vane, *Physiol. Rev.*, **54**, 1007, (1974).
(8) P. J. Piper, J. R. Vane, and J. H. Wyllie, *Nature*, **225**, 600 (1970).
(9) E. R. Block and A. B. Fisher, *J. Appl. Physiol.*, **43**, 254 (1977).
(10) K. S. Hilliker and R. A. Roth, *Biochem. Pharmacol.*, **29**, 253 (1980).
(11) R. H. Briant, E. W. Blackwell, F. M. Williams, D. S. Davies, and C. T. Dollery, *Xenobiotica*, **3**, 787 (1973).
(12) F. C. P. Law, *Drug Metab. Disp.*, **6**, 154 (1978).
(13) H. Uehleke, in *Proc. Eur. Soc. Study Drug Toxicity*, vol. X, Excerpta Medica, Amsterdam, The Netherlands 1969, p. 94.
(14) H. M. Mehendale and E. A. El-Bassiouni, *Drug Metab. Disp.*, **3**, 543 (1975).
(15) W. Dalbey and E. Bingham, *Toxicol. Appl. Pharmacol.*, **43**, 267 (1978).
(16) H. Vadi, B. Jernstrom, and S. Orrenius, *Carcinogenesis*, **1**, 45 (1976).
(17) N. G. Zampaglione and G. J. Mannering, *J. Pharmacol. Exp. Ther.*, **185**, 676 (1973).
(18) R. A. Roth and D. A. Wiersma, *Clin. Pharmacokinet.*, **4**, 355 (1979).
(19) M. K. Cassidy and J. B. Houston, *J. Pharm. Pharmacol.*, **32**, 57 (1980).
(20) M. K. Cassidy and J. B. Houston, *Biochem. Pharmacol.*, **29**, 471 (1980).
(21) J. M. Collins, R. L. Dedrick, F. G. King, J. L. Speyer, and C. E. Myers, *Clin. Pharmacol. Ther.*, **28**, 235 (1980).
(22) P. W. Armstrong, J. A. Armstrong, and G. S. Marks, *Circulation*, **62**, 160 (1980).
(23) E. Jahnchen, H. Bechtold, W. Kasper, F. Kersting, H. Just, J. Heykants, and T. Meinertz, *Clin. Pharmacol. Ther.*, **26**, 187 (1979).
(24) R. E. Kates and C. V. Leier, *ibid.*, **24**, 537 (1978).
(25) N. Benowitz, R. P. Forsyth, K. L. Melmon, and M. Rowland, *ibid.*, **16**, 87 (1974).
(26) J. R. Gillette and K. S. Pang, *ibid.*, **22**, 623 (1977).
(27) M. R. Boyd, L. T. Burka, B. J. Wilson, and H. A. Sasame, *J. Pharmacol. Exp. Ther.*, **207**, 677 (1978).

ACKNOWLEDGMENTS

The encouragement of Dr. Ted Gram, National Cancer Institute, in the preparation of this report is appreciated.

Comparison of Serum Bilirubin Levels in Humans and Two Monogastric Animal Species After a Single Administration of Sulfisoxazole

ROBERT L. SUBER*§x, JOHN C. GUDAT‡, and GEORGE T. EDDS*

Received January 27, 1981, from the *Department of Preventive Medicine and Toxicology, and the ‡Department of Pathology, Clinical Chemistry, University of Florida, Gainesville, FL 32610. §Present address: National Center for Toxicological Research, Pathology Services Project, Jefferson, AR 72079. Accepted for publication May 29, 1981.

Abstract □ Administration of sulfonamides during periods of hepatobiliary failure or hepatic immaturity increases the toxic potential of unconjugated or indirect bilirubin. A small but statistically significant increase of indirect, or unconjugated bilirubin was noted in dogs after oral administration of sulfisoxazole (100 mg/kg). A similar increase was not observed in swine after oral or intravenous administration of sulfisoxazole (100 mg/kg) or in humans (~28 mg/kg) after oral administration or in dogs (100 mg/kg) after intravenous administration. Total and conjugated bilirubin showed small but statistically significant increases and were significantly correlated in dogs after oral and intravenous administration of sulfisoxazole (100 mg/kg) and in swine after oral administration of sulfisoxazole (100 mg/kg). There was a significant negative correlation between conjugated and indirect bilirubin, while total bilirubin increased in dogs after oral and intravenous administration of sulfisoxazole. These data illustrate a difference in species and administration route when attempting to assess the potential toxicity of bilirubin.

Keyphrases □ Sulfisoxazole—comparison of serum bilirubin levels after a single administration, dogs, pigs, humans □ Bilirubin—serum levels after a single administration of sulfisoxazole, dogs, pigs, humans □ Toxicity—potential, indirect bilirubin serum levels after a single administration of sulfisoxazole

Sulfisoxazole [4-amino-*N*-(3,4-dimethyl-5-isoxazolyl)]-benzenesulfonamide is a white-yellowish, odorless, slightly bitter, crystalline powder with a pK of 4.9 (1). It is distributed in the extracellular fluid and fails to enter cells (2–5) resulting in a plasma concentration which is three times higher than that produced by an equal quantity of sulfanilamide (4). Sulfonamides, as a class of chemotherapeutic agents, are considered to be toxic since they may precipitate in the kidney, producing crystalluria (5). The infrequency of renal toxicosis (crystalluria) with sulfisoxazole is due to the exceptionally high water solubility of the free and conjugated (acetyl) fractions within the physiological pH range (6, 7).

Clinical toxicities have been induced by sulfisoxazole competing for the same binding sites as warfarin (8) and furosemide (9, 10), inducing hemolytic anemia due to glucose-6-phosphate dehydrogenase deficiency (11), inhibition of anticoagulant factor VIII (12), hypersensitivity (13), anorexia (14), agranulocytosis (14), and aplastic anemia (14). A case of myocarditis, myositis, and vasculitis associated with severe eosinophilia following sulfisoxazole therapy has been reported (15). Kernicterus has been reported in premature infants with increased levels of serum bilirubin after treatment with sulfisoxazole (4, 16, 17).

Kernicterus occurred when unconjugated or indirect bilirubin was less than 20 mg% in 24 infants, less than 17 mg% in 15 infants, and less than 15 mg% in 11 infants. These occurrences were enhanced by prior acidosis, hypercapnia, and hypothermia (4).

Plasma samples from six adult patients showed that sulfisoxazole concentrations above 5 mg/100 ml had a significant displacing effect on bilirubin *in vitro* (18). When comparing the displacing effects of salicylic acid, salicyluric acid, and aspirin at sulfisoxazole concentrations of 10 mg/100 ml, the most pronounced effect was observed when sulfisoxazole displaced bilirubin from plasma sam-

0022-3549/82/0100-0070$01.00/0

(3) T. R. Devereux, G. E. R. Hook, and J. R. Fouts, *Drug Metab. Disp.*, **7**, 70 (1979).
(4) G. E. R. Hook and J. R. Bend, *Life Sci.*, **18**, 279, (1976).
(5) T. E. Gram, *Drug Metab. Rev.*, **2**, 1 (1973).
(6) D. A. Wiersma and R. A. Roth, *J. Pharmacol. Exp. Ther.*, **212**, 97 (1980).
(7) Y. S. Bakhle and J. R. Vane, *Physiol. Rev.*, **54**, 1007, (1974).
(8) P. J. Piper, J. R. Vane, and J. H. Wyllie, *Nature*, **225**, 600 (1970).
(9) E. R. Block and A. B. Fisher, *J. Appl. Physiol.*, **43**, 254 (1977).
(10) K. S. Hilliker and R. A. Roth, *Biochem. Pharmacol.*, **29**, 253 (1980).
(11) R. H. Briant, E. W. Blackwell, F. M. Williams, D. S. Davies, and C. T. Dollery, *Xenobiotica*, **3**, 787 (1973).
(12) F. C. P. Law, *Drug Metab. Disp.*, **6**, 154 (1978).
(13) H. Uehleke, in *Proc. Eur. Soc. Study Drug Toxicity*, vol. X, Excerpta Medica, Amsterdam, The Netherlands 1969, p. 94.
(14) H. M. Mehendale and E. A. El-Bassiouni, *Drug Metab. Disp.*, **3**, 543 (1975).
(15) W. Dalbey and E. Bingham, *Toxicol. Appl. Pharmacol.*, **43**, 267 (1978).
(16) H. Vadi, B. Jernstrom, and S. Orrenius, *Carcinogenesis*, **1**, 45 (1976).
(17) N. G. Zampaglione and G. J. Mannering, *J. Pharmacol. Exp. Ther.*, **185**, 676 (1973).
(18) R. A. Roth and D. A. Wiersma, *Clin. Pharmacokinet.*, **4**, 355 (1979).
(19) M. K. Cassidy and J. B. Houston, *J. Pharm. Pharmacol.*, **32**, 57 (1980).
(20) M. K. Cassidy and J. B. Houston, *Biochem. Pharmacol.*, **29**, 471 (1980).
(21) J. M. Collins, R. L. Dedrick, F. G. King, J. L. Speyer, and C. E. Myers, *Clin. Pharmacol. Ther.*, **28**, 235 (1980).
(22) P. W. Armstrong, J. A. Armstrong, and G. S. Marks, *Circulation*, **62**, 160 (1980).
(23) E. Jahnchen, H. Bechtold, W. Kasper, F. Kersting, H. Just, J. Heykants, and T. Meinertz, *Clin. Pharmacol. Ther.*, **26**, 187 (1979).
(24) R. E. Kates and C. V. Leier, *ibid.*, **24**, 537 (1978).
(25) N. Benowitz, R. P. Forsyth, K. L. Melmon, and M. Rowland, *ibid.*, **16**, 87 (1974).
(26) J. R. Gillette and K. S. Pang, *ibid.*, **22**, 623 (1977).
(27) M. R. Boyd, L. T. Burka, B. J. Wilson, and H. A. Sasame, *J. Pharmacol. Exp. Ther.*, **207**, 677 (1978).

ACKNOWLEDGMENTS

The encouragement of Dr. Ted Gram, National Cancer Institute, in the preparation of this report is appreciated.

Comparison of Serum Bilirubin Levels in Humans and Two Monogastric Animal Species After a Single Administration of Sulfisoxazole

ROBERT L. SUBER*§x, JOHN C. GUDAT‡, and GEORGE T. EDDS*

Received January 27, 1981, from the *Department of Preventive Medicine and Toxicology, and the ‡Department of Pathology, Clinical Chemistry, University of Florida, Gainesville, FL 32610. §Present address: National Center for Toxicological Research, Pathology Services Project, Jefferson, AR 72079. Accepted for publication May 29, 1981.

Abstract □ Administration of sulfonamides during periods of hepatobiliary failure or hepatic immaturity increases the toxic potential of unconjugated or indirect bilirubin. A small but statistically significant increase of indirect, or unconjugated bilirubin was noted in dogs after oral administration of sulfisoxazole (100 mg/kg). A similar increase was not observed in swine after oral or intravenous administration of sulfisoxazole (100 mg/kg) or in humans (~28 mg/kg) after oral administration or in dogs (100 mg/kg) after intravenous administration. Total and conjugated bilirubin showed small but statistically significant increases and were significantly correlated in dogs after oral and intravenous administration of sulfisoxazole (100 mg/kg) and in swine after oral administration of sulfisoxazole (100 mg/kg). There was a significant negative correlation between conjugated and indirect bilirubin, while total bilirubin increased in dogs after oral and intravenous administration of sulfisoxazole. These data illustrate a difference in species and administration route when attempting to assess the potential toxicity of bilirubin.

Keyphrases □ Sulfisoxazole—comparison of serum bilirubin levels after a single administration, dogs, pigs, humans □ Bilirubin—serum levels after a single administration of sulfisoxazole, dogs, pigs, humans □ Toxicity—potential, indirect bilirubin serum levels after a single administration of sulfisoxazole

Sulfisoxazole [4-amino-*N*-(3,4-dimethyl-5-isoxazolyl)]-benzenesulfonamide is a white-yellowish, odorless, slightly bitter, crystalline powder with a pK of 4.9 (1). It is distributed in the extracellular fluid and fails to enter cells (2–5) resulting in a plasma concentration which is three times higher than that produced by an equal quantity of sulfanilamide (4). Sulfonamides, as a class of chemotherapeutic agents, are considered to be toxic since they may precipitate in the kidney, producing crystalluria (5). The infrequency of renal toxicosis (crystalluria) with sulfisoxazole is due to the exceptionally high water solubility of the free and conjugated (acetyl) fractions within the physiological pH range (6, 7).

Clinical toxicities have been induced by sulfisoxazole competing for the same binding sites as warfarin (8) and furosemide (9, 10), inducing hemolytic anemia due to glucose-6-phosphate dehydrogenase deficiency (11), inhibition of anticoagulant factor VIII (12), hypersensitivity (13), anorexia (14), agranulocytosis (14), and aplastic anemia (14). A case of myocarditis, myositis, and vasculitis associated with severe eosinophilia following sulfisoxazole therapy has been reported (15). Kernicterus has been reported in premature infants with increased levels of serum bilirubin after treatment with sulfisoxazole (4, 16, 17).

Kernicterus occurred when unconjugated or indirect bilirubin was less than 20 mg% in 24 infants, less than 17 mg% in 15 infants, and less than 15 mg% in 11 infants. These occurrences were enhanced by prior acidosis, hypercapnia, and hypothermia (4).

Plasma samples from six adult patients showed that sulfisoxazole concentrations above 5 mg/100 ml had a significant displacing effect on bilirubin *in vitro* (18). When comparing the displacing effects of salicylic acid, salicyluric acid, and aspirin at sulfisoxazole concentrations of 10 mg/100 ml, the most pronounced effect was observed when sulfisoxazole displaced bilirubin from plasma sam-

0022-3549/82/0100-0070$01.00/0

Table I—Mean Control Values of Serum Bilirubin in Humans, Dogs, and Swine [a]

	Total Bilirubin, mg/dl	Conjugated Bilirubin, mg/dl	Indirect Bilirubin, mg/dl
Humans	0.54 ± 0.10	0.41 ± 0.05	0.13 ± 0.02
Dogs	0.21 ± 0.06	0.08 ± 0.04	0.13 ± 0.03
Swine	0.35 ± 0.04	0.19 ± 0.06	0.15 ± 0.05

[a] The mean value ± 1 *SD* of eight samples before oral and intravenous administration of sulfisoxazole in six dogs and six swine. The mean value ± 1 *SD* for humans are calculated from time zero samples for six human subjects.

ples of six adults and 13 infants *in vitro* (18). The displacement of bilirubin is due to competition for similar binding sites on the albumin molecule (19).

Considering these observations and the importance of sulfisoxazole as an antibiotic in treating urinary tract infections, this study was initiated to define a non-rodent animal model which could be used in drug-safety screening of sulfonamides.

EXPERIMENTAL

Model—The trial consisted of six male human volunteers 25–30 years old, weighing 70–80 kg; three female dogs ~2 years old, weighing 20.0 ± 1.0 kg; and six female pigs ~3 months old, weighing 20.0 ± 1.0 kg. The human volunteers were administered 2.0 g of sulfisoxazole in a single oral dose and blood samples were taken at 0, 1, 2, 4, 6, and 8 hr after administration. The dogs were administered 100 mg/kg by intravenous and oral routes in two replicates for each route with a 30-day rest period between each administration. The pigs also were administered 100 mg/kg by intravenous and oral routes with a 21-day rest period between administration. Blood samples were taken at 0.5, 1, 2, 3, 4.5, 6, 9, 12, 22, 32, 44, 56, and 72 hr after intravenous administration and 0, 1, 2, 4, 6, 8, 10, 12, 14, 23, 32, 44, 56, 76, and 96 hr after oral administration in dogs and swine. All animals were maintained on a commercial diet[1,2] with *ad libitum* access to water and were housed in metabolism cages.

Materials—A 12.5% solution of sulfisoxazole[3] was prepared with lithium hydroxide. The solution was filtered and placed in sterile 50-ml ampuls[4]. This solution was used for both the oral and intravenous administration of the drug in dogs and swine and for oral administration to the human subjects. Due to the potential toxicity of intravenous sulfisoxazole administration and its removal from the drug market, intravenous administration of the drug to humans was not allowed[5].

Blood samples were taken from the cephalic vein in dogs and humans and from the anterior vena cava in swine. Human samples were drawn directly into 7-ml sterile silicone-coated tubules[6]. Ten-milliliter samples were taken by a sterile syringe with a 20-gauge needle from the dogs and pigs and transferred to sterile silicone-coated tubes[6]. The samples were centrifuged (2000×*g*) for 10 min, the serum extracted, protected from light, refrigerated, and analyzed within 30 min for total and conjugated (glucuronidated) bilirubin.

Serum Bilirubin—Serum was analyzed for total and conjugated (direct or glucuronidated) bilirubin on a discrete automatic analyzer[7] using a commercial standard[8].

The conjugated method is a modification of the Van den Bergh diazo reaction (20). Under acidic conditions, *p*-nitrobenzenediazonium tetrafluoroborate is coupled to the glucuronidated bilirubin which is measured as an end point reaction at 540 and 600 nm. The normal range in humans is considered to be 0.00 to 0.36 mg/dl[8].

The total bilirubin (the conjugated and unconjugated fractions) was determined also using a derivation of the Van den Bergh reaction (20). A surfactant[9] was used to solubilize the unconjugated (free) bilirubin, which along with the water-soluble glucuronidated bilirubin reacts with *p*-nitrobenzenediazonium tetrafluoroborate in an acid medium to measure an end point reaction at 540 and 600 nm. The normal total bilirubin concentration in humans is <1.5 mg/dl[8]; in dogs, the normal level is <0.5 mg/dl (17); and in swine is <0.6 mg/dl (21).

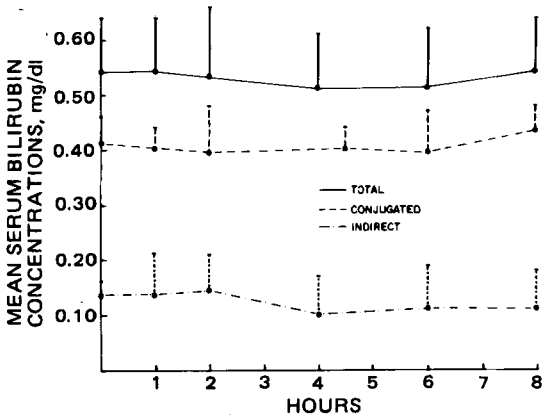

Figure 1—*Serum bilirubin concentrations in humans after oral administration of sulfisoxazole (mean ± 1* SD).

Interferences in these methods are due to hemolyzed samples and light degradation of the bilirubin. All analyses were conducted within 30 min of sampling on serum which was kept in a cool, dark environment.

Total, conjugated, and indirect bilirubin were analyzed for statistical differences[10]. The ANOVA program also produced a correlation coefficient (*R*) for parameters with a significant correlation.

RESULTS

Due to the lack of metabolic heterogenicity of humans, dogs, and swine, each species was used as its own control. The mean values for serum bilirubin were then used as initial or baseline values (Table I).

Humans, Oral Administration—An analysis of variance evaluation after oral administration of sulfisoxazole resulted in no statistical difference in mean total, conjugated, and indirect bilirubin levels (Fig. 1). The lack of significance could be due to the low therapeutic dose (2.0 g, ~28 mg/kg) administered to the human subjects, the fact that humans are able to reduce the *in vivo* effects of sulfisoxazole on the hepato-biliary system, or the sampling period being too short, and additional samples should have been taken over a longer trial period.

Dogs, Intravenous Administration—The mean total bilirubin concentration in six dogs administered sulfisoxazole intravenously exhibited statistically significant ($p < 0.01$) linear increases at 4.5 ($p < 0.05$), 6.0 ($p < 0.1$), 9.0 ($p < 0.01$), and 12.0 ($p < 0.01$) hr with the maximum levels occurring at 6 and 12 hr (Fig. 2). By the next sampling period (22 hr), the mean total bilirubin concentration had decreased to levels which were not significantly different from control values until the 56-hr sampling period ($p < 0.01$).

The mean conjugated bilirubin levels also showed statistically significant increases at 4 hr ($p < 0.01$) and continued throughout the sampling period ($p < 0.01$). There was a significant ($p < 0.01$) maximum mean

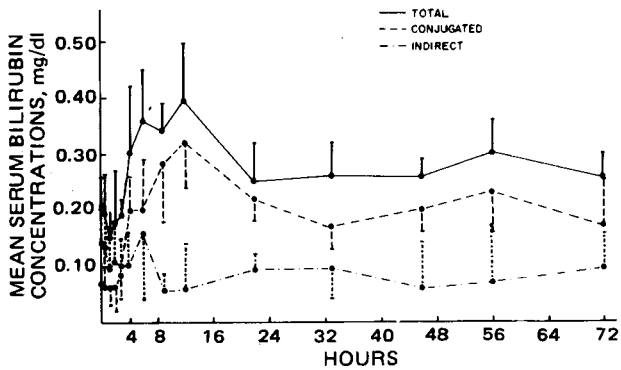

Figure 2—*Serum bilirubin concentrations in dogs after intravenous administration of sulfisoxazole (mean ± 1* SD).

[1] Purina Dog Chow, Ralston Purina, St. Louis, Mo.
[2] Swine Feed 18% protein, University of Florida, Gainesville, Fla.
[3] Hoffmann-LaRoche, Nutley, N.J.
[4] Wheaton, Scientific Products, Ocala, Fla.
[5] Human Research Committee of the University of Florida.
[6] Vacutainer, Becton-Dickinson, Rutherford, N.J.
[7] ACA, Dupont Instruments, Wilmington, Del.
[8] Dade Division, American Hospital Supply, Miami, Fla.
[9] Tween 20, Dupont Instruments, Wilmington, Del.
[10] ANOVA program (22), Northeast Regional Computer Center, University of Florida.

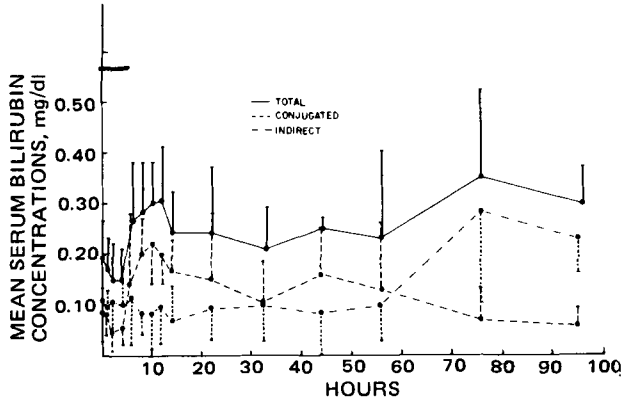

Figure 3—*Serum bilirubin concentrations in dogs after oral administration of sulfisoxazole (mean ± 1 SD).*

conjugated bilirubin concentration at 12 hr, which coincided with the maximum mean total bilirubin concentration (Fig. 2). A second increase was observed at 56 hr ($p < 0.01$) which coincided with the second increase in total bilirubin (Fig. 2). The mean indirect bilirubin concentration (Fig. 2) was not significantly different from the control level throughout the sampling period.

The mean total bilirubin was significantly correlated with mean conjugated bilirubin ($R = 0.75, p = 0.0001$) and with mean indirect bilirubin ($R = 0.31, p = 0.004$) after intravenous administration. The significant correlation of total and conjugated bilirubin is undoubtedly due to the concomitant increase in glucuronidation activity as total bilirubin levels increased. If the glucuronidation enzyme system is not capacity limited, the possibility of kernicterus due to increased indirect bilirubin is minimized after intravenous administration of sulfisoxazole in the dog. This enzyme system acts to maintain a reduced or limited indirect bilirubin concentration and reduces the toxicity of displaced protein-bound bilirubin or increased heme degradation. This was further emphasized by the significant negative correlation of conjugated and indirect bilirubin ($R = -0.39, p = 0.0002$). As the level of conjugated bilirubin increased, the potentially toxic indirect bilirubin level decreased.

A second explanation would be that sulfisoxazole alters the function of the normal hepatocyte to increase conjugated bilirubin regurgitation into the general circulation, instead of being excreted into the bile. The resulting increase in total bilirubin would be the result of the increased level of regurgitated, conjugated bilirubin, along with the normal level of indirect bilirubin.

Dogs, Oral Administration—When sulfisoxazole was administered orally to dogs, there was a significant linear increase in mean total ($p < 0.01$), conjugated ($p < 0.001$), and indirect ($p < 0.0001$) bilirubin (Fig. 3). Total bilirubin reached its first significant peak at 12 hr ($p < 0.01$) and a higher concentration at 76 hr ($p < 0.01$) (Fig. 3). The mean total bilirubin levels were significantly increased at 8 ($p < 0.05$), 10 ($p < 0.01$), and 12 ($p < 0.01$) hr. A second higher peak occurred at 76 hr ($p < 0.01$) and remained greater than the control levels at the end of the sampling period, 96 hr ($p < 0.01$) (Fig. 3). The mean conjugated bilirubin levels also increased linearly ($p < 0.001$) during the sampling period. Significant increases ($p < 0.05$) were observed at 8, 10, and 12 hr (Fig. 3), the same

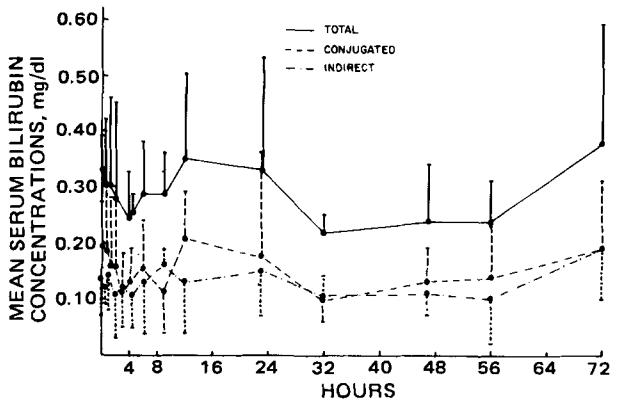

Figure 4—*Serum bilirubin concentrations in swine after intravenous administration of sulfisoxazole (mean ± 1 SD).*

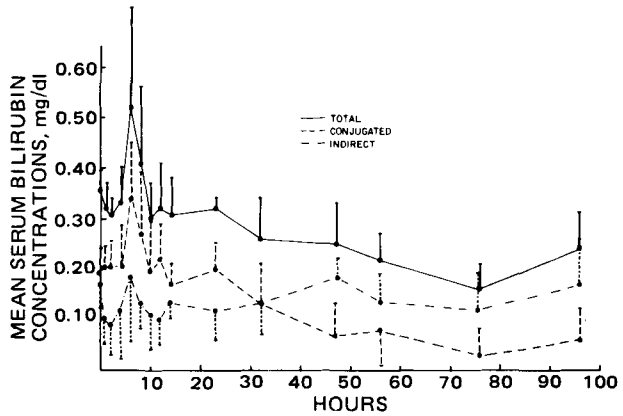

Figure 5—*Serum bilirubin concentrations in swine after oral administration of sulfisoxazole (mean ± 1 SD).*

periods in which total bilirubin was significantly increased. After the 12-hr period, the mean conjugated bilirubin had returned to levels which were not significantly different from control levels. The mean conjugated bilirubin reached its maximum concentration (0.22 mg/dl) at 10 hr, while the maximum total bilirubin (0.31 mg/dl) occurred at the 12-hr sampling period (Fig. 3). The mean indirect bilirubin was not significantly different from control levels until the 76- and 96-hr periods ($p < 0.01$). Mean indirect bilirubin reached a maximum of 0.28 mg/dl at 76 hr but had begun to decline by the end of the trial.

Total bilirubin was significantly correlated with conjugated bilirubin ($R = 0.06, p = 0.0001$) and with indirect bilirubin ($R = 0.56, p = 0.00001$) while conjugated bilirubin was also negatively correlated with indirect bilirubin ($R = -0.31, p = 0.003$). The significant correlation of total and conjugated bilirubin is explained by an increase in glucuronidation as increased heme degradation or increased indirect bilirubin occurs. It may also be due to regurgitation of conjugated bilirubin into the general circulation. The significant correlation of indirect and total bilirubin illustrated that the glucuronidation activity could not account for conjugation of all the bilirubin present. The negative correlation of indirect and conjugated bilirubin is supportive evidence that toxic, indirect bilirubin levels can be reduced to prevent kernicterus, if glucuronidation activity can be stimulated.

Swine, Intravenous Administration—Analysis of variance using mean bilirubin concentrations revealed no statistical difference among the six pigs or during time intervals for total, conjugated, or indirect serum bilirubin after intravenous administration of sulfisoxazole. The mean total conjugated and indirect bilirubin were increasing at the end of the trial but were not significantly different from control levels (Fig. 4).

Total bilirubin was significantly correlated with conjugated bilirubin ($R = 0.86, p = 0.0001$) and with indirect bilirubin ($R = 0.61, p = 0.0001$) after intravenous administration of sulfisoxazole.

Swine, Oral Administration—After oral administration of sulfisoxazole, mean total bilirubin was significantly increased ($p < 0.01$) to 0.52 mg/dl at 6 hr (Fig. 5). A parallel significant ($p < 0.01$) increase was also observed in mean conjugated bilirubin at 6 hr, 0.34 mg/dl (Fig. 5). A significant ($p < 0.0001$) linear decrease occurred over the trial period in conjugated bilirubin. Mean indirect bilirubin was not significantly different from control values at any time after oral administration of sulfisoxazole. However, indirect bilirubin levels did exceed conjugated levels after the 32-hr sampling period and remained at an increased level throughout the remainder of the trial (Fig. 5).

Total bilirubin was significantly correlated with conjugated bilirubin ($R = 0.81, p = 0.0001$) and with indirect bilirubin ($R = 0.42, p = 0.0001$) after oral administration of sulfisoxazole.

Comparison of Bilirubin Levels in Dogs, Swine, and Humans—Control values for total and conjugated bilirubin were higher in humans than in swine and lowest in dogs (Table I). The indirect bilirubin levels in all three species were similar.

A significant increase in total bilirubin occurred in dogs at 12 hr (Fig. 2) after intravenous administration of sulfisoxazole but did not occur in swine (Fig. 4) after administration of the same dose. After oral administration of sulfisoxazole, a significant increase in total bilirubin occurred in dogs (Fig. 3) and swine (Fig. 5) at 6 and 12 hr, respectively, with another increase in dogs at 76 hr. In humans, this increase was not observed over the same time period, probably due to the difference in the oral dosage (Fig. 1).

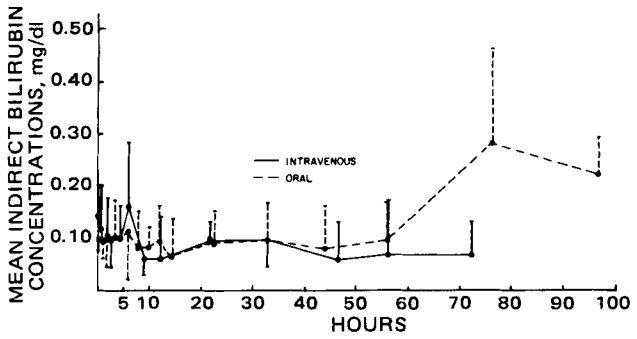

Figure 6.—*Comparison of the indirect bilirubin concentrations in dogs after intravenous and oral administration of sulfisoxazole (mean ± 1* SD).

Initially, total bilirubin levels were higher in swine than in dogs (Table I) but after intravenous administration of sulfisoxazole, total bilirubin was significantly ($p < 0.01$) higher in dogs between 3 and 15 hr (Fig. 2). Total bilirubin levels after oral administration were higher in swine than in dogs until the 56 hr period when the levels in dogs were significantly increased ($p = < 0.01$) (Fig. 3). Even after administration of sulfisoxazole, the total bilirubin increases in dogs and swine did not reach the control or treated levels in humans.

Conjugated bilirubin levels were not significantly increased in swine after intravenous administration of sulfisoxazole even though the control levels were greater in swine than in dogs. Conjugated bilirubin levels were significantly increased in dogs after intravenous administration of sulfisoxazole, exceeded the levels in swine after 3 hr, and reached a maximum at 12 hr after administration. After oral administration of sulfisoxazole, conjugated bilirubin levels were elevated in swine at 6 hr and showed a statistically significant increase in dogs at 10 hr after administration of the drug. The conjugated bilirubin levels in dogs and swine after intravenous or oral administration of sulfisoxazole did not reach the control or treated conjugated bilirubin levels in humans at any of the sampling periods.

Potentially toxic indirect bilirubin showed a statistically significant, but clinically small, increase after oral administration of sulfisoxazole in dogs (Fig. 6). There were no statistically significant increases in indirect bilirubin after oral administration in humans or swine or after intravenous administration of sulfisoxazole to dogs or swine.

DISCUSSION

Small but statistically significant increases in total and conjugated bilirubin occurred when sulfisoxazole was administered orally to dogs and swine but only when administered intravenously to dogs. The maximum increases occurred at different times, depending on species and route of administration. This species variation is further reflected by the indirect bilirubin exceeding conjugated bilirubin levels in dogs and swine when sulfisoxazole was administered orally. While toxic levels of bilirubin have not been established, these results show that the oral route of administration does increase the potentially toxic, indirect bilirubin concentration at a time far removed from the initial single dose in dogs and swine.

The small but statistically significant increase of total and conjugated bilirubin, after oral administration of sulfisoxazole, suggests that the absorption of the oral dosage form may cause the hepatocytes to increase the normal rate of heme degradation or to increase conjugated bilirubin regurgitation into the general circulation. This suggestion is supported by the intravenous dose given to dogs increasing only the total and conjugated bilirubin and not significantly affecting the indirect bilirubin level.

The lack of significant effects in humans and the lack of correlation between humans and dogs or swine could be due to the shorter sampling period in humans, the reduced dosage given to humans, or the species variation which exists even though all are monogastric.

When comparing the correlation coefficient of total and conjugated bilirubin in dogs ($R = 0.75, p = 0.0001$) and swine ($R = 0.85, p = 0.0001$) after intravenous administration, these parameters are more closely correlated in the pig. This is also true for the significant correlation of indirect and total bilirubin in dogs ($R = 0.31, p = 0.004$) and swine ($R = 0.61, p = 0.0001$) after intravenous administration of the drug. When sulfisoxazole is administered orally, the total and conjugated bilirubin levels are more closely correlated in swine ($R = 0.81, p = 0.0001$) than in dogs ($R = 0.60, p = 0.0001$) but indirect bilirubin is more closely correlated to total bilirubin in dogs ($R = 0.56, p = 0.0001$) than in swine ($R = 0.42, p = 0.0001$). In addition, conjugated and indirect bilirubin are negatively correlated after intravenous ($R = -0.39, p = 0.0002$) and oral ($R = -0.31, p = 0.003$) administration only in the dog.

It is evident that the route of sulfisoxazole administration affects the bilirubin level differently in these three species of animals. The potentially toxic indirect bilirubin level is significantly increased only after oral administration in one of the three species (dogs). This observation would be consistent with the first-pass effect (23) which states that oral administration of drugs results in peripheral venous concentrations exclusively *via* the hepatic portal system. This phenomenon, coupled with the reduced or impaired metabolic capability of the dog, would explain the increase in unconjugated bilirubin in this one-animal model. As a non-rodent model, the dog presents an acceptable model to be used in the preliminary evaluation of potentially-toxic, drug-induced effects on bilirubin metabolism after oral administration of the compound.

REFERENCES

(1) "*The Merck Index*," 9th ed., Merck and Co., Rahway, N.J., 1976, p. 1160.

(2) E. K. Marshall, *Proc. Soc. Exp. Biol. Med.*, **68,** 472 (1948).

(3) L. Weinstein, M. A. Madoff, and C. M. Samet, *N. Engl. J. Med.*, **263,** 793 (1960).

(4) L. Stern, B. Doray, G. Chan, and D. Schiff, *Birth Defects* **12,** 255 (1976).

(5) L. S. Goodman and A. Gilman, "The Pharmacological Basis of Therapeutics," Macmillan, New York, N.Y., 1970, p. 1177.

(6) E. H. Loughlin and W. G. Mullin, *Antibiot. Chemother.*, **5,** 609 (1955).

(7) D. Rudman, T. J. Bixler, and A. E. DelRio, *J. Pharmacol. Exp. Ther.*, **176,** 271 (1971).

(8) T. H. Self, W. Evans, and T. Ferguson, *Circulation*, **52,** 528 (1975).

(9) J. Prandota and A. W. Pruitt, *Clin. Pharmacol. Ther.*, **17,** 159 (1975).

(10) S. Shankaran and R. L. Poland, *J. Pediatr.*, **90,** 642 (1977).

(11) F. Meister, L. Endsley, and J. D. Schmidt, *J. Iowa Med. Soc.*, **65,** 465 (1975).

(12) J. C. Vera, E. B. Herzig, H. S. Sise, and M. J. Bauer, *J. Am. Med. Assoc.*, **232,** 1038 (1975).

(13) C. F. Cairy, *J. Am. Vet. Med. Assoc.*, **122,** 468 (1953).

(14) E. M. Yow, *Am. Pract. Dig. Treat.*, **4,** 521 (1953).

(15) L. Ellman, L. Miller, and J. Rappeport, *J. Am. Med. Assoc.*, **230,** 1004 (1974).

(16) W. A. Silverman, D. H. Anderon, W. A. Blanc, and D. N. Crozier, *Pediatrics*, **18,** 614 (1956).

(17) F. Bloom, "The Blood Chemistry of the Dog and Cat," Gamma, New York, N.Y., 1960, pp. 102–110.

(18) S. Øie and G. Levy, *Clin. Pharmacol. Ther.*, **21,** 627 (1977).

(19) G. B. Odell, *Ann. N.Y. Acad. Sci.*, **226,** 225 (1973).

(20) A. A. H. Van den Bergh and P. Miller, *Biochem. Z.*, **77,** 90 (1916).

(21) B. M. Mitruka and H. M. Rawnsley, "Clinical Biochemical and Hematological Reference Values in Normal Experimental Animals," Masson, New York, N.Y., 1977, pp. 149, 161.

(22) A. J. Barr and J. H. Goodnight, "Statistical Analysis System," North Carolina State University, Raleigh, N.C., 1972.

(23) M. Gibaldi and D. Perrier, "Pharmacokinetics," Marcel Dekker, New York, N.Y., 1975, pp. 232–250.

ACKNOWLEDGMENTS

This research was sponsored by the Environmental Protection Agency under Grant Number R804570-01-0.

The authors would like to thank Hoffmann–LaRoche, Nutley, N.J. for the generous supply of sulfisoxazole.

Reversed-Phase High-Pressure Liquid Chromatographic Determination of Serum Methotrexate and 7-Hydroxymethotrexate

ROBERT G. BUICE [x] **and PARAMJEET SIDHU**

Received February 2, 1981, from the *College of Pharmacy, University of Tennessee Center for the Health Sciences, Memphis, TN 38163.* Accepted for publication May 29, 1981.

Abstract □ A reversed-phase high-pressure liquid chromatographic method for determining methotrexate and 7-hydroxymethotrexate in human serum is presented. A mobile phase of acetate buffer (0.2 *M*, pH 5.5 with 0.03 *M* ethylenediaminetetraacetate), methanol, and acetonitrile (85.3:8.4:6.3), passed through a μBondapak C_{18} column at 1.5 ml/min produced excellent resolution of sharp, symmetrical bands. An improved extraction process, using a sample preparation cartridge, resulted in analytical recoveries in excess of 90% for methotrexate and 70% for 7-hydroxymethotrexate, permitting the determination of serum concentrations of 2.20 and 2.13 × 10^{-7} *M*, respectively, using only 200 μl of serum. UV detection at 313 nm provided adequate sensitivity for each component. While the reproducibility for 7-hydroxymethotrexate was approximately equal to previous methods, that for methotrexate was greatly improved. Serum methotrexate data at selected time points following high dose methotrexate therapy are presented.

Keyphrases □ Methotrexate—reversed-phase high-pressure liquid chromatographic determination □ 7-Hydroxymethotrexate—reversed-phase high-pressure liquid chromatographic determination □ High-pressure liquid chromatography—determination of methotrexate and 7-hydroxymethotrexate.

The effectiveness of high dose methotrexate therapy followed by leucovorin rescue was greatly enhanced by the observation that patients at high risk of serious toxicity might be detected by monitoring serum methotrexate (I) concentrations (1). Numerous analytical methods of I have been reported, including a spectrophotofluorometric method (2), several radioimmunoassays (3–7), a competitive protein binding method (8), an enzyme inhibition method (9), and a ligand-binding procedure (10). While recent work (11, 12) established the specificity of several such methods within certain concentration limits, potential cross-reactivity with I metabolites still raises doubt about these and other similar assay methods.

BACKGROUND

The major potentially-interfering metabolite of I, 7-hydroxymethotrexate (IV), has been reported in high concentrations in patient urine (13) and serum (14). Moreover, since the relatively low aqueous solubility of IV has caused some concern that this metabolite might be responsible for nephrotoxicity (13), it also should be monitored. More recently (11), in high dose methotrexate patients, a minor metabolite, 2,4-diamino-10-methylpteroic acid (III), was detected in later (48 hr) serum samples in concentrations that might impede quantitation of low I concentrations.

This potential cross-reactivity from metabolites, coupled with the possible need to quantitate certain metabolites, initiated the development of several high-pressure liquid chromatography (HPLC) methods (13–20). While these methods provide reasonable sensitivities, all require relatively large biological fluid samples (1–3 ml) and only one (19) reports an acceptable reproducibility for I (±3% at 10^{-5} *M*).

Moreover, most of these methods employ lengthy extractions with analytical recoveries varying from 40% (18) to 70% (15). Donehower *et al.* (11) used preparative HPLC and reported a 90% recovery of I, although a large serum sample (3 ml) was required. Lankelma and Poppe (17) used on-column concentration and reported a 70.2% analytical recovery of I, although again, a large serum sample (3 ml) was required.

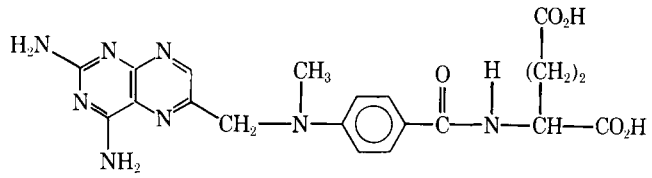

I

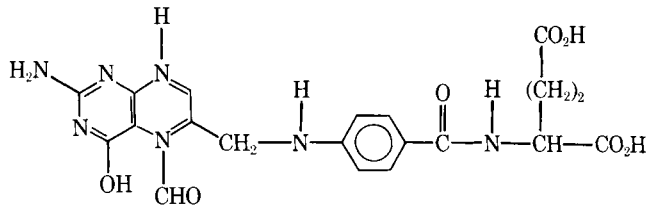

II

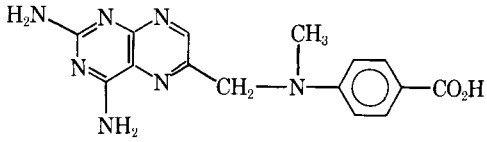

III

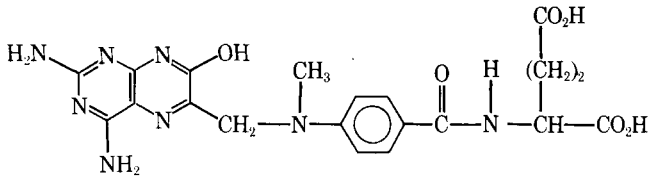

IV

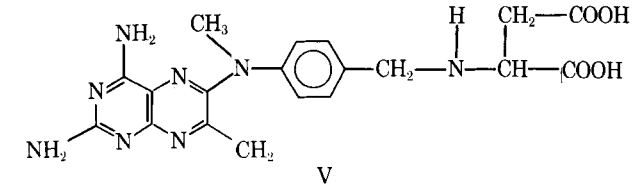

V

Another study (15), included no internal standard, but reported a day-to-day variation as high as 13.4%. Finally, other reported HPLC chromatograms (14, 16, 20) show poor resolution of I and IV. The present report describes an improved and relatively simple HPLC method for the quantitation of I and IV in the serum of patients receiving methotrexate therapy.

EXPERIMENTAL

Materials and Methods—Methanol and acetonitrile, used for the mobile phase, were HPLC grade solvents. Acetate buffer for the mobile phase was prepared using deionized water and reagent grade sodium acetate. All other chemicals were reagent grade. Analytical samples of I[1], leucovorin calcium[1] (II), III[1], IV[2], and the internal standard, *N*-[4-

[1] Lederle Laboratories, Pearl River, N.Y.
[2] Dr. David Johns, National Cancer Institute, Bethesda, Md.

0022-3549/82/0100-0074$01.00/0

Table I—HPLC Conditions and Correlation Coefficients for each Calibration Curve

Curve	Sample Time, hr	Concentration Range[a], μg/ml	Internal Standard[b], μg/ml	Reconstitution Volume / Injection Volume, μl
a	0 (I)	10–100	100.0	200/80
b	0 (IV)	1–10	5.0	200/40
c	12	1–10	5.0	200/100
d	24	0.1–1	0.5	100/80

Curve	Sample Time, hr	Detector Sensitivity	Correlation Coefficients ± *SEM* I	Correlation Coefficients ± *SEM* IV
a	0 (I)	0.500	0.99993 $n = 1$	
b	0 (IV)	0.010		0.98842 $n = 1$
c	12	0.050	0.99372 ± 0.00562 $n = 3$	0.98794 ± 0.00173 $n = 3$
d	24	0.005	0.99955 ± 0.00032 $n = 3$	0.99392 ± 0.00391 $n = 3$

[a] Molar concentration of I = (μg/ml) × (2.2×10^{-6}); molar concentration of IV = (μg/ml) × (2.13×10^{-6}). [b] Prior to Sep Pak treatment, 200 μl of this solution was added to each serum sample.

[(2,4-diamino-6-quinazolinyl)methylamino]benzoyl]aspartic acid[3] (V), were used as received.

Blood samples were obtained from patients at selected time points (0, 12, and 24 hr) following completion of 6-hr high dose methotrexate infusions (3500–5000 mg/m^2). Although it was not possible to obtain a sample from every patient at each preselected time point, a total of five samples were obtained at postinfusion time (0 hr), 11 at 12 hr, and six at 24 hr. Samples were centrifuged and the serum was stored at −5° until required for assay.

Serum concentrations of I and IV were determined using an HPLC system equipped with a 30-cm × 4-mm i.d. reversed-phase column[4]. Separation was followed by UV absorbance detection at 313 nm. A mobile phase consisting of buffer A (0.2 *M* acetate buffer, pH 5.5 with 0.03 *M* ethylenediaminetetraacetate), methanol, and acetonitrile (85.3:8.4:6.3) was passed through the column at a flow rate of 1.5 ml/min. Prior to analysis, the serum samples were processed by a reversed-phase sample preparation cartridge[5].

To each 200-μl serum sample was added 200 μl of internal standard (Table I), 400 μl of tromethamine (0.01 *M*, pH 9), and 1 ml of water. This mixture was vortexed 60 sec and passed through a sample preparation cartridge which had been pretreated with 10 ml of methanol and 10 ml of buffer B (0.2 *M* acetate buffer, pH 5.5). The cartridge was then treated with an additional 5 ml of buffer B, 1 ml of 0.1 *N* NaOH, and another 1 ml of buffer B. The cartridge was vacuum dried and the compounds of interest were eluted with 2 ml of methanol. The methanol was evaporated to dryness under nitrogen and the residue reconstituted in the mobile phase for injection. Analytical recoveries exceeded 90% for I and 70% for IV in the 10^{-7} *M* concentration range.

Four separate calibration curves were required to cover a concentration range of 2.20×10^{-7}–2.20×10^{-4} *M*. Conditions needed for each curve are presented in Table I. The large differences in I and IV concentrations in 0-hr samples required that each compound be determined from separate 200-μl portions of serum (calibration curves a and b). All other I and IV concentrations (12 and 24 hr) were determined simultaneously on single 200-μl serum samples. All samples were assayed in duplicate. Zero and 12-hr samples were quantitated using ratios of peak areas determined by a calculating integrator[6]. Ratios of peak heights were used to quantitate each compound in the 24-hr samples. Fresh calibration curves for I and IV were prepared daily in serum. Correlation coefficients of these curves are presented in Table I.

RESULTS

While most previous methods employed either methanol or acetonitrile as the organic portion of the mobile phase (11, 14, 15, 20), the present system attained maximum resolution of I, IV, and internal standard by combining these solvents. A flow rate of 1.5 ml/min resulted in a symmetrical band for each compound. Faster flow rates produced slightly sharper bands but reduced resolution. Representative HPLC chromatograms resulting from the quantitation of I and IV in 12- and 24-hr patient samples are presented in Fig. 1. Data from all sample determinations, together with percent deviations of duplicates, are presented in Table II.

Although metabolite III was previously reported in later (48 hr) samples, none was detected in any samples of the present study. Moreover, injections of analytical samples clearly show that III, due to its long retention time on this system (28.1 min), cannot interfere with the present assay. Ordinarily, no interference from II would be anticipated since rescue therapy is normally initiated 24-hr postinfusion (1). Furthermore, the retention of II on this system (4.3 min) was much shorter than either of the compounds of interest.

As illustrated in Fig. 1, no interfering bands appeared in the serum blanks of 12-hr samples (calibration curve c). As anticipated, quantitation of samples containing higher concentrations of I and IV (calibration

Table II—Data Resulting from Duplicate Determinations of Each Serum Sample and Percent Difference

I Duplicate Determinations A	I Duplicate Determinations B	Percent Difference	IV Duplicate Determinations A	IV Duplicate Determinations B	Percent Difference
0 hr Molar Concentration × 10^4					
3.04	3.00	1	0.22	0.25	12
2.89	2.97	3	0.32	0.35	9
2.38	2.34	2	0.46	0.61	25
4.69	4.72	1	0.28	0.29	3
3.26	3.28	1	0.31	0.34	9
12 hr Molar Concentration × 10^6					
7.97	8.10	2	13.7	16.6	17
3.78	3.78	0	4.8	4.5	6
6.93	6.86	1	15.8	18.7	16
5.35	5.35	0	6.8	6.1	10
2.02	2.22	9	3.9	4.2	7
2.42	2.51	4	11.0	8.5	23
2.49	2.49	0	7.1	7.2	1
2.22	2.49	11	8.0	7.4	8
7.74	8.10	4	21.3	20.7	3
3.21	3.59	11	7.5	12.7	41
8.10	8.18	1	9.2	9.4	2
24 hr Molar Concentration × 10^7					
7.04	7.39	5	41.5	43.7	5
9.68	9.46	2	40.5	30.5	25
1.09	1.08	1	30.2	21.7	28
4.62	4.18	10	24.3	23.0	5
9.68	9.90	2	31.1	26.2	16
2.64	2.64	0	20.9	19.0	9

[3] Drug Synthesis and Chemistry Branch, Division of Cancer Treatment, National Cancer Institute, Bethesda, Md.

[4] Model U6K injector, Model 6000A solvent delivery system, μBondapak C_{18} column with guard column, and model 440 UV absorbance detector, Waters Associates, Milford, Mass.

[5] C_{18} Sep Pak cartridge, Waters Associates, Milford, Mass.

[6] Hewlett-Packard 3352B laboratory data system.

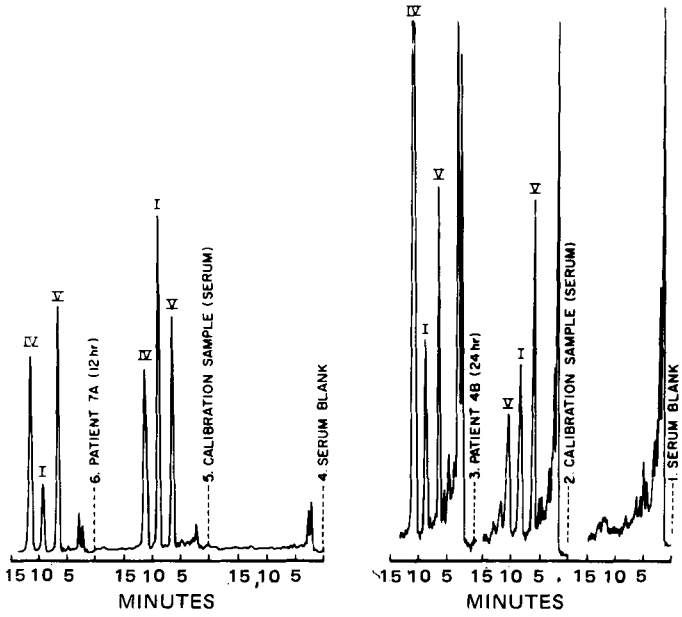

Figure 1—*Representative HPLC chromatograms of curve d serum blank (1), curve d calibration sample (2), 24-hr patient serum sample containing I (9.68 × 10^{-7} M) and IV (5.26 × 10^{-6} M) (3), curve c serum blank (4), curve c calibration sample (5), and 12-hr patient serum sample containing I (2.42 × 10^{-6} M) and IV (1.75 × 10^{-5} M) (6).*

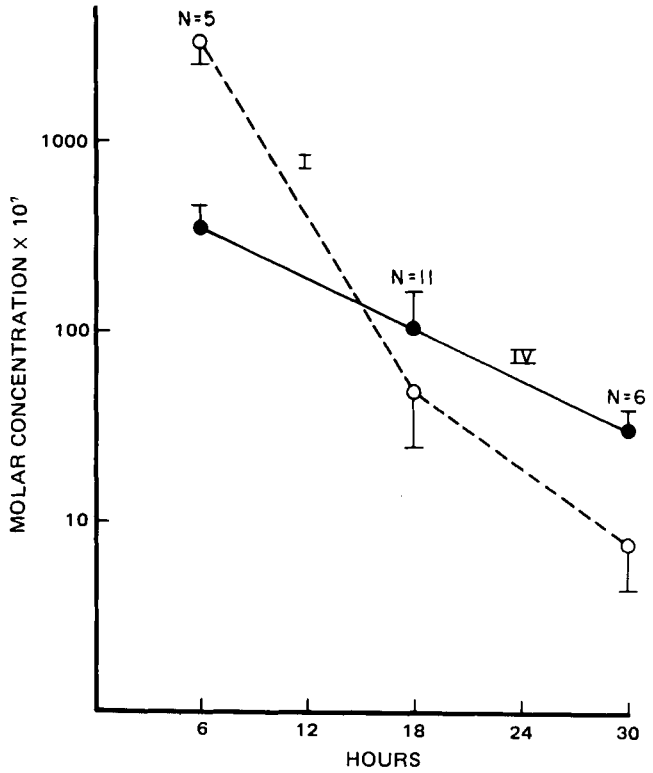

Figure 2—*Serum I (○) and IV (●) concentrations (mean ±SD) at selected time points following initiation of 6-hr high dose infusions (3500–5000 mg/m²).*

curves a and b) involved no interference from serum. Several low concentration (10^{-7}–10^{-6} *M*) samples, while showing no serum interference with I, did reveal a minute serum band slightly overlapping IV. Since the overlap was extremely slight, contribution to the peak height of IV was considered insignificant (Fig. 1).

Attempts to quantitate 24-hr serum samples using ratios of peak areas consistently resulted in poor reproducibility for I and IV. This appears to be characteristic of this calculating integrator in the absence of a completely horizontal baseline. Therefore, all 24-hr samples were quantitated using ratios of peak heights. Patient serum concentration data (mean ±*SD*) determined by this method are presented in Fig. 2.

The reproducibility of the method and the durability of the sample preparation cartridge were simultaneously evaluated by conducting multiple determinations on a single, spiked serum sample (10^{-6} *M* I) using the same cartridge. In duplicate studies, the first six consecutive determinations consistently produced a coefficient of variation which was less than 3%, although over the six repetitions all peak heights were reduced ~10%, suggesting a slightly declining cartridge efficiency. However, in the present study all patient samples were assayed in duplicate with each repetition using a new cartridge. No cartridge was reused.

DISCUSSION

The described method separates all three compounds of interest and produces sharp, symmetrical bands. UV detection at 313 nm, instead of at 254 nm, results in a twofold increase in assay sensitivity to IV, while sensitivity to I is approximately equal at either wavelength. This is consistent with previous reports (14, 20).

The high extraction efficiency resulting from this sample preparation procedure permitted the quantitation of serum I and IV concentrations as low as 2.20 and 2.13 × 10^{-7} *M*, respectively, using only 200 μl of serum. Previously reported methods require 1 ml of serum or more. These data suggest that the present method is readily adaptable to small animal pharmacokinetic studies. Moreover, the small volume of serum required makes the method highly useful in patient pharmacokinetic studies that require large numbers of data points, often from patients who are weakened by disease.

Data presented in Table II show excellent reproducibility for I, although that for IV shows no improvement over previously reported work. This is further evidenced by the calibration curve correlation coefficients given in Table I. The small contaminant which slightly overlapped the IV band in a few 10^{-7} *M* patient samples did not appear to influence reproducibility, suggesting that reproducibility differences in I and IV result from the extraction process.

This procedure results in only minimal column stress since ~800 injections of serum extracts may be made before the column begins to degenerate. Since a sample preparation cartridge can be used up to four times with no significant difference in assay results, the expense of this extraction is relatively small.

REFERENCES

(1) W. E. Evans, C. D. Pratt, R. H. Taylor, L. F. Barker, and W. R. Crom, *Cancer Chemother. Pharmacol.*, **3,** 161 (1979).

(2) J. M. Kinkade, Jr., W. R. Vogler, and P. G. Dayton, *Biochem. Med.*, **10,** 337 (1974).

(3) C. Bohuon, F. Dubrey, and C. Boudene, *Clin. Chim. Acta* **57,** 263 (1974).

(4) J. Hendel, L. J. Sarek, and E. F. Hvidberg, *Clin. Chem.*, **22,** 813 (1976).

(5) L. Levine and E. Powers, *Res. Commun. Chem. Pathol. Pharmacol.*, **9,** 543 (1974).

(6) V. Raso, *Cancer Treat. Rep.*, **61,** 585 (1977).

(7) V. Raso and R. Schreiber, *Cancer Res.*, **35,** 1407 (1975).

(8) C. E. Myers, M. E. Lippman, H. M. Eliot, and B. A. Chabner, *Proc. Natl. Acad. Sci. USA*, **72,** 3683 (1975).

(9) L. C. Falk, D. R. Clark, S. M. Kalman, and T. F. Long, *Clin. Chem.*, **22,** 785 (1976).

(10) S. P. Rothenberg, M. da Costa, and M. P. Igbal, *Cancer Treat. Rep.*, **61,** 575 (1977).

(11) R. C. Donehower, K. R. Hande, J. C. Drake, and B. A. Chabner, *Clin. Pharmacol. Ther.*, **26,** 63 (1979).

(12) R. G. Buice, W. E. Evans, J. Karas, C. A. Nicholas, P. Sidhu, A. B. Straughn, M. C. Meyer, and W. R. Crom, *Clin. Chem.*, **26,** 1902 (1980).

(13) J. L. Wisnicki, W. P. Tong, and D. B. Ludlum, *Cancer Treat. Rep.*, **62,** 529 (1978).

(14) J. L. Cohen, G. H. Hisayasu, A. R. Barrientos, M. S. B. Nayer, and K. K. Chan, *J. Chromatogr.*, **181,** 478 (1980).

(15) C. Canfell and W. Sadee, *Cancer Treat. Rep.*, **64,** 165 (1980).

(16) S. K. Howell, Y. M. Wang, R. Hosoya, and W. W. Sutow, *Clin.*

Chem., **26**, 734 (1980).
(17) J. Lankelma and H. Poppe, *J. Chromatogr.*, **149**, 587 (1978).
(18) J. A. Nelson, B. A. Harris, W. J. Decker, and D. Farquhar, *Cancer Res.*, **37**, 3970 (1977).
(19) E. Watson, J. L. Cohen, and K. K. Chan, *Cancer Treat. Rep.*, **62**, 381 (1978).
(20) Y. M. Wang, S. K. Howell, and J. A. Benvenuto, *J. Liq. Chromatogr.*, **3**, 1071 (1980).

ACKNOWLEDGMENTS

Supported by NCI Grant CA-16518-06.

Theoretical and Experimental Studies of Transport of Micelle-Solubilized Solutes

GREGORY E. AMIDON *x, WILLIAM I. HIGUCHI, and NORMAN F. H. HO

Received February 9, 1981, from the *University of Michigan, Ann Arbor, MI 48109.* Accepted for publication April 27, 1981.
*Present address: Pharmacy Research, The Upjohn Company, Kalamazoo, MI 49001.

Abstract □ A physical model describing the simultaneous diffusion of free solute and micelle-solubilized solute across the aqueous boundary layer, coupled with partitioning and diffusion of free solute through a lipoidal membrane, is derived. *In vitro* experiments utilizing progesterone and polysorbate 80 showed excellent agreement between theoretical predictions based on independently determined parameters and experimental results. The physical model predicts that micelles can assist the transport of solubilized solute across the aqueous diffusion layer, resulting in a higher solute concentration at the membrane surface than would be predicted if micelle diffusion is neglected. At high surfactant concentrations, the aqueous diffusion layer resistance can be eliminated and the activity of the solute at the membrane can approach the bulk solute activity. This mechanism could explain observed enhanced absorption rates *in vivo* when both micelle solubilization occurs and the aqueous diffusion layer is an important transport barrier. The importance of determining and defining the thermodynamic activity of the diffusing solute is emphasized.

Keyphrase □ Diffusion—transport of micelle-solubilized solutes, theoretical and experimental □ Solutes—micelle solubilized, transport, theoretical and experimental □ Micelles—theoretical and experimental transport, solutes

The effects of micelle solubilization on the solubility and intestinal absorption of nonpolar solutes are well documented (1–8). Investigations have been performed to delineate the role of surfactants in diffusional transport. As a result of these studies, it is clear that several factors must be considered, such as the thermodynamic activity of the solute, diffusivities of the free solute and micelles, membrane permeability, and the importance of the aqueous diffusion layer in determining the overall transport rate.

BACKGROUND

In a diffusional process (*e.g.*, intestinal absorption), a difference in the thermodynamic activity determines the direction of and driving force for the net transport of mass. Therefore, when micelle solubilization occurs and the thermodynamic activity of solute is lowered, a decreased diffusional rate is expected. On this basis, decreased absorption rates of salicylic acid in the presence of polysorbate 60 from rat intestinal segments were explained (1).

However there are numerous examples of increased absorption rates *in vivo* when solubilizing agents are present (2, 3). For example, the serum blood levels of indoxole when administered in a polysorbate 80 solution to humans were three to four times higher than comparable doses with an aqueous suspension or hard capsule (4). It was shown (5, 6), however, that membrane permeabilities may change in the presence of surfactant, possibly resulting in a net increase in the absorption rate even with a decreased thermodynamic activity of solute in bulk aqueous solution.

Another reason for enhanced absorption in the presence of solubilizing agents is associated with the diffusion of solute in the aqueous phase (*i.e.*, within the aqueous diffusion layer). Westergaard and Dietschy (7) pointed out that, in addition to the importance of bulk solute concentration and membrane permeability in determining absorption rates, the aqueous boundary layer is an important barrier to transport *in vivo* and should be evaluated. They concluded that the apparent functions of the micelle were to overcome the diffusion layer resistance *in vivo* and to deliver a maximum solute concentration to the membrane surface. It was also suggested (8) that the diffusion coefficient of the free solute–micelle complex is important in quantitatively assessing absorption in the presence of micelles.

Thus, it is clear that an evaluation of the aqueous diffusion layer and the physicochemical events occurring within it is necessary in the development of a realistic physical model. Furthermore, micellar diffusion, membrane permeation, and the thermodynamic activity of the solute in the surfactant solution need to be included in any complete analysis. This report presents a comprehensive physical model incorporating all of the principles just discussed. *In vitro* experiments along with independent determinations of all physicochemical parameters defined in the physical model were carried out utilizing progesterone and the nonionic surfactant polysorbate 80. Therefore, theoretical predictions based on independent estimates of the important parameters and experimentally determined fluxes can be compared.

The physical model is defined for two hydrodynamic conditions: the

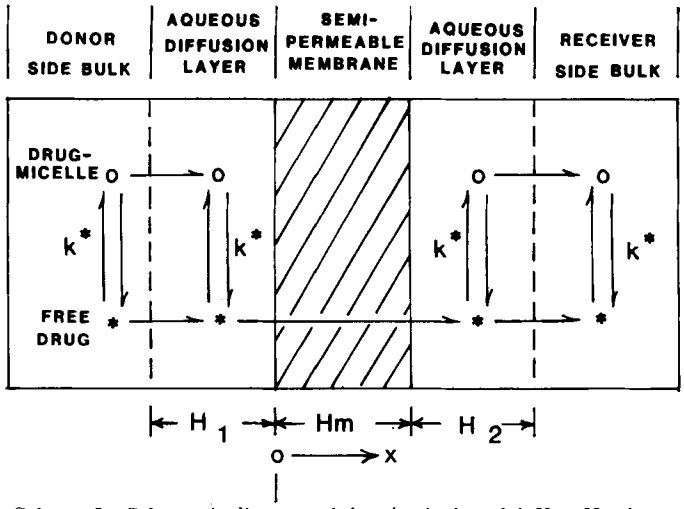

Scheme I—Schematic diagram of the physical model. Key: H_1, *donor side aqueous diffusion layer thickness;* H_m, *semipermeable membrane thickness;* H_2, *receiver side diffusion layer thickness; and* k*, *micelle-free solute equilibrium distribution coefficient.*

[1] Dow Corning, Midland, Mich.

0022-3549/82/0100-0077$01.00/0

Chem., **26**, 734 (1980).
(17) J. Lankelma and H. Poppe, *J. Chromatogr.*, **149**, 587 (1978).
(18) J. A. Nelson, B. A. Harris, W. J. Decker, and D. Farquhar, *Cancer Res.*, **37**, 3970 (1977).
(19) E. Watson, J. L. Cohen, and K. K. Chan, *Cancer Treat. Rep.*, **62**, 381 (1978).
(20) Y. M. Wang, S. K. Howell, and J. A. Benvenuto, *J. Liq. Chromatogr.*, **3**, 1071 (1980).

ACKNOWLEDGMENTS

Supported by NCI Grant CA-16518-06.

Theoretical and Experimental Studies of Transport of Micelle-Solubilized Solutes

GREGORY E. AMIDON *x, WILLIAM I. HIGUCHI, and NORMAN F. H. HO

Received February 9, 1981, from the *University of Michigan, Ann Arbor, MI 48109.* Accepted for publication April 27, 1981.
*Present address: Pharmacy Research, The Upjohn Company, Kalamazoo, MI 49001.

Abstract □ A physical model describing the simultaneous diffusion of free solute and micelle-solubilized solute across the aqueous boundary layer, coupled with partitioning and diffusion of free solute through a lipoidal membrane, is derived. *In vitro* experiments utilizing progesterone and polysorbate 80 showed excellent agreement between theoretical predictions based on independently determined parameters and experimental results. The physical model predicts that micelles can assist the transport of solubilized solute across the aqueous diffusion layer, resulting in a higher solute concentration at the membrane surface than would be predicted if micelle diffusion is neglected. At high surfactant concentrations, the aqueous diffusion layer resistance can be eliminated and the activity of the solute at the membrane can approach the bulk solute activity. This mechanism could explain observed enhanced absorption rates *in vivo* when both micelle solubilization occurs and the aqueous diffusion layer is an important transport barrier. The importance of determining and defining the thermodynamic activity of the diffusing solute is emphasized.

Keyphrase □ Diffusion—transport of micelle-solubilized solutes, theoretical and experimental □ Solutes—micelle solubilized, transport, theoretical and experimental □ Micelles—theoretical and experimental transport, solutes

The effects of micelle solubilization on the solubility and intestinal absorption of nonpolar solutes are well documented (1–8). Investigations have been performed to delineate the role of surfactants in diffusional transport. As a result of these studies, it is clear that several factors must be considered, such as the thermodynamic activity of the solute, diffusivities of the free solute and micelles, membrane permeability, and the importance of the aqueous diffusion layer in determining the overall transport rate.

BACKGROUND

In a diffusional process (*e.g.*, intestinal absorption), a difference in the thermodynamic activity determines the direction of and driving force for the net transport of mass. Therefore, when micelle solubilization occurs and the thermodynamic activity of solute is lowered, a decreased diffusional rate is expected. On this basis, decreased absorption rates of salicylic acid in the presence of polysorbate 60 from rat intestinal segments were explained (1).

However there are numerous examples of increased absorption rates *in vivo* when solubilizing agents are present (2, 3). For example, the serum blood levels of indoxole when administered in a polysorbate 80 solution to humans were three to four times higher than comparable doses with an aqueous suspension or hard capsule (4). It was shown (5, 6), however, that membrane permeabilities may change in the presence of surfactant, possibly resulting in a net increase in the absorption rate even with a decreased thermodynamic activity of solute in bulk aqueous solution.

Another reason for enhanced absorption in the presence of solubilizing agents is associated with the diffusion of solute in the aqueous phase (*i.e.*, within the aqueous diffusion layer). Westergaard and Dietschy (7) pointed out that, in addition to the importance of bulk solute concentration and membrane permeability in determining absorption rates, the aqueous boundary layer is an important barrier to transport *in vivo* and should be evaluated. They concluded that the apparent functions of the micelle were to overcome the diffusion layer resistance *in vivo* and to deliver a maximum solute concentration to the membrane surface. It was also suggested (8) that the diffusion coefficient of the free solute–micelle complex is important in quantitatively assessing absorption in the presence of micelles.

Thus, it is clear that an evaluation of the aqueous diffusion layer and the physicochemical events occurring within it is necessary in the development of a realistic physical model. Furthermore, micellar diffusion, membrane permeation, and the thermodynamic activity of the solute in the surfactant solution need to be included in any complete analysis. This report presents a comprehensive physical model incorporating all of the principles just discussed. *In vitro* experiments along with independent determinations of all physicochemical parameters defined in the physical model were carried out utilizing progesterone and the nonionic surfactant polysorbate 80. Therefore, theoretical predictions based on independent estimates of the important parameters and experimentally determined fluxes can be compared.

The physical model is defined for two hydrodynamic conditions: the

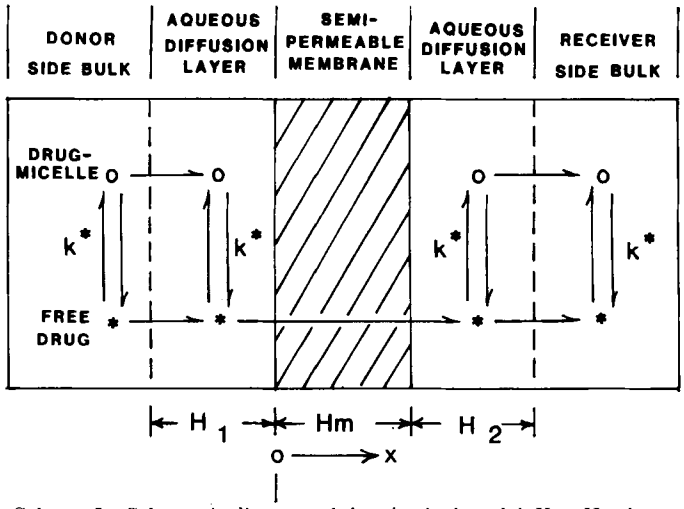

Scheme I—Schematic diagram of the physical model. Key: H_1, *donor side aqueous diffusion layer thickness;* H_m, *semipermeable membrane thickness;* H_2, *receiver side diffusion layer thickness; and* k*, *micelle-free solute equilibrium distribution coefficient.*

[1] Dow Corning, Midland, Mich.

0022-3549/82/0100-0077$01.00/0

stagnant diffusion layer case and the more well-defined hydrodynamic case for the surface of a rotating disk. For this latter situation, the fluid flow within the aqueous diffusion layer is well defined (9) and more easily controlled; it provides insight into actual events occurring within the diffusion layer and places the physical model on a more sound theoretical basis. For hydrodynamic conditions that are not ideal (*i.e.*, many *in vivo* absorption situations), the stagnant diffusion layer approach permits an evaluation of the aqueous diffusion layer resistance to diffusion.

A rotating-membrane diffusion cell similar to that used by Albery *et al.* (10) was employed for the present *in vitro* diffusion experiments. Proper design provides for well-defined hydrodynamics on each side of the rotating semipermeable membrane. Dimethicone (dimethylpolysiloxane[1]) membranes were utilized since they have been shown to maintain their integrity in the presence of surfactants (11) and buffers (12) and are quite permeable to the solutes investigated.

THEORY

Description of Model—The physical model involving the simultaneous diffusion of both free solute and solute solubilized in micelles is shown in Scheme I. Two aqueous compartments are separated by a semipermeable, lipid-like membrane, which permits only the passage of free solute. The donor compartment contains free solute, surfactant, and solute solubilized by the surfactant. It is assumed that the receiver compartment is at an equivalent surfactant concentration. This assumption is not necessary but simplifies the mathematics.

Furthermore, equilibrium between free solute and that solute solubilized in the micelle is assumed to occur at each point in the aqueous phase and in the diffusion layer. This equilibrium distribution coefficient is denoted by k^*; for the present model, it is assumed to be a constant.

The bulk of each aqueous phase is assumed to be well mixed by convection and, therefore, of uniform concentration in each compartment. Adjacent to the membrane is a region of relatively stagnant solution. It is primarily within this region (the aqueous diffusion layer) that concentration gradients of species may exist between the well-stirred bulk and the membrane surface. Under ideal hydrodynamic conditions, such as those of a rotating disk[2], the fluid flow near the surface can be mathematically described and an explicit relationship for the effective diffusion layer thickness can be obtained (13). When hydrodynamic conditions are not well defined, a stagnant diffusion layer model can be used.

Both free solute and micelles that may contain solubilized solute are assumed to diffuse independently across the aqueous diffusion layer. However, only free solute is assumed to partition into and diffuse through the membrane. Therefore, the components of the micelle are conserved in each compartment so that the surfactant concentration is assumed to be constant throughout each bulk phase and the diffusion layers.

Stagnant Diffusion Layer Model—When the aqueous diffusion layer is assumed to be a stagnant solvent layer, the steady-state flux equation for each diffusion layer ($i = 1, 2$) can be written as the sum of the flux of the micelle-solubilized solute and the free solute:

$$J_1 = \frac{D_1^*}{H_1}(C_{b1}^* - C_{s1}^*) + \frac{D_1'}{H_1}(C_{b1}' - C_{s1}') \qquad \text{(Eq. 1)}$$

$$J_2 = \frac{D_2^*}{H_2}(C_{s2}^* - C_{b2}^*) + \frac{D_2'}{H_2}(C_{s2}' - C_{b2}') \qquad \text{(Eq. 2)}$$

where J is the steady-state flux; D is diffusivity; H is effective diffusion layer thickness; C is concentration; the asterisk and prime superscripts denote the micelle-solubilized species and the free solute, respectively; and the subscripts b and s denote the bulk and membrane surface for the donor, 1, and receiver, 2, sides.

The following free solute–micelle-solubilized solute equilibrium is assumed to hold above the critical micelle concentration (CMC) of the surfactant:

$$k^* = \frac{C_i^*}{C_i'(SAA)} \qquad \text{(Eq. 3)}$$

where k^* is the equilibrium distribution coefficient, C_i^* and C_i' are the micelle-solubilized solute concentration and free solute concentration per liter of solution, and (SAA) is the surfactant concentration[3]. This relationship permits the free solute concentration (thermodynamic activity) to be calculated when micelles are present.

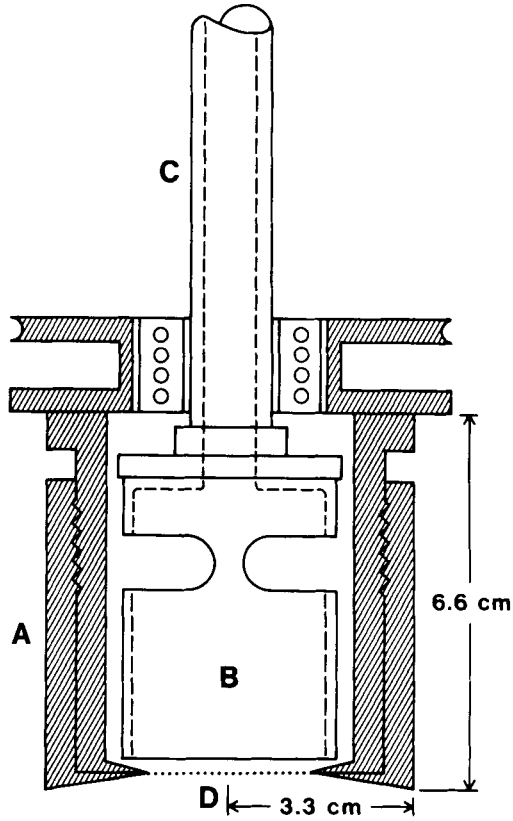

Figure 1—*Schematic diagram of rotating-membrane diffusion cell. Key: A, outer stainless steel cylinder; B, stationary cylindrical baffle; C, sampling port; and D, semipermeable membrane.*

The total bulk and surface concentration for each aqueous compartment can be written:

$$C_{bi} = C_{bi}^* + C_{bi}' = C_{bi}'[1 + k^*(SAA)] \qquad \text{(Eq. 4)}$$

$$C_{si} = C_{si}^* + C_{si}' = C_{si}'(1 + k^*(SAA)] \qquad \text{(Eq. 5)}$$

Eqs. 1 and 2 can be rewritten:

$$J_1 = P_1(C_{b1} - C_{s1}) \qquad \text{(Eq. 6)}$$

$$J_2 = P_2(C_{s2} - C_{b2}) \qquad \text{(Eq. 7)}$$

where P is permeability and:

$$P_i = \frac{D_{\text{eff}}}{H_i} \qquad \text{(Eq. 8)}$$

The effective diffusion coefficient, D_{eff}, is defined as:

$$D_{\text{eff}} = \frac{D_i' + k^*(SAA)D_i^*}{[1 + k^*(SAA)]} \qquad \text{(Eq. 9}a\text{)}$$

An identical way of expressing the effective diffusion coefficient is:

$$D_{\text{eff}} = f'D' + f^*D^* \qquad \text{(Eq. 9}b\text{)}$$

where f' and f^* are the fractions of the total solute in the free form and solubilized form, respectively.

It is evident from Eq. 9*b* that the diffusivity of each aqueous diffusion layer becomes essentially the diffusivity for the micelle-solubilized solute, D^*, when the surfactant concentration is large. At premicellar concentrations and low micellar concentrations, the diffusivity is essentially the diffusivity for free solute, D'.

The steady-state flux of solute through the semipermeable membrane (J_m) can be written as:

$$J_m = \frac{D_m}{H_m}(C_{m1}' - C_{m2}') \qquad \text{(Eq. 10)}$$

where C_{m1}' and C_{m2}' are the free solute concentrations in the membrane at each interface and D_m is the solute diffusivity in the membrane of thickness H_m.

[2] Other geometries such as flow across a flat surface or laminar flow down a tube provide equally well-defined hydrodynamics.

[3] Here (SAA) is equivalent to the concentration of micelles in solution. Therefore, $(SAA) = (SAA)_T - \text{CMC}$, where $(SAA)_T$ is the total surfactant concentration. For surfactants with low CMC values (such as polysorbate 80, CMC $\simeq$ 0.006%): $(SAA) \simeq (SAA)_T$.

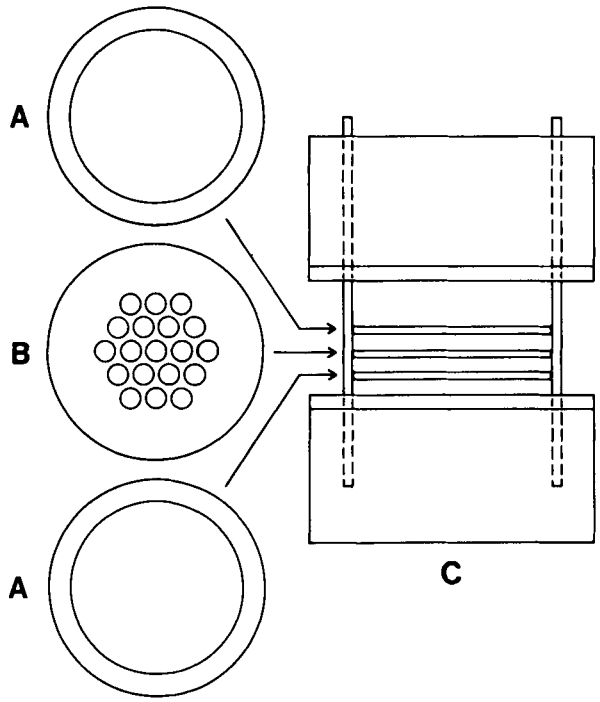

Figure 2—*Membrane support and spacers (each 50-μm thick).*

The membrane–aqueous phase partition coefficient, K, is:

$$K = \frac{C'_{mi}}{C'_{si}} \qquad \text{(Eq. 11)}$$

Combining Eqs. 10 and 11 gives:

$$J_m = \frac{KD_m}{H_m}(C'_{s1} - C'_{s2}) \qquad \text{(Eq. 12)}$$

When the surfactant concentration is the same on each side,[4] the membrane flux can be written in terms of the total solute concentration:

$$J_m = P_m(C_{s1} - C_{s2}) \qquad \text{(Eq. 13)}$$

where:

$$P_m = \frac{KD_m}{H_m[1 + k^*(SAA)]} \qquad \text{(Eq. 14)}$$

The membrane permeability is a function of the surfactant concentration since it is related to the free solute concentration at the membrane surface.

At steady state, the flux of solute through each region must be equal; therefore:

$$J_1 = J_m = J_2 \qquad \text{(Eq. 15)}$$

and:

$$J = P_{\text{eff}}(C_{b1} - C_{b2}) \qquad \text{(Eq. 16)}$$

where the effective permeability coefficient, P_{eff}, is:

$$P_{\text{eff}} = \frac{1}{\frac{1}{P_1} + \frac{1}{P_m} + \frac{1}{P_2}} \qquad \text{(Eq. 17)}$$

The total solute concentration at each interface is given by:

$$C_{s1} = \frac{\left(\frac{1}{P_m} + \frac{1}{P_2}\right)C_{b1} + \left(\frac{1}{P_1}\right)C_{b2}}{\frac{1}{P_1} + \frac{1}{P_m} + \frac{1}{P_2}} \qquad \text{(Eq. 18)}$$

[4] This assumption is not necessary but simplifies the mathematics that follow.

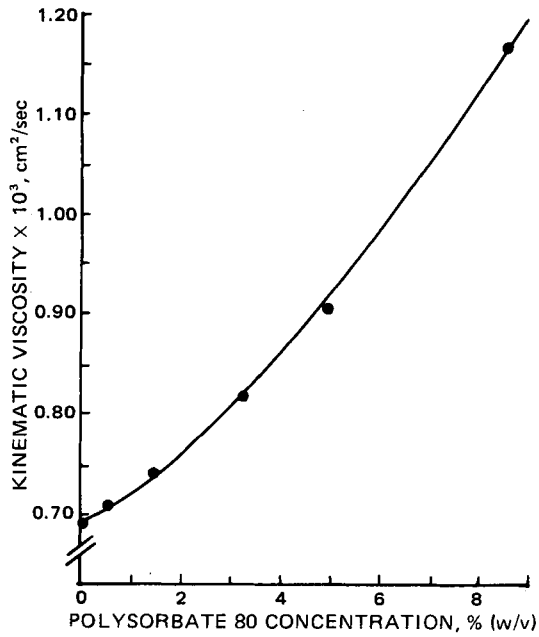

Figure 3—*Kinematic viscosity of polysorbate 80 solutions at 37°.*

$$C_{s2} = \frac{\left(\frac{1}{P_2}\right)C_{b1} + \left(\frac{1}{P_1} + \frac{1}{P_m}\right)C_{b2}}{\frac{1}{P_1} + \frac{1}{P_m} + \frac{1}{P_2}} \qquad \text{(Eq. 19)}$$

Convective Diffusion Layer Model—For the ideal hydrodynamics near the surface of a rotating disk, the convective diffusion equation for mass transfer can be solved (13). The solution predicts solvent movement even immediately adjacent to the rotating surface. Therefore, instead of a stagnant diffusion layer, a dynamic convective diffusion layer is more appropriate. Within this layer (normally ≤50 μm) and extending out into the bulk, there is a gradual transition from an essentially diffusional process at the disk surface to one in which the major transport mechanism is convection.

Under these rotating-disk conditions, the effective diffusion layer thickness is:

$$H = 1.61\nu^{1/6}D^{1/3}\omega^{-1/2} \qquad \text{(Eq. 20)}$$

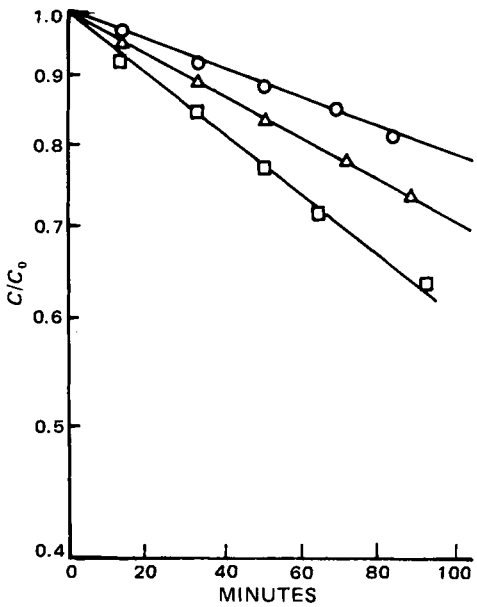

Figure 4—*Semilogarithmic plot of the fraction of radiolabeled capric acid remaining in the donor phase with time when both the donor and receiver side diffusion layers are important. Key:* ○, *60 rpm;* △, *120 rpm; and* □, *300 rpm.*

Table I—Effective Diffusion Coefficients of Progesterone–Polysorbate 80 Solutions

Polysorbate 80 Concentration, % (w/v)	$D_{eff} \times 10^6$, cm^2/sec Trace Concentrations	$D_{eff} \times 10^6$ cm^2/sec Saturated Solutions	$D^* \times 10^6$, cm^2/sec Estimated
0.0	8.50	—	—
0.103	—	6.52	4.68
0.116	6.22	—	4.35
0.514	3.58	—	2.67
0.56	—	2.51	1.49
0.942	3.22	—	2.69
1.96	2.13	—	1.82
2.03	—	1.76	1.46
5.04	1.56	—	1.43

and the steady-state mass flux of solute, J, through the convective diffusion layer can be written:

$$J = \frac{D\,\Delta C}{H} = 0.62D^{2/3}\nu^{-1/6}\omega^{1/2}(C_b - C_s) \qquad \text{(Eq. 21)}$$

where D is the aqueous diffusion coefficient, ν is the kinematic viscosity, and ω is the disk rotation speed in radians per second.

For the simultaneous convective diffusion of free solute and micelle-solubilized solute, Eq. 21 can be modified to:

$$J = 0.62D_{eff}^{2/3}\nu^{-1/6}\omega^{1/2}(C_b - C_s) \qquad \text{(Eq. 22)}$$

where the effective diffusion coefficient, D_{eff}, is defined in Eq. 9*a*.

When the flux of solute through the convective diffusion layer on each side of the semipermeable membrane is given by Eq. 22 and the membrane permeability coefficient is given by Eq. 13, the following equation predicts the total flux of solute (J):

$$J = P_{eff}(C_{b1} - C_{b2}) \qquad \text{(Eq. 23)}$$

where:

$$P_{eff} = \frac{1}{\frac{1}{P_1^c} + \frac{1}{P_m} + \frac{1}{P_2^c}} \qquad \text{(Eq. 24)}$$

and the permeability of each convective diffusion layer, P_i^c, is:

$$P_i^c = \frac{D_{eff}}{H_i} = 0.62D_{eff}^{2/3}\nu^{-1/6}\omega^{1/2} \qquad \text{(Eq. 25)}$$

Both D_{eff} and ν may be functions of surfactant concentration. For simplicity, it is assumed here, as it was in the stagnant diffusion layer model, that the surfactant concentrations in both the donor and receiver sides are equal.

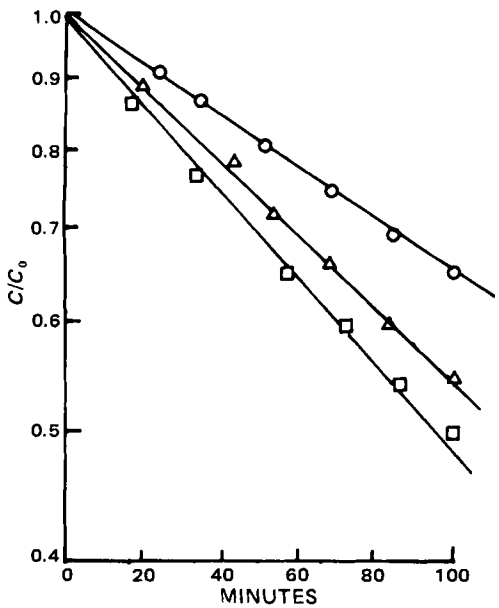

Figure 5—*Semilogarithmic plot of the fraction of radiolabeled capric acid remaining in the donor phase when the receiver side diffusion layer resistance is eliminated by adjustment of pH. Key: ○, 60 rpm; △, 120 rpm; and □, 300 rpm.*

Table II—Reproducibility of Effective Permeability Coefficient Determinations

	Rotation Speed, radians/sec		
	6.28 (60 rpm)	12.57 (120 rpm)	31.42 (300 rpm)
n	5	8	5
$P_{eff} \times 10^4$	6.58	9.77	13.67
$SD \times 10^4$	0.370	0.589	0.733
CV, %	5.6	6.0	5.4

Equation 24 can be rewritten as:

$$\frac{1}{P_{eff}} = \frac{1}{P_1^c} + \frac{1}{P_m} + \frac{1}{P_2^c} \qquad \text{(Eq. 26)}$$

and, using Eq. 25, the following can be derived:

$$\frac{1}{P_{eff}} = 2\left[\frac{\nu^{1/6}}{0.62D_{eff}^{2/3}}\right]\omega^{-1/2} + \frac{1}{P_m} \qquad \text{(Eq. 27)}$$

If one diffusion layer is eliminated, then Eq. 27 reduces to:

$$\frac{1}{P_{eff}} = \left[\frac{\nu^{1/6}}{0.62D_{eff}^{2/3}}\right]\omega^{-1/2} + \frac{1}{P_m} \qquad \text{(Eq. 28)}$$

Thus, Eqs. 27 and 28 offer a convenient way of testing the validity of Eq. 20 for the diffusion layer thickness on each side of the semipermeable membrane.

Diffusion Cell and Membrane Preparation—A diagram of the rotating-membrane diffusion cell is shown in Fig. 1. An outer stainless steel cylinder is connected to a variable-speed motor by a pulley and belt system. In this way, the outer cylinder can be rotated at a variety of speeds with ease. A stationary cylindrical baffle attached to the hollow sampling port is suspended inside the outer cylinder. To allow proper fluid flow inside the cell, two grooves ~1-cm wide are cut 3 cm from the bottom of the inner baffle, which is open.

The outer cylinder can be further disassembled by unscrewing to allow the membrane to be positioned at the bottom of the cell and screwed tightly into place. In addition, at each edge of the membrane, the cylinder is beveled at an angle of ~10° so that fluid flow at the edge is not dis-

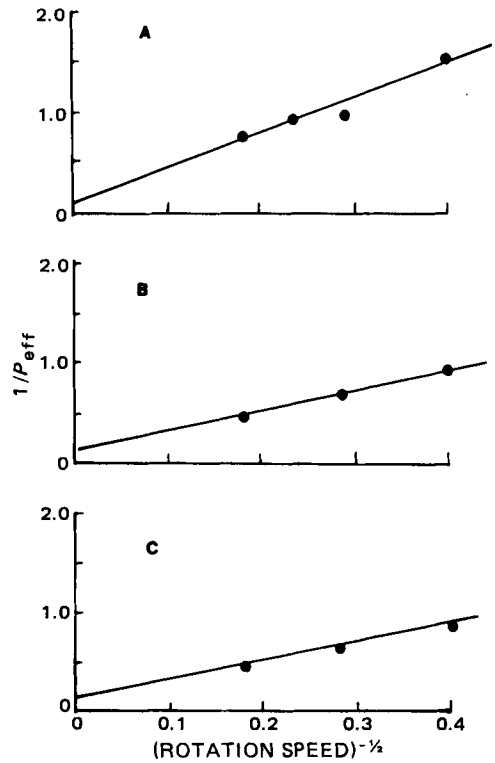

Figure 6—*Permeability coefficient dependence on rotation speed when both donor and receiver side diffusion layer resistances are important (A), outer diffusion layer resistance is eliminated (B), and inner diffusion layer resistance is eliminated (C).*

turbed (10). The cell is immersed in an outer solution of 450 ml, while the inner volume is 70 ml.

Dimethicone, a two-component room temperature vulcanizing dimethyl polysiloxane rubbber, was used as the model membrane. This material forms a nonpolar continuum and is lipid-like in nature, so partitioning and membrane diffusion rather than pore permeation occurs. Unlike more conventional lipid-impregnated membrane filters, it has been shown to be impermeable to ions and buffers and is unaffected by surfactants. These properties, along with the relatively simple procedure for preparing these membranes in the laboratory, indicated it would be a good candidate for model studies.

The membranes were prepared by mixing the catalyst with elastomer base and applying a vacuum to eliminate air bubbles. Then the elastomer was applied to both sides of the membrane support screen shown in Fig. 2. A spacer was placed on each side of the support and was compressed using an appropriate form at 1362 kg (3000 lb) of pressure.

The support and spacers were each 50-μm thick, resulting in a total membrane thickness of ~150 μm. The holes in the support were 0.556 cm in diameter. Preliminary observations using membranes without the supporting structure indicated that the membrane would not remain sufficiently rigid during the experiments. Since this would disturb the hydrodynamics at the surface and affect the diffusion layer thickness, a support was necessary. The membranes were measured with a micrometer at several places to obtain an average thickness.

Each membrane was allowed to cure for ~12 h. They were each removed and soaked in double-distilled water for ~15 min before use. The total area of membrane exposed to the solutions during the experiments was 6.16 cm^2, and the area of the holes through the support screen was 4.36 cm^2.

EXPERIMENTAL

Materials—Commercially available progesterone[5], radiolabeled progesterone[6], and radiolabeled capric acid[7] were used as received. The purity of the radioactive materials was checked periodically using TLC and were shown to be >98%. Polysorbate 80[8] and all other chemicals were used as received. Double-distilled water, degassed by boiling, was the only solvent used in preparing the permeant solutions.

Preparation of Solutions—All surfactant solutions were prepared by weighing polysorbate 80 into an appropriately sized volumetric flask and diluting with double-distilled water, previously degassed by bringing to a near boil, to obtain the correct percent weight/volume concentration of surfactant at 37°. This solution was allowed to equilibrate at 37° overnight before use. Saturated solutions were prepared by adding excess progesterone to surfactant solutions and equilibrating overnight. Before use, these solutions were filtered through two glass fiber filter papers[9] to eliminate particulates. Radioactive solutions were prepared by adding an aliquot of radiolabeled material to the test solution ~15 min before the experiment was begun.

Solubility Determination—The solubility of progesterone at several polysorbate 80 concentrations was determined by sealing ~5 ml of surfactant solution and excess progesterone in 15-ml ampuls and shaking in a 37° waterbath for 48 hr. Aliquots of equilibrated samples were filtered[9], diluted in ethanol USP, and assayed spectrophotometrically[10] at 240 nm. An identical solution, containing no progesterone and prepared in the same way, was used as a blank, and the absorbance was compared to a series of standards.

Viscosity and Density Determinations—The specific gravity of surfactant solutions was determined at 37° using a 25-ml pycnometer; the corresponding density, ρ, was calculated by calibrating the pycnometer with water (ρ = 0.993 g/cm^3 at 37°). Determinations of the kinematic viscosity, ν, were made with a viscometer[11]. The viscosity, η, was calculated from:

$$\nu = \eta/\rho \qquad \text{(Eq. 29)}$$

Diffusion Coefficient Determinations—Aqueous diffusion coefficients at 37° were determined using a small-volume diaphragm cell (14, 15). The apparatus consisted of two well-stirred reservoirs separated by two silver filter membranes[12]. Each membrane was 50-μm thick with a pore diameter of 1.2 μm. This pore diameter was large enough to permit the facile passage of micelles. The diffusion cell constant was determined using 0.1% benzoic acid in 0.01 *N* HCl for which the aqueous diffusion coefficient was known to be 1.4 × 10^{-5} cm^2/sec (16).

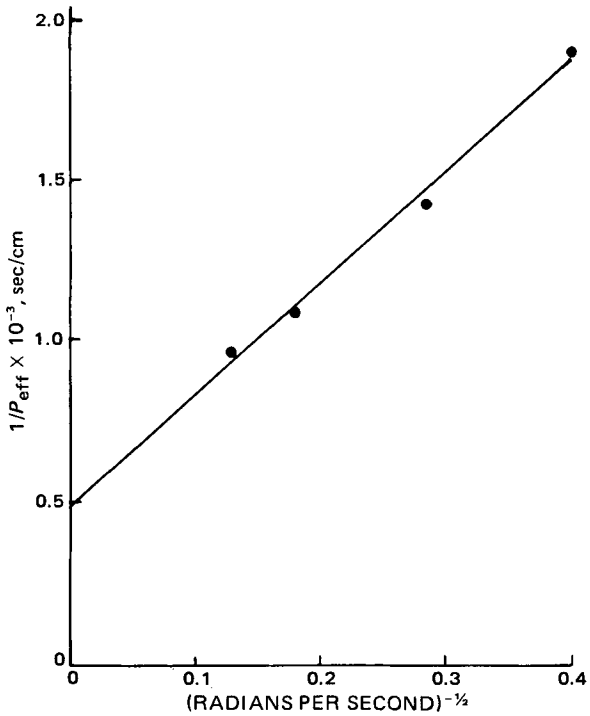

Figure 7—*Permeability coefficient dependence on rotation speed for progesterone.*

Subsequently, either the diffusion coefficient or the effective diffusion coefficient of progesterone in the presence of micelles was determined. Utilization of Eq. 9 permits the diffusion coefficient of the micelle to be factored out of the effective diffusion coefficient.

The effective diffusion coefficient was determined: (a) when only trace amounts of radiolabeled progesterone were present and (b) with surfactant solutions saturated with progesterone and containing sufficient radiolabeled progesterone to permit assay. In this way, any change in diffusivity with a change in progesterone concentration could be determined. All samples were assayed by adding the radioactive sample to 10 ml of liquid scintillation fluid[13] and counting in a liquid scintillation counter[14].

Diffusion Cell Characterization—To test the applicability of Eq. 20 to each side of the rotating membrane, radiolabeled capric acid was used. Since initial experiments showed this solute to have high membrane permeability, it was well suited for testing each diffusion layer separately by adjusting the pH in the donor and receiver solutions. For example, at sufficiently high pH in the receiver compartment, the diffusion of hydroxide ion from the bulk to the membrane surface essentially induces ionization of the permeant at the membrane surface. This results in "sink" conditions at the membrane surface being maintained with respect to the unionized species. If the membrane is impermeable to the ionized species, the receiver side diffusion layer resistance is eliminated or "shorted out." In this manner, the receiver side diffusion layer can be eliminated and the applicability of Eq. 20 to the donor side diffusion layer can be tested.

Prior to the start of each experiment, the prewashed membrane was positioned in the diffusion cell, which had been preheated in an oven to 37°. Then 70 ml of an appropriate solution (either 0.01 *N* HCl or 0.1 *M* phosphate buffer at pH 7.2) was added to the inner compartment. A visual inspection for leaks around the membrane was made. The diffusion cell was then immersed in an outer solution of 450 ml contained in a water-jacketed beaker to maintain the temperature of the outer solution and the diffusion cell at 37° for the duration of the experiment. The cell was rotated at 60, 120, or 300 rpm; 0.10-ml samples were withdrawn from both donor and receiver sides periodically. Assay for capric acid was by

[5] Aldrich Chemical Co., Milwaukee, Wis.
[6] Amersham Corp., Arlington Heights, Ill.
[7] California Bionuclear Corp., Sun Valley, Calif.
[8] Atlas Chemical Industries, Wilmington, Del.
[9] Whatman Filters, W&R Balston Ltd., England.
[10] Hitachi model 139, Hitachi Ltd., Tokyo, Japan.
[11] Size 25, Cannon-Fenske.
[12] Flowtronics, Philadelphia, Pa.
[13] ACS, Amersham Corp., Arlington Heights, Ill., and Aquasol, New England Nuclear, Boston, Mass.
[14] Model LS200, Beckman Instruments, Fullerton, Calif.

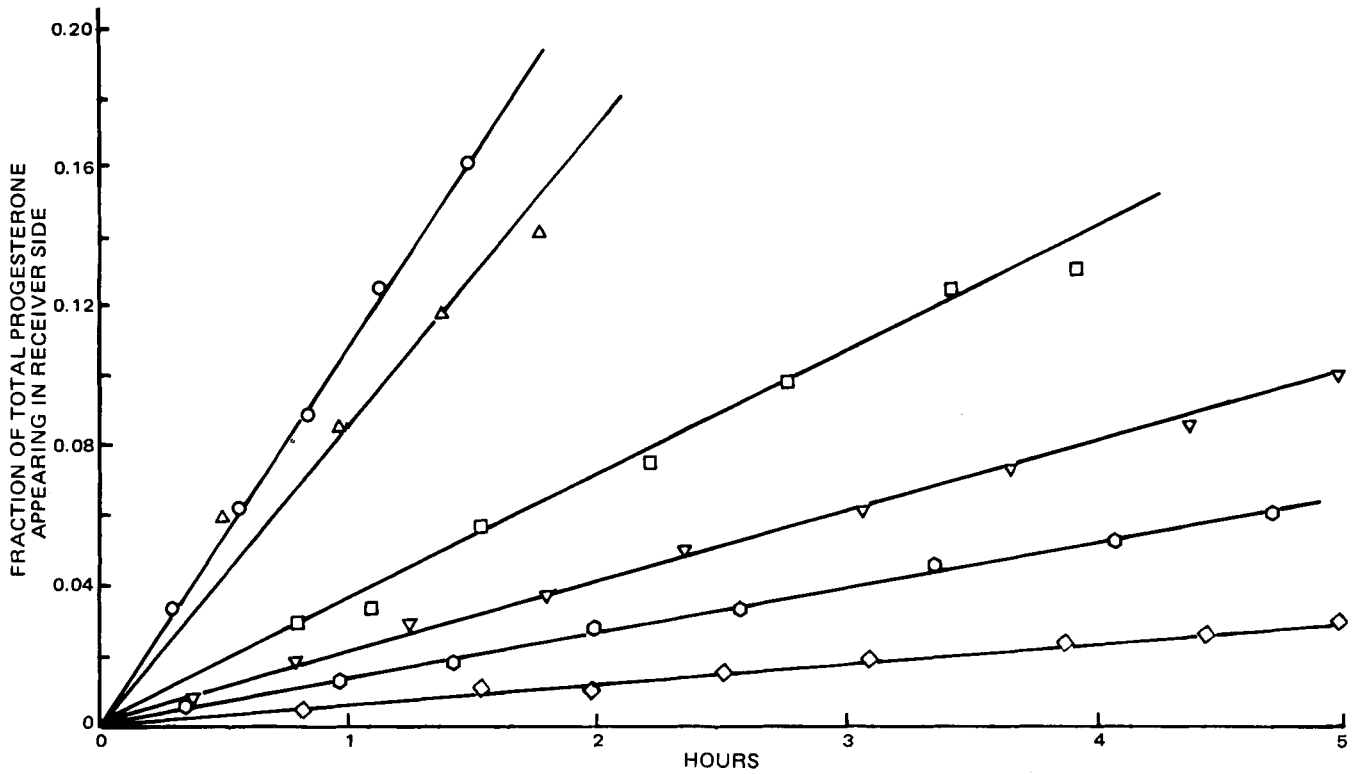

Figure 8—*Appearance of radiolabeled progesterone in the receiver compartment for constant initial concentration studies. Key (polysorbate 80 concentration):* ○, *0%;* △, *0.1%;* □, *0.5%;* ▽, *1.05%;* ○, *2.09%; and* ◇, *5.0%.*

liquid scintillation counting, and samples were corrected for quench if necessary. A series of steady-state experiments could be done in succession by completely replacing the receiver solution with fresh solution at the end of a run and, if necessary, replenishing the donor compartment with test permeant solution.

Micelle Solubilization Studies—The rotating-membrane diffusion cell was utilized for all transport experiments. The inner compartment served as the donor phase and the volume was 70 ml. The outer compartment volume was either 420 or 450 ml, depending on the experiment performed. Samples were taken using either a 100 or 500-μl Eppendorf micropipet[15]. Radioactive samples were assayed by liquid scintillation counting. Correction for quench was done when necessary. Nonradioactive progesterone was assayed by high-pressure liquid chromatography (HPLC) utilizing reversed-phase chromatography[16].

Two types of experiments were conducted to demonstrate clearly the influence of progesterone concentration on transport in the presence of polysorbate 80. Constant initial solute concentration experiments were carried out by adding an aliquot of radiolabeled progesterone (approximately the same concentration for each experiment) to 70 ml of surfactant solution, and saturated solution experiments were performed by adding surfactant solutions previously saturated with nonradiolabeled progesterone to the donor compartment. An identical surfactant solution with no progesterone was used as the receiver phase in each case.

In all experiments, samples were taken from the donor and receiver phases and assayed by liquid scintillation counting or HPLC. All experiments were conducted at 37° and a rotation speed of 60 rpm.

RESULTS AND DISCUSSION

The aqueous solubility of progesterone at 37° was determined to be 12.0 μg/ml, and the total solubility of progesterone increased linearly with increasing surfactant concentration over the range studied. The slope of the line is related to the micelle-free solute equilibrium distribution coefficient, k^*, by:

$$C_T = C^* + C' = C'[1 + k^*(SAA)] \qquad \text{(Eq. 30)}$$

The slope of the line was 1.26×10^{-1} mg/ml percent and corresponded to a value of 10.5 for the equilibrium distribution coefficient. This result is consistent with independent but less reliable measurements conducted in this laboratory using dialysis tubing.

The kinematic viscosity is shown in Fig. 3. The density increased linearly with surfactant concentration from a value of 0.993 g/cm^3 for pure water at 37° to 1.002 g/cm^3 for an 8.5% (w/v) polysorbate 80 solution.

The effective diffusion coefficients at several surfactant concentrations, as determined by using the small-volume diaphragm cell, are presented in Table I. The effective diffusion coefficient decreased as the surfactant concentration increased due to incorporation of more solute into the micelles. The effective diffusion coefficient was determined for both tracer levels of progesterone and saturated solutions. As shown, there was little difference between the diffusion coefficients at comparable surfactant concentrations and it is concluded that D_{eff} does not vary significantly with progesterone concentration.

By utilizing Eq. 9*a*, the diffusion coefficient of the micelle–solute complex (D^*) can be evaluated if the micelle-free solute equilibrium coefficient (k^*) and the free solute diffusion coefficient (D') are known. These values are shown in Table I, assuming a free solute diffusivity of 8.5×10^{-6} cm^2/sec and a micelle-free solute equilibrium coefficient of 10.5. For the progesterone–polysorbate 80 system under investigation, D^* is not constant.

Diffusion Cell Characterization—Typical results of the rate of loss of radiolabeled capric acid from the donor phase for three rotation speeds are shown in Fig. 4 when both the donor and receiver phases are 0.01 *N* HCl solutions. The diffusion layers on each side of the semipermeable membrane, thus, are important barriers to transport. The rate of loss of capric acid from the donor phase, for the same three rotation speeds, with 0.1 *M* phosphate buffer at pH 7.2 as the receiver side solution is shown in Fig. 5. The donor side diffusion layer is the only diffusion layer offering resistance to diffusion in this second case.

The effective permeability of the diffusional resistance under quasi-steady-state conditions can be conveniently assessed from the slope of the semilogarithmic plots by:

$$\ln (C_t/C_0) = \frac{-A}{V} P_{eff} t \qquad \text{(Eq. 31)}$$

where C_t is the concentration of solute remaining in the donor phase at time t, C_0 is the initial concentration, V is the volume of the donor phase, and A the area of the membrane available for transport. The area in these studies is the area of the holes in the membrane support (4.36 cm^2). Equation 31 can be modified to correct for any buildup of solute in the receiver compartment when necessary.

[15] Brinkmann Instruments, Westbury, N.Y.

[16] Model 440 equipped with μBondapack C_{18} column, Waters Associates, Milford, Mass.

Table III—Theoretical and Experimental Slopes of $1/P_{eff}$ *versus* $\omega^{-1/2}$ Plots

pH			Theoretical	Experimental	*SD*
Inner	Outer	*n*	Slope × 10^{-3}	Slope × 10^{-3}	× 10^{-3}
2.0[a]	2.0	5	3.672	3.56	0.44
2.0[a]	7.2	5	1.836	1.87	0.30
7.2	2.0[a]	3	1.836	1.62	0.18

[a] Denotes donor compartment.

The reproducibility of the effective permeability coefficient determinations utilizing the rotating-membrane diffusion cell is shown in Table II. Duplicate experiments in which both donor and receiver compartments were prepared from 0.01 *N* HCl solutions were performed. The average permeability and the standard deviation determmined at 60, 120, and 300 rpm are given. The coefficient of variation for each speed was between 5 and 6%. These deviations include sampling and assay errors as well as some variations in membrane thickness. Each experiment was done with a new membrane. Generally, the observed reproducibility compares with that observed for published work with other diffusion cell systems, indicating satisfactory reproducibility for each experiment.

The applicability of Eq. 20 to the diffusion layer thickness on each side of the membrane can be tested by utilizing Eqs. 27 and 28. Figure 6 depicts the results obtained when the inverse of the permeability is plotted against the inverse square root of the rotation speed for three different conditions. Both the donor and receiver side diffusion layers are important in Fig. 6A, and Eq. 27 should apply. The theoretical slope is 3.672 × 10^3, assuming a diffusion coefficient for capric acid (17) of 7.5 × 10^{-6} cm^2/sec and a kinematic viscosity of 6.96 × 10^{-3} cm^2/sec. Figures 6B and 6C show the results obtained when the outer and inner diffusion layer resistance are eliminated by buffering at pH 7.2. Consequently, Eq. 28 should apply. The theoretical slope is half of that for Eq. 27 or 1.836 × 10^3. The intercept corresponding to the inverse of the membrane permeability should be the same in each case.

Table III presents results from duplicate experiments like those given in Fig. 6. The average slope of 3.56 × 10^3 agrees quite closely with the theoretical prediction of 3.672 × 10^3 when both diffusion layers are included. When the outer or inner diffusion layer is eliminated, the average of the experimentally determined slope is 1.87 or 1.62 × 10^3, respectively. The Student *t* test for significance of difference between two means at the 5% level of confidence indicates there is no statistical difference between the latter two slopes. The 11–16% coefficient of variation for each case can be attributed in part to the 5–6% variation observed in each determination.

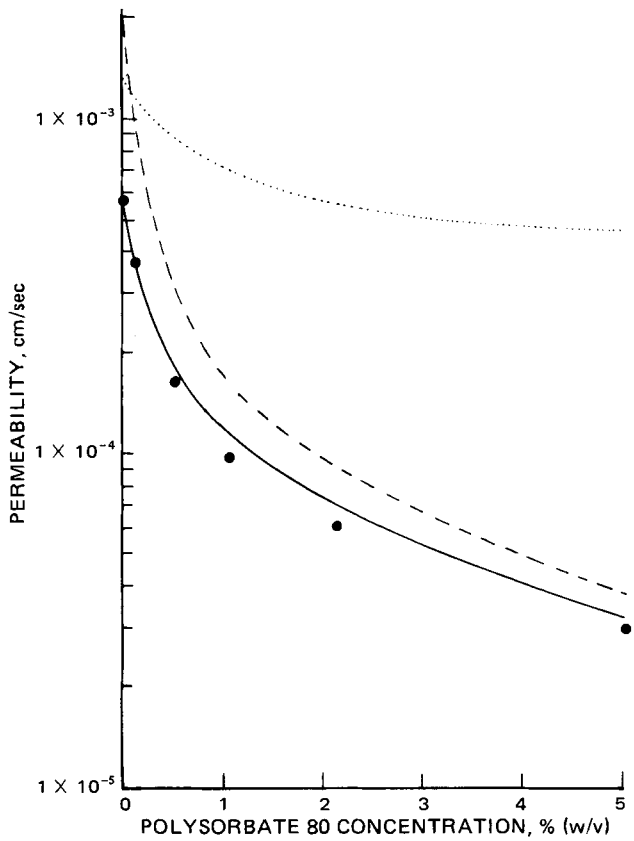

Figure 9—*Theoretical predictions of* P_{eff} (—), P_m (- - -), *and* P_i (· · ·) *as a function of polysorbate 80 concentration based on independent estimates of the physicochemical parameters. Key:* ●, *experimentally determined* P_{eff}.

Table IV—Experimentally Determined Permeability Coefficients and Fluxes from Constant Initial Concentration and Saturated Solution Studies

Polysorbate 80 Concentration, %	Constant Initial Concentration Case, P_{eff} × 10^4, cm/sec	Saturated Solution Case	
		Flux from Saturated Solution × 10^9, g/cm^2 sec	P_{eff} × 10^4, cm/sec
0	5.87	7.05	5.87
0.1	3.75	—	—
0.126	—	9.42	2.89
0.5	1.65	—	—
0.52	—	14.65	1.78
1.05	0.965	—	—
2.04	—	16.98	0.62
2.09	0.612	—	—
5.0	0.30	—	—

Because of the close agreement between theory and experiment, these results indicate that the aqueous diffusion layer thickness on each side of the rotating membrane is equal within the limits of experimental error. Therefore, Eq. 20 applies for each diffusion layer thickness. This diffusion cell system also has the advantage of permitting easy and quantitative control of the aqueous diffusion layer thickness and gives more insight into the events occurring within it. The ability to extrapolate to infinite rotation speed also permits the diffusion layer resistance to be factored out, thereby permitting an estimate of the membrane permeability coefficient.

Equation 27 can be utilized to determine the membrane permeability coefficient and the aqueous diffusion coefficient of progesterone, and results are presented in Fig. 7. The membrane permeability coefficient is estimated from the intercept to be 2.0 × 10^{-3} cm/sec for a 190-μm thick membrane. The aqueous diffusion coefficient, estimated from the slope in Fig. 7, is 8.5 × 10^{-6} cm^2/sec. This value is close to the diffusion coefficient of 7.9 × 10^{-6} cm^2/sec as determined by the small-volume diaphram cell method.

Micelle Solubilization Studies—The appearance of radiolabeled progesterone in the receiver compartment is shown in Fig. 8 for several polysorbate 80 concentrations. In these studies, the donor compartment contained approximately equivalent initial concentrations of radiolabeled progesterone. A decreasing slope as the surfactant concentration is increased is seen, reflecting a decreasing permeability. The effective permeability coefficients as determined from the slope of the lines in Fig. 8 are given in Table IV and are included in Fig. 9 along with theoretical estimates from the model. The theoretical estimates were based on Eqs. 24 and 25 and independent estimates of all relevant physicochemical parameters.

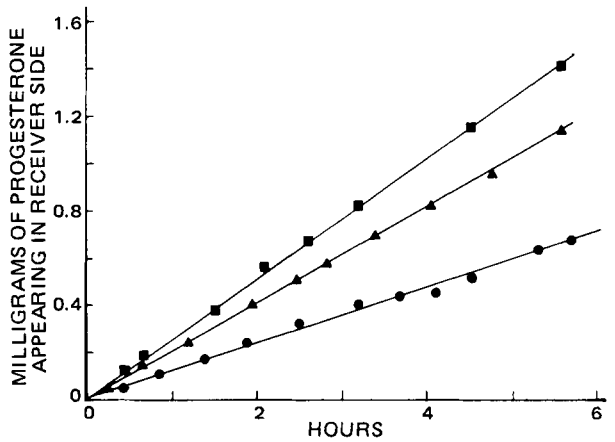

Figure 10—*Appearance of progesterone in the receiver compartment from saturated solutions. Key: (polysorbate 80 concentration)* ■, *2.04%;* ▲, *0.52%; and* ●, *0.126%.*

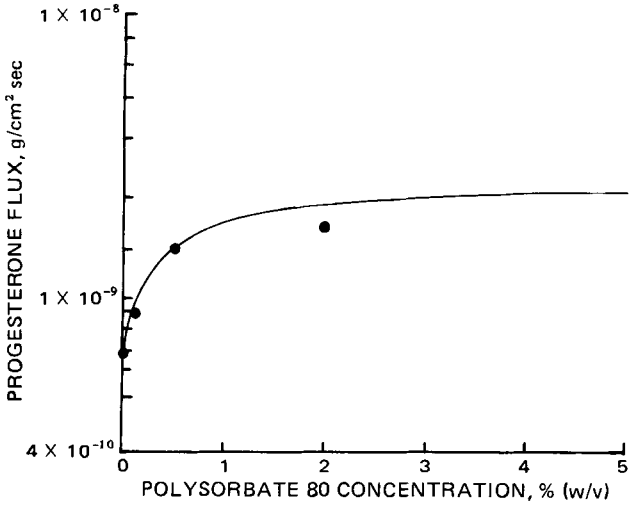

Figure 11—*Flux of progesterone from saturated solutions as a function of polysorbate 80 concentration. Key: —, theory; and ●, experimental.*

There is very good agreement between experimental results and the theoretical model. The predicted change in the permeability coefficient of the aqueous diffusion layer resistance is also included (P_i). It approaches a limiting value at high surfactant concentrations, corresponding to the permeability coefficient of the diffusion layer when only micelles are transported. The effective permeability coefficient continues to decrease, however, since the thermodynamic activity of progesterone continues to decrease with increasing surfactant. The theoretical curve labeled P_m is obtained when the aqueous diffusion layer is completely neglected.

The decreasing flux as a function of surfactant concentration is a result of the decreasing aqueous permeability coefficient and also the decreasing thermodynamic activity of progesterone. The decreasing effective permeability coefficient is in part the result of the changing aqueous diffusion layer permeability coefficient given in Eqs. 8 and 25. As the surfactant concentration increases, more progesterone is incorporated within the micelle and most of the progesterone diffuses through the diffusion layer solubilized in the micelle. The smaller diffusivity of the micelle determines the aqueous permeability coefficient at high surfactant concentrations. The thermodynamic activity of progesterone is also affected by the surfactant concentration since the concentration of free progesterone in the aqueous phase is lower due to micelle solubilization. This situation is reflected in the membrane permeability, P_m, and also in the bulk aqueous phase through Eq. 4.

Saturated Solution Studies—The rate of appearance of progesterone in the receiver side is shown in Fig. 10 for three surfactant concentrations. The donor phase was presaturated with progesterone, and the appearance of solute in the reciever side was followed using HPLC. The corresponding fluxes of progesterone from each of these saturated solutions is shown in Fig. 11, and the corresponding effective permeability coefficients are tabulated in Table IV. The solid line in Fig. 11 is the theoretical prediction based upon Eqs. 23 and 24 and is included to show the close agreement between experimental results and theoretical predictions based on the physical model and independent estimates of the relevant physicochemical parameters.

As was the case for the constant initial progesterone concentration studies, the effective permeability coefficient for the trilaminar resistance decreases with increasing surfactant concentration. However, a larger total bulk solute concentration, C_{b1}, is possible due to micelle solubilization. For the progesterone–polysorbate 80 case, the increased solubility of progesterone offsets the decreased permeability; the net result is an increase in flux as the surfactant concentration increases. In effect, the micelles act as carriers of solute across the aqueous diffusion layer to the membrane surface. In this way, the diffusion layer resistance can be eliminated or shorted out. At high surfactant concentrations, saturated solution conditions can be reached at the membrane surface and the membrane is the only resistance to diffusion. For progesterone, this plateau occurs at ~2% polysorbate 80 and there is little further increase in flux.

REFERENCES

(1) G. Levy and R. H. Reuning, *J. Pharm. Sci.*, **53**, 1471 (1964).

(2) C. L. Gantt, N. Gachman, and J. M. Dyniewics, *Lancet*, **1**, 486 (1961).

(3) C. H. Jones, P. J. Culver, G. D. Drummey, and A. E. Ryan, *Ann. Intern. Med.*, **29**, 1 (1948).

(4) J. G. Wagner, E. S. Gerard, and D. G. Kaiser, *Clin. Pharmacol. Ther.*, **7**, 610 (1966).

(5) G. Levy and J. A. Anello, *J. Pharm. Sci.*, **57**, 101 (1968).

(6) G. B. Dermer, *J. Ultrastructure Res.*, **20**, 311 (1967).

(7) H. Westergaard and J. M. Dietschy, *J. Clin. Invest.*, **58**, 97 (1976).

(8) N. E. Hoffman and W. J. Simmonds, *Biochim. Biophys. Acta*, **241**, 331 (1971).

(9) T. Karman, *Z. Angew. Math. Mech.*, **1**, 244 (1921).

(10) W. J. Albery, J. F. Burke, E. B. Leffler, and J. Hadgraft, *J. Chem. Soc. Faraday Trans.*, **1**, **72**, 1618 (1976).

(11) E. G. Lovering and D. B. Black, *J. Pharm. Sci.*, **63**, 671 (1974).

(12) E. R. Garrett and P. B. Chemburkar, *ibid.*, **57**, 944 (1968).

(13) V. G. Levich, "Physicochemical Hydrodynamics," Prentice-Hall, Englewood Cliffs, N.J., 1962.

(14) M. M. Kreevoy and E. M. Wewerka, *J. Phys. Chem.*, **71**, 4150 (1967).

(15) K. H. Keller, E. R. Canales, and S. S. Yun, *ibid.*, **75**, 379 (1971).

(16) S. Prakongpan, Ph.D. thesis, University of Michigan, Ann Arbor, Mich., 1974.

(17) D. E. Bidstrup and C. J. Geankoplis, *J. Chem. Eng. Data*, **8**, 170 (1963).

High-Performance Liquid Chromatographic Determination of Suprofen in Drug Substance and Capsules

AVINASH L. LAGU *, RICHARD YOUNG, EUGENE McGONIGLE, and PHILIP A. LANE ˣ

Received March 2, 1981, from the *Pharmaceutical Analysis Section, Ortho Pharmaceutical Corporation, Raritan, NJ 08869.* Accepted for publication May 15, 1981. *Present address: Eli Lilly and Co., Indianapolis, IN 46206.

Abstract □ A rapid, simple, stability-indicating assay procedure for suprofen, a new analgesic agent, in suprofen drug substance and in capsules was developed using high-performance liquid chromatography. Suprofen was extracted from the sample matrix with methanol and diluted with internal standard solution, and an aliquot was chromatographed on a reversed-phase column using acetonitrile–pH 3.0 buffer solution as the mobile phase. The selectivity of the chromatographic system for intact suprofen was demonstrated by resolving suprofen from synthetic intermediates, potential impurities, and reaction products resulting from accelerated stress conditions. The method is linear, quantitative, and reproducible. Either peak height or peak area ratios can be used for quantitation.

Keyphrases □ Suprofen—high-performance liquid chromatographic determination in drug substance and capsules □ High-performance liquid chromatography—determination of suprofen in drug substance and capsules □ Analgesics—high-performance liquid chromatographic determination of suprofen in drug substance and capsules

Suprofen, α-methyl-4-(2-thienylcarbonyl)benzeneacetic acid (I), is a potent, new analgesic agent (1, 2) and inhibitor of prostaglandin synthetase (3, 4). Two analytical methods were previously reported for suprofen drug substance; a TLC method (5) was used to monitor suprofen stability and a high-performance liquid chromatographic (HPLC) method (6) was used to determine suprofen and its known metabolites in plasma.

This paper describes a rapid, simple, stability-indicating HPLC method for suprofen in suprofen drug substance and in capsules containing either 100 or 200 mg of suprofen.

EXPERIMENAL

Apparatus—The liquid chromatograph[1], equipped with a constant-displacement pump[2] and a UV detector[3] (254 nm), was operated at ambient temperature. Chromatograms were traced on a strip-chart recorder[4] or drawn by computer[5]. All analyses were performed using a 3.9-mm × 30-cm reversed-phase column[6]. Generally, an automatic sampler[7] was used to inject samples onto the column, but a septumless injector[8] or a fixed-loop injector[9] was also used. Peak height and peak area integrations and calculations were performed by computer[5].

Materials—All chemicals were reagent grade unless noted otherwise and were purchased from commercial sources. 4-Nitrobenzoic acid[10], acetonitrile[11], and methanol[11] were used without additional purification.

Chromatographic Conditions—The mobile phase was acetonitrile–pH 3.0 buffer solution (3:2). The pH 3.0 buffer solution was prepared by adding a 0.02 *M* dibasic sodium phosphate heptahydrate solution to a 0.01 *M* citric acid monohydrate solution until the solution pH was between 2.97 and 3.04. At least 500 ml of this solution was passed through a 0.22-μm filter[12], and 400 ml was thoroughly mixed with 600 ml of acetonitrile. The solution was sonified[13] for 15 min to degas the mixture and then equilibrated in the HPLC system at a rate of 0.5 ml/min.

Internal Standard Solution—The internal standard was 4-nitrobenzoic acid prepared as a 1.2 mg/ml solution in methanol.

Standard Solution—Suprofen standard, ~50 mg, was accurately weighed and transferred into a 25-ml volumetric flask; then it was dissolved and diluted to volume with methanol. Five milliliters of this solution was pipetted into a 10-ml volumetric flask. The flask was then diluted to volume with internal standard solution.

Standard Chromatogram—Two microliters of the standard solution were injected into the liquid chromatograph. The peak heights and peak areas obtained were used in the calculations for suprofen.

Suprofen Synthetic Intermediates, Impurities, and Reaction Products from Accelerated Stress Studies—α-Hydroxy-α-methyl-4-(2-thienylcarbonyl)benzeneacetic acid (II), 4-carboxy-α-methylbenzeneacetic acid (III), methyl-α-methyl-4-(2-thienylcarbonyl)benzeneacetic acid (IV), ethyl-4-(2-thienylcarbonyl)benzene (V), 4-acetyl-α-methylbenzeneacetic acid (VI), α-methyl-4-(2-thienylcarbonyl)benzene acetonitrile (VII), (1-bromoethyl)-4-(2-thienylcarbonyl)benzene (VIII), diethyl-2-methyl-2-[4-(2-thienylcarbonyl)phenyl]-1,3-propanedioate (IX), 4-fluorophenyl-2-thienylmethanone (X), α-methyl-4-(2-thienylcarbonyl)benzene acetamide (XI), 2-fluorophenyl-2-thienylmethanone (XII), 3-fluorophenyl-2-thienylmethanone (XIII),

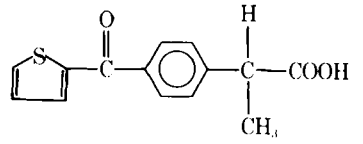

I

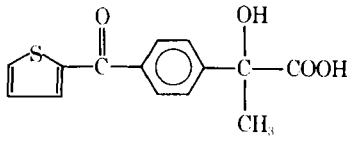

II

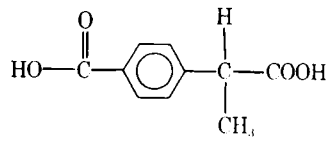

III

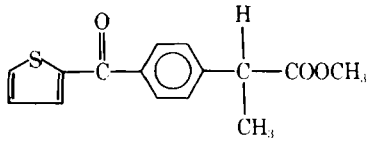

IV

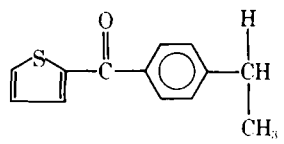

V

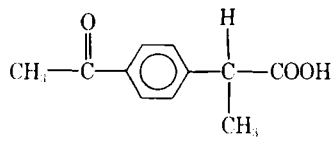

VI

[1] Model ALC 202, Waters Associates, Milford, Mass.
[2] Model M-6000, Waters Associates, Milford, Mass.
[3] Model 440, Waters Associates, Milford, Mass.
[4] Omniscribe recorder model B5117-IX, Houston Instruments, Austin, Tex.
[5] Model 3354C, Hewlett-Packard, Avondale, Pa.
[6] μBondapak C_{18}, Waters Associates, Milford, Mass.
[7] WISP autosampler model 710A, Waters Associates, Milford, Mass.
[8] Model U6K, Waters Associates, Milford, Mass.
[9] Model 7125, Rheodyne Inc., Cotati, Calif.
[10] Catalog No. N1179-5, Aldrich Chemical Co., Milwaukee, Wis.
[11] Distilled in glass, Burdick & Jackson, Muskegon, Mich.
[12] Millipore filter type GC.
[13] Model SC-200T, Sonicar Instrument Corp., Copiaque, N.Y.

0022-3549/82/0100-0085$01.00/0

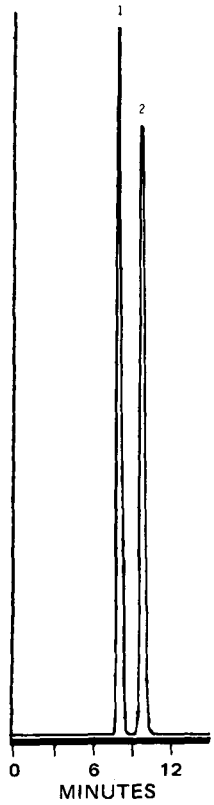

Figure 1—*Typical chromatogram obtained from a suprofen(I) capsule sample. Key: peak 1, internal standard; and peak 2, suprofen.*

α-methyl-4-(5-chloro-2-thienylcarbonyl)benzeneacetic acid (XIV), 2-[4-(2-thienylcarbonyl)phenoxy]propanoic acid (XV), methyl-4-(2-thienylcarbonyl)benzene (XVI), and 4,4-carbonylbis(α-methylbenzeneacetic acid) (XVII) were obtained[14] and chromatographed as methanolic solutions (~2 mg/ml).

Accelerated Stress Studies—Accelerated degradation of suprofen was accomplished by several methods:

1. Suprofen drug substance (50.6 mg) was heated at its melting point of 124° for 1 hr in an oil bath.
2. Suprofen drug substance (50.5 mg) was dispersed in 5.0 ml of 1 *N* HCl and kept at 50° for 72 hr.
3. Suprofen drug substance (50.6 mg) was dispersed in 5.0 ml of 1 *N* NaOH and kept at 50° for 72 hr.
4. Suprofen drug substance (50.2 mg) was dispersed in 5.0 ml of 3% hydrogen peroxide solution and kept at 50° for 72 hr.

After 72 hr, the acid and base samples were neutralized and diluted to 25.0 ml with methanol. The excess peroxide was destroyed by gently heating the solution and then diluting to 25.0 ml with methanol. The sample heated at its melting point was made to 25.0 ml with methanol.

TLC Studies—TLC evaluation of the accelerated stress samples was carried out by spotting the equivalent of 100 μg of suprofen on silica gel plates[15] and developing them 15 cm in tanks lined with adsorbent paper in each of the following systems: System I, *n*-hexane–chloroform–methanol–strong ammonia (50:30:20:1), suprofen R_f 0.18; System II, *n*-hexane–dioxane–acetic acid (80:20:1), suprofen R_f 0.12; and System III, chloroform–methanol–methyl ethyl ketone (40:30:30), suprofen R_f 0.48. Visualization was by short wavelength UV light (254 nm).

Suprofen Recovery Studies—To simulate 100 mg of suprofen capsules, an accurately known amount of suprofen drug substance was transferred to a 50- ml volumetric flask containing 120 ± 2 mg of placebo. For 200-mg suprofen capsules, an accurately known amount of suprofen drug substance was transferred to a 100-ml volumetric flask containing 135 ± 2 mg of placebo. For both studies, 10 individual synthetic samples were prepared. The 200-mg study was conducted by two different operators on different days. Methanol was added to the flasks, which were then shaken[16] for 15 min. After the flasks were made to volume with methanol and thoroughly mixed, a portion of the solution was filtered[17]

[14] Janssen Pharmaceutica, Beerse, Belgium.
[15] Silica gel 60F-254, 0.25-mm thickness plates, E. Merck, Darmstadt, West Germany.
[16] Model 75 wrist action shaker, Burrel Corp., Pittsburgh, Pa.
[17] Millipore filter type FHLP, 0.22 μm pore size.

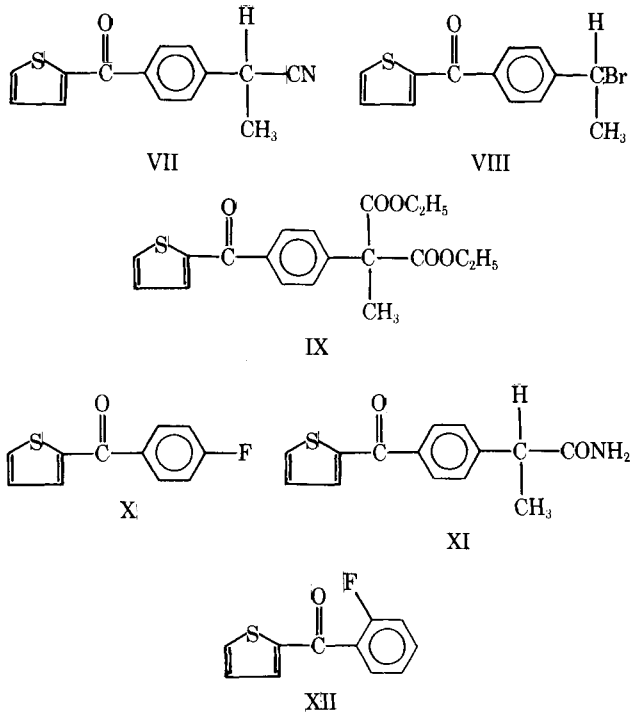

using a syringe equipped with a Swinny adapter. A 5.0-ml aliquot of the filtrate was pipetted into a 10-ml volumetric flask, which was then diluted to volume with internal standard solution. Then 2-μl portions were injected into the liquid chromatograph using either manual or automated injection techniques.

The suprofen recovery was calculated from:

$$\text{percent suprofen} = \frac{R_{sam}}{R_{std}} \times \frac{W_{std}}{W_{sam}} \times D \times 100 \qquad \text{(Eq. 1)}$$

where R_{sam} and R_{std} is the peak area or peak height ratio of suprofen to the internal standard for the sample and standard, respectively; W_{std} is the weight of suprofen standard; W_{sam} is the amount of suprofen taken; and D is a dilution factor, which is equal to 2 for the 100-mg spiked placebo capsules and 4 for the 200-mg spiked capsules.

Suprofen in Capsules—The contents of 20 suprofen capsules were weighed to determine the average capsule fill weight (C_{avg}) and were thoroughly mixed. For 100-mg suprofen capsules, duplicate 220 ± 3-mg

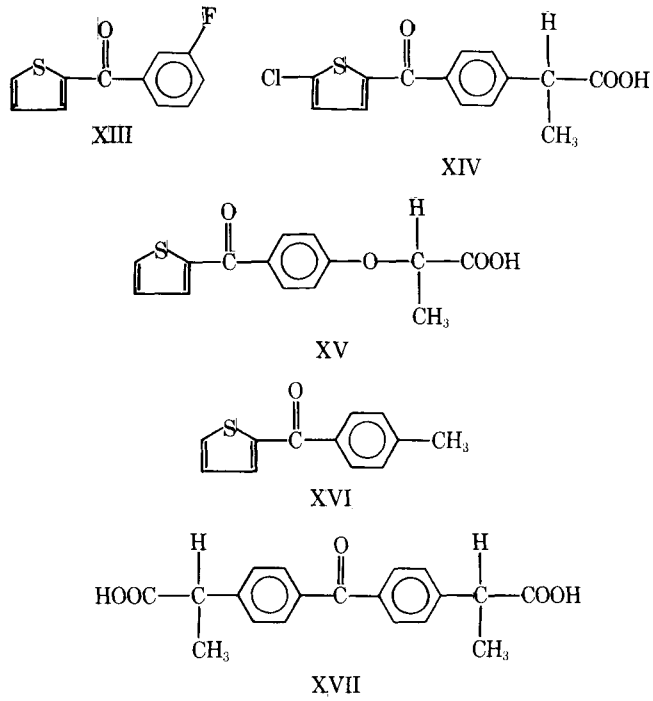

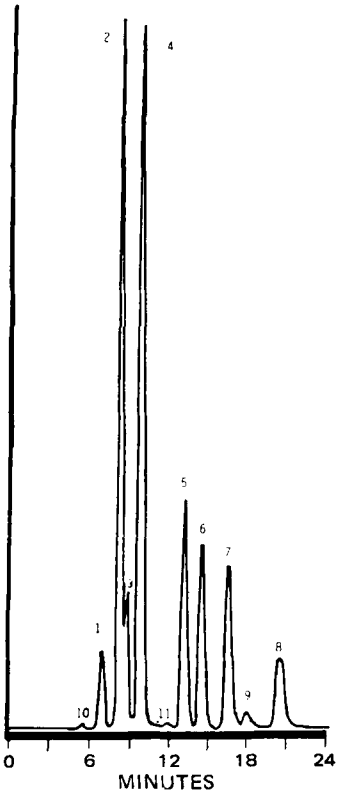

Figure 2—*Chromatogram showing separation of I from various structurally related compounds. Key: peak 1, III; peak 2, XV; peak 3, XVII; peak 4, I; peak 5, VII; peak 6, XVI; peak 7, X; and peak 8, IX. Peak 9 is an impurity in IX. Peaks 10 and 11 are unknown impurities.*

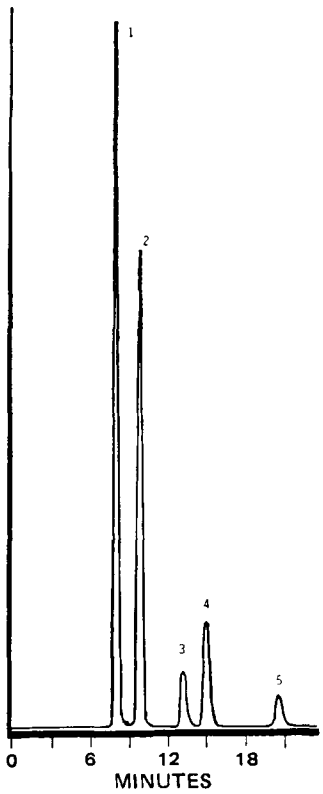

Figure 3—*Chromatogram showing separation of I from various structurally related compounds. Key: peak 1, VI; peak 2, I; peak 3, XIV; peak 4, XIII; and peak 5, VIII.*

samples were accurately weighed and transferred to a 50-ml volumetric flask. For 200-mg suprofen capsules, duplicate 335 ± 3-mg samples were accurately weighed and transferred to a 100-ml volumetric flask. The samples were assayed as already described and calculated as follows:

$$\text{milligrams of suprofen per capsule} = \frac{R_{sam}}{R_{std}} \times \frac{W_{std}}{W_{sam}} \times D \times C_{avg} \quad \text{(Eq. 2)}$$

Suprofen Drug Substance—The suprofen content of suprofen drug substance was determined by treating it like a suprofen standard solution. If samples are assayed for purity, the internal standard need not be added, although a fixed-loop injector should be used. The suprofen content may be calculated using Eq. 1 with a dilution factor (D) equal to 1.

System Suitability—The chromatographic system is considered to be performing satisfactorily if the internal standard has a retention time of 6.5–8.0 min, suprofen has a retention time of 9.0–11.0 min, and the calculated resolution between the two compounds is at least 2.0.

RESULTS AND DISCUSSION

The resolving power of the chromatographic system was demonstrated by chromatographing suprofen and a structurally related series of compounds that arise from various synthetic schemes as intermediates (V and VII–X), potential impurities (II, IV, and XI–XVII), or reaction products (III and VI) resulting from stress studies. The resolution of suprofen and the internal standard in a typical capsule sample is demonstrated in Fig. 1. Several mixtures of suprofen and the structurally related compounds were prepared and chromatographed to show the resolution obtained. The chromatograms resulting from these mixtures are shown in Figs. 2–4. Compounds II, VI, and XI were not totally resolved from the internal standard; if their presence in the sample is suspected, the internal standard should be deleted and the sample reinjected using a fixed-loop injector. Each compound was chromatographed with suprofen, and the relative retention time and resolution (R) were calculated with respect to suprofen (Table I).

Suprofen drug substance that was thermally stressed at its melting point afforded 97.8% recovery of suprofen with no extraneous peaks observed in its chromatogram. The sample subjected to peroxide oxidation afforded 97.4% recovery of suprofen. The chromatogram of this sample showed an extra peak with a retention time of 5.5 min. The suprofen sample subjected to acid hydrolysis afforded quantitative recovery of suprofen and did not show any extra chromatographic peaks. The sample subjected to base hydrolysis turned yellow during the 72-hr interval and afforded 92.8% recovery of suprofen. The chromatogram of this sample showed two extra small peaks at 6 and 7 min.

The stressed samples were qualitatively examined by TLC for any additional unknown spots using basic (System I), acidic (System II), and aprotic (System III) solvent systems. TLC evaluation was chosen because

Table I—Chromatographic Data for Suprofen and Structurally Related Compounds

Compound	Relative Retention Time	Resolution (R)
I	1.0	—
II	0.78	2.0
III	0.71	3.7
IV	1.54	5.3
V	2.12	8.6
VI	0.81	2.5
VII	1.34	3.4
VIII	2.11	8.3
IX	2.10	9.4
X	1.49	4.7
XI	0.86	1.8
XII	1.39	3.9
XIII	1.53	5.6
XIV	1.36	3.5
XV	0.91	1.1
XVI	1.71	6.1
XVII	0.84	1.9

Table II—Suprofen Recovery: 100-mg Dose Using Peak Height Ratio

Operator 1[a]			Operator 2[b]		
Suprofen Added, mg	Suprofen Found, mg	Recovery, %	Suprofen Added, mg	Suprofen Found, mg	Recovery, %
100.6	103	102	102.6	106	103
100.4	103	103	101.4	101	99.6
101.1	102	101	100.4	100	99.6
100.2	102	102	101.8	104	102
100.2	98.6	98.4	102.0	102	100

[a] Average recovery = 101 ± 1.76% (SD), and percent deviation = ±1.74%. [b] Average recovery = 101 ± 1.56% (SD), and percent deviation = ±1.55%.

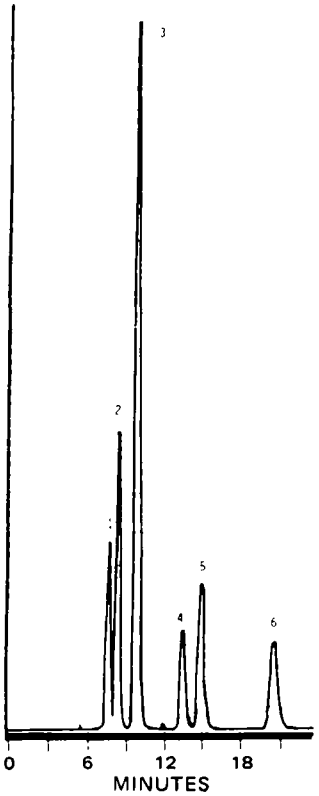

Figure 4—*Chromatogram showing separation of I from various structurally related compounds. Key: peak 1, II; peak 2, XI; peak 3, I; peak 4, XII; peak 5, IV; and peak 6, V.*

all substances present in the stressed sample would be carried through the TLC system. If an unknown UV-absorbing substance in the sample did not migrate in the system, it would still be detectable at the origin. Qualitatively, each of the three systems afforded identical results. The thermally stressed sample and the acid hydrolysis sample showed only the presence of suprofen. The peroxide-stressed sample, in addition to suprofen, showed a faint origin spot, which was in qualitative agreement with the HPLC results, which showed one extra peak. The base hydrolysis sample showed two extra spots, a small origin spot and a spot that was not totally resolved from suprofen. These results were also in qualitative agreement with the HPLC findings.

Since the HPLC system resolved suprofen from its synthetic intermediates, potential impurities, and reaction products from accelerated stress studies, showed drug loss due to decomposition in accelerated stress studies, and showed the presence of the same number of additional peaks from those studies compared to TLC, it was concluded that the method was stability indicating for suprofen.

Using peak height ratios, the detector response was demonstrated to be linear over the range of 0.0997–2.00 $\mu g/\mu l$ of suprofen (10–200% of label claim). Linear regression analysis of the data yielded a slope of 0.978, an intercept of −0.00995, and a coefficient of determination (r^2) of 0.9996. Using area ratios, the detector response was linear over the range of 0.200–1.50 $\mu g/\mu l$ of suprofen (20–150% of label claim). Linear regression analysis of the data yielded a slope of 1.01, an intercept of +0.00194, and coefficient of determination of 0.9999. Thus, the detector response was linear with either peak height ratios or peak area ratios.

The results of recovery studies conducted by two operators on 100 and 200-mg suprofen spiked placebo capsules are shown in Tables II and III,

Table III—Suprofen Recovery: 200-mg Dose Using Peak Height Ratio

Operator 1[a]			Operator 2[b]		
Suprofen Added, mg	Suprofen Found, mg	Recovery, %	Suprofen Added, mg	Suprofen Found, mg	Recovery, %
200.1	199	99.4	199.8	193	96.6
200.8	200	99.6	200.1	200	100
200.5	197	98.3	200.2	199	99.4
200.0	198	99.0	201.3	206	102
201.7	200	99.2	201.6	200	99.2
200.6	201	100	200.3	198	98.9
201.7	201	99.7	199.8	202	101
200.9	200	99.6	202.3	201	99.4
202.2	202	99.9	200.4	200	99.8
201.5	199	98.8	202.3	200	98.9

[a] Average recovery = 99.4 ± 0.53%, and percent deviation = ±0.53%. [b] Average recovery = 99.5 ± 1.42%, and percent deviation = ±1.42%.

Table IV—Analysis of Suprofen Capsules Using Peak Height and Peak Area Ratios

Capsule Sample, mg	Suprofen by Peak Height, mg	Suprofen by Peak Area, mg	Height/ Area[a]
100	96.9	96.7	1.002
	98.1	97.6	1.005
	97.2	96.5	1.007
	101	99.7	1.013
200	199	199	1.000
	196	196	1.000
	195	195	1.000
	197	197	1.000

[a] Theoretical height/area ratio = 1.000.

respectively, using peak height ratios to quantitate suprofen. Quantitative recovery of suprofen was obtained at both concentration levels. The overall recovery for the 30 samples was 100 ± 1.45%. The equivalence of quantitating suprofen by either peak area ratios or peak height ratios is shown in Table IV, where actual suprofen capsules were assayed and quantitated by both techniques. As shown, the ratio of the peak height result to the peak area result was essentially unity, indicating no difference between peak area and peak height results.

REFERENCES

(1) F. C. Colpaert, C. J. Niemegeers, and P. A. Janssen, *Arch. Int. Pharmacodyn. Ther.*, **220**, 329 (1976).

(2) R. Capetola, D. Shriver, and M. Rosenthale, *Pharmacologist*, **20**, 270 (1978).

(3) P. A. Janssen, *Arzneim.-Forsch.*, **25**, 1495 (1975).

(4) F. Awouters, C. J. Niemegeers, F. M. Lenaerts, and P. A. Janssen, *J. Pharm. Pharmacol.*, **30**, 41 (1978).

(5) J. F. Van Rompoy, W. J. Pattyn, and P. J. Demoen, *Arzneim.-Forsch.*, **25**, 1501 (1975).

(6) K. B. Alton and J. E. Patrick, *J. Pharm. Sci.*, **67**, 985 (1978).

ACKNOWLEDGMENTS

The authors thank Mr. Derral Mayberry, Mrs. Joan McMahon, Mrs. Andrea Lanni, and Mr. Robert Gargiullo for help in performing the experiments.

Measurements of Ionization Constants and Partition Coefficients of Guanazole Prodrugs

ABDULGADER A. ALHAIDER, CYNTHIA D. SELASSIE, SWEE-ONG CHUA, and ERIC J. LIEN ˣ

Received January 22, 1981, from the *Section of Biomedicinal Chemistry, School of Pharmacy, University of Southern California, Los Angeles, CA 90033.* Accepted for publication May 15, 1981.

Abstract □ A series of guanazole prodrugs, which are less water soluble than the parent compound and have relatively higher molecular weights, was recently synthesized, and their antineoplastic activities were measured *in vitro*. In the present work, the ionization constants and partition coefficients of these compounds were measured for the first time. In contrast to guanazole, which is a weak base, guanazole prodrugs have been shown to be weak to moderate acids due to the electronic effects of the acyl group and the heterocyclic ring. Possible tautomeric and resonance structures are presented to account for the pKa values observed. Both the inductive and resonance effects of the substituent are important in determining the values of the ionization constant. The preparation of the prodrugs not only altered the lipophilicity but also drastically changed the acid–base property of the parent compound. The observed true partition coefficient values in most guanazole prodrugs studied were higher than those calculated from the π-constants. Under highly ionized conditions, the small amount of water in the octanol layer has a significant effect in trapping a substantial amount of the ionized species in the octanol layer and gives rise to a higher log P value than expected. Under nonionized conditions, intramolecular hydrogen bonding plays an important factor in electron delocalization and reduction of hydrogen bonding with water molecules, causing the nonionized species of the guanazole prodrugs to be more lipophilic than expected.

Keyphrases □ Guanazole–prodrugs, ionization constants and partition coefficients □ Ionization constants—guanazole prodrugs □ Partition coefficients—guanazole prodrugs □ Prodrugs—guanazole, ionization constants and partition coefficients □ Antitumor agents—guanazole prodrugs

Guanazole, a known ribonucleotide reductase inhibitor was shown to have antitumor activity against the murine leukemias L-1210 and K-1964, carcinoma, and reticulum cell sarcoma A-RCS (1). Brockman *et al.* found that guanazole acts by inhibiting the incorporation of adenine, hypoxanthine, and uridine into DNA to a much greater extent than into RNA (2).

BACKGROUND

Guanazole has been shown to be effective clinically in patients with acute and chronic myelogenous leukemias (3). In addition to the side effects observed in therapy with guanazole, such as hematological toxicity and some myelosuppression (4, 5), guanazole has some biopharmaceutical disadvantages. Pharmacokinetic studies on guanazole have shown that 95% of the drug was excreted in the urine of mice within 3 hr and most of it was unchanged (6). It also has a very short half-life: 30 min in mice (7), 68 min in rats (8), and 5 hr in humans (8, 9). Thus, a high dose or continuous administration is necessary to obtain the required therapeutic effect. The short half-life of guanazole can be attributed to its high polarity and its low molecular weight.

To circumvent these problems, a series of new guanazole prodrugs was prepared by acylation of guanazole by various organic anhydrides and acid chlorides (10). The antineoplastic activity *in vitro* against leukemia L-1210 has already been studied. The results showed that four of the prodrugs had comparable or greater *in vitro* activity than guanazole itself. (*In vivo* testing is presently being conducted by the National Cancer Institute.)

To carry out structure–activity relationship studies to serve as guidelines for further molecular modification, it is necessary to have pertinent physicochemical parameters for the guanazole prodrugs. However, these properties of the new compounds are not available in the literature. This need prompted the investigation of the ionization constants (pKa) and partition coefficients (log P) since these are the most important physicochemical constants used in structure–activity relationship studies (11).

Guanazole prodrugs have a triazole structure with two ionization sites, deprotonation and protonation. However, under the present experimental conditions, pKa values represent only the deprotonation process. Since the optical properties of the undissociated forms differ from those of the dissociated forms, UV spectroscopy was utilized to measure the pKa values of the prodrugs.

The partition coefficient (log P) may be measured at a pH in which the drug is partially ionized and partially nonionized (12, 13). However, the ionized form of a molecule does not partition into octanol (13). The true partition coefficient may be calculated from the observed value, the buffer pH, and the pKa of the compound. Therefore, the apparent partition coefficient is pH dependent (14–16) and should be converted to the "true" (corrected) partition coefficient, which is pH independent as indicated by the following:

$$P_{corr} = \frac{C_o}{C_a(1-\alpha)} = \frac{P_{app}}{(1-\alpha)} \qquad \text{(Eq. 1)}$$

where P_{corr} is the corrected partition coefficient, P_{app} is the apparent partition coefficient, C_o is the concentration of the drug in the organic phase, C_a is the concentration of the drug in the aqueous phase, and α is the degree of ionization calculated from the Henderson–Hasselbalch equation (17) as follows. For acids:

$$\alpha = \frac{1}{1 + \text{antilog}\,(\text{pKa} - \text{pH})} \qquad \text{(Eq. 2)}$$

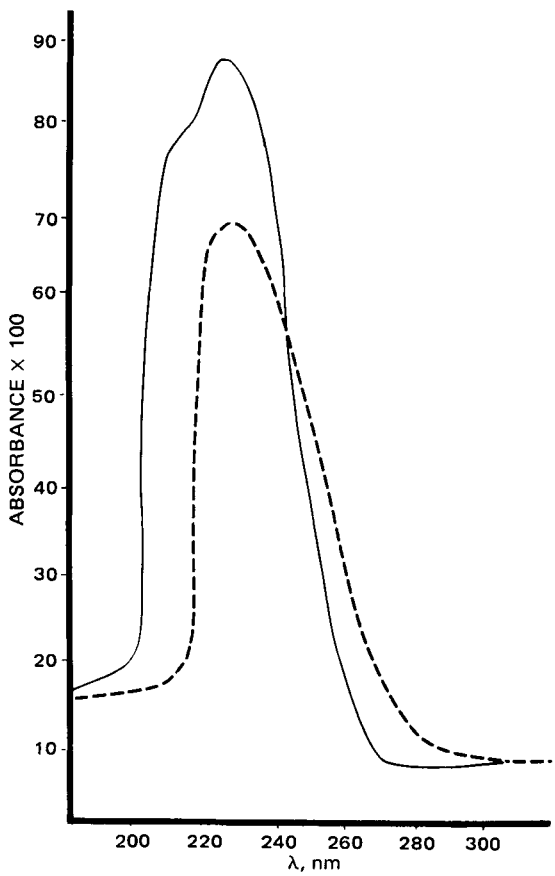

Figure 1—*UV spectrum of 3,5-diacetamido-1,2,4-triazole. Key: —, pH 4.50; and - - -, pH 12.50.*

0022-3549/82/0100-0089$01.00/0

Table I—Structural Formulas of Guanazole Prodrugs

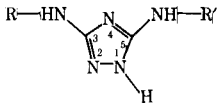

	Chemical Name	R	R′
I	3,5-Diacetamido-1,2,4-triazole	$COCH_3$	$COCH_3$
II	3,5-Dipropionamido-1,2,4-triazole	$COCH_2CH_3$	$COCH_2CH_3$
III	3,5-Dibutyramido-1,2,4-triazole	$COCH_2CH_2$-CH_3	$COCH_2CH_2$-CH_3
IV	3,5-Di(trifluoroacetamido)-1,2,4-triazole	$COCF_3$	$COCF_3$
V	3-Amino,5-heptafluorobutyramido-1,2,4-triazole	H	COC_3F_7
VI	3,5-Dibenzamido-1,2,4-triazole	COC_6H_5	COC_6H_5
VII	3,5-Di(*p*-nitrobenzamido)-1,2,4-triazole	$COC_6H_4NO_2$	$COC_6H_4NO_2$

For bases:

$$\alpha = \frac{1}{1 + \text{antilog}\,(\text{pH} - \text{pKa})} \qquad \text{(Eq. 3)}$$

An aqueous phase with a suitable buffering system is required to enhance the dissolution and ionization or to maintain a particular pH with an organic solvent. However, the effects of buffer species on the apparent partition coefficient were not studied until recently (12). It was found that phosphate buffer is the best system for measuring the true partition coefficient for quantitative structure–activity relationship work for both acidic and neutral drugs whenever the drug is soluble in this system. For many drugs, it is necessary to correct for the discrepancies when different buffer systems are used.

Due to the limited solubility, the phosphate buffer is not suitable for some of the prodrugs studied. It was also observed that the degree of ionization of some prodrugs is very high with most of the buffer systems. Accordingly, the small amount of water molecules in the octanol layers may trap a reasonable amount of the ionized species, giving rise to a higher log *P* value than predicted (12, 18).

EXPERIMENTAL

Materials—A UV spectrometer[1] equipped with a digital recorder, a pH meter[2], and an automatic electrobalance[3] were used. Buffer solutions such as hydrochloric acid–potassium chloride (pH 1.0–2.5), acetate (pH 3.6–5.9), phosphate (pH 6.0–8.0), tromethamine (pH 7.2–9.0), borate (pH 9.2–10.7), and bicarbonate (pH 9.28–10.1) were prepared as reported (19). They were then stored as 0.1 *N* solutions and diluted to the proper ionic strength (17, 20). The pH values were then adjusted by using 0.1 *N* HCl or 0.1 *N* NaOH.

Compounds—Guanazole prodrugs (Table I) were synthesized previously (10). Guanazole (3,5-diamino-1,2,4-triazole) was obtained commercially[4]. The melting point (158°) of salicylic acid[5] was determined to check for purity.

Purification of Octanol—Octanol[6] was purified by shaking with 1 *N* sodium hydroxide, 1 *N* sulfuric acid, and 5% sodium bicarbonate and then drying with excess anhydrous magnesium sulfate and fractional distillation (21, 22). The purified solvent did not show any UV-absorbing impurities (200–800 nm) for the boiling range of 192–195°.

Determination of Ionization Constants—A previously described procedure (17) was used for the determination of ionization constants. Its accuracy was checked with an authentic sample of salicylic acid (at 25°), and the result (2.94) was in close agreement with that reported (2.97) (23). The concentration of the buffers utilized for compounds I–VII was 0.05 *M*.

Determination of Apparent and True (or Corrected) Partition Coefficients—An accurate weight of the drug under investigation was dissolved in a suitable buffer solution to make up the stock solution (100 ml). The problem of low solubility was circumvented by the use of 2% C_2H_5OH, 1% $(CH_3)_2SO$, or 0.05 *N* NaOH (pH 12.4). Aliquots of the stock solution were partitioned between the 1-octanol–aqueous system (each phase being presaturated with the other) in 50-ml glass-stoppered bottles. These two phases were vigorously shaken by hand to ensure rapid distribution. The bottles were then placed in a horizontal bottle shaker for 3–4 hr at room temperature (25 ± 1°), followed by centrifugation of 10 ml of the aqueous layer for 20 min. Alternatively, the partitioned phases were centrifuged for 1 hr at 2000 rpm after 2 min of vigorous shaking.

Standard curves were run from duplicate samples using two separate weighings of the drug. In most cases, a 1:1 (v/v) ratio of 1-octanol to buffer (25 ml:25 ml) was used. The drug concentration in the aqueous phase after centrifugation was measured from UV absorbance and deduced from the standard curve. The apparent partition coefficient was calculated from the equation:

$$P_{app} = C_{octanol}/C_{aqueous} \qquad \text{(Eq. 4)}$$

where $C_{octanol}$ and $C_{aqueous}$ are the prodrug concentrations in the octanol and aqueous phases, respectively. Based on the apparent partition coefficient and its corresponding pH and pKa values, the true or corrected partition coefficient value was calculated from Eq. 1.

[1] Perkin-Elmer double-beam Coleman 124.
[2] Beckman model 3500.
[3] CAHN 25.
[4] Aldrich Chemical Co.
[5] Mallinckrodt Chemical Works.
[6] Fisher Chemicals.

Table II—Ionization Constants and the Apparent and Corrected Partition Coefficients of Guanazole Prodrugs

Compound	pKa	Log *P* Calc.	$1 - \alpha$	Observed Log P_{app}	Observed Log P_{corr}
I	9.35	−2.70	0.989637	−1.02	−1.01
II	9.34	−1.48	0.991776	−0.06	−0.07
III	9.34[a]	−0.54	0.990040	0.78	0.79
IV	5.90	−1.56	0.034265	−0.86	0.62
V	6.10	0.96	0.047727	0.23	1.54
VI	10.21	0.50	0.006415	−0.95	1.25
VII	8.64	0.44	0.953309	0.53	0.55

[a] The pKa of the dipropionated form was used.

RESULTS AND DISCUSSION

The ionization constants and both the apparent and true (corrected) partition coefficients of Compounds I–VII were measured for the first time in this study and are listed in Table II.

Dedichen (24) first measured the basicity constants of 1,2,4-triazole and some of its 2-amino-3,5-dialkyl substituted products. The applicability of Hammett's equation to the triazole ring was shown previously (25, 26). In addition, it was found (27) that basicity increases in the presence of an electron-donating group but decreases in the presence of an electron-withdrawing group. By employing the Hückel approach in conjunction with the linear combination of atomic orbitals–molecular orbital (LCAO–MO) method, the protonation center in 1*H*-1,2,4-triazole was shown to be the N-4 ring nitrogen atom (28). The basicity constants of a series of 5-(3)-substituted 3-(5)-amino-1,2,4-triazoles was determined by potentiometric titration (29). A high degree of quantitative correlation between the pKa values and the Hammett constants was found. Furthermore, the pKa from 3,5-diamino-1,2,4-triazole was 4.43, which was attributed to the conjugate acid of N-4 of the triazole ring (29). On the other hand, the ionization constants of the deprotonation of the heteroimino group of a series of 1,2,4-triazole derivatives were measured previously (30) and were in the range of 6.10–11.08. Consequently, it appears

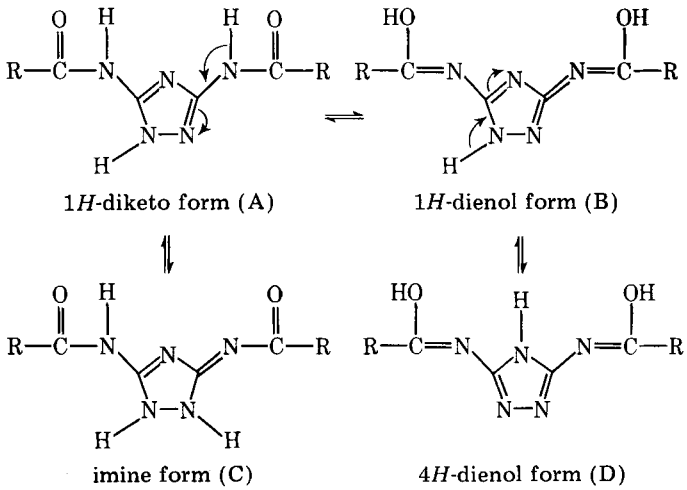

Scheme I

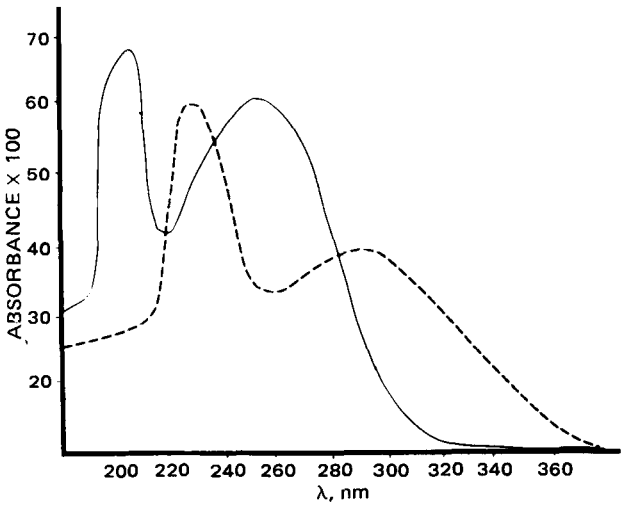

Figure 2—*UV spectrum of 3,5-dibenzamido-1,2,4-triazole. Key: —, pH 5.00; and - - -, pH 12.50.*

that the pKa values determined in this study (Table II) belong to the deprotonation process of the weakly acidic amido —NHCO— group or the 1,2,4-triazole ring rather than to the protonation of any basic nitrogen.

This finding was utilized in determining the percent ionization at the pH values used to measure the ionization constants of the compounds.

Some work has been published on the tautomerism of 1,2,4-triazole derivatives (26, 31, 32); however, nothing has yet been reported concerning the tautomeric isomers of guanazole derivatives. Nevertheless, a theoretical postulate can be drawn for the possible tautomeric isomers of guanazole derivatives as shown in Scheme I.

It has been shown (33) by IR spectral comparison of amidine analogs that alkyl groups (Y) tend to prefer attachment to the amino system 2A rather than to 2B but that the reverse is true for aryl groups.

Chua *et al.* (34) quantified the energy differences between the two possible tautomers by applying the basicity method (35), which depends on the formation of the cation for both the tautomeric forms A and B, and comparing their basicities to fixed models of A and B. From their findings, it appears likely that the tautomeric structure A is the predominant structure for I–III. On the other hand, the tautomeric structures B and C are more likely for IV–VII.

Apparently, there are two different kinds of tautomerism: the imino and keto-enol types. Furthermore, there are four possibilities for dissociation. A comparison of the UV spectra of the neutral and the anion species is important in determining the dissociation site. It was found (27) that the splitting off of a proton attached to the heteronitrogen atom of 3-nitro-1,2,4-triazole-5-carboxylic acid causes a marked (50 nm) bathochromic shift in the UV spectrum while dissociation at the carboxyl group of 1-methyl-5-nitro-1,2,4-triazole-3-carboxylic acid gives a very small (5 nm) bathochromic shift.

The UV spectrum of I (Fig. 1) at various pH values shows a negligible bathochromic shift (4 nm) of the B band of the triazole ring. Therefore, the dissociation process and the possible canonical forms of I–III can be represented by Scheme II.

Likewise, the UV spectra of the neutral and the anionic species of VI is shown in Fig. 2. For the neutral form, there are two absorption maxima, one at 260 nm, which is characteristic of the aromatic ring and is analogous to the K-band (36), and one at 215 nm for the B-band, which is characteristic of the heteroaromatic ring. The splitting off of the proton causes a very strong bathochromic shift of 20 and 40 nm for the B- and K-bands, respectively. Therefore, the removal of the proton causes a delocalization of electrons in both rings, which indicates a possible pathway for the deprotonation process and the resulting resonance structures (Scheme III).

The UV spectrum of VII is shown in Fig. 3. There is a red shift (14 nm) for the K-band as compared to VI, which is attributable to the electron-withdrawing activity of the nitro group. However, the B-band remains

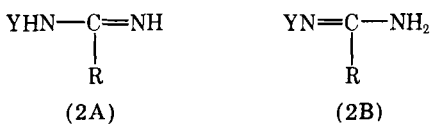

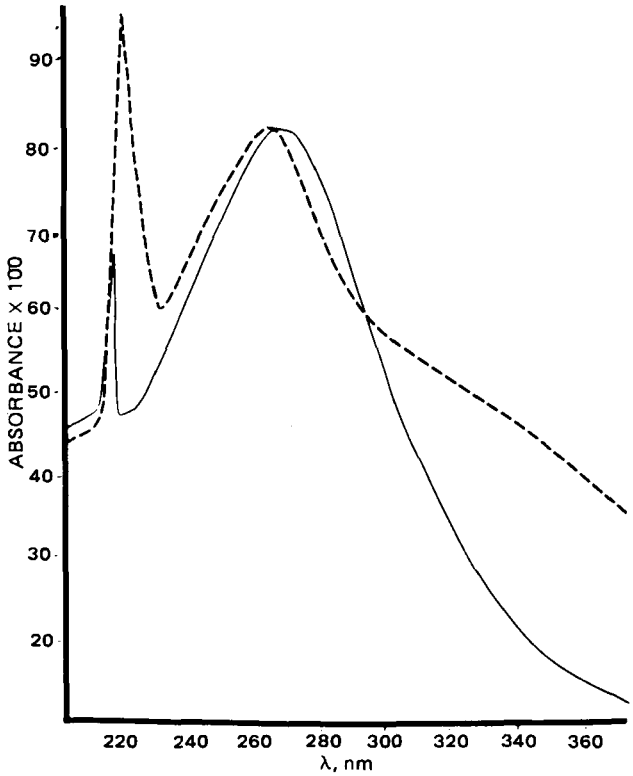

Figure 3—*UV spectrum of 3,5-di(p-nitrobenzamido)-1,2,4-triazole. Key: —, pH 4.50; and - - -, pH 12.50.*

the same as that of VI. Deprotonation causes the solution to change from colorless to yellowish, but a negligible change is observed for both the K- and B-bands. The contributing structures for the visible absorption may be illustrated as shown in Scheme IV.

From Table II, it appears that there is a substantial dependence of the ionization constants on the electronic character of the substituent. The inductive and resonance effects both contribute to the ionization constant in a collective manner.

It was shown (11) that changing the electronic properties of the substituent groups may affect the prototropic equilibria and result in a more active tautomeric form of a particular drug. This investigation found that, in contrast to guanazole which is a weak base, guanazole prodrugs range from weak to moderate acids. Preparation of the prodrugs not only altered the lipophilicity but also drastically changed the acid–base property of the parent compound.

Table II shows the measured and calculated values of the partition coefficients of the prodrugs examined. It was shown (37) that log P is not entirely additive. It has been suggested (38) that the additivity of π-values will break down when there is mutual interaction between substituents (intramolecular hydrogen bonding, steric, and field effects) or when a substituent cannot be dissolved to its maximal potential (39).

The nature of the interaction between guanazole derivatives and both octanol and water can be illustrated by Scheme V.

The preferred interaction of guanazole with the aqueous or organic layers probably would be determined in part by the electronic properties of the X substituent. Electron-withdrawing groups would inhibit hydrogen bonding of the type shown on the right side of Scheme V due to the delocalization of the lone-pair electrons but enhance hydrogen bonding of the type shown on the left side of Scheme V. Octanol, being more nucleophilic than water (40), would compete more effectively in binding with the hydrogen of the amino nitrogen. The differences between the observed and calculated values of log P in Table II can be rationalized in part from the substituent effect on the availability of the lone-pair electrons.

Although the true partition coefficient takes into account the ionization of the drug at a given pH, the assumption that the ionized species of an ionizable drug is insoluble in the nonaqueous layer may be incorrect. First, the small amount of water in the octanol layer is expected to accommodate some concentration of the ionized species (12, 18). Thus, the observed log P would be higher than the calculated value. The partition coefficients of ring-substituted aspirin were measured at different pH values (18). It was found that the discrepancies between the observed and

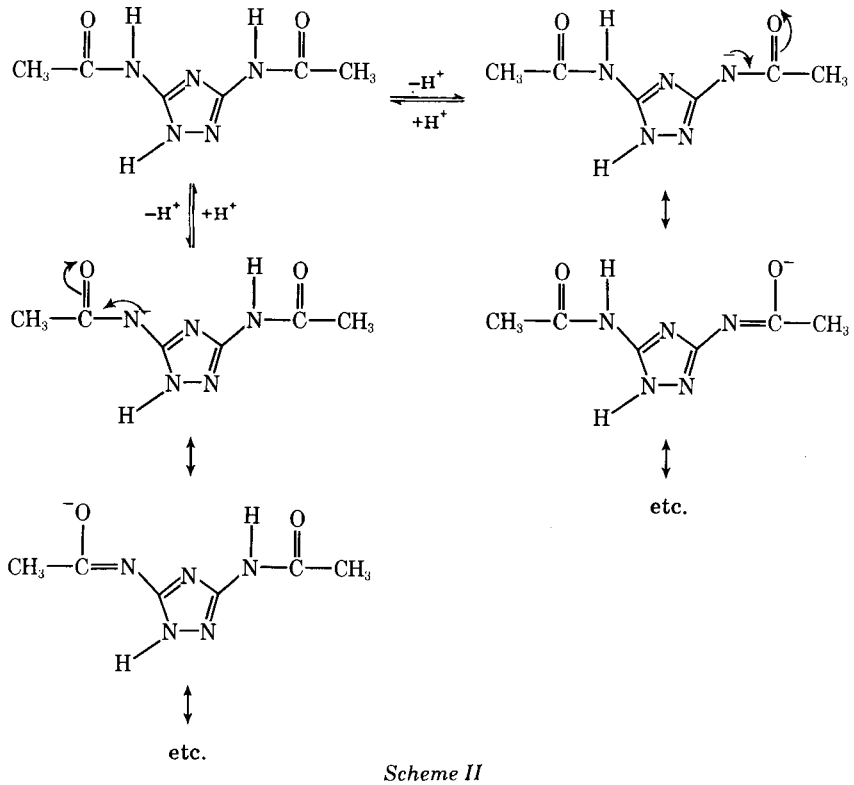

Scheme II

calculated values correlated well with the calculated lipophilicities, which was attributed to ion-pair formation with buffer counterions (41).

Second, the ionized species may have a different conformation than that of the nonionized form. The partition coefficient (log P = 4.33) of salicylic acid in a 1-octanol–bicarbonate buffer (pH 9.20) system has been shown to be very different from that in a 1-octanol–acetate (pH 4.00) system (log P = 2.87). Wang and Lien (12) considered the first factor as well as the effect of the ionic strength of the buffer to rationalize such a deviation. The difference in the intramolecular hydrogen bonding between the ionized and the nonionized forms may also play a significant role. At a pH of 9.2, the deprotonated form of salicylic acid is predominant (Scheme VI).

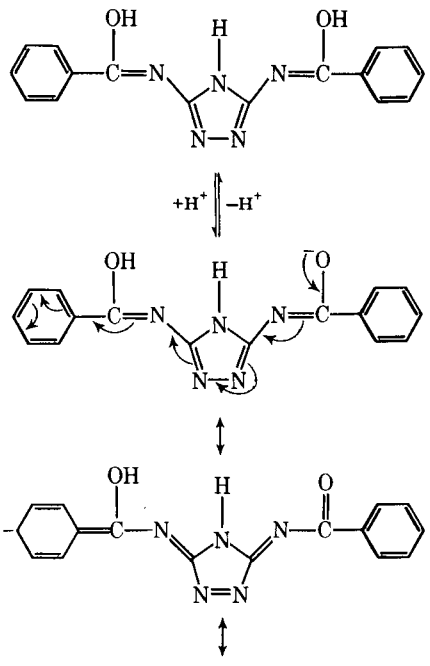

Scheme III

Therefore, the ionized form is more capable of intramolecular hydrogen bonding than the nonionized form and gives rise to a higher log P. However, the ionized form also has a higher preference to a hydrogen bond with water molecules than the nonionized form. This decreases the log P. The net effect on log P depends on the buffer species used as well as the pH value.

Compared to the calculated values, the higher values of the observed log P for I–III can be attributed to both the inductive effect of the substituent and the intramolecular hydrogen bonding between the carbonyl group and the triazole ring. Compounds IV–VI, with a high degree of ionization (low $1 - \alpha$ values) at the given pH values, may be trapped by the small amount of water molecules in the octanol layer, giving a higher log P value. Compound VII has an observed log P value only slightly higher than the expected value.

Compound VII can be considered a nitrobenzene derivative substituted at position 4. It can be considered similar to a dinitro-benzene derivative where each nitro group can nullify the effect of the other, resulting in a smaller difference between the observed and calculated log P. Furthermore, at pH 7.40, the degree of ionization of VII is relatively small (5%). Accordingly, the amount of ionized drug trapped by the small amount of water in the octanol layer is negligible. The observed value of log P did not deviate significantly from the calculated value.

The partition coefficient of salicylic acid was measured utilizing two different procedures:

1. After 2 min of vigorous shaking, the two layers were partitioned for 3–4 hr at 25° in a bottle shaker, and the aqueous layer was centrifuged for 20 min.
2. After 2 min of vigorous shaking, the two layers were centrifuged together for 30–45 min in a centrifuge tube.

The apparent partition coefficients from both methods were identical. However, the pH values, after partitioning from the first and second methods, were 8.90 and 9.20, respectively. Therefore, the true partition coefficient was lower in the first method (4.33 *versus* 4.63). The difference can be attributed to the efficiency of the first method over that of the second in getting clear separation of the aqueous from octanol layer or to the temperature effect that might happen under the longer period of centrifugation in the second method.

Selection of the proper method depends on the compounds being investigated and the volume ratio (42). The first method should be more desirable for a compound that needs a long period of time to reach equilibrium, *i.e.*, phenol (43). For highly ionized compounds, it is advisable to have an efficient separation to minimize any emulsification or clouding of the phases.

In this study, the separation of the two layers with phosphate buffer

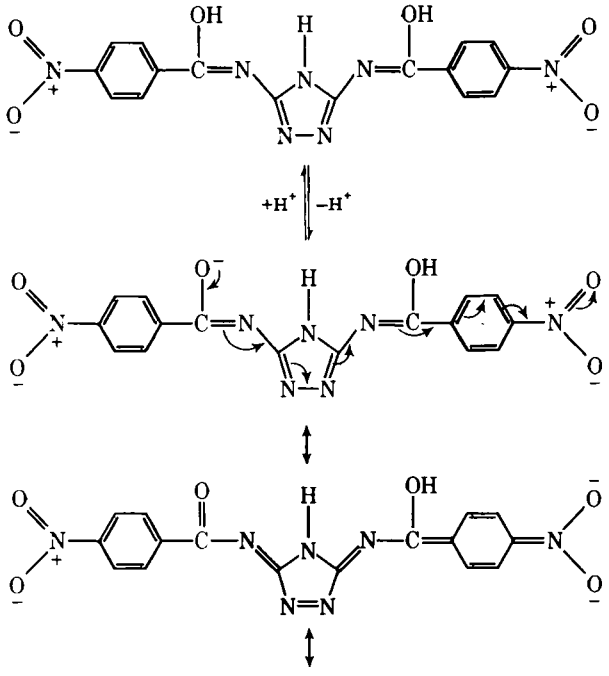

etc.

Scheme IV

was more efficient than other systems used under the same experimental conditions. This finding is in agreement with earlier data (12).

Distribution coefficients (D) of ionizable compounds have been used in structure–activity correlations (43). From the mathematical formula for D, it can be shown that D is the same as the apparent partition coefficient:

$$D = AH_1/(AH_w + A^-)$$

$$(P_{app} = C_o/C_w = AH_1/(AH_w + A^-)$$

$$D/(1 - \alpha) = AH_1/(AH_w + A^-)(1 - \alpha) = AH_1/AH_w = P_{corr}$$

where α = degree of ionization = $A^-/(AH_w + A^-)$. AH_1 and AH_w and the free acid concentration in the lipid and the water layer, respectively, and A^- is the concentration of the anion in the water layer.

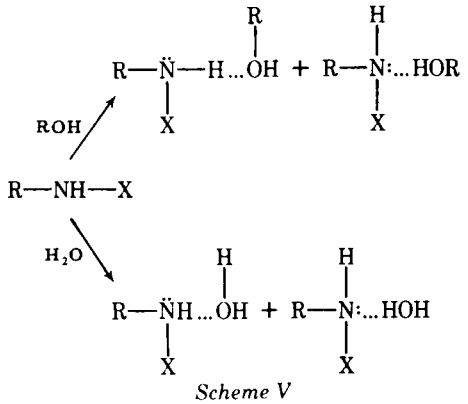

Scheme V

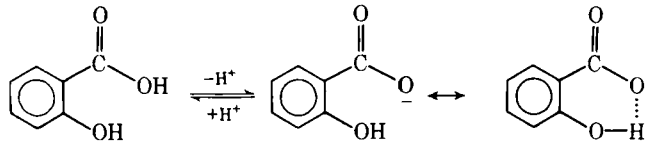

nonionized form ionized form intramolecular hydrogen bonded form

Scheme VI

REFERENCES

(1) M. Hahn and R. Adamson, *Pharmacologist*, **12**, 282 (1970).

(2) R. W. Brockman, S. Shaddix, L. W. Russell, Jr., and F. M. Schabel, *Cancer Res.*, **30**, 2358 (1970).

(3) J. Hewlelt, G. Bodey, C. Coltman, E. Freireich, A. Haut, and K. McCredie, *Clin. Pharmacol. Ther.*, **14**, 271 (1973).

(4) D. Yaker, J. Holland, R. Ellison, and A. Freeman, *Cancer Res.*, **33**, 972 (1973).

(5) V. Land, J. Falleta, C. McMillan, and T. Williams, *Cancer Chemother. Rep.*, **58**, 715 (1972).

(6) M. Hahn, R. Adamson, I. Zarembox, and J. Block, *J. Proc. Am. Assoc. Cancer Res.*, **13**, 105 (1972).

(7) N. Gerber, R. Seibert, D. Desiderio, R. Thompson, and M. Lane, *Clin. Pharmacol. Ther.*, **14**, 264 (1970).

(8) C. Dave and L. Caballes, *J. Pharm. Sci.*, **63**, 347 (1974).

(9) C. Dave, J. Mattern, and D. Higby, *Proc. Am. Assoc. Cancer Res.*, **14**, 86 (1973).

(10) C. Selassie, Ph.D. thesis, University of Southern California, Los Angeles, Calif., 1979.

(11) C. R. Ganellin, in "Drug Action at the Molecular Level," G. C. K. Roberts, Ed., University Park Press, Baltimore, Md., 1977, pp. 1–39.

(12) P. Wang and E. Lien, *J. Pharm. Sci.*, **69**, 662 (1980).

(13) Y. Martin, "Quantitative Drug Design," Dekker, New York, N.Y., 1978.

(14) A. Leo, C. Hansch, and D. Elkins, *Chem. Rev.*, **71**, 525 (1971).

(15) D. Gupta and E. Cadwallader, *J. Pharm. Sci.*, **57**, 2140 (1968).

(16) R. Rekker, in "Biological Activity and Chemical Structure," J. A. Keverling Buisman, Ed., Elsevier, Amsterdam, The Netherlands, 1977, pp. 231–238.

(17) A. Albert and E. Serjeant, in "The Determination of Ionization Constants," Chapman and Hall, London, England, 1972.

(18) J. Dearden and E. George, *J. Pharm. Pharmacol.*, **30**, 499 (1978).

(19) G. Gomori, in "Methods in Enzymology," S. P. Colowick and W. D. Kaplan, Eds., Academic, New York, N.Y., 1955.

(20) A. Perrin, *Austr. J. Chem.*, **16**, 572 (1963).

(21) P. Purcell, E. Bass, and M. Clayton, in "Strategy of Drug Design: A Guide to Biological Activity," Wiley, New York, N.Y., 1973, p. 126.

(22) R. Smith, C. Hansch, and M. Arres, *J. Pharm. Sci.*, **64**, 599 (1975).

(23) D. Newton and R. Kluza, *Drug Intel. Clin. Pharm.*, **12**, 546 (1978).

(24) G. Dedichen, *Chem. Ber.*, **39**, 1849 (1906).

(25) F. Kroger and W. Freiberg, *Z. Chem.*, **5**, 381 (1965).

(26) W. Freiberg and F. Kroger, *Chimia*, **21**, 159 (1967).

(27) L. Bagal and M. Pevzner, *Khimiya Geterotsikl. Soedin. Sb.*, **6**, 558 (1970).

(28) V. Minkin, S. Pozharshii, and Y. Ostrunmov, *ibid.*, **2**, 551 (1966).

(29) M. Voronkov, T. Kashik, V. Makarskii, V. Lopyrev, S. Ponomareva, and E. Shibanova, *Dokl. Akad. Nauk SSSR*, **227**, 5, 1116 (1976).

(30) M. Pevzner and P. Kofman, *Zh. Org. Khim.*, **14**, 10, 2024 (1978).

(31) D. Kalikham, V. Lopyrev, E. Shibanova, A. Pestunorich, and M. Varonkov, *Izv. Akad. Nauk SSSR, Ser. Khim.*, **10**, 2390 (1977).

(32) A. Magnestian, V. Haverbeke, and R. Flammang, *Org. Mass Spectrosc.*, **6**, 1139 (1972).

(33) D. Prevorsek, *J. Phys. Chem.*, **66**, 769 (1962).

(34) S. Chua, M. Cook, and A. Katritzky, *J. Chem. Soc. Perkin II*, **1974**, 546.

(35) G. Schwenker and K. Bosl, *Arch. Pharm.*, **303**, 980 (1970).

(36) P. Silverstein, G. Bassler, and T. Morrill, in "Spectrometric Identification of Organic Compounds," 3rd ed., Wiley, New York, N.Y., 1974.

(37) C. Hansch, A. Leo, and D. Nikaitani, *J. Org. Chem.*, **37**, 3090 (1972).

(38) A. Cammarata, *J. Med. Chem.*, **12**, 314 (1969).

(39) J. Dearden and Y. Ohara, *Eur. J. Med. Chem. Chim. Ther.*, **13**, 415 (1978).

(40) T. Fujita, J. Iwasa, and C. Hansch, *J. Am. Chem. Soc.*, **86**, 5175 (1964).

(41) P. Moser, K. Jakel, P. Krupp, R. Menassa, and A. Sallman, *Eur. J. Med. Chem.*, **10**, 613 (1975).

(42) C. Craig, H. Hodehoom, F. Carpenter, and V. Vingneaud, *J. Biol. Chem.*, **168**, 665 (1947).

(43) R. A. Scherrer and S. M. Howard, *J. Med. Chem.*, **20**, 53 (1977).

ACKNOWLEDGMENTS

Presented in part at the Medicinal Chemistry and Pharmacognosy Section, APhA Academy of Pharmaceutical Sciences, St. Louis, Mo. meeting, March 1981.

S.-O. Chua is on leave from the University Sains Malaysia, Penang, Malaysia.

Heterogeneity of Biochemical Actions among Vasodilators

FORREST C. GREENSLADE, CYNTHIA K. SCOTT ˣ, KATHRYN L. NEWQUIST, KATHRYN M. KRIDER, and MARK CHASIN

Received December 22,1980, from the *Division of Biochemical Research, Ortho Pharmaceutical Corporation, Raritan, NJ 08869.* Accepted for publication May 14, 1981.

Abstract □ Thirty-four vasodilators were screened in several *in vitro* biochemical assays related to smooth muscle excitation–contraction coupling, binding to β_1^-, β_2^-, and α-adrenergic receptors, inhibition of phosphodiesterase activity, and antagonism of calcium accumulation. Isoproterenol and perhexiline only exhibited binding to β-adrenergic sites. Ergocryptine, tolazoline, and amotriphene only bound to α-adrenergic receptors. Leniquinsin, papaverine, proquazone, dioxyline, hoquizil, quazodine, and theophylline were active only as phosphodiesterase inhibitors. Isoxsuprine, nylidrin, and bencyclane bound to α- and β-receptors. Pentoxifylline bound to β_1-sites and inhibited phosphodiesterase. Cyclandelate bound to β_2-sites and blocked calcium accumulation. Cinnarizine and flunarizine antagonized calcium accumulation and bound to α-sites. Prazosin bound to α-sites and inhibited phosphodiesterase. Ethaverine and dipyridamole were inhibitors of phosphodiesterase and calcium accumulation. Nafronyl bound to β_2- and α-sites and antagonized calcium accumulation. Mebeverine bound to β_2- and α-receptors and inhibited phosphodiesterase activity and calcium accumulation. Verapamil bound to α-sites, and blocked phosphodiesterase and calcium accumulation. Quinazosin bound to β_2- and α-receptors and antagonized both phosphodiesterase activity and calcium accumulation. Vasodilators that were inactive in all assays included niacin, nicotinyl alcohol, inositol nicotinate, amyl nitrite, sodium nitroprusside, diazoxide, hydralazine, and protoveratrine. Vasodilators should not be considered as a single drug class since they act on various mechanisms related to coupling of neuronal excitation to muscular contractility.

Keyphrases □ Vasodilators—biochemical mechanisms □ Adrenergic receptors—α, β_1, and β_2, effect of various vasodilators □ Calcium—effect of various vasodilators on intracellular accumulation, red blood cells □ Phosphodiesterase—inhibition by various vasodilators

The treatment of cardiovascular diseases such as hypertension (1, 2), angina pectoris, cardiac failure (3, 4), and certain peripheral vascular diseases (1, 5, 6) utilizes drugs that produce vasodilation. Vasodilation results from an increase in the internal diameter of blood vessels, presumably through relaxation of vascular smooth muscle. Significant progress has been made in elucidating the biochemical mechanisms controlling smooth muscle contractility. Molecular events in that process include the interaction of catecholamines with specific adrenergic receptors of the smooth muscle cell membrane, the activities of enzymes that regulate cellular levels of cyclic AMP, the control of cellular calcium-ion transport and storage, and the interaction of calcium with the contractile proteins of the smooth muscle cell (7–9).

By using this concept of excitation–contraction coupling in smooth muscle as a working hypothesis, the mechanism of action of various vasodilators has been studied. Thirty-four vasodilators (1, 2, 5, 10, 11) were tested in three types of *in vitro* screening models: (*a*) binding to α- and β-adrenergetic receptor sites, (*b*) inhibition of cyclic AMP phosphodiesterase, and (*c*) inhibition of intracellular calcium accumulation. The results suggest that vasodilator drugs interact with a variety of distinct events in the excitation–contraction coupling mechanisms of vascular smooth muscle.

EXPERIMENTAL

Adrenergic Radioreceptor Assays—*β-Adrenergic Receptor Binding Assays*—Sarcolemma-enriched membranes from guinea pig hearts were prepared as described previously (12). Guinea pigs were killed by cervical dislocation, and the hearts were immediately placed in ice-cold physiological saline. Hearts (20–25 g) were minced in 10 volumes of 2.5 m*M* imidazole buffer (pH 7.4) containing 0.1 m*M* ethylenediaminetetraacetic acid (I) and briefly homogenized with a tissue homogenizer. The homogenate was centrifuged for 1 min at 22×*g*.

The supernatant fraction was rehomogenized and recentrifuged five times. The pooled supernatant fractions were passed through three layers of cheesecloth and centrifuged at 1600×*g* for 20 min. The resulting pellet was resuspended in 200 ml of 10 m*M* [tris(hydroxymethyl)aminomethane hydrochloride] buffer (II), pH 7.5, containing 0.1 *M* sucrose and homogenized using a conical polytef[1]/glass tissue grinder. The homogenate was centrifuged at 1600×*g* for 20 min.

These resuspension, homogenization, and centrifugation steps were then repeated. The pellet was resuspended in 50 ml of 0.4 *M* sucrose in 10 m*M* II (pH 7.5) and osmotically shocked by slow dilution into 1 liter of 0.25 m*M* I in 5 m*M* II (pH 7.0) buffer. The membranes were collected by centrifugation at 1600×*g* for 30 min, and the pellet was suspended in 20 ml of 0.4 *M* sucrose in 10 m*M* II (pH 7.5). The suspension was diluted with three volumes of a 13 m*M* II buffer (pH 7.0) containing 1.3 *M* KCl, 2.6 m*M* I, and 0.4 *M* sucrose. After stirring for ~16 hr at 4°, the extract was diluted with an equal volume of buffer [1 *M* KCl–2 m*M* I–10 m*M* II (pH 7.0)]. After centrifugation at 1600×*g* for 30 min, the pellet was washed three times in 100 ml of 0.1 *M* sucrose in 10 m*M* II (pH 7.0) buffer. The final pellet was suspended in 0.1 *M* sucrose and stored in liquid nitrogen.

Bronchial tree membranes were prepared from either fresh guinea pig lungs or lungs stored at −100°. Bronchial trees were exposed by combing through the lungs several times with a steel animal hairbrush to strip them of alveolar tissue. Extraneous tissue was removed by scraping with a scalpel. The bronchial trees were placed in a small volume of ice-cold II (pH 7.4) containing 1 m*M* $MgCl_2$ and 0.25 *M* sucrose. Then they were finely minced and homogenized by four 10-sec bursts with a tissue homogenizer.

The homogenate was filtered through a single layer of cheesecloth, and the filtrate was centrifuged for 10 min at 400×*g*. The pellet was discarded, and the supernate was centrifuged for 10 min at 20,000×*g*. The resulting pellet was washed in 50 m*M* II (pH 7.5) containing 10 m*M* $MgCl_2$ and centrifuged at 28,000×*g* for 10 min. The pellet was resuspended in 75 m*M*

[1] Teflon.

0022-3549/82/0100-0094$01.00/0

(43) R. A. Scherrer and S. M. Howard, *J. Med. Chem.*, **20**, 53 (1977).

ACKNOWLEDGMENTS

Presented in part at the Medicinal Chemistry and Pharmacognosy Section, APhA Academy of Pharmaceutical Sciences, St. Louis, Mo. meeting, March 1981.

S.-O. Chua is on leave from the University Sains Malaysia, Penang, Malaysia.

Heterogeneity of Biochemical Actions among Vasodilators

FORREST C. GREENSLADE, CYNTHIA K. SCOTT ˣ, KATHRYN L. NEWQUIST, KATHRYN M. KRIDER, and MARK CHASIN

Received December 22,1980, from the *Division of Biochemical Research, Ortho Pharmaceutical Corporation, Raritan, NJ 08869.* Accepted for publication May 14, 1981.

Abstract □ Thirty-four vasodilators were screened in several *in vitro* biochemical assays related to smooth muscle excitation–contraction coupling, binding to β_1^-, β_2^-, and α-adrenergic receptors, inhibition of phosphodiesterase activity, and antagonism of calcium accumulation. Isoproterenol and perhexiline only exhibited binding to β-adrenergic sites. Ergocryptine, tolazoline, and amotriphene only bound to α-adrenergic receptors. Leniquinsin, papaverine, proquazone, dioxyline, hoquizil, quazodine, and theophylline were active only as phosphodiesterase inhibitors. Isoxsuprine, nylidrin, and bencyclane bound to α- and β-receptors. Pentoxifylline bound to β_1-sites and inhibited phosphodiesterase. Cyclandelate bound to β_2-sites and blocked calcium accumulation. Cinnarizine and flunarizine antagonized calcium accumulation and bound to α-sites. Prazosin bound to α-sites and inhibited phosphodiesterase. Ethaverine and dipyridamole were inhibitors of phosphodiesterase and calcium accumulation. Nafronyl bound to β_2- and α-sites and antagonized calcium accumulation. Mebeverine bound to β_2- and α-receptors and inhibited phosphodiesterase activity and calcium accumulation. Verapamil bound to α-sites, and blocked phosphodiesterase and calcium accumulation. Quinazosin bound to β_2- and α-receptors and antagonized both phosphodiesterase activity and calcium accumulation. Vasodilators that were inactive in all assays included niacin, nicotinyl alcohol, inositol nicotinate, amyl nitrite, sodium nitroprusside, diazoxide, hydralazine, and protoveratrine. Vasodilators should not be considered as a single drug class since they act on various mechanisms related to coupling of neuronal excitation to muscular contractility.

Keyphrases □ Vasodilators—biochemical mechanisms □ Adrenergic receptors—α, β_1, and β_2, effect of various vasodilators □ Calcium—effect of various vasodilators on intracellular accumulation, red blood cells □ Phosphodiesterase—inhibition by various vasodilators

The treatment of cardiovascular diseases such as hypertension (1, 2), angina pectoris, cardiac failure (3, 4), and certain peripheral vascular diseases (1, 5, 6) utilizes drugs that produce vasodilation. Vasodilation results from an increase in the internal diameter of blood vessels, presumably through relaxation of vascular smooth muscle. Significant progress has been made in elucidating the biochemical mechanisms controlling smooth muscle contractility. Molecular events in that process include the interaction of catecholamines with specific adrenergic receptors of the smooth muscle cell membrane, the activities of enzymes that regulate cellular levels of cyclic AMP, the control of cellular calcium-ion transport and storage, and the interaction of calcium with the contractile proteins of the smooth muscle cell (7–9).

By using this concept of excitation–contraction coupling in smooth muscle as a working hypothesis, the mechanism of action of various vasodilators has been studied. Thirty-four vasodilators (1, 2, 5, 10, 11) were tested in three types of *in vitro* screening models: (*a*) binding to α- and β-adrenergetic receptor sites, (*b*) inhibition of cyclic AMP phosphodiesterase, and (*c*) inhibition of intracellular calcium accumulation. The results suggest that vasodilator drugs interact with a variety of distinct events in the excitation–contraction coupling mechanisms of vascular smooth muscle.

EXPERIMENTAL

Adrenergic Radioreceptor Assays—*β-Adrenergic Receptor Binding Assays*—Sarcolemma-enriched membranes from guinea pig hearts were prepared as described previously (12). Guinea pigs were killed by cervical dislocation, and the hearts were immediately placed in ice-cold physiological saline. Hearts (20–25 g) were minced in 10 volumes of 2.5 m*M* imidazole buffer (pH 7.4) containing 0.1 m*M* ethylenediaminetetraacetic acid (I) and briefly homogenized with a tissue homogenizer. The homogenate was centrifuged for 1 min at 22×*g*.

The supernatant fraction was rehomogenized and recentrifuged five times. The pooled supernatant fractions were passed through three layers of cheesecloth and centrifuged at 1600×*g* for 20 min. The resulting pellet was resuspended in 200 ml of 10 m*M* [tris(hydroxymethyl)aminomethane hydrochloride] buffer (II), pH 7.5, containing 0.1 *M* sucrose and homogenized using a conical polytef[1]/glass tissue grinder. The homogenate was centrifuged at 1600×*g* for 20 min.

These resuspension, homogenization, and centrifugation steps were then repeated. The pellet was resuspended in 50 ml of 0.4 *M* sucrose in 10 m*M* II (pH 7.5) and osmotically shocked by slow dilution into 1 liter of 0.25 m*M* I in 5 m*M* II (pH 7.0) buffer. The membranes were collected by centrifugation at 1600×*g* for 30 min, and the pellet was suspended in 20 ml of 0.4 *M* sucrose in 10 m*M* II (pH 7.5). The suspension was diluted with three volumes of a 13 m*M* II buffer (pH 7.0) containing 1.3 *M* KCl, 2.6 m*M* I, and 0.4 *M* sucrose. After stirring for ~16 hr at 4°, the extract was diluted with an equal volume of buffer [1 *M* KCl–2 m*M* I–10 m*M* II (pH 7.0)]. After centrifugation at 1600×*g* for 30 min, the pellet was washed three times in 100 ml of 0.1 *M* sucrose in 10 m*M* II (pH 7.0) buffer. The final pellet was suspended in 0.1 *M* sucrose and stored in liquid nitrogen.

Bronchial tree membranes were prepared from either fresh guinea pig lungs or lungs stored at −100°. Bronchial trees were exposed by combing through the lungs several times with a steel animal hairbrush to strip them of alveolar tissue. Extraneous tissue was removed by scraping with a scalpel. The bronchial trees were placed in a small volume of ice-cold II (pH 7.4) containing 1 m*M* $MgCl_2$ and 0.25 *M* sucrose. Then they were finely minced and homogenized by four 10-sec bursts with a tissue homogenizer.

The homogenate was filtered through a single layer of cheesecloth, and the filtrate was centrifuged for 10 min at 400×*g*. The pellet was discarded, and the supernate was centrifuged for 10 min at 20,000×*g*. The resulting pellet was washed in 50 m*M* II (pH 7.5) containing 10 m*M* $MgCl_2$ and centrifuged at 28,000×*g* for 10 min. The pellet was resuspended in 75 m*M*

[1] Teflon.

0022-3549/82/0100-0094$01.00/0

Table I—Vasodilators with Affinity for β-Adrenergic Binding Sites

Compound	Structure	IC_{50}, μM: Adrenergic Receptor Binding β_{1}(Heart)[a]	β_2(Lung)[b]	(Uterus)[c]	PDE[d]	Ca^{2+} [e]
Propranolol	Control	0.05	0.07	100	—[f]	—
Atenolol	Control	5.5	30	—	—	—
Isoproterenol	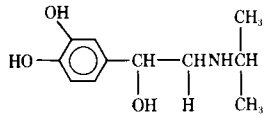	0.6	1.5	—	—	—
Perhexiline	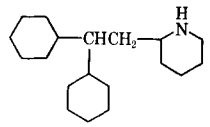	10	4	—	—	—

[a] Competition for binding of [^{3}H]dihydroalprenolol to specific binding sites on guinea pig heart membranes. [b] Competition for binding of [^{3}H]dihydroalprenolol to specific binding sites on guinea pig lung membranes. [c] Competition for binding of [^{3}H]dihydroergocryptine to specific binding sites on rabbit uterine membranes. [d] Inhibition of rat brain phosphodiesterase activity. [e] Inhibition of $^{45}Ca^{2+}$ accumulation in human red blood cells. [f] Indicates no activity at highest concentration tested (150 μM).

Table II—Vasodilators with Affinity for α-Adrenergic Binding Sites [a]

Compound	Structure	IC_{50}, μM: Adrenergic Receptor Binding β_1 (Heart)	β_2 (Lung)	α (Uterus)	PDE	Ca^{2+}
Phentolamine	Control	—	—	0.025	—	—
Phenoxybenzamine	Control	—	—	0.15	—	3
Ergocryptine	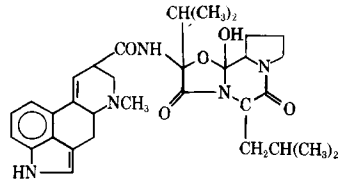	—	—	0.06	—	—
Tolazoline	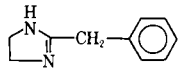	—	—	4	—	—
Amotriphene	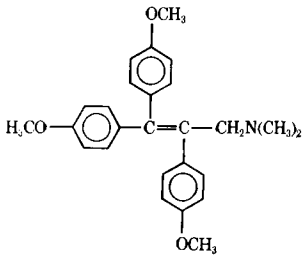	—	—	150	—	—

[a] See footnotes to Table I.

II (pH 8.1) containing 25 m*M* $MgCl_2$ and collected by centrifugation at 28,000×*g*. The final pellet was suspended in the same buffer and stored in liquid nitrogen.

The β-adrenergic binding assays were conducted according to the method of Mukherjee *et al.* (13). The frozen membrane preparation was thawed and maintained on ice. The incubation mixture contained 25 μl of the test drug, 50 μl of [^{3}H]dihydroalprenolol[1] (40,000 cpm; 9 nmoles), and 100 μl of the membrane preparation. A 15-min incubation at 37° was initiated by the addition of the membrane preparation and vortexing. The incubation was terminated by adding 5 ml of ice-cold 75 m*M* I containing 25 m*M* $MgCl_2$ (pH 8.1) and immediately collecting the membranes on glass fiber filter disks. The membranes were washed five times with 5 ml of the same ice-cold buffer. The filter disks were dried in an oven and counted in a scintillation solution[2]. Along with each set of test compounds, incubations were conducted with 1.5×10^{-4} *M* propranolol. Binding of [^{3}H]dihydroalprenolol at this high concentration of propranolol was considered to represent nonspecific binding to β-adrenergic receptor sites.

α-Adrenergic Receptor Binding Assay—Membranes were prepared from frozen type II mature rabbit uteri according to the method of Willliams *et al.* (14). After thawing, fat was removed and endometrial cells were scraped free with a scalpel. Uteri were sliced, finely minced with scissors in a solution containing 0.25 *M* sucrose, 5 m*M* II (pH 7.4), and 1 m*M* $MgCl_2$, and then homogenized four times. After filtration through cheesecloth, the homogenate was centrifuged at 400×*g* for 10 min. The supernatant liquid was then centrifuged for 10 min at 39,000×*g*. The resulting pellet was homogenized using a polytef/glass tissue grinder in 50 m*M* II (pH 7.4) containing 10 m*M* $MgCl_2$. The resuspended pellet was centrifuged for 10 min at 39,000×*g*, and the resulting pellet was washed with the same buffer. The final pellet was homogenized in the same buffer and used fresh in the binding assay.

The incubation consisted of 25 μl of test drug, 50 μl of [^{3}H]dihydroergocryptine[3] (~40,000 cpm, 2 pmoles), and 100 μl of the membrane preparation. A 15-min incubation, conducted at 25°, was terminated by addition of 5 ml of room temperature 10 m*M* $MgCl_2$ in 50 m*M* II (pH 7.5). Membranes were collected by fiber filtration and washed with 5 ml of the same buffer at room temperature. Phentolamine at 1.5×10^{-4} *M* was used to define nonspecific binding to the membranes.

[2] Aquasol, New England Nuclear.

[3] 9,10-[9,10-^{3}H(N)], specific activity 24 Ci/nmole, New England Nuclear.

Table III—Vasodilators that Inhibit Phophodiesterase Activity [a]

Compound	Structure	IC_{50}, μM					
		Adrenergic Receptor Binding			PDE		
		β_1 (Heart)	β_2 (Lung)	α (Uterus)	(Brain)	(Artery)	Ca^{2+}
Etazolate	Control	—	—	—	4	NT[b]	—
Leniquinsin	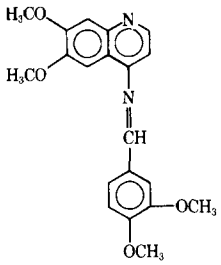	—	—	—	2.8	7.6	—
Papaverine	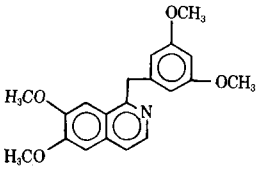	—	—	—	3.1	NT[b]	—
Proquazone	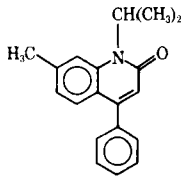	—	—	—	4.4	19	—
Dioxyline	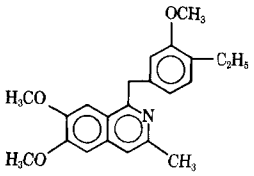	—	—	—	5.4	1.1	—
Hoquizil	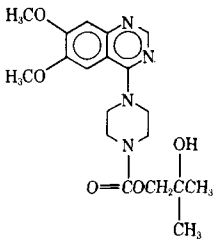	—	—	—	18	15	—
Quazodine	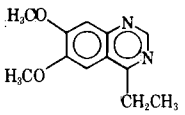	—	—	—	20	48	—
Theophylline	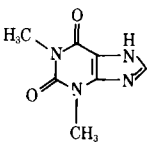	—	—	—	240	NT[b]	—

[a] See footnotes to Table I. [b] Not tested.

Phosphodiesterase Assay—Phosphodiesterase was prepared from rat brain or Cynomolgus monkey abdominal artery by the method of Chasin and Harris (15). Tissues were homogenized in 5–10 volumes of 0.05 *M* II (pH 7.5), and the homogenates were centrifuged for 20 min at 39,000×*g*. The supernate was adjusted to 50% saturation by slow addition of an equal volume of neutral, saturated ammonium sulfate. The precipitate was allowed to form for 1 hr in an ice bath and was collected by centrifugation at 39,000×*g* for 20 min. The precipitate was dissolved in a minimum volume of 0.05 *M* II (pH 7.5) and dialyzed overnight against 20 volumes of the same buffer. The enzyme preparation was stored at 4°.

The enzyme inhibition assay was conducted in plastic scintillation vials. A small drop was produced in the bottom of the vial, which contained 50 μl of II, 50 μl of the [^{3}H]cyclic AMP substrate solution, 50 μl of test drug, and 50 μl of diluted enzyme preparation in 1 mg of bovine serum albumin and 1 mg of snake venom nucleotidase/ml of 0.05*M* II buffer at pH 8.0. The vials were incubated for 10 min at 37° with vigorous shaking. The reaction was terminated by the addition of 0.5 ml of washed anion-exchange resin (200–400 mesh, 50% settled volume).

The phosphodiesterase activity was measured as [^{3}H]adenosine using a modified Bray's scintillation cocktail.

Calcium Transport Assay—The assay for inhibition of calcium accumulation was conducted as described by Scott *et al.* (16). Blood was obtained in heparin from healthy human volunteers, and the red blood

cells were collected by centrifugation at 270×*g*. The cells were washed four times and resuspended in 10 m*M* II (pH 7.3) containing 135 m*M* NaCl, 4.5 m*M* KCl, and 15 m*M* chlorine chloride (III). The cells (400 μl packed red blood cells), 10 μl of test drug solution, and 490 μl of III were preincubated in 12 × 75-mm plastic tubes at 24° for 1 hr. A 100-μl solution of [^{45}Ca]calcium chloride[4] (~1 × 10^6 cpm, specific activity 9.85 mCi/mg) was added, and the tubes were incubated with moderate shaking for 30 min at 37°.

The incubation was terminated by addition of 2 ml of 0.1 m*M* lanthanum chloride in III. Tubes were centrifuged at 270×*g* for 10 min, and the supernate was removed. The cells were washed in 2 ml of buffer and recentrifuged, and the supernate was again removed. Each tube was vortexed, and 200 μl was transferred to a glass scintillation vial. A 200-μl aliquot of 60% perchloric acid was added, the vials were shaken, and then 400 μl of 50% hydrogen peroxide was added with shaking. The vials were heated to 70–80° for 30 min. After cooling, 8 ml of ethylene glycol monomethyl ether was added to each vial, followed by 10 ml of a toluene-phosphor solution (6g of 2,5-diphenyloxazole/liter of scintillation grade toluene). Radioactivity was measured by liquid scintillation spectroscopy.

Drugs—Drugs used as standards in these assays included niacin[5], pentoxifylline[6], dipyridamole[7], amiquinsin[8], leniquinsin[8], dioxyline[9], protoveratrine[9], amylnitrite[9], nicotinyl alcohol[10], sodium nitroprusside[10], cyclandelate[11], cinnarizine[12], flunarizine[12], verapamil[13], nafronyl[14], quazodine[15], ethaverine[16], prazosin[17], quinazosin[17], hoquizil[17], mebeverine[18], diazoxide[19], etazolate hydrochloride[20], phenoxybenzamine[21], bencyclane[22], papaverine[23], nylidrin[23], and amotriphene[24]. Other drugs were obtained commercially.

Drugs were dissolved immediately prior to assay in distilled water, using dimethyl sulfoxide or dimethylformamide as solubilization aids if necessary.

RESULTS

Table I shows the compounds that exhibited binding only to β-adrenergic receptors. Two control compounds were run as assay validation standards. In the competition assays using guinea pig heart and lung membranes and [^{3}H]dihydroalprenolol as the radioligand, the nonselective β-adrenergic antagonist propranolol had high binding affinity. The cardioselective β-blocker atenolol had lower affinity for sites on both heart and lung membranes than did propranolol, the affinity being higher for heart membrane binding sites than for lung membrane sites. The binding sites on guinea pig heart and lung membranes labeled by [^{3}H]-dihydroalprenolol have been characterized as β_1- and β_2-adrenergic, respectively (17).

Two vasodilators exhibited binding affinity for β-adrenergic receptors. Isoproterenol had the highest affinity for both β_1- and β_2-receptors. Perhexiline had lower affinity. Neither compound showed measurable affinity for α-adrenergic receptors. The compounds did not inhibit cyclic AMP phosphodiesterase activity, nor did they block Ca^{2+} accumulation.

Table II shows the vasodilator compounds that bound only to α-adrenergic binding sites. The standard α-antagonist phentolamine had high affinity, and phenoxybenzamine also bound to α-sites. In addition, phenoxybenzamine inhibited the accumulation of calcium 45 into erythrocytes. Ergocryptine and tolazoline also had relatively high affinity for α-adrenergic receptors, while amotriphene exhibited marginal affinity. The three compounds were inactive in the other assays.

Table III lists the active compounds in the phosphodiesterase inhibition assay. The potent phosphodiesterase inhibitor etazolate hydrochloride served as a control standard. Leniquinsin was the most potent of the vasodilators tested with rat brain phosphodiesterase. Papaverine, proquazone, and dioxyline were slightly less potent. Hoquizil and quazodine were less potent, and theophylline was the least potent of the active agents tested. All active compounds tested inhibited phosphodiesterase activity in Cynomolgus monkey abdominal artery. This group of vasodilators was inactive in all other assays.

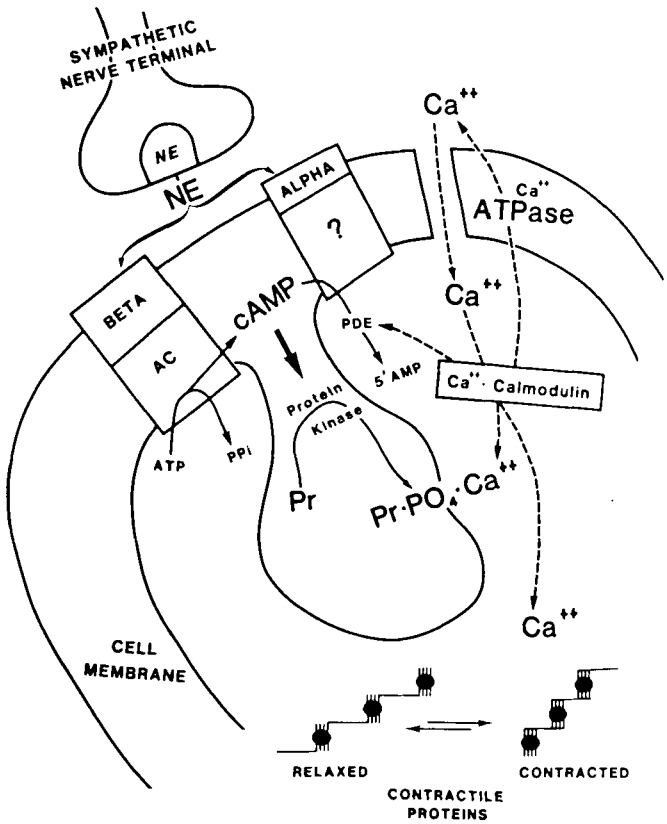

Figure 1—*Possible mechanisms of vascular smooth muscle excitation–contraction coupling.*

Thirteen vasodilators tested were active in more than one assay (Table IV). Isoxyprine, nylidrin, and bencyclane bound to β_1-, β_2-, and α-adrenergic receptors. Pentoxifylline had a low level of affinity for β_1-receptors, and it also inhibited phosphodiesterase activity. Cyclandelate bound to β_2-adrenergic receptors and inhibited accumulation of calcium.

Two compounds, cinnarizine and flunarizine, inhibited accumulation of calcium 45 ion in human red blood cells. Both compounds exhibited some affinity for α-sites. As previously reported (18, 19), prazosin bound to α-receptors. Ethaverine and dipyridamole were phosphodiesterase inhibitors and also inhibited calcium 45 ion accumulation.

Nafronyl was active in three assays. It had low binding affinity for β_2- and α-receptors and inhibited calcium accumulation. Mebeverine also bound to β_2- and α-receptors and inhibited phosphodiesterase activity. Verapamil bound to α-receptors and inhibited both phosphodiesterase activity and calcium 45 ion accumulation.

One compound, quinazosin, was active in four of the five assays. Quinazosin bound to β_2- and α-receptors. It also inhibited phosphodiesterase activity and calcium 45 ion accumulation.

Niacin, nicotinyl alcohol, inositol niacinate, amyl nitrite, sodium nitroprusside, diazoxide, hydralazine, and protoveratrine were inactive in all five assays at the highest concentration listed (150 μ*M*).

DISCUSSION

Vasodilation results from relaxation of vascular smooth muscle and leads to enhanced blood flow and/or reduced peripheral resistance (4, 20). Pharmacologically, vasodilators have been classed in two groups. One group acts indirectly on sympathetic innervation to the arterioles, thereby relieving functional vasoconstriction, and the other acts directly on the smooth muscle of the arterioles. Drugs classically categorized as sympathetic depressants include centrally acting agents such as the dihy-

[4] New England Nuclear.
[5] Supplied by Abbott Laboratories.
[6] Suppliedby Albert-Roussel.
[7] Supplied by Boehringer-Ingelheim.
[8] Supplied by Eaton.
[9] Supplied by Eli Lilly.
[10] Supplied by Hoffmann–La Roche.
[11] Supplied by Ives.
[12] Supplied by Janssen.
[13] Sujpplied by Knoll.
[14] Supplied by Lipha.
[15] Supplied by Mead-Johnson.
[16] Supplied by Parke-Davis.
[17] Supplied by Charles Pfizer.
[18] Supplied by Philips Duphar.
[19] Supplied by Schering-Plough.
[20] Supplied by Squibb.
[21] Supplied by Smith Kline and French.
[22] Supplied by Thiemann.
[23] Supplied by U.S. Vitamin.
[24] Supplied by Winthrop.

Table IV—Vasodilators with Multiple Activities [a]

Compound	Structure	IC_{50}, μM					
		Adrenergic Receptor Binding			PDE		
		β_1 (Heart)	β_2 (Lung)	α (Uterus)	(Brain)	(Artery)	Ca^{2+}
Isoxsuprine	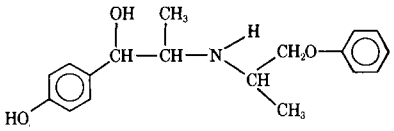	15	57	3	—	NT[b]	—
Nylidrin	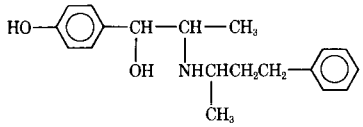	20	10	50	—	NT[b]	—
Bencyclane	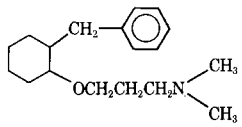	3.5	1.5	15	—	NT[b]	—
Pentoxifylline	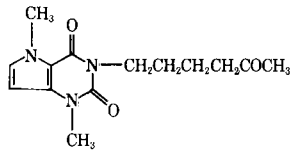	85	—	—	48	NT[b]	—
Cyclandelate	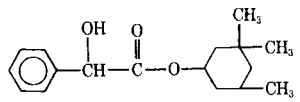	—	16	—	—	NT[b]	31
Cinnarizine	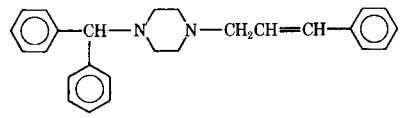	—	—	7	—	NT[b]	19
Flunarizine	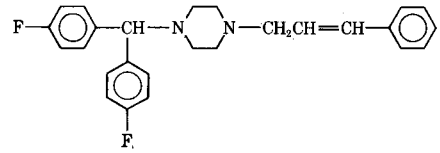	—	—	25	—	NT[b]	46
Prazosin	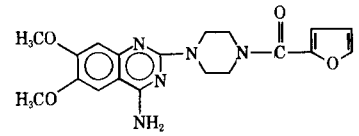	—	—	1.0	26	30	—
Ethaverine	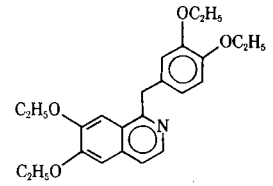	—	—	—	1.5	1.6	11
Dipyridamole	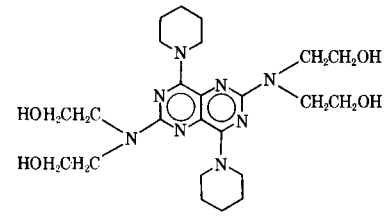	—	—	—	4.2	20	5.6
Mafronyl	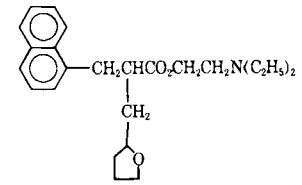	—	75	50	—	NT[b]	2.5

Table IV—*Continued*

Compound	Structure	IC$_{50}$, μM Adrenergic Receptor Binding β_1 (Heart)	β_2 (Lung)	α (Uterus)	PDE (Brain)	(Artery)	Ca^{2+}
Nebeverine	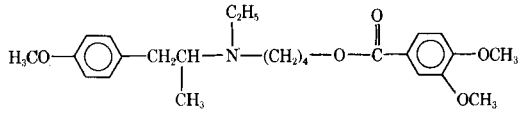	—	10	20	74	100	—
Verapamil	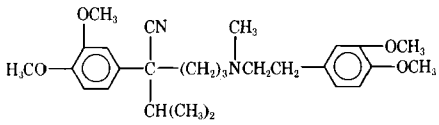	—	—	2.5	28	64	87
Quinazosin	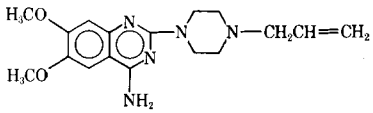	—	15	1.5	84	140	13

[a] See footnotes to Table I. [b] Not tested.

droergot alkaloids, ganglionic blocking drugs (e.g., pentolinium and mecamylamine), and agents such as guanethidine, which block norepinephrine release at neuroeffector junctions. Drugs categorized as acting on smooth muscle include β-adrenergic stimulating agents such as isoproterenol, isoxsuprine, and nylidrin and α-adrenergic blocking agents such as phenoxybenzamine and tolazoline. Other direct acting vasodilators presumably act on contractile mechanisms of the smooth muscle cell (5).

The biochemical mechanisms that underlie the coupling of sympathetic nervous excitation and smooth muscle contractility are beginning to be understood. Figure 1 shows an hypothesized pathway involving a complex series of biochemical events (7, 8, 21–23), by which adrenergic neurotransmitters regulate smooth muscle contractility. With respect to vasodilation, the following pathway is proposed:

1. Norepinephrine binds to specific β-adrenergic sites on the muscle cell surface.
2. The increased activity of a closely coupled enzyme, adenylate cyclase, elevates cellular cyclic AMP levels.
3. The cellular content of cyclic AMP regulates the activity of a second enzyme, cyclic AMP-dependent protein kinase, which functions to phosphorylate (and thus activates) certain proteins in the sarcoplasmic reticulum. The activated proteins in the sarcoplasmic reticulum control the storage and release of Ca^{2+} ions, which ultimately regulate the contraction of the actin–myosin fibrils of the muscle cell.
4. The heat-stable protein calmodulin binds calcium and activates phosphodiesterase to return cellular cyclic AMP levels back to normal. Simultaneously, calmodulin activates the calcium-stimulated ATP phosphohydrolase (the so-called calcium pump) to return intracellular levels of calcium to baseline levels.

The biochemical events elicited by stimulating α-adrenergic sites are less well understood. Three hypotheses have been proposed:

1. α-Receptor stimulation may inhibit adenylate cyclase or stimulate cyclic AMP phosphodiesterase activity, leading to a decrease in cellular cyclic AMP levels.
2. α-Receptor stimulation causes increased guanylate cyclase activities and increased cyclic GMP levels, leading to physiological actions opposing cyclic AMP.
3. α-Receptors function as calcium ionophores, resulting in increased Ca^{2+} influx.

Most of the vasodilators tested were active in one or more of the assays and thus might be expected to act at some specific point in the described excitation-contraction coupling pathways for vascular smooth muscle. The compounds that were inactive in these assays may act on related mechanisms. For example, papaverine, nitroglycerin, diazoxide, and hydralazine all increased the cyclic AMP content in vascular smooth muscle (24). Furthermore, Chidsey and Gottlieb (20) reviewed studies that suggested that certain vasodilators (diazoxide, minoxidil, and sodium nitroprusside) interfere with some calcium movements responsible for initiation or maintenance of contractile state. These vasodilators might alter the availability of calcium ion to contractile proteins through compartmentalization rather than modification of cellular content.

Several vasodilators exhibit multiple activities. Nylidrin and isoxsuprine, vasodilators classically described as β-adrenergic stimulants, showed affinity for β-receptors. However, these compounds also exhibited affinities for α-receptors. The multiple activities of these drugs is consistent with earlier work (25), which showed that isoxsuprine relaxed a variety of nonvascular smooth muscles through mechanisms independent of β-receptors. These investigators suggested that, in addition to its sympathomimetic action, isoxsuprine may have a papaverine-like, direct effect as well as an adrenergic blocking action. Although radioreceptor assays do not distinguish between agonists and antagonists, these results suggest that this compound more likely acts by blocking α-adrenergic receptors than by inhibiting phosphodiesterase activity. Furthermore, work reviewed by Coffman (6) indicated that the effects of isoxsuprine and nylidrin are not completely antagonized by β-adrenergic blocking agents.

Previous findings (18) indicate that prazosin interacts with both the active site of phosphodiesterase and with α-receptors (18). Subsequent data suggest that prazosin binds to two different populations of binding sites, possibly relating to pre- and postsynaptic α-receptors (19).

The α-blocking agent phenoxybenzamine also was found to be an inhibitor of Ca^{2+} accumulation. The acknowledged calcium antagonist verapamil (26) also exhibited affinity for α-receptors, as well as phosphodiesterase inhibition. The finding that several vasodilators exhibited activity in two of three assays (α-receptor, phosphodiesterase inhibition, and calcium accumulation) suggests a close relationship of three biochemical steps. On the other hand, the finding that some vasodilators were only active in one of these three assays supports the contention that these are closely related but independent mechanisms.

The mechanisms closest to the control of contractile protein function evidently involve the transport, storage, and cellular content of calcium ion. Cinnarizine and flunarizine, for example, inhibit accumulation of calcium ion in human red blood cells (18) and have been reported to produce long-lasting inhibition of calcium-induced contraction in isolated vascular preparations of rat and rabbit (11). Other vasodilators such as papaverine, nafronyl, bencyclane, cyclandelate, dihydroergotamine, xanthinol niacinate, and pentoxifylline were reported by the same investigators to be less potent as inhibitors of Ca^{2+}-induced vasospasms. In this regard, flunarizine appears to possess a degree of selectivity in that (in contrast to the majority of reports) it had little effect on spontaneous myogenic activity (11). Flunarizine also prevents blood hyperviscosity induced by ischemic occlusion (26, 27), an effect apparently related to changes in red blood cell flexibility (28). This drug's vasodilator activity and its effects on red blood cell deformability both probably result from inhibition of Ca^{2+} accumulation (16).

With respect to vasodilation, drug actions in the smooth muscle cell resulting in reduced Ca^{2+} available for interaction with the troponin–actin–myosin complex lead to relaxation of the muscle and dilation of the blood vessel.

The biochemical screening models used in this study were predicted on our working hypothesis and were established to ascertain whether vasodilator drugs might have their effects on specific points in these pathways. Several vasodilators previously were shown to act through cyclic AMP-related mechanisms. Papaverine, for example, is a well-

accepted model compound of a vasodilator acting through cyclic AMP phosphodiesterase inhibition (29, 30), and isoproterenol has been shown to elevate cyclic AMP levels through stimulation of adenylate cyclase. It is clear that elevated intracellular cyclic AMP levels can lead to vasodilation and that compounds that interact with either the α-adrenergic receptor or cyclic AMP phosphodiesterase may be potential vasodilators.

The presence of calcium is a necessary component of smooth muscle contraction. Several workers showed that agents that normally contract vascular smooth muscle *in vitro* cannot cause contraction when calcium is omitted from the incubation or when calcium accumulation into the tissue is blocked. Therefore, agents capable of inhibiting calcium accumulation (*e.g.* flunarizine) may act by preventing vasoconstriction and result in a net vasodilation *in vivo* (31).

It is not certain how directly the results using biochemical screening models can be extrapolated to *in vivo* conditions involving vascular smooth muscle. However, several general findings provide a basis for further experimentation and future working hypotheses.

Vasodilators must be considered a heterogeneous drug class. For example, from a therapeutic point of view, vasodilators used in the treatment of hypertension and peripheral vascular disease require different pharmacological properties. In the treatment of peripheral vascular disease, reduction of blood pressure is undesirable, whereas it is obviously a criterion for vasodilators used in hypertension (1). The optimal requirements for peripheral and cerebral vasodilators may also differ.

The actions of vasodilators clearly involve heterogeneous physiological and biochemical mechanisms related to smooth muscle contractility. It is proposed that both the therapeutic utility and side-effect pattern of a vasodilator will depend on the specific profile of the excitation–contraction coupling mechanisms altered by the drug. Additional research on this series of drugs and on future compounds will provide more specific criteria for classifying vasodilator drugs.

REFERENCES

(1) "New Antihypertensive Drugs," A. N. Richards, Ed., Spectrum, New York, N.Y., 1976, pp. 527, 533.

(2) J. Kock-Weser, *Arch. Intern. Med.*, **133,** 1017 (1974).

(3) E. Braunwald, *N. Engl. J. Med.*, **297,** 331 (1977).

(4) J. N. Cohn and J. A. Franciosa, *ibid.*, **297,** 254 (1977).

(5) "Drugs of Choice," W. Modell, Ed., C. V. Mosby, New York, N.Y., 1974, pp. 391, 398.

(6) J. D. Coffman, *N. Engl. J. Med.* **300,** 713 (1974).

(7) H. P. Bar, *Adv. Cyclic Nucleotide Res.*, **4,** 195 (1974).

(8) M. J. Berridge, *ibid.*, **6,** 1 (1975).

(9) H. Rasmassen, P. Jensen, W. Lake, N. Friedman, and D. B. P. Goodman, *ibid.*, **5,** 275 (1975).

(10) W. C. Cutting, "Handbook of Pharmacology," Appleton-Century-Crofts, New York, N.Y., 1969, pp. 201, 233, 243.

(11) J. M. Van Neuten, J. Van Beek, and P. A. J. Janssen, *Arch. Int. Pharmacodyn. Ther.*, **232,** 42 (1978).

(12) F. C. Greenslade and K. L. Newquist, *ibid.*, **233,** 270 (1978).

(13) C. Mukherjee, M. Caron, M. Coverston, and R. Lefkowitz, *J. Biol. Chem.*, **250,** 4869 (1975).

(14) L. T. Williams, D. Mullikin, and R. J. Lefkowtiz, *ibid.*, **251,** 6915 (1976).

(15) "Methods in Cyclic Nucleotide Research," M. Chasin, Ed., Dekker, New York, N.Y., 1972, pp. 69, 198.

(16) C. K. Scott, F. J. Persico, K. Carpenter, and M. Chasin, *Angiology*, **31,** 320 (1980).

(17) K. L. Newquist, F. C. Greenslade, M. Chasin, and F. J. Persico, *Fed. Proc. Fed. Am. Soc. Exp. Biol.*, **37,** 683 (1978).

(18) C. K. Scott, K. M. Krider, K. L. Newquist, M. Chasin, and F. C. Greenslade, *ibid.*, **37,** 351 (1978).

(19) F. C. Greenslade, C. K. Scott, M. Chasin, S. M. Madison, and A. J. Tobia, *Biochem. Pharmacol.*, **28,** 2409 (1979).

(20) C. A. Chidsey and T. B. Gottlieb, *Prog. Cardiovasc. Dis.*, **17,** 99 (1974).

(21) "Stimulus Secretion Coupling in the Gastrointestinal Tract," R. M. Case, and H. Boebell, Eds., Park Press, New York, N.Y., 1976, pp. 33, 47.

(22) M. E. Maguire, E. M. Ross, and A. G. Gilman, *Adv. Cyclic Nucleotide Res.*, **8,** 1 (1977).

(23) M. L. Steer, *Clin. Endocrinol. Metab.*, **6,** 577 (1977).

(24) R. Anderson, *Acta Pharmacol. Toxicol.*, **32,** 321 (1973).

(25) P. M. Lish, K. W. Dungan, and E. L. Peters, *J. Pharmacol. Exp. Ther.*, **129,** 191 (1960).

(26) R. Manhold, R. Steiner, W. Haas, and R. Kaufmann, *Naunyn-Schmiedebergs Arch. Pharmacol.*, **302,** 217 (1978).

(27) F. DeClerck, J. DeCree, J. Brugmans, and D. Wellens, *Arch. Int. Pharmacodyn. Ther.*, **230,** 321 (1977).

(28) R. J. Weed, P. L. Lacele, E. W. Merrill, G. Craib, A. Gregory, F. Karch, and F. Pickens, *J. Clin. Invest.*, **48,** 795 (1969).

(29) W. R. Kukovetz and G. Poech, *Arch. Pharmacol. Exp. Pathol.*, **267,** 189 (1979).

(30) M. S. Amer and W. E. Kreighbaum, *J. Pharm. Sci.*, **64,** 1 (1975).

(31) J. M. Van Neuten, "Mechanism of Vasodilation," Satellite Symposium, 27th International Congress in Physiological Science, Karger, Basel, Switzerland, 1978, pp. 137, 143.

Liposome Disposition *In Vivo* II: Dose Dependency

MARK E. BOSWORTH and C. ANTHONY HUNT ˣ

Received August 28, 1980, from the *School of Pharmacy, University of California, San Francisco, CA 94143.* Accepted for publication May 18, 1981.

Abstract □ The dose-dependent disposition of extruded multilamellar (diameter ~1 μm) negatively charged liposomes containing entrapped [^{14}C]inulin was studied in mice. Mice received 1500, 300, or 15 μmoles of liposomal lipid/kg iv. Carbon 14 levels were measured in the blood, liver, spleen, and carcass for 72 hr. A pronounced saturation effect, consistent with the known dose behavior of other colloids, was seen at early times; it was manifested by higher dose values in the blood and spleen but by lower liver values as the dose increased. This dose effect was attenuated in the liver but was maintained in the spleen at later times, and percent dose values approached plateau values in all tissues for all doses at later times. [^{14}C]Inulin was used as the liposomal marker because of its inability to enter cells (or, presumably, leave them if delivered there by liposomes) in its free form. An early decline in carbon 14 levels (over the first 48 hr) was seen in the liver for the low and medium doses. Because of the known ability of blood factors to cause liposomes to leak their contents, this decline was interpreted as being a loss of [^{14}C]inulin from extracellularly bound liposomes during this period. Moreover, the plateau carbon 14 levels at later times were interpreted as approximating the true level of intracellular inulin delivery by the liposomes.

Keyphrases □ Liposomes—disposition *in vivo*, dose dependency □ Disposition—of liposomes, dose dependency □ Pharmacokinetics—liposome disposition *in vivo*, dose dependency

Recently, there has been considerable interest in liposomes (phospholipid vesicles) as an *in vivo* drug delivery system. There are now ample data showing that liposome encapsulation can drastically alter the blood kinetics and tissue distribution of numerous compounds. Their potential uses in drug therapy, which were recently reviewed

0022-3549/82/0100-0100$01.00/0

accepted model compound of a vasodilator acting through cyclic AMP phosphodiesterase inhibition (29, 30), and isoproterenol has been shown to elevate cyclic AMP levels through stimulation of adenylate cyclase. It is clear that elevated intracellular cyclic AMP levels can lead to vasodilation and that compounds that interact with either the α-adrenergic receptor or cyclic AMP phosphodiesterase may be potential vasodilators.

The presence of calcium is a necessary component of smooth muscle contraction. Several workers showed that agents that normally contract vascular smooth muscle *in vitro* cannot cause contraction when calcium is omitted from the incubation or when calcium accumulation into the tissue is blocked. Therefore, agents capable of inhibiting calcium accumulation (*e.g.* flunarizine) may act by preventing vasoconstriction and result in a net vasodilation *in vivo* (31).

It is not certain how directly the results using biochemical screening models can be extrapolated to *in vivo* conditions involving vascular smooth muscle. However, several general findings provide a basis for further experimentation and future working hypotheses.

Vasodilators must be considered a heterogeneous drug class. For example, from a therapeutic point of view, vasodilators used in the treatment of hypertension and peripheral vascular disease require different pharmacological properties. In the treatment of peripheral vascular disease, reduction of blood pressure is undesirable, whereas it is obviously a criterion for vasodilators used in hypertension (1). The optimal requirements for peripheral and cerebral vasodilators may also differ.

The actions of vasodilators clearly involve heterogeneous physiological and biochemical mechanisms related to smooth muscle contractility. It is proposed that both the therapeutic utility and side-effect pattern of a vasodilator will depend on the specific profile of the excitation–contraction coupling mechanisms altered by the drug. Additional research on this series of drugs and on future compounds will provide more specific criteria for classifying vasodilator drugs.

REFERENCES

(1) "New Antihypertensive Drugs," A. N. Richards, Ed., Spectrum, New York, N.Y., 1976, pp. 527, 533.

(2) J. Kock-Weser, *Arch. Intern. Med.*, **133,** 1017 (1974).

(3) E. Braunwald, *N. Engl. J. Med.*, **297,** 331 (1977).

(4) J. N. Cohn and J. A. Franciosa, *ibid.*, **297,** 254 (1977).

(5) "Drugs of Choice," W. Modell, Ed., C. V. Mosby, New York, N.Y., 1974, pp. 391, 398.

(6) J. D. Coffman, *N. Engl. J. Med.* **300,** 713 (1974).

(7) H. P. Bar, *Adv. Cyclic Nucleotide Res.*, **4,** 195 (1974).

(8) M. J. Berridge, *ibid.*, **6,** 1 (1975).

(9) H. Rasmassen, P. Jensen, W. Lake, N. Friedman, and D. B. P. Goodman, *ibid.*, **5,** 275 (1975).

(10) W. C. Cutting, "Handbook of Pharmacology," Appleton-Century-Crofts, New York, N.Y., 1969, pp. 201, 233, 243.

(11) J. M. Van Neuten, J. Van Beek, and P. A. J. Janssen, *Arch. Int. Pharmacodyn. Ther.*, **232,** 42 (1978).

(12) F. C. Greenslade and K. L. Newquist, *ibid.*, **233,** 270 (1978).

(13) C. Mukherjee, M. Caron, M. Coverston, and R. Lefkowitz, *J. Biol. Chem.*, **250,** 4869 (1975).

(14) L. T. Williams, D. Mullikin, and R. J. Lefkowtiz, *ibid.*, **251,** 6915 (1976).

(15) "Methods in Cyclic Nucleotide Research," M. Chasin, Ed., Dekker, New York, N.Y., 1972, pp. 69, 198.

(16) C. K. Scott, F. J. Persico, K. Carpenter, and M. Chasin, *Angiology*, **31,** 320 (1980).

(17) K. L. Newquist, F. C. Greenslade, M. Chasin, and F. J. Persico, *Fed. Proc. Fed. Am. Soc. Exp. Biol.*, **37,** 683 (1978).

(18) C. K. Scott, K. M. Krider, K. L. Newquist, M. Chasin, and F. C. Greenslade, *ibid.*, **37,** 351 (1978).

(19) F. C. Greenslade, C. K. Scott, M. Chasin, S. M. Madison, and A. J. Tobia, *Biochem. Pharmacol.*, **28,** 2409 (1979).

(20) C. A. Chidsey and T. B. Gottlieb, *Prog. Cardiovasc. Dis.*, **17,** 99 (1974).

(21) "Stimulus Secretion Coupling in the Gastrointestinal Tract," R. M. Case, and H. Boebell, Eds., Park Press, New York, N.Y., 1976, pp. 33, 47.

(22) M. E. Maguire, E. M. Ross, and A. G. Gilman, *Adv. Cyclic Nucleotide Res.*, **8,** 1 (1977).

(23) M. L. Steer, *Clin. Endocrinol. Metab.*, **6,** 577 (1977).

(24) R. Anderson, *Acta Pharmacol. Toxicol.*, **32,** 321 (1973).

(25) P. M. Lish, K. W. Dungan, and E. L. Peters, *J. Pharmacol. Exp. Ther.*, **129,** 191 (1960).

(26) R. Manhold, R. Steiner, W. Haas, and R. Kaufmann, *Naunyn-Schmiedebergs Arch. Pharmacol.*, **302,** 217 (1978).

(27) F. DeClerck, J. DeCree, J. Brugmans, and D. Wellens, *Arch. Int. Pharmacodyn. Ther.*, **230,** 321 (1977).

(28) R. J. Weed, P. L. Lacele, E. W. Merrill, G. Craib, A. Gregory, F. Karch, and F. Pickens, *J. Clin. Invest.*, **48,** 795 (1969).

(29) W. R. Kukovetz and G. Poech, *Arch. Pharmacol. Exp. Pathol.*, **267,** 189 (1979).

(30) M. S. Amer and W. E. Kreighbaum, *J. Pharm. Sci.*, **64,** 1 (1975).

(31) J. M. Van Neuten, "Mechanism of Vasodilation," Satellite Symposium, 27th International Congress in Physiological Science, Karger, Basel, Switzerland, 1978, pp. 137, 143.

Liposome Disposition *In Vivo* II: Dose Dependency

MARK E. BOSWORTH and C. ANTHONY HUNT ˣ

Received August 28, 1980, from the *School of Pharmacy, University of California, San Francisco, CA 94143.* Accepted for publication May 18, 1981.

Abstract □ The dose-dependent disposition of extruded multilamellar (diameter ~1 μm) negatively charged liposomes containing entrapped [^{14}C]inulin was studied in mice. Mice received 1500, 300, or 15 μmoles of liposomal lipid/kg iv. Carbon 14 levels were measured in the blood, liver, spleen, and carcass for 72 hr. A pronounced saturation effect, consistent with the known dose behavior of other colloids, was seen at early times; it was manifested by higher dose values in the blood and spleen but by lower liver values as the dose increased. This dose effect was attenuated in the liver but was maintained in the spleen at later times, and percent dose values approached plateau values in all tissues for all doses at later times. [^{14}C]Inulin was used as the liposomal marker because of its inability to enter cells (or, presumably, leave them if delivered there by liposomes) in its free form. An early decline in carbon 14 levels (over the first 48 hr) was seen in the liver for the low and medium doses. Because of the known ability of blood factors to cause liposomes to leak their contents, this decline was interpreted as being a loss of [^{14}C]inulin from extracellularly bound liposomes during this period. Moreover, the plateau carbon 14 levels at later times were interpreted as approximating the true level of intracellular inulin delivery by the liposomes.

Keyphrases □ Liposomes—disposition *in vivo*, dose dependency □ Disposition—of liposomes, dose dependency □ Pharmacokinetics—liposome disposition *in vivo*, dose dependency

Recently, there has been considerable interest in liposomes (phospholipid vesicles) as an *in vivo* drug delivery system. There are now ample data showing that liposome encapsulation can drastically alter the blood kinetics and tissue distribution of numerous compounds. Their potential uses in drug therapy, which were recently reviewed

0022-3549/82/0100-0100$01.00/0

(1, 2), are a direct result of these kinetic properties.

BACKGROUND

When the fate of intravenously administered liposomes is followed (*e.g., via* an entrapped aqueous space marker), the marker (and presumably the liposomes) accumulate to a significant extent in organs that contain cells of the reticuloendothelial system. This accumulation occurs principally in the liver and spleen where, depending on the liposome type, animal species, and postadministration time, up to 90% of the injected dose of the marker may be found.

The significance of this reticuloendothelial localization was noted by other investigators (3). The reticuloendothelial system is a diffuse system with cells positioned along the vasculature in the liver, spleen, and bone marrow, in the lung alveoli, and in the tissue interstices. One of its functions is to phagocytize colloidal and particulate material such as effete red blood cells, denatured proteins, cellular debris, foreign organisms, and exogenously administered substances such as colloidal carbon or gold (the term "colloid" can arbitrarily encompass suspensions with particle sizes ranging from 10 Å to several microns).

An extensive literature exists on the *in vivo* fate of these "inert" colloids (e.g., carbon and gold) (4). After intravenous administration, they are taken up primarily by reticuloendothelial cells in the liver and spleen by a two-step process, first involving binding to the cell and then phagocytosis; the latter step is presumed to take place quickly after the binding (5). In fact, this assumption is made whenever the blood disappearance rate of one of these colloids is used as a general indicator of reticuloendothelial system function (4). This dose-dependent process exhibits saturability in two respects. First, as the dose (*i.e.*, number of particles) is increased, the rate of colloid removal from the blood is decreased (6). Second, the tissue distribution changes with the dose (5). At very low, nonsaturating doses, for which blood flow to the reticuloendothelial tissues is the rate-limiting factor in the removal of the colloid from the blood, 95% or more of the colloid dose is taken up by the liver and the rest by the spleen. As the dose increases, the spleen takes up an increasingly larger fraction of the dose due to the saturation of the liver uptake. At extremely high doses, the lung and bone marrow can take up significant fractions also, in what amounts to a system-wide mobilization in response to a saturating dose (7).

Because liposomes are colloidal, and because of their well-documented reticuloendothelial system localization, it is reasonable to expect them to behave similarly to other colloids. The present study examined the possible dose dependency of liposome blood kinetics and tissue distribution. Other researchers reported limited evidence that suggests that liposome disposition may be dose dependent (8–10). The possibility of a time dependence in the dose effect was examined in the present study by following blood and tissue levels for 72 hr. An appropriate liposome marker, [^{14}C]inulin, was used to assess the extent to which the liposomes delivered their entrapped contents intracellularly.

EXPERIMENTAL

Chemicals—Purified egg yolk lecithin, sodium dipalmitoyl phosphatidate, cholesterol, and α-tocopherol (vitamin E) were chromatographic grade[1]. [Carboxy-^{14}C]inulin[2] was 2.3 μCi/mg, and scintillation reagents[3,4] were used. All other chemicals were analytical reagent grade or better. Phosphate-buffered saline (I) contained 92 m*M* sodium chloride, 23 m*M* dibasic sodium phosphate, and 11 m*M* monobasic sodium phosphate. Prior to use, phosphatidic acid was obtained by chloroform extraction of a solution of sodium phosphatidate in 0.4 *N* HCl with 20% methanol.

Preparation of Liposomes—Liposomes were prepared essentially as previously described (10) and were composed of egg lecithin, phosphatidic acid, cholesterol, and α-tocopherol in the molar ratios 4:1:1:0.05. The lipids were dissolved in chloroform, mixed in a round-bottom flask, and subsequently evaporated to dryness under vacuum. The buffer (I) containing 5 m*M* [^{14}C]inulin was added to the dried lipid to give a concentration of 37.5 μmoles of lipid/ml and then was agitated by hand (at room temperature after nitrogen sparging) until all of the lipid was suspended. This suspension was then placed in a 25-mm stirred ultrafiltration cell[5] fitted with a 1.0-μm pore size polycarbonate membrane[6] and extruded twice at a flow rate of ~10 ml/min, controlled by nitrogen pressure.

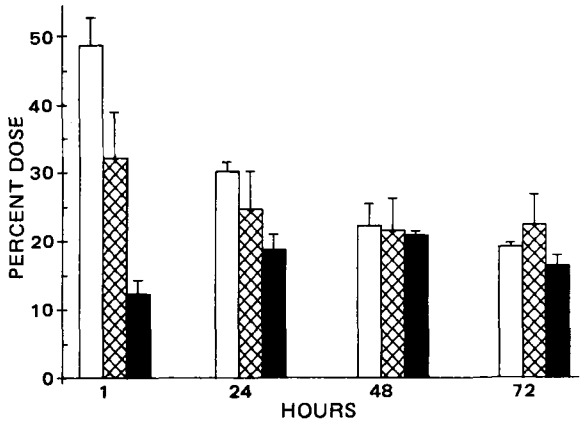

Figure 1—*Percent of injected carbon 14 dose in the liver for low (□), medium (▨), and high (■) doses at four times [mean ± 1* SD (n = *3, 10, and 4 for low, medium, and high doses, respectively)]. Equality of low and high doses was tested, and the differences between doses were statistically significant at 1 and 24 hr but not at 48 and 72 hr (one-tailed unpaired* t *test, α 0.05).*

Liposomes for the high dose were concentrated by adding 0.3 ml of 50% (w/v) sucrose to 1.1 ml of liposomes, centrifuging at 12,000 × *g* for 15 min, removing the upper concentrated liposome layer, and resuspending it in I to give a final concentration of 112.5 μmoles of lipid/ml. Liposomes were dialyzed overnight at 5° against I in dialysis cells fitted with 0.8-μm pore size membranes[6] to remove nonentrapped inulin and to improve the size distribution by removing the smallest liposomes (11). At least 10 buffer changes were done for each cell during the dialysis.

Tissue Distribution Studies—Liposomes were taken off dialysis and kept at 5° throughout the injection period. Male ICR mice, 18–24 g, were injected with 37.5, 7.5, or 0.375 μmoles of lipid/mouse (high, medium, and low doses, respectively) intravenously *via* the tail vein with 0.25–0.35-ml injection volumes. Mice receiving imperfect injections were not used. To determine the percentage of free inulin in each dose, a sample was applied to a 5 × 120-mm column of Sephadex[7] G-200-120 equilibrated and subsequently eluted with I; the eluate fractions were analyzed by scintillation counting, and the percent of inulin entrapped was calculated based on the carbon 14 recovered in the void volume and free inulin fractions.

Mice were anesthetized with ether at 1, 24, 48, or 72 hr after injection, and ~0.5–1.0 ml of blood was quickly removed from the jugular vein with a heparinized syringe. The mice were then sacrificed; the livers, spleens (and, in some instances, the brain, kidneys, and lungs) were removed and frozen for later analysis. In some cases, an aliquot of the blood was cen-

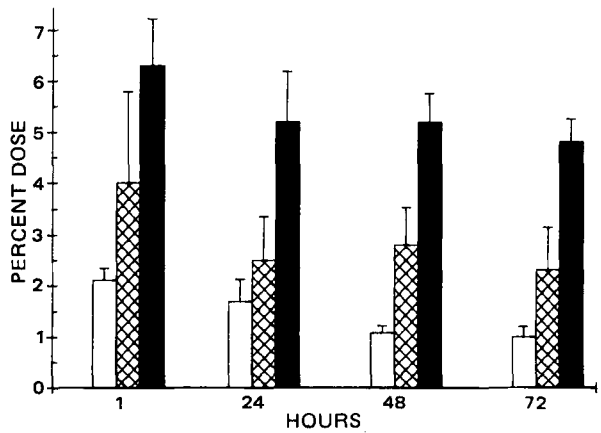

Figure 2—*Percent of injected carbon 14 dose in the spleen for low (□), medium (▨), and high (■) doses at four times [mean ± 1* SD (n = *3, 10, and 4 for low, medium, and high doses, respectively)]. Equality of low and high doses was tested, and the differences between doses were statistically significant at all time points (one-tailed unpaired t test, *α 0.05).*

[1] Sigma Chemical Co., St. Louis, Mo.
[2] New England Nuclear, Boston, Mass.
[3] Carbosorb and Permafluor V, Packard Instrument Co., Downer's Grove, Ill.
[4] PCS, Amersham, Arlington Heights, Ill.
[5] Millipore, Bedford, Mass.
[6] Nucleopore, Pleasanton, Calif.
[7] Pharmacia Fine Chemicals, Sweden.

Table I—Data [a] for Various Organs at 1 hr after Liposome Doses

Dose	Blood Levels, percent dose/ 1.0 ml (Ref.)	Percent Entrapped in Blood	Lungs	Kidneys	Brain
Low	0.39 ± 0.1 (3)	[b]	0.09	—	—
Medium	1.1 ± 0.71 (9)	10.1 ± 2.0 (3)	0.23 ± 0.04 (4)	0.825 ± 0.28 (4)	0.095, 0.18
High	10.4 ± 1.1 (4)	93, 95	0.75, 0.97	—	—

[a] Percent dose: mean ± 1 *SD* (*n*), or individual values where $n \leq 2$. [b] Blood values were too low to measure.

trifuged and a plasma sample was applied to a Sephadex column as described previously to determine the percent entrapped.

Tissue Analysis for Total Radioactivity—Duplicate aliquots of liver (0.14–0.24 g), spleen (0.04–0.08 g), whole blood (0.2 ml), and the radiolabeled liposome dose (0.05 ml) were transferred to preweighed combustion cups, which were reweighed and then allowed to air dry. The remaining carcass was placed in a container with 75 ml of water and homogenized using a wet milling device[8]. Duplicate samples of the resulting slurry (1.3–2.0 g) were weighed into combustion cups and allowed to air dry for 24 hr. Dried samples were analyzed for total carbon 14 by scintillation counting following combustion in a sample oxidizer[9].

Combustions were carried out in series, samples alternating with empty combustion cups or combustion cups containing a known amount of [^{14}C]inulin. Counts per minute were subsequently corrected for variations in quench by use of a quench curve. Results for duplicate samples were averaged, and the total radioactivity in the liver, spleen, carcass, and 1.0 ml of blood was calculated and converted to percent dose. Analysis of experimental samples and control samples of known radioactivity showed that the duplicate determinations were consistently within 5% of their mean.

***In Vivo* Clearance of Free Inulin**—In a separate study, similar doses of [^{14}C]inulin in identical volumes of I were administered to mice, which were subsequently sacrificed and analyzed as described to determine the *in vivo* clearance of free inulin.

RESULTS

Free inulin was cleared rapidly by the kidney. Its half-life in blood after intravenous injection was 10–15 min, with 0.5% of the dose remaining in blood, 2.5% in the liver, and 0.15% in the spleen at 1 hr. Carcass values at 1 hr averaged 6.9%, due presumably to residual inulin in the bladder; this value was minimized by urine removal from the bladder prior to freezing the carcass. The 24-hr value for the carcass was <1%. Thus, the presence of free inulin after the liposome doses may have contributed slightly to the 1-hr carcass data but was negligible at later times and in all other tissues.

Table I shows the 1-hr carbon 14 levels for various organs and blood, as well as the percent entrapped in blood, following the liposome doses.

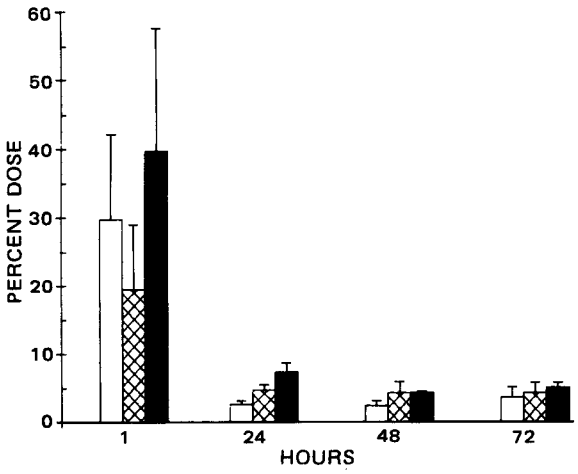

Figure 3—*Percent of injected carbon 14 dose in the carcass. Significant differences between doses were found at 24 and 48 hr but not at 1 and 72 hr (symbols and other details as in Fig. 1).*

[8] Brunwell Scientific, Rochester, N.Y.
[9] Packard Instrument Co., Downer's Grove, Ill.

Blood values, expressed as percent dose per 1.0 ml, exhibited a definite dose dependency; the values at 24, 48, and 72 hr were identical to background in all cases. Lung, brain, and kidney levels, done only in limited cases as controls, were negligible.

The other principal tissues of interest are the liver, spleen, and carcass. Figure 1 shows the results for the liver; a definite dose effect, seen as higher relative levels for the lower doses, is shown at the 1-hr time point. This effect completely diminished by 72 hr, and a similar plateau was approached by all three doses. The spleen results (Fig. 2) also showed a dose dependency but one that differed from that in the liver; the effect was maintained over the 72 hr, and higher relative levels were seen as the dose was increased. The carcass results (Fig. 3), show evidence of a dose effect at later time, which was significant at the 24- and 48-hr time points; the levels fell rapidly after 1 hr and reached a plateau. Figure 4 shows the results for the totals *in vivo*; here there is no evidence for a dose effect, and all values approach a similar plateau[10].

The reproducibility of the radioactivity measurements was also assessed. The average percent difference between duplicate samples was 6.07%, with a standard deviation of 4.23%.

DISCUSSION

The results can best be evaluated by comparison with the results one would expect for inert colloids and for liposomes (based on certain preconceived notions). Figure 5 depicts these expected dose study results. Curves A and B are plots of percent of injected dose found in all reticuloendothelial tissues *versus* time for low and high doses, respectively, of a colloid such as gold. The delayed uptake for the higher dose reflects the saturation phenomenon already mentioned. In both cases, however, all of the dose is eventually found in reticuloendothelial tissues.

The liposome case is different for two important reasons. First, it is now well known that certain factors in blood can destabilize liposomes with respect to the leaking out of their entrapped contents (13, 14). When this "leakiness" effect occurs, a significant portion of the entrapped

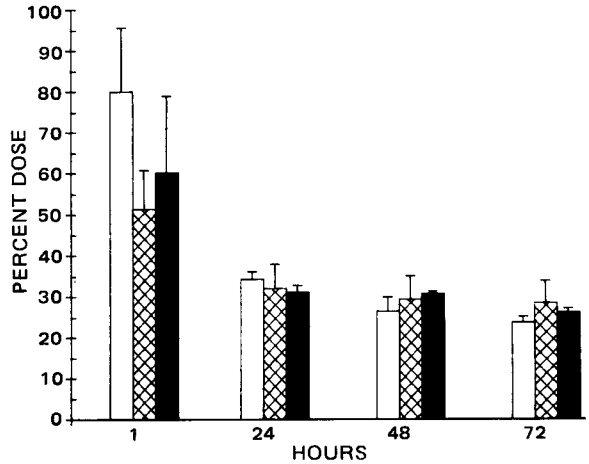

Figure 4—*Percent of injected carbon 14 dose found* in vivo *at four times. No evidence for a dose effect was seen here (symbols and other details as in Fig. 1).*

[10] In a subsequent series of studies, the mole fraction of cholesterol in the liposomes was increased to 50%, which results in liposomes with substantially increased stability in plasma (12). Following the same protocol used here and using liposome of the same size and dose, the total percent dose *in vivo* at 1 hr was 105 (*SD* ± 13%, $n = 5$); eventual plateau levels in liver and spleen were approached more slowly than in these studies.

marker can be released quickly into the blood, resulting in a <100% distribution of the marker to reticuloendothelial tissues.

The second reason is more important as far as evaluating liposome tissue distribution and concerns the nature of the entrapped marker. Most compounds that have been entrapped in liposomes have physical properties that preclude their use as accurate indicators of intracellular delivery by liposomes because these compounds are often capable of entering and leaving the target cells on their own or are metabolized to compounds that can. The resulting situation is depicted in curve E of Fig. 5, in which the tissue levels rise and fall with time due to the exit of the marker. This pattern has, in fact, been almost universally observed when tissue levels have been taken after administration of liposome-entrapped compounds.

The principal disadvantage with such data is that it is impossible to ascertain what fraction of the dose was delivered to the tissue in question. It was felt, however, that these data could be gotten using the appropriate entrapped marker. [^{14}C]Inulin was chosen because its size and polarity prevent it from entering cells on its own (or leaving, if it is delivered there *via* liposomes). It also has simple kinetics and is not metabolized. In short, it is a marker compound that should remain in the tissue to which it is delivered. The result should be tissue levels that reach plateaus at later times but, because of the leakiness effect, approach values of <100%. This situation is depicted for two different doses in curves C and D of Fig. 5.

The results of this study lead to several general conclusions. In all of the principal tissues studied (liver, spleen, carcass, totals *in vivo*) and for all doses, the levels approach plateaus at later times. This evidence supports the hypothesis that tissue level plateaus would be seen with a marker compound such as inulin; an argument will be presented later as to why these plateaus approximate the true level of intracellular delivery of the inulin by the liposomes. Furthermore, there is a pronounced dose effect at early times that is lost (in the liver) at the later times. This dose effect is consistent with that seen for other colloids such as carbon or gold; *i.e.*, the liposomes are subject to saturation kinetics, manifested by elevated relative blood and spleen levels and depressed relative liver levels as the dose increases.

As is the case for other colloids, the liver is the dominant organ in liposome disposition; because of its large blood flow and high clearance capacity relative to the other vascular reticuloendothelial tissues (*i.e.*, spleen and bone marrow), the extent to which the liver disposition of the liposomes is saturated determines the amount of colloid that is taken up by the other tissues. In other words, a delayed liver uptake results in elevated blood levels over a longer time, allowing the spleen, which is thought to have a higher cellular intrinsic activity for colloid uptake (4), to sequester a large fraction of the injected dose. The carcass values reported here (*i.e.*, everything but blood, liver, and spleen) include the bone marrow, and perhaps the slight dose effect seen in the carcass is due to uptake by the marrow.

These results also raise some intriguing questions. It is obvious that the data for the liver do not fit the predictions as depicted by curves C and D of Fig. 5. Only the high dose data fit the expected pattern of a continuous rise of the tissue levels to the eventual plateau. However, the data for the low and medium doses show a pattern with an early decline in levels followed by the plateau. Such a decline can be accounted for in only two ways.

First, a fraction of the marker that has been delivered to the cells at early times somehow partitions out of the cells at later times. However, the assumption was made earlier that the inulin marker, once delivered inside cells, would not partition out. The second explanation is that the marker levels in the liver at early times are not entirely constituted of intracellular inulin. Since the blood levels at 1 hr are very low for these two doses and since the half-life for removal of free inulin from the blood is very fast, a significant fraction of the inulin in the liver at 1 hour must be located in extracellularly bound liposomes.

It is the hypothesis of the present study that the following events occur in the liver disposition of the liposomes. If one postulates the presence of extracellularly bound liposomes, one must contend with the long-held belief that for colloids, removal from the blood can be considered the equivalent of intracellular uptake (*i.e.*, uptake occurs rapidly after binding). Data are available that show that these two phases of uptake are separable under specialized conditions *in vitro* (15), but only recently has evidence been reported that unambiguously shows that, *in vivo*, a colloid's binding to and uptake into Kuppfer cells can be very distinct events, separated by long periods of time (16, 17). In fact, Kavet and Brain (18), in their recent review on the quantification of endocytosis, emphasized that "... ingestion is not a necessary consequence of attachment. Thus, particles may become cell-associated without being interiorized and unless detected as such may be falsely included with the intracellular compartment."

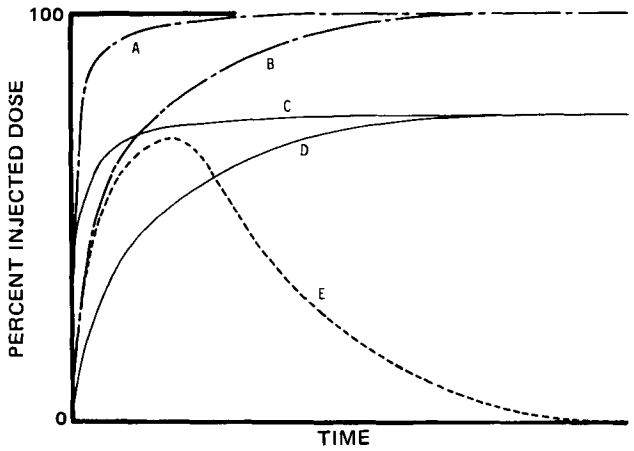

Figure 5—*Expected results for a plot of percent dose in reticuloendothelial time after intravenous administration of two different doses of colloidal gold (curves A and B), two different doses of liposome-entrapped [^{14}C]inulin (curves C and D), or a liposome-entrapped marker that can partition out of cells (curve E). These curves assume that cellular uptake of colloid occurs rapidly after binding to the tissue.*

This fact is crucial in the case of liposomes since it is very likely that extracellularly bound liposomes are just as susceptible to the destabilizing influences of blood as are free-floating liposomes. Thus, what is suggested is that: (a) tissue levels measured after administration of a liposome-entrapped marker may include substantial levels of extracellularly bound, liposome-entrapped marker, even several hours after the dose is given, and (b) these tissue levels may decline because of the slow release of marker from extracellular liposomes due to the destabilizing effect of blood.

One final piece of evidence must be considered, however, to explain completely the disposition of the three doses. Recent evidence suggests that the blood destabilizing effect may itself be saturable (13, 14); *i.e.*, as larger numbers of liposomes are incubated with a given volume of blood, a smaller fraction of the total liposome-entrapped marker is released. The liver data are thus explained as follows. In the low dose case, the liver quickly binds most of the liposome-entrapped insulin dose (part of the inulin is released from the liposomes on the initial mixing of the dose with the blood so that the initial liver value is probably <100% of the dose). However, because the intracellular uptake is slow, the bound liposomes continue to release inulin until they are taken up inside the cells. Thus, what is seen is a decline in liver levels over time until the remaining inulin is entirely intracellular and the plateau is reached[11].

In the high dose case, the initial liver binding is saturated so the relative liver levels (*i.e.*, on a percent dose basis) are low and blood levels are high. Thus, the levels of extracellular liposomes (circulating and bound) remain elevated for longer periods and are exposed to the blood's destabilizing factors longer. However, since this latter system is probably also saturated [it was calculated that the ratio of milligrams of lipid to milliliters of blood is similar to that causing saturation in *in vitro* systems (12)], the liposomes leak their contents at a relatively much slower rate. The net result is that the slowing down of the two processes of uptake (a combination of binding and endocytosis) and blood-induced liposome leakiness are offsetting effects. Thus, at later times the relative amount of inulin taken up inside cells is similar for the two doses (the medium dose is apparently an intermediate effect).

As mentioned previously, the dose behavior of the spleen conforms to the present expectations in that higher relative levels are seen as the dose increases. However, this effect, unlike that in the liver, is still evident at 72 hr. Two factors may be responsible: (*a*) the amount of colloid available to the spleen initially is largely a function of the amount bound by the liver, and (*b*) the actual intracellular uptake may be faster in the spleen so that most of what was initially bound there was also endocytosed. The carbon 14 levels in several other tissues (brain, lungs, and kidneys) were also measured (Table I). However, since the initial experiments indicated

[11] The composition of the liposomes used here was selected because of its intermediate stability in plasma (10, 14). It was conjectured that liposomes without cholesterol would rapidly lose a large fraction of their contents after injection, whereas maximally stable liposomes may result in tissue levels of carbon 14 that decline too slowly to confirm a specific final plateau level.

that very little of the dose could be found in these tissues, they were not analyzed routinely.

The liposomes used were fairly large in size (average size ~1 μm) and had a relatively narrow size distribution. This was accomplished by the use of two techniques in the sizing procedure, extrusion through 1.0-μm pore-size membranes (19) followed by dialysis against 0.8-μm membranes (11). It was felt that the excellent reproducibility seen in the tissue levels (the high dose studies were done on two separate occasions, and the medium dose study on three) was evidence of the liposome batch-to-batch reproducibility that these sizing techniques afford. The lipid composition used in the study was chosen based on *in vitro* liposome–plasma stability studies (14). The object was to choose a composition such that the liposomes were stable enough to retain most of their entrapped contents *in vivo*, yet unstable enough so that if significant long-term extracellular liposome tissue binding did take place, the marker would be released in a reasonable period (~72 hr) and thus would not be included as part of a plateau tissue level value. The decline in liver levels for the low and medium doses took place over the first 24–36 hr, which was fast enough to allow observation of the plateaus by 72 hr.

CONCLUSIONS

The results of this study have several general implications. First, it is obvious that the liposomal dose (or liposome number) is an extremely important determinant of *in vivo* disposition. It is unfortunate that *in vivo* work is still appearing in which the liposome dose is not given and is difficult or impossible to determine from the other details given [the dose in terms of micromoles of lipid/kg of body weight is currently acceptable, but the ideal would be the additional specification of liposome size and number (20)].

Second, the present data suggest that, after administration of a liposome-entrapped marker, a significant fraction of the marker may be located in extracellularly bound liposomes for long periods. Therefore, a general reinterpretation of the significance of tissue levels for most compounds administered in liposomes is needed. Specifically, tissue levels cannot be taken as an indicator of the intracellular delivery of the entrapped compound by the liposomes.

The present data suggest, however, that tissue level plateaus after administration of a liposome-entrapped compound such as inulin may be a valid indicator of intracellular delivery. This would be important for several reasons. It is necessary information for potential entrapped compounds so large or polar that their cellular uptake in the free form is zero. Moreover, for compounds that can penetrate cells to a limited extent and whose efficacy (and intracellular delivery) can benefit from a localized liposomal extracellular slow release effect, it is still important to know what fraction is delivered to cells *via* liposomes because the drug's intracellular destination may be different by different entry routes.

Finally, it is apparent that the *in vivo* system is very complex, with at least two saturable processes affecting liposome disposition and uptake by the reticuloendothelial system (which includes binding and endocytosis) and the destabilizing factors in blood. These processes compete, and their interplay determines the total organ binding and intracellular delivery of a liposome-entrapped compound. In this study, the complexity of this interplay was evidenced by the time dependence of the dose effect such that levels in the tissues approached similar relative values at later times. This finding, however, may not be true in general since the relative magnitudes of these saturable processes probably depend on (and vary at different rates with) liposome physical properties and the animal's physiological properties. These reasons make it even more important that the dose behavior of a given liposome type be well studied so that its therapeutic efficacy can be optimized.

REFERENCES

(1) H. K. Kimelberg and E. G. Mayhew, *CRC Crit. Rev. Toxicol.*, **6,** 25 (1978).

(2) D. Papahadjopoulos, *Annu. Rep. Med. Chem.*, **14,** 250 (1979).

(3) D. Papahadjopoulos, Ed., *Ann. N.Y. Acad. Sci.*, **308,** (1978).

(4) T. Saba, *Arch. Intern. Med.*, **126,** 1031 (1970).

(5) B. N. Halpern, in "Symposium on the Physiopathology of the Reticuloendothelial System," B. N. Halpern, B. Benacerraf, and J. F. Delafresnaye, Eds., 1955.

(6) G. Biozzi, B. Benacerraf, and B. N. Halpern, *Br. J. Exp. Pathol.*, **34,** 441 (1953).

(7) R. N. Baillif, *Ann. N.Y. Acad. Sci.*, **88,** 3 (1960).

(8) V. J. Caride, W. Taylor, J. A. Cramer, and A. Gottschalk, *J. Nucl. Med.*, **17,** 1067 (1976).

(9) G. Gregoriadis, D. E. Nerunjun, and R. Hunt, *Life Sci.*, **21,** 357 (1977).

(10) R. M. Abra, M. E. Bosworth, and C. A. Hunt, *Res. Commun. Chem. Pathol. Pharmacol.*, **29,** 349 (1980).

(11) M. Bosworth and C. A. Hunt, Abstracts, APhA Academy of Pharmaceutical Sciences, **9,** 94 (1979).

(12) C. A. Hunt and M. E. Bosworth, in "Drug Therapeutics: Concepts for Physicians," 1981 ed., K. C. Helman, Ed., Elsevier, North Ireland, New York, N.Y., 1981, pp. 157–174.

(13) M. C. Finkelstein and G. Weissman, *Biochim. Biophys. Acta*, **587,** 202 (1979).

(14) C. A. Hunt and S. Tsang, Abstracts, American Association for the Advancement of Science, 145th National Meeting, 1979, p. 128.

(15) M. Rabinovitch, *Exp. Cell. Res.*, **46,** 19 (1967).

(16) K. J. Donald, *Pathology*, **4,** 295 (1972).

(17) E. H. Bloch, in "Kuppfer Cells and Other Liver Sinusoidal Cells," E. Wisse and D. L. Knook, Eds., Elsevier Biomedical Press, Amsterdam, The Netherlands, 1977.

(18) R. I. Kavet and J. D. Brain, *J. Reticuloendothel. Soc.*, **27,** 201 (1980).

(19) F. Olson, C. A. Hunt, F. C. Szoka, W. J. Vail, and D. Papahadjopoulos, *Biochim. Biophys. Acta*, **557,** 9 (1979).

(20) C. Pidgeon and C. A. Hunt, *J. Pharm. Sci.*, **70,** 173 (1981).

ACKNOWLEDGMENTS

Abstracted in part from a dissertation submitted by M. E. Bosworth to the University of California in partial fulfillment of the Doctor of Philosophy degree requirements.

Supported by Health and Human Sciences Grants G-24612 and GM-26691, US Army Contract DAMD17-79C9045, the University of California at San Francisco patent fund, and a University of California Regents Fellowship.

The authors are grateful to Dr R. M. Abra and Dr. C. Pidgeon for helpful discussions and to the Chemical/Biological Information-Handling Program, National Institutes of Health, for use of the PROPHET computer system.

Phase Equilibria of Nafcillin Sodium–Water

JOSEPH B. BOGARDUS

Received November 28, 1980, from the *College of Pharmacy, University of Kentucky, Lexington, KY 40506.* Accepted for publication May 20, 1981

Abstract □ The phase diagram for the binary system nafcillin sodium–water, was determined using differential scanning calorimetry (DSC) and polarized light microscopy. In the temperature range of −20–30°, three crystalline forms and an amphiphilic liquid crystalline phase were detected. The stable crystalline form of nafcillin sodium (form α) and water exhibit a eutectic mixture containing 28% drug (w/w) at −1°. In more dilute solutions a lower temperature eutectic (−5°) occurs. The composition and form of nafcillin sodium in this eutectic are not known. The form in the −5° eutectic was found to be metastable above 28% concentration and converted to form α. Two other crystalline forms were observed at 9° (form β) and 22° (form γ) at concentrations above 40%. The crystalline forms could not be further characterized due to their transient nature and existence in highly concentrated mixtures. A lamellar mesophase is present near ambient temperature in mixtures containing more than 55% nafcillin sodium. The phase equilibria were highly susceptible to supercooling. Temperature cycling methods were devised which gave reproducible DSC data and allowed construction of the phase diagram.

Keyphrases □ Nafcillin sodium—phase equilibria in water □ Phase diagram—nafcillin sodium–water binary system □ Crystals—forms of nafcillin sodium in aqueous solutions, determined by differential scanning calorimetry and polarized light microscopy □ Differential scanning calorimetry—determination of phase diagram for nafcillin sodium–water system □ Polarized light microscopy—determination of phase diagram for nafcillin sodium–water system

In the drug phase, polymorphic forms and solvates can have a large influence on solubility and dissolution properties (1). Liquid crystalline phases can also occur in pharmaceutical systems, although few examples of mesophase formation by drug compounds have been reported (2, 3). In the solution phase, the influence of salt forms and ionic equilibria on solubility is well understood (4). The difficulties involved in solubility determination for highly insoluble substances was recently studied (5). For such compounds the dissolution rate may strongly retard the approach to equilibrium.

Problems also occur in determining the solubility of compounds which are moderately to highly soluble in water. Nucleation and crystallization of metastable solutions are often inhibited by high solute concentrations or the presence of impurities. The potential for solute-solute interactions becomes greater as drug concentration increases. For example, doxycycline hydrochloride forms a dimer in moderately concentrated solutions which accounts for approximately half of the apparent solubility of the compound in water (6).

In the present investigation phase equilibria of a water-soluble antibiotic, nafcillin sodium (I), with water were studied. Preliminary observations using the polarizing microscope indicated that highly concentrated I–water mixtures formed an amphiphilic liquid crystalline phase. The present study was initiated to further investigate this unusual phase behavior and to determine the phase diagram.

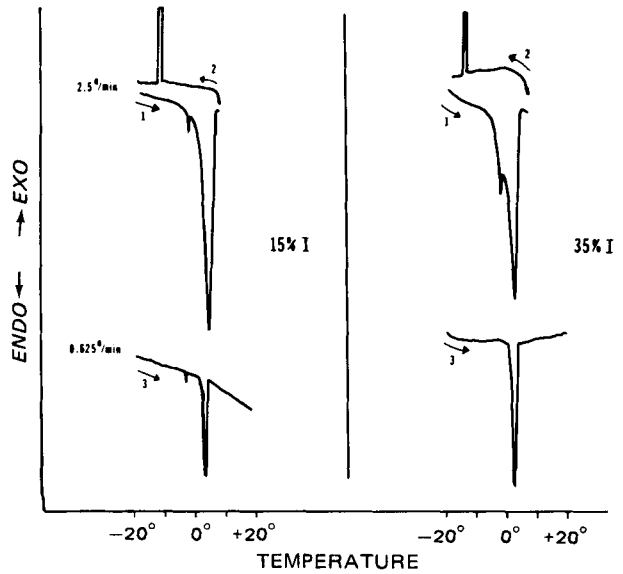

Figure 1—*DSC scans for 15 and 35% nafcillin sodium–water mixtures. Scans 1 and 2 were run at 2.5°/min while scan 3 was obtained at 0.625°/min. Prior to scan 1 the samples were cooled from ambient temperaure to −20° at 2.5°/min.*

EXPERIMENTAL

Transition temperatures were determined using a differential scanning calorimeter[1]. Solutions of I and water were prepared by weight at room temperature and one drop was placed in the aluminum sample pan using a capillary pipet. After sealing, the pan was placed in the sample holder and an empty pan was used as the reference. The low-temperature cell cover supplied with the instrument was filled with dry ice and acetone for cooling the detector cell, which was continuously purged with dry nitrogen. Samples were used within 4 hr to avoid possible effects due to penicillin hydrolysis.

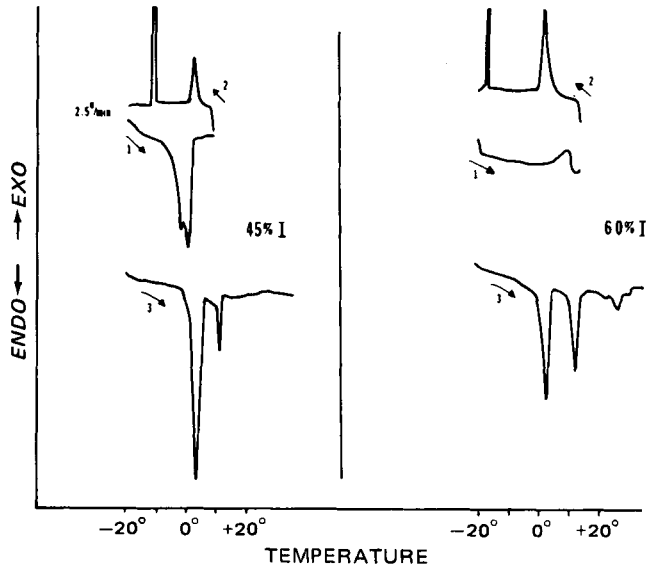

Figure 2—*DSC scans for 45 and 60% nafcillin sodium–water mixtures. All scans were run at 2.5°/min. Prior to scan 1 the samples were cooled from ambient temperature to −20° at 2.5°/min.*

[1] DSC-1B, Perkin-Elmer, Norwalk, Conn.

0022-3549/82/0100-00105$01.00/0

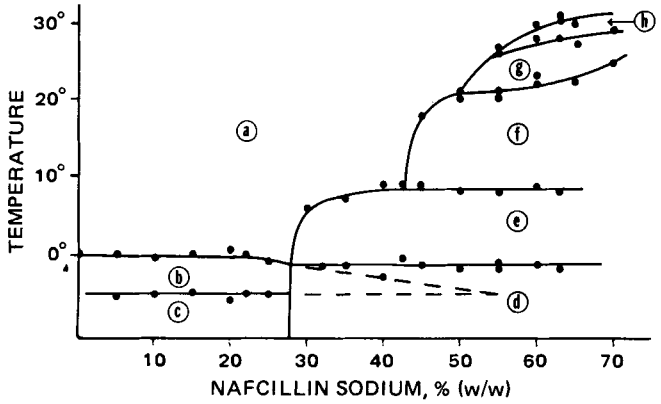

Figure 3—*Phase diagram for nafcillin sodium–water. The dashed line indicates a possible pathway for formation of the −5° eutectic. Phase regions are:* a, *isotropic solution;* b, *ice and solution;* c, *eutectic mixture of ice and low temperature form of nafcillin sodium;* d, *eutectic mixture of ice and crystalline Form α;* e, *solution and Form α;* f, *solution and Form β;* g, *solution and Form γ;* h, *solution and lamellar mesophase.*

Temperature calibration was checked using water, cyclohexane (mp 6.5°), benzene (mp 5.5°), and indium (mp 157°). At the slowest scanning rate, 0.625°/min, the melting transition of water occurred over a 3° range. This behavior was attributed to inefficiency of heat transfer in the system and the large heat of fusion of water. Under the same conditions, the hydrocarbons and indium gave much narrower peaks. The transition temperature was chosen to be the temperature at which ~10% of the total peak height of a transition had occurred. This convention was adopted to allow comparison of large and small transitions in a single scan and to account for variation in sample weight. This method gave melting points for the standards equal to literature values (7). The instrument output was plotted using an X–Y recorder.

The DSC measures the differential heat (millicalories per second) required to keep the sample and reference at the same temperature. Thus, less heat per unit time is required when scanning slowly than when scanning rapidly. The scanning rate is not indicated on the X–Y recorder but the longer time required to scan a peak at a slower scan rate will cause the apparent peak area to be smaller.

A polarizing microscope[2] with a camera attachment was used to observe and photograph the phases. Samples were either equilibrated in a test tube and quickly transferred to a slide for observation or cooled directly on the microscope slide. Although the temperature could not be closely controlled using these methods, the crystalline forms and phase transitions were clearly and reproducibly observed.

Nafcillin sodium monohydrate was used as received[3]. Distilled water which had been redistilled from an all-glass apparatus was used.

RESULTS

The thermal behavior of I–water mixtures was investigated up to 70% I (w/w). At this concentration high viscosity and poor reproducibility prevented further study. Figures 1 and 2 show representative DSC scans over the concentration range studied. Considerable difficulty was encountered in obtaining reproducible data due to the tendency of cooled solutions to supersaturate. The repetitive scanning sequence shown in the figures induced crystallization and provided reproducible DSC data. The transition temperatures from the equilibrium data (scan 3) were used to construct the phase diagram shown in Fig. 3.

After the outline of the phase diagram was established the phases were examined microscopically to determine the nature of the physical changes associated with the thermal processes. Several phase regions were photographed under polarized light and the results are shown in Figs. 4–9. Further identification, such as isolation and spectrometric analysis, was not possible due to the narrow temperature range of existence for the phases.

DISCUSSION

DSC Analysis of Nafcillin Sodium–Water Mixtures—The 15% I scans (Fig. 1) are representative of data obtained in the 5–28% concentration range. A small sharp endotherm occurred at −5° on the shoulder of a large broad endotherm at 0° (scan 1). At the upper temperature limit (6°) the scanning direction was reversed and the sample recooled to −20° (scan 2). This cooling resulted in an exothermic transition between −10 and −20°. The exact temperature of the exotherm varied between samples and was concentration dependent. In some runs a small shoulder was detected on the low temperature side of the exotherm indicating the reversibility of the −5° transition.

Upon warming the sample a second time (scan 3) the −5° endotherm was unchanged although the large endotherm occurred over a narrower temperature range. The apparently smaller area of the transition in scan 3 is due to a fourfold reduction in scanning rate compared to scans 1 and 2. The thermal data at this concentration are typical of a simple eutectic transition followed by melting of crystalline ice at 0°. The melting of an eutectic in a binary system at constant pressure is invariant according to the Gibbs Phase Rule. In DSC this results in an endothermic transition during heating which proceeds until one of the three phases disappears. Solubility equilibrium of the remaining phases, ice and solution, is mo-

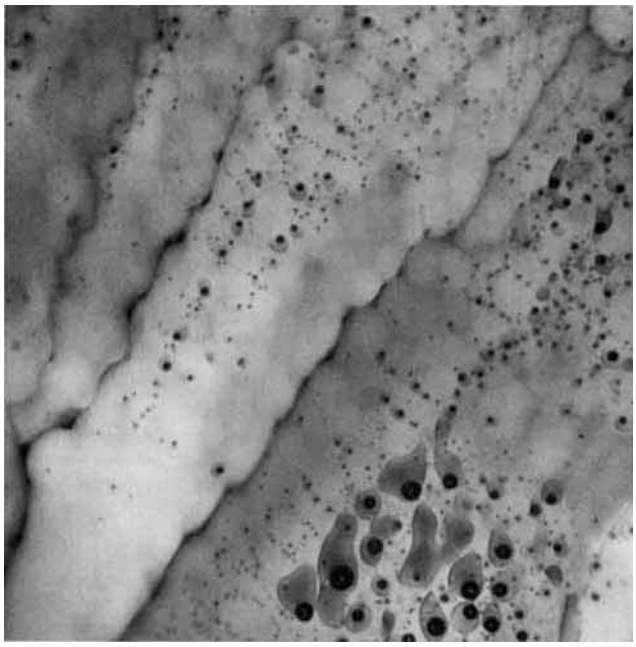

Figure 4—*Region* c, *eutectic mixture of ice and low temperature form of I. Long axis ≃ 400 μm (Initial concentration = 30%).*

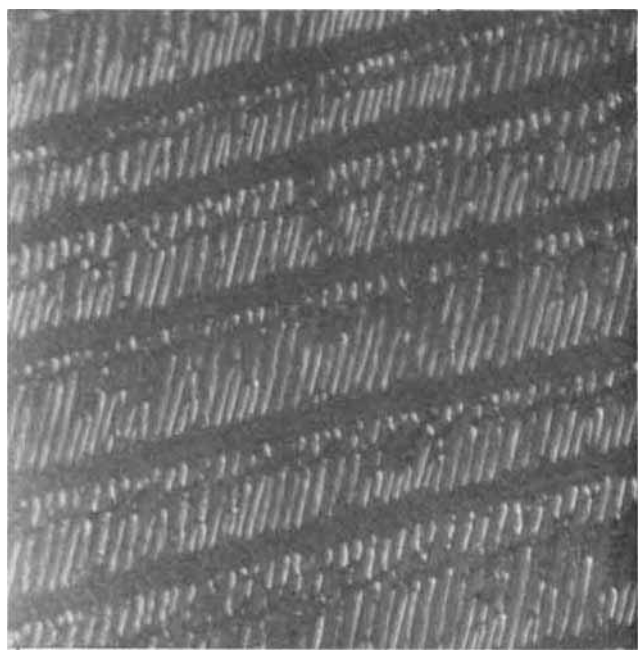

Figure 5—*Region* b, *ice and solution. Long axis ≃ 400 μm (Initial concentration = 25%).*

[2] Zetopan, Reichert, Vienna, Austria.
[3] Wyeth, Philadelphia, Pa.

Figure 6—*Region* e, *form* α *and solution. Long axis* $\simeq$*400* μ*m (Initial concentration = 60%).*

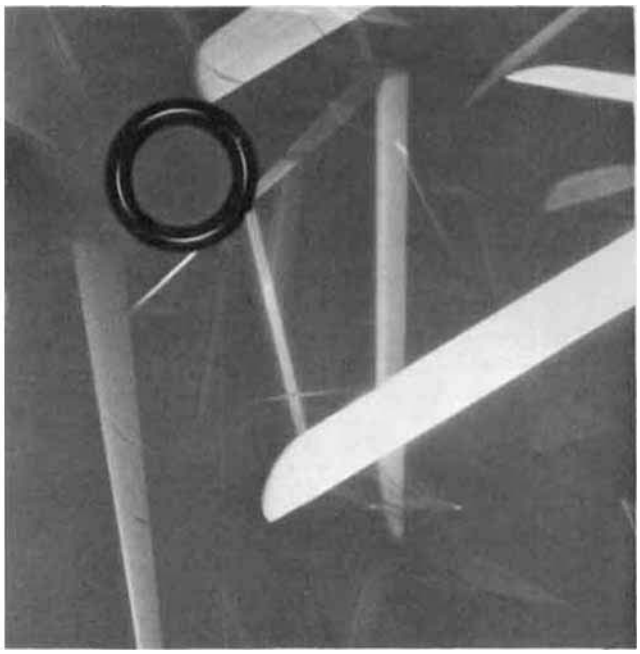

Figure 8—*Region* g, *solution and Form* γ *(needles). Long axis* $\simeq$*400* μ*m (Initial concentration = 60%).*

novariant at constant pressure resulting in a gradual endothermic transition over a wider range of temperature.

The lack of significant freezing point depression in this system is due to the surface activity of I. The critical micelle concentration of I is approximately 20–30 mg/ml (8). Thus, under the conditions of the present study, I is largely present in the system as micelles resulting in minimal freezing point depression of water.

At 35% I (Fig. 1, right side), the data in scans 1 and 2 are qualitatively similar to the 15% mixture. The temperature of the ice-melting endotherm in scan 1 is slightly depressed due to the higher concentration. A major difference exists between the two concentrations. Although present in scan 1, the −5° eutectic point is absent in scan 3. These data indicate that at 35% I the −5° eutectic is metastable since it occurs in the first warming cycle (scan 1) but not in the second (scan 3).

The method employed for scans 1 and 2 (warming to 6–8° and refreezing) was found to be necessary to eliminate the −5° endotherm in scan 3. If the sample is warmed to room temperature (instead of 6–8°) and refrozen, a profile similar to scan 1 is repeatedly obtained. In some runs at this concentration, a small endotherm at 7–8° can be detected. This endotherm becomes prominent at higher concentrations, as shown in Fig. 2. These data can only be explained by the existence of a less soluble (more stable) form of I, different from that present in the −5° eutectic.

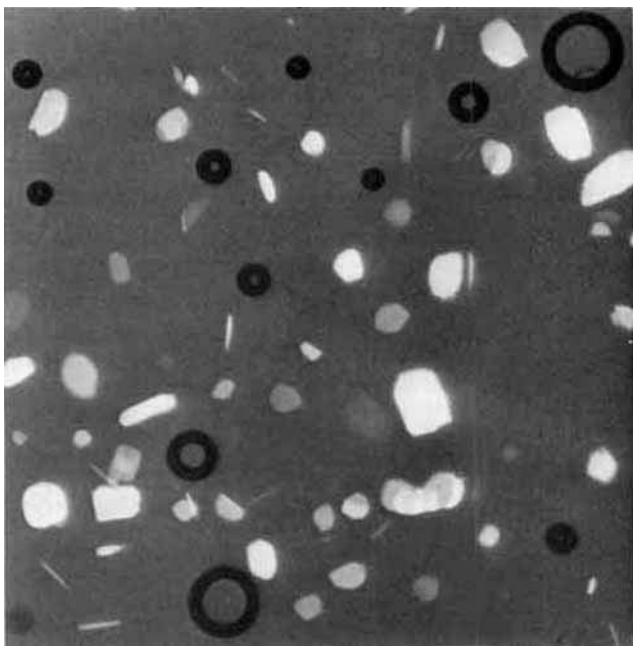

Figure 7—*Region* f, *form* β *(plates) and solution contaminated with Form* γ *(needles). Long axis* $\simeq$*400* μ*m (Initial concentration = 60%).*

The thermal behavior of 45% I solutions is shown in Fig. 2. Scan 1 is again similar to that found at lower concentrations having an apparent −5° eutectic closely followed by the apparent ice-melting endotherm. In the cooling cycle, scan 2, an exotherm occurs at about 2° in addition to the exotherm at −12°. In scan 3 the system is quite different from the lower concentrations. The −5° metastable eutectic is eliminated during scans 1 and 2 and endotherms at −1° and 9° are observed.

At this concentration the −1° transition is due to the dissolving of the eutectic mixture of ice and I. The peak areas indicate that most of the sample is present as the eutectic mixture. Microscopic studies show that the form of I in this eutectic is not the same as that found below 28% concentration. The two-phase region above the eutectic temperature contains crystalline I (denoted form α) and solution.

At 9° the undissolved form α undergoes an endothermic transformation to another crystalline phase, form β. The newly formed crystals of form β at 45% I gradually dissolve and the system becomes an isotropic solution above 18°. These relationships may be seen more clearly in the phase diagram, Fig. 3.

At 60% I (Fig. 2, right side), transitions in scan 1 are absent below 5°. At this temperature, a broad exotherm–endotherm pair occurs due to crystallization and subsequent dissolution of form α I. The cooling process (scan 2) shows a large exotherm due to crystallization of form α in addition to the exotherm for formation of the ice–form α eutectic at −17°. The effect of scan 1 was to induce crystallization of form α allowing the stable eutectic to deposit upon cooling. The warming curve (scan 3) contains the eutectic transition at −1° followed by conversion of form α to form β at 9°. The amount of form α converted to form β is larger at 60% than it was as 45% based on the peak areas. These processes are followed by three small endotherms attributed to the conversion at 22° of form β to a third crystalline phase, form γ, the possible transformation of form γ to a lamellar liquid crystalline phase at 27°, and the dissolution of the liquid crystalline phase to form isotropic solution at 30°.

The small size of the higher temperature endotherms is due to the lower concentrations of crystalline or liquid crystalline material remaining in the systems, since most of the sample is present as an isotropic solution. These conclusions were confirmed microscopically.

Phase Diagram—The various regions of the phase diagram are identified in the legend for Fig. 3.

Regions b *and* c—Freezing of dilute (<28%) aqueous I solutions first causes ice to crystallize below approximately 0° and the system (region

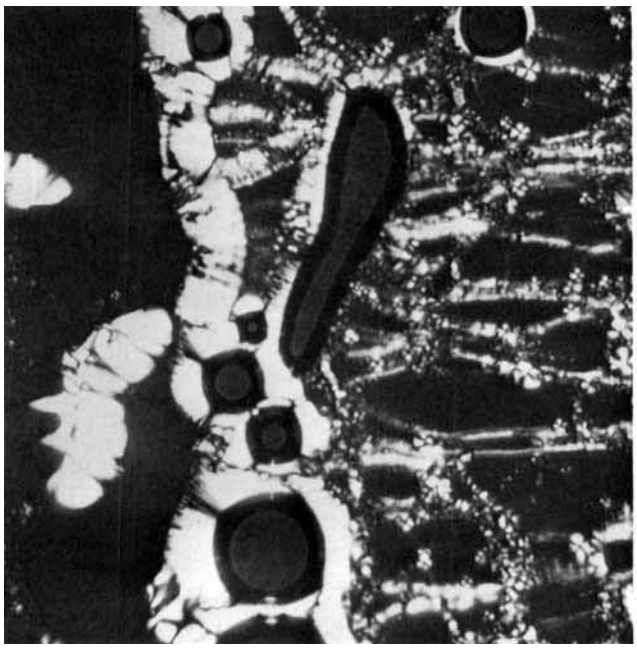

Figure 9—*Region* h, *solution and lamellar mesophase. Long axis* ≃*400 μm (Initial concentration = 60%).*

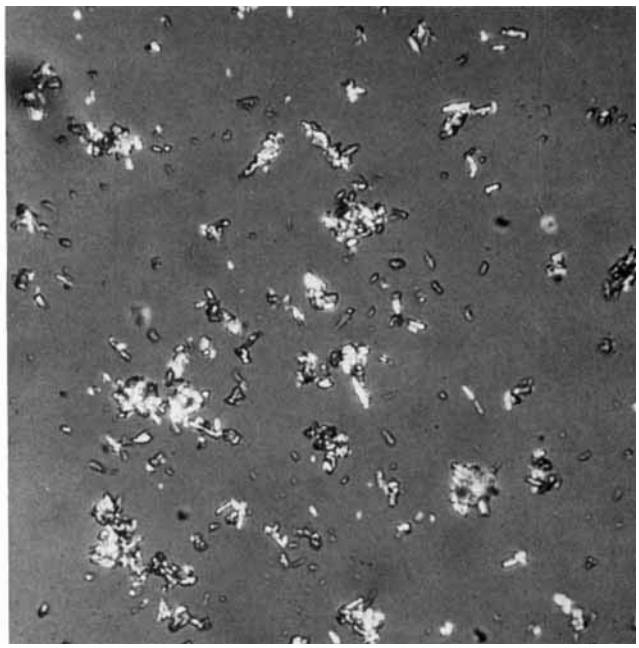

Figure 10—*Nafcillin sodium monohydrate used to prepare all samples. Long axis* ≃*400 μm.*

b) contains ice and solution. Further cooling leads to the −5° eutectic (region *c*), which is stable below 28% I. Above this concentration, the −5° eutectic is easily formed on cooling, indicated by the horizontal dashed line. But between −5 and −1°, the system is not stable and form α crystallizes. The diagonal dashed line shows a possible metastable extension of the ice–solution equilibrium line to the eutectic temperature. The eutectic is expected to contain at least 50% I.

Attempts were made to determine the nature of I in the −5° eutectic. Region *c*, shown in Fig. 4, has a silvery appearance. Figure 5 is a photograph of region *b*, ice and solution, taken just after melting of the eutectic. In the herringbone pattern, the dark channels are solution and the bright lines are ice.

The form of I in this eutectic has the thermodynamic properties of a phase. The sharp and constant eutectic temperature over a wide concentration range indicates that the phase has a fixed composition independent of the initial concentration. If I were in a glassy or amorphous state, no eutectic transition would occur. Only a broad endotherm for melting of ice would be expected (9). Possible explanations for the nature of I in this eutectic are that it is a liquid crystalline mesophase, crystalline forms β or γ, or an unknown crystalline form.

The first explanation, a liquid crystalline phase, is thought to be most consistent with the physical chemical properties of the system. Microscopy does not show discrete crystals, but instead a silvery appearance is observed. During crystallization of ice, the micelles are concentrated into increasingly smaller volumes of solution. The limit of condensation of the micelles would occur at some critical point and the result would probably be a liquid crystalline phase. This hypothesis is the basis of the "R" theory of Winsor (10) in which micellar and liquid crystalline structural features are unified into an order of progression from dilute to concentrated systems. At saturation, micellar solutions usually form amphiphilic liquid crystalline phases (10). Thus, the crystallization of ice from solution follows the horizontal 0° line up to 28% I, as shown in Fig. 3. Instead of forming form α and the eutectic at −1°, the crystallization of ice proceeds and the system continues to be two phases indicated by the diagonal dashed line in the phase diagram. The eventual limit is the formation of the −5° eutectic, which is expected to occur above 50% I.

The existence of the −5° eutectic may be a consequence of the micellar structures in solution. The shape and size of the micelles can change as a function of concentration or ionic strength (11). It is possible that at low concentrations, crystallization of form α would not be favorable because of incompatible micellar structure. At higher concentrations the micelles may become more similar in structure to the packing in form α allowing crystallization to take place.

Regions d *and* e—The eutectic temperature of water–form α mixtures is −1°, shown by the horizontal boundary of region *d* from 28 to 65% I (Fig. 3). It is the point of intersection of the ice–solution and form α–solution phase boundaries. Thus, at concentrations below 28%, ice crystallizes first on cooling the isotropic solution, whereas form α crystallizes first between 28 and 40%.

The crystalline nature of form α is shown in Fig. 6. The sample in Fig. 6 was equilibrated by immersing a test tube containing isotropic solution in an ice–water bath which caused the sample temperature to be in region *e*. Stirring induced crystallization and at this temperature the sample is a thick paste. A small amount of sample was then applied to a precooled slide and photographed immediately.

Crystals of form α are typically splinter-like with high birefringence. The rounded edges are due to dissolution of the crystals into the surrounding isotropic solutions as the sample becomes warmer.

The upper boundary temperature for region *e* (form α and solution) is 9° from 35 to 65% I. Between 28 and 43% I, equilibrium of form α with isotropic solution occurs. At 9° and 43% I, however, an intersection point occurs and the system is invariant. The three phases in equilibrium are form α, form β, and solution. The remaining fraction of form α in suspension is unstable and upon warming to 9°, it converts endothermically to form β. The system is invariant at this temperature until all form α is converted to form β. Such a transformation is called an incongruent melting point (12).

The phenomena of incongruent melting points is common in binary alloys as well as in aqueous solutions of hydrated salts. In phase equilibria, an incongruent melting point occurs when a compound is physically unstable and decomposes (transforms) at a temperature below its melting point; that is, it has no true melting point. Common salts with incongruent melting points are sodium chloride, calcium chloride, and sodium sulfate.

Sodium sulfate decahydrate forms a simple eutectic with water at −1.3° (12). The hydrated salt is in equilibrium with saturated solution up to 32.4°. At this temperature (the incongruent melting point), the decahydrate is unstable and converts to the anhydrous crystalline form. Thus, the invariant system contains the decahydrate, anhydrate, and solution. Thermal arrest occurs until the transformation is complete.

The analogous phase behavior of I and inorganic salts suggests that the observed crystalline forms differ in the degree of hydration in the crystalline state. This proposal is consistent with the small range of temperature in which the forms are stable. The similar crystal energies can be rationalized by small changes in spatial arrangement or solvation resulting in different crystalline forms. The alternate explanation of polymorphism cannot be ruled out at present.

Regions f *and* g—Form β is in equilibrium with solution in region *f* (9–22°, <43% I). The crystal habit of this form (Fig. 7) consists of brightly colored, reflective plates with rectangular faces. The rounded edges are due to dissolution as the slide warmed under the microscope. Samples

of this form are usually contaminated with needle-shaped crystals, which are the higher temperature form γ. This was shown by the following experiment. A tube containing 60% I at 15° containing needles and plates was slowly warmed in a water bath. As the temperature increased, samples were periodically taken and observed with the microscope. The sample temperature was directly monitored with a thermometer and a thermal arrest occurred at 22°, consistent with the DSC data. At this temperature, the plates gradually disappeared and the number of needles increased due to the transformation of form β to form γ. These forms are also related by an incongruent melting point.

When a sample at ambient temperature is cooled to 10–20° to induce crystallization of form β, a small amount of metastable form γ is often obtained, since the temperature region for form γ is passed during cooling. The high viscosity of the system and small difference in stability of the forms allows the metastable form γ to remain in suspension at a temperature where form β is the stable crystalline form. Form γ can be removed from mixtures by warming to near 22° and recooling. If samples of form β are rapidly warmed, the crystals dissolve directly to isotropic solution without the intermediacy of form γ or the mesophase.

Figure 8 shows the acicular habit of form γ which is present between 22 and 26°, above 50% I. These crystals are difficult to grow and were prepared by repeatedly cooling the sample below 22° and warming to obtain the large crystals shown. Form γ is a small fraction of the total sample which is largely isotropic solution.

Region h—When I and water are mixed on a microscope slide at room temperature, a layer of liquid crystalline phase forms on the interface between solid and saturated solution. The mesophase is also easily formed by peripheral evaporation of a drop of solution placed between slide and cover slip. Figure 9 shows the liquid crystalline phase formed from a 60% I sample. Its microscopic texture clearly identifies it as a lamellar mesophase (13). It is indistinguishable from authentic samples prepared with lecithin or docusate sodium. Growth tends to occur on the surfaces of bubbles causing the high birefringence (10). The oily streak texture shown in Fig. 9 is also characteristic of lamellar forms (13). Light pressure on the cover slip causes the viscous phase to flow showing that it is not a solid crystalline phase.

The thermal characteristics of the mesophase could only be approximated by DSC. The slow and erratic nature of its formation and the small thermal changes involved make the boundaries of region *h* uncertain. In addition, the relationship between form γ and the mesophase is not clear since it is difficult to obtain reliable data at such high concentrations. Microscopic samples have been observed in which the mesophase and needles of form γ are present simultaneously so that the conditions for formation of these phases must be quite similar.

In a lamellar mesophase, the amphiphilic molecules are arranged in bilayers with polar groups oriented to the aqueous regions separating the layers. This arrangement was proved for a number of substances using small angle X-ray scattering data (10). The hydrophobic portions form the interior of the bilayers and the thickness of the bilayer is about 40 Å. The lamellar mesophase commonly appears in aqueous systems containing fatty acid soaps, surfactants, and phospholipids. It is only one of several known amphiphilic liquid crystalline phases.

Relationship of the Low Temperature Forms with the Monohydrate—The form of I in commercial use is a monohydrate. Figure 10 shows the bulk form of I used to prepare all samples. It would be reasonable to expect that this crystalline form would be the same as one of the forms identified in this study. Seeding experiments, however, indicate that they are not related. Small amounts of monohydrate were seeded into supersaturated solutions at the temperatures of the three other forms. In each case the seed dissolved, although it did so more slowly at the lower temperatures. Crystallization eventually occurred but control samples indicated that seeding had no effect. The monohydrate appears to be a higher energy form (more soluble) than forms α, β, or γ.

Implications in Freeze-Drying—Although nafcillin sodium is not supplied in a freeze-dried form, several comments should be made regarding the importance of such equilibria in freeze-drying processes. Simple freezing may cause the drug to be present in a metastable state. This may lead to difficulties in the drying process as well as poor physical properties of the dried material (9, 14). These problems are especially serious when the drug is present at high concentration. Gatlin and DeLuca (14) have shown that the physical state of cefazolin sodium and nafcillin sodium in the dried product could be changed by thermal treatment prior to freeze-drying. If processed directly, the frozen drug solutions led to amorphous products, whereas if the frozen solutions were warmed to near the eutectic temperature and refrozen the resulting products were crystalline. The warming–cooling cycle in the frozen state induced crystallization of the drug which was amorphous after the initial freezing.

A single crystalline drug form should not always be expected in frozen or subambient systems. Equilibria beyond the usual eutectic state can occur with drugs in a small temperature range. The nafcillin sodium–water phase diagram shows that the initial drug concentration is an important factor. The form of I in the −5° eutectic (0–28% I) is different from the form α crystals found at higher concentrations. It is expected that this would lead to differences in the respective freeze-dried products.

Depending upon the cooling conditions above 0° the crystalline form of I can easily be altered. Forms β or γ can crystallize and allow little or no form α, the stable form at low temperatures, to be present in the frozen state. This is possible because the forms are similar in energy. In some cases, thermal treatments of the solution may be necessary in the 0–20° range to initiate crystallization of the form desired for freeze-drying.

REFERENCES

(1) E. Shefter and T. Higuchi, *J. Pharm. Sci.*, **52,** 781 (1963).

(2) A. R. Mlodozeniec, *J. Soc. Cosmet. Chem.*, **29,** 659 (1978).

(3) J. S. G. Cox, G. D. Woodward, and W. C. McCrone, *J. Pharm. Sci.*, **60,** 1458 (1971).

(4) S. F. Kramer and G. L. Flynn, *ibid.*, **61,** 1896 (1972).

(5) T. Higuchi, F. L. Shih, T. Kimura, and J. H. Rytting, *ibid.*, **68,** 1267 (1979).

(6) J. B. Bogardus and R. K. Blackwood, Jr., *ibid.*, **68,** 188 (1979).

(7) "The Merck Index," 8th ed., Merck and Co., Rahway, N.J., 1968.

(8) S. C. Penzotti, Jr., and J. W. Poole, *J. Pharm. Sci.*, **63,** 1803 (1974).

(9) L. R. Rey, *Ann. N.Y. Acad. Sci.*, **85,** 510 (1960).

(10) P. A. Winsor, *Chem. Rev.*, **68,** 1 (1968).

(11) F. M. Menger, *Acc. Chem. Res.*, **12,** 111 (1979).

(12) S. Glasstone, "Textbook of Physical Chemistry," 2nd ed., Van Nostrand, New York, N.Y., 1946, chap. 10.

(13) F. B. Rosevear, *J. Am. Oil Chem. Soc.*, **31,** 628 (1954).

(14) L. Gatlin and P. P. DeLuca, *J. Parenter. Drug Assoc.*, **34,** 398 (1980).

ACKNOWLEDGMENTS

Supported in part by a Merck Grant for Faculty Development.

The author thanks Dr. DeLuca and Dr. Gatlin for sharing their unpublished data, which was the stimulus for the present investigation. The technical assistance of Robert Perrone is gratefully acknowledged.

Rapid and Simple GLC Determination of Valproic Acid and Ethosuximide in Plasma of Epileptic Patients

ROBERTO RIVA[x], FIORENZO ALBANI, and AGOSTINO BARUZZI

Received September 24, 1980, from the *Institute of Neurology, School of Medicine, University of Bologna, Via Ugo Foscolo, Bologna, Italy.* Accepted for publication May 13, 1981.

Abstract □ A GLC method for the determination of valproic acid and ethosuximide in plasma was developed. The procedure involved a single solvent extraction of drugs from acidified plasma samples, followed by a GLC injection of the unconcentrated organic phase. This rapid, sensitive, specific, and reproducible method has been used for 2 years for the routine determination of plasma levels of valproic acid and ethosuximide in epileptic patients who receive other antiepileptic drugs simultaneously.

Keyphrases □ Valproic acid—GLC determination in plasma of epileptic patients □ Ethosuximide—GLC determination in plasma of epileptic patients □ Antiepileptic agents—GLC determination of valproic acid and ethosuximide in plasma □ GLC—determination of valproic acid and ethosuximide in human plasma

The use of valproic acid in the treatment of primary generalized epilepsy (particularly petit mal epilepsy) has been reported (1–3). Optimal plasma concentrations of valproic acid are between 40–50 and 100 μg/ml of plasma (1), and the importance of monitoring valproic acid in epileptic patients was discussed (4, 5).

Ethosuximide was introduced 25 years ago in the clinical therapy of petit mal epilepsy (6). There have been several studies (7–9) on the therapeutic use of ethosuximide in epilepsy and on the importance of monitoring plasma ethosuximide concentrations.

Numerous GLC methods are available for the determination of valproic acid (10–18) and ethosuximide concentrations (17, 19–21) in human plasma. However, almost all of these methods require evaporation to concentrate the drugs. This step is crucial because these drugs (particularly valproic acid) are very volatile. A microextractive technique without evaporation of the organic phase is sometimes used to avoid irregular evaporation or decreased sensitivity due to volatility. However, these techniques require a high level of precision due to the minute volumes used.

This report describes a GLC method without evaporation, utilizing 1 ml of plasma. This method has been used in this laboratory for more than 2 years for routine analyses.

EXPERIMENTAL

Reagents—Stock solutions of valproic acid[1] and ethosuximide[2] were prepared by dissolving the drugs in water. Caproic acid[3] (marker for valproic acid) and α,α-dimethyl-β-methyl succinimide[4] (marker for ethosuximide) were dissolved in chloroform[3]. Stock solutions were stored at 4°.

Apparatus—The gas chromatograph[5] was equipped with a flame-ionization detector and a recorder–integrator[6]. The glass column, 1 m long × 3-mm i.d., was packed with 10% diethylene glycol–succinate–phosphate, on 80–100-mesh Supelcoport[7]. The following flow rates were used: hydrogen, 15 ml/min; air, 250 ml/min; and carrier gas (nitrogen), 40 ml/min. The temperature of the column was 145° for valproic acid and 190° for ethosuximide, and the injector temperature was 225° for both drugs.

Extraction Procedure—To 1 ml of plasma containing unknown concentrations of the drugs was added 0.5 ml of 1 *N* HCl and 0.5 ml of chloroform containing 100 μg/ml of caproic acid or 100 μg/ml of α,α-dimethyl-β-methyl succinimide. After being shaken gently for 15 min and centrifuged at 2500 rpm for 10 min, the aqueous phase was discarded and 1–2 μl of the organic phase was injected into the chromatograph.

Plasma samples from patients taking both drugs were extracted into chloroform containing both markers. Calibration curves were prepared by adding exact volumes (5, 10, 20, 40, 100, and 200 μl) of a standard so-

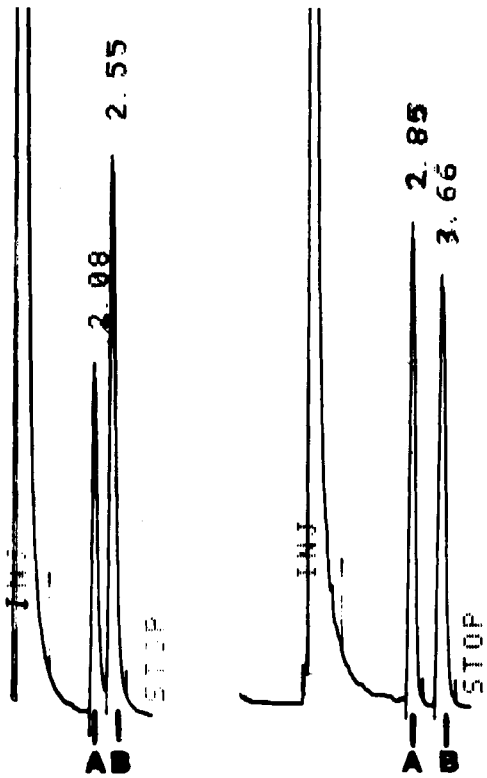

Figure 1—*Response obtained with extract from plasma of a patient being treated with phenobarbital, carbamazepine, and valproic acid (A, caproic acid; and B, valproic acid) (left) and with phenytoin, nitrazepam, and ethosuximide (A, α,α-dimethyl-β-methyl succinimide; and B, ethosuximide) (right).*

[1] Sigma-Tau, Rome, Italy.
[2] Parke-Davis, Milan, Italy.
[3] Carlo Erba, Milan, Italy.
[4] Aldrich-Europe, Beerse, Belgium.
[5] Model Fractovap 2350, Carlo Erba, Milan, Italy.
[6] Model HP 3380A, Hewlett-Packard, Avondale, Pa.
[7] Catalog Number 1-1999, Supelco Inc., Bellefonte, PA 16823.

0022-3549/82/0100-0110$01.00/0

Table I—Reproducibility of Valproic Acid and Ethosuximide Analyses in Human Plasma Samples

Amount Added, μg/ml	Valproic Acid			Ethosuximide		
	Amount Found, μg/ml[a]	*SD*	*CV*, %	Amount Found, μg/ml[a]	*SD*	*CV*, %
10	9.9	0.43	4.3	10.0	0.42	4.2
30	29.9	1.27	4.2	30.2	1.29	4.3
60	60.3	2.04	3.4	60.3	2.10	3.5
100	100.1	3.00	3.0	100.2	3.41	3.4

[a] Mean of 10 determinations.

lution of valproic acid or ethosuximide (1 mg/ml) to 1 ml of drug-free plasma. These plasma samples were treated as already described for samples containing unknown concentrations.

RESULTS AND DISCUSSION

Typical chromatograms of extracts from plasma of two patients undergoing multiple antiepileptic drug therapy, one receiving valproic acid and the other receiving ethosuximide, are shown in Fig. 1. There was no interference from endogenous plasma compounds or from other antiepileptic drugs.

Calibration curves from plasma extract showed a linear correlation between concentration and the respective reading: $y = 0.044x - 0.039$, $r = 0.995$, for valproic acid; and $y = 0.023x - 0.034$, $r = 0.992$, for ethosuximide. To calculate these curves, a least-squares linear regression method was used. The minimal concentration detectable for both drugs was ~1–2 μg/ml of plasma.

Analytical recoveries of substances were established as follows. Various amounts (5, 10, 20, 40, 100, and 200 μg) of valproic acid or ethosuximide were dissolved in 1 ml of drug-free plasma. After acidification, plasma samples were extracted into 0.5 ml of pure chloroform. Then 0.2 ml of a solution containing the marker (100 μl/ml) in chloroform was added to 0.2 ml of the organic phase.

A series of external standards was prepared by adding 0.5 ml of the marker solution (100 μg/ml) to 0.5 ml of chloroform containing various amounts (5, 10, 20, 40, 100, and 200 μg) of valproic acid or ethosuximide.

Analytical recoveries were calculated by comparing peak area ratios of the extracted standards to the ratios of the external standards. Expressed as concentrations in micrograms per milliliter, they were as follows (theoretical values of 5, 10, 20, 40, 100, and 200): 5.0, 10.1, 20.3, 40.7, 102.3, and 202.8 for valproic acid and 4.4, 8.9, 18.0, 35.6, 88.8, and 176.4 for ethosuximide.

Reproducibility was determined by performing 10 replicate analyses of four control samples containing 10, 30, 60, and 100 μg/ml of both drugs on different days over 4 months. The results are shown in Table I.

The total time required to analyze 22 plasma samples (plasma samples from 16 patients and six calibrators) was ~1.6 hr.

This method has been utilized for 2 years, analyzing ~1600 plasma samples from patients being treated with valproic acid and ~250 plasma samples from patients being treated with ethosuximide. Only ~30 samples contained both drugs.

If these drugs appear together in the same plasma, they may be extracted simultaneously, as described, and injected onto the column at two different temperatures. At the highest temperature (190°), valproic acid and its marker elute in front of the solvent; at the lowest temperature (145°), ethosuximide and its marker have a retention time of 20 and 16 min, respectively.

REFERENCES

(1) D. Simon and J. K. Penry, *Epilepsia*, **16**, 549 (1975).

(2) R. M. Pinder, R. N. Brogden, T. M. Speicht, and G. S. Avery, *Drugs*, **13**, 81 (1977).

(3) D. B. Calne, in "Clinical Neuropharmacology," vol. 4, H. L. Klavans, Ed., Raven, New York, N.Y., 1979, pp. 31–38.

(4) F. Schobben, E. van der Kleijn, and F. J. M. Gabreels, *Eur. J. Clin. Pharmacol.*, **8**, 97 (1975).

(5) A. Baruzzi, B. Bordo, L. Bossi, D. Castelli, M. Gerna, G. Tognoni, and P. Zagnoni, *Int. J. Clin. Pharmcol.*, **15**, 403, (1977).

(6) F. T. Zimmerman, *N.Y. State J. Med.*, **56**, 1460 (1956).

(7) J. K. Penry, R. J. Porter, and F. E. Dreifuss, in "Antiepileptic Drugs," D. M. Woodbury, J. K. Penry, and R. P. Schmidt, Eds., Raven, New York, N.Y., 1972, pp. 431–441.

(8) T. R. Browne, F. E. Dreifuss, P. R. Dyken, D. J. Goode, J. K. Penry, R. J. Porter, B. J. White, and P. T. White, *Neurology*, **25**, 515 (1975).

(9) A. L. Sherwin, in "Antiepileptic Drugs: Quantitative Analysis and Interpretation," C. E. Pippenger, J. K. Penry, and H. Kutt, Eds., Raven, New York, N.Y., 1978, pp. 283–295.

(10) T. B. Vree and E. van der Kleijn, *J. Chromatogr.*, **121**, 150 (1976).

(11) W. Loscher, *Epilepsia*, **18**, 225 (1977).

(12) L. J. Dusci and L. P. Hackett, *J. Chromatogr.*, **132**, 145 (1977).

(13) C. J. Jensen and R. Gugler, *ibid.*, **137**, 188 (1977).

(14) A. J. Fellemberg and A. C. Pollard, *Clin. Chim. Acta*, **81**, 203 (1977).

(15) H. J. Kupferberg, in "Antiepileptic Drugs: Quantitative Analysis and Interpretation," C. E. Pippenger, J. K. Penry, and H. Kutt, Eds., Raven, New York, N.Y., 1978, pp.147–151.

(16) B. N. Swanson, R. C. Harland, R. G. Dickinson, and N. Gerber, *Epilepsia*, **19**, 541 (1978).

(17) W. Godolphin and J. Thoma, *Clin. Chem.* **24**, 483 (1978).

(18) A. Hulshoff and H. Roseboom, *Clin. Chim. Acta*, **93**, 9 (1979).

(19) R. Heipertz, H. Piltz, and K. Eickoff, *ibid.*, **77**, 307 (1977).

(20) A. Sengupta and M. A. Peat, *J. Chromatogr.*, **137**, 206 (1977).

(21) C. D. Harvey and A. L. Sherwin, in "Antiepileptic Drugs: Quantitative Analysis and Interpretation," C. E. Pippenger, J. K. Penry, and H. Kutt, Eds., Raven, New York, N.Y., 1978, pp. 87–93.

GLC Determination of Bromperidol in Tablets

ROBERT P. MARTIN ˣ, STEVEN W. K. LUM, EUGENE J. McGONIGLE, and H. R. GUBLER *

Received February 2, 1981, from the *Research Laboratories, Ortho Pharmaceutical Corporation, Raritan, NJ 08869.* Accepted for publication May 14, 1981. *Present address: Cilag-Ltd., Schaffhausen, Switzerland.

Abstract □ A GLC procedure for the determination of bromperidol in 3-, 6-, and 10-mg tablets is described. The method is stability indicating in the presence of compounds structurally related to bromperidol and stress reaction products of bromperidol.

Keyphrases □ Bromperidol—GLC determination in tablets □ GLC—method for determining bromperidol in tablets □ Tranquilizers—bromperidol, determination by GLC, tablets

Bromperidol is a new, potent, neuroleptic formulated in 3-, 6-, and 10-mg tablets; its chemical structure is similar to haloperidol. Analytical methods for haloperidol have included TLC (1), paper chromatography (2), spectrophotometry (3–5), titrimetry (6), polarography, and gas chromatography (7, 8), but only limited resolution data have been submitted for these methods. A TLC and a high-performance liquid chromatographic method for the determination of bromperidol were reported (9). These procedures are selective for bromperidol in the presence of three possible impurities and several other butyrophenones, but resolution from stress reaction products was not demonstrated, limiting data to support stability-indicating properties.

This paper describes a rapid, stability-indicating GLC procedure applicable to the determination of bromperidol in 3-, 6-, and 10-mg tablets. Selectivity in the presence of stress reaction products of bromperidol and other structurally related compounds is demonstrated.

EXPERIMENTAL

Reagents and Chemicals—Reagent grade octacosane (internal standard), cyclohexane, ethyl acetate, and sodium hydroxide were used.

Instrumentation and Apparatus—The gas chromatograph[1] was equipped with an autosampler, a flame-ionization detector, and on-column injection. A laboratory data system[2] was used to carry out peak integration or peak height measurement. However, peak heights could also be determined manually using an attenuation setting of 4×10^3 in combination with a 10-mv strip-chart recorder (1.5 min/cm).

Chromatographic Conditions—A 0.9-m (3 ft) × 2-mm i.d. glass column, packed with 3% SE-30 on 80–100-mesh Gas Chrom Q[3], was conditioned for 24 hr at 240° with a helium flow of ~30 ml/min. For sample determinations, the column temperature was adjusted to 230° with a detector temperature of 300° and an injection port temperature of 250°. The carrier gas was helium at a flow rate of 40 ml/min. Oxygen and hydrogen were maintained at 240 and 35 ml/min, respectively.

Preparation of Internal Standard—Approximately 100 mg of octacosane was accurately weighed into a 100-ml volumetric flask, dissolved in 10.0 ml of cyclohexane, and diluted to volume with ethyl acetate (for a concentration of 1 mg/ml).

Preparation of Bromperidol Standard Solution—Approximately 24 mg of a suitable bromperidol reference standard was accurately weighed into a stoppered 50-ml centrifuge tube and dissolved in 20.0 ml of the internal standard solution. Then 20.0 ml of 0.1 *M* NaOH was added. After shaking for 30 min, the mixture was centrifuged to ensure phase separation.

[1] Hewlett-Packard model 5710A.
[2] Hewlett-Packard model 3354.
[3] Supelco, Bellefonte, Pa.

Table I—Determination of Bromperidol in the Presence of Placebo Tablets (n = 6)

Amount Added, mg	Average Amount Found, mg	Recovery, %	*RSD*, %	Range, mg
3.010	3.037	100.9	0.2	3.028–3.043
6.021	6.155	102.2	0.2	6.112–6.208
10.11	10.21	101.0	1.2	10.00–10.33

Table II—Maximum Error at 90 and 110% of Label Claim Resulting from the Use of a Single Standard (100% Claim) Instead of a Calibration Curve

Formulation, mg	Maximum Error, % 90% of Label	110% of Label
3	0.21	−0.18
6	−0.02	0.07
10	0.69	−0.56

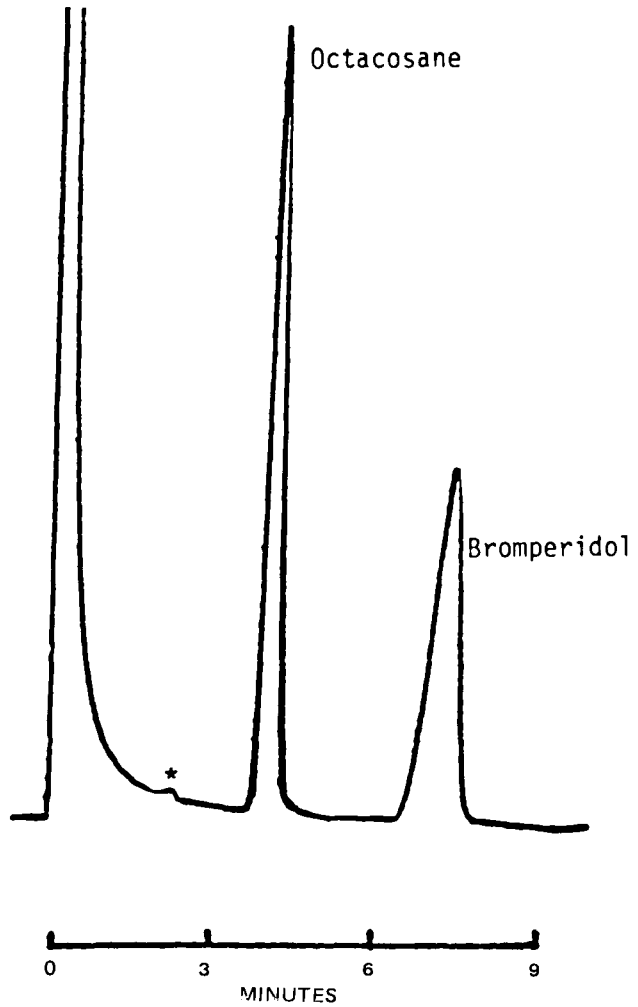

Figure 1—*Typical chromatogram of octacosane (1 mg/ml), and bromperidol (1.2 mg/ml). (*Impurity in octacosane.)*

0022-3549/82/0100-0112$01.00/0

Table III—Determination of Bromperidol in Bromperidol Tablets by GLC and by Spectrophotometry

Experimental Lot	Whole Tablet GLC Determination Using Peak Areas: Average Bromperidol, mg/120-mg tablet	*n*	*RSD*, %	Range, mg	Ground Composite GLC Determination (20 Tablets) Using Peak Areas: Average Bromperidol, mg/120-mg tablet	*n*	*RSD*, %	Range, mg	UV Determination, Average Bromperidol, mg/120-mg Tablet
1	3.05	6	0.3	3.04–3.07	3.03	6	0.3	3.02–3.05	3.03
2	6.10	6	1.1	6.03–6.22	6.20	6	0.5	6.14–6.23	6.06
3	10.19	10	0.4	10.14–10.25	—	—	—	—	9.95

Table IV—Comparison of Determinations of Bromperidol in Tablets by GLC Based on Peak Heights to Similar Determinations Based on Peak Areas

3-mg Tablets (Lot 1)		6-mg Tablets (Lot 2)		10-mg Tablets (Lot 3)	
Peak Height	Peak Area	Peak Height	Peak Area	Peak Height	Peak Area
3.04	3.04	6.37	6.14	10.0	9.88
2.99	3.05	6.20	6.22	10.2	9.99
3.02	3.05	6.18	6.22	10.2	10.1
3.03	3.07	6.12	6.20	10.2	10.0
3.05	3.05	6.19	6.22	10.2	9.89
3.08	3.05	6.12	6.22	10.2	9.87
Average 3.04	3.05	6.20	6.20	10.2	9.96
RSD, % 1.0	0.3	1.5	0.5	0.8	0.9

Table V—Relative Retention Time and Weight Response of Compounds Structurally Related to Bromperidol

Compound	Relative Retention Time	Relative Weight Response
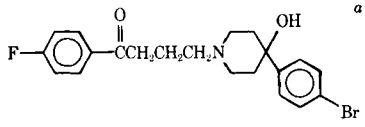 [a]	1.00	1.00
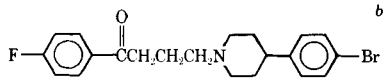 [b]	0.57	1.47
	0.80	0.95
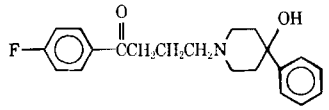	0.41	1.11
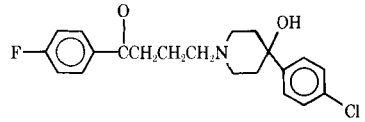	1.22	0.34
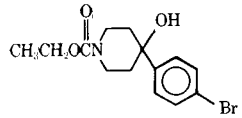	0.15	0.90
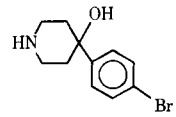	0.05	0.53
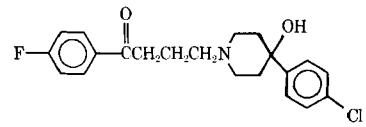	0.74	0.93
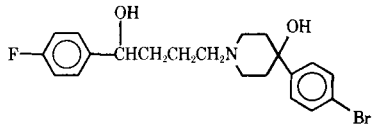	0.90	0.45
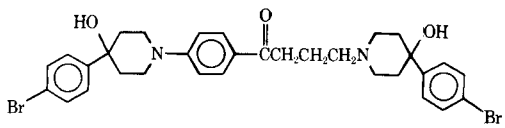	NO [c]	—
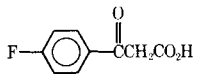	NO	—
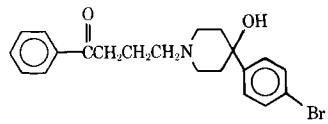	NO	—
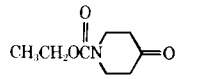	NO	—
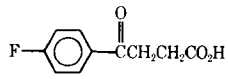	NO	—
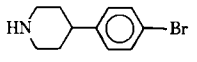	NO	—
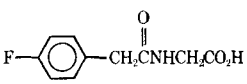	NO	—

[a] Bromperidol. [b] Octacosane. [c] Not observed.

RESULTS AND DISCUSSION

Accuracy and precision were demonstrated in two ways. First, placebo tablets in the presence of known concentrations of bromperidol were assayed by the desired procedure. Results obtained for six replicate determinations of synthetic preparations representative of 3-, 6-, and 10-mg bromperidol tablets show average recoveries of 100.9 ± 0.2, 102.2 ± 0.2, and 101.0 ± 1.2%, respectively (Table I). No interference was encountered from the excipients. A typical chromatogram is shown in Fig. 1.

For each formulation, the area response was linear with concentration. Table II presents the maximum error at 90 and 110% of label claim resulting from the use of a single standard representative of 100% of label claim instead of a calibration curve. Since the maximum error was within the precision of the method, the use of a standard at the nominal concentration in place of a series of concentrations was justified.

Accuracy and precision were also evaluated by comparing results obtained using the described procedure with results obtained by an independent UV spectrophotometric procedure. In the latter method, the

drug was extracted from the tablet matrix using isopropyl alcohol–0.1 *M* hydrochloric acid (9:1) and diluted to a final bromperidol concentration of 15 μg/ml with isopropyl alcohol–0.1 *M* hydrochloric acid. The bromperidol present in the sample was calculated by comparing the absorbance of the sample at 242 nm to a similarly prepared solution of standard at a known concentration. Table III shows the agreement between results obtained by both procedures using actual 3- and 6-mg bromperidol tablets. Equivalent results were obtained independent of whether ground composites or whole tablets were assayed. Table III also shows data collected on representative 10-mg tablet lots.

The data in Table IV demonstrate that peak heights can be used interchangeably with peak areas for quantitation. These data were determined using individual determinations of 3-, 6-, and 10-mg tablets calculated by both techniques. Overall results as well as differences between individual results were within experimental error.

To demonstrate the stability-indicating properties of the method, the chromatographic response of several compounds structurally related to bromperidol were compared to bromperidol and octacosane (the internal standard) to establish resolution properties. Each compound was dissolved in ethyl acetate–cyclohexane (9:1), and the resulting solutions were chromatographed. Besides bromperidol, only seven compounds produced discernible peaks. All compounds were chromatographed individually; Table V presents the relative retention times and weight responses relative to bromperidol (the first compound). Compounds not observed were concluded to have either eluted with the solvent front or been strongly retained by the packing. However, none of the compounds interfered with the determination of bromperidol.

To defend further the resolution properties of the method and, therefore, the stability-indicating properties, a weighed amount of bromperidol drug substance was heated in a capillary tube at 260° (melting point of bromperidol is 158°). After ~30 min at this extreme temperature, the sample was partially discolored near the top of the tube; analysis for bromperidol indicated a drug loss of ~25%. However, no extra peaks were observed in the resulting chromatogram. Examination of the analytical regions of the resultant chromatogram using GLC–mass spectrometry indicated that thermal stress reaction products of bromperidol did not elute with the drug or internal standard.

In addition to the thermal stress experiment, an accurately weighed 25-mg sample of bromperidol was mixed with 2 ml of 30% hydrogen peroxide and allowed to stand for 1 hr. The sample was mixed with 10 ml of methanol to consume excess peroxide and evaporated to dryness under nitrogen. GLC analysis of the residue indicated as little as 10% intact drug remaining. Examination of the oxidized sample of bromperidol by GLC–mass spectrometry in the analytical regions indicated that reaction products of bromperidol did not elute with the internal standard or bromperidol.

This GLC method is specific for bromperidol in the presence of structurally related compounds and stress reaction products of bromperidol. In addition, the procedure is accurate, reproducible, and suitable for stability or release analyses of bromperidol tablets.

REFERENCES

(1) A. Noirfalise, *J. Chromatogr.*, **20,** 61 (1965).

(2) H. Soep, *Nature*, **192,** 67 (1961).

(3) A. Haemers and W. Van den Bossche, *J. Pharm. Pharmacol.*, **21,** 531 (1969).

(4) J. Tyfezynska, *Diss. Pharm. Pharmacol.*, **20,** 459 (1968).

(5) P. J. A. W. Demoen, *J. Pharm. Sci.*, **50,** 350 (1961).

(6) J. Volke, L. Wasilewska, and A. Ryvolova-Kejharova, *Pharmazie*, **26,** 399 (1971).

(7) F. Marcucci, L. Airoldi, E. Mussini, and S. Garattini, *J. Chromatogr.*, **59,** 174 (1971).

(8) I. A Zingales, *ibid.*, **54,** 15 (1971).

(9) E. Van den Eeckhout, G. A. Bens, and P. De Moerloose, *ibid.*, **193,** 255 (1980).

ACKNOWLEDGMENTS

The work of Mr. C. Shaw, who performed the GLC–mass spectrometry, is gratefully acknowledged.

High-Performance Liquid Chromatograhic Determination of Metoprolol in Plasma

M. T. ROSSEEL *x, F. M. BELPAIRE *, I. BEKAERT ‡, and M. G. BOGAERT *

Received November 28, 1980, from the **Heymans Institute of Pharmacology and the ‡Department of Cardiology, University of Gent Medical School, De Pintelaan 135, B-9000 Gent, Belgium.* Accepted for publication May 20,1981.

Abstract □ A high-performance liquid chromatographic method is presented for the determination of metoprolol in human plasma. Metoprolol was extracted from plasma by a single extraction procedure with 4-methylpropranolol as the internal standard. Chromatography was done on a reversed-phase column with fluorescence detection. The minimum detectable concentration was 5.0 ng/ml of plasma. The standard curve was linear in the range evaluated, 10–300 ng/ml. The within-run coefficient of variation was 2.3–6.0%, and the day-to-day variation was 6.8%. The method is free from interference by major metoprolol metabolites.

Keyphrases □ Metoprolol—high-performance liquid chromatographic analysis in plasma □ β-Adrenergic blocking agents—metoprolol, high-performance liquid chromatographic analysis in plasma □ High-performance liquid chromatography—analysis of metoprolol in plasma

Metoprolol is a cardioselective β-adrenergic blocking agent used in the treatment of hypertension and angina. Analysis of metoprolol in plasma has been performed with electron-capture GLC after derivatization (1, 2), and a GC–mass spectroscopy method was recently developed (3).

This report describes a high-performance liquid chromatographic (HPLC) method for the determination of metoprolol in plasma using reversed-phase ion-pair chromatography with fluorescence detection. The same approach has been used for other β-adrenergic blocking drugs such as propranolol (4, 5), atenolol (6, 7), and sotalol (8).

EXPERIMENTAL

Reagents—The following were used: metoprolol tartrate[1], α-hydroxymetoprolol[1], and *O*-desmethylmetoprolol[1] as the *p*-hydroxybenzoic acid salts; and 4-(2-hydroxy-3-isopropylaminopropoxy)phenylacetic acid[1], 2-hydroxy-3-(4-methyoxyethylphenoxy)propanoic acid[1], and 4-methylpropranolol[2] as the hydrochloride salts. Methanol[3] was HPLC grade. 1-Heptanesulfonic acid[4] in acetic acid was used. Glass double-distilled water was passed through a 0.45-μm filter[5]. Methylene chloride was reagent grade and distilled just before use.

Instrument Conditions—The microprocessor-controlled high-per-

[1] Hässle, Mölndal, Sweden
[2] Imperial Chemical Industries, Macclesfield, England.
[3] Burdick & Jackson Laboratories, Muskegon, Mich.
[4] Reagent B-7, Waters Associates, Milford, Mass.
[5] Type HA Millipore Corp., Bedford, Mass.

0022-3549/82/0100-0114$01.00/0

drug was extracted from the tablet matrix using isopropyl alcohol–0.1 *M* hydrochloric acid (9:1) and diluted to a final bromperidol concentration of 15 μg/ml with isopropyl alcohol–0.1 *M* hydrochloric acid. The bromperidol present in the sample was calculated by comparing the absorbance of the sample at 242 nm to a similarly prepared solution of standard at a known concentration. Table III shows the agreement between results obtained by both procedures using actual 3- and 6-mg bromperidol tablets. Equivalent results were obtained independent of whether ground composites or whole tablets were assayed. Table III also shows data collected on representative 10-mg tablet lots.

The data in Table IV demonstrate that peak heights can be used interchangeably with peak areas for quantitation. These data were determined using individual determinations of 3-, 6-, and 10-mg tablets calculated by both techniques. Overall results as well as differences between individual results were within experimental error.

To demonstrate the stability-indicating properties of the method, the chromatographic response of several compounds structurally related to bromperidol were compared to bromperidol and octacosane (the internal standard) to establish resolution properties. Each compound was dissolved in ethyl acetate–cyclohexane (9:1), and the resulting solutions were chromatographed. Besides bromperidol, only seven compounds produced discernible peaks. All compounds were chromatographed individually; Table V presents the relative retention times and weight responses relative to bromperidol (the first compound). Compounds not observed were concluded to have either eluted with the solvent front or been strongly retained by the packing. However, none of the compounds interfered with the determination of bromperidol.

To defend further the resolution properties of the method and, therefore, the stability-indicating properties, a weighed amount of bromperidol drug substance was heated in a capillary tube at 260° (melting point of bromperidol is 158°). After ~30 min at this extreme temperature, the sample was partially discolored near the top of the tube; analysis for bromperidol indicated a drug loss of ~25%. However, no extra peaks were observed in the resulting chromatogram. Examination of the analytical regions of the resultant chromatogram using GLC–mass spectrometry indicated that thermal stress reaction products of bromperidol did not elute with the drug or internal standard.

In addition to the thermal stress experiment, an accurately weighed 25-mg sample of bromperidol was mixed with 2 ml of 30% hydrogen peroxide and allowed to stand for 1 hr. The sample was mixed with 10 ml of methanol to consume excess peroxide and evaporated to dryness under nitrogen. GLC analysis of the residue indicated as little as 10% intact drug remaining. Examination of the oxidized sample of bromperidol by GLC–mass spectrometry in the analytical regions indicated that reaction products of bromperidol did not elute with the internal standard or bromperidol.

This GLC method is specific for bromperidol in the presence of structurally related compounds and stress reaction products of bromperidol. In addition, the procedure is accurate, reproducible, and suitable for stability or release analyses of bromperidol tablets.

REFERENCES

(1) A. Noirfalise, *J. Chromatogr.*, **20,** 61 (1965).

(2) H. Soep, *Nature*, **192,** 67 (1961).

(3) A. Haemers and W. Van den Bossche, *J. Pharm. Pharmacol.*, **21,** 531 (1969).

(4) J. Tyfezynska, *Diss. Pharm. Pharmacol.*, **20,** 459 (1968).

(5) P. J. A. W. Demoen, *J. Pharm. Sci.*, **50,** 350 (1961).

(6) J. Volke, L. Wasilewska, and A. Ryvolova-Kejharova, *Pharmazie*, **26,** 399 (1971).

(7) F. Marcucci, L. Airoldi, E. Mussini, and S. Garattini, *J. Chromatogr.*, **59,** 174 (1971).

(8) I. A Zingales, *ibid.*, **54,** 15 (1971).

(9) E. Van den Eeckhout, G. A. Bens, and P. De Moerloose, *ibid.*, **193,** 255 (1980).

ACKNOWLEDGMENTS

The work of Mr. C. Shaw, who performed the GLC–mass spectrometry, is gratefully acknowledged.

High-Performance Liquid Chromatograhic Determination of Metoprolol in Plasma

M. T. ROSSEEL *x, F. M. BELPAIRE *, I. BEKAERT ‡, and M. G. BOGAERT *

Received November 28, 1980, from the **Heymans Institute of Pharmacology and the ‡Department of Cardiology, University of Gent Medical School, De Pintelaan 135, B-9000 Gent, Belgium.* Accepted for publication May 20,1981.

Abstract □ A high-performance liquid chromatographic method is presented for the determination of metoprolol in human plasma. Metoprolol was extracted from plasma by a single extraction procedure with 4-methylpropranolol as the internal standard. Chromatography was done on a reversed-phase column with fluorescence detection. The minimum detectable concentration was 5.0 ng/ml of plasma. The standard curve was linear in the range evaluated, 10–300 ng/ml. The within-run coefficient of variation was 2.3–6.0%, and the day-to-day variation was 6.8%. The method is free from interference by major metoprolol metabolites.

Keyphrases □ Metoprolol—high-performance liquid chromatographic analysis in plasma □ β-Adrenergic blocking agents—metoprolol, high-performance liquid chromatographic analysis in plasma □ High-performance liquid chromatography—analysis of metoprolol in plasma

Metoprolol is a cardioselective β-adrenergic blocking agent used in the treatment of hypertension and angina. Analysis of metoprolol in plasma has been performed with electron-capture GLC after derivatization (1, 2), and a GC–mass spectroscopy method was recently developed (3).

This report describes a high-performance liquid chromatographic (HPLC) method for the determination of metoprolol in plasma using reversed-phase ion-pair chromatography with fluorescence detection. The same approach has been used for other β-adrenergic blocking drugs such as propranolol (4, 5), atenolol (6, 7), and sotalol (8).

EXPERIMENTAL

Reagents—The following were used: metoprolol tartrate[1], α-hydroxymetoprolol[1], and *O*-desmethylmetoprolol[1] as the *p*-hydroxybenzoic acid salts; and 4-(2-hydroxy-3-isopropylaminopropoxy)phenylacetic acid[1], 2-hydroxy-3-(4-methyoxyethylphenoxy)propanoic acid[1], and 4-methylpropranolol[2] as the hydrochloride salts. Methanol[3] was HPLC grade. 1-Heptanesulfonic acid[4] in acetic acid was used. Glass double-distilled water was passed through a 0.45-μm filter[5]. Methylene chloride was reagent grade and distilled just before use.

Instrument Conditions—The microprocessor-controlled high-per-

[1] Hässle, Mölndal, Sweden
[2] Imperial Chemical Industries, Macclesfield, England.
[3] Burdick & Jackson Laboratories, Muskegon, Mich.
[4] Reagent B-7, Waters Associates, Milford, Mass.
[5] Type HA Millipore Corp., Bedford, Mass.

0022-3549/82/0100-0114$01.00/0

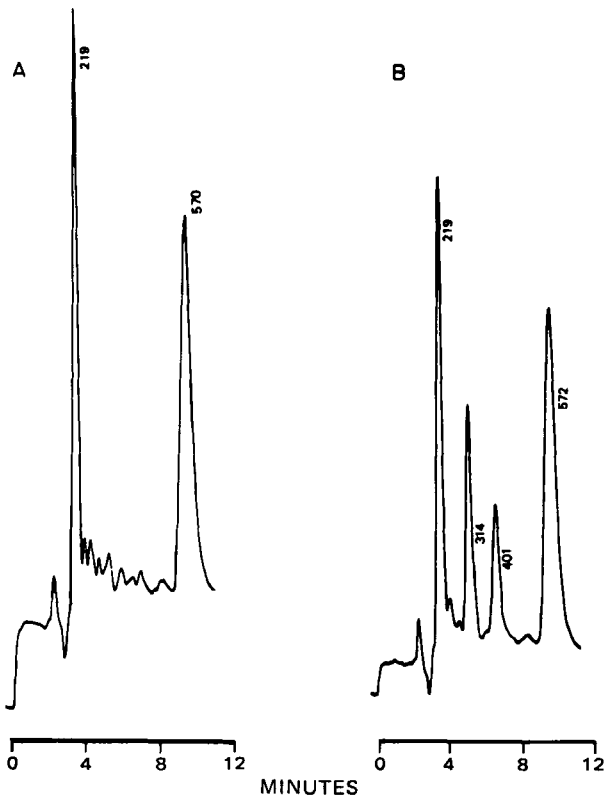

Figure 1—*Liquid chromatograms of 1-ml plasma extracts. Key: A, blank plasma sample of a cardiac patient spiked with 30 ng/ml of the internal standard (570 sec); and B, plasma of the same patient 4 hr after oral intake of 100 mg of metoprolol and spiked with 30 ng/ml of the internal standard. Retention times were 401 and 572 sec for metoprolol and the internal standard, respectively. The plasma metoprolol concentration in this patient was calculated to be 46 ng/ml. The peak at 314 sec is probably α-hydroxymetoprolol.*

formance liquid chromatograph[6] was equipped with a fluorescence detector[7]. The effluent was monitored at an excitation wavelength of 220 nm with a 295-nm UV interference filter to set the emission wavelength.

A reversed-phase column[8] (25-cm long × 4-mm i.d.) was maintained at 40°. The flow rate of the helium-degassed mobile phase was 1.0 ml/min. Samples were injected into the chromatograph *via* an injector[9] equipped with a 10-μl loop.

Mobile Phase—1-Heptanesulfonic acid (25 ml) in acetic acid was mixed with 1 liter of distilled water (Solvent A), and 25 ml of the same acid solution was mixed with 1 liter of methanol (Solvent B). The mobile phase was a mixture of Solvents A and B (15:85 v/v).

Procedure—One milliliter of plasma, 30 μl of the internal standard solution (1 μg/ml in methanol), 0.5 ml of 1.0 *N* NaOH, and 4 ml of methylene chloride were added to a 10-ml glass-stoppered centrifuge tube. The mixture was vortexed for 30 sec and then centrifuged for 5 min at 5000 rpm. The organic phase was transferred to a 6-ml glass-stoppered conical tube, evaporated to dryness under nitrogen at room temperature, and reconstituted in 15 μl of the mobile phase. An aliquot of this solution was injected.

RESULTS AND DISCUSSION

The efficiency of the extraction recovery for metoprolol (100 ng/ml) was 76.9% with a coefficient of variation of 3.1%. Over the 10–300-ng/ml plasma range studied, the standard curve was linear. The standard curves analyzed over 1 month (n=11) gave a mean regression (±*SD*) of y = 0.0104 (±0.0008)x + 0.0054 (±0.0050) with r = 0.9987 (±0.0011), where y is the metoprolol peak height divided by the 4-methylpropranolol peak height and x is the concentration of metoprolol (nanograms of free base per milliliter).

Table I—Within-Run Accuracy and Precision for Metoprolol [a]

Concentration, ng/ml	Mean Result, %	*CV*,%
30	103.1	6.0
50	105.6	5.3
100	100.9	2.3

[a] n = 5.

The reproducibility of the method was demonstrated by a day-to-day coefficient of variation of 6.8% (n=11) using pooled plasma spiked with metoprolol (50 ng/ml) and analyzed over 1 month. The within-run coefficients of variation and accuracy are given in Table I.

The detection limit of this assay with the described instrumentation and procedure was ~5 ng/ml of plasma.

Assay of samples spiked with a number of commonly used cardiovascular drugs showed that procainamide interferes with the internal standard. Plasma samples obtained from 40 cardiac patients taking drugs such as nitrates and other antianginal agents, antiarrhythmic agents, diuretics, antibiotics, theophylline, aspirin, dipyridamole, and benzodiazepines were analyzed. Only in quinidine-treated patients was there a problem since quinidine metabolites interfered with metoprolol on the chromatogram.

An example of the chromatogram obtained from the plasma of a cardiac patient is shown in Fig. 1 along with the chromatogram of plasma of the same patient sampled 4 hr after receiving 100 mg of metoprolol orally.

The metabolites of metoprolol, α-hydroxymetoprolol, *O*-desmethylmetoprolol, 4-(2-hydroxy-3-isopropylaminopropoxy)phenylacetic acid, and 2-hydroxy-3-(4-methoxyethylphenoxy)propanoic acid, eluted at 322, 342, 312, and 215 sec, respectively, which separated them from metoprolol (411 sec) and the internal standard (587 sec). Only the two basic metabolites, α-hydroxymetoprolol and *O*-desmethylmetoprolol, were recovered from extracted spiked plasma. In humans, *O*-desmethylmetoprolol concentrations are low, but α-hydroxymetoprolol concentrations can be detected (9–11). In some patient samples, a peak was seen that could be attributed to α-hydroxymetoprolol (Fig. 1).

The described HPLC assay provides a specific, sensitive, and quantitative method for the determination of metoprolol in plasma.

REFERENCES

(1) M. Ervik, *Acta Pharmacol. Toxicol.*, **36,** 136 (1975).

(2) P. H. Degen and W. Riess, *J. Chromatogr.*, **121,** 72 (1976).

(3) M. Ervik, K.-J. Hoffmann, and K. Kylberg-Hansen, *Biomed. Mass Spectrom.*, in press (1980).

(4) A. M. Taburet, A. A. Taylor, J. R. Mitchell, D. E. Rollins, and J. L. Pool, *Life Sci.*, **24,** 209 (1979).

(5) M. T. Rosseel and M. G. Bogaert, *J. Pharm. Sci.*, **70,** 688 (1981).

(6) O. H. Weddle, E. N. Amick, and W. D. Mason, *ibid.*, **67,** 1033 (1978).

(7) Y.-G. Yee, P. Rubin, and T. F. Blaschke, *J. Chromatogr.*, **171,** 357 (1979)

(8) M. A. Lefebvre, J. Girault, M. Cl. Saux, and J. B. Fourtillan, *J. Pharm. Sci.*, **69,** 1216 (1980).

(9) K.-U. Seiler, K. J. Schuster, G.-J. Meyer, W. Niedermayer, and O. Wassermann, *Clin. Pharmacokinet.*, **5,** 192 (1980).

(10) K.-J. Hoffmann, C.-G. Regårdh, M. Aurell, M. Ervik, and L. Jordö, *ibid.*, **5,** 181 (1980).

(11) C. P. Quarterman, M. J. Kendall, and D. B. Jack, *J. Chromatogr.*, **183,** 92 (1980).

ACKNOWLEDGMENTS

Supported in part by Grant 3.9001.79 from the Fund for Medical Scientific Research.

[6] Spectra Physics, SP-8000, Eindhoven, The Netherlands.
[7] F.S. 970, Schoeffel Instruments Corp., West Germany.
[8] Lichrosorb 10 RP 8, Chrompack, Merksem, Belgium.
[9] Spectra Physics, SP 8000 automatic injector, Eindhoven, The Netherlands.

Stability of Phenylpropanolamine Hydrochloride in Liquid Formulations Containing Sugars

R. H. BARRY, M. WEISS ˣ, J. B. JOHNSON, and E. DeRITTER

Received July 28, 1980, from *Hoffmann-La Roche Inc., Nutley, NJ 07110.* Accepted for publication May 15, 1981

ABSTRACT □ Stability studies with a decongestant syrup formulation containing phenylpropanolamine hydrochloride in a sugar vehicle indicated a loss of phenylpropanolamine hydrochloride. To ascertain the biological significance of this indicated chemical loss, the degraded formulation was administered to human volunteers and the urinary excretion of phenylpropanolamine hydrochloride was determined. The excretion and chemical assay patterns were in good agreement, indicating that the sugar vehicle was both chemically and biologically incompatible with phenylpropanolamine hydrochloride. A control formulation made with phenylpropanolamine hydrochloride in a sorbitol vehicle showed good chemical stability and urinary excretion patterns. Further studies showed chemical losses with phenylpropanolamine hydrochloride in the presence of fructose, dextrose, and 5-(hydroxymethyl)-2-furaldehyde but not with levulinic acid. Possible mechanisms for the sugar–phenylpropanolamine hydrochloride interaction are discussed.

Keyphrases □ Phenylpropanolamine hydrochloride—stability in liquid formulations containing sugars □ Stability—of phenylpropanolamine hydrochloride in liquid formulations containing sugars □ Adrenergic agents—phenylpropanolamine hydrochloride, stability in liquid formulations containing sugars

While formulating a decongestant syrup containing phenylpropanolamine hydrochloride, it was observed that the stability pattern indicated a loss of phenylpropanolamine hydrochloride. Initial formulations contained sucrose with either corn syrup or an invert sugar composition in the vehicle.

Since it was surmised that the sugars had interacted with the phenylpropanolamine hydrochloride, stability experiments were done with phenylpropanolamine hydrochloride in aqueous vehicles containing dextrose, fructose, and sucrose–corn syrup, with a sorbitol vehicle as the control. In addition, 5-(hydroxymethyl)-2-furaldehyde and levulinic acid were tested since these compounds are produced from the hydrolysis of dextrose and fructose.

To ascertain the biological significance of the indicated chemical loss of phenylpropanolamine hydrochloride, a urinary excretion study was performed using the initial formulation in the sucrose–corn syrup vehicle. After storage at 5 and 55° for 1 month, comparisons were made with a formulation containing sorbitol.

EXPERIMENTAL

Analytical Methods—Initially, the phenylpropanolamine hydrochloride[1] in the sucrose[2]–corn syrup[3] formulations was determined using the ion-pair–methyl orange procedure (1, 2). For subsequent experiments using dextrose[4], fructose[4], 5-(hydroxymethyl)-2-furaldehyde[5], and levulinic acid[5], phenylpropanolamine hydrochloride was determined by the ninhydrin procedure of Burke *et al.* (3). A periodate oxidation method (4) was used for the determination of phenylpropanolamine hydrochloride in urine.

Urinary Excretion Tests—All preparations were given orally to nonfasted subjects. Pooled urine samples were collected for 24 hr prior to dosage for measurements of blank excretion values. After the morning dosage, urine was collected for 24 hr. Urinary phenylpropanolamine hydrochloride was determined by a reported method (4).

In agreement with earlier results (4), the present experiments indicated that 90–100% of a 50-mg phenylpropanolamine hydrochloride dose was excreted by humans in the urine. With the 15–25-mg doses administered in the present experiment, only 70–80% was excreted. A relatively constant amount of phenylpropanolamine hydrochloride apparently is metabolized and not recovered in the urine (*e.g.*, 10% of a 50-mg dose equals 5 mg, which is 20% of a 25-mg dose).

Table I—Effect of Sucrose and Corn Syrup on Phenylpropanolamine Hydrochloride Stability

	Formula			
	1	2	3	4
Phenylpropanolamine hydrochloride, % (w/v)	0.15	0.15	0.15	0.15
Sucrose, % (w/v)	40	—	—	40
Corn syrup, % (w/v)	—	40	—	—
Sorbitol, % (w/v)	—	—	40	—
Initial pH	6.0	6.0	5.9	4.5
Retention of phenylpropanolamine hydrochloride (3 days/70°), %	93	54	97	67

RESULTS

The assay data in Table I show that the phenylpropanolamine hydrochloride losses in the presence of sucrose and corn syrup were significant after 3 days at 70°. The sucrose effect was much greater at pH 4.5 than at pH 6. Practically no change occurred with sorbitol.

The data in Table II compare the effect of dextrose and fructose (the hydrolytic cleavage products of sucrose) on phenylpropanolamine hydrochloride stability at pH 4, 6, and 7. As pH increased, the degradation rate and degree of color development increased. At pH 4, there was only a slight rise in pH, whereas pH decreased at pH 6 and 7. Precipitation was noted in all samples after 1 week of storage at 70° and was visibly greater at pH 6 and 7 than at pH 4. The magnitude of these changes was significantly greater for dextrose than for fructose. Formula 5, containing 5 mg of phenylpropanolamine hydrochloride/ml, 35% sucrose, 15% corn syrup, 11% ethanol, and 20% propylene glycol, was the formulation used for the human excretion studies reported in Table III.

Table IV shows the effects of 5-(hydroxymethyl)-2-furaldehyde and levulinic acid on phenylpropanolamine hydrochloride stability at pH 4, 6, and 7 and on sorbitol at pH 6. Sorbitol had no effect, and levulinic acid had no significant effect. In contrast, there was a loss of phenylpropanolamine hydrochloride from interaction with 5-(hydroxymethyl)-2-furaldehyde. While no pH changes occurred, the solution darkened and a dark precipitate developed. Recovery of this precipitate by centrifugation indicated that it was water insoluble, methanol soluble, and very slowly soluble in chloroform. By comparison, precipitates from dextrose–phenylpropanolamine hydrochloride solutions were water insoluble and methanol soluble but appeared to be chloroform insoluble.

Table III shows the urinary excretion data from formulations containing phenylpropanolamine hydrochloride. The first formulation (A-5°) initially contained 24.4 mg of phenylpropanolamine hydrochloride/5 ml in the sugar vehicle already described. After 1 month at 55° (A-55°), ~38% of the phenylpropanolamine hydrochloride was lost with 15.2 mg/5 ml retained. Formulation B, which assayed 26.8 mg of phenylpropanolamine hydrochloride/10 ml, was made in a sorbitol vehicle and was stable.

In all three cases, the amount of phenylpropanolamine hydrochloride recovered in the 24-hr urine samples was in proportion to the amount of "undegraded" phenylpropanolamine hydrochloride administered, or ~71–78% of the dose.

[1] NF XIV, Ganes Chemical Works.
[2] USP XIX.
[3] Globe 1132, Corn Products Division, CPC International
[4] Anhydrous, Aldrich Chemical Co.
[5] Ninety-nine percent, Aldrich Chemical Co.

0022-3549/82/0100-0116$01.00/0

Table II—Effect of Sucrose–Corn Syrup, Dextrose, Fructose, and pH on Phenylpropanolamine Hydrochloride Stability

	Formula						
	5	6	7	8	9	10	11
Ingredients[a]							
Phenylpropanolamine hydrochloride, % (w/v)	0.5	1.0	1.0	1.0	1.0	1.0	1.0
Sucrose, % (w/v)	35	—	—	—	—	—	—
Corn syrup, % (w/v)	15	—	—	—	—	—	—
Dextrose, % (w/v)	—	10	10	10	—	—	—
Fructose, % (w/v)	—	—	—	—	10	10	10
Buffer type	Citrate	Citate	Phosphate	Phosphate	Citrate	Phosphate	Phosphate
Normality	0.29	0.25	0.28	0.23	0.25	0.28	0.23
Physical stability							
Changes in optical density after 1 week at 70°[b]	—	0.414	1.745	1.832	0.2	0.85	1.438
Chemical stability							
pH							
Initial	6	4	6	7	4	6	7
1 week/70°	—	4.2	4.55	4.35	4.1	5.2	5.3
4 weeks/55°	5.25	4.2	4.8	4.6	4.2	5.7	6.05
Percent retention of phenylpropanolamine hydrochloride after							
1 week/70°	—	84	55	45	91	71	63
1 month/55°	65	87	57	43	87	79	73
16 weeks/45°	—	93	64	55	—	84	77
3.5 months/45°	65	—	—	—	—	—	—
3.5 months/37°	85	—	—	—	—	—	—
Percent loss of phenylpropanolamine hydrochloride per week at room temperature[c]	0.26	0.09	0.62	1.37	0.07	0.17	0.46

[a] The vehicles also contained 20% propylene glycol, 11% ethanol, 5% glycerin, and distilled water. [b] Measured at 315 nm using the 5° sample as a blank. Changes were due to formation of colored degradation products. [c] Calculated from losses observed at elevated temperatures using Arrhenius plots.

Table III—Assay and Urinary Excretion of Phenylpropanolamine Hydrochloride

Formulation	Phenylpropanolamine Hydrochloride Assay	24-hr Urinary Excretion Pattern			
		Percent Phenylpropanolamine Retained	Amount Given, ml	Amount Excreted, mg	Percent of Retained Dose Excreted[a]
A-5° (sucrose–corn syrup vehicle, Formula 1 of Table I), 1 month 5°	24.4 mg/5 ml	100	5	19	78
A-55° (same as A-5°), 1 month 55°	15.2 mg/5 ml	62	5	10.8	71
B (sorbital vehicle)	26.8 mg/10 ml	100	10	19	71

[a] Five subjects.

Table IV—Effect of 5-(Hydroxymethyl)-2-furaldehyde, Sorbitol, and Levulinic Acid on Phenylpropanolamine Hydrochloride Stability

	Formula								
	12	13	14	15	16	17	18	19	20
Phenylpropanolamine hydrochloride, % (w/v)	0.2	0.2	0.2	0.2	0.2	0.2	0.2	0.2	0.2
5-(Hydroxymethyl)-2-furaldehyde, % (w/v)	0.142	0.142	0.142	0.142	—	—	—	—	—
Sorbitol, % (w/v)	—	—	—	—	10	—	—	—	—
Levulinic acid	—	—	—	—	—	0.18	0.18	0.18	0.18
Buffer type	Phosphate	Citrate	Phosphate	Phosphate	Phosphate	Phosphate	Citrate	Phosphate	Phosphate
Normality	0.42	0.25	0.28	0.23	0.28	0.43	0.34	0.3	0.39
Initial[a] pH	6	4	6	7	6	5.65	4	6	7
Percent retention after									
7 days 70°	79	95	100	100	101	—	100	100	100
14 days 70°	—	85	76	97.5	—	—	—	95	—
4 weeks 55°	—	93	87	87	98	100	—	—	98
3.5 months 55°	85	—	—	—	—	—	—	—	—

[a] No significant changes observed after storage at elevated temperatures.

DISCUSSION

The analytical data reported here indicate that there was an interaction of phenylpropanolamine hydrochloride with sugars containing aldose or ketose functional groups or with 5-(hydroxymethyl)-2-furaldehyde, a degradation product of dextrose or fructose. Levulinic acid, another possible degradation product, was unreactive. Sucrose *per se* is not expected to be reactive with phenylpropanolamine hydrochloride until hydrolysis to carbonyl-containing cleavage products occurs as a function of time, temperature, and pH of the vehicle. As expected, there was no chemical loss of phenylpropanolamine hydrochloride in sorbitol solutions.

If phenylpropanolamine hydrochloride combines with the carbonyl groups of the aldose or ketose sugars or with a reactive carbonyl degradation product, the resulting interaction product may or may not undergo biological transformation after ingestion to release phenylpropanolamine hydrochloride. The urinary excretion data, although limited, appear to suggest that the interaction product does not revert to free phenylpropanolamine hydrochloride after ingestion. If degraded phenylpropanolamine hydrochloride were converted *in vivo* to free phenylpropanolamine hydrochloride, the group ingesting this dose (containing 62% of the amount found in A-5°, the refrigerated control) would have excreted ~19 mg of phenylpropanolamine hydrochloride rather than 10.8 mg.

Possible Interaction Mechanisms—While the present study did not attempt to elucidate the nature of the interaction of phenylpropanol-

amine hydrochloride with the aldose or ketose sugars, the literature was reviewed with regard to the various possibilities concerning this interaction.

Oxazolidine Formation—β-Amino alcohols, such as ephedrine (5–8), pseudoephedrine (5, 7–9), phenylpropanolamine (9–11), and phenylephrine (12, 13), can form oxazolidines with aliphatic and aromatic aldehydes and ketones. The elimination of water from the reaction between the carbonyl group and the vicinal amino and hydroxyl groups of the amino alcohol is usually accomplished by azeotropic distillation (9, 10) or with a dehydrating agent (13) but can occur in an aqueous medium (11). Oxazolidine formation depends on thermodynamic and steric factors. In some cases, the product may exist as a mobile tautomeric system with the corresponding Schiff base (9, 11).

Stability of oxazolidines to hydrolysis is reportedly variable (6, 9). However, oxazolidines usually can be cleaved by heating with acids to yield the amino alcohol and the carbonyl compound (5, 6, 11, 13). The oxazolidine from the interaction of ephedrine and benzaldehyde was marketed in an oily nasal inhalant and was presumably active topically (6). Oxazolidine formation from interaction of sympathomimetic β-amino alcohols with aldose and ketose sugars or with 5-(hydroxymethyl)-2-furaldehyde has not been reported. 5-(Hydroxymethyl)-2-furaldehyde is readily formed by the acid-catalyzed hydrolysis of glucose or fructose (14) or by heating glucose in water (15).

Tetrahydroisoquinoline Formation—Cyclization of norphenylephrine [1-(3-hydroxyphenyl)-2-amino-ethanol] with various carbonyl compounds (*via* a Pictet–Spengler type of reaction but requiring no acidic catalyst) was reported (16) to yield tetrahydroisoquinolines and not oxazolidines as previously reported. The reaction probably proceeds *via* a Schiff base intermediate and appears to be characteristic of β-amino alcohols with a phenolic hydroxyl *para* to the site of cyclization. Similarly, tetrahydroisoquinolines can be formed in sucrose-coated tablets of norphenylephrine (17) from 5-(hydroxymethyl)-2-furaldehyde and levulinic acid, products of the thermal decomposition of sucrose.

The formation of isoquinolines from interaction of phenylpropanolamine and aldose or ketose sugars or their decomposition products has not been reported. This possibility seems remote since a phenolic group in the benzene nucleus is apparently required to promote cyclization.

Browning (Carbonyl–Amine) Reactions—Nonenzymic browning reactions involving the carbonyl group of aldose or ketose sugars with primary or secondary amines are well known (18, 19). The browning of lactose, galactose, dextrose, dextrates, and 5-(hydroxymethyl)-2-furaldehyde with *dl*-amphetamine, its *N*-methyl derivatives, and *d*-amphetamine was studied extensively (20–26). The carbonyl group of the sugar or 5-(hydroxymethyl)-2-furaldehyde and the amine presumably form colored products *via* a Schiff base-type reaction or by formation of glycosyl amines, *N*-glycosides, or certain compounds formed by Amadori rearrangement (27). Isoglucosamines (amino ketones, not Schiff base), if formed by rearrangement, would be expected to be resistant to hydrolysis unlike the glycosamines, most of which easily darken and undergo further decomposition (27).

No experimental data indicate which of the foregoing interaction possibilities is the principal one involved in the phenylpropanolamine hydrochloride–sugar interaction. It is felt that Schiff base formation probably occurred under the test condition with further rearrangement(s) to produce a compound(s) that did not revert to free phenylpropanolamine hydrochloride either *in vivo* or *in vitro*.

REFERENCES

(1) T. Higuchi and J. I. Bodin, "Pharmaceutical Analysis," Interscience, New York, N.Y., 1961, pp. 413–418.

(2) K. A. Connors, "Textbook on Pharmaceutical Analysis," 2nd ed., Wiley–Interscience, New York, N.Y., 1961, p. 514.

(3) D. Burke, V. S. Venturella, and B. Z. Senkowski, *J. Pharm. Sci.*, **50,** 232 (1961).

(4) K. R. Heimlich, D. R. MacDonnell, T. L. Flanagan, and P. D. O'Brien, *ibid.*, **50,** 232 (1961).

(5) E. H. Stuart, U.S. pats. 1,749,361 and 1,749,452 (1930).

(6) L. H. Welch, *J. Assoc. Off. Ag. Chem.*, **30,** 467 (1947).

(7) L. Neelakantan, *J. Org. Chem.*, **36,** 2253, 2256 (1971).

(8) L. Neelakantan and J. A. Molin-Case, *ibid.*, **36,** 2761 (1971).

(9) E. Bergmann, *Chem. Rev.*, **53,** 310 (1953).

(10) M. Senkus, *J. Am. Chem. Soc.*, **67,** 1515 (1945).

(11) L. Neelakantan and H. Kostenbauder, *J. Pharm. Sci.*, **65,** 740 (1976).

(12) H. Bretschneider, *Monatsch.*, **77,** 117 (1947).

(13) S. Yuan and N. Bodor, *J. Pharm. Sci.*, **65,** 929 (1976).

(14) M. L. Wolfram, R. D. Schuetz, and L. Cavalieri, *J. Am. Chem. Soc.*, **70,** 514 (1948).

(15) B. Scallet and J. Gardner, *ibid.*, **67,** 1934 (1945).

(16) T. Kametani, K. Fukumoto, H. Agui, H. Yagi, K. Kigasawa, H. Sugahara, M. Hiragi, T. Hayasaka, and H. Ishimaru, *J. Chem. Soc. C*, **1968,** 112.

(17) K. Kigazawa, N. Ikari, K. Ohkubo, H. Iimura, and S. Haga, *J. Pharm. Soc., Jpn.*, **93,** 925 (1973).

(18) W. Pigman, "The Carbohydrates: Chemistry, Biochemistry, Physiology," Academic, New York, N.Y., 1957, pp. 406, 412.

(19) R. S. Shallenberger and G. G. Birch, "Sugar Chemistry," AVI Publishing, West Port, Conn., 1975, p. 169.

(20) R. A. Castello and A. M. Mattocks, *J. Pharm. Sci.*, **51,** 106 (1962).

(21) C. A. Brownley and L. Lachman, *ibid.*, **53,** 452 (1964).

(22) R. N. Duvall, K. T. Koshy, and J. W. Pyles, *ibid.*, **54,** 607 (1965).

(23) R. N. Duvall, K. T. Koshy, and R. E. Dashiell, *ibid.*, **54,** 1196 (1965).

(24) K. T. Koshy, R. N. Duvall, A. E. Troup, and J. W. Pyles, *ibid.*, **54,** 549 (1965).

(25) S. M. Blaug and W. Huang, *ibid.*, **61,** 1770 (1972).

(26) *Ibid.*, **63,** 1415 (1974).

(27) J. Stanek, "The Monosaccharides," Academic, New York, N.Y., 1963, pp. 451, 454, 456.

ACKNOWLEDGMENTS

Presented in part at the Basic Pharmaceutics Section, APhA Academy of Pharmaceutical Sciences, Montreal meeting, May 1978.

The authors thank M. Araujo and J. Scheiner for excellent technical assistance.

Synthesis of 7,7-Diaryl-4,5,6,7-tetrahydroimidazo-[4,5-*c*]pyridines

R. L. WILLIAMS ˣ **and SANDRA NEERGAARD**

Received April 6, 1981, from the *Department of Chemical Sciences, Old Dominion University, Norfolk, VA 23508.* Accepted for publication June 2, 1981.

Abstract □ The synthesis and characterization of various 7,7-diaryl-4,5,6,7-tetrahydroimidazo-[4,5-*c*]pyridines are reported. Convulsant activity was observed with a dipyridyl compound.

Keyphrases □ Histamine—condensation reactions to form 7,7-diaryl-4,5,6,7-tetrahydroimidazo-[4,5-*c*]pyridines □ Spirocyclic-4,5,6,7-tetrahydroimidazo-[4,5-*c*]pyridines—synthesis and characterization □ Convulsants—activity in rats, synthesized dipyridyl compound

As part of a continuing research program in the condensation reactions of histamine (I) with various carbonyl compounds, the synthesis of several novel diaryl-4,5,6,7-tetrahydroimidazo-[4,5-*c*]pyridines will be described. While a variety of condensation products were previously described (1–3), an examination of this Pictet-Spengler type reaction of histamine with diaryl ketones has not been reported.

In general, previously reported methods for the condensation of histamine with aldehydes involved the reaction of histamine dihydrochloride in a basic media with the appropriate aldehyde. Good yields of the aldehyde and ketone condensation products can also be realized by refluxing histamine free base with the desired carbonyl compounds in *n*-butanol. Under these conditions, the Schiff-base intermediates undergo ring closure at the C-5 position of the imidazole ring and the products can then be isolated by removal of the reaction solvent.

This rather simple synthesis has been successfully adapted to include examples of both acyclic and, more recently, cyclic ketones such as 9-fluorenone and 1,8-diazafluorene (Scheme I). The resulting 7-spirocyclic-4,5,6,7-tetrahydroimidazo-[4,5-*c*]pyridines (V and VI) as well as the acyclic ketone analogs (II–IV) have all been characterized by NMR, IR, and elemental analysis (Tables I and II).

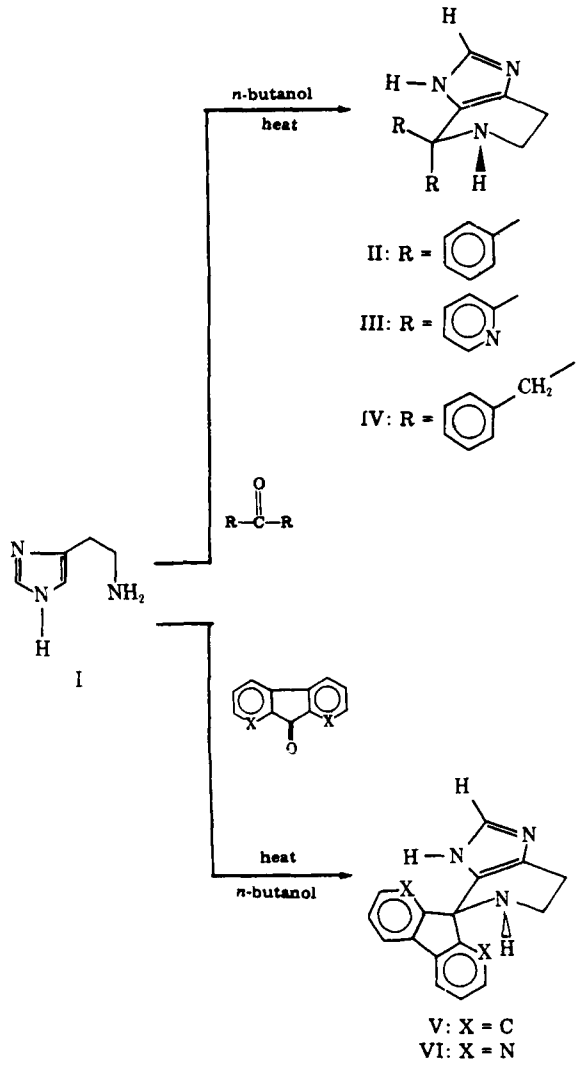

Scheme I

Table I—Physical Data for Diaryl-4,5,6,7-tetrahydroimidazo-[4,5-*c*]pyridines

Compound	Melting Point Free Base	Yield, %	Formula	Analysis, % Calc.	Found
II	100–105°	50	$C_{18}H_{17}N_3$	C 78.54	78.34
				H 6.14	6.36
				15.27	15.36
III	220–222°	66	$C_{16}H_{15}N_5$	C 69.31	69.19
				H 5.41	5.38
				N 25.27	25.65
IV	218–219°	60	$C_{20}H_{21}N_3$	C 79.48	79.46
				H 6.94	6.95
				N 13.89	13.97
V	258°	69	$C_{18}H_{15}N_3$	C 79.41	79.35
				H 5.15	5.51
				N 15.44	15.41
VI	250° (dec.)	41	$C_{16}H_{15}N_5Cl_2$ (dihydrochloride)	C 55.36	54.95
				H 4.08	4.34
				N 20.17	20.01

0022-3549/82/0100-0119$01.00

Table II—Spectral Data for Diaryl-4,5,6,7-tetrahydroimidazo-[4,5-c]pyridines

Compound	IR Spectrum (KBr): ν_{max}, cm^{-1}	^{1}H-NMR Spectrum (deuterodimethylsulfoxide), ppm
II	3100–2800 (bd), 1610, 750, and 695	2.5 (t, 2H, C-4, CH_2), 2.7 (t, 2H, C-5, CH_2), and 7.16–7.4 (m, 11H, Ar, C-2)
III	3250–2850 (bd), 1610, 775, and 745	2,6 (t, 2H, C-4, CH_2), 2.9 (t, 2H, C-5, CH_2), 7.2 (m, 2H, Ar), 7.6 (5H, Ar, C-2), and 8.3 (2H, Ar)
IV	3100–2600 (bd), 1610, 750, and 695	2.16 (t, 2H, C-4, CH_2), 2.7 (t, 2H, C-5, CH_2), 2.9 (d, 2H, CH_2), 3.4 (d, 2H, CH_2), 7.2 (m, 10H, Ar), and 7.6 (S, 1H, C-2)
V	3200–2850 (bd), 1620 and 745	3.3 (t, 2H, C-4, CH_2), 3.75 (t, 2H, C-5, CH_2), 8.06 (S, 1H, C-2), and 7.6 (m, 8H, Ar)
VI	3200–2800 (bd), 1620, 1580, 790, and 755	2.6 (t, 2H, C-4, CH_2), 3.1 (t, 2H, C-5, CH_2), 6.8 (m, 2H, Ar), 7.8 (m, 3H, Ar, C-2), and 8.3 (m, 2H, Ar)

RESULTS AND DISCUSSIONS

The condensation of histamine free base (I) and a variety of aromatic and heteromatic ketones has given rise to a series of novel 4,5,6,7-tetrahydroimidazo-[4,5-c]pyridines. The proposed structures are supported by pertinent spectral data and are consistent with ring closure at C-5 of the imidazole ring with concomitant loss of the characteristic aromatic proton at 6.9 ppm.

A preliminary gross behavioral evaluation of each of these compounds in mice at three different dose levels (33, 54, and 66 mg/kg) has shown that the dipyridyl compound (III) exhibits a marked degree of convulsant activity. None of the other compounds were found to produce convulsions at the same dose levels. Research is currently in progress to establish the possible mode of action of this novel heterocyclic system.

EXPERIMENTAL[1]

All syntheses were carried out by dissolving the appropriate ketone in *n*-butanol and treating the stirred solution with one equivalent of histamine-free base in *n*-butanol. The solutions were refluxed and monitored using TLC (cellulose; *n*-butanol–acetic acid–water, 4:1:1) until no further ketone could be detected. Removal of the solvent under reduced pressure followed by repeated dilutions with methanol and then with acetone caused the precipitation of the crude free bases of the condensation products. The resulting free bases were converted to their corresponding hydrochlorides which could be recrystallized from ethanol–acetone.

REFERENCES

(1) D. Heyl, E. Luz, S. Harris, and K. Folkess, *J. Am. Chem. Soc.*, **70**, 3669 (1943).

(2) F. Stocker, M. Fordice, J. Larson, and T. H. Thorestenson, *J. Org. Chem.*, **31**, 2380 (1966).

(3) G. Habermehl and W. Ecsy, *Heterocycles*, **5**, 127 (1976).

ACKNOWLEDGMENTS

The authors acknowledge the financial support of Old Dominion University.

[1] Melting points for all compounds are uncorrected and were determined on a Thomas-Hoover melting point apparatus. IR spectra were recorded on a Perkin-Elmer 137 spectrometer. NMR spectra were recorded on a Varian T-60 spectrometer in deuterodimethylsulfoxide using tetramethylsilane as the internal standard. All C, H, and N analyses were performed by the M-H-W Laboratories, Phoenix, Ariz.

Quality Control of Phenylbutazone II: Analysis of Phenylbutazone and Its Decomposition Products in Drugs by High-Pressure Liquid Chromatography

H. FABRE ˣ, B. MANDROU, and H. EDDINE

Received June 2, 1980, from the *Laboratoire de Chimie Analytique, Faculté de Pharmacie, 34060 Montpellier Cedex, France.* Accepted for publication June 17, 1981.

Abstract □ A rapid, sensitive, accurate, and reproducible procedure for the simultaneous separation and determination of phenylbutazone and three major degradation products is proposed using reversed-phase high-pressure liquid chromatography and UV detection. The method is ~20 times more sensitive than TLC and allows an accurate determination of degradation products without decomposition during the analysis.

Keyphrases □ Phenylbutazone—analysis by high-pressure liquid chromatography, decomposition products □ High-pressure liquid chromatography—analysis of phenylbutazone and its decomposition products □ Degradation—phenylbutazone, analysis by high-pressure liquid chromatography

An earlier report (1) outlined the difficulties relative to the establishment of an analytical procedure to detect the intermediate products of oxidation and hydrolysis of phenylbutazone (I). These products are 4-hydroxyphenylbutazone (II), *N*-(2-carboxycaproyl)hydrazobenzene (III), and *N*-(2-carboxy-2-hydroxycaproyl)hydrazobenzene (IV). GLC and TLC are not reliable procedures to monitor the stability of I, because artifacts are formed. TLC can only be used with special precautions as a qualitative and quantitative test to determine I–IV (1).

Reversed-phase high-pressure liquid chromatography (HPLC) is often used in stability studies because it is selective and rapid, and it is particularly recommended when the compound is easily oxidized and when extraction procedures may be degradative. No sample preparation is required for aqueous solutions and reversed-phase HPLC is especially attractive for injections of I because I undergoes decomposition in aqueous medium. Re-

0022-3549/82/0100-0120$01.00/0

Table II—Spectral Data for Diaryl-4,5,6,7-tetrahydroimidazo-[4,5-c]pyridines

Compound	IR Spectrum (KBr): ν_{max}, cm^{-1}	^{1}H-NMR Spectrum (deuterodimethylsulfoxide), ppm
II	3100–2800 (bd), 1610, 750, and 695	2.5 (t, 2H, C-4, CH_2), 2.7 (t, 2H, C-5, CH_2), and 7.16–7.4 (m, 11H, Ar, C-2)
III	3250–2850 (bd), 1610, 775, and 745	2,6 (t, 2H, C-4, CH_2), 2.9 (t, 2H, C-5, CH_2), 7.2 (m, 2H, Ar), 7.6 (5H, Ar, C-2), and 8.3 (2H, Ar)
IV	3100–2600 (bd), 1610, 750, and 695	2.16 (t, 2H, C-4, CH_2), 2.7 (t, 2H, C-5, CH_2), 2.9 (d, 2H, CH_2), 3.4 (d, 2H, CH_2), 7.2 (m, 10H, Ar), and 7.6 (S, 1H, C-2)
V	3200–2850 (bd), 1620 and 745	3.3 (t, 2H, C-4, CH_2), 3.75 (t, 2H, C-5, CH_2), 8.06 (S, 1H, C-2), and 7.6 (m, 8H, Ar)
VI	3200–2800 (bd), 1620, 1580, 790, and 755	2.6 (t, 2H, C-4, CH_2), 3.1 (t, 2H, C-5, CH_2), 6.8 (m, 2H, Ar), 7.8 (m, 3H, Ar, C-2), and 8.3 (m, 2H, Ar)

RESULTS AND DISCUSSIONS

The condensation of histamine free base (I) and a variety of aromatic and heteromatic ketones has given rise to a series of novel 4,5,6,7-tetrahydroimidazo-[4,5-c]pyridines. The proposed structures are supported by pertinent spectral data and are consistent with ring closure at C-5 of the imidazole ring with concomitant loss of the characteristic aromatic proton at 6.9 ppm.

A preliminary gross behavioral evaluation of each of these compounds in mice at three different dose levels (33, 54, and 66 mg/kg) has shown that the dipyridyl compound (III) exhibits a marked degree of convulsant activity. None of the other compounds were found to produce convulsions at the same dose levels. Research is currently in progress to establish the possible mode of action of this novel heterocyclic system.

EXPERIMENTAL[1]

All syntheses were carried out by dissolving the appropriate ketone in *n*-butanol and treating the stirred solution with one equivalent of histamine-free base in *n*-butanol. The solutions were refluxed and monitored using TLC (cellulose; *n*-butanol–acetic acid–water, 4:1:1) until no further ketone could be detected. Removal of the solvent under reduced pressure followed by repeated dilutions with methanol and then with acetone caused the precipitation of the crude free bases of the condensation products. The resulting free bases were converted to their corresponding hydrochlorides which could be recrystallized from ethanol–acetone.

REFERENCES

(1) D. Heyl, E. Luz, S. Harris, and K. Folkess, *J. Am. Chem. Soc.*, **70**, 3669 (1943).

(2) F. Stocker, M. Fordice, J. Larson, and T. H. Thorestenson, *J. Org. Chem.*, **31**, 2380 (1966).

(3) G. Habermehl and W. Ecsy, *Heterocycles*, **5**, 127 (1976).

ACKNOWLEDGMENTS

The authors acknowledge the financial support of Old Dominion University.

[1] Melting points for all compounds are uncorrected and were determined on a Thomas-Hoover melting point apparatus. IR spectra were recorded on a Perkin-Elmer 137 spectrometer. NMR spectra were recorded on a Varian T-60 spectrometer in deuterodimethylsulfoxide using tetramethylsilane as the internal standard. All C, H, and N analyses were performed by the M-H-W Laboratories, Phoenix, Ariz.

Quality Control of Phenylbutazone II: Analysis of Phenylbutazone and Its Decomposition Products in Drugs by High-Pressure Liquid Chromatography

H. FABRE ˣ, B. MANDROU, and H. EDDINE

Received June 2, 1980, from the *Laboratoire de Chimie Analytique, Faculté de Pharmacie, 34060 Montpellier Cedex, France.* Accepted for publication June 17, 1981.

Abstract □ A rapid, sensitive, accurate, and reproducible procedure for the simultaneous separation and determination of phenylbutazone and three major degradation products is proposed using reversed-phase high-pressure liquid chromatography and UV detection. The method is ~20 times more sensitive than TLC and allows an accurate determination of degradation products without decomposition during the analysis.

Keyphrases □ Phenylbutazone—analysis by high-pressure liquid chromatography, decomposition products □ High-pressure liquid chromatography—analysis of phenylbutazone and its decomposition products □ Degradation—phenylbutazone, analysis by high-pressure liquid chromatography

An earlier report (1) outlined the difficulties relative to the establishment of an analytical procedure to detect the intermediate products of oxidation and hydrolysis of phenylbutazone (I). These products are 4-hydroxyphenylbutazone (II), *N*-(2-carboxycaproyl)hydrazobenzene (III), and *N*-(2-carboxy-2-hydroxycaproyl)hydrazobenzene (IV). GLC and TLC are not reliable procedures to monitor the stability of I, because artifacts are formed. TLC can only be used with special precautions as a qualitative and quantitative test to determine I–IV (1).

Reversed-phase high-pressure liquid chromatography (HPLC) is often used in stability studies because it is selective and rapid, and it is particularly recommended when the compound is easily oxidized and when extraction procedures may be degradative. No sample preparation is required for aqueous solutions and reversed-phase HPLC is especially attractive for injections of I because I undergoes decomposition in aqueous medium. Re-

0022-3549/82/0100-0120$01.00/0

Table I—Retention Time Values for Phenylbutazone and Degradation Compounds

Compound	Retention Time, sec	Retention Time Relative to I	Retention Time Relative to V
I	509	1.00	1.58
II	824	1.62	2.55
III	242	0.48	0.75
IV	138	0.27	0.43
V	323	0.64	1.00
lidocaine[a]	562	1.10	1.74

[a] Evidenced with 1 g/liter of lidocaine solution.

Table II—Minimum Amount Detectable and Sensitivity for I–V at λ 237–267 nm

Compound	Minimum Amount Detectable, μg		Sensitivity	
	λ = 237 nm	λ = 267 nm	λ = 237 nm	λ = 267 nm
I	8.9×10^{-3}	6.5×10^{-3}	15,225	19,000
II	6.5×10^{-3}	40.0×10^{-3}	19,951	4200
III	2.0×10^{-3}	7.8×10^{-3}	20,600	6000
IV	1.8×10^{-3}	9.4×10^{-3}	19,000	3000
V	3.7×10^{-3}	—	12,770	2043

Table III—Recovery Data from Laboratory Prepared Injections

	Amount Added, mg	Amount Found, mg	Relative Error, %
Placebo	—	—	—
Placebo +I	1000.00	1013.00	1.30
Placebo +I	1000.00	1009.48	0.95
+II	5.00	5.14	2.80
+III	5.00	5.03	0.60
+IV	5.00	5.13	2.60
Placebo +I	1000.00	1030.70	3.07
+II	20.00	19.02	−4.90
+III	20.00	19.99	−0.05
+IV	20.00	20.08	0.40
Placebo +I	1000.00	999.99	0.00
+II	30.00	28.92	−3.60
+III	30.00	30.11	0.38
+IV	30.00	29.29	−2.37

versed-phase HPLC was recently reported (2) to determine I and II metabolites in biological fluids, but there are no literature references relative to the determination of I and its main degradation products *in vitro*. The present study reports a rapid, sensitive, and accurate procedure for simultaneously quantitating I–IV, and an application for injections with lidocaine is given.

EXPERIMENTAL

Material and Reagents—A high-pressure liquid chromatograph[1] with a variable-wavelength UV detector[2], a 10-μl automatic loop injection system, an integrator, and a reversed-phase column[3] were used. Compounds I–IV were used as received[4]. Tromethamine, citric acid, and dimethyl phthalate (V) were analytical reagent grade. Acetonitrile was HPLC reagent grade. Injections (1 g of phenylbutazone, and 50 mg of lidocaine/5 ml of aqueous solvent) were commercial formulations[5]. Distilled water was filtered through a 0.45-μm filter[6]. The *mobile phase* was

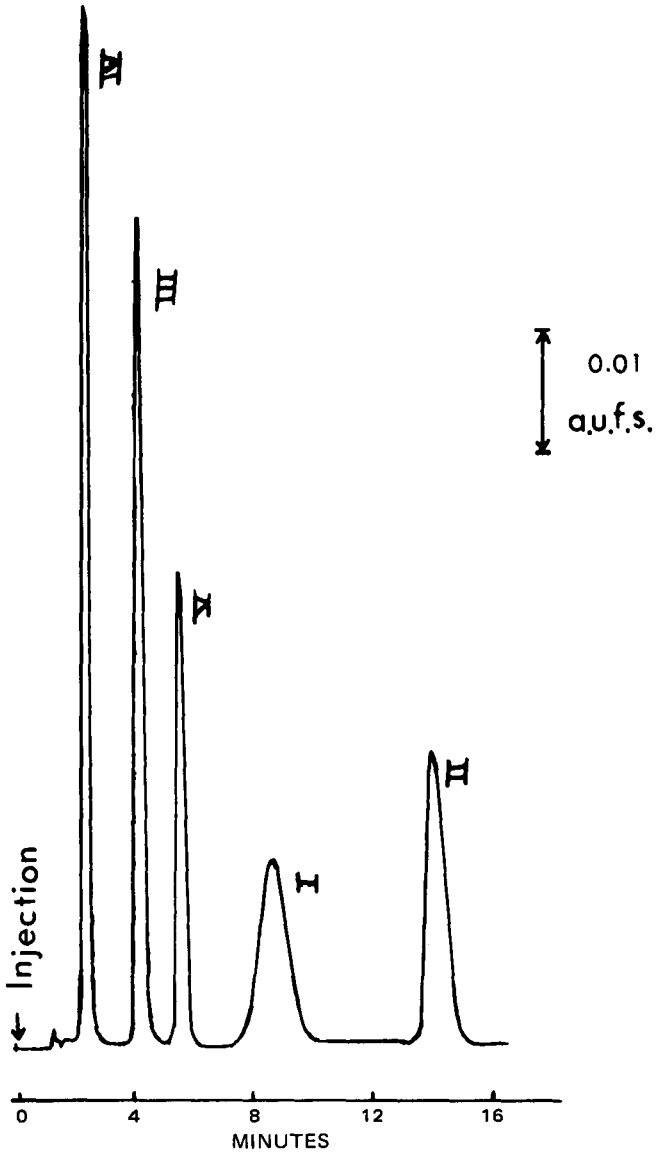

Figure 1—*Chromatogram of a standard solution of I (65.0 μg/ml), II (52.5 μg/ml), III (58.0 μg/ml), IV (68.0 μg/ml), and V (59.6 μg/ml). The mobile phase was 0.1 M tromethamine citrate buffer (pH 5.25)–acetonitrile (60:40); flow was 1.8 ml/min; and pressure was 83 bars. Detector sensitivity 0.1 aufs; chart recorder speed was 0.5 cm/min; and λ = 237 nm.*

0.1 *M* tromethamine citrate buffer[7] (pH 5.25)–acetonitrile (60:40); the mixture was previously degassed.

Standard Solutions—A mixed stock standard solution was prepared in the mobile phase, using I–IV (1000 μg of each per ml). This solution was suitably diluted and an equal volume of internal standard solution (100 μg/ml of V in the mobile phase) was added to give a concentration of 12.5–125 μg of each compound/ml.

Test Solutions—Recoveries of I–IV were carried out on laboratory prepared injections (analogous to commercial formulations) with and without added amounts of II, III, and IV (0.5, 2, and 3.0%, respectively, with respect to I). These solutions and the commercial formulations were suitably diluted in the mobile phase and internal standard was added to match the calibration graph.

Chromatography—Duplicate injections (10 μl) of each solution were injected under the following isocratic conditions: flow rate, 1.8 ml/min;

[1] Spectra-Physics SP 8000.
[2] Schoeffel model SF 770.
[3] 5-μm RP 18, 25-cm length × 4.6-mm diameter, laboratory-made column.
[4] Courtesy of Geigy Laboratories, Basel, Switzerland.
[5] Geigy Laboratories. Injections did not have the same reference numbers as those previously used (1).
[6] Millipore.

[7] Made by dissolving 24.2 g of tromethamine in 70 ml of water, adjusting the pH to 4.7 with citric acid, and diluting to 100 ml with water. The pH 5.25 buffer solution was prepared with a 5-ml aliquot diluted to 100 ml.

pressure, 83 ± 2 bars; chart speed, 0.5 cm/min, detector sensitivity, 0.04–0.1 aufs; and oven temperature, 20°. The chromatograms were recorded at 237 nm.

RESULTS AND DISCUSSION

The maximum absorbance wavelengths in the mobile phase were 267 (I) and 237 (II–IV). A weak absorbance of V was observed at 267 nm; 237 nm was most suitable for the simultaneous determination of I–V. In injections, lidocaine did not absorb at 237 and 267 nm at the concentration used (125 μg/ml) for the determination of II–IV.

A chromatogram of a standard solution is shown in Fig. 1 and Table I lists the retention times of each compound.

Figure 1 and Table I show a good resolution of each compound. The resolution obtained was always better than 1 for I–V.

A calibration graph was plotted of peak area ratio of the solute to the internal standard against solute concentration. The calibration graph was linear in the concentration range studied and went through the origin, using peak areas as well as peak heights. The correlation coefficients of the linear regression analysis were always better than 0.999 using peak areas as well as peak heights.

The minimum amount detectable, defined as the amount (in micrograms) that gives a peak height equal to twice the background, and the sensitivity, defined as the change in area value (measured at the maximum detector sensitivity) resulting from a concentration change of one unit (milligrams per liter) are given in Table II.

The repeatability tested by five replicates and evaluated by the coefficient of variation was 0.978 (I), 1.064 (II), 1.210 (III), and 1.510% (IV). The average data of duplicate assays for recovery studies on laboratory prepared injections with and without added amounts of II–IV are given in Table III.

A comparative separation of I–IV was carried out on a silica column[8]. With hexane–chloroform–methanol–formic acid (400:200:20:1) as a mobile phase, retention times were ~4 (I), 8 (II), 12 (III), 17 (IV), and 25 min for benzenesulfonamide used as an internal standard. Reversed-phase HPLC was faster (14 min) and more convenient than normal HPLC. The insignificant amounts of II–IV (probably present in the reference drug) detected by injecting 10 μl of a concentrated solution of I (2.5 g/liter) and the accuracy obtained for the determination of trace II–IV reveal that reversed-phase HPLC allows the determination of I–IV without decomposition during analysis.

With GLC, artifact peaks were observed when degradation products were present, and it is suggested (3) that the breakdown of the degradates occurs at the injection port maintained at 230°. HPLC is achieved at ambient temperature and prevents this drawback.

With TLC, a significant oxidation of I on the plate was observed during analysis (1). The iron present in the silica coating was responsible (1) for the accelerated air oxidation of I. The absence of degradation with the HPLC procedure is consistent with this hypothesis. The analysis time (13 min), the absence of air exposure, and the presence of citric acid (chelating agent for iron) in the mobile phase (used as an eluting agent and as a solvent in the preparation of solutions) contribute to prevent the degradation of I.

A commercial injection formulation was analyzed by the proposed HPLC procedure. Compound I was 1000.2 mg (100.0% of the labeled strength), III was 14.92 mg (1.49% with respect to theoretical I content), IV was 21.8 mg (2.18% with respect to theoretical I content), and II was not detected. The results are in agreement with other data (4) that shows II is so readily hydrolyzed into IV that it cannot be found in alkaline solution, and the major products of I degradation in injections are III and IV.

Reversed-phase HPLC is a sensitive (20 times more than TLC) and convenient procedure that can be used to evaluate the purity of phenylbutazone and to monitor its stability in pharmaceutical formulations. Because the metabolites of I have been identified as similar to the degradation products *in vitro*, the method is suggested to be applicable to pharmacokinetic studies.

[8] 30 μm Zorbax Sil, 30-cm length.

REFERENCES

(1) H. Fabre and B. Mandrou, *J. Pharm. Sci.*, **70**, 460 (1981), and references therein.

(2) T. Marunaka, T. Shibata, Y. Minami, and Y. Umeno, *J. Chromatogr.*, **183**, 331 (1980).

(3) J. R. Watson, F. Matsui, R. C. Lawrence, and P. M. J. McConnell, *J. Chromatogr.*, **76**, 141 (1973).

(4) D. V. C. Awang, A. Vincent, and F. Matsui, *J. Pharm. Sci.*, **62**, 1673 (1973).

COMMUNICATIONS

Active Conformation of Polycyclic Antidepressants

Keyphrases □ Antidepressants, polycyclic—active conformation □ Conformation, active—of polycyclic antidepressants

To the Editor:

A 300-MHz ^{1}H-NMR study of a series of polycyclic (tetracyclic and pentacyclic) antidepressant agents of the amitriptyline type indicated a preferred conformation in solution in which the alkylamino side chain is folded toward the polycyclic skeleton and its positively charged dimethylammonium ion is oriented above the adjacent aromatic ring.

Amitriptyline (I) and imipramine, prototype tricyclic antidepressant drugs, are potent inhibitors of active reuptake of biogenic amines in nerve endings. The therapeutic effects of these drugs may be related to this activity[1] (1–5). Reuptake inhibition may lead to an accumulation of neurotransmitters, *e.g.*, norepinephrine and serotonin, at the receptor site and to a subsequent increase in activity. The preferred conformation of the tricyclic antidepressant at the biogenic amine uptake jump may be crucial to their antidepressant activity.

Of particular significance is the conformation of the alkylamino side chain *vis-à-vis* the tricyclic skeleton (6, 7). X-ray structure determinations (8–13) indicated that in the crystalline state the side chain is almost fully extended, away from the tricyclic skeleton. However, it was suggested (6, 14) that the active conformation of the alkylamino side chain in polycyclic antidepressants is folded toward the aromatic ring. We present evidence for the amitriptyline-type series in favor of this hypothesis and

[1] For the state of the art of the mode of action of tricyclic antidepressants, see Horn (5).

0022-3549/82/0100-0122$01.00/0

pressure, 83 ± 2 bars; chart speed, 0.5 cm/min, detector sensitivity, 0.04–0.1 aufs; and oven temperature, 20°. The chromatograms were recorded at 237 nm.

RESULTS AND DISCUSSION

The maximum absorbance wavelengths in the mobile phase were 267 (I) and 237 (II–IV). A weak absorbance of V was observed at 267 nm; 237 nm was most suitable for the simultaneous determination of I–V. In injections, lidocaine did not absorb at 237 and 267 nm at the concentration used (125 μg/ml) for the determination of II–IV.

A chromatogram of a standard solution is shown in Fig. 1 and Table I lists the retention times of each compound.

Figure 1 and Table I show a good resolution of each compound. The resolution obtained was always better than 1 for I–V.

A calibration graph was plotted of peak area ratio of the solute to the internal standard against solute concentration. The calibration graph was linear in the concentration range studied and went through the origin, using peak areas as well as peak heights. The correlation coefficients of the linear regression analysis were always better than 0.999 using peak areas as well as peak heights.

The minimum amount detectable, defined as the amount (in micrograms) that gives a peak height equal to twice the background, and the sensitivity, defined as the change in area value (measured at the maximum detector sensitivity) resulting from a concentration change of one unit (milligrams per liter) are given in Table II.

The repeatability tested by five replicates and evaluated by the coefficient of variation was 0.978 (I), 1.064 (II), 1.210 (III), and 1.510% (IV). The average data of duplicate assays for recovery studies on laboratory prepared injections with and without added amounts of II–IV are given in Table III.

A comparative separation of I–IV was carried out on a silica column[8]. With hexane–chloroform–methanol–formic acid (400:200:20:1) as a mobile phase, retention times were ~4 (I), 8 (II), 12 (III), 17 (IV), and 25 min for benzenesulfonamide used as an internal standard. Reversed-phase HPLC was faster (14 min) and more convenient than normal HPLC. The insignificant amounts of II–IV (probably present in the reference drug) detected by injecting 10 μl of a concentrated solution of I (2.5 g/liter) and the accuracy obtained for the determination of trace II–IV reveal that reversed-phase HPLC allows the determination of I–IV without decomposition during analysis.

With GLC, artifact peaks were observed when degradation products were present, and it is suggested (3) that the breakdown of the degradates occurs at the injection port maintained at 230°. HPLC is achieved at ambient temperature and prevents this drawback.

With TLC, a significant oxidation of I on the plate was observed during analysis (1). The iron present in the silica coating was responsible (1) for the accelerated air oxidation of I. The absence of degradation with the HPLC procedure is consistent with this hypothesis. The analysis time (13 min), the absence of air exposure, and the presence of citric acid (chelating agent for iron) in the mobile phase (used as an eluting agent and as a solvent in the preparation of solutions) contribute to prevent the degradation of I.

A commercial injection formulation was analyzed by the proposed HPLC procedure. Compound I was 1000.2 mg (100.0% of the labeled strength), III was 14.92 mg (1.49% with respect to theoretical I content), IV was 21.8 mg (2.18% with respect to theoretical I content), and II was not detected. The results are in agreement with other data (4) that shows II is so readily hydrolyzed into IV that it cannot be found in alkaline solution, and the major products of I degradation in injections are III and IV.

Reversed-phase HPLC is a sensitive (20 times more than TLC) and convenient procedure that can be used to evaluate the purity of phenylbutazone and to monitor its stability in pharmaceutical formulations. Because the metabolites of I have been identified as similar to the degradation products *in vitro*, the method is suggested to be applicable to pharmacokinetic studies.

[8] 30 μm Zorbax Sil, 30-cm length.

REFERENCES

(1) H. Fabre and B. Mandrou, *J. Pharm. Sci.*, **70**, 460 (1981), and references therein.

(2) T. Marunaka, T. Shibata, Y. Minami, and Y. Umeno, *J. Chromatogr.*, **183**, 331 (1980).

(3) J. R. Watson, F. Matsui, R. C. Lawrence, and P. M. J. McConnell, *J. Chromatogr.*, **76**, 141 (1973).

(4) D. V. C. Awang, A. Vincent, and F. Matsui, *J. Pharm. Sci.*, **62**, 1673 (1973).

COMMUNICATIONS

Active Conformation of Polycyclic Antidepressants

Keyphrases □ Antidepressants, polycyclic—active conformation □ Conformation, active—of polycyclic antidepressants

To the Editor:

A 300-MHz ^{1}H-NMR study of a series of polycyclic (tetracyclic and pentacyclic) antidepressant agents of the amitriptyline type indicated a preferred conformation in solution in which the alkylamino side chain is folded toward the polycyclic skeleton and its positively charged dimethylammonium ion is oriented above the adjacent aromatic ring.

Amitriptyline (I) and imipramine, prototype tricyclic antidepressant drugs, are potent inhibitors of active reuptake of biogenic amines in nerve endings. The therapeutic effects of these drugs may be related to this activity[1] (1–5). Reuptake inhibition may lead to an accumulation of neurotransmitters, *e.g.*, norepinephrine and serotonin, at the receptor site and to a subsequent increase in activity. The preferred conformation of the tricyclic antidepressant at the biogenic amine uptake jump may be crucial to their antidepressant activity.

Of particular significance is the conformation of the alkylamino side chain *vis-à-vis* the tricyclic skeleton (6, 7). X-ray structure determinations (8–13) indicated that in the crystalline state the side chain is almost fully extended, away from the tricyclic skeleton. However, it was suggested (6, 14) that the active conformation of the alkylamino side chain in polycyclic antidepressants is folded toward the aromatic ring. We present evidence for the amitriptyline-type series in favor of this hypothesis and

[1] For the state of the art of the mode of action of tricyclic antidepressants, see Horn (5).

0022-3549/82/0100-0122$01.00/0

Table I—^{1}H-NMR $N(CH_3)_2$ Chemical Shifts [a] of I–VI Hydrochlorides in Deuterochloroform (2.4×10^{-5} mole/ml) at 23° and 300 MHz [b]

Compound	$\delta(Z)$	$\delta(E)$	$\Delta\delta = \delta(E) - \delta(Z)$
II	2.633		0
III	2.635	2.693	0.058
IV	2.610	2.706	0.096
V	2.657	2.691	0.034
VI	2.596	2.635	0.039
I	2.680		0

[a] In parts per million relative to tetramethylsilane. [b] Spectra of isomeric mixtures of III–VI were recorded on a Bruker WH-300 spectrometer, FT mode.

establish that the alkylammonium terminus of the side chain is oriented toward and above the plane of the aromatic ring.

The following polycyclic antidepressants were synthesized and evaluated as antidepressants according to their ability to inhibit serotonin uptake into human blood platelets: 6-(3-dimethylaminopropylidene)-13,14-dihydro-6*H*-cyclohepta[1,2-*b*:4,5-*b*′]dinaphthalene (II), 7-(3-dimethylaminopropylidene)-14,15-dihydro-7*H*- cyclohepta[1,2-*a*:4,5-*b*′]dinaphthalene (III), 5-(3-dimethylaminopropylidene)-12,13-dihydro- 5*H* -benzo[4,5]cyclohepta[1,2-*b*]naphthalene (IV), 7-(3-dimethylaminopropylidene) - 12,13-dihydro-7*H*-benzo[4,5]cyclohepta-[1,2-*a*]naphthalene (V), and 7-(3-dimethylaminopropylidene) - 7*H*-benzo[4,5]cyclohepta[1,2 - *a*]naphthalene (VI). These naphthalene variations of the amitriptyline theme that showed comparable activity to the parent drug[2] offered a favorable opportunity to study the conformation of the alkylamino side chain *vis-à-vis* the aromatic ring in solution.

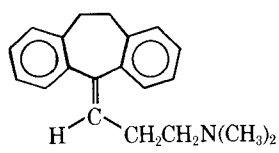

I

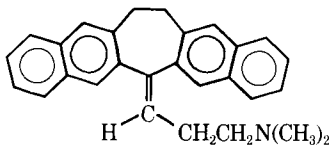

II

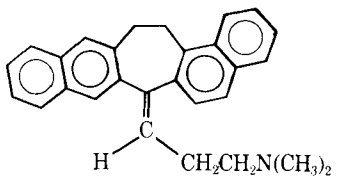

E-III

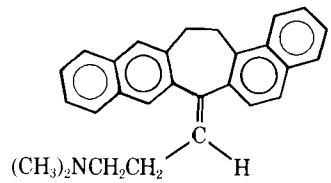

Z-III

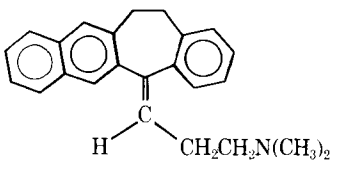

E-IV

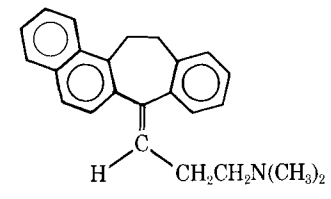

E-V

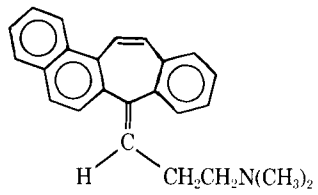

E-VI

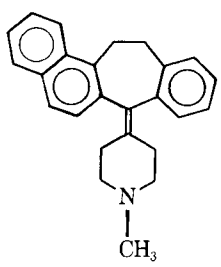

VII

The 300-MHz ^{1}H-NMR chemical shifts of the dimethylamino groups [$\delta N(CH_3)_2$] of I–VI hydrochloride salts in deuterochloroform solution are recorded in Table I. Under the conditions of a superconducting magnet, small differences of chemical shifts (0.001 ppm) in very dilute solutions are detectable and significant. Consider the two symmetric systems, I and II. The long range effect of the naphthalene nuclei in II (as compared with the benzene rings of I) is manifested in the shielding of 0.047 ppm. The unsymmetrical structure of III–VI may exhibit π diastereoisomerism (geometrical isomerism). The presence in each case of the *E* and *Z* isomers is reflected in the ^{1}H-NMR spectrum, which exhibits two vinylic triplets [*e.g.*, δ_1(III) 6.028 (J = 5.9 Hz), δ_2(III) 5.884 (J = 5.9 Hz), $\Delta\delta$ 0.144]. The expected nonequivalence is probably due to an inductive effect and to the proximity of the vinylic proton to the corresponding aromatic nucleus. More significantly, in each pair of *E*, *Z* isomers, the remote dimethylamino protons are also magnetically nonequivalent, leading to two singlets representing the *E* and *Z* isomers.

The barriers for conformational inversion of the seven-membered ring in amitriptyline-type drugs are low. A dynamic NMR study of II revealed a $\Delta G_c^{\neq}$ value of 15.6 kcal/mole (in deuteroacetonitrile). In the more rigid 5-(3-dimethylaminopropylidene)-5*H*-dibenzo[*a*,*d*]cycloheptene, $\Delta G_c^{\neq}$ equals 22.6 kcal/mole (15). Thus, it is unlikely that the two $N(CH_3)_2$ absorptions in each of compounds III–VI are due to two different conformations of the same geometrical isomer. The magnetic nonequivalence of the *N*-methyl groups cannot be ascribed to an inductive effect in view of the number of bonds separating the *N*-methyl protons from the structural perturbation (*E versus Z*) in the polycyclic skeleton. The spatial magnetic environment of the *E*-$N(CH_3)_2$ and *Z*-$N(CH_3)_2$ protons apparently are not identical, thus leading to the observed shifts. The *E*,*Z* assignments (Table I) are based on comparison with the symmetrical drugs I and II. The data indicate that whenever the alkylamino side chain is *Z* to the naphthalene nucleus, δ-$N(CH_3)_2$ is shielded relative to an alkylamino side chain *Z* to the benzene nucleus (II *versus* I, *E*-IV *versus* *Z*-IV, and *E*-V *versus* *Z*-V). In the linearly annelated derivative (*Z*-IV), the long range diamagnetic shielding effect of the naphthalene nucleus is more pronounced than in the angularly annelated derivative *Z*-V, indicating a variation in the proximity of the side chain to the naphthalene (also note *Z*-III *versus* *E*-III).

The observed diamagnetic effect as revealed in the shielding of the *N*-methyl protons is attributed to a preferred conformer of the alkylamino side chain *vis-à-vis* the polycyclic skeleton. The side chain is folded toward the polycyclic system, and the dimethylamino group is oriented above and not in the plane of the aromatic ring (Fig. 1). Such geometry permits interaction between the ammonium-ion terminus and the aromatic π-electron cloud so that the *N*-methyl groups are exposed to the diamagnetic ring current of the aromatic ring. Consistently with

[2] The synthesis of II–VI (hydrochlorides) and their structure–activity relationships will be reported elsewhere.

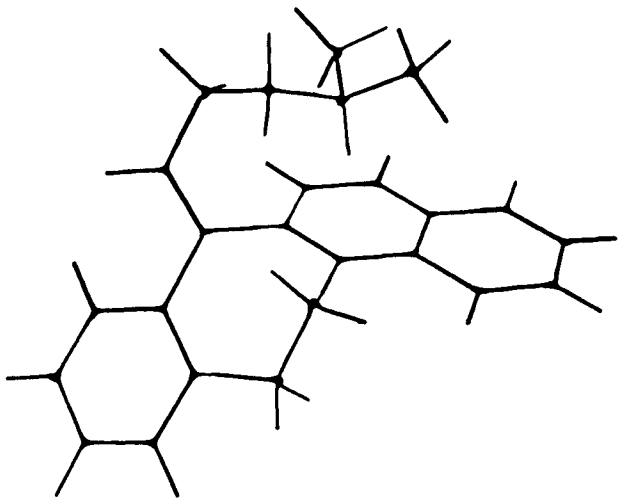

Figure 1—*Preferred conformation of Z-V.*

this picture, the *N*-methylpiperidinylidene analogs of III–VI [*e.g.*, 7-(1-methyl-4-piperidinylidene)-12,13-dihydro-7*H*-benzo[4,5]cyclohepta[1,2-*a*]naphthalene (VII)], in which the nitrogen atoms are rigidly immobilized and positioned away from the polycyclic skeletons, were found to be inactive as inhibitors of serotonin uptake into human blood platelets. The rather considerable difference in $\Delta\delta$ values between IV [$\delta(E\text{-IV}) - \delta(Z\text{-IV}) = 0.096$ ppm] and I–II [$\delta(\text{I}) - \delta(\text{II}) = 0.047$ ppm] should be noted. This difference may be rationalized by considering the conjugation effect of the remote aromatic cycle (*trans* to the side chain) on the diamagnetic ring current of the adjacent aromatic cycle (*cis* to the side chain). The delocalization of the π-electron cloud into the *trans*-aromatic cycle (*via* the exocyclic double bond) weakens the diamagnetic effect of the *cis*-aromatic cycle. This diminution is more pronounced in II (*trans*-naphthalene) than in *Z*-IV (*trans*-benzene) and in *E*-IV than in I. In fact, the order of the net diamagnetic ring current effect is *Z*-IV > II > I > *E*-IV, with the strongest shielding produced by *Z*-IV with its *cis*-naphthalene, *trans*-benzene configuration.

The higher shielding effect in VI relative to V [$\delta(Z\text{-V}) - \delta(Z\text{-VI}) = 0.061$ ppm; $\delta(E\text{-V}) - \delta(E\text{-VI}) = 0.056$ ppm] may be due to the different geometries of the two polycyclic systems. The CH=CH bridge in VI flattens the ring system somewhat, drawing the aromatic surface nearer to the alkylamino side chain. However, the difference in $\Delta\delta$ values between V and VI is very small. It may be concluded that the impact of the *E*,*Z* parameter on the net diamagnetic shielding (due to spatial orientation and conjugation) does not vary significantly from V to VI. A potential energy map for the antidepressant iprindole (as a free base) shows a conformer in which the side chain is folded back toward the plane of the tricyclic system (16). Likewise, in the potent antidepressant *N*,*N*-dimethylspiro[5*H*-dibenzo[*a*,*d*]cyclohepten-5,1′-cyclohexane]-4′ amine, the cyclohexane ring may adopt a boat conformation in which the *N*-methyl group is oriented above the aromatic ring (12, 17).

In a recent conformational structure–activity relationship study of compounds related to tricyclic antidepressants, the projected height of the nitrogen atom over the plane of the nearest aromatic ring seemed to be the most important structural feature (7). The $C^{\gamma}H_2C^{\beta}H_2C^{\alpha}H_2N(CH_3)_2$ side chain of imipramine hydrochloride in a nonaqueous medium (such as deuterochloroform) was shown to exist almost entirely in one fixed conformation with a *gauche* C^{α}–C^{β} and a *trans* C^{β}–C^{γ} fragment (18). The less flexible amitriptyline-type ring system with its rigid exocyclic double bond may be responsible for the preferred active conformation in which the alkylamino side chain is not only folded toward the polycyclic skeleton but its positively charged dimethylammonium ion is oriented above the most adjacent aromatic ring. This effect is manifested even in deuteromethanol solution, which resembles the aqueous physiological environment in which the polycyclic antidepressant agents function: $\Delta\delta(CD_3OD) = \delta(E\text{-III}) - \delta(Z\text{-III}) = 0.045$ ppm. Thus, the preferred conformation of the polycyclic antidepressants in solution is at variance with the conformation in the crystalline state.

(1) A. Carlsson, J. Jonason, and M. Lindqvist, *J. Pharm. Pharmacol.*, **21**, 769 (1969).

(2) L. L. Iversen, *Biochem. Pharmacol.*, **23**, 1927 (1974).

(3) A. S. Horn, *Postgr. Med. J., Suppl. 3*, **52**, 25 (1976).

(4) B. Bopp and J. H. Biel, *Life Sci.*, **14**, 415 (1974).

(5) A. S. Horn, *Postgr. Med. J., Suppl. 1*, **56**, 9 (1980).

(6) M. Wilhelm, *Pharmacol. J.*, **214**, 414 (1975); "Medicinal Chemistry V," J. Mathieu, Ed., Elsevier, Amsterdam, The Netherlands, 1977, p. 173.

(7) T. De Paulis, D. Kelder, S. B. Ross, and N. E. Stjernström, *Mol. Pharmacol.*, **14**, 596 (1978).

(8) K. Hoogsteen, *Acta Crystallogr.*, **21**, A116 (1966).

(9) J. M. Bastian and H. P. Weber, *Helv. Chim. Acta*, **54**, 293 (1971).

(10) J. R. Rodgers, O. Kennard, A. S. Horn, and L. Riva di Sanseverino, *Acta Crystallogr.*, **B30**, 1970 (1974).

(11) M. L. Post, O. Kennard, and A. S. Horn, *Nature*, **252**, 493 (1974); *Acta Crystallogr.*, **B31**, 1008 (1975).

(12) J. R. Rodgers, A. S. Horn, and O. Kennard, *J. Pharm. Pharmacol.*, **27**, 859 (1975).

(13) J. P. Reboul and B. Cristau, *Eur. J. Med. Chem. Chim. Ther.*, **12**, 71 (1977); *Ann. Pharm. Fr.*, **36**, 179 (1978).

(14) R. Sarges, B. K. Koe, A. Weissman, and J. P. Schaefer, *J. Pharmacol. Exp. Ther.*, **191**, 393 (1974).

(15) A. Ebnother, E. Jucker, and A. Stoll, *Helv. Chim. Acta*, **48**, 1237 (1965).

(16) A. S. Horn, O. Kennard, W. D. S. Motherwell, M. L. Post, and J. R. Rodgers, in "Molecular and Quantum Pharmacology," E. D. Bergmann and B. Pullman, Eds., Riedel, Dordrecht, Holland, 1974, pp. 105–118.

(17) B. Carnmalm, E. Jacupovic, L. Johansson, T. de Paulis, R. Rämsby, N. E. Stjernström, A. L. Renyi, S. B. Ross, and S. O. Ögren, *J. Med. Chem.*, **17**, 65 (1974).

(18) R. J. Abraham, L. J. Kricka, and A. Ledwith, *J. Chem. Soc. Perkin. II*, **1974**, 1648.

Yael Asscher
David Avnir
Avner Rotman‡
Israel Agranat ˣ

Department of Organic Chemistry
The Hebrew University of Jerusalem
Jerusalem 91904, Israel
‡ Department of Membrane Research
The Weizmann Institute of Science
Rehovot 76100, Israel

Received March 9, 1981.

Accepted for publication June 25, 1981.

Supported by the Israel Center for Psychobiology–Charles E. Smith Family Foundation.

We thank Professor A. S. Horn (The University, Groningen, The Netherlands) for enlightening discussions.

Potential Errors in Determining Freundlich and Langmuir Constants from Adsorption Isotherms

Keyphrases □ Adsorbents—determination of Freundlich and Langmuir constants, potential errors □ Freundlich constants—potential errors in determination □ Langmuir constants—potential errors in determination

To the Editor:

Numerous pharmaceuticals have been shown to be adsorbed on various adsorbents such as charcoal and kaolin (1–4). Adsorption data are generally presented as Freundlich constants (Eq. 1) and/or Langmuir constants (Eq. 2):

$$\frac{x}{m} = kC^n \quad \text{(Eq. 1)}$$

$$\frac{x}{m} = \frac{\alpha C}{1 + \beta C} \quad \text{(Eq. 2)}$$

where x/m is the amount of drug (grams) adsorbed per gram of adsorbent, C is the equilibrium concentration of unbound drug, k and n are Freundlich constants, and α and β are Langmuir constants.

Freundlich constants are obtained from the logarithmic form of Eq. 1:

$$\log \frac{x}{m} = \log k + n \log C \quad \text{(Eq. 3)}$$

Equation 3 is a straight line equation. When experimental data are plotted as log x/m *versus* log C, the slope equals n and the intercept yields log k. The use of log–log graph paper is popular in plotting such data. Ganjian *et al.* (5) recently utilized log–log graphs to evaluate Freundlich constants for cimetidine adsorption on charcoal, talc, kaolin, and magnesium trisilicate. The intercept was evaluated by directly reading values on the y-axis (*i.e.*, log x/m) where the x-axis shows a value of 1.0. According to Eq. 3, this is correct when the value of C equals 1.0 (log C = 0). Hence, Eq. 3 reduces to

$$\log \frac{x}{m} = \log k \quad \text{(Eq. 4)}$$

and since log–log paper is used, the intercept values read are k values.

Although the x-axis shows the printed value of 1.0 on log–log graph paper, any exponent value of concentration must be considered. In this plot (Fig. 1, Ref. 5), the value of C at the printed value of 1.0 equals 1.0×10^{-5} M. Ganjian *et al.* read the intercept value at the 1.0×10^{-5} M value of C. This is incorrect. To read intercept values graphically, the authors need at least 6-cycle logarithmic graph paper to obtain a value of C = 1.0. The value of an intercept could also be obtained by solving Eq. 3 for log k. Using values obtained by these authors (Table I, Ref. 5) and citing kaolin as an example:

$$\log (4.02 \times 10^{-4}) = \log k + n \log (1 \times 10^{-5})$$

$$= 5.12 \times 10^{-1}$$

The values so obtained are listed in Table I. The value of n remains unaffected. The order of adsorbents according to k value and the value of k are dramatically changed.

Table I—Corrected Freundlich Constants for Adsorption of Cimetidine onto Various Adsorbents

Adsorbent	n[a]	$k \times 10^4$, g(adsorbed)/g(adsorbent)	Corrected Value[b], $k \times 10^1$
Kaolin	0.621	4.02	5.12
Magnesium trisilicate	0.943	3.43	178
Talc	0.384	2.91	0.24
Charcoal	0.347	256	13.91

[a] Reported values (Table I, Ref. 5). [b] The value k evaluated at C = 1.0 M.

Table II—Effect of Equilibrium Concentration Units on the Freundlich Constant

Adsorbent	Freundlich Constant k, g(adsorbed)/g(adsorbent) C, moles/liter	C, g/liter	C, mg %
Kaolin	5.12×10^{-1}	1.65×10^{-2}	9.45×10^{-4}
Magnesium trisilicate	1.78×10^{1}	9.67×10^{-2}	1.26×10^{-3}
Talc	2.42×10^{-2}	2.89×10^{-3}	4.94×10^{-4}
Charcoal	1.39	2.04×10^{-1}	4.13×10^{-2}

The second potential error lies with the usage of proper units. Although concentration is generally expressed in molar or molal quantities, Freundlich isotherms are generally obtained by expressing C values as milligrams percent or grams percent. Since k is an adsorbent capacity when C = 1, the choice of units is particularly important. Using a unit molar concentration when the experimental range is $\sim 1 \times 10^{-5}$ M yields an order of adsorbents that does not coincide with the experimental results of evaluation using other techniques, *e.g.*, Langmuir's equation.

The Freundlich constant k can be readily calculated at any unit concentration. If C is converted into another concentration, C', using a factor f, then Eq. 1 is rewritten as:

$$\frac{x}{m} = \frac{k}{f^n} C'^n f^n \quad \text{(Eq. 5)}$$

where $k/f^n = k'$, a Freundlich constant using another unit concentration. For kaolin, the difference between Freundlich constants calculated using moles/liter and g/liter is $252.34^{0.621}$ (molecular weight of cimetidine = 252.34 g). Similarly, other values can be calculated.

Table II shows the effect of units on the Freundlich constant k. The order of adsorbents according to adsorption capacity (k) can be visually observed from Freundlich isotherms. The order of adsorbents according to the corrected value is magnesium trisilicate > charcoal > kaolin > talc. If isotherm slopes can be visually imagined extending 6 cycles to the right, this order is correct, at least theoretically. However, this order does not reflect its proper order within the experimental range. This result is best achieved by use of other appropriate units such that a unit equilibrium concentration falls reasonably within the experimental range. An equilibrium concentration of 1 mg % (3.962×10^{-5} M) falls well within the range of experimental data. The order obtained is charcoal > magnesium trisilicate > kaolin > talc. This order coincides well with the experimental data.

The Langmuir equation (Eq. 2) can be rearranged to yield the following linear equation.

$$\frac{C}{\frac{x}{m}} = \frac{1}{\alpha} + \frac{\beta}{\alpha} C \quad \text{(Eq. 6)}$$

The plot of $C/(x/m)$ *versus* C yields the value of α from

0022-3549/82/0100-0125$01.00/0

the reciprocal of an intercept and β can be evaluated from the slope.

A visual observation of the intercepts of a Langmuir isotherm (Fig. 2, Ref. 5) shows the order of adsorbents according to α to be charcoal > talc > kaolin > magnesium trisilicate. The calculated values (Table II, Ref. 5) show the order to be charcoal > kaolin > talc > magnesium trisilicate. The discrepancy arises because the calculated value of α for talc is in error[1] and should be ~71.4 (based on an estimated $1/\alpha$ value of 1.4×10^{-2} from Fig. 2, Ref. 5). The corrected values will show that the order coincides well with visually observed intercept values.

It should be noted that, for Langmuir plots, the use of units other than moles/liter for C will not change the order of adsorbents according to α values, since α is evaluated when C equals zero. However, numerical values of α will change.

It is to be expected that the order of adsorbents would be retained regardless of the equation utilized. This would be true if the adsorption isotherms did not cross over, as in this case. The difference in order is due to the fact that the Freundlich constant k is evaluated at unit equilibrium concentration and the Langmuir constant α is evaluated at zero equilibrium concentration. If the isotherms crossed over between zero and a unit concentration, the order of adsorbents would be different.

(1) D. R. Sanvordeker and E. Z. Dajani, *J. Pharm. Sci.*, **64**, 1877 (1975).
(2) E. M. Sellers, V. Knouw, and L. Dolman, *ibid.*, **66**, 1640 (1977).
(3) D. O. Cooney, *ibid.*, **67**, 426 (1978).
(4) B. C. Walker, W. H. Thomas, and B. R. Hajratwala, *Proc. Univ. Otago Med. Sch.*, **57**, 77 (1979).
(5) F. Ganjian, A. J. Cutie, and T. Jochsberger, *J. Pharm. Sci.*, **69**, 352 (1980).

B. R. Hajratwala
Faculty of Pharmacy
Wayne State University
Detroit, MI 48202

Received June 8, 1981
Accepted for publication July 27, 1981

[1] There is also a typographical error in Table II, Ref. 5. Units of α should be given (adsorbed) per gram (adsorbent) and *not* gram (adsorbed) per milligram (adsorbent).

Potential Errors in Determining Freundlich and Langmuir Constants from Adsorption Isotherms: A Response

Keyphrases □ Adsorbents—determination of Freundlich and Langmuir constants, potential errors, reply □ Freundlich constants—potential errors in determination, reply □ Langmuir constants—potential errors in determination, reply

To The Editor:

In a recent publication (1) we calculated Freundlich and Langmuir constants for the adsorption of cimetidine on various adsorbents. A number of points in this article have been criticized by Hajratwala (2) and we wish to respond to some of these criticisms.

We believe the author has incorrectly assumed that the intercepts on which our values were based were read directly from the graph. Actually, both intercepts and slopes were calculated using standard linear regression methods. We also fail to see why 6-cycle paper would be necessary in any case. In addition, we feel that the calculation of the parameters based on a single point, as the author has done, is inappropriate. The accuracy of the values obtained is questionable given the closeness of the logarithmic values employed.

With respect to the use of units, we wish to point out that physical chemistry texts (3, 4) employ molarity as the unit for concentration in determining Freundlich parameters, not milligrams percent or grams percent as suggested by Hajratwala. Indeed, we are puzzled as to why this should make a difference in any case. We agree that utilizing different units will yield different values for the constants. However, one need only state which units are used and this should not affect the relative order of constants.

Finally, we acknowledge the error in Table II as pointed out by the author. The value for α is indeed 70.4 (the intercept being 1.42×10^{-2}) and the correct value of β is 15.2 $\times 10^4$ M^{-1}. We regret the miscalculation. There is a typographical error in Table II as Hajratwala notes; however, we feel that this was a misreading. The correct units are neither g(adsorbed)/mg(adsorbent) as printed nor g(adsorbed)/g (adsorbent) as stated by Hajratwala, but g(adsorbed)/M-g(adsorbent). The capital "M" (for molarity) was obviously misread as a lower case "m."

(1) F. Ganjian, A. J. Cutie, and T. Jochsberger, *J. Pharm. Sci.*, **69**, 352 (1980).
(2) B. R. Hajratwala, *ibid.*, **71**, 125 (1982).
(3) S. H. Maron and J. B. Lando, "Fundamentals of Physical Chemistry," Macmillan, New York, N.Y., 1974, p. 762.
(4) D. P. Shoemaker and C. W. Garland, "Experiments in Physical Chemistry," McGraw-Hill, New York, N.Y., 1967, p. 262.

T. Jochsberger
A. J. Cutie
Division of Pharmaceutics and Industrial Sciences
Arnold & Marie Schwartz College of Pharmacy and Health Sciences
Long Island University
Brooklyn, NY 11201

Received July 30, 1981.
Accepted for publication September 22, 1981

1-Aryl-3,3-dialkyltriazenes with Antitrypanosomal Activity

Keyphrases □ Antitrypanosomal agents—1-aryl-3,3-dialkyltriazenes □ Antitumor agents—1-alkyl-3,3-dialkyltriazenes □ Triazenes, substituted—antitrypanosomal and antitumor activity

To the Editor:

We recently reported the activity of 1-(*p*-tolyl)-3-acetyl-3-methyltriazene (I), against *Trypanosoma rhodesiense* in the mouse (1). We now wish to report that a number of 1-aryl-3-alkyl-3-methyltriazenes (II) have shown significant activity against these parasites in the mouse model.

The synthesis and characterization of the 1-aryl-3-

0022-3549/82/0100-0126$01.00/0

the reciprocal of an intercept and β can be evaluated from the slope.

A visual observation of the intercepts of a Langmuir isotherm (Fig. 2, Ref. 5) shows the order of adsorbents according to α to be charcoal > talc > kaolin > magnesium trisilicate. The calculated values (Table II, Ref. 5) show the order to be charcoal > kaolin > talc > magnesium trisilicate. The discrepancy arises because the calculated value of α for talc is in error[1] and should be ~71.4 (based on an estimated $1/\alpha$ value of 1.4×10^{-2} from Fig. 2, Ref. 5). The corrected values will show that the order coincides well with visually observed intercept values.

It should be noted that, for Langmuir plots, the use of units other than moles/liter for C will not change the order of adsorbents according to α values, since α is evaluated when C equals zero. However, numerical values of α will change.

It is to be expected that the order of adsorbents would be retained regardless of the equation utilized. This would be true if the adsorption isotherms did not cross over, as in this case. The difference in order is due to the fact that the Freundlich constant k is evaluated at unit equilibrium concentration and the Langmuir constant α is evaluated at zero equilibrium concentration. If the isotherms crossed over between zero and a unit concentration, the order of adsorbents would be different.

(1) D. R. Sanvordeker and E. Z. Dajani, *J. Pharm. Sci.*, **64**, 1877 (1975).
(2) E. M. Sellers, V. Knouw, and L. Dolman, *ibid.*, **66**, 1640 (1977).
(3) D. O. Cooney, *ibid.*, **67**, 426 (1978).
(4) B. C. Walker, W. H. Thomas, and B. R. Hajratwala, *Proc. Univ. Otago Med. Sch.*, **57**, 77 (1979).
(5) F. Ganjian, A. J. Cutie, and T. Jochsberger, *J. Pharm. Sci.*, **69**, 352 (1980).

B. R. Hajratwala
Faculty of Pharmacy
Wayne State University
Detroit, MI 48202

Received June 8, 1981
Accepted for publication July 27, 1981

[1] There is also a typographical error in Table II, Ref. 5. Units of α should be given (adsorbed) per gram (adsorbent) and *not* gram (adsorbed) per milligram (adsorbent).

Potential Errors in Determining Freundlich and Langmuir Constants from Adsorption Isotherms: A Response

Keyphrases □ Adsorbents—determination of Freundlich and Langmuir constants, potential errors, reply □ Freundlich constants—potential errors in determination, reply □ Langmuir constants—potential errors in determination, reply

To The Editor:

In a recent publication (1) we calculated Freundlich and Langmuir constants for the adsorption of cimetidine on various adsorbents. A number of points in this article have been criticized by Hajratwala (2) and we wish to respond to some of these criticisms.

We believe the author has incorrectly assumed that the intercepts on which our values were based were read directly from the graph. Actually, both intercepts and slopes were calculated using standard linear regression methods. We also fail to see why 6-cycle paper would be necessary in any case. In addition, we feel that the calculation of the parameters based on a single point, as the author has done, is inappropriate. The accuracy of the values obtained is questionable given the closeness of the logarithmic values employed.

With respect to the use of units, we wish to point out that physical chemistry texts (3, 4) employ molarity as the unit for concentration in determining Freundlich parameters, not milligrams percent or grams percent as suggested by Hajratwala. Indeed, we are puzzled as to why this should make a difference in any case. We agree that utilizing different units will yield different values for the constants. However, one need only state which units are used and this should not affect the relative order of constants.

Finally, we acknowledge the error in Table II as pointed out by the author. The value for α is indeed 70.4 (the intercept being 1.42×10^{-2}) and the correct value of β is 15.2 $\times 10^4$ M^{-1}. We regret the miscalculation. There is a typographical error in Table II as Hajratwala notes; however, we feel that this was a misreading. The correct units are neither g(adsorbed)/mg(adsorbent) as printed nor g(adsorbed)/g (adsorbent) as stated by Hajratwala, but g(adsorbed)/M-g(adsorbent). The capital "M" (for molarity) was obviously misread as a lower case "m."

(1) F. Ganjian, A. J. Cutie, and T. Jochsberger, *J. Pharm. Sci.*, **69**, 352 (1980).
(2) B. R. Hajratwala, *ibid.*, **71**, 125 (1982).
(3) S. H. Maron and J. B. Lando, "Fundamentals of Physical Chemistry," Macmillan, New York, N.Y., 1974, p. 762.
(4) D. P. Shoemaker and C. W. Garland, "Experiments in Physical Chemistry," McGraw-Hill, New York, N.Y., 1967, p. 262.

T. Jochsberger
A. J. Cutie
Division of Pharmaceutics and Industrial Sciences
Arnold & Marie Schwartz College of Pharmacy and Health Sciences
Long Island University
Brooklyn, NY 11201

Received July 30, 1981.
Accepted for publication September 22, 1981

1-Aryl-3,3-dialkyltriazenes with Antitrypanosomal Activity

Keyphrases □ Antitrypanosomal agents—1-aryl-3,3-dialkyltriazenes □ Antitumor agents—1-alkyl-3,3-dialkyltriazenes □ Triazenes, substituted—antitrypanosomal and antitumor activity

To the Editor:

We recently reported the activity of 1-(*p*-tolyl)-3-acetyl-3-methyltriazene (I), against *Trypanosoma rhodesiense* in the mouse (1). We now wish to report that a number of 1-aryl-3-alkyl-3-methyltriazenes (II) have shown significant activity against these parasites in the mouse model.

The synthesis and characterization of the 1-aryl-3-

0022-3549/82/0100-0126$01.00/0

the reciprocal of an intercept and β can be evaluated from the slope.

A visual observation of the intercepts of a Langmuir isotherm (Fig. 2, Ref. 5) shows the order of adsorbents according to α to be charcoal > talc > kaolin > magnesium trisilicate. The calculated values (Table II, Ref. 5) show the order to be charcoal > kaolin > talc > magnesium trisilicate. The discrepancy arises because the calculated value of α for talc is in error[1] and should be ~71.4 (based on an estimated $1/\alpha$ value of 1.4×10^{-2} from Fig. 2, Ref. 5). The corrected values will show that the order coincides well with visually observed intercept values.

It should be noted that, for Langmuir plots, the use of units other than moles/liter for C will not change the order of adsorbents according to α values, since α is evaluated when C equals zero. However, numerical values of α will change.

It is to be expected that the order of adsorbents would be retained regardless of the equation utilized. This would be true if the adsorption isotherms did not cross over, as in this case. The difference in order is due to the fact that the Freundlich constant k is evaluated at unit equilibrium concentration and the Langmuir constant α is evaluated at zero equilibrium concentration. If the isotherms crossed over between zero and a unit concentration, the order of adsorbents would be different.

(1) D. R. Sanvordeker and E. Z. Dajani, *J. Pharm. Sci.*, **64**, 1877 (1975).
(2) E. M. Sellers, V. Knouw, and L. Dolman, *ibid.*, **66**, 1640 (1977).
(3) D. O. Cooney, *ibid.*, **67**, 426 (1978).
(4) B. C. Walker, W. H. Thomas, and B. R. Hajratwala, *Proc. Univ. Otago Med. Sch.*, **57**, 77 (1979).
(5) F. Ganjian, A. J. Cutie, and T. Jochsberger, *J. Pharm. Sci.*, **69**, 352 (1980).

B. R. Hajratwala
Faculty of Pharmacy
Wayne State University
Detroit, MI 48202

Received June 8, 1981
Accepted for publication July 27, 1981

[1] There is also a typographical error in Table II, Ref. 5. Units of α should be given (adsorbed) per gram (adsorbent) and *not* gram (adsorbed) per milligram (adsorbent).

Potential Errors in Determining Freundlich and Langmuir Constants from Adsorption Isotherms: A Response

Keyphrases □ Adsorbents—determination of Freundlich and Langmuir constants, potential errors, reply □ Freundlich constants—potential errors in determination, reply □ Langmuir constants—potential errors in determination, reply

To The Editor:

In a recent publication (1) we calculated Freundlich and Langmuir constants for the adsorption of cimetidine on various adsorbents. A number of points in this article have been criticized by Hajratwala (2) and we wish to respond to some of these criticisms.

We believe the author has incorrectly assumed that the intercepts on which our values were based were read directly from the graph. Actually, both intercepts and slopes were calculated using standard linear regression methods. We also fail to see why 6-cycle paper would be necessary in any case. In addition, we feel that the calculation of the parameters based on a single point, as the author has done, is inappropriate. The accuracy of the values obtained is questionable given the closeness of the logarithmic values employed.

With respect to the use of units, we wish to point out that physical chemistry texts (3, 4) employ molarity as the unit for concentration in determining Freundlich parameters, not milligrams percent or grams percent as suggested by Hajratwala. Indeed, we are puzzled as to why this should make a difference in any case. We agree that utilizing different units will yield different values for the constants. However, one need only state which units are used and this should not affect the relative order of constants.

Finally, we acknowledge the error in Table II as pointed out by the author. The value for α is indeed 70.4 (the intercept being 1.42×10^{-2}) and the correct value of β is 15.2 $\times 10^4$ M^{-1}. We regret the miscalculation. There is a typographical error in Table II as Hajratwala notes; however, we feel that this was a misreading. The correct units are neither g(adsorbed)/mg(adsorbent) as printed nor g(adsorbed)/g (adsorbent) as stated by Hajratwala, but g(adsorbed)/M-g(adsorbent). The capital "M" (for molarity) was obviously misread as a lower case "m."

(1) F. Ganjian, A. J. Cutie, and T. Jochsberger, *J. Pharm. Sci.*, **69**, 352 (1980).
(2) B. R. Hajratwala, *ibid.*, **71**, 125 (1982).
(3) S. H. Maron and J. B. Lando, "Fundamentals of Physical Chemistry," Macmillan, New York, N.Y., 1974, p. 762.
(4) D. P. Shoemaker and C. W. Garland, "Experiments in Physical Chemistry," McGraw-Hill, New York, N.Y., 1967, p. 262.

T. Jochsberger
A. J. Cutie
Division of Pharmaceutics and Industrial Sciences
Arnold & Marie Schwartz College of Pharmacy and Health Sciences
Long Island University
Brooklyn, NY 11201

Received July 30, 1981.
Accepted for publication September 22, 1981

1-Aryl-3,3-dialkyltriazenes with Antitrypanosomal Activity

Keyphrases □ Antitrypanosomal agents—1-aryl-3,3-dialkyltriazenes □ Antitumor agents—1-alkyl-3,3-dialkyltriazenes □ Triazenes, substituted—antitrypanosomal and antitumor activity

To the Editor:

We recently reported the activity of 1-(*p*-tolyl)-3-acetyl-3-methyltriazene (I), against *Trypanosoma rhodesiense* in the mouse (1). We now wish to report that a number of 1-aryl-3-alkyl-3-methyltriazenes (II) have shown significant activity against these parasites in the mouse model.

The synthesis and characterization of the 1-aryl-3-

0022-3549/82/0100-0126$01.00/0

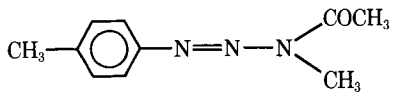

I

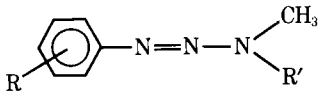

R′ = alkyl

II

alkyl-3-methyltriazenes were reported previously (2, 3). The triazenes were tested against *T. rhodesiense* (Wellcome CT strain) in the mouse (ICR/HA Swiss) (4). Test and control mice were 6 weeks old and weighed 28–30 g. No differences in response between male and female mice have been reported. Each mouse was infected with an intraperitoneal injection of 0.05 ml of a 1:50,000 dilution of heparinized heart blood drawn from donor mice infected 3 days earlier.

Drugs were administered subcutaneously as a single dose in peanut oil 2 hr after injection. Untreated mice died between 4.2 and 4.5 days after injection. Surviving animals were observed for 30 days and mice surviving after this time were considered cured. The surviving mice were not checked for parasitemia. Test data are given in Table I. The activities of some of the compounds against Sarcoma-180 in the mouse are also included.

The activities reported in Table I suggest that triazenes have curative effects against *T. rhodesiense* in mice. However, high doses are required to produce these effects. It has been suggested that similarities exist between some metabolic pathways of the predominant bloodstream form of the African trypanosome and tumor cells (5) and it was shown that a number of anticancer agents are active against *T. rhodesiense* (6). This correlation was also suggested by the data in Table I when a comparison was made of those activities for the compounds on which both types of data were determined. Compounds 2 and 4 are active in both test systems. Compounds 1 and 3 also were reported to be active against murine leukemia L-1210 in the mouse while the *p*-phenyl analog of II (compound 5) is inactive against *T. rhodesiense*, S-180, and L-1210 (7).

Table I—Activity of II against *T. rhodesiense* Infection in Mice

	R	R′	Dose, mg/kg ip	Antitrypanosomal Activity[a]	Anticancer Activity[b]
1	*p*-COOH	CH_3	424	4/5	
			424[c]	5/5	
2	*m*-COOH	CH_3	424	1/5	3.01[d]
3	*p*-NHCO-CH_3	CH_3	424	2/5	
			212	1/5	
			424[c]	2/5	
4	*p*-NO_2	CH_3	424	3/5	3.43[d]
			212	1/5	
			424[c]	3/5	
5	*p*-C_6H_5	CH_3	424	Inactive	Inactive
6	*m*-CF_3	CH_3	424	Inactive	3.18[e]
7	*m*-Cl	CH_3	424	Inactive	3.16[e]
8	*p*-COOH	$CH_2C_6H_5$	424	Inactive	Inactive[e]
9	*p*-COOH	$CH_2C_6H_4$-*p*-CH_3	424	Inactive	3.25[e]
10	*p*-COOH	$CH_2C_6H_4$-*p*-OCH_3	424	Inactive	Inactive[e]
11	*p*-COOH	$CH_2C_6H_4$-*p*-NO_2	424	Inactive	Inactive[e]
12	*p*-COOH	$CH_2C_6H_4$-*p*-CN	424	Inactive	Weakly active[e]
13	*p*-CN	$CH_2C_6H_4$-*p*-CH_3	424	Inactive	Inactive[e]
14	*p*-CN	$CH_2C_6H_4$-*p*-Cl	424	Inactive	Inactive[e]

[a] Cures per five treated animals. [b] Activity is given as $-\log C$; C is the moles/kg required to give an increase life span of 130% of control. Tumor was S-180 in the mouse. [c] Duplicate. [d] From reference 2. [e] From reference 3.

The exact mechanism of the anticancer action of the trianzenes is not known but it is known that the 3,3-dialkyltriazenes undergo extensive metabolic *N*-dealkylation to produce alkylating intermediates (8). This metabolic pathway to activation could be host-mediated or it could also be present in the African trypanosome and be involved in the mechanism of action of the triazenes against this parasite. The antitrypanosomal activities of triazenes are being studied further.

(1) W. J. Dunn, III, J. Powers, J. B. Kaddu, and A. R. Njogu, *J. Pharm. Sci.*, **69**, 1465 (1980).

(2) W. J. Dunn, III, S. Callijas, and M. J. Greenberg, *J. Med. Chem.*, **19**, 1299 (1976).

(3) W. J. Dunn, III and M. J. Greenberg, *J. Pharm. Sci.*, **66**, 1416 (1977).

(4) L. Rane, D. S. Rane, and K. E. Kinnamon, *Am. J. Trop. Med. Hyg.*, **25**, 395 (1976).

(5) P. Borst, *Trans. R. Soc. Trop. Med. Hyg.*, **71**, 3 (1977); C. J. Bacchi, H. C. Nathan, S. H. Hunter, P. P. McCann, and A. Sjoerdsma, *Science*, **210**, 332 (1980).

(6) K. E. Kinnamon, E. A. Steck, and D. S. Rane, *Antimicrob. Agents Chemother.*, **15**, 157 (1979).

(7) G. J. Hathaway, K. H. Kim, S. R. Milstein, C. R. Schmidt, N. R. Smith, and F. R. Quinn, *J. Med. Chem.*, **21**, 563 (1978).

(8) R. Preussman and H. Hengy, *Biochem. Pharmacol.*, **18**, 1 (1969).

W. J. Dunn, III ˣ
Michael Greenberg
Janice Powers
College of Pharmacy
Department of Medicinal Chemistry
University of Illinois at the Medical Center
Chicago, IL 60612

Received July 10, 1981.

Accepted for publication September 4, 1981.

Supported in part by the UNDP/World Bank/World Health Organization Special Program for Research and Training in Tropical Diseases.

We thank Dr. T. Sweeney, Walter Reed Army Institute of Research, for obtaining the antitrypanosomal test data reported in Table I.

Comparison of Equilibrium Times in Dialysis Experiments Using Spiked Plasma or Spiked Buffer

Keyphrases □ Equilibrium dialysis—comparison of spiked plasma and spiked buffer □ Protein binding—effect of spiked plasma and spiked buffer on equilibrium dialysis

To the Editor:

When the plasma protein binding of a drug is to be determined using equilibrium dialysis *in vitro*, the drug can be added to either the buffer side or the plasma side of a dialysis cell. Adding drug to the plasma will dilute the plasma proteins if the drug has to be added as a solution. Adding the drug solution to the buffer avoids this difficulty. However, the approach to equilibrium is slower when the buffer is spiked than when the plasma is spiked. Under conditions where the equilibrium conditions can change

0022-3549/82/0100-0127$01.00/0

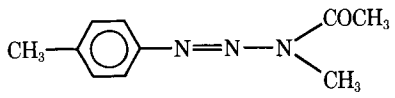

I

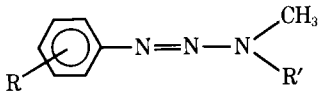

R′ = alkyl

II

alkyl-3-methyltriazenes were reported previously (2, 3). The triazenes were tested against *T. rhodesiense* (Wellcome CT strain) in the mouse (ICR/HA Swiss) (4). Test and control mice were 6 weeks old and weighed 28–30 g. No differences in response between male and female mice have been reported. Each mouse was infected with an intraperitoneal injection of 0.05 ml of a 1:50,000 dilution of heparinized heart blood drawn from donor mice infected 3 days earlier.

Drugs were administered subcutaneously as a single dose in peanut oil 2 hr after injection. Untreated mice died between 4.2 and 4.5 days after injection. Surviving animals were observed for 30 days and mice surviving after this time were considered cured. The surviving mice were not checked for parasitemia. Test data are given in Table I. The activities of some of the compounds against Sarcoma-180 in the mouse are also included.

The activities reported in Table I suggest that triazenes have curative effects against *T. rhodesiense* in mice. However, high doses are required to produce these effects. It has been suggested that similarities exist between some metabolic pathways of the predominant bloodstream form of the African trypanosome and tumor cells (5) and it was shown that a number of anticancer agents are active against *T. rhodesiense* (6). This correlation was also suggested by the data in Table I when a comparison was made of those activities for the compounds on which both types of data were determined. Compounds 2 and 4 are active in both test systems. Compounds 1 and 3 also were reported to be active against murine leukemia L-1210 in the mouse while the *p*-phenyl analog of II (compound 5) is inactive against *T. rhodesiense*, S-180, and L-1210 (7).

Table I—Activity of II against *T. rhodesiense* Infection in Mice

	R	R′	Dose, mg/kg ip	Antitrypanosomal Activity[a]	Anticancer Activity[b]
1	*p*-COOH	CH_3	424	4/5	
			424[c]	5/5	
2	*m*-COOH	CH_3	424	1/5	3.01[d]
3	*p*-NHCO-CH_3	CH_3	424	2/5	
			212	1/5	
			424[c]	2/5	
4	*p*-NO_2	CH_3	424	3/5	3.43[d]
			212	1/5	
			424[c]	3/5	
5	*p*-C_6H_5	CH_3	424	Inactive	Inactive
6	*m*-CF_3	CH_3	424	Inactive	3.18[e]
7	*m*-Cl	CH_3	424	Inactive	3.16[e]
8	*p*-COOH	$CH_2C_6H_5$	424	Inactive	Inactive[e]
9	*p*-COOH	$CH_2C_6H_4$-*p*-CH_3	424	Inactive	3.25[e]
10	*p*-COOH	$CH_2C_6H_4$-*p*-OCH_3	424	Inactive	Inactive[e]
11	*p*-COOH	$CH_2C_6H_4$-*p*-NO_2	424	Inactive	Inactive[e]
12	*p*-COOH	$CH_2C_6H_4$-*p*-CN	424	Inactive	Weakly active[e]
13	*p*-CN	$CH_2C_6H_4$-*p*-CH_3	424	Inactive	Inactive[e]
14	*p*-CN	$CH_2C_6H_4$-*p*-Cl	424	Inactive	Inactive[e]

[a] Cures per five treated animals. [b] Activity is given as $-\log C$; C is the moles/kg required to give an increase life span of 130% of control. Tumor was S-180 in the mouse. [c] Duplicate. [d] From reference 2. [e] From reference 3.

The exact mechanism of the anticancer action of the trianzenes is not known but it is known that the 3,3-dialkyltriazenes undergo extensive metabolic *N*-dealkylation to produce alkylating intermediates (8). This metabolic pathway to activation could be host-mediated or it could also be present in the African trypanosome and be involved in the mechanism of action of the triazenes against this parasite. The antitrypanosomal activities of triazenes are being studied further.

(1) W. J. Dunn, III, J. Powers, J. B. Kaddu, and A. R. Njogu, *J. Pharm. Sci.*, **69**, 1465 (1980).

(2) W. J. Dunn, III, S. Callijas, and M. J. Greenberg, *J. Med. Chem.*, **19**, 1299 (1976).

(3) W. J. Dunn, III and M. J. Greenberg, *J. Pharm. Sci.*, **66**, 1416 (1977).

(4) L. Rane, D. S. Rane, and K. E. Kinnamon, *Am. J. Trop. Med. Hyg.*, **25**, 395 (1976).

(5) P. Borst, *Trans. R. Soc. Trop. Med. Hyg.*, **71**, 3 (1977); C. J. Bacchi, H. C. Nathan, S. H. Hunter, P. P. McCann, and A. Sjoerdsma, *Science*, **210**, 332 (1980).

(6) K. E. Kinnamon, E. A. Steck, and D. S. Rane, *Antimicrob. Agents Chemother.*, **15**, 157 (1979).

(7) G. J. Hathaway, K. H. Kim, S. R. Milstein, C. R. Schmidt, N. R. Smith, and F. R. Quinn, *J. Med. Chem.*, **21**, 563 (1978).

(8) R. Preussman and H. Hengy, *Biochem. Pharmacol.*, **18**, 1 (1969).

W. J. Dunn, III ˣ
Michael Greenberg
Janice Powers
College of Pharmacy
Department of Medicinal Chemistry
University of Illinois at the Medical Center
Chicago, IL 60612

Received July 10, 1981.

Accepted for publication September 4, 1981.

Supported in part by the UNDP/World Bank/World Health Organization Special Program for Research and Training in Tropical Diseases.

We thank Dr. T. Sweeney, Walter Reed Army Institute of Research, for obtaining the antitrypanosomal test data reported in Table I.

Comparison of Equilibrium Times in Dialysis Experiments Using Spiked Plasma or Spiked Buffer

Keyphrases □ Equilibrium dialysis—comparison of spiked plasma and spiked buffer □ Protein binding—effect of spiked plasma and spiked buffer on equilibrium dialysis

To the Editor:

When the plasma protein binding of a drug is to be determined using equilibrium dialysis *in vitro*, the drug can be added to either the buffer side or the plasma side of a dialysis cell. Adding drug to the plasma will dilute the plasma proteins if the drug has to be added as a solution. Adding the drug solution to the buffer avoids this difficulty. However, the approach to equilibrium is slower when the buffer is spiked than when the plasma is spiked. Under conditions where the equilibrium conditions can change

0022-3549/82/0100-0127$01.00/0

with time, as is seen with quinidine (1), it is important to realize the difference in the time to approach equilibrium between adding drug to plasma and buffer.

For the following discussion, the associating and dissociation rates are assumed to be fast in comparison to the diffusion across the dialysis membrane. Furthermore, it is also assumed that there is the same volume V on both sides of the dialysis membrane, and no net flux of water takes place. In addition, the rate of transfer across the membrane is assumed to be covered by a clearance term Cl_T, which is the same in both directions, and the unbound concentration on each side. The binding is assumed to be linear and no net loss of drug occurs during dialysis.

The rate of change in the buffer side can be expressed by:

$$\frac{dA_B}{dt} = -Cl_T C_B + Cl_T \alpha C_p \qquad \text{(Eq. 1)}$$

where A_B is the amount on the buffer side, α is the unbound fraction in plasma, C_B the buffer concentration, and C_p the plasma concentration of drug. The rate of change in the plasma side is expressed by:

$$\frac{dA_p}{dt} = -Cl_T \alpha C_p + Cl_T C_B \qquad \text{(Eq. 2)}$$

where A_p is the amount on the plasma side.

When the drug initially is placed on the plasma side, the concentration on the buffer side is then described by:

$$C_B = \frac{C_0 \alpha}{1+\alpha}\left[1 - e^{-(k_T\alpha + k_T)t}\right] \qquad \text{(Eq. 3)}$$

where t is time, C_0 initial concentration, and k_T the ratio Cl_T/V.

When the drug initially is placed on the buffer side, the buffer side concentration is described by:

$$C_B = \frac{C_0}{1+\alpha}\left[\alpha + e^{-(k_T\alpha + k_T)t}\right] \qquad \text{(Eq. 4)}$$

In both cases the concentration approaches the equilibrium concentration $(C_0\,\alpha)/(1+\alpha)$ when $t \to \infty$. One can determine from Eqs. 3 and 4 the time that is needed to reach a value that is only a fraction, δ, away from the equilibrium concentration; *i.e.*, the time required to reach a buffer concentration of $[(C_0\,\alpha)/(1+\alpha)]\,(1-\delta)$ if the drug is placed initially on the plasma side and $[(C_0\,\alpha)/1+\alpha]\,(1+\delta)$ if it is placed initially on the buffer side. The ratio of the times to reach these concentration is then:

$$R = \frac{t_B}{t_p} = \frac{\ln\left\{\left[\left(\frac{C_0\alpha}{1+\alpha}\right)(1+\delta)\Big/\frac{C_0}{1+\alpha}\right] - \alpha\right\}}{-(k_T\,\alpha + k_T)} \qquad \text{(Eq. 5)}$$

$$\frac{\ln\left\{\left[-\frac{C_0\,\alpha}{1+\alpha}(1-\delta)\Big/\frac{C_0\,\alpha}{1+\alpha}\right] + 1\right\}}{-(k_T\,\alpha + k_T)} \qquad \text{(Eq. 5)}$$

where t_p and t_B are the times to reach equilibrium when the drug is initially added to the plasma and buffer side, respectively. Cancelling the common terms gives:

$$R = \frac{t_B}{t_p} = \frac{\ln\delta + \ln\alpha}{\ln\delta} = 1 + \frac{\ln\alpha}{\ln\delta} \qquad \text{(Eq. 6)}$$

Equation 6 indicates that the closer to the true equilibrium value one wants to be, the closer the ratio is to unity. The stronger the binding and the larger the deviation from the true equilibrium concentration, the greater the advantage of spiking the plasma side.

(1) T. W. Guentert and S. Øie, *J. Pharm. Sci.*, in press.

Svein Øie ˣ
Theodor W. Guentert
School of Pharmacy
University of California
San Francisco, CA 94143

Received May 11, 1981.
Accepted for publication July 28, 1981.
T. W. Guentert is grateful for a postdoctoral fellowship received from the Swiss National Science Foundation.

Stability of Heparin and Other Fractions of Glycosaminoglycan Sulfates in Human Digestive Juices

Keyphrases □ Heparin—stability in human digestive juices □ Glycosaminoglycan sulfates—stability in human digestive juices □ Absorption, intestinal—stability of heparin and glycosaminoglycan sulfates

To the Editor:

The oral administration of heparin has been a subject of controversy (1) because of its uncertain absorption in the GI tract and its stability in digestive juices. Its N-sulfate groups are easily hydrolyzed in an acidic medium, with consequent impairment of biological activity. Some authors (2) also affirmed that intestinal flora degrades and metabolizes heparin.

However, according to recent studies (3, 4), some fractions of glycosaminoglycan sulfates, strictly correlated to heparin, exerted antithrombotic and hypolipidemic activities after oral administration. Furthermore, it was proved that intestinal absorption took place when some fractions of glycosaminoglycan sulfates, labeled with fluorescein (5), were administered intraduodenally (6).

Special excipients to suppress ionization of the functional groups of glycosaminoglycan sulfates and, thus, to promote their GI absorption (7) were studied. It was found that, if biopolymer is administered in micellar suspension with monoolein and bile salts, the intestinal absorption of heparin greatly increases with increasing mucosa permeability (8). For example, the rectal administration to rats of heparin and other glycosaminoglycan sulfates in a 2-mg/kg dose in an oily emulsion prolonged the time of coagulation; only 1 mg/kg, administered by the same route, activated the lipoprotein lipase-inducing system (9).

To evaluate if and to what extent human digestive juices can degrade glycosaminoglycan sulfates, we investigated the stability and biological activity of heparin and a standardized mixture[1] of fractions of glycosaminoglycan sulfates, containing a heparin-like substance with a low molecular weight and condroitin sulfate B, in cat and human gastric and duodenal juices.

Glycosaminoglycan sulfates and heparin were incubated at concentrations of 190 and 238 USP/ml, respectively, for up to 3 hr in digestive juices[2] at 37°. To evaluate the in-

[1] Sulodexide.
[2] Gastric juice of the cat was obtained by a Heidenhain gastric pouch. Human gastric juice was obtained from a probe of five volunteers who had previously been given an injection of 3 U of cholecystokinin kg/hr iv.

0022-3549/82/0100-0128$01.00/0

with time, as is seen with quinidine (1), it is important to realize the difference in the time to approach equilibrium between adding drug to plasma and buffer.

For the following discussion, the associating and dissociation rates are assumed to be fast in comparison to the diffusion across the dialysis membrane. Furthermore, it is also assumed that there is the same volume V on both sides of the dialysis membrane, and no net flux of water takes place. In addition, the rate of transfer across the membrane is assumed to be covered by a clearance term Cl_T, which is the same in both directions, and the unbound concentration on each side. The binding is assumed to be linear and no net loss of drug occurs during dialysis.

The rate of change in the buffer side can be expressed by:

$$\frac{dA_B}{dt} = -Cl_T C_B + Cl_T \alpha C_p \qquad \text{(Eq. 1)}$$

where A_B is the amount on the buffer side, α is the unbound fraction in plasma, C_B the buffer concentration, and C_p the plasma concentration of drug. The rate of change in the plasma side is expressed by:

$$\frac{dA_p}{dt} = -Cl_T \alpha C_p + Cl_T C_B \qquad \text{(Eq. 2)}$$

where A_p is the amount on the plasma side.

When the drug initially is placed on the plasma side, the concentration on the buffer side is then described by:

$$C_B = \frac{C_0 \alpha}{1+\alpha}\left[1 - e^{-(k_T\alpha + k_T)t}\right] \qquad \text{(Eq. 3)}$$

where t is time, C_0 initial concentration, and k_T the ratio Cl_T/V.

When the drug initially is placed on the buffer side, the buffer side concentration is described by:

$$C_B = \frac{C_0}{1+\alpha}\left[\alpha + e^{-(k_T\alpha + k_T)t}\right] \qquad \text{(Eq. 4)}$$

In both cases the concentration approaches the equilibrium concentration $(C_0\,\alpha)/(1+\alpha)$ when $t \to \infty$. One can determine from Eqs. 3 and 4 the time that is needed to reach a value that is only a fraction, δ, away from the equilibrium concentration; *i.e.*, the time required to reach a buffer concentration of $[(C_0\,\alpha)/(1+\alpha)]\,(1-\delta)$ if the drug is placed initially on the plasma side and $[(C_0\,\alpha)/1+\alpha]\,(1+\delta)$ if it is placed initially on the buffer side. The ratio of the times to reach these concentration is then:

$$R = \frac{t_B}{t_p} = \frac{\ln\left\{\left[\left(\frac{C_0\alpha}{1+\alpha}\right)(1+\delta)\Big/\frac{C_0}{1+\alpha}\right] - \alpha\right\}}{-(k_T\,\alpha + k_T)} \qquad \text{(Eq. 5)}$$

$$\frac{\ln\left\{\left[-\frac{C_0\,\alpha}{1+\alpha}(1-\delta)\Big/\frac{C_0\,\alpha}{1+\alpha}\right] + 1\right\}}{-(k_T\,\alpha + k_T)} \qquad \text{(Eq. 5)}$$

where t_p and t_B are the times to reach equilibrium when the drug is initially added to the plasma and buffer side, respectively. Cancelling the common terms gives:

$$R = \frac{t_B}{t_p} = \frac{\ln\delta + \ln\alpha}{\ln\delta} = 1 + \frac{\ln\alpha}{\ln\delta} \qquad \text{(Eq. 6)}$$

Equation 6 indicates that the closer to the true equilibrium value one wants to be, the closer the ratio is to unity. The stronger the binding and the larger the deviation from the true equilibrium concentration, the greater the advantage of spiking the plasma side.

(1) T. W. Guentert and S. Øie, *J. Pharm. Sci.*, in press.

Svein Øie ˣ
Theodor W. Guentert
School of Pharmacy
University of California
San Francisco, CA 94143

Received May 11, 1981.
Accepted for publication July 28, 1981.
T. W. Guentert is grateful for a postdoctoral fellowship received from the Swiss National Science Foundation.

Stability of Heparin and Other Fractions of Glycosaminoglycan Sulfates in Human Digestive Juices

Keyphrases □ Heparin—stability in human digestive juices □ Glycosaminoglycan sulfates—stability in human digestive juices □ Absorption, intestinal—stability of heparin and glycosaminoglycan sulfates

To the Editor:

The oral administration of heparin has been a subject of controversy (1) because of its uncertain absorption in the GI tract and its stability in digestive juices. Its N-sulfate groups are easily hydrolyzed in an acidic medium, with consequent impairment of biological activity. Some authors (2) also affirmed that intestinal flora degrades and metabolizes heparin.

However, according to recent studies (3, 4), some fractions of glycosaminoglycan sulfates, strictly correlated to heparin, exerted antithrombotic and hypolipidemic activities after oral administration. Furthermore, it was proved that intestinal absorption took place when some fractions of glycosaminoglycan sulfates, labeled with fluorescein (5), were administered intraduodenally (6).

Special excipients to suppress ionization of the functional groups of glycosaminoglycan sulfates and, thus, to promote their GI absorption (7) were studied. It was found that, if biopolymer is administered in micellar suspension with monoolein and bile salts, the intestinal absorption of heparin greatly increases with increasing mucosa permeability (8). For example, the rectal administration to rats of heparin and other glycosaminoglycan sulfates in a 2-mg/kg dose in an oily emulsion prolonged the time of coagulation; only 1 mg/kg, administered by the same route, activated the lipoprotein lipase-inducing system (9).

To evaluate if and to what extent human digestive juices can degrade glycosaminoglycan sulfates, we investigated the stability and biological activity of heparin and a standardized mixture[1] of fractions of glycosaminoglycan sulfates, containing a heparin-like substance with a low molecular weight and condroitin sulfate B, in cat and human gastric and duodenal juices.

Glycosaminoglycan sulfates and heparin were incubated at concentrations of 190 and 238 USP/ml, respectively, for up to 3 hr in digestive juices[2] at 37°. To evaluate the in-

[1] Sulodexide.
[2] Gastric juice of the cat was obtained by a Heidenhain gastric pouch. Human gastric juice was obtained from a probe of five volunteers who had previously been given an injection of 3 U of cholecystokinin kg/hr iv.

0022-3549/82/0100-0128$01.00/0

Table I—Activities of Glycosaminoglycan Sulfates after Incubation in Human Digestive Juices

Substance	Time of incubation, min	Residual activity[a] Lipasemic	Anticoagulant
	In Human Gastric Juice, pH 1.4		
Heparin	0	100	100
	5	97	—
	15	95	97
	60	93	100
	180	93	98
Standardized extracts of glycosaminoglycans	0	100	100
	5	—	—
	15	97	107
	60	98	110
	180	105	109
	In Human Duodenal Juice, pH 8.5		
Heparin	0	100	100
	5	—	—
	15	95	97
	60	—	—
	180	98	92
Standardized extracts of glycosaminoglycans	0	100	100
	5	87	102
	15	92	94
	60	98	100
	180	95	96

[a] The values are expressed as percent of initial activity.

fluence of dilution, stability tests were carried out in which the concentrations of heparin and the standardized mixture of glycosaminoglycan sulfates were 19 and 23.8 USP/ml, respectively. Anticoagulant and lipoprotein–lipase-inducing activities were measured in relation to the time of incubation by means of *in vitro* and *in vivo* quantitative methods. Lipoprotein–lipase activity was measured by a turbidimetric method[3].

Anticoagulant action *in vivo* was evaluated by thrombin time with an aliquot of the same plasma used for the determination of lipoprotein–lipase releasing action *in vivo* by the ediol method. All coagulation times were determined automatically.

The biological activity pattern of heparin and other glycosaminoglycan sulfates remained unchanged during the experimental time period, although some variability in biological assessment occurred (Table I).

The confirmed biological activity shows that the nature and conformation of even the more labile chemical groups of glycosaminoglycan sulfates remain unaltered, despite being incubated in chemically and enzymatically aggressive environments such as digestive juices.

(1) L. B. Jaques and J. M. Mahadoo, *Semin. Thromb. Hemostasis*, **4**, 298 (1978).

(2) A. A. Salyers, *Am. J. Clin. Nutr.* **31**, 128 (1978); *Ibid.*, **32**, 158 (1979).

(3) A. K. Sim, "Fifth International Congress on Thromboembolism," Bologna, Italy, May 29–June 2, 1978.

(4) R. Niada, M. Mantovani, and R. Pescador, *Pharmacol. Res. Commun.*, **11**, 349 (1979).

(5) K. Nagasawa and H. Uchiyama, *Biochim. Biophys. Acta*, **544**, 430 (1978).

(6) J. R. Vercellotti, "Hearing on Hypolipidemic Drugs" (Rome, Italy, June 2–3, 1980), Raven, New York, N.Y., in press.

(7) T. K. Sue, L. B. Jaques, and E. Yuen, *Can. J. Physiol. Pharmacol.*, **54**, 613 (1976).

(8) Y. Tokunaga, S. Muranishi, and H. Sezaki, *J. Pharmacobio-Dyn.*, **1**, 28 (1978).

(9) G. P. Corbelli, L. Stanzani, and P. I. Bianchini, "VII International Symposium on Drugs Affecting Lipid Metabolism," Milan, Italy, May 28–31, 1980.

(10) P. Bianchini, B. Osima, and G. Guidi, *Biochem. Exp. Biol.*, **10**, 243 (1972).

[3] This method is based on the capability of rat plasma, treated with glycosaminoglycan sulfates previously (10 min before), to clear an artificial fatty ediol–water suspension. The clearing effect is proportional to the administered amount of glycosaminoglycan sulfates (10).

Mario Brufani
Cattedra di Chimica Farmaceutica
Gruppo di Chimica Biologica
e Strutturistica Chimica
Università di Roma
Rome, Italy

Gianpaolo Corbelli
Giuseppe Mascellani[x]
Luciano Stanzani
Laboratori Ricerche Alfa Farmaceutici S.P.A.
Via Ragazzi del'99 n.5
40133 Bologna, Italy

Received December 15, 1980.
Accepted for publication May 14, 1981.

Adsorption of Methotrexate onto Glassware and Syringes

Keyphrases □ Methotrexate—adsorption onto glassware and syringes □ Adsorption—methotrexate onto glassware and syringes

To the Editor:

Methotrexate, a potent antifolate, is a widely used antineoplastic agent (1). With the advent of high-dose therapy and citrovorum-factor rescue, monitoring of plasma concentrations of methotrexate is recommended (1–4). However, the potential interference of active metabolites, such as 7-hydroxymethotrexate and 4-amino-4-deoxy-N^{10}-methylpteroic acid, renders many assay methods nonspecific (5). A need for re-evaluation of past pharmacokinetic studies has been advocated (6). Hence, development of specific and sensitive assay methods is required. In our recent development of a high-performance liquid chromatographic (HPLC) assay for methotrexate and its metabolites in biological fluids (7), erratic results were often found when series dilutions of methotrexate in water-miscible organic solvents such as methanol were made. These organic solvents were used to enhance the aqueous solubility of methotrexate (8).

Additional studies were carried out to explore the potential interaction between methotrexate and glassware or syringes. This communication reports the results of our preliminary adsorption studies, and discusses its implication in quantitative analysis.

Stock solutions (0.1 mg/ml) of methotrexate were prepared in distilled water, methanol, or 80% ethanol (with 20% water, v/v) using 100-ml volumetric flasks[1]. Series dilutions were made to concentrations of 50, 10, and 1 μg/ml. After mixing and equilibration overnight, the methotrexate concentration was determined directly by the HPLC method described earlier (7). A cation-exchange

[1] Kimax, Fisher Co., Chicago, Ill.

0022-3549/82/0100-0129$01.00/0

Table I—Activities of Glycosaminoglycan Sulfates after Incubation in Human Digestive Juices

Substance	Time of incubation, min	Residual activity[a] Lipasemic	Anticoagulant
	In Human Gastric Juice, pH 1.4		
Heparin	0	100	100
	5	97	—
	15	95	97
	60	93	100
	180	93	98
Standardized extracts of glycosaminoglycans	0	100	100
	5	—	—
	15	97	107
	60	98	110
	180	105	109
	In Human Duodenal Juice, pH 8.5		
Heparin	0	100	100
	5	—	—
	15	95	97
	60	—	—
	180	98	92
Standardized extracts of glycosaminoglycans	0	100	100
	5	87	102
	15	92	94
	60	98	100
	180	95	96

[a] The values are expressed as percent of initial activity.

fluence of dilution, stability tests were carried out in which the concentrations of heparin and the standardized mixture of glycosaminoglycan sulfates were 19 and 23.8 USP/ml, respectively. Anticoagulant and lipoprotein–lipase-inducing activities were measured in relation to the time of incubation by means of *in vitro* and *in vivo* quantitative methods. Lipoprotein–lipase activity was measured by a turbidimetric method[3].

Anticoagulant action *in vivo* was evaluated by thrombin time with an aliquot of the same plasma used for the determination of lipoprotein–lipase releasing action *in vivo* by the ediol method. All coagulation times were determined automatically.

The biological activity pattern of heparin and other glycosaminoglycan sulfates remained unchanged during the experimental time period, although some variability in biological assessment occurred (Table I).

The confirmed biological activity shows that the nature and conformation of even the more labile chemical groups of glycosaminoglycan sulfates remain unaltered, despite being incubated in chemically and enzymatically aggressive environments such as digestive juices.

(1) L. B. Jaques and J. M. Mahadoo, *Semin. Thromb. Hemostasis*, **4**, 298 (1978).

(2) A. A. Salyers, *Am. J. Clin. Nutr.* **31**, 128 (1978); *Ibid.*, **32**, 158 (1979).

(3) A. K. Sim, "Fifth International Congress on Thromboembolism," Bologna, Italy, May 29–June 2, 1978.

(4) R. Niada, M. Mantovani, and R. Pescador, *Pharmacol. Res. Commun.*, **11**, 349 (1979).

(5) K. Nagasawa and H. Uchiyama, *Biochim. Biophys. Acta*, **544**, 430 (1978).

(6) J. R. Vercellotti, "Hearing on Hypolipidemic Drugs" (Rome, Italy, June 2–3, 1980), Raven, New York, N.Y., in press.

(7) T. K. Sue, L. B. Jaques, and E. Yuen, *Can. J. Physiol. Pharmacol.*, **54**, 613 (1976).

(8) Y. Tokunaga, S. Muranishi, and H. Sezaki, *J. Pharmacobio-Dyn.*, **1**, 28 (1978).

(9) G. P. Corbelli, L. Stanzani, and P. I. Bianchini, "VII International Symposium on Drugs Affecting Lipid Metabolism," Milan, Italy, May 28–31, 1980.

(10) P. Bianchini, B. Osima, and G. Guidi, *Biochem. Exp. Biol.*, **10**, 243 (1972).

[3] This method is based on the capability of rat plasma, treated with glycosaminoglycan sulfates previously (10 min before), to clear an artificial fatty ediol–water suspension. The clearing effect is proportional to the administered amount of glycosaminoglycan sulfates (10).

Mario Brufani
Cattedra di Chimica Farmaceutica
Gruppo di Chimica Biologica
e Strutturistica Chimica
Università di Roma
Rome, Italy

Gianpaolo Corbelli
Giuseppe Mascellani[x]
Luciano Stanzani
Laboratori Ricerche Alfa Farmaceutici S.P.A.
Via Ragazzi del'99 n.5
40133 Bologna, Italy

Received December 15, 1980.
Accepted for publication May 14, 1981.

Adsorption of Methotrexate onto Glassware and Syringes

Keyphrases □ Methotrexate—adsorption onto glassware and syringes □ Adsorption—methotrexate onto glassware and syringes

To the Editor:

Methotrexate, a potent antifolate, is a widely used antineoplastic agent (1). With the advent of high-dose therapy and citrovorum-factor rescue, monitoring of plasma concentrations of methotrexate is recommended (1–4). However, the potential interference of active metabolites, such as 7-hydroxymethotrexate and 4-amino-4-deoxy-N^{10}-methylpteroic acid, renders many assay methods nonspecific (5). A need for re-evaluation of past pharmacokinetic studies has been advocated (6). Hence, development of specific and sensitive assay methods is required. In our recent development of a high-performance liquid chromatographic (HPLC) assay for methotrexate and its metabolites in biological fluids (7), erratic results were often found when series dilutions of methotrexate in water-miscible organic solvents such as methanol were made. These organic solvents were used to enhance the aqueous solubility of methotrexate (8).

Additional studies were carried out to explore the potential interaction between methotrexate and glassware or syringes. This communication reports the results of our preliminary adsorption studies, and discusses its implication in quantitative analysis.

Stock solutions (0.1 mg/ml) of methotrexate were prepared in distilled water, methanol, or 80% ethanol (with 20% water, v/v) using 100-ml volumetric flasks[1]. Series dilutions were made to concentrations of 50, 10, and 1 μg/ml. After mixing and equilibration overnight, the methotrexate concentration was determined directly by the HPLC method described earlier (7). A cation-exchange

[1] Kimax, Fisher Co., Chicago, Ill.

0022-3549/82/0100-0129$01.00/0

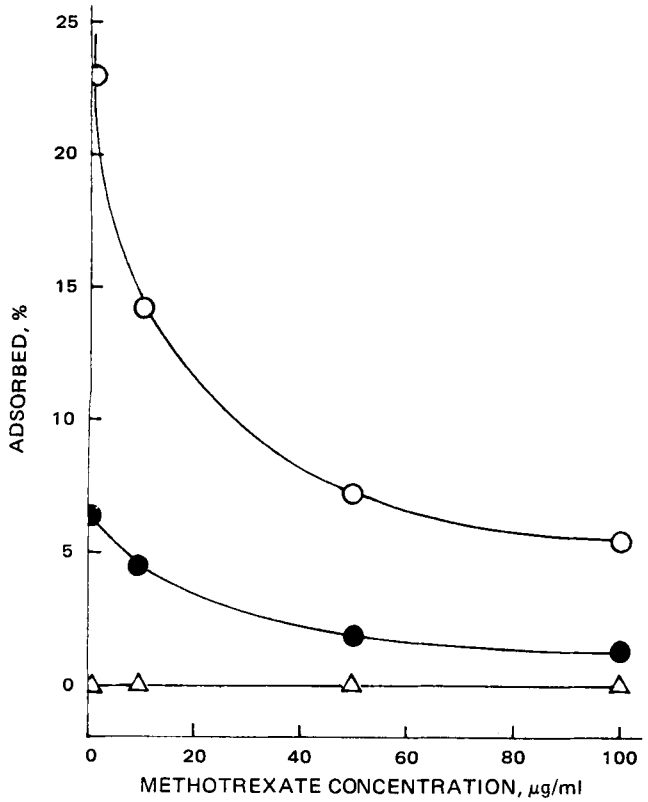

Figure 1—*Effect of concentration and diluent on methotrexate adsorption onto a volumetric flask. Key: ○, methanol; ●, 80% ethanol; and △, water.*

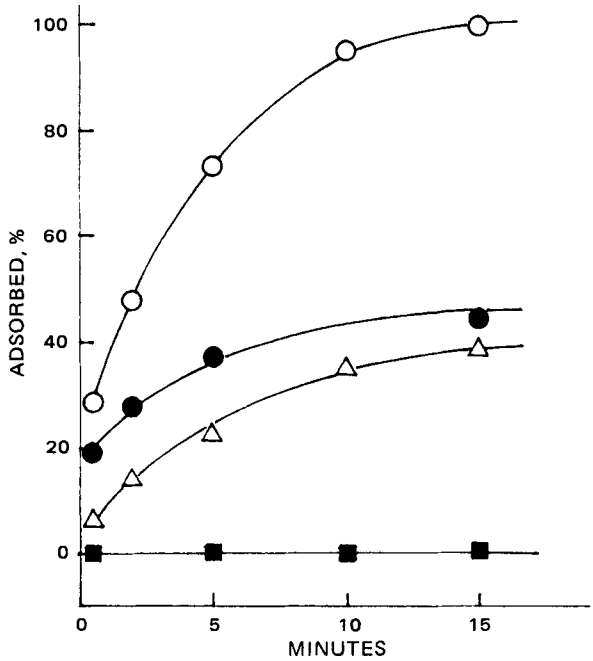

Figure 2—*Effect of exposure time on methotrexate adsorption by the syringe. Key: ○, methanol (0.1 μg/ml); ●, methanol (10 μg/ml); △, 80% ethanol (10 μg/ml); and ■, water (0.1 μg/ml).*

column[2] was used. The mobile phase was prepared by mixing 10 parts of acetonitrile with 90 parts of 0.02 *M* monobasic ammonium phosphate solution acidified with phosphoric acid (0.2%) to pH 2.7. The flow rate was set at 2 ml/min; the retention time for methotrexate was 7 min. *p*-Aminobenzoic acid was used as an internal standard to ensure the proper series dilution and HPLC injection; it was dissolved together with methotrexate in the preparation of stock solutions. No adsorption problem with *p*-aminobenzoic acid was encountered. Experiments were run at least in duplicate.

Figure 1 shows that the extent of adsorption was solvent and concentration dependent. The aqueous solution had no adsorption problem. However, methotrexate showed significant adsorption onto the flask in methanol or 80% ethanol. For example, the adsorption of methotrexate at 1 μg/ml was ~23% in methanol and 7% in 80% ethanol. As shown in Fig. 1, the percentage of methotrexate lost to the volumetric flask increased as the concentration decreased. It is possible that the extent of adsorption may be much greater when the concentration is <1 μg/ml (9).

Further evidence for methotrexate adsorption onto the glassware was supported by the following study. After adsorption equilibration overnight, various drug solutions were withdrawn into syringes[3]. The methotrexate concentrations in the syringes were then measured as a function of time. As shown in Fig. 2, the adsorption of methotrexate increased with the length of contact time in the 15-min period of the study. Again, methotrexate showed a higher degree of adsorption in methanol as compared with the 80% ethanol solution. The extent of adsorption also increased as methotrexate concentration decreased. It appears that the phenomenon of drug adsorption onto syringes used for the HPLC analysis has never been reported in the literature. Adsorption of butaperazine onto quartz cells was reported earlier (10).

A previous study (9) showed that the pH of the solution may influence the magnitude of adsorption. Our preliminary results showed that the adsorption of methotrexate in alcoholic solutions was reduced at lower (pH 2–4) or higher (pH 8–9) pH values.

It should be pointed out that the syringes used in this study were used not only in the preparation of drug standard solutions but also for sample delivery in HPLC assays. If methotrexate is prepared in solvents other than water, serious errors in the determination of the drug concentrations may result. Our preliminary findings also showed that 4-amino-4-deoxy-N^{10}-methylpteroic acid, a methotrexate metabolite (8), had a similar adsorption problem. The results of the present study clearly indicate that the potential adsorption of methotrexate and its metabolites onto glassware and other contact surfaces should be considered as a source of variability in quantitative analysis.

(1) W. A. Bleyer, *Cancer*, **41**, 36 (1978).

(2) A. Nirenberg, C. Mosende, B. Mehta, A. L. Gisolfi, and G. Rosen *Cancer Treat. Rep.*, **61**, 779 (1977).

(3) R. G. Stoller, K. R. Hande, S. A. Jacobs, and B. A. Chabner, *N. Engl. J. Med.*, **297**, 630 (1977).

(4) C. Perez, Y. M. Wang, W. W. Sutow, and J. Herson, *Cancer Clin. Trials*, **1**, 107 (1978).

(5) R. G. Buice, W. E. Evans, C. A. Nicholas, P. Sidhu, A. B. Straughn, M. C. Meyer, and W. R. Crom, *Clin. Chem.*, **26**, 1902 (1980).

(6) S. K. Howell, Y. M. Wang, R. Hosoya, and W. W. Sutow, *ibid.*,

[2] Partisil PXS 10/25 SCX, 25 cm × 4.6-mm i.d., Whatman Inc. Clifton, NJ 07014.

[3] Hamilton Co., Reno, Nev.

26, 734 (1980).
(7) M. L. Chen and W. L. Chiou, *J. Chromatogr. Bio. Appl.*, in press.
(8) R. C. Donehower, K. R. Hande, J. C. Drake, and B. A. Chabner, *Clin. Pharmacol. Ther.*, **26**, 63 (1979).
(9) P. Moorhatch and W. L. Chiou, *Am. J. Hosp. Pharm.*, **31**, 72 (1974).
(10) K. Chang and W. L. Chiou, *J. Pharm. Sci.*, **65**, 630 (1976).

Mei-Ling Chen
Win L. Chiou
Department of Pharmacy
College of Pharmacy
University of Illinois at the Medical Center
Chicago, IL 60612

Received June 29, 1981.
Accepted for publication August 26, 1981.

Pharmacokinetic and Biopharmaceutic Parameters During Enterohepatic Circulation of Drugs

Keyphrases □ Enterohepatic circulation—model, evaluation of pharmacokinetic parameters □ Pharmacokinetics—evaluation of parameters, enterohepatic circulation model

To the Editor:

As research in the area of enterohepatic circulation continues in this laboratory, several aspects of its impact on the interpretation of pharmacokinetic and biopharmaceutic studies have become apparent. Simulation techniques have been used to investigate the effect of enterohepatic circulation on various pharmacokinetic and biopharmaceutic parameters under various conditions.

The simple first-pass perfusion model in Scheme I was used for the simulations. In the model, V_H and V_S are the effective hepatic and systemic volumes[1], Q_H is the blood flow to the liver, and Cl_H and Cl_{HR} are the irreversible and recirculating hepatic organ clearances, respectively. The biliary excretion component was assumed to be continuous in the present model to avoid the complexities associated with gallbladder storage and subsequent excretion into the duodenum. The more complex model was addressed previously (1) and will be investigated further, but the concepts presented here are generally applicable to both situations. For the purpose of the oral absorption simulations, the absorption rate constant, k_A, was set at 0.693 hr^{-1}. Simulations were performed under conditions of intact enterohepatic circulation (k_{BA} = 1.0) and under conditions of bile duct cannulation, *i.e.*, interrupted enterohepatic circulation (k_{BA} = 0.0).

Blood concentration–time data following intravenous and oral doses were simulated using several sets of parameter values. Representative examples from the total number of simulations are presented in Tables I–III. The

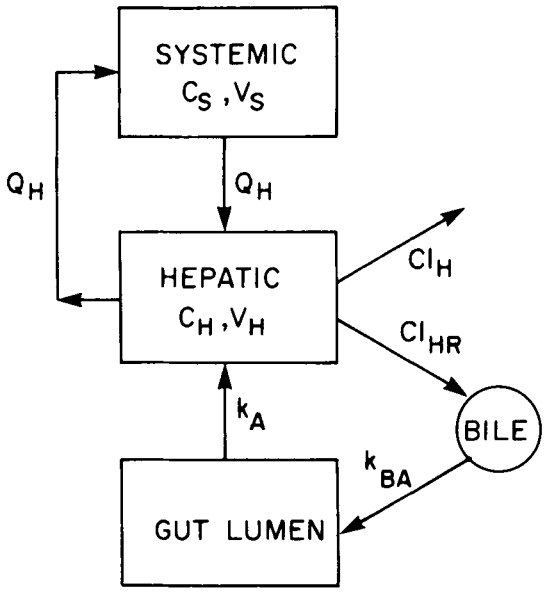

Scheme I—Pharmacokinetic first-pass perfusion model used to describe the systemic blood concentrations of drugs that undergo enterohepatic recycling. Key: Q_H, hepatic blood flow; Cl_H and Cl_{HR}, irreversible and recirculating hepatic organ clearances, respectively; and k_A and k_{BA}, the absorption and bile transport processes, respectively.

effect of enterohepatic circulation on blood clearance (Cl_B), oral clearance (Cl_O), elimination half-life ($t_{1/2\beta}$), and the volume of distribution ($V_{d_{area}}$) are presented in Table I. The influence of enterohepatic circulation on the time (T_{max}) of the maximum observed blood concentration (C_{max}) and the elimination half-life following oral dosing are presented in Table II. Table III contains the blood clearance (Cl_B) and oral clearance (Cl_O) parameters along with the absolute bioavailability under intact (F_I) as well as bile duct-cannulated (F_C) conditions. In addition, the ratio of the area under the curves following intravenous doses (AUC_{IV}) under intact and bile-duct-cannulated conditions (R_{IV}) as well as the ratio of the area under the curves following oral doses (AUC_O) under intact and bile duct-cannulated conditions (R_O) are presented in Table III.

The results of these simulations indicate that enterohepatic circulation increases the apparent volume distribution and prolongs the half-life of elimination when compared to identical blood clearances without it. The more extensive the recycling, the more prolonged the half-life and greater the volume increase (Table I). The data presented in Table II indicate that the pharmacokinetic complexities associated with enterohepatic circulation are affected by the effective hepatic and systemic volumes of distribution. The time (T_{max}) of the maximum observed blood concentrations (C_{max}) following oral doses are a function of both the interrelationship of systemic to hepatic effective volumes of distribution as well as the extent of enterohepatic circulation (Table II).

For example, comparison of cases G–I with cases J–L in Table II indicates that when the effective systemic volume of distribution is smaller than the effective hepatic volume of distribution, more extensive recycling results in longer elimination half-lives and lower C_{max} values, but results

[1] Effective volume is the product of the physiological volume of the organ or pooled tissues times its retention factor.

0022-3549/82/0100-0131$01.00/0

26, 734 (1980).
(7) M. L. Chen and W. L. Chiou, *J. Chromatogr. Bio. Appl.*, in press.
(8) R. C. Donehower, K. R. Hande, J. C. Drake, and B. A. Chabner, *Clin. Pharmacol. Ther.*, **26**, 63 (1979).
(9) P. Moorhatch and W. L. Chiou, *Am. J. Hosp. Pharm.*, **31**, 72 (1974).
(10) K. Chang and W. L. Chiou, *J. Pharm. Sci.*, **65**, 630 (1976).

Mei-Ling Chen
Win L. Chiou
Department of Pharmacy
College of Pharmacy
University of Illinois at the Medical Center
Chicago, IL 60612

Received June 29, 1981.
Accepted for publication August 26, 1981.

Pharmacokinetic and Biopharmaceutic Parameters During Enterohepatic Circulation of Drugs

Keyphrases □ Enterohepatic circulation—model, evaluation of pharmacokinetic parameters □ Pharmacokinetics—evaluation of parameters, enterohepatic circulation model

To the Editor:

As research in the area of enterohepatic circulation continues in this laboratory, several aspects of its impact on the interpretation of pharmacokinetic and biopharmaceutic studies have become apparent. Simulation techniques have been used to investigate the effect of enterohepatic circulation on various pharmacokinetic and biopharmaceutic parameters under various conditions.

The simple first-pass perfusion model in Scheme I was used for the simulations. In the model, V_H and V_S are the effective hepatic and systemic volumes[1], Q_H is the blood flow to the liver, and Cl_H and Cl_{HR} are the irreversible and recirculating hepatic organ clearances, respectively. The biliary excretion component was assumed to be continuous in the present model to avoid the complexities associated with gallbladder storage and subsequent excretion into the duodenum. The more complex model was addressed previously (1) and will be investigated further, but the concepts presented here are generally applicable to both situations. For the purpose of the oral absorption simulations, the absorption rate constant, k_A, was set at 0.693 hr^{-1}. Simulations were performed under conditions of intact enterohepatic circulation (k_{BA} = 1.0) and under conditions of bile duct cannulation, *i.e.*, interrupted enterohepatic circulation (k_{BA} = 0.0).

Blood concentration–time data following intravenous and oral doses were simulated using several sets of parameter values. Representative examples from the total number of simulations are presented in Tables I–III. The

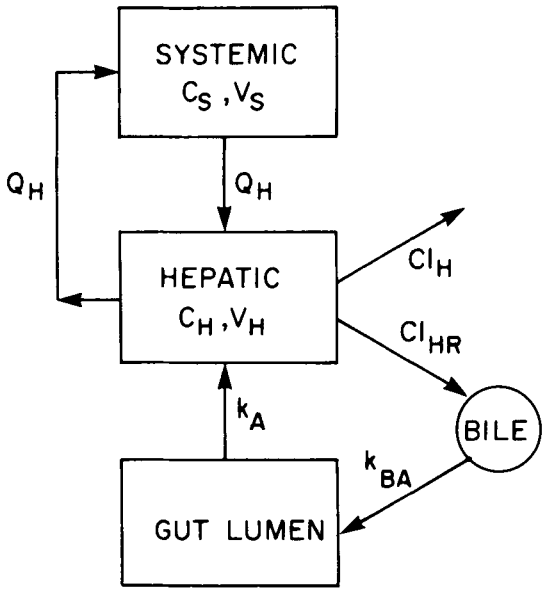

Scheme I—Pharmacokinetic first-pass perfusion model used to describe the systemic blood concentrations of drugs that undergo enterohepatic recycling. Key: Q_H, hepatic blood flow; Cl_H and Cl_{HR}, irreversible and recirculating hepatic organ clearances, respectively; and k_A and k_{BA}, the absorption and bile transport processes, respectively.

effect of enterohepatic circulation on blood clearance (Cl_B), oral clearance (Cl_O), elimination half-life ($t_{1/2\beta}$), and the volume of distribution ($V_{d_{area}}$) are presented in Table I. The influence of enterohepatic circulation on the time (T_{max}) of the maximum observed blood concentration (C_{max}) and the elimination half-life following oral dosing are presented in Table II. Table III contains the blood clearance (Cl_B) and oral clearance (Cl_O) parameters along with the absolute bioavailability under intact (F_I) as well as bile duct-cannulated (F_C) conditions. In addition, the ratio of the area under the curves following intravenous doses (AUC_{IV}) under intact and bile-duct-cannulated conditions (R_{IV}) as well as the ratio of the area under the curves following oral doses (AUC_O) under intact and bile duct-cannulated conditions (R_O) are presented in Table III.

The results of these simulations indicate that enterohepatic circulation increases the apparent volume distribution and prolongs the half-life of elimination when compared to identical blood clearances without it. The more extensive the recycling, the more prolonged the half-life and greater the volume increase (Table I). The data presented in Table II indicate that the pharmacokinetic complexities associated with enterohepatic circulation are affected by the effective hepatic and systemic volumes of distribution. The time (T_{max}) of the maximum observed blood concentrations (C_{max}) following oral doses are a function of both the interrelationship of systemic to hepatic effective volumes of distribution as well as the extent of enterohepatic circulation (Table II).

For example, comparison of cases G–I with cases J–L in Table II indicates that when the effective systemic volume of distribution is smaller than the effective hepatic volume of distribution, more extensive recycling results in longer elimination half-lives and lower C_{max} values, but results

[1] Effective volume is the product of the physiological volume of the organ or pooled tissues times its retention factor.

0022-3549/82/0100-0131$01.00/0

Table I—Effect of Enterohepatic Circulation on Various Pharmacokinetic Parameters

Parameters								
Simulated					Calculated			
V_H, liters	V_S, liters	Q_H, liters/hr	Cl_H, liters/hr	Cl_{HR}, liters/hr	Cl_B, liters/hr	Cl_O, liters/hr	$t_{1/2\beta}$, hr	V_{darea}, liters
100	100	90	10	0	9	10	14.3	185
100	100	90	10	20	9	10	17.8	231
100	100	90	10	80	9	10	28.3	367
100	100	90	10	260	9	10	58.9	765
100	100	90	30	0	22.5	30	5.0	164
100	100	90	30	60	22.5	30	8.8	286
100	100	90	60	0	36.0	60	2.8	143
100	100	90	60	30	36.0	60	3.8	200

Table II—Effect of Enterohepatic Circulation on Various Biopharmaceutic Parameters

	Parameters							
	Simulated					Calculated		
Case	V_H, liters	V_S, liters	Q_H, liters/hr	Cl_H, liters/hr	Cl_{HR}, liters/hr	T_{max}, hr	C_{max}, U/liters	$t_{1/2\beta}$, hr
A	100	100	90	10	0	5	395	14.3
B	100	100	90	10	20	5	331	17.8
C	100	100	90	10	260	4	112	58.9
D	10	100	90	10	0	4	620	8.3
E	10	100	90	10	20	4	474	11.9
F	10	100	90	10	260	4	124	52.8
G	100	10	90	10	0	4	663	7.6
H	100	10	90	10	20	3	524	11.4
I	100	10	90	10	260	1	159	52.7
J	100	1000	90	10	0	8	78.5	83.3
K	100	1000	90	10	20	10	74.5	86.4
L	100	1000	90	10	260	20	49.6	125

Table III—Simulated Effects of Enterohepatic Circulation and Bile Duct Cannulation on Clearance, Bioavailability, and Administration Route Differences

	Parameters										
	Simulated					Calculated					
Recirculation status[a]	V_H, liters	V_S, liters	Q_H, liters/hr	Cl_H, liters/hr	Cl_{HR}, liters/hr	Cl_B, liters/hr	Cl_O, liters/hr	F_I	F_C	R_{IV}	R_O
I	100	100	90	10	0	9.0	10.0	0.900	0.900	1.000	1.000
I	100	100	90	30	0	22.5	30.0	0.750	0.750	1.000	1.000
I	100	100	90	60	0	36.0	60.0	0.600	0.600	1.000	1.000
I	100	100	90	30	60	22.5	30.0	0.750	0.500	0.500	0.333
C				90	0	45.0	90.0				
I	100	100	90	60	30	36.0	60.0	0.600	0.500	0.800	0.667
C				90	0	45.0	90.0				
I	100	100	90	10	20	9.0	10.0	0.900	0.750	0.400	0.333
C				30	0	22.5	30.0				
I	100	100	90	10	80	9.0	10.0	0.900	0.500	0.200	0.111
C				90	0	45.0	90.0				
I	100	100	90	10	260	9.0	10.0	0.900	0.250	0.133	0.037
C				270	0	67.5	270.0				

[a] I, intact, uncannulated; and C, cannulated.

in earlier T_{max} values. However, when the effective systemic volume of distribution is larger than the effective hepatic volume, more extensive recycling not only results in longer elimination half-lives and lower C_{max} values, but also in much later T_{max} values. For comparison with case L, the T_{max} value is 8 hr for a drug with an elimination half-life of 125 hr, but without enterohepatic circulation.

The importance of recycling on estimates of the absolute bioavailability of a drug is shown by comparing the absolute bioavailability simulated in intact, uncannulated (F_I), and bile duct-cannulated (F_C) animals. It is apparent that bioavailability in cannulated animals is less than or equal to the bioavailability in uncannulated animals. This observation is supported by the fact that the ratios of areas under the oral curves (R_O) are decreased more extensively by bile duct cannulation than are the ratios of the areas under the intravenous curves (R_{IV}).

Although enterohepatic circulation affects the shapes of the blood concentration–time curves by increasing the apparent volume of distribution and half-life (Table I) and by altering the C_{max} and T_{max} values (Table II), it will not alter the areas under the blood concentration–time curves unless the enterohepatic circulation is interrupted (Table III) or altered in some way. An interruption can result from bile duct cannulation in the experimental setting, from the oral ingestion of ion-exchange resins, or from changes in the intestinal contents and microflora that may decrease or inhibit drug reabsorption.

Thus, enterohepatic circulation influences the bio-

pharmaceutic and pharmacokinetic parameters associated with a drug. The process needs to be better understood to allow reasonable interpretation of the pharmacokinetic data obtained for drugs that are recycled. The data presented here reflect the simplest case; discontinuous recycling, which is associated with gall bladder storage and emptying, is even more complex (1).

(1) W. A. Colburn, *J. Pharmacokinet. Biopharm.*, in press.

Wayne A. Colburn
Department of Pharmacokinetics and Biopharmaceutics
Hoffmann-La Roche Inc.
Nutley, NJ 07110

Received July 17, 1981.
Accepted for publication September 22, 1981.

BOOKS

REVIEWS

Basic Clinical Pharmacokinetics. By MICHAEL E. WINTER, with BRIAN S. KATCHER and MARY ANNE KODA-KIMBLE. Applied Therapeutics, P.O. Box 31-747, San Francisco, CA 94131. 1980. 231 pp. 14.8 × 22.7 cm. Price $22.00.

Pharmacokinetics and biopharmaceutics are well-established disciplines. Their contributions in describing drug disposition, and predicting plasma drug concentrations and changes in drug concentrations are generally recognized. During the past decade, evaluation of drug concentrations in biological fluids has found wide acceptance as part of drug therapy monitoring. The authors view this book as a practical guideline for the clinician in evaluating drug monitoring.

The book is divided into two parts. The first part gives a brief overview of the basic principles of pharmacokinetics dealing with bioavailability, rate of administration, desired plasma concentration, volume of distribution, clearance, elimination, steady-state concentrations, interpretation of plasma drug concentrations, selection of appropriate equations, and creatinine clearance. At the end of the first part, a very instructive diagram is given for evaluation and interpretation of plasma levels. This diagram will be very helpful for any clinician confronted with blood level data interpretation.

Part 2 discusses the clinical pharmacokinetics of drugs usually monitored by a clinical pharmacokinetics service. The following drugs are covered: digoxin, lidocaine, procainamide, quinidine, theophylline, gentamicin, phenobarbital, and phenytoin. For each of these drugs, therapeutic and toxic plasma levels, bioavailability, if applicable, and the most important pharmacokinetic parameters (*i.e.*, volume of distribution, clearance, and elimination half-life) are covered. Where applicable, the influence of age, disease, and other concomitantly given drugs on drug disposition is discussed.

This section, which is well referenced, is followed by a selection of typical clinical cases, along with the pharmacokinetic approach for solution. The calculations are listed stepwise so that even one who is inexperienced in pharmacokinetics can easily follow. This section will be of great value to anyone interested in or practicing clinical pharmacokinetics, as well as for teaching undergraduate and graduate students. Although only a few drugs are discussed in detail, once one masters these problem cases, the principles can be applied and tailored to many more drugs.

The book contains three appendixes: I, nomograms for calculating body surface area of children and adults; II, a listing of equations used throughout the text; and III, a glossary of terms and abbreviations.

In summary, this is a well-written and well-designed text which incorporates the most important basic principles of basic and clinical pharmacokinetics. As such, the book will be of great value to all those involved in clinical pharmacokinetics and drug monitoring, particularly those who are entering the field. The authors have to be congratulated for writing such a well-organized guideline to the practical approach of drug level monitoring.

Reviewed by W. A. Ritschel
College of Pharmacy and College of Medicine, University of Cincinnati Medical Center Cincinnati, OH 45267

GC/MS Assays for Abused Drugs in Body Fluid. NIDA Research Monograph 32. By RODGER L. FOLTZ, ALLISON F. FENTIMAN, and RUTH B. FOLTZ. National Institute on Drug Abuse, Division of Research, 5600 Fishers Lane, Rockville, MD 20857. 1980. 202 pp. 14 × 23 cm. Price $5.00. (Available from Superintendent of Documents, U.S. Government Printing Office, Washington, DC 20402. Specify GPO stock no. 017-024-01015-4.)

This monograph, prepared by authors who are well versed in the areas of analytical methodology and drug abuse, should be valuable to investigators interested in quantitating drugs in biological fluids. This work is actually a compilation of assays used for measuring the levels of drugs most often misused.

This volume (13 chapters) includes an introduction and a discussion of experimental considerations and operations common to all of the assays (Chapter 2), and each remaining chapter is devoted to a particular drug that is commonly abused. The inclusion of Chapter 2 (which deals with the basics of obtaining internal standards, preparing calibration curves, sample extractions, performance evaluation of the gas chromatograph–mass spectrometer, *etc.*) is an ideal approach since it greatly reduces excessive repetition that would have been required in each of the succeeding chapters. The authors recommend that investigators concentrate on Chapter 2 along with the specific chapter for the drug in question.

Each succeeding chapter is devoted to one of the following drugs of abuse: phencyclidine, methaqualone, methadone, Δ^9-tetrahydrocannabinol and two of its metabolites (11-hydroxy-Δ^9-THC and 11-nor-9-carboxy-Δ^9-THC), cocaine and its major metabolite (benzoylecgonine), morphine, diazepam and its major metabolite (*N*-desmethyldiazepam), amphetamine, methamphetamine, 2,5-dimethoxy-4-methylamphetamine, and mescaline. Each chapter begins with a brief historical description of the drug followed by a synopsis of its pharmacological effects. A discussion on pharmacokinetics and metabolism examines which biological fluid should be chosen for assay and whether metabolites should be quantitated. Then the sensitivity and selectivity of most of the techniques (*e.g.*, spectrometry, gas chromatography, and radioimmunoassay)

pharmaceutic and pharmacokinetic parameters associated with a drug. The process needs to be better understood to allow reasonable interpretation of the pharmacokinetic data obtained for drugs that are recycled. The data presented here reflect the simplest case; discontinuous recycling, which is associated with gall bladder storage and emptying, is even more complex (1).

(1) W. A. Colburn, *J. Pharmacokinet. Biopharm.*, in press.

Wayne A. Colburn
Department of Pharmacokinetics and Biopharmaceutics
Hoffmann-La Roche Inc.
Nutley, NJ 07110

Received July 17, 1981.
Accepted for publication September 22, 1981.

BOOKS

REVIEWS

Basic Clinical Pharmacokinetics. By MICHAEL E. WINTER, with BRIAN S. KATCHER and MARY ANNE KODA-KIMBLE. Applied Therapeutics, P.O. Box 31-747, San Francisco, CA 94131. 1980. 231 pp. 14.8 × 22.7 cm. Price $22.00.

Pharmacokinetics and biopharmaceutics are well-established disciplines. Their contributions in describing drug disposition, and predicting plasma drug concentrations and changes in drug concentrations are generally recognized. During the past decade, evaluation of drug concentrations in biological fluids has found wide acceptance as part of drug therapy monitoring. The authors view this book as a practical guideline for the clinician in evaluating drug monitoring.

The book is divided into two parts. The first part gives a brief overview of the basic principles of pharmacokinetics dealing with bioavailability, rate of administration, desired plasma concentration, volume of distribution, clearance, elimination, steady-state concentrations, interpretation of plasma drug concentrations, selection of appropriate equations, and creatinine clearance. At the end of the first part, a very instructive diagram is given for evaluation and interpretation of plasma levels. This diagram will be very helpful for any clinician confronted with blood level data interpretation.

Part 2 discusses the clinical pharmacokinetics of drugs usually monitored by a clinical pharmacokinetics service. The following drugs are covered: digoxin, lidocaine, procainamide, quinidine, theophylline, gentamicin, phenobarbital, and phenytoin. For each of these drugs, therapeutic and toxic plasma levels, bioavailability, if applicable, and the most important pharmacokinetic parameters (*i.e.*, volume of distribution, clearance, and elimination half-life) are covered. Where applicable, the influence of age, disease, and other concomitantly given drugs on drug disposition is discussed.

This section, which is well referenced, is followed by a selection of typical clinical cases, along with the pharmacokinetic approach for solution. The calculations are listed stepwise so that even one who is inexperienced in pharmacokinetics can easily follow. This section will be of great value to anyone interested in or practicing clinical pharmacokinetics, as well as for teaching undergraduate and graduate students. Although only a few drugs are discussed in detail, once one masters these problem cases, the principles can be applied and tailored to many more drugs.

The book contains three appendixes: I, nomograms for calculating body surface area of children and adults; II, a listing of equations used throughout the text; and III, a glossary of terms and abbreviations.

In summary, this is a well-written and well-designed text which incorporates the most important basic principles of basic and clinical pharmacokinetics. As such, the book will be of great value to all those involved in clinical pharmacokinetics and drug monitoring, particularly those who are entering the field. The authors have to be congratulated for writing such a well-organized guideline to the practical approach of drug level monitoring.

Reviewed by W. A. Ritschel
College of Pharmacy and College of Medicine, University of Cincinnati Medical Center Cincinnati, OH 45267

GC/MS Assays for Abused Drugs in Body Fluid. NIDA Research Monograph 32. By RODGER L. FOLTZ, ALLISON F. FENTIMAN, and RUTH B. FOLTZ. National Institute on Drug Abuse, Division of Research, 5600 Fishers Lane, Rockville, MD 20857. 1980. 202 pp. 14 × 23 cm. Price $5.00. (Available from Superintendent of Documents, U.S. Government Printing Office, Washington, DC 20402. Specify GPO stock no. 017-024-01015-4.)

This monograph, prepared by authors who are well versed in the areas of analytical methodology and drug abuse, should be valuable to investigators interested in quantitating drugs in biological fluids. This work is actually a compilation of assays used for measuring the levels of drugs most often misused.

This volume (13 chapters) includes an introduction and a discussion of experimental considerations and operations common to all of the assays (Chapter 2), and each remaining chapter is devoted to a particular drug that is commonly abused. The inclusion of Chapter 2 (which deals with the basics of obtaining internal standards, preparing calibration curves, sample extractions, performance evaluation of the gas chromatograph–mass spectrometer, *etc.*) is an ideal approach since it greatly reduces excessive repetition that would have been required in each of the succeeding chapters. The authors recommend that investigators concentrate on Chapter 2 along with the specific chapter for the drug in question.

Each succeeding chapter is devoted to one of the following drugs of abuse: phencyclidine, methaqualone, methadone, Δ^9-tetrahydrocannabinol and two of its metabolites (11-hydroxy-Δ^9-THC and 11-nor-9-carboxy-Δ^9-THC), cocaine and its major metabolite (benzoylecgonine), morphine, diazepam and its major metabolite (*N*-desmethyldiazepam), amphetamine, methamphetamine, 2,5-dimethoxy-4-methylamphetamine, and mescaline. Each chapter begins with a brief historical description of the drug followed by a synopsis of its pharmacological effects. A discussion on pharmacokinetics and metabolism examines which biological fluid should be chosen for assay and whether metabolites should be quantitated. Then the sensitivity and selectivity of most of the techniques (*e.g.*, spectrometry, gas chromatography, and radioimmunoassay)

pharmaceutic and pharmacokinetic parameters associated with a drug. The process needs to be better understood to allow reasonable interpretation of the pharmacokinetic data obtained for drugs that are recycled. The data presented here reflect the simplest case; discontinuous recycling, which is associated with gall bladder storage and emptying, is even more complex (1).

(1) W. A. Colburn, *J. Pharmacokinet. Biopharm.*, in press.

Wayne A. Colburn
Department of Pharmacokinetics and Biopharmaceutics
Hoffmann-La Roche Inc.
Nutley, NJ 07110

Received July 17, 1981.
Accepted for publication September 22, 1981.

BOOKS

REVIEWS

Basic Clinical Pharmacokinetics. By MICHAEL E. WINTER, with BRIAN S. KATCHER and MARY ANNE KODA-KIMBLE. Applied Therapeutics, P.O. Box 31-747, San Francisco, CA 94131. 1980. 231 pp. 14.8 × 22.7 cm. Price $22.00.

Pharmacokinetics and biopharmaceutics are well-established disciplines. Their contributions in describing drug disposition, and predicting plasma drug concentrations and changes in drug concentrations are generally recognized. During the past decade, evaluation of drug concentrations in biological fluids has found wide acceptance as part of drug therapy monitoring. The authors view this book as a practical guideline for the clinician in evaluating drug monitoring.

The book is divided into two parts. The first part gives a brief overview of the basic principles of pharmacokinetics dealing with bioavailability, rate of administration, desired plasma concentration, volume of distribution, clearance, elimination, steady-state concentrations, interpretation of plasma drug concentrations, selection of appropriate equations, and creatinine clearance. At the end of the first part, a very instructive diagram is given for evaluation and interpretation of plasma levels. This diagram will be very helpful for any clinician confronted with blood level data interpretation.

Part 2 discusses the clinical pharmacokinetics of drugs usually monitored by a clinical pharmacokinetics service. The following drugs are covered: digoxin, lidocaine, procainamide, quinidine, theophylline, gentamicin, phenobarbital, and phenytoin. For each of these drugs, therapeutic and toxic plasma levels, bioavailability, if applicable, and the most important pharmacokinetic parameters (*i.e.*, volume of distribution, clearance, and elimination half-life) are covered. Where applicable, the influence of age, disease, and other concomitantly given drugs on drug disposition is discussed.

This section, which is well referenced, is followed by a selection of typical clinical cases, along with the pharmacokinetic approach for solution. The calculations are listed stepwise so that even one who is inexperienced in pharmacokinetics can easily follow. This section will be of great value to anyone interested in or practicing clinical pharmacokinetics, as well as for teaching undergraduate and graduate students. Although only a few drugs are discussed in detail, once one masters these problem cases, the principles can be applied and tailored to many more drugs.

The book contains three appendixes: I, nomograms for calculating body surface area of children and adults; II, a listing of equations used throughout the text; and III, a glossary of terms and abbreviations.

In summary, this is a well-written and well-designed text which incorporates the most important basic principles of basic and clinical pharmacokinetics. As such, the book will be of great value to all those involved in clinical pharmacokinetics and drug monitoring, particularly those who are entering the field. The authors have to be congratulated for writing such a well-organized guideline to the practical approach of drug level monitoring.

Reviewed by W. A. Ritschel
College of Pharmacy and College of Medicine, University of Cincinnati Medical Center Cincinnati, OH 45267

GC/MS Assays for Abused Drugs in Body Fluid. NIDA Research Monograph 32. By RODGER L. FOLTZ, ALLISON F. FENTIMAN, and RUTH B. FOLTZ. National Institute on Drug Abuse, Division of Research, 5600 Fishers Lane, Rockville, MD 20857. 1980. 202 pp. 14 × 23 cm. Price $5.00. (Available from Superintendent of Documents, U.S. Government Printing Office, Washington, DC 20402. Specify GPO stock no. 017-024-01015-4.)

This monograph, prepared by authors who are well versed in the areas of analytical methodology and drug abuse, should be valuable to investigators interested in quantitating drugs in biological fluids. This work is actually a compilation of assays used for measuring the levels of drugs most often misused.

This volume (13 chapters) includes an introduction and a discussion of experimental considerations and operations common to all of the assays (Chapter 2), and each remaining chapter is devoted to a particular drug that is commonly abused. The inclusion of Chapter 2 (which deals with the basics of obtaining internal standards, preparing calibration curves, sample extractions, performance evaluation of the gas chromatograph–mass spectrometer, *etc.*) is an ideal approach since it greatly reduces excessive repetition that would have been required in each of the succeeding chapters. The authors recommend that investigators concentrate on Chapter 2 along with the specific chapter for the drug in question.

Each succeeding chapter is devoted to one of the following drugs of abuse: phencyclidine, methaqualone, methadone, Δ^9-tetrahydrocannabinol and two of its metabolites (11-hydroxy-Δ^9-THC and 11-nor-9-carboxy-Δ^9-THC), cocaine and its major metabolite (benzoylecgonine), morphine, diazepam and its major metabolite (*N*-desmethyldiazepam), amphetamine, methamphetamine, 2,5-dimethoxy-4-methylamphetamine, and mescaline. Each chapter begins with a brief historical description of the drug followed by a synopsis of its pharmacological effects. A discussion on pharmacokinetics and metabolism examines which biological fluid should be chosen for assay and whether metabolites should be quantitated. Then the sensitivity and selectivity of most of the techniques (*e.g.*, spectrometry, gas chromatography, and radioimmunoassay)

that have been applied to the analysis of the drug are presented. However, quantitation by gas chromatography–mass spectrometry–single-ion monitoring, which is far more reliable and sensitive than most other methods, is emphasized. A detailed description of gas chromatographic–mass spectrometric methodology is provided. In addition, each chapter has its own reference section, which provides ample documentation.

This monograph enables the investigator to choose the best analytical method for a particular drug based on the materials and equipment available. In addition, the design of basic experimental protocols should be greatly facilitated with the information contained within this volume. Although this book is intended for those in the field of drug abuse, it should be helpful to anyone interested in undertaking an analysis of any drug by gas chromatography–mass spectrometry.

Reviewed by Billy R. Martin
Department of Pharmacology
Medical College of Virginia
Virginia Commonwealth University
Richmond, VA 23298

Pharmacological and Biochemical Properties of Drug Substances, Vol. 3. Edited by MORTON E. GOLDBERG. American Pharmaceutical Association, 2215 Constitution Ave., N.W., Washington, D.C., 20037. 1981. 495 pp. 16 × 24 cm. Price $39.00 (Vols. 1–3, $90.00).

The third volume of this series presents 16 new monographs on a variety of therapeutic agents and topics, bringing the total number of monographs in this series to 52. Most of these reviews (in this volume as well as in the previous two) are concerned with specific drugs and are extensively referenced.

Although Dr. Goldberg's own research has emphasized central nervous system pharmacology, the book covers a wide variety of therapeutic classes such as cardiovascular agents, chemotherapeutic agents, and pulmonary/antiallergy agents, to name a few. The members of the editorial board also are cited for various areas of expertise.

Volume 3 contains three monographs covering topical steroid therapy, eicosanoids and pulmonary function, and one entitled, "Assessing Drug Concentration/Effect Correlations: Implications for Research and Therapy."

The author encourages readers to write to him or one of the editors if it is felt that a drug or topic deserves consideration for future volumes.

Staff review

NOTICES

An Introduction to Hazard and Operability Studies. The Guide Word Approach. By R. ELLIS KNOWLTON. Chematics International Ltd., 1770 Burrard St., Vancouver, B.C., Canada, V6J 3G7. 1981. 43 pp. 17 × 24 cm. Price $7.00.

Ap-GI—2nd International Conference on Pharmaceutical Technology. Paris—3–5 June 1980. Association de Pharmacie Galenique Industrielle, Rue JB, Clement 92290. Chatenay-Malabry, France. 15 × 24 cm. (each book). Price 800 FF complete set of five books, incl. taxes.

Arzneistoffe. (Lehrbuch der Pharmazeutischen Chemie). By WALTER SCHUNACK, KLAUS MAYER, and MANFRED HAAKE. Frieder Viewen & Sohn, Verlagsgesellschaft mbH, Postfach 5829, D-6200, Wiesbaden 1, West Germany. 1981. 608 pp. 17.5 × 24.5 cm. Price DM 68.00.

Basics of Electroorganic Synthesis. By DEMETRIOS K. KYRIACOU. Wiley, One Wiley Drive, Somerset, NJ 08873. 1981. 153 pp. 15 × 23 cm. Price $27.50.

Behavioral Pharmacology. 2nd Ed. By SUSAN D. IVERSEN and LESLIE L. IVERSEN. Oxford University Press, 200 Madison Ave., New York, NY 10016. 1981. 305 pp. 15 × 23 cm. Price $17.95 cloth and $10.95 paper.

Biomedical and Dental Applications of Polymers: Polymer Science and Technology Vol. #14. Edited by CHARLES G. GEBELEIN and FRANK F. KOBLITZ. Plenum, 227 W. 17th St., New York, NY 10011. 1980. 492 pp. 16 × 25 cm.

Breastfeeding: Program, Policy, and Research Issues. Edited by EDWARD C. BAER and BEVERLY WINIKOFF. A Special Issue of Studies in Family Planning, Vol. 12, No. 4. Population Council, 1 Dag Hammarskjold Plaza, New York, NY 10017. 1981. 206 pp. 21 × 28 cm. Price, no charge for single copies, multiple copies, $2.50 each.

Cellular Receptors for Hormones and Neurotransmitters. Edited by DENNIS SCHULSTER and ALEXANDER LEVITZKI. Wiley, 605 Third Ave., New York, NY 10016. 1980. 412 pp. 15 × 23 cm. Price $70.00.

Enzymes as Drugs. Edited by JOHN S. HOLCENBERG and JOSEPH ROBERTS. Wiley, 605 Third Ave., New York, NY 10016. 1981. 455 pp. 15 × 23 cm. Price $59.50.

Hagers Handbuch der Pharmazeutischen Praxis: Vollstandige (Vierte) Neuausgabe. By P. H. LIST and L. HORHAMMER. Springer-Verlag, 44 Hartz Way, Secaucus, NJ 07094. 1980. 628 pp. 16 × 24 cm. Price $100.30.

Hospital Pharmacy. 4th ed. By WILLIAM E. HASSAN, Jr. Lea & Febiger, 600 Washington Square, Philadelphia, PA 19106. 1981. 588 pp. 15 × 24 cm. Price $29.50, Canada $35.50.

IARC Monographs on the Evaluation of the Carcinogenic Risk of Chemicals to Humans. Some Pharmaceutical Drugs. Vol. 24. International Agency for Research on Cancer. World Health Organization, 1211 Geneva 27, Switzerland. 1980. 337 pp. 17 × 24 cm. Price U.S. $25.00 (Sw. fr. 40).

Immunostimulation. By L. CHEDID, P. A. MIESCHER, and H. J. MUELLER-EBERHARD. Springer-Verlag New York, 44 Hartz Way, Secaucus, NJ 07094. 1980. 236 pp. 16 × 24 cm. Price $22.50.

International Journal of Quantum Chemistry. Quantum Biology Symposium No. 7. (Proceedings of the International Symposium on Quantum Biology and Quantum Pharmacology). Held at Palm Coast, Fla., March 5–8, 1980. By PER-OLOV LOWDIN and JOHN R. SABIN. Wiley, 605 Third Ave., New York, NY 10016. 1980. 434 pp. 15 × 23 cm. Price $40.00.

Liquid Chromatography In Clinical Analysis. Edited by POKAR M. KABRA and LAURENCE J. MARTON. The Humana Press Inc., Crescent Manor, P.O. Box 2148, Clifton, NJ 07015. 1981. 466 pp. 15 × 23 cm. Price $55.00. $65.00 foreign.

Manual of Antibiotics and Infectious Diseases. 4th ed. By JOHN E. CONTE, Jr., and STEVEN L. BARRIERE. Lea & Febiger, 600 Washington Square, Philadelphia, PA 19106. 1981. 233 pp. 14 × 22 cm. Price $17.50. Canada $21.00.

Manual of Clinical Pharmacology. Edited by DAVID ROBERTSON and CRAIG R. SMITH. The Williams & Wilkins Co., 428 E. Preston St., Baltimore, MD 21202. 1981. 350 pp. 17 × 25 cm. Price $17.00.

Monoamine Oxidase Inhibitors. The State of the Art. Edited by M. B. H. YOUDIM and E. S. PAYKEL. Wiley, 605 Third Ave., New York, NY 10016. 1980. 214 pp. 15 × 23 cm. Price $39.00.

Pharmaceuticals and Health Policy. (International Perspectives on Provision and Control of Medicines). Edited by RICHARD BLUM, ANDREW HERXHEIMER, CATHERINE STENZIL, and JASPER WOODCOCK. Holmes & Meier Publishers, Inc., 30 Irving Place, New York, NY 10003. 1981. 14 × 22 cm. Price $37.50.

Pharmacology: An Introduction to Drugs. 2nd Ed. By MICHAEL C. GERALD. Prentice-Hall, Inc., Englewood Cliffs, NJ 07632. 1981. 686 pp. 15 × 23 cm. Price $20.95.

SRS-A and Leukotrienes. (Proceedings of the Annual Symposium of the Institute of Basic Medical Sciences Royal College of Surgeons of England. 24th Sept. 1980). Edited by PRISCILLA J. PIPER. Wiley, One Wiley Drive, Somerset, NJ 08873. 282 pp. 15 × 23 cm. Price $45.00.

that have been applied to the analysis of the drug are presented. However, quantitation by gas chromatography–mass spectrometry–single-ion monitoring, which is far more reliable and sensitive than most other methods, is emphasized. A detailed description of gas chromatographic–mass spectrometric methodology is provided. In addition, each chapter has its own reference section, which provides ample documentation.

This monograph enables the investigator to choose the best analytical method for a particular drug based on the materials and equipment available. In addition, the design of basic experimental protocols should be greatly facilitated with the information contained within this volume. Although this book is intended for those in the field of drug abuse, it should be helpful to anyone interested in undertaking an analysis of any drug by gas chromatography–mass spectrometry.

Reviewed by Billy R. Martin
Department of Pharmacology
Medical College of Virginia
Virginia Commonwealth University
Richmond, VA 23298

Pharmacological and Biochemical Properties of Drug Substances, Vol. 3. Edited by MORTON E. GOLDBERG. American Pharmaceutical Association, 2215 Constitution Ave., N.W., Washington, D.C., 20037. 1981. 495 pp. 16 × 24 cm. Price $39.00 (Vols. 1–3, $90.00).

The third volume of this series presents 16 new monographs on a variety of therapeutic agents and topics, bringing the total number of monographs in this series to 52. Most of these reviews (in this volume as well as in the previous two) are concerned with specific drugs and are extensively referenced.

Although Dr. Goldberg's own research has emphasized central nervous system pharmacology, the book covers a wide variety of therapeutic classes such as cardiovascular agents, chemotherapeutic agents, and pulmonary/antiallergy agents, to name a few. The members of the editorial board also are cited for various areas of expertise.

Volume 3 contains three monographs covering topical steroid therapy, eicosanoids and pulmonary function, and one entitled, "Assessing Drug Concentration/Effect Correlations: Implications for Research and Therapy."

The author encourages readers to write to him or one of the editors if it is felt that a drug or topic deserves consideration for future volumes.

Staff review

NOTICES

An Introduction to Hazard and Operability Studies. The Guide Word Approach. By R. ELLIS KNOWLTON. Chematics International Ltd., 1770 Burrard St., Vancouver, B.C., Canada, V6J 3G7. 1981. 43 pp. 17 × 24 cm. Price $7.00.

Ap-GI—2nd International Conference on Pharmaceutical Technology. Paris—3–5 June 1980. Association de Pharmacie Galenique Industrielle, Rue JB, Clement 92290. Chatenay-Malabry, France. 15 × 24 cm. (each book). Price 800 FF complete set of five books, incl. taxes.

Arzneistoffe. (Lehrbuch der Pharmazeutischen Chemie). By WALTER SCHUNACK, KLAUS MAYER, and MANFRED HAAKE. Frieder Viewen & Sohn, Verlagsgesellschaft mbH, Postfach 5829, D-6200, Wiesbaden 1, West Germany. 1981. 608 pp. 17.5 × 24.5 cm. Price DM 68.00.

Basics of Electroorganic Synthesis. By DEMETRIOS K. KYRIACOU. Wiley, One Wiley Drive, Somerset, NJ 08873. 1981. 153 pp. 15 × 23 cm. Price $27.50.

Behavioral Pharmacology. 2nd Ed. By SUSAN D. IVERSEN and LESLIE L. IVERSEN. Oxford University Press, 200 Madison Ave., New York, NY 10016. 1981. 305 pp. 15 × 23 cm. Price $17.95 cloth and $10.95 paper.

Biomedical and Dental Applications of Polymers: Polymer Science and Technology Vol. #14. Edited by CHARLES G. GEBELEIN and FRANK F. KOBLITZ. Plenum, 227 W. 17th St., New York, NY 10011. 1980. 492 pp. 16 × 25 cm.

Breastfeeding: Program, Policy, and Research Issues. Edited by EDWARD C. BAER and BEVERLY WINIKOFF. A Special Issue of Studies in Family Planning, Vol. 12, No. 4. Population Council, 1 Dag Hammarskjold Plaza, New York, NY 10017. 1981. 206 pp. 21 × 28 cm. Price, no charge for single copies, multiple copies, $2.50 each.

Cellular Receptors for Hormones and Neurotransmitters. Edited by DENNIS SCHULSTER and ALEXANDER LEVITZKI. Wiley, 605 Third Ave., New York, NY 10016. 1980. 412 pp. 15 × 23 cm. Price $70.00.

Enzymes as Drugs. Edited by JOHN S. HOLCENBERG and JOSEPH ROBERTS. Wiley, 605 Third Ave., New York, NY 10016. 1981. 455 pp. 15 × 23 cm. Price $59.50.

Hagers Handbuch der Pharmazeutischen Praxis: Vollstandige (Vierte) Neuausgabe. By P. H. LIST and L. HORHAMMER. Springer-Verlag, 44 Hartz Way, Secaucus, NJ 07094. 1980. 628 pp. 16 × 24 cm. Price $100.30.

Hospital Pharmacy. 4th ed. By WILLIAM E. HASSAN, Jr. Lea & Febiger, 600 Washington Square, Philadelphia, PA 19106. 1981. 588 pp. 15 × 24 cm. Price $29.50, Canada $35.50.

IARC Monographs on the Evaluation of the Carcinogenic Risk of Chemicals to Humans. Some Pharmaceutical Drugs. Vol. 24. International Agency for Research on Cancer. World Health Organization, 1211 Geneva 27, Switzerland. 1980. 337 pp. 17 × 24 cm. Price U.S. $25.00 (Sw. fr. 40).

Immunostimulation. By L. CHEDID, P. A. MIESCHER, and H. J. MUELLER-EBERHARD. Springer-Verlag New York, 44 Hartz Way, Secaucus, NJ 07094. 1980. 236 pp. 16 × 24 cm. Price $22.50.

International Journal of Quantum Chemistry. Quantum Biology Symposium No. 7. (Proceedings of the International Symposium on Quantum Biology and Quantum Pharmacology). Held at Palm Coast, Fla., March 5–8, 1980. By PER-OLOV LOWDIN and JOHN R. SABIN. Wiley, 605 Third Ave., New York, NY 10016. 1980. 434 pp. 15 × 23 cm. Price $40.00.

Liquid Chromatography In Clinical Analysis. Edited by POKAR M. KABRA and LAURENCE J. MARTON. The Humana Press Inc., Crescent Manor, P.O. Box 2148, Clifton, NJ 07015. 1981. 466 pp. 15 × 23 cm. Price $55.00. $65.00 foreign.

Manual of Antibiotics and Infectious Diseases. 4th ed. By JOHN E. CONTE, Jr., and STEVEN L. BARRIERE. Lea & Febiger, 600 Washington Square, Philadelphia, PA 19106. 1981. 233 pp. 14 × 22 cm. Price $17.50. Canada $21.00.

Manual of Clinical Pharmacology. Edited by DAVID ROBERTSON and CRAIG R. SMITH. The Williams & Wilkins Co., 428 E. Preston St., Baltimore, MD 21202. 1981. 350 pp. 17 × 25 cm. Price $17.00.

Monoamine Oxidase Inhibitors. The State of the Art. Edited by M. B. H. YOUDIM and E. S. PAYKEL. Wiley, 605 Third Ave., New York, NY 10016. 1980. 214 pp. 15 × 23 cm. Price $39.00.

Pharmaceuticals and Health Policy. (International Perspectives on Provision and Control of Medicines). Edited by RICHARD BLUM, ANDREW HERXHEIMER, CATHERINE STENZIL, and JASPER WOODCOCK. Holmes & Meier Publishers, Inc., 30 Irving Place, New York, NY 10003. 1981. 14 × 22 cm. Price $37.50.

Pharmacology: An Introduction to Drugs. 2nd Ed. By MICHAEL C. GERALD. Prentice-Hall, Inc., Englewood Cliffs, NJ 07632. 1981. 686 pp. 15 × 23 cm. Price $20.95.

SRS-A and Leukotrienes. (Proceedings of the Annual Symposium of the Institute of Basic Medical Sciences Royal College of Surgeons of England. 24th Sept. 1980). Edited by PRISCILLA J. PIPER. Wiley, One Wiley Drive, Somerset, NJ 08873. 282 pp. 15 × 23 cm. Price $45.00.

that have been applied to the analysis of the drug are presented. However, quantitation by gas chromatography–mass spectrometry–single-ion monitoring, which is far more reliable and sensitive than most other methods, is emphasized. A detailed description of gas chromatographic–mass spectrometric methodology is provided. In addition, each chapter has its own reference section, which provides ample documentation.

This monograph enables the investigator to choose the best analytical method for a particular drug based on the materials and equipment available. In addition, the design of basic experimental protocols should be greatly facilitated with the information contained within this volume. Although this book is intended for those in the field of drug abuse, it should be helpful to anyone interested in undertaking an analysis of any drug by gas chromatography–mass spectrometry.

Reviewed by Billy R. Martin
Department of Pharmacology
Medical College of Virginia
Virginia Commonwealth University
Richmond, VA 23298

Pharmacological and Biochemical Properties of Drug Substances, Vol. 3. Edited by MORTON E. GOLDBERG. American Pharmaceutical Association, 2215 Constitution Ave., N.W., Washington, D.C., 20037. 1981. 495 pp. 16 × 24 cm. Price $39.00 (Vols. 1–3, $90.00).

The third volume of this series presents 16 new monographs on a variety of therapeutic agents and topics, bringing the total number of monographs in this series to 52. Most of these reviews (in this volume as well as in the previous two) are concerned with specific drugs and are extensively referenced.

Although Dr. Goldberg's own research has emphasized central nervous system pharmacology, the book covers a wide variety of therapeutic classes such as cardiovascular agents, chemotherapeutic agents, and pulmonary/antiallergy agents, to name a few. The members of the editorial board also are cited for various areas of expertise.

Volume 3 contains three monographs covering topical steroid therapy, eicosanoids and pulmonary function, and one entitled, "Assessing Drug Concentration/Effect Correlations: Implications for Research and Therapy."

The author encourages readers to write to him or one of the editors if it is felt that a drug or topic deserves consideration for future volumes.

Staff review

NOTICES

An Introduction to Hazard and Operability Studies. The Guide Word Approach. By R. ELLIS KNOWLTON. Chematics International Ltd., 1770 Burrard St., Vancouver, B.C., Canada, V6J 3G7. 1981. 43 pp. 17 × 24 cm. Price $7.00.

Ap-GI—2nd International Conference on Pharmaceutical Technology. Paris—3–5 June 1980. Association de Pharmacie Galenique Industrielle, Rue JB, Clement 92290. Chatenay-Malabry, France. 15 × 24 cm. (each book). Price 800 FF complete set of five books, incl. taxes.

Arzneistoffe. (Lehrbuch der Pharmazeutischen Chemie). By WALTER SCHUNACK, KLAUS MAYER, and MANFRED HAAKE. Frieder Viewen & Sohn, Verlagsgesellschaft mbH, Postfach 5829, D-6200, Wiesbaden 1, West Germany. 1981. 608 pp. 17.5 × 24.5 cm. Price DM 68.00.

Basics of Electroorganic Synthesis. By DEMETRIOS K. KYRIACOU. Wiley, One Wiley Drive, Somerset, NJ 08873. 1981. 153 pp. 15 × 23 cm. Price $27.50.

Behavioral Pharmacology. 2nd Ed. By SUSAN D. IVERSEN and LESLIE L. IVERSEN. Oxford University Press, 200 Madison Ave., New York, NY 10016. 1981. 305 pp. 15 × 23 cm. Price $17.95 cloth and $10.95 paper.

Biomedical and Dental Applications of Polymers: Polymer Science and Technology Vol. #14. Edited by CHARLES G. GEBELEIN and FRANK F. KOBLITZ. Plenum, 227 W. 17th St., New York, NY 10011. 1980. 492 pp. 16 × 25 cm.

Breastfeeding: Program, Policy, and Research Issues. Edited by EDWARD C. BAER and BEVERLY WINIKOFF. A Special Issue of Studies in Family Planning, Vol. 12, No. 4. Population Council, 1 Dag Hammarskjold Plaza, New York, NY 10017. 1981. 206 pp. 21 × 28 cm. Price, no charge for single copies, multiple copies, $2.50 each.

Cellular Receptors for Hormones and Neurotransmitters. Edited by DENNIS SCHULSTER and ALEXANDER LEVITZKI. Wiley, 605 Third Ave., New York, NY 10016. 1980. 412 pp. 15 × 23 cm. Price $70.00.

Enzymes as Drugs. Edited by JOHN S. HOLCENBERG and JOSEPH ROBERTS. Wiley, 605 Third Ave., New York, NY 10016. 1981. 455 pp. 15 × 23 cm. Price $59.50.

Hagers Handbuch der Pharmazeutischen Praxis: Vollstandige (Vierte) Neuausgabe. By P. H. LIST and L. HORHAMMER. Springer-Verlag, 44 Hartz Way, Secaucus, NJ 07094. 1980. 628 pp. 16 × 24 cm. Price $100.30.

Hospital Pharmacy. 4th ed. By WILLIAM E. HASSAN, Jr. Lea & Febiger, 600 Washington Square, Philadelphia, PA 19106. 1981. 588 pp. 15 × 24 cm. Price $29.50, Canada $35.50.

IARC Monographs on the Evaluation of the Carcinogenic Risk of Chemicals to Humans. Some Pharmaceutical Drugs. Vol. 24. International Agency for Research on Cancer. World Health Organization, 1211 Geneva 27, Switzerland. 1980. 337 pp. 17 × 24 cm. Price U.S. $25.00 (Sw. fr. 40).

Immunostimulation. By L. CHEDID, P. A. MIESCHER, and H. J. MUELLER-EBERHARD. Springer-Verlag New York, 44 Hartz Way, Secaucus, NJ 07094. 1980. 236 pp. 16 × 24 cm. Price $22.50.

International Journal of Quantum Chemistry. Quantum Biology Symposium No. 7. (Proceedings of the International Symposium on Quantum Biology and Quantum Pharmacology). Held at Palm Coast, Fla., March 5–8, 1980. By PER-OLOV LOWDIN and JOHN R. SABIN. Wiley, 605 Third Ave., New York, NY 10016. 1980. 434 pp. 15 × 23 cm. Price $40.00.

Liquid Chromatography In Clinical Analysis. Edited by POKAR M. KABRA and LAURENCE J. MARTON. The Humana Press Inc., Crescent Manor, P.O. Box 2148, Clifton, NJ 07015. 1981. 466 pp. 15 × 23 cm. Price $55.00. $65.00 foreign.

Manual of Antibiotics and Infectious Diseases. 4th ed. By JOHN E. CONTE, Jr., and STEVEN L. BARRIERE. Lea & Febiger, 600 Washington Square, Philadelphia, PA 19106. 1981. 233 pp. 14 × 22 cm. Price $17.50. Canada $21.00.

Manual of Clinical Pharmacology. Edited by DAVID ROBERTSON and CRAIG R. SMITH. The Williams & Wilkins Co., 428 E. Preston St., Baltimore, MD 21202. 1981. 350 pp. 17 × 25 cm. Price $17.00.

Monoamine Oxidase Inhibitors. The State of the Art. Edited by M. B. H. YOUDIM and E. S. PAYKEL. Wiley, 605 Third Ave., New York, NY 10016. 1980. 214 pp. 15 × 23 cm. Price $39.00.

Pharmaceuticals and Health Policy. (International Perspectives on Provision and Control of Medicines). Edited by RICHARD BLUM, ANDREW HERXHEIMER, CATHERINE STENZIL, and JASPER WOODCOCK. Holmes & Meier Publishers, Inc., 30 Irving Place, New York, NY 10003. 1981. 14 × 22 cm. Price $37.50.

Pharmacology: An Introduction to Drugs. 2nd Ed. By MICHAEL C. GERALD. Prentice-Hall, Inc., Englewood Cliffs, NJ 07632. 1981. 686 pp. 15 × 23 cm. Price $20.95.

SRS-A and Leukotrienes. (Proceedings of the Annual Symposium of the Institute of Basic Medical Sciences Royal College of Surgeons of England. 24th Sept. 1980). Edited by PRISCILLA J. PIPER. Wiley, One Wiley Drive, Somerset, NJ 08873. 282 pp. 15 × 23 cm. Price $45.00.

A publication of the
American Pharmaceutical Association—
the National Professional Society
of Pharmacists

JOURNAL OF PHARMACEUTICAL SCIENCES

INDEX TO AUTHORS
INDEX TO SUBJECTS

VOLUME 71
JANUARY TO DECEMBER, 1982

Published monthly under the supervision of the Board of Trustees

Renewed Attention Regarding Drug Stability

An interview with an aeronautical engineer was recently published in a general circulation magazine. What made the interview unusual was the subject matter: namely, lighter-than-air vehicles, otherwise known as dirigibles, zeppelins, or just plain "balloons."

The engineer brought out the usefulness of such aircraft to harvest logs out of dense forests, to deliver construction materials to otherwise inaccessible sites such as mountain tops, to bring heavy beams or piers into place in constructing bridges or tall buildings, and an assortment of other such uses. But he also lamented the fact that the entire field of lighter-than-air craft has been virtually ignored for the past 40 years as the appeal and glamour of air travel has moved, in turn, from propeller planes, to jet aircraft, to rockets, and to space vehicles.

All of this is just human nature; people's attention and interest are naturally drawn to the new, the exciting, the complex. Thirty years ago, we used the "times tables" to perform our simple multiplications; 20 years ago, we used a slide rule for this purpose; 10 years ago, we were using pocket calculators; today, we have small computers to do the job for us.

In light of this trend, it is not surprising that the pharmaceutical research community has shown less interest in the chemical and physical stability of drug substances and of drug products than in bioavailability, pharmacokinetics, drug metabolism, bioequivalence, and the other new and more glamorous areas of research. These latter areas have captured the drug researchers' fancy and have been accorded the lion's share of interest for at least the past 10 to 15 years.

But just as in the case of lighter-than-air vehicles, there is much to be learned concerning drug stability, as well as much to be done in the way of potentially important applications of that knowledge.

We were particularly reminded of this situation when we reviewed a document issued by the World Health Organization in late Summer 1981. The paper was entitled, "Stability of Pharmaceutical Substances and Simple Methods of Detecting Their Degradation," and it was prepared by Dr. M. Perez of the Analytical Laboratories of Roussel-Uclaf in Romainville, France.

The paper is the second in a series and details the results of a stability survey conducted on an additional 132 pharmaceutical substances. The practical significance of such research was indicative in the finding that 59 of the substances in this latest study were determined to be degradable under the conditions employed, while the remaining 73 substances were judged to be stable under the standardized adverse conditions utilized.

Even more recently, we have read announcements or reports that indicate a renewed interest in drug stability on the part of several pharmaceutical groups in this country.

For example, in October 1981, the United States Pharmacopeia, the American Society of Hospital Pharmacists, and the Food and Drug Administration jointly announced that they would be proceeding to undertake a "program to learn more about the shelf-life stability of drugs under actual market conditions." The program is to be titled "The Drug Stability Testing Program," and it is based on the success of a pilot stability study conducted on digoxin tablets during the preceding year. The results of the latter study, and a description of the study procedure, were published in the December 1981 issue of the *American Journal of Hospital Pharmacy*.

In November 1981, the Extension Services in Pharmacy at the University of Wisconsin announced that their annual Industrial Pharmacy Management Conference, to be presented in late March 1982, would be devoted to the theme "Dating of Pharmaceuticals, Update 1982." This conference will attempt to examine and review all that has happened on this subject since it was initially addressed as the theme of the first Wisconsin conference when this pharmacy management series was launched in 1969.

Finally, in December 1981, the American College of Apothecaries adopted a resolution titled "Uniform Expiration Dating for Pharmaceuticals." The body of the resolution lends support to the proposal for nationwide uniform dating as a part of FDA's Good Manufacturing Practices regulations—all of this out of recognition of the variable stability among drugs and the importance of stability information in ensuring quality pharmaceuticals for the patient.

None of these individual actions or programs is particularly dramatic. Indeed, some of them are not even new.

Nevertheless, they are significant because they address an important subject that has been largely neglected in recent years. Consequently, we applaud such efforts. Moreover, we encourage all within the pharmaceutical community to give their moral and professional support to these and to similar efforts directed at (a) elucidating more information concerning drug stability and instability and (b) the application of this information for the benefit of patients and those practitioners who serve them.

—EDWARD G. FELDMANN
American Pharmaceutical Association
Washington DC, 20037

0022-3549/82/0200-0135$01.00/0

JOURNAL OF PHARMACEUTICAL SCIENCES

FEBRUARY 1982
VOLUME 71 NUMBER 2

LITERATURE SURVEY

Vitamin D: An Update

K. THOMAS KOSHY

Received from *The Agricultural Division, The Upjohn Company, Kalamazoo, MI 49001.*

Keyphrases □ Vitamin D—an update, literature survey □ Literature surveys—vitamin D, an update

CONTENTS

This article reviews the current status of the most promising areas of research and development on vitamin D during the last 15 years. Many pharmacists are involved in the manufacture and sale of vitamin D preparations, yet few are aware of the enormous scientific effort that was expended to find that vitamin D is inactive *per se* and that its biological activity is primarily due to one of its metabolites. Since this metabolite acts in true hormonal fashion vitamin D is now considered by biochemists as a prohormone. The findings of the mode of action of vitamin D are well documented.

In the early 1920's, cod liver oil was known to cure rickets and xerophthalmia. The name vitamin D was given to the antirachitic substance in cod liver oil (1–3), and differentiated from vitamin A by the fact that vitamin A activity in the oil was lost by heating while that of vitamin D was not. Hess and Steenbock discovered, independently (4–7), that the antirachitic activity of this vitamin could be induced by UV irradiation of rachitic animals or their food. Steenbock's discovery that antirachitic activity could be induced by irradiation of foods, particularly of the sterol fraction, ultimately led to the identification of the structure of vitamin D and to the eradication of rickets as a major medical problem (5, 6, 8).

It was later discovered that vitamin D occurs in two active forms, ergocalciferol and cholecalciferol. Ergocalciferol is the synthetic form derived by the irradiation of ergosterol and is designated as vitamin D_2 (9, 10). Cholecalciferol, the natural form, was identified (11, 12) and designated as vitamin D_3. Vitamins D_2 and D_3 are equally active in humans and other mammals, but D_2 is virtually inactive in birds. Thus, poultry feeds must be fortified with D_3.

BIOSYNTHESIS OF VITAMIN D_3

Vitamin D_3 is synthesized in the skin from 7-dehydrocholesterol (7-DHC) when the skin is exposed to sunlight. Okano *et al.* (13) first demonstrated this when they irradiated skins from vitamin D-deficient rats and isolated vitamin D_3 from saponified skin extracts. The sequence of steps leading to the cutaneous photosynthesis of vitamin D_3 from 7-DHC was recently demonstrated (14). In Caucasian skin, all of the epidermal strata contain 7-DHC, but the highest concentration is in the stratum basale and the stratum spinosum.

When irradiated, 7-DHC is photochemically converted by a fast reaction to previtamin D_3 throughout the epidermis and the dermis. Once formed in the skin, previtamin D_3 is isomerized to D_3 by a slow nonphotochemical rearrangement at a rate dictated by skin temperature. At

0022-3549/82/0200-0137$01.00/0

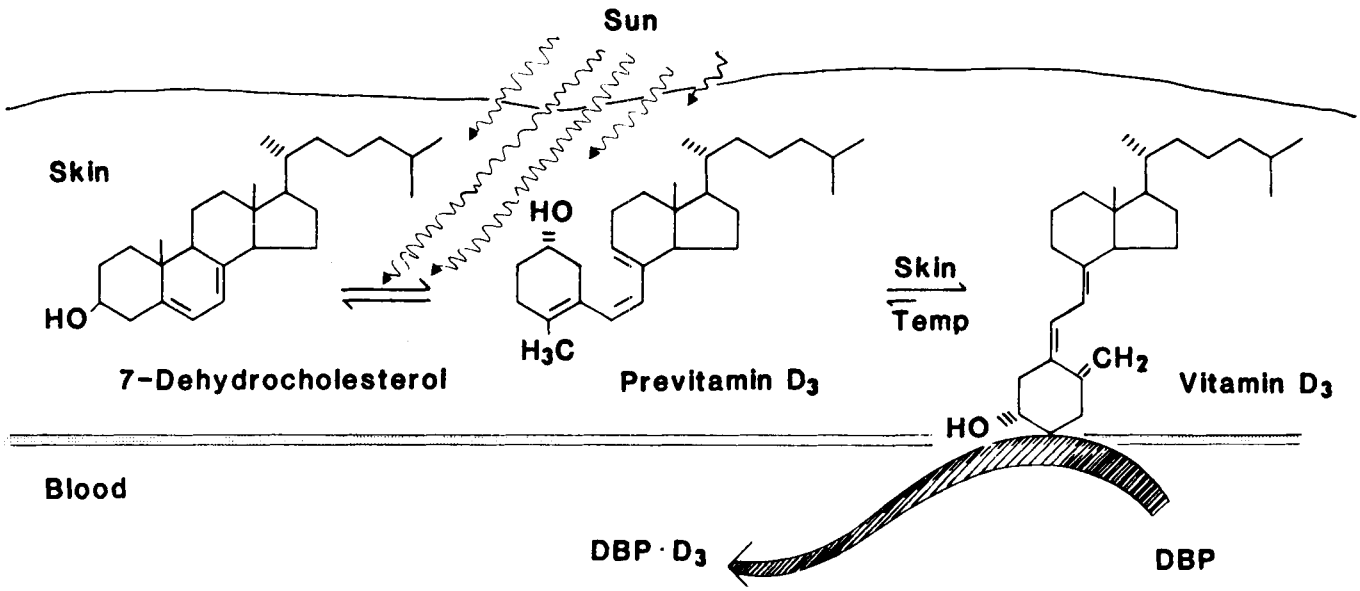

Scheme I—Diagram of the formation of previtamin D_3 in the skin, its thermal conversion to vitamin D_3, and transport by binding proteins (DBP) in plasma into the general circulation (Ref. 14).

37 ± 1° this thermal reaction is more rapid *in vivo* than *in vitro*. This difference is presumed to be due to the removal of vitamin D_3 by a specific binding protein from the skin into the circulating blood. Thus the skin serves as the site for the synthesis of 7-DHC, a reservoir for the storage of the primary photoproduct, previtamin D_3, and the organ where the slow thermal conversion of previtamin D_3 to D_3 occurs. The third process permits the skin to continuously synthesize D_3 and release it into the circulation for up to 3 days after a single exposure to sunlight. Scheme I illustrates this sequence of events.

COMMERCIAL VITAMIN D

Vitamins D_2 and D_3 are prepared commercially by irradiation of the provitamins ergosterol and 7-DHC, respectively. The resulting previtamins are isolated and heated under carefully controlled conditions to produce the respective vitamins. A number of by-products are formed during these irradiation and heating steps, some of which are removed during the final cleanup steps. Scheme II shows the known degradation products (15, 16) that may be present in the synthetic vitamin D concentrates. Some of the by-products have biological activity, but others such as lumisterol, the suprasterols, and the pyro- and isopyrocalciferols have no antirachitic activity. Tachysterol and *trans*-vitamin D have only slight antirachitic activity. Thus, biological activity is primarily due to vitamin D and previtamin D (17). The biological activity of previtamin D is attributed to its *in vivo* conversion to vitamin D (18).

Vitamin D is a 9,10-seco steroid and is treated as such in the numbering of its carbon skeleton. The important aspects of vitamin D chemistry center about its *cis*-triene structure. This structure gives vitamin D and related compounds a characteristic UV absorption maximum at 265 nm and a minimum at 228 nm. An index of purity of the vitamin D compounds is a value of 1.8 for the ratio of the absorbance at 265 nm to that at 228 nm. The *cis*-triene structure makes vitamin D and related compounds susceptible to oxidation and other chemical transformations. Under even mild acidity, it isomerizes to form the 5,6-*trans*-isomer and isotachysterol. Upon mild heating, the 5,6-*trans*-vitamin D is converted to isovitamin D. At higher temperatures, vitamin D is converted to the pyro, isopyro and the supra forms. All of these transformation products have lower biological activity than vitamin D.

It was mentioned earlier that vitamin D exists in thermal equilibrium with previtamin D. Studies showed that the amount of previtamin formed and the rate of equilibration markedly increased with time between 0 and 100° (19, 20). Vitamin D concentrates are available commercially in a resin form, as a solution in peanut oil, and as a dry concentrate in a gelatin beadlet matrix. The vitamin D concentrates usually contain other fat soluble vitamins, especially vitamin A. Therefore, in the analysis of vitamin D concentrates and multivitamin products, the vitamin D must be released and separated from other fat-soluble vitamins prior to its determination. This is accomplished by an alkaline saponification followed by suitable chromatographic steps to purify the vitamin D from interfering ingredients.

Because of the thermal equilibrium with previtamin D, there is disagreement regarding the optimum saponification conditions. Most published reports show optimum saponification for 20–30 min under refluxing conditions. Thompson *et al.* (21), in their procedure for the analysis of vitamin D in fortified milk at the level of 8.8–11.7 ng/g, found that saponification overnight at room temperature produced negligible loss of vitamin D.

The instability of vitamin D has been a challenge in the isolation, identification, and quantitation of its metabolites from biological samples in which their concentrations are in the range of 0.02–30 ng/g of the tissues. However, there now are fairly reliable methods for the isolation and analysis of all major metabolites of vitamin D. Vitamin D and its metabolites can be kept stable in the dry form in an inert atmosphere and protected from light in a freezer. In solution it is stable in nonacidic vegetable oils and in certain organic solvents containing an antioxidant such as α-tocopherol (Vitamin E) and stored in the same conditions as the dry form.

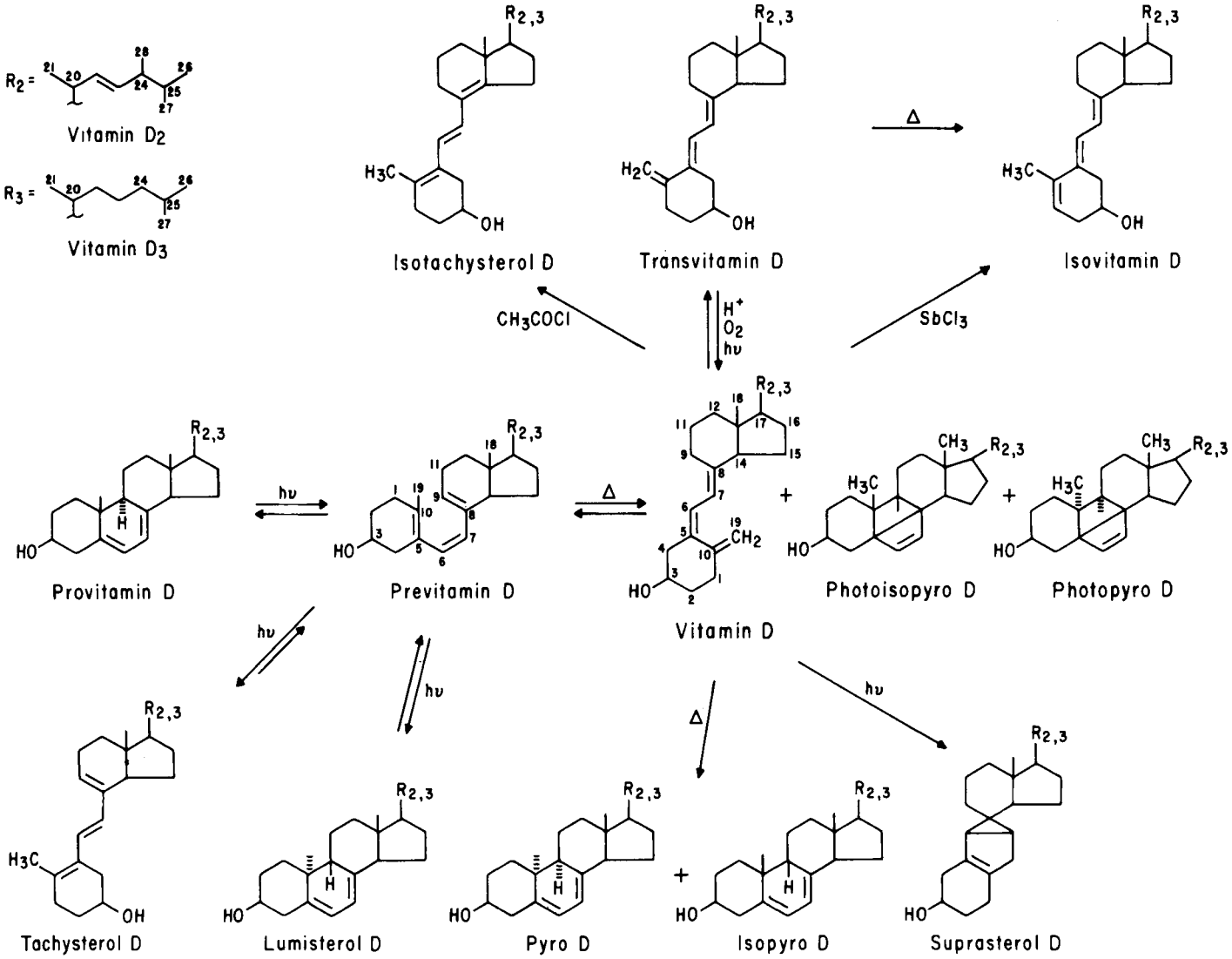

Scheme II—Photochemical, thermal, and chemical reaction pathways in the synthesis of vitamin D (Refs. 15, 16, and 176).

The original reference standard of vitamin D was a solution of irradiated ergosterol in olive oil. The present international standard is a solution of pure crystalline cholecalciferol in olive oil containing 0.025 μg/1 mg of solution. One international unit (IU) is equivalent to 0.025 μg of crystalline D_3 or 1 μg of D_3 is equivalent to 40 IU. The USP reference standards are crystalline ergocalciferol or cholecalciferol packed in sealed ampuls. The USP standards and the international standards are equivalent in that 1 μg of each is equivalent to 40 IU.

METABOLITES OF VITAMIN D_3

For 30 years following its discovery, relatively little was known about the synthesis of vitamin D or its metabolic fate in humans. It was thought that vitamin D acted directly on the target tissues of intestine and bone. However, the time lag reported by Carlsson (22) between the administration of vitamin D_3 and its physiological response appeared to argue against this concept. After intravenous administration of 10 IU of vitamin D_3, there was a lag of 10–12 hr before intestinal calcium transport response occurred (23). This led investigators to suspect that vitamin D_3 was metabolically altered before it became biologically active.

The transport of vitamin D in blood has been studied in considerable detail in animals. It has been shown that the chylomicrons and lipoproteins of the blood are initially important in the transport of vitamin D (24, 25). It was found (25) that upon incubation of blood with radioactive vitamin D or immediately following injection into blood, as much as 50% of the radioactivity in the blood was associated with the lipoprotein fractions. However, as time passed there was progressive shift of the radioactivity from the lipoprotein to the α_2-globulin fraction. The nature of the binding between vitamin D and this protein fraction is not known, but it appears that the vitamin is not easily dissociated from this protein. It was shown (26) that with time, after vitamin D absorption, there is a decreasing association of vitamin D with lipoproteins and an increased association with other protein fractions. The association of vitamin D activity with α_1- and α_2-globulin fractions of plasma was clearly demonstrated (27, 28).

25-Hydroxyvitamin D_3—Major developments in the metabolic study of vitamin D_3 came after radiolabeled compounds with high specific activities were synthesized. Selective ^3H-labeled and random ^{14}C-labeled vitamin D_3

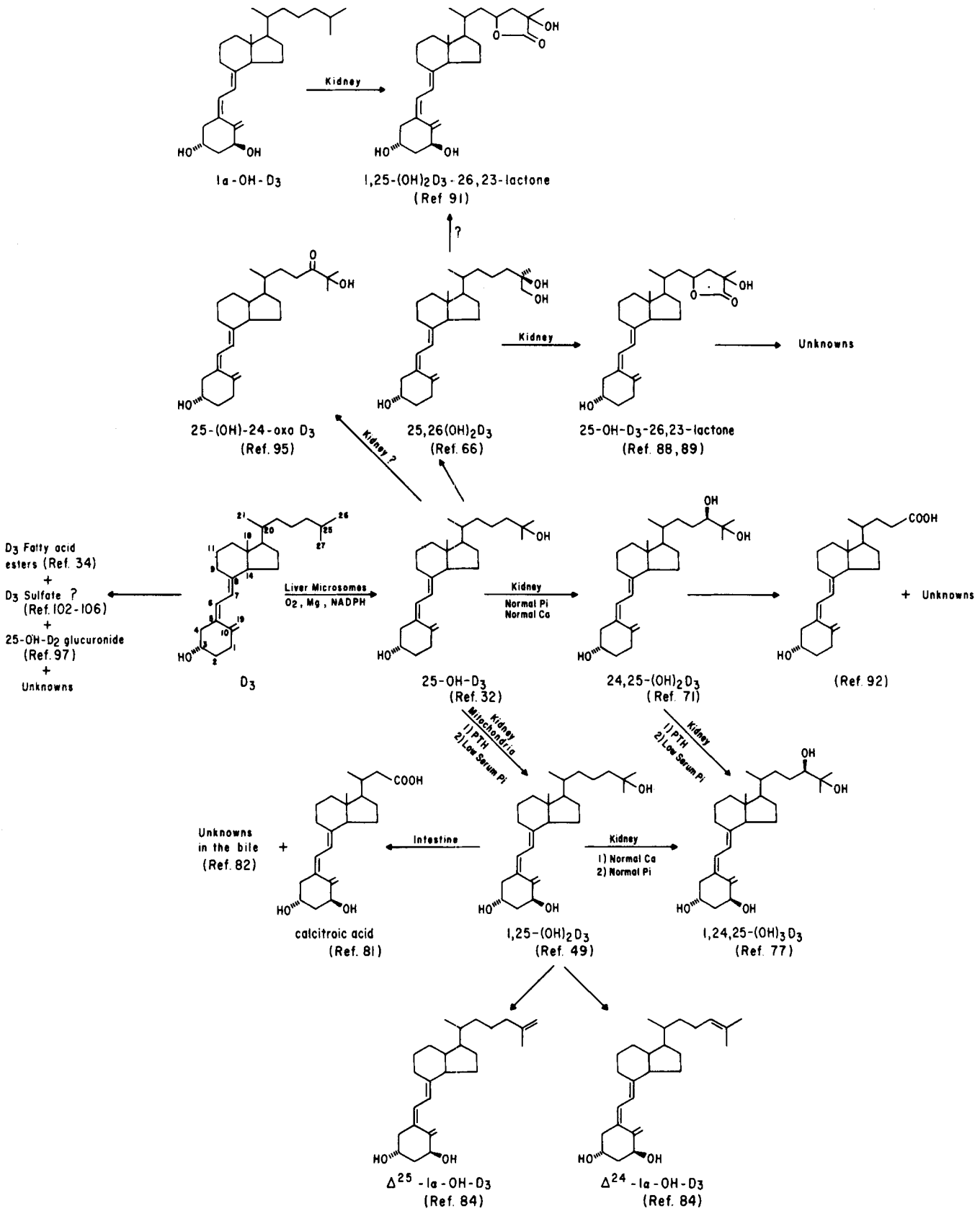

Scheme III—Schematic pathway of vitamin D metabolism.

were prepared in the mid-1960's and used successfully in the isolation and identification of its major metabolites. Other factors that contributed to this success were the development of milder extraction procedures and novel chromatographic techniques.

Norman *et al.* (29) administered [^{3}H]vitamin D orally and intraperitoneally to rats and then extracted the kidney and intestinal tissues with a mixture of methanol–chloroform as described by Bligh and Dyer (30). After chromatography on silicic acid columns and thin-layer

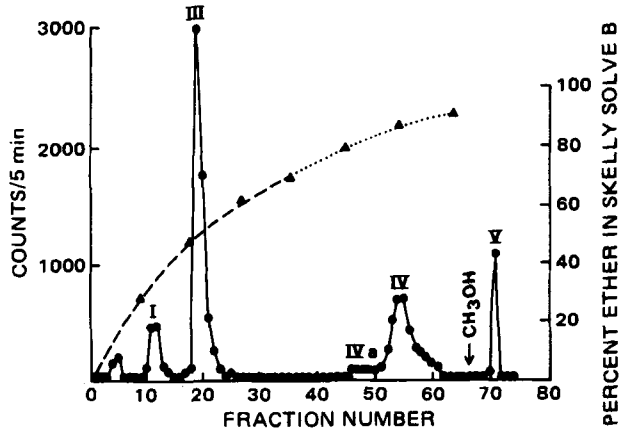

Figure 1—*Silicic acid chromatography of vitamin D_3 and its metabolites. Peaks III and I are vitamin D and its esters, respectively. Peaks IVa and V are unidentified at this time, and peak IV is 25-hydroxyvitamin D_3. (Ref. 32).*

plates, at least three other chloroform-soluble radioactive compounds were detected, all of which showed partial vitamin D activity. The aqueous methanol-soluble radioactive compounds were totally without vitamin D activity.

Biologically active metabolites of vitamin D were found (31) in the bone, liver, and serum of rats that had been given [^{3}H]vitamin D. As before (29), the aqueous-soluble metabolites from the tissues and the feces did not have vitamin D activity. At least three biologically active metabolites were isolated from the chloroform-soluble portion of the extract. One of these, designated as peak IV, was found in large amounts in the liver, blood, and bone. In 1938 Blunt *et al.* (32) conducted the classic experiment which led to the identification of this major metabolite as 25-hydroxy-vitamin D_3 (25-OH-D_3).

In this experiment, one hog was dosed with [^{3}H]vitamin D_3 and 800 ml of serum was collected when the peak IV radioactivity was expected to peak. Four other hogs were maintained on a diet supplemented with 250,000 IU of vitamin D_3 daily for 26 days. The plasma from these hogs (6.8 liters) was treated with ammonium sulfate to precipitate the proteins, which were then extracted with methanol–chloroform. This extract was combined with a similar extract from the serum of the hog that had received the [^{3}H]vitamin D_3 and subjected to chromatography on a 25-g silicic acid column eluted with an ether–Skellysolve B gradient followed by ether and finally stripping the column with methanol. This chromatographic system is reproduced in Fig. 1, which shows the radioactivity profile of the column eluate in order of increasing polarity of the metabolites. Peaks III and I are vitamin D_3 and its fatty acid esters, respectively.

The column eluate representing peak IV was purified further on a partition column using diatomaceous earth[1] as the solid support, 80:20 methanol–water as the stationary phase and Skellysolve B as the mobile phase. In this manner, 1.3 mg of the pure metabolite was obtained. This metabolite was positively identified as 25-OH-D_3 (32) by using GLC, UV, NMR, and mass spectrometry. This discovery was a milestone in the subsequent identification of other metabolites and in our current understanding of the physiological roles of these metabolites. Scheme III shows the metabolic pathway of vitamin D and all its currently known metabolites.

Two other groups of investigators (33, 34) independently found clues to the metabolic hydroxylation of vitamin D. It was soon established that 25-hydroxylation of vitamin D_3 takes place primarily in the liver (35, 36) and that 25-OH-D_3 is the major form of the circulating vitamin in human plasma (37) and is the primary metabolite of vitamin D_2 (38). This metabolite has been chemically synthesized (39).

Although the liver is the major site of 25-hydroxylation of vitamins D_2 and D_3, there is evidence suggesting that it is not the only site. It was shown (40) that homogenates of small intestine and kidney from the chick are capable of hydroxylating vitamin D_3 at position C-25. It was also shown (41) that hepatectomized rats can convert vitamin D_3 to 25-OH-D_3. Initially it was believed that the D_3-25-hydroxylase was located in the mitochondrial fraction of liver cells; however, careful investigation demonstrated that it is principally located in the liver microsomes, and that the enzymatic reaction is supported by reduced NADPH, molecular oxygen, and magnesium (42).

Initially, 25-OH-D_3 was considered to be the main biologically active metabolite of vitamin D. But soon it was discovered that physiological concentrations of 25-OH-D_3, like vitamin D_3, are incapable of stimulating either intestinal calcium transport or bone calcium mobilization (43–45).

1,25-Dihydroxyvitamin D_3—Earlier work (46) showed that the exhaled water from rats dosed with [1α-^{3}H]vitamin D_3 contained less radioactivity than the air from others dosed with vitamin D_3 labeled at the [24,25,26,27-$^3H_9$]-, [7-^{3}H]-, [6-^{3}H]-, and [3-^{3}H]- positions. Lawson *et al.* (34, 47), investigating the nature and localization of vitamin D metabolites by using [4-^{14}C,1α-^{3}H]-vitamin D_3, discovered a metabolite of vitamin D in the chick intestinal nuclei which was more polar than 25-OH-D_3 and which had lost its tritium group from position C-1. This metabolite, designated as peak P, was found in varying amounts in liver, kidney, bone, and blood and was localized in the intestinal nuclei.

It was postulated that the peak P metabolite was similar to the fraction designated "peak 4B" by Haussler *et al.* (33). The peak P metabolite had at least three times the biological activity of an equivalent amount of vitamin D_3 and was derived from 25-OH-D_3. However, the site of its synthesis was not obvious. Another study (48) established that this active metabolite was 1-oxygenated 25-OH-D_3 and that it was produced in the kidney. A short time later, Lawson *et al.* (49) identified peak P to be 1α,25-dihydroxyvitamin D_3 [1,25-$(OH)_2D_3$]. This finding was confirmed by other investigators (50, 51) who found that 1,25-$(OH)_2D_3$ was part of peak V in the silicic acid column profile of vitamin D metabolites shown in Fig. 1.

It is now known that the formation of 1,25-$(OH)_2D_3$ is feedback regulated depending on the need for calcium in the blood. It is also known that 25-OH-D_3 is the main circulating form of all the known metabolites of vitamin D_3. There is as yet no reliable data on the concentration of vitamin D_3 in the blood, but it is believed to be very low (~2–3 ng/ml). The blood level of 25-OH-D_3 was initially determined by competitive protein binding methods

[1] Celite.

(52–54) which showed values of 15–38 ng/ml in normal humans. Since then, more reliable and precise high-performance liquid chromatographic (HPLC) methods have been developed (55–58) but the mean values were in the same range.

The endogenous level of 25-OH-D_3 in the cow was determined by HPLC (59, 60). It was generally in the range of 40–58 ng/ml of serum or plasma (mean 48 ± 5 ng/ml, n = 24), which is higher than that in the human. Following a single intravenous dose of 4 mg of 25-OH-D_3 to a cow, the average serum level declined from a high of 227 ng/ml at 1-hr postinjection, to 51 ng/ml after 51 days, showing an elimination half-life of ~10 days (61). These and other studies have confirmed the earlier findings that 25-OH-D_3 is the major circulating form of vitamin D in the blood of humans and cows.

The concentration of 1,25-$(OH)_2D_3$ in the human serum is very low, between 20 and 40 pg/ml. The concentration is determined by ligand binding methods after extensive cleanup of the serum extract. The most recent procedures use fractionization of the extract by HPLC to purify 1,25-$(OH)_2D_3$ from interfering materials prior to quantitation. Mean plasma values of 35 ± 3 (62), 34 ± 11 (63), and 31 ± 9 (64) pg/ml were reported in normal healthy adults. None was detected in the blood of anephric men (64), confirming that 1-hydroxylation takes place in the kidney. At the present time, 1,25-$(OH)_2D_3$ is considered to be the most potent known metabolite of vitamin D controlling calcium and phosphorus absorption from the intestine and mobilization of these elements from the bone when necessary.

Other Metabolites of Vitamin D_3—*25,26-Dihydroxyvitamin D_3*—It became known during the isolation and identification of 25-OH-D_3 that there were other metabolites in certain tissues and blood following administration of physiological doses of radioactive vitamin D. Suda *et al.* (65) prepared extracts of hog plasma containing these metabolites in a manner similar to the one used by Blunt *et al.* (32). The peak V portion in Fig. 1 was resolved into at least three components, designated V*a*, V*b*, and V*c*, on a second silicic acid column. The V*c* portion was rechromatographed on a diatomaceous earth[1] partition column specially designed for peak V metabolites (66). The V*c* peak was resolved into four peaks. The major peak V*c*3 was further purified on a Sephadex LH-20 column and a radiochemically pure fraction was obtained. This fraction was identified as 25,26-dihydroxyvitamin D [25,26-$(OH)_2D_3$]. This metabolite was about one-half as active as 25-OH-D_3 in the stimulation of intestinal calcium transport. The concentration of this metabolite is very low in the normal human; a value of 0.8 ± 0.4 ng/ml has been reported (67).

24,25-Dihydroxyvitamin D_3—Omdahl and DeLuca (68) reported that the inhibition of intestinal calcium transport due to dietary strontium results from a block of the kidney hydroxylase which produces 1,25-$(OH)_2D_3$ from 25-OH-D_3. They also found that when the synthesis of 1,25-$(OH)_2D_3$ was suppressed, a new metabolite appeared which behaved like the peak V*a* metabolite already described. This metabolite is made exclusively by the kidney (69, 70) and was identified as 24,25-dihydroxyvitamin D_3-[24,25-$(OH)_2D_3$] (71). This metabolite can be produced *in vitro* by incubating 25-OH-D_3 with kidney mitochondria from chickens fed a high calcium diet. It can also be produced *in vivo* in hogs.

Although the structure of 24,25-$(OH)_2D_3$ was determined (71) and confirmed by synthesis (72), the stereochemical configuration of the 24-hydroxyl group was not known. Tanaka *et al.* (73) showed that the trimethylsilyl ethers of 24*R*- and 24*S*-$(OH)_2D_3$ could be separated by HPLC and that the biologically active form was 24*R*,25-$(OH)_2D_3$. The concentration of this metabolite in the plasma of normal animals and humans is low. For example, Taylor *et al.* (74) reported a value of 1.68 ± 0.82 ng/ml among seven normal volunteers. In these subjects, the 25-OH-D_3 level was 8.8–35.7 ng/ml. Other investigators (62, 63, 67) have reported values of ~2 ng/ml of plasma.

It was demonstrated (75, 76) that under normal or hypercalcemic conditions, 24,25-$(OH)_2D_3$ is the major circulating metabolite of 25-OH-D_3. Like 1,25-$(OH)_2D_3$, it is capable of supporting growth, elevating serum calcium, and calcifying bones of rats on a normal calcium, normal phosphorus diet. Their data also demonstrated that 24,25-$(OH)_2D_3$ is capable of inducing intestinal calcium transport at dose levels similar to 1,25-$(OH)_2D_3$. The one major difference is that unlike the latter, 24,25-$(OH)_2D_3$ has little ability to mobilize calcium from the bone. The finding that nephrectomy blocks the biological activity of 24,25-$(OH)_2D_3$ led to the discovery that this metabolite can serve as a substrate for 25-OH-D_3-1-hydroxylase in the kidney, yielding a new, more polar metabolite, 1,24,25-trihydroxyvitamin D_3.

1,24,25-Trihydroxyvitamin D_3—1,24,25-trihydroxyvitamin D_3 [1,24,25-$(OH)_3D_3$] was first prepared (77) *in vitro* from tritium-labeled 24,25-$(OH)_2D_3$ by incubation with chicken kidney homogenates. A total of 50 μg of the labeled compound was incubated in 0.5 μg (120,000 dpm/μg) portions with 1.5 ml of the kidney homogenate at 37° for 30 min. The homogenates were combined and extracted as in previous experiments (71). The extract was subjected to several column chromatographic steps to obtain a radiochemically pure metabolite more polar than the starting material. This metabolite was identified as 1,24,25-$(OH)_3D_3$ by UV and mass spectrometry, and its reactivity to periodate treatment.

The biological activity of 1,24,25-$(OH)_3D_3$ parallels the biological activity reported for 24,25-$(OH)_2D_3$ (76). It is preferentially more active in inducing intestinal calcium transport than in mobilizing calcium from bone and is ~60% as effective as vitamin D_3 in the cure of rachitic lesions. Although on a weight basis it is less active both in the magnitude and duration of response than 1,25-$(OH)_2D_3$, it is probably much more active than 24,25-$(OH)_2D_3$ (77). There is no conclusive data on the concentration of 1,24,25-$(OH)_3D_3$ in the blood. It is known to be lower than that of 1,25-$(OH)_2D_3$ and, therefore, in the low picogram per milliliter range in the plasma.

1α-OH-24,25,26,27-Tetranor-D_3-23-carboxylic Acid (Calcitroic Acid)—During the studies on the metabolism of 1,25-$(OH)_2D_3$, the possibility that it might be converted to more active forms was investigated. In 1976, 26,27-^{14}C-labeled 25-OH-D_3 was synthesized and enzymatically converted to the corresponding 1,25-$(OH)_2D_3$ compound (78). When injected into vitamin D-deficient animals, this compound lost up to 20% of its 26,27-^{14}C in the expired air as carbon-14 dioxide within 24 hr, demonstrating the ex-

istence of a side-chain oxidation reaction of 1,25-$(OH)_2D_3$ (78, 79). This side-chain oxidation appeared to require 1α-hydroxylated metabolites, since nephrectomy abolished carbon-14 dioxide expiration from radiolabeled 25-OH-D_3 but did not affect the amount of carbon dioxide 14 expired from 1,25-$(OH)_2$[26,27-^{14}C]D_3-dosed rats (79). Removal of the jejunum, ileum, and colon drastically reduced the carbon-14 dioxide expired by these rats, implicating an intestinal site of side-chain oxidation (80).

In vivo experiments (81) using doses of 3α-^{3}H- and 26,27-^{14}C-labeled, 1,25-$(OH)_2D_3$ were conducted with examination of tissue extracts for metabolites relatively enriched in tritium. This study culminated in the isolation and identification of the major side-chain oxidized metabolite of 1,25-$(OH)_2D_3$ as 1α,3β-dihydroxy-24,25,26,27-tetranor-D_3-23-carboxylic acid, which was named calcitroic acid.

Calcitroic acid was found in the liver and intestinal tissue, but very little was present in the blood. The amount of calcitroic acid in the organic soluble extracts of the liver and intestine accounted for only 4–6% of the administered dose. It was recently found (82) that the water-soluble metabolites in rat bile are predominantly acids. As much as 13% of the dose present in bile after 24 hr was calcitroic acid. This means that substantial amounts of unknown metabolites of 1,25-$(OH)_2D_3$ remain in bile.

The function of the side-chain oxidation of 1,25-$(OH)_2D_3$ is not known. One possibility is that side-chain oxidation and biliary excretion are a route for inactivation and excretion of 1,25-$(OH)_2D_3$. Alternatively, metabolites of 1,25-$(OH)_2D_3$ in bile may be reabsorbed by the intestine and have biological function there (82). Calcitroic acid was chemically synthesized from 24-oxocholesterol acetate and its biological activity compared with 1,25-$(OH)_2D_3$ (83). It stimulated intestinal calcium transport 6 hr after intravenous administration, but the response was significantly less than that of an identical base of 1,25-$(OH)_2D_3$. It had no effect in the mobilization of calcium from the bone.

Δ^{24}-1α-Hydroxy- and Δ^{25}-1α-Hydroxyvitamin D_3—Onisko *et al.* (84), in their study of the metabolism of 1α,25-dihydroxy[3α-^{3}H]vitamin D_3 in the rat, found two minor radioactive compounds in the bile. These were identified as Δ^{24}-1α-hydroxyvitamin D_3 and Δ^{25}-1α-hydroxyvitamin D_3. The two compounds were present in the same ratio that is obtained by standard chemical dehydrations of the 25-hydroxy group. It is assumed that the isomers arise *via* a nonenzymatic elimination process in bile. The biological significance of these products is not known.

25-Hydroxyvitamin D_3-26,23-lactone—During the course of developing an assay procedure for 24,25-$(OH)_2D_3$ and 25,26-$(OH)_2D_3$ in human plasma, a previously unidentified compound was detected in chick plasma (85, 86). This compound was a contaminant in the assay of 24,25-$(OH)_2D_3$ or 25,26-$(OH)_2D_3$ when only a single chromatographic column was used for pre-assay purification; however, it could be resolved by HPLC on a microparticulate silica column (87). This metabolite was extracted from the plasma of chickens and was identified (88) as 25-hydroxyvitamin D_3-26,23-lactone (25-OH-D_3-26,23-lactone) from its UV, mass, Fourier transform IR, and PMR spectra. Hollis *et al.* (89) found that 25,26-$(OH)_2D_3$ is the precursor for 25-OH-D_3-26,23-lactone and the transformation takes place in the kidney, but its biological importance is not yet known.

1α,25-Dihydroxyvitamin D_3-26,23-lactone—After the discovery of 25-OH-D_3-26,23-lactone, Tanaka *et al.* (90) investigated if 1,25-$(OH)_2D_3$ would undergo a similar transformation to the corresponding lactone. They found that kidney extracts from chicks given large doses of vitamin D_3 readily converted 1,25-$(OH)_2D_3$ to 1,24-25-$(OH)_3D_3$, but produced only trace amounts of the lactone. However, when they incubated 25-OH-D_3-26,23-lactone with kidney homogenates from rachitic chickens known to be rich in 1-hydroxylase activity and deficient in other vitamin D hydroxylases, they isolated a compound which was identified as 1α,25-dihydroxyvitamin D_3-26,23-lactone [1,25-$(OH)_2D_3$-26,23-lactone]. They postulated that because 1α-hydroxylase activity is generally low under the conditions in which the lactone is formed, the *in vivo* 26,23-lactonization of 1,25-$(OH)_2D_3$ would likely be minimal.

Another investigator (91) fed the synthetic analog of vitamin D_3, 1α-hydroxyvitamin D_3 (1α-OH-D_3), to rats and isolated 1,25-$(OH)_2D_3$-26,23-lactone from the blood. The biological potency or significance of this metabolite is not established, and to the author's knowledge, it has not yet been isolated from human blood.

*25,26,27-Tris-*nor*-vitamin D_3-24-carboxylic Acid*—It was pointed out earlier that when 1-hydroxylation is inhibited, 25-OH-D_3 is metabolized to 24,25-$(OH)_2D_3$ (71), which in turn acts as the precursor for 1,24,25-$(OH)_3D_3$ (77). Recently, 24,25-$(OH)_2$ was found to rapidly metabolize to an acid with the loss of three terminal carbons on the side chain. This compound was identified as 25,26,27-tris-*nor*-vitamin D_3-24-carboxylic acid (92). The biological significance of this metabolite is not known.

25-Hydroxy-24-oxocholecalciferol—During the course of investigating renal 24-hydroxylase activity, it was found (93) that kidney homogenates from chicks supplemented with vitamin D_3 metabolized 25-OH[26,27-$^3H_6$]D_3 *in vitro* to three unknowns designated A, C, and E. Production of unknown A increased in parallel with the increase in the amount of 25-$(OH)D_3$ added as a substrate, while that of unknown C was fairly constant irrespective of substrate increase (94). Unknown A was less polar than 25-OH-D_3. This unknown was identified (95) as 25-hydroxy-24-oxocalciferol. The biological significance of this metabolite is unknown, and to this author's knowledge, there has been no confirmation of its presence *in vivo* in humans or animals.

25-Hydroxyvitamin D_2-25-β-D-glucuronic Acid—Previous studies (96) showed that the principal route of excretion of vitamin D metabolites in humans is through the bile. But the identity of most of the biliary metabolites is unknown. Avioli *et al.* (96) also found that in human subjects administered [^{3}H]vitamin D_3, only 8–9% of the biliary radioactivity was extractable with chloroform and that biliary excretion of vitamin D_3 was negligible. Upon treatment with β-glucuronidase, an additional 40% of the biliary radioactivity became chloroform soluble, but only ~5% of the liberated radioactivity appeared to be free vitamin D_3.

Examination of the biliary metabolites of vitamin D_2 in chickens revealed that the major metabolite was 25-hy-

droxyvitamin D_2-25-β-D-glucuronic acid (25-OH-D_2-25-glucuronide) (97). It has long been known that vitamin D_2 is much less active than vitamin D_3 in the chicken while the two forms are equally active in mammals. It was shown earlier (98) that vitamin D_2 is more rapidly removed from the chick blood than vitamin D_3 and excreted into the bile.

It was also reported (99) that the two forms of the vitamin are hydroxylated at C-25 equally by chick liver preparations. Several studies have long established that 25-OH-D_3 is the main circulating form of vitamin D_3 in humans and cows (55–61). But other studies (100, 101) demonstrated that the chick is unable to raise the blood levels of 25-OH-D_2 and other D_2 metabolites to the D_3 metabolite levels. Based on these facts, one may conclude that the facile formation of 25-OH-D_2-25-glucuronide in chicks and its removal from circulation is the reason that chicks and other birds discriminate against vitamin D_2. LeVan *et al.* (97) reported from their preliminary experiments that chicks dosed with [^{3}H]vitamin D_3 produce only small amounts of the 25-glucuronide. Experiments are in progress in their laboratories to see whether the 25-glucuronides of vitamin D metabolites occur in mammalian bile or if this pathway is peculiar to avian species.

Vitamin D Sulfate—Initial experiments with radiolabeled vitamin D showed very little radioactivity in the aqueous portion after the kidney, intestine, serum, or plasma was extracted with a mixture of chloroform and methanol (29, 31). However, the formation of water-soluble conjugates from vitamin D or its metabolites has always been suspected. Thus, several investigators reported the presence of vitamin D sulfate (D-sulfate) in human (102–104) and cow milk (102, 104, 105).

Lakdawala and Widdowson (103) collected milk from 34 women from 3–8 days postpartum and analyzed for D-sulfate. The D-sulfate concentration was 17.8 ng/ml between the 3rd and 5th days and 10.0 ng/ml between the 6th and 8th days, respectively. These authors noted that even in winter, breast milk protected the infants from rickets whereas cow milk did not. Sahashi *et al.* (102) found the concentration of D-sulfate in cow milk and human milk to be 204 and 950 IU/liter (5 and 24 ng/ml), respectively. These figures were all based on a nonspecific colorimetric method.

Very recently, (106) a more specific HPLC method was used for the analysis of human milk whey from six Caucasian mothers between 1 and 8 days postpartum using 1α,2α-[^{3}H]vitamin D sulfate as a tracer to monitor the recovery of the endogenous D-sulfate. No endogenous D-sulfate was found in any of the samples (detection limit, 1 ng/ml). This result was contradictory to that reported by others (102–105). Hollis's (106) contention was that the primary source of antirachitogenic activity in human milk is due to nonconjugated metabolites of vitamin D, primarily 25-OH-D_3. Yet, according to another report by Hollis *et al.* (107), the nonconjugated metabolites in human and cow milk are very low; human milk contained 320 ± 80 pg/ml (n = 5) of 25-OH-D_3. The concentrations of 24,25-$(OH)_2D_3$ and 1,24,25-$(OH)_3D_3$ in the same samples were 42 ± 3 and 12 ± 2 pg/ml, respectively. These results are puzzling when one considers the fact that the large majority of infants in the world are raised primarily on breast milk for up to 6–8 months without any gross manifestations of vitamin D deficiency.

Unidentified Metabolites of Vitamin D_3—Leading investigators are certain that there are many unidentified metabolites of vitamin D. For example, according to Onisko *et al.* (84), there remain substantial amounts of unknown metabolites of 1,25-$(OH)_2D_3$ in the bile. These are water-soluble, negatively-charged compounds, which are rendered chloroform-soluble after methylation. These are likely to be due to unknown carboxylic acid metabolites.

Most of the experiments leading to the discovery of the currently known metabolites have followed the injection of radioactive vitamin D_3 as a single dose to rachitic animals. Experiments with administration of radioactive vitamin D_3 daily for 1–2 weeks (108), have led to the discovery of a number of new metabolites of vitamin D_3, both polar and nonpolar, that have yet to be identified. Whether any of these will have important functions or whether they represent biochemical curiosities or inactivation products remains to be seen.

METABOLITES OF VITAMIN D_2

The only chemical difference between vitamins D_2 and D_3 is in the side chain. Vitamin D_2 has an extra methyl group on the 24th carbon and a double bond between the 22nd and 23rd carbons (Scheme II). The virtual inactivity of vitamin D_2 in birds has long been known. However, the major metabolic pathways of the two forms of vitamin D in birds and mammals are analogous. Thus, 25-OH-D_2 was isolated and identified from porcine blood (38). The 25-OH-D_2 is further converted in the kidney to 1,25-$(OH)_2D_2$, which was isolated and identified (109). The hydroxylases that act on the vitamin D_3 series have been shown to act on vitamin D_2 compounds as well (110). Thus, the liver possesses vitamin D_2-25-hydroxylase and the kidney possesses 1α-hydroxylase. The current opinion is that the primary metabolites of vitamin D_2 would undergo further metabolism like vitamin D_3, but little work has been carried out with humans or animals, primarily because of the unavailability of suitable radiolabeled tracers.

SUMMARY OF THE METABOLIC SCHEME OF VITAMIN D

The currently known metabolic pathway of vitamin D is shown in Scheme III. Vitamin D_3 from the diet or that generated in the skin is absorbed into the blood. There is as yet no reliable figure on its concentration in blood. A portion of the vitamin D is converted into fatty acid esters (34) which are distributed in all vital organs and blood. The fatty acid esters have lower biological potency than vitamin D. Not much research has been conducted on the role of fatty acid esters in the total picture of vitamin D metabolism. A portion of the vitamin D is believed to be available in lactating mammals as D-sulfate (102–105), but this theory has been contradicted by other investigators (106, 107).

Vitamin D is stored to a considerable extent in the body. The liver is thought to be a storage organ, but more recent studies have shown that fat is the major storage site (111). Depletion of vitamin D in the animals depends on the turnover of the fat depots, which usually takes considerable time.

Vitamin D_3 *per se* has no biological activity. It is hydroxylated at carbon 25 to 25-OH-D_3 (35, 36) in the liver. The liver 25-hydroxylase system requires NADPH, mo-

lecular oxygen, and magnesium and is located in the microsomal fraction. Initially, it was thought that this 25-hydroxylation was feed-back regulated (112) to reduce the chances of toxicity to over-intake of vitamin D_3. However, later studies (113) with rats that received weekly or triweekly doses of vitamin D_3 showed that the amount of 25-OH-D_3 in plasma correlated with an increase in vitamin D intake, irrespective of the dose administered. Thus, it seems that vitamin D is efficiently mobilized to 25-OH-D_3 in the liver and then bound to a plasma-binding protein where it acts as a reservoir in the blood. However, other 25-hydroxylases are also present in the liver. These act on cholesterol, dihydrotachysterol, and other analogs of vitamin D such as 1α-hydroxyvitamin D_3 (114–116).

The major circulating form of vitamin D metabolites in the blood is 25-OH-D_3 (37, 55–58). It is transported to the kidney by a specific protein and further hydroxylated on carbon C-1 to 1,25-$(OH)_2D_3$ or on C-24 to 24,25-$(OH)_2D_3$ depending on the circumstances. Under conditions of hypocalcemia, the parathyroid glands are stimulated to secrete parathyroid hormone (PTH), which in turn stimulates synthesis of 1,25-$(OH)_2D_3$. The 1,25-$(OH)_2D_3$ immediately proceeds to the intestine where it functions to stimulate intestinal calcium absorption without PTH. In addition, 1,25-$(OH)_2D_3$ together with the PTH hormone functions to mobilize calcium from previously formed bone. These two functions result in the elevation of serum calcium to normal levels that suppress PTH secretion and, hence, 1,25-$(OH)_2D_3$. Like hypocalcemia, hypophosphatemia directly stimulates synthesis of 1,25-$(OH)_2D_3$, which then independently stimulates the elevation of serum inorganic phosphate.

The mechanism of action of 1,25-$(OH)_2D_3$ was proved (50, 117) after techniques were developed for making [^{3}H]-1,25-$(OH)_2D_3$ from [^{3}H]-25-OH-D_3 *in vitro* from kidney homogenates. Using this technique, these investigators were able to correlate the presence of 1,25-$(OH)_2D_3$ in the intestine and bone, which accounted for 98 and 80% of the total radioactivity in the respective target tissues, with the simultaneous induction of intestinal calcium transport and bone calcium mobilization. These data strongly supported the earlier findings that 1,25-$(OH)_2D_3$ is the biologically active form of vitamin D_3 responsible for maintaining calcium and phosphorus homeostasis and that no further metabolism is required.

Under normocalcemic or hypercalcemic conditions, renal 1α-hydroxylation is inhibited and side-chain hydroxylation of 1,25-$(OH)_2D_3$ occurs, resulting in the formation of the most polar metabolite known so far, 1,24*R*,25-$(OH)_3D_3$ (77). Under these conditions 25-OH-D_3 also undergoes side-chain oxidation to form 24*R*,25-$(OH)_2D_3$ (71) and 25,26-$(OH)_2D_3$ (66). Of these two, 24*R*,25-$(OH)_2D_3$ is the more prominent. There is evidence suggesting that the intracellular concentration of phosphorus is a more important regulator than PTH for determining whether the hydroxylation of 25-OH-D_3 in the kidney occurs on either the C-1α or the C-24 positions (118). The ability of 24*R*,25-$(OH)_2D_3$ to stimulate both intestinal calcium transport and a weak bone mineralization response is believed to be dependent on its 1α-hydroxylation in the kidney to form 1,24*R*,25-$(OH)_3D_3$.

Thus, under normal conditions, one of the end products of both 1,25- and 24*R*,25-dihydroxyvitamin D is the same, *i.e.*, 1,24*R*,25-$(OH)_3D_3$. 1,24*R*,25-$(OH)_3D_3$ is only ~10% as active as 1,25-$(OH)_2D_3$ on a molar basis. It is more effective in stimulating calcium transport than bone mineralization (77, 119).

The low biological activity of 24*R*,25-$(OH)_2D_3$ and 1,24*R*,25-$(OH)_3D_3$ and their rapid metabolism and excretion in the chick prompted speculation that the purpose of 24-hydroxylation of 25-OH-D_3 and 1,25-$(OH)_2D_3$ is to introduce a hydroxyl group proximal to the 25 position to provide facile oxidative cleavage (120). Yet, it is puzzling that these two 24-hydroxylated metabolites are prominent circulating metabolites. Recently, it was reported (121) that small doses of 24*R*,25-$(OH)_2D_3$ increased intestinal calcium transport in anephric patients, suggesting that the compound *per se* is active and 1α-hydroxylation is not absolutely necessary.

When the body does not need 24*R*,25-$(OH)_2D_3$ or 1,24*R*,25-$(OH)_3D_3$, the former is converted to 25,26,27-tris-*nor*-vitamin D_3-24-carboxylic acid (92). The 25,26-$(OH)_2D_3$ undergoes more extensive transformations. After it was synthesized, its biological activity was studied in vitamin D-deficient rats and their nephrectomized counterparts. The results suggested that, like 24*R*,25-$(OH)_2D_3$, it requires renal 1α-hydroxylation before it can stimulate an intestinal calcium transport response (122). As discussed earlier it is also oxidized to calcitroic acid (81) and to 25-OH-D_3-26,23-lactone (88).

VITAMIN D AS A PROHORMONE

Vitamin D is virtually absent from the plant world and is found only in specific substances such as fish liver oils, egg yolk, and to a very small degree, in unfortified milk. A notable exception to this is the existence of conjugated forms of 1,25-$(OH)_2D_3$ in the South American plant *Solanum glaucophyllum* and *Cestrum diurnum* in the southern United States (123, 124). Vitamin D is unique in that under normal circumstances it is formed in the skin in sufficient quantities when humans and animals are exposed to sunshine, and extra supplementation is unnecessary. The previtamin D_3 that is formed in the skin is slowly released into the body as vitamin D_3. This process permits the skin to continuously synthesize and release vitamin D_3 into circulation for up to 3 days after a single exposure to sunlight (Scheme I and Ref. 14).

Because of changes in modern lifestyle and because the urban areas around the world are contaminated with UV-absorbing materials, it may be that insufficient amounts of vitamin D are produced in the skin. Vitamin D_3 is also unique in that it has to be metabolized in sequence to 25-OH-D_3 and to 1,25-$(OH)_2D_3$ or to some as yet unidentified metabolite before it becomes physiologically active, not only in its ability to prevent and cure rickets, but also to maintain calcium and phosphorus homeostasis. In this respect, 25-OH-D_3 only acts as a precursor for 1,25-$(OH)_2D_3$ and also for 24*R*,25-$(OH)_2D_3$ which is also biologically active.

Since 1,25-$(OH)_2D_3$ acts on tissues remote from its production site, it meets the criteria and definition of a hormone. In true hormonal form, its biogenesis is regulated by hypocalcemia or hypophosphatemia. PTH plays a vital role in the biochemistry of vitamin D_3. If 1,25-$(OH)_2D_3$ is accepted as a hormone, then vitamin D_3 can be considered as a prohormone and 25-OH-D_3 as a prehormone. Since the

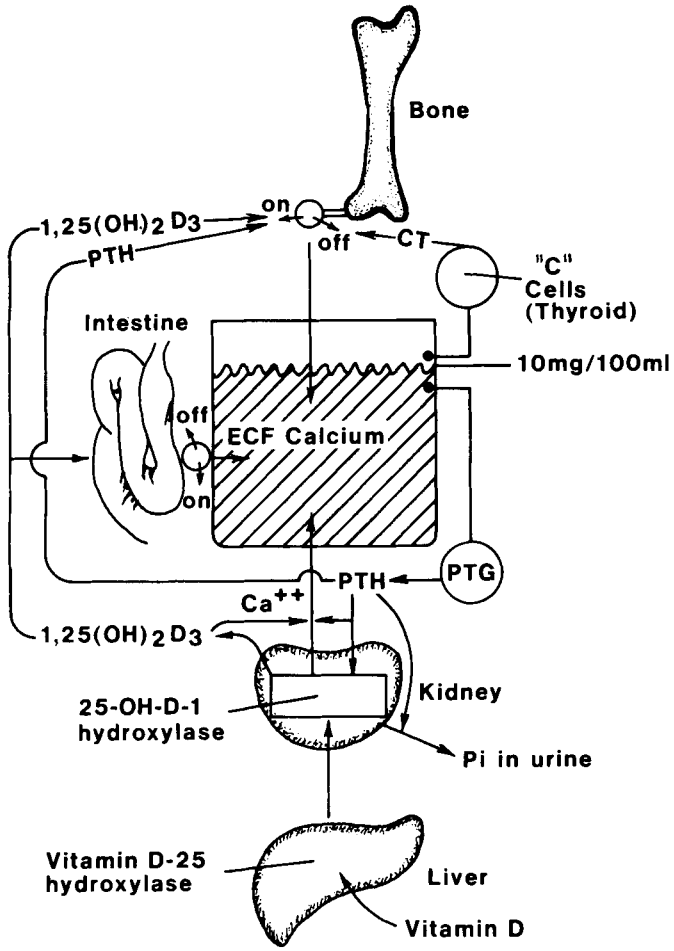

Figure 2—*Diagram of the calcium homeostatic mechanisms involving the vitamin D endocrine system (Ref. 132).*

kidney is the sole site of manufacture of 1,25-$(OH)_2D_3$, the kidney can be considered as the endocrine organ.

REGULATION OF CALCIUM HOMEOSTASIS AND VITAMIN D METABOLISM

The normal serum calcium level is maintained at ~10 mg/100 ml of ionized calcium. The accompanying anion is inorganic phosphorus. When the calcium level falls, the parathyroid glands which serve as the hypocalcemic detection organ are immediately stimulated to produce PTH. PTH is transported to the kidney, liver, and bone (125, 126). In the kidney it causes a phosphate diuresis which is vitamin D independent (127). PTH also stimulates renal reabsorption of calcium. Whether vitamin D is involved in this process is not absolutely established, but available evidence suggests that it is dependent on the existent serum 1,25-$(OH)_2D_3$ (128, 129).

Another, less rapid, calcium-conserving process occurs when PTH stimulates renal 25-OH-D-1-hydroxylase to produce 1,25-$(OH)_2D_3$ (130) and 1,24*R*,25-$(OH)_3D_3$; 1,25-$(OH)_2D_3$ stimulates intestinal calcium absorption without PTH involvement (128, 129). PTH is initially secreted in response to hypocalcemia within minutes, and its lifetime is measured in minutes (125, 126). In contrast, the action of 1,25-$(OH)_2D_3$ requires hours and its lifetime is measured in hours. Thus, PTH serves in a short-term renal process for restoring the calcium level, whereas the action of 1,25-$(OH)_2D_3$ is more prolonged. In the bone, the secreted PTH, together with 1,25-$(OH)_2D_3$, stimulate the transfer of calcium from the bone fluid compartment to the extracellular fluid compartment and into general circulation.

The three sources of calcium described restore serum calcium to the normal level, at which time PTH secretion is suppressed, shutting down the entire calcium mobilizing system. On the other hand, in cases of hypercalcemia, C cells of the thyroid secrete calcitonin, which suppresses mobilization of calcium from the bone and probably stimulates excretion of calcium and phosphorus in the kidney (131). In this manner the vitamin D endocrine system efficiently controls calcium homeostasis as shown in Fig. 2 (132).

In addition to phosphate, PTH, and 1,25-$(OH)_2D_3$, sex-related regulatory phenomena are known to affect calcium absorption. For example, there is a great need for calcium in egg-laying birds. Egg-laying birds have a high level of 1-hydroxylase activity in their kidneys, while nonlaying mature females or males have little 1-hydroxylase activity but higher 24*R*-hydroxylase activity (133, 134). During pregnancy and lactation, plasma 1,25-$(OH)_2D_3$ is elevated in both rats and humans (135, 136) to meet increased calcium demand. Growth hormone and prolactin are believed to provide the stimuli for increased 1-hydroxylase activity (137). These data suggest that sex hormones and other endocrine systems are also involved in the calcium regulatory processes.

Several review articles discuss the biogenesis of vitamin D, its metabolism, the mechanism of action of the metabolites in maintaining calcium and phosphorus homeostasis, and the clinical applications of vitamin D metabolites (132, 138–149).

CLINICAL APPLICATIONS OF VITAMIN D METABOLITES

It is beyond the scope of this article to go into a detailed discussion of the clinical applications of vitamin D metabolites. Of all the metabolites, 25-OH-D_3 and 1,25-$(OH)_2D_3$ are the most important and both are available commercially as prescription products in the United States and West European and Scandinavian countries. The clinical uses of these two compounds are for bone diseases related to abnormal calcium and phosphorus deficiencies in the blood.

As already mentioned, 25-OH-D_3 is the major circulating form of vitamin D_3 and has to be converted to 1,25-$(OH)_2D_3$ to function in the restoration of calcium and phosporus serum levels. The normal serum level of 25-OH-D_3 is 20–40 ng/ml, whereas that of 1,25-$(OH)_2D_3$ is only 20–40 pg/ml. The serum level of 25-OH-D_3 can go up depending on the vitamin D intake or exposure to sunshine, whereas that of 1,25-$(OH)_2D_3$ is constant and regulated according to the calcium level in the serum. In addition, 25-OH-D_3 is much less toxic than 1,25-$(OH)_2D_3$; therefore, 25-OH-D_3 is preferred in all calcium deficiency diseases where renal 1-hydroxylase activity is not impaired by lack of PTH stimulation or the inability of the kidney to produce this enzyme.

Since the discovery of the major metabolites of vitamin D_3, several synthetic analogs were made and researched not only to elucidate the mechanism of vitamin D_3 metabolism, but also as possible substitutes for 25-OH-D_3 and

1,25-$(OH)_2D_3$. Of these, the most prominent one is 1α-hydroxyvitamin D_3 (1α-OH-D_3) which is hydroxylated very readily in the liver to 1,25-$(OH)_2D_3$ (150). Except for a few specific diseases, the rationale for the use of these D_3 metabolites in the treatment of bone diseases is clouded by the interplay of the other less active metabolites and also by the several hormones and enzymes involved in the bone mineralization and bone formation processes. For example, 24,25-$(OH)_2D_3$ was until recently considered as the first of a series of metabolites in the excretionary route for 25-OH-D_3. In normocalcemic animals, 24-25-$(OH)_2D_3$ is the predominant dihydroxylated metabolite, and even though only a few humans have been treated to date with this metabolite, it was reported (149, 151) that it may have an important adjunctive role in the treatment of bone diseases.

Rickets—Rickets was originally thought of as a bone disease, but later found to be a blood disease in the sense that it appeared when the calcium and phosphorus levels in the blood were low. This led scientists to believe that the product of calcium and phosphorus concentrations in the blood was the determining factor in the production of rickets and this measure was used as a diagnostic test. With the mandatory practice of fortifying fresh and evaporated milk, rickets as a nutritional disease has almost been eliminted in the western world.

In addition to vitamin D-deficiency rickets, there are the vitamin D-dependent and vitamin D-resistant hypophosphatemic rickets. Vitamin D-dependent rickets is an inherited disease in children that occurs even when the patients take the daily requirement of vitamin D. These children develop aminoaciduria. The disease is treated by high doses of vitamin D (152), pharmacological doses of 25-OH-D_3 (153), or as little as 1 μg/day of 1,25-$(OH)_2D_3$ (153, 154). It is now believed that this disease is a defect of 1-hydroxylation of 25-OH-D_3. The cure with large doses of vitamin D_3 or 25-OH-D_3 is probably due to the 25-OH-D_3 interacting directly with the receptors.

Vitamin D-resistant hypophosphatemic rickets is more common and is characterized by low blood phosphorus, normal calcium serum concentration, and either normal or reduced intestinal calcium absorption. Studies using a strain of mice having the same genetic and phenotypic characteristics as the human in the development of this disease demonstrated that there is a generalized defect in phosphate transport reactions, especially in the kidney and the intestine (155, 156). Patients with this disease are given large doses of phosphate to counteract the large losses in the urine. Large doses of phosphate can bring about excessive secretion of PTH, which has to be corrected by the administration of 1,25-$(OH)_2D_3$ or 1α-OH-D_3. Thus, the treatment of this type of rickets is a complicated system of checks and balances.

Hypoparathyroidism—PTH secreted by the parathyroid gland senses hypocalcemia (Scheme III). Hypoparathyroid patients do not have this ability and therefore do not metabolize 25-OH-D_3 to 1,25-$(OH)_2D_3$. As a result, the serum calcium levels drop while inorganic phosphate may rise. Previously, such patients were treated with large doses of vitamin D, but now these cases can be treated better with 1,25-$(OH)_2D_3$ or 1α-OH-D_3 at doses of 0.68–2.7 μg/day plus sufficient dietary calcium (157–159). These small doses caused a marked increase in serum calcium concentration and urinary calcium excretion, without significant changes in renal calcium clearance or urinary hydroxyproline excretion. These results suggest that the correction of hypocalcemia involved primarily a stimulation of intestinal calcium absorption rather than a stimulation of skeletal calcium absorption.

Pseudohypothyroidism—Pseudohypothyroid patients secrete sufficient amounts of PTH in response to hypocalcemia, but the kidney and bone do not respond. The result is that patients become hypocalcemic in the presence of large circulating levels of PTH. These patients are treated satisfactorily with oral 1,25-$(OH)_2D_3$ or 1α-OH-D_3 plus calcium. In pharmacological amounts 25-OH-D_3 has also been used successfully for this condition.

Renal Osteodystrophy—Patients with renal osteodystrophy have lost the ability to make 1,25-$(OH)_2D_3$, the calcium-mobilizing hormone. This disease is complicated by the fact that the kidney fails to excrete phosphate, thereby causing a secondary hyperparathyroidism. This in turn can cause excessive erosion of bone calcium giving rise to osteitis fibrosa. Inadequate amounts of 1,25-$(OH)_2D_3$ may also lead eventually to bone resistance to PTH (160). Patients with renal osteodystrophy have been successfully treated with 1,25-$(OH)_2D_3$, 25-OH-D_3, and 1α-OH-D_3 (161–164).

Both 25-OH-D_3 and 1,25-$(OH)_2D_3$ are approved in the United States for the treatment and management of patients undergoing renal dialysis for diseases associated with chronic renal failure or hypocalcemia. At the present time, these are the only clinical conditions for which the two compounds have received approval from the Food and Drug Administration.

The cause for renal osteodystrophy is multifunctional, involving more than excess PTH and/or 1,25$(OH)_2D_3$ deficiency. The exact reasons for the development of one form of bone disease *versus* another remains to be clarified. Although the availability of vitamin D metabolites has substantially improved the therapeutic outlook, the relative merits of 1,25-$(OH)_2D_3$ and 25-OH-D_3 in the management of this bone malfunction remain controversial.

Three predominant forms of renal osteodystrophy are recognized. These are osteitis fibrosa, osteomalacia, and a combination of the two. From available but unpublished clinical data, one might make the following conclusions.

1. Osteitis fibrosa patients with serum calcium <10 mg/dl and phosphorus <5 mg/dl respond about equally to either 1,25-$(OH)_2D_3$ or 25-OH-D_3. Patients on 1,25-$(OH)_2D_3$ treatment may require closer observation because the fluctuation in serum calcium is probably greater than during treatment with 25-OH-D_3. Treatment with either compound is contraindicated for patients with serum calcium >11 mg/dl. If the hypercalcemia is marginal (10–11 mg/dl), 25-OH-D_3 is preferable to 1,25-$(OH)_2D_3$ because it may be less likely to cause an abrupt rise in serum calcium.

2. For patients with pure osteomalacia and serum phosphorus levels <5 mg/dl, 25-OH-D_3 is clearly the treatment of choice. If the calcium level in these patients is >10 mg/dl, a low calcium diet may permit sufficient doses of 25-OH-D_3 to be administered without provoking significant hypercalcemia (>11 mg/dl).

3. In patients with mixed osteomalacia and osteitis fibrosa (serum phosphorus <5 mg/dl), positive responses

have been reported with both 1,25-$(OH)_2D_3$ and 25-OH-D_3. Overall mineralization might be promoted better with 25-OH-D_3 than with 1,25-$(OH)_2D_3$. This is probably because of the role played by 24,25-$(OH)_2D_3$ (149, 151) generated from 25-OH-D_3 in the bone formation process.

Steroid-Induced Osteoporosis—Administration of glucocorticoids results in the thinning of the bones or osteoporosis. The exact reason for this disease is not known. Even though reports on the effect of glucocorticoids on the metabolism of vitamin D conflict, some indicate that administration of either 25-OH-D_3 or 1,25-$(OH)_2D_3$ is beneficial in correcting this problem (165).

Postmenopausal and Senile Osteoporosis—There is convincing evidence that sex hormones may affect vitamin D metabolism and calcium absorption (133–137). It has been shown that intestinal calcium absorption and serum levels of 1,25-$(OH)_2D_3$ diminish with age (165, 166). It has also been suggested that osteoporotic patients may have lower levels of 1,25-$(OH)_2D_3$ in their plasma than controls (167). In addition, there is evidence that the intestinal calcium absorption of osteoporotic patients can be enhanced by 1,25-$(OH)_2D_3$, but not by vitamin D_3 itself. This suggests that age- and sex-related factors prevent the metabolism of vitamin D_3 to its active forms. Several clinical trials are ongoing with 25-OH-D_3, 1,25-$(OH)_2D_3$, and 1α-OH-D_3 for the treatment of this fairly common disorder.

In one study (168), oral administration of 25-OH-D_3 for 3 months to six patients with postmenopausal osteoporosis was effective in raising low intestinal calcium absorption and in augmenting the production of 1,25-$(OH)_2D_3$ and 24,25-$(OH)_2D_3$. If 24,25-$(OH)_2D_3$ is important for bone formation as has been suggested (149, 151) then 25-OH-D_3 may be preferred over 1,25-$(OH)_2D_3$, since the latter is not converted to 24,25-$(OH)_2D_3$ in the body.

Anticonvulsant Drug-Induced Osteomalacia—There is a high incidence of osteomalacia among patients treated with the antiepileptic drug combination of phenytoin[2] and phenobarbital. This condition is generally treated with vitamin D (~4000 IU daily). It is obvious that this disease can be treated with lower doses of the more active metabolites. Stamp *et al.* (169) reported good results with 25-OH-D_3.

Hepatic Disorders—Since vitamin D is first hydroxylated in the liver, it seems that 25-OH-D_3 would be indicated for people with hepatic disorders. Cirrhosis of the liver does not appear to cause markedly reduced 25-OH-D_3 levels in the blood. If patients with hepatic disorders also have bone diseases associated with low serum calcium levels, it is quite likely that they would benefit from 25-OH-D_3 administration.

TOXICITY OF VITAMIN D AND ITS METABOLITES

Vitamin D_3 is toxic at high doses. Since it is converted in sequence to 25-OH-D_3 and to 1,25-$(OH)_2D_3$, and since 1,25-$(OH)_2D_3$ is the most biologically active form, it is not surprising that the margin of safety is lowest for 1,25-$(OH)_2D_3$ and highest for vitamin D_3. The recommended daily intake of vitamin D is 400 IU (10 μg). There is a considerable safety factor between the normal intake and the toxic dose, yet there are diseases like sarcoidosis and idiopathic hypercalcemia in which patients are overly sensitive to vitamin D. However, because there is an ample concentration of 25-OH-D_3 in normal human blood, there is no need to take more than 400 IU/day unless recommended by a physician. Continued daily intake exceeding 100,000 IU produces toxic manifestation. The symptoms include generalized weakness, nausea, vomiting, constipation, polyuria, dehydration, and elevated serum calcium and phosphorus levels. These adverse effects are reversible if the vitamin is withdrawn in time.

The crucial steps in the metabolism of vitamin D_3 are tightly controlled and feedback regulated. However, large doses of vitamin D_3 can overcome control of the 25-hydroxylation step. Haddad and Stamp (170) found a concentration of >600 ng/ml of 25-OH-D_3 in the serum of patients on long-term treatment with 5 mg (200,000 IU) of vitamin D for hypoparathyroidism or sex-linked hypophosphatemic rickets. So it is possible that the toxic effect of excessive intake of vitamin D_3 in normal individuals may be due to the abnormally high level of 25-OH-D_3 in the blood. The toxic symptoms are calcification of the heart, lungs, kidneys, and other soft tissues. Large doses of vitamin D will cause a marked demineralization of the bone at the same time that it causes hypercalcemia and nephrocalcinosis.

ANALYSIS OF VITAMIN D AND ITS METABOLITES

Biological and Chemical Methods—Biological and chemical methods are the oldest and probably the most widely accepted methods for the analysis of vitamin D. The biological methods can be divided into three groups: curative, prophylactic, and those based on calcium absorption into the blood stream. All are based on the administration of measured doses of a standard vitamin D preparation to a group of test animals and comparison of the biological responses with a similar group given the substance under test. A third group of test animals is used as controls. However, these methods are costly, do not distinguish vitamin D from other biologically active isomers and metabolites, and individual variations in the responses of the test animals are high. These tests and specific methods are detailed elsewhere (171–173).

The most widely used chemical method is the antimony trichloride colorimetric method. Antimony trichloride also reacts with vitamin A, and because vitamin A occurs along with D in many biological samples and is also an ingredient in many commercial products, it is necessary to remove it and other interfering substances prior to reaction with the reagent. This is generally achieved by saponification with alcoholic potassium hydroxide, extraction of the unsaponifiable fraction with petroleum ether, and cleanup on chromatographic columns. The procedure for the determination of vitamin D in pharmaceutical preparations is detailed elsewhere (172).

This method is applicable with suitable modifications to biological samples like fish liver oils, fortified milk, *etc.*, but the colorimetric procedures are being replaced when possible by more specific instrumental methods, usually HPLC. To the author's knowledge, there are no reported colorimetric procedures for vitamin D metabolites.

GLC—Although GLC procedures have been used extensively for the determination of numerous physiologically important steroids and hormones, only a few inves-

[2] Dilantin, Parke-Davis.

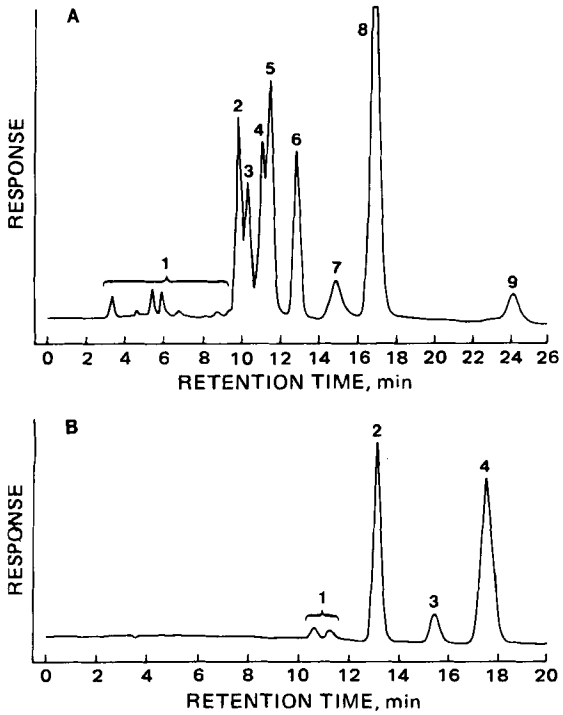

Figure 3—*Chromatogram of a synthetic mixture of photochemical isomers and reaction products of vitamin D_3 (A). Key: 1, unknowns; 2,* trans-*vitamin D_3; 3, previtamin D_3; 4, lumisterol$_3$; 5, isotachysterol$_3$; 6,* p-*dimethylaminobenzaldehyde (internal standard); 7, tachysterol$_3$; 8, vitamin D_3; and 9, 7-dehydrocholesterol. Chromatogram of a typical vitamin D_3 resin (B). Key: 1, resin impurities; 2,* p-*dimethylaminobenzaldehyde (internal standard); 3, tachysterol$_3$; and 4, vitamin D_3 (Ref. 176).*

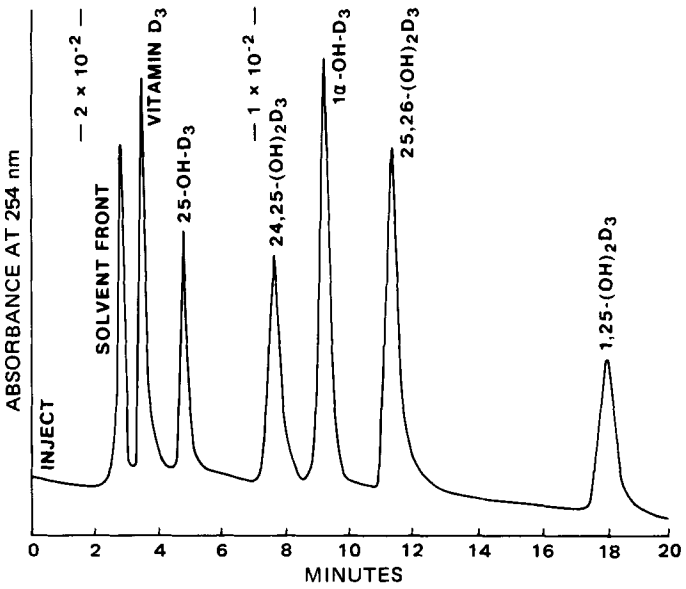

Figure 4—*Chromatogram of vitamin D_3 and its metabolites. A mixture of 40 ng of vitamin D_3, 30 ng of 25-OH-D_3, 25 ng of 24,25-$(OH)_2D_3$, 40 ng of 1α-OH-D_3, 40 ng of 25,26-$(OH)_2D_3$, and 25 ng of 1,25-$(OH)_2D_3$ were injected in 10 μl of 10% isopropanol in Skellysolve B using a U-6 K injector (Waters). With 10% isopropanol in Skellysolve B at 3000 psi pressure and two Zorbax-SIL (DuPont) (2.1 mm × 25 cm) columns in series, a flow rate of 0.5 ml/min was achieved (Ref. 177).*

tigators have attempted to develop similar techniques for vitamin D. The major problems with the GLC analysis of vitamin D are due to its open ring structure incorporating three conjugated double bonds in a 5,6-*cis* configuration. The 5,6-*cis* double bond causes less controllable thermal cyclization into the pyro- and isopyrocalciferols at operating GLC temperatures, resulting in two peaks. Another reason for the lack of interest in GLC analysis is that vitamin D concentration in biological systems is low and the samples generally contain structurally similar compounds requiring extensive sample cleanup. GLC methods for vitamin D analysis were reviewed previously (174, 175). In recent years, HPLC has become the most popular technique for analyzing vitamin D and 25-OH-D_3 and also serves as an important purification step prior to the ligand-binding methods for 1,25-$(OH)_2D_3$,24,25-$(OH)_2D_3$, and 25,26-$(OH)_2D_3$.

Competitive Protein-Binding Methods—It was once believed that 25-OH-D_3 was the most important biologically active metabolite of vitamin D. This belief, coupled with the fact that 25-OH-D_3 is the most abundant of all metabolites in the blood, stimulated a great deal of interest in its analysis.

Proteins with high binding capacity for 25-OH-D_3 were discovered and were utilized in the development of several competitive protein-binding assay procedures (52–54). Similar competitive protein binding methods are also available for vitamin D_3 and its more polar metabolites with much lower concentrations in the blood.

Several different binding proteins have been discovered with either greater binding capacity or greater specificity for a particular metabolite. Under standardized conditions, competitive protein-binding methods are used extensively because the sample volume is very small (0.1–1 ml), sensitivity is unattainable by other methods, sample manipulation is minimal, and a large number of samples can be analyzed simultaneously. The disadvantages are interference from related compounds that compete with the binding-proteins and lack of precision. The interference from related compounds is now minimized greatly by the use of HPLC.

HPLC—The main advantage of HPLC over GLC is that the problems associated with thermal cyclization and degradation are eliminated. Vitamin D and related compounds have a molar extinction coefficient of ~15,000 at 254 nm which allows the use of the most common and stable spectrophotometric detector available for HPLC. Therefore, HPLC is currently the technique of choice for vitamin D analysis. It is invaluable for the analysis of 25-OH-D_3 in biological samples and is also used extensively for purifying the more polar metabolities prior to their analysis by ligand binding methods. Since HPLC is nondestructive the fractions of interest can be collected and used for further tests if necessary.

The photochemical and thermal byproducts of vitamin D synthesis are shown in Scheme II. Until the advent of HPLC it was almost impossible to determine the actual vitamin D content of such a complex synthetic mixture. The separation achieved by Tartivita *et al.* (176) is shown in Fig. 3. Figure 3A is the chromatogram of a crude synthetic mixture and Fig. 3B is of commercial vitamin D in the resin form. These chromatograms were obtained on a 30-cm × 4-mm i.d. commercial microparticulate silica column. The mobile phase was a 70:30:1 mixture of chloroform (free from ethanol and water), *n*-hexane, and tetrahydrofuran at a flow rate of 1 ml/min. Using this system, vitamin D_3 was quantitated in a resin sample containing

Table I—Representative HPLC Systems for the Analysis of Vitamin D and Metabolites

Column No.	Mobile Phase	Compounds Separated or Analyzed	Sample Matrix	Reference
1[a], 50 cm × 2.1 mm	10% isopropanol in Skellysolve B	All known metabolites of D_2 and D_3	Synthetic mixture	177
2[b], 5 μm, 25 cm × 2.1 mm	Acetonitrile–methanol–water (90:5:5)	25-OH-D_3	Human serum	55
2, 5 μm, 22 cm × 6.2 mm	1.5% Water in methanol	D_2 and D_3	Human serum	58
1, 5 μm, 22 cm × 6.2 mm	9% Water in methanol	25-OH-D_3 and 25-OH-D_2	Human serum	58
3[c], 10 μm, 60 cm × 6 mm	*n*-Hexane–isopropanol (88:12)	1,25-$(OH)_2$D	Human serum	62
1, 22 cm × 6.2 mm	10% Isopropanol in hexane	25-OH-D, 24,25-$(OH)_2$D, 1,25-$(OH)_2$D	Human serum	63
1, 25 cm × 4.6 mm	Isopropanol–hexane (1:24 v/v)	25-OH-D and 25-OH-D_3	Human serum	64
1, 25 cm × 4.6 mm	Isopropanol–hexane (1:9 v/v)	24,25-$(OH)_2$D, 25,26-$(OH)_2$D and 1,25-$(OH)_2$D	Human serum	64
2, 25 cm × 4.6 mm	Water–methanol (1:49 v/v)	D_2 and D_3	Human serum	64
1, 6 μm, 25 cm × 6.2 mm	*n*-Hexane–isopropanol–methanol (87:10:3)	25-OH-D_3, 24,25-$(OH)_2D_3$ and 1,25-$(OH)_2D_3$	Human serum	178
1, 25 cm × 4.5 mm	10% Isopropanol in hexane	25-OH-D, 24,25-$(OH)_2$D, 25,26-$(OH)_2$D, 1,25-$(OH)_2$D	Human serum	67
1, 25 cm × 4.5 mm	2.5% Isopropanol in hexane	25-OH-D_2 and 25-OH-D_3	Human serum	67
4[d], 25 cm × 2.6 mm	Acetonitrile–methanol (1:1)	D_3	Fortified milk	179
5[e], 10 μm, 25 cm × 4 mm	1.25% Isopropanol in cyclohexane	D_3	Instant nonfat dried milk	180
6[f], 50 cm × 4.6 mm	Chloroform–*n*-hexane–acetic acid (70:30:1)	D_3	Cod liver oil	181
7[g], 25 m × 3 mm	5% Water in methanol	D_3	Cod liver oil	182
3, 30 cm × 4 mm	0.4% Ethanol in chloroform	D_3	Livestock feed supplement	183
8[h], 25 cm × 4.2 mm	5% Water in methanol	D_3	Livestock feed supplement	184
5, 25 cm × 4.2 mm	30% Chloroform in *n*-hexane	D_3	Livestock feed supplement	185
2, 5 μm, 25 cm × 2.1 mm	Acetonitrile–methanol–water (90:5:5)	25-OH-D_3	Bovine tissues and chicken egg yolk	186, 187
3, 30 cm × 4 mm	Chloroform–hexane–tetrahydrofuran (70:30:1)	Photochemical and thermal isomers	Synthetic mixture and commercial D_3 resin	176
9[i], 5–10 μm, 20–30 cm × 4.6 mm	0.3–0.53% Amyl alcohol in *n*-hexane	D	Commercial D resin powder	188
9, 5–10 μm, 15–60 cm × 3–6.25 mm	0.15–0.7% Amyl alcohol in *n*-hexane	D	Multivitamin preparations	189

[a] Zorbax-Sil, Dupont de Nemours, Wilmington, Del. [b] Zorbax ODS, Dupont de Nemours, Wilmington, Del. [c] μPorasil, Waters Associates, Milford, Mass. [d] ODS-HC-Sil-X-1, Perkin-Elmer Corp., Norwalk, Conn. [e] Lichrosorb NH_2, E. M. Reagents, Montreal, Canada. [f] Partasil, 10 PXS, Whatman, Inc., Clifton, N.J. [g] Lichrosorb 10, RP_{18}, Chromapack, Holland. [h] μBondapack C_{18}, Waters Associates, Milford, Mass. [i] Microparticulate silica

20×10^6 IU/g with a relative standard deviation of 1.37%.

HPLC has been frequently used for the quantitative analysis of 25-OH-D_3 in human serum (55–58). It has also been used extensively for the separation of minor constituents into purer fractions prior to their determination by any one of the appropriate protein-binding assays. Figure 4 shows the separation of a synthetic mixture of all the important metabolites of vitamin D_3 obtained by Jones and DeLuca (177). This separation was achieved using two 25-cm × 2.1-mm i.d. microparticulate silica columns in series and 10% isopropanol in Skellysolve B as the mobile phase at a flow rate of 0.5 ml/min. On the same column, they showed the difficult separation of 25-OH-D_3 from 25-OH-D_2 using 2.5% isopropranol in Skellysolve B at a flow rate of 0.7 ml/min

HPLC also has been used for the analysis of vitamin D and all its metabolites in a variety of matrixes. These include milk and milk products, cod liver oil, animal feed supplements, vitamin D concentrates, multivitamin preparations, chicken egg yolk, cow tissues (liver, kidney, and muscle), cow blood, and human blood. A summary of representative HPLC systems from the literature is shown in Table I.

CONCLUSION

After three decades of comparative inactivity, a surge of interest in vitamin D during the last 15 years has resulted in our understanding of the biogenesis of vitamin D_3, the identification of the major metabolites, the establishment of the metabolic pathway, and the hormonal nature of the metabolites. Vitamin D_3 *per se* is now known to be biologically inactive, while 1,25-$(OH)_2D_3$ (or some other as yet unidentified metabolite) has been established as the principal hormone responsible for maintaining calcium and phosphorus homeostasis. The kidney is the endocrine organ in the vitamin D hormonal functions. Extensive research is still underway in elucidating the role of other endocrine organs in the regulation of vitamin D metabolism and its physiological functions. Other unanswered questions deal with the mechanisms of (*a*) the active forms of vitamin D in the transport of calcium from the intestine into general circulation, (*b*) bone calcium mobilization, and (*c*) renal control of phosphorus concentration in the blood. Meanwhile, two principal metabolites, 25-OH-D_3 and 1,25-$(OH)_2D_3$, are available as prescription products in several western countries for the treatment of vitamin D deficiency diseases.

REFERENCES

(1) E. V. McCollum, N. Simmonds, J. E. Becker, and P. G. Shipley, *J. Biol. Chem.*, **53**, 293 (1922).

(2) *Bull. Johns Hopkins Hosp.*, **33**, 229 (1922).

(3) *J. Biol. Chem.*, **65**, 97 (1925).

(4) A. F. Hess, M. Weinstock, and F. D. Helman, *J. Biol. Chem.*, **63**, 305 (1925).

(5) H. Steenbock and A. Black, *ibid.*, **61**, 405 (1924).

(6) H. Steenbock, *Science*, **60**, 224 (1924).

(7) H. Steenbock and M. T. Nelson, *J. Biol. Chem.*, **62**, 209 (1924).

(8) H. Steenbock and A. Black, *ibid.*, **64**, 263 (1925).

(9) F. A. Askew, R. B. Bourdillon, H. M. Bruce, R. G. C. Jenkins, and T. A. Webster, *Proc. R. Soc. London, Ser. B.*, **107,** 76 (1931).

(10) A. Windaus, A. Linsert, A. Lüttringhaus, and G. Weidlich, *Justus Liebigs Ann. Chem.*, **492,** 226 (1932).

(11) A. Windaus, F. Schenck, and F. Von Werder, *Hoppe-Seylers Z. Physiol. Chem.*, **241,** 100 (1936).

(12) F. Schenck, *Naturwissenschaften*, **25,** 159 (1937).

(13) T. Okano, M. Yasumura, K. Mizuno, and Y. Kobayashi, *J. Nutr. Sci. Vitaminol.*, **23,** 165 (1977).

(14) M. F. Holick, J. A. MacLaughlin, M. B. Clark, S. A. Holick, J. T. Potts, Jr., R. R. Anderson, I. H. Blank, J. A. Parrish, and P. Elias, *Science*, **210,** 203 (1980).

(15) G. M. Sanders, J. Pot, and E. Havinga, *Fortschr. Chem. Org. Naturst.*, **27,** 131 (1969).

(16) H. Steuerle, *J. Chromatogr.*, **115,** 447 (1975).

(17) H. F. DeLuca, *Am. J. Med.*, **57,** 1 (1974).

(18) K. H. Hanewald, M. P. Rappoldt, and J. R. Roborgh, *Rec. Trav. Chim.*, **80,** 1003 (1961).

(19) K. H. Hanewald, F. J. Mulder, and K. J. Keuning, *J. Pharm. Sci.*, **57,** 1308 (1968).

(20) J. A. K. Buisman, K. H. Hanewald, F. J. Mulder, J. R. Roborgh, and K. J. Keuning, *ibid.*, **57,** 1326 (1968).

(21) J. N. Thompson, W. B. Maxwell, and M. L'Abbe, *J. Assoc. Off. Anal. Chem.*, **60,** 998 (1977).

(22) A. Carlsson, *Acta Physiol. Scand.*, **26,** 212 (1952).

(23) H. F. DeLuca, in "The Fat Soluble Vitamins," H. F. DeLuca and J. W. Suttie, Eds., The University of Wisconsin Press, Madison, Wis., 1969, p. 3.

(24) D. Schachter, J. D. Finkelstein, and S. Kowarski, *J. Clin. Invest.*, **43,** 787 (1964).

(25) H. Rikkers and H. F. DeLuca, *Am. J. Physiol.*, **213,** 380 (1967).

(26) P. S. Chen, Jr., and K. Lane, *Arch. Biochem. Biophys.*, **112,** 70 (1965).

(27) W. C. Thomas, Jr., H. G. Morgan, T. B. Connor, L. Haddock, C. E. Bills, and T. E. Howard, *J. Clin. Invest.*, **38,** 1078 (1959).

(28) P. De Crousaz, B. Blanc, and I. Antener, *Helv. Odontol. Acta*, **9,** 151 (1965).

(29) A. W. Norman, J. Lund, and H. F. DeLuca, *Arch. Biochem. Biophys.*, **108,** 12 (1964).

(30) E. G. Bligh and W. J. Dyer, *Can. J. Biochem. Physiol.*, **37,** 911 (1959).

(31) J. Lund and H. F. DeLuca, *J. Lipid Res.*, **7,** 739 (1966).

(32) J. W. Blunt, H. F. DeLuca, and H. F. Schnoes, *Biochemistry*, **7,** 3317 (1968).

(33) M. R. Haussler, J. F. Myrtle, and A. W. Norman, *J. Biochem.*, **243,** 4055 (1968).

(34) D. E. M. Lawson, P. W. Wilson, and E. Kodicek, *Biochem. J.*, **115,** 269 (1969).

(35) G. Ponchon, A. L. Keenan, and H. F. DeLuca, *J. Clin. Invest.*, **48,** 2032 (1969).

(36) M. Horsting and H. F. DeLuca, *Biochem. Biophys. Res. Commun.*, **36,** 251 (1969).

(37) E. B. Mawer, G. A. Lumb, and S. W. Stanbury, *Nature*, **222,** 482 (1969).

(38) T. Suda, H. F. DeLuca, H. K. Schnoes, and J. W. Blunt, *Biochemistry*, **8,** 3515 (1969).

(39) J. W. Blunt and H. F. DeLuca, *ibid.*, **8,** 671 (1969).

(40) G. Tucker, III, R. E. Gagnon, and M. R. Haussler, *Arch. Biochem. Biophys.*, **155,** 47 (1973).

(41) E. B. Olson, J. C. Knutson, M. H. Bhattacharya, and H. F. DeLuca, *J. Clin. Invest.*, **57** 1213 (1976).

(42) M. H. Bhattacharya and H. F. DeLuca, *Arch. Biochem. Biophys.*, **160,** 58 (1974).

(43) I. T. Boyle, L. Miravet, R. W. Gray, M. F. Holick, and H. F. DeLuca, *Endocrinology*, **90,** 605 (1972).

(44) M. F. Holick, M. Garabedian, and H. F. DeLuca, *Science*, **176,** 1146 (1972).

(45) R. G. Wong, J. F. Myrtle, H. C. Tsai, and A. W. Norman, *J. Biol. Chem.*, **247,** 5728 (1972).

(46) R. K. Callow, E. Kodicek, and G. Thompson, *Proc. R. Soc. Ser. B.*, **164,** 1 (1966).

(47) D. E. M. Lawson, P. W. Wilson, and E. Kodicek, *Nature*, **222,** 171 (1969).

(48) D. R. Fraser and E. Kodicek, *ibid.*, **228,** 764 (1970).

(49) D. E. M. Lawson, D. R. Fraser, E. Kodicek, H. R. Morris, and D. H. Williams, *ibid.*, **230,** 228 (1971).

(50) C. A. Frolick and H. F. DeLuca, *Arch. Biochem. Biophys.*, **147,** 143 (1971).

(51) M. F. Holick, H. K. Schnoes, and H. F. DeLuca, *Proc. Natl. Acad. Sci., USA*, **68,** 803 (1971).

(52) J. G. Haddad and K. J. Chyu, *J. Clin. Endocrinol. Metab.*, **33,** 992 (1971).

(53) R. Belsey, H. F. DeLuca, and J. T. Potts, Jr., *ibid.*, **33,** 554 (1971).

(54) F. Bayard, P. Bec, and J. P. Louvet, *Eur. J. Clin. Invest.*, **2,** 195 (1972).

(55) K. T. Koshy and A. L. VanDerslik, *Anal. Lett.*, **10,** 523 (1977).

(56) T. J. Gilbertson and R. P. Stryd, *Clin. Chem.*, **23,** 1700 (1977).

(57) J. A. Eisman, R. M. Shepard, and H. F. DeLuca, *Anal. Biochem.*, **80,** 298 (1977).

(58) G. Jones, *Clin. Chem.*, **24,** 287 (1978).

(59) K. T. Koshy and A. L. VanDerSlik, *Anal. Biochem.*, **74,** 282 (1976).

(60) *Ibid.*, **85,** 283 (1978).

(61) F. R. Frank, M. L. Ogilvie, K. T. Koshy, T. J. Kakuk, and N. A. Jorgensen, "Vitamin D, Biochemical, Chemical and Clinical Aspects Related to Calcium Metabolism," Proceedings of the 3rd Workshop on Vitamin D, Asilomar, Pacific Grove, Calif., 1977, Walter de Gruyter, Berlin, New York, 1977, p. 577

(62) P. W. Lambert, B. J. Syverson, C. D. Arnaud, and T. C. Spelsberg, *J. Steroid Biochem.*, **8,** 929 (1977).

(63) A. E. Caldas, R. W. Gray, and J. Lemann, Jr., *J. Clin. Med.*, **91,** 840 (1978).

(64) R. M. Shepard, R. L. Horst, A. J. Hamstra, and H. F. DeLuca, *Biochem. J.*, **182,** 55 (1979).

(65) T. Suda, H. F. DeLuca, H. K. Schnoes, Y. Tanaka, and M. F. Holick, *Biochemistry*, **9,** 24 (1970).

(66) T. Suda, H. F. DeLuca, H. K. Schnoes, G. Ponchon, Y. Tanaka, and M. F. Holick, *ibid.*, **9,** 2917 (1970).

(67) R. L. Horst, R. M. Shepard, N. A. Jorgensen, and H. F. DeLuca, *J. Lab. Clin. Med.*, **93,** 277 (1979).

(68) J. L. Omdahl and H. F. DeLuca, *Science*, **174,** 949 (1971).

(69) I. T. Boyle, R. W. Gray, J. L. Omdahl, and H. F. DeLuca, in III, *International Symposium Endocrinology*, Wm. Heinemann Medical Books, Ltd, London, England, 1972, pp. 468–476.

(70) J. L. Omdahl, R. W. Gray, I. T. Boyle, J. Knutson, and H. F. DeLuca, *Nature New Biol.*, **237,** 63 (1972).

(71) M. F. Holick, H. K. Schnoes, H. F. DeLuca, R. W. Gray, I. T. Boyle, and T. Suda, *Biochemistry*, **11,** 4251 (1972).

(72) H. Y. Lam, H. K. Schnoes, H. F. DeLuca, and T. C. Chen, *ibid.*, **12,** 4851 (1973).

(73) Y. Tanaka, H. F. DeLuca, N. Ikekawa, M. Morisaki, and N. Koizumi, *Arch. Biochem. Biophys.*, **170,** 620 (1975).

(74) C. M. Taylor, S. E. Hughes, and P. deSilva, *Biochem. Biophys. Res. Commun.*, **70,** 1243 (1976).

(75) I. T. Boyle, R. W. Gray, and H. F. DeLuca, *Proc. Natl. Acad. Sci. USA*, **68,** 2131 (1971).

(76) I. T. Boyle, J. L. Omdahl, R. W. Gray, and H. F. DeLuca, *J. Biol. Chem.*, **248,** 4174 (1973).

(77) M. F. Holick, A. Kleiner-Bossaller, H. K. Schnoes, P. M. Kasten, I. T. Boyle, and H. F. DeLuca, *ibid.*, **248,** 6691 (1973).

(78) D. Harnden, R. Kumar, M. F. Holick, and H. F. DeLuca, *Science*, **193,** 493 (1976).

(79) R. Kumar, D. Harnden, and H. F. DeLuca, *Biochemistry*, **15,** 2420 (1976).

(80) R. Kumar and H. F. DeLuca, *Biochem. Biophys. Res. Commun.*, **76,** 253 (1977).

(81) R. P. Esvelt, H. K. Schnoes, and H. F. DeLuca, *Biochemistry*, **18,** 3977 (1979).

(82) B. L. Onisko, R. P. Esvelt, H. K. Schnoes, and H. F. DeLuca, *ibid.*, **19,** 4124 (1980).

(83) N. Koizumi, M. Morisaki, N. Ikekawa, Y. Tanaka, and H. F. DeLuca, *J. Steroid Biochem.*, **10,** 261 (1979).

(84) B. L. Onisko, R. P. Esvelt, H. K. Schnoes, and H. F. DeLuca, *Biochemistry*, **19,** 4124 (1980).

(85) R. L. Horst, R. M. Shepard, N. A. Jorgensen, and H. F. DeLuca, *J. Lab. Clin. Med.*, **93,** 277 (1979).

(86) R. M. Shepard, R. L. Horst, A. J. Hamstra, and H. F. DeLuca, *Biochem. J.*, **182,** 55 (1979).

(87) R. L. Horst, *Biochem. Biophys. Res. Commun.*, **89,** 286 (1979).

(88) J. K. Wichmann, H. F. DeLuca, H. K. Schnoes, R. L. Horst, R. M. Shepard, and N. A. Jorgensen, *Biochemistry*, **18,** 4775 (1979).
(89) B. W. Hollis, B. A. Roos and P. W. Lambert, *Biochem. Biophys. Res. Commun.*, **95,** 520 (1980).
(90) Y. Tanaka, J. K. Wichmann, H. E. Paaren, H. F. Schnoes, and H. F. DeLuca, *Proc. Natl. Acad. Sci., U.S.A.*, **77,** 6411 (1980).
(91) N. Ohnuma, K. Bannai, H. Yamaguchi, Y. Hashimoto, and A. W. Norman, *Arch. Biochem. Biophys.*, **204,** 387 (1980).
(92) H. F. DeLuca and H. K. Schnoes, in "Proceedings of the Fourth Workshop on Vitamin D," Walter de Gruyter, Berlin, 1979.
(93) Y. Takasaki, N. Horiuchi, and T. Suda, *Biochem. Biophys. Res. Commun.*, **85,** 601 (1978).
(94) T. Suda, Y. Takasaki, and N. Horiuchi, "Basic Research and its Clinical Application," Walter de Gruyter, Berlin, New York, 1979, pp. 579–586.
(95) Y. Takasaki, N. Horiuchi, N. Takahashi, E. Abe, T. Shinki, and T. Suda, *Biochem. Biophys. Res. Commun.*, **95,** 177 (1980).
(96) L. V. Avioli, S. W. Lee, J. E. McDonald, J. Lund, and H. F. DeLuca, *J. Clin. Invest.*, **46,** 983 (1967).
(97) L. W. LeVan, H. K. Schnoes, and H. F. DeLuca, *Biochemistry*, **20,** 222 (1981).
(98) M. H. Imrie, P. F. Neville, A. W. Snellgrove, and H. F. DeLuca, *Arch. Biochem. Biophys.*, **120,** 525 (1967).
(99) G. Jones, L. A. Baxter, H. F. DeLuca, and H. K. Schnoes, *Biochemistry*, **15,** 713 (1976).
(100) G. Jones, H. K. Schnoes, and H. F. DeLuca, *J. Biol. Chem.*, **251,** 24 (1976).
(101) D. Drescher, H. F. DeLuca, and M. H. Imrie, *Arch. Biochem. Biophys.*, **130,** 657 (1969).
(102) Y. Sahashi, T. Suzuki, M. Higaki, and T. Asano, *J. Vitaminol.*, **13,** 33 (1967).
(103) D. R. Lakdawala and E. M. Widdowson, *Lancet*, **1,** 167 (1977).
(104) E. Leerbeck and H. Sondergaard, *Br. J. Nutr.*, **44,** 7 (1980).
(105) N. LeBoulch, C. Gulat-Marnay, and Y. Raoul, *Int. J. Nutr. Res.*, **44,** 167 (1974).
(106) B. W. Hollis, B. A. Roos, D. H. Draper, and P. W. Lambert, *J. Nutr.*, **111,** 384 (1981).
(107) B. W. Hollis, B. A. Roos, D. H. Draper, and P. W. Lambert, *Clin. Res.*, **28,** 395a (1980).
(108) M. L. Ribovich and H. F. DeLuca, *Arch. Biochem. Bioophys.*, **188,** 145 (1978).
(109) G. Jones, H. K. Schnoes, and H. F. DeLuca, *Biochemistry*, **14,** 1250 (1975).
(110) G. Jones, H. K. Schnoes, and H. F. DeLuca, *J. Biol. Chem.*, **251,** 24 (1976).
(111) S. J. Rosenstreich, C. Rich, and W. Volwiler, *J. Clin. Invest.*, **50,** 679 (1971).
(112) M. H. Bhattacharya and H. F. DeLuca, *J. Biol. Chem.*, **248,** 2969 (1973).
(113) M. B. Clark and J. T. Potts, Jr., *Calcif. Tissue Res., Suppl.* **22,** 29 (1977).
(114) M. H. Bhattacharya and H. F. DeLuca, *J. Biol. Chem.*, **248,** 2974 (1973).
(115) M. Fukushima, Y. Suzuki, Y. Tohira, I. Matsunaga, K. Ochi, H. Nagano, Y. Nishii, and T. Suda, *Biochem. Biophys. Res. Commun.*, **66,** 632 (1975).
(116) M. F. Holick, T. Tavela, S. A. Holick, H. K. Schnoes, H. F. DeLuca, and M. B. Gallagher, *J. Biol. Chem.*, **251,** 1020 (1976).
(117) C. A. Frolick and H. F. DeLuca, *J. Clin. Invest.*, **51,** 2900 (1972).
(118) Y. Tanaka and H. F. DeLuca, *Arch. Biochem. Biophys.*, **154,** 566 (1973).
(119) M. W. Walling, D. L. Hartenbower, J. W. Coburn, and A. W. Norman, *Arch. Biochem. Biophys.*, **182,** 251 (1977).
(120) M. F. Holick, L. A. Baxter, P. K. Schraufrogel, T. Tavela, and H. F. DeLuca, *J. Biol. Chem.*, **251,** 397 (1976).
(121) J. A. Kanis, G. Heynen, R. G. G. Russell, R. Smith, R. J. Walton, and G. T. Warner, in "Vitamin D: Biochemical, Chemical and Clinical Aspects Related to Calcium Metabolism," A. W. Norman, K. Schaefer, J. W. Coburn, H. F. DeLuca, D. Fraser, H. G. Grigoliet, and D. V. Herrath, Eds., Walter DeGruyter, New York, 1977, pp. 113–122.
(122) L. Miravet, J. Redel, M. Carre, M. L. Queille, and P. Bordier, *Calcif. Tissue Res.*, **21,** 145 (1976).
(123) R. H. Wasserman, J. D. Henion, M. R. Haussler, and T. A. McCain, *Science*, **194,** 853 (1976).
(124) R. H. Wasserman, R. A. Corradino, L. Krook, M. R. Hughes, and M. R. Haussler, *J. Nutr.*, **106,** 457 (1976).
(125) J. E. Zull and D. W. Repke, *J. Biol. Chem.*, **247,** 2195 (1972).
(126) M. W. Neuman, W. F. Neuman, and K. Lane, *Calcif. Tissue Res.*, **18,** 289 (1975).
(127) L. R. Forte, G. A. Nickols, and C. S. Anast, *J. Clin. Invest.*, **57,** 559 (1976).
(128) R. A. L. Sutton and J. H. Dirks, *Fed. Proc., Fed. Am. Soc. Exp. Biol.*, **37,** 2112 (1978).
(129) T. H. Steele, J. E. Engle, Y. Tanaka, R. S. Lorenc, K. L. Dudgeon, and H. F. DeLuca, *Am. J. Physiol.*, **229,** 489 (1975).
(130) M. Garabedian, M. F. Holick, H. F. DeLuca, and I. T. Boyle, *Proc. Natl. Acad. Sci., USA*, **69,** 1673 (1972).
(131) R. Maier, in "Endocrinology 1973," S. Taylor, R. B. Welbourn, C. C. Booth, and M. Szelke, Eds., Heinemann Medical Books, 1974, pp. 184–189.
(132) H. F. DeLuca, *Nutr. Rev.*, **37,** 161 (1979).
(133) A. D. Kenny, *Am. J. Physiol.*, **230,** 1609 (1976).
(134) Y. Tanaka, L. Castello, and H. F. DeLuca, *Proc. Natl. Acad. Sci. USA*, **73,** 2701 (1976).
(135) A. Boass, S. U. Toverud, T. A. McCain, J. W. Pike, and M. R. Haussler, *Nature*, **267,** 630 (1977).
(136) M. R. Haussler, "Nutrition and Drug Interrelations Nutrition Foundation," Monograph Series International Symposium on Nutrition and Drug Interrelations, Ames, Iowa, 1976 J. N. Hathcock and J. Coon, Eds., Academic, New York, 1978, p. 717.
(137) E. Spanos and I. MacIyntyre, *Lancet* **I,** 840 (1977).
(138) "The Fat Soluble Vitamins," H. F. DeLuca and J. W. Suttie, Eds., University of Wisconsin Press, Madison, Wis., 1969, pp. 1–177.
(139) R. H. Wasserman and R. A. Corradino, in "Vitamins and Hormones," vol. 31, R. S. Harris, P. L. Munson, E. Diczfalusy, and J. Glover, Eds., Academic, New York, 1973, pp. 43–103.
(140) D. E. M. Lawson and J. S. Emtage, in *ibid.*, vol. 32, 1974, pp. 277–298.
(141) R. H. Wasserman, R. A. Corradino, C. S. Fullmer, and A. N. Taylor, in *ibid.*, pp. 299–324.
(142) A. W. Norman, in *ibid.*, pp. 325–384.
(143) H. K. Schnoes and H. F. DeLuca, in *ibid.*, pp. 385–406.
(144) A. W. Norman and H. Henry, *Recent Prog. Horm. Res.*, **30,** 431 (1974).
(145) H. F. DeLuca, in "Monographs on Endocrinology," vol. 13, F. Gross, M. M. Grumbach, A. Labhart, M. B. Lipsett, T. Mann, L. T. Samuels, and J. Zander, Eds., Springer-Verlag, Berlin, Heidelberg, New York, 1979.
(146) H. F. DeLuca, in "Handbook of Lipid Research 2, The Fat Soluble Vitamins," H. F. DeLuca, Ed., Plenum, New York, London, 1978, pp. 69–132.
(147) H. F. DeLuca, *J. Steroid Biochem.*, **11,** 35 (1979).
(148) "Vitamin D, Basic Research and Its Clinical Application; Proceedings of the Fourth Workshop on Vitamin D," A. W. Norman, K. Schaefer, D. V. Herrath, *et al.*, Eds., Walter de Gruyter, Berlin, New York, 1979.
(149) H. Rasmussen and P. Bordier, *Metab. Bone Dis. Relat. Res.*, **1,** 7 (1978).
(150) M. F. Holick, E. J. Semmler, H. Schnoes, and H. F. DeLuca, *Science*, **180,** 190 (1973).
(151) A. Ornoy, D. Goodwin, D. Noff, and S. Edelstein, *Nature*, 276 (1978).
(152) A. Prader, R. Illig, and E. Heierli, *Helv. Paediatr. Acta*, **16,** 452 (1961).
(153) D. Fraser, S. W. Kooh, H. P. Kind, M. F. Holick, Y. Tanaka, and H. F. DeLuca, *N. Engl. J. Med.*, **289,** 817 (1973).
(154) T. M. Reade, C. R. Scriver, F. H. Glorieux, B. Nogrady, E. Delvin, R. Poirier, M. F. Holick, and H. F. DeLuca, *Pediatr. Res.*, **9,** 593 (1975).
(155) E. M. Eicher, J. L. Southard, C. R. Scriver, and F. H. Glorieux, *Proc. Natl. Acad. Sci. USA*, **73,** 4667 (1976).
(156) P. J. A. O'Doherty, H. F. DeLuca, and E. M. Eicher, *Biochem. Biophys. Res. Commun.*, **71,** 617 (1976).
(157) S. W. Kooh, D. Fraser, H. F. DeLuca, M. F. Holick, R. E. Belsey, M. B. Clark, and T. M. Murray, *N. Engl. J. Med.*, **293,** 840 (1975).
(158) R. M. Neer, M. F. Holick, H. F. DeLuca, and J. T. Potts, Jr., *Metabolism*, **24,** 1403 (1975).
(159) R. G. Russell, R. Smith, R. J. Walton, C. Preston, R. Basson, R. G. Henderson, and A. W. Norman, *Lancet* **2,** 14 (1974).
(160) S. G. Massry, J. W. Coburn, D. B. N. Lee, J. Jowsey, and C. R. Kleeman, *Ann. Intern. Med.*, **78,** 357 (1973).
(161) D. S. Silverberg, K. B. Bettcher, J. B. Dossector, T. R. Overton,

M. F. Holick, and H. F. DeLuca, *Can. Med. Assoc. J.*, **112**, 190 (1975).
(162) J. C. M. Chan, S. B. Oldham, M. F. Holick, and H. F. DeLuca, *J. Am. Med. Assoc.*, **234**, 47 (1975).
(163) S. L. Teitelbaum, J. M. Bone, P. M. Stein, J. J. Gilden, M. Bates, V. C. Boisseau, and L. V. Avioli, *ibid.*, **235**, 164 (1976).
(164) H. M. Frost, D. L. Griffith, W. S. S. Jee, D. B. Kimmel, R. P. McCandlis, and S. L. Teitelbaum, *Metab. Bone Dis. Relat. Res.*, **2**, 285 (1981).
(165) B. L. Riggs and J. C. Gallagher, in "Vitamin D: Biochemical, Chemical and Clinical Aspects Related to Calcium Metabolism," A. W. Norman, K. Schaefer, J. W. Coburn, H. F. DeLuca, D. Fraser, H. G. Grigoleit, and D. vonHerrath, Eds., Walter de Gruyter, Berlin, New York, 1977, pp. 639–648.
(166) R. P. Heany, in *ibid.*, pp. 627–633.
(167) C. Gallagher, L. Riggs, J. Eisman, S. Arnaud, and H. F. DeLuca, *Clin. Res.*, **24**, 360 A (1976).
(168) S. Lawoyin, J. E. Zerwekh, K. Glass, and C. Y. C. Pak, *J. Clin. Endocrinol. Metab.*, **50**, 593 (1980).
(169) T. C. B. Stamp, J. M. Round, D. J. F. Rowe, and J. G. Haddad, *Br. Med. J.*, **4**, 9 (1972).
(170) J. G. Haddad and T. C. B. Stamp, *Am. J. Med.*, **57**, 57 (1974).
(171) H. F. DeLuca and J. W. Blunt, in "Methods in Enzymology, in vol. XVIII, Part C, D. B. McCormick and L. D. Wright, Eds., Academic, New York, London, 1971, p. 709.
(172) "The United States Pharmacopeia," 20th rev., Mack Publishing Co., Easton, Pa., 1980, p. 934.
(173) "Official Methods of Analysis," 13th ed., Association of Official Analytical Chemists, 1980, p. 770.
(174) P. P. Nair, in "Advances in Lipid Research," vol. 4, R. Paoletti and D. Kritchevsky, Eds., Academic, New York, London, 1966, pp. 227–256.
(175) A. S. Sheppard, A. R. Prosser, and W. D. Hubbard, *J. Am. Oil Chem. Soc.*, **49**, 619 (1972).
(176) K. A. Tartivita, J. P. Sciarello, and B. C. Rudy, *J. Pharm. Sci.*, **65**, 1024 (1976).
(177) G. Jones and H. F. DeLuca, *J. Lipid Res.*, **16**, 448 (1975).
(178) G. Jones, *J. Chromatogr.*, **221**, 27 (1980).
(179) S. K. Henderson and A. F. Wickroski, *J. Assoc. Off. Anal. Chem.*, **61**, 1130 (1978).
(180) H. Cohen and B. Wakeford, *ibid.*, **63**, 1163 (1980).
(181) S. L. Ali, *Fresenius Z. Anal. Chem.*, **293**, 131 (1978).
(182) E. Egaas and G. Lambertsen, *Int. J. Vitam. Nutr. Res.*, **49**, 35 (1978).
(183) A. C. Ray, J. N. Dwyer, and J. C. Reagor, *J. Assoc. Off. Anal. Chem.*, **60**, 1296 (1977).
(184) H. Cohen and M. Lapointe, *J. Agr. Food Chem.*, **26**, 1210 (1978).
(185) H. Cohen and M. Lapointe, *J. Chromatogr. Sci.*, **17**, 510 (1979).
(186) K. T. Koshy and A. L. VanDerSlik, *J. Agr. Food Chem.*, **25**, 1246 (1977).
(187) *Ibid.*, **27**, 180 (1979).
(188) E. J. DeVries, F. J. Mulder, and B. Borsje, *J. Assoc. Off. Anal. Chem.*, **64**, 58 (1981).
(189) F. J. Mulder, E. J. DeVries, and B. Borsje, *ibid.*, **64**, 61 (1981).

ACKNOWLEDGMENTS

The author wishes to thank D. W. Knuth of The Upjohn Company for his help in the preparation of this article. He also wishes to acknowledge Prof. H. F. DeLuca of The University of Wisconsin, Madison, Wisconsin whose extensive research and writings on this subject were very helpful as resource material.

RESEARCH ARTICLES

Quantitation of Lipophilic Chloroethylnitrosourea Cancer Chemotherapeutic Agents

ROBERT J. WEINKAM‡x and TSUI-YUN J. LIU*

Received February 27, 1981, from the **Brain Tumor Research Center, Department of Neurological Surgery, School of Medicine, University of California, San Francisco, CA 94143* and the ‡*Department of Medicinal Chemistry, School of Pharmacy, Purdue University, West Lafayette, IN 47907.* Accepted for publication June 2, 1981.

Abstract □ A simple and rapid quantitative method for the derivatization and determination of lipophilic chloroethylnitrosoureas is described. This procedure involves the ether extraction of the chloroethylnitrosourea from plasma and conversion of the parent drug to an *O*-methylcarbamate by reaction in anhydrous methanol. The product *O*-methylcarbamate may be separated with gas chromatography (GC) and detected with nitrogen-specific GC detectors or with mass spectrometry using multiple-ion detection. The lower limit of detection for each method was ~100 ng/ml plasma.

Keyphrases □ Cancer chemotherapeutic agents—lipophilic chloroethylnitrosoureas, quantitation □ Chloroethylnitrosoureas—quantitation by gas chromatography □ Gas chromatography—quantitation of lipophilic chloroethylnitrosourea cancer chemotherapeutic agents

The described assay was applied to 1,3-bis(2-chloroethyl)-1-nitrosourea (carmustine, I), 1-(2-chloroethyl)-3-cyclohexyl-1-nitrosourea (lomustine, II), 1-(2-chloroethyl)-3-(4-*trans*-methylcyclohexyl)-1-nitrosourea (semustine, III), 1-(2-chloroethyl)-3-(2,6-dioxo-3-piperidyl)-1-nitrosourea (IV), and 1-(2-chloroethyl)-3-(4-amino-2-methyl-5-pyrimidinyl)methyl-1-nitrosourea (V)[1]. The clearance curve for IV from rat plasma is presented as an example of the application of this method to the determination of biodistribution parameters.

BACKGROUND

The chloroethylnitrosoureas are a class of highly effective and widely used cancer chemotherapeutic agents (1–3). Analysis of these drugs in plasma at therapeutically significant concentrations has proven to be difficult. Although several methods of analysis have been reported, none are generally applicable to patient pharmacokinetic analyses. As a consequence, only carmustine pharmacokinetics has received detailed study (4).

Chloroethylnitrosoureas are thermally labile and decompose at or below 100° so that the parent compounds cannot be analyzed with gas chromatography (GC) (5). Compounds of this class are readily separated with high-performance liquid chromatography (HPLC) (6); however, the low wavelength and molar absorptivity of the nitrosourea chromophore

[1] These compounds are commonly referred to by their respective code designations BCNU, CCNU, Methyl-CCNU, PCNU, and ACNU.

0022-3549/82/0200-0153$01.00/0

M. F. Holick, and H. F. DeLuca, *Can. Med. Assoc. J.*, **112**, 190 (1975).
(162) J. C. M. Chan, S. B. Oldham, M. F. Holick, and H. F. DeLuca, *J. Am. Med. Assoc.*, **234**, 47 (1975).
(163) S. L. Teitelbaum, J. M. Bone, P. M. Stein, J. J. Gilden, M. Bates, V. C. Boisseau, and L. V. Avioli, *ibid.*, **235**, 164 (1976).
(164) H. M. Frost, D. L. Griffith, W. S. S. Jee, D. B. Kimmel, R. P. McCandlis, and S. L. Teitelbaum, *Metab. Bone Dis. Relat. Res.*, **2**, 285 (1981).
(165) B. L. Riggs and J. C. Gallagher, in "Vitamin D: Biochemical, Chemical and Clinical Aspects Related to Calcium Metabolism," A. W. Norman, K. Schaefer, J. W. Coburn, H. F. DeLuca, D. Fraser, H. G. Grigoleit, and D. vonHerrath, Eds., Walter de Gruyter, Berlin, New York, 1977, pp. 639–648.
(166) R. P. Heany, in *ibid.*, pp. 627–633.
(167) C. Gallagher, L. Riggs, J. Eisman, S. Arnaud, and H. F. DeLuca, *Clin. Res.*, **24**, 360 A (1976).
(168) S. Lawoyin, J. E. Zerwekh, K. Glass, and C. Y. C. Pak, *J. Clin. Endocrinol. Metab.*, **50**, 593 (1980).
(169) T. C. B. Stamp, J. M. Round, D. J. F. Rowe, and J. G. Haddad, *Br. Med. J.*, **4**, 9 (1972).
(170) J. G. Haddad and T. C. B. Stamp, *Am. J. Med.*, **57**, 57 (1974).
(171) H. F. DeLuca and J. W. Blunt, in "Methods in Enzymology, in vol. XVIII, Part C, D. B. McCormick and L. D. Wright, Eds., Academic, New York, London, 1971, p. 709.
(172) "The United States Pharmacopeia," 20th rev., Mack Publishing Co., Easton, Pa., 1980, p. 934.
(173) "Official Methods of Analysis," 13th ed., Association of Official Analytical Chemists, 1980, p. 770.
(174) P. P. Nair, in "Advances in Lipid Research," vol. 4, R. Paoletti and D. Kritchevsky, Eds., Academic, New York, London, 1966, pp. 227–256.
(175) A. S. Sheppard, A. R. Prosser, and W. D. Hubbard, *J. Am. Oil Chem. Soc.*, **49**, 619 (1972).
(176) K. A. Tartivita, J. P. Sciarello, and B. C. Rudy, *J. Pharm. Sci.*, **65**, 1024 (1976).
(177) G. Jones and H. F. DeLuca, *J. Lipid Res.*, **16**, 448 (1975).
(178) G. Jones, *J. Chromatogr.*, **221**, 27 (1980).
(179) S. K. Henderson and A. F. Wickroski, *J. Assoc. Off. Anal. Chem.*, **61**, 1130 (1978).
(180) H. Cohen and B. Wakeford, *ibid.*, **63**, 1163 (1980).
(181) S. L. Ali, *Fresenius Z. Anal. Chem.*, **293**, 131 (1978).
(182) E. Egaas and G. Lambertsen, *Int. J. Vitam. Nutr. Res.*, **49**, 35 (1978).
(183) A. C. Ray, J. N. Dwyer, and J. C. Reagor, *J. Assoc. Off. Anal. Chem.*, **60**, 1296 (1977).
(184) H. Cohen and M. Lapointe, *J. Agr. Food Chem.*, **26**, 1210 (1978).
(185) H. Cohen and M. Lapointe, *J. Chromatogr. Sci.*, **17**, 510 (1979).
(186) K. T. Koshy and A. L. VanDerSlik, *J. Agr. Food Chem.*, **25**, 1246 (1977).
(187) *Ibid.*, **27**, 180 (1979).
(188) E. J. DeVries, F. J. Mulder, and B. Borsje, *J. Assoc. Off. Anal. Chem.*, **64**, 58 (1981).
(189) F. J. Mulder, E. J. DeVries, and B. Borsje, *ibid.*, **64**, 61 (1981).

ACKNOWLEDGMENTS

The author wishes to thank D. W. Knuth of The Upjohn Company for his help in the preparation of this article. He also wishes to acknowledge Prof. H. F. DeLuca of The University of Wisconsin, Madison, Wisconsin whose extensive research and writings on this subject were very helpful as resource material.

RESEARCH ARTICLES

Quantitation of Lipophilic Chloroethylnitrosourea Cancer Chemotherapeutic Agents

ROBERT J. WEINKAM‡x and TSUI-YUN J. LIU*

Received February 27, 1981, from the **Brain Tumor Research Center, Department of Neurological Surgery, School of Medicine, University of California, San Francisco, CA 94143* and the ‡*Department of Medicinal Chemistry, School of Pharmacy, Purdue University, West Lafayette, IN 47907.* Accepted for publication June 2, 1981.

Abstract □ A simple and rapid quantitative method for the derivatization and determination of lipophilic chloroethylnitrosoureas is described. This procedure involves the ether extraction of the chloroethylnitrosourea from plasma and conversion of the parent drug to an *O*-methylcarbamate by reaction in anhydrous methanol. The product *O*-methylcarbamate may be separated with gas chromatography (GC) and detected with nitrogen-specific GC detectors or with mass spectrometry using multiple-ion detection. The lower limit of detection for each method was ~100 ng/ml plasma.

Keyphrases □ Cancer chemotherapeutic agents—lipophilic chloroethylnitrosoureas, quantitation □ Chloroethylnitrosoureas—quantitation by gas chromatography □ Gas chromatography—quantitation of lipophilic chloroethylnitrosourea cancer chemotherapeutic agents

The described assay was applied to 1,3-bis(2-chloroethyl)-1-nitrosourea (carmustine, I), 1-(2-chloroethyl)-3-cyclohexyl-1-nitrosourea (lomustine, II), 1-(2-chloroethyl)-3-(4-*trans*-methylcyclohexyl)-1-nitrosourea (semustine, III), 1-(2-chloroethyl)-3-(2,6-dioxo-3-piperidyl)-1-nitrosourea (IV), and 1-(2-chloroethyl)-3-(4-amino-2-methyl-5-pyrimidinyl)methyl-1-nitrosourea (V)[1]. The clearance curve for IV from rat plasma is presented as an example of the application of this method to the determination of biodistribution parameters.

BACKGROUND

The chloroethylnitrosoureas are a class of highly effective and widely used cancer chemotherapeutic agents (1–3). Analysis of these drugs in plasma at therapeutically significant concentrations has proven to be difficult. Although several methods of analysis have been reported, none are generally applicable to patient pharmacokinetic analyses. As a consequence, only carmustine pharmacokinetics has received detailed study (4).

Chloroethylnitrosoureas are thermally labile and decompose at or below 100° so that the parent compounds cannot be analyzed with gas chromatography (GC) (5). Compounds of this class are readily separated with high-performance liquid chromatography (HPLC) (6); however, the low wavelength and molar absorptivity of the nitrosourea chromophore

[1] These compounds are commonly referred to by their respective code designations BCNU, CCNU, Methyl-CCNU, PCNU, and ACNU.

0022-3549/82/0200-0153$01.00/0

(λ_{max} 232 nm, ϵ 6000) causes this approach to lack sensitivity even when variable-wavelength UV detectors are used. An assay limit of 2–5 μg/ml of plasma was found with II (7, 8). Compound V is an exception to this generalization, as the pyrimidinyl substituent is a superior chromophore (9). Both HPLC and GC analyses are hindered by the fact that the chloroethylnitrosourea group is difficult to derivatize.

Radiolabeled chloroethylnitrosoureas, especially I and II, have been used for the measurement of tissue concentrations of parent drug either without separation (10, 11) or after isolation of unchanged drug with TLC (12) or HPLC[2]. This approach is sensitive but the use of radioactive tracers in patients is limited. The colorimetric assay developed by Loo and Dion (13) has a lower detection limit than HPLC but does not possess sufficient sensitivity to assay patient plasma samples. This assay involves the acid-catalyzed decomposition of nitrosourea to nitrous acid which is subsequently trapped and analyzed using the Bratton–Marshall method (14). This approach lacks the specificity necessary to distinguish between parent drug and biologically active metabolites that retain the nitrosourea moiety.

Recently reported polarographic methods have the requisite sensitivity but are susceptible to interference from plasma components and also lack specificity (15). Patient pharmacokinetic studies of carmustine biodistribution have been performed using direct sample insertion chemical-ionization mass spectrometry (5). The method was successful because of the relatively high lipophilicity and volatility of I and is not applicable to less volatile analogs such as II and IV.

The described analytical procedure may be applied to different chloroethylnitrosourea analogs. The parent nonpolar chloroethylnitrosoureas may be extracted from plasma and converted to a stable *O*-methylcarbamate by reaction in anhydrous basic methanol. The *O*-methylcarbamate products may be separated with GC and detected at high sensitivity with multiple-ion detection mass spectrometry or with nitrogen-specific GC detectors.

EXPERIMENTAL

Materials—Reagents used to convert chloroethylnitrosoureas[3] to *O*-methylcarbamates were 0.2 *M* trimethylanilinium hydroxide in anhydrous methanol[4], 10% freshly distilled triethylamine[5] in anhydrous methanol[5], 10% reagent grade pyridine[5] in anhydrous methanol[5], and 2% sodium methoxide in anhydrous methanol prepared by reacting sodium metal with anhydrous methanol.

Instrument Conditions—GC separations of *O*-methylcarbamate derivatives of chloroethylnitrosoureas were performed on instruments equipped with 1.5 m long, 2-mm i.d. glass columns packed with 3% OV-1 on 100–120 mesh Supelcoport[6]. An instrument equipped with a flame-ionization detector[7] and an instrument equipped with a nitrogen-specific detector[8] used helium carrier gas at a flow rate of 40 ml/min. An instrument interfaced to a mass spectrometer[9] operating in the multiple-ion detection mode and equipped with a chemical-ionization source used methane[10] as a combined carrier and reagent gas. In each case, an injection port temperature of 210° was used. Column oven temperatures were varied according to the nitrosourea derivative being analyzed.

Derivatives of I and II were eluted using linear temperature programming with an initial temperature of 70° increasing 4°/min starting at the time of injection. The derivative of I eluted in ~2 min at 80° and II eluted in ~6.5 min at 95°. Isothermal column oven conditions may be used for other derivatives and derivatives of II and III may be eluted at 110° with retention times of ~2.0 and 3.0 min, respectively. Compounds IV and V may be eluted at 160° as *N*-methyl-*O*-methylcarbamates with retention times of ~2.0 and 3.0 min, respectively. GC–mass spectrometric operations were performed at an ion-source pressure of 1.0 mm methane and temperature of 200°.

Extraction and Derivative Formation—Chloroethylnitrosoureas, 0.05–1.0 μg, were added to 1.0 ml of plasma or to 1.0 ml of 0.05 *M* phosphate buffer (pH 7.4) and extracted with 3.0 ml of ether. The 2.0-ml ether layer was removed and placed into a 3.0-ml cone-shaped interior vial[11] containing 1.0 μg of a reference chloroethylnitrosourea. The ether was evaporated to dryness under a nitrogen stream at ambient temperature. Approximately 50 μl of derivatizing reagent was added. Compounds IV and V were derivatized with 0.2 *M* trimethylanilinium hydroxide in anhydrous methanol[4]. Compounds I–III were derivatized with 2% sodium methoxide in anhydrous methanol. The reagent–chloroethylnitrosourea mixture was heated at 50° for 20 min in the capped cone-shaped vial[11]. Approximately 1 μl of this mixture was injected onto the chromatograph column and the peak height ratios were determined. These peak height ratios were compared with those obtained from the analysis of the same amounts of chloroethylnitrosoureas added directly to ether and avoiding the extraction step to determine extraction efficiency.

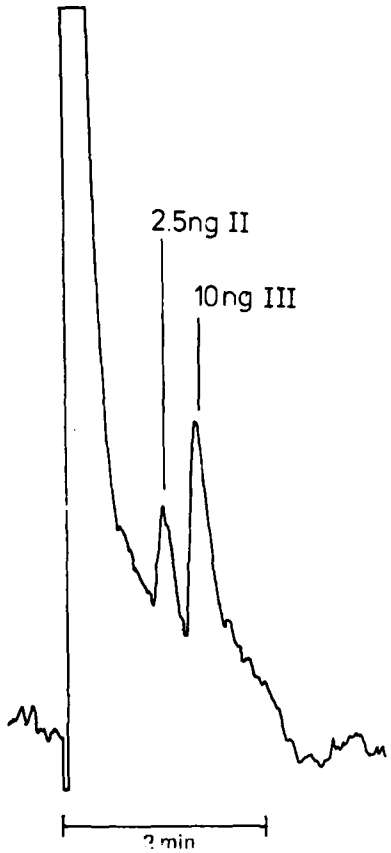

Figure 1—*A chromatogram of O-methylcarbamates derived from II and III. Separations were performed using a 3% OV-1 column at 110° and detected using a nitrogen-specific detector. The amounts injected on-column were calculated from the amounts of II (50 ng) and III (250 ng) extracted from 1 ml of water, derivatized with 20 μl of 2% sodium methoxide in anhydrous methanol and injected assuming 100% conversion at each step.*

Derivatization conditions were optimized by comparison of absolute peak heights obtained from heating derivatizing reagents with chloroethylnitrosoureas at different temperatures and for various times. Optimal peak heights were obtained on heating the reagent mixtures at 50° for 20 min. No decrease in peak heights was observed on heating for longer periods.

Analysis of IV with V as Standard—A 0.1–0.5-ml plasma sample containing IV was mixed[12] with 3.0 ml of ether. The ether (2.0 ml) was removed and placed in a 3.0-ml cone-shaped vial[11] containing 10 μl of a 100 μg/ml stock solution of V in ether (1.0 μg, 3.5 nmoles). The ether was evaporated to dryness under a nitrogen stream at ambient temperature. Approximately 20 μl of 0.2 *M* trimethylanilinium hydroxide in anhydrous methanol[4] was added, mixed, and heated at 50° for 20 min in a capped cone-shaped vial. Approximately 1.0 μl of this mixture was injected onto the column. The eluted peaks were detected with mass spectrometry using multiple-ion detection of ions *m/z* 183.1 for IV and *m/z* 191.1 for V-derived products. The peak height ratio of 183.1/193.1 was determined, and the plasma IV concentration was calculated by reference to a standard curve obtained using the described procedure with known concentrations of IV in plasma. Alternatively, the eluted GC peaks

[2] V. A. Levin and P. Kabra, unpublished results.

[3] Compounds I–IV were obtained from Dr. Robert Engle of the Drug Development Branch, Division of Cancer Treatment, National Cancer Institute and V was obtained from Sayko Co. Ltd., Japan.

[4] Methelute, Pierce Chemical Co.

[5] J. T. Baker Chemical Co.

[6] Supelco, Inc.

[7] Varian Associates model 2100.

[8] Perkin-Elmer model L-14.

[9] Finnigan Corp. model 3200.

[10] Ultra-high purity, Matheson.

[11] American Scientific Products.

[12] Vortex mixer, VWR Scientific Inc.

may be detected with a nitrogen-specific detector and the peak height ratios determined. The plasma concentration was calculated by reference to a standard curve obtained using this detection method.

Analysis of Other Chloroethylnitrosoureas—The described procedure for the analysis of IV may be followed for the analysis of plasma containing V by using IV as a standard.

Compounds I–III may be quantified by mixing 0.1–0.5 ml of plasma containing a chloroethylnitrosourea with 3.0 ml of ether. The ether (2.0 ml) was removed and placed in a 3.0-ml cone-shaped vial containing 1.0 μg of a standard chloroethylnitrosourea. Recommended standards are II for quantification of I or III, and III for quantification of II. Approximately 20 μg of 2% sodium methoxide in anhydrous methanol was added, mixed, and heated at 50° for 20 min in a capped cone-shaped vial. Approximately 1.0 μl of this mixture was injected onto the column.

The eluted peaks were detected with mass spectrometry using multiple-ion detection of ions *m/z* 138.1 or 102.1 for I, *m/z* 158.1 for II, and *m/z* 172.1 for III-derived products. The respective peak height ratios may be determined and used to calculate plasma concentration by reference to a standard curve obtained using the described procedure for analysis of known amounts of sample and reference chloroethylnitrosourea. Eluted GC peaks may be detected using a nitrogen-specific GC detector to obtain the corresponding peak height ratios which may also be used to calculate plasma concentrations.

Clearance from Rat Plasma—Male Fisher-344 rats, 230–290 g, were anesthetized by an intraperitoneal injection of pentobarbital and catheters were inserted into the saphenous artery and vein. After intravenous administration of 100 USP units of heparin sodium, rats were administered 22.2–22.9 mg of IV/kg iv for 20 sec. Samples of arterial blood were removed through the arterial catheter at 1, 2, 4, 6, 10, 15, 30, 60, 90, 120, and 180 min following intravenous administration. Individual 0.2–0.5-ml samples were placed in 1.5-ml capped micro test tubes and centrifuged[13] immediately at 8000×*g* for 30 sec. A known volume (0.1–0.3 ml) of plasma was removed and analyzed as described.

RESULTS AND DISCUSSION

Clinically studied chloroethylnitrosoureas are a class of drugs that share a common reactive nitrosourea moiety but may contain a variety of *N*-substituents, some of which are shown in Scheme I. The described assay employs the known base-catalyzed decomposition reaction of 3-substituted 1-(2-chloroethyl)-1-nitrosoureas to 2-chloroethylazohydroxide and *N*-substituted isocyanates (16–21). In this assay, the decomposition reaction is carried out in anhydrous methanol where the intermediate isocyanates react to yield *N*-substituted-*O*-methylcarbamates (22) as shown in Scheme II. The carbamate products are formed in >90% yield and retain the characteristic R-substituent of the different chloroethylnitrosoureas and their biologically active metabolites (23, 24). The *O*-methylcarbamate derivatives are readily separated by GC and may be detected using a variety of methods.

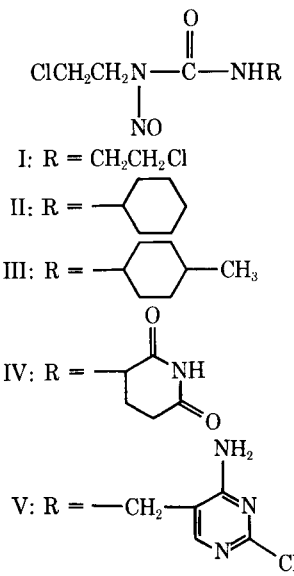

Scheme I—The structure of lipophilic chloroethylnitrosourea cancer chemotherapeutic agents.

[13] Eppendorf model 5412 centrifuge.

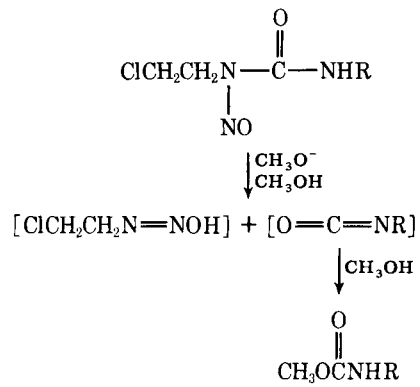

Scheme II—The reaction of chloroethylnitrosourea in basic anhydrous methanol leads to the formation of 2-chloroethyldiazotate and substituted isocyanate. The isocyanate reacts with solvent methanol to give a stable O-methylcarbamate derivative.

The assay procedure requires that the nitrosourea be extracted from plasma. All of the analogs studied (Scheme I) are lipophilic and are readily extracted from aqueous media by organic solvents. The least lipophilic analog, IV, has an octanol/water partition coefficient of 2.3. The extraction efficiency of this compound from 0.5 ml of plasma by a sixfold volume excess of ether is high. When ratios of known amounts of IV to V are plotted against observed peak height ratios, the same slope is obtained from the analyses of known amounts of both compounds following extraction of both components from plasma, and following extraction of IV from plasma using V as a standard. These results confirm that both compounds may be extracted from 0.5 ml of plasma by 3.0 ml of ether in >90% efficiency.

The decomposition of chloroethylnitrosoureas to alkylisocyanates is catalyzed by organic and inorganic bases. Although the choice of catalyst is not critical, 2% sodium methoxide in anhydrous methanol is a convenient reagent compatible with GC nitrogen-specific detectors and with mass spectrometric detection under chemical-ionization conditions. This reagent may be used for the analysis of IV and V as well as the other chloroethylnitrosoureas listed in Scheme I. Trimethylanilinium hydroxide in anhydrous methanol may be used for the analysis of IV and

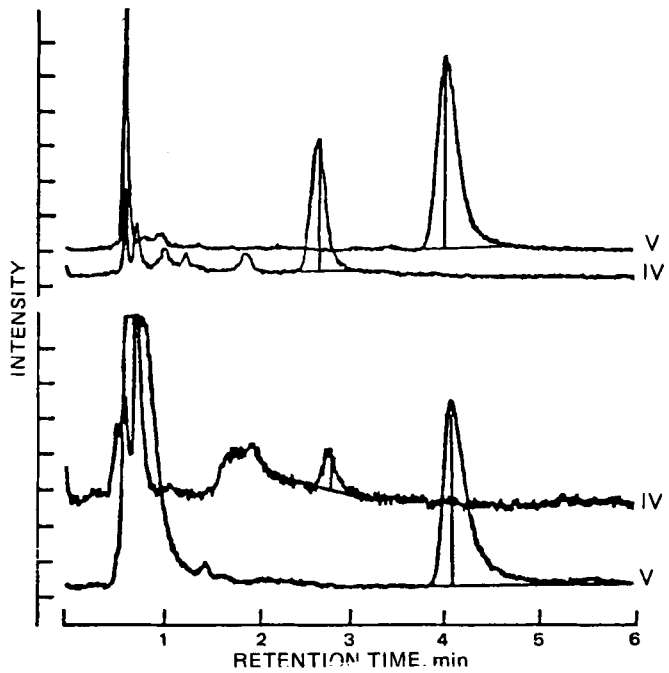

Figure 2—*GC–mass spectrometric selected ion traces for IV and V obtained from rat plasma following the described assay procedure for IV using V as a standard. The upper portion of the figure is the analysis of V in rat plasma following intravenous administration of a 22.5-mg/kg bolus of IV. The lower portion shows the data output operating near the limit of detection in which an estimated 2.0 ng of derivative was injected on-column.*

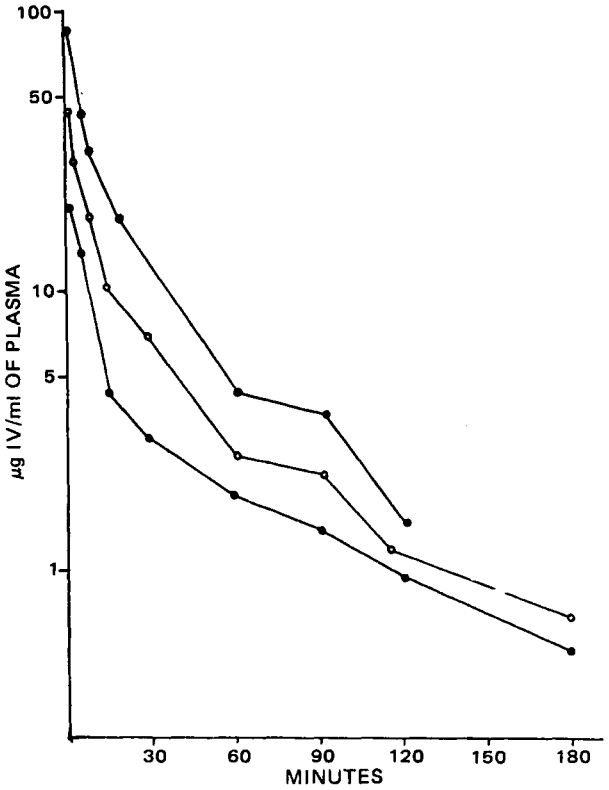

Figure 3—*Plasma clearance curves obtained following the intravenous administration of 22.5-mg/kg bolus of IV to 230–290-g male Fisher-344 rats. Compound IV was analyzed following the procedure using V as a standard. The GC eluate was monitored using mass spectrometry multiple-ion detection.*

V but is not recommended for the analysis of other analogs. This reagent acts as an on-column methylating agent as well as a basic catalyst.

Reaction of a chloroethylnitrosourea at 50° for 20 min in the reagent forms the *O*-methylcarbamate (Scheme II). Injection of the mixture onto the GC column at an injection port temperature of 210° pyrolyzes the trimethylanilinium ion and transfers a methyl group onto the nitrogen of the *O*-methylcarbamate. The resulting *N*,*N*-disubstituted carbamate has good GC characteristics. *N*-Methylation also facilitates chemical-ionization induced fragmentation to the $(MH-HOCH_3)^+$ ion, thereby concentrating the ion current at a single mass and improving detection sensitivity. However, the on-column methylation of I–III and derived *O*-methylcarbamates is not complete under these conditions, so that the use of this reagent leads to partial methylation and generation of two GC peaks for each compound.

GC peak detection was performed using flame-ionization detectors, nitrogen-specific detectors, and multiple-ion detection mass spectrometry. Flame-ionization detection of plasma-extracted I has a detection limit of 100 ng injected on-column. This rather high limit is due, in part, to the poor separation between the volatile I derivative and plasma contaminants. Although the flame-ionization detection limit may be lower for other chloroethylnitrosourea analogs and GC column packings, this method was not pursued because the nitrogen-specific GC detector proved to be a much more sensitive and selective device with approximately the same cost and complexity as the flame-ionization detector.

Figure 1 shows a chromatogram obtained from the rapid elution of 2.5 ng of II- and 10.0 ng of III-derived products injected on-column. This detection limit is well within that needed to perform pharmacokinetic studies and is similar to that observed using mass spectrometric detection. The values for on-column injection were calculated from the amounts of II and III extraction from water, derivatized, and injected, assuming 100% efficiency at each step. The selectivity of the nitrogen-specific detector for compounds containing the C–N bond provides chromatograms of neutral plasma ether extracts that are relatively free from interfering peaks.

Multiple-ion mass spectrometric monitoring of GC peaks is a sensitive and selective detection method. A GC-selected ion trace of IV and V derivatives where IV was extracted from plasma using V as a standard is shown in Fig. 2. The monitored ions are the *N*-methyl-*O*-methylcarbamate derivative $(MH-HOCH_3)^+$ fragment ions *m/z* 183.1 for IV and 193.1 for V. The upper portion of Fig. 2 shows the analysis of a rat plasma sample following administration of IV. The lower portion shows the detection limit of IV at 2 ng injected on-column. This amount was calculated from the amount of IV added to plasma and injected on-column assuming 100% efficiency of extraction, derivatization, and sample transfer. The actual amount of *O*-methylcarbamate injected may be less.

Table I—Plasma Clearance Pharmacokinetic Parameters Calculated [a] from the Clearance Curves Obtained Following a 22.5-mg/kg iv Bolus Dose of IV to 230–290-g Male Fisher-344 Rats

V_1	0.65 (0.36)	liters/kg
V_2	1.07 (0.70)	liters/kg
V_{dss}	1.72 (0.79)	liters/kg
k_{10}	0.061 (0.015)	min^{-1}
k_{12}	0.080 (0.039)	min^{-1}
k_{21}	0.051 (0.014)	min^{-1}
AUC	508 (111)	μg min/ml
Clearance	0.036 (0.011)	liters/min

[a] The data were fit to a two-compartment open model (25). Values presented are the mean ±*SD* of five separate experiments.

The described detection method was used to measure the clearance of IV from rat plasma following intravenous administration of a 22.5 mg/kg bolus. The detection limit in rat plasma was 100 ng/ml using 300-μl plasma sample volumes. Clearance curves were obtained for five animals. Three of these curves are shown (Fig. 3). The clearance curves were fitted to two exponentials using a computer program for nonlinear iterative curve fitting. The data were further analyzed by a two-compartment model for biodistribution (25). Mean pharmacokinetic parameters calculated from the five clearance curves (Table I) illustrate the suitability of the described analytical method for the determination of pharmacokinetic parameters.

Comparison of the biodistribution parameters of IV with those of the more lipophilic analog I (26) show that the volume of distribution and compartment volumes are comparable. The major difference between the two agents is that the area under the clearance curve for I, *AUC* = 359 ± 68 μg min/ml, following administration of a 26 mg/kg iv bolus to male Fisher-344 rats, is significantly less than that for IV. The importance of a prolonged presence of parent drug in plasma is not clear in the case of the chloroethylnitrosoureas because the parent agent must be chemically converted to reactive intermediates and, therefore, cleared from plasma to be active.

CONCLUSIONS

The described assay leads to the formation of chloroethylnitrosourea derivatives that retain the R group characteristic of the analogs in this series. As a consequence, this method has the potential to be applied to the analysis of biologically active hydroxylated II and III metabolites. For example, hydroxylated II metabolites may be extracted from plasma or incubation medium with ether (27) and analyzed by the described procedures since ring-hydroxylated II analogs can be separated as *O*-methylcarbamates on OV-1 GC columns[14].

REFERENCES

(1) S. K. Carter, F. M. Schabel, L. E. Broder, and T. P. Johnston, *Adv. Cancer Res.*, **16**, 273 (1972).

(2) V. DeVita, P. Carbone, A. Owens, G. L. Gold, M. J. Krant, and J. Edmonson, *Cancer Res.*, **25**, 1876 (1965).

(3) V. A. Levin and C. B. Wilson, *Cancer Treat. Rep.*, **60**, 719 (1976).

(4) V. A. Levin, W. Hoffman, and R. J. Weinkam, *Cancer Chemother. Rep.*, **62**, 1305 (1978).

(5) R. J. Weinkam, J. H. C. Wen, D. E. Furst, and V. A. Levin, *Clin. Chem.*, **24**, 45 (1978).

(6) J. A. Montgomery, T. P. Johnston, H. J. Thomas, J. R. Piper, and C. Temple, *Adv. Chromatogr.*, **15**, 169 (1977).

(7) R. J. Weinkam, A. Finn, V. A. Levin, and J. P. Kane, *J. Pharmacol., Exp. Ther.*, **214**, 318 (1980).

(8) J. Hilton and M. D. Walker, *Biochem. Pharmacol.*, **24**, 2153 (1975).

(9) K. Nakamura, M. Asami, K. Kawada, and K. Sasahara, *Ann. Ryst. Sankyo, Res. Lab.*, **29**, 66 (1977).

[14] R. J. Weinkam, unpublished observations.

(10) G. P. Wheeler, B. J. Bowden, and T. C. Herrer, *Cancer Chemother. Rep.*, **42**, (1964).
(11) V. DeVita, C. Denham, J. D. Davidson, and V. T. Oliverio, *Clin. Pharmacol. Ther.*, **8**, 566 (1967).
(12) D. L. Hill, M. C. Kirk, and R. F. Struck, *Cancer Res.*, **35**, 296 (1975).
(13) T. L. Loo and R. L. Dion, *J. Pharm. Sci.*, **54**, 809 (1965).
(14) A. C. Bratton and E. K. Marshall, *J. Biol. Chem.*, **128**, 537 (1939).
(15) I. Bartosek, S. Daniel, and S. Sykara, *J. Pharm. Sci.*, **67**, 1160 (1978).
(16) M. Colvin, J. W. Cowens, R. B. Brundrett, B. S. Kramer, and D. B. Ludlum, *Biochem. Biophys. Res. Commun.*, **60**, 515 (1974).
(17) J. A. Montgomery, R. James, G. S. McCaleb, M. C. Kirk, and T. P. Johnston, *J. Med. Chem.*, **18**, 586 (1975).
(18) D. J. Reed, H. E. May, R. B. Boose, K. M. Gregory, and M. A. Beilstein, *Cancer. Res.* **35**, 568 (1975).
(19) R. B. Brundrett, J. W. Cowens, M. Colvin, and I. Jardin, *J. Med. Chem.*, **19**, 958 (1976).
(20) R. J. Weinkam and H. S. Lin, *ibid.*, **22**, 1193 (1979).
(21) J. W. Lown and L. W. McLaughlin, *Biochem. Pharmacol.*, **28**, 2115 (1979).
(22) F. W. Bollinger, F. N. Hayes, and S. Siegel, *J. Am. Chem. Soc.*, **72**, 5592 (1950).
(23) H. E. May, R. Boose, and D. J. Reed, *Biochem. Biophys. Res. Commun.*, **57**, 426 (1974).
(24) J. Hilton, F. Maldarilli, and S. Sargent, *Biochem. Pharmacol.*, **27**, 1359 (1978).
(25) S. Riegelman, J. Loo, and M. Rowland, *J. Pharm. Sci.*, **57**, 117 (1968).
(26) V. A. Levin, J. Stearns, A. Byrd, A. Finn, and R. J. Weinkam, *J. Pharmacol. Exp. Ther.*, **208**, 1 (1979).
(27) D. J. Reed and H. E. May, in "Microsomes and Drug Oxidation," V. Ullrich, Ed., Pergamon, New York, N.Y., 1977, pp. 680–687.

ACKNOWLEDGMENTS

Supported by National Institutes of Health Grants CA 13525 and Research Career Development Award GM 00007 to Robert J. Weinkam.

The authors also thank Dr. V. Levin for advice in conducting the rat pharmacokinetic experiments and Dr. A. Foster and the Chester Beatty Cancer Research Institute, London, at which the gas chromatograph nitrogen detector experiments were conducted. The Robert J. Weinkam's stay at the Chester Beatty Research Institute was supported by the Burroughs Wellcome Fund.

High-Pressure Liquid Chromatographic Analysis of Indocyanine Green

P. L. RAPPAPORT and J. J. THIESSEN ˣ

Received August 12, 1980, from the *Faculty of Pharmacy, University of Toronto, Toronto, Canada, M5S 1A1.* Accepted for publication May 18, 1981.

Abstract □ The development of a specific high-pressure liquid chromatographic (HPLC) assay, having a quantitative detection limit of 0.4 μg/ml, is described for plasma indocyanine green. In a preliminary study, the HPLC method demonstrated that the traditional spectrophotometric procedure inaccurately quantitates the dye's degradation in aqueous medium since degradation products that absorb light at 770 nm are formed. In a further study, the spectrophotometric method yielded an erroneously low clearance of indocyanine green in the rabbit. In addition, the HPLC assay points to the possibility of metabolite formation of the dye *in vivo*.

Keyphrases □ Indocyanine green—high-pressure liquid chromatographic analysis □ High-pressure liquid chromatography—analysis of indocyanine green □ Dyes—indocyanine green, high-pressure liquid chromatographic analysis

Indocyanine green, an organic anion, has been used to determine cardiac output (1, 2), hepatic blood flow (3–5), and hepatic function (3–9). Analytical methods have been based on the dye's absorbance at 775–800 nm. These procedures employ either direct, continuous measurements of dye in circulating whole blood with a densitometer (1, 2, 10) or standard spectrophotometric analysis of harvested plasma following discrete blood sampling (3–9).

BACKGROUND

In vitro studies (10–12) determined that aqueous solutions of indocyanine green degrade quickly in a concentration-dependent fashion. However, in the presence of plasma or albumin, dye stability is much improved.

In vivo experiments demonstrated a saturable process for indocyanine green uptake by the liver (13, 14) and a biexponential decline in plasma levels for rats, rabbits, dogs, and humans (5, 6, 9, 15). Elimination of unchanged dye by the liver into bile has been thought to be the sole method for indocyanine green clearance. Evidence for this reported absence of metabolites was obtained from paper chromatographic analysis of plasma and bile samples (3, 5, 16, 17).

The reliability of this information depends on the perceived specificity of the spectrophotometric analysis method. Another procedure was needed to examine the existing methods critically. This report describes a high-pressure liquid chromatographic (HPLC) method for analysis of indocyanine green. Preliminary data are presented, highlighting discrepancies between the HPLC and spectrophotometric methods for the determination of *in vitro* dye stability and *in vivo* pharmacokinetics.

EXPERIMENTAL

HPLC Instrumentation—A high-pressure pump[1], a high-pressure injector[2], UV detector[3] (225 nm), and a recorder[4] comprised the chromatographic apparatus. Chromatography was performed on a reversed-phase column[5], using a reversed-phase precolumn[6] to extend column life. The mobile phase, at a flow of 2 ml/min, was composed of 47 parts of acetonitrile[7], 3 parts of methanol[7], and 50 parts 0.05 *M* KH_2PO_4–Na_2HPO_4 buffer[8] (pH 6). A spectrophotometric scan[9] of indocyanine green[10] in reagent grade water[11] showed a peak at 770 nm ($\epsilon = 1.43 \times 10^5$) and another at 210 nm ($\epsilon = 5.17 \times 10^4$). To minimize interference from plasma constituents and to maximize detector performance, a nonoptimal wavelength (225 nm) was used for detection purposes (ϵ ~60% of that at 210 nm).

Preparation of Standards—For the preparation of calibration curves, methanolic solutions of indocyanine green (20, 15, 10, 7, 4, 2, 1, 0.5, 0.2,

[1] Altex model 100.
[2] Valco Universal inlet HPLC valve.
[3] LDC Spectro Monitor I.
[4] Tracor Westronics MT.
[5] Hibar II, C_{18}, 10 μm, 250 × 4.6-mm i.d.
[6] Perisorb, C_{18}, 30–40 μm, 40 × 3.2-mm i.d.
[7] Glass distilled, Burdick & Jackson.
[8] Certified ACS, Fisher Scientific.
[9] Cary model 118, Varian.
[10] Cardio-Green, Hynson, Westcott and Dunning.
[11] Double distilled.

0022-3549/82/0200-0157$01.00/0

(10) G. P. Wheeler, B. J. Bowden, and T. C. Herrer, *Cancer Chemother. Rep.*, **42**, (1964).
(11) V. DeVita, C. Denham, J. D. Davidson, and V. T. Oliverio, *Clin. Pharmacol. Ther.*, **8**, 566 (1967).
(12) D. L. Hill, M. C. Kirk, and R. F. Struck, *Cancer Res.*, **35**, 296 (1975).
(13) T. L. Loo and R. L. Dion, *J. Pharm. Sci.*, **54**, 809 (1965).
(14) A. C. Bratton and E. K. Marshall, *J. Biol. Chem.*, **128**, 537 (1939).
(15) I. Bartosek, S. Daniel, and S. Sykara, *J. Pharm. Sci.*, **67**, 1160 (1978).
(16) M. Colvin, J. W. Cowens, R. B. Brundrett, B. S. Kramer, and D. B. Ludlum, *Biochem. Biophys. Res. Commun.*, **60**, 515 (1974).
(17) J. A. Montgomery, R. James, G. S. McCaleb, M. C. Kirk, and T. P. Johnston, *J. Med. Chem.*, **18**, 586 (1975).
(18) D. J. Reed, H. E. May, R. B. Boose, K. M. Gregory, and M. A. Beilstein, *Cancer. Res.* **35**, 568 (1975).
(19) R. B. Brundrett, J. W. Cowens, M. Colvin, and I. Jardin, *J. Med. Chem.*, **19**, 958 (1976).
(20) R. J. Weinkam and H. S. Lin, *ibid.*, **22**, 1193 (1979).
(21) J. W. Lown and L. W. McLaughlin, *Biochem. Pharmacol.*, **28**, 2115 (1979).
(22) F. W. Bollinger, F. N. Hayes, and S. Siegel, *J. Am. Chem. Soc.*, **72**, 5592 (1950).
(23) H. E. May, R. Boose, and D. J. Reed, *Biochem. Biophys. Res. Commun.*, **57**, 426 (1974).
(24) J. Hilton, F. Maldarilli, and S. Sargent, *Biochem. Pharmacol.*, **27**, 1359 (1978).
(25) S. Riegelman, J. Loo, and M. Rowland, *J. Pharm. Sci.*, **57**, 117 (1968).
(26) V. A. Levin, J. Stearns, A. Byrd, A. Finn, and R. J. Weinkam, *J. Pharmacol. Exp. Ther.*, **208**, 1 (1979).
(27) D. J. Reed and H. E. May, in "Microsomes and Drug Oxidation," V. Ullrich, Ed., Pergamon, New York, N.Y., 1977, pp. 680–687.

ACKNOWLEDGMENTS

Supported by National Institutes of Health Grants CA 13525 and Research Career Development Award GM 00007 to Robert J. Weinkam.

The authors also thank Dr. V. Levin for advice in conducting the rat pharmacokinetic experiments and Dr. A. Foster and the Chester Beatty Cancer Research Institute, London, at which the gas chromatograph nitrogen detector experiments were conducted. The Robert J. Weinkam's stay at the Chester Beatty Research Institute was supported by the Burroughs Wellcome Fund.

High-Pressure Liquid Chromatographic Analysis of Indocyanine Green

P. L. RAPPAPORT and J. J. THIESSEN ˣ

Received August 12, 1980, from the *Faculty of Pharmacy, University of Toronto, Toronto, Canada, M5S 1A1.* Accepted for publication May 18, 1981.

Abstract □ The development of a specific high-pressure liquid chromatographic (HPLC) assay, having a quantitative detection limit of 0.4 μg/ml, is described for plasma indocyanine green. In a preliminary study, the HPLC method demonstrated that the traditional spectrophotometric procedure inaccurately quantitates the dye's degradation in aqueous medium since degradation products that absorb light at 770 nm are formed. In a further study, the spectrophotometric method yielded an erroneously low clearance of indocyanine green in the rabbit. In addition, the HPLC assay points to the possibility of metabolite formation of the dye *in vivo*.

Keyphrases □ Indocyanine green—high-pressure liquid chromatographic analysis □ High-pressure liquid chromatography—analysis of indocyanine green □ Dyes—indocyanine green, high-pressure liquid chromatographic analysis

Indocyanine green, an organic anion, has been used to determine cardiac output (1, 2), hepatic blood flow (3–5), and hepatic function (3–9). Analytical methods have been based on the dye's absorbance at 775–800 nm. These procedures employ either direct, continuous measurements of dye in circulating whole blood with a densitometer (1, 2, 10) or standard spectrophotometric analysis of harvested plasma following discrete blood sampling (3–9).

BACKGROUND

In vitro studies (10–12) determined that aqueous solutions of indocyanine green degrade quickly in a concentration-dependent fashion. However, in the presence of plasma or albumin, dye stability is much improved.

In vivo experiments demonstrated a saturable process for indocyanine green uptake by the liver (13, 14) and a biexponential decline in plasma levels for rats, rabbits, dogs, and humans (5, 6, 9, 15). Elimination of unchanged dye by the liver into bile has been thought to be the sole method for indocyanine green clearance. Evidence for this reported absence of metabolites was obtained from paper chromatographic analysis of plasma and bile samples (3, 5, 16, 17).

The reliability of this information depends on the perceived specificity of the spectrophotometric analysis method. Another procedure was needed to examine the existing methods critically. This report describes a high-pressure liquid chromatographic (HPLC) method for analysis of indocyanine green. Preliminary data are presented, highlighting discrepancies between the HPLC and spectrophotometric methods for the determination of *in vitro* dye stability and *in vivo* pharmacokinetics.

EXPERIMENTAL

HPLC Instrumentation—A high-pressure pump[1], a high-pressure injector[2], UV detector[3] (225 nm), and a recorder[4] comprised the chromatographic apparatus. Chromatography was performed on a reversed-phase column[5], using a reversed-phase precolumn[6] to extend column life. The mobile phase, at a flow of 2 ml/min, was composed of 47 parts of acetonitrile[7], 3 parts of methanol[7], and 50 parts 0.05 *M* KH_2PO_4–Na_2HPO_4 buffer[8] (pH 6). A spectrophotometric scan[9] of indocyanine green[10] in reagent grade water[11] showed a peak at 770 nm ($\epsilon = 1.43 \times 10^5$) and another at 210 nm ($\epsilon = 5.17 \times 10^4$). To minimize interference from plasma constituents and to maximize detector performance, a nonoptimal wavelength (225 nm) was used for detection purposes (ϵ ~60% of that at 210 nm).

Preparation of Standards—For the preparation of calibration curves, methanolic solutions of indocyanine green (20, 15, 10, 7, 4, 2, 1, 0.5, 0.2,

[1] Altex model 100.
[2] Valco Universal inlet HPLC valve.
[3] LDC Spectro Monitor I.
[4] Tracor Westronics MT.
[5] Hibar II, C_{18}, 10 μm, 250 × 4.6-mm i.d.
[6] Perisorb, C_{18}, 30–40 μm, 40 × 3.2-mm i.d.
[7] Glass distilled, Burdick & Jackson.
[8] Certified ACS, Fisher Scientific.
[9] Cary model 118, Varian.
[10] Cardio-Green, Hynson, Westcott and Dunning.
[11] Double distilled.

0022-3549/82/0200-0157$01.00/0

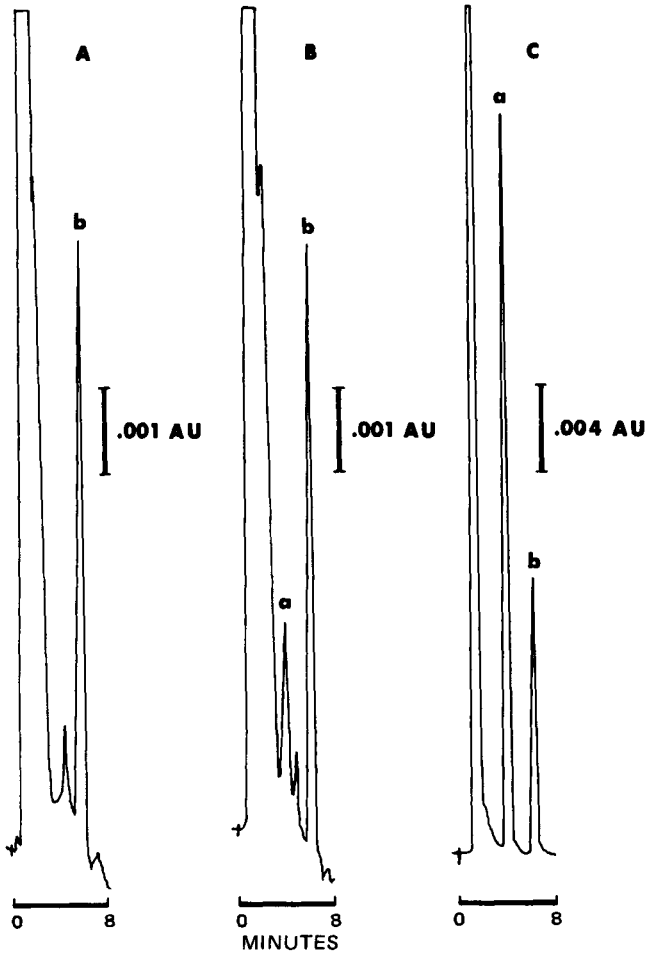

Figure 1—*HPLC chromatograms obtained for indocyanine green (a) and diazepam (b) using an RP-18 column (250 × 4.6-mm i.d.) and a mobile phase of 47% acetonitrile–3% methanol–0.05 M phosphate buffer (pH 6) at 2.0 ml/min. Detection was at 225 nm. Key: A, diazepam (0.15 μg/0.25 ml) in blank rabbit plasma; B, indocyanine green (0.1 μg/0.25 ml) and diazepam (0.15 μg/0.25 ml) in blank rabbit plasma; and C, indocyanine green (10 μg/0.25 ml) and diazepam (1.5 μg/0.25 ml) in blank rabbit plasma.*

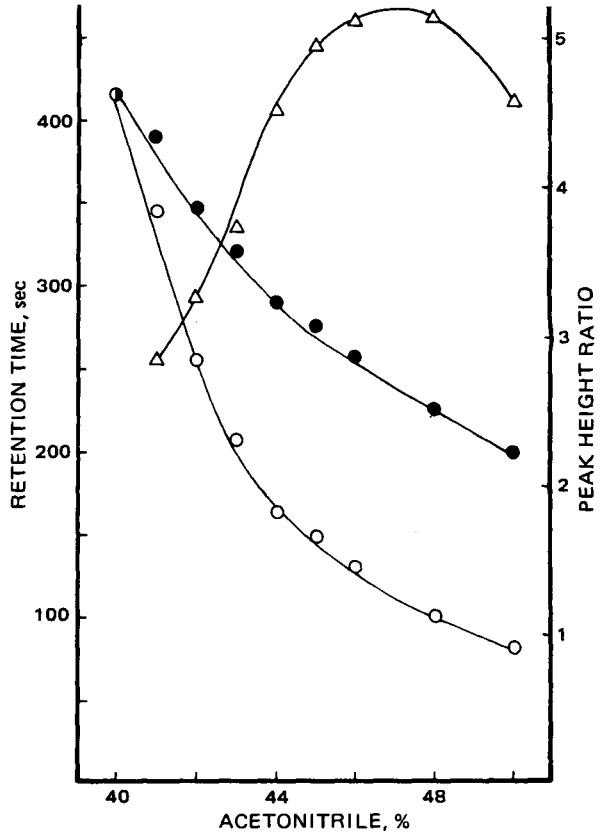

Figure 2—*Effect of acetonitrile concentration in the mobile phase on the retention times of indocyanine green (○) and diazepam (●) and on the indocyanine green/diazepam peak height ratio (△). The aqueous part of the mobile phase was composed of a 0.025 M phosphate buffer (pH 4). The mobile phase was run at 1.6 ml/min on an RP-18 column (250 × 3.2-mm i.d.).*

and 0.1 μg in 0.1 ml) were evaporated to dryness at 40° under a gentle dry nitrogen stream. After this step, standards could be stored in a desiccator under vacuum for 1 week with no detectable degradation. At the time of sample analysis, blank rabbbit plasma (0.25 ml) was added to each tube and allowed to stand for 30 min with intermittent vortexing. After this point, standards were processed in the same manner as *in vivo* samples.

HPLC Sample Preparation—A fixed plasma volume (0.25 ml) was used for all samples. Concentrated samples (>80 μg/ml) were diluted with blank rabbit plasma. Acetonitrile in a 1.6:1 (v/v) ratio with plasma was added in four aliquots (0.1 ml each for 0.25 ml of plasma), with vortexing after each addition. Methanolic diazepam[12] (5, 1.5, or 0.15 μg in 50 μl) was then added as the internal standard, and the mixture was vortexed for 20 sec. The sample was centrifuged(1700×*g*) for 2 min, and a volume of the supernate was injected onto the column. Due to recognized degradation of indocyanine green, the maximum allowable time between sample precipitation and column injection was 30 min.

Spectrophotometric Analysis—The plasma sample (0.25 ml) was diluted with 3.3 ml of reagent grade water. The absorbance of the solution was measured (800 nm) using similarly prepared blank rabbit plasma as the reference.

Stability of Aqueous Solutions—An indocyanine green solution (20 μg/ml in reagent grade water) was exposed to a constant amount of room light (420 lux) at 23°. The solution was sampled periodically to determine the amount of parent dye remaining.

For HPLC analysis, 100 μl of this solution and 100 μl of acetonitrile were added to a tube containing diazepam (0.26 μg). The mixture was vortexed and injected onto the column. Indocyanine green standards were prepared as already described. At the time of analysis, methanolic diazepam (0.26 μg in 0.05 ml) was added to the standards and evaporated. After reconstitution with 0.2 ml of 50% acetonitrile–reagent grade water, the standard was subjected to HPLC analysis.

Spectrophotometric analysis[13] (770 nm) was performed on the solution without a dilution step. The absorbance measurement of a freshly prepared dye solution served as the standard for comparison.

Stability of Plasma Solutions—Standard plasma samples containing 80, 40, 8, 4, or 0.8 μg of indocyanine green in 2.0 ml of fresh blank plasma were prepared as already described. The samples were kept at 6° in polyethylene tubes and 0.25 ml of each was sampled seven times over 10 weeks. A calibration curve, obtained from freshly prepared standards analyzed at the same time as the samples, was used for quantitation of dye degradation.

Indocyanine Green *In Vivo* Study—Indocyanine green was reconstituted with 5% dextrose–water to give a concentration of 8.8 mg/ml. A 25.6-mg/kg dose was administered intravenously[14] to a rabbit over 4 min. Thirteen blood samples (1.5 ml) were collected over 6 hr. Harvested plasma was kept at 6° until analysis later that day.

Calculations—The unknown indocyanine green concentrations in samples analyzed spectrophotometrically or by HPLC were obtained with reference to calibration curves constructed from identically prepared standards. Dye clearance values were calculated using the total area under the indocyanine green concentration *versus* time curve.

RESULTS AND DISCUSSION

Chromatography—Figure 1 illustrates typical chromatograms for blank rabbit plasma and indocyanine green plasma standards. The total

[12] P-1215, Novopharm.

[13] Carl Zeiss spectrophotometer PMQ II.

[14] Model 351 infusion pump, Sage Instruments.

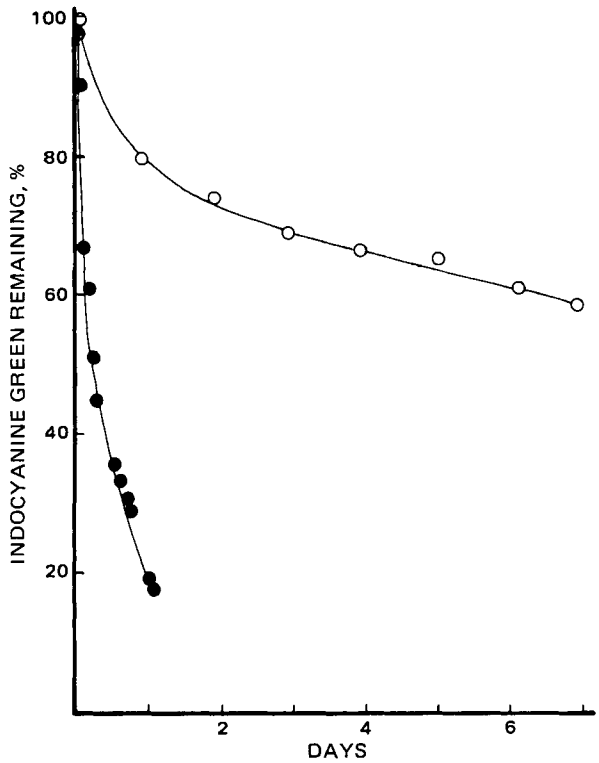

Figure 3—*Degradation profile of aqueous indocyanine green (initial concentration was 20 μg/ml) as examined by HPLC (●) and spectrometric (○) methods.*

retention time was ~7 min, and the quantitative limit of detection for the dye in plasma was 0.4 μg/ml.

The composition of the mobile phase was examined with the following results. The acetonitrile concentration is critical for successful resolution of indocyanine green and diazepam and for optimization of peak shape (Fig. 2). The use of methanol in the ternary solvent system sharpens and reduces the retention time of the internal standard peak without appreciably affecting indocyanine green retention. With respect to the buffer, the salt strength is more important than pH for successful retention of indocyanine green.

The quantitation of indocyanine green in samples varies with the plasma volume (Table I), even when the ratio of precipitant to plasma is constant (1.6:1 v/v). This result may be accounted for by an interfering component in blank rabbit plasma, which exhibits the same retention time as diazepam. Although the diazepam equivalent of this peak only approaches 5% with 0.25-ml samples, the interference is more pronounced with larger sample volumes when the amount of diazepam added remains constant. Therefore, samples with dye concentrations greater than the upper limit of the standard curve (80 μg/ml) were diluted to varying degrees to allow analysis of a constant volume (0.25 ml).

Calibration curves were linear over the concentration range used. The intra-assay coefficient of variation ranged from 2% for 40-μg/ml samples to 8% for 0.4-μg/ml samples (n = 6). The interassay variability was 5–11% for all standards except the 0.4-μg/ml standard, which was 20% (n = 8). The slope variance of standard curves was calculated as 10% (n = 10).

Spectrophotometric Analysis—The lower limit of quantitative detection of indocyanine green in plasma was 2 μg/ml when using 0.25 ml of plasma and the described dilution. The interassay coefficient of variation for all standards was 11–14% (n = 3).

It was reported (18) that different plasma samples yield calibration curves that vary widely, but no explanation for this result has been found. A similar observation was made in this investigation when blank plasma from different rabbits was used. The slopes of calibration curves varied by 32%. This variability is independent of any differences in the inherent absorbance of blank samples at 800 nm. The problem was also not alleviated by protein precipitation using acetonitrile prior to spectrophotometric measurement. Thus, although the source of the variability has not been resolved, it demonstrates a disturbing characteristic of the spectrophotometric method.

Stability Studies of Aqueous Solutions—Once an accurate, reproducible HPLC method for indocyanine green was developed, preliminary studies were conducted to examine the stability of the dye in aqueous solution. Figure 3 illustrates the inadequacy of the spectrophotometric method in the detection of dye degradation in aqueous media. The discrepancy between the two methods results from degradation products of indocyanine green, which absorb a significant amount of light at 770 nm.

Table I—Quantitation Efficiency (Mean ± *SD*) Observed for Indocyanine Green (2 μg) when Added to Plasma Containing 0.735 μg of Diazepam (n = 6)

Plasma Volume, ml	Quantitation Efficiency, %
0.125	91.8 (1.4)
0.25	86.9 (1.8)
0.5	78.5 (2.0)
1.0	72.1 (4.6)

By modifying the mobile phase flow rate, these degradation products can be resolved (Fig. 4). Spectral analysis of the eluate fractions corresponding to these peaks showed that peaks a and b exhibited absorbance at 770 nm. It is unlikely that these peaks represent dye aggregates as described earlier (12, 19), since eluates were below the aggregate-forming concentration (<5 μg/ml) and the ionic strength of the solvent (mobile phase) was constant in all cases. Thus, it was felt that these peaks (Fig. 4) represent products of an irreversible degradation of parent dye. Barbier and DeWeerdt (16) showed two chromatographically distinct species that appear on storage of aqueous dye solution. The "fast" and "slow" fractions exhibited spectral peaks in the visible region at 780 and 783 nm, respectively.

The evidence from these experiments provides another reason why reports using the spectrophotometric method should be questioned.

Dye Stability in Plasma—Standard plasma samples analyzed by the HPLC method exhibited no detectable degradation after 10 weeks of storage at 6°, a finding in agreement with results obtained spectrophotometrically (10, 12).

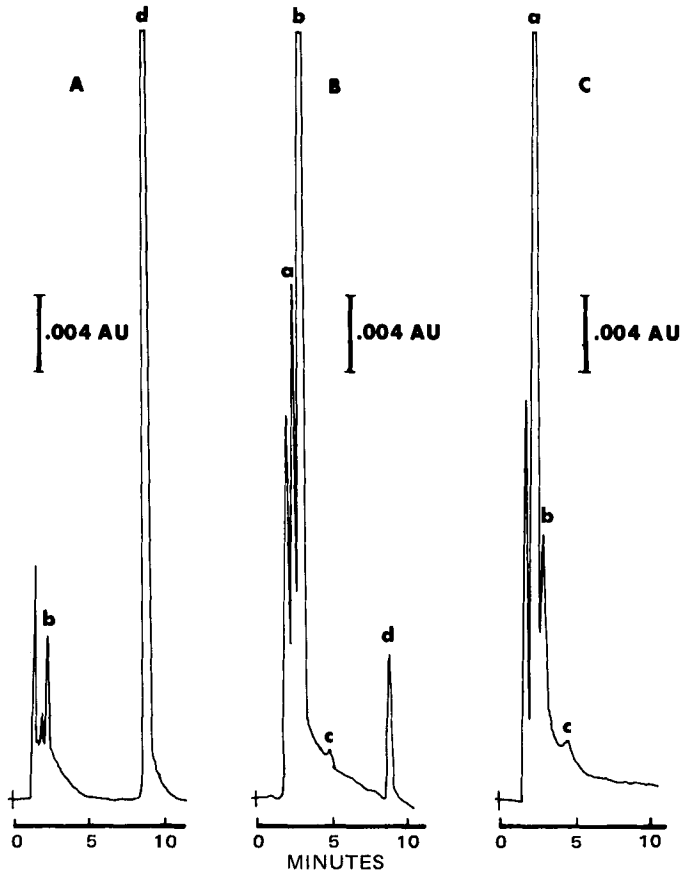

Figure 4—*HPLC chromatograms obtained from aqueous indocyanine green solutions that were freshly prepared (A), 1 day old (B), and 7 days old (C). An RP-18 column (250 × 4.6-mm i.d.) and a mobile phase of 47% acetonitrile–3% methanol–0.05 M phosphate buffer (pH 6) at 1.0 ml/min were employed. Peaks a, b, and c are degradation products of indocyanine green; and peak d is indocyanine green.*

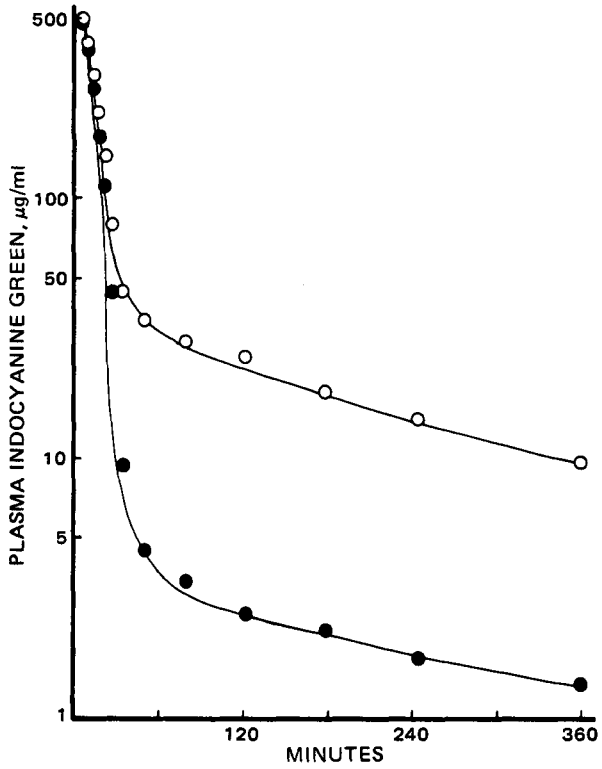

Figure 5—*Plasma indocyanine green observed in a rabbit following a 25.6-mg/kg dose as examined with HPLC (●) and spectrophotometric (○) methods.*

Indocyanine Green *In Vivo* Study—Having established that the HPLC method was more specific for the parent dye in examining aqueous stability, a preliminary study of *in vivo* pharmacokinetics was conducted in a rabbit. Figure 5 illustrates the plasma concentration *versus* time profiles obtained when the same samples were analyzed by the two methods. Initially, indocyanine green concentrations were similar by both procedures. However, after the steep declining phase, their difference became more pronounced. The use of the spectrophotometric method resulted in an erroneously low dye clearance (spectrophotometric method, 1.58 ml/min/kg; HPLC, 2.65 ml/min/kg).

It was questioned whether the observed difference in plasma indocyanine green (Fig. 5) was an artifact or a consequence of the nonspecificity of the spectrophotometric assay. One step in resolving this question was to collect plasma from a rabbit given normal saline rather than indocyanine green. Relative to water, samples collected over 5 hr exhibited an absorbance of 0.0058–0.0067 (790 nm), demonstrating that no time-related changes were found in the inherent absorbance of indocyanine green-free plasma. In view of the plasma stability studies, dye degradation after sample collection was also not responsible for the difference since both analyses were performed on the day of the *in vivo* experiment. It was thus concluded that an *in vivo* degradation product or metabolite of the dye was potentially responsible for the discrepancy seen in Fig. 5.

To evaluate the "metabolite" hypothesis further, the HPLC solvent front eluate was collected for *in vivo* samples, plasma standards, and a plasma blank. It was suspected that the discrepancy noted in Fig. 5 was due to an indocyanine green product eluting in the solvent front (similar to Fig. 4). Spectrophotometric scans of the solvent front eluates of plasma blank and dye standards showed no detectable absorbance in the 600–800-nm region (Fig. 6). However, all solvent front eluates from *in vivo* samples showed some absorbance in this region (Fig. 6). The absorbance pattern was similar to that of parent indocyanine green. However, the ratio of the absorbance at 770 nm to that at 700 nm was 2.4 for the indocyanine green peak eluates and 1.9 for solvent front eluates. For reasons discussed earlier with respect to dye degradation, it is unlikely that the component found in the solvent front eluate represents a dye aggregate. Therefore, it is postulated that indocyanine green undergoes some degradation or metabolism in the body prior to its excretion. The fact that the unknown substance elutes from the HPLC column prior to the parent dye is suggestive of a compound that is more polar than indocyanine green.

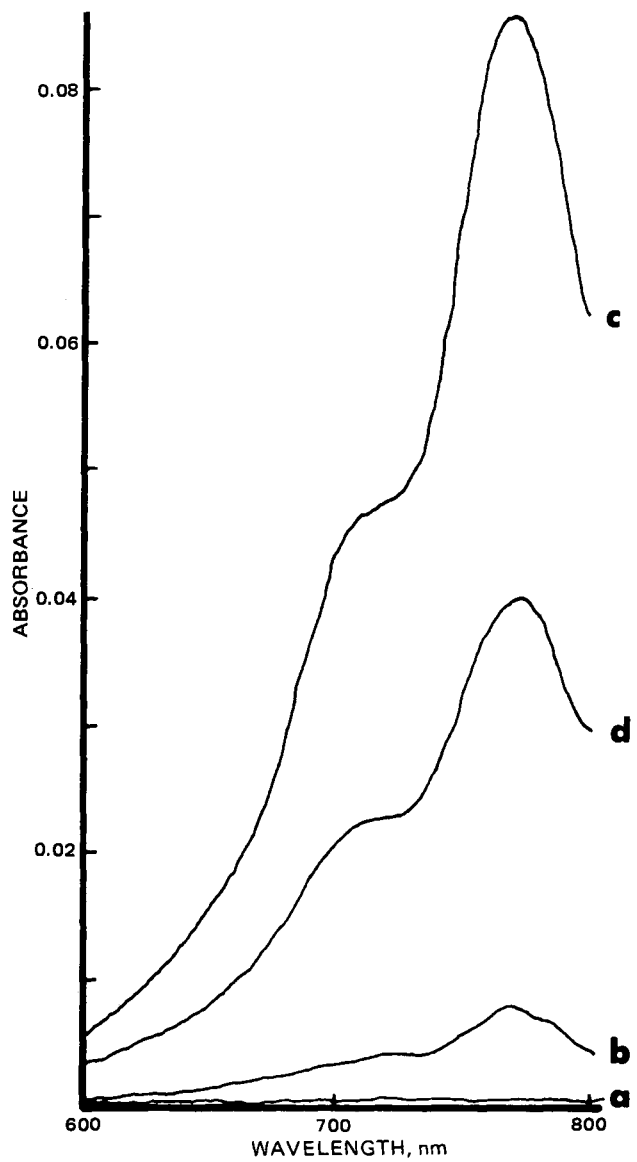

Figure 6—*Spectrophotometric scans of collected HPLC solvent front eluates from processed plasma samples harvested from a rabbit receiving 25.4 mg of indocyanine green/kg. Key: a, instrument baseline (blank solvent in both cells); b, plasma sample 26-min postdose (40 μl of supernate injected); c, plasma sample 120-min postdose (250 μl of supernate injected); and d, plasma sample 360-min postdose (250 μl of supernate injected).*

Only one literature report was found suggesting indocyanine green metabolism. Nambu (20), using ascending chromatography, found three bands in bile samples collected from a dog administered indocyanine green. The three bands exhibited absorbance at 770 nm in a pattern similar to that of the present studies.

The present study demonstrated that the described HPLC method is more specific for indocyanine green then the traditional spectrophotometric methods. This observation demands a reexamination of reports on indocyanine green's stability and *in vivo* pharmacokinetics. Furthermore, the nature of the degradation products/metabolites needs to be elucidated. These aspects are under investigation.

REFERENCES

(1) D. E. Miller, W. L. Gleason, and H. D. McIntosh, *J. Lab. Clin. Med.*, **59**, 345 (1962).

(2) B. Raffestin, J. P. Merillon, C. Masquet, P. Lorente, and R. Gourgon, *Coeur Med. Interne*, **14**, 305 (1975).

(3) J. Caesar, S. Shaldon, L. Chiandussi, L. Guevara, and S. Sherlock, *Clin. Sci.*, **21**, 43 (1961).

(4) B. D. Wiegand, S. G. Ketterer, and E. Rapaport, *Am. J. Dig. Dis.*, **5**, 427 (1960).
(5) G. R. Cherrick, S. W. Stein, C. M. Leevy, and C. S. Davidson, *J. Clin. Invest.*, **39**, 592 (1960).
(6) D. B. Hunton, J. L. Bollman, and H. N. Hoffman, *Gastroenterology*, **39**, 713 (1960).
(7) H. Kojima, *Nagoya J. Med. Sci.*, **40**, 47 (1978).
(8) C. M. Leevy, S. W. Stein, G. R. Cherrick, and C. S. Davidson, *Clin. Res.*, **7**, 290 (1959).
(9) S. Nakagawa, K. Araki, and H. Nagashima, *Kumamoto Med. J.*, **30**, 1 (1977).
(10) I. J. Fox and E. H. Wood, *Mayo Clin. Proc.*, **35**, 732 (1960).
(11) J. Gathje, R. R. Steuer, and K. R. K. Nicholes, *J. Appl. Physiol.*, **29**, 181 (1970).
(12) M. L. J. Landsman, G. Kwant, G. A. Mook, and W. G. Zijlstra, *ibid.*, **40**, 575 (1976).
(13) C. D. Klaassen and G. L. Plaa, *Toxicol. Appl. Pharmacol.*, **15**, 374 (1969).
(14) G. Paumgartner, P. Probst, R. Kraines, and C. M. Leevy, *Ann. N.Y. Acad. Sci.*, **170**, 134 (1970).
(15) E. Rapaport, S. G. Ketterer, and B. D. Wiegand, *Clin. Res.*, **7**, 289 (1959).
(16) F. Barbier and G. A. DeWeerdt, *Clin. Chim. Acta*, **10**, 549 (1964).
(17) H. O. Wheeler, W. I. Cranston, and J. I. Meltzer, *Proc. Soc. Exp. Biol. Med.*, **99**, 11 (1958).
(18) R. Simmons and R. J. Shephard, *J. Appl. Physiol.*, **30**, 502 (1971).
(19) K. J. Baker, *Proc. Soc. Exp. Biol. Med.*, **122**, 957 (1966).
(20) M. Nambu, *Nippon Shokakibyo Gakkai Zasshi*, **63**, 777 (1966).

ACKNOWLEDGMENTS

Supported in part by the Medical Research Council of Canada.
The authors thank Dr. P. E. Coates for constructive discussions and Mrs. S. Selliah and Mr. G. Kieltyka for technical assistance.

Analysis of Oral Suspensions Containing Sulfonamides in Combination with Erythromycin Ethylsuccinate

L. ELROD, Jr.[x], R. D. COX, and A. C. PLASZ

Received March 23, 1981, from the *Analytical Research Department, Abbott Laboratories, North Chicago, IL 60064.*
Accepted for publication May 28, 1981

Abstract □ The sulfonamides and erythromycin ethylsuccinate in combination oral suspensions were determined by high-performance liquid chromatography and automated turbidimetry, respectively. The chromatographic procedure was rapid, specific, and stability-indicating for sulfisoxazole acetyl and the trisulfapyrimidines using a reversed-phase system with UV detection at 254 nm. Erythromycin ethylsuccinate did not interfere with the sulfonamide analysis and these compounds were assayed with relative standard deviations (*RSD*) ranging from ±2.1 to ±3.1%. Erythromycin ethylsuccinate was determined as erythromycin with *RSD* values of ±1.3 or ±3.5% without interference by the sulfonamides present.

Keyphrases □ Sulfonamides—analysis of oral suspensions in combination with erythromycin ethylsuccinate, high-performance liquid chromatography □ Erythromycin ethylsuccinate—analysis of oral suspensions with sulfonamides, high-performance liquid chromatography □ High-performance liquid chromatography—analysis of oral suspensions containing sulfonamides in combination with erythromycin ethylsuccinate

Oral suspensions containing sulfonamides in combination with erythromycin ethylsuccinate have recently been developed for the treatment of acute otitis media. This paper presents the analysis of the sulfonamides and erythromycin ethylsuccinate present in two oral suspensions: erythromycin as erythromycin ethylsuccinate at 200 mg/5 ml and sulfisoxazole as sulfisoxazole acetyl at 600 mg/5 ml (I) and erythromycin as erythromycin ethylsuccinate at 200 mg/5 ml and trisulfapyrimidines: sulfadiazine, sulfamerazine, and sulfamethazine, each at 200 mg/5 ml (II).

Sulfonamide dosage forms are commonly assayed by nitrite titrations or colorimetric methods based on a previous (1) procedure. In mixtures containing more than one sulfonamide or in complex biological matrixes, paper and thin layer chromatography (TLC) have been used to quantitate the individual drugs (2–5). Often these chromatographic separations are followed by the Bratton and Marshall procedure (6–9). The current USP assay (10) of trisulfapyrimidine oral suspensions uses such a procedure and requires several hours to complete.

Use of gas-liquid chromatography (GLC) in the analysis of sulfonamides has been reported (11–14), but derivatization is generally required. High-performance liquid chromatography (HPLC) was used in this study to quantitate the individual sulfonamides. Separations of sulfonamides using ion exchange (15–17), reverse phase (18–24), normal phase (25–28), and ion pairing (29–30) are reported in the recent literature.

Numerous analytical techniques have been reported for the analysis of erythromycin and its various esters. Included are chemical methods based on ultraviolet–visible spectrophotometry (31–34) or fluorometry (35) in addition to GLC (36, 37), TLC (38–41), HPLC (42–45), and microbiological techniques (46–48). Since the microbiological assay is the official methodology required for the determination of erythromycin potency (49), an automated turbidimetric method was employed in this work.

EXPERIMENTAL

Reagents—Acetanilide[1], benzanilide[1], and potassium phosphate[2] (monobasic and dibasic) were obtained commercially and used without further purification. Sulfisoxazole acetyl[3,4], erythromycin base[3], erythromycin ethylsuccinate[5], sulfadiazine[3], sulfamerazine[3], and sulfamethazine[3] were of pharmaceutical quality and were used as received. Acetonitrile[6], chloroform[6], and methanol[6] were HPLC grade. Oral suspensions I[5] and II[5] were prepared from granules prepared in house.

[1] Eastman Kodak Co., Rochester, N.Y.
[2] AR grade, Mallinckrodt, Inc., St. Louis, Mo.
[3] USP Reference Standards, U.S. Pharmacopeia, Rockville, Md.
[4] Hoffmann–LaRoche, Inc., Nutley, N.J.
[5] Abbott Laboratories, North Chicago, Ill.
[6] Burdick & Jackson Laboratories, Muskegon, Mich.

0022-3549/82/0200-0161$01.00/0

(4) B. D. Wiegand, S. G. Ketterer, and E. Rapaport, *Am. J. Dig. Dis.*, **5**, 427 (1960).
(5) G. R. Cherrick, S. W. Stein, C. M. Leevy, and C. S. Davidson, *J. Clin. Invest.*, **39**, 592 (1960).
(6) D. B. Hunton, J. L. Bollman, and H. N. Hoffman, *Gastroenterology*, **39**, 713 (1960).
(7) H. Kojima, *Nagoya J. Med. Sci.*, **40**, 47 (1978).
(8) C. M. Leevy, S. W. Stein, G. R. Cherrick, and C. S. Davidson, *Clin. Res.*, **7**, 290 (1959).
(9) S. Nakagawa, K. Araki, and H. Nagashima, *Kumamoto Med. J.*, **30**, 1 (1977).
(10) I. J. Fox and E. H. Wood, *Mayo Clin. Proc.*, **35**, 732 (1960).
(11) J. Gathje, R. R. Steuer, and K. R. K. Nicholes, *J. Appl. Physiol.*, **29**, 181 (1970).
(12) M. L. J. Landsman, G. Kwant, G. A. Mook, and W. G. Zijlstra, *ibid.*, **40**, 575 (1976).
(13) C. D. Klaassen and G. L. Plaa, *Toxicol. Appl. Pharmacol.*, **15**, 374 (1969).
(14) G. Paumgartner, P. Probst, R. Kraines, and C. M. Leevy, *Ann. N.Y. Acad. Sci.*, **170**, 134 (1970).
(15) E. Rapaport, S. G. Ketterer, and B. D. Wiegand, *Clin. Res.*, **7**, 289 (1959).
(16) F. Barbier and G. A. DeWeerdt, *Clin. Chim. Acta*, **10**, 549 (1964).
(17) H. O. Wheeler, W. I. Cranston, and J. I. Meltzer, *Proc. Soc. Exp. Biol. Med.*, **99**, 11 (1958).
(18) R. Simmons and R. J. Shephard, *J. Appl. Physiol.*, **30**, 502 (1971).
(19) K. J. Baker, *Proc. Soc. Exp. Biol. Med.*, **122**, 957 (1966).
(20) M. Nambu, *Nippon Shokakibyo Gakkai Zasshi*, **63**, 777 (1966).

ACKNOWLEDGMENTS

Supported in part by the Medical Research Council of Canada.
The authors thank Dr. P. E. Coates for constructive discussions and Mrs. S. Selliah and Mr. G. Kieltyka for technical assistance.

Analysis of Oral Suspensions Containing Sulfonamides in Combination with Erythromycin Ethylsuccinate

L. ELROD, Jr.[x], R. D. COX, and A. C. PLASZ

Received March 23, 1981, from the *Analytical Research Department, Abbott Laboratories, North Chicago, IL 60064.*
Accepted for publication May 28, 1981

Abstract □ The sulfonamides and erythromycin ethylsuccinate in combination oral suspensions were determined by high-performance liquid chromatography and automated turbidimetry, respectively. The chromatographic procedure was rapid, specific, and stability-indicating for sulfisoxazole acetyl and the trisulfapyrimidines using a reversed-phase system with UV detection at 254 nm. Erythromycin ethylsuccinate did not interfere with the sulfonamide analysis and these compounds were assayed with relative standard deviations (*RSD*) ranging from ±2.1 to ±3.1%. Erythromycin ethylsuccinate was determined as erythromycin with *RSD* values of ±1.3 or ±3.5% without interference by the sulfonamides present.

Keyphrases □ Sulfonamides—analysis of oral suspensions in combination with erythromycin ethylsuccinate, high-performance liquid chromatography □ Erythromycin ethylsuccinate—analysis of oral suspensions with sulfonamides, high-performance liquid chromatography □ High-performance liquid chromatography—analysis of oral suspensions containing sulfonamides in combination with erythromycin ethylsuccinate

Oral suspensions containing sulfonamides in combination with erythromycin ethylsuccinate have recently been developed for the treatment of acute otitis media. This paper presents the analysis of the sulfonamides and erythromycin ethylsuccinate present in two oral suspensions: erythromycin as erythromycin ethylsuccinate at 200 mg/5 ml and sulfisoxazole as sulfisoxazole acetyl at 600 mg/5 ml (I) and erythromycin as erythromycin ethylsuccinate at 200 mg/5 ml and trisulfapyrimidines: sulfadiazine, sulfamerazine, and sulfamethazine, each at 200 mg/5 ml (II).

Sulfonamide dosage forms are commonly assayed by nitrite titrations or colorimetric methods based on a previous (1) procedure. In mixtures containing more than one sulfonamide or in complex biological matrixes, paper and thin layer chromatography (TLC) have been used to quantitate the individual drugs (2–5). Often these chromatographic separations are followed by the Bratton and Marshall procedure (6–9). The current USP assay (10) of trisulfapyrimidine oral suspensions uses such a procedure and requires several hours to complete.

Use of gas-liquid chromatography (GLC) in the analysis of sulfonamides has been reported (11–14), but derivatization is generally required. High-performance liquid chromatography (HPLC) was used in this study to quantitate the individual sulfonamides. Separations of sulfonamides using ion exchange (15–17), reverse phase (18–24), normal phase (25–28), and ion pairing (29–30) are reported in the recent literature.

Numerous analytical techniques have been reported for the analysis of erythromycin and its various esters. Included are chemical methods based on ultraviolet–visible spectrophotometry (31–34) or fluorometry (35) in addition to GLC (36, 37), TLC (38–41), HPLC (42–45), and microbiological techniques (46–48). Since the microbiological assay is the official methodology required for the determination of erythromycin potency (49), an automated turbidimetric method was employed in this work.

EXPERIMENTAL

Reagents—Acetanilide[1], benzanilide[1], and potassium phosphate[2] (monobasic and dibasic) were obtained commercially and used without further purification. Sulfisoxazole acetyl[3,4], erythromycin base[3], erythromycin ethylsuccinate[5], sulfadiazine[3], sulfamerazine[3], and sulfamethazine[3] were of pharmaceutical quality and were used as received. Acetonitrile[6], chloroform[6], and methanol[6] were HPLC grade. Oral suspensions I[5] and II[5] were prepared from granules prepared in house.

[1] Eastman Kodak Co., Rochester, N.Y.
[2] AR grade, Mallinckrodt, Inc., St. Louis, Mo.
[3] USP Reference Standards, U.S. Pharmacopeia, Rockville, Md.
[4] Hoffmann–LaRoche, Inc., Nutley, N.J.
[5] Abbott Laboratories, North Chicago, Ill.
[6] Burdick & Jackson Laboratories, Muskegon, Mich.

0022-3549/82/0200-0161$01.00/0

Equipment—The chromatographic system consisted of a constant flow pump[7], a septumless injector[8], a UV detector[9] operated at 254 nm, a computing integrator[10] and a strip-chart recorder[11]. The analytical column (4-mm i.d. × 300 mm) was prepacked with fully porous 10-μm silica particles to which octadecylsilane was chemically bonded[12]. Turbidimetric measurements were made with a turbidimeter[13] system containing a dilutor module and a reader module operated at 600 nm.

Sulfonamide Analysis by HPLC—*Mobile Phase*—The mobile phase for I and II consisted of water/acetonitrile (60:40) and water/acetonitrile (80:20), respectively. In preparing the mobile phases, appropriate volumes of acetonitrile were diluted to 1 liter with distilled water. The solutions were filtered through 0.45-μm polycarbonate membranes[14] and degassed under vacuum.

Chromatographic Conditions—The flow rate for I was 1.5 ml/min with a column pressure of ~1800 psi and the detector was operated at 0.32 aufs. The flow rate for II was 1.0 ml/min with a column pressure of ~700 psi and the detector operated at 0.10 aufs. The analytical column was at ambient temperature for all separations.

Internal Standard Solution—A 0.33 mg/ml solution of benzanilide in acetonitrile was prepared as the internal standard for I. A 0.20 mg/ml solution of acetanilide in acetonitrile was prepared as the internal standard for II.

Standard Solution—Approximately 50 mg of sulfisoxazole acetyl was accurately weighed into a 50-ml volumetric flask for I. The drug was dissolved and diluted to volume with the internal standard solution giving a concentration of 1.0 mg/ml. For II, ~20 mg each of sulfadiazine, sulfamerazine, and sulfamethazine were accurately weighed into a 100-ml volumetric flask. The mixture was dissolved and diluted to volume with the internal standard solution giving concentrations of 0.20 mg/ml for each drug.

Sample Preparation—A 1-ml aliquot of I was withdrawn with a disposable syringe and extracted with three 15-ml portions of chloroform. The bottom layers were combined and diluted to 50 ml with chloroform. A portion of the chloroform solution was filtered through a 0.45-μm silver membrane[15] and a 2-ml aliquot of the filtrate was evaporated to dryness under dry nitrogen. The residue was dissolved in 5 ml of the internal standard solution giving a drug concentration of ~0.96 mg/ml.

For II, a 1-ml aliquot of the suspension was withdrawn with a disposable syringe and transferred to a 200-ml volumetric flask containing ~100 ml of methanol/water (60:40). The suspension was mixed for 15 min on a mechanical shaker and diluted to volume with methanol/water (60:40). A portion of the solution was filtered through a 0.45-μm silver membrane[15] and a 1-ml aliquot of the filtrate was evaporated to dryness under nitrogen. The residue was dissolved in 1 ml of the internal standard solution giving concentrations for each drug of ~0.20 mg/ml.

Analysis and Calculation—For I and II, respectively, 5- and 4-μl injections of both the standard and sample preparations were made. Peak area ratios for duplicate injections were calculated and averaged as follows:

$$ST \text{ or } SL = \frac{PA_1}{PA_2} \qquad \text{(Eq. 1)}$$

where ST is the standard peak area ratio, SL is the sample peak area ratio, PA_1 is the peak area of the sulfonamide, and PA_2 is the peak area of the internal standard.

The concentrations of the sulfonamides in 5 ml of suspension were calculated by:

$$\text{sulfonamide content per 5 ml} = \frac{SL}{ST} \times \text{conc} \times 5 \text{ ml} \times DF \qquad \text{(Eq. 2)}$$

where conc is the concentration of sulfonamide standard (mg/ml) and DF is the appropriate dilution factor.

Erythromycin Ethylsuccinate Analysis with Turbidimetric Finish—*Dilution Buffer*—A 20% phosphate buffer was prepared by dissolving 192.6 g of dibasic potassium phosphate and 7.4 g of monobasic potassium phosphate in 1 liter of distilled water. The solution was further diluted 100 ml to 2 liter with distilled water (solution pH 8.0 ± 0.1).

Sample Preparation—A 5-ml aliquot of I or II was transferred to a

[7] Model M6000, Waters Associates, Milford, Mass.
[8] Model U6K, Waters Associates, Milford, Mass.
[9] Model SF 770, Schoeffel Instrument Corp., Westwood, N.J.
[10] Model System I, Spectra-Physics Corp., Santa Clara, Calif.
[11] Recordall Series 5000, Fisher Scientific Co., Pittsburgh, Pa.
[12] μBondapak C_{18}, Waters Associates, Milford, Mass.
[13] Autoturb, Elanco Instruments, Eli Lilly and Co., Indianapolis, Ind.
[14] Nuclepore Corp., Pleasanton, Pa.
[15] Selas Corp. of America, Huntingdon Valley, Pa.

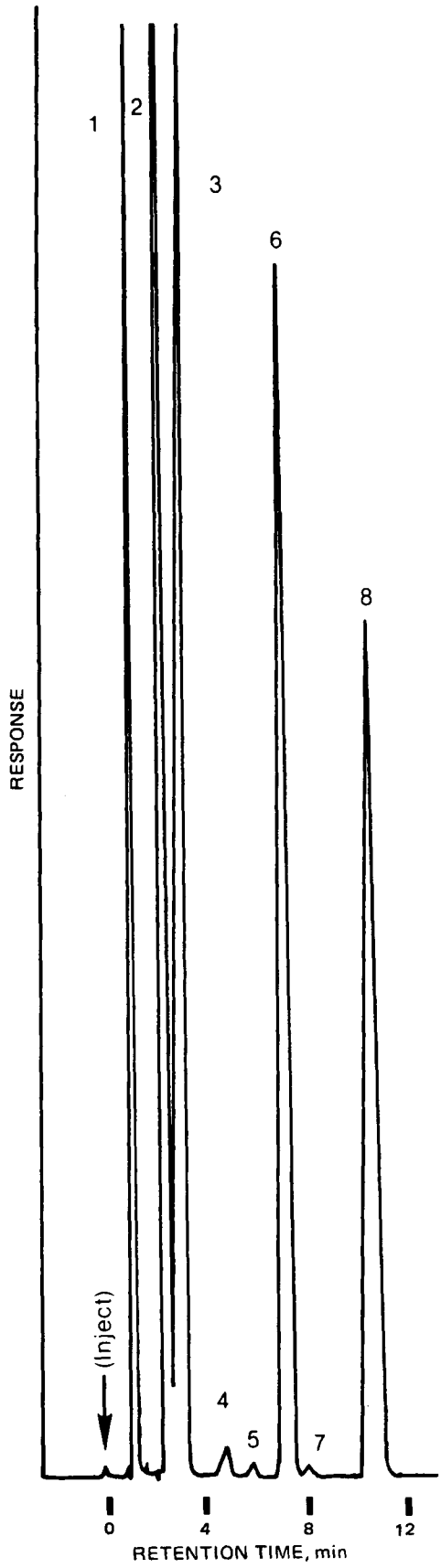

Figure 1—*Chromatogram of a synthetic mixture of sulfisoxazole acetyl (1.0 mg/ml) and three possible degradation products. Key: 1, sulfanilic acid; 2, sulfanilamide; 3, sulfisoxazole; 4, 5, 7, impurities from sulfisoxazole standard; 6, sulfisoxazole acetyl; 8, benzanilide (internal standard).*

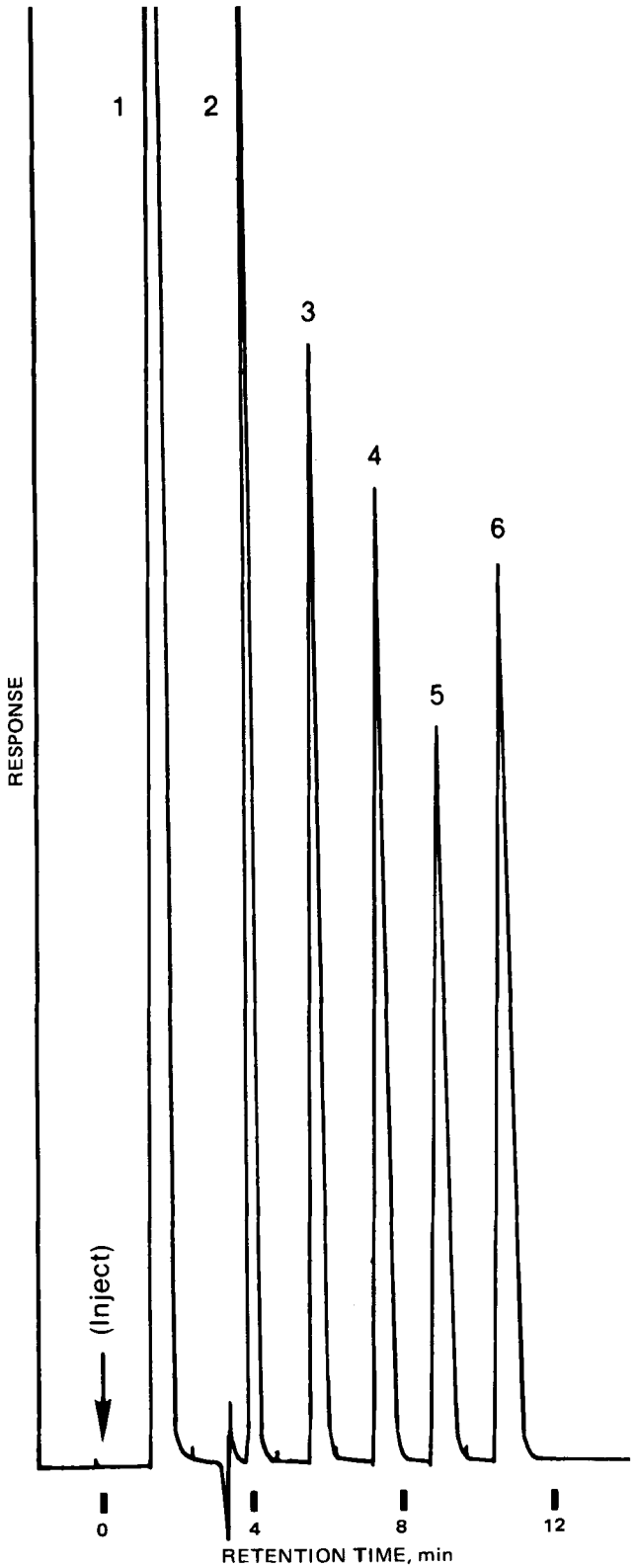

Figure 2—*Chromatogram of a synthetic mixture of trisulfapyrimidines (0.20 mg/ml) and two possible degradation products. Key: 1, sulfanilic acid; 2, sulfanilamide; 3, sulfadiazine; 4, sulfamethazine; 5, sulfamerazine; 6, acetanilide (internal standard).*

high-speed blender containing 195 ml of methanol and was blended for 3 min. The methanolic solution was diluted with the dilution buffer to give a solution containing 100 μg of erythromycin base/ml. This solution was allowed to hydrolyze 16–18 hr at room temperature and diluted to a concentration of 4 μg of erythromycin base/ml with dilution buffer. Sample preparations were performed in quadruplicate.

Table I—Precision Data for Sulfisoxazole Acetyl in I

Sample	Label Claim[a], %
1	105.5
2	110.4
3	110.8
4	107.3
5	110.1
6	106.5
7	106.0
Mean	108.1
SD	±2.3
RSD, %	±2.1

[a] Label claim for I was 600 mg of sulfisoxazole as sulfisoxazole acetyl/5 ml.

Table II—Precision Data for Trisulfapyrimidines in II [a]

Sample	Theoretical Percentage[b]		
	Sulfadiazine	Sulfamethazine	Sulfamerazine
1	105.0	103.5	103.8
2	105.6	104.0	103.5
3	106.6	104.1	103.8
4	100.6	99.6	102.1
5	107.6	109.6	112.2
6	106.7	103.4	107.3
7	104.7	105.3	106.4
8	106.6	105.7	108.0
Mean	105.4	104.4	105.9
SD	±2.2	±2.8	±3.3
RSD, %	±2.1	±2.7	±3.1

[a] Label claim for II was 200 mg of each drug/5 ml. [b] Calculated on a weight basis by accurately weighing suspension sampled and total suspension prepared from granules containing 65.8 mg of each drug/g.

Table III—Standard Addition and Recovery Data for Sulfisoxazole Acetyl in I

Assay Level	Sulfisoxazole Acetyl, mg		
	Added[a]	Recovered	Recovery, %
75%	104.6	106.4	101.7
90%	124.9	125.9	100.8
100%	138.4	138.1	99.8
110%	152.5	151.6	99.4
125%	173.5	172.1	99.2
		Mean	100.2

[a] Weight of drug added per ml with a 1 ml sample preparation.

Assay Procedure and Calculation—Erythromycin determinations were performed turbidimetrically as described for a variety of antibiotics (49).

RESULTS AND DISCUSSION

Sulfonamide Analysis—In the sulfonamide analyses for I and II, high-performance liquid chromatography (HPLC) offered the desired accuracy, sensitivity, and specificity. By operating the UV detector at 254 nm, erythromycin ethylsuccinate carried through with the sample work-up does not interfere in the sulfonamide assay.

In Figs. 1 and 2, respectively, synthetic solutions of sulfisoxazole acetyl (1.0 mg/ml) and trisulfapyrimidines (0.20 mg/ml) are spiked with several possible degradation products and chromatographed. As shown in the figures, the degradation products are well resolved from the drug and internal standard peaks, making the HPLC analyses stability indicating. Figures 3 and 4, respectively, show authentic samples of I and II carried through the HPLC assay procedure. Total elution time for both I and II was ~11 min under the chromatographic conditions chosen.

Linearity of response for the sulfonamides contained in I and II was demonstrated by plotting the peak area ratio of the drugs to the internal standards *versus* drug concentrations (mg/ml). For sulfisoxazole acetyl, detector response was linear to at least 1.5 mg/ml. For the trisulfapyrimidines, detector response was linear to at least 0.30 mg/ml for each compound. The linearity curve for each sulfonamide assayed essentially intersected the origin and the correlation coefficient was >0.999 for each curve.

Precision data for the sulfonamide assay in I and II are presented in Tables I and II, respectively. Analyses for I were performed over a 5-day

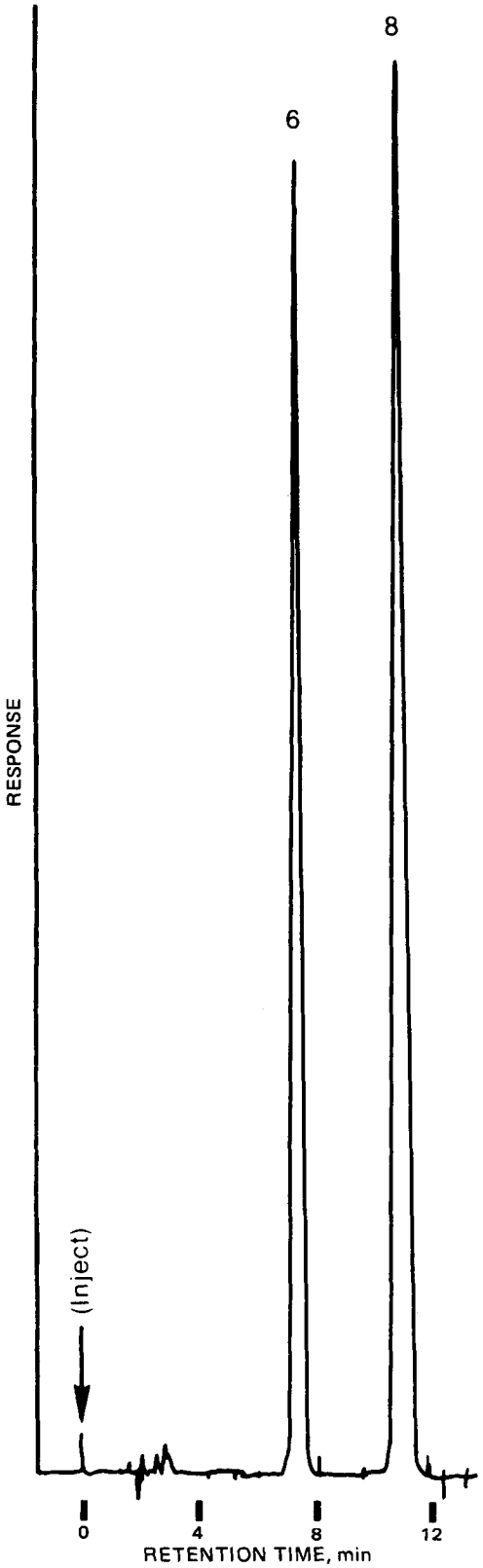

Figure 3—*Chromatogram of an authentic assay preparation of I. Key: 6, sulfisoxazole acetyl; 8, benzanilide (internal standard).*

period by two different analysts, preparing fresh suspensions each day. As shown in Table I, the average assay was 108.1% of the label claim amount, and the relative standard deviation of the procedure was ±2.1%. For II, analyses were performed by two different analysts over a 2-day period, and results were calculated as percent theory on a weight basis. Each sample shown in Table II represents a freshly prepared suspension and as shown, the relative standard deviations ranged from ±2.1 to ±3.1%.

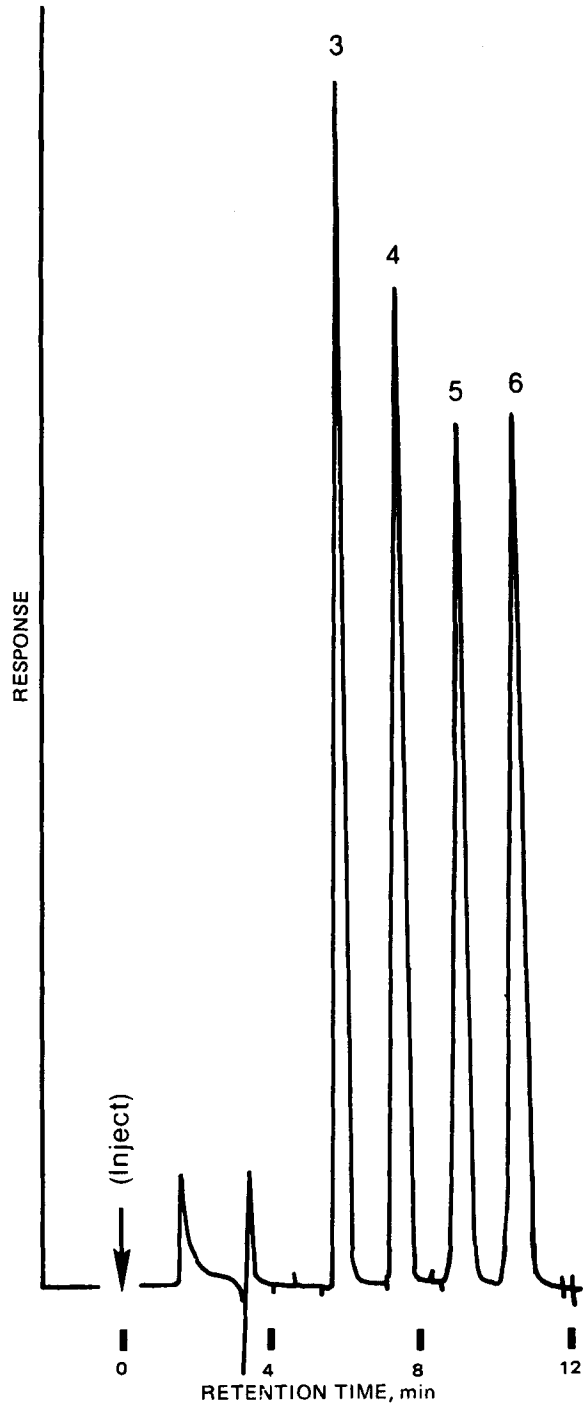

Figure 4—*Chromatogram of an authentic assay preparation of II. Key: 3, sulfadiazine; 4, sulfamethazine; 5, sulfamerazine; 6, acetanilide (internal standard).*

To determine if sulfisoxazole acetyl was recovered quantitatively in the sample preparation of I, portions of the drug were added at 75–125% of the formulation level to a suspension placebo. The resulting mixtures were extracted and assayed as described. The erythromycin ethylsuccinate and excipients were maintained at the same level as for I. The standard addition–recovery results are summarized in Table III and as shown, an average recovery of 100.2% was obtained.

A correlation of the sulfisoxazole acetyl analysis by HPLC and sodium nitrite titration (USP methodology) was made for I to determine if the presence of erythromycin ethylsuccinate or excipients interfered in the titration procedure. Suspensions containing placebo, placebo plus sulfisoxazole acetyl, and placebo plus acetyl sulfisoxazole and erythromycin ethylsuccinate were titrated and simultaneously analyzed for sulfisoxazole acetyl by HPLC. The suspensions were prepared by accurately weighing quantities of each drug substance that would be present in I,

Table IV—Percent Sulfisoxazole Acetyl Recovered by Sodium Nitrite Titration and HPLC in I

Sample	HPLC Analysis	$NaNO_2$ Titration with Potentiometric End-Point[b]	$NaNO_2$ Titrated with Amperometric End-Point[c]
Sulfisoxazole acetyl			
Suspension 1	102.1[a]	102.1[a]	104.6[a]
Suspension 2	102.7[a]	101.1[a]	101.7[a]
I	101.6	108.1	108.5
Placebo	0	0	0
	0	0	—
Placebo + sulfisoxazole acetyl	97.6	98.0	100.2
	98.4	99.2	—
Placebo + sulfisoxazole acetyl + erythromycin ethylsuccinate	98.2	103.6	105.2
	99.0	105.4	—

[a] Percent manufacturer's label claim. [b] Platinum–calomel electrode. [c] Platinum–platinum electrode.

Table V—Erythromycin Precision Data for I and II

Day	Label Claim in I[a,b], %	Label Claim in II[a,b], %
1	96.4	105.0
2	98.9	104.3
2	99.4	—
3	98.2	97.1
4	98.2	98.3
5	100.1	102.6
Mean	98.5	101.5
SD	±1.3	±3.6
RSD, %	±1.3	±3.5

[a] Percent label claim entries are averages of quadruplicate assays. [b] Label claim for I and II was 200 mg of erythromycin as erythromycin ethylsuccinate per 5 ml.

Table VI—Standard Addition and Recovery Data for Erythromycin Ethylsuccinate in I

Erythromycin Added[a], mg	Erythromycin Recovered[a,b], mg	Recovery, %
200.0	198.8	99.4
200.1	193.5	96.7
200.2	192.8	96.3
200.3	193.8	96.8
199.9	195.8	97.9
200.0	198.0	99.0
	Mean	97.7

[a] Milligrams of erythromycin activity (as erythromycin ethylsuccinate) per 5 ml. [b] Obtained from quadruplicate dilutions of a stock methanol sample preparation.

and these suspensions were sampled by weighing an appropriate volume accurately. From the analysis, the weight of suspension sampled and the weight of total suspension prepared, the percent recovery of sulfisoxazole acetyl was calculated. In addition, two commercial sulfisoxazole acetyl suspensions were titrated and simultaneously assayed by HPLC.

In Table IV the results of the sodium nitrite titrations and the HPLC analysis are summarized. For those suspensions containing sulfisoxazole acetyl but no erythromycin ethylsuccinate, the HPLC results and titrations agreed with experimental error. However, for those suspensions containing erythromycin ethylsuccinate, the titration results were invariably higher than the HPLC results. The extent of this high bias ranged from 5.4–7.0% in the sodium nitrite titrations. Placebo alone titrated identically to a solvent blank and no response was observed from the placebo preparations by HPLC. A placebo suspension containing erythromycin ethylsuccinate gave a higher sodium nitrite titer than the placebo alone. A possible explanation for the higher titer in this preparation is the reversible reaction of nitrous acid with the tertiary aliphatic amine group of erythromycin ethylsuccinate (50).

Erythromycin Ethylsuccinate Analysis—Automated turbidimetric analysis for a variety of antibiotics are in wide use. To determine the precision of this technique for I and II, freshly prepared suspensions of each were assayed over 5 days. The precision data are summarized in Table V as percent label claim in terms of erythromycin activity/5 ml of suspension. For I the percent label claim averaged 98.5% with a relative standard deviation of ±1.3%. For II the percent label claim averaged 101.5% with a relative standard deviation of ±3.5%.

To determine if erythromycin ethylsuccinate was recovered quantitatively in the sample preparation of I, accurately weighed quantities of the drug were added to a placebo suspension. Sulfisoxazole acetyl and excipients were at the same levels as in the actual product. The usual sample work-up and analysis was performed using quadruplicate dilutions of the methanol solution. In Table VI, the standard addition–recovery data collected over 5 days by two analysts are presented. As shown, a mean recovery of 97.7% was obtained.

REFERENCES

(1) A. C. Bratton and E. K. Marshall, *J. Biol. Chem.*, **128**, 537 (1939).

(2) D. J. Pietrzyk and E. Chan-Santos, *J. Chromatogr.*, **87**, 543 (1973).

(3) G. L. Biagi, M. Barbaro, M. C. Guerra, G. Cantelli-Forti, and O. Gandolf, *ibid.*, **106**, 349 (1975).

(4) H. R. Klein and W. J. Mader, *J. Pharm. Sci.*, **60**, 448 (1971).

(5) C. W. Sigel, J. L. Woolley, Jr., and C. A. Nichol, *ibid.*, **64**, 973 (1975).

(6) A. K. Fowler, J. P. Merrick, and B. E. Reidel, *Can. Pharm. J.*, **91**, 56 (1958).

(7) T. Bican-Fister and V. Kajganovic, *J. Chromatogr.*, **16**, 503 (1964).

(8) C. A. Brunner, *J. Assoc. Off. Anal. Chem.*, **55**, 194 (1972).

(9) *Ibid.*, **56**, 689 (1973).

(10) "The United States Pharmacopeia," 20th rev., Mack Publishing Co., Easton, Pa., 1980, pp. 831–832.

(11) J. W. Turczan, *J. Pharm. Sci.*, **57**, 142 (1968).

(12) R. J. Daun, *J. Assoc. Off. Anal. Chem.*, **54**, 1277 (1971).

(13) O. Gyllenhaal and H. Ehrsson, *J. Chromatogr.*, **107**, 327 (1975).

(14) N. Nose, S. Kobayashi, A. Hirose, and A. Watanabe, *ibid.*, **123**, 167 (1976).

(15) T. C. Kram, *J. Pharm. Sci.*, **61**, 254 (1972).

(16) R. B. Poet and H. H. Pu, *ibid.*, **62**, 809 (1973).

(17) G. B. Cox and K. Sugden, *Analyst*, **102**, 29 (1977).

(18) J. Owerbach, N. F. Johnson, T. R. Bates, H. J. Pieniaszek, Jr., and W. J. Jusko, *J. Pharm. Sci.*, **67**, 1250 (1978).

(19) R. O. Singletary, Jr., and F. D. Sancillio, *ibid.*, **69**, 144 (1980).

(20) T. J. Goehl, L. K. Mathur, J. D. Strum, J. M. Jaffe, W. H. Pitlick, V. P. Shah, R. I. Poust, and J. L. Colaizzi, *ibid.*, **67**, 404 (1978).

(21) J. P. Sharma, E. G. Perkins, and R. F. Bevill, *ibid.*, **65**, 1606 (1976).

(22) K. Harzer, *J. Chromatogr.*, **155**, 399 (1978).

(23) R. L. Suber and G. T. Edds, *J. Liq. Chromatogr.*, **3**, 257 (1980).

(24) R. W. Bury and M. L. Mashford, *J. Chromatogr.*, **163**, 114 (1979).

(25) D. Seymour and R. D. Rupe, *J. Pharm. Sci.*, **69**, 701 (1980).

(26) H. Umagat, P. F. McGarry, and R. J. Tscherne, *ibid.*, **68**, 922 (1979).

(27) E. C. Jennings and W. C. Landgraf, *ibid.*, **66**, 1784 (1977).

(28) P. H. Cobb and G. T. Hill, *J. Chromatogr.*, **123**, 444 (1976).

(29) C. F. Fischer and U. Klotz, *ibid.*, **162**, 237 (1979).

(30) S. C. Su, A. V. Hartkopk, and B. L. Karger, *ibid.*, **119**, 523 (1976).

(31) J. B. Tepe and C. V. St. John, *Anal. Chem.*, **27**, 744 (1955).

(32) P. E. Manni and J. E. Sinsheimer, *ibid.*, **33**, 1900 (1961).

(33) J. H. Ford, G. C. Prescott, J. W. Hinman, and E. L. Caron, *ibid.*, **25**, 1195 (1953).

(34) R. V. Smith, R. G. Harris, D. D. Maness, and A. Martin, *Microchem. J.*, **23**, 51 (1978).

(35) K. Y. Tserng and J. G. Wagner, *Anal. Chem.*, **48**, 348 (1976).

(36) K. Tsuji and J. H. Robertson, *ibid.*, **43**, 818 (1971).

(37) J. H. Robertson and K. Tsuji, *J. Pharm. Sci.*, **61**, 1633 (1972).
(38) G. Kobrehel, Z. Tamburasev, and S. Djokic, *J. Chromatogr.*, **133**, 415 (1977).
(39) G. Richard, C. Radecka, D. W. Hughes, and W. L. Wilson, *ibid.*, **67**, 69 (1972).
(40) T. T. Anderson, *ibid.*, **14**, 127 (1964).
(41) A. Vilim, M. J. LeBelle, W. L. Wilson, and K. C. Graham, *ibid.*, **133**, 239 (1977).
(42) K. Tsuji and J. F. Goetz, *ibid.*, **147**, 359 (1978).
(43) K. Tsuji, *ibid.*, **158**, 337 (1978).
(44) K. Tsuji and J. F. Goetz, *J. Antibiot.*, **31**, 302 (1978).
(45) S. Omura, Y. Suzuki, A. Hakagawa, and T. Hata, *ibid.*, **26**, 794 (1973).
(46) D. C. Grove and W. H. Randall, "Assay Methods of Antibiotics, A Laboratory Manual," Medical Encyclopedia Publishers, New York, N.Y., 1955, pp. 96–103.
(47) S. C. Bell, J. W. Hamman, and W. E. Grundy, *Appl. Microbiol.*, **17**, 88 (1969).
(48) J. V. Bennett, J. L. Bodie, E. J. Benner, and W. M. Kirby, *ibid.*, **14**, 170 (1966).
(49) "Code of Federal Regulations, Title 21," U.S. Government Printing Office, Washington, D.C., 1980, Parts 436.105 and 436.106.
(50) T. A. Geissman, "Principles of Organic Chemistry," 3rd ed., F. H. Freeman, San Francisco, Calif., 1968, p. 625.

ACKNOWLEDGMENTS

Presented at the APhA Academy of Pharmaceutical Sciences, San Antonio meeting, November 1980.

The authors thank Mr. Tim Porter and staff for their assistance in the validation of this methodology and Ms. Diane Penza for her assistance in preparing the manuscript.

Gas Chromatographic Analysis of Meperidine and Normeperidine: Determination in Blood after a Single Dose of Meperidine

PEYTON JACOB III ‡x, JEAN F. RIGOD ‡, SUSAN M. POND *‡, and NEAL L. BENOWITZ *‡

Received February 13, 1981, from the *Division of Clinical Pharmacology, Department of Medicine, School of Medicine, University of California, San Francisco, CA 94143 and the ‡Division of Clinical Pharmacology, San Francisco General Hospital, San Francisco, CA 94110. Accepted for publication June 25, 1981.

Abstract □ A method is described for the determination of meperidine and its pharmacologically active metabolite, normeperidine, in blood, plasma, and urine using gas chromatography with nitrogen–phosphorus detection. Structural analogs of both meperidine and normeperidine were used as internal standards. Unlike previously reported assays, this procedure was sensitive and convenient enough for use in pharmacokinetic studies of both meperidine and normeperidine following single doses of meperidine. The assay was sensitive to 5 ng of meperidine/ml and 2.5 ng of normeperidine/ml extracted from a 1-ml biological sample. The between-assay coefficients of variation at these concentrations were 9.4 and 10.4%, respectively.

Keyphrases □ Meperidine—gas chromatographic analysis in blood □ Normeperidine—gas chromatographic analysis in blood after single dose of meperidine □ Gas chromatography—analysis of meperidine and normeperidine in blood □ Analgesics—meperidine, gas chromatographic analysis in blood

Normeperidine (I), the *N*-demethylated metabolite of the analgesic drug meperidine (II), is pharmacologically active (1) and may cause seizures in humans (2). Therefore, blood levels of I should be determined when delineating the side effects and drug interactions that occur with II. To carry out such studies after single doses of II, a sensitive and specific gas chromatographic (GC) assay for I and II in biological fluids was developed. The assay allows measurement of II up to 24 hr and I up to 48 hr after a single dose of II.

Previously published methods with adequate sensitivity for the measurement of I in plasma after a single dose have involved GC–mass spectrometry with selected ion monitoring (3, 4), radioimmunoassay (5), or GC using electron-capture detection (6). GC methods with flame-ionization detection (7–10) may be satisfactory for determining therapeutic concentrations of II, but have marginal sensitivity for the determination of plasma I concentrations (7–9) following single doses of the parent drug.

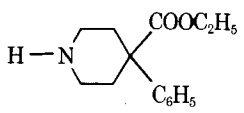

I

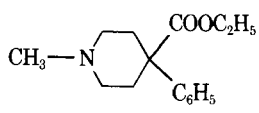

II

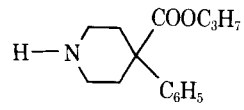

III

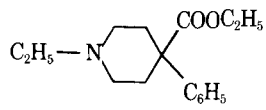

IV

This report describes the GC determination of I and II using a nitrogen–phosphorus detector, which is highly selective toward nitrogen-containing compounds such as II and its derivatives. The assay is significantly faster and more convenient than previously reported GC methods, and is applicable to whole blood, plasma, or urine.

EXPERIMENTAL

Materials—Meperidine hydrochloride and normeperidine hydrochloride were obtained[1]. Heptafluorobutyric anhydride and sodium cyanoborohydride were obtained commercially[2]. Normeperidinic acid *n*-propyl ester (III) was synthesized by a previous method (6). *N*-ethylnormeperidine (IV) was synthesized as will be described. All other chemicals and solvents were analytical reagent grade.

Synthesis of *N*-Ethylnormeperidine Hydrochloride—Sodium cyanoborohydride (100 mg) was added to a solution of normeperidine hydrochloride (250 mg) and acetaldehyde (0.5 ml) in 50 ml of 50% aqueous

[1] Kindly supplied by Sterling-Winthrop Research Institute, Rensselaer, N.Y.
[2] Aldrich Chemical Co., Milwaukee, Wis.

0022-3549/82/0200-0166$01.00/0

(37) J. H. Robertson and K. Tsuji, *J. Pharm. Sci.*, **61**, 1633 (1972).
(38) G. Kobrehel, Z. Tamburasev, and S. Djokic, *J. Chromatogr.*, **133**, 415 (1977).
(39) G. Richard, C. Radecka, D. W. Hughes, and W. L. Wilson, *ibid.*, **67**, 69 (1972).
(40) T. T. Anderson, *ibid.*, **14**, 127 (1964).
(41) A. Vilim, M. J. LeBelle, W. L. Wilson, and K. C. Graham, *ibid.*, **133**, 239 (1977).
(42) K. Tsuji and J. F. Goetz, *ibid.*, **147**, 359 (1978).
(43) K. Tsuji, *ibid.*, **158**, 337 (1978).
(44) K. Tsuji and J. F. Goetz, *J. Antibiot.*, **31**, 302 (1978).
(45) S. Omura, Y. Suzuki, A. Hakagawa, and T. Hata, *ibid.*, **26**, 794 (1973).
(46) D. C. Grove and W. H. Randall, "Assay Methods of Antibiotics, A Laboratory Manual," Medical Encyclopedia Publishers, New York, N.Y., 1955, pp. 96–103.
(47) S. C. Bell, J. W. Hamman, and W. E. Grundy, *Appl. Microbiol.*, **17**, 88 (1969).
(48) J. V. Bennett, J. L. Bodie, E. J. Benner, and W. M. Kirby, *ibid.*, **14**, 170 (1966).
(49) "Code of Federal Regulations, Title 21," U.S. Government Printing Office, Washington, D.C., 1980, Parts 436.105 and 436.106.
(50) T. A. Geissman, "Principles of Organic Chemistry," 3rd ed., F. H. Freeman, San Francisco, Calif., 1968, p. 625.

ACKNOWLEDGMENTS

Presented at the APhA Academy of Pharmaceutical Sciences, San Antonio meeting, November 1980.

The authors thank Mr. Tim Porter and staff for their assistance in the validation of this methodology and Ms. Diane Penza for her assistance in preparing the manuscript.

Gas Chromatographic Analysis of Meperidine and Normeperidine: Determination in Blood after a Single Dose of Meperidine

PEYTON JACOB III ‡x, JEAN F. RIGOD ‡, SUSAN M. POND *‡, and NEAL L. BENOWITZ *‡

Received February 13, 1981, from the *Division of Clinical Pharmacology, Department of Medicine, School of Medicine, University of California, San Francisco, CA 94143 and the ‡Division of Clinical Pharmacology, San Francisco General Hospital, San Francisco, CA 94110. Accepted for publication June 25, 1981.

Abstract □ A method is described for the determination of meperidine and its pharmacologically active metabolite, normeperidine, in blood, plasma, and urine using gas chromatography with nitrogen–phosphorus detection. Structural analogs of both meperidine and normeperidine were used as internal standards. Unlike previously reported assays, this procedure was sensitive and convenient enough for use in pharmacokinetic studies of both meperidine and normeperidine following single doses of meperidine. The assay was sensitive to 5 ng of meperidine/ml and 2.5 ng of normeperidine/ml extracted from a 1-ml biological sample. The between-assay coefficients of variation at these concentrations were 9.4 and 10.4%, respectively.

Keyphrases □ Meperidine—gas chromatographic analysis in blood □ Normeperidine—gas chromatographic analysis in blood after single dose of meperidine □ Gas chromatography—analysis of meperidine and normeperidine in blood □ Analgesics—meperidine, gas chromatographic analysis in blood

Normeperidine (I), the *N*-demethylated metabolite of the analgesic drug meperidine (II), is pharmacologically active (1) and may cause seizures in humans (2). Therefore, blood levels of I should be determined when delineating the side effects and drug interactions that occur with II. To carry out such studies after single doses of II, a sensitive and specific gas chromatographic (GC) assay for I and II in biological fluids was developed. The assay allows measurement of II up to 24 hr and I up to 48 hr after a single dose of II.

Previously published methods with adequate sensitivity for the measurement of I in plasma after a single dose have involved GC–mass spectrometry with selected ion monitoring (3, 4), radioimmunoassay (5), or GC using electron-capture detection (6). GC methods with flame-ionization detection (7–10) may be satisfactory for determining therapeutic concentrations of II, but have marginal sensitivity for the determination of plasma I concentrations (7–9) following single doses of the parent drug.

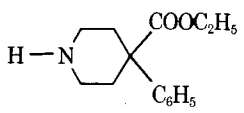

I

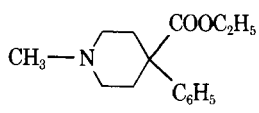

II

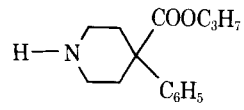

III

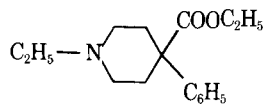

IV

This report describes the GC determination of I and II using a nitrogen–phosphorus detector, which is highly selective toward nitrogen-containing compounds such as II and its derivatives. The assay is significantly faster and more convenient than previously reported GC methods, and is applicable to whole blood, plasma, or urine.

EXPERIMENTAL

Materials—Meperidine hydrochloride and normeperidine hydrochloride were obtained[1]. Heptafluorobutyric anhydride and sodium cyanoborohydride were obtained commercially[2]. Normeperidinic acid *n*-propyl ester (III) was synthesized by a previous method (6). *N*-ethylnormeperidine (IV) was synthesized as will be described. All other chemicals and solvents were analytical reagent grade.

Synthesis of *N*-Ethylnormeperidine Hydrochloride—Sodium cyanoborohydride (100 mg) was added to a solution of normeperidine hydrochloride (250 mg) and acetaldehyde (0.5 ml) in 50 ml of 50% aqueous

[1] Kindly supplied by Sterling-Winthrop Research Institute, Rensselaer, N.Y.
[2] Aldrich Chemical Co., Milwaukee, Wis.

0022-3549/82/0200-0166$01.00/0

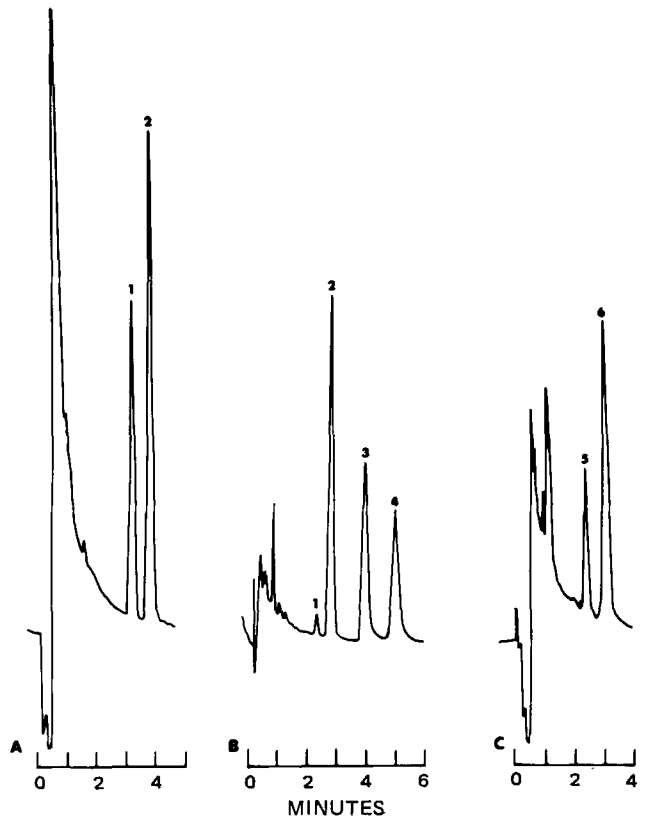

Figure 1—*Chromatograms of extracts containing normeperidine (I) and meperidine (II). Key: A, plasma containing 28 ng of II/ml; B, urine sample containing 108 and 1300 ng/ml of II and I, respectively; and C, plasma containing 10 ng of I/ml. GC conditions are described in the text; and 1 = II; 2 = IV; 3 = I; 4 = III; 5 = heptafluorobutyryl derivative of I; and 6 = heptafluorobutyryl derivative of III.*

ethanol. The solution was stirred and the pH was maintained at 6–7 by the dropwise addition of aqueous sodium acetate. After 2 hr, the pH was adjusted to 2 by the addition of concentrated hydrochloric acid. This procedure was done in a fume hood because hydrogen cyanide is evolved.

The solution was extracted twice with 20-ml portions of methylene chloride. The extracts were discarded and the aqueous phase was brought to pH 12 with aqueous sodium hydroxide. The basic aqueous phase was extracted twice with 20-ml portions of methylene chloride, and the combined extracts were dried over anhydrous potassium carbonate and then evaporated under reduced pressure. The oily residue was dissolved in 3 ml of absolute ethanol, acidified to pH 2 with concentrated hydrochloric acid, and then diluted with 25 ml of anhydrous ether, added in portions with stirring and scratching with a glass rod. The product slowly crystallized and was collected by filtration and air dried. A white crystalline powder (57 mg) was obtained, mp 170.5–172° [lit. (11) mp 171°]. GC analysis indicated a purity of >99.5%.

Instrumentation—GC analyses were performed using an instrument[3] equipped with dual nitrogen–phosphorus detectors. The nitrogen (carrier gas), air, and hydrogen flow rates were 30, 50, and 5 ml/min, respectively. Columns used for II analyses or for simultaneous II and underivatized I analyses (urine) were 1.8 m × 2-mm i.d. glass. The columns were configured for on-column injection, packed with 2% polyethylene glycol and 2% potassium hydroxide on 100–120 mesh chromatographic diatomaceous earth[4], and operated at 190° for determination of II in blood and 205° for simultaneous determination of I and II in urine. Columns used for derivatized I analyses were 1.8 × 2-mm i.d. glass, packed with 3% methyl silicone liquid phase on 100–120 mesh base-deactivated chromatographic diatomaceous earth[5] operated at 205°.

The injection port and detector temperatures were 250 and 300°, respectively. A strip-chart recorder[6] was used for recording chromatograms.

[3] Model 5711A, Hewlett-Packard, Avondale, Pa.
[4] Carbowax, 20 *M* potassium hydroxide on Gas Chrom P, Applied Science Laboratories, State College, Pa.
[5] SP2100 DB, Supelco, Bellefonte, Pa.
[6] Model 9176, Varian Co., Sunnyvale, Calif.

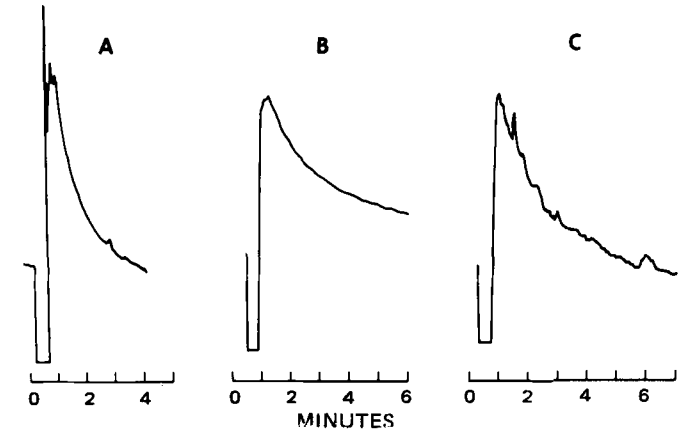

Figure 2—*Chromatograms of extracts of drug-free plasma and urine specimens. Key: A, plasma extracted for II; B, urine extracted for both I and II; and C, plasma extracted for I and derivatized with heptafluorobutyric anhydride.*

All extractions were carried out by agitating for 3 min on a multiple-tube vortex mixer[7]; an analytical evaporator[8] was used for evaporating solvent from extracts with a nitrogen stream.

Assay Procedure—A flow diagram of the extraction procedure is shown in Scheme I. To 1-ml samples of whole blood, plasma, or urine contained in 13-mm × 100-mm culture tubes were added 100-μl aliquots of an aqueous solution of the internal standards, III (for normeperidine) and IV (for meperidine). Methanolic 2 *N* potassium hydroxide (0.5 ml) was added, and the samples were extracted with 3 ml of toluene.

After centrifuging for 5 min, the aqueous layers were frozen by placing the tubes in a dry ice–acetone bath, and the toluene layers were poured into culture tubes containing 0.5 ml of 0.2 *N* sulfuric acid. The tubes were vortexed for 3 min and then centrifuged. The aqueous layers were frozen, the toluene layers discarded, and the aqueous acid layers were allowed to thaw. Aqueous 2 *N* potassium hydroxide (1 ml) was added, and the samples were extracted with 2 ml of toluene and then centrifuged.

At this stage, if the concentrations of I and II were expected to be high

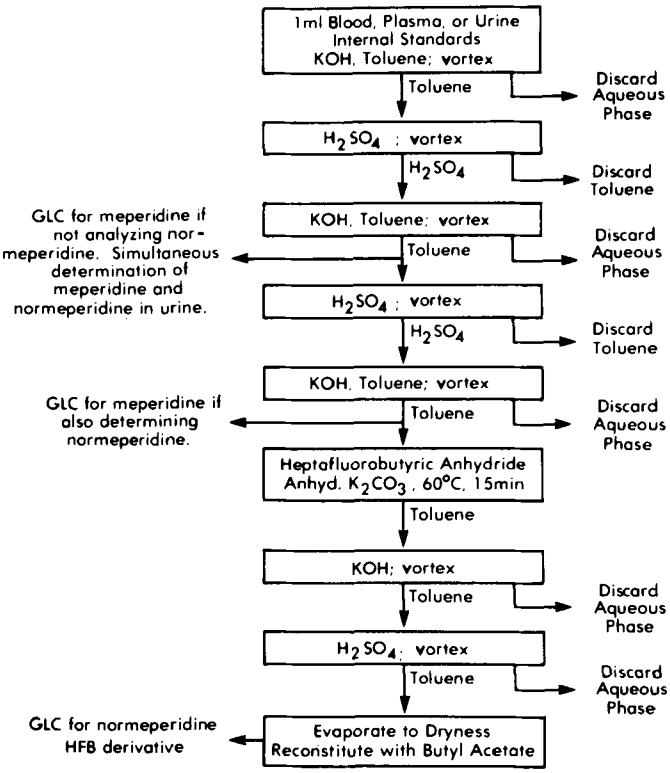

Scheme I—Flow diagram of extraction procedure.

[7] Model VB-1, Kraft Apparatus, Mineola, N.Y.
[8] N-Evap model 111, Organomation Associates, Shrewsbury, Mass.

Table I—Day-to-Day Variations of Identical Plasma Samples

	Meperidine (II)						Normeperidine (I)					
Concentration given, ng/ml	5	10	20	50	100.0	200	2.5	5	10	20	50	100
Concentration found, mean ng/ml	4.9	10.2	20.1	49.6	100.0	202.4	2.3	5.0	10.4	20.8	50.0	98.8
Standard deviation, ng/ml	0.5	0.8	1.3	3.0	6.0	9.6	0.2	0.4	0.5	0.8	1.1	1.9
Coefficient of variation, %	9.4	8.2	6.4	6.1	6.0	4.7	10.4	8.4	5.2	4.0	3.9	1.9

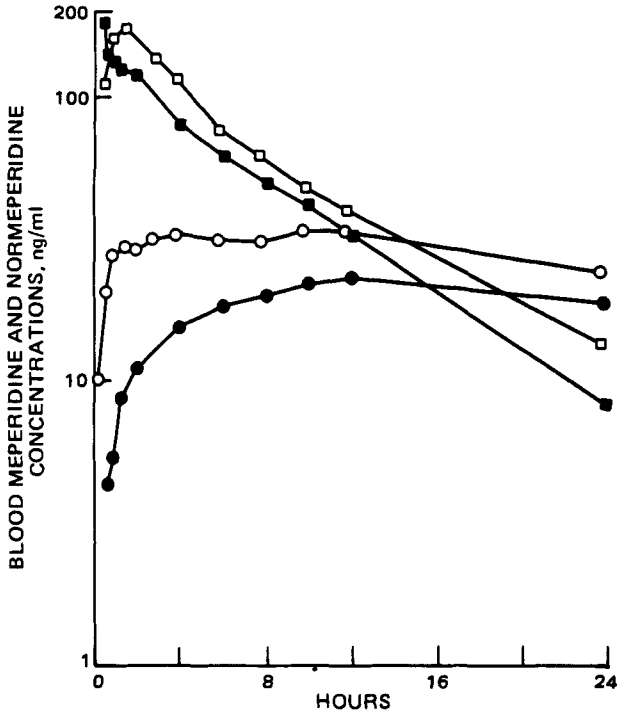

Figure 3—*Blood II (■) and I (●) concentrations following administration of 50 mg iv of II; blood II (□) and I (○) concentrations following administration of 100 mg po of II in a human subject.*

(*e.g.*, as in urine), the toluene extracts were analyzed by GC for both I and II. The retention times were 2.30, 2.75, 4.00, and 4.95 min for II, IV, I, and III, respectively. The extraction recoveries of I and II from urine averaged 70 and 73%, respectively, over the concentration range of 1–20 μg/ml.

The toluene extracts from blood or plasma were back-extracted with 0.5 ml of 0.2 *N* sulfuric acid. The sulfuric acid layers were made basic with 1 ml of 2 *N* aqueous potassium hydroxide and extracted with 0.5 ml of toluene. The toluene layers were transferred to vials containing anhydrous potassium carbonate (~40 mg) to dry the solvent. Aliquots (2–4 μl) of the toluene extracts were injected into the chromatograph for analysis of II. Examples of chromatograms from plasma extracts are presented in Fig. 1. The retention times of II and the internal standard (IV) were 3.30 and 3.85 min, respectively. Extraction recovery from blood over 5–200 ng/ml averaged 67%.

Heptafluorobutyric anhydride (10 μl) was added to the remaining toluene extracts. The tubes were capped and heated at 60° for 15 min on a heating block to derivatize I and its internal standard. After cooling to room temperature, 2 ml of 2 *N* sodium hydroxide was added and the tubes were vortexed for 5 min to destroy excess heptafluorobutyric anhydride. Following centrifugation, the toluene layers were transferred to clean tubes containing 1 ml of 0.2 *N* sulfuric acid.

After extraction for 1 min and centrifugation, the toluene layers were transferred to small vials and evaporated to dryness under a nitrogen stream. Butyl acetate (50 μl) was added to reconstitute the samples, and 2–6 μl was injected into the chromatograph for analysis of I (Fig. 1).

The retention times for the heptafluorobutyryl derivatives of I and III were 2.48 and 3.05 min, respectively. Extraction recoveries from blood averaged 66% over 2.5–100 ng/ml. Chromatograms of blank plasma and urine extracts (Fig. 2) were free from interfering peaks under the extraction conditions employed. The detection limit for each substance was ~1 ng/ml for 1-ml plasma samples.

Standard Curves—Standards were prepared by spiking drug-free blood, plasma, or urine samples with known amounts of drug and internal standard. Standards with at least four different concentrations over the expected range were run with each batch of samples and used to construct standard curves. The amounts of IV added were 2.5 μg for urine and 50 ng for blood or plasma; the amounts of III were 1 μg for urine and 25 ng for blood or plasma. Regression equations relating peak height ratios of standards to their concentrations were used to determine concentrations of I and II. The regression lines were linear over all concentrations studied (0–200 ng/ml for blood, and 0–20 μg/ml for urine) and passed through the origin.

Analytical Variables—Between-run precision was determined by analyzing identical plasma standards with six consecutive runs. Coefficients of variation for six concentrations representative of the therapeutic ranges found in plasma are presented in Table I.

Pharmacokinetic Study in a Human Subject—A healthy male volunteer, age 38 and weight 72 kg, was given 50 mg iv of meperidine hydrochloride over 1 min. One week later, the same subject was given 100 mg po of meperidine hydrochloride in solution. Twelve blood samples were collected over the 24 hr following drug administration and plasma separated for analysis of I and II (Fig. 3).

RESULTS AND DISCUSSION

Losses of basic drugs due to adsorption on glassware and/or GC columns may be variable and reduce the precision of an assay if the internal standard is not chemically similar to the drug being measured. Therefore, an internal standard that is a structural analog of II was used. Sharp peaks and baseline separation of II and IV (the internal standard) were obtained on both polyethylene glycol–potassium hydroxide (Fig. 1) and base-deactivated methyl silicone columns. Good reproducibility was obtained even at concentrations as low as 5 ng/ml (Table I). Consequently, this assay can be used to measure plasma II concentrations for as long as 24 hr after a single dose.

The described procedure is suitable for the analysis of large numbers of samples and its sensitivity should greatly facilitate studies of the kinetic behavior of normeperidine in meperidine drug interactions and in patients with disease states in which normeperidine kinetics may be altered (2).

REFERENCES

(1) J. W. Miller and H. H. Anderson, *J. Pharmacol. Exp. Ther.*, **112**, 191 (1954).

(2) H. H. Szeto, C. E. Inturrisi, R. Houde, S. Saal, J. Cehigh, and M. M. Reidenberg, *Ann. Intern. Med.*, **86**, 738 (1977).

(3) C. Lindberg, M. Berg, L. O. Boreus, P. Hartvig, K.-E. Karlsson, L. Palmer, and A.-M. Thornblack, *Biomed. Mass. Spectrom.*, **5**, 540 (1978).

(4) E. L. Todd, D. T. Stafford, and J. E. Morrison, *J. Anal. Toxicol.*, **3**, 256 (1979).

(5) D. S. Freeman, H. B. Gjika, and H. Van Vanakis, *J. Pharmacol. Exp. Ther.*, **203**, 203 (1977).

(6) P. Hartvig, K.-E. Karlsson, C. Lindberg, and L. O. Boreus, *Eur. J. Clin. Pharmacol.*, **11**, 65 (1977).

(7) U. Klotz, T. S. McHorse, G. R. Wilkinson, and S. Schenker, *Clin. Pharmacol. Ther.*, **16**, 667 (1974).

(8) K. Chan, M. J. Kendall, and M. Mitchard, *J. Chromatogr.*, **89**, 169 (1974).

(9) H. H. Szeto and C. E. Inturrisi, *ibid.*, **125**, 503 (1976).

(10) M. A. Evans and R. D. Harbison, *J. Pharm. Sci.*, **66**, 599 (1977).

(11) E. Walton and M. B. Green, *J. Chem. Soc.*, **1945**, 315.

ACKNOWLEDGMENTS

Supported by Grants DA 01696 and DA 4RG012 from the National Institute on Drug Abuse.

The clinical study was carried out in the General Clinical Research Center RR-00083 at San Francisco General Hospital Medical Center with support by the Division of Research Resources, National Institutes of Health.

Thiamine Whole Blood and Urinary Pharmacokinetics in Rats: Urethan-Induced Dose-Dependent Pharmacokinetics

J. D. PIPKIN* and V. J. STELLA*

Received February 23, 1981, from the *Department of Pharmaceutical Chemistry, The University of Kansas, Lawrence, KS 66045.* Accepted for publication May 20, 1981. * Present address: Squibb Institute for Medical Research, New Brunswick, NJ 08903.

Abstract □ The whole blood pharmacokinetics of thiamine after intravenous administration of thiamine hydrochloride (4, 12, and 36 mg/kg) to rats anesthetized continuously with ether (inhalation) or urethan (1 g/kg ip) were studied. Urinary excretion of thiamine after intravenous administration of thiamine hydrochloride to rats lightly anesthetized with ether was also investigated. At any particular dose, thiamine displayed apparent classical two-compartment model behavior in the time range studied. Under urethan anesthesia, thiamine displayed apparent dose-dependent kinetics as measured by the changes in the pharmacokinetic parameters, AUC, $V_{d(area)}$, $t_{0.5\beta}$, and total body clearance, Cl_{TB}, with dose. However, when ether anesthesia was used, thiamine displayed dose-independent pharmacokinetic behavior. These results suggest that care should be taken in the interpretation of pharmacokinetic data obtained in anesthetized animals, particularly when urethan anesthesia is used.

Keyphrases □ Thiamine—whole blood and urinary pharmacokinetics after urethan and ether administration, rats □ Urethan—effect on whole blood and urinary pharmacokinetics of thiamine □ Anesthetic agents—urethan and ether, effect on whole blood and urinary pharmacokinetics of thiamine, rats □ Pharmacokinetics—of thiamine, effect of urethan and ether administration to rats

Obtaining reliable and accurate blood concentration *versus* time data is crucial in determining a drug's true disposition in any animal species. To minimize pain and discomfort to laboratory animals and provide convenience to the researcher, experiments are often carried out under anesthesia. Reported are some observations on the apparent effects of urethan anesthesia on the pharmacokinetics of thiamine in rats.

Urethan is used as an anesthetic agent for laboratory and agricultural animals. Administered intraperitoneally, it produces a long-lasting narcosis and therefore is used primarily for prolonged, terminal experiments. As opposed to barbituates, urethan has a wide margin of safety and gives a more stable, longer anesthesia (1). Thiamine pharmacokinetics at a dose of 4 mg/kg iv in rats under urethan anesthesia were reported previously (2–4). The present study examined the dose-independent kinetics in unchanged thiamine urinary excretion and the pharmacokinetics of thiamine in whole blood in lightly ether-anesthetized rats. The apparent dose dependency of thiamine pharmacokinetics under urethan anesthesia was also studied.

EXPERIMENTAL

Materials and Methods—Male Sprague-Dawley rats[1], 230–400 g, were used. Prior to intravenous thiamine hydrochloride[2] administration *via* the dorsal penis vein (5) at three dose levels (4, 12, and 36 mg/kg), the rats received either urethan or ether as the anesthetic agent. Urethan[2] was administered intraperitoneally as a 500-mg/ml solution at a dose of 1.0 g/kg; however, some rats required additional urethan, the total not exceeding 2.0 g/kg, to induce continuous anesthesia during the experiment. Ether[3] was administered by inhalation using two different methods. The first method, called light ether anesthesia, involved initially anesthetizing the animal sufficiently to permit the injection and removing the animal to a restraining cage for the remainder of the blood sampling phase. Ether was not administered at any other point in this experiment. The second method used, the "open technique" (6), involved continuous ether; *i.e.*, after initially being anesthetized, the animal was kept unconscious by a constant supply of ether vapors. Forced air was conducted over liquid ether to an open funnel maintained over the nose and mouth of the rat for the remainder of the experiment. Since hypothermia may accompany general anesthesia, each rat's body temperature was monitored by a rectal thermistor probe and the animal was maintained at 37 ± 1° by means of a thermostatically-controlled, heated surgical table. After dosing with thiamine hydrochloride, a total of 10 100-μl blood samples were collected from the tail vein. Free thiamine (nonphosphorylated) in whole blood was determined as previously described (3).

In rats where urinary thiamine was determined, light ether anesthesia was used. Subsequently, the rats were placed in metabolism cages. Urine was collected from the rats at set time intervals after dosing and the free thiamine in urine was determined by standard methods (7–10). The turnover of endogenous thiamine in urine, *i.e.*, urinary excretion of thiamine under conditions of normal dietary intake, was determined in rats over the 24-hr interval prior to intravenous administration of exogenous thiamine hydrochloride. In other words, the rats were placed in individual metabolism cages 24 hr prior to exogenous thiamine administration and urine collected during this period was assayed for thiamine. The amount of thiamine excreted in this 24-hr period for each animal was assumed to be the turnover of endogenous thiamine.

Calculations—The time course of thiamine in blood displayed apparent two-compartment model behavior (Figs. 1–3). Individual rat blood concentration–time profiles were fit to Eq. 1 using two programs, a simplex optimization of the parameters[4] (11, 12), and the NONLIN program (13).

$$C_B = Ae^{-\alpha t} + Be^{-\beta t} \qquad \text{(Eq. 1)}$$

where C_B is the blood levels in μg/ml and A, B, α, and β are standard symbols used to describe classical two-compartment behavior.

The significance of differences between mean pharmacokinetic parameters for each dose was evaluated by a one-tailed t-test, single clas-

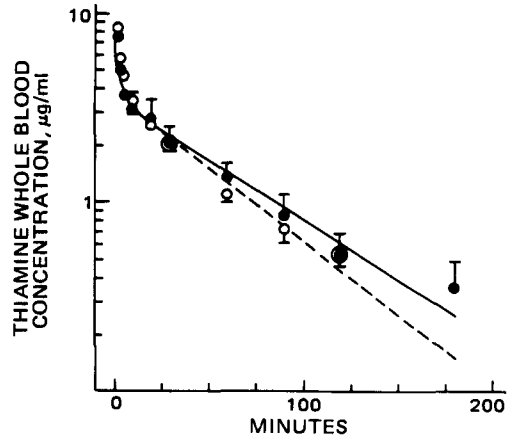

Figure 1—*Thiamine blood levels after treatment with thiamine hydrochloride (4 mg/kg iv) in rats under urethan (○) and light ether anesthesia (●). Concentration of thiamine is expressed as thiamine hydrochloride in micrograms per milliliter.*

[1] ARS/Sprague-Dawley, Madison, Wis.
[2] Sigma Chemical Co., St. Louis, Mo.
[3] Mallinckrodt Chemical Works, St. Louis, Mo.

[4] The program was developed by Dr. W. White, M. Mintun, and various students in the Department of Pharmaceutical Chemistry of the University of Kansas.

0022-3549/82/0200-0169$01.00/0

Table I—Effect of Anesthesia on the Pharmacokinetic Parameters[a] for Thiamine Disposition in Rats after Administration of Thiamine Hydrochloride, 4 mg/kg iv

Parameter	Anesthetic Agent		Statistical Significance of Difference
	Light Ether[b]	Urethan[c]	
A, μg/ml	9.6 ± 2.3	10.3 ± 1.5	
B, μg/ml	3.38 ± 0.60	3.70 ± 0.41	
α, min^{-1}	0.64 ± 0.16	0.469 ± 0.094	
β, min^{-1}	0.0168 ± 0.0016	0.0190 ± 0.0021	
$t_{0.5\beta}$, min	42.2 ± 3.5	41.1 ± 4.4	NS[d]
AUC, μg min/ml	271 ± 48	228 ± 17	NS
AUC/dose, min/ml/kg	0.068 ± 0.012	0.057 ± 0.004	NS
$V_{d(area)}$, ml/kg	1220 ± 180	1090 ± 130	NS
Cl_{TB}, ml/min/kg	17.5 ± 4.1	18.9 ± 1.6	NS

[a] Biexponential parameters determined by fitting blood concentration *versus* time data to Eq. 1 using simplex and NONLIN programs. [b] Mean ± *SE* from five animals. [c] Mean ± *SE* from 11 animals. [d] Not significantly different at $p = 0.05$.

sification Model I ANOVA, and the Student–Newman–Keuls multiple comparison test (14). The exact test applied will be discussed. The parameters calculated (Eqs. 2–5) and compared were area under the curve (AUC), volume of distribution [$V_{d(area)}$], half-life of elimination from blood ($t_{0.5\beta}$), and total body clearance (Cl_{TB}), which were calculated from individual rat blood concentration-time profiles derived by fitting Eq. 1 to the data and employing Eqs. 2–5 (15):

$$AUC_{0\to\infty} = A/\alpha + B/\beta \quad \text{(Eq. 2)}$$

$$V_{d(area)} = \frac{\text{dose}}{\beta(AUC_{0\to\infty})} \quad \text{(Eq. 3)}$$

$$t_{0.5\beta} = 0.693/\beta \quad \text{(Eq. 4)}$$

$$Cl_{TB} = \text{dose}/AUC_{0\to\infty} \quad \text{(Eq. 5)}$$

where $AUC_{0\to\infty}$ is the area under the curve, zero time to infinity.

For urine studies, the doses of thiamine on a milligram per kilogram basis were converted to absolute amounts by using the rat weight. The fraction of the exogenous thiamine dose excreted in the urine was determined by plotting the total amount of thiamine excreted in the 24-hr postdosing minus the amount of thiamine excreted from normal thiamine turnover, determined from the 24-hr predosing, *versus* the dose administered. A linear plot suggests apparent dose-independent elimination kinetics with the slope indicative of the fraction of dose excreted in the urine. Similarly, the fraction of dose excreted in the urine in any time interval may be determined. The terminal half-life for thiamine elimination was determined from a plot of the logarithm of the amount of unchanged drug remaining to be excreted *versus* time. Renal clearance was estimated by dividing the urinary excretion rate by the whole blood concentration at the midpoint of the urine collection period.

RESULTS

Figures 1, 2, and 3 compare the mean blood thiamine concentrations after urethan and light ether anesthesia where thiamine hydrochloride was administered intravenously at 4, 12, and 36 mg/kg, respectively. The curves drawn in Figs. 1–3 were generated by Eq. 1 using the mean pharmacokinetic parameters (Tables I–III) obtained by averaging the parameters determined by computer fitting individual animal blood thiamine concentration *versus* time data.

Tables I–III compare the effects of various anesthetic agents on the pharmacokinetic behavior of thiamine. In addition to the use of light ether anesthesia as a control, continuous ether administration sustaining the rats' unconsciousness throughout the entire sampling period (as was the case with the urethan anesthesia) was used for further comparison at the 36-mg/kg dose. Included in Tables I–III are the parameters A, α, B, β, and the calculated model-dependent parameters, $V_{d(area)}$ and $t_{0.5\beta}$, as well as the model-independent parameters, $AUC_{0\to\infty}$ and Cl_{TB}.

Analyses by an unpaired Student t test of these pharmacokinetic parameters indicated no significant differences between the mean parameters for light ether and urethan anesthesia after intravenous treatment with 4 mg of thiamine hydrochloride/kg. At a dose of 12 mg of thiamine hydrochloride/kg, analyses of pharmacokinetic parameters for light ether and urethan anesthesia by a Student t test indicated highly significant differences between mean $AUC_{0\to\infty}$ ($p < 0.005$), $t_{0.5\beta}$ ($p < 0.1$), and Cl_{TB} ($p < 0.005$), but no significant difference between the mean volumes of distribution.

At a dose of 36 mg of thiamine hydrochloride/kg, the pharmacokinetic parameters for urethan anesthesia were compared with both modes of ether anesthesia, light ether (ether administered only initially), and ether administered continuously. Analyses of variance indicated highly significant differences between mean $AUC_{0\to\infty}$ ($p \ll 0.001$), $t_{0.5\beta}$ ($p \ll 0.001$), and Cl_{TB} ($p \ll 0.001$). No significant difference between the mean volumes of distribution for urethan *versus* light ether anesthesia was seen. When continuous ether-treated animals were compared to those treated with light ether, a significant increase in volume of distribution and Cl_{TB} was noted, but the half-lives were unaffected by the different mode of ether administration.

As shown, urethan markedly affected all of the thiamine pharmaco-

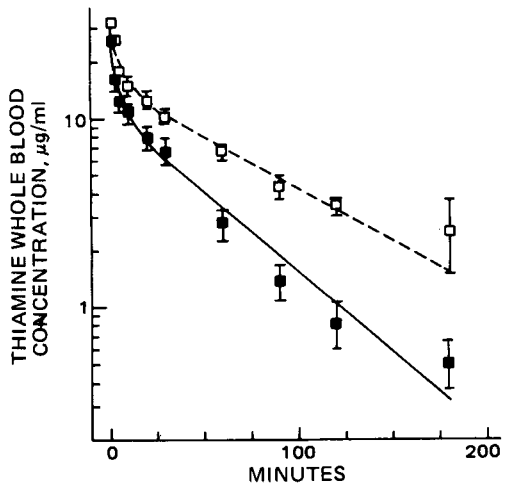

Figure 2—*Thiamine blood levels after treatment with thiamine hydrochloride (12 mg/kg iv) in rats under urethan (□) and light ether anesthesia (■). Concentration of thiamine is expressed as thiamine hydrochloride in micrograms per milliliter.*

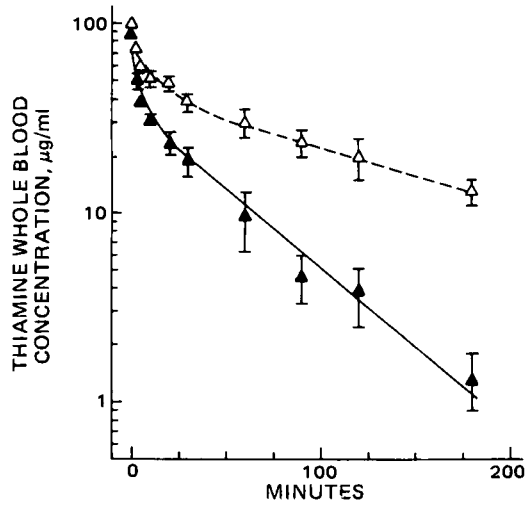

Figure 3—*Thiamine blood levels after treatment with thiamine hydrochloride (36 mg/kg iv) in rats under urethan (△) and light ether anesthesia (▲). Concentration of thiamine is expressed as thiamine hydrochloride in micrograms per milliliter.*

Table II—Effect of Anesthesia on the Pharmacokinetic Parameters[a] for Thiamine Disposition in Rats after Administration of Thiamine Hydrochloride, 12 mg/kg iv

Parameter	Anesthetic Agent		Statistical Significance of Difference
	Light Ether[b]	Urethan[c]	
A, μg/ml	33.0 ± 6.2	36.1 ± 6.1	
B, μg/ml	10.9 ± 1.3	15.1 ± 1.6	
α, min^{-1}	0.57 ± 0.13	0.57 ± 0.10	
β, min^{-1}	0.0201 ± 0.0014	0.0141 ± 0.0014	
$t_{0.5\beta}$, min	35.2 ± 2.2	51.4 ± 4.5	$p < 0.01$[d]
AUC, μg min/ml	627 ± 91	1320 ± 120	$p < 0.005$[d]
AUC/dose, min/ml/kg	0.052 ± 0.008	0.110 ± 0.010	$p < 0.05$[e]
$V_{d(area)}$, ml/kg	1020 ± 110	790 ± 82	NS[f]
Cl_{TB}, ml/min/kg	20.6 ± 2.8	9.6 ± 0.8	$p < 0.005$[d]

[a] Biexponential parameter determined by fitting blood concentration *versus* time data to Eq. 1. [b] Mean ± *SE* for five animals. [c] Mean ± *SE* for seven animals. [d] Parameters under urethan anesthesia significantly different from parameters under light ether anesthesia using one-tailed t test (14) at the level indicated. [e] Parameter under urethan anesthesia significantly different from each value for this parameter in Tables I–III using the Student–Newman–Keuls test (15). [f] Not significantly different at $p = 0.05$.

kinetic parameters (with the exception of the volume of distribution) after intravenous administration of thiamine hydrochloride at 12 and 36 mg/kg. Dose-independent pharmacokinetic parameter changes were observed under light ether anesthesia as demonstrated by comparing the $AUC_{0\to\infty}$/dose. The Student–Newman–Keuls multiple comparison test (15) applied to the mean $AUC_{0\to\infty}$/dose parameter for each anesthetic agent used and at each dose of thiamine hydrochloride, indicated no significant difference among means from light ether-anesthetized animals. This was consistent with results from the urinary excretion studies. The pattern for excretion of thiamine by the renal route is shown in Fig. 4. After taking into account the turnover of endogenous thiamine, ~75% of the exogenous thiamine dose administered was excreted unchanged in the first 2 hr and the amount of thiamine excreted unchanged in 48 hr accounted for 96% of the administered dose as shown in Fig. 5. The urinary excretion rate of thiamine in light ether-anesthetized rats closely parallels the time course of whole blood concentrations, with approximately the same terminal half-life for all the doses studied. In addition, the renal clearance closely correlated with Cl_{TB} for rats anesthetized with ether, since the primary elimination route at these doses is the renal route.

As opposed to the results for thiamine pharmacokinetics after ether anesthesia, the Student–Newman–Keuls test indicated significant differences between mean $AUC_{0\to\infty}$/dose values for urethan and ether-anesthetized animals, and also suggested that differences between the mean $AUC_{0\to\infty}$/dose values at each dose of thiamine hydrochloride for urethan-anesthetized animals were significant.

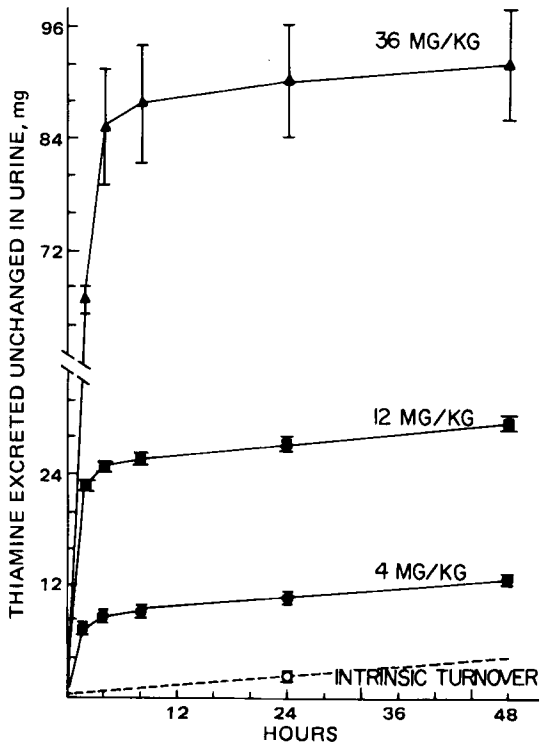

Figure 4—*Cumulative urinary excretion patterns of thiamine after administration of thiamine hydrochloride in rats at 4, 12, and 36 mg/kg iv and the intrinsic turnover of thiamine from the diet.*

DISCUSSION

In the present investigation, urethan anesthesia significantly prolonged the half-life of thiamine in rats after administration of thiamine hydrochloride at 12 and 36 mg/kg relative to the 4-mg/kg dose. Total body clearance significantly decreased, primarily due to the increased half-life (decreased β) and not due to the small changes, if any, in volumes of distribution.

Urinary excretion of unchanged thiamine is the principal elimination route of thiamine in the dose range studied. Since thiamine appears to be exclusively eliminated by the renal route, total body clearance and renal clearance are approximately equal. The total body clearance of thiamine in rats anesthetized with ether (~19 ml/min/kg) is greater than the glomerular filtration rate (10 ml/min/kg) in rats (16). This result is consistent with the known tubular secretion of thiamine and other quaternary ammonium drugs (17–19). Thiamine is also known to be reabsorbed from the renal tubules by a saturable process (19).

The mechanism of urethan alteration of thiamine elimination after thiamine hydrochloride administration is most likely very complex, since urethan changes a number of physiological parameters. It suppresses hematopoiesis and is hepatotoxic (20). Urethan also causes acute changes in blood and blood vessels, hemolysis, and red blood cell breakdown (1). Hemodynamic alterations caused by urethan are slow to occur, and other factors may alter or accelerate these hemodynamic effects (21). It was shown (22) that urethan in anesthetic doses increases the hematocrit,

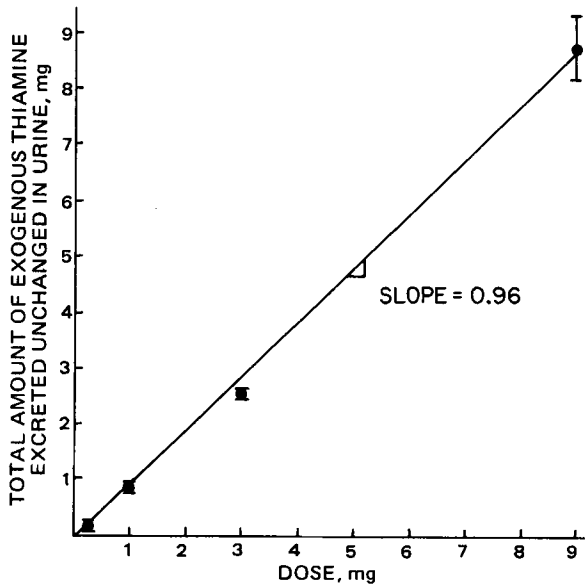

Figure 5—*Plot of the total amount of thiamine excreted unchanged in urine in 48 hr (corrected for the intrinsic turnover of thiamine in 48 hr)* versus *the dose of thiamine hydrochloride administered. The line drawn was generated by least-squares analysis.*

Table III—Effect of Anesthesia on the Pharmacokinetic Parameters [a] for Thiamine Disposition in Rats after Administration of Thiamine Hydrochloride, 36 mg/kg iv

Parameter	Anesthetic Agent			Statistical Significance of Difference
	Light Ether [b]	Continuous Ether [b]	Urethan [c]	
A, μg/ml	142.5 ± 7.6	70.2 ± 5.1	70 ± 10	
B, μg/ml	35.2 ± 5.2	17.9 ± 5.1	43.4 ± 4.1	
α, min^{-1}	0.76 ± 0.20	0.239 ± 0.069	0.232 ± 0.052	
β, min^{-1}	0.019 ± 0.002	0.020 ± 0.004	0.0066 ± 0.0008	
$t_{0.5\beta}$, min	38.1 ± 4.2	37.9 ± 5.6	97.9 ± 7.4	$p \ll 0.001$ [d]
AUC, μg min/ml	2090 ± 290	1304 ± 95	6230 ± 880	$p \ll 0.001$ [d]
AUC/dose, min/ml/kg	0.058 ± 0.008	0.036 ± 0.003	0.173 ± 0.024	$p < 0.05$ [e]
$V_{d(area)}$, ml/kg	830 ± 44	1530 ± 260 ($p < 0.05$) [d]	841 ± 92	NS [f]
Cl_{TB}, ml/min/kg	18.4 ± 2.3	28.0 ± 1.8 ($p < 0.01$) [d]	5.7 ± 1.0	$p \ll 0.001$ [d]

[a] Biexponential parameters determined by fitting blood concentration *versus* time data to Eq. 1. [b] Mean ± SE for five animals. [c] Mean ± SE for six animals. [d] Significantly different from light ether and/or continuous ether using single classification Model I ANOVA (15). [e] Parameter under urethan anesthesia significantly different from each value for this parameter in Tables I–III using the Student–Newman–Keuls test (15). [f] Not significantly different at $p = 0.05$.

decreases blood pressure, increases plasma glucose, and causes local tissue damage to intra-abdominal organs and loss of blood plasma from circulation.

Ether is also known to alter many hemodynamic functions (23). To dramatize these effects, ether was administered continuously in the 36-mg/kg base study. The use of continuous ether anesthesia compared to light ether anesthesia significantly affected only the volume of distribution, and in an increasing direction. As noted, mean pharmacokinetic parameters for thiamine disposition in rats under urethan were significantly different from those in rats under light ether and continuous ether anesthesia.

Hypothermia may accompany general anesthesia due to hemodynamic alterations and general depression of the temperature regulating centers in the hypothalamus (24). Hypothermia was recently shown to alter the pharmacokinetics of pancuronium in the cat (25) and propranolol in the dog and humans (26). It was found (25) that pancuronium was eliminated more slowly and the volume of distribution and total plasma clearance was less in the cat when body temperature was lowered by 10°. Another investigation (26) reported that cooling to 26° markedly reduced the apparent volume of distribution and the total body clearance of propranolol in dogs. Although hypothermia may alter a drug's disposition kinetics, the temperature decreases examined previously were large (≥10°) and in the present investigation the animals under continuous anesthesia were maintained under thermal control.

Most striking and perhaps most consequential to thiamine disposition and elimination may be the pronounced hypocalcemic effect of urethan in rats. This effect was studied (27) with ether and halothane anesthesia. Urethan administered intraperitoneally at anesthetic doses significantly lowered serum calcium within 15 min after injection and this effect lasted for more than 20 hr.

The relationship between calcium and thiamine is well documented. Calcium and magnesium deficiencies alter thiamine distribution in the rat brain and liver. Calcium also plays a significant role in binding thiamine to nerve membrane structure (28–30). Although it is suspected that the hypocalcemic effect of urethan may bear primary consideration in the alteration of thiamine elimination, hemodynamic changes may also contribute.

Since it is not usually necessary to maintain animals under continuous anesthesia during many simple pharmacokinetic studies, the use of urethan or continuous ether anesthesia is no longer common practice. However, for many experiments where significant surgery is required or the animals are exposed to painful techniques, continuous anesthesia is desirable. The results of the present study demonstrate the care which must be taken in the interpretation of pharmacokinetic data otained in anesthetized animals, particularly when urethan anesthesia is used.

REFERENCES

(1) M. M. Bree and B. J. Cohen, *Lab. Anim. Care*, **15**, 254 (1965).

(2) H. Nogami, M. Hanano, S. Awazu, and T. Fuwa, *Chem. Pharm. Bull.*, **18**, 1937 (1970).

(3) J. D. Pipkin and V. J. Stella, *J. Pharm. Sci.*, **67**, 818 (1978).

(4) J. D. Pipkin and V. J. Stella, Abstracts of papers presented before the APhA Academy of Pharmaceutical Sciences, **7** (1), 152 (1977).

(5) M. Virolainen, *Transplantation*, **5**, 1530 (1967).

(6) "Drill's Pharmacology in Medicine," 3rd ed., J. R. DiPalma, Ed., McGraw-Hill, New York, N.Y., 1965, p. 103.

(7) H. N. Haugen, *Scand. J. Clin. Lab. Invest.*, **12**, 384 (1960).

(8) O. Pelletier and R. Madère, *Clin. Chem.*, **18**, 937 (1972).

(9) O. Mickelsen, H. Condiff, and A. Keys, *J. Biol. Chem.*, **160**, 361 (1945).

(10) D. Melnick and H. Field, Jr., *ibid.*, **130**, 97 (1939).

(11) S. L. Morgan and S. N. Deming, *Anal. Chem.*, **46**, 1170 (1974).

(12) S. N. Deming and S. L. Morgan, *ibid.*, **45**, 278A (1973).

(13) C. M. Metzler, G. L. Elfring, and A. J. McEwen, *Biometrics*, **Sept.**, 562 (1974).

(14) M. Gibaldi and D. Perrier, "Pharmacokinetics," Marcel Dekker, New York, N.Y., 1975, pp. 45–88.

(15) R. R. Sokal and F. J. Rohlf, "Biometry," W. H. Freeman, San Francisco, Calif., 1969, pp. 166–172, 226–246.

(16) A. Dittmer, B. Actman, and C. Greebe, "Handbook of Circulation," National Academy of Science, Washington, D.C., 1959, p. 127.

(17) B. R. Rennick, *J. Pharmacol. Exp. Ther.*, **122**, 449 (1958).

(18) G. Malnic, G. A. C. da Silva, R. C. de Angelis, and Z. J. Gomes, *Am. J. Physiol.*, **198**, 1274 (1960).

(19) H. N. Haugen, *Scand. J. Clin. Lab. Invest.*, **13**, 61 (1961).

(20) H. Rosoff, "Handbook of Veterinary Drugs," Springer, New York, N.Y., 1974, pp. 632-633.

(21) T. D. Giles, A. C. Quiroz, and G. E. Burch, *Am. Heart. J.*, **78**, 281 (1969).

(22) C. Van Der Meer, J. A. M. Versluys-Broers, H. A. R. E. Tuynman, and V. A. J. Buur, *Arch. Int. Pharmacodyn. Ther.*, **217**, 257 (1975).

(23) D. G. Vidt, A. Bredemeyer, E. Sapirstein, and L. A. Sapirstein, *Circ. Res.*, **7**, 759 (1959).

(24) L. S. Goodman and A. Gilman, "The Pharmacological Basis of Therapeutics," 3rd ed., Macmillan, New York, N.Y., 1965, chap. 7.

(25) R. D. Miller, S. Agoston, F. Van Der Pol, L. H. D. J. Booi, J. F. Crul, and J. Ham, *J. Pharmacol. Exp. Ther.*, **207**, 532 (1978).

(26) R. G. McAllister, Jr., D. W. Bourne, G. T. Tiong, J. L. Erickson, C. C. Wachtel, and E. P. Todd, *Clin. Pharmacol. Ther.*, **25**, 1 (1979).

(27) T.-C. Peng, C. W. Cooper, and P. L. Munson, *J. Pharmacol. Exp. Ther.*, **182**, 522 (1972).

(28) M. Kimura and Y. Itokawa, *J. Neurochem.*, **28**, 389 (1977).

(29) Y. Itokawa, *Brain Res.*, **94**, 475 (1975).

(30) R. L. Barchi and R. O. Viale, *J. Biol. Chem.*, **251**, 193 (1976).

ACKNOWLEDGMENTS

Supported in part by a Fellowship from the American Foundation for Pharmaceutical Education to J. D. Pipkin, by National Institute of Health Grant NS11998, and General Research Funds from the University of Kansas. The authors thank Laura Inbody-Kenny for her technical assistance.

Binding of Crocetin to Plasma Albumin

THEODORE L. MILLER*x, STEVEN L. WILLETT*, MARYANNE E. MOSS‡§, JOELLE MILLER*¶, and BENJAMIN A. BELINKA, Jr.‡‖

Received December 3, 1980, from the *Department of Chemistry, Ohio Weslyan University, Delaware, OH 43015 and the ‡Department of Chemistry, King's College, Wilkes Barre, PA 18711. Accepted for publication, June 9, 1981. §Present address: Medical College of Pennsylvania, Philadelphia, PA 19129. ¶Present address: College of Medicine, University of Florida, Gainesville, FL 32611. ‖Present address: Department of Chemistry, State University of New York, Binghamton, NY 13901.

Abstract □ The binding of the carotenoid crocetin to human and bovine plasma albumin was studied using absorption and fluorescence techniques. Shifts in the absorption spectrum of crocetin, quenching of the albumin fluorescence, and competitive binding studies all provided information about the binding of crocetin to albumin. These studies suggest that crocetin binds to plasma albumin by occupying the free fatty acid binding sites. The binding constants for the first two binding sites are in the 10^5–10^7 M^{-1} range and are an order of magnitude less than the values reported for other conjugated polyene fatty acids. The importance of this strong plasma albumin binding to the pharmacology of crocetin is discussed.

Keyphrases □ Crocetin—binding to plasma albumin, bovine and human □ Serum protein binding—crocetin, bovine and human serum albumin □ Binding—crocetin, with bovine and human serum albumin

An important function of plasma albumin is to bind metabolites and drugs that are relatively insoluble in aqueous media. The protein complex serves as the transport system that conveys the metabolite or drug to the site of action. Drug binding can influence the therapeutic, pharmacodynamic, and toxicological actions of drugs. The binding of drugs by albumin and plasma protein was reviewed earlier (1, 2).

One of the most important metabolites transported by plasma albumin is free fatty acid, the form in which fat is released from the adipose tissue storage deposits (3). Although the plasma free fatty acid concentration is quite variable, the molar ratio of free fatty acid to albumin in the plasma usually is in the range of 0.5–2.0 and rarely exceeds 3.0 (4, 5). The binding and transport of a drug can be influenced by changes in the plasma free fatty acid concentration. Competitive binding between fatty acids and other organic compounds is examined in a recent review article on fatty acid binding to plasma albumin (6).

BACKGROUND

Crocetin (8,8′-diapocarotenedioic acid) is a dicarboxylic acid that is a member of the class of terpene lipids called carotenoids. Crocetin occurs as the glycoside in varieties of gardenia and members of the crocus family, particularly saffron. It is slightly soluble in aqueous solutions (20 μM at pH 8) that are basic and very soluble in organic bases such as pyridine. Solid crocetin is brick red while solutions are bright yellow.

A recent study demonstrated that the intramuscular injection of crocetin in rabbits fed an atherosclerosis-producing diet resulted in greatly reduced severity of the atherosclerosis (7, 8). The physiological mechanism of crocetin activity is not understood, but there is evidence that it might involve the prevention of hypoxia (8–10). More recently, crocetin has been used to treat cerebral edema in cats (11), to increase fermentation yields (12), for cancer therapy (13, 14), to treat spinal cord injury (15), to treat skin papillomas (16, 17), and to treat hypertension in rats (18).

The original investigations were based on the premise that crocetin would be a free molecular species in plasma solution. It was suggested (8) that a long, rigid molecule of relatively low molecular weight might increase oxygen diffusivity in the plasma. Since crocetin possesses these molecular characteristics, it was selected as a likely candidate for these investigations. Although crocetin has been found to bring about a large increase in oxygen diffusivity in plasma, even in the presence of increased plasma protein levels (8), it was thought that it would bind to plasma albumin and perhaps other plasma components. Absorption and fluorescence techniques were used to study the binding of crocetin to plasma albumin.

EXPERIMENTAL

Crystalline bovine plasma albumin and human plasma albumin were obtained commercially[1]. Solutions of each protein (0.1 mM) were prepared and treated with charcoal[2] in an acidic medium by a previous method (19) to remove endogenous free fatty acids. The albumin–charcoal mixtures were centrifuged[3] for 80 min at 20,200×g and 4°. The pH of the clarified solution was adjusted to 8.0 using 2 M NaOH. Albumin concentrations were determined by measuring UV absorbance of the solution at 280 nm.

The concentrations of the crocetin[4] solutions were determined from the absorbance at 420 nm. A value of 1.1×10^5 liters/mole/cm (420 nm) was found for the molar absorptivity of crocetin in saline solution at pH 8.0. This is similar to the value (114,900 liters/mole-cm) measured for a mixed solvent[5] (25% ethanol in water).

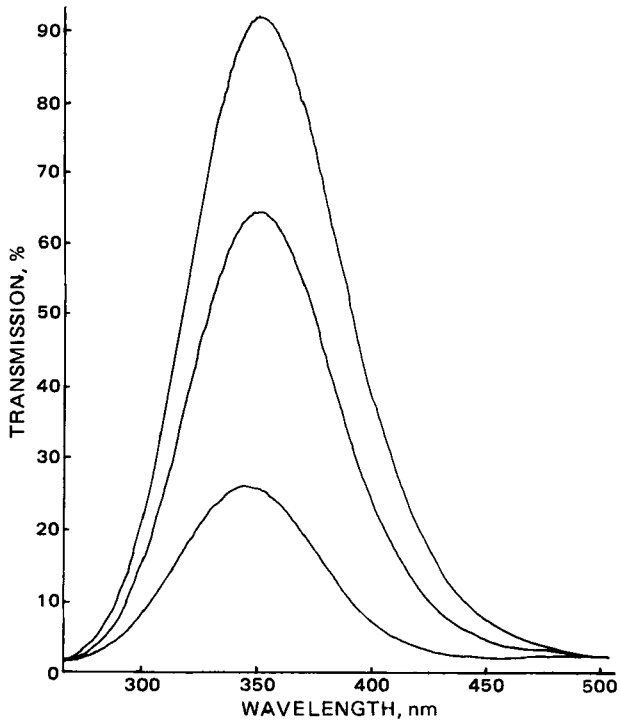

Figure 1—*Fluorescence emission spectrum of bovine plasma albumin in the presence of crocetin. The wavelength of excitation was 280 nm; the media contained 0.53 μM bovine albumin, 0.16 M NaCl, and 0.01 M buffer (pH 8.0); and the molar ratios of crocetin to albumin were 0, 4, and 17 from top to bottom.*

[1] Sigma Chemical Co.
[2] Darco, ICI United States Inc.
[3] Sorvall model SS-33.
[4] Courtesy of John L. Gainer, University of Virginia.
[5] Courtesy of Sterling-Winthrop Research Institute, Rensselaer, N.Y.

0022-3549/82/0200-0173$01.00/0

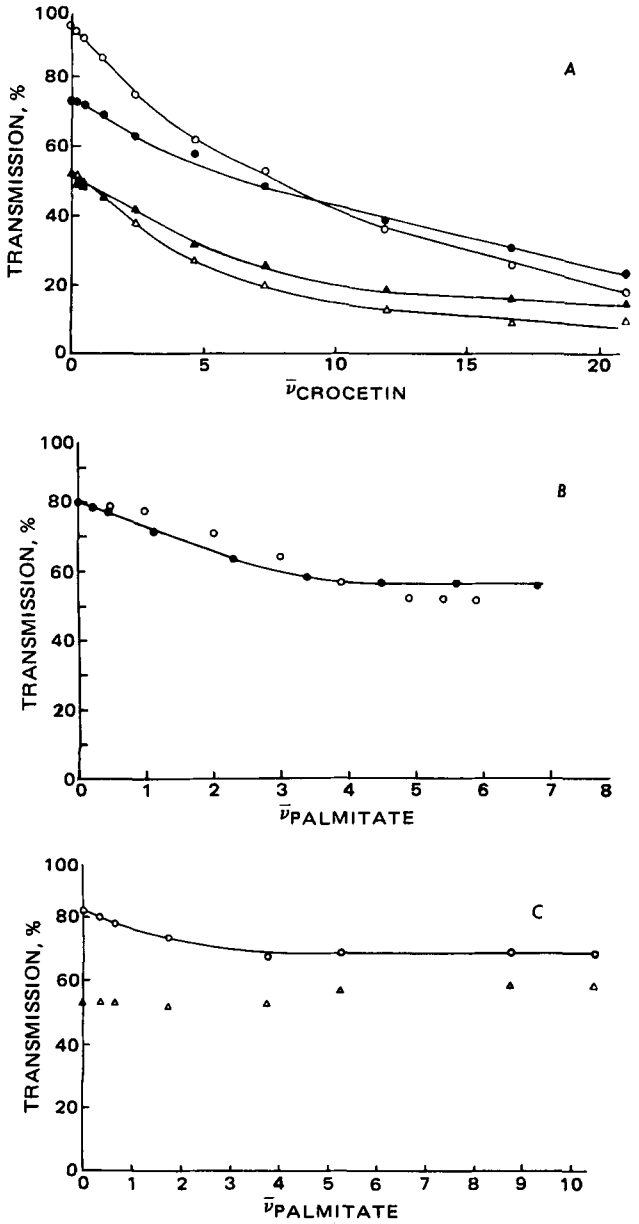

Figure 2—*Fluorescence titration curves for plasma albumin. Excitation was at 280 nm and emission was at 350 nm. Figure 2A shows the quenching of tryptophan emission by crocetin binding to bovine albumin (○) and human albumin (△), to bovine albumin with added palmitate ($\bar{\nu}$ = 4.0) (●), and the human albumin with added palmitate ($\bar{\nu}$ = 3.9) (▲). The bovine and human albumin concentrations were 0.53 and 0.54 μM, respectively. Each data point represents an average of at least two measurements. Figure 2B shows the quenching of tryptophan emission by palmitic acid at pH 8.0 and 0.62 μM bovine albumin (●), and at pH 7.4 and 0.10 mM bovine albumin (○) (pH 7.4 results taken from Ref. 20). Figure 2C shows the quenching of tryptophan emission by palmitate in samples with added crocetin, $\bar{\nu}$ (crocetin) = 1.7 (○) and $\bar{\nu}$ (crocetin) = 7.1 (△). Bovine albumin concentration was 0.64 μM with 0.16 M NaCl and 0.01 M buffer at pH 8.0.*

All absorbance measurements were made with a spectrophotometer[6], and fluorescence measurements were recorded at room temperature with either a spectrophotofluorometer[7] or a fluorometer[8]. Quartz cells (1 cm) were used in all fluorescence measurements. The solutions for the fluorescence titrations were prepared by adding 1.00 ml of albumin (~5 μM) to each of a series of 10-ml volumetric flasks. Various amounts of crocetin (0–9.00 ml of ~10 μM) were added to the flasks which then were diluted to 10.00 ml with buffer. This series gave crocetin to albumin ratios[9] ($\bar{\nu}$) from zero to ~20. All solutions were buffered at pH 8.0 with a 0.01 M tromethamine buffer[10] which contained 0.16 M NaCl.

[6] Either a Cary 219 by Varian or a Beckman model DB-GT.
[7] Turner model 430.
[8] Turner model 110.

Table I—Effect of Crocetin on Albumin Fluorescence in the Presence of Palmitate

Molar Ratio of Crocetin to Bovine Plasma Albumin[a]	Relative Fluorescence	Molar Ratio of Crocetin to Human Plasma Albumin[b]	Relative Fluorescence
0.0	65	0.0	38
0.2	66	0.2	35
0.5	65	0.4	34
1.1	68	0.9	38
2.2	67	1.8	35
4.5	64	3.6	40
6.7	63	5.4	33
11.2	64	9.1	25
15.7	55	12.7	19
20.2	51	16.4	12

[a] For $\bar{\nu}_{palmitate}$ = 9.0, the concentration of bovine albumin was 0.51 μM at pH 8.0. [b] For $\bar{\nu}_{palmitate}$ = 8.0, the concentration of human albumin was 0.53 μM at pH 8.0.

Sodium palmitate solutions were prepared by adding buffer solution to sodium palmitate[1]. The palmitate–albumin solutions were then prepared by adding the warm (60°) standard palmitate solution dropwise to the albumin solutions while they were being stirred magnetically. The final palmitate–albumin solution was used either directly in a palmitate–albumin fluorescence titration or in a competitive palmitate–crocetin binding experiment. For the competitive binding experiment, 2.00 ml of the palmitate–albumin solution was added to a 10-ml volumetric flask. After various amounts of crocetin were added, the solutions were diluted to the mark. In a similar procedure, crocetin–albumin solutions were used in competitive palmitate titrations.

For the difference spectra, 3.00 ml of crocetin (~5 μM) was placed in standard 1-cm cells located in both the sample and reference beams. The difference spectra were recorded after 5-μl aliquots of albumin (~0.5 mM) were added to the sample cell.

All final solutions contained 0.01 M buffer and 0.16 M sodium chloride at pH 8.0. All solutions, including the substrates (crocetin and palmitate) and the substrate–albumin preparations, were optically clear. All measurements were made at room temperature.

RESULTS

The fluorescence emission spectrum of both bovine and human plasma albumin were altered when crocetin was added to the solution. Figure 1 illustrates the alteration for bovine albumin at pH 8.0 and 0.53 μM. The excitation wavelength for these spectra was 280 nm. The relative fluorescence intensity for bovine albumin shifted and was strongly quenched as the crocetin concentration increased. This reduction in relative fluorescence intensity was strictly a reduction in the tryptophan fluorescence from albumin because no emission was observed from either free or albumin-bound crocetin at room temperature. The shift in the wavelength of maximum fluorescence was only from 350 to 345 nm with excess crocetin. The maximum reduction in fluorescence intensity was 81% ($\bar{\nu}$ = 21).

Similar changes in the fluorescence spectrum of human plasma albumin were observed. However, with human albumin, the tyrosine component of the luminescence is much more conspicuous, and it is impossible to determine if the tryptophan fluorescence spectrum is shifted. After excess crocetin is added to human albumin, the tyrosine emission is stronger than the tryptophan emission. The maximum reduction in fluorescence intensity was also 81% ($\bar{\nu}$ = 21) for human albumin.

The extent of binding was evaluated by using the decrease in relative fluorescence intensity at 350 nm (0.54 μM, pH 8.0). The entire fluorescence spectrum was not recorded for most samples.

The decrease in relative fluorescence intensity was nonlinear for both proteins with most of the change occurring before a molar ratio of ~8. The intersection of lines drawn through the linear segments of the curves was used to determine this value. This procedure will also be employed in subsequent evaluations.

Since these fluorescence titrations were performed at an excitation wavelength of 280 nm and an emission wavelength of 350 nm, a filter

[9] The $\bar{\nu}$ value is the molar ratio of total acid (palmitic acid or crocetin) to total albumin present in the solution; ν is the molar ratio of bound acid (palmitic acid or crocetin) to total albumin present in the solution.
[10] G. Frederick Smith Chemical Co.

Table II—Effect of Palmitate on Albumin Fluorescence in the Presence of Crocetin

Molar Ratio of Palmitate to Human Plasma Albumin[a]	Relative Fluorescence
0.0	52
0.3	51
0.7	52
1.7	52
3.5	51
5.3	51
6.6	52
8.3	56
9.2	58

[a] For $\bar{\nu}_{crocetin}$ = 3.5, the concentration of human albumin was 0.54 μM at pH 8.0.

fluorometer[11] gave accurate and reproducible results except in palmitate–albumin solutions where $\bar{\nu}$ was >8. Under these elevated palmitate conditions, the relative fluorescence was higher than anticipated. There was a slight excitation emission crossover with this set of filters and it was assumed that the higher relative intensity values indicate scattering of radiation by palmitate micelles. This hypothesis could also explain why Spector and John (20) observed that the absorbance of free fatty acid–albumin solutions was identical to that of an albumin solution of the same concentration to which no fatty acid was added where the $\bar{\nu}$ did not exceed a critical value (usually 7). This fluorescence anomaly with palmitate did not occur when a spectrophotofluorometer with narrow slits was employed.

Bovine plasma albumin was titrated with palmitate under the same experimental conditions as outlined for crocetin (pH 8.0 and albumin ~0.5 μM). The results for 0.62 μM bovine albumin at pH 8.0 are shown in Fig. 2B. The results reported by Spector and John (20) are also presented (0.10 mM bovine albumin at pH 7.4). The palmitate results for the two experimental conditions are similar. For both data sets most of the change occurred when the molar ratio of palmitate to albumin reached 4. The maximum reduction in fluorescence intensity was 35% for the earlier study and 31% for the present study.

Under their conditions (20–22), 99% or more of the palmitate present in solution is bound to albumin. When the association constant for the fourth binding site ($6.78 \times 10^5\ M^{-1}$) (22) is used in an equilibrium calculation where the first three palmitate ions are assumed to be 100% associated, only 75% of the remaining palmitate should be bound to the albumin at 0.62 μM. However, the observed difference in the magnitude of fluorescence quenching between data sets is <10%, suggesting that the level of palmitate binding at pH 8.0 and 0.62 μM bovine albumin is greater than anticipated from the reported association constant.

A large positive correction like the 432% value calculated for unbound palmitate association in human albumin solution (23) may also be necessary for bovine plasma albumin. These results along with earlier results for octanoate (24) and palmitate (20) indicate that free fatty acid binding is not strongly influenced by pH changes between 7.4 and 8.0. Consequently, the experimental conditions of pH 8.0 and 0.5 μM albumin required in this study should provide a valid assessment of long-chain acid binding to plasma albumin.

Albumin was titrated with crocetin to which palmitate had been added. Both bovine (0.53 μM) and human (0.54 μM) plasma albumin were used in this series of competitive experiments at pH 8.0. First, palmitate was added to bovine albumin ($\bar{\nu}$ = 4.0) and then the solution was titrated with crocetin. The results for this experiment are shown in Fig. 2A and contrasted with the curve for bovine albumin without palmitate. The lower curves in Fig. 2A are for human albumin with palmitate ($\bar{\nu}$ = 3.9) and without palmitate.

In these experiments the maximum reduction in fluorescence intensity was 67 and 71% for bovine and human albumin, respectively. The relative amounts of quenching from $\bar{\nu}$ = 4 to 21 in the experiments without palmitate were 73 and 70% for bovine and human albumin, respectively. The magnitude of fluorescence quenching between $\bar{\nu}$ (crocetin) = 4 to 21 is approximately the same when either palmitate or crocetin is bound to the protein in a 4:1 molar ratio. This observation would tend to imply that crocetin binds to plasma albumin by occupying the four strongest free fatty acid sites. The high-affinity free fatty acid binding sites of albumin were then saturated with palmitate and the solutions were later titrated with crocetin. The results for bovine albumin (0.51 μM, $\bar{\nu}$ = 9.0 for added palmitate) and human albumin (0.53 μM, $\bar{\nu}$ = 8.0 for added palmitate) are given in Table I. No significant change in the relative fluorescence intensity was observed until the crocetin molar ratio became greater than 10. At this point, crocetin started to replace part of the bound palmitate because there was a decrease in relative fluorescence intensity.

[11] Turner filters; 7-54 (excitation) and 7-60 (emission).

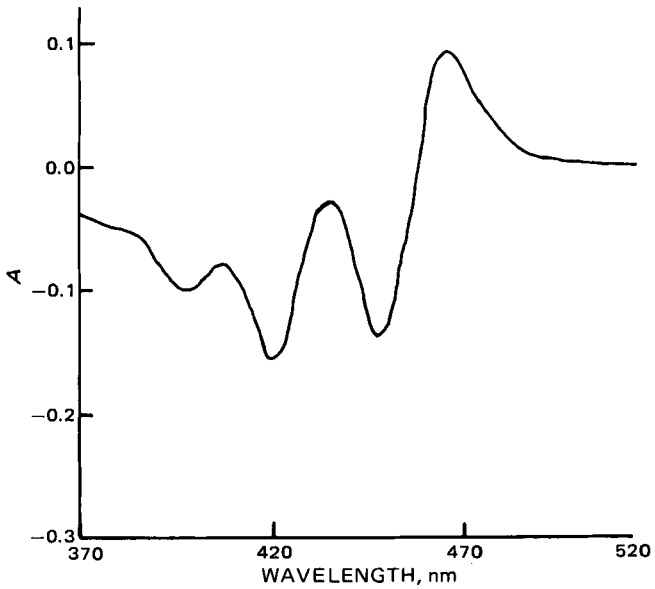

Figure 3—*A typical difference spectrum for the bovine plasma albumin–crocetin system where* ΔA *is the maximum positive absorbance at 465 nm. The bovine plasma albumin–crocetin complex was located in the sample cell and a solution of crocetin with the same concentration was located in the reference cell.*

In a second competitive experiment, albumin was titrated with palmitate to which crocetin had been added. The results for bovine plasma albumin ($\bar{\nu}_{crocetin}$ = 1.7 and 7.1) are shown in Fig. 2C. The maximum reduction in fluorescence intensity ($\bar{\nu}_{crocetin}$ = 1.7) was 16%. The relative amount of quenching from $\bar{\nu}$ = 1.7 to 6.8 in the experiment without crocetin (Fig. 2) was 18%. Most of the change occured before a molar ratio (palmitate to albumin) of 2 was reached. When this value is included with $\bar{\nu}_{crocetin}$ = 1.7, the sum is similar to $\bar{\nu}$ = 3.6 for the palmitate titration without crocetin (Fig. 2B). Thus, the magnitude of fluorescence quenching from $\bar{\nu}_{palmitate}$ = 1.7 to 6.8 was about the same when either crocetin or palmitate was bound to the protein in a 1.7:1 molar ratio. Most of the reduction in fluorescence occurred before $\bar{\nu}$ = 3.6 under both experimental conditions.

For the more concentrated crocetin ($\bar{\nu}$ = 7.1), no change in fluorescence intensity was observed until $\bar{\nu}_{palmitate}$ was ~8. Above 8, a slight increase in intensity was observed. This same observation was made when palmitate was added to human plasma albumin to which crocetin had been added. The results for human albumin ($\bar{\nu}_{crocetin}$ = 3.5) are presented in Table II. There is a very slight increase in the relative fluorescence after $\bar{\nu}_{palmitate}$ reaches 8. The data for these competitive binding experiments support the previous proposition that crocetin binds to the regular free fatty acid binding sites.

Changes in the UV absorption spectra of bovine and human plasma albumin occur when crocetin is added to the solution. There is also a change in the visible absorption spectrum of crocetin when mixed with the proteins. The changes in the UV spectra of proteins have been used to study the binding of lauryl sulfate (25) but at the concentration levels required for crocetin the changes were exceedingly small, which prevented the collection of meaningful data. However, the change in the visible absorption spectrum was used to estimate the binding constants for crocetin.

When bound to either human or bovine plasma albumin, the characteristic absorption spectrum of crocetin was observed, but λ_{max} shifted from 420 nm to longer wavelengths. The magnitude of the shift is proportional to the albumin to crocetin ratio until it reaches a maximum value of ~427 nm. Experimentally, the shift was measured by comparing the spectrum of the crocetin–albumin complex to the spectrum of aqueous crocetin of the same concentration. The difference spectrum was recorded automatically using a double-beam instrument. A typical difference spectrum for the bovine albumin–crocetin system is illustrated in Fig. 3. The magnitude of the spectral shift was recorded as ΔA which is the maximum positive absorbance at 465 nm.

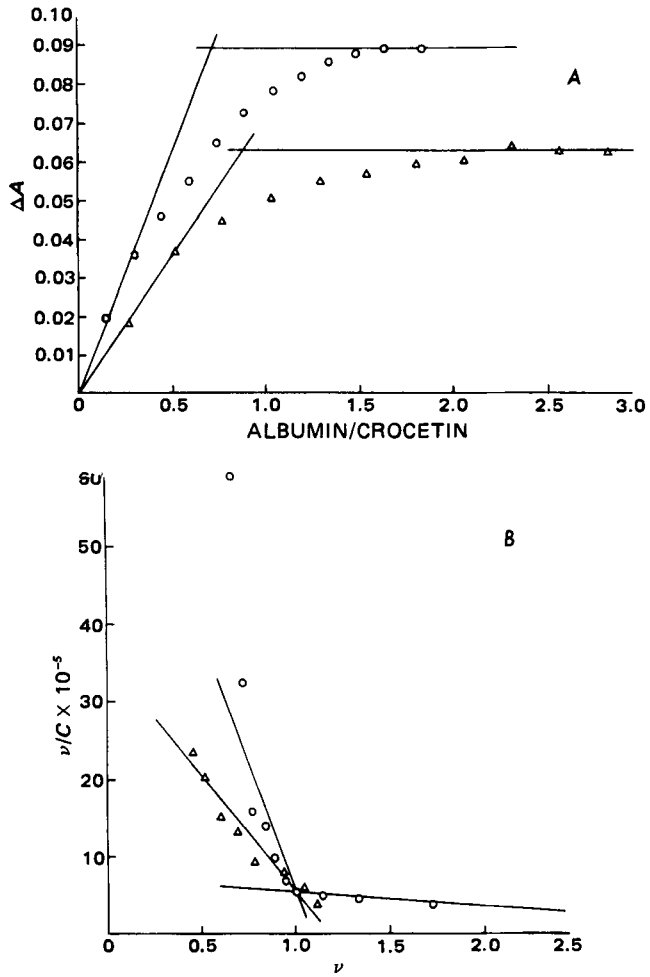

Figure 4—*The changes in the absorption spectra of crocetin (5.0 μM, pH 8.0) on binding albumin. Figure 4A shows the effect of bovine albumin (○) and human albumin (Δ) on the absorption maximum of crocetin as measured by ΔA. The horizontal lines represent ΔA_{max}. Figure 4B shows Scatchard analysis of the data presented in Fig. 4A. Key: ○, bovine albumin; and Δ, human albumin. It was assumed that the maximal ΔA represents 100% binding. The free crocetin concentration is given by C = (1 − $\Delta A/A_{max}$) × 5.0 μM. Albumin was added as microliter aliquots to the sample cell from a stock solution. The lines illustrate the slopes used to determine binding constants.*

Data obtained for crocetin (5.0 μM) binding to bovine albumin and for crocetin (4.2 μM) binding to human albumin at room temperature and pH 8.0 are shown in Fig. 4. The increase in ΔA is shown in Fig. 4A. The initial linear increase in ΔA extrapolates to a maximal value of ~0.7 mole of bovine albumin and 0.9 mole of human albumin/mole of crocetin. There is no additional increase in ΔA when bovine albumin exceeds the ratio of 1.6 moles of albumin/mole of crocetin or human albumin exceeds a ratio of 2. This result was interpreted to indicate that no further binding occurs and that under these experimental conditions, only a vanishingly small amount of free crocetin remains in solution.

A Scatchard plot (26) derived from the data of Fig. 4A is shown in Fig. 4B. It was assumed that maximal ΔA represents 100% binding. Therefore, the percentage of crocetin binding was determined by $\Delta A/\Delta A_{max} \times 100$.

The slope of a Scatchard plot is the binding constant, and a nonlinear curve indicates either nonequivalent binding sites or site–site interactions. Data is limited to the region between $\nu = 0.4$ and 1.7 because of experimental conditions. The slope (binding constant) for bovine albumin at $\nu = 1$ is $9 \times 10^6\ M^{-1}$. The second site has a binding constant on the order of $3 \times 10^5\ M^{-1}$. The fluorescence experiments indicated that there are several additional sites that are not observed under these experimental conditions. The binding data for human albumin is similar, but the slope on the Scatchard plot is not as steep. The slope (binding constant) at $\nu = 1$ is $4 \times 10^6\ M^{-1}$. The second binding site constant could not be evaluated for human albumin.

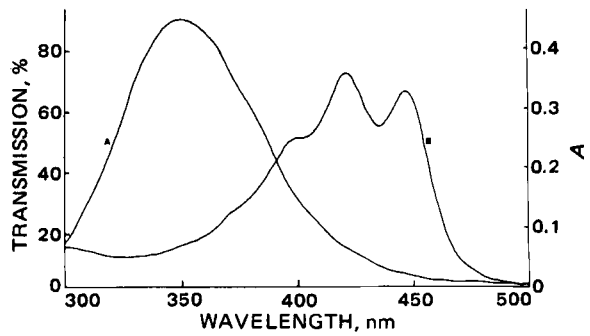

Figure 5—*Fluorescence spectrum of 0.57 μM bovine plasma albumin excited at 280 nm (A). The absorption spectrum of 3.3 μM crocetin (B). Both solutions were prepared with 0.01 M buffer and 0.16 M NaCl at pH 8.*

The experimental strategy of these binding experiments involved varying the albumin concentration while maintaining the crocetin concentration constant. With the addition of 55 μl of albumin to 3.00 ml of crocetin solution, the crocetin concentration was reduced by 1.6%. This small decrease in concentration did not significantly alter the absorbance of the sample. For 55 μl of albumin, the decrease in absorbance at 465 nm was only 0.002, and ΔA was corrected for this small change.

The range of values for the binding of the first 2 moles of crocetin to albumin (10^5–$10^7\ M^{-1}$) was somewhat less than the range of values obtained for the binding of other long-chain fatty acids (6) and conjugated polyene fatty acids (27, 28). Nonetheless, the evidence clearly indicates a similarity in the binding of crocetin and other long-chain fatty acids to plasma albumin.

DISCUSSION

During the preliminary binding studies, some of the properties of crocetin in aqueous solution were examined. Spectrometric titration data at 420 nm indicated that a time-dependent rearrangement occurs. When the time interval between pH and absorbance measurements increased, the equivalence point in the titration curve (*A versus* pH) shifted to a higher pH. On the high pH plateau, the solution was bright yellow; the spectrum observed is shown in Fig. 5. When the pH was lowered into the low pH plateau, a new band at either 297 or 360 nm was observed. Solution conditions determine which band is established after acid is added. Molecular aggregation by either micelle or liquid crystal formation may occur below pH 7.5.

The spectra of buffered crocetin solutions were monitored for 41 days. At pH 7.43, the absorbance dropped more than 50% in 21 hr. By the end of 41 days, the solution was clear with essentially no absorption above 200 nm. The process is reversible because the initial yellow color and spectrum returned when the pH was increased to 8.94 at the end of the 41 days. A much slower irreversible reduction in absorption was observed for a solution buffered at pH 8.66. This reduction is most likely a result of decomposition brought on by the higher hydroxide ion concentration. The hydroxide ion could attack a central carbon–carbon double bond and cause a cleavage of the molecule in a process analogous to the β-carotene–vitamin A process. The reversible loss of color with time is baffling.

The reversible color change and molecular aggregation prevented continuation of the binding study at pH 7.5. The lowest possible value on the high pH plateau was selected (pH 8.0). When the concentration of crocetin is increased above $2 \times 10^{-5}\ M$ at pH 8, a yellow precipitate forms. This restricted the binding studies to the concentration range presented previously. Finally, binding studies by equilibrium dialysis are not possible because crocetin binds very strongly to the dialysis membrane.

Fluorescence spectroscopy is one of the most useful tools for energy transfer studies. The conditions required for long-range energy transfer in proteins have been summarized (29) and energy transfer data has been used to calculate the mean distance between the tryptophan residue of human albumin and conjugated linear polyene fatty acids (28). A prerequisite for energy transfer is that the absorption spectrum of the energy acceptor must overlay the fluorescence spectrum of the donor. Figure 5 shows that this prerequisite is met in the binding of crocetin.

The magnitude of the fluorescence quenching observed for crocetin binding to bovine and human plasma albumin is greater than that observed for long-chain fatty acids. The maximum reduction in fluorescence

intensity for crocetin binding to both proteins was 81%, while the maximum reduction reported for free fatty acid binding was 45% [oleate and other free fatty acids are less than 45% (20)]. However, the degree of quenching is similar to that reported for polyene fatty acids bound to albumin (~68 and 90% for *cis*-eleostearic and *cis*-parinaric acids for bovine albumin, respectively (27), and ~61 and 84%, respectively, for human albumin) (28).

Since crocetin has a carboxyl group at both ends of the hydrocarbon chain, one might anticipate that the structural changes within the nonpolar binding pocket would be more dramatic. This would translate as greater changes in the tryptophan environment and, in turn, greater fluorescence quenching. Because the monocarboxylic polyene acids produce similar quenching and because the strongest hydrophobic interactions probably occur along the carbon chain and not at the deepest point of penetration within the binding pocket, we conclude that radiationless energy transfer causes most of the fluorescence quenching. However, this does not preclude the possibility of greater structural changes when crocetin binds to albumin. The highly efficient energy transfer process conceals any additional quenching due to structural changes, but the blue shift in the fluorescence of bovine albumin illustrates that there are environmental changes that occur as crocetin binds.

The results clearly indicate that crocetin binds strongly to albumin. Competitive binding experiments with palmitate suggest that crocetin binds to the same albumin binding sites that are employed by free fatty acids. When crocetin is added to whole blood *in vitro*, its visible absorption spectrum is red shifted, indicating albumin binding. From these results it is suggested that plasma albumin may serve as the primary transport vehicle for crocetin. Other possibilities, such as plasma lipoprotein transport, cannot be eliminated at this time, but regardless of the transport vehicle, only exceedingly small quantities of free, unbound crocetin can be present in the plasma. Thus, the mechanism by which crocetin reduces the effects of experimental atherosclerosis and increases oxygen diffusivity must reflect strong plasma albumin binding. There are a number of possible mechanisms. First, the increase in oxygen diffusivity could be a direct consequence of crocetin binding to the albumin. An increase in the level of plasma protein results in a large decrease in the diffusion rate of oxygen through blood plasma (10). However, crocetin was found to bring about a large increase in the oxygen diffusivity in plasma, even in the presence of increased plasma protein levels (8). By binding to albumin, crocetin may offset the decrease in diffusivity which would otherwise occur. There are other more indirect mechanisms that may be responsible for crocetin's observed activity. On a purely speculative basis the following possibilities are proposed: (*a*) a rearrangement of crocetin to form a pseudoprostaglandin, initiated by free radical peroxidation, (*b*) crocetin or crocetin–cholesterol liquid crystal formation, (*c*) membrane interactions, or (*d*) perhaps the involvement of the molecular species responsible for the reversible color change.

REFERENCES

(1) M. C. Meyer and D. E. Guttman, *J. Pharm. Sci.*, **57,** 895 (1968).

(2) J. J. Vallner, *ibid.*, **66,** 447 (1977).

(3) A. A. Spector, in "Progress in Biochemical Pharmacology," W. L. Holmes and W. M. Bortz, Eds., **6,** 130 (1971).

(4) D. S. Fredrickson and R. S. Gordon, *J. Clin. Invest.*, **37,** 1504 (1958).

(5) R. J. Havel, A. Naimark, and Borchgrevink, *ibid.*, **42,** 1054 (1963).

(6) A. A. Spector, *J. Lipid Res.*, **16,** 165 (1975).

(7) J. L. Gainer and J. R. Jones, *Experientia*, **31,** 548 (1975).

(8) J. L. Gainer and G. M. Chisolm, III, *Atherosclerosis*, **19,** 135 (1974).

(9) J. D. Pool, J. L. Gainer, and G. M. Chisolm, III, "Atherosclerosis Drug Discovery," *Advances in Expt'l Medicine and Biology*, **67,** 205 (1976), edited by C. E. Day.

(10) G. M. Chisolm, J. L. Gainer, G. E. Stoner, and J. V. Gainer, Jr., *Atherosclerosis*, **15,** 327 (1972).

(11) J. V. Gainer, Jr., U.S. Pat. No. 4,070,460, Jan. 24, 1978.

(12) J. L. Gainer, U.S. Pat. No. 4,038,144 July 29, 1977.

(13) E. S. Wilkins, *Diss. Abstr. Int.* B, **37,** 3529 (1977).

(14) E. S. Wilkins, J. L. Gainer, and M. G. Wilkins, *Experientia*, **33,** 1028 (1977).

(15) J. V. Gainer, Jr., U.S. Pat. No. 4,009,270, Feb. 22, 1977.

(16) J. L. Gainer, U.S. Pat. No. 3,965,261 Apr. 29, 1975.

(17) J. L. Gainer, *Oncology*, **33,** 222 (1976).

(18) J. L. Gainer, U.S. Pat. No. 4,046,880, Apr. 20, 1976.

(19) R. F. Chen, *J. Biol. Chem.*, **242,** 173 (1967).

(20) A. A. Spector and K. M. John, *Arch. Biochem. Biophys.*, **127,** 65 (1968).

(21) A. A. Spector and K. M. John, *Circulation, Suppl. II*, **36,** 38 (1976).

(22) A. A. Spector, J. E. Fletcher, and J. D. Ashbrook, *Biochemistry*, **10,** 3229 (1971).

(23) J. D. Ashbrook, A. A. Spector, E. C. Santos, and J. E. Fletcher, *J. Biol. Chem.*, **250,** 233 (1974).

(24) J. D. Ashbrook, A. A. Spector, and J. E. Fletcher, *ibid.*, **247,** 7038 (1972).

(25) C. C. Bigelow and M. Sonenberg, *Biochemistry*, **1,** 197 (1962).

(26) G. Scatchard, *Ann. N.Y. Acad. Sci.*, **51,** 660 (1949).

(27) L. A. Sklar, B. S. Hudson, and R. D. Simoni, *Biochemistry*, **16,** 5100 (1977).

(28) C. B. Berde, B. S. Hudson, R. D. Simoni, and L. A. Sklar, *J. Biol. Chem.*, **254,** 391 (1979).

(29) I. Z. Steinberg, *Ann. Rev. Biochem.*, **40,** 83 (1971).

ACKNOWLEDGMENTS

The authors gratefully acknowledge the support of this work by the Research Corporation (Cottell College Science Grant, TLM) and the American Heart Association Northeastern Pennsylvania Chapter (Undergraduate Research Grant-In-Aid, MEM). They also thank Michael H. Klapper, The Ohio State University, for making his fluorescence instrument available to us.

Synthesis and Biological Investigations of Some 5*H*-1,3,4-Oxadiazolo[3,2-*a*]pyrimidin-5-ones

FARID S. G. SOLIMAN ˣ, RAGAB M. SHAFIK, and MAGDA DARWISH

Received May 20, 1981, from the *Department of Pharmaceutical Chemistry, Faculty of Pharmacy, University of Alexandria, A.R. Egypt.* Accepted for publication June 16, 1981.

Abstract □ The synthesis of some substituted 7-hydroxy-5*H*-1,3,4-oxadiazolo [3,2-*a*]pyrimidin-5-ones, a class of bicyclics with unexplored pharmacotoxicological properties, is described. Reacting the 2-phenyl derivative with bis(2,4,6-trichlorophenyl)benzylmalonate afforded a linear pyrano-oxadiazolopyrimidinedione. The assigned structures were verified by IR, ^{1}H-NMR, and mass spectral studies. Six compounds of the series were screened for *in vitro* antibacterial and antifungal activities. The effect of four compounds on alkaline phosphatase enzyme was also examined.

Keyphrases □ 5*H*-1,3,4-Oxadiazolo[3,2-*a*]pyrimidin-5-ones—synthesis, screening for antibacterial and antifungal properties and phosphatase inhibition □ ^{1}H-NMR—characterization of 5*H*-1,3,4-oxadiazolo[3,2-*a*]pyrimidin-5-ones □ Mass spectrometry—characterization of 5*H*-1,3,4-oxadiazolo[3,2-*a*]pyrimidin-5-ones

A number of syntheses of substituted 5*H*-1,3,4-oxadiazolo[3,2-*a*]pyrimidin-5-ones (I) have been described in the literature. The 7-hydroxy derivative of I was first produced from 2-amino-1,3,4-oxadiazole and carbon suboxide (1). Ethyl 2-substituted-5-oxo-5*H*-1,3,4-oxadiazolo[3,2-*a*]pyrimidine-6-carboxylates were prepared by fusing 2-amino-5-substituted-1,3,4-oxadiazoles with ethyl ethoxymethylenemalonate and subsequent ring closure of the formed 2-(β,β-dicarbethoxyvinylamino)-1,3,4-oxadiazole derivatives (2). Analogously, 7-methyl-2-substituted-5*H*-1,3,4-oxadiazolo[3,2-*a*]pyrimidin-5-ones have been obtained from 2-aminooxadiazoles and ethyl acetoacetate (2). Reacting 2-amino-1,3,4-oxadiazoles with acetylenemono- or acetylenedicarboxylates afforded the 2-substituted or the 2-substituted-7-carboxylate derivatives of I, respectively (3). 6-Acetyl-2-phenyl-5*H*-1,3,4-oxadiazolo[3,2-*a*]pyrimidin-5-one was obtained *via* interaction of *N'*-2-(5-phenyl-1,3,4-oxadiazolyl)-*N*,*N*-dimethylformamidine with diketene (4). Furthermore, the preparation of some 6,7-dihydro derivatives of I was achieved either by cyclizing 3-(β-chloropropionyl)-2-imino-5-substituted-1,3,4-oxadiazolines (5) or through cycloaddition of diphenylketene with 2-arylideneamino-1,3,4-oxadiazoles (6). On the other hand, class II mesoionic 1,3,4-oxadiazolo[3,2-*a*]pyrimidine-5,6-diones, which can be regarded as isoelectronic and isosteric to xanthines, have been postulated among different bicyclic mesoionic heteroaromatic structures, called mesoionic purinone analogs (7).

There has been no report concerning the bioactivities of such compounds. In contrast, some bioisosteric sulfur analogs derived from 5*H*-1,3,4-thiadiazolo[3,2-*a*]pyrimidin-5-one reportedly possess herbicidal and pesticidal potencies (8). In addition, a number of class-II mesoionic 1,3,4-thiadiazolo[3,2-*a*]pyrimidine-5,7-diones were either shown to display *in vitro* antibacterial activities (9, 10) or acted as inhibitors of adenosine-3',5'-monophosphate phosphodiesterase (11).

As a continuation of previous work (12), the synthesis of various 7-hydroxy-5*H*-1,3,4-oxadiazolo[3,2-*a*]pyrimidin-5-one derivatives was undertaken, and some representative compounds were screened for *in vitro* antimicrobial activity. Because of the potency of the mesoionic

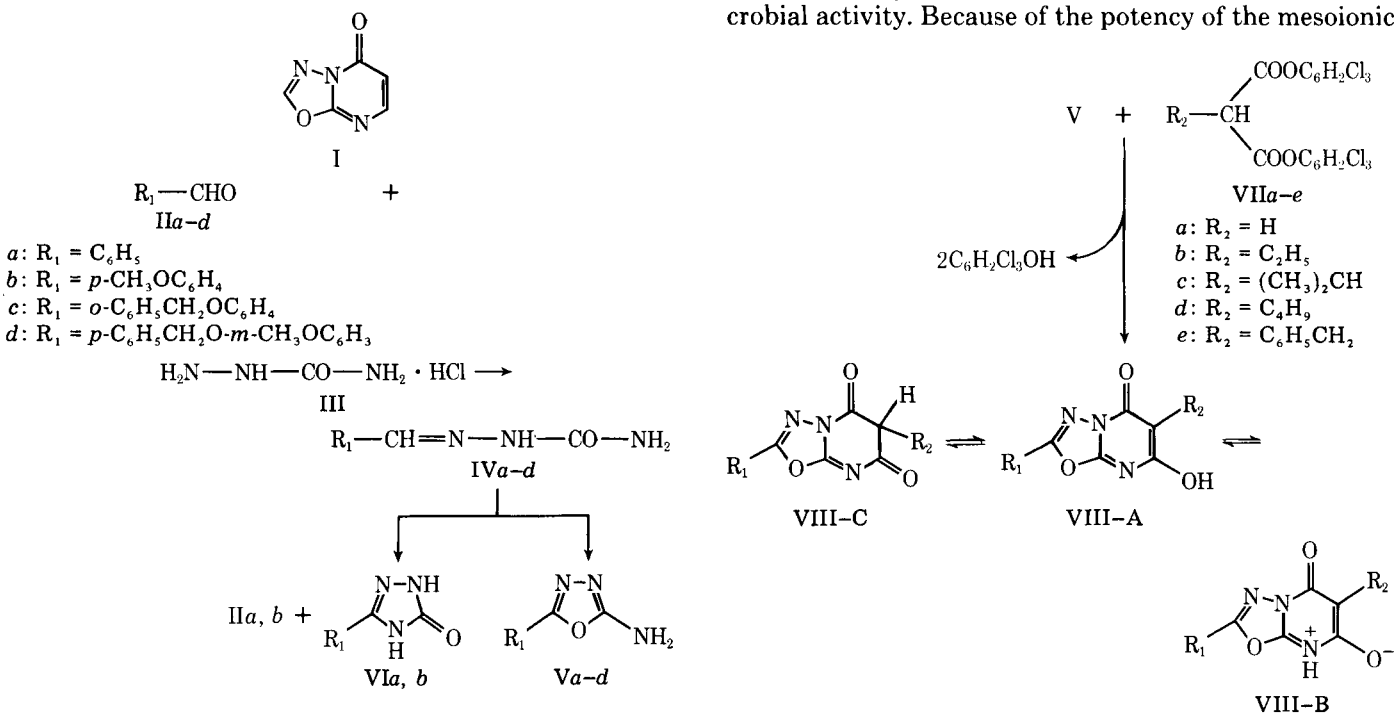

Scheme I

0022-3549/82/0200-0178$01.00/0

Table I—Substituted 7-Hydroxy-5*H*-1,3,4-Oxadiazolo[3,2-*a*]pyrimidin-5-ones (VIII)

Compound	R_1	R_2	Melting Point (Recrystallization Solvent)	Yield, %	Molecular Formula	Analysis, % Calc.	Found	IR,[a] cm^{-1}
VIII*a*	C_6H_5	H	246–248° dec. (ethanol)	88	$C_{11}H_7N_3O_3$	C 57.6 H 3.1 N 18.3	57.3 3.0 18.4	3340–2500 (bm, OH and NH); a split band at 1715 (m, C=O), 1680 (s); 1615 (s); 1580 (s); 1545 (w); 1510 (m, C=N, C=C, and aromatics); 1255 (bs) shouldered at 1220; and 1015 (w, C–O–C)[b]
VIII*b*	C_6H_5	C_2H_5	265–268° dec. (ethanol)	70	$C_{13}H_{11}N_3O_3$	C 60.7 H 4.3 N 16.3	61.0 4.6 16.7	3300–2500 (b, OH and NH)[c]; 1670 (s, C=O) 1635 (w); 1605 (s), 1570 (m); 1540 (bs) shouldered at 1520; and at 1510 (C=N, C=C and aromatics); 1255 (s); and 1025 (m, C–O–C).
VIII*c*	C_6H_5	C_4H_9	208–210° (ethanol–water)	58	$C_{15}H_{15}N_3O_3$	C 63.15 H 5.3 N 14.7	63.3 5.6 14.3	3300–2500 (b, OH and NH)[c]; a split band at 1685 (s, C=O); 1655 (m); 1610 (m); 1560 (s) shouldered at 1575; 1540; and at 1525 (C=N, C=C, and aromatics); 1275 (m); and 1025 (m, C–O–C).
VIII*d*	*p*-$CH_3OC_6H_4$	H	246–248° dec. (ethanol)	85	$C_{12}H_9N_3O_4$	C 55.6 H 3.5 N 16.2	55.9 3.7 16.5	3350–2500 (bm, OH and NH); 1685 (m) shouldered at 1710 (C=O); 1620 (s); 1580 (m); 1550 (w); 1515 (s, C=N, C=C, and aromatics); 1265 (bs); and 1015 (m) (C–O–C)[b].
VIII*e*	*p*-$CH_3OC_6H_4$	C_2H_5	257–258° (ethanol)	83	$C_{14}H_{13}N_3O_4$	C 58.5 H 4.6 N 14.6	59.1 4.6 14.6	3300–2500 (bm) (OH and NH); 1680 (s, C=O), 1620 (s) shouldered at 1635; 1580 (w); 1540 (m), 1520 (s) (C=N, C=C, and aromatics), 1270 (s), and 1020 (m) (C–O–C)[b].
VIII*f*	*p*-$CH_3OC_6H_4$	$C_6H_5CH_2$	256–258° (ethanol)	86	$C_{19}H_{15}N_3O_4$	C 65.3 H 4.3 N 12.0	65.2 4.1 12.1	3350–2500 (bm, OH and NH); 1710 (s, C=O); 1660 (m); 1620 (s); 1575 (m); 1510 (m, C=N, C=C, and aromatics), 1260 (s), and 1020 (m) (C–O–C)[b].
VIII*g*	*o*-$C_6H_5CH_2OC_6H_4$	H	215–217° dec. (ethanol)	89.5	$C_{18}H_{13}N_3O_4$	C 64.5 H 3.9 N 12.5	64.2 4.0 12.0	3200–2400 (b, OH and NH)[d], a split band at 1685 (m, C=O); 1650 (s); 1605 (s), 1585 (w), 1560 (s, C=N, C=C and aromatics); 1265 (s); and 1025 (m, C–O–C).
VIII*h*	*o*-$C_6H_5CH_2OC_6H_4$	$(CH_3)_2CH$	198–199° (methanol–water)	68	$C_{21}H_{19}N_3O_4$	C 66.8 H 5.1 N 11.1	66.8 5.1 10.9	3240–2500 (b, OH and NH)[c]; a split band at 1685 (s, (C=O); 1650 (w); 1610 (m); 1555 (m) shouldered at 1540; 1520; 1495 (m, C=N, C=C and aromatics); 1260 (m); 1025 (m, C–O–C).
VIII*i*	*o*-$C_6H_5CH_2OC_6H_4$	$C_6H_5CH_2$	230–232° (ethanol)	94	$C_{25}H_{19}N_3O_4$	C 70.6 H 4.5 N 9.9	70.3 4.4 10.1	3200–2300 (b, OH and NH)[c]; 1670 (m, C=O); 1605 (s); 1575 (w); 1525 (s, C=N, C=C, and aromatics); 1260 (s); and 1035 (s, C–O–C).
VIII*j*	*p*-$C_6H_5CH_2O$-*m*-$CH_3OC_6H_3$	H	257–259° dec. (dimethylformamide–ethanol)	86	$C_{19}H_{15}N_3O_5$	C 62.5 H 4.1 N 11.5	62.5 4.5 11.1	3400–2500 (bm, OH and NH); a split band at 1720 (m) C=O); 1680 (s); 1620 (s); 1585 (m); 1525 (s) shouldered at 1550 and at 1510 (C=N, C=C and aromatics), 1250 (s) and 1020 (*m*, C–O–C)[b].

[a] The abbreviation b is broad, bm is broad medium, bs is broad strong, m is medium, and s is strong. [b] For potassium bromide disc. [c] Overlapped by the Nujol absorption bond.

thiadiazolopyrimidines, the similarity in structural features of the adopted ring system (I) to xanthines, and the reported association of antimicrobial activities with 1,3,4-oxadiazoles (13, 14) and pyrimidine derivatives (15–17), the effect on alkaline phosphatase enzyme was also studied. The susceptibility of the 1,3,4-oxadiazole moiety to attack with potassium hydroxide (2) and amines (18) may be important to the predicted bioactivity of the prepared compounds.

RESULTS AND DISCUSSION

Chemistry—The reactions outlined in Schemes I and II were followed for the synthesis of the desired compounds. The key intermediates, 2-amino-5-aryl-1,3,4-oxadiazoles (V) were prepared by first condensing the chosen aldehydes (II) with semicarbazide hydrochloride (III) in the presence of sodium acetate followed by oxidative ring closure of the resulting aldehyde semicarbazones (IV) with aqueous iodine–potassium iodide in presence of sodium carbonate (19). A previous report (20) showed that the exclusion of sodium carbonate in the cyclization of IV*a* and IV*b* leads to the formation of the corresponding 5-aryl-2,4-dihy-

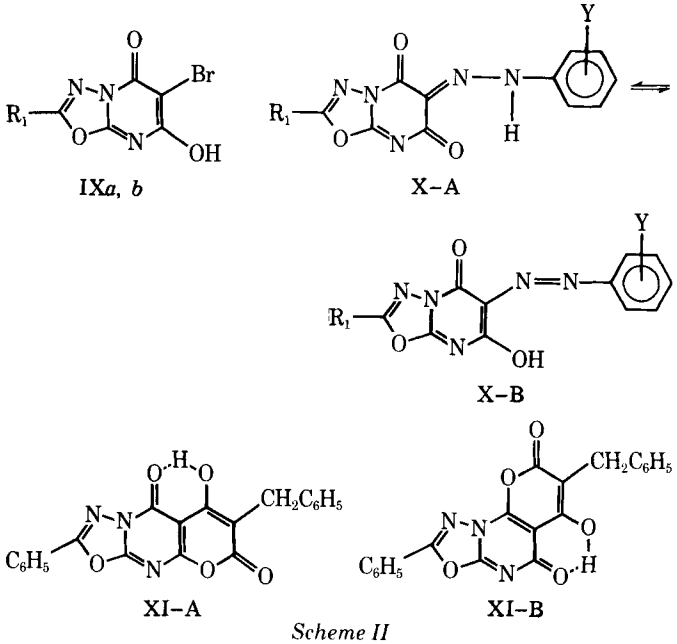

IXa, b X-A X-B XI-A XI-B

Scheme II

dro-3*H*-1,2,4-triazol-3-ones (VI*a*) and (VI*b*) in low yields alongside their parent aldehydes II*a* and II*b*, respectively. The synthesis of the semicarbazones, IV*c* and IV*d*, and their respective oxadiazoles, V*c* and V*d*, have not been reported previously.

Reacting equimolar quantities of V with unsubstituted or monosubstituted bis(2,4,6-trichlorophenyl)malonates (VII) in boiling chlorobenzene afforded high yields of substituted 7-hydroxy-5*H*-1,3,4-oxadiazolo[3,2-*a*]pyrimidin-5-ones (VIII). The reaction involved an intermediate ketene–carboxylate which formed *in situ* from VII at elevated temperatures (21). The IR and ^{1}H-NMR data of VIII (Tables I and II) indicated mostly forms VIII-A and/or VIII-B rather than VIII-C. This is analogous to the structures previously assigned to some related hydroxypyridone systems (22).

The mass spectral data of representative compounds of VIII are recorded in Table II. Compounds VIII*a*, *d*, *e*, and *f* showed molecular ions of relatively low intensity (12–32%). Although the benzoyl cations constituted the base peak of the spectra of VIII*a*, *d*, and *e*, the spectrum of VIII*f* showed the *p*-methoxybenzoyl cation (*m/z* 135) at a lower abundance (56%). All mass spectra showed an ion corresponding to the loss of a fragment (*m/z* 43) from the parent molecule which might be HCNO.

The reactivity of position 6 in the 6-unsubstituted analogs of VIII towards electrophilic attack was considered in order to search for more diverse derivatives. Treatment of VIII*a* or VIII*d* with bromine yielded the corresponding 6-bromo derivatives IX*a* and IX*b*, respectively. Diazocoupling of VIII*a*, *d*, or *g* with either diazotized aniline or an appropriate diazotized sulfonamide in aqueous acetic acid medium provided 6-phenylazo- or 6-(4-substituted sulfonamidophenylazo) derivatives, respectively (X, Table III). The IR (KBr) spectrum of X*a* displayed a broad weak O–H and/or N–H stretching absorption band between 3150–2800 cm^{-1}, suggesting that the azo forms (X-A) exist in equilibrium with their hydrazono tautomers (X-B).

On the other hand, when VIII*a* was condensed with bis(2,4,6-trichlorophenyl)benzylmalonate (VII*e*) in refluxing bromobenzene, a single product was isolated for which the elemental analysis and molecular ion peak coincided with the tricyclic derivative XI-A or XI-B. The linear structure XI-A was shown to be consistent with the IR (KBr) spectrum, since it revealed the tertiary amide–carbonyl stretching absorption at 1690 cm^{-1}. If the angular isomer XI-B was formed it would have displayed this band at a lower frequency.

Determination of Antimicrobial Activity[1]—Compounds VIII*a*, *b*, *d*, *e*, *f*, and *g*[2] were tested for *in vitro* activity against four bacteria: *Staphylococcus aureus* (209 P), *Escherichia coli* (K802N), *Salmonella gallinarum* (595), and *Klebsiella pneumoniae* (SK&F 4200); and three fungi, *Candida albicans* (B-311, BC-759), and *Trichophyton mentagrophytes* (AAB-995). Microtiter twofold broth dilution methods were used to determine the minimum inhibitory concentrations of the compounds in micrograms per milliliter at which the growth of the test cultures are completely suppressed.

The antibacterial activity was determined in trypticase soy broth. The compounds were run at concentrations of 0.2–200 μg/ml. Log cultures of the bacterial strains were diluted so that the inoculum was 10^5 cfu/ml in the test. The microtiter plates were incubated at 37° overnight and observed for inhibition of growth.

The antifungal activity was determined in Sabouraud glucose broth and the compounds were run at concentrations of 0.2–200 μg/ml. Log cultures of the *Candida* strains were used for the inoculum which was 10^5 cfu/ml in the test. Spore suspensions in the glucose broth were prepared from cultures grown on glucose broth agar slants for the *T. mentagrophytes* inoculum. The plates were incubated at 30° and observed for growth at 24 and 48 hr.

Dimethyl sulfoxide–methanol mixture (1:50) was used as the solvent for the compounds. A control without the test compound was included for each organism. Gentamicin and amphotericin B were used as standard antibiotics for comparison against the bacterial and fungal species utilized, respectively.

None of the compounds exhibited antimicrobial activity.

Inhibition of Alkaline Phosphatase[3]—Compounds VIII*d*, *e*, *f*, and *g* were tested for *in vitro* inhibitory activity of alkaline phosphatase following a reported method (23).

Table II—PMR and Mass Spectrometric Data of Some Substituted 5*H*-1,3,4-Oxadiazolo[3,2-*a*]pyrimidin-5-ones (VIII)

Compound	^{1}H-NMR (δppm)	Mass Spectrum: *m/z* Values (Relative abundance, %)
VIII*a*	6.7 (s, 1H, H at C-6), and 7.9–8.75 (m, 5H, aromatic H)[a].	230 (5, M + 1), 229 (32, M^+), 201 (8), 187 (19, M-CH_2=C=O), 186 (85), 161 (24), 145 (37), 138 (14), 118 (21), 112 (11), 106 (14), 105 (100), 91 (23), 89 (19), 77 (27, $C_6H_5^+$).
VIII*d*	3.8 (s, 3H, CH_3O), 5.25 (s, 1H, H at C-6), 7.1 (d, 2H, *J* = 8 Hz, aromatic H), 7.9 (d, 2H, *J* = 8 Hz, aromatic H), and 11.0 (broad, OH).	260 (6, M + 1), 259 (30, M^+), 217 (20, M-CH_2=C=O), 216 (91), 201 (10), 186 (14), 175 (15), 158 (8), 149 (24, *p*-$CH_3OC_6H_4CNO^+$), 136 (14), 135 (100), 134 (8), 133 (45, *p*-$CH_3OC_6H_4$-CN^+), 105 (23).
VIII*e*	1.0 (t, 3H, *J* = 7Hz), CH_3-ethyl), 2.4 (q, 2H, *J* = 7 Hz, CH_2-ethyl), 3.85 (s, 3H, CH_3O), 7.1 (d, 2H, *J* = 8 Hz, aromatic H), 7.9 (d, 2H, *J* = 8 Hz, aromatic H), and 12.0 (broad, OH).	288 (5, M + 1), 287 (12, M^+), 245 (8), 244 (17), 229 (5), 223 (5), 216 (14), 201 (16), 191 (24), 186 (10), 149 (30, *p*-CH_3O-$C_6H_4CNO^+$), 136 (14) 135 (100), 134 (12), 133 (39, *p*-$CH_3OC_6H_5CN^+$), 105 (24), 77 (34), $C_6H_5^+$).
VIII*f*	3.75 (s, 2H, CH_2-benzyl), 3.85 (s, 3H, CH_3O), 7.2 (d, 7H, *J* = 8 Hz, aromatic H), 7.95 (d, 2H, *J* = 8 Hz, aromatic H), and 10.0 (broad, OH).	350 (8, M + 1), 349 (32, M^+, 306 (20), 278 (20), 277 (24), 264 (12), 247 (8), 218 (8, M-C_6H_5-$CH_2\dot{C}$=C=O), 215 (8), 149 (16, *p*-CH_3O-$C_6H_4CNO^+$), 139 (24), 135 (56), 133 (68, *p*-$CH_3OC_6H_5CN^+$), 103 (40), 91 (56, $C_6H_5CH_2^+$), 77 (40, $C_6H_5^+$), 44 (100).

[a] Trifluoroacetic acid was used as solvent.

[1] Conducted by Smith Kline & French Laboratories, Philadelphia, Pa.

[2] Smith Kline & French Nos. 88347, 88350, 88349, 88351, 88355, and 88354, respectively.

[3] Conducted in the Department of Pesticides and Plant Protection, Faculty of Agriculture, University of Alexandria, A.R. Egypt.

Table III—2-Aryl-7-hydroxy-6-(*p*-substituted phenylazo)-5*H*-1,3,4-oxadiazolo[3,2-*a*]pyrimidin-5-ones (X)

Compound	R_1	Y	Melting Point (Recrystallization Solvent)	Yield, %	Molecular Formula	Analysis, % Calc.	Found	IR[b], cm^{-1}
X*a*[a]	C_6H_5	H	268–269° dec. (dimethylformamide–ethanol)	85	$C_{17}H_{11}N_5O_3$	C 61.3 H 3.3 N 21.0	61.0 3.3 21.3	3150–2800 (bw, OH and/or NH), 1735 (s, C=O), 1665 (m), a band split at 1610 (s), 1590 (s), 1575 (s), 1500 (s), 1460 (m, C=N, C=C and aromatics) a band split at 1225 (m) and at 1245 (w), and 1020 (m, C–O–C)[c].
X*b*	*p*-CH_3O-C_6H_4	*p*-H_2NSO_2-	288–290° dec. (dimethylformamide–water)	78.5	$C_{18}H_{14}N_6O_6S$	C 48.9 H 3.2 N 19.0 S 7.25	48.8 3.6 19.1 6.9	3370 (m), 3270 (m, NH and OH)[d], 1725 (s, C=O), 1650 (m), 1615 (s) shouldered at 1575, 1505 (s, C=N, C=C and aromatics), 1320 (m, asymmetric SO_2), 1255 (s, C–O–C), 1150 (s, symmetric SO_2), and 1025 (m, C–O–C).
X*c*	*p*-CH_3O-C_6H_4	*p*- 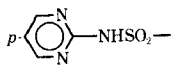 -$NHSO_2$-	304–305° dec. (dimethylformamide–ethanol)	34.5	$C_{22}H_{16}N_8O_6S$	C 50.8 H 3.1 S 6.2	50.6 3.5 6.0	3250–2400 (b, NH and OH)[d], 1720 (m, C=O), 1650 (w), a band split at 1605 (s) and 1575 (s, C=N and aromatics), 1250 (m, C–O–C), 1150 (s, SO_2), and 1030 (m, C–O–C) shouldered at 1010.
X*d*	*o*-C_6H_5-$CH_2OC_6H_4$	*p*-$H_2N-C(=NH)-NHSO_2$-	260° dec. (dimethylformamide–ethanol)	72.5	$C_{25}H_{20}N_8O_6S$	C 53.6 H 3.6 N 20.0 S 5.7	53.4 3.8 20.3 5.7	3500–3100 (m, with several splits, NH and OH)[d], 1715 (m, C=O), a band split at 1650 (m), 1620 (m), 1595 (s), 1580 (s), 1560 (s) and at 1520 (m, C=N, C=C, and aromatics), 1260 (s), and 1025 (s, C–O–C).

[a] ^{1}H-NMR (trifluoroacetic acid) δ: 7.3–8.25 (m, 10H, aromatic H) ppm. [b] b is broad, bm is broad-medium, m is medium, s is strong. [c] For potassium bromide disc. [d] Overlapped by the Nujol absorption band.

The butanol extractable alkaline phosphatase of the human placenta was partially purified as previously described for human liver alkaline phosphatase (24). The enzyme activity was measured at 25° by determining the hydrolysis rate of *p*-nitrophenyl phosphate using the change in absorbance at 410 nm with a spectrophotometer[4]. The reaction mixture contained 1.0 *M* tromethamine hydrochloride (pH 9.4), 10^{-3} *M* substrate, and 50 μl of enzyme in a final volume of 3 ml. The appropriate quantity of the compound dissolved in dimethyl sulfoxide (10^{-2}–10^{-4} *M* concentrations) was incubated with the enzyme in the reaction-buffer at room temperature for 10 min and the reaction was initiated by the addition of the substrate. A control containing dimethyl sulfoxide was included in all determinations.

No inhibition of enzyme activity was observed by any of the compounds tested.

EXPERIMENTAL[5]

Aldehyde Semicarbazones (IV)—These compounds were prepared by treating the appropriate aromatic aldehyde (II) with an equimolar amount of semicarbazide hydrochloride (III) and sodium acetate in aqueous ethanol. The semicarbazones were purified by recrystallization from ethanol.

***o*-Benzyloxybenzaldehyde Semicarbazone (IV*c*)**—The yield was 98% (mp 180–182°); IR: 3440, 3140 shouldered at 3340, 3260, and at 3200 (N–H), 1680 (C=O), 1580 (C=N, and aromatics), 1245, and 1020 (C–O–C) cm^{-1}.

Anal.—Calc. for $C_{15}H_{15}N_3O_2$: C, 66.9; H, 5.6; N, 15.6. Found: C, 66.6; H, 5.6; N, 15.9.

***p*-Benzyloxy-*m*-methoxybenzaldehyde Semicarbazone (IV*d*)**—The yield was 97% (mp 163–164°).

Anal.—Calc. for $C_{16}H_{17}N_3O_3$: C, 64.2; H, 5.7; N, 14.0. Found: C, 64.3; H, 5.8; N, 13.8.

2-Amino-5-aryl-1,3,4-oxadiazoles (V)—These were prepared from IV by a reported method (19).

2-Amino-5-(*o*-benzyloxyphenyl)-1,3,4-oxadiazole (V*c*)—This compound was recrystallized from ethanol, mp 207–209°. The yield was 59%; IR: 3250, 3080 (N–H), 1650 (C=N), 1590 (δN–H and aromatics), 1240, and 1025 (C–O–C) cm^{-1}.

Anal.—Calc. for $C_{15}H_{13}N_3O_2$: C, 67.4; H, 4.9; N, 15.7. Found: C, 67.5; H, 5.2; N, 16.0.

2-Amino-5-(*p*-benzyloxy-*m*-methoxyphenyl)-1,3,4-oxadiazole (V*d*)—This compound was recrystallized from aqueous ethanol, mp 209–210°. The yield was 34%; IR: 3360 (N–H), 1665 (C=N), 1580 shouldered at 1600 (δ N–H and aromatics), 1500, a band split at 1245 and at 1225, and 1030 (C–O–C) cm^{-1}.

Anal.—Calc. for $C_{16}H_{15}N_3O_3$: C, 64.6; H, 5.1; N, 14.1. Found: C, 64.5; H, 4.8; N, 13.6.

Substituted 7-hydroxy-5*H*-1,3,4-oxadiazolo[3,2-*a*]pyrimidin-5-ones (VIII, Table I)—The appropriate bis(2,4,6-trichlorophenyl)-malonate (VII, 1 mmole) was added in one portion to a hot suspension of the amine (V, 1 mmole) in chlorobenzene (15 ml). The mixture was refluxed for 30–60 min. After cooling the crystallized solid was filtered, washed with light petroleum (bp 40–60°), and dried. In some cases, the cooled reaction mixture was treated with an equal volume of light petroleum to precipitate all the product. The compound was recrystallized from the appropriate solvent.

6-Bromo-7-hydroxy-2-phenyl-5*H*-1,3,4-oxadiazolo[3,2-*a*]pyrimidin-5-one (IX*a*)—Bromine (0.05 ml, 1 mmole) was added in one portion to a stirred solution of VIII*a* (0.23 g, 1 mmole) in acetic acid (30 ml) at room temperature. The color of bromine was immediately discharged with liberation of hydrogen bromide and precipitation of the bromo derivative. After 2 hr at room temperature the product was filtered, washed with ethanol, dried, and recrystallized from acetic acid, mp 265–267° dec. The yield was 0.23 g (74.4%).

Anal.—Calc. for $C_{11}H_6BrN_3O_3$: C, 42.9; H, 2.0; Br, 25.9; N, 13.6. Found: C, 42.6; H, 2.2; Br, 26.0; N, 13.6.

6-Bromo-7-hydroxy-2-(*p*-methoxyphenyl)-5*H*-1,3,4-oxadiazolo[3,2-*a*]pyrimidin-5-one (IX*b*)—This compound was prepared by brominating VIII*d* (0.26 g, 1 mmole) with bromine (0.05 ml, 1 mmole) as described for IX*a*. It was recrystallized from acetic acid, mp 248–251° dec. The yield was 0.27 g (79.6%); IR (KBr): 3200–2300 (OH and NH), a band split at 1690 (C=O) and at 1660, a band split at 1615 and at 1600, 1510 shouldered at 1530 (C=N, C=C, and aromatics), 1270, and 1015 (C–O–C) cm^{-1}; mass spectrum: *m/z* (relative abundance, %), 339 (38) (M^+ of ^{81}Br), 338 (15), and 337 (35) (M^+ of ^{79}Br).

Anal.—Calc. for $C_{12}H_8BrN_3O_4$: C, 42.6; H, 2.4; Br, 23.6; N, 12.4. Found: C, 42.7; H, 2.6; Br, 24.0; N, 12.0.

7-Hydroxy-2-phenyl-6-phenylazo-5*H*-1,3,4-oxadiazolo[3,2-*a*]-pyrimidin-5-one (X*a*, Table III)—To a stirred solution of VIII*a* (0.23 g, 1 mmole) in ethanol (10 ml) at 10° was added a cold solution of aniline (0.09 ml, 1 mmole) and sodium nitrite (0.08 g, 1.1 mmole) in 50% aqueous acetic acid (10 ml). After stirring for 1 hr, the reaction mixture was re-

[4] Pye Unicam SP-100.

[5] Melting points were determined in open-glass capillaries and are uncorrected. IR spectra were recorded for Nujol mulls, unless otherwise specified, on a Beckman 4210; or for potassium bromide disks on a Perkin-Elmer 421 spectrophotometer. ^{1}H-NMR spectra were determined on a Varian EM 360 spectrometer using deuterated dimethyl sulfoxide as solvent, unless otherwise indicated, and tetramethylsilane as the internal standard. Mass spectra were obtained using a Varian Mat 111 (80 ev) instrument and peaks of relative intensity below 5% of the base peak were omitted. Microanalysis, for samples dried over phosphorus pentoxide at 70° under reduced pressure, was carried out at the Microanalytical Unit, University of Cairo, A.R. Egypt.

frigerated overnight and a yellow product was collected, washed with water, dried, and recrystallized.

2-Aryl-7-hydroxy-6-(*p*-substituted phenylazo)-5*H*-1,3,4-oxadiazolo [3,2-*a*]pyrimidin-5-ones (X*b–d*, Table III)—The appropriate sulfonamide (1 mmole) was dissolved in acetic acid (20 ml) and the solution was cooled to 5°. A cold solution of sodium nitrite (1.1 mmole) in water (5 ml) was added and the resulting diazonium salt solution was filtered into a stirred solution of the proper VIII (1 mmole) in acetic acid (50–100 ml) at 10°. The reaction mixture was then worked up as described for X*a*, and the yellow crude product crystallized from the suitable solvent.

Reaction of VIII*a* with Bis(2,4,6-trichlorophenyl)benzylmalonate. (VII*e*)—Equimolar amounts of VIII*a* (0.23 g, 1 mmole) and VII*e* (0.55 g, 1 mmole) were refluxed in bromobenzene (25 ml) for 3 hr. The product (XI-A) that separated out on cooling was filtered, washed with light petroleum, and dried. It was recrystallized from a large volume of boiling ethanol, mp 306–308°. The yield was 72%; IR (KBr): 3650–2900 (OH), 1750 (C=O, α-pyrone), 1690 (C=O, amide), a band split at 1620 and 1605, 1585, 1560, 1505 (C=N, C=C, and aromatics), 1255, and 1025 (C–O–C) cm^{-1}; mass spectrum: *m/z* (relative abundance, %) 387 (69) (M^+).

Anal.—Calc. for $C_{21}H_{13}N_3O_5$: C, 65.1; H, 3.4; N, 10.85. Found: C, 65.3; H, 3.7; N, 10.3.

REFERENCES

(1) E. Ziegler and R. Wolf, *Monatsh. Chem.*, **93,** 1441 (1962).

(2) H. Gehlen and B. Simon, *Arch. Pharm.*, **303,** 501 (1970).

(3) P. Henklein, G. Westphal, and R. Kraft, *Tetrahedron*, **29,** 2937 (1973).

(4) M. Sakamoto, K. Miyazawa, and Y. Tomimatsu, *Chem. Pharm. Bull.*, **25,** 3360 (1977).

(5) T. R. Vakula and V. R. Srimivasan, *Indian J. Chem.*, **9,** 901 (1971).

(6) M. Sakamoto, K. Miyazawa, and Y. Tomimatsu, *Chem. Pharm. Bull.*, **24,** 2532 (1976).

(7) R. A. Coburn, R. A. Carapelloti, and R. A. Glennon, *J. Heterocycl. Chem.*, **10,** 479 (1973).

(8) O. Takayuki, T. Eiji, and M. Kazuyuki, *J. Fac. Agric. Kyushu Univ.*, **19,** 91 (1975); through *Chem. Abstr.*, **83,** 127285r (1975).

(9) R. A. Coburn and R. A. Glennon, *J. Pharm. Sci.*, **62,** 1785 (1973).

(10) R. A. Coburn and R. A. Glennon, *J. Med. Chem.*, **17,** 1025 (1974).

(11) R. A. Glennon, M. E. Rogers, R. G. Bass, and S. B. Ryan, *J. Pharm. Sci.*, **67,** 1762 (1978).

(12) F. S. G. Soliman, A. A. B. Hazzaa, and S. A. Shams El-Dine, *Pharmazie*, **33,** 713 (1978).

(13) A. A. Pnomarev and Z. V. Til, *Zh. Obshch. Khim.*, **33,** 2368 (1963); through *Chem. Abstr.*, **59,** 15278b (1963).

(14) I. Mir, M. T. Siddiqui, and A. M. Comrie, *J. Chem. Soc. (C)*, **1971,** 2798.

(15) M. P. V. Boarland, J. F. W. McOmie, and R. N. Timms, *ibid.*, **1952,** 4691.

(16) M. Kawashima, *Chem. Pharm. Bull.*, **7,** 13 (1959).

(17) T. Nishimura, S. Fujita, A. Tanaka, K. Matsumoto, M. Kawakami, H. Fukuyasu, T. Fukuyasu, Y. Kazuno, and T. Watnabe, *Bokin Bobai*, **7,** T 159 (1979); through *Chem. Abstr.*, **91,** 211359r (1979).

(18) H. Gehlen and B. Simon, *Arch. Pharm.*, **303,** 511 (1970).

(19) H. Gehlen and K. Moeckel, *Ann. der Chemie.*, **651,** 133 (1962); through *Chem. Abstr.*, **57,** 3424 (1962).

(20) F. S. G. Soliman, R. M. Shafik, and M. Darwish, *Pharmazie*, **34,** 198 (1979).

(21) E. Ziegler, *Chimia*, **24,** 62 (1970).

(22) T. Kappe and E. Ziegler, *Angew. Chem. (Engl. Ed.)*, **13,** 491 (1974).

(23) M. H. Lee, Y. M. Huang, K. C. Agrawal, and A. C. Sartorelli, *Biochem. Pharmacol.*, **24,** 1175 (1975).

(24) J. M. Trépanier, L. E. Seargeant, and R. A. Stinson, *Biochem. J.*, **155,** 653 (1976).

ACKNOWLEDGMENTS

The authors thank Dr. W. Stadlbauer, Institut für Organische Chemie der Karl-Franzens-Universität, Graz, Austria, for providing samples of active malonic esters and for spectral determinations. They also thank Dr. C. E. Berkoff, Director, Organic Chemistry, Smith Kline & French Laboratories, Philadelphia, Pa., for arranging screening of compounds, and Mr. A. Pavloff, Senior Medicinal Chemist, Research Chemistry, for providing the antimicrobial test report. Thanks are also extended to Professor N. Mansour and Mrs. M. M. Khattab, Department of Pesticides and Plant Protection, Faculty of Agriculture, University of Alexandria, A. R. Egypt, for the alkaline phosphatase screen test.

Influence of Benzalkonium Chloride on the Dissolution Rate Behavior of Several Solid-Phase Preparations of Cholesterol in Bile Acid Solutions

KENNETH M. FELD, WILLIAM I. HIGUCHI ˣ, and CHING-CHIANG SU

Received April 28, 1980, from *The College of Pharmacy, The University of Michigan, Ann Arbor, MI 48109.* Accepted for publication June 2, 1981.

Abstract □ Cholesterol dissolution rate accelerators, such as benzalkonium chloride, function by reducing the interfacial barrier that exists between the negatively-charged bile acid micelle and the negatively-charged cholesterol surface. It has been proposed that this reaction is accomplished by the binding of the positively-charged accelerator to the negatively-charged micelle. An earlier report showed that different solid preparations of cholesterol give different dissolution rates under the same conditions and these differences can be primarily accounted for by variations in the interfacial transport constant (*P*). By using the rotating disk dissolution apparatus and the Levich theory it has been possible to study the dissolution behavior of different cholesterol solid phases as a function of the benzalkonium chloride concentration. It was shown that the ratios of *P* values for the different phases are relatively constant over the range of the accelerator concentrations. This suggests that the accelerators act primarily on the micelle to enhance dissolution rate.

Keyphrases □ Benzalkonium chloride—effect on dissolution of cholesterol preparations in bile acid solutions □ Dissolution—cholesterol preparations, effect of benzalkonium chloride, bile acid solutions □ Cholesterol—effect of benzalkonium chloride on dissolution, bile acid solutions □ Gallstone kinetics—effect of benzalkonium chloride on dissolution of cholesterol preparations in bile acid solutions

Physicochemical studies of gallstone (cholesterol) dissolution kinetics have been performed in these laboratories (1–7). Theoretical treatment (2) showed that *in vivo* dissolution of cholesterol gallstones occurred at much lower rates than expected if dissolution were totally diffusion controlled. It was proposed that interfacial factors may be

0022-3549/82/0200-0182$01.00/0

frigerated overnight and a yellow product was collected, washed with water, dried, and recrystallized.

2-Aryl-7-hydroxy-6-(*p*-substituted phenylazo)-5*H*-1,3,4-oxadiazolo [3,2-*a*]pyrimidin-5-ones (X*b–d*, Table III)—The appropriate sulfonamide (1 mmole) was dissolved in acetic acid (20 ml) and the solution was cooled to 5°. A cold solution of sodium nitrite (1.1 mmole) in water (5 ml) was added and the resulting diazonium salt solution was filtered into a stirred solution of the proper VIII (1 mmole) in acetic acid (50–100 ml) at 10°. The reaction mixture was then worked up as described for X*a*, and the yellow crude product crystallized from the suitable solvent.

Reaction of VIII*a* with Bis(2,4,6-trichlorophenyl)benzylmalonate. (VII*e*)—Equimolar amounts of VIII*a* (0.23 g, 1 mmole) and VII*e* (0.55 g, 1 mmole) were refluxed in bromobenzene (25 ml) for 3 hr. The product (XI-A) that separated out on cooling was filtered, washed with light petroleum, and dried. It was recrystallized from a large volume of boiling ethanol, mp 306–308°. The yield was 72%; IR (KBr): 3650–2900 (OH), 1750 (C=O, α-pyrone), 1690 (C=O, amide), a band split at 1620 and 1605, 1585, 1560, 1505 (C=N, C=C, and aromatics), 1255, and 1025 (C–O–C) cm^{-1}; mass spectrum: *m/z* (relative abundance, %) 387 (69) (M^+).

Anal.—Calc. for $C_{21}H_{13}N_3O_5$: C, 65.1; H, 3.4; N, 10.85. Found: C, 65.3; H, 3.7; N, 10.3.

REFERENCES

(1) E. Ziegler and R. Wolf, *Monatsh. Chem.*, **93,** 1441 (1962).

(2) H. Gehlen and B. Simon, *Arch. Pharm.*, **303,** 501 (1970).

(3) P. Henklein, G. Westphal, and R. Kraft, *Tetrahedron*, **29,** 2937 (1973).

(4) M. Sakamoto, K. Miyazawa, and Y. Tomimatsu, *Chem. Pharm. Bull.*, **25,** 3360 (1977).

(5) T. R. Vakula and V. R. Srimivasan, *Indian J. Chem.*, **9,** 901 (1971).

(6) M. Sakamoto, K. Miyazawa, and Y. Tomimatsu, *Chem. Pharm. Bull.*, **24,** 2532 (1976).

(7) R. A. Coburn, R. A. Carapelloti, and R. A. Glennon, *J. Heterocycl. Chem.*, **10,** 479 (1973).

(8) O. Takayuki, T. Eiji, and M. Kazuyuki, *J. Fac. Agric. Kyushu Univ.*, **19,** 91 (1975); through *Chem. Abstr.*, **83,** 127285r (1975).

(9) R. A. Coburn and R. A. Glennon, *J. Pharm. Sci.*, **62,** 1785 (1973).

(10) R. A. Coburn and R. A. Glennon, *J. Med. Chem.*, **17,** 1025 (1974).

(11) R. A. Glennon, M. E. Rogers, R. G. Bass, and S. B. Ryan, *J. Pharm. Sci.*, **67,** 1762 (1978).

(12) F. S. G. Soliman, A. A. B. Hazzaa, and S. A. Shams El-Dine, *Pharmazie*, **33,** 713 (1978).

(13) A. A. Pnomarev and Z. V. Til, *Zh. Obshch. Khim.*, **33,** 2368 (1963); through *Chem. Abstr.*, **59,** 15278b (1963).

(14) I. Mir, M. T. Siddiqui, and A. M. Comrie, *J. Chem. Soc. (C)*, **1971,** 2798.

(15) M. P. V. Boarland, J. F. W. McOmie, and R. N. Timms, *ibid.*, **1952,** 4691.

(16) M. Kawashima, *Chem. Pharm. Bull.*, **7,** 13 (1959).

(17) T. Nishimura, S. Fujita, A. Tanaka, K. Matsumoto, M. Kawakami, H. Fukuyasu, T. Fukuyasu, Y. Kazuno, and T. Watnabe, *Bokin Bobai*, **7,** T 159 (1979); through *Chem. Abstr.*, **91,** 211359r (1979).

(18) H. Gehlen and B. Simon, *Arch. Pharm.*, **303,** 511 (1970).

(19) H. Gehlen and K. Moeckel, *Ann. der Chemie.*, **651,** 133 (1962); through *Chem. Abstr.*, **57,** 3424 (1962).

(20) F. S. G. Soliman, R. M. Shafik, and M. Darwish, *Pharmazie*, **34,** 198 (1979).

(21) E. Ziegler, *Chimia*, **24,** 62 (1970).

(22) T. Kappe and E. Ziegler, *Angew. Chem. (Engl. Ed.)*, **13,** 491 (1974).

(23) M. H. Lee, Y. M. Huang, K. C. Agrawal, and A. C. Sartorelli, *Biochem. Pharmacol.*, **24,** 1175 (1975).

(24) J. M. Trépanier, L. E. Seargeant, and R. A. Stinson, *Biochem. J.*, **155,** 653 (1976).

ACKNOWLEDGMENTS

The authors thank Dr. W. Stadlbauer, Institut für Organische Chemie der Karl-Franzens-Universität, Graz, Austria, for providing samples of active malonic esters and for spectral determinations. They also thank Dr. C. E. Berkoff, Director, Organic Chemistry, Smith Kline & French Laboratories, Philadelphia, Pa., for arranging screening of compounds, and Mr. A. Pavloff, Senior Medicinal Chemist, Research Chemistry, for providing the antimicrobial test report. Thanks are also extended to Professor N. Mansour and Mrs. M. M. Khattab, Department of Pesticides and Plant Protection, Faculty of Agriculture, University of Alexandria, A. R. Egypt, for the alkaline phosphatase screen test.

Influence of Benzalkonium Chloride on the Dissolution Rate Behavior of Several Solid-Phase Preparations of Cholesterol in Bile Acid Solutions

KENNETH M. FELD, WILLIAM I. HIGUCHI ˣ, and CHING-CHIANG SU

Received April 28, 1980, from *The College of Pharmacy, The University of Michigan, Ann Arbor, MI 48109.* Accepted for publication June 2, 1981.

Abstract □ Cholesterol dissolution rate accelerators, such as benzalkonium chloride, function by reducing the interfacial barrier that exists between the negatively-charged bile acid micelle and the negatively-charged cholesterol surface. It has been proposed that this reaction is accomplished by the binding of the positively-charged accelerator to the negatively-charged micelle. An earlier report showed that different solid preparations of cholesterol give different dissolution rates under the same conditions and these differences can be primarily accounted for by variations in the interfacial transport constant (*P*). By using the rotating disk dissolution apparatus and the Levich theory it has been possible to study the dissolution behavior of different cholesterol solid phases as a function of the benzalkonium chloride concentration. It was shown that the ratios of *P* values for the different phases are relatively constant over the range of the accelerator concentrations. This suggests that the accelerators act primarily on the micelle to enhance dissolution rate.

Keyphrases □ Benzalkonium chloride—effect on dissolution of cholesterol preparations in bile acid solutions □ Dissolution—cholesterol preparations, effect of benzalkonium chloride, bile acid solutions □ Cholesterol—effect of benzalkonium chloride on dissolution, bile acid solutions □ Gallstone kinetics—effect of benzalkonium chloride on dissolution of cholesterol preparations in bile acid solutions

Physicochemical studies of gallstone (cholesterol) dissolution kinetics have been performed in these laboratories (1–7). Theoretical treatment (2) showed that *in vivo* dissolution of cholesterol gallstones occurred at much lower rates than expected if dissolution were totally diffusion controlled. It was proposed that interfacial factors may be

0022-3549/82/0200-0182$01.00/0

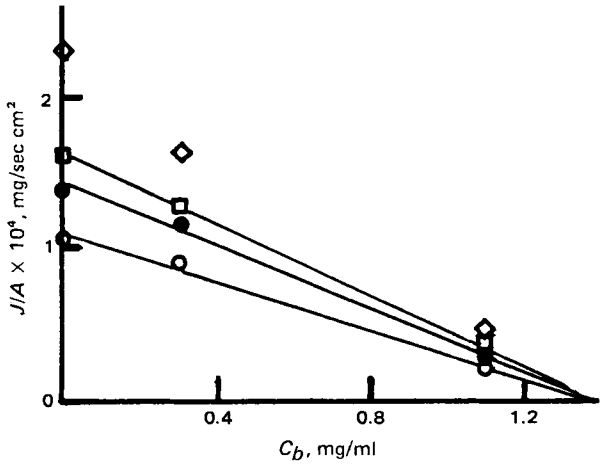

Figure 1—*Dissolution rate* versus *bulk concentration for the normal (I) pellets in 5% sodium cholate, 0.1* M *phosphate buffer, and 0.25% benzalkonium chloride at pH 8.0. Key:* ○, *20;* ●, *50;* □, *150; and* ◇, *450 rpm.*

important *in vivo*. It was also shown (1–3) that *in vitro* dissolution of cholesterol gallstones in simulated and in human bile was dominated by an interfacial barrier at the crystal-solution interface. Kwan *et al.* (6) studied the interfacial process as a function of bile acid type and concentration, bile acid/lecithin ratio, and electrolyte type and concentration. He found that the interfacially-controlled dissolution rate increased with increasing bile acid concentration, increasing bile acid/lecithin ratio, and increasing electrolyte concentration.

BACKGROUND

The elimination of this interfacial barrier by appropriate measures is expected to be clinically significant. Studies by Prakongpan *et al.* (4, 5) showed that when quaternary ammonium compounds were added to the bile acid–lecithin solutions, dissolution rates were enhanced tremendously and approach the diffusion-controlled rates at high concentration. Previous studies (8) on the acceleration effect of primary, secondary, and

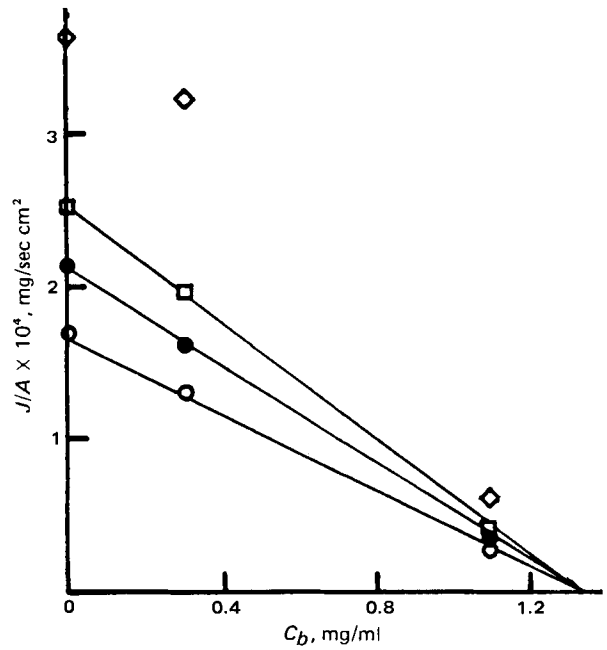

Figure 2—*Dissolution rate* versus *bulk concentration for the rapid (II) pellets in 5% sodium cholate, 0.1* M *phosphate buffer, and 0.25% benzalkonium chloride at pH 8.0. Key:* ○, *20;* ●, *50;* □, *150; and* ◇, *450 rpm.*

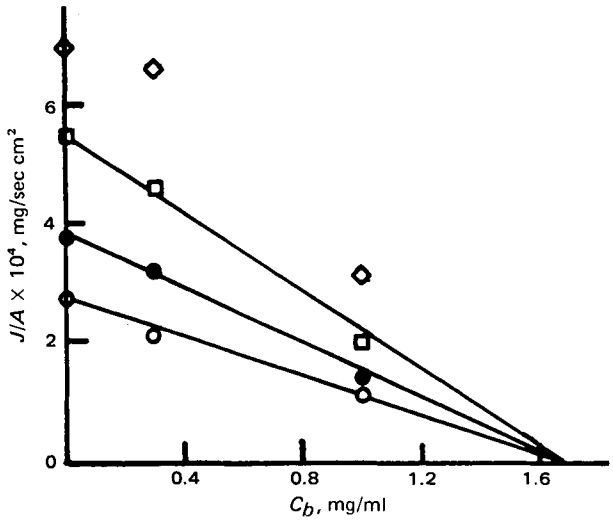

Figure 3—*Dissolution rate* versus *bulk concentration for the melt (III) pellets in 5% sodium cholate, 0.1* M *phosphate buffer, and 0.25% benzalkonium chloride at pH 8.0. Key:* ○, *20;* ●, *50;* □, *150; and* ◇, *450 rpm.*

tertiary amines, quaternary ammonium compounds, steroidal amines, and other surfactants, found that the cationic surfactants and the steroidal amines were effective, but the nonionic and anionic surfactants were not.

Other work (8) led to the following interpretations regarding dissolution mechanisms. Since the surface reaction rate increases with increasing micelle concentration (increasing bile acid concentration) and since the dissolution rate is very sensitive to electrolytes, it was concluded that the micelle is the primary carrier of cholesterol in the rate-limiting step. It was proposed that increasing the counterion concentration results in the reduction of the electrical repulsion which exists between the negatively-charged bile acid micelle and the negatively-charged cholesterol surface. The observation that only cationic surfactants were effective cholesterol dissolution accelerators was interpreted as: (*a*) adsorption of aliphatic long-chain cations on the cholesterol surface aids reduction of the electrical repulsion between the negatively-charged cholesterol surface and the negatively-charged micelle, and/or (*b*) the formation of mixed micelles which reduce the net negative charge on the micelle, thus easing the approach of the micelles to the charged surface.

Patel and Higuchi (9, 10) carried out a systematic study of cholesterol dissolution rate acceleration mechanisms. Using membrane transport

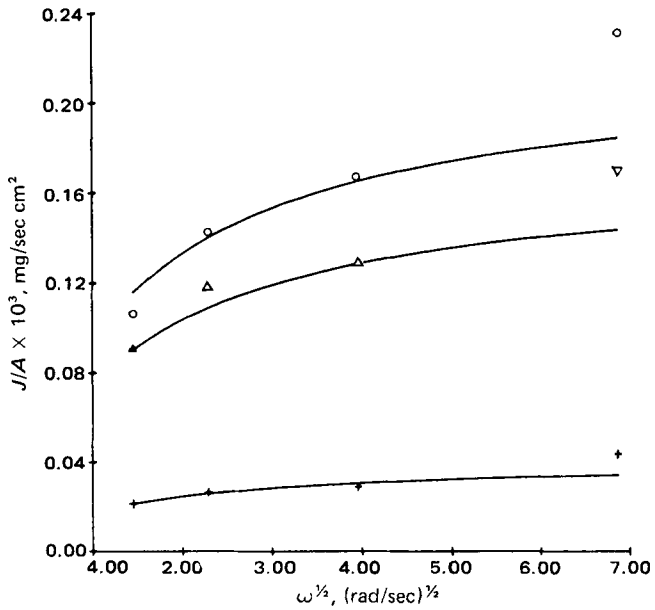

Figure 4—*Best-fit analysis of the normal pellets (I) in 5% sodium cholate, 0.1* M *phosphate buffer, and 0.25% benzalkonium chloride at pH 8.0. Key:* C_b = ○, *0.0;* △, *0.3; and* +, *1.1 mg/ml.*

Table I—Dissolution Rates of the Normal (I) Cholesterol Pellets under Partial Saturation Conditions in 5% Sodium Cholate, 0.1 *M* Phosphate Buffer, and Benzalkonium Chloride at pH 8.0

C_b, mg/ml	rpm	0.0% Benzalkonium Chloride $J/A \times 10^4 \pm$ Range[a], mg/sec cm^2	0.25% Benzalkonium Chloride $J/A \times 10^4 \pm$ Range[a], mg/sec cm^2	0.5% Benzalkonium Chloride $J/A \times 10^4 \pm$ Range[a], mg/sec cm^2
0.0	20	0.58 ± 0.01	1.07 ± 0.08	1.34 ± 0.02
	50	0.67 ± 0.04	1.43 ± 0.01	1.78 ± 0.05
	150	0.72 ± 0.01	1.68 ± 0.08	2.10 ± 0.02
	450	1.07 ± 0.03	2.31 ± 0.01	3.43 ± 0.05
0.2	20	0.52 ± 0.01	—	—
	50	0.54 ± 0.01	—	—
	150	0.59 ± 0.01	—	—
	450	0.88 ± 0.01	—	—
0.3	20	—	0.91 ± 0.03	1.09 ± 0.01
	50	—	1.18 ± 0.03	1.40 ± 0.04
	150	—	1.29 ± 0.03	1.76 ± 0.04
	450	—	1.68 ± 0.04	2.57 ± 0.04
1.1	20	0.14 ± 0.01	0.22 ± 0.01	0.27 ± 0.02
	50	0.15 ± 0.01	0.27 ± 0.01	0.32 ± 0.01
	150	0.16 ± 0.01	0.29 ± 0.01	0.36 ± 0.01
	450	0.22 ± 0.01	0.44 ± 0.04	0.62 ± 0.02

[a] Each J/A value is an average of two experiments and the range refers to the high and low values.

methods, the concentrations of bound and unbound accelerators were determined in the simulated bile acid solutions at low concentrations of accelerators. From the determinations of bound and unbound amine in simulated bile and from data on cholesterol dissolution rate acceleration, it was shown that the amount of bound amine correlated with the efficacy of cholesterol monohydrate dissolution rate acceleration and that the charged form of the amine was important. The electrophoretic mobility of chenodeoxycholate micelles was measured as a function of the amine concentration using the moving boundary electrophoresis method. In addition, particle microelectrophoresis studies showed that there was no significant surface charge variation on cholesterol particles as a function of amine concentration. From an analysis of these data, it was proposed that the predominant mechanism by which the amines enhanced the dissolution rate involved reducing the electrical charge of the bile acid micelles.

The present investigation studied the action of dissolution rate accelerators upon different solid cholesterol phases and attempted to determine the extent to which the donor phase may influence interfacial transfer acceleration kinetics.

THEORY

The rotating disk dissolution rate equation described previously (5) is appropriate for the present study. The following may be used to describe dissolution rate (11):

$$J = \frac{A(C_s - C_b)}{1.612D^{-2/3}\,\nu^{1/6}\,\omega^{-1/2} + 1/P} \qquad \text{(Eq. 1)}$$

where:

J = dissolution rate
A = apparent surface area of the pellet (cm^2)
D = diffusion coefficient (cm^2/sec)
ν = kinematic viscosity (cm^2/sec)
ω = angular velocity of rotation (radians/sec)
C_s = saturation solubility (mg/ml)
C_b = bulk concentration (mg/ml)
P = permeability coefficient (interfacial transport constant, cm/sec)

EXPERIMENTAL

Solutions—Sodium cholate test solutions were prepared by adding equivalent portions of cholic acid with sodium hydroxide. The pH of the solutions was then adjusted to 8.0. Dissolution rate accelerators (benzalkonium chloride) and buffers were added as needed. The solutions were allowed to equilibrate for 1 day before use.

Materials—Commercially obtained cholesterol[1] was recrystallized three times from 95% ethanol. Radioactive cholesterol monohydrate was prepared by mixing 100 μCi of [4-^{14}C]cholesterol with a given amount of the purified cholesterol at 60° in 400 ml of 95% ethanol. The solutions were then allowed to stand undisturbed for 2 days at room temperature. The crystals were filtered and dried *in vacuo* for 24 hr. The purified crystals were stored in the dark and in a container saturated with water vapor at room temperature.

[1] J. T. Baker Co., Phillipsburg, N.J.

Table II—Dissolution Rates of the Rapid Cholesterol (II) Pellets under Partial Saturation Conditions in 5% Sodium Cholate, 0.1 *M* Phosphate Buffer, and Benzalkonium Chloride at pH 8.0

C_b, mg/ml	rpm	0.0% Benzalkonium Chloride $J/A \times 10^4 \pm$ Range[a], mg/sec cm^2	0.25% Benzalkonium Chloride $J/A \times 10^4 \pm$ Range[a], mg/sec cm^2	0.50% Benzalkonium Chloride $J/A \times 10^4 \pm$ Range[a], mg/sec cm^2
0.0	20	0.85 ± 0.02	1.70 ± 0.00	1.94 ± 0.02
	50	0.96 ± 0.05	2.14 ± 0.17	2.59 ± 0.09
	150	1.18 ± 0.03	2.48 ± 0.07	3.33 ± 0.01
	450	1.44 ± 0.04	3.68 ± 0.06	4.51 ± 0.01
0.3	20	0.59 ± 0.02	1.32 ± 0.01	1.43 ± 0.07
	50	0.77 ± 0.00	1.61 ± 0.00	1.99 ± 0.12
	150	0.88 ± 0.02	1.95 ± 0.01	2.59 ± 0.07
	450	1.08 ± 0.10	3.23 ± 0.04	3.62 ± 0.08
1.1	20	0.15 ± 0.02	0.28 ± 0.03	0.36 ± 0.02
	50	0.14 ± 0.01	0.30 ± 0.03	0.42 ± 0.02
	150	0.19 ± 0.02	0.30 ± 0.00	0.51 ± 0.00
	450	0.26 ± 0.01	0.54 ± 0.00	0.82 ± 0.07

[a] See Table I.

Three preparations of cholesterol were used. Normal cholesterol (sample I) was prepared by crystallizing 5 g of cholesterol in 400 ml of 95% ethanol. Rapidly crystallized cholesterol (sample II) was prepared by

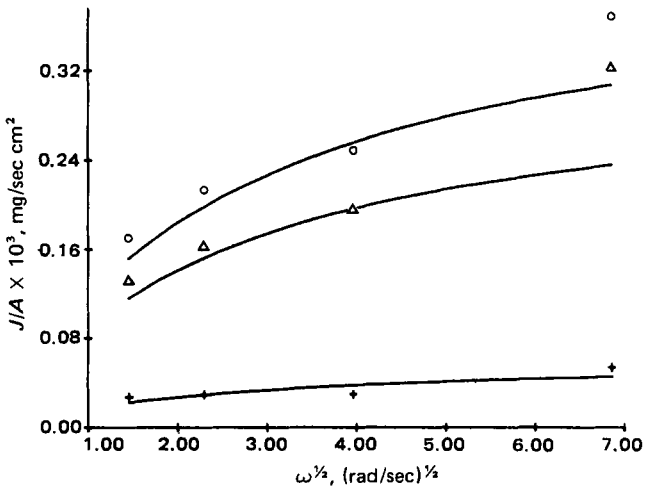

Figure 5—*Best-fit analysis of the rapid (II) pellets in 5% sodium cholate, 0.1* M *phosphate buffer, and 0.25% benzalkonium chloride at pH 8.0. Key:* C_b, ○, *0.0;* △, *0.3; and* +, *1.1 mg/ml.*

Table III—Dissolution Rates of the Melt (III) Pellets under Partial Saturation Conditions in 5% Sodium Cholate, 0.1 *M* Phosphate Buffer, and Benzalkonium Chloride at pH 8.0

C_b, mg/ml	rpm	0.0% Benzalkonium Chloride $J/A \times 10^4 \pm$ Range[a], mg/sec cm^2	0.25% Benzalkonium Chloride $J/A \times 10^4 \pm$ Range[a], mg/sec cm^2	0.5% Benzalkonium Chloride $J/A \times 10^4 \pm$ Range[a], mg/sec cm^2
0.0	20	2.41 ± 0.00	2.74 ± 0.00	3.07 ± 0.00
	50	3.24 ± 0.06	3.73 ± 0.01	3.98 ± 0.14
	150	3.67 ± 0.05	5.48 ± 0.08	6.66 ± 0.15
	450	4.39 ± 0.00	6.91 ± 0.33	10.52 ± 0.22
0.3	20	2.09 ± 0.10	2.17 ± 0.03	2.35 ± 0.05
	50	2.75 ± 0.13	3.21 ± 0.03	3.66 ± 0.19
	150	2.94 ± 0.09	4.60 ± 0.00	5.37 ± 0.11
	450	3.85 ± 0.23	6.53 ± 0.06	8.31 ± 0.46
1.0	20	1.17 ± 0.03	1.13 ± 0.04	1.40 ± 0.08
	50	1.34 ± 0.02	1.45 ± 0.07	1.54 ± 0.02
	150	1.64 ± 0.01	2.00 ± 0.08	2.49 ± 0.02
	450	1.92 ± 0.06	3.11 ± 0.04	3.68 ± 0.06

[a] See Table I.

crystallizing 10 g of cholesterol in 400 ml of 95% ethanol. A melt preparation (III) was obtained by heating sample I at 160° for 10 min. Pellets of each sample were prepared and experiments were run as described previously (5). Cholic acid was recrystallized three times from 95% ethanol and the purity was checked and confirmed by TLC. Benzalkonium chloride[1] was used as received.

Differential scanning calorimetric thermograms were obtained for the three cholesterol samples. Thermograms of samples I and II showed endotherms at 80°, corresponding to the release of water from cholesterol monohydrate. This endotherm was absent from thermograms of sample III. Samples I–III showed endotherms at 150° for melting. In general, these thermograms agree with those obtained previously (12).

Assessment of the Experimental Systems Based on the Solid Preparation Study—Test solutions of 5% sodium cholate, 0.1 *M* phosphate buffer, and 0.0, 0.25, and 0.5% benzalkonium chloride at pH 8.0 were used. These conditions were chosen because the diffusion control/interfacial control ratios would be small to moderate and thus allow for reliable determinations of P values. If a test solution with 1.0% benzalkonium chloride were used, the melt pellets would dissolve ~100% diffusion controlled and the uncertainty in the P value determination would be too great.

RESULTS AND DISCUSSION

The dissolution rates for the various cholesterol pellets were determined in partially saturated solutions at various rotational speeds at 37°. Tables I–III show the dissolution rates as a function of rotational speed and partial saturation for samples I–III. As can be seen, there are significant differences in the dissolution rates among pellet types.

Dynamic solubilities were determined by plotting dissolution rate (J/A) against bulk concentration (C_b). Figures 1–3 show the results of the experiments carried out in 5% sodium cholate, 0.1 *M* phosphate buffer, and 0.25% benzalkonium chloride solutions at pH 8.0. By extrapolation of the data to zero J/A the dynamic solubilities can be determined. This was done with the data in Figs. 1–3 except for the 450-rpm experiments where deviations from Eq. 1 were noted (the possible cause of these deviations is discussed later). Figures 1–3 show a linear decrease in dissolution rate with increasing partial saturation. This indicates that the dissolution kinetics are proportional to ΔC over the entire range of saturation. These figures show that the dynamic solubility is ~1.35, 1.30, and 1.65 mg/ml for the sample I, II, and III pellets, respectively. The tabulated dissolution rates for the three solid preparations in this system are shown in Tables I, II, and III, respectively.

Figures 4–6 show the Levich plots of the described data. The deviations from linearity clearly show the presence of the interfacial barrier in the dissolution process. If cholesterol dissolution were completely diffusion controlled, a plot of J/A *versus* $\omega^{1/2}$ would give a straight line through the origin.

From a best fit analysis (using a kinematic viscosity of 6.99×10^{-3} cm^2/sec), based on a 15% correction (5) of Eq. 1, it was possible to obtain values for C_s, P, and D, where P is the interfacial transport constant and D is the diffusivity. The calculated dissolution rates using the best fit values were compared to the experimental dissolution rates and Figs. 4–6 show the good agreement between the two. The same analysis was done for the three pellet types in 0.0 and 0.50% benzalkonium chloride solutions. Figures 7–9 show the Levich plots for the 0.50% benzalkonium chloride system. Again, a good fit between experiment and theory is seen. It should be noted that the points at 450 rpm ($\omega^{1/2} = 6.86$) were not weighted in this analysis.

A possible explanation for the high J/A value at 450 rpm in some of the experiments is the following. Microscopic examination of individual crystals of cholesterol monohydrate in bile acid solutions showed that

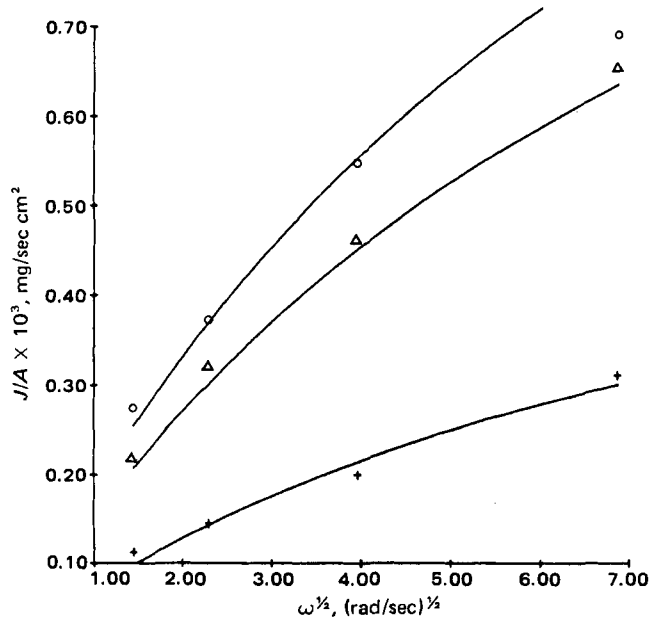

Figure 6—*Best-fit analysis of the melt pellets (III) in 5% sodium cholate, 0.1* M *phosphate buffer, and 0.25% benzalkonium chloride at pH 8.0. Key:* C_b, ○, *0.0;* △, *0.3; and* +, *1.0 mg/ml.*

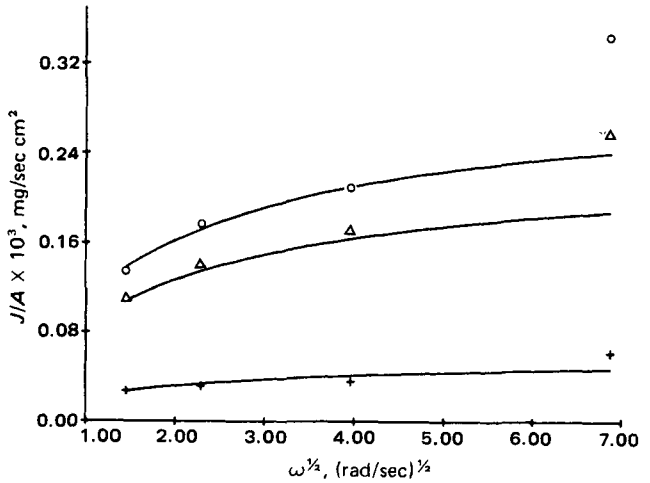

Figure 7—*Best-fit analysis of the normal pellets (I) in 5% sodium cholate, 0.1* M *phosphate buffer, and 0.5% benzalkonium chloride at pH 8.0. Key:* C_b, ○, *0.0;* △, *0.3; and* +, *1.1 mg/ml.*

Table IV—Summary of the Partial Saturation Experiments and the Best-Fit Analysis for the Three Pellet Types in 5% Sodium Cholate, 0.1 *M* Phosphate Buffer, and 0.0% Benzalkonium Chloride at pH 8.0

Pellet	C_s from Extrapolation of Partial Saturation Data	Best-Fit Analysis C_s, mg/ml	$P \times 10^4$, cm/sec	$D \times 10^6$, cm²/sec
I	1.45 (20 rpm)			
	1.45 (50 rpm)			
II	1.45 (150 rpm)	1.45	0.51	1.25
	1.38 (20 rpm)			
	1.36 (50 rpm)			
III	1.37 (150 rpm)	1.37	0.96	1.15
	1.76 (20 rpm)			
	1.72 (50 rpm)			
	1.76 (150 rpm)	1.79	3.32	1.16

surface etching occured. Within 2 hr, a definite saw-tooth pattern developed along the crystal edge. At high rotational speeds in the rotating disk experiments it is possible that the effective surface area might be increased or that some shearing of the peaks along the crystal surface takes place. This reaction, along with normal micellar dissolution, could result in a positive deviation in the apparent dissolution rate from that expected from theory.

Tables IV–VI summarize the results of the partial saturation experiments and the least-squares analysis. It can be seen that the C_s values obtained for the normal pellets (sample I) and the rapid pellets (sample II) are nearly equivalent, while the C_s values obtained for the melt pellets (sample III) was ~20% higher in all cases. It should be noted that the solubilities for samples I and II obtained from the partial saturation experiments agreed with the saturation solubilities of cholesterol (13).

The D values reported here are somewhat smaller than those obtained earlier (14, 15) for bile salt–lecithin systems. Since cholesterol dissolution is essentially surface controlled, the error in determining D values from the present dissolution-rate would be rather large; therefore, significances should not be attached to differences between the D values reported here and those determined using conventional methods (see *Appendix*).

Possible Meaning of *P* in Relation to the Dissolution Process—In general, the solubilization process involves contact of the solvent with the solid surface, where an interaction occurs; this is followed by the transport of the solute or product molecules away from the interface into the bulk. The dissolution of cholesterol in bile acid solutions can be regarded as following this mechanism. The slow or rate-determining step in this process is the approach of the micelle to the cholesterol surface and the subsequent transport of cholesterol molecules into the micellar phase. This process is associated with the interfacial transport constant P.

To understand how the benzalkonium chloride acceleration effects may be dependent on the solid phase of cholesterol, a more detailed consideration of the process is necessary. The model in Fig. 10 is proposed.

Step 1: The micelle moves from the bulk solution through the aqueous diffusion layer to a region close to the pellet surface.

Step 2: Molecules from the solid surface may disengage as a function of their configurations and energies. These molecules remain close to the solid surface and can be thought of as part of the adsorbed layer.

Step 3: Solubilization of these relatively free molecules occurs at the crystal-solution interface as a result of micelle surface "collisions." This solubilization process is a function of a steady-state concentration of the free cholesterol near the surface. The larger the k_1 value, the greater the concentration of free cholesterol and the greater the dissolution value.

Table V—Summary of the Partial Saturation Experiments and the Best-Fit Analysis for the Three Pellet Types in 5% Sodium Cholate, 0.1 *M* Phosphate Buffer, and 0.25% Benzalkonium Chloride at pH 8.0

Pellet	C_s from Extrapolation of Partial Saturation Data	Best-Fit Analysis C_s, mg/ml	$P \times 10^4$, cm/sec	$D \times 10^6$, cm²/sec
I	1.35 (20 rpm)			
	1.35 (50 rpm)			
II	1.33 (150 rpm)	1.35	1.62	1.04
	1.32 (20 rpm)			
	1.30 (50 rpm)			
III	1.28 (150 rpm)	1.29	3.28	1.04
	1.64 (20 rpm)			
	1.65 (50 rpm)			
	1.64 (150 rpm)	1.63	10.62	1.04

Table VI—Summary of the Partial Saturation Experiments and the Best-Fit Analysis for the Three Pellet Types in 5% Sodium Cholate, 0.1 *M* Phosphate Buffer, and 0.50% Benzalkonium Chloride at pH 8.0

Pellet	C_s from Extrapolation of Partial Saturation Data	Best-Fit Analysis C_s, mg/ml	$P \times 10^4$, cm/sec	$D \times 10^6$, cm²/sec
I	1.41 (20 rpm)			
	1.38 (50 rpm)			
II	1.36 (150 rpm)	1.36	2.19	1.08
	1.36 (20 rpm)			
	1.33 (50 rpm)			
III	1.32 (150 rpm)	1.33	4.85	1.08
	1.72 (20 rpm)			
	1.66 (50 rpm)			
	1.66 (150 rpm)	1.63	15.87	1.12

A large k_1 would essentially mean a high concentration of accessible cholesterol for solubilization by the micelles during collision.

In context of the present experiments, k_1 may be related to several factors. A low intrinsic activation energy for molecular disengagement would contribute to a large k_1. A large microscopic surface area at the pellet surface or a high density of active sites may also lead to a large effective k_1. The results of the present study suggest that the activational free energy (or the effective activation free energy) for the cholesterol molecule disengagement from the surface of the melt preparation is lower than that for the monohydrate preparations. This might have arisen from the possibly greater general state of disorganization of the surface molecules in the anhydrous melt, or from other factors such as crystalline defects which may have been more preponderant in the melt preparations.

This description of the dissolution process, together with earlier studies (9) on the influence of long-chain alkyl ammonium ions upon cholesterol dissolution rates in sodium chenodeoxycholate solutions, may be used to examine the present results with benzalkonium chloride. Table VII summarizes the P values and their ratios for all of the experiments. The P_{II}/P_I and the P_{III}/P_I ratios are relatively constant (~2.0 and 7.0, respectively) over the benzalkonium chloride concentration range, up to 0.5%. The ratios change only ~10–15% over a four- to fivefold range of rates.

Constancy in the P_{II}/P_I and the P_{III}/P_I ratios would be consistent with the following analysis. If the relevant surface charge densities for all three cholesterol preparations were essentially the same, and if the addition of benzalkonium chloride to the system did not significantly influence the surface charges, then the mechanism proposed earlier (9, 10) (*i.e.*, the partial neutralization of the negative micellar charge) may dominate and would predict that k_2 (Fig. 10) would be essentially the same in the experiments with all cholesterol samples. Then, if the k_1 values are not influenced by benzalkonium chloride or if k_1 values are affected the same

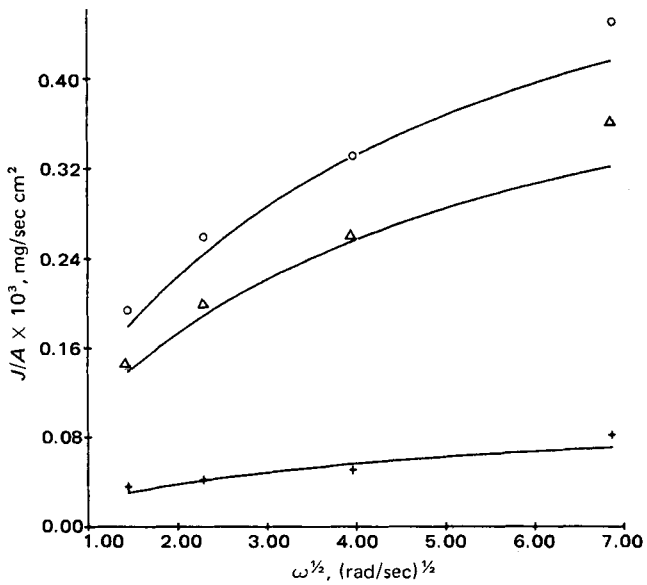

Figure 8—*Best-fit analysis of the rapid (II) pellets in 5% sodium cholate, 0.1* M *phosphate buffer, and 0.5% benzalkonium chloride at pH 8.0. Key:* C_b, ○, *0.0;* △, *0.3; and* +, *1.1 mg/ml.*

Table VII—Summary of the P Values Obtained as a Function of Benzalkonium Chloride Concentration

Percent Benzalkonium Chloride in Solution	$P \times 10^4$, cm/sec				
	I	II	III	P(II)/P(I)	P(III)/P(I)
0.0	0.51	0.96	3.32	1.90	6.53
0.25	1.62	3.28	10.62	2.02	6.55
0.50	2.19	4.85	15.87	2.20	7.25

Table VIII—Summary of the C_s Values Obtained as a Function of Benzalkonium Chloride Concentration

Percent Benzalkonium Chloride in Solution	C_s, mg/ml				
	I	II	III	C_s(II)/C_s(I)	C_s(III)/C_s(I)
0.0	1.45	1.37	1.79	0.95	1.23
0.25	1.35	1.29	1.63	0.96	1.21
0.50	1.36	1.33	1.63	0.97	1.20

(percentage-wise) for all three samples, then constancy of the P ratios should be expected.

A corollary analysis might assume, for example, that there are interactions between benzalkonium chloride and the cholesterol surface to reduce the surface charge density. However, if the initial surface charge densities and the benzalkonium chloride surface effects are essentially the same for all preparations, then again k_2 would be expected to be the same for the three preparations. For this situation, if the initial k_1 values are not affected by the benzalkonium chloride or if they are affected the same, the constancy of the P ratios would again be expected.

The first of these two interpretations may easily explain the behavior difference between sample I and sample II since both of these are cholesterol monohydrates with the same differental scanning colorimetric patterns and essentially the same solubilities (Table VIII). In terms of the proposed model, sample I and sample II might differ only in that their k_1 (or their apparent k_1) values are different because of differing microscopic surface areas or crystallite sizes. The conditions associated with k_2 might be expected to be identical for these two preparations.

The constancy of the P_{III}/P_I ratio is more difficult to predict since sample III is anhydrous cholesterol that had undergone a melting step. The present data suggest, however, that the proposed mechanism may be correct even in this instance; although k_1 may be significantly greater for the melt than for the sample I monohydrate, it is relatively uninfluenced by benzalkonium chloride. The electrical characteristics of the melt pellet surface is similar to that for the monohydrate under the present dissolution kinetics conditions so that the primary effect of benzalkonium chloride is the reduction of the micellar charge and facilitating step 3 *via* the enhancement of k_2.

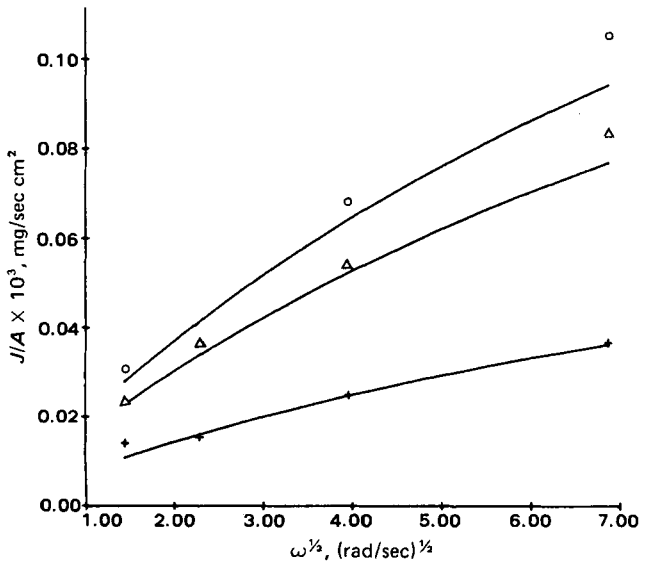

Figure 9—*Best-fit analysis of the melt (III) pellets in 5% sodium cholate, 0.1 M phosphate buffer, and 0.5% benzalkonium chloride at pH 8.0. Key:* C_b, ○, *0.0;* △, *0.3; and* +, *1.0 mg/ml.*

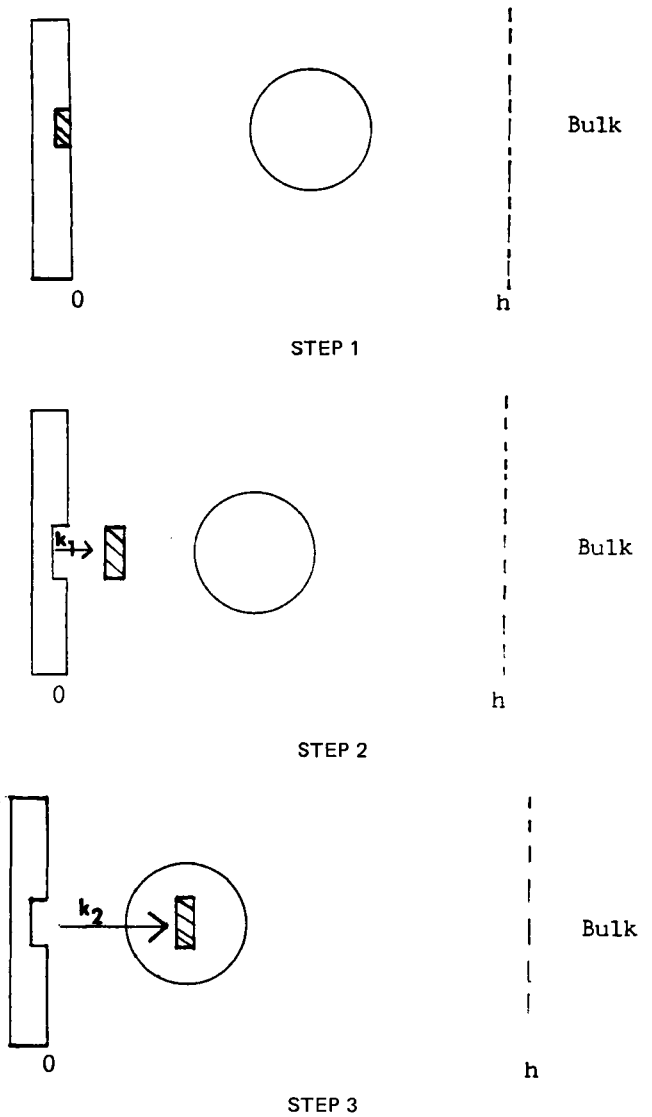

Figure 10—Step 1—*The micelle moves from the bulk solution through the aqueous diffusion layer to a region close to the pellet surface.* Step 2—*Molecules from the solid surface may disengage as a function of their configurations and energies. These molecules remain close to the solid surface and can be considered part of the adsorbed layer.* Step 3—*Solubilization of these relatively free molecules occurs at the crystal-solution interface as a result of micelle surface "collisions." The symbol* k_2 *is the rate constant for the solubilization of the (surface) free cholesterol by the micelle.*

APPENDIX

Sensitivity of the Best Fit Analysis to P—To relate the present results to their sensitivities to P, the parameters C_s and D must be considered. As already shown, there was good agreement between the solubilities obtained from the best fit analysis and those obtained from extrapolation of the partial saturation data. Diffusivities obtained from the best fit analysis were in fairly good agreement with those obtained experimentally. Diffusivity measurements were made at 37° in a small volume diaphragm diffusion cell employing a modified Keller's method (14). The D values determined experimentally in 0.0, 0.25, and 0.50% benzalkonium chloride solutions were 1.52, 1.40, and 1.28×10^{-6} cm^2/sec, respectively. These compare with the best fit D values of 1.25, 1.04, and 1.08×10^{-6} cm^2/sec.

Because of the good agreement between experimental and best fit parameters for C_s and D, an assessment of P can now be made. It must be remembered that as a system approaches total diffusion control, P becomes very large (surface equilibrium is fast) and therefore, $1/P$ becomes small. The smaller the $1/P$ ratio, the less sensitive the best fit results will be to small changes in P. Another look at the systems studied shows that the diffusion control/interfacial control ratios are small to moderate except for the melt pellets in 5% sodium cholate, 0.1 M phosphate buffer, and 0.50% benzalkonium chloride at pH 8.0 where the diffusion control/interfacial control ratio is ~90%. By making small changes in P, the sensitivity of the best fit results can be seen. It can be shown that if P is varied by ±10% there is little change in the best fit results. However, a change in P greater than 10% will result in marked deviation of the experimental results and the theoretical curves. For the case where the diffusion control/interfacial control ratio is ~90%, the uncertainty in P can be as high as 25%.

REFERENCES

(1) W. I. Higuchi, S. Prakongpan, V. Surpuriya, and F. Young, *Science*, **178**, 633 (1972).

(2) W. I. Higuchi, F. Sjuib, D. Mufson, A. P. Simonelli, and A. F. Hofmann, *J. Pharm. Sci.*, **62**, 942 (1973).

(3) W. I. Higuchi, S. Prakongpan, and F. Young, *ibid.*, **62**, 945 (1973).

(4) *Ibid.*, **62**, 1207 (1973).

(5) S. Prakongpan, W. I. Higuchi, K. H. Kwan, and A. M. Molokhia, *J. Pharm. Sci.*, **65**, 685 (1976).

(6) K. H. Kwan, W. I. Higuchi, A. M. Molokhia, and A. F. Hofmann, *ibid.*, **66**, 1094 (1977).

(7) A. M. Molokhia, A. F. Hofmann, W. I. Higuchi, M. Tuchinda, K. Feld, S. Prakongpan, and R. G. Danzinger, *ibid.*, **66**, 1101 (1977).

(8) K. H. Kwan, W. I. Higuchi, A. M. Molokhia, and A. F. Hofmann, *ibid.*, **66**, 1105 (1977).

(9) D. C. Patel and W. I. Higuchi, *J. Colloid Interface Sci.*, **74**, 211 (1980).

(10) *Ibid.*, **74**, 220 (1980).

(11) V. A. Levich, "Physicochemical Hydrodynamics," Prentice-Hall, Englewood Cliffs, N.J., 1962.

(12) C. R. Loomis, G. G. Shipley, and D. M. Small, *J. Lipid Res.*, **20**, 525 (1979).

(13) K. M. Feld, Ph.D. thesis, The University of Michigan, Ann Arbor, Mich., 1980.

(14) K. H. Kwan, Ph.D. thesis, The University of Michigan, Ann Arbor, Mich., 1978.

(15) S. Prakongpan, Ph.D. thesis, The University of Michigan, Ann Arbor, Mich., 1974.

ACKNOWLEDGMENTS

Supported by Grant AM 16694 from the National Institute of Arthritis, Metabolism, and Digestive Diseases.

Particle Size Reduction by a Hammer Mill I: Effect of Output Screen Size, Feed Particle Size, and Mill Speed

B. R. HAJRATWALA

Received May 15, 1981, from the *Pharmaceutics Department, Wayne State University, Detroit, MI 48202.* Accepted for publication June 30, 1981.

Abstract □ A hammer mill is an impact mill commonly used in pharmaceutical manufacturing for reducing particle size for a variety of drugs. Commercial grade ammonium sulfate was milled as a model powder. This salt was sieved to obtain particle size fractions with average diameters of 1.3, 0.9, and 0.72 mm which were used as feed particles. The milled material was analyzed for particle size distribution (PSD) using standard sieves. At a moderate speed (~2500 rpm), the feed size did not result in a significantly changed arithmetic mean diameter, $d_{\bar{x}}$ of milled particles. A new particle size reduction constant, k, is proposed as a result of a linear relationship between $d_{\bar{x}}$ and output screen size, d_{ss}. As d_{ss} decreases, the PSD range of milled particles narrows; as mill speed increases (~5000 rpm), $d_{\bar{x}}$ decreases. The decrease is of a greater magnitude for larger d_{ss} (2 mm) than for a smaller d_{ss} (1 mm). At low speeds (~1000 rpm), the PSD is wider compared to medium and high speeds.

Keyphrases □ Particle size—reduction by hammer mill, effect of output screen size, feed particle size, and mill speed □ Pharmaceutics—particle size reduction by a hammer mill □ Hammer mill—particle size reduction, pharmaceutics

The hammer mill is an impact mill commonly used in pharmaceutical manufacturing for reducing particle size for a variety of drugs (1–3). Milling is an essential unit operation in tablet and capsule manufacture, yet very little has been reported about factors that affect milling (4, 5).

The present report examines the effect of related parameters such as output screen size, feed particle size, and mill speed on particle size reduction by a hammer mill. Commercial grade ammonium sulfate was used as a model substance due to its low cost and large particle size distribution.

EXPERIMENTAL

Equipment—A laboratory bench-type hammer mill[1], USP standard testing sieves[2], and a laboratory sieve vibrator[3] were used. The sieve sizes used were: 2.0, 1.6, 1.0, 0.8, 0.63, 0.4, 0.315, and 0.1 mm for preparation and analysis.

Particle Size Reduction—Ammonium sulfate was sieved to obtain various particle size fractions with average diameters of 1.3, 0.9, and 0.72 mm. Sieve sizes used were 1.6, 1.0, 0.8, and 0.63 mm. The particles were stored at room temperature (25 ± 3°) and at a constant humidity (60 ± 2%, to prevent agglomeration of particles) until required for milling.

[1] Model C580, micro hammer mill, Glen Creston, Stanmore, England.
[2] W. S. Tyler Inc., Mentor, OH 44060.
[3] Model 150, Derrick Inc., Buffalo, N.Y.

0022-3549/82/0200-0188$01.00/0

APPENDIX

Sensitivity of the Best Fit Analysis to P—To relate the present results to their sensitivities to P, the parameters C_s and D must be considered. As already shown, there was good agreement between the solubilities obtained from the best fit analysis and those obtained from extrapolation of the partial saturation data. Diffusivities obtained from the best fit analysis were in fairly good agreement with those obtained experimentally. Diffusivity measurements were made at 37° in a small volume diaphragm diffusion cell employing a modified Keller's method (14). The D values determined experimentally in 0.0, 0.25, and 0.50% benzalkonium chloride solutions were 1.52, 1.40, and 1.28×10^{-6} cm^2/sec, respectively. These compare with the best fit D values of 1.25, 1.04, and 1.08×10^{-6} cm^2/sec.

Because of the good agreement between experimental and best fit parameters for C_s and D, an assessment of P can now be made. It must be remembered that as a system approaches total diffusion control, P becomes very large (surface equilibrium is fast) and therefore, $1/P$ becomes small. The smaller the $1/P$ ratio, the less sensitive the best fit results will be to small changes in P. Another look at the systems studied shows that the diffusion control/interfacial control ratios are small to moderate except for the melt pellets in 5% sodium cholate, 0.1 M phosphate buffer, and 0.50% benzalkonium chloride at pH 8.0 where the diffusion control/interfacial control ratio is ~90%. By making small changes in P, the sensitivity of the best fit results can be seen. It can be shown that if P is varied by ±10% there is little change in the best fit results. However, a change in P greater than 10% will result in marked deviation of the experimental results and the theoretical curves. For the case where the diffusion control/interfacial control ratio is ~90%, the uncertainty in P can be as high as 25%.

REFERENCES

(1) W. I. Higuchi, S. Prakongpan, V. Surpuriya, and F. Young, *Science*, **178**, 633 (1972).

(2) W. I. Higuchi, F. Sjuib, D. Mufson, A. P. Simonelli, and A. F. Hofmann, *J. Pharm. Sci.*, **62**, 942 (1973).

(3) W. I. Higuchi, S. Prakongpan, and F. Young, *ibid.*, **62**, 945 (1973).

(4) *Ibid.*, **62**, 1207 (1973).

(5) S. Prakongpan, W. I. Higuchi, K. H. Kwan, and A. M. Molokhia, *J. Pharm. Sci.*, **65**, 685 (1976).

(6) K. H. Kwan, W. I. Higuchi, A. M. Molokhia, and A. F. Hofmann, *ibid.*, **66**, 1094 (1977).

(7) A. M. Molokhia, A. F. Hofmann, W. I. Higuchi, M. Tuchinda, K. Feld, S. Prakongpan, and R. G. Danzinger, *ibid.*, **66**, 1101 (1977).

(8) K. H. Kwan, W. I. Higuchi, A. M. Molokhia, and A. F. Hofmann, *ibid.*, **66**, 1105 (1977).

(9) D. C. Patel and W. I. Higuchi, *J. Colloid Interface Sci.*, **74**, 211 (1980).

(10) *Ibid.*, **74**, 220 (1980).

(11) V. A. Levich, "Physicochemical Hydrodynamics," Prentice-Hall, Englewood Cliffs, N.J., 1962.

(12) C. R. Loomis, G. G. Shipley, and D. M. Small, *J. Lipid Res.*, **20**, 525 (1979).

(13) K. M. Feld, Ph.D. thesis, The University of Michigan, Ann Arbor, Mich., 1980.

(14) K. H. Kwan, Ph.D. thesis, The University of Michigan, Ann Arbor, Mich., 1978.

(15) S. Prakongpan, Ph.D. thesis, The University of Michigan, Ann Arbor, Mich., 1974.

ACKNOWLEDGMENTS

Supported by Grant AM 16694 from the National Institute of Arthritis, Metabolism, and Digestive Diseases.

Particle Size Reduction by a Hammer Mill I: Effect of Output Screen Size, Feed Particle Size, and Mill Speed

B. R. HAJRATWALA

Received May 15, 1981, from the *Pharmaceutics Department, Wayne State University, Detroit, MI 48202.* Accepted for publication June 30, 1981.

Abstract □ A hammer mill is an impact mill commonly used in pharmaceutical manufacturing for reducing particle size for a variety of drugs. Commercial grade ammonium sulfate was milled as a model powder. This salt was sieved to obtain particle size fractions with average diameters of 1.3, 0.9, and 0.72 mm which were used as feed particles. The milled material was analyzed for particle size distribution (PSD) using standard sieves. At a moderate speed (~2500 rpm), the feed size did not result in a significantly changed arithmetic mean diameter, $d_{\bar{x}}$ of milled particles. A new particle size reduction constant, k, is proposed as a result of a linear relationship between $d_{\bar{x}}$ and output screen size, d_{ss}. As d_{ss} decreases, the PSD range of milled particles narrows; as mill speed increases (~5000 rpm), $d_{\bar{x}}$ decreases. The decrease is of a greater magnitude for larger d_{ss} (2 mm) than for a smaller d_{ss} (1 mm). At low speeds (~1000 rpm), the PSD is wider compared to medium and high speeds.

Keyphrases □ Particle size—reduction by hammer mill, effect of output screen size, feed particle size, and mill speed □ Pharmaceutics—particle size reduction by a hammer mill □ Hammer mill—particle size reduction, pharmaceutics

The hammer mill is an impact mill commonly used in pharmaceutical manufacturing for reducing particle size for a variety of drugs (1–3). Milling is an essential unit operation in tablet and capsule manufacture, yet very little has been reported about factors that affect milling (4, 5).

The present report examines the effect of related parameters such as output screen size, feed particle size, and mill speed on particle size reduction by a hammer mill. Commercial grade ammonium sulfate was used as a model substance due to its low cost and large particle size distribution.

EXPERIMENTAL

Equipment—A laboratory bench-type hammer mill[1], USP standard testing sieves[2], and a laboratory sieve vibrator[3] were used. The sieve sizes used were: 2.0, 1.6, 1.0, 0.8, 0.63, 0.4, 0.315, and 0.1 mm for preparation and analysis.

Particle Size Reduction—Ammonium sulfate was sieved to obtain various particle size fractions with average diameters of 1.3, 0.9, and 0.72 mm. Sieve sizes used were 1.6, 1.0, 0.8, and 0.63 mm. The particles were stored at room temperature (25 ± 3°) and at a constant humidity (60 ± 2%, to prevent agglomeration of particles) until required for milling.

[1] Model C580, micro hammer mill, Glen Creston, Stanmore, England.
[2] W. S. Tyler Inc., Mentor, OH 44060.
[3] Model 150, Derrick Inc., Buffalo, N.Y.

0022-3549/82/0200-0188$01.00/0

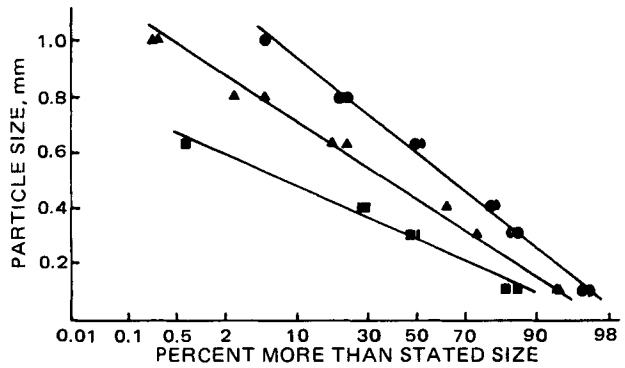

Figure 1—*Effect of varying* d_{ss} *on the particle size distribution. Feed particle size range, 1.6–1.0 mm. Speed setting 4. Key* (d_{ss}): ●, *2.0;* ▲, *1.5; and* ■, *1.0 mm.*

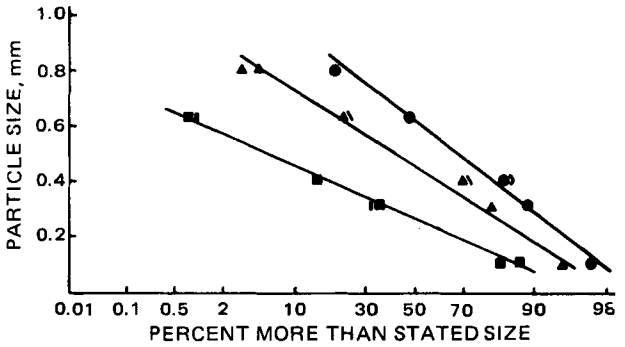

Figure 2—*Effect of varying* d_{ss} *on the particle size distribution. Feed particle size range, 1.0–0.8 mm. Speed setting 4. Key* (d_{ss}): ●, *2.0;* ▲, *1.5; and* ■, *1.0 mm.*

The mill was equipped with three free-swinging hammers with impact edges and variable rotational speed control. The material was fed as 5 g portions.

The total amount milled for each experiment was 50 g. The mill was fitted with round-hole design output screens with 2.0-, 1.5-, or 1.0-mm sizes. They were 3.03-, 3.06-, and 1.23-mm thick, respectively. The milled material was collected in a closed plastic bag and analyzed for particle size distribution using the standard vibrating nested sieve method.

All data were obtained in duplicate and were virtually identical in all cases.

Evaluation of $d_{\bar{x}}$ and σ—The mean diameter, $d_{\bar{x}}$, was obtained from arithmetic probability plots. The particle size at 50% was taken as $d_{\bar{x}}$.

The standard deviation, σ, was also obtained from the arithmetic probability plots. The difference in particle sizes at 84.13 and 50% size was taken as σ.

RESULTS AND DISCUSSION

The rate at which a mill is fed is an important variable. Various amounts of feed material were milled to determine the optimum feed rate. This was determined experimentally by noting the discharge rate (grams per second) of milled material. Five grams was the optimum amount,

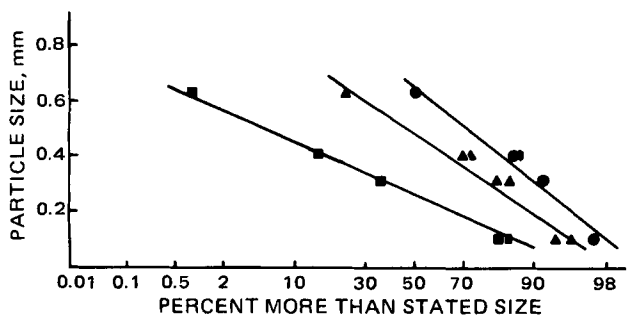

Figure 3—*Effect of varying* d_{ss} *on the particle size distribution. Feed particle size range, 0.8–0.63 mm. Speed setting 4. Key* (d_{ss}): ●, *2.0;* ▲, *1.5; and* ■, *1.0 mm.*

Table I—Effect of Output Screen Size on the Arithmetic Mean and Standard Deviation of the Milled Particles for Various Sizes of Feed Particles at Setting 4 (~2500 rpm)

	Output Screen Size, d_{ss}		
Feed Size Range, mm	2.0 mm $d_{\bar{x}} \pm \sigma$	1.5 mm $d_{\bar{x}} \pm \sigma$	1.0 mm $d_{\bar{x}} \pm \sigma$
1.6–1.0	0.59 ± 0.26	0.43 ± 0.22	0.28 ± 0.15
1.0–0.8	0.61 ± 0.25	0.45 ± 0.21	0.27 ± 0.15
0.8–0.63	0.65 ± 0.26	0.48 ± 0.24	0.26 ± 0.15

Table II—Effect of Milling Speed on Arithmetic Mean and Standard Deviation of the Milled Particles at Varying Output Screen Size [a]

	Milling Speed Setting		
	2	4	8
d_{ss}, mm	$d_{\bar{x}} \pm \sigma$	$d_{\bar{x}} \pm \sigma$	$d_{\bar{x}} \pm \sigma$
2.0	0.88 ± 0.40	0.59 ± 0.26	0.31 ± 0.27
1.0	0.34 ± 0.24	0.28 ± 0.15	0.22 ± 0.15

[a] Feed particle size range, 1.6–1.0 mm.

giving the maximum discharge rate for this mill with ammonium sulfate as the feed material.

This mill had a maximum speed of 6000 rpm. (Any reference to a constant speed implies that the speed setting on the mill was not changed during the experiment). Milling was done at three preselected settings. A low speed (setting 2, ~1000 rpm), a medium speed (setting 4, ~2500 rpm), and a high speed (setting 8, ~5000 rpm) were arbitrary selections.

Effect of Output Screen Size at Moderate Milling Speed—The evaluation of particle size data utilizing histograms has limited use. It is convenient to express data as arithmetic probability or normal probability plots (1).

Figures 1–3 show the effect of output screen size (d_{ss} represents diameter of screen openings) on the particle size distribution of milled product for various sizes of feed material. Although milled material may show a log-normal distribution (4), the particle size distributions for milled particles in this study show a linear relationship on arithmetic probability plots indicating near normal distribution. Some plots show departure from linearity at extremes indicating nonasymptotic distribution; however, the usefulness of the data is not reduced.

Table I shows that the output screen size, d_{ss}, has a significant effect on the arithmetic mean size, $d_{\bar{x}}$, of the milled particles. Since the average feed particle size does not show a significant effect at setting 4, the data can be pooled.

It is expected that decreasing d_{ss} would decrease the particle size of the milled particles, as was confirmed in this study. However, no relationship between d_{ss} and milled particle size has been reported. It is also not known how decreasing d_{ss} would affect the magnitude of σ for the particle size distribution of the milled particles.

A simple relationship may be hypothesized between d_{ss} and $d_{\bar{x}}$ of the milled particles and may be expressed as:

$$d_{\bar{x}} = k/d_{ss} \qquad \text{(Eq. 1)}$$

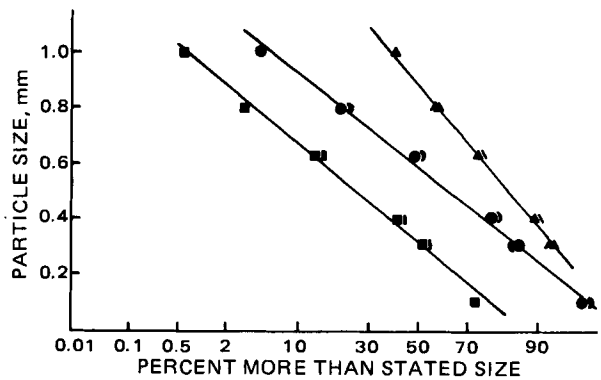

Figure 4—*Effect of varying milling speed on the particle size distribution,* d_{ss} *= 2.0 mm. Feed particle size range, 1.6–1.0 mm. Key (speed):* ▲, *setting 2 (~1000 rpm);* ●, *setting 4 (~2500 rpm); and* ■, *setting 8 (~5000 rpm).*

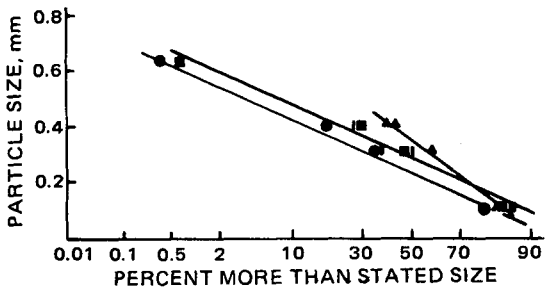

Figure 5—*Effect of varying milling speed on the particle size distribution,* d_{ss} *= 1.0 mm. Feed particle size range, 1.6–1.0 mm. Key (speed): ▲, setting 2 (~1000 rpm); ■, setting 4 (~2500 rpm); and ●, setting 8 (~5000 rpm).*

based on data in Table I where k is a particle size reduction factor. The value of k for Table I data is 0.294 (n = 9, SD = 0.022). This means that $d_{\bar{x}}$ is about one-third less in size than the output screen size, regardless of the feed particle size range used in this experiment, at a moderate milling speed setting of 4 on this mill.

The effect of d_{ss} on the particle size range distribution of milled particles can be seen by comparing its standard deviation. As d_{ss} decreased, σ decreased, *i.e.*, the particle size distribution became narrower. The distributions were unaffected by the feed particle size due to a narrowing of the angle of particle discharge range as output screen size became smaller.

It should be noted that the thickness of the 1-mm output sieve is approximately half of the 2- and 1.5-mm sieves. Decreasing the thickness of the output screen should increase the range of particle discharge angles (6). Thus, the observed data for the 1-mm size should be viewed with caution.

Effect of Milling Speed—The speed at which a mill operates is an important factor in particle reduction. At any given speed, as the material is fed, a mill slows down due to attrition of particles by the hammers until most of the material is discharged and the speed returns to the unloaded speed.

Figures 4 and 5 show the effect of milling speed on the milled product at varying output screen sizes. The arithmetic mean, $d_{\bar{x}}$, and standard deviation (σ) of the milled particles are shown in Table II.

It was expected that milling at higher speeds would further reduce the average particle size of the milled product due to the decreased angle of particle discharge (6). However, the extent of reduction or its effect on the range of particle size distribution of the milled particles has not been reported.

At settings 2, 4, and 8, the mill speeds are ~1000, 2500, and 5000 rpm, respectively. Table II shows that as the mill speed increases, the arithmetic mean of the milled particle decreases. This decrease is of a greater magnitude for the larger output screen size (2 mm) than for the smaller output screen size (1 mm).

At low speeds, the standard deviation of the milled particles is larger compared to medium and high speeds. This is reasonable because at lower speeds the particles are not expected to be discharged at a steeper angle. As the rotational speed increases, the angle of discharge reaches some optimum value, *i.e.*, the particles cannot be discharged at an angle lower than the optimum, and a leveling off of the standard deviation is observed.

Figure 6 shows the effect of output screen size and speed on the average particle size of the milled particles. The feed particle size range was 1.6–1.0 mm.

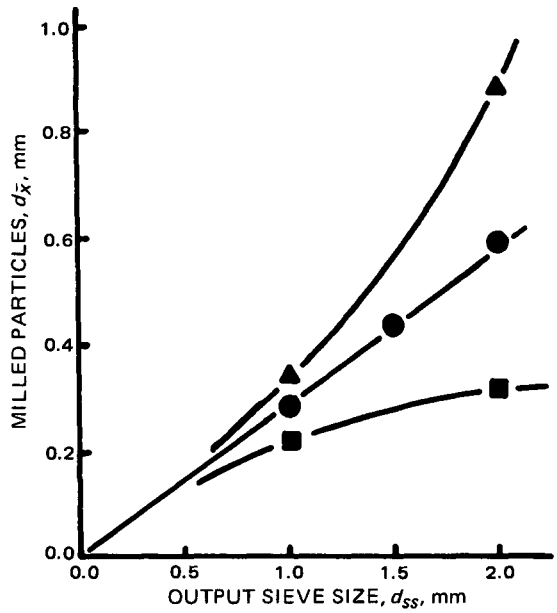

Figure 6—*Effect of* d_{ss} *on* $d_{\bar{x}}$ *of the milled particles at varying milling speeds. Key (speed): ▲, setting 2 (~1000 rpm); ●, setting 4 (~2500 rpm); and ■, setting 8 (~5000 rpm).*

The plot shows that Eq. 1 holds true at a moderate speed in this experimental series, the slope of the line being particle size reduction factor k. Equation 1 does not hold true at a low milling speed (setting 2) or at a high milling speed (setting 8). The equation plot passes through the origin as it would be expected; if the output screen size were zero, then no milled particles would be obtained.

Further work is in progress to determine the mathematical relationship of a change in k and to study milling characteristics of other selected pharmaceuticals.

REFERENCES

(1) E. L. Parrott, in "The Theory and Practice of Industrial Pharmacy," L. Lachman, H. A. Lieberman, and J. L. Kanig, Eds., 2nd ed., Lea & Febiger, Philadelphia, Pa., 1976, pp. 466–485.

(2) S. J. Carter, "Tutorial Pharmacy," 6th ed., Pitman Medical, London, England, 1972, pp. 183–191.

(3) J. T. Carstensen, "Pharmaceutics of Solids and Solid Dosage Forms," Wiley, New York, N.Y., 1977, pp. 111–114.

(4) G. Steiner, M. Patel, and J. T. Carstensen, *J. Pharm. Sci.*, **63**, 1395 (1974).

(5) J. T. Carstensen and M. Patel, *ibid.*, **63**, 1494 (1974).

(6) E. L. Parrott, "Pharmaceutical Technology," Burgess, Minneapolis, Minn., 1971, pp. 42–43.

ACKNOWLEDGMENTS

The technical assistance of Ms. Margaret Sturtevant is gratefully acknowledged. This work was done in part at the Pharmacy Department, University of Otago, Dunedin, New Zealand. The author thanks Dr. W. E. Moore of Pharmaceutics Department, Wayne State University, for helpful suggestions and his astute review of this manuscript.

Solubility and Ionization Characteristics of Doxepin and Desmethyldoxepin

KORAL EMBIL and GEORGE TOROSIAN[x]

Received February 23, 1981, from the *College of Pharmacy, University of Florida, Gainesville, FL 32610.* Accepted for publication June 11, 1981.

Abstract □ The thermodynamic pKa values for doxepin and its metabolite desmethyldoxepin were determined by the solubility method to be 8.96 and 9.75, respectively at 25°. The intrinsic solubilities for doxepin and desmethyldoxepin were linearly dependent upon ionic strength. The intrinsic solubilities at zero ionic strength and 25° were determined to be 1.13×10^{-4} *M* for doxepin and 3.95×10^{-4} *M* for desmethyldoxepin. The solubility experiment was repeated at different temperatures and a constant ionic strength of 0.167 *M*. The change in enthalpy (6.71 kcal/mole) and entropy (−4.16 cal/mole °K) of solution for doxepin was determined from a van't Hoff plot for this nonideal system. The apparent partition coefficient between hexane and water for the doxepin free base was determined to be 13,615 at an ionic strength of 0.067 *M*.

Keyphrases □ Doxepin—solubility and ionization characteristics □ Desmethyldoxepin—solubility and ionization characteristics □ Solubility—of doxepin and desmethyldoxepin, ionization characteristics □ Ionization—of doxepin and desmethyldoxepin, solubility

Doxepin hydrochloride is one of a class of psychotherapeutic agents known as dibenzoxepin tricyclic compounds. To further understand its *in vivo* behavior, the fundamental physicochemical properties of doxepin and one of its metabolites, desmethyldoxepin, were studied. These properties may partially explain the ability of the drug to cross membranes and accumulate and/or distribute in various tissues. The ease of extraction of the drug from biological samples, even at pH values at which the protonated species predominate, may be explained by the magnitude of the partition coefficient and the intrinsic solubility of the free base.

The apparent ionization constants for similar tricyclic compounds were determined earlier using the solubility method (1). Similarly, the solubility method was also used to obtain an apparent pKa value for phenytoin (2).

In this paper, apparent pKa values were determined for doxepin and desmethyldoxepin at different ionic strengths and were used to calculate the thermodynamic pKa values for each compound. In addition, the intrinsic solubilities at zero ionic strength were also determined.

EXPERIMENTAL

Materials—Doxepin and desmethyldoxepin were gifts[1]. Sodium chloride, sodium hydroxide, sodium carbonate, hydrochloric acid, and hexane were all reagent grade and used as obtained.

Determination of pKa—The intrinsic or saturated solubility of doxepin and desmethyldoxepin at different pH values was determined and plotted using the following (3, 4):

$$\mathrm{pH} = \mathrm{pKa} - \log\left(\frac{S}{S_0} - 1\right) \qquad \text{(Eq. 1)}$$

where S_0 is the intrinsic solubility of the free base, and S is total solubility and includes both protonated and unprotonated forms of the drug.

The experiment was carried out by determining the solubility of the compound at several pH values. Ten 15-ml culture tubes with polytef[2]-lined screw caps were silylated[3] and maintained at 25° to minimize the separation of the drug as an oil. Into each pair of tubes, 1 ml of 0.05 carbonate buffer (pH 9.0–10.8) was added.

The solubility for each compound was determined at four to six different pH values at constant ionic strength. The intrinsic solubility (S_0) was obtained by measuring the amount of drug in solution at 25° after the pH was adjusted to 12.6 with sodium hydroxide. This pH provided a ratio in excess of 1000:1 in favor of the unprotonated species. Five milliliters of stock solution (1.0×10^{-3} *M* of doxepin hydrochloride or 4.5×10^{-3} *M* desmethyldoxepin hydrochloride) was added to all tubes, approximating a 10-fold excess of drug as the free base.

The tubes were capped, sealed with paraffin film[4], and equilibrated in a water bath at 25° for 5 hr and centrifuged[5] at 25° and 3000 rpm for 30 min. The supernate was then transferred into a clean culture tube to minimize the redispersion of excess drug present as an oil. The solutions that did not exhibit a Tyndall effect were assayed spectrophotometri-

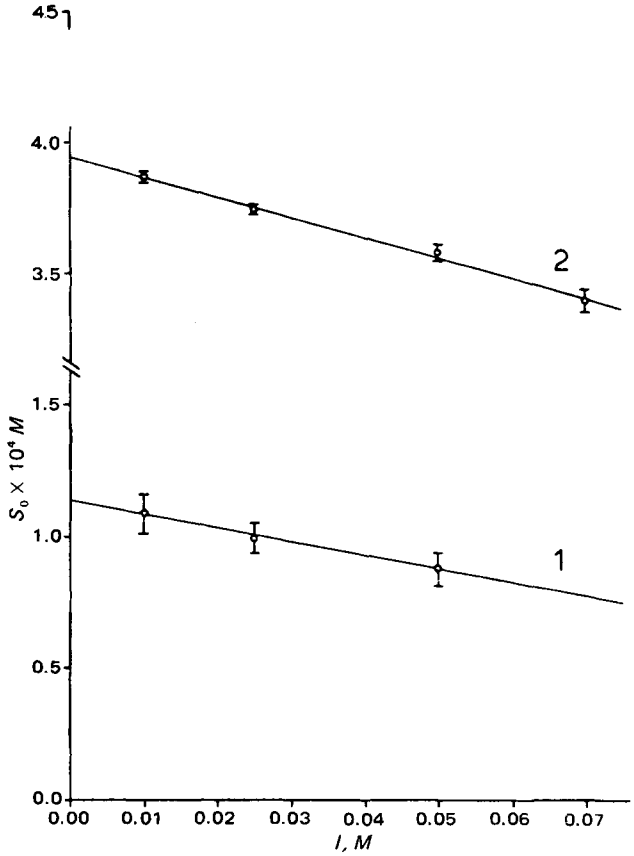

Figure 1—*Plot of intrinsic solubility* (S_0) versus *ionic strength* (I). *Line 1 represents the intrinsic solubility of doxepin at increasing ionic strengths. Each point is an average of five to seven determinations, and the solid line is obtained by least-squares regression. Line 2 represents desmethyldoxepin, each point is the average of two determinations, and the solid line is obtained by least-squares regression. Error bars indicate one standard deviation around the mean.*

[1] Pennwalt Corp., Rochester, NY 14623.

[2] Teflon.

[3] Silyl 8, Pierce Chemical Co., Rockford, Ill.

[4] Parafilm, American Can Co., Dixie/Marathon, Greenwich, CT 06830.

[5] Universal model UV International Equipment Co., Needham Heights, Mass.

0022-3549/82/0200-0191$01.00/0

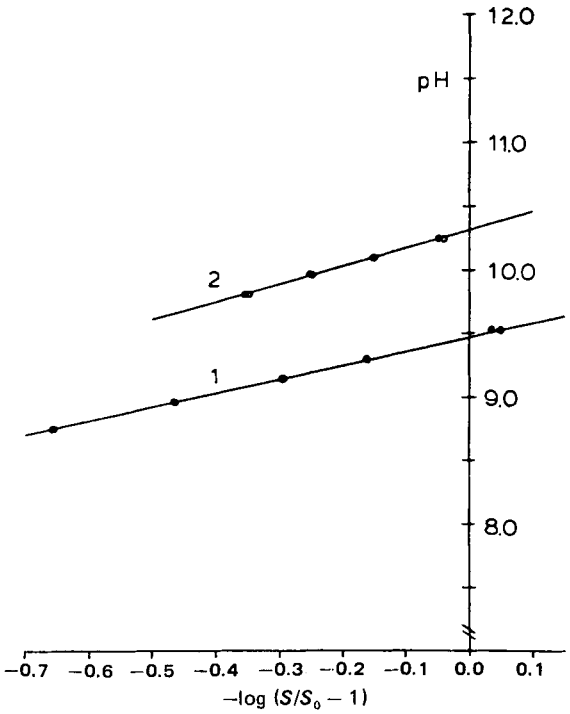

Figure 2—*Typical plot of pH* versus $-log(S/S_0 - 1)$ *for doxepin (Line 1) and desmethyldoxepin (Line 2), obtained at an ionic strength of 0.05 M. Each point represents at least two observations. The solid line in each case represents a least-squares regression through the data points.*

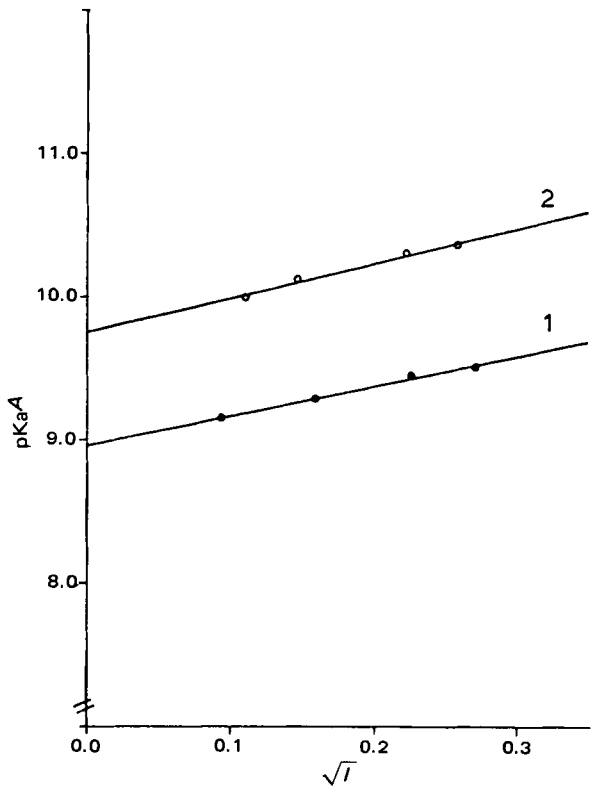

Figure 3—*Plot of apparent pKa* versus $\sqrt{I}$. *Line 1 represents doxepin and line 2 represents desmethyldoxepin. The solid lines are obtained by least-squares regression.*

cally[6] at 292 nm and their pH values were recorded[7]. The absorbances were then converted into concentrations using a standard curve.

Determination of Thermodynamic Parameters—The van't Hoff plot was obtained by determining the intrinsic solubility of doxepin at different temperatures, but at constant ionic strength and plotting the natural log of the mole fractions (X_2) *versus* the reciprocal of the absolute temperatures. The thermodynamic parameters ΔH and ΔS, the change in ethalpy and entropy, respectively, were obtained from the slope and intercept, (5):

$$\ln X_2 = \frac{\Delta S}{R} - \frac{\Delta H}{R}\left(\frac{1}{T}\right) \qquad \text{(Eq. 2)}$$

where R is the gas constant and T is the absolute temperature.

The procedure to determine these parameters was identical to that for the pKa determination, except that 16 tubes were used for each temperature (5, 10, 13, 18, and 25°), and sufficient sodium hydroxide was used to adjust the pH to a constant 12.6. The solutions were brought to temperature (to minimize pressure changes inside the tubes) prior to capping. The tubes were then equilibrated at the selected temperature. After equilibration, the tubes were transferred immediately into a refrigerated centrifuge and spun at 7000 rpm for 40 min at a constant temperature.

The supernate of replicate tubes were combined, transferred into a clean tube and centrifuged[8] at 7000 rpm for an additional 1 hr. The resultant supernate (10 ml) was then spectrophotometrically analyzed as described previously. The data obtained from the doxepin solubilities were converted to mole fractions using the appropriate specific gravity of the solution in question. Specific gravities were determined with a 25-ml pycnometer.

In all cases, the differences in weight per milliliter between the samples and distilled water was less than 1%; hence, the thermodynamic values were obtained from these data without the correction for volume changes upon mixing.

Determination of Partition Coefficient—The conditions were identical to those used in the pKa determination except that four 20-ml tubes were used, each containing 15 ml of doxepin stock solution (7.5×10^{-2} *M*), sufficient sodium hydroxide to obtain a constant pH of 12.6, and 0.5 ml of hexane. After equilibration, the tubes were centrifuged[4] at 2500 rpm for 20 min, and both phases were assayed spectrophotometrically at 292 nm for doxepin content. Saturation of both phases by doxepin was confirmed by repeating the assays at various time intervals during the equilibration period of 5 hr and observing that the drug concentration in both phases remained constant. Excess free base of doxepin was clearly visible in the container forming a separate phase of oil droplets within the aqueous layer. The drug concentration in each phase was calculated, adjusted for volume differences, and used to determine the apparent partition coefficient.

RESULTS AND DISCUSSION

Figure 1 shows the linear relationship of the intrinsic solubility of doxepin and desmethyldoxepin free base obtained at the corresponding ionic strengths. The reduction of the intrinsic solubility with increasing ionic strength may be due to a salting-out effect. The intrinsic solubility at zero ionic strength and 25° was determined from the intercept of the least-squares regression to be 1.13×10^{-4} *M* with a standard error of $\pm 3.12 \times 10^{-6}$ *M* for doxepin and 3.95×10^{-4} *M* with a standard error of $\pm 1.75 \times 10^{-6}$ *M* for desmethyldoxepin.

Tricyclic antidepressants have a high surface activity and it was speculated (1) that they may form micelles. It is therefore possible that the true solubilities may be slightly lower than those indicated. However, discontinuities in the spectrophotometric standard curves which would suggest association, have not been observed over the solubility range. In addition, no Tyndall effect has been detected visually. Therefore, associated species or micelles do not appear to be formed at the concentrations studied for doxepin and desmethyldoxepin.

Figure 2 shows a typical plot of $-\log(S/S_0 - 1)$ *versus* pH (Eq. 1) for doxepin and desmethyldoxepin at an ionic strength of 0.05 *M*. For each compound, the apparent pKa was obtained from the intercept of the least-squares regression line over a range of ionic strengths. For each determination of the apparent pKa, the intrinsic solubility was used at the appropriate ionic strength required. At low ionic strengths of <0.01 *M*, the equation relating pKa to ionic strength (I) is described by (6):

$$pKa^T = pKa^A - 0.505\sqrt{I} \qquad \text{(Eq. 3)}$$

where pKa^T is thermodynamic pKa and pKa^A is apparent pKa.

[6] Beckman DB-GT spectrophotometer connected to a 25.4-cm Beckman recorder.

[7] Beckman Century SS-1 pH meter connected to a model 39030 combination electrode.

[8] Sorvall superspeed RC2-B refrigerated centrifuge fitted with a SS-34 rotor. Sorvall Inc., Newtown, CT 06470.

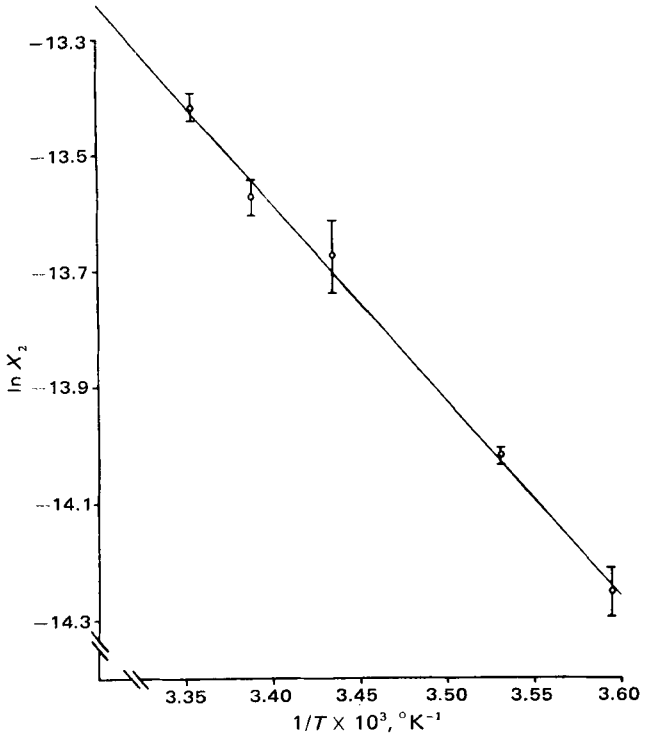

Figure 4—*The van't Hoff plot of ln* X_2 versus 1/T, *in degrees K, for doxepin at an ionic strength of 0.167* M. *Error bars indicate one standard error around the mean with each point representing four to eight determinations.*

Figure 3 shows the least-squares regression line representing the relationship between the apparent pKa values and the square root of the ionic strength of the system at which they were determined (Eq. 3). The y-intercept yields a pKa^T of doxepin at zero ionic strength of 8.96 with a standard error of ±0.05. This value substantially differs from the value of 8.0 (7) but is similar to the apparent pKa of other tricyclics with a similar alkyl side chain, such as chlorpromazine and imipramine whose apparent pKa values are 9.3 and 9.5, respectively (1).

For desmethyldoxepin, a pKa^T value of 9.75 with a standard error of ±0.05 was obtained from the intercept of the least-squares regression line. This value is in the same range as other demethylated tricyclic compounds such as desipramine, whose apparent pKa is 10.2 (1). The increase in the pKa of desmethyldoxepin over that of doxepin may be due to the loss of a methyl group and its replacement by a hydrogen atom on the amine side chain. Hydrogen bonding between the solvent water and the hydrogen atom on the secondary amine of desmethyldoxepin displaces the hydrogen from the nitrogen, causing the nitrogen to be more electron rich, hence, increasing its basic character. This increased basicity leads to a weaker conjugate acid and an increase in pKa (8).

The linearity of the van't Hoff plot ($r^2 = 0.979$) indicates that the number of water molecules necessary for solvation is temperature independent in the range tested. The slope and the intercept of the van't Hoff plot yielded the thermodynamic values for the change in entropy and enthalpy of solution (Fig. 4). The change in enthalpy of solution was 6.71 with a standard error of ±0.19 kcal/mole, a positive value indicating that the system absorbed heat from its surroundings as would be expected from a nonpolar molecule with low aqueous solubility. The change in entropy of solution was −4.16 with a standard error of ±0.64 cal/mole °K.

The apparent partition coefficient for doxepin in hexane–water was determined at pH 12.6 and was 13,615: 1 with a standard deviation of ±360. The high value of the partition coefficient in hexane–water indicates the large lipid solubility of doxepin. The log of the partition coefficient was 4.13 and compares well with other tricyclic psychotherapeutic agents such as imipramine and chlorpromazine whose log octanol–water partition coefficients are 4.62 and 5.32, respectively (9). Preliminary experiments were able to extract 90% of 6.25×10^{-4} *M* doxepin contained in 30 ml of water with a single 3-ml sample of hexane by vortexing for 5 min at pH 7.5. This is 1.5 units below its pKa and the base should be substantially protonated; yet the extraction at a somewhat unfavorable pH took place with ease, apparently due to its large partition coefficient.

However, only 75% of 6.33×10^{-4} *M* desmethyldoxepin was extracted at pH 8.7, 1.3 units below its pKa but otherwise similar conditions. Although the partition coefficient of desmethyldoxepin was not determined in hexane–water, we speculate that it cannot be as large as that of doxepin. Based on our calculations, using a direct proportionality of 90% doxepin with a partition coefficient of 13,615:1 to 75% desmethyldoxepin extracted under similar conditions, the partition coefficient of desmethyldoxepin for hexane–water was estimated to be about 10,000:1.

REFERENCES

(1) A. L. Green, *J. Pharm. Pharmacol.*, **10,** 19 (1967).

(2) P. A. Schwartz, C. T. Rhodes, and J. W. Cooper, *J. Pharm. Sci.*, **66,** 994 (1977).

(3) H. A. Krebs and J. C. Speakman, *J. Chem. Soc.*, **2,** 593 (1945).

(4) H. A. Krebs and J. C. Speakman, *Br. Med. J.*, **47,** (1946).

(5) M. A. Lauffer, "Entropy Driven Processes in Biology," Springer-Verlag, New York, N.Y., 1975, p. 1.

(6) A. Albert and E. P. Serjeant, "Ionization Constants of Acids and Bases," Methuen, London, 1962, p. 59.

(7) Anon., "American Hospital Formulary Service," M. J. Reilly and J. A. Kepler, Eds., American Society of Hospital Pharmacists, Washington, D.C., 1977.

(8) E. M. Arnett and G. W. Mach, *J. Am. Chem. Soc.*, **86,** 2671 (1964).

(9) G. G. Nahas, B. Desoize, and C. Leger, *Proc. Soc. Exp. Biol. Med.*, **160,** 344 (1979).

ACKNOWLEDGMENTS

Supported in part by the National Institute of Child Health and Human Development Grant 1R01HD14075-01.

Nitrogen–Phosphorous Detection of Phencyclidine in Blood Serum

S. STAVCHANSKY ˣ and A. LOPER

Received April 6, 1981 from the *College of Pharmacy, Drug Dynamics Institute, The University of Texas, Austin, TX 78712.* Accepted for publication June 10, 1981.

Abstract □ A method for quantitating phencyclidine in the blood serum of rhesus monkeys with a solvent extraction procedure followed by gas chromatography with nitrogen–phosphorous detection is reported. Phencyclidine was extracted with ether from 0.5 ml of serum (pH 13.5) made basic with 2*M* NaOH, followed by back-extraction into 0.5 *M* sulfuric acid. After the addition of 2 *M* sodium hydroxide, phencyclidine was extracted into a small volume of ether for concentration and injection into the gas chromatograph. The limit of quantitation of phencyclidine in serum was 5 ng/ml. Recovery averaged 51.9 ± 4.3%. Standard curves were linear between 5–50 ng/ml and 100–2000 ng/ml. Comparison between serum and aqueous standards indicated no interference by serum components in the extraction procedure. Pentobarbital, caffeine, and the monohydroxy metabolites of phencyclidine did not interfere with the analysis. This procedure is a rapid and sensitive method for determination of serum phencyclidine levels in animal studies requiring analysis of large numbers of samples.

Keyphrases □ Phencyclidine—analysis using gas chromatography with nitrogen–phosphorous detection, rhesus monkey blood serum □ Gas chromatography—nitrogen–phosphorous detection of phencyclidine in rhesus monkey blood serum □ Drugs of abuse—phencyclidine, analysis using gas chromatography with nitrogen–phosphorus detection, rhesus monkey blood serum

The popularity of phencyclidine [1-(1-phenylcyclohexyl)piperidine] as a drug of abuse has stimulated interest in determination of the drug in body fluids (1, 2). Persons who have ingested phencyclidine (I) often show signs of intoxication even when serum levels are low (10 ng/ml) (3). TLC methods and qualitative, presumptive tests which indicate the presence, but not the concentration, of I in biological matrixes were reported previously (4, 5).

Spectrophotometric quantitation of I after solvent extraction of specimen suffers from the lack of adequate detection limits (4). Homogeneous enzyme immunoassays for I in urine show cross-reactivity with analogs and inactive metabolites of I (6, 7). Radioimmunoassay for I in plasma is sensitive enough for quantitation at plasma levels of ~1 ng/ml (8–10), but some cross-reactivity (2–5%) is seen with hydroxylated metabolites of I in two of these radioimmunoassay procedures (9, 10).

Investigation of an ion-selective electrode for I indicates that potentiometric analysis may provide adequate specificity for the parent drug (11). The reported sensitivity of this electrode is poor compared with radioimmunoassay or gas chromatographic (GC) methods. Preconcentration of sample could possibly lower detection limits; however, this has not been evaluated for use with the phencyclidine-selective electrode.

BACKGROUND

Numerous GLC assays have been used for separation of phencyclidine in biological matrixes. Flame-ionization detection after GC separation of serum extracts cannot provide sufficient sensitivity (4, 12, 13). GC with mass spectrometry lowers detection limits to as little as 5 ng of I/ml in plasma, whole blood, and urine (14–18). Analytical procedures using GC with nitrogen–phosphorous detection provide sensitivity comparable to mass spectrometry (3, 19, 20). However, the solvent extraction procedures reported for sample cleanup prior to separation and subsequent quantitation by nitrogen–phosphorous detection are too laborious for rapid processing of many specimens, or require a larger volume of specimen than is available in studies with small animals.

The analytical procedure reported here combines a rapid extraction procedure for 0.5 ml of blood serum with GC separation and nitrogen–phosphorous detection. This method is particularly useful for analyses in pharmacokinetic studies of phencyclidine in small animals.

EXPERIMENTAL

Apparatus—GC was performed with a gas chromatograph equipped with a nitrogen–phosphorous detector[1]. A 122-cm coiled glass column, 0.2-cm i.d., was silylated with 2% trimethylchlorosilane in hexane and packed with 3% SP-2250-DB on a 100–120 mesh support[2]. The column was conditioned overnight at 250° with a helium flow of 15 ml/min. Gas flows were a helium carrier flow of 25 ml/min and a hydrogen flow of 2.5 ml/min. Air was maintained at a constant pressure of 40 psi. Inlet temperature was 195°, column temperature was 185°, and the detector temperature was 210°. Background current was set at 4×10^{-11} amp.

Reagents—Phencyclidine hydrochloride and two monohydroxy metabolites [4-phenyl-4-piperidinocyclohexanol and 1-(1-phenylcyclohexyl)-4-hydroxypiperidine] were obtained from the National Institute on Drug Abuse. Melting point determinations[3] and electron-impact mass spectrometry[4] were used to confirm identity and purity of the compounds. TLC of phencyclidine produced only one spot on silica gel G, 250-μm plates[5]. Plates were developed with chloroform–ethyl acetate–acetone–triethylamine (38:30:30:2). Spots were visualized by charring with sulfuric acid and heat.

Ketamine hydrochloride[6], caffeine[7], and pentobarbital sodium[8] were used as received. Nanograde ether[9] was distilled in glass each day after

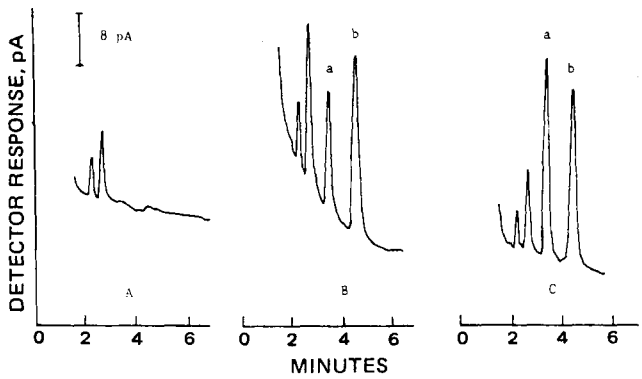

Figure 1—*Chromatograms obtained from extraction and assay of 0.5 ml of blood serum from a rhesus monkey (A), from a 0.5-ml serum sample spiked with 25 ng of phencyclidine and 50 ng of ketamine (B), and from 0.5 ml of serum obtained from a 6.7-kg male rhesus monkey 1.5 hr after intravenous administration of 1.6 mg of phencyclidine/kg (C). Estimated concentration of phencyclidine (a) was 75.4 ng/ml. The concentration of ketamine (b) was 100 ng/ml.*

[1] Tracor model 560 equipped with a model 702 nitrogen–phosphorous detector, Tracor Instruments, Austin, TX 78721.
[2] Supelco, Bellefonte, PA 16823.
[3] Capillary melting point apparatus, Arthur H. Thomas Co., Philadelphia, Pa.
[4] Dupont model 21-491 mass spectrometer.
[5] Analtech, Newark, DE 19711.
[6] Warner-Lambert Co., Ann Arbor, MI 48105.
[7] Sigma Chemical Co., St. Louis, MO 63178.
[8] Robinson, San Francisco, CA 94107.
[9] Mallinckrodt, St. Louis, MO 63147.

0022-3549/82/0200-0194$01.00/0

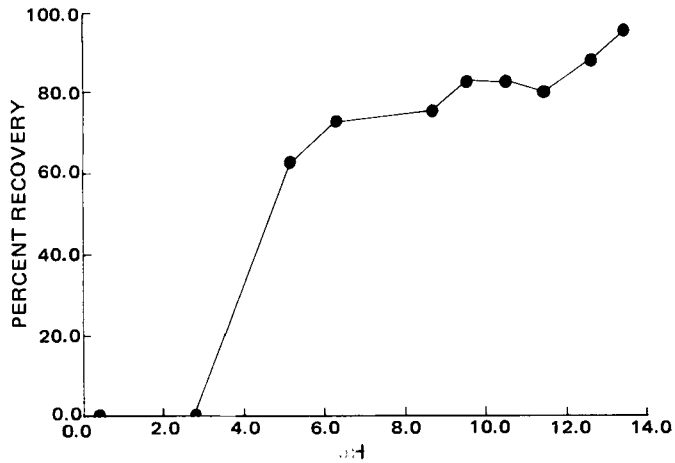

Figure 2—*Recovery of phencyclidine from aqueous solutions of varying pH. Maximum recovery occurs at pH 13.5.*

the addition of aluminum lithium hydride. All other materials were reagent grade.

Procedure—Serum (0.5 ml) obtained from rhesus monkeys was pipetted into a silylated glass tube with a screw cap with an inert liner. For serum phencyclidine concentrations of ~5–20 ng/ml, 50 μl of aqueous ketamine hydrochloride solution (200 ng/ml) was added to each tube as an internal standard. Serum concentrations of 20–100 ng of phencyclidine/ml required 50 μl of aqueous ketamine hydrochloride solution (1 μg/ml), and phencyclidine levels of 100–2000 ng/ml required 50 μl of ketamine solution (10 μg/ml). All stock solutions of phencyclidine and ketamine hydrochloride were prepared with deionized water. Preparation of stock solutions with methanol did not affect extraction and quantitation of phencyclidine and internal standard.

Serum was adjusted to a pH of 13.5 with 0.5 ml of 2 *M* NaOH. Ether (2 ml) was added to each tube. The tubes were placed on a vortex mixer for 60 sec to extract the free bases of phencyclidine and internal standard into the organic phase. The aqueous and organic phases were separated by centrifuging at 3000 rpm for 2 min, and then freezing the aqueous layer in a dry ice–acetone bath. The organic layer was decanted into a second tube containing 0.5 ml of 0.5 *M* H_2SO_4. Phencyclidine and internal standard were back-extracted from the ether into the aqueous layer by vortexing for 30 sec.

Samples were centrifuged at 3000 rpm for 1 min and immersed in a dry ice–acetone bath. The organic layer was discarded, and the aqueous layer was allowed to return to room temperature. The aqueous layer, 0.5 ml of 2 *M* NaOH, and 250 μl of distilled ether were vortexed together for 30 sec and centrifuged for 1 min. After the aqueous phase was frozen in dry ice–acetone, the ether layer was decanted into a conical vial. A small amount of anhydrous potassium carbonate was added to each sample to remove residual moisture. The ether layer was allowed to evaporate to a volume of 10–50 μl. One to five microliters of the sample was injected into the gas chromatograph. After every six injections, a 30-min wait was necessary to allow slow-eluting compounds to be eliminated from the column.

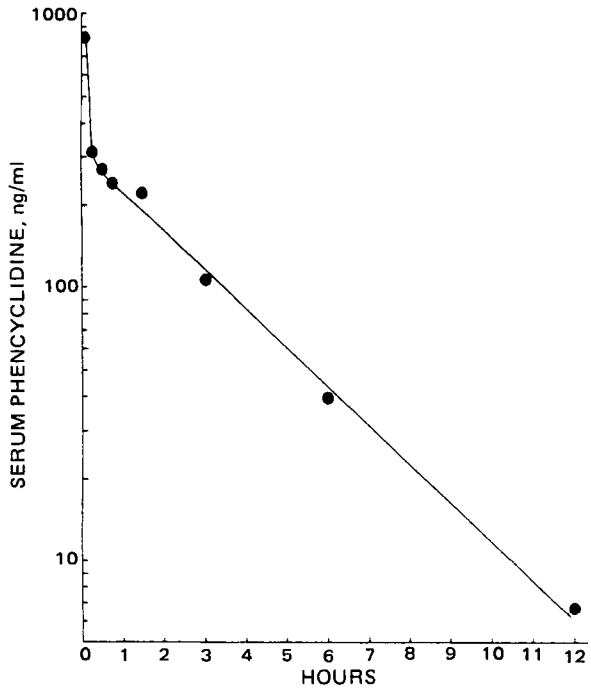

Figure 3—*Semilogarithmic plot of serum levels of phencyclidine in a 5.0-kg male rhesus monkey after administration of a 1.6 mg/kg iv dose.*

Table I—Phencyclidine Recovery from Serum Standards

Phencyclidine Concentration, ng/ml	Mean Recovery[a] ± *SD*, %
4.9	53.7 ± 15.3
9.8	50.5 ± 4.2
48.9	59.5 ± 3.5
97.8	49.1 ± 1.2
489.0	51.2 ± 4.2
978.0	47.5 ± 2.0

[a] Average of six determinations.

A calibration curve was constructed by plotting peak height ratio of phencyclidine to internal standard against the phencyclidine concentration. Serum standards were prepared by addition of appropriate aliquots of aqueous phencyclidine solutions (50 ng/ml, 0.5 μg/ml, or 5 μg/ml) to 0.5 ml of blank serum obtained from dogs or rhesus monkeys. Standard concentrations ranged from 5 to 2000 ng/ml. Standards were extracted and assayed in the same manner as the samples. Standards were also prepared in deionized water and treated identically to serum standards to determine if serum components affected extraction or quantitation of phencyclidine or internal standard.

Recovery of Phencyclidine—Serum standards containing either 4.9, 9.8, 48.9, 97.8, 489.0, or 978.0 ng of phencyclidine/ml and no internal standard were extracted by the same procedure. The final ether extracts were allowed to evaporate to dryness and then reconstituted with 10–100 μl of ethyl acetate containing 2 μg of ketamine/ml. One to five microliters was injected into the gas chromatograph. Peak height ratios of phencyclidine to ketamine were compared with those ratios obtained from ethyl acetate solutions containing 1 or 5 μg of phencyclidine/ml and 2 μg of ketamine/ml.

A profile of phencyclidine recovery *versus* pH of an aqueous solution was constructed. The pH was adjusted with either sulfuric acid or sodium hydroxide solutions. Phencyclidine was present in a concentration of 50 ng/ml. One milliliter of aqueous solution and 2 ml of ether were vortexed for 60 sec and centrifuged at 3000 rpm for 2 min. The ether layer was decanted into a conical vial after freezing the aqueous layer in a dry ice–acetone bath. After evaporation of the ether, samples were reconstituted and treated as already described.

Interference by Other Compounds—Fifty microliters of 1 mg/ml methanolic pentobarbital sodium or caffeine solution was added to 1 ml of deionized water. Methanolic solutions of the two monohydroxy metabolites were used to prepare urine samples containing 1 mg/ml of each metabolite. The resulting samples were extracted and quantitated by the same procedure used for serum to check for interference with phencyclidine or ketamine peaks.

RESULTS AND DISCUSSION

Figure 1 shows representative chromatograms for a serum blank from a male rhesus monkey, a serum blank spiked with phencyclidine, and

Table II—Summary of Linear Regression Analysis of Composite Standard Curves for Phencyclidine in Serum or Water[a]

Standard Curve	Equation	Correlation Coefficient	Standard Error of the Estimate
Serum, 5–50 ng/ml	$y = 0.013x - 0.005$	0.993	0.024
Serum, 100–2000 ng/ml	$y = 0.014x - 0.613$	0.999	0.348
Water, 5–50 ng/ml	$y = 0.014x - 0.005$	0.996	0.020
Water, 100–2000 ng/ml	$y = 0.014x + 0.262$	0.999	0.112

[a] No significant difference between equations for serum and water exists.

Table III—Day-to-Day Coefficient of Variation in Peak Height Ratios for Phencyclidine Serum Standards

Standard Concentration, ng/ml	Number of Determinations	Coefficient of Variation, %
4.9	5	8.3
9.8	5	9.0
14.7	3	6.3
19.6	1	—
48.9	9	4.2
97.8	6	5.5
489.0	5	3.0
685.0	4	8.9
978.0	4	15.7
1958.0	2	8.4

serum obtained 1.5 hr after administration of a 1.6 mg/kg iv dose of phencyclidine to a 6.7-kg male rhesus monkey. Retention times of phencyclidine and internal standard are 3.6 and 4.7 min, respectively. Chromatography of phencyclidine and ketamine at 185° produced good resolution of the two peaks (R = 1.5, 99.7% resolution). Reducing the temperature below 185° produced peak broadening. The lower viscosity of the stationary phase of the SP-2250-DB packing relative to 3% OV-17 allowed operation at lower column temperatures, thus preventing the thermal degradation of phencyclidine to 1-phenylcyclohexene (16). The chromatogram of the serum blank shows two unidentified peaks eluting at 2.3 and 2.7 min. These peaks do not interfere with the analysis. However, small interfering peaks (not evident in this chromatogram) with retention times of 3–5 min were seen with some serum samples. This serum background limited quantitation of phencyclidine in rhesus monkey serum to ~5 ng/ml.

Application of this extraction and quantitation technique to human serum[10] or plasma[11] resulted in a frequent appearance of interfering peaks with retention time of 4–5 min. This interference could not be assigned to pentobarbital, which produced no interfering peaks in the chromatogram, or to caffeine, which produced a peak at 6 min. Extraction and quantitation of the monohydroxy phencyclidine metabolites produced a broad peak at 12 min. Human serum obtained with evacuated collection tubes[12] suitable for trace analysis did not exhibit these large interfering peaks in the chromatogram. This suggests that the interferences seen with serum and plasma extracts might be artifacts of collection or storage. GC–mass spectrometry of extracts containing the interfering substance indicated that it is a basic compound with a probable molecular ion at m/z 86. Further studies are planned to elucidate the structure of this substance.

Hexane and ethyl acetate, as well as ether, were initially evaluated as extracting solvents, since they contained few impurities which interfered with nitrogen–phosphorous detection. However, hexane produced emulsification upon vigorous mixing with serum. The less volatile ethyl acetate (relative to ether) increased the time required to concentrate the final extract.

The percent recovery of phencyclidine from aqueous solutions of varying pH values is shown in Fig. 2. Maximum recovery was 95% at pH 13.5. The single extraction step used in these determinations was not adequate to produce a serum extract free from interference; therefore, phencyclidine was back-extracted into 0.5 M sulfuric acid. Virtually 100% of the phencyclidine should partition into the aqueous layer at this pH (pH < 1) (Fig. 2). Final extraction of phencyclidine from a basified aqueous phase into as small a volume of ether as practical (250 μl) reduced the time required to concentrate the final extract. The average recovery of phencyclidine from serum standards was 51.9 ± 4.3% after the necessary back-extraction steps (Table I).

Linear relationships were found between peak height ratio and phencyclidine serum concentration for concentrations from 5–50 and 100–2000 ng/ml. Above 2000 ng/ml, detector response was no longer linear. The least-squares regression equations are shown in Table II. Statistical analyses (21) indicated no significant difference (p = 0.01) existing between serum and aqueous standard curves at all concentrations. Thus, serum components do not appear to affect the extraction and quantitation procedures. Within-day coefficients of variation in peak height ratios (n = 6) for the 48.9 and 489.0 ng/ml standards were 3.9 and 1.6%, respectively. The day-to-day variation in peak height ratios is presented in Table III. The coefficient of variation is <10% for all but the 978.0 ng/ml standard. The day-to-day coefficient of variation averaged 7.7% over all concentrations.

Serum phencyclidine levels after administration of a 1.6 mg/kg iv dose to a rhesus monkey are shown in Fig. 3. The animal was fasted overnight prior to receiving the dose. After 12 hr, no detectable levels of phencyclidine were present in the serum. The biological half-life, calculated after computer fit of the data to a biexponential equation, was 2.1 hr, which agrees with phencyclidine half-lives in rhesus monkeys reported earlier (14). This rapid extraction procedure, combined with satisfactory detection limits provided by GC with nitrogen–phosphorous detection, is advantageous in animal studies involving numerous small serum samples. In addition, this assay procedure deserves further investigation for clinical use.

[10] Supplied by the Texas State Health Department, Austin, Tex.
[11] Supplied by the Travis County Blood Bank, Austin, Tex.
[12] "Blue-top," siliconized Vacutainer with no additives, Becton-Dickinson, Rutherford, NJ 07070.

REFERENCES

(1) R. H. Cravey, D. Reed, and J. L. Ragle, *J. Anal. Toxicol.*, **3,** 199 (1979).

(2) L. J. Sioris and E. P. Krenzelok, *Am. J. Hosp. Pharm.*, **35,** 1362 (1978).

(3) L. J. Lewellen and E. F. Solomons, *J. Anal. Toxicol.*, **3,** 72 (1979).

(4) R. C. Gupta, I. Lu, G. L. Oei, and G. D. Lundberg, *Clin. Toxicol.*, **8,** 611 (1975).

(5) E. G. Saker and E. T. Solomons, *J. Anal. Toxicol.*, **3,** 220 (1979).

(6) H. Tom, D. S. Kabakoff, C. I. Lin, P. Singh, M. White, P. Westkamper, C. McReynolds, and K. dePorceri-Morton, *Clin. Chem.*, **25,** 1144 (1979).

(7) C. Walberg and R. Gupta, *ibid.*, **25,** 1144 (1979).

(8) B. Kaul and B. Davidow, *Clin. Toxicol.*, **16,** 7 (1980).

(9) L. S. Rosenberg and H. V. Vunakis, *Res. Commun. Chem. Pathol. Pharmacol.*, **25,** 547 (1979).

(10) D. P. Ward and A. J. Trevor, *Life Sci.*, **27,** 457 (1980).

(11) C. R. Martin and H. Freiser, *Anal. Chem.*, **52,** 1772 (1980).

(12) Y. H. Caplan, K. G. Orloff, B. C. Thompson, and R. S. Fisher, *J. Anal. Toxicol.*, **3,** 47 (1979).

(13) J. A. Marshman, M. P. Ramsey, and E. M. Sellers, *Toxicol. Appl. Pharmacol.*, **35,** 129 (1976).

(14) A. E. Wilson and E. F. Domino, *Biomed. Mass Spectrom.*, **5,** 112 (1978).

(15) O. S. Pearce, *Clin. Chem.*, **22,** 1623 (1976).

(16) D. C. K. Lin, A. J. Fentiman, R. L. Foltz, R. D. Forney, and I. Sunshine, *Biomed. Mass Spectrom.*, **2,** 206 (1975).

(17) W. D. MacLeod, D. E. Green, and E. Seet, *Clin. Toxicol.*, **9,** 561 (1976).

(18) D. H. Altmiller, *Lab. Invest.*, **40,** 301 (1979).

(19) D. N. Bailey and J. J. Guba, *Clin. Chem.*, **26,** 437 (1980).

(20) F. N. Pitts, Jr., L. S. Yago, O. Aniline, and A. F. Pitts, *J. Chromatogr.*, **193,** 157 (1980).

(21) J. Neter and W. Wasserman, "Applied Linear Statistical Models," Richard D. Irwin, Homewood, Ill., 1974, p. 160.

ACKNOWLEDGMENTS

The authors thank Dr. Robert Willette of the National Institute on Drug Abuse for supplying the phencyclidine and phencyclidine metabolites. They also are grateful to Dr. Martin L. Black of the Warner-Lambert Company for supplying the ketamine.

Alice Loper is a Fellow of the American Foundation for Pharmaceutical Education.

Mechanism of Action of Granaticin: Inhibition of Ribosomal RNA Maturation and Cell Cycle Specificity

PETER HEINSTEIN

Received December 10, 1980 from the *Department of Medicinal Chemistry and Pharmacognosy, School of Pharmacy and Pharmacal Sciences, Purdue University, W. Lafayette, IN 47907.* Accepted for publication May 21, 1981.

Abstract □ Granaticin, an antibiotic produced by *Streptomyces* species was found to be cytotoxic (ED_{50} 3.2 μg/ml) against human oral epidermoid carcinoma (KB) cells. At ED_{50} concentrations RNA synthesis was inhibited to the greatest extent. Prelabeling of RNA in KB cells, followed by addition of granaticin (2.13 μg/ml) showed that ribosomal RNA maturation was inhibited. The inhibition of the formation of functional ribosomal RNA was determined by sucrose gradient centrifugation and showed that the accumulation of 45S preribosomal RNA was dependent on granaticin concentration and on the time granaticin was in contact with the KB cells. The effect of granaticin (6.3 μg/ml) on KB cells in the different cell cycle phases showed preferential inhibition (93%) of cell survival in the G_2 phase. However, RNA synthesis was only 20% inhibited by granaticin in KB cells in the G_2 phase. From these results, it was concluded that ribosomal RNA maturation was not the only site of action of granaticin toxicity.

Keyphrases □ Granaticin—cytotoxicity, mechanism of action, in human oral epidermoid carcinoma cells □ Cytotoxicity—granaticin, mechanism of action, in human epidermoid carcinoma cells □ Anticancer agents—granaticin, mechanism of action

Granaticin, an antibiotic produced by the *Streptomyces* species was first reported (1) as a fermentation product of *Streptomyces olivaceus*. Its structure was clarified by Keller-Schierlein *et al.* (2). Subsequently, granaticin or its L-rhodinoside, granaticin B, was isolated from *S. violaceoruber* (3), *S. litmogenes* (4), and *S. thermoviolaceus* (5). Granaticin was active against Gram-positive bacteria (6) and showed anticancer activity against P-388 lymphocytic leukemia in mice and cytotoxicity against human oral epidermoid carcinoma (KB) cells (7).

BACKGROUND

Granaticin was reported to inhibit RNA synthesis in bacteria (8). This inhibition was originally attributed to the interaction of granaticin with the DNA template. More recently, the mechanism of action of granaticin in bacteria has been attributed to the inhibition of aminoacylation of leucyl-tRNA by interaction with an aminoacyl-tRNA synthetase (9). It was not determined whether or not this inhibition was due to binding of granaticin to tRNA. Another report (10) showed that granaticin inhibited viral RNA-dependent DNA polymerase isolated from RNA tumor viruses, *i.e.*, Rauscher murine leukemia virus, simian sarcoma virus type 1, and avian myeloblastosis virus. From the sequential addition of granaticin to the reaction, it was proposed that granaticin interacts with the template (RNA) and not the reverse transcriptase. However, direct binding of granaticin to templates was not shown.

Since these results indicated an inhibitory action of granaticin on RNA metabolism, the mechanism of action of granaticin in mammalian cells was studied. In the present study, the effect of granaticin on the formation of functional ribosomal RNA in KB cells, on the uptake of uridine by KB cells and its subsequent phosphorylation, and on the cell cycle traverse of KB cells was investigated.

MATERIAL AND METHODS

Stock solutions of granaticin A[1] were prepared by dissolving 3 mg of granaticin in 0.03 ml of dimethyl sulfoxide and diluting to 10 ml with basal salt solution (11), pH 7.2.

Human oral epidermoid carcinoma cells[2] (KB cells) were grown in monolayer cultures with basal medium supplemented with 10% heat denatured (57°) fetal calf serum containing 100 U of penicillin and 100 g of streptomycin/ml (12, 13). Cells were maintained at 37° in an atmosphere of 5% CO_2 in air and subcultured every 2–3 days. For experiments, cells were detached from the glass support with trypsin–ethylenediaminetetraacetic acid[3], collected by centrifugation, washed and suspended in fresh medium, plated at a density of 5×10^4–1×10^5 cells/ml, and incubated for 3 hr at 37° to allow attachment to the support before an experiment was initiated.

Macromolecular synthesis was measured by the addition of [^{3}H]thymidine[4] (1 μCi/ml cells; 26.1 μCi/μmole) for DNA synthesis, [^{3}H]uridine[4] (1 μCi/ml cells; 22 μCi/μmole) for RNA synthesis, and [^{3}H]lysine[4] (1 μCi/ml cells; 50.4 μCi/μmole) for protein synthesis. Cells were disrupted and the macromolecules were precipitated with an equal volume of ice cold 10% trichloroacetic acid in 0.1 *M* pyrophosphate. The precipitates were collected on glass fiber filters[5], washed three times with trichloroacetic acid in 0.01 *M* pyrophosphate and two times with 0.1 *N* hydrochloric acid, and their radioactivity was determined.

Cell populations synchronized in the S-phase were obtained by a double-thymidine blockade (14–18). KB cells in the different phases were then treated with granaticin and RNA synthesis was measured through the incorporation of [^{3}H]uridine into acid-insoluble fractions. Cell survival after treatment with granaticin (6.2 μg/ml) for 1 hr in different phases of the cell cycle was measured by suspending washed cells in fresh medium. The cell suspension was diluted 1:1000, plated into plastic dishes, and incubated at 37° for 7 days. The number of colonies was determined under a microscope after staining with Giemsa.

The labeling, extraction, and isolation of nucleolar and cytoplasmic ribonucleic acid was described previously (19). KB cells at a concentration of 3.3×10^6 cells/ml were incubated with 1 μCi/ml [^{3}H]uridine (22 μCi/μmole) and 30 ml of medium. Identical incubations contained 2–5 μg of granaticin/ml of medium. Cells were harvested after 1–4 hr at 37°.

The uptake of [^{3}H]uridine and its subsequent conversion to uridine monophosphate, uridine diphosphate, and uridine triphosphate was measured by incubating 1.6–2.4×10^5 KB cells/ml with 1.1 μCi/ml

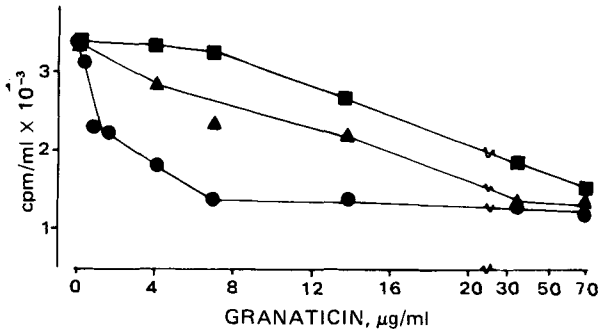

Figure 1—*Effect of granaticin on macromolecular synthesis. KB cells at a concentration of 1×10^5 cells/ml were plated 3 hrs before granaticin was added. DNA synthesis (■) was measured by the incorporation of [^{3}H]thymidine, RNA synthesis (●) was measured by the incorporation of [^{3}H]uridine, and protein synthesis (▲) was measured by the incorporation of [^{3}H]lysine. Granaticin was added 10 min before the radioactive precursor was added. The amount of acid-precipitated radioactivity was measured after the cells were in contact with granaticin for 1 hr.*

[1] Dr. H. G. Floss, Department of Medicinal Chemistry and Pharmacognosy, Purdue University.

[2] American Type Culture Collection (ATCC CL17).
[3] Grand Island Biological Co., Grand Island, N.Y.
[4] Amersham/Searle Corp., Arlington Heights, Ill.
[5] Grade GF/A, Whatman Inc.

0022-3549/82/0200-0197$01.00/0

Table I—Effect of Granaticin on KB Cell Growth

Granaticin[a], μg/ml	Cells/ml × 10^{-5} [b] 24 hr	48 hr	72 hr
0	3.3	4.6	9.3
1.4	3.2	4.0	7.5
6.9	3.0	3.6	5.7
13.8	2.8	2.6	2.4
34.4	0.6	0.7	0.8

[a] Granaticin at the indicated concentrations remained in contact with the cells for 2 hr. The cells were then washed and incubated with fresh medium for 24, 48, and 72 hr. The number of cells remaining were determined by counting an aliquot in an eosinophil counter. Values are the average of three experiments.
[b] Cells were seeded at a concentration of 5 × 10^4 cells/ml 3 hr before granaticin was added.

[^{3}H]uridine (22 μCi/μmole) and with and without 1–2.75 μg of granaticin/ml. Aliquots were removed immediately after the addition of [^{3}H]-uridine and after 2 and 4 hr. The reaction was stopped with an equal volume of ice cold 10% trichloroacetic acid in 0.1 *M* pyrophosphate. The acid soluble fractions were analyzed by TLC followed by scintillation

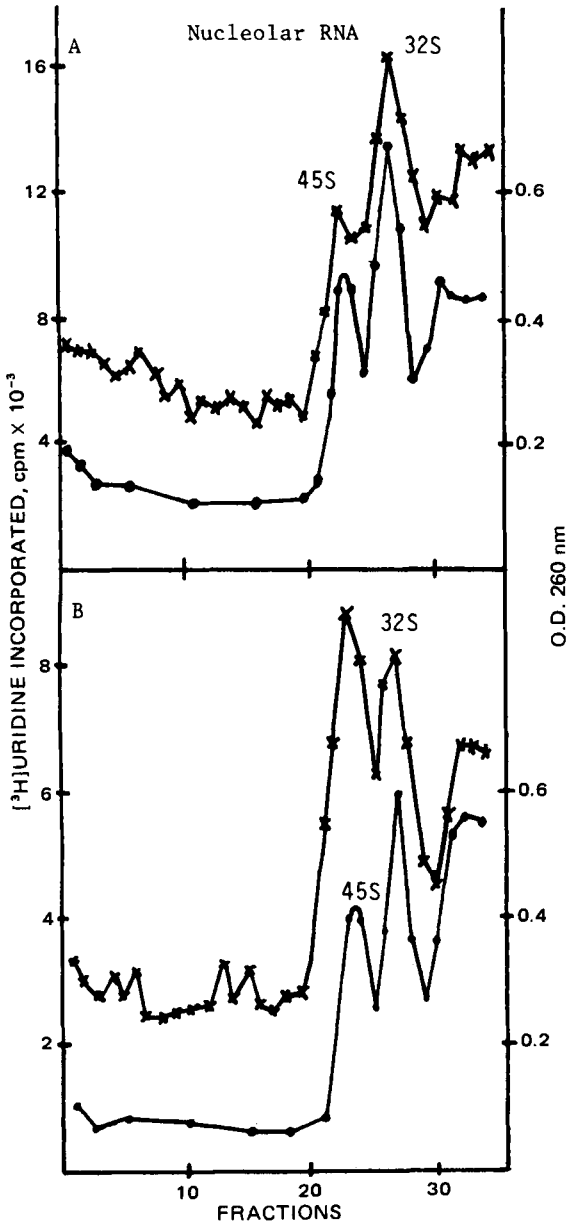

Figure 2—*Sucrose gradient analysis of nuceolar RNA from KB cells. RNA was labeled by the exposure of a total of 1 × 10^8 cells (3 × 10^6 cells/ml) for 1 hr to [^{3}H]uridine in the absence (A) or presence (B) of granaticin (2.13 μg/ml). Fractions were collected through a needle from 15–30% gradients and centrifuged for 12 hr at 20 × 10^3 rpm in an SW 40 rotor.*

counting (20) after the addition of cold uridine mono-, di-, and triphosphate[6] or by the method of Cheung and Suhadolnik (21).

Radioactivity was measured in a liquid scintillation spectrometer[7] in 10 ml of toluene scintillation cocktail or commercial scintillation solution[8] for water-soluble samples.

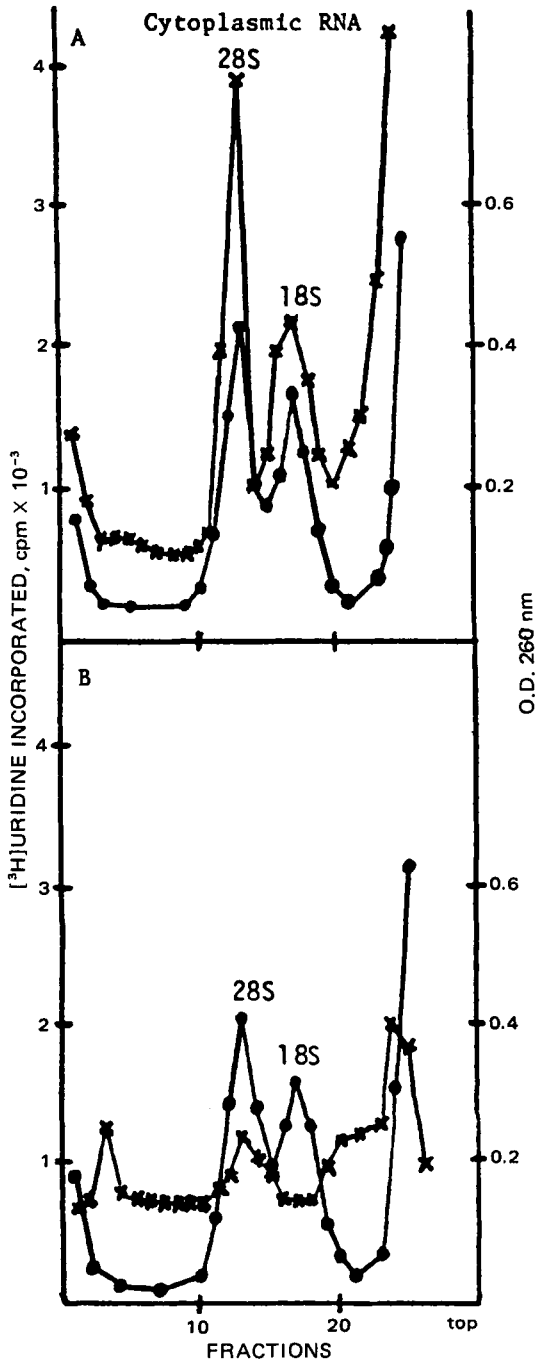

Figure 3—*Sucrose gradient analysis of cytoplasmic RNA from KB cells. Experimental condition was identical to the conditions in Fig. 2, except that the 15–30% sucrose gradients were centrifuged for 16 hr at 22 × 10^3 rpm. (A, control incubation; and B, 2.13 μg of granaticin/ml).*

RESULTS

To determine a concentration of granaticin that would allow study of the inhibition of cellular processes without excessive cell death, the effect of granaticin on cell survival was measured (Table I). Granaticin at a concentration of 1.4 mg/ml for 2 hr caused a 3% reduction in cell numbers

[6] Sigma Chemical Co., St. Louis, Mo.
[7] Beckman Instrument Co. model LS-250.
[8] Aquasol, New England Nuclear, Boston, Mass.

Table II—Effect of Granaticin Concentration and Contact Time on the Maturation of Ribosomal RNA in KB Cells [a]

Granaticin, μg/ml of medium	Incubation, hr	RNA Percent of control [b] 45S	32S	28S	18S
2.16	1	94	48	59	5
2.16	2	86	32	9	0
3.20	1	79	32	42	0
3.20	2	75	11	6	0
5.00	1	53	0	0	0

[a] Cells were seeded at a concentration of 3×10^6 cells/ml and treated with different concentrations of granaticin for 1–2 hr. [b] The radioactivity associated with the 45S, 32S, 28S, and 18S fractions was determined and is expressed as percentage of the radioactivity in control incubations without granaticin, analyzed after 1 and 2 hr.

after 24 hr compared to incubations without granaticin. In addition, the damage to the cells appeared to be permanent, since the reduction in cell number was 14 and 19% after 48 and 72 hr, respectively, at the same granaticin concentration. The cytotoxic effect of granaticin was more pronounced at higher concentrations of the inhibitor (Table I). From these results, concentration of 2 μg of granaticin/ml of cells (in some experiments up to 5 μg/ml) were used for subsequent experiments. In addition, the exposure time of the cells to granaticin was 1–2 hr to minimize cell death.

Synthesis of macromolecules was monitored by measuring the incorporation of radioactively labeled thymidine, uridine, and lysine into acid-insoluble fractions. Addition of granaticin at various concentrations, 10 min before the radioactive precursor was added to the cell cultures, showed (Fig. 1) that the formation of ribonucleic acid was inhibited 50% at a granaticin concentration of ~2 μg/ml. At this same granaticin concentration, DNA and protein synthesis were not appreciably affected.

The ribonucleic acids synthesized in the presence and absence of granaticin were analyzed by differential separation using sucrose gradient centrifugation of the cytoplasmic and nucleolar ribonucleic acids as described previously (19). The results (Figs. 2 and 3) indicated an accumulation of 45S RNA in the nucleoli of granaticin-treated cells (Fig. 3B) compared to untreated control cells (Fig. 2A). Similarly, virtually no 18S and very little 28S RNA apeared in the cytoplasm of granaticin-treated cells (Fig. 3B) compared with untreated cells (Fig. 3A). These results were obtained after 1-hr exposure of the cells to [^{3}H]uridine in the presence or absence of granaticin (2.13 μg/ml/hr). In similar experiments (Table II), KB cells were labeled with [^{3}H]uridine and exposed to granaticin

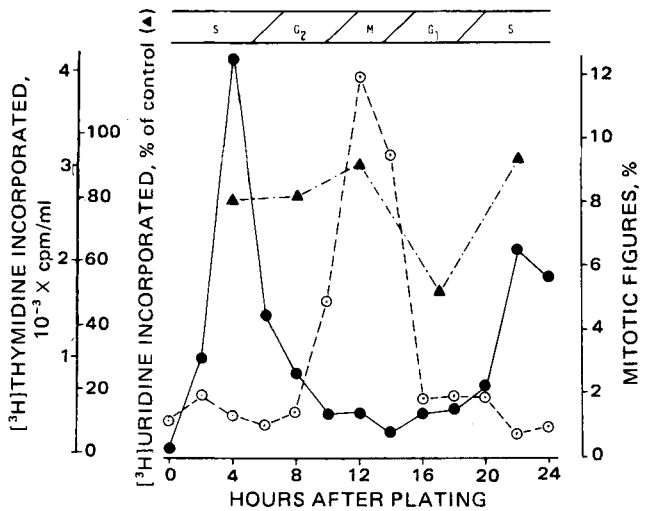

Figure 4—*Traverse of KB cells through the cell cycle after a double-thymidine block. The thymidine was removed at zero hr after plating. Cell-cycle phases were identified through the incorporation of [^{3}H]-thymidine into DNA (●) and through counting of the mitotic figures (⊙) after staining with hematoxylin. The effect of granaticin (6.3 μg/ml for 30 min) on RNA synthesis in KB cells in different phases of the cell cycle was measured by the incorporation of [^{3}H]uridine (▲) (0.4 μCi/ml) reported as percentage of control incubations. Typical values for control incorporations of [^{3}H]uridine into RNA were: S-phase, 780 cpm/mg of protein; G_2-phase, 450 cpm/mg of protein; M-phase 120 cpm/mg of protein; and G_1-phase, 1320 cpm/mg of protein. Each point represents the average of three measurements.*

Table III—Effect of Granaticin on the Uptake and Conversion of [^{3}H]Uridine into Uridine Monophosphate, Uridine Diphosphate, and Uridine Triphosphate [a]

Granaticin, μg/ml	Incubation, hr	Uridine, %	Uridine Monophosphate, %	Uridine Diphosphate, %	Uridine Triphosphate, %
0	0	87.9	6.0	4.0	2.1
0	2	74.0	12.2	10.5	3.3
0	4	72.0	11.4	12.2	4.7
2.75	0	84.7	7.2	5.1	3.0
2.75	2	74.0	11.0	11.3	3.7
2.75	4	70.9	12.9	11.6	4.4

[a] [^{3}H]Uridine (1.1 μCi/ml, 22 μCi/μmole) was added to 1.6–2.4 × 10^5 KB cells/ml and incubated with and without 2.75 μg of granaticin/ml for the time indicated. Separation of uridine and its mono-, di-, and triphosphate ester was by TLC.

concentrations of 3.2 and 5 μg/ml for 1 and 2 hr. The results extend and support the data in Figs. 2 and 3.

Summation of the radioactivity associated with the sucrose gradient fractions representing 45S, 32S, 28S, and 18S RNA, in the control incubation and in incubations of KB cells with granaticin, showed that higher granaticin concentrations (3.2 and 5 μg/ml) have a more drastic effect on the maturation of ribosomal RNA than incubations with 2.16 μg of granaticin/ml of medium (Table II). In addition to granaticin concentration, the incubation time of granaticin with KB cells affected maturation of ribosomal RNA. After a 2-hr incubation at 2.16 or 3.2 μg of granaticin/ml of medium, the inhibition of the formation of functional ribosomal RNA was more pronounced than inhibition after a 1-hr incubation (Table II). At 5 μg of granaticin/ml of medium, no radioactivity was found in 32S, 28S, and 18S ribosomal RNA after a 1-hr incubation (Table II). In all experiments where contact time or granaticin concentration was varied, the maturation of 45S RNA was inhibited to a greater extent than the synthesis of 45S RNA (Table II).

No inhibitory effect of granaticin at a concentration of 2.75 μg/ml for 2 or 4 hr was observed on intracellular accumulation of [^{3}H]uridine and on the subsequent conversion of [^{3}H]uridine to uridine monophosphate, uridine diphosphate, and uridine triphosphate (Table III).

Possible cell cycle specificity of granaticin was investigated in synchronized KB cells. The degree of synchronization was determined by [^{3}H]thymidine incorporation and by counting mitotic figures. A typical profile is reproduced in Fig. 4. Synchronized KB cultures were used to measure [^{3}H]uridine incorporation in the different cell-cycle phases in the presence and absence of granaticin (Fig. 4). Similarly synchronized cell cultures were used to measure the cell survival after treatment with granaticin in the different cell-cycle phases (Fig. 5). [^{3}H]Uridine incor-

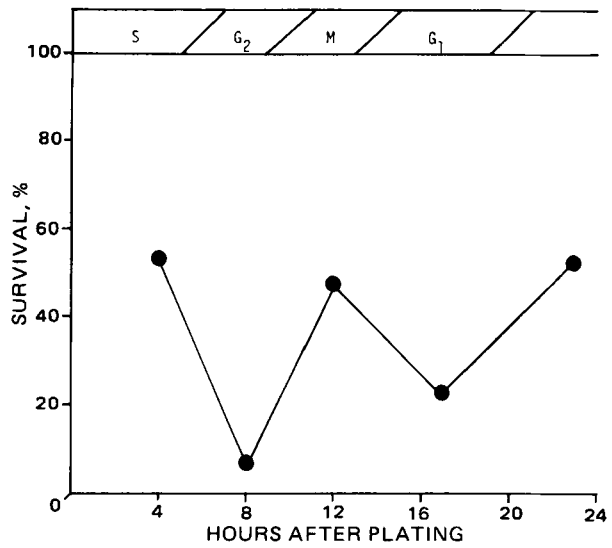

Figure 5—*Effect of granaticin on the survival of synchronized KB cells. Synchronized S-phase KB cells were incubated for 1 hr with 6.3 μg/ml granaticin at 4, 8, 12, 17, and 23 hr after removal of the thymidine block, diluted 1:1000, and grown in monolayers for 7 days. Thereafter, stained colonies were counted and represented as percentage of control incubations without granaticin. Each point represents the average of three measurements.*

poration was inhibited 50% by the addition of granaticin to cells in the G_1-phase (Fig. 4). Little or no effect of granaticin on RNA synthesis was observed in the mitotic and early S-phase and only minimal inhibition (20%) in the late S- and G_2-phases (Fig. 4). However, the effect of granaticin on the cell survival in the different phases was much more pronounced. Almost no cells survived in the G_2-phase (Fig. 5). Similarly, only 25% of the G_1-phase treated cells survived. Survival in the S- and M-phases was ~50% (Fig. 5).

DISCUSSION

In previous studies with bacterial systems granaticin inhibited RNA synthesis *in vivo* (8, 9) and in cell-free incubations (22). In addition, granaticin inhibited reverse transcriptase (10). In both cases, interaction of granaticin with the template was proposed. Although the most recent result with *Bacillus subtilis* (9) indicated that granaticin inhibition was due to the failure to charge leucyl-tRNA, it was not clear if granaticin exerted its inhibitory properties through binding to the tRNA molecule or to the proteins involved in this process. Inhibition of the reverse transcriptase was attributed to the interaction of granaticin with the template (RNA) for this enzyme (10). This conclusion was drawn from sequential addition experiments and, therefore, does not prove interaction of granaticin with the template.

The present results show that RNA synthesis is affected by granaticin at concentrations where protein DNA synthesis is not inhibited. Subsequent analysis of the synthesized RNA showed that maturation of the 45S ribosomal RNA precursor is inhibited. This inhibition was dependent on the granaticin concentration in the incubation mixtures as well as on the duration of incubation. These results may indicate that granaticin binds to 45S RNA and therefore maturation cannot occur. However, similar results would have been obtained if granaticin interacted with one or more of the enzymes (23) involved in the processing of 45S RNA to functional ribosomal RNA.

An indication that granaticin at higher concentrations interacts with other vital processes in mammalian cells was apparent from a comparison of the results of the cell cycle inhibition experiments (Figs. 4 and 5). If inhibition of RNA synthesis was the only site of action of granaticin, then the inhibition of RNA synthesis (Fig. 4) and cell survival (Fig. 5) should have yielded comparable values. Inhibition of RNA synthesis by granaticin in cells in the different phases of the cell cycle was not of the same magnitude as the inhibition of cell growth in the same phases. The magnitude of inhibition in each phase should have been the same if inhibition of RNA synthesis was the only site of action of granaticin toxicity. This type of inhibition was not found. Although 7% of the granaticin-treated G_2-cells did survive (Fig. 5), only 18% inhibition of RNA synthesis was observed in cells treated with granaticin in the same phase (Fig. 4). It should be emphasized that these experiments were done with a granaticin concentration of 6.3 μg/ml. At concentrations of 2 μg/ml, comparable to the inhibition studies in Figs. 2 and 3, this difference in cell survival and inhibition of RNA formation was not apparent.

A number of other compounds inhibit maturation of ribosomal RNA (24). The compounds studied in greatest detail are nucleoside analogs which, in addition to inhibiting the processing of ribosomal RNA, also inhibited *de novo* precursor synthesis (24). Although granaticin cannot be classified as a purine or pyrimidine analog and, therefore, should not inhibit *de novo* nucleoside synthesis, the effect of granaticin on the uptake and phosphorylation of [^{3}H]uridine to the corresponding nucleotides was tested and found to be negative. Camptothecin inhibited ribosomal RNA synthesis (25); however, in this case it appeared to inhibit transcription and not the maturation of preribosomal RNA.

REFERENCES

(1) R. Corbaz, L. Ettlinger, E. Gauemann, Z. Kaldova, W. Keller-Schierlein, F. Knadolfer, B. K. Maunkian, L. Neipp, V. Prelog, P. Reusser, and H. Zaehner, *Helv. Chim. Acta*, **40,** 1262 (1957).

(2) W. Keller-Schierlein, M. Brufani, and S. Barcza, *ibid.*, **51,** 1257 (1968).

(3) S. Barcza, M. Brufani, W. Keller-Schierlein, and H. Zaehner, *ibid.*, **49,** 1736 (1966).

(4) P. Soong and A. A. Au, *Rep. Taiwan Sugar Exp. Stn.* **29,** 33 (1962).

(5) G. Pyrek, M. Mordarski, and A. Zamojski, *Arch. Immunol. Ther. Exp.*, **17,** 827 (1969).

(6) P. Soong, Y. Y. Jen, Y. S. Hsa, and A. A. Au, *Rep. Taiwan Sugar Exp. Stn.*, **34,** 105 (1964).

(7) C. J. Chang, H. G. Floss, P. Soong, and C. T. Chang, *J. Antibiot.*, **28,** 156 (1975).

(8) W. Kersten, H. Kersten, H. Wauke, and A. Ogilvie, *Zentralbl. Bakteriol. Pasasitenk., Infektionskr., Hyg., Abt. 1, Orig.*, **212,** 259 (1970).

(9) A. Ogilvie, K. Wiebauer, and W. Kersten, *Biochem. J.*, **152,** 511 and 517 (1975).

(10) M. L. Sethi, *J. Pharm. Sci.*, **66,** 130 (1977).

(11) J. H. Hanks and R. E. Wallace, *Proc. Soc. Exp. Biol. Med.*, **71,** 196 (1949).

(12) H. Eagle, *ibid.*, **89,** 362 (1955).

(13) G. O. Gey, W. D. Coffman, and M. T. Kubicek, *Cancer Res.*, **12,** 264 (1952).

(14) D. Bootsma, L. Budke, and O. Vas, *Exp. Cell Res.*, **33,** 301 (1964).

(15) G. H. Cohen, R. K. Vaughan, and W. C. Lawrence, *J. Virol.*, **7,** 783 (1971).

(16) T. T. Puck, *Science* **144,** 565 (1964).

(17) T. T. Puck and J. Steffen, *Biophys. J.*, **3,** 379 (1963).

(18) X. Xeros, *Nature (London)*, **194,** 682 (1962).

(19) S. Penman, in "Fundamental Techniques in Virology," K. Habel and N. P. Salzman, Eds., Academic, New York, N.Y., 1969, p.35.

(20) L. M. Allen and P. J. Creaven, *Cancer Res.*, **33,** 3112 (1973).

(21) C. P. Cheung and R. J. Suhadolnik, *Anal. Biochem.*, **83,** 52 (1977).

(22) J. Weiser, I. Janda, K. Mikulik, and J. Tax, *Folia Microbiol.*, **22,** 329 (1977).

(23) R. P. Perry, *Annu. Rev. Biochem.*, **45,** 605 (1976).

(24) J. W. Weiss and H. C. Pitot, *Cancer Res.*, **34,** 581 (1974).

(25) S. B. Horwitz, C.-K. Chang, and A. P. Grollman, *Mol. Pharmacol.*, **7,** 632 (1971).

ACKNOWLEDGMENTS

Supported by a Public Health Service biomedical research support grant.

The technical assistance of Angela Fong and the maintenance of the cell cultures by the Cell Culture Laboratory (Dr. Linda Jacobsen), Purdue University Cancer Center is greatly appreciated. The author thanks Dr. H. G. Floss for the gift of granaticin.

Solubility in Binary Solvent Systems I: Specific *versus* Nonspecific Interactions

WILLIAM E. ACREE, Jr., and J. HOWARD RYTTING ˣ

Received February 24, 1981, from the *Pharmaceutical Chemistry Department, The University of Kansas, Lawrence, KS 66045.* Accepted for publication June 29, 1981.

Abstract □ Solubilities are reported for benzil in carbon tetrachloride–alkane (isooctane, *n*-octane, cyclooctane) systems at 25° and in similar binary mixtures containing cyclohexane plus alkane. The results of these measurements are compared to solution models previously developed for solubility in systems containing specific solute–solvent interactions and to models for purely nonspecific interations. A stoichiometric complexation model based primarily on specific solute–solvent interactions requires several equilibrium constants to mathematically describe the experimental solubilities in binary carbon tetrachloride mixtures. However, there was no direct experimental evidence to suggest complexation between benzil and carbon tetrachloride. In comparison, expressions derived from the Nearly Ideal Binary Solvent (NIBS) model for nonspecific interactions predict experimental solubilities with a maximum deviation of 5% and an overall deviation of 1.0%. The success of the NIBS approach for this system is significant because the mole fraction solubility of benzil changes by a factor of 14 in the carbon tetrachloride–isooctane system.

Keyphrases □ Solubility—binary solvent systems, specific *versus* nonspecific interactions □ Solvent systems—binary, specific *versus* nonspecific interactions, solubility □ Solute–solvent interactions—specific *versus* nonspecific, binary systems

A knowledge of the thermodynamic activity of a drug in a given environment is important in drug design and drug product formulation. The development of an effective drug often involves altering its solubility through either structural modifications or complexation. Ideally, the ability to predict solubility based solely on molecular interactions between the dissolved drug and surrounding solvent molecules is desired. For practical applications, a less fundamental approach must often suffice.

BACKGROUND

Studies of solute–solvent interactions generally have focused on integral thermodynamic properties of binary mixtures. Recently, thermodynamic excess properties of a solute at high dilution in binary solvent mixtures (1–5) have been useful in studying the effects of solution nonideality. Equilibrium constants and enthalpies of hydrogen bond formation have been calculated from the heats of solution of proton donors in mixtures containing a proton acceptor and relatively nonpolar solvent (6, 7). GLC studies on a binary liquid phase provide another method for determining the thermodynamic properties of a solute near infinite dilution, and for investigating association complexes between the solute and one of the solvent components (4, 8–12). Experimental solubilities of iodine and stannic iodide in binary solvent mixtures containing benzene were explained through preferential solvational models (13, 14).

The interpretation of solution nonideality generally has followed two dissimilar lines: the "physical" approach originated by van Laar (15) and the "chemical" approach proposed by Dolezalek (16). The physical approach may be described by a random distribution of molecules throughout the entire solution, while the chemical approach may be characterized by a specific geometric orientation of one molecule with respect to an adjacent molecule.

Even in systems known to contain specific interactions, the need to properly account for nonspecific interactions is recognized. Arnett, *et al.* (7) attempted to separate specific and nonspecific interactions with a "pure base" calorimetric method for determining enthalpies of hydrogen bond formation. The sensitivity of the numerical results to the selection of the model compound and the solvent (17) points out the difficulty in separating physical and chemical contributions of solution nonideality. Bertrand (18) demonstrated that neglecting nonspecific interactions in a chloroform–triethylamine system led to an appreciable error in the enthalpy of complex formation determined with an ideal associated solution model.

Recent solubility determinations of polar organic solutes in binary solvent mixtures containing a polar organic solvent and a nonpolar solvent (such as isooctane) have shown the value of considering nonspecific as well as specific interactions.

For example, do large differences between the solubility of a substance in two pure solvents necessarily indicate complex formation, or can these differences sometimes be just as adequately described with simple mixing models based on nonspecific interactions? One report (19) showed that solubilities of polar nonelectrolytes in polar nonaqueous solvents could not be predicted with the solubility parameter approach of Scatchard and Hildebrand. Another report (20) showed that large differences in the solubilities of polar organic substances could be mathematically described by models that assume stoichiometric solvate species. In many of the systems studied (20), nonspecific interactions were considered unimportant because of the large contributions from specific interactions and the fact that the solubility parameter approach was not adequate.

A zero-parameter equation was developed (3, 5) which predicted solubilities in 35 systems containing naphthalene, stannic iodide, iodine, and benzil as solutes where nonspecific interactions dominate with an average deviation of 2.2% and a maximum deviation of 25%. The maximum deviation occurred in a system (benzil-benzene–cyclohexane) in which complex formation was suggested, and if this system is excluded from calculations, the maximum deviation becomes 6%. The success of the equation is striking because the mole fraction solubility of benzil changes by a factor of 14 in the carbon tetrachloride–*n*-hexane system (5).

The present report describes how nonspecific interactions may contribute significantly to the total nonideality of a solution. Equilibrium constants calculated *via* solvational complexation models may not always represent only specific solute–solvent interactions, but also the failure of the model to properly describe nonspecific interactions. This phenomenon was further examined by measuring additional solubilities for benzil in carbon tetrachloride–alkane (isooctane, *n*-octane, cyclooctane) systems and in similar binary mixtures containing cyclohexane–alkane. These systems were selected primarily because the experimental solubilities of benzil are considerably different in each of the pure solvents. The experimental values in the binary mixtures are interpreted with models for either specific or nonspecific interactions.

EXPERIMENTAL

Reagents—Benzil[1] was recrystallized several times from methanol giving a melting point of 95.0 ± 0.5° [lit. (21) mp 95.2°]. Cyclohexane[2], *n*-heptane[3], *n*-octane[4], isooctane[3], cyclooctane[4], and carbon tetrachloride[5] were all stored over molecular sieves[6] to remove possible trace amounts of water. Binary solvent mixtures were prepared by weight so that compositions could be calculated to 0.0001 mole fraction.

Solubility Determinations—Excess solute and solvent were placed in amber glass bottles and allowed to equilibrate in a constant temperature bath at 25° for several days. Random duplicate samples were allowed to equilibrate for longer periods, but no significant differences in saturation solubility were observed. Aliquots of saturated benzil solutions were transferred through a coarse filter into a tared volumetric flask to determine the amount of sample and then diluted quantitatively with

[1] Eastman.
[2] Purity ≥99.5 Wt %, Phillips Petroleum Co.
[3] Purity ≥99 mol %, Phillips Petroleum Co.
[4] Gold label grade, Aldrich Chemical Co.
[5] Spectranalyzed, Fisher Scientific Co.
[6] Linde, Type 4A.

0022-3549/82/0200-0201$01.00/0

Table I—Mole Fraction Solubilities of Benzil in Several Binary Solvent Mixtures at 25°

Solvent 1 + Solvent 2	X_1^0	$X_{solute}^{sat.}$
CCl_4 + iso-C_8H_{18}	0.0000	0.00587
	0.1676	0.00797
	0.3104	0.01068
	0.4072	0.01360
	0.4096	0.01368
	0.6057	0.02249
	0.6358	0.02463
	0.7246	0.03126
	0.8266	0.04368
	1.0000	0.08082
C_6H_{12} + iso-C_8H_{18}	0.0000	0.00587
	0.2494	0.00670
	0.3791	0.00724
	0.6180	0.00838
	0.7919	0.00935
	0.8704	0.00980
	1.0000	0.01067
C_6H_{12} + C_7H_{16}	0.0000	0.00659
	0.1893	0.00718
	0.3475	0.00778
	0.5774	0.00874
	0.7763	0.00959
	0.8582	0.01001
	1.0000	0.01067
C_6H_{12} + C_8H_{16}	0.0000	0.01454
	0.2260	0.01395
	0.3330	0.01354
	0.5620	0.01266
	0.7548	0.01178
	0.8566	0.01133
	1.0000	0.01068
n-C_8H_{16} + CCl_4	0.0000	0.08082
	0.1081	0.05542
	0.1877	0.04299
	0.2997	0.03077
	0.3750	0.02512
	0.4358	0.02143
	0.5851	0.01535
	0.7129	0.01183
	1.0000	0.00726
C_6H_{12} + *n*-C_8H_{18}	0.0000	0.00726
	0.2468	0.00798
	0.3763	0.00837
	0.5978	0.00911
	0.7892	0.00988
	0.8737	0.01019
	1.0000	0.01068
C_8H_{16} + CCl_4	0.0000	0.08082
	0.1773	0.05762
	0.2575	0.04864
	0.4158	0.03726
	0.5839	0.02768
	0.6524	0.02394
	0.7559	0.02115
	1.0000	0.01454

cyclohexane. Concentrations were determined spectrophotometrically[7] at 390 nm.

Experimental solubilities of benzil in several binary solvent mixtures are given in Table I. The measurements were reproducible to within 1.5%.

THEORETICAL

Stoichiometric Complexation Model—Stoichiometric complexation models have been used frequently to quantitatively explain enhanced solubilities of a polar organic solute in binary mixtures containing an inert hydrocarbon and a polar cosolvent. The basic model assumes complexation between the solute, S, and an interacting cosolvent, L (19,20):

$$S + L \rightleftharpoons SL \overset{+L}{\rightleftharpoons} SL_2 \overset{+L}{\rightleftharpoons} \ldots SL_n$$

Scheme I

Each reaction is described by an appropriate equilibrium constant with concentrations expressed in molarities:

[7] Cary 118.

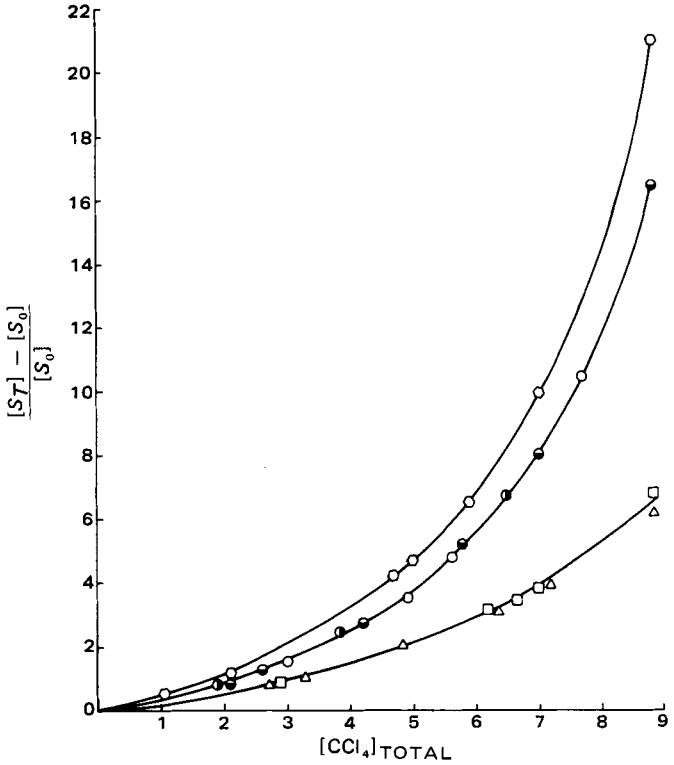

Figure 1—*Graphical determination of* $K_{1:1}$ *from plots of fractional change in solubility* versus *carbon tetrachloride molarity for benzil in several binary solvents consisting of carbon tetrachloride and* ○, n-*octane;* ◒, n-*heptane;* ◑, n-*hexane;* ○, *isooctane;* △, *cyclohexane; and* □, *cyclooctane. Solubilities in solvent mixtures containing cyclohexane,* n-*hexane, and* n-*heptane are from Ref. 5. The basic model requires additional solute–solvent complexes to explain curvature from the linearship. (See Eqs. 5 and 6).*

$$K_{1:1} = \frac{[SL]}{[S_0][L]_f} \qquad \text{(Eq. 1)}$$

$$K_{1:n} = \frac{[SL_n]}{[SL_{n-1}][L]_f} \qquad \text{(Eq. 2)}$$

where $[S_0]$ is the saturation solubility of solute in pure inert hydrocarbon (assumed to represent the free solute concentration in binary mixtures as well) and $[L]_f$ is the free (uncomplexed) ligand.

This particular model assumes only a single solute molecule is present in each complex, but the mathematical form of the resulting equations is not significantly altered by additional solute molecules per complex. The total solubility of solute in any system, $[S_T]$, can be expressed as:

$$[S_T] = [S_0] + K_{1:1}[S_0][L]_f + K_{1:1}K_{1:2}[S_0][L]_f^2 + \ldots \qquad \text{(Eq. 3)}$$

The total concentration of complexing agent, $[L_T]$, is:

$$[L_T] = [L]_f + K_{1:1}[S_0][L]_f + 2K_{1:1}K_{1:2}[S_0][L]_f + \ldots \qquad \text{(Eq. 4)}$$

In the absence of solute, the total concentration of interactive cosolvent $[L_T]$ is equal to $[L]nf$ only if the extent of self-association is negligible. Furthermore, the mathematical form of Eq. 3 predicts that plots of solubility *versus* cosolvent concentration should be concave upward in solvents incapable of self-association.

If only 1:1 complexes are present, Eqs. 3 and 4 can be combined to give:

$$\text{fractional change in solubility} = \frac{[S_T]-[S_0]}{[S_0]} = \frac{K_{1:1}}{1+K_{1:1}[S_0]}[L_T] \qquad \text{(Eq. 5)}$$

A plot of the fractional change in solubility *versus* ligand added gives a straight line. Graphical methods are cumbersome for higher order complexes, and a first approximation often assumes the amount of ligand in complexes is small; $[L_T] = [L]_f$. This additional stipulation enables Eq. 3 to be rewritten as:

$$\frac{[S_T]-[S_0]}{[S_0][L_T]} = K_{1:1} + K_{1:1}K_{1:2}[L_T] \qquad \text{(Eq. 6)}$$

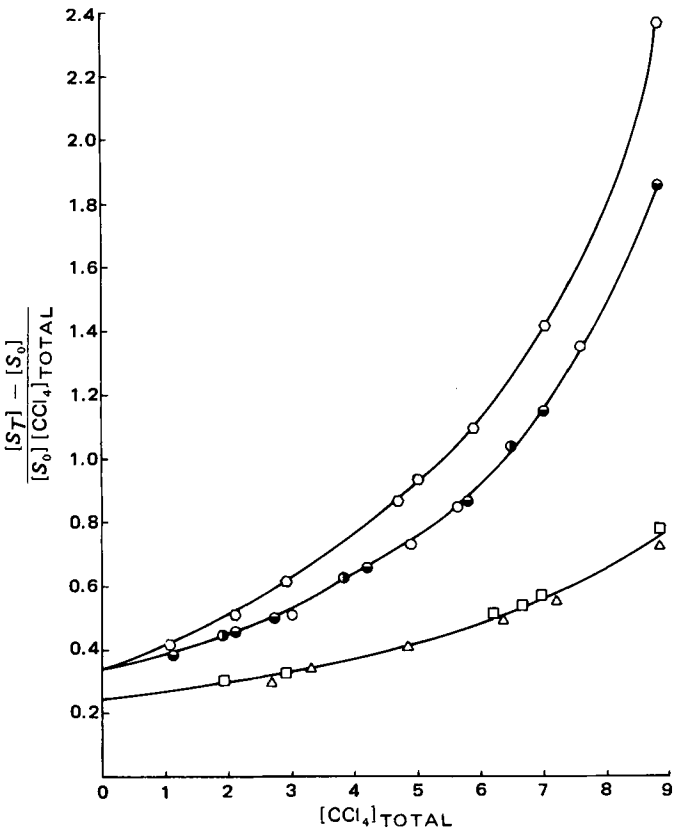

Figure 2—*Determination of* $K_{1:1}$ *and* $K_{1:2}$ *for the interaction of benzil with carbon tetrachloride in several binary solvents at 25°. (See Eq. 6). The binary mixtures contained* ○, *carbon tetrachloride and* n-*octane;* ◒, n-*heptane;* ◑, n-*hexane;* ○, *isooctane;* △, *cyclohexane; and* □, *cyclooctane.*

$K_{1:2}$ is calculated from the slope of the linear portion of $([S_T]-[S_0])/[S_0][L_T]$ *versus* $[L_T]$ and $K_{1:1}$ is determined from the intercept. Applying Eqs. 5 and 6 to systems not involving complexation should theoretically give equilibrium constants of zero. Thus, the model might be expected to distinguish between complexing and noncomplexing systems through the relative magnitudes of calculated equilibrium constants. However, non-negligible K values can be obtained in systems where complexation does not occur.

This particular model includes the basic assumption that the free solute concentration $[S_0]$ is independent of solvent composition, an assumption that is not always supported by experimental evidence. Solubilities of iodine in binary mixtures of *n*-hexane–cyclohexane (0.0460–0.00860 *M*), *n*-hexane–carbon tetrachloride (0.0460–0.116 *M*), and *n*-hexane–chloroform (0.0460–0.176 *M*) depend on solvent composition (22). Yet the violet color of iodine in each of the pure solvents indicates the absence of molecular complexes (23). Similar variations are observed for the benzil solubilities in the binary mixtures of saturated hydrocarbons given in Table I.

Examination of the behavior of Eqs. 3 and 4 in isooctane–cyclohexane mixtures, where association with benzil is considered unlikely, reveals that the equations compensate for variations in $[S_0]$ with solvent composition (0.0353–0.0978 *M*) either by adjusting numerical values of $K_{1:n}$ or by assuming additional solute–solvent complexes. The larger the true variation in the concentration of uncomplexed solute, the larger this compensation becomes. Eventually a point can be reached when the equilibrium constants derived from Eqs. 3 and 4 no longer represent specific solute–solvent interactions, but rather the failure of the particular model to properly describe nonspecific interactions.

Figures 1 and 2 show the graphical determination of potential equilibrium constants calculated from Eqs. 5 and 6 for benzil solubilities in binary mixtures containing carbon tetrachloride. The various cosolvents appear to be grouped along three different curves: one for isooctane, a second for the three normal hydrocarbons (*n*-hexane, *n*-heptane, and *n*-octane), and a third curve for the two cyclic hydrocarbons (cyclohexane and cyclooctane). Presumed equilibrium constants calculated in mixtures containing cyclohexane are not identical to values calculated in

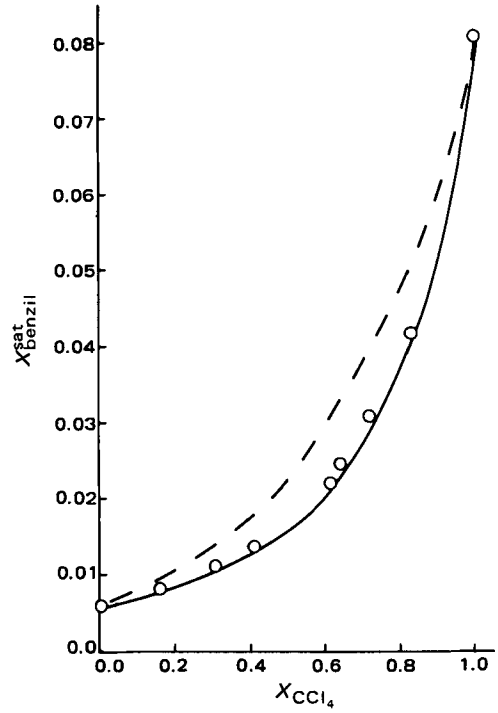

Figure 3—*Comparison between experimental solubilities (*○*) and the NIBS predictions for benzil in binary mixture of carbon tetrachloride and isooctane using Eq. 7 (- - -), and Eqs. 8 and 9 (—). The free energy of mixing data for the binary solvent* ($\Delta\overline{G}^{ex}_{12}$) *is taken from Ref. 40.*

isooctane mixtures. More importantly, the model requires several constants to represent mathematically the experimental data, and yet there appears to be no experimental evidence suggesting complexation between benzil and carbon tetrachloride.

Dipole moment measurements of benzil in benzene and carbon tetrachloride have been interpreted as evidence for specific interactions of benzil with benzene but not with carbon tetrachloride (24). The GLC retention behavior of carbon tetrachloride and chloroform on a benzil stationary phase has been interpreted (25) in terms of London or simple dispersion forces in the case of carbon tetrachloride and in terms of hydrogen bonding in the case of chloroform. Actual numerical values of the equilibrium constants are not reported to avoid the suggestion that a complex is formed between benzil and carbon tetrachloride. Since the *y*-intercept in Fig. 2 gives a presumed $K_{1:1}$, $K_{1:1}$ would range from 0.25–0.35 depending on the choice of cosolvent.

The Nearly Ideal Binary Solvent Model—The Nearly Ideal Binary Solvent (NIBS) approach developed by Bertrand *et al.* was shown to provide reasonable estimates for enthalpies of solution (2), GLC partition coefficients (4, 8), and solubilities (3, 5) in systems containing only nonspecific interactions. However, the approach fails for systems with specific solute–solvent or solvent–solvent interactions. The general expressions, derived from the NIBS model, for predicting solubilities in systems of nonspecific interactions depend on two models of solution nonideality:

$$RT\ln(a_3^{solid}/X_3^{sat}) = (1-X_3^{sat})^2[X_1^0(\Delta\overline{G}_3^{ex})_{X_1^0=1} + X_2^0(\Delta\overline{G}_3^{ex})_{X_2^0=1} - (\Delta\overline{G}_{12}^{ex})] \quad \text{(Eq. 7)}$$

$$RT\ln(a_3^{solid}/X_3^{sat}) = (1-\phi_3^{sat})^2[\phi_1^0(\Delta\overline{G}_3^{ex})_{X_1^0=1} + \phi_2^0(\Delta\overline{G}_3^{ex})_{X_2^0=1} - \overline{V}_3(X_1^0\overline{V}_1 + X_2^0\overline{V}_2)^{-1}(\Delta\overline{G}_{12}^{ex})] \quad \text{(Eq. 8)}$$

$$RT\left[\ln(a_3^{solid}/\phi_3^{sat}) - (1-\phi_3^{sat})\left(1-\frac{\overline{V}_3}{(X_1^0\overline{V}_1 + X_2^0\overline{V}_2)}\right)\right] = (1-\phi_3^{sat})^2[\phi_1^0(\Delta\overline{G}_3^{fh})_{X_1^0=1} + \phi_2^0(\Delta\overline{G}_3^{fh})_{X_2^0=1} - \overline{V}_3(X_1^0\overline{V}_1 + X_2^0\overline{V}_2)^{-1}(\Delta\overline{G}_{12}^{fh})] \quad \text{(Eq. 9)}$$

Equations 7 and 8 are based on the Regular Solution model (23) and Eq. 9 is based on the Flory–Huggins model (26–30). In these expressions, a_3^{solid} is the activity of the solid solute relative to the pure hypothetical supercooled liquid, X_i is mole fraction, ϕ_i is volume fraction, $\overline{V}_i$ is the molar volume of a pure liquid, and $\Delta\overline{G}_{12}^{ex}$ is the molar excess Gibbs free

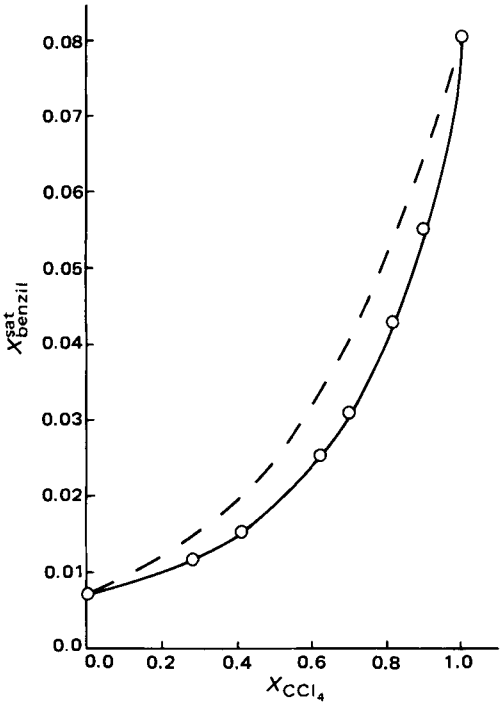

Figure 4—*Comparison between the experimental solubilities (O) and the NIBS predictions for benzil in binary mixtures of carbon tetrachloride and* n*-octane using Eq. 7 (---), and Eqs. 8 and 9 (——). The free energy of mixing for the binary solvent is taken from Ref. 41.*

energy of the binary solvent mixture relative to Raoult's law[8]. The superscript (0) denotes the initial binary solvent composition calculated as if the solute were not present. With these equations, solubility data measured in each pure solvent can be used to calculate the excess partial molar Gibbs-free energy of the solute $[(\Delta\overline{G}_3^{ex})^*_{X_1^0=1}, (\Delta\overline{G}_3^{fh})^*_{X_1^0=1}]$. These quantities are then combined with the excess free energy of the binary solvent to predict solubility in mixed solvents using a reiterative process. The quantity $(1 - X_3^{sat})$ or $(1 - \phi_3^{sat})$ is taken as unity in the first approximation and convergence is quite rapid unless the solubility is large.

Graphical comparisons of experimental and calculated values are shown in Figs. 3 and 4 for benzil in isooctane–carbon tetrachloride and in *n*-octane–carbon tetrachloride mixtures. Properties used in the calculation include: a_3^{solid} (0.224) calculated from the enthalpy of fusion (22.15 cal/g) (21) at the melting point, and $\overline{V}_3$ (183 cm^3/mole) estimated from the density of the liquid at 102° and the coefficient of thermal expansion for benzophenone calculated over 50–95° (31). In general, Eqs. 8 and 9 are comparable with overall average (rms) deviations of 1.4 and 1.0%, respectively and are superior to Eq. 7 which has an average (rms) deviation of 10.0%[9]. These observations are in agreement with earlier findings (2–5) that Eq. 7 is inferior to the other two predictive expressions for systems in which the molar volumes differ substantially.

RESULTS AND DISCUSSION

Although experimental solubilities can be described by equations derived from stoichiometric complexation models, the basic assumption that free solute concentration is independent of solvent composition is not always supported by experimental evidence. Solubilities of benzil in binary mixtures of nonpolar solvents such as isooctane–cyclohexane are found to vary with solvent composition. If carbon tetrachloride is included as a nonpolar solvent for benzil, experimental solubilities exhibit a 22-fold range in carbon tetrachloride–isooctane mixtures. Stoichiometric complexation models that attribute all solubility enhancement to the formation of molecular complexes require several equilibrium constants to describe benzil solubility in binary mixtures containing carbon tetrachloride.

Much smaller ranges have been observed for iodine solubilities in binary mixtures of *n*-hexane–benzene (0.046–0.588 *M*) (32), cyclohexane–benzene (0.083–0.543 *M*)(14), and carbon tetrachloride–benzene (0.116–0.588 *M*) (33) where specific solute–solvent interactions are expected to occur. Charge transfer complexes between iodine and benzene are well documented (34–36). Based on these observations, the range of solubilities encompassed in binary solvent mixtures does not always provide a clear indication of the complexing nature of the system. Caution should be exercised in inferring specific complex formation models in the absence of independent physical evidence for complexation, particularly if the model requires several relatively small equilibrium constants to describe the system.

The success of the NIBS approach in predicting the binary solvent effect on solubilities, covering up to a 14-fold range (mole fraction), suggests the possibility that this model may provide a foundation for approximations of the physical interactions even in a system containing chemical interactions such as association between the solute and a complexing solvent. Extensions of the basic NIBS model to systems containing 1:1 solute–solvent complex were shown to provide reasonable correlations of GLC partition coefficients with a mixed liquid phase (4). Through standard thermodynamic relationships, the expression of the NIBS model for a 1:1 solute–solvent complex (Eq. 25 of Ref. 4) can be applied to the solubility of solid substances, without requiring the solubility of the uncomplexed solute to be independent of solvent composition. Similar models have been suggested (37–39) to study the solubility of gases and solids in complexing systems.

[8] For a binary mixture, the excess molar Gibbs free energy over the predictions of the Flory–Huggins equation is related to the defined excess free energy by: $\Delta\overline{G}_{12}^{fh} = \Delta\overline{G}_{12}^{ex} + RT\,[\ln(X_1^0\overline{V}_1 + X_2^0\overline{V}_2) - X_1^0 \ln \overline{V}_1 - X_2^0 \ln \overline{V}_2]$.

[9] rms deviations (%) $= (100/N^{1/2})\,\{\sum^{n} [\ln(X^{sat}_{calc}/X^{sat}_{exp})]^2\}^{1/2}$. These values were averaged for the six different binary solvent systems. The carbon tetrachloride–cyclooctane system was not included in these calculations because the excess Gibbs free energy was unavailable in the literature.

REFERENCES

(1) E. L. Taylor and G. L. Bertrand, *J. Solution Chem.*, **3**, 479 (1974).
(2) T. E. Burchfield and G. L. Bertrand, *ibid.*, **4**, 205 (1975).
(3) W. E. Acree, Jr., and G. L. Bertrand, *J. Phys. Chem.*, **81**, 1170 (1977).
(4) *Ibid.*, **83**, 2355 (1979).
(5) W. E. Acree, Jr., Ph.D. thesis, University of Missouri-Rolla, 1981.
(6) E. M. Arnett, T. S. S. R. Murty, P. v. R. Schleyer, and L. Joris, *J. Am. Chem. Soc.*, **89**, 5955 (1967).
(7) E. M. Arnett, L. Joris, E. Mitchell, T. S. S. R. Murty, T. M. Gorrie, and P. v. R. Schleyer, *ibid.*, **92**, 2365 (1970).
(8) W. E. Acree, Jr., and J. H. Rytting, *Anal. Chem.*, **52**, 1764 (1980).
(9) C. Eon, C. Pommier, and G. Guiochon, *Chromatographia*, **4**, 241 (1971).
(10) C. Eon, C. Pommier, and G. Guiochon, *J. Phys. Chem.*, **75**, 2632 (1971).
(11) R. J. Laub, D. E. Martire, and J. H. Purnell, *J. Chem. Soc., Faraday Trans.* II, **74**, 213 (1978).
(12) M. W. P. Harbison, R. J. Laub, D. E. Martire, J. H. Purnell, and P. S. Williams, *J. Phys. Chem.*, **83**, 1262 (1979).
(13) A. Purkayastha and J. Walkley, *Can. J. Chem.*, **50**, 834 (1972).
(14) K. Nakanishi and S. Asakura, *J. Phys. Chem.*, **81**, 1745 (1977).
(15) J. J. van Laar, *Z. Phys. Chem.*, **72**, 723 (1910).
(16) F. Dolezalek, *ibid.*, **64**, 727 (1908).
(17) W. C. Duer and G. L. Bertrand, *J. Am. Chem. Soc.*, **92**, 2587 (1970).
(18) G. L. Bertrand, *J. Phys. Chem.*, **79**, 48 (1975).
(19) H. L. Fung and T. Higuchi, *J. Pharm. Sci.*, **60**, 1782 (1971).
(20) B. D. Anderson, J. H. Rytting, and T. Higuchi, *ibid.*, **69**, 676 (1980).
(21) R. C. Weast, "Handbook of Chemistry and Physics," 52nd ed., Chemical Rubber Co., Cleveland, Ohio, 1971.
(22) M. S. Sytilin, *Russ. J. Phys. Chem.*, **48**, 1353 (1974).
(23) J. H. Hildebrand, J. M. Prausnitz, and R. L. Scott, "Regular and Related Solutions," Van Nostrand-Reinhold, New York, N.Y., 1970.
(24) P. A. Hopkins, R. J. W. LeFevre, L. Radom, and G. L. D. Ritchie, *J. Chem. Soc. (B)*, **1971**, 574.
(25) F. Vernon, *J. Chromatogr.*, **63**, 249 (1971).
(26) P. J. Flory, *J. Chem. Phys.*, **10**, 51 (1942).
(27) P. J. Flory, "Principles of Polymer Chemistry," Cornell University Press, New York, N.Y., 1953.
(28) M. L. Huggins, *J. Phys. Chem.*, **46**, 151 (1941).
(29) M. L. Huggins, *Ann. N. Y. Acad. Sci.*, **41**, 1 (1942).

(30) M. L. Huggins, *J. Am. Chem. Soc.*, **64**, 1712 (1942).
(31) J. Timmermans, "Physico-chemical Constants of Pure Organic Compounds," Elsevier, New York, N.Y., 1950.
(32) M. S. Sytilin, *Russ. J. Phys. Chem.*, *48*, 1500 (1974).
(33) S. E. Wood, B. D. Fine, and L. M. Isaacson, *J. Phys. Chem.*, **61**, 1605 (1957).
(34) H. A. Benesi and J. H. Hildebrand, *J. Am. Chem. Soc.*, **70**, 2832, (1948); **71**, 2703 (1949).
(35) R. S. Mulliken, *ibid.*, **72**, 600 (1950); **74**, 811 (1952).
(36) R. S. Mulliken, *J. Phys. Chem.*, **56**, 801 (1952).
(37) T. Nitta and T. Katayama, *J. Chem. Eng. Jpn.*, **6**, 1 (1973); **7**, 310 (1974); **8**, 175 (1975).
(38) T. Nitta, A. Tatsuishi, and T. Katayama, *ibid.*, **6**, 475 (1973).
(39) T. Nitta, Y. Nakamura, H. Ariyasu, and T. Katayama, *ibid.*, **13**, 97 (1980).
(40) R. Battino,, *J. Phys. Chem.*, **72**, 4503 (1968).
(41) D. V. S. Jain and O. P. Yadav, *Indian J. Chem.*, **9**, 342 (1971).

ACKNOWLEDGMENTS

Supported in part by National Institutes of Health Grant GM22357.

Effect of Polyisobutylene on Ethylcellulose-Walled Microcapsules: Wall Structure and Thickness of Salicylamide and Theophylline Microcapsules

S. BENITA and M. DONBROW ˣ

Received November 12, 1980, from the *Department of Pharmacy, School of Pharmacy, Hebrew University-Hadassah Medical School, P.O.B. 12065, Jerusalem, Israel.* Accepted for publication May 20, 1981.

Abstract □ Microcapsules were prepared by the ethylcellulose coacervation process which is based on the differential thermal solubility in cyclohexane. When a protective colloid, polyisobutylene, was present in adequate concentration, individually film-coated core particles formed. However, they were accompanied by small empty coacervate droplets, detectable by microscopic observation. Below the critical colloid concentration, the product had the form of an aggregate, in contrast to individual film-coated microcapsules. Increase of colloid concentration yielded microcapsules of higher drug content, because the coating became progressively thinner; there was a corresponding increase in the release rate of drugs from the microcapsules. Since the initial wall polymer/drug ratio and the particle size are constant, the drug content varied with the thicknesses of the wall membrane. This is shown here by removal of empty coacervate droplets by repeated decantations, enabling determination of drug content by chemical analysis. In contrast to results reported in the literature, in the presence of a protective colloid, microcapsule drug content decreased with decreasing particle size of the drug. This was caused by more complete uptake of the wall polymer on the increased surface of core material. The effect of protective colloid concentration on the apparent loss of wall polymer as empty droplets closely paralleled its effect on the size of stabilized coacervate droplets when core material was absent. It is proposed that stabilized droplet formation is a side reaction when core material is present, causing changes in wall thickness. This reaction not only affects the efficiency of the coating process but may be utilized to control wall thickness. First-order constants for drug release from salicylamide and theophylline microcapsules followed the same pattern as wall thickness and confirmed the validity of the measurements.

Keyphrases □ Polyisobutylene—effect on ethylcellulose-walled microcapsules □ Microencapsulation—effect of polyisobutylene on ethylcellulose-walled microcapsules, wall structure and thickness of salicylamide and theophylline microcapsules □ Coacervation—ethylcellulose effect on polyisobutylene on microencapsulation process

Although ethylcellulose is the most widely used coating material in microencapsulation, the basic coacervation process has been carried out under a variety of conditions (1, 2). Previous experimental results demonstrate that changes in the basic technique, essentially temperature reduction of a hot cyclohexane solution, markedly influence the quality and characteristics of the microcapsules formed. Among variations introduced has been the use of protective colloids such as polyethylene (2, 3), butyl rubber (4, 5), and polyisobutylene (6). Observation of microcapsules prepared in the absence of a protective colloid (7–9) reveals aggregates of coated particles, whereas individual microcapsules consisting of single core particles uniformly coated are formed when a protective colloid is present (3).

Dhruv *et al.* proposed (10, 11) that the extent and integrity of microencapsulation in the gelatin–acacia coacervation system is largely dependent on the coacervate volume, which changes with various experimental parameters in the absence of core material. The effects of polyisobutylene on the basic ethylcellulose coacervation process was recently studied (12). The polyisobutylene concentration was shown to control the phase coacervation volume and the final ethylcellulose coacervate droplet size. The present work investigated the effect of polyisobutylene concentration and particle size of core material on the wall/core ratio and drug release from microcapsules. It was attempted to relate these parameters to the underlying causes revealed by earlier studies.

EXPERIMENTAL

Materials—Ethylcellulose[1] (*N*-type) had an ethoxyl content of 47.5–49.0%. The viscosity of a 5% (w/w) solution in toluene–ethanol (80:20 w/w) was 100 cps[1]. Polyisobutylene[2] had a molecular weight of 380,000. Salicylamide[3] conformed to NF XIV and theophylline[4] conformed to BP 1973.

Preparation of Microcapsules—The method of preparation, developed with modifications from an earlier technique (1), was described elsewhere (12). The core and wall materials[5] were added to the stirred cyclohexane–polyisobutylene solution (250 or 300 rpm). The mixture was then heated to 80°, and allowed to cool at a controlled stirring rate to 45°.

[1] Hercules, Wilmington, Del.
[2] Oppanol B50, BASF, Ludwigshafen, West Germany.
[3] Sigma, Saint Louis, Mo.
[4] May and Baker, Dagenham, England.
[5] The quantities used were always adjusted to 100 g total weight with cyclohexane.

0022-3549/82/0200-0205$01.00/0

(30) M. L. Huggins, *J. Am. Chem. Soc.*, **64**, 1712 (1942).
(31) J. Timmermans, "Physico-chemical Constants of Pure Organic Compounds," Elsevier, New York, N.Y., 1950.
(32) M. S. Sytilin, *Russ. J. Phys. Chem.*, *48*, 1500 (1974).
(33) S. E. Wood, B. D. Fine, and L. M. Isaacson, *J. Phys. Chem.*, **61**, 1605 (1957).
(34) H. A. Benesi and J. H. Hildebrand, *J. Am. Chem. Soc.*, **70**, 2832, (1948); **71**, 2703 (1949).
(35) R. S. Mulliken, *ibid.*, **72**, 600 (1950); **74**, 811 (1952).
(36) R. S. Mulliken, *J. Phys. Chem.*, **56**, 801 (1952).
(37) T. Nitta and T. Katayama, *J. Chem. Eng. Jpn.*, **6**, 1 (1973); **7**, 310 (1974); **8**, 175 (1975).
(38) T. Nitta, A. Tatsuishi, and T. Katayama, *ibid.*, **6**, 475 (1973).
(39) T. Nitta, Y. Nakamura, H. Ariyasu, and T. Katayama, *ibid.*, **13**, 97 (1980).
(40) R. Battino,, *J. Phys. Chem.*, **72**, 4503 (1968).
(41) D. V. S. Jain and O. P. Yadav, *Indian J. Chem.*, **9**, 342 (1971).

ACKNOWLEDGMENTS

Supported in part by National Institutes of Health Grant GM22357.

Effect of Polyisobutylene on Ethylcellulose-Walled Microcapsules: Wall Structure and Thickness of Salicylamide and Theophylline Microcapsules

S. BENITA and M. DONBROW ˣ

Received November 12, 1980, from the *Department of Pharmacy, School of Pharmacy, Hebrew University-Hadassah Medical School, P.O.B. 12065, Jerusalem, Israel.* Accepted for publication May 20, 1981.

Abstract □ Microcapsules were prepared by the ethylcellulose coacervation process which is based on the differential thermal solubility in cyclohexane. When a protective colloid, polyisobutylene, was present in adequate concentration, individually film-coated core particles formed. However, they were accompanied by small empty coacervate droplets, detectable by microscopic observation. Below the critical colloid concentration, the product had the form of an aggregate, in contrast to individual film-coated microcapsules. Increase of colloid concentration yielded microcapsules of higher drug content, because the coating became progressively thinner; there was a corresponding increase in the release rate of drugs from the microcapsules. Since the initial wall polymer/drug ratio and the particle size are constant, the drug content varied with the thicknesses of the wall membrane. This is shown here by removal of empty coacervate droplets by repeated decantations, enabling determination of drug content by chemical analysis. In contrast to results reported in the literature, in the presence of a protective colloid, microcapsule drug content decreased with decreasing particle size of the drug. This was caused by more complete uptake of the wall polymer on the increased surface of core material. The effect of protective colloid concentration on the apparent loss of wall polymer as empty droplets closely paralleled its effect on the size of stabilized coacervate droplets when core material was absent. It is proposed that stabilized droplet formation is a side reaction when core material is present, causing changes in wall thickness. This reaction not only affects the efficiency of the coating process but may be utilized to control wall thickness. First-order constants for drug release from salicylamide and theophylline microcapsules followed the same pattern as wall thickness and confirmed the validity of the measurements.

Keyphrases □ Polyisobutylene—effect on ethylcellulose-walled microcapsules □ Microencapsulation—effect of polyisobutylene on ethylcellulose-walled microcapsules, wall structure and thickness of salicylamide and theophylline microcapsules □ Coacervation—ethylcellulose effect on polyisobutylene on microencapsulation process

Although ethylcellulose is the most widely used coating material in microencapsulation, the basic coacervation process has been carried out under a variety of conditions (1, 2). Previous experimental results demonstrate that changes in the basic technique, essentially temperature reduction of a hot cyclohexane solution, markedly influence the quality and characteristics of the microcapsules formed. Among variations introduced has been the use of protective colloids such as polyethylene (2, 3), butyl rubber (4, 5), and polyisobutylene (6). Observation of microcapsules prepared in the absence of a protective colloid (7–9) reveals aggregates of coated particles, whereas individual microcapsules consisting of single core particles uniformly coated are formed when a protective colloid is present (3).

Dhruv *et al.* proposed (10, 11) that the extent and integrity of microencapsulation in the gelatin–acacia coacervation system is largely dependent on the coacervate volume, which changes with various experimental parameters in the absence of core material. The effects of polyisobutylene on the basic ethylcellulose coacervation process was recently studied (12). The polyisobutylene concentration was shown to control the phase coacervation volume and the final ethylcellulose coacervate droplet size. The present work investigated the effect of polyisobutylene concentration and particle size of core material on the wall/core ratio and drug release from microcapsules. It was attempted to relate these parameters to the underlying causes revealed by earlier studies.

EXPERIMENTAL

Materials—Ethylcellulose[1] (*N*-type) had an ethoxyl content of 47.5–49.0%. The viscosity of a 5% (w/w) solution in toluene–ethanol (80:20 w/w) was 100 cps[1]. Polyisobutylene[2] had a molecular weight of 380,000. Salicylamide[3] conformed to NF XIV and theophylline[4] conformed to BP 1973.

Preparation of Microcapsules—The method of preparation, developed with modifications from an earlier technique (1), was described elsewhere (12). The core and wall materials[5] were added to the stirred cyclohexane–polyisobutylene solution (250 or 300 rpm). The mixture was then heated to 80°, and allowed to cool at a controlled stirring rate to 45°.

[1] Hercules, Wilmington, Del.
[2] Oppanol B50, BASF, Ludwigshafen, West Germany.
[3] Sigma, Saint Louis, Mo.
[4] May and Baker, Dagenham, England.
[5] The quantities used were always adjusted to 100 g total weight with cyclohexane.

0022-3549/82/0200-0205$01.00/0

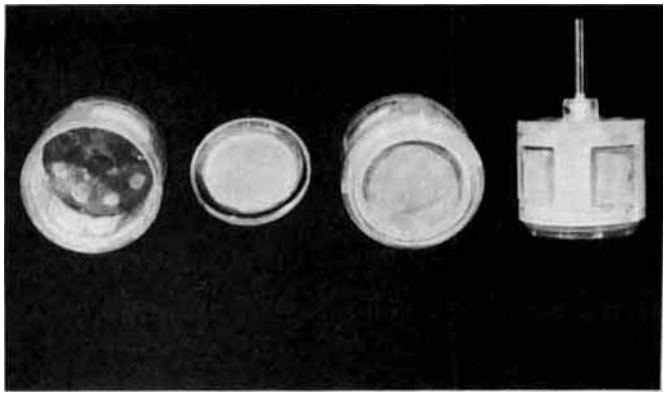

Figure 1—*Rotating basket showing dissembled parts used for release of drugs from microcapsules.*

It was cooled very rapidly using ice to 25° and stirred for another 15 min.

The microcapsules were separated from the solution by decantation and rinsed with three 200-ml portions of cyclohexane to remove any polyisobutylene adsorbed at the microcapsule interface and any empty wall polymer coacervate droplets. They were collected by vacuum filtration and oven-dried at 50° for 30 min, yielding a free-flowing powder.

All batches were duplicated. When the content of active ingredient deviated more than 3–4% between batches, a triplicate was performed. The effect of each experimental parameter was studied while the other parameters were kept constant for each drug. Segregation of the core materials was effected by standard mesh sieves.

Solubility of Drugs in Coating Solution and Drug Losses—Analysis of the clear supernatant layer obtained when the drug suspension was allowed to settle at 80° showed that the solubilities of salicylamide and theophylline in the coating polymer-protective colloid mixture were <0.02 and <0.01%, respectively. The particle size distribution of the core material, checked microscopically, did not appear to change significantly during the microencapsulation process. No uncoated drug particles were observed in the apparatus or in the batch after the process.

Evaluation of the Microcapsules Prepared—*Determination of Microcapsule Content*—The microcapsules were dissolved in chloroform and assayed spectrophotometrically at 306 and 276 nm for salicylamide and theophylline, respectively, using a calibration curve based on standard solutions in chloroform. Ethylcellulose did not absorb in chloroform at these wavelengths.

Determination of Loss of Wall Polymer—The percentage loss was calculated as follows for each batch prepared. The total weight of microencapsulated product obtained, *i.e.*, core and coating material, W_T, in a given batch was obtained from:

$$W_T = W_0/F \qquad \text{(Eq. 1)}$$

where W_0 is the initial amount of drug used and F is the fractional drug content of isolated product, by weight, determined experimentally. The assumption that none of the drug is lost or remains uncapsulated was validated earlier. The weight of the coat in the product, W_{EC}, is given by

$$W_{EC} = W_T - W_0 \qquad \text{(Eq. 2)}$$

If W_{EO} is the initial amount of wall polymer available for microencapsulation, then:

$$\text{percent loss of wall polymer} = \frac{100\,(W_{EO} - W_{EC})}{W_{EO}} \qquad \text{(Eq. 3a)}$$

$$= 100\left[1 + \frac{W_0}{W_{EO}}(1 - 1/F)\right] \qquad \text{(Eq. 3b)}$$

For the case in which $W_0 = W_{EO}$, this simplifies to[6]:

$$\text{percent loss of wall polymer} = 100\,(2 - 1/F) \qquad \text{(Eq. 3c)}$$

For an example, see Table I, 8% (w/w) polyisobutylene. The calculation for a 100-g system is as follows:

[6] The authors acknowledge the reviewer's suggestion to write the equation as a function of the fractional drug content.

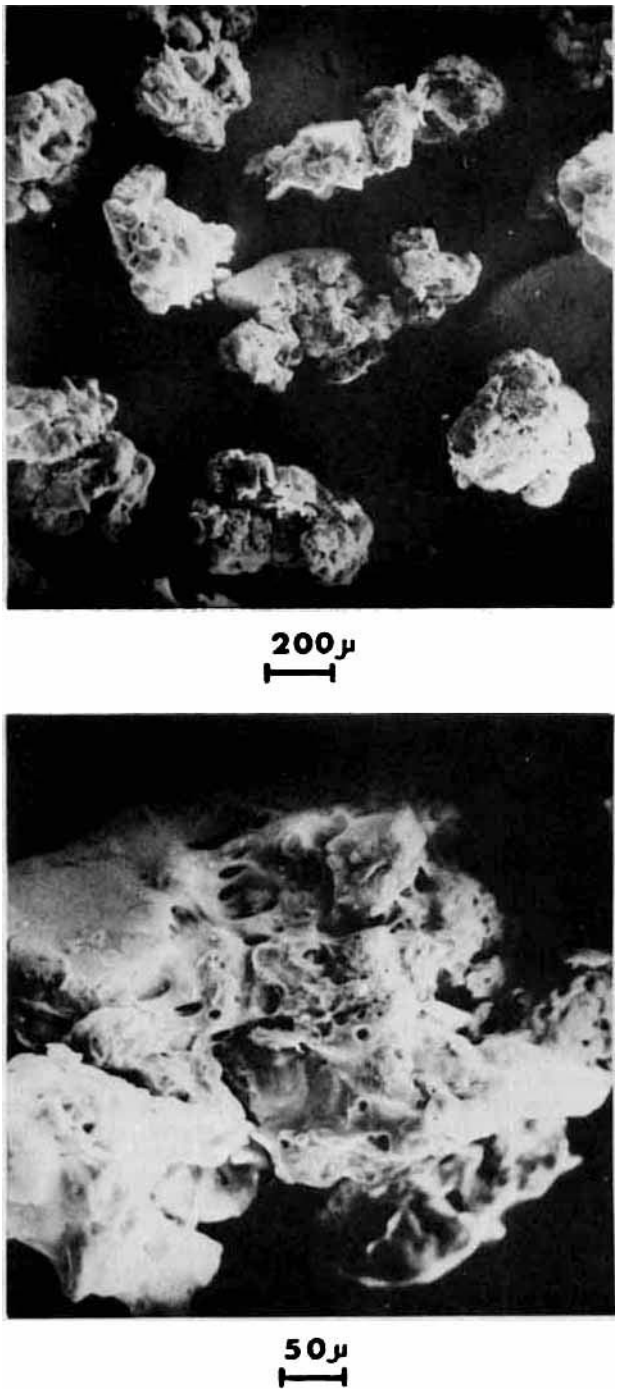

Figure 2—*Scanning electron micrographs of ethylcellulose-microencapsulated salicylamide prepared in the absence of polyisobutylene (5% salicylamide and 5% ethylcellulose at 300 rpm).*

$$W_T = \frac{5}{0.907} = 5.512$$

$$W_{EC} = 5.512 - 5 = 0.512$$

$$\text{ethylcellulose loss} = 89.76\%\ \text{(w/w)}$$

Wall Thickness—The wall thickness of the microcapsules was calculated from the particle size of the core material and the relative densities of the wall and core material. Quantitative expression of the relationship requires use of a shape factor, and because particle shape and size vary widely, even within batches of a single core material, it is generally assumed that the core particles are spherical and the capsule wall is uniform. This enables the use of a simplified model in which the microcapsule is considered to be composed of two spheres. Using the appropriate

Table I—Effect of Polyisobutylene Concentration on Salicylamide Microcapsule Contents and Properties with 5% Salicylamide [a] (100–200 mesh) and 5% Ethylcellulose [a] at 300 rpm

Polyisobutylene[a], %	Drug Content, mean percent ± *SD*	Wall Thickness[b], μm ± *SD*	Ethylcellulose Loss[c], % ± *SD*	Phase Coacervation Volume[d], ml	k_i[e], 10^3 min^{-1}
0	47.6[f]	19.2[f]	0	20	8.03[f]
3	—	—	—	48	—
5	51.2 ± 0.2	17.2 ± 0.1	4.5 ± 0.8	58	1.60
6	50.8 ± 0.9	17.4 ± 0.5	2.9 ± 3.4	59	1.55
7	51.4 ± 1.0	17.0 ± 0.5	5.5 ± 3.8	59	1.62
7.5	66.2 ± 0.4	10.3 ± 0.1	49.0 ± 0.6	—	2.04
8	90.7 ± 0.6	2.4 ± 0.1	89.8 ± 0.6	68	11.2
9	95.1 ± 1.1	1.2 ± 0.3	94.8 ± 1.3	86[g]	18.0

[a] Percentages of materials (w/w) were based on the total weight of the initial suspension containing all the components. [b] Calculated by means of Eq. 4; the standard deviation estimate was based on the drug content analyses. [c] Calculated by means of Eq. 3; the standard deviation estimate was based on the drug content analyses. [d] Parallel experiments performed in the absence of core material (12). [e] First-order release constant. [f] In the absence of polyisobutylene or at low concentrations, the wall polymer separated as an aggregate, both in the absence and presence of core material (see Ref. 12) and the microcapsules formed were of the matrix-coat type. [g] Coacervate phase volume continued to increase above 9% of polyisobutylene.

Table II—Effect of Polyisobutylene Concentration on Theophylline Microcapsule Contents and Properties at Different Particle Sizes [a] with 5% Theophylline and 5% Ethylcellulose at 250 rpm

Polyisobutylene, %	Drug content[b], %	Wall thickness, μm	Ethylcellulose Loss, %	k_i[c], 10^3 min^{-1}
	Particle size, 100–200 mesh			
5	56.7	14.2	23.5	2.58
7	66.0	9.9	48.5	4.75
8	72.0	8.0	61.1	8.15
9	82.4	4.7	78.6	16.85
	Particle size, 60–80 mesh			
5	76.2	12.7	68.7	0.50
8	94.8	2.4	94.5	26.7
9	96.8	1.5	96.7	41.5

[a] See Table I for key. [b] All data show the mean value for two batches (3–7% deviations). [c] Correlation coefficients of the first-order plot (see Fig. 7) were 0.999–0.998.

relationship (13), expressed in terms of fractional drug content[6], a mean spherical wall thickness is estimated as:

$$r_2 - r_1 = \left\{\left[\frac{d_c}{d_{EC}}\left(\frac{1}{F} - 1\right) + 1\right]^{1/3} - 1\right\} r_1 \qquad \text{(Eq. 4)}$$

where r_1, r_2 are the mean radii of the microcapsules and the core particles, and d_{EC}, d_c are the densities of ethylcellulose and the core materials. The densities of the microcapsules and the core and wall materials were determined in cyclohexane using a pycnometer. Dried materials were used and volume adjustment was completed in a few seconds to avoid imbibition and swelling. The results were duplicated exactly and were within 2% of literature values.

Microscopic Studies—Optical[7] and scanning electron microscopy[8] were used to evaluate the quality of the coating obtained under the various conditions used.

Release of Microencapsulated Material—Release of active ingredients from the microcapsules was measured using a rotating basket dissolution apparatus similar to that described in the USP XIX, modified by use of a 100-ml perspex basket in place of the wire mesh, the wall of which was pierced by four windows and covered by a nylon screen (80–100 mesh) bonded permanently by means of epoxy resin to the inner wall, to prevent exit of the microcapsules (Fig. 1). The upper side was pierced by eight holes, sealed with the same nylon screen, and the perspex hollow-ring screw-on base contained a nylon screen insert. The basket was rotated at 100 rpm (±3%) by means of a constant-rate adjustable stirrer[9], using a covered beaker containing 1 liter of water at 37 ± 0.5°. Drug release was determined spectrophotometrically[10] using a flowcell with a pump[11] and automatic recording (sample size, 50–100 mg). There was no turbulence, as checked by measurement of dissolution rate of standard pellets of pure benzoic acid.

The wavelengths used for salicylamide and theophylline were 298 and 272 nm, respectively. Dissolution experiments were duplicated and were closely reproducible.

[7] Tiyoda, Tokyo, Japan.
[8] Cambridge Instrument Co., England.
[9] Fisher Stedi-speed model, Pittsburgh, Pa.
[10] Unicam SP 1800, Pye Unicam Ltd., Cambridge, England.
[11] Model MHRK, Watson-Marlow, Falmouth, England.

Table III—Effect of Particle Size of Salicylamide and Theophylline on Coating Parameters and Release Rates of Drugs from Microcapsules [a]

Particle Size Mesh	Drug Content, %	Wall Thickness, μm	Ethylcellulose EC Loss, %	k_i[b], 10^3 min^{-1}
5% Salicylamide, 7% Polyisobutylene, and 5% Ethylcellulose at 300 rpm				
40–60	89.3	8.3	88.0	2.13
60–80	75.4	13.3	67.3	1.88
100–200	51.5	17.0	5.8	1.60
200–300	50.5	9.8	1.8	5.40
5% Theophylline, 5% Polyisobutylene, and 5% Ethylcellulose at 250 rpm				
60–80	76.2	12.7	68.7	0.50
80–100	67.5	14.1	51.9	0.55
100–200	56.7	14.2	23.5	0.58

[a] See Tables I and II for key. [b] Correlation coefficients, 0.999.

RESULTS AND DISCUSSION

Appearance of Microencapsulated Core Materials—From the preliminary experimental results, it was observed that the presence of polyisobutylene at a minimal concentration was vital to the formation of individual microcapsules. The use of concentrations between 0 and 2% failed to give good reproducible microcapsules. The final product obtained after sieving (1190–840 μm) was composed mainly of large irregular aggregated masses, which were dispersions of core material in ethylcellulose as shown by scanning electron microscopy (Fig. 2). Microscopically, it was impossible to distinguish individually coated particles inside the mass.

Deasy *et al.* (9) obtained a product with surface properties closely similar to the aggregates shown in Fig. 2. The particle size of their product ranged between 1190 and 300 μm, and although an increase in the proportion of finer aggregates was achieved by drastic increase in agitation rate and slowing down of the cooling rate, the nature of the coated particles was essentially unchanged.

The minimum polyisobutylene enabling formation of individually microencapsulated core particles was 3%. However, high turbulence in the system at this concentration, in which the viscosity was low, led to losses of wall polymer by adhesion to the container walls during the cooling phase, while reduced agitation led to adhesion to the stirrer and bottom of the vessel. Such losses were negligible under the experimental conditions used when 5% protective colloid was added.

Photomicrographs (Fig. 3) of salicylamide and theophylline microcapsules in cyclohexane show that each particle was uniformly coated and no aggregation of the microcapsules occurred even after decantation and separation (Fig. 4). The coacervated polymer droplets formed a smooth continuous coat around each particle, markedly different from the surface characteristics of pure salicylamide. Clearly, the presence of an adequate polyisobutylene concentration in the coacervation process

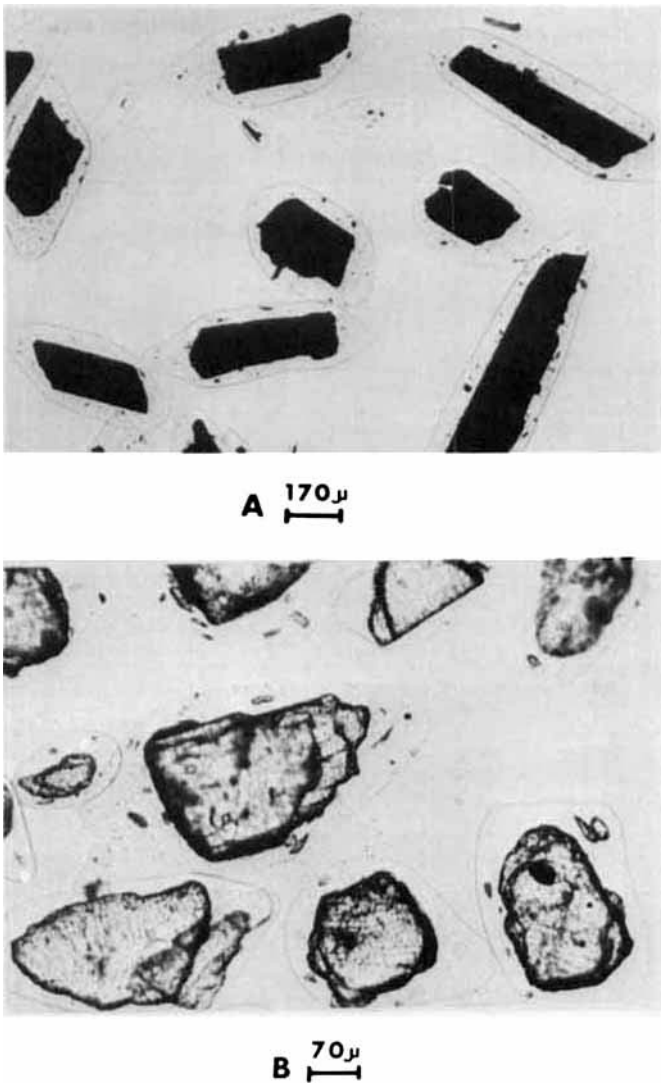

Figure 3—*Photomicrographs of theophylline microcapsules, A (5% theophylline, 5% ethylcellulose, and 5% polyisobutylene at 250 rpm) and salicylamide microcapsules, B (5% salicylamide, 5% ethylcellulose and 5% polyisobutylene at 300 rpm).*

enables formation of such a continuous wall, which may be termed a film-coat, as opposed to the spongy aggregate matrix obtained in the absence of protective colloid or at a low concentration.

These different forms have perhaps not been adequately distinguished in the literature; both are produced by the same basic cooling coacervation method according to the experimental conditions used, and both are described as microcapsules. The particle size of those possessing a matrix-type wall would be expected to be inadequate as a parameter for their characterization and their properties would be expected to vary considerably even at constant particle size, depending on porosity and shape factors and the number of core particles entrapped. On the other hand, in the film-coat type, the shape of the core particle is maintained even when these are highly asymmetrical (Fig. 5). The film thickness appears enlarged in the photomicrographs (Fig. 3) because of swelling of the coat in the original solution or pure cyclohexane. For this reason, no direct measurement of the film thickness could be performed using an optical microscope. Experiments were performed with other solvents such as glycerin and liquid paraffins, but in this case it was difficult to distinguish the wall clearly.

Effect of Polyisobutylene Concentration—In studies of the influence of the protective colloid concentrations, it is not expected that the mean drug content of the microcapsules would change if the initial amounts of wall and core material and the particle size were kept constant, provided the drugs are insoluble in the hot and cold solvent mixtures and the core and wall materials are totally incorporated in the final microcapsules obtained. Alternatively, such losses of core and wall material that do occur should be independent of protective colloid concentration. However, routine microscopic and scanning electron microscopic observation of the products led to detection of varying amounts of empty spherical particles of wall material in the different batches which evidently were solidified coacervate droplets (Fig. 6). They were removed by the repeated decantation to obtain drug-filled microcapsules alone. Since quantitative recovery of empty shells proved to be laborious and some microcapsules were lost in the separation, the drug content of the

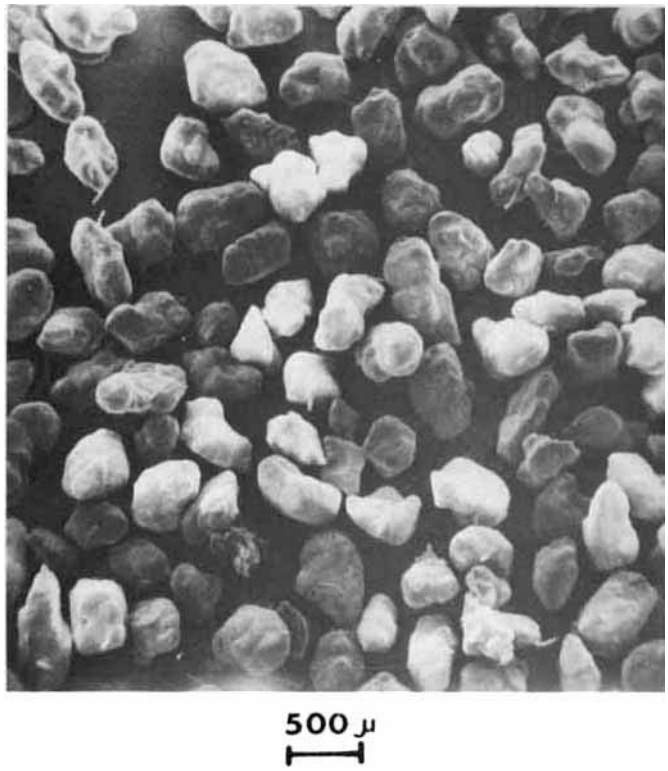

Figure 4—*Scanning electron micrograph of salicylamide microcapsules (see text).*

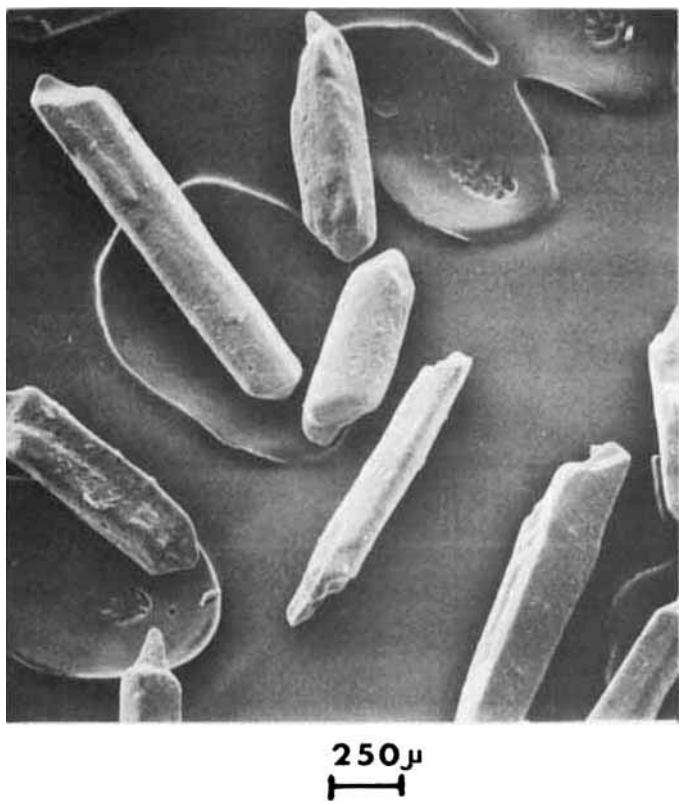

Figure 5—*Scanning electron micrograph of theophylline microcapsules (see text).*

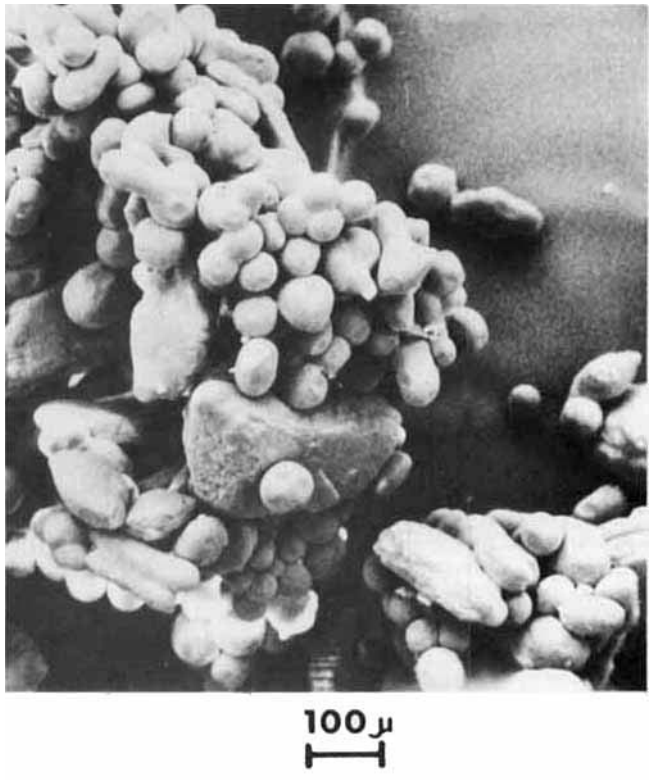

Figure 6—*Scanning electron micrograph of salicylamide microcapsules (250–300 μm) with empty spherical coacervate droplets (40–60 μm).*

purified microcapsules was determined analytically. Then, from the initial quantities of materials used, assuming that all the available drug had been microencapsulated uniformly (as was confirmed by experimental observation) the amount of wall polymer in the microcapsules was calculated and hence the amount "wasted."

This method, described in the experimental section, has not yet been applied to the microencapsulation process. Use of equations for concentric spheres (13) enabled estimation of mean equivalent sphere coat thickness. This calculation probably gives a reasonably true value for salicylamide but a hypothetical one for theophylline due to the crystal shapes (Fig. 3). Repeat batches treated in this way proved to have reproducible drug contents, indicating that stirring conditions, cooling rate, and the separation process were well controlled (Table I).

The drug content of the microcapsules, as seen in Table I, was constant up to 7% of polyisobutylene, but then rose sharply indicating decrease of uptake of wall material by the core particles, which is shown calculated as percentage ethylcellulose loss. The equivalent wall thickness also expresses this trend, and since drug release rate from the microcapsules followed first-order kinetics (Figs. 7A and 7B), release-rate constants[12] were evaluated for the series; they are inversely related to the mean wall thickness in salicylamide (Table I). The same protective colloid effects are evident in the preparation and data of theophylline microcapsules (Table II), although with this core material, the concentration effect is gradual rather than drastic.

Relation to Wall Polymer Coacervation—In considering possible causes of the observed decrease of coating efficiency, it is tempting to assume that excess wall polymer was used, so that decreasing its quantity will eliminate the losses. However, halving the amount of ethylcellulose to 2.5% (w/w) at the 5% level of polyisobutylene, with the other conditions as in Table I, yielded microcapsules which, after purification, contained 87.9% salicylamide, corresponding to 72.4% loss of ethylcellulose, compared with 4.5% loss at 5% wall polymer. Initial studies over a wider range of core and wall concentrations confirms this trend and will be reported upon completion.

In ethylcellulose coacervation studies performed in the absence of core material (12) under the same conditions used in Table I, the phase coacervation volume, which was small at low concentrations of protective colloid, rose sharply at first and flattened out to give a constant value between 5 and 7% of polyisobutylene. Above this level of additive, the

[12] A full analysis of the release kinetics of microcapsules made by this method is the subject of the second part of this investigation.

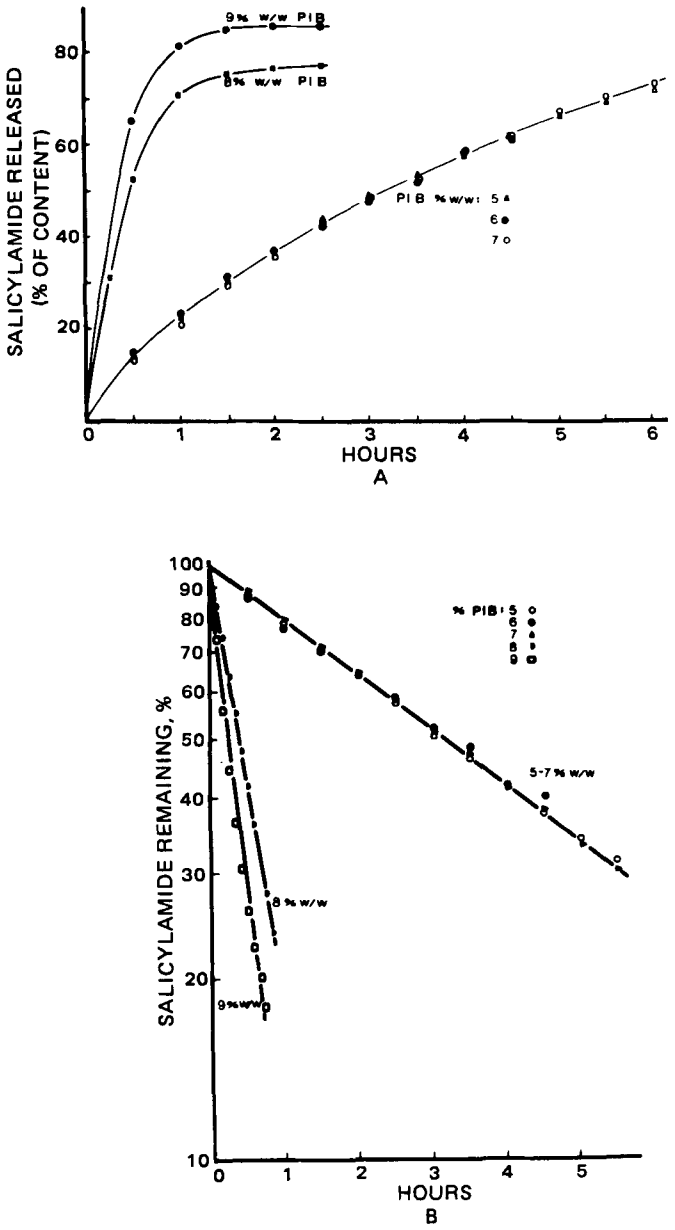

Figure 7—*Salicylamide release from microcapsules prepared using different polyisobutylene concentrations; linear plot (A) and first-order plot (B).*

coacervation volume rose very steeply toward 100% of the total volume, reached at 10% additive. Values (Table I) ran in a manner closely similar to drug content. The coacervate droplet size in the absence of core material was shown to change inversely to the phase coacervation volume (12). The relation of the effects of polyisobutylene on coacervation and microencapsulation parameters are more clearly evident graphically (Fig. 8). Microcapsule wall thickness remained relatively constant as did release rate from the microcapsules and coacervate droplet size at 5–7% polyisobutylene; above this range they changed steeply, with thickness and droplet size falling and release rate rising. The related function, loss of ethylcellulose, followed an inverse pattern to wall thickness. It is clearly indicated that the coating ability for salicylamide falls off drastically as the protective colloid concentration exceeds a critical value, at which the droplet size also undergoes drastic change and the coacervation volume rises (Table I).

It seems that the microcapsule coating process reflects more fundamental changes arising from the coacervation process.

The sudden increase in coacervation volume above 7% in the absence of core material was considered due to a combination of decrease in coacervate drop size and increase in viscosity, the former effect resulting from stabilization of the droplets by adsorption of polyisobutylene as a protective colloid at an earlier stage in droplet growth (12). Such stabi-

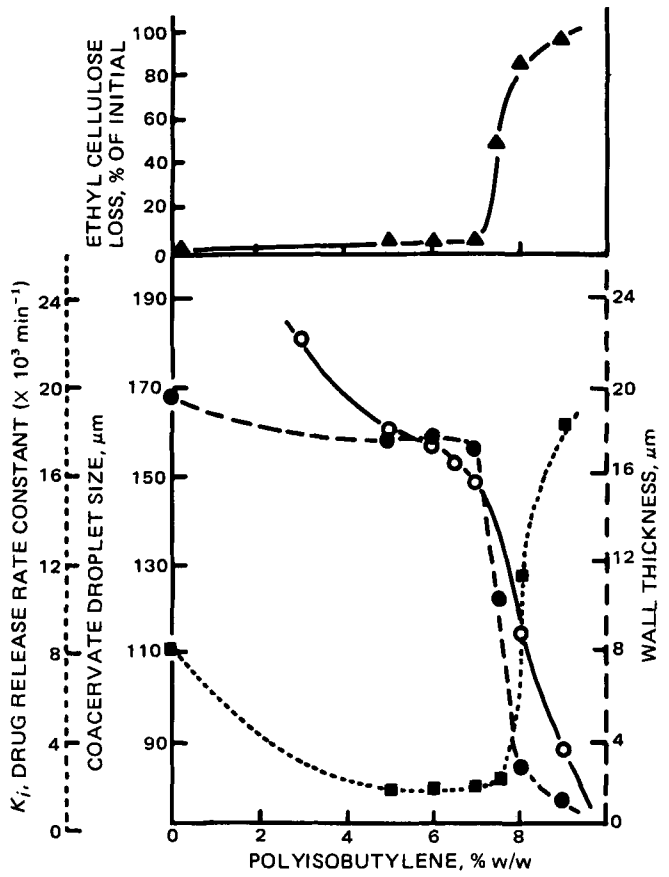

Figure 8—*Effect of polyisobutylene concentration on coacervate and microcapsule parameters (core material: salicylamide; see Table I for conditions). Key: ●, wall thickness; ○, coacervate droplet size; ▲, ethylcellulose loss; and ■, first-order release rate constant* (k_i).

lized coacervate droplets, suspended in the solvent, were unable to coat core material when the two were mixed and stirred together at room temperature. Therefore, it is proposed that the mechanism of the effects observed on increasing the protective colloid concentration above a critical level is that diffusion and growth of wall polymer from the coacervate microdroplets separating out during cooling is inhibited by increase in viscosity, and a larger proportion of droplets are stabilized when they are still small, becoming less available for use in coating.

Effect of Particle Size—The drug content of the microcapsules decreased with reduction in core particle size (Tables II and III). With a fixed amount of core material, particle size reduction leads to increase in the specific surface. The corresponding minimization in the loss of wall polymer may be attributed to the availability of the additional surface for entrapment of separating coacervate droplets. It can also be seen that at equivalent particle sizes there is a tendency for ethylcellulose loss to vary from one drug to another, probably due to differences in particle shape or surface energy[13].

The variation in drug content of the microcapsules as a function of particle size is reflected in the drug release rates, which change inversely with wall thickness[14] (Tables II, III). However, the precise quantitative relationship cannot be tested without allowing for size distribution and shape factors, considerations that are beyond the scope of this study.

The particle size effect fits the mechanism proposed. Considering the coating and stabilization of empty droplets as competitive processes, the former will be favored at the expense of the latter by surface area increase of the core material, which should enhance the rate of uptake of the separating ethylcellulose.

In fact, the results obtained in this work are in contradiction to those published in the literature. It is well accepted that at a constant ratio of coat polymer to drug, decrease of particle size leads to a decrease in wall thickness and an increase in release rate (13). This is true only if in the specific microencapsulation process all the coating polymer is used up in building the wall. Microencapsulation using ethylcellulose coacervated in the presence of protective colloid gives a unique system in which the latter prevents empty stabilized coacervated droplets from interacting with microcapsules, and encourages formation of a continuous uniform film coat which retains the shape of the core material.

The results also show that by means of particle size change, the effective coating efficiency may be varied between high and low levels with consequent change of wall thickness while retaining a true film coating. The question of whether the amount of initial wall material used is in excess or not has a different relevance in a system in which the concentration of protective colloid is one of the major controlling factors in the efficiency of the coating process. By choice of suitable protective colloid concentration or particle size, full efficiency can be achieved without changing the initial wall polymer concentration.

REFERENCES

(1) R. E. Miller, G. O. Fanger, and R. G. McNiff, Union of South Africa pat. 4211-66 (1967).

(2) T. C. Powell and J. L. Anderson, U.S. pat. 3576759 (1971).

(3) P. M. John, H. Minatoya, and F. J. Rosenberg, *J. Pharm. Sci.*, **68,** 475 (1979).

(4) R. E. Miller and J. L. Anderson, U.S. pat. 3155590 (1964).

(5) H. P. Merkle, "Zur Mikroverkapselung Fester Arzneistoffe Mittels Koazervation," Thesis E.P.E., Zurich, 1972.

(6) M. Donbrow and S. Benita, *J. Pharm. Pharmacol.*, **29,** 4P (1977).

(7) N. N. Salib, M. E. Elmen Shawy, and A. A. Ismail, *Pharmazie*, **31,** 721 (1976).

(8) I. Jalsenjak, C. F. Nicolaidou, and J. R. Nixon, *J. Pharm. Pharmacol.*, **28,** 912 (1976).

(9) P. B. Deasy, M. R. Brophy, B. Ecanow, and M. Joy, *ibid.*, **32,** 15 (1980).

(10) A. B. Dhruv, T. C. Needham, and L. A. Luzzi, *Can. J. Pharm. Sci.*, **10,** 33 (1975).

(11) M. Takenaka, Y. Kawashima, and S. Y. Lin, *J. Pharm. Sci.*, **69,** 513 (1980).

(12) S. Benita and M. Donbrow, *J. Colloid Interface Sci.*, **77,** 102 (1980).

(13) J. A. Herbig, in "Encyclopedia of Chemical Technology," 2nd ed., vol. 13, Wiley, New York, N.Y., 1967, p. 436.

ACKNOWLEDGMENTS

Abstracted in part from a thesis submitted by S. Benita to the Hebrew University of Jerusalem in partial fulfillment of the Doctor of Philosophy degree requirements.

The authors acknowledge the generous gift of Oppanol B50 by BASF, Ludwigshafen, West Germany.

[13] Although different stirring rates were employed, this factor was found insufficient to account for the differences between the two drugs.

[14] There is a tendency for release rate to rise as core particle size falls, at equivalent wall thickness, probably due to surface area increase.

Investigation of Digoxin, Quinidine, and Disopyramide Interactions in Rats Utilizing Parotid Saliva, Blood, and Other Tissues

G. JOHN DiGREGORIO[x], ANTHONY J. PIRAINO, EILEEN K. RUCH, and PETER J. BASSECHES

Received February 26, 1981, from the *Hahnemann Medical College and Hospital, Philadelphia, PA 19102.* Accepted for publication June 26, 1981.

Abstract □ Blood, parotid saliva, heart, liver, and kidney concentrations of digoxin and quinidine were determined in rats chronically treated with digoxin and in nontreated (control) rats after the administration of quinidine (20 mg/kg ip) and disopyramide (10 mg/kg ip). The results indicated that digoxin concentrations increased significantly and proportionally in parotid saliva and plasma after quinidine, but did not increase after disopyramide. With the exception of the liver, which showed an increase in digoxin concentrations, tissue concentrations of digoxin did not differ from control animals. In rats pretreated chronically with digoxin, quinidine concentrations in plasma, parotid saliva, or heart tissue did not differ significantly from control animals, but were significantly lower than controls in liver and kidney tissues. The results presented here lend additional support to the hypothesis that the increase in digoxin plasma concentration following quinidine administration is primarily due to interference with renal excretion and displacement of digoxin by quinidine binding sites. Furthermore, it was demonstrated that disopyramide has little or no effect on plasma digoxin levels in rats.

Keyphrases □ Digoxin—interaction with quinidine and disopyramide in parotid saliva, blood, and other tissues □ Quinidine—interaction with digoxin and disopyramide in parotid saliva, blood, and other tissues □ Disopyramide—interaction with digoxin and quinidine in parotid saliva, blood, and other tissues

Considerable attention has been focused on the mechanism of the drug interaction between digoxin and quinidine (1–7). Several mechanisms have been proposed, but because of the limited flexibility of the human model, they cannot be supported by hard experimental evidence. Relatively few animal studies have been employed to evaluate the digoxin–quinidine interaction.

The present investigation evaluated the interaction between digoxin and quinidine and digoxin and disopyramide in rats. Blood, parotid saliva, and tissue concentrations of digoxin were determined in rats pretreated chronically with digoxin and later administered single doses of quinidine or disopyramide. In addition, blood, parotid saliva, and tissue concentrations of quinidine were determined in rats chronically pretreated with digoxin and later administered a single dose of quinidine.

EXPERIMENTAL

Reagents and Materials—all reagents were analytical grade, and all aqueous solutions were made with glass-distilled water. Digoxin[1] and pentobarbital sodium[2] were obtained in the injectable form. Quinidine[3] and disopyramide[4] were obtained in powdered form and appropriate solutions were made. Cannulas for the collection of whole blood and parotid saliva were fabricated from polyethylene 50 and 10 tubing[5]. Samples collected were assayed for digoxin and quinidine content using enzyme immunoassay kits[6] in accordance with the manufacturer's instructions.

Experiment 1—*Comparison of Digoxin Concentrations in Parotid Saliva, Plasma, Heart, Liver, and Kidney Tissues of Rats Administered Quinidine, Disopyramide, and Saline*—Male Wistar rats, 150–170 g, were housed in individual cages and provided with a standard diet of laboratory chow[7] and distilled water containing digoxin (2.5 μg/ml) *ad libitum*. The volume of water consumed and weight gained were recorded daily for each animal. After 8 days of drinking digoxin-containing water, a total of 37 animals were divided into three experimental groups, A, B, and C (Scheme I). These groups were designated to receive saline, quinidine (20 mg/kg ip) and disopyramide (10 mg/kg ip), respectively.

All animals were prepared surgically for collection of parotid saliva and whole blood using pentobarbital (50 mg/kg ip) anesthesia according to an earlier method (8). A tracheotomy was performed and with the aid of a dissecting microscope, the right brachial artery, right femoral artery, and both parotid ducts were surgically exposed for cannulation. The brachial and femoral arteries were cannulated with polyethylene 50 tubing and the parotid ducts were cannulated with tapered polyethylene 10 tubing. The femoral artery was used to obtain blood samples. The brachial artery was used for the constant infusion of the secretagogue, pilocarpine (0.25 mg/ml) at a rate of 0.21 ml/min. The parotid cannulas were directed into a disposable glass culture tube for the collection of saliva.

Following surgery, Group A animals received an intraperitoneal challenge injection of saline, Group B, an intraperitoneal challenge injection of quinidine, and Group C received an intraperitoneal challenge injection of disopyramide. Thirty minutes after the intraperitoneal challenge, the collection of parotid saliva was started and continued over

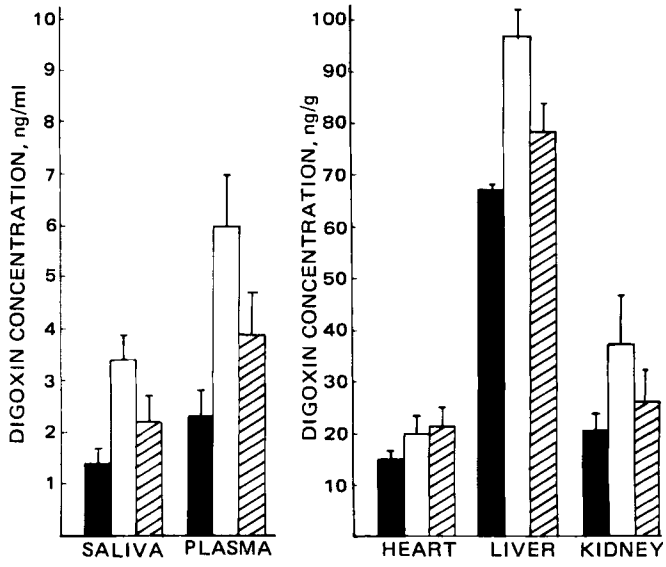

Figure 1—*Comparison of digoxin concentrations in parotid saliva, plasma, heart, liver, and kidney tissues of digoxin chronically treated rats after saline (■, Group A), quinidine (□, Group B), and disopyramide (▨, Group C).*

[1] Lanoxin, Burroughs Wellcome Co., Research Triangle Park, N.C.
[2] Nembutal, Abbott Laboratories, North Chicago, Ill.
[3] Sigma Chemical Co., St. Louis, Mo.
[4] Searle, Chicago, Ill.
[5] Fisher Scientific, King of Prussia, Pa.
[6] EMIT (Enzyme-multiplied immunoassay technique), Syva Co., Palo Alto, Calif.
[7] Ralston Purina, St. Louis, Mo.

0022-3549/82/0200-0211$01.00/0

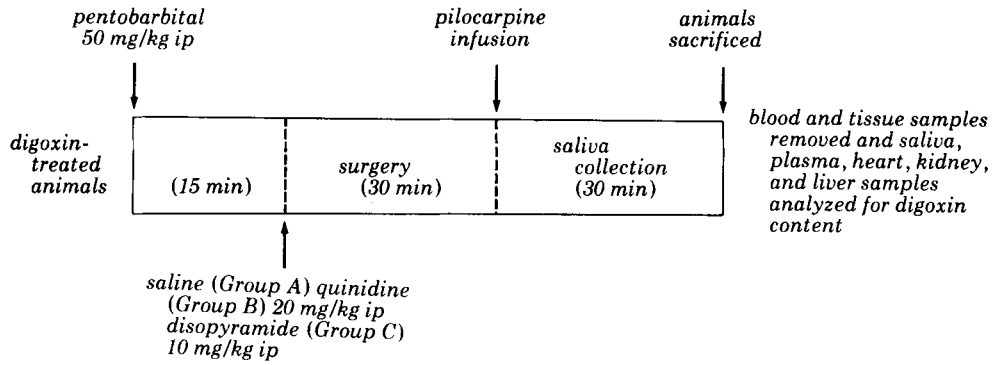

Scheme I—Diagram of experiment 1

the next 30 min. Subsequently, 5 ml of whole blood was removed from the femoral artery and placed in a heparinized tube. The animal was then sacrificed and the heart, liver, and kidneys were removed; whole blood was centrifuged and the plasma was removed. All samples were frozen until the assay. The sequence of these events is presented in Scheme I.

Heart, liver, and kidney samples were weighed and 0.75–1.00 g of tissue was homogenized in 5 ml of 0.9% sodium chloride and mixed with 10 ml of methylene chloride (9). After centrifugation, 5 ml of the organic layer was decanted and evaporated. The residue was dissolved in 5 or 10 ml of distilled water (10). All samples were assayed for digoxin content by enzyme immunoassay.

Experiment 2—*Comparison of Quinidine Concentration in Parotid Saliva, Plasma, Heart, Liver, and Kidney Tissues of Rats Pretreated with Digoxin and Saline*—Male Wistar rats, 150–170 g, were housed in individual cages and given a standard diet of laboratory chow *ad libitum*. Control animals (Group A) were provided tap water *ad libitum*, while experimental animals (Group B) were provided tap water containing digoxin (2.5 μg/ml) *ad libitum* (Scheme II). Water consumption and weight gain were recorded daily for both groups. After 8 days, both groups of rats underwent surgical preparation as described for Experiment 1.

Quinidine (20 mg/kg ip) was administered to Group A and Group B animals. Parotid saliva was collected over 30 min after which each animal was sacrificed and blood, liver, heart, and kidney samples were removed. Samples were handled in a manner similar to that described in Experiment 1. However, in this experiment, samples were assayed for quinidine concentration using enzyme immunoassay.

RESULTS

As described, the rats given digoxin-containing water (2.5 μg/ml) for 8 days were divided into three groups based on the administration of a second drug on the 8th day (Table I): Group A (control animals), which received only digoxin, Group B (quinidine animals), and Group C (disopyramide animals).

Daily digoxin consumption and body weight in these three groups were compared. Using the Student *t* test, no significant differences in the daily digoxin consumption or body weights could be found among any of the groups ($p > 0.05$).

Comparison of Digoxin Concentrations in Parotid Saliva, Plasma, and Heart, Liver, and Kidney Tissues of Rats Administered Quinidine, Disopyramide, and Saline—Digoxin concentrations in the parotid saliva, plasma, liver, kidney, and heart tissues in rats consuming digoxin for 8 days were measured in each of three experimental groups with the following results (Fig. 1).

The digoxin content of saliva and plasma collected from Group A (control) animals was 1.4 ± 0.3 and 2.3 ± 0.5 ng/ml, respectively. Heart, liver, and kidney tissue displayed digoxin concentrations of 14.8 ± 1.7, 67.0 ± 1.0, and 19.7 ± 3.8 ng/g, respectively.

Group B (quinidine treated) rats displayed a digoxin concentration in parotid saliva of 3.4 ± 0.5 ng/ml and a plasma concentration of 6.0 ± 1.0 ng/ml. When the hearts, livers, and kidneys of these animals were homogenized and analyzed they were found to contain 20.0 ± 4.0, 96.4 ± 5.7, and 37.1 ± 9.4 ng/g of digoxin, respectively.

Group C (disopyramide treated) rats displayed saliva and plasma digoxin levels of 2.2 ± 0.5 and 3.9 ± 0.8 ng/ml, respectively. Analysis of their heart, liver, and kidney tissue revealed digoxin levels of 21.7 ± 3.5, 78.4 ± 7.1, and 26.0 ± 6.2 ng/mg, respectively.

When evaluated using the Student *t* test, the digoxin content of parotid saliva, plasma, and liver was significantly higher in Group B rats than in control animals $p < 0.01$, $p < 0.005$, and $p < 0.005$, respectively. No significant differences in digoxin concentration could be found between control rats and Group C animals for any tissue studied ($p > 0.05$).

The mean ratios (±*SE*) between parotid saliva digoxin concentrations and those found in plasma were 0.60 ± 0.10, 0.69 ± 0.11, and 0.68 ± 1.20 for the Group A, B, and C rats, respectively. For Groups A, B, and C, the mean ratios (±*SE*) between the digoxin concentrations found in liver and in plasma were calculated to be 33.8 ± 8.7, 29.0 ± 8.60, and 35.2 ± 10.40; for kidney and plasma, 8.0 ± 1.60, 8.9 ± 2.10, and 8.7 ± 1.70; and finally for heart and plasma, 9.3 ± 2.80, 5.3 ± 1.60, and 7.3 ± 1.80.

Comparison of Quinidine Concentration in Parotid Saliva, Plasma, Heart, Liver, and Kidney Tissues of Rats Pretreated with Digoxin and Saline—Control animals displayed quinidine concentrations (Fig. 2) of 0.3 ± 0.1 ng/ml (parotid saliva) 1.1 ± 0.8 ng/ml (plasma), 1.0 ± 0.2 ng/g (heart), 0.6 ± 0.2 ng/g (liver), and 1.3 ± 0.4 ng/g (kidney). Parotid saliva and plasma were analyzed in Group B rats and found to contain quinidine in concentrations of 0.4 ± 0.04 and 0.9 ± 0.1 ng/ml, respectively. Homogenates of heart, liver, and kidney tissues taken from these animals contained 0.6 ± 0.2, 0.3 ± 0.05, and 0.5 ± 0.1 ng of quinidine/g, respectively. When these quinidine concentrations were compared with those obtained in control animals using the Student *t* test, the following results were noted. No significant variation between the groups was found for quinidine concentrations detected in parotid saliva ($p > 0.05$), plasma ($p > 0.05$), or heart tissue ($p > 0.05$). The quinidine concentrations in the liver and kidney tissue of Group A animals were significantly higher than those of Group B animals ($p < 0.05$).

DISCUSSION

Some controversy exists concerning the mechanism of the interaction reported to occur between quinidine and digoxin. The most frequently

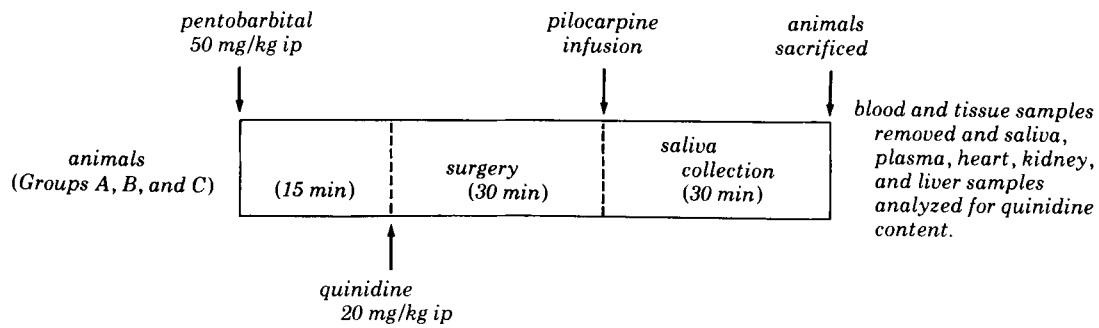

Scheme II—Diagram of experiment 2

Table I—Comparison of Weights and Digoxin Consumption by Three Groups of Rats over 8 Days

Group[a]	n	Weight[b], Mean, g	Digoxin[c] Consumed in 24 hr, ng
A	10	255 ± 4.4	103.0 ± 6.8
B	10	259 ± 4.6	104.0 ± 5.0
C	10	253 ± 7.9	122.2 ± 8.0

[a] Group A animals received digoxin only; Group B received digoxin and quinidine; and Group C received digoxin and disopyramide. [b] Mean (±*SE*) of weights of rats fed over 8 days. [c] Mean (±*SE*) of digoxin consumed per 24 hr from drinking water containing 2.5 μg of digoxin/ml over 8 days.

proposed mechanisms include the displacement of digoxin by quinidine from tissue binding sites (2, 5) and the interference by quinidine with renal digoxin excretion (11).

During the 8 days of digoxin consumption, animals in all groups consumed approximately the same quantity of digoxin. In addition, the mean weights after pretreatment with digoxin did not differ from group to group. The results indicated that during these 8 days, all the animals reacted similarly, so there was little or no intra-individual variation at the time of the experiment.

Results of the present investigation support two possible mechanisms for this interaction: (*a*) quinidine interferes with the renal excretion of digoxin although renal clearance of digoxin has not been measured, and (*b*) quinidine interferes with digoxin tissue binding sites.

Following quinidine administration, digoxin concentrations increased significantly in plasma and parotid saliva compared with control animals. The increases were proportional because the saliva/plasma ratios for control animals and the experimental group did not significantly differ from each other. In liver tissue, digoxin concentrations increased after quinidine administration; however, kidney and heart digoxin concentrations did not significantly differ from those of control animals. The increase in plasma was greater than any of the tissue concentration changes. Subsequently, the liver and cardiac muscle tissue/plasma concentration ratios actually decreased after quinidine administration, whereas the kidney/plasma ratio did not significantly change. These results were similar to other findings (12) where the corresponding digoxin tissue/serum ratios decreased in dogs after quinidine.

Assuming the increase in plasma digoxin concentrations involves an interference with renal digoxin excretion by quinidine, proportional increases in the plasma and parotid saliva digoxin concentrations and possible increases in tissue concentrations would be expected. This hypothesis is supported by previous investigations (13–15) that demonstrated that increasing the plasma concentrations of various drugs causes proportional increases in the free nonprotein-bound plasma drug levels as well as those in the parotid saliva. However, if the increases in plasma digoxin concentration after quinidine administration were due solely to a decrease in plasma protein or tissue digoxin binding, one would anticipate that: (*a*) parotid saliva concentrations would increase to a greater proportion than plasma with a subsequent increase in the saliva/plasma ratio, and/or (*b*) tissue digoxin concentrations would decrease significantly due to the displacement of digoxin by quinidine.

As previously discussed, saliva/plasma ratios did not change from control values, but the liver and cardiac digoxin tissue concentrations showed a tendency to decrease when compared with the plasma concentrations. It is for these reasons that the present results support more than one mechanism for this interaction which may involve tissue binding sites and renal clearance.

Other investigators (1, 16) reported that various antiarrhythmic agents (including disopyramide) had little or no effect on digoxin blood levels. Results also indicate that there are no significant differences between digoxin concentrations in plasma, parotid saliva, and heart, liver, and kidney tissues determined before and after disopyramide administration.

In the second experiment, quinidine concentrations in blood and parotid saliva showed no significant differences between control and digoxin-treated animals. In addition, quinidine concentrations tended

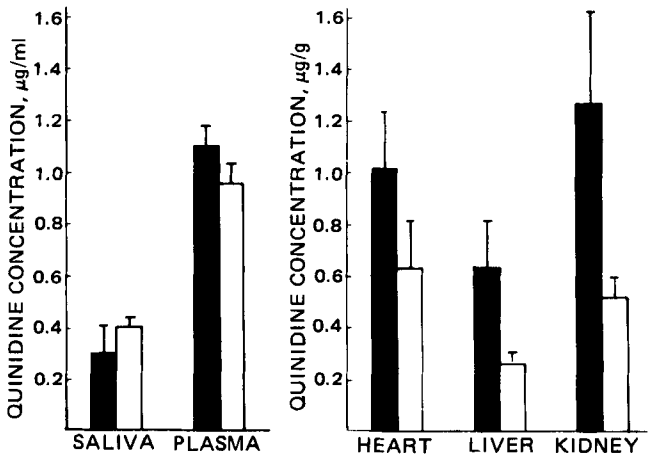

Figure 2—*Comparison of quinidine concentrations in parotid saliva, plasma, heart, liver, and kidney tissues in control rats (■, Group A) and in digoxin chronically treated rats (□, Group B).*

to decrease in liver and kidney tissue. As previously discussed, if the interaction was mainly due to the ability of quinidine to displace digoxin from plasma proteins binding sites, the free plasma concentrations of quinidine or parotid saliva quinidine would be expected to decrease. However, if quinidine significantly occupied tissue binding sites previously occupied by digoxin then the quinidine tissue concentrations would tend to increase over control. In neither instance did the earlier results correlate with an interference of plasma protein or tissue binding. However, if the interaction of quinidine–digoxin was controlled only by a renal mechanism, then quinidine concentrations in plasma and/or parotid saliva would probably not differ from those of controls as observed. However, while one would expect that quinidine concentrations in kidney would increase under this mechanism, the results presented here actually show the opposite effect, suggesting the possibility that more than one mechanism is involved. Studies are in progress to investigate these findings further.

REFERENCES

(1) W. Doering, *N. Engl. J. Med.*, **301**, 300 (1979).

(2) E. Leahey, J. Reiffel, R. Drusin, R. Heissenbuttel, W. Lovejoy, and J. T. Bigger, *J. Am. Med. Assoc.*, **240**, 533 (1978).

(3) T. S. Chen and H. S. Friedman, *ibid.*, **244**, 669 (1980).

(4) T. P. Gibson and H. A. Nelson, *J. Lab. Clin. Med.*, **95**, 417 (1980).

(5) G. Ejvinsson, *Br. Med. J.*, **1**, 279 (1978).

(6) W. D. Hager, P. Fenster, M. Mayershohn, D. Perrier, P. Graves, F. I. Marcus, and S. Goldman, *N. Engl. J. Med.*, **300**, 1238 (1979).

(7) W. S. Burkle and G. R. Matzke, *Am. J. Hosp. Pharm.*, **36**, 968 (1979).

(8) A. J. Piraino, G. J. DiGregorio, and E. K. Ruch, *J. Pharmacol. Methods*, **3**, 1 (1980).

(9) J. Karjalainen, K. Ojala, and P. Reissel, *Acta Pharmacol. Toxicol.*, **34**, 385 (1974).

(10) E. L. Slighton, *J. Forensic Sci.*, **23**, 292 (1978).

(11) W. Doering, *N. Engl. J. Med.*, **301**, 400 (1979).

(12) J. E. Doherty, K. D. Straub, M. L. Murphy, N. Soyza, J. E. Bissett, and J. J. Kane, *Am. J. Cardiol.*, **45**, 1196 (1980).

(13) G. J. DiGregorio, A. J. Piraino, and E. K. Ruch, *Drug Alcohol Depend.*, **3**, 43 (1978).

(14) G. J. DiGregorio, A. J. Piraino, and E. K. Ruch, *Clin. Pharmacol. Ther.*, **24**, 720 (1978).

(15) G. J. DiGregorio and E. K. Ruch, *J. Pharm. Sci.*, **69**, 1457 (1980).

(16) E. B. Leahy, J. A. Reiffel, E. G. V. Giardina, and J. T. Bigger, *Ann. Intern. Med.*, **92**, 605 (1980).

Structure–Activity Relationships Among Substituted *N*-Benzoyl Derivatives of Phenylalanine and Its Analogs in a Microbial Antitumor Prescreen I: Derivatives of *o*-Fluoro-DL-phenylalanine

THEODORE T. OTANI ˣ and MARY R. BRILEY

Received May 15, 1981, from the *Laboratory of Pathophysiology, National Cancer Institute, National Institutes of Health, Bethesda, MD 20205.* Accepted for publication June 11, 1981.

Abstract □ Twelve derivatives of *o*-fluoro-DL-phenylalanine containing fluorine, chlorine, methoxy, and nitro radicals in various positions of the aromatic ring of the benzoyl group were prepared and tested in a *Lactobacillus casei* system. It was found that most substitutions in the benzoyl phenyl ring resulted in a compound exhibiting greater growth-inhibiting activity than the nonsubstituted benzoyl-*o*-fluorophenylalanine. The greatest activity was observed in the *ortho*-substituted fluoro compound and the *meta*- and *para*-substituted chloro and nitro compounds. With the methoxy group, the position of substitution appeared unimportant, since all three methoxy isomers exhibited essentially equal inhibition. Nitro substitution in the *ortho* position had a protective effect in that the product was less active than the unsubstituted benzoyl-*o*-fluoro-DL-phenylalanine.

Keyphrases □ Structure–activity relationships—substituted *N*-benzoyl derivatives of phenylalanine, microbial antitumor prescreen □ Phenylalanine—substituted *N*-benzoyl derivatives, microbial antitumor prescreen □ Antitumor agents, potential—microbial antitumor prescreen, substituted *N*-benzoyl phenylalanine derivatives

Previous studies on the effect of *N*-acylated amino acids and amino acid analogs on the growth of *Lactobacillus casei* in an antitumor prescreen indicate that certain acyl groups could activate an otherwise inert amino acid or amino acid analog to inhibit the growth of the organism (1–4). *N*-Chloroacetyl (1–3) and *N*-trifluoroacetyl (4) derivatives of certain amino acids exhibited modest but significant inhibition. However, among the acyl amino acids studied, the *N*-benzoyl derivatives showed the greatest inhibition, especially the benzoyl derivatives of phenylalanine analogs (5, 6). The nature and the position of the substituent in the aromatic ring of phenylalanine are apparently of some importance in the action, since substituents at various positions in the ring resulted in compounds of different activity. Of the seven benzoyl derivatives of ring-substituted phenylalanine and phenylalanine analogs studied earlier, benzoyl-*p*-chloro- and benzoyl-*m*-fluorophenylalanine showed the greatest inhibition (5, 6). Among the *N*-chloroacetyl derivatives of *p*-halophenylalanines the activity decreased in order from the *p*-iodo through the *p*-bromo and the *p*-chloro to the *p*-fluoro derivatives (7).

This study attempted to find out whether substituents in the aromatic ring of the benzoyl moiety would similarly affect the inhibitory activity of these compounds and whether more potent inhibitors could be devised by combination of the appropriate substituted benzoyl and phenylalanine moieties. Thus, a systematic study was undertaken to observe the effect of varying the substituents (a) to the benzoyl moiety while keeping the amino acid portion constant, and (b) to the amino acid while keeping the benzoyl moiety unchanged.

In this study, the amino acid moiety was *o*-fluoro-DL-phenylalanine, and the aroyl part included 12 ring-substituted benzoyl derivatives[1].

EXPERIMENTAL

o-Fluoro-DL-phenylalanine was obtained commercially[2]. Its purity was checked by paper chromatography in four separate solvent systems (*cf.* Ref. 2), elemental analysis, and by nitrous acid gasometric analysis of primary amino nitrogen (8). When necessary it was recrystallized from water–ethanol. The acylating agents were obtained from commercial sources and purified, by distillation or recrystallization when necessary.

The acyl derivatives were prepared by the Schotten–Baumann procedure (*cf.* Ref. 9). The liquid acylating agents were added in 1.2 mole excess directly into the reaction mixture in six equal portions over a 1-hr period. Solids were added as an ethyl acetate solution, also in six equal portions over a 1-hr period. The reaction in most cases was carried out between 0 and 5°. However, when the acylating agent solidified at that temperature, the reaction was carried out at 10°.

The purity of the prepared acyl derivatives was ascertained by elemental analysis, melting point determination, and by nitrous acid gasometric determination of primary amino nitrogen (8) (Table I).

For the microbiological assay, the acyl compounds were dissolved in one equivalent of sodium hydroxide. In some cases, warming was required to dissolve the compound. At this point, the pH of the test solution was ~6.

A modification was made on the sterilization procedure of the test compounds so that a larger number of compounds could be tested each time. The all-glass filtration procedure for sterilization was replaced with one using sterilizing filter units[3] (0.22-μm pores) attached to plastic syringes[4].

The assay medium was a riboflavin-supplemented riboflavin assay medium[5] containing 0.03 μg of riboflavin[6]/ml in the final assay system.

The system was incubated at 37.5° for 19 hr, and then bacteria growth was terminated by immersing the tubes in boiling water for 10 min. After the suspension was cooled in an ice bath for 10 min, the growth was determined turbidimetrically on a photoelectric colorimeter[7] equipped with a red filter (660 nm).

The organism used was *Lactobacillus casei* 7469[8], which was carried on agar[9], subcultured bimonthly, and transferred to a broth[9] for the preparation of the inoculum. The inoculum was a 1:20 diluted suspension of the washed bacteria in 10 ml of normal saline. Details of the assay procedure were described previously (1).

The extent of growth in the inoculated control (containing no test compound), the inhibitor control (containing 6-mercaptopurine[10]), and in some of the compounds previously studied, varied with different lots

[1] This paper is part of a continuing study of the effect of *N*-acylation of amino acids and of amino acid analogs on the growth of microorganisms used as a prescreen for antitumor activity and is the first of a series of papers describing the inhibitory effect of substituted benzoyl derivatives of various phenylalanine analogs.

[2] ICN Pharmaceuticals, Cleveland, OH 44128.

[3] Millex-GS, Millipore Corp., Bedford, MA 01730.

[4] Plastipak disposable syringes, Becton-Dickinson and Co., Rutherford, NJ 07070.

[5] Difco B325, Difco Laboratories, Detroit, Mich.

[6] Calbiochem-Behring Corp., San Diego, CA 92112.

[7] Klett-Summerson photoelectric colorimeter, Arthur H. Thomas Co., Philadelphia, PA 19105.

[8] The American Type Culture Collection, Rockville, MD 20852.

[9] Micro assay culture agar (Difco B319), Micro inoculum broth (Difco B320) Difco Laboratories, Detroit, Mich.

[10] Sigma Chemical Co., St. Louis, MO 63178.

0022-3549/82/0200-0214$01.00/0

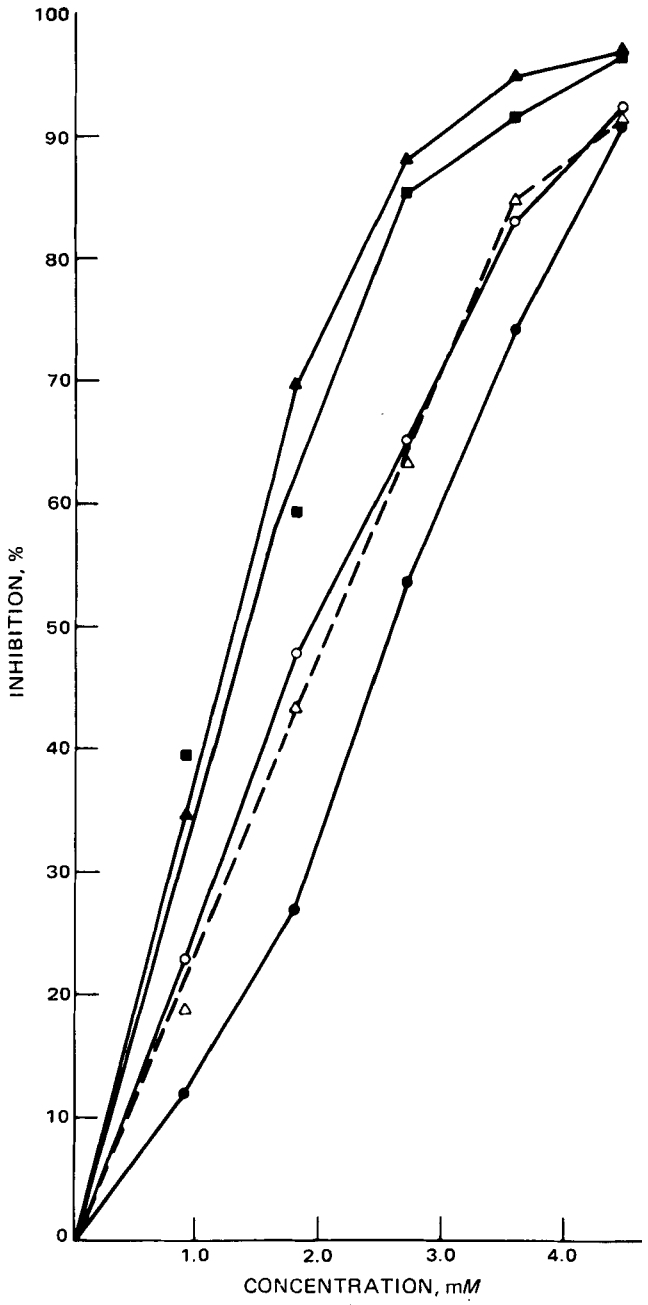

Figure 1—*Inhibition curves of some substituted benzoyl-o-fluoro-DL-phenylalanines: determination of ID_{50}. Key:* ●, *o-fluorobenzoyl-o-fluoro-DL-phenylalanine;* ▲, *m-chlorobenzoyl-o-fluoro-DL-phenylalanine;* ■, *p-chlorobenzoyl-o-fluoro-DL-phenylalanine;* ○, *m-nitrobenzoyl-o-fluoro-DL-phenylalanine; and* △, *p-nitrobenzoyl-o-fluoro-DL-phenylalanine.*

of the riboflavin assay medium used. Therefore, in this study and all subsequent studies of this series, the comparison of the extent of growth was made using medium of the same lot. In addition, the pH of the assay medium was adjusted uniformly to 6.40 by the addition of an appropriate amount of 0.5 *N* HCl before addition of the test compounds. The pH of the final system, determined on an aliquot of the medium containing an equivalent amount of the test compounds as the experimental tubes, was 6.20, and was within 0.1 pH units of the control tubes containing no test compounds.

RESULTS AND DISCUSSION

Most of the substituted *N*-benzoyl derivatives of *o*-fluoro-DL-phenylalanine showed considerable inhibitory activity. Of the 12 compounds tested, nine showed inhibition of ≥50% (Table II). These compounds may be considered to be positive according to the protocol of the microbial antitumor prescreen (10), and will be tested further in mammalian tumor systems.

Of the remaining three compounds, *m*-fluorobenzoyl- and *p*-fluorobenzoyl-*o*-fluoro-DL-phenylalanine, though slightly less active, nevertheless showed almost as much inhibiting activity as the more active chloroacetyl (2, 3) and trifluoroacetyl (4) derivatives studied earlier. The *o*-nitrobenzoyl compound showed about the same activity as most of the active *N*-chloroacetyl amino acids studied previously (3).

Comparison of activity within each group of derivatives (Table II) showed that the nature and the position of the substituents in the benzoyl ring were important to the inhibitory capacity of the compounds. For example, the substitution of a fluorine atom at the *ortho* position in the benzoyl ring of the fluorobenzoyl-*o*-fluoro-phenylalanines resulted in the most active derivative of this series, showing 69% inhibition at 1 mg/ml. Though not as pronounced, fluorine substitution at the *meta* or the *para* position in the benzoyl ring yielded derivatives of appreciable activity (39–47%), the *meta* isomer being slightly more active than the *para* isomer.

With the chlorobenzoyl and nitrobenzoyl derivatives, the *meta* and

Table I—Purity of Benzoyl Ring Substituted Derivatives of *o*-Fluoro-DL-phenylalanine [a]

o-Fluoro-DL-phenylalanine Derivative	Melting Point [b]	Empirical Formula	Analysis [c], %		
				Calc.	Found
o-Fluorobenzoyl	167–168	$C_{16}H_{13}F_2NO_3$	C	62.95	62.72
			H	4.29	4.41
			N	4.59	4.47
			F	12.45	12.86
m-Fluorobenzoyl	168–169	$C_{16}H_{13}F_2NO_3$	C	62.95	62.38
			H	4.29	4.25
			N	4.59	4.35
			F	12.45	12.63
p-Fluorobenzoyl	224	$C_{16}H_{13}F_2NO_3$	C	62.95	62.64
			H	4.29	4.46
			N	4.59	4.61
			F	12.45	12.69
o-Chlorobenzoyl	172–175	$C_{16}H_{13}ClFNO_3$	C	59.73	59.73
			H	4.07	4.11
			N	4.35	4.39
			Cl	11.02	11.13
			F	5.90	5.62
m-Chlorobenzoyl	160–162	$C_{16}H_{13}ClFNO_3$	C	59.73	59.97
			H	4.07	4.16
			N	4.35	4.39
			Cl	11.02	11.17
			F	5.90	6.16
p-Chlorobenzoyl	208–209	$C_{16}H_{13}ClFNO_3$	C	59.73	59.44
			H	4.07	4.07
			N	4.35	4.45
			Cl	11.02	11.02
			F	5.90	5.97
o-Methoxybenzoyl	119–121	$C_{17}H_{16}FNO_4$	C	64.35	64.42
			H	5.08	4.95
			N	4.41	4.42
			F	5.99	5.89
m-Methoxybenzoyl	154–157	$C_{17}H_{16}FNO_4$	C	64.35	63.99
			H	5.08	5.28
			N	4.41	4.53
			F	5.99	6.11
p-Methoxybenzoyl (anisoyl)	168–170	$C_{17}H_{16}FNO_4$	C	64.35	64.85
			H	5.08	5.20
			N	4.41	4.68
			F	5.99	5.63
o-Nitrobenzoyl	177–182	$C_{16}H_{13}FN_2O_5$	C	57.84	57.55
			H	3.94	4.09
			N	8.43	8.30
			F	5.72	5.71
m-Nitrobenzoyl	162–164	$C_{16}H_{13}FN_2O_5$	C	57.84	57.59
			H	3.94	4.11
			N	8.43	8.31
			F	5.72	5.65
p-Nitrobenzoyl	179–182	$C_{16}H_{13}FN_2O_5$	C	57.84	57.58
			H	3.94	3.88
			N	8.43	8.32
			F	5.72	5.83

[a] Van Slyke nitrous acid determination of primary amino nitrogen (8) made on a 1-ml sample containing an equivalent of 0.25–0.30 mg of amino nitrogen (when hydrolyzed) yielded no detectable quantity of nitrogen. [b] Melting points were determined on a Fisher-Johns melting point block and are uncorrected. [c] Elemental analyses were performed by the Microanalytical Laboratory, National Institute of Arthritis, Metabolism, and Digestive Diseases, National Institute of Health, Bethesda, Md.

Table II—Effect of Benzoyl Ring Substituted Derivatives of *o*-Fluorobenzoyl-DL-phenylalanine on the Growth of *L. casei* 7469 [a]

o-Fluoro-DL-phenylalanine Derivative	m*M* Equivalent at 1 mg/ml	Inhibition[b], % 0.1 mg/ml[c]	0.5 mg/ml[c]	1.0 mg/ml[c]
o-Fluorobenzoyl	3.28	5	22	69
m-Fluorobenzoyl	3.28	0	18	47
p-Fluorobenzoyl	3.28	0	11	39
o-Chlorobenzoyl	3.11	6	27	51
m-Chlorobenzoyl	3.11	5	55	90
p-Chlorobenzoyl	3.11	9	57	88
o-Methoxybenzoyl	3.15	6	31	53
m-Methoxybenzoyl	3.15	1	21	53
p-Methoxybenzoyl-(anisoyl)	3.15	5	28	54
o-Nitrobenzoyl	3.01	1	9	17
m-Nitrobenzoyl	3.01	0	36	68
p-Nitrobenzoyl	3.01	0	28	70
Benzoyl	3.48	2	12	31

[a] For details of assay, see Ref. 1. [b] Turbidity readings of the inoculated control tubes (containing no test compound) were 182–194 Klett units. At least three duplicate determinations were made for each compound. The duplicate values in each determination agreed within ±5 Klett units; *e.g.*, the standard deviation of a compound showing a mean value of ~20% inhibition was 2.7 and the standard error was 0.95. [c] Final concentration in assay system.

the *para* isomers were the most active of the three isomers. Hence, *m*-chlorobenzoyl- and *p*-chlorobenzoyl-*o*-fluoro-DL-phenylalanine showed nearly complete inhibition at 1 mg/ml, while the corresponding *o*-derivative showed an inhibition of 51%, and *m*-nitrobenzoyl- and *p*-nitrobenzoyl-*o*-fluoro-DL-phenylalanine exhibited activity of ~70%, while the corresponding *ortho* isomer showed only 17% inhibition.

When the substituent was a methoxy group, the position of substitution in the benzoyl ring appeared unimportant since all three isomers of methoxybenzoylphenylalanine exhibited about the same degree of inhibition (54%).

To allow comparison of relative activities, the degree of inhibition of each compound at 4.47 m*M* was determined (Table III). This concentration is equivalent to 1 mg/ml final concentration in the assay system of *N*-chloroacetyl-D-β-hydroxynorleucine B, the most active *N*-acyl alicyclic amino acid studied earlier (2).

The most active benzoyl ring substituted *o*-fluoro-DL-phenylalanines were *o*-fluorobenzoyl, *m*-chlorobenzoyl, *p*-chlorobenzoyl, *m*-nitrobenzoyl, and *p*-nitrobenzoyl derivatives, all of which showed essentially complete inhibition at 4.47 m*M*.

An inhibition curve was constructed for each of these compounds (Fig. 1). This showed that the most active of these compounds were *m*-chlorobenzoyl- and *p*-chlorobenzoyl-*o*-fluoro-DL-phenylalanine, with ID_{50} values of 1.30 and 1.40, respectively. The next active compounds were the *m*-nitrobenzoyl and *p*-nitrobenzoyl derivatives (ID_{50} 1.95 and 2.10, respectively), and the least active was *o*-fluorobenzoyl-*o*-fluoro-DL-phenylalanine (ID_{50} 2.60). Thus, when the amino acid moiety was phenylalanine containing an electronegative group, *i.e.*, fluorine, in the *ortho* position, a large electronegative group such as chlorine or a nitro group in the *meta* position of the benzoyl ring appeared to increase the inhibitory capacity.

Table III—Comparison of the Effect of Equimolar Concentrations of Benzoyl Ring Substituted Derivatives of *o*-Fluoro-DL-phenylalanine on the Growth of *L. casei* 7469 [a]

Derivative of *o*-Fluoro-DL-phenylalanine	Inhibition[b], %
o-Fluorobenzoyl	94
m-Fluorobenzoyl	61
p-Fluorobenzoyl	54
o-Chlorobenzoyl	66
m-Chlorobenzoyl	97
p-Chlorobenzoyl	96
o-Methoxybenzoyl	76
m-Methoxybenzoyl	75
p-Methoxybenzoyl (anisoyl)	74
o-Nitrobenzoyl	28
m-Nitrobenzoyl	92
p-Nitrobenzoyl	92
Benzoyl	44

[a] Maximum growth in inoculated control tube (containing no test compound) was 182–194 Klett units. For explanation of extent of variation of values, see Table II footnotes. [b] Concentration was 4.47 m*M* and was the final concentration in the assay system. For details of assay, see Ref. 1.

Table IV—Effect of Substituted Benzoic Acids on the Growth of *L. casei* 7469 [a]

Substituted Benzoic Acid	Inhibition[b], %
o-Fluorobenzoic Acid	6
m-Fluorobenzoic Acid	10
p-Fluorobenzoic Acid	7
o-Chlorobenzoic Acid	7
m-Chlorobenzoic Acid	32
p-Chlorobenzoic Acid	32
o-Methoxybenzoic Acid	3
m-Methoxybenzoic Acid	10
p-Methoxybenzoic Acid (anisic acid)	6
o-Nitrobenzoic Acid	9
m-Nitrobenzoic Acid	30
p-Nitrobenzoic Acid	34

[a] See Table II footnotes for details of the assay. [b] Concentration was 4.47 m*M*.

Most of the other seven derivatives showed striking activity (54–76% inhibition). This inhibition was considerably greater than that of compounds with no substituent on the benzoyl ring; benzoyl-*o*-fluoro-DL-phenylalanine inhibited 44%.

The activity of *o*-nitrobenzoyl-*o*-fluoro-DL-phenylalanine (28%), the least active of all the derivatives of the series, was less than that of the unsubstituted benzoyl derivative, *N*-benzoyl-*o*-fluoro-DL-phenylalanine. However, its inhibition was as great as most of the inhibiting chloroacetyl derivatives, which inhibited ~15–35% (3).

Thus, except for *o*-nitrobenzoyl-*o*-fluoro-DL-phenylalanine, all substituents in the benzoyl ring have an inhibitory enhancing effect, whatever the electronic nature of the substituent (*i.e.*, electron-withdrawing or electron-donating).

The position of these substituents in the benzoyl ring appeared to be important, especially when the substituent was strongly electronegative, such as in the chlorine, fluorine, and nitro groups. The data are not yet sufficient to draw conclusions about the relationship between the substituent of the benzoyl ring and that of the phenyl ring of phenylalanine. Only a more restrictive observation applying only to the derivatives of *o*-fluoro-DL-phenylalanine could be made. Subsequent studies will give further information on the role of the amino acid moiety in the inhibitory capacity.

The inhibition is not likely due to the release of hydrolytic products of the substituted benzoyl amino acids, *i.e.*, the release of the ring-substituted benzoic acid or the *o*-fluoro-DL-phenylalanine. Except for *m*-chlorobenzoic acid, *p*-chlorobenzoic acid, *m*-nitrobenzoic acid, and *p*-nitrobenzoic acid, all of which showed ~32–34% inhibition, the substituted benzoic acid had essentially no inhibitory activity (Table IV). For those substituted benzoic acids showing some activity, the benzoyl amino acids containing these groups were decidedly more active than the non-substituted benzoic acid. *o*-Fluoro-DL-phenylalanine was shown to be inactive in this assay system (3). Furthermore, it was demonstrated previously (3) that no notable degree of hydrolysis occurred during incubation.

There is insufficient data to propose a possible inhibition mechanism from these experiments. However, based on earlier studies on proteases (11, 12) where aromatic ring-rich dipeptides were shown to be superior substrates of some of these enzymes, and knowing that proteolytic enzymes are commonly produced by microorganisms, it is reasonable to speculate on the involvement of these aroyl phenylalanine analogs in the inhibition of such enzymes.

REFERENCES

(1) T. T. Otani, *Cancer Chemother. Rep.*, **38**, 25 (1964).
(2) T. T. Otani and M. R. Briley, *J. Pharm. Sci.* **65**, 534 (1976).
(3) *Ibid.*, **67**, 520 (1978).
(4) *Ibid.*, **68**, 496 (1979).
(5) *Ibid.*, **68**, 260 (1979).
(6) *Ibid.*, **68**, 1366 (1979).
(7) *Ibid.*, **70**, 464 (1981).
(8) D. D. Van Slyke, *J. Biol. Chem.*, **83**, 425 (1929).
(9) J. P. Greenstein and M. Winitz, "Chemistry of the Amino Acids," vol. 3, Wiley, New York, N.Y., 1961, p. 1834.
(10) G. E. Foley, R. E. McCarthy, V. M. Binns, E. E. Snell, B. M. Guirard, G. W. Kidder, V. C. Dewey, and P. S. Thayer, *Ann. N.Y. Acad. Sci.*, **76**, 413 (1958).
(11) L. E. Baker, *J. Biol. Chem.*, **193**, 809 (1951).
(12) M. Bergmann and J. S. Fruton, *Adv. Enzymol.*, **1**, 63 (1941).

Potentiometric Study of Molecular Complexes of Weak Acids and Bases Applied to Complexes of α-Cyclodextrin with *para*-Substituted Benzoic Acids

KENNETH A. CONNORS ˣ, SHU-FEN LIN, and ALBERT B. WONG*

Received March 23, 1981, from the *School of Pharmacy, University of Wisconsin, Madison, WI 53706.* Accepted for publication June 15, 1981. *Present address: Elizabeth Arden Research Center, Indianapolis, IN 46285.

Abstract □ The theory of the potentiometric method for studying complexes of ionizable substrates was developed, and graphical techniques are described for obtaining stability constant estimations from the data. The method described is for a system in which the conjugate acid and base forms of the substrate (S) are capable of forming 1:1 (SL) and 1:2 (SL_2) complexes with the ligand (L). It was applied to complexes of α-cyclodextrin (cyclohexaamylose) with 10 *para*-substituted benzoic acid derivatives. Letting K_{11a} and K_{12a} be stability constants for the conjugate acid forms of the substrates, and K_{11b}, K_{12b} for the conjugate base forms, it was found that K_{12b} is zero for all substrates, K_{12a} is zero for seven of the substrates, and $K_{11a} > K_{11b}$ in every case. Hammett plots yielded ρ_{11a} and ρ_{11b} values of −0.31 and 0.77, respectively, which was interpreted to mean that K_{11a} mainly represents binding at the carboxylic acid site, and K_{11b} describes binding at the site of the *para*-substituent. This model of the complexing suggests that K_{12a} represents binding at the *para*-substituent, and therefore K_{12a} should vary roughly with substituent as K_{11b} does; this trend was observed.

Keyphrases □ Complexation—potentiometric study, α-cyclodextrins with *para*-substituted benzoic acids □ Stability constants—α-cyclodextrins with *para*-substituted benzoic acids, potentiometric studies □ α-Cyclodextrins—complexes with *para*-substituted benzoic acids, potentiometric study

If the conjugate acid and base forms of a weak acid–base substrate form cyclodextrin (also called cycloamylose) complexes of different strengths, then addition of cyclodextrin to a solution of the substrate will result in a pH change. Cramer *et al.* (1) reported a change in the apparent dissociation constant of *p*-nitrophenol in the presence of α-cyclodextrin (cyclohexaamylose). A method was described previously based on the measurement of apparent dissociation constants as a function of cyclodextrin concentration in order to extract complex stability constants for both the conjugate acid and base forms of the substrate, assuming 1:1 stoichiometry (2). Miyaji *et al.* (3) developed a similar technique. A potentiometric method for 1:1 and 1:2 stoichiometric systems was also described (4, 5).

Evidence is accumulating (5–7) that in α-cyclodextrin systems both 1:1 and 1:2 complexes must be considered when measuring complex stability constants[1]. The potentiometric method offers a rapid and convenient experimental approach to this problem for ionizable substrates. The present report describes the theory of the method, and examines new graphical techniques for evaluating the stability constants. These techniques are applied to the study of complexing between α-cyclodextrin and a series of *p*-substituted benzoic acids.

THEORY

Let L represent cyclodextrin and HA a neutral weak acid substrate. For 1:1 and 1:2 stoichiometry, there are four complexation equilibria:

$$HA + L \rightleftarrows HAL$$

Scheme I

$$A^- + L \rightleftarrows AL^-$$

Scheme II

$$HAL + L \rightleftarrows HAL_2$$

Scheme III

$$AL^- + L \rightleftarrows AL_2^-$$

Scheme IV

These equilibria have corresponding stability constants:

$$K_{11a} = \frac{[HAL]}{[HA][L]} \quad \text{(Eq. 1)}$$

$$K_{11b} = \frac{[AL^-]}{[A^-][L]} \quad \text{(Eq. 2)}$$

$$K_{12a} = \frac{[HAL_2]}{[HAL][L]} \quad \text{(Eq. 3)}$$

$$K_{12b} = \frac{[AL_2^-]}{[AL^-][L]} \quad \text{(Eq. 4)}$$

where brackets signify molar concentrations, and activity coefficients are assumed to be constant. Thus, the stability constants may be interpreted as thermodynamic quantities with the experimental solvent as the reference state.

There are three acid–base equilibria in this system:

$$HA \rightleftarrows H^+ + A^-$$

Scheme V

$$HAL \rightleftarrows H^+ + AL^-$$

Scheme VI

$$HAL_2 \rightleftarrows H^+ + AL_2^-$$

Scheme VII

They have the acid–base dissociation constants:

$$K_a = \frac{[H^+][A^-]}{[HA]} \quad \text{(Eq. 5)}$$

$$K_{a11} = \frac{[H^+][AL^-]}{[HAL]} \quad \text{(Eq. 6)}$$

$$K_{a12} = \frac{[H^+][AL_2^-]}{[HAL_2]} \quad \text{(Eq. 7)}$$

From Eqs. 1–7 these relationships are found:

$$K_{11a}K_{a11} = K_aK_{11b} \quad \text{(Eq. 8)}$$

$$K_{12a}K_{a12} = K_{a11}K_{12b} \quad \text{(Eq. 9)}$$

Letting S_t and L_t be the total molar concentrations of substrate and ligand, respectively, the mass-balance equations are:

$$S_t = [HA] + [A^-] + [HAL] + [AL^-] + [HAL_2] + [AL_2^-] \quad \text{(Eq. 10)}$$

$$L_t = [L] + [HAL] + [AL^-] + 2[HAL_2] + 2[AL_2^-] \quad \text{(Eq. 11)}$$

For later convenience the quantities A, B, M, and, N are defined:

$$A = 1 + K_{11a}[L] + K_{11a}K_{12a}[L]^2 \quad \text{(Eq. 12)}$$

$$B = 1 + K_{11b}[L] + K_{11b}K_{12b}[L]^2 \quad \text{(Eq. 13)}$$

$$M = K_{11a}[L] + 2K_{11a}K_{12a}[L]^2 \quad \text{(Eq. 14)}$$

$$N = K_{11b}[L] + 2K_{11b}K_{12b}[L]^2 \quad \text{(Eq. 15)}$$

[1] The weak acid–base is the substrate (S), α-cyclodextrin is the ligand (L), and stoichiometric relationships are expressed in the form SL and SL_2, these complexes having 1:1 and 1:2 stoichiometry, respectively.

0022-3549/82/0200-0217$01.00/0

Algebraic combination leads to:

$$S_t = [HA]\left[\frac{A[H^+] + BK_a}{[H^+]}\right] \quad \text{(Eq. 16)}$$

$$L_t = [L] + [HA]\left[\frac{M[H^+] + NK_a}{[H^+]}\right] \quad \text{(Eq. 17)}$$

Eliminating [HA] from Eqs. 16 and 17 gives a general relationship between [L] and L_t:

$$L_t = [L] + S_t\left[\frac{M[H^+] + NK_a}{A[H^+] + BK_a}\right] \quad \text{(Eq. 18)}$$

The electroneutrality equation for this system is:

$$[Na^+] + [H^+] = [OH^-] + [A^-] + [AL^-] + [AL_2^-] \quad \text{(Eq. 19)}$$

where it is supposed that sodium is the counterion to the substrate. Combining Eq. 19 with the preceding expressions gives:

$$[Na^+] + [H^+] - [OH^-] = \frac{S_t BK_a}{A[H^+] + BK_a} \quad \text{(Eq. 20)}$$

The quantity $[Na^+]/S_t$ is the analytical fraction of substrate in the conjugate base form. Equation 20 is the general equation relating hydrogen-ion concentration to free ligand concentration [L]. By means of Eqs. 18 and 20, $[H^+]$ is related to total ligand concentration L_t. In these equations, $[Na^+]$, S_t, and L_t are independent variables; $[H^+]$ and [L] are dependent variables.

Equation 20 can be cast in a more useful form. If $[Na^+] \gg ([H^+] - [OH^-])$, then Eq. 20 becomes:

$$[Na^+] = \frac{S_t BK_a}{A[H^+] + BK_a} \quad \text{(Eq. 21)}$$

For a solution in which L_t is 0, it follows that [L] = 0, A = 1, B = 1, and Eq. 21 becomes:

$$[Na^+]_0 = \frac{S_t K_a}{[H^+]_0 + K_a} \quad \text{(Eq. 22)}$$

A series of measurements of $[H^+]$ as a function of L_t is made at constant S_t and $[Na^+]$; hence $[Na^+] = [Na^+]_0$, and these equations give:

$$\frac{[H^+]_0}{[H^+]} = \frac{A}{B} = C \quad \text{(Eq. 23)}$$

Defining a quantity $\Delta pH = pH - pH_0$:

$$\Delta pH = \log C \quad \text{(Eq. 24)}$$

Equation 24 describes the change in the solution pH as a function of free ligand concentration for fixed $[Na^+]/S_t$. If $[Na^+]/S_t = \frac{1}{2}$, then the pH can be interpreted as pKa′ (apparent dissociation constant), and Eq. 24 becomes $\Delta pKa' = \log C$, or:

$$\Delta pKa' = \log\left[\frac{1 + K_{11a}[L] + K_{11a}K_{12a}[L]^2}{1 + K_{11b}[L] + K_{11b}K_{12b}[L]^2}\right] \quad \text{(Eq. 25)}$$

which is the equation used previously (5) to interpret the cinnamic acid–α-cyclodextrin system. This derivation shows the level of approximation involved in interpreting ΔpH as ΔpKa′.

More generally, the exact Eq. 20 must be used. Defining the operational dissociation constant K_a' by Eq. 26:

$$K_a' = \frac{[H^+]([Na^+] + [H^+] - [OH^-])}{S_t - ([Na^+] + [H^+] - [OH^-])} \quad \text{(Eq. 26)}$$

Substitution into Eq. 26 from Eq. 20 leads to $K_a/K_a' = A/B = C$, or $\Delta pKa' = \log C$. That is, Eq. 25 is general, provided the dissociation constants are evaluated by Eq. 26, which takes into account solvent dissociation. An important feature of this equation is that C is a ratio of polynomials. If $\Delta pK_a' = 0$ at all L_t, then $K_{11a} = K_{11b}$ and $K_{12a} = K_{12b}$.

On chemical grounds, and also by means of Eq. 18, it can be seen that the limits of [L] are $[L] = L_t$ and $[L] = L_t - 2S_t$. In the potentiometric method, S_t must be appreciable in order to provide buffer capacity; hence it is seldom permissible to set $[L] = L_t$, as may often be done in other experimental techniques (such as spectroscopy).

One approach to obtaining the stability constants is to treat them as adjustable parameters, and to curve-fit the data using Eqs. 18 and 25. Although it is possible to achieve good fit to the experimental points (2, 8), it was observed that an apparently infinite number of satisfactory solutions can be obtained in this way (8). Therefore, the curve-fitting approach was abandoned, and graphical techniques leading to unique solutions have been developed.

General Evaluation of Stability Constants—The experimental data consist of ΔpKa′ values measured as a function of L_t, at constant S_t and reaction conditions. Since $\Delta pKa' = \log C$, the quantity C is available. This is related to the stability constants by:

$$C = \frac{1 + K_{11a}[L] + K_{11a}K_{12a}[L]^2}{1 + K_{11b}[L] + K_{11b}K_{12b}[L]^2} \quad \text{(Eq. 27)}$$

The problem is to evaluate the stability constants from these data. Considerable experience with such systems has shown that it is seldom necessary to invoke all four constants, and some important special cases of Eq. 27 suffice to account for most of these systems. These cases are treated in the following section.

To find the stability constants, Eq. 18 must be solved for [L], but this requires the stability constants. The following approach is effective. In this work, the ratio $[Na^+]/S_t = 1/2$, so $[H^+] = K_a$, to a level of accuracy acceptable for the present purpose. Since $C = K_a/K_a'$, this gives $[H^+] = K_a/C$. Substitution into Eq. 18 gives:

$$L_t = [L] + S_t\left[\frac{M}{2A} + \frac{N}{2B}\right] \quad \text{(Eq. 28)}$$

The value of [L] is estimated by combining Eq. 28 with the appropriate special case of Eq. 27. In this development the quantity C is incorporated into the expression for [L] to the greatest extent possible. This has two advantages: first, since the stability constants are needed in the calculation, their introduction in the form of experimental C values ensures that the correct values are being used; and second, the solution of the equation for [L] is usually simplified, since much of the algebraic complexity is possessed by the numerical C values. The particular equations for [L] will be given when the special cases are discussed.

The general approach is to make a plot of C *versus* L_t. From the shape of this curve, the system is tentatively assigned to one of the special cases. The free ligand concentration [L] is calculated, and stability constants are evaluated from the appropriate linear plot. Iterations are carried out until the stability constants are essentially unchanged.

The following treatment considers systems in which C is greater than unity. If C is less than unity, it is convenient to work with its reciprocal, $C' = 1/C$. Then all of the equations are applicable with the subscripts a and b interchanged.

Special Cases—*Case I:* $K_{12a} = 0$, $K_{12b} = 0$—Equation 27 becomes:

$$C = \frac{1 + K_{11a}[L]}{1 + K_{11b}[L]} \quad \text{(Eq. 29)}$$

A plot of C *versus* [L] or L_t will approach a limiting value at high ligand concentration. Diagnosis of Case I behavior is tentative because Eq. 27 also results in this type of curve.

The ligand concentration is calculated with:

$$[L] = L_t - \frac{S_t}{X + 1} \quad \text{(Eq. 30)}$$

where:

$$X = \frac{(C + 1)(R - C)}{(C - 1)(R + C)} \quad \text{(Eq. 31)}$$

and $R = K_{11a}/K_{11b}$. The parameter R is estimated by extrapolating a plot of log C *versus* $1/L_t$ to $1/L_t = 0$, since C approaches R as L_t approaches infinity. A plot is then made according to:

$$\frac{C - 1}{[L]} = K_{11a} - CK_{11b} \quad \text{(Eq. 32)}$$

which is obtained from Eq. 29. The constants K_{11a} and K_{11b} are obtained from this plot, which will be linear for a Case I system. The calculated R is compared with the initial estimate; if they differ significantly, the process is repeated.

Case II: $K_{11b} = 0$, $K_{12a} = 0$, $K_{12b} = 0$—From Eq. 27:

$$C = 1 + K_{11a}[L] \quad \text{(Eq. 33)}$$

where C is a linear function of ligand concentration. Of course, any system will approach linearity at sufficiently low ligand concentration, so L_t must be made large enough to determine if curvature exists. The free ligand concentration is obtained with Eq. 34.

$$[L] = L_t\frac{-(C - 1)S_t}{2C} \quad \text{(Eq. 34)}$$

Case III: $K_{11b} = 0$, $K_{12b} = 0$—Equation 27 becomes:

$$C = 1 + K_{11a}[L] + K_{11a}K_{12a}[L]^2 \quad \text{(Eq. 35)}$$

Table I—Stability Constants for α-Cyclodextrin Complexes of *para*-Substituted Benzoic Acids at 25°

Number	σ^a	X[b]	K_{11a}/M^{-1} ±SD	K_{11b}/M^{-1} ±SD	K_{12a}/M^{-1} ±SD
1	−0.84	$NHCH_3$	1301 (15.9)	6.1 (0.26)	−0.010 (0.14)
2	−0.66	NH_2	1341 (11.1)	9.0 (0.22)	−0.024 (0.10)
3	−0.37	OH	1130 (7.7)	16.6 (0.23)	−0.048 (0.063)
4	−0.27	OCH_3	884 (5.1)	3.5 (0.10)	0.0064 (0.067)
5	−0.17	CH_3	1091 (7.4)	6.6 (0.14)	0.0026 (0.071)
6	0.00	H	722 (9.7)	11.2 (0.35)	−0.0047 (0.13)
7	0.06	F	504 (4.4)	14.2 (0.26)	0.020 (0.081)
8	0.50	CH_3CO	899 (45.0)	60.3 (11.7)	28.8 (1.63)
9	0.66	CN	471 (7.5)	79.2 (4.6)	25.0 (0.47)
10	0.78	NO_2	350 (16.2)	81.0 (9.3)	20.2 (1.14)

[a] Hammett substituent constant. [b] X in X—C_6H_4—COOH.

The plot of C *versus* L_t will reveal curvature that is concave upward; [L] is calculated with:

$$[L] = \frac{2C(L_t - S_t) + 2S_t}{2C - S_t K_{11a}} \quad \text{(Eq. 36)}$$

The linear form of Eq. 35 is:

$$\frac{C-1}{[L]} = K_{11a} + K_{11a}K_{12a}[L] \quad \text{(Eq. 37)}$$

Case IV: $K_{12b} = 0$—Equation 27 becomes:

$$C = \frac{1 + K_{11a}[L] + K_{11a}K_{12a}[L]^2}{1 + K_{11b}[L]} \quad \text{(Eq. 38)}$$

The plot of C *versus* L_t will approach a linear segment of positive slope at high L_t. The equation of this line is:

$$C = R + RK_{12a}[L] \quad \text{(Eq. 39)}$$

where $R = K_{11a}/K_{11b}$. This gives part of the desired information. The concentration [L] is given by:

$$K_{11b}[L]^2 + \left[1 + S_t K_{11b}\left(\frac{3}{2} - \frac{R}{2C}\right) - L_t K_{11b}\right][L] - \left[L_t - \frac{S_t(C-1)}{C}\right] = 0 \quad \text{(Eq. 40)}$$

Several methods have been devised to extract the stability constants. It is a general result from Eq. 27 that:

$$\frac{dC}{d[L]} = \frac{BM - AN}{B^2[L]} \quad \text{(Eq. 41)}$$

Thus the slope at [L] = 0 is equal to $K_{11a} - K_{11b}$. This result, together with the value of R from Eq. 39, gives the stability constants. Another method constructs, on the C *versus* [L] plot, lines such that the quantity $[L]_X$ is found as the value of [L] when $C = R$. Then it is easily shown that:

$$K_{11b} = \frac{R-1}{RK_{12a}[L]_X^2} \quad \text{(Eq. 42)}$$

However, both of these approaches rely on data at very low [L], and it is in this region that the relative error in [L] is the greatest. A better procedure is to measure K_{11b} by a different, independent, experimental method, such as spectroscopy. This will usually be straightforward, the Case IV diagnosis having shown that $K_{12b} = 0$. The linear plot according to Eq. 43 is made:

$$\frac{C-1}{[L]} + CK_{11b} = K_{11a} + K_{11a}K_{12a}[L] \quad \text{(Eq. 43)}$$

This plot is also useful for confirming Case I systems, which should yield a slope equal to zero.

EXPERIMENTAL

Materials—α-Cyclodextrin[2] was dried at 95° for 48 hr. A sample of α-cyclodextrin recrystallized from water and dried under reduced pressure over phosphorus pentoxide for 12 hr (9) gave identical results. The benzoic acids[3] were recrystallized until their melting points agreed with literature values. Water was redistilled from alkaline permanganate.

Procedures—*Potentiometric Studies*—A stock solution of the substrate was prepared such that its final diluted concentration would be 0.003–0.004 M, and the substrate was half-neutralized with 0.10 M NaOH. It was filled to the mark with 0.10 M NaCl.

α-Cyclodextrin was weighed into 5-ml volumetric flasks in amounts to cover its full solubility range. Portions of the substrate stock solution (4.0-ml) were pipetted into each flask, and the solutions were brought to volume with 0.10 M NaCl. They were equilibrated at 25.0°; to ensure adequate mixing, a 10-mm stirring bar was added and driven by a submerged water-driven magnetic stirrer. The solution was transferred to a 5-ml test tube and the combination pH electrode was lowered into the solution (which was protected from contact with the atmosphere). The pH was measured[4] and pKa′ was calculated according to Eq. 26. Reproducibility on duplicate solutions was 0.003 pH units or better. All studies were at 25.0° and ionic strength was 0.10 M.

Substrates with ionizable *para*-substituents (compounds 1–3 in Table I) have pKa values separated sufficiently (10–12) that the measurement of pKa′ for the carboxylic acid group leaves the *para*-substituent in its nonionized state.

Variation of S_t by a factor of 2 resulted in no significant variation in the stability constants.

Spectrophotometric Studies—For Case IV systems, K_{11b} was measured spectrophotometrically[5]. The substrate was dissolved in pH 9.18 tromethamine buffer, ionic strength 0.10 M; S_t was $5.6–8.4 \times 10^{-5}$ M. The data were analyzed by the double-reciprocal linear form with a weighted least-squares treatment (13). The wavelengths of observation were: for CH_3CO—C_6H_4COOH, 253 nm; NC-C_6H_4COOH, 231 and 237 nm; and O_2N-C_6H_4COOH, 265 and 315 nm. Values of K_{11b} were not wavelength dependent.

RESULTS

This potentiometric method was applied to 10 benzoic acid derivatives. All of these compounds gave positive ΔpKa′ values and hence C values greater than unity, apparently a general result for carboxylic acids (2). These systems could be described as Case I or Case IV systems[6].

Figure 1 shows the plot of C *versus* L_t for *p*-hydroxybenzoic acid, a typical Case I system, and Fig. 2 is the corresponding linear plot according to Eq. 32. Figure 3 shows *p*-cyanobenzoic acid, a Case IV system, and Fig. 4 is the linear plot according to Eq. 43. Usually two iterations sufficed to yield final estimates of the stability constants.

Table I shows the stability constants evaluated in this way. For all of these systems, K_{12b} is zero by definition, since they can be adequately described by Cases I or IV. For Case I systems, K_{12a} is zero. However, this assignment can be tested by treating a Case I system as if it were Case IV, making the plot according to Eq. 43. The values of K_{12a} in Table I were evaluated in this way. For compounds 1–7, K_{12a} is clearly not significantly different from zero, whereas substrates 8–10 possess very significant K_{12a} values. For Case I systems, the relative standard deviation of K_{11a} ranges from 0.6–1.3%, and of K_{11b} from 1.4–4.3%. The precision of Case IV systems is poorer, as seems reasonable, since these are three-parameter systems.

DISCUSSION

The Potentiometric Method—For complexing systems in which the

[2] Lot 29C-0425, Sigma Chemical Co.
[3] Aldrich Chemical Co. and Eastman Organic Chemicals.
[4] Orion 701A pH meter equipped with a Sargent-Welch S30072-15 electrode.
[5] Perkin-Elmer model 559 spectrophotometer.
[6] Phenols and amines give negative ΔpK_a values. Some amines have been found to be Case II and Case III systems.

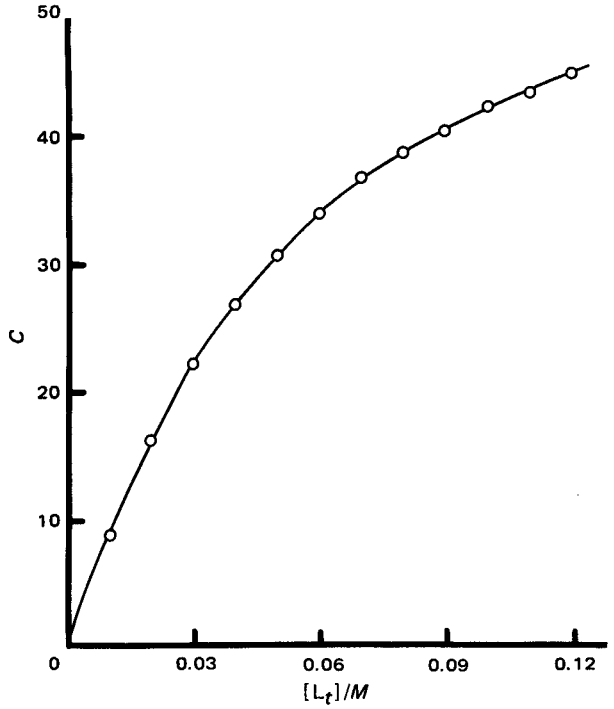

Figure 1—*Plot of* C versus L_t *for the* p-*hydroxybenzoic acid–α-cyclodextrin system.*

full four-parameter equation (Eq. 27) is not required, this potentiometric method with graphical treatment of the data is simple, rapid, and effective. Because of the linear graphing forms, the usual least-squares statistical treatment is appropriate. The error in the abscissa is much smaller than that in the ordinate, as is required by the conventional treatment. The great sensitivity of the quantity $(C - 1)/[L]$ at low [L] values made it necessary to reject some data points at very low [L] in the plots according to Eqs. 32 and 43. At least 10 points were used in every plot.

The assumption that activity coefficients are constant as L_t changes is fundamental to the interpretation of potentiometric data in terms of

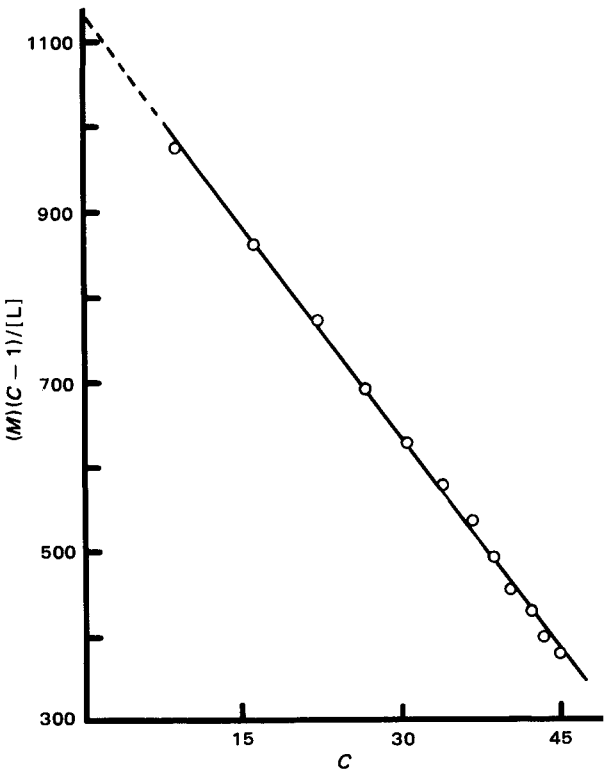

Figure 2—*Plot of Eq. 32 for the* p-*hydroxybenzoic acid–α-cyclodextrin system.*

Table II—Comparison of Stability Constants for the Benzoic Acid–α-Cyclodextrin System [a]

Method	K_{11a}	K_{11b}	Ref.
Competitive spectrophotometry	1050	—	14
Kinetics	—	12.3	15
Thermometry	1000	—	16
Potentiometry	1400	38	2
PMR	233; 800	9.8	17
Potentiometry	751	10.5	4
Solubility	500	—	18
UV spectrophotometry	660	—	18
Competitive spectrophotometry	—	13	19
Potentiometry	722	11.2	This work

[a] At 25°; ionic strengths differ.

1:1 and 1:2 complex formation. It is conceivable that the observation of finite 1:2 stability constants represents a measurement of changing activity coefficients rather than actual 1:2 complexation. Gelb *et al.* (4) described evidence that ionic activity coefficients are not changed as a consequence of changes in cyclodextrin concentration. That K_{12a} for several acids was found to be negligible (Table I) suggests further that activity coefficient changes are not responsible for the observed 1:2 stability constants. Nevertheless, the role of cyclodextrin in modifying the properties of the solvent cannot be overlooked as a possible complicating factor in such studies.

Several studies of the benzoic acid–α-cyclodextrin system were described earlier and are listed chronologically in Table II. The earliest potentiometric result (2) was obtained by curve-fitting, and is now rejected. It is evident that the method proposed in the present paper is capable of generating stability constants consistent with those obtained by other techniques and in other laboratories.

An advantage of potentiometry is that it yields information about the complexing of both the conjugate acid and base forms of the substrate. A limitation is that it can serve as an independent method only when the system includes two (or fewer) complex equilibria, *i.e.*, when the equation

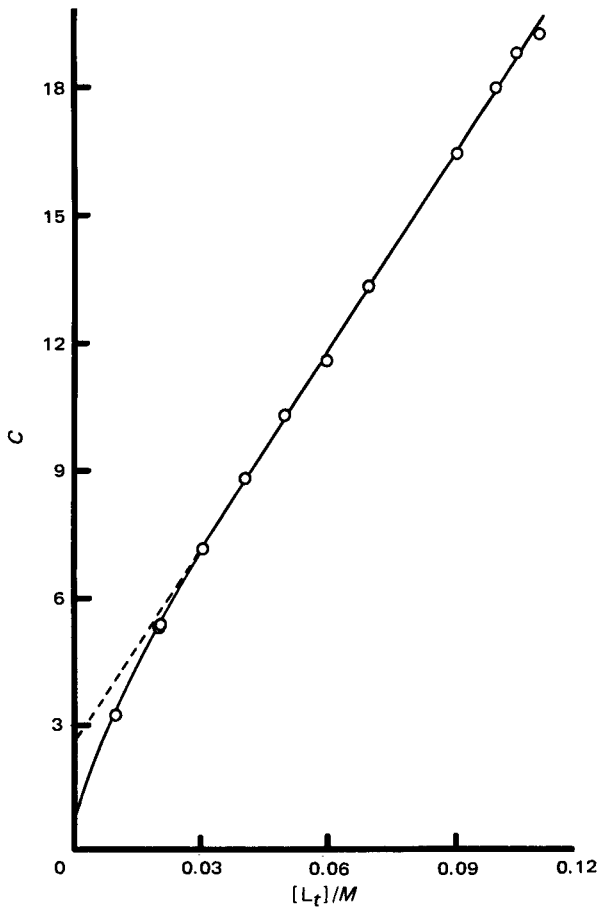

Figure 3—*Plot of* C versus L_t *for the 4-cyanobenzoic acid–α-cyclodextrin system.*

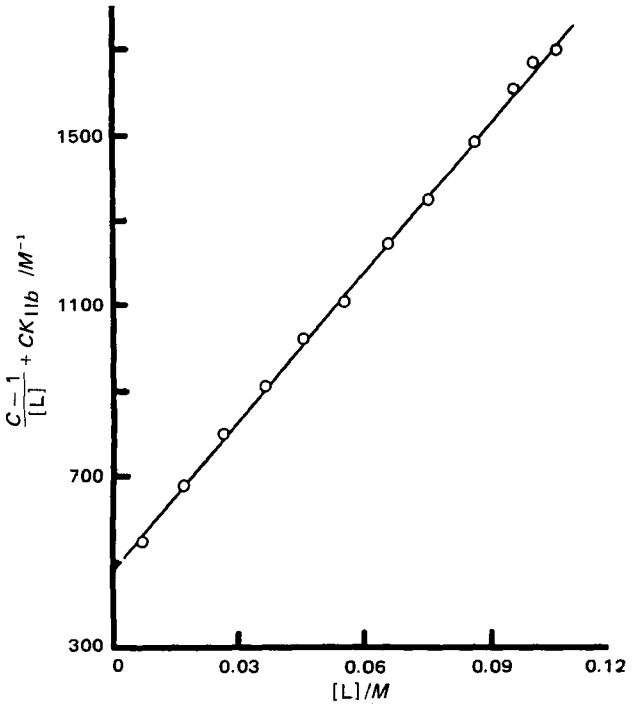

Figure 4—*Plot of Eq. 43 for the 4-cyanobenzoic acid–α-cyclodextrin system.*

has two parameters. For the three-parameter Case IV system, it was judged necessary to make use of a separate experimental determination of one of the parameters. This combination of several techniques is essential if the equation has four parameters, as in the cinnamic acid system (5).

Interpretation of Stability Constants—An earlier report (20) introduced a model of cyclodextrin complex formation helpful in interpreting the present data. The substrate (guest) is symbolized g–G, the lower and upper case letters signifying two binding sites; the cyclodextrin (host) is represented h–H because the two rims of the cavity are chemically different. It was shown that it is possible for four 1:1, four 2:1, and four 1:2 complexes to be present in a system. However, if there are no 2:1 complexes present, it is a reasonable inference that only one end (e.g., H) of the host can be entered. It follows that there can be only two 1:1 complexes (gH and GH) and one 1:2 complex. The 1:2 complex is formed by the addition of a host molecule to either of the 1:1 complexes.

The observed K_{11} value for the system is the sum of the stability constants for the isomeric 1:1 complexes, hence:

$$K_{11} = K_{gH} + K_{GH} \qquad \text{(Eq. 44)}$$

The 1:2 complex can be formed *via* the gH or the GH route:

$$gH + h\text{–}H \overset{K'}{\rightleftarrows} GHHg$$

Scheme VIII

$$GH + h\text{–}H \overset{K''}{\rightleftarrows} GHHg$$

Scheme IX

The observed 1:2 stability constant is given by (20):

$$K_{12} = \frac{K'K''}{K' + K''} \qquad \text{(Eq. 45)}$$

It is also seen that:

$$\frac{K'}{K''} = \frac{K_{GH}}{K_{gH}} \qquad \text{(Eq. 46)}$$

Writing $K' = aK_{GH}$, with Eq. 46, it follows that $K'' = aK_{gH}$. Combination with Eq. 45 gives:

$$K_{12} = \frac{aK_{gH}K_{GH}}{K_{gH} + K_{GH}} \qquad \text{(Eq. 47)}$$

The factor a is a measure of the extent of interaction between the two sites in a 1:2 complex. If the two binding sites are independent, $a = 1$ and

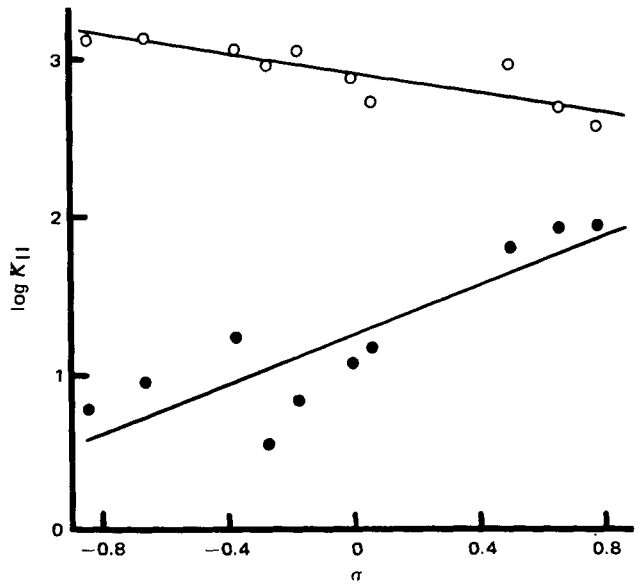

Figure 5—*Hammett plots of* K_{11a} (○) *and* K_{11b} (●) *data from Table I.*

the isomeric stability constants K_{gH} and K_{GH} can be evaluated with Eqs. 44 and 47. For the *para*-substituted benzoic acids it seems improbable that the sites are independent because of their proximity (the two sites being the X-end and the COOH-end of the molecule). Nevertheless, the model is useful in describing the nature of K_{11} and K_{12}, since it shows that K_{12} is actually a constant for the formation of a 1:1 complex from an already formed 1:1 complex. The model leads to interpretations in terms of binding sites.

Figure 5 is a Hammett plot of the K_{11a} and K_{11b} data in Table I. The obvious result is that these quantities vary with substituent constant in opposite ways. The slopes (rho values) are −0.31 (0.07 *SD*) for K_{11a} and +0.77 (0.17 *SD*) for K_{11b}. Casu and Ravà (14) studied K_{11a} for some of these acids; their constants are significantly different from those in Table I, but the general behavior is the same, namely that rho is negative. Electron-withdrawing X groups decrease complex stability in the conjugate acid series.

This behavior is explicable if K_{11a} primarily represents binding at the COOH-end of the substrate molecule. The binding interaction will be increased by an increase in electron density at the binding site, and will be associated with a negative rho value. This hypothesis is supported by PMR data on benzoic acid (17), which indicate that the carboxyl group enters the cavity.

The value of K_{11b} is always smaller than K_{11a} for the same substrate. This also is consistent with the view that K_{11a} represents mainly COOH-site binding. Upon ionization of this group, its affinity for the cavity will be greatly decreased because of the high polarity of COO^- and the nonpolarity (relative to the solvent) of the cavity. Therefore K_{11b} represents binding at the remaining site, namely X. Thus the more electron-withdrawing the X group, the larger is K_{11b}. Since K_{11b} describes X-site binding, the correlation with σ for X is not expected to be as precise as when the substituent is distant from the reaction site.

If K_{11a} describes COOH-site binding (mainly), then K_{12a} must represent mainly binding at the X-site. Therefore, this model predicts that K_{12a} should respond to X-substituent effects the same way that K_{11b} does, since they describe roughly the same process. Table I shows that this is indeed the case, in a general way; both K_{11b} and K_{12a} tend to increase together, and to tend in the opposite sense to K_{11a} along the σ scale.

The Hammett plot suggests that if a substituent with sufficiently large σ were available, K_{11b} would become larger than K_{11a}. This might not result in $\Delta pKa'$ becoming negative, however, because K_{12a} will also increase.

These correlations clearly show trends rather than highly precise relationships, and factors other than electronic density must play a role. For example, K_{11b} for substrates 1–3 seems anomalously high. These are the only X groups capable of functioning as hydrogen-bond donors, and this capability may increase complex stability. The trend in K_{12a} for compounds 8–10 appears to oppose that for K_{11b}, and this may be the result of some additional factor, which could be size, shape, polarity, or polarizability. In fact, K_{12a} for these substrates seems to be a resultant

of the electronic density effect measured by σ, and the X-site polarity as measured by group dipole moments. These moments are, for X = $COCH_3$, 3.00 D; CN, 4.39; and NO_2, 4.21 (21). An increase in site polarity will tend to decrease the site binding constant (20), and both K_{11b} and K_{12a} may reflect this effect superimposed on the electron density effect.

This model of complexing suggests that K_{12} values are especially useful, leading to the question: Why is K_{12} ever equal to zero (for a two-site substrate)? According to Eq. 47, K_{12} can be zero only if $a = 0$ or if one of the site binding constants (K_{gH} or K_{GH}) is zero. This leads to the following argument. If the given site assignments are correct, K_{12b} represents binding at the COO^- site (since K_{11b} mainly describes X-site binding), and it was found that $K_{12b} = 0$ for all substrates. The existence of finite K_{12a} values (substrates 8–10) means that a is finite for these acid substrates, and suggests that it will also be finite in the corresponding base substrates. It follows that K_{12b} is zero as a consequence of the site binding constant for COO^- being zero. Letting K_{gHb} represent this quantity, and K_{GHb} the site binding constant for the X-site in the conjugate base series, it follows that:

$$K_{11b} = K_{gHb} + K_{GHb} = K_{GHb} \qquad \text{(Eq. 48)}$$

i.e., K_{11b} can be identified solely with the binding at site X.

Extension to the acid series requires the assumption that K_{GHb} for binding to X in the base series is identical with K_{GHa} for binding to X in the acid series. If approximately so, then $K_{11a} = K_{gHa} + K_{GHa} = K_{gHa} + K_{GHb} = K_{gHa} + K_{11b}$, and the site binding constant K_{gHa} for the COOH site is given approximately by $K_{11a} - K_{11b}$.

With these estimates of K_{gHa} ($K_{11a} - K_{11b}$) and K_{GHa} (K_{11b}), Eq. 47 leads to estimates of a for these substrates, since:

$$K_{12a} = \frac{aK_{gHa}K_{GHa}}{K_{gHa} + K_{GHa}} = \frac{aK_{11b}(K_{11a} - K_{11b})}{K_{11a}} \qquad \text{(Eq. 49)}$$

For compound number 8, $a = 0.51$; number 9, $a = 0.38$; and number 10, $a = 0.33$. Because of the several approximations, these calculations are unlikely to be accurate, but they are reasonable in magnitude. The interpretation of complex stability data in terms of this model and Eqs. 44 and 47 seems to be a potentially useful means for describing, understanding, and perhaps predicting complex formation behavior.

REFERENCES

(1) F. Cramer, W. Saenger, and H.-Ch. Spatz, *J. Am. Chem. Soc.*, **89,** 14 (1967).

(2) K. A. Connors and J. M. Lipari, *J. Pharm. Sci.*, **65,** 379 (1976).

(3) T. Miyaji, Y. Kurono, K. Uekama, and K. Ikeda, *Chem. Pharm. Bull.*, **24,** 1155 (1976).

(4) R. I. Gelb, L. M. Schwartz, R. F. Johnson, and D. A. Laufer, *J. Am. Chem. Soc.*, **101,** 1869 (1979).

(5) K. A. Connors and T. W. Rosanske, *J. Pharm. Sci.*, **69,** 173 (1980).

(6) R. I. Gelb, L. M. Schwartz, C. T. Murray, and D. A. Laufer, *J. Am. Chem. Soc.*, **100,** 3553 (1978).

(7) R. I. Gelb, L. M. Schwartz, and D. A. Laufer, *ibid.*, **100,** 5875 (1978).

(8) A. B. Wong, Ph.D. thesis, University of Wisconsin, Madison, Wis., 1980.

(9) K. Uekama, M. Otagiri, Y. Kanie, S. Tanaka, and K. Ikeda, *Chem. Pharm. Bull.*, **23,** 1421 (1975).

(10) R. N. Mattoo, *Trans. Faraday Soc.*, **52,** 1462 (1956).

(11) P. O. Lumme, *Suomen Kemist.*, **30B,** 168 (1957).

(12) J. Johnston, *Proc. R. Soc. London*, **A78,** 82 (1906).

(13) P. A. Kramer and K. A. Connors, *Am. J. Pharm. Educ.*, **33,** 193 (1969).

(14) B. Casu and L. Ravà, *Ric. Sci.*, **36,** 733 (1966).

(15) R. L. VanEtten, J. F. Sebastian, G. A. Clowes, and M. L. Bender, *J. Am. Chem. Soc.*, **89,** 3242 (1967).

(16) E. A. Lewis and L. D. Hansen, *J. Chem. Soc., Perkin Trans.*, **II,** 2081 (1973).

(17) R. J. Bergeron, M. A. Channing, and K. A. McGovern, *J. Am. Chem. Soc.*, **100,** 2878 (1978).

(18) T. W. Rosanske, Ph.D. thesis, University of Wisconsin, Madison, Wis., 1979.

(19) R. I. Gelb, L. M. Schwartz, B. Cardelino, and D. A. Laufer, *Anal. Biochem.*, **103,** 362 (1980).

(20) T. W. Rosanske and K. A. Connors, *J. Pharm. Sci.*, **69,** 564 (1980).

(21) E. S. Gould, "Mechanism and Structure in Organic Chemistry," Holt, Rinehart and Winston, New York, N.Y., 1959, p. 62.

Reversed-Phase Ion-Pair Chromatography of Tetracycline, Tetracycline Analogs, and Their Potential Impurities

JÖRGEN HERMANSSON[x] and MATS ANDERSSON

Received December 17, 1980, from the *National Board of Health and Welfare, Department of Drugs, Division of Pharmacy, Box 607, S-751 25 Uppsala, Sweden.* Accepted for publication May 15, 1981.

Abstract □ Methods are presented for the separation of tetracycline, tetracycline analogs, and their potential impurities by reversed-phase ion-pair chromatography. The mobile phase consisted of a phosphate buffer with tripropylamine or *N,N*-dimethyloctylamine as counterions and acetonitrile as the organic modifier. The chromatographic properties of the tetracyclines were significantly improved by addition of the tertiary amines. The best result was obtained with *N,N*-dimethyloctylamine as the counterion, which gave good separation efficiency and peak symmetry for most of the substances studied. Addition of the tertiary amines to the mobile phase also significantly affected the capacity factors of the tetracyclines. Stability studies of the tetracyclines showed a fast degradation of chlortetracycline to isochlortetracycline and of lymecycline to tetracycline in phosphate buffer solutions of different pH. The purity of pharmaceutical preparations of tetracyclines was also investigated.

Keyphrases □ Tetracycline—potential impurities of the drug and its analogs, reversed-phase ion-pair chromatography □ High-performance liquid chromatography—tetracycline, tetracycline analogs, and their potential impurities □ Counterions—*N,N*-dimethyloctylamine, tripropylamine, in reversed-phase ion-pair chromatography of tetracycline, tetracycline analogs, and their possible impurities

The most important impurities in tetracycline and tetracycline analogs are the epimerized, dehydrated, and epimerized dehydrated forms of the tetracyclines. Thus, quatrimycin (epitetracycline), anhydrotetracycline, and epianhydrotetracycline are the most frequently found impurities in tetracycline. Epianhydrotetracycline has been reported to be toxic in humans, but the exact safety level in pharmaceutical preparations is not known. Permitted concentrations of epianhydrotetracycline and other impurities are fixed by the European Pharmacopoeia.

BACKGROUND

Various chromatographic techniques, such as TLC (1, 2) and paper chromatography (3), have been used to analyze tetracycline, but they are

0022-3549/82/0200-0222$01.00/0

of the electronic density effect measured by σ, and the X-site polarity as measured by group dipole moments. These moments are, for X = $COCH_3$, 3.00 D; CN, 4.39; and NO_2, 4.21 (21). An increase in site polarity will tend to decrease the site binding constant (20), and both K_{11b} and K_{12a} may reflect this effect superimposed on the electron density effect.

This model of complexing suggests that K_{12} values are especially useful, leading to the question: Why is K_{12} ever equal to zero (for a two-site substrate)? According to Eq. 47, K_{12} can be zero only if $a = 0$ or if one of the site binding constants (K_{gH} or K_{GH}) is zero. This leads to the following argument. If the given site assignments are correct, K_{12b} represents binding at the COO^- site (since K_{11b} mainly describes X-site binding), and it was found that $K_{12b} = 0$ for all substrates. The existence of finite K_{12a} values (substrates 8–10) means that a is finite for these acid substrates, and suggests that it will also be finite in the corresponding base substrates. It follows that K_{12b} is zero as a consequence of the site binding constant for COO^- being zero. Letting K_{gHb} represent this quantity, and K_{GHb} the site binding constant for the X-site in the conjugate base series, it follows that:

$$K_{11b} = K_{gHb} + K_{GHb} = K_{GHb} \qquad \text{(Eq. 48)}$$

i.e., K_{11b} can be identified solely with the binding at site X.

Extension to the acid series requires the assumption that K_{GHb} for binding to X in the base series is identical with K_{GHa} for binding to X in the acid series. If approximately so, then $K_{11a} = K_{gHa} + K_{GHa} = K_{gHa} + K_{GHb} = K_{gHa} + K_{11b}$, and the site binding constant K_{gHa} for the COOH site is given approximately by $K_{11a} - K_{11b}$.

With these estimates of K_{gHa} ($K_{11a} - K_{11b}$) and K_{GHa} (K_{11b}), Eq. 47 leads to estimates of a for these substrates, since:

$$K_{12a} = \frac{aK_{gHa}K_{GHa}}{K_{gHa} + K_{GHa}} = \frac{aK_{11b}(K_{11a} - K_{11b})}{K_{11a}} \qquad \text{(Eq. 49)}$$

For compound number 8, $a = 0.51$; number 9, $a = 0.38$; and number 10, $a = 0.33$. Because of the several approximations, these calculations are unlikely to be accurate, but they are reasonable in magnitude. The interpretation of complex stability data in terms of this model and Eqs. 44 and 47 seems to be a potentially useful means for describing, understanding, and perhaps predicting complex formation behavior.

REFERENCES

(1) F. Cramer, W. Saenger, and H.-Ch. Spatz, *J. Am. Chem. Soc.*, **89,** 14 (1967).

(2) K. A. Connors and J. M. Lipari, *J. Pharm. Sci.*, **65,** 379 (1976).

(3) T. Miyaji, Y. Kurono, K. Uekama, and K. Ikeda, *Chem. Pharm. Bull.*, **24,** 1155 (1976).

(4) R. I. Gelb, L. M. Schwartz, R. F. Johnson, and D. A. Laufer, *J. Am. Chem. Soc.*, **101,** 1869 (1979).

(5) K. A. Connors and T. W. Rosanske, *J. Pharm. Sci.*, **69,** 173 (1980).

(6) R. I. Gelb, L. M. Schwartz, C. T. Murray, and D. A. Laufer, *J. Am. Chem. Soc.*, **100,** 3553 (1978).

(7) R. I. Gelb, L. M. Schwartz, and D. A. Laufer, *ibid.*, **100,** 5875 (1978).

(8) A. B. Wong, Ph.D. thesis, University of Wisconsin, Madison, Wis., 1980.

(9) K. Uekama, M. Otagiri, Y. Kanie, S. Tanaka, and K. Ikeda, *Chem. Pharm. Bull.*, **23,** 1421 (1975).

(10) R. N. Mattoo, *Trans. Faraday Soc.*, **52,** 1462 (1956).

(11) P. O. Lumme, *Suomen Kemist.*, **30B,** 168 (1957).

(12) J. Johnston, *Proc. R. Soc. London*, **A78,** 82 (1906).

(13) P. A. Kramer and K. A. Connors, *Am. J. Pharm. Educ.*, **33,** 193 (1969).

(14) B. Casu and L. Ravà, *Ric. Sci.*, **36,** 733 (1966).

(15) R. L. VanEtten, J. F. Sebastian, G. A. Clowes, and M. L. Bender, *J. Am. Chem. Soc.*, **89,** 3242 (1967).

(16) E. A. Lewis and L. D. Hansen, *J. Chem. Soc., Perkin Trans.*, **II,** 2081 (1973).

(17) R. J. Bergeron, M. A. Channing, and K. A. McGovern, *J. Am. Chem. Soc.*, **100,** 2878 (1978).

(18) T. W. Rosanske, Ph.D. thesis, University of Wisconsin, Madison, Wis., 1979.

(19) R. I. Gelb, L. M. Schwartz, B. Cardelino, and D. A. Laufer, *Anal. Biochem.*, **103,** 362 (1980).

(20) T. W. Rosanske and K. A. Connors, *J. Pharm. Sci.*, **69,** 564 (1980).

(21) E. S. Gould, "Mechanism and Structure in Organic Chemistry," Holt, Rinehart and Winston, New York, N.Y., 1959, p. 62.

Reversed-Phase Ion-Pair Chromatography of Tetracycline, Tetracycline Analogs, and Their Potential Impurities

JÖRGEN HERMANSSON[x] and MATS ANDERSSON

Received December 17, 1980, from the *National Board of Health and Welfare, Department of Drugs, Division of Pharmacy, Box 607, S-751 25 Uppsala, Sweden.* Accepted for publication May 15, 1981.

Abstract □ Methods are presented for the separation of tetracycline, tetracycline analogs, and their potential impurities by reversed-phase ion-pair chromatography. The mobile phase consisted of a phosphate buffer with tripropylamine or *N,N*-dimethyloctylamine as counterions and acetonitrile as the organic modifier. The chromatographic properties of the tetracyclines were significantly improved by addition of the tertiary amines. The best result was obtained with *N,N*-dimethyloctylamine as the counterion, which gave good separation efficiency and peak symmetry for most of the substances studied. Addition of the tertiary amines to the mobile phase also significantly affected the capacity factors of the tetracyclines. Stability studies of the tetracyclines showed a fast degradation of chlortetracycline to isochlortetracycline and of lymecycline to tetracycline in phosphate buffer solutions of different pH. The purity of pharmaceutical preparations of tetracyclines was also investigated.

Keyphrases □ Tetracycline—potential impurities of the drug and its analogs, reversed-phase ion-pair chromatography □ High-performance liquid chromatography—tetracycline, tetracycline analogs, and their potential impurities □ Counterions—*N,N*-dimethyloctylamine, tripropylamine, in reversed-phase ion-pair chromatography of tetracycline, tetracycline analogs, and their possible impurities

The most important impurities in tetracycline and tetracycline analogs are the epimerized, dehydrated, and epimerized dehydrated forms of the tetracyclines. Thus, quatrimycin (epitetracycline), anhydrotetracycline, and epianhydrotetracycline are the most frequently found impurities in tetracycline. Epianhydrotetracycline has been reported to be toxic in humans, but the exact safety level in pharmaceutical preparations is not known. Permitted concentrations of epianhydrotetracycline and other impurities are fixed by the European Pharmacopoeia.

BACKGROUND

Various chromatographic techniques, such as TLC (1, 2) and paper chromatography (3), have been used to analyze tetracycline, but they are

0022-3549/82/0200-0222$01.00/0

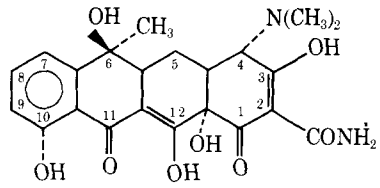

I

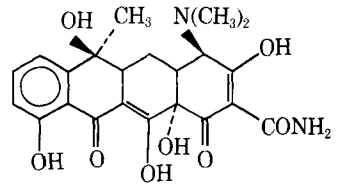

II

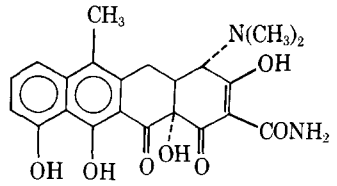

III

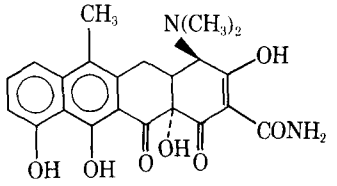

IV

usually not sensitive enough to allow detection of small amounts of impurities with good precision.

Ion-exchange column chromatography has also been used for analysis of tetracycline and tetracycline analogs, but the separation efficiency is not good with typical plate height (H) values >5 mm (4, 5). However, better results were reported with various reversed-phase systems (6–9). The mobile phases used in these methods have pH values between 1.5 and 5. Tetracyclines were reported to undergo epimerization between pH 3 and 5, and dehydration at low pH (10–12). This means that chromatography of tetracyclines in mobile phases with pH between 1.5 and 5 is unsuitable due to possible formation of degradation products during the chromatographic run, or during the dissolution process of tetracycline preparations.

The present report describes studies of reversed-phase ion-pair chromatographic systems using mobile phases of pH 8.0. These chromatographic systems can be used for separation and quantitation of

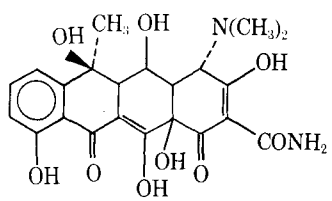

V

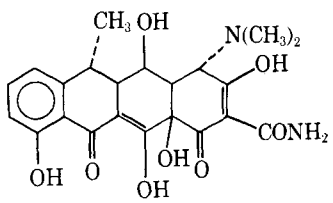

VI

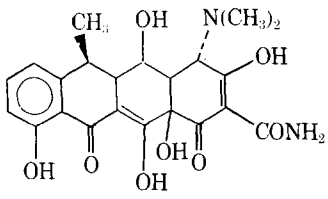

VII

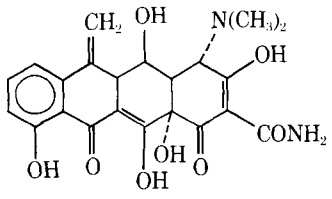

VIII

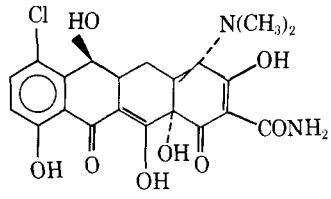

IX

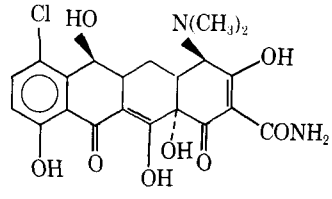

X

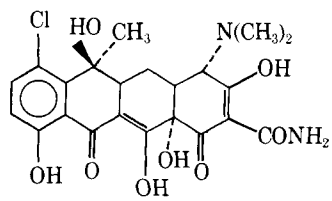

XI

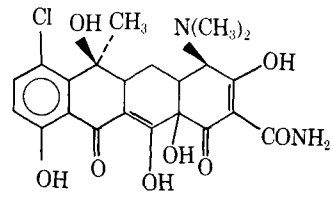

XII

tetracycline, tetracycline analogs, and related impurities. The purpose of this work was to develop chromatographic systems suitable to use in the study of small amounts of impurities (<0.1 %) in pharmaceutical preparations of tetracycline and tetracycline analogs.

EXPERIMENTAL

Apparatus—The high-performance liquid chromatographic system consisted of a high-pressure pump[1] and injection port[2]. UV detection was utilized with a detector[3] set at 280 nm. Columns (150 × 4.5-mm i.d.) were made of No. 316 stainless steel with a polished inner surface and equipped with modified end connections[4] and stainless steel frits[5] (2 μm).

Chemicals—The following chemicals were analytical grade and were used as supplied: acetonitrile[6], tripropylamine[7], and *N,N*-dimethyloctylamine[8]. All other chemicals used were analytical reagent grade and were used without further purification.

Samples of drug substances were obtained directly from the manufacturer or collected in the factory by drug inspectors. The drug preparations were bought in Swedish pharmacies. In most cases, reference samples of potential impurities were provided by the drug manufacturers. The following substances were used: tetracycline (I), quatrimycin (epitetracycline, II), anhydrotetracycline (III), epianhydrotetracycline (IV), oxytetracycline (V), doxycycline (VI), 6-epidoxycycline (VII), methacycline (VIII), demeclocycline (IX), epidemethylchlortetracycline (X), chlortetracycline (XI), epichlortetracycline (XII), isochlortetracycline (XIII), epianhydrochlortetracycline (XIV), anhydrochlortetracycline (XV), and lymecycline (XVI).

Column Packing—The columns were packed by a modification of the ordinary balanced-density slurry technique described previously (13). The support[9] was suspended in chloroform, and acetone was used as the driving liquid in the pump which was operated at 5000 psi. After packing, the column was washed with hexane followed by acetonitrile before equilibration with the mobile phase.

Chromatographic Technique—The chromatographic analyses were performed at room temperature. The mobile phases were prepared from 0.05 or 0.1 M monobasic sodium phosphate and the pH was adjusted to 8.2 (for the tripropylamine systems) or 8.0 (for the *N,N*-dimethyloctylamine system) with sodium hydroxide after addition of tripropylamine or *N,N*-dimethyloctylamine. An appropriate amount of acetonitrile was added and the mobile phase was thermostated at room temperature and degassed in an ultrasonic bath before use. The interstitial volume of the column, V_m, was obtained by injection of water.

Four different mobile phases were used for the purity control of the tetracyclines.

Mobile Phase A—A mixture of 0.1 M monobasic sodium phosphate, 30% acetonitrile, and 0.0194 M *N,N*-dimethyloctylamine was adjusted to pH 8.0 with sodium hydroxide.

Mobile Phase B—Mobile phase B contained 0.05 M monobasic sodium

[1] Waters model 6000, Milford, Mass.
[2] Valco model CV-UHPa 7000 psi injector equipped with a 20-μl loop, Santa Clara, Calif.
[3] Waters model 440, Milford, Mass.
[4] Crawford Fitting Co., Solon, Ohio.
[5] Altex, Berkeley, Calif.
[6] Rathburn Chemicals, Walkerburn Ltd, Peebleshire, Scotland.
[7] Fluka AG, Chemische Fabrik, Buchs, Switzerland.
[8] ICN Pharmaceuticals, Plainview, N.Y.
[9] LiChrosorb RP-8 (5 μm), E. Merck, Darmstadt, W. Germany.

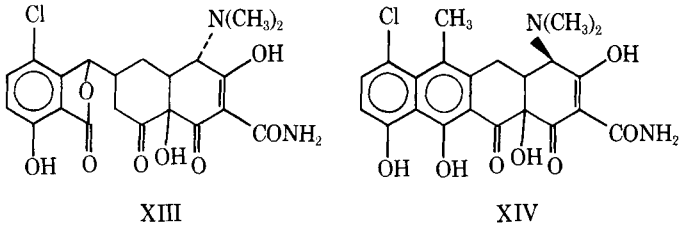

XIII XIV

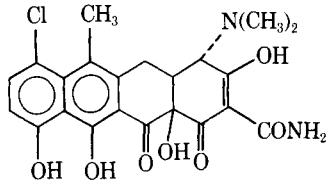

XV

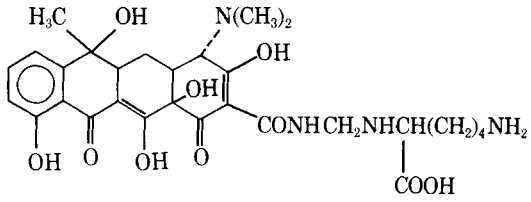

XVI

phosphate, 35% acetonitrile, and 0.0097 *M* *N,N*-dimethyloctylamine adjusted to pH 8.0 with sodium hydroxide.

Mobile Phase C—This phase contained 0.1 *M* monobasic sodium phosphate, 20% acetonitrile, and 0.0194 *M* *N,N*-dimethyloctylamine adjusted to pH 8.0 with sodium hydroxide.

Mobile Phase D—A mixture of 0.1 *M* monobasic sodium phosphate, 28% acetonitrile, and 0.0194 *M* *N,N*-dimethyloctylamine was adjusted to pH 8.0 with sodium hydroxide.

Calculation of Chromatographic Parameters—The chromatographic behavior of the tetracycline substances is expressed by the capacity factor, the plate height, and the asymmetry factor. The capacity factor, k', is calculated by:

$$k' = (t_R - t_m)/t_m \quad \text{(Eq. 1)}$$

where t_R and t_m are elution times for retained and unretained solutes, respectively. The plate height, H, is obtained from the chromatogram by:

$$H = (L/16)(w_t/t_R)^2 \quad \text{(Eq. 2)}$$

where L is the column length and w_t is the peak width at the baseline. The asymmetry factor was calculated by drawing a perpendicular to the baseline from the vertex formed by the two peak tangent lines. The back part of the peak baseline divided by the front part gives the asymmetry factor.

Standard Solutions for Chromatographic Experiments—Standard solutions were freshly prepared just before use. The substances were dissolved in mobile phases which did not contain the tertiary amine. Twenty microliters of the solutions were injected.

Tetracycline Preparations—Tablets, dragees, capsules, suspensions, and ampuls were used for this investigation. Five tablets or dragees were ground and put into a 250-ml volumetric flask. Methanol (200 ml) was added and the flask was sonicated for 10 min in an ultrasonic bath and the contents were diluted to 250 ml with methanol. An appropriate amount of this solution was then centrifuged and an aliquot was taken out and diluted with methanol to give a final concentration of 20 μg/ml (used for quantitation of active substance in the drug preparations) or 1 mg/ml (used for quantitation of impurities in the drug preparations) of active substance. One milliliter of this solution was evaporated with nitrogen at 40° and the residue was dissolved in 1.0 ml of the mobile phase (without addition of the tertiary amine). Twenty microliters of this solution were then injected on the column. The substance in the capsules was accurately weighed and dissolved in the same way and to the same concentration as for tablets and dragees. Ampuls were also handled in the same way. An aliquot of the suspensions (~10 ml) was accurately weighed and put into a volumetric flask and extracted with 100 ml of 0.1 *M* HCl in an ultrasonic bath for 10 min and finally diluted to 150 ml with

Table I—Influence of Tripropylamine Concentration on Selectivity [a]

Selectivity (α)	Tripropylamine Concentration, *M*			
	0	0.032	0.063	0.095
II				
I	2.7	3.0	2.8	2.8
IV	0.7	1.5	1.9	1.8
III	2.3	2.7	3.0	3.2

[a] Mobile phase: pH 8.2 phosphate buffer, 20% acetonitrile with varying concentrations of tripropylamine.

Table II—Influence of the *N,N*-Dimethyloctylamine Concentration on Selectivity [a]

Selectivity (α)	*N,N*-Dimethyloctylamine Concentration, *M*				
	0	0.0097	0.0194	0.0292	0.039
II					
I	2.0	2.1	2.1	1.9	1.8
IV	0.8	2.5	4.2	5.0	5.6
III	1.5	3.9	4.7	5.3	—

[a] Mobile phase: pH 8.2 phosphate buffer, 28% acetonitrile with varying concentrations of *N,N*-dimethyloctylamine.

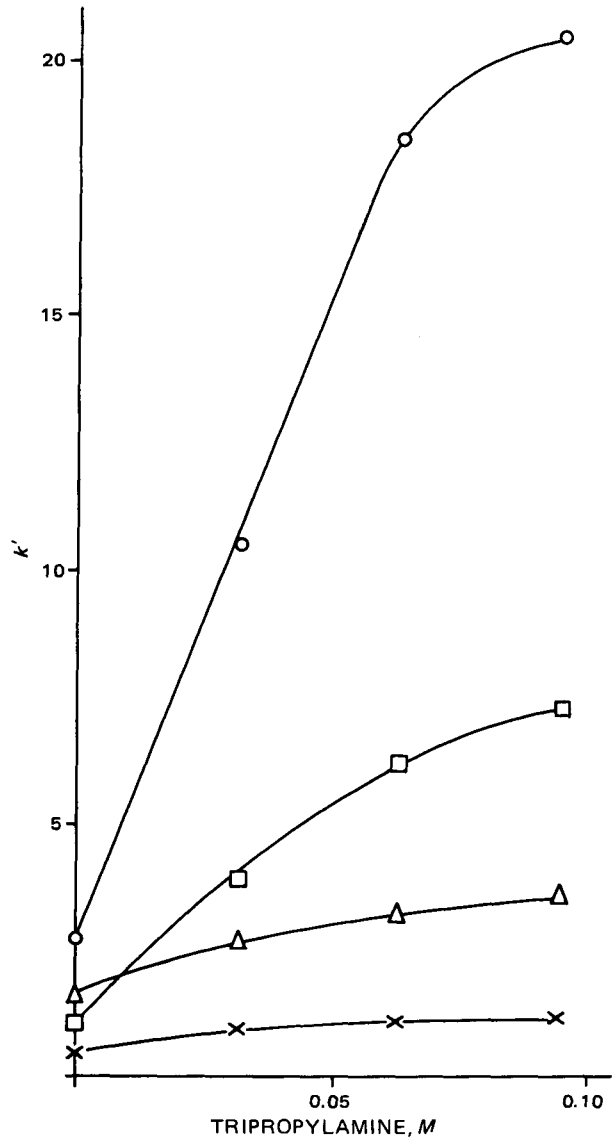

Figure 1—*Regulation of the capacity factors by addition of tripropylamine. The mobile phase consisted of pH 8.2 sodium phosphate buffer containing 20% (v/v) acetonitrile and tripropylamine at a flow rate of 1 ml/min. Key: ×, II; △, I; □, IV; and ○, III.*

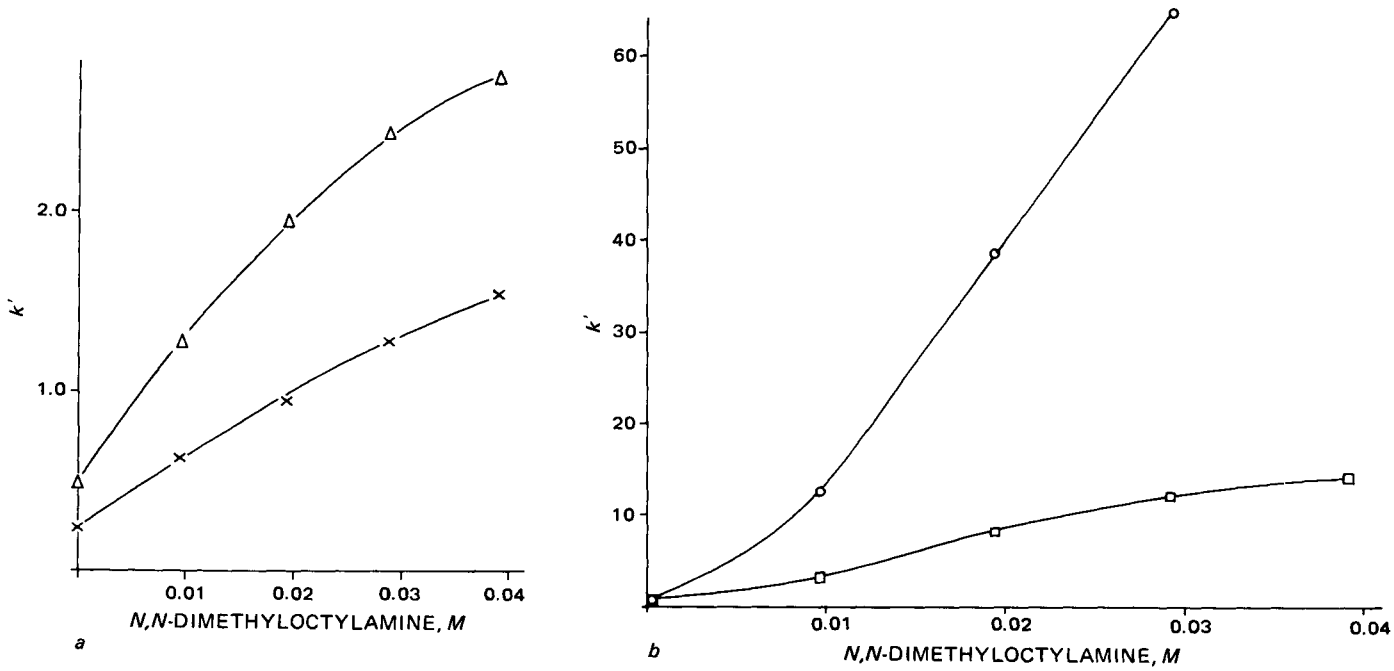

Figure 2a and 2b—*Regulation of the capacity factors by addition of* N,N-*dimethyloctylamine. The mobile phase contained sodium phosphate buffer at pH 8.2 containing 28% (v/v) acetonitrile and* N,N-*dimethyloctylamine. Key: See Fig. 1.*

0.1 *M* HCl. An aliquot of this solution was then handled in the same way as for tablets and dragees.

Drug Substances—Drug substances were dissolved as described for tetracycline preparations to a final concentration of ~1 mg/ml. A 20-μl aliquot was injected onto the column.

RESULTS AND DISCUSSION

Compounds I–IV were used as model compounds in the present study. Tetracycline has three ionization stages in the pH range of 1–12. The first pKa 3.30 involves the ionization of the acidic hydroxy group at the 3-position; the pKa values for the dimethyl amino function and the hydroxy group at position 12 are 7.68 and 9.69, respectively (14). This makes it possible to utilize ion-pair chromatography with a cationic counterion like a tertiary or quaternary amine with a mobile phase at pH 8.0 (15, 16).

Regulation of the Capacity Factor by Addition of Counter Ion—Chromatographic studies of I and its potential impurities were performed using a phosphate buffer at pH 8.2 or 8.0 and acetonitrile as organic modifier in the mobile phase. Tripropylamine and *N,N*-dimethyloctylamine were used as counterions. Twenty percent (v/v) acetonitrile was used in the tripropylamine systems and 28% in the *N,N*-dimethyloctylamine system.

One advantage of reversed-phase ion-pair chromatography is the presence of the counterion in the mobile phase, which makes it possible to regulate the capacity factor by changing the type or the concentration of the counterion. Figures 1, 2a, and 2b illustrate the regulation of the capacity factor of I, II, and the dehydrated forms III and IV by increasing the concentration of tripropylamine from zero to 0.095 *M*, and *N,N*-dimethyloctylamine from zero to 0.039 *M*. It can be seen that I and III have higher capacity factors than their corresponding epi forms, II and IV, respectively. A likely cause of this effect is that I and III have conformations which favor the formation of internal hydrogen bonding, giving the molecule a more hydrophobic character. The possibility of regulating the capacity factor of I and II is rather limited both with tripropylamine and *N,N*-dimethyloctylamine as counterions, while the capacity factors for the dehydrated substances are influenced to a large extent by the increasing concentration of counterion. The possibility of

Table III—Chromatographic Data of Tetracyclines

Compound	Mobile Phase A, k'	H, mm	Asymmetry Factor	Mobile Phase B, k'	Mobile Phase C, k'	Mobile Phase D, k'
Tetracycline (I)	1.3	0.02	1.0			
Quatrimycin (II)	0.7	0.05	1.2			
Epianhydrotetracycline (IV)	4.3	0.03	1.2			
Anhydrotetracycline (III)	17.2	0.03	1.3			
Oxytetracycline (V)	1.1	0.08	1.0	0.5		1.5
Unidentified 1	7.0					
Unidentified 2						2.1
Unidentified 3				3.3		
Doxycycline (VI)	3.4	0.07	1.0			
6-Epidoxycycline (VII)	1.6	0.18	1.7			
Demeclocycline (IX)	1.9	0.07	0.8			
Epidemethylchlortetracycline (X)	1.3	0.04	0.9		3.4	
Epianhydrodemethylchlortetracycline	9.9	0.03	1.0	2.0		
Anhydrodemethylchlortetracycline	40.5	0.04	1.0	10.0		
Unidentified					2.4	
Chlortetracycline (XI)	2.6	0.09	1.0			
Epichlortetracycline (XII)	1.5	0.40	0.2		5.0	
Isochlortetracycline (XIII)	3.9	0.05	0.8		17.0	
Epianhydrochlortetracycline (XIV)	11.1	0.04	1.0	2.2		
Anhydrochlortetracycline (XV)	48.9	0.04	0.9	6.7		
Unidentified					3.5	
Methacycline (VIII)	2.1	0.06	1.1			
Unidentified					5.9	

[a] Flow rate = 1.0 ml/min.

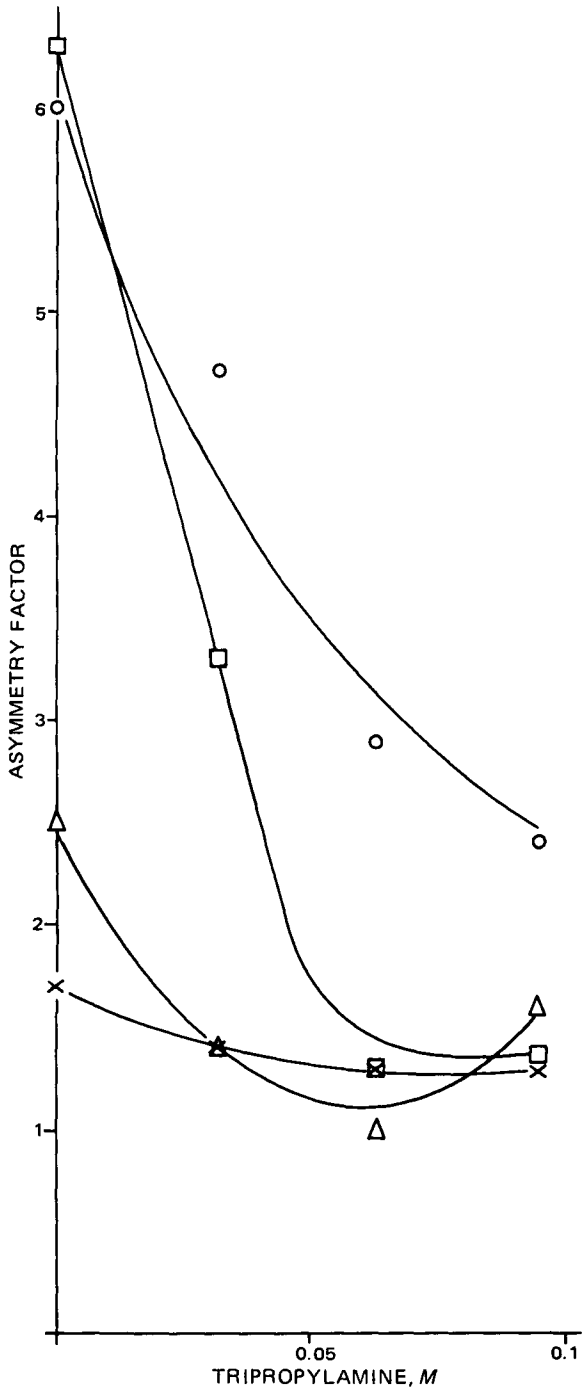

Figure 3—*Effect of the concentration of tripropylamine on peak symmetry. Key: See Fig. 1.*

regulating the capacity factors of the tetracyclines is more pronounced with *N,N*-dimethyloctylamine than with tripropylamine as counterion. This may be partly an effect of one more methylene group in *N,N*-dimethyloctylamine than in tripropylamine giving the *N,N*-dimethyloctylamine ion-pairs a more hydrophobic character.

Selectivity Change by Varying the Counterion Concentration—The influence of the nature and the concentration of the counterion on the separation factor α, is demonstrated in Tables I and II. The selectivity between II and I is better in the tripropylamine system, while the selectivity between IV and III is better in the *N,N*-dimethyloctylamine system. However, the separation factors for I and II are sufficiently large even in the *N,N*-dimethyloctylamine system to permit baseline separation at all *N,N*-dimethyloctylamine concentrations. It can also be seen that the selectivity between II and I is almost uninfluenced by an increase in the counterion concentration, while the selectivities between I and IV and also between IV and III increase with increasing counterion concentration. This effect on the separation selectivity is more

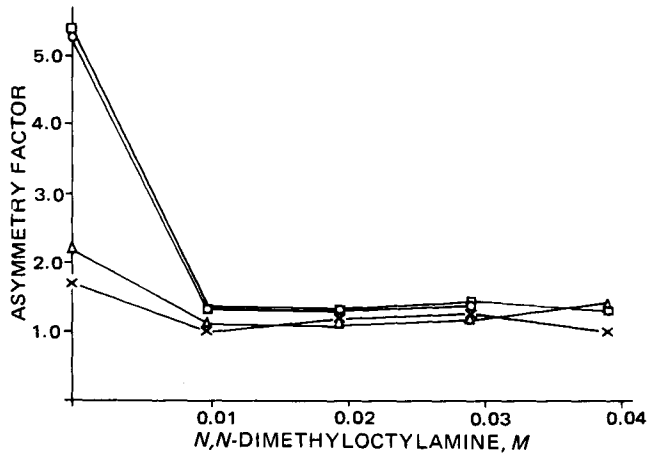

Figure 4—*Effect of the concentration of* N,N-*dimethyloctylamine on peak symmetry. Key: See Fig. 1.*

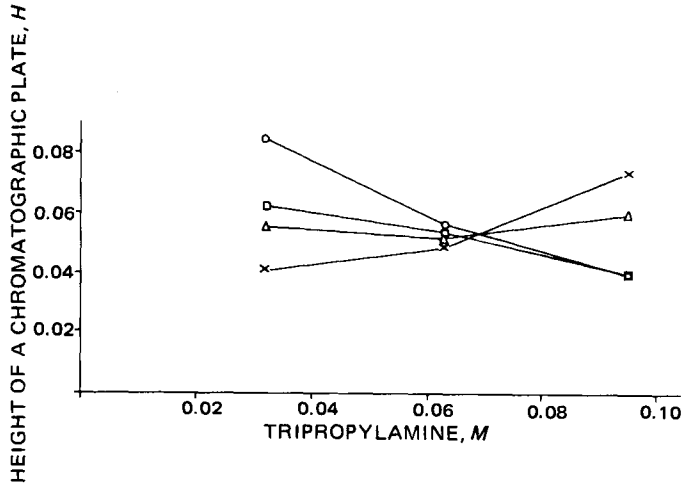

Figure 5—*Effect of the concentration of tripropylamine on separation efficiency. Key: See Fig. 1.*

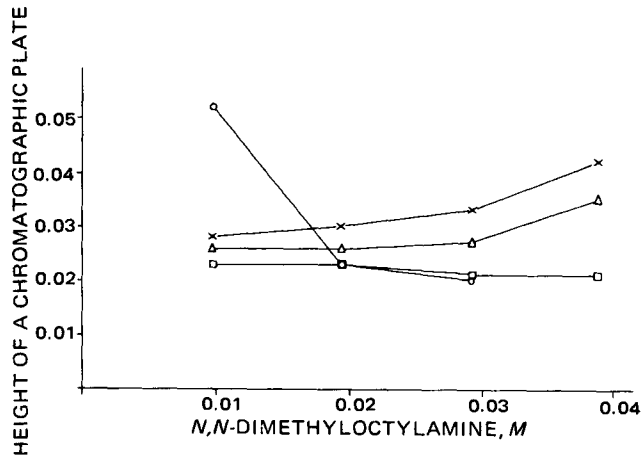

Figure 6—*Effect of the concentration of* N,N-*dimethyloctylamine on the separation efficiency. Key: See Fig. 1.*

pronounced with *N,N*-dimethyloctylamine than with tripropylamine as counterion.

Peak Symmetry and Separation Efficiency—Figure 3 demonstrates the variation in peak symmetry of the tetracyclines with increasing concentration of tripropylamine. Compounds III and IV show considerable tailing without the addition of the tertiary amine. However, tailing is significantly reduced by increasing the concentration of tripropylamine and the asymmetry factors; I, II, and IV are <2 with a tripropylamine concentration of 0.095 *M*, while III at this tripropylamine concentration still show significant tailing.

Table IV—Purity of Tetracycline Substances and Drug Preparations on the Swedish Market

Substances	Smallest Amount of Impurity, %		Largest Amount of Impurity, %		Impurity Limits in Substance, %
	Substance	Drug Preparation	Substance	Drug Preparation	Ph. Eur.
Tetracycline (I)					
Quatrimycin (II)	1.8	1.6	8.4	7.7	4.0
Chlortetracycline (XI)	n.d[a]	n.d	0.4	0.4	2.0
Epianhydrotetracycline (IV)	<0.1	n.d	0.5	0.3	0.5
Anhydrotetracycline (III)	0.1	0.2	1.9	2.2	0.5
Oxytetracycline (V)					
Unidentified 1[b]	<0.1	0.3	0.6	0.6	
Unidentified 2[b]	n.d	0.1	<0.1	0.5	
Unidentified 3[b]	n.d	<0.1	<0.1	0.2	
Doxycycline (VI)					
6-Epidoxycycline (VII)	0.2	0.1	0.9	0.6	
Methacycline (VIII)	<0.1	n.d	0.2	0.3	
Demeclocycline (IX)					
Epidemethylchlortetracycline (X)	2.0	2.1	4.0	3.8	
Epianhydrodemethylchlortetracycline	n.d.	n.d	n.d	n.d	
Anhydrodemethylchlortetracycline	n.d.	n.d	n.d	n.d	
Unidentified[c]	2.0	1.6	2.0	1.6	
Chlortetracycline (XI)					
Epichlortetracycline (XII)	n.d		n.d		
Isochlortetracycline (XIII)	~0.5		~0.5		
Epianhydrochlortetracycline (XIV)	n.d		n.d		
Anhydrochlortetracycline (XV)	0.1		0.1		
Unidentified[d]	5.2		5.2		
Methacycline (VIII)					
Unidentified[e]	0.2	0.3	0.2	0.3	

[a] n.d. = not detected. [b] Amount impurity calculated by using the molar absorptivity of V. [c] Amount impurity calculated using the molar absorptivity of epianhydrodemethylchlortetracycline. [d] Amount impurity calculated by using the molar absorptivity of XI. [e] Amount impurity calculated by using the molar absorptivity of VIII.

A much more pronounced effect on the peak symmetry of the tetracyclines was observed by the addition of *N,N*-dimethyloctylamine to the mobile phase. Figure 4 shows the variation in the asymmetry factor of I and its potential impurities with increasing *N,N*-dimethyloctylamine concentration in the mobile phase. With a *N,N*-dimethyloctylamine concentration as low as 0.01 *M*, all four tetracyclines have an asymmetry factor of <1.5. Positive effects on peak symmetry by addition of *N,N*-dimethyloctylamine were demonstrated for hydrophobic amines like imipramine, desipramine (17), and zimelidine and its metabolites (18), when chromatographed in the cationic forms. The separation efficiency of the tetracyclines is considerably improved by addition of the tertiary amines, tripropylamine, or *N,N*-dimethyloctylamine, to the mobile phase in accordance with peak symmetry. Relations between *H* and the concentration of the tertiary amines are demonstrated in Figs. 5 and 6.

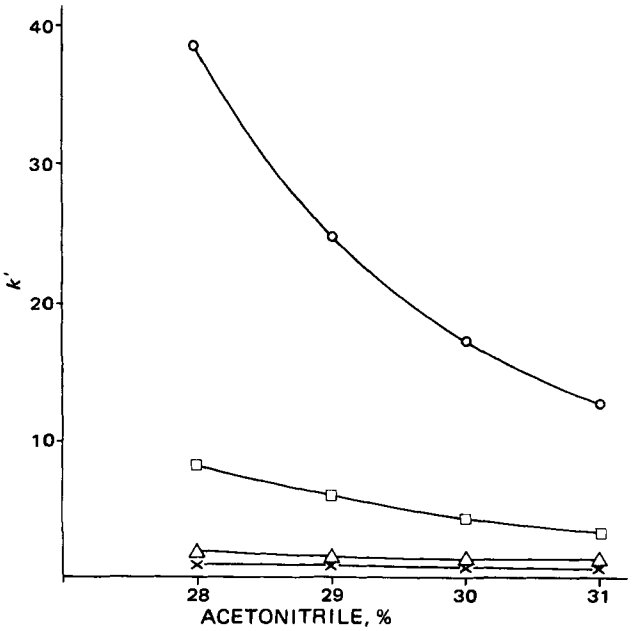

Figure 7—*Regulation of capacity factors by varying the acetonitrile concentration. The mobile phase contained a pH 8.0 sodium phosphate buffer with 0.0194* M N,N-*dimethyloctylamine and varying concentrations of acetonitrile. Key: See Fig. 1.*

Regulation of the Capacity Factor for Varying Acetonitrile Concentration—From the data presented, it follows that chromatography of the tetracyclines as *N,N*-dimethyloctylamine ion-pairs gives better chromatographic performance than when using tripropylamine as the counterion. A *N,N*-dimethyloctylamine concentration of ~0.02 *M* was sufficient to give good separation efficiency and symmetrical peaks of I–IV. Accordingly, in the following studies, the *N,N*-dimethyloctylamine system was used. From Fig. 1 it can be seen that the capacity factors of dehydrated III and IV are rather high with a *N,N*-dimethyloctylamine concentration of 0.02 *M* and 28% acetonitrile in pH 8.2 phosphate buffer.

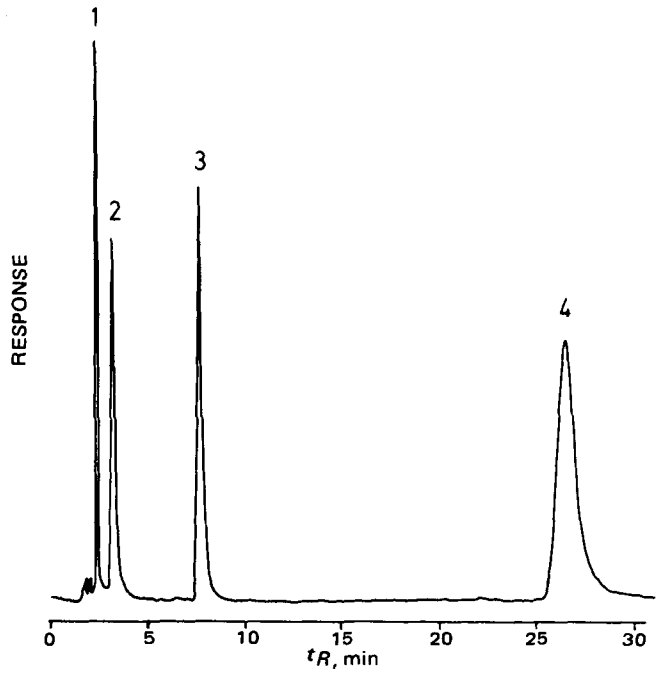

Figure 8—*Separation of I and its impurities. The mobile phase consisted of pH 8.0 sodium phosphate buffer containing 0.0194* M N,N-*dimethyloctylamine and 30% (v/v) acetonitrile at a flow rate of 1 ml/min. Key: 1, II (240 ng); 2, I (268 ng); 3, IV (246 ng); and 4, III (650 ng).*

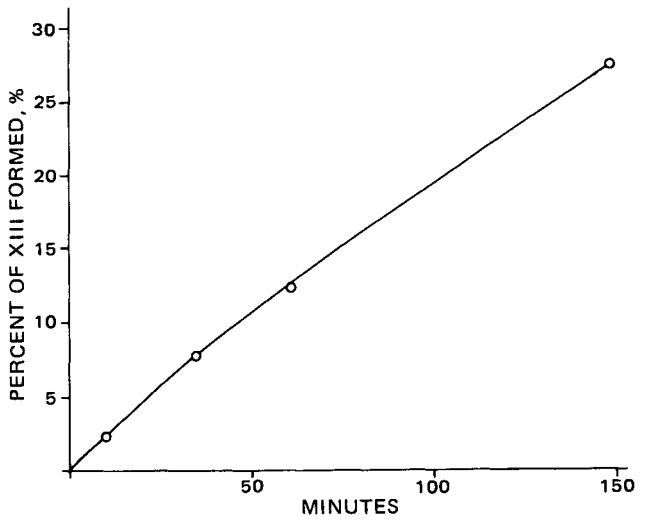

Figure 9—*Degradation rate of XI to XIII. Initial concentration of XI was 1.076 mg/ml, dissolved in mobile phase C without addition of tertiary amine.*

To optimize the separation time of the four tetracycline substances without loss of selectivity and peak symmetry, the influence of the acetonitrile concentration in the mobile phase on the capacity factor was determined. The results are demonstrated in Fig. 7. As expected, there is a drastic decrease of the capacity factor of III with a small increase in the acetonitrile concentration, but the capacity factors of I, II, and IV are influenced only to a limited extent. Figure 8 shows a separation of I, II, III, and IV by using a mobile phase consisting of 30% acetonitrile in pH 8.0 phosphate buffer and 0.0194 *M* *N,N*-dimethyloctylamine as the counterion.

Chromatography of Tetracycline Analogs and Potential Impurities—A suitable mobile phase composition to separate tetracycline analogs from their impurities was found to be pH 8.0 phosphate buffer with 30% acetonitrile and 0.0194 *M* *N,N*-dimethyloctylamine as the counterion (mobile phase A). The chromatographic data presented in Table III indicate that some of the substances have rather high capacity factors in mobile phase A, giving high retention times. Three alternative mobile phases were used, allowing regulation of the capacity factors over a wide range. Capacity factors for some of the tetracyclines in mobile phases B–D are also presented in Table III.

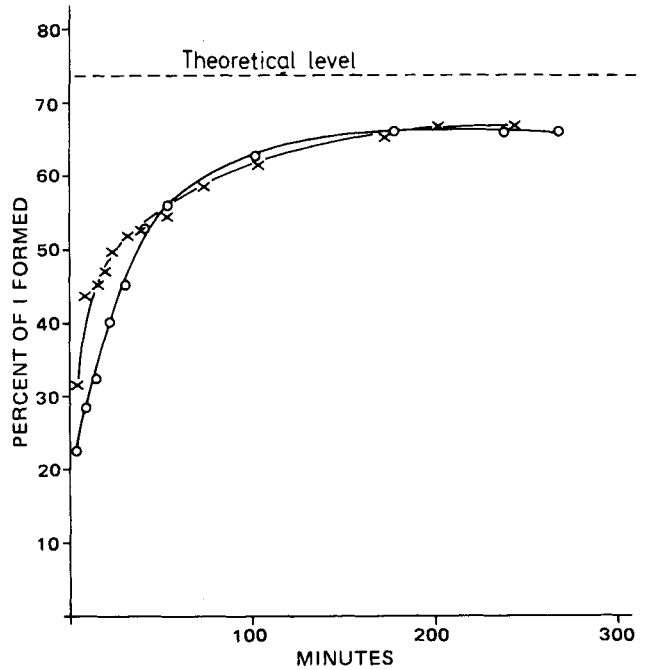

Figure 10—*Degradation rate of XVI to I. Key: ×, XVI (0.994 mg/ml) dissolved in pH 2.2 phosphate buffer; and ○, XVI (1.005 mg/ml) dissolved in pH 7.5 phosphate buffer.*

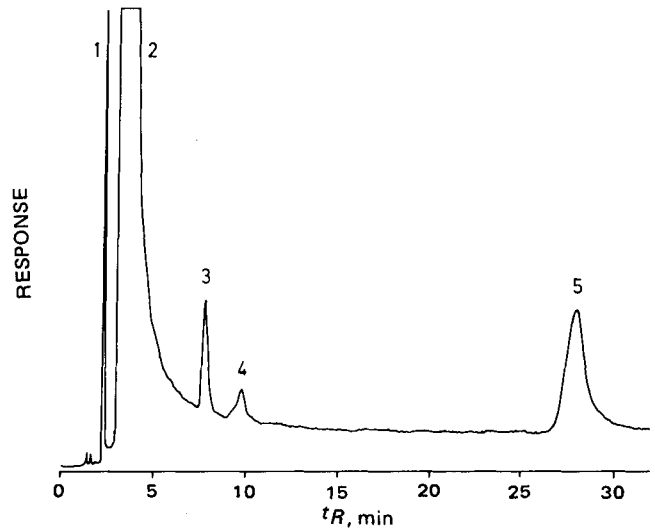

Figure 11—*Separation of I and its impurities from a tablet extract. Conditions were the same as in Fig. 8. Injection of 20 μl of a tablet extract with an initial concentration of 1.231 mg/ml is shown. Key: 1, II; 2, I; 3, IV (0.15%); 4, unknown impurity or tablet constituent; and 5, III.*

Stability of Tetracyclines—Tetracyclines have been reported (16) to undergo some degradation reactions like dehydration (at low pH) and epimerization between pH 3 and 5 in water solution. Stability tests of the tetracyclines were performed to exclude the possibility that the detected impurities were artifacts due to degradation during the chromatographic run, and to learn how to handle the dissolved substances before injection on the column. The commercial tetracyclines containing potential impurities were dissolved in the mobile phase without addition of the tertiary amine. A concentration of ~1 mg/ml of the tetracyclines was used, which allowed detection of the impurities to <0.1%. Repeated injections of the solutions were made over a minimum of 70 min, and the quantity of impurity was measured.

Two of the studied tetracycline substances showed significant degradation during the experimental period. Figure 9 shows the rate of rearrangement of XI to XIII. This study was performed by using a solution of XI with an initial concentration of 1.076 mg/ml. The substance was dissolved in mobile phase C without addition of the tertiary amine.

Figure 10 shows the degradation rate of XVI to I measured as percent I produced at pH 2.2 and 7.5 (phosphate buffer). The initial concentrations of (XVI) were 0.994 and 1.005 mg/ml, respectively. Mobile phase A was used for the quantitation of I produced. The molecular weights of I and XVI are 444 and 602.6, respectively, which means that 73.7% I produced corresponds to fully degraded XVI. The discrepancy between the theoretical and the observed I levels is not yet clearly understood. Compound XVI is a condensation product of I, lysine, and formaldehyde.

The described experiments show a fast degradation rate of XVI at acidic and neutral pH. This degradation means that there is a potential risk of formaldehyde liberation during therapy with XVI preparations. The liberation of formaldehyde during the degradation of XVI was determined by preparing the 2,4-dinitrophenylhydrazone derivative of formaldehyde followed by quantitation on a normal-phase column. Due to the fast degradation of XI and XVI, use of the described method is not recommended in the purity control of the drug substances.

Purity Control of Tetracycline Substances and Pharmaceutical Preparations—Figure 11 demonstrates the separation of tetracycline tablet extract containing small amounts of the impurities II, IV (0.15%), and III (0.6%). Table IV summarizes the content of impurities found in tetracycline, tetracycline analogs, and pharmaceutical preparations. There is good correlation of the impurity levels found in the drug substances and in the pharmaceutical preparations.

The precision of the method was evaluated to some extent by analyzing six samples containing 1 μg of III/ml. The relative SD was 6.5% at this concentration level. A concentration of 1 μg/ml corresponds to 0.1% impurity by injection of a tetracycline solution containing 1 mg/ml, which was the usual concentration of tetracycline used in the purity control studies.

Standard curves constructed by plotting peak areas *versus* sample concentrations show good linearity in the concentration range for all substances, with correlation coefficients >0.9994 in all cases.

REFERENCES

(1) A. A. Fernandez, V. T. Noceda, and E. S. Carrera, *J. Pharm. Sci.*, **58,** 443 (1969).

(2) P. P. Ascione and G. P. Chrekian, *ibid.*, **59,** 1480 (1970).

(3) E. Addison and R. G. Clark, *J. Pharm. Pharmacol.*, **15,** 268 (1963).

(4) J. P. Sharma, G. D. Koritz, E. G. Perkins, and R. F. Bevill, *J. Pharm. Sci.*, **66,** 1319 (1977).

(5) A. G. Butterfield, D. W. Hughes, W. L. Wilson, and N. J. Pound, *ibid.*, **64,** 316 (1975).

(6) J. H. Knox and J. Jurand, *J. Chromatogr.*, **110,** 103 (1975).

(7) *Ibid.*, **186,** 763 (1979).

(8) J. H. Knox and A. Pryde, *J. Chromatogr.*, **112,** 171 (1975).

(9) A. P. De Leenheer and H. I. C. F. Nelis, *ibid.*, **140,** 293 (1977).

(10) T. D. Sokoloski, L. A. Mitscher, P. H. Yuen, J. V. Juvarkar, and B. Hoener, *J. Pharm. Sci.*, **66,** 1159 (1977).

(11) B. Hoener, T. D. Sokoloski, L. A. Mitscher, and L. Malspeis, *ibid.*, **63,** 1901 (1974).

(12) K. D. Schlecht and C. W. Frank, *ibid.*, **62,** 258 (1973).

(13) R. E. Majors, *Anal. Chem.*, **44,** 1722 (1972).

(14) C. R. Stephens, K. Murai, K. J. Brunings, and R. B. Woodward, *J. Am. Chem. Soc.*, **78,** 4155 (1956).

(15) J. Hermansson, *J. Chromatogr.*, **152,** 437 (1978).

(16) K.-G. Wahlund, *ibid.*, **115,** 411 (1975).

(17) A. Sokolowski and K-G. Wahlund, *ibid.*, **189,** 299 (1980).

(18) D. Westerlund and E. Erixon, *ibid.*, **185,** 593 (1979).

ACKNOWLEDGMENTS

The authors are grateful to Mr. S. Eriksson for skillful drawing of the figures and to Mr. B. Wiese for technical assistance.

Hydration and Percutaneous Absorption III: Influences of Stripping and Scalding on Hydration Alteration of the Permeability of Hairless Mouse Skin to Water and *n*-Alkanols

CHARANJIT R. BEHL *x, MICHAEL BARRETT, GORDON L. FLYNN, TAMIE KURIHARA, KENNETH A. WALTERS, OLIVIA G. GATMAITAN, NANCY HARPER, WILLIAM I. HIGUCHI, NORMAN F. H. HO, and CARL L. PIERSON

Received January 19, 1981, from the *College of Pharmacy and Medical School, University of Michigan, Ann Arbor, MI 48109.* Accepted for publication June 10, 1981. *Present address: Pharmaceutical Research, Roche Laboratories, Hoffmann-La Roche Inc., Nutley, NJ 07110.

Abstract □ The influence of hydration on the permeability of stripped and scalded skins of hairless mice was investigated *in vitro* using water and *n*-alkanols as test permeants. Irrespective of pretreatment, the permeation rates of water, methanol, and ethanol were unaffected by aqueous immersion of skin sections in a diffusion cell, consistent with earlier data on unprocessed skins. The permeation rates of butanol and hexanol also were insensitive to hydration, differing from earlier studies on normal, intact skin in which both solutes' rates doubled after 10 hr of soaking. Following both pretreatments, the permeability of octanol declined over the first 5–10 hr of maceration, but remained invariant thereafter. The decline was most pronounced for the scalded skins. With untreated skin, octanol permeability initially increased and then declined before assuming a constant value. This study indicates that the barrier properties of the epidermis and dermis are not particularly sensitive to extended hydration except in the case of octanol. Scalding at 60° for 60 sec rapidly hydrates the skin, altering tissue permeability to about the same extent as a 10-hr (or longer) immersion in water at 37°. Octanol's unique hydration profile is explained by locating the origin of permeability decline in tissue beneath the horny exterior of the skin.

Keyphrases □ Permeability—of hairless mouse skin to water and *n*-alkanols after stripping and scalding □ Absorption, percutaneous—influence of stripping and scalding on permeability of water and *n*-alkanols, hairless mouse skin □ Hydration—alteration of permeability of stripped and scalded mouse skin to water and *n*-alkanols

It is known that the permeability of intact hairless mouse skin is altered by aqueous maceration, and that increases in permeation rates upon extended immersion of the skin in saline are a function of chemical structure for small, nonelectrolyte penetrants. Thus, the processes of hydration are complex, and probably involve more than one isolated phase of the skin membrane. A more thorough understanding of such hydration phenomena will add to the mechanistic understanding of the skin's barrier behavior.

Recently, effects of hydration on hairless mouse skin permeability were examined using water and *n*-alkanols as test permeants (1). These *in vitro* studies showed that hydration-induced permeability increases were a function of the penetrant lipophilicity. The permeabilities of the polar solutes, water, methanol, and ethanol, were not changed by hydration, while the permeabilities of the moderately lipophilic compounds, butanol and hexanol, asymptotically doubled in 10 hr of hydration. Permeation rates of the more lipophilic heptanol also increased to an asymptote, but only by ~50% in 10 hr. Octanol, the most lipophilic solute, showed an initial increase of ~50% in 5 hr, but then declined by ~25% by the 10th hr, undergoing a net increase in permeability of ~25%.

The skin hydration studies were extended to the Swiss mouse using water, methanol, ethanol, and butanol as permeants (2). In contrast to the hairless mouse skin results, water permeability increased up to 30 hr of hydration, and showed signs of leveling off between 30 and 43 hr. The permeabilities of methanol and ethanol also increased, but plateaued by 15 hr. Permeation rates of butanol increased over the first 15 hr and then declined almost linearly up to 48 hr. The hydration effect profile differences between the Swiss mouse and its hairless counterpart are

Standard curves constructed by plotting peak areas *versus* sample concentrations show good linearity in the concentration range for all substances, with correlation coefficients >0.9994 in all cases.

REFERENCES

(1) A. A. Fernandez, V. T. Noceda, and E. S. Carrera, *J. Pharm. Sci.*, **58,** 443 (1969).

(2) P. P. Ascione and G. P. Chrekian, *ibid.*, **59,** 1480 (1970).

(3) E. Addison and R. G. Clark, *J. Pharm. Pharmacol.*, **15,** 268 (1963).

(4) J. P. Sharma, G. D. Koritz, E. G. Perkins, and R. F. Bevill, *J. Pharm. Sci.*, **66,** 1319 (1977).

(5) A. G. Butterfield, D. W. Hughes, W. L. Wilson, and N. J. Pound, *ibid.*, **64,** 316 (1975).

(6) J. H. Knox and J. Jurand, *J. Chromatogr.*, **110,** 103 (1975).

(7) *Ibid.*, **186,** 763 (1979).

(8) J. H. Knox and A. Pryde, *J. Chromatogr.*, **112,** 171 (1975).

(9) A. P. De Leenheer and H. I. C. F. Nelis, *ibid.*, **140,** 293 (1977).

(10) T. D. Sokoloski, L. A. Mitscher, P. H. Yuen, J. V. Juvarkar, and B. Hoener, *J. Pharm. Sci.*, **66,** 1159 (1977).

(11) B. Hoener, T. D. Sokoloski, L. A. Mitscher, and L. Malspeis, *ibid.*, **63,** 1901 (1974).

(12) K. D. Schlecht and C. W. Frank, *ibid.*, **62,** 258 (1973).

(13) R. E. Majors, *Anal. Chem.*, **44,** 1722 (1972).

(14) C. R. Stephens, K. Murai, K. J. Brunings, and R. B. Woodward, *J. Am. Chem. Soc.*, **78,** 4155 (1956).

(15) J. Hermansson, *J. Chromatogr.*, **152,** 437 (1978).

(16) K.-G. Wahlund, *ibid.*, **115,** 411 (1975).

(17) A. Sokolowski and K-G. Wahlund, *ibid.*, **189,** 299 (1980).

(18) D. Westerlund and E. Erixon, *ibid.*, **185,** 593 (1979).

ACKNOWLEDGMENTS

The authors are grateful to Mr. S. Eriksson for skillful drawing of the figures and to Mr. B. Wiese for technical assistance.

Hydration and Percutaneous Absorption III: Influences of Stripping and Scalding on Hydration Alteration of the Permeability of Hairless Mouse Skin to Water and *n*-Alkanols

CHARANJIT R. BEHL *x, MICHAEL BARRETT, GORDON L. FLYNN, TAMIE KURIHARA, KENNETH A. WALTERS, OLIVIA G. GATMAITAN, NANCY HARPER, WILLIAM I. HIGUCHI, NORMAN F. H. HO, and CARL L. PIERSON

Received January 19, 1981, from the *College of Pharmacy and Medical School, University of Michigan, Ann Arbor, MI 48109.* Accepted for publication June 10, 1981. *Present address: Pharmaceutical Research, Roche Laboratories, Hoffmann-La Roche Inc., Nutley, NJ 07110.

Abstract □ The influence of hydration on the permeability of stripped and scalded skins of hairless mice was investigated *in vitro* using water and *n*-alkanols as test permeants. Irrespective of pretreatment, the permeation rates of water, methanol, and ethanol were unaffected by aqueous immersion of skin sections in a diffusion cell, consistent with earlier data on unprocessed skins. The permeation rates of butanol and hexanol also were insensitive to hydration, differing from earlier studies on normal, intact skin in which both solutes' rates doubled after 10 hr of soaking. Following both pretreatments, the permeability of octanol declined over the first 5–10 hr of maceration, but remained invariant thereafter. The decline was most pronounced for the scalded skins. With untreated skin, octanol permeability initially increased and then declined before assuming a constant value. This study indicates that the barrier properties of the epidermis and dermis are not particularly sensitive to extended hydration except in the case of octanol. Scalding at 60° for 60 sec rapidly hydrates the skin, altering tissue permeability to about the same extent as a 10-hr (or longer) immersion in water at 37°. Octanol's unique hydration profile is explained by locating the origin of permeability decline in tissue beneath the horny exterior of the skin.

Keyphrases □ Permeability—of hairless mouse skin to water and *n*-alkanols after stripping and scalding □ Absorption, percutaneous—influence of stripping and scalding on permeability of water and *n*-alkanols, hairless mouse skin □ Hydration—alteration of permeability of stripped and scalded mouse skin to water and *n*-alkanols

It is known that the permeability of intact hairless mouse skin is altered by aqueous maceration, and that increases in permeation rates upon extended immersion of the skin in saline are a function of chemical structure for small, nonelectrolyte penetrants. Thus, the processes of hydration are complex, and probably involve more than one isolated phase of the skin membrane. A more thorough understanding of such hydration phenomena will add to the mechanistic understanding of the skin's barrier behavior.

Recently, effects of hydration on hairless mouse skin permeability were examined using water and *n*-alkanols as test permeants (1). These *in vitro* studies showed that hydration-induced permeability increases were a function of the penetrant lipophilicity. The permeabilities of the polar solutes, water, methanol, and ethanol, were not changed by hydration, while the permeabilities of the moderately lipophilic compounds, butanol and hexanol, asymptotically doubled in 10 hr of hydration. Permeation rates of the more lipophilic heptanol also increased to an asymptote, but only by ~50% in 10 hr. Octanol, the most lipophilic solute, showed an initial increase of ~50% in 5 hr, but then declined by ~25% by the 10th hr, undergoing a net increase in permeability of ~25%.

The skin hydration studies were extended to the Swiss mouse using water, methanol, ethanol, and butanol as permeants (2). In contrast to the hairless mouse skin results, water permeability increased up to 30 hr of hydration, and showed signs of leveling off between 30 and 43 hr. The permeabilities of methanol and ethanol also increased, but plateaued by 15 hr. Permeation rates of butanol increased over the first 15 hr and then declined almost linearly up to 48 hr. The hydration effect profile differences between the Swiss mouse and its hairless counterpart are

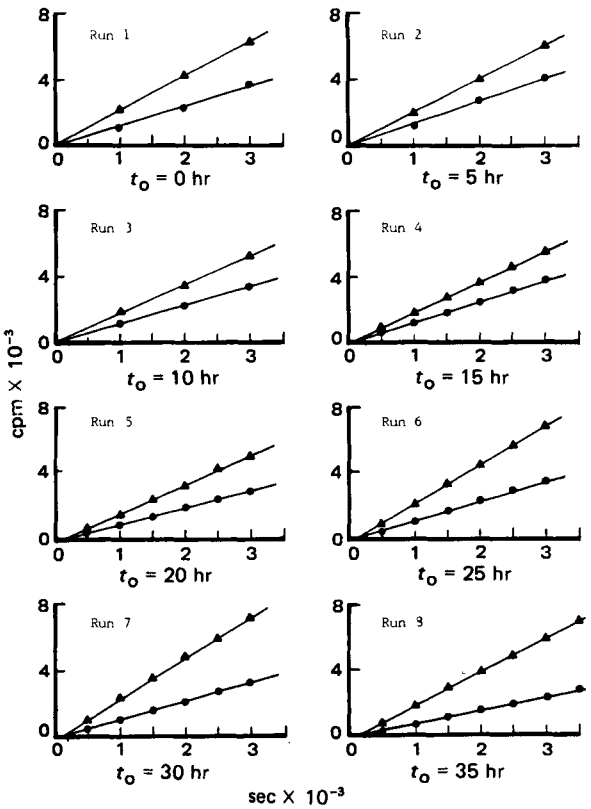

Figure 1—*Series of amount penetrated (cpm) versus time profiles for a set of eight sequential permeation runs on a single piece of stripped (25×) skin. The initial time of hydration for each run in terms of the total elapsed time (t_0) is indicated under each plot. This is one set of data for the methanol–butanol series. Key: ●, methanol; and ▲, butanol.*

apparently due to the abundant follicular presence in the Swiss species.

In both of the previous studies, unaltered full thickness skins consisting of the stratum corneum, the viable epidermis and the dermis were employed. It is well known that different strata of the skin control permeation rates of different solutes, depending on the relative oil/water partition coefficients of the permeants (3–5). Therefore, it is likely that different layers of the skin are responsible for the observed hydration-induced permeability increases or lack of increases. The present study was undertaken to study the influences of hydration on hairless mouse skins that were either scalded to alter thermally the properties of the stratum corneum (6) or stripped to completely remove the stratum corneum.

EXPERIMENTAL

Chemicals—[^{3}H]water[1], [^{3}H]methanol[1], [^{14}C]ethanol[2], [^{14}C]hexanol[2], [^{14}C]heptanol[2], and [^{14}C]octanol[2] were used as received. The radiochemicals were diluted into 0.9% sodium chloride irrigation medium[3] (saline) to prepare solutions for the permeation experiments. The final chemical concentrations in the diffusional medium were 10^{-4} *M* or lower.

Animals—Male hairless mice, SKH-hr^{-1} strain[4], were given free access to food and water. The mice were housed individually in shoebox cages to prevent them from damaging each other's skin; bedding was changed at least once a week. They were visually examined at least once a day to ascertain their general health.

[1] New England Nuclear, Boston, MA 02218.
[2] International Chemical and Nuclear Corp., Irvine, CA 92664.
[3] Abbott Laboratories, North Chicago, IL 60064.
[4] Skin Cancer Hospital, Temple University, Philadelphia, PA 19140.

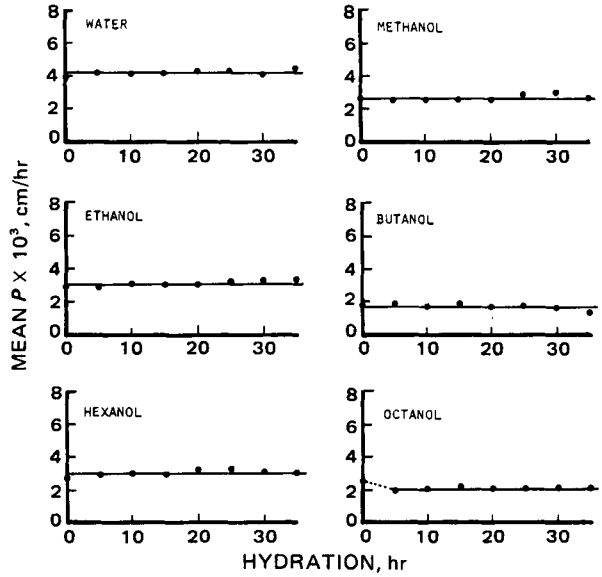

Figure 2—*Plots of average permeability coefficients (P) of the stripped (25×) skins versus hydration time for water, methanol, ethanol, butanol, hexanol, and octanol.*

Scalding Procedure—The dorsal surface of a mouse freshly sacrificed by spinal dislocation was scalded for 60 sec at 60° by immersing the dorsum in water contained in a jacketed apparatus through which water (60°) was perfused from a constant-temperature water bath (6). Both the abdominal and the dorsal surfaces were scalded before running the permeation experiments. Since scalding softens the stratum corneum, extra care was exercised in handling the skin. The skins were excised and mounted in diffusion cells within a few minutes after scalding, and the permeation experiment was started within 30 min.

Stripping Procedure—The abdominal surface of a mouse, freshly sacrificed by spinal dislocation, was stripped 25 times with adhesive tape (5, 7), using a fresh piece of tape each time. The abdominal surfaces were stripped with the adhesive tape because this site is easier to strip than the back. This choice did not affect the results because no site-to-site variations were observed in previous hydration-induced permeability alterations (1). Since removal of the stratum corneum causes the skin to shrink and fold over itself, making it difficult to handle and to excise from the animal, great care was observed in processing the stripped skins.

Radioisotopic Assay—The concentration of the radiolabeled permeant was determined by placing discrete samples in a cocktail[5] and assaying on a liquid scintillation counter[6]. Whenever possible, the technique of dual labels (1, 2, 4, 6–11) was used to economize the study and improve experimental precision.

Permeation Procedure—Two-compartment glass diffusion cells were employed to determine skin permeability. The mouse age was controlled (age 60 days) as much as possible, to avoid any age-related effects (4). The

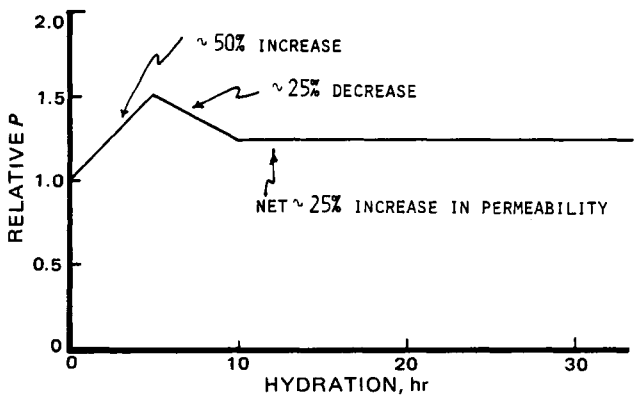

Figure 3—*Changes in octanol permeation rate as a function of hydration time. Data for this plot were abstracted from Ref. 1.*

[5] Aquasol, New England Nuclear, Boston, MA 02218.
[6] Beckman Liquid Scintillation Counter, Model LS 9000, Beckman Instruments, Fullerton, Calif.

Table I—Summary of Results of Stripped Abdominal Skins

Hydration, hr	$P \times 10^3$, cm/hr: Water[a] Mouse 1, 60 days; 31.0 g	Mouse 2, 60 days; 31.0 g	Mouse 3, 60 days; 26.0 g	Mean $P \times 10^3$ [b], cm/hr
~0	382.0	—	—	382.0
5	420.0	—	—	420.0
10	409.7	—	—	409.7
15	424.6	—	—	424.6
20	434.2	—	—	434.2
25	429.5	—	—	429.5
30	415.5	—	—	415.5
35	444.8	—	—	444.8
Mean ± *SD*				420.0 ± 18.9

Hydration, hr	Methanol: Mouse 1, 117 days; 37.0 g	Mouse 2, 117 days; 37.0 g	Mouse 3, 117 days; 35.0 g	Mean $P \times 10^3$ ± *SD*, cm/hr
~0	269.0	255.0	239.7	254.6 ± 14.7
5	254.8	258.0	238.8	250.5 ± 10.3
10	249.0	223.0	264.6	245.5 ± 21.0
15	274.0	247.1	251.7	257.6 ± 14.4
20	290.0	215.9	244.6	250.2 ± 37.4
25	[c]	289.4	291.9	290.7 ± 1.8
30	[c]	300.8	302.4	301.6 ± 1.1
35	[c]	277.1	259.7	268.4 ± 12.3
Mean ± *SD*				264.9 ± 20.7

Hydration, hr	$P \times 10^3$ cm/hr: Ethanol Mouse 1, 60 days; 31.0 g	Mouse 2, 60 days; 31.0 g	Mouse 3, 60 days; 26.0 g	Mean $P \times 10^3$ [b], ± *SD*, cm/hr
~0	276.5	303.3	261.2	280.3 ± 21.3
5	303.7	263.0	285.1	283.9 ± 20.4
10	317.5	344.6	273.0	311.7 ± 36.2
15	319.9	259.5	339.4	306.3 ± 41.7
20	328.8	259.4	336.2	308.1 ± 42.4
25	330.8	278.8	370.1	326.6 ± 45.8
30	333.9	291.5	370.1	331.8 ± 39.4
35	339.9	314.2	373.3	342.5 ± 29.6
Mean ± *SD*				311.4 ± 22.0

Hydration, hr	Butanol: Mouse 1, 117 days; 37.0 g	Mouse 2, 117 days; 37.0 g	Mouse 3, 117 days; 37.0 g	Mean $P \times 10^3$ ± *SD*, cm/hr
~0	181.0	188.0	189.7	186.2 ± 4.6
5	198.0	200.3	177.7	192.0 ± 12.4
10	190.0	155.0	188.2	177.7 ± 19.7
15	193.0	197.6	158.1	182.9 ± 21.6
20	195.0	147.5	153.1	165.2 ± 26.0
25	169.0	171.6	169.5	170.0 ± 1.4
30	157.0	154.7	156.3	156.0 ± 1.2
35	139.0	114.8	115.5	123.1 ± 13.8
Mean ± *SD*				169.1 ± 22.0

Hydration, hr	$P \times 10^3$ cm/hr: Hexanol Mouse 1, 60 days; 34.0 g	Mouse 2, 60 days; 25.0 g	Mouse 3, 60 days; 32.5 g	Mean $P \times 10^3$ [b], ± *SD*, cm/hr
~0	227.1	353.2	226.4	268.9 ± 73.0
5	205.1	411.0	262.2	292.8 ± 106.3
10	205.1	430.0	262.2	299.1 ± 116.9
15	219.8	417.8	223.4	287.0 ± 113.3
20	237.9	455.5	282.0	325.1 ± 115.0
25	258.1	436.0	273.4	322.6 ± 98.7
30	263.2	406.4	263.3	311.0 ± 82.6
35	261.0	411.7	255.5	309.4 ± 88.6
Mean ± *SD*				302.5 ± 19.6

Hydration, hr	Octanol: Mouse 1, 60 days; 35.0 g	Mouse 2, 60 days; 30.0 g	Mouse 3, 60 days; 27.0 g	Mean $P \times 10^3$ ± *SD*, cm/hr
0	244.4	216.0	283.7	248.0 ± 34.0
5	189.3	193.0	200.3	194.2 ± 5.6
10	230.9	188.9	194.1	204.6 ± 22.9
15	236.9	225.5	201.3	221.2 ± 18.2
20	231.1	195.6	195.0	207.2 ± 20.7
25	208.8	200.2	208.4	205.8 ± 4.9
30	224.2	207.8	198.5	210.2 ± 13.0
35	213.9	210.2	202.2	208.8 ± 6.0
Mean ± *SD*				207.4 ± 8.0

[a] Skins of Mouse 2 and Mouse 3 were damaged after ~5 hr of experiment. [b] The standard deviations represent mouse-to-mouse variability, not in the estimate of hydration-induced alterations (or lack of them). [c] The skins were damaged.

external medium of diffusion was normal saline. The half-cell contents were stirred at 150 rpm and all permeation experiments were carried out at 37°. The half-cell facing the stratum corneum was always the donor chamber and the half-cell facing the dermis was always the receiver chamber. Therefore, net diffusion was from the stratum corneum to the dermis side. Complete hydration profiles were obtained on each piece of skin by running six to nine sequential experiments, with thorough rinsing between runs (1).

Data Analysis—The data were plotted as receiver compartment concentration (in counts per minute) *versus* time. The permeability coefficients were calculated from (1):

$$P = \frac{V}{A}\frac{(dC/dt)}{\Delta C} \qquad \text{(Eq. 1)}$$

where:

P = the permeability coefficient (centimeters per hour)
A = the diffusional area (~0.6 cm^2)
ΔC = the concentration difference across the membrane, which was taken to be equal to the donor concentration (counts per minute)
V = the half-cell volume (1.4 ml)
dC/dt = the quasisteady-state slope (counts per minute per cubic centimeter per hour)

RESULTS

Figure 1 contains a representative set of eight subplots obtained in sequential permeation experiments carried out on one piece of skin over 35 hr using [^{3}H]methanol and [^{14}C]butanol as dual permeants. A linear relationship between the receiver concentration *versus* time was obtained, indicating a good approximation of steady-state transport conditions. This permeation behavior is consistent with that reported for the intact, unaltered skins of hairless (1) and Swiss (2) mice. Slopes of these linear plots were used to compute permeability coefficients.

Table I contains a summary of results for the stripped abdominal skins. Three mice were used for each of the permeants, and eight sequential permeation experiments were run on each skin.

Data from sequential runs performed on scalded skins were processed as indicated in Fig. 1. One of the experiments, the methanol/butanol set, was of long duration (>40 hr) and involved nine separate experiments on each piece of tissue spaced at 5-hr intervals. Table II contains a summary of results for the scalded skins.

Two skins, one abdominal and one dorsal, were employed for each of the permeants, and [^{3}H]methanol was used as a copermeant with all alkanols. The individual permeability coefficients of the abdominal and the dorsal skins are quite similar, indicating that the data are not a function of the anatomical site. This observation is consistent with the earlier studies where the abdominal and the dorsal permeabilities were found to converge beyond the age of ~50 days (4).

Since methanol was used as a reference permeant, it is possible to normalize the data for ethanol, butanol, hexanol, and octanol to methanol permeability at a given hydration time. This procedure levels out animal-to-animal variability and results in more precise data. The standard deviations associated with the average ratios are much smaller than those associated with the average permeability values (Table II).

DISCUSSION

In vitro diffusion through membranes from body tissues or from synthetic materials is one of the most general means of characterizing the physicochemical attributes of physiological and synthetic barriers. With

Table II—Summary of Results of Pre-scalded Skins

Hydration, hr	$P \times 10^3$, cm/hr: Abdominal	Dorsal	Abdominal	Dorsal	Average $P \times 10^3 \pm SD$, cm/hr:		Average Ratio $\pm SD$
	Methanol[a]		Ethanol[a]		Methanol	Ethanol	P_{c_2}/P_{c_1}
~0	3.7	3.8	3.1	3.1	3.8 ± 0.1	3.1 ± 0.0	0.8 ± 0.0
5	3.4	3.4	2.8	2.9	3.4 ± 0.0	2.9 ± 0.1	0.9 ± 0.1
10	3.7	4.0	3.1	3.2	3.9 ± 0.2	3.2 ± 0.1	0.8 ± 0.0
15	4.0	4.2	3.4	3.5	4.1 ± 0.1	3.5 ± 0.1	0.9 ± 0.1
20	4.1	4.4	3.2	3.4	4.3 ± 0.2	3.3 ± 0.1	0.8 ± 0.0
25	4.1	4.6	3.2	3.3	4.4 ± 0.4	3.3 ± 0.1	0.8 ± 0.0
Mean ± *SD*					4.0 ± 0.4	3.2 ± 0.2	0.8 ± 0.1
Hydration, hr	Methanol[b]		Butanol[b]		Methanol	Butanol	P_{c_4}/P_{c_1}
~0	3.0	2.6	9.7	11.9	2.8 ± 0.3	10.8 ± 1.6	3.9 ± 1.0
5	3.3	2.7	9.7	11.5	3.0 ± 0.4	10.6 ± 1.3	3.8 ± 1.2
10	3.1	2.8	10.4	9.5	3.0 ± 0.2	10.0 ± 0.6	3.4 ± 0.0
15	3.8	2.7	10.3	12.9	3.3 ± 0.8	11.6 ± 1.8	3.8 ± 1.5
20	3.2	2.9	10.1	13.1	3.1 ± 0.2	11.6 ± 2.1	3.9 ± 0.9
25	3.0	2.9	9.4	13.5	3.0 ± 0.1	11.5 ± 2.9	3.9 ± 1.1
30[c]	—	2.8	—	12.7	3.0 ± 0.3[d]	11.3 ± 2.0[d]	3.9 ± 1.1[d]
35[c]	—	2.8	—	12.9	3.0 ± 0.3[d]	11.3 ± 2.1[d]	3.9 ± 1.1[d]
40[c]	—	2.7	—	12.7	3.0 ± 0.4[d]	11.3 ± 2.0[d]	3.9 ± 1.1[d]
Mean ± *SD*					3.0 ± 0.1	11.1 ± 0.5	3.8 ± 0.2
Hydration, hr	Methanol[e]		Hexanol[e]		Methanol	Hexanol	P_{c_6}/P_{c_1}
~0	2.6	3.0	42.0	53.2	2.8 ± 0.3	47.6 ± 7.9	17.0 ± 1.1
5	2.2	2.6	35.2	43.3	2.4 ± 0.3	39.3 ± 5.7	16.4 ± 0.5
10	2.5	2.6	36.1	40.3	2.6 ± 0.1	38.2 ± 3.0	15.0 ± 0.8
15	2.6	2.7	37.3	45.3	2.7 ± 0.1	41.3 ± 5.7	15.7 ± 1.8
20	2.8	2.7	40.7	45.3	2.8 ± 0.1	43.0 ± 3.3	15.7 ± 1.6
25	2.8	2.7	38.7	46.0	2.8 ± 0.1	42.3 ± 5.2	15.4 ± 2.3
Mean ± *SD*					2.7 ± 0.2	42.0 ± 3.3	15.9 ± 0.7
Hydration, hr	$P \times 10^3$, cm/hr: Abdominal	Dorsal			Average $P \times 10^3 \pm SD$, cm/hr:		Average Ratio $\pm SD$
	Methanol[f]		Octanol[f]		Methanol	Octanol	P_{c_8}/P_{c_1}
0	2.7	2.1	129.6	94.0	2.4 ± 0.4	111.8 ± 25.1	46.4 ± 2.3
5	2.2	2.8	87.5	100.2	2.5 ± 0.4	93.9 ± 9.0	37.8 ± 2.8
10	1.8	2.2	68.3	76.2	2.0 ± 0.3	72.3 ± 5.6	36.3 ± 2.3
15	2.2	2.3	78.7	77.0	2.3 ± 0.1	77.9 ± 1.2	35.5 ± 1.9
20	2.1	2.6	75.5	70.7	2.4 ± 0.4	73.1 ± 3.4	31.6 ± 6.2
25	2.2	2.8	78.7	80.6	2.5 ± 0.4	79.7 ± 1.3	32.3 ± 4.9
30	1.8	2.9	72.6	91.9	2.4 ± 0.8	82.3 ± 13.6	36.0 ± 6.1
Mean ± *SD*					2.4 ± 0.2	77.1 ± 4.3[g]	34.3 ± 2.2[g]

[a] Mouse age, 77 days; mouse weight, 20 g. [b] Mouse age, 54 days; mouse weight, 19.5 g. [c] The abdominal skins were damaged. [d] The abdominal data at 0, 5, 10, 15, 20, and 25 hr of hydration were averaged and combined with the dorsal data at 30, 35, and 40 hr of hydration. [e] Mouse age, 102 days; mouse weight, 33.0 g. [f] Mouse age, 102 days; mouse weight, 31.5 g. [g] Averages of data at hydration times of 10, 15, 20, 25 and 30 hr.

a judicious choice of permeants, the mass transfer mechanisms of the membranes can be determined and related fundamentally to permeant chemical structure. However, all such research presumes the membranes in question to be physically stable over the experimental time frame. However, diffusional experiments are by their nature lengthy, and over the extended membrane contact time with usually liquid external media there is ample opportunity for solvation to modify basic membrane integrity. Therefore, the effects of solvation must be considered during the assessment of barrier properties.

In the case of biological membranes, the media bathing the tissue is usually aqueous and made osmotically physiological with salts. It is the influence of such aqueous solutions that must be assessed. Since biological membranes are polyphasic, with each distinct phase presumably having a unique hydration sensitivity, a full understanding of hydration phenomena promises to be of mechanistically interpretive value. Certain skin preparations such as tape-stripped skin may be useful for simulating the influences of abrasive and disease related damage on the permeability of skin. Thus, the stability of processed skins to solvation are also of interest.

Effect of Hydration on Permeability of Stripped Skin—The skin becomes exceedingly permeable as a result of the stripping procedure used, which effectively removes the entire stratum corneum. Table III contains a comparative list of the average permeability coefficients of normal skins (abstracted from earlier studies) and stripped skins. The stripping procedure made the skin most permeable to water; a more than 300-fold increase was noted. Both methanol and ethanol demonstrate about half as much enhancement.

As the permeants become more lipophilic, the ratio drops almost exponentially, indicating a declining role of the stratum corneum with increased lipoidal characteristics of the permeants. The permeability coefficients for the alkanols through the stripped skin decline by only a factor of two from methanol to octanol, in contrast to the systematically increasing permeability coefficients of normal skin. The former pattern is *prima facie* evidence that transport of these compounds through the dermis and residual epidermis does not involve a lipid/water partitioning step. This evidence reaffirms conclusions previously made by these authors and by Scheuplein and Blank (12).

With the possible exception of octanol, there does not appear to be any change in permeability of the stripped skin sections to water or the *n*-alkanols over >35 hr of hydration (Fig. 2). It was previously reported (1)

Table III—Permeabilities of Stripped and Unaltered Skins of Hairless Mice

Compound	$P \times 10^3$, cm/hr: Skin[a] Unaltered[b]	Stripped	Ratio, $P_{stripped}/P_{unaltered}$
Water	1.3 ± 0.2	420.0 ± 18.9	323.0
Methanol	2.0 ± 0.4	269.4 ± 25.2	134.7
Ethanol	2.1 ± 0.1	311.4 ± 22.0	148.3
Butanol	10.8 ± 2.2	169.1 ± 22.0	15.7
Hexanol	38.8 ± 15.6	302.5 ± 19.6	7.8
Octanol	97.8 ± 13.5	207.4 ± 8.0	2.1

[a] Hydrated skins. [b] Abstracted from Ref. 1.

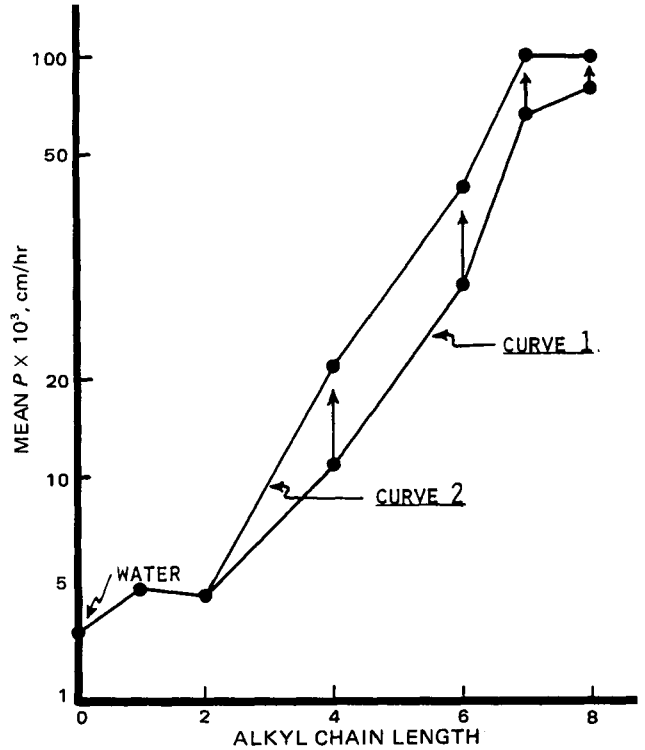

Figure 4—*Semilogarithmic plots of average permeability coefficients* versus *alkyl chain length for skins in their natural state of hydration (curve 1) and for skins which were exposed to saline in the diffusion cells for a minimum of 10 hr. Raw data for these plots were abstracted from Ref. 1.*

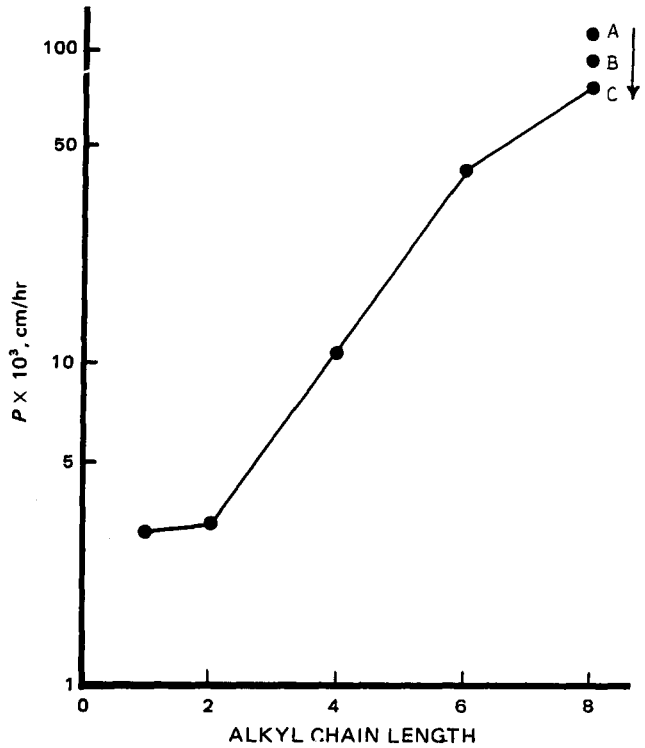

Figure 5—*Semilogarithmic plot of average permeability coefficients* (P *values*) versus *alkyl chain length for the scalded (60°; 60 sec) skins. Data for methanol, ethanol, butanol, and hexanol obtained at different times of hydration, were averaged. The individual permeabilities of octanol at ~0 and 5 hr of hydration are presented (points A and B, respectively). The remaining octanol data by hydration times of 10, 15, 20, 25, and 30 hr were averaged (point C).*

that the permeability coefficients of butanol and hexanol doubled over 10 hr of soaking. Considering the large increases in absolute permeability coefficients of the permeants caused by stripping and the hydration insensitivity of the membrane to their permeation after stipping, it appears that the effect of water with intact skin originates in the horny layer.

Because both butanol and hexanol increase exponentially on the log *P versus* alkyl chain length plot, it is evident that the effects are within the lipoid region of the stratum corneum. Whether they represent a physicochemical change in the diffusional medium or a physical rearrangement of the critical phase cannot be determined at this time. For the length of time they were carried out, the data for methanol are consistent with earlier studies where its permeation rate was found to be invariant in both abdominally and dorsally isolated dermis for hydration times of up to 800 hr (8).

The data for octanol may be interpreted differently. Its hydration–permeability profile, previously reported (1), is mechanistically revealing (Fig. 3). There is a 50% increase in permeation rates in the first 5 hr of hydration, and a 25% decrease by the 10th hr, followed by invariant permeability thereafter. To aid the discussion, data from previous hydration effect studies (1) were abstracted and are presented (Fig. 4) in terms of the alkyl chain profiles of the unhydrated skins (curve 1) and the hydrated skins (curve 2). Both curve 1 and curve 2 contain the following three segments: (*a*) a lower plateau evident for the polar solutes, water, methanol, and ethanol, signifying that their permeation occurs through some sort of highly polar, presumably aqueous pores present in the stratum corneum (4); (*b*) a steep rise in the permeability coefficients between ethanol and heptanol, which is linear when the data are obtained in the fully hydrated state (curve 2). [This segment demonstrates that the permeation process of these penetrants is controlled by their partitioning into the lipid regions of the stratum corneum (3, 4)]; and (*c*) the beginning of a second plateau near octanol, meaning that a third mechanism becomes important for the more hydrophobic compounds.

This mechanism has a permeation rate that is controlled by aqueous tissue resistance encountered in the viable epidermis and the dermis (3–5); *i.e.*, at an alkyl chain length of eight, the rate-controlling stratum changes from the horny layer to the viable epidermis and dermis. Based on this information and previous observations that octanol permeability increases somewhat with incremental stripping of the skin (7), it can be concluded that the control rate of octanol transport is significantly biphasic. Due to the wide difference in lipophilicity, it is reasonable that the stratum corneum and the dermis might influence the permeability of octanol (a transition compound) in an opposite manner, as a function of hydration time. Therefore, the initial increase in the permeability coefficients of octanol (Fig. 3) may be due to maceration of the stratum corneum. (Both competing processes occur simultaneously.)

If this argument is true, hydration of the stripped skin should slightly decrease its permeability to octanol. The hydration profile depicted in Fig. 2 indicates that this is probably the case. There seems to be some decrease in octanol permeability in the first 5 hr of hydration. This is less evident based on the stripped skin data alone but a statistically significant and similar effect is noted with scalded skin. It is curious that the other alkanols studied are not, as far as can be judged, similarly affected in stripped skin. At the present time, it is not possible to ascribe the ob-

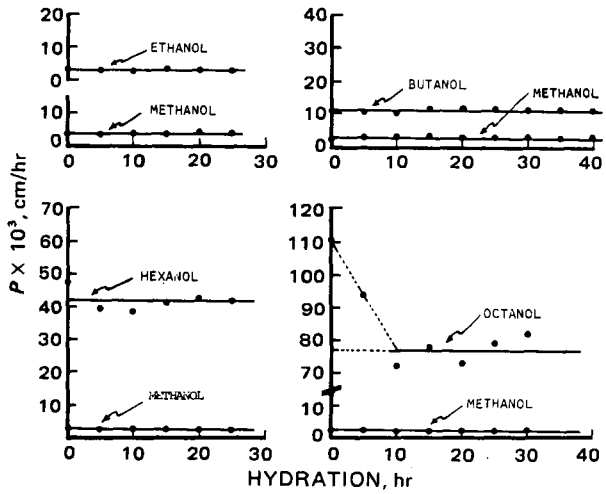

Figure 6—*Plots of average permeability coefficients* (P) *of the scalded (60°, 60 sec) skins* versus *time of hydration for methanol, ethanol, butanol, hexanol, and octanol. Methanol was used as a copermeant with all other alkanols to serve as a control solute.*

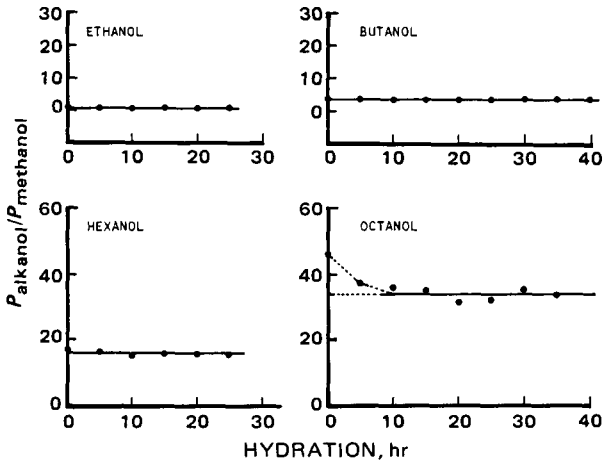

Figure 7—*Plots of normalized permeabilities (permeability of alkanol/permeability of methanol) of ethanol, butanol, hexanol, and octanol versus time of hydration.*

served octanol effect to any specific property of the molecule, *i.e.*, hydrophobicity or molecular size.

Effects of Hydration on Permeability of Scalded Skins—Figure 5 graphically illustrates the alkyl chain length profiles of the scalded skin permeabilities. Since no definite hydration–permeability trends are apparent through hexanol, data obtained at different hydration times were averaged for water, methanol, ethanol, butanol, and hexanol and these averages are plotted. Data for octanol were averaged only after 10 hr of hydration when its skin permeability coefficient was stabilized.

Octanol permeabilities at ~0 and 5 hr of hydration are also displayed in Fig. 5. A smooth sigmoidal curve is obtained when the points representing the fully equilibrated skin permeabilities are joined. This plot contains the three segments of curve 2 (Fig. 4) discussed previously, *i.e.*, the lower plateau, steep rise in the P values, and a second plateau. The absolute numbers plotted in Fig. 4 (curve 2) and in Fig. 5 are also, in agreement within ±50%. This close qualitative and quantitative parallelism between the two situations is significant and indicates that permeation in the normal, fully hydrated skin, and the scalded skin, occurs *via* the same mechanism.

There did not appear to be any significant increases or decreases caused by aqueous immersion in the permeability of scalded hairless mouse skin to the *n*-alkanols through hexanol. Neither the averages of the actual permeability coefficients (Fig. 6) nor their ratios to concurrently studied methanol permeability coefficients (Fig. 7) varied with hydration time. Water, methanol, and ethanol were previously shown to be unaffected by hydration in normal skin (1) but there were measurable hydration-associated increases in the permeabilities of butanol and hexanol (and heptanol). These were obliterated by scalding. The conclusion that scalding rapidly hydrates the skin was substantially reinforced by these extended studies. Moreover, the absolute permeability coefficients of the scalded skins were close in magnitude to those reported for fully hydrated normal skin. Therefore, 60-sec scalding not only rapidly hydrates the skin, but alters its permeability to about the same extent as does the 10 hr (or longer) aqueous soaking at 37°. This conclusion can aid in the interpretation of burned skin permeability data regardless of whether the skin is scalded (6, 9) or branded (10, 11).

Octanol appeared to behave differently. Its permeation rates gradually declined between 0 and 10 hr of hydration, and remained mostly unaltered thereafter. In view of the discussion and the theory of the switching-over of the rate-controlling mechanisms presented in the earlier section, it can be hypothesized that the observed decline probably was due to the effects of hydration on the epidermis–dermis. The data reported here further support the tentative interpretation presented to explain the up and down trends observed in octanol hydration–permeability profiles (1).

REFERENCES

(1) C. R. Behl, G. L. Flynn, T. Kurihara, N. Harper, W. M. Smith, W. I. Higuchi, N. F. H. Ho, and C. L. Pierson, *J. Invest. Dermatol.*, **75,** 346 (1980).

(2) C. R. Behl, M. Barrett, and G. L. Flynn, *J. Pharm. Sci.*, in press.

(3) H. H. Durrheim, G. L. Flynn, W. I. Higuchi, and C. R. Behl, *ibid.*, **69,** 781 (1980).

(4) C. R. Behl, G. L. Flynn, T. Kurihara, W. M. Smith, N. Harper, O. G. Gatmaitan, C. L. Pierson, W. I. Higuchi, and N. F. H. Ho, Basic Pharmaceutics Abstract 82, presented at the 126th Annual Meeting of the American Pharmaceutical Association, April 21–26, 1979, Anaheim, Calif.

(5) G. L. Flynn, H. H. Durrheim, and W. I. Higuchi, *J. Pharm. Sci.*, **70,** 52 (1981).

(6) C. R. Behl, G. L. Flynn, T. Kurihara, W. M. Smith, O. G. Gatmaitan, W. I. Higuchi, N. F. H. Ho., and C. L. Pierson, *J. Invest. Dermatol.*, **75,** 340 (1980).

(7) R. Meyer, C. R. Behl, and G. L. Flynn, Presented at the 128th American Pharmaceutical Association Annual Meeting, Basic Pharmaceutics Section, St. Louis, Mo., March 29, 1981.

(8) C. R. Behl, G. L. Flynn, W. M. Smith, T. Kurihara, K. A. Walters, O. G. Gatmaitan, W. I. Higuchi, C. L. Pierson, and N. F. H. Ho, Basic Pharmaceutics Abstract 53, presented at the 27th Annual Meeting of APhA Academy of Pharmaceutical Sciences, Kansas City, Mo., Nov. 1980.

(9) G. L. Flynn, C. R. Behl, K. A. Walters, O. G. Gatmaitan, A. Wittkowski, T. Kurihara, N. F. H. Ho, W. I. Higuchi, and C. L. Pierson, Basic Pharmaceutics Abstract #52, presented at the 27th Annual Meeting of APhA Academy of Pharmaceutical Sciences, Kansas City, Mo., November 1980.

(10) C. R. Behl, G. L. Flynn, M. Barrett, K. A. Walters, E. E. Linn, Z. Mohamed, T. Kurihara, and C. L. Pierson, Basic Pharmaceutics Abstract 80, presented at the 127th Annual Meeting of the American Pharmaceutical Association, Washington, D.C., April 1980.

(11) C. R. Behl, G. L. Flynn, M. Barrett, E. E. Linn, C. L. Pierson, W. I. Higuchi, and N. F. H. Ho, Basic Pharmaceutics Abstract 81, presented at the 127th Annual Meeting of the American Pharmaceutical Association, Washington, D.C., April, 1980.

(12) R. J. Scheuplein and I. H. Blank, *J. Invest. Dermatol.*, *60*, 286 (1971).

ACKNOWLEDGMENTS

Presented, in part, at the Basic Pharmaceutics Section, APhA Academy of Pharmaceutical Sciences, Washington, D.C. meeting, April 1980, and the APhA Academy of Pharmaceutical Sciences, Kansas City, Mo. meeting, November 1979.

Supported by National Institutes of Health Grant GM 24611.

Glucosylated Albumin and Its Influence on Salicylate Binding

K. A. MEREISH, H. ROSENBERG[x], and J. COBBY

Received March 27, 1981, from the *College of Pharmacy, University of Nebraska Medical Center, Omaha, NE 68105.* Accepted for publication June 16, 1981.

Abstract □ Human serum albumin was incubated at 37° in 0.01 *M* phosphate buffer (pH 7.4) under sterile conditions for up to 10 days with labeled [^{14}C]glucose (1–25 mg/ml). Glucose incorporated into albumin was calculated following extensive dialysis of the incubation mixture. The results indicated that glucose reacted with albumin by a nonenzymatic process involving Schiff base formation and Amadori rearrangement to a stable ketoamine derivative. The degree of glucosylation was dependent on the reaction time, glucose concentration, and pH. Glucosylation was enhanced when albumin was fatty acid free. Glucosylated albumin was separated from unmodified albumin by cation exchange chromatography on carboxymethylcellulose and quantitated colorimetrically with 2-thiobarbituric acid. Salicylate binding studies revealed that the glucosylated component had a decreased salicylate binding capacity accompanied by a reduction in the number of classes of binding sites.

Keyphrases □ Albumin, serum—effect of glucosylation on salicylate binding, human □ Glucosylation—human serum albumin, effect on salicylate binding □ Binding—salicylate, effect of glucosylation of human serum albumin

It is generally recognized that the major threat to life and function posed by diabetes mellitus is the insidious development of long-term complications such as atherosclerosis, microangiopathic vascular disease, and neuropathy (1, 2). Many investigators speculate that frequent lapses in diabetic control are associated with an increased incidence and rate of progression of the diabetic complications. Although the mechanism by which hyperglycemia may lead to these complications is unknown, recent attention has been focused on the nonenzymatic condensation of glucose with proteins to yield stable covalent adducts (3). Such nonenzymatic glucosylation could result in altered protein structure, function, stability, and immunological response (2).

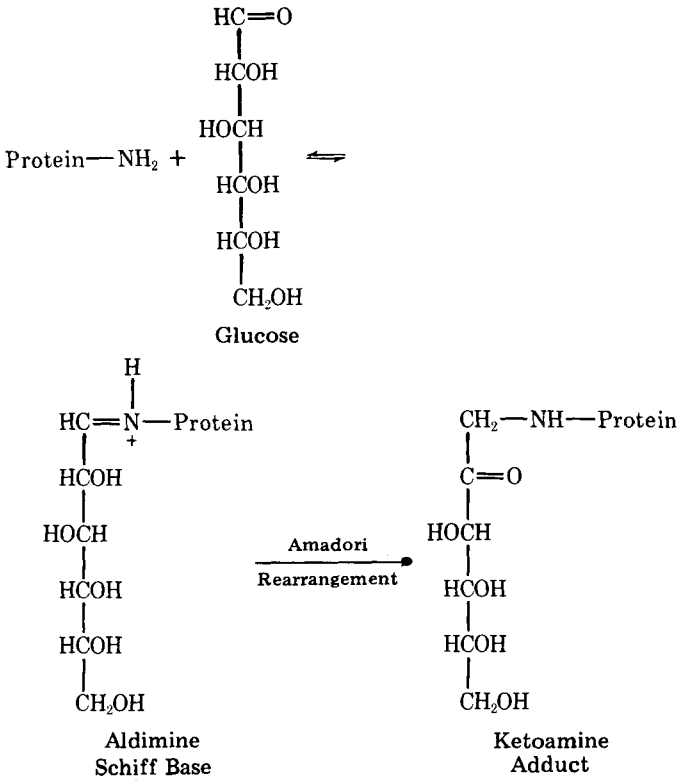

Scheme I—Proposed nonenzymatic reaction sequence involved in the formation of glycosylated proteins.

BACKGROUND

The demonstration of increased amounts of the glucosylated form of hemoglobin A (hemoglobin Alc) in diabetics was the first example of posttranslational protein modification correlated with elevated blood glucose concentrations (3). Evidence was recently published linking the development of corneal opalescence in diabetes with glucosylation of lens crystallins (4, 5). The nonenzymatic glucosylation of human serum proteins (6–8), insulin (9), and collagen (10) were also reported. Mechanistically, the nonenzymatic interaction of glucose and protein occurs by way of a ketoamine linkage involving the free amino group at the *N*-terminus or the ϵ-amino groups of lysine residues (Scheme I).

To establish a closer link between hyperglycemia and secondary complications of diabetes, experiments were initiated to compare the extent to which fatty acid-free albumin and albumin bound with fatty acids are susceptible to glucosylation *in vitro*. The hypothesis that enhanced rates of nonenzymatic protein glucosylation may contribute to the pathophysiology of diabetes is valid if such glucosylation is accompanied by altered protein function. To determine whether the glucosylation of albumin could result in altered protein function, salicylate binding to glucosylated, partially glucosylated, and nonglucosylated albumin was compared.

EXPERIMENTAL

Preparation of Glucosylated Albumin—Albumin[1] (Fraction V) solutions of 47.5 mg/ml were prepared in 0.01 *M* phosphate buffer, pH 7.4. Following the addition of D-[^{14}C]glucose[2] to final concentrations

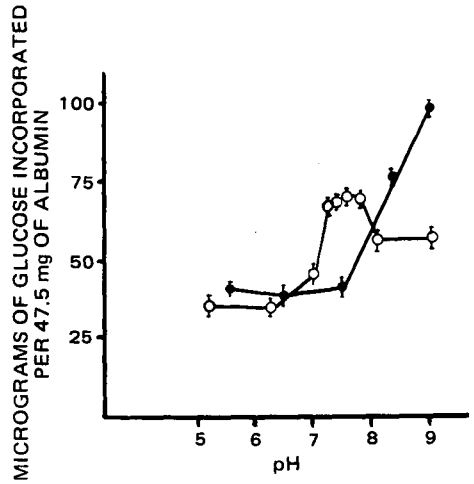

Figure 1—*Dependence of glucose incorporation into albumin on pH and composition of incubation buffer. Albumin (47.5 mg/ml) was incubated at 37° in 0.01 M phosphate buffer (○) and 0.1 M tromethamine buffer (●) containing 10 mg/ml (1 μCi) of [^{14}C]glucose. After 24 hr, samples with the indicated pH were dialyzed, lyophilized, and counted for radioactivity. Values are the means of four determinations ±SD.*

[1] Sigma Chemical Co., St. Louis, Mo.
[2] New England Nuclear, Boston, Mass.

0022-3549/82/0200-0235$01.00/0

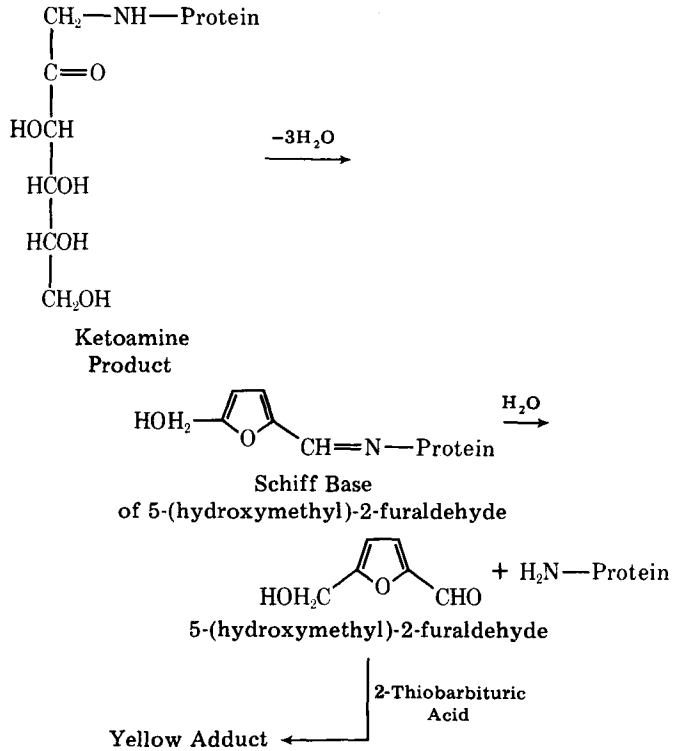

Scheme II—Detection of ketoamine adducts of proteins.

ranging from 1–25 mg/ml, the solutions were sterilized by ultrafiltration and incubated for up to 10 days in capped, sterile vials at 37°. At the end of each incubation period, 1-ml samples were removed and dialyzed against several 1000-fold volumes of distilled water for 24 hr at 4°. A portion of the dialysate was monitored for the presence of free glucose by the glucose oxidase method[3]. The remainder was lyophilized and counted for radioactivity. Incubated samples were compared to control samples which were prepared by dissolving identical quantities of albumin and [^{14}C]glucose in phosphate buffer and immediately dialyzing against distilled water for 24 hr.

Influence of pH on the Glucosylation of Albumin—Albumin (47.5 mg/ml) was incubated at 37° in 0.01 *M* phosphate buffer and 0.1 tromethamine buffer containing 10 mg/ml of D-[^{14}C]glucose (1 μCi). The pH of the reaction solutions was varied from 5.0–9.0. After 24 hr of incubation, the samples were dialyzed, lyophilized, and counted for radioactivity.

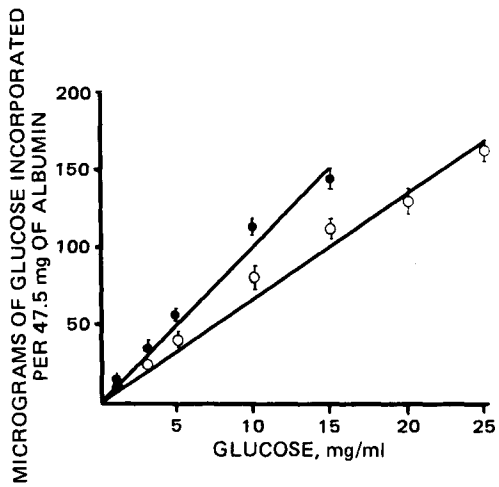

Figure 2—*Incorporation of glucose into albumin and fatty acid-free albumin as a function of glucose concentration. Albumin (○) and fatty acid-free albumin (●) were incubated at 37° in 0.01* M *phosphate buffer, pH 7.4, containing the indicated concentrations of [^{14}C]glucose. After 24 hr the incubated samples were dialyzed, lyophilized, and counted for radioactivity. Values are the means of four determinations* ±SD.

[3] Glucose oxidase kit, Sigma Chemical Co., St. Louis, Mo.

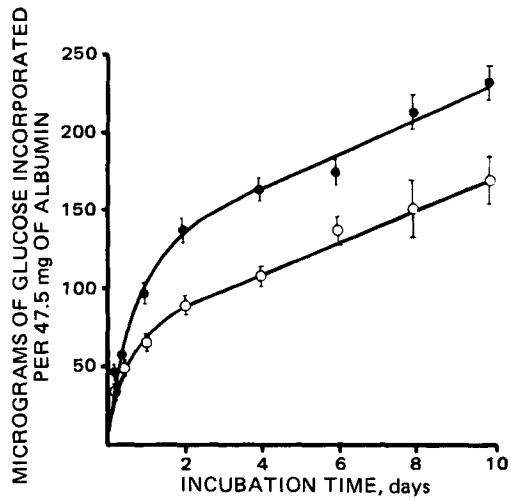

Figure 3—*Incorporation of glucose into albumin and fatty acid-free albumin as a function of incubation time. Albumin (○) and fatty acid-free albumin (●) were incubated at 37° in 0.01* M *phosphate buffer, pH 7.4, containing 10 mg/ml [^{14}C]glucose. Aliquots were removed at the indicated times, dialyzed, lyophilized, and counted for radioactivity. Values are the means of four determinations* ±SD.

Galactosylation of Albumin—Albumin (47.5 mg/ml) was incubated with 1 μCi of D-[6-^{3}H]galactose (1 mg/ml) in 0.01 *M* phosphate buffer, pH 7.4, at 37°. After 36 hr the reaction samples were treated as described previously.

Glucosylation of Albumin with D-[2-^{3}H] and D-[5-^{3}H]glucose—Albumin (47.5) mg/ml) was incubated with 1 μCi D-[2-^{3}H]glucose (10 mg/ml) in 0.01 *M* phosphate buffer, pH 7.4 at 37°. In an identical incubation, albumin was reacted with 1μCi D-[5-^{3}H]glucose (10 mg/ml). After 36 hr of incubation, the reaction samples were treated as described previously.

Thiobarbituric Acid Test for Glucosylated Protein—Glucosylated protein was detected using a modification of the thiobarbituric acid procedure of Flückiger and Winterhalter (11). This assay measures 5-(hydroxymethyl)-2-furaldehyde released upon hydrolysis of ketoamine adducts of proteins (Scheme II).

Samples of glucosylated albumin (5 mg) were placed in 15-ml culture tubes and dissolved in distilled water (1 ml). After the addition of 1.0 *N* oxalic acid (0.5 ml), the tubes were gently shaken, capped, and placed in a heating block at 100° for 5 hr. The tubes were subsequently cooled and

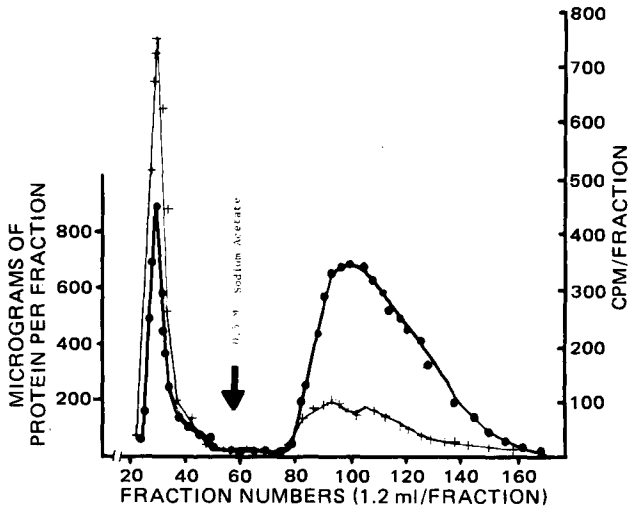

Figure 4—*Separation of human serum albumin into glucosylated and nonglucosylated components by chromatography on carboxymethylcellulose. Samples in 0.01* M *sodium acetate, pH 4.65, were applied to a column (17 × 2 cm) of carboxymethylcellulose and eluted using a 200-ml gradient of 0.01–0.5* M *sodium acetate, pH 4.65. Elution with 0.5* M *sodium acetate is indicated by the arrow.*

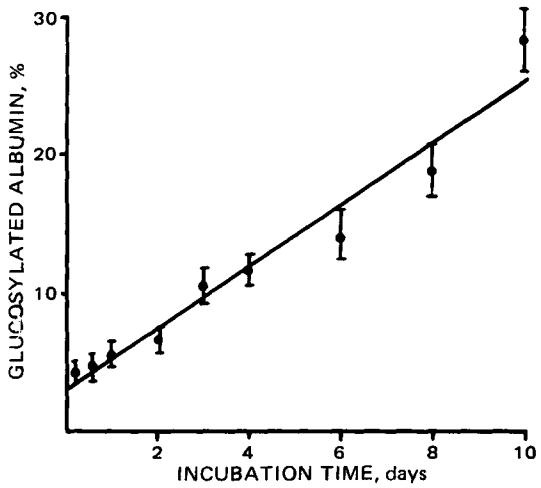

Figure 5—*Percentage glucosylated albumin as a function of incubation time. Albumin (47.5 mg/ml) was incubated at 37° in 0.01* M *phosphate buffer, pH 7.4, containing 10 mg/ml glucose. Aliquots were removed at the indicated times, dialyzed, lyophilized, and 10 mg was subjected to carboxymethylcellulose chromatography to separate the glucosylated fraction. Values are the means of four determinations* ±SD.

cold 40% trichloroacetic acid (0.25 ml) was added to precipitate the protein. The contents were then centrifuged at 2000×*g* for 10 min. An aliquot (1 ml) of the supernate was removed and added to a solution of 0.05 *M* aqueous 2-thiobarbituric acid (0.5 ml). After mixing and an incubation period of 15 min at 37°, the absorbance of each sample was measured at 443 nm.

Chromatographic Separation of Glucosylated and Nonglucosylated Albumin—Glucosylated and nonglucosylated albumin were separated using cation exchange chromatography on carboxymethylcellulose (6). Carboxymethylcellulose was suspended in 0.01 *M* sodium acetate buffer, pH 4.65, and packed in a 30 × 1.7-cm column to a length of 20 cm. Samples (50 mg) in the sodium acetate buffer were applied to the column and eluted with a 200-ml gradient of 0.01–0.5 *M* sodium acetate buffer, pH 4.65. Fractions (1 ml) were collected and assayed for protein content by an earlier method (12). An aliquot (0.1 ml) of each fraction was monitored for radioactivity.

Utilizing larger columns, 1-g quantities of glucosylated and nonglucosylated albumin were separated for use in the salicylate binding studies. Separated fractions were dialyzed against water for 24 hr and then lyophilized prior to their use in salicylate binding studies.

Salicylate Binding Capacity of Glucosylated and Nonglucosylated Albumin—The salicylate binding properties of nonglucosylated, 5–10% glucosylated, 25–30% glucosylated, and 100% glucosylated albumin were compared by the equilibrium dialysis method[4]. Albumin (47.5 mg/ml) was dialyzed against 1.2, 1.0, 0.8, 0.6, 0.5, 0.4, 0.25, and 0.125 mg/ml sodium salicylate. After 2.5 hr of dialysis, the solutions were acidified and extracted with 1 ml of chloroform. The concentration of salicylate in the chloroform extracts was assayed at 310 nm (13).

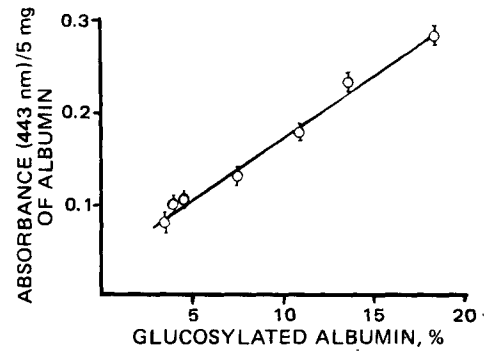

Figure 6—*Formation of 5-(hydroxymethyl)-2-furaldehyde from glucosylated albumin. Albumin (47.5 mg/ml) was incubated at 37° in 0.01* M *phosphate buffer, pH 7.4, containing 10 mg/ml of glucose. Aliquots were removed at different times, dialyzed and lyophilized. Ten milligrams was subjected to carboxymethylcellulose chromatography to determine the percentage of glucosylated albumin formed. Another 5 mg was subjected to the 2-thiobarbituric acid test. Values are the means of four determinations* ±SD.

[4] Dianorm multiple dialyzing system, Medizinisch-Wissenschaffliche Institute, Zurich, Switzerland.

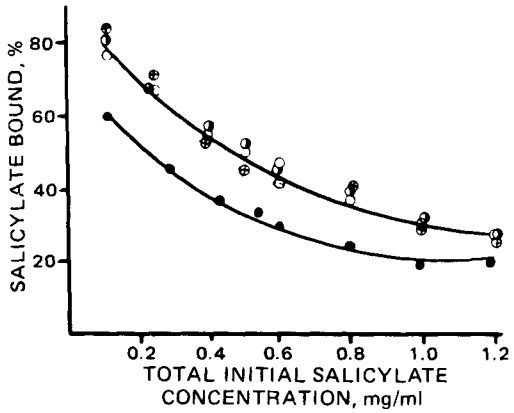

Figure 7—*Salicylate bound to nonglucosylated, partially glucosylated, and completely glucosylated human serum albumin. Percent salicylate bound to partially glucosylated (5–10%, ⊕; 25–35%, ◑), nonglucosylated (○), and completely glucosylated (●) human serum albumin.*

RESULTS AND DISCUSSION

Incubation of [^{14}C]glucose with human serum albumin at physiological pH, temperature, and albumin concentration resulted in the incorporation of labeled glucose into protein. This radioactivity was not removed by extensive dialysis against distilled water, suggesting a covalent linkage between glucose and albumin. To determine the nature of the linkage between glucose and albumin, the glucosylated albumin was treated with oxalic acid, resulting in the release of 5-(hydroxymethyl)-2-furaldehyde, which was detected by the characteristic colored adduct formed with 2-thiobarbituric acid (Scheme II). Formation of 5-(hydroxymethyl)-2-furaldehyde is characteristic of monosaccharides bound to protein by a ketoamine linkage (3).

Additional evidence for the ketoamine linkage was provided by studies in which albumin was separately incubated with 1 μCi of D-[2-^{3}H]glucose and D-[5-^{3}H]glucose having identical specific activities. In the case of glucose labeled in the 5-position, the glucosylated albumin had a specific activity of 670 cpm/mg of albumin. In contrast, albumin incubated with glucose labeled in the 2-position showed a specific activity of 267 cpm/mg of albumin. These results indicated loss of the label from the 2-position of the sugar, thus implying the occurrence of an Amadori rearrangement during the reaction. Obviously, glucosylation of albumin occurred by the same mechanism as in the formation of hemoglobin Alc; that is, glucose reacted with the amino groups of albumin to form aldimine linkages, which subsequently underwent an Amadori rearrangement to form the more stable ketoamine linkages (Scheme I).

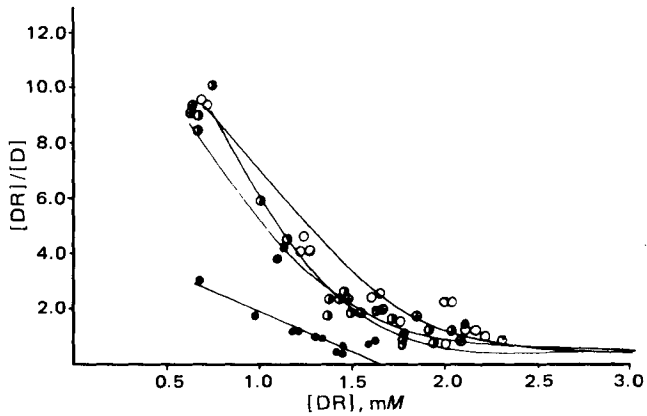

Figure 8—*Rosenthal plot for salicylate bound to nonglucosylated, partially glucosylated, and completely glucosylated human serum albumin. [DR], bound salicylate (*m*M); [D], unbound salicylate (*m*M). Key: ⊕, 5–10% glucosylated albumin; ◑, 25–30% glucosylated albumin; ○, nonglucosylated albumin; and ●, completely glucosylated albumin.*

The degree of nonenzymatic glucosylation of human serum albumin was dependent on the pH and composition of the incubation buffer (Fig. 1). The reaction between glucose and albumin most likely occurs by means of a nucleophilic attack by an unprotonated amino group on the glucose molecule. At physiological pH, few of the primary groups exist in the unprotonated state. This situation may account for the relatively slow rate of the glucosylation reaction.

At physiological pH and temperature, human serum albumin as well as fatty acid-free albumin incorporated labeled glucose in a concentration-dependent manner (Fig. 2). However, at every glucose concentration employed, glucose incorporation into fatty acid-free albumin was significantly greater than that incorporated by albumin bound with fatty acids. Perhaps common sites were utilized in the covalent binding of glucose and the ionic binding of fatty acids. In diabetes, the increased levels of albumin glucosylation may adversely affect fatty acid transport and, thus, may contribute to the pathogenesis of the disease.

The rate of glucose incorporation into albumin and fatty acid-free albumin was also dependent on the reaction time (Fig. 3). In both cases, during the initial 2 days of incubation the rate of glucose uptake was faster than in the succeeding days. This indicated that some sites on the albumin molecule were more easily glucosylated than others. The initial rate of glucose incorporation into fatty acid-free albumin was considerably faster than into albumin. This suggests that the process of defatting the albumin resulted in the release of additional sites that were capable of being glucosylated. However, the preparation of fatty acid-free albumin was accomplished at a pH below 3.0 for a period of not less than 8 hr (14, 15). This treatment may have caused the hydrolysis of glucose molecules already covalently bound to albumin, thereby releasing additional sites for glucosylation.

Nonenzymatic glycosylation of albumin by means of a ketoamine linkage can occur with hexoses other than glucose. Calculations based on the amount of radioactivity incorporated into albumin revealed that 9.95 μg of galactose and 8.8 μg of glucose were bound to albumin following identical incubations in which galactose and glucose (1 mg/ml) were reacted separately with albumin (47.5 mg/ml) under physiological conditions for 36 hr. This incorporation of galactose into albumin is not surprising in view of the reported glycosylation of hemoglobin with other sugars and sugar–phosphates (3).

Glucosylated albumin was readily separated from unmodified albumin by cation exchange chromatography on carboxymethylcellulose (Fig. 4). Prior to the *in vitro* incubation with glucose, albumin was found to be 5–10% glucosylated as determined by the chromatographic separation of the glucosylated from nonglucosylated components. In addition, the percentage of glucosylated albumin increased proportionally with time (Fig. 5).

Figure 6 illustrates the results obtained when glucosylated albumin is subjected to the 2-thiobarbituric acid test. It is evident that 5-(hydroxymethyl)-2-furaldehyde generation is directly dependent on the percentage of glucosylated albumin formed, suggesting the basis for a practical colorimetric assay to monitor the degree of diabetic control. Until now, only hemoglobin Alc has been considered as a diagnostic indicator for the long-term control of diabetes. Measurement of glucosylated albumin may be more advantageous, since the half-life for albumin is only 20 days (16) compared with 120 days for erythrocytes. Assuming that glucosylated and nonglucosylated albumin have the same turnover rate, one would expect fluctuations in blood glucose to be detected more sensitively by changes in glucosylated albumin than in glucosylated hemoglobin. Moreover, unlike hemoglobin Alc values, the amount of glucosylated albumin is not influenced by hemolytic disorders.

The results obtained from the salicylate binding studies indicate that the percentage of salicylate bound to totally glucosylated albumin is significantly lower than that for nonglucosylated or partially glucosylated albumin (Fig. 7). Analysis of the data by means of a Rosenthal plot (17) suggests that nonglucosylated and partially glucosylated albumin possess more than one class of binding sites, whereas 100% glucosylated albumin appears to possess only one class of binding sites (Fig. 8). The fact that the glucosylated component of albumin has a significantly decreased capacity to bind salicylate may have little significance for the diabetic, since the glucosylated fraction comprises a relatively small proportion of total albumin. Even at 25–30% glucosylation, there is no significant decrease in the salicylate binding capacity.

REFERENCES

(1) P. K. Bondy and P. Felig, *Med. Clin. North Am.*, **55,** 889 (1971).

(2) A. E. Renold, D. H. Mintz, W. A. Muller, and G. F. Cahill, in "The Metabolic Basis of Inherited Disease," J. B. Stanbury, J. B. Wyngaarden, and D. S. Fredrickson, Eds., 4th ed., McGraw-Hill, New York, N.Y., 1978, pp. 80–109.

(3) H. F. Bunn, K. H. Gabbay, and P. M. Gallop, *Science*, **200,** 21 (1978).

(4) V. J. Stevens, C. A. Rouzer, V. M. Monnier, and A. Cerami, *Proc. Natl. Acad. Sci. USA*, **75,** 2918 (1978).

(5) A. Cerami, V. J. Stevens, and V. M. Monnier, *Metabolism*, **28,** 431 (1979).

(6) J. F. Day, S. R. Thorpe, and J. W. Baynes, *J. Biol. Chem.*, **254,** 595 (1979).

(7) R. Dolhofer and O. H. Wieland, *FEBS Lett.*, **103,** 282 (1979).

(8) C. E. Guthrow, M. A. Morris, J. F. Day, S. R. Thorpe, and J. W. Baynes, *Proc. Natl. Acad. Sci. USA*, **76,** 4258 (1979).

(9) R. Dolhofer and O. H. Wieland, *FEBS Lett.*, **100,** 133 (1979).

(10) H. Rosenberg, J. B. Modrak, J. M. Hassing, W. A. Al-Turk, and S. J. Stohs, *Biochem. Biophys. Res. Commun.*, **91,** 498 (1979).

(11) R. Flückiger and K. H. Winterhalter, *FEBS Lett.*, **71,** 356 (1976).

(12) O. H. Lowry, N. J. Rosebrough, A. L. Farr, and R. J. Randall, *J. Biol. Chem.*, **193,** 256 (1971).

(13) "The National Formulary," XIII ed., Mack Publishing Co., Easton, Pa., 1970, pp. 66–68.

(14) D. S. Goodman, *Science*, **125,** 1296 (1957).

(15) E. J. Williams and J. F. Foster, *J. Am. Chem. Soc.*, **81,** 865 (1959).

(16) H. E. Schultzer and J. F. Heremans, "Molecular Biology of Human Proteins," Elsevier, New York, N.Y., 1966, pp. 450–517.

(17) R. F. Mais, S. Keresztes-Nagy, J. F. Zaroslinski, and Y. T. Oester, *J. Pharm. Sci.*, **63,** 1423 (1974).

Effect of Carboxylic Acids on Permeation of Chlorpromazine Through Dimethyl Polysiloxane Membrane

M. R. GASCO ˣ, M. TROTTA, and M. E. CARLOTTI

Received February 19, 1981, from the *Istituto di Chimica Farmaceutica e Tossicologica dell'Università di Torino, Corso Raffaello 31, Torino, Italy.* Accepted for publication July 2, 1981.

Abstract □ The effect of carboxylic acids on the permeation of chlorpromazine was investigated through a dimethyl polysiloxane nonpolar membrane. The permeability of the diffusate, at pH 5.8, increases considerably in the presence of carboxylic acids or phosphate, probably due to an ion-pair formation between the relative anions and chlorpromazine.

Keyphrases □ Chlorpromazine—permeation through a dimethyl polysiloxane membrane, effect of carboxylic acids □ Diffusion—chlorpromazine, through a dimethyl polysiloxane membrane, effect of carboxylic acids □ Carboxylic acids—effect on chlorpromazine diffusion through a dimethyl polysiloxane membrane

Previously reported studies (1–3) on the diffusion and permeation of drugs through polymeric membranes have contributed much to the knowledge of drug diffusion; a dimethyl polysiloxane polymer would be useful to investigate drug permeation through a membrane.

The permeation of molecules through a nonpolar membrane in the presence of other molecular species, has been studied previously (2, 4, 5). Many factors, including complex and ion-pair formation (6, 7), can influence the physiological availability of drugs. Nakano (8) studied the influence of a variety of substances, such as adsorbents and excipients, on the permeation of chlorpromazine through a model membrane. All the examined compounds, dissolved in citrate or dimethylglutarate buffers, decrease the permeation of the drug.

The present study examined the variation of chlorpromazine permeation through a nonpolar membrane in the presence of many acids to understand the effect of different organic anions on drug permeability. The selected carboxylic acids, the majority of them being physiological, had different structures.

EXPERIMENTAL

Materials—Nonreinforced dimethyl polysiloxane[1] sheeting in a labeled thickness of 5 ml (12.5×10^{-3} cm), thoroughly rinsed and treated as described previously (2), was used.

Chlorpromazine hydrochloride[2] as well as, citric[3], tartaric[3], acetic[3], glutaric[3], adipic[3], isocitric[4], oxaloacetic[4], malic[3], α-ketoglutaric[3], succinic[3], fumaric[3], and aconitic[4] acids were obtained commercially.

Instruments—A pH meter[5], a spectrophotometer[6], and a plate tensiometer[7] were used.

Determination of Critical Micelle Concentration (CMC)—The CMC of chlorpromazine in the presence of bicarboxylic acids was determined by measurement of surface tension with a plate tensiometer at 37 ± 0.5° in 50×10^{-3} *M* solution of acid. The ionic strength was maintained at 0.146 *M* by adding sodium chloride.

Diffusion Studies—The diffusion cell was constructed according to one used previously (9). The glass cell consisted of donor and receptor compartments (the volume of each compartment was 22 ml) and a membrane (available area was 3.14 cm^2) placed between them. Twenty-two milliliters of 0.01 *N* HCl was added to one arm and an equal volume of the test solution was placed in the other arm. The concentration of diffusible chlorpromazine in the desorbing solution was kept to a zero value to maintain diffused chlorpromazine in a dissociated form. The diffusing solutions were always corrected with sodium hydroxide or with hydrochloric acid, according to the desired pH, since preliminary experiments showed that phosphate and carboxylate anions can change drug permeation considerably. All solutions were warmed in a jacketed container maintained at 37 ± 0.1°. The content of each compartment was rotated by a magnet attached to an electric motor; the rotating speed was ~300 rpm.

Analytical Methods—At scheduled times an aliquot (0.5 ml) of the receptor solution was pipetted out for UV determination, and the same volume of 0.01 *N* HCl was added to the receptor compartment to replace the reduced volume. The 0.5-ml aliquot of the desorbing solution was transferred into a volumetric flask, and 4.5 ml of water was added. The drug concentrations were determined spectrophotometrically at 254 nm (log ε 4.49) for more diluted solutions and at 305 nm (log ε 3.63) for more concentrated solutions, or when additives interfered with the measurement at 254 nm.

Determination of the Apparent Diffusion Constant—Equation 1, derived by Garrett and Chemburkar (1) for a steady-state diffusion, was used to obtain the apparent diffusion constant *D*:

$$D = \frac{C_1 X V}{t C_2 S} \qquad \text{(Eq. 1)}$$

where C_1 is the concentration of diffusate in the desorbing solution, X is the thickness of the membrane, S is the available area of membrane, V is the volume of the desorbing solution, and C_2 is the concentration of the diffusate.

Diffusion Studies with Increasing Phosphate Concentration—Solutions at pH 5.8 with 2×10^{-3} *M* chlorpromazine and increasing phosphate concentrations ($1–70 \times 10^{-3}$ *M*) were prepared. The steady-state diffusion of chlorpromazine through the membrane was studied at 37° (Fig. 1).

Diffusion Studies of Chlorpromazine at Various pH—The solutions of chlorpromazine were kept at a concentration of 2×10^{-3} *M* when the pH range was within 3.5–6.0 and at a concentration of 5×10^{-4} *M* when the pH was >6.0. The required pH was obtained with hydrochloric acid or sodium hydroxide. The steady-state diffusion of chlorpromazine from these solutions through a 5-ml thick dimethyl polysiloxane membrane into 22 ml of 0.01 *N* HCl was studied at 37°. The pH values of diffusing solutions were noted before and after the experiments and were unchanged. The samples were removed at intervals of 20 min over a 2-hr period (Fig. 2, curve a).

In another series of tests, the effect of phosphate on the steady-state diffusion of chlorpromazine was studied at different pH. Diffusing 2 ×

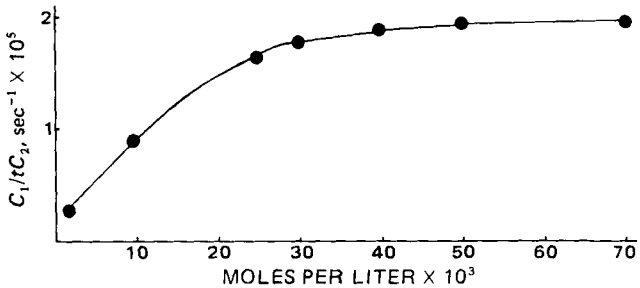

Figure 1—*Specific concentration rate increase of chlorpromazine (in the presence of phosphate) through a membrane into 0.01* M *HCl solution* versus *phosphate concentration.*

[1] Silastic, Dow Corning.
[2] Rhone-Poulenc.
[3] Merck.
[4] Fluka.
[5] Orion model 701/A.
[6] Perkin-Elmer EPS-3T.
[7] Dognon Abribat.

0022-3549/82/0200-0239$01.00/0

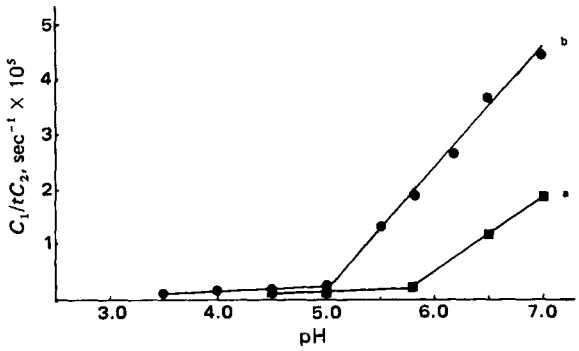

Figure 2—*Specific concentration rate of chlorpromazine through a membrane into 0.01 M HCl desorbing solution at 37° versus the pH of the diffusing drug solution. Key: a, without phosphate; and b, with a phosphate concentration 25 times the molarity of chlorpromazine.*

10^{-3} *M* chlorpromazine solutions in the pH range 3.5–6.0 and 5×10^{-4} *M* at pH >6.0, each containing phosphate concentration 25 times the molarity of the drug, were prepared (Fig. 2, curve b) and examined.

Diffusion Studies of Chlorpromazine in the Presence of Carboxylates—Experiments relative to the permeation of chlorpromazine in the presence of carboxylates were carried out at pH 5.8 and 37°. The diffusing solutions contained $1–3 \times 10^{-3}$ *M* of chlorpromazine and a carboxylate concentration 25 times the molarity of the drug.

RESULTS AND DISCUSSION

Effect of Phosphate on the Diffusion Rate of Chlorpromazine—The rate of steady-state diffusion through dimethyl polysiloxane membranes of an almost constant concentration (C_2) of chlorpromazine increases with the increasing phosphate concentration (Fig. 1). The specific diffusion rate of chlorpromazine is invariant at an acid concentration 21 times higher than the molarity of the drug. The permeation increase could be ascribed to ion-pair formation between chlorpromazine and the phosphate anions. An ion-pair interaction between dialkylaminoalkylphenothiazines and pteridines was also verified (10). The same interaction was proved between phosphate and antidepressive tricyclic drugs (11).

These results show that it is impossible to study the influence of a carboxylic anion on the permeability of chlorpromazine in the presence of other anions (such as phosphate). Therefore, all diffusion experiments were carried out without buffering the solutions, but using only hydrochloric acid or sodium hydroxide to adjust the pH.

Effect of pH on the Diffusion Rates—The diffusion of chlorpromazine varies according to pH. As shown by Fig. 2, curve a, chlorpromazine diffusion is very low at low pH values, because with a pKa of 9.3 (12), it is almost completely ionized. As pH increases, the chlorpromazine diffusion rate also increases, owing to the formation of undissociated hydrochloride. Figure 2, curve b, shows that the specific diffusion rates of chlorpromazine, in the presence of a constant excess of phosphate in the pH 5.5–7.0 range, are higher than those obtained using only the drug as a consequence of the formation of an ion-pair.

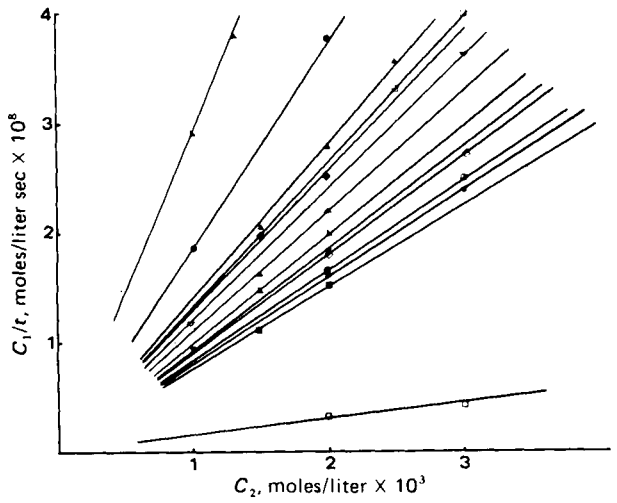

Figure 3—*Rates (C_1/t) of concentration increase in 22 ml of 0.01 N HCl desorbing solution versus chlorpromazine solution concentrations in the presence of carboxylic acid at a concentration 25 times the molarity of the drug. Key: □, none; ■, aconitic; ★, adipic; △, malic; ○, isocitric; ◇, malonic; ▼, fumaric; ◺, tartaric; ▲, glutaric; ▽, citric; ◆, α-ketoglutaric; □, acetic; ◢, succinic; ●, phosphoric; and ◭, oxaloacetic acids.*

Table I—Apparent Diffusion Constants of Chlorpromazine through a Dimethyl Polysiloxane Membrane in the Presence of Various Acids at a Concentration 25 Times Higher than That of the Drug at 37°

Acid	C_1/tC_2[a] ×10^5, sec^{-1}	Apparent Diffusion Constant $D \times 10^{10}$, liter cm/sec
None	0.15	1.31
Aconitic	0.74	6.48
Adipic	0.80	7.01
Malic	0.83	7.25
Isocitric	0.84	7.35
Malonic	0.92	8.05
Fumaric	0.93	8.14
Tartaric	1.00	8.75
Glutaric	1.10	9.62
Citric	1.13	9.89
α-Ketoglutaric	1.28	11.21
Acetic	1.34	11.73
Succinic	1.38	12.08
Phosphoric	1.91	16.72
Oxaloacetic	2.91	25.42

[a] Specific rate of concentration increase of desorbing solution.

Effect of Carboxylates on Rate Diffusion of Chlorpromazine—Since the rate of steady-state diffusion of an almost constant concentration (C_2) of chlorpromazine increased in the presence of oxaloacetic acid, the permeation rate of chlorpromazine was determined in the presence of other carboxylic acids. The linear dependence of the diffusion rates for the same membrane area, thickness, and volume of the diffusing solution, showed that rate diffusion through the membrane was directly proportional to the concentration of the diffusing drug. The lag times are negligible.

Rates of chlorpromazine concentration increase in 22 ml of 0.01 *N* HCl desorbing solution, C_1/t, are shown in Fig. 3 as a function of the respective concentration C_2 of the drug in the diffusing solution.

Apparent diffusion constants (D) were computed from the specific rates and are summarized in Table I. From D values it can be observed that the effect of permeation varies among the carboxylic acids. The apparent diffusion constant (D) depended on the acid concentrations up to a maximum of 21 times that of the drug and afterward remained invariant for all examined solutions where the acid concentration was 25 times higher than that of the drug.

The difference in the drug permeability in the presence of acids could also be explained by an ion-pair formation, probably dependent on D for its stability. To understand the behavior of the acids, the apparent diffusion constants of chlorpromazine in the presence of bicarboxylic acids were plotted against the chlorpromazine critical micelle concentration (CMC), determined in the presence of a fixed concentration of the same

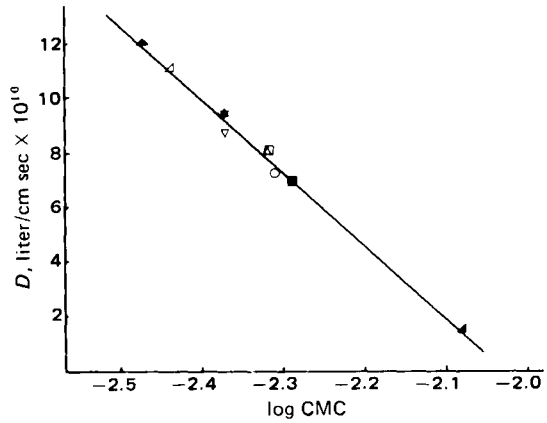

Figure 4—*Apparent diffusion constant D of chlorpromazine into 0.01 N HCl desorbing solution in the presence of bicarboxylic acids versus log CMC of chlorpromazine determined in 50 × 10^{-3} M solution of the same acid (μ = 0.146 M). Key: ◢, sodium chloride; ■, adipic; ○, malic; □, malonic; △, fumaric; ▽, tartaric; ★, glutaric; ◺, oxoglutaric; and ▲, succinic acids.*

acid. The CMC describes the lipophilicity of amphiphilic substances (13); the CMC value of chlorpromazine in the presence of acid could be an indirect measure of the lipophilicity of the ion-pair. Figure 4 shows an almost linear correlation between D and the CMC for the different bicarboxylic acids.

Chlorpromazine was selected for this study since it is representative of many tricyclic drugs and its behavior toward carboxylic acids may be important in GI absorption. Ion-pair formation between chlorpromazine and dietary carboxylic acids (such as citric, tartaric, and acetic acid) would give a favorable absorption in GI lumen. Furthermore, these findings could be useful for the development of dosage forms. It was shown (14) that certain drugs can be absorbed in their undissociated state, either directly or by ion-pair or complex formation. The behavior of chlorpromazine in humans might also be ascribed to the interactions of the drug with some of the physiological acids studied.

REFERENCES

(1) E. R. Garrett and P. B. Chemburkar, *J. Pharm. Sci.*, **57**, 949 (1968).

(2) M. Nakano and N. K. Patel, *ibid.*, **59**, 77 (1970).

(3) G. L. Flynn and J. Roseman, *ibid.*, **60**, 1788 (1971).

(4) R. H. Reuning and G. J. Levy, *ibid.*, **58**, 79 (1969).

(5) T. R. Bates, J. Galownia, and W. H. Johns, *Chem. Pharm. Bull.*, **18**, 656 (1970).

(6) G. Levy and E. J. Mroszczak, *J. Pharm. Sci.*, **57**, 235 (1968).

(7) T. Higuchi, A. Michaelis, and A. Hurwitz, *Anal. Chem.*, **39**, 974 (1967).

(8) M. Nakano, *J. Pharm. Sci.*, **60**, 571 (1971).

(9) K. Juni, M. Nakano, and T. Arita, *Chem. Pharm. Bull.*, **25**, 2807 (1977).

(10) M. R. Gasco, M. E. Carlotti, and M. Trotta, *Pharm. Acta Helv.*, **56**, 55 (1981).

(11) A. Tilly, *Acta Pharm. Suec.*, **12**, 89 (1975).

(12) A. L. Green, *J. Pharm. Pharmacol.*, **19**, 89 (1966).

(13) E. Tomlinson, S. S. Davis, and G. I. Mukhayer, in "Solution Chemistry of Surfactants," vol. 2, Mittal, Ed. 1980, pp. 889.

(14) M. J. Cho, and R. Schnabel, *J. Pharm. Sci.*, **64**, 1894 (1975).

Effect of Albumin Conformation on the Binding of Phenylbutazone and Oxyphenbutazone to Human Serum Albumin

A. ABD ELBARY*, J. J. VALLNER ˣ, and C. W. WHITWORTH

Received March 9, 1981, from the *School of Pharmacy, University of Georgia, Athens, GA 30602.* Accepted for publication June 29, 1981. *Present address: Faculty of Pharmacy, Cairo University, Cairo, Egypt.

Abstract □ The binding of phenylbutazone (I) and oxyphenbutazone (II) to human serum albumin over pH 6.9–9.3 was studied by difference spectrophotometry and equilibrium dialysis. At each pH tested, there was higher binding affinity of I to human serum albumin than II. Equilibrium dialysis showed that over the pH 7–8.2 range both agents had a single high-affinity site and several sites of lower affinity, with the highest binding constant and number of binding sites at pH 7.4 for both I and II. Both techniques showed that the affinity of both drugs to albumin was higher for the neutral form than for the basic form and this transition occurred in both cases around the neutral region (7–7.4). Both the ionized and unionized forms of I and II participated in the binding. In the neutral region, magnesium ion increased the affinity of both drugs to albumin while chloride ion decreased it slightly.

Keyphrases □ Phenylbutazone—effect of albumin conformation on binding to human serum albumin □ Oxyphenbutazone—effect of albumin conformation on binding to human serum albumin □ Albumin, human serum—effect of conformation on binding of phenylbutazone and oxyphenbutazone □ Binding—of phenylbutazone and oxyphenbutazone, effect of albumin conformation, human serum albumin

Drug–protein binding studies are important for prediction of drug dynamics in the body (1). The affinity of such interaction can possibly be used to correlate therapeutic and toxicological effects, as well as drug distribution and excretion. Most *in vitro* drug–protein interaction studies are conducted in isotonic pH 7.4 buffer. Data reduction in terms of binding constants assumes that for a partially ionized drug each species is bound with equivalent affinity (2).

It was reported (3) that conformational changes occur in serum albumin over pH 6–9. Zurawski and Foster (4) established that two conformational states exist in bovine serum albumin over this pH region. They called the form at neutral pH (pH 6–7) the "N" form and the form at higher pH (around pH 9) the "B" (base) form. Thus, the conformational change that occurs is the N to B or B to N transition. It was recently shown (5–7) that the same conformational change occurs in human serum albumin over pH 6–9. The N to B transition is seemingly dependent on pH but may also occur to some extent with ionic strength of the buffer and buffer ion composition. Calcium ion and chloride ion affect this transition (5–10) as well as the binding of drug to the protein.

BACKGROUND

While the macromolecule conformation changes with varying pH, ionization of the drug may also occur over such a pH range. A method was presented recently (2) to distinguish which species of a partially ionized acidic or basic drug bind to the protein and to enable determination of the binding site constant (3) for the interaction. In addition, this method aids in the detection of significant changes in the protein binding site that may result from pH perturbation. Since the blood pH in patients may vary between 6.8 and 7.8 (11), significant changes in drug binding to albumin or other plasma proteins could take place with a change in blood or local change in organ (*e.g.*, liver) pH. This pH range could not be predicted in any one individual; at best these pH differences usually would be only a few tenths of a pH unit (*i.e.*, respiratory acidosis or alkalosis).

The present study used equilibrium dialysis and UV difference spectroscopy to investigate the effect of albumin conformational state on the binding of phenylbutazone and oxyphenbutazone to human serum albumin at various pH values.

EXPERIMENTAL

Materials—The human serum albumin used was previously investigated for purity[1] (12). Phenylbutazone (I) and its metabolite oxyphen-

[1] Armour Pharmaceutical Co., Kankakee, Ill.

0022-3549/82/0200-0241$01.00/0

acid. The CMC describes the lipophilicity of amphiphilic substances (13); the CMC value of chlorpromazine in the presence of acid could be an indirect measure of the lipophilicity of the ion-pair. Figure 4 shows an almost linear correlation between D and the CMC for the different bicarboxylic acids.

Chlorpromazine was selected for this study since it is representative of many tricyclic drugs and its behavior toward carboxylic acids may be important in GI absorption. Ion-pair formation between chlorpromazine and dietary carboxylic acids (such as citric, tartaric, and acetic acid) would give a favorable absorption in GI lumen. Furthermore, these findings could be useful for the development of dosage forms. It was shown (14) that certain drugs can be absorbed in their undissociated state, either directly or by ion-pair or complex formation. The behavior of chlorpromazine in humans might also be ascribed to the interactions of the drug with some of the physiological acids studied.

REFERENCES

(1) E. R. Garrett and P. B. Chemburkar, *J. Pharm. Sci.*, **57**, 949 (1968).

(2) M. Nakano and N. K. Patel, *ibid.*, **59**, 77 (1970).

(3) G. L. Flynn and J. Roseman, *ibid.*, **60**, 1788 (1971).

(4) R. H. Reuning and G. J. Levy, *ibid.*, **58**, 79 (1969).

(5) T. R. Bates, J. Galownia, and W. H. Johns, *Chem. Pharm. Bull.*, **18**, 656 (1970).

(6) G. Levy and E. J. Mroszczak, *J. Pharm. Sci.*, **57**, 235 (1968).

(7) T. Higuchi, A. Michaelis, and A. Hurwitz, *Anal. Chem.*, **39**, 974 (1967).

(8) M. Nakano, *J. Pharm. Sci.*, **60**, 571 (1971).

(9) K. Juni, M. Nakano, and T. Arita, *Chem. Pharm. Bull.*, **25**, 2807 (1977).

(10) M. R. Gasco, M. E. Carlotti, and M. Trotta, *Pharm. Acta Helv.*, **56**, 55 (1981).

(11) A. Tilly, *Acta Pharm. Suec.*, **12**, 89 (1975).

(12) A. L. Green, *J. Pharm. Pharmacol.*, **19**, 89 (1966).

(13) E. Tomlinson, S. S. Davis, and G. I. Mukhayer, in "Solution Chemistry of Surfactants," vol. 2, Mittal, Ed. 1980, pp. 889.

(14) M. J. Cho, and R. Schnabel, *J. Pharm. Sci.*, **64**, 1894 (1975).

Effect of Albumin Conformation on the Binding of Phenylbutazone and Oxyphenbutazone to Human Serum Albumin

A. ABD ELBARY*, J. J. VALLNER ˣ, and C. W. WHITWORTH

Received March 9, 1981, from the *School of Pharmacy, University of Georgia, Athens, GA 30602.* Accepted for publication June 29, 1981. *Present address: Faculty of Pharmacy, Cairo University, Cairo, Egypt.

Abstract □ The binding of phenylbutazone (I) and oxyphenbutazone (II) to human serum albumin over pH 6.9–9.3 was studied by difference spectrophotometry and equilibrium dialysis. At each pH tested, there was higher binding affinity of I to human serum albumin than II. Equilibrium dialysis showed that over the pH 7–8.2 range both agents had a single high-affinity site and several sites of lower affinity, with the highest binding constant and number of binding sites at pH 7.4 for both I and II. Both techniques showed that the affinity of both drugs to albumin was higher for the neutral form than for the basic form and this transition occurred in both cases around the neutral region (7–7.4). Both the ionized and unionized forms of I and II participated in the binding. In the neutral region, magnesium ion increased the affinity of both drugs to albumin while chloride ion decreased it slightly.

Keyphrases □ Phenylbutazone—effect of albumin conformation on binding to human serum albumin □ Oxyphenbutazone—effect of albumin conformation on binding to human serum albumin □ Albumin, human serum—effect of conformation on binding of phenylbutazone and oxyphenbutazone □ Binding—of phenylbutazone and oxyphenbutazone, effect of albumin conformation, human serum albumin

Drug–protein binding studies are important for prediction of drug dynamics in the body (1). The affinity of such interaction can possibly be used to correlate therapeutic and toxicological effects, as well as drug distribution and excretion. Most *in vitro* drug–protein interaction studies are conducted in isotonic pH 7.4 buffer. Data reduction in terms of binding constants assumes that for a partially ionized drug each species is bound with equivalent affinity (2).

It was reported (3) that conformational changes occur in serum albumin over pH 6–9. Zurawski and Foster (4) established that two conformational states exist in bovine serum albumin over this pH region. They called the form at neutral pH (pH 6–7) the "N" form and the form at higher pH (around pH 9) the "B" (base) form. Thus, the conformational change that occurs is the N to B or B to N transition. It was recently shown (5–7) that the same conformational change occurs in human serum albumin over pH 6–9. The N to B transition is seemingly dependent on pH but may also occur to some extent with ionic strength of the buffer and buffer ion composition. Calcium ion and chloride ion affect this transition (5–10) as well as the binding of drug to the protein.

BACKGROUND

While the macromolecule conformation changes with varying pH, ionization of the drug may also occur over such a pH range. A method was presented recently (2) to distinguish which species of a partially ionized acidic or basic drug bind to the protein and to enable determination of the binding site constant (3) for the interaction. In addition, this method aids in the detection of significant changes in the protein binding site that may result from pH perturbation. Since the blood pH in patients may vary between 6.8 and 7.8 (11), significant changes in drug binding to albumin or other plasma proteins could take place with a change in blood or local change in organ (*e.g.*, liver) pH. This pH range could not be predicted in any one individual; at best these pH differences usually would be only a few tenths of a pH unit (*i.e.*, respiratory acidosis or alkalosis).

The present study used equilibrium dialysis and UV difference spectroscopy to investigate the effect of albumin conformational state on the binding of phenylbutazone and oxyphenbutazone to human serum albumin at various pH values.

EXPERIMENTAL

Materials—The human serum albumin used was previously investigated for purity[1] (12). Phenylbutazone (I) and its metabolite oxyphen-

[1] Armour Pharmaceutical Co., Kankakee, Ill.

0022-3549/82/0200-0241$01.00/0

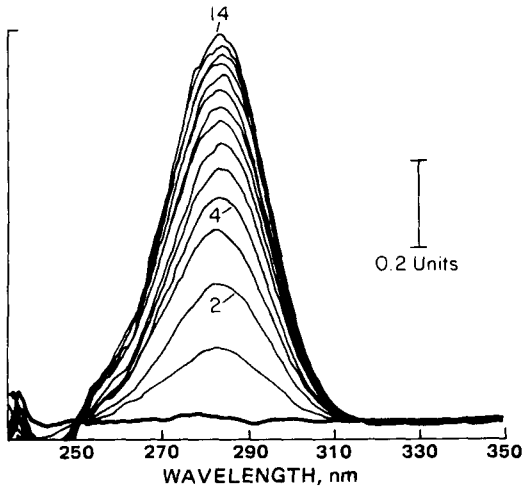

Figure 1—*Difference spectrophotometric titration of 1.45 × 10^{-5} M albumin with I at pH 8.2. Each curve represents the addition of 10 μl of I solution (1.5 × 10^{-3} M) to 3 ml (initially) of buffer in the reference compartment and to 3 ml of albumin in the sample compartment. The numbers 2, 4, and 14 indicate the number of increments added.*

butazone (II) were obtained commercially[2]. All other chemicals were analytical grade[3,4] and all solutions were prepared in deionized water.

Binding Studies—Binding studies of I and II to human serum albumin were carried out using UV difference spectroscopy and equilbirium dialysis techniques. In all binding studies, the albumin (1.45 × 10^{-5} *M*) was dissolved in phosphate buffer adjusted to various pH values, *i.e.*, 6.8, 7.0, 7.4, 7.8, and 8.2, and pH 9.3 borate buffer. All buffer solutions were made isotonic using sodium chloride or magnesium chloride.

Difference Spectrophotometry—The tandem technique (13) was employed in the split-beam mode[5]. Identical 10-μl increments[6] of either I or II (1.50 × 10^{-3} *M*) were added to the buffer cell in the reference beam and to the albumin cell in the sample beam to give final concentrations of I or II of 4.97 × 10^{-6}–6.4 × 10^{-5} *M*, representing drug to protein ratios of 0.34–4.4. To maintain a constant albumin concentration in each beam after drug addition, a volume of albumin equal to that of the drug added, but twice the concentration of the albumin already in the cell, was added to the protein cell. Drug concentration was kept constant by the addition of an identical volume of buffer to the buffer cell in the reference compartment. Resulting difference spectra were subsequently recorded.

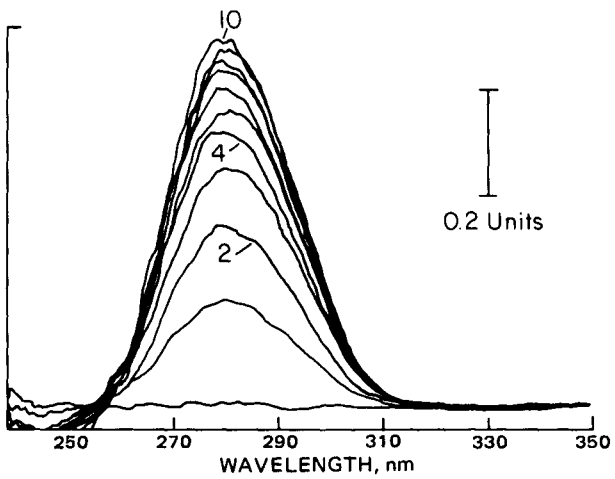

Figure 2—*Difference spectrophotometric titration of 1.45 × 10^{-5} M albumin with II at pH 7. Each curve represents the addition of 10 μl of II solution (1.5 × 10^{-3}) to 3 ml (initially) of buffer in the reference compartment and to 3 ml of albumin in the sample compartment. The numbers 2, 4, and 10 indicate the number of increments added.*

[2] Ciba-Geigy, Summit, N.J.
[3] J. T. Baker Chemical Co., Phillipsburg, N.J.
[4] Fisher Scientific Co., Fair Lawn, N.J.
[5] Model 118, Cary spectrophotometer, Varian Instruments, Palo Alto, Calif.
[6] Hamilton Co., Reno, Nev.

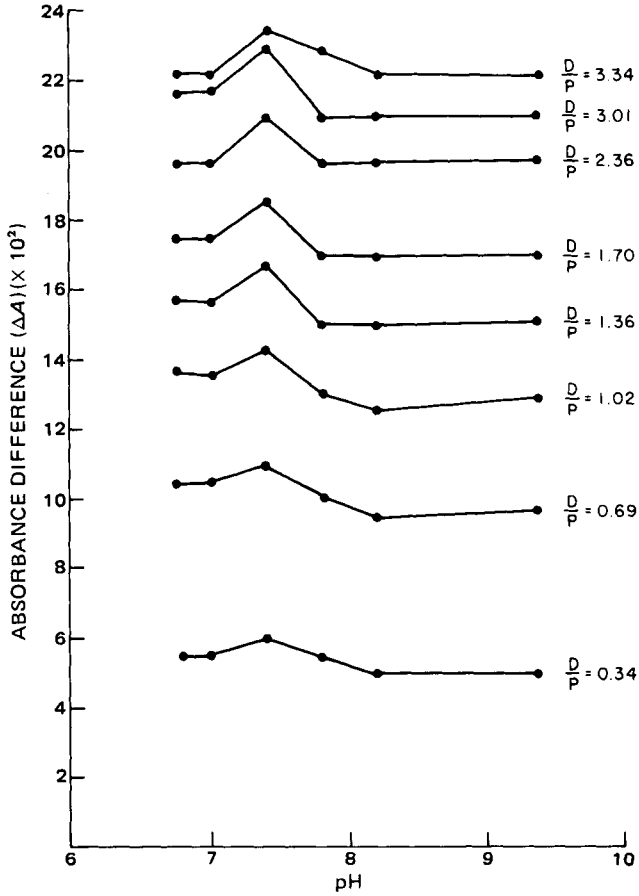

Figure 3—*Effect of pH on the absorbance differences (ΔA) of I–albumin complex.*

Equilibrium Dialysis—Equilibrium dialysis experiments were performed with an equilibrium dialyzer[7] using cell compartments of 10 ml total volume. Hydrated cellulose membranes[8] were prepared and used as suggested by the manufacturer. The concentrations of I or II used ranged from 7.6 × 10^{-6} to 1.5 × 10^{-3} *M*. Equilibrium was achieved within 4 hr for the lowest concentration and took as long as 15 hr for the highest concentration. Determination of the free drug was carried out spectrophotometrically; both I and II had a maximum at 264 nm in phosphate buffer. Standard calibration curves were constructed for each drug at each pH. Control experiments were conducted using buffer solution instead of protein.

Effect of Chloride and Magnesium Ions—The binding of I and II to albumin was also studied in phosphate buffer containing no sodium chloride and in phosphate buffer containing 1 × 10^{-3} *M* magnesium chloride. The equilibrium dialysis technique was used and phosphate buffers of pH 7.4 and 7.8 were selected for I and II, respectively.

RESULTS AND DISCUSSION

Both I and II were shown to bind to human serum albumin at different pH by the technique of difference spectroscopy and equilibrium dialysis. Examples of difference absorption spectra obtained for the association of I and II with albumin are shown in Figs. 1 and 2. In the case of I, the spectra were characterized by positive peaks at 282 ± 2 nm and negative troughs at 244 ± 2 nm. In the case of II, the spectra were characterized by a positive peak at 280 ± 2 nm and negative peak at 244 ± 2 nm. Families of curves were generated by incremental addition of I or II to albumin. At each pH examined, the absorbance difference spectra (Δ*A*) of I was larger than II. This indicates that I has a higher affinity for albumin than II (since their molar absorptivities are equivalent).

Absorbance difference curves at different pH were generated by plotting the change in absorbance measured as the difference in intensity of the peak (280 or 282 nm) and trough (244 nm) for I and II, respectively,

[7] Dianorm, Diachema AG, Ruschlikon, Switzerland.
[8] Diachema AG, Ref. 10.14, m.w. cut-off 5000, and diameter 63.

Table I—Primary Association Constant of Phenylbutazone (I) and Oxyphenbutazone (II) and Number of Sites Calculated at Different pH from Scatchard Plots

pH	K_1, liters/mole		N_1		N_2 ($N_t - N_1$)		K_2	
	I	II	I	II	I	II	I	II
7.0		$2.20 \pm 0.15 \times 10^5$		1.42		6.2		$4.76 \pm 0.84 \times 10^3$
7.4	$5.06 \pm 0.86 \times 10^5$	$3.53 \pm 0.74 \times 10^5$	1.25	1.30	8.1	8.0	$5.63 \pm 0.61 \times 10^3$	$4.20 \pm 0.19 \times 10^3$
7.8	$2.96 \pm 0.57 \times 10^5$	$1.97 \pm 0.64 \times 10^5$	1.30	1.25	3.5	2.7	$7.08 \pm 1.03 \times 10^3$	$9.70 \pm 0.84 \times 10^3$
8.2	$1.92 \pm 0.74 \times 10^5$	$1.62 \pm 0.31 \times 10^5$	1.55	1.45	3.5	4.0	$5.60 \pm 5.1 \times 10^3$	$7.67 \pm 0.59 \times 10^3$

versus pH (Figs. 3 and 4). These figures indicate that a change in pH influences the difference spectra produced as a result of the drug-protein interaction. In the case of I (Fig. 3) the curves indicate a maxima in the difference spectra at pH 7.4. The absorbance difference is slightly higher in the slightly acidic region over that observed in alkali.

This difference may indicate that I is bound more to albumin in the neutral region. In the case of II (Fig. 4), the effect of changing pH on the difference spectra was more pronounced. At all drug–albumin ratios used, the absorbance difference was larger in the neutral or slightly acidic region than in the alkaline region. An abrupt decrease occurred around pH 7–7.4. This decrease was more pronounced at higher drug–albumin ratios. The inflection points of these curves was at pH 7.8 indicative of the greatest change. This higher value of ΔA obtained in the neutral region indicates that II has a higher affinity to the N form of the albumin.

Data obtained from the equilibrium dialysis studies were plotted according to Scatchard (14) (Figs. 5 and 6). Each plot is curved and, therefore, the data were analyzed in terms of two classes of binding sites using the computer program of Perrin *et al.* (15). Results of the Scatchard plot analysis are given in Table I. There is a single high affinity binding site for both I and II and several sites of lower interaction potential (Table I). It should be pointed out that the range of I and II concentrations used in the binding studies varied considerably, from 7×10^{-6} to 1×10^{-3} M; previous literature reports use a narrower concentration range.

Considering the effect of pH on the association constants of I and II, Table I shows that K for both drugs decreases with increasing pH. In addition, at pH 7.4 the largest number of sites seems to be present. At each pH used, the association constant of I was larger than that of II.

Other workers calculated similar albumin association constants for both I and II. Solmon *et al.* (16) reported that albumin has only one binding site for I with an affinity constant of 1.17×10^5 M^{-1}. However, the concentration of I used by these workers was always less than that of albumin. Chignell (17) showed that albumin had three binding sites for I, one binding site of high affinity ($K = 1 \times 10^5$ M^{-1}), and two others with lower affinity ($K = 4 \times 10^4$ M^{-1}). For II he reported two association constants $k_1 = 2.28 \times 10^5$ M^{-1} and $k_2 = 3.7 \times 10^4$ M^{-1}. Two association constants were also reported (18) for I, $k_1 = 2.37 \times 10^{-5}$ M^{-1} $k_2 = 4.56 \times 10^4$ M^{-1}, and for II, $k_2 = 2.32 \times 10^5$ M^{-1} and $k_3 = 1.16 \times 10^4$ M^{-1}. The report indicated that K for II was very large and the affinity constants (K_2 and K_3) calculated assumed $n_1 = 1$; the first molar equivalent of II was so strongly bound as to be virtually removed from solution.

The pKa of I and II are 4.5 and 4.7, respectively (19). To determine whether the ionized and/or unionized species of these two drugs is bound to albumin, the method recently reported (2) for the determination of the site binding constant of each species of a partially ionized drug was applied to the equilibrium dialysis data. The method appeared applicable over the pH range examined for each compound and indicated that both species of I and II were responsible for the binding. The site binding constants for the ionized species were 1.40×10^5 and 1.16×10^5 for I and II, respectively. The site binding constants for the unionized species of I and II were much greater, approaching 2.93×10^8 and 1.18×10^8, respectively. However, the overall affinity or binding constant would be expected to be only somewhat greater than ionized drug since only a very small proportion of each drug is present in the unionized form, consequently adding little to the overall constant. Alternatively, it may be possible that a conformational change in the protein occurs and is re-

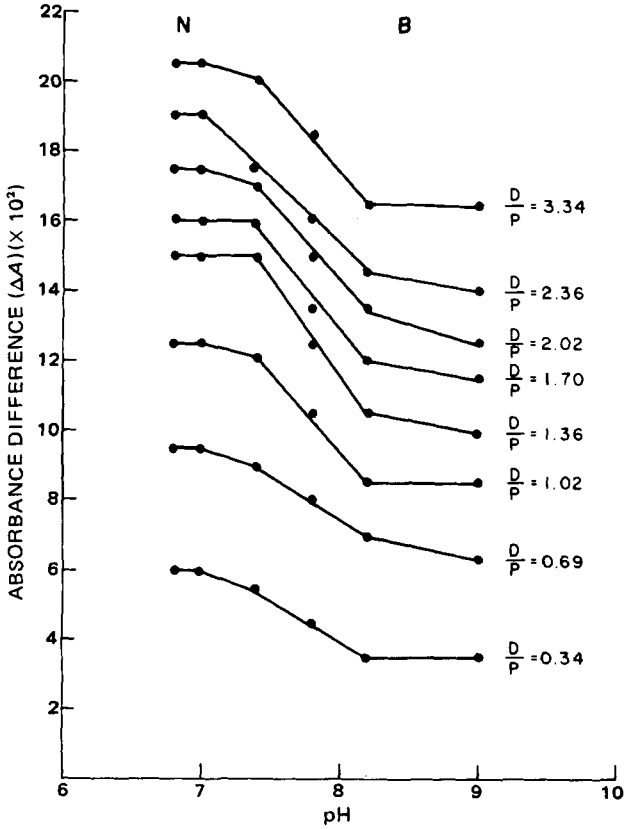

Figure 4—*Effect of pH on the absorbance differences (ΔA) of II–albumin complex.*

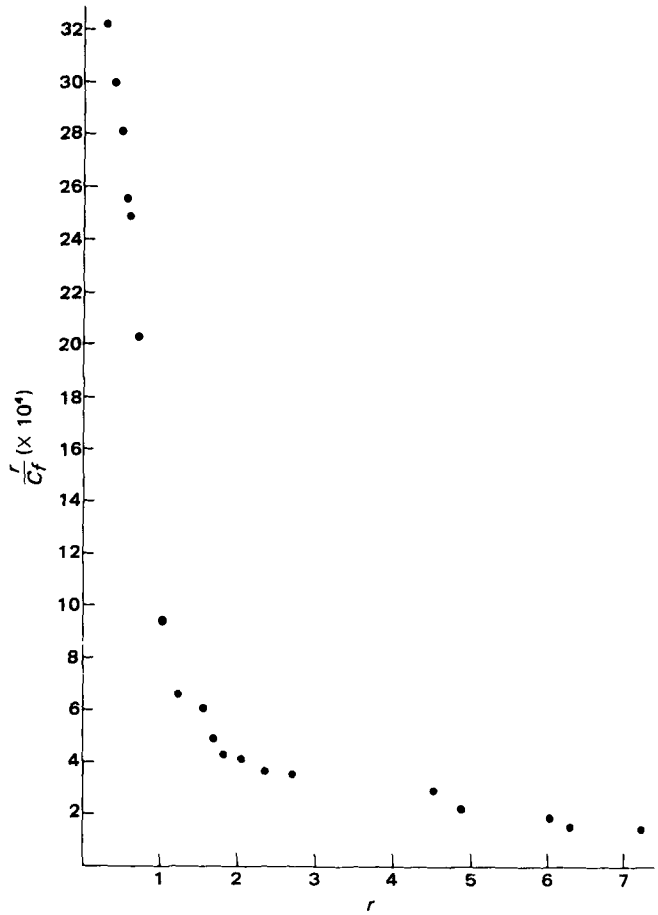

Figure 5—*Scatchard plot of dialysis data for the interaction of I with albumin at pH 7.4. Key:* r, *moles of drug bound per mole of albumin; and* C_f, *free drug concentration.*

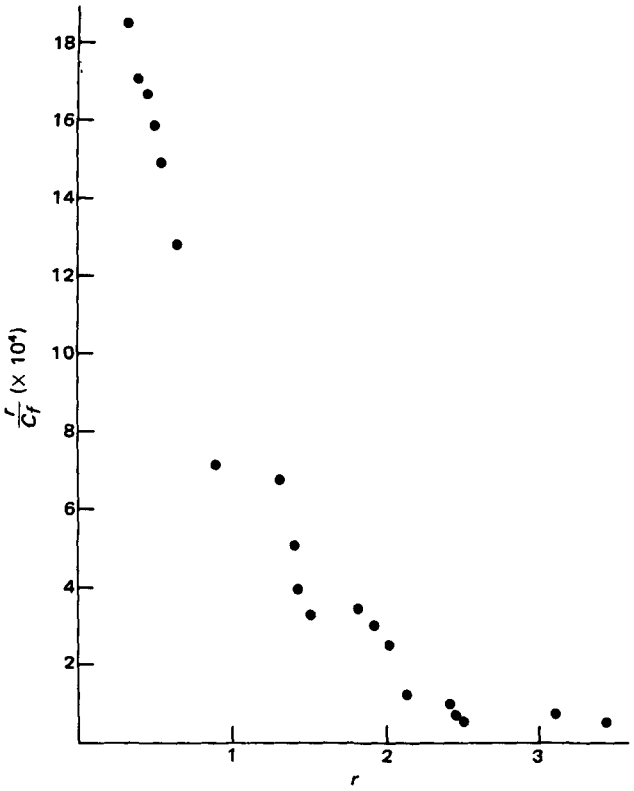

Figure 6—*Scatchard plot of dialysis data for the interaction of II with albumin at pH 7.8. Key:* r, *moles of drug bound per mole of albumin; and* C_f, *free drug concentration.*

sponsible for marked differences in affinity between various drug forms.

The effect of chloride and magnesium ions on the binding of I and II to albumin was opposite in nature. Chloride ions reduced the amount of drug bound. This was most evident in the neutral pH region for both drugs. The mechanism is possibly one of displacement of drug from albumin as postulated earlier (6, 10). Magnesium ion increased the binding of both drugs in the same pH region. The increase was as much as 10% in the presence of magnesium at pH 7.4. Cations, especially divalent cations, have been found to affect the N to B transition of the protein (6, 7) and this is possibly the reason for the increased binding. The effects of both chloride and magnesium ions were greater on the high affinity sites than on the sites in the second class of binding.

The UV difference spectroscopy and equilibrium dialysis data indicated that albumin has a higher affinity for I than II at each pH examined. Oxyphenbutazone is less hydrophobic (more polar) than phenylbutazone, and the importance of hydrophobic interactions in the binding of drugs to protein was noted previously (17, 20, 21).

With either method of examining binding it is evident that pH affects the affinity of the interaction. It is also apparent that the binding affinity of each drug is higher in the neutral region (N form of protein) than in the alkaline region (B form). This fact, coupled with the results of absorbance difference *versus* pH which show a marked transition (inflection) in the neutral pH region, indicate that the N to B transition of albumin may be responsible for the changes in the affinity of the complex with pH.

REFERENCES

(1) B. K. Martin, *Nature*, **207**, 274 (1975).

(2) D. L. Parsons and J. J. Vallner, *Acta Pharm. Suec.*, **17**, 12 (1980).

(3) W. J. Leonard, K. K. Vijai, and J. F. Foster, *J. Biol. Chem.*, **238**, 1984 (1973).

(4) V. R. Zurawski and J. F. Foster, *Biochemistry*, **13**, 3465 (1974).

(5) J. Wilting, M. M. Weideman, A. C. Roomer, and J. H. Perrin, *Biochim. Biophys. Acta*, **579**, 469 (1979).

(6) J. Wilting, W. F. Van Der Giesen, L. H. M. Janssen, M. Weideman, M. Otagiri, and J. H. Perrin, *Biol. Chem.*, **255**, 3032 (1980).

(7) J. Jacobsen and T. Faerch, *Biochim. Biophys. Acta*, **623**, 199 (1980).

(8) S. Katz and I. M. Klotz, *Arch. Biochem. Biophys.*, **44**, 351 (1953).

(9) B. H. M. Harmsen, S. H. de Bruin, L. H. M. Janssen, J. F. Rodrigues de Miranda, and G. A. J. Vanos, *Biochemistry*, **10**, 3217 (1971).

(10) L. H. M. Janssen and T. H. A. Nelen, *J. Biol. Chem.*, **254**, 4300 (1979).

(11) K. Diem and C. Lentzer, "Wissenschaftliche Tabellen," 7th ed., 556, Ciba-Geigy AB, Basel, Switzerland, 1976.

(12) J. H. Perrin and J. J. Vallner, *J. Pharm. Sci.*, **64**, 1508 (1975).

(13) A. S. Brill and H. E. Sandberg, *Biophys. J.*, **8**, 669 (1968).

(14) Scatchard, *Ann. N.Y. Acad. Sci.*, **51**, 660 (1949).

(15) J. G. Perrin, J. J. Vallner, and S. Wold, *Biochim. Biophys. Acta*, **371**, 482 (1974).

(16) H. H. Solmon, J. J. Schrage, and D. Williams, *Biochem. Pharmacol.*, **17**, 143 (1968).

(17) C. F. Chignell, *Mol. Pharmacol.*, **5**, 244 (1969).

(18) A. Rosen, *Biochem. Pharmacol.*, **19**, 2075 (1970).

(19) A. B. Gutman, P. G. Dayton, T. F. Yii, L. Berger, W. Chen, L. E. Sican, and J. J. Burns, *Am. J. Med.*, **29**, 1017 (1960).

(20) F. Helmer, K. Kiehs, and C. Hansch, *Biochemistry*, **7**, 2858 (1968).

(21) W. Scholtan, *Arzneim.-Forsch.*, **18**, 505 (1968).

Pharmacokinetics of Hydrochlorothiazide in Fasted and Nonfasted Subjects: A Comparison of Plasma Level and Urinary Excretion Methods

RASHMI H. BARBHAIYA*§, WILLIAM A. CRAIG‡, H. PERRI CORRICK-WEST*, and PETER G. WELLING*x

Received March 30, 1981, from the *School of Pharmacy, Veterans Administration Hospital, and the ‡School of Medicine, University of Wisconsin, Madison, WI 53706. Accepted for publication July 1, 1981. §Present address: Department of Drug Metabolism and Pharmacokinetics, Bristol Laboratories, Syracuse, NY 13201.

Abstract □ The bioavailability of hydrochlorothiazide from 50-mg oral tablet doses was examined in healthy male volunteers under fasting and nonfasting conditions. Bioavailability was examined from plasma levels and urinary excretion of unchanged drug. The pharmacokinetics of hydrochlorothiazide in plasma could be described in terms of a triexponential function, and the mean drug half-lives determined from the three exponents were 1.0, 2.2, and 9.0 hr. Changing the accompanying fluid volume had no significant effect on hydrochlorothiazide absorption in fasted subjects. Plasma drug levels were significantly reduced in nonfasted individuals, compared with those in fasted individuals. A similar trend was observed in the urinary excretion of hydrochlorothiazide, but differences between treatments were not significant ($p > 0.05$). Mean 48-hr urinary recovery of hydrochlorothiazide was 70.5% of the dose in nonfasted subjects, and 73.5 and 75.0% of the dose in fasted subjects receiving the drug with 20 and 250 ml of water, respectively. The cumulative urinary excretion of hydrochlorothiazide correlated poorly ($r = 0.27$) with areas under plasma drug level curves, although the correlation between the means of these values for each of the three treatments was high ($r = 0.996$). Close similarity was observed between urinary excretion rates of hydrochlorothiazide and the time course of drug concentrations in plasma.

Keyphrases □ Hydrochlorothiazide—pharmacokinetics, fasted and nonfasted subjects □ Pharmacokinetics—hydrochlorothiazide, fasted and nonfasted subjects □ Diuretics—hydrochlorothiazide, pharmacokinetics in fasted and nonfasted subjects

High-pressure liquid chromatographic (HPLC) procedures were described to measure hydrochlorothiazide in plasma and urine (1). Preliminary clinical data obtained in that study indicated that the elimination of hydrochlorothiazide from plasma is biphasic in nature, and that its urinary excretion rate closely resembles its concentration profile in plasma.

This report describes studies in which previously described methods (1) were used to examine the plasma levels and urinary excretion of hydrochlorothiazide following single oral doses to healthy male subjects, under fasting and nonfasting conditions, and with large and small accompanying fluid volumes.

EXPERIMENTAL

Subjects—Eight male volunteers[1], 23–35 years of age (mean 28) and weighing 64–84 kg (mean 78) participated in the study after passing a physical examination and giving informed consent. No subject had a history of drug allergy.

Protocols—Subjects were instructed to take no drugs for 1 week before, and no drugs other than hydrochlorothiazide during the study. No caffeine-containing beverages were permitted from 1 day before each hydrochlorothiazide dose until the end of the plasma and urine sampling periods.

Hydrochlorothiazide[2] was administered as three single-dose oral treatments: treatment A, one 50-mg tablet with 250 ml of water, following overnight fast; treatment B, one 50-mg tablet with 20 ml of water, following overnight fast; and treatment C, one 50-mg tablet with 250 ml of water, immediately following a standard breakfast.

The treatments were administered according to a randomized crossover design, and subjects received each treatment 1 week apart.

Subjects were instructed to eat no food after 8 pm, and no liquid after 10 pm, on the day preceding each study. No further food apart from the breakfast in treatment C was permitted until 4 hr after each drug dose. After that time normal eating and drinking were permitted.

On a treatment morning, 250 ml of water was ingested on arising, at least 1 hr before dosing. The drug was administered at 8 am, the tablets being swallowed whole. No further liquid intake was permitted until 4-hr postdose. The standard breakfast consisted of cornflakes with milk, ~150 ml of orange juice, two poached eggs, two slices of toast, and a cup of caffeine-free coffee.

Blood samples (10 ml) were taken from a forearm vein into vacuum tubes[3] (containing heparin as anticoagulant) immediately before and then serially through 24-hr postdose. Urine was collected immediately before and then quantitatively at intervals through 48-hr postdose. Plasma was separated from blood by centrifugation, and plasma and urine samples were stored at −20° until assayed, generally within 2 weeks.

Analytical—Concentrations of hydrochlorothiazide in plasma and urine were determined by the HPLC methods described previously (1). The methods are linearly sensitive to hydrochlorothiazide concentrations of 2–100 μg/ml in urine, and 10–750 ng/ml in plasma. The coefficients of variation from multiple determinations within these concentration ranges were within 10% of the mean.

Analysis of the Data—Plasma hydrochlorothiazide concentrations

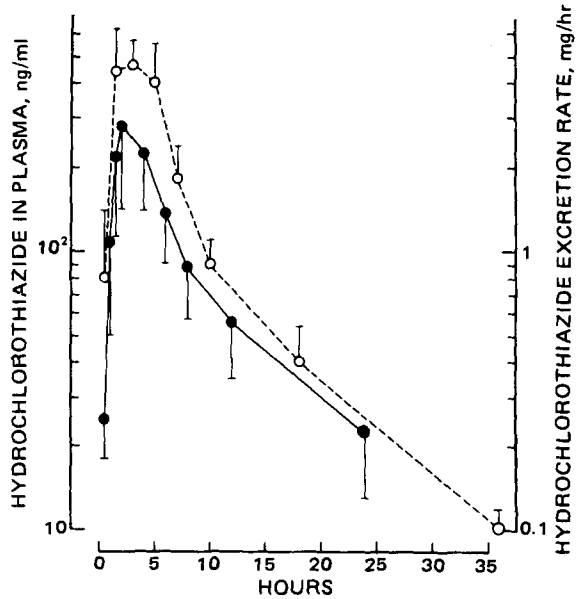

Figure 1—*Mean plasma concentrations (●) and urinary excretion rates, (○) of hydrochlorothiazides following treatment A, 50-mg tablet dose with 250 ml of water on a fasted stomach. Error bars indicate ±1* SD.

[1] Technical staff and graduate students.

[2] Hydrodiuril 50-mg tablets, lot B0686, Merçk Sharp and Dohme, West Point, Pa.

[3] Vacutainer.

0022-3549/82/0200-0245$01.00/0

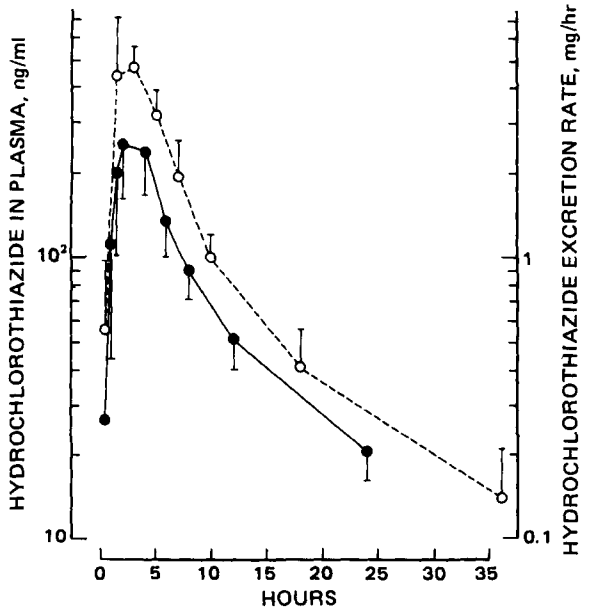

Figure 2—*Mean plasma concentrations (●) and urinary excretion rates (○) of hydrochlorothiazide following treatment B, 50-mg tablet dose with 20 ml of water on a fasted stomach.*

from each individual subject were fitted to a triexponential function of the form:

$$C = Xe^{-\alpha t} + Ye^{-\beta t} + Ze^{-\gamma t} \qquad \text{(Eq. 1)}$$

where C is the drug concentration in plasma at time t and other values are constants.

Initial estimates of parameter values were obtained by standard graphical methods. Improved estimates, together with statistical analysis, were obtained by nonlinear regression using the NREG computer program (2). Plasma hydrochlorothiazide levels at each sampling time, urinary excretion data, and pharmacokinetic parameter values were examined for subject and treatment effects by analysis of variance for crossover design. When significant treatment effects were obtained by analysis of variance, differences between treatments were examined by Tukey's test (3).

Reagents—The sources of reagents and solvents were described previously (1).

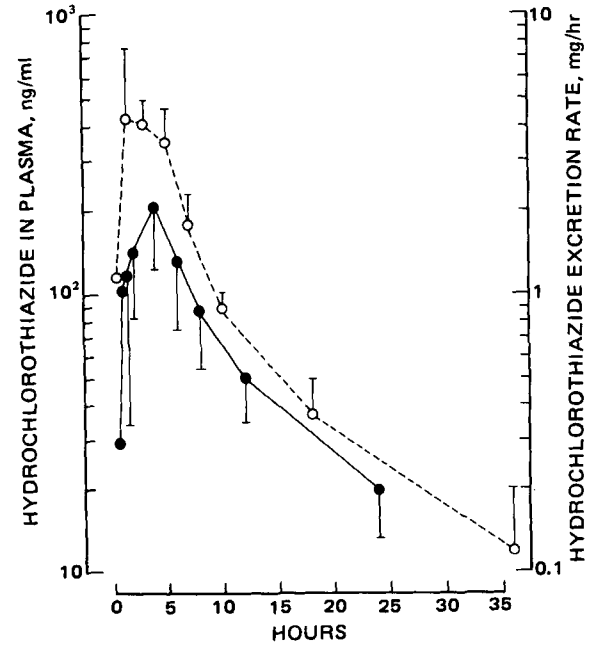

Figure 3—*Mean plasma concentrations (●) and urinary excretion rates (○) of hydrochlorothiazide following treatment C, 50-mg tablet dose with 250 ml of water immediately following a standard meal.*

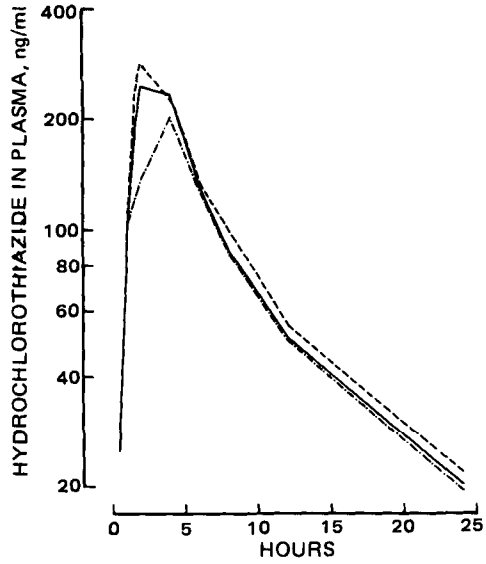

Figure 4—*Mean plasma concentrations of hydrochlorothiazide following treatments A (– –), B (—), and C (– · – ·).*

RESULTS

Plasma Hydrochlorthiazide Levels—The mean plasma hydrochlorothiazide concentration curves from the three treatments are shown in Figs. 1–3. For comparison between treatments, the curves are combined in Fig. 4.

The mean plasma drug profiles obtained from the two fasting treatments were almost identical. Mean peak drug concentrations of 310 and 291 ng/ml were obtained ~2.5-hr postdosing from treatments A and B, respectively (Table I). After this time, the drug levels declined rapidly to 12 hr, and at a slower rate to 24 hr.

The nonfasting dose of hydrochlorothiazide yielded drug profiles in plasma similar to the fasting treatments, but the drug concentrations tended to be lower. Plasma drug levels from treatment C were significantly lower ($p < 0.05$) than those from treatment A at 2 hr, and from treatment B at 4 hr. From Table I, the C_{max} and AUC^{24} values from treatment C were significantly lower than those from treatment A, while treatment B yielded intermediate values.

Analysis of individual drug curves in terms of Eq. 1 yielded the numerical values for the rate constants α, β, and γ shown in Table II. Almost identical mean values were obtained for each of the constants from the different treatments. The mean coefficients of determination, r^2, obtained from nonlinear regression analysis $[(\Sigma obs^2 - \Sigma dev^2)/\Sigma obs^2]$ were 0.91 ± 0.03, 0.93 ± 0.06, and 0.92 ± 0.08 for treatments A, B, and C, respectively.

Urinary Excretion of Hydrochlorothiazide—The mean cumulative urinary recovery of hydrochlorothiazide at each collection interval is shown in Fig. 5. The 24- and 48-hr mean recovery values are given in Table I. Overall recovery of hydrochlorothiazide was 75.0, 73.5, and 70.5% of the dose from treatments A, B, and C, respectively. While urinary recovery exhibited a similar trend to plasma levels, there were no significant

Table I—Pharmacokinetic Parameter Values (±1 *SD*, *n* = 8) for Hydrochlorothiazide

Parameter	Value: Treatment A	Value: Treatment B	Value: Treatment C	Statistical Significance
C_{max}[a], ng/ml	310 ± 130	291 ± 80	241 ± 66	$\overline{A\ B\ C}$
T_{max}[b], hr	2.4 ± 1.8	2.6 ± 1.2	2.9 ± 1.5	NSD[c]
AUC^{24}[d], ng hr/ml	2097 ± 717	2018 ± 450	1777 ± 384	$\overline{A\ B\ C}$
AU^{24}[e], %	69.0 ± 8.5	66.7 ± 8.6	64.3 ± 6.1	NSD
Au^{48}[f], %	75.0 ± 8.4	73.5 ± 10.1	70.5 ± 9.3	NSD
R_{cl}[g], ml/min	307 ± 124	292 ± 93	320 ± 100	NSD

[a] Maximum concentration of hydrochlorothiazide in plasma. [b] Time of C_{max}. [c] No significant differences. [d] Area under hydrochlorothiazide concentration curve in plasma from zero to 24 hr, calculated by trapezoidal rule. [e] Cumulative 24-hr urinary excretion of hydrochlorothiazide. [f] Cumulative 48-hr urinary excretion of hydrochlorothiazide. [g] Renal clearance of hydrochlorothiazide, calculated by dividing Au^{24} by AUC^{24}.

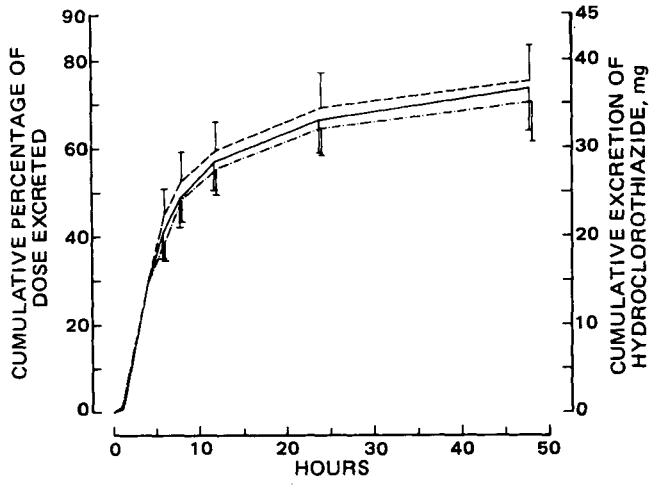

Figure 5—*Mean cumulative excretion of hydrochlorothiazide in urine following treatments A (– –), B (—), and C (– · – ·).*

differences in the urinary recovery from the different treatments. The renal clearance of hydrochlorothiazide was ~300 ml/min, and there were no significant treatment effects in this value.

DISCUSSION

Information on the pharmacokinetics and bioavailability of the thiazide diuretics has been restricted by a lack of suitable analytical procedures. Early studies utilized colorimetry (4) but HPLC methods are now favored because of their greater sensitivity and specificity (5). Plasma hydrochlorothiazide concentrations are approximately 100-fold lower than those in urine, and previous studies concerning plasma drug levels have used gas chromatography with electron-capture detection (6–8).

The HPLC procedures used in this study are suitable for analysis of both urine and plasma hydrochlorothiazide levels following single therapeutic doses. Initial studies using these assay procedures (1) indicated that elimination of hydrochlorothiazide from plasma was biphasic. They also suggested that, while there is poor agreement between the areas under plasma level curves and cumulative urinary excretion of hydrochlorothiazide (9, 10), there is close similarity between the time course of plasma drug levels and urinary excretion rates.

The present study confirms these observations. While the biphasic decline of drug levels in plasma is based largely on data points obtained at 12 and 24 hr, this elimination pattern was reported previously (1, 9). The half-lives calculated from the mean values of γ, α, and β in Table II are ~1.0, 2.2, and 9.0 hr, respectively, and these values were unaffected by the different treatments. The largest of these, the terminal half-life for hydrochlorothiazide in plasma, is similar to values reported previously (1, 10).

The mechanism underlying biphasic elimination of hydrochlorothiazide from plasma is unclear. Hydrochlorothiazide accumulates in erythrocytes, but equilibrium of drug between plasma water and blood cells is reached in 4 hr after an oral dose (10). The pattern of hydrochlorothiazide elimination from plasma is different from that of chlorothiazide. In the case of hydrochlorothiazide, biphasic elimination is clearly evident in individual subjects, as shown in Fig. 6. However, in the case of chlorothiazide, while mean plasma levels could be described by a triexponential function, profiles in individual subjects were erratic and exhibited a sawtooth effect (11, 12).

The plasma drug levels obtained from the different treatments showed that the efficiency of hydrochlorothiazide absorption from oral tablets was not markedly influenced by fluid volume, but decreased when the drug was taken after a meal. The urinary excretion data showed a similar trend, but the treatment effects on drug excretion were not significant.

Table II—Values of Rate Constants (±1 *SD*, $n = 8$) Obtained by Fitting Individual Plasma Hydrochlorothiazide Profiles to Eq. 1

Treatment	Rate Constant, hr^{-1}		
	α	β	γ
A	0.32 ± 0.08	0.078 ± 0.18	0.67 ± 0.22
B	0.32 ± 0.08	0.078 ± 0.18	0.65 ± 0.52
C	0.28 ± 0.09	0.078 ± 0.011	0.74 ± 0.52

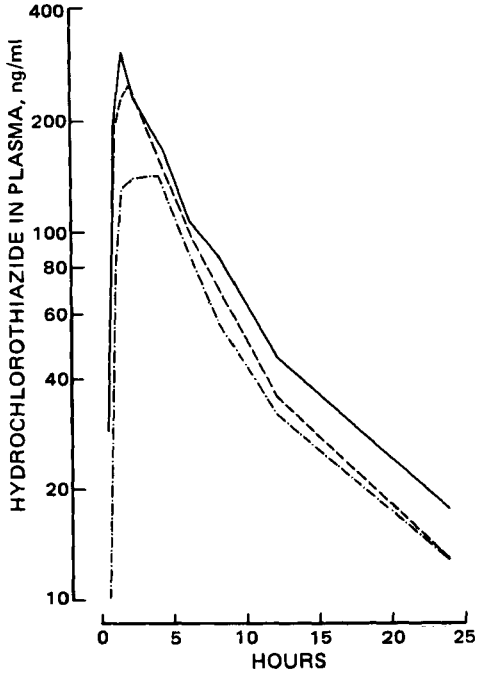

Figure 6—*Plasma concentrations of hydrochlorothiazide in one subject following treatments A (– –), B (—), and C (– · – ·).*

These results are inconsistent with a previous report in which hydrochlorothiazide absorption was increased by food (7). Procedural differences between the studies may account for this. In the present study, both fasted and nonfasted subjects were permitted normal food intake after 4-hr postdosing. In the previous study, fasted subjects received no solid food until 10-hr postdosing, while nonfasted subjects received three regular meals during that period. Prolonged abstinence from food by the fasted subjects may have affected drug absorption due to altered GI secretion and motility. The previous study also employed a higher dose of hydrochlorothiazide (75 mg).

The different effects of food on the GI absorption of hydrochlorothiazide and chlorothiazide (11) are possibly related to dose size. Chlorothiazide was shown to be poorly absorbed from 250 and 500 mg doses; less than 25% of the administered dose was recovered in urine (12, 13). Absorption was improved to only a small extent when chlorothiazide was administered as a solution, compared to tablets (12, 13), but doubled when chlorothiazide tablets were administered immediately following a meal (11). However, hydrochlorothiazide was efficiently absorbed from 50–75-mg oral doses (6–9).

The poor bioavailability of oral chlorothiazide may be due to saturable and site-specific absorption (5, 11). The structural similarity of the two compounds suggests that hydrochlorothiazide may be absorbed by a mechanism similar to chlorothiazide, but the lower dose of hydrochlorothiazide precludes saturation of the absorption mechanism. While food may increase the bioavailability of oral chlorothiazide by reducing the rate at which drug is presented to the absorption site (11), this mechanism would be less important for lower doses of hydrochlorothiazide. The inhibitory effects of food appear to dominate with this compound (14, 15), but these effects are small and are unlikely to be clinically significant.

The negligible effect of altered fluid volume on hydrochlorothiazide absorption was unexpected. Hydrochlorothiazide has a low aqueous solubility (9), and large accompanying fluid volumes have been shown to increase the absorption of a number of lipophilic drugs (16). Previously, increased absorption has been attributed to more efficient drug dissolution or faster stomach emptying (14). In the case of hydrochlorothiazide, these effects appear to be negligible. This is possibly related to the efficient absorption of hydrochlorothiazide in general; an increase in absorption due to increased fluid volume would be difficult to detect. It could be speculated that any potential increase in drug release in the GI tract may be offset by saturable absorption, but other studies would be needed to confirm this.

Although an official dissolution test exists for hydrochlorothiazide tablets (17), there have been differing reports on the ability of *in vitro* dissolution rates to accurately predict *in vivo* drug bioavailability (18, 19).

Correlations between individual areas under hydrochlorothiazide

plasma curves and cumulative excretion in the present study were poor. Correlation coefficients between AUC^{24} and Au^{48} (48-hr urinary excretion), and between C_{max} and Au^{48} for all subjects were 0.25 and 0.27, respectively. Poor correlations between these parameters, which have been reported previously (9, 10), appear to be due to the variability of individual data and to the relatively small treatment effects, rather than to the lack of a true relationship. The correlation coefficient between mean AUC^{24} and Au^{48} values, and between mean C_{max} and Au^{48} values for each treatment were 0.996 and 0.997, respectively.

The previous suggestion that the rate of hydrochlorothiazide excretion in urine closely resembles the time course of plasma levels (1) is confirmed in this study. Mean urinary excretion rates of hydrochlorothiazide are plotted together with plasma levels in Figs. 1–3. In each case, the overall urinary excretion rates exhibited a similar triphasic pattern to those in plasma.

The high renal clearance of hydrochlorothiazide suggests that, like chlorothiazide, it is eliminated by both renal filtration and active secretion.

REFERENCES

(1) R. H. Barbhaiya, T. A. Phillips, and P. G. Welling, *J. Pharm. Sci.*, **70**, 291 (1981).

(2) "MACC Nonlinear Regression Routines," Academic Computer Center, University of Wisconsin, Madison, Wis., 1972.

(3) J. Neter and W. Wasserman, "Applied Linear Statistical Models," Richard D. Irwin, Homewood, Ill., 1974, p. 275.

(4) R. E. Shepherd, J. C. Price, and L. A. Luzzi, *J. Pharm. Sci.*, **61**, 1152 (1972).

(5) D. E. Resetarits and T. E. Bates, *J. Pharmacokinet. Biopharm.*, **7**, 463 (1979).

(6) B. Beermann and M. Groschinsky-Grind, *Eur. J. Clin. Pharmacol.*, **13**, 385 (1978).

(7) *Ibid.*, **13**, 125 (1978).

(8) L. Backman, B. Beermann, M. Groschinsky-Grind, and D. Hallberg, *Clin. Pharmacokinet.*, **4**, 63 (1979).

(9) B. Beermann, M. Groschinsky-Grind, and A. Rosen, *Clin. Pharmacol. Ther.*, **19**, 531 (1976).

(10) B. Beermann and M. Groschinsky-Grind, *Eur. J. Clin. Pharmacol.*, **12**, 297 (1977).

(11) P. G. Welling and R. H. Barbhaiya, *J. Pharm. Sci.*, in press.

(12) V. P. Shah, V. K. Prasad, B. E. Cabana, and P. Sojka, *Curr. Ther. Res.*, **24**, 366 (1978).

(13) A. B. Straughn, A. P. Melikian, and M. C. Meyer, *J. Pharm. Sci.*, **68**, 1099 (1979).

(14) P. G. Welling, *J. Pharmacokinet. Biopharm.*, **5**, 291 (1977).

(15) R. D. Toothaker and P. G. Welling, *Prog. Drug Metab.*, **4**, 131 (1980).

(16) P. G. Welling, in "Progress in Drug Metabolism," J. W. Bridges and L. F. Chasseaud, Eds. Wiley, New York, N.Y., 1980, p. 131.

(17) "The United States Pharmacopeia," 20th rev. U.S. Pharmacopeial Convention Inc., Rockville, MD 20852, 1980, p. 378.

(18) I. J. McGilveray, R. D. Hossie, and G. L. Mattock, *Can. J. Pharm. Sci.*, **8**, 13 (1973).

(19) K. A. Shah and T. E. Needham, *J. Pharm. Sci.*, **68**, 1486 (1979).

ACKNOWLEDGMENTS

Supported by Grant GM 20327, National Institutes of Health.

Pharmacokinetic Comparison of Sublingual Lorazepam with Intravenous, Intramuscular, and Oral Lorazepam

DAVID J. GREENBLATT ˣ, MARCIA DIVOLL, JEROLD S. HARMATZ, and RICHARD I. SHADER

Received May 21, 1981, from the *Division of Clinical Pharmacology, Departments of Psychiatry and Medicine, Tufts University School of Medicine* and the *New England Medical Center Hospital, Boston, MA 02111.* Accepted for publication July 7, 1981.

Abstract □ Ten healthy volunteers received single 2-mg doses of lorazepam on five occasions in random sequence. Modes of administration were: A, intravenous injection; B, deltoid intramuscular injection; C, oral tablets in the fasting state; D, sublingual dosage of oral tablets in the fasting state; and E, sublingual dosage of specially formulated tablets in the fasting state. Kinetic variables were determined from multiple plasma lorazepam concentrations meaured during 48 hr postdose. After intravenous lorazepam, mean (±*SE*) values were: elimination half-life ($t_{1/2\beta}$), 12.9 (±0.8) hr; volume of distribution, 1.3 (±0.07) liters/kg; total clearance, 1.21 (±0.1) ml/min/kg. Absorption of intramuscular lorazepam was rapid. Peak plasma levels were reached at 1.15 hr after dosage, with absorption half-life averaging 14.2 (±4.7) min. Absorption of oral and sublingual lorazepam tended to be less rapid than intramuscular injection, although differences were not significant. Times of peak concentration were 2.37, 2.35, and 2.25 hr postdose for trials C, D, and E, respectively; values of absorption half-life were 32.5, 28.5, and 28.7 min. Absolute systemic availability for trials B, C, D, and E averaged 95.9, 99.8, 94.1, and 98.2%, respectively; none of these differed significantly from 100%. Values of $t_{1/2\beta}$ were highly replicable within individuals regardless of the administration route. Thus, sublingual lorazepam is completely absorbed and is a suitable administration route in clinical practice.

Keyphrases □ Lorazepam—sublingual, pharmacokinetics compared with intravenous, intramuscular, and oral dosage forms □ Pharmacokinetics—sublingual lorazepam, comparison with intravenous, intramuscular, and oral dosage forms □ Dosage forms—sublingual lorazepam, pharmacokinetics compared with intravenous, intramuscular, and oral dosage forms

Lorazepam is a 3-hydroxy-1,4-benzodiazepine derivative in clinical use as an antianxiety and sedative agent (1, 2). Clinical situations may arise in which oral administration of a sedative is unwise or not possible, and intravenous dosage is precluded because a physician is not available. In such circumstances, intramuscular injection usually is the only alternative. The present study assessed the pharmacokinetics of lorazepam given sublingually to determine the possible clinical role of this administration route as an alternative to oral or intramuscular administration.

EXPERIMENTAL

Subjects—Ten healthy male and female volunteers, 24–39 years of age, participated after giving written informed consent (Table I). They were free of any identifiable medical disease. Subject 10 was taking oral contraceptive steroids, but no other medications were being used on a regular basis.

0022-3549/82/0200-0248$01.00/0

plasma curves and cumulative excretion in the present study were poor. Correlation coefficients between AUC^{24} and Au^{48} (48-hr urinary excretion), and between C_{max} and Au^{48} for all subjects were 0.25 and 0.27, respectively. Poor correlations between these parameters, which have been reported previously (9, 10), appear to be due to the variability of individual data and to the relatively small treatment effects, rather than to the lack of a true relationship. The correlation coefficient between mean AUC^{24} and Au^{48} values, and between mean C_{max} and Au^{48} values for each treatment were 0.996 and 0.997, respectively.

The previous suggestion that the rate of hydrochlorothiazide excretion in urine closely resembles the time course of plasma levels (1) is confirmed in this study. Mean urinary excretion rates of hydrochlorothiazide are plotted together with plasma levels in Figs. 1–3. In each case, the overall urinary excretion rates exhibited a similar triphasic pattern to those in plasma.

The high renal clearance of hydrochlorothiazide suggests that, like chlorothiazide, it is eliminated by both renal filtration and active secretion.

REFERENCES

(1) R. H. Barbhaiya, T. A. Phillips, and P. G. Welling, *J. Pharm. Sci.*, **70**, 291 (1981).

(2) "MACC Nonlinear Regression Routines," Academic Computer Center, University of Wisconsin, Madison, Wis., 1972.

(3) J. Neter and W. Wasserman, "Applied Linear Statistical Models," Richard D. Irwin, Homewood, Ill., 1974, p. 275.

(4) R. E. Shepherd, J. C. Price, and L. A. Luzzi, *J. Pharm. Sci.*, **61**, 1152 (1972).

(5) D. E. Resetarits and T. E. Bates, *J. Pharmacokinet. Biopharm.*, **7**, 463 (1979).

(6) B. Beermann and M. Groschinsky-Grind, *Eur. J. Clin. Pharmacol.*, **13**, 385 (1978).

(7) *Ibid.*, **13**, 125 (1978).

(8) L. Backman, B. Beermann, M. Groschinsky-Grind, and D. Hallberg, *Clin. Pharmacokinet.*, **4**, 63 (1979).

(9) B. Beermann, M. Groschinsky-Grind, and A. Rosen, *Clin. Pharmacol. Ther.*, **19**, 531 (1976).

(10) B. Beermann and M. Groschinsky-Grind, *Eur. J. Clin. Pharmacol.*, **12**, 297 (1977).

(11) P. G. Welling and R. H. Barbhaiya, *J. Pharm. Sci.*, in press.

(12) V. P. Shah, V. K. Prasad, B. E. Cabana, and P. Sojka, *Curr. Ther. Res.*, **24**, 366 (1978).

(13) A. B. Straughn, A. P. Melikian, and M. C. Meyer, *J. Pharm. Sci.*, **68**, 1099 (1979).

(14) P. G. Welling, *J. Pharmacokinet. Biopharm.*, **5**, 291 (1977).

(15) R. D. Toothaker and P. G. Welling, *Prog. Drug Metab.*, **4**, 131 (1980).

(16) P. G. Welling, in "Progress in Drug Metabolism," J. W. Bridges and L. F. Chasseaud, Eds. Wiley, New York, N.Y., 1980, p. 131.

(17) "The United States Pharmacopeia," 20th rev. U.S. Pharmacopeial Convention Inc., Rockville, MD 20852, 1980, p. 378.

(18) I. J. McGilveray, R. D. Hossie, and G. L. Mattock, *Can. J. Pharm. Sci.*, **8**, 13 (1973).

(19) K. A. Shah and T. E. Needham, *J. Pharm. Sci.*, **68**, 1486 (1979).

ACKNOWLEDGMENTS

Supported by Grant GM 20327, National Institutes of Health.

Pharmacokinetic Comparison of Sublingual Lorazepam with Intravenous, Intramuscular, and Oral Lorazepam

DAVID J. GREENBLATT ˣ, MARCIA DIVOLL, JEROLD S. HARMATZ, and RICHARD I. SHADER

Received May 21, 1981, from the *Division of Clinical Pharmacology, Departments of Psychiatry and Medicine, Tufts University School of Medicine* and the *New England Medical Center Hospital, Boston, MA 02111.* Accepted for publication July 7, 1981.

Abstract □ Ten healthy volunteers received single 2-mg doses of lorazepam on five occasions in random sequence. Modes of administration were: A, intravenous injection; B, deltoid intramuscular injection; C, oral tablets in the fasting state; D, sublingual dosage of oral tablets in the fasting state; and E, sublingual dosage of specially formulated tablets in the fasting state. Kinetic variables were determined from multiple plasma lorazepam concentrations meaured during 48 hr postdose. After intravenous lorazepam, mean (±*SE*) values were: elimination half-life ($t_{1/2\beta}$), 12.9 (±0.8) hr; volume of distribution, 1.3 (±0.07) liters/kg; total clearance, 1.21 (±0.1) ml/min/kg. Absorption of intramuscular lorazepam was rapid. Peak plasma levels were reached at 1.15 hr after dosage, with absorption half-life averaging 14.2 (±4.7) min. Absorption of oral and sublingual lorazepam tended to be less rapid than intramuscular injection, although differences were not significant. Times of peak concentration were 2.37, 2.35, and 2.25 hr postdose for trials C, D, and E, respectively; values of absorption half-life were 32.5, 28.5, and 28.7 min. Absolute systemic availability for trials B, C, D, and E averaged 95.9, 99.8, 94.1, and 98.2%, respectively; none of these differed significantly from 100%. Values of $t_{1/2\beta}$ were highly replicable within individuals regardless of the administration route. Thus, sublingual lorazepam is completely absorbed and is a suitable administration route in clinical practice.

Keyphrases □ Lorazepam—sublingual, pharmacokinetics compared with intravenous, intramuscular, and oral dosage forms □ Pharmacokinetics—sublingual lorazepam, comparison with intravenous, intramuscular, and oral dosage forms □ Dosage forms—sublingual lorazepam, pharmacokinetics compared with intravenous, intramuscular, and oral dosage forms

Lorazepam is a 3-hydroxy-1,4-benzodiazepine derivative in clinical use as an antianxiety and sedative agent (1, 2). Clinical situations may arise in which oral administration of a sedative is unwise or not possible, and intravenous dosage is precluded because a physician is not available. In such circumstances, intramuscular injection usually is the only alternative. The present study assessed the pharmacokinetics of lorazepam given sublingually to determine the possible clinical role of this administration route as an alternative to oral or intramuscular administration.

EXPERIMENTAL

Subjects—Ten healthy male and female volunteers, 24–39 years of age, participated after giving written informed consent (Table I). They were free of any identifiable medical disease. Subject 10 was taking oral contraceptive steroids, but no other medications were being used on a regular basis.

0022-3549/82/0200-0248$01.00/0

Table I—Subject Characteristics and Kinetics of Intravenous Lorazepam

Subjects				Lorazepam Kinetics				
Number	Age, years	Sex	Wt, kg	$t_{1/2\alpha}$, min	$t_{1/2\beta}$, hr	V_1, liters/kg	V_d, liters/kg	Clearance, ml/min/kg
1	33	F	61.4	2.8	10.9	0.39	1.24	1.32
2	24	M	70.5	3.3	7.2	0.44	1.09	1.76
3	38	M	77.3	12.0	13.1	0.30	1.08	0.96
4	29	F	61.4	1.1	15.9	0.32	1.28	0.93
5	34	M	79.5	12.6	12.2	0.53	1.59	1.51
6	25	M	63.6	13.0	14.2	0.79	1.60	1.29
7	29	M	68.1	11.2	15.2	0.58	1.19	0.91
8	32	F	50.0	10.7	14.4	1.02	1.42	1.14
9	25	F	54.5	18.6	13.9	0.50	0.99	0.82
10	26	F	57.7	1.0	12.2	0.37	1.49	1.42
			Mean (±*SE*)	8.7 (±1.9)	12.9 (±0.8)	0.52 (±0.07)	1.30 (±0.07)	1.21 (±0.10)

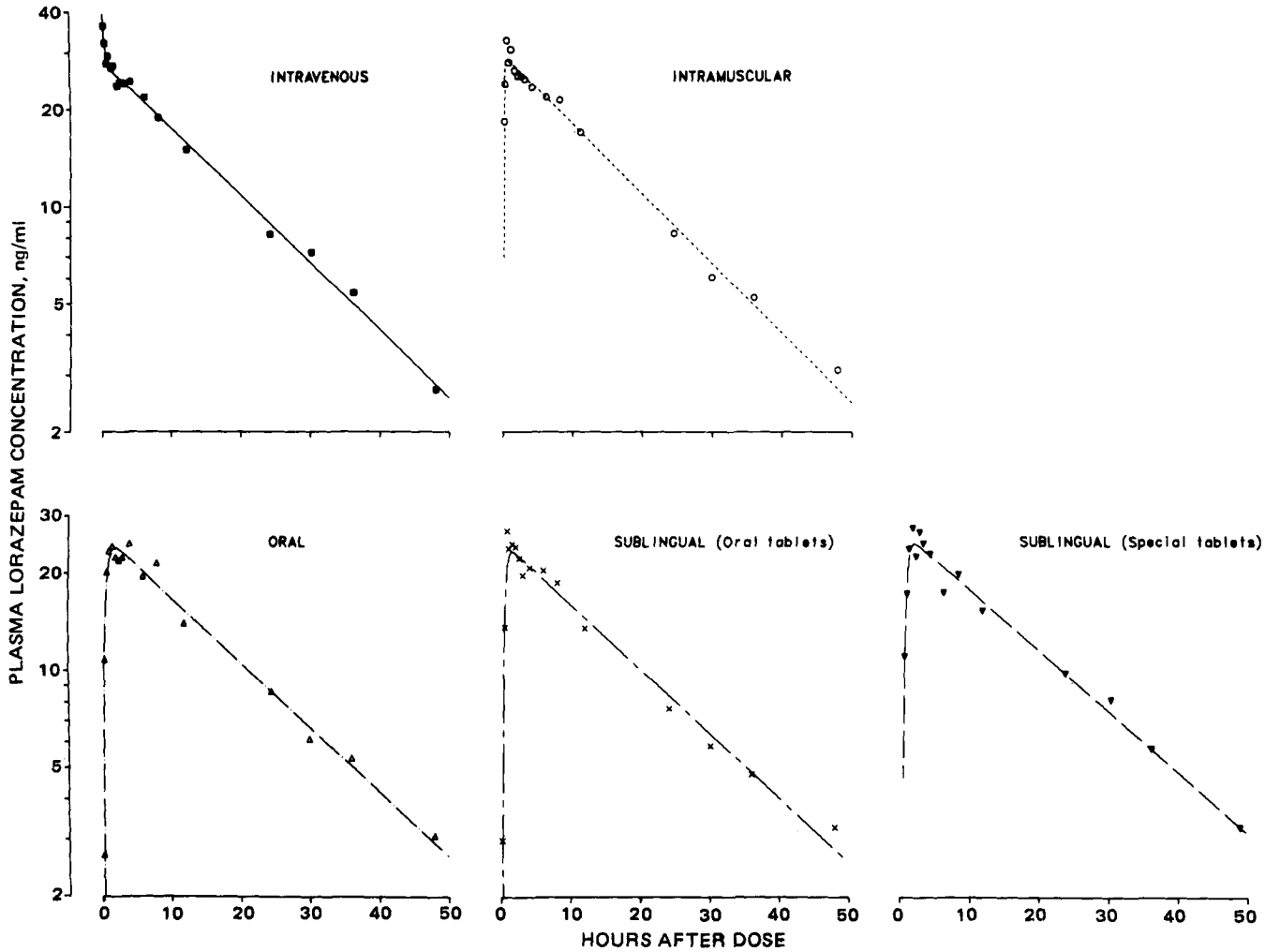

Figure 1—*Plasma lorazepam concentrations and pharmacokinetic functions of best fit following administration of lorazepam to subject 8 by each of the five administration routes.*

Design—A randomized, single-dose, five-way crossover design was utilized. Each subject received single 2-mg doses of lorazepam[1] on five occasions separated by at least 1 week. The administration modes were:

A. Intravenous lorazepam, 1 ml of a 2 mg/ml injectable preparation, infused into an antecubital vein over a 30-sec period.
B. Intramuscular lorazepam, 1 ml of the 2 mg/ml injectable preparation, given by a physician as a single deltoid intramuscular injection.
C. Oral lorazepam, administered as two standard 1-mg tablets (*in vitro* dissolution rate, 80% in 1 hr) with 100–200 ml of tap water.
D. Sublingual lorazepam, administered as two standard 1-mg oral tablets placed under the tongue and held for 15 min.
E. Sublingual lorazepam, administered as two special 1-mg sublingual tablets (*in vitro* dissolution rate, 84% in 1 hr) placed under the tongue and held for 15 min.

For trials A and B, no restrictions were placed upon the ingestion of food or liquid. For trials C, D, and E, subjects fasted overnight prior to drug administration and remained fasting for 3 hr postdose.

Procedure—Venous blood samples were drawn into heparinized tubes from an indwelling butterfly cannula or by separate venipuncture, prior to lorazepam administration, and at the following times after each dose: 5 min, and 0.25, 0.5, 0.75, 1.0, 1.5, 2.0, 2.5, 3, 4, 6, 8, 12, 24, 30, 36, and 48 hr. After intravenous dosage, a sample was also drawn just after the

[1] Ativan, Wyeth Laboratories, Radnor, Pa.

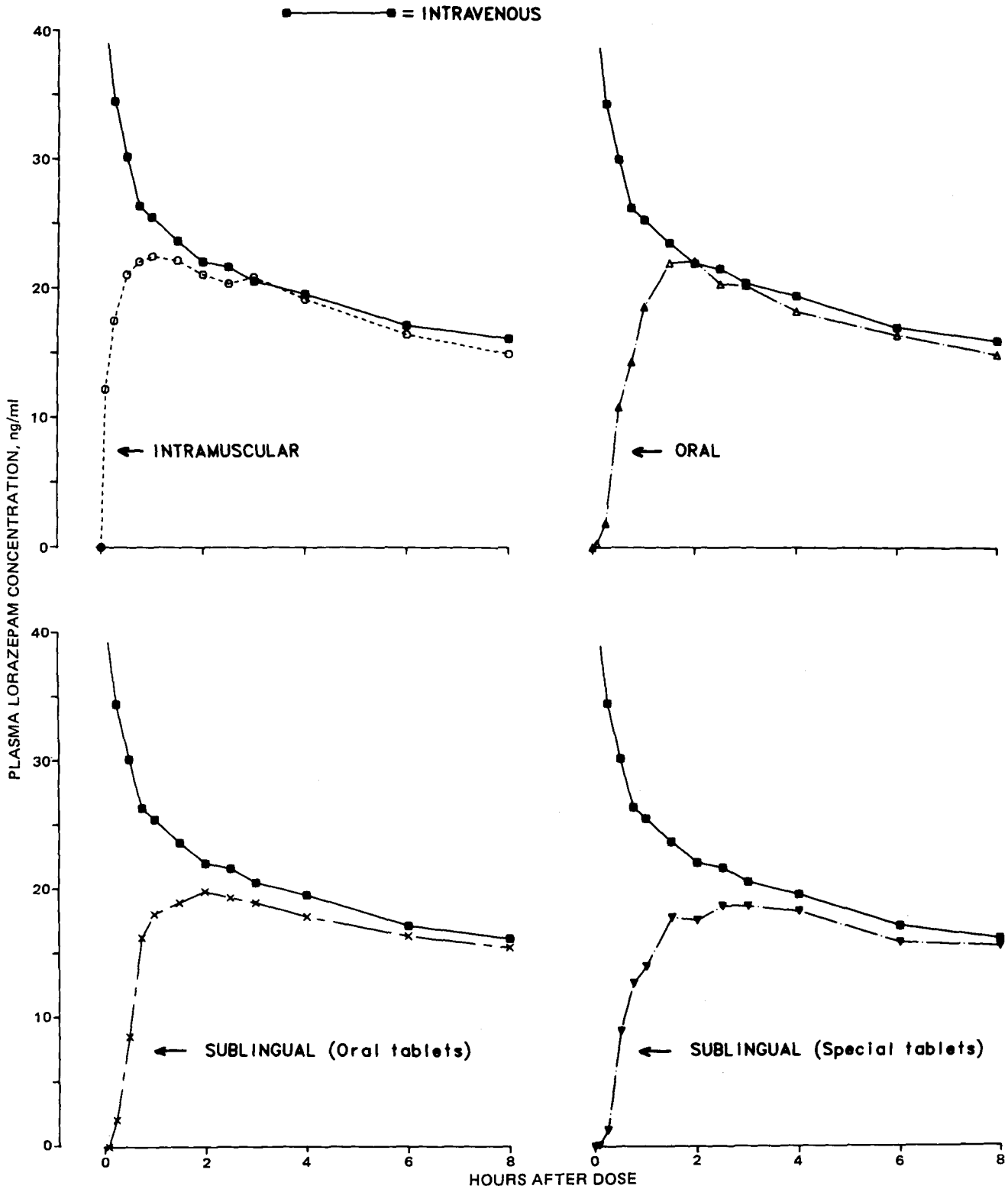

Figure 2—*Plasma lorazepam concentrations for the first 8 hr after dosage by the four extravascular administration routes compared with that observed after intravenous dosage. Each point is the mean for all 10 subjects at the corresponding time.*

infusion. Blood samples were centrifuged, and the plasma was separated and stored at −20° until assay.

Analysis of Plasma Samples—Lorazepam concentrations in all plasma samples were determined by electron-capture GLC after addition of oxazepam as the internal standard (2–4).

Analysis of Data—Plasma lorazepam concentrations following each subject trial were analyzed using iterative nonlinear least-squares regression techniques described previously (5, 6). Data points were fitted to a linear sum of exponential terms. After intravenous lorazepam, coefficients and exponents from the fitted function were used to calculate the following kinetic variables: initial (α) distribution half-life ($t_{1/2\alpha}$), elimination half-life ($t_{1/2\beta}$), volume of central compartment (V_1), total volume of distribution using the area method (V_d), total clearance, and total area under the plasma concentration curve from time zero to infinity (AUC).

After the four extravascular modes of administration, fitted functions were used to calculate the apparent half-life of absorption, lag time elapsing prior to the start of absorption (t_0), and elimination half-life ($t_{1/2\beta}$). The area under the plasma concentration curve from time zero until the last detectable plasma concentration was calculated using the

Table II—Effect of Route of Administration on Lorazepam Pharmacokinetics

Variable	Mean (±SE) Values[a] for Trial A Intravenous	B Intramuscular	C Oral	D Sublingual	E Sublingual	Value of F Two-Way ANOVA	Value of P
Peak plasma concentration, ng/ml	—	26.0 (±1.9)	24.9 (±2.4)	23.3 (±2.8)	20.7 (±1.7)	2.50	0.081
Time of peak concentration, hr postdose	—	1.15 (±0.3)	2.37 (±0.32)	2.35 (±0.7)	2.25 (±0.33)	2.32	0.098
Lag time, min	—	0	11.8 (±2.1)	22.7 (±5.1)	14.9 (±3.5)	3.29[b]	0.061
Absorption half-life, min	—	14.2 (±4.7)	32.5 (±3.8)	28.5 (±8.4)	28.7 (±7.6)	1.97	0.142
Elimination half-life, hr	12.9 (±0.8)	13.1 (±1.1)	14.1 (±1.0)	13.2 (±0.7)	14.4 (±1.0)	1.63	0.187
Systemic availability, percentage of intravenous	—	95.9 (±4.0)	99.8 (±5.7)	94.1 (±6.5)	98.2 (±5.8)	0.56	0.648

[a] Individual values are available on request. [b] Does not include value for trial B.

trapezoidal method. To this was added the residual area extrapolated to infinity, calculated at the last detectable plasma concentration divided by β, yielding the total *AUC*.

Statistical Analysis—Two-way analysis of variance was used to analyze differences in kinetic variables among the various treatments. The absolute systemic availability (completeness of absorption) of the four extravascular routes of lorazepam administration were calculated by dividing each subject's total *AUC* for a particular route of administration by the corresponding value of *AUC* following intravenous lorazepam administration to the same individual.

RESULTS

Intravenous Lorazepam (trial A)—Disappearance of lorazepam from plasma following intravenous injection was described by a linear sum of two exponential terms for subjects 1–9, and by a sum of three exponentials for subject 10. Mean kinetic variables for lorazepam were: $t_{1/2\alpha}$, 8.7 min; $t_{1/2\beta}$, 12.9 hr; V_1, 0.52 liters/kg; V_d, 1.30 liters/kg; and total clearance, 1.21 ml/min/kg (Table I).

Intramuscular Lorazepam (trial B)—All subjects noted mild to moderate local discomfort associated with the injection. This was transient and resolved shortly after the injection without specific treatment.

Peak lorazepam concentrations averaged 26 ng/ml, and were reached an average of 1.5 hr postdose (Table II, Figs. 1 and 2). In all subjects, peak plasma concentrations were reached within 3 hr of dosage. In no case did a lag time elapse prior to the start of absorption. The mean value of absorption half-life was 14.2 min (Fig. 3), and that of $t_{1/2\beta}$ was 13.1 hr. Absolute systemic availability of intramuscular lorazepam averaged 96% of the intravenous value; this was not significantly different from 100% (Table II, Fig. 4).

Oral Lorazepam (trial C)—Peak plasma lorazepam concentrations averaged 25 ng/ml and were attained an average of 2.4 hr postdose (Table II, Figs. 1 and 2). A lag time elapsed prior to the start of absorption in nine of the 10 subjects; the mean lag time was 11.8 min. The mean value of absorption half-life was 32.5 min (Fig. 3), and that of $t_{1/2\beta}$ was 14.1 hr. Mean systemic availability was 99.8% (Table II, Fig. 4).

Sublingual Lorazepam (trial D)—Peak plasma lorazepam concentrations after sublingual administration of the standard oral tablets averaged 23.3 ng/ml and were attained an average of 2.3 hr after dosage (Table II, Figs. 1 and 2). A lag time elapsed prior to the start of absorption in nine of the 10 subjects; the mean lag time was 22.7 min. The mean absorption half-life was 28.5 min, and $t_{1/2\beta}$ averaged 13.2 hr. Mean systemic availability was 94.1%.

Sublingual Lorazepam (trial E)—The kinetic profile of sublingual lorazepam administered as special tablets was very similar to that following sublingual administration of standard oral tablets described for trial D. Peak plasma concentrations averaged 20.7 ng/ml and were attained at 2.25 hr after dosage. A lag time elapsed prior to administration in eight of 10 subjects, and averaged 14.9 min. Absorption half-life averaged 28.7 min, while $t_{1/2\beta}$ averaged 14.4 hr. Mean systemic availability was 98%.

Comparison among Administration Routes—Values of $t_{1/2\beta}$ were highly consistent within subjects among the five trials (Table II, Fig. 5). Two-way analysis of variance indicated that differences attributable to administration route did not approach significance.

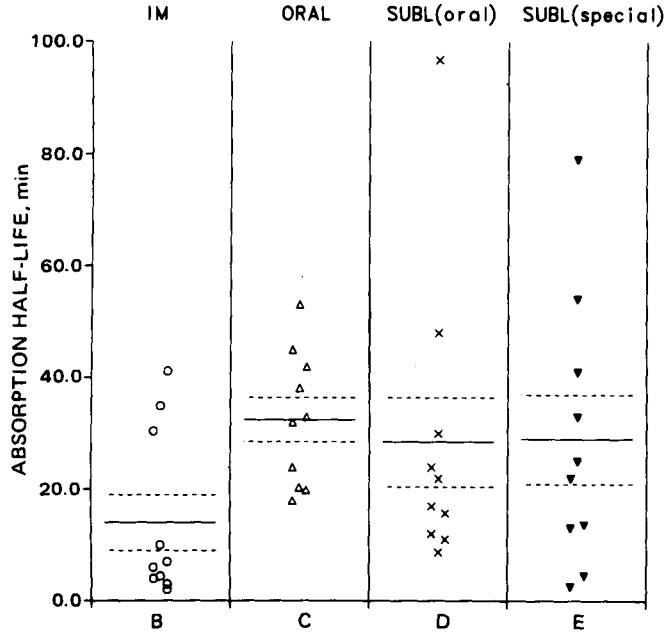

Figure 3—*Lorazepam absorption half-life following each of the four extravascular administration routes. Individual and mean (±SE) values for all subjects are shown. See Table II for statistical analysis.*

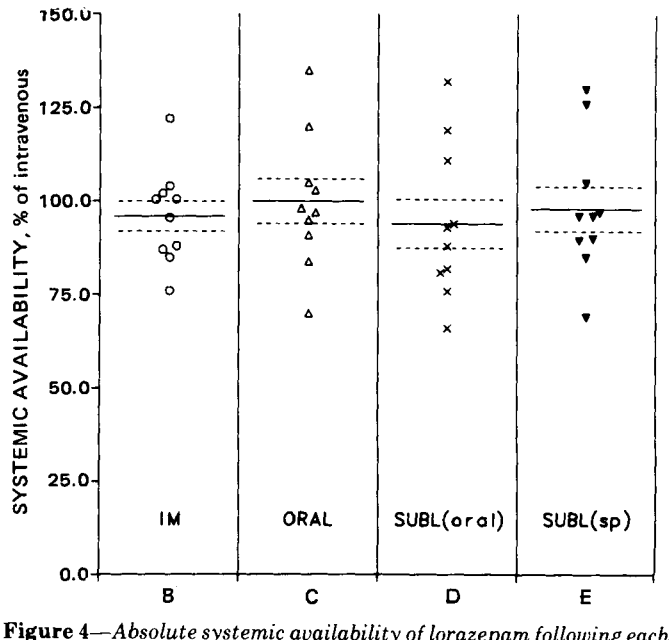

Figure 4—*Absolute systemic availability of lorazepam following each of the four extravascular administration routes. Individual and mean (±SE) values for all subjects are shown. See Table II for statistical analysis.*

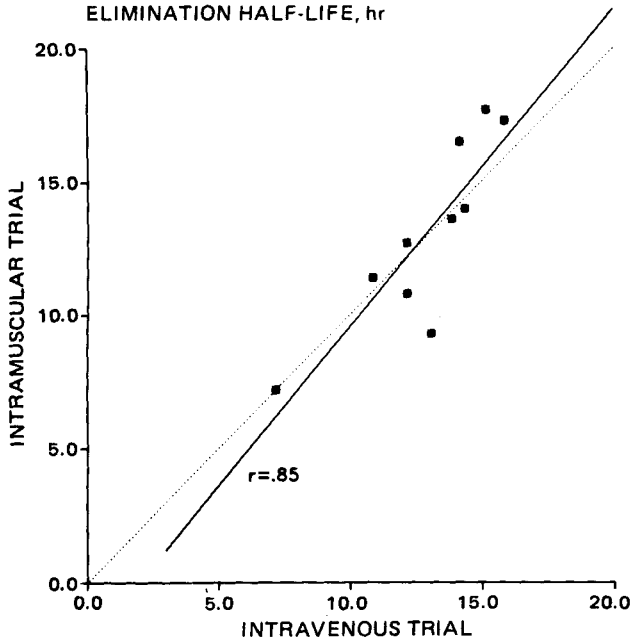

Figure 5—*Values of lorazepam elimination half-life following intravenous (trial A) and intramuscular (trial B) administration routes to the 10 subjects. Solid line was determined by least-squares regression analysis; dotted line is the line of identity.*

Differences among the four extravascular trials in peak plasma lorazepam concentrations and time of peak concentration approached but did not attain significance ($0.05 < p < 0.1$). Both variables indicated a trend for higher peak plasma levels reached sooner after the dose following intramuscular injection then after oral or sublingual administration. However, differences among trials C, D, and E were minimal (Table II). A similar trend was observed in absorption half-life. Although differences among the four extravascular trials did not reach significance, absorption half-life following intramuscular injection (trial B) was only half as long as that following the oral and sublingual routes (Table II, Fig. 3). However, differences among trials C, D, and E were minimal. Finally, no lag times were observed following intramuscular injection, whereas a lag time elapsed prior to the start of absorption in the majority of subjects following oral or sublingual administration.

Absolute systemic availability among the four extravascular modes of administration were highly comparable (Table II, Fig. 4). Mean values for trials B, C, D, and E were 96, 100, 94, and 98%, respectively. Differences among the four routes did not approach significance. Furthermore, in no case did the mean value of absolute systemic availability differ significantly from 100%.

DISCUSSION

The kinetic profile of lorazepam in the present study is similar to that reported previously from this laboratory (5–7) and elsewhere (2, 8, 9). In the present group of subjects, the range of values for $t_{1/2\beta}$ was 7–21 hr. This is similar to the range of 8–24 hr noted previously using different healthy young volunteers (5–7). It is also important to note that values of $t_{1/2\beta}$ were highly replicable within a given subject upon repeated administration of lorazepam.

The kinetics of intramuscular and oral lorazepam also are similar to patterns described previously (5–7). Deltoid intramuscular injection of lorazepam leads to rapid absorption of the drug; the completeness of absorption from the injection site is very close to 100%. Absorption of oral lorazepam is somewhat slower than that of intramuscular injection, probably due to the time required for drug dissolution and gastric emptying. Absorption of orally administered lorazepam was close to 100%.

The pattern of lorazepam absorption following sublingual administration resembles that of oral lorazepam. In the majority of cases, a lag time elapsed prior to the start of absorption, after which first-order absorption proceeded with a half-life averaging ~29 min. As in the case of oral lorazepam, the completeness of absorption of sublingual lorazepam, whether administered as standard oral tablets or specially-formulated tablets, was nearly 100%.

Thus, the rate and completeness of lorazepam absorption following sublingual administration are comparable to that observed following oral dosage on an empty stomach. In clinical terms, sublingual and oral dosage of lorazepam are likely to be therapeutically equivalent. Sublingual administration could also substitute for intramuscular injection, although the onset of clinical activity following the sublingual route may be slightly slower than that observed after intramuscular injection. Findings from the present study of sublingual lorazepam apply only to the tablet preparations studied. More rapid absorption of sublingual lorazepam might occur with formulations having more rapid dissolution rates.

REFERENCES

(1) B. Ameer and D. J. Greenblatt, *Drugs*, **21**, 161 (1981).

(2) D. J. Greenblatt, *Clin. Pharmacokinet.*, **6**, 89 (1981).

(3) D. J. Greenblatt, K. Franke, and R. I. Shader, *J. Chromatogr.*, **146**, 311 (1978).

(4) D. J. Greenblatt, M. Divoll, J. S. Harmatz, and R. I. Shader, *J. Pharmacol. Exp. Ther.*, **215**, 86 (1980).

(5) D. J. Greenblatt, R. I. Shader, K. Franke, D. S. MacLaughlin, J. S. Harmatz, M. D. Allen, A. Werner, and E. Woo, *J. Pharm. Sci.*, **68**, 57 (1979).

(6) D. J. Greenblatt, M. D. Allen, D. S. MacLaughlin, D. H. Huffman, J. S. Harmatz, and R. I. Shader, *J. Pharmacokinet. Biopharm.*, **7**, 159 (1979).

(7) D. J. Greenblatt, M. D. Allen, A. Locniskar, J. S. Harmatz, and R. I. Shader, *Clin. Pharmacol. Ther.*, **26**, 103 (1979).

(8) J. W. Kraus, P. V. Desmond, J. P. Marshall, R. F. Johnson, S. Schenker, and G. R. Wilkinson, *ibid.*, **24**, 411 (1978).

(9) R. V. Patwardhan, G. W. Yarborough, P. V. Desmond, R. F. Johnson, S. Schenker, and K. V. Speeg, *Gastroenterology*, **79**, 912 (1980).

ACKNOWLEDGMENTS

Supported in part by Grant MH-34223 from the United States Public Health Service, by a Clinical Pharmacology Unit Developmental Grant from the Pharmaceutical Manufacturers' Association Foundation, and by a grant-in-aid from Wyeth Laboratories, Radnor, Pa.

The authors are grateful for the assistance of Ann Locniskar, Lawrence J. Moschitto, Ann M. Zumbo, Dr. Dean S. MacLaughlin, Dr. Darrell R. Abernethy, Dr. Hans H. Koepke, and the staff of the Clinical Study Unit, New England Medical Center Hospital (supported by USPHS Grant RR-24040).

DNA-Binding Specificity and RNA Polymerase Inhibitory Activity of Bis(aminoalkyl)anthraquinones and Bis(methylthio)vinylquinolinium Iodides

WILLIAM O. FOYE ˣ, OPA VAJRAGUPTA*, and SISIR K. SENGUPTA‡

Received November 21, 1980, from the *Samuel M. Best Research Laboratory, Massachusetts College of Pharmacy and Allied Health Sciences, Boston, MA 02115.* Accepted for publication June 9, 1981. *Present address: School of Pharmacy, Mahidol University, Bangkok, Thailand. ‡Present address: Boston University Medical Center, Boston, MA 02118.

Abstract □ The determination of DNA-binding specificities for a series of bis(methylthio)vinylquinolinium iodides and two bis(aminoalkyl)-anthraquinones was accomplished by spectral analysis, equilibrium dialysis, elevation of melting temperature, and inhibition of DNA function as a template for *Escherichia coli* RNA-polymerase transcription activity *in vitro*. Studies of complex formation were carried out by comparison of difference spectra of the compounds in the presence of native double-stranded DNA and separated-strand DNA. Base specificity of the interaction between DNA and the compounds was demonstrated for both series, particularly for the anthraquinones, for the guanine–cytosine base pair. Comparison of the difference spectra of the compounds in the presence of DNA with varied base-pair ratios showed a strong preference of the anthraquinones for the guanine–cytosine base pair, but the quinolinium compounds showed no preference. The linear-binding isotherm for the quinolinium compounds indicated one type of binding site, while two types of binding sites were apparent for the anthraquinones. Since only one anthraquinone was active in leukemia tests, factors other than DNA binding must account for the activity of the antileukemic derivative.

Keyphrases □ DNA—binding specificity of bis(aminoalkyl)anthraquinones and bis(methylthio)vinylquinolinium iodides □ Bis(aminoalkyl)anthraquinones—DNA binding specificity and RNA polymerase inhibition □ Bis(methylthio)vinylquinolinium iodides—DNA binding specificity and RNA polymerase inhibition

A series of 1-methylquinolinium-2-dithioacetic acid zwitterions (1, 2) and derivatives (3) showed appreciable anticancer activity against P-388 lymphocytic leukemia growth in mice. Since the structures of these compounds differ in several respects from those of other antileukemic agents, no obvious clue to a possible mechanism of anticancer action was apparent. However, the planar nature of the quinoline ring suggested binding to DNA as a possible factor in their action, and accordingly, DNA binding studies were carried out. At the same time, two structurally similar anthraquinone derivatives (4), one having good antileukemic activity and the other inactive, were measured and examined for any differences in their binding ability. Chloroquine, a known intercalating agent for DNA, was used as a control substance.

The methods used to determine DNA binding ability involved spectral analysis, equilibrium dialysis, elevation of melting temperature, and *in vitro* inhibition of cell-free RNA transcription. In addition, studies of complex formation of the compounds with DNA were carried out using native double-strand and single-strand DNA, and also using DNA from various sources with different base-pair ratios. Absorption spectra of the compounds in the presence of DNA with different base-pair ratios were compared to determine any base-pair specificities in the DNA binding. It was thought that use of several different techniques could provide more information on DNA binding than one method alone.

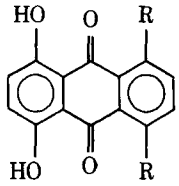

I: R = $NH(CH_2)_2NH(CH_2)_2OH \cdot 2\,HCl \cdot 5\,H_2O$
II: R = $NH(CH_2)_4N(CH_3)_2$

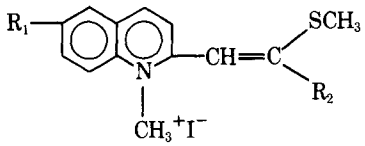

III: R_1 = H, R_2 = SCH_3
IV: R_1 = CH_3, R_2 = SCH_3
V: R_1 = OCH_3, R_2 = SCH_3

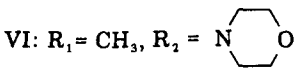

EXPERIMENTAL[1]

Materials — 5,8-Dihydroxy-1,4-bis[2-(hydroxyethyl)aminoethyl] amino-9,10-anthracenedione (I) and 5,8-dihydroxy-1,4-bis[4-(dimethylaminobutyl)amino]-9,10-anthracenedione(II) were used. 1-Methyl-2-bis(2-methylthio)vinylquinolinium iodide(III), 1,6-dimethyl-2-bis(2-methylthio)vinylquinolinium iodide(IV), 1-methyl-6-methoxy-2-bis(2-methylthio)vinylquinolinium iodide(V), and 1,6-dimethyl-2-[2-methylthio-2-(1-morpholino)vinyl]quinolinium iodide (VI) were previously reported (3). Chloroquine (VII), calf thymus DNA type I sodium salt [43% guanosine–cytidine (G–C)], *Escherichia coli* DNA type VIII (50% G–C), *Clostridium perfringens* DNA type XII (27% G–C), *Micrococcus lysodeikticus* DNA type XI (72% G–C), bovine serum albumin, RNA polymerase type I from *E. coli*, adenosine 5′-triphosphate disodium salt (ATP), cytidine 5′-triphosphate sodium salt type III (CTP), uridine 5′-triphosphate sodium salt type III (UTP), and guanosine 5′-triphosphate sodium salt type III (GTP) were all obtained commercially[2]. Tromethamine[3] and [8-^{14}C]adenosine 5′-triphosphate tetrasodium salt[4], [8-^{14}C]ATP, (40 Ci/mmole) were also obtained commercially.

Spectral Analysis—Stock solutions of the compounds were made 1 × 10^{-4} *M* in 5 m*M* tromethamine hydrochloric acid buffer, pH 7.4. Beer's law curves were prepared from the regressed absorbance values, and solutions of 1.5–3.5 × 10^{-5} *M* were scanned in the UV and visible regions. Molar absorptivities are listed in Table I. Spectra were observed in the presence of calf thymus DNA solutions at concentrations of 1.5 × 10^{-5}–5 × 10^{-4} *M*, and are shown in Figs. 1 and 2 for the anthraquinones.

Equilibrium Dialysis—These experiments were carried out using an earlier method (5) with 5-ml glass dialysis cells and a membrane with

[1] Absorption spectra were taken with a Beckman DB spectrophotometer. Melting temperatures were measured with a Gilford 250 spectrophotometer equipped with a baseline reference compensator, analog multiplexer No. 6046 and a No. 2527 thermoprogrammer. Measurement of inhibition of DNA function as a template for *E. coli* RNA polymerase was done using a Packard Tricarb LSC model 3320 liquid scintillation spectrometer.

[2] Sigma Chemical Co., St. Louis, Mo.

[3] Trizma compounds 8.2 and 7.5, Sigma Chemical Co., St. Louis, Mo.

[4] New England Nuclear Corp., Boston, Mass.

0022-3549/82/0200-0253$01.00/0

Table I—Molar Absorptivities [a]

Compound	Absorption Maximum, nm	ϵ_{max}
I	608	18,630
II	610	18,490
III	402	25,480
IV	402	16,870
V	404	20,060
VI	434	30,245
VII	338	13,225

[a] Observed in 5 m*M* tromethamine hydrochloric acid buffer (pH 7.4).

a molecular weight limit of 12,000[5]. Solutions of calf thymus DNA ranging from 1.0×10^{-5} to 1.5×10^{-3} *M* were made in 5 m*M* tromethamine hydrochloric acid buffer (pH 7.4), and a concentration of 1×10^{-4} *M* of compound was prepared in the same medium. Concentrations at equilibrium (24 hr, 25°) were measured by absorption spectra and determinations for each compound were made in duplicate or triplicate. Concentrations of free and bound species were calculated as previously described (6, 7). The correlation coefficient for each compound tested was >0.91. Binding parameters K_{app} and B_{app} are listed in Table II.

Melting Temperature Determination—The temperature in a heated cell was increased at the rate of 1°/min. The concentration of calf thymus DNA was 1.0×10^{-4} *M* nucleotide phosphorus, and the buffer was 5 m*M* tromethamine hydrochloric acid (pH 7.4). Concentrations of compounds used were 1×10^{-4} and 1×10^{-5} *M* for the anthraquinones and 1×10^{-4} *M* for the quinolinium compounds. Absorbance was measured at 260 nm. The temperature at which 50% hyperchromicity is attained (T_m) for the compounds tested is recorded in Table III.

Inhibition of *E. coli* RNA Polymerase—Stock solution H was prepared from: tromethamine hydrochloric acid (1.376 g); potassium chloride (2.795 g); 2-mercaptoethanol (0.195 g); magnesium chloride (0.508 g); bovine serum albumin (0.125 g); and distilled water to make 100 ml.

Stock solution I was prepared from: ATP sodium salt (0.117 g); CTP sodium salt (0.109 g); UTP sodium salt (0.105 g); GTP sodium salt (0.114 g); and distilled water to make 10 ml.

Stock solution J contained [8-^{14}C]ATP (0.01 mCi, 0.13 mg/0.5 ml, 30 μl), and distilled water to make 200 μl.

Stock solution K consisted of 100 units of *E. coli* RNA polymerase diluted with 60% glycerol–40% tromethamine hydrochloric acid buffer containing 0.2 m*M* 1,4-dithiothreitol, 0.01 m*M* ethylenediaminetetraacetic acid, and 10 m*M* magnesium chloride to give 2 units/10 μl. It was stored below 0°.

Stock solution L was prepared from calf thymus DNA solution, 5 m*M* in nucleotide phosphorus (absorption coefficient at 260 nm of 6600 M^{-1}/cm, 0.083 g); ethylenediaminetetraacetic acid (0.056 g); and 5 m*M* tromethamine hydrochloric acid buffer (pH 7.4) to make 50 ml. Solution L was stored below 0°. Other DNA solutions were prepared in the same way.

The liquid scintillation solution contained 2,5-diphenyloxazole (6.000 g); 1,4-bis[2-(5-phenyloxazolyl)]benzene (0.200 g); toluene (1400 ml); and methanol (600 ml).

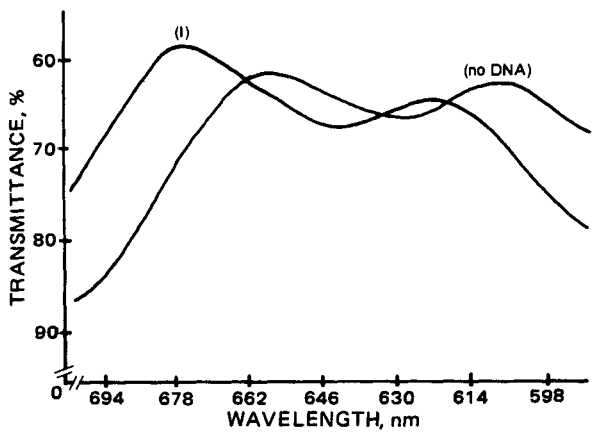

Figure 1—*Influence of DNA on the visible spectrum of I. DNA was used at a concentration of* 25.0×10^{-5} M.

[5] UM-10 Diaflo, Amicon Corp.

Table II—Equilibrium Constants for Binding of I–VII to Calf Thymus DNA [a]

Compound	K_{app}	B_{app}
I	1.31×10^6	0.341
II	2.61×10^6	0.341
III	7.47×10^4	0.063
IV	1.31×10^3	0.075
V	1.05×10^3	0.085
VI	8.70×10^4	0.077
VII	8.08×10^5	0.138

[a] Determined in 5 m*M* tromethamine hydrochloric acid buffer (pH 7.4).

The gain setting for maximum efficiency of the scintillation spectrometer was determined at 40%. The activity of RNA polymerase was determined by measuring the amount of [8-^{14}C]ATP rendered acid insoluble as determined by the filter paper disk assay of Bollum (8).

The assay mixture contained in 0.125 ml consisted of pH 8.0 tromethamine hydrochloric acid buffer (5.000 μmoles); magnesium chloride (1.250 μmoles); potassium chloride (18.750 μmoles); 2-mercaptoethanol (1.250 μmoles); CTP sodium salt (0.019 μmole); GTP sodium salt (0.019 μmole); UTP sodium salt (0.019 μmole); [8-^{14}C]ATP tetrasodium salt (6,500 cpm) (0.019 μmole); calf thymus DNA, (5.000 μg); and bovine serum albumin, (62.500 μg).

DNA (5.0 μg) solutions were preincubated with each compound (1.0×10^{-5}–5.0×10^{-5} *M*) in 25 μl of 5 m*M* tromethamine hydrochloric acid buffer (pH 7.4) for 10 min at 37° prior to the assay of RNA polymerase activity. The reference blank contained DNA in buffer solution.

The assay mixture was prepared by adding 50 μl of solution H, 10 μl of solution I, 10 μl of solution J, 20 ml of distilled water, 5.0 μl of preincubated DNA and the test compound in 25 μl, and 10 μl of *E. coli* RNA polymerase solution (2 units). The mixture was incubated for 10 min at 37°, and the enzyme reaction was terminated by the addition of 25 μl of cold 5% trichloroacetic acid containing 1% tetrasodium pyrophosphate and by chilling in an ice water bath for 15 min.

The acid insoluble material from a 100-μl aliquot of each incubation mixture was spotted uniformly on a 2.5-cm circular millipore filter (0.45 μm pore size), kept at room temperature for 15 min, and washed three times by being swirled in 10 ml of 5% trichloroacetic acid containing 1% tetrasodium pyrophosphate, followed by two washings each of 2.5% trichloroacetic acid and 95% ethanol. Filters were dried and placed in 15 ml of scintillation liquid. Radioactivity was counted in the scintillation spectrometer and all assays were run in triplicate. Inhibition of RNA polymerase activity by the test compounds was recorded (Tables IV and V).

Comparison of Absorption Spectra of Compounds in the Presence of Native Double-Stranded DNA and Separated-Strand DNA—One milliliter of a test compound solution (2.0–5.0×10^{-4} *M*, in tromethamine hydrochloric acid buffer, pH 7.4) was added to 1 ml of either native double-stranded calf thymus DNA (1.25×10^{-4}–5.0×10^{-4} *M*) or to 1 ml of separated-strand DNA solution. Strand separation was done by heating calf thymus DNA solution at 98° for 30 min and immediately

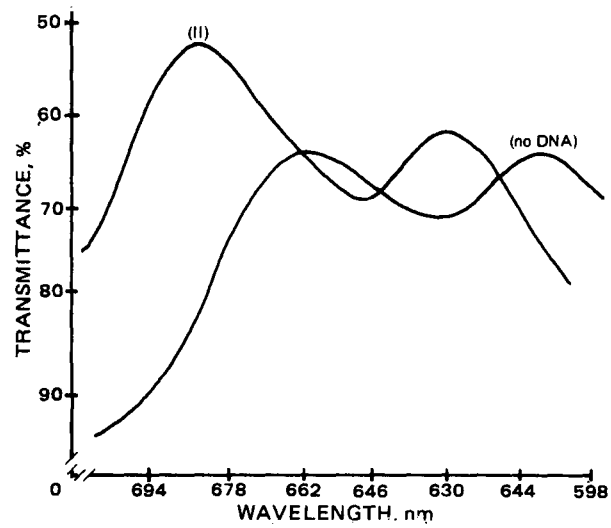

Figure 2.—*Influence of DNA on the visible spectrum II; DNA was used at a concentration of* 40.0×10^{-5} M.

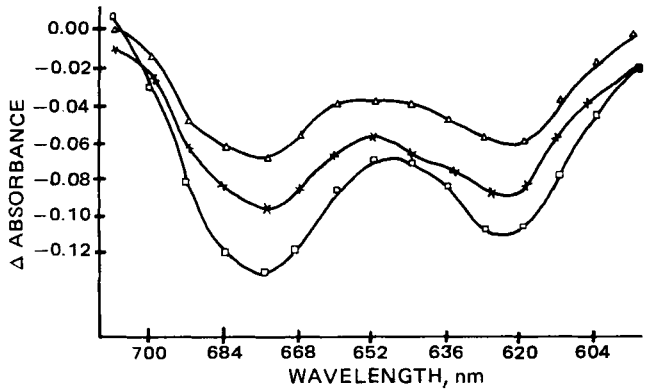

Figure 3—*Difference spectra of free and DNA-bound test compounds. The concentration used was 2.0 × 10⁻⁵ M I and the DNA concentration used was 1.25 × 10⁻⁵ M. Key:* △, C. perfringens *DNA; X, calf thymus DNA; and* □, M. lysodeikticus *DNA.*

cooling the solution at 0°. The control solution used was 5 m*M* tromethamine hydrochloric acid buffer, pH 7.4. Difference spectra were recorded in the visible region.

Inhibition of DNA Function as Template for *E. coli* RNA Polymerase with Varied Base Ratio DNA–DNA from the following sources was used: *C. perfringens* (27% G–C); calf thymus (43% G–C); *E. coli* (50% G–C); and *M. lysodeikticus* (72% G–C). RNA polymerase activity was measured as described and results are tabulated in Table VI. Concentrations used were 1×10^{-4} *M* for the anthraquinones and 1.5×10^{-3} *M* for the quinolinium compounds.

Comparison of Absorption Spectra of Compounds in the Presence of Varied Base Ratio DNA. One milliliter of a test compound solution (2.0×10^{-5}–5.0×10^{-4} *M* in 5 m*M* tromethamine hydrochloric acid buffer, pH 7.4) was added to 1 ml of the various DNA solutions (1.25×10^{-5} *M*, based on phosphorus). The buffer (5 m*M*, pH 7.4) was used as a control. Difference spectra were recorded in the visible region, and the data are plotted in Figs. 3 and 4 for the anthraquinones.

DISCUSSION

Spectral Analysis—The interaction of the compounds with calf thymus DNA resulted in a consistent bathochromic/hypochromic shift in the visible spectrum around 20–30 nm for the anthraquinones and 20–50 nm for the quinolinium compounds. In comparison, chloroquine showed an average shift of 10 nm in the presence of calf thymus DNA.

Equilibrium Dialysis—These experiments using calf thymus DNA were done at ambient temperature at pH 7.4. For determining binding parameters, Scatchard plots were employed using the expression:

$$r/C_f = K_{app}(B_{app} - r) \qquad \text{(Eq. 1)}$$

where r is the ratio of bound compound to DNA nucleotide phosphorus, C_f is the concentration of free compound, K_{app} is the apparent binding constant, and B_{app} is the apparent number of binding sites per nucleotide phosphorus. The binding parameters K_{app} and B_{app} are shown in Table II. These values were obtained from the nearly linear portion of the isotherm at small values of r for a strong binding.

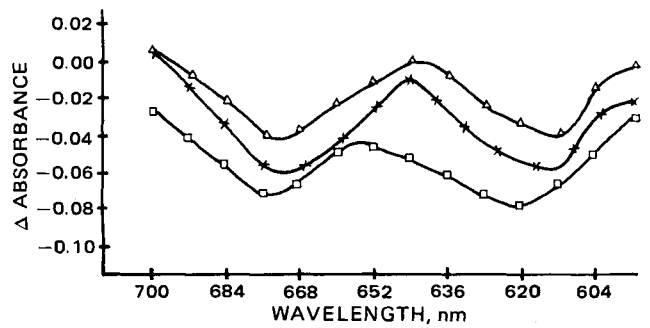

Figure 4—*Difference spectra of free and DNA-bound test compounds. The concentration used was 2.0 × 10⁻⁵ M II and the DNA concentration used was 1.25 × 10⁻⁵ M. Key:* △, C. perfringens *DNA; X, calf thymus DNA;* and □, M lysodeikticus *DNA.*

Table III—Melting Temperature Determination [a]

Compound	T_m	ΔT_m
DNA (calf thymus) [b]	62.0°	
I [b]	72.0°	10.0°
II [b]	74.0°	12.0°
I [c]	>100.0°	>38.0°
II [c]	>100.0°	>38.0°
III [b]	69.5°	7.5°
IV [b]	71.5°	9.5°
V [b]	71.0°	9.0°
VI [b]	70.0°	8.0°
VII [b]	76.0°	14.0°

[a] Measured at 260 nm with a temperature rise of 1°/min. [b] 1.0×10^{-4} *M*. [c] 1.0×10^{-5} *M*.

Table IV—Inhibition of *E. coli* RNA Polymerase by the Anthraquinones on Calf Thymus DNA as Substrate

Concentration, *M*	Inhibition, % I	Inhibition, % II
2.0×10^{-4}	89.01	90.26
1.0×10^{-4}	79.03	79.20
6.0×10^{-5}	40.39	68.38
2.0×10^{-5}	31.80	35.92
1.0×10^{-5}	26.69	10.44
1.0×10^{-6}	0.00	0.00

Table V—Inhibition of *E. coli* RNA Polymerase by the Methylthiovinylquinolinium Iodides on Calf Thymus DNA as Substrate

Concentration, *M*	Inhibition, % III	IV	V	VII	VIII
5.0×10^{-3}					60.00
4.0×10^{-3}	50.08	67.44	52.18	47.08	
2.0×10^{-3}	35.28	57.66	26.05	35.98	35.12
1.0×10^{-3}	27.40	41.47	18.41	3.37	19.28
1.0×10^{-4}	17.02	8.03	13.28	0.00	0.00
1.0×10^{-5}	13.18	0.00	0.00	0.00	0.00
1.0×10^{-6}	0.00	0.00	0.00	0.00	0.00

Scatchard plots of the binding data for the anthraquinones yielded biphasic curves, which indicates that two binding sites are involved, a stronger and a weaker (Figs. 5 and 6). The stronger binding data were derived from the linear region of the plot at small values of r. The other slope at higher values of r indicates the presence of a weaker binding site. The strong binding is most likely associated with intercalation of the anthraquinone ring into DNA base pairs (9, 10). The weaker binding may be associated with the secondary binding of the side chains by electrostatic interaction with the anionic exterior of the DNA helix.

Association constants for the anthraquinone derivatives are of the same order of magnitude as those found for daunorubicin and doxorubicin (9, 10), lower than that for dactinomycin (11, 12), and greater than that for chloroquine (13). The apparent number of binding sites per nucleotide obtained for the strong binding site is 0.34, indicating that binding of these compounds involves approximately three adjacent phosphate groups on the DNA.

The linear binding isotherms of the quinolinium compounds indicate that only one type of binding site is involved on the DNA helix. The association constants are lower than those obtained for either the anthraquinones or chloroquine. The compounds of this group bind at approximately one of every contiguous 8–12 phosphate groups on the DNA. The binding abilities of the compounds of this type were essentially the same, indicating little effect from the 6-substituents.

Melting Temperature Elevation—Thermal denaturation studies were done at pH 7.4, using calf thymus DNA. The results shown in Table III indicate that all of the compounds bind to and stabilize the DNA helix toward temperature denaturation. Thermal stabilization did not vary much between the members in each series, but the anthraquinones caused a greater T_m increase than either the quinolinium compounds or chloroquine, and much greater than the usual tetracyclic intercalating agents (9). This suggests the possible formation of a covalent bond *via* a radical reaction induced at higher temperature (14).

Inhibition of *E. coli* RNA-Polymerase Activity—Inhibition of DNA function as a template for *E. coli* RNA polymerase was carried out *in vitro* using graded concentrations of the compounds. Results are listed in

Table VI—Inhibition of *E. coli* RNA Polymerase Using Varied DNA Base Ratios

DNA (% G–C)	Inhibition, %						
	I	II	III	IV	V	VI	VIII
C. perfringens (27%)	46.43	41.17	20.79	18.18	14.39	25.21	5.05
Calf thymus (43%)	79.74	78.68	26.52	35.66	26.17	22.58	25.78
E. coli (50%)	81.12	89.49	33.84	36.66	28.24	41.42	45.19
M. lysodeikticus (72%)	97.53	93.86	48.93	40.17	48.94	46.54	51.51

Tables IV and V. The anthraquinones were the stronger inhibitors, giving 80–90% inhibitions at concentrations of 10^{-4} *M*. The quinolinium compounds gave 47–67% inhibitions at concentrations of 10^{-3} *M*, which were comparable to the inhibitory ability of the same concentrations of chloroquine (13).

Studies of Complex Formation—Comparison of the visible absorption spectra of the compounds in the presence of native double-stranded and separated-strand DNA (calf thymus) was made. The difference spectra showed marked quenching in absorptivities in the spectrum of the double-stranded DNA (Figs. 3 and 4) but very little change in the spectrum of the separated-strand DNA. The requirement for double-stranded DNA with all the compounds tested indicated that the double-helical structure is necessary for strong binding, and that both strands are involved.

Base specificity for the interaction between DNA and the compounds tested was clearly demonstrated by the inhibition of DNA function as measured by inhibition of *E. coli* RNA-polymerase activity with different base ratios of guanosine and cytidine. The extent of transcription inhibition is shown in Table VI. It is apparent that there is a preference for the G–C base pair, since the degree of inhibition is greatest, with both series of compounds, with the DNA source having the highest G–C base pair ratio. The anthraquinones appeared to have a greater preference for this base pair than the quinolinium compounds, as indicated by extent of inhibition.

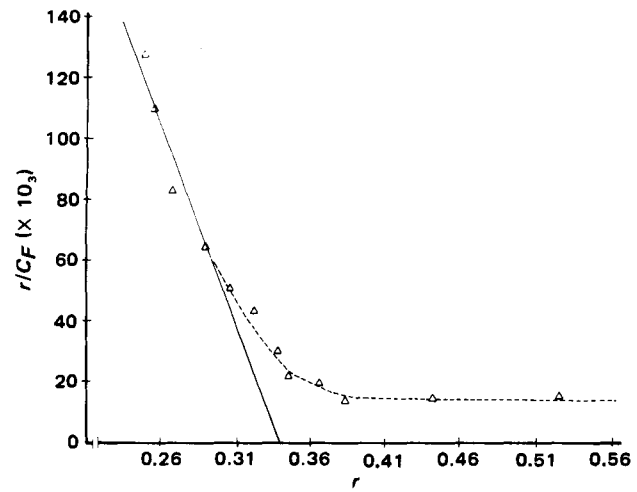

Figure 5—*Scatchard plot of I.*

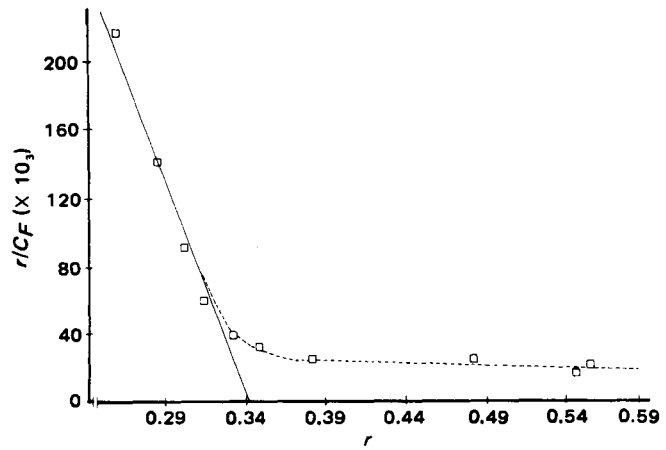

Figure 6—*Scatchard plot of II.*

Comparison of the absorption spectra of the compounds in the presence of the varied DNA base ratios was also carried out to further delineate the tendency toward base-pair specificity in DNA binding. The difference spectra for the anthraquinones (Figs. 3 and 4) revealed a proportionality to the G–C contents of the DNA species used, but the quinolinium derivatives showed no difference in depressive effect on the extinction coefficients in the spectra, indicating no G–C specificity. This illustrates the advantage of employing more than one method of measurement.

A probable mode of action of the methylthiovinylquinolinium iodides is an inhibition of nucleic acid biosynthesis with formation of a molecular complex with DNA. Only one type of binding site is apparently involved. The complex formed involves both strands of the DNA double helix and may result from the insertion of the planar ligand between base pairs of the helix, the intercalation model of Muller and Crothers (15) and Lerman (16).

The binding parameters of the four compounds in this series are of the same order of magnitude. Although a marginal preference of G–C base-pair binding was shown by the extent of inhibition of RNA transcription, this was not detectable by comparison of the visible absorption spectra of the compounds in the presence of varied DNA base ratios. One can assume that the biochemical technique is definitely more sensitive and meaningful than the spectral methods for distinguishing those agents with borderline DNA base-pair specificities of binding. The presence of a 6-substituent has little effect on the extent of DNA binding.

The binding studies of the two anthraquinones indicate that both compounds bind to DNA with comparable strength. Binding isotherms indicate two binding sites on DNA for these compounds. The stronger binding is presumed to be intercalation between successive base pairs; the weaker binding is considered to be an electrostatic interaction involving DNA phosphate groups and the amino side chains. Comparison of absorption spectra and the extent of RNA transcription inhibition with varied DNA base ratios show a preference for binding with the G–C base pair. Since the binding parameters of the two anthraquinones are essentially the same, the strong antileukemic activity of the active compound (I) could be due to additional factors such as *in vivo* metabolic activation, pharmacokinetic behavior of biologically active components, or alternative action sites in the cell apparatus other than nuclei (14).

It is apparent from these *in vitro* methods of studying DNA binding ability that some differences in anticancer activity, such as between the anthraquinones and the quinolinium compounds, may be correlated with the relative binding strengths to DNA. On the other hand, these methods may fail to distinguish between active and inactive compounds, as seen with the anthraquinones, where other biological factors may become determinant.

REFERENCES

(1) W. O. Foye, Y. J. Lee, K. A. Shah, and J. M. Kauffman, *J. Pharm. Sci.*, **67**, 962 (1978).

(2) W. O. Foye and J. M. Kauffman, *ibid.*, **68**, 336 (1979).

(3) *Ibid.*, **69**, 477 (1980).

(4) R. E. Wallace, K. C. Murdock, R. B. Angier, and F. E. Durr, *Cancer Res.*, **39**, 1570 (1978).

(5) K. G. Wagner and R. Arav, *Biochemistry*, **7**, 1771 (1968).

(6) G. Scatchard, *Ann. N.Y. Acad. Sci.*, **51**, 660 (1949).

(7) W. O. Foye, M. M. Karkaria, and W. H. Parsons, *J. Pharm. Sci.*, **69**, 84 (1980).

(8) F. J. Bollum, *Proc. Nucleic Acid Res.*, **1**, 296 (1966).

(9) F. Zunio, R. Gambetta, A. DiMarco, and A. Zacchara, *Biochim. Biophys. Acta*, **277**, 489 (1972).

(10) J. C. Double and J. R. Brown, *J. Pharm. Pharmacol.*, **27**, 502 (1975).

(11) W. Gilbert, C. E. Smith, D. Neville, and G. Felsenfeld, *J. Mol. Biol.*, **11**, 445 (1965).

(12) S. K. Sengupta and D. Schaer, *Biochim. Biophys. Acta*, **521**, 89 (1978).

(13) R. L. O'Brien, J. L. Allison, and F. E. Hahn, *ibid.*, **129**, 622 (1966).

(14) N. R. Bachur, S. L. Gordon, and M. V. Gee, *Mol. Pharmacol.*, **13**,

901 (1977).
(15) W. Muller and D. M. Crothers, *J. Mol. Biol.*, **35**, 251 (1968).
(16) L. S. Lerman, *ibid.*, **3**, 18 (1961).

ACKNOWLEDGMENTS

Abstracted from a thesis submitted by O. Vajragupta to the Massachusetts College of Pharmacy and Allied Health Sciences in partial fulfillment of Doctor of Philosophy degree requirements.

The authors express their appreciation to the John R. and Marie K. Sawyer Memorial Fund and the Gillette Company for financial assistance, and to National Cancer Institute Grant CA 26281 to Sisir K. Sengupta. They also thank Dr. K. C. Murdock of Lederle Laboratories for the gift of the anthraquinone derivatives used in this study.

Antitumor Agents XLVII: The Effects of Bisbrusatolyl Malonate on P-388 Lymphocytic Leukemia Cell Metabolism

IRIS H. HALL ˣ, Y. F. LIOU, K. H. LEE, M. OKANO, and STEPHEN G. CHANEY *

Received February 19, 1981, from the *Division of Medicinal Chemistry, School of Pharmacy, and the *Department of Biochemistry, School of Medicine, University of North Carolina at Chapel Hill, NC 27514.* Accepted for publication July 15, 1981.

Abstract □ Bisbrusatolyl malonate, which was shown previously to be active against P-388 lymphocytic leukemia cell growth, was investigated for inhibitory effects on nucleic acid and protein synthesis. DNA and RNA synthesis as well as protein synthesis were markedly inhibited at 10, 25, and 50 μmole final concentrations *in vitro*. The major sites of inhibition of nucleic acid synthesis appeared to be DNA polymerase, messenger and transfer RNA polymerases, orotidine-5′-monophosphate decarboxylase, phosphoribosyl pyrophosphate amino transferase, and dihydrofolate reductase. Moderate inhibition of nucleotide kinase activities and oxidative phosphorylation processes occurred after drug treatment. Cyclic adenosine monophosphate levels were reduced. Protein synthesis was inhibited during the elongation step of peptide synthesis. The data suggested that bisbrusatolyl malonate interfered with the peptide bond formation. However, the ongoing polypeptide synthesis must be completed before the drug can bind to the ribosome effectively.

Keyphrases □ Bisbrusatolyl malonate—effects on P-388 lymphocytic leukemia cell metabolism □ Antitumor agents—effects of bisbrusatolyl malonate on P-388 lymphocytic leukemia cell metabolism □ RNA—synthesis, effect of bisbrusatolyl malonate, P-388 lymphocytic leukemia cells □ DNA—synthesis, effect of bisbrusatolyl malonate, P-388 lymphocytic leukemia cells □ Protein synthesis—effect of bisbrusatolyl malonate, P-388 lymphocytic leukemia cells

Antineoplastic activity against P-388 lymphocytic leukemia growth was established previously for bisbrusatolyl esters (1, 2). One of these derivatives, bisbrusatolyl malonate at 0.6 mg/kg/day ip, gave T/C % values of 271, 197, and 188 in BDF_1 male mice (2) in a P-388 tumor model sensitive to quassinoids (2). This agent was shown to suppress *in vitro* DNA synthesis by 45%, RNA synthesis by 48%, and protein synthesis by 83% at 10 μM concentration after 90 min incubation. A number of enzymes involved in nucleic acid metabolism, *e.g.*, DNA polymerase and dihydrofolate reductase, were inhibited *in vitro* by this ester (2). A detailed study of the effects of bisbrusatolyl malonate on P-388 lymphocytic leukemia cellular metabolism was conducted and its effects on nucleic acid and protein metabolism are now reported.

EXPERIMENTAL

Bisbrusatolyl malonate (I) was synthesized and characterized previously in the literature (2). The P-388 lymphocytic leukemia tumor line was maintained in DBA/2 male mice (~20 g). For the *in vitro* studies,

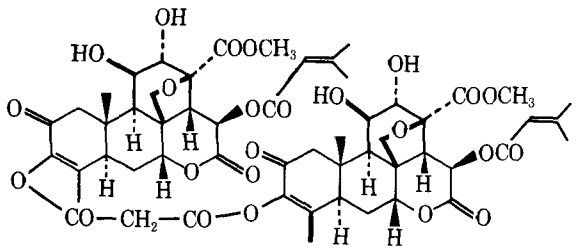

I

P-388 cells were harvested from the peritoneal cavity 10 days after administering 10^6 P-388 lymphocytic leukemia cells intraperitoneally into BDF_1 male mice (~20 g) on day 0 (3). In the *in vivo* studies, BDF_1 male mice were inoculated with 10^6 P-388 cells intraperitoneally, and on days 7, 8, and 9 the mice were administered 0.6 mg/kg/day bisbrusatolyl malonate intraperitoneally. The biochemical studies were performed on cells harvested from the peritoneal cavity on day 10.

The *in vitro* incorporation studies (4) were conducted using 1 μCi [6-^{3}H]thymidine (21.8 Ci/mmole), [6-^{3}H]uridine (22.4 Ci/mmole), or [4,5-^{3}H(N)]L-leucine (56.5 Ci/mmole) with 10^6 P-388 cells in minimum essential medium, pH 7.2, in a total volume of 1 ml, incubated for 60 min at 37°. Thymidine incorporation into DNA was terminated with perchloric acid containing pyrophosphate which was filtered on glass fiber paper by vacuum suction. RNA and protein assays were terminated with trichloroacetic acid and collected on nitrocellulose membranes by vacuum suction. The acid-insoluble precipitates on the filter papers were placed in scintillation vials and counted. *In vivo* thymidine incorporation into DNA was determined by injecting into the animal 10 μCi of [^{3}H]-methylthymidine (24.7 Ci/mmole) intraperitoneally 1 hr before sacrifice. The DNA was isolated (5) and the [^{3}H]thymidine content determined in scintillation fluid[1] and corrected for quenching. The DNA concentration was determined by the diphenylamine reaction using calf thymus DNA as the standard. The results were expressed as dpm/mg of DNA isolated. Uridine incorporation into RNA was determined in an analogous manner with 10 μCi of [^{3}H]uridine (20 Ci/mmole) and the RNA extracted (6). Leucine incorporation into protein was determined by the method of Sartorelli (7) with 10 μCi[^{3}H]L-leucine (56.5 Ci/mmole). The control values for DNA synthesis were 202,098 dpm/mg of DNA, 235,360 dpm/mg of RNA for RNA synthesis, and 99,102 dpm/mg of protein isolated for leucine incorporation.

On day 10 after *in vivo* administration of the drug, the number of tumor cells per milliliter and the 0.4% trypan blue uptake were determined with a hemocytometer (8). The *in vitro* UV binding studies were conducted with I (50 μg/ml) incubated with DNA (38 μg/ml) in 0.1 *M* phosphate

[1] Fisher Scintiverse.

0022-3549/82/0200-0257$01.00/0

901 (1977).
(15) W. Muller and D. M. Crothers, *J. Mol. Biol.*, **35**, 251 (1968).
(16) L. S. Lerman, *ibid.*, **3**, 18 (1961).

ACKNOWLEDGMENTS

Abstracted from a thesis submitted by O. Vajragupta to the Massachusetts College of Pharmacy and Allied Health Sciences in partial fulfillment of Doctor of Philosophy degree requirements.

The authors express their appreciation to the John R. and Marie K. Sawyer Memorial Fund and the Gillette Company for financial assistance, and to National Cancer Institute Grant CA 26281 to Sisir K. Sengupta. They also thank Dr. K. C. Murdock of Lederle Laboratories for the gift of the anthraquinone derivatives used in this study.

Antitumor Agents XLVII: The Effects of Bisbrusatolyl Malonate on P-388 Lymphocytic Leukemia Cell Metabolism

IRIS H. HALL ˣ, Y. F. LIOU, K. H. LEE, M. OKANO, and STEPHEN G. CHANEY *

Received February 19, 1981, from the *Division of Medicinal Chemistry, School of Pharmacy, and the *Department of Biochemistry, School of Medicine, University of North Carolina at Chapel Hill, NC 27514.* Accepted for publication July 15, 1981.

Abstract □ Bisbrusatolyl malonate, which was shown previously to be active against P-388 lymphocytic leukemia cell growth, was investigated for inhibitory effects on nucleic acid and protein synthesis. DNA and RNA synthesis as well as protein synthesis were markedly inhibited at 10, 25, and 50 μmole final concentrations *in vitro*. The major sites of inhibition of nucleic acid synthesis appeared to be DNA polymerase, messenger and transfer RNA polymerases, orotidine-5′-monophosphate decarboxylase, phosphoribosyl pyrophosphate amino transferase, and dihydrofolate reductase. Moderate inhibition of nucleotide kinase activities and oxidative phosphorylation processes occurred after drug treatment. Cyclic adenosine monophosphate levels were reduced. Protein synthesis was inhibited during the elongation step of peptide synthesis. The data suggested that bisbrusatolyl malonate interfered with the peptide bond formation. However, the ongoing polypeptide synthesis must be completed before the drug can bind to the ribosome effectively.

Keyphrases □ Bisbrusatolyl malonate—effects on P-388 lymphocytic leukemia cell metabolism □ Antitumor agents—effects of bisbrusatolyl malonate on P-388 lymphocytic leukemia cell metabolism □ RNA—synthesis, effect of bisbrusatolyl malonate, P-388 lymphocytic leukemia cells □ DNA—synthesis, effect of bisbrusatolyl malonate, P-388 lymphocytic leukemia cells □ Protein synthesis—effect of bisbrusatolyl malonate, P-388 lymphocytic leukemia cells

Antineoplastic activity against P-388 lymphocytic leukemia growth was established previously for bisbrusatolyl esters (1, 2). One of these derivatives, bisbrusatolyl malonate at 0.6 mg/kg/day ip, gave T/C % values of 271, 197, and 188 in BDF_1 male mice (2) in a P-388 tumor model sensitive to quassinoids (2). This agent was shown to suppress *in vitro* DNA synthesis by 45%, RNA synthesis by 48%, and protein synthesis by 83% at 10 μM concentration after 90 min incubation. A number of enzymes involved in nucleic acid metabolism, *e.g.*, DNA polymerase and dihydrofolate reductase, were inhibited *in vitro* by this ester (2). A detailed study of the effects of bisbrusatolyl malonate on P-388 lymphocytic leukemia cellular metabolism was conducted and its effects on nucleic acid and protein metabolism are now reported.

EXPERIMENTAL

Bisbrusatolyl malonate (I) was synthesized and characterized previously in the literature (2). The P-388 lymphocytic leukemia tumor line was maintained in DBA/2 male mice (~20 g). For the *in vitro* studies,

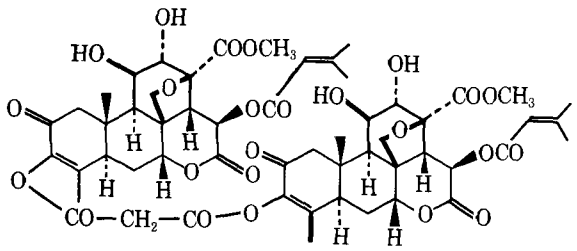

I

P-388 cells were harvested from the peritoneal cavity 10 days after administering 10^6 P-388 lymphocytic leukemia cells intraperitoneally into BDF_1 male mice (~20 g) on day 0 (3). In the *in vivo* studies, BDF_1 male mice were inoculated with 10^6 P-388 cells intraperitoneally, and on days 7, 8, and 9 the mice were administered 0.6 mg/kg/day bisbrusatolyl malonate intraperitoneally. The biochemical studies were performed on cells harvested from the peritoneal cavity on day 10.

The *in vitro* incorporation studies (4) were conducted using 1 μCi [6-^{3}H]thymidine (21.8 Ci/mmole), [6-^{3}H]uridine (22.4 Ci/mmole), or [4,5-^{3}H(N)]L-leucine (56.5 Ci/mmole) with 10^6 P-388 cells in minimum essential medium, pH 7.2, in a total volume of 1 ml, incubated for 60 min at 37°. Thymidine incorporation into DNA was terminated with perchloric acid containing pyrophosphate which was filtered on glass fiber paper by vacuum suction. RNA and protein assays were terminated with trichloroacetic acid and collected on nitrocellulose membranes by vacuum suction. The acid-insoluble precipitates on the filter papers were placed in scintillation vials and counted. *In vivo* thymidine incorporation into DNA was determined by injecting into the animal 10 μCi of [^{3}H]-methylthymidine (24.7 Ci/mmole) intraperitoneally 1 hr before sacrifice. The DNA was isolated (5) and the [^{3}H]thymidine content determined in scintillation fluid[1] and corrected for quenching. The DNA concentration was determined by the diphenylamine reaction using calf thymus DNA as the standard. The results were expressed as dpm/mg of DNA isolated. Uridine incorporation into RNA was determined in an analogous manner with 10 μCi of [^{3}H]uridine (20 Ci/mmole) and the RNA extracted (6). Leucine incorporation into protein was determined by the method of Sartorelli (7) with 10 μCi[^{3}H]L-leucine (56.5 Ci/mmole). The control values for DNA synthesis were 202,098 dpm/mg of DNA, 235,360 dpm/mg of RNA for RNA synthesis, and 99,102 dpm/mg of protein isolated for leucine incorporation.

On day 10 after *in vivo* administration of the drug, the number of tumor cells per milliliter and the 0.4% trypan blue uptake were determined with a hemocytometer (8). The *in vitro* UV binding studies were conducted with I (50 μg/ml) incubated with DNA (38 μg/ml) in 0.1 *M* phosphate

[1] Fisher Scintiverse.

0022-3549/82/0200-0257$01.00/0

Table I—*In Vitro* Effects of Bisbrusatolyl Malonate on Nucleic Acid and Protein Synthesis of P-388 Lymphocytic Leukemia Cells after 60-min Incubation

	% Control, whole cells		
	DNA Synthesis	RNA Synthesis	Protein Synthesis
Control (0.05% polysorbate 80)	100 ± 6[a]	100 ± 5[b]	100 ± 5[c]
Bisbrusatolyl malonate			
10 μM	58 ± 3[d]	78 ± 5[d]	52 ± 6[d]
25 μM	54 ± 7[d]	65 ± 6[d]	18 ± 3[d]
50 μM	57 ± 6[d]	92 ± 7	8 ± 2[d]
	% Control homogenized cells		
	DNA Synthesis	RNA Synthesis	Protein Synthesis
Control (0.05% polysorbate 80)	100 ± 7	100 ± 8	100 ± 6
Bisbrusatolyl malonate			
10 μM	59 ± 6[d]	72 ± 5	48 ± 4[d]

[a] 37659 dpm/10^6 cells/hr. [b] 42981 dpm/10^6 cells/hr. [c] 77421 dpm/10^6 cells/h. [d] $p \leq 0.001$.

buffer (pH 7.2) from 0–24 hr and measured over the range of 200–340 nm (8).

The *in vitro* enzymatic studies were conducted with I present in a final concentration of 10 μM. The *in vitro* and *in vivo* enzymatic assays have been described previously (4). Nuclear DNA polymerase activity was determined on isolated P-388 cell nuclei (9) using the incubation medium of Sawada *et al.* (10), except that [^{3}H]methylthymidine triphosphate (78.1 Ci/mmole) was used. The insoluble nucleic acids were collected on glass fiber papers. The control value was 24,568 dpm/mg of nuclear protein. Messenger, ribosomal, and transfer RNA polymerase enzymes were isolated using different concentrations of ammonium sulfate (11), and the individual polymerase activities were measured using [5,6-^{3}H]-uridine-5-triphosphate (23.2 Ci/mmole). Insoluble ribonucleic acids were collected on nitrocellulose filters (11, 12). Control values for messenger, ribosomal, and transfer RNA polymerase activities were 1807, 2987, and 2270 dpm/mg of nucleic protein, respectively. Ribonucleotide reductase activity was measured by a previous method (13) using [^{14}C]cytidine-5′-diphosphate (25 Ci/mmole). The deoxyribonucleotides were separated from ribonucleotides by polyethyleneiminecellulose TLC. The control value for the reductase was 22,392 dpm/mg of protein. Deoxythymidine kinase, deoxythymidylate monophosphate kinase, and deoxythymidylate diphosphate kinase activities were measured by spectrophotometric assay (14) based on the disappearance of nadide at 340 nm. Control values using a postnuclear supernate (600×*g* for 10 min) were a change in absorbance of 0.365, 0.182, and 0.368 o.d. units/hr/mg of protein, respectively. Enzymes of the pyrimidine synthetic pathway were also measured. Carbamyl phosphate synthetase activity was determined by a previous method (15). The colorimetric determination of citrulline was also performed according to a previous method (16), resulting in 3.26 mg of citrulline formed/hr/μg of protein. Aspartate carbamyl transferase activity was carried out in the presence of aspartate transcarbamylase (15) and the colorimetric determination (17) of the carbamyl aspartate that formed resulted in 0.301 μmole formed/hr/mg of protein. Orotidine-5′-phosphate decarboxylase activity was measured using a 16,300×*g* (20 min) supernate by a technique (18) using [^{14}C]carbonyl orotidine-5′-monophosphate (34.9 mCi/mmole). The control value was 39,059 dpm/mg of protein. Thymidylate synthetase activity was determined by a method (19) utilizing a postmitochondrial supernate (9000×*g* for 10 min) with 5 μCi of [5-^{3}H]deoxyuridine monophosphate (11 Ci/mmole), giving a control value of 12,374 dpm/hr/mg of protein. Dihydrofolate reductase activity was determined using a 600×*g* (10 min) supernate by a spectrophotometric method (20) based on the disappearance of reduced nadide resulting in a value of 0.761 o.d. unit/hr/mg of protein for 10-day P-388 cells. [^{14}C]-Formate incorporation into purines was measured by a method (21) using 0.5 μCi of [^{14}C]formic acid (4.95 mCi/mmole). Purine separation was achieved by silica gel TLC eluting with *n*-butanol–acetic acid–water (4:1:5). Using guanine and adenine standards, the appropriate spots were scraped and the radioactivity determined. The control value for purine synthesis was 10,621 dpm/mg of protein. Phosphoribosyl pyrophosphate amino transferase activity was determined by a spectrophotometric method (22) at 340 nm using a 600×*g* (10 min) supernate, resulting in a control value of 0.806 o.d. unit/hr/mg of protein. Inosinic acid dehydrogenase activity was determined by a spectrophotometric method (23) at 340 nm. The control value for 10-day P-388 cells was 0.133 o.d. unit/min/μg of protein for a 600×*g* (10 min) supernate. Deoxyribonuclease activity was measured at pH 5.0 by a modification of the deDuve method (24). Ribonuclease and acid cathepsin activities were determined at pH 5.0 by a previous method (25). The control deoxyribonuclease activity was 1.72 μg of DNA hydrolyzed/min/mg of protein; ribonuclease activity was 7.24 μg RNA hydrolyzed/min/mg of protein. Cathepsin activity was 65.7 μg of azocasein hydrolyzed/min/mg of protein for 10-day P-388 cells.

Table II—*In Vitro* Effects of Bisbrusatolyl Malonate on Enzymatic Activities of P-388 Lymphocytic Leukemia Cells

Enzyme (n = 6)	% Control: Control (0.05% Polysorbate 80)	% Control: Bisbrusatolyl Malonate, 10 μM
Deoxyribonucleic acid polymerase	100 ± 12	43 ± 8[a]
Messenger ribonucleic acid polymerase	100 ± 8	75 ± 11[b]
Ribosomal ribonucleic acid polymerase	100 ± 3	84 ± 10[b]
Transfer ribonucleic acid polymerase	100 ± 3	66 ± 7[a]
Ribonucleotide reductase	100 ± 12	88 ± 9
d-Thymidine kinase	100 ± 7	72 ± 5[a]
d-Thymidine monophosphate kinase	100 ± 13	50 ± 6[a]
d-Thymidine diphosphate kinase	100 ± 6	79 ± 9[b]
Carbamyl phosphate synthetase	100 ± 3	85 ± 8[b]
Aspartate carbamoyltransferase	100 ± 9	107 ± 12
Orotidine-5′-phosphate decarboxylase	100 ± 11	69 ± 4[a]
Thymidylate synthetase	100 ± 11	82 ± 6[c]
Dihydrofolate reductase	100 ± 13	71 ± 10[b]
^{14}C-Formate incorporation into purines	100 ± 6	45 ± 6[a]
Phosphoribosyl pyrophosphate aminotransferase	100 ± 3	69 ± 5[a]
Inosinic acid dehydrogenase	100 ± 12	94 ± 10
Deoxyribonuclease	100 ± 8	33 ± 7[a]
Ribonuclease	100 ± 5	16 ± 7[a]
Cathepsin	100 ± 7	72 ± 6[a]
Histone phosphorylation	100 ± 5	111 ± 6
Nonhistone phosphorylation	100 ± 5	89 ± 4[b]
S-Adenosyl-L-methionine methyl transferase	100 ± 6	53 ± 7
Oxidative phosphorylation processes		
Succinate		
State 4	100 ± 4	84 ± 3[a]
State 3	100 ± 3	76 ± 5[a]
α-ketoglutarate		
State 4	100 ± 5	71 ± 3[a]
State 3	100 ± 4	78 ± 3[a]

$p \leq 0.005$. [c] $p \leq 0.010$.

Histone phosphorylation was determined by injecting 10 μCi of [γ-^{32}P]adenosine triphosphate (27 Ci/mmole) intraperitoneally. The nuclei were isolated 1 hr later and the histone chromatin protein extracted (26). Nonhistone chromatin phosphorylation by nucleic protein kinase was determined on isolated nuclei (9), utilizing 2 mmoles of [γ-^{32}P]adenosine triphosphate. Chromatin protein was collected on nitrocellulose membrane filters (27) and cyclic adenosine triphosphate levels were determined with a commercial radioimmunoassay kit[2] using iodine 125. Methyl transferase activity was determined by a method (28) using 0.05 μCi of [$^{14}CH_3$]*S*-adenosyl-L-methionine (53 mCi/mmole). The control value for histone phosphorylation was 1211 dpm/mg of chromatin protein isolated; nonhistone phosphorylation was 2391 dpm/mg of protein, and cyclic adenosine phosphate was 1.25 pmoles/10^6 cells. Methyl transferase activity for the control was 217 dpm/mg of protein. Oxidative phosphorylation studies were carried out on 9-day P-388 cells (29). Oxygen consumption was measured with a Clark electrode connected to an oxygraph. The reaction vessel contained 55 μmoles of sucrose, 22 μmoles of monobasic potassium phosphate, 22 μmoles of potassium chloride, 90 μmoles of succinate or 60 μmoles of α-ketoglutarate as substrate, and 22 μmoles of adenosine triphosphate. The final I concentration was 10 μmoles. After the basal metabolic level (state 4) was reached, 0.257 μmole of adenosine diphosphate was added to the vessel to obtain the adenosine diphosphate-stimulated respiration rate (state 3). Basal respiration (state 4) using succinate as substrate resulted in 11.44 μl O_2 consumed/min/mg of protein and 10.0/μl of O_2 consumed/min/mg of protein using α-ketoglutarate. The adenosine diphosphate stimulated respiration rate for succinate was 20.76, and for α-ketoglutarate 10.17 μl of O_2 consumed/min/mg of protein.

The studies on the effects of I on protein synthesis were conducted on P-388 cells harvested on day 10. P-388 lymphocytic leukemia lysates were

[2] Becton Dickinson.

Table III—Effects of Bisbrusatolyl Malonate on P-388 Lymphocytic Leukemia Cells *In Vivo*

	Control	Bisbrusatolyl Malonate, 0.6 mg/kg/day, days 7, 8, 9
Incorporation Studies		
Thymidine into DNA	100 ± 9	41 ± 5[a]
Uridine into RNA	100 ± 8	53 ± 9[a]
Leucine into protein	100 ± 4	34 ± 7[a]
Enzymatic Studies		
DNA polymerase	100 ± 8	44 ± 7[a]
Messenger RNA polymerase	100 ± 6	61 ± 5[a]
Ribosomal RNA polymerase	100 ± 6	83 ± 6[b]
Transfer RNA polymerase	100 ± 7	50 ± 7[a]
Ribonucleotide reductase	100 ± 6	108 ± 8
d-Thymidine kinase	100 ± 5	68 ± 4
d-Thymidine monophosphate kinase	100 ± 8	63 ± 6[a]
d-Thymidine diphosphate kinase	100 ± 10	77 ± 8[b]
Carbamyl phosphate synthetase	100 ± 8	102 ± 7
Aspartate carbamyl transferase	100 ± 12	100 ± 8
Orotidine monophosphate decarboxylase	100 ± 10	27 ± 3[a]
Thymidylate synthetase	100 ± 6	89 ± 5
Dihydrofolate reductase	100 ± 11	12 ± 7[a]
[^{14}C]Formate incorporation into purines	100 ± 12	55 ± 11[a]
Phosphoribosyl pyrophosphate aminotransferase	100 ± 4	59 ± 7[a]
Inosinic acid dehydrogenase	100 ± 10	100 ± 8
Histone phosphorylation	100 ± 12	136 ± 13[b]
Non-histone phosphorylation	100 ± 4	79 ± 7[a]
Cyclic adenosine monophosphate levels	100 ± 8	20 ± 5[a]
Oxidative Phosphorylation Studies		
Succinate		
State 4	100 ± 4	75 ± 7[a]
State 3	100 ± 4	66 ± 4[a]
α-ketoglutarate		
State 4	100 ± 3	72 ± 5[a]
State 3	100 ± 5	70 ± 2[a]
Number cells × 10^6/ml ascites fluid	100 ± 6	44 ± 5[a]

[a] $p \leq 0.001$. [b] $p \leq 0.005$. [c] $p \leq 0.010$.

prepared by the method of Kruh *et al.* (30). The following were isolated from P-388 lysates by literature techniques: run-off ribosomes (31), pH 5 enzyme (30), and uncharged transfer RNA (32).The P-388 lymphocytic leukemia cell initiation factors for protein synthesis were prepared by the method of Majumdar (33) O^{3}H methionyl transfer RNA was prepared from P-388 cell transfer RNA (tRNA) by a previous method (34). The effect of I on endogenous protein synthesis (35) of P-388 lysates was carried out in a reaction mixture (0.5 ml) containing 10 m*M* tromethamine hydrochloride (pH 7.6), 76 m*M* KCl, 1 m*M* adenosine triphosphate, 0.2 m*M* guanosine triphosphate, 15 m*M* phosphocreatine, 2 m*M* $MgCl_2$, 1 m*M* dithiothreitol, 0.1 m*M* of each of the 19 essential amino acids, 0.9 mg/ml creatine phosphokinase, and 20 μCi [^{3}H]leucine (56.5 Ci/mmole). An aliquot of the reaction mixture was incubated at 30°. After 90 sec of incubation, I or the standards pyrocatechol violet or emetine was added to a final concentration of 100 μ*M*. At 1-min intervals, 50-μl aliquots were removed from the reaction tubes and spotted on filter papers[3] and then treated for 10 min in boiling 5% trichloroacetic acid, followed by 10 min in cold 5% trichloroacetic acid and washed with cold 5% trichloroacetic acid, ether–ethanol (1:1), and ether. The filter papers were dried and counted in scintillation fluid.

The effects of I, pyrocatechol violet, and emetine on the ribosome profile (35) of P-388 cell lysate were assayed using the described reaction medium (500 μl). Following drug addition (100 μ*M* final concentration) the reaction was incubated for 4 min at 37°. The reaction was terminated in ice and gradient buffer [1 ml of tromethamine hydrochloride (pH 7.6) 10 m*M* KCl, and 1.5 m*M* $MgCl_2 \cdot 6H_2O$] was added. The mixture was layered over 36 ml of 10–25% linear sucrose gradient (35), prepared in gradient buffer, and centrifuged for 165 min at 25,000 rpm in a swinging bucket rotor[4] at 4°. The absorbance profile at 260 nm was determined using a flow cell (light path 0.2 cm) attached to a spectrophotometer[5].

The reaction mixture (50 μl) for the polyuridine directed polyphenylalanine synthesis (36) contained 50 m*M* tromethamine hydrochloride (pH 7.6), 12.5 m*M* magnesium acetate, 80 m*M* KCl, 5 m*M* phospho-

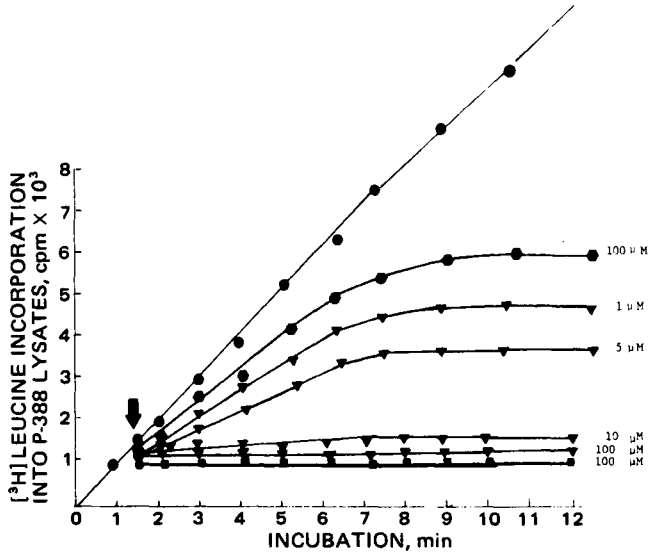

Figure 1—*Effects of bisbrusatolyl malonate on the protein synthesis of P-388 lysates using endogenous mRNA. Key:* ●, *control;* ●, *pyrocatechol violet;* ▼, *bisbrusatolyl malonate; and* ■, *emetine.*

creatine, 0.05 mg/ml creatine phosphokinase, 0.36 mg/ml polyuridine[6] (A_{280}/A_{260} = 0.34), 0.5 μCi [^{14}C]phenylalanine (536 mCi/mmole) 75 μg uncharged P-388 cell transfer RNA, 70 μg of P-388 cell pH 5 enzyme preparation, and 0.9 A_{260} of P-388 cell run-off ribosomes. After incubation for 20 min at 30°, a 35-μl aliquot was spotted on filter paper[3] and processed as described previously.

The reaction medium (200 μl) used to measure the formation of the 80S initiation complex and the methionyl puromycin reaction (37) contained 15 m*M* tromethamine hydrochloride (pH 7.6), 80 m*M* KCl, 1 m*M* adenosine triphosphate, 0.5 m*M* guanosine triphosphate, 20 m*M* phosphocreatine, 0.2 mg/ml creatine phosphokinase, 3 m*M* magnesium acetate, 0.1 m*M* ethylenediaminetetraacetic acid, 1 m*M* dithiothreitol, 0.1 m*M* of each of the 19 essential amino acids, 3 mg of P-388 cell lysates, 100 μg/ml chlortetracycline[7], 3 × 10^5 cpm [^{3}H]methionine-transfer ribonucleic acid$_f$ (Met-tRNA$_f$), and 20 μg/ml polyadenosine–uridine–guanosine (poly AUG) and 5 μl of drug. The incubation was carried out at 23° and after 2 min aliquots were withdrawn to analyze for 80S complex formation. Puromycin (10 μg/ml) was then added to the reaction medium. The incubation was continued for another 6 min and aliquots were withdrawn to analyze for reaction of the 80S complex with puromycin. All aliquots (50 μl) were diluted to 250 μl with buffer [20 m*M* tromethamine hydrochloride (pH 7.6), 80 m*M* KCl, 3 m*M* magnesium acetate, 1 m*M* dithiothreitol, and 0.1 m*M* ethylenediaminetetraacetic acid], layered on 11.8 ml of a 15–30% linear sucrose gradient, and centrifuged for 3 hr at 36,000 rpm in a swinging bucket rotor[8]. Fractions (0.4 ml) were collected and precipitated with 10% trichloroacetic acid on filter papers and counted.

The reaction mixtures (75 μl) for the ternary complex formation (37) contained 21.4 m*M* tromethamine hydrochloride (pH 8.0), 80 m*M* KCl,

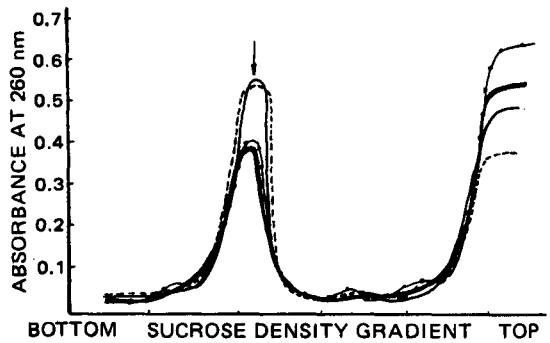

Figure 2—*P-388 ribosome profile. Key: – – –, bisbrusatolyl malonate; ——, pyrocatechol violet; ——, emetine, and – · – · –, control.*

[3] Whatman No. 3.
[4] Beckman SW27.
[5] Gilford.
[6] Miles Laboratory, Inc.
[7] Sigma Chemical Co.
[8] Beckman SW40 rotor.

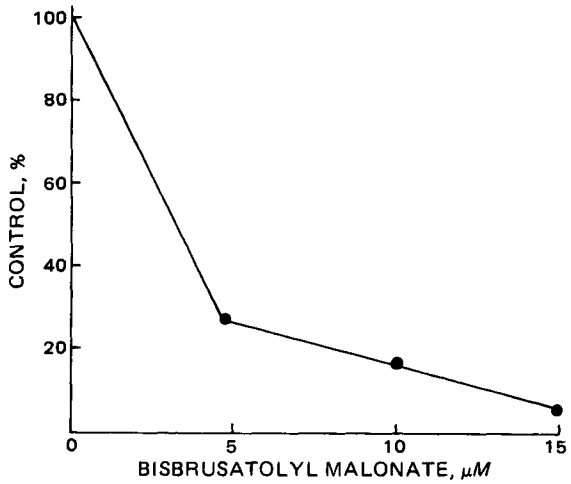

Figure 3—*Effect of various concentrations of bisbrusatolyl malonate on polyuridine directed poly[^{14}C]phenylalanine synthesis in P-388 run-off ribosomes.*

0.26 m*M* guanosine triphosphate, 21.4 m*M* dithiothreitol, 10 μg of bovine serum albumin, 5 pmoles of P-388 cell [^{3}H]methionine-transfer ribonucleic acid$_f$ (Met-tRNA$_f$, 1 × 10^4 cpm), 100 A_{260}/ml of crude P-388 cell initiation factors, and 10 μl of drug or standard. The incubation was conducted for 5 min at 37° and terminated by the addition of 3 ml of cold buffer [21.4 m*M* tromethamine hydrochloride (pH 8.0), 80 m*M* KCl, 2.14 m*M* dithiothreitol]. The samples were filtered through 0.45 μm filters[9], washed twice in buffer, and counted.

The reaction mixture (75 μl) for the 80S initiation complex (38) formation contained 1.9 m*M* magnesium acetate, 5 A_{260}/ml polyadenosine–uridine–guanosine[5], and 100 A_{260}/ml of 80S P-388 cell ribosomes in addition to the components necessary for the ternary complex formation reaction. Incubation was 10 min at 37° which was then cooled to 4° and titrated to 5 m*M* with magnesium acetate. After 5 min at 4°, the samples were diluted with cold buffer [21.4 m*M* tromethamine hydrochloride (pH 8.0) 80 m*M* KCl, 5 m*M* magnesium acetate, and 2.14 m*M* dithiothreitol] and filtered as indicated for the ternary complex formation experiment.

Amino acid-transfer RNA activation steps were determined by a previous method (39). The reaction medium contained 0.1 m*M* tromethamine hydrochloride (pH 7.4), 0.2 m*M* adenosine triphosphate, 0.3 mg/ml pH 5 enzyme from P-388 cells, and 2.5 μCi/ml of [^{14}C]phenylalanine (536 mCi/mmole), [^{3}H]leucine (56.5 Ci/mmole), or [^{3}H]methionine (80.0 Ci/mmole) in a total volume of 1 ml. After incubation at 37° for 20 min, 2 ml of ice cold 10% trichloroacetic acid was added and the activated amino acid-transfer RNA collected on nitrocellulose filters.

RESULTS AND DISCUSSION

In vitro incubation of I at 10-, 25-, and 50-μ*M* concentrations indicated that DNA synthesis was inhibited by relatively the same degree (42–46%) for all three concentrations employed (Table I). RNA synthesis was inhibited at 10 and 25 μ*M* but not at 50 μ*M*. The inhibition of protein synthesis *in vitro* followed a dose response curve for the doses employed in this study. Homogenized and whole cells demonstrated approximately the same degree of inhibition of DNA, RNA, and protein synthesis at 10 μ*M* final concentration of drug indicating that I inhibition of macromolecular synthesis was not due to the inhibition of radiolabeled precursor transport across the tumor cell membrane. The *in vitro* effects of I at 10 μ*M* on several of the enzymes required for nucleic acid synthesis (Table II) indicated that the major inhibition sites are at DNA polymerase, thymidine monophosphate kinase, purine synthesis, and methyl transferase, all of which were suppressed ~50% by I *in vitro*. Minor sites of *in vitro* inhibition included RNA polymerase, thymidine kinase, orotidine monophosphate decarboxylase, dihydrofolate reductase, phosphoribosyl pyrophosphate amino transferase, and oxidative phosphorylation processes, both basal and adenosine diphosphate stimulated respiration using succinate or α-ketoglutarate as substrate.

Examination of the effects of I on lysosomal hydrolytic enzymatic activities indicated that lysosomal membranes were stabilized by the drug. Thus, nucleases and proteolytic enzymatic activities of the lysosomes of the P-388 cells would not play a decreased role in nucleic acid and protein turnover, thereby resulting in erroneous incorporation values of radiolabeled precursors into synthetic macromolecules.

In vivo administration (Table III) of I at 0.6 mg/kg on days 7, 8, and 9 showed that the incorporation of thymidine, uridine, and leucine into DNA, RNA, and protein were drastically reduced (*i.e.*, at least 50% for nucleic acids and 66% for protein synthesis). Examination of the enzymes involved in nucleic acid synthesis indicated that DNA polymerase activity was inhibited 56%, messenger RNA polymerase activity was inhibited by 39%, and transfer RNA polymerase was inhibited by 50%. The suppression of the nucleic acid polymerase activities would indicate that template activity is interfered with by the drug binding in some manner. However, the UV spectrophotometric studies indicated only marginal interaction between DNA and I after incubation for 24 hr. Nucleotide kinase activity was inhibited moderately (23–37%). Orotidine-5′-monophosphate decarboxylase was inhibited significantly, inhibition being far greater *in vivo* (73%) than *in vitro* (31%). This difference may be due to a metabolite or may reflect slow binding between enzyme and drug. No other enzyme in the pyrimidine pathway was inhibited by I. Purine synthesis was inhibited 45%; one of the key regulatory sites of purine synthesis, phosphoribosyl pyrophosphate amino transferase was inhibited 41%. However, another enzyme that plays a significant role in one carbon transfer for both pyrimidine and purines, dihydrofolate reductase, was 88% inhibited *in vivo* whereas *in vitro* it was only 29% inhibited. Cyclic adenosine triphosphate levels were inhibited by 80%. Oxidative phosphorylation after *in vivo* administration of the drug was moderately inhibited (34–25%). Although a moderate loss of energy from this process could influence all synthetic pathways of the tumor cell. The number of tumor cells per milliliter was reduced by 56% after dosing for 3 days with I at 0.6 mg/kg.

In comparison to brusatol's effects on P-388 lymphocytic leukemia cell metabolism at 100 μg/kg/day (4), I was found to inhibit DNA polymerase and dihydrofolate reductase activities more effectively than brusatol both *in vivo* and *in vitro*. Furthermore, I inhibited thymidine nucleotide kinases enzymatic activities where no inhibition of the kinases was observed

Table IV—Effects of Bisbrusatolyl Malonate on Ternary and 80S Complex Formation

	Concentration, μ*M*	Complex Formation, pmole	Percent of Control
Ternary Complex Formulation			
Control		2.10	100
+ Emetine	100	2.02	96
+ Pyrocatechol violet	100	0.21	10
+ Bisbrusatolyl malonate	25	1.81	86
80S Initiation Complex Formation			
Control		1.82	100
+ Emetine	100	1.49	82
+ Pyrocatechol violet	100	0.36	20
+ Bisbrusatolyl malonate	25	1.51	83

Table V—Effects of Bisbrusatolyl Malonate on Amino Acid Transfer RNA Activation in P-388 Lymphocytic Leukemia Cells

Inhibitor	Concentration	Amino Acid Transfer RNA Formation, pmol	Percent of Control
[^{14}C]Phenylalanine-transfer RNA			
Control	—	1.05	100
+ Emetine	100	0.97	92
+ Pyrocatechol violet	100	0.98	93
+ Bisbrusatolyl malonate	50	0.97	92
]^{3}H]Leucyl-transfer RNA			
Control	—	1.83	100
+ Emetine	100	1.74	95
+ Pyrocatechol violet	100	1.72	94
+ Bisbrusatolyl malonate	50	1.76	96
[^{3}H]Methionyl-transfer RNA			
Control	—	1.62	100
+ Emetine	100	1.54	95
+ Pyrocatechol violet	100	1.57	97
+ Bisbrusatolyl malonate	50	1.52	94

[9] Millipore.

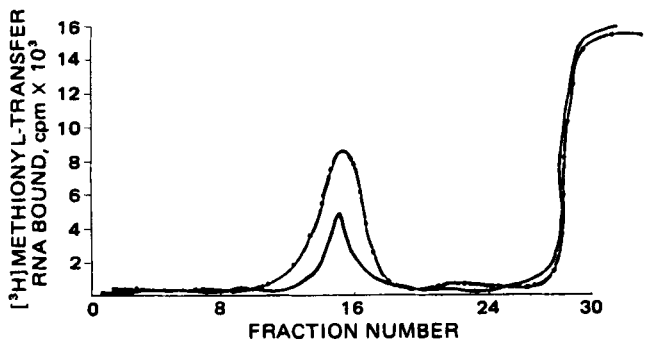

Figure 4—*Formation of the 80S initiation complex of P-388 cell system (linear sucrose gradient centrifugation). Key: ——, control; - · - · -, bisbrusatolyl malonate.*

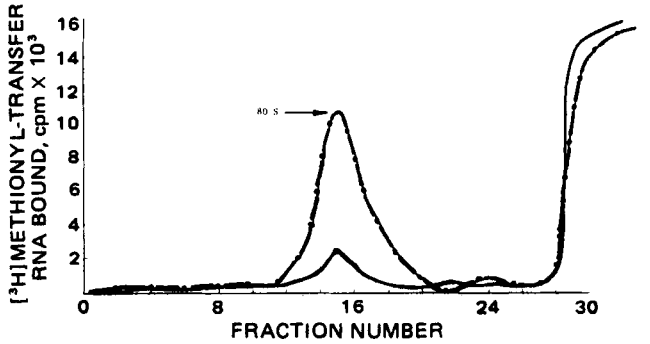

Figure 5—*Formation of the methionyl puromycin reaction of P-388 cell system (linear sucrose gradient centrifugation). Key: ——, control and puromycin; - · - · -, bisbrusatolyl malonate and puromycin.*

with brusatol. Brusatol caused a massive increase in cyclic adenosine monophosphate levels which was not observed for I. Brusatol caused a greater magnitude of inhibition of nucleic acid and protein synthesis in P-388 cells than I; however, this greater suppression did not correlate with increased antileukemic activity (T/C % = 158) for brusatol.

When the effect on protein synthesis of the P-388 cells was examined in detail, I clearly mimicked the action of brusatol and bruceantin. Previous studies with bruceantin in a yeast system (40) and brusatol in a rabbit reticulocyte system (41) have shown that these drugs bind preferentially to the free 80S subunit and subsequently inhibit any peptidyl transferase reaction. Thus, they allowed elongation of preformed polypeptide chains and formation of a new 80S initiation complex, but prevented utilization of that 80S initiation complex in the elongation steps of protein synthesis. The malonate ester has a similar mode of action.

Figure 1 shows that at a 1 μM concentration there is a lag of 6–7 min before inhibition by I becomes fully effective. This behavior is similiar to the initiation inhibitor pyrocatechol violet and suggests that preformed polypeptide chains are being completed prior to the onset of inhibition. This hypothesis is further confirmed by examining the ribosome profile following drug treatment of lysates prelabeled with [^{3}H]leucine (Fig. 2). At 1 μM, I causes accumulation of an 80S peak (presumably the 80S initiation complex). Since no radioactivity is associated with this peak, it is evident that 1 μM I also allows completion and release of the prelabeled polypeptide chain. These results are comparable to what one might expect to see from an initiation inhibitor (pyrocatechol violet). However, at higher concentrations (10 and 100 μM) I mimics the elongation inhibitors emetine and tetracycline. That is, inhibition occurs without any lag (Fig. 1) and results in freezing the preformed polypeptide chain on the ribosome (Fig. 2). This observation is consistent with previous data showing that at low concentrations, bruceantin binds only to free 80S subunits; however, at sufficiently high concentrations, it will also bind directly to the 80S elongation complex (41).

Further evidence that I acts as an elongation inhibitor comes from studies on polyuridine directed polyphenylalanine synthesis. Figure 3 shows the inhibition curve for polyphenylalanine synthesis carried out with purified run-off ribosomes isolated from 10-day P-388 cells. Clearly, the drug is effective as an inhibitor of polyuridine directed and endogenous protein synthesis. Since polyuridine directed protein synthesis does not require normal initiation or termination reactions, these data strongly suggest that I is an elongation inhibitor.

Confirmation of this hypothesis comes from detailed studies of the individual initiation and elongation steps. The initiation steps of protein synthesis were evaluated using a fractionated P-388 cell system. Bisbrusatolyl malonate (Table IV) had little or no effect on the formation of either the ^{3}H-ternary complex[10] or the 80S ^{3}H-initiation complex[11]. Bisbrusatolyl malonate also had no effect on the amino acid transfer RNA activation reactions with phenylalanine, leucine, and methionine (Table V).

Finally, the formation of the 80S initiation complex[11] and peptide bond formation were assayed as described previously (41). Addition of polyadenine–uridine–guanosine (poly AUG) to the P-388 lysate resulted in the formation of a detectable 80S initiation complex which was not inhibited by the addition of I (Fig. 4). Addition of puromycin to this reaction mixture caused formation of methionyl puromycin and consequent release of [^{3}H]methionine from the 80S complex (Fig. 5). This reaction was completely blocked by I.

[10] eIF·GTP[^{3}H]methionyl-transfer RNA.
[11] 80S·AUG·eIF·GTP[^{3}H]methionyl-transfer RNA.

In conclusion, I does not significantly affect the individual initiation steps leading to the formation of stable 80S initiation complex in P-388 cells. However, it does inhibit both polyuridine directed polyphenylalanine synthesis and the formation of the first peptide bond between puromycin and the [^{3}H]methionyl transfer RNA bound to the initiation complex. The data derived from these experiments suggests that I is a potent inhibitor of the peptidyl transferase reaction. The apparent runoff of polyribosomes to the 80S ribosomes suggests that the ribosome must complete its elongation and termination cycles before this drug can bind and usually must complete the initiation steps before the bound drug becomes an effective inhibitor. This pattern of inhibition is almost identical to that observed previously with the other quassinoids, bruceantin and brusatol (40), in rabbit reticulocytes and yeast cells.

In P-388 lymphocytic leukemia cells, I is a potent inhibitor of nucleic acids synthesis by inhibiting key sites in pyrimidine and purine synthesis and DNA and RNA polymerase activities. In addition, it is a potent inhibitor of protein synthesis by inhibiting the elongation step of polypeptide synthesis.

REFERENCES

(1) K. H. Lee, M. Okano, and I. H. Hall, *J. Pharm. Sci.*, in press.

(2) I. H. Hall, K. H. Lee, M. Okano, D. Sims, T. Ibuka, Y. F. Liou, and Y. Imakura, *ibid.*, **70**, 1147 (1981).

(3) R. I. Geran, N. H. Greenberg, M. M. MacDonald, A. M. Schumacher, and B. J. Abbott, *Cancer Chemother. Rep.*, **3**, 9 (1972).

(4) I. H. Hall, K. H. Lee, S. A. ElGebaly, Y. Imakura, Y. Sumida, and R.Y. Wu, *J. Pharm. Sci.*, **68**, 883 (1979).

(5) C. B. Chae, J. L. Irvine, and C. Piantadosi, *Proc. Am. Assoc. Cancer Res.*, **9**, 12 (1968).

(6) R. G. Wilson, R. H. Bodner, and G. E. MacWhorter, *Biochim. Biophys. Acta*, **378**, 260 (1975).

(7) A. C. Sartorelli, *Biochem. Biophys. Res. Commun.*, **27**, 26 (1967).

(8) I. H. Hall, K. H. Lee, E. C. Mar, C. O. Starnes, and T. G. Waddell, *J. Med. Chem.*, **20**, 333 (1977).

(9) W. C. Hymer and E. L. Kuff, *J. Histochem. Cytochem.*, **12**, 359 (1964).

(10) H. Sawada, K. Tatsumi, M. Sasada, S. Shirakowa, T. Nakumura, and G. Wakisaka, *Cancer Res.*, **34**, 3341 (1974).

(11) I. H. Hall, G. L. Carlson, G. S. Abernethy, and C. Piantadosi, *J. Med. Chem.*, **17**, 1253 (1974).

(12) K. M. Anderson, I. S. Mendelson, and G. Guzik, *Biochim. Biophys. Acta*, **383**, 56 (1975).

(13) E. C. Moore and R. B. Hurlbert, *J. Biol. Chem.*, **241**, 4802 (1966).

(14) F. Maley and S. Ochoa, *ibid.*, **233**, 1538 (1958).

(15) S. M. Kalman, P. H. Duffield, and T. Brzozwski, *Am. Biol. Chem.*, **24**, 1871 (1966).

(16) R. M. Archibald, *J. Biol. Chem.*, **156**, 121 (1944).

(17) S. B. Koritz and P. P. Cohen, *ibid.*, **209**, 145 (1954).

(18) S. H. Appel, *ibid.*, **243**, 3924 (1968).

(19) A. Kampf, R. L. Barfknecht, P. J. Schaffer, S. Osaki, and M. P. Mertes, *J. Med. Chem.*, **19**, 903 (1976).

(20) Y. K. Ho, T. Hakala, and S. F. Zakrzewski, *Cancer Res.*, **32**, 1023 (1972).

(21) M. K. Spassova, G. C. Russev, and E. V. Golovinsky, *Biochem. Pharmacol.*, **25**, 923 (1976).

(22) J. B. Wyngaarden and D. M. Ashton, *J. Biol. Chem.*, **234**, 1492

(1959).
(23) B. Magasanik, *Methods Enzymol.*, **6**, 106 (1963).
(24) I. H. Hall, K. S. Ishaq, and C. Piantadosi, *J. Pharm. Sci.*, **63**, 625 (1974).
(25) Y. S. Cho-Chung and P. M. Gullino, *J. Biol. Chem.*, **248**, 4743 (1973).
(26) A. Raineri, R. C. Simsiman, and R. K. Boutwell, *Cancer Res.*, **33**, 134 (1973).
(27) Y. M. Kish and L. J. Kleinsmith, *Methods Enzymol.*, **40**, 201 (1975).
(28) R. T. Borchardt, J. A. Huber, and Y. S. Wu, *J. Med. Chem.*, **19**, 1094 (1976).
(29) S. A. ElGebaly, I. H. Hall, K. H. Lee, Y. Sumida, Y. Imakura, and R. Y. Wu, *J. Pharm. Sci.*, **68**, 887 (1979).
(30) J. Kruh, L. Grossman, and K. Moldave, *Methods Enzymol.*, **12**, 732 (1968).
(31) M. H. Schreier and T. Staehelin, *J. Mol. Biol.*, **73**, 329 (1973).
(32) J. M. Ravel, R. D. Mosteller, and B. Hardesty, *Proc. Natl. Acad. Sci. USA*, **56**, 701 (1966).
(33) A. Majumdar, S. Reynolds, and N. K. Gupta, *Biochem. Biophys. Res. Commun.*, **67**, 689 (1975).
(34) K. Takeishi, T. Ukita, and S. Nishimura, *J. Biol. Chem.*, **243**, 5761 (1968).
(35) L. L. Liao, S. M. Kupchan, and S. B. Horwitz, *Mol. Pharmacol.*, **12**, 167 (1976).
(36) A. Jimenez, L. Sanchez, and D. Vasquez, *Biochim. Biophys. Acta*, **383**, 427 (1975).
(37) J. Carter and M. Cannon, *Eur. J. Biochem.*, **84**, 103 (1978).
(38) S. H. Reynolds, A. Majumdar, A. Das Gupta, S. Palmieri, and N. K. Gupta, *Arch. Biochem. Biophys.*, **184**, 328 (1977).
(39) K. Moldane, *Methods Enzymol.*, **6**, 757 (1963).
(40) W. Willingham, E. A. Stafford, S. H. Reynolds, S. G. Chaney, K. H. Lee, M. Okano, and I. H. Hall, *Biochim. Biophys. Acta*, **654**, 169 (1981).
(41) M. Fresno, A. Gonzales, D. Vasquez, and A. Jimenez, *ibid.*, **518**, 104 (1978).

ACKNOWLEDGMENTS

Supported by American Cancer Society Grant CH-19 (K. H. Lee and I. H. Hall) and National Cancer Institute Grants CA-22929 and CA-17625 (in part) (K. H. Lee) and CA-26466 (S. G. Chaney, I. H. Hall, K. H. Lee).

NOTES

Improved and Rapid High-Performance Liquid Chromatographic Assay for 13-*cis*-Retinoic Acid or All-*trans*-retinoic Acid

RICKEY SHELLEY, J. C. PRICE ˣ, H. WON JUN, D. E. CADWALLADER, and A. C. CAPOMACCHIA

Received June 11, 1980, from the *Department of Pharmaceutics, School of Pharmacy, University of Georgia, Athens, GA 30602.* Accepted for publication May 15, 1981.

Abstract □ A rapid, specific, and sensitive reversed-phase high-performance liquid chromatographic (HPLC) assay for the quantitative determination of all-*trans*- retinoic acid (I) or 13-*cis*-retinoic acid (II) in rat serum without extraction or lyophilization is described. Chromatographic separation from retinol, serum components, and retinol acetate standard was achieved on octadecylsilane-coated particles with acetonitrile–1% ammonium acetate as the eluent. Serum samples (100 μl) containing as little as 10 ng of retinoid were analyzed. Serum level profiles of rats dosed with the retinoids demonstrated the utility of the assay and indicated elimination half-lives of 0.58 and 0.92 hr for I and II, respectively.

Keyphrases □ High-performance liquid chromatography—assay for 13-*cis*-retinoic acid and all-*trans*-retinoic acid □ 13-*cis*-Retinoic acid—high-performance liquid chromatographic analysis □ All-*trans*-retinoic acid—high-performance liquid chromatographic analysis

High-performance liquid chromatographic (HPLC) assay procedures for all-*trans*-retinoic acid (I) or 13-*cis*-retinoic acid (II) in serum samples differ markedly in sample preparation. One previously reported method employed lyophilization followed by extraction with methanol before analysis by reversed-phase chromatography. By this method as little as 50 ng of retinoic acid was detected in 0.5 ml of human plasma samples (1). Another report (2) showed a sensitivity limit of 25 ng/ml of plasma with reversed-phase chromatography after extraction of samples containing 1 ml of plasma with a mixture of hexane, methylene chloride, and isopropanol. In another study (3), 0.5 ml of serum was extracted with ethyl acetate, followed by evaporation and dissolution of the residue in mobile phase. Normal-phase adsorption chromatography was employed to achieve a sensitivity of 10–20 ng/ml of serum. A fourth method (4) required no extraction step and had a detection limit of 100 ng of retinoic acid when 400 μl of serum was mixed with methanol and centrifuged for 20 min and the supernatant liquid was analyzed directly by reversed-phase chromatography.

The present study describes a simple timesaving method for determining serum I or II by reversed-phase liquid chromatography with no extraction or lyophilization steps. Only 100 μl of serum is required, and many samples can be analyzed in a short time. Sensitivity compares favorably with other reported assay procedures.

EXPERIMENTAL

Reagents—All-*trans*-retinoic acid[1] (I), 13-*cis*-retinoic acid[2] (II), and all-*trans*-retinol acetate[3] (III) were used as received. All other chemicals

[1] Eastman Kodak, Rochester, N.Y.
[2] Hoffmann-La Roche, Nutley, N.J.
[3] Sigma Chemical Co., St. Louis, Mo.

0022-3549/82/0200-0262$01.00/0

(1959).
(23) B. Magasanik, *Methods Enzymol.*, **6**, 106 (1963).
(24) I. H. Hall, K. S. Ishaq, and C. Piantadosi, *J. Pharm. Sci.*, **63**, 625 (1974).
(25) Y. S. Cho-Chung and P. M. Gullino, *J. Biol. Chem.*, **248**, 4743 (1973).
(26) A. Raineri, R. C. Simsiman, and R. K. Boutwell, *Cancer Res.*, **33**, 134 (1973).
(27) Y. M. Kish and L. J. Kleinsmith, *Methods Enzymol.*, **40**, 201 (1975).
(28) R. T. Borchardt, J. A. Huber, and Y. S. Wu, *J. Med. Chem.*, **19**, 1094 (1976).
(29) S. A. ElGebaly, I. H. Hall, K. H. Lee, Y. Sumida, Y. Imakura, and R. Y. Wu, *J. Pharm. Sci.*, **68**, 887 (1979).
(30) J. Kruh, L. Grossman, and K. Moldave, *Methods Enzymol.*, **12**, 732 (1968).
(31) M. H. Schreier and T. Staehelin, *J. Mol. Biol.*, **73**, 329 (1973).
(32) J. M. Ravel, R. D. Mosteller, and B. Hardesty, *Proc. Natl. Acad. Sci. USA*, **56**, 701 (1966).
(33) A. Majumdar, S. Reynolds, and N. K. Gupta, *Biochem. Biophys. Res. Commun.*, **67**, 689 (1975).
(34) K. Takeishi, T. Ukita, and S. Nishimura, *J. Biol. Chem.*, **243**, 5761 (1968).
(35) L. L. Liao, S. M. Kupchan, and S. B. Horwitz, *Mol. Pharmacol.*, **12**, 167 (1976).
(36) A. Jimenez, L. Sanchez, and D. Vasquez, *Biochim. Biophys. Acta*, **383**, 427 (1975).
(37) J. Carter and M. Cannon, *Eur. J. Biochem.*, **84**, 103 (1978).
(38) S. H. Reynolds, A. Majumdar, A. Das Gupta, S. Palmieri, and N. K. Gupta, *Arch. Biochem. Biophys.*, **184**, 328 (1977).
(39) K. Moldane, *Methods Enzymol.*, **6**, 757 (1963).
(40) W. Willingham, E. A. Stafford, S. H. Reynolds, S. G. Chaney, K. H. Lee, M. Okano, and I. H. Hall, *Biochim. Biophys. Acta*, **654**, 169 (1981).
(41) M. Fresno, A. Gonzales, D. Vasquez, and A. Jimenez, *ibid.*, **518**, 104 (1978).

ACKNOWLEDGMENTS

Supported by American Cancer Society Grant CH-19 (K. H. Lee and I. H. Hall) and National Cancer Institute Grants CA-22929 and CA-17625 (in part) (K. H. Lee) and CA-26466 (S. G. Chaney, I. H. Hall, K. H. Lee).

NOTES

Improved and Rapid High-Performance Liquid Chromatographic Assay for 13-*cis*-Retinoic Acid or All-*trans*-retinoic Acid

RICKEY SHELLEY, J. C. PRICE ˣ, H. WON JUN, D. E. CADWALLADER, and A. C. CAPOMACCHIA

Received June 11, 1980, from the *Department of Pharmaceutics, School of Pharmacy, University of Georgia, Athens, GA 30602.* Accepted for publication May 15, 1981.

Abstract □ A rapid, specific, and sensitive reversed-phase high-performance liquid chromatographic (HPLC) assay for the quantitative determination of all-*trans*- retinoic acid (I) or 13-*cis*-retinoic acid (II) in rat serum without extraction or lyophilization is described. Chromatographic separation from retinol, serum components, and retinol acetate standard was achieved on octadecylsilane-coated particles with acetonitrile–1% ammonium acetate as the eluent. Serum samples (100 μl) containing as little as 10 ng of retinoid were analyzed. Serum level profiles of rats dosed with the retinoids demonstrated the utility of the assay and indicated elimination half-lives of 0.58 and 0.92 hr for I and II, respectively.

Keyphrases □ High-performance liquid chromatography—assay for 13-*cis*-retinoic acid and all-*trans*-retinoic acid □ 13-*cis*-Retinoic acid—high-performance liquid chromatographic analysis □ All-*trans*-retinoic acid—high-performance liquid chromatographic analysis

High-performance liquid chromatographic (HPLC) assay procedures for all-*trans*-retinoic acid (I) or 13-*cis*-retinoic acid (II) in serum samples differ markedly in sample preparation. One previously reported method employed lyophilization followed by extraction with methanol before analysis by reversed-phase chromatography. By this method as little as 50 ng of retinoic acid was detected in 0.5 ml of human plasma samples (1). Another report (2) showed a sensitivity limit of 25 ng/ml of plasma with reversed-phase chromatography after extraction of samples containing 1 ml of plasma with a mixture of hexane, methylene chloride, and isopropanol. In another study (3), 0.5 ml of serum was extracted with ethyl acetate, followed by evaporation and dissolution of the residue in mobile phase. Normal-phase adsorption chromatography was employed to achieve a sensitivity of 10–20 ng/ml of serum. A fourth method (4) required no extraction step and had a detection limit of 100 ng of retinoic acid when 400 μl of serum was mixed with methanol and centrifuged for 20 min and the supernatant liquid was analyzed directly by reversed-phase chromatography.

The present study describes a simple timesaving method for determining serum I or II by reversed-phase liquid chromatography with no extraction or lyophilization steps. Only 100 μl of serum is required, and many samples can be analyzed in a short time. Sensitivity compares favorably with other reported assay procedures.

EXPERIMENTAL

Reagents—All-*trans*-retinoic acid[1] (I), 13-*cis*-retinoic acid[2] (II), and all-*trans*-retinol acetate[3] (III) were used as received. All other chemicals

[1] Eastman Kodak, Rochester, N.Y.
[2] Hoffmann-La Roche, Nutley, N.J.
[3] Sigma Chemical Co., St. Louis, Mo.

0022-3549/82/0200-0262$01.00/0

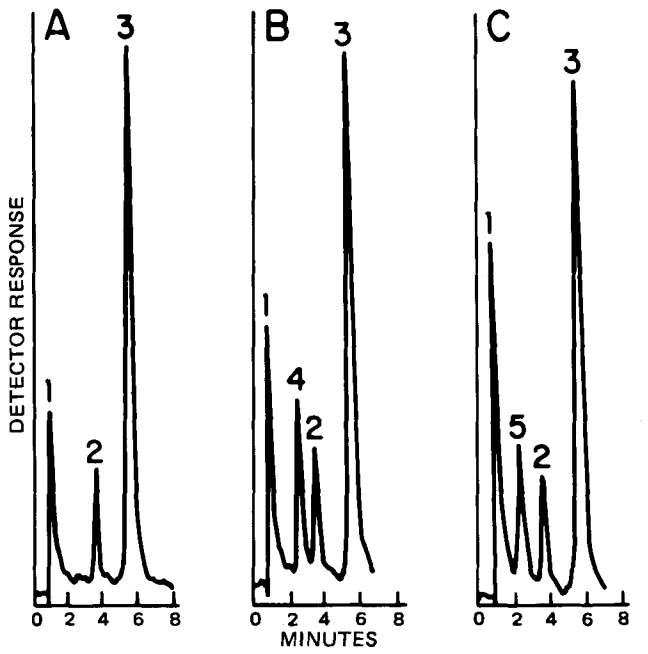

Figure 1—*Chromatograms of: A, normal rat serum with added internal standard; B, rat serum containing 15 ng of I plus internal standard; and C, rat serum containing 15 ng of II plus internal standard. Key: 1, solvent; 2, retinol (present in all serum samples); 3, internal standard; 4, I; and 5, II.*

and reagents were high grade, commercially available materials.

Chromatography—Analyses were performed on a liquid chromatograph[4] operated at ambient temperature and equipped with a UV detector (340 nm). Separations were performed on a 3.2-mm × 25-cm reversed-phase column containing 5-μm octadecylsilane-coated particles[5]. A guard column, containing 30–40 μm octadecylsilane-coated pelicular material, was employed to protect the main column. Samples were introduced into the column through a 100-μl sample loop by way of a loop filler port and sample injection valve. Chromatograms were traced on a strip-chart recorder (20 cm/hr), and peak heights were determined by an integrator–peak detector.[6] The mobile phase was acetonitrile–1% ammonium acetate solution (75:25 v/v).

Calibration—Stock solutions (0.1 mg/ml) of I and II were prepared in acetonitrile and stored at −10°. In addition, an internal standard stock solution (10 μg/ml) of III was prepared. Periodic chromatographic and spectrophotometric analyses showed that these stock solutions could be stored without alteration for 1 month at −10°. Similar stability was reported previously (5).

Blood from untreated male white rats[7] was collected from the tails (6) in serum separation tubes and centrifuged to generate a serum pool. The serum was immediately transferred to 15-ml screw-capped vials and frozen. Known amounts of I stock solutions and 50 μl of the internal standard solution were added to 100 μl of drug-free serum samples in 15-ml screw-capped test tubes.

Each sample was further diluted with acetonitrile to a final volume of 400 μl to achieve I concentrations of 0.1–7.5 μg/ml (10–750 ng/100-μl sample) and a constant III concentration of 5.0 μg/ml. Samples of II and the internal standard were obtained in the same manner. The samples were shaken vigorously on a vortex mixer, and the precipitate was separated by centrifugation (2 min at 3500 rpm). The resulting supernatant liquid was injected onto the chromatograph for analysis. In a separate calibration, water was substituted for serum in essentially the same procedure to determine whether the serum had significantly affected the assay.

Calibration curves of the peak height ratios (retinoic acid to internal standard) *versus* the retinoid concentration were prepared from the analysis of the serum and water samples at each concentration of I and II.

Serum Level Profiles—Serum concentrations of the retinoids of the male rats, weighing an average of 390 g, were determined after intravenous injection into the tail vein using the described method. All rats were fasted for 24 hr before injection. Injected retinoids were in saline solution. For I, six rats were given a bolus intravenous injection of 1.0 mg; blood samples were taken from each rat at 0.5, 1, 2, 3, 4, and 5 hr after injection. For II, eight rats received 1.25 mg iv; blood samples were taken at 0.5, 1, 1.75, 2.5, 3.25, 4, and 4.75 hr after injection. Samples were taken and analyzed as described for the calibration experiments.

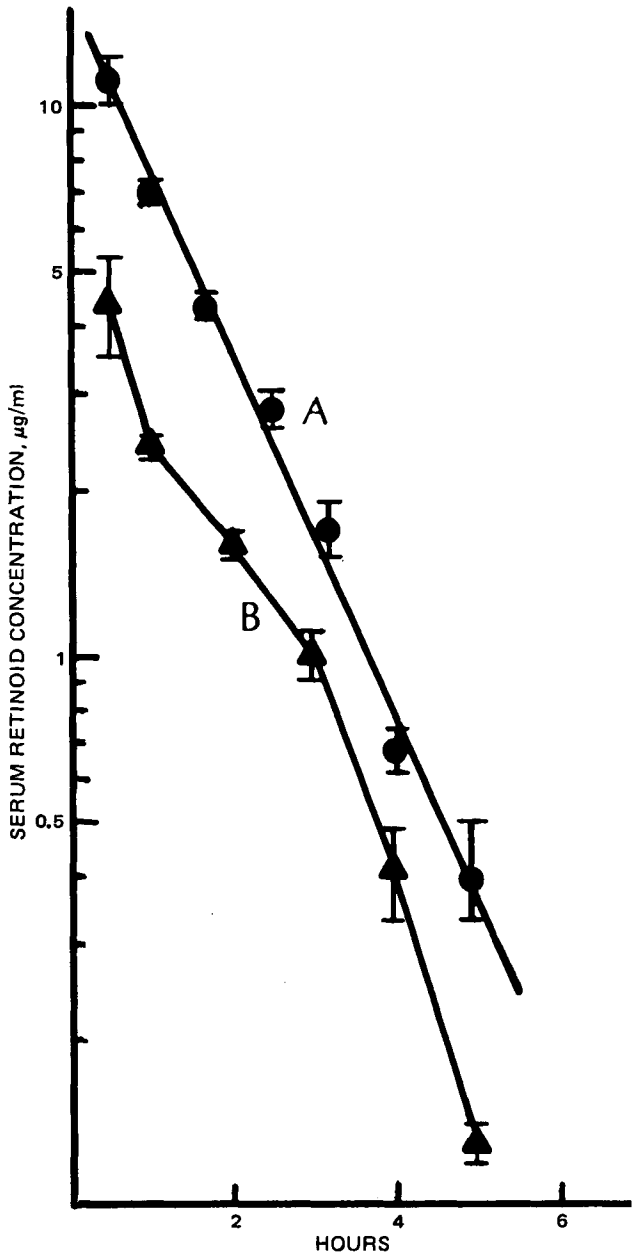

Figure 2—*Average serum concentrations of II (A) and I (B) following rapid intravenous injections of 1.25 and 1.0 mg, respectively. Each point represents data averaged from at least six rats. Bars show the standard deviation of the data.*

RESULTS AND DISCUSSION

Chromatograms of serum containing the internal standard and the internal standard plus I or II are shown in Fig. 1. All serum chromatograms showed the presence of retinol, which did not interfere with the assay. No other interfering peaks were observed.

Separation of all I from the internal standard, retinol (present in all serum samples), and the solvent front was obtained after adjusting the mobile phase of acetonitrile–1% ammonium acetate to a ratio of 75:25 (v/v) and the flow rate to 1.6 ml/min. The 1% ammonium acetate aqueous solution was needed to obtain complete separation of I from the solvent

[4] Altex model 2100 pump with model 153 UV detector, Altex Scientific, Berkeley, Calif.
[5] Spherisorb ODS, Phase Separations Ltd., Hauppauge, N.Y.
[6] Minigrator, Spectra-Physics, Santa Clara, Calif.
[7] Sprague-Dawley strain.

Table I—Retinoic Acid Assay Calibration

Number of Samples[a]	Retinoid[b] in Sample, ng	Retinoid Detected,[c] ng	Sample Concentration, ng/ml	Peak Height Ratio ± *SD* Retinoic Acid I	Retinoic Acid II
9	10	2.5	100	0.045 ± 0.015	0.055 ± 0.02
3	20	5.0	200	0.077 ± 0.002	—
9	40	10	400	0.143 ± 0.010	0.157 ± 0.02
3	60	15	600	0.217 ± 0.002	—
9	80	20	800	0.297 ± 0.016	0.308 ± 0.038
3	100	25	1000	0.375 ± 0.007	—
9	150	37.5	1500	0.601 ± 0.016	0.581 ± 0.037
3	300	75	3000	1.231 ± 0.037	—
9	450	112.5	4500	1.821 ± 0.048	1.594 ± 0.088
3	600	150	6000	2.431 ± 0.061	—
9	750	187.5	7500	3.021 ± 0.098	2.678 ± 0.103

[a] Samples of nine were determined over 3 weeks, three samples per week. [b] Contained in 0.1 ml of rat serum. [c] Detected quantity represents the calculated theoretical quantity of retinoid injected into the chromatograph.

front (Fig. 1B). Under these conditions, the retention times for I, retinol, and III were 3.0, 3.9, and 5.9 min, respectively. In addition to the spiked serum samples, a drug-free sample was run to determine if there were any absorbing substances in the region of I (Fig. 1A). Separation of II from the internal standard, retinol, and the solvent front was achieved under the same conditions as for I (Fig. 1C). The retention time for II was 2.6 min.

The results of calibration procedures for I and II in rat serum samples are shown in Table I. Linear regression analysis of chromatogram peak height ratios of sample to standard *versus* concentration showed correlation coefficients of 0.9999 for both I and II for a sample size of 10–750 ng (100–7500 ng/ml). At a sample size of 10 ng of retinoic acid, the standard deviations for data pooled from 3 different days were ±33% for I and ±36% for II and probably represent the lower working limits for the assay. At the 80-ng sample size, reproducibility was much better, with standard deviations of 7 and 13%, respectively, for the two acids. Single-day determinations usually showed lower standard deviations.

The peak height ratios of retinoids to the internal standard at each concentration for the serum and water samples were compared to determine the percent recovery of I and II from the serum samples. The recoveries of I and II were 102.9 ± 5.6% and 91.7 ± 5%, respectively.

Figure 2 shows the applicability of the assay to monitor serum levels in rats after single doses of the retinoids. Both serum level profiles showed log-linear elimination phases with correlation coefficients of ~0.99. The elimination half-lives of I and II were 0.58 and 0.92 hr, respectively. The elimination curve for I, possibly indicating saturation or storage, tends to confirm previous observations (7).

REFERENCES

(1) C. A. Frolik, T. E. Tavela, G. L. Peck, and M. B. Sporn, *Anal. Biochem.*, **86**, 743 (1978).

(2) J. G. Besner and R. Leclaire, *J. Chromatogr.*, **183**, 346 (1980).

(3) C. V. Puglisi and J. A. F. DeSilva, *ibid.*, **152**, 421 (1978).

(4) C. C. Wang, S. Campbell, R. L. Furner, and D. K. Hill, *Drug Metab. Dispos.*, **8**, 8 (1980).

(5) R. Hanni, D. Hervouet, and A. Busslinger, *J. Chromatogr.*, **162**, 615 (1979).

(6) S. T. Nerenberg and D. Zedler, *J. Lab. Clin. Med.*, **85**, 523 (1975).

(7) B. N. Swanson, C. A. Frolik, D. W. Zaharevitz, P. P. Roller, and M. B. Sporn, *Biochem. Pharmacol.*, **30**, 107 (1981).

ACKNOWLEDGMENTS

Supported by Contract N01 CP 85663 from the National Cancer Institute, National Institutes of Health.

The assistance of Mr. Richard Rabek is gratefully acknowledged.

Quantitative Analysis of Ethynodiol Diacetate and Ethinyl Estradiol/Mestranol in Oral Contraceptive Tablets by High-Performance Liquid Chromatography

G. CARIGNAN, B. A. LODGE ˣ, and W. SKAKUM

Received August 6, 1980, from the *Bureau of Drug Research, Health Protection Branch, Health and Welfare Canada, Tunney's Pasture, Ottawa, Ontario, K1A 0L2, Canada.* Accepted for publication July 7, 1981.

Abstract □ A procedure is described for the assay of ethynodiol diacetate and ethinyl estradiol/mestranol by HPLC using two UV detectors at 210 and 280 nm. The system was acetonitrile 38% (v/v) in water as mobile phase on a 250 × 3.2-mm i.d. RP-2 column, with butylated hydroxytoluene as the internal standard. There was >99% recovery from synthetic preparations and the coefficient of variation was <2.0% for formulations.

Keyphrases □ Oral contraceptives—quantitative analysis of ethynodiol, estradiol, and mestranol by high-performance liquid chromatography □ Ethynodiol—quantitative analysis by high-performance liquid chromatography, oral contraceptive tablets □ Ethinyl estradiol—quantitative analysis by high-performance liquid chromatography, oral contraceptive tablets □ Mestranol—quantitative analysis by high-performance liquid chromatography, oral contraceptive tablets □ High-performance liquid chromatography—quantitative analysis of ethynodiol, estradiol, and mestranol in oral contraceptive tablets

Ethynodiol diacetate is a synthetic steroid showing progestogenic activity. It is used in oral contraceptives in admixture with either ethinyl estradiol or mestranol. Compendial procedures (1–3) are limited to raw material or to single ingredient formulations, except the USP XX (1) which describes the analysis of the ethynodiol diace-

0022-3549/82/0200-0264$01.00/0

Table I—Retinoic Acid Assay Calibration

Number of Samples[a]	Retinoid[b] in Sample, ng	Retinoid Detected,[c] ng	Sample Concentration, ng/ml	Peak Height Ratio ± *SD* Retinoic Acid I	Retinoic Acid II
9	10	2.5	100	0.045 ± 0.015	0.055 ± 0.02
3	20	5.0	200	0.077 ± 0.002	—
9	40	10	400	0.143 ± 0.010	0.157 ± 0.02
3	60	15	600	0.217 ± 0.002	—
9	80	20	800	0.297 ± 0.016	0.308 ± 0.038
3	100	25	1000	0.375 ± 0.007	—
9	150	37.5	1500	0.601 ± 0.016	0.581 ± 0.037
3	300	75	3000	1.231 ± 0.037	—
9	450	112.5	4500	1.821 ± 0.048	1.594 ± 0.088
3	600	150	6000	2.431 ± 0.061	—
9	750	187.5	7500	3.021 ± 0.098	2.678 ± 0.103

[a] Samples of nine were determined over 3 weeks, three samples per week. [b] Contained in 0.1 ml of rat serum. [c] Detected quantity represents the calculated theoretical quantity of retinoid injected into the chromatograph.

front (Fig. 1B). Under these conditions, the retention times for I, retinol, and III were 3.0, 3.9, and 5.9 min, respectively. In addition to the spiked serum samples, a drug-free sample was run to determine if there were any absorbing substances in the region of I (Fig. 1A). Separation of II from the internal standard, retinol, and the solvent front was achieved under the same conditions as for I (Fig. 1C). The retention time for II was 2.6 min.

The results of calibration procedures for I and II in rat serum samples are shown in Table I. Linear regression analysis of chromatogram peak height ratios of sample to standard *versus* concentration showed correlation coefficients of 0.9999 for both I and II for a sample size of 10–750 ng (100–7500 ng/ml). At a sample size of 10 ng of retinoic acid, the standard deviations for data pooled from 3 different days were ±33% for I and ±36% for II and probably represent the lower working limits for the assay. At the 80-ng sample size, reproducibility was much better, with standard deviations of 7 and 13%, respectively, for the two acids. Single-day determinations usually showed lower standard deviations.

The peak height ratios of retinoids to the internal standard at each concentration for the serum and water samples were compared to determine the percent recovery of I and II from the serum samples. The recoveries of I and II were 102.9 ± 5.6% and 91.7 ± 5%, respectively.

Figure 2 shows the applicability of the assay to monitor serum levels in rats after single doses of the retinoids. Both serum level profiles showed log-linear elimination phases with correlation coefficients of ~0.99. The elimination half-lives of I and II were 0.58 and 0.92 hr, respectively. The elimination curve for I, possibly indicating saturation or storage, tends to confirm previous observations (7).

REFERENCES

(1) C. A. Frolik, T. E. Tavela, G. L. Peck, and M. B. Sporn, *Anal. Biochem.*, **86**, 743 (1978).

(2) J. G. Besner and R. Leclaire, *J. Chromatogr.*, **183**, 346 (1980).

(3) C. V. Puglisi and J. A. F. DeSilva, *ibid.*, **152**, 421 (1978).

(4) C. C. Wang, S. Campbell, R. L. Furner, and D. K. Hill, *Drug Metab. Dispos.*, **8**, 8 (1980).

(5) R. Hanni, D. Hervouet, and A. Busslinger, *J. Chromatogr.*, **162**, 615 (1979).

(6) S. T. Nerenberg and D. Zedler, *J. Lab. Clin. Med.*, **85**, 523 (1975).

(7) B. N. Swanson, C. A. Frolik, D. W. Zaharevitz, P. P. Roller, and M. B. Sporn, *Biochem. Pharmacol.*, **30**, 107 (1981).

ACKNOWLEDGMENTS

Supported by Contract N01 CP 85663 from the National Cancer Institute, National Institutes of Health.

The assistance of Mr. Richard Rabek is gratefully acknowledged.

Quantitative Analysis of Ethynodiol Diacetate and Ethinyl Estradiol/Mestranol in Oral Contraceptive Tablets by High-Performance Liquid Chromatography

G. CARIGNAN, B. A. LODGE ˣ, and W. SKAKUM

Received August 6, 1980, from the *Bureau of Drug Research, Health Protection Branch, Health and Welfare Canada, Tunney's Pasture, Ottawa, Ontario, K1A 0L2, Canada.* Accepted for publication July 7, 1981.

Abstract □ A procedure is described for the assay of ethynodiol diacetate and ethinyl estradiol/mestranol by HPLC using two UV detectors at 210 and 280 nm. The system was acetonitrile 38% (v/v) in water as mobile phase on a 250 × 3.2-mm i.d. RP-2 column, with butylated hydroxytoluene as the internal standard. There was >99% recovery from synthetic preparations and the coefficient of variation was <2.0% for formulations.

Keyphrases □ Oral contraceptives—quantitative analysis of ethynodiol, estradiol, and mestranol by high-performance liquid chromatography □ Ethynodiol—quantitative analysis by high-performance liquid chromatography, oral contraceptive tablets □ Ethinyl estradiol—quantitative analysis by high-performance liquid chromatography, oral contraceptive tablets □ Mestranol—quantitative analysis by high-performance liquid chromatography, oral contraceptive tablets □ High-performance liquid chromatography—quantitative analysis of ethynodiol, estradiol, and mestranol in oral contraceptive tablets

Ethynodiol diacetate is a synthetic steroid showing progestogenic activity. It is used in oral contraceptives in admixture with either ethinyl estradiol or mestranol. Compendial procedures (1–3) are limited to raw material or to single ingredient formulations, except the USP XX (1) which describes the analysis of the ethynodiol diace-

0022-3549/82/0200-0264$01.00/0

Table I—Capacity Factor (K^1) for the Steroids and Other Substances

Substance	K^1
Ethinyl estradiol	3.85
Mestranol	8.08
Ethynodiol diacetate	22.65
Butylated hydroxytoluene	16.54
Unknown No. 1	8.33
Unknown No. 2	11.62
Ethynodiol diacetate acidic degradation product	27.82
Ethynodiol diacetate basic degradation products	1. 3.57 2. 8.62

tate–ethinyl estradiol mixtures.

Ethynodiol diacetate has been quantitatively assayed by argentimetric titration of its ethinyl group (2), by UV determination after its acidic conversion to a conjugated diene (1), by colorimetric reaction with antimony trichloride (3), and by GLC analysis (4).

The estrogenic components have been analyzed using such methods as argentimetry (2), colorimetry (1, 3, 5), fluorometry (2), UV spectrophotometry (6), GLC (6), TLC with fluorescent detection (7), and high-performance liquid chromatography (HPLC) (8–10).

This paper describes a simple, rapid HPLC procedure to assay quantitatively mixtures of ethynodiol diacetate with either ethinyl estradiol or mestranol using simultaneous measurements of UV absorption at 210 and 280 nm.

EXPERIMENTAL

Apparatus—A modular HPLC system consisting of a pump[1] operated at 1.75 ml/min, two variable-wavelength UV detectors (set at 210 and 280 nm, respectively)[2,3], and a 7000-psi loop injector[4] (equipped with a 20-μl loop) were used. The column (250 × 3.2-mm i.d.) was ethylsilane chemically bonded to totally porous, irregularly shaped microparticulate silica[5].

Peak retention times and areas were obtained with two reporting integrators[6].

Reagents—Ethynodiol diacetate, ethinyl estradiol, and mestranol were USP reference standards. Butylated hydroxytoluene[7] was recrystallized from methanol, acetonitrile was HPLC grade[8], and water was double-distilled in glass.

Mobile Phase—Acetonitrile 38% (v/v) in water (filtered through a membrane[9] and degassed while filtering under a vacuum not exceeding 500 mm Hg) was used.

Internal Standard Solution—A solution of butylated hydroxytoluene in aqueous acetonitrile (80% v/v) was prepared at a concentration of 50 μg/ml.

Standard Preparations—*Ethynodiol Diacetate–Ethinyl Estradiol Standard*—A solution of ethynodiol diacetate with ethinyl estradiol in internal standard solution was prepared at the same concentration as in the sample preparation (based on label claim).

Ethynodiol Diacetate–Mestranol Standard—A solution of ethynodiol diacetate with mestranol in internal standard solution was prepared at the same concentration as in the sample preparation (based on label claim).

Sample Preparation—Not less than 20 tablets were weighed and finely powdered (60 mesh). An amount of powder equivalent to one tablet was accurately weighed into a 15-ml centrifuge tube with a polytef-lined cap. Two milliliters of internal standard solution were added. The tube was capped and vigorously shaken for 30 min. The tube was then centrifuged to obtain a clear solution.

[1] Constametric II, Laboratory Data Control, Riviera Beach, FL 33404.
[2] Spectromonitor I, Laboratory Data Control, Riviera Beach, FL 33404.
[3] Schoeffel model SF 770, Westwood, NJ 07675.
[4] Rheodyne septumless valve injector model 7120, Berkeley, CA 94710.
[5] RP-2 Express series, Altex Inc., Berkeley, CA 94710.
[6] HP 3385A automation systems, Hewlett-Packard, Avondale, PA 19311.
[7] Koch-Light Laboratory, Colnbrook, England S13 0B7.
[8] Fisher Scientific, Fair Lawn, NJ 07410.
[9] FH 0.2 μm, Millipore Inc., Bedford, MA 01730.

Table II—Standard Curves for Ethinyl Estradiol, Mestranol, and Ethynodiol Diacetate

Steroid	Weight Range Injected, mg	Wavelength, nm	Curve, $y = mx + b$	Correlation Coefficient
Ethinyl estradiol	0.2–1.2	210	0.827×-0.003	0.9999
		280	0.835×-0.022	0.9998
Mestranol	0.2–1.2	210	$0.895 \times +0.002$	0.9996
		280	0.784×-0.013	0.9998
Ethynodiol diacetate	2.0–12	210	0.303×-0.007	0.9999

Recovery Study—Sufficient inert materials (4.67 g of lactose, 4.67 g of cornstarch, 0.5 g of povidone, 0.1 g of calcium stearate) to make a total weight of 10 g (after drying) were added to a solution in 10 ml of alcohol of about 2.5 mg of ethinyl estradiol, 5.0 mg of mestranol, and 50.0 mg of ethynodiol diacetate, each accurately weighed. This mixture was shaken to homogenize, then dried at room temperature using reduced pressure.

A 200-mg portion of this synthetic preparation was treated as in sample preparation.

Procedure—Aliquots (20 μl) of standard preparation or sample preparation (synthetic preparation) were successively injected into the chromatograph. The peak area ratios of ethynodiol diacetate and the estrogen to the internal standard were calculated on the 210-nm detector and the peak area ratio of the estrogen to internal standard was calculated on the 280-nm detector for both standard and sample preparations. The quantities of active ingredients per tablet were calculated using the following formula:

$$C_u = 2 \times C_s \times \frac{R_u}{R_s} \times \frac{W_t}{W_u} \qquad \text{(Eq. 1)}$$

where:

C_u = active ingredient per tablet, milligrams
C_s = concentration of active ingredient in standard preparation, milligrams per milliliter
R_u = area ratio of active ingredient to internal standard in sample preparation
R_s = area ratio of active ingredient to internal standard in standard preparation
W_u = weight of sample taken, milligrams
W_t = average weight per tablet, milligrams

RESULTS AND DISCUSSION

All chromatograms were as expected with respect to the shape of the peaks, and complete baseline resolution was achieved between the solvent front, ethinyl estradiol, mestranol, internal standard, and ethynodiol diacetate (Table I). An unidentified impurity definitely not either of the monoacetates (as determined by basic degradation) or either of the diene degradation products (as determined by acidic degradation), was detected while analyzing the ethynodiol diacetate–ethinyl estradiol formulations. It had a retention close to that of mestranol. Several solvent systems on different reversed-phase columns failed to improve separation. Spectrometric study showed its absorption maximum was at ~235 nm with no absorption at 280 nm. This impurity was found in all commercial formulations studied (two manufacturers), and it appeared to be an ethynodiol diacetate degradation product.

To overcome the problem of the same impurity (No. 1, Table I) appearing in ethynodiol diacetate–mestranol formulations, detection using 280-nm wavelength seemed more appropriate for the estrogenic component. However, since ethynodiol diacetate has no measurable absorbance at 280 nm, it was necessary to use 210 nm for its determination. A second impurity (K^1 = 11.62) did not conflict with other components in the mixture.

Linearity of response *versus* concentration was studied for the three steroids at both wavelengths (Table II). All standard curves were found to be linear in the concentration ranges studied and passed close to the origin. Their correlation coefficients were nearly ideal (>0.9996).

Table III shows the accuracy of the procedure for a synthetic preparation. Recovery was >98% for each steroid at its determination wavelength, and reproducibility was excellent (*RSD* <1.3%).

Quantitative analysis of three commercial dosage forms are listed in Table IV. All results are within compendial limits (90–110%). Coefficients of variation are <2.0%. A difference of 2.4% is reported for mestranol

Table III—Recovery of Steroids from a Synthetic Preparation

Steroid	Added, μg	Recovery at 210 nm[a] μg	%	CV	Recovery at 280 nm[a] μg	%	CV
Ethinyl estradiol	51.86	50.98	98.3	1.3	51.96	100.2	1.1
Mestranol	100.23	98.97	99.0	1.0	99.78	99.8	1.1
Ethynodiol diacetate	1015.5	1008.6	99.3	0.7	—	—	—

[a] Average of five determinations.

Table IV—Assay of Commercial Tablets[a]

Steroid	Wavelength Setting, nm	Product A % Label Claimed	CV	Product B % Label Claimed	CV	Product C % Label Claimed	CV
Ethinyl estradiol	210	99.9	1.2	101.3	1.3	—	—
	280	101.3	1.9	102.5	1.8	—	—
Mestranol	210	—	—	—	—	103.2	1.3
	280	—	—	—	—	100.8	0.8
Ethynodiol diacetate	210	96.5	0.9	95.2	0.9	92.4	0.5

[a] Average of 10 determinations.

analyses between the two wavelengths used, whereas analysis of the synthetic formulation revealed a variation of 0.8%, which is relatively minor. Variations reported for ethinyl estradiol (~1.5%) are the same for tablets and the synthetic formulation.

CONCLUSIONS

This HPLC procedure, using dual wavelength detection, is fast and accurate. It has been specially designed for single dosage form analysis as required in the USP–NF content uniformity test, and would advantageously replace the long, open-column chromatography procedure.

REFERENCES

(1) "The United States Pharmacopeia," 20th rev., Mack Publishing Co., Easton, Pa., 1980.

(2) "British Pharmacopoeia," Her Majesty's Stationery Office, London, England, 1973.

(3) R. Pasini and G. Gavazzi, *J. Pharm. Sci.*, **58**, 872 (1969).

(4) R. Mestres and J. L. Berges, *Trav. Soc. Pharm. Montpellier*, **32**, 313 (1972).

(5) M. A. Korany, M. Abdel-Salam, and A. M. Wahbi, *Analyst*, **102**, 683 (1977).

(6) A. P. Shroff and J. Grodsky, *J. Pharm. Sci.*, **56**, 460 (1967).

(7) M. Amin and M. Hassenbach, *Analyst*, **104**, 407 (1979).

(8) K. R. Bagon and E. W. Hammond, *ibid.*, **103**, 156 (1978).

(9) G. L. Schmidt, F. L. Vandemark, and W. Slavin, *Anal. Biochem.*, **91**, 636 (1978).

(10) R. W. Roos, *J. Pharm. Sci.*, **67**, 1735 (1978).

Effect of the pH–Zero Point of Charge Relationship on the Interaction of Ionic Compounds and Polyols with Aluminum Hydroxide Gel

DHIREN N. SHAH *, JOSEPH R. FELDKAMP ‡, JOE L. WHITE ‡, and STANLEY L. HEM *x

Received December 12, 1980, from the **Department of Industrial and Physical Pharmacy and the* ‡*Department of Agronomy, Purdue University, West Lafayette, IN 47907.* Accepted for publication June 26, 1981.

Abstract □ The adsorption of magnesium nitrate, docusate sodium, and mannitol by chloride-containing aluminum hydroxide gel or aluminum hydroxycarbonate gel can be directly related to the surface charge characteristics of the aluminum hydroxide gel as determined by the pH–zero point of charge (ZPC) relationship. Magnesium cation is completely adsorbed under pH conditions where the gel has a negative surface charge, *i.e.*, when the pH is above the ZPC. Docusate sodium is more strongly adsorbed when the pH–ZPC relationship causes the surface charge of aluminum hydroxycarbonate gel to be positive indicating adsorption of the docusate anion. However, adsorption also occurred when the pH was above the ZPC suggesting that adsorption of the hydrophobic portion of docusate anion by van der Waals forces also contributes to the overall adsorption mechanism. Mannitol is adsorbed under all pH conditions. However, greater adsorption occurs when the pH is above the ZPC. Maximum hydrogen bonding is believed to occur when mannitol acts as the proton donor and the negative aluminum hydroxycarbonate gel surface serves as the proton acceptor.

Keyphrases □ Aluminum hydroxide—gel, adsorption of ionic compounds and polyols, effect of pH–zero point of charge □ Aluminum hydroxycarbonate—gel, adsorption of ionic compounds and polyols, effect of pH–zero point of charge □ Adsorption—ionic compounds and polyols to aluminum hydroxide and aluminum hydroxycarbonate, effect of pH–zero point of charge

The zero point of charge (ZPC) is an important property of colloidal systems possessing a pH-dependent surface charge. The ZPC is the pH at which the net surface charge is zero; at this pH the densities of the positive and negative charges are equal. The apparent surface charge can be controlled by adjusting the pH to be either below or above the ZPC to produce a positive or negative surface charge, respectively (1). A recent study demonstrated the impor-

0022-3549/82/0200-0266$01.00/0

Table III—Recovery of Steroids from a Synthetic Preparation

Steroid	Added, μg	Recovery at 210 nm[a] μg	%	CV	Recovery at 280 nm[a] μg	%	CV
Ethinyl estradiol	51.86	50.98	98.3	1.3	51.96	100.2	1.1
Mestranol	100.23	98.97	99.0	1.0	99.78	99.8	1.1
Ethynodiol diacetate	1015.5	1008.6	99.3	0.7	—	—	—

[a] Average of five determinations.

Table IV—Assay of Commercial Tablets[a]

Steroid	Wavelength Setting, nm	Product A % Label Claimed	CV	Product B % Label Claimed	CV	Product C % Label Claimed	CV
Ethinyl estradiol	210	99.9	1.2	101.3	1.3	—	—
	280	101.3	1.9	102.5	1.8	—	—
Mestranol	210	—	—	—	—	103.2	1.3
	280	—	—	—	—	100.8	0.8
Ethynodiol diacetate	210	96.5	0.9	95.2	0.9	92.4	0.5

[a] Average of 10 determinations.

analyses between the two wavelengths used, whereas analysis of the synthetic formulation revealed a variation of 0.8%, which is relatively minor. Variations reported for ethinyl estradiol (~1.5%) are the same for tablets and the synthetic formulation.

CONCLUSIONS

This HPLC procedure, using dual wavelength detection, is fast and accurate. It has been specially designed for single dosage form analysis as required in the USP–NF content uniformity test, and would advantageously replace the long, open-column chromatography procedure.

REFERENCES

(1) "The United States Pharmacopeia," 20th rev., Mack Publishing Co., Easton, Pa., 1980.

(2) "British Pharmacopoeia," Her Majesty's Stationery Office, London, England, 1973.

(3) R. Pasini and G. Gavazzi, *J. Pharm. Sci.*, **58**, 872 (1969).

(4) R. Mestres and J. L. Berges, *Trav. Soc. Pharm. Montpellier*, **32**, 313 (1972).

(5) M. A. Korany, M. Abdel-Salam, and A. M. Wahbi, *Analyst*, **102**, 683 (1977).

(6) A. P. Shroff and J. Grodsky, *J. Pharm. Sci.*, **56**, 460 (1967).

(7) M. Amin and M. Hassenbach, *Analyst*, **104**, 407 (1979).

(8) K. R. Bagon and E. W. Hammond, *ibid.*, **103**, 156 (1978).

(9) G. L. Schmidt, F. L. Vandemark, and W. Slavin, *Anal. Biochem.*, **91**, 636 (1978).

(10) R. W. Roos, *J. Pharm. Sci.*, **67**, 1735 (1978).

Effect of the pH–Zero Point of Charge Relationship on the Interaction of Ionic Compounds and Polyols with Aluminum Hydroxide Gel

DHIREN N. SHAH *, JOSEPH R. FELDKAMP ‡, JOE L. WHITE ‡, and STANLEY L. HEM *x

Received December 12, 1980, from the **Department of Industrial and Physical Pharmacy and the* ‡*Department of Agronomy, Purdue University, West Lafayette, IN 47907.* Accepted for publication June 26, 1981.

Abstract □ The adsorption of magnesium nitrate, docusate sodium, and mannitol by chloride-containing aluminum hydroxide gel or aluminum hydroxycarbonate gel can be directly related to the surface charge characteristics of the aluminum hydroxide gel as determined by the pH–zero point of charge (ZPC) relationship. Magnesium cation is completely adsorbed under pH conditions where the gel has a negative surface charge, *i.e.*, when the pH is above the ZPC. Docusate sodium is more strongly adsorbed when the pH–ZPC relationship causes the surface charge of aluminum hydroxycarbonate gel to be positive indicating adsorption of the docusate anion. However, adsorption also occurred when the pH was above the ZPC suggesting that adsorption of the hydrophobic portion of docusate anion by van der Waals forces also contributes to the overall adsorption mechanism. Mannitol is adsorbed under all pH conditions. However, greater adsorption occurs when the pH is above the ZPC. Maximum hydrogen bonding is believed to occur when mannitol acts as the proton donor and the negative aluminum hydroxycarbonate gel surface serves as the proton acceptor.

Keyphrases □ Aluminum hydroxide—gel, adsorption of ionic compounds and polyols, effect of pH–zero point of charge □ Aluminum hydroxycarbonate—gel, adsorption of ionic compounds and polyols, effect of pH–zero point of charge □ Adsorption—ionic compounds and polyols to aluminum hydroxide and aluminum hydroxycarbonate, effect of pH–zero point of charge

The zero point of charge (ZPC) is an important property of colloidal systems possessing a pH-dependent surface charge. The ZPC is the pH at which the net surface charge is zero; at this pH the densities of the positive and negative charges are equal. The apparent surface charge can be controlled by adjusting the pH to be either below or above the ZPC to produce a positive or negative surface charge, respectively (1). A recent study demonstrated the impor-

0022-3549/82/0200-0266$01.00/0

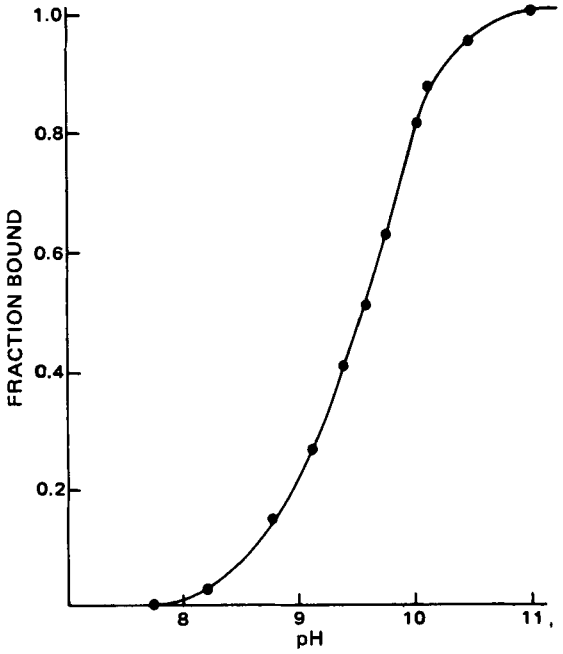

Figure 1—*Effect of pH on the fraction of magnesium cation bound by a chloride-containing aluminum hydroxide gel.*

tant effect which the relationship between pH and ZPC exerts on the physical properties of aluminum hydroxide gel (2). The present study investigates the influence that the surface charge characteristics of aluminum hydroxide and aluminum hydroxycarbonate gel have on the adsorption of ionic solutes such as magnesium nitrate or docusate sodium as well as mannitol, a neutral polyol.

EXPERIMENTAL[1]

The chloride-containing aluminum hydroxide gel was prepared by reacting aluminum chloride and potassium hydroxide as described previously (2). The ZPC of this gel was determined by a titration procedure (2) and was found to be 9.65. The bulk pH was 8.00 when diluted with distilled water to 3% equivalent aluminum oxide. Two aluminum hydroxycarbonate gels were obtained commercially. Aluminum hydroxycarbonate gel number 1 had a ZPC of 6.95 and a bulk pH of 6.5 at 3% equivalent aluminum oxide, while gel 2 had a ZPC of 6.32 and a bulk pH of 6.25 under the same conditions.

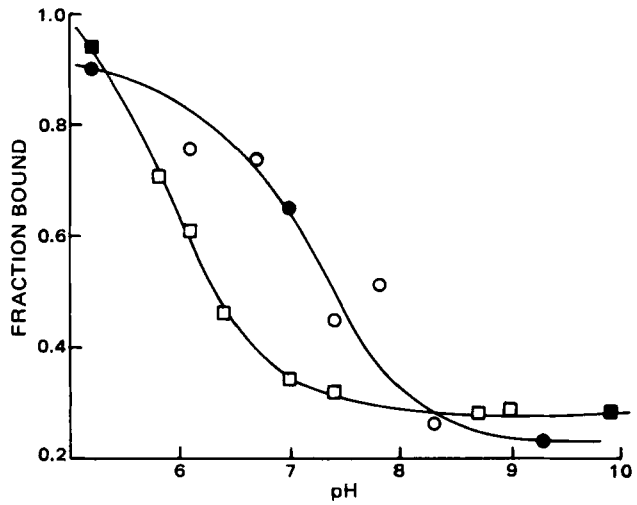

Figure 2—*Effect of pH on the fraction of docusate anion bound by gel 1 (○, ●) and gel 2 (□, ■). The open data points were determined without adjusting the ionic strength and the closed data points were determined at a constant ionic strength of* 5×10^{-3}.

[1] All chemicals used were either official or reagent grade.

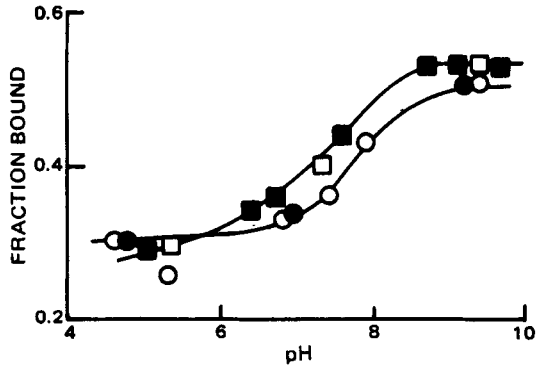

Figure 3—*Effect of pH on the fraction of mannitol bound by gel 1 (○, ●) and gel 2 (□, ■). The open data points were determined without adjusting the ionic strength and the closed data points were determined at a constant ionic strength of* 5×10^{-3}.

The fraction of magnesium nitrate, docusate sodium, or mannitol adsorbed by the aluminum hydroxide gel at different pH conditions was determined by first adjusting portions of the gel to the desired pH by addition of 0.1 *N* HCl or 0.1 *N* KOH. The maximum change in ionic strength due to the pH adjustment was 5×10^{-3}. A second series of samples was prepared at an ionic strength of 5×10^{-3} by adding an appropriate quantity of potassium chloride to each sample following pH adjustment. No significant difference in adsorption was observed between the first series in which the ionic strength varied up to 5×10^{-3} and the second series in which all samples had an ionic strength of 5×10^{-3}. Adsorption is normally related to ionic strength, but the small quantities of acid or base needed to adjust the pH did not cause a large enough ionic strength differential to significantly affect adsorption. Thus, the data at constant and variable ionic strength were pooled.

Following pH adjustment, an adsorbate solution was added to produce a mixture containing 9.8×10^{-2} *M* equivalent aluminum oxide and either 6×10^{-4} *M* $Mg(NO_3)_2$, 3.2×10^{-4} *M* docusate sodium, or 3×10^{-2} *M* mannitol. The docusate sodium concentration was selected to be below the critical micelle concentration which was reported to be 6.8×10^{-4} *M* in water (3). The mixtures were equilibrated by shaking at 25° for 2 hr, the pH was determined, the sample was centrifuged at 15,000 rpm (27,000 × *g*) for 30 min, and the supernate was analyzed. Magnesium was determined by chelatometric titration (4), docusate sodium was determined by the official assay (5), and mannitol was determined by a microcolorimetric method (6).

RESULTS AND DISCUSSION

The fraction of magnesium cation adsorbed by the chloride-containing aluminum hydroxide gel was strongly pH dependent (Fig. 1). Virtually no adsorption occurred below pH 8, while complete adsorption of magnesium cation occurred at pH 11. It is interesting to note that 50% of the magnesium cation was adsorbed at pH 9.65 which corresponds to the ZPC of the chloride-containing aluminum hydroxide gel. Thus adsorption of magnesium cation can be directly related to the surface charge as predicted from the pH–ZPC relationship. At pH conditions below the ZPC, the positively-charged aluminum hydroxide surface will not interact with the magnesium cation, while a strong attraction occurs when the pH is above the ZPC, producing a negative surface charge. A sigmoidal adsorption curve is commonly observed for the adsorption of transition metal ions on various metal oxide surfaces (7, 8).

The adsorption of the anionic surface active agent, docusate sodium, is somewhat more complex, but a strong dependence on the pH–ZPC relationship is evident in Fig. 2. Gel 1 had a ZPC of 6.95, while the ZPC of gel 2 was 6.32. In both cases, the ZPC corresponded approximately with the midpoint of the fraction bound curve with greater adsorption occurring when the pH was below the ZPC. However, a minimum of ~20% of the docusate anion was adsorbed even under pH conditions where the apparent surface charge of the aluminum hydroxycarbonate gel was negative.

Although docusate sodium is known to hydrolyze in alkaline solutions (9), the amount of degradation occurring at pH 10 during 4 hr (the time required for the fraction bound study) was negligible. It is believed that adsorption of the hydrophobic portion of docusate anion occurred even though repulsive forces exist between the negatively-charged hydrophilic

portion of docusate anion and the negatively-charged aluminum hydroxycarbonate surface.

The adsorption of polyols, although occurring by hydrogen bonding rather than electrostatic attraction (10, 11), was also affected by the pH–ZPC relationship (Fig. 3). The extent of mannitol adsorption by either gel 1 or 2 is much less than was observed for the adsorption of the magnesium cation or the docusate anion, reflecting the weaker adsorption mechanism of hydrogen bonding in comparison to electrostatic attraction. However, the fraction of mannitol adsorbed increased from ~30% at pH conditions below the ZPC to 50% when the pH was above the ZPC. Hydrogen bonding occurs more readily when mannitol serves as the proton donor and the negatively-charged oxygen at the aluminum hydroxycarbonate gel surface serves as the proton acceptor. This condition exists when the pH is above the ZPC and coincides with the region of maximum adsorption of mannitol.

The results of this study suggest that the pH–ZPC relationship will provide a useful guideline for predicting adsorption reactions in the formulation of antacid dosage forms and may also be useful in predicting drug interactions arising from the coadministration of drugs and aluminum hydroxide-containing antacids.

REFERENCES

(1) R. G. Gast, in "Minerals in Soil Environments," J. B. Dixon and S. B. Weed, Eds., Soil Science Society of America, Madison, Wis., 1977, pp. 27–73.

(2) J. R. Feldkamp, D. N. Shah, S. L. Meyer, J. L. White, and S. L. Hem, *J. Pharm. Sci.*, **70**, 638 (1981).

(3) L. I. Osipow, "Surface Chemistry: Theory and Industrial Applications," Reinhold, New York, N.Y. 1962, pp 169.

(4) "The United States Pharmacopeia," 20th rev., United States Pharmacopeial Convention, Inc. Rockville, Md., 1980, p. 1072.

(5) *Ibid.*, p. 262.

(6) J. M. Bailey, *J. Lab. Clin. Med.*, **54**, 158 (1959).

(7) F. Dalang and W. Stumm, in "Colloid Interface Science," (Proc. 50th Int. Conf.), **4**, 157–163 (1976).

(8) R. O. James and T. W. Healy, *J. Colloid Interface Sci.*, **40**, 42 (1972).

(9) "The Merck Index," 9th ed., Merck and Co., Rahway, N.J., 1976, p. 438.

(10) D. N. Shah, J. L. White, and S. L. Hem, *J. Pharm. Sci.*, **70**, 1101 (1981).

(11) S. L. Nail, J. L. White, and S. L. Hem, *ibid.*, **65**, 1195 (1976).

ACKNOWLEDGMENTS

Supported in part by William H. Rorer, Inc.

This report is Journal Paper 8303, Purdue University Agricultural Experiment Station, West Lafayette, IN 47907.

COMMUNICATIONS

TLC and GLC Determination of Aromatic Amine Impurities in Bulk *p*-Aminobenzoic Acid and in Its Potassium and Sodium Salts

Keyphrases □ *p*-Aminobenzoic acid—aromatic amine impurities determined by GLC and TLC □ TLC—determination of aromatic amine impurities in *p*-aminobenzoic acid □ GLC—determination of aromatic amine impurities in *p*-aminobenzoic acid

To the Editor:

The current USP monograph (1) for *p*-aminobenzoic acid lacks a requirement for limiting the amount of aromatic amine impurities in the finished bulk drug. The carcinogenicity of these possible amine impurities prompted this laboratory to adapt the derivatization and GLC technique of Bruce and Maynard (2) to identify and quantitate these compounds. A TLC confirmatory test using a portion of the underivatized sample solution was also developed.

A finely ground 5-g sample of bulk *p*-aminobenzoic acid or its salts, in a 50-ml stoppered centrifuge tube, was extracted by shaking with 25 ml of benzene for 5 min. After centrifuging, the benzene layer was transferred to a separator and extracted with two 15-ml portions of 2% aqueous sodium bicarbonate. The aqueous layers were discarded, and the benzene layer was dried through anhydrous sodium sulfate.

A 2-ml portion of the extract was derivatized in a separator with 25 μl of heptafluorobutyric anhydride. After 30 min at room temperature, 10 ml of benzene was added, the organic layer was washed with three 10-ml portions of water, and the water was discarded. The benzene layer was diluted to 50 ml with benzene and 5 μl was injected into a gas chromatograph equipped with a 15-μCi ^{63}Ni-electron-capture detector, a 1.8 m × 4-mm i.d. spiral glass tube packed with 6% OV-101 and 9% OV-210 (1:1) coated on acid-washed silanized high-performance flux calcined diatomite support (100–120 mesh). Inlet, column, and detector temperatures were 225, 140, and 325°, respectively. Argon–methane (95:5) at a flow rate of 50 ml/min was used as the carrier gas.

For TLC, 5 ml of the dried benzene sample extract was evaporated to 200 μl, and 20 μl was applied to a silica gel GF plate. After 10-cm development with benzene–ethyl acetate–acetic acid (90:5:5), the plate was sprayed with 1% *p*-dimethylaminobenzaldehyde in ethanol containing 5% HCl.

Table I lists the TLC R_f values for the 10 amines used in this study. The GLC retention times for the corre-

Table I—TLC and GLC Data for 10 Aromatic Amines

Amine	TLC[a] R_f Free Amine	GLC[b] Retention Time, min[c]	Approximate Nanograms for HSD[d]
Aniline[e]	0.07	1.2	0.05
o-Toluidine	0.28	1.7	0.10
p-Toluidine	0.19	2.0	0.10
p-Chloroaniline	0.42	3.1	0.10
2-Methyl-5-chloroaniline	0.67	4.4	0.10
Diphenylamine	0.85	11.9	0.80
2-Chloro-5-nitroaniline	0.74	15.0	0.40
Benzocaine[e]	0.45	16.8	0.40
p-Nitroaniline	0.42	17.9	0.40
2-Methyl-5-nitroaniline	0.55	26.0	0.40

[a] 20 × 20 cm 0.25-mm thick silica gel GF plates, Mallinckrodt Chemical Works, St. Louis, Mo. [b] Tracor 560, Tracor Inc., Austin, Tex. [c] Heptafluorobutyric anhydride derivative. [d] Nanograms for half-scale deflection (HSD) at GLC detector setting of 7 namp, and attenuation at 5. [e] Found in commercial samples.

0022-3549/82/0200-0268$01.00/0

portion of docusate anion and the negatively-charged aluminum hydroxycarbonate surface.

The adsorption of polyols, although occurring by hydrogen bonding rather than electrostatic attraction (10, 11), was also affected by the pH–ZPC relationship (Fig. 3). The extent of mannitol adsorption by either gel 1 or 2 is much less than was observed for the adsorption of the magnesium cation or the docusate anion, reflecting the weaker adsorption mechanism of hydrogen bonding in comparison to electrostatic attraction. However, the fraction of mannitol adsorbed increased from ~30% at pH conditions below the ZPC to 50% when the pH was above the ZPC. Hydrogen bonding occurs more readily when mannitol serves as the proton donor and the negatively-charged oxygen at the aluminum hydroxycarbonate gel surface serves as the proton acceptor. This condition exists when the pH is above the ZPC and coincides with the region of maximum adsorption of mannitol.

The results of this study suggest that the pH–ZPC relationship will provide a useful guideline for predicting adsorption reactions in the formulation of antacid dosage forms and may also be useful in predicting drug interactions arising from the coadministration of drugs and aluminum hydroxide-containing antacids.

REFERENCES

(1) R. G. Gast, in "Minerals in Soil Environments," J. B. Dixon and S. B. Weed, Eds., Soil Science Society of America, Madison, Wis., 1977, pp. 27–73.

(2) J. R. Feldkamp, D. N. Shah, S. L. Meyer, J. L. White, and S. L. Hem, *J. Pharm. Sci.*, **70**, 638 (1981).

(3) L. I. Osipow, "Surface Chemistry: Theory and Industrial Applications," Reinhold, New York, N.Y. 1962, pp 169.

(4) "The United States Pharmacopeia," 20th rev., United States Pharmacopeial Convention, Inc. Rockville, Md., 1980, p. 1072.

(5) *Ibid.*, p. 262.

(6) J. M. Bailey, *J. Lab. Clin. Med.*, **54**, 158 (1959).

(7) F. Dalang and W. Stumm, in "Colloid Interface Science," (Proc. 50th Int. Conf.), **4**, 157–163 (1976).

(8) R. O. James and T. W. Healy, *J. Colloid Interface Sci.*, **40**, 42 (1972).

(9) "The Merck Index," 9th ed., Merck and Co., Rahway, N.J., 1976, p. 438.

(10) D. N. Shah, J. L. White, and S. L. Hem, *J. Pharm. Sci.*, **70**, 1101 (1981).

(11) S. L. Nail, J. L. White, and S. L. Hem, *ibid.*, **65**, 1195 (1976).

ACKNOWLEDGMENTS

Supported in part by William H. Rorer, Inc.

This report is Journal Paper 8303, Purdue University Agricultural Experiment Station, West Lafayette, IN 47907.

COMMUNICATIONS

TLC and GLC Determination of Aromatic Amine Impurities in Bulk *p*-Aminobenzoic Acid and in Its Potassium and Sodium Salts

Keyphrases □ *p*-Aminobenzoic acid—aromatic amine impurities determined by GLC and TLC □ TLC—determination of aromatic amine impurities in *p*-aminobenzoic acid □ GLC—determination of aromatic amine impurities in *p*-aminobenzoic acid

To the Editor:

The current USP monograph (1) for *p*-aminobenzoic acid lacks a requirement for limiting the amount of aromatic amine impurities in the finished bulk drug. The carcinogenicity of these possible amine impurities prompted this laboratory to adapt the derivatization and GLC technique of Bruce and Maynard (2) to identify and quantitate these compounds. A TLC confirmatory test using a portion of the underivatized sample solution was also developed.

A finely ground 5-g sample of bulk *p*-aminobenzoic acid or its salts, in a 50-ml stoppered centrifuge tube, was extracted by shaking with 25 ml of benzene for 5 min. After centrifuging, the benzene layer was transferred to a separator and extracted with two 15-ml portions of 2% aqueous sodium bicarbonate. The aqueous layers were discarded, and the benzene layer was dried through anhydrous sodium sulfate.

A 2-ml portion of the extract was derivatized in a separator with 25 μl of heptafluorobutyric anhydride. After 30 min at room temperature, 10 ml of benzene was added, the organic layer was washed with three 10-ml portions of water, and the water was discarded. The benzene layer was diluted to 50 ml with benzene and 5 μl was injected into a gas chromatograph equipped with a 15-μCi ^{63}Ni-electron-capture detector, a 1.8 m × 4-mm i.d. spiral glass tube packed with 6% OV-101 and 9% OV-210 (1:1) coated on acid-washed silanized high-performance flux calcined diatomite support (100–120 mesh). Inlet, column, and detector temperatures were 225, 140, and 325°, respectively. Argon–methane (95:5) at a flow rate of 50 ml/min was used as the carrier gas.

For TLC, 5 ml of the dried benzene sample extract was evaporated to 200 μl, and 20 μl was applied to a silica gel GF plate. After 10-cm development with benzene–ethyl acetate–acetic acid (90:5:5), the plate was sprayed with 1% *p*-dimethylaminobenzaldehyde in ethanol containing 5% HCl.

Table I lists the TLC R_f values for the 10 amines used in this study. The GLC retention times for the corre-

Table I—TLC and GLC Data for 10 Aromatic Amines

Amine	TLC[a] R_f Free Amine	GLC[b] Retention Time, min[c]	Approximate Nanograms for HSD[d]
Aniline[e]	0.07	1.2	0.05
o-Toluidine	0.28	1.7	0.10
p-Toluidine	0.19	2.0	0.10
p-Chloroaniline	0.42	3.1	0.10
2-Methyl-5-chloroaniline	0.67	4.4	0.10
Diphenylamine	0.85	11.9	0.80
2-Chloro-5-nitroaniline	0.74	15.0	0.40
Benzocaine[e]	0.45	16.8	0.40
p-Nitroaniline	0.42	17.9	0.40
2-Methyl-5-nitroaniline	0.55	26.0	0.40

[a] 20 × 20 cm 0.25-mm thick silica gel GF plates, Mallinckrodt Chemical Works, St. Louis, Mo. [b] Tracor 560, Tracor Inc., Austin, Tex. [c] Heptafluorobutyric anhydride derivative. [d] Nanograms for half-scale deflection (HSD) at GLC detector setting of 7 namp, and attenuation at 5. [e] Found in commercial samples.

0022-3549/82/0200-0268$01.00/0

sponding heptafluorobutyric anhydride derivatives are also reported with the approximate nanogram amounts of the parent amine needed for half-scale deflection at the electron-capture detector settings.

Eight samples of *p*-aminobenzoic acid, two samples of its sodium salt, and one sample of its potassium salt were analyzed in duplicate. Salt forms from three different lots contained no detectable aromatic amine impurities. Four of the acid samples contained benzocaine at levels of 3–65 ppm, while one sample of the acid contained 25 ppm of aniline. The TLC procedure confirmed the presence of both amine impurities. The derivatized samples were analyzed by GC–mass spectrometry and the mass spectral patterns of the samples matched those of derivatized standards of aniline and benzocaine.

The presence of benzocaine as an impurity was unexpected and cannnot be explained without knowledge of the synthesis process employed by the manufacturer. The aniline found in one sample could have been a contaminant of toluene used as a starting material for the synthesis of the *p*-aminobenzoic acid. The presence of aniline is significant because of its possible harmful effects on the body.

In synthesizing *p*-aminobenzoic acid, the process usually starts with toluene, followed by nitration, reduction, and oxidation reactions. The reported analytical procedure will determine the primary aromatic amine impurities formed in the synthesis of *p*-aminobenzoic acid or its salts. The 10 amines listed in Table I were added at levels of 1–5 ppm to the uncontaminated lots of free acid and recoveries of 90% or better were achieved using the derivatization technique.

(1) "The United States Pharmacopeia," 20th rev., Mack Publishing Co., Easton, Pa, 1980, p. 29.

(2) R. B. Bruce and W. R. Maynard, *Anal. Chem.*, **41**, 977 (1969).

Edward J. Wojtowicz
Food and Drug Administration
599 Delaware Avenue
Buffalo, NY 14202

Received January 16, 1981.
Accepted for publication September 23, 1981.
The author acknowledges Robert P. Barron, Division of Drug Chemistry, Food and Drug Administration, Washington, D.C. for mass spectral identification of the impurities found in the sample.

The Antitumor and Mammalian Xanthine Oxidase Inhibitory Activity of 5-Methyl-6-substituted Pyrrolo(2,3-*d*)pyrimidine-2,4-diones

Keyphrases □ Antitumor agents—potential, 5-methyl-6-substituted pyrrolo(2,3-*d*)pyrimidine-2,4-diones □ Xanthine oxidase—potential inhibitors, 5-methyl-6-substituted pyrrolo(2,3-*d*)pyrimidine-2,4-diones

To the Editor:

Gout is a disease that is a consequence of hyperuricemia. The objective of drug therapy in gout is to ameliorate inflammatory arthritis and to control serum urate concentration to <6 mg/100 ml. The two drug treatments currently used to decrease urate levels are the blocking of uric acid renal tubular reabsorption with probenecid or sulfinpyrazone and to block the enzymatic activity of xanthine oxidase. This enzyme catalyzes the oxidation of hypoxanthine to xanthine and xanthine to uric acid.

Table I—The Xanthine Oxidase Inhibitory Constant (K_i) of 5-Methyl-6-substituted Pyrrolo(2,3-*d*)pyrimidine-2,4-diones and Allopurinol

R[a]	K_i[b], *M*
$-CH_3$	1.5×10^{-5}
$-C_2H_5$	*NA*[c]
$-CH_2CH(CH_3)_2$	*NA*
$-C_6H_5$	4.0×10^{-6}
$-CH_2C_6H_5$	*NA*
$-CH_2C_6H_4$-*p*-OH	*NA*
Allopurinol	8.0×10^{-8}

[a] R refers to structure II in the text. [b] Inhibitory constant. [c] No activity.

Allopurinol (I) is used currently as a xanthine oxidase inhibitor. A series of substituted pyrrolo(2,3-*d*)pyrimidine-2,4-diones (II) was synthesized (1) and tested for inhibition of xanthine oxidase activity. A drug as potent as allopurinol would provide an alternative therapy for the gout patient.

The activity of buttermilk xanthine oxidase (1, 2) was measured *in vitro* by a previous method (2). [The activity of xanthine oxidase from humans is similar to that obtained from cow's milk (2).] The assay was performed at pH 8.0 in 0.1 *M* sodium phosphate buffer. Allopurinol[1], the pyrrolo(2,3-*d*)pyrimidine-2,4-diones, and hypoxanthine[2] were dissolved in 0.1 *M* sodium phosphate buffer, pH 8.0. Uric acid production was monitored at 300 nm in a UV spectrophotometer[3] at 36° after 1 μl (0.035 units) of xanthine oxidase was added to each reaction mixture. The hypoxanthine concentration varied from 0.06 to 0.10 m*M*, and the inhibitor concentration varied from 0 to 5×10^{-2} m*M*. The inhibitor constant (K_i) for each drug was determined by using a Dixon plot where 1/Vr is plotted against inhibitor concentration (3). Allopurinol was used as the standard xanthine oxidase inhibitor.

Table I lists the K_i for allopurinol and the six pyrrolo(2,3-*d*)pyrimidine-2,4-diones that were tested. Only two of the tested compounds showed any *in vitro* inhibition. The phenyl substituted compound had the most activity but it was low compared to allopurinol.

Because of the similarity of these compounds to normal purines, one compound, 5,6-dimethylpyrrolo(2,3-*d*)-pyrimidine-2,4-dione, was tested for *in vivo* activity against two transplantable mouse lymphoid tumor systems: H-5 ascites tumor[4] in A/J male mice[5] and L-1210 leukemia[6] in $B6D2F_1$ male mice[5].

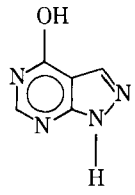

(I)

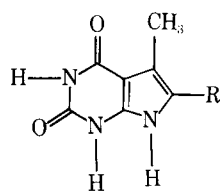

(II)

[1] Sigma Chemical Co., Saint Louis, MO 63178.
[2] Gilford Model 222A Photometer.
[3] From Buttermilk, grade III.
[4] A gift from Dr. J. Wynn, University of South Carolina.
[5] Jackson Laboratories, Bar Harbor, Ma.
[6] A gift from Dr. C. Bauguess, University of South Carolina.

0022-3549/82/0200-0269$01.00/0

sponding heptafluorobutyric anhydride derivatives are also reported with the approximate nanogram amounts of the parent amine needed for half-scale deflection at the electron-capture detector settings.

Eight samples of *p*-aminobenzoic acid, two samples of its sodium salt, and one sample of its potassium salt were analyzed in duplicate. Salt forms from three different lots contained no detectable aromatic amine impurities. Four of the acid samples contained benzocaine at levels of 3–65 ppm, while one sample of the acid contained 25 ppm of aniline. The TLC procedure confirmed the presence of both amine impurities. The derivatized samples were analyzed by GC–mass spectrometry and the mass spectral patterns of the samples matched those of derivatized standards of aniline and benzocaine.

The presence of benzocaine as an impurity was unexpected and cannnot be explained without knowledge of the synthesis process employed by the manufacturer. The aniline found in one sample could have been a contaminant of toluene used as a starting material for the synthesis of the *p*-aminobenzoic acid. The presence of aniline is significant because of its possible harmful effects on the body.

In synthesizing *p*-aminobenzoic acid, the process usually starts with toluene, followed by nitration, reduction, and oxidation reactions. The reported analytical procedure will determine the primary aromatic amine impurities formed in the synthesis of *p*-aminobenzoic acid or its salts. The 10 amines listed in Table I were added at levels of 1–5 ppm to the uncontaminated lots of free acid and recoveries of 90% or better were achieved using the derivatization technique.

(1) "The United States Pharmacopeia," 20th rev., Mack Publishing Co., Easton, Pa, 1980, p. 29.

(2) R. B. Bruce and W. R. Maynard, *Anal. Chem.*, **41**, 977 (1969).

Edward J. Wojtowicz
Food and Drug Administration
599 Delaware Avenue
Buffalo, NY 14202

Received January 16, 1981.
Accepted for publication September 23, 1981.
The author acknowledges Robert P. Barron, Division of Drug Chemistry, Food and Drug Administration, Washington, D.C. for mass spectral identification of the impurities found in the sample.

The Antitumor and Mammalian Xanthine Oxidase Inhibitory Activity of 5-Methyl-6-substituted Pyrrolo(2,3-*d*)pyrimidine-2,4-diones

Keyphrases □ Antitumor agents—potential, 5-methyl-6-substituted pyrrolo(2,3-*d*)pyrimidine-2,4-diones □ Xanthine oxidase—potential inhibitors, 5-methyl-6-substituted pyrrolo(2,3-*d*)pyrimidine-2,4-diones

To the Editor:

Gout is a disease that is a consequence of hyperuricemia. The objective of drug therapy in gout is to ameliorate inflammatory arthritis and to control serum urate concentration to <6 mg/100 ml. The two drug treatments currently used to decrease urate levels are the blocking of uric acid renal tubular reabsorption with probenecid or sulfinpyrazone and to block the enzymatic activity of xanthine oxidase. This enzyme catalyzes the oxidation of hypoxanthine to xanthine and xanthine to uric acid.

Table I—The Xanthine Oxidase Inhibitory Constant (K_i) of 5-Methyl-6-substituted Pyrrolo(2,3-*d*)pyrimidine-2,4-diones and Allopurinol

R[a]	K_i[b], *M*
$-CH_3$	1.5×10^{-5}
$-C_2H_5$	*NA*[c]
$-CH_2CH(CH_3)_2$	*NA*
$-C_6H_5$	4.0×10^{-6}
$-CH_2C_6H_5$	*NA*
$-CH_2C_6H_4$-*p*-OH	*NA*
Allopurinol	8.0×10^{-8}

[a] R refers to structure II in the text. [b] Inhibitory constant. [c] No activity.

Allopurinol (I) is used currently as a xanthine oxidase inhibitor. A series of substituted pyrrolo(2,3-*d*)pyrimidine-2,4-diones (II) was synthesized (1) and tested for inhibition of xanthine oxidase activity. A drug as potent as allopurinol would provide an alternative therapy for the gout patient.

The activity of buttermilk xanthine oxidase (1, 2) was measured *in vitro* by a previous method (2). [The activity of xanthine oxidase from humans is similar to that obtained from cow's milk (2).] The assay was performed at pH 8.0 in 0.1 *M* sodium phosphate buffer. Allopurinol[1], the pyrrolo(2,3-*d*)pyrimidine-2,4-diones, and hypoxanthine[2] were dissolved in 0.1 *M* sodium phosphate buffer, pH 8.0. Uric acid production was monitored at 300 nm in a UV spectrophotometer[3] at 36° after 1 μl (0.035 units) of xanthine oxidase was added to each reaction mixture. The hypoxanthine concentration varied from 0.06 to 0.10 m*M*, and the inhibitor concentration varied from 0 to 5×10^{-2} m*M*. The inhibitor constant (K_i) for each drug was determined by using a Dixon plot where 1/Vr is plotted against inhibitor concentration (3). Allopurinol was used as the standard xanthine oxidase inhibitor.

Table I lists the K_i for allopurinol and the six pyrrolo(2,3-*d*)pyrimidine-2,4-diones that were tested. Only two of the tested compounds showed any *in vitro* inhibition. The phenyl substituted compound had the most activity but it was low compared to allopurinol.

Because of the similarity of these compounds to normal purines, one compound, 5,6-dimethylpyrrolo(2,3-*d*)-pyrimidine-2,4-dione, was tested for *in vivo* activity against two transplantable mouse lymphoid tumor systems: H-5 ascites tumor[4] in A/J male mice[5] and L-1210 leukemia[6] in $B6D2F_1$ male mice[5].

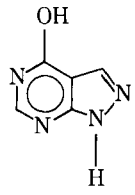

(I)

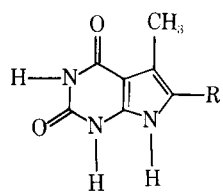

(II)

[1] Sigma Chemical Co., Saint Louis, MO 63178.
[2] Gilford Model 222A Photometer.
[3] From Buttermilk, grade III.
[4] A gift from Dr. J. Wynn, University of South Carolina.
[5] Jackson Laboratories, Bar Harbor, Ma.
[6] A gift from Dr. C. Bauguess, University of South Carolina.

0022-3549/82/0200-0269$01.00/0

Ascites fluid (0.1 ml) from a tumor-bearing mouse and containing 10^5 cells[7] was injected intraperitoneally on day zero. Each experimental group contained six male mice (20–25 g) (4). The drug was injected intraperitoneally on days 1, 5, and 9 at a 120-mg/kg dose. The T/C was 85.4% for the L-1210 leukemia and 83.5% for the H-5 ascites tumor. A 360-mg/kg dose at day 1 or 40 mg/kg on days 1–9 in the L-1210 tumor also gave a T/C of 85.4%. A T/C value ≤85% indicates that the compound is probably producing a toxic response (4). This compound did not cause any deaths in control A/J or $B6D2F_1$ mice at the doses used, nor did it cause any visible toxicity, such as weight loss.

The probable toxic response of this compound in tumor-bearing mice hindered the testing of other substituted pyrrolo(2,3-*d*)pyrimidine-2,4-diones for antitumor activity.

(1) S. R. Etson, R. J. Mattson, and J. W. Sowell, Sr., *J. Heterocycl. Chem.*, **16**, 929 (1979).
(2) F. Bergman and S. Dikstein, *J. Biol. Chem.*, **223**, 765, (1956).
(3) H. N. Christensen and G. A. Palmer, "Enzyme Kinetics," 2nd ed., W. B. Saunders, Philadelphia, Pa., 1974, p. 82.
(4) B. J. Abbott, *Cancer Chemother. Rep. Part 3*, **3**, 2 (1972).

*Charles J. Betlach**x
J. Walter Sowell, Sr.
College of Pharmacy
University of South Carolina
Columbia, SC 29208

* Present address: Massachusetts College of Pharmacy and Allied Health Sciences, Boston, MA 02115.

[7] Cells were counted on an improved Neubauer ultraplane spot lite counting chamber (Scientific Products).

Studies on Herbal Remedies I: Analysis of Herbal Smoking Preparations Alleged to Contain Lettuce (*Lactuca sativa* L.) and Other Natural Products

Keyphrases □ Pharmacognosy—analysis of smoking preparations alleged to contain lettuce (*Lactuca sativa* L.) □ Psychotropics—alleged, analysis of lettuce (*Lactuca sativa* L.) in smoking preparations

To the Editor:

In this communication we would like to draw attention to the availability in health food stores and other outlets of three so-called "narcotic substitute" smoking products[1] that allegedly contain distillates of lettuce. Preparation 1 ("Hashish") and preparation 2 ("Opium") are recommended by their manufacturer for legal, social smoking, while preparation 3 ("Hash Oil") is suggested for application to marijuana cigarettes to enhance potency and taste. According to the package inscriptions, all three preparations contain "*Lactuca sativa*" (Garden Lettuce) and "*Turnera diffusa*" (Damiana) distillates. In addition, preparation 1 is claimed to be fortified with African Yohimbe bark, and preparation 2 with *Lactuca virosa* (Wild Lettuce) and *Nepeta cataria* (Catnip) distillates, as well as Chinese ginseng root. Ingredient proportions are not stated on the package labels.

It was suggested to us[2] that the smoking of preparation 2, without additives, may have been responsible for producing apparent psychotropic effects experienced by two teenagers. In an attempt to provide a rationale for this observation, the literature was searched for any ethnomedical and biological activities of Garden and Wild Lettuce and Damiana, and to whether or not any of the known constituents of these plants belong to classes of psychotropic substances.

Extracts of both *L. sativa* and *L. virosa* have been claimed to possess narcotic properties (1, 2), while the latter plant has been associated with hypnotic and sedative effects (3). Experimentally, extracts of *L. sativa* have exhibited *in vitro* antitubercular properties (4) and hypotensive activity in dogs (5). *T. diffusa* extracts reputedly show mild stimulant (2), purgative (3), and aphrodisiac (1, 3) activities.

An early study indicated that *L. sativa* and *L. virosa* contain a mydriatic alkaloid, which was identified as the tropane derivative hyoscyamine on the basis of the melting point of its aurochloride (6). The presence of a mydriatic alkaloid, although disputed, was presumably confirmed in later studies on *L. virosa* (7, 8). *L. virosa* has been shown to contain *N*-methyl-β-phenethylamine (9), and *T. diffusa* has been stated to contain the xanthine derivative, caffeine (10). Tropane alkaloids, phenethylamines, and xanthines were recently classified, respectively, as deliriant psychodysleptics, visionary psychodysleptics, and excitatory psychoanaleptics (11).

All three preparations were examined phytochemically to determine if any of these amines could be detected. Three extraction procedures, namely, a general alkaloidal method (12), and methods for the specific extraction of phenethylamines (13) and caffeine (14), were applied to 2-g portions of each product. No alkaloidal spots corresponding to reference hyoscyamine, *N*-methyl-β-phenethylamine[3], or caffeine were detected by TLC on silica gel using several solvent systems (15). Dragendorff's reagent, as well as other reagents useful for the detection of phenethylamines (ninhydrin) (15) and xanthines (iodine and ferric chloride) (15) were used for plate visualization.

Therefore, it appears that any psychotropic effects experienced by the smoking of these lettuce-Damiana distillates are not due to the presence of tropane alkaloids, phenethylamines, or xanthine bases.

(1) "The Dispensatory of the United States of America," 19th ed., H. C. Wood, J. P. Remington, and S. P. Sadtler, Eds., J. B. Lippincott, Philadelphia, Pa., 1907, pp. 686, 1471.
(2) R. K. Seigel, *J. Am. Med. Assoc.*, **236**, 473 (1976).
(3) "Extra Pharmacopoeia (Martindale)," 25th ed., R. G. Todd, Ed., Pharmaceutical Press, London, U.K., 1967, pp. 1518, 1531.
(4) F. K. Fitzpatrick, *Antibiot. Chemother.*, **4**, 528 (1954).
(5) L. Sollero, O. M. da Fonseca, W. B. Mors, A. A. de Figueiredo, and N. Sharapin, *Ciênc. Cult. (Sao Paulo)*, **20**, 33 (1968).
(6) T. S. Dymond, *J. Chem. Soc.*, **61**, 90 (1892).
(7) E. M. Farr and R. Wright, *Pharm. J.*, **72**, 186 (1904).
(8) Editorial, *ibid.*, **72**, 195 (1904).
(9) P. Marquardt, H.-G. Classen, and K.-A. Schumacher,

[1] Preparations 1–3 described in this report are Lettucenes 1–3, Woodley Herber, Okemos, MI 48864.

[2] Our attention was drawn to this problem by C. R. Sherwood, A. J. Canfield Co., Chicago, IL 60619.

[3] We are grateful to Prof. J. L. McLaughlin, Purdue University, W. Lafayette, Ind., for a reference sample of *N*-methyl-β-phenethylamine hydrochloride.

0022-3549/82/0200-0270$01.00/0

Ascites fluid (0.1 ml) from a tumor-bearing mouse and containing 10^5 cells[7] was injected intraperitoneally on day zero. Each experimental group contained six male mice (20–25 g) (4). The drug was injected intraperitoneally on days 1, 5, and 9 at a 120-mg/kg dose. The T/C was 85.4% for the L-1210 leukemia and 83.5% for the H-5 ascites tumor. A 360-mg/kg dose at day 1 or 40 mg/kg on days 1–9 in the L-1210 tumor also gave a T/C of 85.4%. A T/C value ≤85% indicates that the compound is probably producing a toxic response (4). This compound did not cause any deaths in control A/J or $B6D2F_1$ mice at the doses used, nor did it cause any visible toxicity, such as weight loss.

The probable toxic response of this compound in tumor-bearing mice hindered the testing of other substituted pyrrolo(2,3-*d*)pyrimidine-2,4-diones for antitumor activity.

(1) S. R. Etson, R. J. Mattson, and J. W. Sowell, Sr., *J. Heterocycl. Chem.*, **16**, 929 (1979).
(2) F. Bergman and S. Dikstein, *J. Biol. Chem.*, **223**, 765, (1956).
(3) H. N. Christensen and G. A. Palmer, "Enzyme Kinetics," 2nd ed., W. B. Saunders, Philadelphia, Pa., 1974, p. 82.
(4) B. J. Abbott, *Cancer Chemother. Rep. Part 3*, **3**, 2 (1972).

*Charles J. Betlach**x
J. Walter Sowell, Sr.
College of Pharmacy
University of South Carolina
Columbia, SC 29208

* Present address: Massachusetts College of Pharmacy and Allied Health Sciences, Boston, MA 02115.

[7] Cells were counted on an improved Neubauer ultraplane spot lite counting chamber (Scientific Products).

Studies on Herbal Remedies I: Analysis of Herbal Smoking Preparations Alleged to Contain Lettuce (*Lactuca sativa* L.) and Other Natural Products

Keyphrases □ Pharmacognosy—analysis of smoking preparations alleged to contain lettuce (*Lactuca sativa* L.) □ Psychotropics—alleged, analysis of lettuce (*Lactuca sativa* L.) in smoking preparations

To the Editor:

In this communication we would like to draw attention to the availability in health food stores and other outlets of three so-called "narcotic substitute" smoking products[1] that allegedly contain distillates of lettuce. Preparation 1 ("Hashish") and preparation 2 ("Opium") are recommended by their manufacturer for legal, social smoking, while preparation 3 ("Hash Oil") is suggested for application to marijuana cigarettes to enhance potency and taste. According to the package inscriptions, all three preparations contain "*Lactuca sativa*" (Garden Lettuce) and "*Turnera diffusa*" (Damiana) distillates. In addition, preparation 1 is claimed to be fortified with African Yohimbe bark, and preparation 2 with *Lactuca virosa* (Wild Lettuce) and *Nepeta cataria* (Catnip) distillates, as well as Chinese ginseng root. Ingredient proportions are not stated on the package labels.

It was suggested to us[2] that the smoking of preparation 2, without additives, may have been responsible for producing apparent psychotropic effects experienced by two teenagers. In an attempt to provide a rationale for this observation, the literature was searched for any ethnomedical and biological activities of Garden and Wild Lettuce and Damiana, and to whether or not any of the known constituents of these plants belong to classes of psychotropic substances.

Extracts of both *L. sativa* and *L. virosa* have been claimed to possess narcotic properties (1, 2), while the latter plant has been associated with hypnotic and sedative effects (3). Experimentally, extracts of *L. sativa* have exhibited *in vitro* antitubercular properties (4) and hypotensive activity in dogs (5). *T. diffusa* extracts reputedly show mild stimulant (2), purgative (3), and aphrodisiac (1, 3) activities.

An early study indicated that *L. sativa* and *L. virosa* contain a mydriatic alkaloid, which was identified as the tropane derivative hyoscyamine on the basis of the melting point of its aurochloride (6). The presence of a mydriatic alkaloid, although disputed, was presumably confirmed in later studies on *L. virosa* (7, 8). *L. virosa* has been shown to contain *N*-methyl-β-phenethylamine (9), and *T. diffusa* has been stated to contain the xanthine derivative, caffeine (10). Tropane alkaloids, phenethylamines, and xanthines were recently classified, respectively, as deliriant psychodysleptics, visionary psychodysleptics, and excitatory psychoanaleptics (11).

All three preparations were examined phytochemically to determine if any of these amines could be detected. Three extraction procedures, namely, a general alkaloidal method (12), and methods for the specific extraction of phenethylamines (13) and caffeine (14), were applied to 2-g portions of each product. No alkaloidal spots corresponding to reference hyoscyamine, *N*-methyl-β-phenethylamine[3], or caffeine were detected by TLC on silica gel using several solvent systems (15). Dragendorff's reagent, as well as other reagents useful for the detection of phenethylamines (ninhydrin) (15) and xanthines (iodine and ferric chloride) (15) were used for plate visualization.

Therefore, it appears that any psychotropic effects experienced by the smoking of these lettuce-Damiana distillates are not due to the presence of tropane alkaloids, phenethylamines, or xanthine bases.

(1) "The Dispensatory of the United States of America," 19th ed., H. C. Wood, J. P. Remington, and S. P. Sadtler, Eds., J. B. Lippincott, Philadelphia, Pa., 1907, pp. 686, 1471.
(2) R. K. Seigel, *J. Am. Med. Assoc.*, **236**, 473 (1976).
(3) "Extra Pharmacopoeia (Martindale)," 25th ed., R. G. Todd, Ed., Pharmaceutical Press, London, U.K., 1967, pp. 1518, 1531.
(4) F. K. Fitzpatrick, *Antibiot. Chemother.*, **4**, 528 (1954).
(5) L. Sollero, O. M. da Fonseca, W. B. Mors, A. A. de Figueiredo, and N. Sharapin, *Ciênc. Cult. (Sao Paulo)*, **20**, 33 (1968).
(6) T. S. Dymond, *J. Chem. Soc.*, **61**, 90 (1892).
(7) E. M. Farr and R. Wright, *Pharm. J.*, **72**, 186 (1904).
(8) Editorial, *ibid.*, **72**, 195 (1904).
(9) P. Marquardt, H.-G. Classen, and K.-A. Schumacher,

[1] Preparations 1–3 described in this report are Lettucenes 1–3, Woodley Herber, Okemos, MI 48864.

[2] Our attention was drawn to this problem by C. R. Sherwood, A. J. Canfield Co., Chicago, IL 60619.

[3] We are grateful to Prof. J. L. McLaughlin, Purdue University, W. Lafayette, Ind., for a reference sample of *N*-methyl-β-phenethylamine hydrochloride.

0022-3549/82/0200-0270$01.00/0

Arzneim.-Forsch., **26**, 2001 (1976).
(10) X. A. Domínguez and M. Hinojosa, *Planta Med.*, **30**, 68 (1976).
(11) J. L. Díaz, *Ann. Rev. Pharmacol. Toxicol.*, **17**, 647 (1977).
(12) N. R. Farnsworth and K. L. Euler, *Lloydia*, **26**, 186 (1962).
(13) M. N. Graziano, G. E. Ferraro, and J. D. Coussio, *ibid.*, **34**, 453 (1971).
(14) R. Ikan, "Natural Products. A Laboratory Guide," Academic, London and New York, 1969, p. 183.
(15) "Thin-Layer Chromatography. A Laboratory Handbook," E. Stahl, Ed., Springer-Verlag, New York-Heidelberg-Berlin, 1969, pp. 432, 499, 548.

Zei-Jing Huang
A. Douglas Kinghorn[x]
Norman R. Farnsworth
Department of Pharmacognosy and Pharmacology, College of Pharmacy
University of Illinois
at the Medical Center
Chicago, IL 60612

Received June 8, 1981.
Accepted for publication August 8, 1981

BOOKS

REVIEWS

Burger's Medicinal Chemistry, 4th Ed., Part III. Edited by MANFRED E. WOLFF. Wiley, 605 Third Ave., New York, NY 10016. 1981. 1354 pp. 18.5 × 26 cm. Price $100.00.

This book is part of an excellent series in the medicinal chemistry field. With contributions by a number of knowledgeable and literate authors, the contents include drugs acting on the central nervous system, the autonomic nervous system, the cardiovascular system, and the renal system. The book is a well-balanced blend of the theoretical and practical aspects of the field and its potential application to new discoveries.

Each chapter is well planned, emphasizes biochemical rationale, structure–function relationships, and metabolism, and is adequately referenced to provide the reader with sources of more detailed information. This text is also characterized by thoughtful attention to pedagogy, since the prose does more than fill the space between structures and equations. The book contains many useful tables, graphs, and other illustrations and is replete with numerous structures.

Professor Wolff has assembled an informative and excellent text, so it is regrettable that the major limitation of this potentially useful text appears to be its price. Overall, the present volume together with Parts I and II of the series offers a high quality and useful source of information with broad application across the biomedical sciences. Professor Wolff upholds the series' reputation as one of the classic and indispensable reference works for those in teaching and research.

Reviewed by Claude Piantadosi
School of Pharmacy
University of North Carolina
Chapel Hill, NC 27514

Principles of Medicinal Chemistry. Edited by WILLIAM O. FOYE. Lea & Febiger, 600 S. Washington Square, Philadelphia, PA 19106. 1981. 931 pp. 18 × 26 cm. Price $45.50. (Canada $54.50).

This book assembles 39 chapters of information associated with textbooks intended for undergraduate courses in organic medicinal chemistry. The first six chapters give effective coverage of general introductory principles; thereafter, with the exception of Chapters 27–29 (which provide good introductions to drugs of plant origin and subsequent chapters on chemotherapeutic agents), the book proceeds systematically through major pharmacological or therapeutic classes of drugs.

Discussions are generally restricted to organic agents, although actions of some inorganic agents such as iodine and iodides, sodium nitroprusside, and gold sodium thiosulfate are cited. The last chapter is also an exception to the overall organic medicinal chemical content in that it incorporates a very good introduction to radiopharmaceuticals. Finally, there is an appendix containing useful compilations of pKa values for a number of drugs and pH values for body fluids.

The authors of the chapters dealing with the pharmacological classes of agents have used a variety of formats to cover their topics. In general, they discuss pharmacological actions, absorption, distribution, metabolism and excretion, clinical uses, and structure–activity relationships and give appropriate examples. Often this information is set out against a background survey of biochemistry pertaining to the group under consideration. In some of these chapters, the explanations of the agents' pharmacological actions, based on the structural reasons for their ability to fit into a biochemical sequence, are impressive. The overall quality of these chapters, despite differing organizational styles, is very good.

While the individual chapters impress as compact, self-contained entities, some readers may notice instances of redundancy. For example, the scheme for catabolism for certain neurotransmitters is repeated in detail in several chapters and the pharmacology of a number of therapeutic agents is given several times. It is possible that such repetition cannot be avoided in a multiauthored work. In addition, while background pharmacology, biochemistry, and the clinical uses of the agents are almost always thoroughly treated, chemical properties such as acidity, basicity, and chemical stability are sometimes not discussed. Perhaps inclusion of such coverage would not only help students appreciate some pharmaceutically important properties but would also help them relate structure and chemical properties to absorption, distribution, metabolism, excretion, and biological actions.

In summary, all chapters bear evidence of careful scholarly preparation. They are generally thorough and current in their coverage and are quite readable. The book meets its objectives very well and should afford excellent reading for medicinal chemists, pharmacologists, and students in pharmacy and related disciplines.

Reviewed by Eugene Isaacson
Idaho State University
College of Pharmacy
Pocatello, ID 83201

Toxicants and Drugs: Kinetics and Dynamics. By ELLEN J. O'FLAHERTY. Wiley, 605 Third Ave., New York, NY 10016. 1981, 398 pp. 16 × 24 cm. Price $42.50.

This useful book approaches a complex subject with a disarming frankness not usually found in such texts. In the preface, the author states that the first chapter reviews algebra and calculus at a level designed to give nonmathematicians—even antimathematicians!—confidence that they can "do" kinetics. After hopefully instilling such confidence and expertise, the reader is eventually lead into sophisticated concepts relating to disposition in saturable and nonlinear systems, the plateau principle of chronic exposure, receptor theory, pharmacodynamics and dose–response relationships. The book is a gem. A useful list of definitions of various symbols is included as a separate section and as an added bonus, a number of interesting problems taken from examples in the

Arzneim.-Forsch., **26**, 2001 (1976).
(10) X. A. Domínguez and M. Hinojosa, *Planta Med.*, **30**, 68 (1976).
(11) J. L. Díaz, *Ann. Rev. Pharmacol. Toxicol.*, **17**, 647 (1977).
(12) N. R. Farnsworth and K. L. Euler, *Lloydia*, **26**, 186 (1962).
(13) M. N. Graziano, G. E. Ferraro, and J. D. Coussio, *ibid.*, **34**, 453 (1971).
(14) R. Ikan, "Natural Products. A Laboratory Guide," Academic, London and New York, 1969, p. 183.
(15) "Thin-Layer Chromatography. A Laboratory Handbook," E. Stahl, Ed., Springer-Verlag, New York-Heidelberg-Berlin, 1969, pp. 432, 499, 548.

Zei-Jing Huang
A. Douglas Kinghorn[x]
Norman R. Farnsworth
Department of Pharmacognosy and Pharmacology, College of Pharmacy
University of Illinois
at the Medical Center
Chicago, IL 60612

Received June 8, 1981.
Accepted for publication August 8, 1981

BOOKS

REVIEWS

Burger's Medicinal Chemistry, 4th Ed., Part III. Edited by MANFRED E. WOLFF. Wiley, 605 Third Ave., New York, NY 10016. 1981. 1354 pp. 18.5 × 26 cm. Price $100.00.

This book is part of an excellent series in the medicinal chemistry field. With contributions by a number of knowledgeable and literate authors, the contents include drugs acting on the central nervous system, the autonomic nervous system, the cardiovascular system, and the renal system. The book is a well-balanced blend of the theoretical and practical aspects of the field and its potential application to new discoveries.

Each chapter is well planned, emphasizes biochemical rationale, structure–function relationships, and metabolism, and is adequately referenced to provide the reader with sources of more detailed information. This text is also characterized by thoughtful attention to pedagogy, since the prose does more than fill the space between structures and equations. The book contains many useful tables, graphs, and other illustrations and is replete with numerous structures.

Professor Wolff has assembled an informative and excellent text, so it is regrettable that the major limitation of this potentially useful text appears to be its price. Overall, the present volume together with Parts I and II of the series offers a high quality and useful source of information with broad application across the biomedical sciences. Professor Wolff upholds the series' reputation as one of the classic and indispensable reference works for those in teaching and research.

Reviewed by Claude Piantadosi
School of Pharmacy
University of North Carolina
Chapel Hill, NC 27514

Principles of Medicinal Chemistry. Edited by WILLIAM O. FOYE. Lea & Febiger, 600 S. Washington Square, Philadelphia, PA 19106. 1981. 931 pp. 18 × 26 cm. Price $45.50. (Canada $54.50).

This book assembles 39 chapters of information associated with textbooks intended for undergraduate courses in organic medicinal chemistry. The first six chapters give effective coverage of general introductory principles; thereafter, with the exception of Chapters 27–29 (which provide good introductions to drugs of plant origin and subsequent chapters on chemotherapeutic agents), the book proceeds systematically through major pharmacological or therapeutic classes of drugs.

Discussions are generally restricted to organic agents, although actions of some inorganic agents such as iodine and iodides, sodium nitroprusside, and gold sodium thiosulfate are cited. The last chapter is also an exception to the overall organic medicinal chemical content in that it incorporates a very good introduction to radiopharmaceuticals. Finally, there is an appendix containing useful compilations of pKa values for a number of drugs and pH values for body fluids.

The authors of the chapters dealing with the pharmacological classes of agents have used a variety of formats to cover their topics. In general, they discuss pharmacological actions, absorption, distribution, metabolism and excretion, clinical uses, and structure–activity relationships and give appropriate examples. Often this information is set out against a background survey of biochemistry pertaining to the group under consideration. In some of these chapters, the explanations of the agents' pharmacological actions, based on the structural reasons for their ability to fit into a biochemical sequence, are impressive. The overall quality of these chapters, despite differing organizational styles, is very good.

While the individual chapters impress as compact, self-contained entities, some readers may notice instances of redundancy. For example, the scheme for catabolism for certain neurotransmitters is repeated in detail in several chapters and the pharmacology of a number of therapeutic agents is given several times. It is possible that such repetition cannot be avoided in a multiauthored work. In addition, while background pharmacology, biochemistry, and the clinical uses of the agents are almost always thoroughly treated, chemical properties such as acidity, basicity, and chemical stability are sometimes not discussed. Perhaps inclusion of such coverage would not only help students appreciate some pharmaceutically important properties but would also help them relate structure and chemical properties to absorption, distribution, metabolism, excretion, and biological actions.

In summary, all chapters bear evidence of careful scholarly preparation. They are generally thorough and current in their coverage and are quite readable. The book meets its objectives very well and should afford excellent reading for medicinal chemists, pharmacologists, and students in pharmacy and related disciplines.

Reviewed by Eugene Isaacson
Idaho State University
College of Pharmacy
Pocatello, ID 83201

Toxicants and Drugs: Kinetics and Dynamics. By ELLEN J. O'FLAHERTY. Wiley, 605 Third Ave., New York, NY 10016. 1981, 398 pp. 16 × 24 cm. Price $42.50.

This useful book approaches a complex subject with a disarming frankness not usually found in such texts. In the preface, the author states that the first chapter reviews algebra and calculus at a level designed to give nonmathematicians—even antimathematicians!—confidence that they can "do" kinetics. After hopefully instilling such confidence and expertise, the reader is eventually lead into sophisticated concepts relating to disposition in saturable and nonlinear systems, the plateau principle of chronic exposure, receptor theory, pharmacodynamics and dose–response relationships. The book is a gem. A useful list of definitions of various symbols is included as a separate section and as an added bonus, a number of interesting problems taken from examples in the

Arzneim.-Forsch., **26**, 2001 (1976).
(10) X. A. Domínguez and M. Hinojosa, *Planta Med.*, **30**, 68 (1976).
(11) J. L. Díaz, *Ann. Rev. Pharmacol. Toxicol.*, **17**, 647 (1977).
(12) N. R. Farnsworth and K. L. Euler, *Lloydia*, **26**, 186 (1962).
(13) M. N. Graziano, G. E. Ferraro, and J. D. Coussio, *ibid.*, **34**, 453 (1971).
(14) R. Ikan, "Natural Products. A Laboratory Guide," Academic, London and New York, 1969, p. 183.
(15) "Thin-Layer Chromatography. A Laboratory Handbook," E. Stahl, Ed., Springer-Verlag, New York-Heidelberg-Berlin, 1969, pp. 432, 499, 548.

Zei-Jing Huang
A. Douglas Kinghorn[x]
Norman R. Farnsworth
Department of Pharmacognosy and Pharmacology, College of Pharmacy
University of Illinois
at the Medical Center
Chicago, IL 60612

Received June 8, 1981.
Accepted for publication August 8, 1981

BOOKS

REVIEWS

Burger's Medicinal Chemistry, 4th Ed., Part III. Edited by MANFRED E. WOLFF. Wiley, 605 Third Ave., New York, NY 10016. 1981. 1354 pp. 18.5 × 26 cm. Price $100.00.

This book is part of an excellent series in the medicinal chemistry field. With contributions by a number of knowledgeable and literate authors, the contents include drugs acting on the central nervous system, the autonomic nervous system, the cardiovascular system, and the renal system. The book is a well-balanced blend of the theoretical and practical aspects of the field and its potential application to new discoveries.

Each chapter is well planned, emphasizes biochemical rationale, structure–function relationships, and metabolism, and is adequately referenced to provide the reader with sources of more detailed information. This text is also characterized by thoughtful attention to pedagogy, since the prose does more than fill the space between structures and equations. The book contains many useful tables, graphs, and other illustrations and is replete with numerous structures.

Professor Wolff has assembled an informative and excellent text, so it is regrettable that the major limitation of this potentially useful text appears to be its price. Overall, the present volume together with Parts I and II of the series offers a high quality and useful source of information with broad application across the biomedical sciences. Professor Wolff upholds the series' reputation as one of the classic and indispensable reference works for those in teaching and research.

Reviewed by Claude Piantadosi
School of Pharmacy
University of North Carolina
Chapel Hill, NC 27514

Principles of Medicinal Chemistry. Edited by WILLIAM O. FOYE. Lea & Febiger, 600 S. Washington Square, Philadelphia, PA 19106. 1981. 931 pp. 18 × 26 cm. Price $45.50. (Canada $54.50).

This book assembles 39 chapters of information associated with textbooks intended for undergraduate courses in organic medicinal chemistry. The first six chapters give effective coverage of general introductory principles; thereafter, with the exception of Chapters 27–29 (which provide good introductions to drugs of plant origin and subsequent chapters on chemotherapeutic agents), the book proceeds systematically through major pharmacological or therapeutic classes of drugs.

Discussions are generally restricted to organic agents, although actions of some inorganic agents such as iodine and iodides, sodium nitroprusside, and gold sodium thiosulfate are cited. The last chapter is also an exception to the overall organic medicinal chemical content in that it incorporates a very good introduction to radiopharmaceuticals. Finally, there is an appendix containing useful compilations of pKa values for a number of drugs and pH values for body fluids.

The authors of the chapters dealing with the pharmacological classes of agents have used a variety of formats to cover their topics. In general, they discuss pharmacological actions, absorption, distribution, metabolism and excretion, clinical uses, and structure–activity relationships and give appropriate examples. Often this information is set out against a background survey of biochemistry pertaining to the group under consideration. In some of these chapters, the explanations of the agents' pharmacological actions, based on the structural reasons for their ability to fit into a biochemical sequence, are impressive. The overall quality of these chapters, despite differing organizational styles, is very good.

While the individual chapters impress as compact, self-contained entities, some readers may notice instances of redundancy. For example, the scheme for catabolism for certain neurotransmitters is repeated in detail in several chapters and the pharmacology of a number of therapeutic agents is given several times. It is possible that such repetition cannot be avoided in a multiauthored work. In addition, while background pharmacology, biochemistry, and the clinical uses of the agents are almost always thoroughly treated, chemical properties such as acidity, basicity, and chemical stability are sometimes not discussed. Perhaps inclusion of such coverage would not only help students appreciate some pharmaceutically important properties but would also help them relate structure and chemical properties to absorption, distribution, metabolism, excretion, and biological actions.

In summary, all chapters bear evidence of careful scholarly preparation. They are generally thorough and current in their coverage and are quite readable. The book meets its objectives very well and should afford excellent reading for medicinal chemists, pharmacologists, and students in pharmacy and related disciplines.

Reviewed by Eugene Isaacson
Idaho State University
College of Pharmacy
Pocatello, ID 83201

Toxicants and Drugs: Kinetics and Dynamics. By ELLEN J. O'FLAHERTY. Wiley, 605 Third Ave., New York, NY 10016. 1981, 398 pp. 16 × 24 cm. Price $42.50.

This useful book approaches a complex subject with a disarming frankness not usually found in such texts. In the preface, the author states that the first chapter reviews algebra and calculus at a level designed to give nonmathematicians—even antimathematicians!—confidence that they can "do" kinetics. After hopefully instilling such confidence and expertise, the reader is eventually lead into sophisticated concepts relating to disposition in saturable and nonlinear systems, the plateau principle of chronic exposure, receptor theory, pharmacodynamics and dose–response relationships. The book is a gem. A useful list of definitions of various symbols is included as a separate section and as an added bonus, a number of interesting problems taken from examples in the

Arzneim.-Forsch., **26**, 2001 (1976).
(10) X. A. Domínguez and M. Hinojosa, *Planta Med.*, **30**, 68 (1976).
(11) J. L. Díaz, *Ann. Rev. Pharmacol. Toxicol.*, **17**, 647 (1977).
(12) N. R. Farnsworth and K. L. Euler, *Lloydia*, **26**, 186 (1962).
(13) M. N. Graziano, G. E. Ferraro, and J. D. Coussio, *ibid.*, **34**, 453 (1971).
(14) R. Ikan, "Natural Products. A Laboratory Guide," Academic, London and New York, 1969, p. 183.
(15) "Thin-Layer Chromatography. A Laboratory Handbook," E. Stahl, Ed., Springer-Verlag, New York-Heidelberg-Berlin, 1969, pp. 432, 499, 548.

Zei-Jing Huang
A. Douglas Kinghorn[x]
Norman R. Farnsworth
Department of Pharmacognosy and Pharmacology, College of Pharmacy
University of Illinois
at the Medical Center
Chicago, IL 60612

Received June 8, 1981.
Accepted for publication August 8, 1981

BOOKS

REVIEWS

Burger's Medicinal Chemistry, 4th Ed., Part III. Edited by MANFRED E. WOLFF. Wiley, 605 Third Ave., New York, NY 10016. 1981. 1354 pp. 18.5 × 26 cm. Price $100.00.

This book is part of an excellent series in the medicinal chemistry field. With contributions by a number of knowledgeable and literate authors, the contents include drugs acting on the central nervous system, the autonomic nervous system, the cardiovascular system, and the renal system. The book is a well-balanced blend of the theoretical and practical aspects of the field and its potential application to new discoveries.

Each chapter is well planned, emphasizes biochemical rationale, structure–function relationships, and metabolism, and is adequately referenced to provide the reader with sources of more detailed information. This text is also characterized by thoughtful attention to pedagogy, since the prose does more than fill the space between structures and equations. The book contains many useful tables, graphs, and other illustrations and is replete with numerous structures.

Professor Wolff has assembled an informative and excellent text, so it is regrettable that the major limitation of this potentially useful text appears to be its price. Overall, the present volume together with Parts I and II of the series offers a high quality and useful source of information with broad application across the biomedical sciences. Professor Wolff upholds the series' reputation as one of the classic and indispensable reference works for those in teaching and research.

Reviewed by Claude Piantadosi
School of Pharmacy
University of North Carolina
Chapel Hill, NC 27514

Principles of Medicinal Chemistry. Edited by WILLIAM O. FOYE. Lea & Febiger, 600 S. Washington Square, Philadelphia, PA 19106. 1981. 931 pp. 18 × 26 cm. Price $45.50. (Canada $54.50).

This book assembles 39 chapters of information associated with textbooks intended for undergraduate courses in organic medicinal chemistry. The first six chapters give effective coverage of general introductory principles; thereafter, with the exception of Chapters 27–29 (which provide good introductions to drugs of plant origin and subsequent chapters on chemotherapeutic agents), the book proceeds systematically through major pharmacological or therapeutic classes of drugs.

Discussions are generally restricted to organic agents, although actions of some inorganic agents such as iodine and iodides, sodium nitroprusside, and gold sodium thiosulfate are cited. The last chapter is also an exception to the overall organic medicinal chemical content in that it incorporates a very good introduction to radiopharmaceuticals. Finally, there is an appendix containing useful compilations of pKa values for a number of drugs and pH values for body fluids.

The authors of the chapters dealing with the pharmacological classes of agents have used a variety of formats to cover their topics. In general, they discuss pharmacological actions, absorption, distribution, metabolism and excretion, clinical uses, and structure–activity relationships and give appropriate examples. Often this information is set out against a background survey of biochemistry pertaining to the group under consideration. In some of these chapters, the explanations of the agents' pharmacological actions, based on the structural reasons for their ability to fit into a biochemical sequence, are impressive. The overall quality of these chapters, despite differing organizational styles, is very good.

While the individual chapters impress as compact, self-contained entities, some readers may notice instances of redundancy. For example, the scheme for catabolism for certain neurotransmitters is repeated in detail in several chapters and the pharmacology of a number of therapeutic agents is given several times. It is possible that such repetition cannot be avoided in a multiauthored work. In addition, while background pharmacology, biochemistry, and the clinical uses of the agents are almost always thoroughly treated, chemical properties such as acidity, basicity, and chemical stability are sometimes not discussed. Perhaps inclusion of such coverage would not only help students appreciate some pharmaceutically important properties but would also help them relate structure and chemical properties to absorption, distribution, metabolism, excretion, and biological actions.

In summary, all chapters bear evidence of careful scholarly preparation. They are generally thorough and current in their coverage and are quite readable. The book meets its objectives very well and should afford excellent reading for medicinal chemists, pharmacologists, and students in pharmacy and related disciplines.

Reviewed by Eugene Isaacson
Idaho State University
College of Pharmacy
Pocatello, ID 83201

Toxicants and Drugs: Kinetics and Dynamics. By ELLEN J. O'FLAHERTY. Wiley, 605 Third Ave., New York, NY 10016. 1981, 398 pp. 16 × 24 cm. Price $42.50.

This useful book approaches a complex subject with a disarming frankness not usually found in such texts. In the preface, the author states that the first chapter reviews algebra and calculus at a level designed to give nonmathematicians—even antimathematicians!—confidence that they can "do" kinetics. After hopefully instilling such confidence and expertise, the reader is eventually lead into sophisticated concepts relating to disposition in saturable and nonlinear systems, the plateau principle of chronic exposure, receptor theory, pharmacodynamics and dose–response relationships. The book is a gem. A useful list of definitions of various symbols is included as a separate section and as an added bonus, a number of interesting problems taken from examples in the

literature are provided at the end of each chapter. Some helpful hints but no answers are given, however.

No doubt pharmacokineticists will differ with the author in some of her interpretations, but this should not be viewed as particularly unusual nor detrimental. No one, however, could argue with the avowed purpose of the book, which is "to bridge the gap between pure mathematical theory, at the one extreme, and the indiscriminate application of simple standard models to data that they may not adequately describe, at the other." To this end, the author has made a notable contribution. Researchers in pharmacology, toxicology, and drug metabolism will find it a valuable addition to their bookshelf.

Reviewed by Howard B. Hucker
Department of Drug Metabolism
Merck Institute for Therapeutic Research
West Point, PA 19486

Psychotropic Drugs. Plasma Concentration and Clinical Response. Edited by GRAHAM D. BURROWS and TREVOR R. NORMAN. Dekker, 270 Madison Ave., New York, NY 10016. 1981. 528 pp. 15 × 23 cm. Price $68.00 (20% higher outside the U.S. and Canada).

This book is well written and highly readable, with an avowed purpose of presenting all evidence, pro and con, of the relationship between plasma concentrations and clinical response of psychotropic drugs. Never mind that we have to wait until Chapter 5 before the question is first addressed—the preceding chapters are useful summaries of the mechanism of action, methodology, and pharmacokinetics of tricyclic antidepressants and antipsychotic agents.

If this puts the reader in a mood to skip around before settling down to read the book straight through, then he or she may as well read the last chapter first—a perceptive overview of the subject by Hollister. His rather pessimistic estimation of the value of measuring plasma concentrations may disappoint some readers, but be sure to judge his reasons fairly before dismissing his conclusions. We learn, for example, that the rationale behind measurement of plasma concentrations of antianxiety drugs has been for pharmacokinetics and not for monitoring treatment. This is corroborated in the chapter on benzodiazepines.

Perusal of the remaining chapters in this interesting book—on zimelidine, lithium, antipsychotic agents, butyrophenones, sedatives, hypnotics, and anticonvulsants—is revealing since, with only one exception, the various authors conclude that the relationships between plasma concentration and clinical response showed "no consensus," were "questionable" or "futile," or "correlate poorly" or that the measurements were "naive" or "uninformative." The exception is, of course, lithium. This all might make one long for the simpler days of the sulfonamides and clear correlations between plasma concentrations, therapeutic response, and side effects.

As minor criticisms of the book, this reviewer found Chapter 8 on chlorpromazine to be too exhaustive in its historical treatment and too vituperative in defense of the author's own analytical method. In addition, separate chapters on zimelidine and pharmacokinetics of tricyclic antidepressants and cerebrospinal fluid seem unnecessary.The terminology "plasma levels" also appears, which smacks of jargon, yet attempts to eliminate it will be a losing battle.

The book, in general, will be valuable to pharmacologists, clinicians, drug metabolism scientists, and analytical chemists in this field.

Reviewed by Howard B. Hucker
Merck Institute for Therapeutic Research
West Point, PA 19486

Adrenergic Activators and Inhibitors. Part II. (Handbook of Experimental Pharmacology, Vol. 54/II.) Edited by L. SZEKERES. Springer-Verlag, 44 Hartz Way, Secaucus, NJ 07094. 1981. 936 pp. 17 × 25 cm. Price $224.20.

This book is the second part of the latest volume in the well-known *Handbook* series and contains two sections and 14 chapters. The first section covers the effects of autonomic drugs on organ systems other than the nervous and cardiovascular systems. There are chapters on the respiratory system, skeletal muscles, digestive system, endocrine glands, genitals, kidneys, urinary tract, eyes, and sweat glands. The second section covers kinetics, toxic effects, biotransformation, and clinical implications. All types of adrenergic drugs are covered in great detail, including receptor agonists and blocking agents, indirect-acting agonists, false transmitters, and neuron-blocking agents.

As expected, this handbook is well-referenced. The material presented is fairly up to date, with the latest references dating from 1978. There are more than 10,000 items in the author index and about 13,500 separate entries in the subject index.

Each chapter includes some discussion of functional anatomy, location and classification of receptors, and general effects of the drug types of interest. Species variation in drug response are fully covered. In fact, some unusual and exotic species are included. For example, the apocrine sweat glands of the camel, the black rhinoceros, and the slow loris are described.

It may be unfair to criticize the second part of a two-set volume without seeing the first part. However, there are some obvious deficiencies. For example, in the chapter on the respiratory system, there is an obvious error of calculation in a table showing the selectivity index for metaproterenol. There is no mention of the effects of beta blockers on childbirth. In the chapter on the kidney, only receptor agonists and blocking agents are covered; the other types of adrenergic drugs are not considered. However, these minor deficiencies do not detract from the quality of this book.

This volume is an invaluable resource for all researchers in pharmacology and, together with Volume I, should be available to every serious student of pharmacology.

Reviewed by Raymond P. Ahlquist
Department of Pharmacology
Medical College of Georgia
Augusta, GA 30902

literature are provided at the end of each chapter. Some helpful hints but no answers are given, however.

No doubt pharmacokineticists will differ with the author in some of her interpretations, but this should not be viewed as particularly unusual nor detrimental. No one, however, could argue with the avowed purpose of the book, which is "to bridge the gap between pure mathematical theory, at the one extreme, and the indiscriminate application of simple standard models to data that they may not adequately describe, at the other." To this end, the author has made a notable contribution. Researchers in pharmacology, toxicology, and drug metabolism will find it a valuable addition to their bookshelf.

Reviewed by Howard B. Hucker
Department of Drug Metabolism
Merck Institute for Therapeutic Research
West Point, PA 19486

Psychotropic Drugs. Plasma Concentration and Clinical Response. Edited by GRAHAM D. BURROWS and TREVOR R. NORMAN. Dekker, 270 Madison Ave., New York, NY 10016. 1981. 528 pp. 15 × 23 cm. Price $68.00 (20% higher outside the U.S. and Canada).

This book is well written and highly readable, with an avowed purpose of presenting all evidence, pro and con, of the relationship between plasma concentrations and clinical response of psychotropic drugs. Never mind that we have to wait until Chapter 5 before the question is first addressed—the preceding chapters are useful summaries of the mechanism of action, methodology, and pharmacokinetics of tricyclic antidepressants and antipsychotic agents.

If this puts the reader in a mood to skip around before settling down to read the book straight through, then he or she may as well read the last chapter first—a perceptive overview of the subject by Hollister. His rather pessimistic estimation of the value of measuring plasma concentrations may disappoint some readers, but be sure to judge his reasons fairly before dismissing his conclusions. We learn, for example, that the rationale behind measurement of plasma concentrations of antianxiety drugs has been for pharmacokinetics and not for monitoring treatment. This is corroborated in the chapter on benzodiazepines.

Perusal of the remaining chapters in this interesting book—on zimelidine, lithium, antipsychotic agents, butyrophenones, sedatives, hypnotics, and anticonvulsants—is revealing since, with only one exception, the various authors conclude that the relationships between plasma concentration and clinical response showed "no consensus," were "questionable" or "futile," or "correlate poorly" or that the measurements were "naive" or "uninformative." The exception is, of course, lithium. This all might make one long for the simpler days of the sulfonamides and clear correlations between plasma concentrations, therapeutic response, and side effects.

As minor criticisms of the book, this reviewer found Chapter 8 on chlorpromazine to be too exhaustive in its historical treatment and too vituperative in defense of the author's own analytical method. In addition, separate chapters on zimelidine and pharmacokinetics of tricyclic antidepressants and cerebrospinal fluid seem unnecessary.The terminology "plasma levels" also appears, which smacks of jargon, yet attempts to eliminate it will be a losing battle.

The book, in general, will be valuable to pharmacologists, clinicians, drug metabolism scientists, and analytical chemists in this field.

Reviewed by Howard B. Hucker
Merck Institute for Therapeutic Research
West Point, PA 19486

Adrenergic Activators and Inhibitors. Part II. (Handbook of Experimental Pharmacology, Vol. 54/II.) Edited by L. SZEKERES. Springer-Verlag, 44 Hartz Way, Secaucus, NJ 07094. 1981. 936 pp. 17 × 25 cm. Price $224.20.

This book is the second part of the latest volume in the well-known *Handbook* series and contains two sections and 14 chapters. The first section covers the effects of autonomic drugs on organ systems other than the nervous and cardiovascular systems. There are chapters on the respiratory system, skeletal muscles, digestive system, endocrine glands, genitals, kidneys, urinary tract, eyes, and sweat glands. The second section covers kinetics, toxic effects, biotransformation, and clinical implications. All types of adrenergic drugs are covered in great detail, including receptor agonists and blocking agents, indirect-acting agonists, false transmitters, and neuron-blocking agents.

As expected, this handbook is well-referenced. The material presented is fairly up to date, with the latest references dating from 1978. There are more than 10,000 items in the author index and about 13,500 separate entries in the subject index.

Each chapter includes some discussion of functional anatomy, location and classification of receptors, and general effects of the drug types of interest. Species variation in drug response are fully covered. In fact, some unusual and exotic species are included. For example, the apocrine sweat glands of the camel, the black rhinoceros, and the slow loris are described.

It may be unfair to criticize the second part of a two-set volume without seeing the first part. However, there are some obvious deficiencies. For example, in the chapter on the respiratory system, there is an obvious error of calculation in a table showing the selectivity index for metaproterenol. There is no mention of the effects of beta blockers on childbirth. In the chapter on the kidney, only receptor agonists and blocking agents are covered; the other types of adrenergic drugs are not considered. However, these minor deficiencies do not detract from the quality of this book.

This volume is an invaluable resource for all researchers in pharmacology and, together with Volume I, should be available to every serious student of pharmacology.

Reviewed by Raymond P. Ahlquist
Department of Pharmacology
Medical College of Georgia
Augusta, GA 30902

literature are provided at the end of each chapter. Some helpful hints but no answers are given, however.

No doubt pharmacokineticists will differ with the author in some of her interpretations, but this should not be viewed as particularly unusual nor detrimental. No one, however, could argue with the avowed purpose of the book, which is "to bridge the gap between pure mathematical theory, at the one extreme, and the indiscriminate application of simple standard models to data that they may not adequately describe, at the other." To this end, the author has made a notable contribution. Researchers in pharmacology, toxicology, and drug metabolism will find it a valuable addition to their bookshelf.

Reviewed by Howard B. Hucker
Department of Drug Metabolism
Merck Institute for Therapeutic Research
West Point, PA 19486

Psychotropic Drugs. Plasma Concentration and Clinical Response. Edited by GRAHAM D. BURROWS and TREVOR R. NORMAN. Dekker, 270 Madison Ave., New York, NY 10016. 1981. 528 pp. 15 × 23 cm. Price $68.00 (20% higher outside the U.S. and Canada).

This book is well written and highly readable, with an avowed purpose of presenting all evidence, pro and con, of the relationship between plasma concentrations and clinical response of psychotropic drugs. Never mind that we have to wait until Chapter 5 before the question is first addressed—the preceding chapters are useful summaries of the mechanism of action, methodology, and pharmacokinetics of tricyclic antidepressants and antipsychotic agents.

If this puts the reader in a mood to skip around before settling down to read the book straight through, then he or she may as well read the last chapter first—a perceptive overview of the subject by Hollister. His rather pessimistic estimation of the value of measuring plasma concentrations may disappoint some readers, but be sure to judge his reasons fairly before dismissing his conclusions. We learn, for example, that the rationale behind measurement of plasma concentrations of antianxiety drugs has been for pharmacokinetics and not for monitoring treatment. This is corroborated in the chapter on benzodiazepines.

Perusal of the remaining chapters in this interesting book—on zimelidine, lithium, antipsychotic agents, butyrophenones, sedatives, hypnotics, and anticonvulsants—is revealing since, with only one exception, the various authors conclude that the relationships between plasma concentration and clinical response showed "no consensus," were "questionable" or "futile," or "correlate poorly" or that the measurements were "naive" or "uninformative." The exception is, of course, lithium. This all might make one long for the simpler days of the sulfonamides and clear correlations between plasma concentrations, therapeutic response, and side effects.

As minor criticisms of the book, this reviewer found Chapter 8 on chlorpromazine to be too exhaustive in its historical treatment and too vituperative in defense of the author's own analytical method. In addition, separate chapters on zimelidine and pharmacokinetics of tricyclic antidepressants and cerebrospinal fluid seem unnecessary.The terminology "plasma levels" also appears, which smacks of jargon, yet attempts to eliminate it will be a losing battle.

The book, in general, will be valuable to pharmacologists, clinicians, drug metabolism scientists, and analytical chemists in this field.

Reviewed by Howard B. Hucker
Merck Institute for Therapeutic Research
West Point, PA 19486

Adrenergic Activators and Inhibitors. Part II. (Handbook of Experimental Pharmacology, Vol. 54/II.) Edited by L. SZEKERES. Springer-Verlag, 44 Hartz Way, Secaucus, NJ 07094. 1981. 936 pp. 17 × 25 cm. Price $224.20.

This book is the second part of the latest volume in the well-known *Handbook* series and contains two sections and 14 chapters. The first section covers the effects of autonomic drugs on organ systems other than the nervous and cardiovascular systems. There are chapters on the respiratory system, skeletal muscles, digestive system, endocrine glands, genitals, kidneys, urinary tract, eyes, and sweat glands. The second section covers kinetics, toxic effects, biotransformation, and clinical implications. All types of adrenergic drugs are covered in great detail, including receptor agonists and blocking agents, indirect-acting agonists, false transmitters, and neuron-blocking agents.

As expected, this handbook is well-referenced. The material presented is fairly up to date, with the latest references dating from 1978. There are more than 10,000 items in the author index and about 13,500 separate entries in the subject index.

Each chapter includes some discussion of functional anatomy, location and classification of receptors, and general effects of the drug types of interest. Species variation in drug response are fully covered. In fact, some unusual and exotic species are included. For example, the apocrine sweat glands of the camel, the black rhinoceros, and the slow loris are described.

It may be unfair to criticize the second part of a two-set volume without seeing the first part. However, there are some obvious deficiencies. For example, in the chapter on the respiratory system, there is an obvious error of calculation in a table showing the selectivity index for metaproterenol. There is no mention of the effects of beta blockers on childbirth. In the chapter on the kidney, only receptor agonists and blocking agents are covered; the other types of adrenergic drugs are not considered. However, these minor deficiencies do not detract from the quality of this book.

This volume is an invaluable resource for all researchers in pharmacology and, together with Volume I, should be available to every serious student of pharmacology.

Reviewed by Raymond P. Ahlquist
Department of Pharmacology
Medical College of Georgia
Augusta, GA 30902

A publication of the
American Pharmaceutical Association—
the National Professional Society
of Pharmacists

JOURNAL OF PHARMACEUTICAL SCIENCES

INDEX TO AUTHORS
INDEX TO SUBJECTS

VOLUME 71
JANUARY TO DECEMBER, 1982

Published monthly under the supervision of the Board of Trustees

Toward a Standardized ID System for Drugs

In his writings, and particularly in *1984*—the well-known novel predicting the totality of government bureaucratic involvement in society and our private lives—George Orwell forecast that numbers would gradually replace names as the common means of identifying virtually everyone and everything.

We are now only a couple of years away from that fateful date, and already we see that much of what Orwell predicted has come to pass. For example, it seems more important today for a person to have a Social Security number than it is to have a name. Just try filing your income tax, or getting a driver's license, or registering in college, or opening an interest-bearing account, or cashing a check, or filing a health insurance claim form, and so on *ad infinitum*, without giving a Social Security number. One quickly finds that, if not impossible, it is very difficult at best. But yet, none of these activities has even a remote bearing on Social Security or the intended purpose in issuing Social Security numbers.

Numerous other examples—from the universal price codes appearing on packaged food products, to long-distance direct dial telephone numbers, to nine-digit zip codes, to personal charge account numbers—can be cited from everyday life that also illustrate how numbers and numeric codes have virtually taken over how we now operate in daily living.

All this is happening because, whether we like it or not, these systems generally work. They provide fast access, ready location, foolproof identification, ease of information storage, and similar advantages. As we move closer to the computerized age, such benefits will continue to grow in both kind and degree.

But one area has somehow remained outside of, or at most on the fringes of, our otherwise successful efforts to manage various affairs and activities by developing and applying useful and logical numbering systems.

That area is drug identification. True, we do have a "National Drug Code," and NDC numbers do appear in drug company catalogs, on product labels, and in a few other places. But NDC numbers are not in wide use and it is clearly evident that they are not now—and never will become—an adequate and useful substitute for the drug or drug product name in a manner comparable to Social Security numbers as identifiers for people.

Why is this?

Even a cursory familiarity with the NDC system makes the answer clearly evident. Namely, the NDC numbering system has virtually no consistency or standardization.

Each NDC number is comprised of three segments: the first segment is unique to the manufacturer, and that portion is reasonably satisfactory (although such things as company mergers have created some room for improvement even there); the second segment is used to identify the drug entity; and the third segment identifies the dosage form. It is in these latter two portions of the NDC numbering system that there is absolutely no consistency or standardization.

Each individual drug company is completely free to use whatever number it wishes to identify the drug and the dosage form. The result, of course, is that there is no uniformity because everyone uses a different number to identify both the same drug moiety and the same dosage form.

How much better it would be if the system were standardized so that a single, uniform number was applied to tetracycline, and similarly that another single, uniform number was used to designate 250-mg capsules. The composite NDC number then would be light years more useful as a means of drug identification, of simplifying such public health measures as poison prevention and treatment, of inventorying and stocking pharmacy shelves, of processing drug reimbursement claims, of more rational drug prescribing, and so on.

Washington rumors are that federal budgetary squeezes may cause the Food and Drug Administration to close down its office that runs the NDC system, thereby abandoning the system itself. Undoubtedly, had the present NDC numbering system been more effective, it would have enjoyed much greater use, thereby making its elimination less attractive to the budget-cutters.

In a concurrent development, the National Association of Pharmaceutical Manufacturers—the so-called "generic manufacturers association"—recently recommended to FDA that a set of uniform drug identification numbers based on the active ingredients be established at the federal level. This proposal was primarily prompted by legislation or regulations being adopted at the state level concerning drug product identification. The NAPM even went a step further with its suggestion by generating a proposed alpha numeric "ID list" covering over 600 drug entities in specific dosage forms.

Based upon our review, the NAPM identification scheme itself is not as useful as it would be if drug entity and dosage form were two separate components of the composite ID number, and if each of these two elements were standardized separately.

However, that really is only a detail of implementation. The key point is the recommendation that *the system itself be standardized.* In that, they have our wholehearted support.

Critics will claim that the NAPM has its self-interest reasons for urging the adoption of such a standardized system. That is true; just as it is also true that the brand name segment of the drug industry had its self-interest motives for opposing a standardized approach years ago when the NDC system was originally developed.

The important consideration now is the broader picture of all that can be done using today's and tomorrow's computer technology if only there were a compatible drug numbering system. It is ironic that the industry that was so far-sighted as to pioneer in the use of the metric system on a commercial level is now the laggard in permitting full adaptation to a standardized drug numbering system, with its associated technological benefits.

Clearly, it is a time for statesmanship in the board rooms of the nation's major drug companies.

—EDWARD G. FELDMANN
American Pharmaceutical Association
Washington, DC 20037

0022-3549/82/0300-0273$01.00/0

JOURNAL OF PHARMACEUTICAL SCIENCES

MARCH 1982
VOLUME 71 NUMBER 3

RESEARCH ARTICLES

Effects of Phenobarbital on the Distribution Pharmacokinetics and Biological Half-Lives of Model Nonmetabolizable Organic Anions in Rats

DENNIS J. SZYMANSKI * and JANARDAN B. NAGWEKAR ˣ

Received August 6, 1980, from the *Pharmaceutics Division, College of Pharmacy and Allied Health Professions, Wayne State University, Detroit, MI 48202.* Accepted for publication July 6, 1981. *Present address: Travenol Laboratories, Inc., Morton Grove, IL 60053.

Abstract □ The blood level pharmacokinetics of model nonmetabolizable and nonprotein bound anionic compounds (pKa 3.3–3.4), namely, benzoylformic acid (I), D-(−)-mandelic acid (II), and *p*-methyl benzoylformic acid (III), which are excreted in the urine in the unchanged form, were studied in control and phenobarbital-treated rats to determine the effects of phenobarbital on distribution and elimination pharmacokinetic parameters. These compounds were used, also, because they represent three different compartment models in the untreated rats: a three-compartment open model (I), a two-compartment open model (II), and a one-compartment open model (III). The three-compartment open model (I) in the control rats was reduced to a two-compartment open model with only one kinetically distinguishable peripheral tissue compartment in the phenobarbital-treated rats. The pharmacokinetics of II were described by a two-compartment open model in both control and phenobarbital-treated rats but the apparent distribution volumes of the central and peripheral compartments were found to be significantly smaller in phenobarbital-treated rats. One-compartment open model pharmacokinetics were observed for III in both the control and phenobarbital-treated rats with no significant difference in apparent distribution volumes. The transmembrane transport of these compounds, which exist in the body fluids as anions, was previously reported to occur *via* the aqueous pores of the tissue cell membranes. The decrease in the apparent distribution volumes of these organic anions in the phenobarbital-treated rats was explained in terms of the possible effect of phenobarbital in increasing the protein and phospholipid concentrations of the cell membranes of tissues other than liver. This narrows the size of the aqueous pores of the central and tissue compartment cell membranes and hinders the diffusion of these compounds through the aqueous pores. Regardless of the compartment model displayed by these compounds, the biological half-life of each compound was significantly shorter in the phenobarbital-treated rats than in the control rats. This effect was attributed to the possible induction effect of phenobarbital on the renal tubular secretion carrier mechanism of these compounds in rats.

Keyphrases □ Phenobarbital—effect on pharmacokinetics of nonmetabolizable organic anions, rats □ Pharmacokinetics—effect of phenobarbital, nonmetabolizable organic anions, rats □ Nonmetabolizable organic anions—effect of phenobarbital on pharmacokinetics, rats

It has been shown in humans and animals that concomitant administration of many metabolizable drugs with phenobarbital results in a decrease in their biological half-lives as well as in pharmacological activity (1, 2). In most instances these effects are attributed to the enzyme-inducing property of phenobarbital which results in the increased rate of metabolism of concomitantly administered drugs. The enzyme-inducing property of phenobarbital is due to its ability to increase the synthesis of drug-metabolizing enzymes in the liver (1–3).

BACKGROUND

Phenobarbital was shown to increase general protein synthesis by its direct action on the hepatic endoplasmic reticulum (4, 5) and to increase the concentration of microsomal phospholipids by reducing their rate of catabolism (6) and/or by increasing their rate of biosynthesis (5). The liver appears to have been extensively investigated for these effects of phenobarbital and, in keeping with the objective of such studies, mainly metabolizable drugs have been used in these investigations. The kidney has been infrequently investigated to show the effect of phenobarbital (7).

In addition to the effect in the liver and kidney, phenobarbital may also increase protein and phospholipid concentrations in other tissues. Since proteins and phospholipids are the major components of tissue plasma membranes, it is conceivable that chronic administration of phenobarbital might alter the transmembrane transport or distribution of certain concomitantly administered drugs into various tissues. Consequently, this may decrease the biological half-lives of these drugs and affect pharmacological responses. This consideration is important because, for a drug to exert pharmacological activity, it must first reach its site(s) of action.

The extent of pharmacological response to a drug is dependent not only on the drug–receptor interaction but also on the drug concentration at the receptor site(s). It is known that the distribution rate of a drug to the site(s) of action is governed by many processes occurring simultaneously; these processes include metabolism, binding to plasma and/or tissue proteins, and renal and nonrenal excretion.

Studies of the effect of phenobarbital on the distribution pharmacokinetics of drugs would be difficult if conducted with concomitantly administered drugs that are subject to metabolism and binding to plasma and/or tissue proteins. These factors may obscure and complicate identification of the effect of phenobarbital on the distribution pharmacokinetic parameters of the drugs.

0022-3549/82/0300-0275$01.00/0

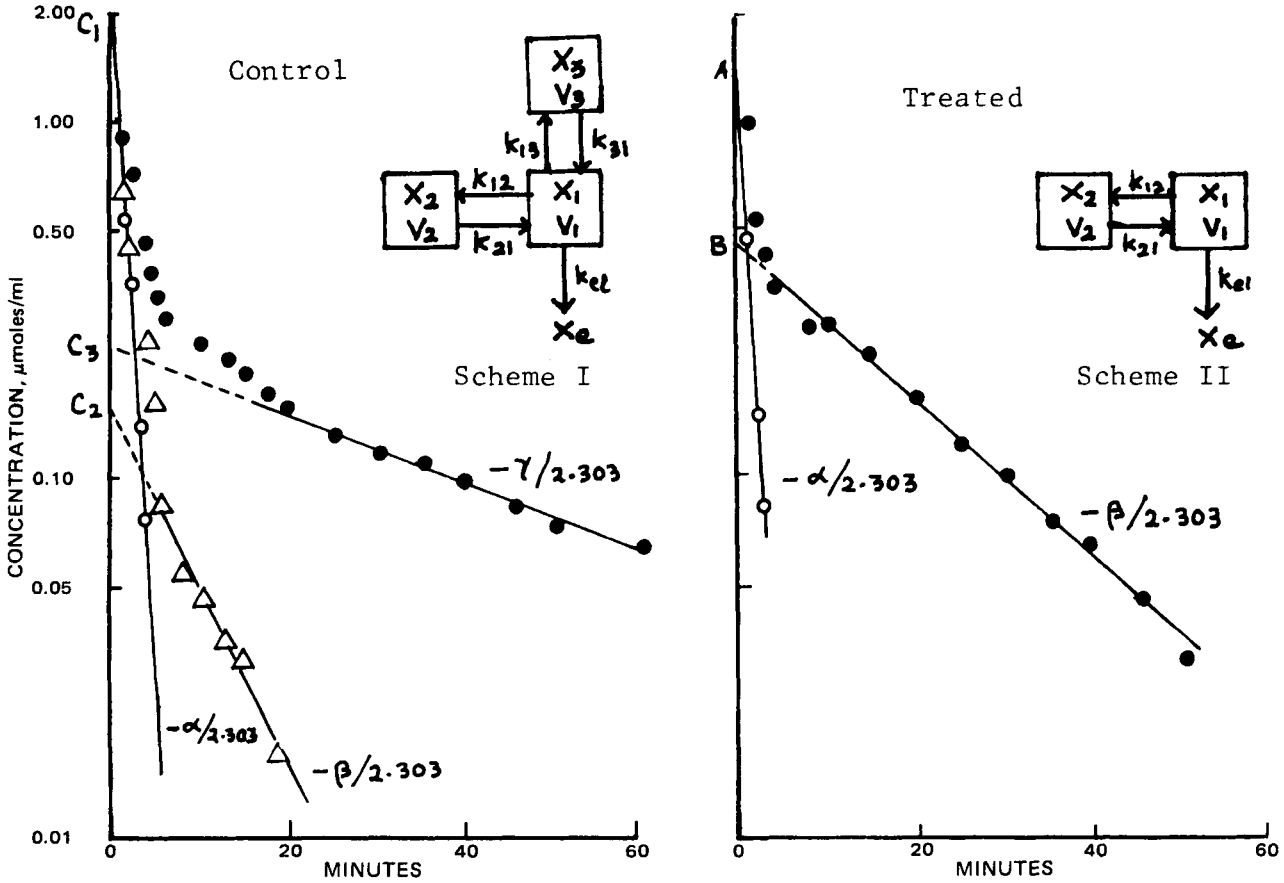

Figure 1—*Semilogarithmic plots showing blood concentrations of benzoylformic acid declining triexponentially in control rats and biexponentially in phenobarbital-treated rats following intravenous administration.*

Scheme I—Three-compartment open model; Scheme II—Two-compartment open model. Key: ●, observed data points; △, ○, data points obtained upon feathering by the residual method.

To demonstrate the effect of phenobarbital on the distribution and biological half-lives of certain compounds, the pharmacokinetics of benzoylformic acid (I), D-(−)-mandelic acid (II), and *p*-methyl benzoylformic acid (III) were studied. These compounds served as model compounds since they are neither metabolized, bound to plasma proteins, nor reabsorbed in the renal tubules. They are excreted in the urine of rats entirely in the unchanged form (8–10). Second, these compounds (pKa 3.3–3.4, referred to in this study as organic anions because they remain completely ionized in the blood) distribute between the body compartments by diffusion through the "aqueous pores" of cell membranes, which presumably are lined with proteins and phospholipids (10). Consequently, it was reasonable to assume that any alteration in the composition of tissue cell membranes might reduce the transmembrane transport of these anions due to a possible decrease in mean pore size. Third, these compounds are represented by three distinctly different compartment models in untreated rats. The pharmacokinetics of I, II, and III have been described (10) by a three-compartment open system, a two-compartment open system, and a one-compartment open system, respectively.

EXPERIMENTAL

Materials—The following were used: D-(−)-mandelic acid[1], mp 131–133°, $[\alpha]_D^{25°}$ − 153°; benzoylformic acid[1], mp 67–69°; *p*-methyl benzoylformic acid, mp 97–99°, synthesized by the method of Kindler *et al.* (11); and sodium phenobarbital[2] USP, granular.

Methodology—Male Sprague–Dawley rats weighing between 170 and 230 g (most weighed ~200 g) were used in the study. The pharmacokinetics of I, II, and III were studied in phenobarbital-treated rats and in control rats. To pretreat the rats, 2 ml of isotonic solution containing a 20-mg/kg dose of sodium phenobarbital was administered intraperitoneally daily to each rat for 5 days in the study of II, 4 days in the study of I, and 3 days in the study of III. The control rat used in each study was pretreated daily with 2 ml normal saline intraperitoneally for 5, 4, and 3 days, respectively.

Food, but not water, was withheld from the rats 12–14 hr prior to the study as well as during the course of the experiment. A given compound was injected intravenously to the rats 24 hr after the last dose of sodium phenobarbital in each study. Five milliliters of normal saline was administered intraperitoneally to each rat 20 min prior to the intravenous administration of the substrate compound being studied to be consistent with previous procedures (8–10). The rat was anesthetized with ether for less than a minute prior to the intravenous injection of a fixed dose of the compound in a 2-ml isotonic solution. The fixed doses of I, II, and III used were 7.5 mg (~250 μmoles/kg), 5 mg (~165 μmoles/kg), and 5 mg (~151 μmoles/kg), respectively. Each compound was injected as its sodium salt by adding equivalent amounts of sodium hydroxide. The solutions were made isotonic with sodium chloride. One blood sample was obtained from each rat upon its decapitation at predetermined time after the administration of the compound. After decapitation, blood was collected in 30-ml beakers which were previously coated with 0.2 ml (40 U) of heparin to prevent coagulation. The blood samples were analyzed on the same day that they were collected.

Because of the voluminous work involved in extracting a compound from numerous blood samples and then analyzing it by GC, blood samples for the pharmacokinetic studies of I and II were collected in two or three portions on two or three different days, each portion involving 5–8 rats. Each portion represented a proper distribution of blood sampling times. For instance, in the control study of II, one study portion included 2-, 4-, 8-, 10-, 15-, 25-, and 50-min blood sampling times and the other study portion included 3-, 5-, 20-, 30-, and 40-min blood sampling times. In the control study of I, one study portion included 2-, 4-, 6-, 8-, 15-, 25-, 45-, and 60-min blood sampling times, the second portion included 1-, 3-, 5-, 10-, and 40-min blood sampling times, and the third study portion included 13-, 18-, 20-, 30-, 35-, and 50-min blood sampling times. For each study portion, a standard curve for the compound was prepared for quantitative determination of the blood samples. In the case of III, all

[1] Aldrich Chemical Co., Milwaukee, Wis.
[2] Merck and Co., Rahway, N.J.

Table I—Pharmacokinetic Parameters for Benzoylformic Acid Estimated and Derived by NONLIN Least-Squares Fitting in Control Rats (Three-Compartment Model) and 4-Day Phenobarbital-Treated Rats (Two-Compartment Model)

Parameter	Control (Three-Compartment)	Treated (Two-Compartment)	Statistical Significance of Difference (p)
V_1, ml/kg	178.95 ± 13.15	151.30 ± 10.35	N.S.
k_{12}, min^{-1}	0.2474 ± 0.0640	0.5312 ± 0.0413	
k_{21}, min^{-1}	0.1821 ± 0.0410	0.2706 ± 0.0139	
k_{13}, min^{-1}	0.1051 ± 0.0241		
k_{31}, min^{-1}	0.0761 ± 0.0281		
K_{el}, min^{-1}	0.1041 ± 0.0083	0.1574 ± 0.0112	<0.001
α, min^{-1}	0.5812	0.9125 ± 0.1465	
β, min^{-1}	0.1068	0.0466 ± 0.0063	
γ, min^{-1}	0.0234 ± 0.0029		
V_2, ml/kg	278.90	297.00 ± 34.25	
V_3, ml/kg	344.65		
V_{ss}, ml/kg	802.50	448.30 ± 35.78	
$K_{el}V_1$, ml/min/kg	18.63 ± 2.02	23.81 ± 2.35	N.S.
$t_{1/2}$ elimination phase, min	29.62 ± 3.67	14.87 ± 2.01	<0.005
Correlation, r	0.997	0.998	

blood samples were obtained in a single study portion since each group of control and phenobarbital-treated rats involved only seven blood samples.

GLC Analysis—I, II, and III were quantitatively determined by GC using a flame ionization detector[3]. These procedures were essentially the same as those described previously (10).

Phenobarbital Pretreatment—*Mandelic Acid (II)*—A 5-day pretreatment schedule for rats with phenobarbital was chosen because numerous literature reports have indicated that a maximum drug metabolizing enzyme induction effect of phenobarbital is produced within ~3 days of pretreatment with a daily 20–100-mg/kg ip dose of phenobarbital. It was felt that if there was an effect of phenobarbital, a 5-day treatment period would be adequate to produce a maximum effect on the pharmacokinetic behavior of II.

Since phenobarbital treatment influenced the pharmacokinetics of II, it was of interest to determine if the maximum effect of phenobarbital on the pharmacokinetics of the compound was produced in a 5-day treatment. Therefore, the pharmacokinetics of II were also studied in rats treated with a daily 20-mg/kg ip dose of phenobarbital for 1 day and for 10 days.

Benzoylformic Acid (I)—It was noted that a substantial effect of phenobarbital on the pharmacokinetics of II could occur in rats even after a 1-day treatment and that a maximum effect occurred after a 5-day treatment. Possibly, the maximum effect of phenobarbital on the pharmacokinetics of the compound might have occurred after treating rats with phenobarbital for less than 5 days. To determine this possibility with I, the pharmacokinetics were studied in 4-day phenobarbital-treated rats. Additional pharmacokinetic studies of the compound were carried out in 6- and 10-day phenobarbital treated rats where each rat received a daily 20-mg/kg ip dose of phenobarbital.

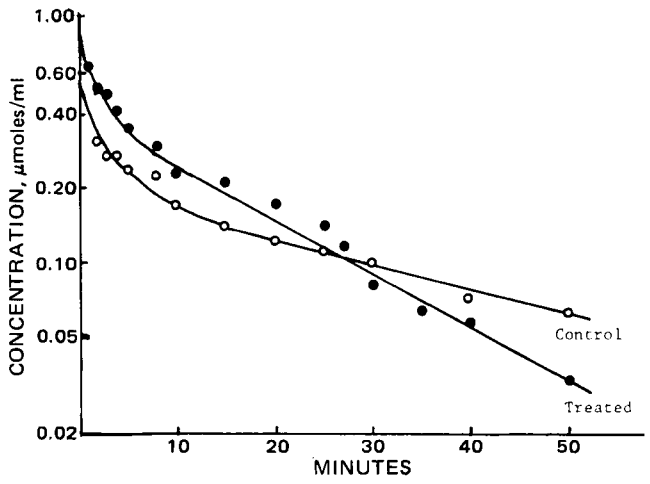

Figure 2—*Biexponential semilogarithmic plots of blood concentrations of mandelic acid obtained in control (○) and phenobarbital-treated (●) rats. The solid lines are the NONLIN least-squares regression lines for the data of respective groups of rats.*

[3] Hewlett-Packard Model 5720.

p-Methyl Benzoylformic Acid (III)—Since the maximum effects of phenobarbital on the pharmacokinetic parameters of II and I were observed in rats after 4 to 5 days of phenobarbital treatment, it was thought possible that the maximum effect of phenobarbital treatment on the pharmacokinetic parameters of III would be observed in less than 4 days of phenobarbital treatment. Therefore, the pharmacokinetics of III were studied in 3-day phenobarbital-treated rats.

To determine if the maximum effect on the pharmacokinetic parameters of the compound was produced after a 3-day phenobarbital treatment, additional pharmacokinetic studies of the compound were carried out in 5-day phenobarbital-treated rats. In that study, each rat also received a daily 20 mg/kg ip dose of phenobarbital.

Overall Urinary Recovery of the Tested Compounds in Phenobarbital-Treated Rats—Studies were done to determine if intravenous doses of II (5 mg), I (7.5 mg), and III (5 mg) are recovered in the urine of phenobarbital-treated rats entirely in the unchanged form. After administering intravenous doses of II, I, and III to rats treated with phenobarbital (20 mg/kg ip) for 5, 4, and 3 days, respectively, urine samples were collected for 12–24 hr for II and I and for 3–5 hr for III.

Binding of Tested Compounds by Blood from Phenobarbital-Treated Rats—The fact that I, II, and III are negligibly bound to whole blood of untreated rats has been demonstrated previously (8, 10). Therefore, the binding of these compounds was studied only with blood from rats treated with phenobarbital for 3–5 days. These determinations were carried out at 37° by the equilibrium dialysis method previously described for these compounds (10). The amount of a given compound used in these studies was calculated on the basis of its apparent distribution volume of the central compartment determined in the phenobarbital-treated rats from the blood level studies described later.

RESULTS

In previous demonstrations (8, 10), all of the intravenously administered doses of I, II, and III were recovered unchanged in untreated rat

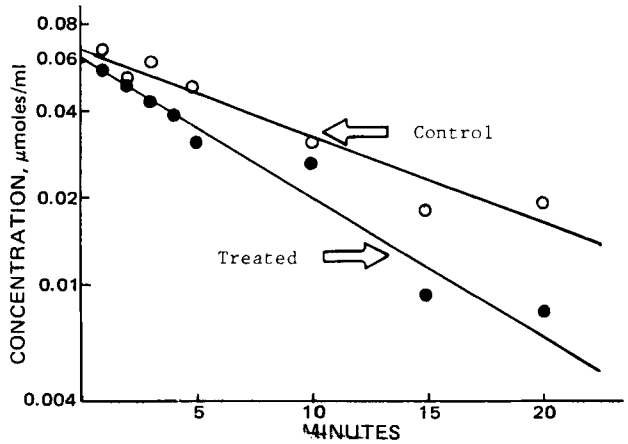

Figure 3—*Monoexponential semilogarithmic plots of blood concentrations of p-methyl benzoylformic acid obtained in control (○) and phenobarbital-treated (●) rats. The solid lines are the least-squares regression lines for the data of respective groups of rats.*

Table II—Comparison of Two-Compartment Model Pharmacokinetic Parameters Determined for Benzoylformic Acid in 4-, 6-, and 10-Day Phenobarbital-Treated Rats

Parameter	Duration of Phenobarbital Treatment		
	4 Days	6 Days	10 Days
V_1, ml/kg	151.30 ± 10.35	145.60 ± 10.80	150.25 ± 10.60
k_{12}, min^{-1}	0.5312 ± 0.0413	0.4593 ± 0.0431	0.3777 ± 0.0563
k_{21}, min^{-1}	0.2706 ± 0.0149	0.2214 ± 0.0109	0.2339 ± 0.0253
K_{el}, min^{-1}	0.1574 ± 0.0112	0.1646 ± 0.0107	0.1571 ± 0.0093
α, min^{-1}	0.9125 ± 0.1465	0.7998 ± 0.0674	0.7176 ± 0.1249
β, min^{-1}	0.0466 ± 0.0063	0.0456 ± 0.0010	0.0512 ± 0.0063
V_2, ml/kg	297.00 ± 34.25	302.05 ± 39.03	242.62 ± 47.85
V_{ss}, ml/kg	448.30 ± 35.78	447.65 ± 40.49	392.87 ± 49.00
$K_{el}V_1$, ml/min/kg	23.81 ± 2.35	23.96 ± 2.36	23.60 ± 2.16
$t_{1/2\beta}$, min	14.87 ± 2.01	15.19 ± 0.33	13.53 ± 1.66
Correlation, r	0.998	0.997	0.994

urine. In the present study, virtually 100% of the dose of each compound administered to phenobarbital-treated rats was recovered unchanged in the urine, indicating negligible metabolism of the compounds in the rats. The urinary recoveries of II, I, and III were 99.13 ± 0.12(n = 3), 99.47 ± 0.3(n = 4), and 98.1 ± 1.0%(n = 5), respectively.

Negligible binding of the tested compounds to plasma proteins in untreated rats has been demonstrated previously (8, 10). From the equilibrium dialysis studies, the binding of these compounds to the whole blood of phenobarbital-treated rats varied from 0.4 to 3.3%, which is negligible.

Pharmacokinetics of I in Control and Phenobarbital-Treated Rats—The blood level data obtained for I in the control and phenobarbital-treated rats were plotted on semilogarithmic graph paper. Since these plots indicated multiexponential concentration decline of the compound, they were resolved into all possible linear exponential segments upon feathering the data by the method of residuals. While the data for the control rats could be resolved into three linear exponential segments, the data for the phenobarbital-treated rats could be resolved into only two linear exponential segments. This indicates that I shows characteristics of a three-compartment model in the control rats (Scheme I, Fig. 1), as was observed previously in saline-untreated rats (10). But I shows characteristics of a two-compartment model in the phenobarbital-treated rats (Scheme II, Fig. 1).Therefore, the blood levels of the compound obtained in the control rats and the phenobarbital-treated rats were analyzed according to the three-compartment model kinetics and two-compartment model kinetics, respectively. As shown in Schemes I and II, the fact that elimination of I occurs from the central compartment only by urinary excretion (10) is asserted by demonstrating that the intravenous dose of the compound is completely recovered in the urine.

In Schemes I and II, X_1, X_2, and X_3 represent the amounts of I at time t in the central compartment, tissue compartment I, the tissue compartment II, respectively; V_1, V_2, and V_3 represent the apparent distribution volume for the compound in the respective compartments. The variable X_e is the amount of the compound excreted in the urine up to time t. The variable K_{el} is the apparent first-order rate constant of elimination of the compound from the central compartment, and k_{12}, k_{21}, k_{13}, and k_{31} are the apparent first-order rate constants for the transfer of the compound between the given compartments.

The general solution for the three-compartment open model is given by the following equation (12):

$$C = C_1 e^{-\alpha t} + C_2 e^{-\beta t} + C_3 e^{-\gamma t} \qquad \text{(Eq. 1)}$$

where C is the concentration of the compound in the blood at any time t. The concentrations in Fig. 1 are normalized on the basis of the intravenous dose of 7.5 mg of I/200 g rat body weight. The preliminary estimates of the intercepts (C_1, C_2, and C_3) and slopes ($-\alpha/2.303$, $-\beta/2.303$, and $-\gamma/2.303$) due to the three linear exponential segments (Fig. 1) were obtained by the least-squares method. Using the preliminary estimates of C_1, C_2, C_3, α, β, and γ, the initial estimates of K_{el}, k_{12}, k_{21}, k_{13}, and k_{31} were obtained using the appropriate well-known equations (12). The preliminary estimate of V_1 was obtained from V_1 = dose/$C_1 + C_2 + C_3$. Using the initial estimates of these rate constants and V_1, the blood level data of the control rats were analyzed by the NONLIN least-squares program (13) and refined estimates of V_1, k_{12}, k_{21}, k_{13}, k_{31}, and K_{el} with their standard deviations and those of α, β, and γ without their standard deviations were obtained. Using the estimated values of these parameters, the values of V_2 and V_3 were calculated using the appropriate equations (12). Values of V_{ss} ($V_1 + V_2 + V_3$), blood clearance or body clearance ($K_{el}V_1$), and elimination phase ($t_{1/2} = 0.693/\gamma$) were calculated. The estimated and derived pharmacokinetic parameters are listed in Table I. The apparent volume of the central compartment (V_1) refers to the blood volume and the fluid volume of highly perfused tissues which are readily accessible to the compound, and V_2 and V_3 refer to the apparent volumes of fluids of the "shallow" and "deep" tissues, respectively.

The general solution for the two-compartment open model is given by the following equation:

$$C = A e^{-\alpha t} + B e^{-\beta t} \qquad \text{(Eq. 2)}$$

where C is the concentration of the compound in the blood at time t. Preliminary estimates of the intercepts (A and B) and slopes ($-\alpha/2.303$ and $-\beta/2.303$) for the two linear exponential segments (Fig. 1) were obtained by the least-squares method. Using the preliminary estimates of A, B, α, and β, the initial estimates of k_{12}, k_{21}, and K_{el} were obtained by using known equations (12). The preliminary estimate of V_1 was obtained from V_1 = intravenous dose/$A + B$. Using the initial estimates of k_{12}, k_{21}, K_{el}, and V_1, the blood level data of I obtained in the phenobarbital-treated rats were analyzed by the NONLIN least-squares program (13) and the refined estimates of V_1, k_{12}, k_{21}, and K_{el} with their standard deviations and those of α and β without their standard deviations were obtained. Using the estimated values of these parameters, V_2 [V_1 (k_{12}/k_{21})] was calculated. The values of V_{ss} ($V_1 + V_2$), elimination phase ($t_{1/2} = 0.693/\beta$), and body clearance ($K_{el}V_1$) were also calculated. The estimated and derived pharmacokinetic parameters of the compound obtained in the 4-day phenobarbital-treated rats are listed in Table I and those obtained in the 6- and 10-day phenobarbital-treated rats are listed in Table II.

Pharmacokinetics of II—The semilogarithmic graphical analysis

Table III—Pharmacokinetic Parameters Estimated and Derived for the Two-Compartment Model by NONLIN Least-Squares Fitting for Mandelic Acid in Control and 5-Day Phenobarbital-Treated Rats

Parameter	Control	Treated	Statistical Significance of Difference (p)
V_1, ml/kg	447.85 ± 15.60	190.15 ± 26.85	<0.001
k_{12}, min^{-1}	0.0535 ± 0.0075	0.1912 ± 0.0479	<0.001
k_{21}, min^{-1}	0.0854 ± 0.0080	0.2542 ± 0.0385	<0.001
K_{el}, min^{-1}	0.0377 ± 0.0021	0.0949 ± 0.0114	<0.001
α, min^{-1}	0.1561 ± 0.0458	0.4913 ± 0.1343	<0.05
β, min^{-1}	0.0206 ± 0.0056	0.0491 ± 0.0095	<0.05
V_2, ml/kg	280.55 ± 48.31	143.00 ± 46.47	<0.05
V_{ss}, ml/kg	728.40 ± 50.77	333.15 ± 53.67	<0.001
$K_{el}V_1$, ml/min/kg	16.88 ± 1.11	18.04 ± 3.34	N.S.
$t_{1/2\beta}$, min	33.64 ± 8.40	14.11 ± 2.73	<0.05
Correlation, r	0.995	0.989	

Table IV—Comparison of Two-Compartment Model Pharmacokinetic Parameters Determined for Mandelic Acid in 1-, 5-, and 10-Day Phenobarbital-Treated Rats

Parameters	Duration of Phenobarbital Treatment		
	1 Day	5 Days	10 Days
V_1, ml/kg	162.35 ± 15.55	190.15 ± 26.85	165.90 ± 11.45
k_{12}, min^{-1}	0.1937 ± 0.0270	0.1912 ± 0.0479	0.2019 ± 0.0191
k_{21}, min^{-1}	0.1120 ± 0.0121	0.2542 ± 0.0385	0.1927 ± 0.0114
K_{el}, min^{-1}	0.0973 ± 0.0095	0.0949 ± 0.0114	0.1093 ± 0.0071
α, min^{-1}	0.3739 ± 0.0713	0.4913 ± 0.1343	0.4580 ± 0.0532
β, min^{-1}	0.0292 ± 0.0036	0.0491 ± 0.0095	0.0460 ± 0.0035
V_2, ml/kg	280.75 ± 56.34	143.00 ± 46.47	173.80 ± 22.73
V_{ss}, ml/kg	443.10 ± 58.43	333.15 ± 53.67	339.70 ± 25.47
$K_{el}V_1$, ml/min/kg	15.79 ± 2.16	18.04 ± 3.34	18.13 ± 1.71
$t_{1/2\beta}$, min	23.73 ± 2.92	14.11 ± 2.73	15.06 ± 1.15
Correlation (r)	0.997	0.989	0.996

Table V—Comparison of the One-Compartment Model Pharmacokinetic Parameters Determined for *p*-Methyl Benzoylformic Acid in Control Rats and in 3- and 5-Day Phenobarbital-Treated Rats

Parameters	Control	Duration of Phenobarbital Treatment		Statistical Significance of Difference (p)	
		3 Days	5 Days	3-Day[a]	5-Day[a]
V_d, ml/kg	222.35 ± 25.85	251.28 ± 29.65	242.47 ± 11.18	N.S.	N.S.
K_{el}, min^{-1}	0.0689 ± 0.0092	0.1053 ± 0.0106	0.1049 ± 0.0047	<0.05	<0.01
$K_{el}V_d$, ml/min/kg	15.33 ± 2.71	26.46 ± 4.10	26.45 ± 1.69	<0.05	<0.01
$t_{1/2}$, min	10.06 ± 1.34	6.58 ± 0.66	6.61 ± 0.29	<0.05	<0.05
Correlation (r)	0.971	0.982	0.993		

[a] Compared to the control.

of blood level data obtained for II both in the control and the phenobarbital rats indicated that blood levels of the compound declined biexponentially (Fig. 2). Therefore, these data were analyzed according to two-compartment model kinetics, with the elimination of the compound occurring from the central compartment. The blood concentrations in Fig. 2 are normalized on the basis of the 5 mg iv dose/200 g rat body weight; the blood level data were treated with Eq. 2. The preliminary estimates of the intercepts (A and B) and slopes ($-\alpha/2.303$ and $-\beta/2.303$) due to the two resolved linear exponential segments were obtained by the least-squares method. Using the estimates of A, B, α, and β, the initial estimates of V_1, k_{12}, k_{21}, and K_{el} were obtained by the method described previously. The refined estimates of V_1, k_{12}, k_{21}, and K_{el} with their standard deviations and those of α and β without their standard deviations were obtained using the NONLIN least-squares program (13). Using computer estimated values of these parameters, the estimates of V_2, V_{ss}, elimination phase ($t_{1/2}$), and $K_{el}V_1$ were calculated. The estimated and derived pharmacokientic parameters of II obtained in the control rats and the 5-day phenobarbital-treated rats are listed in Table III and those obtained in the 1-day and 10-day phenobarbital-treated rats are listed in Table IV.

Pharmacokinetics of III—The blood levels of III in both the control rats and the phenobarbital-treated rats declined monoexponentially (Fig. 3), indicating a one-compartment open model. The concentrations in Fig. 3 are normalized on the basis of the 5 mg iv dose of III/200 g rat body weight. The blood level data were treated according to the following equation:

$$\log C = \log C_0 - K_{el}t/2.303 \qquad \text{(Eq. 3)}$$

where C is the concentration of the compound at time t, C_0 is the concentration of the compound at zero time, and K_{el} is the apparent first-order rate constant of elimination of the compound. Values of C_0 for the compound were determined from the intercepts obtained by extrapolating the respective least-squares lines to zero time (Fig. 3). The volumes of distribution and the biological half-lives ($t_{1/2}$) were calculated according to the equations V_d = intravenous dose/C_0 and $t_{1/2} = 0.693/K_{el}$. The value of K_{el} was calculated from the slope ($-K_{el}/2.303$) of the least-squares lines. The pharmacokinetic parameters thus determined for the compound in the control rats as well as in the 3- and 5-day phenobarbital-treated rats are listed in Table V. The body clearance ($K_{el}V_d$) of the compound was also calculated.

Statistical Considerations and Treatment—Since only one blood sample was obtained from a rat at a given time following the intravenous administration of the compound under study, each data point in Figs. 1–3 and other pharmacokinetic studies represents the concentration of the compound in a single rat. This procedure was the same as that employed in previous pharmacokinetic studies (10) of these compounds in saline-untreated rats where the correlation coefficient observed between the concentration and time values was >0.991. There were reasons for using this procedure, instead of performing the study in a single rat by collecting the blood samples over the duration of the study following intravenous administration of a compound.

If a complete pharmacokinetic study of a compound were performed in a single rat, the total volume of blood that would have been withdrawn would have amounted to as high as 6 ml. The sensitivity of the assay procedures for these compounds at low intravenous doses would have necessitated the withdrawal of 0.2–0.3 ml of blood in each sampling during the initial period and 0.5–0.7 ml of blood in each sampling during the later period of the kinetic study. This would have been true especially in the case of I and II which confer upon the body the characteristics of multicompartment models. Withdrawal of such a high blood volume (about 40% of the total blood volume of a 200 g rat) would have been undesirable. In conjunction with the blood level pharmacokinetic studies carried out previously (10), the pharmacokinetics of these compounds were also studied from urinary excretion data (14) by performing (unlike in the blood level studies) complete pharmacokinetic studies in individual rats, since the sensitivity of the same assay procedure used for blood samples was not prohibitive in the quantitative determination of the amounts of compounds excreted in the urine. In these urinary excretion studies (14) a minimum subject-to-subject variation was observed in the excretion rates and elimination phase half-lives of these compounds, thereby supporting the assumption that rats showed minimum variations in the blood concentrations and half-lives of the compounds.

Therefore, in each pharmacokinetic study, a single blood concentration value of the compound was obtained per rat per time with the basic assumptions of the regression model that the single concentration variate corresponding to a given time is independently and normally distributed and the samples along the regression line have a common variance (15). The high correlation coefficient values between the two variates, concentration and time, support this assumption.

The standard deviation values indicated in Tables I–IV for the pharmacokinetic parameters V_1, k_{12}, k_{21}, k_{13}, k_{31}, and K_{el} of I and V_1, k_{12}, k_{21}, and K_{el} of II are the computer estimated values. According to the NONLIN least-squares program, the computer also estimated the values of α, β, and γ, but without their standard deviations. The standard deviations of these parameters and other derived pharmacokinetic parameters of I and II were estimated by the following procedures:

To estimate the standard deviation of β, the data points of a given study obtained exclusively in the elimination β-phase were plotted according to the equation $\ln C = \ln B - \beta t$. The standard deviation ($\hat{\sigma}c, t$) about the least-squares regression line thus obtained was estimated by the following formula (16):

$$\hat{\sigma}c,t = \left[\frac{\Sigma(\ln C)^2 - \frac{(\Sigma \ln C)^2}{n} - \beta^2\left\{\Sigma t^2 - \frac{(\Sigma t)^2}{n}\right\}}{n-2}\right]^{1/2}$$

The standard deviation of the slope ($\hat{SD}\beta$) was then calculated by the formula (16):

$$\hat{SD}\beta = \frac{\hat{\sigma}c,t}{\sqrt{\Sigma t^2 - \frac{(\Sigma t)^2}{n}}}$$

The standard deviations of α ($= K_{el}k_{21}/\beta$), V_2 ($= k_{12}V_1/k_{21}$), body clearance ($BC = K_{el}V_1$), V_{ss} ($= V_1 + V_2$), and $t_{1/2\beta}$, (0.693/β) were estimated by the general approximate formulas (17, 18):

$$\sigma\alpha = [\{(\sigma K_{el}/K_{el})^2 + (\sigma k_{21}/k_{21})^2 + (\sigma\beta/\beta)^2\}(\alpha)^2]^{1/2}$$

$$\sigma V_2 = [\{(\sigma k_{12}/k_{12})^2 + (\sigma V_1/V_1)^2 + (\sigma k_{21}/k_{21})^2\}(V_2)^2]^{1/2}$$

$$\sigma BC = [\{(\sigma K_{el}/K_{el})^2 + (\sigma V_1/V_1)^2\}(BC)^2]^{1/2};\ \sigma V_{ss} = [\sigma V_1^2 + \sigma V_2^2]^{1/2}$$

and

$$\sigma t_{1/2\beta} = 0.693 \cdot \sigma\beta/\beta^2$$

In the case of I a direct comparison of V_2, V_3, α, and β, the pharmacokinetic parameters of a three-compartment model in control rats, cannot be made with V_2, α, and β, the parameters of a two-compartment model in phenobarbital-treated rats. For this reason, and because of the complex equations from which V_2 and V_3 are obtained (12) for the three-compartment model, no attempt was made to determine the standard deviations of V_2, V_3, α, and β for I in control rats. However, because it is appropriate to compare the three-compartment parameters γ, $t_{1/2\gamma}$, and body clearance ($K_{el}V_1$) with the equivalent two-compartment parameters β, $t_{1/2\beta}$ and body clearance ($K_{el}V_1$), respectively, the standard deviations of these parameters were determined as described and used for determining statistical differences between the corresponding parameters (Table I).

In the case of III, which followed one-compartment model kinetics, the standard deviation of K_{el} was obtained as follows. First, the standard deviation ($\hat{\sigma}c,t$) about the least-squares regression line from the plot of ln$C$ *versus* t was obtained by (16):

$$\hat{\sigma}c,t = \left[\frac{\Sigma(\ln C)^2 - \frac{(\Sigma \ln C)^2}{n} - K_{el}^2\left\{\Sigma t^2 - \frac{(\Sigma t)^2}{n}\right\}}{n-2}\right]^{1/2}$$

The standard deviation of the slope ($\hat{SD}_{K_{el}}$) was then calculated from (16):

$$\hat{SD}_{K_{el}} = \frac{\hat{\sigma}c,t}{\sqrt{\Sigma t^2 - \frac{(\Sigma t)^2}{n}}}$$

The standard deviation of concentration of the compound at zero time (C_0) was estimated from the standard deviation of the slope of a least-squares regression line obtained by plotting C *versus* $e^{-K_{el}t}$ according to the equation $C = C_0e^{-K_{el}t}$.

For the three compounds used in the study, statistically significant differences between corresponding pharmacokinetic parameters obtained in the control and phenobarbital-treated rats were determined using t test statistics at $p \leq 0.05$.

DISCUSSION

Benzoylformic Acid (I)—The three-compartment model noted for I with two kinetically distinguishable peripheral tissue compartments in the control rats was reduced to a two-compartment model with one kinetically distinguishable peripheral tissue compartment in the 4-day phenobarbital-treated rats as well as in 6- and 10-day phenobarbital-treated rats. The pharmacokinetic parameters determined for the compound in 6- and 10-day phenobarbital-treated rats (Table II) were very similar to those determined in 4-day phenobarbital-treated rats. This indicates that the maximum effects of phenobarbital treatment on the pharmacokinetic parameters of the compound were indeed produced after a 4-day treatment with phenobarbital.

Since different compartment models are observed in the control and phenobarbital-treated rats, V_1, K_{el}, γ, $k_{el}V_1$, and $t_{1/2}$ elimination phase are the only pharmacokinetic parameters obtained for the compound in control rats which may be compared with the corresponding pharmacokinetic parameters in the phenobarbital-treated rats. It was observed that K_{el} and β of I in phenobarbital-treated rats were significantly greater than K_{el} and γ in the control rats. The $t_{1/2}$ of the compound in phenobarbital-treated rats was significantly shorter than that in control rats. Although there was a tendency for V_1 to decrease and $K_{el}V_d$ to increase in the phenobarbital-treated rats, these changes were not significant ($p = 0.05$) (Table I).

Mandelic Acid (II)—Table III shows that, except for $K_{el}V_1$, all pharmacokinetic parameters of II in the phenobarbital-treated rats were significantly different from those in the control rats. The parameters V_1, V_2, V_{ss}, and $t_{1/2\beta}$ decreased, and K_{el}, α, and β increased in the phenobarbital-treated rats compared with the corresponding parameters in the control rats.

The comparison of the pharmacokinetic parameters (Table IV) of the compound in the 1- and 10-day phenobarbital-treated rats with those of the 5-day treated rats indicated that the effects of phenobarbital treatment are seen on certain parameters even after a 1-day treatment with phenobarbital, but the maximum effects on all parameters were certainly obtained after a 5-day phenobarbital treatment. The pharmacokinetic parameters obtained in the 10-day phenobarbital-treated rats were not significantly different from those obtained in the 5-day phenobarbital-treated rats. Some of the pharmacokinetic parameters noted in the 10-day phenobarbital-treated rats are very similar to those in the 5-day phenobarbital-treated rats.

***p*-Methyl Benzoylformic Acid (III)**—Table V shows that the pharmacokinetic parameters of III from the 5-day phenobarbital-treated rats were very similar to those obtained in the 3-day phenobarbital-treated rats, indicating that the maximum pharmacokinetic effects were produced in 3-day phenobarbital-treated rats.

Except for V_d, all pharmacokinetic parameters of III determined in 3-day phenobarbital-treated rats were significantly different from those determined in the control rats. The values of K_{el} and $K_{el}V_d$ increased and $t_{1/2}$ decreased in phenobarbital-treated rats as compared with control rats.

Effects of Phenobarbital Treatment on the Pharmacokinetic Parameters of the Compounds—The effect of phenobarbital treatment on some pharmacokinetic parameters of the compounds studied seemed to depend on whether the compound conferred the characteristics of a one-, two-, or three-compartment model on the body. The effect on some other pharmacokinetic parameters appeared to be model independent. These effects are as follows:

1. The biological half-lives ($t_{1/2}$) of all compounds were significantly shorter in the phenobarbital-treated rats than those in the control rats.
2. The elimination rate constants (K_{el}) of the compounds from the central compartment were significantly greater in phenobarbital-treated rats than in the control rats.
3. The disposition rate constants (β) in phenobarbital-treated rats, which are a function of elimination and distribution of the compounds, were significantly greater than the corresponding disposition rate constants in the control rats (γ in the case of I and β in the case of II).
4. The distributive phases observed for I and II were shorter in the phenobarbital-treated rats than in the control rats.
5. A reduction in the apparent distribution volumes of the peripheral tissue compartments for I in phenobarbital-treated rats became evident by the fact that a three-compartment model in the control rats was reduced to a two-compartment model in the phenobarbital-treated rats. In the case of II (which displayed two-compartment model characteristics in both control and phenobarbital-treated rats), the apparent distribution volume of the peripheral tissue compartment (V_2) was significantly smaller in the phenobarbital-treated rats than that in the control rats.
6. The apparent distribution volume of the central compartment (V_1) of II was significantly smaller in the phenobarbital-treated rats than in the control rats. However, V_1 of I (three-compartment in control rats) and V_d of III observed in the phenobarbital-treated rats were not found to be significantly different from those observed in the control rats.
7. The body clearance ($K_{el}V_d$) of III was significantly greater in phenobarbital-treated rats than in the control rats. In the case of I and II, although there was a tendency for body clearance ($K_{el}V_1$) to be greater in the phenobarbital-treated rats, such increases were not significantly different, most probably because the increase in K_{el} was offset by a simultaneous decrease of V_1.

Thus, the major effects produced by the phenobarbital treatment were to shorten the biological half-lives of the compounds used, irrespective of the pharmacokinetic model displayed, and to reduce the apparent distribution volumes of the peripheral tissue compartments of the compounds which displayed multicompartment model pharmacokinetics.

The known *in vivo* effects of phenobarbital treatment are to induce drug metabolizing microsomal enzymes (1, 3), to increase the bile flow (19, 20), and increase the liver (21) and kidney (7) blood flows. These effects potentially can shorten the biological half-lives of compounds, but since the compounds used in this study were not metabolized and were excreted in the urine entirely in the intact form by the phenobarbital-treated rats, the enzyme induction effect was not expected to influence their biological half-lives. The increase in the biliary flow and liver blood flow was also expected to have little or no effect on the kinetic dispositions of these compounds. Since the increased blood flow to the kidney is compensated by the autoregulation of the kidney to yield a constant blood flow to the glomerulus (7), no effect on the glomerular filtration rates of the compounds is expected. However, recent reports (7) have shown that the renal tubular secretion rates of *p*-aminohippuric acid increased in phenobarbital-treated rats. This effect was attributed to the increase in the renal tubular transport system available for the compound in rats. Since I, II, and III are secreted by the renal tubules of rats (9, 22), the contribution of this factor in increasing K_{el} of the compounds or in shortening their biological half-lives is possible.

The effects of phenobarbital treatment on the distribution pharmacokinetic parameters of the compounds that displayed multicompartment pharmacokinetics appear to be consistent with the hypothesis that phenobarbital treatment of rats may also increase the concentration of proteins and phospholipids in the membranes of tissue cells other than those of liver and kidney. Consequently, the rate of diffusion of the ionic species of the compounds through the aqueous pores of the tissue cell membranes decreases. One mechanism which has been widely recognized (23–29) for transmembrane transport of solutes is diffusion through aqueous pores. Previous pharmacokinetic studies (10, 22) of I, II, and several of their *para*-alkylated homologs, showed that the alkyl groups in these model organic anions decreased the apparent distribution volumes of the peripheral tissue compartments in rats, instead of increasing such distribution volumes as might have been expected due to the presence of lipophilic alkyl groups. Therefore, it was proposed (10, 22) that the distribution of these organic anions from the central compartment to the peripheral tissue compartments occurs mainly through aqueous pores of the tissue cell membranes.

No direct evidence has been obtained to show that the concentration of proteins and phospholipids of various tissue cell membranes increased resulting in reduction of the aqueous pore size of the membranes. However, the rationalization of the results of this study on the basis of the following considerations supports this possible effect of phenobarbital treatment in rats. It was previously indicated(10, 22) that the anionic forms of the compounds studied interact with the components (proteins and phospholipids) of the lining of aqueous pores while diffusing through them by means of intermolecular forces such as electrostatic interaction, hydrogen bonding, and hydrophobic bonding. By considering the slight differences in the chemical structures of these anions, the variations in the composition of cell membranes of various tissue cells (30), the possible differences in the degree of intermolecular interactions with aqueous pore lining, and the heteroporosity (31–33) of the membranes, the existence of a three-compartment open model for I and a two-compartment open model for II was explained (10).

It is also recognized that the membranes of most organs are heteroporous, with pore size ranging from 8 to 320 Å, with a mean pore size range of 70–120 Å (31–33), and that only about one-fourth of the total pore size constitutes the effective space for the diffusion of solute molecules through a pore (34). Therefore, the possible phenobarbital treatment induced reduction in the aqueous pore size would be expected to cause greater intermolecular interactions of the anions with the constituents of the pore lining and cause a decrease in the penetration of the anions into the tissue. This may decrease the apparent distribution volume occupied by the anions in that tissue.

The two peripheral tissue compartments noted for I in the control rats, were thought to be due to those organs whose aqueous pores exhibit weak hydrogen bonding with the I molecules and due to those organs whose aqueous pores exhibit strong hydrogen bonding with the I molecules (10, 22). In the phenobarbital-treated rats, only one peripheral tissue compartment was kinetically distinguishable. This may be due to the phenobarbital affecting the size of aqueous pores in the two tissue compartments such that the strengths of hydrogen bonding of the I anions with the aqueous linings of one tissue compartment were similar to those of the other tissue compartment.

It may be pointed out that the decrease in the distribution volumes observed in the phenobarbital-treated rats is for the compounds that display multicompartment characteristics and exist in the blood in the ionized form. Such changes in the distribution volume may not be observed for multicompartment model compounds that exist in the blood in the nonionized form. These compounds generally have greater membrane solubility and are expected to diffuse through the entire membrane surface of which aqueous pores constitute only a fractional surface area. Furthermore, if the shortening of the biological half-lives of these compounds is due to the stimulation by phenobarbital of their renal tubular secretion mechanism, changes in the biological half-lives may not be observed for compounds not involved in renal tubular secretion but are excreted in the urine due to glomerular filtration. Studies with model drugs supporting these hypotheses are presented elsewhere (35).

REFERENCES

(1) A. H. Conney, *Pharmacol. Rev.*, **19,** 317 (1967).

(2) H. Remer, *Eur. J. Clin. Pharmacol.*, **5,** 116 (1972).

(3) E. A. Sotaniemi, *Pharmacology*, **10,** 306 (1973).

(4) L. Shuster, *Nature*, **189,** 314 (1961).

(5) D. L. Young, G. Powell, and W. O. McMillan, *J. Lipid Res.*, **12,** 1 (1971).

(6) J. L. Holtzman and J. R. Gillette, *Biochem. Biophys. Res. Commun.*, **24,** 639 (1966).

(7) E. E. Ohnhaus and H. Siegl, *Arch. Int. Pharmacodyn. Ther.*, **223,** 107 (1976).

(8) E. J. Randinitis, M. Barr, H. C. Wormser, and J. B. Nagwekar, *J. Pharm. Sci.*, **59,** 806 (1970).

(9) E. J. Randinitis, M. Barr, and J. B. Nagwekar, *ibid.*, **59,** 813, (1970).

(10) Y. M. Amin and J. B. Nagwekar, *ibid.*, **64,** 1804 (1975).

(11) K. Kindler, W. Metzendorf, and Dschi-Yin-Kevok, *Chem. Ber.*, **76B,** 308 (1943).

(12) A. Resigno and G. Segre, in "Drug and Tracer Kinetics," Blaisdell, Waltham, Mass., 1966, p. 94.

(13) C. M. Metzler, "NONLIN, A Program to Estimate the Parmameters in a Nonlinear System of Equations," The Upjohn Co., Kalamazoo, Mich., 1969.

(14) Y. M. Amin and J. B. Nagwekar, *J. Pharm. Sci.*, **65,** 1341 (1976).

(15) R. R. Sokal and F. J. Rohlf, in "Biometry: The Principles and Practice of Statistics in Biological Research," Freeman, San Francisco, Calif., 1969, p. 410.

(16) B. W. Brown and M. Hollander, in "Statistics: A Biomedical Introduction," Wiley, New York, N.Y., 1977, p. 269–275.

(17) W. E. Deming, in "Statistical Adjustment of Data," Dover, New York, N.Y., 1938, p. 37–48.

(18) P. Armitage, in "Statistical Methods in Medical Research," Wiley, New York, N.Y., 1971, p. 97.

(19) C. D. Klassen, *J. Pharmacol. Exp. Ther.*, **175,** 289 (1970).

(20) T. Javor, A. Gogl, T. Horvath, and I. Tenyi, *Drug Metab. Dispos.*, **1,** 424 (1973).

(21) E. E. Ohnhaus, S. S. Thorgerson, D. S. Davis, and A. Brekenridge, *Biochem. Pharmacol.*, **20,** 2561 (1971).

(22) Y. M. Amin and J. B. Nagwekar, *J. Pharm. Sci.*, **64,** 1813 (1975).

(23) W. D. Stein, in "The Movements of Molecules Across Cell Membranes," Academic, New York, N.Y., 1967, p. 314.

(24) A. K. Solomon, *J. Gen. Physiol.*, **51,** 335S (1968).

(25) W. Van Alphen, N. Van Selm, and B. Lughtenberg, *Molec. Gen. Genet.*, 75 (1978).

(26) A. M. Schindler and A. S. Iborall, *Biophys. J.*, **13,** 804 (1973).

(27) H. N. Christensen, in "Biological Transport," 2nd ed., Benjamin, Reading, Mass., 1975, pp. 31–33.

(28) L. Orci, A. Perrelet, F. Malaisse-Lagae, and P. Vassalli, *J. Cell Sci.*, **25,** 157 (1977).

(29) M. Bundgaard, *Ann. Rev. Physiol.*, **42,** 325 (1980).

(30) A. Goldstein, L. Aronow, and S. M. Kalman, in "Principles of Drug Action, The Basis of Pharmacology," Wiley, New York, N.Y., 1974, pp. 129–225.

(31) C. Cron, *Pfluegers Arch.*, **336,** 656 (1972).

(32) J. R. Pappenheimer, K. M. Rankin, and L. M. Borrero, *Am. J. Physiol.*, **167,** 13 (1951).

(33) K. Welch and V. Friedman, *Brain*, **83,** 454 (1960).

(34) E. Middleton, *J. Membrane Biol.*, **34,** 93 (1977).

(35) J. B. Nagwekar and S. Kundu, *J. Pharm. Sci.*, in press.

ACKNOWLEDGMENTS

Abstracted in part from a dissertation submitted by D. J. Szymanski to the Graduate School, Wayne State University, in partial fulfillment of the Doctor of Philosophy degree requirements.

Ascorbic Acid Absorption in Humans: A Comparison among Several Dosage Forms

SUSANNA YUNG ‡, MICHAEL MAYERSOHN *x, and J. BARRY ROBINSON ‡

Received May 11, 1981, from the * *Department of Pharmaceutical Sciences, College of Pharmacy, University of Arizona, Tucson, AZ 85721* and the ‡ *Faculty of Pharmacy, University of Toronto, Toronto, Ontario, Canada.* Accepted for publication July 20, 1981.

Abstract □ There have been few studies conducted to determine the efficiency of ascorbic acid absorption in humans. Differences in the extent of its absorption among individuals may contribute to the outcome of clinical trials. Ascorbic acid absorption in four subjects was investigated from several oral dosage forms containing 1 g of the vitamin (solution, tablet, chewable tablet, and timed-release capsule). Approximately 85% of an intravenous dose was recovered in the urine as ascorbic acid and its major metabolites. In contrast, only ~30% of the dose was recovered from the solution and tablet forms. A considerably smaller fraction of the dose (~14%) was recovered from the timed-release capsule. There was considerable intersubject variation in ascorbic acid absorption and there appeared to be good and poor absorbers of the vitamin. Consideration should be given to the influence of the extent of ascorbic acid absorption on the results of clinical trials.

Keyphrases □ Ascorbic acid—comparison of absorption of several dosage forms, humans □ Absorption—ascorbic acid, comparison of several dosage forms, humans □ Vitamin C—comparison of absorption of several dosage forms, humans

Since the claim (1–3) that the daily consumption of large quantities of ascorbic acid may have beneficial effects for such conditions as the common cold, numerous investigations have been conducted to evaluate the efficacy of large doses of this vitamin for reducing the frequency and duration of cold symptoms (4–8). The results of these studies remain controversial (9, 10) although there is at least some tentative support for the clinical claims. Several studies have been criticized for lack of adequate control and for poor experimental design, factors which may have substantially influenced their results and conclusions. Perhaps equally as important is an understanding and the proper control of variables that may affect the absorption or bioavailability of the vitamin from the oral form. At present little is known about the absorption and disposition of ascorbic acid administered exogenously. Since ascorbic acid appears to be absorbed in humans by a specialized process (11, 12), the rate and extent of its absorption may be influenced by the relative efficiency of different oral dosage forms, size of the dose, and physiological conditions along the GI tract. The present study was designed to examine ascorbic absorption from various commercially available oral dosage forms.

EXPERIMENTAL

Protocol—Four healthy adult subjects participated in the study (three males and one female, 25–32 years of age) after giving informed written consent. Each subject ingested 1 g of ascorbic acid/day for a period of not less than 2 weeks prior to the experiments, in order to saturate body stores of the vitamin. Saturation of body stores was determined in the following manner. After the 2-week dosing period, 1 g of ascorbic acid (powder dissolved in water) was ingested on an empty stomach. Total urine was collected for the subsequent 24 hr and assayed for total vitamin. This procedure was repeated 3–7 days later. Between these two test doses the subjects ingested 1 g of ascorbic acid/day. The body stores were accepted as being saturated if the total amount of vitamin excreted during 24 hr from each test dose was within ±10% of each other.

Two days prior to and during an experimental day the subjects avoided the ingestion of ascorbic acid either in the form of vitamin preparations or foods known to be high in ascorbic acid content. One day prior to the experiment, blank urine samples were obtained by collecting total urine for several hours during two collection periods (one in the morning and one in the afternoon). The bladder was voided at the beginning of the collection period and the exact time of the collection interval and urine volume was noted.

On the experimental day the subjects ingested the assigned dosage form of the vitamin on an empty stomach after an overnight fast. Food was withheld for the next 3–4 hr. The dosage forms were ingested with 200 ml of water. The chewable tablets were thoroughly chewed prior to swallowing. The dosage forms ingested were:

A. 1 g of ascorbic acid powder dissolved in water[1]
B. 1 g of ascorbic acid tablets[2] (two 500-mg tablets)
C. 1 g of ascorbic acid chewable tablets[3] (two 500-mg tablets)
D. 1 g of ascorbic acid timed-release capsules[4] (two 500-mg capsules)

Each subject was randomly assigned to a specific schedule for ingestion of the different dosage forms according to a 4 × 4 Latin square design. In addition to the above dosage forms, 1 g of ascorbic acid was given intravenously 1 week after the completion of these experiments. The injectable solution[5] (4 ml) was injected into an arm vein over 3–4 min (500 mg/2-ml vial).

The bladder was voided immediately after drug administration. Urine was then collected during frequent and known time intervals during the subsequent 24 hr. The total volume of each collection was recorded and a 15-ml aliquot was taken and transferred to a vial which contained sufficient metaphosphoric acid such that a 4% solution of the acid was obtained with 15 ml of urine. The vial was shaken to dissolve the acid and stored in a refrigerator and assayed within 4 days. After the 24-hr collection period, the subjects resumed daily ingestion of 1 g of ascorbic acid until 2 days prior to the next experiment. A period of 1 week elapsed between successive experiments.

Analytical—All dosage forms were assayed to determine ascorbic acid

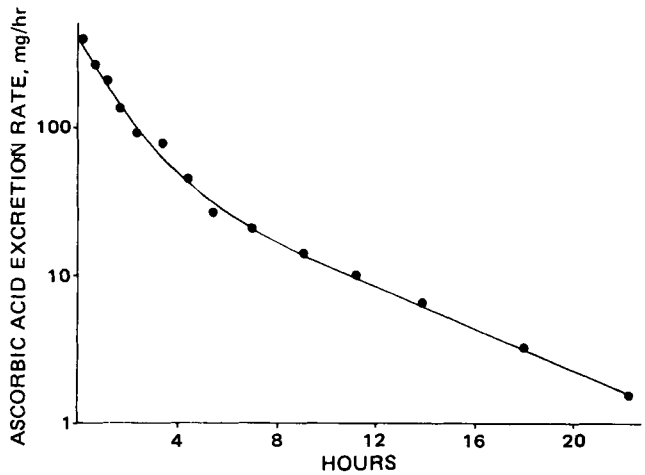

Figure 1—*Urinary excretion rate of ascorbic acid as a function of time in one subject after the intravenous injection of 1 g of ascorbic acid. The solid line represents the best fit of the data.*

[1] Lot 53808, BDH Chemicals, Ltd., Toronto, Ontario, Canada.
[2] Lot 509731, Novopharm Ltd., Scarborough, Ontario, Canada.
[3] Lot 505434, Novopharm Ltd., Scarborough, Ontario, Canada.
[4] Lot NDC 0817-0015-25, Ascorbicap, ICN Pharmaceuticals, Cincinnati, Ohio.
[5] Lot 7509-1, Sterilab Corp., Ltd., Downsview, Ontario, Canada.

0022-3549/82/0300-0282$01.00/0

Table I—Bioavailability of Ascorbic Acid from Various Dosage Forms

Subject	Percentage of Dose Recovered: Dosage Form: Solution	Tablet	Chewable Tablet	Timed-Release Capsule	Intravenous
1	16.1	10.7	12.2	6.2	81.3
2	34.9	44.2	26.1	17.4	84.6
3	23.4	19.0	24.6	10.9	85.7
4	54.2	45.3	58.8	22.6	87.3
Mean	32.1	29.8	30.4	14.2	84.7
±*SD*	16.6	17.6	19.9	7.2	2.5

content according to USP methods (13). Urine was assayed by the 2,4-dinitrophenylhydrazine method outlined by Pelletier (14) to determine concentrations of ascorbic acid and its two major metabolites, dehydroascorbic acid and diketogulonic acid. This assay method is based upon the formation of a colored osazone from dehydroascorbic and diketogulonic acids and it offers a means of differentiating the three compounds. The final solutions were measured colorimetrically at 520 nm. Concentrations of the compounds were determined from previously prepared standard curves and amounts excreted during a collection interval were calculated from the product of concentration and urine volume. The urinary excretion data were corrected for blank values determined from the urine samples collected on the day prior to each experiment.

Data Analysis—Urinary excretion data were used to calculate ascorbic acid excretion rate as a function of time. Initial estimates of the absorption rate constant (K_a) and the elimination rate constant (K) were obtained from semilogarithmic graphs of excretion rate *versus* time by the method of residuals. Using these initial estimates, the data obtained after the oral administration of ascorbic acid were fit by nonlinear regression analysis employing the equation appropriate for a one-compartment model and assuming first-order absorption and elimination. Since the urinary excretion data suggested the existence of a lag time (T_{lag}) between the time of dosing and the time when ascorbic acid excretion began, the equation incorporated T_{lag} as a parameter to be estimated. The computer-generated values for the above parameters were used to calculate the maximum excretion rate (ER_{max}) and the time of occurrence of this maximum (T_{max}). The excretion rate *versus* time data obtained after intravenous administration of the vitamin were fit to the equation appropriate for a two-compartment model. Initial estimates of the coefficients and exponents of the equation were obtained graphically using the method of residuals. These data were then fit by nonlinear regression analysis as already mentioned.

The bioavailability or extent of ascorbic acid absorption from each of the forms administered was determined from the total amount of the vitamin excreted into the urine during 24 hr (*i.e.*, the sum of ascorbic, dehydroascorbic, and diketogulonic acids). This value was then corrected for the actual dose ingested based on the assay of the dosage forms. Similarly, since ER_{max} depends on the actual dose ingested, this value was corrected for the actual assayed content of the vitamin. The extent of absorption was expressed either as a percentage of the dose recovered or as a percentage of the intravenous dose recovered.

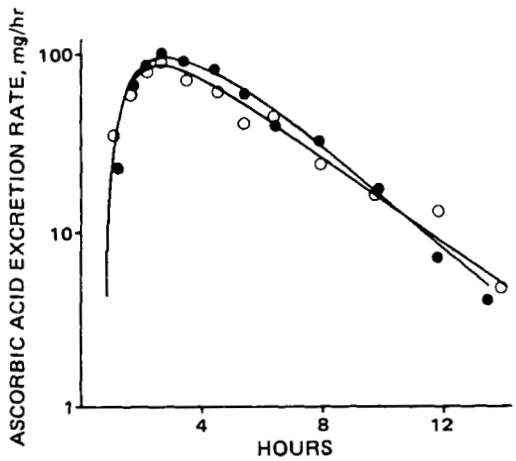

Figure 2—*Urinary excretion rate of ascorbic acid as a function of time in one subject after the ingestion of 1 g of ascorbic acid as a solution (●) or as a tablet (○). The solid lines represent the best fit of the data.*

Table II—Maximum Ascorbic Acid Excretion Rate (ER_{max}) from Various Dosage Forms

Subject	Maximum Excretion Rate, mg/hr: Dosage Form: Solution	Tablet	Chewable Tablet	Timed-Release Capsule
1	35.8	20.2	25.5	6.4
2	54.5	49.7	45.5	24.0
3	46.9	43.0	43.5	16.6
4	96.2	77.5	98.1	30.1
Mean	58.4	47.6	53.1	19.3
±*SD*	26.4	23.6	31.3	10.2

The percentage availability of ascorbic acid, ER_{max} and T_{max}, were statistically analyzed to determine any differences among the dosage forms examined. These data were analyzed according to a 4 × 4 Latin square design (15). Variance ratios were calculated for comparisons among dosage forms, subjects, and sequence of administration. Scheffe's test (16) was also employed to contrast these parameters.

RESULTS AND DISCUSSION

Standard curves for ascorbic acid in urine were linear and reproducible over the concentration range of 2–40 μg/ml. By repetitively assaying urine containing a known concentration of ascorbic acid (with 4% metaphosphoric acid and stored in a refrigerator) it was determined that the vitamin was stable for at least 4 days.

The mean assayed contents of ascorbic acid determined from 20 samples of the oral dosage forms were (expressed as percent of label claim): powder, 99.9%; tablet, 107.8%; chewable tablet, 101.2%; and timed-released capsule, 104.3%. The injectable solution contained 108.7% of the label claim based on the assay of three vials. The urinary excretion data were corrected for these values of actual ascorbic acid content.

The results of the intravenous experiments were previously reported elsewhere (17). Figure 1 is a representative graph of ascorbic acid excretion rate as a function of time after intravenous administration to one subject. The data appear to be consistent with a two-compartment model. The average elimination $t_{1/2}$ associated with the log-linear terminal exponential phase (β-phase) was 3.5 hr (range, 2.7–4.3 hr). The percentage of the intravenous dose recovered in the urine averaged 84.7% (range, 81.3–87.3%) as shown in Table I. Figures 2–4 are representative graphs of ascorbic acid excretion rate as a function of time after the oral ingestion of the various dosage forms studied. For comparison, the data obtained from the oral solution are included in each graph. The excretion rate–time profiles are similar for the oral solution, tablets, and chewable tablets. A comparable pattern is not seen, however, for the timed-release preparation. In the latter case, the rate of absorption and ER_{max} are considerably smaller compared with the other oral dosage forms.

The bioavailability of the vitamin from these dosage forms is summarized in Table I. The solution, tablet, and chewable tablet are absorbed to approximately the same extent (~30% of the dose) although there is considerable intersubject variation in the percentage of the dose recov-

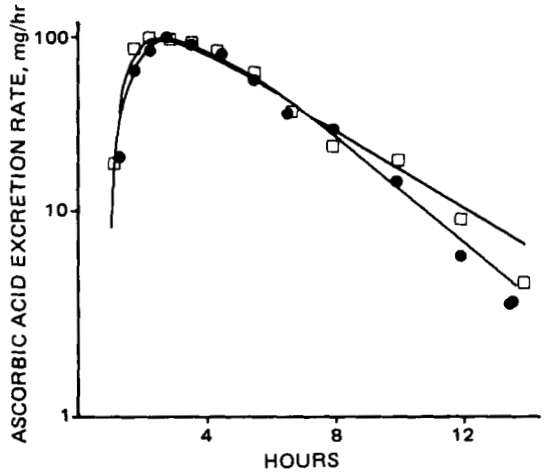

Figure 3—*Urinary excretion rate of ascorbic acid as a function of time in one subject after the ingestion of 1 g of ascorbic acid as a solution (●) or as a chewable tablet (□). The solid lines represent the best fit of the data.*

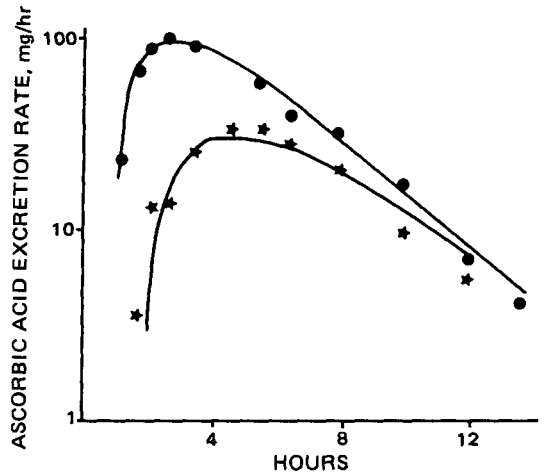

Figure 4—*Urinary excretion rate of ascorbic acid as a function of time in one subject after the ingestion of 1 g of ascorbic acid as a solution (●) or as a timed-release capsule (★). The solid lines represent the best fit of the data.*

ered. Absorption from the timed-release capsule is considerably less than from the other dosage forms (~14% of the dose). Based on analysis of variance there is a statistically significant difference among subjects with respect to the percentage of the oral dose recovered ($p < 0.01$) but there was not a statistical difference with respect to sequence of administration ($p > 0.25$). Percentage recoveries among the oral dosage forms were not statistically different ($0.05 < p < 0.10$), probably as a result of the large variation in these values among the subjects. Since the urinary recovery data suggested that the timed-release capsule was considerably different from the other oral dosage forms, Scheffe's test (16) was used to compare the means obtained from the timed-release capsule *versus* the other forms. As with the analysis of variance, the difference was close to but did not reach statistical significance.

A comparison of maximum ascorbic acid excretion rate (ER_{max}) among the different dosage forms is presented in Table II. These values have been normalized for the assayed content of ascorbic acid in each form. Analysis of variance indicated significant differences among the products ($p < 0.01$) and among subjects ($p < 0.01$), while there was no significant difference with respect to sequence of administration ($p > 0.25$). The timed-release capsule had a substantially lower ER_{max} value compared to the other oral dosage forms.

Table III summarizes the times needed to achieve maximum excretion rates (T_{max}). Consistent with a slower absorption rate noted for the timed-release capsule, T_{max} for this form was significantly prolonged ($p < 0.01$) compared with the other oral dosage forms. There were no statistically significant differences among subjects or as a result of administration sequence.

Prior to the evaluation of ascorbic acid absorption from the various dosage forms examined, all subjects were shown to be saturated with the vitamin. This approach is necessary in evaluating the absorption of the vitamin from urinary excretion data, since the retention of the vitamin in the body is influenced by the nutritional status of the individual (18–20).

The urinary recovery values of the vitamin were very similar among the subjects after intravenous administration. An average of 85% of the dose was ultimately recovered in the urine. The remainder of the dose may be accounted for by other minor metabolites of the vitamin not detected by the assay method (*e.g.*, oxalic acid and ascorbate-2-sulfate) (21, 22) or a portion of the dose may remain in the ascorbate pool.

In contrast to the intravenous data, there was considerable variation in the urinary recovery of the vitamin after oral ingestion (Table I). With any given oral dosage form there is large variation in the excretion of the vitamin among the subjects. There appeared to be a trend in this variation in that subject 1 consistently excreted less vitamin and subject 4 consistently excreted more vitamin than the other subjects. While the conclusions presented here are necessarily limited by the number of subjects that participated, the data suggest that there may be "poor" and "good" absorbers of ascorbic acid. This trend is best supported by the oral solution data where there are no dosage form effects (*e.g.*, disintegration and dissolution processes) to mask the inherent ability to absorb the vitamin. When dissolved in water the vitamin is presented to absorption sites of the GI tract in a form optimal for absorption.

Table III—Time of Maximum Ascorbic Acid Excretion Rate (T_{max}) from Various Dosage forms

	Time of Maximum Excretion Rate, hr			
	Dosage Form			
Subject	Solution	Tablet	Chewable Tablet	Timed-Release Capsule
1	3.1	2.3	2.6	4.9
2	2.3	3.8	2.4	3.8
3	2.1	2.5	3.1	3.5
4	3.0	2.7	2.5	4.5
Mean	2.6	2.9	2.7	4.2
±*SD*	0.5	0.6	0.3	0.6

It was suggested that ascorbic acid is absorbed in humans by a specialized transport mechanism (11, 12). Differences among individuals in the values of the parameters associated with this transport process may partially account for the variation noted in the extent of absorption. Furthermore, differences in physiological variables along the gut (*e.g.* gastric emptying rate) may contribute to this intersubject variation. The absolute absorption of the vitamin from oral solution may be calculated by the ratio of urinary recoveries from the solution to the intravenous dose. Approximately 40% of the dose ingested as a solution is absorbed (range, 20–62%). Compounds transported by specialized processes are generally absorbed only at certain sites along the GI tract. This has been shown, for example, for riboflavin where absorption proceeds from the upper regions of the small intestine (23). The same observation is likely to apply to ascorbic acid. As a result, factors altering gastric emptying and intestinal transit rates (*e.g.*, food and drugs) may influence the efficiency of absorption from the oral dosage form. This effect was adequately illustrated for riboflavin (23, 24) and appears to be the case for ascorbic acid as well (25).

The urinary recovery data indicated that the vitamin was absorbed to approximately the same extent from the solution, tablet, and chewable tablet. The timed-release capsule, however, was absorbed to a much smaller extent compared with the other oral forms. The absolute percentage of the dose absorbed from this capsule was ~17%, which is less than one-half the amount absorbed from the solution (~40%). Several reasons may be suggested to account for the poor absorption of the vitamin from the timed-release capsule. The vitamin may be incompletely released from the formulation resulting in reduced absorption compared with a solution. An additional explanation may be that, to be well absorbed, the vitamin must be released from the formulation and be in solution before the vitamin passes its sites of maximal absorption. Since timed-release formulations are designed to release a compound slowly over an extended period of time, a substantial portion of the dose of the vitamin may not have been released before passing this site. This would be particularly true if, as it appears (26), the major site for absorption is in the upper region of the small intestine.

Further insight into the absorption of ascorbic acid may be obtained by reference to Tables II and III. While the ER_{max} values are similar among the solution, tablet, and chewable tablet forms, the timed-release capsule provides considerably smaller values (Table II). These smaller values for the capsule indicate slower and less complete absorption of the vitamin. The slower and prolonged rate of absorption in contrast to the solution is illustrated in Fig. 4. Also consistent with this slower rate of absorption is the fact that it takes longer for the timed-release capsule to achieve the maximum excretion rate compared with the other oral forms (Table III and Fig. 4). The average value of T_{max} for the timed-release product (4.2 hr) is similar to the value of 4.9 hr reported (27) for a different timed-release formulation of ascorbic acid. Consistent with this discussion are the differences in the apparent first-order absorption rate constant among the dosage forms. The apparent absorption rate constants for the solution (1.4 hr^{-1}), tablet (1.4 hr^{-1}), and chewable tablet (1.3 hr^{-1}) forms are about three times larger than that for the timed-release product (0.4 hr^{-1}).

The results of this study are consistent with the findings of Richards *et al.* (28) who reported greater ascorbic acid plasma concentrations after oral administration of a nonsustained-release product compared with those achieved with a sustained-release product. Similar results were reported by Allen (29) who examined the same timed-release product used in this study. In that study, however, there was no crossover among subjects and the body store of the vitamin was relatively low. The latter point is supported by the small recovery of the vitamin in urine (~3% of the dose for the regular capsule and 1% for the timed-release product). The present findings disagree, however, with those of Zetler *et al.* (27) who measured ascorbic acid blood concentrations and urinary excretion

after oral ingestion of a capsule and a sustained-release product. Their results indicated that the extent of absorption from the sustained-release product was almost twice that from a regular capsule. In addition, ~98% of the sustained-release dose was absorbed compared to an intravenous dose. The latter value is unusually high and we are not aware of any study where an oral dose of ascorbic acid is virtually completely absorbed. Another discrepancy is that the ascorbic acid half-life was determined (27) to be ~11 hr prior to saturation and 29 hr after saturation. These values are considerably greater than those reported for the half-life of the vitamin after exogenous administration (11, 17, 26, 30). The reason for the substantial differences in half-life and availability from the timed-release products reported here and by Zetler *et al.* (27) is not known.

The results of this study indicate that ascorbic acid absorption is incomplete after oral ingestion and that there is considerable intersubject variation in the extent of absorption. In addition, absorption of the vitamin is considerably less efficient from the timed-release capsule examined here compared with the other oral forms. These findings have several implications. From a practical point of view, efficient oral therapy with the vitamin can be achieved by dissolving powdered ascorbic acid in water. In addition, for the specific manufacturers' products examined in this study, tablets and chewable tablets appear comparable to a solution of the vitamin. This conclusion may not apply to tablets made by all manufacturers but that can only be determined from the evaluation of other products in a manner used in the present study. The timed-release capsule examined here appears to be a more expensive and less reliable means of providing oral vitamin therapy compared with other more conventional dosage forms. This conclusion may apply to similar dosage forms which attempt to delay or sustain the release of the vitamin; therefore, bioavailability studies for such forms are essential.

A question that remains to be answered is to what extent does variation in ascorbic acid absorption influence the results of large-scale trials designed to examine the clinical effects of the vitamin? To the authors' knowledge no consideration has been given to absorption as a parameter potentially influencing the findings of such studies. Investigators pursuing such trials should give some consideration to the possible influence of variation in ascorbic acid absorption on clinical outcome.

REFERENCES

(1) L. Pauling, "Vitamin C and the Common Cold," Freeman, San Francisco, Calif., 1970.

(2) L. Pauling, *Proc. Natl. Acad. Sci., USA*, 68 2678 (1971).

(3) L. Pauling, *Am J. Clin. Nutr.*, **24**, 1294 (1971).

(4) T. W. Anderson, D. B. W. Reid, and G. H. Beaton, *Can. Med. Assoc. J.*, **107**, 503 (1972).

(5) T. W. Anderson, G. Suranyi, and G. H. Beaton, *ibid.*, **111**, 31 (1974).

(6) T. W. Anderson, G. H. Beaton, P. N. Corey, and L. Spero, *ibid.*, **112**, 823 (1975).

(7) T. R. Karlowski, T. C. Chalmers, L. D. Frenkel, A. Z. Kapikian, T. L. Lewis, and J. M. Lynch, *J. Am. Med. Assoc.*, **231**, 1038 (1975).

(8) T. L. Lewis, T. R. Karlowski, A. Z. Kapikian, J. M. Lynch, G. W. Schaffer, and D. A. George, *Ann. N.Y. Acad. Sci.*, **258**, 505 (1975).

(9) T. C. Chalmers, *Am. J. Med.*, **58**, 532 (1975).

(10) M. H. M. Dykes and P. Meier, *J. Am. Med. Assoc.* **231**, 1073 (1975).

(11) W. Kubler and J. Gehler, *Int. Z. Vitaminforsch.*, **40**, 442 (1970).

(12) M. Mayersohn, *Eur. J. Pharmacol.* **19**, 140 (1972).

(13) "The United States Pharmacopeia," 19th rev. Mack Publishing Co., Easton, Pa. 1974, pp. 36–38.

(14) O. Pelletier, *J. Lab. Clin. Med.*, **72**, 674 (1968).

(15) G. W. Snedecor and W. G. Cochran, "Statistical Methods," Iowa State University Press, Ames, Iowa, 1973, pp 312–317.

(16) *Ibid.*, 1973, pp 268–271.

(17) S. Yung, M. Mayersohn, and J. B. Robinson, *J. Pharm. Sci.*, **67**, 1491 (1978).

(18) J. M. Faulkner and F. H. L. Taylor, *J. Clin Invest.*, **17**, 69 (1938).

(19) L. J. Harris and S. N. Ray, *Lancet*, **1**, 71 (1935).

(20) S. W. Johnston and S. S. Zilva, *Biochem. J.*, **28**, 1393 (1934).

(21) E. M. Baker, D. C. Hammer, S. C. March, B. M. Tolbert, and J. E. Canhan, *Science*, **173**, 826 (1971).

(22) B. M. Tolbert, M. Downing, R. W. Carlson, M. K. Knight, and E. M. Baker, *Ann. N.Y. Acad. Sci.*, **258**, 48 (1975).

(23) G. Levy and W. J. Jusko, *J. Pharm. Sci.*, **55**, 285 (1966).

(24) W. J. Jusko and G. Levy, *ibid.*, **56**, 58 (1967).

(25) S. Yung, M. Mayersohn, and J. B. Robinson, *Life Sci.*, **28**, 2505 (1981).

(26) J. S. Stewart and C. C. Booth, *Clin. Sci.*, **27**, 15 (1964).

(27) G. Zetler, G. Seidel, C. P. Siegers, and H. Ivens, *Eur. J. Clin. Pharmacol.*, **10**, 273 (1976).

(28) T. W. Richards, E. Cheraskin, and W. M. Ringsdorf, *Int. J. Vitam. Res.*, **39**, 407 (1969).

(29) E. S. Allen, *Curr. Ther. Res.*, **11**, 745 (1969).

(30) J. Gehler and W. Kubler, *Int. Z. Vitaminforsch.*, **40**, 454 (1970).

Mass Spectral Fragmentation of 24,24-Diphenyl-23-ene Derivatives of Cholic Acid

JERRY RAY DIAS

Received December 8, 1980, from the *Department of Chemistry, University of Missouri–Kansas City, Kansas City, MO 64110.* Accepted for publication June 30, 1981.

Abstract □ After electron impact in the mass spectrometer, 24,24-diphenyl-23-ene derivatives of cholic acid ejected the 17-sidechain as an ionized 1,1-diphenyl-butadiene derivative, and the 12α-acetoxy group activated this loss. This contrasts markedly with the mass spectrometric fragmentation of typical sterols having unsaturated 17-sidechains that are also devoid of functionality on the C-ring.

Keyphrases □ Mass spectra—fragmentation of 24, 24-diphenyl-23-ene derivatives of cholic acid □ Cholic acid—24, 24-diphenyl-23-ene derivatives, fragmentation by mass spectra □ Derivatives—24, 24-diphenyl-23-ene derivatives of cholic acid, mass spectral fragmentation

During the course of other investigations (1), a number of 24,24-diphenyl-23-ene derivatives of cholic acid having structural similarities to known biologically active compounds were prepared. Since the Barbier–Wieland 17-sidechain degradation is used extensively in steroid-terpenoid synthesis (2, 3) and electron impact induced loss of the 17-sidechain is of both fundamental and diagnostic importance (4–6), the observations concerning mass spectral cleavage processes of the Barbier–Wieland modified 17-sidechain of steroids and terpenoids are summarized.

RESULTS AND DISCUSSION

The preparation of the compounds in this study was unexceptional. However, isolation of pure diene (IV*a*–IV*d*) was difficult because unreacted monoene was invariably present. Also, it is likely that *E* and *Z*

0022-3549/82/0300-0285$01.00/0

after oral ingestion of a capsule and a sustained-release product. Their results indicated that the extent of absorption from the sustained-release product was almost twice that from a regular capsule. In addition, ~98% of the sustained-release dose was absorbed compared to an intravenous dose. The latter value is unusually high and we are not aware of any study where an oral dose of ascorbic acid is virtually completely absorbed. Another discrepancy is that the ascorbic acid half-life was determined (27) to be ~11 hr prior to saturation and 29 hr after saturation. These values are considerably greater than those reported for the half-life of the vitamin after exogenous administration (11, 17, 26, 30). The reason for the substantial differences in half-life and availability from the timed-release products reported here and by Zetler *et al.* (27) is not known.

The results of this study indicate that ascorbic acid absorption is incomplete after oral ingestion and that there is considerable intersubject variation in the extent of absorption. In addition, absorption of the vitamin is considerably less efficient from the timed-release capsule examined here compared with the other oral forms. These findings have several implications. From a practical point of view, efficient oral therapy with the vitamin can be achieved by dissolving powdered ascorbic acid in water. In addition, for the specific manufacturers' products examined in this study, tablets and chewable tablets appear comparable to a solution of the vitamin. This conclusion may not apply to tablets made by all manufacturers but that can only be determined from the evaluation of other products in a manner used in the present study. The timed-release capsule examined here appears to be a more expensive and less reliable means of providing oral vitamin therapy compared with other more conventional dosage forms. This conclusion may apply to similar dosage forms which attempt to delay or sustain the release of the vitamin; therefore, bioavailability studies for such forms are essential.

A question that remains to be answered is to what extent does variation in ascorbic acid absorption influence the results of large-scale trials designed to examine the clinical effects of the vitamin? To the authors' knowledge no consideration has been given to absorption as a parameter potentially influencing the findings of such studies. Investigators pursuing such trials should give some consideration to the possible influence of variation in ascorbic acid absorption on clinical outcome.

REFERENCES

(1) L. Pauling, "Vitamin C and the Common Cold," Freeman, San Francisco, Calif., 1970.

(2) L. Pauling, *Proc. Natl. Acad. Sci., USA*, 68 2678 (1971).

(3) L. Pauling, *Am J. Clin. Nutr.*, **24**, 1294 (1971).

(4) T. W. Anderson, D. B. W. Reid, and G. H. Beaton, *Can. Med. Assoc. J.*, **107**, 503 (1972).

(5) T. W. Anderson, G. Suranyi, and G. H. Beaton, *ibid.*, **111**, 31 (1974).

(6) T. W. Anderson, G. H. Beaton, P. N. Corey, and L. Spero, *ibid.*, **112**, 823 (1975).

(7) T. R. Karlowski, T. C. Chalmers, L. D. Frenkel, A. Z. Kapikian, T. L. Lewis, and J. M. Lynch, *J. Am. Med. Assoc.*, **231**, 1038 (1975).

(8) T. L. Lewis, T. R. Karlowski, A. Z. Kapikian, J. M. Lynch, G. W. Schaffer, and D. A. George, *Ann. N.Y. Acad. Sci.*, **258**, 505 (1975).

(9) T. C. Chalmers, *Am. J. Med.*, **58**, 532 (1975).

(10) M. H. M. Dykes and P. Meier, *J. Am. Med. Assoc.* **231**, 1073 (1975).

(11) W. Kubler and J. Gehler, *Int. Z. Vitaminforsch.*, **40**, 442 (1970).

(12) M. Mayersohn, *Eur. J. Pharmacol.* **19**, 140 (1972).

(13) "The United States Pharmacopeia," 19th rev. Mack Publishing Co., Easton, Pa. 1974, pp. 36–38.

(14) O. Pelletier, *J. Lab. Clin. Med.*, **72**, 674 (1968).

(15) G. W. Snedecor and W. G. Cochran, "Statistical Methods," Iowa State University Press, Ames, Iowa, 1973, pp 312–317.

(16) *Ibid.*, 1973, pp 268–271.

(17) S. Yung, M. Mayersohn, and J. B. Robinson, *J. Pharm. Sci.*, **67**, 1491 (1978).

(18) J. M. Faulkner and F. H. L. Taylor, *J. Clin Invest.*, **17**, 69 (1938).

(19) L. J. Harris and S. N. Ray, *Lancet*, **1**, 71 (1935).

(20) S. W. Johnston and S. S. Zilva, *Biochem. J.*, **28**, 1393 (1934).

(21) E. M. Baker, D. C. Hammer, S. C. March, B. M. Tolbert, and J. E. Canhan, *Science*, **173**, 826 (1971).

(22) B. M. Tolbert, M. Downing, R. W. Carlson, M. K. Knight, and E. M. Baker, *Ann. N.Y. Acad. Sci.*, **258**, 48 (1975).

(23) G. Levy and W. J. Jusko, *J. Pharm. Sci.*, **55**, 285 (1966).

(24) W. J. Jusko and G. Levy, *ibid.*, **56**, 58 (1967).

(25) S. Yung, M. Mayersohn, and J. B. Robinson, *Life Sci.*, **28**, 2505 (1981).

(26) J. S. Stewart and C. C. Booth, *Clin. Sci.*, **27**, 15 (1964).

(27) G. Zetler, G. Seidel, C. P. Siegers, and H. Ivens, *Eur. J. Clin. Pharmacol.*, **10**, 273 (1976).

(28) T. W. Richards, E. Cheraskin, and W. M. Ringsdorf, *Int. J. Vitam. Res.*, **39**, 407 (1969).

(29) E. S. Allen, *Curr. Ther. Res.*, **11**, 745 (1969).

(30) J. Gehler and W. Kubler, *Int. Z. Vitaminforsch.*, **40**, 454 (1970).

Mass Spectral Fragmentation of 24,24-Diphenyl-23-ene Derivatives of Cholic Acid

JERRY RAY DIAS

Received December 8, 1980, from the *Department of Chemistry, University of Missouri–Kansas City, Kansas City, MO 64110.* Accepted for publication June 30, 1981.

Abstract □ After electron impact in the mass spectrometer, 24,24-diphenyl-23-ene derivatives of cholic acid ejected the 17-sidechain as an ionized 1,1-diphenyl-butadiene derivative, and the 12α-acetoxy group activated this loss. This contrasts markedly with the mass spectrometric fragmentation of typical sterols having unsaturated 17-sidechains that are also devoid of functionality on the C-ring.

Keyphrases □ Mass spectra—fragmentation of 24, 24-diphenyl-23-ene derivatives of cholic acid □ Cholic acid—24, 24-diphenyl-23-ene derivatives, fragmentation by mass spectra □ Derivatives—24, 24-diphenyl-23-ene derivatives of cholic acid, mass spectral fragmentation

During the course of other investigations (1), a number of 24,24-diphenyl-23-ene derivatives of cholic acid having structural similarities to known biologically active compounds were prepared. Since the Barbier–Wieland 17-sidechain degradation is used extensively in steroid-terpenoid synthesis (2, 3) and electron impact induced loss of the 17-sidechain is of both fundamental and diagnostic importance (4–6), the observations concerning mass spectral cleavage processes of the Barbier–Wieland modified 17-sidechain of steroids and terpenoids are summarized.

RESULTS AND DISCUSSION

The preparation of the compounds in this study was unexceptional. However, isolation of pure diene (IV*a*–IV*d*) was difficult because unreacted monoene was invariably present. Also, it is likely that *E* and *Z*

0022-3549/82/0300-0285$01.00/0

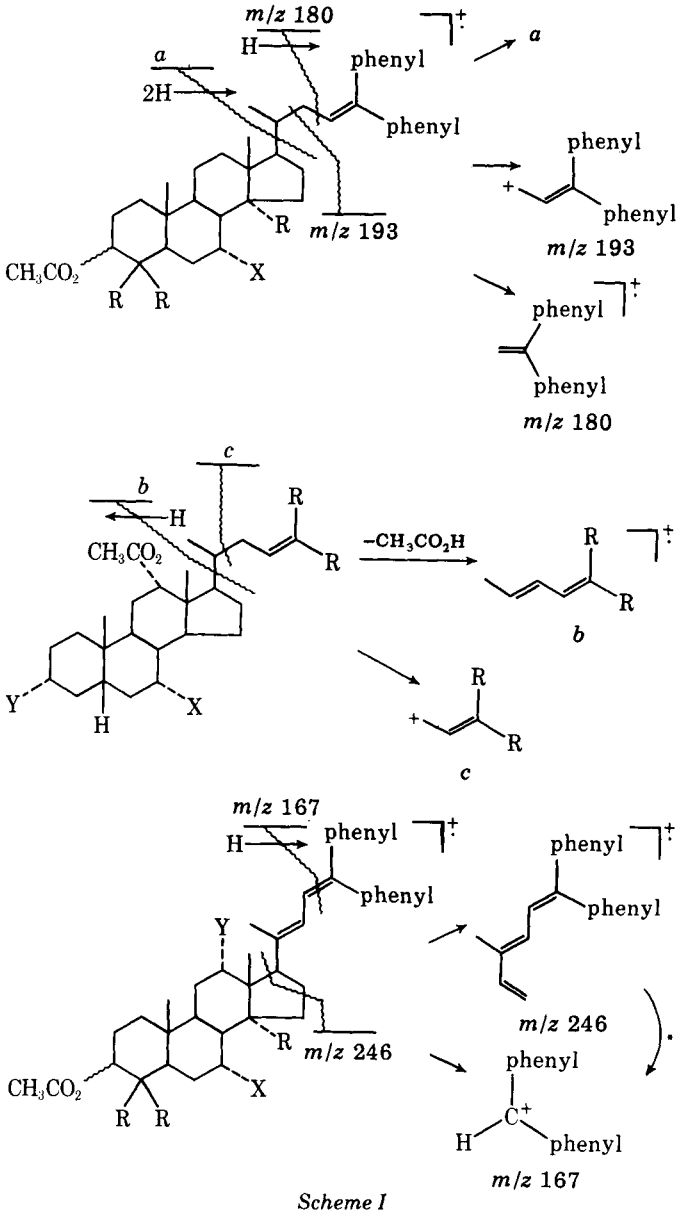

Scheme I

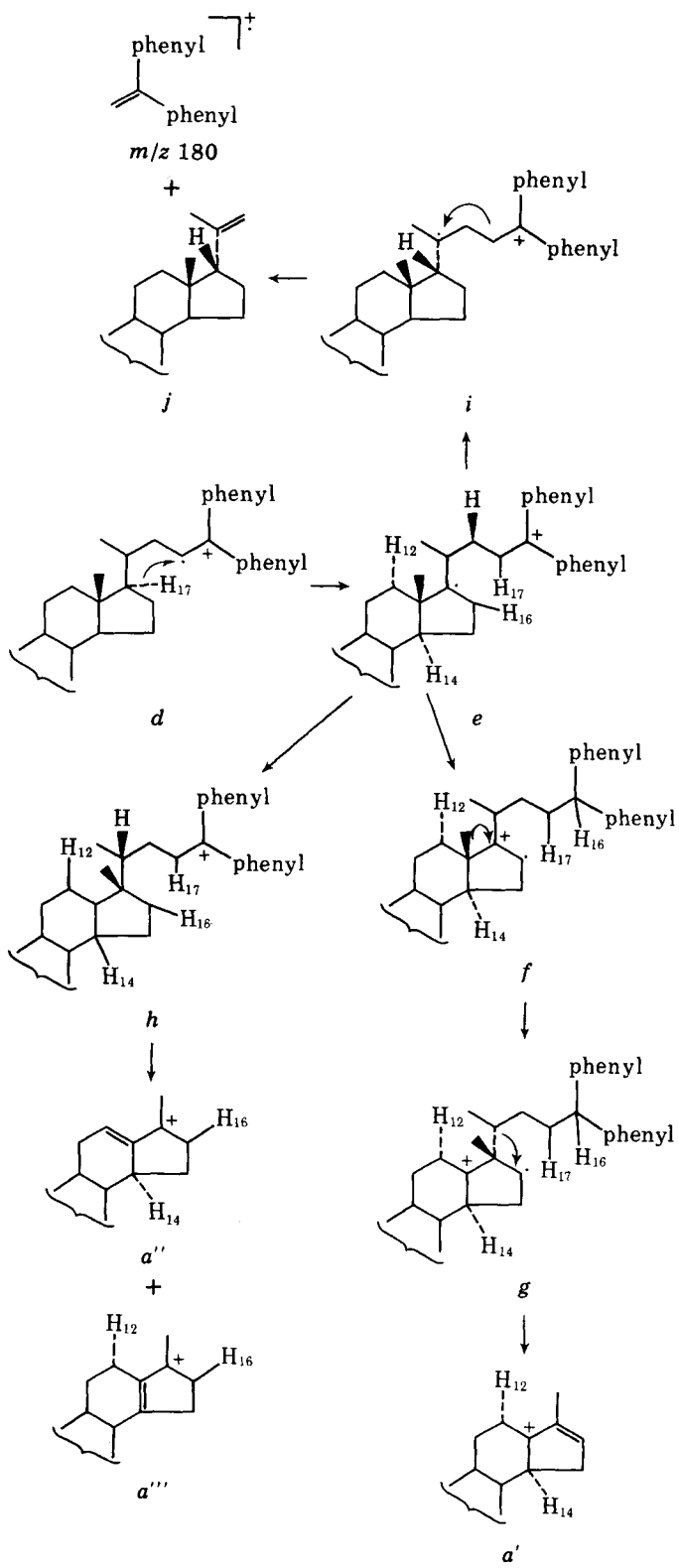

Scheme II

17-sidechain diene isomers may be coproducts, but this could not be verified experimentally. The propensity for acid catalyzed elimination of the 7α-acetoxy group as acetic acid for both the monoenes and dienes has been previously noted (1, 3). Table I summarizes the mass spectral data for compounds I–VIII.

Scheme I summarizes the characteristic fragmentations of 24,24-diphenyl-23-ene derivatives of cholic acid. If no functionality exists on the C-ring of the monoene, then ion *a*, the allyl carbocation (*m/z* 193), and ionized α,α-stilbene are the predominant ions observed in the mass spectra. The genesis of ion *a* was previously elucidated (4). Typical sterols having no B-ring or C-ring functionality and either a saturated or unsaturated 17-sidechain exhibit 17-sidechain and D-ring cleavage processes in which there is a drift of hydrogen atoms from the steroid skeleton to the departing neutral fragment (7). Placing functionality on the B- or C-rings (*e.g.*, an oxo group at positions 6 or 12) reverses the direction of hydrogen atom drift so that hydrogen moves from the 17-sidechain toward the steroid skeleton. The former process results in increased unsaturation in the steroid framework and corresponding charge residence in that unit upon scission, whereas the latter process produces increased unsaturation in the 17-sidechain unit and frequently results in greater charge residence in that fragment. Thus, ion *a* in Scheme I emanates from hydrogen migration to the 17-sidechain from the steroid skeleton followed by scission at the 17–20 bond; ion *b* emanates from hydrogen migration from the 17-sidechain to the steroid skeleton followed by 17–20 bond scission, where the reversal of hydrogen migration in the latter is induced by the presence of the 12α-acetoxy group. Otherwise, the process not regulated by hydrogen migration, simple allylic scission (*m/z* 193 and ion *c*), appears to be relatively unaltered in 24,24-diphenyl-23-enes either possessing or not possessing C-ring functionalization by the 12α-acetoxy group.

The specific mechanism for the genesis of ion *a* is presented in Scheme II. Charge localization on the olefinic 17-sidechain triggers site specific C-17 hydrogen transfer through a 5-membered ring to give the highly stable ion-radical *e* (4). The second itinerant hydrogen originated from positions C-12, C-14, and C-16 (4). Direct transfer of C-16 hydrogen to C-24 gives ion *f* which can undergo a 1,2-methyl shift to give ion *g*. Simple

Table I—Partial Monoisotopic Mass Spectra (70 ev) of 24,24-Diphenyl-23-ene Derivatives of Cholic Acid

Compound	$[M]^+$	$[M-2CH_3CO_2H]^+$	$[M-3CH_3CO_2H]^+$	$[M-CH_3CO_2H]^+$	$[M-CH_2CH{=}CR_2-CH_3CO_2H]^+$	$[M-CH_3CHCH_2CH_2CHR_2-CH_3CO_2H]^+$
Ia	596 (1)	536 (10)	476 (5)	—	—	—
Ib	596 (1)	536 (8)	476 (3)	—	343 (3)	313 (14)
Ic	610 (15)	550 (11)	490 (10)	—	357 (5)	—
Id	654 (3)	594 (7)	534 (4)	474 (3)	341 (7)[a]	—
IIa	724,722 (2, 3)	664,662 (4, 6)	604,602 (3, 5)	544,542 (2, 3)	341 (4)[a]	—
IIb	714 (6)	654 (4)	594 (2)	534 (2)	—	—
III	640 (5)	580 (18)	520 (39)	460 (14)	—	—
IVa	594 (8)	534 (44)	474 (5)	—	—	—
IVb	594 (6)	534 (3)	474 (2)	—	—	—
IVc	550 (44)	490 (6)	—	—	—	—
IVd	610 (13)	592 (10)[b]	532 (32)[b]	472 (6)[b]	—	—
V	536 (3)	476 (10)	—	—	—	313 (56)[c]
VI	594 (14)	534 (19)	474 (6)	—	341 (28)	311 (6)
VII	580 (3)	520 (2)	—	—	327 (29)	297 (6)
VIII	578 (9)	518 (3)	—	—	—	—

Compound	$[M-CH_2CH{=}CR_2-2CH_3CO_2H]^+$	$[M-CH_3CHCH_2CH_2CHR_2-2CH_3CO_2H]^+$	$[CH_2{=}C(CH_3){-}CH{=}CHCH{=}CR_2]^+$	$[CH_3CH{=}CH{-}CH{=}CR_2]^+$	$[CH{=}CH{-}CH{=}CR_2]^+$	$[CH_2CH{=}CR_2]^+$
Ia	283 (4)	253 (6)	246 (2)	220 (100)	205 (9)	193 (12)
Ib	283 (62)	253 (100)	246 (6)	—	—	193 (91)
Ic	297 (54)	—	246 (5)	220 (58)	205 (24)	193 (100)
Id	281 (12)[a]	—	—	220 (100)	205 (14)	193 (22)
IIa	281 (11)[a]	—	—	290,288 (64, 100)	275,273 (2, 3)	263,261 (12, 18)
IIb	—	—	—	280 (41)	265 (7)	253 (100)
III	—	—	—	206 (12)[d]	—	207 (100)[d]
IVa	—	—	246 (11)	220 (26)	205 (11)	193 (11)
IVb	—	—	246 (55)	220 (62)	205 (22)	193 (15)
IVc	—	—	246 (15)	220 (20)	205 (19)	193 (30)
IVd	—	—	246 (23)	220 (34)	205 (25)	193 (16)
V	283 (42)[c]	253 (100)[c]	246 (11)	220 (12)	205 (5)	193 (96)
VI	281 (100)	251 (18)	—	220 (24)	205 (13)	193 (68)
VII	—	—	—	—	—	193 (22)
VIII	—	—	246 (100)	220 (46)	205 (11)	—

Compound	$[CH_2{=}CR_2]^+$	$[R_2CH]^+$	Miscellaneous	Metastable Transitions
Ia	180 (4)	167 (3)	—	191 (220 → 205)
Ib	180 (72)	167 (21)	373 (1, $[M-CH_3CHCH_2CH_2CHPh_2]^+$), 314 (16)	423 (536 → 476), 233.5 (596 → 373)
Ic	180 (84)	167 (22)	—	574.5 (610 → 592), 515 (550 → 532), 496 (612 → 550) 455 (490 → 472), 436.5 (550 → 490), 332 (610 → 443)
Id	180 (7)	167 (12)	401 (1)	191 (220 → 205)
IIa	—	237,235 (6, 10)	253, 255 (30, 10, [228, 290 → 253, 255]$^+$)	488-90 (602,4 → 542,4), 259-61 (288, 90 → 273, 5) 222-4 (288, 90 → 253, 5)
IIb	240 (18)	227 (37)	145 (35)	82 (253 → 145)
III	180 (20)	167 (12)	129 (43)	466 (580 → 520), 407 (520 → 460)
IVa	—	167 (100)	—	
IVb	—	167 (100)	255 (17, [m-2HOAc—$CH_3C{=}CHCH{=}CR_2]^+$), 231 (13, [246—CH_3]$^+$)	480 (594 → 534), 217 (246 → 231), 191 (220 → 205), 113.5 (246 → 167)
IVc		167 (100)	299 (20), 259 (12), 231 (12)	515 (550 → 532), 437 (550 → 490)
IVd	180 (24)	167 (100)	550 (2), 490 (3), 365 (13), 305 (7)	575 (610 → 592), 478 (592 → 532)
V	180 (22)	167 (23)	521 (3), 461 (8), 115 (65)	446.5 (476 → 461), 506.5 (536 → 521), 68.5 (193 → 115)
VI	—	167 (13)	115 (40)	504 (534 → 519), 480 (594 → 534), 444 (474 → 459), 421 (534 → 474) 232 (341 → 281), 68.5 (193 → 115)
VII	180 (100)	—	357(17,[M-$CH_3CHCH_2CH_2C-HR_2]^+$), 343 [10]	247 (357 → 297)
VIII	—	167 (57)	231 (13, [246-CH_3]$^+$)	217 (246 → 231), 191 (220 → 205), 113.5 (246 → 167)

[a] Add one more CH_3CO_2H loss to column heading. [b] Replace one CH_3CO_2H by H_2O in column heading. [c] Delete one CH_3CO_2H in column heading. [d] Subtract or add a CH_2 group to the column heading.

scission of ion *g* leads to the allylic carbocation *a'*. Alternatively, a 1,2-methyl shift in ion *e* gives ion *h* where the tertiary radical at C-12 activates α-hydrogens at both the C-12 and C-14 positions, and their transfer to C-24 followed by simple scission at 17–20 leads to allylic ions *a''* and *a'''*, respectively. An ion analogous to the *m/z* 180 ion was not observed, and no doubt its presence in the spectra of Ib, V, and VII results from the stabilizing effects of the phenyl groups. A 1,2-hydrogen shift from C-20 to C-17 converts ion *e* into ion *i*, which can undergo simple scission to give olefin *j* and the *m/z* 180 ion.

The introduction of a 12α-acetoxy group into the C-ring of 24,24-diphenyl-23-enes results in a dramatic alteration of their mass spectral breakdown and is emphasized by comparing the mass spectra of Ia *versus*

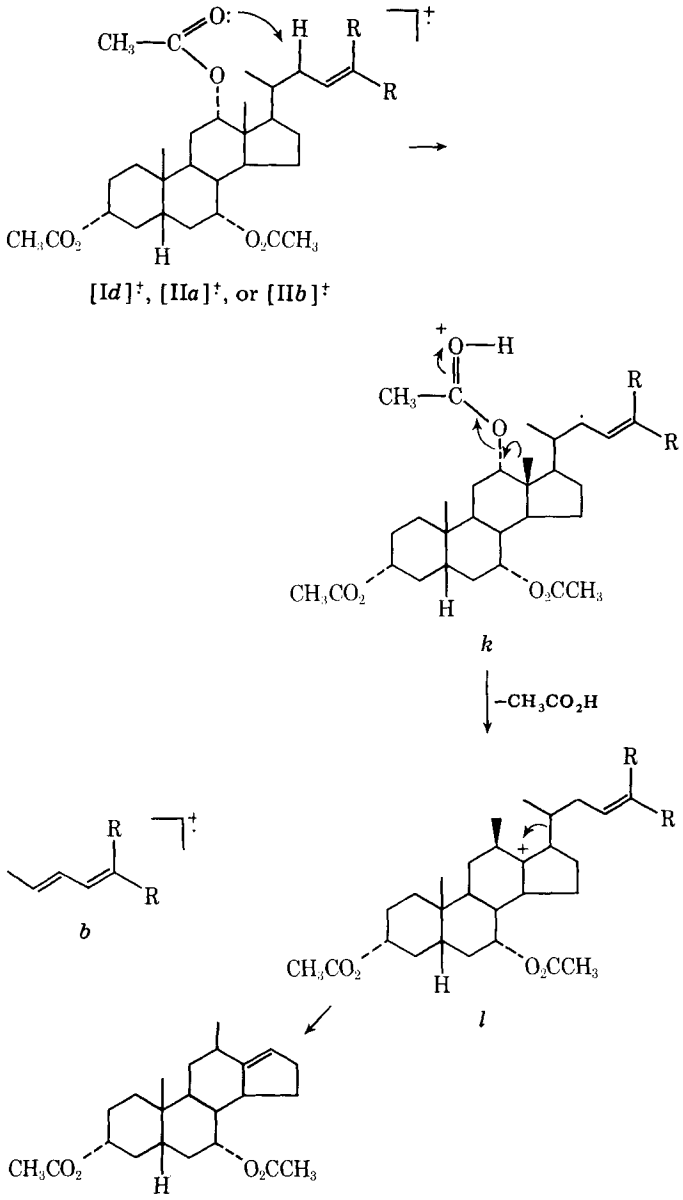

Scheme III

Ib. By selectively labeling with acetate-d_3, prior work demonstrated that in the consecutive loss of three acetic acid molecules from the molecular ion of methyl 3α,7α,12α-triacetoxy-5β-cholan-23-oate, that the first loss of acetate comes from the 12α-acetoxy group, the second from the 7α-acetoxy, and the third from the 3α-acetoxy group (8). A plausible mechanism for the formation of 1,1-biphenyl-1,3-butadiene ions (*b*) from the 17-sidechain in the mass spectra of Ia, Id, IIa, IIb, III, and VI could involve prior elimination of acetic acid from the 12α-acetoxy group to produce an 11–12 double bond which then triggers this process. However, Dreiding models suggests that it is sterically possible to transfer the activated C-22 hydrogen directly to the 12α-acetoxy carbonyl (Scheme III) through a nine-membered ring (an eight-membered ring for III) to generate the resonance stabilized ion *k*. Precedence for long-range activated hydrogen transfer to the 12α-acetoxy group in other cholic acid derivatives after electron impact has been provided (9). Extrusion of acetate from ion *k* simultaneous to 1,2-methyl shift would produce the tertiary carbocation *l* which can decompose *via* simple scission to give ion *b*.

Loss of the allyl radical ($\cdot CH_2CH{=}CR_2$) from the 17-sidechain was observed in all the monoenes and indicates that some charge localization occurs at the 12–17 bond. This is probably responsible for the 281 base peak in the mass specrum of VI, since the 8–14 double bond should activate ionization of this bond

$$[(VI)^{+} \rightarrow m/z\ 401 \xrightarrow{-CH_3CO_2H} m/z\ 341 \xrightarrow{-CH_3CO_2H} m/z\ 281].$$

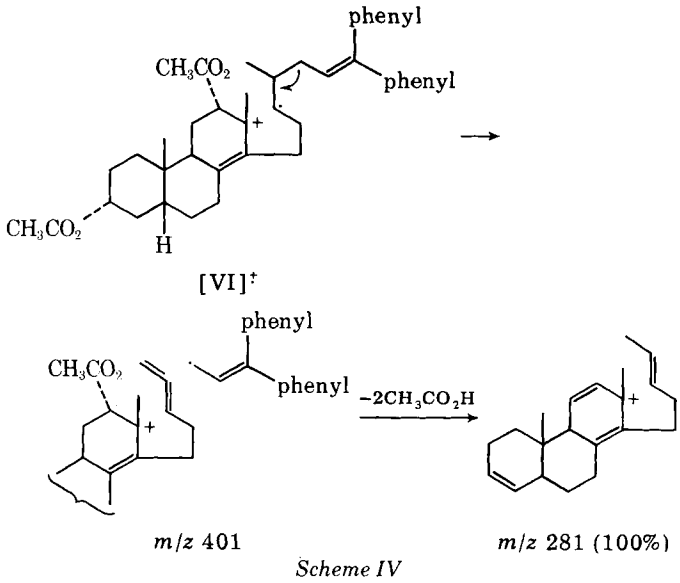

Scheme IV

Prior mass spectral work established that the dominant consecutive loss of one, two, and three acetic acid molecules from the 12α, 7α, and 3α-acetoxy groups of methyl cholate triacetate after electron impact led to increasingly more stable daughter ions since the relative intensities of the $[M\text{-}CH_3CO_2H]^{+}$, $[M\text{-}2CH_3CO_2H]^{+}$, and $[M\text{-}3CH_3CO_2H]^{+}$ ion peaks dramatically increased in that order (8). This observation permitted tracing of the probable movement of positive charge from the region of the D-ring to that of the A-ring. The fact that the mass spectral ions $[M\text{-}CH_3CO_2H]^{+}$, $[M\text{-}2CH_3CO_2H]^{+}$, and $[M\text{-}3CH_3CO_2H]^{+}$ are of low intensity and decrease in that order in relative intensity for Id, IIa, and IIb (Table I) provides evidence for extensive localization of charge on or near the 24,24-diphenyl-23-ene moiety. Since the critical energy for bond cleavage in a mass spectral ion is lower in the vicinity of positive charge and because there is a quasi-equilibrium fluctuation of excitation energy over the total charged molecule, it was observed that fragmentation in these compounds (I–VIII) is dominated by hydrogen migration and bond scission in the region of the 17-sidechain, which is the site of charge localization.

Simple D-ring scission of dienes IVa to IVd and VIII led to an *m/z* 246 hexatriene ion of obvious stability. Metastable peaks (Table I) corresponding to the degradation of the *m/z* 246 ion to *m/z* 167 (m* 113.5) were observed in the spectra of IVb and VIII. A plausible mechanism (Scheme V) for the formation of the dominant *m/z* 167 ion involves an orbital symmetry allowed 1,5-hydrogen shift to form ion *m* which decomposes

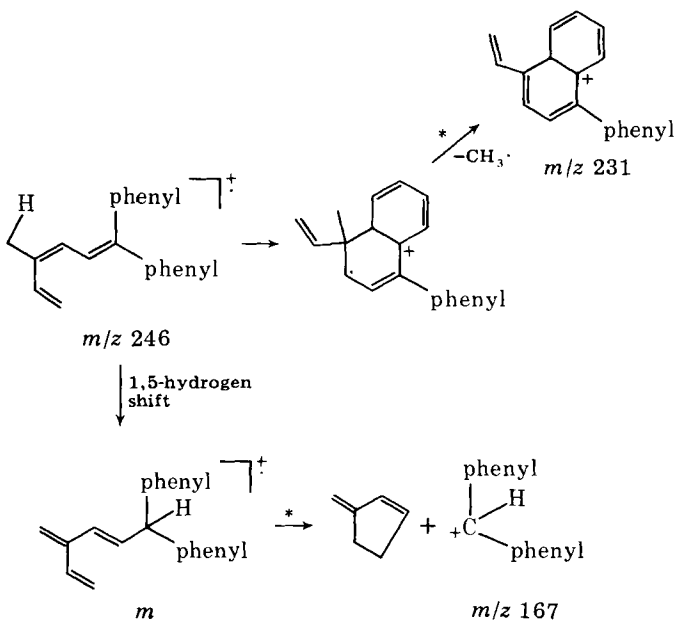

Scheme V

to m/z 167. The m/z 167 related ions in the spectra of the monoenes have a nominal relative abundance and no doubt have an alternate genesis.

Unidirectional migration of two hydrogens from the unsubstituted C- and D-rings of the steroid skeleton to the unsaturated 17-sidechain where charge is initially localized precedes the loss of the 17-sidechain as a neutral radical. In the presence of a 12α-acetate group, this process is superseded by the migration of a hydrogen from the ion-radical containing 17-sidechain to the C-ring acetate substituted steroid system producing an ionized butadiene derivative. Simple scission fragmentation processes occurring near the site of charge localization and not involving hydrogen migration in steroid systems should be less affected (than processes involving hydrogen migration) by the presence of local ring substituents that do not significantly alter the charge distribution in the ion.

EXPERIMENTAL

IR data, reported in inverse centimeters (cm^{-1}), were obtained as chloroform solutions; ^{1}H-NMR data[1], reported in ppm (δ) from tetramethylsilane, were obtained in chloroform-*d*. Mass spectra[2] were obtained at an ionization voltage of 12 and 70 ev (Table I), source temperature of 180°, and a trap current of 10 μamp.

Column chromatography was performed using silica gel[3], and TLC was performed on silica gel HF_{254}[3]. The latter was usually developed with 4:1 hexane–ethyl acetate. TLC was visualized by viewing under a UV lamp and charring by brief heating after spraying the TLC plate with 2% ceric sulfate in 2 *N* sulfuric acid. All reactions were monitored by TLC. In general, the dienes had slightly smaller R_f values than the corresponding monoenes and the deoxycholate analogs had larger R_f values than the corresponding chenodeoxycholate analogs. The order of decreasing R_f value for the monoenes coincided with the order of increasing electron density in the phenyl moiety; *p*-chlorophenyl II *a* (largest R_f), diphenyl I*d*, and *p*-methoxyphenyl II*b* (smallest R_f, gives characteristic red color upon brief charring with ceric sulfate).

The synthesis of compounds I*a*, I*b*, I*d*, IV*b*, V, VI, VII, and VIII have already been described (1, 3, 10).

3α,7α-Diacetoxy-12-oxo-24,24-diphenyl-5β-chol-23-ene(I*c*)—Saponification of 3α,7α,12α-triacetoxy-24,24-diphenyl-5β-chol-23-ene (5 g) was achieved by heating at reflux with potassium hydroxide (10 g) and methanol (165 ml) for 2 hr. This was diluted with water and extracted with ether. The ether extract was washed with 5% HCl and concentrated on a rotary evaporator. The dry residue of triol (4 g) was selectively acetylated to the 3α,7α-diacetate by dissolving it in benzene (20 ml) and pyridine (5 ml) and reacting at room temperature with acetic anhydride (5 ml) for 12 hr. The isolated 3α,7α-diacetoxy-12α-ol (4.2 g) was dissolved in acetone (150 ml), cooled on an ice bath, and oxidized dropwise with Jones reagent. Chromatography of the isolated 3α,7α-diacetoxy-12-one I*c* yielded 83% of pure product: mp 186–188° (melts at 115° and solidifies again and then melts at 186–188°); ^{1}H-NMR: δ 7.23 (s, 10H, phenyl H), 6.15 (t, 1H, C-23), 4.97 (peak, 1H, 7β-H), 4.57 (hump, 1H, 3β-H), 2.00 (s, 6H, 3α,7α-acetates), and 1.02 (s, 6H, C-18, and C-19).

3α,7α,12α-Triacetoxy-24,24-di(*p*-chlorophenyl)-5β-chol-23-ene(II*a*)—A Grignard reagent of 4-bromochlorobenzene (45 g) and magnesium (5.8 g) was prepared in dry ether (100 ml). Methyl cholate (10 g) dissolved in dry tetrahydrofuran (100 ml) was added dropwise to the Grignard reagent. After heating at reflux for 48 hr, the contents of the reaction were poured into ice (400 g) containing 36% HCl (70 ml), the organic layer was separated, and the aqueous phase was extracted with ether. The combined ether extracts were dried over anhydrous sodium sulfate and concentrated on a rotary evaporator to yield 15.7 g of crude tetraol. This tetraol was heated at reflux in a mixture of acetic anhydride (50 ml) and acetic acid (100 ml) for 6 hr, and then the acetic acid/anhydride solvent was slowly distilled off until the volume was reduced to 30 ml. The residue was steam distilled to remove the biphenyl side-product, and the isolated product was chromatographed through silica by gradient elution with hexane–ethyl acetate to yield 11 g of II*a*:mp 180–182°; $\bar{\nu}_{max}$ 2960 (strong, C-H stret), 1730 and 1250 (strong, acetate), and 1590 (weak, olefin stret); ^{1}H-NMR δ 6.94 (4 peak multiplet, 8 H, aromatic H), 4.53 (hump, 1 H, 3β-H), 2.10 (s, 3H, 12α-acetate), 2.05 (s, 3H, 7α-acetate), 2.03 (s, 3H, 3α-acetate), 0.92 (s, 3H, C-10), and 0.73 (s, 3H, C-18).

[1] Varian, models A-60 and T-60.
[2] Nuclide 12-90-G single focusing instrument.
[3] MCB Grade 62 and E. Merck.

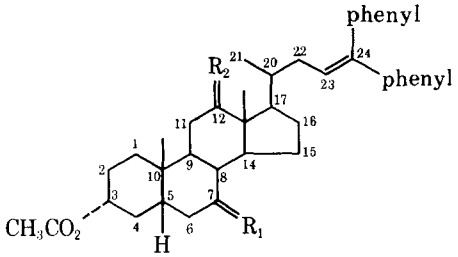

I*a*: $R_1 = H_2$, R_2 = α-OAc, β-H
I*b*: R_1 = α-OAc, β-H, R_2H_2
I*c*: R_1 = α-OAc, β-H, R_2O
I*d*: R_1 = α-OAc, β-H, R_2α-OAc, β-H

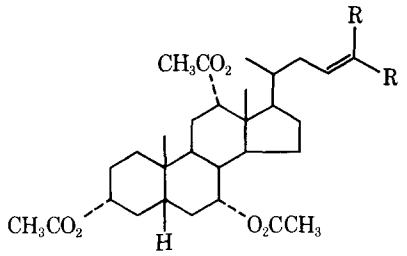

II*a*: R = *p*-ClC_6H_4
II*b*: R = *p*-$CH_3OC_6H_4$

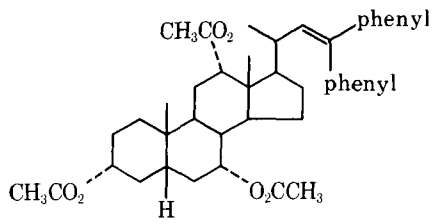

III

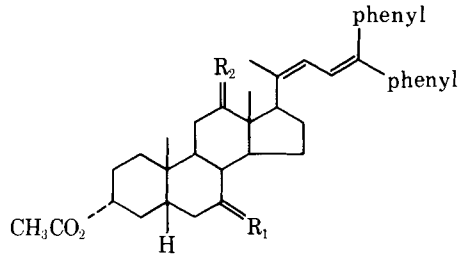

IV*a*: $R_1 = H_2$, R_2 = α-acetate, β-H
IV*b*: R_1 = α-acetate, β-H, H_2
IV*c*: $R_1 = H_2$, O
IV*d*: R_1 = α-acetate, β-H, α-OH, β-H

3α,7α,12α-Triacetoxy-24,24-di(*p*-methoxyphenyl)-5β-chol-23-ene (II*b*)—A solution of 4-methoxyphenylmagnesium bromide was prepared from *p*-bromophenol (100 g), magnesium (913 g), and dry tetrahydrofuran (300 ml). Methyl cholate (23 g) in dry benzene (150 ml) was added dropwise to the red-colored Grignard. After heating the reaction mixture at reflux for 24 hr, the reaction was halted, worked up, and purged of 4,4′-bismethoxybiphenyl by steam distillation. The 60 g of carbinol product thus obtained was heated at reflux in acetic anhydride/acetic acid (1:2, 400 ml) for 6 hr. Then the acetic anhydride/acetic acid solution was slowly distilled to a volume of 100 ml. The isolated product was column chromatographed through silica gel to yield 36 g of a glassy solid which refused to crystallize but was pure by TLC: ^{1}H-NMR δ 7.0 (m, 8H, phenyl H, 5.90 (t, 1H, C-23), 5.05 (peak, 1H, 12β-H), 4.98 (peak, 1H, 7β-H), 4.54 (hump, 1H, 3β-H), 3.81 (s, 3H, OCH_3), 3.76 (s, 3H, OCH_3), 2.11 (s, 3H, 12α- acetate), 2.07 (s, 3H, 7α-acetate), 2.02 (s, 3H, 7α-acetate), 0.92 (s, 3H, C-19), and 0.73 (s, 3H, C-18).

3α,7α,12α-Triacetoxy-23,23-diphenyl-24-nor-5β-chol-22-ene (III)—Methyl norcholate (2.0 g) dissolved in dry benzene (10 ml) was added dropwise to phenylmagnesium bromide (10 equivalents) in ether (25 ml), and tetrahydrofuran (10 ml). After heating at reflux for 24 hr, the reaction mixture was poured into ice (100 g) containing 36% HCl (5

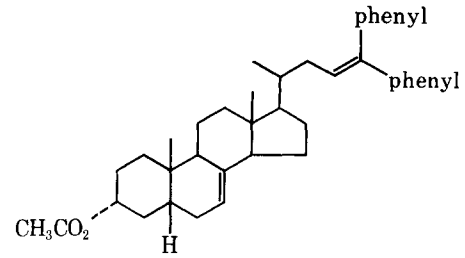

V

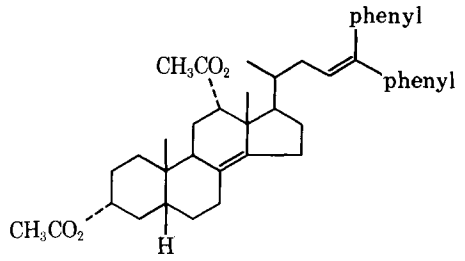

VI

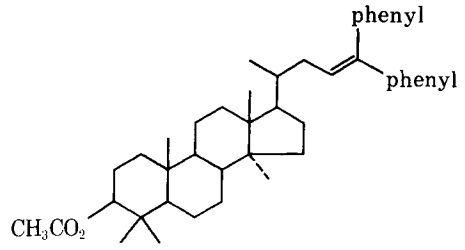

VII

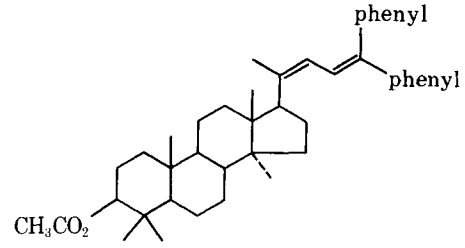

VIII

ml). This aqueous mixture was steam distilled to remove the biphenyl side product. The isolated carbinol (3.1 g) was heated at reflux with acetic anhydride (26 ml) and acetic acid (52 ml) for 3 hr, and then the volume of the acetic anhydride/acetic acid was reduced to 20 ml by slow distillation. Column chromatography of the crude triacetate through silica gel with hexane–ethyl acetate yielded 1.8 g of desired product: mp 109–111°; ^{1}H-NMR δ 7.20 (s, 10H, phenyl H), 5.80 (d, J = 10 Hz, 1H, C-22), 4.98 (peak, 1H, 12β-H), 4.88 (peak, 1H, 7β-H), 4.53 (hump, 1H, 3β-H), 2.15 (s, 3H, 12α-acetate), 2.07 (s, 3H, 7α-acetate), 2.02 (s, 3H, 3α-acetate), 0.95 (d, J = 6 Hz, 3H, C-20), 0.88 (s, 3H, C-19), and 0.52 (s, 3H, C-18).

3α,7α-Diacetoxy-12α-hydroxy-24,24-diphenyl-5β-chola-20(22),23-diene (IV*d*)—3α,7α,12α-Triacetoxy-24,24-diphenyl-5β-chola-20(22),23-diene was saponified and selectively acetylated to yield the title compound (IV*d*) after chromatography: mp 164–166°; ^{1}H-NMR δ 7.28 (s, 10H, phenyl H), 6.97 (d, J = 11 Hz, 1H, C-23), 6.03 (d, J = 11 Hz, 1H, C-22), 4.9 (peak, 1H, 7β-H), 4.53 (hump, 1H, 3β-H), 3.60 (peak, 1H, 12β-H), 2.03 (s, 3H, 7α-acetate), 2.02 (s, 3H, 3α-acetate), 1.95 (s, 3H, C-21), 0.92 (s, 3H, C-19), and 0.56 (s, 3H, C-18).

3α-Acetoxy-12-oxo-24,24-diphenyl-5β-chola-20(22),23-diene (IV*c*)—Monoene I*a* was synthesized by a published method [^{1}H-NMR δ 7.18 (s, 10H, phenyl H), 6.06 (t, 1H, C-23), 5.06 (peak 1H, 12β-H), 4.67 (hump, 1H, 3β-H), 2.07 (s, 3H, 12α-acetate), 2.01 (s, 3H, 3α-acetate), 0.91 (s, 3H, C-19), and 0.72 (s, 3H, C-18)]. The volume of a mixture of monoene I*a* (10.5 g) and carbon tetrachloride (400 ml) was reduced to 300 ml by distillation, *N*-bromosuccinimide (4.1 g) was added, and the mixture was photolyzed with a sun lamp (100 watts)while heating at reflux for 1 hr. The resulting mixture was filtered and heated at reflux for an additional 3 hr to complete the hydrogen bromide elimination. Column chromatography of the crude product through silica gel by gradient elution with hexane–ethyl acetate yielded 10 g of material that contained some unreacted monoene (<10% by NMR) but mainly comprised of diene IV*a*: ^{1}H-NMR δ 7.22 (s, 10H, phenyl H), 6.88 (d, J = 11 Hz, 1H, C-23), 5.92 (d, J = 11 Hz, 1H, C-22), 4.82 (peak, 1H, 7β-H), 4.57 (hump, 1H, 3β-H), 2.14 (s, 3H, 7α-acetate), 2.02 (s, 3H, 3α-acetate), 1.92 (s, 3H, C-23), 0.90 (s, 3H, C-19), and 0.60 (s, 3H, C-18). Saponification of IV*a* was achieved by heating at reflux with potassium hydroxide (10 g) and methanol (200 ml) for 3 hr. The reaction mixture was poured into ice (600 g) and the solid was collected by filtration. The dry solid was selectively acetylated by reacting with acetic anhydride (25 ml) and pyridine (25 ml) in benzene (125 ml) for 24 hr. Column chromatography produced 8 g of 3α-acetoxy-12α-hydroxy-24,24-diphenyl-5β-chola-20(22),23-diene: ^{1}H-NMR δ 7.30 (s, 10H, phenyl H), 6.98 (d, J = 11 Hz, 1H, C-23), 6.05 (d, J = 11 Hz, 1H, C-22), 4.75 (hump, 1H, 3β-H), 3.78 (peak, 1H, 12β-H), 2.02 (s, 3H, 3α-acetate), 1.97 (s, 3H, C-21), 0.93 (s, 3H, C-19), and 0.57 (s, 3H, C-18). Jones oxidation of this product was carried out in cold (5°) acetone (800 ml) to yield 4.0 g of IV*c*: mp 190–192°; $\bar{\nu}_{max}$ 1730 and 1240 (acetate), 1705 (12-oxo), and 1630 cm^{-1} (weak C=C stret); ^{1}H-NMR δ 7.23 (s, 10H, phenyl H), 6.90 (d, J = 11 Hz, 1H, C-23), 6.04 (d, J = 11 Hz, 1H, C-22), 4.67 (hump, 1H, 3β-H), 1.99 (s, 6H, 3α-acetate and C-20), 1.01 (s, 3H, C-18), and 0.88 (s, 3H, C-19).

Also, 0.8 g of 3,12-dioxo-24,24-diphenyl-5β-chola-20(22),23-diene [^{1}H-NMR δ 7.28 (s, 10H, phenyl H), 6.94 (d, J = 11 Hz, 1H, C-23), 6.07 (d, J = 11 Hz, 1H, C-22), 2.02 (s, 3H, C-21), 1.10 (s, 3H, C-18), and 0.92 (s, 3H, C-19)], and 1.2 g of 3α-acetoxy-12-oxo-5β-pregnan-20-one [^{1}H-NMR δ 4.68 (hump, 1H, 3β-H), 3.32 (t, 1H, 17α-H), 2.25 (s, 3H, C-21), 2.00 (s, 3H, 3α-acetate), 1.03 (s, 3H, C-18), and 0.95 (s, 3H, C-19)] were obtained.

3α,12α-Diacetoxy-24,24-diphenyl-5β-chol-23-ene (1*a*)—The synthesis of I*a* has been described (10); mass spectrum (12 ev), *m/z* (%): 596 (1, $[M]^+$), 536 (11, $[M-CH_3CO_2H]^+$), 476 (5, $[M-2CH_3CO_2H]^+$), 461 (1, $[M-2CH_3CO_2H-CH_3]^+$), 283 (6, $[M-2CH_3CO_2H-C_{15}H_{13}]^+$), 256 (9, $[M-CH_3CO_2H-C_{14}H_{12}]^+$), 246[3], 220 (100, $[C_{15}H_{13}]^+$), 205 (10, $[220-CH_3]^+$)*, 193 (10, $[C_{15}H_{13}]^+$), 180 (5, $[C_{14}H_{12}]^+$), and 167 (3, $[C_{13}H_{11}]^+$).

3α,7α-Diacetoxy-24,24-diphenyl-5β-chol-23-ene (1*b*)(1)—Mass spectrum (12 ev), *m/z* (%): 569 (1, $[M]^+$), 536 (7, $[M-CH_3CO_2H]^+$), 476 (3, $[M-2CH_3CO_2H]^+$), 343 (5, $[M-CH_3CO_2H-C_{15}H_{13}]^+$), 314[28], 313 (23, $[M-CH_3CO_2H-C_{17}H_{19}]^+$), 253 (100, $[M-2CH_3CO_2H-C_{17}H_{19}]^+$), 193 (33, $[C_{15}H_{13}]^+$), 180 (56, $[C_{14}H_{12}]^+$), and 149 [73].

3β-Acetoxy-24,24-diphenyl-5α-lanost-23-ene (VII)—Mass spectrum (12 ev), *m/z* (%): 580 (2, $[M]^+$), 565 (1, $[M-CH_3]^+$), 387 (2, $[M-C_{15}H_{13}]^+$), 357 (36, $[M-C_{17}H_{19}]^+$), 343[15], 327 (33, $[M-C_{15}H_{13}-CH_3CO_2H]^+$), 297 (6, $[M-C_{17}H_{19}-CH_3CO_2H]^+$), 283[3], 259[2], 231[3], 222[15], 217[15], 193 (22, $[C_{15}H_{13}]^+$), 180 (100, $[C_{14}H_{12}]^+$), 163[5], 149[4], 135[4], and 122[5].

REFERENCES

(1) J. R. Dias and B. Nassim, *Steroids*, **35**, 405 (1980).

(2) G. R. Pettit, P. Hofer, W. Bowyer, T. R. Kasturi, R. Bansal, R. Kadunce, and B. Green, *Tetrahedron*, **19**, 1143 (1963).

(3) J. R. Dias and R. Ramachandra, *J. Org. Chem.*, **42**, 1613 (1977).

(4) S. Wyllie and C. Djerassi, *ibid.*, **33**, 305 (1968).

(5) I. Massey and C. Djerassi, *ibid.*, **44**, 2448 (1979).

(6) C. Djerassi, N. Theobald, W. C. M. C. Kokke, C. S. Pak, and M. K. Carlson, *Pure Appl. Chem.*, **51**, 1815 (1979).

(7) C. Djerassi, *ibid.*, **50**, 171 (1978).

(8) J. R. Dias and B. Nassim, *Org. Mass. Spectrom.*, **13**, 402 (1978).

(9) J. R. Dias, R. Ramachandra, and B. Nassim, *ibid.*, **13**, 307 (1978).

(10) B. Riegel, R. Moffett, and A. McIntosh, *Org. Syn., Coll. Vol. III*, 234 (1955).

ACKNOWLEDGMENTS

This work was partially supported by the UMKC Research Council.

The author thanks Mr. Rickey Barbarash and Barbara J. Dias for their technical assistance. Also, the author expresses his appreciation to Professor G. R. Pettit for supplying a sample of compounds VII and VIII. The author thanks Dr. Marvin J. Karten, Contraceptive Development Branch, CPR, NICHD, National Institutes of Health, Bethesda, Md., for providing the biological assays.

A preliminary account of this work was presented at the 14th Midwest Regional Meeting of the ACS, Fayetteville, Ark., Oct. 26–27, 1978.

The Synthesis and Analgesic Activities of Some Spiro[indan-1,3′-pyrrolidine] Derivatives Designed as Rigid Analogs of Profadol

P. A. CROOKS *x and **R. SOMMERVILLE**

Received February 18, 1981, from the *Department of Pharmacy, University of Manchester, Manchester M13 9PL, England.* Accepted for publication July 17, 1981. * Present address: College of Pharmacy, University of Kentucky, Lexington, KY 40506.

Abstract □ Aromatic hydroxylated derivatives of spiro[indan-1,3′-pyrrolidine], designed as conformationally restricted analogs of profadol, were synthesized and pharmacologically evaluated in mice for analgesia and other central nervous system activities. None of the compounds synthesized were as potent as profadol in writhing and hot plate tests, but the 4-hydroxy derivative exhibited codeine-level analgesia in the tests.

Keyphrases □ Profadol—rigid analogs, spiro[indan-1,3′-pyrrolidine] derivatives, synthesis and analgesic activity □ Analgesic activity—evaluation of some spiro[indan-1,3′-pyrrolidine] derivatives, synthesis □ Spiro[indan-1,3′-pyrrolidine] derivatives—synthesis and evaluation for analgesic activity

As part of this laboratory's interest in the use of spiro-compounds as analgesic receptor probes (1–3), a series of spiro[tetralin-1,3′-pyrrolidine] (I) derivatives, designed as conformationally and rotationally restricted analogs of the analgesic drug, profadol (II), were synthesized recently and their analgesic activities determined. The present report describes the synthesis and analgesic activities of some structurally related spiro[indan-1,3′-pyrrolidine] (III) derivatives in which conformational flexibility is restricted more than in I.

EXPERIMENTAL[1]

Chemistry—*Ethyl 4-Methoxy-indanylidenecyanoacetate* (*IV*b)—A mixture of 4-methoxy-1-indanone (16.2 g, 0.1 mole), ethyl cyanoacetate (12.43 g, 0.11 mole), ammonium acetate (15.4 g, 0.2 mole), and acetic acid (48 g, 0.8 mole) in benzene (100 ml) was heated under reflux with a Dean and Stark water trap for 24 hr. The cooled reaction mixture was washed with water (3 × 100 ml), the washings extracted with benzene (2 × 50 ml) and the combined benzene liquors dried (magnesium sulfate) and concentrated to give crude product. Recrystallization from ethanol gave an analytical sample (Table I); NMR (dimethyl sulfoxide-d_6): δ 1.38 (t, 3H, OCH_2CH_3), 2.98 (m, 2H, indan-3 protons), 3.52 (m, indan-2 protons), 3.86 (s, 3H, OCH_3), 4.32 (q, 2H, OCH_2CH_3), 7.00 (1H, m, indan-5 proton), 7.29 (1H, m, indan-6 proton), and 8.26 (1H, m, indan-7 proton) ppm; IR: 2215 (C≡N) and 1720 (C=O) cm^{-1}.

Compounds IV*a*, IV*c*, and IV*d* were prepared similarly from the appropriately substituted 1-indanone[2] (Table I). The IR and NMR spectra were consistent with their assigned structures.

4-Methoxy-1-cyano-1-cyanomethylindane (*IVf*)—A solution of potassium cyanide (16.2 g, 0.25 mole) in water (50 ml) was added to a stirred solution of IV*b* (24.5 g, 0.1 mole) in absolute ethanol (200 ml) and the contents stirred at 65° for 16 hr. The mixture was then evaporated to dryness *in vacuo*, the residue suspended in water (200 ml) and extracted with ether (3 × 200 ml). The ether extracts were washed with water (2 × 50 ml), dried (magnesium sulfate), and the solvent evaporated to give a brown oil. This oil was vacuum distilled to give IV*f*, a colorless oil that crystallized on standing. Recrystallization from ethanol gave an analytical sample (Table I); NMR (deuterochloroform): δ 2.40 (m, 2H, indan-2 protons), 2.86 (s, 2H, CH_2CN), 2.97 (m, 2H, indan-3 protons), 3.80 (s, 3H, OCH_3), 6.83 (m, 1H, indan-5 proton), 7.12 (m, 1H, indan-6 proton), and 7.33 (m, 1H, indan-7 proton) ppm; IR: 2255 and 2240 (both C≡N) cm^{-1}.

Compounds IV*e*, IV*g*, and IV*h* were prepared similarly from IV*a*, IV*c*, and IV*d*, respectively. IR and NMR spectra were consistent with the assigned structures.

4-Methoxy spiro[indan-1,3′-pyrrolidine-2′,5′-dione] (*IVj*)—A suspension of IV*f* (21.2 g, 0.1 mole) in acetic acid (50 ml) and 78% (v/v) sulfuric acid (20 ml) was heated in an oil bath at 125° for 1 hr. The acetic acid was removed by *in vacuo* distillation and the resulting mass was suspended in water (50 ml) and extracted with ethyl acetate (3 × 300 ml). The organic phase was washed with saturated sodium bicarbonate solution (2 × 200 ml) and water (100 ml) and then dried (magnesium sul-

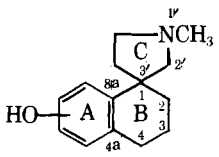

I

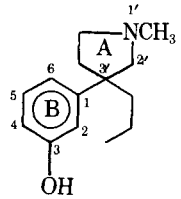

II

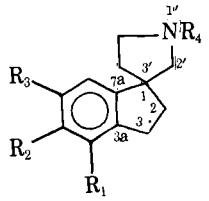

III

IIIa: $R_1 = R_2 = R_3 = R_4 = H$
IIIb: $R_1 = R_2 = R_3 = H$; $R_4 = CH_3$
IIIc: $R_1 = OCH_3$; $R_2 = R_3 = R_4 = H$
IIId: $R_1 = OCH_3$; $R_2 = R_3 = H$; $R_4 = CH_3$
IIIe: $R_1 = R_3 = R_4 = H$; $R_2 = OCH_3$
IIIf: $R_1 = R_3 = H$; $R_2 = OCH_3$; $R_4 = CH_3$
IIIg: $R_1 = R_2 = R_4 = H$; $R_3 = OCH_3$
IIIh: $R_1 = R_2 = H$; $R_3 = OCH_3$; $R_4 = CH_3$
IIIi: $R_1 = OH$; $R_2 = R_3 = R_4 = H$
IIIj: $R_1 = OH$; $R_2 = R_3 = H$; $R_4 = CH_3$
IIIk: $R_1 = R_3 = R_4 = H$; $R_2 = OH$
IIIl: $R_1 = R_3 = H$; $R_2 = OH$; $R_4 = CH_3$
IIIm: $R_1 = R_2 = R_4 = H$; $R_3 = OH$
IIIn: $R_1 = R_2 = H$; $R_3 = OH$; $R_4 = CH_3$

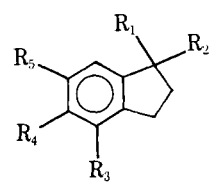

IV*a*–IV*l*
(Table I)

[1] Melting points were determined on a Reichert hot stage microscope and are uncorrected. IR spectra were determined as Nujol mulls on a Perkin-Elmer 237 spectrophotometer, and NMR spectra were determined on a Perkin-Elmer R12B instrument using tetramethylsilane as the internal standard.

[2] 1-Indanone and 5-methoxy-1-indanone were purchased from Aldrich Chemical Corp., 4-methoxy-1-indanone was prepared by the method of London and Razdan (4), and 6-methoxy-1-indanone was prepared by the method of House and Hudson (5).

0022-3549/82/0300-0291$01.00/0

Table I—Physical and Analytical Data for 1,1-Disubstituted Indane Derivatives

Compound	R_1	R_2	R_3	R_4	R_5	Yield, %	Melting Point	Formula	Analysis, % Calc.	Found
IV*a*	$=C(CN)CO_2C_2H_5$		H	H	H	61.7	103–104°	$C_{14}H_{13}NO_2$	C 74.0	74.2
									H 5.7	5.5
									N 6.2	6.1
IV*b*	$=C(CN)CO_2C_2H_5$		$-OCH_3$	H	H	33.1	175–178°	$C_{15}H_{15}NO_3$	C 70.0	70.0
									H 5.9	5.9
									N 5.4	5.3
IV*c*	$=C(CN)CO_2C_2H_5$		H	$-OCH_3$	H	50.8	165–167° (subl.)	$C_{15}H_{15}NO_3$	C —	70.1
									H —	6.0
									N —	5.3
IV*d*	$=C(CN)CO_2C_2H_5$		H	H	$-OCH_3$	20.4	137–139°	$C_{15}H_{15}NO_3$	C —	70.1
									H —	6.0
									N —	5.3
IV*e*	CN	CH_2CN	H	H	H	83.5	54–56°	$C_{12}H_{10}N_2$	C 79.1	79.4
									H 5.5	5.5
									N 15.4	15.4
IV*f*	CN	CH_2CN	$-OCH_3$	H	H	84.7	71.5–73°	$C_{13}H_{12}N_2O$	C 73.6	74.0
									H 5.7	5.8
									N 13.2	13.2
IV*g*	CN	CH_2CN	H	OCH_3	H	57.7	52–55°	$C_{13}H_{12}N_2O$	C —	73.4
									H —	5.8
									N —	12.8
IV*h*	CN	CH_2CN	H	H	OCH_3	50.8	86–88°	$C_{13}H_{12}N_2O$	C —	74.1
									H —	5.9
									N —	13.0
IV*i*	$-CONHCOCH_2-$		H	H	H	69.7	151–153°	$C_{12}H_{11}NO_2$	C 71.6	71.7
									H 5.5	5.55
									N 7.0	6.8
IV*j*	$-CONHCOCH_2-$		OCH_3	H	H	61.6	187–189°	$C_{13}H_{13}NO_3$	C 67.5	67.4
									H 5.7	5.7
									N 6.1	6.0
IV*k*	$-CONHCOCH_2-$		H	OCH_3	H	66.7	174–176°	$C_{13}H_{13}NO_3$	C —	67.4
									H —	5.4
									N —	6.1
IV*l*	$-CONHCOCH_2-$		H	H	OCH_3	73.0	154–156°	$C_{13}H_{13}NO_3$	C —	67.6
									H —	5.7
									N —	5.8

fate). Evaporation of the solvent gave the crude product which was recrystallized from absolute ethanol to give an analytical sample (Table I); NMR (dimethyl sulfoxide-d_6): δ 1.87–2.80 (m, 2H, indan-2 protons), 2.89–3.26 (m, 2H, indan-3 protons), 2.03 (s, 2H, pyrrolidine-4′ protons), 3.79 (s, 3H, OCH_3), 6.68 (m, 1H, indan-5 proton), 6.74 (m, 1H, indan-7 proton), 7.21 (m, 1H, indan-6 proton), and 8.50 (broad s, 1H, exchangeable with deuterium oxide, −NH) ppm; IR: 3190, 3075, 1780, 1725, and 1695 cm^{-1}.

Compounds IV*i*, IV*k*, and IV*l* were prepared similarly from IV*e*, IV*g*, and IV*h*, respectively; IR and NMR spectra were consistent with the assigned structures.

4-Methoxy spiro[indan-1,3′-pyrrolidine] (*III*c)—Finely divided IV*j* (23.1 g, 0.1 mole) was added slowly to a stirred suspension of aluminum lithium hydride (11.25 g, 0.3 mole) in dry tetrahydrofuran and the mixture refluxed for 24 hr. The excess aluminum lithium hydride was decomposed by careful addition of water, anhydrous magnesium sulfate was added, and the suspension was filtered. The filtrate was evaporated *in vacuo* to give a pale yellow oil which was distilled *in vacuo* to give III*c;* NMR (deuterochloroform): δ 1.78–2.22 (m, 4H, indan C-2 and C-4′ protons), 2.05 (s, 1H, exchangeable with deuterium oxide, NH), 2.69–2.97 (m, 2H, C-3 protons), 2.90 (s, 2H, C-2′ protons), 2.07–3.29 (m, 2H, C-5′ protons), 3.76 (s, 3H, OCH_3), 6.66 (m, 1H, C-5 proton), 6.80 (m, 1H, C-7 proton), and 7.17 (m, 1H, C-6 proton) ppm. The base was converted to the fumarate salt which was recrystallized from ethanol–ether to give an analytical sample (Table II).

Compounds III*a*, III*c*, and III*g* were prepared in a similar manner from IV*i*, IV*k*, and IV*l*, respectively and converted to the hydrochloride or fumarate salts (Table II). IR and NMR spectra were consistent with the assigned structures.

*4-Methoxy-*N*-methyl spiro[indan-1,3′-pyrrolidine]* (*III*d)—A solution of III*c* (2.0 g, 0.01 mole) in formic acid (2.3 g, 0.05 mole) and 40% formaldehyde solution (2 ml, 0.02 mole) was heated with stirring at 95° for 24 hr. The reaction mixture was diluted with 5% hydrochloric acid (5 ml) and extracted with ether (2 × 10 ml). The aqueous phase was made basic with concentrated ammonia solution, and extracted with ether (3 × 20 ml). The combined layers were washed with water (10 ml), dried (magnesium sulfate), and the solvent evaporated. The resulting oil was distilled *in vacuo* to give pure III*d;* NMR (deuterochloroform): δ 1.88–2.30 (m, 4H, C-2 and C-4′ protons), 2.35 (s, 3H, N—CH_3), 2.50–2.98 (m, 4H, C-3 and C-5′ protons), 2.64 (s, 2H, C-2′ protons), 3.77 (s, 3H, OCH_3), 6.64 (m, 1H, C-5 proton), 6.90 (m, 1H, C-7 proton), and 7.20 (m, 1H, C-6 proton) ppm. The base was converted to the fumarate salt which was recrystallized from ethanol–ether to give an analytical sample (Table II).

Compounds III*b*, III*f*, and III*h* were prepared in a similar manner from III*a*, III*e*, and III*g*, respectively, and converted to either their hydrochloride or fumarate salts (Table II). Their IR and NMR spectra were consistent with the assigned structures.

4-Hydroxy spiro[indan-1,3′-pyrrolidine]hydrobromide (*III*i)—A solution of III*c* (2.0 g, 0.01 mole) in 48% aqueous hydrobromic acid (25 ml) was refluxed under nitrogen for 1.5 hr. The yellow-brown solution was chilled to give buff crystals of III*i* which were recrystallized from ethanol–ether, giving an analytical sample (Table II); NMR (deuterium oxide): δ 1.80–2.20 (m, 4H, C-2 and C-4′ protons), 2.55–2.90 (m, 2H, C-3 protons), 3.21 (s, 2H, C-2′ protons), 3.24–3.68 (m, 2H, C-5′ protons), 6.51 (m, 1H,C-5 proton), 6.69 (m, 1H, C-7 proton), and 7.02 (m, 1H, C-6 proton) ppm; IR: 3210 (–OH), 2720 (NH) cm^{-1}.

Compounds III*j*–III*n* were prepared similarly from the appropriately substituted spiro[indan-1,3′-pyrrolidine]. Their IR and NMR spectra were all consistent with the assigned structures (Table II).

Pharmacology—Analgesia was determined by the acetic acid writhing test (6) in groups of six mice. Each group was dosed orally with either vehicle[3] or the compound under test and injected intraperitoneally 30 min later with dilute acetic acid (0.4 ml, 0.25%). Compounds showing analgesia at 50 mg/kg in that test were also tested for analgesia by the hot-plate method (7) (Table II).

Locomotor activity was determined using a battery of photobeam cages (30 × 12 × 9-cm) traversed by a beam of light. Interruptions of the beam were counted automatically. Groups of 10 mice were dosed and placed singly in the cages. After 45 min the total number of interruptions recorded and the percentage of inhibition or increase in movement relative to controls were determined.

Reversal of reserpine-induced hypothermia was assessed in groups of

[3] The testing vehicle used was "Dispersol," ICI Ltd., Pharmaceuticals Division, Macclesfield, UK, which consists of Lissapol NX (Ex ICI Dyestuffs Division, nonylphenol–ethylene oxide concentrate) (0.1%), "Lissapol" C** (sodium salt of sulfated cetyl/oleyl alcohol mixture) (0.1%), "Dispersol" OG** (polyglyceryl ricinoleate) (0.1%), and water (99.7%).

Table II—Physical, Chemical, and Pharmacological Data for Spiro[indan-1,3′-pyrrolidine] Derivatives

Compound	Yield, %	Melting Point	Formula	Analysis, % Calc.	Analysis, % Found	Writhing Test (Mice) ED_{50}, mg/kg po[a]
III*a* HCl	79.3	122–125°	$C_{12}H_{15}N$·HCl	C 68.7 H 7.7 N 6.7	68.7 7.6 6.6	>50
III*b* HCl	86.4	219–221°	$C_{13}H_{17}N$·HCl	C 69.8 H 8.1 N 6.3	69.7 8.2 6.4	13.9 (11.1–16.3)[b,c]
III*c* fumarate	98.9	188–195°	$C_{13}H_{17}NO{\cdot}C_4H_4O_4$	C 63.9 H 6.6 N 4.4	64.1 6.6 4.5	31.3 (23.2–39.6)[d]
III*d* fumarate	89.2	150–155°	$C_{14}H_{19}NO{\cdot}C_4H_4O_4$	C 64.9 H 6.9 N 4.2	65.1 7.1 4.2	*NA*
III*e* fumarate	89.8	168–175°	$C_{13}H_{17}NO{\cdot}C_4H_4O_4$	C 63.9 H 6.6 N 4.4	64.0 6.6 4.3	*NA*
III*f* fumarate	81.9	146–150°	$C_{14}H_{19}NO{\cdot}C_4H_4O_4$	C 64.9 H 6.9 N 4.2	64.7 6.7 3.8	*NA*
III*g* fumarate	92.4	124–130°	$C_{13}H_{17}NO{\cdot}C_4H_4O_4$	C 63.9 H 6.6 N 4.4	64.1 6.6 4.25	*NA*[e]
III*h* fumarate	93.5	140–147°	$C_{14}H_{19}NO{\cdot}C_4H_4O_4$	C 64.9 H 6.9 N 4.2	64.7 6.7 4.0	30.1 (19.1–38.2)[d]
III*i* HBr	75.2	181–187°	$C_{12}H_{15}NO$·HBr	C 53.4 H 6.0 N 5.2	53.3 6.1 5.3	12.5 (8.9–15.1)[f]
III*j* HBr	75.2	231–237°	$C_{13}H_{17}NO$·HBr	C 54.9 H 6.4 N 4.9	55.1 6.4 4.7	*NA*
III*k* HBr	92.8	222–229°	$C_{12}H_{15}NO$·HBr	C 53.4 H 6.0 N 5.2	53.6 6.1 5.2	>50
III*l* HBr	57.3	272–278°	$C_{13}H_{17}NO$·HBr	C 54.9 H 6.4 N 4.9	54.9 6.3 4.9	>50[g]
III*m* HBr	87.9	263–267°	$C_{12}H_{15}NO$·HBr	C 53.4 H 6.0 N 5.2	53.2 5.9 5.0	*NA*
III*n* HBr	94.3	182–187°	$C_{13}H_{17}NO$·HBr	C 54.9 H 6.4 N 4.9	54.8 6.3 4.9	*NA*
Morphine						1.4 (0.7–3.6)[h]

[a] Confidence limits in parentheses. [b] Effective at 30 mg/kg in reversing pentylenetetrazol-induced convulsions in mice. [c] Failed to exhibit a normal dose-response curve in the hot-plate test. [d] Not active at 50 mg/kg po in hot-plate test. [e] Exhibited central stimulant activity at 30 mg/kg in mice. [f] ED_{50} = 16.8 (11.6–25.3) mg/kg po in hot-plate test. [g] Caused a 90% reduction in motility at 30 mg/kg in mice. [h] ED_{50} = 3.8 (2.2–6.5) mg/kg po in hot-plate test. *NA* Not active at 100 mg/kg.

six mice as described previously (8) and based on the method of Askew (9).

Anticonvulsant activity was measured in groups of six mice subjected to the application of maximal electroshock (20 mamp for 0.22 sec *via* aural clip electrodes) or administration of the chemical convulsant, pentylenetetrazol (160 mg/kg subcutaneously). In each case, tonic extensor spasm was used as the end-point.

Impairment of motor coordination was assessed by measuring the ability of groups of six mice to balance on a stationary 1.3-cm diameter metal rod. Individual animals were placed on the rod and observed throughout the subsequent 20 sec. The time each mouse remained upon the rod was recorded and converted to a score. If the mouse balanced for the entire 20 sec, a score of 0 was given; if the mouse fell off after T sec, a score of $20 - T$ was given. Mice that fell off the rod on their first attempt were replaced for three more trials, providing a maximum possible score of 80. The mean score per mouse was determined and compared by standard statistical procedures with corresponding values obtained for groups treated with vehicle alone.

RESULTS

Chemistry—The syntheses of compounds IV*a*–IV*l* and III*a*–III*h* were carried out using procedures similar to those described previously for the preparation of the spiro[tetralin-1,3′-pyrrolidine] derivatives (3), but utilizing the appropriately substituted 1-indanone in place of the corresponding 1-tetralone. The appropriate 1-tetralone was condensed with ethylcyanoacetate to give the 1-indanylidenecyanoacetate derivative (IV*a*–IV*d*), which was reacted with potassium cyanide to give the corresponding 1-cyano-1-(cyanomethyl)indane (IV*e*–IV*h*). Treatment of compounds IV*e*–IV*h* with an acetic acid–sulfuric acid mixture gave the corresponding spiro[indan-1,3′-pyrrolidine-2′,5′-dione] derivatives (IV*i*–IV*l*). These compounds were then reduced with aluminum lithium hydride in tetrahydrofuran to give the appropriately substituted spiro[indan-1,3′-pyrrolidine] (III). *O*-Demethylation of compounds III*c*–III*h* was carried out under nitrogen in refluxing 48% hydrobromic acid containing 1% phosphoric acid. *N*-Methylation of compounds III*a*, III*c*, III*e*, and III*g* was accomplished in formic acid–formaldehyde solution (Tables I and II).

Pharmacology—Compounds III*b* and III*i* were the most active compounds in the series, exhibiting codeine-level analgesia, whereas compound III*j* showed no analgesic activity. None of the other hydroxylated derivative (III*k*–III*n*) showed any significant analgesic activity, although compound III*l* caused marked reduction in motility in mice at a 30-mg/kg dose, whereas compound III*g* exhibited central stimulant properties at 30 mg/kg in mice. Compound III*b* protected mice against pentylenetetrazol induced convulsions at 30 mg/kg. Compounds III*a*–III*n* were inactive in the maximal electroshock test, in reserpine antagonism tests, and did not produce any impairment of coordination in the stationary rod test.

DISCUSSION

An important feature of profadol (II) structure is the rotational freedom present in the molecule which allows a number of rotameric forms as the aromatic ring is rotated about the C1–C3′ bond. Thus, the weak analgesic activity exhibited by compounds of structure I possibly results from these compounds adopting conformations that are noncomplimentary with the receptor. Spiro[indan-1,3′-pyrrolidine] (III) derivatives may be regarded as profadol analogs, which are more conformationally rigid than the spiro system (I), since aromatic ring rotation is severely

restricted in III as a result of the reduction of ring B to a five-membered ring. Thus, compounds III*j*, III*l*, and III*n* represent interesting rigid analogs of II. Furthermore, molecular model examination of III*j* and morphine shows the phenolic and tertiary amino groups, and the aromatic ring in both compounds to be almost stereosuperimposable. In addition, it was of interest to find a patent describing some 3-hydroxyspiro[indan-1,3'-pyrrolidine] derivatives as orally active analgesics (10). Profadol is thought to interact with the analgesic receptor in the half-chair conformation (11).

Although the spiro systems I and III represent structural analogs in which the profadol molecule is fixed in a conformation related to the morphine molecule, these compounds exhibit only weak or insignificant analgesic properties. Thus, other structural features appear to be important in profadol-receptor interaction. The inability of these spiro analogs to enhance or maintain the analgesic properties of profadol may be related to a decreased fit of these compounds at the receptor due to the rigid orientation of the B ring in these compounds, which represents a fixed, and perhaps undesirable, conformation of the 3-propyl group in II.

REFERENCES

(1) P. A. Crooks and H. E. Rosenberg, *J. Med. Chem.*, **21**, 585 (1978).

(2) P. A. Crooks and H. E. Rosenberg, *J. Chem. Soc., Perkin I*, **1979**, 2719.

(3) P. A. Crooks and R. Szyndler, *J. Med. Chem.*, **23**, 679 (1980).

(4) J. D. London and R. K. Razdan, *J. Chem. Soc.*, **1954**, 4299.

(5) H. O. House and C. B. Hudson, *J. Org. Chem.*, **35**, 647 (1970).

(6) C. Vander Wende and S. Margolin, *Fed. Proc., Fed. Am. Soc. Exp. Biol.*, **15**, 494 (1956).

(7) J. A. J. Jannsen and A. H. Ingeneau, *J. Pharm. Pharmacol.*, **9**, 381 (1957).

(8) D. T. Greenwood and A. R. Sommerville, *Psychopharmacologia*, **24**, 231 (1972).

(9) B. M. Askew, *Life Sci.*, **2**, 725 (1963).

(10) J. M. Bastian, K. Hasspacker, and M. Strasser, *Ger. Offen.*, 2,241,027 (1973); through *Chem. Abstr.*, **78**, 159422W (1974).

(11) A. S. Horn and J. R. Rodgers, *Nature (London)*, **260**, 795 (1976).

ACKNOWLEDGMENTS

The authors are grateful to Imperial Chemical Industries, Ltd. for effecting pharmacological evaluations and to the Pharmaceutical Society of Great Britain for awarding a research scholarship to R. Sommerville.

Quantitation of Hydroxyprogesterone Caproate, Medroxyprogesterone Acetate, and Progesterone by Reversed-Phase High-Pressure Liquid Chromatography

V. DAS GUPTA

Received March 20, 1981, from the *University of Houston, College of Pharmacy, Houston, TX 77030.* Accepted for publication June 29, 1981.

Abstract □ A high-pressure liquid chromatographic method for the quantitation of hydroxyprogesterone caproate, medroxyprogesterone acetate, and progesterone in pharmaceutical dosage forms was developed. The method gave accurate, precise, and reproducible results. The excipients present in the dosage forms did not interfere with the assay procedure except benzyl benzoate in progesterone injection. The percent relative standard deviations based on six injections were 1.6, 2.5, and 2.7% for hydroxyprogesterone caproate, medroxyprogesterone acetate, and progesterone, respectively. The stability of progesterone in ethanol–propylene glycol–water (10:50:40) was studied. The loss in potency of progesterone, even after 487 days of storage at 50°, was <10%.

Keyphrases □ Hydroxyprogesterone caproate—quantitation by reversed-phase high-pressure liquid chromatography □ Medroxyprogesterone acetate—quantitation by reversed-phase high-pressure liquid chromatography □ Progesterone—quantitation by reversed-phase high-pressure liquid chromatography □ High-pressure liquid chromatography—quantitation of hydroxyprogesterone caproate, medroxyprogesterone acetate, and progesterone

The pharmaceutical dosage forms of hydroxyprogesterone caproate (I), medroxyprogesterone acetate (II), and progesterone (III) are used extensively. The USP method (1) for the quantitative determination of I in dosage forms is based on a reaction with isoniazid. The color produced is measured spectrophotometrically.

For dosage forms of II, the USP method (2) requires normal phase high-pressure liquid chromatography (HPLC) with a porous silica column. The quantitation of III requires reversed-phase chromatography (3). The 1-m column for this procedure has to be packed with octadecylsilane chemically bonded to silica gel. The USP method (3) appears to be a modification of a procedure recommended previously (4).

This investigation attempted to develop a reversed-phase HPLC method (with prepacked column) suitable for the quantitation of I, II, and III in pharmaceutical dosage forms. The stability of III in some aqueous systems was also determined.

EXPERIMENTAL

Reagents and Chemicals—All reagents and chemicals were ACS, USP, or NF grade and were used as received. 17-Hydroxyprogesterone[1], hydroxyprogesterone caproate[1], medroxyprogesterone acetate[2], and progesterone[3] were used without further purification.

Apparatus—The chromatograph[4] was connected to a multiple-wavelength detector[5], a recorder[6], and an integrator[7]. All pH values were determined using a pH meter[8].

Column—The column[9] (30 cm × 4-mm i.d.) was of a semipolar material consisting of a monomolecular layer of cyanopropylsilane permanently bonded by silicone–carbon bonds.

Chromatographic Conditions—The mobile phase contained 30%

[1] E. R. Squibb & Sons, Princeton, N.J.
[2] The Upjohn Co., Kalamazoo Mich.
[3] Aldrich Chemical Co., Milwaukee, Wis.
[4] Model ALC 202 equipped with a U6K universal injector, Waters Associates, Milford, Mass.
[5] Spectroflow monitor SF770, Schoeffel Instruments Corp., Westwood, N.J.
[6] Omniscribe 5213-12, Houston Instruments, Austin, Tex.
[7] Autolab minigrator, Spectra-Physics, Santa Clara, Calif.
[8] Model 4500 digital pH meter, Beckman Instruments, Irvine, Calif.
[9] μBondapak/CN, Waters Associates, Milford, Mass.

0022-3549/82/0300-0294$01.00/0

restricted in III as a result of the reduction of ring B to a five-membered ring. Thus, compounds III*j*, III*l*, and III*n* represent interesting rigid analogs of II. Furthermore, molecular model examination of III*j* and morphine shows the phenolic and tertiary amino groups, and the aromatic ring in both compounds to be almost stereosuperimposable. In addition, it was of interest to find a patent describing some 3-hydroxyspiro[indan-1,3'-pyrrolidine] derivatives as orally active analgesics (10). Profadol is thought to interact with the analgesic receptor in the half-chair conformation (11).

Although the spiro systems I and III represent structural analogs in which the profadol molecule is fixed in a conformation related to the morphine molecule, these compounds exhibit only weak or insignificant analgesic properties. Thus, other structural features appear to be important in profadol-receptor interaction. The inability of these spiro analogs to enhance or maintain the analgesic properties of profadol may be related to a decreased fit of these compounds at the receptor due to the rigid orientation of the B ring in these compounds, which represents a fixed, and perhaps undesirable, conformation of the 3-propyl group in II.

REFERENCES

(1) P. A. Crooks and H. E. Rosenberg, *J. Med. Chem.*, **21**, 585 (1978).

(2) P. A. Crooks and H. E. Rosenberg, *J. Chem. Soc., Perkin I*, **1979**, 2719.

(3) P. A. Crooks and R. Szyndler, *J. Med. Chem.*, **23**, 679 (1980).

(4) J. D. London and R. K. Razdan, *J. Chem. Soc.*, **1954**, 4299.

(5) H. O. House and C. B. Hudson, *J. Org. Chem.*, **35**, 647 (1970).

(6) C. Vander Wende and S. Margolin, *Fed. Proc., Fed. Am. Soc. Exp. Biol.*, **15**, 494 (1956).

(7) J. A. J. Jannsen and A. H. Ingeneau, *J. Pharm. Pharmacol.*, **9**, 381 (1957).

(8) D. T. Greenwood and A. R. Sommerville, *Psychopharmacologia*, **24**, 231 (1972).

(9) B. M. Askew, *Life Sci.*, **2**, 725 (1963).

(10) J. M. Bastian, K. Hasspacker, and M. Strasser, *Ger. Offen.*, 2,241,027 (1973); through *Chem. Abstr.*, **78**, 159422W (1974).

(11) A. S. Horn and J. R. Rodgers, *Nature (London)*, **260**, 795 (1976).

ACKNOWLEDGMENTS

The authors are grateful to Imperial Chemical Industries, Ltd. for effecting pharmacological evaluations and to the Pharmaceutical Society of Great Britain for awarding a research scholarship to R. Sommerville.

Quantitation of Hydroxyprogesterone Caproate, Medroxyprogesterone Acetate, and Progesterone by Reversed-Phase High-Pressure Liquid Chromatography

V. DAS GUPTA

Received March 20, 1981, from the *University of Houston, College of Pharmacy, Houston, TX 77030.* Accepted for publication June 29, 1981.

Abstract □ A high-pressure liquid chromatographic method for the quantitation of hydroxyprogesterone caproate, medroxyprogesterone acetate, and progesterone in pharmaceutical dosage forms was developed. The method gave accurate, precise, and reproducible results. The excipients present in the dosage forms did not interfere with the assay procedure except benzyl benzoate in progesterone injection. The percent relative standard deviations based on six injections were 1.6, 2.5, and 2.7% for hydroxyprogesterone caproate, medroxyprogesterone acetate, and progesterone, respectively. The stability of progesterone in ethanol–propylene glycol–water (10:50:40) was studied. The loss in potency of progesterone, even after 487 days of storage at 50°, was <10%.

Keyphrases □ Hydroxyprogesterone caproate—quantitation by reversed-phase high-pressure liquid chromatography □ Medroxyprogesterone acetate—quantitation by reversed-phase high-pressure liquid chromatography □ Progesterone—quantitation by reversed-phase high-pressure liquid chromatography □ High-pressure liquid chromatography—quantitation of hydroxyprogesterone caproate, medroxyprogesterone acetate, and progesterone

The pharmaceutical dosage forms of hydroxyprogesterone caproate (I), medroxyprogesterone acetate (II), and progesterone (III) are used extensively. The USP method (1) for the quantitative determination of I in dosage forms is based on a reaction with isoniazid. The color produced is measured spectrophotometrically.

For dosage forms of II, the USP method (2) requires normal phase high-pressure liquid chromatography (HPLC) with a porous silica column. The quantitation of III requires reversed-phase chromatography (3). The 1-m column for this procedure has to be packed with octadecylsilane chemically bonded to silica gel. The USP method (3) appears to be a modification of a procedure recommended previously (4).

This investigation attempted to develop a reversed-phase HPLC method (with prepacked column) suitable for the quantitation of I, II, and III in pharmaceutical dosage forms. The stability of III in some aqueous systems was also determined.

EXPERIMENTAL

Reagents and Chemicals—All reagents and chemicals were ACS, USP, or NF grade and were used as received. 17-Hydroxyprogesterone[1], hydroxyprogesterone caproate[1], medroxyprogesterone acetate[2], and progesterone[3] were used without further purification.

Apparatus—The chromatograph[4] was connected to a multiple-wavelength detector[5], a recorder[6], and an integrator[7]. All pH values were determined using a pH meter[8].

Column—The column[9] (30 cm × 4-mm i.d.) was of a semipolar material consisting of a monomolecular layer of cyanopropylsilane permanently bonded by silicone–carbon bonds.

Chromatographic Conditions—The mobile phase contained 30%

[1] E. R. Squibb & Sons, Princeton, N.J.
[2] The Upjohn Co., Kalamazoo Mich.
[3] Aldrich Chemical Co., Milwaukee, Wis.
[4] Model ALC 202 equipped with a U6K universal injector, Waters Associates, Milford, Mass.
[5] Spectroflow monitor SF770, Schoeffel Instruments Corp., Westwood, N.J.
[6] Omniscribe 5213-12, Houston Instruments, Austin, Tex.
[7] Autolab minigrator, Spectra-Physics, Santa Clara, Calif.
[8] Model 4500 digital pH meter, Beckman Instruments, Irvine, Calif.
[9] μBondapak/CN, Waters Associates, Milford, Mass.

0022-3549/82/0300-0294$01.00/0

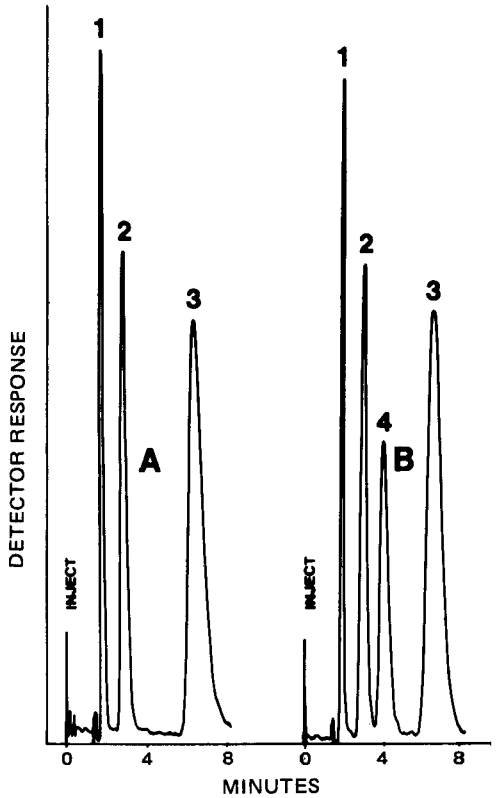

Figure 1—*Sample chromatograms. Peaks 1–3 are from the solvent, internal standard (17-hydroxyprogesterone) and I, respectively. Peak 4 in chromatogram B is from benzyl benzoate. Key: A, standard solution; and B, injection of I. The chromatographic conditions are given in the text.*

by volume (40% by volume for I) of methanol in 0.02 *M* aqueous solution of monobasic potassium phosphate. The temperature was ambient and the flow rate was 2.0 ml/min. The detector was set at 0.04 (254 nm) and the chart speed was 30.5 cm/hr.

Solution Preparation—The stock solutions of I, II, and III were prepared by dissolving 100.0 mg of the compound in enough ethanol to make 100.0 ml. The standard solutions were prepared as needed by diluting the stock solutions either with ethanol or dilute ethanol (50% by volume in water). Before final dilution, an appropriate quantity of the internal standard (17-hydroxyprogesterone for I and hydrocortisone for II and III) was added. The final concentration of the internal standard was always 20 μg/ml. The stock solutions of internal standards were also prepared by dissolving 100.0 mg of the substance in enough ethanol to make 100.0 ml.

Preparation of Progesterone Solutions for Stability Studies—A 10.0-ml quantity of the III solution (10.0 mg/ml in ethanol) was mixed with 50.0 ml of propylene glycol and the mixture was brought to volume (100.0 ml) with either water or a 0.125 *M* phosphate buffer of an appropriate pH value.

After the initial assays, the solutions were divided into two parts and stored in amber bottles[10] (60-ml capacity) at 25 and 50°.

Assay Solutions—One milliliter of the commercially available hydroxyprogesterone caproate injection (250 mg/ml) was diluted to 100.0 ml with ethanol. In addition to I, the injection also contained 46% of benzyl benzoate and castor oil *q.s.*; a 1.2 ml of this solution was mixed with 1.0 ml of the internal standard (a 1.0 mg/ml solution of 17-hydroxyprogesterone in ethanol) and the mixture was brought to volume (50.0 ml) with ethanol.

Medroxyprogesterone Acetate Suspension (400 mg/ml)—A 2.0-ml quantity of the well-shaken suspension was diluted to 1000.0 ml (to 250 ml when the concentration of II in suspension was 100 mg/ml) with ethanol. Then 2.5 ml of the clear mixture was further diluted to 50.0 ml (before diluting, 1.0 ml of the internal standard was added) with ethanol. In addition to II, the suspension contained (per milliliter) polyethylene glycol 4000, 20.3 mg; sodium sulfate anhydrous, 11 mg; and myristyl-γ-picolinium chloride, 1.7 mg.

[10] Made of Sera glass, Brockway Glass Co., Brockway, Pa.

Table I—Assay Results of Dosage Forms

Type of Dosage Form	Active Ingredient	Percent of the Label Claim Found[a] (Proposed HPLC Method)	USP XX–NF XV Method
Injection	I	99.2	100.1
Injection (different lot)	I	100.8	100.7
Synthetic mixture similar to above injection	I	100.2	100.1
Suspension	II	98.6	—[b]
Suspension (different lot)	II	99.2	—[b]
Tablets	II	99.1	—[b]
Tablets (different lot)	II	100.7	—[b]
Injection	III	132.8[c]	—[b]
Suspension	III	95.6	—[b]
Suspension (different lot)	III	96.3	—[b]
Synthetic mixture similar to above suspension	III	99.7	—[b]

[a] Average of three assays. Reproducibility on different days was within ±1.5%. [b] Not assayed using USP–NF method which is also based on HPLC. [c] Results are high because of interference from benzyl benzoate with the assay procedure.

Medroxyprogesterone Acetate Tablets (10 mg/Tablet)—Ten tablets were ground to a fine powder and stirred with ~50 ml of ethanol. The mixture was transferred to a 100-ml volumetric flask and more ethanol rinses were added to bring it to volume. The mixture was filtered[11], 20 ml of the filtrate was rejected and then 2.0 ml of the filtrate was mixed with 1.0 of the internal standard (hydrocortisone solution in

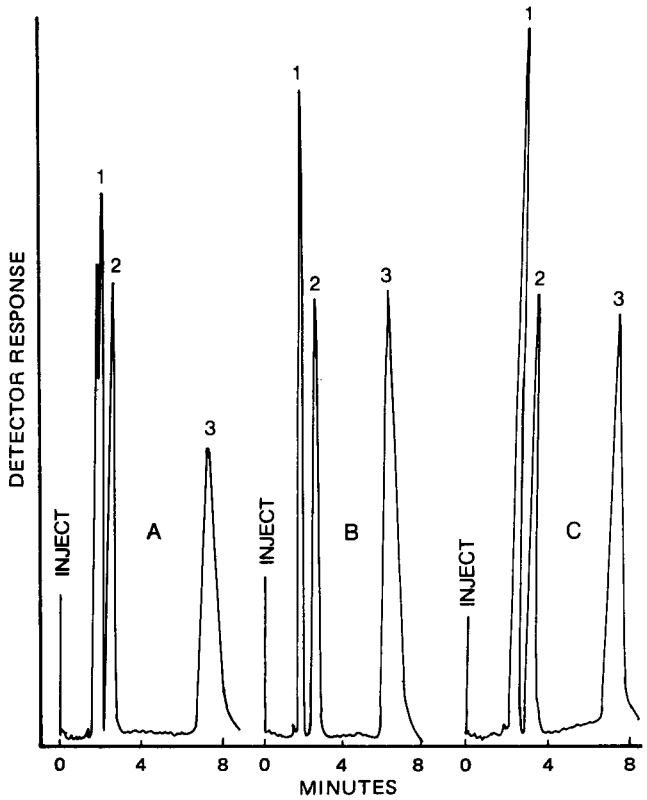

Figure 2—*Sample chromatograms. Peaks 1 and 2 are from the solvent and the internal standard (hydrocortisone), respectively. Peak 3 in chromatogram A is from II and in chromatograms B and C from III. Key: A, suspension of II; B, standard solution of III in ethanol; and C, suspension of III. The chromatographic conditions are given in the text.*

[11] Whatman No. 1 filter paper.

Table II—Assay Results[a] of Aqueous Solutions of Progesterone Compounded for Stability Studies

Solution[b]	pH (±0.1)[c]	Assay Results after (days) Based on 100% on Day 0				
		48	120	240	360	487
1 (Unbuffered)	5.7	99.3	100.1	99.7	98.9	99.4
2 (Buffered)	5.0	99.9	99.5	98.9	97.4	92.5
3 (Buffered)	5.6	100.2	100.1	100.1	99.8	94.9
4 (Buffered)	6.6	99.9	101.0	100.1	99.1	95.2
5 (Buffered)	7.5	100.8	100.8	99.7	98.1	95.2

[a] For samples stored at 50°. The results of samples stored at 25° did not indicate any decomposition, even in 487 days. [b] All other solutions were diluted with 0.125 *M* KH_2PO_4 solution of an appropriate pH value except solution 1, which was diluted with water. [c] pH values of the solutions.

ethanol, 1 mg/ml), and the mixture was brought to volume (50.0 ml) with ethanol. The list of the excipients was not disclosed on the label.

Progesterone Aqueous Suspension (50 mg/ml)—The suspension was shaken well, and 2.0 ml was transferred to a 100-ml volumetric flask and brought to volume with ethanol. The mixture was filtered[11] if necessary, and 2.0 ml of the clear solution was mixed with 1.0 ml of the internal standard (1 mg/ml solution of hydrocortisone in ethanol) and brought to volume (50.0 ml) with ethanol. In addition to III, the suspension contained (per milliliter) sodium carboxymethylcellulose, 2 mg; methylcellulose, 0.3 mg; dioctyl sodium sulfosuccinate, 0.15 mg; and thimerosal, 0.08 mg.

Progesterone Injection (50 mg/ml)—A 2.0-ml quantity of the injection was extracted with ethanol (85% by volume in water) according to the procedure recommended by King *et al.* (4), and the extracts were brought to volume (100.0 ml) with 85% ethanol. A 2.0-ml quantity of the clear solution was further diluted to 50.0 ml with dilute ethanol (50% by volume in water). Before diluting, 1.0 ml of the internal standard was added as already described. In addition to III, the injection contained 20% benzyl benzoate, 0.5% phenol, and peanut oil *q.s.*

Progesterone Solutions for Stability Studies—A 2.0-ml quantity of the solution was mixed with 1.0 ml of the internal standard and the mixture was brought to volume (50.0 ml) with dilute ethanol.

Assay Procedure—A 20.0-μl aliquot of the assay solution was injected into the chromatograph using the described conditions. For comparison, an identical volume of the appropriate standard solution was injected after the assay solution eluted. The standard solutions contained identical concentrations of the drug (based on label claim of the assay) and the internal standard and were diluted using the identical solvent (ethanol or dilute ethanol).

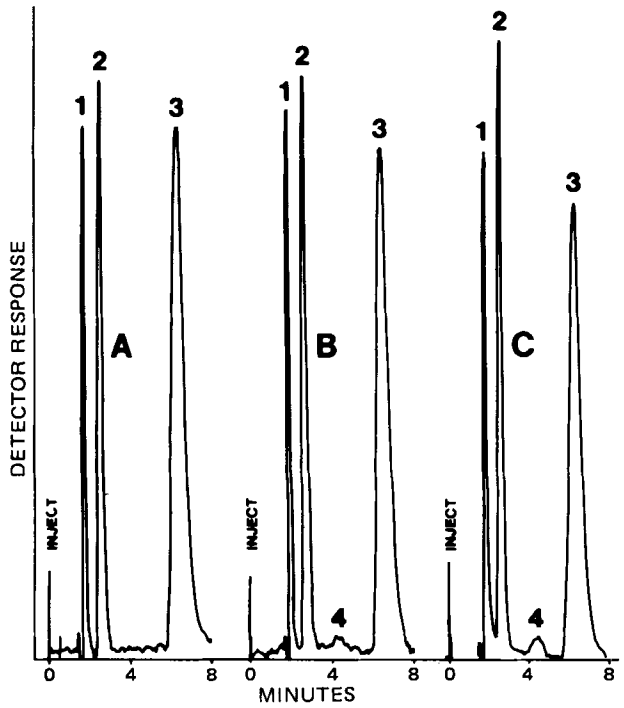

Figure 3—*Sample chromatograms. Peaks 1–3 are from the solvent, hydrocortisone (internal standard), and III, respectively. Peak 4 in chromatograms B and C is from the decomposition product of III. Key: A, standard solution of III in 50% ethanol; B, solution 3 (Table II) after 487 days of storage at 50°; and C, solution of III after boiling with 1* N *NaOH. The chromatographic conditions are given in the text.*

Preliminary studies were conducted to determine the interferences from the excipients with the assay procedure. No interference was found except from benzyl benzoate present in progesterone injection.

Calculations—Since preliminary investigations indicated that peak heights (also the peak areas) were directly related to the concentrations (ranges tested were 0.4–1.6 μg for I and 0.4–1.2 μg for II and III), the results were calculated using

$$\text{percent of label claim} = \frac{(R_{ph})_a}{(R_{ph})_s} \times 100 \qquad \text{(Eq. 1)}$$

where $(R_{ph})_a$ is the ratio of the peak heights of the drug in the assay solution and the internal standard and $(R_{ph})_s$ for the standard solution of identical concentrations. The results are presented in Tables I and II and Figs. 1–3.

Other Experiments—A 2.0-ml quantity of the stock solution of III was mixed with either 2.0 ml of ~0.1 *N* NaOH or 0.1 *N* HCl solution and allowed to stand for 24 hr. The internal standard was then added, and the mixture was brought to volume (50.0 ml) with dilute ethanol and assayed.

In another experiment, 2.0 ml of the stock solution of III was mixed with 1.0 ml of ~1 *N* NaOH solution and 20 ml of dilute ethanol. The mixture was boiled for ~5 min on a hot plate and cooled to room temperature. The internal standard was then added, and the mixture was brought to volume and assayed. The result is presented in Fig. 3C.

RESULTS AND DISCUSSION

Hydroxyprogesterone Caproate—The assay results (Table I) indicate that the proposed HPLC method can be adopted for the quantitative determination of I in injectables. The castor oil and benzyl benzoate present in the injection did not interfere with the assay procedure. Benzyl benzoate gave a separate peak between the internal standard and the drug (peak 2 in Fig. 1B).

No preliminary procedure to extract I from the injectable solution was required. The percent relative standard deviation based on six injections was 1.6. The method was reproducible.

Medroxyprogesterone Acetate—The assay results (Table I) indicate that HPLC is a reliable method for the quantitation of II in suspension and tablets. A very simple procedure was required to extract II from the tablets, while the suspension did not require preliminary extraction. None of the excipients present in suspension (polyethylene glycol 4000, sodium sulfate, and myristyl-γ-picolinium chloride) interfered with the assay procedure (Fig. 2A). The chromatogram obtained from tablets was similar to Fig. 2A.

The percent relative standard deviation based on six injections was 2.5% and the assay method was reproducible.

Progesterone—The assay results of suspensions (Table I) indicate that the HPLC method can be used for the quantitation of III in suspension. However, in the case of injection, the benzyl benzoate interfered. It had the same retention time as of III; therefore, the assay results were high (Table I).

The excipients present in the suspension (sodium carboxymethylcellulose, methylcellulose, dioctyl sodium sulfosuccinate, and thimerosal) did not interfere with assay procedure (Fig. 2C). The percent relative standard deviation based on six injections was 2.7% and the method was reproducible.

The stability results (Table II) indicate that progesterone is a very stable compound in the vehicle (ethanol, 10%; propylene glycol, 50%; and water, 40%) studied. Even in 487 days of storage at 50°, the decomposition in all the solutions was <10%. This is equal to at least 5 years of storage at room temperature. The samples which were stored at room temperature did not decompose at all, even in 487 days.

In other experiments, the progesterone did not decompose in 24 hr on treating with 0.1 *N* HCl and with 0.1 *N* NaOH, the loss in potency was ~4%. On boiling with 1 *N* NaOH for 5 min, the sample lost slightly more than 16% of the potency. An additional peak between the peaks of the

internal standard (hydrocortisone) and III was obtained (Fig. 3C) in the chromatogram.

REFERENCES

(1) "USP XX-NF XV," U.S. Pharmacopeial Convention, Rockville, MD, 1980, p. 386.

(2) *Ibid.*, p. 468.

(3) *Ibid.*, pp. 666–667.

(4) R. H. King, L. T. Grady, and J. T. Reamer, *J. Pharm. Sci.*, **63**, 1591 (1974).

A Time-Lag Model for Pharmacokinetics of Drugs Subject to Enterohepatic Circulation

JEAN-LOUIS STEIMER*x, YVES PLUSQUELLEC‡, ANNE GUILLAUME*, and JEAN-FRANÇOIS BOISVIEUX*

Received August 1, 1980, from the **INSERM U 194, Département de Biomathématiques, 91, Bd de l'Hôpital, F-75634 Paris Cedex 13, France and the ‡Laboratorie d'Algèbre, Département de Mathématiques, Université Paul-Sabatier, F-31000 Toulouse, France.* Accepted for publication June 29, 1981.

Abstract □ A two-compartment model with time lag is proposed to describe the pharmacokinetics of drugs subject to enterohepatic circulation. The basic model, including two compartments for body and GI tract, respectively, with elimination occurring from both compartments, was previously proposed. The assumption that the reabsorption of a drug molecule is delayed after its biliary excretion is expressed by the addition of a time lag in the transfer from the first to the second compartment. Computer simulation of the model for intravenous bolus injection and oral intake of the drug was performed through first-order numerical integration. Several qualitative results concerning changes in pharmacokinetics due to modifications in biliary excretion, in reabsorption, or in elimination are identical with predictions using the basic model. However, several qualitative and quantitative results were significantly different. The pharmacokinetics, though remaining linear, are no longer biexponential. Initial decay after intravenous injection was not affected by modifications in reabsorption or elimination from intestine. Predictions based on the time-delay model agree with existing experimental evidence concerning pharmacokinetics of substances undergoing enterohepatic cycling. Delayed recirculation may lead to rebounds in plasma level profiles as well as after intravenous and oral administration. The half-life of the drug is significantly prolonged even when the kinetic processes involved in recirculation remain unchanged.

Keyphrases □ Pharmacokinetics—time-lag model, enterohepatic drug circulation □ Models, pharmacokinetic—enterohepatic drug circulation, time-lag model □ Enterohepatic circulation—drugs, pharmacokinetics, time-lag model

When a substance is taken up by the liver and excreted into the bile, it may be either eliminated through the GI tract or reabsorbed and carried to the liver *via* the portal blood stream. This second process is known as enterohepatic cycling. This phenomenon affects both endogenous and exogenous substances.

BACKGROUND

A two-compartment model was previously developed (1) representing the body and the GI tract. Qualitative modifications in pharmacokinetic time-profiles and parameters for drugs subject to enterohepatic cycling due to changes in biliary excretion and reabsorption rates are well depicted by this model.

Predictions of the two-compartment model agree with previous experimental results (1, 2). However, some discrepancies, such as the evidence of a secondary peak in the time course of serum concentrations, remain. Such a secondary peak was reported (3) appearing after intravenous, oral, and intraportal administration of morphine in rats. An eight-compartment model for morphine pharmacokinetics was proposed. The GI tract compartment of Harrison and Gibaldi (1) is split into a catenary system of three compartments forming a loop connected with the central compartment. Experimental evidence for a secondary peak in plasma radioactivity time profiles, as well as subsequent very slow elimination kinetics exist for labeled vitamin D_3 in humans (4) and rats (5). The main active metabolite of vitamin D_3 undergoes enterohepatic cycling (6).

A modification of the two-compartment enterohepatic recirculation model is proposed to take into account these previous experimental findings. The basic assumption is that a time-delay exists between the excretion of a given molecule of the substance into bile and its reabsorption from the intestine. This time lag may be due to delayed biotransformation in the liver, to the storage of the substance in the gallbladder (*e.g.*, in humans), or simply to its transport in bile, at a limited flow-rate, from the site of excretion to the site of reabsorption. The corresponding time-delay model proposed here exhibits qualitative agreement with the two basic observations on pharmacokinetics of drugs subject to enterohepatic circulation: first, the occurrence of "rebounds" in serum level profiles after intravenous and oral administration of drug; and second, the slow terminal kinetics of the drug when recirculation occurs, even when the processes of deconjugation and reabsorption are not rate-limiting.

THEORETICAL

Mathematical Formulation—The model presented in Scheme I is a two-compartment system differing from the basic model of Harrison

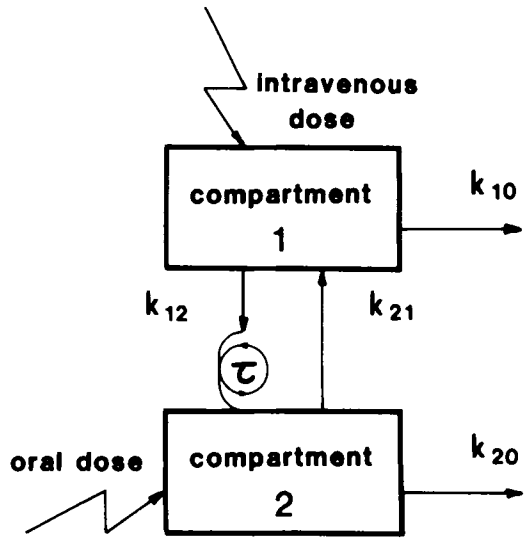

Scheme I—Time-lag pharmacokinetic model for a drug subject to enterohepatic circulation. Compartment 1 represents the body including the liver. Compartment 2 represents the GI tract. Existence of a time delay is assumed after biliary excretion, before reabsorption can occur.

0022-3549/82/0300-0297$01.00/0

internal standard (hydrocortisone) and III was obtained (Fig. 3C) in the chromatogram.

REFERENCES

(1) "USP XX-NF XV," U.S. Pharmacopeial Convention, Rockville, MD, 1980, p. 386.

(2) *Ibid.*, p. 468.

(3) *Ibid.*, pp. 666–667.

(4) R. H. King, L. T. Grady, and J. T. Reamer, *J. Pharm. Sci.*, **63**, 1591 (1974).

A Time-Lag Model for Pharmacokinetics of Drugs Subject to Enterohepatic Circulation

JEAN-LOUIS STEIMER*x, YVES PLUSQUELLEC‡, ANNE GUILLAUME*, and JEAN-FRANÇOIS BOISVIEUX*

Received August 1, 1980, from the **INSERM U 194, Département de Biomathématiques, 91, Bd de l'Hôpital, F-75634 Paris Cedex 13, France and the ‡Laboratorie d'Algèbre, Département de Mathématiques, Université Paul-Sabatier, F-31000 Toulouse, France.* Accepted for publication June 29, 1981.

Abstract □ A two-compartment model with time lag is proposed to describe the pharmacokinetics of drugs subject to enterohepatic circulation. The basic model, including two compartments for body and GI tract, respectively, with elimination occurring from both compartments, was previously proposed. The assumption that the reabsorption of a drug molecule is delayed after its biliary excretion is expressed by the addition of a time lag in the transfer from the first to the second compartment. Computer simulation of the model for intravenous bolus injection and oral intake of the drug was performed through first-order numerical integration. Several qualitative results concerning changes in pharmacokinetics due to modifications in biliary excretion, in reabsorption, or in elimination are identical with predictions using the basic model. However, several qualitative and quantitative results were significantly different. The pharmacokinetics, though remaining linear, are no longer biexponential. Initial decay after intravenous injection was not affected by modifications in reabsorption or elimination from intestine. Predictions based on the time-delay model agree with existing experimental evidence concerning pharmacokinetics of substances undergoing enterohepatic cycling. Delayed recirculation may lead to rebounds in plasma level profiles as well as after intravenous and oral administration. The half-life of the drug is significantly prolonged even when the kinetic processes involved in recirculation remain unchanged.

Keyphrases □ Pharmacokinetics—time-lag model, enterohepatic drug circulation □ Models, pharmacokinetic—enterohepatic drug circulation, time-lag model □ Enterohepatic circulation—drugs, pharmacokinetics, time-lag model

When a substance is taken up by the liver and excreted into the bile, it may be either eliminated through the GI tract or reabsorbed and carried to the liver *via* the portal blood stream. This second process is known as enterohepatic cycling. This phenomenon affects both endogenous and exogenous substances.

BACKGROUND

A two-compartment model was previously developed (1) representing the body and the GI tract. Qualitative modifications in pharmacokinetic time-profiles and parameters for drugs subject to enterohepatic cycling due to changes in biliary excretion and reabsorption rates are well depicted by this model.

Predictions of the two-compartment model agree with previous experimental results (1, 2). However, some discrepancies, such as the evidence of a secondary peak in the time course of serum concentrations, remain. Such a secondary peak was reported (3) appearing after intravenous, oral, and intraportal administration of morphine in rats. An eight-compartment model for morphine pharmacokinetics was proposed. The GI tract compartment of Harrison and Gibaldi (1) is split into a catenary system of three compartments forming a loop connected with the central compartment. Experimental evidence for a secondary peak in plasma radioactivity time profiles, as well as subsequent very slow elimination kinetics exist for labeled vitamin D_3 in humans (4) and rats (5). The main active metabolite of vitamin D_3 undergoes enterohepatic cycling (6).

A modification of the two-compartment enterohepatic recirculation model is proposed to take into account these previous experimental findings. The basic assumption is that a time-delay exists between the excretion of a given molecule of the substance into bile and its reabsorption from the intestine. This time lag may be due to delayed biotransformation in the liver, to the storage of the substance in the gallbladder (*e.g.*, in humans), or simply to its transport in bile, at a limited flow-rate, from the site of excretion to the site of reabsorption. The corresponding time-delay model proposed here exhibits qualitative agreement with the two basic observations on pharmacokinetics of drugs subject to enterohepatic circulation: first, the occurrence of "rebounds" in serum level profiles after intravenous and oral administration of drug; and second, the slow terminal kinetics of the drug when recirculation occurs, even when the processes of deconjugation and reabsorption are not rate-limiting.

THEORETICAL

Mathematical Formulation—The model presented in Scheme I is a two-compartment system differing from the basic model of Harrison

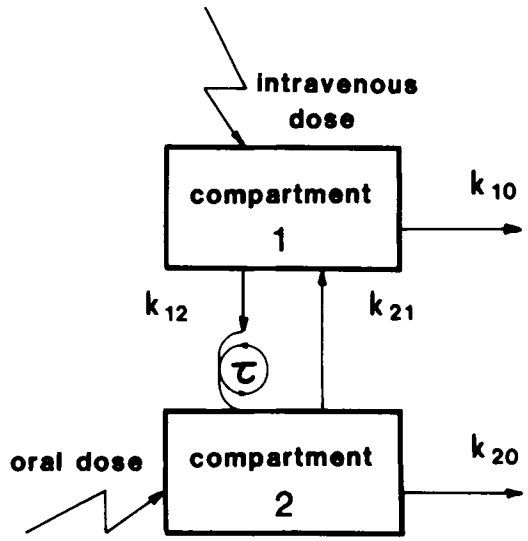

Scheme I—Time-lag pharmacokinetic model for a drug subject to enterohepatic circulation. Compartment 1 represents the body including the liver. Compartment 2 represents the GI tract. Existence of a time delay is assumed after biliary excretion, before reabsorption can occur.

0022-3549/82/0300-0297$01.00/0

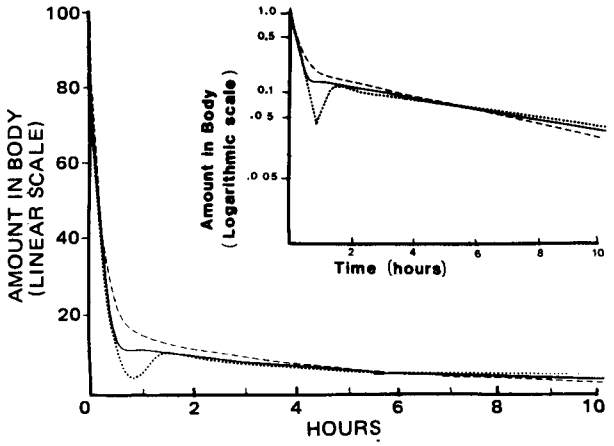

Figure 1—*Effect of time lag on pharmacokinetic profile after intravenous injection. For all curves,* $k_{12} = 3.0$, $k_{10} = 1.0$, $k_{21} = 1.0$, *and* $k_{20} = 0.0\ hr^{-1}$. *Key: - - -,* $\tau = 0$ *(no time lag);* ——, $\tau = 0.4$ *hr; and . . .,* $\tau = 0.8$ *hr.*

and Gibaldi (1) by the addition of a time lag on the transfer pathway from compartment 1 to compartment 2. In this model, compartment 1 represents the whole body, including the liver, while compartment 2 describes the GI tract.

The transfer processes are supposed to be governed by first-order kinetics and are denoted respectively by k_{10} for the nonbiliary elimination process, k_{20} for the biotransformation in the GI tract and the fecal excretion, and k_{21} for the reabsorption process.

The important characteristic of the model lies in the addition of a time delay occurring in series with the conventional k_{12} coefficient, thus implying that the drug leaving compartment 1 at time t enters compartment 2 at time $t + \tau$.

The corresponding mathematical formulation is:

$$\frac{dA_1(t)}{dt} = -(k_{10} + k_{12})A_1(t) + k_{21}A_2(t) \qquad \text{(Eq. 1}a\text{)}$$

$$\frac{dA_2(t)}{dt} = -(k_{20} + k_{21})A_2(t) + k_{12}A_1(t - \tau) \qquad \text{(Eq. 1}b\text{)}$$

Due to the existence of this time delay, the initial conditions take a special form; to calculate the solutions of Eqs. 1*a* and 1*b* starting from arbitrary time t_0, one has to define:

$$A_1(t) \text{ for } t_0 - \tau \leq t \leq t_0 \qquad \text{(Eq. 2}a\text{)}$$

and

$$A_2(t) \text{ for } t = t_0 \qquad \text{(Eq. 2}b\text{)}$$

To be more general, it is also possible to account for any input either in compartment 1 or compartment 2 or both by adding appropriate terms in Eqs. 1*a* and 1*b*. In the present study the single intravenous injection of a given dose D of drug, and the single oral intake of the same dose are considered.

In both cases, the mathematical formulation is described by Eqs. 1*a* and 1*b* with the corresponding initial conditions. For intravenous administration:

$$\begin{gathered} A_1(0) = D \\ A_1(t) = 0 \quad \text{for } -\tau \leq t < 0 \\ A_2(0) = 0 \end{gathered} \qquad \text{(Eq. 3)}$$

and for oral administration:

$$\begin{gathered} A_1(t) = 0 \quad \text{for } -\tau \leq t \leq 0 \\ A_2(0) = D \end{gathered} \qquad \text{(Eq. 4)}$$

Simulation of the Model—Two models were studied: model I corresponds to an intravenous single dose and is described by Eqs. 1*a*, 1*b*, and 3; model II corresponds to an oral single dose and is described by Eqs. 1*a*, 1*b*, and 4.

In both cases, the explicit analytical solutions can only be derived in a recurrent manner on successive time intervals. The results obtained for the models on the first two intervals of duration τ are given in the *Appendix*. It must be emphasized that the derived expressions increase in complexity when t gets larger in such a way that they rapidly become intractable in practice.

The simulation of the models, and more generally of Eqs. 1*a* and 1*b* with appropriate input and initial conditions, has to be carried out through numerical integration.

The method proposed in this study is the first-order Euler method, which calculates the values of $A_1(t)$ and $A_2(t)$ at discrete times $t_j = jh$, where h is a small time increment and j is any positive integer; the time lag should also be a multiple integer of h. The corresponding recursive equations are given by:

$$A_1(t_{j+1}) = (1 - hK_1)A_1(t_j) + hk_{21}A_2(t_j) \qquad \text{(Eq. 5}a\text{)}$$

$$A_2(t_{j+1}) = (1 - hK_2)A_2(t_j) + hk_{12}A_1(t_j - \tau) \qquad \text{(Eq. 5}b\text{)}$$

where

$$K_1 = k_{10} + k_{12} \text{ and } K_2 = k_{20} + k_{21}.$$

Sensitivity Study—Theoretical sensitivity analysis of the whole pharmacokinetic profile through partial differentiation of $A_1(t)$ with respect to the parameters is difficult in the present case, since no explicit analytical expression is available for the complete solution. The study of the influence of modifications in the microconstants k_{12}, k_{21}, k_{10}, and k_{20} and in the time lag τ was performed numerically using repeated computer simulations.

The reference parameter values are those used by Harrison and Gibaldi (1), *i.e.*, $k_{12} = 3.0$, $k_{21} = 1.0$, and $k_{20} = 0.0\ hr^{-1}$. Modified values of the microconstants and values of τ, from 0.0 to 1.0 hr, are indicated for each computer simulation under the corresponding figure or in the text.

With respect to terminal kinetics, general algebraic results can be given. Assuming the final phase of the decay is exponential, the terminal rate constant β' is the solution of the following equation, whose derivation is given in the *Appendix:*

$$(\beta')^2 - \beta'(k_{12} + k_{10} + k_{21} + k_{20}) + (k_{12} + k_{10})(k_{21} + k_{20}) - k_{12}k_{21}\exp(\beta'\tau) = 0 \qquad \text{(Eq. 6)}$$

Because of the term $\exp(\beta'\tau)$, Eq. 6 cannot be solved explicitly for β'. Accordingly, values of β' and of the terminal half-life ($T^{\beta'}_{1/2}$) were obtained numerically for each computer-simulated pharmacokinetic profile. Nevertheless, the equation can be used to investigate the dependency of β' on the microconstants and the time lag. Analytical sensitivity study of β' is explained in the *Appendix*.

Note also that for $\tau = 0$, Eq. 6 reduces to the customary equation for determination of α and β for the basic two-compartment open model for enterohepatic circulation without time delay (1, 2). Furthermore, if k_{12} is interchanged with k_{21}, and k_{10} is interchanged with k_{20} at the same time, the equation remains identical. Hence, the value of β' is not modified.

RESULTS

The case where there is no time delay between biliary excretion and drug reabsorption has been studied extensively (1, 2). This presentation is therefore restricted to the case where the time lag is of the same order of magnitude as the time constants of the first-order kinetics accounting for distribution and elimination.

Modifications in the serum level profile due to changes in the time lag τ (all microconstants being unchanged) are presented in Fig. 1. When τ is zero, the amount in the body shows biexponential monotonic decrease. When τ becomes larger, a plateau ($\tau = 0.4$) is obtained first, and for greater values ($\tau = 0.8$) a significant rebound appears in the time profile. Three periods may be distinguished on the pharmacokinetic profile:

1. From zero to τ, the amount in the body decreases monoexponentially (by analogy with conventional notation, the term α'-phase is proposed).
2. When distribution is achieved, the amount in the body again decreases exponentially with constant β' (the β'-phase).
3. Between these two extreme periods, there exists a transient phase where the influence of the time lag is most apparent (τ-phase).

Although the simulated curves displayed in Fig. 1 correspond to maximum enterohepatic cycling ($k_{20} = 0$), the qualitative results remain the same even when the drug is partly eliminated through the intestine ($k_{20} \neq 0$). When a time lag is present, the entire pharmacokinetic profile is modified, in the so-called initial distribution phase as well as in the terminal elimination phase. Further increase in τ gives rise to other peaks in the drug level profile so that the duration of the transient phase becomes longer. Hence, the whole distribution phase (including the α'-phase

and the τ-phase) is time-lag sensitive with respect to its profile and also to its duration. Furthermore, the hybrid constant β', which describes the terminal phase, decreases when τ is enhanced (*Appendix*) regardless of the combination of microconstants. Figure 1 shows how terminal kinetics slow down when the time lag increases. For example, values of $T_{1/2}^{\beta'}$ for $\tau = 0$, $\tau = 0.4$, and $\tau = 0.8$ hr (Fig. 1) are respectively 3.3, 4.2, and 5.1 hr; there is a 50% increase in terminal half-life between the two extreme cases.

The effects of modifications in biliary excretion on the pharmacokinetics of drugs subject to enterohepatic cycling when the basic model ($\tau = 0$) is considered have been described previously (1, 2). Existence of a significant time delay between excretion and reabsorption slightly modifies the conclusions. The decay in the initial phase is slower when k_{12} is reduced, regardless of other parameter values. The influence of modifications in k_{12} on β', and therefore on the terminal half-life $T_{1/2}^{\beta'}$, are less simple. If $k_{20} < k_{10}$, *i.e.*, when nonbiliary elimination from the body is predominant, a decrease in biliary excretion leads to an increase in β', and therefore shortens the half-life of the drug. For the curves displayed in Fig. 2 ($k_{10} = 0.5$, $k_{20} = 0.2$ hr^{-1}), the half-lives are 4.5, 3.1, and 2.2 hr for k_{12} values of 3.0, 1.0, and 0.33 hr^{-1}, respectively. More precisely, an increase in k_{12} will always decrease β' if $k_{20} < k_{10} + \Delta_1$, where Δ_1 (a quantity depending on k_{10}, k_{21}, and τ) is zero for the basic model and strictly positive when a time lag exists (*Appendix*). On the other hand, if $k_{20} > k_{10} + \Delta_1$, *i.e.*, when the intestine plays the dominant role in elimination, the opposite results are obtained. In this case, the reduction in k_{12} leads to the reduction in β'. However, this effect is markedly less than in the first case ($k_{20} < k_{10}$). For the same set of k_{12} values, the values computed for $T_{1/2}^{\beta'}$ when $k_{10} = 0.2$ and $k_{20} = 0.5$ hr^{-1} are 3.0, 3.1, and 3.3 hr, respectively. Regardless of the relative magnitudes of k_{10} and k_{20}, the pharmacokinetic profile becomes increasingly smooth when k_{12} decreases (Fig. 2). However, note that the initial decrease is strictly monoexponential for the duration of the time delay (1.0 hr for these simulations), even when no rebound is apparent.

The influence of reabsorption on drug disposition was analytically studied by Chen and Gross (2). They showed that enhancement in reabsorption (increase in k_{21}) produces the same effects on terminal kinetics as reduction in biliary excretion (decrease in k_{12}); the effect may be an increase or a decrease of the half-life, depending on which of the parameters, k_{10} or k_{20}, is the greatest. Predictions of the time-lag model are identical with those of the basic model when either $k_{10} < k_{20}$ or $k_{10} > k_{20} + \Delta_2$, where $\Delta_2 > 0$ if $\tau > 0$ (*Appendix*). Enhancement of the reabsorption rate k_{21} will increase the half-life in the first case and reduce $T_{1/2}^{\beta'}$ in the second case. However, if k_{10} is such that $k_{20} < k_{10} < k_{20} + \Delta_2$, increased reabsorption will produce a longer, not shorter, half-life. The curves shown in Fig. 3 are associated with parameter values such that the double inequality holds. Terminal half-lives $T_{1/2}^{\beta'}$ are 3.0, 3.1, and 3.3 hr when k_{21} is set equal to 0.33, 1.0, and 3.0 hr^{-1}, respectively. Predictions based on the time-lag model also differ from those of Chen and Gross (2) when the initial decay is considered. The three simulated curves displayed in Fig. 3 are superimposed during the 1st hr. When a time lag is present, the pharmacokinetics after intravenous injection are insensitive to modifications in reabsorption until τ has elapsed. Influence of reabsorption is only apparent in the transient and terminal phase of the pharmacokinetic profile.

Existence of the rebound is independent of the relative magnitude of rate constants k_{12} and k_{21}. It may be observed either with high biliary excretion and moderate reabsorption ($k_{12} = 3.0$, $k_{21} = 1.0$; Fig. 2) or with moderate biliary excretion and high reabsorption ($k_{12} = 1.0$, $k_{21} = 3.0$; Fig. 3). A slight decrease in either k_{12} or k_{21} implies reduction in the amplitude of the peak; further decrease leads to complete disappearance of this peak.

The influence of both elimination processes (*e.g.*, through the kidney and the intestine) was studied through modifications in rate constants k_{10} and k_{20} (Fig. 4). The first extreme case appears when enterohepatic recirculation is complete ($k_{20} = 0$). When k_{10} varies, both α' and β' vary accordingly; however, the transient τ-phase is modified to a lesser extent. The semi-logarithmic diagram (Fig. 4*a*) does not give an entirely satisfactory description of the time process. Although the minimum (A_1 min) and the peak (A_1 max) both occur when k_{10} is reduced, the magnitude of the gap between these two values remains almost constant and is even slightly increased when k_{10} decreases. The second extreme case is when the substance is not subject to nonbiliary elimination from the body ($k_{10} = 0$). When k_{20} varies, the initial decay remains the same; the α'-phase is insensitive to modifications in k_{20} as well as in k_{21} (Fig. 4*b*). In any case, the terminal half-life $T_{1/2}^{\beta'}$ is longer when either k_{10} or k_{20} is reduced, regardless of the other parameters' values (*Appendix*). If elimination occurs through both the kidney and the intestine, the corresponding pharmacokinetic profile is intermediate between the two extremes.

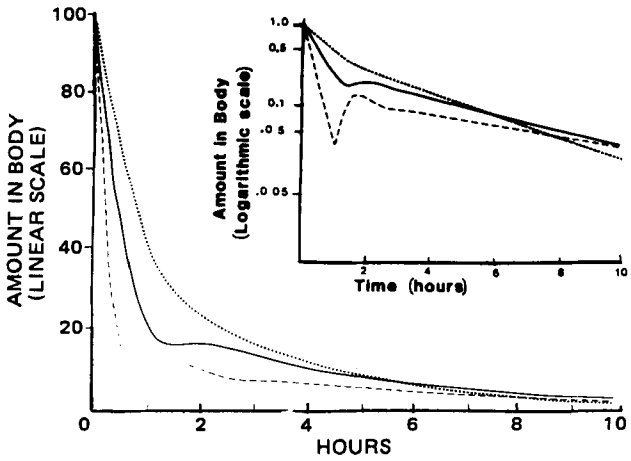

Figure 2—*Effect of biliary excretion on pharmacokinetic profile without modification in time lag. For all curves,* $k_{10} = 0.5$, $k_{21} = 1.0$, $k_{20} = 0.2$ hr^{-1}, *and* $\tau = 1.0$ hr ($k_{20} < k_{10} + \Delta_1$). *Key:* - - -, $k_{12} = 3.0$ hr^{-1}; —, $k_{12} = 1.0$ hr^{-1}; *and* . . ., $k_{12} = 0.33$ hr^{-1}.

The time-delay model may also reveal what happens after oral intake of the drug. The relationship between pharmacokinetic profiles after intravenous and oral administration of a substance is shown in Fig. 5 for the basic model of enterohepatic circulation (1) and the model with time lag ($k_{20} = 0$, $k_{12} > k_{21}$). The oral profile is smoother than the intravenous in both cases. How the increase in time lag affects the pharmacokinetic profile is further depicted in Fig. 6, where $k_{21} > k_{12}$. When the reabsorption rate is greater than the biliary excretion rate, somewhat sharper time profiles (Fig. 6) than in the reverse case are observed. Nevertheless, the conclusions are the same whenever $k_{12} > k_{21}$ (Fig. 5) or $k_{12} < k_{21}$ (Fig. 6). When the delay is present in the enterohepatic cycle, the terminal half-life is prolonged. When τ increases, the τ-phase becomes first apparent ($\tau = 0.4$) and evident afterward ($\tau = 0.8$), although the gap between the local minimum and the secondary peak is less than in the corresponding intravenous case. Furthermore, the customary first peak, though occurring sooner, is of lesser magnitude than in the standard case where no time delay is present.

DISCUSSION

The influence of a delay for drugs subject to enterohepatic circulation was investigated through computer simulation. The time-lag model is a modification of a two-compartment model first proposed by Harrison and Gibaldi (1). Predictions of the time-lag model on the influence of cholestasis on pharmacokinetics show qualitative agreement with results obtained through an analytical parameter sensitivity study of the basic model (2). However, changes in reabsorption or in intestinal elimination lead to different results. The basic model predicts that the α-phase is

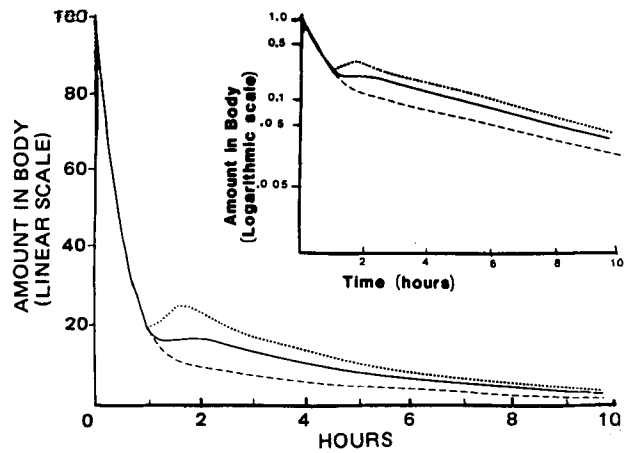

Figure 3—*Effect of reabsorption on pharmacokinetic profile without modification in time lag. For all curves,* $k_{12} = 3.0$, $k_{10} = 0.5$, $k_{20} = 0.2$ hr^{-1}, *and* $\tau = 1.0$ hr ($k_{20} < k_{10} < k_{20} + \Delta_2$). *Key:* . . ., $k_{21} = 3.0$ hr^{-1}; —, $k_{21} = 1.0$ hr^{-1}; *and* - - -, $k_{21} = 0.33$ hr^{-1}.

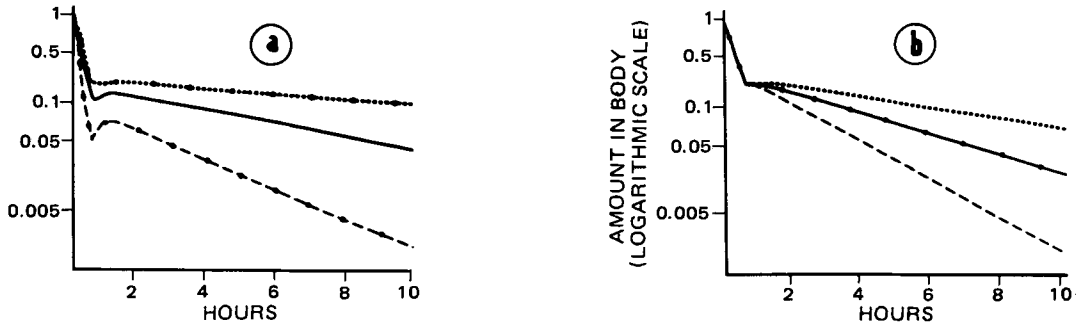

Figure 4—*Effect of both elimination processes on pharmacokinetic profile without modification in time lag. Parameters* k_{12}, k_{21}, *and* τ *are identical for all simulations* ($k_{12} = 3.0$, $k_{21} = 1.0\ hr^{-1}$; *and* $\tau = 0.5\ hr$). *(a) Nonbiliary elimination only* ($k_{20} = 0.0\ hr^{-1}$). *Key:* · ● ·; $k_{10} = 0.33\ hr^{-1}$; —, $k_{10} = 1.0\ hr^{-1}$; *and* –●–, $k_{10} = 3.0\ hr^{-1}$. *(b) Elimination from intestine only* ($k_{10} = 0.0\ hr^{-1}$). *Key:* . . ., $k_{20} = 0.25\ hr^{-1}$, —●—, $k_{20} = 0.50\ hr^{-1}$; *and* - - -, $k_{20} = 1.0\ hr^{-1}$.

modified when either the reabsorption rate k_{21} or the intestinal elimination rate k_{20} changes. Instead, when a significant delay is present in the enterohepatic cycling process, modifications in reabsorption or in intestinal elimination do not affect the initial decay of the plasma level after intravenous injection of the drug.

Further basic differences between both models become apparent when pharmacokinetic profiles are considered after intravenous injection as well as after oral intake of the drug. When a time lag is present, the time profile is not biexponential. For the same values of the microconstants, the time-lag model exhibits both a more rapid decay in the initial phase and a slower disappearance rate for the terminal phase than the basic model. An increase of ~50% in the terminal half-life value is not uncommon for the range of values of microconstants and time lag studied here. In addition to monoexponential initial and terminal kinetics, the time-lag model shows specific behavior in the transient phase. Delayed reabsorption may lead to uncommon patterns such as rebounds, or secondary peaks in plasma level profiles after intravenous injection or oral intake of the drug. Although apparently uncharacteristic, phenomenon of this kind were described for substances undergoing enterohepatic circulation such as morphine (3) and the main metabolite of vitamin D_3 (4–6). The eight-compartment model devised previously to describe morphine pharmacokinetics gives an adequate description of the data (3). It accounts for both rebounds in the measured levels and slow terminal kinetics, two basic features often connected with significant enterohepatic circulation. The overall rate-limiting step in the model (3) is morphine reabsorption from the GI tract; this result may be specific for that drug. In spite of its relative complexity as compared with the eight-compartment model, the time-lag model may produce slow terminal kinetics even when the overall rate-limiting step does not belong to the enterohepatic cycling loop. Existence of a time delay in recirculation prolongs the terminal half-life of the drug by much more than the time lag itself.

Nevertheless, the time-lag model is certainly a rough approximation of the underlying process. A representation of all complex physiological processes involved in enterohepatic circulation of a substance by two first-order rate constants with an additional time lag (presumably due to transport delay) is an oversimplification.

Furthermore, the assumption that the time lag is constant for the duration of the pharmacokinetic experiment may also be an approximation. The delay may be a function of time following slight modifications in bile flow, or may show discontinuous variations in some species due to sudden emptying of the gallbladder. Furthermore, the successive steps of hepatic conjugation, biliary excretion of the metabolite, deconjugation in the GI tract, and reabsorption of the parent drug have been summarized by means of only two first-order rate constants. Although the two-compartment time-lag model is a simplification, it seems to be a reasonable compromise, since it exhibits satisfactory qualitative agreement with existing data.

Enterohepatic recirculation is not the only pharmacokinetic process where time-lag models have been shown to be valuable. Evidence for time-delayed response also exists for various drugs after oral intake. However, pharmacokinetic analysis is somewhat simpler in the latter case because the absorption phase (as opposed to the distribution phase) is affected. Nevertheless, time-lag models may be useful for pharmacokinetic interpretation and substitutes for conventional standard compartment models that fail to describe the data. However, even when a significant time-delay exists, evidence for it may be difficult to demonstrate. Secondary peaks in plasma level profiles may not be observable on all pharmacokinetic data in a series of experiments. Sensitivity analysis of the time-lag model has shown that moderate changes in microconstants and time lag among the sample subjects may lead to important variations in the shapes of time profiles. Predefined standard sampling, a basic requirement in most experimental protocols may be, in some cases, inappropriate for detection of kinetic peculiarities. A combination of uncertainties resulting from interindividual variability, sampling, and measurement errors frequently makes it a difficult task, in practice. To decide whether a given uncommon feature is an artifact or a relevant kinetic pattern, inspection of data may not be sufficient. Additional arguments based on physiological knowledge should exist for the introduction of a time lag in a mathematical model for drug pharmacokinetics.

A present theoretical limitation should be stressed. Computer simulation is a basic requirement for investigation, analysis, fitting to data, and predictive use of the pharmacokinetic model when time lags are present in disposition kinetics. Less analytical results can be obtained in linear time-lag pharmacokinetics, as in nonlinear pharmacokinetics. While powerful numerical integration methods exist for the latter case (7), algorithms higher than first order for simulation of time-lag differential equations are not commonly available. The development of appropriate numerical methods is, therefore, a primary condition for routine use of time-lag models in pharmacokinetic analysis.

APPENDIX

Explicit Solutions of Model I and II for Initial Phase—These results are obtained through straightforward integration of models I and II on successive intervals of duration τ. In each interval, $A_1(t - \tau)$ is considered the forcing term of Eqs. 1*a* and 1*b* submitted to the appropriate initial conditions. For this reason, the complexity of the solution increases rapidly and explicit solutions are presented only for the first two τ intervals.

Model I: Single Intravenous Injection of a Dose (D)—Denoting $K_1 = k_{10} + k_{12}$ and $K_2 = k_{20} + k_{21}$ for $0 \leq t \leq \tau$:

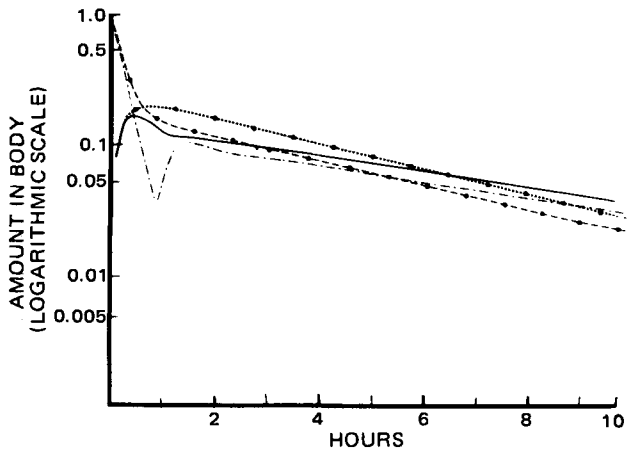

Figure 5—*Pharmacokinetic profiles after intravenous dose and oral dose. For all curves,* $k_{12} = 3.0$, $k_{10} = 1.0$, $k_{21} = 1.0$, *and* $k_{20} = 0.0\ hr^{-1}$. *Key: Without time lag* ($\tau = 0$): –●–, *intravenous; and* · ● ·, *oral. With time lag* ($\tau = 0.8\ hr$): - - -, *intravenous; and* —, *oral.*

$$A_1(t) = D\exp(-K_1 t) \quad \text{(Eq. A1}a\text{)}$$

$$A_2(t) = 0 \quad \text{(Eq. A1}b\text{)}$$

For $\tau \leq t \leq 2\tau$:

$$A_1(t) = D\exp(-K_1 t) + D\frac{k_{12}k_{21}}{K_2 - K_1}\left[\left(t - \tau - \frac{1}{K_2 - K_1}\right) \times \exp[-K_1(t-\tau)] + \frac{1}{K_2 - K_1}\exp[-K_2(t-\tau)]\right] \quad \text{(Eq. A2}a\text{)}$$

$$A_2(t) = D\frac{k_{12}}{K_2 - K_1}\left[\exp[-K_1(t-\tau)] - \exp[-K_2(t-\tau)]\right] \quad \text{(Eq. A2}b\text{)}$$

Model II: Single Oral Intake of a Dose (D)—For $0 \leq t \leq \tau$:

$$A_1(t) = D\frac{k_{21}}{K_2 - K_1}\left[\exp(-K_1 t) - \exp(-K_2 t)\right] \quad \text{(Eq. A3}a\text{)}$$

$$A_2(t) = D\exp(-K_2 t) \quad \text{(Eq. A3}b\text{)}$$

and for $\tau \leq t \leq 2\tau$:

$$A_1(t) = D\frac{k_{21}}{K_2 - K_1}[\exp(-K_1 t) - \exp(-K_2 t)] + D\frac{k_{12}(k_{21})^2}{(K_2 - K_1)^2}\left[\left(t - \tau - \frac{2}{K_2 - K_1}\right)\exp[-K_1(t-\tau)] + \left(t - \tau + \frac{2}{K_2 - K_1}\right)\exp[-K_2(t-\tau)]\right] \quad \text{(Eq. A4}a\text{)}$$

$$A_2(t) = D\exp(-K_2 t) + D\frac{k_{12}k_{21}}{K_2 - K_1}\left[\frac{1}{K_2 - K_1}\exp[-K_1(t-\tau)] - \left(t - \tau + \frac{1}{K_2 - K_1}\right)\exp[-K_2(t-\tau)]\right] \quad \text{(Eq. A4}b\text{)}$$

These expressions are especially useful to validate the numerical approximations to be used on the time interval $[0, 2\tau]$.

Approximation of the Solution of Models I and II for Large Time Values—In the range of the parameter values used in the different simulations, it has been observed that for t greater than a given time t^* which depends on the time-lag τ, the decrease of amount of drug in body is monoexponential. For $t > t^*$:

$$A_1(t) = A_1^* \exp(-\beta' t) \quad \text{(Eq. A5}a\text{)}$$

and

$$A_2(t) = A_2^* \exp(-\beta' t) \quad \text{(Eq. A5}b\text{)}$$

From Eqs. A5a and A5b are derived:

$$\ln[A_1(t)] = \ln A_1^* - \beta' t \quad \text{(Eq. A6}a\text{)}$$

$$\ln[A_2(t)] = \ln A_2^* - \beta' t \quad \text{(Eq. A6}b\text{)}$$

Division of both state equations (Eqs. 1a and 1b) by $A_1(t)$ and $A_2(t)$, respectively, leads to:

$$\frac{dA_1(t)}{A_1(t)dt} = -(k_{10} + k_{12}) + k_{21}\frac{A_2(t)}{A_1(t)} \quad \text{(Eq. A7}a\text{)}$$

$$\frac{dA_2(t)}{A_2(t)dt} = -(k_{20} + k_{21}) + k_{12}\frac{A_1(t-\tau)}{A_2(t)} \quad \text{(Eq. A7}b\text{)}$$

Equations A7a and A7b may be rewritten as:

$$\frac{d[\ln A_1(t)]}{dt} = -(k_{10} + k_{12}) + k_{21}\frac{A_2^*}{A_1^*} \quad \text{(Eq. A8}a\text{)}$$

and:

$$\frac{d[\ln A_2(t)]}{dt} = -(k_{20} + k_{21}) + k_{12}\frac{A_1^*}{A_2^*}\exp(\beta'\tau) \quad \text{(Eq. A8}b\text{)}$$

Therefore:

$$-\beta' = -(k_{10} + k_{12}) + k_{21}\frac{A_2^*}{A_1^*} \quad \text{(Eq. A9}a\text{)}$$

and:

$$-\beta' = -(k_{20} + k_{21}) + k_{12}\exp(\beta'\tau)\frac{A_1^*}{A_2^*} \quad \text{(Eq. A9}b\text{)}$$

Elimination of the ratio A_2^*/A_1^* from Eqs. A9a and A9b leads to the algebraic equation to be solved for β':

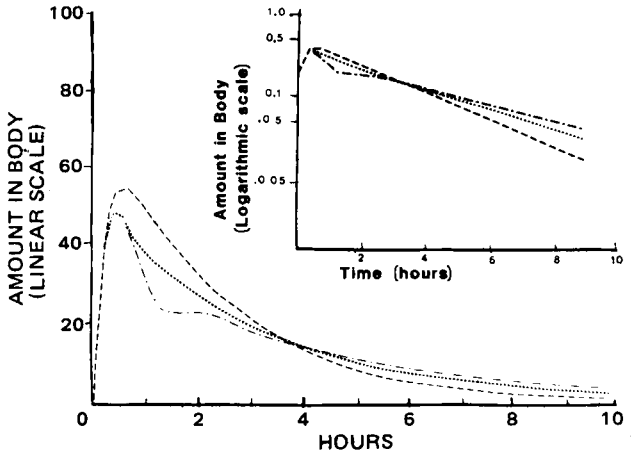

Figure 6—*Effect of time lag on pharmacokinetic profile after oral intake of the drug. For all curves,* $k_{12} = 1.0$, $k_{10} = 0.5$, $k_{21} = 3.0$, *and* $k_{20} = 0.2\ hr^{-1}$. *Key: ---,* $\tau = 0$ *hr; . . .,* $\tau = 0.5$ *hr; and -·-,* $\tau = 1.0$ *hr.*

$$(\beta')^2 - \beta'(k_{12} + k_{10} + k_{21} + k_{20}) + (k_{12} + k_{10})(k_{21} + k_{20}) - k_{12}k_{21}\exp(\beta'\tau) = 0 \quad \text{(Eq. A10)}$$

With $K_1 = k_{10} + k_{12}$ and $K_2 = k_{20} + k_{21}$, Eq. A10 can be rewritten as:

$$f(\beta') \triangleq (\beta' - K_1)(\beta' - K_2) - k_{12}k_{21}\exp(\beta'\tau) = 0 \quad \text{(Eq. A11)}$$

Function f is positive for $\beta' = 0$ and negative for $\beta' = K_1$ and $\beta' = K_2$. Furthermore, its derivative is negative for β' less than the minimum of K_1 and K_2. So f has one unique root on [0, min (K_1, K_2)]. This is the smallest root for β' and the relevant one for large time values.

Sensitivity Analysis of β'—*Sensitivity* versus *the Time Lag* (τ)—Assuming all microconstants to be kept at a fixed value, the partial derivative of β' with respect to τ is deduced from the differentiation of f. Hence:

$$(2\beta' - K_1 - K_2)\frac{\partial\beta'}{\partial\tau} - k_{12}k_{21}\exp(\beta'\tau)\left(\tau\frac{\partial\beta'}{\partial\tau} + \beta'\right) = 0 \quad \text{(Eq. A12).}$$

and:

$$\frac{\partial\beta'}{\partial\tau}[2\beta' - K_1 - K_2 - k_{12}k_{21}\tau\exp(\beta'\tau)] = \beta' k_{12}k_{21}\exp(\beta'\tau) \quad \text{(Eq. A13)}$$

If $\beta' < K_1$ and $\beta' < K_2$, the coefficient of $\partial\beta'/\partial\tau$ is negative. Furthermore, the second member of (Eq. A13) is positive. Therefore:

$$\frac{\partial\beta'}{\partial\tau} < 0 \quad \text{(Eq. A14)}$$

For any value of the microconstants, β' decreases when τ increases and vice versa. Accordingly, the half-life increases when the time lag is enhanced, regardless of the combination of microconstants.

Sensitivity versus *the Transfer Rate Constants* k_{12} *and* k_{21}—When partial differentiation of β' with respect to k_{12} is considered, an equation similar to Eq. A13 is obtained. In the present case, the second member is equal to $\beta' - K_2 + k_{21}\exp(\beta'\tau)$. The sign of $\partial\beta'/\partial k_{12}$ is the opposite sign of the previous expression. In abbreviated form:

$$\text{sign}(\partial\beta'/\partial k_{12}) = -\text{sign}[\beta' - K_2 + k_{21}\exp(\beta'\tau)] \quad \text{(Eq. A15)}$$

After replacement of $k_{21}\exp(\beta'\tau)$ according to Eq. A11, multiplication by k_{12} (positive) and division by $(\beta' - K_2)$ (negative), it follows that:

$$\text{sign}\left(\frac{\partial\beta'}{\partial k_{12}}\right) = \text{sign}(\beta' - k_{10}) \quad \text{(Eq. A16)}$$

According to the definition of function f (Eq. A11) and to its properties on the interval [0, min (K_1, K_2)], the sign of $(\beta' - k_{10})$ verifies:

$$\beta' - k_{10} > 0 \Leftrightarrow f(k_{10}) > 0 \quad \text{(Eq. A17}a\text{)}$$

$$\beta' - k_{10} < 0 \Leftrightarrow f(k_{10}) < 0 \quad \text{(Eq. A17}b\text{)}$$

As:

$$f(k_{10}) = k_{12}k_{21}[1 - \exp(k_{10}\tau)] + k_{12}(k_{20} - k_{10}) \quad \text{(Eq. A18)}$$

We get the following results for $\partial\beta'/\partial k_{12}$:

$$\frac{\partial\beta'}{\partial k_{12}} < 0 \text{ if } k_{20} < k_{10} + \Delta_1 \quad \text{(Eq. A19a)}$$

$$\frac{\partial\beta'}{\partial k_{12}} = 0 \text{ if } k_{20} = k_{10} + \Delta_1 \quad \text{(Eq. A19b)}$$

$$\frac{\partial\beta'}{\partial k_{12}} > 0 \text{ if } k_{20} > k_{10} + \Delta_1 \quad \text{(Eq. A19c)}$$

where $\Delta_1 = k_{21}[\exp(k_{10}\,\tau) - 1]$.

Note that the test condition does not depend on k_{12} itself. Sensitivity analysis of β' *versus* k_{21} relies on similar algebraic manipulations. Therefore:

$$\frac{\partial\beta'}{\partial k_{21}} < 0 \text{ if } k_{10} < k_{20} + \Delta_2 \quad \text{(Eq. A20a)}$$

$$\frac{\partial\beta'}{\partial k_{21}} = 0 \text{ if } k_{10} = k_{20} + \Delta_2 \quad \text{(Eq. A20b)}$$

$$\frac{\partial\beta'}{\partial k_{21}} > 0 \text{ if } k_{10} > k_{20} + \Delta_2 \quad \text{(Eq. A20c)}$$

where $\Delta_2 = k_{12}[\exp(k_{20}\tau) - 1]$.

Clear-cut results can be given in some cases. If $k_{20} < k_{10}$, $\partial\beta'/\partial k_{12}$ is always negative and if $k_{20} > k_{10}$, the same is true for $\partial\beta'/\partial k_{21}$, regardless of the combination of other parameters. For other cases, the test condition should be computed and applied.

Sensitivity versus *the Elimination Rate Constants* k_{10} *and* k_{20}—Differentiation of f with respect to β' and k_{10} leads to:

$$\frac{\partial\beta'}{\partial k_{10}}[2\beta' - K_1 - K_2 - k_{12}k_{21}\,\tau\exp(\beta'\tau)] = \beta' - K_2 \quad \text{(Eq. A21)}$$

As β' is less than K_2, the second member is negative in the present case. Hence:

$$\frac{\partial\beta'}{\partial k_{10}} > 0 \quad \text{(Eq. A22)}$$

Similarly it can be shown that:

$$\frac{\partial\beta'}{\partial k_{20}} > 0 \quad \text{(Eq. A23)}$$

Therefore, an increase in elimination processes, through either k_{10} or k_{20} will always increase β' and shorten the half-life $T^{\beta'}_{1/2}$.

REFERENCES

(1) L. I. Harrison and M. Gibaldi, *J. Pharm. Sci.*, **65,** 1346 (1976).

(2) H. S. G. Chen and J. F. Gross, *ibid.*, **68,** 792 (1979).

(3) B. E. Dahlström and L. K. Paalzow, *J. Pharmacokinet. Biopharm.*, **6,** 505 (1978).

(4) L. V. Avioli, S. W. Lee, J. E. MacDonald, J. Lund, and H. F. De Luca, *J. Clin. Invest.*, **46,** 983 (1967).

(5) G. Ponchon and H. F. De Luca, *J. Clin. Invest.*, **48,** 1273 (1969).

(6) S. B. Arnaud, R. S. Goldsmith, P. W. Lambert, and V. L. W. Go, *Proc. Soc. Exp. Biol. Med.*, **149,** 570 (1975).

(7) J. D. Lambert, in "The State of the Art in Numerical Analysis," D. Jacobs, Ed., Academic, New York, N.Y., 1977, pp. 451–500.

ACKNOWLEDGMENTS

Presented in part at the "Premier Congrès Européen de Biopharmacie et Pharmacocinétique," Clermont-Ferrand, France, April 1–3, 1981.

Supported in part by a grant from the Caisse Mutuelle Provinciale des Professions Libérales and by funds from the Laboratoire d'Algèbre, Université Paul-Sabatier, F-31000 Toulouse, France.

The authors thank Professor L. Bousquet, Département de Mathématiques, Faculté de Médecine, F-31000 Toulouse Rangueil for computational help at the early stages of the study, Professor S. Guillemant, Laboratoire de Biochimie Médicale, Hôpital de la Pitié, F-75013 Paris for vitamin D_3 data, and the reviewer for helpful comments. The help of Mr. Subra and Mr. Depardieu is also acknowledged.

Combined Water-Soluble Carriers for Coprecipitates of Tolbutamide

M. J. MIRALLES, J. W. McGINTY, and A. MARTIN ˣ

Received January 19, 1981, from the *Drug Dynamics Institute, College of Pharmacy, University of Texas, Austin, TX 78712.* Accepted for publication July 23, 1981.

Abstract □ A study was conducted on the influence of single and combined carriers on the dissolution rate of tolbutamide from its coprecipitates. All of the water-soluble carriers investigated enhanced the dissolution rate of tolbutamide, but the combination of 40% polyethylene glycol 6000–60% dextrose as the carrier for a 1:1 coprecipitate yielded the most rapid dissolution of tolbutamide. Other carriers used were polyethylene glycol 6000, polyethylene glycol 4000, dextrose, and mannitol, alone or combined in various proportions.

Keyphrases □ Tolbutamide—coprecipitates, combined water-soluble carriers, dissolution □ Solubility—combined water-soluble carriers for coprecipitates of tolbutamide, dissolution □ Dissolution—effect of combined water-soluble carriers, coprecipitates of tolbutamide

The rate at which a drug dissolves from its intact or disintegrated and deaggregated form in the GI tract is often responsible for the rate at which the drug appears in the blood, *i.e.*, the absorption rate of the drug. When this is the case, dissolution is said to be the rate-limiting process.

BACKGROUND

The sulfonylurea compounds employed as oral hypoglycemic compounds are considered to be poorly water soluble. Variation in the dissolution rates of these compounds has been reported (1). The influence of *in vitro* dissolution rates on the rate of decline of blood sugar levels has also been studied (2). Varley (3) investigated two formulations of tolbutamide, both generically equivalent in terms of chemical content and USP specifications; he found they were not equivalent as measured by availability of drug to the patient (serum drug levels) or on the basis of therapeutic efficacy (hypoglycemic response). Levy (4) found marked variation in the dissolution rates of two brands of tolbutamide tablets and recommended that patients should not change the brand of the drug they were taking unless the dose of the new brand was established. Another report (5) showed a correlation between percentage of the tolbutamide dose excreted in the urine as its metabolite and the surface area of tolbutamide in the dosage form.

The influence of povidone and polyethylene glycol 6000 on the dissolution rate of tolbutamide was studied (6). It was found that both carriers favorably increased the dissolution rate of the drug and that a complex formed between the drug and povidone but not between tolbutamide and polyethylene glycol. Later it was found (7) that the solid dispersion of

0022-3549/82/0300-0302$01.00/0

We get the following results for $\partial\beta'/\partial k_{12}$:

$$\frac{\partial\beta'}{\partial k_{12}} < 0 \text{ if } k_{20} < k_{10} + \Delta_1 \quad \text{(Eq. A19a)}$$

$$\frac{\partial\beta'}{\partial k_{12}} = 0 \text{ if } k_{20} = k_{10} + \Delta_1 \quad \text{(Eq. A19b)}$$

$$\frac{\partial\beta'}{\partial k_{12}} > 0 \text{ if } k_{20} > k_{10} + \Delta_1 \quad \text{(Eq. A19c)}$$

where $\Delta_1 = k_{21}[\exp(k_{10}\,\tau) - 1]$.

Note that the test condition does not depend on k_{12} itself. Sensitivity analysis of β' *versus* k_{21} relies on similar algebraic manipulations. Therefore:

$$\frac{\partial\beta'}{\partial k_{21}} < 0 \text{ if } k_{10} < k_{20} + \Delta_2 \quad \text{(Eq. A20a)}$$

$$\frac{\partial\beta'}{\partial k_{21}} = 0 \text{ if } k_{10} = k_{20} + \Delta_2 \quad \text{(Eq. A20b)}$$

$$\frac{\partial\beta'}{\partial k_{21}} > 0 \text{ if } k_{10} > k_{20} + \Delta_2 \quad \text{(Eq. A20c)}$$

where $\Delta_2 = k_{12}[\exp(k_{20}\tau) - 1]$.

Clear-cut results can be given in some cases. If $k_{20} < k_{10}$, $\partial\beta'/\partial k_{12}$ is always negative and if $k_{20} > k_{10}$, the same is true for $\partial\beta'/\partial k_{21}$, regardless of the combination of other parameters. For other cases, the test condition should be computed and applied.

Sensitivity versus *the Elimination Rate Constants* k_{10} *and* k_{20}—Differentiation of f with respect to β' and k_{10} leads to:

$$\frac{\partial\beta'}{\partial k_{10}}[2\beta' - K_1 - K_2 - k_{12}k_{21}\,\tau\exp(\beta'\tau)] = \beta' - K_2 \quad \text{(Eq. A21)}$$

As β' is less than K_2, the second member is negative in the present case. Hence:

$$\frac{\partial\beta'}{\partial k_{10}} > 0 \quad \text{(Eq. A22)}$$

Similarly it can be shown that:

$$\frac{\partial\beta'}{\partial k_{20}} > 0 \quad \text{(Eq. A23)}$$

Therefore, an increase in elimination processes, through either k_{10} or k_{20} will always increase β' and shorten the half-life $T^{\beta'}_{1/2}$.

REFERENCES

(1) L. I. Harrison and M. Gibaldi, *J. Pharm. Sci.*, **65,** 1346 (1976).

(2) H. S. G. Chen and J. F. Gross, *ibid.*, **68,** 792 (1979).

(3) B. E. Dahlström and L. K. Paalzow, *J. Pharmacokinet. Biopharm.*, **6,** 505 (1978).

(4) L. V. Avioli, S. W. Lee, J. E. MacDonald, J. Lund, and H. F. De Luca, *J. Clin. Invest.*, **46,** 983 (1967).

(5) G. Ponchon and H. F. De Luca, *J. Clin. Invest.*, **48,** 1273 (1969).

(6) S. B. Arnaud, R. S. Goldsmith, P. W. Lambert, and V. L. W. Go, *Proc. Soc. Exp. Biol. Med.*, **149,** 570 (1975).

(7) J. D. Lambert, in "The State of the Art in Numerical Analysis," D. Jacobs, Ed., Academic, New York, N.Y., 1977, pp. 451–500.

ACKNOWLEDGMENTS

Presented in part at the "Premier Congrès Européen de Biopharmacie et Pharmacocinétique," Clermont-Ferrand, France, April 1–3, 1981.

Supported in part by a grant from the Caisse Mutuelle Provinciale des Professions Libérales and by funds from the Laboratoire d'Algèbre, Université Paul-Sabatier, F-31000 Toulouse, France.

The authors thank Professor L. Bousquet, Département de Mathématiques, Faculté de Médecine, F-31000 Toulouse Rangueil for computational help at the early stages of the study, Professor S. Guillemant, Laboratoire de Biochimie Médicale, Hôpital de la Pitié, F-75013 Paris for vitamin D_3 data, and the reviewer for helpful comments. The help of Mr. Subra and Mr. Depardieu is also acknowledged.

Combined Water-Soluble Carriers for Coprecipitates of Tolbutamide

M. J. MIRALLES, J. W. McGINTY, and A. MARTIN ˣ

Received January 19, 1981, from the *Drug Dynamics Institute, College of Pharmacy, University of Texas, Austin, TX 78712.* Accepted for publication July 23, 1981.

Abstract □ A study was conducted on the influence of single and combined carriers on the dissolution rate of tolbutamide from its coprecipitates. All of the water-soluble carriers investigated enhanced the dissolution rate of tolbutamide, but the combination of 40% polyethylene glycol 6000–60% dextrose as the carrier for a 1:1 coprecipitate yielded the most rapid dissolution of tolbutamide. Other carriers used were polyethylene glycol 6000, polyethylene glycol 4000, dextrose, and mannitol, alone or combined in various proportions.

Keyphrases □ Tolbutamide—coprecipitates, combined water-soluble carriers, dissolution □ Solubility—combined water-soluble carriers for coprecipitates of tolbutamide, dissolution □ Dissolution—effect of combined water-soluble carriers, coprecipitates of tolbutamide

The rate at which a drug dissolves from its intact or disintegrated and deaggregated form in the GI tract is often responsible for the rate at which the drug appears in the blood, *i.e.*, the absorption rate of the drug. When this is the case, dissolution is said to be the rate-limiting process.

BACKGROUND

The sulfonylurea compounds employed as oral hypoglycemic compounds are considered to be poorly water soluble. Variation in the dissolution rates of these compounds has been reported (1). The influence of *in vitro* dissolution rates on the rate of decline of blood sugar levels has also been studied (2). Varley (3) investigated two formulations of tolbutamide, both generically equivalent in terms of chemical content and USP specifications; he found they were not equivalent as measured by availability of drug to the patient (serum drug levels) or on the basis of therapeutic efficacy (hypoglycemic response). Levy (4) found marked variation in the dissolution rates of two brands of tolbutamide tablets and recommended that patients should not change the brand of the drug they were taking unless the dose of the new brand was established. Another report (5) showed a correlation between percentage of the tolbutamide dose excreted in the urine as its metabolite and the surface area of tolbutamide in the dosage form.

The influence of povidone and polyethylene glycol 6000 on the dissolution rate of tolbutamide was studied (6). It was found that both carriers favorably increased the dissolution rate of the drug and that a complex formed between the drug and povidone but not between tolbutamide and polyethylene glycol. Later it was found (7) that the solid dispersion of

0022-3549/82/0300-0302$01.00/0

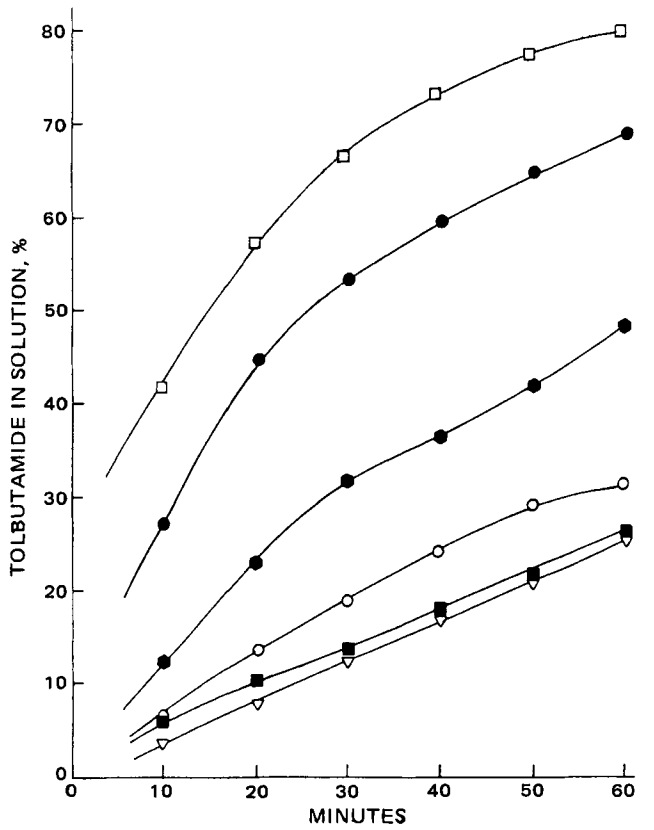

Figure 1—*Dissolution profiles of tolbutamide from its coprecipitates using single carriers. Total amount of tolbutamide: 62.5 mg. Key: ▽, tolbutamide recrystallized from methanol; ■, tolbutamide USP; ○, tolbutamide with mannitol; ●, tolbutamide with dextrose; ●, tolbutamide with polyethylene glycol 6000; and □, tolbutamide with polyethylene glycol 4000.*

tolbutamide in polyethylene glycol and in povidone increased the absorption of the drug and shortened its peak time from 3 hr to <1 hr. Recent reports (8, 9) compared the effect of polyethylene glycol and polyoxyethylene stearate on the dissolution rate and solution properties of tolbutamide from solid dispersions. Sugar combinations have been employed to increase the dissolution rates of hydrocortisone and prednisone (10).

In the present study, the coprecipitation technique was applied to enhance the dissolution rate of tolbutamide. Single and combined water-soluble carriers were utilized and their effects on dissolution rates were compared.

EXPERIMENTAL

Materials—Tolbutamide[1], polyethylene glycol 6000[2], polyethylene glycol 4000[2], dextrose anhydrous[3], and mannitol[3] were obtained commercially.

Preparation of Tolbutamide Coprecipitates—Quantities to make 1:1 coprecipitates of tolbutamide and carrier(s) were weighed accurately and dissolved in a sufficient volume of methanol[4]. The temperature was raised to 37°, and the solvent was allowed to evaporate under the hood, stirring continuously. When evaporation was almost complete, the resulting coprecipitate was removed from the container using a spatula, and placed *in vacuo* for 24 hr. The coprecipitates were sieved and the 100–200 mesh fraction was separated and kept in a desiccator for analysis and dissolution studies. The tolbutamide coprecipitate compositions are shown in Table I.

Dissolution Profiles of Tolbutamide and Tolbutamide Coprecipitates—The dissolution rate studies of tolbutamide and its coprecipitates were done in a dissolution apparatus[5] at 25 ± 0.5°. Nine-hundred

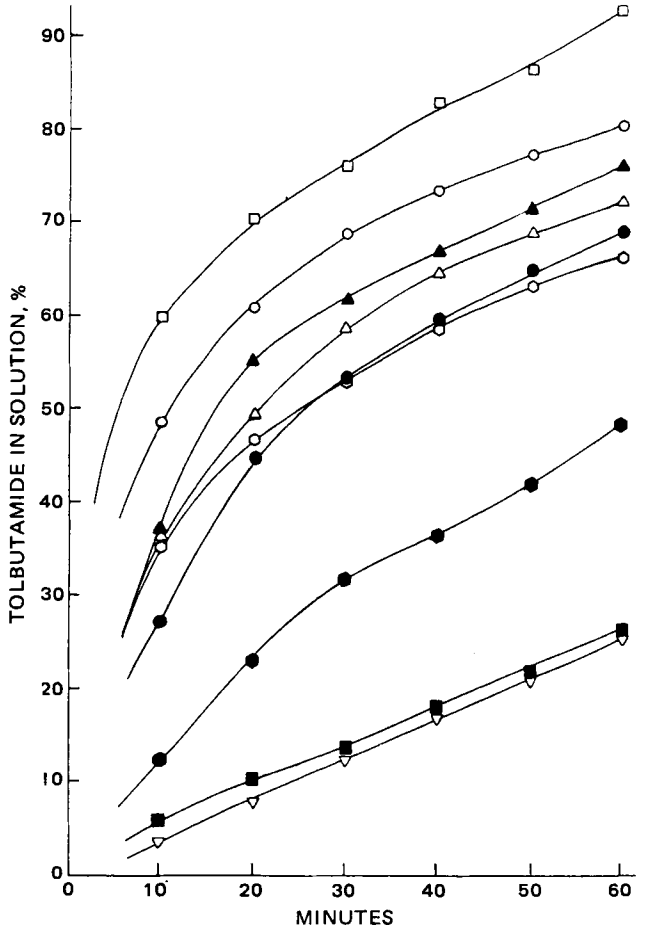

Figure 2—*Dissolution profiles of tolbutamide from its coprecipitates in polyethylene glycol 6000–dextrose carrier systems. Total amount of tolbutamide: 62.5 mg. Key: ▽, tolbutamide recrystallized from methanol; ■, tolbutamide USP; ●, tolbutamide with dextrose; ○, tolbutamide with 20% polyethylene glycol 6000–80% dextrose; ●, tolbutamide with polyethylene glycol 6000; △, tolbutamide with 60% polyethylene glycol 6000–40% dextrose; ▲, tolbutamide with 70% polyethylene glycol 6000–30% dextrose; ○, tolbutamide with 80% polyethylene glycol 6000–20% dextrose; and □, tolbutamide with 40% polyethylene glycol 6000–60% dextrose.*

milliliters of deionized water was placed in the vessels, the paddle stirring speed was set at 150 rpm, and 125 mg of the coprecipitate or 62.5 mg of the drug were added to the medium after the temperature was reached. The paddle was placed 2.5 cm from the bottom of the vessel. A glass filter[6] was attached to a 3-way stopcock[7] and this was attached to a glass syringe. One milliliter of filtrate was removed every 10 min and diluted to 10 ml with deionized water. The volume in the vessel was replaced with deionized water after each sample was taken. The absorbances of the solutions were measured in a spectrophotometer[8] at 230 nm using deionized water as the blank. None of the carriers interfered with the measurement of the absorbances at this wavelength.

RESULTS AND DISCUSSION

Tolbutamide Content of the Coprecipitates—The tolbutamide coprecipitates were assayed by spectrophotometry at λ_{max} = 230 nm using a 5% (v/v) dilution of methanol in deionized water as the blank. The drug content of the tolbutamide coprecipitates was within the 48.9–51.9% (w/w) range.

Dissolution Profiles of Tolbutamide Alone and from Its Coprecipitates—The dissolution profiles of tolbutamide alone, (100/200 mesh, and tolbutamide recrystallized from methanol and sieved to a 100/200 mesh) and with tolbutamide coprecipitates containing single carriers,

[1] The Upjohn Co., Kalamazoo, Mich.
[2] Union Carbide Corp., New York, N.Y.
[3] Matheson Coleman and Bell Manufacturing Chemists, Norwood, Ohio.
[4] Fisher Scientific Co., Fair Lawn, N.J.
[5] Easi-Lift model 72SL dissolution apparatus, Hanson Research Corp., Northridge, Calif.
[6] Kimble model 28630 gas dispersion tube, size 12-C, Owens-Illinois, Toledo, Ohio.
[7] K-75 three-way stopcock, Pharmaseal Inc., Toa Alta, Puerto Rico.
[8] Beckman model 25 spectrophotometer, Beckman Instruments Inc., Fullerton, Calif.

Table I—Composition of 1:1 Tolbutamide Coprecipitates

Polyethylene Glycol 6000, %	Dextrose, %
100	0
80	20
70	30
60	40
40	60
20	80
0	100
Polyethylene glycol 4000, %	**Mannitol, %**
100	0
80	20
60	40
50	50
40	60
20	80
0	100

are shown in Fig. 1. The dissolution profiles of tolbutamide from the two combination carrier systems (polyethylene glycol 6000–dextrose and polyethylene glycol 4000–mannitol) are shown in Figs. 2 and 3, respectively. Each point in these plots corresponds to the average of six determinations. The dissolution studies of tolbutamide from its coprecipitates showed that the presence of the water-soluble carrier enhanced the dissolution rate of the drug in all cases as compared with plain and recrystallized tolbutamide. From Fig. 1 it can be seen that the increase in the dissolution rate of tolbutamide was more pronounced when polyethylene glycol 4000 was used as the carrier than when polyethylene glycol 6000 was the drug vehicle. Dextrose alone and mannitol alone produced little increase in dissolution rate, but the combination of these carriers with polyethylene glycol 6000 and polyethylene glycol 4000 produced a large increase in dissolution rate of the drug in all proportions studied. The combination of 40% polyethylene glycol 6000–60% dextrose produced the highest dissolution rate of tolbutamide from its coprecipitates. If single carriers were desired, polyethylene glycol 4000 would be the carrier of choice with 44% of drug released after 10 min of the dissolution test. When carrier combinations were studied, ~60% of the drug was dissolved after 10 min for a coprecipitate of the drug in 40% polyethylene glycol 6000–60% dextrose. Approximately the same results were obtained when 50% polyethylene glycol 4000–50% mannitol was employed. It can be seen from Figs. 1–3 that the amount of the drug dissolved increased more than 15 times during the first 10 min of the dissolution study as compared with the dissolution of recrystallized tolbutamide; it was ~3 times higher after 1 hr when the drug was dispersed in a 40% polyethylene glycol 6000–60% dextrose mixture. When mannitol was the carrier, the amount dissolved increased only ~1.5 times indicating that mannitol, in the ratio of drug to carrier investigated (1:1), was a poor carrier for tolbutamide. Polyethylene glycol 6000 has been extensively used as a water-soluble carrier for slightly soluble drugs and has been claimed as a universal carrier. However, in this case the amount of drug dissolved increased only ~5 times as compared with the dissolution of recrystallized tolbutamide.

It is important to point out that only the 1:1 coprecipitates were investigated and that the enhancement of dissolution rates of tolbutamide from its coprecipitates would be expected to increase when the ratio of drug to carrier is diminished.

CONCLUSIONS

The 100–200 mesh fraction of the 1:1 coprecipitates of tolbutamide with dextrose, mannitol, polyethylene glycol 6000, polyethylene glycol 4000, and combinations of polyethylene glycol 6000–dextrose and polyethylene glycol 4000–mannitol in different proportions showed a faster dissolution *in vivo* than plain tolbutamide or tolbutamide recrystallized from methanol.

The use of combined carriers in the preparation of the coprecipitates of tolbutamide constituted an advantage over the formulation of the solid dispersions in a single carrier. The carrier combination consisting of 40% polyethylene glycol 6000–60% dextrose provided the fastest dissolution of the drug from its coprecipitate. Since polyethylene glycol 4000 alone produced a faster dissolution of tolbutamide than polyethylene glycol 6000 alone, and dextrose alone gave a faster dissolution of the drug than did mannitol alone, it is probable that combinations of polyethylene glycol 4000–dextrose would result in a better carrier system for tolbutamide. Further investigation is needed to support this suggestion.

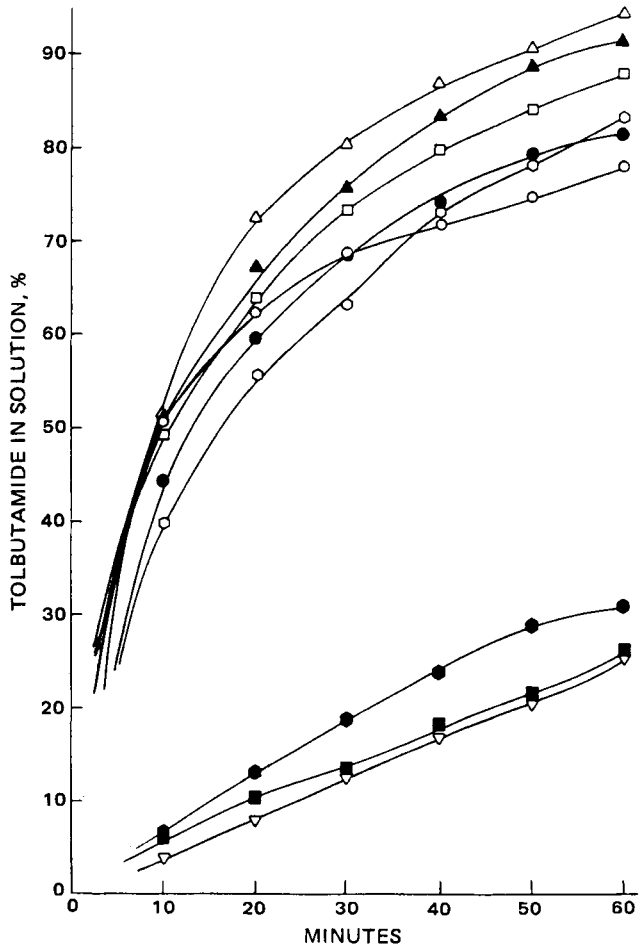

Figure 3—*Dissolution profiles of tolbutamide from its coprecipitates in polyethylene glycol 4000–mannitol carrier systems. Total amount of tolbutamide: 62.5 mg. Key: ▽, tolbutamide recrystallized from methanol; ■, tolbutamide USP; ●, tolbutamide with mannitol; ○, tolbutamide with 20% polyethylene glycol 4000–80% mannitol; ●, tolbutamide with polyethylene glycol 4000; ○, tolbutamide with 80% polyethylene glycol 4000–20% mannitol; □, tolbutamide with 40% polyethylene glycol 4000–60% mannitol; ▲, tolbutamide with 60% polyethylene glycol 4000–40% mannitol; △, tolbutamide with 50% polyethylene glycol 4000–50% mannitol.*

REFERENCES

(1) J. F. Nash, J. A. Galloway, A. D. Garner, D. W. Johnson, I. W. Kleber, and B. A. Rodda, *Can. J. Pharm. Sci.*, **12**, 59 (1977).

(2) E. Nelson, E. L. Knoechel, W. E. Hamlin, and J. G. Wagner, *J. Pharm. Sci.*, **51**, 509 (1962).

(3) A. B. Varley, *J. Am. Med. Assoc.*, **206**, 1745 (1968).

(4) G. Levy, *J. Can. Med. Assoc.*, **90**, 978 (1964).

(5) E. Nelson, S. Long, and J. G. Wagner, *J. Pharm. Sci.*, **53**, 1224 (1964).

(6) S. A. Said, H. M. El-Fatatry, and A. S. Geneidi, *Aust. J. Pharm. Sci.*, **NS3**, 42 (1974).

(7) S. A. Said and S. F. Saad, *ibid.*, **NS4**, 121 (1975).

(8) R. Kaur, D. J. W. Grant, and T. Eaves, *J. Pharm. Sci.*, **69**, 1317 (1980).

(9) *Ibid.*, **69**, 1321 (1980).

(10) L. V. Allen, Jr., R. S. Levinson, and D. Martono, *J. Pharm. Sci.*, **67**, 979 (1978).

ACKNOWLEDGMENTS

This work was supported in part by an endowed professorship provided to A. Martin by Coulter R. Sublett.

M. J. Miralles expresses her gratitude to the Venezuelan government for providing her with continuous financial support over the time this investigation was conducted.

Synthesis and Characterization of Iodoazidobenzylpindolol

ABBAS RASHIDBAIGI and ARNOLD E. RUOHO ˣ

Received April 13, 1981, from the *Department of Pharmacology, University of Wisconsin Medical School, Madison, WI 53706.* Accepted for publication July 15, 1981.

Abstract □ A high affinity β-adrenergic ligand, iodoazidobenzylpindolol, was synthesized and characterized. The absorption spectrum of this compound changed markedly upon photolysis, consistent with decomposition of the azide group. This compound has a K_D of 5–7 × 10^{-10} *M* for the duck erythrocyte ghost β-adrenergic receptor when measured in a competitive binding assay.

Keyphrases □ Iodoazidobenzylpindolol—synthesis and characterization, β-adrenergic receptor competitive binding assay □ β-Adrenergic blocking agents—iodoazidobenzylpindolol, synthesis and characterization □ Photoaffinity labeling—iodoazidobenzylpindolol label for β-adrenergic receptor binding sites

To identify the polypeptides that comprise the catecholamine receptor, suitable derivatives of β-receptor ligands must be available for forming covalent bonds in the binding site. This method for specifically tagging a binding site in an otherwise heterogeneous mixture of binding sites utilizing chemically reactive site-directed ligands has been described as affinity labeling (1–3) or the more recently used method of "photoaffinity labeling" (4–7).

The present study describes the synthesis and characterization of a potent β-adrenergic ligand containing an azide functional group. This compound, which is called iodoazidobenzylpindolol (VI), has been used as a photoaffinity label for β-adrenergic receptor binding site(s) (8).

EXPERIMENTAL[1]

Materials—2-Nitropropane[2], *p*-nitrobenzylchloride[2], thallium trichloride[3], nitromethane[4], *m*-nitrophenol[5], L-alprenolol-D-tartrate[5], and DL-propranolol hydrochloride[5] were all pure grade. DL-[^{125}I]Iodohydroxybenzylpindolol was synthesized according to a slightly modified method of Brown (9) from hydroxybenzylpindolol[6].

Instruments—Photolysis was performed with a high-pressure mercury lamp[7]. Melting points were determined on a capillary melting-point apparatus[8]. The IR spectra were obtained on a grating spectrophotometer[9] as potassium bromide disks. NMR spectra were determined on a 90 MHz Fourier transform spectrometer[10]. The chemical shifts reported are relative to an internal tetramethylsilane standard. Mass spectra were run on a spectrometer[11] at 70 ev.

Synthesis of 4-(2,3-Epoxypropoxy)indole (II)—6-Nitrosalicylaldehyde was prepared from *m*-nitrophenol according to the method of Ando and Emoto (10), with an overall yield of 7.2%. 5-Nitro-1,3-benzodioxane was purified by vacuum distillation (instead of column chromatography) at 1-mm Hg followed by crystallization in ethanol. In the process, 7-nitro-1,3-benzodioxane was removed and discarded.

4-Hydroxyindole (I)—Compound I was prepared from 6-nitrosalicylaldehyde according to the method of Beer *et al.* (11), with an overall yield of 26.0%.

4-(2,3-Epoxypropoxy)indole (II)—4-Hydroxyindole (I) (722 mg, 5.43 mmoles) was added to a solution of sodium hydroxide (216 mg, 5.40 mmoles) in 5 ml of water. Freshly distilled epichlorhydrin, 0.54 ml, was then added under nitrogen, and the reaction was stirred for 22 hr at ambient temperature. The mixture was extracted with ether, decolorized with activated charcoal, and dried over anhydrous sodium sulfate. The ether extract was evaporated to give 570 mg (55.5%) of an oily product. This compound was purified further using a silica gel column[5] (60–200 mesh) equilibrated with petroleum ether. The product was eluted from the column with increasing amounts of chloroform to give a white solid material (II); mp 64–65° [lit. (12), 65–67°]; NMR (deuterochloroform): δ 8.60–8.35 (s, 1H, indole-NH), 7.0–6.3 (m, 5H, aromatic H), and 4.3–2.5 (m, 5H, CH_2, epoxide-H) ppm; mass spectrum: *m/z* 189 (M^+).

Anal.—Calc. for $C_{11}H_{11}NO_2$: C, 69.84; H, 5.82; N, 7.41. Found: C, 70.00; H, 6.02; N, 7.45.

Synthesis of 1-(*p*-Azido-*m*-iodophenyl)-2-methyl-2-propylamine (V)—2-Methyl-2-nitro-1-(*p*-nitrophenyl)propane was prepared according to the method of Hass *et al.* (13), with an overall yield of 47%.

1-(p-Aminophenyl)-2-methyl-2-propylamine (III)—2-Methyl-2-nitro-1-(*p*-nitrophenyl)propane (10 g, 44.6 mmoles) was dissolved in 150 ml of 50% ethanol–water. Zinc powder (42.5 g, 654 mmoles) was mixed with the above solution. While heating the mixture very slowly with fast mechanical stirring, hydrochloric acid (25 ml of 37% mixed with 40 ml of 50% ethanol–water) was added dropwise. The mixture was refluxed for 1 hr after addition of hydrochloric acid and stirring continued during refluxing. After cooling the mixture, a yellow solution was separated from the zinc and was adjusted to pH 9.0 using 2 *N* potassium hydroxide. The amino compound, 1-(*p*-aminophenyl)-2-methyl-2-propylamine (III), was extracted with ether. The ether solution was dried under anhydrous sodium sulfate followed by evaporation of ether and distillation of the compound under vacuum. A yellow solid, 3.45 g (48%), was collected; mp 81–82° [lit. (13), 84–85°]; R_f 0.17 on silica gel plates[12] in chloroform–methanol (70:30); IR (potassium bromide): 3500, 3350, and 3200 cm^{-1} (NH_2); NMR (deuterochloroform): δ 6.7 (d, 2H, aromatic H, *J* = 3 Hz), 6.4 (d, 2H, aromatic H, *J* = 3 Hz), 2.45 (s, 2H, CH_2), and 1.0 (s, 6H, CH_3); mass spectrum: *m/z* 164 (M^+). The dihydrochloride salt of this compound was prepared by passing hydrogen chloride gas through an ether solution.

1-(p-Amino-m-iodophenyl)-2-methyl-2-propylamine (IV)—1-(*p*-Amino-phenyl)-2-methyl-2-propylamine dihydrochloride (III) (1.66 g, 7.0 mmoles) was dissolved in 200 ml of sodium acetate buffer (pH 4.0, 0.1 *M*). To this solution was added sodium iodide (1.05 g, 7.0 mmoles). Thallium trichloride (2.6 g, 7.0 mmoles) in 50 ml of distilled water was slowly added to the above solution under nitrogen. The mixture was heated on a steam bath for 1 hr under nitrogen, then sodium sulfite (0.88 g, 7.0 mmoles) in 20 ml of water was added. The reaction mixture was made alkaline using sodium bicarbonate and extracted with ether. The compound (IV), 0.76 g (37%), was purified using a silicic acid (325 mesh) column, eluting with increasing concentrations of methanol in chloroform. The compound was oily with a brownish color and an R_f of 0.30 on silica gel plate in chloroform–methanol (70:30). NMR (deuterochloroform): δ 7.4 (d, 1H, aromatic H *ortho* to I), 7.0–6.6 (m, 2H, aromatic H), 2.5 (s, 2H, CH_2), 1.1 (s, 6H, CH_3) ppm, and NH exchangeable with deuterium oxide; mass spectrum: *m/z* 290 (M^+).

Anal.—Calc. for $C_{10}H_{15}IN_2$: C, 41.38; H, 5.17, N, 9.66. Found: C, 41.16; H, 5.31, N, 9.42.

1-(p-Azido-m-iodophenyl)-2-methyl-2-propylamine (V)—1-(*p*-Amino-*m*-iodophenyl)-2-methyl-2-propylamine (IV) (220 mg, 0.758 mmoles) was dissolved in 6.2 ml of water containing 0.207 ml of 96% sulfuric acid. The mixture was cooled in crushed ice, and sodium nitrite (58 mg, 0.840 mmoles) in 8 ml of water was added dropwise while stirring the mixture. When the addition was completed, the reaction was allowed to proceed for 15 min, then sodium azide (54 mg, 0.83 mmoles) in 1 ml of water was added. After another 15 min, the mixture was made alkaline

[1] Elemental analyses were performed by the Galbraith Laboratories, Knoxville, Tenn.
[2] Aldrich Chemical Co., Milwaukee, Wis.
[3] K & K Laboratories, Plainview, N.Y.
[4] Fisher Scientific Co., Itasca, Ill.
[5] Sigma Chemical Co., St. Louis, Mo.
[6] A gift from Sandoz Pharmaceutical Co., East Hanover, N.J.
[7] AH-6 lamp from Advanced Radiation Corp., Santa Clara, Calif.
[8] Buchi, Switzerland.
[9] Model 700, Perkin-Elmer Corp., Norwalk, Conn.
[10] HX-90 Fourier transform NMR spectrometer, Bruker Instruments, Inc., Billerica, Mass.
[11] Model 1015 Finnigam spectrometer with Finnigam 6000 data system.
[12] Silica gel GF254, Type 60, E. Merck, was used to prepare plates with a 0.5-mm thickness.

0022-3549/82/0300-0305$01.00/0

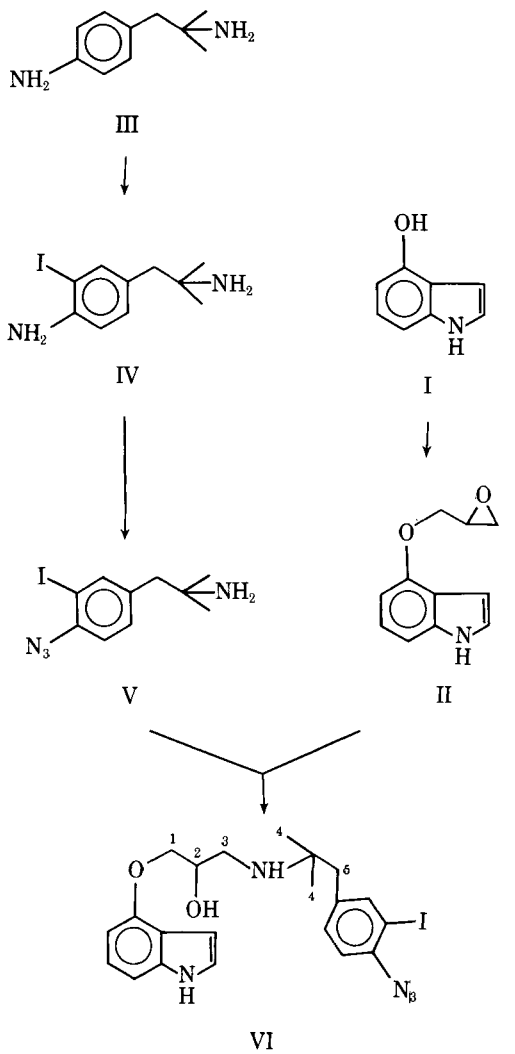

Scheme I—Synthetic scheme for iodoazidobenzylpindolol (VI).

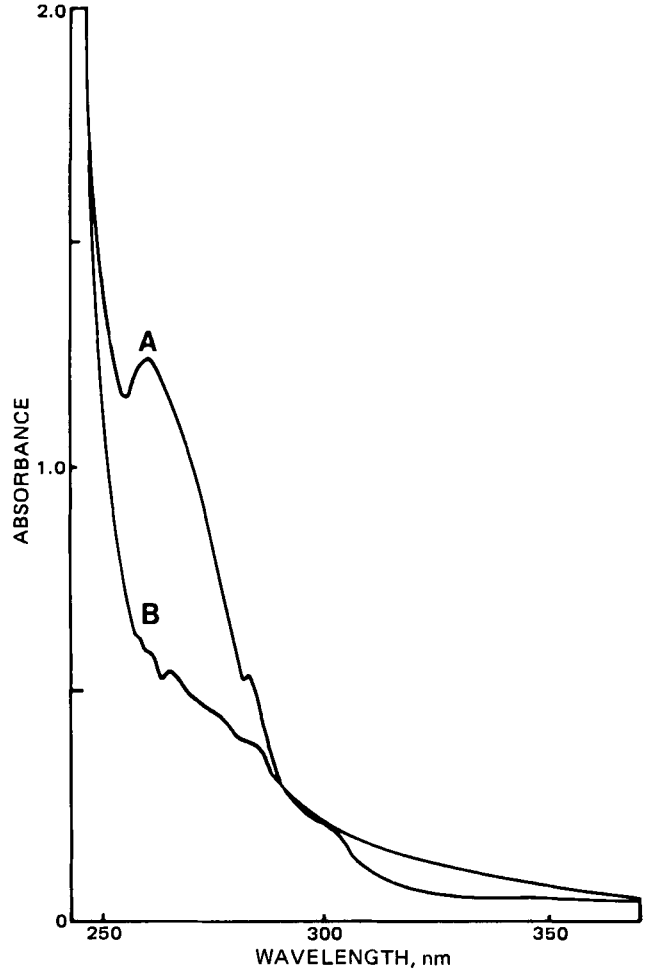

Figure 1—*Ultraviolet spectra for iodoazidobenzylpindolol (VI) before and after photolysis. A, VI (5.7×10^{-5} M) in ethanol; B, VI (5.7×10^{-5} M) photolyzed for 5 sec in ethanol using a high-pressure mercury lamp.*

using sodium bicarbonate and extracted with ether. All reactions were performed in the dark, and 72 mg (30%) of the oily product was purified by preparative TLC using silica gel in chloroform–methanol (70:30) with an R_f of 0.59; IR (potassium bromide): 2150 cm^{-1} (N_3); NMR (deuterochloroform): δ 7.60 (d, 1H, aromatic H *ortho* to I), 7.26–6.97 (m, 2H, aromatic H), 2.5 (s, 2H, CH_2), and 1.1 (s, 6H, CH_3) ppm.

Synthesis of DL-1-(Indol-4-yloxy)-3-[1-*p*-(azido-*m*-iodophenyl)-2-methyl-2-propylamine]-2-propanol (Iodoazidobenzylpindolol, VI)—4-(2,3-Epoxypropoxy)indole (II) (56 mg, 0.296 mmoles) and 1-(*p*-azido-*m*-iodophenyl)-2-methyl-2-propylamine (V) (35 mg, 0.110 mmoles) were dissolved in 1.5 ml of absolute ethanol. The reaction was heated in a sealed tube at 60° in the dark for 7 days. The products of the reaction mixture were separated on preparative silica gel plates with benzene–acetonitrile–triethylamine (100:75:1) to yield 44 mg (78.8%) of a solid compound (VI) with an R_f of 0.39 and a mp of 70–73° (dec. at 140–150°); IR (potassium bromide): 2150 cm^{-1} (N_3); NMR (deuterochloroform): δ 8.9 (s, 1H, indole-NH), 7.78 (d, 1H, aromatic H *ortho* to I), 7.57–6.45 (m, 7H, aromatic H), 4.20 [m, 5H, NH, OH, CH_2(1), CH(2)]; deuterium oxide exchange: 4.10 [m, 3H, CH_2(1), CH(2)], 3.01 [m, 2H, CH_2(3)], 2.70 [s, 2H, CH_2(5)], and 1.12 [s, 6H, CH_3(4)] ppm; UV (ethanol): 300, 288, and 262 nm (Fig. 1A) with ϵ262 = 19,000 and ϵ288 = 6920 M^{-1} cm^{-1}.

Anal.—Calc. for $C_{21}H_{24}IN_5O_2$: C, 49.90; H, 4.75; N, 13.86. Found: C, 50.03; H, 5.24; N, 13.10.

The %H and %N values differ by 0.5 and 0.7%, respectively, from the calculated values. This is probably due to decomposition that occurred before analysis, resulting from exposure of the compound to light.

Preparation of Duck Erythrocyte Ghosts—All steps were performed at 4°. Heparinized whole duck blood was diluted in an equal volume of washing buffer (145 m*M* NaCl, 10 m*M* tromethamine[5], 20 m*M* glucose, pH 7.4). The cells were centrifuged at 500×*g* and the supernate and buffy coat were removed. The packed cells were washed twice more in washing buffer and then lysed by stirring in lysis buffer (10 m*M* tromethamine, 4 m*M* magnesium chloride, pH 7.4). The resulting lysate was centrifuged at 20,000×*g* and the supernate was removed. The ghosts were stored at −80° at a concentration of ~15 mg/ml. The protein content of the ghosts was determined by the Lowry method (14) using bovine serum albumin as a standard.

[^{125}I]Iodohydroxybenzylpindolol Competitive Binding Assay—Nucleated duck ghosts were diluted to a protein concentration of 3–4 mg/ml with 50 m*M* tromethamine buffer, pH 7.4, containing 10 m*M* magnesium chloride. Each condition in the incubation contained ~0.2 mg of nucleated ghosts in 0.1 ml of total incubation volume, various concentrations of the competitive ligands, and 0.6 n*M* [^{125}I]iodohydroxybenzylpindolol. Incubation proceeded for 30 min at 32°. The binding was terminated by diluting 35-μl aliquots in duplicate into 10 ml of lysis buffer at 35°, filtering quickly (10 sec) through a glass fiber filter paper[13] under vacuum, and washing with an additional 10 ml of lysis buffer (5 sec) at 27°. The filter papers were counted using a gamma counter[14] with 70% efficiency, and the amount of bound [^{125}I]iodohydroxybenzylpindolol was determined.

The amount of nonspecific binding in all experiments was determined by incubating membranes and [^{125}I]iodohydroxybenzylpindolol in the presence of 1 μ*M* (L)-alprenolol. Nonspecific binding was generally 5–10% of the total binding and was subtracted from all experimental values. The K_D for each ligand was calculated from the equation (15):

$$K_D = IC_{50}/(1 + L/K_L) \qquad \text{(Eq. 1)}$$

where IC_{50} is the concentration of nonradioactive ligand which half maximally inhibits [^{125}I]iodohydroxybenzylpindolol binding, L is the concentration of [^{125}I]iodohydroxybenzylpindolol in the incubation, and

[13] GF/A Whatman glass microfilter paper, England.
[14] Model 5230, Packard Instrument, Downers Grove, Ill.

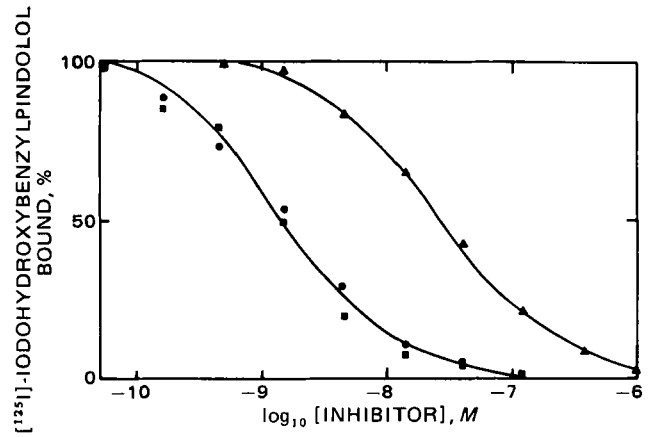

Figure 2—*Competitive inhibition of specific β-receptor binding of [125I]iodohydroxybenzylpindolol by DL-iodoazidobenzylpindolol (VI), DL-hydroxybenzylpindolol, and DL-propranolol. Data for each compound were obtained in duplicate, and the mean was plotted as percent of initial specific binding of [125I]-iodohydroxybenzylpindolol. Key: DL-iodoazidobenzylpindolol, ●; DL-hydroxybenzylpindolol, ■; and DL-propranolol, ▲.*

K_L is the equilibrium dissociation constant of [125I]iodohydroxybenzylpindolol determined from Scatchard analysis (16) (5×10^{-10} *M*).

RESULTS

Synthesis of Iodoazidobenzylpindolol (VI)—The synthetic scheme for the compound is summarized in Scheme I. The indole-containing epoxide (II) was prepared in a straightforward manner from 4-hydroxyindole (I). The epoxide was reacted with a primary amine to generate the final product (VI). The primary amine that was used in this synthesis contained an aralkyl structure, since it is known that affinity for the β-receptor is increased by increasing the size of substituents on the amino nitrogen (17). This final product, VI, has several structural features that are noteworthy: (*a*) the compound contains an indole ring structure which is characteristic of pindolol (12, 18); (*b*) the propanolamine structure which is characteristic of adrenergic compounds; and (*c*) an alkyl chain terminating with an aromatic group. Iodoazidobenzylpindolol (VI) is an analogue of iodohydroxybenzylpindolol (19), in which the phenolic hydroxyl on the aralkyl chain is replaced by an azido group and an iodine atom is *ortho* to the azido group rather than on the indole ring. An important synthetic reaction to generate 1-(*p*-amino-*m*-iodophenyl)-2-methyl-2-propylamine (IV) was the use of thallium trichloride and sodium iodide to incorporate iodine covalently. This type of reaction was reported previously for the preparation of iodinated polynucleotides (20) and nucleotides (21). In these cases, covalent iodine incorporation was followed by using carrier-free [125I]sodium iodide. This reaction demonstrated that the iodine-containing nucleotides could substitute for the parent nucleotides in polymers synthesized by either DNA or RNA polymerase (21). Chemical characterization of the reaction products was not performed.

Iodoazidobenzylpindolol (VI) has three absorption maxima (262, 288, and 300 nm). The main absorption occurs at 262 nm, whereas the 288 and 300 nm absorbances are secondary peaks (Fig. 1A). The photosensitivity of VI is shown in Fig. 1. After a 5-sec photolysis of VI in ethanol using a 1 kw mercury lamp, the ultraviolet absorption at 262, 288, and 300 nm were all reduced in a manner consistent with the decomposition of the azide group (Fig. 1B).

Biological Characterization of Iodoazidobenzylpindolol (VI)—To determine the binding characteristics of VI to the β-adrenergic receptor, intact duck erythrocyte ghosts were utilized. The β-receptor in this system has been thoroughly characterized for [3H]-L-dihydroalprenolol binding and has been partially purified 5000–10,000-fold over detergent extracts[15]. The apparent equilibrium dissociation constants (K_D) were determined by a previous method (15) utilizing competitive inhibition of [125I]iodohydroxybenzylpindolol binding. Iodoazidobenzylpindolol (VI) and hydroxybenzylpindolol possess the same affinity for the duck erythrocyte β-receptor with an apparent K_D calculated to be 0.5–0.7 n*M* (Fig. 2). From Scatchard analysis (16), it was found that the K_D for [125I]iodohydroxybenzylpindolol is 0.5 n*M* under the same conditions (data not shown). DL-Propranolol inhibited [125I]iodohydroxybenzylpindolol binding with a calculated K_D of 12.5 n*M* (Fig. 2), the same as previously reported for other β-adrenergic receptor systems (22).

[15] Y. Shing, A. Abramson, and A. E. Ruoho, submitted for publication.

DISCUSSION

The successful chemical synthesis of an azide derivative of pindolol, a potent β-adrenergic ligand, was performed. The compound was synthesized from 4-(2,3-epoxypropoxy)indole (II), which was prepared in good yield from *m*-nitrophenol. Thallium trichloride and sodium iodide were used to produce 1-(*p*-amino-*m*-iodophenyl)-2-methyl-2-propylamine (IV). This reaction allowed covalent incorporation of iodine into the phenyl ring *ortho* to the amine functional group which could then be readily converted to the azide derivative of V.

Iodoazidobenzylpindolol (VI) has as high an affinity as hydroxybenzylpindolol for the duck erythrocyte β-adrenergic receptor, and contains an azide functional group which can be incorporated into the β-adrenergic receptor binding site(s) upon photolysis (8). To minimize photodestruction of the biological samples and release of iodine, the majority of the light of wavelength <300 nm was filtered out. Successful photoincorporation of 4-[125I]iodobenzene-1-azide (23) and 5-[125I]iodonapthyl-1-azide (24) have also been reported for probing the lipid bilayer of biological membrane and labeling of the α-subunit of the sodium–potassium adenosinetriphosphatase (25).

REFERENCES

(1) L. Wofsy, H. Metzger, and S. J. Singer, *Biochemistry*, **1**, 1031 (1962).

(2) S. J. Singer, *Adv. Protein Chem.*, **22**, 1 (1967).

(3) B. R. Baker, "Design of Active-Site Directed Irreversible Enzyme Inhibitors," Wiley, New York, N.Y., 1967, p. 17.

(4) V. Chowdry and F. H. Westheimer, *Ann. Rev. Biochem.*, **48**, 293 (1979).

(5) H. Kiefer, J. Lindstrom, E. S. Lennox, and S. J. Singer, *Proc. Natl. Acad. Sci. USA*, **67**, 1688 (1970).

(6) A. E. Ruoho, H. Kiefer, P. Roeder, and S. J. Singer, *ibid.*, **70**, 2567 (1977).

(7) H. Baley and J. R. Knowles, *Methods Enzymol.*, **46**, 69 (1977).

(8) A. Rashidbaigi and A. E. Ruoho, *Proc. Natl. Acad. Sci. USA*, **78**, 1609 (1981).

(9) E. M. Brown, G. D. Aurbach, D. Hauser, and F. Troxler, *J. Biol. Chem.*, **251**, 1232 (1976).

(10) M. Ando and S. Emoto, *Bull. Chem. Soc. Jpn.*, **46**, 2903 (1973).

(11) R. J. S. Beer, K. Clarke, H. G. Khorana, and A. Robertson, *J. Chem. Soc. London*, **1948**, 1605.

(12) F. Seemann, E. Wiskoff, P. Nilaus, and F. Troxler, *Helv. Chim. Acta*, **54**, 2411 (1971).

(13) H. B. Hass, E. J. Berry, and M. L. Bender, *J. Am. Chem. Soc.*, **71**, 2290 (1949).

(14) O. H. Lowry, N. J. Rosebrough, A. L. Farr, and R. J. Randall, *J. Biol. Chem.*, **193**, 265 (1951).

(15) Y. Cheng and W. H. Prusoff, *Biochem. Pharmacol.*, **22**, 3099 (1973).

(16) G. Scatchard, *Ann. N.Y. Acad. Sci.*, **51**, 660 (1948).

(17) C. Mukherjee, M. G. Caron, D. Mullikin, and R. J. Lefkowitz, *Mol. Pharmacol.*, **12**, 16 (1976).

(18) A. F. Crowther, R. Howe, B. J. McLaughlin, K. B. Mallion, B. S. Roa, L. H. Smith, and R. W. Turner, *J. Med. Chem.*, **15**, 260 (1972).

(19) C. F. Bearer, R. D. Kanapp, A. J. Kaumann, T. L. Swartz, and L. Birnbaumer, *Mol. Pharmacol.*, **17**, 328 (1980).

(20) S. L. Commerford, *Biochemistry*, **10**, 1993 (1971).

(21) N. H. Scherberg and S. Refetoff, *Biochim. Biophys. Acta*, **340**, 446 (1974).

(22) B. B. Wolfe, T. K. Harden, and P. B. Molinoff, *Ann. Rev. Pharmacol. Toxicol.*, **17**, 575 (1977).

(23) A. Klip and C. Gitler, *Biochem. Biophys. Res. Commun.*, **60**, 1155 (1974).

(24) T. Bercovici and C. Gitler, *Biochemistry*, **17**, 1484 (1978).

(25) S. J. D. Karlish, P. L. Jorgensen, and C. Gitler, *Nature*, **269**, 715 (1977).

ACKNOWLEDGMENTS

This study was supported by Grant NS-12392 from the National Institute of Neurological and Communicative Disorders and Stroke. Arnold Ruoho is a recipient of a Research Career Development Award (NS-00158) from the National Institutes of Health.

Phosphorus–Nitrogen Compounds XXIII: Oncolytic Phosphorylated Imines

LINDLEY A. CATES ˣ and VEN-SHUN LI

Received March 18, 1981, from the *Department of Medicinal Chemistry and Pharmacognosy, College of Pharmacy, University of Houston, Houston, TX 77004.* Accepted for publication July 22, 1981.

Abstract □ A series of 15 amidine, iminopiperidine, iso(thio)urea, and guanidine derivatives and six 2,5-dihydro-1,3,5,2-triazaphosphorines were synthesized. Most of the compounds were tested for ability to react with L-cysteine and for antitumor activity against sarcoma 180 and P-388 murine tumor systems. Three acyclic phosphorylated imines and one triazaphosphorine showed activity in the former model to indicate that the P(O)N=C grouping serves as an oncolytic moiety. All agents condensed with L-cysteine with the active antitumor compounds displaying a tendency for relatively higher reactivity with this amino acid.

Keyphrases □ Phosphorus–nitrogen compounds—oncolytic phosphorylated imines □ Antitumor agents, potential—phosphorylated imines □ Phosphorylated imines—amidine, iminopiperidine, iso(thio)-urea, and guanidine derivatives, synthesis and screening for anticancer activity

A number of synthetic and naturally occurring products possessing α,β-unsaturated carbonyl moieties or their congeners are reported to produce an oncolytic effect *via* a type of Michael-condensation with biologically important nucleophiles. Since compounds that contain a P(O)-N=C grouping would be expected to undergo a similar reaction, a series of cyclic and acyclic phosphorylated imines were synthesized and tested for their ability to condense with L-cysteine and for anticancer activity.

BACKGROUND

Recently, there have been several investigations of conjugated systems that possess anticancer properties. Among those reported are phenyl nonenones (1, 2), styryl ketones (3–6), α-methylene lactams and lactones (7–9), and cyclopentenones (10, 11). Each compound contains a carbonyl function with a lateral overlap between two π-bond systems to produce a molecular orbital encompassing all four atoms. A valence bond representation of the system is $^{+}C—C=C—O^{-}$ where the β-carbon bond carries a positive charge and is subject to nucleophilic attack.

A related system contains an azomethine lactone grouping (IV) arising from the dehydration of carbinolamide derivatives (III) which were synthesized during an investigation of the "eastern zone" of maytansine (12). The dehydration rate of these tertiary alcohols to the conjugated system correlated with their ability to react with DNA bases and to show antineoplastic activity. The carbinolamides also undergo 1,4-addition with alcohols and ethanethiol in the presence of trace acid (13).

The only reported α,β-unsaturated system containing a phosphorus atom and concerned with anticancer activity is a proposed metabolite of cyclophosphamide (14). Iminophosphamide(VI) is thought to arise from the dehydration of 4-hydroxycyclophosphamide(V), providing an alternative explanation for the presence of 4-ethoxycyclophosphamide in microsomal incubation mixtures of V treated with ethanol.

Cyclophosphamide remains the most used and investigated chemotherapeutic of this chemical type. Studies, including those involving metabolism, have not completely accounted for this superior effectiveness. It can be speculated that the P(O)N=C moiety of VI may provide alkylating properties in addition to those of the nitrogen mustard group.

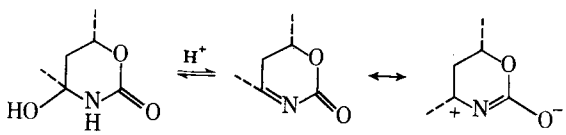

III IV

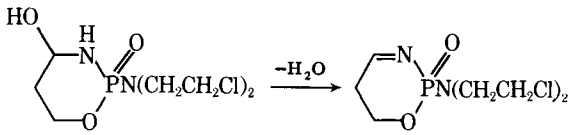

V VI

This functionality may permit the *in vivo* formation of substituted derivatives as stable, and less toxic transport forms. Support for this latter hypothesis is given by studies with 4(*S,R*) sulfido cyclophosphamide derivatives as stabilized forms of activated V (15).

The biological nucleophile most frequently associated with 1,4-addition to α,β-unsaturated system is L-cysteine, alone or as part of a protein molecule (16). However, correlation between L-cysteine and cytotoxicity was not observed in certain sesquiterpene lactones (17) and α-methylene lactones (9).

With this in mind, a series of acyclic(I) and cyclic(II) phosphorylated imines were synthesized for an investigation of their antitumor and L-cysteine addition properties (Table I).

EXPERIMENTAL

All solvents used were spectranalyzed or reagent grade. Melting points were determined by the capillary method (oil bath) and are corrected to reference standards. IR[1] (potassium bromide or neat for Ic), UV[2], and mass[3] spectra were recorded. ^{1}H-NMR[4] (in deuterochloroform) and ^{13}C-NMR[5] (in dimethylsulfoxide-d_6) spectra were measured in parts per million with tetramethylsilane as the internal standard. Elemental microanalyses were performed[6]. Silica gel 60 (70–230 mesh) was used for column chromatography and silica gel GHLF[7] was used for TLC.

Seven compounds [Ie, If, Ij, Ik (18), Ig, Ih (19), and In (20)] were prepared using literature methods employing the usual reaction of phosphoro(di)chloridates with compounds possessing imino groups or their salts. The catalytic hydrogenolysis of Ij gave Ia (18). Compounds Ib, Ii, Il, and Im were synthesized from *N*-methyl-1-chloro-*N'*-(dichlorophosphinyl)formamidine according to the procedure of Derkach and Narbut (21), while the triazaphosphorines IIa–IId were prepared by a novel reaction involving an intramolecular cyclization of bis imides (20). Compound Ic was prepared previously (22) from triethylphosphite and ethyl *N*-chloroacetamidine and isolated by vacuum distillation (bp 49–50°, 0.08 mm Hg). Compound Ic was synthesized using 4.7 g (0.05 mole) of acetamidine hydrochloride and 8.6 g (0.05 mole) of diethyl phosphorochloridate in the presence of 11.1 g (0.11 mole) of triethylamine and the product purified by chromatography. A solution of the chloridate in 50 ml of methylene chloride was added dropwise with stirring under nitrogen to the amidine salt and triethylamine in methylene chloride (100

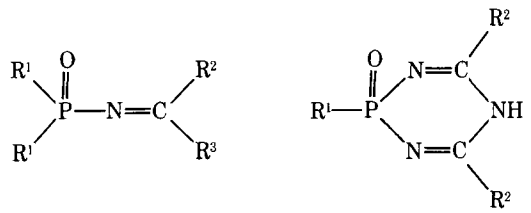

I II

[1] Perkin-Elmer 282 spectrophotometer.
[2] Perkin-Elmer 200 spectrophotometer.
[3] Hewlett-Packard 58930 GC/MS with 5933A data system.
[4] Varian Associates T-60 spectrometer.
[5] By Dr. G. E. Martin, employing a Varian Associates XL-100 spectrometer.
[6] Atlantic Microlab, Inc., Atlanta, Ga.
[7] Analtech.

0022-3549/82/0300-0308$01.00/0

Table I—Acyclic (I) and Cyclic (II) Phosphorylated Imines

Compound	R^1	R^2	R^3	Melting Point or Boiling Point/mm	Formula
I*a*	HO	CH_3	NH_2	166–167°[a]	$C_2H_7N_2O_3P$
I*b*	CH_3O	CH_3O	CH_3NH	74–75°/0.15[b]	$C_5H_{13}N_2O_4P$
I*c*	C_2H_5O	CH_3	NH_2	54–56°[c]	$C_6H_{15}N_2O_3P$
I*d*	C_2H_5O	C_6H_5	C_6H_5NH	122–123°	$C_{16}H_{21}N_2O_3P$
I*e*	C_6H_5O	NH_2	NH_2	117–118°[d]	$C_{13}H_{14}N_3O_3P$
I*f*	C_6H_5O	CH_3	NH_2	86–87°[e]	$C_{14}H_{15}N_2O_3P$
I*g*	C_6H_5O	CH_3S	NH_2	76–77°[f]	$C_{14}H_{15}N_2O_3PS$
I*h*	C_6H_5O	CH_3O	NH_2	78–79°[g]	$C_{14}H_{15}N_2O_4P$
I*i*	C_6H_5O	C_6H_5O	CH_3NH	84–85°[h]	$C_{20}H_{19}N_2O_4P$
I*j*	$C_6H_5CH_2O$	CH_3	NH_2	90.5–91.5°[i]	$C_{16}H_{19}N_2O_3P$
I*k*	$C_6H_5CH_2O$	H	NH_2	110–112°[j]	$C_{15}H_{17}N_2O_3P$
I*l*	n-C_4H_9NH	n-C_4H_9NH	CH_3NH	95–97°	$C_{14}H_{34}N_5OP$
I*m*	C_6H_5NH	C_6H_5NH	CH_3NH	163–166°[k]	$C_{20}H_{22}N_5OP$
I*n*	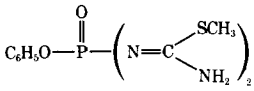			114–114.5°[l]	$C_{10}H_{15}N_4O_2PS_2$
I*o*	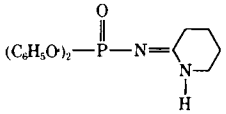			131.5–132°	$C_{17}H_{19}N_2O_3P$
II*a*	C_2H_5O	CH_3		231–232[l]	$C_6H_{12}N_3O_2P$
II*b*	C_2H_5O	C_6H_5		198–200°[l]	$C_6H_{12}N_3O_2P$
II*c*	C_6H_5O	CH_3		303–305°[l]	$C_{10}H_{12}N_3O_2P$
II *d*	C_6H_5	CH_3		270–272°[l]	$C_{10}H_{12}N_3OP$
II *e*	$(ClCH_2CH_2)_2N$	CH_3		191–192°	$C_8H_{15}Cl_2N_4OP$
II *f*	$(ClCH_2CH_2)_2N$	C_6H_5		171–173°	$C_{18}H_{19}Cl_2N_4OP$

[a] Lit. mp 161°; ref. 18. [b] Lit. bp 100–103°/0.6 mm; ref. 21. [c] See *Experimental*. [d] Lit. mp 118°; ref. 18. [e] Lit. mp 86–87°; ref. 18. [f] Lit. mp 78°; ref. 19. [g] Lit. mp 80°; ref. 18. [h] Lit. mp 86–87°; ref. 21. [i] Lit. mp 92.5°; ref. 18. [j] Lit. mp 116; ref. 18. [k] Lit. mp 149–150°; ref. 21. [l] Reference 20.

ml) at 0°. The reaction mixture was stirred to room temperature over a 2-hr period and refluxed for 12 hr. The mixture was filtered, spin evaporated, and the residue dried under vacuum. This material was extracted with benzene, filtered, and the residue dried under vacuum. The crude product was chromatographed with 10% methanol in chloroform to yield the pure material; IR: 3380, 3180 (NH_2), 1658 (N=C), and 1200 (P=O) cm^{-1}; ^{1}H-NMR: 1.32 (t, 6H, $2CH_3$), 2.15 (s, 3H, CH_3), 4.05 (m, 4H, $2CH_2$), and 7.12, 7.40 (2bs, 2H, NH_2) ppm; mass spectrum: *m/z*, 194 (M^+) (36.8%) and 195 (M^{+1})(6.0%).

***N*-(Diethoxyphosphinyl)phenylbenzamidine (I*d*)**—To a solution of 4.9 g (0.1 mole) of *N*-phenylbenzamidine and 10.1 g (0.1 mole) of triethylamine in 250 ml of ether was added a solution of 4.3 g (0.025 mole) of diethyl phosphorochloridate in 50 ml of ether, dropwise with stirring. The mixture was refluxed for 4 hr and filtered. The filtrate was concentrated by spin evaporation to yield, after drying in a vacuum desiccator, an analytically pure product; ^{1}H-NMR: 6.69–7.69 (m, 10H, aromatic), 3.59–4.28 (p, J = 7 Hz, 4H, $2CH_2$), and 1.20 (t, J = 7 Hz, 6H, $2CH_3$).

Anal.—Calc. for $C_{13}H_{14}N_3O_3P$: C, 61.34; H, 6.37; N, 8.43. Found: C, 61.43; H, 6.39; N, 8.42.

***N*-(Diphenoxyphosphinyl)-3-iminopiperidine (I*o*)**—A solution of 26.9 g (0.1 mole) of diphenyl phosphorochloridate in 100 ml of benzene was added dropwise with stirring at 5–10° to a solution of 13.4 g (0.01 mole) of 2-iminopiperidine hydrochloride and 30.3 g (0.3 mole) of triethylamine in 150 ml of benzene. The mixture was refluxed for 3 hr, at which time only two spots developed on a TLC plate (50% benzene in chloroform) at the origin (I_2 vapor) and at R_f 0.41 (UV and I_2 vapor). The mixture was cooled and filtered. Recrystallization of the residue from benzene produced a pure product. ^{13}C-NMR: pyridine carbons, 17.8 and 19.8 (C-4 and C-5), 28.1 (J = 7.1 Hz, C-3), 42.3 (C-6), and 169.3 (J = 4.6 Hz, C-1), 125.4 (C-4), 129.9 (C-3), and 150.0 (J = 7.3 Hz, C-1).

Anal.—Calc. for $C_{17}H_{19}N_2O_3P$: C, 61.81; H, 5.80; N, 8.48. Found: C, 61.89; H, 5.81; N, 8.47.

2-(Bis-*n*-butylaminophosphinyl)-1-*n*-butyl-3-methylguanidine (I*l*)—To a solution of 6.67 g (0.066 mole) of triethylamine and 4.82 g (0.066 mole) of *n*-butylamine in 20 ml of benzene, precooled to −10° and under a nitrogen atmosphere, was slowly added a solution of 4.10 g (0.02 mole) of *N*-methyl-1-chloro-*N'*-(dichlorophosphinyl)formamidine (21) in 60 ml of benzene. The reaction mixture was stirred at room temperature for 12 hr, filtered, the filtrate washed three times with water, and the benzene layer dried over anhydrous potassium carbonate. The benzene was removed under reduced pressure to yield a glassy solid. The crude product was purified by column chromatography using chloroform–ether (9:1) as the eluent. Recrystallization from methylene chloride–ether gave a white solid; IR: 3280 (NH), 1630 (C=N), and 1120, 1090 (P=O) cm^{-1}; ^{1}H-NMR: 0.65–1.60 (m, 21H, 3 $CH_3CH_2CH_2$), 1.80–2.40 (m, 2H, 2 NHP=O), 2.40–3.30 (m, 9H, CH_3N and 3 CH_2N), and 5.30–6.25 (bd, 2H, 2 NHC=N) ppm; mass spectrum: *m/z*, 247 (100), 191 (48), 149 (44), and 319 (M^+, 41).

Anal.—Calc. for $C_{14}H_{34}N_5OP$: C, 52.62; H, 10.73; N, 21.92. Found: C, 52.56; H, 10.72; N, 21.88.

2-Bis(2-chloroethyl)amino-4,6-dimethyl-2,5-dihydro-1,3,5,2-triazaphosphorine-2-oxide (II*e*)—To a mixture of 4.7 g (0.05 mole) of acetamidine hydrochloride and 1.1 g (0.11 mole) of triethylamine in 250 ml of methylene chloride was added, with stirring, cooling at 5–10°, and under a nitrogen atmosphere, 6.5 g (0.025 mole) of *N*-bis(2-chloroethyl)phosphoramidic dichloride. The reaction mixture was refluxed for 18 hr and filtered. The filtrate was spin evaporated and the residue dried under vacuum. The remaining material was extracted with acetone, the solvent removed by spin evaporation, and the crude product chromatographed with 20% methanol in chloroform to give a crystalline solid. This material was recrystallized from chloroform to yield the pure product; IR: 3260 (NH), 1630, 1660 (C=N), and 1210 (P=O) cm^{-1}; ^{1}H-NMR: 2.16 (s, 6H, $2CH_3$) and 2.95–3.75 (m, 8H, $4CH_2$) ppm; mass spectrum: *m/z*, 284 (M^+, 1.9) and 286 (M^{+2}, 1.0).

Anal.—Calc. for $C_8H_{15}Cl_2N_4OP$: C, 33.79; H, 5.32; N, 19.71. Found: C, 33.63; H, 5.39; N, 19.64.

2-Bis(2-chloroethyl)amino-4,6,diphenyl-2,5-dihydro-1,3,5,2-triazaphosphorine-2-oxide (II*f*)—The method employed was the same as for II*e* with the use of 7.8 g (0.05 mole) of benzamidine hydrochloride instead of acetamidine hydrochloride and except for the chromatographic and recrystallization procedures. The first elution was stepwise with 100 ml of chloroform followed by 2, 5, and 10% of methanol in chloroform. Recrystallization from methylene chloride gave the pure product; IR: 1610, 1630 (C=N), 1580 (C=C), and 1200 (P=O) cm^{-1}; ^{1}H-NMR: 3.0–3.7 (m, 8H, $4CH_2$), 7.2–8.9 (m, 10H, aromatic), and 11.5 (bs, 1H, NH) ppm; mass spectrum: *m/z*, 408 (M^+, 1.8) and 410 (M^{+2}, 0.8).

Anal.—Calc. for $C_{18}H_{19}Cl_2N_4OP$: C, 52.80; H, 4.68; N, 13.69. Found: C, 52.76; H, 4.73; N, 13.66.

An improved method for the preparation of *N*-bis(2-chloroethyl)-phosphoramidic dichloride for use in the synthesis of II*e* and II*f* was devised. A previous procedure (23) employed vacuum distillation to get this product, whereas a slightly higher yield was obtained using recrystallization for the purification step. A suspension of 50.0 g (0.28 mole) of bis(2-chloroethyl)amine hydrochloride, purified by washing with acetone, in 213.8 g (1.37 moles) of freshly distilled phosphorus oxychloride was refluxed at 135–140° in an oil bath for 15 hr or until a clear mixture was obtained. Excess phosphorus oxychloride was removed under vacuum. The residue was dissolved in warm acetone, filtered, the filtrate spin

Table II—Antitumor Testing

	Sarcoma 180		P-388[a]	
	mg/kg	T/C%[b]	mg/kg	T/C%
I *a*	200	144[c]	200[d]	100
I *b*	400	93	100[e]	110
I *c*	100	132	—	—
I *d*	400	89	100[e]	99
I *f*	100	97	50[f]	104
I *g*	400	112	—	—
I *h*	400	128	200[e]	100
I *i*	400	95	100[e]	93
I *j*	100	110	200[d]	97
I *k*	50	100	100[d]	101
I *l*	50	89	25[g]	108
I *m*	400	89	200[e]	86
I *n*	400	93	—	—
I *o*	25	122	25[e]	99
II *a*	200	109	200[d]	95
II *c*	—	—	200[d]	106
II *d*	200	109	200[d]	92
II *e*	100	144[c]	500[h]	104

[a] Performed by contractors of the National Cancer Institute, National Institutes of Health, according to general screening procedures; Ref. 24. In each case the results from the highest, nontoxic dose are shown. [b] Average survival time (treated/control) × 100. [c] 1 cure/6 mice. [d] Administered five times, every other day, beginning with Day 1. [e] Administered nine times, each day, beginning with Day 1. [f] Results of the repeat study. [g] Administered three times, four days apart, beginning with Day 1. [h] Administered once on Day 1.

evaporated, and the residue dried under vacuum. This material (71.0 g) was refluxed for 0.5 hr with 400 ml of ether, the suspension filtered to remove ether insoluble substances, and the filtrate concentrated to give two crops of pure product totaling 60.8 g (83.8%) melting at 53–55° [lit. (23) mp 54–56°].

A modified procedure of Cassady *et al.* (9) was employed for the measurement of L-cysteine addition. To 2.0 ml of 1.25×10^{-4} *M* L-cysteine in 0.05 *M* phosphate buffer (pH 7.4) under nitrogen atmosphere in a 1-cm cell was added 50 μl of a 10^{-2} *M* solution of the test compound or cyclopentenone in tetrahydrofuran. The reference cell contained 2.0 ml of the L-cysteine solution and 50 μl of tetrahydrofuran. After 4 min, 0.1 ml of 10^{-2} *M* 2,2′-dithiopyridine in tetrahydrofuran was added to each cell, the cells inverted to affect mixing, and the absorbance read at 343 nm. The method was done in triplicate, the values averaged, and the deviations between the three values were calculated. The absorbances of the test compounds were converted to values relative to cyclopentenone, arbitrarily set at 100.

Pharmacological Testing—Groups of six female Swiss albino mice weighing 20 ± 2 g were injected intraperitoneally with 0.1 ml of ascites fluid from donor mice bearing 7-day tumor growths and containing ~7.5×10^6 Sarcoma 180 cells. After 24 hr (Day 1) the control group was intraperitoneally administered 0.2 ml of vehicle consisting of 2% polyoxyethylene (20) sorbitan monooleate in normal saline, and test groups were similarly dosed with 0.2-ml solutions or suspensions of the compounds in vehicle. The injections were repeated every other day for a total of five doses. Animals surviving 30 days from Day 1 were considered to be cured and were calculated as 30-day survivors in the calculation of average survival times (treated/controls × 100). Control groups survived an average of 15.4 ± 2.7 (first study) and 16.5 ± 3.2 (second study) days. Prior to tumor testing the maximum nontoxic dose of each compound, up to 400 mg/kg, was estimated by similar injections of female albino mice with the above preparations.

RESULTS AND DISCUSSION

The only chemistry deemed appropriate for discussion concerns compound Io. Although it was assumed that phosphorylation occurs at the more basic imino nitrogen of 2-iminopiperidine, this starting material also possesses a secondary amine nitrogen capable of substitution. The only product isolated was converted to the hydrochloride salt and both it and 2-iminopiperidine hydrochloride were subjected to ^{13}C-NMR spectral analysis. The pertinent chemical shifts and couplings occurred as singlets at 25.3 and 116.5 ppm, which were assigned to C-2 and C-3 of the piperidine ring, respectively, for the starting material and as doublets at 28.1 and 169.3 ppm for the same carbon atoms in the product. If the piperidino nitrogen were phosphorylated, additional splitting of the ring carbon atoms at the 5- and 6-positions would be expected.

The effect of the compounds on the survival times of mice bearing Sarcoma 180 and P-388 ascites cells is shown in Table II. The Sarcoma 180 testing was done in two sets of experiments, while the P-388 screening was done periodically over a 1-year period. The initial Sarcoma 180 study involved Id, Ig–Ii, and Ik–Im. Four compounds, Id, Ii, Il, and Im possessed bulky substituents on the imino carbon atom. The inactivity of these agents led to speculation that adverse steric or solubility factors were involved. However, Ig and Il, whose toxicity required reduction to a lower dose, also gave negative results. The positive effect of Ih and the initial presumptive activity of If against P-388 (which was not confirmed in later testing) prompted the synthesis of compounds possessing methyl or methoxy and amino or methylamino groups as the two imino carbon substituents. Subsequently, the remaining derivatives, principally those with the aforementioned substituents and several with increased hydrophilicity, were synthesized and tested. Activity was found with IIe > Ia > Ic > Ih and borderline effects with Io and IIa, based on T/C % values. Each of these four active compounds possess methyl, methoxy and amino, or NH grouping on the imino, or comparable, carbon atom. Of the three active imido derivatives, the highest activity was found in those with the greatest hydrophilicity, Ia and Ic. Compound IIe, bearing a nitrogen mustard moiety had the greatest activity, but the effects produced by Ia, Ic, and Ih establish the P(O)N=C system as a new oncolytic grouping, probably acting through an alkylating mechanism. Although seven and ten different atoms or groups were used for R1 and attached to the imino carbon atom, respectively, it is believed that substituents providing optimum electronic, steric, and solubility characteristics leading to the most active derivatives of this nature have yet to be found.

Table III—L-Cysteine Addition

Compound	Relative Reactivity
Cyclopentenone	100.0 ± 8.1
I *g*	79.4 ± 3.6
I *a*	77.3 ± 1.1
II *a*	77.1 ± 5.1
I *k*	74.0 ± 2.2
I *n*	74.0 ± 2.2
I *f*	65.0 ± 6.7
I *c*	64.5 ± 3.3
I *o*	61.7 ± 1.1
I *l*	59.2 ± 3.9
II *e*	54.9 ± 1.1
I *j*	50.4 ± 1.1
II *d*	50.4 ± 1.1
II *b*	49.3 ± 4.5
I *i*	47.1 ± 6.7
I *h*	47.1 ± 2.3
I *e*	40.4 ± 4.5
I *d*	33.6 ± 6.7

Seventeen compounds were also investigated for ability to condense with L-cysteine (Table III). Some derivatives, *e.g.* Im, were not sufficiently soluble for use in the procedure. Of the antitumor agents tested, Ia, IIa, and Ic were among the seven compounds possessing the highest degree of reactivity with the amino acid while Ih gave anomalous results. Based on this evidence, there is no precise correlation between biological and chemical activities but there appears to be some relationship between these effects.

REFERENCES

(1) J. R. Dimmock, P. J. Smith, I. M. Noble, and W. R. Pennekoek, *J. Pharm. Sci.*, **67**, 1536 (1978).

(2) J. R. Dimmock, C. B. Nyathi, and P. J. Smith, *ibid.*, **67**, 1543 (1978).

(3) N. W. Hamon, D. L. Bassenlowski, D. E. Wright, J. R. Dimmock, and L. M. Noble, *ibid.*, **67**, 1539 (1978).

(4) C. B. Nyathi, U. S. Gupta, and J. R. Dimmock, *ibid.*, **68**, 1383 (1979).

(5) J. R. Dimmock, N. W. Hamon, L. M. Noble, and D. E. Wright, *ibid.*, **68**, 1033 (1979).

(6) J. R. Dimmock, C. B. Nyathi, and P. J. Smith, *ibid.*, **68**, 1216 (1979).

(7) M. J. Kornet, *ibid.*, **68**, 350 (1979).

(8) I. H. Hall, K.-H. Lee, C. O. Starnes, S. A. Eigebaly, T. Ibuka, Y.-S. Wu, T. Kimura, and M. Haruna, *ibid.*, **67**, 1235 (1978).

(9) J. M. Cassady, S. R. Byrn, I. K. Stamos, S. M. Evans, and A. McKenzie, *J. Med. Chem.*, **21**, 815 (1978).

(10) K.-H. Lee, T. Ibuka, E.-C. Mar, and I. H. Hall, *ibid.*, **21**, 698 (1978).

(11) K.-H. Lee, E.-C. Mar, M. Okamoto, and I. H. Hall, *ibid.*, **21**, 819 (1978).
(12) J. W. Lown, K. C. Majumdar, A. I. Meyers, and A. Hecht, *Bioorg. Chem.*, **6**, 453 (1977).
(13) A. I. Meyers and C.-C. Shaw, *Tetrahedron Lett.*, **9**, 717 (1974).
(14) C. Fenselau, M.-N. N. Kan, S. S. Rao, A. Myles, O. M. Friedman, and M. Colvin, *Cancer Res.*, **37**, 2538 (1977).
(15) G. Peter and H.-J. Hohorst, *Cancer Chemother. Pharmacol.*, **3**, 181 (1979).
(16) S. M. Kupchan, D. C. Fessler, M. A. Eakin, and T. J. Giacobbe, *Science*, **168**, 376 (1970).
(17) S. M. Kupchan, M. A. Eakin, and A. M. Thomas, *J. Med. Chem.*, **14**, 1147 (1971).
(18) F. Cramer and A. Vollmar, *Chem. Ber.*, **91**, 911 (1958).
(19) *Ibid.*, **91**, 919 (1958).
(20) V.-S. Li and L. A. Cates, *J. Heterocycl. Chem.*, **18**, 503 (1981).
(21) G. I. Derkach and A. V. Narbut, *J. Gen. Chem. USSR*, **36**, 330 (1966).
(22) G. I. Derkach and M. V. Kolotilo, *ibid.*, **36**, 85 (1966).
(23) O. M. Friedman and A. M. Seligman, *J. Am. Chem. Soc.*, **76**, 655 (1954).
(24) R. I. Geran, N. H. Greenberg, M. M. MacDonald, A. M. Schumacher, and B. J. Abbott, *Cancer Chemother. Rep., Part 3*, **3**, 1 (1972).

ACKNOWLEDGMENTS

This investigation was supported by Grant CA24970-02, from the National Cancer Institute, National Institutes of Health.

Presented in part at the Medicinal Chemistry and Pharmacognosy Section, 29th National Meeting, APhA Academy of Pharmaceutical Sciences, San Antonio, Tex., November, 1980.

Synthesis and Antimicrobial Activity of Triorganotin 5-Nitro-2-furoates

EUGENE J. KUPCHIK *x, MICHAEL A. PISANO ‡, STEPHEN M. WHALEN *, and JOSEPH LYNCH ‡

Received June 29, 1981, from the **Department of Chemistry and the ‡Department of Biological Sciences, St. John's University, New York, NY 11439.* Accepted for publication July 27, 1981.

Abstract □ Five triorganotin 5-nitro-2-furoates were synthesized by reacting 5-nitro-2-furoic acid with either the corresponding bis(triorganotin) oxide or the corresponding triorganotin hydroxide. The IR spectrum of each compound was obtained over the 4000–200-cm^{-1} range, and some of the bands were assigned. One compound, tri-*n*-butyltin 5-nitro-2-furoate, was an excellent antifungal agent, completely inhibiting the growth of six of ten test fungi at a concentration of 1 μg/ml. The new compounds were also investigated for antibacterial activity and were especially inhibitory toward Gram-positive species. Two of the compounds completely inhibited the Gram-negative bacterium *Escherichia coli* at a concentration of 100 μg/ml.

Keyphrases □ Organometallics—triorganotin compounds, synthesis, tested for antifungal and antibacterial activity □ Tin—triorganotin compounds, synthesis and evaluation as antifungal and antibacterial agents □ Antifungal agents, potential—triorganotin compounds, synthesis □ Antibacterials, potential—triorganotin compounds, synthesis

Many biocidal applications have been found or suggested for organotin compounds (1, 2). The specific organotin compounds currently used in agriculture were reviewed recently (3–5). Their use in agriculture as fungicides and pesticides is of special interest because they degrade to nontoxic inorganic compounds and, therefore, appear to pose little threat to the environment (6–10). Recently, a series of diorganotin dihalide complexes was shown to exhibit antitumor activity (11).

It was reported previously that *N*-substituted *N*-(triphenylstannyl)cyanamides (I) are better antifungal agents than *N*-substituted *N'*-cyano-*S*-(triphenylstannyl)isothioureas (II) and *N*-substituted *N'*-cyano-*O*-(triphenylstannyl)isoureas (III) (12). The I compounds were similar in activity to ethyl *N*-aryl-*S*-(triphenylstannyl)isothiocarbamates (IV). Triethylammonium (organocyanoamino)chlorotriphenylstannates (V), which are the triethylammonium chloride complexes of the I compounds, reportedly exhibit higher antifungal activity than the I compounds (12). Although all of the compounds mentioned inhibited Gram-positive bacteria, they showed little inhibitory activity toward Gram-negative bacteria. In this respect, they resemble numerous other organotin compounds (13–16). One purpose of the present study was to synthesize some organotin compounds that might inhibit both Gram-positive and Gram-negative bacteria. Since 5-nitro-2-substituted furans are known to inhibit both Gram-positive and Gram-negative bacteria (17–19), the antibacterial activity of some triorganotin 5-nitro-2-furoates (VI) was studied. The antifungal activity of these

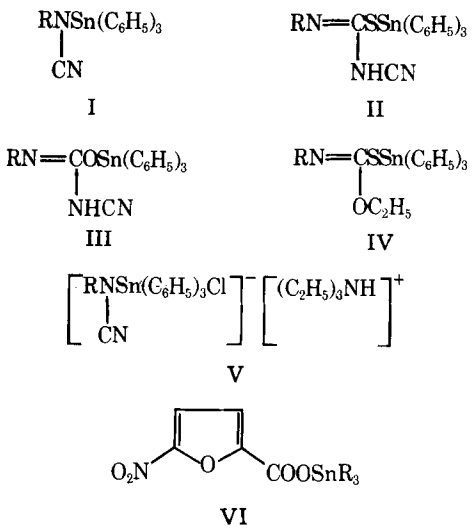

0022-3549/82/0300-0311$01.00/0

(11) K.-H. Lee, E.-C. Mar, M. Okamoto, and I. H. Hall, *ibid.*, **21**, 819 (1978).
(12) J. W. Lown, K. C. Majumdar, A. I. Meyers, and A. Hecht, *Bioorg. Chem.*, **6**, 453 (1977).
(13) A. I. Meyers and C.-C. Shaw, *Tetrahedron Lett.*, **9**, 717 (1974).
(14) C. Fenselau, M.-N. N. Kan, S. S. Rao, A. Myles, O. M. Friedman, and M. Colvin, *Cancer Res.*, **37**, 2538 (1977).
(15) G. Peter and H.-J. Hohorst, *Cancer Chemother. Pharmacol.*, **3**, 181 (1979).
(16) S. M. Kupchan, D. C. Fessler, M. A. Eakin, and T. J. Giacobbe, *Science*, **168**, 376 (1970).
(17) S. M. Kupchan, M. A. Eakin, and A. M. Thomas, *J. Med. Chem.*, **14**, 1147 (1971).
(18) F. Cramer and A. Vollmar, *Chem. Ber.*, **91**, 911 (1958).
(19) *Ibid.*, **91**, 919 (1958).
(20) V.-S. Li and L. A. Cates, *J. Heterocycl. Chem.*, **18**, 503 (1981).
(21) G. I. Derkach and A. V. Narbut, *J. Gen. Chem. USSR*, **36**, 330 (1966).
(22) G. I. Derkach and M. V. Kolotilo, *ibid.*, **36**, 85 (1966).
(23) O. M. Friedman and A. M. Seligman, *J. Am. Chem. Soc.*, **76**, 655 (1954).
(24) R. I. Geran, N. H. Greenberg, M. M. MacDonald, A. M. Schumacher, and B. J. Abbott, *Cancer Chemother. Rep., Part 3*, **3**, 1 (1972).

ACKNOWLEDGMENTS

This investigation was supported by Grant CA24970-02, from the National Cancer Institute, National Institutes of Health.

Presented in part at the Medicinal Chemistry and Pharmacognosy Section, 29th National Meeting, APhA Academy of Pharmaceutical Sciences, San Antonio, Tex., November, 1980.

Synthesis and Antimicrobial Activity of Triorganotin 5-Nitro-2-furoates

EUGENE J. KUPCHIK *x, MICHAEL A. PISANO ‡, STEPHEN M. WHALEN *, and JOSEPH LYNCH ‡

Received June 29, 1981, from the **Department of Chemistry and the ‡Department of Biological Sciences, St. John's University, New York, NY 11439.* Accepted for publication July 27, 1981.

Abstract □ Five triorganotin 5-nitro-2-furoates were synthesized by reacting 5-nitro-2-furoic acid with either the corresponding bis(triorganotin) oxide or the corresponding triorganotin hydroxide. The IR spectrum of each compound was obtained over the 4000–200-cm^{-1} range, and some of the bands were assigned. One compound, tri-*n*-butyltin 5-nitro-2-furoate, was an excellent antifungal agent, completely inhibiting the growth of six of ten test fungi at a concentration of 1 μg/ml. The new compounds were also investigated for antibacterial activity and were especially inhibitory toward Gram-positive species. Two of the compounds completely inhibited the Gram-negative bacterium *Escherichia coli* at a concentration of 100 μg/ml.

Keyphrases □ Organometallics—triorganotin compounds, synthesis, tested for antifungal and antibacterial activity □ Tin—triorganotin compounds, synthesis and evaluation as antifungal and antibacterial agents □ Antifungal agents, potential—triorganotin compounds, synthesis □ Antibacterials, potential—triorganotin compounds, synthesis

Many biocidal applications have been found or suggested for organotin compounds (1, 2). The specific organotin compounds currently used in agriculture were reviewed recently (3–5). Their use in agriculture as fungicides and pesticides is of special interest because they degrade to nontoxic inorganic compounds and, therefore, appear to pose little threat to the environment (6–10). Recently, a series of diorganotin dihalide complexes was shown to exhibit antitumor activity (11).

It was reported previously that *N*-substituted *N*-(triphenylstannyl)cyanamides (I) are better antifungal agents than *N*-substituted *N'*-cyano-*S*-(triphenylstannyl)isothioureas (II) and *N*-substituted *N'*-cyano-*O*-(triphenylstannyl)isoureas (III) (12). The I compounds were similar in activity to ethyl *N*-aryl-*S*-(triphenylstannyl)isothiocarbamates (IV). Triethylammonium (organocyanoamino)chlorotriphenylstannates (V), which are the triethylammonium chloride complexes of the I compounds, reportedly exhibit higher antifungal activity than the I compounds (12). Although all of the compounds mentioned inhibited Gram-positive bacteria, they showed little inhibitory activity toward Gram-negative bacteria. In this respect, they resemble numerous other organotin compounds (13–16). One purpose of the present study was to synthesize some organotin compounds that might inhibit both Gram-positive and Gram-negative bacteria. Since 5-nitro-2-substituted furans are known to inhibit both Gram-positive and Gram-negative bacteria (17–19), the antibacterial activity of some triorganotin 5-nitro-2-furoates (VI) was studied. The antifungal activity of these

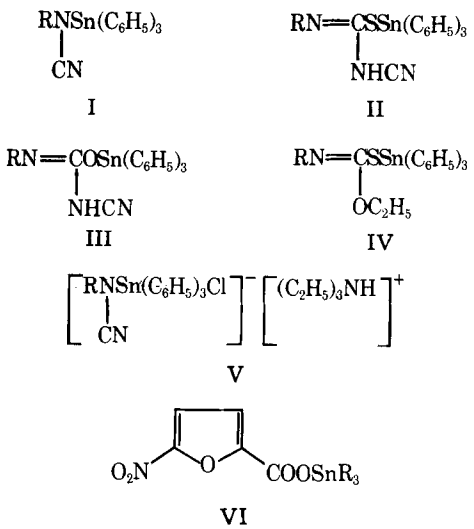

0022-3549/82/0300-0311$01.00/0

Table I—Triorganotin 5-Nitro-2-furoates

Compound	R	Yield, %[a]	Melting Point[b]	Formula	Analysis, % Calc.	Found
VI*a*	C_6H_5	90	111.8–112.5°	$C_{23}H_{17}NO_5Sn$	C 54.59	54.51
					H 3.39	3.59
					N 2.77	2.90
					Sn 23.45	23.09
VI*b*	n-C_4H_9	97	68–69.7°	$C_{17}H_{29}NO_5Sn$	C 45.77	45.60
					H 6.55	6.63
					N 3.14	3.28
					Sn 26.61	26.67
VI*c*	cyclo-C_6H_{11}	97	154.8–156°	$C_{23}H_{35}NO_5Sn$	C 52.70	52.92
					H 6.73	6.98
					N 2.67	2.82
					Sn 22.64	22.57
VI*d*	$CH_2C(CH_3)_2C_6H_5$	93	79.3–80°	$C_{35}H_{41}NO_5Sn$	C 62.33	62.56
					H 6.13	6.26
					N 2.08	2.13
					Sn 17.60	17.84
VI*e*	CH_3	94	190–192°	$C_8H_{11}NO_5Sn$	C 30.04	30.15
					H 3.47	3.74
					N 4.38	4.43
					Sn 37.12	36.89

[a] Based on material melting within 5° of the analytical sample. [b] Refers to the analytical sample.

Table II—IR Spectra of Triorganotin 5-Nitro-2-furoates[a]

Compound	C=O[b]	C—O	SnR_3[c] ν_{as}	ν_s
VI*a*	1613s	1355s	268s[d]	234s
VI*b*	1610s	1350s	605w	510w
VI*c*	1613s	1353s	610w	510w
VI*d*	1613s	1353s	610m	510w
VI*e*	1615s[e]	1345s	558m	510w

[a] Values are expressed in centimeters^{-1}; s = strong, m = medium, and w = weak. The data for 4000–400 cm^{-1} were obtained using potassim bromide pellets. The data for 400–200 cm^{-1} were obtained using mineral oil. [b] Refs. 22 and 23. [c] Refs. 24 and 25. [d] A strong band was present at 280 cm^{-1}. [e] A strong band was present at 1630 cm^{-1}.

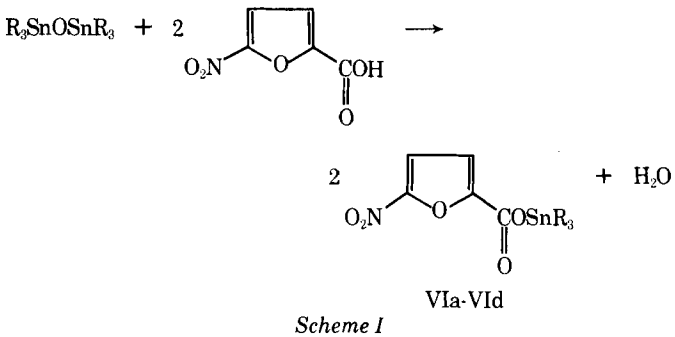

Scheme I

compounds was compared also to that of the I–V compounds.

RESULTS AND DISCUSSION

Synthesis—Compounds VI*a*–VI*e* (Table I) were prepared by reacting 5-nitro-2-furoic acid with either the corresponding bis(triorganotin) oxide (VI*a*–VI*d*) (Scheme I) or the corresponding triorganotin hydroxide (VI*e*) (Scheme II). The compounds were identified by elemental analysis (Table I) and IR (Table II). Their IR spectra are considerably different from those of organic esters. Whereas the C=O stretching vibration of normal saturated organic esters occurs in the range 1750–1730 cm^{-1} (20), the C=O stretching vibration of the organotin esters in Table II occurs in the range 1630–1610 cm^{-1}. This shift to lower frequency may be due to intermolecular or intramolecular coordination between the carbonyl oxygen and the tin atom. Interestingly, this shift occurred even for compound VI*d*, which has bulky neophyl groups around the tin atom. The organotin esters contained both the ν_{as}(SnC) and the ν_a(SnC) bands indicating that the triorganotin groups may be nonplanar in these compounds (21).

Biological Results—Compound VI*b* was the best antifungal agent of the VI compounds (Table III), completely inhibiting the growth of six of the ten test fungi at 1 μg/ml and all of the test fungi at 10 μg/ml. Compound VI*b* was the best antifungal agent of the I–VI compound series. Compound VI*a* was the second best antifungal agent of the VI

Table III—Antifungal Activity of Triorganotin 5-Nitro-2-furoates[a]

Compound	*Aspergillus niger* (ATCC 12845) 1[b]	10	100	*Chaetomium globosum* (ATCC 6205) 1	10	100	*Cladosporium carpophilum* (ATCC 12117) 1	10	100	*Fusarium moniliforme* (ATCC 10052) 1	10	100	*Myrothecium verrucaria* (ATCC 9095) 1	10	100
VI*a*	+	2+	2+	+	+	+	2+	2+	2+	+	+	+	+	2+	2+
VI*b*	2+	2+	2+	2+	2+	2+	2+	2+	2+	+	2+	2+	2+	2+	2+
VI*c*	+	+	+	+	+	+	−	+	+	+	+	+	+	+	+
VI*d*	−	−	−	−	+	+	−	−	−	−	−	−	−	+	+
VI*e*	−	+	+	−	+	+	+	2+	2+	−	+	+	+	+	2+

Compound	*Penicillium notatum* (ATCC 9179) 1	10	100	*Rhizopus stolonifer* (ATCC 10404) 1	10	100	*Saccharomyces cerevisiae* (ATCC 9896) 1	10	100	*Trichoderma viride* (ATCC 8678) 1	10	100	*Trichophyton mentagrophytes* (ATCC 9129) 1	10	100
VI*a*	+	2+	2+	+	+	+	−	+	+	+	+	+	+	2+	2+
VI*b*	+	2+	2+	+	2+	2+	2+	2+	2+	2+	2+	2+	+	2+	2+
VI*c*	+	+	2+	−	+	+	−	−	−	+	+	+	+	+	+
VI*d*	−	+	+	−	−	−	−	−	−	−	−	−	+	+	+
VI*e*	−	+	2+	+	+	+	−	−	−	+	+	+	+	+	+

[a] A − indicates no inhibition of growth, + indicates partial inhibition of growth, and 2+ indicates complete inhibition of growth. [b] Indicates concentration of compounds employed in micrograms per milliliter.

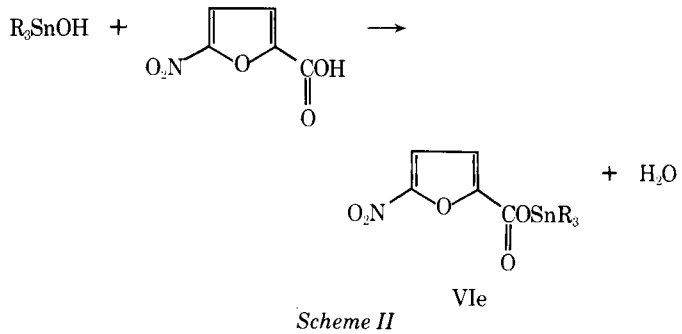

VIe

Scheme II

compounds, partially inhibiting the growth of all of the test fungi, except *Saccharomyces cerevisiae*, at 1 μg/ml and completely inhibiting the growth of five of the ten test fungi at 10 μg/ml. Compound VI*e* was a generally better antifungal agent than compound VI*c*. Compound VI*e* completely inhibited the growth of *Cladosporium carpophilum* at 10 μg/ml and *Penicillium notatum* at 100 μg/ml. Compound V*c*, on the other hand, inhibited completely the growth of only one fungus (*Penicillium notatum*) at 100 μg/ml. Compounds VI*e* and VI*c* were inactive toward *Saccharomyces cerevisiae* at all concentrations. The poorest antifungal agent of the VI compound series was VI*d*, which was completely inactive toward six of the ten test fungi at all concentrations. The inactivity of VI*d* may be due to the bulky neophyl groups attached to the tin atom in this compound.

The antibacterial activity of the VI compounds is shown in Table IV. Compounds VI*a* and VI*b* both completely inhibited the Gram-positive bacteria *Bacillus megaterium* and *Staphylococcus aureus* at the minimum concentration of organotin compound (1 μg/ml). The activity of compounds VI*a* and VI*b* towards *S. aureus* was identical to that previously observed for the II, IV, and V compounds. The one previously tested III compound, on the other hand, could only completely inhibit this bacterium at 100 μg/ml. Compound VI*e* was the least active of the VI compounds toward the two Gram-positive bacteria. Compound VI*e* was the least active of the II–VI compounds toward *S. aureus*. Compounds VI*b* and VI*e* were the only series VI compounds to show activity toward the Gram-negative bacteria *Pseudomonas aerusginosa* and *Escherichia coli*. Compounds VI*b* and VI*e* both completely inhibited *E. coli* at 100 μg/ml. The one previously tested III compound was inactive toward this bacterium at 100 μg/ml. The II, IV, and V compounds only inhibited growth of this bacterium partially at 100 μg/ml. Compound VI*e* was able to completely inhibit *P. aeruginosa* at 100 μg/ml, while compound VI*b* could only partially inhibit this bacterium at 100 μg/ml.

EXPERIMENTAL[1]

Triphenyltin 5-Nitro-2-furoate (VI*a*)—A mixture of bis(triphenyltin) oxide (11.38 g, 0.01589 mole), 5-nitro-2-furoic acid (5.00 g, 0.0318 mole), and benzene (100 ml) was refluxed for 19 hr. The mixture was filtered, and the benzene was evaporated from the filtrate to give 14.41 g (90%) of VI*a*, mp 111–132°. Four recrystallizations from heptane–benzene (7:5) gave the analytical sample, mp 111.8–112.5°.

Tri-*n*-butyltin 5-Nitro-2-furoate (VI*b*)—A mixture of bis(tri-*n*-butyltin) oxide (10.43 g, 0.01750 mole), 5-nitro-2-furoic acid (5.50 g, 0.0350 mole), and benzene (100 ml) was refluxed for 19 hr. The mixture was filtered, and the benzene was evaporated from the filtrate to give 15.18 g (97%) of VI*b*, mp 62.0–67.0°. Four recrystallizations from heptane gave the analytical sample, mp 68–69.7°.

Tricyclohexyltin 5-Nitro-2-furoate (VI*c*)—A mixture of bis(tricyclohexyltin) oxide (26) (11.96 g, 0.1590 mole), 5-nitro-2-furoic acid (5.00 g, 0.0318 mole), and benzene (100 ml) was refluxed for 16 hr. The mixture was filtered, and the benzene was evaporated from the filtrate to give 16.09 g (97%) of VI*c*, mp 147–155.5°. Four recrystallizations from heptane gave the analytical sample, mp 154.8–156°.

Trineophyltin 5-Nitro-2-furoate (VI*d*)—A mixture of bis(trineophyltin) oxide (27) (2.63 g, 0.00250 mole), 5-nitro-2-furoic acid (0.78 g, 0.0050 mole), and benzene (25 ml) was refluxed for 26.5 hr. The mixture was filtered, and the benzene was evaporated from the filtrate to give 3.14 g (93%) of VI*d*, mp 74–78°. Three recrystallizations from heptane gave the analytical sample, mp 79.3–80°.

Trimethyltin 5-Nitro-2-furoate (VI*e*)—A mixture of trimethyltin hydroxide (9.20 g, 0.0509 mole), 5-nitro-2-furoic acid (8.00 g, 0.0509 mole), and benzene (75 ml) was refluxed for 19 hr. The precipitate was collected on a filter paper and dried to give 15.30 g (94%) of VI*e*, mp 188.2–195.5°. Three recrystallizations from benzene gave the analytical sample, mp 190–192°.

Biological Methods—The compounds were individually dissolved in tetrahydrofuran. The preparation of sterile solutions of the compounds, the fungi employed, the antifungal testing procedures, and the determination of growth inhibition were reported previously (28).

The compounds were also investigated for antibacterial activity according to the procedure reported earlier (28).

[1] Melting points were determined with a Mel-Temp capillary melting point apparatus and are uncorrected. IR data were obtained with a Perkin-Elmer model 283 spectrophotometer. The far IR data were obtained with a Perkin-Elmer model FIS-3 spectrophotometer. The benzene used as a solvent in the synthesis of the organotin esters was dried over sodium ribbon. The water produced in the reactions was removed with the aid of a Dean-Stark trap. Elemental analyses were performed by Schwarzkopf Microanalytical Laboratory, Woodside, N.Y.

Table IV—Antibacterial Activity of Triorganotin 5-Nitro-2-furoates

Compound	*Pseudomonas aeruginosa*[a]			*Escherichia coli*			*Bacillus megaterium*			*Staphylococcus aureus*		
	1[b]	10	100	1	10	100	1	10	100	1	10	100
VI*a*	–	–	–	–	–	–	2+	2+	2+	2+	2+	2+
VI*b*	–	–	+	–	–	2+	2+	2+	2+	2+	2+	2+
VI*c*	–	–	–	–	–	–	+	2+	2+	+	2+	2+
VI*d*	–	–	–	–	–	–	+	2+	2+	–	2+	2+
VI*e*	–	–	2+	–	–	2+	+	+	+	–	–	+

[a] Bacteria were obtained from the culture collection of the Department of Biological Sciences, St. John's University. [b] Indicates concentration of compounds employed in micrograms per milliliter; – indicates no inhibition of growth, + indicates partial inhibition of growth, and 2+ indicates complete inhibition of growth.

REFERENCES

(1) J. S. Thayer, *J. Organometal. Chem.*, **76**, 265 (1974).

(2) "Organotin Compounds: New Chemistry and Applications," J. J. Zuckerman, Ed., American Chemical Society, Washington, D.C., 1976.

(3) B. Sugavanam, *Tin Its Uses*, **126**, 4 (1980).

(4) F. E. Smith, *ibid.*, **126**, 6 (1980).

(5) S. Haynes, *ibid.*, **127**, 12 (1981).

(6) K.-D. Freitag and R. Bock, *Pestic. Sci.*, **5**, 731 (1974).

(7) R. D. Barnes, A. T. Bull, and R. C. Poller, *ibid.*, **4**, 305 (1973).

(8) M. E. Getzendaner and H. B. Corbin, *J. Agr. Food Chem.*, **20**, 881 (1972).

(9) R. Bock and K.-D. Freitag, *Naturwissenschaften*, **59**, 165 (1972).

(10) A. J. Chapman and J. W. Price, *Int. Pestic. Control*, **1**, 11 (1972).

(11) A. J. Crowe and P. J. Smith, *Chem. Ind. (London)*, 200 (1980).

(12) E. J. Kupchik, M. A. Pisano, A. M. Carroll, J. R. Lumpp, and J. A. Feiccabrino, *J. Pharm. Sci.*, **69**, 340 (1980).

(13) A. K. Sijpesteijn, *Meded. Landbouwhogesch. Opzoekingsst. Staat Gent*, **24**, 850 (1959).

(14) A. K. Sijpesteijn, J. G. A. Luijten, and G. J. M. van der Kerk, in "Fungicides, An Advanced Treatise," D. C. Torgeson, Ed., Academic, New York, N.Y., 1969, chap. 7.

(15) A. K. Sijpesteijn, F. Rijkens, J. G. A. Luijten, and L. C. Willemsens, *Antonie van Leeuwenhoek*, **28**, 346 (1962).

(16) J. G. A. Luijten, in "Organotin Compounds," vol. 3, A. K. Sawyer, Ed., Dekker, New York, N.Y., 1972, chap. 12.

(17) A. P. Dunlop and F. N. Peters. "The Furans," Reinhold, New York, N.Y., 1953, p. 164.

(18) "Introduction to the Nitrofurans," vol. 1, Eaton Laboratories, New York, N.Y., 1958.

(19) J. H. S. Foster and A. D. Russell, in "Inhibition and Destruction of the Microbial Cell," W. B. Hugo, Ed., Academic, New York, N.Y., 1971, chap. 3 F.

(20) L. J. Bellamy, "The Infrared Spectra of Complex Molecules," 3rd ed., vol. 1, Wiley, New York, N.Y., 1975, p. 204.

(21) R. Okawara and M. Wada, *Adv. Organometal. Chem.*, **5**, 137 (1967).

(22) J. G. A. Luijten and G. J. M. van der Kerk, *Rec. Trav. Chim. Pays-Bas*, **82**, 90 (1963).

(23) R. Okawara and M. Ohara, *J. Organometal. Chem.*, **1**, 360 (1964).

(24) N. S. Dance, W. R. McWhinnie, and R. C. Poller, *J. Chem. Soc. Dalton Trans.*, **1976**, 2349.
(25) R. C. Poller, "The Chemistry of Organotin Compounds," Academic, New York, N.Y., pp. 222, 227.
(26) J. G. A. Luijten and G. J. M. van der Kerk, "Investigations in the Field of Organotin Chemistry," Tin Research Institute, Greenford, Middlesex, England, 1955, reprinted 1959, p. 111.
(27) W. T. Reichle, *Inorg. Chem.*, **5**, 87 (1966).
(28) E. J. Kupchik, M. A. Pisano, D. K. Parikh, and M. A. D'Amico, *J. Pharm. Sci.*, **63**, 621 (1974).

Morphine Pharmacokinetics: GLC Assay *versus* Radioimmunoassay

DONALD R. STANSKI *x, LENNART PAALZOW ‡, and PER OLOF EDLUND ‡

Received April 22, 1981, from the **Department of Anesthesiology and Medicine, Clinical Pharmacology, Stanford University School of Medicine, Stanford, CA 94305*, and the ‡*Department of Pharmacology, Central Research and Control Laboratory, National Corporation of Swedish Pharmacies, Solna, Sweden.* Accepted for publication July 15, 1981.

Abstract □ The validity of a radioimmunoassay (RIA) for research on the pharmacokinetics of morphine has been questioned because of the possible measurement of cross-reactive metabolites. An RIA using antiserum derived from the 3-*O*-carboxymethylmorphine hapten was compared with a specific GLC assay in the measurement of plasma morphine concentrations in humans. The ratio of values for morphine concentrations measured using RIA and those measured using GLC was determined. The RIA values resulted in a 27% overestimation of this ratio. This overestimation did not significantly affect the values for terminal elimination half-life, volume of distribution at steady state, or total body clearance that were derived using results from each assay and model-independent pharmacokinetic techniques.

Keyphrases □ Morphine—pharmacokinetic determination from radioimmunoassay and GLC assay compared □ Pharmacokinetics—morphine, determination from radioimmunoassay and GLC assay compared □ Radioimmunoassay—morphine, comparison with GLC assay, pharmacokinetics □ GLC—morphine, comparison with radioimmunoassay, pharmacokinetics

The radioimmunoassay (RIA) for morphine, first described by Spector *et al.* (1, 2), has been used to characterize the pharmacokinetic profile of morphine (3, 4). A major concern in using any immunoassay for pharmacokinetic research is its accuracy in measuring the true drug concentration. For antibody generated in one laboratory (at morphine concentrations of 20 ng/ml), at least eight times more morphine-3-glucuronide than morphine was required to produce equivalent displacement of the labeled dihydromorphine (5). At 40 ng/ml, more than 32 times more morphine-3-glucuronide was required for an equivalent displacement. Similar results were obtained when relatively high morphine concentrations (1.8–3.1 μg/ml) were measured in rats using the RIA and a specific fluorometric assay (6). This concentration range markedly exceeds that occurring after therapeutic doses in humans. Catlin (7) questioned the validity of RIA for pharmacokinetic analysis, demonstrating a variability in the specificity of the antibody and interference from morphine metabolites that can result in discrepant interpretations.

Because of the limited sensitivity of currently available analytical methods for measuring morphine, it previously has not been possible to validate the accuracy of RIA for morphine in humans because of the low plasma concentrations (1–50 ng/ml) of morphine attained following pharmacological doses of morphine (0.15 mg/kg). A new specific and sensitive GLC assay was used to reevaluate plasma samples of morphine obtained in a previous pharmacokinetic study that were originally analyzed by RIA. The morphine concentrations measured by the different assays were then compared.

EXPERIMENTAL

Plasma Analysis—Plasma samples that were analyzed in a previous study on morphine pharmacokinetics using RIA were reevaluated using a specific GLC morphine assay. The analysis was undertaken on five of the six subjects who had received 10 mg of intravenous morphine sulfate and on four of the five subjects who had received 10 mg of intramuscular morphine sulfate. All samples had remained frozen at −30° until the time of assay. The GLC assays were performed ~2 years after the RIA measurements. There was no evidence of sample deterioration during this time. Demographic characteristics of the patient population and the drug administration protocol were described earlier (4).

Morphine concentrations in plasma were quantitated using RIA and rabbit antimorphine antisera[1] as described previously (4). The detection limit of this assay was 1 ng/ml, and the pooled coefficient of variation was 8.3% for a series of two to three identical samples containing known concentrations of morphine ranging from 1.0 to 45 ng/ml. Although the specificity of the antisera was not assessed, previous reports of antisera from the same source described its relative affinity for morphine, morphine metabolites, and other opiate alkaloids (5). Morphine concentrations in plasma were also determined using the GLC method described by Edlund (8). The detection limit of the assay was 1 ng/ml. The coefficient of variation of the assay was 4 and 10% at 62 and 0.8 ng/ml, respectively.

Data Analysis—Three analyses were performed on the data to determine differences between the two assays and the consequences of these differences on the derived pharmacokinetic values for morphine. The first analysis used linear regression through the origin (9) to compare the morphine concentrations measured with the two assays. Only plasma morphine concentrations <60 ng/ml were used, which included 118 of 138 possible data pairs. The distribution of the 20 data points in the 70–350-ng/ml concentration range was not sufficiently uniform for accurate regression analysis. The excluded data points represented the high morphine concentrations that occurred immediately after the 2-min rapid intravenous infusion. To determine the possible influence of metabolites on the RIA at low concentrations, linear regression through the origin was performed on only those concentrations measured 1 hr after drug administration. In both regression analyses, the 95% confidence interval of the slope was computed to determine if the slope differed significantly from 1.

In the second data analysis, the relative precision and bias of the RIA, as compared with the GLC morphine assay, were determined using approaches suggested previously (10). Relative precision measures the deviation or prediction error of the morphine concentration determined using the RIA compared to the value measured by GLC. This prediction error may have a systematic component called relative bias. The relative bias is the degree to which the typical RIA prediction is either too high

[1] Obtained from Dr. Sidney Spector, Roche Institute of Molecular Biology, Nutley, N.J.

0022-3549/82/0300-0314$01.00/0

(24) N. S. Dance, W. R. McWhinnie, and R. C. Poller, *J. Chem. Soc. Dalton Trans.*, **1976**, 2349.
(25) R. C. Poller, "The Chemistry of Organotin Compounds," Academic, New York, N.Y., pp. 222, 227.
(26) J. G. A. Luijten and G. J. M. van der Kerk, "Investigations in the Field of Organotin Chemistry," Tin Research Institute, Greenford, Middlesex, England, 1955, reprinted 1959, p. 111.
(27) W. T. Reichle, *Inorg. Chem.*, **5**, 87 (1966).
(28) E. J. Kupchik, M. A. Pisano, D. K. Parikh, and M. A. D'Amico, *J. Pharm. Sci.*, **63**, 621 (1974).

Morphine Pharmacokinetics: GLC Assay *versus* Radioimmunoassay

DONALD R. STANSKI *x, LENNART PAALZOW ‡, and PER OLOF EDLUND ‡

Received April 22, 1981, from the **Department of Anesthesiology and Medicine, Clinical Pharmacology, Stanford University School of Medicine, Stanford, CA 94305*, and the ‡*Department of Pharmacology, Central Research and Control Laboratory, National Corporation of Swedish Pharmacies, Solna, Sweden.* Accepted for publication July 15, 1981.

Abstract □ The validity of a radioimmunoassay (RIA) for research on the pharmacokinetics of morphine has been questioned because of the possible measurement of cross-reactive metabolites. An RIA using antiserum derived from the 3-*O*-carboxymethylmorphine hapten was compared with a specific GLC assay in the measurement of plasma morphine concentrations in humans. The ratio of values for morphine concentrations measured using RIA and those measured using GLC was determined. The RIA values resulted in a 27% overestimation of this ratio. This overestimation did not significantly affect the values for terminal elimination half-life, volume of distribution at steady state, or total body clearance that were derived using results from each assay and model-independent pharmacokinetic techniques.

Keyphrases □ Morphine—pharmacokinetic determination from radioimmunoassay and GLC assay compared □ Pharmacokinetics—morphine, determination from radioimmunoassay and GLC assay compared □ Radioimmunoassay—morphine, comparison with GLC assay, pharmacokinetics □ GLC—morphine, comparison with radioimmunoassay, pharmacokinetics

The radioimmunoassay (RIA) for morphine, first described by Spector *et al.* (1, 2), has been used to characterize the pharmacokinetic profile of morphine (3, 4). A major concern in using any immunoassay for pharmacokinetic research is its accuracy in measuring the true drug concentration. For antibody generated in one laboratory (at morphine concentrations of 20 ng/ml), at least eight times more morphine-3-glucuronide than morphine was required to produce equivalent displacement of the labeled dihydromorphine (5). At 40 ng/ml, more than 32 times more morphine-3-glucuronide was required for an equivalent displacement. Similar results were obtained when relatively high morphine concentrations (1.8–3.1 μg/ml) were measured in rats using the RIA and a specific fluorometric assay (6). This concentration range markedly exceeds that occurring after therapeutic doses in humans. Catlin (7) questioned the validity of RIA for pharmacokinetic analysis, demonstrating a variability in the specificity of the antibody and interference from morphine metabolites that can result in discrepant interpretations.

Because of the limited sensitivity of currently available analytical methods for measuring morphine, it previously has not been possible to validate the accuracy of RIA for morphine in humans because of the low plasma concentrations (1–50 ng/ml) of morphine attained following pharmacological doses of morphine (0.15 mg/kg). A new specific and sensitive GLC assay was used to reevaluate plasma samples of morphine obtained in a previous pharmacokinetic study that were originally analyzed by RIA. The morphine concentrations measured by the different assays were then compared.

EXPERIMENTAL

Plasma Analysis—Plasma samples that were analyzed in a previous study on morphine pharmacokinetics using RIA were reevaluated using a specific GLC morphine assay. The analysis was undertaken on five of the six subjects who had received 10 mg of intravenous morphine sulfate and on four of the five subjects who had received 10 mg of intramuscular morphine sulfate. All samples had remained frozen at −30° until the time of assay. The GLC assays were performed ~2 years after the RIA measurements. There was no evidence of sample deterioration during this time. Demographic characteristics of the patient population and the drug administration protocol were described earlier (4).

Morphine concentrations in plasma were quantitated using RIA and rabbit antimorphine antisera[1] as described previously (4). The detection limit of this assay was 1 ng/ml, and the pooled coefficient of variation was 8.3% for a series of two to three identical samples containing known concentrations of morphine ranging from 1.0 to 45 ng/ml. Although the specificity of the antisera was not assessed, previous reports of antisera from the same source described its relative affinity for morphine, morphine metabolites, and other opiate alkaloids (5). Morphine concentrations in plasma were also determined using the GLC method described by Edlund (8). The detection limit of the assay was 1 ng/ml. The coefficient of variation of the assay was 4 and 10% at 62 and 0.8 ng/ml, respectively.

Data Analysis—Three analyses were performed on the data to determine differences between the two assays and the consequences of these differences on the derived pharmacokinetic values for morphine. The first analysis used linear regression through the origin (9) to compare the morphine concentrations measured with the two assays. Only plasma morphine concentrations <60 ng/ml were used, which included 118 of 138 possible data pairs. The distribution of the 20 data points in the 70–350-ng/ml concentration range was not sufficiently uniform for accurate regression analysis. The excluded data points represented the high morphine concentrations that occurred immediately after the 2-min rapid intravenous infusion. To determine the possible influence of metabolites on the RIA at low concentrations, linear regression through the origin was performed on only those concentrations measured 1 hr after drug administration. In both regression analyses, the 95% confidence interval of the slope was computed to determine if the slope differed significantly from 1.

In the second data analysis, the relative precision and bias of the RIA, as compared with the GLC morphine assay, were determined using approaches suggested previously (10). Relative precision measures the deviation or prediction error of the morphine concentration determined using the RIA compared to the value measured by GLC. This prediction error may have a systematic component called relative bias. The relative bias is the degree to which the typical RIA prediction is either too high

[1] Obtained from Dr. Sidney Spector, Roche Institute of Molecular Biology, Nutley, N.J.

0022-3549/82/0300-0314$01.00/0

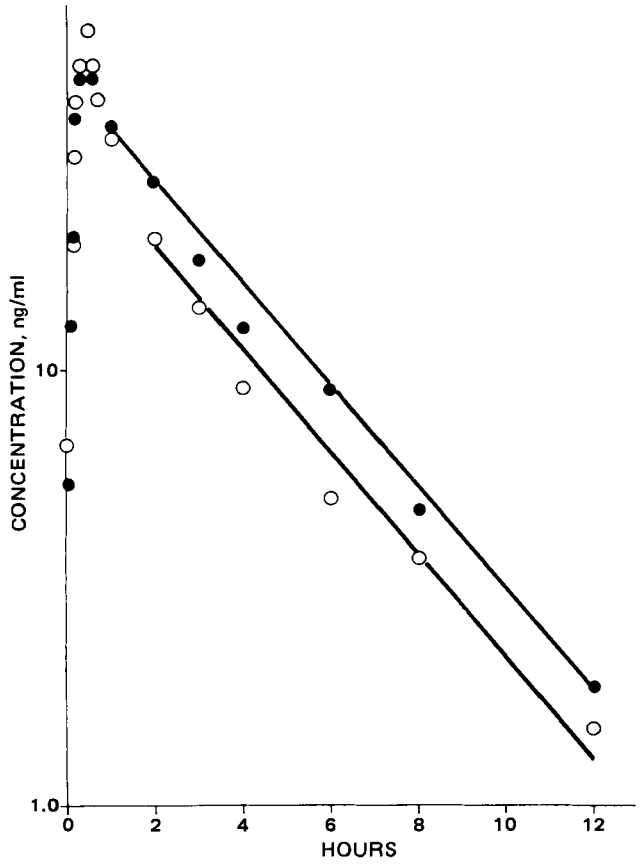

Figure 1—*Plasma concentration data determined by RIA (●) and GLC (○) versus time, for one subject receiving morphine sulfate 10 mg intramuscularly. Lines represent the terminal elimination phases characterized by linear regression.*

or too low. A measure of relative precision is the mean squared prediction error (*MSE*):

$$MSE = \frac{1}{n}\sum_{i=1}^{n}(\text{RIA} - \text{GLC})^2 \qquad \text{(Eq. 1)}$$

where n is the number of data points.

A measure of relative bias is the sample mean prediction error (*ME*):

$$ME = \frac{1}{n}\sum_{i=1}^{n}(\text{RIA} - \text{GLC}) \qquad \text{(Eq. 2)}$$

In the following relationship, the *MSE* is composed of bias (*ME*) and random, nonsystematic error:

$$MSE = ME^2 + \frac{1}{n}\sum_{i=1}^{n}[(\text{RIA} - \text{GLC}) - ME]^2 \qquad \text{(Eq. 3)}$$

in which the last term of the equation is an estimate of the variance of the prediction error and thus a measure of the random error. The relative precision (*MSE*), bias (*ME*), and their 95% confidence interval, along with the proportion of the precision that was bias and random error, were determined using all the values for morphine plasma concentrations that were <60 ng/ml and all the values for 1 hr after drug administration.

In the third data analysis, pharmacokinetic parameters for each individual patient were computed. Model-independent approaches were

Table I—Comparison of Relative Assay Precession and Bias

	All Data <60 ng/ml	Data after 1 hr
Relative precession (*MSE*), ng/ml	27.8	20.4
95% confidence bounds	18.1–37.5	13.6–27.2
Relative bias (*ME*), ng/ml	1.97	3.21
95% confidence bounds	1.02–2.92	2.41–4.01
Components of the *MSE*		
Relative bias, %	14	50
Random error, %	86	50

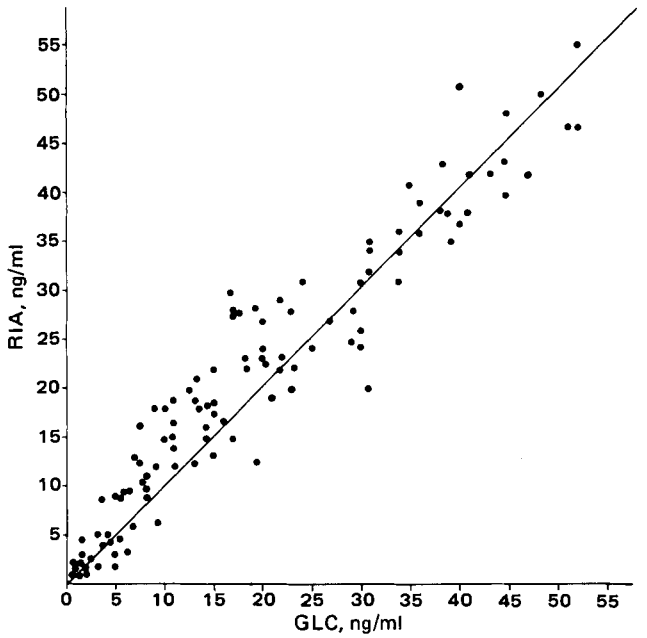

Figure 2—*Regression through the origin using all the morphine concentrations below 60 ng/ml as determined by RIA and GLC. The line represents linear regression.*

applied to the morphine concentration data derived from the two assays. Linear regression of the log plasma concentration *versus* time data was used to determine the apparent terminal elimination half-life. The plasma concentration values that occurred 1 hr after drug administration (*i.e.*, when distribution or absorption was complete) were used. Total body clearance was determined by dividing the dose by the area under the plasma concentration *versus* time curve, determined by the linear trapezoid rule. Complete bioavailability was assumed for intramuscular administration of morphine on the basis of a previous study (4) that demonstrated comparable area under the curves from intravenous and intramuscular administration in the same subject. A model-independent estimate of the volume of distribution at steady state was determined

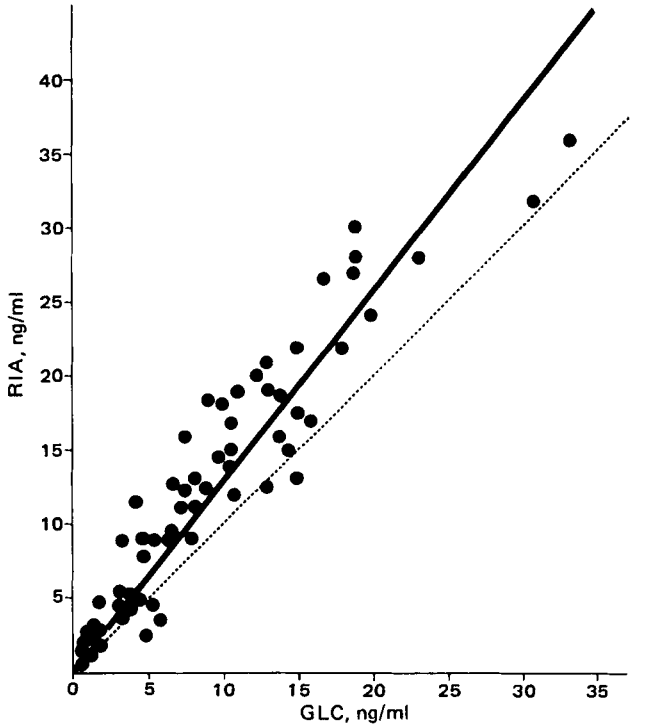

Figure 3—*Regression through the origin of the morphine concentrations as determined by RIA and GLC. Only the values obtained 1 hr after drug administration were used. Linear regression (—) and identity (- - - -) are also shown.*

Table II—Pharmacokinetic Parameters Derived from RIA and GLC Assays

Subject	Age, yr	Weight, kg	Dose, mg	Elimination Half-Life, min			Total Body Clearance, ml/kg/min			Volume of Distribution at Steady-State, liters/kg		
				RIA	GLC	Difference	RIA	GLC	Difference	RIA	GLC	Difference
1	25	64	10 iv	169	190	−21	11.4	15.8	−4.4	2.48	3.35	−0.87
2	28	84	10 iv	159	159	0	14.4	13.8	+0.6	2.72	2.51	+0.21
3	29	80	10 iv	198	233	−35	14.7	17.4	−2.7	3.73	4.48	−0.75
4	28	64	10 iv	184	157	+27	17.1	23.9	−6.7	3.57	3.44	+0.13
4	28	64	10 im	158	153	+5	12.3	14.7	−2.4	2.56	2.11	+0.45
5	34	75	10 iv	183	288	−105	12.3	13.2	−0.9	2.07	4.89	−2.82
5	34	75	10 im	166	234	−68	11.3	12.1	−0.8	2.46	3.28	−0.81
6	29	100	10 im	161	195	−34	12.0	15.0	−3.0	2.97	2.81	+0.16
7	32	76	10	158	161	−3	11.1	11.5	−0.4	2.30	2.44	−0.14
Mean	29.7	75.7		170	197	−26	13.0	15.2	−2.3	2.76	3.25	−0.49
±*SD*	3.0	11.6		14	47	41	2.0	3.7	2.3	0.56	0.89	1.0

using the first statistical moment described by Benet and Galeazzi (11). An appropriate correction for the intramuscular absorption phase was made in the calculation of the volume of distribution at steady state. A paired Student *t* test was used to determine if there was a significant ($p \leq 0.05$) difference in the pharmacokinetic parameters derived from the RIA and GLC assays.

RESULTS AND DISCUSSION

Examining the individual curves of plasma morphine concentration *versus* time in four of five subjects receiving intravenous morphine, and in three of the four receiving intramuscular morphine, the RIA gave consistently higher plasma concentrations than the GLC assay for time periods 1 hr after drug administration. Figure 1 represents the plasma morphine concentrations determined by the two assays in a subject who received intramuscular morphine.

In the first data analysis, when all plasma concentrations <60 ng/ml were compared (118 data pairs) using regression through the origin, the slope of the regression line was 1.03 and the 95% confidence interval was 0.993–1.064 (Fig. 2). This indicates that the ratio of RIA/GLC morphine concentrations did not differ significantly from 1 when measured with the two assays. When only the data after 1 hr were evaluated (66 data pairs), the slope of the regression through the origin was 1.27 and the 95% confidence interval was 1.23–1.30, indicating that the ratio of RIA/GLC plasma concentrations differs significantly from 1 (Fig. 3). This results in a 27% overestimation of the true morphine concentration by RIA.

In the second data analysis (Table I), the measures of RIA *versus* GLC assay relative precision (*MSE*) and bias (*ME*) are given. The relative biases differ significantly from zero for all plasma morphine concentrations <60 ng/ml and for plasma morphine concentrations 1 hr after drug administration. The plasma concentration data 1 hr after drug administration represents a greater portion of the *MSE* than can be attributed to bias relative to all the plasma morphine concentration data <60 ng/ml.

From the third data analysis, Table II shows the individual pharmacokinetic parameters derived by model-independent techniques for each patient and assay. The GLC assay resulted in a longer mean apparent elimination half-life, higher mean total plasma clearance, and a larger mean apparent volume of distribution at steady state. These differences were not statistically significant when evaluated with a paired *t* test.

Comparison of the morphine concentration determined by RIA and GLC demonstrated a 27% overestimation of the true morphine concentration by RIA at time intervals 1 hr after drug administration. The RIA was significantly less precise than the GLC assay, and had a greater systematic bias for morphine concentrations obtained 1 hr after drug administration. While the morphine antiserum samples have less affinity for morphine metabolites (specifically the main metabolite, morphine-3-glucuronide), they can affect the accurate measurement of morphine with the RIA in several ways. The standard curves for morphine and morphine-3-glucuronide are not parallel, resulting in dose-dependent inhibition ratios of morphine to morphine-3-glucuronide (7). In addition, there is also evidence that the elimination half-life of morphine-3-glucuronide is longer than that of the parent drug in rabbits (7) and humans (3). A previous report (12) showed that morphine metabolites present at concentrations 8–12 times higher than the true morphine concentration 1 hr after drug administration. Overestimation of the true morphine concentration 1 hr after drug administration probably results from cross-reaction of morphine-3-glucuronide with the antiserum samples when true morphine concentrations are lower than the metabolite concentrations.

Overestimation of plasma morphine concentrations by the RIA did not affect derived pharmacokinetic values. The elimination half-life calculated using the values from the GLC assay did not differ markedly from that determined using RIA values. The higher clearance and larger volume of distribution of morphine calculated using the results of the GLC assay reflect the lower plasma concentrations measured by GLC. While statistical differences were not present for the morphine elimination half-lives, clearances, and volumes of distribution derived from the two assays, the variability (standard deviation) of the mean of differences between individual pharmacokinetic values derived from each assay was large and the sample size was small. Both variability and sample size contribute to the probability of detecting a difference in the statistical analysis.

The major mechanism by which morphine is removed from the body is hepatic metabolism. Morphine's high hepatic extraction ratio (13, 14) indicates that clearance is very dependent on hepatic blood flow. The difference in mean total morphine clearance between the two assays (12.9 *versus* 15.3 ml/kg/min) was relatively small given the variability in hepatic perfusion that can exist in humans. The difference in mean volume of distribution between the two assays (2.76 *versus* 3.25 liters/kg) was also small. The differences in derived values for pharmacokinetics between the two assays was minimal and does not affect the interpretation of the fate of morphine in the human body.

Overestimation of the morphine concentration by RIA can be minimized by use of antiserum samples that exhibit minimal cross-reactivity with morphine-3-glucuronide (15, 16).

REFERENCES

(1) S. Spector, *J. Pharmacol. Exp. Ther.*, **178**, 253 (1971).

(2) S. Spector and C. Parker, *Science*, **168**, 1347 (1970).

(3) B. A. Berkowitz, S. H. Ngai, J. C. Yang, J. Hempstead, and S. Spector, *Clin. Pharmacol. Ther.*, **17**, 629 (1975).

(4) D. R. Stanski, L. Lowenstein, and D. J. Greenblatt, *ibid.*, **24**, 52 (1978).

(5) B. A. Berkowitz, K. Cerreta, and S. Spector, *J. Pharmacol. Exp. Ther.*, **191**, 527 (1974).

(6) H. Kupferberg, A. Burkhalter, and E. L. Way, *ibid.*, **145**, 247 (1964).

(7) D. H. Catlin, *ibid.*, **200**, 224 (1977).

(8) P. O. Edlund, *J. Chromatogr.*, **206**, 109 (1981).

(9) J. Neter and W. Wasserman, "Applied Linear Statistical Models," R. D. Irwin, Inc., Homewood, Ill., 1974, p. 156.

(10) L. B. Sheiner and S. L. Beal, *J. Pharmacokinet. Biopharm.*, **9**, 503 (1981).

(11) L. Z. Benet and R. Galeazzi, *J. Pharm. Sci.*, **68**, 1071 (1979).
(12) M. R. Murphy and C. C. Hug, *Anesthesiology*, **54**, 187 (1981).
(13) K. Iwamoto and C. D. Klaassen, *J. Pharmacol. Exp. Ther.*, **200**, 236 (1977).
(14) B. Dahlström and L. Paalzow, *J. Pharmacokinet. Biopharm.*, **6**, 505 (1978).
(15) A. R. Gintzler, E. Mohacsi, and S. Spector, *Eur. J. Pharmacol.*, **38**, 149 (1976).
(16) J. W. Findlay, R. F. Butz, and R. M. Welch, *Res. Commun. Chem. Pathol. Pharmacol.*, **17**, 595 (1977).

ACKNOWLEDGMENTS

The authors gratefully acknowledge the assistance of Dr. David J. Greenblatt and Dr. Edward Lowenstein in gathering the pharmacokinetic data.

Peak Homogeneity Determination for the Validation of High-Performance Liquid Chromatographic Assay Methods

G. T. CARTER ˣ, R. E. SCHIESSWOHL, H. BURKE, and R. YANG

Received April 10, 1981, from the *Physical and Analytical Chemistry Department, Ciba-Geigy Corporation, Suffern, NY 10901.* Accepted for publication July 27, 1981.

Abstract □ To validate high-performance liquid chromatographic assay procedures with regard to specificity, methods were developed to determine the homogeneity of the chromatographic peaks. These methods employed a rapid-scanning UV-visible spectrophotometer to monitor the chromatographic effluent. The absorption data were processed to nullify the signal due to the drug substance specifically, while allowing the detection of coincident impurities. Results from three model systems indicated the ability of these methods to detect as little as 0.1% of a coincident impurity.

Keyphrases □ High-performance liquid chromatography—validity, determination of peak homogeneity □ Impurities—high-performance liquid chromatography, determination by measurement of peak homogeneity □ UV spectrometry—use in determination of peak homogeneity of high-performance liquid chromatographic assays

The use of high-performance liquid chromatography (HPLC) for quantitative analyses of pharmaceuticals has been increasing rapidly (1). HPLC offers excellent sensitivity, accuracy, and precision, as well as convenience. Perhaps the most significant advantage of HPLC is the specificity obtained, since the drug substance is assayed following separation from any impurities. It is this specificity which has led to the acceptance of HPLC methods for stability-indicating assays. Naturally, the validity of such procedures is dependent on the homogeneity of the chromatographic peak of interest. In ordinary practice, a procedure is considered sound in this regard if the chromatographic peak representing the drug-substance is resolved from all known or theoretical synthetic impurities as well as decomposition products (2). Such indirect methods do not actually examine the homogeneity of the peak and are limited in scope to compounds previously identified as potential impurities. However, homogeneity, within specified limits, can be shown for any chromatographic technique, if it can be demonstrated that a critical physical property of the peak in question does not change with time. For example, GC peak homogeneity can be shown by using rapid-scanning mass spectrometers as specific detectors to demonstrate the constancy of the mass spectrum of the eluting peak with time (3, 4).

This report presents a similar method which evaluates the homogeneity of HPLC peaks directly, by monitoring the constancy of the UV–visible (UV/VIS) absorption spectrum of the moving eluting substance without the use of a stopped-flow apparatus, which examines only a small portion of the peak of interest. Specifically, it is the ratio between absorbances at specified wavelengths in the absorption spectrum of the eluted peak which is examined. Homogeneity is demonstrated by the fact that for sufficiently dilute solutions of a pure substance, the ratio of absorbances should remain constant, regardless of concentration throughout the chromatographic peak. To accomplish this, a rapid-scanning, microcomputer controlled UV/VIS spectrophotometer was employed to examine the chromatographic effluent. Several reports have appeared (5–9) concerning the use of rapid-scanning spectrophotometers as detectors for HPLC. This report represents the first application of these detectors for HPLC method validation in pharmaceutical analysis. Results obtained for three model systems are described; each of these systems contains a drug substance: carbamazepine (I), desipramine (II), or estrone (III), plus a representative impurity designed to coelute.

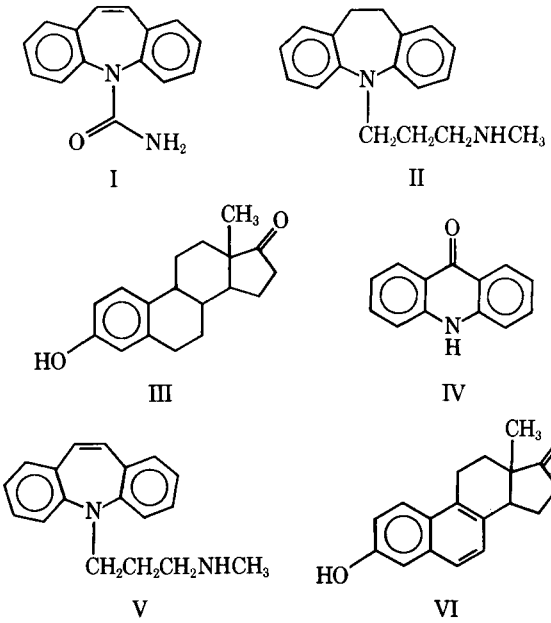

0022-3549/82/0300-0317$01.00/0

(11) L. Z. Benet and R. Galeazzi, *J. Pharm. Sci.*, **68**, 1071 (1979).
(12) M. R. Murphy and C. C. Hug, *Anesthesiology*, **54**, 187 (1981).
(13) K. Iwamoto and C. D. Klaassen, *J. Pharmacol. Exp. Ther.*, **200**, 236 (1977).
(14) B. Dahlström and L. Paalzow, *J. Pharmacokinet. Biopharm.*, **6**, 505 (1978).
(15) A. R. Gintzler, E. Mohacsi, and S. Spector, *Eur. J. Pharmacol.*, **38**, 149 (1976).
(16) J. W. Findlay, R. F. Butz, and R. M. Welch, *Res. Commun. Chem. Pathol. Pharmacol.*, **17**, 595 (1977).

ACKNOWLEDGMENTS

The authors gratefully acknowledge the assistance of Dr. David J. Greenblatt and Dr. Edward Lowenstein in gathering the pharmacokinetic data.

Peak Homogeneity Determination for the Validation of High-Performance Liquid Chromatographic Assay Methods

G. T. CARTER ˣ, R. E. SCHIESSWOHL, H. BURKE, and R. YANG

Received April 10, 1981, from the *Physical and Analytical Chemistry Department, Ciba-Geigy Corporation, Suffern, NY 10901.* Accepted for publication July 27, 1981.

Abstract □ To validate high-performance liquid chromatographic assay procedures with regard to specificity, methods were developed to determine the homogeneity of the chromatographic peaks. These methods employed a rapid-scanning UV-visible spectrophotometer to monitor the chromatographic effluent. The absorption data were processed to nullify the signal due to the drug substance specifically, while allowing the detection of coincident impurities. Results from three model systems indicated the ability of these methods to detect as little as 0.1% of a coincident impurity.

Keyphrases □ High-performance liquid chromatography—validity, determination of peak homogeneity □ Impurities—high-performance liquid chromatography, determination by measurement of peak homogeneity □ UV spectrometry—use in determination of peak homogeneity of high-performance liquid chromatographic assays

The use of high-performance liquid chromatography (HPLC) for quantitative analyses of pharmaceuticals has been increasing rapidly (1). HPLC offers excellent sensitivity, accuracy, and precision, as well as convenience. Perhaps the most significant advantage of HPLC is the specificity obtained, since the drug substance is assayed following separation from any impurities. It is this specificity which has led to the acceptance of HPLC methods for stability-indicating assays. Naturally, the validity of such procedures is dependent on the homogeneity of the chromatographic peak of interest. In ordinary practice, a procedure is considered sound in this regard if the chromatographic peak representing the drug-substance is resolved from all known or theoretical synthetic impurities as well as decomposition products (2). Such indirect methods do not actually examine the homogeneity of the peak and are limited in scope to compounds previously identified as potential impurities. However, homogeneity, within specified limits, can be shown for any chromatographic technique, if it can be demonstrated that a critical physical property of the peak in question does not change with time. For example, GC peak homogeneity can be shown by using rapid-scanning mass spectrometers as specific detectors to demonstrate the constancy of the mass spectrum of the eluting peak with time (3, 4).

This report presents a similar method which evaluates the homogeneity of HPLC peaks directly, by monitoring the constancy of the UV–visible (UV/VIS) absorption spectrum of the moving eluting substance without the use of a stopped-flow apparatus, which examines only a small portion of the peak of interest. Specifically, it is the ratio between absorbances at specified wavelengths in the absorption spectrum of the eluted peak which is examined. Homogeneity is demonstrated by the fact that for sufficiently dilute solutions of a pure substance, the ratio of absorbances should remain constant, regardless of concentration throughout the chromatographic peak. To accomplish this, a rapid-scanning, microcomputer controlled UV/VIS spectrophotometer was employed to examine the chromatographic effluent. Several reports have appeared (5–9) concerning the use of rapid-scanning spectrophotometers as detectors for HPLC. This report represents the first application of these detectors for HPLC method validation in pharmaceutical analysis. Results obtained for three model systems are described; each of these systems contains a drug substance: carbamazepine (I), desipramine (II), or estrone (III), plus a representative impurity designed to coelute.

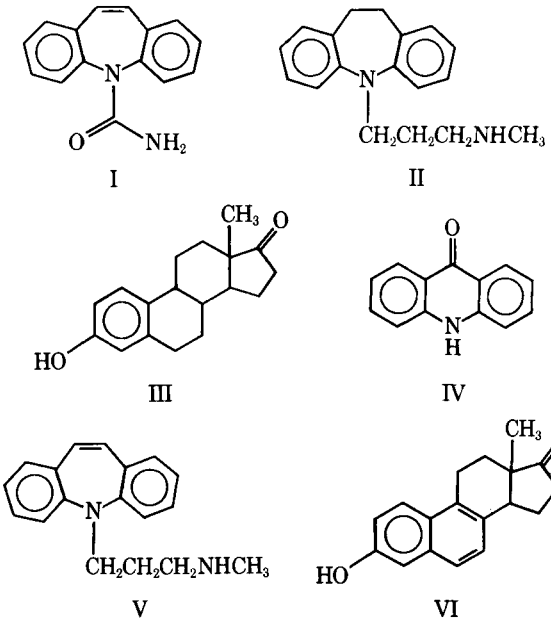

0022-3549/82/0300-0317$01.00/0

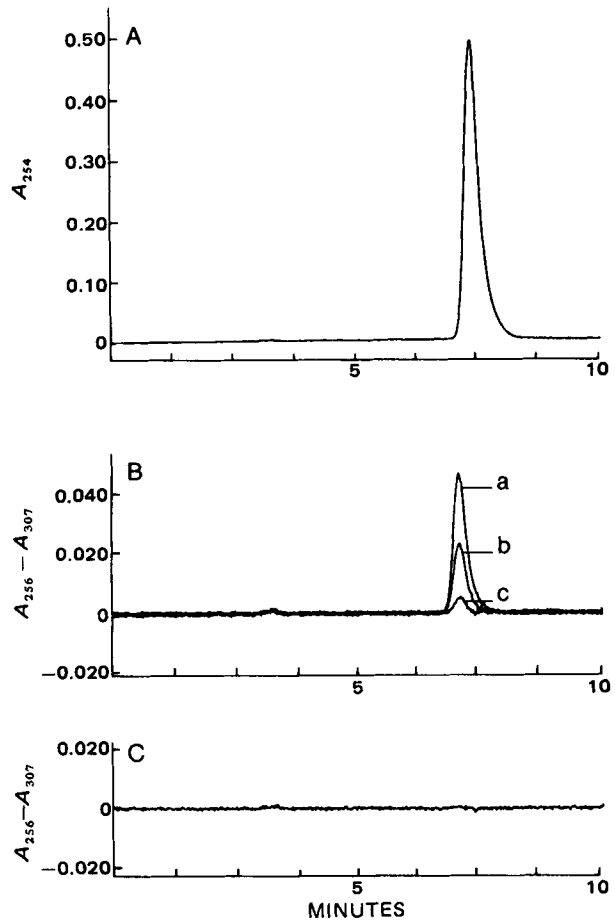

Figure 1—*A) Chromatogram of carbamazepine containing 1% acridone; B) chromatograms of carbamazepine containing (a) 1% acridone, (b) 0.5% acridone, and (c) 0.1% acridone; C) baseline chromatogram obtained for pure carbamazepine. Approximately 5 μg of carbamazepine was injected in 2.5 μl of mobile phase in all cases.*

EXPERIMENTAL

Materials—Carbamazepine[1] (I), acridone[1] (IV), desipramine[1] (II), 5-(3-methylaminopropyl)-5*H*-dibenz[*b*,*f*]azepine[1] (V), estrone[2] (III), and equilenin[2] (VI) were used in the model systems. Spectrophotometric grade solvents[3] were used in all mobile phases. The ion-pairing reagent was prepared by dissolving 5.5 g of sodium heptane sulfonate[4] in 50 ml of distilled water and diluting to 100 ml with glacial acetic acid. All mobile phases were passed through membrane filters[5] prior to use.

Apparatus—All analyses were performed using a high-performance liquid chromatograph[6] equipped with a standard injector, a 3.9 mm × 30-cm reversed-phase column and a fixed wavelength UV absorption detector. The outlet line from the detector was connected *via* a low dead-volume coupling to a quartz micro flow cell[7] (volume, 8 μl, light path, 1 cm) mounted on the optical bench of the rapid-scanning UV/VIS spectrophotometer[8]. The spectrophotometer's built-in microcomputer (16-bit word, 32K words of memory) processed the spectral data in real time. Full-range spectra (200–800 nm) were recorded *versus* air as the blank on the chromatographic effluent, computations were made, and the resultant data were plotted[9] every second to generate the chromatograms shown.

Peak Homogeneity—The methods employed to detect inhomogeneities in chromatographic peaks are designed to specifically nullify the signal due to the drug substance, while allowing the detection of other

[1] Ciba-Geigy Corp., Suffern, NY 10901.
[2] Sigma Chemical Co., St. Louis, MO 63178.
[3] Fisher Scientific Co., Fair Lawn, NJ 07410.
[4] Eastman Organic Chemicals, Rochester, NY 14650.
[5] Millipore Corp., Bedford, MA 01730.
[6] Model 6000A solvent delivery system, U6K injector, μ-Bondapak C_{18} column, and Model 440 detector, Waters Associates, Milford, MA 01757.
[7] Model 178.32, Hellma Cells, Inc., Jamaica, NY 11424.
[8] Model 8450A, Hewlett-Packard, Palo Alto, CA 94304.
[9] Model 7245A, Hewlett-Packard, San Diego, CA 92127.

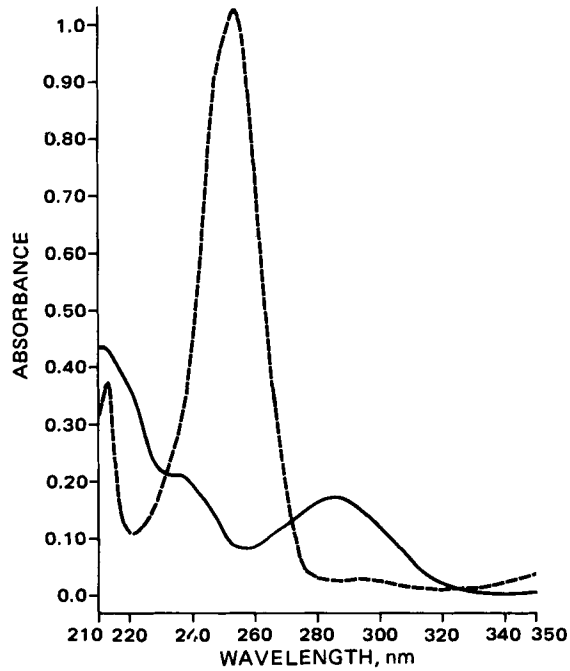

Figure 2—*UV absorption spectra of carbamazepine (—) and acridone (- - - -) obtained as 10 μg/ml solutions in mobile phase.*

compounds. The strict proportionality between absorbances at two wavelengths in the absorption spectrum of the pure drug substance was used, as given:

$$\frac{A_{\lambda_1}}{A_{\lambda_2}} = k_{1,2} \qquad \text{(Eq. 1)}$$

This equation can also be expressed as the null relationship of Eq. 2:

$$A_{\lambda_1} - k_{1,2}A_{\lambda_2} = 0 \qquad \text{(Eq. 2)}$$

which provides a basis for eliminating the response due to the drug-substance. By recording this difference *versus* retention time, a chromatogram which is void of any signal resulting from the elution of the drug substance is obtained. In the simplest case, two wavelengths of equal absorbance (*i.e.* when $k_{1,2} = 1.0$) have been chosen from the absorption spectrum of the drug substance.

In some cases it was advantageous to compare the average absorbance over two or more wavelengths with the absorbance at another single wavelength. The average absorbance over two wavelengths, λ_1 and λ_2, is related to the absorbance at a third wavelength, λ_3. The proportional relationships between the individual wavelengths obtained from Eq. 1 are:

$$A_{\lambda_1} = k_{1,3}A_{\lambda_3} \qquad \text{(Eq. 3)}$$

and

$$A_{\lambda_2} = k_{2,3}A_{\lambda_3} \qquad \text{(Eq. 4)}$$

Addition of these two equations and dividing by 2 gives an expression for the average absorbance at λ_1 and λ_2, $\overline{A}_{\lambda_{1,2}}$:

$$\overline{A}_{\lambda_{1,2}} = \frac{A_{\lambda_1} + A_{\lambda_2}}{2} = A_{\lambda_3}\frac{(k_{1,3} + k_{2,3})}{2} \qquad \text{(Eq. 5}a\text{)}$$

This is more simply written as:

$$\overline{A}_{\lambda_{1,2}} = k'A_{\lambda_3} \qquad \text{(Eq. 5}b\text{)}$$

where $k' = (k_{1,3} + k_{2,3})/2$. Equation 5*b* is then rearranged to give a null relationship similar to Eq. 2.

Comparison of average absorbances of two or more sets of wavelengths is a useful technique. In the simplest case, the average absorbance at λ_1 and λ_2, $\overline{A}_{\lambda_{1,2}}$, is related to the average absorbance at λ_3 and λ_4, $\overline{A}_{\lambda_{3,4}}$. Two equations relate $\overline{A}_{\lambda_{1,2}}$ to the absorbances at the individual wavelengths λ_3 and λ_4:

$$\overline{A}_{\lambda_{1,2}} = k'A_{\lambda_3} = k''A_{\lambda_4} \qquad \text{(Eq. 6)}$$

where $k'' = (k_{1,4} + k_{2,4})/2$. Addition of these equations and division by

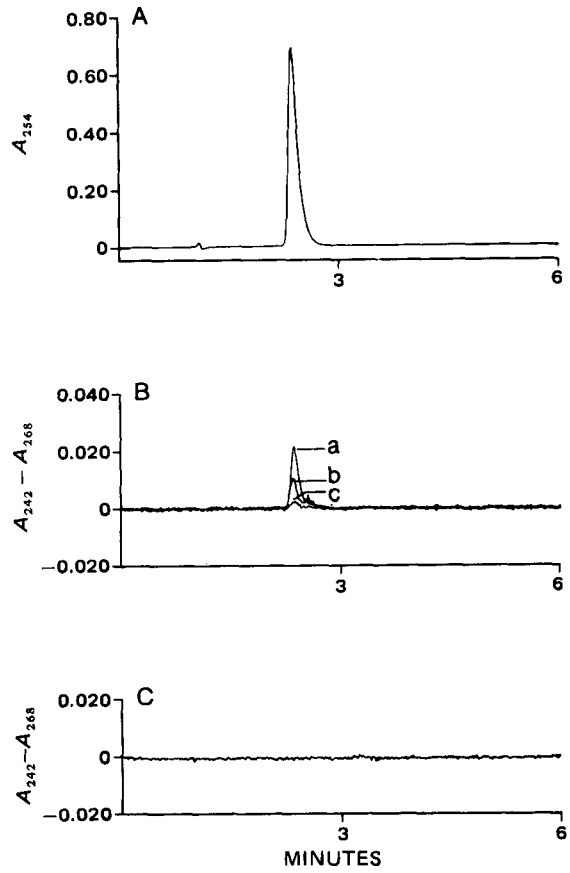

Figure 3—*A) Chromatogram of desipramine containing 1% V; B) chromatograms of desipramine containing (a) 1% V, (b) 0.5% V, and (c) 0.1% V; C) baseline chromatogram obtained for pure desipramine. Approximately 10 μg of desipramine was injected in 5 μl of mobile phase in all cases.*

2 gives Eq. 7, which expresses $\overline{A}_{\lambda_{1,2}}$ as a function of A_{λ_3} and A_{λ_4}:

$$\overline{A}_{\lambda_{1,2}} = \frac{k'A_{\lambda_3} + k''A_{\lambda_4}}{2} \qquad \text{(Eq. 7)}$$

As seen from Eq. 7, $\overline{A}_{\lambda_{1,2}}$ is directly proportional to $\overline{A}_{\lambda_{3,4}}$ only when $k' = k''$:

$$\overline{A}_{\lambda_{1,2}} = k'\frac{(A_{\lambda_3} + A_{\lambda_4})}{2} = k'\overline{A}_{\lambda_{3,4}} \qquad \text{(Eq. 8)}$$

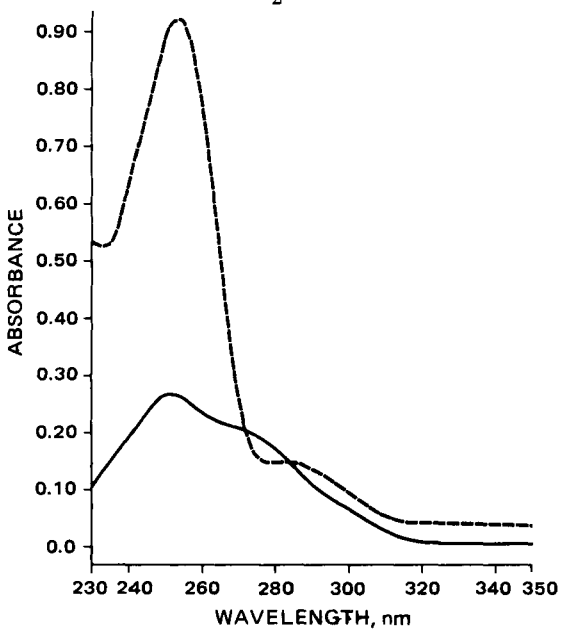

Figure 4—*UV absorption spectra of desipramine(—) and V (- - - -) obtained as 10 μg/ml solutions in mobile phase.*

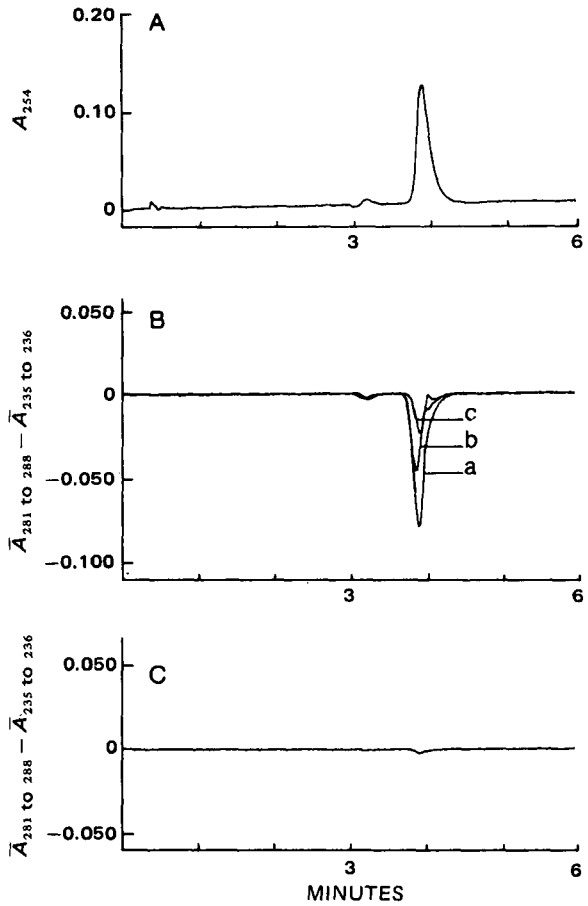

Figure 5—*A) Chromatogram of estrone containing 1% equilenin; B) chromatograms of estrone containing (a) 1% equilenin, (b) 0.5% equilenin, and (c) 0.1% equilenin; C) baseline chromatogram obtained for pure estrone. Approximately 20 μg of estrone was injected in 10 μl mobile phase in all cases.*

Rearrangement of this equation gives the null relationship:

$$\overline{A}_{\lambda_{1,2}} - k'\overline{A}_{\lambda_{3,4}} = 0 \qquad \text{(Eq. 9)}$$

when $k' = k''$. The implication of the requirement that $k' = k''$ in Eq. 9 is that the absorbances at λ_3 and λ_4 must be equal. In practice, this requirement is not a major limitation due to the broad nature of the UV/VIS absorption spectra of most organic compounds. Thus, a range of wavelengths at absorption maxima or minima have essentially equal absorbances, and on all but the steepest curves adjacent wavelengths (within 1–2 nm) have absorbances close enough to be considered equal in these comparisons.

When null relationships are applied to the absorption data obtained as the drug substance elutes from the column, inhomogeneities in the peak result in positive or negative deviations from the baseline. Homogeneity is indicated by a flat baseline.

RESULTS AND DISCUSSION

Carbamazepine—A standard chromatogram (absorbance at 254 nm *versus* time) of carbamazepine containing 1% (w/w) of acridone (IV), a potential impurity, is shown in Fig. 1A. The composition of the mobile phase [methanol–water (55:45); flow rate, 1.0 ml/min] was adjusted to cause the two materials to overlap at a retention time of 7.4 min, since they are readily separable in other mobile phases. Under these conditions, no indication of inhomogeneity in the carbamazepine peak was observed. To detect the acridone, the response derived from the carbamazepine was removed by manipulation of the spectral data. The UV spectrum of carbamazepine (Fig. 2) contains two points of equal absorbance at 256 and 307 nm. To nullify the signal of carbamazepine, the difference in absorbance at these two wavelengths is plotted *versus* time. The resulting chromatogram for pure carbamazepine is shown in Fig. 1C, which reveals a flat baseline. Examination of the UV spectrum of acridone (Fig. 2) shows a strong absorbance at 256 nm and essentially no absorbance at 307 nm,

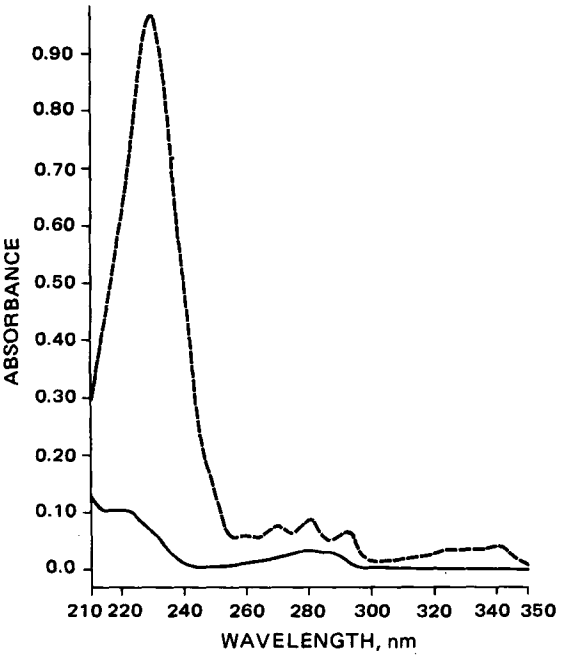

Figure 6—*UV absorption spectra of estrone (—) and equilenin (- - - -) obtained as 4 μg/ml solutions in mobile phase.*

which indicates a positive response should be observed for acridone when this absorbance difference is monitored. The 1% solution used to generate the chromatogram of Fig. 1A gives chromatogram *a* in Fig. 1B. Chromatograms *b* and *c* of Fig. 1B result from the analyses of carbamazepine solutions containing 0.5 and 0.1% acridone, respectively.

Desipramine—A completely analogous method was used to evaluate the homogeneity of the desipramine chromatographic peak in conjunction with its potential by-product (10) 5-(3-methylaminopropyl)-5*H*-dibenz[*b*,*f*]azepine (V). As shown in Fig. 3A, both materials chromatograph with a retention time of 2.5 min under the conditions chosen [mobile phase, acetonitrile/water/ion-pairing reagent/triethylamine (500:500:20:2); flow rate, 2.5 ml/min]. Referring to the UV spectrum of desipramine (Fig. 4), approximately equal absorbances were noted at 242 and 268 nm. Subtraction of the absorbances at these two wavelengths effectively eliminates the response from desipramine, as shown in the chromatogram of Fig. 3C. Samples of desipramine spiked with V at levels of 1.0, 0.5, and 0.1% gave the chromatograms shown in Fig. 3B. The positive signal results from the greater absorbance exhibited by V at 242 nm as compared with 268 nm (Fig. 4).

Estrone—Estrone preparations commonly contain the estrogen equilenin (VI) (11). Using a mobile phase of methanol and water (85:15) and a flow rate of 1.0 ml/min both substances elute at 3.9 min as shown in Fig. 5A. In this case, the relationship of Eq. 9 was applied, as the average absorbance from 235 to 236 nm was subtracted from the average absorbance between 281 and 288 nm (refer to the UV spectrum in Fig. 6) to give the baseline shown in Fig. 5C. When the spiked samples (1.0, 0.5, and 0.1% equilenin) are measured, negative peaks are observed (Fig. 5B), as equilenin has a greater absorbance in the low wavelength range (Fig. 6).

In each of the three systems, the lack of homogeneity created by the addition of low levels of a coeluting substance is apparent. Comparison of the chromatograms for the three 1% mixtures shown in Figs. 1B, 3B, and 5B reveals a range of responses from ~0.02*A* to 0.08*A*. These differences in intensity are related to the absorption characteristics of the particular impurity, the detection method employed and the amount of sample analyzed. The effect of the detection method can be appreciated by considering desipramine. Greater sensitivity for V could be obtained by using Eq. 10 as the null relationship since 255 nm is the absorption maximum of this impurity (Fig. 4):

$$A_{255\text{ nm}} - kA_{280\text{ nm}} = 0 \qquad \text{(Eq. 10)}$$

where:

$$k = \frac{A_{255\text{ nm}}\text{ (desipramine)}}{A_{280\text{ nm}}\text{ (desipramine)}} \qquad \text{(Eq. 11)}$$

The results obtained for these model systems illustrate the potential of the technique for the rapid determination of the homogeneity of HPLC

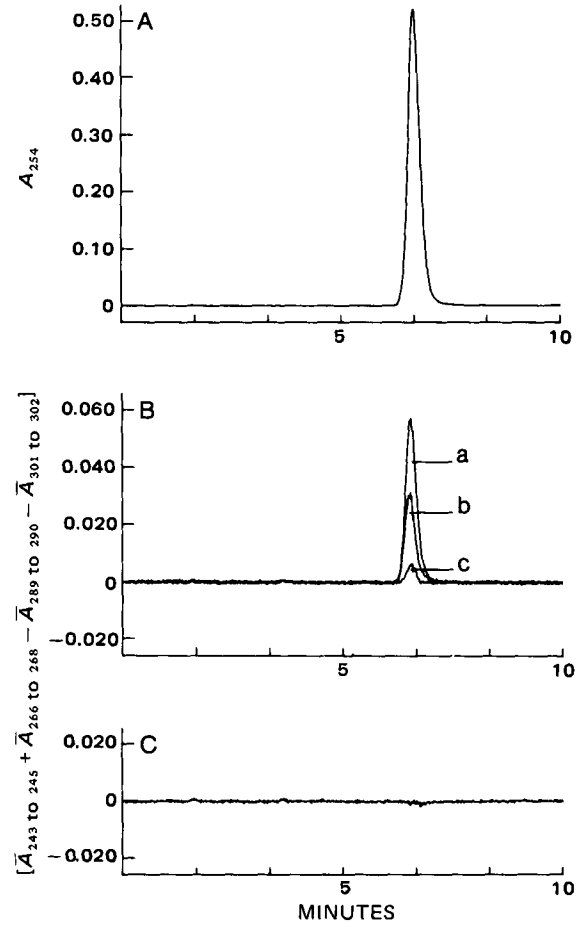

Figure 7—*A) Chromatogram of carbamazepine containing 1% acridone; B) chromatograms of carbamazepine containing (a) 1% acridone, (b) 0.5% acridone, and (c) 0.1% acridone; C) baseline chromatogram obtained for pure carbamazepine. Approximately 5 μg of carbamazepine was injected in 2.5 μl of mobile phase in all cases.*

peaks. Application of these principles to validate HPLC assay procedures is straightforward. The UV/VIS absorption spectrum of the drug substance is measured in the appropriate mobile phase in the flow cell as the material is chromatographed, to eliminate interference from any resolved contaminants. From these data, the nullifying relationship is constructed. The drug-substance is then rechromatographed and the null relationship is monitored *versus* retention time. Homogeneity is indicated if no significant deviation from zero is observed as the drug substance elutes. Hence, from the standpoint of specificity, the chromatographic method is valid.

An erroneous indication of peak homogeneity is possible in the described test if an exactly coincident impurity gives rise to a signal equal in half-width to that of the drug substance. In this case, the contribution from the impurity's absorbance to the total absorbance is proportionally the same throughout the peak. This situation is unlikely in pharmaceutical analysis. Although chromatographic theory (12) predicts equal band widths for substances of identical retention time, impurities typically are present in such small amounts relative to the drug substance (*i.e.*, less than 1%) that they have much narrower effective band widths. The presence of the narrow peak under the envelope of the drug substance is detected readily by these methods.

To bolster the initial indication of peak homogeneity, additional comparison studies should be done. These experiments use the null relationship generated on the original sample to examine the homogeneity of other samples of the drug substance containing increased levels of impurities (and those containing lower levels, if available). Such samples could be derived from purification steps (mother liquors, chromatographic fractions, *etc.*) or as products of accelerated decomposition experiments. These studies are particularly important for stability-indicating assays. Any deviation in the baseline as the drug substance elutes signifies a potential problem in the HPLC method. An invariant baseline represents further evidence of peak homogeneity and essentially eliminates the possibility of a coincident impurity of equal half-width in the

original sample.

Although the method outlined is an independent one, which does not require prior knowledge of possible interfering substances, care must be taken to ensure its generality. The inclusion of just two wavelengths in the detection method, as in Eq. 2, ignores absorbances from contaminants at all other wavelengths. A material which has the same ratio of absorbances at these two wavelengths as the drug-substance (or zero absorbance at each) would not be detected, regardless of the nature of its absorbances at other wavelengths. To enable the detection of the widest range of interfering substances, absorption values across the entire spectral region of interest should be compared. This can be accomplished by either sequential application of the simple relationship of Eq. 2, varying the wavelengths each time, or by using an extended expression which includes the absorbances at several wavelengths.

The latter approach is illustrated in Fig. 7 for the carbamazepine system. Figure 7A shows the unresolved chromatographic peak due to carbamazepine and acridone (1%). To detect the acridone, the multiwavelength expression of Eq. 12 was plotted *versus* retention time:

$$\overline{A}_{243\text{ nm}-245\text{ nm}} + \overline{A}_{266\text{ nm}-268\text{ nm}} - \overline{A}_{289\text{ nm}-290\text{ nm}} - \overline{A}_{301\text{ nm}-302\text{ nm}} = 0 \quad \text{(Eq. 12)}$$

For simplicity, wavelength ranges were chosen whose absorbance values will cancel without the use of proportionality constants. As shown in Fig. 7B, the results are comparable in terms of sensitivity to those given in Fig. 1, and the cancellation of the response due to pure carbamazepine is equally complete (Fig. 7C). The major benefit of this approach is in the generality obtained in one operation. A standard method, which includes sufficient wavelengths to be of wide scope, would be the use of absorbances at 20 nm intervals across a broad spectral region (~200 nm).

One concern is the degree of homogeneity indicated in these methods by a flat baseline. Two limitations imposed by the apparatus described under *Experimental*, are the experimentally determined response threshold of ±0.001*A* and the photometric linearity constraint. This latter restriction requires maximum absorbance values of ~1.0 *A* for wavelengths used in the null relationship, to preserve optimum photometric linearity. Thus, the maximum amount of drug substance analyzed, which governs the relative level of impurities found, is determined by this photometric limitation and by the chromatographic constraint against overloading the column. Given these instrumental restrictions, there are three principal factors which affect the response level of a given impurity: the intensity of its absorption (molar absorptivity), the degree of similarity between its absorption spectrum and that of the drug substance, and the detection method (null relationship) employed. In the case of unknown materials, absorption characteristics are unknown quantities, and the detection method cannot be tailored to attain the maximum response. Because of this, the use of multiple expressions containing data obtained at several wavelengths is recommended. An *a priori* detection limit cannot be stated for all possible impurities. However, these methods can ensure >99% homogeneity in most cases.

REFERENCES

(1) R. K. Gilpin, *Anal. Chem.*, **51**, 257R (1979).

(2) F. Volpe, J. Zintel, and D. Spiegel, *J. Pharm. Sci.*, **68**, 1264 (1979).

(3) C. Fenselau, *Anal. Chem.*, **49**, 563A (1977).

(4) H. B. Woodruff, P. C. Tway, and L. J. Cline Love, *ibid.*, **53**, 81 (1981).

(5) M. S. Denton, T. P. DeAngelis, A. M. Yacynych, W. R. Heineman, and T. W. Gilbert, *ibid.*, **48**, 20 (1976).

(6) M. J. Milano, S. Lam, and E. Grushka, *J. Chromatogr.*, **125**, 315 (1976).

(7) R. E. Dessy, W. D. Reynolds, W. G. Nunn, C. A. Titus, and G. F. Moler, *ibid.*, **126**, 347 (1976).

(8) A. E. McDowell and H. L. Pardue, *Anal. Chem.*, **49**, 1171 (1977).

(9) L. N. Klatt, *J. Chromatogr. Sci.*, **17**, 225 (1979).

(10) K. Adank and T. Schmidt, *Chimia*, **23**, 299 (1969).

(11) "The United States Pharmacopeia," 20th rev., U.S. Pharmacopeial Convention, Rockville, Md., 1979, pp. 300–301.

(12) L. R. Snyder and J. J. Kirkland, "Introduction to Modern Liquid Chromatography," 2nd ed., Wiley, New York, N.Y., 1979, pp. 27–34.

Kinetics and Stability of a Multicomponent Organophosphate Antidote Formulation in Glass and Plastic

PETER ZVIRBLIS and ROBERT I. ELLIN[x]

Received March 17, 1980, from the *U.S. Army Biomedical Laboratory, Aberdeen Proving Ground, MD 21010.* Accepted for publication July 20, 1981.

Abstract □ An aqueous solution of trimedoxime bromide, atropine, and benactyzine hydrochloride was formulated to have maximum stability as an antidote in organophosphorus poisoning. The stability of the mixture in glass and plastic cartridges was determined. Glass cartridges were more desirable than plastic; there was less vapor loss, color formation, and anomolous reaction. Trimedoxime was stable, losing 1.4% of its potency after 1 year at 25° and atropine was more stable than trimedoxime. Considerable degradation of benactyzine occurred; 20% of its potency was lost after 1 year at 25°. Equations for predicting the shelf life of each ingredient at selected temperatures are presented.

Keyphrases □ Benactyzine—in formulation, kinetics and stability in glass and plastic □ Atropine—in formulation, kinetics and stability in glass and plastic □ Trimedoxime—in formulation, kinetics and stability in glass and plastic

The administration of atropine with and without oxime is a common therapy for poisoning by organophosphorus anticholinesterase pesticides such as parathion[1] and malathion[1], and for other organophosphorus compounds such as isopropylmethylphosphonofluoridate (sarin) and pinacolyl methylphosphonofluoridate (soman). Atropine is used to overcome cholinergic stimulation from the anticholinesterases, and oxime reactivates and restores the activity of the enzyme. A recent report claims that the effectiveness of a therapy could be enhanced significantly by simultaneous administration of the cholinolytic drugs,

[1] Parathion, *O,O*-diethyl-*O*-(4-nitrophenyl)phosphorothioate; malathion, *O,O*-dimethyl-*S*-(1,2-dicarbethoxyethyl)phosphorodithioate; trimedoxime bromide, pyridinium-1,1′-(1,3-propanediyl)bis(4-(hydroxyimino)methyl)-dibromide; and benactyzine, α-hydroxy-α-penylbenzeneacetic acid 2-(diethylamino)ethyl ester.

0022-3549/82/0300-0321$01.00/0

original sample.

Although the method outlined is an independent one, which does not require prior knowledge of possible interfering substances, care must be taken to ensure its generality. The inclusion of just two wavelengths in the detection method, as in Eq. 2, ignores absorbances from contaminants at all other wavelengths. A material which has the same ratio of absorbances at these two wavelengths as the drug-substance (or zero absorbance at each) would not be detected, regardless of the nature of its absorbances at other wavelengths. To enable the detection of the widest range of interfering substances, absorption values across the entire spectral region of interest should be compared. This can be accomplished by either sequential application of the simple relationship of Eq. 2, varying the wavelengths each time, or by using an extended expression which includes the absorbances at several wavelengths.

The latter approach is illustrated in Fig. 7 for the carbamazepine system. Figure 7A shows the unresolved chromatographic peak due to carbamazepine and acridone (1%). To detect the acridone, the multiwavelength expression of Eq. 12 was plotted *versus* retention time:

$$\overline{A}_{243\text{ nm}-245\text{ nm}} + \overline{A}_{266\text{ nm}-268\text{ nm}} - \overline{A}_{289\text{ nm}-290\text{ nm}} - \overline{A}_{301\text{ nm}-302\text{ nm}} = 0 \quad \text{(Eq. 12)}$$

For simplicity, wavelength ranges were chosen whose absorbance values will cancel without the use of proportionality constants. As shown in Fig. 7B, the results are comparable in terms of sensitivity to those given in Fig. 1, and the cancellation of the response due to pure carbamazepine is equally complete (Fig. 7C). The major benefit of this approach is in the generality obtained in one operation. A standard method, which includes sufficient wavelengths to be of wide scope, would be the use of absorbances at 20 nm intervals across a broad spectral region (~200 nm).

One concern is the degree of homogeneity indicated in these methods by a flat baseline. Two limitations imposed by the apparatus described under *Experimental*, are the experimentally determined response threshold of ±0.001*A* and the photometric linearity constraint. This latter restriction requires maximum absorbance values of ~1.0 *A* for wavelengths used in the null relationship, to preserve optimum photometric linearity. Thus, the maximum amount of drug substance analyzed, which governs the relative level of impurities found, is determined by this photometric limitation and by the chromatographic constraint against overloading the column. Given these instrumental restrictions, there are three principal factors which affect the response level of a given impurity: the intensity of its absorption (molar absorptivity), the degree of similarity between its absorption spectrum and that of the drug substance, and the detection method (null relationship) employed. In the case of unknown materials, absorption characteristics are unknown quantities, and the detection method cannot be tailored to attain the maximum response. Because of this, the use of multiple expressions containing data obtained at several wavelengths is recommended. An *a priori* detection limit cannot be stated for all possible impurities. However, these methods can ensure >99% homogeneity in most cases.

REFERENCES

(1) R. K. Gilpin, *Anal. Chem.*, **51**, 257R (1979).

(2) F. Volpe, J. Zintel, and D. Spiegel, *J. Pharm. Sci.*, **68**, 1264 (1979).

(3) C. Fenselau, *Anal. Chem.*, **49**, 563A (1977).

(4) H. B. Woodruff, P. C. Tway, and L. J. Cline Love, *ibid.*, **53**, 81 (1981).

(5) M. S. Denton, T. P. DeAngelis, A. M. Yacynych, W. R. Heineman, and T. W. Gilbert, *ibid.*, **48**, 20 (1976).

(6) M. J. Milano, S. Lam, and E. Grushka, *J. Chromatogr.*, **125**, 315 (1976).

(7) R. E. Dessy, W. D. Reynolds, W. G. Nunn, C. A. Titus, and G. F. Moler, *ibid.*, **126**, 347 (1976).

(8) A. E. McDowell and H. L. Pardue, *Anal. Chem.*, **49**, 1171 (1977).

(9) L. N. Klatt, *J. Chromatogr. Sci.*, **17**, 225 (1979).

(10) K. Adank and T. Schmidt, *Chimia*, **23**, 299 (1969).

(11) "The United States Pharmacopeia," 20th rev., U.S. Pharmacopeial Convention, Rockville, Md., 1979, pp. 300–301.

(12) L. R. Snyder and J. J. Kirkland, "Introduction to Modern Liquid Chromatography," 2nd ed., Wiley, New York, N.Y., 1979, pp. 27–34.

Kinetics and Stability of a Multicomponent Organophosphate Antidote Formulation in Glass and Plastic

PETER ZVIRBLIS and ROBERT I. ELLIN[x]

Received March 17, 1980, from the *U.S. Army Biomedical Laboratory, Aberdeen Proving Ground, MD 21010.* Accepted for publication July 20, 1981.

Abstract □ An aqueous solution of trimedoxime bromide, atropine, and benactyzine hydrochloride was formulated to have maximum stability as an antidote in organophosphorus poisoning. The stability of the mixture in glass and plastic cartridges was determined. Glass cartridges were more desirable than plastic; there was less vapor loss, color formation, and anomolous reaction. Trimedoxime was stable, losing 1.4% of its potency after 1 year at 25° and atropine was more stable than trimedoxime. Considerable degradation of benactyzine occurred; 20% of its potency was lost after 1 year at 25°. Equations for predicting the shelf life of each ingredient at selected temperatures are presented.

Keyphrases □ Benactyzine—in formulation, kinetics and stability in glass and plastic □ Atropine—in formulation, kinetics and stability in glass and plastic □ Trimedoxime—in formulation, kinetics and stability in glass and plastic

The administration of atropine with and without oxime is a common therapy for poisoning by organophosphorus anticholinesterase pesticides such as parathion[1] and malathion[1], and for other organophosphorus compounds such as isopropylmethylphosphonofluoridate (sarin) and pinacolyl methylphosphonofluoridate (soman). Atropine is used to overcome cholinergic stimulation from the anticholinesterases, and oxime reactivates and restores the activity of the enzyme. A recent report claims that the effectiveness of a therapy could be enhanced significantly by simultaneous administration of the cholinolytic drugs,

[1] Parathion, *O,O*-diethyl-*O*-(4-nitrophenyl)phosphorothioate; malathion, *O,O*-dimethyl-*S*-(1,2-dicarbethoxyethyl)phosphorodithioate; trimedoxime bromide, pyridinium-1,1′-(1,3-propanediyl)bis(4-(hydroxyimino)methyl)-dibromide; and benactyzine, α-hydroxy-α-penylbenzeneacetic acid 2-(diethylamino)ethyl ester.

0022-3549/82/0300-0321$01.00/0

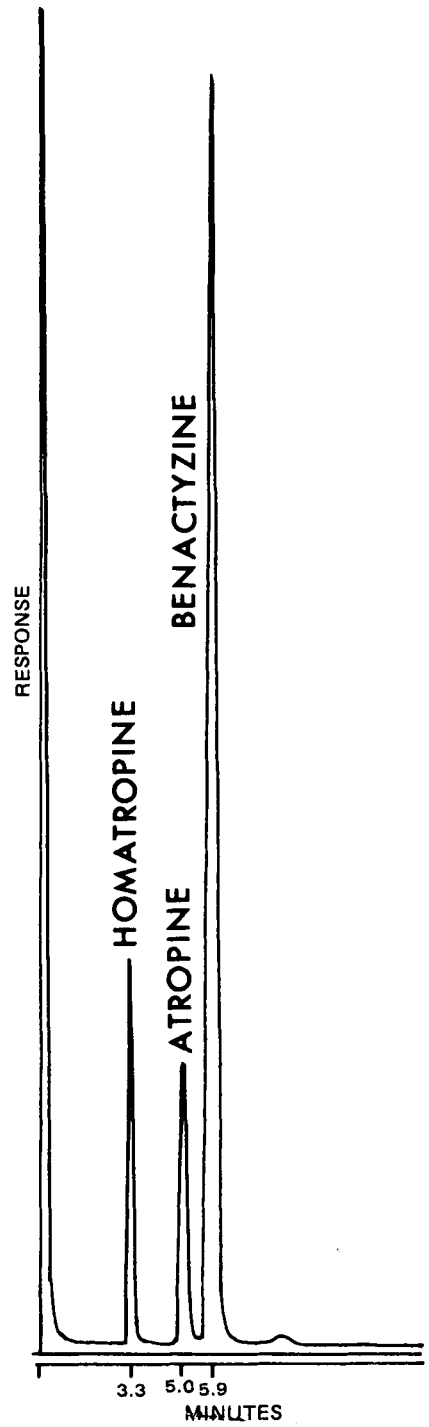

Figure 1—*Chromatogram of atropine and benactyzine with the internal standard, homatropine.*

atropine, and benactyzine[1] (1). This investigation was initiated in answer to the need of the United States Defense Forces for a stable and ready-for-use antidote that would be effective against a variety of organophosphorus compounds. Studies were conducted with a three-drug combination containing trimedoxime bromide[1], atropine sulfate, and benactyzine hydrochloride. The stability of aqueous solutions of the multicomponent mixture, in prefilled glass or plastic cartridges for a semiautomatic injector device, was studied.

The kinetics of hydrolysis of atropine and trimedoxime bromide in dilute aqueous solution in the pH range 0.5–

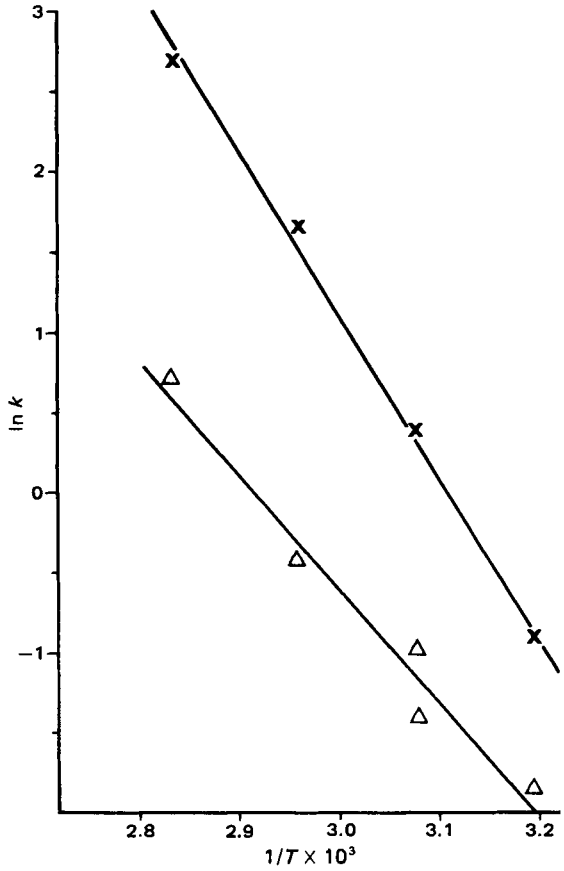

Figure 2—*Effect of temperature on net weight loss. Key: △, glass cartridges; ×, plastic cartridges.*

13.0 and at various temperatures were reported previously (2–4). Another report (5) studied the stability of benactyzine in the pH range 2.1–6.3 at 37°. A mixture of the three drugs (trimedoxime bromide, atropine sulfate, and benactyzine hydrochloride) was prepared at pH 2.8 to maximize the overall stability of the active ingredients of the multicomponent formulation.

EXPERIMENTAL

Materials—Cartridges were either glass (USP type 1) or polypropylene resins. Cartridge seals were butyl rubber.

The ingredients in the cartridge were: trimedoxime bromide, 20 mg/ml; atropine sulfate USP, 0.5 mg/ml; benactyzine hydrochloride, 2.05 mg/ml; methylparaben USP, 0.5 mg/ml; and propylparaben, 0.05 mg/ml[2]. All ingredients are dissolved in USP Water for Injection. Dilute hydrochloric acid USP, ~0.5 ml/liter, was used to adjust the pH to 2.8. Each cartridge was filled to 2.0 ml. The open ends of the cylindrical cartridges were stoppered with tight-fitting gray butyl rubber plugs.

Storage—The glass and plastic cartridge assemblies were wrapped individually in aluminum foil. They were then placed in a horizontal position in constant temperature ovens at either 80° for 3 weeks, 65° for 7 weeks, 52° for 3 months; in a water-jacketed incubator at 40° for 4 months; or in a refrigerator at 5° for 4 months. Some assemblies stored at 65° were placed vertically to determine whether the storage position had any influence. The physical appearance of the assembly cartridges, the net weight of the contents, pH, and the concentrations of benactyzine, trimedoxime, and atropine were studied. Samples were removed from storage at intervals for assessment and analysis. Differences found between glass and plastic cartridges were evaluated using a t test to determine significance at 95% confidence limits (6). The data for both types

[2] Reference standards of trimedoxime bromide and benactyzine hydrochloride are available upon request to Contracting Officer, Defense Personnel Support Center, Directorate of Medical Material, 2800 South 20th Street, Philadelphia, PA 19401.

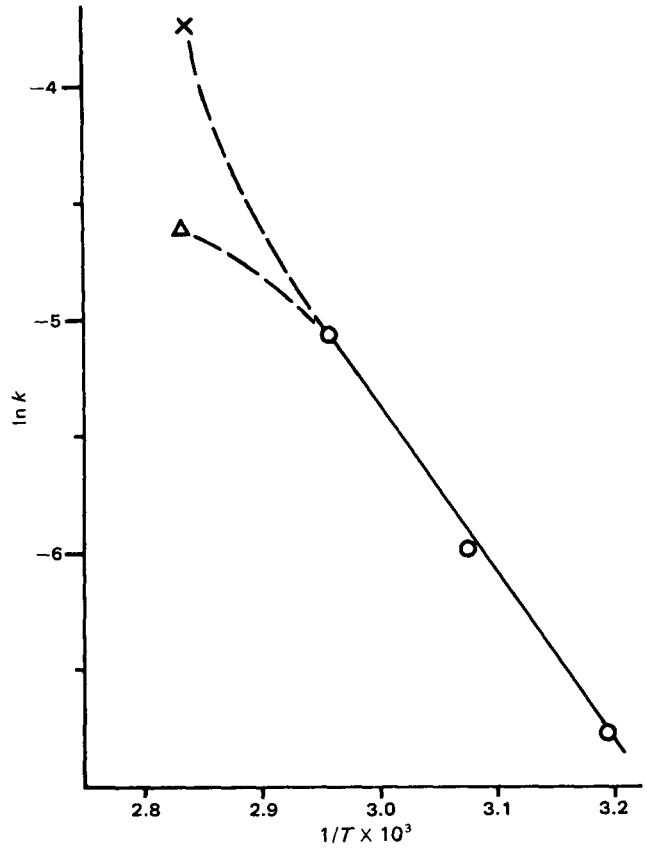

Figure 3—*Influence of temperature on pH decrease. Key: △, glass cartridges; ×, plastic cartridges. Values at 80° deviate significantly from the Arrhenius plot.*

of cartridges were combined where no statistically significant difference was shown.

Assay—*Benactyzine Hydrochloride and Atropine Sulfate*—One milliliter of each antidote mixture was pipetted into 10-ml glass tubes with polytef-lined screw caps. Internal standard[3] (1.0 ml), chloroform (1.0 ml), and 7% sodium carbonate (1.0 ml) were added successively. The tubes were capped immediately, shaken vigorously for 2 min, and the layers were allowed to separate. Approximately 2–3 μl of the chloroform layer was injected into the chromatograph.

The gas chromatographic analysis was done on a 1.2 m × 4-mm i.d. glass column with a 100/120-mesh Gas Chrom Q with 3% OV-17 column support and coating. The column temperature was 200° isothermal, the injection port temperature 190°, and the detector temperature 220°. The carrier gas was helium at a flow rate of 80 ml/min. The detector had an 80 ml/min hydrogen flow, and a 450 ml/min air flow. A typical chromatogram is shown in Fig. 1.

Trimedoxime Bromide (*4*)—Fifty microliters of the cartridge solution was added to 14.0 ml of deionized water; 100 μl of this dilution was added to 10.0 ml of 0.05 *N* NaOH and the resulting mixture was scanned between 400 and 300 nm. The absorbance at the peak near 346 nm was compared to that of a standard solution and the trimedoxime concentration was determined. In a series of samples, a blank and a standard solution were run at the beginning and end of the series. In larger groups, a standard solution was also interspersed between every 8–10 samples. The standard solution was 20 mg of trimedoxime/ml, 0.05% methylparaben, and 0.005% propylparaben in 10^{-3} *M* HCl. This solution was filtered through a 0.22 μm filter and stored at 5°.

RESULTS

The cartridges stored at 5° were assumed to yield baseline values. Over the period of the study there were no changes in the concentrations of trimedoxime, atropine, and benactyzine at 5°. The solutions from these cartridges were clear and faintly yellow, a color characteristic of trimedoxime solutions. No statistically significant differences between the glass and plastic cartridges were demonstrated at this temperature for any of

[3] Homotropine hydrobromide USP, 0.5 ng/ml in 10^{-3} *N* hydrochloric acid.

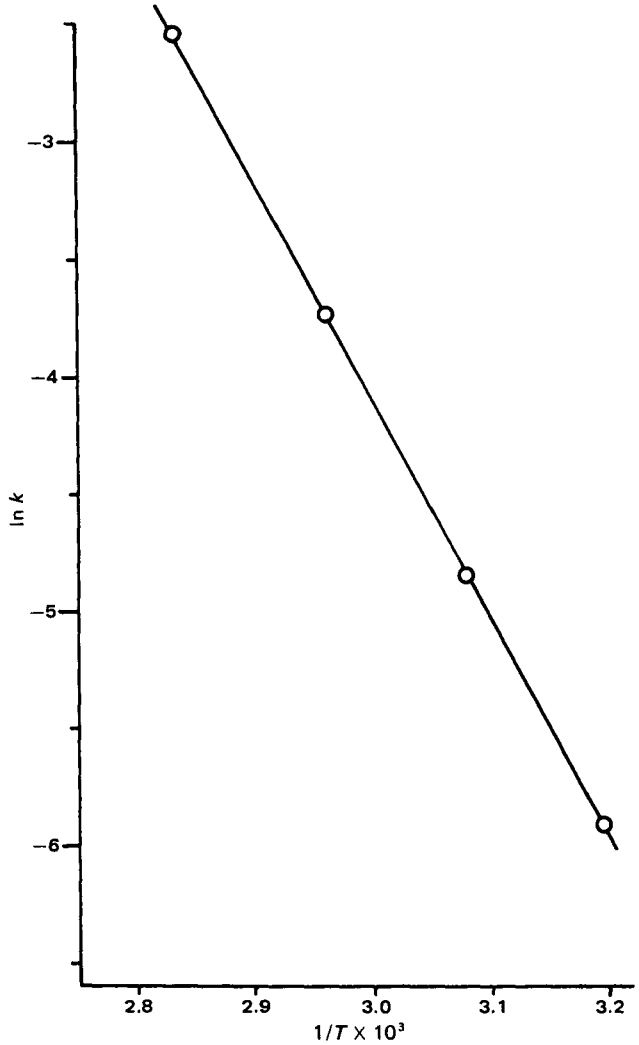

Figure 4—*Influence of temperature on the degradation rates of benactyzine.*

the factors studied except net weight. The average weight of the ejected contents for the plastic cartridge was 14 mg less than that for the glass cartridge at 5°.

The solutions stored at elevated temperatures in both the glass and the plastic cartridges remained clear throughout the study. Solutions in glass cartridges developed a trace of yellow color at 80°. Solutions in the plastic cartridge developed color much faster. At the end of each storage period the solutions were bright yellow at 80°, moderately yellow at 65°, light yellow at 52°, and at 40° contained a trace of yellow. One sample at 40° was very dark yellow, and had a pH of 2.5, (~0.2 units lower than expected).

No physical change was observed in glass cartridges throughout the study. In several plastic cartridges stored at 80°, the pressure generated was sufficient to move the rubber plunger toward the open end of the cartridge. The plastic cartridges became stained with a narrow brown ring at the interface of the plunger and the solution. In the cartridges where the plunger had moved, the stain was diffused over the path of the plunger movement. The stain was apparent in less than 1 week at 80 and 65°, in ~1 month at 52°, and in ~4 months at 40°.

No significant differences were demonstrated when the cartridges were stored in a vertical position (either end up) at 65° when compared with those stored in a horizontal position.

Reaction velocities of the various stability-related factors are influenced by temperature. This is expressed by the Arrhenius equation in its integrated form:

$$\ln k = A - E/RT \qquad \text{(Eq. 1)}$$

where k is the specific rate constant; E is the energy of activation; R is the gas constant (1.987 cal/deg mole); T is the absolute temperature; and A is a frequency factor.

The data were used to determine the best value of k at each tempera-

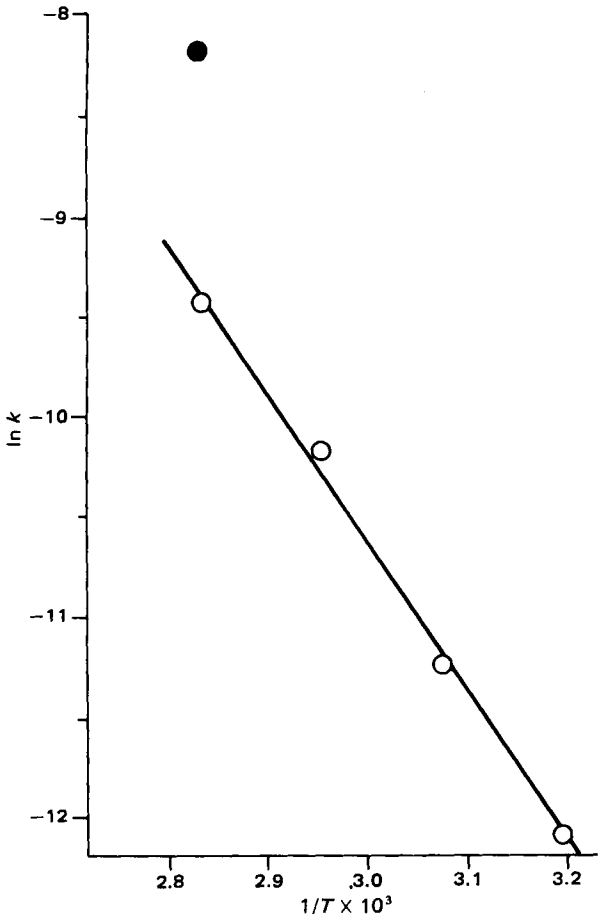

Figure 5—*Influence of temperature on the degradation rates of trimedoxime. The value for plastic cartridges at 80° (●) deviates significantly from the Arrhenius plot.*

ture. The best line of ln k *versus* $1/T$ was fitted by the least-squares method and the intercept (A) and the slope ($-E/R$) were determined.

Weight Loss—Loss of water from the solution in the cartridges, presumably occurring through the rubber closures and the walls of the plastic cartridge, would be reflected in a change in volume. Since the loss was small, measuring the change in weight was considered a more sensitive method of determining the loss than measuring the volume differences. The rate of weight loss in the glass and plastic cartridges was determined at each temperature, using the equation:

$$w = w_0 - kt \qquad \text{(Eq. 2)}$$

where w_0 is the weight in milligrams at the zero intercept, k is the rate of weight loss in milligrams per day[4]; and t is the time in days.

The effect of temperature on weight loss was significantly different between the two types of cartridges. The activation energies for the weight loss in the glass and plastic containers were 14.1 ± 1.6 (SE) and 20.1 ± 0.9 (SE) kcal, respectively. The Arrhenius plot for the glass and plastic cartridges is shown in Fig. 2.

Change in pH—The pH of the solutions in the cartridges decreased with storage time and can be expressed by the equation:

$$\text{pH} = \text{pH}_0 - kt \qquad \text{(Eq. 3)}$$

where pH_0 is the pH at time zero; k is in pH units per day; and t is time in days.

The rate of decrease in pH was significantly different between the glass and plastic cartridges at 80°. At this temperature the rate was lower for the glass cartridge than would be predicted from the other three temperature points, and higher for the plastic cartridge. No significant pH differences between glass and plastic cartridges were found at the lower temperatures. The best values for k are plotted in Fig. 3 and are expressed by the equation:

[4] The unit for k is generally expressed in concentration rather than weight. The authors feel that by expressing water loss in weight, rather than concentration, the data would be more meaningful.

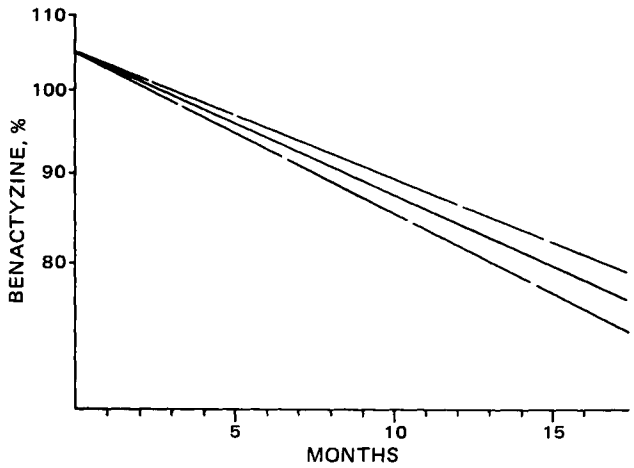

Figure 6—*Predicted disappearance of benactyzine hydrochloride at 25°. The solid line is the predicted thermal degradation rate of benactyzine in the injector at 105% fill. The dashed lines encompass the 95% confidence limits of the predicted rate.*

$$\ln k = 16.1455 - 14{,}300/RT \qquad \text{(Eq. 4)}$$

where the units for k are pH units/day. The standard error for the energy of activation is 690 calories.

Active Ingredients—*Benactyzine Hydrochloride*—The degradation of benactyzine in the mixture can be described adequately by the first-order rate equation:

$$\ln C = \ln C_0 - kt \qquad \text{(Eq. 5)}$$

where C is in milligrams per milliliter, C_0 is concentration at zero time, and t is time in days. There were no statistically significant differences between the glass and plastic cartridges for either C_0 or k.

The effect of temperature on the degradation rate is illustrated in Fig. 4, where the equation is expressed by:

$$\ln k = 23.7461 - 18{,}460/RT \qquad \text{(Eq. 6)}$$

where the unit of k is day^{-1} and the standard error for the activation energy is 150 calories.

Atropine Sulfate—No statistically significant disappearance of atropine sulfate in either glass or plastic cartridges could be demonstrated at any temperature during the term of this study.

Trimedoxime Bromide—The decrease in trimedoxime concentration is expressed by the zero-order equation:

$$C = C_0 - kt \qquad \text{(Eq. 7)}$$

where C is in moles per liter, C_0 is the concentration at zero time, k is in milligrams per day, and t is time in days.

A significant difference between the k values for glass and plastic

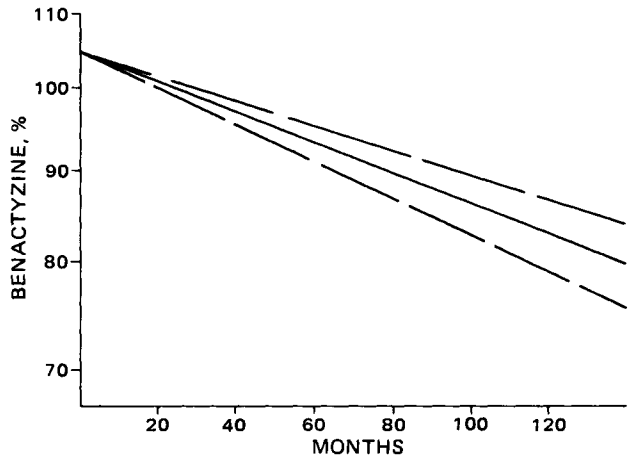

Figure 7—*Predicted disappearance of benactyzine hydrochloride at 5°. The solid line is the predicted thermal degradation rate of benactyzine in the injector at 105% fill. The dashed lines encompass the 95% confidence limits of the predicted rate.*

Table I—Predicted Shelf Life of Benactyzine in Multicomponent Formulation

Temperature	90% Shelf Life	75% Shelf Life
5°	4.5 years	12.3 years
15°	1.4 years	3.9 years
25°	5.9 months	1.3 years
40°	1.3 months	3.6 months
60°	0.2 months	0.6 months

cartridges was found only at 80°. No significant differences were found with regard to k or C_0 at other temperatures. The data for plastic cartridges at 80° were excluded in calculating the regression equation in Fig. 5. The line is expressed by

$$\ln k = 18.0100 - 14{,}900/RT \qquad \text{(Eq. 8)}$$

where k is in moles per liter-day. The standard error for the activation energy is 880 calories.

DISCUSSION

Glass cartridges were found to be more suitable than plastic as containers for trimedoxime, atropine, and benactyzine formulations. Benactyzine is the least stable of the active ingredients in the antidote formulation. Results of this study show that benactyzine degrades ~20% after 1 year at 25° in either plastic or glass. The usefulness of the injector could be prolonged by storage at 5°, where the predicted decrease in benactyzine is 10% after 5 years. Figures 6 and 7 illustrate the enhanced shelf life of benactyzine when filled at 105% of label and stored at 25 or 5°. Predicted shelf life at various temperatures is presented in Table I.

The trimedoxime in the injector is very stable; about 1.4% degradation would occur after 1 year at 25°. Solutions of trimedoxime can exist in equilibrium with its hydrolysis products (7, 8). The degradation rate of trimedoxime in plastic cartridges at 80° was faster then expected. The unusual drop in pH at 80° (Fig. 3), greater than expected based on temperature studies, could shift the equilibrium of trimedoxime and consequently account for the increased degradation rate in plastic.

Atropine sulfate in the medication is quite stable. According to kinetic studies of atropine in solution at pH 2.8, its half-life would be about 200 years at 25° and about 2 years at 80° (2, 3).

The pH values in glass were homogeneous at all temperatures. There was some heterogeneity of pH in the plastic cartridge; *i.e.*, 2 of 23 samples stored at 5° had a pH of about 2.95; one sample at 80° had a pH of 3.01, 0.5 units more than expected. A sample at 40° had a pH of 2.51, 0.2 units lower than expected. The decrease in pH with storage time was consistent with temperatures of 65° and below. At 80°, the decrease in pH was slower than expected, suggesting abstraction of hydrogen ion by the rubber in the cartridge. In the plastic cartridge, the pH decreased at a considerably faster rate than expected; this observation suggests a reaction caused by some material in plastic at this temperature. At 25° the drop in pH, probably due to the formation of benzilic acid, is predicted to be less than 0.15 units after 1 year of storage.

Vapor transmission from the cartridges at ambient temperature is low; it is estimated that water loss would be about 1%/year for the glass cartridge and about 2%/year for the plastic cartridge at 25°.

REFERENCES

(1) J. Schenk, W. Löffler, and N. Weger, *Arch. Toxicol.*, **36,** 71 (1976).

(2) P. Zvirblis, I. Socholitsky, and A. A. Kondritzer, *J. Am. Pharm. Assoc. Sci. Ed.*, **45,** 450 (1956).

(3) A. A. Kondritzer and P. Zvirblis, *ibid.*, **46,** 521 (1957).

(4) R. I. Ellin, D. E. Easterday, P. Zvirblis, and A. A. Kondritzer, *J. Pharm. Sci.*, **55,** 1263 (1966).

(5) J. P. Jefferies and J. I. Phillips, *J. Pharm. Pharmacol.*, **86,** 907 (1956).

(6) G. W. Snedecor, "Statistical Methods," 4th ed., Iowa State College Press, Ames, Iowa, 1953.

(7) R. I. Ellin, J. S. Carlese, and A. A. Kondritzer, *J. Pharm. Sci.*, **51,** 141 (1962).

(8) I. Christenson, *Acta Pharm. Suec.*, **9,** 351 (1972).

ACKNOWLEDGMENTS

The opinions or assertions contained herein are the private views of the authors and are not to be construed as official or as reflecting the views of the Army or the Department of Defense.

Factors Influencing the Apparent Protein Binding of Quinidine

THEODOR W. GUENTERT * and SVEIN ØIE ‡

Received September 26, 1980, from the *Department of Pharmacy, School of Pharmacy, University of California at San Francisco, Medical Center, San Francisco, CA 94143.* Accepted for publication July 8, 1981.

*Present address: Pharmazeutisches Institut, Universitaet Basel, Totengaesslein 3, CH-4051 Basel, Switzerland.

Abstract □ Various factors influencing the apparent protein binding of quinidine were examined. Different binding values in rabbit plasma were obtained by equilibrium dialysis techniques employing three commonly used buffers. Binding values comparable to those found by ultrafiltration were achieved after dialysis against isotonic phosphate buffer for ~4 hr. Dialysis beyond 8 hr gave an increased free fraction with time. The reported effect of *in vitro* added heparin on plasma protein binding could be prevented by reducing the final concentration in blood from 20 to 5 U/ml, a concentration still sufficient to prevent clotting of the blood sample. Daily freezing and thawing of plasma samples over 1 week did not alter the binding of quinidine. The samples were stable for at least 2 months at −20°.

Keyphrases □ Binding, protein—quinidine, factors influencing binding, rabbit plasma □ Quinidine—factors influencing protein binding, rabbit plasma □ Plasma protein binding—quinidine, factors influencing binding, rabbits

A wide range of protein binding values for quinidine have been reported. Mean unbound fractions of 0.10–0.29 were observed in normal volunteers (1–5), while mean values of 0.19–0.42 were found for patients with cirrhosis (2, 3). Although interindividual differences in binding properties may contribute significantly to the variability in these results, differences in the blood collection method and in the binding determination could be important contributing factors. Ultrafiltration and equilibrium dialysis have been used previously for quinidine binding determinations. In equilibrium dialysis, various investigators have used different temperatures, equilibrium

0022-3549/82/0300-0325$01.00/0

Table I—Predicted Shelf Life of Benactyzine in Multicomponent Formulation

Temperature	90% Shelf Life	75% Shelf Life
5°	4.5 years	12.3 years
15°	1.4 years	3.9 years
25°	5.9 months	1.3 years
40°	1.3 months	3.6 months
60°	0.2 months	0.6 months

cartridges was found only at 80°. No significant differences were found with regard to k or C_0 at other temperatures. The data for plastic cartridges at 80° were excluded in calculating the regression equation in Fig. 5. The line is expressed by

$$\ln k = 18.0100 - 14{,}900/RT \qquad \text{(Eq. 8)}$$

where k is in moles per liter-day. The standard error for the activation energy is 880 calories.

DISCUSSION

Glass cartridges were found to be more suitable than plastic as containers for trimedoxime, atropine, and benactyzine formulations. Benactyzine is the least stable of the active ingredients in the antidote formulation. Results of this study show that benactyzine degrades ~20% after 1 year at 25° in either plastic or glass. The usefulness of the injector could be prolonged by storage at 5°, where the predicted decrease in benactyzine is 10% after 5 years. Figures 6 and 7 illustrate the enhanced shelf life of benactyzine when filled at 105% of label and stored at 25 or 5°. Predicted shelf life at various temperatures is presented in Table I.

The trimedoxime in the injector is very stable; about 1.4% degradation would occur after 1 year at 25°. Solutions of trimedoxime can exist in equilibrium with its hydrolysis products (7, 8). The degradation rate of trimedoxime in plastic cartridges at 80° was faster then expected. The unusual drop in pH at 80° (Fig. 3), greater than expected based on temperature studies, could shift the equilibrium of trimedoxime and consequently account for the increased degradation rate in plastic.

Atropine sulfate in the medication is quite stable. According to kinetic studies of atropine in solution at pH 2.8, its half-life would be about 200 years at 25° and about 2 years at 80° (2, 3).

The pH values in glass were homogeneous at all temperatures. There was some heterogeneity of pH in the plastic cartridge; *i.e.*, 2 of 23 samples stored at 5° had a pH of about 2.95; one sample at 80° had a pH of 3.01, 0.5 units more than expected. A sample at 40° had a pH of 2.51, 0.2 units lower than expected. The decrease in pH with storage time was consistent with temperatures of 65° and below. At 80°, the decrease in pH was slower than expected, suggesting abstraction of hydrogen ion by the rubber in the cartridge. In the plastic cartridge, the pH decreased at a considerably faster rate than expected; this observation suggests a reaction caused by some material in plastic at this temperature. At 25° the drop in pH, probably due to the formation of benzilic acid, is predicted to be less than 0.15 units after 1 year of storage.

Vapor transmission from the cartridges at ambient temperature is low; it is estimated that water loss would be about 1%/year for the glass cartridge and about 2%/year for the plastic cartridge at 25°.

REFERENCES

(1) J. Schenk, W. Löffler, and N. Weger, *Arch. Toxicol.*, **36,** 71 (1976).

(2) P. Zvirblis, I. Socholitsky, and A. A. Kondritzer, *J. Am. Pharm. Assoc. Sci. Ed.*, **45,** 450 (1956).

(3) A. A. Kondritzer and P. Zvirblis, *ibid.*, **46,** 521 (1957).

(4) R. I. Ellin, D. E. Easterday, P. Zvirblis, and A. A. Kondritzer, *J. Pharm. Sci.*, **55,** 1263 (1966).

(5) J. P. Jefferies and J. I. Phillips, *J. Pharm. Pharmacol.*, **86,** 907 (1956).

(6) G. W. Snedecor, "Statistical Methods," 4th ed., Iowa State College Press, Ames, Iowa, 1953.

(7) R. I. Ellin, J. S. Carlese, and A. A. Kondritzer, *J. Pharm. Sci.*, **51,** 141 (1962).

(8) I. Christenson, *Acta Pharm. Suec.*, **9,** 351 (1972).

ACKNOWLEDGMENTS

The opinions or assertions contained herein are the private views of the authors and are not to be construed as official or as reflecting the views of the Army or the Department of Defense.

Factors Influencing the Apparent Protein Binding of Quinidine

THEODOR W. GUENTERT * and SVEIN ØIE ‡

Received September 26, 1980, from the *Department of Pharmacy, School of Pharmacy, University of California at San Francisco, Medical Center, San Francisco, CA 94143.* Accepted for publication July 8, 1981.

*Present address: Pharmazeutisches Institut, Universitaet Basel, Totengaesslein 3, CH-4051 Basel, Switzerland.

Abstract □ Various factors influencing the apparent protein binding of quinidine were examined. Different binding values in rabbit plasma were obtained by equilibrium dialysis techniques employing three commonly used buffers. Binding values comparable to those found by ultrafiltration were achieved after dialysis against isotonic phosphate buffer for ~4 hr. Dialysis beyond 8 hr gave an increased free fraction with time. The reported effect of *in vitro* added heparin on plasma protein binding could be prevented by reducing the final concentration in blood from 20 to 5 U/ml, a concentration still sufficient to prevent clotting of the blood sample. Daily freezing and thawing of plasma samples over 1 week did not alter the binding of quinidine. The samples were stable for at least 2 months at −20°.

Keyphrases □ Binding, protein—quinidine, factors influencing binding, rabbit plasma □ Quinidine—factors influencing protein binding, rabbit plasma □ Plasma protein binding—quinidine, factors influencing binding, rabbits

A wide range of protein binding values for quinidine have been reported. Mean unbound fractions of 0.10–0.29 were observed in normal volunteers (1–5), while mean values of 0.19–0.42 were found for patients with cirrhosis (2, 3). Although interindividual differences in binding properties may contribute significantly to the variability in these results, differences in the blood collection method and in the binding determination could be important contributing factors. Ultrafiltration and equilibrium dialysis have been used previously for quinidine binding determinations. In equilibrium dialysis, various investigators have used different temperatures, equilibrium

0022-3549/82/0300-0325$01.00/0

times, and buffers in their studies (1, 4, 6–9). A significant influence of the ionic composition of the buffer on the extent of apparent protein binding determined by dialysis has been found (10, 11). Woo and Greenblatt (9) demonstrated higher binding at room temperature than at body temperature which could explain differences in results obtained by different investigators. However, no information is available on the time course of equilibrium or whether the dialysis time affects the quinidine binding. Recent studies suggest that the addition of heparin to blood samples may alter the plasma protein binding of quinidine (11).

To determine the influence of the dialysis medium and the equilibrium time on the apparent protein binding of quinidine, the protein binding in rabbit plasma was measured by dialyzing the plasma against various buffers. The influence of heparin *in vitro* at two different concentration levels and *in vivo* was established. Furthermore, the stability of a spiked rabbit plasma sample under conditions of repeated freezing and thawing was tested over 2 months.

EXPERIMENTAL

Assay—Quinidine concentrations in plasma and buffer from equilibrium dialysis were determined using a modification of a previously reported specific high-pressure liquid chromatography (HPLC) method (12). A 50-μl sample of plasma or a 200-μl sample of buffer was mixed with 200 μl (plasma) or 100 μl (buffer) of methanol containing 193 ng of hydroquinine[1]/ml as internal standard. Plasma samples were centrifuged in a microhematocrit centrifuge[2] at ~12,000×*g*. A 20-μl aliquot of the sample was then injected onto a C_{18} μBondapak column[3] of 30-cm length and 3.9-mm bore, connected to an HPLC pump[4]. The mobile phase consisted of methanol[5]–water–phosphoric acid[5] 85% (27.0:72.95:0.05) at a flow rate of 2 ml/min. Quantitation was achieved by means of fluorescence detection[6] with excitation at 245 nm and emission at 440 nm (cutoff filter). Standard curves were prepared daily using peak height ratios of various quinidine[7] concentrations in plasma or buffer prepared as above.

Equilibrium Dialysis—Aliquots (700 μl) of plasma or serum were dialyzed against 700 μl of buffer in a 1-ml dialysis cell[8]. A dialysis membrane[9] with an average pore radius of 24 Å, pretreated by soaking in distilled water (10 min), ethanol (15 min), and buffer (120 min), was used in these studies. The cells were incubated in a shaker bath[10] at 37° during the dialysis. At the end of the planned equilibrium time (6 hr ± 20 min, when not otherwise stated) the plasma or serum and buffer were removed from the half-cells and assayed for quinidine within 24 hr (stored at 4° until assayed). The ratio of quinidine concentrations in the buffer to the plasma or serum was taken as the free fraction of drug in the biological sample.

A blank serum or plasma sample was dialyzed in each binding experiment to assess the presence of endogenous or exogenous compounds that might interfere with the quinidine measurement.

Ultrafiltration—Protein determination using ultrafiltration was carried out with 3 ml of plasma or serum in a stirred cell[11] using an ultrafiltration filter with a molecular weight cutoff of 25,000[12]. The filtration was accomplished using a positive pressure of 3.5 atm with a gas mixture of 1.4% CO_2 in nitrogen at 37° in an incubator. The filtrate was collected in a polyethylene tubing[13]. Volumes of 100-μl aliquots were sampled from the tubing and assayed for quinidine immediately. Filtration was continued until subsequent aliquots of filtrate contained comparable amounts of drug.

Table I—Influence of Storage with Frequent Freezing and Thawing on Plasma Protein Binding of Quinidine

Sample	Free Fraction of Drug, Day 0	Day 2	Day 4	Day 7	Day 60
1	0.20	0.21	0.21	0.17	0.17
2	0.21	0.23	0.22	0.21	0.17
3	0.19	0.21	0.22	0.21	0.20
4	0.18	0.21	0.22	0.18	—
Mean	0.20	0.22	0.22	0.19	0.18
CV[a]	6.6	4.7	2.3	10.7	9.6

[a] Coefficient of variation in percent.

Sample Stability—To determine the influence of storage at −20° with frequent freezing and thawing on the protein binding, a large sample of rabbit plasma was spiked with quinidine[7] at a concentration of 2 μg/ml. A blank sample was kept separate but treated identically to the spiked portion. The samples were stored frozen with daily thawing and freezing for the first week. Protein binding was determined in 700-μl aliquots (quadruplicate) of the spiked sample by equilibrium dialysis [Krebs–Ringer bicarbonate buffer (14)] immediately after drawing the blood from the animal and again after 2, 4, and 7 days. An additional determination was made after 2 months.

Influence of Buffer Composition and Equilibration Time—The dependence of the apparent protein binding value determined by equilibrium dialysis on buffer composition and equilibrium time was evaluated in three experiments. A large sample of freshly drawn pooled rabbit plasma (stabilized with 5 U of heparin/ml) was spiked with 1 μg of quinidine/ml. Aliquots (700 μl) were dialyzed using 12 separate cells for each buffer. The cells were removed after 1, 2 (duplicates), 3, 4, 6 (duplicates), 8, 12, 18, and 24 (duplicates) hr and analyzed by HPLC. The buffers used were Krebs–Ringer bicarbonate and phosphate buffer pH 7.4, both prepared according to Umbreit *et al.* (14) and isotonic phosphate buffer pH 7.4 (0.107 *M* Na_2HPO_4, 0.024 *M* KH_2PO_4 in double-distilled water). The samples containing Krebs–Ringer bicarbonate solutions were dialyzed in a 5% CO_2–95% O_2 atmosphere, the other in a normal atmosphere.

Quinidine binding in the sample was also determined by ultrafiltration ($n = 6$). The first 200 μl of ultrafiltrate was discarded and the unbound concentration was determined in the subsequent aliquots. The concentration in these subsequent aliquots varied less than 2%.

Influence of Heparin—Blank rabbit serum was spiked with quinidine to a concentration of 0.4 μg/ml and with heparin[14] to final concentrations of 0, 5, and 20 U/ml. Protein binding was determined in triplicate by equilibrium dialysis and the values found in the heparinized samples were compared to those found in the nonheparinized samples (Student *t* test).

To test for an indirect effect of heparin *in vivo*, 450 U/kg was injected into a rabbit. Blood samples (3 ml) were collected immediately before injection and after 5, 10, 30, 60, and 180 min. Only the 0- and 180-min samples coagulated within 2 hr and allowed collection of serum; in the other samples the clear supernate after centrifugation was taken for analysis. All samples collected were spiked with 1 μg of quinidine/ml and protein binding was determined using equilibrium dialysis (duplicates) with the Krebs–Ringer bicarbonate buffer.

Concentration Dependence—Rabbit serum was spiked with quinidine at concentration of 250, 750, 1875, and 3000 ng/ml. Protein binding was determined in the samples (triplicates) using equilibrium dialysis with the Krebs–Ringer bicarbonate buffer.

RESULTS AND DISCUSSION

The assay used for quinidine measurements was fast and precise. The number of samples that can be analyzed in 1 day is only limited by the retention time of the compounds on the HPLC column (quinidine, 3.6 min; hydroquinine, 6.0 min). Because no extraction step was involved in the sample preparation there was little variability in repeated determinations of the same sample. For quinidine in plasma or serum the coefficient of variation (*CV*) in duplicated determinations was between 0.18 and 3.9% ($n = 6$) at 0.5 μg/ml and between 0.76 and 1.2% ($n = 2$) at

[1] Prepared by hydrogenation of quinine (Fluka AG, Chemische Fabrik, CH-9470 Buchs, Switzerland).
[2] Model MB, International Equipment Co., Needham Heights, Mass.
[3] Waters Associates, Milford, Mass.
[4] Model 110, Altex Scientific, Berkeley, Calif.
[5] AR grade, Mallinckrodt, St. Louis, Mo.
[6] Schoeffel Instrument Corp., Westwood, N.J.
[7] Fluka AG, Chemische Fabrik, CH-9470 Buchs, Switzerland; hydroquinidine free material prepared by method of Thron and Dirscherl (13).
[8] Technilabs Instruments, Pequannacock, N.J.
[9] VWR Scientific Inc., San Francisco, Calif.
[10] Braun-Melsungen AG, West Germany.
[11] Millipore Co., Bedford, Mass.
[12] Pellicon Type PS, Millipore Co., Bedford, Mass.
[13] Intramedic, 1.57-mm i.d., 2.08-mm o.d., Clay Adams, Parsippany, N.Y.
[14] Heparin sodium injection USP 1000 U/ml, Invenex.

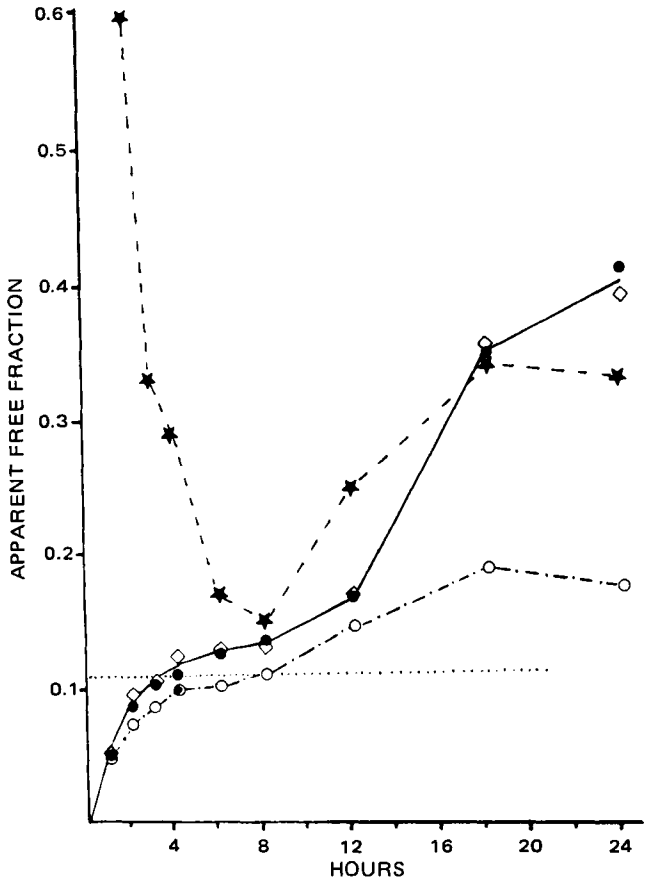

Figure 1—*Influence of buffer composition and equilibration time on apparent free fraction of quinidine in rabbit plasma. Key: ◊, spiked plasma dialyzed against Krebs–Ringer bicarbonate buffer; ●, spiked plasma dialyzed against Krebs–Ringer phosphate buffer; ○, spiked plasma dialyzed against isotonic phosphate buffer; ★ spiked Krebs–Ringer phosphate buffer dialyzed against rabbit plasma; and ·····, ultrafiltration of spiked plasma.*

1 μg/ml. Similar low variability was also observed in duplicate determinations of buffer samples: 0.94–6.3% (n = 4) at 50 ng/ml and 1.7–4.3% (n = 5) at 100 ng/ml. Standard curves were prepared daily by spiking blank plasma or water with various amounts of quinidine. The curves were linear with a CV for concentration-normalized peak height ratios of 4.5–7.5% in plasma and 2.0–5.8% in water.

A great deal of attention has been directed to the stability of biological samples when protein binding is to be measured. Denaturation of a major binding component under the storage conditions could influence the apparent free fraction of drug in the samples. Because freezing of biological fluids collected in pharmacokinetic studies is the most common form of storage, the influence of frequent freezing and thawing on the protein binding of quinidine in rabbit plasma was determined. Table I summarizes the result of a 2-month stability test. There was no significant change or trend in the free fraction of quinidine over a 1-week period with daily freezing and thawing of the sample, and no difference in the extent of binding could be detected after storage of the plasma in the freezer over a 2-month period. These results are in agreement with other findings (9).

The apparent free fraction of quinidine in a test sample was compared using equilibrium dialysis with three different buffers. Because little information exists regarding the time course of the equilibration process of quinidine, studies for each buffer were established. Samples equilibrated for 2, 6, and 24 hr were run in duplicate to allow estimation of the variability in the protein binding determination. Ultrafiltration of the same spiked plasma sample provided an independent estimate of the unbound drug concentration and yielded a value for the free fraction of 0.11.

In the dialysis experiments (Fig. 1), no clear equilibrium was reached for any one of the buffers even after 18–24 hr of dialysis. The values of the free fraction measured at these times exceeded the value of 0.11 determined by ultrafiltration and the samples showed turbidity. However, there appeared to be a temporary plateau discernible in the binding

Table II—Unbound Fraction of Quinidine in Plasma at Various Concentration Levels

Total Quinidine Concentration, ng/ml	Unbound Fraction[a]
250	0.11 (2.8%)
750	0.14 (5.1%)
1875	0.11 (14%)
3000	0.13 (3.2%)

[a] Mean (coefficient of variation).

curves between ~4 and 8 hr with unbound fraction similar to those obtained by ultrafiltration. Therefore, it can be concluded that equilibrium between the free quinidine concentration in plasma and in buffer was established after 4–6 hr, and that a second event causing displacement of drug from the protein or a particularly noticeable reduction of the binding capacity took place when dialysis extended beyond 8 hr. A second, much higher plateau in the equilibration curve was seemingly approached after 18–24 hr.

To further verify the use of the plateau at 4–8 hr as being representative of quinidine binding in plasma, the equilibrium time experiment was repeated using Krebs–Ringer phosphate buffer. However, in this instance the buffer side and not the plasma side was spiked. The result is shown in Fig. 1. After an initial rapid decline in the apparent drug free fraction, a trough value was attained after 8 hr at which time the apparent free fraction increased again, identically to the experiment using spiked plasma samples. The same plateau values were not attained as when the plasma side was spiked and only approached after 8 hr. This is readily explained by the general phenomenon that spiked buffer samples approach equilibrium at a slower rate than spiked plasma samples (15).

These experiments strongly indicate that under the given conditions the equilibrium is reached after 4–6 hr, and beyond 8 hr secondary effects occur that decrease the binding. Special care should be taken when using extended equilibrium times, particularly if the buffer side is spiked when assessing the binding. For example, in a study of demethylchlorimipramine protein binding (16), no apparent equilibrium was found even after 19 hr of dialysis when spiking the buffer side. However, a trough level was observed after 6 hr, after which the apparent free fraction started to increase again. It is possible that the 6-hr trough levels better represent the true unbound levels than the 19-hr dialysis values.

The reason for this phenomenon is not clear. Due to the increasing turbidity of the buffer samples, it is felt that microbiological growth took place, causing either drug displacement or binding protein degradation. This phenomenon is being investigated further.

Krebs–Ringer bicarbonate and Krebs–Ringer phosphate buffers gave higher unbound fraction values than isotonic phosphate buffer after 6 hr. This is consistent with previous findings (10, 11) that chloride displaces quinidine from plasma proteins. The Krebs–Ringer buffers contain chloride (128 mmoles/liter) while isotonic phosphate buffer does not. Because the Krebs–Ringer buffers contain a chloride concentration close to *in vivo* plasma levels, the use of these buffers would be expected to give values close to the *in vivo* unbound levels. However, the ultrafiltration values are closer to the values obtained by use of the isotonic phosphate buffer and therefore do not confirm this assumption.

Figure 1 shows that the increase in the apparent free fraction beyond 8 hr is less pronounced using the isotonic phosphate buffer. For practical reasons it may be more advantageous to use the isotonic phosphate buffer in binding determinations by equilibrium dialysis rather than Krebs–Ringer buffers, although the latter should be the buffer of choice on a theoretical basis.

Heparin is widely used clinically as an anticoagulant, *in vitro* for plasma collection methods, and *in vivo* for blood exchange techniques and for patients undergoing cardiopulmonary bypass or cardiac catheterization. It also has been shown to influence the protein binding or binding determination of various drugs including quinidine (1, 17, 18). The binding of quinidine to serum proteins was unaffected by a heparin concentration of 5 U/ml ($p > 0.10$) but significantly decreased in the presence of 20 U of heparin/ml ($p < 0.05$). Because 5 U of heparin/ml is sufficient to prevent coagulation *in vitro*, the influence of anticoagulant on protein binding could be prevented merely by reducing its concentration.

The effect of injected heparin was immediate with the strongest increase in the free fraction of drug in the first sample (collected at 5 min) and an exponential decline thereafter. Even after 3 hr, the binding of quinidine to proteins had not yet reached the pre-experimental value.

Although the amount of heparin injected may not be large compared to therapeutically administered doses, it is much more than would reach the general circulation by using indwelling heparinized catheters. The effect of lower amounts should be carefully assessed prior to studies using such catheters not only if protein binding determinations are planned, but in kinetic studies in general. This is important because altered protein binding can have a profound effect on kinetic parameters such as clearance (19) and apparent volume of distribution (20) or the interpretation of such data.

An earlier report (12) raised the possibility that protein binding of quinidine, at least in rabbits, might be capacity limited. However, Table II shows that there is no such effect discernible over the concentration range of 250–3000 ng/ml. Similarly, a previous study (9) found no concentration-dependence in the binding of quinidine to human serum over the clinically relevant range.

REFERENCES

(1) K. M. Kessler, R. C. Leech, and J. F. Spann, *Clin. Pharmacol. Ther.*, **25**, 204 (1979).

(2) M. Perez-Mateo and S. Erill, *Eur. J. Clin. Pharmacol.*, **11**, 225 (1977).

(3) M. Affrime and M. M. Reidenberg, *ibid.*, **8**, 267 (1975).

(4) D. Fremstad, O. G. Nilsen, L. Storstein, J. Amlie, and S. Jacobsen, *ibid.*, **15**, 187 (1979).

(5) R. E. Kates, T. D. Sokoloski, and T. J. Comstock, *Clin. Pharmacol. Ther.*, **23**, 30 (1978).

(6) O. G. Nilsen and S. Jacobsen, *Biochem. Pharmacol.*, **24**, 995 (1978).

(7) O. G. Nilsen, D. Fremstad, and S. Jacobsen, *Eur. J. Pharmacol.*, **33**, 131 (1975).

(8) D. Fremstad, K. Bergerud, J. F.W. Haffner, and P. K. M. Lunde, *ibid.*, **10**, 441 (1976).

(9) E. Woo and D. J. Greenblatt, *J. Pharm. Sci.*, **68**, 466 (1979).

(10) H. L. Conn and R. J. Luchi, *J. Pharmacol. Exp. Ther.*, **133**, 76 (1961).

(11) O. G. Nilsen, *Biochem. Pharmacol.*, **25**, 1007 (1976).

(12) T. W. Guentert and S. Øie, *J. Pharmacol. Exp. Ther.*, **215**, 165 (1980).

(13) H. Thron and W. Dirscherl, *Justus Liebigs Ann. Chem.*, **515**, 252 (1935).

(14) W. W. Umbreit, R. H. Burris, and J. F. Stauffer, "Manometric Techniques and Tissue Metabolism," Burgess, Minneapolis, Minn., 1951, p. 149.

(15) S. Øie and T. W. Guentert, *J. Pharm. Sci.*, in press.

(16) L. Bertilsson, R. Braithwaite, G. Tybring, M. Garle, and O. Borgå, *Clin. Pharmacol. Ther.*, **26**, 265 (1979).

(17) M. Wood, D. G. Shand, and A. J. J. Wood, *ibid.*, **25**, 103 (1979).

(18) D. Fremstad and K. Bergerud, *ibid.*, **20**, 120 (1976).

(19) G. Levy and A. Yacobi, *J. Pharm. Sci.*, **63**, 805 (1974).

(20) A. Yacobi and G. Levy, *ibid.*, **66**, 567 (1977).

ACKNOWLEDGMENT

T. W. Guentert is grateful for a postdoctoral fellowship received from the Swiss National Science Foundation.

Antineoplastic Effects of N^6-(Δ^2-Isopentenyl)adenosine against L-1210 Mouse Lymphocytic Leukemic Cells Using a Polymeric Delivery System

YUNIK CHANG ˣ **and BRUCE HACKER**

Received May 27, 1981, from the *Departments of Pharmaceutics and Pharmacology, Northeast Louisiana University, Monroe, LA 71209.* Accepted for publication July 24, 1981.

Abstract □ N^6-(Δ^2-Isopentenyl)adenosine (I), a nucleoside previously shown to be cytotoxic against several types of tumor cells, was impregnated in silicone polymer monolithic disc devices for release *in vitro* against lymphocytic mouse leukemia cells. Plotting the cumulative amount of N^6-(Δ^2-isopentenyl)adenosine released per unit area of the device *versus* the square root of time revealed a linear relationship. However, the higher loading dose tended to rapidly release any drug deposited on the polymer surface. The optimum loading dose of the device for the most effective antileukemic activity in 24 hr was calculated based on a plot of the release rate *versus* the square root of an initial loading dose. The silicone polymer–I delivery system enabled a sustained and controllable release of additional agent. It was thus possible to achieve virtually total inhibition of leukemic cell replication using the polymeric delivery system. Increased concentrations of I, without the use of the polymeric system, resulted in maximum 24 hr inhibition of only ~81%, followed by a decline in overall antileukemic activity. It is possible to achieve a more predictable release rate of N^6-(Δ^2-isopentenyl)adenosine and corresponding antileukemic activity using a polymeric delivery system against L-1210 mouse leukemic cells *in vitro*. The relative data indicate the ED_{50} concentrations to be considerably less using the polymeric delivery system.

Keyphrases □ Delivery systems—impregnated silicone polymer, N^6-(Δ^2-isopentenyl)adenosine □ Release rates—impregnated silicone polymer delivery system, N^6-(Δ^2-isopentenyl)adenosine □ N^6-(Δ^2-Isopentenyl)adenosine—antineoplastic, improved delivery using impregnated silicone polymer

N^6-(Δ^2-Isopentenyl)adenosine (I), a nucleoside previously shown to be both an inhibitor and cytotoxic to human leukemic myeloblast and sarcoma-180 cells (1), was prepared entrapped in the polymeric delivery form of a silicone polymer[1] monolithic disk to evaluate its relative antineoplastic properties.

Earlier studies demonstrated that I, found also in several isoaccepting species of tRNA, can interfere with the transport of unmodified nucleosides through the cytoplasmic membrane of mouse embryo cells at the level of the transmembrane translocation function (2). This membrane transport inhibition is believed to be responsible for its ability to alter RNA synthesis in phytohemagglutinin-stimulated mouse spleen lymphocytes as well as to be immunosuppressive in nature (3). In the latter context, it was possible to prepare an antibody with serologic specificity for I (4). Previous studies (5) demonstrated that L-1210 mouse leukemic cells possess the necessary

[1] Silastic, 382 Medical Grade Elastomer, Dow Corning Corp., Midland, Mich.

0022-3549/82/0300-0328$01.00/0

Although the amount of heparin injected may not be large compared to therapeutically administered doses, it is much more than would reach the general circulation by using indwelling heparinized catheters. The effect of lower amounts should be carefully assessed prior to studies using such catheters not only if protein binding determinations are planned, but in kinetic studies in general. This is important because altered protein binding can have a profound effect on kinetic parameters such as clearance (19) and apparent volume of distribution (20) or the interpretation of such data.

An earlier report (12) raised the possibility that protein binding of quinidine, at least in rabbits, might be capacity limited. However, Table II shows that there is no such effect discernible over the concentration range of 250–3000 ng/ml. Similarly, a previous study (9) found no concentration-dependence in the binding of quinidine to human serum over the clinically relevant range.

REFERENCES

(1) K. M. Kessler, R. C. Leech, and J. F. Spann, *Clin. Pharmacol. Ther.*, **25**, 204 (1979).

(2) M. Perez-Mateo and S. Erill, *Eur. J. Clin. Pharmacol.*, **11**, 225 (1977).

(3) M. Affrime and M. M. Reidenberg, *ibid.*, **8**, 267 (1975).

(4) D. Fremstad, O. G. Nilsen, L. Storstein, J. Amlie, and S. Jacobsen, *ibid.*, **15**, 187 (1979).

(5) R. E. Kates, T. D. Sokoloski, and T. J. Comstock, *Clin. Pharmacol. Ther.*, **23**, 30 (1978).

(6) O. G. Nilsen and S. Jacobsen, *Biochem. Pharmacol.*, **24**, 995 (1978).

(7) O. G. Nilsen, D. Fremstad, and S. Jacobsen, *Eur. J. Pharmacol.*, **33**, 131 (1975).

(8) D. Fremstad, K. Bergerud, J. F.W. Haffner, and P. K. M. Lunde, *ibid.*, **10**, 441 (1976).

(9) E. Woo and D. J. Greenblatt, *J. Pharm. Sci.*, **68**, 466 (1979).

(10) H. L. Conn and R. J. Luchi, *J. Pharmacol. Exp. Ther.*, **133**, 76 (1961).

(11) O. G. Nilsen, *Biochem. Pharmacol.*, **25**, 1007 (1976).

(12) T. W. Guentert and S. Øie, *J. Pharmacol. Exp. Ther.*, **215**, 165 (1980).

(13) H. Thron and W. Dirscherl, *Justus Liebigs Ann. Chem.*, **515**, 252 (1935).

(14) W. W. Umbreit, R. H. Burris, and J. F. Stauffer, "Manometric Techniques and Tissue Metabolism," Burgess, Minneapolis, Minn., 1951, p. 149.

(15) S. Øie and T. W. Guentert, *J. Pharm. Sci.*, in press.

(16) L. Bertilsson, R. Braithwaite, G. Tybring, M. Garle, and O. Borgå, *Clin. Pharmacol. Ther.*, **26**, 265 (1979).

(17) M. Wood, D. G. Shand, and A. J. J. Wood, *ibid.*, **25**, 103 (1979).

(18) D. Fremstad and K. Bergerud, *ibid.*, **20**, 120 (1976).

(19) G. Levy and A. Yacobi, *J. Pharm. Sci.*, **63**, 805 (1974).

(20) A. Yacobi and G. Levy, *ibid.*, **66**, 567 (1977).

ACKNOWLEDGMENT

T. W. Guentert is grateful for a postdoctoral fellowship received from the Swiss National Science Foundation.

Antineoplastic Effects of N^6-(Δ^2-Isopentenyl)adenosine against L-1210 Mouse Lymphocytic Leukemic Cells Using a Polymeric Delivery System

YUNIK CHANG ˣ **and BRUCE HACKER**

Received May 27, 1981, from the *Departments of Pharmaceutics and Pharmacology, Northeast Louisiana University, Monroe, LA 71209.* Accepted for publication July 24, 1981.

Abstract □ N^6-(Δ^2-Isopentenyl)adenosine (I), a nucleoside previously shown to be cytotoxic against several types of tumor cells, was impregnated in silicone polymer monolithic disc devices for release *in vitro* against lymphocytic mouse leukemia cells. Plotting the cumulative amount of N^6-(Δ^2-isopentenyl)adenosine released per unit area of the device *versus* the square root of time revealed a linear relationship. However, the higher loading dose tended to rapidly release any drug deposited on the polymer surface. The optimum loading dose of the device for the most effective antileukemic activity in 24 hr was calculated based on a plot of the release rate *versus* the square root of an initial loading dose. The silicone polymer–I delivery system enabled a sustained and controllable release of additional agent. It was thus possible to achieve virtually total inhibition of leukemic cell replication using the polymeric delivery system. Increased concentrations of I, without the use of the polymeric system, resulted in maximum 24 hr inhibition of only ~81%, followed by a decline in overall antileukemic activity. It is possible to achieve a more predictable release rate of N^6-(Δ^2-isopentenyl)adenosine and corresponding antileukemic activity using a polymeric delivery system against L-1210 mouse leukemic cells *in vitro*. The relative data indicate the ED_{50} concentrations to be considerably less using the polymeric delivery system.

Keyphrases □ Delivery systems—impregnated silicone polymer, N^6-(Δ^2-isopentenyl)adenosine □ Release rates—impregnated silicone polymer delivery system, N^6-(Δ^2-isopentenyl)adenosine □ N^6-(Δ^2-Isopentenyl)adenosine—antineoplastic, improved delivery using impregnated silicone polymer

N^6-(Δ^2-Isopentenyl)adenosine (I), a nucleoside previously shown to be both an inhibitor and cytotoxic to human leukemic myeloblast and sarcoma-180 cells (1), was prepared entrapped in the polymeric delivery form of a silicone polymer[1] monolithic disk to evaluate its relative antineoplastic properties.

Earlier studies demonstrated that I, found also in several isoaccepting species of tRNA, can interfere with the transport of unmodified nucleosides through the cytoplasmic membrane of mouse embryo cells at the level of the transmembrane translocation function (2). This membrane transport inhibition is believed to be responsible for its ability to alter RNA synthesis in phytohemagglutinin-stimulated mouse spleen lymphocytes as well as to be immunosuppressive in nature (3). In the latter context, it was possible to prepare an antibody with serologic specificity for I (4). Previous studies (5) demonstrated that L-1210 mouse leukemic cells possess the necessary

[1] Silastic, 382 Medical Grade Elastomer, Dow Corning Corp., Midland, Mich.

0022-3549/82/0300-0328$01.00/0

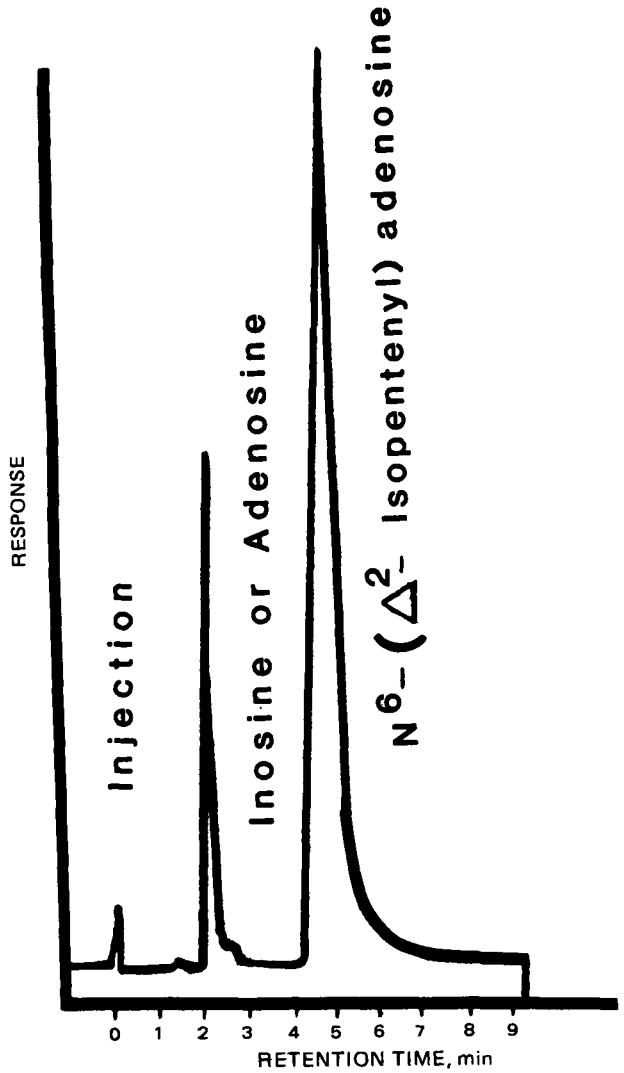

Figure 1—*High-pressure liquid chromatogram of a sample prepared by adding inosine or adenosine to the cultured sample containing 182 μg of I/ml.*

enzyme systems to phosphorylate I to the nucleotide level *in vitro*. It is not yet certain whether this biotransformation is a prerequisite for its antileukemic property.

The chemical reactions, biosynthesis, and metabolism of I, as well as its structural and functional role with respect to tRNA has been extensively reviewed (6). The importance of the intact allylic double bond moiety of the side chain of the purine, in addition to the ribose group of the nucleoside I, is generally recognized as being essential for antileukemic activity.

Table I—Preliminary Determination of Optimum Concentration of N^6-(Δ^2-Isopentenyl)adenosine (without Silicone Polymer) Required to Inhibit the Growth of Cultured L-1210 Mouse Leukemic Cells

Experimental Series[a]	Time after Addition of I to Culture Medium: Concentration of I in Culture Medium[b], μg/ml (4 hr)	Change in Total Cell Number[c], % (4 hr)	Concentration of I in Culture Medium, μg/ml (24 hr)	Change in Total Cell Number, % (24 hr)
A (control)	0	+24.3	0	+141.3
B (182 μg I/ml)	143	−25.1	140	−67.2
C (320 μg I/ml)	253	−61.3	250	−81.2

[a] Each T-flask contained 5 ml of growth medium containing RPMI 1640 plus 10% FCS, L-1210 cells and initial concentrations of I as indicated; cultures were conducted in triplicate. [b] Performed using HPLC. [c] Initial numbers of cells in control and treated cultures were $2 \times 10^5 \pm 6\%$ per ml of growth medium.

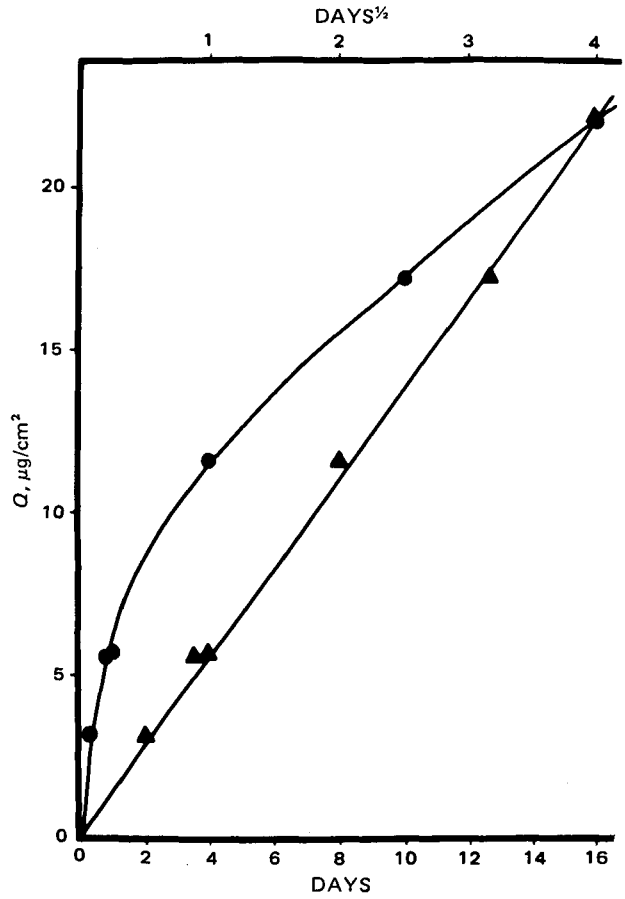

Figure 2—*Release of I in phosphate buffered saline solution from silicone polymer sheet containing 3% (w/w) I (points indicate the average of two experiments). Key:* ●, Q versus t; *and* ▲, Q versus $t^{1/2}$.

Although I has antineoplastic and cytotoxic effects against leukemic cells when administered to humans, it is known to be susceptible to enzyme degradation. Chheda *et al.* (7) showed that the biological half-life of I after intravenous administration was 4 hr. Other results (8) indicated that adenosine deaminase catalyzes conversion of I to inosine. It was also reported (9) that elevated adenosine deaminase activity in human blood significantly facilitates I degradation.

The present study developed a polymeric delivery system capable of releasing the optimum amount of I in a given interval of time required for most effective antileukemic activity.

EXPERIMENTAL

Preparation of N^6-(Δ^2-Isopentenyl)adenosine—I was prepared according to procedures described previously (2, 4, 5). Samples for analytical comparison using enzymatic and chromatographic techniques were described earlier (5).

Isolation and Propagation of L-1210 Mouse Leukemic Cells—Lymphocytic mouse leukemias were first described by Law *et al.* (10). Drug-sensitive and certain resistant sublines were propagated and cryopreserved (11) for *in vivo* and cell culture experiments. Parent lines were initially provided by other institutes[2,3]. Parent L-1210 mouse leukemic cells were grown to various densities as suspension cultures in tissue

[2] Dr. A. E. Bogden, Mason Research Inst., Worcester, Mass.
[3] Dr. H. Harder, Oral Roberts University Medical Center, Tulsa, Okla.

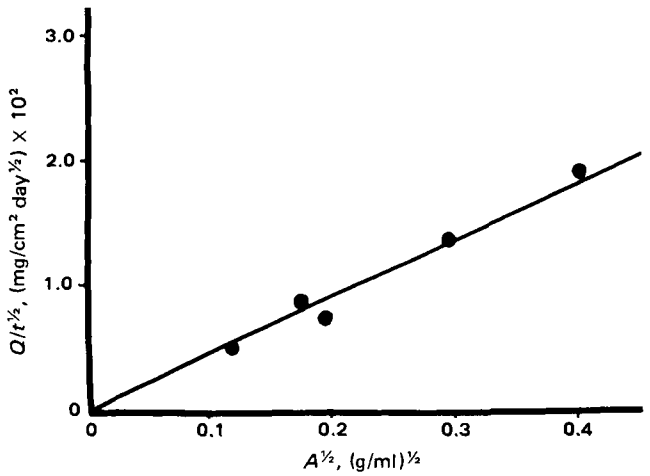

Figure 3—*Effect of the square root loading dose ($A^{1/2}$) in the silicone polymer sheet on the release rate of I ($Q/t^{1/2}$).*

culture flasks[4] containing 5.0 ml of growth medium[5]. Incubations were done at 37° under controlled conditions using a digital incubator[6] containing a 5% carbon dioxide–air atmosphere with a 98% relative humidity. Cells were visually monitored daily to assess general growth characteristics and to ensure the absence of contaminants using an inverted microscope–video system designed and interfaced in this laboratory and described elsewhere (12). Cell number and viability values were determined using Turk's solution and trypan blue exclusion methods, respectively, in hemocytometer cells (11).

Preparation of Isopentenyl Adenosine–Silicone Polymer Monolithic Sheets—N^6-(Δ^2-Isopentenyl)adenosine–silicone polymer sheets were prepared by mixing the required amounts of I into the silicone polymer and polymerizing with catalyst[7]. The mixture was then spread in a thin film on a glass plate and left overnight before the release study. The concentration of I in the polymeric delivery devices was calculated based on the weight-ratio of the drug and polymer used. Sheets of I–silicone for the cell culture media were sterilized using ethylene oxide sterilization[8]. Before use, each preparation was left at room temperature at atmospheric conditions overnight to eliminate residual ethylene oxide effects on the culture medium. Preliminary experiments indicated that equivalent quantities of the silicone polymer without I were not cytotoxic to normal growth of L-1210 cells.

Determination of Antineoplastic Activity of I against L-1210 Lymphocytic Leukemic Cells—Mouse L-1210 leukemic cells were grown in supplemented growth medium at several initial cell concentrations. Aliquots were removed using aseptic techniques for the determinations of cell number, and for centrifugation–filtration to obtain filtrates for assessing I concentration by high-pressure liquid chromatography (HPLC). Cell numbers in each culture flask were determined initially and after the introduction of I–silicone preparations or sterile-filtered solutions of I. These solutions were prepared by dissolving various quantities of solid I in 0.1–0.5-ml volumes of growth medium, and sterile-filtered using individual microunits[9]. After introducing small-volume aliquots of I solutions or I–silicone, aliquots of cell suspensions were removed during continuous incubation conditions and subjected to centrifugation–filtration. The latter consisted of using a centrifugal microfilter device fitted with 0.2-μm regenerated cellulose filters[10] to centrifuge and filter cell suspensions to get a cell-free filtrate.

Determination of I Released from the Polymer Sheet—Polymer sheets of known sizes were suspended on a chrome wire in 100-ml portions of phosphate-buffered saline solution, pH 7.4. The solution was covered to minimize evaporation. Throughout the diffusion experiment, the solution was stirred constantly to reduce boundary-layer effects. Fresh portions of phosphate-buffered saline solution replaced spent medium at each sampling time. For the quantitation of I released, aliquots (30 μl) of the eluting solution were applied onto a high-pressure liquid chromatograph[11]. All determinations of release rates were performed at least in duplicate.

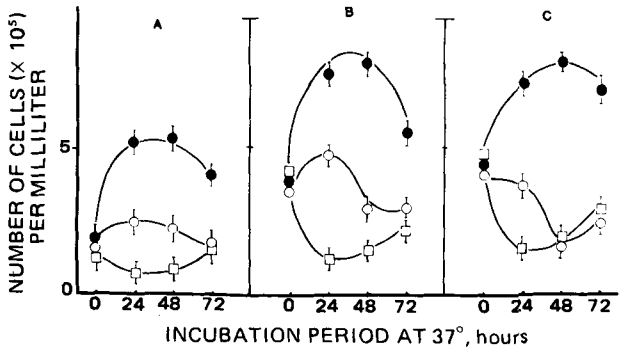

Figure 4—*The antileukemic effect of I using a silicone polymeric delivery system and varying numbers of cultured L-1210 mouse leukemia cells (A, 0.01 ml; B, 0.02 ml; C, 0.03 ml of 24-hr cell stock). Key: ●, control cultures; ○, I–silicone (5 mg I per 200-mg silicone polymer sheet); □, I (40 μg/ml).*

High-Pressure Liquid Chromatographic Procedure—The HPLC separation was performed using a reversed-phase column[12] with a flow rate of 1.0 ml/min using methanol[13]–water (3:2) as the mobile phase. Column effluent was pumped through a variable wavelength detector[14] monitored at 269 nm at ambient temperature. The detector sensitivity for phosphate buffer saline sample and cell culture sample was set at 0.05 and 0.5 aufs respectively. All quantitative determinations were made based on the standard curve obtained by plotting the peak height or electronic integrator response against the concentration of I.

RESULTS AND DISCUSSION

Monolithic sheet devices of I–silicone polymer were prepared that release I at the concentration range for >95% destruction of leukemic cells in the culture medium within 24 hr. The pattern of antileukemic activities of intact I and the I–silicone polymer system were compared.

High-Pressure Liquid Chromatography System—HPLC analysis of I in diffusion samples of phosphate buffered saline solution or cell culture medium was sensitive enough for the diffusion study and provided rapid, quantitative results. The results shown in Fig. 1 show a typical HPLC chromatogram of I in diffusion sample. Retention time of I was 5.0 min. Injection with several possible degradation products such as inosine, xanthine, or hypoxanthine showed no interference with I. These possible degradation products had retention times <5.0 min.

The released concentration of I in 100 ml of phosphate buffered saline solution was ~1–3 μg/ml. The standard curve for I was linear over the concentration range of 0.2–30 μg/ml. The correlation coefficient for the standard curve was 0.99 (n = 7). Standard solution injected at each time of diffusion sample assay showed no significant deviation from the standard curve during a set of experiments.

Since the total volume of cell culture medium was 5.0 ml, the concentration of I in the sample was high enough to change the detector sensitivity 0.5 aufs. The cell culture sample was filtered through cellulose filters before the injection on the HPLC column. The loss of I due to the filtration procedure was found to be negligible. The residual culture base peaks appeared close to the solvent.

Release of I from Silicone Polymer Matrix—Release time profiles of I were obtained with different loading doses on the same size silicone polymer sheets, each having an exposed surface area of 12.0 cm² and 0.35 ± 0.05 mm thick. All the experimental data were analyzed according to Eq. 1 (13, 14) on the basis of the diffusion controlled transport in a polymer matrix:

$$Q = [D(2A - C_s)C_s t]^{1/2} \qquad \text{(Eq. 1)}$$

where Q is the cumulative amount of drug released per unit area of devices (g/cm²) at time t, A is the amount of drug dispersed in a unit volume of device (g/cm³), D is the diffusivity of the drug in the matrix, and C_s is the solubility of the drug in the matrix phase. Based on Eq. 1, the cumulative amount of drug released (Q) from unit area should increase linearly with the square root of time.

[4] Falcon Plastics, 25 cm², No. 3012.
[5] RPMI-1640 medium including L-glutamine, supplemented with 10% fetal bovine serum (all products of Grand Island Biological Co., Grand Island, N.Y.).
[6] Model 3029, Forma Scientific, Marrietta, Ohio.
[7] Dow Corning Catalyst M., Dow Corning Corp., Midland, Mich.
[8] Steri-Vac Gas Sterilizer, 3M Co., St. Paul, Minn.
[9] Nalgene filter unit (cat. no. 120-0020;0.12μm), Sybron-Nalge Co., Rochester, N.Y.
[10] Bioanalytical System, West Lafayette, Ind.; Schleicher-Schuell filters.
[11] Varian 5020, Varian Instrument Co., Palo Alto, Calif.
[12] Micropak MCH-10(30 × 0.4 cm i.d.), Varian Instrument Co., Palo Alto, Calif.
[13] HPLC grade, Fisher Scientific Co., Fair Lawn, N.J.
[14] UV-50, Varian Instrument Co., Palo Alto, Calif.

Table II—Antileukemic Effect of N^6-(Δ^2-Isopentenyl)adenosine against Cultured L-1210 Leukemic Cells within 24 hr Using an Optimized Silicone Polymeric Delivery System

Experimental Series[a]	Time after Addition of I–Silicone Polymer Device: Concentration of I in Culture Medium[b], μg/ml (4 hr)	Change in Total Cell Number[c], % (4 hr)	Concentration of I in Culture Medium, μg/ml (24 hr)	Change in Total Cell Number, % (24 hr)
A (control)	0	+22.4[b]	0	+130.6
B (46 mg I/235-mg silicone device; 8 cm^2)	230	−37.2	350	−83.6
C (92 mg I./470-mg silicone device; 16 cm^2)	325	−56.1	456	−98.1

[a] Each T-flask contained 5 ml of growth medium containing RPMI 1640 plus 10% FCS, L-1210 cells, and I–silicone polymer; cultures were conducted in duplicate. [b] Performed using HPLC. [c] Initial numbers of cells were $2 \times 10^5 \pm 5\%$ per ml of growth medium.

Figure 2 shows the plots of Q *versus* t and Q *versus* $t^{1/2}$ obtained from I–silicone sheet containing 3% I. The release rate of drug decreased with time. The linear relationship between Q and $t^{1/2}$ was observed as expected. All other systems showed this type of release pattern. However, at the high loading dose, the Q *versus* $t^{1/2}$ plot showed intercept values on Q axis. The intercept value increased with increased loading dose. This may be due to the rapid release of drug deposited on the surface of the devices. Such a rapid initial drug release was reported previously (15).

The prediction of optimum loading dose in silicone polymer devices to get the effective minimum concentration of I in culture medium was attempted. The slope of Q *versus* $t^{1/2}$ is defined as:

$$Q/t^{1/2} = [D(2A - C_s)C_s]^{1/2} \quad \text{(Eq. 2)}$$

In the case where $2A \gg C_s$, Eq. 2 may be written as:

$$Q/t^{1/2} = (2D\,C_s)^{1/2}\,A^{1/2} \quad \text{(Eq. 3)}$$

indicating the linear relationship of $Q/t^{1/2}$ *versus* $A^{1/2}$. Experimentally, this linear relationship was observed as shown in Fig. 3. The slope, $(2D\,C_s)^{1/2}$ was calculated as 0.0482 with a linear coefficient of 0.986. The ratio of the matrix device volume to its weight was 0.85 ± 0.05. By relating this factor to Fig. 3, the approximate loading dose for the optimum concentrations of I to be released from a device was calculated.

Antineoplastic Effects of I Against L-1210 Mouse Lymphocytic Leukemic Cells—In preliminary experiments to assess the effectiveness of the silicone polymeric delivery system for releasing low concentrations of I certain salient features were uncovered. The I–silicone device initially containing 5 mg of I gave approximately the same concentration after 24 hr as adding I directly; the I–silicone system showed ~38% inhibition compared to ~65% for the direct addition method. On the other hand, the cytotoxic effects of the I–silicone system against L-1210 cells was comparable within 48–72 hr. At 72 hr, at the highest concentration of cells used (Fig. 4C), the pattern was reversed, with the I–silicone system becoming the more inhibitory of the two. In these experiments (and those depicted in Tables I and II), inhibition of cells in fresh medium appeared to be more permanent or irreversible for cells in cultures where I was introduced in the form of I–silicone. In contrast, those cells surviving the direct addition of I allowed for the recovery of viable cells when propagated in fresh medium. This suggested that the exposure time of L-1210 cells to I, which is limited directly to the timing of its release, is important with respect to the permanency of inhibition. This conclusion was supported by data presented in Tables I and II where at higher I–silicone concentration (92 mg/470 mg), inhibition was virtually complete (98.1%). The few surviving cells were deformed, did not exclude trypan blue dye, and did not transfer successfully to fresh medium. This inhibition level was not achievable with any concentration of I using the direct addition method. Recently, the National Cancer Institute group concluded that the pharmacokinetics of drug release and exposure time is important for another adenosine analog, sangivamycin, against Sarcoma-180 (16).

These data suggest that although comparable concentrations of I may be achieved using direct addition, the I–silicone delivery technique appears to produce a timed, controllable, and sustained release which optimizes inhibition by I against L-1210 lymphocytic leukemia. The use of the polymeric delivery systems with other antitumor agents, especially where enzyme degradation or inactivation of the drug is possible, may offer a better means of administering labile drug agents.

REFERENCES

(1) J. T. Grace, M. T. Hakala, R. H. Hall, and J. Blakeslee, *Proc. Am. Assoc. Cancer Res.*, **8**, 23 (1967).

(2) J. D. Hare and B. Hacker, *Physiol. Chem. Phys.*, **4**, 275 (1972).

(3) B. Hacker and T. L. Feldbush, *Cancer*, **27**, 1384 (1971).

(4) B. Hacker, H. Vunakis, and L. Levine, *J. Immunol.*, **108**, 1726 (1972).

(5) B. Hacker, *Biochim. Biophys. Acta*, **224**, 635 (1960).

(6) R. H. Hall, *Prog. Nucleic Acid Res. Mol. Biol.*, **10**, 57 (1970).

(7) G. B. Chheda and A. Mittelman, *Biochem. Pharmacol.*, **21**, 27 (1972).

(8) B. M. Chassy and R. J. Suhadolnik, *J. Biol. Chem.*, **242**, 3655 (1967).

(9) R. H. Hall and G. Mintsioulis, *J. Biochem.*, **73**, 739 (1973).

(10) L. W. Law, T. B. Dunn, and P. J. Doyle, *J. Natl. Cancer Inst.*, **10**, 179, (1949).

(11) B. Hacker and C. Doty, *Cryobiology*, **12**, 463 (1975).

(12) T. T. Martinez, G. A. Collins, and M. J. A. Walker, *Prostaglandins*, **14**, 450 (1972).

(13) T. Higuchi, *J. Pharm. Sci.*, **50**, 874 (1961).

(14) *Ibid.*, **52**, 1145 (1963).

(15) Y. W. Chien, H. J. Lambert, and D. E. Grant, *J. Pharm. Sci.*, **63**, 365 (1974).

(16) P. S. Ritch, R. I. Glazer, R. E. Cunningham, and S. E. Shackney, *Cancer Res.*, **41**, 1784 (1981).

Viscosity Change after Dilution with Solutions of Water–Oil–Water Emulsions and Solute Permeability Through the Oil Layer

MINORU TOMITA *, YOSHIRO ABE *, and TAMOTSU KONDO ‡x

Received November 6, 1980, from the **Department of Applied Chemistry, Faculty of Engineering, Keio University, Kohoku-ku, Yokohama, Japan 223* and the ‡*Faculty of Pharmaceutical Sciences, Science University of Tokyo, Shinjuku-ku, Tokyo, Japan 162.* Accepted for publication July 22, 1981.

Abstract □ A water-in-oil-in-water (W/O/W) multiple phase emulsion was prepared by a two-step emulsification procedure. The oil phase consisted of paraffin oil and sorbitan monooleate. The inner aqueous phase and the outer aqueous phase were 0.5% glucose solution and 3% polysorbate 80 solution, respectively. Viscosity measurements were carried out on the W/O/W emulsion after diluting it with a number of solutions. A given sequence for the solutes that would increase the emulsion viscosity after dilution was determined. This sequence was identical with that obtained with the solutes in an independent permeability experiment using a planar membrane composed of sorbitan monooleate alone. As a result, it was suggested that solutes as well as water can permeate the oil layer of vesicles of the emulsion to change the vesicle volume, thereby causing a change in the emulsion viscosity.

Keyphrases □ Emulsions—water–oil–water, viscosity change after dilution with solutions, permeability through the oil layer □ Permeability—solutes, through oil layer of water–oil–water emulsions □ Viscosity—changes, water–oil–water emulsions after dilution with solutions

Recently, a great deal of work has been done on preparation methods and applications of water-in-oil-in-water type multiple phase emulsions (denoted hereafter as W/O/W emulsions). Matsumoto *et al.* (1–3) reported a systematic procedure for the preparation of W/O/W emulsions. It was shown that an anticancer agent is localized at the cancer site for prolonged periods when administered in the form of a W/O/W emulsion, with the drug dissolved in inner aqueous phase (4–8). The application of W/O/W emulsions in foods (9) and cosmetics (10) also has been described.

In the application of W/O/W emulsions, it is necessary to estimate their stability experimentally. Viscosity has been claimed as a convenient method to determine stability (11). Although the viscosity of W/O/W emulsions is affected by a number of factors, the most important is the osmotic pressure gradient between the inner aqueous phase and the outer aqueous phase. This may produce changes in the volume of the inner aqueous phase due to the migration of water and/or solutes through the oil layer. In fact, the initial viscosity rise of some W/O/W emulsions on aging was explained by assuming the permeation of water containing a solute through the oil layer, from the outer aqueous phase to the inner aqueous phase due to the osmotic pressure gradient between the two phases (12). The present study will try to show that the viscosity change of W/O/W emulsions after dilution with solutions is interpreted more reasonably by assuming that solutes as well as water can permeate the oil layer.

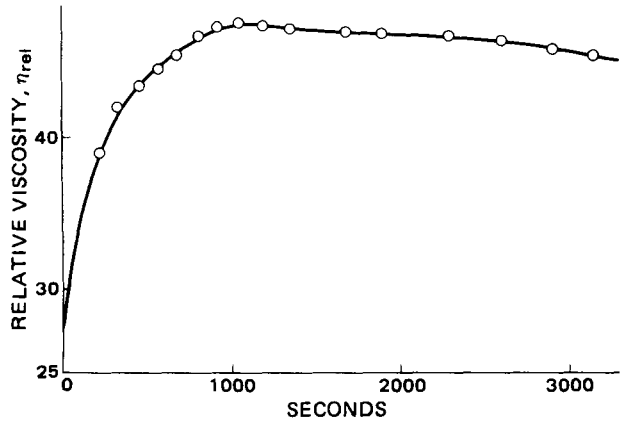

Figure 1—*Viscosity change of W/O/W emulsion after dilution with water.*

EXPERIMENTAL

Preparation of W/O/W Emulsions—The W/O/W emulsion was prepared by a two-step emulsification procedure according to Matsumoto *et al.* (1). Sorbitan monooleate[1] (8 g) and liquid paraffin[2] (10 g) were mixed thoroughly in a 100-ml beaker with a pin-mixer[3]. The stirring bar of the mixer was two six-pin blades which were fixed in a pile with a stainless steel bar. The rotation speed was maintained at 196 rpm by a constant speed stirrer[4]. As the mixture was being stirred, 30 ml of 0.5% (w/v) aqueous glucose solution was added slowly into the beaker at a constant rate. Addition of the glucose solution was controlled at a 3 ml/min rate by a pump[5]. The W/O emulsion formed was then stirred for 10 more min. It took 100 min for the first emulsification.

Thirty-five grams of the newly prepared W/O emulsion was dispersed into 35 ml of 3% aqueous solution of polysorbate 80 [6] using a homogenizer. The blade was a part of another homogenizer[7], and consisted of a fixed outer blade and an inner rotatable blade. The viscous W/O emulsion was torn and dispersed when passed through the narrow gap between the

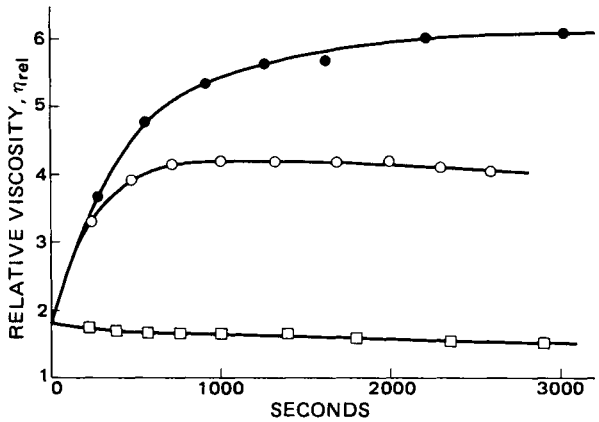

Figure 2—*Viscosity changes of W/O/W emulsion after dilution with aqueous potassium chloride solutions. Key:* ●, *water;* ○, 10^{-3} M; *and* □, 10^{-2} M.

[1] Tokyo Kasei Co., Tokyo.
[2] Kokusan Chemical Works, Tokyo.
[3] National Mfg. Ltd., Lincoln, Neb.
[4] Tokyo Rikakikai Co., Tokyo.
[5] Kuramochi Kagaku Kikai Mfg. Ltd., Tokyo.
[6] Nikko Chemicals Co., Tokyo.
[7] Polytron PCU-2, Kinematica Co., Basel, Switzerland.

0022-3549/82/0300-0332$01.00/0

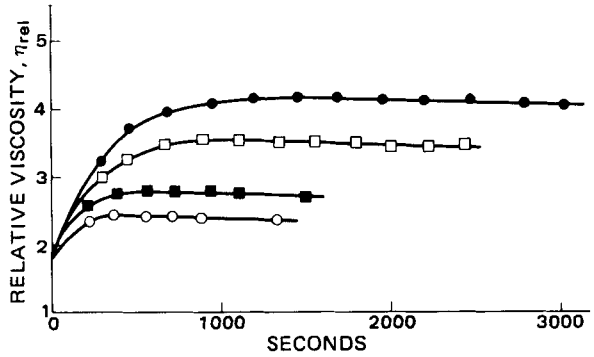

Figure 3—*Viscosity changes of W/O/W emulsion after dilution with aqueous sucrose solutions. Key:* ●, 1×10^{-3} M; □, 2×10^{-3} M; ■, 4×10^{-3} M; *and* ○, 6×10^{-3} M.

blades. The blade was connected to the constant speed stirrer used in the first emulsification since slow rotation was necessary. The rotation speed was set at 324 rpm and it took ~10 min to complete the second emulsification. The W/O/W emulsion prepared was denoted Sample A.

Viscometry of W/O/W Emulsion—The viscosity of W/O/W emulsions was measured with a capillary viscometer[8] in a constant temperature water bath maintained at 25 ± 0.1°. The time course was started at the time of Sample A dilution with water or an aqueous solution. The measurement time was taken as the average of the start and finish time of each liquid addition. All diluents were kept at 25° beforehand. As the ratio of diluent volume to Sample A weight was not constant for all runs, it is noted where necessary.

Planar Membrane Experiment—To determine if solutes can migrate through the oil layer, the following planar membrane experiment was done using an apparatus consisting of two acrylic chambers separated by a millipore filter[9] to which sorbitan monooleate was applied. Sorbitan monooleate acts not only as a W/O emulsifying agent, but as water solubilizer in oil. Liquid paraffin was omitted because it made the applied liquid easy to detach from the millipore filter. The millipore filter was compatible with the surfactant without swelling or dissolving. Its thickness was measured as 150 μm. The diameter of the diaphragm was 2.5 cm, and therefore the membrane area was 4.91 cm^2. Water and a solution (200 ml each), were placed in the two cells, respectively, and the whole apparatus was immersed in a thermostated water bath (30°). Since the cells were clear and transparent after each run, sorbitan monooleate was probably not removed from the millipore filter.

Fluxes for electrolytes were measured with a conductance meter equipped with platinum electrodes immersed in the water in one of the cells. In the conductometry, it was necessary to keep room temperature at 19 ± 1° throughout the measurement to obtain reproducible data. Measurements were taken every 30 min. Conventional colorimetric methods were employed for determining the fluxes of nonelectrolytes. Every hour, 3 ml of sample was withdrawn and then an equal volume of water previously kept at 30° was added to the cell to prevent hydrostatic pressure differences from being created.

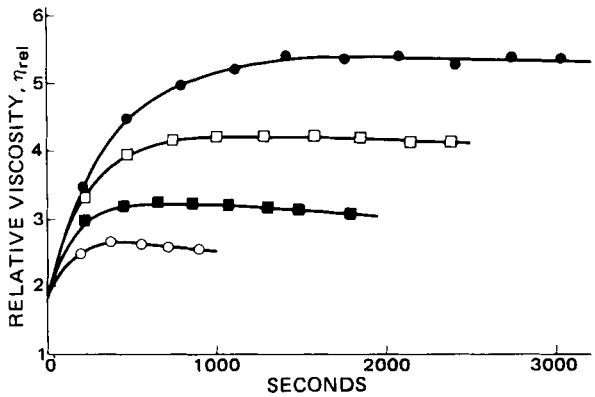

Figure 4—*Viscosity changes of W/O/W emulsion after dilution with aqueous glucose solutions. Key:* ●, 1×10^{-3} M; □, 2×10^{-3} M; ■, 4×10^{-3} M; *and* ○, 6×10^{-3} M.

[8] Ostwald type.
[9] Type GSWP 02500.

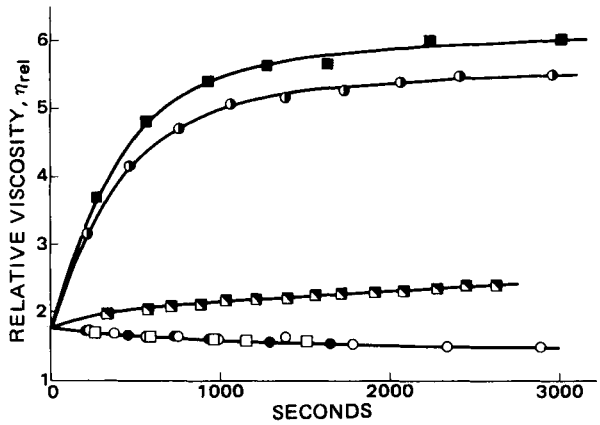

Figure 5—*Viscosity changes of W/O/W emulsion after dilution with a variety of aqueous solutions. Key:* ■, *water;* ◑, 2×10^{-2} M *urea;* ◪, 10^{-2} M *KSCN;* ○, 10^{-2} M *KCl;* ●, 2×10^{-2} M *glucose; and* □, $2/3 \times 10^{-2}$ M $CaCl_2$.

RESULTS AND DISCUSSION

Figure 1 shows the viscosity change with time for a W/O/W emulsion after dilution with water, in which the ratio of Sample A weight to diluent volume was 1:1.

The viscosity increased with time to a maximum and then decreased monotonically. A similar viscosity change was obtained even with the original emulsion. Matsumoto and Kohda (2) also reported this type of viscosity change for their W/O/W emulsions, the inner and outer aqueous phases of which were glucose solution and water, respectively. This viscosity change was ascribed to the volume change of vesicles in the W/O/W emulsions (2). To deal with this phenomenon quantitatively, an appropriate equation which correlates the relative viscosity to the volume fraction of vesicles should be known. However, it is impossible to determine an equation that would be appropriate, since the volume fraction changes on aging from the time of preparation and also changes on dilution. Hence, the volume change of vesicles in W/O/W emulsions can only be estimated qualitatively by means of viscometry, light scattering measurement, photomicroscopy, etc. For example, vesicle swelling after dilution of the original sample was confirmed by photomicroscopy. Similar observations were reported for a water/*n*-heptane/water emulsion (13).

Figures 2–4 show viscosity changes caused by dilution with aqueous potassium chloride, sucrose, and glucose solutions of various concentrations, respectively. In these cases the ratio of Sample A weight to diluent volume was 1:4.

The rate of viscosity change decreases with increasing concentration of solute in the diluent, and the viscosity falls even below its initial value when the emulsion is diluted with 10^{-2} *M* potassium chloride. These findings may be explained by the osmotic pressure difference between the inner aqueous phase and the outer aqueous phase as suggested previously (12, 14). The oil layer of vesicles in the W/O/W emulsion has a permeability to water, and the amount and direction of water movement depend on the osmotic pressure gradient. Figure 5 shows the viscosity change produced by dilution with a variety of aqueous solutions which have identical π values in the equation:

$$\pi = zcRT \qquad \text{(Eq. 1)}$$

where π is osmotic pressure, c is the concentration of solute, R and T are the usual gas constants, and z is an integer which is 1 for nonelectrolytes, 2 for uni-univalent electrolytes, and 3 for calcium chloride. The ratio of Sample A weight to diluent volume is 1:4. The equation gives the osmotic pressure of the outer aqueous phase when the oil layer has ideal semipermeability to the solute.

Urea and potassium thiocyanate increase viscosity, while potassium chloride, glucose, and calcium chloride decrease it. This suggests that solutes which produce a greater increase in viscosity contribute to a smaller degree to the osmotic pressure of the outer phase. In other words, these latter solutes can more or less permeate the oil layer. Therefore, the permeability sequence for the solutes is: urea > potassium thiocyanate > potassium chloride > glucose > calcium chloride.

Tanaka and coworkers[10] found a dependency of W/O/W emulsion

[10] Personal communication.

Table I—Permeability Coefficients Evaluated from Planar Membrane Experiments

Solute	Permeability Coefficient (30°), cm/sec × 10^9
Urea	440
Potassium thiocyanate	21.9
Cesium chloride	3.76
Rubidium chloride	2.84
Potassium chloride	2.37
Sodium chloride	2.19
Lithium chloride	1.77

viscosity at the time of preparation on the species of solute enclosed in the inner aqueous phase. For example, potassium chloride shows a much higher viscosity than potassium thiocyanate. Although it was suggested[10] that potassium thiocyanate prevents formation of W/O/W to give a lower viscosity, this can also be explained in terms of the permeability difference between the two salts. Since potassium thiocyanate, which is more permeable than potassium chloride, would contribute to the osmotic pressure of the inner aqueous phase less than potassium chloride, there would be less movement of water from the outer to the inner aqueous phase, thus giving a lower viscosity.

Table I lists the permeability coefficients calculated for some solutes from the fluxes determined in the planar membrane experiment. The sequence of permeability coefficient values in the table is identical with that obtained in the viscometry of the W/O/W emulsion. Furthermore, the absolute values of the permeability coefficient for sodium chloride and urea are in good agreement with those obtained with phospholipid bilayer membranes (15, 16). The sequence for alkali chlorides is also identical with that obtained with the lipid bilayers (15).

It would be reasonable to conclude that solutes can permeate the oil layer of vesicles in the W/O/W emulsion, probably due to a large total surface area of the vesicles, even though there is a considerable difference in composition between the oil layer and the planar membrane. Water would act as the carrier of solutes across the oil layer, presumably in the solubilized form.

Matsumoto *et al.* (1) proposed to measure the yield of W/O/W emulsion by a dialysis method. That is, when the emulsion containing a solute in the inner aqueous phase is dialyzed against distilled water, the concentration of the solute in the water should correspond to the yield. However, if the solute can permeate the oil layer of vesicles in the emulsion, there is no way to distinguish the solute diffused from the inner aqueous phase from the solute that leaked out as a result of vesicle destruction. The dialysis method cannot give correct yield. Moreover, if a high solute concentration in the water and a low emulsion viscosity are found (as in the case where a highly permeable solute is used) it could be incorrectly concluded that the solute has prevented the formation of a W/O/W emulsion.

REFERENCES

(1) S. Matsumoto, Y. Kita, and D. Yonezawa, *J. Colloid Interface Sci.*, **57,** 353 (1976).

(2) S. Matsumoto, M. Kohda, and S. Murata, *ibid.*, **62,** 149 (1977).

(3) Y. Kita, S. Matsumoto, and D. Yonezawa, *J. Chem. Soc. Jpn.*, **1977,** 748.

(4) C. J. Benoy, L. A. Elson, and R. Schneider, *Br. J. Pharmacol.*, **45,** 135 (1972).

(5) T. Takahashi, M. Mizuno, Y. Fujita, S. Ueda, B. Nishizawa, and S. Majima, *Gann*, **64,** 345 (1978).

(6) T. Takahashi, U. Satoshi, K. Kono, and S. Majima, *Cancer*, **38,** 1507 (1976).

(7) T. Takahashi, K. Kono, and T. Yamaguchi, *J. Exp. Med.*, **123,** 235 (1977).

(8) M. Hashida, M. Egawa, S. Muranishi, and H. Sezaki, *J. Pharmacokinet. Biopharm.*, **5,** 225 (1977).

(9) S. Matsumoto, Y. Ueda, Y. Kita, and D. Yonezawa, *Agr. Biol. Chem.*, **42,** 739 (1978).

(10) H. Fukuda and M. Tanaka, Japanese pat. 134,029 (1977).

(11) Y. Kita, S. Matsumoto, and D. Yonezawa, *J. Colloid Interface Sci.*, **62,** 87 (1977).

(12) S. Matsumoto and M. Kohda, *ibid.*, **73,** 13 (1980).

(13) S. Matsumoto, T. Inoue, M. Kohda, and K. Ikura, *ibid.*, **77,** 555 (1980).

(14) Y. Kita, S. Matsumoto, and D. Yonezawa, *J. Chem. Soc. Jpn.*, **1978,** 11.

(15) V. K. Miyamoto and T. E. Thompson, *J. Colloid Interface Sci.*, **25,** 16 (1967).

(16) R. E. Wood, F. P. Wirth, Jr., and H. E. Morgan, *Biochim. Biophys.* **163,** 171 (1968).

ACKNOWLEDGMENTS

The authors express their thanks to Dr. Minako Tanaka of the Lion Co., Tokyo, for her valuable discussion.

Ion Chromatographic Determination of the Principal Inorganic Ion in Bulk Antibiotic Salts

J. W. WHITTAKER * and P. R. LEMKE ˣ

Received May 13, 1981, from *Pfizer Inc., Quality Control Division, Groton, CT 06340.* Accepted for publication July 28, 1981. *Present address: IBM Instrument Inc., Orchard Park, P.O. Box 332, Danbury, CT 06810.

Abstract □ Two ion-chromatographic procedures were developed for determining the principal inorganic ions in bulk antibiotic salts. The anion system enables sulfate determination in sulfate salts of polymyxin, neomycin, streptomycin, and dihydrostreptomycin, with typical analysis times of 8 min/sample and a relative precision of ±2% (95% confidence interval). The cation system is applicable to sodium or potassium analysis in the respective penicillin salts in 9–16 min with a relative precision of ±2.5%. These methods offer speed, specificity, and easy sample preparation compared with traditional assays.

Keyphrases □ Ion chromatography—determination of inorganic ion in bulk antibiotic salts □ Antibiotics—determination of inorganic ion in salts using ion chromatography □ Inorganic ion—determination in salts of various antibiotics by ion chromatography

Bulk antibiotic salts can be characterized by the determination of their principal components for the purposes of quality assurance. An accurate assay is required for both the pharmacologically active organic ion and the inorganic counterion. For the organic moiety, many specific chromatographic assays (1) are applicable to bulks. However,

0022-3549/82/0300-0334$01.00/0

Table I—Permeability Coefficients Evaluated from Planar Membrane Experiments

Solute	Permeability Coefficient (30°), cm/sec × 10^9
Urea	440
Potassium thiocyanate	21.9
Cesium chloride	3.76
Rubidium chloride	2.84
Potassium chloride	2.37
Sodium chloride	2.19
Lithium chloride	1.77

viscosity at the time of preparation on the species of solute enclosed in the inner aqueous phase. For example, potassium chloride shows a much higher viscosity than potassium thiocyanate. Although it was suggested[10] that potassium thiocyanate prevents formation of W/O/W to give a lower viscosity, this can also be explained in terms of the permeability difference between the two salts. Since potassium thiocyanate, which is more permeable than potassium chloride, would contribute to the osmotic pressure of the inner aqueous phase less than potassium chloride, there would be less movement of water from the outer to the inner aqueous phase, thus giving a lower viscosity.

Table I lists the permeability coefficients calculated for some solutes from the fluxes determined in the planar membrane experiment. The sequence of permeability coefficient values in the table is identical with that obtained in the viscometry of the W/O/W emulsion. Furthermore, the absolute values of the permeability coefficient for sodium chloride and urea are in good agreement with those obtained with phospholipid bilayer membranes (15, 16). The sequence for alkali chlorides is also identical with that obtained with the lipid bilayers (15).

It would be reasonable to conclude that solutes can permeate the oil layer of vesicles in the W/O/W emulsion, probably due to a large total surface area of the vesicles, even though there is a considerable difference in composition between the oil layer and the planar membrane. Water would act as the carrier of solutes across the oil layer, presumably in the solubilized form.

Matsumoto *et al.* (1) proposed to measure the yield of W/O/W emulsion by a dialysis method. That is, when the emulsion containing a solute in the inner aqueous phase is dialyzed against distilled water, the concentration of the solute in the water should correspond to the yield. However, if the solute can permeate the oil layer of vesicles in the emulsion, there is no way to distinguish the solute diffused from the inner aqueous phase from the solute that leaked out as a result of vesicle destruction. The dialysis method cannot give correct yield. Moreover, if a high solute concentration in the water and a low emulsion viscosity are found (as in the case where a highly permeable solute is used) it could be incorrectly concluded that the solute has prevented the formation of a W/O/W emulsion.

REFERENCES

(1) S. Matsumoto, Y. Kita, and D. Yonezawa, *J. Colloid Interface Sci.*, **57,** 353 (1976).

(2) S. Matsumoto, M. Kohda, and S. Murata, *ibid.*, **62,** 149 (1977).

(3) Y. Kita, S. Matsumoto, and D. Yonezawa, *J. Chem. Soc. Jpn.*, **1977,** 748.

(4) C. J. Benoy, L. A. Elson, and R. Schneider, *Br. J. Pharmacol.*, **45,** 135 (1972).

(5) T. Takahashi, M. Mizuno, Y. Fujita, S. Ueda, B. Nishizawa, and S. Majima, *Gann*, **64,** 345 (1978).

(6) T. Takahashi, U. Satoshi, K. Kono, and S. Majima, *Cancer*, **38,** 1507 (1976).

(7) T. Takahashi, K. Kono, and T. Yamaguchi, *J. Exp. Med.*, **123,** 235 (1977).

(8) M. Hashida, M. Egawa, S. Muranishi, and H. Sezaki, *J. Pharmacokinet. Biopharm.*, **5,** 225 (1977).

(9) S. Matsumoto, Y. Ueda, Y. Kita, and D. Yonezawa, *Agr. Biol. Chem.*, **42,** 739 (1978).

(10) H. Fukuda and M. Tanaka, Japanese pat. 134,029 (1977).

(11) Y. Kita, S. Matsumoto, and D. Yonezawa, *J. Colloid Interface Sci.*, **62,** 87 (1977).

(12) S. Matsumoto and M. Kohda, *ibid.*, **73,** 13 (1980).

(13) S. Matsumoto, T. Inoue, M. Kohda, and K. Ikura, *ibid.*, **77,** 555 (1980).

(14) Y. Kita, S. Matsumoto, and D. Yonezawa, *J. Chem. Soc. Jpn.*, **1978,** 11.

(15) V. K. Miyamoto and T. E. Thompson, *J. Colloid Interface Sci.*, **25,** 16 (1967).

(16) R. E. Wood, F. P. Wirth, Jr., and H. E. Morgan, *Biochim. Biophys.* **163,** 171 (1968).

ACKNOWLEDGMENTS

The authors express their thanks to Dr. Minako Tanaka of the Lion Co., Tokyo, for her valuable discussion.

Ion Chromatographic Determination of the Principal Inorganic Ion in Bulk Antibiotic Salts

J. W. WHITTAKER * and P. R. LEMKE ˣ

Received May 13, 1981, from *Pfizer Inc., Quality Control Division, Groton, CT 06340.* Accepted for publication July 28, 1981. *Present address: IBM Instrument Inc., Orchard Park, P.O. Box 332, Danbury, CT 06810.

Abstract □ Two ion-chromatographic procedures were developed for determining the principal inorganic ions in bulk antibiotic salts. The anion system enables sulfate determination in sulfate salts of polymyxin, neomycin, streptomycin, and dihydrostreptomycin, with typical analysis times of 8 min/sample and a relative precision of ±2% (95% confidence interval). The cation system is applicable to sodium or potassium analysis in the respective penicillin salts in 9–16 min with a relative precision of ±2.5%. These methods offer speed, specificity, and easy sample preparation compared with traditional assays.

Keyphrases □ Ion chromatography—determination of inorganic ion in bulk antibiotic salts □ Antibiotics—determination of inorganic ion in salts using ion chromatography □ Inorganic ion—determination in salts of various antibiotics by ion chromatography

Bulk antibiotic salts can be characterized by the determination of their principal components for the purposes of quality assurance. An accurate assay is required for both the pharmacologically active organic ion and the inorganic counterion. For the organic moiety, many specific chromatographic assays (1) are applicable to bulks. However,

0022-3549/82/0300-0334$01.00/0

Table I—Instrument Conditions for the Ion Chromatographic Analysis of Antibiotic Bulks

	Anion System	Cation System
Columns	3 × 150-mm anion separator	3 × 150-mm cation precolumn
		6 × 250-mm cation separator
	6 × 250-mm anion suppressor	9 × 250-mm cation suppressor
Mobile phase	0.003 *M* $NaHCO_3$/0.0024 *M* Na_2CO_3	0.005 *N* HNO_3
Flow rate	2.25 ml/min	3.0 ml/min
Pressure	400–600 psi	360–580 psi
Detector sensitivity	100 μMHO	10 μMHO
Regeneration solution	1 *N* H_2SO_4	1 *N* NaOH
Regeneration flow rate	2.25 ml/min	2.25 ml/min

Table II—Sample Preparation for Inorganic Ion Analysis

Ion	Antibiotic	Target Weight, mg	Sample Concentration Injected, g/ml	Typical Ion Concentrations, g/ml
K^+	Potassium benzyl penicillin	950	285	30
	Potassium phenoxymethyl penicillin	990	297	30
Na^+	Monosodium indanyl carbenicillin monohydrate	1000	200	9
	Sodium carbenicillin	1000	200	11
SO_4^{2-}	Neomycin sulfate	25	30	7
	Dihydrostreptomycin sulfate	50	60	12
	Streptomycin sulfate	50	60	12
	Polymyxin sulfate	50	60	10

for the inorganic ion portion of the salt, only the traditional volumetric, gravimetric, or colorimetric methods are available (2). The classical assays are generally time consuming, cumbersome, and lack specificity.

The present study reports a rapid and specific inorganic analysis technique which is applicable to a variety of antibiotic salts. The technique was termed ion chromatography by Small (3), in reporting the use of a mobile phase suppressor column as part of an ion-exchange system with conductivity detection. A comparison between suppressed and nonsuppressed ion chromatography and the development of ion chromatography were discussed in a recent review (4). Suppressed ion chromatography was chosen for bulk antibiotic analysis because the conductivity detector response is independent of the counterion species. A standard set of conditions applies to the analysis of various anions or cations and to a variety of sample types. Ion chromatography is specific for the ion of interest, and sample preparation only involves dissolving the salt in the mobile phase. Analysis times are generally shorter than those of traditional assays, and the methodology can be automated.

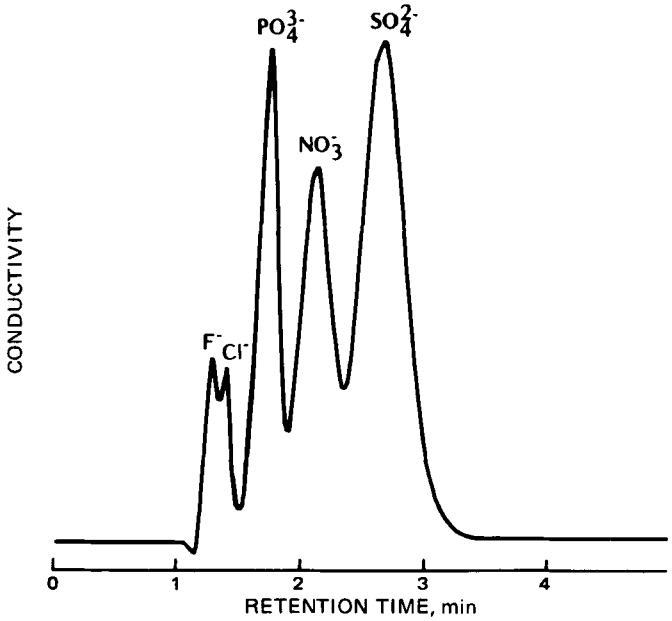

Figure 1—*Chromatogram demonstrating the resolution of standard anions utilizing a 3 × 150-mm separator column.*

Table III—Reproducibility of Sulfate Analysis by Ion Chromatography

Antibiotic	SO_4^{2-}, %[a]	Relative Precision, %[b] Manual	Automated
Polymyxin sulfate	17.12 ± 0.10	1.6	2.5
Streptomycin sulfate	18.12 ± 0.04	0.6	2.3
Dihydrostreptomycin sulfate	18.79 ± 0.07	1.0	0.8
Neomycin sulfate	27.73 ± 0.17	0.6	3.0

[a] Confidence interval, 1 *SD*. [b] Confidence interval, 95%.

Table IV—Reproducibility of Cation Analysis by Ion Chromatography

Cation	Anion	Cation, %[a]
K^+	Benzyl penicillin	10.53 ± 0.26
K^+	Phenoxymethyl penicillin	10.20 ± 0.24
Na^+	Indanyl carbenicillin	4.57 ± 0.12
Na^+	Carbenicillin monohydrate	5.40 ± 0.14

[a] Confidence interval, 95%.

EXPERIMENTAL

Apparatus—A commercially available ion chromatograph[1] containing a 100-μl loop-type injector and conductivity detector with a dual pen strip chart recorder[2] or computing integrator[3] was used. The autosampler[4] employed a 50-μl injector loop connected after the manual injection loop and before the first separator column. The prepacked chromatographic columns were obtained commercially[5], and 0.22-μm disposable filters were used to treat sample solutions[6].

Materials—Reagent grade inorganic salts were sufficiently pure to be used as obtained. All water was passed through a mixed bed deionizer and an activated carbon unit[7].

Method—The analysis conditions and instrument settings are shown in Table I. The bulk antibiotic was dried, and a sample weighing approximately the amount specified in Table II was dissolved and diluted with mobile phase to prepare the sample stock solutions. A working solution was prepared by diluting the stock solution with mobile phase to obtain the final sample concentrations (Table II).

The chromatographic system required equilibration for ~1 hr, until

[1] Dionex model 14 ion chromatograph.
[2] Honeywell dual channel/dual pen variable input recorder.
[3] Spectra Physics model 4100 computing integrator.
[4] Micromeritics model 725 autosampler.
[5] Dionex Corp., Sunnyvale, Calif.
[6] Millipore Millex-GS 0.22 μm.
[7] Continental water conditioning system models 350 and 350A.

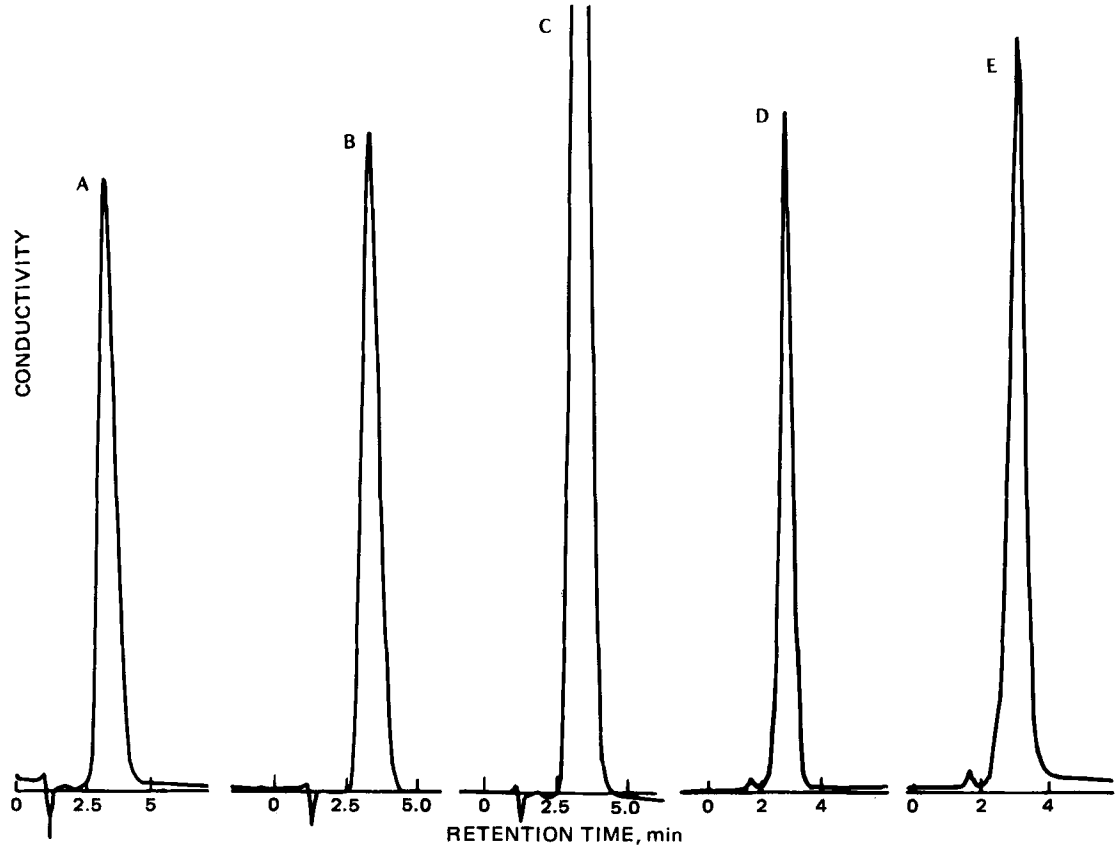

Figure 2—*Chromatograms obtained during sulfate analysis. The sodium sulfate standard chromatogram (A), is indistinguishable from the sulfate component of the organic salts neomycin (B), dihydrostreptomycin (D), and polymyxin (E), and from the spike of sodium sulfate into neomycin sulfate (C).*

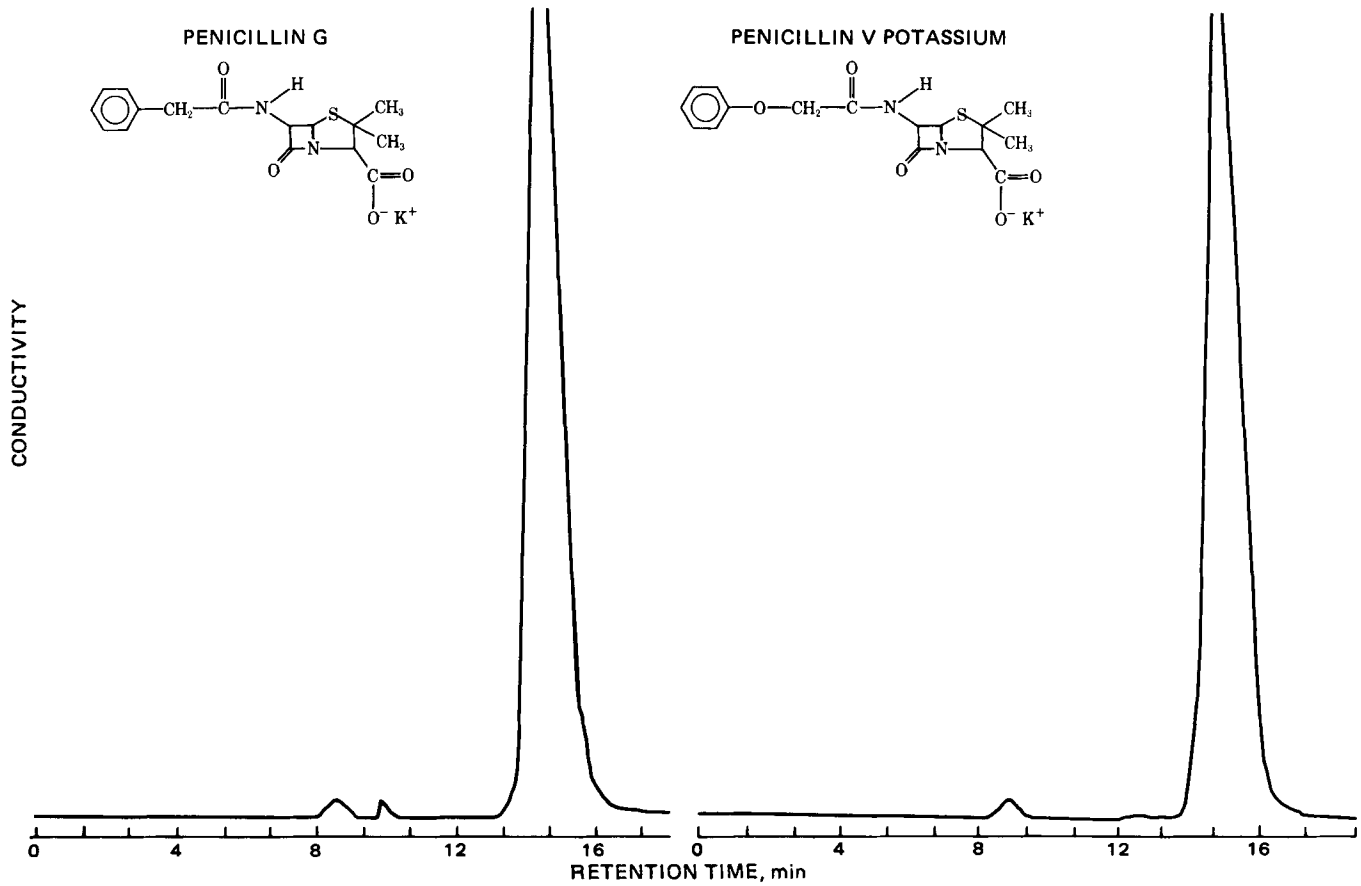

Figure 3—*Chromatograms demonstrating potassium determination in potassium phenoxymethyl penicillin and potassium benzyl penicillin.*

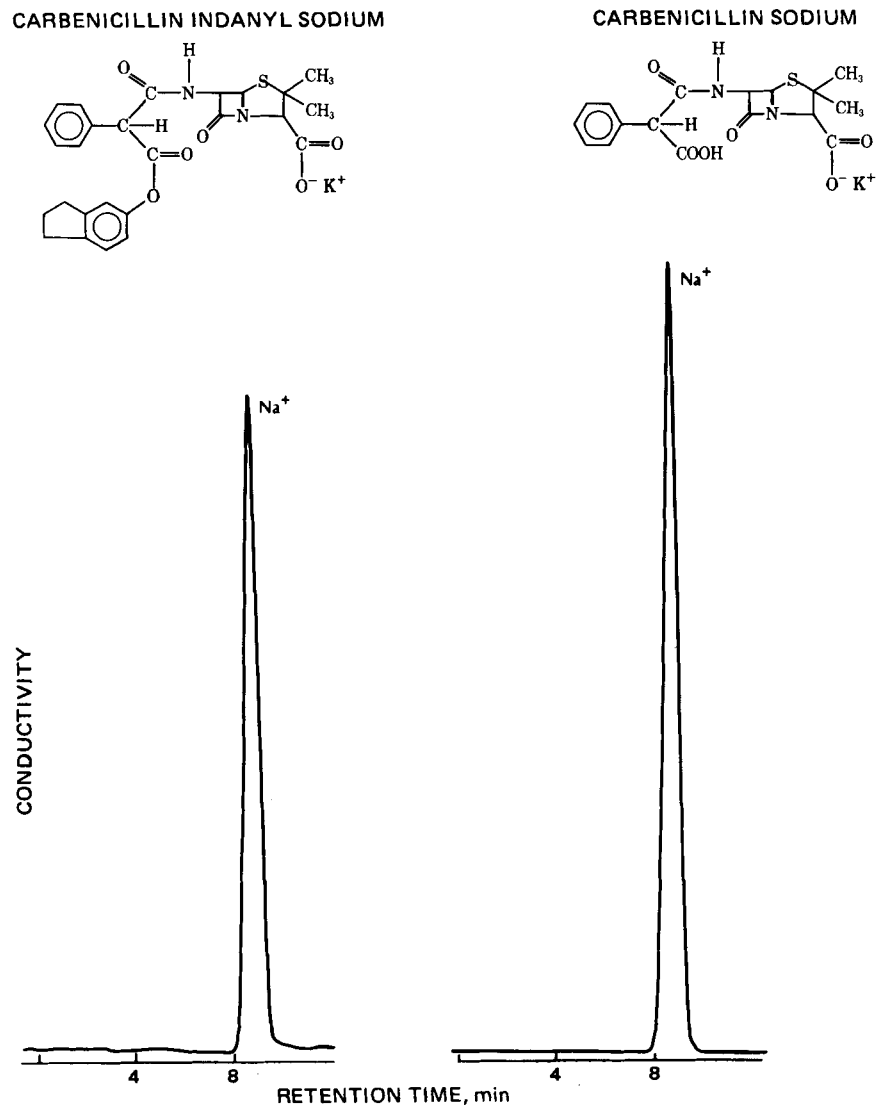

Figure 4—*Chromatograms demonstrating sodium determination in monosodium indanyl carbenicillin (MIC) and monosodium carbenicillin (MSC).*

a stable baseline was obtained. Duplicate injections of the working standard were made, and the peak retention time and response reproducibility were compared with previously determined values in order to check the suitability of the instrument system.

Sample solutions were injected through the disposable filter into the ion chromatograph or autosampler vial. For the autosampler, sample and rinse solutions were alternately injected.

After 5–6 samples were injected, the system was recalibrated by reinjecting the working standard. The sample concentrations can be calculated using either peak height or peak area measurement techniques.

RESULTS AND DISCUSSION

Anion Analysis—The anion system was identical with the systems generally recommended for common anion analysis, (5, 6) except that a short (3 × 150 mm) separator anion exchange column was employed. This short separator column enabled rapid analysis with adequate resolution (Fig. 1). In bulk antibiotic salts, potentially interfering ions are present in only small amounts, thereby minimizing the need for large separator columns and long analysis times.

In the event that simultaneous analyses of the major ion and some trace ion are desired, a longer separator column could be employed. For example, a system that can analyze both 0.1–0.4% bisulfite and 13–38% sulfate in a sulfate salt was developed using both a 3 × 150-mm and a 3 × 500-mm separator column. The bisulfite eluted with a relative retention time of 0.75 (9 min) to sulfate (12 min). Glycerin (1%) was used to stabilize the bisulfite; the glycerin had no effect on the chromatography.

Typical chromatograms (Fig. 2) obtained during sulfate analysis show that the sulfate peak in the antibiotic salt was indistinguishable from that of the sodium sulfate standard.

Linearity—Standards containing 5–20 μg/ml sulfate gave a linear response by both peak height and peak area computation. This range encompasses the theoretical sulfate content for the antibiotic salts, which are 26.9% for neomycin, 19.7% for streptomycin, 19.7% for dihydrostreptomycin, and 16.6% for polymyxin.

Reproducibility—The assay precision was determined by 5–6 replicate analyses of the same antibiotic lot. The precision values (Table III) include variations due to weighing and sample preparation. The manual analyses exhibited better precision than the automated analyses; although the precision of the automated method was adequate, no attempt was made to improve its precision. The precision of the automated method became unacceptable if a sample rinse was not employed to prevent carry over of the sulfate from the previous injection. The automated ion chromatograph was successfully employed for the analysis of all of the sulfated antibiotics in overnight runs.

Equivalency—Two classical methods for sulfate determination can be applied to sulfate analysis in antibiotics: the traditional barium gravimetric method (7) and a volumetric (8) method. The latter has been proposed for incorporation into the *European Pharmacopeia* monograph for polymyxin sulfate. To compare these methods and the ion chromatography technique, various lots of polymyxin sulfate were assayed by both the classical and ion chromatographic methods. For eight lots assayed by both gravimetric and ion chromatography, the average relative difference was −0.6 ±1.1% (confidence interval: 1 *SD*). Similarly, for 14 lots examined by the volumetric and ion chromatographic methods, the difference was −0.3 ±2.7%. The data indicate no apparent bias between

the methods. In both cases, the ion chromatographic method is more rapid and involves less sample manipulation than the traditional assays.

Cation Analysis—An ion chromatographic method, similar to the method reported for the determination of cations in ambient air aerosols (9), was successfully applied to the analysis of various penicillins (Figs. 3 and 4). The cation system, like the anion system, is independent of the nature of the counter-ion.

Linearity—Standards containing 5–15 μg/ml sodium and 10–40 μg/ml potassium gave linear responses by both peak height and peak area computation (Figs. 3 and 4). These ranges encompass the theoretical cation content for the antibiotic salts. The stoichiometric potassium level is 10.07% in penicillin V potassium (potassium phenoxymethyl penicillin) and 10.50% in penicillin G (potassium benzyl penicillin). Theoretical sodium levels in the sodium salts are 4.45% in carbenicillin indanyl sodium and 5.49% in carbenicillin sodium monohydrate. The sample concentrations (Table II) were chosen to give a similar response for both cations so that samples could be batched.

Reproducibility—Typical precisions of the ion chromatographic cation determination are shown in Table IV. These experiments include the complete replicate analysis of the same bulk lot.

Equivalency—No compendial requirement exists for the potassium content of the penicillins; however, both assays agreed well with the theoretical values.

The ion chromatographic sodium analysis was compared with sodium content determined by ashing six different antibiotic lots in the presence of sulfuric acid and measuring the remaining sodium sulfate gravimetrically. For carbenicillin sodium monohydrate, the relative difference was $-1.0 \pm 3.3\%$ (confidence interval: 1 *SD*). Carbenicillin indanyl sodium by ion chromatography was $3.9 \pm 4.3\%$ greater than the analysis by the residue on ignition method. Since both differences are smaller than the confidence interval, there was no apparent bias between methods.

REFERENCES

(1) R. K. Gilpin, *Anal. Chem.*, **51**, 257R (1979).

(2) "The United States Pharmacopeia XX–National Formulary XV," United States Pharmacopeial Convention, Rockville, Md., 1980.

(3) H. Small, T. Stevens, and W. Bauman, *Anal. Chem.*, **47**, 1801 (1975).

(4) C. A. Pohl and E. L. Johnson, *J. Chromatogr. Sci.*, **18**, 442 (1980).

(5) J. D. Mulik, E. Estes, and E. Sawicki, in "Ion Chromatographic Analysis of Environmental Pollutants," E. Sawicki, J. D. Muilk, and E. Wittgenstein, Eds., Ann Arbor, Mich., 1978, chap. 4.

(6) T. S. Long and A. L. Reinsvold, *Jt. Conf. Sens. Environ. Pollut. (Conf. Proc.), 4th*, 1977 (Pub. 1978), 624.

(7) B. J. Heinrich, M. D. Grimes, and J. E. Puckett "Treatise on Analytical Chemistry," I. M. Kolthoff, P. J. Elving, and E. B. Sandell, Eds., vol. 7, part II, New York, N.Y., 1961, p. 103.

(8) "European Pharmacopeia," vol. II, 1971, p. 344; Proposed Revision Polymyxin Sulfate Monograph, PA/PH/EXP. 7/T (78) 26, 1st rev.

(9) "Ion Chromatography–A New Analytical Technique for the Assay of Sulfate and Nitrate in Ambient Aerosols," National Bureau of Standards Special Publication 464, U.S. Government Printing Office, Washington, D.C., 1977.

ACKNOWLEDGMENTS

Presented in part at the 31st Pittsburgh Conference, Atlantic City, N.J., March 1980.

Antitumor Agents XLV: Bisbrusatolyl and Brusatolyl Esters and Related Compounds as Novel Potent Antileukemic Agents

KUO-HSIUNG LEE *x, MASAYOSHI OKANO *, IRIS H. HALL *, DAVID A. BRENT ‡, and BERND SOLTMANN ‡

Received April 6, 1981, from the **Department of Medicinal Chemistry, School of Pharmacy, University of North Carolina, Chapel Hill, NC 27514* and the ‡Wellcome Research Laboratories, Burroughs Wellcome Co., Research Triangle Park, NC 27709. Accepted for publication July 15, 1981.

Abstract □ A series of new bisbrusatolyl and brusatolyl esters and related compounds were synthesized and tested for *in vivo* antileukemic activity against a quassinoid sensitive strain of P-388 lymphocytic leukemia in BDF_1 mice. The bisbrusatolyl malonate, succinate, glutarate, adipate, and sebacate were as active or more active than brusatol. The C-3 esters of brusatol and bruceantin were also found to be as active or more active than brusatol or bruceantin in general. The free hydroxyl groups at C-11 and C-12 as well as the enone double bond in ring A of both bisbrusatolyl and brusatolyl esters are required for antileukemic activity. The presence of a double bond in the ester side chain contributes to the enhanced activity of these esters.

Keyphrases □ Brusatol—bisbrusatolyl and bisbrusatolyl esters, synthesis, potential antileukemic agents □ Antitumor agents—potential, bisbrusatolyl and bisbrusatolyl esters, synthesis □ Antileukemic agents—potential, bisbrusatolyl and bisbrusatolyl esters, synthesis, tested against P-388 lymphocytic leukemia

The structural requirements for antineoplastic activity (particularly in the P-388 mouse lymphocytic leukemic system) of quassinoids bruceantin (I), holacanthone, glaucarubolone, 6α-senecioyloxychaparrinone, and related compounds have recently been reviewed (1–6). It was concluded that the Δ^3-2-oxo moiety in ring A, the lactone moiety in ring D, the ester groups at either C-6 or C-15, the methyleneoxy bridge, and the hydroxyl moieties at either C-1 or C-3, and at C-12 are required for biological activity.

The isolation of novel antileukemic glycosides bruceoside-A and bruceoside-B, as well as their subsequent hydrolysis product brusatol (II) (7, 8) provided the opportunity for developing brusatol related compounds into future clinically active anticancer agents. Brusatol is structurally identical to bruceantin (I) [currently in the Phase II clinical trial as an anticancer agent by the National Cancer Institute (9)] except for a slight difference in the C-15 ester side chain. The C-15 ester moiety in I is important for its potent antileukemic activity and probably serves as a carrier group in processes such as membrane transport of the drug into intact cells or complex formation as previously suggested (2, 6, 10). The importance of the ester group which contributes to the enhanced antileukemic activity is also seen in other naturally oc-

0022-3549/82/0300-0338$01.00/0

the methods. In both cases, the ion chromatographic method is more rapid and involves less sample manipulation than the traditional assays.

Cation Analysis—An ion chromatographic method, similar to the method reported for the determination of cations in ambient air aerosols (9), was successfully applied to the analysis of various penicillins (Figs. 3 and 4). The cation system, like the anion system, is independent of the nature of the counter-ion.

Linearity—Standards containing 5–15 μg/ml sodium and 10–40 μg/ml potassium gave linear responses by both peak height and peak area computation (Figs. 3 and 4). These ranges encompass the theoretical cation content for the antibiotic salts. The stoichiometric potassium level is 10.07% in penicillin V potassium (potassium phenoxymethyl penicillin) and 10.50% in penicillin G (potassium benzyl penicillin). Theoretical sodium levels in the sodium salts are 4.45% in carbenicillin indanyl sodium and 5.49% in carbenicillin sodium monohydrate. The sample concentrations (Table II) were chosen to give a similar response for both cations so that samples could be batched.

Reproducibility—Typical precisions of the ion chromatographic cation determination are shown in Table IV. These experiments include the complete replicate analysis of the same bulk lot.

Equivalency—No compendial requirement exists for the potassium content of the penicillins; however, both assays agreed well with the theoretical values.

The ion chromatographic sodium analysis was compared with sodium content determined by ashing six different antibiotic lots in the presence of sulfuric acid and measuring the remaining sodium sulfate gravimetrically. For carbenicillin sodium monohydrate, the relative difference was $-1.0 \pm 3.3\%$ (confidence interval: 1 *SD*). Carbenicillin indanyl sodium by ion chromatography was $3.9 \pm 4.3\%$ greater than the analysis by the residue on ignition method. Since both differences are smaller than the confidence interval, there was no apparent bias between methods.

REFERENCES

(1) R. K. Gilpin, *Anal. Chem.*, **51**, 257R (1979).

(2) "The United States Pharmacopeia XX–National Formulary XV," United States Pharmacopeial Convention, Rockville, Md., 1980.

(3) H. Small, T. Stevens, and W. Bauman, *Anal. Chem.*, **47**, 1801 (1975).

(4) C. A. Pohl and E. L. Johnson, *J. Chromatogr. Sci.*, **18**, 442 (1980).

(5) J. D. Mulik, E. Estes, and E. Sawicki, in "Ion Chromatographic Analysis of Environmental Pollutants," E. Sawicki, J. D. Muilk, and E. Wittgenstein, Eds., Ann Arbor, Mich., 1978, chap. 4.

(6) T. S. Long and A. L. Reinsvold, *Jt. Conf. Sens. Environ. Pollut. (Conf. Proc.), 4th*, 1977 (Pub. 1978), 624.

(7) B. J. Heinrich, M. D. Grimes, and J. E. Puckett "Treatise on Analytical Chemistry," I. M. Kolthoff, P. J. Elving, and E. B. Sandell, Eds., vol. 7, part II, New York, N.Y., 1961, p. 103.

(8) "European Pharmacopeia," vol. II, 1971, p. 344; Proposed Revision Polymyxin Sulfate Monograph, PA/PH/EXP. 7/T (78) 26, 1st rev.

(9) "Ion Chromatography–A New Analytical Technique for the Assay of Sulfate and Nitrate in Ambient Aerosols," National Bureau of Standards Special Publication 464, U.S. Government Printing Office, Washington, D.C., 1977.

ACKNOWLEDGMENTS

Presented in part at the 31st Pittsburgh Conference, Atlantic City, N.J., March 1980.

Antitumor Agents XLV: Bisbrusatolyl and Brusatolyl Esters and Related Compounds as Novel Potent Antileukemic Agents

KUO-HSIUNG LEE *x, MASAYOSHI OKANO *, IRIS H. HALL *, DAVID A. BRENT ‡, and BERND SOLTMANN ‡

Received April 6, 1981, from the **Department of Medicinal Chemistry, School of Pharmacy, University of North Carolina, Chapel Hill, NC 27514* and the ‡Wellcome Research Laboratories, Burroughs Wellcome Co., Research Triangle Park, NC 27709. Accepted for publication July 15, 1981.

Abstract □ A series of new bisbrusatolyl and brusatolyl esters and related compounds were synthesized and tested for *in vivo* antileukemic activity against a quassinoid sensitive strain of P-388 lymphocytic leukemia in BDF_1 mice. The bisbrusatolyl malonate, succinate, glutarate, adipate, and sebacate were as active or more active than brusatol. The C-3 esters of brusatol and bruceantin were also found to be as active or more active than brusatol or bruceantin in general. The free hydroxyl groups at C-11 and C-12 as well as the enone double bond in ring A of both bisbrusatolyl and brusatolyl esters are required for antileukemic activity. The presence of a double bond in the ester side chain contributes to the enhanced activity of these esters.

Keyphrases □ Brusatol—bisbrusatolyl and bisbrusatolyl esters, synthesis, potential antileukemic agents □ Antitumor agents—potential, bisbrusatolyl and bisbrusatolyl esters, synthesis □ Antileukemic agents—potential, bisbrusatolyl and bisbrusatolyl esters, synthesis, tested against P-388 lymphocytic leukemia

The structural requirements for antineoplastic activity (particularly in the P-388 mouse lymphocytic leukemic system) of quassinoids bruceantin (I), holacanthone, glaucarubolone, 6α-senecioyloxychaparrinone, and related compounds have recently been reviewed (1–6). It was concluded that the Δ^3-2-oxo moiety in ring A, the lactone moiety in ring D, the ester groups at either C-6 or C-15, the methyleneoxy bridge, and the hydroxyl moieties at either C-1 or C-3, and at C-12 are required for biological activity.

The isolation of novel antileukemic glycosides bruceoside-A and bruceoside-B, as well as their subsequent hydrolysis product brusatol (II) (7, 8) provided the opportunity for developing brusatol related compounds into future clinically active anticancer agents. Brusatol is structurally identical to bruceantin (I) [currently in the Phase II clinical trial as an anticancer agent by the National Cancer Institute (9)] except for a slight difference in the C-15 ester side chain. The C-15 ester moiety in I is important for its potent antileukemic activity and probably serves as a carrier group in processes such as membrane transport of the drug into intact cells or complex formation as previously suggested (2, 6, 10). The importance of the ester group which contributes to the enhanced antileukemic activity is also seen in other naturally oc-

0022-3549/82/0300-0338$01.00/0

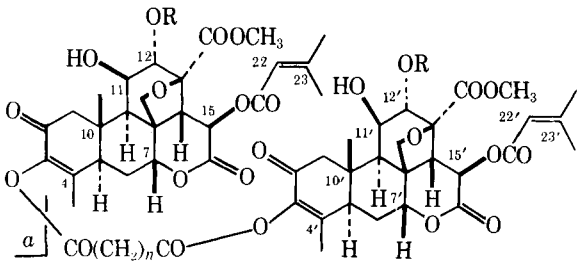

III: n = 1; R = H
IV: n = 2; R = H
V: n = 3; R = H
VI: n = 4; R = H
VII: n = 8; R = H
VIII: n = 2; R = $COCH_3$
IX: n = 3; R = $COCH_3$
X: n = 4; R = $COCH_3$

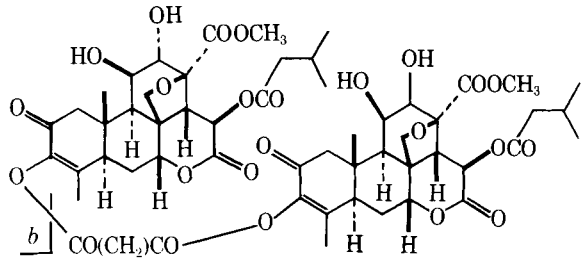

XI: n = 1
XII: n = 3

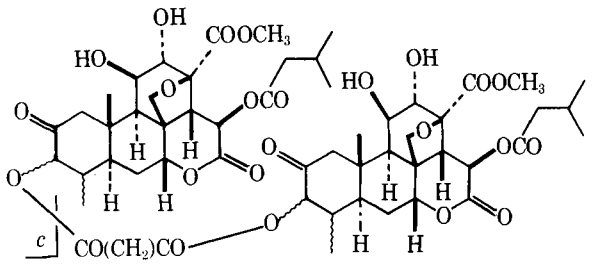

XIII

curring antitumor agents (11).

In view of the overall structural requirements for the antileukemic activity of I, any major degradation of the intact I molecule might thus lead to the less active or inactive compounds. However, a minor modification by combining two intact active quassinoids *via* a diester linkage (such as I or II) might yield highly active antileukemic agents with reduced toxicity as observed with bishelenalinyl malonate and related esters (1, 11). An initial examination of the antileukemic activity of bisbrusatolyl malonate (III) and bisbrusatolyl succinate (IV) against a quassinoid-sensitive strain of P-388 lymphocytic leukemia indicated that III and IV were more potent and less toxic than brusatol (11). For example, the optimal T/C % value for III was 272 at 0.6 mg/kg, while for II it was 158 at 0.125 mg/kg. The synthesis and antileukemic activity of bisbrusatolyl and brusatolyl esters and related compounds are now reported.

CHEMISTRY

Bisbrusatolyl esters III–VII were prepared by reacting brusatol II with malonic dichloride, succinic dichloride, glutaric dichloride, adipic dichloride, and sebacic dichloride, respectively, in pyridine–benzene or pyridine–chloroform mixed solvent at room temperature. The monoacetates (VIII–X) of the bisbrusatolyl esters IV–VI were prepared by acetylation using acetic anhydride–pyridine and worked up as usual. Catalytic hydrogenation of the C-15 ester side chain of III and V with palladium-on-carbon in ethanol gave rise to the corresponding bis-dihydro derivatives XI and XII, respectively. The bistetrahydrobrusatolyl succinate (XIII) was prepared by esterification of tetrahydrobrusatol (XXXV), obtained by catalytic hydrogenation of II, with succinic dichloride.

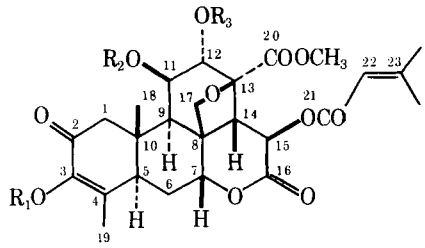

I: R_1 = R_2 = R_3 = H; CO 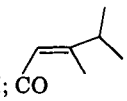 replaces CO  (bruceantin)
II: R_1 = R_2 = R_3 = H (brusatol)

XIV: R_1 = CO ; R_2 = R_3 = H
XV: R_1 = $CO(CH_2)_3CH_3$; R_2 = R_3 = H
XVI: R_1 = $COCH_2CH_2COOCH_2CH_3$; R_2 = R_3 = H

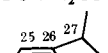

XVII: R_1 = CO ; R_2 = R_3 = H

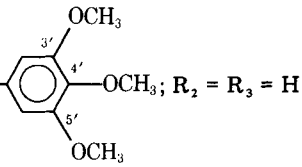

XVIII: R_1 = CO–; R_2 = R_3 = H

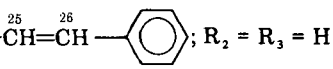

XIX: R_1 = CO–CH=CH–; R_2 = R_3 = H

XX: R_1 = CO ; R_2 = H; R_3 = $COCH_3$
XXI: R_1 = $CO(CH_2)_3CH_3$; R_2 = H; R_3 = $COCH_3$
XXII: R_1 = $COCH_2CH_2COOCH_2CH_3$; R_2 = H; R_3 = $COCH_3$

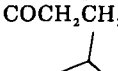

XXIII: R_1 = CO ; R_2 = H; R_3 = $COCH_3$

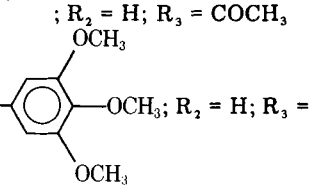

XXIV: R_1 = CO–; R_2 = H; R_3 = $COCH_3$

XXV: R_1 = CO ; R_2 = R_3 = $COCH_3$
XXVI: R_1 = $CO(CH_2)_3CH_3$; R_2 = R_3 = $COCH_3$
XXVII: R_1 = $COCH_2CH_2COOCH_2CH_3$; R_2 = R_3 = $COCH_3$

Encouraged by the potent antileukemic activity and reduced toxicity demonstrated by the bisbrusatolyl esters (III–VII) resulting from esterification of the C-3 hydroxyl group of the diosphenol ring A, it was decided to further investigate the C-3 esters of brusatol (II). Thus, various C-3 esters, such as senecioate (XIV), valerate (XV), ethyl succinate (XVI), 3,4-dimethyl-2-pentenoate (XVII), 3′,4′,5′-trimethoxybenzoate (XVIII), and cinnamate (XIX), were prepared by esterification of II with a corresponding acyl chloride in pyridine–benzene or pyridine–chloroform mixed solvent at room temperature. Esterification of II with cinnamoyl chloride under these conditions yielded a C-3, C-11 dicinnamate (XXXI) in addition to the C-3 cinnamate (XIX). Esterification of bruceantin (I)

in an analogous manner afforded its C-3, 3,4-dimethyl-2-pentenoate ester (XXXIII).

Esterification of C-3, C-11, and C-12 hydroxyl groups is greatly affected by the reaction temperature and time. The C-11 hydroxyl group is sterically hindered and resistant to esterification under mild reaction conditions like those for the selective esterification of C-3. In general, it is required to heat the reaction mixture up to ~60° for esterification of C-11 and C-12 hydroxyl groups other than those involving acetylation. However, for esterification of the C-3 hydroxyl group, the reaction may be run at room temperature. The introduction of a C-3 ester was confirmed by examining the UV spectrum which should show the disappearance of a diosphenol chromophore at λ_{max} 278 nm. Confirmation of the presence of ester moieties at C-11 and C-12 was achieved by observing the downfield shift of H-11 and H-12 resulting from such esterification.

The mono- (XX–XXIV), di- (XXV–XXIX), and tri- (XXX) acetates of II were prepared by acetylation of the corresponding esters XIV–XIX with acetic anhydride in pyridine. The tri-ester (XXXII) was prepared by treating II with 3,4-dimethyl-2-pentenoyl chloride in dry benzene under reflux for 24 hr. The dihydro- (XXXIV) and tetrahydro- (XXXV) brusatol were prepared by catalytic hydrogenation of II with palladium-on-carbon. Sodium borohydride reduction of XXXV gave rise to the lactol (XXXVI). Spectral data (Table I) of all compounds (II–XXXIV) were in accord with the assigned structures.

XXVIII: R_1 = 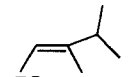 ; $R_2 = R_3 = COCH_3$

XXIX: R_1 = CO—CH=CH—  ; $R_2 = R_3 = COCH_3$

XXX: $R_1 = R_2 = R_3 = COCH_3$

XXXI: $R_1 = R_2$ = CO—CH=CH—  ; $R_3 = H$

XXXII: $R_1 = R_2 = R_3$ = 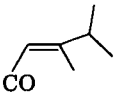

XXXIII: R_1 = 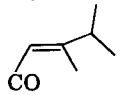 ; $R_2 = R_3 = H$;

C_{15}-OCO 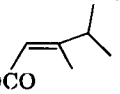 replaces C_{15}-OCO 

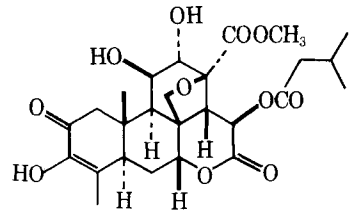

XXXIV

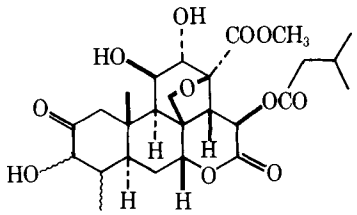

XXXV

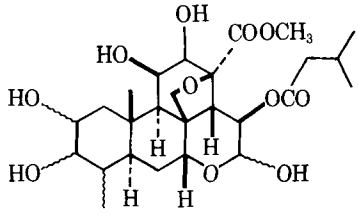

XXXVI

DISCUSSION

The preliminary evaluations of the antileukemic activity of compounds II–XXXVI were carried out in a quassinoid sensitive strain of P-388 lymphocytic leukemia in BDF_1 mice which were described previously (11). A comparison of the T/C % values for the antileukemic activity of the compounds listed in Table II disclosed that the bisbrusatolyl esters (III–VII) possessed equal or more potent activity than brusatol at 0.6 mg/kg (compare T/C% of 272, 217, 176, 176, and 143 for III, IV, V, VI, and VII, respectively, to 149 for II). Compound III followed a dose response curve and demonstrated potent antileukemic activity (T/C = 213, 272, and 215% at doses of 1.0 mg, 0.6 mg, and 0.3 mg/kg/day, respectively). At comparable dose levels, brusatol was either much less active or more toxic. Monoacetylation of the 12- and 12′-hydroxyl groups of the bisesters (IV–VI) resulted in less active or inactive compounds (VIII–X), suggesting that the presence of such hydroxyl groups at the 12- and 12′-positions are required for antileukemic activity. Reduction of the senecioate ester double bonds of III and V afforded the corresponding bisdihydro derivatives XI and XII, in which XI (T/C = 132%) and XII (T/C = 147%) were less active than III and V. Saturation of the diosphenol double bond, as in the case of bistetrahydrobrusatolyl succinate (XIII), gave rise to an inactive compound.

Compounds XIV–XIX were various C-3 esters of brusatol (II). Again it was observed that the esters were more active or as active as II at 0.6 mg/kg/day (compare T/C of 185–130% of XIV–XIX to 149% of II). Similarly, the C-3, 3,4-dimethyl-2-pentenoate ester of bruceantin (*i.e.*, XXXIII), demonstrated a T/C of 194% at the same testing dose. Acetylation of compounds XIV–XIX either at the 12-hydroxyl moiety or at both the 11- and 12-hydroxyl groups yielded compounds XX–XXIV and XXV–XXIX, respectively, which showed no activity. The 11,12-diacetates of 3-cinnamoyl brusatol (XXIX) and of 3-acetyl brusatol (XXX), as well as the 3,11,12-tri-3,4-dimethyl-2-pentenoyl brusatol (XXXII) were all found to be inactive. However, the 3,11-dicinnamoyl brusatol (XXXI) in which the 12-hydroxyl group was free was found to give a T/C of 133% indicating the importance of a free hydroxyl group at position 12 for significant antileukemic activity. Reduction of the ester double bond of II yielded dihydrobrusatol (XXXIV), which did not decrease the activity. However, destruction of the enone system in ring A gave rise to XXXV which was much less active. Further reduction of the carbonyl at C-2 and C-16 yielded the inactive lactol (XXXVI).

EXPERIMENTAL[1]

Brusatol (II)—A solution of bruceoside-A (7, 8) (101 g, 0.148 mole) in 3 *N* sulfuric acid–methanol (1:1, 2000 ml) was stirred at 65° for 20 hr. The hydrolyzed product was extracted with chloroform to give a brown resinous substance (76.9 g). Column chromatography of this substance on silica gel yielded crude brusatol (67.7 g, 86%), which was further recrystallized from acetone to give II as colorless crystals: mp 274–277°.

[1] Unless otherwise specified, melting points were determined on a Thomas–Hoover melting point apparatus and were uncorrected. IR spectra were recorded on a Perkin-Elmer 257 grating spectrophotometer. PMR spectra were measured with a Varian XL-100 instrument (tetramethylsilane). Electron impact mass spectra were determined on an AEI MS-902 instrument at 70 eV using a direct inlet system. The field desorption mass spectra were obtained on a Varian MAT 731 mass spectrometer interfaced to a VG 2200 Datasystem (13). All spectra were run in a cyclic scanning mode with a steady increase of the emitter current from 0–50 mA. The sample was coated on the field desorption wire using the dipping technique. The solution used for dipping contained 5–10 μg of sample/μl of acetone. All samples desorbed at emitter currents between 22 and 26 mA. Compounds XIV–XXXII gave intense $[M]^+$ and/or $[M + H]^+$ ions. The esters of the dicarboxylic acids gave no molecular ions. Rather, these compounds were protonated on the ester oxygen and gave an ion due to simple cleavage, *e.g.* $[a + H]^+$. Some showed only ions which were produced by the net loss of water from this simple cleavage ion. Silica gel for column chromatography refers to Mallinckrodt Silica AR CC7-Special; silica gel for preparative TLC refers to Merck precoated silica gel GF-254 (0.25 mm, 5 × 20 cm) developed with suitable solvent systems and visualized by spraying with 1% cesium sulfate—10% sulfuric acid solution followed by heating or by use of an UV lamp. Pyridine and chloroform used as solvents for reactions were predried on molecular sieve and anhydrous calcium chloride, respectively. Elemental analyses were performed by Integral Microlab, Inc., Raleigh, N.C. All compounds (II–XXXVI) reported gave either satisfactory elemental or mass spectral (high resolution electron impact or field desorption) analyses (Table III). Also, all new compounds have been rigorously purified to homogeneity by TLC in at least three solvent systems. High resolution mass spectrometry was used in lieu of combustion elemental analysis in many cases due to the limited supply of natural brusatol.

Table I—NMR Spectra of Bisbrusatolyl and Brusatolyl Esters and Related Compounds[a]

Compd	—CH_2CO—	H-15 (15′)	H-22 (22′)	H-7 (7′)	H-11 (11′)	H-12 (12′)	$COOCH_3$	CH_3-23 (23′)	CH_3-4 (4′)	CH_3-10 (10′)	H-17 (17′)	H-1 (1′), H-6 (6′)	H-14 (14′)	Misc.
II		6.26 d (13)	5.64 m	4.80 m	4.25 m	4.22 m	3.80 s	2.20 d (1.5) 1.93 d (1.5)	1.84 d (2)	1.39 s	4.76 d (8) 3.80 d (8)	2.98 d (16) 2.40 d (16)	3.12 d (13)	
III	3.79 bs[b]	6.26 d (13)	5.66 m	4.83 m	4.30 m	4.22 m	3.79 bs[b]	2.18 d (1.5) 1.92 d (1.5)	1.84 s	1.48 s	4.76 d (8) 3.82 d (8)	3.00 d (16) 2.44 d (16)	3.16 d (13)	
IV	2.95 t (6)	6.24 d (13)	5.66 m	4.83 m	4.27 m	4.21 m	3.78 s	2.18 bs 1.94 bs	1.78 bs	1.47 bs	4.76 d (8) 3.78 d (8)	2.95[b] 2.44 d (16)	3.17 d (13)	
V	2.71 (t-like)	6.24 d (13)	5.67 m	4.85 m	4.30 m	4.23 m	3.78 s	2.19 bs 1.93 bs	1.79 bs	1.48 s	4.77 d (8) 3.80 d (8)	2.97 d (16) 2.42 d (16)	3.17 d (13)	
VI	2.60 (t-like)	6.21 d (13)	5.65 m	4.83 m	4.26 m	4.21 m	3.78 s	2.19 bs 1.94 bs	1.80 bs	1.49 s	4.75 d (8) 3.80 d (8)	2.96 d (16) 2.42 d (16)	3.18 d (13)	
VII	2.52 t (6)	6.24 d (13)	5.65 m	4.83 m	4.28 m	4.22 m	3.79 s	2.18 bs 1.92 bs	1.78 bs	1.48 s	4.76 d (8) 3.80 d (8)	2.98 d (16) 2.40 d (16)	3.18 d (13)	1.35 m (Methylene)
VIII	2.96 (t-like)	6.01 d (13)	5.64 m	4.82 m	4.12 m	5.31 m	3.76 s	2.10 bs 1.95 bs	1.80 bs	1.48 bs	4.78 d (8) 3.80 d (8)	2.94 d (16) 2.40 d (16)	3.30 d (13)	2.02 s ($OCOCH_3$)
IX	2.70 t (6)	6.04 d (13)	5.65 m	4.85 m	4.15 d (5)	5.33 m	3.75 s	2.18 bs 1.93 bs	1.79 bs	1.47 s	4.80 d (8) 3.80 d (8)	2.92 d (16) 2.38 d (16)	3.30 d (13)	2.00 s ($OCOCH_3$)
X	2.60 (t-like)	6.06 d (13)	5.64 m	4.82 m	4.14 m	5.32 m	3.76 bs	2.20 bs 1.94 bs	1.81 bs	1.50 s	4.78 d (8) 3.82 d (8)	2.94 d (16) 2.40 d (16)	3.30 d (13)	2.03 s ($OCOCH_3$)
XI	3.85[b]	6.33 d (13)		4.79 m	4.26 m	4.21 m	3.85[b]	0.94 (6)	1.83 bs	1.47 bs	4.76 d (8) 3.85[b]	2.98 d (16) 2.44 d (16)	3.08 d (13)	
XII	2.70 t (6)	6.30 d (13)		4.78 m	4.21 m	4.21 m	3.83 s[b]	0.97 (6)	1.79 bs	1.47 s	4.74 d (8) 3.83 m[b]	2.80 d (16) 2.38 d (16)	3.08 d (13)	
XIII	3.50 m	6.33 d (13)		4.70 m	4.21 m	4.21 m	3.84 bs	0.99 (6)	0.99 d (6)	1.45 s	4.66 d (8) 3.76 d (8)	2.76 d (16) 2.18 d (16)	3.08 d (13)	
XIV		6.23 d (13)	5.66 m	4.84 m	4.30 m	4.24 m	3.78 s	2.20 bs 1.93 bs	1.80 s	1.52 s	4.76 d (8) 3.78 d (8)	2.99 d (16) 2.44 d (16)	3.20 d (13)	5.91 m (H-25); 2.20 bs, 1.97 bs (CH_3-26)
XV		6.22 d (13)	5.64 m	4.82 m	4.27 m	4.21 m	3.77 s	2.17 bs 1.92 bs	1.78 s	1.48 s	4.74 d (8) 3.78 d (8)	2.96 d (16) 2.54 d (16)	3.17 d (13)	0.93 t (7) (terminal CH_3)
XVI		6.22 d (13)	5.65 m	4.83 m	4.27 m	4.16 m	3.78 s	2.19 bs 1.93 bs	1.81 s	1.47 s	4.74 d (8) 3.78 d (8)	2.96 d (16) 2.42 d (16)	3.18 d (13)	4.16 q (7), 1.26 t (7) (ethyl ester)
XVII		6.22 d (13)	5.65 m	4.83 m	4.28 m	4.22 m	3.77 s	2.18 bs 1.92 d (1.5)	1.79 s	1.51 s	4.75 d (8) 3.78 d (8)	2.98 d (16) 2.42 d (16)	3.18 d (13)	5.90 m (H-25); 2.16 bs (CH_3-26) 1.10 d (7) (CH_3-27)
XVIII		6.29 d (13)	5.66 m	4.84 m	4.30 d (5)	4.23 m	3.79 s	2.19 d (1.5) 1.93 d (1.5)	1.85 s	1.58 s	4.79 d (8) 3.93[b]	3.04 d (16) 2.46 d (16)	3.17 d (13)	7.42 s (phenyl) 3.93 s (OCH_3)
XIX		6.28 d (13)	5.66 m	4.82 m	4.30 m	4.23 m	3.80 s	2.21 d (1.5) 1.94 d (1.5)	1.86 s	1.56 s	4.78 d (8) 3.80 d (8)	3.03 d (16) 2.46 d (16)	3.18 d (13)	7.55–7.45 m (phenyl); 6.61 d (16) and 7.85 d (16) (H-25, H-26)
XX		6.02 d (13)	5.65 m	4.84 m	4.14 d (5)	5.32 m	3.74 s	2.19 bs 1.93 d (1.5)	1.80 s	1.52 s	4.80 d (8) 3.80 d (8)	2.96 d (16) 2.38 d (16)	3.30 d (13)	5.91 m (H-25); 2.19 bs, 1.96 bs (CH_3-23 and -26); 2.01 s ($OCOCH_3$)
XXI		6.00 d (13)	5.62 m	4.81 m	4.12 d (5)	5.30 m	3.73 s	2.17 bs 1.92 bs	1.77 bs	1.47 s	4.77 d (8) 3.78 d (8)	2.94 d (16) 2.36 d (16)	3.29 d (13)	0.92 t (7) (terminal CH_3) 2.00 s ($OCOCH_3$)
XXII		5.98 d (13)	5.62 m	4.80 m	4.10[b]	5.29 m	3.74 s	2.18 bs 1.93 d (1.5)	1.80 bs	1.47 s	4.76 d (8) 3.78 d (8)	2.93 d (16) 2.34 d (16)	3.28 d (13)	4.14 q (7) 1.25 t (7) (ethyl ester); 2.01 s ($OCOCH_3$)
XXIII		6.04 d (13)	5.65 m	4.84 m	4.14 d (5)	5.32 m	3.76 s	2.19 bs 1.94 bs	1.81 s	1.53 s	4.80 d (8) 3.80 d (8)	2.96 d (16) 2.39 d (16)	3.31 d (13)	5.92 m (H-25); 2.16 bs (CH_3-26); 2.03 s ($OCOCH_3$)
XXIV		6.05 d (13)	5.65 m	4.85 m	4.16 m	5.34 m	3.76 s	2.18 bs 1.92 bs	1.84 s	1.56 s	4.80 d (8) 3.76 s (8)	3.00 d (16) 2.42 d (16)	3.15 d (13)	7.42 s (phenyl), 3.92 bs (OCH_3) 2.02 s ($OCOCH_3$)

continued on next page

Table I—*Continued*

Compd	—CH_2CO—	H-15 (15′)	H-22 (22′)	H-7 (7′)	H-11 (11′)	H-12 (12′)	$COOCH_3$	CH_3-23 (23′)	CH_3-4 (4′)	CH_3-10 (10′)	H-17 (17′)	H-1 (1′), H-6 (6′)	H-14 (14′)	Misc.
XXV		6.10 d (13)	5.65 m	4.87 m	5.24 d (5)	5.34 m	3.75 s	2.19 bs 1.94 d (1.5)	1.81 d (2)	1.36 s	4.78 d (8) 3.85 d (8)	3.10 d (16) 2.52 d (16)	3.28 d (13)	5.91 m (H-25); 2.19 bs, 1.97 bs (CH_3-23 and -26) 2.04 s, 2.12 s ($OCOCH_3$)
XXVI		6.07 d (13)	5.62 m	4.84 m	5.22 d (5)	5.31 m	3.71 s	2.17 d (1.5) 1.92 d (1.5)	1.78 d (2)	1.31 s	4.75 d (8) 3.83 d (8)	3.08 d (16) 2.38 d (16)	3.26 d (13)	0.93 t (7) (terminal CH_3), 2.02 s ($OCOCH_3$) 2.10 s ($OCOCH_3$)
XXVII		6.06 d (13)	5.62 m	4.83 m	5.21 d (5)	5.31 m	3.72 s	2.19 d (1.5) 1.92 d (1.5)	1.81 d (2)	1.30 s	4.74 d (8) 3.82 d (8)	2.92 d (16) 2.48 d (16)	3.26 d (13)	4.15 q (7) 1.25 t (7) (ethyl ester); 2.03 s, 2.11 s ($OCOCH_3$)
XXVIII		6.10 d (13)	5.65 m	4.88 m	5.25 d (5)	5.35 m	3.74 s	2.20 bs 1.94 d (1.5)	1.82 s	1.37 s	4.79 d (8) 3.86 d (8)	3.10 d (16) 2.52 d (16)	3.29 d (13)	5.92 m (H-25); 2.16 bs (CH_3-26); 2.05 s, 2.13 s ($OCOCH_3$)
XXIX		6.13 d (13)	5.66 m	4.89 m	5.27 d (5)	5.36 m	3.74 s	2.21 d (1.5) 1.94 d (1.5)	1.86 s	1.37 s	4.80 d (8) 3.87 d (8)	3.14 d (16) 2.43 d (16)	3.30 d (13)	7.54–7.46 m (phenyl); 6.61 d (16), 7.85 d (16) (H-25, H-26); 2.05 s, 2.16 s ($OCOCH_3$)
XXXI		6.26 d (13)	5.68 m	4.92 m	5.53 d (5)	4.23 m	3.77 s	2.21 bs 1.94 bs	1.85 s	1.43 s	4.88 d (8) 3.90 d (8)	3.14 d (16) 2.45 d (16)	3.29 d (13)	7.53–7.44 m (phenyl); 6.59 d (16), 7.82 d (16) (H-25, H-26 of C_3); 6.41 d (16) 7.70 d (16) (H-25, H-26 of C_{11})
XXXII		6.14 d (13)	5.70 m	4.86 m	5.31 d (5)	5.30 m	3.69 m	2.18 bs 1.90 bs	1.80 bs	1.32 s	4.82 d (8) 3.84 d (8)	2.92 d (16) 2.36 d (16)	3.30 d (13)	5.87 m (H-25); 2.17 bs (CH_3-26 of C_3); 1.10 d (7) (CH_3-27 of C_3) 2.14 bs, 2.13 bs (CH_3-26 of C_{11} and C_{12}); 1.08 d (7), 1.06 d (7) (CH_3-27 of C_{11} and C_{12})

[a] Run in $CDCl_3$ at 100 MHz, and values are parts per million. Multiplicities are indicated by the usual symbols: d, doublet; t, triplet; m, multiple whose center is given; bs, slightly broadened singlet. Figures in parentheses are coupling constants in hertz. [b] Overlapped signals.

The identity of II as brusatol was confirmed by a direct comparison (mixed melting point, TLC, and IR, PMR, and mass spectra) with an authentic sample.

Synthesis of III–VII—3,3-Bisbrusatolyl malonate (III), succinate (IV), glutarate (V), adipate (VI), and sebacate (VII) were synthesized. Esterification was accomplished by treating II (~0.2 mmole) in dry pyridine (2 ml) with a solution of the corresponding malonyl (0.348 mmole), succinyl (0.738 mmole), glutaryl (0.74 mmole), adipyl (0.74 mmole), and sebacyl (0.215 mmole) dichlorides in dry chloroform (2 ml) and cooling with ice. After the mixture was stirred at room temperature for 19, 19, 40, 20, and 20 hr, respectively, it was shaken with dilute sulfuric acid to remove pyridine. The product was extracted with chloroform and purified by preparative TLC (chloroform–acetone 1:1).

III: pale blue crystals (19% yield); mp 191–193°; UV (ethyl alcohol) 221 nm (log ϵ 4.38); IR (potassium bromide) 3450 (OH), 1730, 1720 (ester and lactone CO), 1680 (α,β-unsaturated CO), and 1645 (C=C) cm^{-1}.

IV: colorless crystals (61% yield); mp 248–250°; UV (ethyl alcohol) 221 nm (log ϵ 4.45); IR (potassium bromide) 3480 (OH), 1730, 1710 (ester and lactone CO), 1680 (α,β-unsaturated CO), and 1645 (C=C) cm^{-1}.

V: colorless crystals (39% yield); mp 166–168°; UV (ethyl alcohol) 221 nm (log ϵ 4.45); IR (potassium bromide) 3440 (OH), 1740, 1715 (ester and lactone CO), 1680 (α,β-unsaturated CO), and 1640 (C=C) cm^{-1}.

VI: colorless crystals (53% yield); mp 239–241°; IR (potassium bromide) 3480 (OH), 1725 (ester and lactone CO), 1675 (α,β-unsaturated CO), and 1640 (C=C) cm^{-1}.

Table II—Antileukemic Activity of Bisbrusatolyl and Brusatolyl Esters and Related Compounds against P-388 Lymphocytic Leukemia Cell Growth in BDF_1 Mice

Compound	Dose, mg/kg/day intraperitoneally	Average Days Survived of Treated/Control	T/C, %[a]
II	0.6	14.2/9.5	149
	0.3	14.3/9.5	150
	0.25	14.5/9.5	153
	0.125	15.0/9.5	158
	0.100	12.8/9.5	134
III	1.0	20.2/9.5	213
	0.6	25.8/9.5	272
	0.3	20.4/9.5	215
	0.25	15.5/9.5	163
	0.125	11.0/9.5	116
	0.100	11.0/9.5	116
IV	0.6	20.6/9.5	217
V	0.6	16.7/9.5	176
VI	0.6	16.8/9.5	176
VII	0.6	13.6/9.5	143
VIII	0.6	11.2/9.5	118
IX	0.6	11.6/9.5	122
X	0.6	9.21/9.5	97
XI	0.6	12.5/9.5	132
XII	0.6	13.9/9.5	147
XIII	0.6	10.7/9.5	113
XIV	0.6	17.6/9.5	185
XV	0.6	15.7/9.5	166
XVI	0.6	15.3/9.5	161
XVII	0.6	14.2/9.5	149
XVIII	0.6	12.3/9.5	130
XIX	0.6	13.0/9.5	137
XX	0.6	9.8/9.5	103
XXI	0.6	9.9/9.5	104
XXII	0.6	11.4/9.5	120
XXIII	0.6	9.9/9.5	105
XXIV	0.6	10.6/9.5	112
XXV	0.6	9.8/9.5	103
XXVI	0.6	10.3/9.5	109
XXVII	0.6	10.4/9.5	109
XXVIII	0.6	10.2/9.5	107
XXIX	0.6	9.0/9.5	95
XXX	0.6	9.7/9.5	102
XXXI	0.6	11.2/9.5	118
XXXII	0.6	12.6/9.5	133
XXXIII	0.6	18.4/9.5	194
XXXIV	0.6	14.2/9.5	150
XXXV	0.6	11.4/9.5	120
XXXVI	0.6	10.2/9.5	107
5-Fluorouracil	12.5	15.7/9.5	166

[a] A compound is active if it exhibits a T/C $\geq$ 125% (12).

VII: colorless crystals (79% yield); mp 173–175°; UV (ethyl alcohol) 220 nm (log ϵ 4.60); IR (potassium bromide) 3450 (OH), 1730, 1715 (ester and lactone CO), and 1650 (C=C) cm^{-1}.

General Method for the Synthesis VIII–X—12,12′-Diacetoxy-3,3′-bisbrusatolyl succinate (VIII), glutarate (IX), and adipate (X) were synthesized. These 12,12′-diacetates were prepared by acetylation of the corresponding IV–VI with dry pyridine–acetic anhydride (1:1) for 18–24 hr at room temperature with stirring followed by workup with preparative TLC (chloroform–acetone 1:1) purification.

VIII: colorless crystals (42% yield); mp 204–206°; IR (potassium bromide) 3480 (OH), 1735 (ester and lactone CO), 1685 (α,β-unsaturated CO), 1640 (C=C), and 1220 ($OCOCH_3$) cm^{-1}.

IX: colorless crystals (85% yield); mp 213–215°; IR (potassium bromide) 3440 (OH), 1740 (ester and lactone CO), 1680 (α,β-unsaturated CO), 1640 (C=C), and 1220 ($OCOCH_3$) cm^{-1}.

X: colorless crystals (44% yield); mp 248–250°; IR (potassium bromide) 3490 (OH), 1730 (ester and lactone CO), 1680 (α,β-unsaturated CO), 1640 (C=C), and 1215 ($OCOCH_3$) cm^{-1}.

General Method for the Synthesis of XI and XII—3,3′-Bis-22,23-dihydrobrusatolyl malonate (XI) and glutarate (XII) were synthesized. A solution of III (36.7 mg, 0.0331 mmole) and V (30 mg, 0.0264 mmole) in absolute ethanol (3 and 2 ml, respectively) was hydrogenated in the presence of prereduced 10% palladium-on-charcoal (48 and 47 mg, respectively and at 65 and 70° for 8 and 48 hr, respectively). Compounds XI and XII were obtained by eluting the reaction mixture with ethanol through a column containing anhydrous magnesium sulfate.

XI: colorless crystals (48% yield); mp 208–210°; IR (potassium bromide) 3480 (OH), 1740 (ester and lactone CO), 1680 (α,β-unsaturated CO), and 1640 (C=C) cm^{-1}.

XII: colorless crystals (83% yield); mp 223–225°; IR (potassium bromide) 3420 (OH), 1730, 1720 (ester and lactone CO), 1680 (α,β-unsaturated CO), and 1640 (C=C) cm^{-1}.

Synthesis of XIII—3,3′-Bis-3,4,22,23-tetrahydrobrusatolyl succinate (XIII) was synthesized. A solution of IV (32.65 mg, 0.0291 mmole) in ethanol (2 ml) was hydrogenated in the presence of prereduced 10% palladium-on-charcoal (58 mg) at 60° for 44 hr until the disappearance of UV absorption at λ_{max} ~220 nm. The product was purified directly by preparative TLC (chloroform–acetone 1:1) to yield XIII as colorless crystals (21.65 mg, 66%): mp 280° (dec.); IR (potassium bromide) 3430 (OH), 1735, and 1725 (ester and lactone CO) cm^{-1}.

General Method for the Synthesis of XIV–XIX and XXXI—Brusatol-3-yl senecioate (XIV), valerate (XV), ethyl succinate (XVI), 3,4-dimethyl-2-pentenoate (XVII), 3′,4′,5′-trimethoxybenzoate (XVIII), cinnamoate (XIX), and brusatol-3,11-diyl dicinnamoate (XXXI) were synthesized. These esters were prepared by treatment of II (105 mg, ~0.2 mmole) in dry pyridine (2 ml) with a solution of the corresponding senecioyl (171 mg, 1.44 mmoles), valeryl (170 mg, 1.41 mmoles), ethyl succinyl (64 mg, 0.43 mmole), 3,4-dimethyl-2-pentenoyl (106.4 mg, 0.726 mmole), 3′,4′,5′-trimethoxybenzoyl (154 mg, 0.67 mmole, in 10 ml of dry benzene), and cinnamoyl (166.6 mg, 1.00 mmole) chlorides in dry chloroform (2 ml) under cooling with ice. After the mixture was stirred at room temperature for 2, 24, 20, 28, 50, and 24 hr, respectively, and worked up in a manner analogous to the synthesis of III–VII, it was subjected to preparative TLC using chloroform–acetone 10:1 for XIV, XVII, XIX, and XXXI, and chloroform–acetone 1:1 for XV, XVI, and XVIII.

XIV: colorless crystals (83 mg, 66% yield); mp 143–145°; IR (potassium bromide) 3400 (OH), 1725, 1710 (ester and lactone CO), 1675 (α,β-unsaturated CO), and 1635 (C=C) cm^{-1}.

XV: colorless crystals (81 mg, 64% yield); mp 156–158°; IR (potassium bromide) 3480 (OH), 1740 (ester and lactone CO), 1680 (α,β-unsaturated CO), and 1640 (C=C) cm^{-1}.

XVI: colorless crystals (115 mg, 90% yield); mp 198–200°; IR (potassium bromide) 3460 (OH), 1730, 1715 (ester and lactone CO), 1680 (α,β-unsaturated CO), and 1640 (C=C) cm^{-1}.

XVII: colorless crystals (83 mg, 65% yield); mp 145–147°; IR (potassium bromide) 3400 (OH), 1720, 1710 (ester and lactone CO), 1670 (α,β-unsaturated CO), and 1635 (C=C) cm^{-1}.

XVIII: colorless crystals (124 mg, 82% yield); mp 147–149°; IR (potassium bromide) 3460 (OH), 1730, 1710 (ester and lactone CO), 1680 (α,β-unsaturated CO), and 1640 (C=C) cm^{-1}.

XIX: colorless crystals (103 mg, 80% yield); mp 253–255°; IR (potassium bromide) 3400 (OH), 1730, 1710 (ester and lactone CO), 1690 (α,β-unsaturated CO), and 1630 (C=C) cm^{-1}.

XXXI: colorless crystals (16.4 mg, 11% yield); mp 168–170°; IR (potassium bromide) 3400 (OH), 1730, 1720 (ester and lactone CO), 1680 (α,β-unsaturated CO), and 1630 (C=C) cm^{-1}.

General Method for Synthesis of XX–XXX—12-Acetoxybrusatol-

Table III—Analytical Data of Bisbrusatolyl and Brusatolyl Esters and Related Compounds

Compound	Empirical Formula	Theory, % C	Theory, % H	Found, % C	Found, % H	Characteristic Ions[a] in the Field Desorption Mass Spectrum
III	$C_{55}H_{64}O_{24}$ (1108)					520 $[a + H]^+$
IV	$C_{56}H_{66}O_{24}$ (1122)					502 $[a + H - H_2O]^+$
V	$C_{57}H_{68}O_{24}$ (1136)					502 $[a + H - H_2O]^+$
VI	$C_{58}H_{70}O_{24}$ (1150)					502 $[a + H - H_2O]^+$
VII	$C_{62}H_{78}O_{24}$ (1206)					502 $[a + H - H_2O]^+$
VIII	$C_{60}H_{70}O_{26}$ (1206)					544 $[a + H - H_2O]^+$
	$C_{60}H_{70}O_{26}H_2O$	58.92	5.89	58.98	5.89	
IX	$C_{61}H_{72}O_{26}$ (1220)					544 $[a + H - H_2O]^+$
	$C_{61}H_{72}O_{26}\frac{1}{2}H_2O$	59.56	5.94	59.59	5.95	
X	$C_{62}H_{74}O_{26}$ (1234)					544 $[a + H - H_2O]^+$
XI	$C_{55}H_{68}O_{24}$ (1112)					522 $[b + H]^+$
XII	$C_{57}H_{72}O_{24}$ (1140)					522 $[b + H]^+$
XIII	$C_{56}H_{74}O_{24}$ (1130)					506 $[c + H - H_2O]^+$
XIV	$C_{31}H_{38}O_{12}$ (602)					602 M^+
XV	$C_{31}H_{40}O_{12}$ (604)					605 $[M + H]^+$
XVI	$C_{32}H_{40}O_{14}$ (648)					649 $[M + H]^+$
XVII	$C_{33}H_{42}O_{12}$ (630)					631 $[M + H]^+$
XVIII	$C_{36}H_{42}O_{15}$ (714)					714 M^+
	$C_{36}H_{42}O_{15}\frac{1}{2}H_2O$	59.75	5.94	59.53	5.94	
XIX	$C_{35}H_{38}O_{12}$ (650)					650 M^+
XX	$C_{33}H_{40}O_{13}$ (644)					644 M^+
XXI	$C_{33}H_{42}O_{13}$ (646)					646 M^+
XXII	$C_{34}H_{42}O_{15}$ (690)					691 $[M + H]^+$
XXIII	$C_{35}H_{44}O_{13}$ (672)					672 M^+
XXIV	$C_{38}H_{44}O_{16}$ (756)					756 M^+
	$C_{38}H_{44}O_{16}\frac{1}{2}H_2O$	59.60	5.88	59.99	5.38	
XXV	$C_{35}H_{42}O_{14}$ (686)					686 M^+
XXVI	$C_{35}H_{44}O_{14}$ (688)					688 M^+
XXVII	$C_{36}H_{44}O_{16}$ (732)					732 M^+
XXVIII	$C_{37}H_{46}O_{14}$ (714)					714 M^+
XXIX	$C_{39}H_{42}O_{14}$ (734)					734 M^+
	$C_{39}H_{42}O_{14}\frac{1}{2}H_2O$	62.98	5.78	63.00	5.80	
XXX	$C_{32}H_{38}O_{14}$	59.43	5.92	59.13	6.20	
XXXI	$C_{44}H_{44}O_{13}$ (780)					780 M^+
XXXII	$C_{47}H_{62}O_{14}$ (850)					850 M^+

[a] The most intense ion is reported.

3-yl senecioate (XX), 11,12-diacetoxybrusatol-3-yl senecioate (XXV), 12-acetoxybrusatol-3-yl valerate (XXI), 11,12-diacetoxybrusatol-3-yl valerate (XXVI), 12-acetoxy-brusatol-3-yl ethyl succinate (XXII), 11,12-diacetoxybrusatol-3-yl ethyl succinate (XXVII), 12-acetoxybrusatol-3-yl 3,4-dimethyl-2-pentenoate (XXIII), 11,12-diacetoxybrusatol-3-yl 3,4-dimethyl-2-pentenoate (XXVIII), 12-acetoxybrusatol-3-yl 3′,4′,5′-trimethoxybenzoate (XXIV), 11,12-diacetoxybrusatol-3-yl cinnamoate (XXIX), and 11,12-diacetoxybrusatol-3-yl acetate (XXX) were synthesized. Acetylation of XIV (58.8 mg, 0.098 mmole), XV (49 mg, 0.081 mmole), XVI (69 mg, 0.106 mmole), XVII (84 mg, 0.133 mmole), and XVIII (25 mg, 0.0342 mmole) with 2 ml of dry pyridine–acetic anhydride (1:1) at room temperature for 21–24 hr yielded the corresponding 12 mono- and 11,12 diacetates XX, XXV, XXI, XXVI, XXII, XXVII, XXIII, XXVIII, and XXIV, respectively. Similar acetylation of XIX (50 mg, 0.0769 mmole) for 68 hr gave XXIX. Compound XXX was prepared according to a literature method (14). All of these acetates (XX–XXIX) were purified by preparative TLC using 1:1 chloroform–acetone for XX, XXV, XXII, XXVII, XXIII, and XXVIII, and 10:1 chloroform–acetone for XXI, XXVI, XXIV, and XXIX.

XX: colorless crystals (26.7 mg, 42% yield); mp 180–182°; IR (potassium bromide) 3440 (OH), 1740, 1720 (ester and lactone CO), 1680 (α,β-unsaturated CO), 1635 (C=C), and 1220 ($OCOCH_3$) cm^{-1}.

XXV: colorless crystals (9.1 mg, 14% yield); mp 126–128°; IR (potassium bromide) 1730, 1710 (ester and lactone CO), 1680 (α,β-unsaturated CO), 1635 (C=C), and 1215 ($OCOCH_3$) cm^{-1}.

XXI: colorless crystals (31 mg, 59% yield); mp 116–118°; IR (potassium bromide) 3480 (OH), 1735 (ester and lactone CO), 1680 (α,β-unsaturated CO), 1640 (C=C), and 1222 ($OCOCH_3$) cm^{-1}.

XXVI: colorless crystals (15 mg, 27% yield); mp 169–170°; IR (potassium bromide) 1740 (ester and lactone CO), 1680 (α,β-unsaturated CO), 1640 (C=C), 1220, and 1135 ($OCOCH_3$) cm^{-1}.

XXII: colorless crystals (52.2 mg, 71% yield); mp 170–172°; IR (potassium bromide) 3440 (OH), 1730, 1720 (ester and lactone CO), 1680 (α,β-unsaturated CO), 1635 (C=C), and 1220 ($OCOCH_3$) cm^{-1}.

XXVII: colorless crystals (22.85 mg, 29% yield); mp 218–220°; IR (potassium bromide) 1730 (ester and lactone CO), 1680 (α,β-unsaturated CO), 1645 (C=C), and 1220 ($OCOCH_3$) cm^{-1}.

XXIII: colorless crystals (46.2 mg, 52% yield); mp 178–180°; IR (potassium bromide) 3440 (OH), 1735, 1720 (ester and lactone CO), 1680 (α,β-unsaturated CO), 1635 (C=C), and 1225 ($OCOCH_3$) cm^{-1}.

XXVIII: colorless crystals (14.8 mg, 16% yield); mp 160–162°; IR (potassium bromide) 1750, 1720 (ester and lactone CO), 1680 (α,β-unsaturated CO), 1640 (C=C), and 1220 ($OCOCH_3$) cm^{-1}.

XXIV: colorless crystals (8.1 mg, 31% yield); mp 178–180°; IR (potassium bromide) 3440 (OH), 1730, 1720 (ester and lactone CO), 1680 (α,β-unsaturated CO), 1640 (C=C), and 1210 ($OCOCH_3$) cm^{-1}.

XXIX: colorless crystals (27.1 mg, 48% yield); mp 268–270° (dec.); IR (potassium bromide) 1735, 1720 (ester and lactone CO), 1690 (α,β-unsaturated CO), 1630 (C=C), and 1220 ($OCOCH_3$) cm^{-1}.

General Synthesis of XXXII—Brusatol-3,11,12-triyl 3,4-dimethyl-2-pentenoate (XXXII) was synthesized. To a solution of 3,4-dimethyl-2-pentenoic acid chloride (107 mg, 0.728 mmole) in dry benzene (10 ml) was added II (104 mg, 0.20 mmole). The mixture was refluxed for 24 hr and purified by preparative TLC (chloroform–acetone, 10:1).

XXXII: colorless crystals (159.5 mg, 94% yield); mp 98–101°; IR (potassium bromide) 1720 (ester and lactone CO), 1685 (α,β-unsaturated CO), and 1635 (C=C) cm^{-1}.

Bruceantin-3-yl 3,4-Dimethyl-2-pentenoate (XXXIII)—Compound XXXIII was prepared according to the method of Okano and Lee (15).

22,23-Dihydrobrusatol (XXXIV)—This was prepared according to the method of Sim *et al.* (14).

Synthesis of XXXV—A solution of XXXIV (190 mg) in absolute ethanol (10 ml) was shaken with hydrogen at 65° and atmospheric pressure for 48 hr with 10% palladium-on-charcoal (200 mg). The filtered solution was evaporated to yield colorless crystals of 3,4,22,23-tetrahydrobrusatol (XXXV) after purification by preparative TLC.

XXXV: mp 252–253°; IR (potassium bromide) 3440 (OH), and 1715

(ester and lactone CO) cm^{-1}. PMR ($CDCl_3$) δ 0.99 (d, J = 6 Hz, 9H, CH_3-4 and two CH_3-23), 1.40 (s, CH_3-10), 3.86 (s, $COOCH_3$), and 6.40 (d, J = 13 Hz, H-15).

Anal.—Calc. for $C_{26}H_{36}O_{11}$: *m/z* 524.2255 (M^+). Found: *m/z* 524.2259.

Compound XXXV could also be prepared by hydrogenation of II (504 mg) in 90% ethanol (100 ml) with platinum oxide (50 mg) in water at room temperature and atmospheric pressure. The reaction mixture was filtered by use of a silica gel column. The filtered solution was evaporated to yield colorless XXXV (498 mg).

Synthesis of XXXVI—To a solution of XXXV (66 mg) in methyl alcohol (10 ml) was added a solution of sodium borohydride (2 mg) in water (5 ml). The mixture was stirred at room temperature for 23 hr and then subjected to preparative TLC (chloroform-acetone 1:1) to give 2-hydroxy-2-deoxytetrahydrobrusatol lactol (XXXVI) as colorless crystals (31.6 mg).

XXXVI: mp 121–123°; IR (potassium bromide) 3440 (OH), 1715 (ester CO), 1040 (cyclic *sec*-OH); PMR ($CDCl_3$) δ 0.91 (d, J = 6 Hz, 9H, CH_3-4 and two CH_3-23), 1.50 (s, CH_3-10), 3.81 (s, $COOCH_3$), 4.13 (m, H-12), 4.20 (m, H-11), 4.60 (m, H-2 and H-3) and 5.52 (m, H-15 and H-16).

Anal.—Calc. for $C_{26}H_{40}O_{11}$: *m/z* 528.2571 (M^+). Found: *m/z* 528.2573.

REFERENCES

(1) K. H. Lee, T. Ibuka, D. Sims, O. Muraoka, H. Kiyokawa, I. H. Hall, and H. L. Kim, *J. Med. Chem.*, **24,** 924 (1981). (Presented in part at the Second Chemical Congress of North American Continent, Las Vegas, Nev., August 1980.)

(2) S. M. Kupchan, R. W. Britton, J. A. Lacadie, M. F. Ziegler, and C. W. Sigel, *J. Org. Chem.*, **40,** 648 (1975).

(3) M. Suffness and J. Douros, in "Methods in Cancer Research," Vol. XVI, V. J. De Vita and H. Busch, Eds., Academic New York, N.Y. 1979, chap. III.

(4) M. E. Wall and M. C. Wani, *J. Med. Chem.*, **21,** 1186 (1979).

(5) S. M. Kupchan, J. A. Lacadie, G. A. Howie, and B. R. Sickles, *ibid.*, **19,** 1130 (1976).

(6) M. E. Wall and M. C. Wani, *Ann. Rev. Pharmacol. Toxicol.*, **17,** 117 (1977).

(7) K. H. Lee, Y. Imakura, and H. C. Huang, *J. Chem. Soc. Chem. Commun.*, **1977,** 69.

(8) K. H. Lee, Y. Imakura, Y. Sumida, R. Y. Wu, and I. H. Hall, *J. Org. Chem.*, **44,** 2180 (1979).

(9) National Cancer Institute, *DCT Bulletin*, **1979,** July, p. 4.

(10) L. L. Liao, S. M. Kupchan, and S. B. Horwitz, *Mol. Pharmacol.* **12,** 167 (1976).

(11) I. H. Hall, K. H. Lee, M. Okano, D. Sims, T. Ibuka, Y. F. Liou, and Y. Imakura, *J. Pharm. Sci.*, **70,** 1147 (1981).

(12) R. I. Geran, N. H. Greenberg, M. M. MacDonald, A. M. Schumacher, and B. J. Abbott, *Cancer Chemother. Rep. Part 3*, **3,** 1 (1972).

(13) C. Sweeley, B. Soltmann, and J. F. Holland, "High Performance Mass Spectrometry Chemical Application," ACS Symposium Series No. 70, 1978, p. 209.

(14) K. Y. Sim, J. J. Sims, T. A. Geissman, *J. Org. Chem.*, **33,** 429 (1968).

(15) M. Okano and K. H. Lee, *ibid.*, **46,** 1138 (1981).

ACKNOWLEDGMENTS

Supported by U.S. Public Health Service Research Grants CA-22929 and CA-17625 from the National Cancer Institute.

The authors thank Dr. D. L. Harris, Department of Chemistry, University of North Carolina at Chapel Hill for PMR spectra, Dr. David Rosenthal and Mr. Fred Williams of the Research Triangle Center for Mass Spectrometry for the electron-impact mass spectral data, and Mr. Chris Ledbetter and Miss Erma Mallory for technical assistance.

Antitumor Agents XLVI: *In Vitro* Effects of Esters of Brusatol, Bisbrusatol, and Related Compounds on Nucleic Acid and Protein Synthesis of P-388 Lymphocytic Leukemia Cells

IRIS H. HALL ˣ, Y. F. LIOU, M. OKANO, and K. H. LEE

Received February 19, 1981, from the *Division of Medicinal Chemistry, School of Pharmacy, University of North Carolina at Chapel Hill, NC 27514.* Accepted for publication July 15, 1981.

Abstract □ A series of esters of brusatol, bisbrusatol, and bruceantin were shown to have potent antileukemic activity. Antineoplastic activity was correlated with the ability of the compounds to suppress DNA and protein synthesis in P-388 lymphocytic leukemia cells. Compounds with high T/C% values successfully inhibited DNA polymerase activity and purine synthesis. The ability to inhibit protein synthesis during the elongation process also correlated positively with high antileukemic activity in this series of quassinoids. Dihydrofolate reductase activity and basal and adenosine diphosphate stimulated respiration of P-388 cells were also inhibited.

Keyphrases □ Brusatol—esters, *in vitro* effects on nucleic acid and protein synthesis, P-388 lymphocytic leukemia cells □ Bisbrusatol—esters, *in vitro* effects on nucleic acid and protein synthesis, P-388 lymphocytic leukemia cells □ Antitumor agents—*in vitro* effects of brusatol, bisbrusatol, and related compounds on nucleic acid and protein synthesis, P-388 lymphocytic leukemia cells

Bruceantin was first isolated from *Brucea antidysenterica* (1, 2) and is currently in Phase II clinical trials as an antineoplastic agent (3, 4). Brusatol, a derivative of bruceantin, was prepared by Lee *et al.* (5, 6) and shown to be active against P-388 lymphocytic leukemia cell growth (7). This laboratory demonstrated that bruceantin and brusatol reduced nucleic acid and protein synthesis (7, 8), purine synthesis (7), and oxidative phosphorylation processes (8) of P-388 cells. Based on the observation that a number of potent antileukemic agents have an ester in their structure, a series of brusatol related esters as well

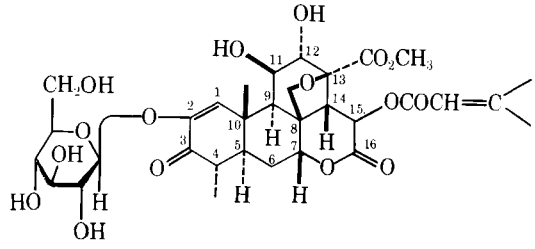

I: Bruceoside-A

0022-3549/82/0300-0345$01.00/0

(ester and lactone CO) cm^{-1}. PMR ($CDCl_3$) δ 0.99 (d, J = 6 Hz, 9H, CH_3-4 and two CH_3-23), 1.40 (s, CH_3-10), 3.86 (s, $COOCH_3$), and 6.40 (d, J = 13 Hz, H-15).

Anal.—Calc. for $C_{26}H_{36}O_{11}$: *m/z* 524.2255 (M^+). Found: *m/z* 524.2259.

Compound XXXV could also be prepared by hydrogenation of II (504 mg) in 90% ethanol (100 ml) with platinum oxide (50 mg) in water at room temperature and atmospheric pressure. The reaction mixture was filtered by use of a silica gel column. The filtered solution was evaporated to yield colorless XXXV (498 mg).

Synthesis of XXXVI—To a solution of XXXV (66 mg) in methyl alcohol (10 ml) was added a solution of sodium borohydride (2 mg) in water (5 ml). The mixture was stirred at room temperature for 23 hr and then subjected to preparative TLC (chloroform-acetone 1:1) to give 2-hydroxy-2-deoxytetrahydrobrusatol lactol (XXXVI) as colorless crystals (31.6 mg).

XXXVI: mp 121–123°; IR (potassium bromide) 3440 (OH), 1715 (ester CO), 1040 (cyclic *sec*-OH); PMR ($CDCl_3$) δ 0.91 (d, J = 6 Hz, 9H, CH_3-4 and two CH_3-23), 1.50 (s, CH_3-10), 3.81 (s, $COOCH_3$), 4.13 (m, H-12), 4.20 (m, H-11), 4.60 (m, H-2 and H-3) and 5.52 (m, H-15 and H-16).

Anal.—Calc. for $C_{26}H_{40}O_{11}$: *m/z* 528.2571 (M^+). Found: *m/z* 528.2573.

REFERENCES

(1) K. H. Lee, T. Ibuka, D. Sims, O. Muraoka, H. Kiyokawa, I. H. Hall, and H. L. Kim, *J. Med. Chem.*, **24,** 924 (1981). (Presented in part at the Second Chemical Congress of North American Continent, Las Vegas, Nev., August 1980.)

(2) S. M. Kupchan, R. W. Britton, J. A. Lacadie, M. F. Ziegler, and C. W. Sigel, *J. Org. Chem.*, **40,** 648 (1975).

(3) M. Suffness and J. Douros, in "Methods in Cancer Research," Vol. XVI, V. J. De Vita and H. Busch, Eds., Academic New York, N.Y. 1979, chap. III.

(4) M. E. Wall and M. C. Wani, *J. Med. Chem.*, **21,** 1186 (1979).

(5) S. M. Kupchan, J. A. Lacadie, G. A. Howie, and B. R. Sickles, *ibid.*, **19,** 1130 (1976).

(6) M. E. Wall and M. C. Wani, *Ann. Rev. Pharmacol. Toxicol.*, **17,** 117 (1977).

(7) K. H. Lee, Y. Imakura, and H. C. Huang, *J. Chem. Soc. Chem. Commun.*, **1977,** 69.

(8) K. H. Lee, Y. Imakura, Y. Sumida, R. Y. Wu, and I. H. Hall, *J. Org. Chem.*, **44,** 2180 (1979).

(9) National Cancer Institute, *DCT Bulletin*, **1979,** July, p. 4.

(10) L. L. Liao, S. M. Kupchan, and S. B. Horwitz, *Mol. Pharmacol.* **12,** 167 (1976).

(11) I. H. Hall, K. H. Lee, M. Okano, D. Sims, T. Ibuka, Y. F. Liou, and Y. Imakura, *J. Pharm. Sci.*, **70,** 1147 (1981).

(12) R. I. Geran, N. H. Greenberg, M. M. MacDonald, A. M. Schumacher, and B. J. Abbott, *Cancer Chemother. Rep. Part 3*, **3,** 1 (1972).

(13) C. Sweeley, B. Soltmann, and J. F. Holland, "High Performance Mass Spectrometry Chemical Application," ACS Symposium Series No. 70, 1978, p. 209.

(14) K. Y. Sim, J. J. Sims, T. A. Geissman, *J. Org. Chem.*, **33,** 429 (1968).

(15) M. Okano and K. H. Lee, *ibid.*, **46,** 1138 (1981).

ACKNOWLEDGMENTS

Supported by U.S. Public Health Service Research Grants CA-22929 and CA-17625 from the National Cancer Institute.

The authors thank Dr. D. L. Harris, Department of Chemistry, University of North Carolina at Chapel Hill for PMR spectra, Dr. David Rosenthal and Mr. Fred Williams of the Research Triangle Center for Mass Spectrometry for the electron-impact mass spectral data, and Mr. Chris Ledbetter and Miss Erma Mallory for technical assistance.

Antitumor Agents XLVI: *In Vitro* Effects of Esters of Brusatol, Bisbrusatol, and Related Compounds on Nucleic Acid and Protein Synthesis of P-388 Lymphocytic Leukemia Cells

IRIS H. HALL ˣ, Y. F. LIOU, M. OKANO, and K. H. LEE

Received February 19, 1981, from the *Division of Medicinal Chemistry, School of Pharmacy, University of North Carolina at Chapel Hill, NC 27514.* Accepted for publication July 15, 1981.

Abstract □ A series of esters of brusatol, bisbrusatol, and bruceantin were shown to have potent antileukemic activity. Antineoplastic activity was correlated with the ability of the compounds to suppress DNA and protein synthesis in P-388 lymphocytic leukemia cells. Compounds with high T/C% values successfully inhibited DNA polymerase activity and purine synthesis. The ability to inhibit protein synthesis during the elongation process also correlated positively with high antileukemic activity in this series of quassinoids. Dihydrofolate reductase activity and basal and adenosine diphosphate stimulated respiration of P-388 cells were also inhibited.

Keyphrases □ Brusatol—esters, *in vitro* effects on nucleic acid and protein synthesis, P-388 lymphocytic leukemia cells □ Bisbrusatol—esters, *in vitro* effects on nucleic acid and protein synthesis, P-388 lymphocytic leukemia cells □ Antitumor agents—*in vitro* effects of brusatol, bisbrusatol, and related compounds on nucleic acid and protein synthesis, P-388 lymphocytic leukemia cells

Bruceantin was first isolated from *Brucea antidysenterica* (1, 2) and is currently in Phase II clinical trials as an antineoplastic agent (3, 4). Brusatol, a derivative of bruceantin, was prepared by Lee *et al.* (5, 6) and shown to be active against P-388 lymphocytic leukemia cell growth (7). This laboratory demonstrated that bruceantin and brusatol reduced nucleic acid and protein synthesis (7, 8), purine synthesis (7), and oxidative phosphorylation processes (8) of P-388 cells. Based on the observation that a number of potent antileukemic agents have an ester in their structure, a series of brusatol related esters as well

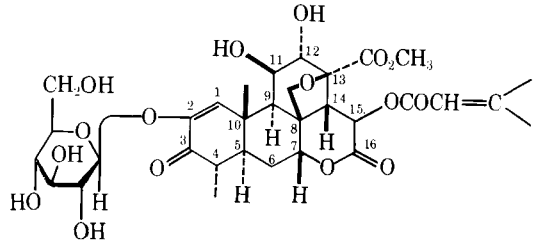

I: Bruceoside-A

0022-3549/82/0300-0345$01.00/0

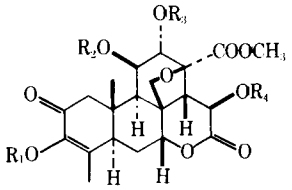

II: Brusatol: $R_1 = R_2 = R_3 = H$, $R_4 =$ 

III: Bruceantin: $R_1 = R_2 = R_3 = H$, $R_4 =$ 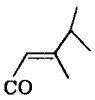

IV: Brusatol triacetate: $R_1 = R_2 = R_3 = COCH_3$, $R_4 =$ 

V: Bruceolide: $R_1 = R_2 = R_3 = R_4 = H$

VI: 3-(3,4-Dimethyl-2-pentenoyl)bruceolide:

$R_1 =$ 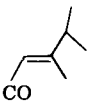 , $R_2 = R_3 = R_4 = H$

VII: 3-(3,4-Dimethyl-2-pentenoyl)bruceantin:

$R_1 = R_4 =$ 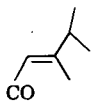 , $R_2 = R_3 = H$

VIII: 12-Acetyl-3,15-disenecioyl bruceolide:

$R_1 = R_4 =$ 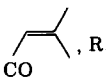 , $R_2 = H$, $R_3 = COCH_3$

IX: 3,15-Disenecioyl bruceolide:

$R_1 = R_4 =$ 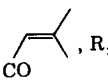 , $R_2 = R_3 = H$

as bisbrusatolyl esters and related moieties were synthesized. These compounds were tested for antineoplastic activity and were active against P-388 lymphocytic leukemia growth (10). These ester derivatives of brusatol were examined for their *in vitro* effects on nucleic acid and protein synthesis of P-388 cells and the results are now reported.

EXPERIMENTAL

The compound bruceoside-A (I) was originally isolated from *Brucea javanica* (5). Brusatol (II) was obtained by treating bruceoside-A with 3*N* H_2SO_4–methanol (1:1) to hydrolyze the glycosidic linkage (5, 6). Bruceantin (III) was obtained from bruceoside-A by synthetic methods (11). The chemical synthesis, purification, and physical characterization

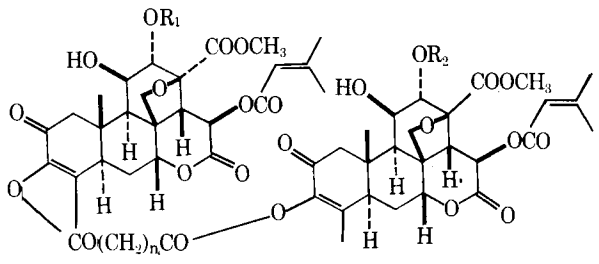

X: Bis-12,12′-diacetyl brusatolyl succinate: $R_1 = R_2 = COCH_3$, n = 2

XI: Bisbrusatolyl adipate: $R_1 = R_2 = H$, n = 4

XII: Bisbrusatolyl glutarate: $R_1 = R_2 = H$, n = 3

XIII: Bisbrusatolyl succinate: $R_1 = R_2 = H$, n = 2

XIV: Bisbrusatolyl malonate: $R_1 = R_2 = H$, n = 1

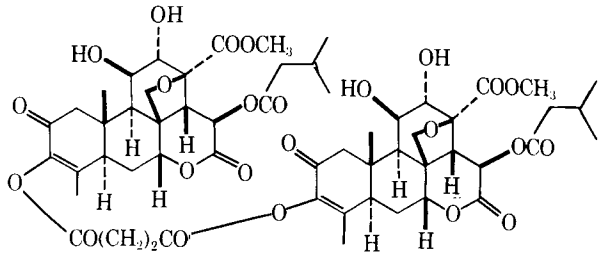

XV: Bisdihydrobrusatolyl succinate

of compounds IV–XIX, *i.e.*, brusatol esters, bisbrusatolyl esters, and related derivatives, were reported recently by this laboratory (10, 11).

Antileukemic Screen—The UNC P-388 lymphocytic leukemia tumor line was maintained in DBA/2 male mice (~20 g) by inoculation with 10^6 P-388 cells on day 0, intraperitoneally. The tumor was transferred on day 8 to BDF_1 male mice (~18 g) for the testing of new agents. Test drugs were suspended by homogenization in 0.05% polysorbate 80 and administered 0.6 mg/kg intraperitoneally on days 1–14, utilizing 5-fluorouracil as a standard (12).

***In Vitro* Incorporation Studies**—BDF_1 ($C_{57}B1/6 \times DBA/j$) male mice were inoculated with 10^6 tumor cells as previously described. On day 9, the P-388 ascites cells were collected from the peritoneal cavity. *In vitro* incorporation studies (8) were carried out using 10^6 P-388 cells in minimum essential medium in 10% fetal calf serum and either 1 μCi of [6-^{3}H] thymidine (21.8 Ci/mmole), [6-^{3}H]uridine (22.4 Ci/mmole) or [4,5-^{3}H(N)]-L-leucine (56.5 Ci/mmole) in a total volume of 1 ml and incubated for 90 min at 37°. The final concentration of I–XIX was 10 μ*M*. Thymidine incorporation into DNA was terminated with perchloric acid containing pyrophosphate which was filtered on glass fiber paper by vacuum suction. The control value was 137,346 dpm/10^6 cells/90 min. RNA and protein incorporation assays were terminated with trichloroacetic acid and the macromolecule was collected on nitrocellulose membrane filter paper. The acid insoluble precipitates on the filter papers were placed in scintillation vials and counted in a toluene–oxtoxynol scintillation fluid. The control value for uridine incorporation was 36,442 dpm/10^6 cells/90 min and for leucine incorporation into protein the value was 8477 dpm/10^6 cells/90 min. Nuclear DNA polymerase activity was determined on isolated P-388 lymphocytic leukemia cell nuclei. The incubation medium was that used by Sawada *et al.* (13) except that [^{14}C]thymidine triphosphate (78.1 Ci/mmole) was used; the insoluble nucleic acids were collected on glass fiber paper discs[1], resulting in a control value of 24,568 dpm/mg nucleic protein. [^{14}C]Formic acid incorporation into purines was measured using 0.5 μCi of [^{14}C]formic acid (4.95 mCi/mmole) (14). The reaction medium was spotted on silica gel TLC plates and eluted with *n*-butanol–acetic acid–water (4:1:5). Using adenosine and guanosine as standards, the plates were scraped and the radioactivity determined. The control value was 10,621 dpm/mg of protein. Dihydrofolate reductase was determined by a spectrophotometric method (15) based on the rate of disappearance of 0.1 μmole of reduced NADP. The control resulted in an absorbance difference of 0.760 o.d. unit/hr/mg of protein using a 600×*g* (10 min) supernate.

Utilizing a test system (7) that differentiates between initiation and elongation inhibitors of protein synthesis, P-388 tumor cells were homogenized and incubated in tromethamine buffer (pH 7.6) containing KCl, $MgCl_2$, adenosine triphosphate, guanosine triphosphate, phosphoenolpyruvate, pyruvate kinase, dithiothreitol, the 19 basic amino acids, and [^{3}H]leucine (56.5 Ci/mmol) for 0–14 min at 37°. Test drugs were added at 10 μ*M* concentration to the incubation medium 90 sec after initiating the experiment. Samples were taken from the assay medium at 1 min intervals and spotted on filter paper[2]. The reaction was terminated with trichloroacetic acid and the protein extracted and counted. The test drugs were compared to the standards pyrocatechol violet, an initiator inhibitor, and emetine, an elongation inhibitor of protein synthesis at 75 μmoles. Oxidative phosphorylation studies were carried out on 9 day P-388 cells (9). Oxygen consumption was measured with an oxygen electrode[3] connected to an oxygraph. The reaction vessel contained 55 μmoles of sucrose, 22 μmoles of monobasic potassium phosphate, 22 μmoles of potassium chloride, 90 μmoles of succinate or 60 μmoles of α-ketoglutarate as substrate, and 22 μmoles of adenosine triphosphate. Test drugs were present in a final concentration of 10 μ*M*. After the basal metabolic level (state 4) was obtained, 0.257 μmole of

[1] GF/F.
[2] Whatman No. 3.
[3] Clark.

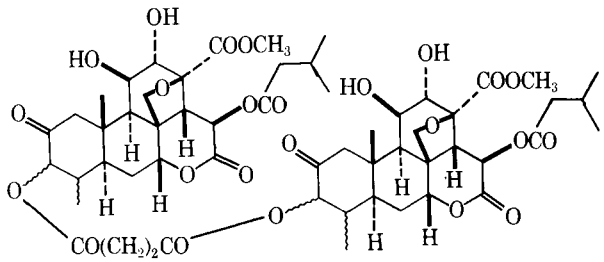

XVI: Bistetrahydrobrusatolyl succinate

adenosine diphosphate was added to the vessel to obtain the adenosine diphosphate-stimulated respiration rate (state 3). The control values for states 4 and 3 respiration were 11.44 and 20.76 μl of oxygen consumed/min/mg of protein, respectively, using succinate as substrate. When α-ketoglutarate was used as substrate, states 4 and 3 respiration were 10.01 and 19.17 μl of oxygen consumed/min/mg of protein.

RESULTS

Using a dose of 0.6 mg/kg/day, compounds II, III, V–VII, IX, XI–XV, and XVIII demonstrated significant inhibitory activity against P-388 lymphocytic leukemia cell growth in BDF_1 mice. The bisbrusatolyl esters (XI–XIV) were in general more potent than brusatol (II), especially the succinate (XIII) and the malonate (XIV) with T/C = 217 and 272%, respectively. Reduction of the C-15 ester double bond did not decrease the activity (compare XV to XIII and XVIII to III). However, saturation of the diosphenol double bond gave either less active or inactive compounds

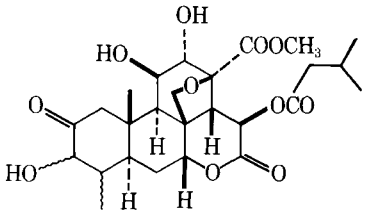

XVII: Tetrahydrobrusatol

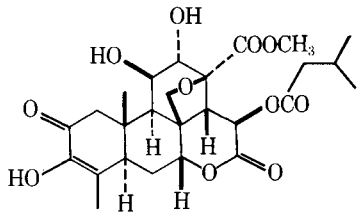

XVIII: Dihydrobrusatol

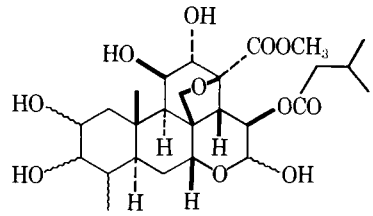

XIX: 2-Hydroxy-2-deoxotetrahydrobrusatol lactol

(XVI, XVII, and XIX). Esterification of II at C-3 afforded VII and IX which were more active than II. Acetylation of hydroxyl groups at C-11 and C-12 gave compounds (IV, VIII, and X) which were either less active or inactive, indicating the importance of these hydroxyl groups for enhanced antileukemic activity.

Examination of the *in vitro* incorporation studies in P-388 lymphocytic leukemia cells demonstrated that compounds II, III, VII, IX, XI–XIV, and XVIII suppressed thymidine incorporation into DNA 41–59%. These same compounds inhibited uridine incorporation into RNA 16–59%. L-Leucine incorporation into protein was suppressed more than 70% by XIV and VIII and more than 50% by II and IX. Compounds III, V, VII, XI, XII, XV, and XVIII caused at least 40% inhibition of protein synthesis of P-388 cells.

Detailed examination of a number of enzymatic activities which are known to be suppressed by quassinoids subsequently followed. Nucleic DNA polymerase activity in P-388 was inhibited at least 50% by compounds XI, XII, and XIV and at least 40% by compounds II, III, VII, and IX. Purine synthesis was inhibited more than 50% by compounds III, VII, IX, and XIII–XV and more than 40% by II, X, XI, and XII. Dihydrofolate reductase activity was suppressed at least 40% by compounds I, III, IV, XI, XIII, XIV, and XV. The elongation process of protein synthesis compared with the emetine standard was inhibited greater than 60% by II, VII, XI, XIII, XIV, IX, and XII at 10 μ*M*. The quassinoids inhibited ongoing polypeptide synthesis. Oxidative phosphorylation processes were not inhibited as significantly as other metabolic events. However, state 4 (basal) respiration with succinate as the substrate was inhibited greater than 15% by compounds II, III, V–VII, IX, XI–XIII, XV, and XVIII. With α-ketoglutarate as the substrate, compounds II, III, VI, VII, IX–XV, XVII, and XVIII caused 15% state 4 inhibition. Adenosine diphosphate-stimulated respiration was inhibited 15% using succinate as substrate by compounds II, III, V, IX, XI, XII, XIV, and XVIII and by compounds II, III, VII, IX, XI–XV, XVII, and XVIII using α-ketoglutarate as substrate.

DISCUSSION

The quassinoids demonstrated that protein and nucleic acid metabolism were inhibited in a manner which correlated positively with their antileukemic activity when tested against P-388 lymphoid leukemia growth. Compounds with the higher T/C % values had a greater ability

Table 1—*In Vitro* Effects of Quassinoids on Nucleic Acid and Protein Synthesis of P-388 Lymphocytic Leukemia Cells

Drug, 10 μ*M* (*n* = 6)	% Control			*In Vivo* 0.6 mg/kg/day, T/C %
	Thymidine into DNA	Uridine into RNA	L-Leucine into Protein	
I Bruceoside A	65 ± 4[a]	72 ± 5[a]	54 ± 5[a]	118
II Brusatol	51 ± 5[a]	44 ± 4[a]	44 ± 3[a]	149
III Bruceantin	41 ± 3[a]	53 ± 4[a]	57 ± 3[a]	162
IV Brusatol triacetate	98 ± 7	94 ± 6	89 ± 6	102
V Bruceolide	74 ± 6	100 ± 7	60 ±4[a]	139
VI 3-(3,4-Dimethyl-2-pentonyl) bruceolide	91 ± 4[b]	106 ± 5	64 ± 4[a]	131
VII 3-(3,4-Dimethyl-2-pentonyl) bruceantin	53 ± 6[a]	69 ± 3[a]	59 ± 5[a]	194
VIII 12-Acetyl-3,15-disenecioyl bruceolide	112 ± 5	91 ± 4[b]	78 ± 6[a]	103
IX 3,15-Disenecioyl bruceolide	56 ± 4[a]	53 ± 5[a]	38 ± 3[a]	185
X Bis-12,12′-diacetyl brusatolyl succinate	98 ± 5	87 ± 6[c]	75 ± 4[a]	118
XI Bisbrusatolyl adipate	59 ± 3[a]	61 ± 5[c]	60 ± 5[a]	176
XII Bisbrusatolyl glutarate	55 ± 6[a]	75 ± 5[a]	57 ± 4[a]	176
XIII Bisbrusatolyl succinate	45 ± 3[a]	41 ± 4[a]	28 ± 4[a]	217
XIV Bisbrusatolyl malonate	55 ± 5[a]	52 ± 3[a]	17 ± 3[a]	272
XV Bisdihydrobrusatolyl succinate	62 ± 3[a]	60 ± 5[a]	57 ± 4[a]	193
XVI Bistetrahydrobrusatolyl succinate	111 ± 5	83 ± 5[a]	66 ± 5[a]	113
XVII Tetrahydrobrusatol	89 ± 6[b]	108 ± 6	76 ± 3[a]	120
XVIII Dihydrobrusatol	54 ± 5[a]	61 ± 5[a]	58 ± 4[a]	150
XIX 2-Hydroxy-2-deoxotetrahydrobrusatol lactol	88 ± 4[c]	93 ± 4	60 ± 4[a]	107
XX 0.05% Polysorbate 80 water	100 ± 5	100 ± 4	100 ± 6	100

[a] $p \leq 0.001$. [b] $p \leq 0.010$. [c] $p \leq 0.005$.

Table II—*In Vitro* Effects of Quassinoids on Specific Processes of Nucleic Acid and Protein Synthesis and Respiration

Drugs, 10 μM ($n = 6$)	% Control							
	DNA Polymerase Activity	[^{14}C]Formate into Purines	Dihydrofolate Reductase Activity	Elongation Process of Protein Synthesis	Oxidative Phosphorylation			
					Succinate		α-Ketoglutarate	
					State 4	State 3	State 4	State 3
I	89 ± 6[a]	82 ± 6[b]	50 ± 4[b]	54 ± 6[b]	86 ± 4[b]	99 ± 7	85 ± 4[b]	93 ± 4
II	57 ± 5[b]	58 ± 4[b]	64 ± 5[b]	28 ± 3[b]	80 ± 3[b]	78 ± 5[b]	69 ± 3[b]	74 ± 4[b]
III	56 ± 7[b]	49 ± 4[b]	47 ± 4[b]	77 ± 4[b]	81 ± 5[b]	81 ± 4[b]	82 ± 4[b]	75 ± 3[b]
IV	79 ± 8[b]	93 ± 3	55 ± 8[b]	60 ± 5[b]	87 ± 3[b]	95 ± 3	86 ± 2[c]	114 ± 5
V	74 ± 7[b]	86 ± 5[c]	65 ± 4[b]	64 ± 6[b]	80 ± 4[b]	81 ± 4[b]	87 ± 5[c]	89 ± 4[c]
VI	77 ± 6[b]	81 ± 4[b]	81 ± 7[c]	57 ± 5[b]	82 ± 5[b]	90 ± 5[a]	82 ± 4[b]	89 ± 5[c]
VII	56 ± 5[b]	17 ± 2[b]	87 ± 6[a]	33 ± 4[b]	72 ± 3[b]	89 ± 3[b]	64 ± 6[b]	67 ± 3[b]
VIII	91 ± 4	91 ± 4	69 ± 7[b]	78 ± 4[b]	98 ± 5[b]	89 ± 5[c]	95 ± 6	92 ± 5
IX	58 ± 3[b]	46 ± 5[b]	58 ± 6[b]	53 ± 6[b]	66 ± 3[b]	72 ± 4[b]	67 ± 4[b]	72 ± 5[b]
X	91 ± 7	81 ± 5[b]	72 ± 5[b]	67 ± 5[b]	89 ± 3[c]	92 ± 6	83 ± 5[b]	101 ± 4
XI	47 ± 6[b]	55 ± 5[b]	65 ± 5[b]	38 ± 3[b]	83 ± 2[b]	73 ± 5[b]	68 ± 4[b]	73 ± 4[b]
XII	47 ± 5[b]	55 ± 6[b]	65 ± 4[b]	46 ± 4[b]	83 ± 3[b]	77 ± 5[b]	70 ± 4[b]	68 ± 5[b]
XIII	70 ± 6[b]	43 ± 5[b]	53 ± 3[b]	35 ± 4[b]	73 ± 4[b]	89 ± 6[c]	57 ± 4[b]	64 ± 6[b]
XIV	43 ± 4[b]	45 ± 4[b]	50 ± 2[b]	20 ± 3[b]	85 ± 5[b]	76 ± 5[b]	70 ± 5[b]	76 ± 5[b]
XV	78 ± 5[b]	43 ± 3[b]	59 ± 4[b]	31 ± 5[b]	75 ± 6[b]	90 ± 4[c]	52 ± 5[b]	61 ± 4[b]
XVI	72 ± 4[b]	100 ± 7	64 ± 5[b]	70 ± 4[b]	91 ± 4	90 ± 5[c]	94 ± 4	96 ± 6
XVII	91 ± 5	108 ± 4	62 ± 4[b]	89 ± 4[c]	87 ± 3[b]	85 ± 3[b]	83 ± 6[b]	70 ± 3[b]
XVIII	81 ± 4[b]	69 ± 3	—	64 ± 5[b]	61 ± 5[b]	62 ± 5[b]	70 ± 4[a]	74 ± 4[b]
XIX	85 ± 3[b]	96 ± 5	—	80 ± 6[b]	90 ± 6	96 ± 4	102 ± 3	86 ± 5[c]
XX	100 ± 5	100 ± 6	100 ± 7	100 ± 4	100 ± 5	100 ± 4	100 ± 5	100 ± 4

[a] $P \leq 0.010$. [b] $P \leq 0.001$. [c] $P \leq 0.005$.

to suppress protein synthesis (compounds XIII, XIV, XV, XI, and VII). The elongation step of translocation appeared to be affected preferentially over initiation events of protein synthesis. This observation is consistent with previous data for compound II on rabbit reticulocyte protein synthesis and compound III on yeast. The inhibition of DNA and RNA was also positively correlated with antineoplastic activity although DNA synthesis was suppressed slightly less than the inhibition of protein synthesis. Nuclear DNA polymerase activity was inhibited ~50% by compounds with T/C % >150 although there were exceptions. Purine synthesis inhibition correlated more positively with inhibition of nucleic acid synthesis and antineoplastic activity than inhibition of DNA polymerase activity by these quassinoids. Dihydrofolate reductase activity was affected in a similar manner although the regulatory enzyme of purine synthesis, phosphoribosyl pyrophosphate aminotransferase, was identified as being inhibited when these drugs are administered *in vivo*. However, only marginal inhibitory effects were observed after *in vitro* (6) incubation of the quassinoids with this regulatory enzyme. Surprisingly, 3-(3,4-dimethyl-2-pentonyl) bruceantin (VII) inhibited purine synthesis 83%, apparently at some site other than dihydrofolate reductase. The inhibition of purine synthesis by VII probably contributes significantly to the T/C % = 194. Previously, data indicated that quassinoids affected anaerobic and aerobic respiration of P-388 cells and that state 4 and state 3 respiration were inhibited ~50% by quassinoids at 0.015 mM. However, at 0.010 mM concentrations, the effect on oxidative phosphorylation was not as dramatic. Basal and coupled oxidative phosphorylation was inhibited ~15% by those compounds possessing a T/C % ≥125 in the antineoplastic screen. Reduction of oxidative phosphorylation processes would reduce the available energy for macromolecular synthesis in rapidly dividing cells, thus possibly indirectly affecting nucleic acid and protein synthetic pathways. Hence, it may be concluded that the optimum structural requirements for potent antileukemic activity and metabolic inhibition of P-388 cells are (*a*) bis-esters of brusatol with an ester carbon chain length of one or two and (*b*) a C-3, C-15 disenecioate or di-3,4-dimethyl-2-pentenoate side chain of bruceolide. Both types of structure require an enone system in ring A and a free hydroxyl group at positions C-11 and C-12.

REFERENCES

(1) S. M. Kupchan, R. W. Britton, J. A. Lacadie, M. F. Ziegler, and C. W. Sigel, *J. Org. Chem.*, **40**, 648 (1975).

(2) L.-L. Liao, S. M. Kupchan, and S. B. Horwitz, *Mol. Pharmacol.*, **12**, 167 (1976).

(3) A. Y. Bedikian, M. Valdivieso, G. P. Bodey, W. K. Murphy, and E. J. Freireich, *Cancer Treat. Rep.*, **63**, 1843 (1979).

(4) M. B. Garnick, R. H. Blum, G. P. Canellos, R. J. Mayer, L. Parker, A. T. Skarin, F. P. Li, I. C. Henderson, and E. Frei, *ibid.*, **63**, 1929 (1979).

(5) K. H. Lee, Y. Imakura, and H. C. Huang, *J. Chem. Soc. Chem. Commun.*, **1979**, 69.

(6) K. H. Lee, Y. Imakura, Y. Sumida, R. Y. Wu, I. H. Hall, and H. C. Huang, *J. Org. Chem.*, **44**, 2180 (1979).

(7) W. Willingham, E. A. Stafford, S. H. Reynolds, S. G. Chaney, K. H. Lee, M. Okano, and I. H. Hall, *Biochim. Biophys. Acta*, **654**, 169 (1981).

(8) I. H. Hall, K. H. Lee, S. A. ElGebaly, Y. Imakura, Y. Sumida, and R. Y. Wu, *J. Pharm. Sci.*, **68**, 883 (1979).

(9) S. A. ElGebaly, I. H. Hall, K. H. Lee, Y. Sumida, Y. Imakura, and R. Y. Wu, *ibid.*, **68**, 887 (1979).

(10) K. H. Lee, M. Okano, I. H. Hall, D. A. Brent, and B. Soltmann, *ibid.*, in press.

(11) M. Okano and K. H. Lee, *J. Org. Chem.*, **46**, 118 (1981).

(12) R. I. Geran, N. H. Greenberg, M. M. MacDonald, A. M. Schumacher, and B. J. Abbott, *Cancer Chemother. Rep., Part 3*, **3**, 1 (1972).

(13) H. Sawada, K. Tatsumi, M. Sasada, S. Shirakawa, T. Nakumura, and G. Wakisaka, *Cancer Res.*, **34**, 3341 (1974).

(14) M. K. Spassova, G. C. Russev, and E. V. Golovinsky, *Biochem. Pharmacol.*, **25**, 923 (1976).

(15) Y. K. Ho, T. Hakala, and S. F. Zakrzewski, *Cancer Res.*, **32**, 1023 (1972).

ACKNOWLEDGMENTS

Supported by American Cancer Society Grant CH-19 (K.H. Lee and I. H. Hall) and National Cancer Institute Grants CA-22929 and CA-17625 (in part) (K. H. Lee).

Fluorescence Stability of Human Albumin Solutions

D. L. PARSONS

Received June 24, 1981, from the *Department of Pharmaceutical Sciences, College of Pharmacy, University of Arizona, Tucson, AZ 85721.* Accepted for publication July 23, 1981. Present address: School of Pharmacy, Auburn University, Auburn, AL 36849.

Abstract □ The fluorescence stability on aging of three types of human albumin solutions was investigated. For the first 8 hr after preparation, the magnitude of the fluorescence of the albumin solutions examined did not undergo the large fluctuations with time that had been previously observed for bovine albumin solutions. The fluorescence intensity of each of the human albumin solutions examined appeared to undergo a small but consistent decrease with time for the length of each study. Based on these results, the practice of preparing human albumin solutions several hours prior to use simply to achieve fluorescence stability is unnecessary.

Keyphrases □ Fluorescence, stability—human albumin solutions □ Human albumin—evaluation of fluorescence stability □ Stability, fluorescence—human albumin solutions

The quenching of the intrinsic fluorescence of serum albumin and other proteins upon the binding of a ligand has been used for many years to study ligand–macromolecule interactions (1). In such studies it is important to correct the collected data for variations in fluorescence intensity that are due to factors other than the ligand–macromolecule interaction, such as the inner filter effect. Another factor that may affect the magnitude of the intrinsic fluorescence of a protein molecule is the age of the protein solution. The magnitude of the fluorescence of freshly prepared solutions of crystallized bovine serum albumin at pH 7.45 varies regularly as a function of time until the solutions are ~5-hr old (2). Fluorescence values for one bovine serum albumin solution varied from an initial value of ~72–65 after 2 hr, and to 85 after 3 hr before stabilizing at a value of 78 after 5 hr. To avoid these time-dependent fluctuations in fluorescence intensity, solutions of bovine serum albumin were not used for ligand binding studies until they were 5–6-hr old. It was suggested that these fluctuations in fluorescence intensity may be the result of a slow obtainment of equilibrium among various conformational species of this protein or to hydration of the bovine serum albumin molecules followed by a rearrangement to native structures. Similar events, which were termed conformational oscillations, were observed for other protein macromolecules (3).

BACKGROUND

In most ligand binding studies utilizing quenching of intrinsic fluorescence of human serum albumin, the possible effect of time was not discussed. However, the results of the study of the fluorescence stability of bovine serum albumin (2) have been applied to studies utilizing human serum albumin. In one binding study, solutions of both bovine and human serum albumin were not used for fluorescence quenching studies until the solutions were at least 6-hr old (4). In another study, measurements of the fluorescence of human serum albumin solutions were not taken until the solutions were 2–3-hr old (5), even though this is the time period when bovine serum albumin appears to undergo the greatest fluctuations in fluorescence (2). A different approach to the problem of fluorescence stability was used in another binding study (6). A reference solution of human albumin was used to correct the fluorometer for drifts in instrument response and for variations in intrinsic protein fluorescence during the titration of a second cell of human albumin with ligand. The magnitude of any variation observed in the fluorescence of these albumin solutions with time was not given. Of course, any variation observed in the magnitude of fluorescence in this study could be the result of instrument drift and/or photodecomposition rather than, or in addition to, the variation in intrinsic albumin fluorescence. In addition, if serum albumin undergoes large fluctuations in fluorescence with time as a result of a time-dependent obtainment of an equilibrium conformation, the binding of ligand could also be time dependent.

Since most ligand binding studies are currently conducted utilizing human, rather than bovine, serum albumin, the stability of the magnitude of fluorescence of human albumin solutions was investigated. The fluorescence stability of three types of human albumin was investigated, since any observed fluctuations in fluorescence could be the result of a time-dependent obtainment of an equilibrium conformation. The time required to obtain this equilibrium conformation could possibly depend on the method used to purify the protein.

EXPERIMENTAL

Materials—Fraction V[1], crystalline[2], and fatty acid-free fraction V[3] human albumin, and propranolol hydrochloride[4] were used as received. Human albumin solutions were prepared using 0.1 *M* phosphate buffer (pH 7.4). The buffer was prepared from analytical grade dibasic sodium phosphate[5], monobasic potassium phosphate[5], and water purified by reverse osmosis followed by distillation.

Methods—Measurements of the magnitude of fluorescence of 2×10^{-6} *M* solutions of human albumin were made at various time intervals after preparation on a spectrofluorometer[6] at excitation and emission wavelengths of 283 and 351 nm, respectively. Excitation and emission slit widths of 2 and 10 nm, respectively, were used for all fluorescence measurements. The fluorescence sample cells had a pathlength of 1 cm and were oriented in the same direction in the cell holder for each fluorescence measurement during an experiment. The zero time point was set as the time at which the human albumin was first brought into contact with the buffer solution. No fluorescence measurements were made for the following 30 min to ensure complete dissolution of the protein.

Fluorescence measurements were made at ambient temperature (23.4 ± 0.6°). However, the temperature of the cell compartment of the spectrofluorometer was found to increase steadily for the first 2 hr after the instrument was turned on. Therefore, an instrument warm-up time of at least 2 hr was used before any fluorescent measurements were taken. After temperature equilibration, the cell compartment temperature was ~4° higher than room temperature. A time of 5 min was found to be sufficient for the temperature equilibration of samples placed inside the cell compartment. The effect of fluctuations in ambient temperature was apparently less than random error, since changes in the magnitude of fluorescence did not follow the variations in temperature observed during these studies.

A solution of propranolol hydrochloride (1.3 μg/ml) in 0.01 *N* HCl was used as a reference solution for each fluorescence measurement to correct for drifts in spectrofluorometer response and to correct for variations in

[1] Lot 903653, Calbiochem-Behring Corp.
[2] Lot 001395, Calbiochem-Behring Corp.
[3] Lot 15, Miles Laboratories, Inc.
[4] Ayerst Laboratories, Inc.
[5] Fisher Scientific Co.
[6] Model 650-10M, Perkin-Elmer Corp.

0022-3549/82/0300-0349$01.00/0

Table I—Results of Linear Regression Analysis of the Fluorescence Stability Data

Human Albumin	r^2	y-Intercept	Slope	95% Confidence Interval of the Slope
Fraction V	0.179	64.3	-2.14×10^{-3}	-7.79×10^{-4} to -3.49×10^{-3}
Crystalline	0.466	51.9	-3.76×10^{-3}	-2.88×10^{-3} to -4.63×10^{-3}
Fatty acid-free fraction V	0.202	42.3	-2.45×10^{-3}	-1.48×10^{-3} to -3.43×10^{-3}
Fraction V[a]	0.464	63.7	-3.18×10^{-3}	-1.67×10^{-3} to -4.69×10^{-3}

[a] Based on the data of Fig. 2.

the fluorescence sample cells used. No detectable change in the magnitude of the fluorescence of the reference solution occurred after 3 hr of continuous irradiation at the wavelength and slit width of excitation used in this study. The total irradiation time of the reference solution was not more than 15 min in subsequent experiments.

To prevent photodecomposition of the protein solutions, aliquots of the same solution of human albumin were irradiated in the spectrofluorometer only once for the few seconds required for a fluorescence measurement. Except as otherwise noted, fluorescence sample cells were rinsed six times with water followed by two rinses in spectrophotometric grade acetone between each use.

RESULTS AND DISCUSSION

The fluorescence intensities of human albumin solutions were determined at various times for 480 min after preparation. The results obtained for fraction V, crystalline, and fatty acid-free fraction V human albumin are presented in Fig. 1. The three data points obtained at each time point were obtained for three different protein solutions. To allow sufficient drying time after rinsing, two different fluorescence sample cells had to be used for each albumin solution when fluorescence measurements were made every 15 min for crystalline and fatty acid-free fraction V human albumin. In an attempt to decrease data variability, fluorescence measurements were only made every 30 min using the same fluorescence sample cell for each solution of fraction V human albumin.

The three types of human albumin were quite different with respect to the magnitude of their fluorescence. The magnitude of the fluorescence of each type of albumin was not corrected for differences in moisture content and purity. The greater fluorescence of fraction V as compared to the crystalline form of human albumin was observed previously for bovine serum albumin (4). The fatty acid-free fraction V human albumin exhibited the smallest fluorescence intensity of the human albumins examined. This decrease in fluorescence intensity may not be related to the decrease in the fatty acid content of the preparation. The fluorescence intensities of two crystalline human albumin preparations were found to differ, but the preparation containing the lowest content of fatty acid was more fluorescent (7). The difference in the emission spectra for three different crystalline human albumin samples which had equal absorbance values at the wavelength of excitation was apparently due to impurities other than fatty acids (8).

The magnitude of the fluorescence of the three types of human albumin examined in this study did not undergo the large fluctuations with time that had been previously observed for a bovine albumin solution (2). Therefore, it is not necessary to prepare these albumin solutions several hours prior to fluorescence measurements to allow the intrinsic protein fluorescence to stabilize. Of course, the proteins examined could have undergone conformational changes during this time period which were not reflected by changes in fluorescence intensity.

While large fluctuations in fluorescence intensity with time were not observed with the human albumin solutions used in this study, the magnitude of the fluorescence of the solutions appeared to undergo a small but continuous decrease with time for the length of each study. Much of the variability in the data for each type of protein was due to differences between the individual protein solutions used. For each type of human albumin at each time point, one albumin solution consistently had the highest fluorescence intensity while another albumin solution consistently had the lowest fluorescence. The apparent decrease in the magnitude of the fluorescence of each human albumin solution observed 480 min after preparation is not much greater than the experimental

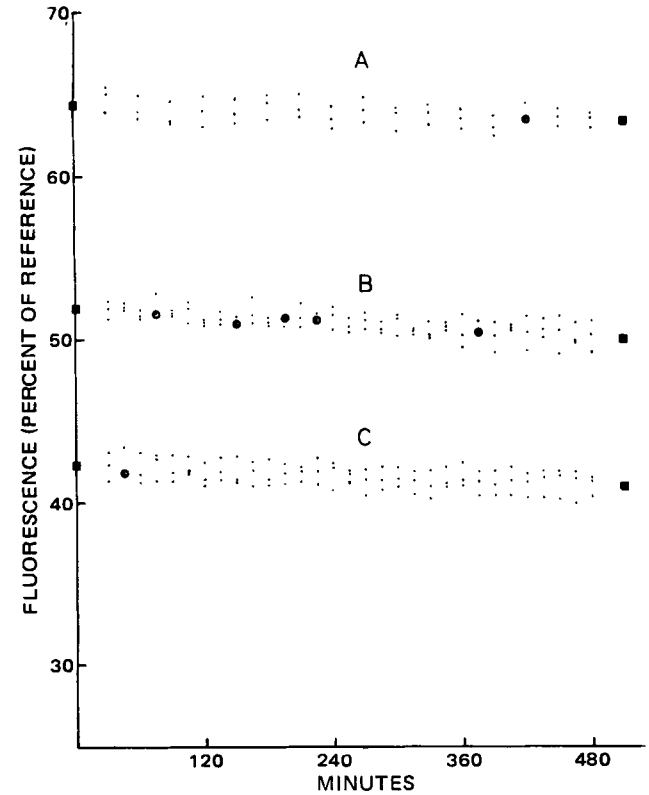

Figure 1—*The magnitude of fluorescence of human albumin solutions upon aging, where ● represents two identical experimental points and ■ represents the linear regression line of the data. Key: A, fraction V; B, crystalline; and C, fatty acid-free fraction V.*

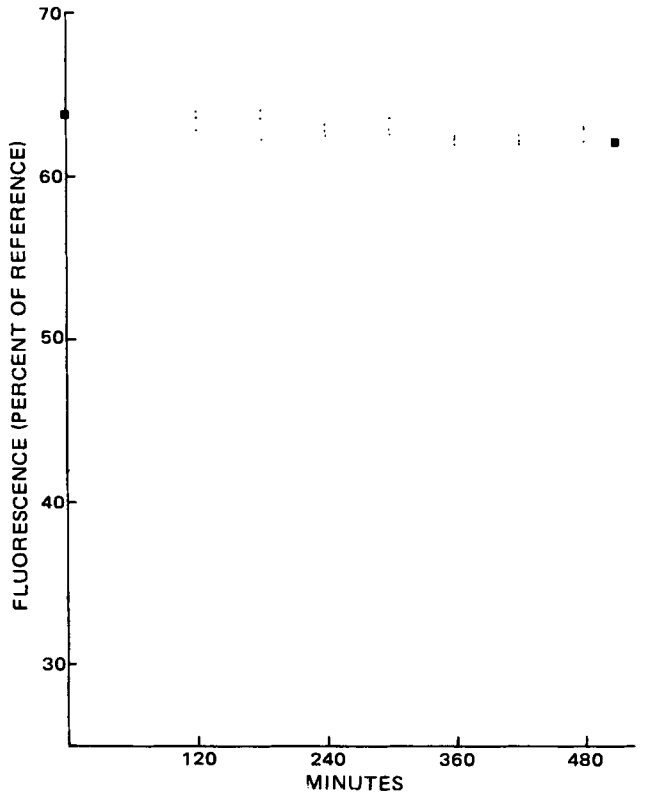

Figure 2—*The magnitude of fluorescence of fraction V human albumin solutions upon aging when fluorescence sample cells are cleaned with sulfuric acid–dichromate solution between measurements. Key: ■, the linear regression line of the data.*

variability observed in the fluorescence intensity of the different albumin solutions at each time point.

The results of linear regression analysis of the data for each type of human albumin are presented in Table I. While the r^2 value for each set of data is very low, the slope of each set of data does have a small negative value and zero is not included in the 95% confidence interval of the slope. The points at $t = 0$ and $t = 510$ min in Fig. 1 represent the linear least-squares fit of the experimental data. The actual lines were not drawn so that the experimental data could be examined without obstruction.

To determine if the small decrease in fluorescence intensity with time was due to inadequate washing of fluorescence sample cells between sample measurements, the experiment with fraction V human albumin was repeated. In this second study, fluorescence measurements were taken every hour to decrease the use of each sample cell. After each fluorescence measurement the cells were rinsed once with water, filled with sulfuric acid–dichromate cleaning solution for 15 min and rinsed using the procedure used in the previous experiments. The results are presented in Fig. 2. The fluorescence intensities of the solutions again appeared to undergo a small decrease with time. The results of linear regression analysis of the data are presented in Table I. The slope has a small negative value which is within the 95% confidence interval of the slope previously obtained for fraction V human albumin. As observed previously, zero is not within the 95% confidence interval of the slope. Thus, this different method of sample cell treatment between fluorescence measurements had no significant effect on the apparent decrease in fluorescence intensity of these protein solutions with time.

In conclusion, the intrinsic fluorescence intensity of each of the solutions of human albumin examined in this study was very stable for the first 8 hr after preparation. Based on these results, the practice of preparing solutions of human albumin several hours prior to use simply to achieve fluorescence stability is unnecessary. Since the fluorescence intensity of each of the albumin solutions examined underwent a small, consistent decrease with time, it may be advisable to use a reference solution of human albumin, as described previously (6), to correct binding data obtained from the quenching of intrinsic human albumin fluorescence by ligand.

REFERENCES

(1) C. F. Chignell, *Methods Pharmacol.*, **2**, 33 (1972).

(2) N. A. Attallah and G. L. Lata, *Biochim. Biophys. Acta*, **168**, 321 (1968).

(3) S. E. Shnoll and E. P. Chetverikova, *ibid.*, **403**, 89 (1975).

(4) D. V. Parke and W. E. Lindup, *Ann. N.Y. Acad. Sci.*, **226**, 200 (1973).

(5) H. Uchida and M. Hanano, *Chem. Pharm. Bull.*, **22**, 1571 (1974).

(6) R. L. Levine, *Clin. Chem.*, **23**, 2292 (1977).

(7) D. S. Lukas and A. G. DeMartino, *J. Clin. Invest.*, **48**, 1041 (1969).

(8) R. F. Chen, *J. Biol. Chem.*, **242**, 173 (1967).

ACKNOWLEDGMENTS

The author thanks Ms. M. DiMatteo for technical assistance.

Separation of Penicillin and Its Major Degradation Products by Ion-Pair Reversed-Phase High-Pressure Liquid Chromatography

ISAAC GHEBRE-SELLASSIE *, STANLEY L. HEM ‡, and ADELBERT M. KNEVEL *x

Received March 12, 1981, from the **Department of Medicinal Chemistry and Pharmacognosy and the ‡Department of Industrial and Physical Pharmacy, School of Pharmacy and Pharmacal Sciences, Purdue University, West Lafayette, IN 47907.* Accepted for publication June 11, 1981.

Abstract □ An ion-pair reversed-phase high-pressure liquid chromatographic technique capable of separating penicillin and its major degradation products within 8 min was developed. The influence of pH, counterion concentration, buffer concentration, and organic modifier content was studied and the observed behavior of the compounds during the chromatographic process was discussed.

Keyphrases □ Penicillin—major degradation products, separation by ion-pair reversed-phase high-pressure liquid chromatography □ High-pressure liquid chromatography—ion-pair reversed-phase, separation of penicillin and its major degradation products □ Degradation products—penicillin, separation by ion-pair reversed-phase high-pressure liquid chromatography

Various analytical methods for the detection, separation, and/or quantification of penicillin in the presence of its degradation products have been reported (1–7). The most recent papers deal with anion-exchange chromatography (5), reversed-phase chromatography (6), and NMR spectroscopy (7). NMR generally lacks sensitivity while the chromatographic approaches result in relatively long analysis times. However, the availability of small-particle size packings for reversed-phase chromatography suggests that very high chromatographic efficiencies and shorter analysis times can be expected with this procedure (8, 9). The present paper describes a high-pressure liquid chromatographic (HPLC) method that utilizes an ion-pair reversed-phase technique to separate penicillin and its three major degradation products: penillic acid, penicilloic acid, and penilloic acid in <8 min.

EXPERIMENTAL

Chemicals and Reagents—Penicillin G potassium[1] and tetrabutylammonium chloride[2] were obtained commercially and used without further treatment. Penillic acid, penicilloic acid, and penilloic acid were synthesized by standard methods (10). Acetonitrile was HPLC grade[3] while all other chemicals were either USP or reagent grade. Double-distilled water was used to prepare buffer solutions.

Apparatus—A liquid chromatograph[4] equipped with a fixed-wavelength UV absorbance detector set at 254 nm was used. A commercial stainless steel column[5] (150-mm × 4.6-mm i.d.) prepacked with 5-μm particles, with the silanol groups chemically bonded to a monomolecular layer of octadecylsilane, was used. A strip-chart recorder[6] recorded the detector output.

Chromatographic Conditions—The mobile phase was composed of acetonitrile, phosphate buffer, and a counterion. The ion-pair reagent, tetrabutylammonium chloride, was dissolved in the phosphate buffer

[1] Sigma Chemical Co., St. Louis, Mo.
[2] Aldrich Chemical Co., Milwaukee, Wis.
[3] Waters Associates, Milford, Mass.
[4] Model ALC 202, Waters Associates, Framingham, Mass.
[5] Ultrasphere-ODS, Beckman Instruments, Irvine, Calif.
[6] Omniscribe recorder, Houston Instruments, Houston, Tex.

0022-3549/82/0300-0351$01.00/0

variability observed in the fluorescence intensity of the different albumin solutions at each time point.

The results of linear regression analysis of the data for each type of human albumin are presented in Table I. While the r^2 value for each set of data is very low, the slope of each set of data does have a small negative value and zero is not included in the 95% confidence interval of the slope. The points at $t = 0$ and $t = 510$ min in Fig. 1 represent the linear least-squares fit of the experimental data. The actual lines were not drawn so that the experimental data could be examined without obstruction.

To determine if the small decrease in fluorescence intensity with time was due to inadequate washing of fluorescence sample cells between sample measurements, the experiment with fraction V human albumin was repeated. In this second study, fluorescence measurements were taken every hour to decrease the use of each sample cell. After each fluorescence measurement the cells were rinsed once with water, filled with sulfuric acid–dichromate cleaning solution for 15 min and rinsed using the procedure used in the previous experiments. The results are presented in Fig. 2. The fluorescence intensities of the solutions again appeared to undergo a small decrease with time. The results of linear regression analysis of the data are presented in Table I. The slope has a small negative value which is within the 95% confidence interval of the slope previously obtained for fraction V human albumin. As observed previously, zero is not within the 95% confidence interval of the slope. Thus, this different method of sample cell treatment between fluorescence measurements had no significant effect on the apparent decrease in fluorescence intensity of these protein solutions with time.

In conclusion, the intrinsic fluorescence intensity of each of the solutions of human albumin examined in this study was very stable for the first 8 hr after preparation. Based on these results, the practice of preparing solutions of human albumin several hours prior to use simply to achieve fluorescence stability is unnecessary. Since the fluorescence intensity of each of the albumin solutions examined underwent a small, consistent decrease with time, it may be advisable to use a reference solution of human albumin, as described previously (6), to correct binding data obtained from the quenching of intrinsic human albumin fluorescence by ligand.

REFERENCES

(1) C. F. Chignell, *Methods Pharmacol.*, **2**, 33 (1972).

(2) N. A. Attallah and G. L. Lata, *Biochim. Biophys. Acta*, **168**, 321 (1968).

(3) S. E. Shnoll and E. P. Chetverikova, *ibid.*, **403**, 89 (1975).

(4) D. V. Parke and W. E. Lindup, *Ann. N.Y. Acad. Sci.*, **226**, 200 (1973).

(5) H. Uchida and M. Hanano, *Chem. Pharm. Bull.*, **22**, 1571 (1974).

(6) R. L. Levine, *Clin. Chem.*, **23**, 2292 (1977).

(7) D. S. Lukas and A. G. DeMartino, *J. Clin. Invest.*, **48**, 1041 (1969).

(8) R. F. Chen, *J. Biol. Chem.*, **242**, 173 (1967).

ACKNOWLEDGMENTS

The author thanks Ms. M. DiMatteo for technical assistance.

Separation of Penicillin and Its Major Degradation Products by Ion-Pair Reversed-Phase High-Pressure Liquid Chromatography

ISAAC GHEBRE-SELLASSIE *, STANLEY L. HEM ‡, and ADELBERT M. KNEVEL *x

Received March 12, 1981, from the **Department of Medicinal Chemistry and Pharmacognosy and the ‡Department of Industrial and Physical Pharmacy, School of Pharmacy and Pharmacal Sciences, Purdue University, West Lafayette, IN 47907.* Accepted for publication June 11, 1981.

Abstract □ An ion-pair reversed-phase high-pressure liquid chromatographic technique capable of separating penicillin and its major degradation products within 8 min was developed. The influence of pH, counterion concentration, buffer concentration, and organic modifier content was studied and the observed behavior of the compounds during the chromatographic process was discussed.

Keyphrases □ Penicillin—major degradation products, separation by ion-pair reversed-phase high-pressure liquid chromatography □ High-pressure liquid chromatography—ion-pair reversed-phase, separation of penicillin and its major degradation products □ Degradation products—penicillin, separation by ion-pair reversed-phase high-pressure liquid chromatography

Various analytical methods for the detection, separation, and/or quantification of penicillin in the presence of its degradation products have been reported (1–7). The most recent papers deal with anion-exchange chromatography (5), reversed-phase chromatography (6), and NMR spectroscopy (7). NMR generally lacks sensitivity while the chromatographic approaches result in relatively long analysis times. However, the availability of small-particle size packings for reversed-phase chromatography suggests that very high chromatographic efficiencies and shorter analysis times can be expected with this procedure (8, 9). The present paper describes a high-pressure liquid chromatographic (HPLC) method that utilizes an ion-pair reversed-phase technique to separate penicillin and its three major degradation products: penillic acid, penicilloic acid, and penilloic acid in <8 min.

EXPERIMENTAL

Chemicals and Reagents—Penicillin G potassium[1] and tetrabutylammonium chloride[2] were obtained commercially and used without further treatment. Penillic acid, penicilloic acid, and penilloic acid were synthesized by standard methods (10). Acetonitrile was HPLC grade[3] while all other chemicals were either USP or reagent grade. Double-distilled water was used to prepare buffer solutions.

Apparatus—A liquid chromatograph[4] equipped with a fixed-wavelength UV absorbance detector set at 254 nm was used. A commercial stainless steel column[5] (150-mm × 4.6-mm i.d.) prepacked with 5-μm particles, with the silanol groups chemically bonded to a monomolecular layer of octadecylsilane, was used. A strip-chart recorder[6] recorded the detector output.

Chromatographic Conditions—The mobile phase was composed of acetonitrile, phosphate buffer, and a counterion. The ion-pair reagent, tetrabutylammonium chloride, was dissolved in the phosphate buffer

[1] Sigma Chemical Co., St. Louis, Mo.
[2] Aldrich Chemical Co., Milwaukee, Wis.
[3] Waters Associates, Milford, Mass.
[4] Model ALC 202, Waters Associates, Framingham, Mass.
[5] Ultrasphere-ODS, Beckman Instruments, Irvine, Calif.
[6] Omniscribe recorder, Houston Instruments, Houston, Tex.

0022-3549/82/0300-0351$01.00/0

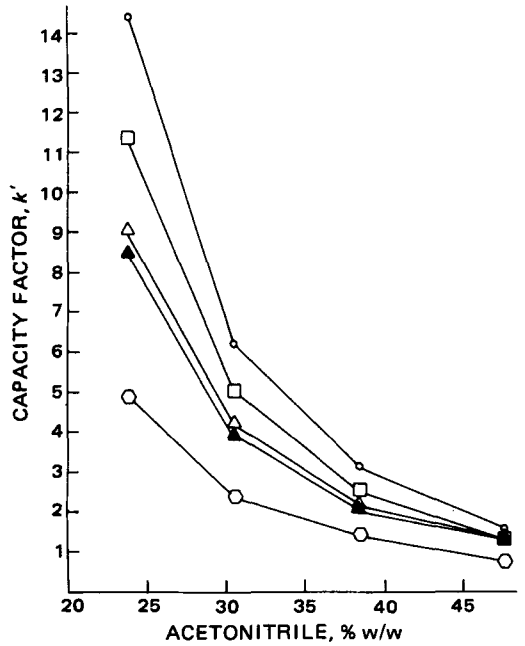

Figure 1—*Plots of the capacity factor* versus *the acetonitrile concentration in the mobile phase. Key:* ○, *penicillin;* □, *penicilloic acid;* △,▲, *penilloic acid; and* ○, *penillic acid.*

and the pH was adjusted with 1 *M* phosphoric acid before the required volume of acetonitrile was added. The mixture was filtered through a 0.45-μm filter[7] and degassed prior to use. The column was operated at ambient temperatures. Samples were introduced *via* an injection port[8] fitted with a 20-μl loop. The flow rate and the chart speed were 1.5 ml/min and 0.51 cm/min, respectively. The sensitivity range of the detector was set at 0.16 aufs.

RESULTS AND DISCUSSION

Penicillin and its major degradation products contain carboxylic acid functional groups with pH-dependent ionic states. Consequently, in the past, anion-exchange chromatography was usually used for the separation

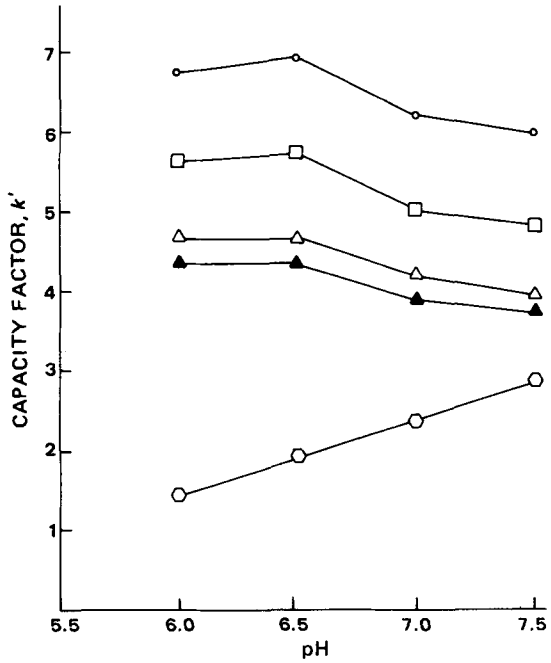

Figure 2—*Plots of the capacity factor* versus *the mobile phase pH. Key:* ○, *penicillin;* □, *penicilloic acid;* △,▲, *penilloic acid; and* ○, *penillic acid.*

[7] Millipore Corp., Bedford, Mass.
[8] Rheodyne model 70-10, Rheodyne, Berkeley, Calif.

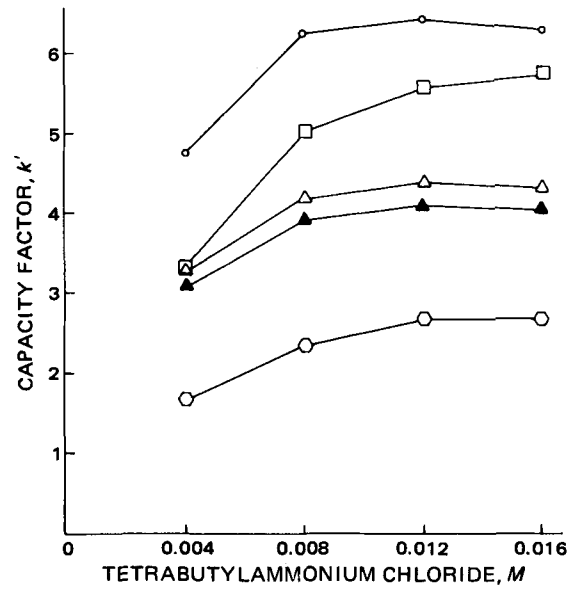

Figure 3—*Plots of the capacity factor* versus *the concentration of the ion-pair reagent in the mobile phase. Key:* ○, *penicillin;* □, *penicilloic acid;* △,▲, *penilloic acid; and* ○, *penillic acid.*

of these compounds. A reversed-phase mode utilizing an ion-suppression technique also was employed to achieve separation. However, in addition to having long analysis times, both methods use mobile phases with pH values less than optimum with respect to the stabilities of the compounds being analyzed.

The ion-pair reversed-phase technique reported here combines the advantages of both methods and also utilizes mobile phases with pH values compatible with the chemical stabilities of the solutes (10, 11). The pH range selected (6.0–7.5) satisfies the requirement that bonded-phase columns not be used at high pH while also maximizing the ionization of the solutes, despite the reported rise in pKa values as organic modifiers are added to aqueous solutions (12).

The effects of pH, counterion concentration, acetonitrile content, and phosphate buffer concentration on the capacity factors (k') and separation selectivities were studied (Figs. 1–4). The k' values of penicillin and its major decomposition products were affected substantially by a change in the percent composition of acetonitrile in the mobile phase (Fig. 1).

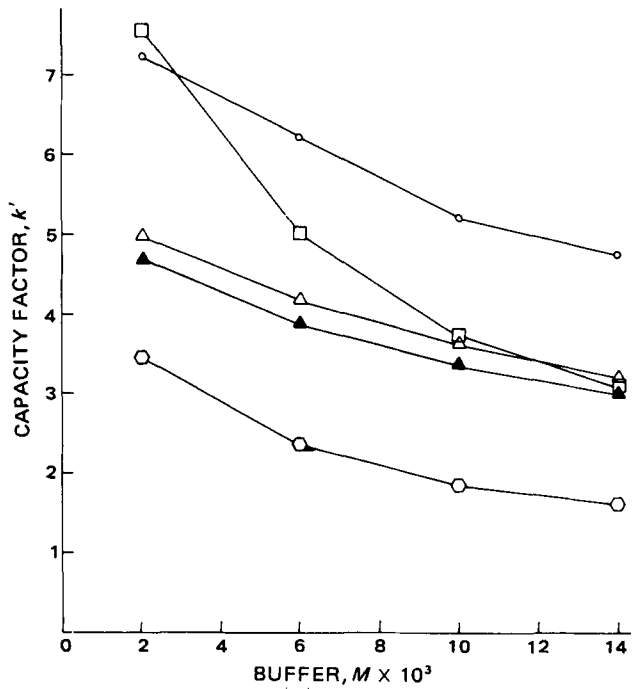

Figure 4—*Plots of the capacity factor* versus *the phosphate buffer concentration in the mobile phase. Key:* ○, *penicillin;* □, *penicilloic acid;* △,▲, *penilloic acids; and* ○, *penillic acid.*

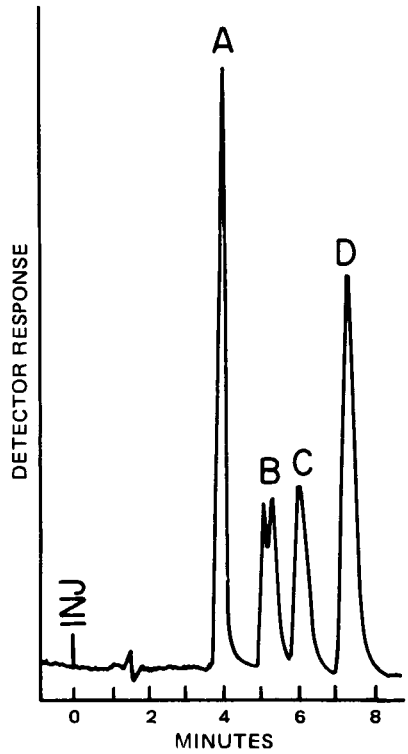

Figure 5—*Ion-pair reversed-phase high-pressure liquid chromatogram of penicillin and its major degradation products. Key: A, penillic acid; B, penilloic acid; C, penicilloic acid; and D, penicillin.*

At high acetonitrile concentrations, all four compounds gave sharp and symmetrical peaks; however, the capacity factors were so close to each other that the resolution was inadequate. Lowering the acetonitrile content improved the resolution significantly. Even the single peak of penilloic acid was partially resolved into two peaks which presumably represent the 5*R* and 5*S*, diastereoisomers of the compound (7).

Maximum k' values for penicillin, penicilloic acid, and penilloic acid were obtained between pH 6.0 and 6.5, when the compounds were completely ionized and ion-pair formation was at a maximum (Fig. 2). As the pH of the mobile phase increased, the k' values of the three anionic compounds decreased, presumably because hydroxyl ions compete with them and reduce the number of ion-pairs that would be formed (13). Although the penillic acid pK_1 and pK_2 values were similar to the ionization constants of the other three compounds (14), its capacity factor increased proportionally with an increase in pH.

Initially, the k' values of the sample molecules increased as the concentration of the ion-pair reagent was raised, but leveled off at higher concentrations (Fig. 3). This was expected because, once all sample anions form ion-pairs, the excess counterions would have no direct effect on retention. However, the ionic strength of the mobile phase increases and, in turn, varies the capacity factors. At low concentrations of ion-pair reagent, the retention times of the compounds are greatly reduced since the number of counterions available is insufficient for maximum ion-pair formation.

Furthermore, an increase in buffer concentration in the mobile phase led to a significant decrease in k' values of penicillin and its degradation products (Fig. 4). This was thought to be due mainly to the phosphate ions tying up the counterions, which would otherwise form ion-pairs with sample molecules. The simultaneous increase in ionic strength also influences the k' values of sample anions.

Logarithmic plots of the capacity factors and the four parameters studied showed linear relationships with correlation coefficients >0.99. The slopes of the curves in each graph were not always the same, clearly indicating the array of selectivities offered by the chromatographic system.

The composition of the mobile phase used to develop the chromatogram in Fig. 5 was determined by these studies. A pH of 7.5 was chosen because the peaks of the compounds were significantly removed from the solvent front and the compounds that eluted last had the lowest k' value compared to those at other pH values. Both 0.008 and 0.012 *M* tetrabutylammonium chloride yielded excellent resolution of the four compounds, but the former concentration was selected because it gave better resolution between the penicillin and penicilloic acid peaks, thus reducing the probability of overlap that might occur at high penicillin concentrations. A 0.006 *M* buffer concentration in the mobile phase offered the best selectivity and was taken as the optimum value. A 30% acetonitrile concentration was used since it provided maximum separation and reasonable analysis time.

The described chromatographic method could be extended to include other degradation products of penicillin. The four compounds studied were selected primarily for two reasons: (*a*) penicilloic acid, penillic acid, and penilloic acid are of prime importance in stability studies since they are major decomposition products of penicillin in acidic and basic media, and (*b*) since penicillin and penilloic acid are monocarboxylic acids, and penicilloic and penillic acids are dicarboxylic acids, a detailed study of their behavior in ion-pair reversed-phase chromatography could assist in the application of this analytical method for other degradation products of penicillin and similar compounds of pharmaceutical interest.

REFERENCES

(1) S. G. Pan, *Anal. Chem.*, **25,** 1438 (1954).

(2) A. H. Thomas and R. A. Broadridge, *Analyst*, **95,** 459 (1970).

(3) J. Birner, *J. Pharm. Sci.*, **59,** 757 (1970).

(4) P. E. Manni, R. A. Lipper, J. M. Blaha, and S. L. Hem, *J. Chromatogr.*, **76,** 512 (1973).

(5) J. M. Blaha, A. M. Knevel, and S. L. Hem, *J. Pharm. Sci.*, **64,** 1384 (1975).

(6) W. A. Vadino, E. T. Sugita, R. L. Schnaare, H. V. Ando, and P. J. Niebergall, *ibid.*, **68,** 1316 (1979).

(7) J. P. Degelaen, S. L. Loukas, J. Feeney, G. C. K. Roberts, and A. S. V. Burgen, *J. Chem. Soc. Perkin II*, **1979,** 86.

(8) E. R. White, M. A. Carroll, J. E. Zarembo, and A. D. Bender, *J. Antibiot.*, **28,** 205 (1975).

(9) E. R. White, M. A. Carroll, and J. E. Zarembo, *ibid.*, **30,** 811 (1977).

(10) "The Chemistry of Penicillin," H. T. Clark, J. R. Johnson, and R. Robinson, Eds., Princeton University Press, Princeton, N.J., 1949.

(11) P. Finholt, G. Jurgensen, and H. Kristiansen, *J. Pharm. Sci.*, **54,** 387 (1965).

(12) F. Salto, J. G. Prieto, and M. T. Alemany, *ibid.*, **69,** 501 (1980).

(13) L. R. Snyder and J. J. Kirkland, "Introduction to Modern Liquid Chromatography," 2nd ed., Wiley, New York, N.Y., 1979, p. 468.

(14) "Antibiotics II," H. W. Florey et al., Eds., Oxford University Press, London, England, 1949.

ACKNOWLEDGMENTS

Supported in part by the Purdue Research Foundation and the Biomedical Research Support Grant S07 RR 05586-11.

Interaction of Theobromine with Sodium Benzoate

JUZIRO NISHIJO ˣ and IKUKO YONETANI

Received March 30, 1981, from the *Kobe Women's College of Pharmacy, Motoyama-Kitamachi, Higashinada-ku, Kobe 658, Japan.* Accepted for publication June 22, 1981.

Abstract □ The interaction of theobromine with sodium benzoate was investigated by PMR spectroscopy. The interaction of theobromine with pentadeuterated benzoic acid (benzoic acid-d_5) was examined in the same manner but to a lesser degree. Chemical shifts of theobromine protons were determined as a function of sodium benzoate concentration in deuterium oxide at 30 and 15°. Signals of both methyl groups of theobromine underwent significant upfield shifts when sodium benzoate was added to a theobromine solution. This fact suggests that a complex is formed by vertical stacking or plane-to-plane stacking. The same results were obtained for benzoic acid-d_5.

Keyphrases □ Theobromine—interaction with sodium benzoate □ Sodium benzoate—interaction with theobromine □ Diuretics—theobromine, interaction with sodium benzoate

Xanthine derivatives such as theophylline and caffeine form a 1:1 complex with sodium benzoate in aqueous solution. The physicochemical properties relating to this complex formation were studied by various methods including calorimetry (1), a solubility method (2), and by PMR spectroscopy (^{1}H-NMR) (3, 4). In the present study, the interaction of theobromine(I), a xanthine derivative, with either sodium benzoate(II) or pentadeuterated benzoic acid (benzoic acid-d_5)(III) was studied by ^{1}H-NMR in deuterium oxide.

EXPERIMENTAL

Materials—Reagent grade theobromine[1] and sodium benzoate JP were used without further purification. Benzoic acid-d_5 (>99.0% pure) and deuterium oxide (99.8%) were used as received[2].

Methods—To examine whether self-association of theobromine takes place, 1.9×10^{-4}–2.6×10^{-3} *M* theobromine was prepared. The concentration of theobromine was maintained constant while that of benzoic acid-d_5 was varied from 1.0×10^{-3} to 3.0×10^{-2} *M* and that of sodium benzoate varied from zero to 1 *M*. ^{1}H-NMR spectra were recorded[3] in duplicate at probe temperatures of 30 ± 0.5° or 15 ± 0.5°. External tetramethylsilane was used as the reference and as the source of a lock signal[4].

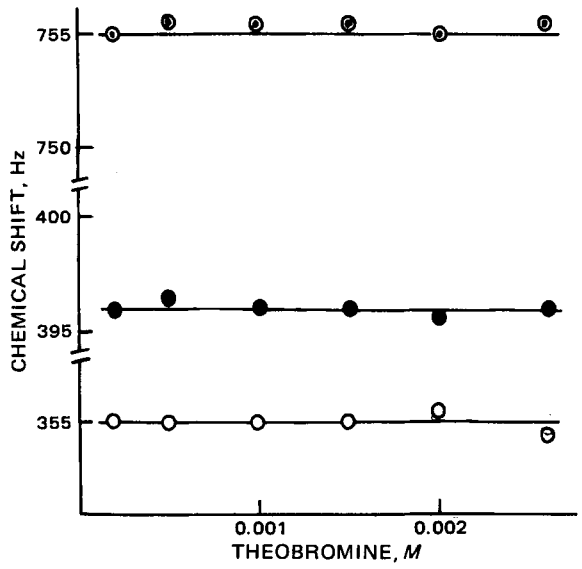

Figure 1—*Concentration dependence of theobromine proton chemical shifts. Key:* ⊙, *8-H;* ●, *7-CH_3; and* ○, *3-CH_3.*

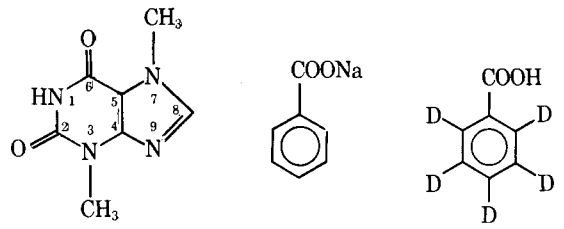

I II III

Bulk susceptibility corrections were tried, but it was found that they were not necessary. In the theobromine-sodium benzoate system, the corrections were too small in comparison with the large induced chemical shift changes due to complexation (4) and in the theobromine-benzoic acid-d_5 system and the study of theobromine self-asasociation, the volume magnetic susceptibilities of the samples were equal to deuterium oxide for the low concentrations of theobromine and benzoic acid-d_5. Chemical shifts were reproducible to better than 0.5 Hz.

RESULTS AND DISCUSSION

The ^{1}H-NMR spectrum of the 1.5×10^{-3} *M* deuterium oxide solution of theobromine has three signals of relative intensities 1:3:3, at 8.36, 4.40, and 3.94 ppm (from external tetramethylsilane), corresponding to the proton at C-8 and to the 7- and 3-methyl protons, respectively, at 30°. The self-associations of theophylline (5) and caffeine (6) in aqueous solution is known, but theobromine self-association has not been reported.

Initially, ^{1}H-NMR spectra of theobromine in deuterium oxide were recorded at 30°. The results (Fig. 1), show that none of the theobromine proton chemical shifts changed regardless of the theobromine concentration and, therefore, no theobromine self-association appears to occur

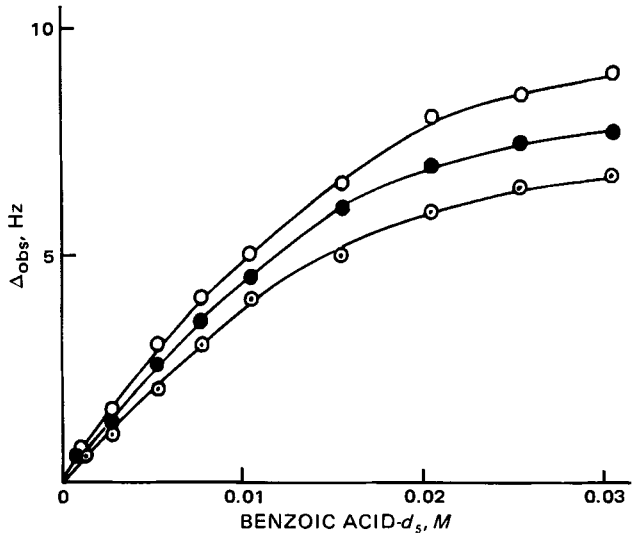

Figure 2—*Induced chemical shift changes for theobromine protons as a function of benzoic acid-*d_5. *Key:* ○, *3-CH_3;* ●, *7-CH_3; and* ⊙, *8-H.*

[1] Tokyo Kasei Kogyo Co., Ltd.
[2] Merck, West Germany.
[3] Nichiden-Varian type NV-21 spectrometer, 90 MHz, FT mode.

0022-3549/82/0300-0354$01.00/0

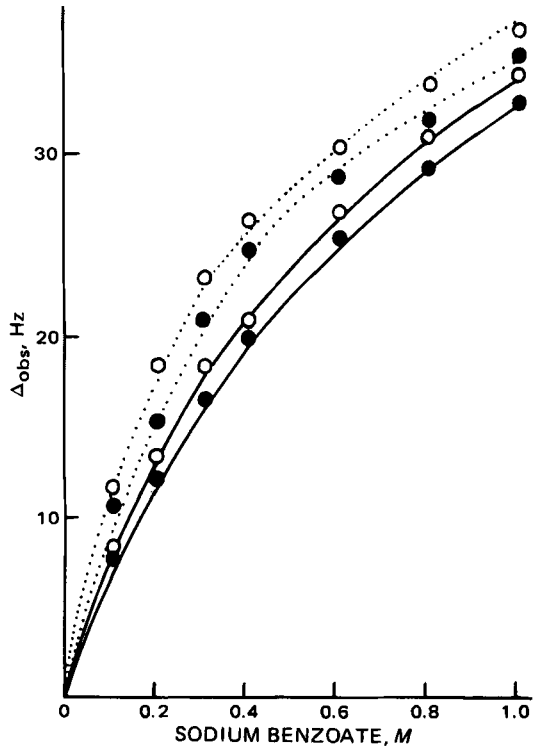

Figure 3—*Induced chemical shift changes for theobromine protons as a function of sodium benzoate concentration. Key: —, 30°; . . ., 15°; ○, 3-CH_3; and ●, 7-CH_3.*

within the concentration range examined. Because of poor theobromine solubility in water, it is thought that theobromine molecules exist mostly in a monomer state.

^{1}H-NMR spectra of the solution containing both theobromine in a fixed concentration of 1.5×10^{-3} *M* benzoic acid-d_5 at various concentrations were recorded at 30°. Signals for the proton at C-8, and the 7- and 3-methyl protons of theobromine, shifted upfield with an increase in the benzoic acid-d_5 concentration. The extent of the upfield shift of the 3-methyl protons was larger than that of the 7-methyl protons and that of the 7-methyl protons was larger than that of the proton at C-8 (Fig. 2).

The upfield shifts of the 3- and 7-methyl signal, and the proton signal at C-8 in the presence of benzoic acid-d_5 suggest that theobromine and benzoic acid form a complex in which the 3- and 7-methyl groups, and the C-8 proton in the theobromine molecule are located over the benzene ring of benzoic acid. The relative small upfield shift of the C-8 proton signal may be caused by compensation with a downfield shift, resulting from the addition of a proton arising from benzoic acid-d_5 to nitrogen at the 9 position of theobromine. However, the addition of a proton seems to occur very sparingly because benzoic acid is weakly acidic with a pKa of 4.19 (7) at 25°. The pKa assigned to nitrogen at the 9-position of theobromine is 0.45 (8) at 18°.

To confirm this theory, the pH of an aqueous solution of 1.5×10^{-3} *M* theobromine was measured at 18° in the presence of 2.0×10^{-2} *M* benzoic acid. Using this value (pH 3.05), theobromine and protonated theobromine were in a molar ratio of 500:1 and the theory was proven valid. Consequently, the 3-methyl protons are nearer the axis of the benzene ring than the 7-methyl protons, which in turn are nearer the axis than the C-8 proton.

^{1}H-NMR spectra of the solution containing both 1.5×10^{-3} *M* theobromine and sodium benzoate at various concentrations were measured (Fig. 3). The signals of the 3- and 7-methyl protons shifted upfield with an increase in the sodium benzoate concentration, the extent of the upfield shift of the 3-methyl protons being slightly larger than that of the 7-methyl protons. The signal of the proton at C-8 could not be measured because of the overlap with the signals of benzene protons of sodium benzoate. These results suggest that the formation of a complex between theoxyline and benzoic acid or sodium benzoate involves vertical stacking or plane-to-plane stacking. It was similarly reported (4) that theobromine interacts with sodium benzoate to form a complex by vertical stacking or plane-to-plane stacking.

Table I—Apparent Thermodynamic Parameters for Complex Formation of Theobromine with Sodium Benzoate in Deuterium Oxide

Parameter	15°		30°
K, M^{-1}	2.6[a]		1.4[a]
ΔG, kcal/mole	−0.55		−0.20
ΔH, kcal/mole		−7.1	
ΔS, kcal/mole degree	0.023		0.023

[a] Average value calculated from 3-CH_3 and 7-CH_3 of theobromine.

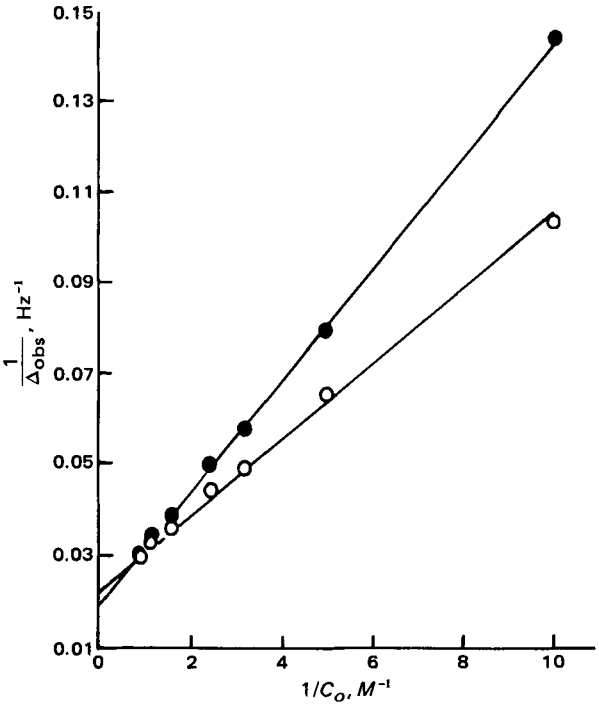

Figure 4—*Plots of theobromine 7-CH_3 versus $C_b{}^{-1}$ of sodium benzoate. Key: ●, 30°; and ○, 15°.*

Following an earlier procedure (9), the apparent formation constant *K* was calculated using Eq. 1, assuming a 1:1 complex:

When $C_b \gg C_a$

$$\frac{1}{\Delta_{obs}} = \frac{1}{K(\delta_c - \delta_a)} + \frac{1}{\delta_c - \delta_a} \qquad \text{(Eq. 1)}$$

where:

K = apparent formation constant
C_a = theobromine concentration
C_b = sodium benzoate concentration
δ_c = chemical shift of theobromine proton in the complex form
δ_a = chemical shift of theobromine proton in the uncomplex form
Δ_{obs} = the difference between the observed chemical shift and δa

The results are shown in Fig. 4 and the apparent formation constant is listed in Table I. The results of the interaction of theobromine with sodium benzoate at 15 and 30° are shown in Figs. 3 and 4 and Table I. As the apparent formation constant *K* was varied depending on temperature, the enthalpy change of complex formation (ΔH), the free energy change (ΔG), and the entropy change (ΔS) were calculated (Table I).

It was concluded that the complex formation of theobromine with sodium benzoate is an exothermic reaction accompanied by reduction of entropy.

REFERENCES

(1) P. Rohdenwald and M. Baumeister, *J. Pharm. Pharmacol.*, **21**, 861 (1969).

(2) T. Higuchi and D. A. Lach, *J. Am. Pharm. Assoc., Sci. Ed.*, **43**, 524 (1954).

(3) H. Stamm, *Arch. Pharm.*, **302**, 174 (1969).

(4) A. L. Thakkar and L. G. Tensmeyer, *J. Pharm. Sci.*, **63**, 1319 (1974).
(5) A. L. Thakkar, L. G. Tensmeyer, and W. L. Wilham, *Chem. Commun.*, **1970**, 524.
(6) A. L. Thakkar, L. G. Tensmeyer, and W. L. Wilham, *J. Pharm. Sci.*, **60**, 1267 (1971).
(7) "Merck Index," 9th ed., M. Windholz, Ed., 1976, p. 142.
(8) *Ibid.*, p. 1195.
(9) M. W. Hanna and A. L. Ashbaugh, *J. Phys. Chem.*, **68**, 811 (1961).

ACKNOWLEDGMENTS

The authors thank Dr. M. Sugiura for ^{1}H-NMR measurements.

Antileukemic Activity of Tetrazole Analogs of Phenylalanine Derivatives

C. M. DARLING

Received February 18, 1981, from the *Auburn University School of Pharmacy, Department of Pharmacal Sciences, Auburn, AL 36849.* Accepted for publication June 9, 1981.

Abstract □ Eleven tetrazole analogs of substituted phenylalanines were prepared and tested for antitumor activity using P-388 lymphocytic leukemia cells in mice. None of the compounds exhibited significant activity (T/C %, < 125).

Keyphrases □ Antileukemic activity—tetrazole analogs of substituted phenylalanines against P-388 lymphocytic leukemia □ Phenylalanines, substituted—tetrazole analogs, preparation and screening for antileukemic activity □ Tetrazole—analogs of substituted phenylalanines, preparation and screening for antileukemic activity

The demand for nutrients differs between tumor cells and normal cells (1). Since rapidly proliferating cancer cells take up nutrients more rapidly, they may be selectively "starved" by substituting nonfunctional amino acid derivatives for the normal substrate. *N*-Chloroacetyl derivatives of *para*-substituted phenylalanines were reported (2) to have significant growth inhibitory activity in a microbial antitumor prescreen.

Recent reviews (3, 4) indicated that no reports have appeared for testing tetrazole analogs of amino acids for antineoplastic activity. Studies of the biological activity of 5-substituted tetrazoles have been prompted by a close similarity between the acidity of the tetrazole group and the carboxylic acid group, and the fact that the tetrazole function appears to be metabolically more stable (3).

The chemically similar tetrazole ring system (5) has been used to replace the carboxyl group in several amino acids (6–8). These *in vitro* studies suggested that the tetrazole analog may serve as substrate inhibitor of the respective amino acid in certain enzymatic reactions. The purpose of this study was to determine whether tetrazole analogs of certain phenylalanine derivatives would exhibit antileukemic action in mice.

Table I—Aryl-Substituted Ethyl 2-Acetamido-2-cyano-3-phenylpropanoates

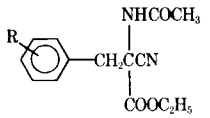

Compound	R	Melting Point	Yield, %	Formula	Analysis, %	Calc.	Found
					C	60.43	61.07
I	2F	94–96°	65.8	$C_{14}H_{15}FN_2O_3$	H	5.43	5.51
					N	10.07	10.07
					C	58.35	58.46
II[a]	2Cl	145–8°	28.6	$C_{15}H_{17}ClN_2O_3$	H	5.55	5.61
					N	9.07	9.04
					C	49.57	49.63
III	2Br	150–152°	68.7	$C_{14}H_{15}BrN_2O_3$	H	4.46	4.51
					N	8.26	8.24
					C	43.54	43.61
IV	2I	174–176°	67.5	$C_{14}H_{15}IN_2O_3$	H	3.92	3.96
					N	7.25	7.23
					C	62.06	62.12
V	$2OCH_3$	142–144°	92.8	$C_{15}H_{18}N_2O_4$	H	6.25	6.31
					N	9.65	9.67
					C	62.06	62.01
VI	$4OCH_3$	164–167°	57.1	$C_{15}H_{18}N_2O_4$	H	6.25	6.29
					N	9.65	9.63
					C	49.57	49.41
VII	4Br	165–168°	62.7	$C_{14}H_{15}BrN_2O_3$	H	4.46	4.52
					N	8.26	8.24

[a] Isopropyl ester (the analytical sample was inadvertently recrystallized from isopropyl alcohol resulting in transesterification).

0022-3549/82/0300-0356$01.00/0

(4) A. L. Thakkar and L. G. Tensmeyer, *J. Pharm. Sci.*, **63**, 1319 (1974).
(5) A. L. Thakkar, L. G. Tensmeyer, and W. L. Wilham, *Chem. Commun.*, **1970**, 524.
(6) A. L. Thakkar, L. G. Tensmeyer, and W. L. Wilham, *J. Pharm. Sci.*, **60**, 1267 (1971).
(7) "Merck Index," 9th ed., M. Windholz, Ed., 1976, p. 142.
(8) *Ibid.*, p. 1195.
(9) M. W. Hanna and A. L. Ashbaugh, *J. Phys. Chem.*, **68**, 811 (1961).

ACKNOWLEDGMENTS

The authors thank Dr. M. Sugiura for ^{1}H-NMR measurements.

Antileukemic Activity of Tetrazole Analogs of Phenylalanine Derivatives

C. M. DARLING

Received February 18, 1981, from the *Auburn University School of Pharmacy, Department of Pharmacal Sciences, Auburn, AL 36849.* Accepted for publication June 9, 1981.

Abstract □ Eleven tetrazole analogs of substituted phenylalanines were prepared and tested for antitumor activity using P-388 lymphocytic leukemia cells in mice. None of the compounds exhibited significant activity (T/C %, < 125).

Keyphrases □ Antileukemic activity—tetrazole analogs of substituted phenylalanines against P-388 lymphocytic leukemia □ Phenylalanines, substituted—tetrazole analogs, preparation and screening for antileukemic activity □ Tetrazole—analogs of substituted phenylalanines, preparation and screening for antileukemic activity

The demand for nutrients differs between tumor cells and normal cells (1). Since rapidly proliferating cancer cells take up nutrients more rapidly, they may be selectively "starved" by substituting nonfunctional amino acid derivatives for the normal substrate. *N*-Chloroacetyl derivatives of *para*-substituted phenylalanines were reported (2) to have significant growth inhibitory activity in a microbial antitumor prescreen.

Recent reviews (3, 4) indicated that no reports have appeared for testing tetrazole analogs of amino acids for antineoplastic activity. Studies of the biological activity of 5-substituted tetrazoles have been prompted by a close similarity between the acidity of the tetrazole group and the carboxylic acid group, and the fact that the tetrazole function appears to be metabolically more stable (3).

The chemically similar tetrazole ring system (5) has been used to replace the carboxyl group in several amino acids (6–8). These *in vitro* studies suggested that the tetrazole analog may serve as substrate inhibitor of the respective amino acid in certain enzymatic reactions. The purpose of this study was to determine whether tetrazole analogs of certain phenylalanine derivatives would exhibit antileukemic action in mice.

Table I—Aryl-Substituted Ethyl 2-Acetamido-2-cyano-3-phenylpropanoates

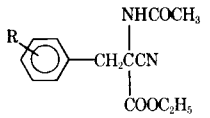

Compound	R	Melting Point	Yield, %	Formula	Analysis, %	Calc.	Found
					C	60.43	61.07
I	2F	94–96°	65.8	$C_{14}H_{15}FN_2O_3$	H	5.43	5.51
					N	10.07	10.07
					C	58.35	58.46
II[a]	2Cl	145–8°	28.6	$C_{15}H_{17}ClN_2O_3$	H	5.55	5.61
					N	9.07	9.04
					C	49.57	49.63
III	2Br	150–152°	68.7	$C_{14}H_{15}BrN_2O_3$	H	4.46	4.51
					N	8.26	8.24
					C	43.54	43.61
IV	2I	174–176°	67.5	$C_{14}H_{15}IN_2O_3$	H	3.92	3.96
					N	7.25	7.23
					C	62.06	62.12
V	$2OCH_3$	142–144°	92.8	$C_{15}H_{18}N_2O_4$	H	6.25	6.31
					N	9.65	9.67
					C	62.06	62.01
VI	$4OCH_3$	164–167°	57.1	$C_{15}H_{18}N_2O_4$	H	6.25	6.29
					N	9.65	9.63
					C	49.57	49.41
VII	4Br	165–168°	62.7	$C_{14}H_{15}BrN_2O_3$	H	4.46	4.52
					N	8.26	8.24

[a] Isopropyl ester (the analytical sample was inadvertently recrystallized from isopropyl alcohol resulting in transesterification).

0022-3549/82/0300-0356$01.00/0

Table II—Aryl-Substituted Ethyl 1-Acetamido-1-tetrazol-5-yl-2-phenylpropanoates

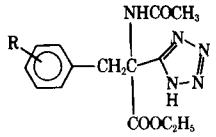

Compound	R	Melting Point	Yield, %	Formula	Analysis, %	
					Calc.	Found
VIII	2F	131–133°	9.6	$C_{14}H_{16}FN_5O_3 \cdot \frac{1}{2}H_2O$	C 50.91 H 5.19 N 21.20	51.20 4.99 21.35
IX	2Cl	65–68°	79.3	$C_{14}H_{16}ClN_5O_3$	C 49.78 H 4.77 N 20.73	49.71 4.94 20.53
X	2Br	71–74°	63.3	$C_{14}H_{16}BrN_5O_3$	C 43.99 H 4.22 N 18.32	43.74 5.25 16.13
XI	2I	163–165°	52.2	$C_{14}H_{16}IN_5O_3$	C 39.18 H 3.76 N 16.32	38.50 3.83 16.18
XII	$2OCH_3$	95–100°	30.0	$C_{15}H_{19}N_5O_4$	C 54.05 H 5.75 N 21.01	53.29 5.97 20.76
XIII	$4OCH_3$	100–102°	17.2	$C_{15}H_{19}N_5O_4 \cdot H_2O$	C 51.28 H 6.02 N 19.93	51.19 6.00 20.16
XIV	4Br	90–92°	63.7	$C_{14}H_{16}BrN_5O_3 \cdot H_2O$	C 42.01 H 4.53 N 17.50	41.87 4.57 17.52

Table III—Aryl-Substituted 5-(1-Amino-2-phenylethyl)tetrazoles

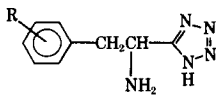

Compound[a]	R	Melting[b] Point	Yield, %	Formula	Analysis, %	
					Calc.	Found
XV	2F	270°	46.5	$C_9H_{10}FN_5$	C 52.17 H 4.86 N 33.80	51.91 4.92 33.68
XVI	2Cl	284°	34.7	$C_9H_{10}ClN_5$	C 48.33 H 4.51 N 31.31	48.34 4.53 31.26
XVII	2Br	273°	62.3	$C_9H_{10}BrN_5$	C 40.32 H 3.76 N 26.12	40.51 3.43 26.26
XVIII	2I	270°	62.2	$C_9H_{10}IN_5$	C 34.30 H 3.20 N 22.22	34.46 2.92 22.27
XIX	$2OCH_3$	280°	26.1	$C_{10}H_{13}N_5O$	C 54.78 H 5.98 N 31.94	54.69 5.99 31.91
XX	$4OCH_3$	280°	26.3	$C_{10}H_{13}N_5O$	C 54.78 H 5.98 N 31.94	54.81 5.63 32.15
XXI	4OH	290°	76.6	$C_9H_{11}N_5O \cdot \frac{1}{2}H_2O$	C 50.46 H 5.65 N 32.69	49.91 5.43 32.58
XXII	4Br	269°	70.7	$C_9H_{10}BrN_5$	C 40.32 H 3.76 N 26.12	40.19 3.79 26.16
XXIII	3F[c]				—	—
XXIV	4Cl[c]				—	—
XXV	$4CH_3$[c]				—	—

[a] All racemates. [b] All compounds melted with decomposition. [c] Reference 6.

EXPERIMENTAL[1]

Aryl-substituted Ethyl 2-Acetamido-2-cyano-3-phenylpropanoates (I–VII)—A previously reported method (6) was used to prepare intermediates I–VII. Physical and chemical data are shown in Table I.

NMR data agreed with the proposed structures. The NMR spectra (dimethyl sulfoxide-d_6, tetramethylsilane internal standard) showed the following common absorption peaks: δ 1.00–1.20 (t, 3H, CCH_3), 1.90–2.10 (s, 3H, $COCH_3$), 3.35–3.55 (s, 2H, aryl CH_2C), 4.00–4.20 (q, 2H, OCH_2C), and 7.10–7.90 (4H, the pattern varied depending on the ring substituent) ppm. Each spectrum integrated for the correct number of protons. The spectra of V and VI exhibited an additional absorption peak at δ 3.70 (s, 3H, OCH_3). The isopropyl ester of II showed absorption peaks for isopropyl at δ 1.10 [m, 6H, $C(CH_3)_2$] and 4.90 (m, 1H, CH) ppm.

Aryl-substituted Ethyl 1-Acetamido-1-tetrazol-5-yl-2-phenylpropanoates (VIII–XIV)—Intermediates VIII–XIV were prepared

[1] Elemental analyses were performed by Atlantic Microlab, Atlanta, Ga. NMR data were recorded on a Varian T-60A spectrophotometer. Melting points were taken in open capillary tubes and are uncorrected.

using a previous procedure (6) and Table II lists their physical and chemical data.

In agreement with the proposed structures, the NMR data exhibited the common absorption peaks (dimethyl sulfoxide-d_6, tetramethylsilane internal standard): δ 1.10–1.20 (t, 3H, CCH_3), 1.90–2.00 (s, 3H, $COCH_3$), 3.65–3.85 (s, 2H, aryl CH_2C), 4.10–4.20 (q, 2H, OCH_2C), and 6.80–7.30 (m,4H, aromatic) ppm. The spectra of XII and XIII showed a singlet at δ 3.60 ppm that integrated for 5 protons (aryl CH_2 and aryl OCH_3).

Aryl-substituted 5-(1-Amino-2-phenylethyl)tetrazoles XV–XXII)—Compounds XV–XX and XXII were prepared by a previously reported method (6). Compound XXI was prepared by modification of a previously reported method (9). A mixture of compound XX (3.0 g, 0.014 mole) in 48% hydrogen bromide (50 ml) was heated at reflux under nitrogen for 4 hr. The mixture was concentrated under reduced pressure. The residue was dissolved in distilled water and the pH was adjusted to 7 with concentrated ammonium hydroxide. After standing at room temperature for 12 hr, the product was filtered, air dried, and recrystallized from *N,N*-dimethylformamide, 2.2 g (76.6%), mp 290° dec. Table III contains physical and chemical data for XV–XXII.

Assignments of the common NMR absorption peaks are (10% sodium deuteroxide): δ 2.95–3.10 (m, 2H, aryl CH_2), 4.30–4.50 (m, 1H, CCH), and 6.70–7.20 (m, 4H, aromatic) ppm. There was an additional absorption peak for XIX and XX at δ 3.40 (s, 3H, aryl OCH_3) ppm.

Anticancer Screening—The tetrazole analogs of substituted phenylalanines were screened for anticancer activity[2] using P-388 lymphocytic leukemia cells in mice of either sex. On day zero, mice were inoculated intraperitoneally with 10^6 leukemic cells. Twenty-four hours later, a test compound was administered intraperitoneally once daily for the first 9 days or in three injections on every 4th day (XVI, XXIII). The test results were recorded on the 30th day.

[2] Developmental Therapeutics Program, Division of Cancer Treatment, National Cancer Institute, Silver Spring, MD 20910.

RESULTS AND DISCUSSIONS

All compounds were tested for antileukemic activity at doses of 25, 50, 100, and 200 mg/kg (some in triplicate). For compounds XVI, XVIII, and XIX, the T/C% was near or greater than 125. For all other compounds, the T/C% was < 125 (all mice died when compounds XX and XXIII were administered at 200 mg/kg). Compounds XVI, XVIII, and XIX were retested at 400 mg/kg (in duplicate) and exhibited a T/C% < 125. None of the compounds exhibited significant antileukemic activity.

REFERENCES

(1) S. C. Harvey, in "Remington's Pharmaceutical Sciences," A. Osol, Ed., 16th ed., Mack Publishing, Easton, Pa., 1980, p. 1081.
(2) T. T. Otani and M. R. Briley, *J. Pharm. Sci.*, **70,** 464 (1981).
(3) R. N. Butler, *Adv. Heterocycl. Chem.*, **21,** 323 (1977).
(4) H. Singh, A. S. Chawla, V. K. Kapoor, D. Paul, and R. K. Malhotra, *Prog. Med. Chem.*, **17,** 151 (1980).
(5) F. R. Benson, *Chem. Rev.*, **41,** 1 (1947).
(6) H. R. McNeil, B. B. Williams, Jr., and C. M. Darling, *J. Pharm. Sci.*, **66,** 1642 (1977).
(7) J. M. McManus and R. M. Herbst, *J. Org. Chem.*, **24,** 1643 (1959).
(8) J. K. Elwood, R. M. Herbst, and G. L. Kilgour, *J. Biol. Chem.*, **240,** 2073 (1965).
(9) J. G. Cannon, G. J. Hatheway, J. P. Long, and F. M. Sharabi, *J. Med. Chem.*, **19,** 987 (1976).

Analysis of Commercial Pilocarpine Preparations by High-Performance Liquid Chromatography

MICHAEL V. DRAKE ˣ, JAMES J. O'DONNELL, and ROBERT P. SANDMAN

Received May 11, 1981, from the *Department of Ophthalmology, University of California, San Francisco, CA 94143.* Accepted for publication July 15, 1981.

Abstract □ Pilocarpine, isopilocarpine, pilocarpic acid, and isopilocarpic acid can be measured effectively by high-performance liquid chromatography (HPLC). Previous reports have differed on the degree of contamination of commercial pilocarpine preparations with isopilocarpine and pilocarpic acid. This report describes a study of commercial pilocarpine in which no significant contamination was found.

Keyphrases □ Pilocarpine—analysis of commercial preparations by high-performance liquid chromatography □ High-performance liquid chromatography—analysis of commercial pilocarpine □ Ocular agents—pilocarpine, analysis by high-performance liquid chromatography

Several assays have been reported for pilocarpine, isopilocarpine, pilocarpic acid, and isopilocarpic acid using high-pressure liquid chromatography (HPLC) (1–4). The earliest of these reports includes the results of a study done on commercial pilocarpine samples, which showed that in one case, contamination with isopilocarpine was as high as 25% (1). An effort to corroborate this study failed, due to technical difficulties (2). Modifications of the original HPLC method were used in a recent study of commercial pilocarpine preparations and no significant contamination with the isopilocarpine isomer or the degradation products, pilocarpic acid or isopilocarpic acid, was found (5). The present report describes a similar study.

EXPERIMENTAL

Each locally available commercial pilocarpine preparation was obtained through prescription from a retail pharmacy. Letters were sent to all other manufacturers[1] of pilocarpine asking for a 1% sample of their product to be used for animal experimentation. Nine fresh samples of pilocarpine were obtained. Each sample was diluted with HPLC grade water to a concentration of 0.10%. Pilocarpine hydrochloride[2] and isopilocarpine hydrochloride[3] standards were obtained commercially in powder form. Pilocarpic acid and isopilocarpic acid were prepared by the hydrolysis of pilocarpine and isopilocarpine in 0.1 *N* NaOH, respectively. These were diluted to make 0.10% standard solutions.

The mobile phase was prepared by dissolving 50 g of monobasic potassium phosphate in a solution of 900 ml of water and 30 ml of methanol. The solution pH was adjusted to 2.5 with 85% phosphoric acid, and the total volume was brought to 1 liter with water. Separation was achieved by isocratic reversed-phase chromatography[4] on an RP-C18 10μm column[5], (flow rate 1.5 ml/min) at ambient temperature. Detection was by optical absorbance at 216 nm[6]. Peak heights of standard preparations were compared with peak heights of the unknown commercial prepara-

[1] Listed in the "Pharmaceutical Drug Topic Redbook" (6) as of January 1979.
[2] Mallinckrodt, St. Louis, Mo.
[3] Aldrich, Milwaukee, Wis.
[4] Model 310 high-performance liquid chromatograph, Altex Scientific, Berkeley, Calif.
[5] Lichrosorb RP-C18 (10 μm) in 4.6 × 250-mm column, Altex Scientific, Berkeley, Calif.
[6] Model 785 variable-wavelength detector, Micromeritics Instrument Corp., Norcross, Va.

0022-3549/82/0300-0358$01.00/0

using a previous procedure (6) and Table II lists their physical and chemical data.

In agreement with the proposed structures, the NMR data exhibited the common absorption peaks (dimethyl sulfoxide-d_6, tetramethylsilane internal standard): δ 1.10–1.20 (t, 3H, CCH_3), 1.90–2.00 (s, 3H, $COCH_3$), 3.65–3.85 (s, 2H, aryl CH_2C), 4.10–4.20 (q, 2H, OCH_2C), and 6.80–7.30 (m,4H, aromatic) ppm. The spectra of XII and XIII showed a singlet at δ 3.60 ppm that integrated for 5 protons (aryl CH_2 and aryl OCH_3).

Aryl-substituted 5-(1-Amino-2-phenylethyl)tetrazoles XV–XXII)—Compounds XV–XX and XXII were prepared by a previously reported method (6). Compound XXI was prepared by modification of a previously reported method (9). A mixture of compound XX (3.0 g, 0.014 mole) in 48% hydrogen bromide (50 ml) was heated at reflux under nitrogen for 4 hr. The mixture was concentrated under reduced pressure. The residue was dissolved in distilled water and the pH was adjusted to 7 with concentrated ammonium hydroxide. After standing at room temperature for 12 hr, the product was filtered, air dried, and recrystallized from *N,N*-dimethylformamide, 2.2 g (76.6%), mp 290° dec. Table III contains physical and chemical data for XV–XXII.

Assignments of the common NMR absorption peaks are (10% sodium deuteroxide): δ 2.95–3.10 (m, 2H, aryl CH_2), 4.30–4.50 (m, 1H, CCH), and 6.70–7.20 (m, 4H, aromatic) ppm. There was an additional absorption peak for XIX and XX at δ 3.40 (s, 3H, aryl OCH_3) ppm.

Anticancer Screening—The tetrazole analogs of substituted phenylalanines were screened for anticancer activity[2] using P-388 lymphocytic leukemia cells in mice of either sex. On day zero, mice were inoculated intraperitoneally with 10^6 leukemic cells. Twenty-four hours later, a test compound was administered intraperitoneally once daily for the first 9 days or in three injections on every 4th day (XVI, XXIII). The test results were recorded on the 30th day.

[2] Developmental Therapeutics Program, Division of Cancer Treatment, National Cancer Institute, Silver Spring, MD 20910.

RESULTS AND DISCUSSIONS

All compounds were tested for antileukemic activity at doses of 25, 50, 100, and 200 mg/kg (some in triplicate). For compounds XVI, XVIII, and XIX, the T/C% was near or greater than 125. For all other compounds, the T/C% was < 125 (all mice died when compounds XX and XXIII were administered at 200 mg/kg). Compounds XVI, XVIII, and XIX were retested at 400 mg/kg (in duplicate) and exhibited a T/C% < 125. None of the compounds exhibited significant antileukemic activity.

REFERENCES

(1) S. C. Harvey, in "Remington's Pharmaceutical Sciences," A. Osol, Ed., 16th ed., Mack Publishing, Easton, Pa., 1980, p. 1081.
(2) T. T. Otani and M. R. Briley, *J. Pharm. Sci.*, **70,** 464 (1981).
(3) R. N. Butler, *Adv. Heterocycl. Chem.*, **21,** 323 (1977).
(4) H. Singh, A. S. Chawla, V. K. Kapoor, D. Paul, and R. K. Malhotra, *Prog. Med. Chem.*, **17,** 151 (1980).
(5) F. R. Benson, *Chem. Rev.*, **41,** 1 (1947).
(6) H. R. McNeil, B. B. Williams, Jr., and C. M. Darling, *J. Pharm. Sci.*, **66,** 1642 (1977).
(7) J. M. McManus and R. M. Herbst, *J. Org. Chem.*, **24,** 1643 (1959).
(8) J. K. Elwood, R. M. Herbst, and G. L. Kilgour, *J. Biol. Chem.*, **240,** 2073 (1965).
(9) J. G. Cannon, G. J. Hatheway, J. P. Long, and F. M. Sharabi, *J. Med. Chem.*, **19,** 987 (1976).

Analysis of Commercial Pilocarpine Preparations by High-Performance Liquid Chromatography

MICHAEL V. DRAKE ˣ, JAMES J. O'DONNELL, and ROBERT P. SANDMAN

Received May 11, 1981, from the *Department of Ophthalmology, University of California, San Francisco, CA 94143.* Accepted for publication July 15, 1981.

Abstract □ Pilocarpine, isopilocarpine, pilocarpic acid, and isopilocarpic acid can be measured effectively by high-performance liquid chromatography (HPLC). Previous reports have differed on the degree of contamination of commercial pilocarpine preparations with isopilocarpine and pilocarpic acid. This report describes a study of commercial pilocarpine in which no significant contamination was found.

Keyphrases □ Pilocarpine—analysis of commercial preparations by high-performance liquid chromatography □ High-performance liquid chromatography—analysis of commercial pilocarpine □ Ocular agents—pilocarpine, analysis by high-performance liquid chromatography

Several assays have been reported for pilocarpine, isopilocarpine, pilocarpic acid, and isopilocarpic acid using high-pressure liquid chromatography (HPLC) (1–4). The earliest of these reports includes the results of a study done on commercial pilocarpine samples, which showed that in one case, contamination with isopilocarpine was as high as 25% (1). An effort to corroborate this study failed, due to technical difficulties (2). Modifications of the original HPLC method were used in a recent study of commercial pilocarpine preparations and no significant contamination with the isopilocarpine isomer or the degradation products, pilocarpic acid or isopilocarpic acid, was found (5). The present report describes a similar study.

EXPERIMENTAL

Each locally available commercial pilocarpine preparation was obtained through prescription from a retail pharmacy. Letters were sent to all other manufacturers[1] of pilocarpine asking for a 1% sample of their product to be used for animal experimentation. Nine fresh samples of pilocarpine were obtained. Each sample was diluted with HPLC grade water to a concentration of 0.10%. Pilocarpine hydrochloride[2] and isopilocarpine hydrochloride[3] standards were obtained commercially in powder form. Pilocarpic acid and isopilocarpic acid were prepared by the hydrolysis of pilocarpine and isopilocarpine in 0.1 *N* NaOH, respectively. These were diluted to make 0.10% standard solutions.

The mobile phase was prepared by dissolving 50 g of monobasic potassium phosphate in a solution of 900 ml of water and 30 ml of methanol. The solution pH was adjusted to 2.5 with 85% phosphoric acid, and the total volume was brought to 1 liter with water. Separation was achieved by isocratic reversed-phase chromatography[4] on an RP-C18 10μm column[5], (flow rate 1.5 ml/min) at ambient temperature. Detection was by optical absorbance at 216 nm[6]. Peak heights of standard preparations were compared with peak heights of the unknown commercial prepara-

[1] Listed in the "Pharmaceutical Drug Topic Redbook" (6) as of January 1979.
[2] Mallinckrodt, St. Louis, Mo.
[3] Aldrich, Milwaukee, Wis.
[4] Model 310 high-performance liquid chromatograph, Altex Scientific, Berkeley, Calif.
[5] Lichrosorb RP-C18 (10 μm) in 4.6 × 250-mm column, Altex Scientific, Berkeley, Calif.
[6] Model 785 variable-wavelength detector, Micromeritics Instrument Corp., Norcross, Va.

0022-3549/82/0300-0358$01.00/0

Table I—Commercial Pilocarpine Samples (1%) Compared with a Fresh Pilocarpine Standard

Sample	Percent of Labeled Amount of Pilocarpine Actually Found	Percent Isopilocarpine Found
1	100	1.1
2	99	2.6
3	100	5.5
4	95	5.7
5	101	4.9
6	105	4.0
7	104	1.1
8	102	0.9
9	98	—

tions. There was slight peak tailing; the minimum amount of isopilocarpine detectable in the presence of pilocarpine was 1 part in 100.

RESULTS AND DISCUSSION

Isopilocarpine eluted first at ~10 min followed by pilocarpine, pilocarpic acid, and isopilocarpic acid. The entire process was complete in 20 min. The concentration of pilocarpine found by HPLC analysis was within 5% of the concentration stated by the manufacturer on the label in all cases. The amount of isopilocarpine present ranged from 0.0 to 5.7% of the pilocarpine present (Table I). Pilocarpic acid or isopilocarpic acid were not found in significant quantities in any sample. These results agree with a recent study (5) and are in contrast to another report (1).

There are several possible explanations for the disagreement between this study and the earlier study (1). The official USP method for determining the purity of pilocarpine preparations at the time of the previous report did not effectively distinguish between pilocarpine and isopilocarpine (7). It is possible that pharmaceutical industry standards for purity of pilocarpine preparations have been modified such that they now exceed standards. Another possible explanation is that fresh samples of pilocarpine were used, and degradation products which would have appeared after prolonged storage were not present in these samples.

The results of this study and the study by Noordam *et al.* (5) illustrate the effectiveness of HPLC for pilocarpine assay. Because these newer methods are capable of providing more accurate analysis of pilocarpine than the current official USP method, it is reasonable to consider modifying the USP to reflect more current technology.

REFERENCES

(1) T. Urbanyi, A. Piedmont, E. Willis, and G. Manning, *J. Pharm. Sci.*, **65**, 257 (1976).

(2) J. D. Weber, *J. Assoc. Off. Anal. Chem.*, **59**, 1409 (1976).

(3) A. Noordam, K. Waliszewski, C. Olieman, L. Maat, and H. C. Beyerman, *J. Chromatogr.*, **153**, 271 (1978).

(4) J. J. O'Donnell, R. Sandman, and M. V. Drake, *J. Pharm. Sci.*, **69**, 1096 (1980).

(5) A. Noordam, L. Maat, and H. C. Beyerman, *ibid.*, **70**, 96 (1981).

(6) "Pharmaceutical Drug Topics Red Book," Medical Economics, Oradell, N.J., 1978.

(7) "The United States Pharmacopeia," 19th rev., Mack Publishing Co., Easton, Pa., 1975, pp. 384–386.

ACKNOWLEDGMENTS

Supported by National Eye Institute Grant Ey-02162 and by the UCSF Academic Senate Committee on Research, Research Grant 2-503302-37864.

Novel Method of Derivatization of an Amidinourea (Lidamidine) for GLC Analysis

C. M. WON ˣ, J. J. ZALIPSKY, D. M. PATEL, and W. M. GRIM

Received February 20, 1981, from the *Analytical & Physical Chemistry Department, Research & Development Division, William H. Rorer, Inc., Fort Washington, PA 19034.* Accepted for publication June 9, 1981.

Abstract □ A new quantitative GLC method for analysis of lidamidine hydrochloride (I) was developed. The method was based on derivatization of I to 1-(2,6-dimethylphenyl)-4-methylamino-dihydro-1,3,5-triazin-2-one (II) using dimethylformamide dimethylacetal reagent. Compound II was synthesized and characterized by IR, NMR, mass spectrometry, and elemental analysis. The assigned structure was in agreement with characterization analyses. Cyclization of I to a triazinone using dimethylformamide dimethylacetal reagent presented a new route for the preparation of II.

Keyphrases □ Lidamidine—derivatization to a triazinone for GLC analysis □ GLC—derivatization of lidamidine to a triazinone for GLC analysis □ Triazinones—derivatization of lidamidine for GLC analysis

The arylamidinoureas are a family of compounds pharmacologically active on the GI tract, and the cardiovascular and central nervous systems. They also demonstrate local anesthetic activity[1]. Among a series of substituted arylamidinoureas, lidamidine hydrochloride, *N*-(2,6 - dimethylphenyl) - *N'* - [imino(methylamino)methyl]urea hydrochloride (I), exhibited promising antidiarrheal activity. Extensive pharmacological, toxicological, and biochemical studies of I have been reported (1–6). The chemical synthesis (7), the hydrolysis kinetics, and the physical and chemical parameters of I were also reported (8).

Stability-indicating high-performance liquid chromatographic (HPLC) methods[1] were developed to analyze I quantitatively in the presence of impurities or hydrolysis products. A direct GLC method to quantitate I failed because of its low volatility and/or thermal instability. The separation of amidinoureas by the GLC method required derivatization of the functional groups. Derivatization attempts by conventional silylation and acylation methods were unsuccessful.

For the derivatization of primary amines, dimethylformamide dimethylacetal reagent is used to form the *N*-dimethylaminoethylene derivative (9). When substituted guanidines were derivatized by dimethylformamide dimethylacetal, the resultant *N*-dimethylaminoethylene derivative underwent further cyclization reactions to form

[1] William H. Rorer, Inc., internal communication.

0022-3549/82/0300-0359$01.00/0

Table I—Commercial Pilocarpine Samples (1%) Compared with a Fresh Pilocarpine Standard

Sample	Percent of Labeled Amount of Pilocarpine Actually Found	Percent Isopilocarpine Found
1	100	1.1
2	99	2.6
3	100	5.5
4	95	5.7
5	101	4.9
6	105	4.0
7	104	1.1
8	102	0.9
9	98	—

tions. There was slight peak tailing; the minimum amount of isopilocarpine detectable in the presence of pilocarpine was 1 part in 100.

RESULTS AND DISCUSSION

Isopilocarpine eluted first at ~10 min followed by pilocarpine, pilocarpic acid, and isopilocarpic acid. The entire process was complete in 20 min. The concentration of pilocarpine found by HPLC analysis was within 5% of the concentration stated by the manufacturer on the label in all cases. The amount of isopilocarpine present ranged from 0.0 to 5.7% of the pilocarpine present (Table I). Pilocarpic acid or isopilocarpic acid were not found in significant quantities in any sample. These results agree with a recent study (5) and are in contrast to another report (1).

There are several possible explanations for the disagreement between this study and the earlier study (1). The official USP method for determining the purity of pilocarpine preparations at the time of the previous report did not effectively distinguish between pilocarpine and isopilocarpine (7). It is possible that pharmaceutical industry standards for purity of pilocarpine preparations have been modified such that they now exceed standards. Another possible explanation is that fresh samples of pilocarpine were used, and degradation products which would have appeared after prolonged storage were not present in these samples.

The results of this study and the study by Noordam *et al.* (5) illustrate the effectiveness of HPLC for pilocarpine assay. Because these newer methods are capable of providing more accurate analysis of pilocarpine than the current official USP method, it is reasonable to consider modifying the USP to reflect more current technology.

REFERENCES

(1) T. Urbanyi, A. Piedmont, E. Willis, and G. Manning, *J. Pharm. Sci.*, **65**, 257 (1976).

(2) J. D. Weber, *J. Assoc. Off. Anal. Chem.*, **59**, 1409 (1976).

(3) A. Noordam, K. Waliszewski, C. Olieman, L. Maat, and H. C. Beyerman, *J. Chromatogr.*, **153**, 271 (1978).

(4) J. J. O'Donnell, R. Sandman, and M. V. Drake, *J. Pharm. Sci.*, **69**, 1096 (1980).

(5) A. Noordam, L. Maat, and H. C. Beyerman, *ibid.*, **70**, 96 (1981).

(6) "Pharmaceutical Drug Topics Red Book," Medical Economics, Oradell, N.J., 1978.

(7) "The United States Pharmacopeia," 19th rev., Mack Publishing Co., Easton, Pa., 1975, pp. 384–386.

ACKNOWLEDGMENTS

Supported by National Eye Institute Grant Ey-02162 and by the UCSF Academic Senate Committee on Research, Research Grant 2-503302-37864.

Novel Method of Derivatization of an Amidinourea (Lidamidine) for GLC Analysis

C. M. WON ˣ, J. J. ZALIPSKY, D. M. PATEL, and W. M. GRIM

Received February 20, 1981, from the *Analytical & Physical Chemistry Department, Research & Development Division, William H. Rorer, Inc., Fort Washington, PA 19034.* Accepted for publication June 9, 1981.

Abstract □ A new quantitative GLC method for analysis of lidamidine hydrochloride (I) was developed. The method was based on derivatization of I to 1-(2,6-dimethylphenyl)-4-methylamino-dihydro-1,3,5-triazin-2-one (II) using dimethylformamide dimethylacetal reagent. Compound II was synthesized and characterized by IR, NMR, mass spectrometry, and elemental analysis. The assigned structure was in agreement with characterization analyses. Cyclization of I to a triazinone using dimethylformamide dimethylacetal reagent presented a new route for the preparation of II.

Keyphrases □ Lidamidine—derivatization to a triazinone for GLC analysis □ GLC—derivatization of lidamidine to a triazinone for GLC analysis □ Triazinones—derivatization of lidamidine for GLC analysis

The arylamidinoureas are a family of compounds pharmacologically active on the GI tract, and the cardiovascular and central nervous systems. They also demonstrate local anesthetic activity[1]. Among a series of substituted arylamidinoureas, lidamidine hydrochloride, *N*-(2,6 - dimethylphenyl) - *N'* - [imino(methylamino)methyl]urea hydrochloride (I), exhibited promising antidiarrheal activity. Extensive pharmacological, toxicological, and biochemical studies of I have been reported (1–6). The chemical synthesis (7), the hydrolysis kinetics, and the physical and chemical parameters of I were also reported (8).

Stability-indicating high-performance liquid chromatographic (HPLC) methods[1] were developed to analyze I quantitatively in the presence of impurities or hydrolysis products. A direct GLC method to quantitate I failed because of its low volatility and/or thermal instability. The separation of amidinoureas by the GLC method required derivatization of the functional groups. Derivatization attempts by conventional silylation and acylation methods were unsuccessful.

For the derivatization of primary amines, dimethylformamide dimethylacetal reagent is used to form the *N*-dimethylaminoethylene derivative (9). When substituted guanidines were derivatized by dimethylformamide dimethylacetal, the resultant *N*-dimethylaminoethylene derivative underwent further cyclization reactions to form

[1] William H. Rorer, Inc., internal communication.

0022-3549/82/0300-0359$01.00/0

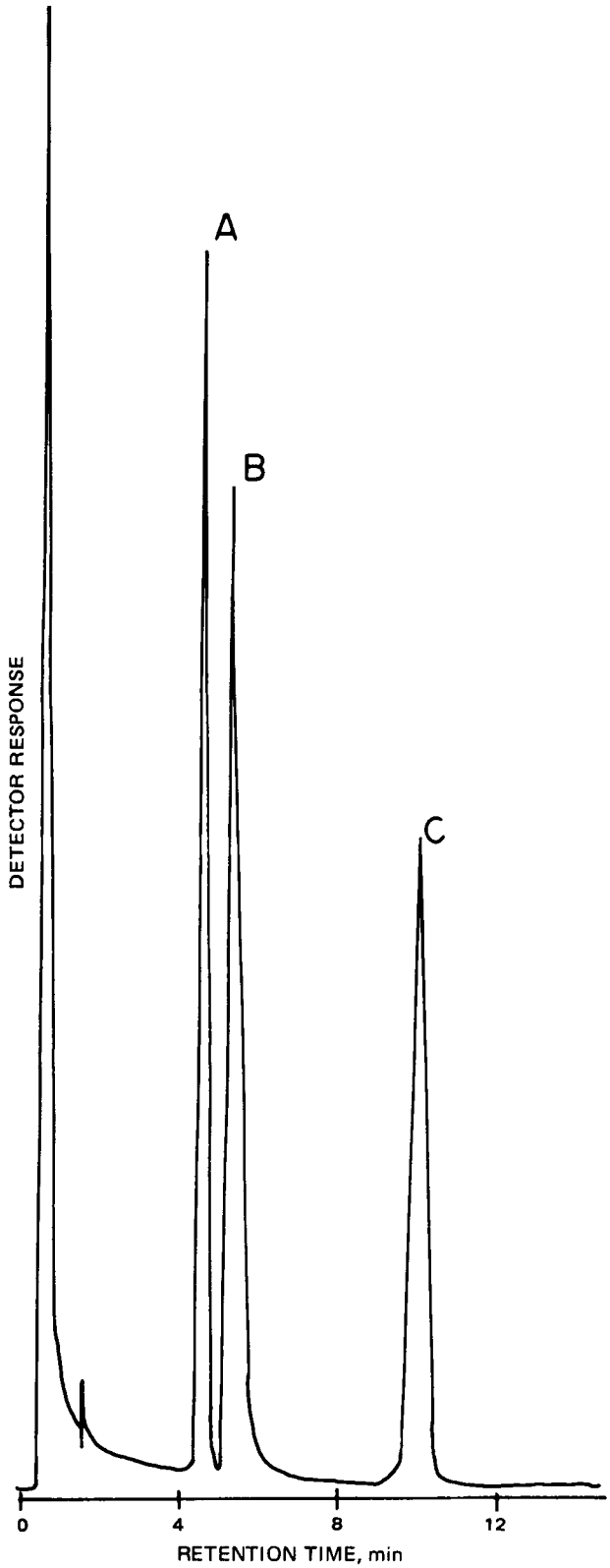

Figure 1—*Chromatogram of internal standard triphenylethylene (A); derivative II (B); and internal standard tetraphenylethylene (C).*

triazine derivatives (10). Biguanides are also known to undergo similar cyclization reactions on derivatization by trifluoroacetic anhydride (11) and *p*-nitrobenzoyl chloride (12).

Dimethylformamide dimethylacetal was used to derivatize I with the hope that a similar reaction would occur and a stable derivative could be formed. The resultant derivative was a triazinone-type compound, which involved cyclization of I during the derivatization.

EXPERIMENTAL

Materials—*N*,*N*-Dimethylformamide dimethylacetal[2], *N*,*N*-dimethylformamide[3], triphenylethylene[4], and tetraphenylethylene[4] were used without further purification.

Instrumentation—A gas chromatograph[5] and an electronic integrator[6] equipped with a flame-ionization detector were used. The 183-cm × 4-mm i.d. glass column was packed with 10% methyl silicone gum[7] on 80–100 mesh diatomaceous earth[8]. The injection port, column, and detector temperatures were maintained isothermally at 270, 250, and 270°, respectively. Nitrogen was used as the carrier gas at a flow rate of 45 ml/min.

Derivatization—Approximately 10 mg of I and 3 mg of an internal standard (triphenylethylene or tetraphenylethylene) were weighed accurately and placed into a 1-ml hypodermic vial and dissolved in 1 ml of *N*,*N*-dimethylformamide. Using a syringe, 0.1 ml of *N*,*N*-dimethylformamide dimethylacetal reagent was added to the vial. The vial was sealed with a silicone rubber septum, shaken, and put in an oven at 110° for 20 min. An aliquot (2 μl) was injected into a gas chromatograph.

Isolation of the Derivative (II)—The derivative was prepared in larger quantity for isolation and characterization. Approximately 200 mg of I was placed in a hypodermic vial and dissolved in 1 ml of acetonitrile. To the solution was added 0.2 ml of *N*,*N*-dimethylformamide dimethylacetal reagent. The vial was sealed and heated at 105° for 15 min in an oven. Seven identical preparations in the separate vials were made. The contents of the vials were pooled and placed in a round-bottom flask and evaporated to dryness under reduced pressure. The resultant solid residue was dissolved in a mixture of 30 ml of chloroform and 20 ml of water in a 60-ml separator and shaken vigorously. The aqueous layer was discarded and the chloroform layer was washed with another 20 ml of water. To the chloroform solution was added 10 g of anhydrous sodium sulfate. The solution was swirled, decanted into a flask, and evaporated to dryness. The white solid residue was recrystallized from 2-pentanone and dried in a desiccator over phosphorus pentoxide under vacuum for 1 hr.

Characterization of the Derivative (II)—The IR spectrum of a potassium bromide dispersion of II was obtained using an IR spectrophotometer[9]. The NMR spectrum[10] was obtained in deuterated chloroform solution with tetramethylsilane as an internal standard. The chemical-ionization mass spectrum[11] was obtained with methane as a reagent gas.

RESULTS AND DISCUSSION

Figure 1 shows a typical chromatogram of II and the internal standards. To establish optimum derivatization time and temperature, a sample containing I and triphenylethylene, an internal standard, was mixed with *N*,*N*-dimethylformamide dimethylacetal and the peak area ratio of II to the internal standard was followed for 3 hr at room temperature. However, the derivatization was not complete during this time period at room temperature. The same experiment at an elevated temperature (110°) showed that the derivatization was complete within 16 min. Dimethylformamide was chosen as the solvent because it is a relatively good solvent for both I and triphenylethylene or tetraphenylethylene and has a high boiling point.

To evaluate the response linearity of the GLC process, I was derivatized at various concentrations (0.9, 1.8, 2.7, and 3.6 mg) in the presence of triphenylethylene (0.7 mg) and then injected into the GLC. A plot of the peak area ratio of II to the internal standard against the concentration of I showed a linear relationship. The linear plot showed a negative intercept indicating column adsorption of II.

Scheme I shows the most probable pathway in the preparation of II. The structure of II was elucidated from IR, NMR, and mass spectrometric analyses. In addition, elemental analysis was performed on the sample.

[2] Applied Science Laboratories.
[3] Fisher Scientific Co.
[4] Eastman Kodak Co.
[5] Hewlett-Packard, 7620A.
[6] Hewlett-Packard, 3370A.
[7] SE-30, Analabs.
[8] Chromosorb W-HP, John-Manville Products Corp.
[9] Perkin-Elmer model 283B.
[10] Varian model T-60.
[11] Finnigan 3300 mass spectrometer.

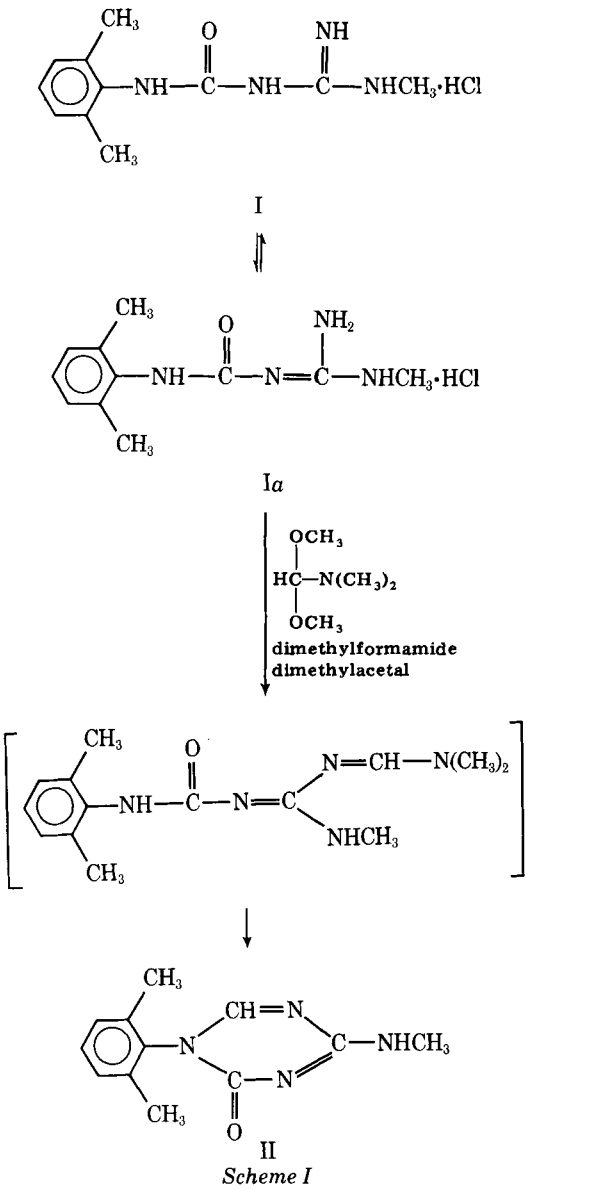

Scheme I

The IR spectrum of II showed a band at 3300 cm^{-1} representing —NH stretch of a secondary amine, a strong band at 1620 cm^{-1}, and a doublet at 1700 cm^{-1}, indicating carbonyl and —C=N stretches.

The NMR spectrum of II showed six protons of two methyl groups on the aromatic ring at 2.20 ppm (singlet), three protons of the methyl group (NH—CH_3) at 3.10 ppm (doublet), three protons of the aromatic ring at 7.26 ppm (singlet), and one proton (—N=CH—N=) at 7.75 ppm (singlet). The spectrum also reveals additional small signals at 3.15 ppm (doublet) and at 7.95 ppm (singlet). The appearance of the additional signals indicates that II can exhibit tautomerism causing protons of the NH—CH_3 and —N=CH—N= groups to be magnetically nonequivalent and therefore in different environments.

The chemical-ionization mass spectrum of II showed mass peaks at *m/z* 231 (M + 1), 259 (M + 29) and 271 (M + 41) which are characteristic peaks formed with methane as a reagent gas. The spectrum confirmed the molecular weight of the derivative as 230.

Based on the spectral data, the structure of the derivative is 1-(2,6-dimethylphenyl)-4-methylamino-dihydro-1,3,5-triazine-2-one. The elemental analysis of the derivative was in agreement with the chemical composition.

Anal.—Calc. for $C_{12}H_{14}N_4O$: C, 62.59; H, 6.13; N, 24.33. Found: C, 62.54; H, 6.14; N, 24.28.

The derivatization process is shown in Scheme I. The amidinourea moiety of I can be drawn in many tautomeric configurations, one of which is Ia. The tautomer would react with *N,N*-dimethylformamide dimethylacetal to form the *N*-dimethylaminoethylene derivative, an intermediate, which imparts structural stability by ring closure to form II. The cyclization of I to a triazinone using *N,N*-dimethylformamide dimethylacetal reagent presents a new route for the preparation of II (13).

REFERENCES

(1) G. N. Mir, R. L. Alioto, J. W. Sperow, J. R. Eash, J. B. Krebs, and J. Yelnosky, *Arzneim.-Forsch.*, **28,** 1448 (1978).

(2) G. N. Mir, J. W. Sperow, J. B. Krebs, J. R. Eash, G. S. Rowles, and J. Yelnosky, *ibid.*, **28,** 1454 (1978).

(3) R. L. Riley, G. N. Mir, G. S. Rowles, J. W. Sperow, R. L. Alioto, and J. Yelnosky, *ibid.*, **28,** 1461 (1978).

(4) G. N. Mir, J. W. Sperow, R. L. Riley, R. L. Alioto, G. W. Nuss, B. J. Chou, and J. Yelnosky, *ibid.*, **28,** 1466 (1978).

(5) B. J. Chou, G. N. Mir, W. R. Brown, W. R. Rapp, and J. Yelnosky, *ibid.*, **28,** 1471 (1978).

(6) A. F. DeLong, G. P. Martin, A. Polk, V. Carter, and T. Herczeg, *ibid.*, **28,** 1477 (1978).

(7) G. H. Douglas, J. Diamond, W. L. Studt, G. N. Mir, R. L. Alioto, K. Auyang, B. J. Burns, J. Cias, P. R. Darkes, S. A. Dodson, S. O'Connor, N. J. Santora, C. T. Tsuei, J. J. Zalipsky, and H. K. Zimmerman, *ibid.*, **28,** 1435 (1978).

(8) J. J. Zalipsky, C. M. Won, and D. M. Patel, *ibid.*, **28,** 1441 (1978).

(9) J. P. Thenot and E. C. Horning, *Anal. Lett.*, **5,** 519 (1972).

(10) H. Bredereck, F. Effenberger, and A. Hofmann, *Chem. Ber.*, **97,** 61 (1964).

(11) S. B. Matin, J. H. Karam, P. H. Forsham, and J. B. Knight, *Biomed. Mass Spectrom.*, **1,** 320 (1974).

(12) M. S. F. Ross, *J. Chromatogr.*, **133,** 408 (1977).

(13) C. M. Won, J. J. Zalipsky, and D. M. Patel, U.S. pat. 4,225,315.

Evaluation of ^{99m}Tc-Labeled Iminodiacetic Acid Derivatives of Substituted 2-Aminopyrroles as Hepatobiliary Imaging Agents in Rats II

BERNARD W. GRAHAM ˣ, CARL M. DEJULIIS, RONALD J. MATTSON, and J. WALTER SOWELL, SR.

Received March 20, 1981, from the *College of Pharmacy, University of South Carolina, Columbia SC 29208.* Accepted for publication July 28, 1981.

Abstract □ The synthesis and biodistribution properties of ^{99m}Tc-labeled 5-substituted *N*-(3-cyano-4-methyl-2-pyrrylcarbamoylmethyl)iminodiacetic acids and a similar series of N^1-methyl analogs are described. These compounds were compared with ^{99m}Tc-labeled *N*-(2,6-dimethylphenylcarbamoylmethyl)iminodiacetic acid for hepatobiliary activity in the rat. The effects of structural modifications on biological activity are also reported.

Keyphrases □ Imaging agents—^{99m}Tc-labeled iminodiacetic acid derivatives of substituted 2-aminopyrroles, rats □ Iminodiacetic acid—^{99m}Tc labeled derivatives of 2-substituted aminopyrroles, as hepatobiliary imaging agents in rats □ 2-Aminopyrroles—substituted, ^{99m}Tc-labeled derivatives, as hepatobiliary imaging agents in rats

Diseases of the gall bladder and biliary tract are a major health problem. Visualization of the hepatobiliary system in humans can be used in the differential diagnosis of these diseases. The use of radiopharmaceuticals as diagnostic tools for the dynamic evaluation of the hepatobiliary system was initiated by Taplin *et al.* (1) when they introduced the rose bengal sodium iodine 131 test.

BACKGROUND

Rose bengal sodium iodine 131 has many drawbacks because of the physical characteristics of the iodine 131 label. Recently, many technetium 99*m* complexes have been produced and studied as possible replacements for rose bengal sodium iodine 131. These technetium 99*m* complexes include penicillamine (2), dihydrothioctic acid (3), tetracycline (4), mercaptoisobutyric acid (5), and pyridoxalamine acids (6). Among the most promising of the agents are the iminodiacetic acid derivatives (7), such as *N*-(2,6-dimethylphenylcarbamoylmethyl)iminodiacetic acid (I). Many analogs of I have been synthesized by altering the lipophilic substituent on the benzene ring and many of these analogs are being investigated clinically in humans. To date, however, no ideal hepatobiliary agent has been introduced because all of these complexes are adversely affected by elevated serum bilirubin levels.

To make a more effective hepatobiliary agent more needs to be known about the structure–activity relationship. It was reported previously (8) that a chelate must have a molecular weight between 300 and 1000, exist as an organic anion, contain at least two aromatic rings, and bind to albumin to be effective as a hepatobiliary scintigraphic agent. Another report (9) proposed a bichelate structure for ^{99m}Tc–I with a molecular weight of the lidocaine derivative that favors biliary excretion. One of the first attempts at indicating a structure–activity relationship of the lidocaine analogs (10) reported a linear relationship between the biliary excretion in mice and the natural logarithm of the absolute value of the molecular weight of the technetium 99*m* chelate divided by the net charge on the chelate.

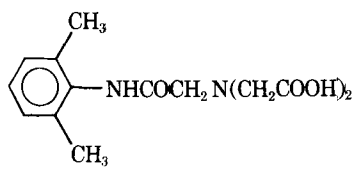

I

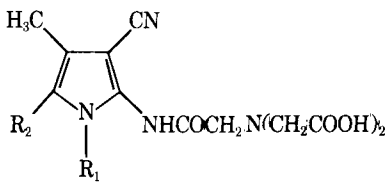

II: R_1 = H
III: R_1 = CH_3

Recently, the synthesis and the biodistribution properties of ^{99m}Tc-labeled 2-aminopyrrole analogs of I were reported (11). The activity exhibited by these compounds prompted the synthesis and evaluation of other 5-substituted *N*-(3-cyano-4-methyl-2-pyrrylcarbamoylmethyl)-iminodiacetic acids (II) and a similar series of N^1-methyl analogs (III). All of the derivatives were labeled with technetium 99*m* and compared with ^{99m}Tc–I for hepatobiliary activity in rats. The effects of N^1-methylation and the effects of C-5 substitution on biological activity are reported (Table I).

EXPERIMENTAL[1]

Chemistry—*N-(3-Cyano-1,4,5-trimethyl-2-pyrrylcarbamoylmethyl)-iminodiacetic Acid (IIIa)*—The procedure for the synthesis of IIIa is given as a general method for II*a–e* and III*b–f*. A modified procedure of Callery *et al.* (12) was used. A solution of 2-chloroacetamido-3-cyano-1,4,5-trimethylpyrrole (6.77 g, 0.03 mole) (13), disodium iminodiacetic acid monohydrate (5.85 g, 0.03 mole), and sodium hydroxide (1.2 g, 0.03 mole) in 100 ml methanol–water (3:1) was refluxed with stirring for 3 hr. The solution was stirred at ambient temperature overnight, diluted with water (100 ml), and the methanol removed *in vacuo*. The resulting suspension was diluted with additional water (50 ml), warmed gently, and filtered. After acidification of the filtrate to pH 3 by dropwise addition of concentrated hydrochloric acid, the precipitate was collected and dried. The crude product (7.25 g, 75.0%) was recrystallized from water to yield a light lavender powder (homogeneous on TLC, methanol, R_f 0.57), mp 184–185° dec., IR (KBr): 3300, 3020, 2860, 2210, 1680 (broad), 1560, 1410, 1350, and 970 cm^{-1}; NMR (dimethyl sulfoxide-d_6): δ 2.00 (s, 3H, CH_3 at C_4), 2.07 (s, 3H, CH_3 at C_5), 3.27 (s, 3H, CH_3 at N_1), 3.53 (s, 6H, —CH_2—alpha to amino group), 7.80–9.20 (broad s, 3H, amide NH and COOH) ppm.

N-(2,6-Dimethylphenylcarbamoylmethyl)iminodiacetic acid (I)—A solution of 1-chloroacetamido-2,6-dimethylbenzene (5.93 g, 0.03 mole), disodium iminodiacetic acid monohydrate (5.85 g, 0.03 mole), and sodium hydroxide (1.2 g 0.03, mole) in 100 ml of methanol–water (3:1) was refluxed with stirring for 4.5 hr. The methanol was removed *in vacuo* and the crude product (5.5 g, 69%) was isolated according to the procedure described for III*a*. The product was recrystallized from water to yield white crystals, mp 216–217° [lit. mp 215–216° (4)]; IR (KBr): 3180, 1750, 1610, 1530, 1215, 1155, and 770 cm^{-1}.

Anal.—Calc. for $C_{14}H_{18}N_2O_5$: C, 57.13; H, 6.16; N, 9.52. Found: C, 57.16; H, 6.18; N, 9.51.

Labeling with Technetium 99*m*—The iminodiacetic acid derivatives (I, II*a–e*, III*a–f*) were labeled by a stannous chloride reduction of sodium (^{99m}Tc) pertechnetate (IV) eluate from a molybdenum 99–technetium

[1] IR spectral data were determined on a Beckman Acculab 4 Spectrophotometer using the potassium bromide technique. NMR spectra were determined on a Hitachi-Perkin-Elmer R24 high-resolution spectrometer with tetramethylsilane as the internal reference. Melting points were obtained using a Thomas-Hoover capillary apparatus and are uncorrected. TLC was performed using Eastman Chromatogram sheets, type 6060 (silica gel), and the sheets were developed in an iodine chamber. Carbon, hydrogen, and nitrogen values were obtained from analysis performed by Atlantic Microlabs, Inc., Atlanta, Ga.

0022-3549/82/0300-0362$01.00/0

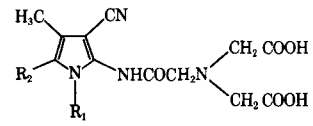

Table I—Data for Various *N*-(3-Cyano-4-methyl-2-pyrrylcarbamoylmethyl)iminodiacetic Acids

Compound	R_1	R_2	Yield, %	Recrystallization Solvent	Melting Point	R_f[a]	Formula	Analysis, % Calc.	Found
IIa[b]	—H	—CH_3							
IIb	—H	—iso-C_4H_9	63.5	water	163–166.5° dec.	0.37	$C_{16}H_{22}N_4O_5$	C 54.84 H 6.33 N 15.99	54.87 6.33 15.98
IIc	—H	—$CH_2CH_2SCH_3$	57.0	dimethyl sulfoxide–acetone–ether (1:4:1)	184–186° dec.	0.41	$C_{15}H_{20}N_4O_5S$	C 48.90 H 5.47 N 15.21 8.70	48.71 5.54 15.14 8.66
IId[b]	—H	—$CH_2C_6H_5$							
IIe	—H	—$CH_2C_6H_4$-p-OH	50.0	water	111.5–115°	0.28	$C_{19}H_{20}N_4O_6$ · 0.5 H_2O	C 55.74 H 5.17 N 13.69	55.63 5.29 13.82
IIIa	—CH_3	—CH_3	75.0	water	184–186° dec.	0.57	$C_{14}H_{18}N_4O_5$	C 52.17 H 5.63 N 17.38	52.03 5.63 17.33
IIIb	—CH_3	—iso-C_4H_9	73.5	water	170–171° dec.	0.57	$C_{17}H_{24}N_4O_5$	C 56.03 H 6.64 N 15.38	56.04 6.65 15.37
IIIc	—CH_3	—$CH_2CH_2SCH_3$	60.9	water	144–145°	0.57	$C_{16}H_{22}N_4O_5S$	C 50.25 H 5.80 N 14.65 S 8.39	50.42 5.86 14.75 8.41
IIId	—CH_3	—C_6H_5	60.7	water	162–165° dec.	0.62	$C_{19}H_{20}N_4O_5$	C 59.37 H 5.24 N 14.58	59.30 5.27 14.57
IIIe	—CH_3	—$CH_2C_6H_5$	73.6	water	168–169° dec.	0.55	$C_{20}H_{22}N_4O_5$	C 60.29 H 5.57 N 14.06	60.06 5.65 13.99
IIIf	—CH_3	—CH_2—C_6H_4-p-OCH_3	73.9	water	171–172° dec.	0.62	$C_{21}H_{24}N_4O_6$	C 58.87 H 5.65 N 13.07	58.62 5.72 13.02

[a] Methanol. [b] Data previously reported in ref. 11.

Table II—Parameters for the Blood Elimination Equation of ^{99m}Tc in the Rat following Intravenous Injection of ^{99m}Tc-Labeled Iminodiacetic Acid Derivatives[a]

	A	α	*B*	β	R^2
I	0.63 (0.02)	0.23 (0.02)	0.36 (0.02)	0.013 (0.00013)	99.8
IIa[b]	0.73 (0.04)	0.52 (0.04)	0.27 (0.02)	0.023 (0.003)	98.2
IIb	0.73 (0.03)	0.50 (0.03)	0.27 (0.01)	0.019 (0.001)	99.7
IIc	0.67 (0.02)	0.32 (0.01)	0.33 (0.01)	0.0104 (0.0011)	99.7
IId[b]	0.81 (0.03)	0.69 (0.05)	0.19 (0.01)	0.027 (0.002)	97.8
IIe	0.79 (0.03)	0.58 (0.03)	0.21 (0.01)	0.023 (0.002)	99.5
IIIa	0.54 (0.03)	0.43 (0.04)	0.44 (0.01)	0.015 (0.001)	99.7
IIIb	0.57 (0.03)	0.37 (0.03)	0.43 (0.01)	0.013 (0.001)	99.7
IIIc	0.56 (0.03)	0.25 (0.02)	0.43 (0.02)	0.012 (0.001)	99.7
IIId	0.67 (0.02)	0.26 (0.02)	0.33 (0.01)	0.016 (0.001)	99.8
IIIe	0.58 (0.03)	0.28 (0.03)	0.42 (0.02)	0.011 (0.001)	99.7
IIIf	0.56 (0.02)	0.26 (0.02)	0.44 (0.01)	0.008 (0.001)	99.9

[a] Standard error in parentheses. [b] Data previously reported in ref. 11.

99*m* generator[2] in an aqueous solution. Ten milligrams of each compound were dissolved in minimal amounts of sodium hydroxide (1 *N*). This solution was back titrated with hydrochloric acid (0.05 *N*) to pH 7. Seven millicuries of IV in 0.2 ml was added and the resulting solution was purged with nitrogen for 5 min. After purging, 0.1 ml of freshly prepared stannous chloride solution[3] (1 mg/ml) was added and the solution was kept at room temperature for 20 min. The molar ratio of ligand to tin varied from 52:1 to 77:1. The final solution was passed through a millipore filter into a sterile evacuated vial.

The radiochemical purities of technetium 99*m* labeled IIc, IIe, IIIa, and IIIc compounds were determined using instant TLC[4] with a chloroform–acetone (70:30) solvent system. The radiochemical purities of 99*m* Tc-labeled I, IIa, IIb, IId, IIId, IIIe, and IIIf compounds were determined using instant TLC with methyl–ethyl ketone, 85% methanol, and saline solvent systems. Examination of the chromatographic strips revealed the bound fraction to be 95% or greater for all of the radiopharmaceuticals.

***In Vivo* Studies**—Fasting, nonhydrated, male Sprague-Dawley[5] rats, 175–250 g, were used. The left jugular vein was exposed and cannulated for each animal after anesthetizing with pentobarbital sodium (30 mg/kg). The animal was then positioned over a rectilinear scanner[6] modified to record the counts arising from the cardiac pool. Following the injection of 0.25 mCi of the ^{99m}Tc-labeled compound into the cannula, sequential counts were obtained for the duration of the study. These counts were used to model the disappearance of the radioactivity from the blood.

Each animal was sacrificed 1 hr after injection of the radiopharmaceutical by overanesthesia with ether. Selected organs were removed from the animal and assayed for radioactivity. The results are reported as the percentage of the total injected radioactivity.

RESULTS

The disappearance of the radioactivity from the blood is described by a two-compartment open model. The computer-fitted equation[7] used to describe the data is:

$$C_B = A \exp(-\alpha t) + B \exp(-\beta t) \qquad \text{(Eq. 1)}$$

where C_B refers to the fraction of the dose retained in the blood (biological) and t is time (min). The parameters for Eq. 1 and the correlation

[2] CintiChem, Union Carbide Corp., Tuxedo, N.Y.
[3] The stannous chloride solution was prepared daily by dissolving 15 mg of $SnCl_2 \cdot 2H_2O$ in 15 ml of hydrochloric acid (0.05 *N*).
[4] ITLC SG, Gelman Instrument Co., Ann Arbor, Mich.
[5] GIBCO Animal Research Laboratories, Madison, Wis.
[6] Magnascanner 500, Picker Instruments, Cleveland, Ohio.
[7] NLIN, SAS 76, Raleigh, N.C.

Table III—Percent of Administered Radioactivity at 1 hr after Intravenous Injection of ^{99m}Tc-Labeled Iminodiacetic Acid Derivatives in Selected Organs of the Rat[a]

	GI Tract	Liver	Spleen	Kidneys	Lung	Heart	Carcass
I	64.7	3.89	0.06	4.11	0.19	0.07	27.0
	(5.83)	(0.55)	(0.02)	(0.59)	(0.07)	(0.04)	(4.70)
IIa[b]	38.0	8.00	0.07	11.1	0.30	0.02	44.0
	(2.40)	(0.21)	(0.05)	(3.41)	(0.18)	(0.01)	(2.80)
IIb	72.9	6.06	0.08	5.92	0.21	0.05	14.8
	(2.71)	(1.43)	(0.01)	(0.60)	(0.05)	(0.01)	(1.26)
IIc	75.2	5.50	0.04	6.80	0.16	0.05	12.0
	(2.24)	(1.43)	(0.01)	(0.07)	(0.03)	(0.02)	(1.56)
IId[b]	81.5	6.72	0.15	2.34	0.20	0.07	9.90
	(2.48)	(0.91)	(0.08)	(0.35)	(0.03)	(0.02)	(0.92)
IIe	76.1	4.67	0.07	3.04	0.20	0.07	15.8
	(2.29)	(1.02)	(0.01)	(0.21)	(0.02)	(0.01)	(1.20)
IIIa	21.9	11.3	0.14	6.8	0.38	0.16	59.3
	(3.60)	(4.70)	(0.09)	(0.6)	(0.08)	(0.09)	(3.61)
IIIb	53.3	10.8	0.04	4.03	0.24	0.06	31.4
	(11.8)	(2.41)	(0.01)	(1.22)	(0.03)	(0.03)	(9.57)
IIIc	58.1	6.40	0.06	2.81	0.26	0.09	32.0
	(3.69)	(1.59)	(0.01)	(0.27)	(0.02)	(0.02)	(3.73)
IIId	78.6	4.00	0.03	1.63	0.17	0.03	15.3
	(1.94)	(0.40)	(0.01)	(0.02)	(0.04)	(0.01)	(1.62)
IIIe	69.1	6.62	0.07	2.37	0.49	0.14	20.6
	(0.47)	(0.72)	(0.01)	(0.24)	(0.08)	(0.01)	(0.52)
IIIf	59.6	11.8	0.12	2.23	0.54	0.19	24.9
	(2.59)	(2.41)	(0.01)	(0.37)	(0.04)	(0.09)	(2.20)

[a] Standard error in parentheses. [b] Data previously reported in reference 11.

coefficient (R^2) for each parameter are listed in Table II. The data represents the combined data for three rats for each compound.

Table III shows the distribution of technetium 99*m* in selected organs and tissues of the rat 1 hr after intravenous injection. The data are expressed as a percentage of the injected dose and represent the average of three rats for each compound. The carcass values represent the remainder after the removal of the other organs and include the bladder, which accounted for much of the activity.

This experiment was a completely randomized block design which permitted the calculation of differences between the ^{99m}Tc-labeled pyrrole derivatives IIa–*e*, IIIa–*f*, and ^{99m}Tc–I. Differences were tested by two-sided Student *t* tests at a 90% confidence level. Student *t* statistics between ^{99m}Tc–I and the ^{99m}Tc-labeled iminodiacetic acid derivatives of 5-substituted 2-aminopyrroles were computed for the β phases of the blood curves, the percentage of injected radioactivity in the GI tracts, carcasses, livers, and kidneys.

The results show that ^{99m}Tc–IIa, ^{99m}Tc–II*d*, and ^{99m}Tc–IIIa are different from ^{99m}Tc–I. When ^{99m}Tc–IIa and ^{99m}Tc–IIIa were compared with ^{99m}Tc–I, these complexes showed less of the radioactivity accumulating in the GI tract and more remaining in the carcass at 1 hr after injection. A comparison between ^{99m}Tc–II*d* and ^{99m}Tc–I showed that ^{99m}Tc–II*d* had less radioactivity remaining in the carcass and more accumulating in the GI tract.

The experimental design allowed testing of the effects of N^1-methylation and C-5 substitution on the pyrrole ring by a two-way analysis of variance. The analysis of variance was performed on the β phase rate constants and on the percentages of radioactivity in the carcass, GI tract, liver, and kidneys.

The results show that N^1-methylation significantly decreased the rate constant, increased the accumulation of radioactivity in the carcass and kidneys, and decreased the accumulation of technetium 99*m* in the GI tract. One possible explanation for these results is that these chelates are in the structure proposed by Loberg and Fields (9) and that the technetium 99*m* labeled compounds IIa–*e* can undergo intramolecular hydrogen bonding between the N^1 hydrogen and the carbonyl group at position 2. The N^1-methyl series (IIIa–*f*) cannot undergo this intramolecular hydrogen bonding. Therefore, the free carbonyl group of compounds IIIa–*f* can interact with water to a greater extent through intermolecular hydrogen bonding which reduces protein binding and biliary excretion.

The two-way analysis of variance also revealed that the C-5 substitution effect was significant for the rate constant and the percentages of radioactivity in the carcass, GI tract, and kidneys.

Since the C-5 substitution was significant for these measured parameters, correlation analysis between the molecular weight of the C-5 substituent and the amount of radioactivity found in the GI tract was performed.

The correlation analysis revealed that when the C-5 substituent of either the N^1-H series (II) or the N^1-methyl series was aliphatic, increasing the molecular weight of the technetium 99*m* complex increased biliary excretion. The correlation coefficient for the N^1-H aliphatic series is 0.86; for the N^1-methyl series it is 0.77. When the C-5 substituent was aromatic, an increase in molecular weight of the technetium 99*m* complex decreased biliary excretion. For the N^1-H series, the correlation coefficient is −0.90; for the N^1-methyl series it is −0.62.

REFERENCES

(1) B. V. Taplin, O. M. Meredith, and H. Kade, *J. Lab. Clin. Med.*, **45,** 665 (1955).

(2) M. Tubis, G. T. Krishnamurthy, J. S. Endow, and W. H. Blahd, *J. Nucl. Med.*, **13,** 652 (1972).

(3) A. K. Tonkin and F. H. DeLand, *ibid.*, **15,** 539 (1974).

(4) C. P. Fliegel, M. K. Dewanjee, L. B. Holman, M. A. Davis, and S. Treves, *Radiology*, **110,** 407 (1974).

(5) T. H. Lin, A. Khentigen, and H. S. Winchell, *J. Nucl. Med.*, **15,** 613 (1974).

(6) R. J. Baker, J. C. Bellen, and P. M. Ronai, *ibid.*, **16,** 720 (1975).

(7) E. Harvey, M. Loberg, and M. Cooper, *ibid.*, **16,** 533 (1975).

(8) G. Firnau, *Eur. J. Nucl. Med.*, **1,** 137 (1976).

(9) M. D. Loberg and A. T. Fields, *Int. J. Appl. Radiol. Isotop.*, **29,** 167 (1978).

(10) D. Burns, L. Marzilli, D. Sowa, D. Baum, and H. N. Wagner, *J. Nucl. Med.*, **18,** 624 (1977).

(11) C. M. DeJuliis, B. W. Graham, R. J. Mattson, and J. W. Sowell, Sr., *J. Pharm. Sci.*, **69,** 731 (1980).

(12) P. S. Callery, W. C. Faith, M. D. Loberg, A. T. Fields, E. G. Harvey, and M. D. Cooper, *J. Med. Chem.*, **19,** 962 (1976).

(13) J. W. Sowell, Sr., A. J. Block, M. E. Derrick, J. J. Freeman, J. W. Kosh, R. J. Mattson, P. F. Mubarak, and P. A. Tenthorey, *J. Pharm. Sci.*, **70,** 135 (1981).

ACKNOWLEDGMENTS

Abstracted in part from a thesis submitted by C. M. DeJuliis to the Graduate School of the University of South Carolina in partial fulfillment of Master of Science degree requirements.

Antibacterial N-[ω,ω'-Bis(alicyclic and aryl)-*sec*-alkyl]-1,3-diamino-2-propanol Dihydrochloride Salts

NATHANIEL GRIER ˣ, RICHARD A. DYBAS, ROBERT A. STRELITZ, BRUCE E. WITZEL, and EUGENE L. DULANEY

Received February 9, 1981, from the *Merck Sharp & Dohme Research Laboratories, Rahway NJ 07065.* Accepted for publication July 27, 1981.

Abstract □ A series of 14 antibacterial N-[ω,ω'-bis(cycloalkyl, bicyclo[2.2.1]heptyl, and substituted phenyl)-*sec*-alkyl]-1,3-diamino-2-propanol dihydrochloride salts were synthesized as potential topical antiseptics and disinfectants. Four derivatives which were particularly effective against *Pseudomonas aeruginosa* encompassed the three diverse ring-type substituents and an 8-n-pentadecyl moiety. The calculated Hansch hydrophobic parameter (π) for the N-substituents of the more efficient compounds were in the range 7.0–9.0 and correlated with minimal inhibitory activity as a parabola for all of the products under the assay conditions. The potencies against Gram-positive and other Gram-negative bacteria were comparable to benzalkonium chloride and chlorhexidine.

Keyphrases □ Antibacterials—potential, N-[ω,ω'-Bis(alicyclic and aryl)-*sec*-alkyl]-1,3-diamino-2-propanol dihydrochloride salts □ *Pseudomonas aeruginosa*—effect of potential antiseptics and disinfectants □ Hansch hydrophobic parameter—correlation with efficiencies of potential antibacterials

Antimicrobial agents have been sought from among N-mono-(1), N,N'-bis(mono)- (2, 3), and disubstituted 1,3-diamino-2-propanol salt derivatives (4). The present report describes the synthesis of N-substituted *sec*-alkyl compounds of the first type, the *in vitro* antibacterial assay, and a potential structure–activity relationship. This study is part of an effort to develop antiseptics and disinfectants especially effective against *Pseudomonas aeruginosa* (5). The cell envelope of Gram-negative bacteria presents a permeability barrier which includes high lipid content, anionic lipopolysaccharides, and proteins (porins) apparently able to form molecular size-limiting channels trans-outer membrane (6). Variation of the *sec*-alkyl group by symmetrical substitution of the ω,ω' carbon atoms with alicyclic or aryl moieties provided products with differences in lipophilicity, geometry, and surfaces with proton or electron enrichment. Interestingly, a recent report noted that single methyl branching introduced on a long-chain alkyl group in several tertiary amines, caused a loss of inhibitory action for Gram-negative bacteria but not toward Gram-positive bacteria (7).

RESULTS AND DISCUSSION

Syntheses—The dihydrochloride salts I*a*–I*n* were prepared by condensation of the requisite symmetrical alkanone and 1,3-diamino-2-propanol to form the Schiff base, followed by reduction of the carbon–nitrogen double bond by catalytic hydrogenation or with sodium borohydride, and neutralization with hydrogen chloride in diethyl ether, 2-propanol, or binary mixtures (2, 8, 9). Yields were 40–90%. Compounds I*d* (5) and I*l* (9) were reported previously. The ketone-starting materials for I*a*, I*b*, and I*f* were purchased[1] or were obtained from earlier N-substituted triamine and tetramine syntheses (5), for I*c–e*, I*h–l*, and were known for I*m* (10). The preparation of ketones required for I*g* and I*n* is described under *Experimental.*

Microbiology—The minimal inhibitory concentrations of the compounds were determined by an agar dilution method. Stock solutions of the 14 compounds containing 1 or 10 mg/ml in dimethyl sulfoxide were added to melted sterile nutrient agar[2] to give the desired final concentrations, and 10 ml was pipetted into Petri plates. The concentrations tested were 200, 100, 80, 60, 50, 40, 30, 20, 10, 8, 6, 4, 2, and 1 μg/ml (5, 11). The dimethyl sulfoxide had no inhibitory effect on the test bacteria. The test bacteria were shaken at 220 rpm for 20 hr at 37° in 10 ml of brain–heart broth[2], diluted to 10^{-3} in fresh brain–heart broth, and spot inoculated onto the surfaces of the agar plates containing the test compounds. The number of colony-forming units in each inoculated spot was $\sim 10^5$. The plates were scored after a 20-hr incubation at 37°. The minimum inhibitory concentration is the lowest concentration of compound that completely inhibited growth by macroscopic examination. All assays were run in duplicate. The results are shown in Tables I and II.

The more potent pseudomonad inhibitors of the series (Table I) represented practically all substituent variations; namely, linear alkyl (I*b*), alicyclic (I*d* and I*e*), and electron-donor substituted aryl (I*i*). The efficiency, comparable to chlorhexidine, could be linked to the lipid–water partition property and apparently was not sensitive to steric, electronic, and bulk factors. However, no attempt was made to analyze structure–activity relationships by molecular connectivity (12) or polarizability parameters (13).

Structure–Activity—The calculated hydrophobic parameter, π, (14) for the $[R(CH_2)_n]^2$ groups of the best inhibitors was in the range 7–9. Regression analysis using the least-squares method indicated, within 95% confidence limits, a parabolic relationship with minimal inhibitory concentration for both pseudomonad strains and provided the predicted curves: minimum inhibitory concentration (μg/ml) = 1340.68 (±279.13) − 343.39 (±78.11) π + 22.40 (±5.25) π^2 for strain MB418 (n = 14, r = 0.8048, and s = 55.65) (Fig. 1); minimum inhibitory concentration (μg/ml) = 1343.55 (±285.83) − 346.38 (±79.99) π + 22.69 (±5.38) π^2 for strain MB2245 (n = 14, r = 0.7985, and s = 56.90); where n is the number of assayed compounds used, r is the correlation coefficient, and s the standard deviation from the regression line.

Use of a lipid group-calculated π for correlation purposes (the polar base moiety remaining constant in the series) avoided problems associated with whether the active molecular species was neutral, ionic (15), or metal chelated (16).

The broad spectrum assay (Table II) showed a similar ordering in which compounds with high inhibitory potency for Gram-negative bacteria (*e.g., Escherichia coli*) were comprised of diverse substituent groups.

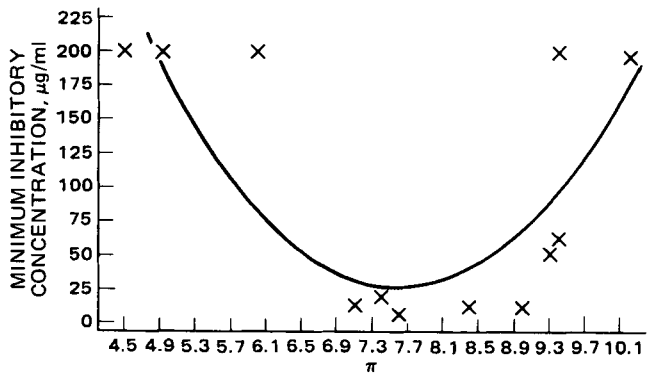

Figure 1—*The calculated Hansch hydrophobic parameter (x) for the lipoidal substituent, $[R(CH_2)_n]_2$ (Table I), of* N-*substituted 1,3-diamino-2-propanol dihydrochlorides and* in vitro *minimal inhibitory concentration; (—) regression analysis predicted curve:* P. aeruginosa *MB418.*

[1] Aldrich Chemical Co.

[2] Difco, brain–heart infusion agar.

0022-3549/82/0300-0365$01.00/0

Table I—*N*-(Substituted *sec*-alkyl)-1,3-diamino-2-propanol Dihydrochloride Salts: Physicochemical and Antipseudomonad Screen Data {$[R(CH_2)_n]_2CHNHCH_2CHOHCH_2NH_2 \cdot 2HCl$}

Compound	R	*n*	Melting Point[a]	Minimum Inhibitory Concentration μg/ml *Pseudomonas aeruginosa* MB 418	MB 2245	$[R(CH_2)_n]_2$ π[b]	Empirical Formula	Analysis Calc.	Found
I*a*	Methyl	3	203–205[c]	>200	>200	4.5	$C_{12}H_{30}Cl_2N_2O$	C 49.80	49.67
								H 10.45	10.22
								Cl 24.50	24.52
								N 9.68	9.50
I*b*	Methyl	6	273–276	6	6	7.6	$C_{18}H_{42}Cl_2N_2O$	C 57.88	58.02
								H 11.33	11.65
								N 7.50	7.18
I*c*	Cyclohexyl	1	262–264[c]	80	40	6.1	$C_{18}H_{38}Cl_2N_2O$	C 58.53	58.63
								H 10.37	10.63
								N 7.58	7.18
I*d*	Cyclohexyl	2	254–255[c]	10	8	7.1	$C_{20}H_{42}Cl_2N_2O$	C 60.45	60.04
								H 10.65	10.82
								N 7.05	7.06
I*e*	3,3-Dimethyl-bicyclo[2.2.1]-heptan-2-yl	2	236–237[c]	10	10	9.0	$C_{26}H_{50}Cl_2N_2O$	C 65.40	65.55
								H 10.55	10.95
								N 5.86	5.68
I*f*	Phenyl	1	185–186	>200	>200	4.9	$C_{18}H_{26}Cl_2N_2O$	C 60.50	60.70
								H 7.33	7.48
								Cl 19.84	19.47
								N 7.84	8.17
I*g*	4-Phenylphenyl	2	241–243[d]	>200	>200	9.4	$C_{32}H_{38}Cl_2N_2O$	C 71.50	71.48
								H 7.13	7.27
								N 5.21	5.03
I*h*	4-Methylphenyl	2	265–267	40	50	6.9	$C_{20}H_{34}Cl_2N_2O$	C 64.09	63.94
								H 8.25	8.16
								N 6.74	6.39
I*i*	4-(1-Methylethyl)phenyl	2	260–262	10	10	8.4	$C_{26}H_{42}Cl_2N_2O$	C 66.60	66.65
								H 9.02	9.23
								Cl 15.10	14.89
								N 5.97	6.00
I*j*	4-(1-Methylethyl)phenyl	3	244–246[c]	60	60	9.4	$C_{28}H_{46}Cl_2N_2O$	C 67.59	67.58
								H 9.32	9.69
								N 5.63	5.70
I*k*	4-(1,1-Dimethylethyl)phenyl	2	270–272[e]	50	50	9.3	$C_{28}H_{46}Cl_2N_2O$	C 67.59	67.34
								H 9.32	9.60
								N 5.63	5.55
I*l*	4-(1,1-Dimethylethyl)phenyl	3	267–269[c]	>200	>200	10.3	$C_{30}H_{50}Cl_2N_2O$	C 68.53	67.99
								H 9.59	9.46
								Cl 13.48	13.19
								N 5.33	5.12
I*m*	4-Methoxyphenyl	2	240–242	200	200	6.0	$C_{22}H_{34}Cl_2N_2O$	C 59.32	59.43
								H 7.69	7.91
								N 6.29	6.40
I*n*	4-Chlorophenyl	2	263–265[e]	20	20	7.4	$C_{20}H_{28}Cl_4N_2O$	C 52.88	52.86
								H 6.21	6.46
								Cl 31.22	31.20
								N 6.17	6.00
	Benzalkonium chloride			>200	>200				
	Chlorhexidine			6	8				

[a] Salts were crystallized or recrystallized from isopropanol except as otherwise noted. [b] Hansch hydrophobic parameter (14). [c] Purified by column chromatography of the base on silica gel (1 g:75 g) with methylene chloride–methanol–ammonium hydroxide (35:4:1), conversion to the dihydrochloride in ether with dry HCl in 2-propanol (29% w/w), and isolation upon precipitation or by solvent removal. [d] Recrystallized from ether–2-propanol. [e] Ethanol.

Several of the most lipophilic salts were highly effective against the nine genera; I*j* at ≤6 μg/ml and I*k* exhibited similar patterns, but they were only moderately active for the two *Pseudomonas* strains, suggesting a more critical partitioning requirement.

Many examples of antibacterial activity–lipophilicity parabolic findings have been reported previously for homologs of inhibitors (17). Several explanations have been proposed. Highly hydrophilic compounds in a series cannot penetrate a cell envelope lipid barrier, whereas the more hydrophobic members remain entrapped in the lipid phase and fail to reach target sites. These postulates may account for each low activity side of the parabolic curve, with molecule size and colloidal associations as other possible contributors. More recent studies using quaternary ammonium salts of increasing alkyl chain length, in a simple salts test medium with and without varying sensitivity mutants of *Ps. aeruginosa*, indicate a positive linear correlation between lipophilicity and antimicrobial activity (18). However, the probable test medium imposed artifactual results of the present work may better anticipate activities under conditions of potential use. Preliminary *in vitro* and *in vivo* antibacterial studies on skin (excised and intact cow udder) with Table I derivatives appear to confirm the findings[3].

[3] To be published elsewhere.

EXPERIMENTAL

Melting points were taken in open capillary tubes[4] and are uncorrected. IR spectra for solids were run as mulls in mineral oil[5]. NMR spectra[6] (60 MHz) were obtained in dimethyl sulfoxide-d_6 with tetramethylsilane as an internal standard. Spectral data for all reported compounds appeared consistent with assigned structures. TLC was performed on precoated gel GF glass plates (250 μm)[7], using dioxane–methanol–ammonium hydroxide (15:4:1) as the developing solvent for the diamine hydrochloride salts and ether–petroleum ether (1:1) or hexane–ethyl acetate (1:1) mixtures for ketones (iodine staining). The amine salts were colorless solids, easily hydrated, and were dried for 4 hr at 60–80° (0.05 mm) before analysis. All hydrogenations were run at 20–25° and 2.8–3.5 kg/cm^2 until theoretical hydrogen uptake, requiring from 1 to 4 hr. After catalyst removal by filtration, the solvent was distilled *in vacuo*.

Ketones—1,5-Bis(aryl)-1,4-pentadien-3-ones were prepared by literature methods.

Bis(4-chlorophenyl) Derivative—A mixture of 4-chlorobenzaldehyde

[4] Thomas-Hoover melting point apparatus.
[5] Perkin-Elmer 137 spectrometer.
[6] Varian A-60 spectrometer.
[7] Analtech.

Table II—*In Vitro* Antibacterial Assay

Compound	Minimal Inhibitory Concentration, μg/ml								
	S. aureus[a]	*S. pyogenes*[b]	*B. bronchiseptica*[c]	*K. aerogenes*[d]	*B. subtilis*[e]	*C. pseudodiphtherium*[f]	*P. multocida*[g]	*E. coli*[h]	*S. schottmuelleri*[i]
I*a*	—[j]	60	60	—	—	200	200	—	—
I*b*	6	2	2	6	6	2	2	6	6
I*c*	40	1	6	80	40	6	20	20	50
I*d*	4	2	2	6	4	2	2	8	8
I*e*	6	1	6	2	6	1	4	6	6
I*f*	—	200	50	200	—	50	60	—	—
I*g*	6	4	8	200	6	60	50	60	200
I*h*	30	4	4	30	30	30	6	40	40
I*i*	40	4	6	2	4	2	6	40	40
I*j*	6	2	2	6	6	4	4	6	6
I*k*	8	2	4	20	4	2	2	8	8
I*l*	6	4	40	200	6	6	6	40	8
I*m*	60	40	40	200	40	60	40	80	200
I*n*	2	1	1	20	6	1	1	2	20
Benzalkonium chloride[k]	1	1	8	6	6	1	1	—	200
Chlorhexidine	1	1	1	2	1	1	1	2	6

[a] Merck Bacteria (MB); genus and strain, Staphylococcus MB 2865. [b] Streptococcus MB 3738. [c] Bordetella MB 3551. [d] Klebsiella MB 1503. [e] Bacillus MB 964. [f] Corynebacterium MB 261. [g] Pasturella MB 7. [h] Escherichia MB 2884. [i] Salmonella MB 2837. [j] Greater than 200 μg/ml. [k] Hyamine 3500, Rohm & Haas, which contains alkyl (50% C-14, 40% C-12, 10% C-16) dimethylbenzylammonium chloride as an 80% solution in ethanol.

(15.2 g, 0.11 mole) and acetone (3.1 g, 0.05 mole) in 60 ml of ethanol was added dropwise (15 min) to a solution of sodium hydroxide (12 g, 0.3 mole) in 120 ml of water diluted with 100 ml of ethanol. The temperature during addition was maintained at 10–13° and then at 20–25° for 4 hr. The precipitated solids were filtered, washed with water, and air dried. Recrystallization of 0.2 g of the yellow product (13.5 g, 83%) from benzene gave pure bis(4-chlorobenzal)acetone (0.14 g); mp 191–193° [lit. (19) mp 193–194°].

1,5-Bis(4-chlorophenyl)-3-pentanone—A mixture of the di-unsaturated ketone (6 g, 0.02 mole) and 2.5 g of Raney nickel in 100 ml of ethanol was shaken at 20° under 3.5 kg/cm^2 hydrogen for 2 hr until near theoretical uptake was observed. The catalyst was filtered and the solvent was removed by distillation. The residual oil was dissolved in 400 ml of methylene chloride and chromatographed on a column containing 450 g of silica gel. The product was obtained in fractions four and five (400 ml each) as a solid (4 g, 75%) after solvent removal. One gram was recrystallized from 5 ml of 2-propanol to yield colorless plates (0.7 g); mp 65–67°, IR: 1690 (C=O) cm^{-2}.

Anal.—Calc. for $C_{17}H_{16}Cl_2O$: C, 66.46; H, 5.25; Cl, 23.08. Found: C, 66.58; H, 5.20; Cl, 23.02.

***N*-(ω,ω'-Disubstituted *sec*-alkyl)-1,3-diamino-2-propanol Dihydrochlorides (I*a*–I*n*)**—Schiff bases were obtained by condensation of ω,ω'-disubstituted alkanones with 1,3-diamino-2-propanol in refluxing toluene and azeotropic water removal (5), or by reaction in ethanol without water separation. The carbon–nitrogen double bond was reduced catalytically with hydrogen or with sodium borohydride. Both procedures are exemplified with the preparations, I*i* and I*m*. Table I lists the physical and analytical data.

1-Amino -3- {[3-[4-(1-methylethyl)phenyl] -1- [2-[4-(1-methylethyl)phenyl]ethyl]-propyl}amino}-2-propanol Dihydrochloride (I*i*)—A solution of 1,5-bis[4-(1-methylethyl)-phenyl]-3-pentanone (6.4 g, 0.02 mole) in 20 ml of ethanol was added dropwise (45 min) to a stirred solution of 1,3-diamino-2-propanol (10.8 g, 0.12 mole) in 80 ml of ethanol maintained at 90°. The resulting solution was heated at 90° for 12 hr, diluted with 50 ml of ethanol and cooled to 5°. Sodium borohydride (1.2 g, 0.03 mole) was added portionwise (10 min), and the reaction mixture, after 2 hr at 5°, was stirred for 2 hr at 20°. The solvent was removed *in vacuo* and the residual oil partitioned between 75 ml of ether and 75 ml of water. The ether solution was washed with 75 ml of brine, dried over sodium sulfate and concentrated *in vacuo*. The residual base was dissolved in 15 ml of 2-propanol, the solution cooled to 5° and mixed with 25 ml of 2-propanol saturated with hydrogen chloride. The solids, after mixing at 5° for 6 hr, were filtered and recrystallized from 35 ml of 95% 2-propanol to yield 6.9 g of Ic; NMR (dimethyl sulfoxide-d_6): δ 3.47 ppm [quintet, 1H of *sec*-alkyl(—CH_2)$_2$C*H*—NH—].

1-Amino -3- [3-(4-methoxyphenyl) -1- [2-(4-methoxyphenyl)ethyl]propylamino]-2-propanol Dihydrochloride (I*m*)—Powdered 1,5-bis(4-methoxyphenyl)-3-pentanone (6.0 g, 0.02 mole) was added slowly (30 min) to a stirred solution of 1,3-diamino-2-propanol (9.0 g, 0.1 mole) in 100 ml of ethanol maintained at 90°. After 12 hr the solution was cooled to 20°, diluted with 50 ml of ethanol, and mixed with 0.75 g of platinum oxide. Hydrogenation was run at 20–25° and 3.5 kg/cm^2 hydrogen. Within 2.5 hr, theoretical uptake was observed, and the reaction mixture was shaken an additional 0.5 hr. The catalyst was removed by filtration and the solvent distilled *in vacuo*. The residual oil was dissolved in 100 ml of ether. The product precipitated when mixed with 5 ml of 2-propanol which was previously saturated with hydrogen chloride. After 3 hr of mixing, the salt was filtered to yield 7.9 g (89%) of I*n* which was recrystallized from 2-propanol; NMR (dimethyl sulfoxide-d_6): δ 3.24 ppm [quintet, 1 H of *sec*-alkyl(—CH_2)$_2$C*H*—NH—].

REFERENCES

(1) A. Rancurel and G. Grenier, W. German pat. 2,606,106 (1976).

(2) C. H. Gleason, British pat. 987,438 (1965).

(3) E. Jeney and T. Zsolnai, *Zentr. Bakteriol., Parasitenk. Infektionskr. Abt I Orig.*, **192,** 358 (1964).

(4) D. Mlynarcik, I. Lacko, and F. Devinsky, *Experientia*, **35,** 1044 (1979).

(5) N. Grier, R. A. Dybas, R. A. Strelitz, B. E. Witzel, and E. L. Dulaney, *J. Med. Chem.*, **22,** 1409 (1979).

(6) T. C. Y. Lo, *Can. J. Biochem.*, **57,** 289 (1979).

(7) M. D. Culler, J. Bitman, M. J. Thompson, W. E. Robbins, and S. R. Dutky, *J. Dairy Sci.*, **62,** 584 (1979).

(8) H. A. Cyba, U.S. pat. 3,189,613 (1965).

(9) R. A. Dybas, N. Grier, and B. E. Witzel, U.S. pat. 4,172,094 (1979).

(10) E. M. Richardson and E. E. Reid, *J. Am. Chem. Soc.*, **62,** 413 (1940).

(11) N. Grier and R. A. Strelitz, *J. Pharm. Sci.*, **65,** 616 (1976).

(12) L. H. Hall and L. B. Kier, *ibid.*, **67,** 1743 (1978).

(13) M. Charton and B. I. Charton, *J. Org. Chem.*, **44,** 2284 (1979).

(14) A. Leo, C. Hansch, and D. Elkins, *Chem. Rev.*, **71,** 525 (1971).

(15) A. Panthananickal, C. Hansch, and A. Leo, *J. Med. Chem.*, **22,** 1267 (1979).

(16) T. G. Appleton and J. R. Hall, *Inorg. Chem.*, **11,** 117 (1972).

(17) C. Hansch and J. M. Clayton, *J. Pharm. Sci.*, **62,** 1 (1973).

(18) M. R. W. Brown and E. Tomlinson, *ibid.*, **68,** 146 (1979).

(19) R. E. Lutz, T. A. Martin, J. F. Codington, T. M. Amacker, R. K. Allison, N. H. Leake, R. J. Rowlett, Jr., J. D. Smith, and J. W. Wilson, III, *J. Org. Chem.*, **14,** 982 (1949).

ACKNOWLEDGMENTS

The authors thank Jack Gilbert and associates of Microanalytical Services for elemental analyses and Dr. L. Oppenheimer for the statistical evaluation.

Intraocular Penetration of Topically Applied [^{14}C]Fosfonet Sodium in Rabbits

BARBARA A. BOPP,[x] WALTER W. HUNTER, and DAVID J. ANDERSON

Received February 2, 1981, from the *Drug Metabolism Department, Abbott Laboratories, North Chicago, IL 60064.* Accepted for publication July 30, 1981.

Abstract □ The intraocular penetration of [^{14}C]fosfonet was studied following topical application of 25 mg of an ointment containing 5% [^{14}C]fosfonet sodium onto the intact and abraded eyes of New Zealand white rabbits. Radioactivity penetrated rapidly through the abraded cornea and entered the anterior chamber. The concentration of fosfonet in the aqueous humor peaked at 7.2 μg/ml by 90 min. Assuming an aqueous humor volume of 300 μl, this level would correspond to approximately 0.2% of the applied dose. The highest concentration of fosfonet found in the abraded cornea was 0.3 μg/mg, or 0.4% of the applied dose. The half-lives for the elimination of fosfonet from the aqueous humor and cornea were about 2.5 and 2.7 hr, respectively. The fosfonet levels in the iris were extremely low throughout the 6-hr period. The penetration of [^{14}C]fosfonet through the intact cornea was considerably less than that found in the abraded eye. The peak concentrations of fosfonet in the aqueous humor and cornea of the intact eye were 0.26 μg/ml and 0.02 μg/mg, respectively, and occurred within 10 min of application of the ointment.

Keyphrases □ [^{14}C]Fosfonet sodium—intraocular penetration □ Ocular agents—[^{14}C]fosfonet, aqueous humor, ophthalmic bioavailability, rabbit eye □ Antiherpetic agent—effect of [^{14}C]fosfonet on rabbit cornea

Shipkowitz *et al.* (1) first reported that fosfonet sodium (disodium phosphonoacetate) inhibited the replication of herpes viruses both in tissue cultures and in experimental animal models. Fosfonet was effective in reducing the severity of the corneal lesions in rabbits when applied topically in concentrations of 0.5 to 5% starting 2 hr after virus inoculation. Subsequent studies demonstrated that 5% fosfonet, either as a solution or an ointment, was as effective as 0.5% idoxuridine in the treatment of established herpetic keratitis in rabbits (2–4) and was superior to idoxuridine in inhibiting the replication of the virus (3). Furthermore, it was found (4) that fosfonet was also effective against idoxuridine-resistant keratitis when applied topically on rabbit eyes and against herpetic iritis when administered to rabbits either intravenously or subconjunctively but not topically.

Fosfonet is relatively nontoxic to rabbit eyes. It was reported (4) that 5% fosfonet was not toxic to the corneal epithelium of rabbits when applied 6 times a day for 5 days. Similarly, rabbit eyes were treated with a 5% fosfonet ointment 4 times a day for 42 days and no evidence of toxicity in clinical and histopathological studies was found (3). Although fine punctate lesions of the superficial corneal epithelium were observed (2) when a 5% fosfonet solution was applied to normal rabbit eyes 8 times a day for 3 days, the lesions disappeared within 48 hr after treatment was stopped and were no more severe than those encountered with idoxuridine.

Because of its potential usefulness in treating herpetic keratitis, this study was performed to investigate the intraocular penetration of [^{14}C]fosfonet after topical application of an ointment containing 5% fosfonet sodium onto the intact or abraded eyes of rabbits. Since removal of the corneal epithelium frequently enhances the intraocular penetration of drugs and the integrity of the corneal epithelium may be disrupted in ocular herpes infections, it was of special interest to study the intraocular penetration of fosfonet in eyes with corneal abrasions.

Table I—Aqueous Humor, Cornea, and Iris Concentrations following Topical Application of a 5% [^{14}C]Fosfonet Sodium Ointment (25 mg) onto Abraded Eyes of New Zealand White Rabbits

Time after Application	Aqueous Humor[a]			Cornea[a]		Iris[a]	
	%/ml	%	μg/ml	%	μg/mg	%	μg/mg
10 min	0.31 ± 0.05	0.09 ± 0.01	2.94 ± 0.47	0.40 ± 0.06	0.27 ± 0.04	<0.01 —	0.02 ± <0.01
20 min	0.40 ± 0.05	0.12 ± 0.02	3.76 ± 0.48	0.41 ± 0.05	0.27 ± 0.03	0.01 ± <0.01	0.02 ± <0.01
40 min	0.70 ± 0.08	0.21 ± 0.02	6.61 ± 0.79	0.41 ± 0.07	0.28 ± 0.04	0.01 ± <0.01	0.02 ± 0.01
1 hr	0.69 ± 0.10	0.21 ± 0.03	6.53 ± 0.91	0.30 ± 0.04	0.22 ± 0.02	<0.01 —	0.01 ± <0.01
1.5 hr	0.76 ± 0.10	0.23 ± 0.03	7.23 ± 0.91	0.34 ± 0.08	0.23 ± 0.05	0.01 ± <0.01	0.02 ± <0.01
2 hr	0.67 ± 0.08	0.20 ± 0.02	6.36 ± 0.79	0.28 ± 0.03	0.18 ± 0.02	<0.01 —	0.01 ± <0.01
3 hr	0.59 ± 0.09	0.18 ± 0.03	5.61 ± 0.87	0.21 ± 0.03	0.13 ±0.02	<0.01 —	0.01 ± <0.01
4 hr	0.42 ± 0.09	0.12 ± 0.03	3.97 ± 0.83	0.17 ± 0.02	0.10 ±0.01	<0.01 —	0.01 ± <0.01
6 hr	0.21 ± 0.03	0.06 ± 0.01	2.01 ± 0.31	0.12 ± 0.01	0.07 ± 0.01	<0.01 —	<0.01 —

[a] Mean ± standard error of 10–12 determinations, based on total radioactivity and expressed as micrograms of fosfonet, assuming a 25-mg dose of the ointment corresponding to 1250 μg of fosfonet sodium or 950 μg of fosfonet. Concentrations expressed per milliliter aqueous humor or milligram dry weight of cornea or iris. The percentage in aqueous humor was calculated from the %/ml, assuming a total aqueous humor volume of 0.30 ml.

EXPERIMENTAL

Materials—Fosfonet sodium was labeled with carbon 14 in the carboxylic position. Radiochemical and chemical purity was established by thin layer and anion exchange chromatography and mass spectrometry. A lanolin–petrolatum based ointment[1] containing 5% [^{14}C]fosfonet sodium was prepared and had a final activity of 0.16 μCi/mg ointment.

Animals—Male New Zealand white rabbits, weighing 2.3–4.0 kg, were used. Prior to use, the animals were maintained in standard laboratory animal cages and allowed food and water *ad libitum*. During the study, the rabbits were placed in restraining cages which held them in a normal upright position. All animals were acclimated to these conditions by being placed in the restrainers for successively longer periods of time twice a day for 3 days.

Corneal abrasions were made by anesthetizing the eye with 0.5% tetracaine hydrochloride[2] and then gently scraping the cornea with a scalpel blade to remove the epithelial surface. Fluorescein staining was performed in preliminary studies to assess the abrading technique. Extreme care was exercised to avoid damaging the corneal stroma or the conjunctiva, and any animal that had visible signs of damage (*e.g.*, bleeding) was not used in the study. About 1.5–2 hr elapsed between abrading and dosing the eye.

While holding the eyelids open and after the nictitating membrane had receded, the ointment (~25 mg) was applied onto the corneal surface and into the pocket formed by the lower lid and the globe. The eyelids were

[1] Composition of the ointment in % by weight: Solution containing 50% (w/v) fosfonet disodium monohydrate, 15.3%; anhydrous lanolin, 22.6%; 17% benzalkonium chloride, 0.01%; white petrolatum, 62.1%.

[2] Abbott Laboratories, North Chicago, Ill.

0022-3549/82/0300-0368$01.00/0

Table II—Aqueous Humor and Cornea Concentrations following Topical Application of a 5% [^{14}C]Fosfonet Sodium Ointment (25 mg) onto Intact Eyes of New Zealand White Rabbits

Time After Application	Aqueous Humor[a]			Cornea[a]	
	%/ml	%	μg/ml	%	μg/mg
10 min	0.03 ± 0.01	0.008 ± 0.002	0.26 ± 0.08	0.04 ± 0.01	0.02 ± <0.01
20 min	0.01 ± <0.01	0.002 ± <0.001	0.06 ± 0.01	0.02 ± <0.01	0.01 ± <0.01
40 min	0.01 ± <0.01	0.004 ± 0.001	0.12 ± 0.03	0.03 ± <0.01	0.01 ± <0.01
1 hr	0.01 ± <0.01	0.003 ± <0.001	0.08 ± 0.01	0.02 ± <0.01	0.01 ± <0.01
1.5 hr	0.02 ± 0.01	0.006 ± 0.002	0.20 ± 0.07	0.02 ± 0.01	0.01 ± <0.01
2 hr	0.02 ± 0.01	0.005 ± 0.003	0.16 ± 0.10	0.01 ± <0.01	0.01 ± <0.01
3 hr	0.02 ± <0.01	0.005 ± <0.001	0.16 ± 0.02	0.02 ± <0.01	0.01 ± <0.01
4 hr	0.02 ± 0.01	0.005 ± 0.002	0.15 ± 0.05	0.01 ± <0.01	0.01 ± <0.01
6 hr	0.02 ± 0.01	0.005 ± 0.002	0.16 ± 0.05	0.01 ± <0.01	<0.01 —

[a] Mean ± standard error of six determinations, based on total radioactivity and expressed as micrograms of fosfonet, assuming a 25-mg dose of the ointment corresponding to 1250 μg of fosfonet sodium or 950 μg of fosfonet. Concentrations expressed per milliliter aqueous humor or milligram dry weight of cornea. The percentage in aqueous humor was calculated from the %/ml, assuming a total aqueous humor volume of 0.30 ml.

then released and gently manipulated to spread the ointment over the cornea. Generally both eyes of each rabbit were used, but the dosing schedule was adjusted so that the eyes represented two different, but not successive, time points. At selected times after dosing, the rabbits were sacrificed by injecting an overdose of a solution[3] containing sodium pentobarbital, sodium secobarbital, and mephenesin into the marginal ear vein. The cornea and sclera were thoroughly rinsed with physiological saline[4] and gently wiped dry with a tissue. An aqueous humor sample (0.1–0.2 ml) was withdrawn from the anterior chamber. The optic nerve and blood vessels were then clamped with a hemostat, and the corneal surface was again rinsed with saline. The cornea and iris were removed by cutting around the corneal-scleral limbus, and the iris was separated from the cornea. Both tissues were thoroughly rinsed in saline, allowed to dry for several days at room temperature, and weighed.

In some animals, ointment was applied to both eyes at the same time, and blood samples were withdrawn from the central artery of an ear at selected times after dosing. The heparinized blood samples were centrifuged and the plasma was saved for radioassay.

Radioassay—An aliquot of the aqueous humor samples was applied to an absorbant paper disc[5] encased in a cellophane combustion envelope[6]. The tissue and plasma samples were placed in combustion cones[7] containing cellulose powder[8]. All samples were then burned in a sample oxidizer[9], and radioassay was accomplished by liquid scintillation spectrometry[10]. Correction for quenching was made by automatic external standardization. All levels were based on total radioactivity and were expressed as micrograms of fosfonet. To correct for the small and statistically insignificant differences in the milligrams of ointment applied, the results were expressed as adjusted concentrations based on a 25.0-mg dose.

RESULTS

The drug concentrations in the aqueous humor, cornea, and iris at various times after topical application of the [^{14}C]fosfonet sodium ointment onto the abraded eyes of New Zealand white rabbits are presented in Table I. The radioactivity appeared to penetrate rapidly through the abraded cornea and enter the aqueous humor. The concentration of fosfonet in the aqueous humor ~2.9 μg/ml by 10 min, reached 6.6 μg/ml by 40 min, and peaked at 7.2 μg/ml by 90 min. Thereafter, the levels in the aqueous humor declined slowly, with a half-life of ~2.5 hr, as determined by linear regression analysis. The peak concentration of fosfonet in the abraded cornea was ~0.3 μg/mg dry weight and remained relatively constant through at least 40 min. The half-life for the disappearance of radioactivity from the cornea was ~2.7 hr. The levels of fosfonet in the iris were very low throughout the study, never exceeding 0.02 μg/mg.

The penetration of fosfonet through the intact cornea (Table II) was considerably less than that found in the abraded eyes. The peak levels in both the aqueous humor and cornea of the intact eyes were reached by 10 min but were only 0.26 μg/ml and 0.02 μg/mg, respectively. The concentrations in the iris were consistently less than 0.01 μg/mg.

The systemic absorption of fosfonet appeared to be quite limited. In rabbits with an intact corneal epithelium, the plasma concentrations at times ranging from 10 min to 24 hr never reached 0.01 μg/ml, while the levels in the rabbits with abraded corneas averaged 0.01–0.02 μg/ml.

DISCUSSION

The results of this study were based on total radioactivity but were expressed as micrograms of fosfonet. Since previous studies[11] in these laboratories had indicated that intravenously administered [^{14}C]fosfonet was excreted unchanged in the urine of rabbits, it is reasonable to assume that most of the radioactivity did represent the parent drug. It was also assumed that the radioactivity found in each eye came from transcorneal penetration and not from the systemic circulation. The low plasma levels of radioactivity suggested that this assumption was also valid. The plasma levels appeared to be slightly higher in the rabbits with abraded corneas than those with an intact corneal epithelium, possibly due to the greater penetration of fosfonet into the abraded eye. However, it was more striking that the drug levels in the systemic circulation were exceedingly low.

Generally, less than 1% of the instilled dose of most drugs crosses the cornea and enters the anterior chamber (5). For example, it was reported (6) that ~0.1–0.2% of an instilled dose of a tritiated pilocarpine nitrate solution was found in the aqueous humor of intact rabbit eyes. If the total volume of aqueous humor in a rabbit eye is assumed to be 300 μl (7, 8), then ~0.23% of the applied fosfonet dose would be present in the aqueous humor of the abraded eyes at the time of the peak concentration (1.5 hr). In contrast, less than 0.01% of the dose would have penetrated through the intact cornea and entered the aqueous humor. Comparison of the areas under the aqueous humor concentration–time curves indicated that the amount of drug penetrating through the intact cornea was only about 3% of that found in the aqueous humor of the abraded eyes. Removal of the corneal epithelium enhances the rate and degree of penetration, especially with water soluble or polar compounds (9). Therefore, the marked difference in the penetration of fosfonet through the intact and abraded corneas is not surprising. However, it should be noted that the integrity of the corneal epithelium is one factor that might markedly affect the intraocular penetration and possibly the therapeutic efficacy of fosfonet.

Most drugs achieve peak concentrations in the cornea and aqueous humor in a short time, thus appearing to penetrate rapidly into the ocular tissues. However, recent studies with pilocarpine nitrate have shown that the short time required to reach the peak concentrations is primarily dependent on the rapid parallel elimination of the drug from the precorneal area and that the actual absorption rates for the cornea and aqueous humor are lower than expected from the concentration–time profiles (10–13). With fosfonet, the peak concentrations in both the intact and abraded corneas were reached within 10 min, the shortest time interval studied. The peak concentration in the aqueous humor of the intact eye was also reached within 10 min, but there was considerable fluctuation in the aqueous humor levels during the first two hr. In contrast, the aqueous humor concentrations in the abraded eye peaked considerably later (1.5 hr). The reasons for the difference in the peak concentration times are not known. More work is required to determine fosfonet pharmacokinetics in intact and abraded eyes and to assess other factors that might influence the time needed to reach peak concentrations.

It was found (4) that fosfonet was effective in treating experimental herpetic iritis in rabbits when administered systemically or subconjunctively but not topically. The low fosfonet levels in the iris were consistent with the lack of beneficial effects of topically applied fosfonet in herpetic iritis in rabbits. However, stromal disease and iritis are difficult to treat effectively with the topical application of most other antiviral agents as well (14).

[3] Repose; Diamond Laboratories, Des Moines, Ia.
[4] Abbott Laboratories, North Chicago, Ill.
[5] Schleicher and Schuell, Keene N.H.
[6] Ivers-Lee Co., West Caldwell, N.J.
[7] Packard Instrument Co., Downers Grove, Ill.
[8] Whatman, Inc., Clifton, N.J.
[9] Model 306 Sample Oxidizer, Packard Instrument Co., Downers Grove, Ill.
[10] Model 3380 Liquid Scintillation Spectrometer, Packard Instrument Co., Downers, Grove, Ill.

[11] Dr. G. Ikeda, Abbott Laboratories, North Chicago, Ill. (unpublished results).

REFERENCES

(1) N. L. Shipkowitz, R. R. Bower, R. N. Appell, C. W. Nordeen, L. R. Overby, W. R. Roderick, J. B. Schleicher, and A. M. Von Esch, *Appl. Microbiol.*, **26**, 264 (1973).

(2) D. D. Gerstein, C. R. Dawson, and J. O. Oh, *Antimicrob. Agents Chemother.*, **7**, 285 (1975).

(3) Y. J. Gordon, H. Lahav, S. Photious, and Y. Becker, *Br. J. Ophthalmol.*, **61**, 506 (1977).

(4) R. F. Meyer, E. D. Varnell, and H. E. Kaufman, *Antimicrob. Agents Chemother.*, **9**, 308 (1976).

(5) T. F. Patton and J. R. Robinson, *J. Pharm. Sci.*, **64**, 267 (1975).

(6) S. S. Chrai and J. R. Robinson, *Am. J. Ophthalmol.*, **77**, 735 (1974).

(7) "Blood and Other Body Fluids," P. L. Altman and D. S. Dittmer, Eds., Federation of American Societies for Experimental Biology, Bethesda, Md., 1971, p. 480.

(8) J. M. Conrad and J. R. Robinson, *J. Pharm. Sci.*, **66**, 219 (1977).

(9) H. Benson, *Arch. Ophthalmol.*, **91**, 313 (1974).

(10) M. C. Makoid, J. W. Sieg, and J. R. Robinson, *J. Pharm. Sci.*, **65**, 150 (1976).

(11) J. W. Sieg and J. R. Robinson, *J. Pharm. Sci.*, **65**, 1817 (1976).

(12) *Ibid.*, **66**, 1222 (1977).

(13) M. C. Makoid and J. R. Robinson, *J. Pharm. Sci.*, **68**, 435 (1979).

(14) H. E. Kaufman, *J. Infect. Dis.*, **133**, A96 (1976).

ACKNOWLEDGMENTS

The authors thank Dr. Joseph Robinson of the University of Wisconsin, Madison, Wisconsin, for his helpful advice and for demonstrating the techniques used in this study.

COMMUNICATIONS

Unusual Cholesterol Solubility in Water/Glyceryl-1-monooctanoate Solutions

Keyphrases □ Cholesterol—unusual solubility in water/glyceryl-1-monooctanoate solutions □ Glyceryl-1-monooctanoate—aqueous solutions, unusual solubilities of cholesterol □ Gallstones—cholesterol, solubility in water/glyceryl-1-monooctanoate solutions

To the Editor:

Glyceryl-1-monooctanoate (monooctanoin) (I) has been recently used in humans for dissolution of cholesterol gallstones in the common bile duct (1, 2). The solvent is slowly infused into the bile duct for several days, usually *via* a T-tube left in place following cholecystectomy. The high cholesterol solubility in I, 11.7% (w/v) at 37°, was reported in a systematic study of cholesterol solubility in organic solvents by Flynn *et al.* (3). Optimum cholesterol solubility appeared to occur when the solvent (*n*-alkanols or fatty acid ethyl esters) had a total carbon chain length of about seven atoms.

The present study was initiated to determine if cholesterol was involved in formation of liquid crystalline phases in aqueous I solutions. Larsson found that highly purified I and water formed a lamellar liquid crystalline phase at 37° when the water content was between 8 and 45% (4). Such equilibria could be important in gallstone dissolution since I would be in contact with bile during the infusion procedure and with moisture during handling. But when water/I mixtures were prepared with the same type of I used in the reported gallstone dissolution studies[1], only isotropic phases were observed by polarizing microscopy[2]. This apparent discrepancy is thought to be caused by the presence of about 30% of the corresponding diglyceride in the commercial material (1, 5). Diglycerides or triglycerides are more hydrophobic and do not form lyotropic mesophases (4). The solubility of water in the commercial sample of I was determined visually to be ~18–20% (w/w) at 37°. An exact value is not meaningful, since each batch will vary somewhat in its fatty acid distribution and diglyceride content. Above this concentration simple emulsions were formed rather than liquid crystalline phases.

Cholesterol is known to crystallize in anhydrous and monohydrate forms (6) and the anhydrous form is ~50% more soluble in aqueous bile salt solutions (7). Since either of these crystalline forms could possibly exist in aqueous I solutions, the cholesterol solubility in such solvent mixtures was determined (Fig. 1). Suspensions of anhydrous cholesterol[3] or cholesterol monohydrate (recrystallized from aqueous ethanol) were prepared in aqueous I solutions and equilibrated using a vibratory mixer[4] in a constant-temperature bath. The suspensions at equilibrium were observed with the polarizing microscope and quickly filtered through 0.45 μm membranes[5] which had been equilibrated at the test temperature. The two crystal forms were microscopically identified by their characteristic habits (6). The filtrates were analyzed for cholesterol by HPLC (8) with detection at 205 nm and for water content by Karl Fischer titrimetry[6].

Cholesterol solubility increased to a maximum and then decreased over the range of water concentration studied. The solubility was independent of the sampling time and crystal form initially present, indicating that equilibrium had been attained. An explanation cannot be offered for the higher solubility found in the present investigation compared to previous reports (3).

Immediate microscopic inspection of the suspensions showed that at water concentrations below the apparent

[1] Capmul 8210, Capitol City Products, Columbus, Ohio.
[2] Zetopan, Reichert, Vienna, Austria.
[3] Sigma Chemical Co., St. Louis, Mo.
[4] Vibromixer E1, Chemapec, Woodbury, N.Y.
[5] Millipore, Bedford, Mass.
[6] Auto-aquatrator, Precision Scientific, Chicago, Ill.

0022-3549/82/0300-0370$01.00/0

REFERENCES

(1) N. L. Shipkowitz, R. R. Bower, R. N. Appell, C. W. Nordeen, L. R. Overby, W. R. Roderick, J. B. Schleicher, and A. M. Von Esch, *Appl. Microbiol.*, **26**, 264 (1973).

(2) D. D. Gerstein, C. R. Dawson, and J. O. Oh, *Antimicrob. Agents Chemother.*, **7**, 285 (1975).

(3) Y. J. Gordon, H. Lahav, S. Photious, and Y. Becker, *Br. J. Ophthalmol.*, **61**, 506 (1977).

(4) R. F. Meyer, E. D. Varnell, and H. E. Kaufman, *Antimicrob. Agents Chemother.*, **9**, 308 (1976).

(5) T. F. Patton and J. R. Robinson, *J. Pharm. Sci.*, **64**, 267 (1975).

(6) S. S. Chrai and J. R. Robinson, *Am. J. Ophthalmol.*, **77**, 735 (1974).

(7) "Blood and Other Body Fluids," P. L. Altman and D. S. Dittmer, Eds., Federation of American Societies for Experimental Biology, Bethesda, Md., 1971, p. 480.

(8) J. M. Conrad and J. R. Robinson, *J. Pharm. Sci.*, **66**, 219 (1977).

(9) H. Benson, *Arch. Ophthalmol.*, **91**, 313 (1974).

(10) M. C. Makoid, J. W. Sieg, and J. R. Robinson, *J. Pharm. Sci.*, **65**, 150 (1976).

(11) J. W. Sieg and J. R. Robinson, *J. Pharm. Sci.*, **65**, 1817 (1976).

(12) *Ibid.*, **66**, 1222 (1977).

(13) M. C. Makoid and J. R. Robinson, *J. Pharm. Sci.*, **68**, 435 (1979).

(14) H. E. Kaufman, *J. Infect. Dis.*, **133**, A96 (1976).

ACKNOWLEDGMENTS

The authors thank Dr. Joseph Robinson of the University of Wisconsin, Madison, Wisconsin, for his helpful advice and for demonstrating the techniques used in this study.

COMMUNICATIONS

Unusual Cholesterol Solubility in Water/Glyceryl-1-monooctanoate Solutions

Keyphrases □ Cholesterol—unusual solubility in water/glyceryl-1-monooctanoate solutions □ Glyceryl-1-monooctanoate—aqueous solutions, unusual solubilities of cholesterol □ Gallstones—cholesterol, solubility in water/glyceryl-1-monooctanoate solutions

To the Editor:

Glyceryl-1-monooctanoate (monooctanoin) (I) has been recently used in humans for dissolution of cholesterol gallstones in the common bile duct (1, 2). The solvent is slowly infused into the bile duct for several days, usually *via* a T-tube left in place following cholecystectomy. The high cholesterol solubility in I, 11.7% (w/v) at 37°, was reported in a systematic study of cholesterol solubility in organic solvents by Flynn *et al.* (3). Optimum cholesterol solubility appeared to occur when the solvent (*n*-alkanols or fatty acid ethyl esters) had a total carbon chain length of about seven atoms.

The present study was initiated to determine if cholesterol was involved in formation of liquid crystalline phases in aqueous I solutions. Larsson found that highly purified I and water formed a lamellar liquid crystalline phase at 37° when the water content was between 8 and 45% (4). Such equilibria could be important in gallstone dissolution since I would be in contact with bile during the infusion procedure and with moisture during handling. But when water/I mixtures were prepared with the same type of I used in the reported gallstone dissolution studies[1], only isotropic phases were observed by polarizing microscopy[2]. This apparent discrepancy is thought to be caused by the presence of about 30% of the corresponding diglyceride in the commercial material (1, 5). Diglycerides or triglycerides are more hydrophobic and do not form lyotropic mesophases (4). The solubility of water in the commercial sample of I was determined visually to be ~18–20% (w/w) at 37°. An exact value is not meaningful, since each batch will vary somewhat in its fatty acid distribution and diglyceride content. Above this concentration simple emulsions were formed rather than liquid crystalline phases.

Cholesterol is known to crystallize in anhydrous and monohydrate forms (6) and the anhydrous form is ~50% more soluble in aqueous bile salt solutions (7). Since either of these crystalline forms could possibly exist in aqueous I solutions, the cholesterol solubility in such solvent mixtures was determined (Fig. 1). Suspensions of anhydrous cholesterol[3] or cholesterol monohydrate (recrystallized from aqueous ethanol) were prepared in aqueous I solutions and equilibrated using a vibratory mixer[4] in a constant-temperature bath. The suspensions at equilibrium were observed with the polarizing microscope and quickly filtered through 0.45 μm membranes[5] which had been equilibrated at the test temperature. The two crystal forms were microscopically identified by their characteristic habits (6). The filtrates were analyzed for cholesterol by HPLC (8) with detection at 205 nm and for water content by Karl Fischer titrimetry[6].

Cholesterol solubility increased to a maximum and then decreased over the range of water concentration studied. The solubility was independent of the sampling time and crystal form initially present, indicating that equilibrium had been attained. An explanation cannot be offered for the higher solubility found in the present investigation compared to previous reports (3).

Immediate microscopic inspection of the suspensions showed that at water concentrations below the apparent

[1] Capmul 8210, Capitol City Products, Columbus, Ohio.
[2] Zetopan, Reichert, Vienna, Austria.
[3] Sigma Chemical Co., St. Louis, Mo.
[4] Vibromixer E1, Chemapec, Woodbury, N.Y.
[5] Millipore, Bedford, Mass.
[6] Auto-aquatrator, Precision Scientific, Chicago, Ill.

0022-3549/82/0300-0370$01.00/0

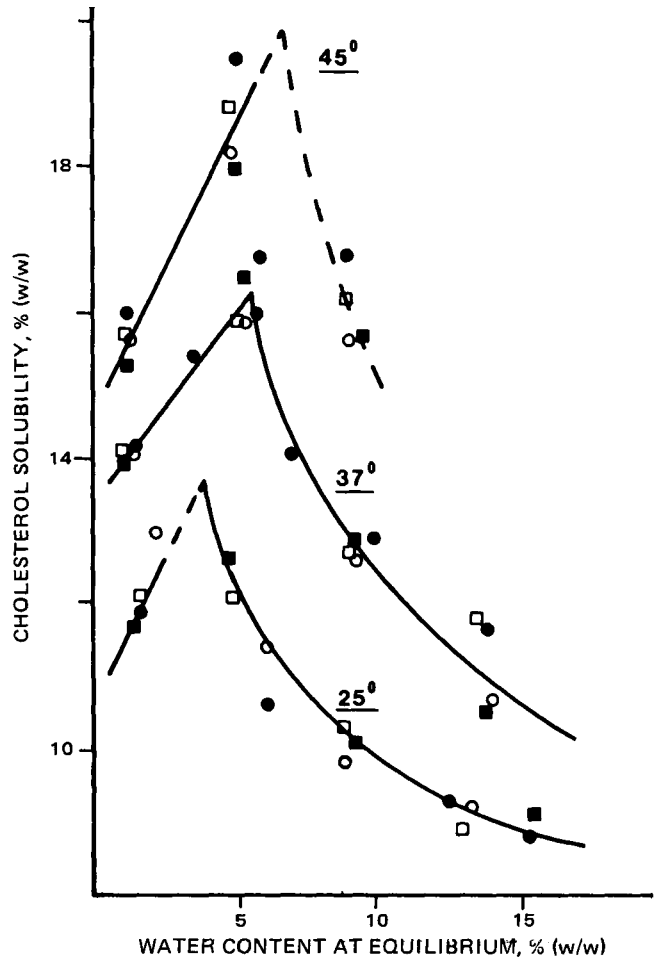

Figure 1—*Solubility of cholesterol in aqueous I solutions at 25, 37, and 45°. Key: Circles, initial solid phase was cholesterol monohydrate; squares, initial solid was anhydrous cholesterol; open symbols, 5 days; closed symbols, 7 days equilibration.*

solubility maxima, anhydrous cholesterol was present. Conversely, cholesterol monohydrate was present at water concentrations above the solubility maxima. In samples at 37° with 5.2% water, both forms were simultaneously observed. The maxima at 25 and 45° were not directly observed and the profiles are indicated by dashed lines.

When suspensions initially containing anhydrous cholesterol and about 5% water at 37 or 45° were cooled to room temperature, cholesterol monohydrate crystallized. The conversion process took place slowly on the microscope slide for several days until the anhydrous crystals were completely eliminated. Suspensions containing 1–2% water, however, remained as the anhydrous form when treated identically.

The concentration units used in this study may be misleading. A concentration of 5% (w/w) water would correspond to ~2.8 *M* and cholesterol concentrations of 14–16% are 0.36–0.41 *M*. The mole fractions for a system containing 5% water and 16% cholesterol are 0.44 and 0.07, respectively. The comparisons show that on a mole fraction basis the systems contain more water than indicated by simple concentration units.

The progression of the apparent maxima to higher water concentrations with increasing temperature (Fig. 1) is related to the heats of solution of the two crystalline forms. The ΔH^s_{anh} = 2.8 kcal/mole for the anhydrous form was estimated from the average of the slopes of ln (solubility) *versus* T^{-1} plots at water concentrations of 0 (extrapolated), 1.0, and 3.0% according to the van't Hoff relationship. For cholesterol monohydrate ΔH^s_{hydr} = 4.1 kcal/mole was estimated from the data at 9% water. The difference in these values represents the enthalpy of hydration of the crystalline anhydrous form to the monohydrate in aqueous I:

$$\text{anhydrous} + H_2O \rightleftharpoons \text{hydrate}, \Delta H = -1.3 \text{ kcal/mole}$$

This value is consistent with literature data for enthalpies of hydration which range from 1–4 kcal/mole for monohydrates (9–11). Therefore, the solubility of the monohydrate is more sensitive to temperature than is that of the anhydrous form.

The maximum cholesterol concentration occurs at the unique point at which the solubilities of the two forms are equal. As temperature increases, more added water is necessary to compensate for the greater effect of temperature on the monohydrate solubility. In this way the solubility maxima occur at higher water concentrations as temperature increases. This process is illustrated by a suspension of the two forms at 25° (solubility = 13.4%, water ≃3.5%) that is warmed to 37°. If excess solid is present and the forms behave independently, the solubility of the monohydrate should increase to 17.5%, the anhydrous form would increase to 16.1%, and the concentration of water would be slightly higher. Dissolution of the monohydrate causes the cholesterol concentration to be above the solubility of the anhydrous form and crystallization occurs. This process continues until the solid monohydrate is exhausted and the system is a suspension of anhydrous cholesterol. Addition of water to the anhydrous cholesterol suspension would cause solubility to increase slightly until the water causes crystallization of the monohydrate. The system would then be at the solubility maximum at 37°. Conversely, cooling of a suspension of both forms from 37 to 25° would result in a suspension containing only cholesterol monohydrate.

Igimi and Carey (7) reported solubility–temperature data for the two forms of cholesterol in aqueous sodium chenodeoxycholate solutions. From van't Hoff plots of these data, ΔH^s_{anh} (0.71 kcal/mole), ΔH^s_{hydr} (1.04 kcal/mole), and a difference (heat of hydration) of −0.33 kcal/mole were calculated. The poor agreement between the data in water/I and chenodeoxycholate solutions can not be explained at present, although the enthalpies for the bile salt solutions appear to be unusually low.

These preliminary data show that the maxima of cholesterol solubility in aqueous I solutions and its temperature dependence are due to the thermodynamics of interconversion of anhydrous and monohydrate crystalline forms. However, the reason for the increase in solubility of anhydrous cholesterol by small amounts of added water is not known. Addition of water to solutions containing cholesterol generally would be expected to *decrease* solubility. Further studies are in progress to investigate this behavior and determine the effect of water on dissolution rates of cholesterol and gallstones in aqueous I solutions.

(1) J. L. Thistle, G. L. Carlson, A. F. Hofmann, N. F. LaRusso, R. L. MacCarty, G. L. Flynn, W. I. Higuchi, and V. K. Babayan, *Gastroen-*

terology, **78**, 1016 (1980).
(2) E. Mack, E. M. Patzer, A. B. Crummy, A. F. Hofmann, and V. K. Babayan, *Arch. Surg.*, **116**, 341 (1981).
(3) G. L. Flynn, Y. Shah, S. Prakongpan, K. H. Kwan, W. I. Higuchi, and A. F. Hofmann, *J. Pharm. Sci.*, **68**, 1090 (1979).
(4) K. Larsson, *Z. Phys. Chem.*, **56**, 173 (1967).
(5) Product Specifications, Capmul 8210, Capitol City Products Co., Columbus, Ohio.
(6) C. R. Loomis, G. G. Shipley, and D. M. Small, *J. Lipid Res.*, **20**, 525 (1979).
(7) H. Igimi and M. C. Carey, *ibid.*, **22**, 254 (1981).
(8) E. Hansbury and T. J. Scallen, *ibid.*, **19**, 742 (1978).
(9) E. Shefter and T. Higuchi, *J. Pharm. Sci.*, **52**, 781 (1963).
(10) D. A. Wadke and G. R. Reier, *ibid.*, **61**, 868 (1972).
(11) K. Sekiguchi, M. Kanke, Y. Tsuda, K. Ishida, and Y. Isuda, *Chem. Pharm. Bull.*, **21**, 1592 (1973).

Joseph B. Bogardus
College of Pharmacy
University of Kentucky
Lexington, KY 40506

Received August 10, 1981.
Accepted for publication October 5, 1981.

Noncompartmental Determination of the Steady-State Volume of Distribution for Any Mode of Administration

Keyphrases □ Pharmacokinetics—noncompartmental determination of the steady-state volume of distribution for any mode of administration □ Volume of distribution—steady-state, noncompartmental determination for any mode of administration

To the Editor:

The analysis of concentration–time data by pharmacokinetic methods traditionally involves the use of compartmental models. The interpretation of this analysis, represented by a linear equation in the form of a sum of coefficient and exponential terms, provides useful insight into drug disposition. In recent years, however, there has been a move away from the traditional approach to an alternative method referred to as model-independent data analysis. There are reasons to recommend the latter approach; there is no need to ascribe the data to a specific model, and as a result it is not necessary to have a sophisticated computer and nonlinear regression programs available. The model-independent approach assumes only that all dispositional processes may be described by first-order kinetics with elimination occurring from the rapidly equilibrating or central compartment. This approach may also be termed an area analysis, since the useful parameters of clearance and volumes of distribution (V_{ss} and V_β or V_{area}) are based on determination of the total area under the plasma concentration–time curve (AUC) and total area under the first moment of the plasma concentration–time curve ($AUMC$). The areas generally are determined using the linear or logarithmic trapezoidal rule and extrapolation techniques. The elimination rate constant and half-life are determined from linear regression of the terminal (*i.e.*, post-absorption, post-distribution) concentration–time data.

Benet and Galeazzi (1) applied techniques of tracer kinetics, and used moment analysis (2, 3) to obtain the volume of distribution at steady state, V_{ss}, following an intravenous bolus injection. The purpose of this communication is to extend their analysis to permit calculation of V_{ss} for any mode of administration.

The mean transit time for a drug in the body, $\bar{t}_b$, is a function of the mean transit time for the response to the input (in), usually measured as plasma concentration, $\bar{t}_{b+in}$, and the mean transit time of the input, $\bar{t}_{in}$ (4):

$$\bar{t}_b = \bar{t}_{b+in} - \bar{t}_{in} \qquad \text{(Eq. 1)}$$

Mean transit or residence time for the response to the input, *i.e.*, plasma concentration, is given by:

$$\bar{t}_{b+in} = \int_0^\infty tC\,dt \Big/ \int_0^\infty C\,dt = AUMC/AUC \qquad \text{(Eq. 2)}$$

while the mean transit time for the input is given by (5):

$$\bar{t}_{in} = \int_0^\infty X\,dt/\text{dose} \qquad \text{(Eq. 3)}$$

where dose is the dose administered, and $\int_0^\infty X\,dt$ is the total area under the amount *versus* time curve for the input. For example, if a drug is administered as a zero-order infusion:

$$X = \text{dose} - k_0 t \qquad \text{(Eq. 4)}$$

In Eq. 4, X is the amount remaining to be infused at time t, and k_0 is the zero-order infusion rate. Administration by a first-order process (*e.g.*, extravascular administration) results in the following expression for X, the amount remaining to be administered:

$$X = F\,\text{dose}\,e^{-k_a t} \qquad \text{(Eq. 5)}$$

where k_a is an apparent first-order rate constant, and F is the fraction of the administered dose ultimately reaching the systemic circulation. Integration of Eqs. 4 and 5 yields:

$$\int_0^T X\,dt = k_0 T^2/2 \qquad \text{(Eq. 6)}$$

and

$$\int_0^\infty X\,dt = F\,\text{dose}/k_a \qquad \text{(Eq. 7)}$$

respectively. In Eq. 6, T is the duration of the infusion and is the upper limit of the integral, *i.e.*, T is equivalent to infinity.

Substitution for $\bar{t}_{b+in}$ and $\bar{t}_{in}$, according to Eqs. 2 and 3, respectively, in Eq. 1 gives the following expression for drug transit time in the body:

$$\bar{t}_b = AUMC/AUC - \int_0^\infty X\,dt/\text{dose} \qquad \text{(Eq. 8)}$$

Since V_{ss} is equal to the product of clearance (dose/AUC) and transit time (1), that is:

$$V_{ss} = \frac{\text{dose}}{AUC}\bar{t}_b \qquad \text{(Eq. 9)}$$

Equations 8 and 9 can be readily used to calculate V_{ss} following any mode of administration. Where there is a single mode of administration, Eqs. 8 and 9 can be readily solved for V_{ss}. For the case where drug is administered as a single bolus, $\int_0^\infty X\,dt = 0$,

$$V_{ss} = \frac{\text{dose}}{AUC}\bar{t}_b = \frac{\text{dose}}{AUC}\left(\frac{AUMC}{AUC}\right) = \text{dose}\,\frac{AUMC}{AUC^2} \qquad \text{(Eq. 10)}$$

This is the same equation as derived by Benet and Galeazzi

0022-3549/82/0300-0372$01.00/0

terology, **78**, 1016 (1980).
(2) E. Mack, E. M. Patzer, A. B. Crummy, A. F. Hofmann, and V. K. Babayan, *Arch. Surg.*, **116**, 341 (1981).
(3) G. L. Flynn, Y. Shah, S. Prakongpan, K. H. Kwan, W. I. Higuchi, and A. F. Hofmann, *J. Pharm. Sci.*, **68**, 1090 (1979).
(4) K. Larsson, *Z. Phys. Chem.*, **56**, 173 (1967).
(5) Product Specifications, Capmul 8210, Capitol City Products Co., Columbus, Ohio.
(6) C. R. Loomis, G. G. Shipley, and D. M. Small, *J. Lipid Res.*, **20**, 525 (1979).
(7) H. Igimi and M. C. Carey, *ibid.*, **22**, 254 (1981).
(8) E. Hansbury and T. J. Scallen, *ibid.*, **19**, 742 (1978).
(9) E. Shefter and T. Higuchi, *J. Pharm. Sci.*, **52**, 781 (1963).
(10) D. A. Wadke and G. R. Reier, *ibid.*, **61**, 868 (1972).
(11) K. Sekiguchi, M. Kanke, Y. Tsuda, K. Ishida, and Y. Isuda, *Chem. Pharm. Bull.*, **21**, 1592 (1973).

Joseph B. Bogardus
College of Pharmacy
University of Kentucky
Lexington, KY 40506

Received August 10, 1981.
Accepted for publication October 5, 1981.

Noncompartmental Determination of the Steady-State Volume of Distribution for Any Mode of Administration

Keyphrases □ Pharmacokinetics—noncompartmental determination of the steady-state volume of distribution for any mode of administration □ Volume of distribution—steady-state, noncompartmental determination for any mode of administration

To the Editor:

The analysis of concentration–time data by pharmacokinetic methods traditionally involves the use of compartmental models. The interpretation of this analysis, represented by a linear equation in the form of a sum of coefficient and exponential terms, provides useful insight into drug disposition. In recent years, however, there has been a move away from the traditional approach to an alternative method referred to as model-independent data analysis. There are reasons to recommend the latter approach; there is no need to ascribe the data to a specific model, and as a result it is not necessary to have a sophisticated computer and nonlinear regression programs available. The model-independent approach assumes only that all dispositional processes may be described by first-order kinetics with elimination occurring from the rapidly equilibrating or central compartment. This approach may also be termed an area analysis, since the useful parameters of clearance and volumes of distribution (V_{ss} and V_β or V_{area}) are based on determination of the total area under the plasma concentration–time curve (AUC) and total area under the first moment of the plasma concentration–time curve ($AUMC$). The areas generally are determined using the linear or logarithmic trapezoidal rule and extrapolation techniques. The elimination rate constant and half-life are determined from linear regression of the terminal (*i.e.*, post-absorption, post-distribution) concentration–time data.

Benet and Galeazzi (1) applied techniques of tracer kinetics, and used moment analysis (2, 3) to obtain the volume of distribution at steady state, V_{ss}, following an intravenous bolus injection. The purpose of this communication is to extend their analysis to permit calculation of V_{ss} for any mode of administration.

The mean transit time for a drug in the body, $\bar{t}_b$, is a function of the mean transit time for the response to the input (in), usually measured as plasma concentration, $\bar{t}_{b+in}$, and the mean transit time of the input, $\bar{t}_{in}$ (4):

$$\bar{t}_b = \bar{t}_{b+in} - \bar{t}_{in} \qquad \text{(Eq. 1)}$$

Mean transit or residence time for the response to the input, *i.e.*, plasma concentration, is given by:

$$\bar{t}_{b+in} = \int_0^\infty tC\,dt \Big/ \int_0^\infty C\,dt = AUMC/AUC \qquad \text{(Eq. 2)}$$

while the mean transit time for the input is given by (5):

$$\bar{t}_{in} = \int_0^\infty X\,dt/\text{dose} \qquad \text{(Eq. 3)}$$

where dose is the dose administered, and $\int_0^\infty X\,dt$ is the total area under the amount *versus* time curve for the input. For example, if a drug is administered as a zero-order infusion:

$$X = \text{dose} - k_0 t \qquad \text{(Eq. 4)}$$

In Eq. 4, X is the amount remaining to be infused at time t, and k_0 is the zero-order infusion rate. Administration by a first-order process (*e.g.*, extravascular administration) results in the following expression for X, the amount remaining to be administered:

$$X = F\,\text{dose}\,e^{-k_a t} \qquad \text{(Eq. 5)}$$

where k_a is an apparent first-order rate constant, and F is the fraction of the administered dose ultimately reaching the systemic circulation. Integration of Eqs. 4 and 5 yields:

$$\int_0^T X\,dt = k_0 T^2/2 \qquad \text{(Eq. 6)}$$

and

$$\int_0^\infty X\,dt = F\,\text{dose}/k_a \qquad \text{(Eq. 7)}$$

respectively. In Eq. 6, T is the duration of the infusion and is the upper limit of the integral, *i.e.*, T is equivalent to infinity.

Substitution for $\bar{t}_{b+in}$ and $\bar{t}_{in}$, according to Eqs. 2 and 3, respectively, in Eq. 1 gives the following expression for drug transit time in the body:

$$\bar{t}_b = AUMC/AUC - \int_0^\infty X\,dt/\text{dose} \qquad \text{(Eq. 8)}$$

Since V_{ss} is equal to the product of clearance (dose/AUC) and transit time (1), that is:

$$V_{ss} = \frac{\text{dose}}{AUC}\bar{t}_b \qquad \text{(Eq. 9)}$$

Equations 8 and 9 can be readily used to calculate V_{ss} following any mode of administration. Where there is a single mode of administration, Eqs. 8 and 9 can be readily solved for V_{ss}. For the case where drug is administered as a single bolus, $\int_0^\infty X\,dt = 0$,

$$V_{ss} = \frac{\text{dose}}{AUC}\bar{t}_b = \frac{\text{dose}}{AUC}\left(\frac{AUMC}{AUC}\right) = \text{dose}\,\frac{AUMC}{AUC^2} \qquad \text{(Eq. 10)}$$

This is the same equation as derived by Benet and Galeazzi

0022-3549/82/0300-0372$01.00/0

Table I—Equations for $\int_0^\infty X\,dt$ and $\int_0^\infty X\,dt$/Dose for Various Modes of Drug Administration

Mode of Administration	$\int_0^\infty X\,dt$	$\int_0^\infty X\,dt$/dose
Intravenous bolus	0	0
Intravenous infusion	$k_0T^2/2$[a]	$T/2$
First-order input	F dose/k_a[b]	$1/k_a$
Simultaneous bolus plus infusion	$k_0t^2/2$	$k_0T^2/2(k_0T + \text{dose}_{iv})$[c]
Two consecutive infusions	$(k_0T^2/2)_1 + (k_0T^2/2)_2$[d]	$\frac{(k_0T^2/2)_1 + (k_0T^2/2)_2}{(k_0T)_1 + (k_0T)_2}$[c]

[a] See Eqs. 4 and 6. [b] See Eqs. 5 and 7. [c] See Eq. 13. [d] Subscript 1 refers to the first infusion, and subscript 2 refers to the second infusion.

(1). Substitution of $k_0T^2/2$ for $\int_0^\infty Xdt$ (see Eq. 6) in Eq. 8, and recognizing that k_0T equals dose, yields the following equation for V_{ss} for infusion data (6):

$$V_{ss} = \frac{\text{dose}}{AUC}\left(\frac{AUMC}{AUC} - \frac{T}{2}\right) = \text{dose}\,\frac{AUMC}{AUC^2} - \frac{T\ \text{dose}}{2\,AUC} \quad \text{(Eq. 11)}$$

If a case were to arise where input was first-order:

$$V_{ss} = \frac{F\ \text{dose}}{AUC}\left(\frac{AUMC}{AUC} - \frac{1}{k_a}\right) = F\ \text{dose}\,\frac{AUMC}{AUC^2} - \frac{F\ \text{dose}}{k_a\,AUC} \quad \text{(Eq. 12)}$$

If a value of F is not available, V_{ss}/F rather than V_{ss} would be calculated. As is apparent, information other than areas is required to determine V_{ss} where input is other than a bolus.

Administration of drug by multiple modes, for example, a simultaneous bolus plus an infusion, or consecutive infusions, may yield concentration–time data from which it may be desirable to estimate V_{ss}. Equation 9 in conjunction with a more general form of Eq. 8 may be used:

$$\bar{t}_b = \frac{AUMC}{AUC} - \frac{\sum \int_0^\infty X dt}{\sum \text{dose}} \quad \text{(Eq. 13)}$$

Table II—Calculation of V_{ss} for Various Modes of Administration[a]

Mode of Administration	AUC, (μg/ml) hr	$AUMC$, (μg/ml) hr^2	$\frac{AUMC}{AUC}$[b] hr	$\frac{\sum \int_0^\infty X\,dt}{\sum \text{dose}}$ hr	V_{ss}[c] L
IV bolus, 500 mg	1000.0[d]	25002.5[e]	25.0	0	25.0
IV infusion, 250 mg/hr over 2 hr	1000.0	26002.5[f]	26.0	1.0	25.0
First-order administration, 500 mg, $F = 1$, $k_a = 1.4\ \text{hr}^{-1}$	1000.0	25716.8[g]	25.7	0.7	25.0
Bolus plus infusion, 500 mg bolus plus 250 mg/hr over 2 hr	2000.0	51005.0[h]	25.5	0.5	25.0
Two consecutive infusions, 250 mg/hr over 2 hr followed by 41.67 mg/hr over 6 hr	1500.0	40003.7[i]	26.7	1.7	25.0

[a] Calculations based on equation, $C = A_1e^{-\lambda_1 t} + A_2e^{-\lambda_2 t}$, where $A_1 = 60.9545$ μg/ml, $\lambda_1 = 5.0605\ \text{hr}^{-1}$, $A_2 = 39.0459$ μg/ml and $\lambda_2 = 0.03952\ \text{hr}^{-1}$ following a 500-mg bolus dose. [b] See Table I. [c] See Eq. 13. [d] $AUC = \sum_{i=1}^{n} A_i/\lambda_i$. [e] $AUMC = \sum_{i=1}^{n} A_i/\lambda_i^2$. [f] $AUMC = \sum_{i=1}^{n} A_1/\lambda_i^2 + T\,AUC/2$. [g] $AUMC = N/k_a^2 + k_aA_1/\lambda_1^2(k_a - \lambda_1) + k_aA_2/\lambda_2^2(k_a - \lambda_2)$, where $N = k_a$ dose $(k_{21} - k_a)/V_c(\lambda_1 - k_a)(\lambda_2 - k_a)$. [h] Equals c plus d. [i] Use c for two different infusion rates, and add the resulting numbers. Note that only one-half the dose was given on the second infusion.

In Eq. 13, *AUMC* and *AUC* are the total areas under the resulting t C *versus* time and C *versus* time curves, and can be determined in the same manner as outlined for intravenous bolus data (1). The second term on the right hand side of Eq. 13 can be readily solved as the numerator is simply the sum of the $\int_0^\infty Xdt$ values for each mode of administration, and the denominator is the total dose administered by all modes of administration. Examples are illustrated in Table I.

The V_{ss} was determined for the various modes of administration outlined in Table I, utilizing the same data as employed by Benet and Galeazzi (1). All calculations were performed from explicit equations and are presented in Table II. Explicit equations were used to illustrate the validity of the relationships presented here. Estimation of the areas, *AUC* and *AUMC*, from time zero to the first point of the postabsorption and/or postdistribution phase with the linear or logarithmic trapezoidal rule, and from this latter point to time infinity using explicit equations (1) would yield values which vary from the theoretical values. Such variability is primarily due to inherent errors in the methods used to estimate the areas. However, the values obtained would be as reliable as those calculated using traditional methods of data analysis.

(1) L. Z. Benet and R. L. Galeazzi, *J. Pharm. Sci.*, **68**, 1071 (1979).

(2) K. Yamaoka, T. Nakagawa, and T. Uno, *J. Pharmacokinet. Biopharm.*, **6**, 547 (1978).

(3) S. Riegelman and P. Collier, *ibid.*, **8**, 509 (1980).

(4) N. A. Lassen and W. Perl, "Tracer Kinetic Methods in Medical Physiology," Raven Press, New York, N.Y. 1979, pp. 86–88.

(5) *Ibid.*, pp. 76–80.

(6) J. A. Gambertoglio, S. L. Barriere, E. T. Lin, and J. E. Conte, Jr., *Antimicrob. Agents Chemother.*, **18**, 952 (1980).

Donald Perrier [x]
Michael Mayersohn
Department of Pharmaceutical Sciences
College of Pharmacy
The University of Arizona
Tucson, AZ 85721

Received September 21, 1981.
Accepted for publication November 24, 1981
Supported in part by NIH Grant HL24559 and NIDA Grant DA02680.

Albumin Does Not Mediate the Removal of Taurocholate by the Rat Liver

Keyphrases □ Albumin—effect on removal of taurocholate from liver □ Taurocholate—removal from liver not mediated by albumin

To the Editor:

In a recent article by Forker and Luxon (1), the authors discuss what they refer to as a contradiction in liver extraction as a function of albumin concentration and taurocholate free concentration. The authors have failed to relate their experimental observations to a fundamental clearance concept (2):

0022-3549/82/0300-0373$01.00/0

Table I—Equations for $\int_0^\infty X\,dt$ and $\int_0^\infty X\,dt$/Dose for Various Modes of Drug Administration

Mode of Administration	$\int_0^\infty X\,dt$	$\int_0^\infty X\,dt$/dose
Intravenous bolus	0	0
Intravenous infusion	$k_0T^2/2$[a]	$T/2$
First-order input	F dose/k_a[b]	$1/k_a$
Simultaneous bolus plus infusion	$k_0t^2/2$	$k_0T^2/2(k_0T + \text{dose}_{iv})$[c]
Two consecutive infusions	$(k_0T^2/2)_1 + (k_0T^2/2)_2$[d]	$\frac{(k_0T^2/2)_1 + (k_0T^2/2)_2}{(k_0T)_1 + (k_0T)_2}$[c]

[a] See Eqs. 4 and 6. [b] See Eqs. 5 and 7. [c] See Eq. 13. [d] Subscript 1 refers to the first infusion, and subscript 2 refers to the second infusion.

(1). Substitution of $k_0T^2/2$ for $\int_0^\infty Xdt$ (see Eq. 6) in Eq. 8, and recognizing that k_0T equals dose, yields the following equation for V_{ss} for infusion data (6):

$$V_{ss} = \frac{\text{dose}}{AUC}\left(\frac{AUMC}{AUC} - \frac{T}{2}\right) = \text{dose}\,\frac{AUMC}{AUC^2} - \frac{T\ \text{dose}}{2\,AUC} \quad \text{(Eq. 11)}$$

If a case were to arise where input was first-order:

$$V_{ss} = \frac{F\ \text{dose}}{AUC}\left(\frac{AUMC}{AUC} - \frac{1}{k_a}\right) = F\ \text{dose}\,\frac{AUMC}{AUC^2} - \frac{F\ \text{dose}}{k_a\,AUC} \quad \text{(Eq. 12)}$$

If a value of F is not available, V_{ss}/F rather than V_{ss} would be calculated. As is apparent, information other than areas is required to determine V_{ss} where input is other than a bolus.

Administration of drug by multiple modes, for example, a simultaneous bolus plus an infusion, or consecutive infusions, may yield concentration–time data from which it may be desirable to estimate V_{ss}. Equation 9 in conjunction with a more general form of Eq. 8 may be used:

$$\bar{t}_b = \frac{AUMC}{AUC} - \frac{\sum \int_0^\infty X dt}{\sum \text{dose}} \quad \text{(Eq. 13)}$$

Table II—Calculation of V_{ss} for Various Modes of Administration[a]

Mode of Administration	AUC, (μg/ml) hr	$AUMC$, (μg/ml) hr^2	$\frac{AUMC}{AUC}$[b] hr	$\frac{\sum \int_0^\infty X\,dt}{\sum \text{dose}}$ hr	V_{ss}[c] L
IV bolus, 500 mg	1000.0[d]	25002.5[e]	25.0	0	25.0
IV infusion, 250 mg/hr over 2 hr	1000.0	26002.5[f]	26.0	1.0	25.0
First-order administration, 500 mg, $F = 1$, $k_a = 1.4\ \text{hr}^{-1}$	1000.0	25716.8[g]	25.7	0.7	25.0
Bolus plus infusion, 500 mg bolus plus 250 mg/hr over 2 hr	2000.0	51005.0[h]	25.5	0.5	25.0
Two consecutive infusions, 250 mg/hr over 2 hr followed by 41.67 mg/hr over 6 hr	1500.0	40003.7[i]	26.7	1.7	25.0

[a] Calculations based on equation, $C = A_1e^{-\lambda_1 t} + A_2e^{-\lambda_2 t}$, where $A_1 = 60.9545$ μg/ml, $\lambda_1 = 5.0605\ \text{hr}^{-1}$, $A_2 = 39.0459$ μg/ml and $\lambda_2 = 0.03952\ \text{hr}^{-1}$ following a 500-mg bolus dose. [b] See Table I. [c] See Eq. 13. [d] $AUC = \sum_{i=1}^{n} A_i/\lambda_i$. [e] $AUMC = \sum_{i=1}^{n} A_i/\lambda_i^2$. [f] $AUMC = \sum_{i=1}^{n} A_1/\lambda_i^2 + T\,AUC/2$. [g] $AUMC = N/k_a^2 + k_aA_1/\lambda_1^2(k_a - \lambda_1) + k_aA_2/\lambda_2^2(k_a - \lambda_2)$, where $N = k_a$ dose $(k_{21} - k_a)/V_c(\lambda_1 - k_a)(\lambda_2 - k_a)$. [h] Equals c plus d. [i] Use c for two different infusion rates, and add the resulting numbers. Note that only one-half the dose was given on the second infusion.

In Eq. 13, *AUMC* and *AUC* are the total areas under the resulting t C *versus* time and C *versus* time curves, and can be determined in the same manner as outlined for intravenous bolus data (1). The second term on the right hand side of Eq. 13 can be readily solved as the numerator is simply the sum of the $\int_0^\infty Xdt$ values for each mode of administration, and the denominator is the total dose administered by all modes of administration. Examples are illustrated in Table I.

The V_{ss} was determined for the various modes of administration outlined in Table I, utilizing the same data as employed by Benet and Galeazzi (1). All calculations were performed from explicit equations and are presented in Table II. Explicit equations were used to illustrate the validity of the relationships presented here. Estimation of the areas, *AUC* and *AUMC*, from time zero to the first point of the postabsorption and/or postdistribution phase with the linear or logarithmic trapezoidal rule, and from this latter point to time infinity using explicit equations (1) would yield values which vary from the theoretical values. Such variability is primarily due to inherent errors in the methods used to estimate the areas. However, the values obtained would be as reliable as those calculated using traditional methods of data analysis.

(1) L. Z. Benet and R. L. Galeazzi, *J. Pharm. Sci.*, **68**, 1071 (1979).

(2) K. Yamaoka, T. Nakagawa, and T. Uno, *J. Pharmacokinet. Biopharm.*, **6**, 547 (1978).

(3) S. Riegelman and P. Collier, *ibid.*, **8**, 509 (1980).

(4) N. A. Lassen and W. Perl, "Tracer Kinetic Methods in Medical Physiology," Raven Press, New York, N.Y. 1979, pp. 86–88.

(5) *Ibid.*, pp. 76–80.

(6) J. A. Gambertoglio, S. L. Barriere, E. T. Lin, and J. E. Conte, Jr., *Antimicrob. Agents Chemother.*, **18**, 952 (1980).

Donald Perrier [x]
Michael Mayersohn
Department of Pharmaceutical Sciences
College of Pharmacy
The University of Arizona
Tucson, AZ 85721

Received September 21, 1981.
Accepted for publication November 24, 1981
Supported in part by NIH Grant HL24559 and NIDA Grant DA02680.

Albumin Does Not Mediate the Removal of Taurocholate by the Rat Liver

Keyphrases □ Albumin—effect on removal of taurocholate from liver □ Taurocholate—removal from liver not mediated by albumin

To the Editor:

In a recent article by Forker and Luxon (1), the authors discuss what they refer to as a contradiction in liver extraction as a function of albumin concentration and taurocholate free concentration. The authors have failed to relate their experimental observations to a fundamental clearance concept (2):

0022-3549/82/0300-0373$01.00/0

$$E = \frac{F_f Cl_I}{Q + F_f Cl_I} \quad \text{(Eq. 1)}$$

Equation 1 can be rearranged to yield:

$$Cl_I = \frac{E\,Q}{F_f\,(1 - E)} \quad \text{(Eq. 2)}$$

where F_f is the free fraction (rather than free concentration) of drug in perfusate, E is the extraction ratio, Q is perfusate flow, and Cl_I is intrinsic clearance by the perfused organ. Using Eq. 2 and the mean data presented by the authors in Tables I and II of their paper (1), (*e.g.*, Q = 4.81 ml/min/g when F_f = 0.57 and E = 0.97 and Q = 4.55 ml/min/g when F_f = 0.11 and E = 0.86), it is apparent that the intrinsic organ clearances are comparable, *i.e.*, Cl_I = 273 and 254 ml/min/g, respectively. The similarity of these intrinsic clearance values indicates that the data generated by Forker and Luxon are consistent with, rather than divergent from, conventional pharmacokinetic theory and that liver uptake can be predicted using free fraction in perfusate and Eq. 2. Therefore, it is apparent that albumin does not mediate the removal of taurocholate by rat liver.

(1) E. L. Forker and B. A. Luxon, *J. Clin. Invest.*, **67**, 1517 (1981).
(2) G. R. Wilkinson and D. G. Shand, *Clin. Pharmacol. Ther.*, **18**, 377 (1975).

Wayne A. Colburn
Department of Pharmacokinetics and Biopharmaceutics,
Hoffmann-La Roche, Inc.
Nutley, NJ 07110

Received October 22, 1981.
Accepted for publication, December 9, 1981.

Effect of Plasma Protein Binding on Clearance of Drugs Metabolized by Michaelis–Menten Kinetics

Keyphrases □ Plasma protein binding—effect on clearance of drugs metabolized by Michaelis–Menten kinetics □ Michaelis–Menten kinetics—drug metabolism, effect of plasma protein binding

To the Editor:

It is generally known that restrictively bound drugs exhibit increasing clearances as the unbound concentration increases (1–3). However, the applicability of this concept to restrictively bound drugs which are subject to Michaelis–Menten rather than first-order kinetics has not received much attention. Consider a drug cleared exclusively by the liver. If the enzymes mediating its metabolism are saturable and metabolism is further limited by availability of unbound drug, the intrinsic clearance of unbound drug can be described as (4):

$$Cl'_{int} = \frac{V_{max}}{K_m + \alpha \overline{C}_{ss}} \quad \text{(Eq. 1)}$$

where Cl'_{int} is intrinsic clearance of unbound drug, V_{max} is the maximum velocity of the drug metabolizing enzyme, K_m is the concentration of unbound drug in plasma when the rate of metabolism is $V_{max}/2$, $\overline{C}_{ss}$ is the average steady-state plasma concentration of total drug, and α is the unbound fraction[1]. Equation 1 can be rewritten as follows:

$$Cl'_{int} = \frac{V_{max}}{\alpha\left[\frac{K_m}{\alpha} + \overline{C}_{ss}\right]} \quad \text{(Eq. 2)}$$

For a restrictively bound drug eliminated by a single clearing organ, organ clearance and total clearance can be defined in terms of intrinsic organ clearance and the unbound fraction of drug (5) as follows:

$$Cl_{tot} = Cl'_{int}\,\alpha \quad \text{(Eq. 3)}$$

Equation 2 can be rewritten in terms of Cl_{tot} as follows:

$$Cl_{tot} = \frac{V_{max}\alpha}{\alpha\left[\frac{K_m}{\alpha} + \overline{C}_{ss}\right]} \quad \text{(Eq. 4)}$$

which simplifies to:

$$Cl_{tot} = \frac{V_{max}}{\frac{K_m}{\alpha} + \overline{C}_{ss}} \quad \text{(Eq. 5)}$$

Equation 5 shows that Cl_{tot} will increase as α increases, but the magnitude of the increase depends on the values of V_{max}, K_m, and $\overline{C}_{ss}$. Moreover, for a drug such as phenytoin which is restrictively bound and metabolized by a saturable oxidase, the reported values for K_m (6) are really apparent K_m values rather than true K_m values, since they are calculated on the basis of total rather than unbound concentrations. Actual K_m would be given by:

$$K_m = K_{m\ app}\alpha \quad \text{(Eq. 6)}$$

where $K_{m\ app}$ is the apparent K_m. Thus, it should be noted that for a restrictively bound drug:

$$Cl_{tot} = \frac{V_{max}}{K_{m\ app} + \overline{C}_{ss}} \quad \text{(Eq. 7)}$$

The impact of changes in α on Cl_{tot} become more pronounced as K_m increases as shown in Fig. 1. The relationship between Cl'_{tot}/Cl_{tot} *versus* α is unaffected by changes in V_{max}.

Several investigators have shown increased clearances for phenytoin corresponding to increases in the free fraction of the drug. Shand *et al.* (7) perfused phenytoin through isolated rat liver, varying the albumin concentration of the perfusate and consequently the unbound fraction. Their data show a relationship between Cl_{tot} and α similar to that in Fig. 2. Gugler and coworkers (8) reported a doubling of the free fraction and Cl_{tot} in six hypoalbuminemic nephrotic patients compared with six control subjects. However, average steady-state concentrations of total drug were 6.8 and 2.9 mg/liter for controls and nephrotics, respectively, well below the concentrations necessary to saturate the phenytoin oxidase. When $\overline{C}_{ss} \ll K_m/\alpha$, Eq. 7 simplifies to:

$$Cl_{tot} = \alpha\frac{V_{max}}{K_m} \quad \text{(Eq. 8)}$$

If plasma levels are sufficiently high so that metabolism

[1] Cl'_{int} is intrinsic clearance of unbound drug as defined by Wilkinson and Shand [G. Wilkinson and D. Shand, *Clin. Pharmacol. Ther.* 18, 377 (1975)], and is equivalent to Cl_{int} of Rowland *et al.* (4).

0022-3549/82/0300-0374$01.00/0

$$E = \frac{F_f Cl_I}{Q + F_f Cl_I} \quad \text{(Eq. 1)}$$

Equation 1 can be rearranged to yield:

$$Cl_I = \frac{E\,Q}{F_f\,(1 - E)} \quad \text{(Eq. 2)}$$

where F_f is the free fraction (rather than free concentration) of drug in perfusate, E is the extraction ratio, Q is perfusate flow, and Cl_I is intrinsic clearance by the perfused organ. Using Eq. 2 and the mean data presented by the authors in Tables I and II of their paper (1), (*e.g.*, Q = 4.81 ml/min/g when F_f = 0.57 and E = 0.97 and Q = 4.55 ml/min/g when F_f = 0.11 and E = 0.86), it is apparent that the intrinsic organ clearances are comparable, *i.e.*, Cl_I = 273 and 254 ml/min/g, respectively. The similarity of these intrinsic clearance values indicates that the data generated by Forker and Luxon are consistent with, rather than divergent from, conventional pharmacokinetic theory and that liver uptake can be predicted using free fraction in perfusate and Eq. 2. Therefore, it is apparent that albumin does not mediate the removal of taurocholate by rat liver.

(1) E. L. Forker and B. A. Luxon, *J. Clin. Invest.*, **67**, 1517 (1981).
(2) G. R. Wilkinson and D. G. Shand, *Clin. Pharmacol. Ther.*, **18**, 377 (1975).

Wayne A. Colburn
Department of Pharmacokinetics and Biopharmaceutics,
Hoffmann-La Roche, Inc.
Nutley, NJ 07110

Received October 22, 1981.
Accepted for publication, December 9, 1981.

Effect of Plasma Protein Binding on Clearance of Drugs Metabolized by Michaelis–Menten Kinetics

Keyphrases □ Plasma protein binding—effect on clearance of drugs metabolized by Michaelis–Menten kinetics □ Michaelis–Menten kinetics—drug metabolism, effect of plasma protein binding

To the Editor:

It is generally known that restrictively bound drugs exhibit increasing clearances as the unbound concentration increases (1–3). However, the applicability of this concept to restrictively bound drugs which are subject to Michaelis–Menten rather than first-order kinetics has not received much attention. Consider a drug cleared exclusively by the liver. If the enzymes mediating its metabolism are saturable and metabolism is further limited by availability of unbound drug, the intrinsic clearance of unbound drug can be described as (4):

$$Cl'_{int} = \frac{V_{max}}{K_m + \alpha \overline{C}_{ss}} \quad \text{(Eq. 1)}$$

where Cl'_{int} is intrinsic clearance of unbound drug, V_{max} is the maximum velocity of the drug metabolizing enzyme, K_m is the concentration of unbound drug in plasma when the rate of metabolism is $V_{max}/2$, $\overline{C}_{ss}$ is the average steady-state plasma concentration of total drug, and α is the unbound fraction[1]. Equation 1 can be rewritten as follows:

$$Cl'_{int} = \frac{V_{max}}{\alpha\left[\frac{K_m}{\alpha} + \overline{C}_{ss}\right]} \quad \text{(Eq. 2)}$$

For a restrictively bound drug eliminated by a single clearing organ, organ clearance and total clearance can be defined in terms of intrinsic organ clearance and the unbound fraction of drug (5) as follows:

$$Cl_{tot} = Cl'_{int}\,\alpha \quad \text{(Eq. 3)}$$

Equation 2 can be rewritten in terms of Cl_{tot} as follows:

$$Cl_{tot} = \frac{V_{max}\alpha}{\alpha\left[\frac{K_m}{\alpha} + \overline{C}_{ss}\right]} \quad \text{(Eq. 4)}$$

which simplifies to:

$$Cl_{tot} = \frac{V_{max}}{\frac{K_m}{\alpha} + \overline{C}_{ss}} \quad \text{(Eq. 5)}$$

Equation 5 shows that Cl_{tot} will increase as α increases, but the magnitude of the increase depends on the values of V_{max}, K_m, and $\overline{C}_{ss}$. Moreover, for a drug such as phenytoin which is restrictively bound and metabolized by a saturable oxidase, the reported values for K_m (6) are really apparent K_m values rather than true K_m values, since they are calculated on the basis of total rather than unbound concentrations. Actual K_m would be given by:

$$K_m = K_{m\ app}\alpha \quad \text{(Eq. 6)}$$

where $K_{m\ app}$ is the apparent K_m. Thus, it should be noted that for a restrictively bound drug:

$$Cl_{tot} = \frac{V_{max}}{K_{m\ app} + \overline{C}_{ss}} \quad \text{(Eq. 7)}$$

The impact of changes in α on Cl_{tot} become more pronounced as K_m increases as shown in Fig. 1. The relationship between Cl'_{tot}/Cl_{tot} *versus* α is unaffected by changes in V_{max}.

Several investigators have shown increased clearances for phenytoin corresponding to increases in the free fraction of the drug. Shand *et al.* (7) perfused phenytoin through isolated rat liver, varying the albumin concentration of the perfusate and consequently the unbound fraction. Their data show a relationship between Cl_{tot} and α similar to that in Fig. 2. Gugler and coworkers (8) reported a doubling of the free fraction and Cl_{tot} in six hypoalbuminemic nephrotic patients compared with six control subjects. However, average steady-state concentrations of total drug were 6.8 and 2.9 mg/liter for controls and nephrotics, respectively, well below the concentrations necessary to saturate the phenytoin oxidase. When $\overline{C}_{ss} \ll K_m/\alpha$, Eq. 7 simplifies to:

$$Cl_{tot} = \alpha\frac{V_{max}}{K_m} \quad \text{(Eq. 8)}$$

If plasma levels are sufficiently high so that metabolism

[1] Cl'_{int} is intrinsic clearance of unbound drug as defined by Wilkinson and Shand [G. Wilkinson and D. Shand, *Clin. Pharmacol. Ther.* 18, 377 (1975)], and is equivalent to Cl_{int} of Rowland *et al.* (4).

0022-3549/82/0300-0374$01.00/0

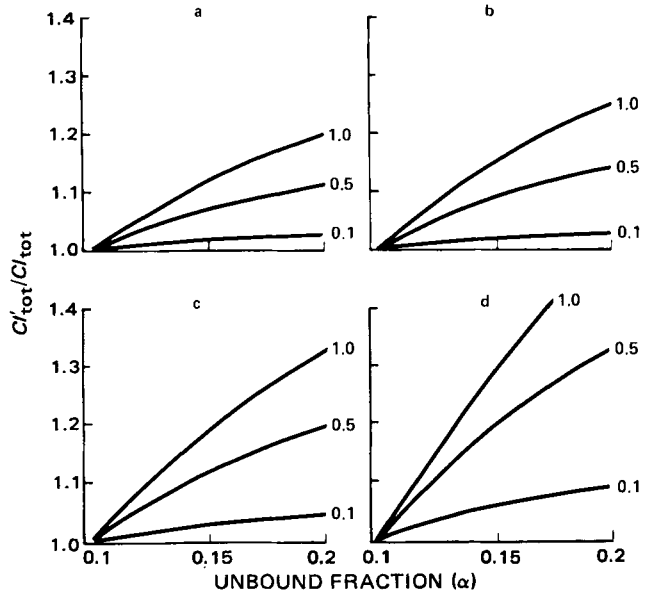

Figure 1—*Impact of α on the clearance of a restrictively bound drug metabolized by Michaelis–Menten kinetics.* Cl'_{tot} *is clearance when* $\alpha > 0.1$. Cl_{tot} *is clearance at* $\alpha = 0.1$. *Actual* K_m *values are shown for each curve.* $\bar{C}_{ss}$ *is 20, 15, 10, and 5 mg/liters for graphs a, b, c, and d, respectively.*

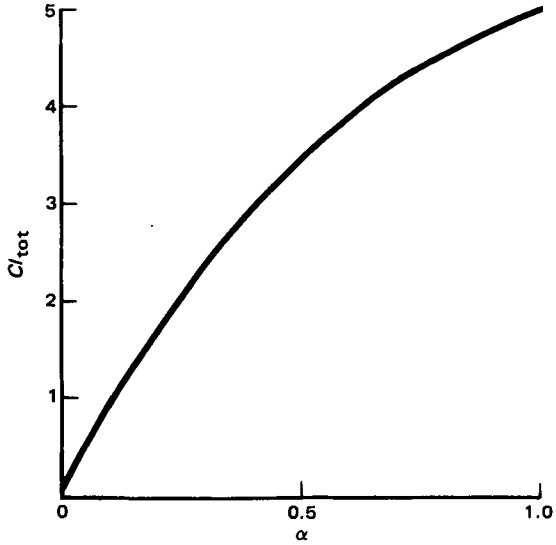

Figure 2—*Relationship between steady-state clearance and magnitude of unbound fraction for a restrictively bound drug metabolized by Michaelis–Menten kinetics.* $\bar{C}_{ss} = 1$ *mg/liter,* $V_{max} = 10$ *mg/hr, and* $K_m = 1$ mg/liter.

is no longer operating by apparent first-order kinetics, the changes in Cl_{tot} will no longer be directly proportional to α. As shown in Fig. 1, a doubling of α will only increase Cl_{tot} slightly, and the extent of the increase will also depend on the actual value of K_m and $\bar{C}_{ss}$.

While clearance changes in a complex manner with altered protein binding, the changes in total and unbound drug concentration are simple. The rate of drug administration required to achieve a targeted average steady-state plasma level is:

$$R_{in} = \frac{V_{max}\bar{C}_{ss}}{\frac{K_m}{\alpha} + \bar{C}_{ss}} \qquad \text{(Eq. 9)}$$

where R_{in} represents the rate of drug administration. If, for example, protein binding were altered by hepatitis, cirrhosis, uremia, heparinization, or drug interaction such that α increased while the rate of administration remained unchanged, the relationship between the total steady-state plasma concentration of drug before and after the change in binding would be:

$$\bar{C}'_{ss} = \frac{\bar{C}_{ss}}{a} \qquad \text{(Eq. 10)}$$

where a is the ratio of altered α to original α, $\bar{C}_{ss}$ is the total plasma concentration before the change, and $\bar{C}'_{ss}$ is the total plasma concentration after the change in binding. From Eq. 10 it is apparent that the average steady-state concentration of free drug is not altered by the change in binding.

The recommendations for adjusting the doses of restrictively bound drugs that are cleared by hepatic metabolism apply to drugs metabolized by either apparent first-order or Michaelis–Menten kinetics when binding is decreased. Though clearance increases, the average steady-state concentration of unbound drug does not. Decreasing the dose and the dosing interval so that the dosing rate remains constant will help to contain peak and trough levels of unbound drug within therapeutic limits.

(1) A. Yacobi, J. Udall, and G. Levy, *Clin. Pharmacol. Ther.*, **19**, 552 (1976).

(2) T. Blaschke, *Clin. Pharmacokinet.*, **2**, 32 (1977).

(3) G. Levy, *J. Pharm. Sci.*, **65**, 1264 (1976).

(4) M. Rowland, T. Blaschke, P. Meffin, and R. Williams, in "The Effect of Disease States on Drug Pharmacokinetics," L. Benet, Ed., American Pharmaceutical Association, Washington, D.C., 1976, pp. 53–75.

(5) R. Williams and L. Benet, *Ann. Rev. Pharmacol. Toxicol.*, **20**, 389 (1980).

(6) T. Ludden, J. Allen, W. Valutsky, A. Vicuna, J. Nappi, S. Hoffman, J. Wallace, D. Lalka, and J. McNay, *Clin. Pharmacol. Ther.*, **21**, 287 (1977).

(7) D. Shand, R. Cotham, and G. Wilkinson, *Life Sci.*, **19**, 125 (1976).

(8) R. Gugler, D. Shoeman, D. Huffman, J. Cohlmia, and D. Azarnoff, *J. Clin. Invest.*, **55**, 1182 (1975).

Kenneth Bachmann[x]
Timothy J. Sullivan
College of Pharmacy
University of Toledo
Toledo, OH 43606

Received May 29, 1981.
Accepted for publication October 6, 1981.

REVIEWS

Physical Chemical Properties of Drugs. By SAMUEL H. YALKOWSKY, ANTHONY A. SINKULA, and SHRI C. VALVANI. Dekker, 270 Madison Ave., New York, NY 10016. 1980. 361 pp. 14 × 23 cm. Price $45.00 (20% higher outside U.S. and Canada).

An understanding of the chemical properties of a drug is necessary for understanding its activity since covalent bonding at the reaction site sometimes is (and metabolism always is) an important consideration. However, over the past two decades more sophisticated analytical tools, *e.g.*, NMR and X-ray crystallography, have focused our attention on the fact that it is the wide variety of weaker physicochemical forces that nature uses to define a drug for a very specific purpose. Therefore, there recently has been a concerted effort to measure and report these physical constants.

Actual application of appropriate constants to drug design has been limited by two factors: measurement of these constants has not kept pace with the need, and application methodology has lagged behind in certain areas. This volume does a great deal to remedy both shortcomings. Chapters 1, 5, 8, 9, and 10 describe calculation procedures for pKa, partition coefficient (octanol/water), solubility parameter, molecular connectivity, and molecular surface areas, respectively. Chapters 2, 3, 6, and 7 focus on the more effective use of pKa, hydrophobicity, solubility, and thermodynamic considerations in drug improvement. Chapter 4 points out important limitations in the Hansch approach to structure–activity relationships.

This book does not in any important way duplicate others presently available in this field. It can be highly recommended to anyone with a strong commitment in drug design, as well as to students in advanced courses in that discipline. This book should be very valuable to anyone involved in modeling environmental transport and fate.

Reviewed by Albert J. Leo
Pomona College Medicinal Chemistry Project
Seaver Chemistry Laboratory
Claremont, CA 91711

Pharmaceutical Dosage Forms: Tablets Vol. 2. Edited by HERBERT A. LIEBERMAN and LEON LACHMAN. Dekker, 270 Madison Avenue, New York, NY 10016, 1981. 520 pp. 18 × 25.5 cm Price $59.75. (A special student price of $24.50 for five or more copies through a college or university bookstore in the United States or Canada.)

The second volume of this set lives up to the promise of the first. Whereas the first volume emphasizes the distinction between the types of tablets with details on the manufacturing of each, this volume discusses each unit process completely. As before, each chapter develops without a dependency on the nuances of other sections.

The first four chapters cover mixing, drying, size reduction, and compression. Chapter five is really two chapters, one on the characterization of granulations, and the other on the evaluation of finished tablets. The final chapter is a review of tablet press tooling. The types of punches, terminology, control, and problem solving are all discussed in excellent detail.

Chapter six, "Bioavailability in Tablet Technology," is over one-third of this volume. This does seem excessive. Most relevant background biopharmaceutic and pharmacokinetic concepts are reviewed in detail from the everted gut technique, pH partition, dissolution, and compartmental modeling, to multiple dosing kinetics. There are excellent sections of dissolution evaluation and bioavailability assessment, with liberal referencing to the Federal Register. Examples are given of virtually everything discussed, and yet there is no discussion of the FDA's statistical criteria of bioavailability of bioequivalence or of their criteria for the setting of a dissolution specification for generic bioavailability. These were needed more than some portions of the existing chapter when considering where this chapter is presented.

Nevertheless, this set, when completed, will probably be the state-of-the-art for many years to come.

Reviewed by John H. Wood
School of Pharmacy
Medical College of Virginia
Virginia Commonwealth University
Richmond, VA 23298

REVIEWS

Physical Chemical Properties of Drugs. By SAMUEL H. YALKOWSKY, ANTHONY A. SINKULA, and SHRI C. VALVANI. Dekker, 270 Madison Ave., New York, NY 10016. 1980. 361 pp. 14 × 23 cm. Price $45.00 (20% higher outside U.S. and Canada).

An understanding of the chemical properties of a drug is necessary for understanding its activity since covalent bonding at the reaction site sometimes is (and metabolism always is) an important consideration. However, over the past two decades more sophisticated analytical tools, *e.g.*, NMR and X-ray crystallography, have focused our attention on the fact that it is the wide variety of weaker physicochemical forces that nature uses to define a drug for a very specific purpose. Therefore, there recently has been a concerted effort to measure and report these physical constants.

Actual application of appropriate constants to drug design has been limited by two factors: measurement of these constants has not kept pace with the need, and application methodology has lagged behind in certain areas. This volume does a great deal to remedy both shortcomings. Chapters 1, 5, 8, 9, and 10 describe calculation procedures for pKa, partition coefficient (octanol/water), solubility parameter, molecular connectivity, and molecular surface areas, respectively. Chapters 2, 3, 6, and 7 focus on the more effective use of pKa, hydrophobicity, solubility, and thermodynamic considerations in drug improvement. Chapter 4 points out important limitations in the Hansch approach to structure–activity relationships.

This book does not in any important way duplicate others presently available in this field. It can be highly recommended to anyone with a strong commitment in drug design, as well as to students in advanced courses in that discipline. This book should be very valuable to anyone involved in modeling environmental transport and fate.

Reviewed by Albert J. Leo
Pomona College Medicinal Chemistry Project
Seaver Chemistry Laboratory
Claremont, CA 91711

Pharmaceutical Dosage Forms: Tablets Vol. 2. Edited by HERBERT A. LIEBERMAN and LEON LACHMAN. Dekker, 270 Madison Avenue, New York, NY 10016, 1981. 520 pp. 18 × 25.5 cm Price $59.75. (A special student price of $24.50 for five or more copies through a college or university bookstore in the United States or Canada.)

The second volume of this set lives up to the promise of the first. Whereas the first volume emphasizes the distinction between the types of tablets with details on the manufacturing of each, this volume discusses each unit process completely. As before, each chapter develops without a dependency on the nuances of other sections.

The first four chapters cover mixing, drying, size reduction, and compression. Chapter five is really two chapters, one on the characterization of granulations, and the other on the evaluation of finished tablets. The final chapter is a review of tablet press tooling. The types of punches, terminology, control, and problem solving are all discussed in excellent detail.

Chapter six, "Bioavailability in Tablet Technology," is over one-third of this volume. This does seem excessive. Most relevant background biopharmaceutic and pharmacokinetic concepts are reviewed in detail from the everted gut technique, pH partition, dissolution, and compartmental modeling, to multiple dosing kinetics. There are excellent sections of dissolution evaluation and bioavailability assessment, with liberal referencing to the Federal Register. Examples are given of virtually everything discussed, and yet there is no discussion of the FDA's statistical criteria of bioavailability of bioequivalence or of their criteria for the setting of a dissolution specification for generic bioavailability. These were needed more than some portions of the existing chapter when considering where this chapter is presented.

Nevertheless, this set, when completed, will probably be the state-of-the-art for many years to come.

Reviewed by John H. Wood
School of Pharmacy
Medical College of Virginia
Virginia Commonwealth University
Richmond, VA 23298

A publication of the
American Pharmaceutical Association—
the National Professional Society
of Pharmacists

JOURNAL OF PHARMACEUTICAL SCIENCES

INDEX TO AUTHORS
INDEX TO SUBJECTS

VOLUME 71
JANUARY TO DECEMBER, 1982

Published monthly under the supervision of the Board of Trustees

Fulfilling Member Expectations

For a number of reasons, most of which are not really pertinent to this editorial and which would be very complex to explain in the limited space available here, the American Pharmaceutical Association is in the initial process of assessing and reassessing the products and services that it provides to its membership. Essentially, the Association is attempting to ascertain how well its present activities, projects, and products meet the desires and needs of today's pharmacists and of APhA members in particular.

Moreover, this is not always an all-or-none matter. Perhaps it is just a case that shifting interests or membership orientation calls for expanding a certain activity or project; alternatively, for the same reasons, the budget and resources involving another area may need to be cut back from current levels. But in the case of some projects, it may be concluded that a partial reduction is not a suitable remedy, and total elimination may be the only logical solution.

As an illustration, the huge costs associated with updating the data base for APhA's Drug Interactions Evaluation Program and the skyrocketing costs of paper and printing—coupled with less in the way of clinically significant new information and diminishing practitioner interest—led the APhA Board of Trustees recently to decide against the publication of a complete new edition of its *Evaluations of Drug Interactions*. At the same time, however, the Board also directed staff to continue to explore other communication approaches for drug interactions information, including computerized systems that might be more economically viable.

This incident is not an isolated example of APhA changing its approach in providing some member service. During the past 10 years, there have been any number of such modifications, to wit: in the publications area, the Association's newsletter was doubled in frequency to become a weekly, thereby making it a speedier communications vehicle; several different approaches were tried with regard to supplying news of the Annual Meeting and disseminating the Association's Annual Report; mid-year, regional, and specialized meetings of each of the Association's three subdivisions have been sponsored in addition to the traditional APhA Annual Meeting; innovative poster sessions, audiovisual learning programs, scientific exhibits, and assorted other departures from conventional meeting formats have been experimented with and largely implemented; and books, journals, and meetings have all been condensed and either severely edited or restructured to make them more concise in an effort to save time and money for all concerned. Many of these experiments have proven to be highly successful; on the other hand, in a few cases the reception has been dismal despite every reason to have expected an enthusiastic member reaction.

Nor has APhA been alone in such efforts and their outcome. Other professional, technical, and scientific membership societies have been likewise searching for new and alternative ways to meet contemporary membership needs and expectations. Although few such groups have attempted as many innovations and have been quite as daring as APhA in departures from the conventional "tried and true," we believe that each organization in its own way strives to satisfy the perceived desires of its members.

And, as Shakespeare would have put it, therein lies the rub! No survey, no questionnaire, no Gallup poll, or whatever, really can tell the organization anything, or give it any meaningful guidance, unless the membership has a pretty clear idea of what it wants, what it will use, and what it is willing to support and pay for.

Just this past week, this writer received a questionnaire from the American Chemical Society, an organization in which we have long maintained personal membership. Over the years, the ACS has done a conscientious job of trying to be responsive to its membership, and this latest questionnaire was largely devoted to exploring member preferences in ACS's continuing education programs.

In completing the questionnaire, we were struck by our own ambivalent feelings and reactions. When the question was asked about our interest in, or desire for, a CE program in a new computerized format, we impulsively wanted to express our positive reaction. But yet, our own working experience in conducting such surveys gave us pause to stop and critically ask ourselves the question, "In all honesty, would we *really* order it, pay for it, and use it?" And in this case we concluded that our answer was, "No, we really wouldn't."

The message of this editorial is to suggest that all of us need to reflect in a similar fashion when we are asked for our opinions by our professional organizations.

We know for a fact that the officers and staff of APhA, as well as its Academy of Pharmaceutical Sciences and the other APhA subdivisions, all are making a sincere effort to provide meaningful membership services in the most cost-effective manner. But they can only be responsive in direct proportion to the accuracy with which the membership articulates its true desires and its willingness to utilize and pay for those services when they are subsequently offered.

The best chef in the world can do little to please the diner's palate unless and until the diner selects from the menu a specific dish that will appeal to that particular diner.

—EDWARD G. FELDMANN
American Pharmaceutical Association
Washington, DC 20037

0022-3549/82/0400-0377$01.00/0

JOURNAL OF PHARMACEUTICAL SCIENCES

APRIL 1982
VOLUME 71 NUMBER 4

LITERATURE SURVEY

Experimental Methods in Cancer Therapeutics

KENNETH J. WIDDER *¶x, **ANDREW E. SENYEI** ‡¶, and **BARRY SEARS** §

Received from the *Department of Pathology, Duke University Medical Center, Durham, N.C., the ‡Department of Obstetrics and Gynecology, University of California at Irvine, Orange, Calif., and the §National Magnet Laboratory, Massachusetts Institute of Technology, Cambridge, Mass. ¶Present address: Kendrew Biosystems, Inc., San Diego, Calif.

Keyphrases □ Liposomes—as drug carriers, cancer therapeutics, literature survey □ Albumin—magnetically responsive microspheres, cancer therapeutics, literature survey □ Cancer therapeutics—experimental methods, literature survey

CONTENTS

During the last 10 years, the search for methods of selectively targeting antineoplastic agents has increased significantly. Because of the lack of tumor specificity of systemically administered antitumor drugs, toxic side effects are common, often resulting in greater harm to the host tissue than to the neoplastic process. Currently, the therapeutic index of most antineoplastic agents used in systemic therapy remains marginal, despite efforts to achieve tumor specificity. Despite various chemical modifications of chemotherapeutic agents (e.g., altering their partition coefficient, attaching immunologic ligands, or altering charge density), only variable success has been achieved in increasing specificity. An alternative approach for increasing the effectiveness of antitumor drugs is to alter their distribution in the body by incorporating them into particulate carriers, which theoretically can be concentrated at the tumor site. In this way, the toxicity of the drug for the tumor might be enhanced while the systemic toxicity is minimized.

Two major approaches for achieving this goal are discussed in this article. The first consists of new types of liposomes which impart an element of selectivity to desired target sites; the second consists of magnetically responsive drug-carrying microspheres which are capable of being targeted to tissue sites by use of an external magnetic field. A detailed comparison of all the various methods of drug delivery has been reviewed elsewhere (1).

BACKGROUND

The goal of any drug delivery system involves the altering of the pharmacokinetics and physiological disposition of the drug in question in order to obtain a higher therapeutic index. This can be accomplished either by decreasing the toxicity of the drug or by increasing its efficacy. In treating neoplastic disease, these concentrations become essential. Since the biochemical differences between normal and transformed cells are minimal and are difficult to exploit (2), the chemical synthesis of more efficacious drugs has not been entirely fruitful. Cancer therapy currently involves the administration of toxic drugs with a relatively small safety margin. Any drug delivery system that could significantly increase the therapeutic index of an antitumor drug would have a major impact in cancer treatment.

Many approaches have been tried in attempts to design a "magic bullet" for cancer. Implanted drug reservoirs give a more uniform dosage rate of the entrapped drug. The pharmacokinetics of the drug and its eventual disposition, however, remain identical to those of the free drug administered *via* normal methods. Covalently attaching antitumor agents to antibodies specific for the tumor has been suggested as a method of achieving tumor specificity. The results so far are only suggestive of potential applicability (3, 4). This approach is limited further by the extent that the attachment of the drug to the antibody de-

0022-3549/82/0400-0379$01.00/0

creases the immunological specificity of the antibody. The most encouraging prospect of increasing the therapeutic index of antitumor drugs is to encapsulate them inside macromolecular carriers that can circulate within the body. In theory, macromolecular carriers can be localized at the tumor site with high specificity, thereby increasing the therapeutic index of the encapsulated drug. Two such macromolecular carriers have been exploited recently in the targeting of drugs. The first, the liposome, is an assembly of phospholipids held together by noncovalent forces. The other carrier is the magnetically responsive albumin microsphere which can be targeted to tissue sites *via* external magnetic fields. We will critically evaluate the current experimental data for both of these systems and then speculate on their future clinical use in treating cancer.

LIPOSOMES

Liposomes form spontaneously when dry phospholipids are hydrated with an aqueous solution. These structures, which are held together by noncovalent forces, consist of concentric bilayers of phospholipids that are separated by an aqueous space (5, 6). Within this aqueous space, water soluble compounds such as antitumor drugs can be stored. Drug-containing lipsosomes can be separated from nonsequestered drug by centrifugation of the liposomes or by gel filtration. However, all phospholipids do not form liposomes; in fact only very few naturally occurring phospholipids form liposomes that are stable under physiological conditions. Phosphatidylcholine, the most abundant natural phospholipid, readily forms stable liposomes, whereas phosphatidylethanolamine, the second most abundant natural phospholipid, does not. Furthermore, phospholipid liposomes only form if they are hydrated above a temperature that corresponds to the physical transition of the phospholipid from a crystal-like (*i.e.*, gel) state to a liquid crystalline state. This temperature, which is dependent on the fatty acid composition of the phospholipid, is known as the transition temperature. Liposomes formed under these conditions are multilamellar bilayers that range from 1 to 5 μm in diameter. Upon sonication, these multilamellar bilayers are reduced in size to 0.02 μm in diameter. Other size ranges between these two extremes are possible *via* polycarbonate filter extrusion techniques (5).

The potential use of liposomes as drug delivery systems for antineoplastic agents has been summarized in many articles (6–10). This review will attempt to update and critically evaluate recent experimental results using liposomes in treating neoplastic disease and to anticipate potential new approaches in this area that may be useful in the future.

Physiological Fate of Liposomes—It is now appreciated that the simple encapsulation of an antitumor drug in unsonicated dispersions of phosphatidylcholine is a relatively naive approach to greater *in vivo* drug specificity. This is partly due to the complexity of the interaction of both the plasma and the reticuloendothelial system with liposomes. In the former case, the drug is released from the liposome so that its fate becomes that of the free drug. In the latter, the rapid removal of liposomes and their associated antitumor drug by fixed macrophages of the liver and spleen limits the number of liposomes capable of reaching a target site.

In the rush to demonstrate the ability of liposomes to treat neoplastic disease, few controlled studies have been conducted into the physiological fate of systemically injected liposomes. Such studies would require having liposomes of defined size and composition. Without this definition, relatively simple experiments such as *in vitro* exchange of cholesterol between sonicated phosphatidylcholine vesicles, can be misinterpreted (11). Rigorous studies on the physiological fate of liposomes require the use of radioactive phospholipids rather than easily obtained commercial radioactive markers such as cholesterol or cholesteryl esters. Such markers exchange readily with blood components (12) or are metabolized in the plasma to components that can exchange easily (13) resulting in an erroneous interpretation of carrier distribution. It is also essential to determine whether actual mass transfer of the phospholipid from the liposome is observed or simply the exchange of radioactive phospholipid equivalents with other blood components. Finally, the structural integrity of the liposome and the associated antitumor drug in the systemic circulation should be verified. Due to the complexity of such experiments, few studies exist that fulfill these criteria. The most complete work is that of Tall (14) in which all of these experimental parameters are examined. This particular study is important in that it gives insight into the molecular modification of liposomes by the lipoprotein apoproteins.

A wide variety of lipoproteins circulate in the plasma. Lipoprotein particles are responsible for transporting highly insoluble lipids such as triglycerides and cholesteryl esters to their site of utilization. The protein moieties of the lipoproteins, known as apoproteins, appear to play a role in the structural integrity of the lipoprotein particle as well as functioning as a recognition signal for various receptors in the body.

Apoproteins, especially apo A, can leave their respective lipoprotein particles and associate with phospholipid liposomes. With apo A, this association can eventually lead to the disruption of liposomal integrity (15–17) and the release of the associated water soluble antitumor agent. It has become clear that the inclusion of cholesterol in the liposome bilayer minimizes the interaction of apo A with phospholipid liposomes *in vitro* (18). However, the inclusion of cholesterol may not significantly alter the physiological fate of most of the liposomes *in vivo* (14).

The effect of another apoprotein, apo E, on phospholipid liposomes is often unappreciated. Apo E is associated with the uptake of chylomicron and very low density lipoprotein (VLDL) remnants in the liver (19, 20). Its association with phospholipids either as liposomes (21) or as phospholipid–triglyceride emulsions (22) is well documented. One hypothesis is that apo E may have a higher affinity for cholesterol-rich liposomes than for cholesterol-poor liposomes. If so, the cholesterol rich liposomes *in vivo* would be taken up by the hepatic receptor that recognizes apo E. Tall indicates that this may be the case (14). Therefore, the physiological fate of most cholesterol rich liposomes *in vivo* may be the liver, even though the fractional amount of the liposomes that remains in the plasma may appear to be structurally intact (18).

It is also well documented that the inclusion of choles-

terol in a liposome will reduce the rate of leakage of entrapped drugs. The reduction in the rate of loss of an antitumor agent from such cholesterol rich liposomes can be beneficial to the efficacy of cell cycle sensitive drugs such as cytarabine (23–25). Cytarabine entrapped within liposomes is sequestered from the plasma and is not subject to rapid metabolism; hence, the liposome acts as a long-lived depot for the drug. For other noncell cycle-dependent drugs, however, large increases in the efficacy of encapsulated drug regardless of the composition of the liposome, has not been observed (26), probably because most of the drug is removed to distant sites before the tumor can be reached. Thus, the inclusion of cholesterol in the liposome only decreases the permeability of the drug from a liposome and does not appear to significantly alter liposome tissue distribution.

The unresolved basic problem is how to gain greater target specificity for the drug. The most exploited way is to reduce the size of the liposome to that of a small unilamellar vesicle with a diameter of ~200 Å. This size reduction increases the plasma lifetime of the liposome compared to unsonicated dispersions (27), thereby increasing the possibility that greater tumor localization can be achieved compared to larger liposomes. The reduction in size of the liposome, however, also decreases the amount of interior aqueous space, thereby limiting the amount of water soluble antitumor drug that can be encapsulated. Moreover, the *in vitro* stability of small unilamellar vesicles is less than that of larger liposomes, either as large unilamellar vesicles or as unsonicated dispersions. The reduction in the size of the liposome while increasing plasma circulation time does not appear to alter extensively the physiological fate of the liposome (*i.e.*, localization primarily in the liver and the spleen).

Incorporation of Glycolipids—One new approach to alter the tissue distribution of liposomes is the inclusion of natural and synthetic glycolipids into the liposomes. Taking advantage of the asialo galactose receptor in the liver, vesicles containing an exposed galactose moiety accumulated to an even greater extent in the liver than liposomes without such glycolipids (28). On the other hand, the presence of a sialic acid group on the glycolipid slightly retards the accumulation of the such liposomes in the liver (29). Using a variety of synthetic glycolipids, such as amino mannose derivatives, Baldeschwieler and coworkers have shown that enhancement of vesicle stability can occur along with a highly altered tissue distribution, especially to the lung (30, 31). More recent studies have indicated that the same amino mannose derivatives enhance the uptake of liposomes by macrophages (32). Whether or not such altered stability and different tissue location have any beneficial effects for cancer chemotherapy remains to be tested. These results indicate that suitable modifications of the liposomal surface can dramatically alter *in vivo* characteristics.

Incorporation of Immunoglobulins—Another new methodology that has received much attention is the use of immunoglobulins to direct liposomes and the associated antitumor drug to a specific site. In theory, suitable tumor-specific antibodies can be bound to the liposomal surface and then can impart the necessary tissue specificity so that targeting can be achieved. An early study indicated that specificity could be achieved *in vitro* (33). Although internalization of the liposome and its associated antitumor drug was demonstrated, the studies were done with highly phagocytic cells. As attractive as this potential may be, there are factors that must be critically assessed. First, as shown by Weinstein and coworkers, the increased binding of a liposome containing the appropriate hapten to a cell, mediated by the $F(ab)_2$ fragment of an IgG specific antibody, does not ensure internalization of the liposome and its associated antitumor drug into nonphagocytic cells (34). Even the localization of liposomes containing methotrexate near tumor cells *in vitro* does not enhance the cytotoxic behavior of methotrexate (34). Recent studies have indicated that sonicated vesicles containing methotrexate and a surface-oriented hapten can be internalized into highly phagocytic cells having an F_c receptor by prior reaction of the lysosomes with antihapten IgG antibody (35). However, the therapeutic uses of this technique may be limited to highly phagocytic cells. Moreover, many normal cells also have F_c receptors that appear to be needed for carrier internalization (35).

Other workers have shown that IgG or $F(ab)_2$ fragments can be covalently linked to liposomes *via* oxidized glycolipids present in the bilayer of the liposome (36). Using $F(ab)_2$ fragments specific for red cells, a high degree of binding to red cells has been observed (37). Likewise, monoclonal antibodies can be rendered hydrophobic and linked to the liposome with subsequent *in vitro* specificity (38) or can be covalently linked *via* phosphatidylethanolamine in the liposome (39). Nonetheless, the mere increased binding to the target cell does not ensure greater efficacy of the associated antitumor drug, even *in vitro* (34). Therapeutic uses of antibody-directed liposomes must also be considered based on work demonstrating the physiological fate of purified ^{131}I-labeled anticarcinoembryonic antigen administered to patients with colorectal carcinomas. It has been shown that although diagnostic specificity (*i.e.*, higher radioactivity in tumor tissue compared to normal adjacent tissue) is observed, only 0.1% of the injected antibody localizes in the resected tumor (40). Such low absolute specificity raises a question for the potential use of antibodies as a way of targeting liposomes and their associated antitumor drugs to a tumor, since the carcinoembryonic antigen is one of the most characterized tumor markers. Also, since solid tumors are known to shed their antigens into the plasma, much of the liposome–antibody complex would most likely bind with circulating antigens, severely limiting the number of liposomes capable of binding to antigens on the tumor surface (40). Finally, there remains the problem of whether the liposome–antibody complex can leave the plasma compartment and enter into the extravascular compartment. If the liposome complex is being simply removed from the circulation by the fixed macrophages of the liver and spleen, then there is little liklihood that the liposome will encounter the bulk of the tumor. On the other hand, if the liposome–antibody complex can leave the vascular system at the tumor site, or enter the lymphatic circulation, then the possibility exists that the complex can interact with the tumor. The problem of the cellular uptake of the liposome and its associated antitumor drug *in vivo* remains the same as discussed for the *in vitro* studies.

Use of Biological Factors—A more novel approach to the problem of tissue specificity is the use of biological

factors to stimulate the body's immune system to attack tumor sites. The use of interferon as an immuno-modulating agent has received much attention, but its use has failed to produce uniformly positive results (41). Attempts have been made to restrict biological response modifiers selectively at the site of tumors. One example of this approach is the encapsulation of lymphokines within phospholipid liposomes (42). Liposomes, composed of phosphatidylcholine and phosphatidylserine, were shown to localize in the lung after intravenous injection. Such localization allowed the alveolar macrophages to phagocytose the liposomes and their associated macrophage activating factor. Thus, by activating the alveolar macrophages, metastases, which have migrated to the lung from a primary tumor, can be attacked with high efficiency, but only if the primary tumor had been excised from the animal (43). Further experiments indicated that macrophage activating factor can be replaced by the synthetic immuno-potentiating compound muramyl dipeptide with similar results (44). This approach indicates that if one can localize biological response modifiers such as macrophage activating factor and muramyl dipeptide to macrophages in the lung, substantial efficacy can be observed under certain conditions (*i.e.*, removal of the primary tumor). In a similar approach, immune RNA has been encapsulated in liposomes coated with antilymphocyte antibody studies. The phagocytosis of these liposomes by lymphocytes *in vitro* resulted in enhanced cytotoxicity to tumor cells (45). The *in vivo* utility of a system using antibodies to target liposomes to lymphocytes to enhance chemotherapy, has the same limitations as outlined previously.

Thus far, most attempts at targeting liposomes to selected tissues *in vivo* has relied on size, glycolipids, or antibodies. Even if successful, unless the tumor cells in the target tissue are highly endocytic, the contents of the liposome are unlikely to enter the target cell unless they leak from the liposome. That is to say, the free drug must still enter the target cell. Another novel approach is the localization of the free antitumor drug at a desired site by using the physical parameters of the liposome phospholipid composition to increase the permeability of the drug.

Use of Transition Temperature—It has been shown that at the transition temperature, when the phospholipids of a liposome undergo a physical transition from the gel to liquid crystalline state, there is a dramatic increase in the permeability of the liposomal membrane (46). An encapsulated drug will leak out more rapidly at this transition temperature than at temperatures slightly higher or lower. Liposomes with entrapped methotrexate have been designed to have a transition temperature near 42° (47). Localized heating of the target tissue can raise the internal tissue temperature high enough to reach 42°, causing a large efflux of the encapsulated methotrexate from the liposome as the carrier enters the heated tissue. As the liposome is removed from the target site *via* the circulatory system, the permeability of the drug from the liposomes decreases rapidly due to the decrease in local temperature. Recent experimental results indicated that high density lipoproteins are necessary to destabilize the liposomes at the phase transition temperature (48). Theoretically this process can be repeated during every circulatory pass of the liposome thereby delivering the drug at high localized concentrations at the target site. A variation of this approach is to incorporate *N*-palmitoyl homocysteine into liposomes. By adjusting the composition of the liposome, one can increase the permeability of an encapsulated drug with decreasing external pH (49). This approach assumes that the pH near the tumor site will be sufficiently lower than that of normal tissue, hence giving a selective release of the drug at that site. Such a theoretical concept remains to be demonstrated *in vivo*. In both approaches, this type of targeting is a transient phenomenon, and while it does not localize the drug in high concentrations at the desired site, it does give greater concentration of the free drug at the target site than can be achieved with conventional administration. With the heat sensitive liposomes, some therapeutic benefit has been observed (47).

Current experimental evidence indicates there is much to accomplish in order to demonstrate the necessary increased efficacy of antitumor agents in liposomes before contemplating potential clinical use. Nonetheless, there are a number of theoretical factors that should be part of an ideal lipid-based drug delivery system. It must be stable *in vivo*; *i.e.*, it should be resistant to the interaction of apoproteins of the plasma lipoproteins on the vesicle surface, resulting in structural destabilization or hepatic localization (especially *via* apo E). The carrier should have a small size (less than 300 Å) in order to penetrate into the extravascular space or lymphatic circulation, thereby giving the drug and carrier maximum opportunity to interact with tumor cells. Furthermore, this small size will enhance the possibility of endocytosis of the lipid-based carrier in a similar fashion to low-density lipoproteins, especially by cells that are not highly phagocytic (50). Finally, the carrier should be able to be localized with high specificity to any desired part of the organism *in vivo*. It is unlikely that immunological means will be able to accomplish this final goal.

MAGNETICALLY RESPONSIVE ALBUMIN MICROSPHERES

By using magnetically responsive albumin microspheres as a drug carrier, an entirely different approach to drug targeting can be considered (51). Microspheres composed of a denatured human serum albumin matrix serve as the vehicle in which a chemotherapeutic agent and ultrafine particles of magnetite (Fe_3O_4), are entrapped. Because of the magnetic material within the microspheres, they are susceptible to the effects of a magnetic field.

Albumin microspheres alone have some of the major problems discussed previously regarding liposomes; namely, clearance by the fixed macrophages of the liver and spleen and the lack of target site specificity. However, magnetically responsive drug-carrying microspheres infused into an artery supplying a tumor can be retained within the capillaries of tumor by an external magnet over the tumor site. Retention of the microspheres in the microvasculature can be achieved by taking advantage of the difference in the linear flow velocity of blood in a large artery (15–30 cm/sec) *versus* that in capillaries (0.05 cm/sec). Since the linear flow velocity of the microspheres is much slower within the capillaries, a much smaller magnetic field is sufficient to retain them within these vessels. By targeting the microspheres in this manner, they can be focused to a desired site with high specificity with

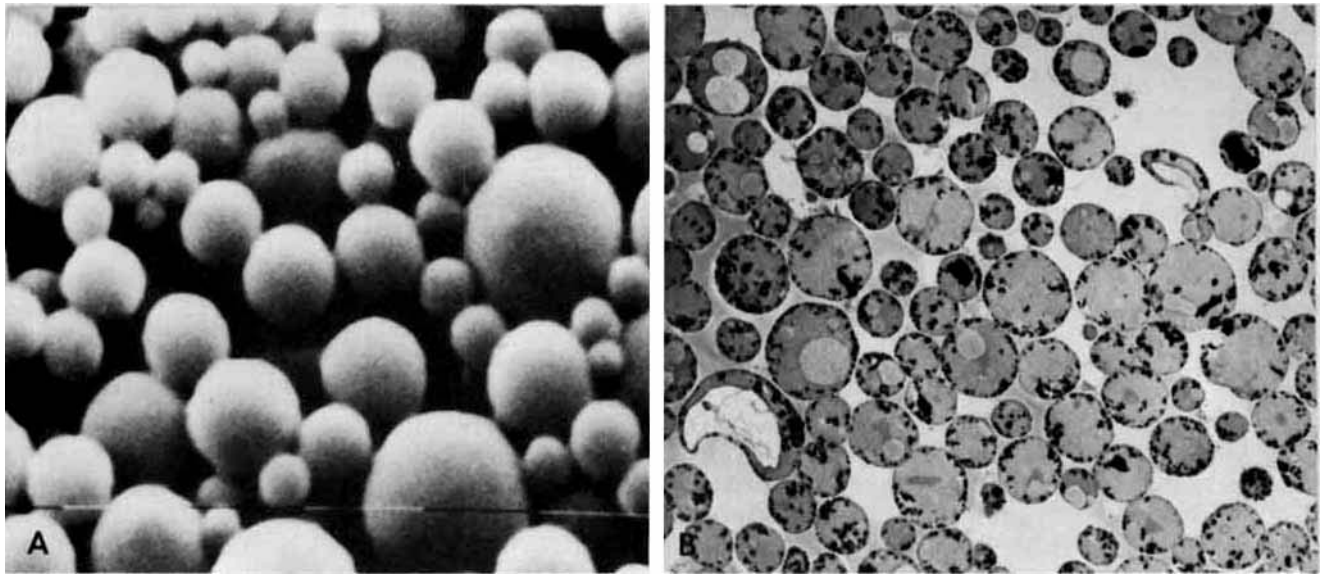

Figure 1—*Scanning electron photomicrograph (A) of microspheres showing an average diameter of ~1 μm. The largest sphere in the photomicrograph is 1.5 μm. Calibration bars represent 1 μm (×15,000). Transmission electron microscopy (B) reveals albumin microspheres containing clusters of Fe_3O_4 in a peripheral orientation (×8500). Drug is entrapped within the albumin matrix.*

subsequent decrease in clearance by mononuclear phagocytes. Restriction of the microspheres within the capillary circulation is essential for two reasons. First, drug diffusion occurs maximally in capillaries and venules; second, the microspheres from the microvasculature must transit into the extravascular space. By doing so, an extra-vascular depot would be created for sustained drug release within the target area. The drug released from the microspheres would saturate the tumor environment with a high local drug concentration. In addition, there is the possibility that the microspheres could be internalized by adjacent tumor cells as a result of increased tumor cell phagocytic activity (52, 53). By this mechanism, cytotoxic drugs released from microspheres would do so intracellularly and in high concentration resulting in cell death. Problems of drug resistance due to the inability of the drug to be transported across the cell membrane may be surmounted.

Preparation—Magnetically responsive albumin microspheres are prepared by a water-in-oil phase separation emulsion polymerization (54). Essentially, this consists of forming, in a small aqueous volume, a solution of albumin and water soluble chemotherapeutic agent (*e.g.*, adriamycin) to which an aqueous suspension of magnetite (Fe_3O_4) is added. This aqueous suspension is then added to a larger volume of oil and the mixture homogenized to generate proteinaceous spheres. These spheres are hardened either by heating the oil above 100° or by adding hydrophobic cross-linking agents to the emulsion. Microspheres are isolated by sequential washings in ether to remove residual oil and are stored as a powder at 4°.

Microspheres range in size from 0.2 to 1.35 μm in diameter with an average of 1.0 μm (Fig. 1A). By transmission electron microscopy it was determined that each albumin sphere contains clumps of Fe_3O_4 distributed largely around the periphery of the spheres (Fig. 1B).

Adriamycin was used in early studies of this approach because of its range of efficacy against a variety of tumors but was limited clinically due to its cardiotoxicity. It must be stressed, however, that virtually any water soluble chemotherapeutic agent may be successfully entrapped within the microspheres, giving them a broad potential range of utility.

Since optimal drug delivery *in vivo* necessitates predominantly capillary-level retention of the targeted microspheres, an *in vitro* system capable of simulating linear flow velocities of blood in various sized vessels was used to study the retention of microspheres using various magnetic parameters (55). Results (Fig. 2) demonstrated, at a magnetic field strength of 8000 Oe and using linear flow velocities comparable to those found in the microvasculature (*i.e.*, 0.05 cm/sec), virtually 100% of microspheres were magnetically retained, while microspheres in flow velocities comparable to those in medium sized arteries were not influenced by the magnetic field. Curve B illustrates the shift in the retention curve obtained when more magnetic material was entrapped within the microspheres. Studies on the effect matrix stabilization (chemical cross linking *versus* heating) indicated that the slow release of adriamycin could be manipulated without extensive loss

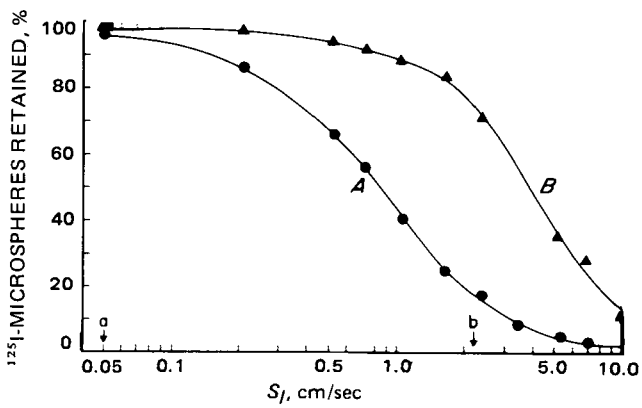

Figure 2—*Magnetic retention of heat-stabilized ^{125}I-microspheres suspended in 0.15 N NaCl at various rates of laminar flow (S_l = linear flow velocity). Curve A represents microspheres containing 20% Fe_3O_4 (w/w); curve B represents microspheres containing 50% Fe_3O_4. Increased microsphere iron content causes the retention curve to shift to the right. Physiological rates of blood flow are indicated for capillaries (a) and medium-sized arteries (b).*

Table I—*In Vivo* Localization of ^{125}I-Labeled Magnetic Albumin

Magnetic Field Strength, Oersteds	Number of Animals	Distribution Percentages								
		Tail Segment Number				Organ				
		1	2	3	4	Liver	Spleen	Kidney	Lung	Heart
0 (control)	10	0	0	0	0	76–85	3–9	<1	6–19	<1
4000	5	0	0	0–3	0	72–85	3–7	<1	5–18	<1
6000	5	0	0–4	10–25	0	57–70	2–8	<1	6–18	<1
8000	10	0	0–3	37–65	0–2	30–48	2–6	<1	3–17	<1

of drug activity (56).

***In Vivo* Testing**—After determining optimal *in vitro* characteristics, *in vivo* testing was undertaken to assess the validity of magnetic targeting. Initially, attempts were made to target microspheres to normal cutaneous and subcutaneous tissue in the tail of Sprague-Dawley rats (51). For experimental purposes, the tail was demarcated into four approximately equal segments with segment 1 being proximal. A permanent bipolar magnet was placed adjacent to tail segment 3, which was regarded as the target site. The ventral caudal artery was exposed by a cut-down procedure at the base of the tail (segment 1) and a polyethylene catheter was inserted 1.5 cm proximal to the target site. Microspheres labeled with iodine 125 were infused at a rate that corresponded to the rate of blood flow in this artery. After 30 min with the magnet in place, rats were sacrificed and organs counted for iodine 125 gamma radiation. The tail was cut into the designated segments and each was counted individually. In separate experiments animals were sacrificed 24 hr after magnetic localization.

Results of these experiments are shown in Table I. Increasing magnetic field strength resulted in increased retention of the drug carrier selectively in tail segment 3, the target site. Using an 8000 Oe magnetic field, ~50% of the infused microspheres were selectively retained in tail segment 3. Animals sacrificed 24 hr after targeting of microspheres demonstrated a similar 50% retention of injected carrier at the target site. No necrosis or evidence of obstructed blood flow was observed in these animals prior to sacrifice. Electron microscopy performed on skin from tail segment 3 demonstrated microspheres within endothelial cells as well as lodged between adjacent endothelial cells (51). Thus, ultrastructural evidence indicated that some targeted microspheres were able to exit from the vascular compartment to set up a potential extravascular drug depot.

The amount of adriamycin at the target site was evaluated in the same rat model system (57). Experimental animals were sacrificed at various time intervals after exposure of the target site to an 8000 Oe magnetic field.

Table II—*In Vivo* Distribution of Carrier-Delivered and Free Adriamycin

Form of Drug	Dose mg/kg	Magnetic Field[a]	Tissue Concentrations, μg/gm[b]	
			Target Tail Skin	Pooled Organs[c]
Carrier-delivered	0.05	0	<1	<1
	0.05	+	3.9	<1
Free	0.05	0	<1	<1
	5.00	0	5.5	15.0

[a] A magnetic field of 8000 Oe was placed over tail segment 3 (target area) for 5 min. [b] Limits of detection, ≤1 μg of drug/g of tissue (wet weight). [c] Organs consisted of liver, spleen, kidneys, lungs, and heart. Adriamycin was found predominantly in the liver.

Adriamycin was solubilized from tail skin and organs and assessed quantitatively by spectrophotofluorometry. In animals sacrificed 5 min after carrier infusion, 3.9 μg of adriamycin/g of tissue was localized in the target tail skin. No drug was detectable in the nontarget tail segments or in the liver. By contrast, a 100-fold higher dose of systemically administered unencapsulated adriamycin was required to obtain comparable local tissue concentrations (Table II). In similar experiments where animals were sacrificed 60 min after carrier infusion, an equivalent adriamycin concentration of 3.7 μg/g was found at the target site with no detectable levels of drug found in adjacent tail segments or in any of the visceral organs examined. In animals receiving 100 times the adriamycin dose (5 mg/kg, iv), the amount of adriamycin at the target site 60 min after administration was only 50% of that delivered by the microspheres. Thus, after 60 min, using 0.1% of the free intravenous dose, adriamycin targeted *via* magnetic microspheres yielded approximately twice the local adriamycin concentration at the preselected site with no detectable systemic distribution as compared to the intravenously administered drug.

The microspheres were next tested for efficacy in the treatment of established rat tumors (58). The ascites form of Yoshida rat sarcoma was chosen due to its known sensitivity to adriamycin and because of its aggressive biological behavior. The solid form of the tumor can be obtained by inoculating tumor cells subcutaneously. Tumor nodules appeared ~3 days after implantation. Average time of death of untreated animals was found to be 16 days post-tumor inoculation.

Prior to microsphere experiments, animals were inoculated with tumor cells in the lateral aspect of the tail and treated with adriamycin intravenously to assess tumor sensitivity to the drug. Animals received either intravenous normal saline, 0.5 mg of adriamycin/kg, or 5.0 mg of adriamycin/kg on days 1, 5, and 9 postinoculation of the tumor. Animals were assessed for tumor size, weight change, and life span.

Only animals receiving the multiple high-dose regimen (5 mg/kg) showed any evidence of tumor sensitivity to the drug as demonstrated by reduction of tumor growth. Furthermore, animals receiving the 5 mg/kg dosage regimen, had an average weight loss of 12 g, demonstrating evidence of systemic toxicity. It should be noted, however, that no difference in life span was noted between any treatment group. In summary, animals receiving multiple doses of adriamycin at 5 mg/kg demonstrated some inhibition of tumor growth; however, these animals also demonstrated evidence of systemic toxicity and no enhancement of life span was noted.

Once tumor sensitivity had been established, experiments were designed to treat the Yoshida sarcoma with adriamycin targeted *via* magnetic microspheres. Again,

Table III—Effect of Magnetic Microspheres Containing Adriamycin on Yoshida Sarcoma-Bearing Rats

	Untreated Control	Adriamycin, 5 mg/kg iv	Adriamycin, 5 mg/kg ia	Adriamycin 0.5 mg/kg, ia	Placebo Microspheres with Magnet	Microspheres Bearing 0.5 mg/kg Adriamycin No Magnet	Microspheres Bearing 0.5 mg/kg Adriamycin With Magnet
Initial tumor size, mm	36.2	19.4	26.8	25.7	29.3	27.8	28.7
Final tumor size, mm	46.4	38.4	41.9	44.5	46.9	48.5	5.0
Deaths, %	90	100	80	100	80	100	0
Regressions, %	11	0	0	0	0	0	92
Total remissions, %	0	0	0	0	0	0	75
Metastases, %	89	100	80	100	80	100	0

animals were inoculated with the tumor cells into the lateral aspect of the tail, but unlike sensitivity experiments, animals were used for experiments 6–8 days *after* tumor implantation. By the time of experimental use, tumors were not only measurable, but occasionally, showed evidence of necrosis. Regardless of the type of therapy given, animals received only single-dose treatment 6–8 days after tumor inoculation.

The experimental group consisted of 12 animals which received drug-bearing microspheres at a dose of 0.5 mg of adriamycin/kg with the tumor exposure to the magnetic field for 30 min. The method of microsphere infusion into the ventral caudal artery was identical to that described previously. The following groups of animals constituted the control groups: 10 animals received placebo microspheres (without drug) infused in the same manner with exposure of the tumor to the magnetic field; another group received drug-bearing microspheres, but no magnetic field was applied. Finally, free adriamycin was administered intra-arterially (*via* the ventral caudal artery) at 0.5 and 5 mg/kg and intravenously at 5 mg/kg. Animals were observed for weight change, tumor size, and death. All animals were sacrificed 29 days after treatment. Complete autopsies were performed and organs were examined both grossly and microscopically for evidence of tumor.

Results of single-dose therapy with magnetically responsive microspheres are presented in Table III. Tumor size increased markedly in all animals treated with free adriamycin, regardless of the administration route or the dose. Control animals receiving either no treatment, placebo microspheres, or drug-bearing microspheres without localization, also demonstrated a significant increase in tumor size. In contrast, there was a significant (92%) decrease in tumor size in animals receiving adriamycin containing microspheres (0.5 mg/kg) with the magnet placed adjacent to the tumor. The weights of all control animals increased during the course of the experiments, indicating no evidence of systemic toxicity. Animals receiving targeted therapy also showed an increase in weight.

In all groups of animals, except those receiving magnetically localized adriamycin microspheres, there was an 80–100% mortality rate and an 80–100% incidence of distant metastases during the 29 days the animals were observed. In contrast, no deaths or metastases occurred in animals treated with the single dose of magnetically targeted microspheres containing adriamycin. Moreover, 75% of the animals in this group had complete tumor remission as confirmed by microscopic examination of the tissues. An additional 17% had significant tumor regression. The remaining animal showed no change in tumor size and was alive at the end of the experimental period. In comparison, there were no remissions in any control group with the exception of a slight decrease in tumor size in one animal from the untreated control group.

In prior experiments performed to assess tumor susceptibility to adriamycin, it was found that the tumor would respond only when the therapeutic regimen consisted of multiple dose intravenous adriamycin (5 mg/kg) given on days 1, 5, and 9 after tumor inoculation. Animals thus treated showed some evidence of tumor regression. However, these animals also experienced weight loss suggestive of toxicity due to the drug. More importantly, survival was not enhanced in animals treated in this fashion compared with untreated controls. In contrast, a single dose of adriamycin, when administered in magnetically responsive microspheres and targeted to the tumor site, achieved 75% total remissions with no deaths or histologic evidence of metastases in experimental animals. These animals were treated after tumor load was evident (6–8 days after tumor inoculation) and with only a single dose of 0.5 mg of adriamycin/kg as compared to multiple-dose therapy. Evidence of tumor necrosis was histologically evident as early as 3 days after treatment.

It is important to note that none of the rats treated with targeted therapy had any histological evidence of metastatic disease. This was perhaps related to the timing of the therapy, though tumor nodules were large and rapidly growing at the time of experimental use. The metastatic potential of the tumor at the time of treatment, however, may well have been limited. It is believed that the spread of metastases begins ~7–8 days after tumor inoculation, with tumor neovascularization beginning at day 2–3[1]. Alternatively, destruction of the tumor cells by adriamycin, along with subsequent decrease in tumor load and inhibited secretion of soluble low molecular weight tumor product inhibitors (59) may have tilted the immunological balance toward an active host response.

Thus, the potential of magnetic microspheres to enhance the therapeutic index of an antineoplastic agent has been demonstrated. The increase in the therapeutic index appears to come from both decreased toxicity and increased efficacy. Nonetheless, several questions remain to be resolved before the advent of clinical use. The first and foremost involves the external magnetic field used in targeting. The magnetic microspheres are held in place by the magnetic field gradient and not just the strength of the magnetic field. Magnetic field gradients drop off dramatically from the magnet pole face. The localization of microspheres to a tumor present subcutaneously allows maximum magnetic field gradients to be imposed on the

[1] Dr. Judah Folkman, personal communication.

target site. Other target sites may be too distant to allow the retention of the magnetic microspheres to take place. The theoretical problem of focusing magnetic field gradients at sites external to the magnet face is formidable. This problem must be solved if widespread clinical use is to be expected.

The second problem is that the magnetic microsphere must be administered intra-arterially as opposed to intravenously. An intravenous administration would result in the clearance of the microspheres by mononuclear phagocytes before reaching the target site. Intra-arterial administration involves a necessary cut-down, and hence some morbidity. This problem may possibly be overcome by altering the surface characteristics of the microspheres to allow them to bypass the phagocytic cells upon intravenous administration. Results in this area would be applicable to liposomes. Finally, this carrier may be applicable only for water soluble antitumor drugs. This problem is relatively minor, since currently, most antitumor drugs are water soluble.

Nonetheless, given the above limitations, the magnetic microspheres have given the most dramatic demonstration to date of the ability to direct antitumor drugs to a target site resulting in increased efficacy of the incorporated drug.

CONCLUSIONS

Drug carriers offer significant promise for the selective delivery of toxic chemotherapeutic agents in the treatment of cancer. Liposomes have been explored to a considerable degree for use as drug carriers in the treatment of neoplasms. Though some interesting results have been obtained in this area, liposomes generally have failed to perform as a practical method for drug delivery *in vivo*. Their usefulness is restricted, mainly due to a lack of target site specificity and their rapid clearance by mononuclear phagocytes in the liver and spleen. Approaches that take advantage of specific cell receptors *via* antibodies or glycolipids show some potential for achieving specificity; however, major obstacles remain in the application of these approaches. In contrast, a magnetically responsive drug delivery system is capable of a significant degree of *in vivo* targeting as well as a controllable release of drug at the microvascular level.

It is the authors' view that magnetically responsive drug carriers, either as a lipid or protein base, may have significant clinical relevance in the treatment of neoplastic disease. Each type of magnetically responsive carrier would have certain advantages. Protein microspheres would be useful for water-soluble drugs and can serve as long-lived localized drug depots. Magnetically responsive lipid base systems would be most applicable to water insoluble antitumor drugs. They may also have a smaller size than the protein microspheres, and hence a longer circulatory lifetime. Whichever type of magnetically responsive carrier is developed, the potential for targeting *via* external magnetic fields offers a new approach to a longstanding challenge in cancer chemotherapy. Although problems remain to be solved, the experimental results to date justify optimism.

REFERENCES

(1) K. J. Widder, A. E. Senyei, and D. F. Ranney, in "Advances in Pharmacology and Chemotherapy," S. Garattini *et al.*, Eds., vol. 16, Academic, New York, N.Y. 1979, pp. 213–271.

(2) G. F. Rowland, G. J. O'Neill, and D. A. L. Davies, *Nature (London)*, **255,** 487 (1975).

(3) J. D. Everall, P. Dowd, D. A. L. Davies, G. J. O'Neill, and G. F. Rowland, *Lancet*, **1,** 1105 (1977).

(4) T. Ghose, S. T. Norvell, A. Guclu, A. Bodcertha, J. Tai, and A. S. McDonald, *J. Natl. Cancer Inst.*, **58,** 845 (1977).

(5) F. Szoka, F. Olson, T. Heath, W. Vail, E. Mayhew, and D. Papahadjopoulos, *Biochim. Biophys. Acta*, **601,** 559 (1980).

(6) G. Gregoriadis, *N. Engl. J. Med.*, **295,** 704 (1976).

(7) *Ibid.*, **295,** 765 (1976).

(8) R. E. Pagano and J. N. Weinstein, *Ann. Rev. Biophys. Bioeng.*, **7,** 435 (1978).

(9) "Drug Carriers in Biology and Medicine," G. Gregoriadis, Ed., Academic, New York, N.Y., 1979.

(10) "Liposomes in Biological Systems," G. Gregoriadis and A. C. Allison, Eds., Wiley, New York, N.Y., 1980.

(11) J. M. Backer and E. A. Dawidowicz, *Biochim. Biophys. Acta*, **551,** 260 (1979).

(12) K. R. Bruckdorfer, J. M. Graham, and C. Green, *Eur. J. Biochem.*, **4,** 512 (1968).

(13) Y. Stein, G. Halperin, and O. Stern, *FEBS Lett.*, **111,** 104 (1980).

(14) A. R. Tall, *J. Lipid Res.*, **21,** 354 (1980).

(15) L. Krupp, A. V. Chobanian, and P. I. Brescher, *Biochem. Biophys. Res. Commun.*, **72,** 1251 (1976).

(16) G. Scherphof, E. Roerdink, M. Waite, and J. Parks, *Biochim. Biophys. Acta*, **542,** 29 (1978).

(17) T. M. Allen, *Biochim. Biophys. Acta*, **640,** 385 (1981).

(18) C. Kirby, J. Clarke, and G. Gregoriadis, *Biochem. J.*, **186,** 591 (1980).

(19) E. Windler, Y. Chao, and R. J. Havel, *J. Biol. Chem.*, **255,** 5475 (1980).

(20) *Ibid.*, 8303 (1980).

(21) R. J. Havel, Y. Chao, E. Windler, L. Otite, and L. S. Guao, *Proc. Natl. Acad. Sci. USA*, **77,** 4349 (1980).

(22) S. F. Robinson and S. H. Quarfordt, *Lipids*, **14,** 343 (1979).

(23) T. Obayashi, S. Tsukayoshi, and Y. Sakurai, *Gann*, **66,** 719 (1975).

(24) E. Mayhew, Y. M. Rustum, F. Szoka, and D. Papahadjopoulos, *Cancer Treat. Rep.*, **63,** 1923 (1979).

(25) R. Ganapathi, A. Krishan, I. Wodinski, C. G. Zubrod, and L. J. Lesko, *Cancer Res.*, **40,** 630 (1980).

(26) J. A. Todd, A. M. Levine, and A. T. Zolten, *J. Natl. Cancer Inst.*, **64,** 715 (1980).

(27) R. L. Juliano and D. Stamp, *Biochem. Biophys. Res. Commun.*, **63,** 651 (1975).

(28) A. Surolia and B. K. Bachwatt, *Biochim. Biophys. Acta*, **497,** 760 (1977).

(29) M. M. Jonah, E. A. Cerny, and Y. E. Rahman, *ibid.*, **541,** 321 (1978).

(30) M. M. Mauk, R. C. Gamble, and J. D. Baldeschwieler, *Science*, **207,** 309 (1980).

(31) M. M. Mauk, R. C. Gamble, and J. D. Baldeschwieler, *Proc. Natl. Acad. Sci. USA*, **77,** 4430 (1980).

(32) P. Wu, G. W. Tin, and J. D. Baldeschwieler, *ibid.*, **78,** 2033 (1981).

(33) G. Gregoriadis and D. Neerunjun, *Biochem. Biophys. Res. Commun.*, **65,** 537 (1975).

(34) J. N. Weinstein, R. Blumenthal, S. O. Sharrow, and P. A. Henkart, *Biochim. Biophys. Acta*, **509,** 272 (1978).

(35) L. D. Leserman, J. N. Weinstein, R. Blumenthal, and W. D. Terry, *Proc. Natl. Acad. Sci. USA*, **77,** 4089 (1980).

(36) T. D. Heath, B. A. Macker, and D. Papahadjopoulos, *Biochim. Biophys. Acta*, **640,** 66 (1981).

(37) T. D. Heath, R. T. Fraley, and D. Papahadjopoulos, *Science*, **210,** 539 (1980).

(38) A. Huang, L. Huang, and S. J. Kennel, *J. Biol. Chem.*, **255,** 8015 (1980).

(39) L. D. Leserman, J. Barbet, F. Kourilsky, and J. N. Weinstein, *Nature (London)*, **288,** 602 (1980).

(40) J. Mach, S. Carrel, M. Forni, J. Ritschard, A. Donath, and P. Alberto, *N. Engl. J. Med.*, **303,** 5 (1980).

(41) M. Sun, *Science*, **212,** 141 (1981).

(42) I. J. Fidler, A. Roz, W. E. Folger, R. Kirsch, P. Bugelshi, and G. Poste, *Cancer Res.*, **40,** 4460 (1980).

(43) I. J. Fidler, *Science*, **208**, 1469 (1980).
(44) I. J. Fidler, S. Sore, W. E. Folger, and Z. L. Barnes, *Proc. Natl. Acad. Sci. USA*, **78**, 1680 (1981).
(45) W. E. Magee, J. H. Grovenberger, and D. E. Thor, *Cancer Res.*, **38**, 1173 (1979).
(46) M. B. Yatvin, J. N. Weinstein, W. H. Dennis, and R. Blumenthal, *Science*, **202**, 1290 (1978).
(47) J. N. Weinstein, R. L. Magin, R. L. Cysyk, and D. S. Zaharko, *Cancer Res.*, **40**, 1388 (1980).
(48) J. N. Weinstein, R. D. Klausner, T. Innerarity, E. Ralston, and R. Blumenthal, *Biochim. Biophys. Acta*, in press.
(49) M. B. Yatvin, W. Kreutz, B. A. Horwitz, and M. Shinitzky, *Science*, **210**, 1253 (1980).
(50) J. L. Goldstein, R. G. W. Anderson, and M. S. Brown, *Nature (London)*, **279**, 679 (1979).
(51) K. J. Widder, A. E. Senyei, and D. G. Scarpelli, *Proc. Soc. Exp. Biol. Med.*, **58**, 141 (1978).
(52) H. Busch, E. Fujwara, and D. C. Firszt, *Cancer Res.*, **21**, 371 (1961).
(53) S. Cohen, S. M. Beiser, and K. C. Hsu, *ibid.*, **21**, 1510 (1961).
(54) K. J. Widder, G. Flouret, and A. E. Senyei, *J. Pharm. Sci.*, **68**, 79 (1979).
(55) A. Senyei, K. Widder, and G. Czerlinski, *J. Appl. Phys.*, **49**, 3578 (1978).
(56) K. J. Widder, A. E. Senyei, and D. F. Ranney, *Cancer Res.*, **40**, 3512 (1980).
(57) A. E. Senyei, S. D. Reich, and K. J. Widder, *J. Pharm. Sci.*, **70**, 389 (1981).
(58) K. J. Widder, R. M. Morris, G. Poore, D. P. Howard, and A. E. Senyei, *Proc. Natl. Acad. Sci USA*, **78**, 579 (1981).
(59) R. Snyderman and M. C. Pike, *Am. J. Pathol.*, **88**, 727 (1977).

RESEARCH ARTICLES

Properties, Stability, Assay, and Preliminary Pharmacokinetics of the Immunomodulatory 1,2-*O*-Isopropylidene-3-*O*-3′(*N*′,*N*′-dimethylamino-*n*-propyl)-D-glucofuranose Hydrochloride

EDWARD R. GARRETT ˣ, ACHIEL VAN PEER, HELMY MAHROUS, and WALDTRAUT SCHUERMANN

Received May 14, 1981, from *The Beehive, College of Pharmacy, J. Hillis Miller Health Center, University of Florida, Gainesville, FL 32610.* Accepted for publication August 14, 1981.

Abstract □ 1,2-*O*-Isopropylidene-3-*O*-3′(*N*′,*N*′-dimethylamino-*n*-propyl)-D-glucofuranose hydrochloride (I) is a new agent with claimed immunomodulatory action and antiviral activity. Thin-layer chromatographic procedures and identifying tests were developed to separate the drug, its synthetic precursors, and solvolytic products, and were applied to stability studies. It is stable in 0.1 *N* NaOH at 60° where its acid solvolysis product, 3-*O*-3′-(*N*′,*N*′-dimethylamino-*n*-propyl)-D-glucose is readily degraded. The partition coefficient of I (pK_a = 9.28) between chloroform and plasma was 6.4 ± 0.2 *SEM* between pH 10.5 and 11.0. Plasma and urine (0.5 ml) adjusted to pH 11.0 were extracted with 10 ml of chloroform and the extract evaporated. The reconstituted residue in 50 μl of benzene, with the diisopropylaminoethyl analog of I as an internal standard, was derivatized with 50 μl of heptafluorobutyric anhydride at 60° for 45 min and was evaporated and reconstituted in 100 μl of benzene to be assayed for I by GLC with electron capture detection with a sensitivity of 5 ng/0.5 ml of biological fluid. The procedure was applied to pharmacokinetics in the dog and a two-compartment body model was observed with a terminal half-life of 103–130 min. At the 40-mg dose, 60–64% was excreted renally unchanged and 20–34% as unidentified metabolities. At the 200-mg dose 82–85% was excreted renally unchanged and 15–17% as unidentified metabolites. The respective renal clearances of I were 135 and 163 ml/min. The respective total clearances of I were 204 and 191 ml/min. These metabolites were apparently unextracted with chloroform from biological fluids at pH 11 and the liquid scintillation counting (LSC) assay of extracted radiolabeled I appeared synonomous with the GLC assay of I in such fluids.

Keyphrases □ Pharmacokinetics—new immunomodulatory and antiviral agent, dogs □ GLC, electron capture—pharmacokinetics of a new immunomodulatory and antiviral agent, dogs □ Immunomodulatory agent—pharmacokinetics of a new immunomodulatory and antiviral agent, dogs

It has been shown (1–7) that 1,2-*O*-isopropylidene-3-*O*-3′-(*N*′,*N*′-dimethylamino - *n* - propyl)-D-glucofuranose hydrochloride, I, exhibits immunomodulatory action and antiviral activity and that it possesses pro host action in which cellular immune response is augmented and macrophages are activated (8, 9). The advantageous therapeutic action is to potentiate protective responses of the immune system(6) without the inhibition of vital cell actions with their concomitant toxicities (4).

Compound I is a substituted monosaccharide of low toxicity, widely different in structure than the clinically used nonsteroidal anti-inflammatory agents with high incidences of toxicity. An interesting argument for this possible activity of the 3-substituted monosaccharide (1–8) is that it mimics the immunological activity of the cell walls of mycobacteria with its positive cyclic guanosine monophosphate action and without its negative cyclic adenosine monophosphate effect on proliferation.

The procedure for the synthesis of I, is outlined in Scheme I. The diisopropylidene derivative of D-glucose, IV, is prepared by the addition of acetone. It is subsequently conjugated with *N*′,*N*′-dimethylamino propanol, II, in the 3 position. Compound I is then prepared by selective acid hydrolysis of the 5,6-*O*-isopropylidene group.

0022-3549/82/0400-0387$01.00/0

(43) I. J. Fidler, *Science*, **208**, 1469 (1980).
(44) I. J. Fidler, S. Sore, W. E. Folger, and Z. L. Barnes, *Proc. Natl. Acad. Sci. USA*, **78**, 1680 (1981).
(45) W. E. Magee, J. H. Grovenberger, and D. E. Thor, *Cancer Res.*, **38**, 1173 (1979).
(46) M. B. Yatvin, J. N. Weinstein, W. H. Dennis, and R. Blumenthal, *Science*, **202**, 1290 (1978).
(47) J. N. Weinstein, R. L. Magin, R. L. Cysyk, and D. S. Zaharko, *Cancer Res.*, **40**, 1388 (1980).
(48) J. N. Weinstein, R. D. Klausner, T. Innerarity, E. Ralston, and R. Blumenthal, *Biochim. Biophys. Acta*, in press.
(49) M. B. Yatvin, W. Kreutz, B. A. Horwitz, and M. Shinitzky, *Science*, **210**, 1253 (1980).
(50) J. L. Goldstein, R. G. W. Anderson, and M. S. Brown, *Nature (London)*, **279**, 679 (1979).
(51) K. J. Widder, A. E. Senyei, and D. G. Scarpelli, *Proc. Soc. Exp. Biol. Med.*, **58**, 141 (1978).
(52) H. Busch, E. Fujwara, and D. C. Firszt, *Cancer Res.*, **21**, 371 (1961).
(53) S. Cohen, S. M. Beiser, and K. C. Hsu, *ibid.*, **21**, 1510 (1961).
(54) K. J. Widder, G. Flouret, and A. E. Senyei, *J. Pharm. Sci.*, **68**, 79 (1979).
(55) A. Senyei, K. Widder, and G. Czerlinski, *J. Appl. Phys.*, **49**, 3578 (1978).
(56) K. J. Widder, A. E. Senyei, and D. F. Ranney, *Cancer Res.*, **40**, 3512 (1980).
(57) A. E. Senyei, S. D. Reich, and K. J. Widder, *J. Pharm. Sci.*, **70**, 389 (1981).
(58) K. J. Widder, R. M. Morris, G. Poore, D. P. Howard, and A. E. Senyei, *Proc. Natl. Acad. Sci USA*, **78**, 579 (1981).
(59) R. Snyderman and M. C. Pike, *Am. J. Pathol.*, **88**, 727 (1977).

RESEARCH ARTICLES

Properties, Stability, Assay, and Preliminary Pharmacokinetics of the Immunomodulatory 1,2-*O*-Isopropylidene-3-*O*-3′(*N*′,*N*′-dimethylamino-*n*-propyl)-D-glucofuranose Hydrochloride

EDWARD R. GARRETT ˣ, ACHIEL VAN PEER, HELMY MAHROUS, and WALDTRAUT SCHUERMANN

Received May 14, 1981, from *The Beehive, College of Pharmacy, J. Hillis Miller Health Center, University of Florida, Gainesville, FL 32610.* Accepted for publication August 14, 1981.

Abstract □ 1,2-*O*-Isopropylidene-3-*O*-3′(*N*′,*N*′-dimethylamino-*n*-propyl)-D-glucofuranose hydrochloride (I) is a new agent with claimed immunomodulatory action and antiviral activity. Thin-layer chromatographic procedures and identifying tests were developed to separate the drug, its synthetic precursors, and solvolytic products, and were applied to stability studies. It is stable in 0.1 *N* NaOH at 60° where its acid solvolysis product, 3-*O*-3′-(*N*′,*N*′-dimethylamino-*n*-propyl)-D-glucose is readily degraded. The partition coefficient of I (pK_a = 9.28) between chloroform and plasma was 6.4 ± 0.2 *SEM* between pH 10.5 and 11.0. Plasma and urine (0.5 ml) adjusted to pH 11.0 were extracted with 10 ml of chloroform and the extract evaporated. The reconstituted residue in 50 μl of benzene, with the diisopropylaminoethyl analog of I as an internal standard, was derivatized with 50 μl of heptafluorobutyric anhydride at 60° for 45 min and was evaporated and reconstituted in 100 μl of benzene to be assayed for I by GLC with electron capture detection with a sensitivity of 5 ng/0.5 ml of biological fluid. The procedure was applied to pharmacokinetics in the dog and a two-compartment body model was observed with a terminal half-life of 103–130 min. At the 40-mg dose, 60–64% was excreted renally unchanged and 20–34% as unidentified metabolities. At the 200-mg dose 82–85% was excreted renally unchanged and 15–17% as unidentified metabolites. The respective renal clearances of I were 135 and 163 ml/min. The respective total clearances of I were 204 and 191 ml/min. These metabolites were apparently unextracted with chloroform from biological fluids at pH 11 and the liquid scintillation counting (LSC) assay of extracted radiolabeled I appeared synonomous with the GLC assay of I in such fluids.

Keyphrases □ Pharmacokinetics—new immunomodulatory and antiviral agent, dogs □ GLC, electron capture—pharmacokinetics of a new immunomodulatory and antiviral agent, dogs □ Immunomodulatory agent—pharmacokinetics of a new immunomodulatory and antiviral agent, dogs

It has been shown (1–7) that 1,2-*O*-isopropylidene-3-*O*-3′-(*N*′,*N*′-dimethylamino - *n* - propyl)-D-glucofuranose hydrochloride, I, exhibits immunomodulatory action and antiviral activity and that it possesses pro host action in which cellular immune response is augmented and macrophages are activated (8, 9). The advantageous therapeutic action is to potentiate protective responses of the immune system(6) without the inhibition of vital cell actions with their concomitant toxicities (4).

Compound I is a substituted monosaccharide of low toxicity, widely different in structure than the clinically used nonsteroidal anti-inflammatory agents with high incidences of toxicity. An interesting argument for this possible activity of the 3-substituted monosaccharide (1–8) is that it mimics the immunological activity of the cell walls of mycobacteria with its positive cyclic guanosine monophosphate action and without its negative cyclic adenosine monophosphate effect on proliferation.

The procedure for the synthesis of I, is outlined in Scheme I. The diisopropylidene derivative of D-glucose, IV, is prepared by the addition of acetone. It is subsequently conjugated with *N*′,*N*′-dimethylamino propanol, II, in the 3 position. Compound I is then prepared by selective acid hydrolysis of the 5,6-*O*-isopropylidene group.

0022-3549/82/0400-0387$01.00/0

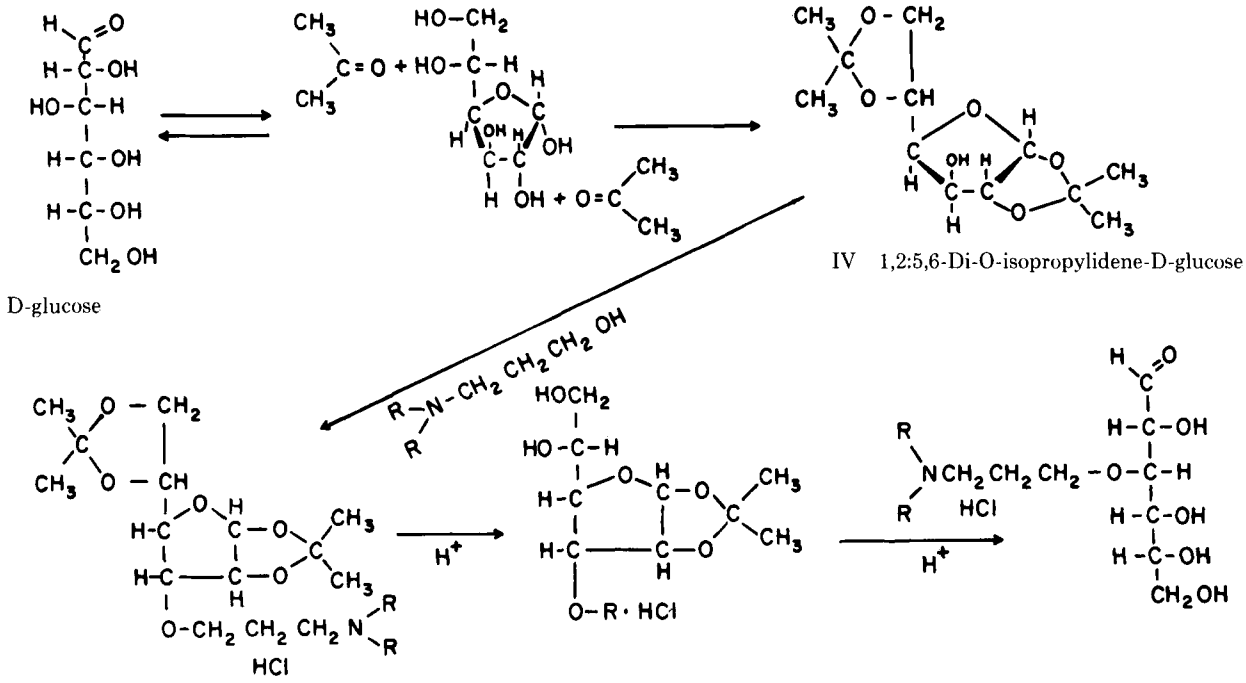

D-glucose

IV 1,2:5,6-Di-O-isopropylidene-D-glucose

II 1,2:5,6-Di-O-isopropylidene-3-O-3′-(N′,N′-dimethylamino-n-propyl)-D-glucofuranose (R = CH_3)

I R = $-CH_2CH_2CH_2-N(CH_3)_2$ 1,2-O-isopropylidene-3-O-3′(N′,N′-dimethylamino-n-propyl)-D-glucofuranose hydrochloride

V di-isopropylaminoethyl analog of I R = $-CH_2-CH_2-N(i-C_3H_7)_2$ (internal standard)

III 3-O-3′-N′,N′-dimethylamino-n-propyl)-D-glucose hydrochloride R = CH_3

Scheme I—Synthesis and Hydrolysis of I

Excessive acid hydrolysis could give the dimethylaminopropylglucose, III. The radiolabeled compound I was prepared with randomly labeled [^{14}C]D-glucose.

These studies present thin-layer chromatographic (TLC) procedures to separate I from its synthetic precursors and its solvolysis products. They were applied to studies of the acid-base stabilities of these compounds. Dissociation constants and partition coefficients as functions of pH were determined. A sensitive GLC method was developed for the assay of I where the heptafluorobutyryl derivative was detected by electron capture. This procedure was applied to preliminary pharmacokinetic studies of intravenously administered I in the dog and compared to the assay of radiolabeled I in the monitored biological fluids.

EXPERIMENTAL

Materials—The following analytical grade materials were used: acetic acid[1], sodium acetate[1], sodium phosphate dibasic[1], potassium phosphate monobasic[1], sodium carbonate[1], sodium bicarbonate[1], ammonium hydroxide[1], phosphoric acid[2], sulfuric acid[1], volumetric concentrates of sodium hydroxide[3] and hydrochloric acid[3], nanograde benzene[1], *n*-butyl alcohol[1], chloroform suitable for GC[4], methylene chloride[1], absolute alcohol[5], ethyl acetate[4], nanograde hexane[1], isopentyl alcohol[6], methanol[4], *n*-propanol[2], heptafluorobutyric anhydride[7], and a silylating agent[8].

Precoated silica gel plates[9] were used for TLC separation. The following spray reagents were used: 1% ninhydrin[8] in alcohol, 4% 2,3,5-triphenyl-2H-tetrazolium chloride[10] in methanol, 3.5% *p*-anisidine hydrochloride[10] in *n*-butyl alcohol–alcohol–water (4:1:1), 3% copper acetate[2] in 18% phosphoric acid. TLC plates were also placed in tanks containing resublimed iodine[11].

1,2-*O*-Isopropylidene- 3 -*O*-3′(*N*′-*N*′-dimethylamino-*n*-propyl)-D-glucofuranose hydrochloride (I), the diethylaminoisopropyl analog of I, [1,2-*O*-isopropylidene-3-*O*-3′(*N*′,*N*′-diethylaminoisopropyl)-D-glucofuranose hydrochloride] (VI), and the GLC internal standard diisopropylaminoethyl analog of I, [1,2-*O*-isopropylidene-3-*O*-3′(*N*′,*N*′-diisopropylaminoethyl)-D-glucofuranose hydrochloride] (V) were received as hydrochlorides[12]. Diisopropylidene glucose[12], IV (mp 106°) (1,2,5,6-di-*O*-isopropylidene-D-glucose), monoisopropylidene glucose[12] [VII (mp 154–155°) 1,2-*O*-isopropylidene-D-glucose], dimethylamino-*n*-propyl-D-glucose hydrochloride[12] [III (mp 131–133°), 3-*O*-3′(*N*′,*N*′-dimethylamino-*n*-propyl)-D-glucose hydrochloride], glucose[2], and lactose[13] were also used as standards for TLC.

Radiolabeled I, randomly ^{14}C-labeled in the glucose component[14] (324.0 mCi/mmole), was used to prepare doses for the pharmacokinetic study. [^{14}C]Urea[15] (55 mCi/mmole) was the internal standard for the radioactive assay. A toluene-based scintillation cocktail[16] was used in the radioactive assays.

Apparatus—A gas chromatograph[17] equipped with a ^{63}Ni-electron capture detector was used. Silylated 1.83-m glass columns were packed with 4% SE 30 and 6% OV 210 on 100/120 chromosorb W-HP[7]. The column temperature was maintained at 190°; injector temperature was 230°, and detector temperature 300°. The flow rate of the carrier gas (95%

[1] Mallinckrodt Inc., Saint Louis, MO 63147.
[2] J. T. Baker Chemical Co., Phillipsburg, N.J.
[3] Ricca Chemical Co., Arlington, TX 76012.
[4] Burdick and Jackson Laboratories, Muskegon, MI 49442.
[5] U.S. Industrial Chemicals Co., New York, NY 10016.
[6] Allied Chemical, Morristown, N.J.
[7] Supelco Inc., Bellefonte, PA 16823.
[8] Silyl 8, a silylating agent and ninhydrin, Pierce Chemical Co., Rockford, IL 61105.
[9] Silica gel 60, E. Merck Laboratories, Elmsford, NY 10523.
[10] Eastman Kodak Co., Rochester, NY 14650.
[11] Fisher Scientific Co., Fair Lawn, NJ 07410.
[12] Greenwich Pharmaceuticals, Greenwich, CT 06830. (The I used was Lot 3646.)
[13] Strategic Medical Research Corp., Chicago, IL 60680.
[14] Lot #1141-220, New England Nuclear, Boston, MA 02118.
[15] Lot #921885, ICN Pharmaceuticals, Irvine, CA 92715.
[16] Scinti Verse, Fisher Scientific Co., Fair Lawn, NJ 07410.
[17] Model Sigma I Perkin-Elmer, Norwalk, CT 06856.

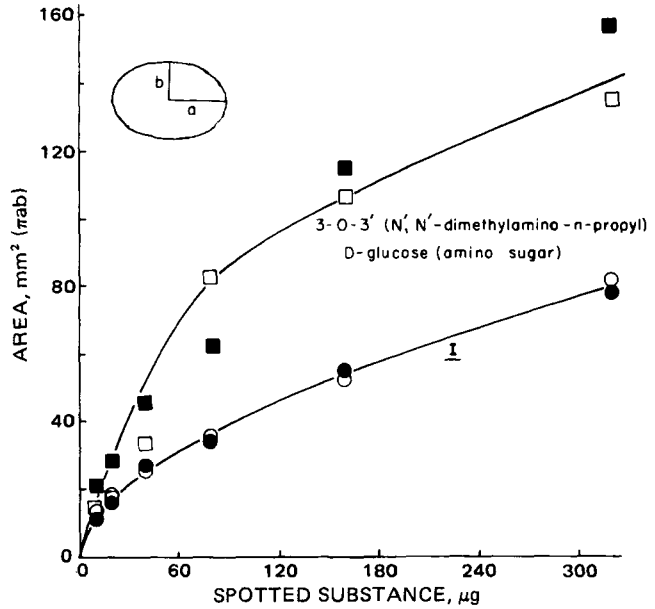

Figure 1—*Quantitative TLC analyses, Area = πab versus μg, of I (○, ●), and 3-O-3′(N′,N′-dimethylamino-n-propyl)D-glucose hydrochloride, III (□, ■) as developed in n-propanol–ethyl acetate–water–NH_4OH (6:1:4:1). Key: open symbols are for the areas of the elliptical spots determined from the product of the orthogonal radii, a × b and π from ninhydrin visualization; closed symbols are from visualization after charring with 50% H_2SO_4. Various volumes of 10-μg/μl materials were spotted at the origin with successive application and drying.*

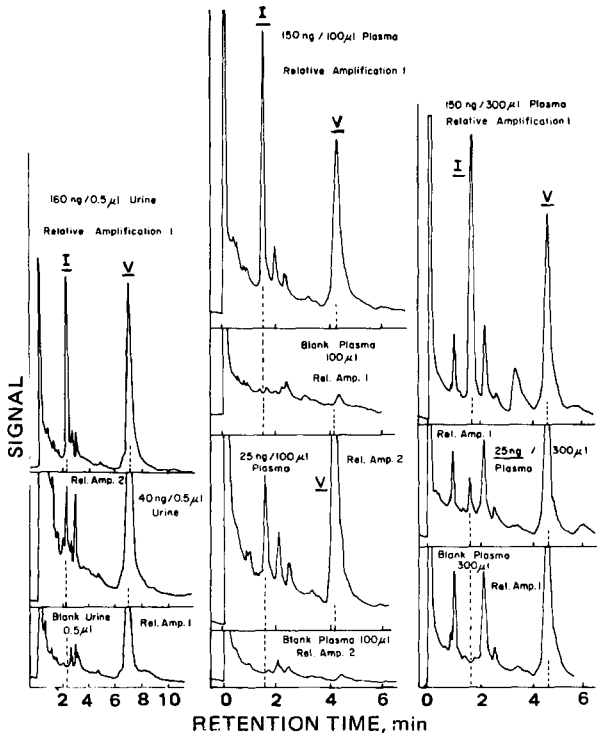

Figure 2—*Typical GLC chromatograms of heptafluorobutyrylated I, and the internal standard diisopropylaminoethyl analog of I, (V) in plasma and urine as well as derivatized blank urine and plasma samples, detected by electron capture. The signals are labeled as to their relative amplification for comparison. The vertical dashed lines represent the retention times of derivatized I and internal standard. The amounts and volumes of biological samples assayed are given.*

argon–5% methane) was 30 ml/min.

Radioactivity of samples was determined with a liquid scintillation counter[18].

GLC Assay of I—A solution (0.05 ml) of internal standard [10 μg diisopropylaminoethyl analog of I hydrochloride (V)/ml of distilled water] was added to an aliquot (<0.5 ml) of urine or plasma, which was diluted to 0.5 ml with distilled water. After adjustment to pH 11.0 with 0.1 *N* NaOH (>50 μl), the solution was extracted with 5 ml of water-saturated chloroform. The samples were shaken for 15 min and centrifuged[19] at 3000 rpm for 15 min.

The aqueous phase was removed by aspiration and 4 ml of the chloroform phase was transferred into 5-ml silylated reaction vials[7] and evaporated to dryness under a nitrogen stream[20] at room temperature. Benzene (50 μl) and heptafluorobutyric anhydride (50 μl) were added to derivatize the extracted I and the diisopropylaminoethyl analog, V, with shaking for 45 min at 60° in heating blocks[21]. The cooled reaction vials contents were evaporated (30 min) under a nitrogen stream at room temperature. The residue was reconstituted in 100 μl benzene and 1 μl was injected into the gas chromatograph.

Calibration curves were prepared using the same amounts of blank urine or plasma spiked with 0, 20, 40, 60, 80, 100, 120, 140, and 160 ng of I.

Thin-Layer Chromatography (TLC)—Glass plates coated with silica gel were used to separate the following materials (50 μg) using the system *n*-propanol–ethyl acetate–water–NH_4OH, 6:1:4:1. The following R_f values were obtained: diisopropylidene glucose (IV), 0.83; I (0.58); monoisopropylidene glucose (VII), 0.54; glucose, 0.32; diethylaminoisopropyl analog of I, (VI), 0.27; dimethylaminopropylglucose (III), 0.20; and lactose, 0.20. Compounds I and III could be detected by iodine vapor on the plate. Compound I could be detected as a purple spot when the plate was sprayed with 1% ninhydrin in ethanol, and VI and III gave burnt yellow colors after heating the plates 10–15 min at 110°. The compounds IV and VII, could not be detected with this reagent although the glucose spot gave a yellow coloration. Glucose compounds III and VI gave an orange spot when sprayed with 4% tetrazolium hydrochloride in methanol after heating 5 min at 110° or a brown spot when sprayed with 3.5% *p*-anisidine in *n*-butanol–ethanol–water (4:1:1) after heating 10 min at 110°, while I gave no coloration.

All spots could be visualized with 3% copper acetate in 18% phosphoric acid after heating for 30 min at 110° or after charring with 50% sulfuric acid for 10–15 min at 120°.

Preliminary Studies of Extractability by TLC—Several organic solvents (5 ml) were used to extract 10 mg of I from 3 ml of pH 10 aqueous solution and 10 mg of III from 2 ml of pH 10 aqueous solution. The mixtures were vortexed for 30 sec and centrifuged for 5 min at 2000 rpm. Aliquots of the organic layer (100 μl) were spotted on the silica gel plates and the developed spots at the R_f of I were visualized by charring with 50% sulfuric acid spray and compared with developed spots after the application of standard I and dimethylaminopropylglucose solutions.

Hexane and hexane with 2% isopentyl alcohol extracts showed no detectable spots at the R_f of I, whereas benzene and hexane with 10 and 20% isopentyl alcohol showed small faint spots of I. The chloroform and methylene chloride extracts of I gave spots of the same size and intensity as the developed standard. Benzene extracts of I gave spots but at less intensity than with chloroform. Compound III was apparently not significantly extracted in any of these solvents as no spot was apparent from the organic extracts at the R_f of standard III.

Quantitative Analysis by TLC—Amounts (1–32 μl, 10–320 μg) of I and III were spotted on several TLC plates and developed in the system. One plate was visualized with ninhydrin (purple for I, orange for III) and one plate was visualized after spraying with 50% sulfuric acid and charring. The areas were estimated from the product of the horizontal and vertical radii times π. Plots of these areas *versus* spotted amounts for the two visualizations are given in Fig. 1.

Stability Estimates by TLC—Solutions (10 mg/ml) of I and III were prepared in water, 0.1 and 1.0 *N* NaOH, and 0.1 and 1.0 *N* HCl and maintained at 30 and 60°. Aliquots (20 μl) of these solutions were spotted on the TLC plates at intervals, and the developed spots visualized after spraying with ninhydrin and/or by charring with 50% sulfuric acid. The samples in alkali were neutralized with acid before spotting.

Potentiometric Titrations of I—Compound I (29 mg, 0.08486 meq) was dissolved in 20 ml water which contained 200 μl of 1.839 *N* NaOH and potentiometrically titrated with 1.967 *N* HCl with a microburette. Similar solutions without I were titrated similarly and the pH was plotted against the difference in milliliters necessary to achieve the same pH values. A typical potentiometric titration curve by this method (10) was

[18] Tricarb 460 CD, Packard Instrument Co., Downers Grove, IL 60515.

[19] International Centrifuge, International Equipment Co., Needham Heights, MA 02194.

[20] The Meyer N-Evap, Organomation Associates Inc., Shrewsburry, MA 01545.

[21] Reacti-therm Heating Modules, Pierce Chemical Co., Rockford, IL 61105.

Table I—Organic/Aqueous Partition Coefficients of 500 ng of I Between V_{org} ml of Chloroform and V_{aq} ml of Buffer or Plasma at Room Temperature

pH	V_{aq}	V_{org}	k'	k^a
			Buffer Solutions	
7.34	0.5	11.0	0.064	5.63
7.52	1.0	10.0	0.070	4.11
7.72	1.0	5.0	0.153	5.70
8.07	1.0	1.0	0.319	5.50
9.29	1.0	1.0	3.75	7.41
9.61	1.0	10.0	3.23	4.74
10.07	20.0	1.0	4.66	5.42
10.44	20.0	1.0	5.63	6.02
11.02	5.0	1.0	6.10	6.10
				Average 5.63 ± 0.31 *SEM*
			Dog Plasma	
10.10	5.0	1.0	8.4[b]	
10.5	5.0	1.0	6.0	
10.5	5.0	1.0	6.5	
11.0	5.0	1.0	6.7	
11.0	5.0	1.0	6.2	
			Average 6.35 ± 0.16 *SEM*	

[a] $k = (1 + 10^{-pH}/K'_a)\,k'$ where $K'_a = 5.25 \times 10^{-10}$. [b] Omitted from average.

obtained. The pH at half titration between the two inflection points gave pK'_a values of 9.20 and 9.28 and the apparent equivalent weight of the titrated I was 380 (theoretical, 342).

Partition Coefficient—A stock solution of the base of I was prepared in chloroform by the extraction of 0.20 ml of a sodium carbonate buffer solution (pH 10) containing 100 μg of I with 10 ml of chloroform. This 10 μg/ml solution of free base (as I equivalent) was diluted 10-fold to give a stock solution of 1.00 μg of I as the free base in 1.00 ml of chloroform.

Partition studies between appropriate volume ratios of water-saturated chloroform and buffer solutions of various pH values were effected by shaking the mixture for 15 min and then centrifuging. Higher relative volumes of the organic phase were used at the lower pH values and of the aqueous phase at higher pH values (Table I). Aliquots (0.9 of the respective volumes) of the aqueous and organic phases were taken. The organic phase was evaporated to dryness under nitrogen, derivatized, assayed by the GLC method, and the peak height ratio (PHR_{org}) to the internal standard diisopropylaminoethyl analog of I, (V) determined. The volume of aqueous phase taken was adjusted to pH 11.0 with NaOH and extracted with 10 ml chloroform and 9 ml of $CHCl_3$, taken to dryness, derivatized, assayed by the GLC method, and the peak height ratio (PHR_{aq1}) to V determined. The extracted aqueous phase was re-extracted with chloroform and the reclaimed I was assayed (PHR_{aq2}).

Preparation of the Pharmacokinetic Dose—A volume of 2.8 ml of the I-[^{14}C]glucose solution, containing 1.5 mg of I-[^{14}C]glucose hydrochloride with a labeled specific activity of 324.0 mCi/mmol, was mixed with 58.5 mg of I for the 40-mg dose, or with 298.5 mg of I for the 200-mg dose, and with 12.2 ml of sterile isotonic saline. Aliquots (10.00 ml) were injected as intravenous bolus over 20 sec into the dog. The theoretical specific activity was 8.10 mCi/mmol of I for the 40-mg dose and 1.62 mCi/mmole of the 200-mg dose.

The experimental specific activity was determined by mixing 10.00 μl of the prepared dosing solution with 10 ml of liquid scintillation fluid. The capped vials[22] were adapted to the dark for at least 6 hr before counting in the liquid scintillation counter. Experimental specific activities were 7.82 ± 0.03 (*SEM*) mCi/mmole and 1.554 ± 0.004 (*SEM*) mCi/mmole for the 40- and 200-mg dosing, respectively, and were used in the assays.

Counting Efficiencies—Counting efficiency in samples was estimated by the internal standard method. Selected samples of blank and drug-affected plasma or urine and samples of aqueous and organic phase after extraction of plasma and urine were counted before and after the addition of 22,000 dpm of internal standard [^{14}C]urea with a specific activity of 55 mCi/mmole. All capped vials[22] were dark-adapted for at least 6 hr before counting in the liquid scintillation counter. The counting efficiencies in the systems approached 100%, 99.0 ± 0.6 (*SEM*) % in blank and in drug-containing biological fluids. There were no significant quenching effects of 10–200 μl of dog urine or dog plasma when such amounts were added to 10 ml of liquid scintillation fluid.

Total Radioactivity—The total radioactivity of a plasma or urine sample was determined from the addition of 0.01–0.2 ml of plasma or urine to 10 ml of liquid scintillation fluid. The capped vials were dark-adapted for at least 6 hr before counting in the liquid scintillation counter.

The values (counts per minute) were converted to disintegrations per minute (dpm) by dividing by the counting efficiency after subtracting background. The total concentration of radio-labeled substances as I equivalents was calculated by dividing the dpm values by the specific activity and by taking into account the volume of plasma or urine assayed.

Determination of Radiolabeled Substances After Extraction of Plasma or Urine—Plasma (0.025–0.5 ml) or urine (0.005–0.5 ml) was transferred into a 15-ml silylated centrifuging tube. Distilled water was added to a volume of 0.5 ml, and the pH was adjusted to ~11.5 with sodium hydroxide solution (0.1 *N* or 1 *N*). The mixture was extracted with 5 ml of water-saturated chloroform by shaking for 10 min. The phases were separated by centrifugation at 3000 rpm for 10 min. An aliquot of the aqueous phase (0.3 ml) was transferred into a scintillation vial and liquid scintillation fluid (10 ml) was added. The counting efficiency of the aqueous phase was 99.0 ± 0.4 (*SEM*)% for plasma and 93.1 ± 0.5 (*SEM*)% for urine. An aliquot of the organic phase (4 ml) was evaporated in a scintillation vial under nitrogen at room temperature. Liquid scintillation fluid (10 ml) was added to the residue. The capped vials were dark-adapted and counted. The counting efficiency was calculated by the internal standard method already described. The counting efficiency was 96.7 ± 0.4 (*SEM*)% for the organic extract of plasma and 93.8 ± 0.8 (*SEM*)% for that of urine.

Concentrations, C_I^{LSC}, of I in biological fluids were calculated from liquid scintillation counting (LSC) by dividing the disintegrations per minute per milliliter of organic extract by the extraction efficiency (f_1 = 0.984) and by the experimentally determined specific activity of I (f_2), which was 50,304 dpm/μg for the 40-mg dose and 9995 dpm/μg for the 200-mg dose. Thus, when the ratio, r, of milliliters of organic phase to milliliters of biological fluid is known, C_I^{LSC} can be determined as follows:

C_I^{LSC} = concentration of I as hydrochloride in biological fluid

$$= \frac{\text{dpm/ml organic phase}}{f_1 \times f_2} \times r \quad \text{(Eq. 1)}$$

There are two methods to calculate the concentrations of radiolabeled substances in plasma or urine which cannot be assigned to I *per se*, presumably the metabolite concentration, C_M. This is the concentration in the aqueous phase of compounds that are not I expressed in equivalents of I as the hydrochloride after extraction of I from plasma or urine. The direct method for calculation, C_M^{direct}, is to divide the disintegrations per minute per milliliter of the aqueous phase after extraction by the specific activity of I (f_2) and to subtract the unextracted concentration of I that remained in the aqueous phase:

C_M^{direct} = apparent metabolite concentration as equivalents of the hydrochloride of I in biological sample

$$= \frac{\text{dpm/ml of extracted aqueous phase}}{f_2} - (1 - f_1)C_I^{LSC} \quad \text{(Eq. 2)}$$

[22] Kimble, Division of Owens-Illinois, Toledo, OH 43668.

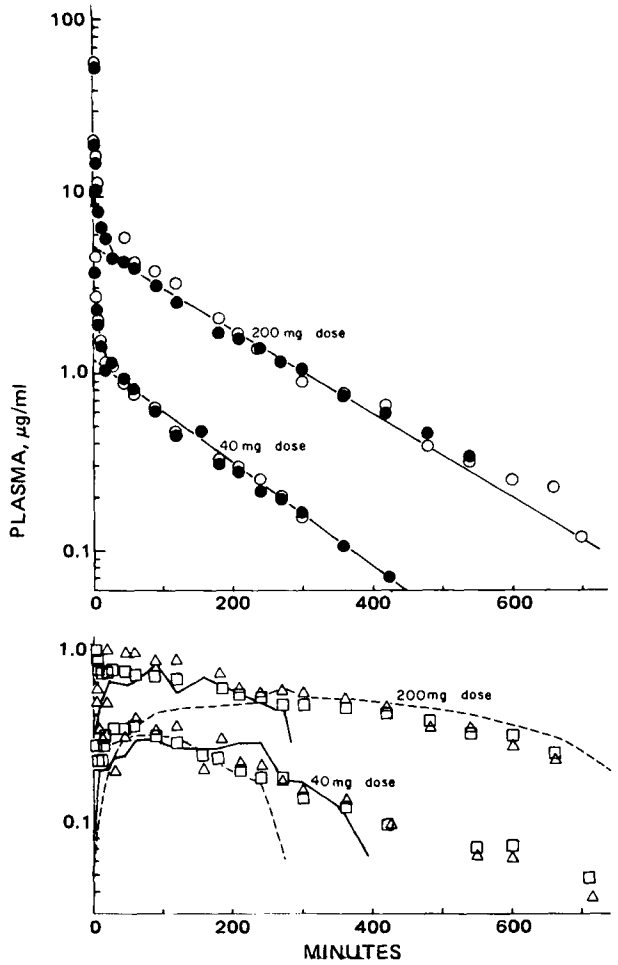

Figure 3—*Semilogarithmic plots of plasma levels of I (○, ●) and apparent total metabolite (□, △) in equivalents of I as the hydrochloride* versus *time for the 40- and 200-mg intravenous doses in the same dog. The symbols represent the GLC assayed I concentrations (C_I^{GLC}, ○) and the LSC assayed I concentrations (C_I^{LSC}, Eq. 1, ●) obtained from radioactivity measurement of the organic extract. The lines, $C = \Sigma A_i e^{-\alpha_i t}$, drawn through the I data were calculated from the parameters given in Table II. The plotted apparent plasma metabolite concentrations were obtained by direct LSC assay of the extracted plasma (C_M^{direct}, Eq. 2, □) and from the difference between the total plasma radioactivity count and that due to I concentrations in plasma (C_M^{diff}, Eq. 3, △). The solid lines drawn through the data were calculated apparent plasma metabolite level values based on the direct LSC assay of the previously extracted urine samples (Eq. 2) in accordance with Eq. 14 using $Cl_{met}^{tot} - Cl_x = 30.4$ and 18.5 ml/min, and $V_M = 4037$ and 3728 ml for the data of the 40- and 200-mg doses, respectively. The dashed line through the 200-mg dose data was also based on this direct LSC assay of previously extracted urine (Eq. 2) but used $Cl_{met}^{tot} - Cl_x = 27.3$ ml/min with $V_M = 16{,}852$ ml in Eq. 14. The dashed line through the 40-mg dose data was based on the urine assays conducted by taking the differences between total radioactivity and that due to I (Eq. 3) where $Cl_{met}^{tot} - Cl_x = 42.2$ ml/min and $V_M = 4078$ ml.*

The alternative difference method for estimating C_M^{diff} is to subtract the concentration, C_I^{LSC}, of I calculated from Eq. 1 from the apparent concentration, C_{tot}, estimated from the liquid scintillation counting of unextracted urine or plasma:

$$C_M^{diff} = \text{apparent metabolite concentration as I (hydrochloride) equivalents in biological sample} = \frac{\text{dpm/ml of unextracted plasma or urine}}{f_2} - C_I^{LSC} \quad \text{(Eq. 3)}$$

Pharmacokinetic Studies in the Dog—The selected dog had physiological values in the normal range: white cell count, 19,900 cells/mm^3; sedimentation rate, 5 min/hr; and packed cell volume, 43%. Tests for microfilaria were negative. The pharmacokinetics of ^{14}C-radiolabeled I in this dog were studied with intravenous bolus doses of 40- and then 200-mg after a 2-month interval.

Table II—Pharmacokinetics of Intravenous I in a 20-kg Dog

Dose (D_o), mg	40	200
Specific activity, dpm/μg	50304	9995
A^a, μg/ml	3.4	11.5
B^a	1.19	5.30
α^a, min^{-1} ($t_{1/2}$, min)	0.195 (3.6)	0.160 (4.3)
$10^3\beta^a$	6.68 (104)	5.44 (127)
β^b	6.36 (109)	5.18 (134)
Clearances, ml/min		
Cl_{tot}^{I} [c]	204.4	191.2
Cl_{ren}^{I} [d]	135	163
Cl_{met}^{tot} [e]	69.4	28.2
$Cl_{met}^{tot} - Cl_x^I$	42.4[g], 30.4[h]	27.3[h,i], 18.5[h,j]
Cl_x^k	27[g], 39[h]	0.9[h,i], 9.7[h,j]
Cl_{ren}^{M} [d]	103.0[g], 67.0[h]	101[g], 76[h]
Apparent distribution volumes[l]		
V_C^I [m]	8.7	11.9
V_d^I [n]	30.6	35.1
$V_{dextrap}^I$ [o]	33.6	37.7
V_M^p [f]	4.08[g], 4.04[f]	3.28[h,i], 18.5[h,j]
Disposition, fraction of dose[q]		
ΣU_∞^I/Dose	0.60[r], 0.64[s]	0.82[r], 0.85[s]
ΣU_∞^M/Dose	0.34[g], 0.18[h]	0.168[g], 0.145[h]
ΣU^{tot}/Dose	0.94[g,r], 0.98[g,s]	0.99[g,r], 1.02[g,s]
	0.78[h,r], 0.82[h,s]	0.97[h,r], 1.00[h,s]

[a] Parameters estimated from best fit of [I] (as hydrochloride) in plasma against time (Fig. 3) in accordance with $[I] = Ae^{-\alpha t} + Be^{-\beta t}$. [b] Estimated from Σ^- plot of $\log(\Sigma U_\infty^I - \Sigma U^I) = -\beta/2.303\, t + \log \Sigma U_\infty^I$ (Fig. 4). [c] Total clearance of I, Dose/AUC_∞, where AUC_∞ is the total area under I plasma level–time plot. [d] Renal clearance of I (or total metabolite) consistent with $\Sigma U = Cl_{ren} AUC$ (Fig. 5) where AUC is the area under I (or metabolite) plasma level–time plot for the time when the cumulative amount of I (or metabolite) in the urine, ΣU, was measured. The values for I were consistent with the renal clearance plots of Fig. 6. [e] The total metabolic clearance is the difference between the total and renal clearances of I, $Cl_{tot}^I - Cl_{ren}^I$. [f] Determined from intercept and slope of linear plots in accordance with Eq. 13, $\Sigma U^M/AUC^I = -V_M[M]/AUC^I + Cl_{met}^{tot} - Cl_x$ (Fig. 7). [g] From plots in Figs. 5 and 7 for ΣU^M data based on urinary amounts of metabolite calculated from the differences between total urine radioactivity count and that due I in urine (Eq. 3). [h] From plots in Figs. 5 and 7 for ΣU^M data based on urinary amounts of metabolite calculated from the direct LSC assay of I-extracted urine (Eq. 2). [i] Data from linear fitting in Fig. 7 of 200-mg dose data between 27 and 250 min. [j] Data from linear fitting in Fig. 7 of 200-mg dose data between 250 and 850 min. [k] Clearance of I by processes other than renal or the metabolic process that produced metabolites into the circulating body fluids to be subsequently renally excreted as metabolite. [l] Referenced to total concentrations in plasma. [m] Apparent volume of central compartment for I, Dose/$(A + B)$. [n] Apparent overall volume of distribution for I, Cl_{tot}^I/β. [o] Apparent extrapolated distribution volume for I on presumption of one-compartment body model, Dose/B. [p] Apparent overall distribution volume for metabolite. [q] Estimated from asymptotes of ΣU *versus* time plots of Fig. 5. [r] Based on GLC assay of urine. [s] Based on LSC assay of organic extract of urine (Eq. 1).

The dog was trained for several days before the experiments. He was placed on a table in a standing position and was restrained by separate straps around the forelegs and hindlegs and fixed to a horizontal bar above.

The day before the experiment the dog was weighed. Body weight was 18.6 kg at the first 40-mg dose and 20.9 kg at the 200-mg dose.

After intramuscular administration of 0.75 ml of ketamine hydrochloride[23] equivalent to 100 mg/ml ketamine, one external jugular vein of the neck was exposed and cannulated under sterile conditions with 30 cm of a catheter[24]. At least 20 cm was inserted into the vein. The incision was closed after the patency of the cannula was verified and it was filled with heparinized saline. Heparinized saline (100 units/ml) was prepared by adding 3 ml of heparin[25] (1000 units/ml) to 30 ml of bacteriostatic sodium chloride solution[26]. The dog was transferred to a metabolism cage and fasted overnight with water, *ad libitum*.

On the following day the dog was restrained on the table in the standing position. The dog was water-loaded orally 30 to 60 min before drug administration with 150 ml of tap water and was continuously infused with 0.9% NaCl solution (1 ml/min)[27] *via* a three-way stopcock[28] into the

[23] Ketaset, Veterinary Products, Bristol Lab., Syracuse, NY 13201.
[24] Intracath, intravenous placement unit, catheter size 16 GA, catheter length 12 inch, needle size 14 GA, Deseret Pharmaceutical Co., Sandy, UT 84070.
[25] Lipo-Hepin, 1000 U.S.P. units per ml (heparin sodium for injection), Riker Lab. Inc., North Ridge, CA 91324.
[26] Bacteriostatic sodium chloride inj. U.S.P., Invenex, Chagrin Falls, OH 44022.
[27] Sodium chloride injection U.S.P. McGaw Laboratories, Irvine, CA 92714.
[28] Pharmaseal Inc., Toa Alta, PR 00758.

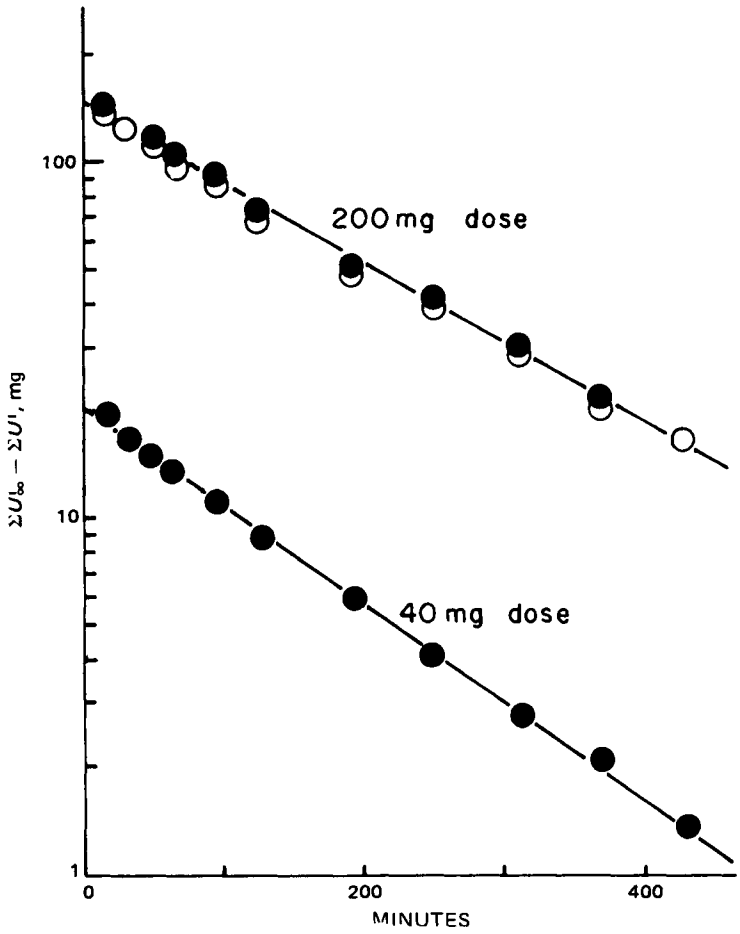

Figure 4—*Semilogarithmic plots of amounts of I not-yet-excreted* versus *time where* ΣU^I_∞ *is 25.74 mg for the 40-mg dose* ($\beta = 6.45 \times 10^{-3}$ *min) and is 170.4 mg for the 200-mg dose* ($\beta = 5.18 \times 10^{-3}$ *min). Key: (○) data obtained from GLC assay of urine; (●) data from LSC assay of the organic phase of extracted urine.*

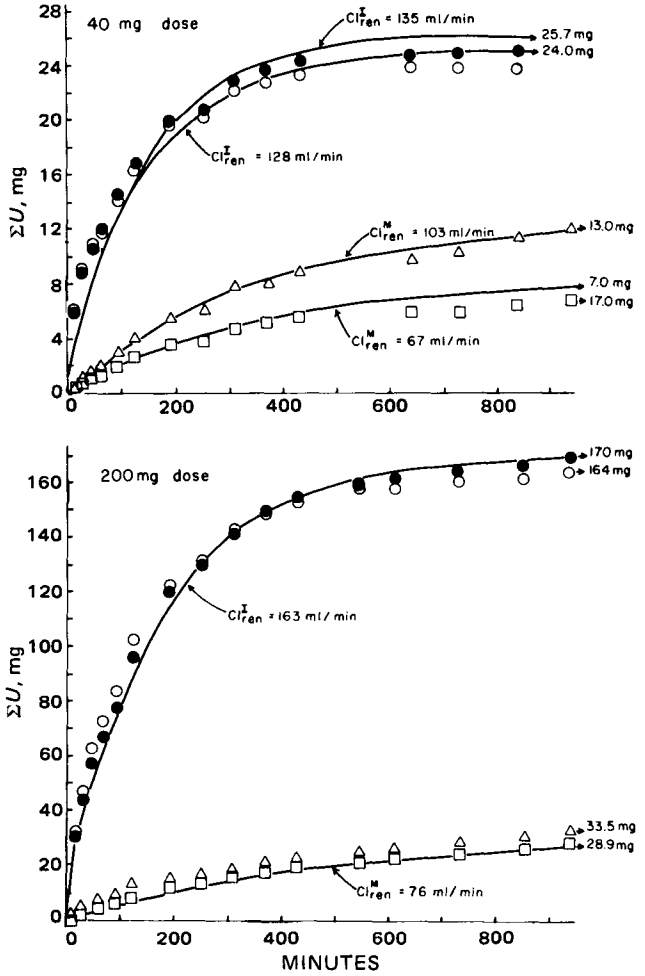

Figure 5—*Plots of the experimental values of cumulative I,* ΣU^I*, and the total metabolite,* ΣU^M*, in urine against time. The curves through the data points are the theoretical values calculated from* $\Sigma U^I = Cl^I_{ren} AUC^I$ *and* $\Sigma U^M = Cl^M_{ren} AUC^M$ *for the labeled renal clearances of I,* Cl^I_{ren}*, and total metabolite,* Cl^M_{ren}*, is plasma where* AUC^I *and* AUC^M *are their respective areas under plasma level–time curves at the time when the cumulative amounts in the urine,* ΣU*, were measured. Key: (○) data obtained by GLC assay of I in urine; (●) data from LSC assay of I in the organic phase of extracted urine (Eq. 1). The total metabolites excreted in urine were assayed by the direct LSC assay of I-extracted urine (Eq. 2, ⊡) and from the difference between the total urine radioactivity count and that due to I in urine (Eq. 3, △).*

catheterized jugular vein. A transurethral catheter[29] was placed under sterile conditions to collect bladder urine.

The saline drip was halted before the drug administration and a 10-ml blank blood sample was withdrawn from the jugular catheter *via* the three-way stopcock into a sterile, disposable syringe[30] after the dead space of the catheter (0.5 ml) had been filled with undiluted blood. The saline drip was reconnected. The blood samples taken at intervals were transferred immediately to 15-ml tubes[31] containing 143 USP units of sodium heparin and were carefully mixed and centrifuged[32] at 1500 rpm for 10 min. The plasma was transferred to a 15-ml tube[31] without additive with a Pasteur pipet and the tube was stoppered and frozen.

Urine was collected before and after the drug administration at intervals *via* the transurethral catheter using a sterile 20-ml syringe[30].

A ^{14}C-labeled I solution of a known amount and specific activity was injected into the jugular vein catheter over 20 sec. The dosing syringe and catheter were flushed with 10 ml of sterile saline into the jugular.

Blood was sampled at 1, 3, 5, 8, 13, 20, 30, 45, 60, 90, 120, 150, 180, 210, 240, 270, 300, 360, 420, 480, 540, 600, 660, 750, 840, 1360, 1590, 1800, 2040, 2270, and 2840 min. Adequate volumes of blood were withdrawn: 2 ml for the first 30 min samples, 3 ml for samples between 30 and 150 min, 4 ml for samples between 150 and 300 min, and 5 ml for all subsequent samples. Hematocrits were determined using a microhematocrit centrifuge and reader[33] on selected blood samples prior to centrifugation. An aliquot of plasma was removed to measure total carbon 14. The remaining plasma was stored in the freezer.

Urine was collected from the transurethral catheter at approximately 15, 30, 45, 60, 90, 120, 190, 250, 310, 370, 430, 490, 540, 610, 730, 850, 1380, 1590, 1800, 2040, 2280, and 2800 min. The volume and pH of each thoroughly mixed urine collect were measured immediately after the withdrawal from the catheter. An aliquot of the fresh urine was transferred to a 15-ml tube and was diluted in a ratio of 1:10, 1:20, 1:50, or 1:100 with distilled water, dependent on the sample time and the volume of each urine collected. Appropriate volumes of undiluted and diluted urine were removed to determine total carbon 14. The remaining urine collections were divided into 10-ml portions and stored in the freezer.

The dog was returned to the metabolism cage 14 hr after the drug administration.

[29] Urine catheter, 8FR, 16 inch long, Davol Inc., Providence, RI 02901.
[30] Monoject, St. Louis, MO 63103.
[31] Vacutainer tubes, Becton-Dickinson and Co., Rutherford, NJ 07070.
[32] Safeguard Centrifuge, Clay Adams Co., Inc., New York, N.Y.
[33] IEC MB Centrifuge, Damon/IEC Division, Needham Heights, MA 02194.

RESULTS AND DISCUSSION

Properties of I—Compound I as the hydrochloride is a white crystalline solid, mp 181–183°, mw 341.74, mass spectrum: m/z 305 (m^+).

Anal—Calc % for $C_{14}H_{28}O_6ClN$: C = 49.19; H, 8.19; N, 4.09; Cl, 10.39; O, 28.11. Found: C, 49.31; H, 8.38; N, 3.06; Cl, 10.50; O, 27.9%.

It is highly soluble in water and soluble in methanol and hot ethanol. It is recrystallized from methanol. The free amine from aqueous solutions of I buffered at pH 10 was determined by TLC of the organic extracts to be highly extracted in chloroform and methylene chloride, less efficiently extracted in benzene, and relatively nonextracted in hexane; although, hexane plus 10 and 20% isopentyl alcohol showed small faint spots of I. The dimethylaminopropylglucose, III, was not significantly extracted

by any of these solvents. Compound I has an apparent pK'_a of 9.28 by potentiometric titration, and the optical rotation of a 10% aqueous solution at pH 7 is $-24.5 \pm 0.5°$ and an index of refraction of $n_D^{23°} = 1.3465$. The optical rotation of III is $+37.0 \pm 0.5°$. The infrared spectrum of I (KBr disc) shows the presence of a split OH-band in the 3400 cm^{-1} region and characteristic bands in 1000–1400 cm^{-1} for isopropylidene groups. It cannot be readily differentiated from II and IV, although IV can be removed from acid solutions of I by chloroform extraction.

The compounds I, III, IV, and V can be separated from each other by TLC by the system *n*-propanol–ethyl acetate–water–NH_4OH, 6:1:4:1.

Stability Estimates by TLC—Compound I gave the same spot with the same developed color intensity as the standard on being subjected to 0.1 and 1.0 *N* NaOH at both 30 and 60° for 3, 24, 50, and 400 hr. The dimethylaminopropylglucose, III, $R_f = 0.20$, produced two additional spots at R_f values of 0.13 and 0.37 on being subjected to 0.1 *N* NaOH at 30° for 3 hr whereas, in 1.0 *N* NaOH, most of the amino sugar spot of 0.20 had been transformed to that at $R_f = 0.37$ at 3 hr. The developed spot assigned to compound III had disappeared at 24 hr in both 0.1 and 1.0 *N* NaOH at 30°.

Compound III gave the same spot with the same developed color intensity as the standard on being subjected to 0.1 and 1.0 *N* HCl at both 30 and 60° for 3, 24, 50, and 400 hr. Compound I ($R_f = 0.52$) produced a considerable quantity of the open chain dimethylaminopropylglucose (III) in 1 hr at 30° in 0.1 *N* HCl and was completely transformed to III in 1 hr at 60 and 30° in 1.0 *N* HCl.

Thus, compound I has high stability in 0.1 and 1 *N* NaOH, whereas III is rapidly degraded. I is rapidly degraded in 0.1 and 1 *N* HCl to stable III by splitting of the ether linkages to liberate acetone. The alkaline degradation products of III showed compounds with high UV spectrophotometric absorbances at <550 nm whereas undegraded III had no absorbance down to 210 nm.

Partition Coefficients and Extraction Efficiency of I from Aqueous Solutions and Plasma by Chloroform—The apparent partition coefficients, k', was calculated for chloroform extraction of the aqueous phase at a given pH value by:

$$k' = \frac{[I]_{org}}{[I]_{aq}} = \frac{(PHR)_{org} \times 1/\gamma_1}{[(PHR)_{aq_1} + (PHR)_{aq_2}] \times 1/\gamma_2 \times 1/\gamma_3} \times \frac{V_{aq}}{V_{org}} \quad \text{(Eq. 4)}$$

where the peak height ratios determined for I relative to V were PHR_{org} for the assay of a γ_1 fraction of the volume of the organic phase, and PHR_{aq} for the assay of a γ_3 fraction of the volume of chloroform used to extract a γ_2 fraction of the volume of the aqueous phase. The PHR_{aq_1} and PHR_{aq_2} were the peak height ratios for the first and second extractions of the previously equilibrated aqueous phase. These two extractions accounted for practically all of the I partitioned into the buffer or plasma when a volume of V_{aq} milliliters of buffer or plasma were initially equilibrated with V_{org} milliliters of chloroform (Table I).

This apparent partition coefficient can be defined as:

$$k' = \frac{[I]_{org}}{[I]_{aq}} = \frac{[\text{I as base}]_{org}}{[\text{I as base}]_{aq} + [\text{protonated I}]_{aq}} \quad \text{(Eq. 5)}$$

Since:

$$1/k' = \frac{[\text{I as base}]_{aq}}{[\text{I as base}]_{org}} + \frac{[\text{protonated I}]_{aq}}{[\text{I as base}]_{org}} = 1/k + \frac{[\text{protonated I}]_{aq}}{[\text{I as base}]_{org}} \quad \text{(Eq. 6)}$$

where k is the intrinsic partition coefficient for the free base of I between the organic and aqueous phases, and:

$$[\text{protonated I}]_{aq} = [\text{I as base}]_{aq} [H^+]/K'_a \quad \text{(Eq. 7)}$$

where $K'_a = 5.25 \times 10^{-10}$ is the apparent dissociation constant of I ($pK'_a = 9.28$) and $[H^+] = 10^{-pH}$ is the activity of the hydrogen ion in the extracted buffer solution or plasma. Then by substitution of Eq. 7 into Eq. 6,

$$1/k' = 1/k + \frac{[\text{I as base}]_{aq} [H^+]}{[\text{I as base}]_{org} K'_a} = 1/k + \frac{[H^+]}{kK'_a} \quad \text{(Eq. 8)}$$

It follows that the intrinsic partition coefficient is

$$k = (1 + [H^+]/K'_a)k' \quad \text{(Eq. 9)}$$

and these calculated values are given in Table I.

The standard assay of I in plasma or urine extracts 0.5 ml with 5 ml of chloroform at pH 11.5. Thus, for partition coefficients of 5.63–6.35, 98.4% of I is extracted into the organic phase.

GLC Assay of I—Typical chromatograms of I, and the internal standard diisopropylaminoethyl I are given in Fig. 2 and, for the specified conditions, had retention times of 1.6 and 4.3 min, respectively. The limit of detection was 5–10 ng of I. The regression analysis of the assayed amounts of I in 0.5 ml of plasma or urine against the PHR were effected in accordance with:

$$C \pm s_{C\ PHR} = (m \pm s_m)\text{PHR} + (b \pm s_b) \quad \text{(Eq. 10)}$$

where C is the concentration of I in 0.5 ml of aqueous fluid, PHR is the peak height ratio of I to the internal standard (500 ng of diisopropylaminoethyl analog of I in 0.5 ml of the extracted aqueous phase), m is the slope, b is the intercept, $s_{C\ PHR}$ is the standard error of estimate of concentration/0.5 ml on the PHR, s_m is the standard error of the regression coefficient m, and s_b is the standard error of the intercept b.

The intercepts of such calibration curves were not significantly different from zero. The standard errors of estimates of the concentrations from these calibration curves ranged between 4.9 and 6.3 ng/0.5 ml of assayed fluid.

A typical calibration curve for GLC–electron capture detection of derivatized I with 500 ng of the diisopropylaminoethyl analog of I (V), as the internal standard gave the following regression equation for amounts (A) in 0.5 μl of urine:

$$A \pm 6.34 \text{ ng} = (144.6 \pm 7.1)\ \text{PHR} - 4.6 \pm 5.2 \quad \text{(Eq. 11)}$$

For amounts in 100 μl of plasma,

$$A \pm 4.87 \text{ ng} = (162.0 \pm 6.1)\ \text{PHR} - 10.0 \pm 4.2 \quad \text{(Eq. 12)}$$

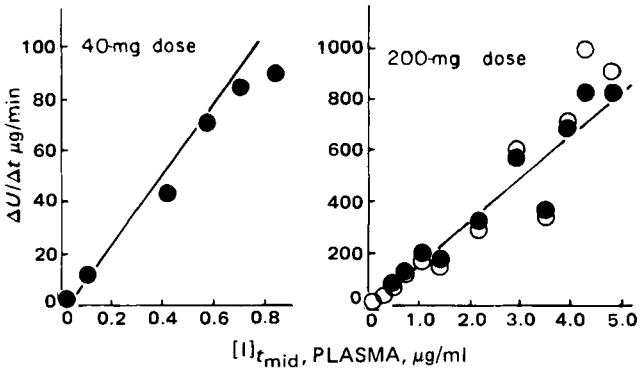

Figure 6—*Renal clearance plots of μg/min of I excreted into the urine versus the plasma levels of I, $[I]_{t_{mid}}$ at the mid-time of the collected interval. Key: (○) data obtained by GLC assay of urine; (●) data from LSC assay of the organic phase of extracted urine (Eq. 1). The lines drawn through the plots are for renal clearances of 135 and 163 ml/min for the 40- and 200-mg I doses, respectively.*

Comparison of GLC and LSC assays—When radiolabeled I was extracted from 0.5 ml of water, plasma, or urine that had been adjusted to pH 11.5 with 5 ml of chloroform, reextraction of the separated aqueous phase with the same amount of chloroform showed less than 2% of the original radioactivity in the second extract. This was consistent with the 1.6% that had been estimated from the measured partition coefficients to be nonextracted under these conditions. The paired assay values of I by GLC and LSC, were highly correlated with a correlation coefficient of $r = 0.995$ for the 40-mg dose for plasma values between 0.15 and 2.6 μg of I/ml of plasma. The paired values were challenged by the Student t test ($t = 1.12$; $df = 13$) and the null hypothesis that the values were the same from both assays could not be rejected. Similarly, the correlation coefficient was 0.991 for the 200-mg dose for plasma values between 0.3 and 4.0 μg I/ml of plasma. The null hypothesis of no difference between the LSC and GLC assays of I in plasma could not be rejected ($t = 1.73$; $df = 9$). The correlation can be observed from Fig. 3.

The correlation coefficients for the paired GLC and LSC urine assays of I were 0.995 and 0.986 at the 40- and 200-mg doses, respectively. The t values for the 40-mg dose were 0.16, $df = 6$, and 1.85, $df = 12$, for the amounts in the urine fractions collected in the interval 0–193 min and 0–732 min, respectively. The t values for the 200-mg dose were 0.25, $df = 11$ and 0.60, $df = 16$, for the amounts in the urine fractions collected between 0–546 min and 0–747 min, respectively.

Thus, it can be concluded that the LSC assay of the radiolabeled I in the chloroform extract of plasma and urine of dogs administered ^{14}C-labeled I intravenously does not give significantly different results than the GLC assay of the extract. Thus, any radiolabeled metabolites that

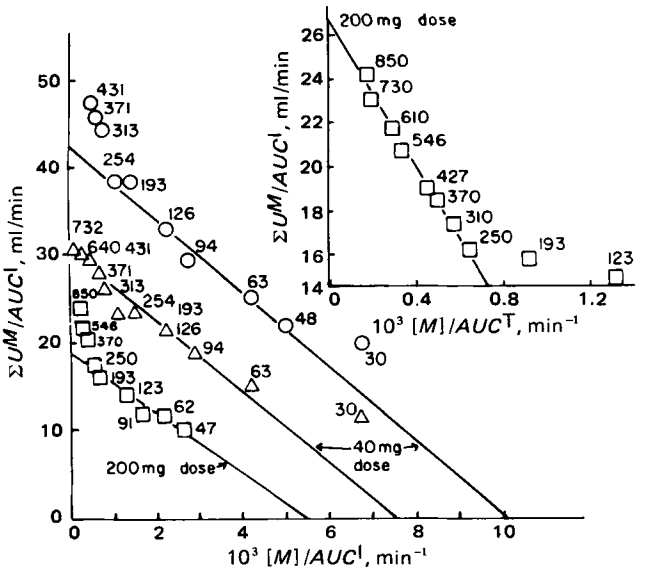

Figure 7—*Plots in accordance with Eq. 13:* $\Sigma U^M/AUC^I = -V_M[M]/AUC^I + Cl^{tot}_{met} - Cl_x$ *where the intercepts of* $Cl^{tot}_{met} - Cl_x$ *and the negative slopes of* V_M, *respectively, were for the 40-mg dose; 42.4 ml/min and 4078 ml when the urinary amounts of metabolite,* U^M, *were calculated from the difference between total urine radioactivity count and that due I in urine (Eq. 3, ⊙); 30.4 ml/min and 4037 ml when the urinary amounts of metabolite,* U^M, *were calculated from the direct LSC assay of I-extracted urine (Eq. 2, △). The respective values for the 200-mg dose when the urinary amounts of metabolite,* U^M, *were calculated from the direct LSC assay of I-extracted urine (Eq. 2, ⊡) were 27.3 ml/min and 3278 ml when the data between 47 and 250 min were fitted linearly and 18.5 ml/min and 16,850 ml when the data between 250 and 850 min were fitted linearly (see insert).*

may exist in the plasma or urine are not readily or significantly extracted into chloroform under the conditions used.

Preliminary Pharmacokinetics of I in the Dog—The pharmacokinetic parameters are listed in Table II. Details of their calculations and the definitions of the symbols have been given in other publications (11, 12). These preliminary studies indicate that the plasma level–time curve of intravenously administered I in the dog conforms to a two-compartment body model (Fig. 3) which can be characterized by the sum of two exponentials. The respective half-lives of the two phases are 3.6–4.3 and 104–127 min. The respective estimated terminal half-lives from the urine sigma minus plot (Fig. 4) and the plasma level–time curves (Fig. 3) were the same (Table II). These limited studies do not permit the definitive conclusion that I may have dose dependent kinetics and a potentially saturable elimination process even though the higher dose had a longer half-life.

The apparent distribution volumes of I, in reference to total concentration in plasma for the central compartment (V_C) and equilibrated tissues (V_d), were 8.7–11.9 and 31–35 liters, respectively.

Clearances—The total clearances of I were similar for both the 40- and 200-mg doses, 204 and 191 ml/min (Table II). The renal clearances for these respective doses were 135 and 163 ml/min (Figs. 5 and 6) indicative of excess tubular secretion in addition to glomerular filtration, since a 12-kg dog has an inulin (glomerular filtration) clearance of 51 ± 12 ml/min (13). The possibility of saturable tubular reabsorption could explain the apparent variation of renal clearance with dose if it were substantiated by further studies.

The extra-renal clearances, Cl^{tot}_{met}, are thus estimable from the differences between the total and renal clearances and are 69.4 and 28.2 ml/min at the 40- and 200-mg doses, respectively, and do indicate a possible saturable metabolism with dose-dependent pharmacokinetics.

Urinary Recoveries—The urinary recovery of unchanged I was 60–64 and 82–85% at the 40- and 200-mg doses, respectively. This was consistent with the fact of higher renal clearance of I at the higher dose. Whereas the calculated total amounts of radiolabeled metabolites excreted in the urine at the higher 200-mg dose, *i.e.*, radiolabeled amounts not extractable into chloroform at pH 11.5, were reasonably the same when calculated from both the direct assay of extracted urine 15% (Eq. 2); and the differences between total urine radioactivity and that due I 17% (Eq. 3). This was not true for the 40-mg dose. The respective values at this dose were 18 and 34%. The only explanation other than technological for this discrepancy would be that some radiolabeled metabolite was extracted into the organic phase in sufficiently small amounts so that statistics of identity between the GLC and LSC analyses of I in this phase were not significantly perturbed.

The total urine recovery of I and its metabolite was 100 ± 2% at the 200-mg dose. It was 96 ± 2 and 80 ± 2% for the 40-mg dose when the difference (Eq. 2) and direct (Eq. 3) assays for metabolites were used, respectively.

Attempted Estimates of Pharmacokinetic Properties of Metabolites—If only one metabolite, M, were produced from I, and if this metabolite in the systemic circulation were only renally excreted, the following equation would be valid for constant clearances (12):

$$\Sigma U^M/AUC^I = -V_M[M]/AUC^I + Cl^{tot}_{met} - Cl_x \qquad \text{(Eq. 13)}$$

where [M] and ΣU^M are the respective plasma concentrations of metabolite and the cumulative amount of metabolite excreted into the urine at time, t, corresponding to the area under the plasma level-time curve of I, AUC^I, to that time; where V_M is the estimated overall apparent distribution volume of the metabolite; and where $C^{tot}_{met} - Cl_x$ is the clearance of I to systematically circulating metabolite.

The V_M and $Cl^{tot}_{met} - Cl_x$ values can be estimated from the slope and intercept, respectively, of plots of the quotients in Eq. 13 (Fig. 7). The discrepancy in the estimates of ΣU^M by the direct and difference methods of radiolabeled metabolites in urine for the 40-mg dose gave different values for $Cl^{tot}_{met} - Cl_x$ of 30.4 and 42.4 ml/min, respectively; even though the apparent distribution volumes, V_M, for the metabolite were the same, 4.0 liters. As a consequence, the residual clearances of I, $Cl_x = Cl^{tot}_{met} - (Cl^{tot}_{met} - Cl_x)$, which could be due to metabolite partitioning or I excretion into the bile, differed also (Table II). The estimated values of these parameters for the 200-mg dose depended on where the data were presumed to be linear (Fig. 7). The assumption of validity for the early time data (<250 min) gave a V_M value of 3.3 liters nearest that obtained for the same time range of data for the 40-mg dose. The assumption of validity of the terminal data (>250 min) in Fig. 7 gave an extremely high apparent volume of distribution for the metabolite, a V_M of 18.5 liters.

Rearrangement of Eq. 13 and use of these estimated parameters permit the estimation of theoretical plasma levels of a possible metabolite in accordance with:

$$[M]_{calc} = \frac{(Cl^{tot}_{met} - Cl_x)AUC_I - \sum U^M}{V_M} \qquad \text{(Eq. 14)}$$

and the lines drawn through the experimental plasma concentrations of apparent metabolite were calculated on these premises (Fig. 3). The fact that the parameters chosen from Fig. 7 for the early time intervals gave reasonable fits for the early time, but not the latter (also compare the two fits of metabolite plasma levels at the 200-mg dose), is a strong indication that either the simple hypothesis of a single metabolite being formed from I is invalid or that the formed metabolite is partitioned into bile and undergoes an enterohepatic recirculation which elevates its terminal plasma levels above the theoretical value calculated from Eq. 14.

REFERENCES

(1) P. Gordon, B. Ronson, and S. V. Kulkarni, *Am. Soc. Microbiol.*, **74,** 165 (1973).

(2) P. Gordon, B. Ronson, and D. P. Mucha, *Fed. Proc. Fed. Am. Soc. Exp. Biol.*, **32,** 807 (1975).

(3) P. Gordon, B. Ronson, and D. P. Mucha, *Am. Soc. Microbiol.*, **75,** 6 (1975).

(4) J. A. Majde and P. Gordon, "Immunomodulation by 1,2,-*O*-Isopropylidene-3-*O*-3′-(*N*′,*N*′-dimethylamino-*n*-propyl)-D-glucofuranose SM-1213, a Drug with Antiviral Activity." Presented at the 16th Interscience Conference on Antimicrobial Agents and Chemotherapy, Abstract, Chicago, Ill. (1976).

(5) J. A. Majde and P. Gordon "Maintenance of Immuno Responsiveness During Subclinical Herpes Virus Infection in Mice by SM-1213, a Drug with Antiviral Activity." Presented at the 17th Interscience Conference on Antimicrobial Agents and Chemotherapy, New York, N.Y. (1977).

(6) P. Gordon, T. Hashimoto, and J. A. Majde, "*In Vitro* and *In Vivo* Enhancement of Leukocyte Functions by 1,2-*O*-Isopropylidene-3-*O*-3′-(*N*′,*N*′-dimethylamino-*n*-propyl)-D-glucofuranose (SM 1213), a Microbicidal Immunomodulator." Presented at the 18th Interscience Conference on Antimicrobial Agents and Chemotherapy, Atlanta, Ga. (1978).

(7) P. Gordon and H. Shinhai, *Am. Soc. Microbiol.*, **79,** 14 (1979).

(8) J. W. Hadden, *Cancer Treat. Rep.*, **62**, 1981 (1978).
(9) J. W. Hadden, A. England, J. R. Sadlik, and E. M. Hadden, *Int. J. Immunopharmacol.*, **1**, 17 (1979).
(10) T. V. Parke and W. W. Davis, *Anal. Chem.*, **26**, 642 (1954).
(11) E. R. Garrett and A. J. Jackson, *J. Pharm. Sci.*, **68**, 753 (1979).
(12) E. R. Garrett and T. Gürkan, *ibid.*, **69**, 1116 (1980).
(13) H. M. Smith, "Principles of Renal Physiology," Oxford University Press, New York, N.Y., 1956, p. 32.

ACKNOWLEDGMENTS

Supported in part by grants from Greenwich Pharmaceuticals Inc., Greenwich, Conn. and Kali-Pharma Inc., Elizabeth, N.J.

A. Van Peer thanks the Belgian Foundation for Medicinal Scientific Research for their support.

The technical assistance of Kathy Eberst and Marjorie Rigby is gratefully acknowledged.

Systematic Error Associated with Apparatus 2 of the USP Dissolution Test II: Effects of Deviations in Vessel Curvature from That of a Sphere

DON C. COX*x, CLYDE E. WELLS*, WILLIAM B. FURMAN*, THOMAS S. SAVAGE‡, and ALFRED C. KING§

Received April 16, 1981, from the *Food and Drug Administration: *National Center for Drug Analysis, St. Louis, MO 63101; ‡Los Angeles, CA 90015; and §Winchester Engineering and Analytical Center, Winchester, MA 01890.* Accepted for publication July 23, 1981.

Abstract □ Dissolution vessels made from glass or plastic are recognized by the USP as being suitable for dissolution testing. Glass vessels with a bottom inside curvature flatter than that of a sphere can cause a high bias in dissolution results; vessels with a steeper curvature can cause a low bias. The inside bottom curvature of plastic vessels adhered closely to the curvature of a sphere. The plastic vessels are preferable for use if the drug is not adsorbed and the vessel is not attacked by the dissolution medium. Bias in results between individual positions of a dissolution apparatus was traced to two shafts which were not vertical.

Keyphrases □ Dissolution—systematic error associated with USP dissolution Apparatus 2 □ USP—error associated with dissolution Apparatus 2 □ Apparatus—systematic error associated with USP dissolution Apparatus 2

Only one manufacturer[1] produces a glass, round-bottom vessel (1) suitable for the multiple-spindle drive equipment used for the USP dissolution test (2). The manufacturing process was changed in 1978 in an attempt to improve the vessel. The vessel was formed manually in the older process by using a mold to which the outside of the vessel could conform. These molded vessels vary considerably with respect to weight, inside cylindrical diameter, and inside bottom curvature. In the newer process the vessel is made from large-bore glass tubing, and the bottom of the vessel is shaped manually from the outside. The tubing-produced vessels examined compare closely with respect to weight and inside cylindrical diameter. However, the inside bottom curvature varies from one vessel to the next. Vessels made from the tubing process are in widespread use. Many vessels made from the older process do not pass the USP requirement that the inside diameter be 10.0–10.5 cm.

A plastic vessel[2] formed by injection molding has been available since 1979. The variation in physical dimensions (including bottom curvature) of individual plastic vessels is less than that of glass vessels because of the manner in which they are produced. Both types of vessels are currently recognized by the USP as being suitable for dissolution testing.

The effect of variations in physical dimensions of the vessels on dissolution results was studied. The study of the molded glass vessels was conducted under the test conditions described in the Fourth Supplement to USP XIX (3); *i.e.*, the stirring element consisted of a shaft with a detachable paddle blade positioned on the side of the shaft. The tubing-produced glass vessels and plastic vessels were studied with the currently official stirring element (4). The tubing-produced glass vessels and plastic vessels are compared for their suitability for use in the USP dissolution test for prednisone tablets.

EXPERIMENTAL

A commercial sample of 5-mg prednisone tablets was used to check the performance of dissolution equipment. Dissolution results from these tablets were reported recently (5). The tablets are reasonably uniform in total drug content. A randomly selected 60-tablet subsample gave an overall average result of 97.2% of label claim with a coefficient of variation (CV) of 2.88% in a content-uniformity assay (6). The average weight of the tablets was 143 mg. This tablet sample was referred to as Tablet 1 (7).

In 1979 a commercial sample of 10-mg prednisone tablets, referred to as Tablet 2, was characterized (the supply of Tablet 1 was running low). This second performance standard gave an average result of 100.0% of label claim with a CV of 1.5% when 20 tablets were subjected to content-uniformity assay. The average tablet weight was 225 mg. Both Tablet 1 and Tablet 2 disintegrate within 2 min into coarse, insoluble granules which stay on the bottom of the vessel throughout the test. The granules from three disintegrated units of Tablet 1 visually appear to occupy about the same volume in the bottom of the vessel as the granules from one disintegrated unit of Tablet 2.

Evaluation of Molded Glass Vessels—Three laboratories[3], each using a commercially available six-spindle dissolution apparatus[4], compared dissolution results from four sets of six molded glass vessels. Tablet 1 was used by all three laboratories. The data from this experiment were collected prior to the modification of the apparatus; *i.e.*, the apparatus described in the Fourth Supplement to USP XIX was used. All other experimental data reported in this paper were collected using the current apparatus.

Evaluation of Glass Tubing-Produced Vessels—An apparatus described previously (7) was selected for this experiment. The apparatus

[1] Kimble, Division of Owens-Illinois, Inc., Vineland, NJ 08360.
[2] Eli Lilly and Co., Indianapolis, IN 46206.
[3] Food and Drug Administration laboratories located in Los Angeles, Calif., St. Louis, Mo., and Winchester, Mass.
[4] Hanson Research Corp., Northridge, CA 91324.

0022-3549/82/0400-0395$01.00/0

(8) J. W. Hadden, *Cancer Treat. Rep.*, **62**, 1981 (1978).
(9) J. W. Hadden, A. England, J. R. Sadlik, and E. M. Hadden, *Int. J. Immunopharmacol.*, **1**, 17 (1979).
(10) T. V. Parke and W. W. Davis, *Anal. Chem.*, **26**, 642 (1954).
(11) E. R. Garrett and A. J. Jackson, *J. Pharm. Sci.*, **68**, 753 (1979).
(12) E. R. Garrett and T. Gürkan, *ibid.*, **69**, 1116 (1980).
(13) H. M. Smith, "Principles of Renal Physiology," Oxford University Press, New York, N.Y., 1956, p. 32.

ACKNOWLEDGMENTS

Supported in part by grants from Greenwich Pharmaceuticals Inc., Greenwich, Conn. and Kali-Pharma Inc., Elizabeth, N.J.

A. Van Peer thanks the Belgian Foundation for Medicinal Scientific Research for their support.

The technical assistance of Kathy Eberst and Marjorie Rigby is gratefully acknowledged.

Systematic Error Associated with Apparatus 2 of the USP Dissolution Test II: Effects of Deviations in Vessel Curvature from That of a Sphere

DON C. COX*x, CLYDE E. WELLS*, WILLIAM B. FURMAN*, THOMAS S. SAVAGE‡, and ALFRED C. KING§

Received April 16, 1981, from the *Food and Drug Administration: *National Center for Drug Analysis, St. Louis, MO 63101; ‡Los Angeles, CA 90015; and §Winchester Engineering and Analytical Center, Winchester, MA 01890.* Accepted for publication July 23, 1981.

Abstract □ Dissolution vessels made from glass or plastic are recognized by the USP as being suitable for dissolution testing. Glass vessels with a bottom inside curvature flatter than that of a sphere can cause a high bias in dissolution results; vessels with a steeper curvature can cause a low bias. The inside bottom curvature of plastic vessels adhered closely to the curvature of a sphere. The plastic vessels are preferable for use if the drug is not adsorbed and the vessel is not attacked by the dissolution medium. Bias in results between individual positions of a dissolution apparatus was traced to two shafts which were not vertical.

Keyphrases □ Dissolution—systematic error associated with USP dissolution Apparatus 2 □ USP—error associated with dissolution Apparatus 2 □ Apparatus—systematic error associated with USP dissolution Apparatus 2

Only one manufacturer[1] produces a glass, round-bottom vessel (1) suitable for the multiple-spindle drive equipment used for the USP dissolution test (2). The manufacturing process was changed in 1978 in an attempt to improve the vessel. The vessel was formed manually in the older process by using a mold to which the outside of the vessel could conform. These molded vessels vary considerably with respect to weight, inside cylindrical diameter, and inside bottom curvature. In the newer process the vessel is made from large-bore glass tubing, and the bottom of the vessel is shaped manually from the outside. The tubing-produced vessels examined compare closely with respect to weight and inside cylindrical diameter. However, the inside bottom curvature varies from one vessel to the next. Vessels made from the tubing process are in widespread use. Many vessels made from the older process do not pass the USP requirement that the inside diameter be 10.0–10.5 cm.

A plastic vessel[2] formed by injection molding has been available since 1979. The variation in physical dimensions (including bottom curvature) of individual plastic vessels is less than that of glass vessels because of the manner in which they are produced. Both types of vessels are currently recognized by the USP as being suitable for dissolution testing.

The effect of variations in physical dimensions of the vessels on dissolution results was studied. The study of the molded glass vessels was conducted under the test conditions described in the Fourth Supplement to USP XIX (3); *i.e.*, the stirring element consisted of a shaft with a detachable paddle blade positioned on the side of the shaft. The tubing-produced glass vessels and plastic vessels were studied with the currently official stirring element (4). The tubing-produced glass vessels and plastic vessels are compared for their suitability for use in the USP dissolution test for prednisone tablets.

EXPERIMENTAL

A commercial sample of 5-mg prednisone tablets was used to check the performance of dissolution equipment. Dissolution results from these tablets were reported recently (5). The tablets are reasonably uniform in total drug content. A randomly selected 60-tablet subsample gave an overall average result of 97.2% of label claim with a coefficient of variation (CV) of 2.88% in a content-uniformity assay (6). The average weight of the tablets was 143 mg. This tablet sample was referred to as Tablet 1 (7).

In 1979 a commercial sample of 10-mg prednisone tablets, referred to as Tablet 2, was characterized (the supply of Tablet 1 was running low). This second performance standard gave an average result of 100.0% of label claim with a CV of 1.5% when 20 tablets were subjected to content-uniformity assay. The average tablet weight was 225 mg. Both Tablet 1 and Tablet 2 disintegrate within 2 min into coarse, insoluble granules which stay on the bottom of the vessel throughout the test. The granules from three disintegrated units of Tablet 1 visually appear to occupy about the same volume in the bottom of the vessel as the granules from one disintegrated unit of Tablet 2.

Evaluation of Molded Glass Vessels—Three laboratories[3], each using a commercially available six-spindle dissolution apparatus[4], compared dissolution results from four sets of six molded glass vessels. Tablet 1 was used by all three laboratories. The data from this experiment were collected prior to the modification of the apparatus; *i.e.*, the apparatus described in the Fourth Supplement to USP XIX was used. All other experimental data reported in this paper were collected using the current apparatus.

Evaluation of Glass Tubing-Produced Vessels—An apparatus described previously (7) was selected for this experiment. The apparatus

[1] Kimble, Division of Owens-Illinois, Inc., Vineland, NJ 08360.
[2] Eli Lilly and Co., Indianapolis, IN 46206.
[3] Food and Drug Administration laboratories located in Los Angeles, Calif., St. Louis, Mo., and Winchester, Mass.
[4] Hanson Research Corp., Northridge, CA 91324.

0022-3549/82/0400-0395$01.00/0

Table I—Dissolution Results (Percent of Label Claim) for Tablet 1 from Three Laboratories Using Four Sets [a] of Molded Glass Vessels

	Vessel Set											
	1			2			3			4		
Laboratory	n	$\bar{x}$	$\pm SD$	n	$\bar{x}$	$\pm SD$	n	$\bar{x}$	$\pm SD$	n	$\bar{x}$	$\pm SD$
A	—	—	—	—	—	—	12	52.4	1.82	24	37.5	3.48
B	24	43.2	3.18	—	—	—	24	49.3	1.66	12	42.7	5.90
C	6	40.0	3.94	24	52.0	3.15	—	—	—	—	—	—

[a] Vessel sets 1 and 3 originated from laboratory B. Vessel set 2 originated from laboratory C. Vessel set 4 originated from laboratory A.

Table II—Dissolution Data [a] for Tablet 1 from Glass Tubing-Produced Vessels Rearranged for Two-Way ANOVA

	Position						Vessel	
Vessel	1	2	3	4	5	6	$\bar{x}^b$	$\pm SD^b$
1	51.4	53.7	54.6	60.0	58.6	63.5		
	52.0	52.9	54.8	58.9	60.7	63.4	57.0	4.33
2	53.3	54.9	57.3	57.7	53.2	63.5		
	54.3	55.3	56.9	59.1	54.0	61.0	56.7	3.22
3	56.1	51.5	53.9	62.3	59.5	58.7		
	52.3	52.9	53.1	60.9	59.1	58.7	56.6	3.72
4	54.5	49.8	51.8	61.0	53.8	57.5		
	52.1	51.5	50.5	60.1	55.8	58.1	54.7	3.78
5	53.6	56.2	57.3	62.2	56.1	62.5		
	54.3	55.0	56.2	60.7	58.1	62.4	57.9	3.26
6	56.2	56.1	55.9	60.9	64.4	59.4		
	57.8	57.6	56.5	60.7	59.6	60.7	58.8	2.60
Position $\bar{x}$	54.0	54.0	54.9	60.4	57.7	60.8		
Position SD	1.96	2.30	2.22	1.33	3.29	2.25		

[a] Percent of label claim dissolved at 30 min. [b] Mean and standard deviation of 12 individual tablets.

Table III—Dissolution Data [a] for Tablet 1 from Plastic Vessels Rearranged for Two-Way ANOVA

	Position						Vessel	
Vessel	1	2	3	4	5	6	$\bar{x}^b$	$\pm SD^b$
1	38.4	36.9	38.0	49.0	42.3	48.9		
	38.5	38.4	38.6	46.8	40.3	47.6	42.0	4.73
2	42.3	38.6	39.2	47.8	40.5	51.2		
	37.8	37.8	39.1	49.3	44.0	49.8	43.1	5.11
3	37.1	38.8	38.4	46.0	42.4	45.5		
	38.2	38.5	36.3	51.5	39.9	47.2	41.7	4.82
4	38.8	42.0	42.0	44.3	45.2	49.4		
	39.9	41.3	39.4	51.2	44.5	49.2	43.9	4.16
5	40.5	38.0	40.7	50.7	42.2	46.9		
	39.5	36.7	46.8	51.8	41.0	50.5	43.8	5.30
6	40.8	40.5	47.2	56.3	45.5	54.7		
	44.1	41.6	42.6	52.0	42.7	51.2	46.6	5.60
Position $\bar{x}$	39.7	39.1	40.7	49.7	42.5	49.3		
Position SD	2.01	1.81	3.41	3.24	1.92	2.44		

[a] Percent of label claim dissolved at 30 min. [b] Mean and standard deviation of 12 individual tablets.

can be aligned to conform to USP specifications, but shafts 4 and 6 are not parallel with the other four shafts. Six glass tubing-produced vessels, purchased specifically for this experiment, were numbered one through six and placed in the apparatus. Two sets of six tablets each were subjected to the dissolution test (one tablet per vessel for each set of tablets). The vessels were then moved one position in a clockwise direction, and two more sets of six tablets each were subjected to the test. This procedure was continued until each vessel had been tested twice in each position of the apparatus. A total of 72 tablets was subjected to the test. Twelve dissolution results were associated with each vessel, which had been sequentially placed in all six positions. Likewise, 12 results were associated with each position in which all six vessels had been sequentially placed. The experiment was conducted with Tablet 1 and then with Tablet 2.

Evaluation of Plastic Vessels—The plastic vessels were evaluated in the same manner as the glass tubing-produced vessels; the same apparatus was used. The experiment was conducted with Tablet 1 and then Tablet 2.

Evaluation of Inside Bottom Curvature of Vessels—The water was removed from the bath used with the dissolution apparatus. The empty vessels were placed in position in the base of the apparatus. A slurry of 60 g of plaster of Paris and 50 ml of water was poured into each vessel and allowed to set for 1–2 hr. The vessels were removed from the apparatus, and the plaster casts were removed. The casts retained the exact shape of the bottom inside curvature of the vessels.

RESULTS AND DISCUSSION

The data obtained from different sets of molded glass vessels are given in Table I. With different sets of vessels, a mean difference of 8.8% of label claim was obtained between laboratories B and C for Tablet 1. When the same vessels were used to analyze Tablet 1 in both laboratories, the mean difference between laboratories dropped to 3.2%. When two sets of vessels were exchanged between laboratories A and B, mean results of 52.4 and 49.3% of label claim, respectively, were obtained using one set, and 37.5 and 42.7% of label claim were obtained for laboratories A and B, respectively, using the other set of vessels.

The data indicate that there are significant differences between laboratories, even when the same vessels are used. The bias in results between the laboratories was reduced considerably when the same sets of vessels were available to each laboratory. These vessels vary considerably with respect to flange thickness, inside diameter, and inside bottom curvature. A correlation between the physical dimensions of the vessels and the dissolution data is difficult to make because of this lack of uniformity in all three critical areas. However, when plaster casts were made of the bottom of the vessels originally used by laboratory A, the impressed curvatures came to a distinct blunted point at what would be the bottom of the vessel. These curvatures were steeper than that of a sphere with a diameter equal to the width of the vessel. These vessels also gave the lowest results for Tablet 1.

The data collected in the evaluation of the plastic and glass tubing-

Table IV—Dissolution Data [a] for Tablet 2 from Glass Tubing-Produced Vessels Rearranged for Two-Way ANOVA

Vessel	Position 1	2	3	4	5	6	Vessel $\bar{x}^b$	$\pm SD^b$
1	37.5	36.7	34.9	58.7	45.8	46.5		
	34.9	35.2	33.9	55.1	51.1	48.5	43.2	8.81
2	35.5	35.7	39.3	52.0	37.3	57.0		
	34.8	35.1	33.0	44.6	53.0	51.5	42.4	8.70
3	33.9	35.6	34.5	57.7	36.7	55.0		
	36.2	34.7	33.3	46.6	38.1	53.0	41.3	9.15
4	32.6	38.1	33.7	40.6	42.0	54.0		
	32.3	34.0	38.9	49.0	37.7	47.1	40.0	6.95
5	36.0	39.3	49.8	65.2	39.9	61.0		
	37.1	35.6	52.8	72.0	53.2	58.8	50.1	12.50
6	56.8	49.6	39.6	69.5	57.5	58.2		
	34.0	38.2	51.4	61.5	40.6	64.5	51.8	11.47
Position $\bar{x}$	36.8	37.3	39.6	56.0	44.4	54.6		
Position SD	6.50	4.18	7.49	9.93	7.41	5.62		

[a] Percent of label claim dissolved at 30 min. [b] Mean and standard deviation of 12 individual tablets.

Table V—Dissolution Data [a] for Tablet 2 from Plastic Vessels Rearranged for Two-Way ANOVA

Vessel	Position 1	2	3	4	5	6	Vessel $\bar{x}^b$	$\pm SD^b$
1	35.4	38.3	39.7	42.1	40.8	47.6		
	38.8	37.5	37.2	46.4	45.7	47.5	41.4	4.35
2	36.6	40.9	33.7	42.2	42.6	41.7		
	38.0	34.9	37.5	44.7	35.1	41.9	39.2	3.62
3	40.3	31.8	32.8	44.9	37.1	48.8		
	33.2	40.0	34.4	45.3	41.1	46.9	39.7	5.90
4	39.9	35.3	39.3	45.5	35.5	47.1		
	35.7	33.5	41.9	43.2	39.8	41.1	39.8	4.25
5	38.4	33.0	33.5	44.1	39.7	42.7		
	33.8	33.9	39.2	46.4	37.4	41.4	38.6	4.49
6	34.4	38.4	38.4	47.7	34.5	44.0		
	37.6	32.1	40.1	45.6	36.3	44.7	39.5	4.99
Position $\bar{x}$	36.8	35.8	37.3	44.8	38.8	44.6		
Position SD	2.36	3.12	3.01	1.71	3.40	2.84		

[a] Percent of label claim dissolved at 30 min. [b] Mean and standard deviation of 12 individual tablets.

produced vessels were analyzed by a two-way analysis of variance (ANOVA) (8). The data collected from the test runs[5], rearranged for the ANOVA, are shown in Tables II–V. The data in the rows are for the individual vessels and the data in the columns are for the individual positions on the apparatus. (For example, the data in row one are the dissolution results from vessel one after it had been placed in all six positions; the data in column one are the dissolution results from position one after all six vessels had been rotated to position one.) Table VI shows the results of the ANOVA for each combination of tablet and vessel.

Table VI shows the difference between the mean dissolution results for 72 tablets of Tablet 1 with the glass tubing-produced vessels and with the plastic vessels. Ideally the results should compare closely if both types of vessels are equivalent for use with Apparatus 2. However, the glass vessels give results that are higher by 13.5% of label claim.

Tablet 2 responded in a similar manner, but the overall difference in results is smaller (5.1%). The difference between the mean squares of the data from these two sets of vessels is more pronounced. The total mean square for the Tablet 2 results collected from the glass vessels is over five times that of the plastic vessels.

Each of the mean squares listed in Table VI for Tablet 1 or 2 is an independent estimate of the variance of that particular tablet. These independent estimates differ widely from each other in most instances. The smallest variance is the within-groups mean square, which is the pooled variance of the tablets taken under the most repeatable conditions for each experiment, *i.e.*, the mean of the variances derived from the duplicate results. The square root of the within-groups mean square gives the best estimate of the inherent standard deviation of the tablets. The standard deviation of Tablet 1 is 1.1% of label claim in the glass vessels and 2.0% of label claim in the plastic vessels. The standard deviation of Tablet 2 is 5.5% of label claim in the glass vessels and 2.7% of label claim in the plastic vessels. The overall standard deviations, derived from taking the square root of the respective total mean squares, are 3.6, 5.1, 10.4, and 4.6% of label claim. Thus, Apparatus 2 is not measuring the variation of the tablets. Instead, the tablets are measuring the variations in Apparatus 2.

[5] The data, in the original order taken, are available from the authors upon request.

The within-groups mean square was divided into mean squares associated with the vessels, apparatus position, and the interaction between vessels and apparatus position to obtain the F ratios shown in Table VI. The magnitudes of the F ratios indicate that there are statistically significant differences in the mean dissolution results associated with the individual vessels and apparatus positions. Tablet 1 showed differences between the individual glass vessels and between the individual plastic vessels. Tablet 2 showed differences only between the individual glass vessels. Both tablets showed differences between the apparatus positions. Finally, Tablet 1 revealed a significant interaction between the glass vessels and the apparatus positions.

Tables II–V clearly show where the major sources of the variations are located. The mean results of 12 tablets associated with a position on the dissolution apparatus (the column means) show that positions 4 and 6 give higher results than positions 1, 2, 3, and 5 for each combination of tablet and vessel type. It was established previously (7) that the paddle shafts in positions 4 and 6 were not parallel with the other four shafts. If the other four shafts were made vertical, shafts 4 and 6 would each be misaligned in relation to the vertical axis of the respective vessel. Though misaligned, the shafts still meet the USP specification because each is within 0.2 cm of the vertical axis of its vessel at all points along the shaft. The manufacturers of dissolution equipment must take special care in the design and manufacture of their equipment if this source of variation is to be reduced.

The mean results of 12 tablets associated with the glass vessels in Tables II and IV show that vessel 4 gives the lowest mean and vessels 5 and 6 the highest means for both Tablet 1 and Tablet 2. The rank correlation from the vessel giving the lowest results to the vessel giving the highest results is the same for both samples (vessels 4, 3, 2, 1, 5, 6). The mean results for the plastic vessels from Tablet 1 (Table III) showed statistically significant differences; however, the mean results from Tablet 2 (Table V) were not significantly different. These findings indicate that Tablet 1 is being affected by a characteristic of the plastic vessels to which Tablet 2 does not respond.

Plaster casts were made of the lower bottom curvatures of both sets of vessels. Visual inspection of the casts showed that all six of the glass vessels had a flattened area on the bottom. The flattened area was not uniform from one glass vessel to the next. Vessels 1, 2, and 3, although

Table VI—Results of Two-Way ANOVA from Data Presented in Tables II—V

	Tablet 1				Tablet 2				
	Glass		Plastic		Glass		Plastic		
	Mean Square	*F* Ratio	Mean Square	*F* Ratio	Mean Square	*F* Ratio	Mean Square	*F* Ratio	*F*.95
Vessels (rows)	23.0	18.2	37.8	9.8	288.2	9.5	10.7	1.4	2.5
Apparatus position (columns)	117.6	93.2	278.1	71.6	886.9	29.4	193.3	26.2	2.5
Interaction	7.5	6.0	4.0	1.0	31.3	1.0	7.9	1.1	1.8
Subtotal	25.5		48.0		190.2		34.8		
Within-groups	1.3		3.9		30.2		7.4		
Total	13.2		25.6		109.1		20.9		
Mean for 72 tablets	57.0		43.5		44.8		39.7		

exhibiting a flattened area, possessed some curvature over this area. Vessels 5 and 6 had areas of ~1 cm in diameter that were almost completely flat. Vessel 4 exhibited a curvature similar to vessels 5 and 6, except that there was a small indentation in the middle of the flattened area.

Plaster casts revealed that all six plastic vessels had uniform bottom curvatures which were considerably greater than the curvatures of the glass vessels. The bottom curvatures of the plastic vessels did not vary from one vessel to the next as determined by visual comparison of the plaster casts.

It is known that dissolution rate depends on the surface area of the dissolving substance in contact with the dissolution medium and the velocity of the liquid passing over the substance (9). A tablet which disintegrates fairly rapidly into granules of sufficient specific gravity will appear as a rotating cone-shaped mass of particles on the bottom of the dissolution vessel shortly after being introduced to Apparatus 2 (Fig. 1). If the inner surface of the vessel is symmetrical around the center axis of the paddle, liquid flow in a vessel with a small indentation in the bottom or with a steeper curvature will gather the particles into a more compact mass than in a vessel with a flatter curvature. If the inner surface of the vessel is not symmetrical around the center axis of the paddle, the liquid flow in the vessel will not be symmetrical; the tablet particles will be more agitated, and the conical shape of the mass of particles may be disrupted as the asymmetrical flow of liquid buffets the particles. Asymmetrical liquid flow can be generated by a misaligned paddle, *i.e.*, a paddle whose center axis does not coincide with the cylindrical axis of the vessel, as well as by a vessel that is not symmetrical.

These hypotheses may explain the differences between the tablet results associated with the glass vessels and with apparatus positions. They may also explain the fact that significant interactions exist between the glass vessels and the apparatus positions for Tablet 1. If the individual vessel curvature and paddle misalignment are unique, the liquid flow pattern, and thus the tablet results, will be unique for that combination.

Tablet 1 revealed significant differences which were associated with the plastic vessels. Table III shows that vessel 6 gave higher results than the other five vessels. No physical difference was observed which would account for the higher results in vessel 6. Vessel 6 was obtained at a later time to replace one of the original vessels that was broken before any testing was conducted. As the manufacturing history of none of the vessels is known, this observation may be meaningless; on the other hand, it may point to a subtle difference in manufacture of the plastic vessels.

Since the plastic vessels are physically more uniform than the glass vessels, the plastic vessels are preferable for dissolution testing. The chance for bias in dissolution results between laboratories is less if the plastic vessels are used. The USP specifies that the inside bottom curvature for the dissolution vessels be spherical. Thus, a quantitative determination of vessel curvature for comparison to that of a sphere is required before a conclusion can be reached about the suitability of the vessels for use in the USP dissolution test.

The following relationship exists between the diameter of a circle and a chord parallel to the diameter:

$$D = (L^2/4h) + h \qquad \text{(Eq. 1)}$$

where D is the diameter, L is the chord length, and h is the perpendicular distance from the center of the chord to the circumference of the circle.

A diameter was calculated from the equation for each vessel by determining the values of h and L. A mechanic's depth gauge[6] was used for

Table VII—Physical Measurements [a] Relating to Vessel Curvature

Vessel		h [b]	Diameter	
			Calculated	Measured
Glass	1	11.5	107.9	103.2
	2	11.9	105.1	102.1
	3	11.5	107.9	100.7
	4	10.7	114.3	102.7
	5	9.9	121.9	102.3
	6	10.7	114.3	101.7
Plastic	1	12.3	102.5	101.5
	2	12.7	100.0	101.2
	3	12.3	102.5	101.4
	4	12.7	100.0	101.3
	5	12.7	100.0	101.2
	6	12.7	100.0	101.4

[a] All measurements in mm. Chord length (L) was 66.6 mm in all vessels. [b] Perpendicular distance from center of chord to circumference of circle.

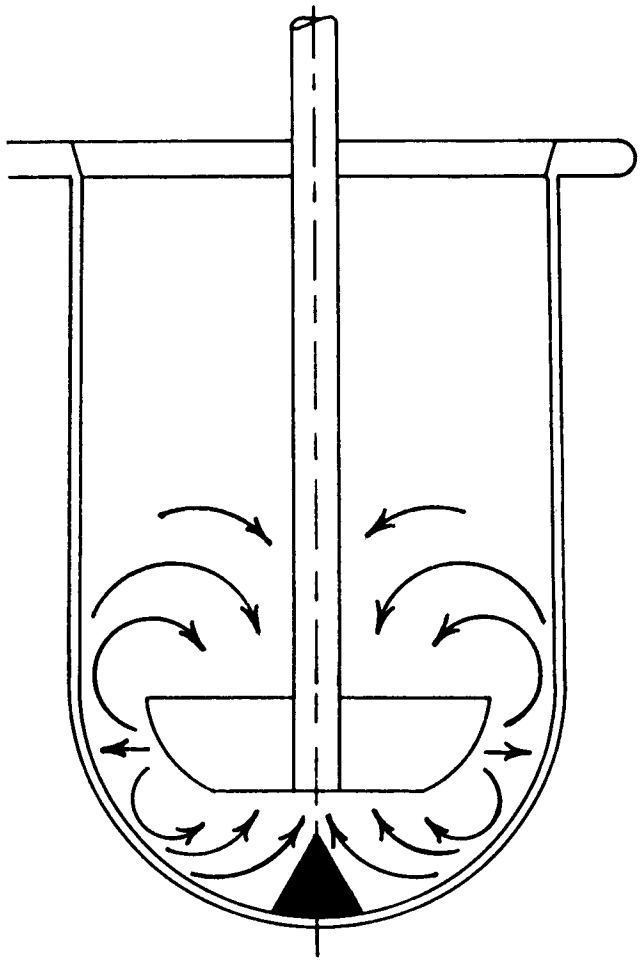

Figure 1—*Vertical cross-sectional view of USP Apparatus 2 illustrating formation of cone-shaped mass of particles due to a symmetrical liquid flow.*

[6] Combination depth and angle gauge, No. 236, L. S. Starrett Co., Athol, MA 01331.

this purpose. The base of the gauge was measured for the chord length (L). The gauge was then set inside the vessel with the ends of the gauge base resting on the curved surface of the vessel. The distance (h) between the base and the bottom of the vessel was taken from the gauge rule. The cylindrical diameter of the vessel was then taken 2 to 3 cm above opposite points where a tangent to the curved bottom of the vessel coincides with the vessel wall. Inside calipers were used for this purpose.

Table VII shows the measurements taken from the vessels and the comparison of the theoretical diameters calculated from these measurements with the actual diameters. The glass vessels possess a flatter curvature than a sphere of the same diameter. The curvature of the plastic vessels closely approximates a sphere of the same diameter. When the results from plastic vessels differ from those obtained from glass vessels, the results from the plastic vessels are more correct, because the plastic vessels conform more closely to the USP specifications.

CONCLUSIONS

Differences in the bottom curvature of dissolution vessels can cause bias in the dissolution results obtained from prednisone tablets. Vessels with a curvature which is less (flatter) than that of a sphere cause a high bias. Vessels with a curvature that is greater (steeper) than that of a sphere cause a low bias. The plastic vessels are more uniform than glass vessels and possess a curvature that more closely approximates the curvature specified in the USP. As such, they are preferable to the glass vessels for use in the dissolution test when the drug is not adsorbed and the vessel is not attacked by the dissolution medium.

The dissolution rate is controlled by the velocity of the liquid passing over the tablet. The liquid velocity at any point in a stirred vessel is controlled by the stirring rate and the geometry of the system. An idealized geometry is defined in the USP. Minor variations from this idealized geometry, such as those discussed in this paper and previously (7), change the liquid velocity in the vicinity of the tablet and, thus, the dissolution results. If the reproducibility of the test is to be improved, equipment must be made available which allows the analyst to adhere to this idealized geometry as closely as possible.

REFERENCES

(1) R. D. Kirchhoefer, *J. Assoc. Off. Anal. Chem.*, **59**, 367 (1976).

(2) "The United States Pharmacopeia," 20th rev., Mack Publishing Co., Easton, Pa., 1980, p. 959.

(3) "Fourth Supplement to USP XIX and NF XIV," The United States Pharmacopeial Convention, Inc., Rockville, Md., 1978, p. 141.

(4) "The United States Pharmacopeia," 20th rev., Mack Publishing Co., Easton, Pa., 1980, p. 655.

(5) D. P. Page, D. C. Cox, M. L. Dow, M. A. Kreienbaum, P. A. McCullen, T. W. Moore, and L. K. Thornton, *FDA By-Lines*, **10**, 57 (1980).

(6) J. F. Brower, *J. Assoc. Off. Anal. Chem.*, **60**, 27 (1977).

(7) D. C. Cox and W. B. Furman, *J. Pharm. Sci.*, **71**, 451 (1981).

(8) W. J. Dixon and F. J. Massey, Jr., "Introduction to Statistical Analysis," McGraw-Hill, New York, N.Y., 1969, pp. 175–181.

(9) F. Langenbucher, *J. Pharm. Sci.*, **58**, 1265 (1969).

ACKNOWLEDGMENT

The authors thank John C. Black for drawing the figure.

HPLC Determination of D and L Moxalactam in Human Serum and Urine

J. A. ZIEMNIAK *‡, D. A. CHIARMONTE ‡, D. J. MINER §, and J. J. SCHENTAG *‡x

Received March 25, 1981, from the **Department of Pharmaceutics, School of Pharmacy, State University of New York at Buffalo;* the ‡*Clinical Pharmacokinetics Laboratory, Millard Fillmore Hospital, Buffalo, N.Y. 14209* and the §*Lilly Research Laboratories, Indianapolis, IN 46285.* Accepted for publication July 24, 1981

ABSTRACT □ A high-pressure liquid chromatographic procedure was developed to determine the D and L isomers of moxalactam in human plasma and urine. After protein precipitation with hydrochloric acid the sample was extracted with ethyl acetate. It was then back extracted into tromethamine buffer (pH 8.0) and washed with octanol. Extraction recovery from plasma ranged from 73–81%. An aliquot of the tromethamine buffer was then injected onto a C_{18}-μBondapak column. The mobile phase was 3% acetonitrile in 0.05 *M* ammonium acetate pH 6.5 buffer. Samples were quantitated by UV detection at 275 nm and 0.01 aufs. The lower limit of detection was 0.5 μg/ml for each isomer. Preliminary stability studies were performed to assess proper sample handling and storage conditions. The procedure was evaluated in a clinical setting to demonstrate its applicability to the study of moxalactam pharmacokinetics in critically ill patients.

Keyphrases □ Moxalactam—determination in human plasma and urine by high-pressure liquid chromatography, D and L isomers □ High-pressure liquid chromatography—determination of moxalactam in human plasma and urine, D and L isomers □ Anti-infectives—moxalactam, high-pressure liquid chromatographic determination, D and L isomers

Moxalactam is a new oxycephalosporin derivative undergoing clinical trials in the United States and Europe. *In vitro* experiments have demonstrated that moxalactam is active against a broad spectrum of microorganisms, including resistant Gram-negative bacteria such as *Pseudomonas aeruginosa* and *Bacteroides fragilis*, some indole-positive *Proteus* species (1), β-lactamase-producing strains of *Enterobacteriaceae* (2), and clinical isolates shown to be cephalosporin resistant (3). Its expanded spectrum of activity compared to conventional β-lactam antibiotics is attributed to replacement of the thio group at the 1 position of the dihydrothiazine nucleus with an oxygen moiety (4).

The pharmacokinetics of moxalactam elimination usually have been evaluated employing standard microbiological techniques (5, 6). However, a more specific analytical procedure was required for pharmacokinetic studies of this compound in critically ill patients. A high-pressure liquid chromatographic (HPLC) assay developed recently, although more specific than microbiological techniques, had limited applicability in the critical care setting[1]. A more specific HPLC analysis was required for studies in seriously ill patients. The present report describes a suitable HPLC procedure for the quantitation of both moxalactam isomers in patient plasma and urine.

[1] D. J. Miner, D. L. Coleman, A. M. Shephend, and T. Hardyn, Antimicrob. Agents Chemother., in press.

0022-3549/82/0400-0399$01.00/0

this purpose. The base of the gauge was measured for the chord length (L). The gauge was then set inside the vessel with the ends of the gauge base resting on the curved surface of the vessel. The distance (h) between the base and the bottom of the vessel was taken from the gauge rule. The cylindrical diameter of the vessel was then taken 2 to 3 cm above opposite points where a tangent to the curved bottom of the vessel coincides with the vessel wall. Inside calipers were used for this purpose.

Table VII shows the measurements taken from the vessels and the comparison of the theoretical diameters calculated from these measurements with the actual diameters. The glass vessels possess a flatter curvature than a sphere of the same diameter. The curvature of the plastic vessels closely approximates a sphere of the same diameter. When the results from plastic vessels differ from those obtained from glass vessels, the results from the plastic vessels are more correct, because the plastic vessels conform more closely to the USP specifications.

CONCLUSIONS

Differences in the bottom curvature of dissolution vessels can cause bias in the dissolution results obtained from prednisone tablets. Vessels with a curvature which is less (flatter) than that of a sphere cause a high bias. Vessels with a curvature that is greater (steeper) than that of a sphere cause a low bias. The plastic vessels are more uniform than glass vessels and possess a curvature that more closely approximates the curvature specified in the USP. As such, they are preferable to the glass vessels for use in the dissolution test when the drug is not adsorbed and the vessel is not attacked by the dissolution medium.

The dissolution rate is controlled by the velocity of the liquid passing over the tablet. The liquid velocity at any point in a stirred vessel is controlled by the stirring rate and the geometry of the system. An idealized geometry is defined in the USP. Minor variations from this idealized geometry, such as those discussed in this paper and previously (7), change the liquid velocity in the vicinity of the tablet and, thus, the dissolution results. If the reproducibility of the test is to be improved, equipment must be made available which allows the analyst to adhere to this idealized geometry as closely as possible.

REFERENCES

(1) R. D. Kirchhoefer, *J. Assoc. Off. Anal. Chem.*, **59**, 367 (1976).

(2) "The United States Pharmacopeia," 20th rev., Mack Publishing Co., Easton, Pa., 1980, p. 959.

(3) "Fourth Supplement to USP XIX and NF XIV," The United States Pharmacopeial Convention, Inc., Rockville, Md., 1978, p. 141.

(4) "The United States Pharmacopeia," 20th rev., Mack Publishing Co., Easton, Pa., 1980, p. 655.

(5) D. P. Page, D. C. Cox, M. L. Dow, M. A. Kreienbaum, P. A. McCullen, T. W. Moore, and L. K. Thornton, *FDA By-Lines*, **10**, 57 (1980).

(6) J. F. Brower, *J. Assoc. Off. Anal. Chem.*, **60**, 27 (1977).

(7) D. C. Cox and W. B. Furman, *J. Pharm. Sci.*, **71**, 451 (1981).

(8) W. J. Dixon and F. J. Massey, Jr., "Introduction to Statistical Analysis," McGraw-Hill, New York, N.Y., 1969, pp. 175–181.

(9) F. Langenbucher, *J. Pharm. Sci.*, **58**, 1265 (1969).

ACKNOWLEDGMENT

The authors thank John C. Black for drawing the figure.

HPLC Determination of D and L Moxalactam in Human Serum and Urine

J. A. ZIEMNIAK *‡, D. A. CHIARMONTE ‡, D. J. MINER §, and J. J. SCHENTAG *‡x

Received March 25, 1981, from the **Department of Pharmaceutics, School of Pharmacy, State University of New York at Buffalo;* the ‡*Clinical Pharmacokinetics Laboratory, Millard Fillmore Hospital, Buffalo, N.Y. 14209* and the §*Lilly Research Laboratories, Indianapolis, IN 46285.* Accepted for publication July 24, 1981

ABSTRACT □ A high-pressure liquid chromatographic procedure was developed to determine the D and L isomers of moxalactam in human plasma and urine. After protein precipitation with hydrochloric acid the sample was extracted with ethyl acetate. It was then back extracted into tromethamine buffer (pH 8.0) and washed with octanol. Extraction recovery from plasma ranged from 73–81%. An aliquot of the tromethamine buffer was then injected onto a C_{18}-μBondapak column. The mobile phase was 3% acetonitrile in 0.05 *M* ammonium acetate pH 6.5 buffer. Samples were quantitated by UV detection at 275 nm and 0.01 aufs. The lower limit of detection was 0.5 μg/ml for each isomer. Preliminary stability studies were performed to assess proper sample handling and storage conditions. The procedure was evaluated in a clinical setting to demonstrate its applicability to the study of moxalactam pharmacokinetics in critically ill patients.

Keyphrases □ Moxalactam—determination in human plasma and urine by high-pressure liquid chromatography, D and L isomers □ High-pressure liquid chromatography—determination of moxalactam in human plasma and urine, D and L isomers □ Anti-infectives—moxalactam, high-pressure liquid chromatographic determination, D and L isomers

Moxalactam is a new oxycephalosporin derivative undergoing clinical trials in the United States and Europe. *In vitro* experiments have demonstrated that moxalactam is active against a broad spectrum of microorganisms, including resistant Gram-negative bacteria such as *Pseudomonas aeruginosa* and *Bacteroides fragilis*, some indole-positive *Proteus* species (1), β-lactamase-producing strains of *Enterobacteriaceae* (2), and clinical isolates shown to be cephalosporin resistant (3). Its expanded spectrum of activity compared to conventional β-lactam antibiotics is attributed to replacement of the thio group at the 1 position of the dihydrothiazine nucleus with an oxygen moiety (4).

The pharmacokinetics of moxalactam elimination usually have been evaluated employing standard microbiological techniques (5, 6). However, a more specific analytical procedure was required for pharmacokinetic studies of this compound in critically ill patients. A high-pressure liquid chromatographic (HPLC) assay developed recently, although more specific than microbiological techniques, had limited applicability in the critical care setting[1]. A more specific HPLC analysis was required for studies in seriously ill patients. The present report describes a suitable HPLC procedure for the quantitation of both moxalactam isomers in patient plasma and urine.

[1] D. J. Miner, D. L. Coleman, A. M. Shephend, and T. Hardyn, Antimicrob. Agents Chemother., in press.

0022-3549/82/0400-0399$01.00/0

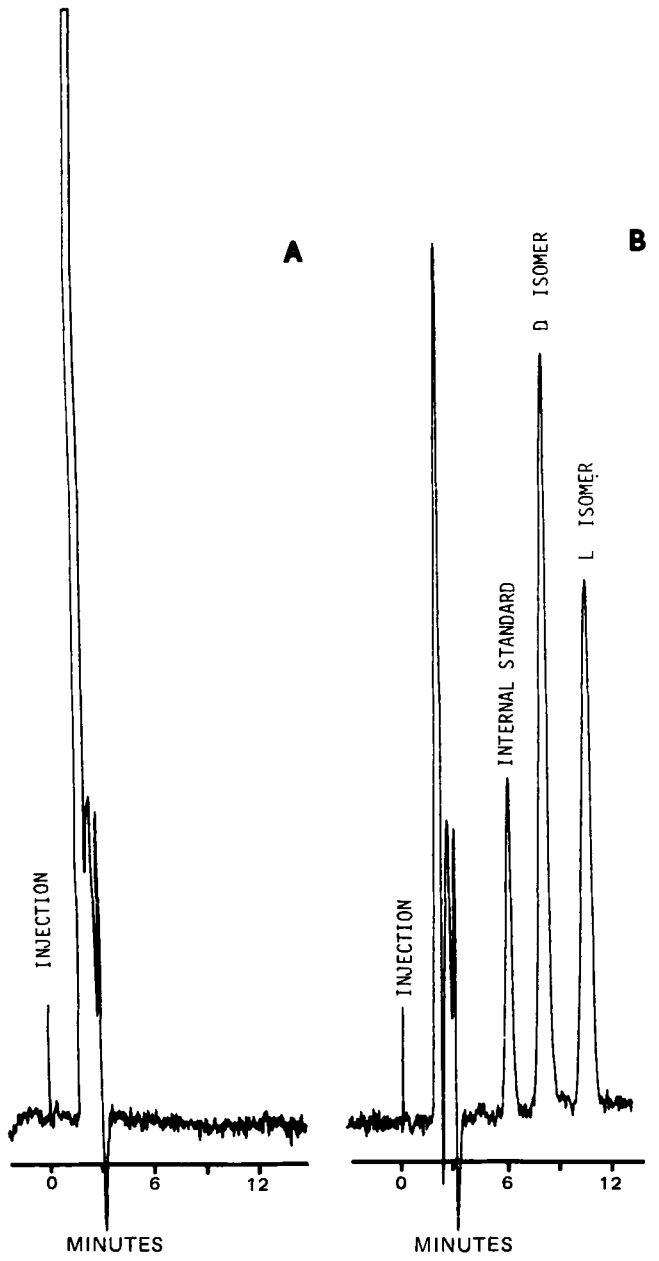

Figure 1—*Chromatograms obtained after extracting 0.5 ml of a blank patient plasma (A) and a moxalactam plasma standard (B). The peak heights of each isomer correspond to a plasma concentration of 10 μg/ml.*

EXPERIMENTAL

Reagents—All chemicals and reagents were analytical grade unless otherwise indicated. Moxalactam was supplied as a lyophylized powder containing a 1:1 mixture of D and L isomers[2]. Allopurinol[3], ammonium acetate, potassium chloride, acetic acid, hydrochloric acid, sodium hydroxide, octanol, tromethamine, glass-distilled acetonitrile[4], methanol, and ethyl acetate[5] were used as received.

Preparation of Stock Solutions—Initial stock solutions of moxalactam were prepared in water and subsequent dilutions made with blank human plasma. Due to the poor aqueous solubility of the internal standard (allopurinol), the drug was first dissolved in 0.1 *N* NaOH and then diluted with water to a final working concentration of 1.5 mg/ml.

Ammonium acetate buffer (0.05 *M*) was adjusted to pH 6.5 with acetic acid. Tromethamine–HCl pH 8.0 and KCl–HCl pH 1.0 buffers (0.05 *M*) were prepared as standard laboratory reagents (7). All buffers were stored at 5° and allowed to reach ambient temperature prior to use.

Extraction Procedure—Two hundred microliters of concentrated hydrochloric acid was added to 0.5 ml of plasma or dilute urine (typically 1:100) containing 0.1 ml of the internal standard solution (allopurinol, 1.5 mg/ml). The mixture was then vortexed, resulting in precipitation of almost all protein present in the sample. After centrifuging at 5000 rpm for 5 min[6], a 0.6-ml portion of the clear supernate was transferred to a 12 × 75-mm polypropylene tube containing 0.5 ml of KCl–HCl pH 1.0 buffer. Three milliliters of HPLC grade ethyl acetate was then added, and the solution was vortexed for 60 sec. After centrifuging[7] at 3000 rpm for 5 min, a 2.9 ml aliquot of the upper ethyl acetate phase was transferred to a second tube containing 0.5 ml of tromethamine–HCl pH 8.0 buffer. This mixture was vortexed for 30 sec, and then centrifuged. The upper organic phase was aspirated and discarded. A 0.4-ml aliquot of the lower aqueous phase was transferred to another tube and washed with 3 ml of octanol by rotation[8] for 1 min. The upper organic phase was discarded after centrifugation, and a 50-μl portion of the lower aqueous phase was used for HPLC analysis. When necessary, the aqueous phase could be stored at 5° for as long as 24 hr prior to HPLC quantitation.

HPLC Conditions—A high-pressure liquid chromatograph[9] equipped with a variable wavelength UV detector[10] and a 10-mv recorder[11] were used. Separation occurred on a C_{18} reverse phase column[12] with a 3% acetonitrile/0.05 *M* ammonium acetate mobile phase at a flow rate of 1.5 ml/min. The column effluent was monitored at 275 nm, and an attenuation of 0.01 aufs was used in all chromatographic procedures.

Recovery Studies—Recovery experiments were performed by adding equivalent amounts of moxalactam to blank plasma and to a solution of mobile phase. Samples were extracted according to the described procedure, except that the internal standard was introduced just prior to injection according to the external standardization method. Recovery was calculated by comparing moxalactam peak-height ratios for the extracted plasma samples with those obtained from direct injection of the mobile phase standard.

Recovery studies were carried out at two concentrations, with five replicate determinations at each concentration. Within- and between-day variation was evaluated at 10 and 80 μg of moxalactam/ml. To assess within-day variation, five aliquots of a single plasma sample were extracted at each concentration. Additional samples were assayed daily over 13 days to assess between-day variation.

Stability Studies—To determine the effects of temperature on the stability of D and L moxalactam, 1.0-ml aliquots of spiked plasma were incubated at −30, 5, 25, and 38°. Samples were periodically assayed for each isomer for up to 40 days. Semilogarithmic plots of each isomer

Table I—Analytical Recovery of D and L Moxalactam from Human Plasma

	Moxalactam, μg/ml	Mean Recovery, %	±*SD*[a]	*CV*, %[b]
D isomer	5.0	81.3	2.6	3.2
(n = 5)	40.0	75.2	2.7	3.5
L isomer	5.0	79.6	5.3	6.7
(n = 5)	40.0	72.8	4.3	5.9

[a] *SD* = standard deviation. [b] *CV* = coefficient of variation, calculated as *SD*/mean.

Table II—Within-Day and Between-Day Variation in the Determination of D and L Moxalactam in Human Plasma

	Within-Day			Between-Day		
	Mean, μg/ml[a]	*SD*[b]	*CV*, %[c]	Mean, μg/ml[a]	*SD*	*CV*, %
D isomer	4.8	0.13	2.8	4.8	0.23	4.7
	41.5	1.5	3.6	39.6	0.60	1.5
L isomer	4.7	0.18	3.9	4.8	0.37	3.6
	41.2	1.3	3.2	39.7	0.70	1.8

[a] n = 5. [b] *SD* = standard deviation. [c] *CV* = coefficient of variation, calculated as *SD*/mean.

[2] Eli Lilly Research Laboratories, Indianapolis, Ind.
[3] Sigma Chemical Co., St. Louis, Mo.
[4] J. T. Baker Chemical Co., Phillipsburg, N.J.
[5] Burdick & Jackson Laboratories, Muskegon, Mich.
[6] Fisher Micro-Centrifuge, Pittsburgh, Pa.
[7] Sorvall GLC-1 Centrifuge, Newton, Conn.
[8] Fisher Roto-Rack, Fisher Scientific Co., Pittsburgh, Pa.
[9] Perkin-Elmer Series II HPLC, Perkin-Elmer Co., Norwalk, Conn.
[10] Schoeffel Variable Wavelength Detector Model 770, Schoeffel Instruments, Westwood, N.J.
[11] Houston Omniscribe Recorder, Houston Instruments, Austin, Tex.
[12] μBondapak-C_{18}, Waters Associates, Milford. Mass.

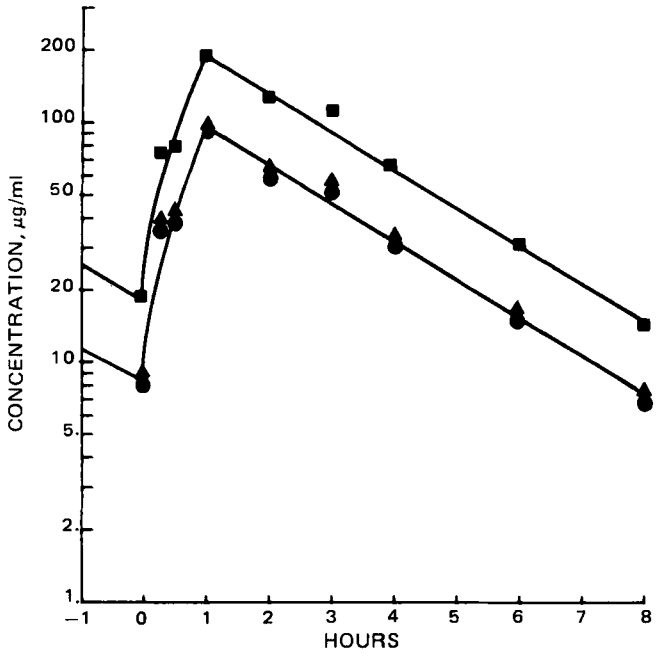

Figure 2—*Plasma concentration versus time profiles for moxalactam (■), its D isomer (▲), and L isomer (●) after intravenous infusion of moxalactam.*

concentration *versus* time were constructed to determine the rate and order of moxalactam degradation. The data were evaluated by means of an Arrhenius plot, and the line of best fit was determined by linear regression analysis.

Pharmacokinetic Study—After getting informed consent, a 10-day course of moxalactam therapy was started in a 60-year old female patient diagnosed as having an abdominal abscess secondary to invasive large bowel cancer. The pathogens involved included *Escherichia coli* and enterococcus, both of which were susceptible to moxalactam *in vitro*. This patient had normal hepatic and renal function, and therefore was given 2 g of intravenous moxalactam every 8 hr. The pharmacokinetic study was conducted on day 6 of therapy to allow steady-state concentrations to be achieved. Plasma and urine samples were obtained throughout a dosing interval and stored at −30° prior to quantitation of D and L moxalactam. The serum concentration *versus* time profiles for moxalactam and each isomer were evaluated by means of nonlinear regression analysis.

RESULTS

Chromatography—Representative chromatograms for a blank patient sample (A) and a spiked plasma standard (B) are presented in Fig. 1. No other peaks were evident in the blank plasma chromatogram even though the patient was receiving numerous medications. Chromatogram B was obtained after extracting 0.5 ml of plasma containing a total moxalactam concentration of 20 μg/ml. A 50-μl aliquot of the final buffer solution was injected onto the column. Allopurinol, the internal standard, had a retention time of 6.0 min, while the D and L isomers of moxalactam had retention times of 7.8 and 10.5 min, respectively. The lower limit of detection for each isomer was 0.5 μg/ml when a 50-μl aliquot of the final buffer phase was injected onto the column.

Calibration curves for each individual isomer were prepared daily by plotting peak-height ratio (isomer/internal standard) *versus* concentration for series of prepared plasma or urine standards. These plots were linear over the 2.5–50-μg/ml concentration range. Samples that exceeded the range of standards were diluted prior to extraction.

Recovery Experiments—The results of the recovery experiments are given in Table I. The overall recovery for both isomers ranged from 73 to 81% over an approximate 10-fold increase in concentration. Although these values are less than quantitative, the recovery was adequate for routine analysis of patient samples. When increased sensitivity was required, the volume ultimately injected onto the column can be increased to as much as 150 μl without deviation from linearity.

Both isomers demonstrate low between- and within-day variation at each of the concentrations evaluated (Table II). The coefficient of variation ranged from 2.8 to 3.9% for the within-day experiments, while the between-day studies yielded coefficients of variation ranging from 1.5 to 4.7%.

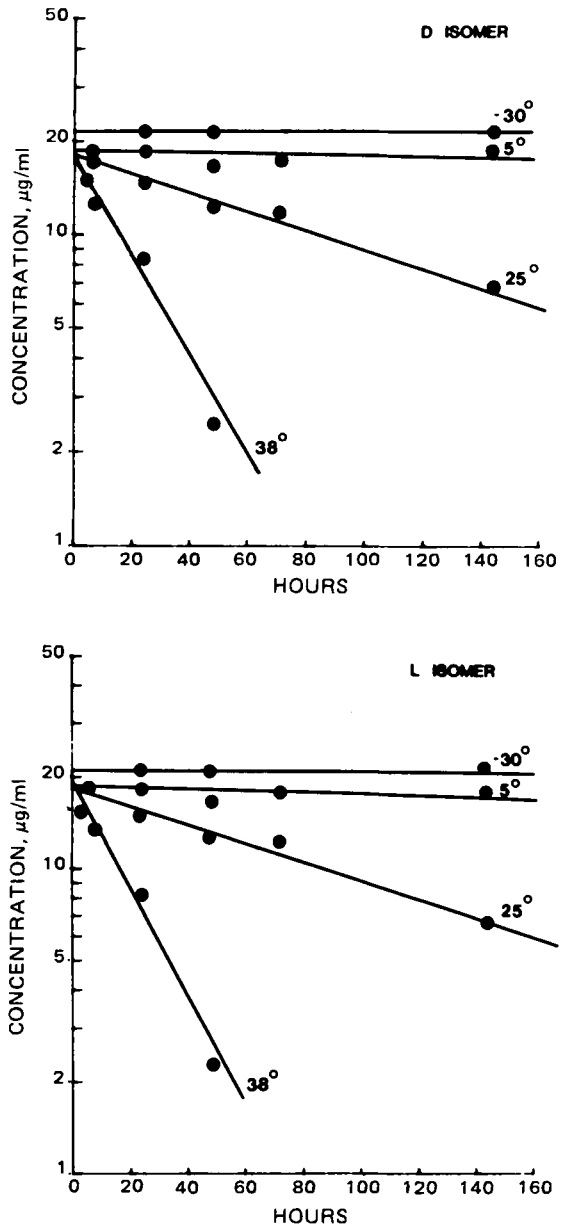

Figure 3—*Effects of temperature on the degradation of D and L moxalactam in human plasma.*

Pharmacokinetic Analysis—Figure 2 is the serum concentration *versus* time profile for moxalactam and its individual isomers in the patient. The subject received 2.0 g of moxalactam by intravenous infusion over 1 hr. The moxalactam concentration is given as the sum of the D and L isomers. The zero plasma sample was obtained immediately before the start of the infusion. The peak concentrations of 95 μg/ml for both isomers were noted at the completion of the infusion period, and concentrations decreased monoexponentially to a minimum of 7 μg/ml. There were no discernible differences in the concentration profile of each isomer.

The data for moxalactam and its isomers were fitted to a one-compartment model with zero order input, by means of nonlinear least-squares regression analysis. Total body clearance of moxalactam calculated as dose/*AUC* was 55.3 ml/min. Total moxalactam and the separate isomers showed similar elimination rates, with half-lives of 1.86, 1.9, and 1.85 hr, respectively.

Stability Studies—Moxalactam is a relatively unstable compound subject to degradation *in vitro*. To assess proper sample handling and storage conditions, the effect of temperature on the degradation rate was evaluated. Figure 3 shows the effect of temperature on the stability of each moxalactam isomer. No differences were observed in the degradation rate for the individual isomers from the two figures. The degradation rate

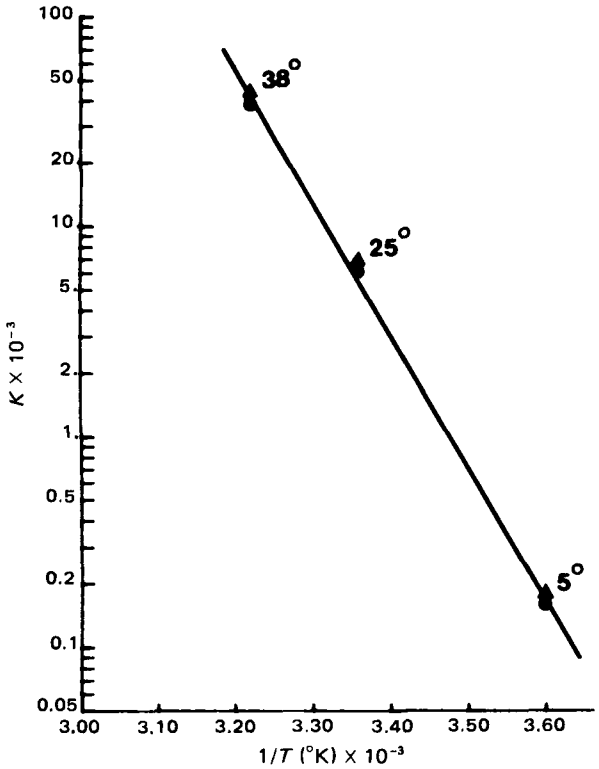

Figure 4—*Arrhenius plot of moxalactam degradation in human plasma. Key:* ▲ *D isomer;* ●, *L isomer.*

is consistent with an apparent first-order process, with the most rapid rate observed at the elevated temperature. Plasma samples were stable over the 40-day test period if frozen at −30°.

An Arrhenius plot was constructed by plotting the apparent first-order rate constant for 10% degradation (K) as a function of the reciprocal of temperature. The data for each isomer are presented in Fig. 4. The relationship was linear over the temperature range of 5–38°, with the slope yielding an activation energy of 29.1 kcal/mole, a value consistent with hydrolysis reactions.

DISCUSSION

Serum moxalactam concentrations have been routinely determined in healthy volunteers using standard microbiological assays (5, 6). The limitation of these assays in a clinical setting is well known, with the most frequently encountered problem being assay interferences from concurrent medications. Additional interferences may arise due to metabolic and/or degradative products of many drugs, or from endogenous substances possessing antibacterial activity. These procedures also cannot measure the individual isomers of moxalactam, whose quantitation may be clinically relevant, as was the case with warfarin (8) and propranolol (9).

An HPLC procedure was reported recently for the determination of D and L moxalactam in serum and urine[1]. This procedure has several short-comings. The extraction procedure, although adequate for samples obtained from select healthy volunteers, was unable to remove interfering substances in samples from critically ill patients. In most instances, extraneous peaks and interferences made quantitation of moxalactam impossible. This method also lacks a suitable internal standard; thus, reproducibility and precision are difficult to achieve. Finally, the previous method requires a separate chromatographic procedure utilizing PIC[13] reagents for the determination of moxalactam in urine.

The present procedure has advantages over existing techniques in that it is more specific than previous methods as well as useful for quantitating both the D and the L isomers of moxalactam. It was tested rigorously during the course of a clinical trial in critically ill patients hospitalized for a variety of disease states including renal and hepatic failure. These patients were receiving numerous concurrent medications and no interferences were seen in any of these samples. Some compounds that were specifically tested and found not to interfere were: cephalothin, cefamandole, cefazolin, cephapirin, cephalexin, caffeine, cimetidine, theophylline, tobramycin, clindamycin, furosemide, dicloxacillin, methicillin, amoxicillin, ampicillin, penicillin G, nafcillin, and trimethoprim.

The effect of disease state on the preferential elimination of one of the isomeric forms of some compounds, such as warfarin and propranolol, is well known. Although the clinical significance of discriminating moxalactam D and L isomers is unknown, this procedure is capable of addressing the question in the course of moxalactam clinical trials.

REFERENCES

(1) T. Yoshida, S. Matsuura, M. Mayama, Y. Kameda, and S. Kuwahara, *Antimicrob. Agents Chemother.*, **17**, 302 (1980).

(2) H. Neu, N. Aswapokee, K. Fu, and P. Aswapokee, *ibid.*, **16**, 141 (1979).

(3) R. N. Jones, P. C. Fuchs, H. M. Sommers, T. L. Gavan, A. L. Barry, and E. H. Gerlach, *ibid.*, **17**, 750 (1980).

(4) K. Matsumoto, Y. Uzuka, T. Nagatake, and H. Shishido, in "Proceedings of 11th International Congress of Chemotherapy and the 19th Interscience Conference on Antimicrobial Agents and Chemotherapy," J. D. Nelson and C. Grassi, Eds., vol. 1, American Society for Microbiology, Washington, D.C., p. 112.

(5) J. Kurihara, K. Matsumoto, Y. Uzuka, H. Shishido, T. Nagatake, H. Yamada, T. Yoshida, T. Oguma, Y. Kimura, and Y. Tochino, in *Ibid.*, p. 110.

(6) J. N. Parsons, J. M. Romano, and M. E. Levison, *Antimicrob. Agents Chemother.*, **17**, 226 (1980).

(7) "Documenta Geigy Scientific Tables," K. Diem and C. Lenter, Eds., Ciba-Geigy Limited, Basle, Switzerland, 1970, p. 280.

(8) L. Goding and B. West, *J. Med. Chem.*, **12**, 517 (1969).

(9) A. Barrett and V. Cullum, *Br. J. Pharmacol.*, **34**, 43 (1968).

ACKNOWLEDGMENTS

Supported in part by NIGMS Grant 20852 from the National Institutes of Health, and in part by a grant from Eli Lilly Company.

[13] Pair ion chromatography.

Carbenicillin Prodrugs: Kinetics of Intestinal Absorption Competing Degradation of the α-Esters of Carbenicillin and Prediction of Prodrug Absorbability from Quantitative Structure–Absorption Rate Relationship

AKIRA TSUJI *×, ETSUKO MIYAMOTO §, TETSUYA TERASAKI *, and TSUKINAKA YAMANA ‡

Received June 8, 1981, from the *Faculty of Pharmaceutical Sciences,‡ Hospital Pharmacy, Kanazawa University, Takara-machi, Kanazawa 920, Japan, and the §School of Pharmacy, Hokuriku University, Kanagawa-machi, Kanazawa 920-11, Japan. Accepted for publication July 17, 1981.

Abstract □ The intestinal absorption of α-esters of carbenicillin disodium, carbenicillin phenyl sodium, and carbenicillin indanyl sodium was investigated using the *in situ* rat intestinal recirculating method. In the *in situ* intestinal lumen at pH 7, two prodrugs were rapidly converted to poorly absorbable carbenicillin, possibly by the action of intestinal nonspecific esterase in competition with the slow absorption of prodrugs. At pH 5, the reduced action of esterase and the increased absorption rate after 3 hr resulted in 50 and 60% absorption of carbenicillin phenyl sodium and carbenicillin indanyl sodium, respectively. The absorption rate constants determined for both prodrugs were in good agreement with the prediction from the quantitative structure–absorption rate relationship derived from the two-compartment aqueous diffusion model.

Keyphrases □ Carbenicillin—prodrugs, kinetics of intestinal absorption, α-esters □ Prodrugs—carbenicillin, kinetics of intestinal absorption, α-esters □ Absorption, intestinal—carbenicillin prodrugs, kinetics

Carbenicillin (II) is very acid unstable and has low lipid solubility; thus, it is poorly absorbed by the GI tract after oral administration and its use is limited to parenteral administration. A series of α-carboxyl esters (I) of carbenicillin was synthesized in an attempt to overcome these disadvantages in the physicochemical properties of II and to increase oral bioavailability. These esters are designed to hydrolyze in the body to liberate II (1). The *in vitro* degradation kinetics of therapeutically useful derivatives of I, phenyl ester (carfecillin, I*a*) and indanyl ester (carindacillin, I*b*), in a wide pH range at 35° and ionic strength of 0.5 were reported previously (2). Bundgaard (3) showed the acid degradation kinetics of the same compounds at 60°. These kinetic data predicted that the β-lactam moiety of both prodrugs is six times more stable than that of II at pH 2.0 and the half-lives of the ester hydrolysis *in vitro* are 8.5 hr for I*a* and 17 hr for I*b* at pH 7.0 and 37° (2).

The present study was undertaken to evaluate the relative importance of parallel rate processes, absorption, and both chemical and enzymatic degradations (possibly proceeding at the absorption sites after oral administration of these esters) by utilizing the *in situ* rat intestinal recirculating method. The physicochemical properties of carbenicillin prodrugs were also evaluated in order to improve the GI absorption rate of the parent antibiotic by application of the structure–absorption rate relationship established previously for β-lactam antibiotics (4).

EXPERIMENTAL

Materials and Reagents—The materials, reagents, and equipment used in this study were, unless otherwise stated, the same as those used previously (2, 4). All isotonic buffer solutions were prepared with the highest reagent grade chemicals available.

Intestinal Absorption Experiments—Male albino rats (Wistar strain) weighing ~200 g, were fasted over a 20-hr period prior to the experiments, but water was given freely. The rats were anesthetized with urethan, 1.3 g/kg ip.

The intestinal recirculating absorption procedure was reported previously (4). The *in situ* loop absorption method was essentially the same as that of Perrier and Gibaldi (5) except for the use of the duodenum and for the ligation of the bile duct.

Each antibiotic solution was prepared with an isotonic buffer of pH 5 or 7 to make a final concentration of 1–4 mg/ml. Aliquots (0.1 ml) of the samples were withdrawn at appropriate intervals, diluted with distilled water, filtered through a 0.45-μm filter[1] to remove any solid materials, and analyzed.

Analytical Procedure—Samples were analyzed by UV spectrometry developed previously to quantify I and II simultaneously in a solution (2).

Table I—Percentage Residue of Carfecillin (Ia) and Carbenicillin (II) in the *In Situ* Rat Small Intestinal Loop [a]

Rat No.	Residual Ia, %	Residual II, %	Disappearance of Total Antibiotics, %
1	38.6	38.2	22.2
2	0.0	80.4	19.6
3	28.8	47.6	23.6
Mean	22.5	55.4	21.8
SD	20.1	22.2	2.0

[a] All experiments were over 1 hr. I*a* was dissolved in isotonic phosphate buffer (pH 7) and injected in a volume of 1 ml (1 mg/ml) into a 5-cm intestinal loop (duodenum).

RESULTS AND DISCUSSION

Disappearance of Prodrugs from *In Situ* Rat Intestinal Loop—It was suggested that I*a* and I*b* are both well absorbed by the GI tract and can be converted rapidly to II during absorption through the mucous membrane and/or in the blood by a nonspecific esterase (1).

The percentage of the residual I*a* and II produced after 1 hr in the *in situ* rat intestinal loop at pH 7 is shown in Table I. From previous kinetic data (2), the rate constant for the ester hydrolysis of I*a* was evaluated at 1.5×10^{-3} min^{-1} for the isotonic and 0.066 *M* phosphate buffer solution (pH 7.0) used in this study. The 55.4 ± 22.2% of *in situ* formation of II at the end of 1 hr was about six times greater than that predicted from the chemical hydrolysis rate of the phenyl ester. Because the percentage disappearance of the total antibiotics (I*a* + II) was 21.8 ± 2.0%, the result suggests that the prodrug I*a* may be absorbed as well as converted to II by the chemical hydrolysis and enzymatic action of nonspecific esterase in the intestinal fluid and/or mucosal surface of the intestine.

Kinetics of Absorption and Metabolism of Prodrugs by the *In Situ* Rat Intestine—To clarify the GI absorption of I from its kinetics, the intestinal absorption experiments were performed using the recirculating perfusion technique. The pH of the perfusion solution was maintained

[1] Sartorius-Membranfilter, GmbH, 34 Göttingen, West Germany.

0022-3549/82/0400-0403$01.00/0

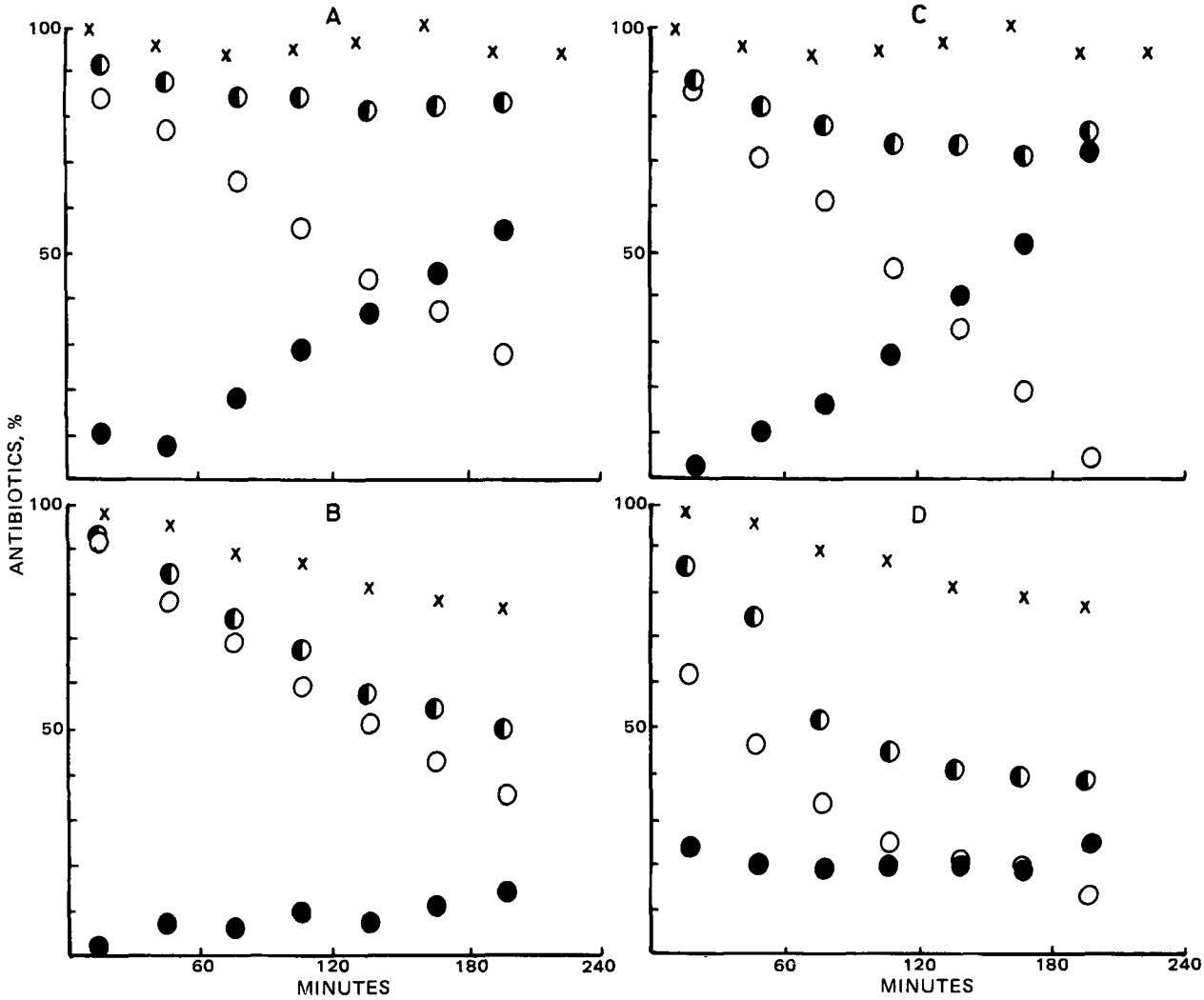

Figure 1—*Time course of absorption and metabolism of carfecillin (Ia) (A and B) and carindacillin (Ib) (C and D) during* in situ *recirculation through the rat small intestine at pH 7.0 (A and C) and pH 5.0 (B and D). Perfusion volume, 15 ml; initial concentration, 4 mg/ml (A and B), 2 mg/ml (C), and 1 mg/ml (D); flow rate, 2 ml/min. Key:* ◐, *total antibiotics;* ○, *prodrug (I); and* ●, *carbenicillin (II). The symbol* (x) *shows the experimental points for II under the same conditions.*

at a constant of pH 5.0 or 7.0 by use of a pH-stat during the absorption experiments.

Results of the lumen content analysis are shown in Fig. 1, indicating that disappearance of I at pH 7.0 proceeds to a similar extent for Ia and Ib, accompanying an increase of II up to ~50–60% after 3 hr in 15-ml of lumen perfusion solution (Figs. 1A and 1C). Interestingly the rates for total loss of I and the formation of II depend markedly on the volume of the perfusion solution. The loss of total antibiotic from 15-ml lumen solution was about 20% for Ib after 3 hr. The disappearance of II was only ~6% after 3 hr under the same condition (Fig. 1A and 1C). The decrease in the total antibiotic may be attributed mostly to the absorption of intact I. However, in the experiments with 40–50 ml of lumen solution, about 35–40% of I loss corresponded to the formation of II; the absorption of the antibiotics was negligible.

At pH 5, on the other hand, absorption was 50% for Ia and 60% for Ib but only 20% for the parent antibiotic II after 3 hr for the 15-ml solution (Figs. 1B and 1D). Under this condition, a relatively small amount (10–20%) of II was produced, probably due to the reduced action of nonspecific esterase.

From these results, the kinetic model for the absorption and metabolism of I may be derived as reported previously (6). I is absorbed by the intestine in an intact form but is partially degraded by two possible processes as shown in Scheme I. One process is a nonenzymatic degradation of β-lactam moiety to produce the penicilloic acid (III) of I and the other is both a nonenzymatic and enzymatic hydrolysis of ester linkage to form the poorly absorbable II. Compound II is also degraded to its penicilloic acid (IV) similarly to form III from I along with the slow absorption by the intestine.

If it is assumed (not being influenced by the volume change of the perfusion solution) that the absorption kinetics obey Fick's law, that enzymatic ester hydrolysis is described by Michaelis–Menten kinetics, and that all β-lactam cleavages obey apparent first-order kinetics, then the rate of each species can be written:

$$\frac{d[\mathrm{I}]}{dt} = -[k_a/V + (k_d)_1 + (k_d)_2][\mathrm{I}] - \frac{k_e(A_e/V)\,[\mathrm{I}]}{K_m + [\mathrm{I}]} \qquad \text{(Eq. 1)}$$

$$\frac{d[\mathrm{II}]}{dt} = (k_d)_1[\mathrm{I}] - [k_a'/V + (k_d)_3]\,[\mathrm{II}] + \frac{k_e(A_e/V)\,[\mathrm{I}]}{K_m + [\mathrm{I}]} \qquad \text{(Eq. 2)}$$

where [I] and [II] represent the concentration of I and II, respectively, at time t, K_m is the Michaelis constant, A_e represents the amount of enzyme, k_e is the degradation rate constant for the formation of II from the drug–enzyme complex, $(k_d)_1$ is the first-order rate constant for the nonenzymatic ester hydrolysis to produce II, $(k_d)_2$ and $(k_d)_3$ are the first-order rate constants for the nonenzymatic β-lactam cleavage reactions of I and II, respectively, k_a and k_a' are the absorption clearance (ml/time) of I and II, and V is the volume of perfusion solution. From Eqs. 1 and 2, Eqs. 3 and 4 can easily be derived (6):

$$k_{app} = k_a/V + (k_d)_2 \qquad \text{(Eq. 3)}$$

$$k_{app} = \frac{[\mathrm{I}]_{t_1} - [\mathrm{I}]_{t_2} + [\mathrm{II}]_{t_1} - [\mathrm{II}]_{t_2} - [k_a'/V + (k_d)_3]\int_{t_1}^{t_2}[\mathrm{II}]dt}{\int_{t_1}^{t_2}[\mathrm{I}]dt} \qquad \text{(Eq. 4)}$$

where subscripts t_1 and t_2 represent the sampling times. The values of

Table II—Absorption Clearance Determined at pH 5 and 7 in the *In Situ* Absorption Experiments through the Rat Small Intestine and the Related Physicochemical Parameters for Carbenicillin Prodrugs (I) and Carbenicillin (II)

	Ia		Ib		II	
	pH		pH		pH	
	5	7	5	7	5	7
Molecular weight[a]		454.5		494.6		378.4
pKa[b]		2.91		2.94		3.06[c]
Log P_u (octanol–water)[b]		2.96		3.77		1.95[d]
P_{app}[e]	7.35	0.0741	50.8	0.512	0.207	0.00549
$10^2 k_u$ (theor)[f], ml/min	3.68	0.05	12.17	0.29	0.37	0.00
$10^2 k_{theor}$[g], ml/min	4.83	1.20	13.32	1.44	1.52	1.15
$10^2 k_{obs}$[h], ml/min	6.6	1.7	13.5	2.3	1.5	0.45[i]

[a] As free acid. [b] Determined at 37° and ionic strength 0.15, from Ref. 8. [c] Determined at 37° and ionic strength 0.5, from Ref. 9. [d] Reference 13. [e] Defined by Eq. 7. [f] Calculated from the first term of the right side in Eq. 5. [g] Calculated from Eq. 5 where k_i = 0.0115 ml/min. [h] Observed value. [i] Total disappearance including possible degradation.

the integrals, which should be equal to the areas under the respective concentration–time curves of I and II, were calculated by the trapezoidal rule.

As shown in Fig. 2, the plots of k_{app} *versus* $1/V$ for both prodrugs gave reasonably straight lines[2]. Absorption clearances at pH 7.0 calculated from the slopes were 0.017 and 0.023 ml/min for I*a* and I*b*, respectively. Despite the 50-fold difference at maximum in the oil–water partition coefficient of the ionized species of I and the other β-lactam antibiotics (7, 8), the absorption clearance of I was very close to that (average 0.012 ml/min) of other monobasic penicillins (4). This supports the fact that the intestinal absorption rate of ionic species of monobasic β-lactam antibiotics is almost independent of their lipophilicity (4).

At pH 5, the absorption clearances were calculated to be 0.066 and 0.135 ml/min for I*a* and I*b*, respectively, according to Eqs. 3 and 4. *In vitro* degradation rate constants of $(k_d)_2 = 9.7 \times 10^{-5}$ min^{-1} and 8.9×10^{-5} min^{-1} for I*a* and I*b* and $(k_d)_3 = 4.3 \times 10^{-4}$ min^{-1}, which were evaluated at 37° and pH 5.0 from the kinetic data (2, 3, 9, 10) were used in the calculations. The absorption clearance of II, k'_a, was determined to be 0.015 ml/min (Fig. 1). The prodrug absorbabilities were ~4 times larger for I*a* and 9 times larger for I*b* than that of the parent drug, II. The increased absorption rate at pH 5 with the increased lipophilicity of I may be due to the enhanced lipoidal membrane transport of undissociated species of I across the aqueous diffusion layer adjacent to the mucosal surface (11).

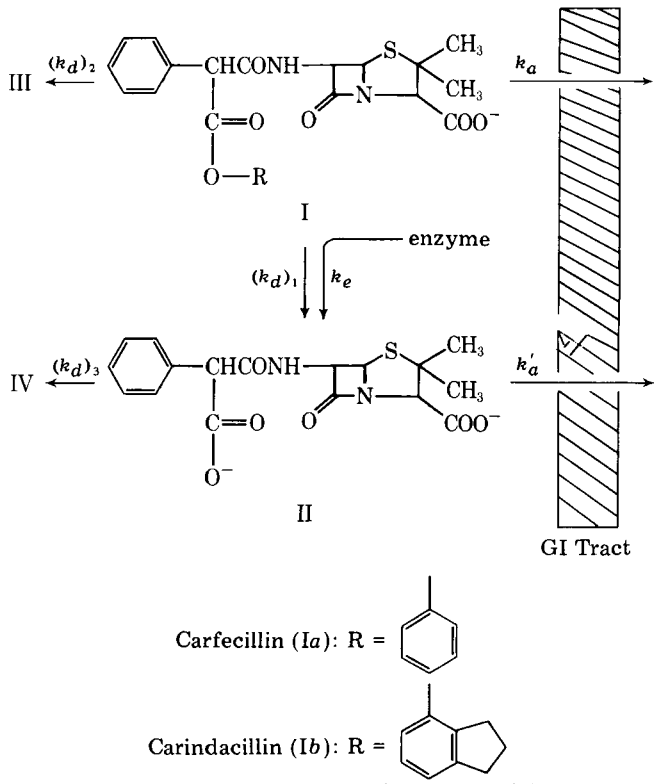

Scheme I—Pathways of simultaneous absorption and degradation of carbenicillin prodrug (I) in the GI.

Prediction of Penicillin Prodrug Absorbability from Quantitative Structure–Absorption Rate Relationship—A previous report (4) established that the theoretical absorption clearance, k_{theor}, for monobasic β-lactam antibiotics was generalized by the sum of the absorption clearances, $k_u + k_i$, for the undissociated and ionized species of the drug as:

$$k_{theor}\ (\text{ml/min}) = \frac{\alpha}{\sqrt{MW}}\left(\frac{f_u P_u}{\beta + f_u P_u}\right) + k_i \qquad \text{(Eq. 5)}$$

where MW is the molecular weight of the undissociated form of antibiotics, P_u is the partition coefficient of the undissociated drug between oil (*e.g.*, octanol) and water, α, and β are constants, and f_u is the fraction of undissociated species as a function of pH expressed as:

$$f_u = \frac{a_H^+}{K_a + a_H^+} \qquad \text{(Eq. 6)}$$

where a_H^+ is the hydrogen-ion activity of perfusion solution and K_a is the dissociation constant of drug. Thus, $f_u P_u$ represents the apparent partition coefficient, P_{app}, as a function of the solution pH:

$$P_{app} = f_u P_u \qquad \text{(Eq. 7)}$$

The first term in Eq. 5 was derived for k_u from the kinetic model of membrane permeation across the lipoidal barrier for the undissociated penicillin species transported through the aqueous diffusion layer adjacent to the GI membrane surface (11). With the parameters[3] α (4.62), β (35.9), and k_i (0.0115) evaluated from the absorption rates (three phenoxy derivatives and four isoxazole derivatives of penicillins) in the same experiments (4), the theoretical absorption clearances of I*a*, I*b*, and II were calculated according to Eqs. 5 and 6 as a function of lumen solution pH[4]. The results are shown in Fig. 3.

In Fig. 3, the k_a–pH profiles for penicillin V, propicillin, and dicloxacillin (4) are redrawn by conversion of the first-order absorption rate constant to its clearance using the volume (9 ml) of the perfusion solution used. The predicted values are in fairly good agreement with the experimental data for carbenicillin prodrugs and the parent drug, as well as

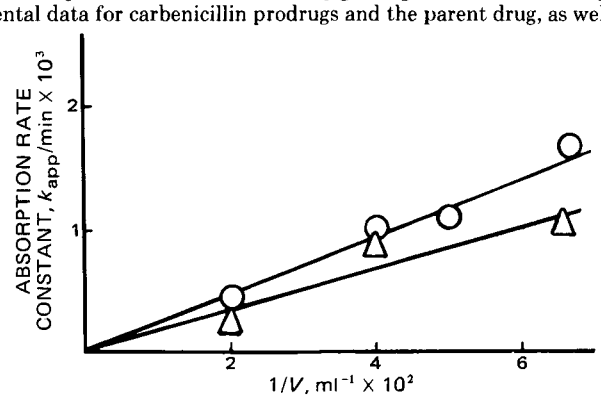

Figure 2—*Effect of the volume of perfusion solution on the absorption rates of carfecillin (Ia, △) and carindacillin (Ib, ○) from the* in situ *rat intestine at pH 7.0 under the same conditions as in Fig. 1.*

[2] For I*b*, k_{app} was reevaluated according to Eqs. 3 and 4 because the calculation in the previous paper (5) neglected the absorption rate of II.

[3] These values were evaluated from Eqs. 6, 12, 14 in Ref. 4 by changing the perfusion solution volume to 9 ml.

[4] The parameters based on these calculations are listed in Table II.

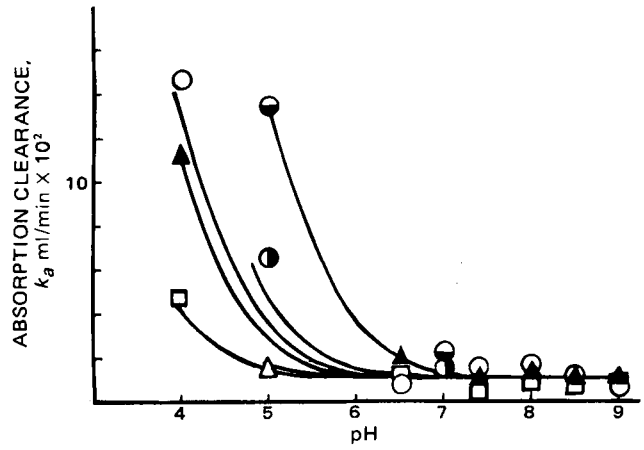

Figure 3—*Plots of the* in situ *rat intestinal absorption clearance,* k_{obs}, *of penicillins* versus *pH of the perfusion solution at 37°. The curves were generated from Eq. 5 with the corresponding parameters listed in Table II and from Ref. 4. Key:* ◒, *carindacillin (Ib);* ◑, *carfecillin (Ia);* ○, *dicloxacillin;* ▲, *propicillin;* □, *penicillin V; and* △, *carbenicillin (II). Data for dicloxacillin, propicillin, and penicillin V were taken from Ref. 4.*

for other antibiotics. The results indicate that the prodrugs, Ia and Ib, are sufficiently lipophilic to be absorbed rapidly from the GI tract by crossing the first barrier of the aqueous diffusion layer in front of the GI membrane surface and the second barrier of the lipid membrane.

The two prodrug chemical modifications of carbenicillin increase both the GI absorption rate and the acid-stability and exhibit sufficient chemical stability of the ester bond in the GI lumen. However, the results suggest that since the ester moieties of Ia and Ib are easily subject to the intestinal enzymatic metabolism, both ester prodrugs may liberate the poorly absorbable II as a result of nonspecific esterase action accompanied by absorption to reduce both bioavailabilities. After oral dosage in humans, 15–30% for Ia and 35–40% for Ib are recovered as II in urine compared with 75–100% after II intravenously (12). The relatively low recovery for I may be attributed to incomplete absorption and/or a first-pass effect. But II itself can not achieve a large urinary recovery after an oral dose.

REFERENCES

(1) J. P. Clayton, M. Cole, S. W. Elson, K. D. Hardy, L. W. Mizen, and R. Sutherland, *J. Med. Chem.*, **18**, 172 (1975).

(2) A. Tsuji, E. Miyamoto, T. Terasaki, and T. Yamana, *J. Pharm. Sci.*, **68**, 1259 (1979).

(3) H. Bundgaard, *Arch. Pharm. Chemi, Sci. Ed.*, **7**, 95 (1979).

(4) A. Tsuji, E. Miyamoto, O. Kubo, and T. Yamana, *J. Pharm. Sci.*, **68**, 812 (1979).

(5) D. Perrier and M. Gibaldi, *ibid.*, **62**, 1486 (1973).

(6) A. Tsuji, E. Miyamoto, I. Kagami, H. Sakaguchi, and T. Yamana, *ibid.*, **67**, 1701 (1978).

(7) T. Yamana, A. Tsuji, E. Miyamoto, and O. Kubo, *ibid.*, **66**, 747 (1977).

(8) A. Tsuji, O. Kubo, E. Miyamoto, and T. Yamana, *ibid.*, **66**, 1675 (1977).

(9) T. Yamana, A. Tsuji, and Y. Mizukami, *Chem. Pharm. Bull.*, **22**, 1186 (1974).

(10) H. Zia, M. Tehrani, and R. Zargarbashi, *Can. J. Pharm. Sci.*, **9**, 112 (1974).

(11) A. Tsuji, E. Miyamoto, N. Hashimoto, and T. Yamana, *J. Pharm. Sci.*, **67**, 1705 (1978).

(12) T. Bergan, *Antibiot. Chemother.*, **25**, 1 (1978).

(13) A. E. Bird, *J. Pharm. Sci.*, **64**, 1671 (1975).

ACKNOWLEDGMENTS

Presented in part at the Pharmaceutical Society of Japan, 97th Annual Meeting, Tokyo, April 1977.

The authors thank Taito Pfizer, Co. and Beecham Yakuhin, Co. for the gift of the antibiotics.

A Dissolution Anomaly Involving Ticrynafen in Simulated Intestinal Fluid without Enzyme

ELISABETH S. RATTIE, JOSEPH G. BALDINUS, LOUIS J. RAVIN ˣ, INA B. SNOW, and MIRZA M. A. BEG

Received March 2, 1981, from the *Research and Development Division, Smith, Kline & French Laboratories, Philadelphia, PA 19101.* Accepted for publication July 20, 1981.

Abstract □ Data are presented showing that the anomalous dissolution behavior of ticrynafen in simulated intestinal fluid without enzyme is due to the presence of potassium ions in the dissolution medium. Solubility studies indicate that an insoluble 1:1 complex is formed between ticrynafen and its potassium salt. This complex apparently creates an insoluble barrier that prevents complete dissolution of ticrynafen. To determine whether this might also occur in clinical use, a three-way cross-over study in 12 subjects was done. Data from this investigation show that concomitant administration of ticrynafen tablets and potassium in the form of a commercial supplement does not adversely affect bioavailability.

Keyphrases □ Ticrynafen—dissolution anomaly in simulated intestinal fluid without enzyme, potassium ions □ Potassium ions—complex with ticrynafen, dissolution anomaly in simulated intestinal fluid without enzyme □ Dissolution—anomaly, ticrynafen in simulated intestinal fluid without enzyme

Considerable effort has been devoted to the development of *in vitro* dissolution test methods that attempt to characterize the *in vitro* dissolution rate-controlled absorption of drugs administered in solid dosage forms. Unfortunately, the lack of understanding surrounding the many variables that can influence the *in vivo* dissolution, and possibly the subsequent absorption, make predictions based on *in vitro* data alone extremely difficult. The nature of the dissolution media can sometimes influence *in vitro* dissolution behavior dramatically and be misleading with regard to *in vivo* performance. The present study shows how the presence of potassium ions in simulated intestinal fluid without enzyme retarded drug dissolution without affecting the *in vivo* performance of ticrynafen[1].

EXPERIMENTAL

Materials—Ticrynafen[2], potassium ticrynafen[2], and 500-mg ticrynafen tablets[1] were obtained. All other chemicals were reagent grade and were used without further purification.

[1] 'Selacryn', Smith, Kline & French Laboratories.
[2] Smith, Kline & French Laboratories.

0022-3549/82/0400-0406$01.00/0

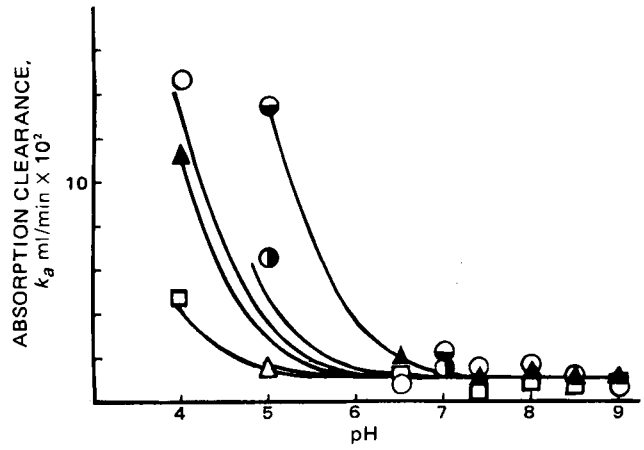

Figure 3—*Plots of the* in situ *rat intestinal absorption clearance,* k_{obs}, *of penicillins* versus *pH of the perfusion solution at 37°. The curves were generated from Eq. 5 with the corresponding parameters listed in Table II and from Ref. 4. Key:* ◒, *carindacillin (Ib);* ◑, *carfecillin (Ia);* ○, *dicloxacillin;* ▲, *propicillin;* □, *penicillin V; and* △, *carbenicillin (II). Data for dicloxacillin, propicillin, and penicillin V were taken from Ref. 4.*

for other antibiotics. The results indicate that the prodrugs, Ia and Ib, are sufficiently lipophilic to be absorbed rapidly from the GI tract by crossing the first barrier of the aqueous diffusion layer in front of the GI membrane surface and the second barrier of the lipid membrane.

The two prodrug chemical modifications of carbenicillin increase both the GI absorption rate and the acid-stability and exhibit sufficient chemical stability of the ester bond in the GI lumen. However, the results suggest that since the ester moieties of Ia and Ib are easily subject to the intestinal enzymatic metabolism, both ester prodrugs may liberate the poorly absorbable II as a result of nonspecific esterase action accompanied by absorption to reduce both bioavailabilities. After oral dosage in humans, 15–30% for Ia and 35–40% for Ib are recovered as II in urine compared with 75–100% after II intravenously (12). The relatively low recovery for I may be attributed to incomplete absorption and/or a first-pass effect. But II itself can not achieve a large urinary recovery after an oral dose.

REFERENCES

(1) J. P. Clayton, M. Cole, S. W. Elson, K. D. Hardy, L. W. Mizen, and R. Sutherland, *J. Med. Chem.*, **18**, 172 (1975).

(2) A. Tsuji, E. Miyamoto, T. Terasaki, and T. Yamana, *J. Pharm. Sci.*, **68**, 1259 (1979).

(3) H. Bundgaard, *Arch. Pharm. Chemi, Sci. Ed.*, **7**, 95 (1979).

(4) A. Tsuji, E. Miyamoto, O. Kubo, and T. Yamana, *J. Pharm. Sci.*, **68**, 812 (1979).

(5) D. Perrier and M. Gibaldi, *ibid.*, **62**, 1486 (1973).

(6) A. Tsuji, E. Miyamoto, I. Kagami, H. Sakaguchi, and T. Yamana, *ibid.*, **67**, 1701 (1978).

(7) T. Yamana, A. Tsuji, E. Miyamoto, and O. Kubo, *ibid.*, **66**, 747 (1977).

(8) A. Tsuji, O. Kubo, E. Miyamoto, and T. Yamana, *ibid.*, **66**, 1675 (1977).

(9) T. Yamana, A. Tsuji, and Y. Mizukami, *Chem. Pharm. Bull.*, **22**, 1186 (1974).

(10) H. Zia, M. Tehrani, and R. Zargarbashi, *Can. J. Pharm. Sci.*, **9**, 112 (1974).

(11) A. Tsuji, E. Miyamoto, N. Hashimoto, and T. Yamana, *J. Pharm. Sci.*, **67**, 1705 (1978).

(12) T. Bergan, *Antibiot. Chemother.*, **25**, 1 (1978).

(13) A. E. Bird, *J. Pharm. Sci.*, **64**, 1671 (1975).

ACKNOWLEDGMENTS

Presented in part at the Pharmaceutical Society of Japan, 97th Annual Meeting, Tokyo, April 1977.

The authors thank Taito Pfizer, Co. and Beecham Yakuhin, Co. for the gift of the antibiotics.

A Dissolution Anomaly Involving Ticrynafen in Simulated Intestinal Fluid without Enzyme

ELISABETH S. RATTIE, JOSEPH G. BALDINUS, LOUIS J. RAVIN ˣ, INA B. SNOW, and MIRZA M. A. BEG

Received March 2, 1981, from the *Research and Development Division, Smith, Kline & French Laboratories, Philadelphia, PA 19101.* Accepted for publication July 20, 1981.

Abstract □ Data are presented showing that the anomalous dissolution behavior of ticrynafen in simulated intestinal fluid without enzyme is due to the presence of potassium ions in the dissolution medium. Solubility studies indicate that an insoluble 1:1 complex is formed between ticrynafen and its potassium salt. This complex apparently creates an insoluble barrier that prevents complete dissolution of ticrynafen. To determine whether this might also occur in clinical use, a three-way cross-over study in 12 subjects was done. Data from this investigation show that concomitant administration of ticrynafen tablets and potassium in the form of a commercial supplement does not adversely affect bioavailability.

Keyphrases □ Ticrynafen—dissolution anomaly in simulated intestinal fluid without enzyme, potassium ions □ Potassium ions—complex with ticrynafen, dissolution anomaly in simulated intestinal fluid without enzyme □ Dissolution—anomaly, ticrynafen in simulated intestinal fluid without enzyme

Considerable effort has been devoted to the development of *in vitro* dissolution test methods that attempt to characterize the *in vitro* dissolution rate-controlled absorption of drugs administered in solid dosage forms. Unfortunately, the lack of understanding surrounding the many variables that can influence the *in vivo* dissolution, and possibly the subsequent absorption, make predictions based on *in vitro* data alone extremely difficult. The nature of the dissolution media can sometimes influence *in vitro* dissolution behavior dramatically and be misleading with regard to *in vivo* performance. The present study shows how the presence of potassium ions in simulated intestinal fluid without enzyme retarded drug dissolution without affecting the *in vivo* performance of ticrynafen[1].

EXPERIMENTAL

Materials—Ticrynafen[2], potassium ticrynafen[2], and 500-mg ticrynafen tablets[1] were obtained. All other chemicals were reagent grade and were used without further purification.

[1] 'Selacryn', Smith, Kline & French Laboratories.
[2] Smith, Kline & French Laboratories.

0022-3549/82/0400-0406$01.00/0

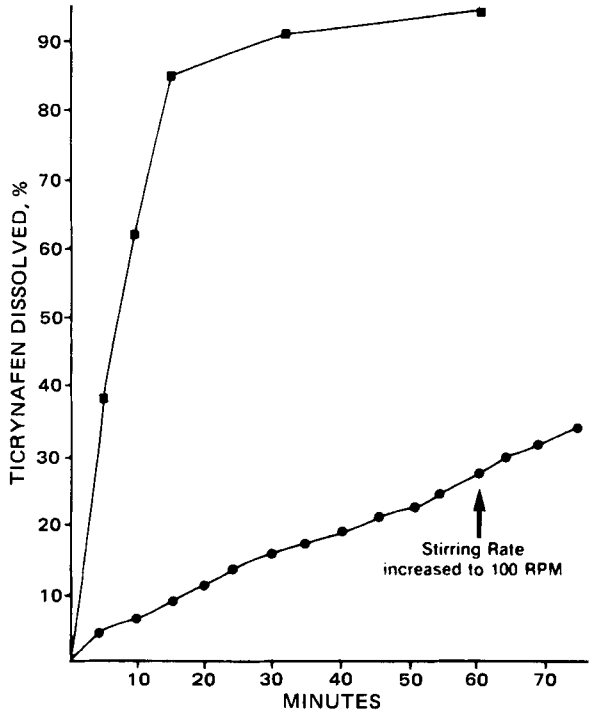

Figure 1—*Effect of stirring rate on the dissolution behavior of 500-mg ticrynafen tablets in simulated intestinal fluid without enzyme. Key: ●, 50 rpm; ■, 100 rpm.*

Dissolution Media—The following dissolution media were used in the dissolution studies: simulated intestinal fluid without enzyme USP (0.05 *M*), 0.05 *M* potassium phosphate buffer (pH 7.5), 0.05 *M* sodium phosphate buffer (pH 7.5), 0.05 *M* tromethamine buffer (pH 7.6). Buffers were freshly prepared prior to all dissolution studies.

Dissolution Methodology—The tablet dissolution profiles were determined in various buffer systems using Method II as described in the official compendia (1). The amount of drug dissolved with time was monitored by circulating the filtered dissolution media through a flow cell in a recording spectrophotometer[3] at 355 nm and returning it to the vessel. The ticrynafen absorbance *versus* time represents the dissolution profile of the tablet. The fractional amount of drug released as a function of time was determined by dividing the absorbance at any particular time by the absorbance after complete dissolution. A standard solution of ticrynafen (500 mg in 900 ml of dissolution medium) was utilized in the flow-cell apparatus to determine the absorbance when the tablet dissolution was complete.

Complexation Studies—A solubility method described previously (2) was utilized. Excess amounts of ticrynafen were placed in screw-capped glass vials. A 10-ml aliquot of various known concentrations of potassium ticrynafen was added to the vials. The samples were rotated overnight in a constant temperature bath at 25 ± 0.5°. An aliquot was removed from the vials, diluted with the appropriate solvent, and analyzed spectrophotometrically at 355 nm.

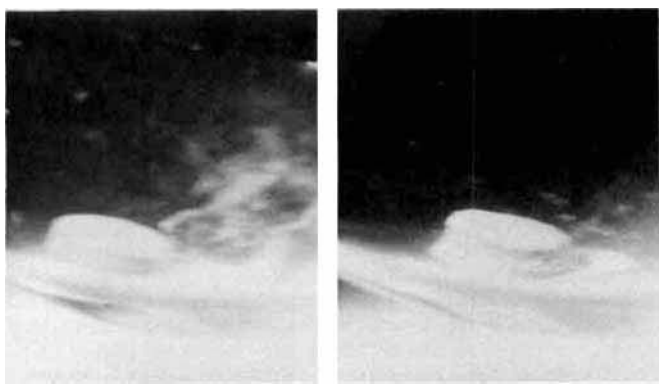

Figure 2—*Ticrynafen tablet (500 mg), initially and after 60 min in simulated intestinal fluid without enzyme.*

[3] Cary 15.

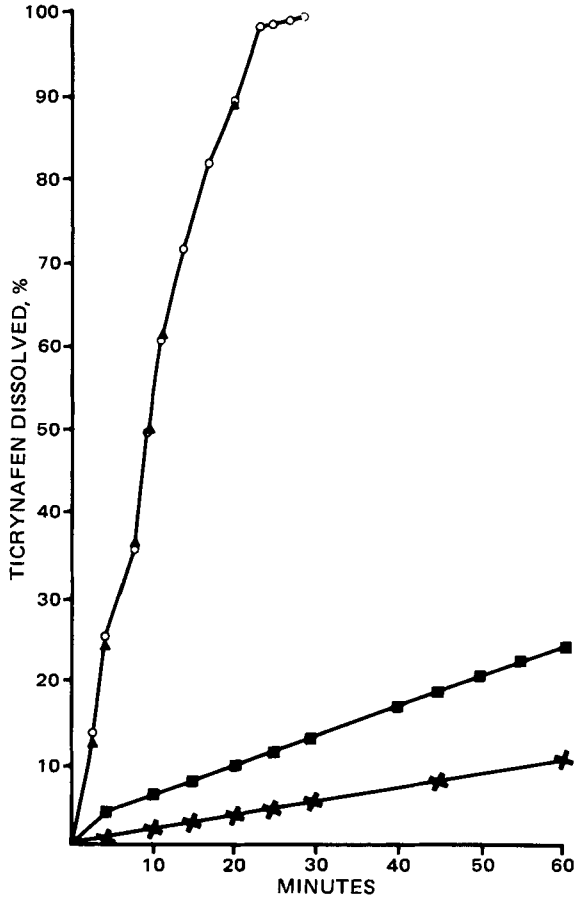

Figure 3—*Dissolution behavior of 500-mg ticrynafen tablets in simulated intestinal fluid without enzyme (■), 0.05 M potassium phosphate solution (×), 0.05 M sodium phosphate solution (○), and 0.05 M tromethamine solution (▲).*

RESULTS AND DISCUSSION

Dissolution Studies—Figure 1 shows the results of dissolution studies conducted with 500-mg ticrynafen tablets by USP Method II in simulated intestinal fluid without enzyme at 37° at 50 and 100 rpm, respectively. There appears to be a marked dependency on agitation. Physical observations during the dissolution test indicate that the tablet appeared to develop a crusty layer at the surface at 50 rpm. This effect is shown in Fig. 2. Since the ticrynafen tablets showed poor dissolution behavior at 50 rpm and developed the crust-like surface, it was thought that something in the system might be causing an interaction that resulted in poor dissolution. The effect also seemed dependent on agitation intensity, since complete tablet dissolution was achieved in 30 min at 100 rpm. In addition, increased agitation intensity had little, if any, effect on the dissolution behavior after the apparent interaction took place.

Additional dissolution studies were then conducted with several alternate buffer systems. Figure 3 shows the results of dissolution studies with 500-mg ticrynafen tablets in 0.05 *M* potassium phosphate, sodium phosphate, and tromethamine buffers and simulated intestinal fluid without enzyme, respectively. It is apparent that the presence of potassium ions in the dissolution media had a significant effect on the dissolution behavior of ticrynafen.

Since ticrynafen is usually administered to patients on concomitant potassium therapy, experiments were conducted to determine what effect

Table I—Summary of Blood Level and Urinary Excretion Data

Regimen	Blood Level *AUC*	Percentages Excreted
Tablet	173.67	30.20
Solution	170.16	30.49
Tablet with 20 meq potassium	165.83	31.55

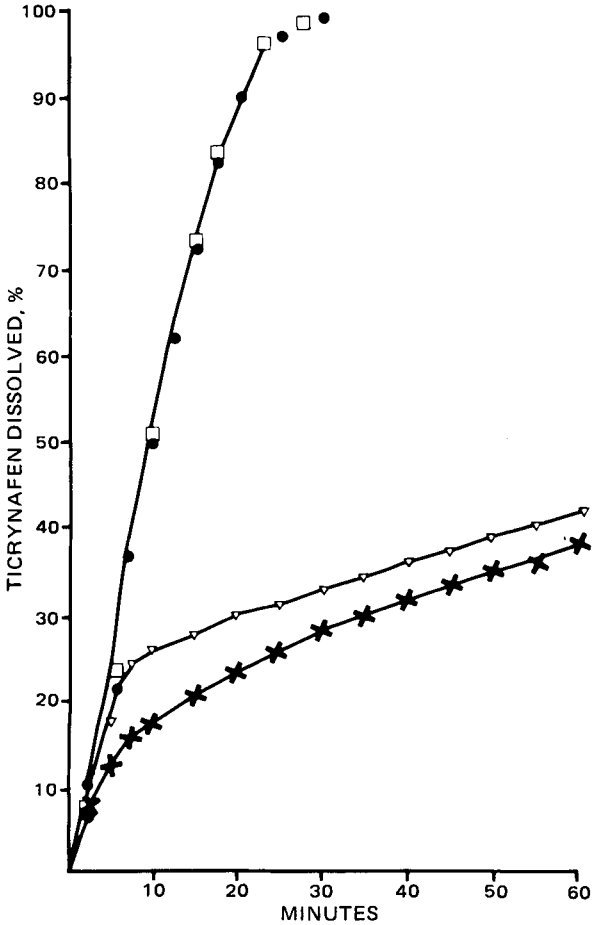

Figure 4—*Effect of the addition of potassium and sodium ions on the dissolution behavior of 500-mg ticrynafen tablets in 0.05* M *tromethamine solution (□), 0.05* M *tromethamine solution with 20 meq potassium added initially (×), 0.05* M *tromethamine solution with 20 meq potassium added after 5 min (▽), 0.05* M *tromethamine solution with 20 meq sodium added after 5 min (●).*

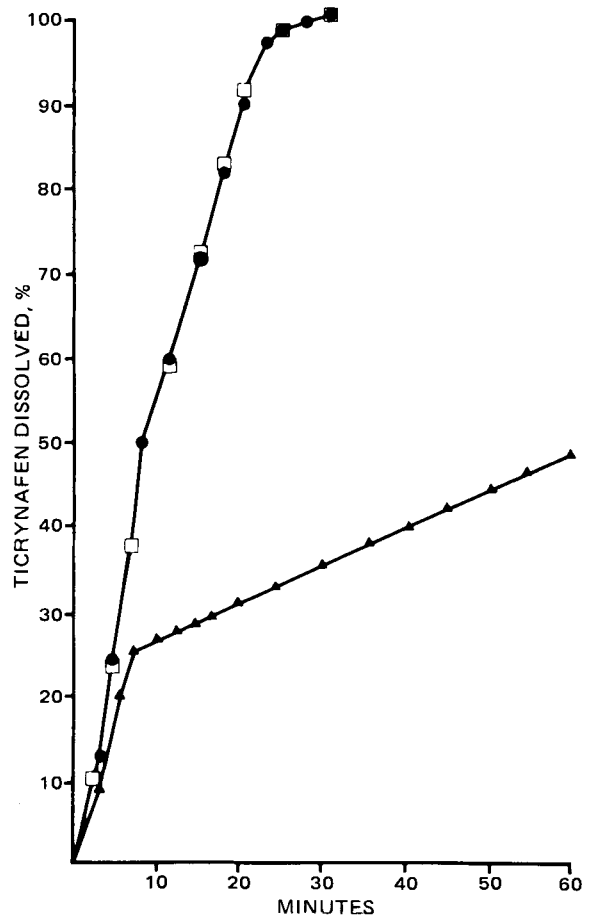

Figure 5—*Effect of the addition of potassium and sodium ions on the dissolution behavior of ticrynafen tablets (500 mg) in 0.05* M *sodium phosphate solution (●), 0.05* M *sodium phosphate solution with 20 meq potassium added after 5 min (▲), 0.05* M *sodium phosphate solution with 20 meq sodium added after 5 min (□).*

the addition of potassium to the tromethamine and sodium phosphate buffer solutions would have immediately and after 5 min on the dissolution behavior of ticrynafen. Sodium ions were also added in a separate experiment. Figures 4 and 5 show the results of these studies. The data indicate that the addition of 20 meq of potassium has a significant effect on the dissolution behavior of ticrynafen and appears to be more pronounced when the potassium ions are added immediately. The addition of 20 meq of sodium has no apparent effect.

To determine if this physicochemical phenomenon was reversible, dissolution studies were done in which 500-mg ticrynafen tablets were placed in 0.05 *M* potassium phosphate buffer. After 15 min the buffer solution was replaced carefully with 0.05 *M* tromethamine buffer solution and the dissolution test was continued for 1 hr. The results of these studies are shown in Fig. 6. It is apparent that this effect is not completely reversible. After changing the medium, dissolution did not proceed at the rate observed in tromethamine buffer. Figure 6 also includes a dissolution study in which the tablet was accidentally disturbed during the transfer of dissolution medium. This apparently created a fresh surface of drug which resulted in increased dissolution. In the case where the tablet was not disturbed the effect was less dramatic. However, in both cases the dissolution of the tablet after the exchange of media did not approach its dissolution in 0.05 *M* tromethamine buffer.

Complexation Studies—Previous reports showed that organic acids can interact with their alkali salts to form soluble and insoluble complex species (3, 4). Since the presence of potassium ions in the dissolution media had such a dramatic effect on the dissolution behavior of ticrynafen it was thought that complex formation might be responsible. Solubility studies were conducted to detect this interaction (Fig. 7). Initially, solubility increased which suggested an interaction had taken place. As more complex formed, the system became saturated with respect to the complex, and precipitated from solution. This is shown by the plateau region in Fig. 7. The pH of the system in this plateau region remained constant even with the continued addition of potassium ticrynafen solution. Since the slope of the initial solubility curve is 2, a complex having a stoichiometry of 1:1 is formed. If no complex was formed this initial slope should be 1, since the appearance of ticrynafen in solution was followed spectrophotometrically.

Samples of the complex were isolated from the saturated solution and analyzed for potassium by atomic absorption spectroscopy. A potassium content of 4.54% was found, which compares favorably with the theoretical potassium content of 4.5% calculated on the basis of a 1:1 complex.

The solubility increases at ~0.01 *M* potassium ticrynafen concentration indicating that the complex is probably soluble in an excess of the potassium ticrynafen solution. This apparently explains the dissolution behavior. During the dissolution of ticrynafen in systems containing potassium ions, a conversion of the free acid to the potassium salt takes place. Apparently, under the conditions of the study, the complex forms at 50 rpm more readily, creating an insoluble barrier which further retards dissolution. However, at 100 rpm the conditions are such that the optimum concentration for the formation of the complex is exceeded rapidly, due to the rapid dissolution of the drug at this agitation intensity.

Bioavailability Studies—Bioavailability studies were conducted to determine the effect of concomitant potassium therapy on the availability of ticrynafen from 500-mg ticrynafen tablets. A three-way cross-over study with a 1-week wash-out period between regimens was conducted in 12 normal, randomly selected adults. The following regimens were tested: (*a*) a 500-mg ticrynafen tablet, (*b*) a solution containing 500 mg of ticrynafen, (*c*) a 500-mg ticrynafen tablet with 20 meq of potassium administered simultaneously (15 ml of a 10% potassium elixir). Blood samples were collected at 0.5, 1, 2, 3, 4, 6, 8, 12, and 24 hr after the administered dose. Urine was collected for 24 hr before and 24 after dosing. Fractional urine collections after administration of the regimens were obtained at 0–4, 4–6, 8–12, and 12–24 hr. The concentration of ticrynafen in plasma and urine samples was determined by an automated high-

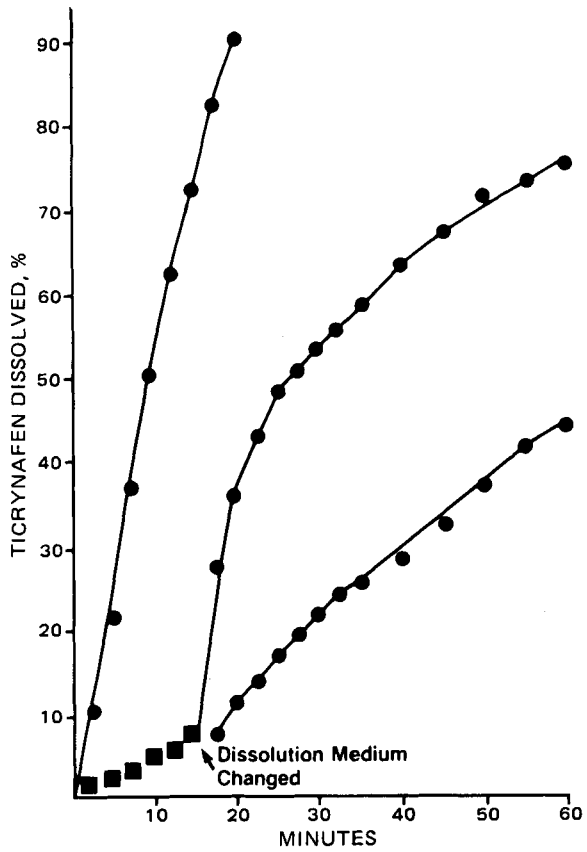

Figure 6—*Effect of media exchange on the dissolution behavior of ticrynafen tablets (500 mg) in 0.05* M *tromethamine solution (●), 0.05 M potassium phosphate solution for 15 min then replaced with 0.05* M *tromethamine solution (■).*

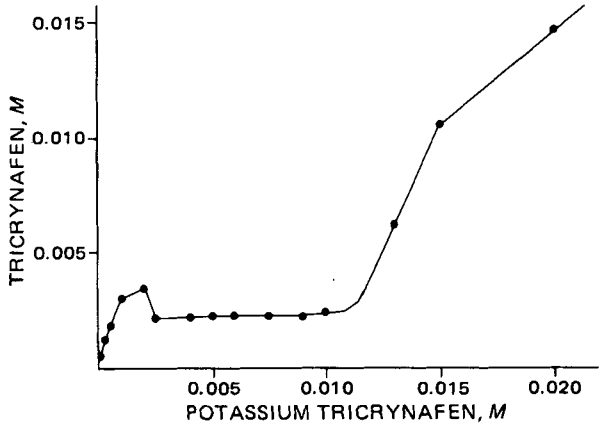

Figure 7—*Effect of potassium ticrynafen on the equilibrium solubility of ticrynafen.*

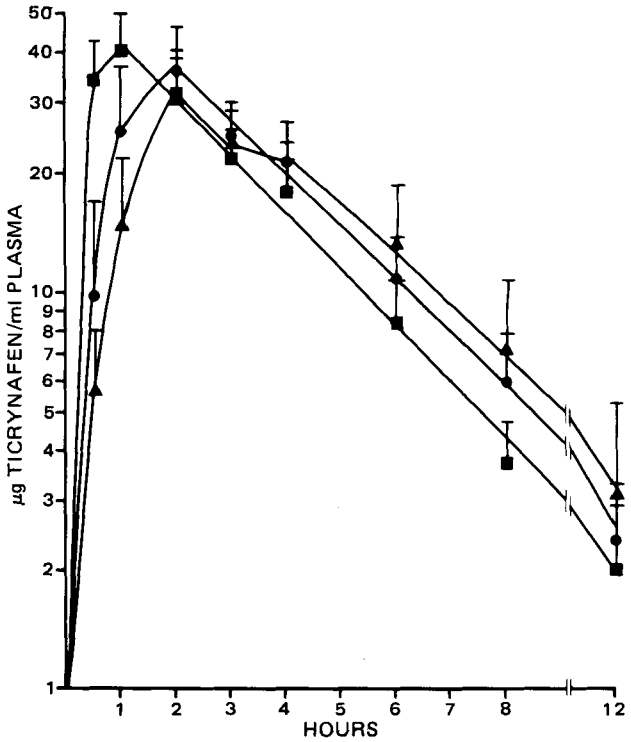

Figure 8—*Mean plasma ticrynafen levels* ± SD *after administration of 500-mg tablet (●), 500-mg solution (■), 500-mg a tablet with 20 meq potassium (▲).*

pressure liquid chromatographic procedure (5). The extraction and analysis of plasma and urine were accomplished in a completely automated fashion using an automatic HPLC system[4]. Figure 8 illustrates the blood level profiles obtained for the various dosage regimens. The area under the blood level curves and the urinary excretion were used as a measure of bioavailability (Table 1). There were no statistically significant differences between the regimen means for the area under the blood level curves or the percentage excreted in the urine when a t test was applied at the 95% confidence interval. Thus, the concomitant use of potassium supplements should not affect the bioavailability of ticrynafen in clinical use.

REFERENCES

(1) "United States Pharmacopeia," 20th rev., Mack Publishing Co., Easton, Pa., p. 959.

(2) T. Higuchi and J. L. Lach, *J. Am. Pharm. Assoc., Sci. Ed.*, **43**, 349 (1954).

(3) T. Higuchi, M. Gupta, and L. W. Busse, *ibid.*, **41**, 122 (1952).

(4) H. R. Valinoti and S. Bolton, *J. Pharm. Sci.*, **51**, 201 (1962).

(5) I. B. Snow, F. Heineman, R. W. Wittendorf, S. M. Ehrlich, Th. A. Handy, W. J. Westlake, and A. R. Maas, *Drug Metab. Rev.*, **12**, 293 (1981).

[4] Technicon (F.A.S.T.)

Metronidazole Phosphate—A Water-Soluble Prodrug for Parenteral Solutions of Metronidazole

M. J. CHO ˣ, R. R. KURTZ, C. LEWIS, S. M. MACHKOVECH, and D. J. HOUSER

Received January 12, 1981, from the *Pharmaceutical Research and Development Division, The Upjohn Company, Kalamazoo, MI 49001.* Accepted for publication July 29, 1981.

Abstract □ To develop a parenteral solution of relatively water-insoluble metronidazole (2-methyl-5-nitro-1*H*-imidazole-1-ethanol), its phosphate ester was synthesized *via* two routes. One route utilized 2-cyanoethyl phosphate and the other utilized pyrophosphoryl tetrachloride. The first method used dicyclohexylcarbodiimide as a coupling agent and the cyanoethyl group was removed under mild alkaline conditions. The second method was a one-step procedure in which free acid of metronidazole phosphate was isolated as a crystalline solid. The solubility of metronidazole in various solvents was determined at 25°. From the pH-dependence of its aqueous solubility, the pKa of the conjugate acid of metronidazole was estimated to be 2.62, which agreed well with the pKa values of other nitroimidazoles. Metronidazole phosphate behaved as a zwitterionic compound in an acidic medium with a minimum solubility at pH 2.0. At pH 7, its solubility was ~50 times that of metronidazole. The phosphate ester was so soluble at pH higher than 7 that it was difficult to measure the solubility accurately. In human serum, the hydrolysis of metronidazole phosphate followed zero-order kinetics at an initial concentration of 0.25 mg/ml or higher, presumably due to enzyme saturation (0.035 mg/ml/hr at 37°). A reversed-phase HPLC procedure was adopted to monitor the appearance of metronidazole and the disappearance of metronidazole phosphate. Subcutaneous administration of metronidazole phosphate to rats produced a blood level of bioactivity comparable to that observed after administration of metronidazole.

Keyphrases □ Metronidazole phosphate—a water-soluble prodrug for parenteral solutions of metronidazole □ Prodrugs—water-soluble, metronidazole phosphate for parenteral solutions of metronidazole □ Solubility—metronidazole phosphate, water-soluble prodrug for metronidazole

Although metronidazole is associated with some controversy regarding its carcinogenicity in rodents and mutagenicity in bacteria (1–6), it is often the drug of choice for the treatment of certain anaerobic infections, particularly *Trichomonas vaginalis* (7–21). Presently, the drug is available in the U.S. only in an oral dosage form (22). Parenteral dosage forms for a single injection are not available, presumably because of the relatively low solubility of metronidazole in water (~10 mg/ml at 25°). Sterile solutions for infusion are, however, available in other countries[1]. These preparations usually call for infusion of 100.0 ml of a 5 mg/ml solution. To overcome the solubility problem in formulating a parenteral solution, a prodrug approach was adopted in the present report. A water-soluble derivative was prepared and administered, which can be quantitatively converted to metronidazole by specific and/or nonspecific hydrolytic enzymes present in the body.

BACKGROUND

For some drugs with alcoholic functional groups, hemiesters of dicarboxylic acids are derivatives with desirable aqueous solubility and facile enzymatic cleavage in the blood. Parenteral dosage forms of hydrocortisone[2], methylprednisolone[2], and chloramphenicol[3] are all hemiester products. In the case of metronidazole, the monosuccinate ester is in the patent literature (23). One disadvantage associated with such monoesters of dicarboxylic acids is that they are not stable enough in aqueous solutions to provide a satisfactory shelflife for a parenteral solution (less than 10% decomposition within 2 years). Even without catalytic species from buffers, spontaneous hydrolysis of a simple ester prevents formulation in aqueous media. In the case of monosuccinates, hydrolysis is expected to be even faster because of the intramolecular catalysis from the remaining carboxylic acid and/or carboxylate anion (24).

The monophosphate of a drug with an alcoholic group carries two phosphoric acid functions with pKa values in the range of 2 and 6.5, and is freely soluble at physiological pH 7.4. In the past, phosphate esters have been used in preparing parenteral dosage forms of certain drug compounds (25) such as clindamycin, lincomycin, diethylstilbestrol, carboxybenzylpenicillin, hydroxysteroids, and trichloroethanol. Since these phosphate esters were found to be active *in vivo*, it was hoped that metronidazole phosphate also would be bioequivalent to or as bioavailable as the parent drug compound. The serum hydrolysis of metronidazole phosphate was studied to confirm that it regenerates metronidazole in the blood stream after intramuscular or intravenous injection within a reasonable period of time. Since phosphate esters are generally quite stable at neutral pH (26), metronidazole phosphate was expected to be stable enough to be prepared as a parenteral solution with an acceptable shelflife at an ambient temperature. The bioavailability of metronidazole from the phosphate ester prodrug was determined in rats.

EXPERIMENTAL

Solubility of Metronidazole and Metronidazole Phosphate—A large excess of metronidazole was added to a series of 7-ml vials containing 5.0 ml of various solvents. They were shaken continuously for 24 hrs in a waterbath at 25 ± 0.2°, and filtered through disposable pipets with tips that were tightly packed with glass wool. An aliquot of the filtrate was evaporated under a nitrogen stream. The residue was redissolved in water and after proper dilution the concentration was determined from the absorbance[4] at 320 nm.

The apparent aqueous solubilities of metronidazole and its monophosphate also were determined at various pH valves in a similar manner. In the latter case, the phosphate ester free acid was used; hence, at higher pH values, a downward pH drift was noted as the solubility equilibrium was attained. In such a case, the desired pH was maintained by intermittently titrating the sample with concentrated sodium hydroxide solution. In both cases, the concentration of solutes was determined by an

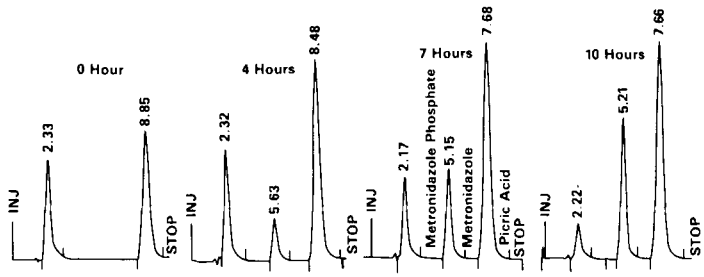

Figure 1—*Reversed-phase HPLC analysis for the serum hydrolysis of metronidazole phosphate to metronidazole at 37°. The samples were obtained after 0, 4, 7, and 10 hr of hydrolysis at an initial concentration 0.50 mg/ml. Numbers by the peaks are the retention times in minutes. Picric acid served as an internal standard.*

[1] Rhone-Poulene (SPECIA), France.
[2] Solu-Cortef and Solu-Medrol, The Upjohn Co., Kalamazoo, Mich.
[3] Chloromycetin, Parke-Davis, Morris Plains, N.J.

[4] Beckman Model DB-G Spectrophotometer.

0022-3549/82/0400-0410$01.00/0

Table I—Solubility of Metronidazole at 25°

Solvent	Solubility, mg/ml
Water	9.50
Ethanol	5.00[a]
Methanol	32.20
Acetone	20.70
Benzene	0.65
Ethyl acetate	6.50
Acetonitrile	17.20
Ether	0.99
Chloroform	4.01
Methylene chloride	4.12
Hexane	$\sim 2.5 \times 10^{-3}$
Dioxane	18.40
Tetrahydrofuran	17.70

[a] "The Merck Index," 8th ed., Merck & Co., Rahway, N.J., 1968, p. 695.

HPLC procedure. Buffers used in this series of experiments were hydrochloric acid, chloroacetate, acetate, and phosphate systems.

Synthesis of Metronidazole Phosphate (Method A)—This method essentially followed the literature procedure in which 2-cyanoethyl phosphate was used in preparing phosphate esters (27). The barium salt of 2-cyanoethyl phosphates (16.16 g, 0.05 mole) was added to a suspension of a cationic exchanger[5] (70 ml in 150 ml water), and stirred until the solution was completed. The entire suspension was poured into a column containing the same resin (50 ml), and the column was eluted with water (300 ml). The eluent plus pyridine (~30 ml) was evaporated under vacuum at 40°, and the residue was dried further by evaporation with anhydrous pyridine. Finally the residue was dissolved in 50 ml of dry pyridine.

Metronidazole (3.42 g, 0.02 mole) and the 2-cyanoethyl phosphate stock solution (40 ml, 0.04 mole) were mixed and concentrated under vacuum. After being dried completely, dicyclohexylcarbodiimide (20.6 g, 0.1 mole)[5] in pyridine (180 ml) was added, and the reaction mixture was kept in the dark at room temperature for 2 days. Water (350 ml) was added and dicyclohexylurea was filtered off 2 hr later. The filtrate was taken up into a cationic exchanger suspension[6] (60 ml), stirred for 20 min, and filtered. After concentration, the filtrate was subject to a silica gel liquid chromatographic separation[7] using methanol–water–acetic acid (100:2:1) as the mobile phase. UV absorption of the eluent was continuously monitored at 320 nm. The fraction between 1.3 and 2.0 liter was combined and concentrated to 20 ml.

The solution was then titrated with ~31 ml of 1.0 *N* KOH over 30 min

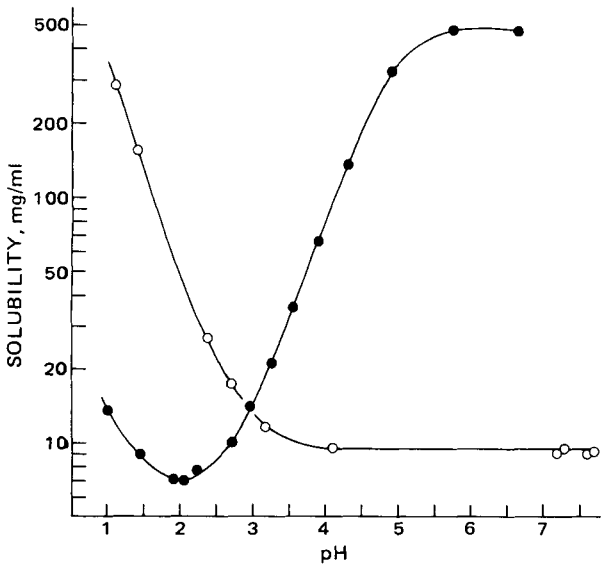

Figure 2—*The pH dependence of the apparent solubility of metronidazole (○) and metronidazole phosphate (●) at 25°. The concentration of the latter was expressed in terms of its equivalence to metronidazole.*

[5] Aldrich Chemical Co., Milwaukee, Wis.
[6] Dowex 50W, 20–50 mesh, H^+ form; Bio-Rad Laboratories, Richmond, Calif.
[7] Three Size C Silica Gel 60 prepacked columns from EM Laboratories.

Table II—pKa Values of Substituted Imidazoles[a]

Compound	pKa
Imidazole	6.953
1-C_2H_5-	7.300
1-CH_3-5-NO_2-	2.130
1-CH_3-4-NO_2-	−0.530
2-CH_3-	7.851
Metronidazole	2.62[b]

[a] From ref. 31. [b] See text.

at 45° maintaining the pH at ~10–11. After another 45 min at 45°, the solution was neutralized with 1.0 *N* HCl. After evaporation, the solid residue was triturated with methanol and filtered. The filtrate was again evaporated to the crude product, which was recrystallized twice from 95% ethanol (3.23 g; 50% yield), mp >180°; NMR (methanol-d_4): δ 7.85 (s, 1H, C-4), 4.5 and 3.9 (t, 2H each, —CH_2—CH_2— at N-1), and 2.5 (s, 3H, C-2) ppm; IR (Nujol) ν_{max}: 3200 (H_2O), 1525 (—NO_2), 1250 (phosphate), and 980 (phosphate) cm^{-1}; Karl Fischer water 6.91%.

Anal.—Calc. for $C_6H_8N_3O_6K_2P \cdot 1.35\ H_2O$: C, 20.50; H, 3.07; N, 11.95; O, 33.45; K, 22.24; P, 8.81. Found: C, 20.07; H, 3.14; N, 10.76; K, 23.04.

Synthesis of Metronidazole Phosphate (Method B)—Pyrophosphoryl tetrachloride was prepared following a literature procedure (28). Metronidazole (5 g, 0.029 mole) was dissolved in tetrahydrofuran (375 ml), stirred, and cooled to −25°. The pyrophosphoryl tetrachloride (12 ml) was then added, and the resulting mixture was stirred at −25° for 1 hr. The mixture was then poured into ice water (200 ml), stirred well, and the solvent was evaporated under vacuum. The resulting oil was triturated with acetonitrile, then seeded and stirred with 95% ethanol (200 ml) to crystallize 6.0 g of metronidazole monophosphate free acid (82% yield), mp 237–238°; IR (Nujol) C_{max}: 3130, 2620, 2300, 1140, 1070, 945, and 865; equivalent weight 125 by titration.

Anal.—Calc. for $C_6H_{10}N_3O_6P$: C, 28.69; H, 4.01; N, 16.73; P, 12.34. Found: C, 28.70; H, 4.20; N, 17.04; P, 12.04.

Metronidazole monophosphate free acid (4.35 g; 0.017 mole) was dissolved in water (40 ml) and titrated with 1.0 *N* KOH to pH 7.20. The resulting solution was freeze-dried to give 6.2 g white powder, which was recrystallized from 95% ethanol to give dipotassium salt hydrate.

Anal.—Calc. for $C_6H_8N_3O_6K_2P \cdot 4H_2O$: C, 17.98; H, 4.50; N, 10.48; P, 7.72. Found: C, 17.99; H, 4.06; N, 11.06; P, 7.88.

Serum Hydrolysis of Metronidazole Phosphate—To each of three 15-ml test tubes with a screw cap were added 0.50, 0.25, or 0.10 ml of a metronidazole phosphate stock solution in water (10.0 mg/ml) and 9.50, 9.75, or 9.90 ml human serum at 37°, respectively. The tubes were shaken immediately and kept at 37 ± 0.2°. At proper intervals, 0.50-ml aliquots were transferred to a series of 10-ml centrifuge tubes containing 2.0 ml of methanol. After being shaken thoroughly, samples were kept at −20° until analysis. Just prior to analysis, 0.05 or 0.20 ml of a picric acid stock solution in water (1.56 mg/ml) was added, mixed thoroughly, and centrifuged. The supernate was analyzed directly by HPLC. A typical res-

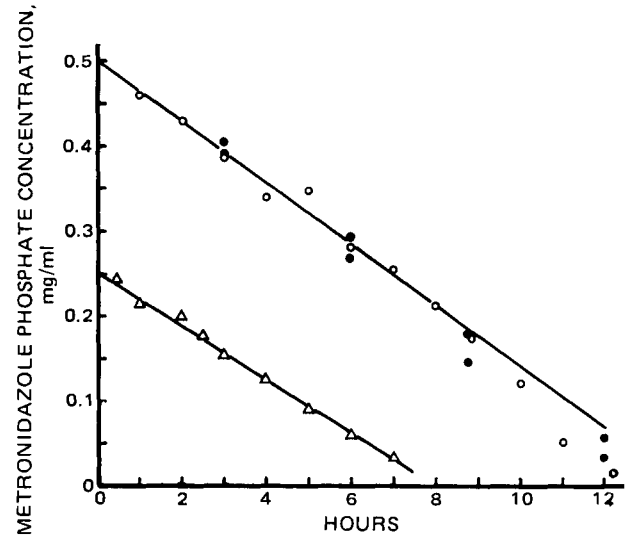

Figure 3—*Serum hydrolysis of metronidazole phosphate at 37° at two initial concentrations. Data obtained from the human serum of two volunteers are represented as open and closed symbols, respectively.*

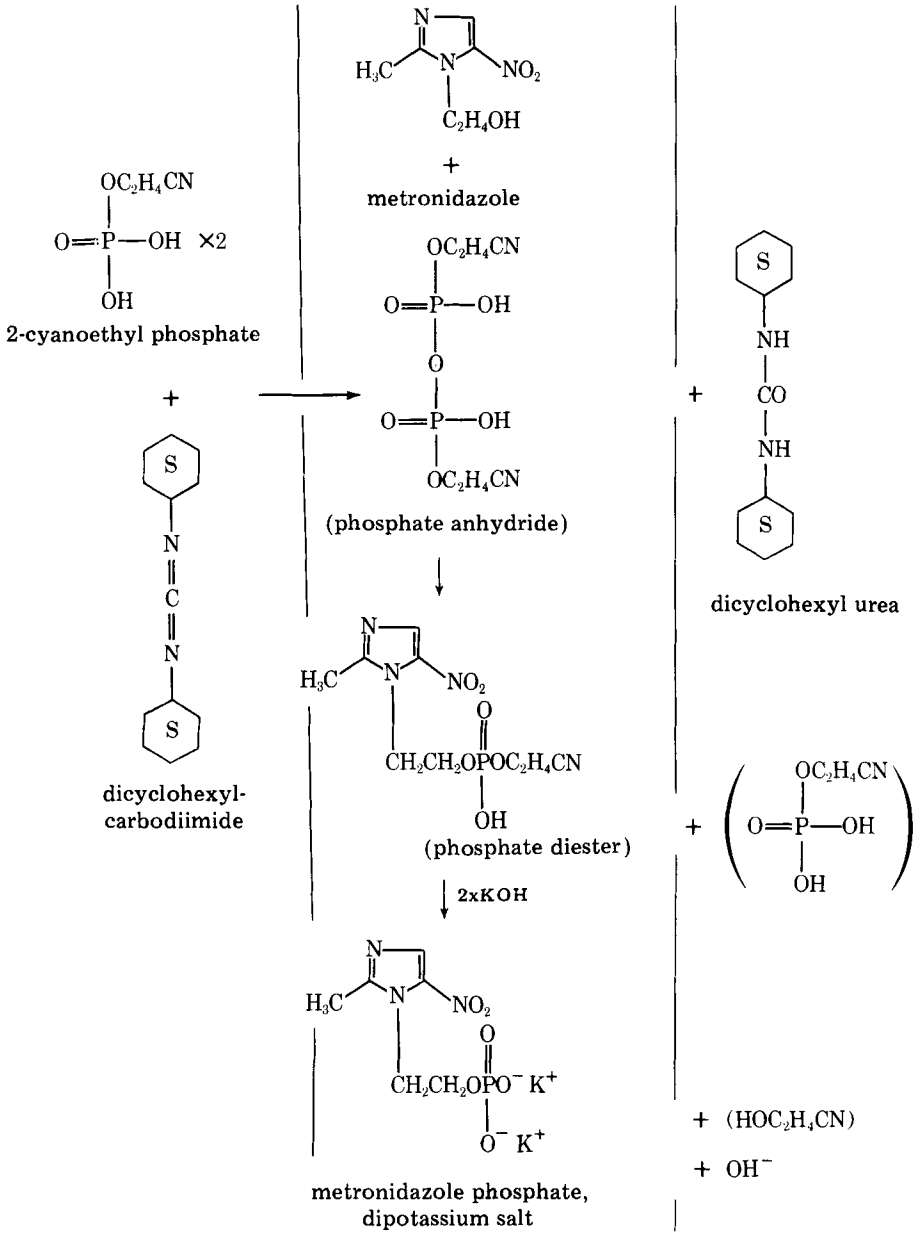

Scheme I—Synthesis of metronidazole phosphate.

olution of metronidazole phosphate and metronidazole is shown in Fig. 1. The following chromatographic conditions were used with a commercially obtained column and equipment[8]: mobile phase, 0.10 *M* phosphate buffer (pH 7.0) and methanol (90:10); pressure, 1500 psi; flow rate, 0.50 ml/min; column temperature 50°; λ, 317 nm; attenuation, 0.08–0.16 absorbance unit; sample size, 5–9 μl.

Bioavailability Studies in Rats—A single 40 mg/kg dose of metronidazole phosphate dipotassium salt was administered subcutaneously to each of three male rats weighing 190–210 g. These animals were fasted (except for water) for 24 hr prior to and during the experiments. Similarly, the parent compound, metronidazole, was administered to three rats. In both cases, the drugs were dissolved in 10% aqueous dimethylformamide.

At a given time after the drug administration, blood was withdrawn by clipping a portion of the tail. Microbiological assay disks[9] were saturated with the blood sample, placed on *C. perfringens*[10] seeded assay agar, and incubated anaerobically at 37°. The size of the inhibition zone was then measured to the nearest millimeter and the metronidazole concentration was determined from a standard curve. The area under a curve on the plot of blood concentration *versus* time was calculated by the trapezoidal rule using a digital computer.

RESULTS AND DISCUSSION

Physical Properties of Metronidazole and Metronidazole Phosphate—The solubility of metronidazole in various solvents is listed in Table I; the average of duplicate determinations is reported. In general, basic polar solvents such as tetrahydrofuran and dioxane dissolve metronidazole well, presumably through hydrogen binding. On the other hand, metronidazole phosphate was found to be freely soluble in water. Its dipotassium salt is also soluble in methanol and hot ethanol.

The pH dependence of the solubility of metronidazole at 25 ± 0.2° is shown in Fig. 2, from which the apparent pKa of metronidazole was estimated as follows: from $S = S_0[1 + K_a/(H^+)]$, in which S and S_0 are the pH dependent apparent and intrinsic solubilities, respectively, $S = 2S_0$ when $(H^+) = K_a$ (30). A value of 2.62 was obtained for the pKa of the protonated N-1. Compared with imidazole (pKa ~7), metronidazole is a much weaker base. This is because of the adjacent —NO_2 group at C-5. Table II lists the pKa values of some structurally related compounds reported in the literature (31). As expected, electron-donating alkyl groups at N-1 or C-2 position of imidazole increase the pKa value but this effect is overridden by the adjacent —NO_2 group (*e.g.*, 1-methyl-5-ni-

[8] DuPont Model 830 HPLC unit was equipped with a DuPont Model 837 spectrophotometer, a Hewlett-Packard Model 3380A integrator, and an automatic injector valve described elsewhere (29). The column used was a Zorbax ODS column from DuPont (2.1 mm i.d. × 30 cm).

[9] S&S Disc (no. 740-E), Schleicher Schuell Co., Keene, N.H.

[10] *C. perfringens* was obtained from Center for Disease Control, Atlanta, Ga. In-house identification number UC-6054.

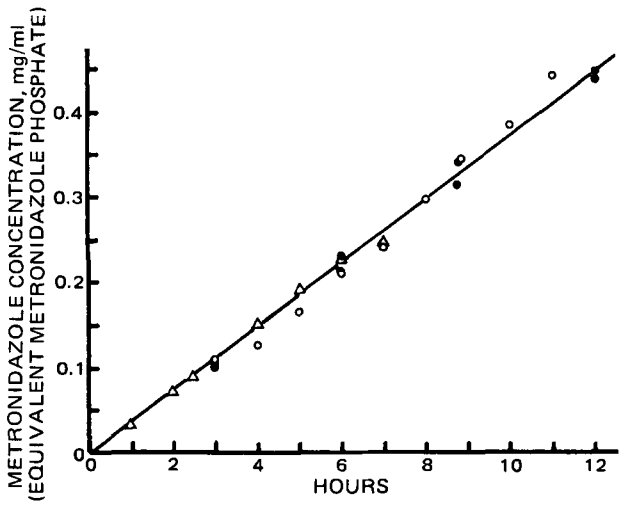

Figure 4—*Appearance of metronidazole from the serum hydrolysis of metronidazole phosphate. Symbols are the same as in Fig. 3.*

troimidazole). Interestingly, the electron-withdrawing effect through an induction effect appears less significantly than through a resonance interaction (*e.g.*, 1-methyl-4- and 5-nitroimidazole).

Since the first pKa of the two remaining phosphoric acid functions should be close to 2 and since that of protonated N-1 is in the range of 2.5, metronidazole phosphate should predominantly exist as a zwitterion at pH ~2.5. Accordingly, the apparent solubility of the prodrug shows its minimum at pH 2 (Fig. 2). Note, however, that the solubility of the prodrug exceeds 730 mg/ml, equivalent to 500 mg of metronidazole/ml, at pH 7.0, approximately 50 times the metronidazole solubility. As pH increases further, the solubility of metronidazole phosphate increases again as the second phosphoric acid undergoes ionization. Thus, it was possible to formulate the prodrug at a concentration of metronidazole desired in clinical studies, in a desired volume, at a physiologically acceptable pH.

During the measurement of the melting point of metronidazole phosphate dipotassium salts, it was noted that the compound undergoes dehydration at ~90°. This process was seen clearly when a sample suspended in silicone oil was heated. Under microscope, the formation of a distinctive water phase from the dehydration was observed as the temperature approached 90°. Thermal gravimetric analysis, differential scanning calorimetry, and Karl Fischer titration were adopted for further characterization. After dehydration, the compound decomposed at ~180°. Such thermal behavior, dehydration of nonstoichiometric amount of water, and gradual decomposition, is commonly found among other salts of phosphate esters (32).

Synthesis of Metronidazole Phosphate—Method A described earlier employed that 2-cyanoethyl phosphate route in which dicyclohexylcarbodiimide was used as a dehydrative coupling reagent (Scheme I). The procedure is well established in the area of nucleotides (27) and was

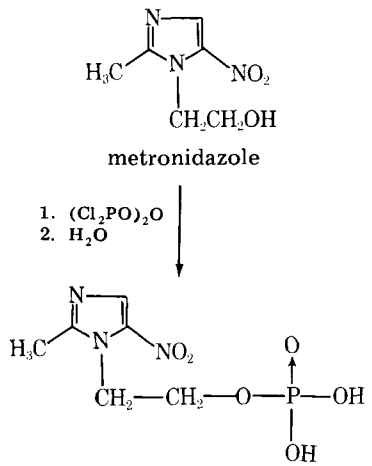

Scheme II—Synthesis of metronidazole phosphate

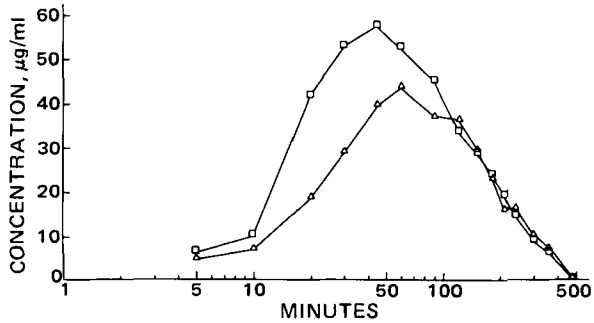

Figure 5—*Blood levels in rats following subcutaneous administration of metronidazole (□) or metronidazole phosphate (△).*

adopted in the synthesis of lincomycin phosphate (32). The procedure was adopted initially in the synthesis of metronidazole phosphate primarily for a feasibility study. Method B, on the other hand, utilizes the high reactivity of pyrophosphoryl tetrachloride (28). This procedure (Scheme II) is simpler and more convenient than Method A.

Biological Properties of Metronidazole Phosphate—The hydrolysis rate of metronidazole phosphate to metronidazole, catalyzed by a number of enzymes, was determined by monitoring the appearance of the latter and the disappearance of the former in whole human serum at 37°. Throughout kinetic experiments, the mass balance was well observed.

As shown in Fig. 3, the disappearance of metronidazole phosphate in serum at 37° follows zero-order kinetics at two initial concentrations, 0.50 and 0.25 mg/ml, with rate constants 0.036 and 0.031 mg/ml/hr (1.10 and 0.95×10^{-4} *M* hr^{-1}), respectively. For a sample with an initial concentration 0.10 mg/ml, no metronidazole phosphate was detected after 3 hr. Limited data obtained within the initial 3 hr appeared to follow first-order kinetics, but this remains to be confirmed.

Serum used for three runs of experiments and with an initial concentration of 0.50 mg/ml was obtained from the two healthy male volunteers. An identical rate constant appears to satisfy both series of data, indicating that the *total* enzyme activity towards metronidazole phosphate does not vary significantly between the two volunteers. Experiments with an initial concentration of 0.25 mg/ml produced a rate constant virtually identical to that obtained with an initial concentration of 0.50 mg/ml, leading to a conclusion that phosphatases and possibly other enzymes that cause the bioconversion are most likely saturated with the substrate at such high substrate concentration. Figure 4, where the appearance of metronidazole in three series of experiments is presented as a function of time, also produces a single zero-order rate constant, 0.037 mg/ml/hr (1.13×10^{-4} *M* hr^{-1}) for the disappearance of the phosphate. This rate constant corresponds to 0.019 mg/ml/hr (1.13×10^{-4} *M* hr^{-1}) in terms of the appearance of metronidazole. The ratio of molecular weight of metronidazole to that of the phosphate is 0.523. The average of three rate constants for the hydrolysis of the phosphate ester reported above, 0.035 mg/ml hr (1.06×10^{-4} *M* hr^{-1}), represents the maximum velocity in the apparent Michaelis–Menten kinetics (33).

As shown in Fig. 5, metronidazole phosphate produced blood levels of bioactivity in rats given 40 mg/kg subcutaneously (metronidazole equivalent) that were comparable to those produced by metronidazole when administered at the same dosage level. The maximum blood level produced by the phosphate ester was 43.3 μg/ml while that produced by metronidazole was 57.4 μg/ml, which occurred 60 and 45 min after administration, respectively. The corresponding ratio of total area under a curve was found to be 0.88:1.00. No conclusive explanation for the slightly (but significant at 95% confidence level) less area under a curve obtained from the phosphate ester than from metronidazole are given in the present report, although it is possible that the phosphate prodrug, being a highly ionic compound, may be readily eliminated intact through the kidney prior to or during the enzymatic conversion to the parent compound. In this aspect, it is interesting to note that the difference in bioavailability occurs during the initial 100 min and that the assumed elimination phase is nearly identical in both cases.

REFERENCES

(1) R. Weltman, *Med. News*, **239**, 1371 (1978).

(2) *FDA Drug Bull.*, **6**, 22 (1976).

(3) W. T. Speck, A. B. Stein, and H. S. Rosenkranz, *J. Natl. Cancer Inst.*, **56**, 283 (1976).

(4) S. C. Cowdrey, *N. Engl. J. Med.*, **293**, 454 (1975).
(5) J. R. Dykers, Jr., *ibid.*, **293**, 454 (1975).
(6) M. S. Legator, T. H. Connor, and M. Stoeckel, *Science*, **188**, 1118 (1975).
(7) H. T. Dihn, S. Kerbaum, and J. Frottier, *Lancet*, **1**, 338 (1978).
(8) H. R. Ingham, J. B. Selkon, and C. M. Roxby, *Br. Med J.*, **2**, 991 (1977).
(9) G. M. Churcher and R. P. Human, *J. Antimicrob. Chemother.*, **3**, 363 (1977).
(10) A. T. Willis, *et al.*, *Br. Med. J.*, **1**, 318 (1976).
(11) S. J. Eykyn and I. Phillips, *ibid.*, **2**, 1418 (1976).
(12) D. F. Busch, V. L. Sutter, and S. M. Finegold, *J. Infect. Dis.*, **133**, 321 (1976).
(13) J. E. Hale, R. M. Perinpanayagam, and G. Smith, *Lancet*, **2**, 70 (1976).
(14) R. L. Willson, *ibid.*, **1**, 304 (1976).
(15) S. M. Finegold, J. G. Bartlett, A. W. Chow, D. J. Flora, S. L. Gorbach, E. J. Harder, and F. P. Tally, *Ann. Intern. Med.*, **83**, 375 (1975).
(16) H. R. Ingham, G. E. Rich, J. B. Selkon, J. H. Hale, C. M. Roxby, M. J. Betty, R. W. G. Johnson, and P. R. Uldall, *J. Antimicrob. Chemother.*, **1**, 235 (1975).
(17) A. W. Chow, V. Petten, and L. B. Guze, *J. Infect. Dis.*, **131**, 182 (1975).
(18) R. Wise, J. M. Andrews, and K. A. Bedford, *J. Antimicrob. Chemother.*, **1**, 439 (1975).
(19) R. M. J. Ingo, J. A. McFadzean, and W. E. Ormerod, *Xenobiotica*, **5**, 223 (1975).
(20) R. Ursing and C. Kamme, *Lancet*, **1**, 775 (1975).
(21) W. M. McCormack, *Clin. Obstet. Gynecol.*, **18**, 57 (1975).
(22) "Physicians' Desk Reference," 31st ed., Medicon Economics Co., Oradell, N.J., 1977, pp. 1447–1448.
(23) Irish pat. 593/3 (to Rhone-Poulenc), April 14, 1963.
(24) T. Higuchi, H. Takechi, I. H. Pitman, and H. L. Fung, *J. Am. Chem. Soc.*, **93**, 539 (1971).
(25) A. A. Sinkula and S. H. Yalkowsky, *J. Pharm. Sci.*, **64**, 181 (1975).
(26) C. A. Bunton, *J. Chem. Educ.*, **45**, 21 (1968).
(27) G. M. Tener, *J. Am. Chem. Soc.*, **83**, 159 (1961).
(28) P. C. Crofts, I. M. Downie, and R. B. Heslop, *J. Chem. Soc.*, **1960**, 3673.
(29) W. F. Beyer and D. Gleason, *J. Pharm. Sci.*, **64**, 1557 (1975).
(30) A. N. Martin, "Physical Pharmacy," Lea & Febiger, Philadelphia, Pa., 1960, p. 373.
(31) D. D. Perrin, "Dissociation Constants of Organic Bases in Aqueous Solution," Butterworth, Washington, D.C., 1965.
(32) W. Morozowich, D. J. Lamb, H. A. Karnes, F. A. McKellar, C. Lewis, K. F. Stern, and E. L. Rowe, *J. Pharm. Sci.*, **58**, 1485 (1969).
(33) M. L. Bender, "Mechanisms of Homogeneous Catalysis from Proton to Proteins," Wiley-Interscience, New York, N.Y., 1971, p. 288.

ACKNOWLEDGMENTS

The authors thank Dr. Walter Morozowich for valuable discussion on the synthesis of phosphate esters in general.

Dose-Dependent Pharmacokinetics of the Antihypertensive 2,3,4,4a-Tetrahydro-1*H*-pyrazino[1,2a]quinoxalin-5-(6*H*)-one in Dogs and Rats

ROGER T. SCHILLINGS *ˣ, SOONG T. CHIANG ‡, and SAMUEL F. SISENWINE *

Received August 5, 1980, from the **Drug Metabolism Subdivision*, ‡*Biostatistics Section, Wyeth Laboratories, Inc., Radnor, PA 19087.* Accepted for publication July 22, 1981.

Abstract □ A sensitive and reproducible GLC assay was developed for determining 2,3,4,4a-tetrahydro-1*H*-pyrazino[1,2a]quinoxalin-5(6*H*)-one (I) in biological fluids, utilizing the electron-capturing capability of the heptafluorobutyryl derivative. After single 2.5- and 10-mg/kg oral and intravenous doses to three dogs, plasma concentration–time data for I were fitted to a biexponential equation and pharmacokinetic parameters were calculated. A dose-dependency for certain parameters, most notably total body clearance (Cl_T), was indicated. The difference in Cl_T for the low and high dose was statistically significant. After single 5-, 25-, and 50-mg/kg intragastric doses were given to rats, the decline in plasma concentrations of I with time followed a monoexponential equation. As with dogs, there was a disproportionate change in kinetic parameters with increasing dose for rats. While simple Michaelis–Menten kinetics were not evident, nonlinearity in biotransformation (intrinsic clearance) appeared to be the cause for the dose-dependent pharmacokinetics.

Keyphrases □ 2,3,4,4a-Tetrahydro-1*H*-pyrazino[1,2a]quinoxalin-5(6*H*)-one—dose-dependent pharmacokinetics, dogs and rats □ Antihypertensive agents — 2,3,4,4a-tetrahydro-1*H*-pyrazino[1,2a]quinoxalin-5(6*H*)-one, dose-dependent pharmacokinetics, dogs and rats □ Pharmacokinetics—dose-dependent, 2,3,4,4a-tetrahydro-1*H*-pyrazino [1,2a]quinoxalin-5(6*H*)-one, dogs and rats

The compound 2,3,4,4a-tetrahydro-1*H*-pyrazino[1,2a]-quinoxalin-5(6*H*)-one (I) is an antihypertensive agent that is effective in lowering blood pressure in hypertensive dogs, cats, and rats[1]. Its synthesis has been described previously (1).

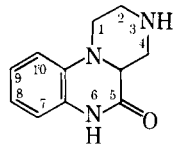

I

For metabolic disposition studies, single intravenous and oral doses of 2.5 and 10 mg/kg were given to normotensive male dogs and intragastric doses of 5, 25, and 50 mg/kg to normotensive male rats. From the resulting data, estimates of pharmacokinetic parameters were determined and the effect of dose on pharmacokinetics was investigated.

EXPERIMENTAL

The hydrochloride salt and free base of I were used and 8-fluoro-2,3,4,4a-tetrahydro-1*H*-pyrazino[1,2a]quinoxalin-5(6*H*)-one hydro-

[1] Dr. R. L. Wendt, Wyeth Laboratories Inc., Radnor, Pa., unpublished results.

0022-3549/82/0400-0414$01.00/0

(4) S. C. Cowdrey, *N. Engl. J. Med.*, **293**, 454 (1975).
(5) J. R. Dykers, Jr., *ibid.*, **293**, 454 (1975).
(6) M. S. Legator, T. H. Connor, and M. Stoeckel, *Science*, **188**, 1118 (1975).
(7) H. T. Dihn, S. Kerbaum, and J. Frottier, *Lancet*, **1**, 338 (1978).
(8) H. R. Ingham, J. B. Selkon, and C. M. Roxby, *Br. Med J.*, **2**, 991 (1977).
(9) G. M. Churcher and R. P. Human, *J. Antimicrob. Chemother.*, **3**, 363 (1977).
(10) A. T. Willis, *et al.*, *Br. Med. J.*, **1**, 318 (1976).
(11) S. J. Eykyn and I. Phillips, *ibid.*, **2**, 1418 (1976).
(12) D. F. Busch, V. L. Sutter, and S. M. Finegold, *J. Infect. Dis.*, **133**, 321 (1976).
(13) J. E. Hale, R. M. Perinpanayagam, and G. Smith, *Lancet*, **2**, 70 (1976).
(14) R. L. Willson, *ibid.*, **1**, 304 (1976).
(15) S. M. Finegold, J. G. Bartlett, A. W. Chow, D. J. Flora, S. L. Gorbach, E. J. Harder, and F. P. Tally, *Ann. Intern. Med.*, **83**, 375 (1975).
(16) H. R. Ingham, G. E. Rich, J. B. Selkon, J. H. Hale, C. M. Roxby, M. J. Betty, R. W. G. Johnson, and P. R. Uldall, *J. Antimicrob. Chemother.*, **1**, 235 (1975).
(17) A. W. Chow, V. Petten, and L. B. Guze, *J. Infect. Dis.*, **131**, 182 (1975).
(18) R. Wise, J. M. Andrews, and K. A. Bedford, *J. Antimicrob. Chemother.*, **1**, 439 (1975).
(19) R. M. J. Ingo, J. A. McFadzean, and W. E. Ormerod, *Xenobiotica*, **5**, 223 (1975).
(20) R. Ursing and C. Kamme, *Lancet*, **1**, 775 (1975).
(21) W. M. McCormack, *Clin. Obstet. Gynecol.*, **18**, 57 (1975).
(22) "Physicians' Desk Reference," 31st ed., Medicon Economics Co., Oradell, N.J., 1977, pp. 1447–1448.
(23) Irish pat. 593/3 (to Rhone-Poulenc), April 14, 1963.
(24) T. Higuchi, H. Takechi, I. H. Pitman, and H. L. Fung, *J. Am. Chem. Soc.*, **93**, 539 (1971).
(25) A. A. Sinkula and S. H. Yalkowsky, *J. Pharm. Sci.*, **64**, 181 (1975).
(26) C. A. Bunton, *J. Chem. Educ.*, **45**, 21 (1968).
(27) G. M. Tener, *J. Am. Chem. Soc.*, **83**, 159 (1961).
(28) P. C. Crofts, I. M. Downie, and R. B. Heslop, *J. Chem. Soc.*, **1960**, 3673.
(29) W. F. Beyer and D. Gleason, *J. Pharm. Sci.*, **64**, 1557 (1975).
(30) A. N. Martin, "Physical Pharmacy," Lea & Febiger, Philadelphia, Pa., 1960, p. 373.
(31) D. D. Perrin, "Dissociation Constants of Organic Bases in Aqueous Solution," Butterworth, Washington, D.C., 1965.
(32) W. Morozowich, D. J. Lamb, H. A. Karnes, F. A. McKellar, C. Lewis, K. F. Stern, and E. L. Rowe, *J. Pharm. Sci.*, **58**, 1485 (1969).
(33) M. L. Bender, "Mechanisms of Homogeneous Catalysis from Proton to Proteins," Wiley-Interscience, New York, N.Y., 1971, p. 288.

ACKNOWLEDGMENTS

The authors thank Dr. Walter Morozowich for valuable discussion on the synthesis of phosphate esters in general.

Dose-Dependent Pharmacokinetics of the Antihypertensive 2,3,4,4a-Tetrahydro-1*H*-pyrazino[1,2a]quinoxalin-5-(6*H*)-one in Dogs and Rats

ROGER T. SCHILLINGS *ˣ, SOONG T. CHIANG ‡, and SAMUEL F. SISENWINE *

Received August 5, 1980, from the **Drug Metabolism Subdivision*, ‡*Biostatistics Section, Wyeth Laboratories, Inc., Radnor, PA 19087.* Accepted for publication July 22, 1981.

Abstract □ A sensitive and reproducible GLC assay was developed for determining 2,3,4,4a-tetrahydro-1*H*-pyrazino[1,2a]quinoxalin-5(6*H*)-one (I) in biological fluids, utilizing the electron-capturing capability of the heptafluorobutyryl derivative. After single 2.5- and 10-mg/kg oral and intravenous doses to three dogs, plasma concentration–time data for I were fitted to a biexponential equation and pharmacokinetic parameters were calculated. A dose-dependency for certain parameters, most notably total body clearance (Cl_T), was indicated. The difference in Cl_T for the low and high dose was statistically significant. After single 5-, 25-, and 50-mg/kg intragastric doses were given to rats, the decline in plasma concentrations of I with time followed a monoexponential equation. As with dogs, there was a disproportionate change in kinetic parameters with increasing dose for rats. While simple Michaelis–Menten kinetics were not evident, nonlinearity in biotransformation (intrinsic clearance) appeared to be the cause for the dose-dependent pharmacokinetics.

Keyphrases □ 2,3,4,4a-Tetrahydro-1*H*-pyrazino[1,2a]quinoxalin-5(6*H*)-one—dose-dependent pharmacokinetics, dogs and rats □ Antihypertensive agents — 2,3,4,4a-tetrahydro-1*H*-pyrazino[1,2a]quinoxalin-5(6*H*)-one, dose-dependent pharmacokinetics, dogs and rats □ Pharmacokinetics—dose-dependent, 2,3,4,4a-tetrahydro-1*H*-pyrazino [1,2a]quinoxalin-5(6*H*)-one, dogs and rats

The compound 2,3,4,4a-tetrahydro-1*H*-pyrazino[1,2a]-quinoxalin-5(6*H*)-one (I) is an antihypertensive agent that is effective in lowering blood pressure in hypertensive dogs, cats, and rats[1]. Its synthesis has been described previously (1).

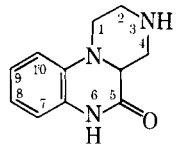

I

For metabolic disposition studies, single intravenous and oral doses of 2.5 and 10 mg/kg were given to normotensive male dogs and intragastric doses of 5, 25, and 50 mg/kg to normotensive male rats. From the resulting data, estimates of pharmacokinetic parameters were determined and the effect of dose on pharmacokinetics was investigated.

EXPERIMENTAL

The hydrochloride salt and free base of I were used and 8-fluoro-2,3,4,4a-tetrahydro-1*H*-pyrazino[1,2a]quinoxalin-5(6*H*)-one hydro-

[1] Dr. R. L. Wendt, Wyeth Laboratories Inc., Radnor, Pa., unpublished results.

0022-3549/82/0400-0414$01.00/0

chloride (II) was the internal standard in the GLC assay. Concentrations of I and II are expressed as free base. Solvents were obtained commercially[2] and were distilled in glass by the manufacturer. Methylene chloride was washed successively with 1 *N* HCl, 1 *N* NaOH, and three times with water before using. Heptafluorobutyrylimidazole[3] (III) was obtained in 1-g ampuls and was used without further purification.

Drug Administration and Sample Collection—Three normotensive, purebred, male beagle dogs (10–14 kg) were used for the study. The dogs were fasted 16 hr prior to each dosing, and feeding was resumed 6 hr after dosing. Compound I was given orally (2.5 or 10 mg/kg) in capsule form and intravenously (2.5 or 10 mg/kg) in saline. Plasma specimens from heparinized whole blood were obtained after each dose at 0.25, 0.50, 1, 2, 4, 6, 8, 12, 24, and 48 hr, and also at 0.08 hr after each intravenous dose. The animals were kept in individual metabolism cages and urine was collected at 0–4, 4–8, 8–12, 12–24, 24–36, 36–48, 48–72, and 72–96 hr after dosing. Plasma and urine were frozen until analysis. Intervals of at least 4 weeks separated each dose.

Male albino rats[4] (250–300 g) were randomly assigned to three treatment groups of 45 animals each, fasted for 16 hr, and given either 5, 25, or 50 mg/kg of I in sterile water by gastric intubation. The animals were fasted except for those to be sacrificed at 24 and 48 hr. At intervals of 0.5, 1, 2, 4, 6, 8, 12, 24, and 48 hr, five animals from each dose group were anesthetized with ether, blood was drawn from the inferior vena cava into heparinized tubes, and the plasma separated by centrifugation. Urine was collected at 0–24 and 24–48 hr after dosing from the five animals who remained in metabolism cages until sacrifice at 48 hr. Plasma and urine were frozen until analysis.

Analytical Procedures—To disposable 16- × 125-mm glass culture tubes[5] (with plastic-lined screw cap) containing a plasma sample (1.0 ml) were added 100 ng of II in 0.05 ml of water and 0.025 ml 1 *N* NH_4OH. Plasma samples less than 1 ml were adjusted to 1 ml with drug-free dog plasma, and water was added to bring the total volume to 2 ml. Ethyl acetate (5 ml) was added to each tube, the tubes were shaken for 5 min on a mechanical rocker-type shaker[6], and centrifuged for 5 min. The organic layer was transferred to another 16- × 125-mm culture tube, and the extraction of the aqueous phase was repeated with 4 ml of ethyl acetate. The combined extracts were mixed[7] with 1 ml of 0.1 *N* H_2SO_4 for 30 sec and centrifuged.

The organic layer was aspirated, and the aqueous phase was washed with 1.5 ml of methylene chloride. Methylene chloride (5 ml) and 1 *N* NH_4OH (0.3 ml) were added to the aqueous phase, and the contents were mixed for 30 sec and centrifuged. The aqueous phase was aspirated, and the organic phase was evaporated to dryness in a 37° water bath under a nitrogen stream. The residue was dissolved in 0.7 ml of toluene, and 50 μl of III was added. The contents were heated at 55° for 15 min and then washed with successive 1 ml portions of 1 *N* NH_4OH, 0.2 *N* H_2SO_4, and water. The washed toluene phase was transferred to a 12- × 75-mm test tube and stored at −20° until analysis by GLC.

A 1 μl volume was injected into the chromatograph. For each analysis, calibration standards were prepared by adding varying amounts (25–400 ng) of I in 0.05–0.1 ml of water to a series of tubes containing 1 ml of drug-free dog plasma. Internal standard, alkali, and water were added to these tubes in the same way as for the plasma samples of unknown concentration.

Aliquots of urine were diluted to 1 ml with water and processed in a manner similar to that for the plasma samples. The calibration standards contained 100–800 ng of I and 200 ng of internal standard in 0.1 ml of control urine. Additional water was added to adjust the total volume to 1 ml.

The samples containing the heptafluorobutyryl derivatives of I and II were chromatographed on a gas chromatograph[8] equipped with a nickel 63 electron-capture detector and a 122- × 0.2-cm glass column packed with 1% Silar 10CP on 100/20 mesh chromosorb W-HP[9]. The column temperature was 240°, the injection port was 250°, and the detector was 350°; the flow of carrier gas (95% argon, 5% methane) was maintained at 26 ml/min.

A calibration curve was constructed daily by plotting the ratio of peak heights for derivatized I to derivatized internal standard *versus* the concentration of the I standard. Unknown concentrations of I were determined from the calibration curve.

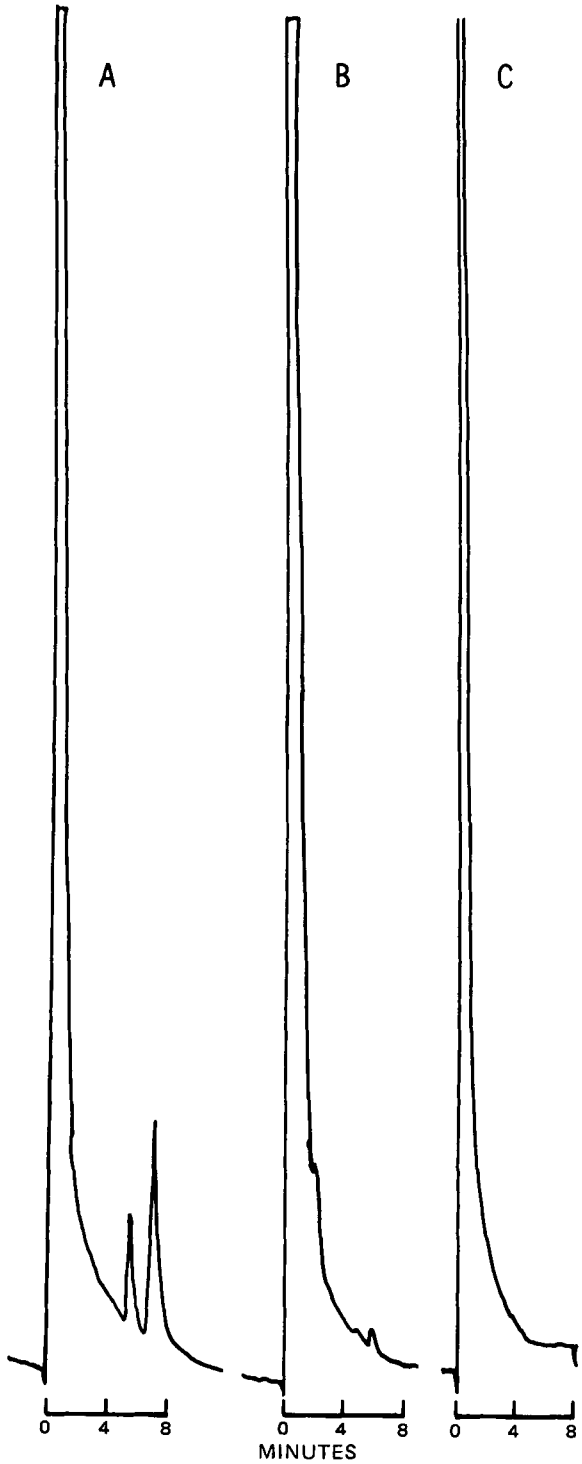

Figure 1—*Gas–liquid chromatograms. Key: A, 50 ng of I (as derivative, t_r = 5.5 min) and 100 ng of II (as derivative, t_r = 7.2 min) in dog plasma extract; B, blank dog plasma extract, 1 ml; C, blank dog urine extract (1 ml).*

Pharmacokinetic Analysis—A two-compartment model was applied to fit simultaneously the intravenous and oral plasma data from each dog at a given dose level according to the equations:

$$C_{iv} = \frac{\text{dose}}{V_c}\left(\frac{k_{21}-\alpha}{\beta-\alpha}e^{-\alpha t} + \frac{k_{21}-\beta}{\alpha-\beta}e^{-\beta t}\right) \quad \text{(Eq. 1)}$$

$$C_{po} = \frac{F\ \text{dose}\ k_a}{V_c}\left[\frac{k_{21}-k_a}{(\beta-k_a)(\alpha-k_a)}e^{-k_a t} + \frac{k_{21}-\alpha}{(k_a-\alpha)(\beta-\alpha)}e^{-\alpha t} + \frac{k_{21}-\beta}{(\alpha-\beta)(k_a-\beta)}e^{-\beta t}\right] \quad \text{(Eq. 2)}$$

[2] Burdick & Jackson Laboratories, Muskegon, Mich.
[3] Pierce Chemical Co., Rockford, Ill.
[4] Charles River CD-1, Strain COBS.
[5] Corning 99449.
[6] Buchler Instruments, Fort Lee, N.J.
[7] Vortex Genie, Scientific Industries.
[8] Model 5710A, Hewlett-Packard.
[9] Supelco, Inc.

Table I—Precision of the GLC Assay of I in Dog Plasma

Concentration of I (Free Base), ng/ml	n	Mean Ratio ± SD	CV, %[a]
	Experiment 1		
25	5	0.234 ± 0.009	4.0
50	5	0.486 ± 0.011	2.3
100	5	0.957 ± 0.010	1.1
200	5	1.916 ± 0.042	2.2
400	5	3.866 ± 0.050	1.3
	Experiment 2		
25	5	0.258 ± 0.018	7.0
50	5	0.503 ± 0.018	3.5
100	5	0.989 ± 0.041	4.1
200	5	2.097 ± 0.050	2.4
400	5	4.194 ± 0.034	0.8

[a] Coefficient of variation.

where C is the plasma concentration at time t, k_a, α, and β are the first-order absorption, distribution, and elimination rate constants, respectively, V_c is the distribution volume of the central compartment, F is the systemic availability of the oral dose, and k_{21} is the intercompartmental distribution rate constant (2).

The initial values of model parameters were estimated using the AUTOAN computer program (3). F was estimated by:

$$AUC_{po} \times \text{body weight}_{iv}/AUC_{iv} \times \text{body weight}_{po} \qquad \text{(Eq. 3)}$$

where AUC is the area under the plasma concentration–time curve between zero and infinity. Equations 1 and 2 were then applied to fit the intravenous and oral plasma data from each dog simultaneously with the aid of the NONLIN computer program (4). The statistical weighting factor in the least-squares procedure was the inverse of the observed plasma concentration and the overall goodness of fit was assessed by the coefficient of determination (r^2). Other parameters calculated were the total body clearance (Cl_T), the volume of distribution at steady state (Vd_{ss}), and after distribution equilibrium (Vd_β), the renal clearance (Cl_R), and the intercepts A and B (2). The fraction of the intravenous dose eliminated as unchanged I in urine was designated as f_{iv}.

The plasma concentration–time data from intragastrically dosed rats were fitted by a one-compartment model according to the equation:

$$C = \frac{FDk_a}{V(k_a - K)}(e^{-Kt} - e^{-k_a t}) \qquad \text{(Eq. 4)}$$

Synthesis of Heptafluorobutyramides—Compound I as free base (200 mg) in 2 ml of ethyl acetate was reacted with 0.5 ml of III at 55°. After completion of the reaction (0.5 hr), the reaction mixture was washed once with 2 ml of 0.2 N H_2SO_4, twice with 2 ml of water, and evaporated to dryness at 55° under a nitrogen stream. The residue was recrystallized from ethanol and gave 150 mg of 3-(2′,2′,3′,3′,4′,4′,4′-heptafluorobutyryl)-2,4,4a-trihydro-1H-pyrazino[1,2a]quinoxalin-5-(6H)-one (IV), mp 188°.

Anal.—Calc. for $C_{15}H_{12}N_3O_2F_7$: C, 45.12; H, 3.03; N, 10.53. Found: C, 45.23; H, 3.14; N, 10.22.

The free base of II was extracted with ethyl acetate from an alkalinized solution of the hydrochloride and then derivatized and crystallized by the described method to give 8-fluoro-3-(2′,2′,3′,3′,4′,4′,4′-heptafluorobutyryl)-2,4,4a-trihydro-1H-pyrazino[1,2 a]quinoxalin-5(6H)-one(V), mp 190°.

Anal.—Calc. for $C_{15}H_{11}N_3O_2F_8$: C, 43.18; H, 2.66; N, 10.07. Found: C, 43.13; H, 2.69; N, 10.07.

Mass Spectrometry—Samples were examined by direct introduction with the mass spectrometer[10] in the electron-impact mode. Source temperature was 150–200° and ionizing potential 70 ev.

Differential Scanning Calorimetry (DSC)—DSC curves were obtained using a differential scanning calorimeter[11]. Samples (1 mg) were heated at the rate of 10°/min in a nitrogen atmosphere.

RESULTS

Analytical—The elemental analysis of IV indicated that a monoheptafluorobutyryl derivative of I was formed. Consistent with the elemental analysis, the mass spectrum of IV exhibited a molecular ion at m/z 399 (base peak) and a major ion at m/z 202 from the loss of the acyl group (C_4F_7O). The thermogram for IV from the differential scanning calorimeter (DSC) showed a single sharp peak at the melting point (188°) of the derivative and no decomposition up to 260°. The DSC curve confirmed the purity of the product and demonstrated the stability of the derivative at the GLC operating conditions.

The retention times (t_r) of IV and V were 5.5 and 7.2 min, respectively. A representative chromatogram from an analysis of 50 ng of I and 100 ng of II in 1 ml of dog plasma is illustrated in Fig. 1A. Chromatograms of blank dog plasma and urine (1 ml each) carried through the GLC assay are shown in Figs. 1B and 1C, respectively. No metabolites of I interfered with the chromatographic detection of IV and V. To determine reproducibility, the mean ratio of the peak heights of IV to V (n = 5) and its coefficient of variation (CV) at concentrations ranging from 25 to 400 ng/ml were determined during two analyses on separate days (Table I). The peak height ratio varied with a CV <7%. The mean ratio was linearly related to I concentration with a correlation coefficient of 0.999 between these two analyses. The recoveries of the drug at each concentration varied from 37 to 39% (CV = 2–13%). A minimum of 12 ng/ml could be quantified using a 2-ml plasma sample.

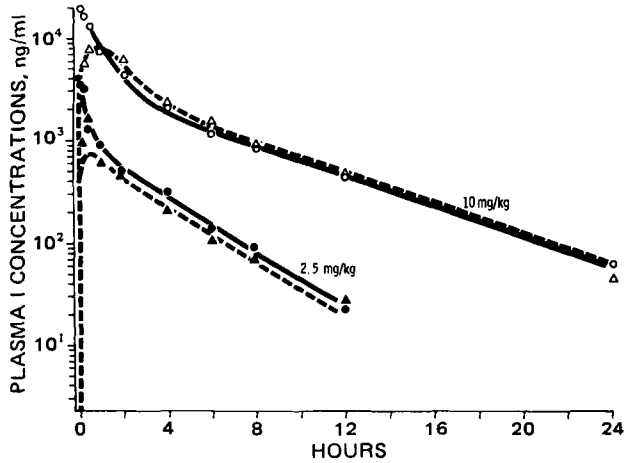

Figure 2—*Mean concentrations of I in the plasma of dogs given intravenous (○) and oral (△) doses of 2.5 and 10 mg/kg.*

Pharmacokinetics of I in Dogs—Concentrations of I in dog plasma after 2.5 and 10 mg/kg iv and oral doses are illustrated in Fig. 2 and the derived pharmacokinetic parameters are listed in Table II. The decline in plasma concentrations followed the biexponential equation for a two-compartment model. After oral administration, observed peak plasma concentrations and standard deviations (C_{max}) were 1667 ± 651 and 7710 ± 6858 ng/ml for the 2.5- and 10-mg/kg doses, respectively, and occurred at 0.5 hr for each dose.

The mean drug recoveries in urine and their standard deviations after

Table II—Pharmacokinetic Parameters of I in Dogs following Single Intravenous and Oral Doses[a]

Parameter	Dose: 2.5 mg/kg, Mean ± SD	Dose: 10 mg/kg, Mean ± SD	Statistical Difference[b], $t(p)$
A, μg/ml	3.44 ± 0.91	19.5 ± 2.4	1.74[c] (NS)
B, μg/ml	0.65 ± 0.98	3.57 ± 0.56	2.81[c] (NS)
Cl_T, ml/min/kg	9.3 ± 0.70	4.70 ± 0.33	8.01 (<0.05)
β, hr^{-1}	0.24 ± 0.03	0.17 ± 0.01	3.35 (NS)
Vd_β, liters/kg	2.3 ± 0.2	1.70 ± 0.1	7.54 (<0.05)
AUC_{iv}, hr ng/ml	4514 ± 331	35620 ± 2584	7.9[c] (<0.05)
AUC_{po}, hr ng/ml	3075 ± 323	33678 ± 6327	5.02[c] (<0.05)
F	0.73 ± 0.05	0.95 ± 0.16	2.42 (NS)
k_{21}, hr^{-1}	0.58 ± 0.19	0.36 ± 0.05	1.92 (NS)
$t_{1/2\beta}$, hr	2.9 ± 0.40	4.10 ± 0.20	3.14 (NS)
k_a, hr^{-1}	3.0 ± 0.80	1.94 ± 2.05	1.57 (NS)
α, hr^{-1}	2.4 ± 1.0	1.36 ± 0.04	1.67 (NS)
$t_{1/2\alpha}$, hr	0.33 ± 0.13	0.51 ± 0.02	1.73 (NS)
V_c, liters/kg	0.61 ± 0.19	0.44 ± 0.04	1.34 (NS)
Vd_{ss}, liters/kg	1.6 ± 0.2	1.08 ± 0.06	3.67 (NS)
Cl_R, ml/min/kg	0.46 ± 0.02	0.62 ± 0.10	1.87 (NS)
f_{iv}, fraction of dose	0.05 ± 0.003	0.13 ± 0.04	3.22 (NS)

[a] The overall goodness of fit of measured plasma data to the generated curves (Fig. 2) was r^2 = 0.93. [b] Paired t test; degrees of freedom = 2. [c] For statistical analysis, these parameters were normalized by dose.

[10] AEI-MS902 equipped with a Data General Nova 3 computer and DS-50s software.

[11] Model 2, Perkin-Elmer Corp.

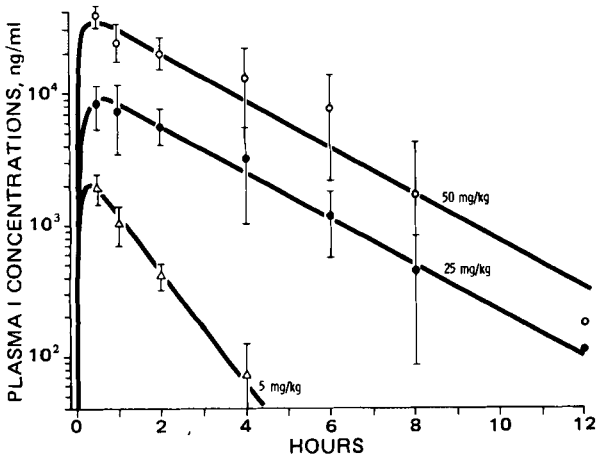

Figure 3—*Mean concentrations of I (±SD) in the plasma of rats given intragastric doses of 5 mg/kg (△), 25 mg/kg (○), and 50 mg/kg (●).*

the 2.5-mg/kg iv and oral doses were 5.0 ± 0.3 and 1.8 ± 0.8 % of the administered dose, respectively. After the 10-mg/kg iv and oral doses 13.4 ± 4.4 and 5.4 ± 0.5% of the administered doses were recovered, respectively.

Pharmacokinetics of I in Rats—Concentrations of I in rat plasma after intragastric administration of 5, 25, and 50 mg/kg are shown in Fig. 3; the estimated pharmacokinetic parameters are listed in Table III. The decline in plasma concentrations after 5, 25, and 50 mg/kg was apparently monoexponential. In the order of increasing dose, the observed peak plasma concentrations ($C_{max} \pm SD$) were 1966 ± 529, 8609 ± 3176, and 38,999 ± 5896 ng/ml and occurred at 0.5 hr for each dose. The mean drug recoveries in urine after the 5, 25, and 50 mg/kg doses were 1.3 ± 0.4, 4.0 ± 2.0, and 6.9 ± 3.7% of the administered dose, respectively.

DISCUSSION

The described GLC assay is highly sensitive and reproducible. The minimum quantifiable concentration was 25 ng/ml for a 1-ml specimen, while a minimum of 12 ng/ml could be quantified in plasma using 2-ml samples.

In dogs, I was quickly absorbed with a Vd_{ss} (1.6 liter/kg) which is 2–3 times larger than the reported total body water of the dog [0.5–0.8 liter/kg (5)]. The calculated availability (F) was high (73% for a 2.5-mg/kg dose and 95% for a 10-mg/kg dose) and increased with increasing dose (Table II). The compound was eliminated rapidly from plasma and was excreted to a small extent into urine, but appears to be eliminated mainly by metabolism. The elimination half-lives in the rat (Table III) were less than those calculated for the dog (Table II), and similar plasma levels of the compound in rats and dogs were observed only when rats received higher doses. This species difference in disposition may account for a longer duration of the compound's hypotensive effect in the dog.[1]

Although linear pharmacokinetic models were used to fit the plasma data for both dogs and rats, the disproportionate increases in AUC with increasing dose indicate that dose-dependent kinetics are in effect. For example, total body clearance in dogs is almost reduced by one-half at the higher dose. However, the elimination of I from plasma does not appear to follow simple Michaelis–Menten kinetics since the elimination is slower after the higher doses than the lower doses in the same concentration range. This pattern suggests product inhibition as pointed out by Perrier *et al.* (6). Thus, the model employed to fit the data yields dose-average pharmacokinetic parameters at each dosage level which may not be operative as a function of specific plasma concentrations. Although the differences in β, $t_{1/2\beta}$, and F at the two doses were below statistical significance (Table II) these differences were assumed to be connected with the statistically significant change in Cl_T. The lack of visible nonlinearity and Michaelis–Menten characteristics precluded fitting the data with a specific nonlinear function. However, the NONLIN-fitted least-square value of Cl_T agreed well with the time-average value obtained from the quotient Dose/AUC_{iv}.

The factor responsible for the nonlinear disposition of I can be assessed further by considering first-pass concepts (7). If complete availability from the dosage form is assumed, then the apparent intrinsic clearance of I can be estimated as:

$$Cl'_{int} = \frac{(1 - f_{iv})_{Dose}}{AUC_{po}} \qquad \text{(Eq. 5)}$$

Table III—Pharmacokinetic Parameters of I in Rats following Single Intragastric Doses

Parameter	Dose, mg/kg 5	25	50
C_{max}, μg/ml	2.0	8.6	39.0
t_{max}, hr	0.5	0.5	0.5
K, hr^{-1}	0.97	0.41	0.41
$t_{1/2}$, hr	0.72	1.7	1.7
V/F, liters/kg	2.0	2.1	1.1
AUC, hr μg/ml	2.6	29.3	116
Cl_T/F, ml/min/kg	32	14	7
Cl_R, ml/min/kg	0.43	0.56	0.49

Table IV—Comparison of Apparent Intrinsic Clearance (Cl'_{int}) and Systemic Availability (F) of I after Oral and Intravenous Doses in Dogs

Dose, mg/kg	Oral Cl'_{int}, ml/min/kg	Oral F^a	Intravenous Cl'_{int}, ml/min/kg	Intravenous F^a
2.5	13.0 ± 1.4	0.76 ± 0.02	11.3 ± 1.1	0.78 ± 0.02
10.0	4.4 ± 1.2	0.90 ± 0.02	4.5 ± 0.6	0.90 ± 0.01

[a] Calculated from Cl'_{int} and Q_H as discussed in text.

where f_{iv} is the fraction of the intravenous dose excreted as unchanged I. Protein binding was not measured so these equations do not yield the true $Cl_{int} = V_{max}/K_m$. The intravenous doses give the body clearance (Cl_T):

$$Cl_T(1 - f_{iv}) = \frac{Q_H\, Cl'_{int}}{Q_H + Cl'_{int}} \qquad \text{(Eq. 6)}$$

where Q_H is hepatic blood flow.

Equation 6 can be rearranged to:

$$Cl'_{int} = \frac{Cl_T(1 - f_{iv})Q_H}{Q_H - Cl_T(1 - f_{iv})}$$

Table IV shows calculated values of Cl'_{int} obtained by both methods. Hepatic blood flow in the dog was assumed to be 40 ml/min/kg (8). The good agreement and diminishment with dose indicates that nonlinearity in I disposition is probably due to a dose-dependent decrease in biotransformation rate. The Cl'_{int} values can be used to estimate values of F, as shown in Table IV, since:

$$F = \frac{Q_H}{Q_H + Cl'_{int}} \qquad \text{(Eq. 7)}$$

The larger F with increasing dose is consistent with the nonlinear Cl'_{int}. The significant decrease in Vd_β with increasing dose could result from changes in elimination (9).

REFERENCES

(1) M. E. Freed and J. R. Potoski, U.S. pat. 4, 089, 958 (1978).

(2) M. Gibaldi and D. Perrier, "Pharmacokinetics," Dekker, New York, N.Y., 1975.

(3) A. J. Sedman and J. G. Wagner, "AUTOAN-A Decision-Making Pharmacokinetic Computer Program," Publication Distribution Service, Ann Arbor, Mich., 1974.

(4) C. M. Metzler, G. K. Elfring, and A. J. McEwen, *Biometrics*, **30**, 562 (1974). Abstract.

(5) P. L. Altman and D. S. Dittmar, "Biological Handbook," Federation of American Societies for Experimental Biology, Washington, D.C., 1974, p. 1989.

(6) D. Perrier, J. J. Ashley, and G. Levy, *J. Pharmacokinet. Biopharm.*, **1**, 231 (1973).

(7) G. R. Wilkinson and D. G. Shand, *Clin. Pharmacol. Ther.*, **18**, 377 (1975).

(8) P. L. Altman and D. S. Dittmar, "Biological Handbook," Federation of American Societies for Experimental Biology, Washington, D.C., 1974, p. 1704.

(9) W. J. Jusko and M. Gibaldi, *J. Pharm. Sci.*, **61**, 1270 (1972).

ACKNOWLEDGMENTS

The authors thank Mr. M. Wassermann for the GLC analyses, Mr. L. Sivieri for the DSC curves, Dr. John Sellstedt for the mass spectra, Dr. William J. Jusko for helpful discussions on the pharmacokinetics, and Mr. Frazer Hadley for reviewing the manuscript. The hydrochloride salts of I and II were obtained from Dr. M. Freed. The free base of I was obtained from Dr. C. Robinson.

Phenethylamine Inhibitors of Partially Purified Rat and Human Pancreatic Lipase

KAREN COMAI ˣ and ANN C. SULLIVAN

Received March 18, 1981, from the *Department of Pharmacology, Hoffmann–La Roche, Nutley, NJ 07110.* Accepted for publication July 23, 1981

Abstract □ Methodology for the preparation of rat and human pancreatic lipase (EC 3.1.1.3) is described, which resulted in good yield of partially purified, stable enzyme useful for kinetic studies. Apparent K_m values for the rat (6.5 m*M*) and human (3.5 m*M*) enzyme were determined with triolein as the substrate. Several compounds of the phenethylamine class were found to be inhibitors of both rat and human pancreatic lipase. The structural feature in the phenethylamine series tested, which appeared to be necessary for lipase inhibition, was a halogenated substituent on the 3 or 4 position of the aromatic ring as in flutiorex, fenfluramine, *N*-benzyl-β-methoxy-3-(trifluoromethyl)phenethylamine (I), chlorphentermine and *p*-chloroamphetamine. A chloro group at the 2 position was ineffective (chlortermine). Alterations in the ethylamine portion of the molecule did not cause significant changes in the inhibitory properties of the active phenethylamines.

Keyphrases □ Phenethylamines—inhibition of pancreatic lipase, rats and humans □ Kinetics—competitive inhibition of pancreatic lipase, rats and humans □ Pancreatic lipase—inhibition by phenethylamines, rats and humans

The anorectic effect of many compounds of the phenethylamine class has been recognized for almost 40 years (1). In addition to anorexia, some phenethylamines show marked effects on lipid metabolism. Amphetamine and fenfluramine have been shown to decrease the postprandial rise in plasma triglycerides in corn oil loaded rats (2–4) and in humans (5), and to elevate plasma free fatty acid concentration (5, 6). Fenfluramine also was reported to inhibit hepatic lipogenesis (2), reduce intestinal motility (4), and interfere with postabsorptive reesterification by inhibiting rat intestinal palmitolyl CoA monolein transferase activity (7). Furthermore, fenfluramine and an analog, benfluorex, were reported to inhibit pancreatic lipase (2, 8, 9). Although these activities were postulated previously (4, 10) to explain (in part) weight reduction by fenfluramine through decreased dietary triglyceride absorption, a study in healthy humans revealed that fenfluramine did not alter fat absorption (11).

In addition to phenethylamines, several chemically unrelated compounds which inhibit the release of free fatty acids from adipose tissue reportedly interfere with postprandial lipemia (12, 13). Barboriak, *et al.* (12) demonstrated that 3,5-dimethylpyrazole, salicylic acid, and nicotinic acid inhibit plasma triglyceride rise in rats given corn oil. In these studies, reduced fat absorption was observed in animals receiving salicylic acid. Another report (13) demonstrated the antilipolytic activity of two α-blockers, phentolamine and phenoxybenzamine. These studies were furthered by examination of inhibitory effect of phentolamine and phenoxybenzamine on rat epididymal fat and pancreatic lipases (14). The epididymal fat lipase appeared to be inhibited by both α-blockers; pancreatic lipase was inhibited by phenoxybenzamine but stimulated by phentolamine.

The present study reports the effectiveness of various phenethylamines and other antilipolytic agents as inhibitors of rat and human pancreatic lipase. A systematic *in vitro* evaluation of representative compounds was initiated using freshly prepared, partially purified preparations of rat and human pancreatic lipase. The results were compared with those obtained with diethyl-*p*-nitrophenyl phosphate, a known active site inhibitor of hog pancreatic lipase (15).

MATERIALS AND METHODS

Pancreatic Lipase Preparations—Rat pancreatic proteins were prepared by adaptation of a method described for the guinea pig pancreas (16). In a representative experiment, six female Sprague-Dawley rats[1], weighing 180–220 g were fed a 20% corn oil diet *ad libitum* for 8 to 10 weeks. This diet was shown to increase pancreatic lipase levels ~50% (17, 18). Prior to sacrifice the rats were fasted for 24 hr to accumulate zymogen granules in the acinar cells of the pancrease (19). The pancrease was removed quickly after sacrifice and immersed in oxygenated Krebs-Ringer bicarbonate. The pancreatic lobules were prepared as described previously (16). Eight lobules corresponding to ~50 mg wet weight per flask were incubated for 4 hr in 5 ml of the oxygenated Krebs-Ringer bicarbonate containing carbachol (10^{-5} *M*), soybean trypsin inhibitor (10 μg/ml), benzamidine (10 m*M*), and phenylmethylsulfonyl fluoride (5 m*M*). After incubation the flask contents were centrifuged at 100,000×*g* for 30 min. The resulting juice was frozen immediately in liquid nitrogen and stored at −70°.

Human pancreatic juice was obtained from a patient with acute pancreatitis whose pancreatic duct had been cannulated. Benzamidine (8.2 m*M*) and soybean trypsin inhibitor (0.5 mg/ml) were added to the collection vessels to deter enzymatic degradation of the lipase. The juice was stored at −70°.

Rat and human pancreatic juices were purified by gel filtration chromatography[2] (2.5 × 100 cm) using 0.05 *M* tromethamine[3] buffer, pH 8 at 25°. Protein profiles were monitored at 280 nm[4]. Active fractions were combined, concentrated[5], and stored in 1-ml aliquots at −70°. These preparations remained fully active for over 6 months and were the source of enzymes for all experiments.

Pancreatic Lipase Assays—Two methods were utilized for the pancreatic lipase assay. The first was developed for use in screening large numbers of compounds and was based on the method of Krauss *et al.* (20). Glycerol tri[1-^{14}C]oleate (32 m*M*) was emulsified in 0.2 *M* tromethamine, pH 8 at 36° containing 0.15 *M* NaCl, bovine serum albumin (15 mg/ml, fatty acid free), and sodium taurocholate (1.4 m*M*) by sonication for three 1-min intervals at 80 watts[6]. The final assay volume was 1.0 ml. The reaction was initiated by the addition of enzyme and was allowed to proceed for 10 min. Under these conditions the reaction was linear for up to 20 min. The liberated free fatty acids were extracted and quantitated in a liquid scintillation counter[7]. The second method used was the titrimetric assay described by Maylie *et al.* (15). An olive oil–sodium taurocholate (1.4 m*M*) emulsion stabilized in 2% gum arabic was the substrate. The molecular weight of triolein (885 g) was used to calculate the substrate concentration. The final assay volume was 3.0 ml. The reaction was initiated by the addition of enzyme. The long-chain fatty acids released at 25° (pH 8) were continuously titrated with the aid of a recording pH-stat[8]. The lipase activity was determined directly from the slope of the linear portion of the curve.

[1] Charles River Breeding Laboratories, Wilmington, Mass.
[2] Sephadex G-200, Pharmacia, Piscataway, N.J.
[3] Trizma, Sigma Chemical Co., St. Louis, Mo.
[4] Uvicord II, LKB, Sweden.
[5] PM10 filter, Amicon Corp., Lexington, Mass.
[6] Labsonic 9100, Labline Instruments, Melrose Park, Ill.
[7] Packard model 3380, Downers Grove, Ill.
[8] Radiometer, Copenhagen, Denmark.

0022-3549/82/0400-0418$01.00/0

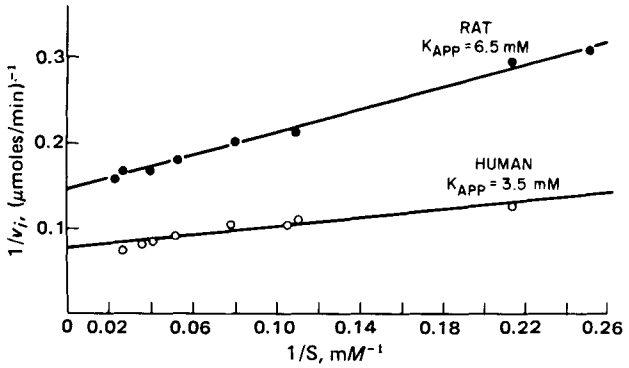

Figure 1—*Lineweaver–Burke plot of rat and human G-200 lipase activity. Assays were run using the described pH-stat method. Key: ●, rat G-200 lipase (protein concentration, 8.6 μg/ml); and ○, human G-200 lipase (protein concentration, 9.2 μg/ml).*

Inhibitors were added to the assays as solutions in either 90% ethanol or water, pH 8; 90% ethanol had no effect on pancreatic lipase activity assayed by either method.

Protein determinations were performed using the Lowry method (21).

Materials—Glycerol tri[1-^{14}C]oleate[9] was used without further purification. Sodium taurocholate, norepinephrine, epinephrine, phenylephrine, bovine serum albumin (fatty acid free), dopamine, phenethylamine, phenylpropanolamine, *l*-ephedrine, *d*-ephedrine, tyramine, and diisopropylfluorophosphate were purchased commercially[10]. Hydroxyamphetamine, amphetamine, phenoxybenzamine and *N*-benzyl-β-methoxy-3-(trifluoromethyl)phenethylamine (I) were used as received[11]. Diethylpropion[12], protokylol[12], metaraminol[13], nordefrin[13], tuaminoheptane[14], cyclopentamine[14], methoxyphenamine[15], clortermine[16], phentermine[17], nylidrin[18], metaproterenol[19], benzphetamine[20], phenmetrazine[21], phentolamine[21], chlorphentermine[22], fenfluramine[23], flutiorex[24], *p*-chloroamphetamine[25], and diethyl-*p*-nitrophenylphosphate[26] were used without further purification.

RESULTS

Characterization of Pancreatic Lipase Activities—Gel filtration of rat and human pancreatic juices by chromatography resulted in partial purification of both enzymes. The enzyme activities emerged 2.2 void volumes for rat lipase and 2.0 void volumes for human lipase resulting in a twofold purification of rat lipase and a sevenfold purification of human lipase.

Molecular weights were determined on the chromatographic column by comparing the elution of the lipases to standard proteins. The rat lipase appeared to have a molecular weight near 37,000; the human lipase molecular weight was ~48,000 (22).

The kinetics of the lipolytic reactions of the two lipase preparations were analyzed using the Michaelis–Menten formula as has been done for hog lipase (23) and phospholipases (24–26). The effects of varying substrate concentration on the initial velocity are shown in Fig. 1. Apparent K_m values obtained for rat and human G-200 lipase were of the order of 6.5 m*M* and 3.5 m*M*, respectively. It is not known whether the similar apparent K_m values are due to enzyme similarities or the physical characteristics of the emulsion assay system.

To determine whether the G-200 preparations contained colipase, purified hog colipase was incubated for 10 min at 37° with both the rat and human G-200 preparations at a ratio of 2 moles pure colipase to 1 mole of enzyme. The enzymic activities were assessed from initial velocity measurements using the pH-stat assay. As seen in Figs. 2A and 2B, there was no enhancement of either rat or human lipase activity after addition of exogenous colipase, indicating the G-200 lipase preparations were saturated with colipase. However, the additional colipase provided some protection of enzymic activity at high taurocholate concentrations (5–14 m*M*).

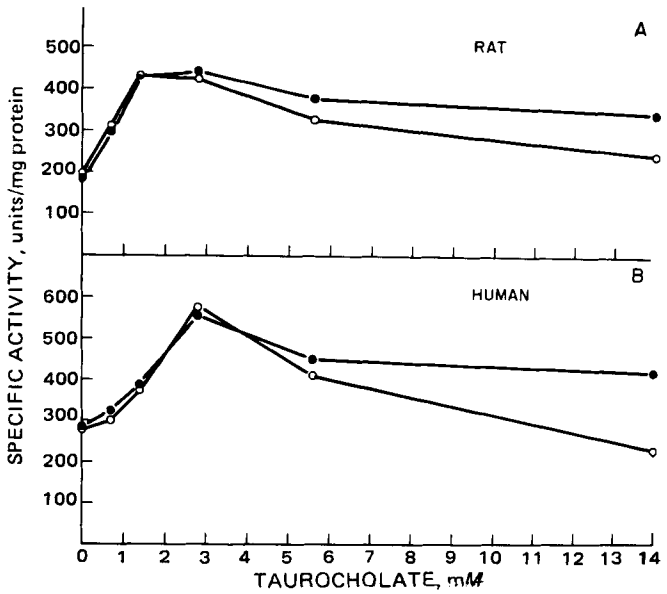

Figure 2—*Effect of added colipase on rat and human G-200 lipase. Two moles of pure colipase per mole of lipase were incubated with lipase for 10 min at 37°. An aliquot of the incubated enzyme–colipase mixture was added to the assay medium and the initial velocity recorded using the pH-stat assay. Key: ○, minus colipase; and ●, added colipase. (A), rat G-200 lipase; and (B), human G-200 lipase.*

Inhibition of Rat G-200 Pancreatic Lipase—Many phenethylamines with central nervous system effects were inactive as inhibitors of pancreatic lipase. Table I shows the results of a structure–activity profile of the phenethylamine series evaluated in the carbon 14 and pH-stat titrimetric assays. All compounds were tested either to 20 m*M* or 100% inhibition. The catecholamines were either ineffective or slightly stimulatory toward rat pancreatic lipase. Interestingly, the five compounds in this series, which exhibited good inhibition, were the compounds related to amphetamine but with halogenated substituents on the 3 or 4 position of the aromatic ring. Inhibition constants summarized in Table I, as determined by a graphical method (27), were calculated for the five active phenethylamines from initial velocity data recorded during the titrimetric assay at 6 and 28 m*M* substrate concentrations. The lines were determined from linear regression analyses of the initial velocity data points which appeared to lie along a straight line. Cooperative and competitive inhibitory phenomena were observed for flutiorex, fenfluramine, and chlorphentermine. Using this method chlorphentermine, flutiorex, fenfluramine, *p*-chloroamphetamine, and I gave K_i values of 1.9, 3.0, 3.3, 6.2, and 11 m*M*, respectively. Analysis of the carbon 14 assay data resulted in K_i values of 9.6 m*M* for chlorphentermine, 6 m*M* for *p*-chloroamphetamine, 3.5 m*M* for flutiorex, 9.0 m*M* for fenfluramine, and 11 m*M* for I (Table I). Variation in the initial velocity was observed at the low substrate concentrations (6 m*M* triolein). However, this was <10% variation in the resulting K_i values. Interestingly, chlortermine, a phenylamine having a chlorine in the 2 position of the benzene ring, was not an inhibitor of rat pancreatic lipase, whereas the 4-chloro derivatives were inhibitors.

Two α-blockers were examined as inhibitors of rat G-200 pancreatic lipase and compared with diethyl-*p*-nitrophenylphosphate. The data were obtained and analyzed in the same manner as was done for the phenethylamines. The results are given in Table II. Phenoxybenzamine, which appeared to be a very strong inhibitor in the carbon 14 screen (0.9 m*M*), was a much weaker inhibitor when evaluated in the titrimetric assay (10 m*M*). This discrepancy was due to the fact that phenoxybenzamine delayed the initial velocity reaction for up to 6 min. However, after the initial lag time the enzymatic reaction proceeded and required relatively high phenoxybenzamine concentrations for inhibition.

Phentolamine was inhibitory in both the carbon 14 and titrimetric

[9] Amersham, Arlington Heights, Ill.
[10] Sigma Chemical Co., St. Louis, Mo.
[11] Smith, Kline & French, Philadelphia, Pa.
[12] Merrell-National Laboratories, Cincinnati, Ohio.
[13] Winthrop Laboratories, New York, N.Y.
[14] Eli Lilly, Indianapolis, Ind.
[15] Ganes Chemical Works, Carlstadt, N.J.
[16] USV Pharmaceuticals, Tuckahoe, N.Y.
[17] Beecham-Messengil Pharmaceuticals, Bristol, Tenn.
[18] Millmaster Chemicals, New York, N.Y.
[19] Boehringer-Ingelheim, Ltd., Elmsford, N.Y.
[20] Upjohn, Kalamazoo, Mich.
[21] Geigy Pharmaceuticals, Ardsley, N.Y.
[22] Warner-Lambert, Morris Plains, N.J.
[23] A. H. Robins, Richmond, Va.
[24] Synthelabo, France.
[25] Leo Pharmaceuticals, Denmark.
[26] Aldrich, Milwaukee, Wis.

Table I—Chemical Structures of Phenethylamines and Inhibitory Properties on Rat Pancreatic Lipase

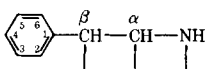

					Pancreatic Lipase Activity	
					^{14}C Assay	Titrimetric Assay
					K_i (mM)	
Flutiorex	3-SCF_3	H	CH_3	C_2H_5	3.5	3.0
Fenfluramine	3-CF_3	H	CH_3	C_2H_5	9.0	3.3
N-Benzyl-β-methoxy-3-(trifluoromethyl)phenethylamine	3-CF_3	OCH_3	H	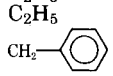	11.0	11.0
Chlorphentermine	4-Cl	H	*a*	H	9.6	1.9
p-Chloroamphetamine	4-Cl	H	CH_3	H	6.0	6.2
					Carbon 14 Assay (10 mM)	
					% of Control	
Phenethylamine		H	H	H	100	
Amphetamine		H	CH_3	H	96	
Methamphetamine		H	CH_3	CH_3	85	
Benzphetamine		H	CH_3	*b*	100	
Phentermine		H	*a*	H	100	
Phenylpropanolamine		OH	CH_3	H	100	
d-Ephedrine		OH	CH_3	CH_3	119	
l-Ephedrine		OH	CH_3	CH_3	112	
Diethylpropion		O	CH_3	$(C_2H_5)_2$	109	
Phenmetrazine		*c*			100	
Methoxyphenamine	2-OCH_3	H	CH_3	CH_3	90	
Clortermine	2-Cl	H	*a*	H	91	
Phenylephrine	3-OH	OH	H	CH_3	90	
Metaraminol	3-OH	OH	CH_3	H	111	
Tyramine	4-OH	H	H	H	117	
Hydroxyamphetamine	4-OH	H	CH_3	H	85	
Nylidrin	4-OH	OH	CH_3	*d*	126	
Isoxsuprine	4-OH	OH	CH_3	*e*	88	
Dopamine	3-OH, 4-OH	H	H	H	80	
Norepinephrine	3-OH,4-OH	OH	H	H	111	
Epinephrine	3-OH,4-OH	OH	H	CH_3	113	
Nordefrin	3-OH,4-OH	OH	CH_3	H	106	
Isoproterenol	3-OH,4-OH	OH	H	$CH(CH_3)_2$	106	
Protokylol	3-OH,4-OH	OH	H	*f*	100	
Metaproterenol	3-OH,5-OH	OH	H	$CH(CH_3)_2$	100	
Cyclopentamine	*g*	H	CH_3	CH_3	84	
Tuaminoheptane	$CH_3(CH_2)_3$	H	CH_3	H	104	

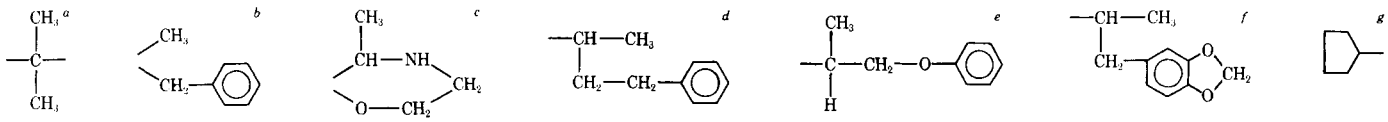

assay. Inhibition constants of 5.8 mM for the former assay and 1.6 mM for the titrimetric assay were determined from Dixon plots (27). Diethyl-p-nitrophenylphosphate, an active site inhibitor of hog lipase (15), gave comparable K_i values for rat G-200 lipase in both the carbon 14 assay (0.1 mM) and the titrimetric assay (0.1 mM). Diisopropylfluorophosphate, an inhibitor of enzymes having an essential serine residue in the active site, produced no inhibition of rat G-200 lipase at 20 mM. This agrees with data obtained with hog lipase (15).

Inhibition of Human G-200 Pancreatic Lipase—The active inhibitors of rat G-200 pancreatic lipase were tested as inhibitors of human G-200 pancreatic lipase using the pH-stat titrimetric assay. Except for minor variations, the inhibitors of rat G-200 lipase were also effective as inhibitors of human G-200 lipase (Table III).

Diethyl-p-nitrophenylphosphate was the most effective inhibitor of both rat and human G-200 lipase giving identical inhibition constants of 0.1 mM. p-Chloroamphetamine was a stronger inhibitor of human G-200 lipase with an inhibition constant of 3.5 mM compared with rat G-200 lipase, 6.2 mM. The other active compounds gave inhibition constants for human G-200 lipase that were comparable or identical to the inhibition constants obtained for rat G-200 lipase.

DISCUSSION

Based on the reported specific activities for purified rat lipase and purified human lipase (28–30), the present preparations of rat and human G-200 lipases were 47 and 65% pure, respectively. A molecular weight of 37,000 was calculated for the rat lipase and agreed with the reported value of 36,000 (28). The human lipase had a calculated molecular weight of 48,000, slightly higher than the reported values of 45,000 (30) and 46,000 (29).

The fact that gel filtration did not appear to separate lipase from colipase was a major advantage of the present preparations. The presence of sufficient colipase for maximum activity with rat or human lipase was demonstrated in the experiments where high taurocholate concentrations (14 mM) did not inhibit significantly and added colipase did not stimulate significantly (Fig. 2).

The reversal of bile salt inhibition of lipase by colipase is most notable using the nonphysiological bile salt, taurodeoxycholate (28, 31, 32) and the nonphysiological substrate, tributyrin (23, 28). With a more physiological substrate (33), taurocholate at concentrations of 1–3 mM stimulated lipase hydrolysis of olive oil whether or not exogeneous colipase was added (Fig. 2). In the absence of exogeneous colipase, taurocholate at concentrations >6 mM produced similar decreases in rat and human lipase activity in agreement with previous results (34). Exogenous colipase protected the activity from this mild inhibition.

The results from conventional kinetic analysis were valuable despite difficulties due to the complex nature of the enzyme systems. The apparent K_m values calculated for rat (6.5 mM) and human (3.5 mM) lipases (Fig. 1) were on the same order as reported by Maylie, *et al.* for hog lipase using olive oil as substrate (23). In that communication, the reported K_m values were 2 mM in the presence and 3.5 mM in the absence of colipase, with 1.6 and 0.4 mM taurodeoxycholate, respectively. These K_m values do not represent the affinity between lipase and triglyceride as would be interpreted in aqueous systems. However, as suggested in another report (35) the K_m values do reflect the affinity of the enzyme molecule for the emulsion interface and could be considered the enzyme–interface dissociation constant, thereby lending a physical concept to the value.

The evaluation of compounds as inhibitors of lipase was validated by the agreement between the two lipase assays. The single-time point carbon 14 assay was valuable since a large number of compounds could be evaluated quickly. However, it did not have the ability to distinguish compounds which delayed the initial velocity from the true enzyme inhibitors. The pH-stat assay, which recorded initial velocities, could distinguish easily between the two types of compounds. Phenoxybenzamine was an inhibitor that caused a long delay in the initial velocity of rat G-200 lipase. Previous studies which indicated that phenoxybenzamine was a potent inhibitor of pancreatic lipase (1 mM resulting in 80% inhibition),

Table II—Inhibition Constants of Non-Phenethylamine Inhibitors of Rat Pancreatic Lipase

Compound	Pancreatic Lipase: Assay Carbon 14 K_i (mM)	Pancreatic Lipase: Titrimetric Assay K_i (mM)
Diethyl-*p*-nitrophenylphosphate	0.1	0.2
Phenoxybenzamine	0.9	10.2
Phentolamine	5.8	1.6
Diisopropylfluorophosphate	No inhibition at 20 mM	

Table III—Comparison of Inhibition Constants of Inhibitors of Rat and Human Pancreatic Lipase

Compound	Pancreatic Lipase: Rat K_i (mM)	Pancreatic Lipase: Human K_i (mM)
Diethyl-*p*-nitrophenylphosphate	0.1	0.1
Phentolamine	1.6	1.1
Chlorphentermine	1.9	2.1
Flutiorex	3.1	2.6
Fenfluramine	3.3	3.8
p-Chloroamphetamine	6.2	3.5
Phenoxybenzamine	10.0	8.9
N-Benzyl-β-methoxy-3-(trifluoromethyl)phenethylamine	11.0	12.0

utilized a single-time point assay and eliminated bile salt from the assay medium (36). Either condition might be responsible for the discrepancy between the present results and those published previously. Because of the complexity of the lipase system, phenoxybenzamine and the other inhibitors may interfere with an organization step in the enzyme–colipase–substrate–bile salt complex, thereby causing the lag time and/or inhibition of the initial velocity. A disruption of the lipase–colipase interaction by fenfluramine has been reported recently (37).

The utility of classical kinetics in studying the competitive inhibitors of lipase was evident in the use of the Dixon plot and resulting K_i values for ranking the efficacy of lipase inhibitors. Cooperative and competitive inhibitory properties were observed for fenfluramine, flutiorex, chlorophentermine, and phentolamine at concentrations >10 mM. A halogenated substituent on the 3 or 4 position of the aromatic ring (flutiorex, fenfluramine, I, chlorphentermine, *p*-chloroamphetamine) appeared to be necessary for lipase inhibition in the phenethylamine series tested (Table I). A chloro group at the 2 position was ineffective (chlortermine). Alterations in the ethylamine portion of the molecule did not cause significant changes in the inhibitory properties of the active phenethylamines. These data confirm the inhibitory effect of fenfluramine on pancreatic lipase (2, 8) and extended the observation to include a structure–activity profile of a number of phenethylamines.

REFERENCES

(1) M. F. Lesses and A. Myerson, *N. Engl. J. Med.*, **218**, 119 (1938).

(2) K. Comai and A. C. Sullivan, *Biochem. Pharmacol.*, **27**, 1987 (1978).

(3) S. Garattini, M. E. Hess, M. T. Tocconi, E. Veneroni, and A. Bizzi, in Advances in Experimental Medicine and Biology," W. L. Holmes, R. Paoletti, and D. Kritchevsky, Eds., Plenum, New York, N.Y., 1972, p. 103.

(4) A. Bizzi, E. Veneroni, and S. Garattini, *Eur. J. Pharmacol.*, **23**, 131 (1973).

(5) G. L. D. Pawn, in "Amphetamines and Related Compounds," E. Costa and S. Garattini, Eds., Raven, New York, N.Y., 1970, p. 641.

(6) J. Duhault and M. Boulanger, *Rev. Fr. Etudes Clin. Biol.*, **X**, 215 (1965).

(7) W. N. Dannenburg, B. C. Kardian, and L. Y. Norrell, *Arch. Int. Pharmacodyn. Ther.*, **201**, 115 (1973).

(8) W. N. Dannenburg and J. W. Ward, *ibid.*, **191**, 58 (1971).

(9) J.-J. Bernier, *Nouv. Presse Med.* **29**, 971 (1975).

(10) S. Garattini, *S. Afr. Med. J., Suppl.*, **45**, 21 (1971).

(11) E. Evans, P. D. Samuel, D. S. Miller, and W. L. Burland, Postgrad. *Med. J., Suppl. 1*, **51**, 115 (1975).

(12) J. J. Barboriak, R. C. Meade, J. Owenby, and R. A. Stiglitz, *Arch. Int. Pharmacodyn. Ther.*, **176**, 249 (1968).

(13) E. Wertheimer, M. Hamosh, and E. Shafrir, *Am. J. Clin. Nutr.*, **8**, 705 (1960).

(14) S. Ramachandran, Y. K. Yip, and S. R. Wagle, *Eur. J. Biochem.*, **12**, 201 (1970).

(15) M. F. Maylie, M. Charles, and P. Desnuelle, *Biochim. Biophys. Acta*, **276**, 162 (1972).

(16) G. A. Scheele and G. E. Palade, *J. Biol. Chem.*, **250**, 2660 (1975).

(17) L. I. Gidez, *J. Lipid Res.*, **14**, 169 (1973).

(18) A. Bucko and Z. Kopec, *Nutr. Dieta*, **10**, 276 (1968).

(19) J. P. Reboud, A. Benabdeljilil, and P. Desnuelle, *Biochim. Biophys. Acta*, **58**, 326 (1962).

(20) R. M. Krauss, H. G. Windmueller, R. I. Levy, and D. S. Fredrikson, *J. Lipid Res.*, **14**, 286 (1973).

(21) O. H. Lowry, N. J. Rosebrough, A. L. Farr, and R. J. Randall, *J. Biol. Chem.*, **193**, 265 (1951).

(22) K. Weber and M. Osborn, *J. Biol. Chem.*, **244**, 4406 (1969).

(23) M. F. Maylie, M. Charles, M. Astier, and P. Desnuelle, *Biochem. Biophys. Res. Commun.*, **52**, 291 (1973).

(24) J. A. Blain, J. D. E. Patterson, C. D. Shaw, and M. Waheed Akhtar, *Lipids*, **11**, 553 (1976).

(25) J. Scandella and A. Kornberg, *Biochemistry*, **10**, 4447 (1971).

(26) D. A. White, D. J. Pounder, and J. N. Hawthorne, *Biochim. Biophys. Acta*, **242**, 99 (1971).

(27) M. Dixon and E. C. Webb, in "Enzymes," Academic, New York, N.Y., 1964, p. 329.

(28) B. Borgstrom and C. Erlanson, *Eur. J. Biochem.*, **37**, 60 (1973).

(29) A. Vandermeers, M. C. Vandermeers-Piret, J. Rathe, and J. Cristophe, *Biochim. Biophys. Acta*, **370**, 257 (1974).

(30) E. Forssell, *Ann. Acad. Sci. Fenn. [Medica]*, **166**, 1 (1974).

(31) "Hawks' Physiological Chemistry," B. L. Oser, Ed., McGraw-Hill, New York, N.Y. 1965, p. 491.

(32) B. Borgstrom and C. Erlanson, *Biochim. Biophys. Acta*, **242**, 509 (1971).

(33) P. Desnuelle and P. Savary, *J. Lipid Res.*, **4**, 369 (1963).

(34) R. G. H. Morgan and N. E. Hoffman, *Biochim. Biophys. Acta*, **248**, 143 (1971).

(35) H. Brockerhoff and R. G. Jensen, in "Lipolytic Enzymes," Academic, New York, N.Y., 1974, p. 15.

(36) K. Santhanam, Y. K. Yip, S. Ramachandran, D. O. Allen, and S. R. Wagle, *Life Sci.*, **10**, 437 (1971).

(37) B. Borgstrom and C. Wollesen, *FEBS Lett.*, **126**, 25 (1981).

ACKNOWLEDGMENTS

The authors are grateful to Dr. George Nardi of Massachusetts General Hospital for the generous gift of human pancreatic juice. Purified hog lipase and colipase were gifts of Dr. M.-F. Maylie-Pfenninger. The authors thank Mrs. SueAnn Grossman for her secretarial assistance in the preparation of this manuscript.

Effects of Phenobarbital on the Distribution Pharmacokinetics and Biological Half-Lives of Model Nonmicrosomal Enzyme Metabolizable Sulfonamides in Rats

JANARDAN B. NAGWEKAR ˣ **and SUBHAS KUNDU** *

Received August 6, 1980, from the *Pharmaceutics Division, College of Pharmacy and Allied Health Professions, Wayne State University, Detroit, MI 48202.* Accepted for publication July 6, 1981. * Present address: Syntex Labs, Inc., Palo Alto, CA 94304.

Abstract □ The pharmacokinetics of sulfisoxazole and sulfanilamide were studied in control rats and in rats treated for 5 days with a daily 100 mg/kg ip dose of phenobarbital. These drugs represent the organic anionic and nonionized drugs, respectively, whose nonmicrosomal enzymatic metabolisms were unstimulated by phenobarbital. Sulfisoxazole showed the characteristics of a two-compartment open model. However, its biological half-life and the apparent distribution volume of the central compartment were significantly lower and the intercompartmental transport rate constants and the urinary excretion rate constant were significantly greater, in phenobarbital treated rats than in control rats. The apparent steady-state distribution volume of sulfisoxazole was smaller in the phenobarbital treated rats at the 90% confidence level. Sulfanilamide showed characteristics of a one-compartment model in both the control and phenobarbital treated rats, but none of the pharmacokinetic parameters of the compound in the phenobarbital treated rats were significantly different from those in the control rats.

Keyphrases □ Phenobarbital—effect on pharmacokinetics of sulfisoxazole and sulfanilamide □ Pharmacokinetics—effect of phenobarbital on sulfisoxazole and sulfanilamide □ Sulfisoxazole—effect of phenobarbital on pharmacokinetics □ Sulfanilamide—effect of phenobarbital on pharmacokinetics □ Sulfonamides—effect of phenobarbital on the pharmacokinetics of sulfisoxazole and sulfanilamide

In a previous paper (1), it was reported that phenobarbital treatment in rats caused a decrease in the apparent distribution volumes of nonmetabolizable model organic anions which gave the body characteristics of multicompartment open models. Regardless of the model followed by the body (one-compartment or multicompartment model), the half-lives of these compounds were shorter in phenobarbital treated rats than in control rats.

BACKGROUND

It is recognized that all drugs do not possess the ideal properties described for the organic anions previously reported (1). Drugs usually are subject to metabolism and binding to plasma proteins and remain in the blood in the ionized and/or nonionized forms. Therefore, the influences of phenobarbital treatment on the distribution volumes of organic anionic drugs which are metabolized and bound to plasma proteins were investigated. However, as an extension of previous work (1), the effect of phenobarbital treatment on the apparent distribution volumes and biological half-lives of drugs, which are metabolized and bound to plasma proteins but whose metabolism and extent of protein binding will not be affected by the microsomal enzymes induced by phenobarbital, were studied. The organic anionic drug chosen was sulfisoxazole (pKa 5.1) and the nonionized drug chosen was sulfanilamide (pKa 10.1). Sulfisoxazole and sulfanilamide are metabolized mainly by acetylation by the nonmicrosomal enzymes (2), which apparently are not induced by phenobarbital treatment. Both the drugs and their metabolites are excreted by the kidney, thereby avoiding the possible influence of increased biliary flow brought about by phenobarbital treatment (3). The protein binding of sulfisoxazole is not affected by phenobarbital treatment (4). Furthermore, while sulfisoxazole is involved in renal tubular secretion, sulfanilamide is excreted in the urine due to glomerular filtration (5).

It was stated previously (1) that the apparent distribution volumes of organic anions, which give the body the characteristics of a multicompartment open model, are likely to be lower in phenobarbital treated rats than in control rats, possibly due to reduction in the aqueous pore size of tissue cell membranes brought about by phenobarbital. It was also postulated that, if the biological half-lives of compounds are shortened in treated rats due to the stimulatory effect of phenobarbital on the renal tubular secretion mechanism (1), then such effects would be expected only for compounds involved in renal tubular secretion and not those excreted in the urine due to glomerular filtration. Therefore, the apparent distribution volume(s) and biological half-life of sulfisoxazole should be reduced in the phenobarbital treated rats but not those of sulfanilamide.

EXPERIMENTAL

Materials—Sulfanilamide[1] (mp 166°), sulfisoxazole[2] (mp 198°), and phenobarbital sodium[1] were USP grade. The other chemical agents used were analytical reagent grade.

Methodology—Male Sprague-Dawley rats weighing between 175 and 210 g (most weighed ~200 g) were used in the study.

Overall urinary excretion studies of the sulfonamides were conducted to determine the effect of phenobarbital treatment on the extent of their metabolism and to select the phenobarbital pretreatment regimen. For the urinary excretion studies of sulfanilamide, 20, 50, and 100-mg/kg ip doses were tried; a given dose was administered to each rat daily for 5–10 consecutive days. The intraperitoneal doses of phenobarbital were dissolved in 5 ml of normal saline. Each control rat was treated with 5 ml normal saline for similar periods of time as the phenobarbital treated rats. Twenty-four hours after the last treatment dose of phenobarbital or normal saline, each rat received a 10-mg iv dose of sulfanilamide *via* the tail vein. The intravenous solution of sulfanilamide (2 ml) was prepared by dissolving 10 mg of the drug in water for injection, adjusting the pH of the solution to 7.4 with sodium hydroxide, and rendering the solution isotonic with sodium chloride. Food was withheld from the rats for 12–14 hr prior to the intravenous administration of the drug and during the study. The rats were anesthetized with ether for ~2 min when the drug was administered. After administering the drug, rats are transferred to urine collection cages described previously (6). Urine samples were carefully collected over the periods of 0–8 and 8–35 hr. These urine samples were analyzed for intact sulfanilamide and its metabolites. The phenobarbital treatment schedule selected was a daily 100-mg/kg ip dose for 5 consecutive days.

Overall urinary excretion studies were also conducted for sulfisoxazole in control rats and rats treated with a daily dose of 100 mg/kg of phenobarbital for 5 consecutive days. The 2 ml of pH 7.4, isotonic solution containing 7 mg of sulfisoxazole was injected intravenously *via* the tail vein to each rat 24 hr after the last dose of phenobarbital or normal saline. Urine samples were collected over a period of 0–10 and 10–52 hr and analyzed for intact sulfisoxazole and its metabolites.

In the sulfanilamide pharmacokinetic study, three sets of studies were carried out on three different days. The first two sets of studies involved six control rats and six phenobarbital treated rats, and the third set involved only 6 phenobarbital treated rats. The third study was carried out to reinforce the finding of the first two sets of studies. In each set, only one blood sample was obtained from a given rat following decapitation at the predetermined time after intravenous administration of sulfanilamide. Blood samples were collected at 0.25, 0.5, 1, 2, 3, and 4 hr from both control and phenobarbital treated rats. The procedure of obtaining one

[1] Merck and Co., Inc., Rahway, N.J.
[2] National Biochemical Corp., Cleveland, Ohio.

0022-3549/82/0400-0422$01.00/0

Table I—Amounts of Intact Sulfanilamide and Its Metabolite(s) Recovered in the Urine in 35 hr Following Intravenous Administration of a 10-mg Dose of Sulfanilamide to Control Rats and Phenobarbital Treated Rats

	Phenobarbital Dose, mg/kg/day	Phenobarbital Treatment, days	Intact, mg	Metabolite(s), mg[a]
		Control		
1	—	—	3.62	6.38
2	—	—	3.61	6.06
3	—	—	3.15	6.01
4	—	—	3.10	6.61
5	—	—	2.92	6.33
6	—	—	3.15	6.38
7	—	—	2.96	6.84
8	—	—	3.08	6.93
9	—	—	2.80	7.00
Mean ± *SD*			3.16 ± 0.28	6.50 ± 0.36
		Phenobarbital Treated		
1	20.0	5	3.40	6.38
2	20.0	5	3.22	6.78
3	20.0	10	3.21	6.69
4	20.0	10	3.29	6.45
5	20.0	10	3.18	6.17
6	50.0	5	2.91	6.33
7	50.0	5	2.71	6.29
8	100.0	5	2.69	6.01
9	100.0	5	2.74	5.96
10	100.0	5	2.85	6.27
11	100.0	5	3.00	5.57
12	100.0	5	2.85	7.05
13	100.0	5	2.84	6.97
Mean[b] ± *SD*			2.82 ± 0.11[c]	6.30 ± 0.59[c]

[a] Expressed as the equivalent amount of sulfanilamide. [b] Mean based on data obtained in rats pretreated with 100 mg/kg/day of phenobarbital for 5 consecutive days. [c] Not significantly different from the corresponding values of the control.

blood sample per rat was described previously for other compounds (1).

In the sulfisoxazole pharmacokinetic study, two sets of studies were carried out on two different days, each set involving 12 control and 12 phenobarbital treated rats. In each set, only one blood sample was obtained from a given rat after decapitation at the predetermined time after the intravenous administration of sulfisoxazole. Blood samples were collected at 0.083, 0.166, 0.25, 0.5, 0.75, 1, 2, 3, 4, 5, 6, and 8 hr from both control and phenobarbital treated rats.

The reason multiple concentration values of a sulfonamide were obtained at a given time period was to further ascertain the assumption of the regression model: each concentration variate corresponding to the given value of time is a sample from a population of independently and normally distributed variates and that the samples along the regression line have a common variance (7).

After decapitation the blood sample from a rat was collected in a 30-ml beaker coated with 0.2 ml (40 U) of heparin to prevent coagulation. Blood samples were analyzed for the intact and total (intact plus metabolites) sulfonamide on the same day they were collected.

Assay of Sulfanilamide and Sulfisoxazole—A general method used for the analysis of a sulfonamide, first developed by Bratton and Marshall (8), was to quantitate intact sulfanilamide or sulfisoxazole and the total (intact plus metabolites) sulfanilamide or sulfisoxazole present in the urine or blood samples with minor modifications. The absorbance of the complex formed between free sulfonamide and Bratton–Marshall reagent was measured on a spectrophotometer[3] at 540 nm for sulfanilamide and 545 nm for sulfisoxazole.

An accurately measured blood sample (1.0–1.5 ml) was transferred to a 150-ml beaker, diluted with 30 ml of water, stirred for 1 min, and the proteins and blood cells precipitated by dropwise addition of 8 ml of 15% trichloroacetic acid. The precipitate was allowed to settle for 2 min and 5 ml of the supernate was transferred to a 10-ml test tube. Sodium nitrite solution (1 ml, 0.1% w/v) was added, and the contents were mixed for 2 sec. Then 1 ml of 0.5% (w/v) sulfamic acid solution was added to the mixture and stirred for 10 sec. Following this, 1 ml of a 0.1% (w/v) Marshall reagent solution was added to the mixture, and it was stirred again for 10 sec. After allowing this mixture (total volume 8.5 ml) to stand for 5 min, the colored solution was filtered and the absorbance of the complex

[3] Beckman Model 24 Spectrophotometer.

Table II—Amounts and Fractions of Intact Sulfisoxazole (f_I) and Its Metabolite (f_m) Recovered in the Urine in 52 hr Following the Intravenous Administration of a 7-mg Dose of Sulfisoxazole to Control Rats and Phenobarbital Treated Rats

	Intact, mg	Metabolite, mg[a]	f_I	f_m
		Control		
1	6.59	0.33	0.95	0.05
2	6.42	0.56	0.92	0.08
3	6.34	0.67	0.90	0.10
4	6.12	0.88	0.87	0.13
5	6.15	0.78	0.89	0.11
Mean ± *SD*	6.32 ± 0.19	0.64 ± 0.21	0.91 ± 0.03	0.09 ± 0.03
		Phenobarbital Treated		
1	5.59	0.98	0.85	0.15
2	6.07	0.87	0.87	0.13
3	6.17	0.83	0.88	0.12
4	6.17	0.43	0.93	0.07
5	6.23	0.73	0.89	0.11
Mean ± *SD*	6.05 ± 0.26	0.77 ± 0.21	0.88 ± 0.03[b]	0.12 ± 0.03[b]

[a] Expressed as the equivalent amount of sulfisoxazole. [b] Not significantly different from the corresponding values of the control.

of the sulfonamide formed was measured at the appropriate wavelength.

The amounts of intact sulfanilamide or sulfisoxazole excreted in the urine samples were determined by the procedure described for blood samples, except that protein precipitation was unnecessary for the urine samples.

The total (intact plus metabolites) amount of sulfanilamide or sulfisoxazole excreted in the urine samples was determined after hydrolyzing the conjugated metabolites of the sulfonamide by heating the samples in the boiling water bath for 2 hr with 4 *N* HCl. The total sulfonamide was then analyzed according to the procedure described above for the intact sulfonamide.

The amount of free sulfonamide present in the unhydrolyzed urine or blood sample or the hydrolyzed urine sample was calculated with a calibration curve prepared for the respective sulfonamide. To prepare a calibration curve, known quantities of a sulfonamide were added to 1-ml volumes of blood obtained from rats not treated with a sulfonamide. The standard blood samples were treated in the same way as the actual blood samples, and their absorbance values were measured on a spectrophotometer at appropriate wavelength.

The absorbance for a given amount of sulfonamide contained in 1 ml of blood or 1 ml of water was identical after treatment by the Bratton–Marshall procedure, indicating that the residual amount of the blood constituents present in the supernate of the blood samples did not contribute to the absorbance. Therefore, the calibration curve of a sulfonamide was prepared from its aqueous solution without involving blood.

The main metabolite of sulfanilamide or sulfisoxazole was reported to be the acetylated form (9, 10). The amount of metabolite (in terms of the equivalent amount of intact sulfonamide) was calculated by subtracting the amount of free sulfonamide in the unhydrolyzed urine samples from the total amount of free sulfonamide in the hydrolyzed urine samples.

pH Determination of Cumulative Urine Samples—Each of four rats was treated with 5 ml normal saline for 5 days, and each of eight rats was treated with a 100-mg/kg ip dose of phenobarbital (in 5 ml normal saline) for 5 days. Each rat received 2 ml of pH 7.4 normal saline solution *via* the tail vein 24 hr after the last treatment dose of phenobarbital or normal saline. Cumulative urine samples were then collected separately from each rat for 7 hr. The pH of each cumulative urine sample was measured with a laboratory pH-meter. The urine pH of control rats varied from 6.35 to 6.50 and that of phenobarbital treated rats varied from 6.28 to 6.45.

RESULTS

Urinary Excretion Data for Sulfanilamide and Sulfisoxazole—The overall urinary excretion data obtained following the intravenous dose of sulfanilamide to the control and phenobarbital treated rats are shown in Table I. Virtually the entire dose of sulfanilamide was recovered in the urine in the intact and the metabolic forms in 35 hours for both the control and phenobarbital treated rats. All excretable intact compound was excreted in the urine in 8 hr and all excretable metabolite(s) were

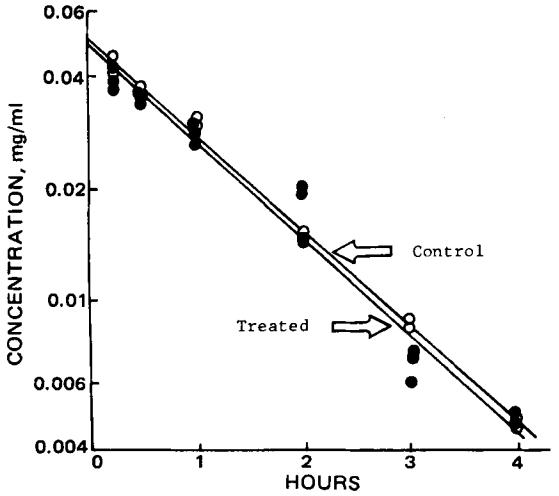

Figure 1—*Monoexponential semilogarithmic plots of blood concentrations of sulfanilamide obtained in control (○) and phenobarbital treated (●) rats. The solid lines are least-squares regression lines for the data of respective groups of rats.*

excreted in the urine in 35 hr. Of the total amount of the metabolites excreted, 80 to 85% was excreted in 8 hr.

To select the daily intraperitoneal dose of phenobarbital and the number of days to pretreat rats with this dose, the data in Table I were considered. The extent of metabolism of the compound in rats treated with a daily phenobarbital dose of 20 mg/kg for 5 days, 20 mg/kg for 10 days, 50 mg/kg for 5 days, or 100 mg/kg for 5 days was practically the same. Therefore, the regimen of phenobarbital treatment adopted in the pharmacokinetic study was a 100-mg/kg ip dose per day for 5 consecutive days. This was 5 times greater than the dose used in a previous study (1). The selection of the high phenobarbital dose was considered advisable since the compounds used in the present study are metabolized and bound to plasma proteins, unlike the nonmetabolized and nonprotein bound compounds used in a previous study (1). It was thought that, if the effects of phenobarbital treatment on sulfonamide distribution pharmacokinetics and biological half-lives were marginal at daily 20-mg/kg doses, more pronounced effects might be seen at daily 100-mg/kg doses. However, no pharmacokinetic studies were carried out at a daily 20-mg/kg dose of phenobarbital to determine if phenobarbital effects at the lower dose were less pronounced than those seen at a daily 100-mg/kg dose.

The overall urinary excretion data obtained following intravenous administration of 7 mg of sulfisoxazole to each control or phenobarbital treated rat are shown in Table II. Practically the entire administered dose of sulfisoxazole was recovered in the urine in intact and metabolic forms for the control and phenobarbital treated rats. There was no significant difference in the amounts of intact drug or metabolites recovered in the urine of the control and phenobarbital treated rats. The fractions of sulfisoxazole recovered in the intact (f_I) and metabolic (f_m) forms, based on the total amount recovered in 52 hr, are also listed in Table II. Of the total amount of sulfisoxazole recovered in the urine during the initial 10-hr period, 80–86% was in the intact form and 9–11% in the metabolic forms in the control and phenobarbital treated rats.

From the data in Tables I and II, a subject-to-subject variation among the control and phenobarbital treated rats in the extent of metabolism of the sulfonamides was minimum.

Pharmacokinetics of Sulfanilamide—The semilogarithmic plots of concentration *versus* time obtained for sulfanilamide in both the control and phenobarbital treated rats were monoexponential (Fig. 1). Therefore, the data were analyzed according to a one-compartment open model.

$$C = C_0 e^{-K_{el}t} \qquad \text{(Eq. 1)}$$

where C is the concentration of intact sulfanilamide at time t, C_0 is the concentration of intact sulfanilamide at time zero, and K_{el} is the apparent first-order rate constant of elimination of the drug. The drug concentrations plotted in Fig. 1 are normalized on the basis of a 10-mg iv dose of the drug per 200 g rat weight. The values of C_0 for the drug were determined from the intercepts obtained by extrapolating the respective least-squares line to time zero (Fig. 1). Values of K_{el} were calculated from the respective slope ($-K_{el}/2.303$) of the least-squares line. The apparent

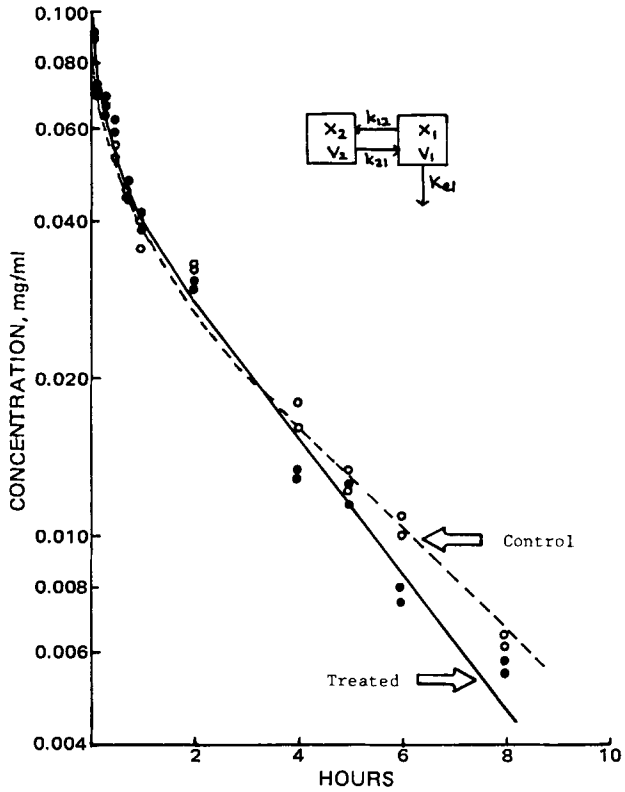

Figure 2—*Biexponential semilogarithmic plots of blood concentrations of sulfisoxazole obtained in control (○) and phenobarbital (●) treated rats. The solid and dotted lines are NONLIN least-squares regression lines for the data of respective group of rats. Insert is Scheme I.*

distribution volumes (V_d) and biological half-lives ($t_{1/2}$) of the drug were calculated in the usual manner (1). The pharmacokinetic parameters determined from these studies are listed in Table III. The standard deviations of all pharmacokinetic parameters were estimated by procedures described previously (1). The values of the parameters determined for the phenobarbital treated rats were not significantly different from those determined for the control rats. In fact, the values of all pharmacokinetic parameters observed are almost identical in the phenobarbital treated rats and the control rats, indicating that phenobarbital treatment had no effect on the distribution and elimination kinetics of sulfanilamide.

Pharmacokinetics of Sulfisoxazole—The semilogarithmic plots of concentration *versus* time for sulfisoxazole in both the control and phenobarbital treated rats indicated biexponential decline of the drug concentration in blood (Fig. 2). Therefore, the data were analyzed according to a two-compartment open model (Scheme I, Fig. 3) with elimination of the drug occurring from the central compartment:

$$C = Ae^{-\alpha t} + Be^{-\beta t} \qquad \text{(Eq. 2)}$$

where C is the concentration of intact sulfisoxazole in the blood at time t and other terms in the equation (and in Scheme I) are described in previous papers (1, 11). The drug concentrations plotted in Fig. 2 are normalized on the basis of a 7-mg iv dose of the drug per 200 g rat weight. Preliminary estimates of the intercepts (A and B) and slopes ($-\alpha/2.303$ and $-\beta/2.303$) for the two linear exponential segments (resolved by the method of residuals) were obtained by a least-squares method described previously (1). Using the preliminary estimates of A, B, α, and β, the initial estimates of V_1, k_{12}, k_{21}, and K_{el} were obtained in the manner described previously (1). Refined estimates of V_1, k_{12}, k_{21}, and K_{el} with their standard deviations, and those of α and β without their standard deviations, were obtained by analyzing the data using the NONLIN least-squares program (12). Using the computer estimated values of these parameters, estimates of V_2, V_{ss}, elimination phase ($t_{1/2}$), and body clearance ($K_{el}V_1$) were calculated as shown previously (1). The estimated and derived parameters are listed in Table IV. Standard deviation values of V_1, k_{12}, k_{21}, and K_{el} are computer estimated values and those of other parameters were estimated by the procedures described previously (1). The values of all pharmacokinetic parameters, except V_2, V_{ss}, and $K_{el}V_1$, determined for sulfisoxazole in phenobarbital treated rats were significantly different from those determined in control rats.

Table III—One-Compartment Model Pharmacokinetic Parameters of Sulfanilamide Determined in Control and Phenobarbital Treated Rats

Parameter	Control	Phenobarbital Treated	Statistical Significance of Difference (p)
C_0, mg/ml	0.054 ± 0.002	0.053 ± 0.003	*NS*[a]
K_{el}, hr^{-1}	0.598 ± 0.020	0.615 ± 0.030	*NS*
$t_{1/2}$, hr	1.16 ± 0.04	1.13 ± 0.06	*NS*
V_d, ml/kg	926.0 ± 34.3	931.0 ± 53.4	*NS*
r	0.996	0.980	

[a] No significant difference.

Rate Constants of Urinary Excretion and Metabolism of Sulfisoxazole—In Scheme I (Fig. 2), K_{el} is the sum of the apparent first-order rate constants of urinary excretion (k_{ex}) and metabolism (k_m) of sulfisoxazole. The values of k_{ex} and k_m can be calculated using the following equations (13):

$$k_{ex} = K_{el} f_I \quad \text{(Eq. 3)}$$

$$k_m = K_{el} f_m \quad \text{(Eq. 4)}$$

$$f_I = \frac{S_{e\infty}}{S_{e\infty} + M_{e\infty}} \quad \text{(Eq. 5)}$$

$$f_m = \frac{M_{e\infty}}{S_{e\infty} + M_{e\infty}} \quad \text{(Eq. 6)}$$

where $S_{e\infty}$ is the amount of sulfisoxazole excreted in the urine in infinite time and $M_{e\infty}$ is the equivalent amount of sulfisoxazole excreted in the urine as metabolite(s) in infinite time (Table II). Using the corresponding values of f_I and f_m from Table II and those of K_{el} in Table IV, the values of k_{ex} and k_m were calculated for control and phenobarbital treated rats (Table V). The standard deviation of k_{ex} and k_m were estimated according to the formulas (14):

$$k_{ex} = [\{(\sigma k_{ex}/k_{ex})^2 + (\sigma f_I/f_I)^2\}(k_{ex})^2]^{1/2} \quad \text{(Eq. 7)}$$

$$k_m = [\{(\sigma k_m/k_m)^2 + (\sigma f_m/f_m)^2\}(k_m)^2]^{1/2} \quad \text{(Eq. 8)}$$

As noted in Table V, according to the t test statistics, k_{ex}, but not k_m, was significantly greater in the phenobarbital treated rats than in the control rats.

DISCUSSION

Phenobarbital treatment did not affect the extent of nonmicrosomal enzymatic metabolism (Table II) or protein binding (4) of sulfisoxazole (which is excreted mainly by the kidney in rats). The significant decrease in the apparent distribution volume of the central compartment and the biological half-life of sulfisoxazole in the phenobarbital treated rats cannot be attributed to the increased hepatic blood flow, microsomal enzyme concentration, and biliary flow usually brought about by chronic phenobarbital treatment. The possibility of a decrease in the biological half-life of sulfisoxazole (pKa 5.1) due to a posssible increase in urine pH of rats was also evaluated. The normal pH of luminal fluids in the proximal tubules of rats was reported to be 6.82 (15). In this study, the pH of the cumulative urine samples collected separately from four control rats for 7 hr varied from 6.35 to 6.5, with an average pH of 6.42. Similarly, the pH of the cumulative urine samples collected separately from eight phenobarbital treated rats for 7 hr varied from 6.28 to 6.45, with an average pH of 6.36. Thus, the urine pH in phenobarbital treated rats was similar to that in the control rats. In the pH ranges measured, sulfisoxazole remains 94–96% in the anionic form. Therefore, the slight variation in urine pH was not expected to influence the half-life of sulfisoxazole in these rats.

Distribution Kinetics—The reduction in the distribution volume of the central compartment of sulfisoxazole in phenobarbital treated rats may be due to a possible decrease in the rate of diffusion of the anionic form of sulfisoxazole through the aqueous pores of the cell membranes of central compartment tissues. This was previously proposed (1) for the anions of mandelic acid, which also displayed the characteristics of a two-compartment model. As observed with mandelic acid, there was a tendency for V_2 and V_{ss} of sulfisoxazole to be lower in the phenobarbital treated rats, but the values of these parameters were not significantly different at the 95% confidence level from those in the control rats. However, V_{ss} of sulfisoxazole in the phenobarbital treated rats was different from that in the control rats at a 90% confidence level.

Table IV—Two-Compartment Model Pharmacokinetic Parameters of Sulfisoxazole Determined in Control and Phenobarbital Treated Rats

Parameter	Control	Phenobarbital Treated	Statistical Significance of Difference (p)
V_1, ml/kg	402.20 ± 12.00	366.35 ± 12.40	<0.05
k_{12}, hr^{-1}	0.5672 ± 0.0611	0.9716 ± 0.0814	<0.001
k_{21}, hr^{-1}	0.8308 ± 0.0845	1.6549 ± 0.1272	<0.001
K_{el}, hr^{-1}	0.4237 ± 0.0174	0.5183 ± 0.0235	<0.005
α, hr^{-1}	1.6021 ± 0.2305	2.8432 ± 0.3400	<0.01
β, hr^{-1}	0.2198 ± 0.0205	0.3017 ± 0.0239	<0.05
V_2, ml/kg	274.58 ± 41.46	215.08 ± 25.45	*NS*
V_{ss}, ml/kg	676.78 ± 43.16	581.43 ± 28.31	*NS*(p=0.1)
$K_{el}V_1$, ml/hr/kg	170.41 ± 8.69	189.88 ± 10.74	*NS*
$t_{1/2\beta}$, hr	3.15 ± 0.29	2.30 ± 0.18	<0.05
r	0.993	0.992	

As rationalized previously (1) for model organic anions, the transmembrane transport of sulfisoxazole anions is assumed to occur through the aqueous pores of cell membranes of the central and tissue compartments. It is likely that the possible increase in protein and phospholipid concentration brought about by phenobarbital pretreatment (1), probably causes a decrease in the pore size of (especially) the small size pores of cell membranes of the central and tissue compartments. This may cause a greater interaction of diffusing sulfisoxazole molecules with the proteins and phospholipids of the aqueous pore lining by intermolecular forces such as hydrogen bonding, hydrophobic bonding, and electrostatic interaction.

Interestingly, k_{12} and k_{21} for the intercompartmental transport of sulfisoxazole and mandelic acid in a previous study (1) were significantly greater in the phenobarbital treated rats than in the control rats, although the rate and extent of penetration of these anions into the deeper regions of the tissues was decreased in the phenobarbital treated rats. This may be rationalized by recognizing that k_{12} and k_{21} are the hybrid overall rate constants of anions which penetrate the tissues by diffusing through aqueous pores of small and large sizes, experiencing a greater transport barrier through the small size aqueous pores. If the very small size aqueous pores have narrowed sufficiently due to phenobarbital treatment and blocked penetration of anions through them in the deeper regions of tissues and decreased the apparent distribution volumes of accessible tissues, the remaining pores are the relatively large size aqueous pores whose resistance to penetration of the anions is not substantially affected. This situation would give a relatively rapid attainment of equilibrium of the reversible intercompartmental transport of the anions, leading to apparent increases in k_{12} and k_{21} values in phenobarbital treated rats.

Elimination Kinetics—The elimination rate constant (K_{el}) of sulfisoxazole, which is involved in renal tubular secretion (4), is increased by the phenobarbital treatment, as were the elimination rate constants of model organic anions (1) involved in renal tubular secretion in rats. Since the model organic anions were not metabolized and were eliminated from the body due to urinary excretion, K_{el} of these compounds were essentially the urinary excretion rate constants (k_{ex}). The increase in k_{ex} of model organic anions was attributed to the possible stimulatory effect of phenobarbital on the renal tubular secretory process (1). The rate constant of elimination of sulfisoxazole (K_{el}) represents the sum of k_{ex} and k_m, and, as noted in Table V, the increase in K_{el} is due to the significant increase in k_{ex} of sulfisoxazole in the phenobarbital treated rats. The increase in k_{ex} of sulfisoxazole anions may also be due to a stimulatory effect of phenobarbital on its renal tubular secretion process. This effect was shown for p-amino hippurate in phenobarbital treated rats (16).

Sulfanilamide—It was proposed (1) that a decrease in the apparent distribution volumes may be observed in phenobarbital treated rats for compounds which exist in the blood in the ionized form, exhibit multicompartment characteristics, and distribute between the compartments mainly by diffusion through the aqueous pores of the tissue cell membranes. It was also postulated (1) that such changes in the apparent distribution volumes are unlikely to be observed for compounds that exist in the blood in the nonionized form and may even display multicompartment characteristics, since they generally have greater membrane solubility and diffuse through the entire membrane surface of which aqueous pores constitute only a fractional surface area. It was further proposed that the increase in the elimination rate constants may be observed in the phenobarbital treated rats even for organic anions whose metabolic process is not stimulated by phenobarbital, but are secreted

Table V—Apparent First-Order Rate Constants of Urinary Excretion (k_{ex}) and Metabolism (k_m) of Sulfisoxazole Calculated for Control and Phenobarbital Treated Rats

	Control	Phenobarbital Treated	Statistical Significance of Difference (p)
k_{ex}, hr^{-1}	0.3838 ± 0.0204	0.4582 ± 0.0260	<0.05
k_m, hr^{-1}	0.0398 ± 0.0130	0.0601 ± 0.0156	*NS*

by the renal tubules, due to the possible stimulatory effect of phenobarbital on the renal tubular secretory mechanism of organic anions such as *p*-amino hippurate (16). As a corollary to this, it was postulated that the elimination rate constants of compounds whose metabolic process if not stimulated by phenobarbital will not be influenced in phenobarbital treated rats if the compounds are excreted in the urine by glomerular filtration.

The results (Table III) obtained for sulfanilamide are supportive of these hypotheses. The apparent distribution volume of sulfanilamide, which not only exists in the blood in the nonionized form but also shows characteristic one-compartment behavior, was not affected by the phenobarbital treatment. Also, K_{el} or $t_{1/2}$ of sulfanilamide, which is not involved in renal tubular secretion but is excreted by glomerular filtration in the urine, is not affected by the phenobarbital treatment.

CONCLUSIONS

The previous (1) and present studies demonstrate that, besides its known drug metabolizing enzyme induction effect, phenobarbital treatment may produce two additional effects on the pharmacokinetics of organic anions displaying multicompartment model characteristics. One effect is the changes in distribution space and rates reflected in such pharmacokinetic parameters as k_{12}, k_{21}, V_1, and V_{ss} of two-compartment model compounds. The other effect is on the renal tubular secretion process, reflected in such pharmacokinetic parameters as k_{ex} and K_{el} of the compounds. The fact that these pharmacokinetic parameters of drugs are independent of their elimination rate constants was pointed out previously (17).

The biological half-lives of multicompartment model compounds are derived from the disposition rate constants of the compounds and are, therefore, a function of both distribution and/or elimination (11). Therefore, the change in the biological half-lives of compounds brought about by phenobarbital treatment reflect the changes in distribution and/or elimination of the compounds.

Although the results of the previous (1) and present studies are consistent with the mechanism conceived previously (1) for the effects of phenobarbital, direct evidence of the increase in the protein and phospholipid concentration of certain target peripheral tissue cell membranes has not been obtained at this time. However, regardless of whether such direct evidence is obtained in the future, further evidence of the effects of phenobarbital treatment on the distribution and elimination pharmacokinetic parameters of other suitable organic anionic drugs should be gathered.

REFERENCES

(1) D. J. Szymanski and J. B. Nagwekar, *J. Pharm. Sci.*, **71**, 275 (1982).

(2) L. S. Goodman and A. Gilman, "The Pharmacological Basis of Therapeutics," 5th ed., Macmillan, New York, N.Y., 1975, p. 17.

(3) C. D. Klassen, *J. Pharmacol. Exp. Ther.*, **175**, 289 (1970).

(4) A. Yacobi and G. Levy, *J. Pharm. Sci.*, **68**, 742 (1979).

(5) R. Hari, K. Sunayashiki, and A. Kamiya, *Chem. Pharm. Bull.*, **26**, 740 (1978).

(6) E. J. Randinitis, M. Barr, H. C. Wormser, and J. B. Nagwekar, *J. Pharm. Sci.*, **59**, 806 (1970).

(7) R. R. Sokal and F. J. Rohlf, in "Biometry: The Principles and Practice of Statistics in Biological Research," W. H. Freeman, San Francisco, Calif., 1969, p. 410.

(8) A. C. Bratton and E. K. Marshall, *J. Biol. Chem.*, **128**, 537 (1939).

(9) M. Yamazaki, M. Aoki, and A. Kamada, *Chem. Pharm. Bull.*, **16**, 721 (1968).

(10) *Ibid.*, **16**, 707 (1968).

(11) M. Gibaldi and D. Perrier, "Pharmacokinetics," vol. 1, Dekker, New York, N.Y., 1975, chap. 2.

(12) C. M. Metzler, "NONLIN: A Program to Estimate the Parameters in a Nonlinear System of Equations," The Upjohn Co., Kalamazoo, Mich., 1969.

(13) K. A. McMahon and W. J. O'Reilly, *J. Pharm. Sci.*, **61**, 518 (1972).

(14) W. E. Deming, in "Statistical Adjustment of Data," Dover, New York, N.Y., 1938, pp. 37–48.

(15) C. F. Rector, N. W. Carter, and D. W. Seldin, *J. Clin. Invest.*, **44**, 278 (1965).

(16) E. E. Ohnhaus and H. Seigl, *Arch. Int. Pharmacodyn. Ther.*, **223**, 107 (1976).

(17) W. J. Jusko and M. Gibaldi, *J. Pharm. Sci.*, **61**, 1270 (1972).

ACKNOWLEDGMENTS

Abstracted in part from a thesis submitted by S. Kundu to the Graduate School, Wayne State University, in partial fulfillment of the Master of Science degree requirements.

A Comparison of Frozen and Reconstituted Cattle and Human Skin as Barriers to Drug Penetration

IAN H. PITMAN ˣ **and SUSAN J. ROSTAS**

Received March 6, 1981, from the *School of Pharmaceutics, Victorian College of Pharmacy, Parkville, Victoria, Australia 3052.* Accepted for publication August 3, 1981.

Abstract □ An *in vitro* study of the permeabilities of frozen and reconstituted cattle skin and human skin to levamisole was done. Cattle skin was 400 times more permeable to levamisole from an organic solvent (largely 2-ethoxyethanol) than was human skin. The diffusion coefficient value of levamisole in cattle skin and the partition coefficient value of levamisole from the organic solvent into the skin suggested that a relatively large amount of drug passed through skin appendages such as hair follicles or sweat/sebaceous ducts. Transcellular transport across the stratum corneum was rate-determining in human skin penetration.

Keyphrases □ Permeability—frozen and reconstituted cattle and human skin *in vitro*, levamisole □ Levamisole—*in vitro* permeability through frozen and reconstituted cattle and human skin □ Dosage forms, topical—levamisole, *in vitro* permeability through frozen and reconstituted cattle and human skin

The use of topical dosage forms for the systemic delivery of drugs to domestic animals was foreshadowed by Rogoff and Kohler (1) when they showed that cattle grubs could be controlled by applying a small volume of a concentrated crufomate solution to a cow's skin. Such dosage forms, which are known as pour-ons or spot-ons, have subsequently been proposed for the systemic delivery of a variety of drugs to sheep and cattle (2–6).

The present report concerns the rate and mechanism by which the anthelmintic levamisole is transported across samples of excised cattle skin that were frozen and reconstituted.

The work was undertaken as part of a program to develop an *in vitro* screen for pour-on formulations. The development of topical drug delivery systems for humans has been greatly facilitated by the use of *in vitro* screens which are based on the realization that strong qualitative agreement exists between the rate at which drugs penetrate excised human skin in *in vitro* experiments and *in vivo* penetration (7). In addition, it was established (8) that it does not matter whether the skin used in the *in vitro* experiments is fresh or frozen or whether stratum corneum, epidermis, or whole skin is used.

EXPERIMENTAL

Preparation of Cattle Skins—Skin was harvested in mid-March (*i.e.*, early fall in Australia) from an 8-month old Hereford calf. As soon as the animal had been sacrificed its hair was clipped[1] as close as possible to the skin without damaging it. Strips of skin were removed from the dorsal thoraco-lumbar region using a dermatome[2] set at 1.1 mm. The strips of skin were immediately labeled, wrapped, and placed on ice. Within 3 hr the skins were placed in a freezer at −30° until required for an experiment. The permeability of skin handled in this way did not change appreciably after at least 12 months storage.

Before starting a skin permeability experiment, a sample was thawed at room temperature in a sealed jar containing paper that was soaked in normal saline. This procedure was adopted to minimize skin dehydration.

Preparation of Human Skin—Skin, and its accompanying subcutaneous fat, was obtained from the upper thigh of humans following leg amputations or from breasts following cosmetic surgery. The skin was frozen, stored, and thawed in the manner described for cattle skin. When the human skin had thawed, the subcutaneous fat and the lower section of the dermis were removed with a scalpel.

Materials—Levamisole[3], mp 61°, was used without further purification. the solvents used in the levamisole formulations were an aqueous borate solution (pH 8.9 buffer) and an organic solvent (solvent A) containing nonaromatic hydrocarbons (15%), polyoxypropylene 15-stearyl ether (12%), and ethoxyethanol (73%). The receptor phase was normal saline.

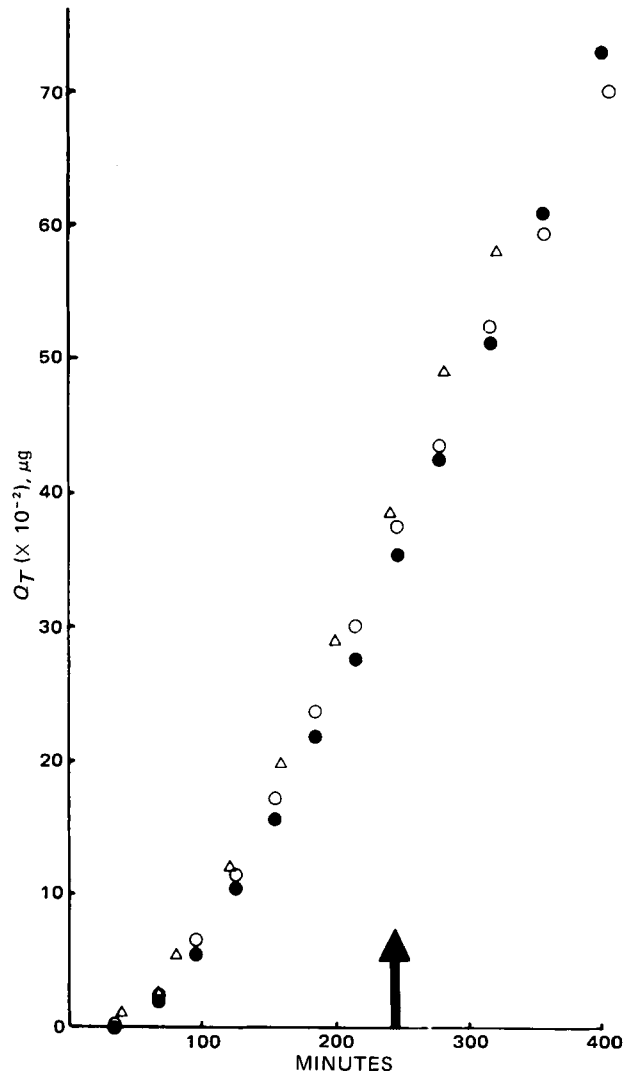

Figure 1—*The quantity of levamisole penetrating 1.45 3 cm² of cattle skin from a 10% solution in solvent A* versus *time using a constant stirring rate throughout (△), a constant stirring rate for 245 min and then half the rate (●), and a constant stirring rate for 245 min and then no stirring except for 4 min prior to taking a reading (○).*

[1] Andis R 400 or Oster A5 Clippers.
[2] Brown Electro Dermatome, Model 902.

[3] ICI Australia Ltd.

0022-3549/82/0400-0427$01.00/0

Table I—Permeability of Cattle Skin to Levamisole from a 10% Solution in Solvent A

$10 \times r^a$, cm	$10^6 \times k_p{}^b$, cm/min	$10^6 \times k_p\, r$, cm^2/min	L^c, min	$10^5 \times D^d$, cm^2/min	$10 \times PC^e$	$10^{-2} \times Q_{200}{}^f$, μg
1.69 (0.10)	42	7.1	118	4.0	1.8	5.1
1.31 (0.03)	94	12.3	104	2.8	4.4	12.8
1.24 (0.05)	93	12.5	96	2.7	4.3	13.9
1.23 (0.05)	110	13.5	99	2.5	5.4	16.1
1.15 (0.03)	113	13.0	100	2.2	5.9	16.1
1.14 (0.08)	120	13.7	80	2.7	5.1	20.1
1.09 (0.03)	164	17.9	76	2.6	6.9	29.7
1.08 (0.02)	141	15.2	63	3.1	4.9	27.1
1.04 (0.05)	165	17.2	79	2.3	7.5	28.9
1.01 (0.03)	144	14.5	90	1.9	7.6	23.2
0.98 (0.05)	164	16.1	72	2.2	7.3	30.2
0.95 (0.04)	187	17.8	68	2.2	8.1	35.3
0.87 (0.02)	177	15.4	43	2.9	5.3	41.4
0.86 (0.06)	187	16.1	62	2.0	8.1	38.3
0.86 (0.03)	219	18.8	65	1.9	9.9	43.7
0.80 (0.03)	206	16.5	58	1.8	9.2	41.8
0.65 (0.03)	286	18.6	30	2.3	8.1	72.1

[a] r = skin thickness and number in parentheses is the spread; [b] k_p = permeability constant; [c] L = lag time; [d] D = diffusion coefficient; [e] PC = partition coefficient; [f] Q_{200} = quantity crossing 1.453 cm^2 in 200 min.

Measurement of Skin Permeability and Calculation of Permeability Constants—The method used for measuring skin permeability and the chemical assay of levamisole have been described previously (9). Skin thickness was measured at the conclusion of an experiment with a tension micrometer. These measuresments were made at the end of an experiment rather than at the beginning to avoid causing mechanical damage to the skin prior to making permeability measurements. The average of five readings taken over the entire surface was recorded.

The permeability constant, k_p (cm/min), was calculated using:

$$k_p = \frac{S \times V}{1.453 \times C} \qquad \text{(Eq. 1)}$$

where S (μg/ml/min) is the slope of the steady-state plot of drug concentration in the receptor compartment *versus* time, V (cm^3) is the volume of the receptor compartment, 1.453 cm^2 is the surface area of the skin, and C (μg/ml) is the concentration of drug applied to the skin surface.

The lag time, L (min), was taken as the intercept on the x-axis of the steady-state plot of drug concentration in the receptor compartment *versus* time.

RESULTS AND DISCUSSION

Permeability of Cattle Skin to Levamisole—*Effect of Rate of Stirring of Receptor Phase*—Figure 1 shows the amounts of levamisole that had penetrated samples of cattle skin (Q_T) from a 10% solution in solvent A. The stirring rate of the receptor phase was different in each experiment. In one experiment, a constant stirring rate was maintained from start to finish. In subsequent experiments, the same rate was maintained for 245 min, and then the stirring rate was either halved or stopped (except for 4 min immediately prior to the removal of an aliquot for assay).

The results of Fig. 1 indicate that the rate of appearance of levamisole in the receptor phase was independent of the stirring rate. This result suggests that transport of levamisole through the skin is the *in vitro* rate-determining process rather than clearance from the skin into the receptor phase (10). Increasing the agitation rate of the receptor phase would decrease the thickness of the unstirred layer of receptor phase adjacent to the skin and would increase the rate of appearance of levamisole in the receptor phase if this were the rate-determining process.

The value of the present report to an understanding of the *in vivo* topical absorption process in domestic animals depends on whether penetration of drug through the skin rather than clearance into a receptor phase is the rate-determining step in both *in vitro* and *in vivo* situations. If this were not the case, the difference in character between stirred normal saline (*in vitro* experiments) and flowing blood (*in vivo* experiments) as receptor phases would reduce the likelihood of correlation between the results of the two types of experiment.

Effect of Skin Sample Thickness—The skin samples from the calf consisted of the epidermis together with varying thicknesses of dermis.

Table II—Permeability of Human Skin to Levamisole from a 0.85% Solution in an Aqueous Buffer at pH 8.9

Donor	$10 \times r^a$, cm	$10^6 \times k_p{}^b$, cm/min	L^c, min	$10^{-2} \times Q_{200}{}^d$, μg
6	1.28 ± 0.04	131	83	2.2
6	1.23 ± 0.06	145	84	2.4
6	0.98 ± 0.19	117	98	1.7
9	1.09 ± 0.18	161	75	1.7
9	0.99 ± 0.08	135	98	2.0
8	0.91 ± 0.05	101	107	1.3
8	0.81 ± 0.01	118	150	0.9

[a] r = skin thickness. [b] k_p = permeability constant. [c] L = lag time. [d] Q_{200} = quantity crossing 1.453 cm^2 in 200 min.

Studies of the penetration of levamisole from its 10% solution in solvent A indicated that steady-state penetration was achieved by 100 min in all cases and was maintained for at least 5–6 hr. Table I shows the permeability constants, lag times, and quantity of levamisole which had penetrated in 200 min through samples of cattle skin 0.65–1.69 mm thick.

There was a strong negative correlation between skin thickness and permeability constant ($\gamma = -0.95$; $0.01\% > P$) and a positive correlation between skin thickness and lag time ($\gamma = +0.90$; $0.01\% > P$). Furthermore, the product of permeability constant and total skin thickness ($k_p r$) was essentially constant for skins whose thickness varied from 0.65–1.1 mm.

These results suggest that the outer 1 mm or so of skin acts like a homogeneous barrier to levamisole penetration. For diffusion of molecules through a homogeneous barrier, the values of k_p and L are related to the skin thickness, r, in the following manner (11):

$$k_p = \frac{D(PC)}{r} \qquad \text{(Eq. 2)}$$

$$L = \frac{r^2}{6D} \qquad \text{(Eq. 3)}$$

where D (cm^2/min) is the diffusion coefficient of the diffusing molecule in the barrier, and PC is the partition coefficeint for the diffusing substance between the barrier and the solvent.

Under conditions where Eqs. 2 and 3 apply, values of the terms $k_p r$ [$= D(PC)$] and $r^2/6L$ ($=D$) should be constant. Values of these terms are included in Table I.

While values of $k_p r$ and $r^2/6L$ do vary with r when it is changed from 1.69 to 0.8 mm, it appears that these terms are essentially constant for skin specimens <1.1 mm thick. This suggests that the portion of the skin from the surface of the stratum corneum down to a depth of ~1 mm can be considered to be a homogeneous barrier when considering levamisole penetration. The mean value of the term $r^2/6L$ throughout this thickness range, 2.1×10^{-5} cm^2/min, is the apparent diffusion coefficient of levamisole in the homogeneous barrier.

The mean value of the term $k_p r$ [$D(PC)$] throughout the barrier with a thickness 0.8–1.09 mm was 17.2×10^{-6} cm^2/min. Thus, on the basis that D was 2.1×10^{-5} cm^2/min, the apparent value of PC between the barrier and the solvent A was 0.84.

Permeability of Human Skin to Levamisole—It has been established (11, 12) that the stratum corneum is the rate-determining barrier to penetration of human skin by most nonelectrolytes of small to medium size molecular weights. This was confirmed for levamisole penetration in human skin by considering the effect of skin sample thickness and the removal of the stratum corneum on permeability.

Table II contains the calculated permeability constants and lag times for penetration of human skin at 37° by levamisole from its 0.85% solution in an aqueous buffer, pH 8.9.

Table III—Effect of Removal of Stratum Corneum on Human Skin Permeability to Levamisole from a 0.85% Solution in an Aqueous Buffer at pH 8.9

Donor	$10 \times r^a$, cm	Treatment	$10^6 \times k_p{}^e$, cm/min	L^f, min	$10^{-2} \times Q_{200}{}^g$, μg
9	1.09	*b*	161	75	1.7
9	0.97	*c*	108	92	1.7
9	0.93	*d*	720	33	17.5
9	0.91	*d*	692	46	15.5

[a] r = skin thickness. [b] treated as in Table II. [c] heated at 60° for 2 min and cooled. [d] as in *c* but stratum corneum peeled off. [e] k_p = permeability constant. [f] L = lag time. [g] Q_{200} = quantity penetrating 1.453 cm^2 in 200 min.

Figure 2—*Micrograph (×80) of a vertical section of calf skin stained with hemotoxylin and eosin.*

The aqueous buffer was used in these experiments instead of solvent A because levamisole only penetrated human skin very slowly from the latter solvent. This is in marked contrast to the situation with cattle skin penetration. Whereas 4180 μg of levamisole penetrated a 0.8 mm thick sample of calf skin in 200 min from solvent A, only 10 μg penetrated through a 0.81-mm sample of human skin in the same time. Only 121 μg of levamisole had penetrated the human skin in 12 hr. Steady-state penetration from the aqueous solution was achieved within 100 min in most cases and was maintained for at least 5 hr.

One problem encountered in interpreting the data in Table II arose because only limited amounts of skin could be obtained from each donor. Hence, in contrast to the situation with cattle skin penetration, insufficient data to permit a statistical analysis of the effect of skin thickness was obtained on skin from a single donor. However, the data suggest that no strong correlation with a negative correlation coefficient exists between human skin thickness and the permeability constant when the former is varied between 0.81 and 1.28 mm. The small amount of data on skin from each donor is more consistent with the conclusion that permeability constants and lag times for diffusion are independent of skin sample thickness. This is in contrast to the cattle skin permeability and is consistent with the proposal that the stratum corneum (*i.e.*, the outer 10 μm of the epidermis) is the rate-determining barrier to penetration.

Table III supports this conclusion. The data relate to the permeability of a skin sample that was heated in 60° water for 2 min prior to the penetration experiment and a similarly treated skin sample whose stratum corneum was peeled off after heating and prior to the permeability experiment.

The results show that heating the skin to 60° and cooling prior to a permeability experiment did not significantly effect the skin permeability. However, removal of the stratum corneum led to a dramatic increase in permeability which confirmed the postulate that this layer is rate determining for penetration of levamisole through human skin which has been frozen and reconstituted.

An estimate of the diffusion coefficient of levamisole in human stratum corneum, D (cm^2/min), and of the partition coefficient of levamisole between water at pH 8.9 and human stratum corneum can be made using Eqs. 1 and 2, a value of 10^{-3} cm for the thickness of the stratum corneum, and values of k_p (cm/min) and L (min) in Table II. For the purpose of this exercise, the data in Table II that were obtained on skin sample 6 were used, *i.e.*, $k_p = 131 \pm 14 \times 10^{-6}$ cm/min and $L = 88 \pm 10$ min. This led to values of $D = 1.9 \times 10^{-9}$ cm^2/min and $PC = 69$.

The value of D is similar to the values that have been reported (11) for water and low molecular weight nonelectrolytes ($3–4 \times 10^{-8}$ cm^2/min) in human stratum corneum.

Levamisole has a pKa value of 7.94 at 37° (9) and, thus, exists to the extent of 90% as a neutral molecule at pH 8.9. The calculated value of PC(69) suggests that the stratum corneum has a much lower polarity than water and is a better solvent for levamisole than water.

Mechanism of Absorption of Levamisole across Cattle Skin—The apparent constancy of the product $k_p r$ for levamisole absorption across cattle skin samples with a thickness of 0.65–1.1 mm suggests that this total skin thickness, rather than the 30 μm stratum corneum (13), is the rate-determining barrier. Values of $k_p r$ tended to decrease when skin with a thickness >1.1 mm was used. It will be argued subsequently that the first 1.1 mm of skin is richly supplied with blood and that drug molecules that penetrate into it would be rapidly absorbed into the blood. Consequently, it is proposed that controlling the rate at which drug molecules pass through the first 1.1 mm will result in control of the rate at which they enter the blood in the *in vivo* situation.

It may be argued that the stratum corneum was removed from the skin samples investigated by either the method of the skin preparation or by solvent A. The first possibility is considered unlikely since fine clipping of hair was shown (14) to remove no more than 4 of 30 layers of bovine stratum corneum. The second possibility is discounted because $k_p r$ was also constant for levamisole penetration through cattle skin from aqueous solutions.

It is proposed that the first 1.0–1.1 mm of the cattle skin used in these experiments is made up of the epidermis with its stratum corneum (60 μm thick) (13) and the highly vascular papillary layer of the dermis.

Histological studies of a variety of cattle skins revealed (15) that the first 1 mm is usually epidermis plus papillary layer of the dermis, and the lower 6 mm is the collagenous reticular layer of the dermis. McEwan-Jenkinson (16) has suggested that the papillary and reticular layers of the dermis of bovine skin meets in the area of the sebaceous gland. Confirmation of this proposition comes from inspection of the micrograph of a dehydrated, paraffin-embedded section of cattle skin (Fig. 2). This section, which is typical of the skin studied, shows that the first 1 mm of skin contains most of the hair follicle and the sebaceous gland associated with it.

It is not clear whether the bulk of the drug is transported through the first 1 mm or so of skin *via* the cells (*i.e.*, transcellular) as in human skin penetration (11) (although in this case it is only the stratum corneum which is rate determining) or *via* the appendages such as the hair follicle, sweat duct or sebaceous duct.

The value of the diffusion coefficient for levamisole in the first 1.0 mm of cattle skin (2.1×10^{-5} cm^2/min) is much closer to those of water and low molecular weight nonelectrolytes through human hair follicles ($0.3–1.2 \times 10^{-5}$ cm^2/min) or sweat ducts ($6.0–12.0 \times 10^{-5}$ cm^2/min) than to the value calculated for levamisole passing through human stratum corneum cells (1.9×10^{-9} cm^2/min). Consequently, it is tempting to postulate that most of the drug is transported *via* the skin appendages in transport across cattle skin.

A major reason why transport *via* skin appendages has only been assigned a minor role in human skin transport is because their density per unit area of skin is very low (40–70 cm^{-2} for hair follicles and 200–250 cm^{-2} for sweat glands) (11). Thus, it would be reasonable to predict that this route would be more favorable in cattle skin penetration because the density of hair follicles is higher ($\simeq$890 cm^{-2}) (17), and each follicle has a sweat gland, sebaceous gland, and the ducts associated with it. However, the greater density of hair follicles in cattle (~15 times the density in human skin) cannot on its own account for the 400-fold increase in the rate at which levamisole crosses cattle skin as compared to human skin. It is possible that penetration *via* the cattle skin appendages is facilitated by the emulsified sebum that is associated with them (18). This emulsion may be a better solvent for levamisole than the sebum which is associated with human hair follicles or the sweat associated with human sweat glands. Studies concerning the role that emulsified sebum plays in cattle skin penetration are currently underway.

If the above postulate is correct, it is likely that the drug would rapidly enter the systemic circulation in live animals because the appendages are richly supplied with blood vessels.

CONCLUSIONS

The first 1 mm or so of frozen and reconstituted cattleskin[4] acts as a homogeneous barrier to penetration of the skin by chemicals. The diffusion coefficient of levamisole in this barrier is close to its expected value in hair follicles or sweat ducts. The results of the present study suggest that polar molecules such as levamisole will penetrate cattle skin much more rapidly than human skin.

REFERENCES

(1) W. M. Rogoff and P. H. Kohler, *J. Econ. Entomol.*, **53**, 814 (1960).

(2) R. O. Drummond and O. H. Graham, *ibid.*, **55**, 255 (1962).

(3) F. C. Loomis, A. Noordehaven, and W. J. Roulston, *ibid.*, **65**, 1638 (1972).

(4) P. J. Brooker and J. Goose, *Vet. Rec.*, **96**, 249 (1975).

(5) D. ap T. Rowlands and J. Berger, *J. S. Afr. Vet. Assoc.*, **48**, 85 (1977).

(6) R. O. Drummond and T. M. Whetstone, *J. Econ. Entomol.*, **67**, 237 (1974).

(7) T. J. Franz, *J. Invest. Dermatol.*, **64**, 190 (1975).

(8) R. B. Stoughton, in "Progress in the Biological Sciences in Relation to Dermatology," A. Rook and R. H. Champion, Eds., Cambridge University Press, 1964.

(9) L. M. Ponting and I. H. Pitman, *Aust. J. Pharm. Sci.*, **8**, 15 (1979).

(10) G. L. Flynn and S. H. Yalkowsky, *J. Pharm. Sci.*, **61**, 838 (1972).

(11) R. J. Scheuplein and I. H. Blank, *Physiol. Rev.*, **51**, 702 (1971).

(12) I. H. Blank and R. J. Scheuplein, *Br. J. Dermatol.*, **81**, 4 (1969).

(13) D. H. Lloyd, W. D. B. Dick, and D. McEwan-Jenkinson, *Res Vet. Sci.*, **26**, 172 (1979).

(14) *Ibid.*, **26**, 250 (1979).

(15) D. F. Dowling, *Aust. J. Agr. Res.*, **6**, 776 (1955).

(16) D. McEwan-Jenkinson, in "Comparative Physiology and Pathology of the Skin," A. J. Rook and G. S. Walton, Eds., Blackwell, Oxford, 1965.

(17) H. G. Turner, T. Nay, and G. T. French, *Aust. J. Agr. Res.*, **13**, 960 (1962).

(18) D. McEwan-Jenkinson, *Proc. R. Soc. Edinburgh*, **79B**, 3 (1980).

[4] It should be noted that freezing the skin could very well alter its cellular geography to such an extent that the results of this study may not reflect properties of intact fresh skin. If this is true, then the value of the present results to *in vivo* behavior will only be realized when *in vivo* experiments are completed. However, the results clearly indicate that frozen and reconstituted cattle skin has very different barrier properties to similarly treated human skin and that the stratum corneum of the former skin does not appear to be the rate-determining barrier to penetration.

ACKNOWLEDGMENTS

Supported in part by ICI Australia Ltd. and ICI Ltd.

Grateful acknowledgment is made to Professor P. Bhathal, University of Melbourne, for assistance with the human skin measurements and to Mr. Ian Ray, Victorian College of Pharmacy and Mr. John Standing, Alfred Hospital, Melbourne for assistance in harvesting animal skins.

Antitumor Agents XLVIII: Structure–Activity Relationships of Quassinoids as *In Vitro* Protein Synthesis Inhibitors of P-388 Lymphocytic Leukemia Tumor Cell Metabolism

Y. F. LIOU, I. H. HALL ˣ, M. OKANO, K. H. LEE, and S. G. CHANEY *

Received April 6, 1981, from the *Division of Medicinal Chemistry, School of Pharmacy, and the *Department of Biochemistry, School of Medicine, University of North Carolina, Chapel Hill, NC 27514.* Accepted for publication August 4, 1981.

Abstract □ A series of brusatol, bisbrusatol, and bruceantin esters were examined for their ability to inhibit protein synthesis in P-388 lymphocytic leukemia cells. Compounds which produced high T/C % values (170–272) resulted in ID_{50} of 5.4–15.5 μM for inhibition of whole cell protein synthesis, ID_{50} of 1.3–13 μM for inhibition of endogenous protein synthesis in cell homogenates, and ID_{50} of 1.9–6 μM for inhibition of polyuridine directed polyphenylalanine synthesis using "runoff" ribosomes and a "pH 5" enzyme preparation. The polyuridine directed polyphenylalanine synthesis requires neither initiation nor termination factors, suggesting that quassinoids are exclusively elongation inhibitors. Bruceantin, brusatol, and bisbrusatolyl malonate allowed a runoff of the polyribosomes to 80S free ribosomes. However, formation of the ternary complex and 80S initiation complex were not inhibited by the quassinoids. Thus, these agents do not affect the individual steps leading to the formation of a stable 80S initiation complex in P-388 cells. Brusatol, bruceantin, and bisbrusatolyl malonate inhibited the formation of the first peptide bond between puromycin and [^{3}H]methionyl-transfer RNA bound to the initiation complex, indicating peptidyl transferase activity is inhibited by the quassinoids in P-388 cells. These studies also suggest that the free 80S ribosome is the site of binding by the quassinoid. Ribosomes actively conducting protein synthesis will continue protein synthesis and terminate before the quassinoids bind. This proves quassinoids are elongation inhibitors of tumor cells. A strong correlation was observed between potent antileukemic activity and the ability to inhibit protein synthesis in P-388 lymphocytic leukemia cells.

Keyphrases □ Protein synthesis—inhibition by quassinoids, P-388 lymphocytic leukemia cells □ Quassinoids—inhibition of protein synthesis, P-388 lymphocytic leukemia cells □ Structure–activity relationships—quassinoids, inhibition of protein synthesis, P-388 lymphocytic leukemia cells □ Antitumor agents—quassinoids, inhibition of protein synthesis, P-388 lymphocytic leukemia cells

Bruceantin, a quassinoid now in phase II clinical trials, was first isolated from *Brucea antidysenterica* (1, 2). Subsequently, bruceoside A was isolated from *Brucea javanica* (3) and brusatol was derived chemically from bruceoside A. It was demonstrated (4) that bruceantin inhibited protein synthesis in HeLa cells by 90% at 2 μM, whereas DNA and RNA synthesis were inhibited 60 and 15%, respectively. Protein synthesis was inhibited 79% in rabbit reticulocytes by bruceantin at 0.1 μM (4). Liao (4) postulated that bruceantin was an initiation inhibitor of

0022-3549/82/0400-0430$01.00/0

CONCLUSIONS

The first 1 mm or so of frozen and reconstituted cattleskin[4] acts as a homogeneous barrier to penetration of the skin by chemicals. The diffusion coefficient of levamisole in this barrier is close to its expected value in hair follicles or sweat ducts. The results of the present study suggest that polar molecules such as levamisole will penetrate cattle skin much more rapidly than human skin.

REFERENCES

(1) W. M. Rogoff and P. H. Kohler, *J. Econ. Entomol.*, **53**, 814 (1960).

(2) R. O. Drummond and O. H. Graham, *ibid.*, **55**, 255 (1962).

(3) F. C. Loomis, A. Noordehaven, and W. J. Roulston, *ibid.*, **65**, 1638 (1972).

(4) P. J. Brooker and J. Goose, *Vet. Rec.*, **96**, 249 (1975).

(5) D. ap T. Rowlands and J. Berger, *J. S. Afr. Vet. Assoc.*, **48**, 85 (1977).

(6) R. O. Drummond and T. M. Whetstone, *J. Econ. Entomol.*, **67**, 237 (1974).

(7) T. J. Franz, *J. Invest. Dermatol.*, **64**, 190 (1975).

(8) R. B. Stoughton, in "Progress in the Biological Sciences in Relation to Dermatology," A. Rook and R. H. Champion, Eds., Cambridge University Press, 1964.

(9) L. M. Ponting and I. H. Pitman, *Aust. J. Pharm. Sci.*, **8**, 15 (1979).

(10) G. L. Flynn and S. H. Yalkowsky, *J. Pharm. Sci.*, **61**, 838 (1972).

(11) R. J. Scheuplein and I. H. Blank, *Physiol. Rev.*, **51**, 702 (1971).

(12) I. H. Blank and R. J. Scheuplein, *Br. J. Dermatol.*, **81**, 4 (1969).

(13) D. H. Lloyd, W. D. B. Dick, and D. McEwan-Jenkinson, *Res Vet. Sci.*, **26**, 172 (1979).

(14) *Ibid.*, **26**, 250 (1979).

(15) D. F. Dowling, *Aust. J. Agr. Res.*, **6**, 776 (1955).

(16) D. McEwan-Jenkinson, in "Comparative Physiology and Pathology of the Skin," A. J. Rook and G. S. Walton, Eds., Blackwell, Oxford, 1965.

(17) H. G. Turner, T. Nay, and G. T. French, *Aust. J. Agr. Res.*, **13**, 960 (1962).

(18) D. McEwan-Jenkinson, *Proc. R. Soc. Edinburgh*, **79B**, 3 (1980).

[4] It should be noted that freezing the skin could very well alter its cellular geography to such an extent that the results of this study may not reflect properties of intact fresh skin. If this is true, then the value of the present results to *in vivo* behavior will only be realized when *in vivo* experiments are completed. However, the results clearly indicate that frozen and reconstituted cattle skin has very different barrier properties to similarly treated human skin and that the stratum corneum of the former skin does not appear to be the rate-determining barrier to penetration.

ACKNOWLEDGMENTS

Supported in part by ICI Australia Ltd. and ICI Ltd.

Grateful acknowledgment is made to Professor P. Bhathal, University of Melbourne, for assistance with the human skin measurements and to Mr. Ian Ray, Victorian College of Pharmacy and Mr. John Standing, Alfred Hospital, Melbourne for assistance in harvesting animal skins.

Antitumor Agents XLVIII: Structure–Activity Relationships of Quassinoids as *In Vitro* Protein Synthesis Inhibitors of P-388 Lymphocytic Leukemia Tumor Cell Metabolism

Y. F. LIOU, I. H. HALL ˣ, M. OKANO, K. H. LEE, and S. G. CHANEY *

Received April 6, 1981, from the *Division of Medicinal Chemistry, School of Pharmacy, and the *Department of Biochemistry, School of Medicine, University of North Carolina, Chapel Hill, NC 27514.* Accepted for publication August 4, 1981.

Abstract □ A series of brusatol, bisbrusatol, and bruceantin esters were examined for their ability to inhibit protein synthesis in P-388 lymphocytic leukemia cells. Compounds which produced high T/C % values (170–272) resulted in ID_{50} of 5.4–15.5 μM for inhibition of whole cell protein synthesis, ID_{50} of 1.3–13 μM for inhibition of endogenous protein synthesis in cell homogenates, and ID_{50} of 1.9–6 μM for inhibition of polyuridine directed polyphenylalanine synthesis using "runoff" ribosomes and a "pH 5" enzyme preparation. The polyuridine directed polyphenylalanine synthesis requires neither initiation nor termination factors, suggesting that quassinoids are exclusively elongation inhibitors. Bruceantin, brusatol, and bisbrusatolyl malonate allowed a runoff of the polyribosomes to 80S free ribosomes. However, formation of the ternary complex and 80S initiation complex were not inhibited by the quassinoids. Thus, these agents do not affect the individual steps leading to the formation of a stable 80S initiation complex in P-388 cells. Brusatol, bruceantin, and bisbrusatolyl malonate inhibited the formation of the first peptide bond between puromycin and [^{3}H]methionyl-transfer RNA bound to the initiation complex, indicating peptidyl transferase activity is inhibited by the quassinoids in P-388 cells. These studies also suggest that the free 80S ribosome is the site of binding by the quassinoid. Ribosomes actively conducting protein synthesis will continue protein synthesis and terminate before the quassinoids bind. This proves quassinoids are elongation inhibitors of tumor cells. A strong correlation was observed between potent antileukemic activity and the ability to inhibit protein synthesis in P-388 lymphocytic leukemia cells.

Keyphrases □ Protein synthesis—inhibition by quassinoids, P-388 lymphocytic leukemia cells □ Quassinoids—inhibition of protein synthesis, P-388 lymphocytic leukemia cells □ Structure–activity relationships—quassinoids, inhibition of protein synthesis, P-388 lymphocytic leukemia cells □ Antitumor agents—quassinoids, inhibition of protein synthesis, P-388 lymphocytic leukemia cells

Bruceantin, a quassinoid now in phase II clinical trials, was first isolated from *Brucea antidysenterica* (1, 2). Subsequently, bruceoside A was isolated from *Brucea javanica* (3) and brusatol was derived chemically from bruceoside A. It was demonstrated (4) that bruceantin inhibited protein synthesis in HeLa cells by 90% at 2 μM, whereas DNA and RNA synthesis were inhibited 60 and 15%, respectively. Protein synthesis was inhibited 79% in rabbit reticulocytes by bruceantin at 0.1 μM (4). Liao (4) postulated that bruceantin was an initiation inhibitor of

0022-3549/82/0400-0430$01.00/0

protein synthesis. However, it was shown (5), using the yeast organism *Saccharomyces cereviseae*, that bruceantin blocks the peptidyl transferase site of the ribosome and inhibits the peptide chain elongation reaction. Interestingly, the drug binds to the free ribosome as opposed to the ribosome actively engaged in protein synthesis (5).

Brusatol has been observed to inhibit DNA, RNA, and protein synthesis of P-388 lymphocytic leukemia cells at 0.015 m*M* concentration resulting in 84, 62, and 86% inhibition, respectively. At 0.005 m*M* the inhibitions are 38, 44, and 60%, respectively (6). Brusatol was shown to be an elongation inhibitor by using the rabbit reticulocyte pro-

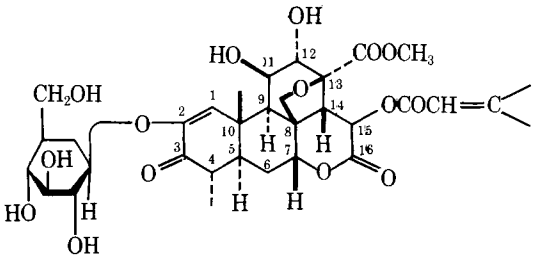

I[bruceoside A]

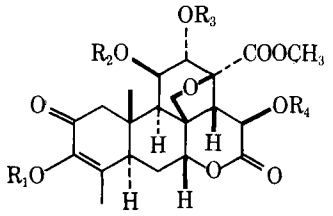

II[brusatol]: $R_1 = R_2 = R_3 = H$, R_4 =

III[bruceantin]: $R_1 = R_2 = R_3 = H$, R_4 =

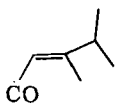

IV[brusatol triacetate]: $R_1 = R_2 = R_3 = COCH_3$, R_4 =

V[bruceolide]: $R_1 = R_2 = R_3 = R_4 = H$

VI[3-(3,4-dimethyl-2-pentenoyl)bruceolide]: R_1 =

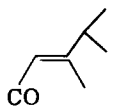

, $R_2 = R_3 = R_4 = H$

VII[3-(3,4-dimethyl-2-pentenoyl)bruceantin]: $R_1 = R_4$ =

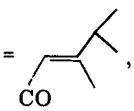

, $R_2 = R_3 = H$

VIII[12-acetyl-3,15-disenecioyl bruceolide]: $R_1 = R_4$ =

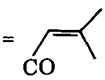

, R_2 = H, $R_3 = COCH_3$

IX[3,15-disenecioyl bruceolide]: $R_1 = R_4$ =

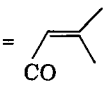

, $R_2 = R_3 = H$

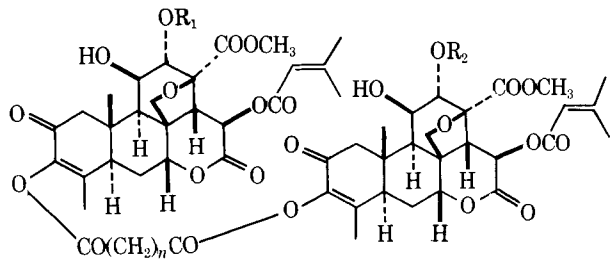

X[bis-12,12′-diacetyl brusatolyl succinate]: $R_1 = R_2 = COCH_3$, n = 2
XI[bisbrusatolyl adipate]: $R_1 = R_2 = H$, n = 4
XII [bisbrusatolyl glutarate]: $R_1 = R_2 = H$, n = 3
XIII[bisbrusatolyl succinate]: $R_1 = R_2 = H$, n = 2
XIV[bisbrusatolyl malonate]: $R_1 = R_2 = H$, n = 1

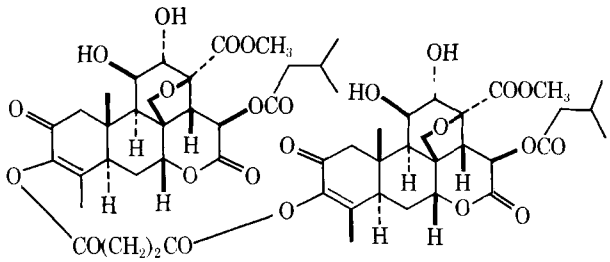

XV[bis-dihydrobrusatolyl succinate]

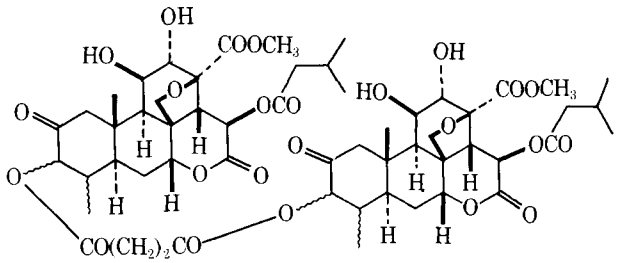

XVI[bis-tetrahydrobrusatolyl succinate]

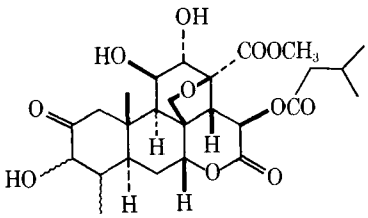

XVII [tetrahydrobrusatol]

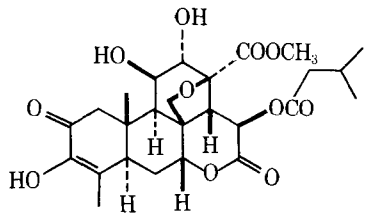

XVIII [dihydrobrusatol]

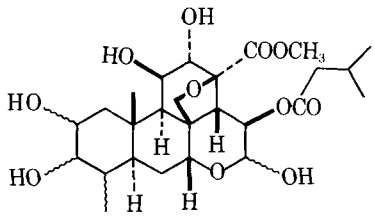

XIX[2-hydroxy-2-deoxotetrahydrobrusatol lactol]

tein synthesis system. Brusatol probably inhibits peptidyl transferase activity (7). Bruceantin and brusatol are active against P-388 lymphocytic leukemia growth *in vivo* between 100 μg/kg to 1 mg/kg depending on the host strain of mice used (8). A series of brusatol esters and bisbrusatolyl esters were synthesized and characterized previously (9).

The present study reports the structure–activity relationships between the antileukemic activity and the ability to suppress protein synthesis elongation processes.

RESULTS AND DISCUSSION

Potent antileukemic activity against P-388-UNC lymphocytic leukemia was observed with compounds VII, IX, XIII, XIV, and XV giving T/C % ≧ 180 at 0.6 mg/kg/day in BDF_1 male mice. The results are comparable with the standard, fluorouracil, at 25 mg/kg/day. Moderate activity (T/C % ≧ 140–176) was observed with compounds II, III, XI, XII, and VIII. The bisbrusatolyl esters (XI–XIV) were more potent than brusatol (II) or bruceoside A (I), respectively, the succinate (XIII) and malonate (XIV) esters with T/C % of 217 and 272, respectively. Reduction of the C_{15} ester double bond did not decrease the antileukemic activity significantly (compare XV to XIII and XVIII to III). However, saturation of the diosphenol double bond resulted in either less activity or an inactive compound (XVI, XVII, and XIX). Esterification of II at the C-3 position gave VII and IX which were more active than II. Compounds formed by acetylation of the hydroxyl groups at C-11 and C-12 possessed little antileukemic activity (IV, VIII, and X).

Whole cell protein synthesis of P-388 cells was inhibited maximally (92%) by compound XIV (Table I) followed by compounds II, IX, and XIII (78–69%) and compounds I, III, V, VII, XII, XV, and XVIII (60–53%) at 15 μ*M* final concentration. The quassinoids followed a dose response from 5–15 μ*M*. Examination of the lysate protein synthesis assay demonstrated that compounds II, IX, XIII, XIV, and XV caused >80% inhibition, whereas compounds VII, XI, and XII resulted in >70% inhibition of protein synthesis (Table II).

Compounds II and III have been previously demonstrated to be elongation inhibitors in normal rabbit reticulocytes and compound XIV in the P-388 tumor line. For this reason a series of experiments were conducted to establish the inhibition mechanism by compounds II and III in the P-388 leukemia cells. A comparison of Fig. 2 with Fig. 1 shows that compounds II, III, and XIV all allow accumulation of the 80S ribosome peak similar to pyrocatechol violet rather than emetine. The result suggests the quassinoids allow completion of the already initiated polypeptide chain synthesis and release of the free 80S ribosome from the polyribosome before totally inhibiting protein synthesis. The quassinoids had little or no effect on the formation of either the ternary complex[1] or the 80S initiation complex[2] (Table III). The quassinoids II, III, and XIV behaved in these assays more like emetine than pyrocatechol violet indicating that they did not inhibit initiation events of polypeptide chain synthesis.

In an additional study, the formation of the 80S initiation complex[2] and peptide bond formation was examined by treating P-388 cell lysates with the elongation inhibitor chlortetracycline, which specifically inhibited binding of the aminoacyl-transfer RNA to the ribosome A site but did not inhibit the peptidyl transferase reaction. When [^{3}H]methionyl-transfer RNA was added to the system, most of the radioactivity was found associated with the 80S initiation complex. Addition of poly-adenosine-uridine-guanosine to the chlortetracycline treated lysate allowed formation of an 80S initiation complex (Fig. 3). The complex then reacted with puromycin followed by the puromycin-induced release of [^{3}H]methionine from the 80S complex (Fig. 4). The quassinoids II, III, and XIV did not appear to inhibit the formation of the 80S initiation complex, but did inhibit puromycin release of methionine indicating that the quassinoids inhibit P-388 peptide bond formation. Examination of the formation of aminoacyl-transfer RNA with phenylalanine, leucine, or methionine indicated that these agents had no effect on the activation of amino acid for incorporation into polypeptides. These studies suggest that the quassinoids are elongation inhibitors of protein synthesis, probably inhibiting peptidyl transferase activity. The quassinoids do not inhibit the synthesis of ongoing polypeptide synthesis but rather appear to bind to free P-388 80S ribosomes. The 80S peak which accumulates in the presence of the quassinoids is actually an 80S initiation complex

[1] eIF·Guanosine triphosphate·[^{3}H]methionyl-transfer RNA.

[2] 80S·Adenosine-uridine-guanosine·eIF·guanosine triphosphate·[^{3}H]methioinyl-transfer RNA.

Table I—Effect of Quassinoids on Protein Synthesis of P-388 Lymphocytic Leukemia

Drugs	Control Protein Synthesis, % Concentration, μM 5	10	15	T/C	ID_{50}
I. Bruceoside A	70	48	42	121	9.7
II. Brusatol	61	44	22	149	7.5
III. Bruceantin	74	57	46	146	13.1
IV. Brusatol triacetate	94	89	79	102	110.0
V. Bruceolide	72	60	40	139	12.1
VI. 3-(3,4-Dimethyl-2-pentenoyl)-bruceolide	68	64	57	131	24.8
VII. 3-(3,4-Dimethyl-2-pentenoyl)-bruceantin	66	59	48	194	13.9
VIII. 12-Acetyl-3,15-disenecioyl bruceolide	91	78	69	103	37.2
IX. 3,15-Disenecioyl bruceolide	52	38	31	185	6.0
X. Bis-12,12′-diacetyl brusatolyl succinate	83	75	67	118	37.0
XI. Bisbrusatolyl adipate	70	60	51	176	15.3
XII. Bisbrusatolyl glutarate	63	57	43	176	11.9
XIII. Bisbrusatolyl succinate	58	40	30	217	6.8
XIV. Bisbrusatolyl malonate	54	17	8	272	5.4
XV. Bisdihydrobrusatolyl succinate	60	57	47	193	13.8
XVI. Bistetrahydrobrusatolyl succinate	75	66	57	113	21.6
XVII. Tetrahydrobrusatol	85	76	56	120	17.8
XVIII. Dihydrobrusatol	72	58	43	150	12.3
XIX. 2-Hydroxy-2-deoxotetrahydrobrusatol lactol	77	70	65	107	48.1
XX. 0.05% Polysorbate·water	100	100	100	100	

rather than true runoff ribosomes. The acceleration of 80S initiation complex has been reported previously with bruceantin in yeast, brusatol in rabbit reticulocytes, and bisbrusatolyl malonate in P-388 cells. Table IV demonstrates that the quassinoids inhibit polyuridine directed synthesis of polyphenylalanine, a study carried out on purified runoff ribosomes isolated from 10-day P-388 cells. Polyuridine directed polyphenylalanine synthesis does not require the normal initiation and termination reactions; consequently, this inhibition is of the elongation type exclusively. Table IV shows that compound XIV caused 92% inhibition at 15 μM. Compounds VII and XIII result in greater than 80% inhibition of polyphenylalanine synthesis, whereas compounds II, IX, XI, and XII caused greater than 75% inhibition at 15 μM.

The structural rquirements for inhibition of protein synthesis of P-388 leukemia cells are bis-esters of brusatol with an alkyl side chain of the ester of 1 or 2 carbons, or a C-3 or C-15 disenecioate or di-3,4-dimethyl-2-pentenoate side chain of bruceolide. Those compounds which demonstrated potent activity possessed an enone system in ring A and free hydroxy groups at C-11 and C-12. The same structural requirements are needed for antileukemic activity and *in vitro* inhibition of protein synthesis of P-388 cells. Analysis of the inhibition of polyuridine directed polyphenylalanine synthesis in Table IV and T/C % values obtained in the antileukemic screen indicated that there was a negative correlation coefficient of 0.84, *i.e.*, the higher the T/C % value obtained for the esters, the greater the degree of inhibition of protein synthesis in P-388 lymphocytic leukemic cells.

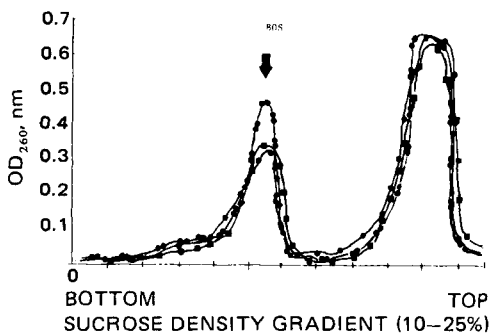

Figure 1—*Effects of pyrocatechol violet and emetine on the P-388 ribosome profile. Key:* ●—●, *control;* —● ●—, *pyrocatechol violet; and* ■—■, *emetine.*

Table II—Effects of Quassinoids on P-388 Lymphocytic Leukemia Cell Lysate Using Endogenous mRNA

Drugs	Control, % 1 μM	10 μM	100 μM	ID_{50}
I. Bruceoside A	76.8	53.8	47.3	38.3
II. Brusatol	76.8	28.4	10.9	6.0
III. Bruceantin	85.8	76.5	61.9	6.0
IV. Brusatol triacetate	87.4	60.2	53.6	125.0
V. Bruceolide	76.4	64.4	55.4	268.0
VI. 3-(3,4-Dimethyl-2-pentenoyl)bruceolide	70.6	57.3	53.9	695.0
VII. 3-(3,4-Dimethyl-2-pentenoyl)bruceantin	54.2	33.1	26.0	1.7
VIII. 12-Acetyl-3,15-disenecioyl bruceolide	91.9	77.6	67.0	125.0
IX. 3,15-Disenecioyl bruceolide	69.6	52.8	16.8	13.0
X. Bis-12,12′-diacetyl brusatolyl succinate	85.7	67.1	62.4	1400.0
XI. Bisbrusatolyl adipate	50.5	37.6	21.5	1.3
XII. Bisbrusatolyl glutarate	69.4	46.1	21.4	6.8
XIII. Bisbrusatolyl succinate	62.0	34.9	18.1	2.7
XIV. Bisbrusatolyl malonate	57.8	19.9	8.7	1.7
XV. Bisdihydrobrusatolyl succinate	57.9	31.3	13.9	2.0
XVI. Bistetrahydrobrusatolyl succinate	84.7	69.9	54.9	122.0
XVII. Tetrahydrobrusatol	89.9	83.9	78.3	1930.0
XVIII. Dihydrobrusatol	69.4	63.8	43.0	50.0
XIX. 2-Hydroxy-2-deoxotetrahydrobrusatol lactol	86.3	79.8	67.1	1120.0
XX. 0.05% Polysorbate·water	100.0	100.0	100.0	

EXPERIMENTAL

Source of Compounds—Bruceoside A (1) originally was isolated from *Brucea javanica* (1, 2). Brusatol (II) was obtained by treating bruceoside A with 3 N H_2SO_4–methanol (1:1) to hydrolyze the glycosidic linkage (3). Bruceantin (III) was obtained from bruceoside A by the synthetic method (20). The chemical synthesis, purification, and physical characteristics of compounds IV–XIX, *i.e.*, brusatol esters, bisbrusatolyl esters, and related derivatives, were reported elsewhere (9).

P-388 Lymphocytic Leukemia Antitumor Screen—The P-388 lymphocytic leukemia cell line was maintained in DBA/2 male mice (~20 g). For the antineoplastic screen, 10^6 cells were injected intraperitoneally into BDF_1 male mice (~20 g) on day 0. Test compounds were homogenized in 0.05% polysorbate 80–water and administered on days 1–14. The average number of days survived for each group was determined and T/C % values were calculated (10). Fluorouracil was used as a positive standard.

Studies of the effects of quassinoid esters on protein synthesis were conducted on P-388 cells harvested on day 10. P-388 lymphocytic leukemia lysates were prepared by the method of Kruh *et al.* (11). The following were isolated from P-388 lysates by literature techniques: runoff ribosomes (12), "pH 5" enzyme (11), and uncharged transfer RNA (13). The P-388 lymphocytic leukemia cell initiation factors for protein synthesis were prepared as decribed previously (14). [^{3}H]Methionyl-transfer RNA was prepared from P-388 cell transfer RNA by the method of Takeishi *et al.* (15). The effects of the brusatol esters on endogenous protein synthesis (4) of P-388 lysates were carried out in a reaction

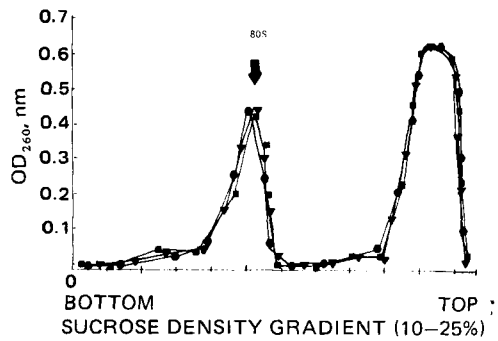

Figure 2—*Effects of brusatol, bruceantin, and bisbrusatolyl malonate on the P-388 ribosomal profile. Key:* ■, *brusatol;* ●, *bruceantin; and* ▼, *bisbrusatolyl malonate.*

Table III—Effects of Bisbrusatolyl Malonate on Ternary and 80S Complex Formation

	Concentration, μM	Complex Formation, pmole	Control, %
Ternary Complex Formation			
Control		2.10	100
+ Emetine	100	2.02	96
+ Pyrocatechol violet	100	0.21	10
III. + Bruceantin	25	2.01	96
II. + Brusatol	25	1.97	94
XIV. + Bisbrusatolyl malonate	25	1.81	86
80S Initiation Complex Formation			
Control		1.82	100
+ Emetine	100	1.49	82
+ Pyrocatechol violet	100	0.36	20
III. + Bruceantin	25	1.64	90
II. + Brusatol	25	1.55	85
XIV. + Bisbrusatolyl malonate	25	1.51	83

mixture (0.5 ml) containing 10 mM tromethamine (pH 7.6), 76 mM KCl, 1 mM adenosine triphosphate, 0.2 mM guanosine triphosphate, 15 mM creatine phosphate, 2 mM $MgCl_2$, 1 mM dithiothreitol, 0.1 mM of each of the essential amino acids, 0.9 mg/ml creatine phosphokinase, and 20 μCi [^{3}H]leucine (56.6 Ci/mmole). An aliquot of the reaction mixture was incubated at 30°. After 90 sec of incubation, test drugs or the standards (pyrocatechol violet or emetine) were added to a final concentration of 1, 10, and 100 μM. At 1-min intervals, 50-μl aliquots were removed from the reaction tubes and spotted on filter papers[3] which were treated for 10 min in boiling 5% trichloroacetic acid, followed by 10 min in cold 5% trichloroacetic acid and washed with cold 5% trichloroacetic acid, ether–ethanol (1:1), and ether. The filter papers were dried and counted in scintillation fluid.

The effects of bruceantin, brusatol, bisbrusatolyl malonate, pyrocatechol violet, and emetine on the ribosome profile (4) of P-388 cell lysates were assayed using the reaction medium described previously (500 μl). Following drug addition to a 100-μM final concentration, the reaction was incubated for 4 min at 37°. The reaction was terminated in ice and gradient buffer consisting of 1 ml of tromethamine (pH 7.6), 10 mM KCl, and 1.5 mM $MgCl_2$-$6H_2O$ was added. The mixture was layered over 36 ml of 10–25% linear sucrose gradient (4), prepared in gradient buffer, and centrifuged for 165 min at 25,000 rpm in a swinging bucket rotor[4] at 4°. The absorbance profile at 260 nm was determined with a flow cell (light path 0.2 cm) attached to a spectrophotometer[5].

The reaction medium for the polyuridine (poly U) directed polyphenylalanine synthesis (16) contained 50 mM tromethamine (pH 7.6), 12.5 mM magnesium acetate, 80 mM KCl, 5 mM creatine phosphate, 0.05 mg/ml creatine phosphokinase, 0.36 mg/ml polyuridine[6] (A_{280}/A_{260} = 0.34), 0.5 μCi [^{14}C]phenylalanine (536 mCi/mmole), 75 μg uncharged P-388 cell transfer RNA, 70 μg of P-388 "pH 5" enzyme preparation, and 0.9 A_{260} of P-388 cell runoff ribosomes. Test drugs I–XIX were present in 5-, 10-, and 15-μM concentrations. Incubation was for 20 min at 30°,

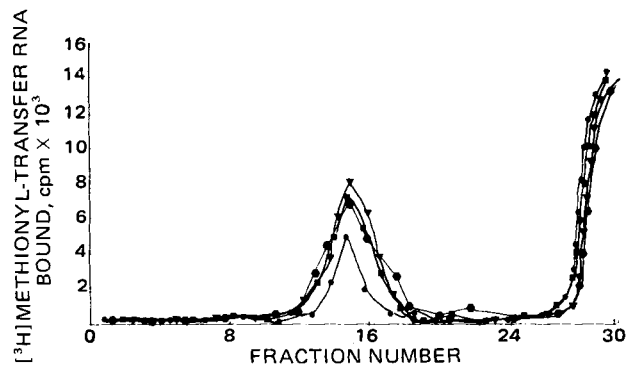

Figure 3—*Formation of the 80S initiation complex of P-388 cell system (linear sucrose gradient centrifugation). Key: ●, control; ■, brusatol; ●, bruceantin; and ▼, bisbrusatolyl malonate.*

[3] Whatman No. 3.
[4] Beckman. SW 27.
[5] Gilford.
[6] Miles Laboratory, Inc.

Table IV—Inhibition by Quassinoids of Polyuridine Directed Polyphenylalanine Syntheses of 10-Day P-388 Cells

Drugs	Control Protein Synthesis, % Concentration, μM 5	10	15	ID_{50}
I. Bruceoside A	76	63	40	12.5
II. Brusatol	54	43	23	6.4
III. Bruceantin	75	58	34	11.5
IV. Brusatol triacetate	92	87	80	90.0
V. Bruceolide	77	55	38	11.6
VI. 3-(3,4-Dimethyl-2-pentenoyl)bruceolide	80	67	45	13.5
VII. 3-(3,4-Dimethyl-2-pentenoyl)bruceantin	44	36	19	2.9
VIII. 12-Acetyl-3,15-disenecioyl bruceolide	90	80	72	46.0
IX. 3,15-Disenecioyl bruceolide	48	39	20	4.4
X. Bis-12,12′-diacetyl brusatolyl succinate	84	71	60	21.5
XI. Bisbrusatolyl adipate	53	41	22	6.0
XII. Bisbrusatolyl glutarate	51	40	22	5.2
XIII. Bisbrusatolyl succinate	39	27	15	2.7
XIV. Bisbrusatolyl malonate	31	18	8	1.9
XV. Bisdihydrobrusatolyl succinate	45	36	21	3.4
XVI. Bistetrahydrobrusatolyl succinate	81	66	50	15.0
XVII. Tetrahydrobrusatol	83	70	48	14.5
XVIII. Dihydrobrusatol	79	65	42	13.0
XIX. 2-Hydroxy-2-2-deoxotetrahydrobrusatol lactol	80	72	65	36.0
XX. 0.05% Polysorbate-water	100	100	100	

after which a 35-μl aliquot was spotted on filter paper[3] and processed as indicated previously.

The reaction medium (200 μl) used to measure the formation of the 80S initiation complex and the methionyl puromycin reaction (17) contained 15 mM tromethamine (pH 7.6), 80 mM KCl, 1 mM adenosine triphosphate, 0.5 mM guanosine triphosphate, 20 mM creatine phosphokinase, 3 mM magnesium acetate, 0.1 mM edetic acid, 1 mM dithiothreitol, 0.1 mM each of the 19 essential amino acids, 3 mg of P-388 cell lysates, 100 μg/ml chlortetracycline[7] 3 × 105 cpm [^{3}H]methionyl-transfer RNA, and 20 μg/ml (polyadenosine–uridine–guanosine); and 5 μl of bruceantin, brusatol, and bisbrusatolyl malonate (25 μmoles). The incubation was carried out at 23° and aliquots were withdrawn after 2 min to analyze for 80S complex formation. Puromycin (10 μg/ml) was then added to the reaction medium. The incubation was continued for another 6 min and aliquots were withdrawn to analyze for reaction of the 80S complex with puromycin. All aliquots (50 μl) were diluted to 250 μl with 20 mM tromethamine (pH 7.6), 80 mM KCl, 3 mM magnesium acetate, 1 mM dithiothreitol, and 0.1 mM edetic acid, layered on 11.8 ml of a 15–30% linear sucrose gradient, and centrifuged for 3 hr at 36,000 rpm in a swinging bucket rotor[8]. Fractions (0.4 ml) were collected and precipitated with 10% trichloroacetic acid on filter papers and counted.

The reaction mixtures (75 μl) for the ternary complex formation[1] (18) contained 21.4 mM tromethamime (pH 8.0), 80 mM KCl, 0.26 mM gua-

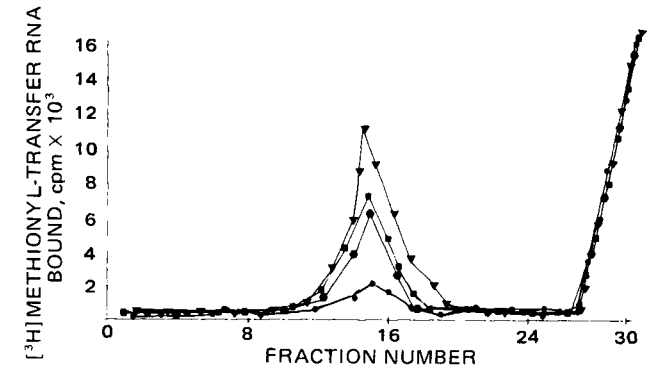

Figure 4—*Effects of quassinoids in the methinoyl puromycin reaction of P-388 cell system (linear sucrose gradient centrifugation). Key: ●, control; ■, brusatol; ●, bruceantin; and ▼, bisbrusatolyl malonate.*

[7] Sigma Chemical Co.
[8] Beckman SW 40.

Table V—Effects of Bisbrusatolyl Malonate on Amino Acid tRNA Activation in P-388 Lymphocytic Leukemia Cells

	Inhibitor	Concentration, μM	Amino Acid t-RNA Formation, pmole	Control, %
	[^{14}C]Phenylalanine-tRNA			
	Control		1.05	100
	+ Emetine	100	0.97	92
	+ Pyrocatechol violet	100	0.98	93
III.	+ Bruceantin	50	0.96	91
II.	+ Brusatol	50	0.95	90
XIV.	+ Bisbrusatolyl malonate	50	0.97	92
	[^{3}H]Leucyl-tRNA			
	Control		1.83	100
	+ Emetine	100	1.74	95
	+ Pyrocatechol violet	100	1.72	94
III.	+ Bruceantin	50	1.68	92
II.	+ Brusatol	50	1.72	94
XIV.	+ Bisbrusatolyl malonate	50	1.76	96
	[^{3}H]Methionyl-tRNA			
	Control		1.62	100
	+ Emetine	100	1.54	95
	+ Pyrocatechol violet	100	1.57	97
III.	+ Bruceantin	50	1.59	96
II.	+ Brusatol	50	1.56	98
XIV.	+ Bisbrusatolyl malonate	50	1.52	94

nosine triphosphate, 2.14 mM dithiothreitol, 10 μg of bovine serum albumin, 5 pmoles of P-388 cell [^{3}H]methionine-transfer RNA (Met-tRNA$_f$, 1×10^4 cpm), 100 A_{260}/ml of crude P-388 cell initiation factors and 10 μl of drug or standard. The incubation was conducted for 5 min at 37° and terminated by addition of 3 ml of cold buffer [21.4 tromethamine (pH 8.0), 80 mM KCl, and 2.14 mM dithiothreitol]. The samples were filtered through 0.45-μm filters, washed twice in buffer, and counted.

The reaction mixture (75 μl) for the 80S initiation complex[2] (18) formation contained, in addition to the components necessary for the ternary complex formation reaction, 1.9 mM magnesium acetate, 5 A_{260}/ml polyadenosine–uridine–guanosine[7], and 100 A_{260}/ml of 80S P-388 cell ribosomes. Incubation was 10 min at 37° which was then cooled to 4° and titrated to 5 mM with magnesium acetate. After 5 min at 4°, the samples were diluted with cold buffer [21.4 mM tromethamine (pH 8.0), 80 mM KCl, 5 mM magnesium acetate, and 2.14 mM dithiothreitol] and filtered as indicated for the ternary complex formation experiment.

Amino acid transfer RNA activation steps were determined by the method of Moldave (19). The reaction medium contained 0.1 mM tromethamine (pH 7.4), 0.2 mM adenosine triphosphate, 0.3 mg/ml "pH 5" enzyme from P-388 cells, and 2.5 μCi/ml of [^{14}C]phenylalanine (536 mCi/mmole), [^{3}H]leucine (56.5 Ci/mmole), or [^{3}H]methionine (80.0 Ci/mmole) in a total volume of 1 ml. After incubation at 37° for 20 min, 2 ml of ice cold 10% trichloroacetic acid was added and the activated amino acid-transfer RNA was collected on nitrocellulose filters.

REFERENCES

(1) S. M. Kupchan, R. W. Britton, J. A. Lacadie, M. F. Ziegler, and C. W. Sigel, *J. Org. Chem.*, **40,** 648 (1975).

(2) M. Suffness and J. Douros, in "Methods in Cancer Research," V. T. DeVita and H. Busch, Eds., Academic, New York, N.Y. 1979, p. 73.

(3) K. H. Lee, Y. Imakura, Y. Sumida, R. Y. Wu, I. H. Hall, and H. C. Huang, *J. Org. Chem.*, **44,** 2180 (1979).

(4) L. L. Liao, S. M. Kupchan, and S. B. Horwitz, *Mol. Pharmacol.*, **12,** 167 (1976).

(5) M. Fresno, A. Jimenez, and D. Vasquez, *Eur. J. Biochem.*, **72,** 323 (1977).

(6) I. H. Hall, K. H. Lee, S. A. ElGebaly, Y. Imakura, Y. Sumida, and R. Y. Wu, *J. Pharm. Sci.*, **68,** 883 (1979).

(7) W. Willingham, E. A. Stafford, S. H. Reynolds, S. G. Chaney, K. H. Lee, M. Okano, and I. H. Hall, *Biochim. Biophys. Acta*, **654,** 169 (1981).

(8) I. H. Hall, K. H. Lee, M. Okano, D. Sims, T. Ibuka, Y. F. Liou, and Y. Imakura, *J. Pharm. Sci.* **70,** 1147 (1981).

(9) K. H. Lee, M. Okano, I. H. Hall, D. A. Brent, and B. Soltmann, *ibid.*, **71,** 338 (1982).

(10) R. I. Geran, N. H. Greenberg, M. M. MacDonald, A. M. Schumacher, and B. J. Abbott, *Cancer Chemother. Rep.*, **3,** 9 (1972).

(11) J. Kruh, L. Grossman, and K. Moldane, *Methods Enzymol.*, **XIIb,** 732 (1968).

(12) M. H. Schreier and T. Staehelin, *J. Mol. Biol.*, **73,** 329 (1973).

(13) J. M. Ravel, R. D. Mosteller, and B. Hardesty, *Proc. Natl. Acad. Sci. USA*, **56,** 701 (1966).

(14) A. Majumdar, S. Reynolds, and N. K. Gupta, *Biochem. Biophys. Res. Commun.*, **67,** 689 (1975).

(15) K. Takeishi, T. Ukita, and S. Nishimura, *J. Biol. Chem.*, **243,** 5761 (1968).

(16) J. Jimenez, A. Sanchez, and D. Vasquez, *Biochim. Biophys. Acta*, **383,** 4271 (1975).

(17) J. Carter and M. Cannon, *Eur. J. Biochem.*, **84,** 103 (1978).

(18) S. H. Reynolds, A. Majumdar, A. Das Gupta, S. Palmieri, and N. K. Gupta, *Arch. Biochem. Biophys.*, **184,** 324 (1977).

(19) K. Moldave, *Methods Enzymol.*, **6,** 757 (1963).

(20) M. Okano and K. H. Lee, *J. Org. Chem.*, **46,** 1183, 1981.

ACKNOWLEDGMENTS

Supported by American Cancer Society Grant CH-19 (K. H. Lee and I. H. Hall) and National Cancer Institute Grants CA 22929 and CA 17625 (in part) (K. H. Lee), and CA 26466 (S. G. Chaney).

The authors thank Dr. E. S. Huang of the Department of Virology, School of Medicine, University of North Carolina at Chapel Hill for the use of the sucrose gradient system and technical assistance for the completion of this research project.

An Isocratic High-Pressure Liquid Chromatographic Determination of Naproxen and Desmethylnaproxen in Human Plasma

J. L. SHIMEK, N. G. S. RAO, and S. K. WAHBA KHALIL ˣ

Received April 24, 1981, from the *College of Pharmacy, North Dakota State University, Fargo, ND 58105.* Accepted for publication August 14, 1981.

Abstract □ An isocratic high-pressure liquid chromatographic method for the determination of naproxen and its desmethyl metabolite in human plasma is presented. A reversed-phase octadecylsilane column was utilized with a mobile phase consisting of 55% methanol and 45% 0.10 *M* acetate buffer, pH 5.0. A spectrofluorometric detector with an excitation wavelength of 253 nm and a band pass filter provided high sensitivity with no interference from normal plasma constituents. The reproducibility and precision of the method were shown by analysis of spiked samples containing 2.5–70 μg/ml of plasma.

Keyphrases □ Naproxen—determination by isocratic high-pressure liquid chromatography, human plasma □ High-pressure liquid chromatography—isocratic, determination of naproxen and desmethylnaproxen in human plasma □ Metabolites—determination of naproxen and its desmethyl metabolite in human plasma, high-pressure liquid chromatography

Naproxen is a nonsteroidal anti-inflammatory drug commonly used for the treatment of arthritis, dysmenorrhea, and for the relief of mild to moderate pain (1). Drugs in this class share many side effects such as GI (2, 3) and renal toxicity (4). Due to the high incidence of side effects, there is interest in the use of patient monitoring as a method of minimizing adverse reactions.

A direct spectrophotometric method lacking specificity due to interference from metabolites and salicylic acid has been reported (5). Several GLC methods also have been reported, all of which require derivation and a minimum 0.5-ml plasma sample (6–10). Quantitation has been performed by high-pressure liquid chromatography (HPLC) (11–14), and methods have been described involving precipitation of plasma protein followed by injection of the supernate (11) and the direct injection of diluted samples (12). The use of ion-pairing has also been described (12). An HPLC method for screening solid dosage forms using dual UV detectors was reported recently (15). Methods capable of determining the metabolite require a 0.5-ml plasma sample (10, 13).

The present report describes a method for the rapid determination of naproxen and its desmethyl metabolite using an isocratic HPLC separation and fluorometric detection. Conditions for the extraction, separation, and detection of naproxen and desmethylnaproxen in a sample size of 0.1-ml plasma are discussed. The applicability of this model was demonstrated by the analysis of plasma from patients receiving oral naproxen.

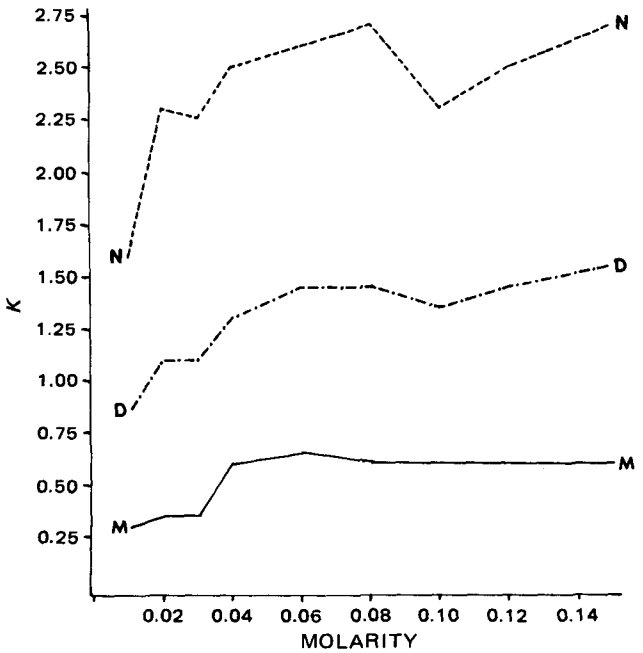

Figure 1—*Effect of molarity of the mobile phase at pH 5 on capacity factor, K'. Key: N, naproxen; M, desmethyl metabolite; and D, diphenylacetic acid (internal standard).*

EXPERIMENTAL

Instrumentation—A high-pressure liquid chromatograph[1] was equipped with a fluorometric detector[2] and an octadecylsilane column[3]

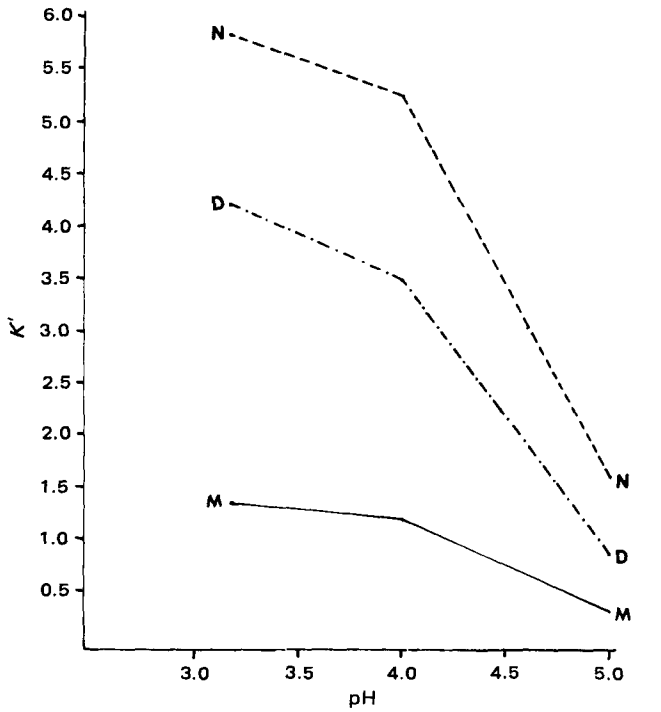

Figure 2—*Effect of pH on the mobile phase at 0.01* M *on capacity factor, K'. Key: N, naproxen; M, desmethyl metabolite; and D, diphenylacetic acid (internal standard).*

[1] Model 202 chromatograph, M6000 pump, and U6K Universal injector, Waters Associates, Milford, Mass.
[2] FS-970, Schoeffel, Westwood, N.J.
[3] Zorbax, Dupont, Wilmington, Del.

0022-3549/82/0400-0436$01.00/0

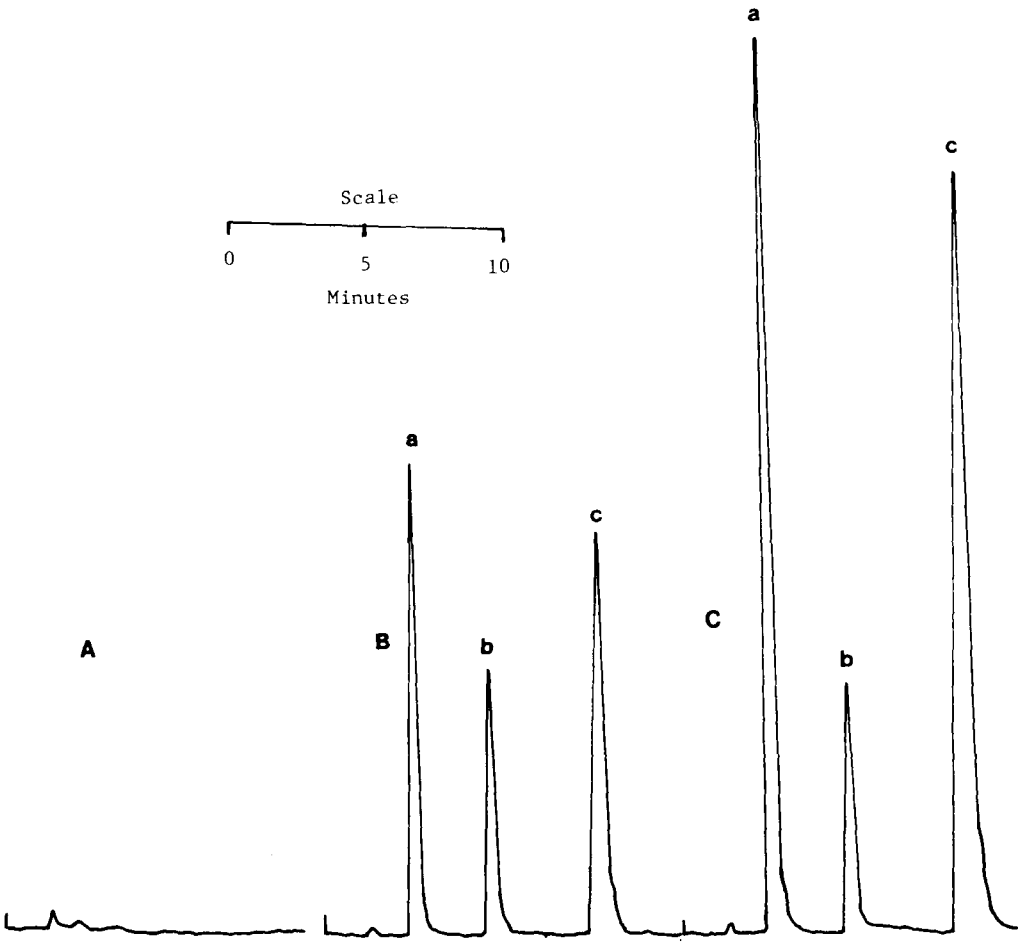

Figure 3—*Typical chromatograms of desmethylnaproxen (a), diphenylacetic acid (b), and naproxen (c) from plasma. Key: A, plasma blank; B, 15 μg drug and metabolite/1.0 ml plasma; and C, 30 μg drug and metabolite/1.0 ml plasma.*

(25 cm × 4.6-mm i.d.). The degassed mobile phase was pumped through the column at 1.5 ml/min (3200–3400 psi) at ambient temperature until a stable baseline was obtained. The fluorometer was set at an excitation wavelength of 253 nm and a band pass filter (230–420 nm) was used.

Chemicals and Reagents—Sodium acetate, sodium phosphate, acetic acid, phosphoric acid, methylene chloride, hexane, chloroform, ethyl acetate, ether, isopropanol, and diphenylacetic acid were reagent grade. HPLC grade methanol was used. Naproxen and desmethylnaproxen were obtained from the manufacturer[4].

Mobile Phases—To study the effect of ionic concentration and pH on retention time, methanol with pH 4 and 5 sodium acetate buffers (0.01, 0.02, 0.03, 0.04, 0.06, 0.08, 0.10, 0.12, and 0.15 *M*) or acetic acid solutions (0.01, 0.02, and 0.3 *M*) were used as mobile phases. All mobile phases were degassed under vacuum.

Extraction Conditions—Plasma containing naproxen and desmethylnaproxen was acidified with one of the following: 1.0 *M* phosphoric acid, 1.0 *M* sulfuric acid, 0.1 *M* phosphate buffer (pH 4), 0.1 *M* phosphate buffer (pH 3), or 0.1 *M* acetate buffer (pH 4). The acidified plasma was extracted with hexane, methylene chloride, chloroform containing 5% isopropanol, ether, or ethyl acetate.

Standard Stock Solution—A solution containing 10 mg each of naproxen and its desmethyl metabolite in 10 ml of methanol was prepared.

Extraction Solution—A solution of 120 mg of the internal standard, diphenylacetic acid, in 250 ml of methylene chloride was prepared (2.4 mg/5 ml).

Analytical Procedure—Spiked plasma standards were prepared by adding an appropriate aliquot of the standard stock solution to 1 ml of heparinized plasma. The spiked plasma was vortexed and 0.1-ml portions were placed in 15-ml screw-capped centrifuge tubes. The plasma was acidified with 0.3 ml of 1.0 *M* phosphoric acid, and 5-ml extraction solution containing the internal standard was added. The tubes were vortexed for 10 sec and centrifuged for 5 min at 3500 rpm. A 4-ml volume of the organic phase was transferred to a concentration tube[5] and evaporated to dryness at ambient temperature under a gentle nitrogen stream. The residue was dissolved in 0.5 ml of methanol and 10 μl was injected[6]. The mobile phase used for the analysis was 55:45 methanol and acetate buffer (pH 5, 0.10 *M*).

Quantitation—A standard curve was constructed by injecting plasma extracts simulating concentrations of the drug and metabolite. The chromatograms were recorded[7] at a chart speed of 0.5 cm/min. The ratios of peak heights (drug or metabolite to internal standard) were calculated and plotted *versus* the concentration in micrograms per milliliter plasma.

Interference—The possible interference of normal plasma constituents was tested by the analysis of blank plasma. The interference of other drugs was tested by direct injection of methanolic drug solution or by the analysis of extracts of plasma samples containing therapeutic concentrations.

Recovery—For the recovery study, plasma standards were prepared as described previously. After evaporation the residue was dissolved in 0.5 ml of methanol containing 360 ng of naproxen or desmethylnaproxen. A 10-μl aliquot containing 7.2 ng was injected onto the column.

Patient Sample Preparation and Analysis—Heparinized plasma samples from patients receiving oral naproxen were processed in duplicate as described previously. The amount of drug and metabolite was calculated by comparison with standards prepared daily.

RESULTS AND DISCUSSION

Increasing buffer molarity had a complex effect on the capacity factors of naproxen, desmethylnaproxen, and the internal standard (Fig. 1). The capacity factor was increased by decreasing pH (Fig. 2). Moreover, at low pH the compounds have a high capacity factor causing very long retention times and band broadening.

[4] Syntex, Palo Alto, Calif.

[5] Concentratube, Laboratory Research Co., Los Angeles, Calif.
[6] Hamilton Co., Reno, Nev.
[7] Model 56, Perkin-Elmer, Norwalk, Conn.

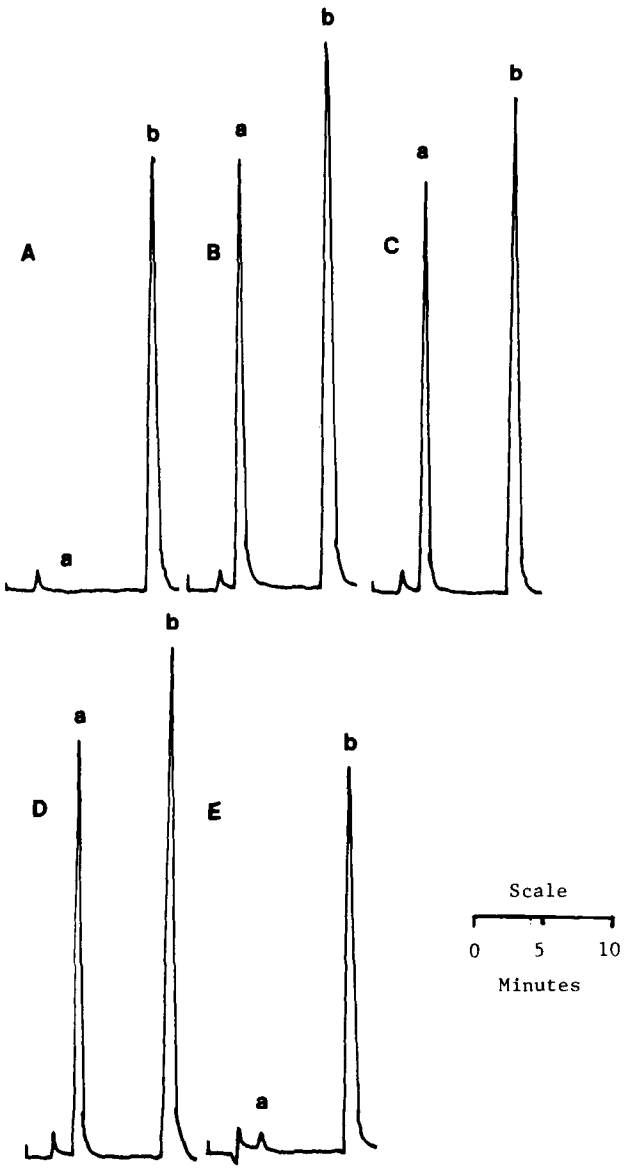

Figure 4—*Chromatograms of plasma extracts containing desmethylnaproxen (40 μg/ml) (a) and naproxen (40 μg/ml) (b). Key: A, hexane; B, methylene dichloride; C, chloroform containing 5% isopropanol; D, ether; and E, ethyl acetate.*

The choice of diphenylacetic acid as internal standard was based on coextractability with the drug and metabolite and an ideal relative retention time. A mobile phase of 55% methanol and 45% acetate buffer (pH 5, 0.10 *M*) gave well resolved, sharp peaks for naproxen, its metabolite and the internal standard, with retention times of 10.0, 3.3, and 5.9 min, respectively (Fig. 3). Under the described conditions 0.5 μg of naproxen or its desmethyl metabolite per milliliter of plasma could be quantitated.

Naproxen can be extracted readily from acidified plasma using organic solvents with a wide range of polarities; however, its desmethyl metabolite cannot be extracted with hexane or ethyl acetate (Fig. 4). The choice of acid or buffer for acidification of plasma can be used to optimize recovery and to minimize interference from plasma constituents, but due to the small sample size required and the small aliquot injected onto the column,

Table I—Statistical Analysis of Linear Regression

Parameter	Naproxen	Metabolite
Range of standards, μg/ml plasma	2.5–70	2.5–70
Correlation coefficient	0.9913	0.9922
Slope	0.1021 ± 0.0029	0.1247 ± 0.0046
Intercept	−0.0327 ± 0.0480	−0.0714 ± 0.0760

Table II—Assay Precision[a]

Theoretical, μg/ml plasma	Naproxen % Found	Naproxen *SE*	Metabolite % Found	Metabolite *SE*
2.5	113.6	0.09	113.6	0.22
5	101.0	0.15	101.8	0.11
10	101.3	0.52	100.3	0.21
15	101.3	0.56	103.6	0.26
20	90.6	0.26	89.8	0.25
30	103.4	0.82	103.4	0.99
40	96.5	0.96	98.7	0.98
50	104.2	0.99	101.5	0.12
70	99.0	1.41	99.6	1.72

[a] $N = 5$.

Table III—Possible Interferences Under Assay Conditions

Drug or Metabolite	Fluorescence at Assay Conditions	Retention Time, min
Acetaminophen	No	—
Caffeine	No	—
Carbamazepine	No	—
Fenoprofen	Yes	>15
Ibuprofen	Yes	>15
Indomethacin	No	—
Des(chlorobenzoyl) metabolite	Yes	Solvent front
Desmethyl metabolite	No	—
Phenobarbital	No	—
Phenytoin	No	—
Primidone	No	—
Quinidine	No	—
Salicylic acid	Yes	Solvent front
Sulindac	No	—
Sulfide metabolite	No	—
Sulfone metabolite	No	—
Theophylline	No	—
Tolmetin	No	—
Metabolite	No	—
Valproic acid	No	—

there was no interference from plasma constituents with any of the acids or buffers tested. Optimum recovery of naproxen (66.6%) and desmethylnaproxen (62.4%) from spiked plasma samples was obtained using 1.0 *M* phosphoric acid to acidify plasma prior to extraction with methylene chloride.

The ratio of peak height of naproxin or its metabolite to the peak height of the internal standard was plotted *versus* concentration. Statistical analysis indicated excellent linearity (Table I) and reproducibility (Table II).

Plasma levels of patients receiving 250-mg doses, two or three times daily were 21.5–65.1 μg/ml. The metabolite was not present in significant amounts since it is not expected to significantly accumulate unless the patient's renal function is compromised (12).

Aspirin and other commonly used drugs did not interfere with the analysis (Table III).

The described method is simple and rapid. Both naproxen and its desmethyl metabolite can be determined in a single isocratic assay with no interference from many commonly used drugs. This method can be recommended for routine patient monitoring and for pharmacokinetic studies.

REFERENCES

(1) E. K. Kastrup, Ed., "Facts and Comparisons," Facts and Comparisons, Inc., St. Louis, Mo., 1981, p. 253L.

(2) W. Golden, *J. Am. Med. Assoc.*, **243**, 408 (1980).

(3) W. R. Barclay, Ed., *ibid.*, **240**, 334 (1978).

(4) R. P. Kimberly, R. E. Bowden, H. R. Keiser, and P. H. Poltz, *Am. J. Med.*, **64**, 804 (1978).

(5) M. Antilla, *J. Pharm. Sci.*, **66**, 433 (1977).

(6) R. Runkel, M. Chaplin, G. Boost, E. Segre, and E. Forchielli, *ibid.*, **61**, 703 (1972).

(7) R. Runkel, E. Forchielli, H. Sevelius, M. Chaplin, and E. Segre, *Clin. Pharmacol. Ther.*, **15**, 261 (1974).

(8) J. P. Desager, M. Vanderbist, and C. Harvengt, *J. Clin. Pharmacol.*, **16**, 189 (1976).

(9) R. Runkel, M. D. Chaplin, and H. Sevelius, *Clin. Pharmacol.*

Ther., **20**, 269 (1976).
(10) S. H. Wan and S. B. Martin, *J. Chromatogr.*, **170**, 473 (1979).
(11) L. J. Dusci and L. P. Hackett, *ibid.*, **172**, 516 (1979).
(12) D. Westlund, A. Theodorsen, and Y. Jaksch, *J. Liq. Chromatogr.*, **2**, 969 (1979).
(13) J. T. Slattery and G. Levy, *Clin. Biochem.*, **12**, 100 (1979).
(14) R. F. Burgoyne and P. R. Brown, *J. Liq. Chromatogr.*, **3**, 101 (1980).
(15) J. K. Baker and E. K. Fifer, *J. Pharm. Sci.*, **69**, 590 (1980).

ACKNOWLEDGMENTS

The authors acknowledge the Veteran's Administration Center, Fargo, N.D., for providing research facilities.

Extended Hildebrand Solubility Approach: Solubility of Tolbutamide, Acetohexamide, and Sulfisomidine in Binary Solvent Mixtures

A. MARTIN ˣ and M. J. MIRALLES

Received March 12, 1981, from the *Drug Dynamics Institute, College of Pharmacy, University of Texas, Austin, TX 78712.* Accepted for publication August 6, 1981.

Abstract □ The extended Hildebrand approach for predicting solubilities of crystalline compounds in solvent mixtures was tested using tolbutamide, acetohexamide, and sulfisomidine in mixed solvents consisting of hexane–absolute ethanol and 95% (v/v) ethyl alcohol–aqueous buffer. The solubility of these drugs was determined at 25 ± 0.2° and then back-calculated using the adhesive energy term, W, to account for solute–solvent interaction. Solubilities were predicted within 13% for tolbutamide, 31% for acetohexamide, and 43% for sulfisomidine, and with considerably better accuracy in most solvent mixtures.

Keyphrases □ Hildebrand solubility approach, extended—tolbutamide, acetohexamide, and sulfisomidine in binary solvent mixtures □ Tolbutamide—solubility in binary solvent mixtures, extended Hildebrand approach □ Acetohexamide—solubility in binary solvent mixtures, extended Hildebrand approach □ Sulfisomidine—solubility in binary solvent mixtures, extended Hildebrand approach

The Hildebrand–Scatchard theory (1) for crystalline solids in regular solution is expressed by:

$$-\log X_2 \simeq \frac{\Delta H_m^f}{2.303\,RT}\left(\frac{T_m - T}{T_m}\right) + \frac{V_2\,(\phi_1)^2}{2.303\,RT}(\delta_1 - \delta_2)^2 \quad \text{(Eq. 1)}$$

where X_2 is the mole fraction solubility, ΔH_m^f is the heat of fusion, T_m is the melting point of the solute expressed in absolute degrees, T is the absolute temperature of the solution, R is the gas constant expressed in cal/°Kmole, V_2 is the molar volume of the solute as a hypothetical supercooled liquid, δ_1 and δ_2 are the solubility parameters of the solvent and the solute, respectively, and ϕ_1 is the volume fraction of the solvent.

An approach (2) was suggested recently to extend regular solution theory to semipolar drugs in pure solvents and in polar binary solvent mixtures (2–4). The extended Hildebrand solubility equation may be written as:

$$-\log X_2 = -\log X_2^i + \frac{V_2\,(\phi_1)^2}{2.303\,RT}(\delta_1^2 + \delta_2^2 - 2W_{calc}) \quad \text{(Eq. 2)}$$

where X_2^i is the ideal solubility of the solute expressed in mole fraction, W_{calc} is the potential energy of solute–solvent interaction, and all other terms are identical with those in Eq. 1. The square of the solubility parameters are referred to as cohesive energy densities, and W may be referred to as an adhesive energy density since it involves both solute and solvent. The units of energy densities are calories per cubic centimeter (cal/cm^3) and for solubility parameters they are the square root of the same unit [(cal/cm^3)$^{1/2}$]. The ideal solubility term, $-\log X_2^i$, constitutes the first right-hand term of Eq. 1. Log X_2^i may be taken as roughly equal to $-\Delta H_m^f/2.303\,RT\,[(T_m - T)/T_m]$ as seen in Eq. 1, or as $\Delta S_m^f/R\,[\log (T/T_m)]$ as used in earlier studies (2–4). Although it has not been established which is more correct, either form provides satisfactory results

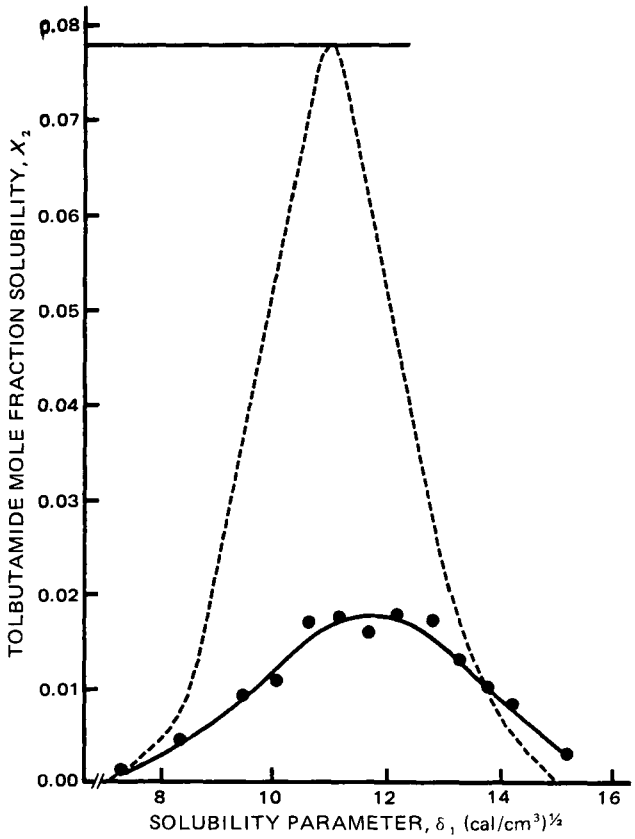

Figure 1—*Solubility profile of tolbutamide in* n*-hexane–absolute ethanol and 95% ethanol–aqueous buffer systems at 25°; δ_2 = 10.98, X_2^i = 0.07218. Key: (- - -) regular solution (Eq. 1); (—) calculated solubility (Eqs. 3*a *and* b*). The horizontal line intersecting the regular solution curve at its peak is the ideal solubility, X_2^i = 0.07218.*

0022-3549/82/0400-0439$01.00/0

Ther., **20**, 269 (1976).
(10) S. H. Wan and S. B. Martin, *J. Chromatogr.*, **170**, 473 (1979).
(11) L. J. Dusci and L. P. Hackett, *ibid.*, **172**, 516 (1979).
(12) D. Westlund, A. Theodorsen, and Y. Jaksch, *J. Liq. Chromatogr.*, **2**, 969 (1979).
(13) J. T. Slattery and G. Levy, *Clin. Biochem.*, **12**, 100 (1979).
(14) R. F. Burgoyne and P. R. Brown, *J. Liq. Chromatogr.*, **3**, 101 (1980).
(15) J. K. Baker and E. K. Fifer, *J. Pharm. Sci.*, **69**, 590 (1980).

ACKNOWLEDGMENTS

The authors acknowledge the Veteran's Administration Center, Fargo, N.D., for providing research facilities.

Extended Hildebrand Solubility Approach: Solubility of Tolbutamide, Acetohexamide, and Sulfisomidine in Binary Solvent Mixtures

A. MARTIN ˣ and M. J. MIRALLES

Received March 12, 1981, from the *Drug Dynamics Institute, College of Pharmacy, University of Texas, Austin, TX 78712.* Accepted for publication August 6, 1981.

Abstract □ The extended Hildebrand approach for predicting solubilities of crystalline compounds in solvent mixtures was tested using tolbutamide, acetohexamide, and sulfisomidine in mixed solvents consisting of hexane–absolute ethanol and 95% (v/v) ethyl alcohol–aqueous buffer. The solubility of these drugs was determined at 25 ± 0.2° and then back-calculated using the adhesive energy term, W, to account for solute–solvent interaction. Solubilities were predicted within 13% for tolbutamide, 31% for acetohexamide, and 43% for sulfisomidine, and with considerably better accuracy in most solvent mixtures.

Keyphrases □ Hildebrand solubility approach, extended—tolbutamide, acetohexamide, and sulfisomidine in binary solvent mixtures □ Tolbutamide—solubility in binary solvent mixtures, extended Hildebrand approach □ Acetohexamide—solubility in binary solvent mixtures, extended Hildebrand approach □ Sulfisomidine—solubility in binary solvent mixtures, extended Hildebrand approach

The Hildebrand–Scatchard theory (1) for crystalline solids in regular solution is expressed by:

$$-\log X_2 \simeq \frac{\Delta H_m^f}{2.303\,RT}\left(\frac{T_m - T}{T_m}\right) + \frac{V_2\,(\phi_1)^2}{2.303\,RT}(\delta_1 - \delta_2)^2 \quad \text{(Eq. 1)}$$

where X_2 is the mole fraction solubility, ΔH_m^f is the heat of fusion, T_m is the melting point of the solute expressed in absolute degrees, T is the absolute temperature of the solution, R is the gas constant expressed in cal/°Kmole, V_2 is the molar volume of the solute as a hypothetical supercooled liquid, δ_1 and δ_2 are the solubility parameters of the solvent and the solute, respectively, and ϕ_1 is the volume fraction of the solvent.

An approach (2) was suggested recently to extend regular solution theory to semipolar drugs in pure solvents and in polar binary solvent mixtures (2–4). The extended Hildebrand solubility equation may be written as:

$$-\log X_2 = -\log X_2^i + \frac{V_2\,(\phi_1)^2}{2.303\,RT}(\delta_1^2 + \delta_2^2 - 2W_{calc}) \quad \text{(Eq. 2)}$$

where X_2^i is the ideal solubility of the solute expressed in mole fraction, W_{calc} is the potential energy of solute–solvent interaction, and all other terms are identical with those in Eq. 1. The square of the solubility parameters are referred to as cohesive energy densities, and W may be referred to as an adhesive energy density since it involves both solute and solvent. The units of energy densities are calories per cubic centimeter (cal/cm^3) and for solubility parameters they are the square root of the same unit [(cal/cm^3)$^{1/2}$]. The ideal solubility term, $-\log X_2^i$, constitutes the first right-hand term of Eq. 1. Log X_2^i may be taken as roughly equal to $-\Delta H_m^f/2.303\,RT\,[(T_m - T)/T_m]$ as seen in Eq. 1, or as $\Delta S_m^f/R\,[\log (T/T_m)]$ as used in earlier studies (2–4). Although it has not been established which is more correct, either form provides satisfactory results

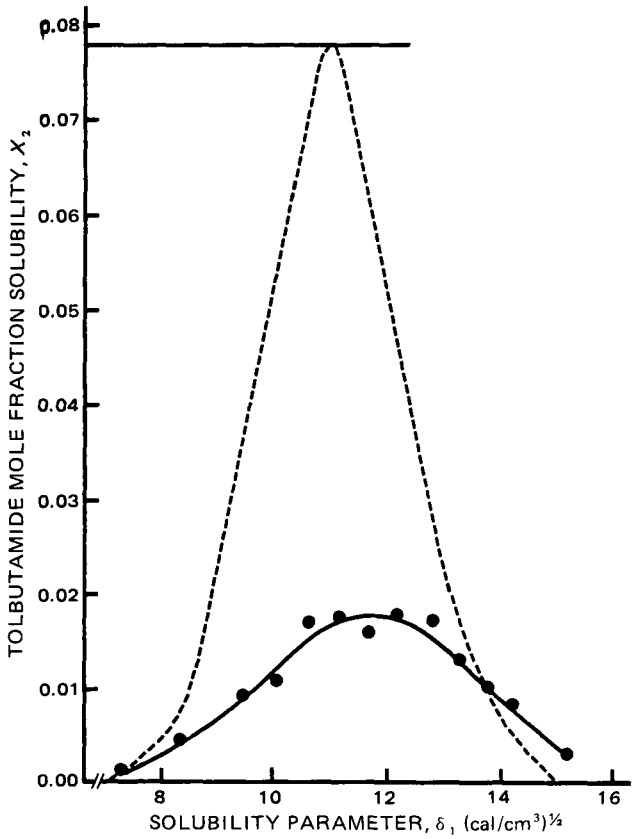

Figure 1—*Solubility profile of tolbutamide in* n*-hexane–absolute ethanol and 95% ethanol–aqueous buffer systems at 25°; δ_2 = 10.98, X_2^i = 0.07218. Key: (- - -) regular solution (Eq. 1); (—) calculated solubility (Eqs. 3*a *and* b*). The horizontal line intersecting the regular solution curve at its peak is the ideal solubility, X_2^i = 0.07218.*

0022-3549/82/0400-0439$01.00/0

Table I—Melting Point, Heat of Fusion, Ideal Solubility, Molar Volume, and Solubility Parameters of I, II, and III

Compound	T_m, °K	ΔH_m^f, cal/mole[a]	X_2^i, (25°)	log X_2^{ib}, (25°)	V_2^c, cm³/mole (25°)	δ_2^c, cal/cm$^{3\ 1/2}$ (25°)
Tolbutamide (I)	404.8	6122	0.072180	−1.1416	209.9	10.98
Acetohexamide (II)	457.0	9819	0.003146	−2.5022	234.4	11.64
Sulfisomidine (III)	515.6	10781	0.000463	−3.3344	181.9	12.80

[a] Determined by differential scanning calorimetry. [b] Calculated from the equation, $-\log X_2^i = (\Delta H_m^f)/2.303\,RT\,[(T_m - T)/T_m]$. [c] Obtained from the method of Fedors (Ref. 5).

Table II—Mole Fraction Solubility of I in *n*-Hexane–Absolute Ethanol and 95% (v/v) Ethanol–Aqueous Buffer Systems at 25°[a]

Solvent Composition	δ_1, cal/cm$^{3\ 1/2}$	Solution Density, g/cm³	V_1, cm²/mole	A	W_{obs}	W_{calc}	log α_2/A (obs)	log α_2/A (calc)	X_{2obs}	X_{2calc}	Percent Error in X_2
100% hexane	7.30	0.6559	131.35	0.15324	81.1643	81.2637	11.5219	11.3230	0.001238	0.001328	−7.27
80 hexane in absolute ethanol	8.39	0.6862	113.12	0.15119	91.5510	91.3535	7.8504	8.2454	0.004694	0.004091	12.85
60% hexane in absolute ethanol	9.48	0.7248	96.67	0.14777	102.2015	102.1887	6.0279	6.0533	0.009283	0.009202	0.87
50% hexane in absolute ethanol	10.03	0.7366	89.26	0.14621	107.7655	107.9390	5.6303	5.2833	0.010845	0.012188	−12.38
40% hexane in absolute ethanol	10.58	0.7608	81.49	0.14099	114.0233	113.8790	4.4502	4.7787	0.017021	0.015499	8.94
30% hexane in absolute ethanol	11.12	0.7705	75.66	0.13979	119.8956	119.8957	4.4235	4.4234	0.017380	0.017380	0.00
20% hexane in absolute ethanol	11.63	0.7895	69.40	0.13964	125.5801	125.7461	4.6570	4.3251	0.016148	0.017966	−11.26
10% hexane in absolute ethanol	12.17	0.8039	62.75	0.13706	132.0865	132.1185	4.4963	4.4324	0.017464	0.017820	−2.04
100% absolute ethanol	12.76	0.8182	58.28	0.13606	139.4080	139.2900	4.5620	4.7980	0.017287	0.016055	7.13
95% (v/v) ethanol	13.24	0.8375	54.96	0.13986	145.2214	145.2856	5.4151	5.2868	0.012620	0.013153	−4.22
95% ethanol in aqueous buffer	13.72	0.8492	52.01	0.14143	151.4441	151.4258	5.9105	5.9473	0.010531	0.010405	1.20
90% ethanol in aqueous buffer	14.20	0.8597	49.38	0.14357	157.8167	157.7104	6.5771	6.7795	0.008206	0.007675	6.47
80% ethanol in aqueous buffer	15.15	0.8838	44.05	0.14357	170.5180	170.5750	9.0469	8.9328	0.003225	0.003354	−4.00

[a] $X_2^i = 0.07218$; $V_2 = 209.9$; $\delta_2 = 10.98$.

in the back-calculation method of the extended solubility approach.

To further test the extended solubility approach for drugs in mixed solvents, solubilities of the hypoglycemic agents, tolbutamide (I) and acetohexamide (II), and a structurally related compound, sulfisomidine (III), were determined in mixtures of *n*-hexane–absolute ethanol, and 95% (v/v) ethanol in an aqueous buffer. The W values of the extended solubility equation are obtained from experimental X_2 using Eq. 2, and then W_{calc} is obtained by regressing W on δ_1 for the solvent mixture in a second degree or higher power series. Log α_2/A may also be regressed against δ_1 to obtain logα_2/A_{calc}.

EXPERIMENTAL

Materials—Tolbutamide[1], acetohexamide[2], sulfisomidine[3], *n*-hexane[4], absolute ethanol[5], 95% ethanol[6], sodium hydroxide[6], and methanol[6] were tested for identity and purity, and otherwise used as received.

Solubility Determination—The solubility of I (δ_2 = 10.98) and II (δ_2 = 11.64) was determined in mixed solvents consisting of *n*-hexane (δ_{1a} = 7.30) and absolute ethanol (δ_{1b} = 12.76), and in 95% ethanol (δ_{1c} = 13.24) mixed with aqueous buffer (δ_{1d} = 22.77, pH = 2.59) in different proportions. The solubility of III (δ_2 = 12.80) was determined in mixed solvents consisting of *n*-hexane and absolute ethanol, and 95% ethanol–aqueous buffer (δ_{1c} = 22.34, pH = 4.9).

About 20 ml of the pure solvent or solvent mixture was introduced into screw-capped vials containing an excess of the drug being studied. The vials were agitated for ~72 hr in a shaker bath maintained at 25 ± 0.2°. After equilibrium was obtained, a filtered aliquot was pipetted, using an automatic micropipette, into a volumetric flask and appropriately diluted with methanol. The solutions were analyzed in a spectrophotometer[7] at 264 nm for I, 247 nm for II, and 281.5 nm for III. The densities of the saturated solutions and solvent mixtures were determined at 25 ± 0.2° using a 10-ml pycnometer. All determinations were made in triplicate.

Water Content—The water content of absolute ethanol and ethanol labeled 95% (v/v) was determined by direct titration[8].

Aqueous Buffer Preparation—The pH of the distilled water used in the preparation of the solvent mixtures was adjusted so that the drugs existed predominantly in their nonionized form; thus, solubility as the ion was not involved. The pH of the buffer solution was measured after preparation and at several intervals to be sure that changes in pH did not occur in the solutions alone or after the drug was added.

Heat of Fusion of I, II, and III—A differential scanning calorimeter[9] was used to determine the heats of fusion of the drugs. The technique and equations utilized in the determination were reported earlier (3).

Solubility Parameter and Molar Volume—The solubility parameters and molar volumes of I, II, and III were calculated using the functional group contribution method of Fedors (5). The solubility parameters of the solutes were verified using the data from solubility studies of the drugs in binary systems (4). The solubility parameter (δ_2) was obtained at peak solubility and was assumed to be equal to the solubility parameter of the solvent mixture (δ_1). In polar solvent mixtures this procedure yields somewhat different solubility parameters depending on the solvent system used.

Other quantities required in predicting the solubility of a drug in solvent mixtures (molar volumes, V; volume fraction of the solvent mixtures, ϕ_1; mole fraction solubility of the solute, X_2; ideal solubility of the solute expressed in mole fraction, X_2^i; solute activity coefficients, α_2; and the adhesive energy density, W) were calculated as described previously (3). The solubility parameters and the molecular weights of absolute ethanol

[1] Upjohn, Kalamazoo, Mich.
[2] Eli Lilly, Indianapolis, Ind.
[3] Sigma Chemical, St. Louis, Mo.
[4] Aldrich Chemical, Wilwaukee, Wis.
[5] Commercial Solvent, Terre Haute, Ind.
[6] Fisher Scientific, Fair Lawn, N.J.
[7] Beckman Model 25 spectrophotometer.
[8] Aquatrator, Precision Scientific Co.
[9] Model 1B, Perkin-Elmer.

Table III—Regression Equations of W_{calc} and log α_2/A_{calc} for I, II, and III in Hexane–Absolute Ethanol and 95% Ethanol–Aqueous Buffer Systems at 25°. [a]

Compound	Equations	
Tolbutamide (I)	$W_{calc} = 32.9064\ (\pm 0.8420) + 4.3342\ (\pm 0.1528)\ \delta_1 + 0.3137\ (\pm 0.0067)\ \delta_1^2$	(Eq. 3a)
	$n = 13 \quad R^2 = 0.999 \quad s = 0.12663 \quad F = 265172 \quad F_{(2,10,0.01)} = 7.56$	
	$\log \alpha_2/A_{calc} = 54.7567\ (\pm 1.6842) - 8.6700\ (\pm 0.3056)\ \delta_1 + 0.3726\ (\pm 0.0135)\ \delta_1^2$	(Eq. 3b)
	$n = 13 \quad R^2 = 0.988 \quad s = 0.25330 \quad F = 420 \quad F_{(2,10,0.01)} = 7.56$	
Acetohexamide (II)	$W_{calc} = 43.0479\ (\pm 1.8180) + 3.7634\ (\pm 0.3300)\ \delta_1 + 0.3460\ (\pm 0.0146)\ \delta_1^2$	(Eq. 4a)
	$n = 10 \quad R^2 = 0.999 \quad s = 0.25268 \quad F = 53040 \quad F_{(2,7,0.01)} = 9.55$	
	$\log \alpha_2/A_{calc} = 49.4027\ (\pm 3.6367) - 7.5282\ (\pm 0.6601)\ \delta_1 + 0.3081\ (\pm 0.0291)\ \delta_1^2$	(Eq. 4b)
	$n = 10 \quad R^2 = 0.962 \quad s = 0.50544 \quad F = 90 \quad F_{(2,7,0.01)} = 9.55$	
Sulfisomidine (III)	$W_{calc} = 93.8825\ (\pm 6.5207) - 5.7575\ (\pm 1.6683)\ \delta_1 + 1.1189\ (\pm 0.1366)\ \delta_1^2 - 0.0186\ (\pm 0.0036)\ \delta_1^3$	(Eq. 5a)
	$n = 12 \quad R^2 = 0.999 \quad s = 0.33165 \quad F = 49488 \quad F_{(3,8,0.01)} = 7.59$	
	$\log \alpha_2/A_{calc} = -23.9294\ (\pm 13.0437) + 11.5170\ (\pm 3.3371)\ \delta_1 - 1.2380\ (\pm 0.2732)\ \delta_1^2 + 0.0371\ (\pm 0.0072)\ \delta_1^3$	(Eq. 5b)
	$n = 12 \quad R^2 = 0.984 \quad s = 0.66342 \quad F = 166 \quad F_{(3,8,0.01)} = 7.59$	

[a] The statistical parameters under each regression equation are n, the number of solvent mixtures used; R^2, the squared multiple correlation coefficient; s, the standard deviation of the sample; F, the Fisher F ratio, which is followed by the tabular value of F with degrees of freedom k and $n - k - 1$ at the 99% level. The value k is the number of independent variables in the equation.

and 95% ethanol were corrected relative to their water content [0.57% (v/v) for absolute ethanol and 5.06% (v/v) for ethanol labeled 95%].

RESULTS AND DISCUSSION

Experimental melting points (T_m), obtained with a capillary apparatus[10], heat of fusion (ΔH_m^f), ideal solubilities (X_2^i), solubility parameters, and molar volumes for I, II, and III are reported in Table I.

The values of observed and calculated solubilities (Eq. 2) of I in hexane–absolute ethanol and 95% ethanol–aqueous buffer are compared in Table II. Solution densities are included to allow calculations of solubilities in mole/liter or gram/cm^3. The experimental solubilities of I, II, and III, expressed as mole fraction *versus* the solubility parameters of the solvent mixtures, are plotted in Figs. 1–3. The ideal solubilities, X_2^i, and the regular solution curve obtained using Eq. 1 are also shown. The regression equations and statistics for W_{calc} and log α_2/A_{calc} are shown in Table III. Earlier studies (3, 4) employed 20–30 data points for regression analysis. The present study shows that about 12 points are adequate for back-calculating the solubility curve.

The regular solution curves of Figs. 1, 2, and 3, do not coincide with the experimentally determined solubilities, indicating that the mixtures do not follow regular solution theory. In contrast, the lines obtained by using the extended Hildebrand approach for the drugs investigated reproduced the solubility of I, II, and III in the solvent mixtures satisfactorily (Figs. 1, 2, and 3). The ideal solubilities of I and II are higher than the peak solubility in mixtures of *n*-hexane–absolute ethanol and 95% ethanol–aqueous buffer. For III the ideal solubility is lower than the experimental solubility in aqueous ethanol, presumably because of solvation of the drug by the mixed solvent.

At the maximum of the solubility curve, the experimental points for II fall below the predicted solubility using the extended Hildebrand approach, but the discrepancy is not great. This may be explained by the presence of small peaks and valleys in the solubility profile of II that the empirical expression for W cannot be expected to reproduce. The presence of peaks and valleys around the maximum solubility is not an uncommon occurrence; prominent peaks were first observed by Paruta and Irani (6) in the solubility of caffeine in a mixture of dioxane and water.

The solubility parameters for I, II, and III were used to position the maxima of the regular solution lines of Figs. 1–3. The maxima do not coincide exactly with the peaks of the experimental curves. Although an accurate knowledge of the solubility parameters of the drugs is important for an understanding of physicochemical properties, the extended solubility method—being a back-calculation procedure—does not depend on absolute values of δ_2 for its success. As reported earlier (3) the method may, in fact, bypass W and δ_2 and yield X_{2calc} by regression of logα_2/A on δ_1, as shown in Table III. In the present study, the results obtained using the Fedors method (5) were accepted as a first approximation as the solubility parameters of the three drugs.

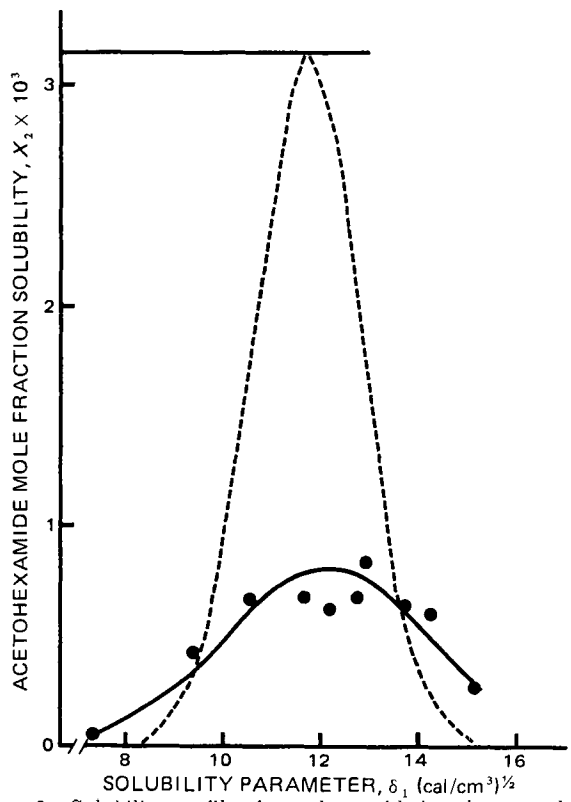

Figure 2—*Solubility profile of acetohexamide in* n*-hexane–absolute ethanol and 95% ethanol–aqueous buffer at 25°; $\delta_2 = 11.64$, $X_2^i = 0.00314$. Key: (- - -) regular solution (Eq. 1); (—) calculated solubility (Eqs. 4a and b). The horizontal line intersecting the regular solution curve at its peak is the ideal solubility, $X_2^i = 0.00314$.*

[10] Thomas Hoover capillary melting point apparatus, A. H. Thomas Co.

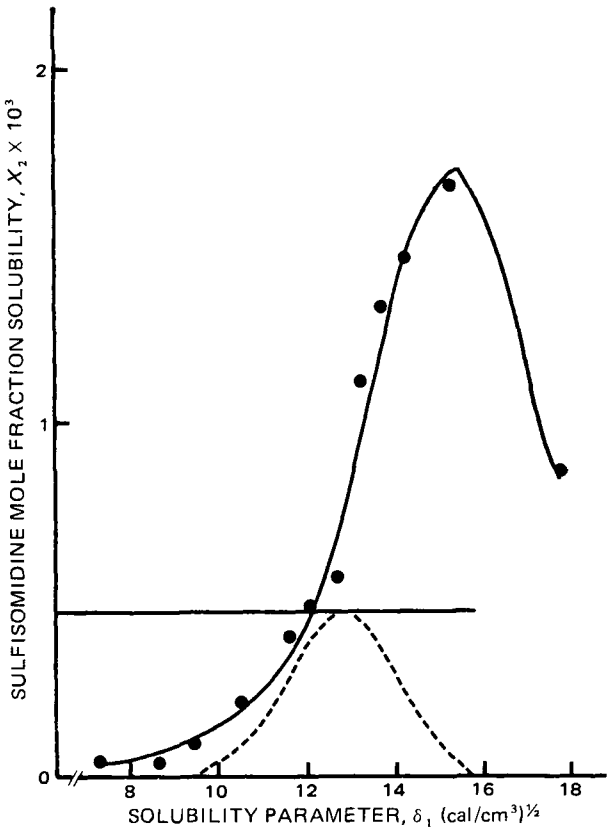

Figure 3—*Solubility profile of sulfisomidine in n-hexane–absolute ethanol and 95% ethanol–aqueous buffer systems at 25°; δ_2 = 12.80. Key: (- - -) regular solubility (Eq. 1); (—) calculated solubility (Eqs. 5a and b). The horizontal line intersecting the peak of the regular solution curve signifies the ideal mole fraction solubility, $X_2^i = 0.463 \times 10^{-3}$.*

CONCLUSIONS

The extended Hildebrand solubility approach (1–3) was tested for its ability to reproduce solubilities of tolbutamide, acetohexamide, and sulfisomidine in mixtures of *n*-hexane–absolute ethanol and 95% ethanol–aqueous buffer. Power series regression (quadratic for I and II and cubic for III) in δ_1 was used to back-calculate W, and from W to calculate solubilities.

Workers in various industries, including the pharmaceutical and cosmetic sciences, have not been able to rely on the Hildebrand equation (Eq. 1) for estimating solubilities in polar solvent systems. According to regular solution theory the solubility of I is predicted to be much larger than actual solubility at $\delta_1 = \delta_2 = 10.98$ (Fig. 1). Conversely, for III the solubility predicted by the Hildebrand approach is grossly underestimated (Fig. 3). The Hildebrand theory provides reasonable, although not always accurate, estimates of solubility in nonpolar solvents but is not successful for polar systems.

The extended Hildebrand solubility approach, replacing the geometric mean $\delta_1\delta_2$ by an adhesive energy density W, and regressing W against the solvent solubility parameter to obtain back-calculated values of solubility, shows one reason why the Hildebrand method (Eq. 1) fails in binary mixtures of polar solvents. Surprisingly, small differences between W and $\delta_1\delta_2$ result in large differences between actual and ideal solubility. For I at $\delta_1 = 11.12$, $\delta_1\delta_2 = 122.0976$, and $W = 119.8957$; $X_2 = 0.017380$, and $X_2^i = 0.072180$. The difference of as little as 1.8% between W of the extended approach and $\delta_1\delta_2$ of the Hildebrand theory yields a 315% solubility difference between experimental solubility and that calculated by the Hildebrand method. In the same mixed solvent, 30% hexane in ethanol, the extended Hildebrand solubility method calculates the correct solubility, $X_{2calc} = 0.01738$ (0.0% error).

Both the Hildebrand and its extended method yield unsatisfactory estimates for solubilities of crystalline drugs in single polar solvents. Unlike binary mixtures, individual solvents show wide differences in molar volume, acid–base characteristics, and other properties. It will be necessary to devise new approaches, such as that suggested by the Hansen partial solubility parameters (7), in order to describe complex drug molecules in single solvents of high, low, and intermediate polarity.

REFERENCES

(1) J. H. Hildebrand and R. L. Scott, "The Solubility of Nonelectrolytes," 3rd. ed., Reinhold, New York, N.Y., 1950, p. 271.

(2) A. Martin, J. Newburger, and A. Adjei, *J. Pharm. Sci.*, **68**, iv (10) (1979).

(3) *Ibid.*, **69**, 487 (1980).

(4) A. Adjei, J. Newburger, and A. Martin, *J. Pharm. Sci.*, **69**, 659 (1980).

(5) R. F. Fedors, *Polym. Eng. Sci.*, **14**, 147 (1974).

(6) A. N. Paruta and S. A. Irani, *J. Pharm. Sci.*, **55**, 1060 (1966).

(7) C. M. Hansen and A. Beerbower, in "Encyclopedia of Chemical Technology," suppl. vol., 2nd ed., A. Standen, Ed., Wiley, New York, N.Y., 1971, pp. 889–910.

ACKNOWLEDGMENTS

Supported in part by an endowed professorship provided to A. Martin by Coulter R. Sublett.

M. J. Miralles wishes to express her gratitude to the Fundacion Gran Mariscal de Ayacucho for providing financial support. The authors appreciate the assistance of P. L. Wu.

O-Methylhydroxylamine as a New Trapping Reagent for Quantitative Studies of 4-Hydroxycyclophosphamide and Aldophosphamide

GERALD ZON *x, SUSAN MARIE LUDEMAN *, EDWARD M. SWEET *, WILLIAM EGAN ‡, and LAWRENCE R. PHILLIPS ‡

Received June 19, 1981, from the **Department of Chemistry, The Catholic University of America, Washington, DC 20064*, and the ‡*Bureau of Biologics, Food and Drug Administration, Bethesda, MD 20205.* Accepted for publication August 14, 1981.

Abstract □ ^{31}P- and ^{1}H-NMR spectroscopy were used to demonstrate that the primary metabolites of the anticancer drug cyclophosphamide (4-hydroxycyclophosphamide and its acyclic tautomer, aldophosphamide) are quantitatively converted by *O*-methylhydroxylamine, at pH 7.4 and 37°, into the *E* and *Z* isomers of aldophosphamide *O*-methyl oxime. These trapping products are readily extracted from aqueous media with either chloroform or ethyl acetate, are stable at pH 6–8 toward oxime hydrolysis and elimination of phosphoramide mustard (a secondary metabolite of cyclophosphamide), and showed no evidence for transoximination with either ketone or aldehyde acceptors. All of these features support the use of aldophosphamide *O*-methyl oxime in quantitative studies related to cyclophosphamide metabolism.

Keyphrases □ Cyclophosphamide—metabolites, 4-hydroxycyclophosphamide, aldophosphamide, trapping with *O*-methylhydroxylamine □ Aldophosphamide—*O*-methyloxime derivative, *E* and *Z* isomers, ^{1}H-NMR identification □ NMR Spectroscopy—^{1}H analysis aldophosphamide *O*-methyloxime identification, ^{31}P analysis, decomposition kinetics

There is considerable interest in the organic chemistry and quantitative analysis of 4-hydroxycyclophosphamide (II) and aldophosphamide (III) (Scheme I), as these primary metabolites of cyclophosphamide (I) are generally believed to play pivotal roles in the oncostatic selectivity of this widely used anticancer prodrug (1, 2). The presence of a hemiaminal moiety in II allows for facile tautomerization with III, which can fragment into acrolein (IV) and phosphoramide mustard (V). The combined alkylating activity of II, III, and V can be quantified using 4-(*p*-nitrobenzyl)pyridine (3), whereas the combined cytotoxicity of low levels of all lethal cyclophosphamide metabolites is measurable [*e.g.*, by an *in vitro* assay employing Walker 256 rat carcinosarcoma cells (4)]. One method for selectively measuring the total concentration of metabolites II and III is their conversion to a relatively stable derivative using reaction conditions which preempt loss of II and III by fragmentation. Reported examples of such trapping products (Scheme I) include 4-ethoxycyclophosphamide (VI) (5), aldophosphamide semicarbazone (VII) (6), aldophosphamide propanediol-1,3-acetal (VIII) (7), and aldophosphamide cyanohydrin (IX) (8). In contrast to these compounds, analytical utilization of 4-sulfidocyclophosphamides (X) must contend with their hydrolytic instability (9). Pulse Fourier-transform NMR spectroscopy is an alternative methodology which offers the unique advantages of providing direct quantitative measurements of II and III as individual solution components.

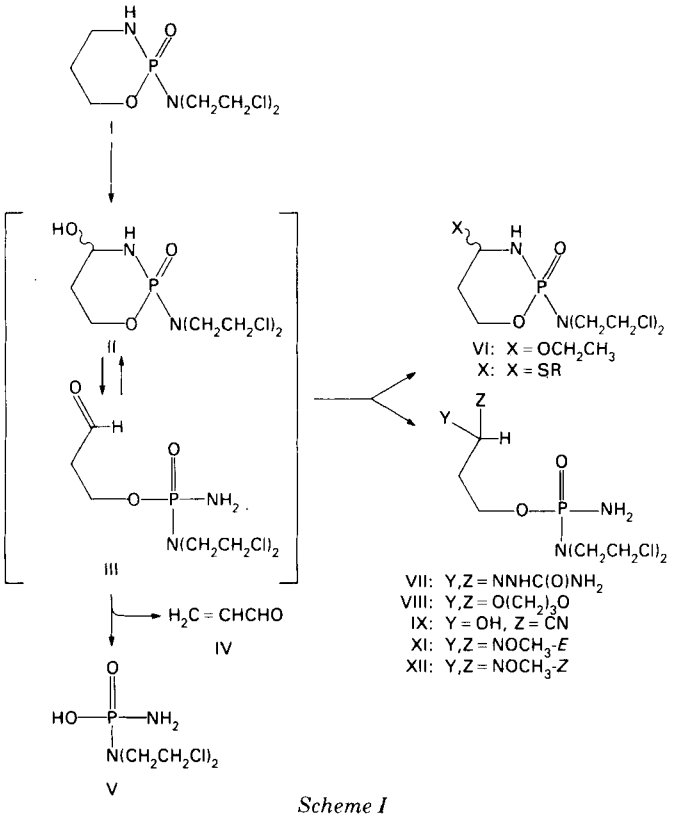

Scheme I

During the NMR kinetic studies of II and III, *O*-methylhydroxylamine, which serves as a derivatizing agent for GC–mass spectrometric analyses of aldoses (10), was conducive to this study because of (*a*) its super-nucleophilicity due to lone-pair repulsion; (*b*) the thermal (GC, GC–mass spectrometric) stability of *O*-methyl oximes; (*c*) the resistance of *O*-methyl oximes toward hydrolytic reversion to aldehydes; (*d*) the availability of *O*-methylhydroxylamine hydrochloride in various stable isotope-enriched (^{2}H, ^{13}C, ^{15}N) and radioactive (^{3}H, ^{14}C) forms; and (*e*) the possibility for chemically induced reformation of aldehyde III. Since all of these features are not applicable to VI–IX, this study reports the formation and characterization of the trapping products derived from the reaction of II/III with *O*-methylhydroxylamine, namely, the *E* (XI) and *Z* (XII) isomers of aldophosphamide *O*-methyl oxime.

EXPERIMENTAL

Hydroxyphosphamide (8), 4-ketocyclophosphamide (XIV) (11), and compound XV (12) were synthesized and compound XIII was prepared and purified by Colvin's[1] method. ^{31}P-Fourier-transform NMR spectra at 40.25 MHz[2] were obtained using 10-mm sample tubes, a 5-kHz spectral window, 8192 data points zero-filled to 16,384, a $\pi/2$ pulse of 18 μsec, low-power ^{1}H-decoupling, and a 2-sec pulse repetition time. Spectra were

[1] M. Colvin, Johns Hopkins University School of Medicine, personal communication.

[2] FX-100 spectrometer, JEOL USA, Inc.

0022-3549/82/0400-0443$01.00/0

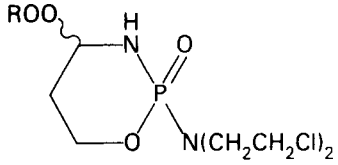

XIII: R = H
XV: R = I-4-yl
XVI: R = $C(CH_3)_3$

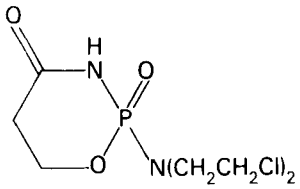

XIV

broadened by 1 Hz due to exponential multiplication prior to Fourier-transform. ^{31}P-Fourier-transform NMR spectra at 121.5 MHz[3] were recorded in a similar manner except for the use of a 20-μsec $\pi/2$ pulse, a 1.4-sec pulse repetition time, and 2.5 Hz of line-broadening. ^{1}H-Fourier-transform NMR spectra at 300 MHz[3] were recorded using 5-mm sample tubes, a 6-kHz spectral window, a 2-μsec $\pi/2$ pulse, a 5.4-sec pulse repetition time, and 0.2 Hz of line-broadening. ^{1}H-NMR spectra at 220 MHz[4] were recorded in the continuous-wave mode. Unless specified otherwise, ^{31}P-chemical shifts (δ, ppm) refer to deuterium oxide solvent and are relative to external 25% H_3PO_4. ^{1}H-Chemical shifts are relative to internal tetramethylsilane. NMR sample temperatures were measured by immersion of a precalibrated copper-constantan thermocouple. Values of pH measured[5] in deuterated water were not corrected for isotope effects (13). Electron-impact mass spectra[6] were scanned from samples introduced *via* a solids' inlet probe; the probe temperature was maintained at 20° for a 2-min period and was then elevated at 120°/min to a final temperature of 325°. Chemical-ionization mass spectra obtained with isobutane were scanned from samples similarly introduced. The ion-source temperature was 180°, the ionizing potential was 70 eV (150 eV for chemical-ionization), the ion-source pressure was 5×10^{-6} torr (10^{-3} torr for chemical ionization), and the ionizing current was 50 μamp.

4-(*tert*-Butylperoxy)cyclophosphamide (XVI)[7]—A solution of cyclophosphamide monohydrate[8] (2.048 g, 7.34 mmole) and *tert*-butyl hydroperoxide (1.0 ml, 70% aqueous solution) in 34 ml of acetone–water 1:2 was cooled with an ice bath, and ozone[9] (25–50 mg/min) was then bubbled into this solution through a glass frit. More acetone (5 ml) was added at 30-min intervals, and more *tert*-butyl hydroperoxide (1 ml) was added at 1.0-hr intervals during the course of the reaction (3 hr). Acetone was removed *in vacuo* on a rotary evaporator at room temperature and the remaining aqueous solution was extracted with methylene chloride (5×25 ml). The combined extracts were dried over anhydrous magnesium sulfate and solvent was then removed *in vacuo* without heating. The residual oil was chromatographed at 6° on a column (2.2×26-cm) of silica gel[10] using acetone–chloroform (2:1) and a flow rate of 8 ml/hr. Product [R_f 0.80, 250-μm silica gel, acetone–chloroform (2:1), iodine visualization] contaminated with *tert*-butyl hydroperoxide (R_f 0.95) and XIV (R_f 0.60) eluted in fractions 7–9 (8 ml/fraction), which were combined and concentrated *in vacuo* to give material (380 mg) for rechromatography in hexane–acetone–chloroform (3:2:1). The two diastereomers of XVI were detected in fractions 12–16 as overlapping TLC components [R_f 0.58 and 0.52, 250-μm silica gel, hexane–acetone–chloroform (3:2:1)]. Removal of solvent from these fractions afforded a pure sample (144 mg) of the faster eluting diastereomer and a mixture (113 mg) of the faster and slower eluting diastereomers; total yield 10% (257 mg). ^{31}P-NMR (40.25 MHz, deuterochloroform) of faster eluting XVI: δ 6.04; for slower eluting XVI, δ 6.44. ^{1}H-NMR (220 MHz, deuterochloroform) of faster eluting XVI: 5.09 (d, J_{HP} = 25 Hz of q, J_{HH} = 3 Hz, 1H, C_4—H), 4.64 (m, 1H, 1-C_6—H), 4.09 (m, 1H, 1-C_6—H), 3.82 (broad s, 1H, NH), 3.59 (t, J_{HH} = 7 Hz, 4H, 2-NCH_2CH_2Cl), 3.41 (m, 4H, 2-NCH_2CH_2Cl), 2.02 (m, 2H, 2-C_5—H), and 1.23 [s, 9H, $C(CH_3)_3$] ppm; electron-impact mass spectrum: *m/z* 57 (55%) $[(CH_3)_3C]^+$, 73 (2%) $[(CH_3)_3CO]^+$, 92 (70%) $(^{35}ClCH_2CH_2NHCH_2)^+$, and 142 (4%) $[(^{35}ClCH_2CH_2)_2NH_2]^+$; chemical-ionization—mass spectrum: *m/z* 93 (38%) $(^{35}ClCH_2CH_2NHCH_2 + 1)^+$, and 143 (100%) $[(^{35}ClCH_2CH_2)_2N + 3]^+$; 349 $(M + 1)^+$ not observed.

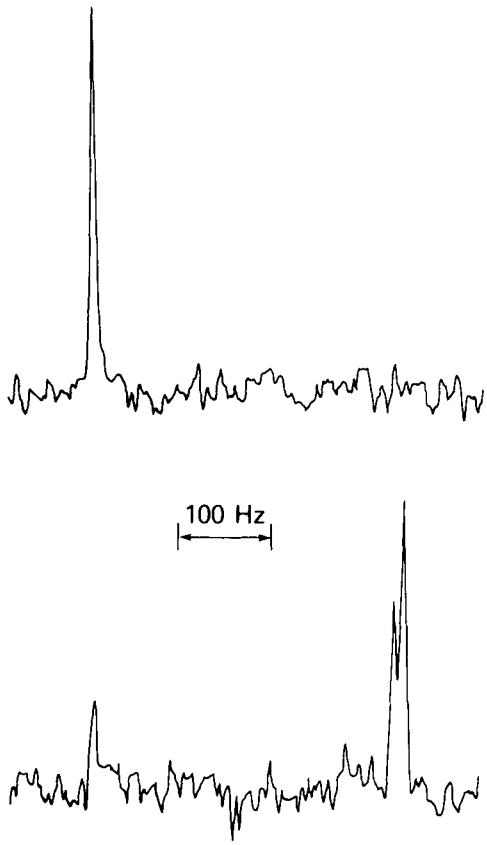

Figure 1—*^{31}P-NMR (40.25 MHz) spectra recorded in 0.05* M *lutidine buffer at 37°; bottom:* cis- *and* trans-*II (δ 12.62, 12.93) and III (δ 20.83); top: ~10 min after reaction with* O*-methylhydroxylamine to form* O*-methyl oximes XI/XII (δ 20.83).*

Reaction of II/III with *O*-Methylhydroxylamine—After recording the ^{31}P-NMR (40.25 MHz) spectrum of a solution of *cis*-XIII (10 mg, 0.034 mmole) in deuterochloroform (2 ml) at 25°, triphenylphosphine (12.5 mg, 0.048 mmole, 1.4 equivalents) was added and the spectrum was recorded after 5 min. The original signal for *cis*-XIII (δ 11.07) was replaced by that of *cis*-II (δ 10.89), and residual triphenylphosphine (δ −6.70) was detected in addition to the triphenylphosphine oxide (δ 27.42) by-product. Solvent was removed *in vacuo* on a rotary evaporator without heating, and the residue was then sonicated for 10 min with lutidine buffer (2 ml of 0.05 *M*, pH 7.4, 5 v/v% deuterium oxide). The filtered solution was clarified by centrifugation and was then analyzed by ^{31}P-NMR before and after (10 min) addition of *O*-methylhydroxylamine hydrochloride (14 mg, 0.170 mmole, 5 equivalents; sample pH adjusted to 7.4 with 1 *N* sodium hydroxide); spectra are shown in Fig. 1. The solution was saturated with sodium chloride and then extracted with deuterochloroform (2×1 ml) for ^{1}H- and ^{31}P-NMR analyses, which showed the presence of XI/XII as a single phosphorus resonance (δ 14.13); XI/XII were not detectable (^{31}P-NMR) in the remaining aqueous layer. Similar results were obtained by ethyl acetate extraction of a duplicate reaction mixture.

Preparative-Scale Isolation of XI/XII, Decomposition of XIII in the Presence of *O*-Methylhydroxylamine—A sample of crude XIII (175 mg, ~0.5 mmole), which contained ~20 moles % XIV by ^{31}P-NMR, was dissolved in water (10 ml) and was then treated with an alkaline solution of *O*-methylhydroxylamine that had been prepared from its hydrochloride salt (100 mg, 1.2 mmoles in 6.2 ml of 0.2 *M* sodium hydroxide). After 24 hr at room temperature, the sodium chloride-saturated

[3] WM-300 spectrometer, Bruker Instruments, Inc.
[4] HR-220 spectrometer, Varian Associates, Inc.
[5] Model PHM 64 pH meter, Radiometer A/S.
[6] Model 2091 GC-MS and 2130 Data System, LKB Instruments, Inc.
[7] Compound XVI has been independently prepared by R. B. Brundrett, Johns Hopkins University School of Medicine.
[8] Aldrich Chemical Co.
[9] Model 03V5-0 ozone generator, Ozone Research & Equipment Corp.
[10] Merck 60, <230 mesh, EM Laboratories.

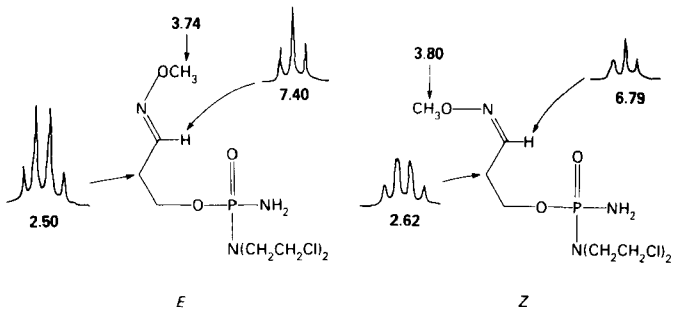

Figure 2—*Structures of* E *and* Z *aldophosphamide* O*-methyl oximes (XI and XII) with* ^{1}*H-NMR (300 MHz) spectral inserts and chemical shifts for the indicated protons.*

reaction mixture was extracted with chloroform (3 × 15 ml) and the combined extract was then dried with anhydrous magnesium sulfate. Removal of chloroform *in vacuo* gave a residue (54 mg) which was subjected to TLC (1000-μm silica gel, acetone–chloroform 1:1) and afforded two overlapping components (R_f 0.1–0.2) identified as a 62:38 mixture of *E* (XI) and *Z* (XII) *O*-methyl oximes of III (17 mg of oil, 12% corrected yield); ^{1}H-NMR (300 MHz, acetone-d_6) for XI and XII, respectively (Fig. 2): δ 7.40 and 6.79 (2-t, J_{HH} = 5.8 and 5.1 Hz, 61:39, 1H total, nonequivalent CH_2CH=N), 4.07 (m, 2H, CH_2O), 3.74 and 3.80 (2-s, 63:37, 3H total, nonequivalent OCH_3), 3.90 (broad s, 2H, NH_2), 3.69 (t, *J* = 7.2 Hz, 4H, 2-NCH_2CH_2Cl), 3.31 (m, 4H, 2-NCH_2CH_2Cl), 2.50 and 2.62 (2-q, J_{HH} = 6.2 and 5.9 Hz, respectively, 61:39, 2H total, nonequivalent CH_2CH=N) ppm; electron-impact–mass spectrum: *m/z* 274 (0.8%) and 276 (0.4%) $(M-CH_3O)^+$, 165 (70%) $[M-(ClCH_2CH_2)_2N]^+$, 142 (3%) $[(^{35}ClCH_2CH_2)_2NH_2]^+$, 92 (87%) $(^{35}ClCH_2CH_2NHCH_2)^+$, and 86 (69%) $(CH_3ON{=}CHCH_2CH_2)^+$; chemical-ionization–mass spectrum: 87 (100%) $(CH_3ON{=}CHCH_2CH_2+1)^+$, 93 (26%) $(^{35}ClCH_2CH_2NHCH_2+1)^+$, 143 (58%) $[(^{35}ClCH_2CH_2)_2N+3]^+$, 308 (39%) and 310 (25%) $(M+3)^+$. Upon standing in a freezer, the initial oily sample of XI/XII crystallized, mp 72–75°.

Anal.—Calc. for $C_8H_{18}N_3O_3PCl_2$: C, 31.38; H, 5.94; N, 13.73. Found: C, 31.34; H, 5.89; N, 13.64.

Decomposition of XV in the Presence of *O*-Methylhydroxylamine—A solution of lutidine buffer (1.75 ml of 0.05 *M*, 5 v/v% deuterium oxide) and *O*-methylhydroxylamine hydrochloride (20 mg, 0.24 mmole), adjusted to pH 7.4 with 1 *N* sodium hydroxide, was sonicated with crystalline XV (10 mg, 0.018 mmole) to achieve rapid dissolution. The sample was placed in the ^{31}P-NMR (121.5 MHz) probe at 37°, and after 10 min of temperature equilibration, the free-induction decay signal for each spectrum (320 pulses, 7.56 min) was automatically accumulated and stored. The average concentration of XV in each frequency-domain spectrum was measured as a relative percentage, using the peak height of XV (δ 12.60) and all other reaction components: XI/XII (δ 20.83), XIII (δ 13.43), and XIV (δ 9.93). A plot of $\ln([XV]_0/[XV]_t)$ *versus* time (*t*) using eight data points was linear over the monitored decomposition period (75%) and gave $\tau_{1/2}$ = 0.5 hr.

Decomposition of XVI in the Presence of *O*-Methylhydroxylamine—The procedure with the faster eluting diastereomer of XVI (15 mg, 0.043 mmole) was the same as that described above for compound XV, except for the use of pyridine buffer (1.30 ml of 0.1 *M*, 5 v/v% deuterium oxide). From the ^{31}P-NMR peak heights of XVI (δ 11.57), XIII (δ 12.84), and XI/XII (δ 20.80) in eight spectra (300 pulses, 10.00 min/spectrum) obtained over 9 hr of monitoring (67% decomposition), a linear plot of $\ln([XVI]_0/[XVI]_t)$ *versus t* gave $\tau_{1/2}$ = 5.2 hr.

Stability Studies with XI/XII—All buffers refer to 0.05 *M* aqueous solutions. An aliquot (0.10 ml) of a stock solution of XI/XII (0.073 *M*) in methanol was added to potassium dihydrogen phosphate (1 ml) at pH 6.00, 7.03, and 8.03, and lutidine (1 ml) at pH 7.01. A standard solution of the oximes was similarly prepared in chloroform (1 ml). Each solution was magnetically stirred at room temperature and was analyzed as a function of time using TLC [250-μm silica gel, acetone–chloroform (3:1)], XI/XII R_f = 0.62. There was no detectable oxime decomposition after 6 days.

An aliquot (25 μl) of a stock solution of XI/XII (0.146 *M*) in methanol was added to both the phosphate buffer at pH 7.03 and the lutidine buffer at pH 7.01, giving an oxime concentration of 7.0 m*M*. The former solution was combined with acetone (15 μl, 0.2 mmole, 55-fold molar excess), while the latter solution was treated with acetaldehyde (10 μl, 0.18 mmole, 48-fold molar excess). Daily TLC monitoring as described showed no evidence of reaction after 6 days at room temperature.

The initial oxime solutions in phosphate buffer at pH 6.00, 7.03, and 8.03, and lutidine buffer at pH 7.01, were each combined after 6 days with aqueous formaldehyde (6 μl of 37 w/w %, 0.073 mmole, 10-fold molar excess) and were stirred at room temperature. TLC analysis showed no detectable oxime decomposition after 4 days.

RESULTS AND DISCUSSION

Triphenylphosphine deoxygenation of 4-hydroperoxycyclophosphamide (XIII) is commonly employed for synthetic entry to *cis*-II, *trans*-II, and III, which give rise to ^{1}H-decoupled, ^{31}P-NMR singlet absorptions at δ 12.63, 12.93, and 20.83, respectively, in 0.05 *M* lutidine buffer at 37° (Fig. 1)[11]. Hydroxyphosphamide (δ 21.01), which is the 3-hydroxypropyl analog of aldophosphamide (III), is a good chemical shift model for ^{31}P-NMR identification of III; however, it should be noted that the proportion of free aldehyde in III *versus* its hydrate (15) has not been established. The absolute and relative signal intensities for *cis*-II, *trans*-II, and III vary (not shown) during the course of their gradual tautomerization and fragmentation of III to give IV and V, which is relatively short-lived and was previously studied by ^{31}P-NMR (16). In contrast to these spectral changes, addition of a 5-fold molar excess of *O*-methylhydroxylamine hydrochloride leads to rapid (<10 min) consumption of II/III with formation of a single resonance (δ 20.83) due to the *E* and *Z* aldophosphamide *O*-methyl oxime (XI and XII) trapping products (Fig. 1)[12]. ^{1}H-NMR analysis of an analytically pure oxime sample, which was obtained from spontaneous decomposition of XIII in the presence of *O*-methylhydroxylamine followed by extraction and TLC, showed resonance doubling (Fig. 2) for three types of protons: CH_3O (singlets), CH_2CH_2CH=N (quartets), and CH_2CH_2CH=N (triplets). Other investigators (17, 18) have compared the ^{1}H-NMR spectra of nine *E/Z* pairs of *O*-methyl oximes, and have concluded that the imino proton (CH=N) in the *E* isomer generally exhibits an ~0.6–0.9 ppm downfield shift relative to the corresponding resonance from the *Z* form. On this basis, the triplets at δ 7.40 and 6.79 (Δδ = 0.61 ppm) are respectively assigned to the *E* (XI) and *Z* (XII) *O*-methyl oximes of III, while averaged signal integrations gave a 62:38 (±1%) *E/Z* product ratio. Selective irradiation of each imino proton triplet led to the observation of a triplet for the corresponding CH_2CH_2CH=N nuclei, while irradiation of the overlapping absorptions for the CH_2O protons led to simultaneous collapse of both CH_2CH_2CH=N quartets into doublets, thus confirming the internal spectral assignments.

The utility of *O*-methylhydroxylamine in simplifying kinetic studies of 4-peroxy derivatives of I and its analogs (2) was exemplified by the spontaneous decomposition of 4-peroxycyclophosphamide (XV) in lutidine buffer (0.05 *M*) containing a 13-fold molar excess of this trapping reagent. ^{31}P-NMR spectra recorded as a function of time at 37° show the gradual disappearance of XV (δ 12.60) with the transient intermediacy of XIII (δ 13.43) and the steady accumulation of XI/XII (δ 20.83), together with the formation of 4-ketocyclophosphamide (XIV, δ 9.93) as a minor by-product (18%). The disappearance of XV obeys a first-order rate law, with $\tau_{1/2}$ = 0.5 hr, whereas other investigators (19), who monitored the time-course for release of acrolein from XV, reported an initial lag phase and postulated a coupled set of homolytic reactions. While the mechanistic origins for these kinetic differences require further investigation, the competing production of XIV is tentatively ascribed to free-radical cage reactions prior to formation of II and then III, which is finally intercepted as XI/XII. Analogous kinetic measurements with diastereomerically pure 4-(*tert*-butylperoxy)cyclophosphamide (XVI) revealed an ~10-fold increase in stability ($\tau_{1/2}$ = 5.2 hr), relative to XV ($\tau_{1/2}$ = 0.5 hr), and the absence of XIV (<1%) during formation of XI/XII. The contrasting results obtained for XV and XVI clearly reveal that the details for spontaneous decomposition of 4-peroxy derivatives of I are more complex than anticipated, *a priori*.

The stability of XI/XII toward either hydrolytic reversion to II/III or fragmentation into IV and V was demonstrated by TLC monitoring of the *O*-methyl oximes in buffered solutions at pH 6, 7, and 8, which showed no evidence of either oxime disappearance or formation of acrolein (IV) after 6 days at room temperature. Treatment of these solutions at pH 7 with excess acetone (55 equivalents), acetaldehyde (48 equivalents), or formaldehyde (10 equivalents) gave no TLC evidence for transoximination.

[11] The ^{31}P-NMR chemical shifts of I and its metabolites in aqueous solution are dependent upon pH, temperature, and the type of buffer (14).

[12] TLC and ^{1}H-NMR analyses of a deuterochloroform extract confirmed the presence of oximes XI and XII, thus ruling out the possibility of catalyzed conversion of II into III, which happens to have the same chemical shift as XI/XII under the stated reaction conditions.

CONCLUSIONS

O-Methylhydroxylamine rapidly reacts with tautomers II and III at neutral pH to quantitatively produce an ~60:40 mixture of the *E* and *Z* isomers of aldophosphamide *O*-methyl oxime, XI and XII. Assuming that oxime formation occurs by condensation of the amine with aldehyde III, it follows that the rate of ring-opening of *cis*- and *trans*-II to give III must be relatively fast, since ^{31}P-NMR analysis of the reaction mixture showed that these hemiaminals are no longer detectable after ~10 min at 37°. The *O*-methyl oximes of III are resistant toward hydrolysis of the oxime functionality, fragmentation into IV and V, and transoximination with either acetone, acetaldehyde, or formaldehyde. In concert, these features lend themselves to the use of *O*-methylhydroxylamine as an effective trapping agent for studies of cyclophosphamide metabolites II and III. Investigations of enzymatic and chemical regeneration of III from XI/XII in the design of new anticancer prodrugs will be reported in another study.

REFERENCES

(1) O. M. Friedman, A. Myles, and M. Colvin, in "Advances in Cancer Chemotherapy," vol. 1, A. Rosowsky, Ed., Marcel Dekker, New York, N.Y., 1979, pp. 143–204.

(2) G. Zon, in "Progress in Medicinal Chemistry," vol. 19, C. P. Ellis, Ed., Elsevier/North-Holland, Amsterdam, The Netherlands, in press.

(3) O. M. Friedman and E. Boger, *Anal. Chem.*, **33**, 906 (1961).

(4) F. A. Weaver, A. R. Torkelson, W. A. Zygmunt, and H. P. Browder, *J. Pharm. Sci.*, **67**, 1009 (1978).

(5) T. A. Connors, P. J. Cox, P. B. Farmer, A. B. Foster, M. Jarman, and J. K. Macleod, *Biomed. Mass Spectrom.*, **1**, 130 (1974).

(6) N. E. Sladek, *Cancer Res.*, **33**, 651 (1973).

(7) H.-R. Schulten, *Cancer Treatment Rep.*, **60**, 501 (1976).

(8) A. Myles, C. Fenselau, and O. M. Friedman, *Tetrahedron Lett.*, **1977**, 2475.

(9) G. Peter and H.-J. Hohorst, *Cancer Chemother. Pharmacol.*, **3**, 181 (1979).

(10) R. A. Laine and C. C. Sweeley, *Carbohydr. Res.*, **27**, 199 (1973).

(11) G. Peter, T. Wagner, and H.-J. Hohorst, *Cancer Treatment Rep.*, **60**, 429 (1976).

(12) J. van der Steen, J. G. Westra, C. Benckhuysen, and H.-R Schulten, *J. Am. Chem. Soc.*, **102**, 5691 (1980).

(13) R. Lumry, E. L. Smith, and R. R. Glantz, *ibid.*, **73**, 4330 (1951).

(14) K. O'Neill and C. P. Richards, in "Annual Reports on NMR Spectroscopy," vol. 10A, G. A. Webb, Ed., Academic, New York, N.Y., 1980, pp. 137–140.

(15) R. F. Struck, *Cancer Treatment Rep.*, **60**, 317 (1976).

(16) T. W. Engle, G. Zon, and W. Egan, *J. Med. Chem.*, **22**, 897 (1979).

(17) G. J. Karabatsos and N. Hsi, *Tetrahedron*, **23**, 1079 (1967).

(18) G. J. Karabatsos and R. A. Taller, *ibid.*, **24**, 3347 (1968).

(19) C. Benckhuysen, J. van der Steen, and E. J. Spanjersberg, *Cancer Treatment Rep.*, **60**, 369 (1976).

ACKNOWLEDGMENTS

This work was supported in part by research grant CA-21345 to Gerald Zon from the National Institutes of Health.

A visiting scientist appointment for Gerald Zon at the Bureau of Biologics, and a Senior Research Associate appointment for Edward M. Sweet at The Catholic University of America are gratefully acknowledged.

The authors thank Dr. R. B. Brundrett of the Johns Hopkins School of Medicine for information regarding the preparation of compound XVI.

Fourier-transform NMR and mass spectroscopy facilities were made available through the cooperation of the Bureau of Biologics, Division of Biochemistry and Biophysics.

High-Performance Liquid Chromatographic Analysis of Hydrocortisone Drug Substance, Tablets, and Enema

MILDA J. WALTERS ˣ **and WALTER E. DUNBAR**

Received January 28, 1981, from the *Food and Drug Administration, Department of Health and Human Services, Detroit, MI 48207.* Accepted for publication August 10, 1981.

Abstract □ Methods for the analysis of hydrocortisone drug substance, tablets, and enema were developed using adsorption high-performance liquid chromatography (HPLC). This HPLC system was shown to be capable of isolating hydrocortisone from its degradation products, synthesis precursor, and related corticosteroids. The accuracy, precision, and linearity of the HPLC assay methods and their applicability to commercial products has been demonstrated.

Keyphrases □ High-performance liquid chromatography—analysis of hydrocortisone drug substance, tablets, and enema □ Hydrocortisone—analysis of drug substance, tablets, and enema using high-performance liquid chromatography □ Degradation products—separation from hydrocortisone, high-performance liquid chromatography

The majority of reported analytical methods for corticosteroids utilize blue tetrazolium (1–10), isoniazid (11), or phenylhydrazine (12, 13) reactions, UV spectrophotometry (14), or high-performance liquid chromatography (HPLC)[1] (15–22).

The methods for determining hydrocortisone products in the last four revisions of the United States Pharmacopeia (USP) (2, 23–25) have employed the blue tetrazolium reaction as the final determinative step. This is preceded by extraction or thin layer chromatographic (TLC) isolation of the active ingredient. Interferences and critical parameters of the reaction have been reported (6–9, 26).

HPLC is rapidly becoming the method of choice for the analysis of many drugs, and numerous applications of this technique to hydrocortisone are reported in the literature. The majority of published methods utilize reversed-phase systems (15–20). Recent reports, however, demonstrate that normal-phase adsorption chromatography offers greater selectivity for closely related corticosteroid structures[2] (21–22).

This study was undertaken to develop an HPLC system suitable for the analysis of hydrocortisone products and to compare the relative advantages of the USP and HPLC methods. Accuracy, precision, specificity, indication of

[1] E. Bunch, Food and Drug Administration, Seattle, Wash., unpublished work (1975).

[2] M. J. Walters, Food and Drug Administration, Detroit, Mich., unpublished work, presented at the 6th Annual Meeting of the Federation of Analytical Chemistry and Spectroscopy Societies (1979).

0022-3549/82/0400-0446$01.00/0

CONCLUSIONS

O-Methylhydroxylamine rapidly reacts with tautomers II and III at neutral pH to quantitatively produce an ~60:40 mixture of the *E* and *Z* isomers of aldophosphamide *O*-methyl oxime, XI and XII. Assuming that oxime formation occurs by condensation of the amine with aldehyde III, it follows that the rate of ring-opening of *cis*- and *trans*-II to give III must be relatively fast, since ^{31}P-NMR analysis of the reaction mixture showed that these hemiaminals are no longer detectable after ~10 min at 37°. The *O*-methyl oximes of III are resistant toward hydrolysis of the oxime functionality, fragmentation into IV and V, and transoximination with either acetone, acetaldehyde, or formaldehyde. In concert, these features lend themselves to the use of *O*-methylhydroxylamine as an effective trapping agent for studies of cyclophosphamide metabolites II and III. Investigations of enzymatic and chemical regeneration of III from XI/XII in the design of new anticancer prodrugs will be reported in another study.

REFERENCES

(1) O. M. Friedman, A. Myles, and M. Colvin, in "Advances in Cancer Chemotherapy," vol. 1, A. Rosowsky, Ed., Marcel Dekker, New York, N.Y., 1979, pp. 143–204.

(2) G. Zon, in "Progress in Medicinal Chemistry," vol. 19, C. P. Ellis, Ed., Elsevier/North-Holland, Amsterdam, The Netherlands, in press.

(3) O. M. Friedman and E. Boger, *Anal. Chem.*, **33**, 906 (1961).

(4) F. A. Weaver, A. R. Torkelson, W. A. Zygmunt, and H. P. Browder, *J. Pharm. Sci.*, **67**, 1009 (1978).

(5) T. A. Connors, P. J. Cox, P. B. Farmer, A. B. Foster, M. Jarman, and J. K. Macleod, *Biomed. Mass Spectrom.*, **1**, 130 (1974).

(6) N. E. Sladek, *Cancer Res.*, **33**, 651 (1973).

(7) H.-R. Schulten, *Cancer Treatment Rep.*, **60**, 501 (1976).

(8) A. Myles, C. Fenselau, and O. M. Friedman, *Tetrahedron Lett.*, **1977**, 2475.

(9) G. Peter and H.-J. Hohorst, *Cancer Chemother. Pharmacol.*, **3**, 181 (1979).

(10) R. A. Laine and C. C. Sweeley, *Carbohydr. Res.*, **27**, 199 (1973).

(11) G. Peter, T. Wagner, and H.-J. Hohorst, *Cancer Treatment Rep.*, **60**, 429 (1976).

(12) J. van der Steen, J. G. Westra, C. Benckhuysen, and H.-R Schulten, *J. Am. Chem. Soc.*, **102**, 5691 (1980).

(13) R. Lumry, E. L. Smith, and R. R. Glantz, *ibid.*, **73**, 4330 (1951).

(14) K. O'Neill and C. P. Richards, in "Annual Reports on NMR Spectroscopy," vol. 10A, G. A. Webb, Ed., Academic, New York, N.Y., 1980, pp. 137–140.

(15) R. F. Struck, *Cancer Treatment Rep.*, **60**, 317 (1976).

(16) T. W. Engle, G. Zon, and W. Egan, *J. Med. Chem.*, **22**, 897 (1979).

(17) G. J. Karabatsos and N. Hsi, *Tetrahedron*, **23**, 1079 (1967).

(18) G. J. Karabatsos and R. A. Taller, *ibid.*, **24**, 3347 (1968).

(19) C. Benckhuysen, J. van der Steen, and E. J. Spanjersberg, *Cancer Treatment Rep.*, **60**, 369 (1976).

ACKNOWLEDGMENTS

This work was supported in part by research grant CA-21345 to Gerald Zon from the National Institutes of Health.

A visiting scientist appointment for Gerald Zon at the Bureau of Biologics, and a Senior Research Associate appointment for Edward M. Sweet at The Catholic University of America are gratefully acknowledged.

The authors thank Dr. R. B. Brundrett of the Johns Hopkins School of Medicine for information regarding the preparation of compound XVI.

Fourier-transform NMR and mass spectroscopy facilities were made available through the cooperation of the Bureau of Biologics, Division of Biochemistry and Biophysics.

High-Performance Liquid Chromatographic Analysis of Hydrocortisone Drug Substance, Tablets, and Enema

MILDA J. WALTERS ˣ **and WALTER E. DUNBAR**

Received January 28, 1981, from the *Food and Drug Administration, Department of Health and Human Services, Detroit, MI 48207.* Accepted for publication August 10, 1981.

Abstract □ Methods for the analysis of hydrocortisone drug substance, tablets, and enema were developed using adsorption high-performance liquid chromatography (HPLC). This HPLC system was shown to be capable of isolating hydrocortisone from its degradation products, synthesis precursor, and related corticosteroids. The accuracy, precision, and linearity of the HPLC assay methods and their applicability to commercial products has been demonstrated.

Keyphrases □ High-performance liquid chromatography—analysis of hydrocortisone drug substance, tablets, and enema □ Hydrocortisone—analysis of drug substance, tablets, and enema using high-performance liquid chromatography □ Degradation products—separation from hydrocortisone, high-performance liquid chromatography

The majority of reported analytical methods for corticosteroids utilize blue tetrazolium (1–10), isoniazid (11), or phenylhydrazine (12, 13) reactions, UV spectrophotometry (14), or high-performance liquid chromatography (HPLC)[1] (15–22).

The methods for determining hydrocortisone products in the last four revisions of the United States Pharmacopeia (USP) (2, 23–25) have employed the blue tetrazolium reaction as the final determinative step. This is preceded by extraction or thin layer chromatographic (TLC) isolation of the active ingredient. Interferences and critical parameters of the reaction have been reported (6–9, 26).

HPLC is rapidly becoming the method of choice for the analysis of many drugs, and numerous applications of this technique to hydrocortisone are reported in the literature. The majority of published methods utilize reversed-phase systems (15–20). Recent reports, however, demonstrate that normal-phase adsorption chromatography offers greater selectivity for closely related corticosteroid structures[2] (21–22).

This study was undertaken to develop an HPLC system suitable for the analysis of hydrocortisone products and to compare the relative advantages of the USP and HPLC methods. Accuracy, precision, specificity, indication of

[1] E. Bunch, Food and Drug Administration, Seattle, Wash., unpublished work (1975).

[2] M. J. Walters, Food and Drug Administration, Detroit, Mich., unpublished work, presented at the 6th Annual Meeting of the Federation of Analytical Chemistry and Spectroscopy Societies (1979).

0022-3549/82/0400-0446$01.00/0

product stability, and applicability to most products on the commercial market were the criteria considered necessary for a suitable HPLC method. Of particular concern was the separation of hydrocortisone (I) from the major degradation products 11β,17-dihydroxyandrost-4-ene-3-one-20-oic acid (II) and 11β-hydroxyandrost-4-ene-3,17-dione (III) (6, 27–29), the common synthesis precursor, hydrocortisone acetate (IV), and the other closely related steroids, cortisone acetate (V), cortisone (VI), prednisone (VII), and prednisolone (VIII).

A silica microparticulate column with a mobile phase of ethylene dichloride containing methanol as modifier with small, controlled amounts of water and acetic acid met all of the listed requirements for an HPLC system. This system was incorporated into the assay procedures developed for hydrocortisone drug substance, tablets, and enema.

EXPERIMENTAL

Reagents and Materials—All solvents used were HPLC grade[3,4]. Glacial acetic acid was analytical reagent grade[5]. USP Reference Standard I, the degradation products II and III[6], acetaminophen[7], and corticosteroids[8] were used without further treatment. The TLC plates were purchased precoated with a 250-μm layer of silica gel with a fluorescent indicator[9]. Polytetrafluoroethylene 0.5-μm porosity membrane filters[10] were used to filter HPLC solvents and samples.

HPLC Determination of I—*Internal Standard Solution*—Two hundred milligrams of acetaminophen (IX) was dissolved in 4 ml of methanol and diluted to 200 ml with ethylene dichloride. The solution was kept in a tightly stoppered flask protected from light.

Standard Solutions—Solution A was prepared by accurately weighing and dissolving ~10 mg of I in 2 ml of methanol in a 50-ml volumetric flask. The internal standard solution (4 ml) was added, and the solution was diluted to volume with methylene chloride.

Solution B was prepared by accurately weighing and dissolving ~8 mg of I in 4 ml of methanol in a 100-ml volumetric flask. Internal standard solution (2 ml) was added and the solution was diluted to volume with chloroform. Solution A was used in the drug substance and tablet assays. Solution B was used to assay the enema.

HPLC System—The liquid chromatograph[11] was equipped with an automatic injector[12] having a 10-μl loop, a 25-cm × 4.6-mm i.d. column packed with spherical, 5–6 μm diameter, porous silica microparticles[13], a 254-nm UV detector[14], and a 10-mv span recorder[15]. The HPLC system was interfaced with a data system[16] for tracking peak areas and performing calculations. The detector was set at 0.5 absorbance units full scale (aufs) which produced peak heights of ~50% of full scale for both I and the internal standard in a 10-μl injection of standard solution A. Mobile solvent A was prepared by mixing 55 ml of a 5% water in methanol solution with 1.0 ml of acetic acid and diluting to 1 liter with ethylene dichloride. The flow rate was 1.5 ml/min and the methanol content was adjusted when needed to obtain a retention time of ~7.5 min for I. An alternate mobile solvent B consisted of 45 ml of 5% water in methanol solution mixed with 1.0 ml of acetic acid and diluted to 1 liter with methylene chloride.

System Suitability Test—The HPLC system was equilibrated by passing mobile solvent through the column for ~0.5 hr. Portions of the standard solution (10 μl) were then introduced. The system was considered suitable when (*a*) the retention times for I and IX were ~7.5 and ~10 min, respectively; (*b*) the resolution[17] R between I and IX was not less than 2.5, the column efficiency[18] N calculated using the I peak was not less than 5000 theoretical plates; and (*c*) the relative standard deviation of the response ratios of the I peak relative to the internal standard IX peak for six consecutive injections did not exceed 1%.

Table I—HPLC Retention of Hydrocortisone and Related Compounds

Compound	Retention Volume, ml	Capacity Factor, k'
Carbon tetrachloride	2.85	0
Benzene	2.85	0
Propylparaben	4.37	0.53
Methylparaben	4.67	0.61
11β-Hydroxyandrost-4-ene-3,17-dione	4.82	0.69
Cortisone acetate	4.88	0.71
Hydrocortisone acetate	5.55	0.95
Methylprednisolone acetate	6.02	1.11
Prednisolone acetate	6.32	1.22
Triamcinolone acetonide	6.89	1.42
Cortisone	6.96	1.44
Prednisone	7.74	1.72
Dexamethasone	10.28	2.60
Hydrocortisone	11.07	2.88
Methylprednisolone	12.84	3.51
Prednisolone	13.58	3.76
Acetaminophen	14.10	3.95
11β,17-Dihydroxyandrost-4-ene-3-one-20-oic acid	15.17	4.32
Triamcinolone	18.42	5.46

Sample Preparation—*Drug Substance*—Approximately 50 mg of sample, previously dried for 3 hr at 105°, was weighed into a 250-ml volumetric flask. Ten milliliters of methanol and 20.0 ml of internal standard solution were added and the solution was diluted to volume with methylene chloride.

Tablet Composite Assay—An accurately weighed portion of a 20-tablet composite equivalent to one tablet was transferred to a volumetric flask of an appropriate size to yield a final I concentration of ~0.2 mg/ml. Two milliliters of methanol per 10 mg of declared I was added and the flask placed in an ultrasonic bath for 2 min. Methylene chloride was then added until the flask was about half full and the flask was returned to the ultrasonic bath for 1 min. An accurately measured volume of internal standard solution equivalent to 4 ml/10 mg of declared I was added. The sample was diluted to volume with methylene chloride and a portion was filtered for HPLC assay.

Tablet Content Uniformity Determination—Each tablet was placed in an Erlenmeyer or volumetric flask of a size selected to yield a final I concentration of ~0.2 mg/ml. The tablet was softened by placing 100 μl of water/10 mg of declared I directly on the tablet and allowing it to soak in for 0.5 hr. Methanol (2 ml/10 mg of declared I) was added and the flask was placed in an ultrasonic bath for 10 min or until the tablet disintegrated. The procedure for tablet composite assay was then followed.

Enema—A sample equivalent to 8 mg of I was accurately weighed by difference into a separatory funnel and I was extracted with four 20-ml portions of chloroform, each portion filtered through chloroform-washed cotton into a 100-ml volumetric flask.

Methanol (4 ml) and internal standard solution (2 ml) were added, the sample was diluted to volume with chloroform, and a portion was filtered for HPLC assay.

Procedure—The HPLC system was allowed to equilibrate by passing the mobile solvent through the column for ~0.5 hr. Standard solution (10-μl portions) were introduced and the response ratios (R_s) of the I peak relative to the internal standard IX were calculated. When the R_s for three consecutive injections agreed within 1%, 10 μl of the sample preparation was injected. The quantity of I in the portion of the sample taken was calculated by the formula I (mg) = $V_u W_s R_u / V_s R_s$, where W_s is milligrams of I in the standard solution, V_s and V_u are the volumes (ml) of internal standard solution in the standard and sample solutions, respectively, and R_u is the response ratio of the peaks (I/IX) in the sample chromatogram.

Validation of HPLC Procedures—*Specificity*—Test solutions

[3] Omnisolv grade methanol, MCB Manufacturing Chemists, Cincinnati, OH 45212.

[4] Distilled in glass methylene chloride, chloroform, and ethylene dichloride Burdick & Jackson Laboratories, Muskegon, MI 49442. The ethylene dichloride purchased from Burdick & Jackson was found to be suitable for use without further treatment; other brands required water washing to remove impurities.

[5] Mallinckrodt, Inc., St. Louis, MO 63147.

[6] Received from Robert E. Graham, Food and Drug Administration, Dallas, TX 75204.

[7] Eastman Kodak, Co., Rochester, NY 14650.

[8] K & K Laboratories, Plainview, NY 11803.

[9] "Redi/Plate," Analtech Inc., distributed by Fisher Scientific Co., Pittsburgh, PA 15238.

[10] TE 36, Schleicher & Schuell, Inc., Keene, NH 03431.

[11] Series 2/1, Perkin-Elmer Corp., Norwalk, CT 06856.

[12] Model 725, Micromeritics Instruments Corp., Norcross, GA 30071.

[13] Zorbax Sil, Dupont Co., Wilmington, DE 19898.

[14] Model 440, Waters Associates, Milford, MA 01757.

[15] Model SR-204, Heath Co., Benton Harbor, MI 49022.

[16] PEP 2, Perkin-Elmer Corp., Norwalk, CT 06856.

[17] $R = 2(t_{r\,IX} - t_{r\,I})/(W_{IX} + W_I)$, where t_r and W are the retention times and peak widths at baseline measured in mm for compounds IX and I.

[18] $N = 16(t_r)^2/W$

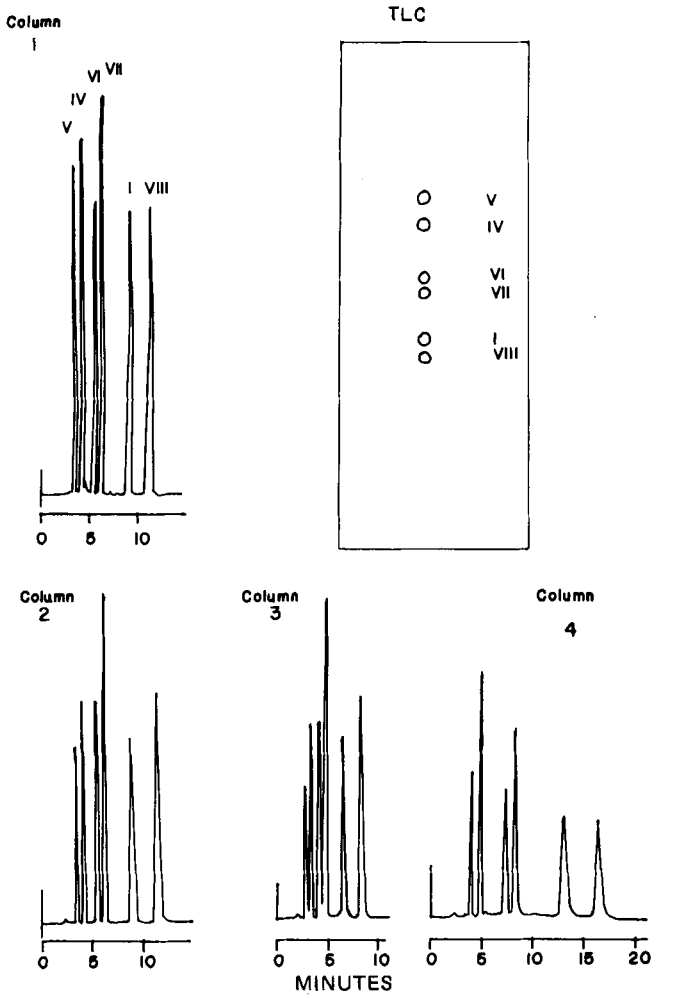

Figure 1—*Chromatographic separation of corticosteroids by four different HPLC columns and by TLC. Key: I, hydrocortisone; V, cortisone acetate; IV, hydrocortisone acetate; VI, cortisone; VII, prednisone; VIII, prednisolone; column 1, 25 cm × 4.6-mm i.d. packed with 5–6 μm diameter spherical silica particles; column 2, 25 cm × 4.6-mm i.d. packed with 5 μm irregular shaped silica; column 3, 30 cm × 3.9-mm i.d. packed with 10 μm, irregular shaped silica; column 4, 10 cm × 8-mm i.d. pressurized cartridge packed with 10 μm diameter, spherical silica particles. All chromatograms were obtained using the same mixture of compounds; the order of elution was the same for all columns.*

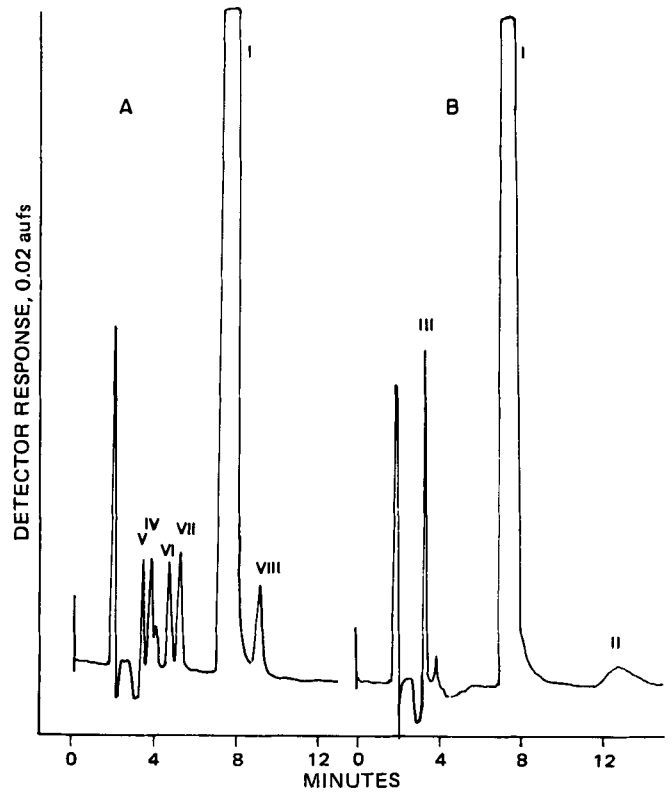

Figure 2—*Chromatograms of hydrocortisone (I) with added (0.5% of each) corticosteroids IV–VIII(A) and degradation products II and III (B).*

containing 0.04–0.2 mg/ml of the compounds listed in Table I, prepared in methylene chloride–methanol (98:2), were introduced into the HPLC system and their respective capacity factors[19] (k') were calculated. A model mixture containing 0.1 mg/ml each of I and IV–VIII in methylene chloride–methanol (98:2) was used to compare the performance of HPLC columns, mobile solvents, and HPLC to TLC.

Precision—Precision of the HPLC system was tested by injecting 36 portions of standard solution A, determining the R_s values for the peaks (I/IX) based on areas as well as heights, and calculating the relative standard deviation. The precision of the respective assay methods was tested by subjecting 10 portions of each of the appropriate sample composites to the entire assay procedure and determining the relative standard deviation of the results.

Accuracy—The accuracy of the assay procedures was tested using synthetic samples. The product formulations were categorized by excipient formulation. Typical formulations were selected for five tablet and two enema products, and placebo mixtures were prepared by combining all ingredients except I. Five portions of each placebo were taken and an accurately weighed amount of I, equivalent to the declared product potency, was added to each portion. These were analyzed by the appropriate HPLC assay procedures and the recovery of I was calculated.

Confirmation of Impurities—(*A*) *Separation of II–VII from I*—Drug substance I (~80 μg) was spotted on a TLC plate previously impregnated with 15% formamide in acetone (30). The chromatogram was developed three times using chloroform as the mobile solvent. The spots were detected by examining in short wavelength (254 nm) UV light followed by spraying with 25% H_2SO_4 in methanol, heating 5 min at 120°, and observing characteristically colored corticosteroid spots in long wavelength (366 nm) UV light. Compound I with added II–VIII at a level of 0.5% each was spotted and developed using the above system. Compounds II–VII were resolved and detected, while VIII was not separated from I at this level.

(*B*) *Separation of VIII from I*—Concentrated solutions (10 mg/ml) of I samples suspected to contain VIII were injected into the HPLC system and eluate portions corresponding to VIII retention were collected. After concentrating by evaporation, the eluate was spotted on a TLC plate and developed with methylene chloride–methanol–water (180:15:1) mobile solvent (2). Prednisolone was detected as in the TLC system described in A.

RESULTS AND DISCUSSION

The USP (2) single steroid assay (included in the I drug substance and tablet monographs) requires a TLC separation, quantitative transfer of portions of the silica layer, extraction, and final quantitation by the blue tetrazolium colorimetric procedure. The USP assay for hydrocortisone enema (2) involves a chloroform extraction followed by blue tetrazolium quantitation. This reaction is not specific for I and because I is not isolated from related steroids in the enema assay the results would include total corticosteroids as well as other compounds which react with this reagent (26). The USP methods for hydrocortisone were found to be tedious and time-consuming, and presented difficulties with the sample preparation of some commercial products[23]. Therefore, it was considered advantageous to develop alternate methods capable of providing equal specificity without these limitations.

HPLC was selected as the technique offering the greatest potential with respect to specificity, speed, and convenience. Adsorption HPLC was utilized due to its capabilities to separate closely related structures. The desired separation of I from its degradation products, precursor (IV), and related steroids (V–VIII) was achieved on a silica column with two equivalent mobile solvent systems (A and B). Though both mobile solvents have the same retention and selectivity for I–VIII, A is less volatile

[19] $k' = (t_r - t_0)/t_0$, where t_0 is the time required to elute unretained component through the system.

Table II—Analysis of Hydrocortisone Drug Substance

Sample	Hydrocortisone Found, %		Impurities Found, %[b]			
	HPLC[a]	USP[a]	Cortisone	Prednisolone	Hydrocortisone Acetate	Unidentified
22	98.6 (0.0)	98.2 (1.3)	0.13	—	—	Trace
23	98.5 (0.4)	98.2 (0.9)	0.26	0.53	0.1	Trace
24	98.8 (0.3)	98.7 (0.4)	0.13	0.57	0.1	Trace
25	97.2 (0.2)	98.2 (1.2)	0.20	—	—	Trace
26	99.1 (0.0)	102.4 (1.1)	0.16	0.31	—	Trace

[a] % by weight on dried basis, average of two determinations (% difference between duplicates). [b] % by weight, trace was estimated to be less than 0.1% based on UV response equivalent to cortisone.

Table III—HPLC Analysis of Synthetic Samples

Product	Formulation Type	HPLC Assay				
		Number of Determinations	Added I, mg[a]	Added I found, %		
				Average	Range	$RSD^{\dagger}$
Tablets	A	5	20	99.4	98.6–98.8	0.48
Tablets	B	5	20	99.0	98.6–99.4	0.30
Tablets	C	5	10	99.7	99.1–100.6	0.56
Tablets	D	5	10	101.2	99.7–101.8	0.84
Tablets	H	5	20	100.2	100.1–100.5	0.21
Average				99.9		
Enema	K	5	8	99.9	99.5–100.4	0.38
Enema	L	5	8	99.1	98.9–99.5	0.24
Average				99.5		

[a] Approximate amount of accurately weighed hydrocortisone (I) added to each portion of placebo.

resulting in a more rugged system and was therefore incorporated into the assay procedures. The selectivity of this HPLC system is illustrated in Table I, which shows the capacity factors (k') for compounds of interest. A good separation was obtained for corticosteroid pairs I and VIII, and VI and VII, which are difficult to resolve by reversed-phase systems (20). Corticosteroid acetates, which eluted close together when mobile solvent A was used, were found to have higher k' values and better resolution when the methanol content of the mobile solvent was decreased to 3.5%. Thus, the same column with slight modifications in the mobile solvent shows a potential for application to corticosteroid products other than those reported here.

A model mixture of I and IV–VIII was used to investigate four silica columns, using resolution (R) between VI and VII as well as efficiency (N) (calculated as theoretical plates based on the I peak) as the criteria for comparison. Columns 1 and 2 were both 25 cm × 4.6-mm i.d. in size. Column 1 was packed with 5–6 μm diameter, spherical silica[13], while column 2 contained irregular-shaped 5-μm silica particles[20]. Column 3 was 30 cm × 3.9-mm i.d. in size packed with 10-μm, irregular-shaped silica[21]. Column 4 was packed with 10-μm spherical silica particles in a 10 cm × 8-mm i.d. plastic cartridge[22] maintained under pressure. The test compounds eluted in the same order through all four columns. Differences were observed in the total elution times and resolution (Fig. 1). The highest efficiency (N = 8300) and resolution (R = 1.56) were obtained with column 1. The performance of column 2 was very similar to 1, while the differences were more apparent with columns 3 and 4 which had 3400 and 3700 theoretical plates, respectively. Compound I was completely resolved on all four columns. Column 1 was used for all analyses reported in this paper.

The six-steroid model mixture was also used to compare the specificity of HPLC to that of the TLC system used in the USP single steroid assay, and Fig. 1 shows that HPLC provides equal or better selectivity for related steroids. Figure 2 demonstrates the system's capability to separate I from its major degradation products, II and III, as well as from its immediate synthesis precursor, IV.

Acetaminophen (IX) was incorporated into the procedures as an internal standard to compensate for possible injection variability and solution volume changes. The relative standard deviation of the response ratios (R_s) for the peaks (I/IX) of 36 replicate injections of standard solution was found to be 0.19% based on peak areas and 0.60% using manually measured peak heights. While the computerized area calculations are preferred due to better precision and a savings of time and effort, manual peak height calculations also gave acceptable results.

The response for I was found to be linear in the tested range of 0.8–3.4 μg, equivalent to 40–170% of the injection amount specified in the method. The internal standard (IX) produced a linear response as did the response ratios for the I peak relative to the internal standard peak over the range of 50–150% of the specified concentrations.

The HPLC assay results for five I drug substance samples (Table II) show reasonable agreement with those obtained by the USP assay. Duplicate assays by the HPLC method agree within <0.5% (average = 0.2%) while the USP duplicates range from 0.4 to 1.3% (average = 1%). An additional portion from each sample was prepared and chromatographed

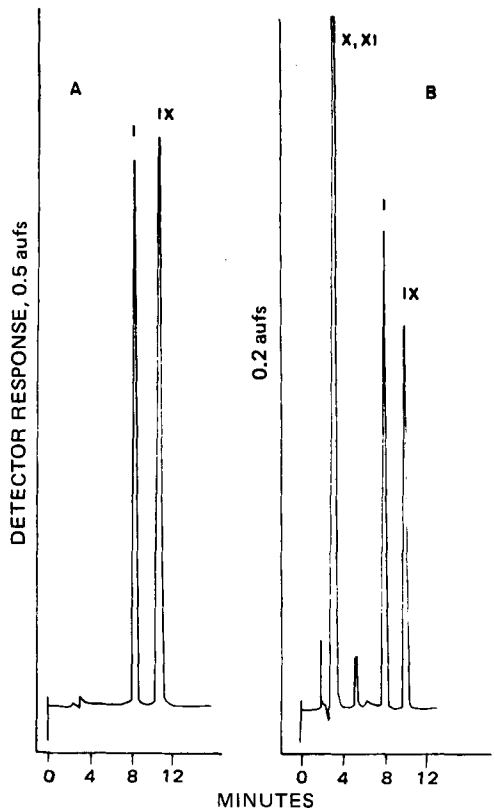

Figure 3—*Typical hydrocortisone (I) assay chromatograms. Key: A, tablets; B, enema; IX, internal standard; X, methylparaben; XI, propylparaben.*

[20] LiChrosorb Si60, E. M. Reagents, Cincinnati, OH 45212.
[21] μ Porasil, Waters Associates, Milford, MA 01757.
[22] RCM Cartridge B, Waters Associates, Milford, MA 01757.
[23] M. J. Walters, Food and Drug Administration, Detroit, Mich., unpublished work (1980).

Table IV—Analysis of Hydrocortisone Tablets

Sample Number	Formulation Category	Declared Potency, mg/tablet	Results, % of Declared Potency			
			USP Assay[a]	HPLC Assay[a]	Content Uniformity of Individual Tablets by HPLC	
					Average[b]	*RSD*, %
1	A	20	91.6	92.5	95.0	2.5
2	B	20	99.3	104.9	105.6	1.4
3	B	20	99.2	101.8	102.2	1.4
4	B	10	95.2	94.8	95.9	1.0
5	B	20	91.8	95.8	95.1	4.6
6	B	20	98.8	100.2	100.4	1.0
7	C	20	90.4	96.6	96.9	1.0
8	C	10	95.8	96.8	96.4	1.5
9	D	20	95.5	97.1	95.4	3.6
10	D	10	97.7	97.7	98.9	3.0
11	E	20	93.7	96.6	96.8	2.1
12	F	20	95.2	95.4	96.5	0.82
13	G	20	96.5	94.4	93.0	2.7
14	H	10	99.6	98.0	97.8	2.3
15	H	20	100.8	100.2	103.0	3.1
16	I	20	92.9	94.6	95.4	1.4
17	I	10	93.8	96.1	96.7	1.6
18	[c]	20	92.6	95.0	96.5	1.1
19	J	5	95.2	100.6	99.9	0.63
20	J	10	100.8	99.2	95.5	0.58
21	J	20	100.4	99.0	99.0	0.67

[a] Average of duplicate determinations. [b] Average of 10 individual tablet assays. [c] Not known.

without the internal standard, and none of the chromatograms showed interfering peaks at the retention corresponding to the internal standard. These solutions were also used to test for the presence of impurities by increasing the detector sensitivity 25-fold, from 0.5 to 0.02 aufs. Chromatograms of reference standard I with degradation products II, III, and the related steroids IV–VIII, each added at a level of 0.5% of I, showed that these impurities are detectable at this level by this procedure (Fig 2). An estimated 0.1–0.3% of cortisone was found in all five samples and 0.3–0.6% of prednisolone was found in three samples of I drug substance (Table II). The presence of cortisone and prednisolone was confirmed by TLC, the latter after subjecting concentrated solutions to HPLC, collecting, and concentrating the appropriate portions of the eluate. Traces of hydrocortisone acetate and unidentified impurities were also detected. No degradation products were found. The total amount of detected impurities was <1% in all samples.

The HPLC system was applied to the analysis of I tablets by introducing a sample preparation step and performing additional validation experiments. The dilutions specified in the sample preparation for tablets result in the same final concentration of I regardless of the dosage level, which ranges from 5 to 20 mg/tablet. Thus, the same standard solution and detector sensitivity can be used.

The recovery of I through the method and the influence of excipients was checked by the synthetic sample approach. Five typical product formulations prepared in the laboratory were assayed. The recovery results (Table III) ranged from 98.6 to 101.8% and the overall mean for a total of 25 determinations was 99.9% with a relative standard deviation of 0.91%. No bias in the method is indicated. The precision for commercial products was checked by assaying 10 composite portions for each of five samples. The results showed good precision with the relative standard deviation for the five samples ranging from 0.27 to 0.78%.

The tablet content uniformity procedure is essentially identical to the assay, the only difference being in the initial sample preparation required to disintegrate the intact tablet. A small amount of water was needed to soften the tablet and enhance the disintegration. The volumes of water and methanol were limited to the specified low levels in order to maintain the equilibrium of the chromatographic system.

Twenty-one commercial tablet products manufactured by 12 different firms were subjected to the HPLC assay and content uniformity procedures. The results are summarized in Table IV along with those obtained by the USP assay. While all the results are within USP limits, 14 of the 21 USP assay results are lower than the HPLC assay with an average difference of 1.45%, suggesting a negative bias in the USP assay. The average difference between results of duplicate determinations was 1.1% for the USP method and 0.49% for the HPLC assay method. The HPLC composite assay results show good agreement with the respective average content uniformity results for 10 individual tablets.

A typical chromatogram is shown in Fig. 3A. A portion of each composite chromatographed without internal standard showed no interferences at the retention volume of IX.

The same HPLC system was applied to the assay of hydrocortisone enema after introducing an appropriate sample preparation step. Since the adsorption HPLC system requires that the water content be maintained at a low and closely controlled level, aqueous enema samples could not be introduced without eliminating the water. An extraction of I into chloroform was found to overcome this problem. Methyl- and propylparabens, present as preservatives, were also extracted into chloroform but were well resolved from I by HPLC (Fig. 3B).

The average recovery for 10 portions of I through the enema assay was 100.2% with a relative standard deviation of 0.65%. The average of 10 recoveries for two synthetic enema formulations was 99.9 and 99.1% with a relative standard deviation of 0.38 and 0.24%, respectively (Table III). Replicate determinations of two commercial enema products resulted in a relative standard deviation of 1.0% in both cases, showing acceptable precision. One of the products was found to have satisfactory potency with good agreement between the HPLC and blue tetrazolium assays, 99.8 and 101.0%, respectively. The second product showed only 82.7% of the labeled I content by HPLC and 86.5% by blue tetrazolium. Since the blue tetrazolium reaction is not specific, it is possible that an impurity in the product may have caused false high results. This suspicion was further reinforced when a small peak at 5.6 min was observed in the sample chromatograms. This peak did not appear in the standard, synthetic sample or the other enema product chromatograms; did not correspond to I–IX; and remains unidentified. The low HPLC assay result was confirmed by subjecting the sample to a reversed-phase HPLC assay using an octyl–silane bonded column and a methanol–water (60:40) mobile solvent.

The presented HPLC methods for the analysis of I drug substance tablets and enema have been shown to be accurate, precise, specific, and applicable to products on the commercial market. It is anticipated that with appropriate sample preparation the same HPLC system will be applicable to other hydrocortisone products.

REFERENCES

(1) W. Mader and R. Buck, *Anal. Chem.*, **24,** 666 (1952).

(2) "The United States Pharmacopeia," 20th rev., Mack Publishing, Easton, Pa., 1980.

(3) F. M. Kunze and J. S. Davis, *J. Pharm. Sci.*, **53,** 1170 (1964).

(4) *Ibid.*, **53,** 1259 (1964).

(5) R. E. Graham, P. A. Williams, and C. T. Kenner, *J. Pharm. Sci.*, **59,** 1472 (1970).

(6) *Ibid.*, **59,** 1152 (1970).

(7) R. E. Graham and C. T. Kenner, *J. Pharm. Sci.*, **62,** 103 (1973).

(8) R. E. Graham, E. R. Biehl, C. T. Kenner, G. H. Luttrell, and D. L. Midleton, *ibid.*, **64,** 226 (1975).

(9) R. M. Otelza, R. S. Wooten, C. T. Kenner, R. E. Graham, and E. R. Biehl, *ibid.*, **66**, 1385 (1977).
(10) R. E. Graham, E. R. Biehl, and C. T. Kenner, *ibid.*, **67**, 792 (1978).
(11) E. Umberger, *Anal. Chem.*, **27**, 768 (1955).
(12) C. C. Porter and R. H. Silber, *J. Biol. Chem.*, **185**, 201 (1950).
(13) R. H. Silber and C. C. Porter, *ibid.*, **210**, 923 (1954).
(14) N. Stroud, N. E. Richardson, D. J. G. Davies, and D. A. Norton, *Analyst*, **105**, 455 (1980).
(15) M. C. Olson, *J. Pharm. Sci.*, **62**, 2001 (1973).
(16) J. Korpi, D. P. Wittmer, B. J. Sandmann, and W. G. Haney, Jr., *ibid.*, **65**, 1087 (1976).
(17) V. Das Gupta, *ibid.*, **67**, 299 (1978).
(18) T. J. Goehl, G. M. Sundaresan, and V. K. Prasad, *ibid.*, **68**, 1374 (1979).
(19) M. D. Smith and D. J. Hoffman, *J. Chromatogr.*, **168**, 163 (1979).
(20) N. W. Thymes, *J. Chromatogr. Sci.*, **15**, 151 (1977).
(21) J. H. M. VanDenBerg, J. Milley, N. Vonk, and R. S. Deelder, *J. Chromatogr.*, **132**, 421 (1977).
(22) S. Hara and S. Hayashi, *ibid.*, **142**, 689 (1977).
(23) "The United States Pharmacopeia," 19th rev., Mack Publishing, Easton, Pa., 1975.
(24) *Ibid.*, 18th rev., 1970.
(25) *Ibid.*, 17th rev., 1965.
(26) J. E. Sinsheimer and E. F. Salim, *Anal. Chem.*, **37**, 566 (1965).
(27) T. Chulski and A. A. Florist, *J. Pharm. Sci.*, **47**, 533 (1958).
(28) U. Westphal, G. J. Chader, and G. B. Harding, *Steroids*, **10**, 155 (1967).
(29) C. Monder and M. C. Walker, *ibid.*, **15**, 1 (1970).
(30) H. Vanderhaege and J. Hoebus, *J. Pharm. Belg.*, **31**, 25 (1976).

ACKNOWLEDGMENTS

The authors thank Robert E. Graham for providing the degradation products and commercial samples, Laura M. Tuck for her analytical work on the enema, and Stephen M. Walters for a constructive editorial review.

NOTES

Systematic Error Associated with Apparatus 2 of the USP Dissolution Test I: Effects of Physical Alignment of the Dissolution Apparatus

DON C. COX[x] and WILLIAM B. FURMAN

Received April 17, 1981, from the *National Center for Drug Analysis, Food and Drug Administration, St. Louis, MO 63101.* Accepted for publication July 23, 1981.

Abstract □ The physical alignment of the paddle and the vessel is critical in obtaining reproducible results from the USP dissolution test with Apparatus 2. Large variations in dissolution results were traced to minor variations in alignment of different apparatuses.

Keyphrases □ Dissolution—USP Apparatus 2, reproducibility of results □ USP—dissolution Apparatus 2, reproducibility of results □ Apparatus—USP dissolution Apparatus 2, reproducibility of results

This laboratory has been recently studying the systematic error associated with Apparatus 2 of the USP dissolution test (1). Collaborative studies conducted by the Academy of Pharmaceutical Sciences[1] and by the Food and Drug Administration (2) showed a wide variation in test results reported by different laboratories. The present report is the first of a series of papers describing sources of systematic error associated with the dissolution test.

The test method first appeared in the Fourth Supplement to USP XIX and NF XIV (3). The stirring element consisted of a shaft with a detachable paddle blade positioned on its side. In the Fifth Supplement of USP XIX and NF XIV, the stirring element was modified to its present configuration: the blade is now rigidly mounted through the diameter of the shaft. The data reported in this paper were collected prior to the modification of the apparatus.

[1] Unpublished data, Dissolution Technology Committee, APhA Academy of Pharmaceutical Sciences.

EXPERIMENTAL

Two commercial samples of 5-mg prednisone tablets (referred to as Tablet 0 and Tablet 1) were used for the evaluation of six dissolution apparatuses. Dissolution data for the two samples from each apparatus were collected using a single set of six glass dissolution vessels[2] and uniform analytical technique. Two appartuses, designated A and B, were designed and built by the Food and Drug Administration. Four apparatuses, designated C, D, E, and F, were commercially available[3]. Each apparatus could test six tablets simultaneously.

The dissolution and analytical methodology is described in the Fourth Supplement to USP XIX and NF XIV (4).

RESULTS AND DISCUSSION

The data collected from the two samples with each apparatus are shown in Table I. The results for apparatuses E and F are considerably higher than those for the other four apparatuses. These discrepancies were traced to minor variations in the vertical alignment of the paddle shafts. The experiment pointed out two deficiencies in the dissolution methodology.

The first deficiency was that the equipment operator could not be certain that the USP alignment specifications were being met: the paddle shaft must be aligned so that its axis is not more than 0.2 cm from the vertical axis of the vessel at any point. Devices adequate to measure and adjust the equipment to meet this requirement were not available initially. Although the apparatus was adjusted to make the drive head parallel with the base, no conscientious effort was made to improve the precision with which a vessel was centered around its shaft.

The second deficiency lay in the design of the apparatus. The support

[2] Kimble, Vineland, N.J.
[3] C: Model 72A, Hanson Research Corp., Northridge, Calif. D, E, and F: Three separate Hanson Model 72R apparatuses.

0022-3549/82/0400-0451$01.00/0

(9) R. M. Otelza, R. S. Wooten, C. T. Kenner, R. E. Graham, and E. R. Biehl, *ibid.*, **66**, 1385 (1977).
(10) R. E. Graham, E. R. Biehl, and C. T. Kenner, *ibid.*, **67**, 792 (1978).
(11) E. Umberger, *Anal. Chem.*, **27**, 768 (1955).
(12) C. C. Porter and R. H. Silber, *J. Biol. Chem.*, **185**, 201 (1950).
(13) R. H. Silber and C. C. Porter, *ibid.*, **210**, 923 (1954).
(14) N. Stroud, N. E. Richardson, D. J. G. Davies, and D. A. Norton, *Analyst*, **105**, 455 (1980).
(15) M. C. Olson, *J. Pharm. Sci.*, **62**, 2001 (1973).
(16) J. Korpi, D. P. Wittmer, B. J. Sandmann, and W. G. Haney, Jr., *ibid.*, **65**, 1087 (1976).
(17) V. Das Gupta, *ibid.*, **67**, 299 (1978).
(18) T. J. Goehl, G. M. Sundaresan, and V. K. Prasad, *ibid.*, **68**, 1374 (1979).
(19) M. D. Smith and D. J. Hoffman, *J. Chromatogr.*, **168**, 163 (1979).
(20) N. W. Thymes, *J. Chromatogr. Sci.*, **15**, 151 (1977).
(21) J. H. M. VanDenBerg, J. Milley, N. Vonk, and R. S. Deelder, *J. Chromatogr.*, **132**, 421 (1977).
(22) S. Hara and S. Hayashi, *ibid.*, **142**, 689 (1977).
(23) "The United States Pharmacopeia," 19th rev., Mack Publishing, Easton, Pa., 1975.
(24) *Ibid.*, 18th rev., 1970.
(25) *Ibid.*, 17th rev., 1965.
(26) J. E. Sinsheimer and E. F. Salim, *Anal. Chem.*, **37**, 566 (1965).
(27) T. Chulski and A. A. Florist, *J. Pharm. Sci.*, **47**, 533 (1958).
(28) U. Westphal, G. J. Chader, and G. B. Harding, *Steroids*, **10**, 155 (1967).
(29) C. Monder and M. C. Walker, *ibid.*, **15**, 1 (1970).
(30) H. Vanderhaege and J. Hoebus, *J. Pharm. Belg.*, **31**, 25 (1976).

ACKNOWLEDGMENTS

The authors thank Robert E. Graham for providing the degradation products and commercial samples, Laura M. Tuck for her analytical work on the enema, and Stephen M. Walters for a constructive editorial review.

NOTES

Systematic Error Associated with Apparatus 2 of the USP Dissolution Test I: Effects of Physical Alignment of the Dissolution Apparatus

DON C. COX[x] and WILLIAM B. FURMAN

Received April 17, 1981, from the *National Center for Drug Analysis, Food and Drug Administration, St. Louis, MO 63101.* Accepted for publication July 23, 1981.

Abstract □ The physical alignment of the paddle and the vessel is critical in obtaining reproducible results from the USP dissolution test with Apparatus 2. Large variations in dissolution results were traced to minor variations in alignment of different apparatuses.

Keyphrases □ Dissolution—USP Apparatus 2, reproducibility of results □ USP—dissolution Apparatus 2, reproducibility of results □ Apparatus—USP dissolution Apparatus 2, reproducibility of results

This laboratory has been recently studying the systematic error associated with Apparatus 2 of the USP dissolution test (1). Collaborative studies conducted by the Academy of Pharmaceutical Sciences[1] and by the Food and Drug Administration (2) showed a wide variation in test results reported by different laboratories. The present report is the first of a series of papers describing sources of systematic error associated with the dissolution test.

The test method first appeared in the Fourth Supplement to USP XIX and NF XIV (3). The stirring element consisted of a shaft with a detachable paddle blade positioned on its side. In the Fifth Supplement of USP XIX and NF XIV, the stirring element was modified to its present configuration: the blade is now rigidly mounted through the diameter of the shaft. The data reported in this paper were collected prior to the modification of the apparatus.

[1] Unpublished data, Dissolution Technology Committee, APhA Academy of Pharmaceutical Sciences.

EXPERIMENTAL

Two commercial samples of 5-mg prednisone tablets (referred to as Tablet 0 and Tablet 1) were used for the evaluation of six dissolution apparatuses. Dissolution data for the two samples from each apparatus were collected using a single set of six glass dissolution vessels[2] and uniform analytical technique. Two appartuses, designated A and B, were designed and built by the Food and Drug Administration. Four apparatuses, designated C, D, E, and F, were commercially available[3]. Each apparatus could test six tablets simultaneously.

The dissolution and analytical methodology is described in the Fourth Supplement to USP XIX and NF XIV (4).

RESULTS AND DISCUSSION

The data collected from the two samples with each apparatus are shown in Table I. The results for apparatuses E and F are considerably higher than those for the other four apparatuses. These discrepancies were traced to minor variations in the vertical alignment of the paddle shafts. The experiment pointed out two deficiencies in the dissolution methodology.

The first deficiency was that the equipment operator could not be certain that the USP alignment specifications were being met: the paddle shaft must be aligned so that its axis is not more than 0.2 cm from the vertical axis of the vessel at any point. Devices adequate to measure and adjust the equipment to meet this requirement were not available initially. Although the apparatus was adjusted to make the drive head parallel with the base, no conscientious effort was made to improve the precision with which a vessel was centered around its shaft.

The second deficiency lay in the design of the apparatus. The support

[2] Kimble, Vineland, N.J.
[3] C: Model 72A, Hanson Research Corp., Northridge, Calif. D, E, and F: Three separate Hanson Model 72R apparatuses.

0022-3549/82/0400-0451$01.00/0

Table I—Comparison of Dissolution Data from Different Apparatuses for Two Samples of 5-mg Prednisone Tablets [a]

Apparatus	Tablet 0[b]		Tablet 1[c]	
	$\bar{x}$	$\pm SD$	$\bar{x}$	$\pm SD$
A	19.9	±6.4	52.6	±5.6
B	19.3	±7.8	53.7	±6.6
C	23.1	±11.5	56.1	±11.5
D	22.1	±9.5	54.5	±3.4
E	29.9	±13.1	63.2	±10.4
F	37.7	±17.0	80.7	±4.0

[a] Results in percent of label claim dissolved at 30 min. [b] $n = 12$. [c] $n = 6$.

Table II—Comparison of Dissolution Data from Two Samples of 5-mg Prednisone Tablets After Realignment of Apparatuses [a]

Apparatus	Tablet 0[b]		Tablet 1[c]	
	$\bar{x}$	$\pm SD$	$\bar{x}$	$\pm SD$
E	19.0	±6.3	48.8	±4.8
F	20.6	±6.8	46.3	±3.3

[a] Results in percent of label claim dissolved at 30 min. [b] $n = 12$. [c] $n = 6$.

Table III—Effect of Verticality of Paddle Shafts on Dissolution Results Obtained from Tablet 1

Condition	Dissolution Results[a]			
	$\bar{x}$	$\pm SD$	$\bar{x}$	$\pm SD$
Shafts in vertical position	50.1	±5.2	48.6	±2.7
Shafts 0.5 degree from vertical position	53.8	±4.6	54.6	±4.2
Shafts realigned to vertical position	50.6	±3.6	—	

[a] Duplicate runs. Results in percent of label claim dissolved at 30 min. $n = 6$.

for the dissolution drive for apparatuses D, E, and F consisted of a keyed center post. The drive could be moved vertically on the post and pivoted up and out of the way to facilitate the changing of vessels between tests. Because of this design the dissolution drives of apparatuses D, E, and F were held less rigidly and precisely over the holes in the base of the apparatus than the dissolution drive of apparatus C.

Alignment procedures were developed for the apparatus. A centering tool, a paddle depth gauge, and a means of holding the vessel in a position centered around the paddle shaft were developed. These procedures and tools (5) were used to realign apparatuses E and F. The dissolution test was repeated on Tablet 0 and Tablet 1. Realignment improved the test results for apparatuses E and F (Table II), which were in closer agreement with the Table I results for the other four apparatuses than before realignment.

Data collected from Tablet 1 after alignment of a commercial apparatus[4] are shown in Table III. The shafts were then tilted ~0.5 degree by raising one side of the drive base by 3 mm. Additional data were collected. The shafts were readjusted to a vertical position, and the test was repeated a third time. The data (Table III) show that the effect of tilting the shafts from a vertical position by only 0.5 degree is substantial and reproducible.

The shafts in a six-spindle apparatus can all be made vertical only if the chucks hold the shafts parallel to each other. The shafts of one of the commercial apparatuses showed small deviations from parallelism. Vernier calipers, capable of measurement to the nearest 0.02 mm, were used to measure the distances between shafts. Measurements were taken in a horizontal plane near the chucks and in a horizontal plane 17 cm below the chucks. The differences in the measurements (Fig. 1) are small but significant. If shafts 1, 2, 3, and 5 are made vertical, shafts 4 and 6 will not be vertical. Shaft 4 in particular will be displaced about 0.5 degree

[4] Model 72RL, Hanson Research Corp.

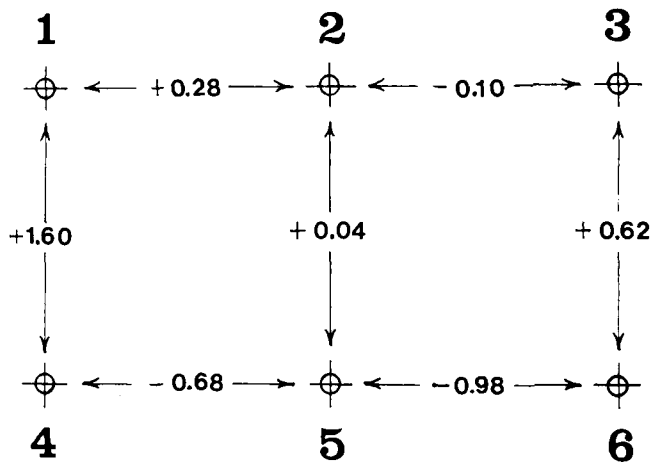

Figure 1—*Deviations (in millimeters) from parallelism of shafts of one commercial apparatus. Measurements were taken where the shafts come out of the chucks and compared to measurements taken 17 cm below the chucks. A positive sign indicates the two shafts are divergent. A negative sign indicates the two shafts are convergent.*

from a vertical position. When Tablet 1 was examined with this apparatus, the data from shafts 4 and 6 were markedly different from those from shafts 1, 2, 3, and 5, and the differences were of the same magnitude as the differences in averages reported in Table III.

Experience has since indicated that an analyst who is new to the dissolution test may interpret the USP requirement for paddle shaft alignment as a requirement to center the tops of the vessels around the shafts to within 0.2 cm. It is equally important that the shafts are precisely vertical. Despite the fact that the top of each vessel was centered around its shaft, minor vertical deviations of shafts caused large changes in the test results from Table 1.

CONCLUSIONS

The liquid flow rates generated in different sections of the vessel are controlled by the location of the paddle in the vessel as well as the rotational rate of the paddle. Dissolution results obtained prior to modification of the paddle blade can differ from results obtained after modification. The system geometry of both paddle designs must be precisely controlled if results from either are to be reproducible. To minimize error resulting from minor variations in the system geometry of Apparatus 2, the base of the apparatus must be horizontal, the shafts must be vertical, each shaft must be positioned along the vertical axis of each vessel, and the paddles must be set at a standarized depth in the vessels. These alignments must be made as precisely as current technology will allow.

REFERENCES

(1) "The United States Pharmacopeia," 20th rev., Mack Publishing, Easton, Pa., 1980, p. 959.

(2) S. Sherken, presented at a Dissolution Workshop-Seminar, Division of Biopharmaceutics, Food and Drug Administration, Washington, D.C., Oct. 1977.

(3) "Fourth Supplement to USP XIX and NF XIV," The United States Pharmacopeial Convention, Inc., Rockville, Md., 1978, p. 194.

(4) *Ibid.*, p. 141.

(5) D. C. Cox, C. C. Douglas, W. B. Furman, R. D. Kirchhoefer, J. W. Myrick, and C. E. Wells, *Pharm. Technol.*, **2**, (4), 41 (1978).

ACKNOWLEDGMENTS

The authors thank John C. Black for drawing the figure.

Reduced Hydrolytic Lability of Epoprostenol in the Presence of Cationic Micelles

M. J. CHO

Received January 12, 1981, from the *Upjohn Co., Kalamazoo, MI 49001.* Accepted for publication July 24, 1981.

Abstract □ The rapid hydrolysis of epoprostenol to 6-keto-prostaglandin $F_{1\alpha}$ is hydronium ion-catalyzed even at pH 10 or higher. In the presence of 1.0% hexadecyltrimethylammonium chloride, the rate was reduced significantly (1580-fold at pH 2 and 283-fold at a physiological pH). This decrease in the hydrolysis rate is attributed to two causes: favorable partitioning of epoprostenol in the micellar phase and electrostatic repulsion between the hydronium ion and the cationic micellar surface.

Keyphrases □ Prostaglandins—epoprostenol, reduced hydrolytic lability in the presence of cationic micelles □ Micelles—reduction of hydrolytic lability of epoprostenol □ Epoprostenol—reduced hydrolytic lability in the presence of cationic micelles

The antiplatelet (anti- and deaggregatory) and vasodilator actions of epoprostenol (I) has brought about not only some potential clinical applications but also "a direct impact on research dealing with the mode of antiaggregatory cyclic AMP activity" (1). Being a vinyl ether, however, I is extremely unstable in aqueous media; half-life ($t_{1/2}$) of its hydrolysis is only several minutes at a physiological pH and 25° (2). Subsequently it was found that the compound is unusually reactive even as a vinyl ether and that the hydronium ion-catalyzed hydrolytic lability of the carboxylate anion is nearly two orders of magnitude greater than that of the free acid or methyl ester (Fig. 1) (3). The instability of this endogenous hormone-like substance has hampered the progress of clinical applications and in the basic research area. The present study reports that in the presence of cationic micelles the hydrolysis rate can be retarded by a factor of 1.5×10^3 at pH 2 and 10^2 at a physiological pH.

EXPERIMENTAL

A UV spectrophotometric[1] procedure was used to follow the hydrolysis of I (2). Essentially, the absorbance change at 235 or 240 nm was monitored continuously immediately after the sodium salt of I (~4 mg) was dissolved in a non-UV absorbing buffer solution (~3 ml) of 0.5 *M* ionic strength in a cell. When the spectral change was scanned continuously, an isosbestic point was observed at 256 nm throughout a kinetic run over the pH range studied. Hexadecyltrimethylammonium chloride[2], was used as received.

RESULTS AND DISCUSSION

Negative micellar catalysis has not been subject to numerous applications in the area of drug formulation development, although stabilization of a drug compound can be achieved in aqueous media (4). This is surprising since micelle-catalyzed organic reactions in aqueous media have been studied extensively as model systems of enzymatic reactions.

Aqueous solutions containing a surface-active agent form molecular aggregates known as micelles when the total concentration reaches a certain value, which is referred to as the critical micellar concentration (CMC). The CMC of hexadecyltrimethylammonium chloride $[(CH_3)_3N^+(CH_2)_{15}CH_3 \cdot Cl^-]$ is $\sim 1.3 \times 10^{-3} M$(5), and hence in a 1.0% $(3.12 \times 10^{-2} M)$ solution (in which the stability of I was investigated), most of the surfactant molecules are engaged in micelles. Since the polarity of the micellar phase can be much lower than that of the bulk aqueous phase, I free acid is expected to partition favorably into the micellar phase. However, as pH increases the apparent fractional concentration of I found inside the micellar phase will decrease because the dynamic equilibrium becomes more favorable for the anion to exist in an aqueous environment.

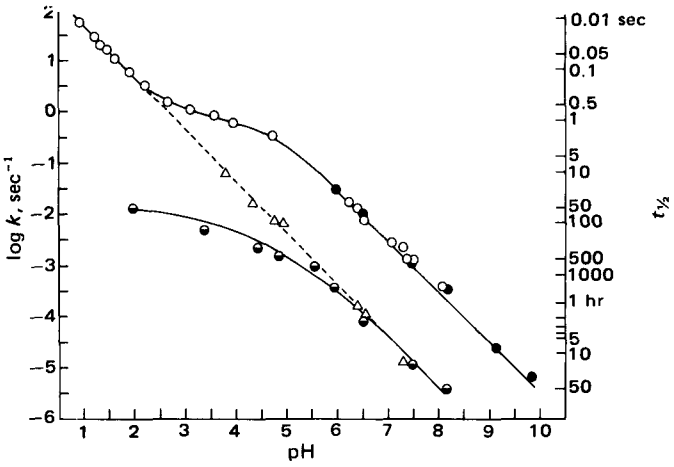

Figure 1—*pH dependence of the hydrolysis rate of I (closed circles from Ref. 2 and open circles from Ref. 3), I methyl ester (triangles from Ref. 3), and in the presence of 1.0% hexadecyltrimethylammonium chloride (half-circles), all at 25°. The former two are the rate constants at zero buffer concentration, and the last one was at 0.5* M *ionic strength.*

From this pH-dependence of the partitioning behavior of I and from

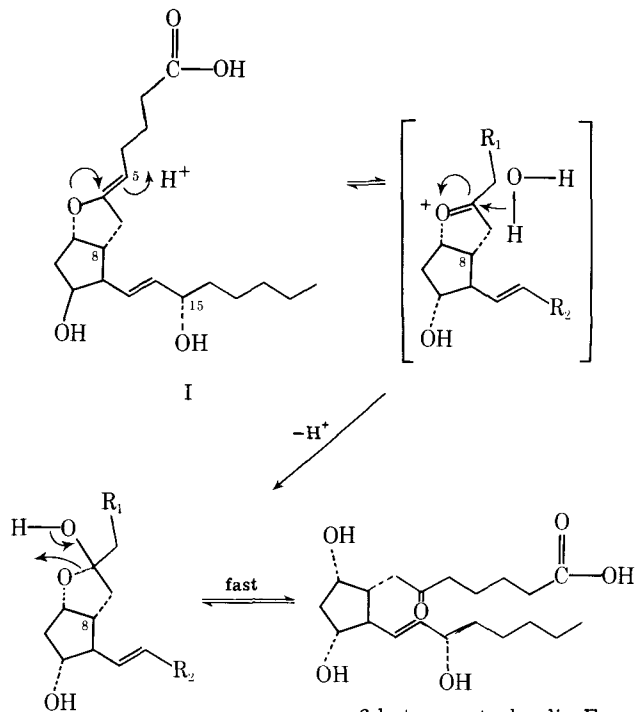

Scheme I—Reaction pathway of I hydrolysis.

[1] Zeiss Model DMR-21 Spectrophotometer
[2] Eastman Kodak Co., Rochester, N.Y.

0022-3549/82/0400-0453$01.00/0

the general belief that the thermodynamic activities of water (reactant) and hydronium ion (catalyst) can be extremely low inside the micellar phase, one would expect the pH-profile of log k_{obs} shown in Fig. 1 (half-filled circles). Note that the overall rate-determining step in the hydrolysis of I is the protonation at C-5, which makes the Δ^5 bond polarized and susceptible to the subsequent water attack (Scheme I) (3). That is, if an intrinsic reactivity is assigned to the free acid present inside the micellar phase, regardless of the pH of the bulk phase, then the pH-profile of the observed rate constant should resemble that of the apparent partition coefficient. This analysis is consistent with what was observed.

In the presence of 1.0% hexadecyltrimethylammonium chloride, the apparent hydrolysis rate at pH below 3 is $\sim 1.5 \times 10^3$ fold slower than in the absence of the surfactant (Fig. 1). At neutral pH values, however, such a comparison can be made only after taking the general acid catalysis by buffer components into consideration. At pH 7.45, for instance, if the data shown in Fig. 1 are compared, only a 62-fold decrease in the rate is obtained. However, the hydrolysis rate shown in Fig. 1 in the absence of the surfactant is the rate extrapolated to zero buffer concentration, whereas that in the presence of the surfactant was obtained in a 0.165 *M* phosphate buffer of 0.50 *M* ionic strength. In an identical buffer system without the surfactant, it was found previously that the hydrolysis is ~4.56 faster than at zero buffer concentration (2). The net effect of 1.0% hexadecyltrimethylammonium chloride is, therefore, a reduction of the hydrolysis rate of ~280-fold; $t_{1/2}$ from 3.5 min to 16.5 hr.

Finally, one should not attempt to interpret the coincidental overlap of the rate constants for the hydrolysis of methyl ester (triangles in Fig. 1) and I in the presence of the surfactant at pH above 6. As discussed previously (4), the latter is a function of the concentration of both substrate and the surfactant present in a given system.

REFERENCES

(1) R. J. Gryglewski, *CRC Crit. Rev. Biochem.*, 291 (1980), and references therein.

(2) M. J. Cho and M. A. Allen, *Prostaglandins*, **15**, 943 (1978).

(3) Y. Chiang, A. J. Kresge, and M. J. Cho, *J. Chem. Soc. Chem. Commun.*, **1979**, 129.

(4) M. J. Cho and M. A. Allen, *Int. J. Pharm.*, **1**, 281 (1978), and references therein.

(5) P. Mukerjee and K. J. Mysels, "Critical Micellar Concentrations of Aqueous Surfactant Systems," U.S. Government Printing Office, Washington, D.C., 1971, p. 136.

Determination of Tissue to Blood Partition Coefficients in Physiologically-Based Pharmacokinetic Studies

GILBERT LAM *, MEI-LING CHEN, and WIN L. CHIOU ˣ

Received May 18, 1981, from the *Department of Pharmacy, College of Pharmacy, University of Illinois at the Medical Center, Chicago, IL 60680.* Accepted for publication August 10, 1981. * Present address: Stine Laboratory, E.I. du Pont Nemours and Co., Inc., Newark, DE 19711.

Abstract □ The partition coefficient between tissue and blood used in physiologically-based pharmacokinetic modeling analysis was investigated using the concept of clearance. New equations were derived and compared with previously reported equations in constant intravenous infusion and bolus injection methods. The importance of differentiating arterial from venous blood is discussed.

Keyphrases □ Partition coefficient—tissue to blood, physiologically-based pharmacokinetics □ Pharmacokinetics—determination of tissue to blood partition coefficients in physiologically-based pharmacokinetic studies □ Blood sampling—differences between arterial and venous blood, physiologically-based pharmacokinetic studies

The formulation of a physiologically-based pharmacokinetic model requires an accurate determination of physiological parameters such as blood flow, organ volume, partition coefficient, and clearance (1). The estimation of the tissue to blood partition coefficients for a compound is of special interest to pharmacokineticists because it can be directly measured in the laboratory. Recently, Chen and Gross (2) pointed out different methods by which tissue to plasma partition coefficients can be determined under specific experimental conditions. The following equations were used in constant infusion and bolus injection studies, respectively:

$$R = \left(1 + \frac{K}{Q}\right)\frac{C_t^\infty}{C_p^\infty} \qquad \text{(Eq. 1)}$$

$$R = \frac{(Q + K)C_t^0}{(QC_p^0 + \alpha V_t C_t^0)} \qquad \text{(Eq. 2)}$$

where R is the partition coefficient of drug between organ tissue and plasma, K was defined as the first-order elimination rate constant [but was used as organ clearance in their calculations (2)], Q is the flow rate of plasma in the organ, C_t^∞ and C_p^∞ are the concentrations of drug in tissue and plasma at steady state, C_t^0 and C_p^0 are the concentrations of drug in tissue and plasma at time zero extrapolated from the terminal phase, α is the terminal rate constant, and V_t is the volume of the organ or tissue. The present study examined Eqs. 1 and 2 from the concept of physiological clearance and derived new equations for the determination of R in constant infusion and bolus injection studies. Flow and concentration in terms of blood were dealt with instead of plasma.

THEORETICAL

The concept of clearance and its applications are well defined in the pharmacokinetic literature (3–7). In an eliminating organ or tissue, it describes the volume of incoming blood completely cleared of drug by the organ per unit time. Conventionally, it is expressed as the organ clearance, CL_s, and is defined as:

$$CL_s = \frac{r}{C_i} \qquad \text{(Eq. 3)}$$

where r is the rate at which the drug is removed from the organ and C_i is the drug concentration in the incoming blood. However, it has been observed that CL_s might be dependent on the blood flow through the organ and the use of intrinsic clearance, CL_i, was proposed to correct for the influence of blood flow (3). CL_i is defined as:

$$CL_i = \frac{r}{C_0} \qquad \text{(Eq. 4)}$$

where C_0 is the effluent venous blood concentration which is in equilibrium with the eliminating organ. It measures the maximum capacity of the organ to eliminate the drug. An important relation obtained from the above clearance equation is:

$$r = CL_s C_i = CL_i C_0 \qquad \text{(Eq. 5)}$$

0022-3549/82/0400-0454$01.00/0

the general belief that the thermodynamic activities of water (reactant) and hydronium ion (catalyst) can be extremely low inside the micellar phase, one would expect the pH-profile of log k_{obs} shown in Fig. 1 (half-filled circles). Note that the overall rate-determining step in the hydrolysis of I is the protonation at C-5, which makes the Δ^5 bond polarized and susceptible to the subsequent water attack (Scheme I) (3). That is, if an intrinsic reactivity is assigned to the free acid present inside the micellar phase, regardless of the pH of the bulk phase, then the pH-profile of the observed rate constant should resemble that of the apparent partition coefficient. This analysis is consistent with what was observed.

In the presence of 1.0% hexadecyltrimethylammonium chloride, the apparent hydrolysis rate at pH below 3 is $\sim 1.5 \times 10^3$ fold slower than in the absence of the surfactant (Fig. 1). At neutral pH values, however, such a comparison can be made only after taking the general acid catalysis by buffer components into consideration. At pH 7.45, for instance, if the data shown in Fig. 1 are compared, only a 62-fold decrease in the rate is obtained. However, the hydrolysis rate shown in Fig. 1 in the absence of the surfactant is the rate extrapolated to zero buffer concentration, whereas that in the presence of the surfactant was obtained in a 0.165 *M* phosphate buffer of 0.50 *M* ionic strength. In an identical buffer system without the surfactant, it was found previously that the hydrolysis is ~4.56 faster than at zero buffer concentration (2). The net effect of 1.0% hexadecyltrimethylammonium chloride is, therefore, a reduction of the hydrolysis rate of ~280-fold; $t_{1/2}$ from 3.5 min to 16.5 hr.

Finally, one should not attempt to interpret the coincidental overlap of the rate constants for the hydrolysis of methyl ester (triangles in Fig. 1) and I in the presence of the surfactant at pH above 6. As discussed previously (4), the latter is a function of the concentration of both substrate and the surfactant present in a given system.

REFERENCES

(1) R. J. Gryglewski, *CRC Crit. Rev. Biochem.*, 291 (1980), and references therein.

(2) M. J. Cho and M. A. Allen, *Prostaglandins*, **15**, 943 (1978).

(3) Y. Chiang, A. J. Kresge, and M. J. Cho, *J. Chem. Soc. Chem. Commun.*, **1979**, 129.

(4) M. J. Cho and M. A. Allen, *Int. J. Pharm.*, **1**, 281 (1978), and references therein.

(5) P. Mukerjee and K. J. Mysels, "Critical Micellar Concentrations of Aqueous Surfactant Systems," U.S. Government Printing Office, Washington, D.C., 1971, p. 136.

Determination of Tissue to Blood Partition Coefficients in Physiologically-Based Pharmacokinetic Studies

GILBERT LAM *, MEI-LING CHEN, and WIN L. CHIOU ˣ

Received May 18, 1981, from the *Department of Pharmacy, College of Pharmacy, University of Illinois at the Medical Center, Chicago, IL 60680.* Accepted for publication August 10, 1981. * Present address: Stine Laboratory, E.I. du Pont Nemours and Co., Inc., Newark, DE 19711.

Abstract □ The partition coefficient between tissue and blood used in physiologically-based pharmacokinetic modeling analysis was investigated using the concept of clearance. New equations were derived and compared with previously reported equations in constant intravenous infusion and bolus injection methods. The importance of differentiating arterial from venous blood is discussed.

Keyphrases □ Partition coefficient—tissue to blood, physiologically-based pharmacokinetics □ Pharmacokinetics—determination of tissue to blood partition coefficients in physiologically-based pharmacokinetic studies □ Blood sampling—differences between arterial and venous blood, physiologically-based pharmacokinetic studies

The formulation of a physiologically-based pharmacokinetic model requires an accurate determination of physiological parameters such as blood flow, organ volume, partition coefficient, and clearance (1). The estimation of the tissue to blood partition coefficients for a compound is of special interest to pharmacokineticists because it can be directly measured in the laboratory. Recently, Chen and Gross (2) pointed out different methods by which tissue to plasma partition coefficients can be determined under specific experimental conditions. The following equations were used in constant infusion and bolus injection studies, respectively:

$$R = \left(1 + \frac{K}{Q}\right)\frac{C_t^\infty}{C_p^\infty} \qquad \text{(Eq. 1)}$$

$$R = \frac{(Q + K)C_t^0}{(QC_p^0 + \alpha V_t C_t^0)} \qquad \text{(Eq. 2)}$$

where R is the partition coefficient of drug between organ tissue and plasma, K was defined as the first-order elimination rate constant [but was used as organ clearance in their calculations (2)], Q is the flow rate of plasma in the organ, C_t^∞ and C_p^∞ are the concentrations of drug in tissue and plasma at steady state, C_t^0 and C_p^0 are the concentrations of drug in tissue and plasma at time zero extrapolated from the terminal phase, α is the terminal rate constant, and V_t is the volume of the organ or tissue. The present study examined Eqs. 1 and 2 from the concept of physiological clearance and derived new equations for the determination of R in constant infusion and bolus injection studies. Flow and concentration in terms of blood were dealt with instead of plasma.

THEORETICAL

The concept of clearance and its applications are well defined in the pharmacokinetic literature (3–7). In an eliminating organ or tissue, it describes the volume of incoming blood completely cleared of drug by the organ per unit time. Conventionally, it is expressed as the organ clearance, CL_s, and is defined as:

$$CL_s = \frac{r}{C_i} \qquad \text{(Eq. 3)}$$

where r is the rate at which the drug is removed from the organ and C_i is the drug concentration in the incoming blood. However, it has been observed that CL_s might be dependent on the blood flow through the organ and the use of intrinsic clearance, CL_i, was proposed to correct for the influence of blood flow (3). CL_i is defined as:

$$CL_i = \frac{r}{C_0} \qquad \text{(Eq. 4)}$$

where C_0 is the effluent venous blood concentration which is in equilibrium with the eliminating organ. It measures the maximum capacity of the organ to eliminate the drug. An important relation obtained from the above clearance equation is:

$$r = CL_s C_i = CL_i C_0 \qquad \text{(Eq. 5)}$$

0022-3549/82/0400-0454$01.00/0

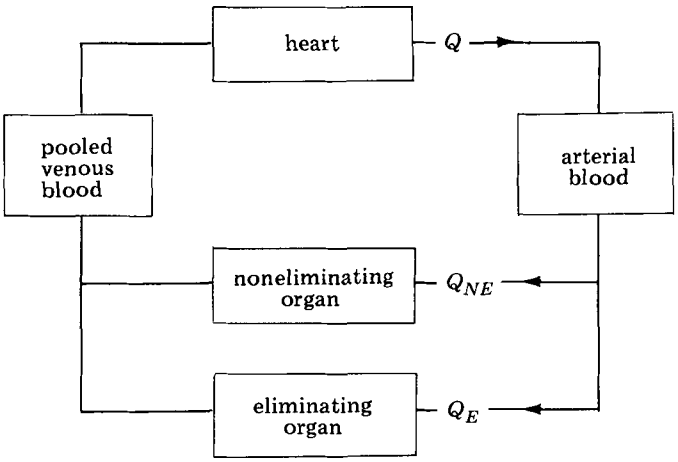

Scheme I—A simplified physiologically-based pharmacokinetic model in mammals.

This relationship describes the rate of removal of the drug from the eliminating organ in terms of either the influent arterial or effluent venous blood concentration. A simplified physiological model (Scheme I) is depicted for discussion purposes. Conventionally, the eliminating organs are the liver and kidney, while the noneliminating organs are the heart, muscle, adipose tissue, bone, etc. The lung is also considered as an eliminating organ for many drugs (8, 9), but due to its anatomical arrangement, it is treated separately. Nevertheless, the same reasoning could be applied to its treatment.

From the mass balance principle, the rate of drug accumulation in any organ can be described by the following equation:

$$V_t \frac{dC_t}{dt} = QC_i - QC_0 - CL_sC_i \qquad \text{(Eq. 6)}$$

In a well-stirred model, one generally assumes rapid equilibrium between organ tissue and its emerging venous blood (3, 10). The partition coefficient between tissue and blood is then defined as the ratio of the amount of drug per gram of the extravascular tissue (C_t) to the concentration of drug in the effluent venous blood:

$$R = \frac{C_t}{C_0} \qquad \text{(Eq. 7)}$$

Substituting into Eq. 6 yields:

$$V_t \frac{dC_t}{dt} = QC_i - \frac{QC_t}{R} - CL_sC_i \qquad \text{(Eq. 8)}$$

Partition coefficients can be estimated based on the conditions imposed by the method of administration, namely, constant infusion, intravenous bolus injection, and first-order absorption (2). Only the first two methods will be examined here.

Constant Infusion—It is apparent that at steady state, the differential term in Eq. 8 will become zero and:

$$R = \frac{QC_t^\infty}{(Q - CL_s)C_i^\infty} \qquad \text{(Eq. 9)}$$

Since $CL_s = QE$, and $C_i^\infty = C_0^\infty/(1 - E)$, where E is the extraction ratio of the organ, Eq. 9 will be reduced to:

$$R = \frac{C_t^\infty}{C_0^\infty} = \frac{C_t^\infty}{C_i^\infty(1 - E)} \qquad \text{(Eq. 10)}$$

In the case of a noneliminating organ, the concentration of the influent blood will be the same as the effluent blood at the steady state (7, 11) and the applicability of Eq. 10 is evident.

Bolus Intravenous Injection—For a linear multicompartmental system, the concentration in each compartment will decay at the same rate after the attainment of pseudo-distribution equilibrium. Both the arterial and the venous blood concentration will be of the form:

$$C = C^0e^{-\alpha t} \qquad \text{(Eq. 11)}$$

at the terminal phase; C^0 and α are the same as defined previously. Substitution of Eq. 11 and its derivative into Eq. 8 yields:

$$-\alpha V_tC_t^0e^{-\alpha t} = QC_i^0e^{-\alpha t} - \frac{QC_t^0}{R}e^{-\alpha t} - CL_sC_i^0e^{-\alpha t} \qquad \text{(Eq. 12)}$$

so that:

$$R = \frac{QC_t^0}{(Q - CL_s)C_t^0 + \alpha V_tC_t^0} \qquad \text{(Eq. 13)}$$

RESULTS AND DISCUSSION

The derived equations provide the theoretical basis for estimating the partition coefficient of drugs between tissue and blood. It is obvious that Eqs. 9 and 13 are different from Eqs. 1 and 2. If CL_iC_0 is in the place of CL_sC_i in Eq. 6, and knowing that $CL_s = CL_iQ/(CL_i + Q)$, the same conclusion can be drawn. The discrepancy between the newly derived and the reported equations lies in the definition of the clearance in the mass balance equation. The effluent concentration, C_0 or C_t/R, in the elimination rate in Eq. 6 should only be used with CL_i.

For constant infusion studies, R can be calculated by simply taking the ratio of the drug concentration in the tissue to the effluent venous blood as indicated in Eq. 10. The arterial blood concentration can also be used if the extraction ratio of the compound by the organ is known. Either arterial or venous blood concentration can be used interchangeably for the R determination of a noneliminating organ.

Equation 13, on the other hand, offers the tool to estimate R from bolus injection data. Its limitation, however, is quite severe because all of the physiological and clearance parameters must be known before applying the equation. It also requires the exclusive use of arterial blood concentration in its application. In the case of a noneliminating organ, Eq. 13 could be reduced to:

$$R = \frac{C_t^0}{C_0^o} = \frac{C_t}{C_0} \qquad \text{(Eq. 14)}$$

By recognizing the fact that $QC_i + \alpha V_tC_t = QC_0$ and $CL_s = 0$. The use of effluent venous blood concentration would then be most appropriate. It is of interest to note that for such an organ, venous blood sampling avoids the cumbersome restrictions dictated by Eq. 13. It also avoids the use of literature physiological parameter values, since errors in them may be compounded in the determination of R.

The previous discussions suggest the importance of the source of blood sampling. As indicated in Eqs. 10 and 14, venous blood concentration can be used for determining R; however, venous blood must be obtained from the outflow of the organ of interest. Since the venous concentrations can vary among organs (11) many venous samples might have to be taken from different organs to satisfy the conditions prescribed by the equations. In reality, venous blood is often obtained from one peripheral vein or the pooled venous blood (such as studies in mice or rats); the validity of such practices appears questionable in light of the arguments presented. In addition, many tissues and blood (plasma) flow parameters are often pooled and scaled accordingly, making the possibility of obtaining venous blood for these tissues almost impossible.

Systemic arterial blood, on the other hand, is generally regarded as homogeneous in the body (7, 11). Sampling it from any site could closely reflect the influent arterial blood concentration in all other organs except for the lung (7, 8). Because of its association with CL_s in Eq. 6, literature clearance data can be used readily without any modifications, since organ clearance is estimated routinely by the quotient of the total amount of drug eliminated from a particular route and the total area under the blood (plasma) level–time curve. In addition, sampling of arterial blood is relatively easy in experimental animals and the advantage of this approach is obvious.

The source of blood sampling is not only important in the determination of R, but may also be significant in the overall successfulness of a physiologically-based pharmacokinetic model. From a mathematical standpoint, the predicted blood (plasma) levels from the system of first-order differential equations are, in fact, those of the arterial blood (12–17). Therefore, it seems only logical to sample arterial blood for comparison with the predicted levels. A brief review of the literature, however, revealed that the source of blood sample could be any one of the following: arterial[lidocaine (12) and procaine (13)], jugular venous [sulfobromophthalein (14) and digoxin (15)], peripheral venous [adriamycin (16)], and total pooled plasma [methotrexate (17)]. It is apparent that no general rule has been adopted in this area. Arterial sampling certainly is justifiable physiologically and should be used. This is particularly true in view of a recent study which showed significant arteriovenous plasma concentration difference for six compounds after intravenous administration to dogs and rabbits (11).

REFERENCES

(1) K. B. Bischoff, in "Chemical Engineering in Medicine and Biology," D. Hershey, Ed., Plenum, New York, N.Y., 1962, p. 417.

(2) H. G. Chen and J. F. Gross, *J. Pharmacokinet. Biopharm.*, **7**, 117 (1979).
(3) M. Rowland, L. Z. Benet, and G. Graham, *ibid.*, **1**, 123 (1973).
(4) M. Rowland, *J. Pharm. Sci.*, **61**, 70 (1972).
(5) G. R. Wilkinson and D. G. Shand, *Clin. Pharmacol. Ther.*, **18**, 377 (1975).
(6) S. Keiding and P. B. Andreason, *Pharmacology*, **19**, 105 (1979).
(7) W. L. Chiou and G. Lam, *Int. J. Clin. Pharmacol. Ther. Toxicol.*, in press.
(8) W. L. Chiou, *J. Pharmacokinet. Biopharm.*, **7**, 527 (1979).
(9) R. A. Roth and D. A. Wiersma, *Clin. Pharmacokinet.*, **4**, 355 (1979).
(10) K. S. Pang and M. Rowland, *J. Pharmacokinet. Biopharm.*, **5**, 625 (1977).
(11) W. L. Chiou, G. Lam, M. L. Chen, and M. G. Lee, *Res. Commun. Chem. Pathol. Pharmacol.*, **32**, 27 (1981) and references therein.
(12) N. Benowitz, R. P. Forsyth, K. L. Melmon, and M. Rowland, *Clin. Pharmacol. Ther.*, **16**, 87 (1974).
(13) R. H. Smith, D. H. Hunt, A.B. Seifen, A. Ferrari, and D. S. Thompson, *J. Pharm. Sci.*, **68**, 1016 (1979).
(14) B. Montandon, R. J. Roberts, and L. J. Fischer, *J. Pharmacokinet. Biopharm.*, **3**, 277 (1975).
(15) L. I. Harrison and M. Gibaldi, *J. Pharm. Sci.*, **66**, 1138 (1977).
(16) P. A. Harris and J. R. Gross, *Can. Chemother. Rep. Part 1*, **59**, 819 (1975).
(17) K. B. Bischoff, R. L. Dedrick, and D. S. Zaharko, *J. Pharm. Sci.*, **59**, 149 (1970).

Conductivity Studies of Suspension Systems in Different States of Aggregation

BERNARD ECANOW ˣ, JUDY M. WEBSTER, and MARTIN I. BLAKE

Received February 8, 1980, from the *College of Pharmacy, Department of Pharmacy, University of Illinois at the Medical Center, Chicago, IL, 60612.* Accepted for publication July 29, 1981.

Abstract □ The electrical conductivity effects of dispersed, coagulated, and flocculated systems were investigated using sulfamerazine powder, an insoluble, hydrophobic drug to prepare the suspension systems. For the dispersed systems, a peak in conductivity was observed at a drug concentration between 5 and 15%. The critical coagulating concentration was defined as the concentration of drug at which a maximum in specific conductance was observed. At this concentration, a maximum number of charged particles were in the system. Coagulated suspensions showed higher conductance values than the dispersed systems at equivalent concentrations; however, the critical coagulating concentration value appeared to be the same. For flocculated suspensions there was an increase in conductance with drug concentration with no perceptible peak conductance value.

Keyphrases □ Conductivity—use in studies of suspension systems in different states of aggregation □ Aggregation states—electrical conductivity effects on dispersed, coagulated, and flocculated systems □ Suspension systems—electrical conductivity effects on dispersed, coagulated, and flocculated systems

As defined in the United States Pharmacopeia (1), suspensions are preparations of finely divided, undissolved drugs in liquid vehicles. Insoluble particles dispersed in a liquid medium have large specific surface areas which render the suspension system thermodynamically unstable. The particles tend to settle and form aggregates which have a reduced surface area and, thus, a decreased surface free energy. This results in a system of greater thermodynamic stability. Two types of aggregation are identified: coagulation and flocculation. Unfortunately, these terms are used frequently in the literature in a way that confuses the nature of the systems being described (2).

Here, a dispersed system in water is described as consisting of primary particles acting as independent entities in the bulk water polar medium. The settling process, in general, is relatively slow with each particle settling separately.

In a coagulated system the aggregated particles, including adsorbed surface films, are in surface contact with each other and each aggregate of particles (coagula) acts as a unit. The particles are held together by film–film bonds. The interstitial water is structured and exhibits nonpolar behavior. Coagulated suspensions tend to form caked systems which can be difficult, if not impossible, to redisperse.

In a flocculated system the aggregated particles are held together by one of several mechanisms: adsorption bridging, chemical bridging, or long-range Van der Waals forces (secondary minimums). The particles settle out as a "floc," a loosely packed aggregate having a network-like structure. A hard cake does not form and the sediment is readily redispersed to the original suspension form. The water medium is bulk polar water.

The classification of these systems was first reported by Ecanow *et al.* (3) and has since been referred to by others (4). The properties of dispersed, coagulated, and flocculated systems have been compared in terms of caking (5), sedimentation rate (6), rheology (3), gas adsorption (7), and filtration rates (8). In the present study, the electrical conductivity effects of these systems were investigated. Sulfamerazine powder, a hydrophobic drug, was used to prepare the suspensions, and docusate sodium (I), an anionic surfactant, rendered the drug particles hydrophilic in the formation of the dispersed and the coagulated systems. Compound I and aluminum chloride were used to form the flocculated systems (9) of sulfamerazine particles.

EXPERIMENTAL

Materials—Sulfamerazine[1] was USP grade and ranged in particle size from 5 to 20 μm. Docusate sodium[2] USP was employed as the surfactant, and aluminum chloride[3] NF served as the flocculating agent. All other chemicals were reagent grade and were used without further treatment.

[1] Sigma Chemical Co., Lot 103C 2660.
[2] Aerosol OT, Fisher Scientific Co., Lot 732561.
[3] Mallinckrodt Chemical Works, Lot WLJD.

0022-3549/82/0400-0456$01.00/0

(2) H. G. Chen and J. F. Gross, *J. Pharmacokinet. Biopharm.*, **7**, 117 (1979).
(3) M. Rowland, L. Z. Benet, and G. Graham, *ibid.*, **1**, 123 (1973).
(4) M. Rowland, *J. Pharm. Sci.*, **61**, 70 (1972).
(5) G. R. Wilkinson and D. G. Shand, *Clin. Pharmacol. Ther.*, **18**, 377 (1975).
(6) S. Keiding and P. B. Andreason, *Pharmacology*, **19**, 105 (1979).
(7) W. L. Chiou and G. Lam, *Int. J. Clin. Pharmacol. Ther. Toxicol.*, in press.
(8) W. L. Chiou, *J. Pharmacokinet. Biopharm.*, **7**, 527 (1979).
(9) R. A. Roth and D. A. Wiersma, *Clin. Pharmacokinet.*, **4**, 355 (1979).
(10) K. S. Pang and M. Rowland, *J. Pharmacokinet. Biopharm.*, **5**, 625 (1977).
(11) W. L. Chiou, G. Lam, M. L. Chen, and M. G. Lee, *Res. Commun. Chem. Pathol. Pharmacol.*, **32**, 27 (1981) and references therein.
(12) N. Benowitz, R. P. Forsyth, K. L. Melmon, and M. Rowland, *Clin. Pharmacol. Ther.*, **16**, 87 (1974).
(13) R. H. Smith, D. H. Hunt, A.B. Seifen, A. Ferrari, and D. S. Thompson, *J. Pharm. Sci.*, **68**, 1016 (1979).
(14) B. Montandon, R. J. Roberts, and L. J. Fischer, *J. Pharmacokinet. Biopharm.*, **3**, 277 (1975).
(15) L. I. Harrison and M. Gibaldi, *J. Pharm. Sci.*, **66**, 1138 (1977).
(16) P. A. Harris and J. R. Gross, *Can. Chemother. Rep. Part 1*, **59**, 819 (1975).
(17) K. B. Bischoff, R. L. Dedrick, and D. S. Zaharko, *J. Pharm. Sci.*, **59**, 149 (1970).

Conductivity Studies of Suspension Systems in Different States of Aggregation

BERNARD ECANOW ˣ, JUDY M. WEBSTER, and MARTIN I. BLAKE

Received February 8, 1980, from the *College of Pharmacy, Department of Pharmacy, University of Illinois at the Medical Center, Chicago, IL, 60612.* Accepted for publication July 29, 1981.

Abstract □ The electrical conductivity effects of dispersed, coagulated, and flocculated systems were investigated using sulfamerazine powder, an insoluble, hydrophobic drug to prepare the suspension systems. For the dispersed systems, a peak in conductivity was observed at a drug concentration between 5 and 15%. The critical coagulating concentration was defined as the concentration of drug at which a maximum in specific conductance was observed. At this concentration, a maximum number of charged particles were in the system. Coagulated suspensions showed higher conductance values than the dispersed systems at equivalent concentrations; however, the critical coagulating concentration value appeared to be the same. For flocculated suspensions there was an increase in conductance with drug concentration with no perceptible peak conductance value.

Keyphrases □ Conductivity—use in studies of suspension systems in different states of aggregation □ Aggregation states—electrical conductivity effects on dispersed, coagulated, and flocculated systems □ Suspension systems—electrical conductivity effects on dispersed, coagulated, and flocculated systems

As defined in the United States Pharmacopeia (1), suspensions are preparations of finely divided, undissolved drugs in liquid vehicles. Insoluble particles dispersed in a liquid medium have large specific surface areas which render the suspension system thermodynamically unstable. The particles tend to settle and form aggregates which have a reduced surface area and, thus, a decreased surface free energy. This results in a system of greater thermodynamic stability. Two types of aggregation are identified: coagulation and flocculation. Unfortunately, these terms are used frequently in the literature in a way that confuses the nature of the systems being described (2).

Here, a dispersed system in water is described as consisting of primary particles acting as independent entities in the bulk water polar medium. The settling process, in general, is relatively slow with each particle settling separately.

In a coagulated system the aggregated particles, including adsorbed surface films, are in surface contact with each other and each aggregate of particles (coagula) acts as a unit. The particles are held together by film–film bonds. The interstitial water is structured and exhibits nonpolar behavior. Coagulated suspensions tend to form caked systems which can be difficult, if not impossible, to redisperse.

In a flocculated system the aggregated particles are held together by one of several mechanisms: adsorption bridging, chemical bridging, or long-range Van der Waals forces (secondary minimums). The particles settle out as a "floc," a loosely packed aggregate having a network-like structure. A hard cake does not form and the sediment is readily redispersed to the original suspension form. The water medium is bulk polar water.

The classification of these systems was first reported by Ecanow *et al.* (3) and has since been referred to by others (4). The properties of dispersed, coagulated, and flocculated systems have been compared in terms of caking (5), sedimentation rate (6), rheology (3), gas adsorption (7), and filtration rates (8). In the present study, the electrical conductivity effects of these systems were investigated. Sulfamerazine powder, a hydrophobic drug, was used to prepare the suspensions, and docusate sodium (I), an anionic surfactant, rendered the drug particles hydrophilic in the formation of the dispersed and the coagulated systems. Compound I and aluminum chloride were used to form the flocculated systems (9) of sulfamerazine particles.

EXPERIMENTAL

Materials—Sulfamerazine[1] was USP grade and ranged in particle size from 5 to 20 μm. Docusate sodium[2] USP was employed as the surfactant, and aluminum chloride[3] NF served as the flocculating agent. All other chemicals were reagent grade and were used without further treatment.

[1] Sigma Chemical Co., Lot 103C 2660.
[2] Aerosol OT, Fisher Scientific Co., Lot 732561.
[3] Mallinckrodt Chemical Works, Lot WLJD.

0022-3549/82/0400-0456$01.00/0

Table I—Specific Conductance Values for Dispersed and Aggregated Suspension Systems

Suspension Concentration, %(w/v)	Conductance, mmho		
	Dispersed System	Coagulated System	Flocculated System
2	0.28 ± 0.018[a]	0.34 ± 0.013	1.19 ± 0.103
5	0.49 ± 0.078	0.68 ± 0.010	2.59 ± 0.370
10	0.62 ± 0.016	0.82 ± 0.013	4.10 ± 0.346
15	0.55 ± 0.038	0.63 ± 0.015	5.40 ± 0.535
20	0.49 ± 0.075	0.58 ± 0.015	6.30 ± 0.770
25	0.40 ± 0.061	0.55 ± 0.006	7.50 ± 0.577
30	0.36 ± 0.052	0.52 ± 0.015	8.25 ± 0.500
35	0.31 ± 0.017	0.37 ± 0.014	9.00 ± 0.000

[a] Mean value based on at least four determinations ± *SD*.

Apparatus—A conductivity apparatus[4] designed for testing suspension systems was used to measure the specific conductances of the suspension systems.

Suspension Systems—Sulfamerazine dispersed suspensions and coagulated systems contained 2, 5, 10, 15, 20, 25, 30, 35% (w/v) sulfamerazine. In each system the concentration of I was one-tenth the sulfamerazine content.

In the flocculated systems the concentrations of sulfamerazine and I were the same as in the previous systems, but, in addition, the concentration of aluminum chloride in each system was equal to 5% that of the sulfamerazine content.

The suspensions were prepared by weighing out the calculated amount of sulfamerazine powder and transferring the powder to a glass mortar. The appropriate volume of a 5% solution of I was added to the mortar and the mixture was triturated until a smooth slurry was formed. The slurry was then transferred to a 100-ml graduated cylinder with additional rinsings of the mortar using distilled water. Sufficient water was added to bring the volume to the 100-ml mark. For the preparation of the flocculated suspensions, the same procedure was followed except that the appropriate volume of a 20% aluminum chloride solution was added to the cylinder prior to filling to the mark with distilled water. The cylinder was then capped with a glass stopper, inverted, and agitated sufficiently to ensure both thorough mixing and the formation of a uniform initial suspension of the powder.

The conductance of the initial suspensions (dispersed systems) was measured immediately by immersing the conductivity cell into each suspension system. The systems were then allowed to settle for 48 ± 2 hr before additional conductivity data were obtained. During the settling period, aggregation took place resulting in the formation of a coagulated system. Before the conductance reading was taken, the cylinder containing the coagulated system was agitated sufficiently to ensure dispersion of the coagula. The conductivity of the dispersed system was then measured immediately. The flocculated systems were treated in the same manner as the coagulated systems. Conductivity readings were measured after thoroughly agitating the system to ensure redispersion of the flocules.

RESULTS AND DISCUSSION

Conductance data for all of the suspension systems are shown in Table I. The data for dispersed systems were analyzed statistically by the Student t test. The t value was 4.131 corresponding to a p value of < 0.005, indicating that conductance is dependent on concentration. Analysis of the data for the coagulated systems by the Student t test produced a t value of 4.102, which corresponds to a p value <0.005. The t value obtained for the flocculated suspensions by comparing concentration with the mean conductance value was 2.837, which corresponded to a p value <0.01.

It was the purpose of this study to observe the electrical conductivity properties associated with different states of suspension aggregation and to note the effect of variable concentration of an insoluble drug on the electrical conductivity of each suspension system. Specific conductance, rather than equivalent conductance, was determined since it is a measure of conductance capacity of all ions present in a unit volume of solution and thus, varies with concentration.

[4] Solu Bridge Soil Tester, Beckman Instruments, Inc., Model RD-B15, Ser. 21034.

The system can be described as follows: The sulfamerazine powder is in the paracolloid particle size range (5–20 μm). Compound I, an anionic surfactant, acts by coating the insoluble drug particles and converting them to hydrophilic particles (9). Therefore, each particle has a negative charge and is surrounded by its own ionic atmosphere. Closely associated with the hydrophilic particles are water molecules from the suspension medium. Sodium ions of I balance the negatively charged particles. Compound I molecules are present in the system as individual ionic species and as micelles, since the critical micelle concentration for I is about 0.07% at 25°. This concentration was exceeded in all suspensions prepared in this study.

It is evident that, for the dispersed suspension system, the conductivity increases with drug concentration at low concentrations of drug. This is expected because the number of charged particles in the system has increased. However, at some concentration between 5 and 15%, a peak in conductance is reached after which the conductance values decrease with increasing drug concentration. This may be explained by the fact that after a peak value is reached, the charged particles begin to aggregate by forming associated particles, or coagula, which results in fewer, but larger, charged species. Because the actual number of charged particles is decreased, the specific conductance will be lower. The concentration of drug in a dispersed or coagulated system at which the specific conductance is a maximum is the critical coagulating concentration. At this concentration there is a maximum number of charged particles in the system which accounts for the maximum in specific conductance.

The coagulated suspensions behaved similarly to that of the dispersed systems. The conductance values for the coagulated systems were consistently higher than the corresponding dispersed systems (Table I). Since the coagulated suspensions consist of fewer and larger charged particles, it would be expected that the specific conductance would be lower than in the dispersed systems (as noted previously in connection with the effect of drug concentration on the conductivity in the dispersed systems). One possible explanation of this behavior is that because the water in the film–film bonds of the coagula is highly structured (nonpolar) (10), electrolytes are squeezed out of the films, thus increasing the concentration of charged species in the polar aqueous medium of the supernate. This, in effect, produces higher conductance values for the coagulated systems.

The data for the flocculated systems show an almost direct linear relationship between conductance and drug concentration. This is in contradistinction to that observed for the dispersed and coagulated systems. In a separate study, a similar relationship was observed with only aluminum chloride and I (the sulfamerazine was excluded). Apparently, the aggregation state of the suspended particles does not affect the conductance of the flocculated system. In this system each suspended drug particle behaves independently. The precise nature of aluminum ion participation in the flocculation process was reported previously (9) and first identified as a chemical bridging reaction.

REFERENCES

(1) "The United States Pharmacopeia," 19th rev., Mack Publishing, Easton, Pa., 1975, p. 704.

(2) V. K. La Mer, *J. Colloid Sci.*, **19,** 291 (1964).

(3) B. Ecanow, B. Gold, and C. Ecanow, *Am. Perfum. Cosmet.*, **84,** 27 (1969).

(4) J. V. Bondi, R. L. Schnaare, P. J. Niebergall, and E. T. Sugita, *J. Pharm. Sci.*, **62,** 1731 (1973).

(5) R. Wilson and B. Ecanow, *ibid.*, **53,** 782 (1964).

(6) B. Ecanow and B. Gold, *Science*, **193,** 919 (1976).

(7) W. F. Stanaszek, R. S. Levinson, and B. Ecanow, *J. Pharm. Sci.*, **63,** 1941 (1974).

(8) A. Dakkuri and B. Ecanow, *Am. Perfum. Cosmet.*, **81,** 33 (1966).

(9) R. Wilson and B. Ecanow, *J. Pharm. Sci.*, **52,** 757 (1963).

(10) B. Ecanow and H. L. Klawans, Jr., in "Models of Human Neurological Diseases," H. L. Klawans, Jr., Ed., Excerpta Medica, Amsterdam, The Netherlands, 1974, pp. 253–286.

ACKNOWLEDGMENTS

Abstracted in part from a thesis submitted by J. M. Webster to the Graduate College, University of Illinois at the Medical Center, in partial fulfillment of the Master of Science degree requirements.

Presystemic Elimination of Drugs: Theoretical Considerations for Quantifying the Relative Contribution of Gut and Liver

R. F. MINCHIN *x and K. F. ILETT

Received November 19, 1980 from the *Department of Pharmacology, University of Western Australia, Nedlands, Western Australia, 6009.* Accepted for publication July 30, 1981. * Present address: National Cancer Institute, Bethesda, MD 20205.

Abstract □ From a consideration of the basic processes involved in drug elimination, the fraction of drug cleared by the gut and by the liver were described as functions of availability and hepatic clearance. For a drug given orally, a plot of the fraction of drug cleared by the gut or liver against α, a proportionality constant relating gut elimination following intravenous administration to that following oral administration, allowed an estimate of the possible contribution of gut and liver to presystemic elimination. This method was dependent only on the measurement of peripheral blood drug concentrations and urine levels. Application of the theory to published data for several drugs known to have a reduced availability after oral administration was used to illustrate the procedure.

Keyphrases □ Liver—relative contribution to presystemic elimination □ Gut—relative contribution to presystemic elimination □ Presystemic elimination—quantification of contribution of gut and liver, theoretical considerations

When given orally, many drugs undergo significant presystemic metabolism in the gut and liver, reducing their pharmacological activity by decreasing systemic availability (1). In experimental animals, the relative contribution of the liver and gut to presystemic elimination can be quantified by measuring portal and peripheral blood drug concentrations following oral and intravenous administration (2–4). However, as pointed out by Routledge and Shand (1), such procedures cannot be readily carried out in humans because of technical and ethical limitations and, therefore it has not been possible to demonstrate which site of metabolism is more important during presystemic elimination in humans. In the present study, a theoretical approach to quantifying the contribution of gut and liver to presystemic elimination was considered and equations derived which, for drugs obeying certain criteria, allowed calculation of the fraction of drug cleared in the gut or liver using clearance and availability estimates obtained by measurement of drug concentrations in systemic blood.

THEORY

The presystemic elimination of a drug in a linear system was considered. Availability (F) can be estimated by:

$$F = \frac{AUC_{oral}\, D_{iv}}{AUC_{iv}\, D_{oral}} = (1 - f_G)(1 - f_L) \qquad \text{(Eq. 1)}$$

where AUC_{oral} and AUC_{iv} are the areas under the blood drug concentration–time curves following an oral (D_{oral}) and an intravenous (D_{iv}) dose respectively, f_G is the fraction of dose cleared in gut, and f_L is the fraction of dose reaching the portal blood system which is cleared by the liver.

When such a drug is given intravenously, elimination may occur in the liver or in the gut if significant diffusion of the drug from the portal blood into the gut wall occurs. The rate of drug elimination in the liver (dE_L/dt) can be described by:

$$\frac{dE_L}{dt} = (Q_L - Q_G)f_L C_1 + Q_G f_L C_G \qquad \text{(Eq. 2)}$$

where Q_L is the total hepatic blood flow, Q_G is the intestinal blood flow, C_1 is the peripheral blood concentration, and C_G is the concentration of drug entering the liver *via* the portal system. The rate of drug elimination in the gut wall following intravenous administration (dE_G/dt) is given by:

$$\frac{dE_G}{dt} = \alpha Q_G f_G C_1 \qquad \text{(Eq. 3)}$$

where $1 \geq \alpha \geq 0$. The proportionality constant, α, allows for the fact that the fraction of drug cleared after entering the gut from the general circulation may not be equal to that cleared after entering the gut from the lumen. Total elimination rate from the splanchnic circulation (dE/dt) can be described by the addition of Eq. 2 and 3.

$$\frac{dE}{dt} = (Q_L - Q_G)f_L C_1 + Q_G f_L C_G + \alpha Q_G f_G C_1 \qquad \text{(Eq. 4)}$$

Since $C_G = (1 - \alpha f_G)C_1$, then:

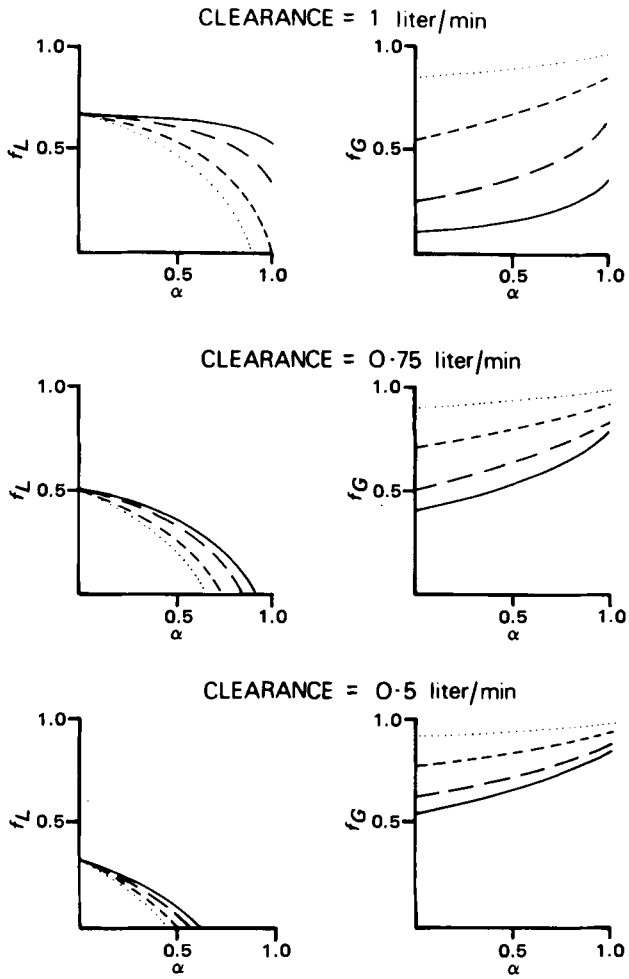

Figure 1—*Dependence of* f_L *and* f_G *on availability, clearance, and* α. *Assuming* Q_L *and* Q_G *to be 1.5 and 1.2 liters/min, respectively,* f_L *and* f_G *were calculated according to Eqs. 8 and 9. Key: Availability = 0.3 (——), 0.25 (— —), 0.15 (– – –), and 0.05 (. . .).*

0022-3549/82/0400-0458$01.00/0

Table I—Kinetic Data for Drugs Known to Undergo Significant Presystemic Elimination

Drug	Availability	Plasma Clearance, liter/min	Blood-Plasma Distribution Ratio	Fraction Excreted in Urine	Hepatic Blood Clearance[a], liters/min	Reference
Imipramine	0.47	1.05	1.34	0.0	0.784	8
Propranolol	0.36	0.702	0.78	0.0	0.90	9
Quinidine	0.795	0.256	0.66	0.276	0.281	10
Pentazocine	0.184	1.38	1.07	0.154	1.09	11
Oxprenolol	0.462	0.372	0.80	0.03	0.457	12
Nortriptyline	0.505	0.527	1.49	0.02	0.347	13
Lidocaine						
Healthy subjects	0.37	0.77	0.83	0.01	0.918	14
Epileptics	0.15	0.85	0.83	0.01	1.014	14
Phenacetin[b]						
Controls	0.452	0.00276	1.06	0.0	0.0026	15
Induced	0.058	0.01763	1.06	0.0	0.0166	15

[a] Calculated as $[1-f_R]Cl_T/\lambda$ where f_R = fraction of drug excreted in urine, Cl_T = total plasma clearance, and λ = blood to plasma distribution ratio. [b] Study undertaken in rats, controls were pretreated with saline, while induced were pretreated with 3-methylcholanthrene; Q_L = 21 ml/min, Q_G = 16.8 ml/min.

$$\frac{dE}{dt} = (Q_L - Q_G)f_L C_1 + Q_G f_L(1 - \alpha f_G)C_1 + \alpha Q_G f_G C_1 \quad \text{(Eq. 5)}$$

Equation 5 simplifies to:

$$\frac{dE}{dt} = C_1[Q_L f_L + \alpha Q_G f_G(1 - f_L)] \quad \text{(Eq. 6)}$$

The term enclosed by the square brackets is equivalent to the classical hepatic clearance constant (Cl_H) where gut and liver are considered as a single functional unit. Thus:

$$Cl_H = Q_L f_L + \alpha Q_G f_G(1 - f_L) \quad \text{(Eq. 7)}$$

From Eq. 1:

$$f_G = 1 - [F/(1 - f_L)] \quad \text{(Eq. 8)}$$

Substituting Eq. 8 into Eq. 7 and rearranging:

$$f_L = \frac{Cl_H - \alpha Q_G(1 - F)}{(Q_L - \alpha Q_G)} \quad \text{(Eq 9)}$$

Exact solutions of f_L, f_G, and α are not possible from the above equations, since the three parameters are described by only two independent equations (Eqs. 8 and 9). However, a plot of f_L and f_G *versus* α for $1 \geq \alpha \geq 0$ may allow some conclusions concerning the overall contribution of gut and liver to the presystemic elimination of a drug to be made.

RESULTS AND DISCUSSION

The proportionality constant α in Eq. 9 relates gut elimination following oral to that following intravenous drug administration. The role of the GI tract in drug metabolism, particularly after intravenous administration, has not been comprehensively investigated. Theoretically, α is equal to unity when the gut contributes equally to the elimination of a drug after its oral and intravenous administration. During absorption, a drug must cross the mucosal epithelium, basement membrane, and the capillary endothelium. Movement of drug in the opposite direction may be equal to or less than the corresponding rate of absorption depending on its physicochemical properties, the pH gradient across the gut wall, the blood flow rate, and the degree of drug binding to blood constituents. All these factors may cause α to be less than unity. For some drugs such as isoproterenol (5, 6) and pentazocine (7) which have been shown to undergo significant biotransformation in the gut following oral administration but not after infusion into the mesenteric arterial blood supply, α is equal to zero.

Using Eqs. 8 and 9, f_L and f_G have been computed at various clearance and availability values for $1 \geq \alpha \geq 0$, Q_L = 1.5 liters/min, and Q_G = 1.2 liters/min (Fig. 1). For a given oral availability, the importance of the liver to overall presystemic elimination decreases, while that for gut increases as clearance is reduced. Furthermore, regardless of the value of α, the gut becomes increasingly more important as availability is reduced at a constant clearance. In general, the liver is the site of greater elimination in systems of relatively high clearance and high availability, whereas the gut is dominant in systems of relatively low clearance and low availability.

Using kinetic data (Table I) obtained from the literature (8–15), curves of *f versus* α were constructed to determine the contribution of gut and

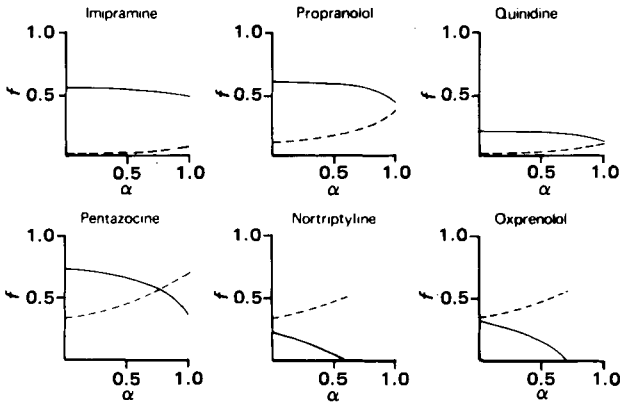

Figure 2—*The* f *versus* α *curves for several drugs known to undergo significant presystemic elimination (see Table I). Key:* —— f_L; *and* — — — f_G.

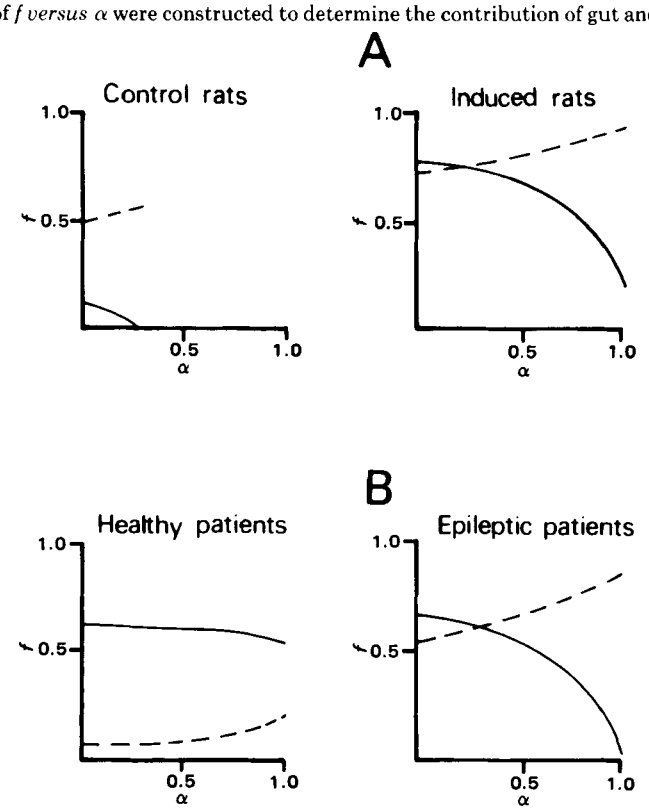

Figure 3—*Effect of induction on the* f versus α *curves for phenacetin (A) and lidocaine (B). For phenacetin, rats were pretreated with saline (controls) or 3-methylcholanthrene (induced) before receiving an oral or intravenous dose of phenacetin. For lidocaine, data were collected from healthy subjects and also from epileptic patients who were receiving enzyme-inducing drugs such as phenobarbital. Key:* —— f_L, *and* — — — f_G.

liver to the presystemic elimination of a number of drugs. Total hepatic clearance was calculated as $(1 - f_R)Cl_T/\lambda$ where f_R is the fraction of drug eliminated unchanged in the urine, Cl_T is the total plasma clearance, and λ is the blood to plasma distribution ratio. For all drugs considered, it was assumed that significant elimination occurred only in gut, liver, and kidney. Total hepatic and intestinal blood flows were assumed to be 1.5 and 1.2 liters/min, respectively (16). For the phenacetin data that were obtained from experiments in rats, Q_L and Q_G were taken to be 21.0 and 16.8 ml/min, respectively, assuming a body weight of 240 g (17).

The contribution of the liver to presystemic elimination was greater than that of the gut for imipramine, propranolol, and quinidine regardless of the value of α (Fig. 2). However, with oxprenolol and nortriptyline, the gut was generally more important. For both these drugs, the boundaries of α were reduced to $0.708 \geq \alpha \geq 0$ and $0.584 \geq \alpha \geq 0$, respectively, since, by definition, $1 \geq f_L \geq 0$ and $1 \geq f_G \geq 0$. Because of the nature of Eqs. 8 and 9, it is possible that plotting f_L and f_G *versus* α will produce curves which suggest that the gut is more important than the liver at one extremity of α ($\alpha \rightarrow 1$), while the reverse is true at the other extremity ($\alpha \rightarrow 0$). This is exemplified by the f *versus* α curves for pentazocine Fig. 2) where the gut eliminated 33% of an oral dose if $\alpha = 0$, but 71% if $\alpha = 1$. In such a case, plotting f_L and f_G against α would not assist in assessing the relative contribution of gut and liver to the reduced availability, and information concerning the magnitude of α would have to be obtained from isolated human gut loops, experiments in patients undergoing portocaval anastomosis, or by extrapolation from animal data.

The use of f *versus* α curves also may reveal how induction or inhibition of enzymatic systems can affect availability. In Fig. 3, the change in f_L and f_G for phenacetin in rats and lidocaine in humans was illustrated before and after induction. For control rats, it could be calculated that at least 88% of the total dose eliminated before reaching the systemic circulation was due to clearance in the gut. After pretreatment with 3-methylcholanthrene, there was a small increase in f_G, but a far more marked increase in f_L for all values of α suggesting that the decrease in availability in induced animals was due to a greater contribution from the liver. However, the change in lidocaine availability from 37% in healthy subjects to only 15% in epileptic patients was primarily due to an increase in gut elimination. It should be noted that f_G may be a function of a number of factors such as gut lumen metabolism, gut wall metabolism, or incomplete absorption. The greater contribution of gut to the presystemic elimination of lidocaine in epileptic patients was also reflected in the lack of any change in plasma half-life (14) which should have been reduced by a significant increase in liver metabolism since f_L was much less than 1 in healthy subjects, (greatest value of f_L was 0.612 for $\alpha = 0$).

Finally, it should be noted that the use of this method in humans is dependent on reliable estimates of Q_L and Q_G. While numerous studies have shown relatively constant estimates for these values in healthy subjects, both may be markedly altered in patients with cardiovascular, hepatic, or renal disease, or by the drug under investigation. For example, the f *versus* α curves for propranolol, oxprenolol, quinidine, and lidocaine should be interpreted cautiously considering the known hemodynamic effects of these drugs. This limitation could be avoided by individual measurement of Q_L and Q_G. Hepatic blood flows may be estimated using well-established invasive techniques (18, 19) which usually involve direct infusion of a radiolabeled inert gas such as xenon or krypton into the liver.

REFERENCES

(1) P. A. Routledge and D. G. Shand, *Ann. Rev. Pharmacol. Toxicol.*, **19,** 447 (1979).

(2) W. A. Colburn, *J. Pharmacokinet. Biopharm.*, **7,** 407 (1979).

(3) K. Iwamoto and C. D. Klaassen, *J. Pharmacol. Exp. Ther.*, **200,** 236 (1977).

(4) M. K. Cassidy and J. B. Houston, *J. Pharm. Pharmacol.*, **32,** 57 (1980).

(5) C. F. George, E. W. Blackwell, and D. S. Davies, *ibid.*, **26,** 265 (1974).

(6) K. F. Ilett, C. T. Dollery, and D. S. Davies, *ibid.*, **32,** 362 (1980).

(7) R. D. Anderson and K. F. Ilett, *Clin. Exp. Pharmacol. Physiol.*, in press.

(8) L. F. Gram and J. Christiansen, *Clin. Pharmacol. Ther.*, **17,** 555 (1975).

(9) D. M. Kornhauser, A. J. J. Wood, R. E. Vestal, G. R. Wilkinson, R. A. Branch, and D. G. Shand, *ibid.*, **23,** 165 (1978).

(10) D. J. Greenblatt, H. J. Pfeifer, H. R. Ochs, K. Franke, D. S. MacLaughlin, T. W. Smith, and J. Koch-Weser, *J. Pharmacol. Exp. Ther.*, **202,** 365 (1977).

(11) M. Ehrnebo, L. O. Boreus, and U. Lonroth, *Clin. Pharmacol. Ther.*, **22,** 888 (1977).

(12) W. D. Mason and N. Winer, *ibid.*, **20,** 401 (1976).

(13) L. F. Gram and K. F. Overo, *ibid.*, **18,** 305 (1976).

(14) E. Perucca and A. Richens, *Br. J. Clin. Pharmacol.*, **8,** 21 (1979).

(15) R. M. Welch, C. R. Hughes, and R. L. Deangelis, *Drug Metab. Dispos.*, **4,** 402 (1976).

(16) N. Benowitz, R. P. Forsyth, K. L. Melmon, and M. Rowland, *Clin. Pharmacol. Ther.*, **16,** 87 (1974).

(17) L. I. Harrison and M. Gibaldi, *J. Pharm. Sci.*, **66,** 1138 (1977).

(18) D. P. Leiberman, R. T. Mathie, A. M. Harper, and L. H. Blumgart, *Br. J. Surg.*, **65,** 578 (1978).

(19) A. M. Holroyd and A. M. Peters, *ibid.*, **67,** 178 (1980).

ACKNOWLEDGMENTS

A preliminary report was presented to the 14th Annual Meeting of the Australasian Society of Clinical and Experimental Pharmacologists, Canberra, 1980.

Pharmacokinetics of Rosoxacin in Human Volunteers

G. B. PARK, J. SANESKI, T. WENG, and J. EDELSON ˣ

Received June 8, 1981, from the *Departments of Drug Metabolism and Disposition, and Biometry, Sterling-Winthrop Research Institute, Rensselaer, NY 12144.* Accepted for publication August 12, 1981.

Abstract □ Reversed-phase liquid chromatography was used to determine plasma rosoxacin concentrations in normal, healthy males, each of whom received one 300 mg capsule of rosoxacin. The plasma data for each subject were described by an open one-compartment body model with first-order absorption, and the pharmacokinetic parameters were determined. The mean (±*SE*) apparent first-order terminal elimination rate constant was 0.203 ± 0.015 hr^{-1} (N = 16), the mean apparent volume of distribution was 0.644 ± 0.050 liters/kg, and the mean apparent plasma clearance was 2.08 ± 0.15 ml/min/kg.

Keyphrases □ Rosoxacin—pharmacokinetics, normal, healthy males □ Pharmacokinetics—rosoxacin, one-compartment body model, oral absorption, normal, healthy males □ Absorption—first-order with open one-compartment body model, pharmacokinetics of rosoxacin, normal, healthy males

Rosoxacin[1], 1-ethyl-1,4-dihydro-4-oxo-7-(4-pyridyl)-3-quinolinecarboxylic acid, is a member of the class of orally active antimicrobial agents which includes nalidixic acid. The metabolic fate and assay methods for this class of compounds has been reviewed (1).

Rosoxacin is effective *in vitro* against a variety of microorganisms (2–5) and has been used clinically for the treatment of gonorrhea (6). Concentrations of rosoxacin, which were higher than the minimum inhibitory concentrations for most Enterobacteriaceae, were found in renal hilar lymph, renal interstitial fluid, prostatic interstitial fluid, prostatic secretion, vaginal and urethral secretions, and cerebrospinal fluid from dogs treated with this compound (7, 8).

The present report describes the results of a pharmacokinetic study in a group of normal, male, human subjects receiving 300 mg of rosoxacin.

EXPERIMENTAL

Human Volunteers—Appropriate institutional review and approval were obtained from the subjects, none of whom had clinical or laboratory findings indicative of renal, hepatic, or cardiac dysfunction. The mean (±*SE*) age of these volunteers was 29.4 ± 1.9 yr; the mean weight was 71.7 ± 1.6 kg and the mean height was 174 ± 1.7 cm. Each of the 16 volunteers received a single 300-mg capsule of rosoxacin. Blood samples were collected before medication and 0.33, 0.67, 1.0, 1.5, 2.0, 2.5, 3.0, 4.0, 5.0, 6.0, 8.0, 10, 12, 15, and 24 hr after treatment. The blood was centrifuged, and the plasma was separated and frozen until assayed.

Assay Procedure—Plasma samples were analyzed by a high-performance liquid chromatographic (HPLC) method developed previously (9). Plasma standards, prepared in control human plasma, were extracted and analyzed with each set of plasma samples from the volunteers. Plasma rosoxacin concentrations were determined by inverse prediction on the linear regression of peak height ratios obtained from plasma and internal standards. The minimum quantifiable level of the assay was estimated as the concentration whose lower 80% confidence limit just encompassed zero[2], and was ~0.13 μg of rosoxacin/ml of plasma.

Three separate modular HPLC systems were used for the analyses. Each consisted of an automatic injector, a pump, a column[3], and a UV detector monitoring the column effluent at 280 nm.

Pharmacokinetic Calculations—The data obtained from the analysis of the human plasma samples were described by a one-compartment open model with first-order absorption by means of an unweighted nonlinear regression procedure (10). This model is described by the equation:

$$C = A[e^{-k_e(t-t_0)} - e^{-k_a(t-t_0)}] \quad \text{(Eq. 1)}$$

where C is the plasma concentration at time t, t_0 is the lag time (before absorption begins), A is a constant, and k_a and k_e are apparent first-order rate constants for absorption and elimination, respectively. The volume of distribution of rosoxacin, V, was calculated by:

$$V = \frac{FDk_a}{A(k_a - k_e)} \quad \text{(Eq. 2)}$$

where F is the fraction of the administered dose (D) which is available to the systemic circulation; the other terms are as defined previously. The total area under the plasma concentration *versus* time curve [AUC_0^∞], time to maximum concentration (t_{max}), maximum concentration (C_{max}), and plasma clearance (Cl_p) for each subject were calculated from:

$$t_{max} = t_0 + \frac{\ln(k_a/k_e)}{k_a - k_e} \quad \text{(Eq. 3)}$$

$$C_{max} = A[e^{-k_e(t_{max}-t_0)} - e^{-k_a(t_{max}-t_0)}] \quad \text{(Eq. 4)}$$

$$AUC_0^\infty = \frac{A(k_a - k_e)}{k_a k_e} \quad \text{(Eq. 5)}$$

$$Cl_p = \frac{FD}{AUC_0^\infty} \quad \text{(Eq. 6)}$$

In addition to the regression-dependent parameters defined previously, the plasma concentration data were analyzed with respect to the following model-independent parameters: the maximum observed plasma concentration (C_{max}^{obs}), the time at which the maximum plasma concentration was observed (t_{max}^{obs}), and the area under the plasma concentration *versus* time curve, 0–24 hr, AUC_0^{24}. The latter was calculated by trapezoidal rule, using all data for the 24-hr study period.

RESULTS AND DISCUSSION

The mean observed plasma rosoxacin concentration data are shown in Fig. 1. Plasma levels declined exponentially with time suggesting a one-compartment body model. Pharmacokinetic parameters for each subject were estimated after computer-fitting of the data by an iterative nonlinear least-squares regression technique (10). For subjects 1 and 6 it was necessary to adjust the lag time such that it corresponded to the

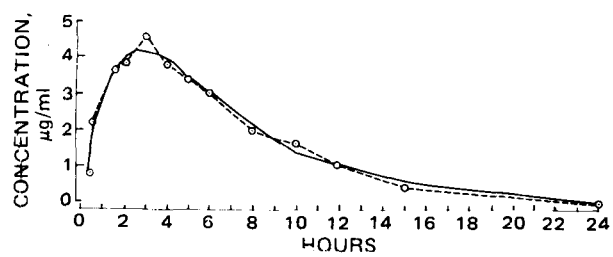

Figure 1—*Plasma concentrations of rosoxacin in human volunteers after oral administration of a single capsule containing 300 mg of rosoxacin. Mean plasma concentration observed in 16 subjects (dotted line) and concentration predicted by the open one-compartment model with oral absorption (solid line).*

[1] Eradicil, Sterling Drug Inc., New York, N.Y.

[2] R. W. Ross and H. Stander, "Some Statistical Problems in Drug Metabolism," paper presented at the Princeton Conference on Applied Statistics, December, 1975.

[3] Partisil-PXS 10/25 PAC column, Whatman, Clifton, N.J.

0022-3549/82/0400-0461$01.00/0

Table I—Pharmacokinetic Parameters Derived from Rosoxacin Plasma Data

	Model-Independent			Regression-Dependent									
Subject Number	t_{max}^{obs}, hr	C_{max}^{obs}, μg/ml	AUC_0^{24}, μg hr/ml	A, μg/ml	k_a, hr^{-1}	k_e, hr^{-1}	t_0, hr	t_{max}, hr	C_{max}, μg/ml	AUC_0^{∞}, μg hr/ml	$t_{1/2}$, hr	$\frac{V}{F}$, liters/kg	$\frac{Cl_p}{F}$, ml/min/kg
1	4.0	6.32	48.1	10.2	1.25	0.176	1.00[a]	3.90	6.38	49.8	3.94	0.458	1.34
2	1.5	4.30	24.6	6.77	1.76	0.241	0.21	1.52	4.26	24.2	2.88	0.740	2.98
3	2.5	3.29	20.8	5.61	1.19	0.225	0.00	1.72	3.09	20.3	3.08	0.877	3.28
4	3.0	5.91	42.4	8.91	1.24	0.171	0.27	2.12	5.60	44.8	4.05	0.603	1.73
5	2.5	5.61	31.2	20.6	0.66	0.328	0.51	2.62	5.15	31.4	2.11	0.380	2.08
6	4.0	3.56	26.6	6.48	1.16	0.214	1.00[a]	4.21	3.60	24.7	3.24	0.866	3.08
7	2.5	3.58	27.1	7.26	0.73	0.200	0.65	3.09	3.24	26.3	3.47	0.732	2.45
8	3.0	6.57	51.4	10.1	1.18	0.160	0.17	2.13	6.37	54.4	4.33	0.539	1.44
9	3.0	5.60	47.8	12.6	0.77	0.195	0.26	2.65	5.91	48.3	3.55	0.425	1.39
10	4.0	4.88	50.3	21.0	0.37	0.195	0.32	3.97	4.89	51.1	3.55	0.492	1.60
11	1.5	5.83	33.3	9.36	1.51	0.235	0.29	1.75	5.62	33.7	2.95	0.466	1.82
12	1.5	4.18	29.6	6.91	1.18	0.196	0.26	2.08	4.03	29.3	3.54	0.697	2.29
13	3.0	2.85	32.4	4.91	0.65	0.115	0.53	3.76	2.79	35.2	6.03	1.016	1.95
14	2.0	4.86	35.0	6.18	1.95	0.154	0.62	2.03	4.58	37.0	4.50	0.858	2.20
15	1.5	4.28	39.4	5.23	3.12	0.117	0.22	1.31	4.43	43.0	5.92	0.758	1.48
16	3.0	5.56	32.6	25.8	0.53	0.325	0.31	2.68	4.68	31.1	2.13	0.393	2.13
Mean	2.66	4.89	35.8	10.5	1.20	0.203	0.41	2.60	4.66	36.5	—	0.644	2.08
SE	0.22	0.30	2.42	1.59	0.17	0.015	0.071	0.23	0.28	2.69	—	0.050	0.15

[a] No meaningful value; the lag time is that time at which the observed plasma concentration first exceeded the minimum quantifiable level.

first time point with measurable rosoxacin concentration, to obtain a reasonable fit of the data. In the other 14 subjects, no adjustment was necessary (Table I). Using the mean parameters, the plasma rosoxacin concentration, C (μg/ml) at time t (hr), is given by:

$$C = 10.5\,[e^{-0.203(t-0.41)} - e^{-1.20(t-0.41)}] \qquad \text{(Eq. 7)}$$

The mean apparent first-order terminal elimination half-life for rosoxacin was ~3.4 hr.

The mean observed concentration data were also described by the model, and a comparison of the observed and predicted concentrations is shown in Fig. 1. The observed, model-independent, parameters are in reasonable agreement with those calculated from the open one-compartment body model with oral absorption, Table I.

The mean apparent volume of distribution was 0.644 liters/kg. This suggests that rosoxacin is distributed into the total body water, which may be responsible for the membrane permeability and relatively high levels of rosoxacin found in tissues (7, 8). This hypothesis will be tested in future studies.

An earlier study of the pharmacokinetics of rosoxacin in the dog (9) reported an apparent first-order terminal elimination half-life of 2 hr and a plasma clearance, corrected for body weight, of 8.6 ml/min/kg. In humans the elimination half-life is longer, ~3.4 hr, and the plasma clearance of rosoxacin, corrected for weight, is slower, 2.08 ml/min/kg.

REFERENCES

(1) J. Edelson, C. Davison, and D. P. Benziger, *Drug Metab. Rev.*, **6**, 105 (1977).

(2) J. R. O'Connor, R. A. Dobson, P. E. Came, and R. B. Wagner, *Curr. Chemother. Infect. Dis.*, **1**, 440 (1980).

(3) R. A. Dobson, J. R. O'Connor, S. A. Poulin, R. B. Kundsin, T. F. Smith, and P. E. Came, *Antimicrob. Agents Chemother.*, **18**, 738 (1980).

(4) I. Braveny and K. Machka, *Arzneim.-Forsch.*, **30**, 1476 (1980).

(5) D. Milatovic, K. Machka, O. Galla, and I. Braveny, *Infection*, **6**, 242 (1978).

(6) B. M. Limson, R. K. Macasaet, J. J. Salem, C. G. Beling, and H. A. Burnham, *Curr. Ther. Res.*, **26**, 842 (1979).

(7) S. Maigaard, N. Frimodt-Möller, U. Hoyme, and P. O. Madsen, *Invest. Urol.*, **17**, 149 (1979).

(8) S. Maigaard, N. Frimodt-Möller, and P. O. Madsen, *Urol. Res.*, **8**, 113 (1980).

(9) M. P. Kullberg, R. Koss, S. O'Neil, and J. Edelson, *J. Chromatogr.*, **173**, 155 (1979).

(10) "SAS User's Guide," J. T. Helwig and K. A. Council, Eds., SAS Institute Inc., Raleigh, N.C., 1979, pp. 317–329.

ACKNOWLEDGMENTS

The authors thank the staffs of the Quincy Research Center and the Department of Drug Metabolism, Sterling-Winthrop Research Institute for their assistance in the collection and analysis, respectively, of the plasma samples.

Toxicity of *Gonyaulax tamarensis* var. *excavata* Cells to the Brine Shrimp *Artemia salina* L.

JOSEPH M. BETZ * ˣ and WALTER J. BLOGOSLAWSKI ‡

Received February 25, 1981, from the **Department of Biology, Philadelphia College of Pharmacy and Science, Philadelphia, PA 19104* and the *‡ National Marine Fisheries Service, Northeast Fisheries Center, Milford Laboratory, Milford, CT 06460.* Accepted for publication August 21, 1981.

Abstract □ Brine shrimp (*Artemia salina* L.) were exposed to concentrations of live *Gonyaulax tamarensis* var. *excavata* cells ranging from 0 to 13,400 cells/ml in unialgal culture. The shrimp ingested the dinoflagellate cells and an LD_{50} determination was made. The shrimp had a 72-hr LD_{50} of 1258 *G. tamarensis* cells/ml, which was calculated to correspond to 73,385 μg/kg of body weight. This figure can be compared with an oral LD_{50} value of 2100 μg/kg for the mouse. Since it requires one-tenth as much toxin to kill a mouse (LD_{50} approximately 0.04 mg) as to kill an *Artemia* (LD_{50} approximately 0.4 mg), the whole cell *G. tamarensis* bioassay is a poor alternative to the current mouse assay.

Keyphrases □ Paralytic shellfish poisoning—toxicity of *Gonyaulax tamarensis* var. *excavata* cells to brine shrimp □ Brine shrimp—toxicity of *Gonyaulax tamarensis* var. *excavata*, potential bioassay for paralytic shellfish poisoning □ Bioassay—potential, toxicity of *Gonyaulax tamarensis* var. *excavata* to brine shrimp, paralytic shellfish poisoning

Paralytic shellfish poisoning is a potentially fatal form of food poisoning caused by ingestion of shellfish that have been feeding on blooms of toxic dinoflagellates (1). Mollusks feeding on the dinoflagellates appear unaffected, the immunity apparently related to a lack of sensitivity of the nerves of bivalve mollusks to the action-potential blocking effects of the toxins (2). Isolated crayfish (*Procambarus clarkii*) (3), spider crab (*Maia squinado*) (4), and American lobster (*Homarus americanus*) (5) nerves have been found to be highly susceptible to the toxins. Controlled feeding of highly toxic clams to lobsters has, however, failed to demonstrate any toxicity to the intact animal (6).

The present study attempted to develop an inexpensive bioassay for paralytic shellfish poison to replace the costly mouse assay, and to determine the LD_{50} value of the gonyautoxins present in the Atlantic dinoflagellate *Gonyaulax tamarensis* var. *excavata*, to a crustacean (*Artemia salina* L.). This was a preliminary step in the investigation of the immunity mechanism of crustaceans to the toxins.

EXPERIMENTAL

Culture of Organisms and Confirmation of Dinoflagellate Toxicity—Experimental media for culture of *Gonyaulax* (*Gonyaulax* medium) were prepared from salt well water[1] and supplemented with 100 mg of KNO_3, 10 mg of K_2HPO_4, 1 mg of $FeCl_3$, and 0.05 mg of Na_2SiO_3/liter. The pH was adjusted to 8.6 with 1 *N* NaOH (7). This solution was sterilized by autoclaving for 15 min at 15 psi. Traces of cyanocobalamin and thiamine solutions which had been filtered through a sterile membrane filter unit were added to the medium aseptically (8).

The culture was initiated by inoculating 1 liter of medium with 1 ml of stock *Gonyaulax tamarensis* var. *excavata*, (Strain IB-72)[2] culture containing 20,000 cells/ml and was then incubated at 20° for 30 days in 3-liter Fernbach flasks. All cultures were incubated under continuous illumination in an environmental chamber. *G. tamarensis* cells in the culture were counted with a hemacytometer slide using appropriate dilutions to count 1-ml samples (6). The toxicity of this *G. tamarensis* strain was confirmed by mouse assay of an extract of the dinoflagellate. Three liters of 25-day *G. tamarensis* culture containing 2500 cells/ml were membrane filtered. The filter pads were then placed into 100 ml of 0.1 *N* HCl to lyse the cells. The clear yellow-green solution was refiltered to remove cellular debris, and the solution assayed using female white mice (9). *Dunaliella salina*[3] (a nontoxic marine phytoflagellate) was extracted and assayed as described. Brine shrimp (*Artemia salina* L.) eggs[4] were hatched and raised to the adult state (10) with *Dunaliella salina* as an additional food source.

Brine Shrimp Assay—The experimental vessels for the study of *G. tamarensis* toxicity to brine shrimp were 125-ml Erlenmeyer flasks which had been loosely stoppered with nonabsorbent cotton and autoclaved at 15 psi for 15 min. The dinoflagellate source was a 29-day *G. tamarensis* culture with an original concentration of 13,400 cells/ml. The experiment was performed using five different dinoflagellate concentrations (13,400, 6700, 3400, 1300, and 135 cells/ml) and a control containing no cells. Each flask was prepared by removing a portion of the stock culture with a sterile pipet and placing the calculated volume containing the appropriate number of cells into an aliquot of diluent (sterile *Gonyaulax* medium) in one of the experimental flasks. Five brine shrimp were then added to each flask, and five flasks were used for each concentration of dinoflagellate cells. The experiment was repeated four times for a total of 100 shrimp at each concentration of cells. After restoppering the flask with its cotton plug, it was examined for cessation of *Artemia* swimming motions at intervals of 20 min, 1, 8, 24, and 72 hr.

Two controls for this portion of the experiment were sterile *Gonyaulax* medium to which no inoculum had been added, and medium from an active culture of *G. tamarensis* (13,400 cells/ml) from which the cells had been removed by membrane filtration. Bioassay data on *G. tamarensis* were used to calculate LD_{50} values by transforming the curve for percent mortality *versus* log dose of toxin (cells/ml) to a straight line by probit

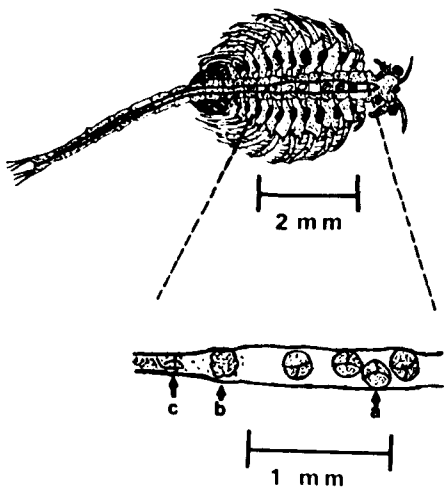

Figure 1—*Partially digested* Gonyaulax tamarensis *var.* excavata *within the digestive tract of a brine shrimp (*Artemia salina *L.). Top—view of* Artemia *with ingested dinoflagellate for size comparison. Bottom—Enlarged section of digestive tract showing phases of dinoflagellate degradation: (a) Intact* G. tamarensis *cells at beginning of tract, (b) cell further along in tract showing swelling and loss of cellular detail, and (c) cell fragments.*

[1] Flower's Oyster Hatchery, Bayville, N.Y.
[2] Dr. Christopher Martin, University of Massachusetts Marine Station, Gloucester, MA 01930.
[3] Carolina Biological Supply Co., Burlington, NC 27215.
[4] Ward's of California, Monterey, CA 93940.

0022-3549/82/0400-0463$01.00/0

Table I—Intraperitoneal Toxicity of Dinoflagellate and *Dunaliella salina* Control Extracts to Mice

Number of Mice	Toxin Source	Average Weight, g	Dilution	pH	Median Toxicity: Mouse, Unit	Median Toxicity: μg/ml	Median Toxicity: μg/100 g Meat
3	GTX ext[a]	10.6	1:5	2.0	1.008	1.09	218[b]
3	*Dunaliella* extract	10.9	1:1	2.0	0.0	0.0	000

[a] GTX ext = *G. tamarensis* cell extract. [b] Calculated theoretical values for purposes of comparison.

Table II—LD_{50} Values for *G. tamarensis* Cells to *Artemia salina* L. at 20 ± 2°

G. tamarensis Concentration, cells/ml	Number of Test Organisms	Number of Test Organisms Dead, hr: 1	8	24	48	72
13,400	100	0	3	38	69	87
6,700	100	0	3	28	69	81
3,400	100	0	0	16	42	61
1,300	100	0	2	16	48	62
135	100	0	1	4	13	39
0[a]	100	0	1	5	12	19
0[b]	100	0	0	1	1	2

	8 hr	24 hr	48 hr	72 hr
LD_{50} (cells/ml) from probit analysis	7.24×10^{10}	36308	5875	1258[c]
95% confidence limits	1.53×10^{12}	45709	9078	2058.7[c]
	3.43×10^{9}	28840	3802	703.6[c]
Slope of probit line	0.28069	0.9345	1.0145	0.8098
	±0.1576	±0.0538	±0.0464	±0.0151

[a] Control using inoculated *Gonyaulax* medium with cells removed by membrane filtration. This value was used in LD_{50} computations. [b] Control using sterile *Gonyaulax* medium. [c] Indicates value obtained by computer.

analysis (11), using a computer program written specifically for the purpose[5].

RESULTS AND DISCUSSION

Confirmation of Toxicity of *G. tamarensis* Culture—The solution obtained from extraction of the dinoflagellate was found to be toxic to mice (Table I). Concentration of toxin as determined by mouse assay was 109 μg/1000 ml of extract. This is 1 μg of saxitoxin equivalent/2294 cells. In the *Dunaliella* control solution, all mice survived.

Brine Shrimp Assay—The two control groups using *Gonyaulax* medium (uninoculated and inoculated with cells removed) gave negligible mortality and a pronounced mortality of 19%, respectively (Table II). This second mortality was taken into account when calculating the LD_{50}.

Mortality in the control group followed a pattern similar to that seen in the experimental group and was probably caused by toxins released into the medium by dinoflagellate cells (12). Brine shrimp added to *G. tamarensis* cells became intoxicated and died. Microscopic examination of the *Artemia* disclosed the presence of dinoflagellate cells within their digestive tracts (Fig. 1). The computer program used for statistical analysis of the data took into account the 19% control mortality (11). Thus, the rate at which *Artemia* were killed (according to this model) depended on the concentration of *G. tamarensis* cells rather than on the rate of dinoflagellate ingestion by the brine shrimp. Further studies on the rate of dinoflagellate ingestion should provide more accurate estimates of oral LD_{50}. Upon intoxication, the *Artemia* underwent a period of hyperactivity during which they evinced a series of contractions (anterior–posterior curling and uncurling motions). This lasted for 1–2 hr and then ceased. Soon after, the shrimp lost their ability to remain near the surface of the medium and sank to the bottom of the container. The vigor of swimming motions decreased gradually and the organism ceased all movements.

The LD_{50} for 72 hr was 1258 cells/ml in 50 ml of medium (Table II). This value was converted to a microgram per kilogram lethal dose by taking the value of 1 μg of toxin/2294 cells and multiplying it by the 20% toxin reduction expected between the 25th and 29th days of culture (13). The corrected value for toxin content per dinoflagellate cells is 1 μg of toxin/2868 cells. This figure yields a toxin content of 0.00035 μg/*G. tamarensis* cell. When this concentration is multiplied by the number of cells per lethal dose (Table II), it is found that the LD_{50} in terms of amount of toxin is 0.4403 mg/*Artemia*.

Since the culture was unialgal but not axenic, decomposition of *Artemia* proceeded rapidly after death, and attempts to obtain shrimp weights were futile unless performed immediately after death. An average *Artemia* weight of 6 mg was used in determining microgram per kilogram LD_{50} values (14). Thus, the toxicity of gonyautoxins to *Artemia salina* L. is ~73,385 μg/kg of body weight. This figure is almost 150 times larger than the oral LD_{50} of 500 μg/kg for man, and 18 times larger than the 4000 μg/kg for the most resistant recorded mammal, a monkey (15). Mice, which are the current assay organisms and are somewhat closer in size to *Artemia* than either of the aforementioned animals, have an oral LD_{50} value of 2100 μg/kg of body weight (15). Thus, one-tenth as much toxin is required to kill a mouse as to kill a brine shrimp (LD_{50} 0.04 mg and 0.4 mg/animal, respectively). This fact, coupled with the 72 hr duration of the test (compared to the 15 min required for the Association of Official Analytical Chemists mouse assay) make the whole cell assay of *G. tamarensis* by *Artemia* a poor alternative to the mouse assay for purposes of routine monitoring of shellfish toxicity.

Attempts to assay both homogenized cells and shellfish extract which had been proven toxic by mouse assay failed due to rapid fungal overgrowth of the test solution. *Artemia* subjected to overgrown extract died rapidly in the presence or absence of paralytic shellfish poison. Concomitant administration of an antifungal agent not only added another variable to the experiment, but also did not sufficiently control fungal growth over the 72 hr required for the test.

The cause of death in cases of saxitoxin intoxication is paralysis of muscular contraction by inhibition of nerve conduction (blockade of Na^+ influx) resulting in a peripheral paralysis of respiratory muscles (16), as opposed to a nonspecific cytolytic factor which physically destroys gill surfaces (as is the case with *Gymnodinium breve* toxin) (13). Absorption of the gonyautoxins is necessary for their activity, detoxification occurring in either the absorptive or metabolic phase of digestion.

Organic extraction procedures similar to those employed for brine shrimp assay of ciguatera toxins (17) were beyond the scope of this study but will be examined in future experiments.

[5] Mr. Joseph Heyes, Philadelphia College of Pharmacy and Science Philadelphia, PA 19104.

REFERENCES

(1) B. W. Halstead and D. A. Courville, "Posionous and Venomous Marine Animals of the World," vol. 1, U.S. Government Printing Office, Washington, D.C., 1965, p. 157.

(2) B. M. Twarog, T. Hidaka, and H. Yamaguchi, *Toxicon*, **10**, 273 (1972).

(3) J. S. D'Arrigo, *J. Membrane Biol.*, **29**, 231 (1976).

(4) P. F. Baker and K. A. Rubinson, *Nature (London)*, **257**, 412 (1975).

(5) J. Baumgold, *J. Neurochem.*, **34**, 327 (1980).

(6) C. M. Yentsch and W. Balch, *Environ. Lett.*, **9**, 249 (1975).
(7) E. J. Schantz, J. M. Lynch, G. Vaynada, K. Matsumoto, and H. Rapoport, *Biochemistry*, **5**, 1191 (1966).
(8) S. H. Hutner and J. J. A. McLaughlin, *Sci. Am.*, **199**, 92 (1958).
(9) "Official Methods of Analysis," 12th ed., Association of Official Analytical Chemists, Washington, D.C., 1975, p. 319.
(10) A. S. Michael, C. G. Thompson, and M. Abramovitz, *Science*, **123**, 463 (1956).
(11) D. J. Finney, "Probit Analysis," 2nd ed., University Press, Cambridge, England, 1962.
(12) A. Prakash, *J. Fish. Res. Board Can.*, **24**, 1589 (1967).
(13) A. W. White and L. Maranda, *ibid.*, **35**, 397 (1978).
(14) N. M. Trieff, M. McShan, D. Grajcer, and M. Alam, *Texas Rep. Biol. Med.*, **31**, 409 (1973).
(15) E. F. McFarren, M. L. Schafer, J. E. Campbell, K. H. Lewis, E. T. Jensen, and E. J. Schantz, *Proc. Natl. Shellfish Assoc.*, **47**, 114 (1956).
(16) M. H. Evans, *Br. J. Exp. Pathol.*, **46**, 245 (1965).
(17) H. R. Granade, P. C. Cheng, and N. J. Doorenbos, *J. Pharm. Sci.*, **65**, 1414 (1976).

ACKNOWLEDGMENTS

The authors thank Dr. Chris Martin, University of Massachusetts Marine Station for dinoflagellate cultures and information on their care; John Hurst, Jr., of the Maine Ocean Science Laboratory for aid in assaying crude mussel extracts during preliminary investigations; Dr. J. E. Campbell, Food and Drug Administration, for paralytic shellfish poisoning standard solution; Drs. Hugo Freudenthal and Bernard Newman of C. W. Post Center of Long Island University, and Dr. Ara Der Marderosian of the Philadelphia College of Pharmacy and Science for their invaluable contributions.

1,4-Bis(4-guanylphenylethyl)benzenes as Potential Antitrypanosomal Agents

BIJAN P. DAS, VERA B. ZALKOW, MARGRET L. FORRESTER, FRANK F. MOLOCK, and DAVID W. BOYKIN ˣ

Received July 13, 1981, from the *Department of Chemistry, Georgia State University, Atlanta, GA 30303.* Accepted for publication August 14, 1981.

Abstract □ A series of 1,4-bis(4-guanylphenylethyl)benzenes, including masked amidines in which the guanyl function is incorporated into a heterocyclic ring, were prepared for screening as potential antitrypanosomal agents. Some of these compounds were active against *Trypanosoma rhodesiense* in mice. The diamidines were prepared by standard methods from 1,4-bis(4-cyanophenylethyl)benzene which was obtained from 1,4-bis(4-cyanostyryl)benzene by diimide reduction. The latter compound was prepared by the Wittig reaction between 4-cyanobenzylphosphonium ylide and terephthaldicarboxaldehyde.

Keyphrases □ Antitrypanosomal agents—potential, 1,4-bis(4-guanylphenylethyl)benzenes □ *Trypanosoma rhodesiense*—1,4-bis(4-guanylphenylethyl)benzenes, activity as antitrypanosomal agents □ Structure–activity relationships—1,4-bis(4-guanylphenylethyl)benzenes as potential antitrypanosomal agents

Aryl diamidines have been known to be useful antitrypanosomal agents for many years (1, 2). The aryl diamidines reported to exhibit antitrypanosomal activity fall into two general, apparently arbitrary, sets: those that have their guanyl functions separated by approximately 12Å and those that are separated by approximately 20Å (3). It is not known if this observation has any significance regarding the interaction of these compounds with their bioreceptor(s). A number of quite active aryl diamidines have been reported which fall into the category of the 12Å set (3–5) and this report describes efforts to synthesize compounds that fall into the 20Å class. Pentamidine (1), congocidin (1), and the terephthanilide amidines (6) are notable examples of the antitrypanosomal compounds that fall into the latter structural class. While pentamidine and the terephthanilide amidines have similar separation of the guanyl functions, they differ in that terephthanilide amidines probably exist in a planar conformation, whereas this is unlikely for pentamidine. The present study attempted to determine the effect on antitrypanosomal activity and binding to the bioreceptor for the terephthanilide amidine types which are conformationally more flexible. To test this point, 1,4-bis(4-guanylphenylethyl)benzene was synthesized along with related compounds in which the conformationally rigid carboxamido groups of the terephthanilide amidines were replaced by the conformationally flexible $-CH_2CH_2-$ units.

RESULTS AND DISCUSSION

The synthesis of the target diamidines was achieved by employing a conventional synthetic approach (Scheme I). The first step involves a Wittig reaction between the 4-cyanobenzylphosphonium ylide and terephthaldicarboxaldehyde to yield a bis-1,4-(4-cyanostyryl)benzene (I), the stereochemistry of which was not determined. The bis styryl

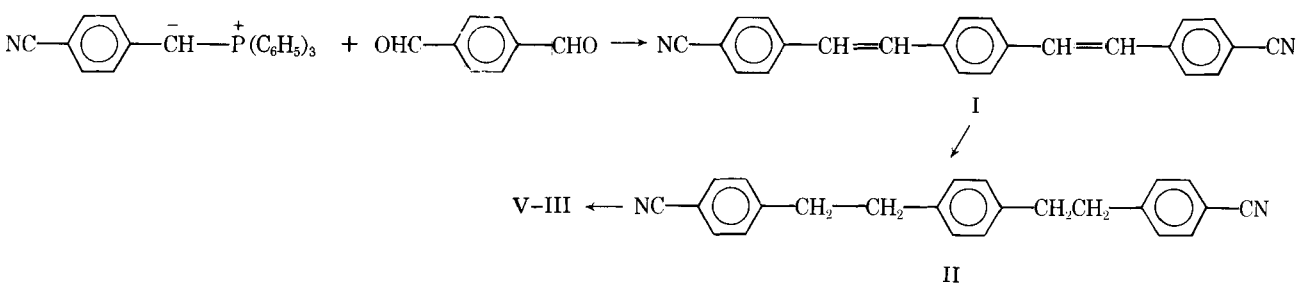

Scheme I

0022-3549/82/0400-0465$01.00/0

(6) C. M. Yentsch and W. Balch, *Environ. Lett.*, **9**, 249 (1975).
(7) E. J. Schantz, J. M. Lynch, G. Vaynada, K. Matsumoto, and H. Rapoport, *Biochemistry*, **5**, 1191 (1966).
(8) S. H. Hutner and J. J. A. McLaughlin, *Sci. Am.*, **199**, 92 (1958).
(9) "Official Methods of Analysis," 12th ed., Association of Official Analytical Chemists, Washington, D.C., 1975, p. 319.
(10) A. S. Michael, C. G. Thompson, and M. Abramovitz, *Science*, **123**, 463 (1956).
(11) D. J. Finney, "Probit Analysis," 2nd ed., University Press, Cambridge, England, 1962.
(12) A. Prakash, *J. Fish. Res. Board Can.*, **24**, 1589 (1967).
(13) A. W. White and L. Maranda, *ibid.*, **35**, 397 (1978).
(14) N. M. Trieff, M. McShan, D. Grajcer, and M. Alam, *Texas Rep. Biol. Med.*, **31**, 409 (1973).
(15) E. F. McFarren, M. L. Schafer, J. E. Campbell, K. H. Lewis, E. T. Jensen, and E. J. Schantz, *Proc. Natl. Shellfish Assoc.*, **47**, 114 (1956).
(16) M. H. Evans, *Br. J. Exp. Pathol.*, **46**, 245 (1965).
(17) H. R. Granade, P. C. Cheng, and N. J. Doorenbos, *J. Pharm. Sci.*, **65**, 1414 (1976).

ACKNOWLEDGMENTS

The authors thank Dr. Chris Martin, University of Massachusetts Marine Station for dinoflagellate cultures and information on their care; John Hurst, Jr., of the Maine Ocean Science Laboratory for aid in assaying crude mussel extracts during preliminary investigations; Dr. J. E. Campbell, Food and Drug Administration, for paralytic shellfish poisoning standard solution; Drs. Hugo Freudenthal and Bernard Newman of C. W. Post Center of Long Island University, and Dr. Ara Der Marderosian of the Philadelphia College of Pharmacy and Science for their invaluable contributions.

1,4-Bis(4-guanylphenylethyl)benzenes as Potential Antitrypanosomal Agents

BIJAN P. DAS, VERA B. ZALKOW, MARGRET L. FORRESTER, FRANK F. MOLOCK, and DAVID W. BOYKIN ˣ

Received July 13, 1981, from the *Department of Chemistry, Georgia State University, Atlanta, GA 30303.* Accepted for publication August 14, 1981.

Abstract □ A series of 1,4-bis(4-guanylphenylethyl)benzenes, including masked amidines in which the guanyl function is incorporated into a heterocyclic ring, were prepared for screening as potential antitrypanosomal agents. Some of these compounds were active against *Trypanosoma rhodesiense* in mice. The diamidines were prepared by standard methods from 1,4-bis(4-cyanophenylethyl)benzene which was obtained from 1,4-bis(4-cyanostyryl)benzene by diimide reduction. The latter compound was prepared by the Wittig reaction between 4-cyanobenzylphosphonium ylide and terephthaldicarboxaldehyde.

Keyphrases □ Antitrypanosomal agents—potential, 1,4-bis(4-guanylphenylethyl)benzenes □ *Trypanosoma rhodesiense*—1,4-bis(4-guanylphenylethyl)benzenes, activity as antitrypanosomal agents □ Structure–activity relationships—1,4-bis(4-guanylphenylethyl)benzenes as potential antitrypanosomal agents

Aryl diamidines have been known to be useful antitrypanosomal agents for many years (1, 2). The aryl diamidines reported to exhibit antitrypanosomal activity fall into two general, apparently arbitrary, sets: those that have their guanyl functions separated by approximately 12Å and those that are separated by approximately 20Å (3). It is not known if this observation has any significance regarding the interaction of these compounds with their bioreceptor(s). A number of quite active aryl diamidines have been reported which fall into the category of the 12Å set (3–5) and this report describes efforts to synthesize compounds that fall into the 20Å class. Pentamidine (1), congocidin (1), and the terephthanilide amidines (6) are notable examples of the antitrypanosomal compounds that fall into the latter structural class. While pentamidine and the terephthanilide amidines have similar separation of the guanyl functions, they differ in that terephthanilide amidines probably exist in a planar conformation, whereas this is unlikely for pentamidine. The present study attempted to determine the effect on antitrypanosomal activity and binding to the bioreceptor for the terephthanilide amidine types which are conformationally more flexible. To test this point, 1,4-bis(4-guanylphenylethyl)benzene was synthesized along with related compounds in which the conformationally rigid carboxamido groups of the terephthanilide amidines were replaced by the conformationally flexible $-CH_2CH_2-$ units.

RESULTS AND DISCUSSION

The synthesis of the target diamidines was achieved by employing a conventional synthetic approach (Scheme I). The first step involves a Wittig reaction between the 4-cyanobenzylphosphonium ylide and terephthaldicarboxaldehyde to yield a bis-1,4-(4-cyanostyryl)benzene (I), the stereochemistry of which was not determined. The bis styryl

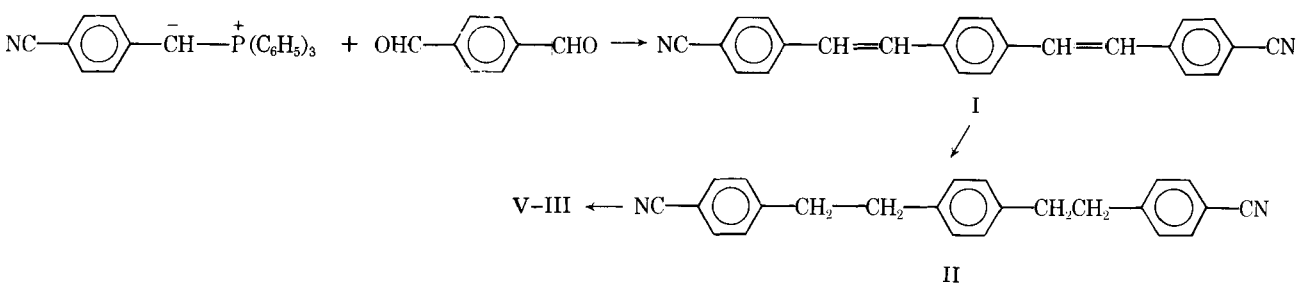

Scheme I

0022-3549/82/0400-0465$01.00/0

Table I—Antitrypanosomal Screening Results [a]

No.	Cures[b] or ΔMST[c] at given Dosage[d], mg/kg															
	640	424	320	212	160	106	80	53	40	26.5	20	13.3	10	5	2.5	1.25
III		5		5		5		3		1		1.30				
IV		2.3*D*		1.6*D*		0.6*D*		0.4*D*		0.5*D*		0.2*D*				
V		T[e]		5		5		4		2		2.4*D*				
VI[f]	5		5		5		5		5		5		5	5	4	1
VII[g]	5		5		5		5		5		5		5	5	4	4

[a] See Ref. 8. Antitrypanosomal testing was done at the Leo Rane Laboratory of the University of Miami under the direction of Dr. A. L. Ager, Jr. [b] A cure is defined as a 30-day increase in survival time of the treated animals over the controls. Five mice were used at each dosage level; hence, five is the maximum number of cures. [c] ΔMST is the increase in mean survival time of test animals *versus* controls in days. ΔMST is differentiated from cures by the use of *D*; *i.e.*, 1.3*D* = 1.6 days. [d] Dosage is in milligrams of compound per kilogram of body weight of the test animal (mice). [e] T = toxic death. [f] Pentamidine. [g] 2,5-Bis(guanylphenyl)furan.

compound I was subjected to a diimide-type reduction by the method of Dewey and Van Tamelen (7) and produced 1,4-bis(4-cyanophenylethyl)benzene (II). The bis-nitrile was converted into the corresponding imidate ester which was used directly to prepare the guanyl derivatives.

The target compounds (III–V) were screened against *Trypanosoma rhodensiense* in mice (8), and the results are shown in Table I. Included for comparison in Table I are test results from the same screening program for pentamidine and 2,5-bis(4-guanylphenyl)furan, a very effective 12Å-type compound reported previously (3). The bis-guanyl compound (III) showed good activity, providing cures down to a dosage level of 26 mg/kg. Its activity was significantly lower than that of pentamidine or the furan derivative included in Table I. Interestingly, the two masked amidines showed markedly different activities. The imidazolinyl compound (IV) was essentially devoid of activity; however, the related pyrimidinyl (V), while toxic at high dosages, was slightly more active than the parent compound III at low dosage levels. In a large number of 12Å types (3–5), the masked amidines have generally shown limited activity.

EXPERIMENTAL[1]

Melting points reported under 300° were taken using an oil-bath melting point apparatus; the melting points of compounds melting above 300° were obtained using a solid block apparatus and all melting points are uncorrected. Satisfactory IR spectra were reported for all new compounds; the expected PMR spectra were recorded on all new compounds in [^{2}H]chloroform or [^{2}H]dimethylsulfoxide (tetramethylsilane standard).

1,4-Bis(*p*-cyanostyryl)benzene (I)—4-Cyanobenzyl triphenylphosphonium bromide (10 g, 0.02 mole) was added, under a nitrogen atmosphere, to a solution containing 0.03 mole of freshly prepared sodium ethoxide in 180 ml of ethanol. The solution was stirred for ~5 min and terephthaldicarboxaldehyde (1.4 g, 0.01 mole) dissolved in 100 ml of ethanol was added dropwise. After addition was complete the reaction mixture was stirred for 3.5 hr under a nitrogen atmosphere during which time crystals appeared. The solid (1.1 g, 17%) was filtered and recrystallized from ethanol mp 280–282°.

Anal.—Calc. for $C_{24}H_{16}N_2$: C, 86.74; H, 4.81. Found: C, 86.66; H, 4.95.

1,4-Bis(*p*-cyanophenylethyl)benzene (II)—*p*-Toluenesulfonylhydrazide (9) (4.0 g, 0.02 mole) in 50 ml of ethylene glycol monomethylether was added in portions to a refluxing suspension of the bis-styryl compound (3.3 g, 0.01 mole) in 100 ml of ethylene glycol monomethylether, under a nitrogen atmosphere. After addition was complete, the mixture was refluxed for 16 hr. The volume of solvent was reduced to ~30 ml and 2.8 g (83%) was obtained on cooling. The product was dissolved in methylene chloride, passed through a short alumina column, and the solvent was evaporated. Recrystallization from chloroform and dimethylsulfoxide gave a solid which melted 208–211°.

Anal.—Calc. for $C_{24}H_{20}N_2$: C, 85.68; H, 5.99; N, 8.33. Found: C, 85.56; H, 5.99; N, 8.27.

1,4-Bis(4′-guanylphenylethyl)benzene Dihydrochloride (III)—The bis-nitrile (1.4 g, 0.004 mole) was dissolved in 100 ml of dioxane and 25 ml of ethanol, cooled in an ice bath, and hydrogen chloride gas was passed through it until the solution was saturated. The mixture was placed in a pressure bottle and shaken for 3 days at room temperature. The solid (imidate ester hydrochloride) that formed was filtered, dried under vacuum, and checked for unreacted starting material by examining the nitrile region of its IR spectra. A suspension of 1.5 g of imidate ester in 100 ml of absolute ethanol was prepared and dry ammonia was passed through the cold suspension until it was saturated. The mixture was shaken at room temperature for 3 days in a pressure bottle. The yellow solid that formed was dissolved in absolute ethanol saturated with hydrogen chloride gas; concentration of the solution gave 1.1 g (63%) of yellow solid which was recrystallized from ethanol, mp 345–346° (dec).

Anal.—Calc. for: $C_{24}H_{28}Cl_2N_4$: C, 65.01; H, 6.32; N, 12.64. Found: C, 64.81; H, 6.37; N, 12.53.

1,4-Bis[4-(2-imidazolinyl)phenylethyl]benzene (IV)—The imidate ester hydrochloride (2.9 g, 0.0054 mole) was suspended in 75 ml ethanol, ethylene diamine (0.65 g, 0.11 mole) was added, and the mixture was refluxed for 16 hr. The solid product was filtered, washed with ethanol, and dried. The solid was dissolved in absolute ethanol and the solution was saturated with dry hydrogen chloride gas. The solution was filtered and then concentrated until crystals began to appear; 1.9 g (78%), mp 298–303° (dec).

Anal.—Calc. for $C_{28}H_{32}Cl_2N_4$: C, 67.87; H, 6.46; N, 11.31. Found: C, 67.41; H, 6.56; N, 11.02.

1,4-Bis[4-(1,4,5,6-tetrahydro-2-pyrimidinyl)phenylethyl]benzene (V)—The imidate ester hydrochloride (1.9 g, 0.0043 mole) was suspended in 75 ml of ethanol and 1,3-propanediamine (0.64 g, 0.009 mole) was added and the mixture was refluxed overnight during which time a solid formed. The solid was washed with ethanol and dried. It was then dissolved in absolute ethanol and the solution was saturated with dry hydrogen chloride gas. The solution was filtered and concentrated until crystals formed; 1.4 g (61%), mp 345–350° (dec.).

Anal.—Calc. for $C_{30}H_{36}Cl_2N_4(0.5)H_2O$: C, 67.66; H, 7.00; N, 10.52. Found: C, 67.55; H, 6.83; N, 10.32.

[1] Elemental analyses were performed by Atlantic Microlab, Atlanta, Georgia.

REFERENCES

(1) E. A. Steck "Chemotherapy of Protozoan Diseases," vol. II, U.S. Government Printing Office, Washington, D.C., 1972, Chapts. 7, 11.

(2) B. A. Newton, "Trypanosomiasis and Leshmaniasis with Special Reference to Chagas Disease," Elsevier, Amsterdam, The Netherlands, 1974, pp. 285–307.

(3) B. P. Das and D. W. Boykin, *J. Med. Chem.*, **20,** 531 (1977).

(4) *Ibid.*, **20,** 1219 (1977).

(5) B. P. Das, R. A. Wallace, and D. W. Boykin, *J. Med. Chem.*, **23,** 578 (1980).

(6) B. S. Gill, *Indian J. Exp. Biol.*, **9,** 397 (1971).

(7) R. S. Dewey and E. E. van Tamelen, *J. Am. Chem. Soc.*, **83,** 3729 (1961).

(8) L. Rane, D. S. Rane, and K. E. Kinnamon, *Am. J. Trop. Med. Hyg.*, **25,** 395 (1976).

(9) L. F. Fieser and M. Fieser, "Reagents for Organic Synthesis," Wiley, New York, N.Y., 1967, p. 1185.

ACKNOWLEDGMENTS

Support of this work by the U.S. Army Medical Research and Development Command under Contract No. DADA17-68-C-8035 is gratefully acknowledged. This is Contribution No. 1596 from the Army Research Program on Malaria. The authors thank Dr. Edgar A. Steck for helpful discussions and advice.

The Interaction of Granaticin with Nucleic Acids and Pyruvate Decarboxylase

GAIL GIBSON-CLAY, STEPHEN R. BYRN, and PETER HEINSTEIN ˣ

Received November 14, 1979, from the *Department of Medicinal Chemistry and Pharmacognosy, School of Pharmacy and Pharmacal Sciences, Purdue University, West Lafayette, IN 47907.* Accepted for publication August 5, 1981.

Abstract □ The interaction of granaticin with two different yeast ribonucleic acids, dialyzed transfer RNA and calf thymus DNA was studied. Contrary to previous reports, no binding of granaticin to DNA or RNA was observed. The visible spectrum of granaticin on direct mixing or equilibrium dialysis of granaticin with RNA or DNA was unchanged. Furthermore, granaticin did not displace acridine orange from DNA in competitive binding studies using fluorescence polarization. However, granaticin was shown to inhibit pyruvate decarboxylase. From the K_i for granaticin (3.8 m*M*) it was concluded that granaticin is as efficient as other 1,4-naphthoquinones in inhibiting pyruvate decarboxylase.

Keyphrases □ Granaticin A—absence of interaction with DNA and RNA, interaction with proteins from the inhibition of pyruvate decarboxylase □ DNA—interaction with granaticin A □ RNA—interaction with granaticin A □ Pyruvate decarboxylase—inhibition by granaticin A in the interaction between granaticin A and protein

Granaticin, isolated from *Streptomyces olivaceus* (1), is a quinone antibiotic which is active against Gram-positive bacteria (2). Also known as litmomycin (3), granaticin has been studied for its interaction with various biochemical species. Previous work proposed that granaticin (*a*) interferes with the charging process of transfer RNA, thereby inhibiting the synthesis of leucyl transfer RNA (4), (*b*) interferes with leucyl transfer RNA synthetase (5), (*c*) inhibits the synthesis of RNA or the function of RNA polymerase, which is not DNA dependent (6), (*d*) inhibits reverse transcriptase by binding to the template RNA (7), and (*e*) appears to inhibit maturation of ribosomal RNA (8). These biological effects of granaticin could be due to the interaction of granaticin with template macromolecules (*i.e.*, DNA and RNA) or with catalytic macromolecules, (*i.e.* proteins).

The inhibition of the reverse transcriptase was attributed to the interaction of granaticin with the RNA template (7). Inhibition of leucyl transfer RNA formation (4) and maturation of RNA may have been due to binding of granaticin to the RNA or to the reaction of granaticin with a protein factor required in the formation of RNA (8).

The purpose of this study was to investigate the binding of granaticin to two different RNA preparations and DNA and to measure the effect of granaticin on enzyme activity.

EXPERIMENTAL

Binding Studies—A stock solution of granaticin A[1] (27.9 μM) was prepared in 0.005 *M* phosphate buffer, pH 7.2, by stirring in the dark for 3 days at 2–37°. The solution was gravity filtered before use. Yeast transfer RNA type III (19.0 mg)[2] (9) was dissolved in 250 ml of 0.005 *M* phosphate buffer, pH 7.2. A fixed amount of granaticin stock solution (15 ml) was directly mixed with varying amounts of RNA solution (2, 5, 8, 10, 15, and 20 ml) and diluted to 100 ml with phosphate buffer. Visible spectra of these samples were recorded[3] scanning from 625–460 nm. The baseline was established by using phosphate buffer in both the sample and reference cells. Control absorption curves were generated using granaticin stock solution (15 ml) diluted to 100 ml with phosphate buffer and RNA solution (2–20 ml, as described above) diluted to 100 ml with phosphate buffer. The same procedure was used to test the interaction of granaticin with RNA type XI[2] (a mixture of messenger and ribosomal RNA) and calf thymus DNA[2].

In a slightly different experimental approach, 1 and 2 ml of an RNA solution (type XI and type III)[2] containing 20 mg of RNA in 10 ml of 0.005 *M* phosphate buffer, pH 7.2, was placed in a dialysis bag[4], sealed, and immersed in 50 ml of a granaticin solution (27.9 μM) in phosphate buffer. The solution was stirred in the dark for 72 hr at 2–37°. Thereafter, visible spectra (625–460 nm) of the RNA–granaticin solution inside the dialysis bag and the granaticin solution outside the dialysis bag were recorded[3]. In control incubations, phosphate buffer replaced the RNA solutions inside the dialysis bag, and in a second incubation the granaticin solution outside the dialysis tubing was replaced with phosphate buffer. Controls were treated the same as the samples.

Competitive Binding Studies[5]—Granaticin, 0.025–25 μg/ml in 0.01 *M* cacodylate[2] buffer, pH 6.7, was used in the competitive binding assay inhibiting the binding of acridine orange[2] to calf thymus DNA type I[2]. This binding is accompanied by an increase in fluorescence polarization. Granaticin and acridine orange (100 μl of a 10-μM solution) were mixed in a cell, and the initial fluorescence polarization (P_0) was measured[6] using excitation and emission filters at 492 and 520 nm, respectively. DNA (equivalent to 35% saturation) was then added to the cell and the final polarization (P) was determined after mixing. Results were expressed as a percentage of maximum binding; maximum binding was expressed as the P–P_0 obtained without granaticin (11).

Enzyme Assays—Pyruvate decarboxylase[2] (2-oxo acid carboxyl-lyase, EC 4.1.1.1, 13 U/mg protein) was assayed in a coupled assay with alcohol dehydrogenase[2] (alcohol:NAD$^+$ oxidoreductase EC 1.1.1.1, 300 U/mg protein) by measuring the oxidation of reduced nadide[2] at 340 nm (12). A typical incubation mixture contained reduced nadide (1.2 μmoles), alcohol dehydrogenase (0.3 U), pyruvate[2] (0–150 μmoles), pyruvate decarboxylase (0.29 U), and granaticin (0, 0.33, 0.42, and 0.52 μmoles) in a total volume of 3.0 ml of 0.2 *M* citrate[2] buffer, pH 6.0. Granaticin was dissolved in 0.2 *M* citrate buffer, pH 6.0 by stirring in the dark for 4 days at 2°. The reagents, except pyruvate decarboxylase, were mixed in a cell and the base line was recorded from 300–380 nm. The spectrophotometer[3] was then set at 340 nm and pyruvate decarboxylase was added, rapidly mixed, and the change in absorbance at 340 nm recorded. Temperature was maintained at 30°.

To ensure that the observed effect of granaticin in the enzyme assay was not due to the inhibition of alcohol dehydrogenase by granaticin, this enzyme was assayed with or without granaticin and without pyruvate decarboxylase. The reaction mixture contained reduced nadide (1.2 μmoles), acetaldehyde[2] (0–114 μmoles), granaticin (0, 0.33, 0.42 and 0.52 μmole, solution prepared as described previously), and alcohol dehydrogenase (0.3 U) in a total volume of 3.0 ml and 0.2 *M* citrate buffer, pH 6.0. The reagents, except the enzyme, were mixed in a cell and the base line recorded from 300–380 nm. The reaction was started by adding alcohol dehydrogenase and the change in absorbance at 340 nm was recorded. Temperature was maintained at 30°.

RESULTS AND DISCUSSION

It was proposed that granaticin binds to transfer RNA (4) and to the template RNA in the reverse transcriptase assay (7); however, these results were based on indirect observations. Therefore, binding of granaticin

[1] Granaticin A was a gift of Dr. H. G. Floss, Department of Medicinal Chemistry and Pharmacognosy, Purdue University.
[2] Sigma Chemical Co., St. Louis, Mo.
[3] Cary model 17 recording spectrophotometer.
[4] Fisher Scientific Co., Spectra/Por 1 Membranes: 6000 to 8000 MWCO.
[5] Analysis was performed by Dr. Carol L. Richardson, Principal Scientist, Meloy Laboratories, Inc., Springfield, Va.
[6] Model Fluoro I, Meloy Laboratories, Inc., Springfield, Va.

0022-3549/82/0400-0467$01.00/0

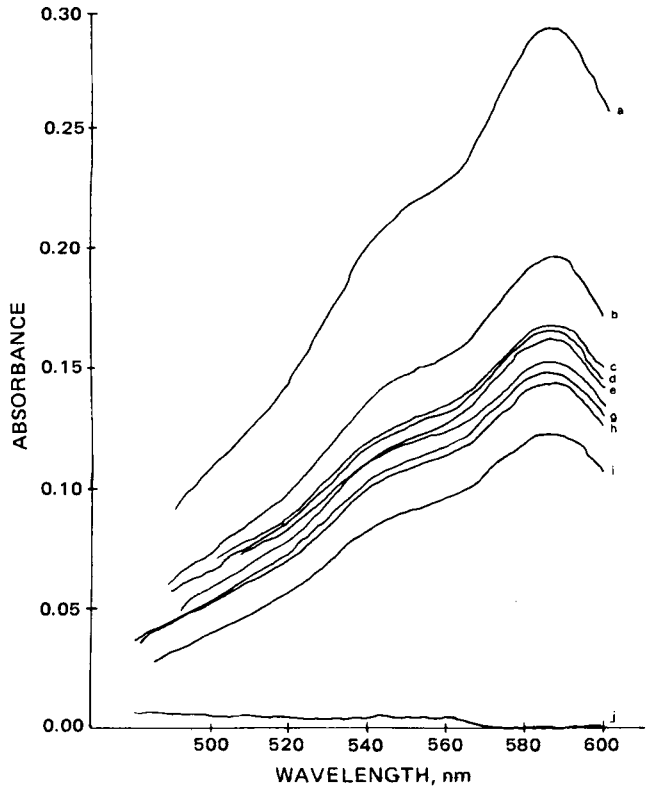

Figure 1—*Visible spectrum of granaticin and RNA type III in a direct mixing experiment. Key: a, 15 ml granaticin + 85 ml buffer; b, 10 ml granaticin + 90 ml buffer; c, 10 ml granaticin + 2 ml RNA type III + 88 ml buffer; d, 10 ml granaticin + 7 ml RNA type III + 83 ml buffer and 10 ml granaticin + 10 ml RNA type III + 80 ml buffer; e, 10 ml granaticin + 5 ml RNA type III + 85 ml buffer; f, 10 ml granaticin + 30 ml RNA type III + 60 ml buffer; g, 10 ml granaticin + 15 ml RNA type III + 75 ml buffer and 10 ml granaticin + 25 ml RNA type III + 65 ml buffer; h, 10 ml granaticin + 20 ml RNA type III + 70 ml buffer; i, 7 ml granaticin + 93 ml buffer; j, buffer only.*

to yeast transfer RNA type III and a mixture of ribosomal RNA and messenger RNA type XI through direct addition and dialysis experiments was attempted. In neither experiment did the absorption spectrum of granaticin exhibit any changes on addition of the RNA. Part of the visible absorption spectrum of granaticin is shown in Fig. 1 (curve a). Neither the peak at 580 nm, nor the shoulder at 550 nm in the granaticin spectrum were changed significantly on addition of RNA. The same results were obtained when granaticin and RNA were mixed or dialyzed for up to 3 days at temperatures that varied from 2 to 37° in different experiments. These results indicate that granaticin does not bind to RNA molecules *in vitro*.

In identical experiments where calf thymus DNA was substituted for RNA, no *in vitro* binding of granaticin to DNA was observed.

The inability of granaticin to interact *in vitro* with nucleic acids is supported by the results of the competitive binding assay (11). Granaticin showed no evidence of displacement of acridine orange from DNA.

Since the inhibitory action of granaticin on reverse transcriptase (7) and on the charging of transfer RNA (4) might be due to the interaction with proteins involved in these processes, and no interaction between RNA or DNA with granaticin was observed, the possibility that granaticin binds to protein (potential nucleophilic reactants) was investigated. The enzyme selected for these experiments was pyruvate decarboxylase, since compounds similar in structure to granaticin, naphthoquinone, and anthraquinone, inhibit this enzyme (13). Pyruvate decarboxylase was assayed at optimum conditions (12) and was coupled to the reduction of acetaldehyde, the product of the pyruvate decarboxylase reaction, by alcohol dehydrogenase resulting in the oxidation of reduced nadide.

Lineweaver–Burk plots ($1/V$ *versus* $1/[S]$) yielded parallel lines which indicated that granaticin is an uncompetitive inhibitor of pyruvate decarboxylase. In a control experiment where only alcohol dehydrogenase was assayed, granaticin had no effect on the enzyme. The K_i for granaticin was calculated to be 3.8 mM. Granaticin is, therefore, as good an inhibitor of pyruvate decarboxylase as 1,4-naphthoquinone (k_i = 4.2 mM) (12), whereas anthraquinone, at twice the concentration, did not inhibit pyruvate decarboxylase (13). Interestingly, granaticin had a half-wave potential of −0.685v (14) compared with a half-wave potential of −0.603v for naphthoquinone (15), but different from the half-wave potential of −0.85v for anthraquinone (16). These values would indicate a bioreductive alkylation (17) of a nucleophilic center in a protein. Additional experiments are required to prove this hypothesis.

It appears that at least one of the inhibiting actions of granaticin on living cells is the interaction of granaticin with proteins and not with RNA or DNA as reported previously (4, 7). However, it should be emphasized that the experimental procedures used in the present report utilized direct binding studies, whereas previous reports (4, 7) used indirect biochemical measurements to conclude that granaticin interacted with RNA and DNA.

REFERENCES

(1) R. Corbaz, L. Ettlinger, E. Gaumann, J. Kalvoda, E. Keller-Schierlein, F. Kradolfer, B. K. Manukian, L. Neipp, V. Prelog, P. Reusser, and H. Zahner, *Helv. Chim. Acta*, **40,** 1262 (1957).

(2) R. H. Thomson, "Naturally Occurring Quinones," 2nd ed., Academic, New York, N.Y., 1971, pp. 298–302.

(3) C.-J. Chang, H. G. Floss, P. Soong, and C.-T. Chang, *J. Antibiot.*, **28,** 156 (1975).

(4) A. Ogilvie, K. Wiebauer, and W. Kersten, *Biochem. J.*, **152,** 511 (1975).

(5) *Ibid.*, **152,** 517 (1975).

(6) W. Kersten, "Progress in Molecular and Subcellular Biology," vol. 2, Springer-Verlag, New York, N.Y., 1971.

(7) M. L. Sethi, *J. Pharm. Sci.*, **66,** 130 (1977).

(8) P. Heinstein, *ibid.*, **71,** 197 (1982).

(9) R. W. Holley, J. Apgar, B. P. Doctor, J. Farrow, M. A. Marini, and S. H. Merrill, *J. Biol. Chem.*, **236,** 200 (1961).

(10) C. L. Richardson, A. D. Grant, S. L. Schpok, W. C. Krueger, and L. H. Li, *Cancer Res.*, **41,** 2235 (1981).

(11) C. L. Richardson, and G. E. Schulman, *Biochim. Biophys. Acta*, **652,** 55 (1981).

(12) H. U. Bermeyer, "Methods of Enzymatic Analysis," vol. 1, Academic, New York, N.Y., 1974, p. 509.

(13) J. L. Webb, "Enzymes and Metabolic Inhibitors," vol. 3, Academic, New York, N.Y., 1966.

(14) G. Gibson, M.S. thesis, Purdue University, West Lafayette, Ind., 1979.

(15) T. Fujinaga, K. Izutsu, and T. Nomura, *J. Electroanal. Chem.*, **29,** 203 (1971).

(16) L. Y. Kheifets, V. D. Bezuglyi, N. S. Dokunikhin, and V. N. Kolokolov, *J. Gen. Chem., USSR*, **37,** 280 (1967).

(17) H. W. Moore, *Science*, **197,** 527 (1977).

ACKNOWLEDGMENTS

Abstracted in part from a thesis submitted by G. Gibson-Clay to the Department of Medicinal Chemistry and Pharmacognosy, Purdue University, in partial fulfillment of the Master of Science degree requirements.

This research was supported by National Institutes of Health grants ES00929 and GM23249.

The authors thank Dr. H. G. Floss for the generous gift of granaticin and Dr. C. L. Richardson, Meloy Laboratories, Inc., Springfield, Va., for including granaticin in the fluorescence polarization assay developed by her.

Distribution Volume Related to Body Weight and Protein Binding

Keyphrases □ Volume of distribution—related to body weight and protein binding □ Pharmacokinetics—distribution volume related to body weight and protein binding

To the Editor:

The physiological approach to drug distribution volume proposed by Gillette (1) has proven very useful for characterizing the dual effects of body size and plasma and tissue binding on steady-state volume of distribution (V_{ss}). Gillette's equation has commonly appeared as:

$$V_{ss} = V_p + \frac{f_{up}}{f_{ut}} V_t \qquad \text{(Eq. 1)}$$

where V_p is plasma volume, V_t is remaining body volume or mass accessible to drug, and f_{up} and f_{ut} are the fractions of unbound drug in plasma and tissues, respectively, which are assumed to be concentration-independent parameters.

Related conceptual models have been proposed by Wagner (2), Øie and Tozer (3), and others (reviewed in Ref. 4) with the assumptions that unbound drug diffusion serves as the equilibrating mechanism throughout body spaces, linear conditions exist, and the drug is bound and/or partitions into various tissue spaces. Equation 1 has been particularly helpful in pharmacokinetics as it rationalizes the meaning and calculation of V_{ss} as an essential "model-independent" parameter (5) and provides a means for estimating tissue binding of drugs. In the latter regard, Gibaldi and McNamara (6) revised Eq. 1 to yield a relationship which allowed calculation of f_{ut} based on assumption of reasonable values of V_p and V_t:

$$f_{ut} = \frac{V_t f_{up}}{V_{ss} - V_p} \qquad \text{(Eq. 2)}$$

The purpose of this communication is to further consider Eq. 1 in terms of the practice of normalizing V_{ss} for body weight and for f_{up}.

The adjustment of V_{ss} for total body weight (TBW) has been proposed as a means of expressing drug distribution in terms of an apparent tissue–plasma distribution or partition coefficient (5, 7):

$$K_D = V_{ss}/\text{TBW} \qquad \text{(Eq. 3)}$$

While further division of V_{ss}/TBW by f_{up} appears logical, the usefulness of the resulting parameter has not been ascertained. For oral dose clearance data, the analogous computation of Dose/f_{up} × AUC yields the intrinsic clearance of unbound drug, a parameter indicative of the V_{max}/K_m ratio for a biotransformation process (8, 9). It would be helpful if V_{ss}/f_{up} had a similar, direct physiological interpretation.

Equation 1 can be rearranged to the following expression upon division by f_{up} and substitution of TBW − V_t for V_p:

$$\frac{V_{ss}}{f_{up}} = \frac{\text{TBW}\, f_{ut} + V_t(f_{up} - f_{ut})}{f_{up} f_{ut}} \qquad \text{(Eq. 4)}$$

Since V_p is small compared to TBW, the approximation can be made that $V_t \simeq$ TBW and Eq. 4 simplifies and rearranges to:

$$K_D^u = V_{ss}\,\text{TBW}^{-1} f_{up}^{-1} = f_{ub}^{-1} \qquad \text{(Eq. 5)}$$

Thus, the calculation of V_{ss}, normalized both for body weight[1] and plasma binding, should yield a reasonable value for the reciprocal of f_{ub}, an estimate of the unbound fraction of drug in the body. This "intrinsic volume" should help in examining factors such as the effects of disease states on plasma and tissue binding of drugs.

While f_{ut} has been viewed (6) as "the average fraction of unbound drug in the extravascular water space weighted for tissue mass" according to Eq. 2, it serves in Eq. 5 as "the average fraction of unbound drug in the body weighted for tissue mass." Neither parameter can be considered more correct without direct quantitation of tissue binding. However, Eq. 5 is proposed for use because of several advantages. It obviates the need to estimate V_p and V_t in different persons or animals as body water spaces. The assumption that drugs are localized only in body water spaces is thereby removed, but the influences of lipid partitioning, active transport, ion trapping caused by pH differences among tissues, and binding to body solids become implicitly included (3, 4). As experimental capabilities for estimating tissue drug binding *in vitro* (4, 10) improve, the value of f_{ub} should prove easier to measure and calculate per unit of total tissue mass than per unit of tissue water.

One major value of Eq 5 is that calculation of K_D^u directly from free drug concentrations in plasma has been rationalized as having intrinsic merit. Equation 1 is difficult to employ when plasma protein binding is nonlinear. For prednisolone (which exhibits marked concentration-dependent binding to transcortin and albumin in plasma) the model-independent calculation of V_{ss} from plasma clearance (Cl) and mean transit time ($\bar{t}$):

$$V_{ss} = Cl\bar{t}/\text{TBW} \qquad \text{(Eq. 6)}$$

yields dose and time-average values of V_{ss} which vary with dose (11). Similar calculations can be made using free drug concentrations (C_u) and area–moment analysis (12) to yield:

$$K_D^u = \frac{\text{dose} \int_0^\infty t C_u dt}{\left(\int_0^\infty C_u dt\right)^2 \text{TBW}} = f_{ub}^{-1} \qquad \text{(Eq. 7)}$$

This approach served as the basis for comparing prednisolone pharmacokinetics in humans and rabbits. As shown in Fig. 1, both species yielded K_D^u values (time and dose average) which centered about 2 liters/kg. Extending the interpretation using Eqs. 5 and 7, the average body binding of the corticosteroid would be ~50%.

A second demonstration of the use of Eqs. 2 and 5 for estimation of drug binding is shown in Table I. Oxaprozin

[1] While K_D^u has units of liters/kg, it can be altered to a dimensionless number more equivalent to f_{ub}^{-1} by converting body weight to volume. Weight is retained here for simplicity.

0022-3549/82/0400-0469$01.00/0

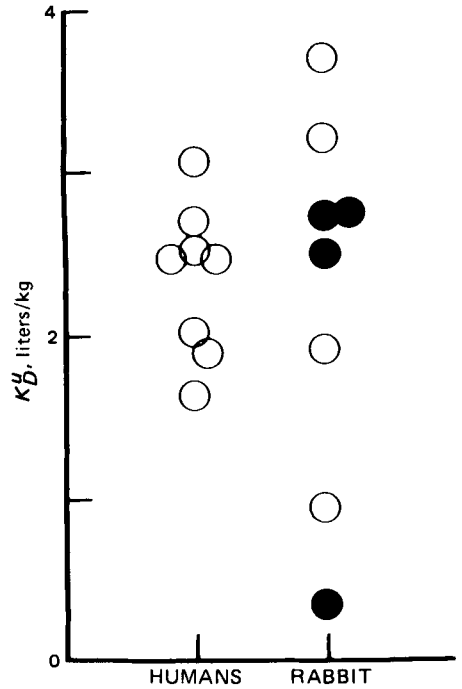

Figure 1—*Steady-state volume of distribution of unbound prednisolone calculated according to Eq. 7 for humans and rabbit.*

Table I—Protein Binding and Distribution Properties of Oxaprozin in Normal and Azotemic Subjects

Subjects	V_{ss}/TBW, liters/kg	f_{up}, %	K_D^u, liters/kg	f_{ut}, % Eq. 2[a]	f_{ub}, % Eq. 5
Normal	0.15 (0.01)	0.078 (0.003)	193 (11)	0.42 (0.03)	0.52 (0.03)
Renal impairment	0.18 (0.01)	0.177 (0.016)	103 (13)	0.79 (0.11)	1.03 (0.12)
Dialysis	0.21 (0.02)	0.283 (0.036)	79 (13)	1.05 (0.21)	1.43 (0.25)

[a] Assumes V_t = extravascular water space (554 ml/kg) and V_p = 46 ml/kg.

pharmacokinetics and binding were examined in subjects with normal and impaired renal function[2]. Direct plasma protein binding studies showed altered binding in plasma in the azotemic patients. The values of f_{ut} and f_{ub} were estimated by the two equations. The proposed equation did not obscure the apparent occurrence of impaired tissue binding in azotemic patients.

It is becoming common practice to calculate intrinsic clearance and the unbound volume of distribution directly from C_u *versus* time data. It is helpful to be able to interpret the resultant value in terms of overall drug binding. The necessary assumption that passive diffusion of unbound drug accounts for equilibration between tissues is retained. These arguments for simplified calculation of K_D^u, however, should not preclude the application of more specific tissue binding models when based on appropriate experimental data.

(1) J. R. Gillette, *Ann. N.Y. Acad. Sci.*, **179,** 43 (1971).
(2) J. G. Wagner, *Eur. J. Clin. Pharmacol.*, **10,** 425 (1976).
(3) S. Øie and T. N. Tozer, *J. Pharm. Sci.*, **68,** 1203 (1979).
(4) W. J. Jusko and M. Gretch, *Drug Metab. Rev.*, **5,** 43 (1976).
(5) W. J. Jusko, in "Applied Pharmacokinetics," W. E. Evans, J. J. Schentag, and W. J. Jusko, Eds., Applied Therapeutics, San Francisco, Calif., 1980, p. 649.
(6) M. Gibaldi and P. J. McNamara, *J. Pharm. Sci.*, **66,** 1211 (1977).
(7) J. Watanabe and A. Kozaki, *Chem. Pharm. Bull.*, **26,** 665 (1978).
(8) G. Levy and A. Yacobi, *J. Pharm. Sci.*, **63,** 805 (1974).
(9) D. G. Shand, R. H. Cotham, and G. R. Wilkinson, *Life Sci.*, **19,** 125 (1976).
(10) B. Fichtl and H. Kurz, *Eur. J. Clin. Pharmacol.*, **14,** 335 (1978).
(11) W. J. Jusko and J. Q. Rose, *Ther. Drug Monit.*, **2,** 169 (1980).
(12) M. L. Rocci and W. J. Jusko, *J. Pharm. Sci.*, **70,** 1201 (1981)

[2] Unpublished data.

William J. Jusko[x]
Department of Pharmaceutics
School of Pharmacy
State University of New York at Buffalo
Amherst, NY 14260

Soong T. Chiang
Department of Biostatistics
Wyeth Laboratories
Philadelphia, PA 19101

Received July 21, 1981.
Accepted for publication November 27, 1981.
Supported in part by Grant No. 24211 from the National Institute of General Medical Sciences, NIH.

Trace Decomposition of Choline

Keyphrases □ Choline—trace decomposition after exposure to high humidity or in unbuffered solutions □ Decomposition—trace, of choline after exposure to high humidity or in unbuffered solutions

To the Editor:

Decomposition of pharmaceuticals to the extent of parts per thousand, or less, usually is considered negligible. Such trace decomposition cannot be ignored where it affects the acceptability of drug products, *i.e.*, where it is manifested as insoluble matter in an injection, as discoloration, or by odor formation. The origin of a characteristic fishy odor in oxtriphylline (choline theophyllinate) exposed to high humidity for protracted periods or in unbuffered solutions led to the studies reported here. This odor, which is characteristic of many choline salts, can be attributed to trace decomposition; trace, because the presence of an odor has no measurable effect on physicochemical properties and decomposition, since quaternary ammonium salts are nonvolatile and would be expected to be odorless on that account.

A decomposition study of choline, measuring intact quaternary ammonium function, showed that it proceeded very slowly in solution at 100°. On heating choline has been reported (1) to yield 85–90% trimethylamine, 5% dimethylamine, 25% ethylene glycol, 4% acetaldehyde, and 10–15% acetylene on a molar basis with excess concentrated potassium hydroxide. The nature of the neutral reaction products would be expected to vary with reaction conditions, but it was assumed in this study that trimethylamine would constitute the bulk of the basic products. Because the amounts of trimethylamine formed were extremely low, a method was developed using microdiffusion to iso-

0022-3549/82/0400-0470$01.00/0

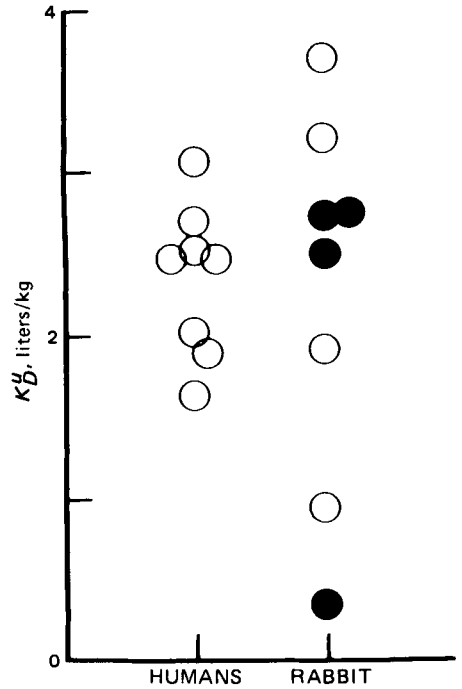

Figure 1—*Steady-state volume of distribution of unbound prednisolone calculated according to Eq. 7 for humans and rabbit.*

Table I—Protein Binding and Distribution Properties of Oxaprozin in Normal and Azotemic Subjects

Subjects	V_{ss}/TBW, liters/kg	f_{up}, %	K_D^u, liters/kg	f_{ut}, % Eq. 2[a]	f_{ub}, % Eq. 5
Normal	0.15 (0.01)	0.078 (0.003)	193 (11)	0.42 (0.03)	0.52 (0.03)
Renal impairment	0.18 (0.01)	0.177 (0.016)	103 (13)	0.79 (0.11)	1.03 (0.12)
Dialysis	0.21 (0.02)	0.283 (0.036)	79 (13)	1.05 (0.21)	1.43 (0.25)

[a] Assumes V_t = extravascular water space (554 ml/kg) and V_p = 46 ml/kg.

pharmacokinetics and binding were examined in subjects with normal and impaired renal function[2]. Direct plasma protein binding studies showed altered binding in plasma in the azotemic patients. The values of f_{ut} and f_{ub} were estimated by the two equations. The proposed equation did not obscure the apparent occurrence of impaired tissue binding in azotemic patients.

It is becoming common practice to calculate intrinsic clearance and the unbound volume of distribution directly from C_u *versus* time data. It is helpful to be able to interpret the resultant value in terms of overall drug binding. The necessary assumption that passive diffusion of unbound drug accounts for equilibration between tissues is retained. These arguments for simplified calculation of K_D^u, however, should not preclude the application of more specific tissue binding models when based on appropriate experimental data.

(1) J. R. Gillette, *Ann. N.Y. Acad. Sci.*, **179,** 43 (1971).
(2) J. G. Wagner, *Eur. J. Clin. Pharmacol.*, **10,** 425 (1976).
(3) S. Øie and T. N. Tozer, *J. Pharm. Sci.*, **68,** 1203 (1979).
(4) W. J. Jusko and M. Gretch, *Drug Metab. Rev.*, **5,** 43 (1976).
(5) W. J. Jusko, in "Applied Pharmacokinetics," W. E. Evans, J. J. Schentag, and W. J. Jusko, Eds., Applied Therapeutics, San Francisco, Calif., 1980, p. 649.
(6) M. Gibaldi and P. J. McNamara, *J. Pharm. Sci.*, **66,** 1211 (1977).
(7) J. Watanabe and A. Kozaki, *Chem. Pharm. Bull.*, **26,** 665 (1978).
(8) G. Levy and A. Yacobi, *J. Pharm. Sci.*, **63,** 805 (1974).
(9) D. G. Shand, R. H. Cotham, and G. R. Wilkinson, *Life Sci.*, **19,** 125 (1976).
(10) B. Fichtl and H. Kurz, *Eur. J. Clin. Pharmacol.*, **14,** 335 (1978).
(11) W. J. Jusko and J. Q. Rose, *Ther. Drug Monit.*, **2,** 169 (1980).
(12) M. L. Rocci and W. J. Jusko, *J. Pharm. Sci.*, **70,** 1201 (1981)

[2] Unpublished data.

William J. Jusko[x]
Department of Pharmaceutics
School of Pharmacy
State University of New York at Buffalo
Amherst, NY 14260

Soong T. Chiang
Department of Biostatistics
Wyeth Laboratories
Philadelphia, PA 19101

Received July 21, 1981.
Accepted for publication November 27, 1981.
Supported in part by Grant No. 24211 from the National Institute of General Medical Sciences, NIH.

Trace Decomposition of Choline

Keyphrases □ Choline—trace decomposition after exposure to high humidity or in unbuffered solutions □ Decomposition—trace, of choline after exposure to high humidity or in unbuffered solutions

To the Editor:

Decomposition of pharmaceuticals to the extent of parts per thousand, or less, usually is considered negligible. Such trace decomposition cannot be ignored where it affects the acceptability of drug products, *i.e.*, where it is manifested as insoluble matter in an injection, as discoloration, or by odor formation. The origin of a characteristic fishy odor in oxtriphylline (choline theophyllinate) exposed to high humidity for protracted periods or in unbuffered solutions led to the studies reported here. This odor, which is characteristic of many choline salts, can be attributed to trace decomposition; trace, because the presence of an odor has no measurable effect on physicochemical properties and decomposition, since quaternary ammonium salts are nonvolatile and would be expected to be odorless on that account.

A decomposition study of choline, measuring intact quaternary ammonium function, showed that it proceeded very slowly in solution at 100°. On heating choline has been reported (1) to yield 85–90% trimethylamine, 5% dimethylamine, 25% ethylene glycol, 4% acetaldehyde, and 10–15% acetylene on a molar basis with excess concentrated potassium hydroxide. The nature of the neutral reaction products would be expected to vary with reaction conditions, but it was assumed in this study that trimethylamine would constitute the bulk of the basic products. Because the amounts of trimethylamine formed were extremely low, a method was developed using microdiffusion to iso-

0022-3549/82/0400-0470$01.00/0

late the amine and gas chromatography with a nitrogen-specific detector to quantify it. Heating solutions of choline in 1 *N* sodium hydroxide at 60° for 14 days produced decomposition products in quantities of parts per million measured as trimethylamine. The rate and extent of decomposition appear to vary directly with the hydroxyl ion concentration of the medium.

Solutions of choline chloride, 2 mg/ml, were prepared in water with 0.01, 0.1, and 1.0 *N* sodium hydroxide. They were filled into 10-ml glass ampuls and sealed, then heated at steam bath temperature, ~100°, for 21 days. Intact choline was estimated by a modification of the Reinecke salt colorimetric method (2), the modification consisting of sparging the solutions with nitrogen gas to remove volatile amines. Three-milliliter portions of the ampule contents were acidified with sulfuric acid, 10 ml of 1% aqueous ammonium reineckate was added to each solution with stirring, and the mixtures were allowed to stand for 10 min. They were chilled in ice water and filtered through fine-frit sintered-glass crucibles. The precipitates were washed with ice water, then dissolved and made up to 10 ml with acetone. Absorbance of the solutions was determined in 1-cm cells at 523 nm, and the choline concentrations were calculated by reference to a standard curve constructed by carrying scalar amounts of choline chloride through the colorimetric procedure. The results support the hypothesis that degradation increases with increase in hydroxyl ion concentration; 96.0% of intact choline remained with water as the medium, 92.9% with 0.01 *N*, 89.8% with 0.1 *N*, and 80.4% in 1.0 *N* alkali.

Although drug decomposition at pH extremes generally is of little practical significance, it is important in this instance, for the pH of a saturated solution of oxtriphylline is >13. In a moist environment, oxtriphylline particles or granulation may be visualized as surrounded with a thin film of saturated solution. In support of this concept, it was found that adjustment of oxtriphylline granulations to a lower degree of alkalinity resulted in an odorless product. (Since the pKa of theophylline is ~8.8, a pH of 11 would afford all of the drug in the anionic form, yet the 100-fold reduction in hydroxyl ion concentration represented by the change from pH 13 to 11 minimizes the extent of decomposition.)

Solutions of choline chloride containing 50 mg/ml were prepared in water with 0.01, 0.1, and 1 *N* sodium hydroxide solutions. Aliquots of 2 ml were pipetted into the outer chamber of microdiffusion cells[1] and 2 ml of 1 *M* citric acid was pipetted into the inner chamber. The cells were sealed with a fine-ground flat glass plate using a minimum amount of stopcock grease and placed in an oven maintained at 60°. They were removed at intervals and allowed to cool to room temperature. A 1-ml portion of the citric acid solution from the inner chamber was pipetted into a 15-ml glass-stoppered centrifuge tube, then 3 ml of 30% chloroform in hexane and 5 ml of 1 *N* sodium hydroxide were added, the tube was stoppered and shaken for 5 min, and then centrifuged to obtain clear, immiscible phases. A 4-μl portion of the upper layer was injected into a gas chromatograph[2] fitted with a nitrogen-specific detector, using a 3.66-m × 2-mm i.d. glass column[3]. Temperatures were 110° for the column, 100° for the injection port, and 150° for the detector. Hydrogen pressure was 3 psi and attenuation × 8. The retention time for authentic trimethylamine was ~2 min and its detection limit ~5 ng on-column. Standard solutions of trimethylamine were prepared by serial dilutions of a 25% aqueous solution. Concentrations of 13.3–266 ng on-column, in 6 increments (3.3–66.5 μg/ml), provided a rectilinear plot of concentration *versus* peak area.

No time-dependent data were obtained for the solution in water or the lower alkali concentrations over a 24-day period; the amount of trimethylamine that diffused into the citric acid solution was ~6 μg (or 12 ng on-column), close to the limit of detection. Losses due to adsorption on glass surfaces or dissolution in the grease seal may be significant at this level. In 1 *N* NaOH, however, the trimethylamine determined was 43 μg after 2 days at 60° and 78 μg after 14 days, when the experiment was terminated. These data, with intermediate points obtained at 4, 7, and 10 days, gave a pseudo first-order rate constant of 7.14×10^{-5} day^{-1}. The amount of trimethylamine determined after 2 weeks at 60° represented <4 ppm of decomposed choline on a molar basis.

(1) A. T. Babyan, L. K. Gamburyan, and E. O. Chukhadzhyan, *Dokl. Akad. Nauk Arm. SSR*, **44**, 29 (1967); through *Chem. Abstr.*, **67**, 43196u (1967).

(2) F. J. Bandelin, *J. Am. Pharm. Assoc., Sci. Ed.*, **37**, 10 (1948).

Lester Chafetz[x]
Jose Philip
Product Development Laboratories
Warner-Lambert Pharmaceutical Research
Morris Plains, NJ 07950

Received October 13, 1981.
Accepted for publication December 16, 1981.

[1] Conway microdiffusion cells, D3318, SGA Scientific, Bloomfield, N.J.
[2] Perkin-Elmer model 900.
[3] 28% Pennwalt 223 and 4% potassium hydroxide on 80/100 mesh Gas Chrom R.

Changes in Plasma Protein Binding of Drugs after Blood Collection from Pregnant Rats

Keyphrases □ Protein binding—plasma, changes after blood collection from pregnant rats □ *In vitro–in vivo* correlation—plasma protein binding changes after blood collection from pregnant rats

To the Editor:

Determinations of drug–protein binding in plasma are associated with a number of potential methodological and technical difficulties. It is, therefore, desirable to confirm the suitability of *in vitro* protein binding measurement procedures by *in vivo* studies, if possible. The steady-state concentration of phenytoin in cerebrospinal fluid is essentially identical to the concentration of free (unbound) phenytoin in plasma so that the ratio of phenytoin concentration in cerebrospinal fluid to the total (free plus bound) concentration of phenytoin in plasma gives an *in vivo* estimate of the free fraction of phenytoin in plasma (1). We have recently used this method in rats to demon-

0022-3549/82/0400-0471$01.00/0

late the amine and gas chromatography with a nitrogen-specific detector to quantify it. Heating solutions of choline in 1 *N* sodium hydroxide at 60° for 14 days produced decomposition products in quantities of parts per million measured as trimethylamine. The rate and extent of decomposition appear to vary directly with the hydroxyl ion concentration of the medium.

Solutions of choline chloride, 2 mg/ml, were prepared in water with 0.01, 0.1, and 1.0 *N* sodium hydroxide. They were filled into 10-ml glass ampuls and sealed, then heated at steam bath temperature, ~100°, for 21 days. Intact choline was estimated by a modification of the Reinecke salt colorimetric method (2), the modification consisting of sparging the solutions with nitrogen gas to remove volatile amines. Three-milliliter portions of the ampule contents were acidified with sulfuric acid, 10 ml of 1% aqueous ammonium reineckate was added to each solution with stirring, and the mixtures were allowed to stand for 10 min. They were chilled in ice water and filtered through fine-frit sintered-glass crucibles. The precipitates were washed with ice water, then dissolved and made up to 10 ml with acetone. Absorbance of the solutions was determined in 1-cm cells at 523 nm, and the choline concentrations were calculated by reference to a standard curve constructed by carrying scalar amounts of choline chloride through the colorimetric procedure. The results support the hypothesis that degradation increases with increase in hydroxyl ion concentration; 96.0% of intact choline remained with water as the medium, 92.9% with 0.01 *N*, 89.8% with 0.1 *N*, and 80.4% in 1.0 *N* alkali.

Although drug decomposition at pH extremes generally is of little practical significance, it is important in this instance, for the pH of a saturated solution of oxtriphylline is >13. In a moist environment, oxtriphylline particles or granulation may be visualized as surrounded with a thin film of saturated solution. In support of this concept, it was found that adjustment of oxtriphylline granulations to a lower degree of alkalinity resulted in an odorless product. (Since the pKa of theophylline is ~8.8, a pH of 11 would afford all of the drug in the anionic form, yet the 100-fold reduction in hydroxyl ion concentration represented by the change from pH 13 to 11 minimizes the extent of decomposition.)

Solutions of choline chloride containing 50 mg/ml were prepared in water with 0.01, 0.1, and 1 *N* sodium hydroxide solutions. Aliquots of 2 ml were pipetted into the outer chamber of microdiffusion cells[1] and 2 ml of 1 *M* citric acid was pipetted into the inner chamber. The cells were sealed with a fine-ground flat glass plate using a minimum amount of stopcock grease and placed in an oven maintained at 60°. They were removed at intervals and allowed to cool to room temperature. A 1-ml portion of the citric acid solution from the inner chamber was pipetted into a 15-ml glass-stoppered centrifuge tube, then 3 ml of 30% chloroform in hexane and 5 ml of 1 *N* sodium hydroxide were added, the tube was stoppered and shaken for 5 min, and then centrifuged to obtain clear, immiscible phases. A 4-μl portion of the upper layer was injected into a gas chromatograph[2] fitted with a nitrogen-specific detector, using a 3.66-m × 2-mm i.d. glass column[3]. Temperatures were 110° for the column, 100° for the injection port, and 150° for the detector. Hydrogen pressure was 3 psi and attenuation × 8. The retention time for authentic trimethylamine was ~2 min and its detection limit ~5 ng on-column. Standard solutions of trimethylamine were prepared by serial dilutions of a 25% aqueous solution. Concentrations of 13.3–266 ng on-column, in 6 increments (3.3–66.5 μg/ml), provided a rectilinear plot of concentration *versus* peak area.

No time-dependent data were obtained for the solution in water or the lower alkali concentrations over a 24-day period; the amount of trimethylamine that diffused into the citric acid solution was ~6 μg (or 12 ng on-column), close to the limit of detection. Losses due to adsorption on glass surfaces or dissolution in the grease seal may be significant at this level. In 1 *N* NaOH, however, the trimethylamine determined was 43 μg after 2 days at 60° and 78 μg after 14 days, when the experiment was terminated. These data, with intermediate points obtained at 4, 7, and 10 days, gave a pseudo first-order rate constant of 7.14×10^{-5} day^{-1}. The amount of trimethylamine determined after 2 weeks at 60° represented <4 ppm of decomposed choline on a molar basis.

(1) A. T. Babyan, L. K. Gamburyan, and E. O. Chukhadzhyan, *Dokl. Akad. Nauk Arm. SSR*, **44**, 29 (1967); through *Chem. Abstr.*, **67**, 43196u (1967).

(2) F. J. Bandelin, *J. Am. Pharm. Assoc., Sci. Ed.*, **37**, 10 (1948).

Lester Chafetz[x]
Jose Philip
Product Development Laboratories
Warner-Lambert Pharmaceutical Research
Morris Plains, NJ 07950

Received October 13, 1981.
Accepted for publication December 16, 1981.

[1] Conway microdiffusion cells, D3318, SGA Scientific, Bloomfield, N.J.
[2] Perkin-Elmer model 900.
[3] 28% Pennwalt 223 and 4% potassium hydroxide on 80/100 mesh Gas Chrom R.

Changes in Plasma Protein Binding of Drugs after Blood Collection from Pregnant Rats

Keyphrases □ Protein binding—plasma, changes after blood collection from pregnant rats □ *In vitro–in vivo* correlation—plasma protein binding changes after blood collection from pregnant rats

To the Editor:

Determinations of drug–protein binding in plasma are associated with a number of potential methodological and technical difficulties. It is, therefore, desirable to confirm the suitability of *in vitro* protein binding measurement procedures by *in vivo* studies, if possible. The steady-state concentration of phenytoin in cerebrospinal fluid is essentially identical to the concentration of free (unbound) phenytoin in plasma so that the ratio of phenytoin concentration in cerebrospinal fluid to the total (free plus bound) concentration of phenytoin in plasma gives an *in vivo* estimate of the free fraction of phenytoin in plasma (1). We have recently used this method in rats to demon-

0022-3549/82/0400-0471$01.00/0

strate that the apparent decrease of phenytoin binding in plasma after heparin administration is an *in vitro* artifact (1) apparently due to increased nonesterified fatty acid concentrations caused by lipolysis in plasma after blood collection (2). On the other hand, there was excellent agreement between the *in vivo* free fraction of phenytoin in the serum of rats who received that drug alone or together with the competitive binding inhibitor salicylic acid, and the *in vitro* free fraction measurements by equilibrium dialysis (1).

More recent studies on pregnant rats yielded *in vivo* plasma free fraction estimates for phenytoin that were considerably lower than the free fraction values determined by *in vitro* equilibrium dialysis. Therefore, experiments were designed to assess these differences. Wistar-Lewis rats, 20 days pregnant and weighing ~320 g, received 14.7 mg/kg phenytoin through a jugular vein cannula by rapid injection followed immediately by an infusion of 195 μg/min/kg for 2 hr. The animals were then anesthetized with ether, and cerebrospinal fluid and 10 ml of blood from the aorta were obtained. The blood was collected in a plastic syringe containing 200 U of heparin. Plasma was separated immediately (10 min centrifugation at 1500×*g*). About 2 ml of plasma was placed in cellophane tubing which was mounted in stoppered plastic centrifuge tubes. They were centrifuged at 750×*g* for 30 min at about 37° in a controlled temperature centrifuge, whose head had been preheated to 37°, and about 0.1 ml ultrafiltrate (tested with trichloroacetic acid for absence of protein) was collected. The time interval between blood collection and the end of the ultrafiltration procedure was ~50 min. Another portion of plasma was placed in a closed glass vial which was rotated in a water-bath at 37° for 6 hr. That plasma was then subjected to ultrafiltration. A third portion of plasma was placed in a dialysis cell and dialyzed for 6 hr (sufficient to reach equilibrium in the case of plasma from normal animals) at 37° against an equal volume of pH 7.4 phosphate buffer (1). All samples were assayed for phenytoin by high-performance liquid chromatography (HPLC) as described previously (1).

Results obtained from studies on nine animals are summarized in Table I. The free fraction values determined by immediate ultrafiltration were similar (~32% higher, on the average) to the *in vivo* estimates. These *in vitro* and *in vivo* free fraction values were strongly correlated ($r = 0.79$, $p < 0.02$). On the other hand, the free fraction values obtained by ultrafiltration after 6 hr were ~133% higher than the *in vivo* estimates and the free fraction values obtained by dialysis were ~63% higher. Clearly, a pronounced decrease in protein binding of phenytoin occurred in plasma from the pregnant rats during 6 hr after blood collection. Additional ultrafiltration studies with plasma incubated at 37° for 4 and 9 hr, respectively, showed that the maximum change in binding had occurred by 4 hr. This change was not prevented by the addition of antibiotics (mixture of penicillin G, streptomycin, and polymyxin B) to the plasma.

Table I—Protein Binding of Phenytoin in Plasma from Pregnant Rats [a]

Total phenytoin in plasma, μg/ml	12.9 ± 2.1
Cerebrospinal fluid/plasma concentration ratio	0.200 ± 0.029
Free fraction by immediate ultrafiltration	0.263 ± 0.027
Free fraction by ultrafiltration after 6 hr at 37°	0.461 ± 0.044
Free fraction by dialysis for 6 hr at 37°	0.322 ± 0.028

[a] Mean ± *SD*, $n = 9$.

Table II—Protein Binding of Salicylate in Plasma from Pregnant and Nonpregnant Rats [a]

	Pregnant Rats	Nonpregnant Rats
Total salicylate in plasma, μg/ml	234 ± 18	295 ± 33
Free fraction by immediate ultrafiltration	0.560 ± 0.081	0.435 ± 0.036
Free fraction by ultrafiltration after 4 hr at 37°	0.763 ± 0.118	0.468 ± 0.037
Free fraction by dialysis for 4 hr at 37°	0.733 ± 0.165	0.385 ± 0.029
Ratio of free fractions by ultrafiltration[b], 4 hr/immediate	1.36 ± 0.09	1.08 ± 0.04
Ratio of free fractions[b], dialysis/immediate ultrafiltration	1.30 ± 0.17	0.886 ± 0.040

[a] Mean ± *SD*, $n = 5$ per group. [b] These ratios are reported because one of the pregnant rats had an unusually low free fraction value in all determinations, thereby causing a relatively large coefficient of variation of the mean free fraction values.

The results of these studies do not mean that *in vivo* drug–protein binding alterations do not occur during pregnancy. The phenytoin concentration ratio, cerebrospinal fluid/plasma, in the pregnant rats is significantly larger than that ratio in nonpregnant rats from the same group of animals studied concurrently[1].

Additional protein binding studies were carried out with salicylic acid, but cerebrospinal fluid–plasma concentration ratios were not obtained because salicylate in cerebrospinal fluid, unlike phenytoin, does not equilibrate with free salicylate in plasma due to the active transport of salicylate from cerebrospinal fluid to blood (1). Twenty-days pregnant Wistar-Lewis rats and nonpregnant female rats (200–250 g) received a rapid intravenous injection of sodium salicylate, 100 mg/kg, and blood was collected 30 min later. Plasma was ultrafiltered immediately and after 4 hr of incubation at 37°, and another portion of plasma was subjected to equilibrium dialysis at 37° for 4 hr as described previously. All assays were carried out by HPLC (1). The results of these studies are summarized in Table II. There were only very small differences between free fraction values obtained by ultrafiltration immediately and 4 hr after blood collection, and between the 4 hr ultrafiltration and equilibrium dialysis free fraction values, in nonpregnant rats. On the other hand, there were considerably larger differences between free fraction values obtained immediately by ultrafiltration as compared with values obtained 4 hr later by ultrafiltration or equilibrium dialysis in plasma from pregnant rats. Results obtained by ultrafiltration at 4 hr and by equilibrium dialysis were essentially identical. These observations also indicate that drug–protein binding in plasma from pregnant animals decreases *in vitro* with time and that the magnitude of such changes in plasma from nonpregnant animals is much smaller.

In summary, drug–protein binding in plasma obtained from pregnant rats can undergo rapid changes (decreases) *in vitro* after blood collection. Similar changes may occur in plasma of other species, including humans, and in plasma from animals with other pathophysiological conditions associated with alterations in drug–protein binding,

[1] Results to be published.

but the rates and magnitudes of these changes may be different. Careful attention will have to be given to the methodology of *in vitro* drug–protein binding determinations if artifactual results are to be avoided.

(1) R. C. Chou and G. Levy, *J. Pharmacol. Exp. Ther.*, in press.
(2) K. M. Giacomini, S. E. Swezey, J. C. Giacomini, and T. F. Blaschke, *Life Sci.*, **27**, 771 (1980).

Ruby C. Chou
Gerhard Levy[x]

Department of Pharmaceutics
School of Pharmacy
State University of New York at Buffalo
Amherst, NY 14260

Received August 7, 1981.
Accepted for publication November 20, 1981.
Supported in part by grant GM 20852 from the National Institutes of General Medical Sciences, National Institutes of Health.

The Loss of Nitroglycerin from Intravenous Administration Sets during Infusion: A Theoretical Treatment

Keyphrases □ Nitroglycerin—loss from intravenous administration sets during infusion □ Administration sets—loss of nitroglycerin during infusion

To the Editor:

In a recent report (1), a model was proposed to explain the loss of nitroglycerin from solution into a plastic bag. Under static conditions, the kinetics describing the loss of drug was biexponential and expressed as:

$$A = \beta e^{-k_3 t} + (A_0 - \beta)e^{-k_1 t} \quad \text{(Eq. 1)}$$

where A is the amount of drug in solution, k is the rate of drug absorption onto the surface of the plastic, k_3 is the diffusion of drug into the plastic, A_0 the initial amount of drug in solution, and β is a constant. With plastic bags, Eq. 1 showed an excellent fit to the experimental data.

During the infusion therapy, the above principles apply to large volume parenteral therapy. However, a dynamic situation exists in the infusion set due to the constant flow of solution through the plastic tubing. A model depicting the loss of nitroglycerin from solution when drug is diluted in a glass bottle (no absorption) and allowed to flow through the infusion set is shown in Scheme I.

In addition, because of the large amount of drug in the bottle, the tubing could become saturated. Thus, the amount of drug lost from solution is also dependent on the amount of drug present in the tubing. (It was assumed that the rate of absorption is not dependent on the amount remaining to be absorbed, $C_0 - C_T$, but on the amount present, C_T. The results appear to support this assumption.) The differential equations, therefore, describing the rate of change of C_0, C_I, C_S, and C_T are:

$$\frac{dC_T}{dt} = k_2 C_T \quad \text{(Eq. 2)}$$

$$\frac{dC_S}{dt} = k_1 C_I - k_{-1} C_S - k_2 C_T \quad \text{(Eq. 3)}$$

$$\frac{dC_I}{dt} = k_0 C_0 - k_1 C_I - k_3 C_I + k_{-1} C_S \quad \text{(Eq. 4)}$$

$$\frac{dC_0}{dt} = 0 \quad \text{(Eq. 5)}$$

To solve for this model, it must be assumed that the supply of drug in the bottle is infinite, and that the amount of drug and solution delivered through the infusion set is insignificant compared to what remains in the bottle. Solving for Eq. 2, then:

$$C_T = C_{T_0} e^{-k_2 t} \quad \text{(Eq. 6)}$$

where C_{T_0} is the saturation concentration in the tubing. To solve Eq. 3, one needs to consider the total mass balance of drug (D) in that:

$$D_0 = D_I + D_B + D_S + D_T \quad \text{(Eq. 7)}$$

where D_0 is the total amount of drug, D_I is the drug in the infusion set (which includes the amount delivered), D_B is the drug in the bottle, D_S is the drug on the surface of the set, and D_T is the amount of drug in the plastic. Since the assumption was made that the amount of drug in the bottle is in infinite supply, then $D_0 \approx D_B$. Since D is the concentration (C) × volume (V), Eq. 7 can be approximated to be:

$$C_I = -\frac{V_S}{V_T} C_S - \frac{V_T}{V_I} C_T \quad \text{(Eq. 8)}$$

Substituting Eqs. 8 and 6 into Eq. 3, and solving for C_S, one obtains the following solution for C_S:

$$C_S = Ae^{-at} - Ae^{-k_2 t} \quad \text{(Eq. 9)}$$

where

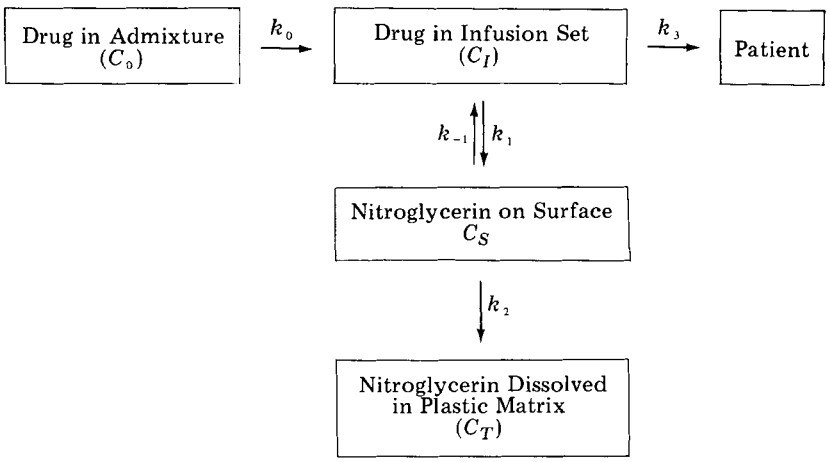

Scheme I

0022-3549/82/0400-0473$01.00/0

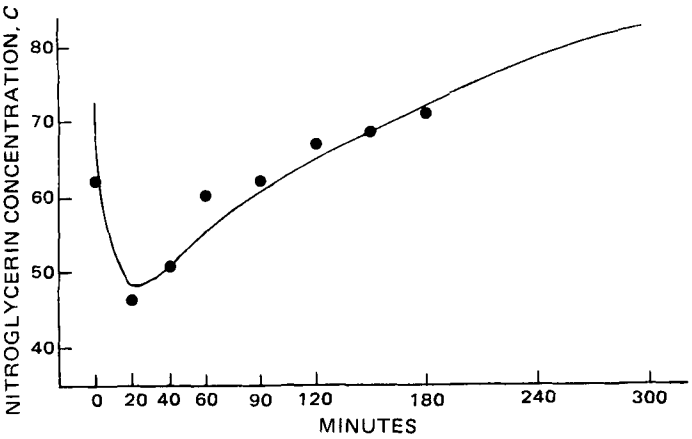

Figure 1—*Nitroglycerin loss: concentration in bottle = 100 μg/ml, flow rate = 1.0 ml/min. Equation describing loss:* $1 - (C/C_0) = 0.327e^{-0.0036t} - 0.270e^{-0.049t} + 1.08e^{-0.91t}$, *where ● is actual data and the smooth curve is computer-fitted data.*

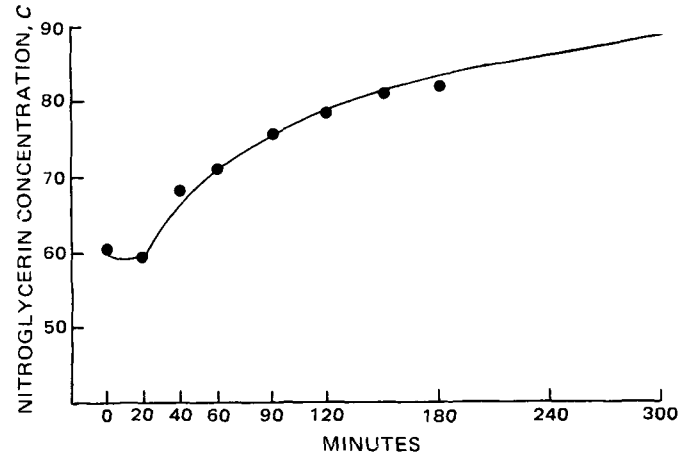

Figure 2—*Nitroglycerin loss: concentration in bottle = 100 μg/ml, flow rate = 0.5 ml/min. Equation describing loss:* $1 - (C/C_0) = 0.201e^{-0.068t} - 0.57e^{-0.004t} + 0.59e^{-0.118t}$, *where ● is actual data and smooth line is computer-fitted data.*

$$A = \frac{k_1 \frac{V_T}{V_I} C_{T_0} + k_2 C_{T_0}}{k_2 - k_{-1} - k_1 \frac{V_S}{V_I}} \qquad \text{(Eq. 10)}$$

and

$$a = k_1 \frac{V_S}{V_I} + k_{-1} \qquad \text{(Eq. 11)}$$

Finally, substituting Eq. 9 into Eq. 4 and solving for C_I:

$$C_I = \frac{k_0 C_0}{k_1 + k_3} - \left(\frac{k_0 C_0}{k_1 + k_3} - \alpha + \beta\right) e^{-(k_1 + k_3)t} + \alpha e^{-at} - \beta e^{-k_2 t} \qquad \text{(Eq. 12)}$$

where

$$\alpha = \frac{k_1 A}{a - k_1 - k_3} \qquad \text{(Eq. 13)}$$

and

$$\beta = \frac{k_1 A}{k_2 - k_1 - k_3} \qquad \text{(Eq. 14)}$$

To further simplify Eq. 12 at the initial phase, prior to adsorption of nitroglycerin, $k_1 = 0$, $k_3 = k_0$, and rearranging Eq. 12:

$$1 - \frac{C_I}{C_0} = \left(\frac{k_0}{k_1 + k_3} - \frac{\alpha + \beta}{C_0}\right) e^{-(k_1 + k_3)t} - \frac{\alpha}{C_0} e^{-at} + \frac{\beta}{C_0} e^{-k_2 t} \qquad \text{(Eq. 15)}$$

The results of the treatment of the infusion data using Eq. 15 is shown in Figs. 1 and 2, using different flow rate conditions. The data were listed using back projection (stripping) technique (2). As predicted by the model, a triexponential loss of nitroglycerin is seen. The model shows that the initial loss is due to adsorption and loss due to infusion, followed by equilibration on the inside surface of the infusion set and, consequently, the rate-limiting adsorption of nitroglycerin by the plastic. The model also shows that when no adsorption/absorption occurs, the concentration of drug delivered is the same as the concentration in the bottle.

All factors affecting nitroglycerin loss have been documented previously for static conditions (1). All these factors apply here, in addition to the loss also being dependent on the flow rate.

(1) A. W. Malick, A. H. Amann, D. M. Baaske, and R. G. Stoll, *J. Pharm. Sci.*, **70**, 798 (1981).

(2) J. G. Wagner, "Fundamentals of Clinical Pharmacokinetics," Drug Intelligence, Hamilton, Ill., 1975.

*Anton H. Amann** ˣ
David M. Baaske
American Critical Care
McGaw Park, IL 60085

Received October 13, 1981.
Accepted for publication November 27, 1981.
* Present address: K-V Pharmaceutical Company, St. Louis, MO 63144.

General Derivation of the Equation for Time to Reach a Certain Fraction of Steady State

Keyphrases □ Pharmacokinetics—derivation of the equation for time to reach a certain fraction of steady state □ Equations—for time to reach a certain fraction of steady state, derivation

To the Editor:

The time to reach a certain fraction of a given steady-state plasma concentration for a drug which exhibits multiexponential characteristics is not a simple function of the terminal disposition rate constant or half-life. Rather, it is a complex function of all coefficients and disposition rate constants in the equation describing the concentration–time curve. A given fraction of steady state is reached sooner with a drug that demonstrates multiexponential behavior than one that demonstrates monoexponential behavior. Recently, Chiou (1, 2) developed a general equation that permits the estimation of fraction of steady state from area ratios. The derivations were based on the superposition principle, or assume constant rate input of drug into the body. The following appears to be a more general approach for the derivation of the area equation.

0022-3549/82/0400-0474$01.00/0

but the rates and magnitudes of these changes may be different. Careful attention will have to be given to the methodology of *in vitro* drug–protein binding determinations if artifactual results are to be avoided.

(1) R. C. Chou and G. Levy, *J. Pharmacol. Exp. Ther.*, in press.
(2) K. M. Giacomini, S. E. Swezey, J. C. Giacomini, and T. F. Blaschke, *Life Sci.*, **27**, 771 (1980).

Ruby C. Chou
Gerhard Levy[x]

Department of Pharmaceutics
School of Pharmacy
State University of New York at Buffalo
Amherst, NY 14260

Received August 7, 1981.
Accepted for publication November 20, 1981.
Supported in part by grant GM 20852 from the National Institutes of General Medical Sciences, National Institutes of Health.

The Loss of Nitroglycerin from Intravenous Administration Sets during Infusion: A Theoretical Treatment

Keyphrases □ Nitroglycerin—loss from intravenous administration sets during infusion □ Administration sets—loss of nitroglycerin during infusion

To the Editor:

In a recent report (1), a model was proposed to explain the loss of nitroglycerin from solution into a plastic bag. Under static conditions, the kinetics describing the loss of drug was biexponential and expressed as:

$$A = \beta e^{-k_3 t} + (A_0 - \beta)e^{-k_1 t} \quad \text{(Eq. 1)}$$

where A is the amount of drug in solution, k is the rate of drug absorption onto the surface of the plastic, k_3 is the diffusion of drug into the plastic, A_0 the initial amount of drug in solution, and β is a constant. With plastic bags, Eq. 1 showed an excellent fit to the experimental data.

During the infusion therapy, the above principles apply to large volume parenteral therapy. However, a dynamic situation exists in the infusion set due to the constant flow of solution through the plastic tubing. A model depicting the loss of nitroglycerin from solution when drug is diluted in a glass bottle (no absorption) and allowed to flow through the infusion set is shown in Scheme I.

In addition, because of the large amount of drug in the bottle, the tubing could become saturated. Thus, the amount of drug lost from solution is also dependent on the amount of drug present in the tubing. (It was assumed that the rate of absorption is not dependent on the amount remaining to be absorbed, $C_0 - C_T$, but on the amount present, C_T. The results appear to support this assumption.) The differential equations, therefore, describing the rate of change of C_0, C_I, C_S, and C_T are:

$$\frac{dC_T}{dt} = k_2 C_T \quad \text{(Eq. 2)}$$

$$\frac{dC_S}{dt} = k_1 C_I - k_{-1} C_S - k_2 C_T \quad \text{(Eq. 3)}$$

$$\frac{dC_I}{dt} = k_0 C_0 - k_1 C_I - k_3 C_I + k_{-1} C_S \quad \text{(Eq. 4)}$$

$$\frac{dC_0}{dt} = 0 \quad \text{(Eq. 5)}$$

To solve for this model, it must be assumed that the supply of drug in the bottle is infinite, and that the amount of drug and solution delivered through the infusion set is insignificant compared to what remains in the bottle. Solving for Eq. 2, then:

$$C_T = C_{T_0} e^{-k_2 t} \quad \text{(Eq. 6)}$$

where C_{T_0} is the saturation concentration in the tubing. To solve Eq. 3, one needs to consider the total mass balance of drug (D) in that:

$$D_0 = D_I + D_B + D_S + D_T \quad \text{(Eq. 7)}$$

where D_0 is the total amount of drug, D_I is the drug in the infusion set (which includes the amount delivered), D_B is the drug in the bottle, D_S is the drug on the surface of the set, and D_T is the amount of drug in the plastic. Since the assumption was made that the amount of drug in the bottle is in infinite supply, then $D_0 \approx D_B$. Since D is the concentration (C) × volume (V), Eq. 7 can be approximated to be:

$$C_I = -\frac{V_S}{V_T} C_S - \frac{V_T}{V_I} C_T \quad \text{(Eq. 8)}$$

Substituting Eqs. 8 and 6 into Eq. 3, and solving for C_S, one obtains the following solution for C_S:

$$C_S = Ae^{-at} - Ae^{-k_2 t} \quad \text{(Eq. 9)}$$

where

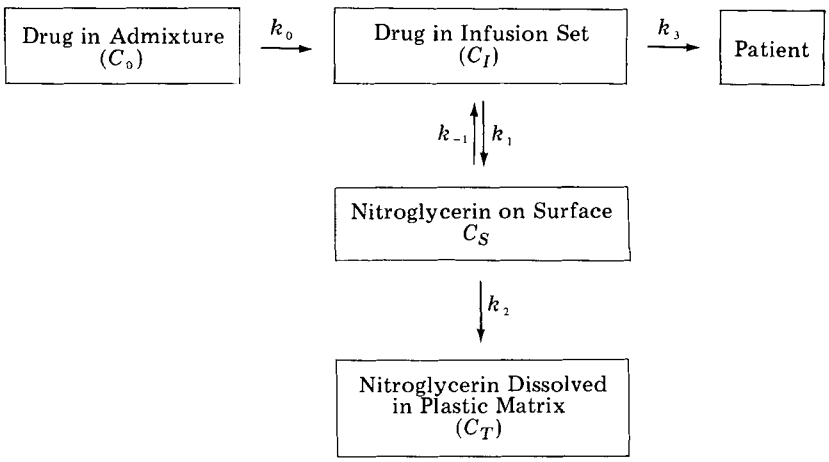

Scheme I

0022-3549/82/0400-0473$01.00/0

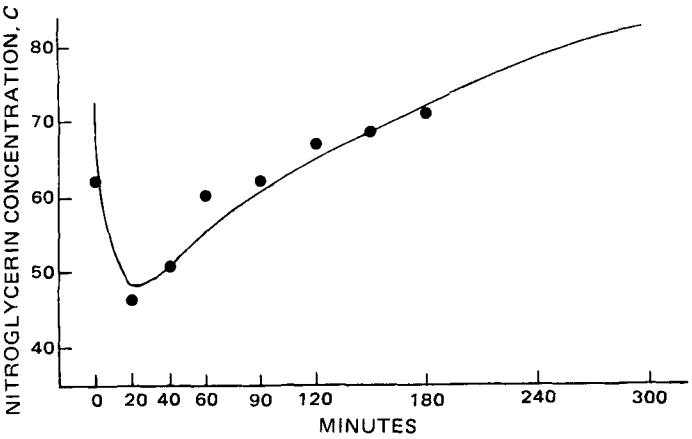

Figure 1—*Nitroglycerin loss: concentration in bottle = 100 μg/ml, flow rate = 1.0 ml/min. Equation describing loss:* $1 - (C/C_0) = 0.327e^{-0.0036t} - 0.270e^{-0.049t} + 1.08e^{-0.91t}$, *where ● is actual data and the smooth curve is computer-fitted data.*

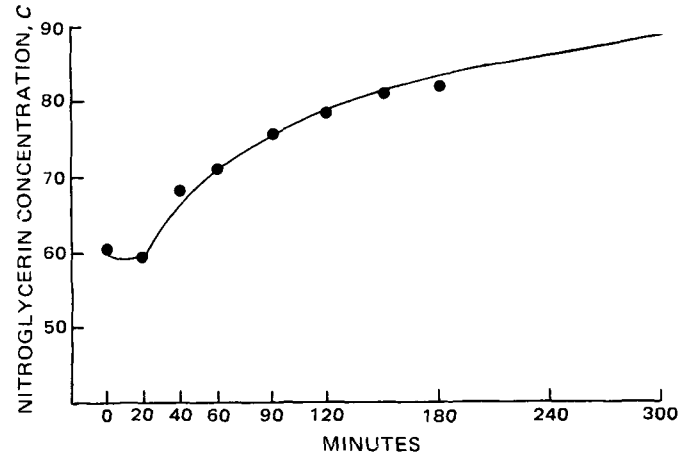

Figure 2—*Nitroglycerin loss: concentration in bottle = 100 μg/ml, flow rate = 0.5 ml/min. Equation describing loss:* $1 - (C/C_0) = 0.201e^{-0.068t} - 0.57e^{-0.004t} + 0.59e^{-0.118t}$, *where ● is actual data and smooth line is computer-fitted data.*

$$A = \frac{k_1 \frac{V_T}{V_I} C_{T_0} + k_2 C_{T_0}}{k_2 - k_{-1} - k_1 \frac{V_S}{V_I}} \qquad \text{(Eq. 10)}$$

and

$$a = k_1 \frac{V_S}{V_I} + k_{-1} \qquad \text{(Eq. 11)}$$

Finally, substituting Eq. 9 into Eq. 4 and solving for C_I:

$$C_I = \frac{k_0 C_0}{k_1 + k_3} - \left(\frac{k_0 C_0}{k_1 + k_3} - \alpha + \beta\right) e^{-(k_1 + k_3)t} + \alpha e^{-at} - \beta e^{-k_2 t} \qquad \text{(Eq. 12)}$$

where

$$\alpha = \frac{k_1 A}{a - k_1 - k_3} \qquad \text{(Eq. 13)}$$

and

$$\beta = \frac{k_1 A}{k_2 - k_1 - k_3} \qquad \text{(Eq. 14)}$$

To further simplify Eq. 12 at the initial phase, prior to adsorption of nitroglycerin, $k_1 = 0$, $k_3 = k_0$, and rearranging Eq. 12:

$$1 - \frac{C_I}{C_0} = \left(\frac{k_0}{k_1 + k_3} - \frac{\alpha + \beta}{C_0}\right) e^{-(k_1 + k_3)t} - \frac{\alpha}{C_0} e^{-at} + \frac{\beta}{C_0} e^{-k_2 t} \qquad \text{(Eq. 15)}$$

The results of the treatment of the infusion data using Eq. 15 is shown in Figs. 1 and 2, using different flow rate conditions. The data were listed using back projection (stripping) technique (2). As predicted by the model, a triexponential loss of nitroglycerin is seen. The model shows that the initial loss is due to adsorption and loss due to infusion, followed by equilibration on the inside surface of the infusion set and, consequently, the rate-limiting adsorption of nitroglycerin by the plastic. The model also shows that when no adsorption/absorption occurs, the concentration of drug delivered is the same as the concentration in the bottle.

All factors affecting nitroglycerin loss have been documented previously for static conditions (1). All these factors apply here, in addition to the loss also being dependent on the flow rate.

(1) A. W. Malick, A. H. Amann, D. M. Baaske, and R. G. Stoll, *J. Pharm. Sci.*, **70**, 798 (1981).

(2) J. G. Wagner, "Fundamentals of Clinical Pharmacokinetics," Drug Intelligence, Hamilton, Ill., 1975.

*Anton H. Amann** ˣ
David M. Baaske
American Critical Care
McGaw Park, IL 60085

Received October 13, 1981.
Accepted for publication November 27, 1981.
* Present address: K-V Pharmaceutical Company, St. Louis, MO 63144.

General Derivation of the Equation for Time to Reach a Certain Fraction of Steady State

Keyphrases □ Pharmacokinetics—derivation of the equation for time to reach a certain fraction of steady state □ Equations—for time to reach a certain fraction of steady state, derivation

To the Editor:

The time to reach a certain fraction of a given steady-state plasma concentration for a drug which exhibits multiexponential characteristics is not a simple function of the terminal disposition rate constant or half-life. Rather, it is a complex function of all coefficients and disposition rate constants in the equation describing the concentration–time curve. A given fraction of steady state is reached sooner with a drug that demonstrates multiexponential behavior than one that demonstrates monoexponential behavior. Recently, Chiou (1, 2) developed a general equation that permits the estimation of fraction of steady state from area ratios. The derivations were based on the superposition principle, or assume constant rate input of drug into the body. The following appears to be a more general approach for the derivation of the area equation.

0022-3549/82/0400-0474$01.00/0

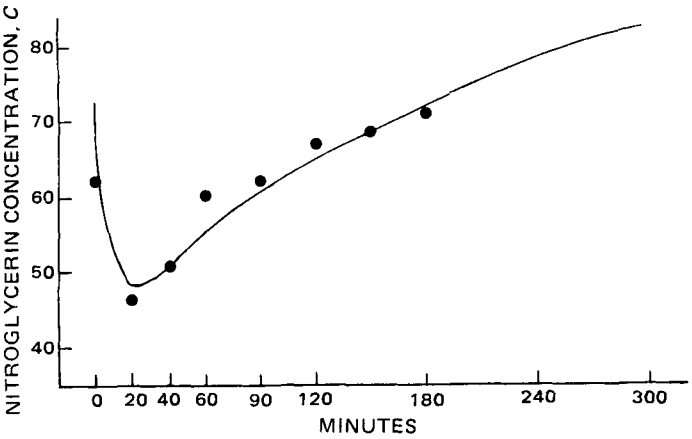

Figure 1—*Nitroglycerin loss: concentration in bottle = 100 μg/ml, flow rate = 1.0 ml/min. Equation describing loss:* $1 - (C/C_0) = 0.327e^{-0.0036t} - 0.270e^{-0.049t} + 1.08e^{-0.91t}$, *where ● is actual data and the smooth curve is computer-fitted data.*

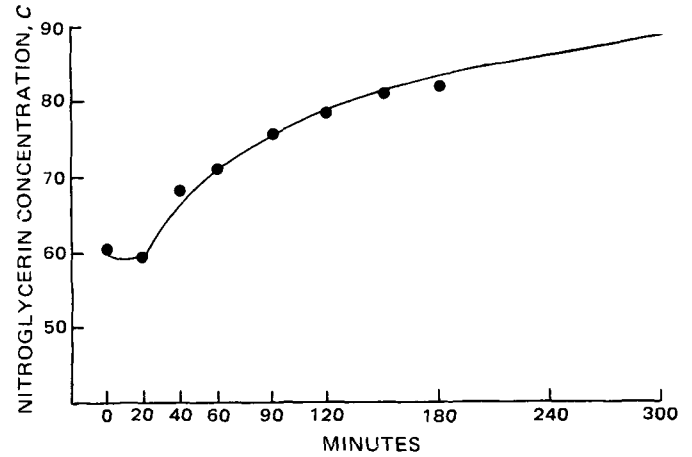

Figure 2—*Nitroglycerin loss: concentration in bottle = 100 μg/ml, flow rate = 0.5 ml/min. Equation describing loss:* $1 - (C/C_0) = 0.201e^{-0.068t} - 0.57e^{-0.004t} + 0.59e^{-0.118t}$, *where ● is actual data and smooth line is computer-fitted data.*

$$A = \frac{k_1 \frac{V_T}{V_I} C_{T_0} + k_2 C_{T_0}}{k_2 - k_{-1} - k_1 \frac{V_S}{V_I}} \qquad \text{(Eq. 10)}$$

and

$$a = k_1 \frac{V_S}{V_I} + k_{-1} \qquad \text{(Eq. 11)}$$

Finally, substituting Eq. 9 into Eq. 4 and solving for C_I:

$$C_I = \frac{k_0 C_0}{k_1 + k_3} - \left(\frac{k_0 C_0}{k_1 + k_3} - \alpha + \beta\right) e^{-(k_1 + k_3)t} + \alpha e^{-at} - \beta e^{-k_2 t} \qquad \text{(Eq. 12)}$$

where

$$\alpha = \frac{k_1 A}{a - k_1 - k_3} \qquad \text{(Eq. 13)}$$

and

$$\beta = \frac{k_1 A}{k_2 - k_1 - k_3} \qquad \text{(Eq. 14)}$$

To further simplify Eq. 12 at the initial phase, prior to adsorption of nitroglycerin, $k_1 = 0$, $k_3 = k_0$, and rearranging Eq. 12:

$$1 - \frac{C_I}{C_0} = \left(\frac{k_0}{k_1 + k_3} - \frac{\alpha + \beta}{C_0}\right) e^{-(k_1 + k_3)t} - \frac{\alpha}{C_0} e^{-at} + \frac{\beta}{C_0} e^{-k_2 t} \qquad \text{(Eq. 15)}$$

The results of the treatment of the infusion data using Eq. 15 is shown in Figs. 1 and 2, using different flow rate conditions. The data were listed using back projection (stripping) technique (2). As predicted by the model, a triexponential loss of nitroglycerin is seen. The model shows that the initial loss is due to adsorption and loss due to infusion, followed by equilibration on the inside surface of the infusion set and, consequently, the rate-limiting adsorption of nitroglycerin by the plastic. The model also shows that when no adsorption/absorption occurs, the concentration of drug delivered is the same as the concentration in the bottle.

All factors affecting nitroglycerin loss have been documented previously for static conditions (1). All these factors apply here, in addition to the loss also being dependent on the flow rate.

(1) A. W. Malick, A. H. Amann, D. M. Baaske, and R. G. Stoll, *J. Pharm. Sci.*, **70**, 798 (1981).

(2) J. G. Wagner, "Fundamentals of Clinical Pharmacokinetics," Drug Intelligence, Hamilton, Ill., 1975.

*Anton H. Amann** ˣ
David M. Baaske
American Critical Care
McGaw Park, IL 60085

Received October 13, 1981.
Accepted for publication November 27, 1981.
* Present address: K-V Pharmaceutical Company, St. Louis, MO 63144.

General Derivation of the Equation for Time to Reach a Certain Fraction of Steady State

Keyphrases □ Pharmacokinetics—derivation of the equation for time to reach a certain fraction of steady state □ Equations—for time to reach a certain fraction of steady state, derivation

To the Editor:

The time to reach a certain fraction of a given steady-state plasma concentration for a drug which exhibits multiexponential characteristics is not a simple function of the terminal disposition rate constant or half-life. Rather, it is a complex function of all coefficients and disposition rate constants in the equation describing the concentration–time curve. A given fraction of steady state is reached sooner with a drug that demonstrates multiexponential behavior than one that demonstrates monoexponential behavior. Recently, Chiou (1, 2) developed a general equation that permits the estimation of fraction of steady state from area ratios. The derivations were based on the superposition principle, or assume constant rate input of drug into the body. The following appears to be a more general approach for the derivation of the area equation.

0022-3549/82/0400-0474$01.00/0

The plasma concentration (C) *versus* time (t) curve for a drug obeying linear kinetics can be described by:

$$C = \sum_{l=1}^{n} A_l e^{-\lambda_l t} \quad \text{(Eq. 1)}$$

following a single dose, or by:

$$C_N = \sum_{l=1}^{n} A_l \left(\frac{1 - e^{-N\lambda_l \tau}}{1 - e^{-\lambda_l \tau}}\right) e^{-\lambda_l t} \quad \text{(Eq. 2)}$$

following the administration of multiple doses at a fixed time interval of τ. In Eq. 2, C_N is the plasma concentration during a dosing interval at any time following the Nth dose. Once steady state is achieved, the concentration (C_{ss}) is given by:

$$C_{ss} = \sum_{l=1}^{n} A_l \left(\frac{1}{1 - e^{-\lambda_l \tau}}\right) e^{-\lambda_l t} \quad \text{(Eq. 3)}$$

The fraction of the steady-state concentration (f_{ss}) can be defined as the ratio of the average plasma concentration during the Nth dosing interval ($\overline{C}_N$) to the average plasma concentration at steady state ($\overline{C}$), that is:

$$f_{ss} = \overline{C}_N / \overline{C} \quad \text{(Eq. 4)}$$

where

$$\overline{C}_N = AUC_N / \tau \quad \text{(Eq. 5)}$$

and

$$\overline{C} = AUC / \tau \quad \text{(Eq. 6)}$$

AUC_N and AUC are the areas under the plasma concentration–time curves during the Nth dosing interval and at steady state, *i.e.* $\int_0^\tau C_N\,dt$ and $\int_0^\tau C_{ss}\,dt$, respectively. Integrating Eqs. 2 and 3 from time zero to τ, substituting these values for AUC_N and AUC in Eqs. 5 and 6, and solving for f_{ss} in Eq. 4 using the resulting values for $\overline{C}_N$ and $\overline{C}$ yields:

$$f_{ss} = \frac{\sum_{l=1}^{n} A_l (1 - e^{-N\lambda_l \tau})/\lambda_l}{\sum_{l=1}^{n} A_l/\lambda_l} \quad \text{(Eq. 7)}$$

This relationship for f_{ss} can be expanded to give

$$f_{ss} = \frac{\sum_{l=1}^{n} A_l/\lambda_l - \sum_{l=1}^{n} A_l e^{-N\lambda_l \tau}/\lambda_l}{\sum_{l=1}^{n} A_l/\lambda_l} \quad \text{(Eq. 8)}$$

The total area under a plasma concentration *versus* time curve following a single dose of a drug equals $\Sigma_{l=1}^{n} A_l/\lambda_l$ (*i.e.*, the integral of Eq. 1), therefore,

$$f_{ss} = \frac{AUC - \sum_{l=1}^{n} A_l e^{-N\lambda_l \tau}/\lambda_l}{AUC} \quad \text{(Eq. 9)}$$

Furthermore, the integral of Eq. 1 from time t to ∞ provides an expression for the area under a plasma concentration *versus* time curve following a single dose from time t to ∞, AUC_t^∞:

$$AUC_t^\infty \sum_{l=1}^{n} A_l e^{-\lambda_l t}/\lambda_l \quad \text{(Eq. 10)}$$

Because $N\tau$ in Eq. 9 equals the time since the beginning of dosing, *i.e.*, t, AUC_t^∞ can be substituted for $\Sigma_{l=1}^{n} A_l e^{-N\lambda_l \tau}/\lambda_l$ in Eq. 9 to yield:

$$f_{ss} = \frac{AUC - AUC_t^\infty}{AUC} = \frac{AUC_0^t}{AUC} \quad \text{(Eq. 11)}$$

Therefore, the fraction of steady state reached at time t after initiation of a multiple dosing regimen can be determined by knowing the areas, AUC and AUC_t^∞ or AUC_0^t obtained from a single dose of the drug. No model has to be assumed to permit the use of Eq. 11 for determining f_{ss}.

(1) W. L. Chiou, *J. Pharm. Sci.*, **68**, 1546 (1979).
(2) W. L. Chiou, *J. Pharmacokinet. Biopharm.*, **8**, 311 (1980).

Donald Perrier[x]
College of Pharmacy
University of Arizona
Tucson, AZ 85721

Milo Gibaldi
School of Pharmacy
University of Washington
Seattle, WA 98195

Received August 13, 1981.
Accepted for publication November 23, 1981.

Hypotensive Activity of *Cecropia obtusifolia*

Keyphrases □ *Cecropia obtusifolia*—ethanol extract, hypotensive activity □ Hypotensive activity—effect of *Cecropia obtusifolia*, ethanol extract

To the Editor:

Cecropia obtusifolia Bertol is a medium-sized tree of the Moraceae family which grows wild in the tropical areas of Mexico. In the traditional medicine of tropical America, different species of *Cecropia* have been credited with a variety of therapeutic properties, such as antitussive, anti-inflammatory, and antidiarrhetic. Since the beneficial effects of extracts of *Cecropia* leaves in the treatment of heart failure were documented in a clinical study (1), it seemed of interest to determine the cardiovascular effects of *C. obtusifolia* in view of its widespread distribution in Mexico.

The material investigated[1] was collected in the area of the botanical station of Los Tuxtlas operated by the Institute of Biology of the University of Mexico and located in the Gulf coast state of Veracruz. Two kilograms of the leaves were ground and extracted with hexane in a Soxhlet apparatus. The residue was then treated with ethanol and the resulting extract dried by lyophilization. One portion of the 104-g extract was used for pharmacological studies; the other for further extraction [shown previously (2)]. The results of this work, which led to the isolation and identification of two compounds, will be reported elsewhere.

The cardiovascular activity of the extract was determined in male Wistar rats anesthetized with a 1.8 g/kg ip dose of urethane. Blood pressure and heart rate were recorded continuously, the former with a transducer connected to a cannulated femoral artery and the latter with a tachograph triggered by the pressure pulse. The extract was dissolved in propylene glycol and diluted with isotonic saline to a final concentration of 10 mg/ml, resulting in a

[1] The plant material used in this investigation was identified as *Cecropia obtusifolia* Bertol (Moraceae) by J. I. Calzada, Institute of Biology, National University of Mexico. A specimen (Number MEXU-237314) representing material collected for this investigation is available for inspection at the Herbarium of the Institute of Biology, National University of Mexico.

0022-3549/82/0400-0475$01.00/0

The plasma concentration (C) *versus* time (t) curve for a drug obeying linear kinetics can be described by:

$$C = \sum_{l=1}^{n} A_l e^{-\lambda_l t} \quad \text{(Eq. 1)}$$

following a single dose, or by:

$$C_N = \sum_{l=1}^{n} A_l \left(\frac{1 - e^{-N\lambda_l \tau}}{1 - e^{-\lambda_l \tau}}\right) e^{-\lambda_l t} \quad \text{(Eq. 2)}$$

following the administration of multiple doses at a fixed time interval of τ. In Eq. 2, C_N is the plasma concentration during a dosing interval at any time following the Nth dose. Once steady state is achieved, the concentration (C_{ss}) is given by:

$$C_{ss} = \sum_{l=1}^{n} A_l \left(\frac{1}{1 - e^{-\lambda_l \tau}}\right) e^{-\lambda_l t} \quad \text{(Eq. 3)}$$

The fraction of the steady-state concentration (f_{ss}) can be defined as the ratio of the average plasma concentration during the Nth dosing interval ($\overline{C}_N$) to the average plasma concentration at steady state ($\overline{C}$), that is:

$$f_{ss} = \overline{C}_N / \overline{C} \quad \text{(Eq. 4)}$$

where

$$\overline{C}_N = AUC_N / \tau \quad \text{(Eq. 5)}$$

and

$$\overline{C} = AUC / \tau \quad \text{(Eq. 6)}$$

AUC_N and AUC are the areas under the plasma concentration–time curves during the Nth dosing interval and at steady state, *i.e.* $\int_0^\tau C_N\,dt$ and $\int_0^\tau C_{ss}\,dt$, respectively. Integrating Eqs. 2 and 3 from time zero to τ, substituting these values for AUC_N and AUC in Eqs. 5 and 6, and solving for f_{ss} in Eq. 4 using the resulting values for $\overline{C}_N$ and $\overline{C}$ yields:

$$f_{ss} = \frac{\sum_{l=1}^{n} A_l (1 - e^{-N\lambda_l \tau})/\lambda_l}{\sum_{l=1}^{n} A_l/\lambda_l} \quad \text{(Eq. 7)}$$

This relationship for f_{ss} can be expanded to give

$$f_{ss} = \frac{\sum_{l=1}^{n} A_l/\lambda_l - \sum_{l=1}^{n} A_l e^{-N\lambda_l \tau}/\lambda_l}{\sum_{l=1}^{n} A_l/\lambda_l} \quad \text{(Eq. 8)}$$

The total area under a plasma concentration *versus* time curve following a single dose of a drug equals $\Sigma_{l=1}^{n} A_l/\lambda_l$ (*i.e.*, the integral of Eq. 1), therefore,

$$f_{ss} = \frac{AUC - \sum_{l=1}^{n} A_l e^{-N\lambda_l \tau}/\lambda_l}{AUC} \quad \text{(Eq. 9)}$$

Furthermore, the integral of Eq. 1 from time t to ∞ provides an expression for the area under a plasma concentration *versus* time curve following a single dose from time t to ∞, AUC_t^∞:

$$AUC_t^\infty \sum_{l=1}^{n} A_l e^{-\lambda_l t}/\lambda_l \quad \text{(Eq. 10)}$$

Because $N\tau$ in Eq. 9 equals the time since the beginning of dosing, *i.e.*, t, AUC_t^∞ can be substituted for $\Sigma_{l=1}^{n} A_l e^{-N\lambda_l \tau}/\lambda_l$ in Eq. 9 to yield:

$$f_{ss} = \frac{AUC - AUC_t^\infty}{AUC} = \frac{AUC_0^t}{AUC} \quad \text{(Eq. 11)}$$

Therefore, the fraction of steady state reached at time t after initiation of a multiple dosing regimen can be determined by knowing the areas, AUC and AUC_t^∞ or AUC_0^t obtained from a single dose of the drug. No model has to be assumed to permit the use of Eq. 11 for determining f_{ss}.

(1) W. L. Chiou, *J. Pharm. Sci.*, **68**, 1546 (1979).
(2) W. L. Chiou, *J. Pharmacokinet. Biopharm.*, **8**, 311 (1980).

Donald Perrier[x]
College of Pharmacy
University of Arizona
Tucson, AZ 85721

Milo Gibaldi
School of Pharmacy
University of Washington
Seattle, WA 98195

Received August 13, 1981.
Accepted for publication November 23, 1981.

Hypotensive Activity of *Cecropia obtusifolia*

Keyphrases □ *Cecropia obtusifolia*—ethanol extract, hypotensive activity □ Hypotensive activity—effect of *Cecropia obtusifolia*, ethanol extract

To the Editor:

Cecropia obtusifolia Bertol is a medium-sized tree of the Moraceae family which grows wild in the tropical areas of Mexico. In the traditional medicine of tropical America, different species of *Cecropia* have been credited with a variety of therapeutic properties, such as antitussive, anti-inflammatory, and antidiarrhetic. Since the beneficial effects of extracts of *Cecropia* leaves in the treatment of heart failure were documented in a clinical study (1), it seemed of interest to determine the cardiovascular effects of *C. obtusifolia* in view of its widespread distribution in Mexico.

The material investigated[1] was collected in the area of the botanical station of Los Tuxtlas operated by the Institute of Biology of the University of Mexico and located in the Gulf coast state of Veracruz. Two kilograms of the leaves were ground and extracted with hexane in a Soxhlet apparatus. The residue was then treated with ethanol and the resulting extract dried by lyophilization. One portion of the 104-g extract was used for pharmacological studies; the other for further extraction [shown previously (2)]. The results of this work, which led to the isolation and identification of two compounds, will be reported elsewhere.

The cardiovascular activity of the extract was determined in male Wistar rats anesthetized with a 1.8 g/kg ip dose of urethane. Blood pressure and heart rate were recorded continuously, the former with a transducer connected to a cannulated femoral artery and the latter with a tachograph triggered by the pressure pulse. The extract was dissolved in propylene glycol and diluted with isotonic saline to a final concentration of 10 mg/ml, resulting in a

[1] The plant material used in this investigation was identified as *Cecropia obtusifolia* Bertol (Moraceae) by J. I. Calzada, Institute of Biology, National University of Mexico. A specimen (Number MEXU-237314) representing material collected for this investigation is available for inspection at the Herbarium of the Institute of Biology, National University of Mexico.

0022-3549/82/0400-0475$01.00/0

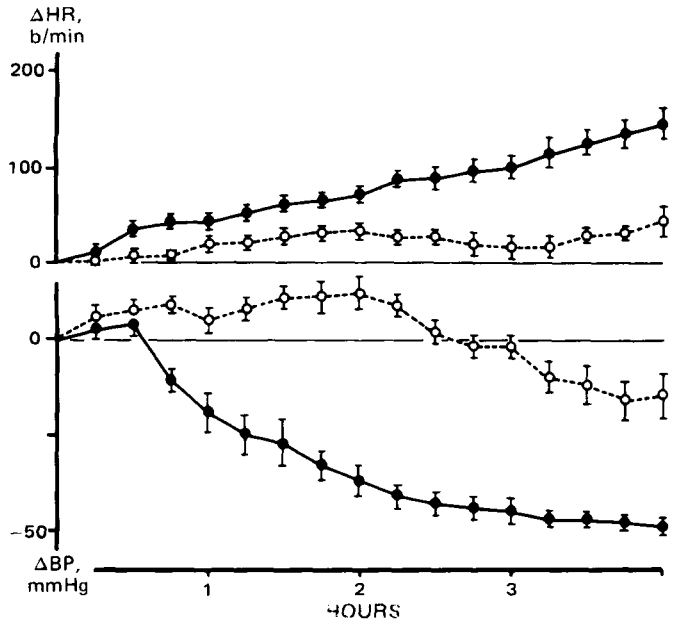

Figure 1—*Influence of a lyophilized ethanol extract of leaves of* Cecropia obtusifolia *on the blood pressure and heart rate of anesthetized rats. Also shown are the changes in these parameters observed in animals receiving the vehicle (15% propylene glycol). Circles correspond to means of six experiments; vertical lines denote standard errors. Key: (●—●) extract, 10 mg/kg; (○- - -○) vehicle.*

propylene glycol concentration of 15%. Groups of six rats received the extract at intravenous doses of 3.1, 10, or 31 mg/kg; an additional group received the vehicle.

The dose of 10 mg/kg produced a slowly developing fall in blood pressure, which began 45 min after injection and reached a maximum at ~3 hr (Fig. 1). This was accompanied by a progressive increase in heart rate. Rats receiving the vehicle showed a slight tachycardia and a decrease in blood pressure toward the end of the 4-hr observation period. The 31-mg/kg dose (not shown) produced a virtually identical hypotensive response and a smaller rise in heart rate; the 3.1-mg/kg dose (not shown) elicited changes similar to those seen in the vehicle-treated animals.

The blood pressure-lowering effect of relatively low doses of lyophilized ethanol extracts of *C. obtusifolia* leaves is interesting in view of its delayed onset and long duration. Such characteristics are theoretically desirable in an agent potentially useful in the treatment of arterial hypertension. Studies are continuing to confirm this effect in more suitable models of hypertension and to identify the active principle involved.

(1) A. Gilbert and P. Carnot, *Bull. Sci. Pharm.*, **11**, 200 (1905).
(2) F. Gstirner and H. Syring, *Arch. Pharm.*, **294**, 783 (1961).

H. Vidrio ˣ
F. García-Márquez
Department of Pharmacology
School of Medicine
J. Reyes
R. M. Soto
Department of Pharmaceutical Chemistry and Natural Products
School of Chemistry
National University of Mexico
Mexico, D. F. 04510

Received October 14, 1981.
Accepted for publication December 31, 1981.

Effect of Propylene Glycol on Subcutaneous Absorption of a Benzimidazole Hydrochloride

Keyphrases □ Propylene glycol—effect on subcutaneous absorption of a benzimidazole hydrochloride □ Absorption, subcutaneous—effect of propylene glycol on subcutaneous absorption of a benzimidazole hydrochloride □ Pharmacokinetics—effect of propylene glycol on subcutaneous absorption of a benzimidazole hydrochloride

To the Editor:

In the field of parenteral preparations, several water-miscible nonaqueous solvents are known to enhance either the stability or solubility of certain drugs. Reviews on the subject are available (1, 2). A third use of these nonaqueous solvents is to alter the absorption rate of the drug from the injection site. Absorption rates of several intramuscularly administered drugs were shown to decrease when the ethanol content of each preparation increased (3). This inhibitory effect was attributed to the combined effects of an increased viscosity of the vehicle and a decreased connective tissue permeability in the presence of ethanol (3). In systems involving propylene glycol, glycerin, or polyethylene glycol 400 as a cosolvent, the viscosity increased was found to be solely responsible for absorption rate reduction of intramuscularly administered isonicotinamide (4). A similar viscosity effect was revealed from a comparison of the duration of action of a prostaglandin administered subcutaneously to beagles in polyethylene glycol 400 and in water (5). However, these past studies investigated only nonionic drugs. Yet, many parenteral drugs are soluble salts of weak acids or weak bases. Very little is known about how the water-miscible nonaqueous solvents might affect the absorption rate of a drug delivered in a salt form. This communication reports the effect of propylene glycol on the subcutaneous absorption of a benzimidazole hydrochloride, 5(6)-isobutylsulfinyl-2-carbomethoxyaminobenzimidazole hydrochloride (I).

An aqueous solution and a propylene glycol–water (1:1) solution of 2-^{14}C-I (1.01 μCi/mg) were made with distilled water and propylene glycol, USP, at 100 mg/ml equivalent to the free base of I. The propylene glycol solutions of 2-^{14}C-I were made at 50 and 75 mg/ml. These solutions were administered subcutaneously to six heifers at 5 mg/kg free base equivalent. The two propylene glycol solutions, 50 and 75 mg/ml, were administered to groups 1 and 2, three heifers in each group, respectively. On the eighth day postinjection, the same groups 1 and 2 were administered the propylene glycol–water solution and the aqueous solution, respectively. In all cases, blood was drawn periodically into heparinized tubes following each administration. Plasma was obtained immediately after collection and frozen until analyzed. Total radioactivity in the plasma was determined by liquid scintillation counting[1]. The results are reported as free base equivalents (Fig. 1). Each point represents a mean plasma concentration of three animals. Vertical bars represent the standard error of each mean.

Figure 1 exhibits an apparent trend of relative absorption rate in the decreasing order for the four injections tested: 75 mg/ml propylene glycol solution >50 mg/ml

[1] LS 8100, Beckman Instruments, Inc.

0022-3549/82/0400-0476$01.00/0

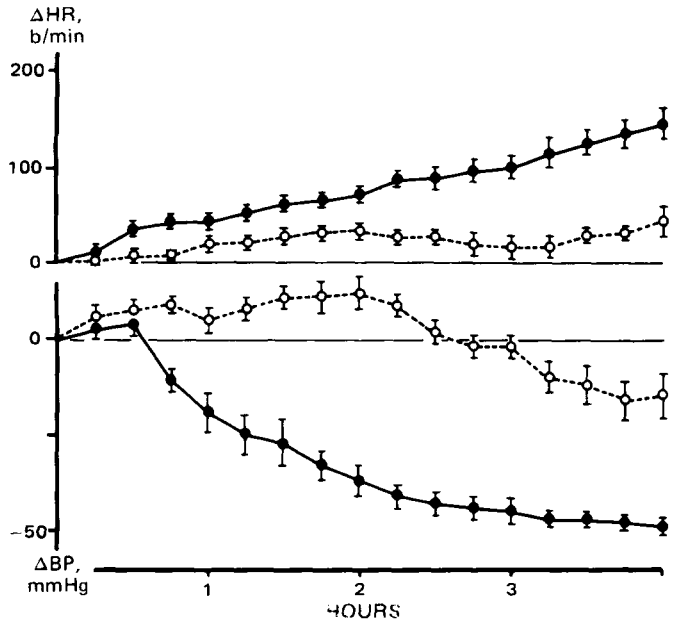

Figure 1—*Influence of a lyophilized ethanol extract of leaves of* Cecropia obtusifolia *on the blood pressure and heart rate of anesthetized rats. Also shown are the changes in these parameters observed in animals receiving the vehicle (15% propylene glycol). Circles correspond to means of six experiments; vertical lines denote standard errors. Key: (●—●) extract, 10 mg/kg; (○- - -○) vehicle.*

propylene glycol concentration of 15%. Groups of six rats received the extract at intravenous doses of 3.1, 10, or 31 mg/kg; an additional group received the vehicle.

The dose of 10 mg/kg produced a slowly developing fall in blood pressure, which began 45 min after injection and reached a maximum at ~3 hr (Fig. 1). This was accompanied by a progressive increase in heart rate. Rats receiving the vehicle showed a slight tachycardia and a decrease in blood pressure toward the end of the 4-hr observation period. The 31-mg/kg dose (not shown) produced a virtually identical hypotensive response and a smaller rise in heart rate; the 3.1-mg/kg dose (not shown) elicited changes similar to those seen in the vehicle-treated animals.

The blood pressure-lowering effect of relatively low doses of lyophilized ethanol extracts of *C. obtusifolia* leaves is interesting in view of its delayed onset and long duration. Such characteristics are theoretically desirable in an agent potentially useful in the treatment of arterial hypertension. Studies are continuing to confirm this effect in more suitable models of hypertension and to identify the active principle involved.

(1) A. Gilbert and P. Carnot, *Bull. Sci. Pharm.*, **11**, 200 (1905).
(2) F. Gstirner and H. Syring, *Arch. Pharm.*, **294**, 783 (1961).

H. Vidrio ˣ
F. García-Márquez
Department of Pharmacology
School of Medicine
J. Reyes
R. M. Soto
Department of Pharmaceutical Chemistry and Natural Products
School of Chemistry
National University of Mexico
Mexico, D. F. 04510

Received October 14, 1981.
Accepted for publication December 31, 1981.

Effect of Propylene Glycol on Subcutaneous Absorption of a Benzimidazole Hydrochloride

Keyphrases □ Propylene glycol—effect on subcutaneous absorption of a benzimidazole hydrochloride □ Absorption, subcutaneous—effect of propylene glycol on subcutaneous absorption of a benzimidazole hydrochloride □ Pharmacokinetics—effect of propylene glycol on subcutaneous absorption of a benzimidazole hydrochloride

To the Editor:

In the field of parenteral preparations, several water-miscible nonaqueous solvents are known to enhance either the stability or solubility of certain drugs. Reviews on the subject are available (1, 2). A third use of these nonaqueous solvents is to alter the absorption rate of the drug from the injection site. Absorption rates of several intramuscularly administered drugs were shown to decrease when the ethanol content of each preparation increased (3). This inhibitory effect was attributed to the combined effects of an increased viscosity of the vehicle and a decreased connective tissue permeability in the presence of ethanol (3). In systems involving propylene glycol, glycerin, or polyethylene glycol 400 as a cosolvent, the viscosity increased was found to be solely responsible for absorption rate reduction of intramuscularly administered isonicotinamide (4). A similar viscosity effect was revealed from a comparison of the duration of action of a prostaglandin administered subcutaneously to beagles in polyethylene glycol 400 and in water (5). However, these past studies investigated only nonionic drugs. Yet, many parenteral drugs are soluble salts of weak acids or weak bases. Very little is known about how the water-miscible nonaqueous solvents might affect the absorption rate of a drug delivered in a salt form. This communication reports the effect of propylene glycol on the subcutaneous absorption of a benzimidazole hydrochloride, 5(6)-isobutylsulfinyl-2-carbomethoxyaminobenzimidazole hydrochloride (I).

An aqueous solution and a propylene glycol–water (1:1) solution of 2-^{14}C-I (1.01 μCi/mg) were made with distilled water and propylene glycol, USP, at 100 mg/ml equivalent to the free base of I. The propylene glycol solutions of 2-^{14}C-I were made at 50 and 75 mg/ml. These solutions were administered subcutaneously to six heifers at 5 mg/kg free base equivalent. The two propylene glycol solutions, 50 and 75 mg/ml, were administered to groups 1 and 2, three heifers in each group, respectively. On the eighth day postinjection, the same groups 1 and 2 were administered the propylene glycol–water solution and the aqueous solution, respectively. In all cases, blood was drawn periodically into heparinized tubes following each administration. Plasma was obtained immediately after collection and frozen until analyzed. Total radioactivity in the plasma was determined by liquid scintillation counting[1]. The results are reported as free base equivalents (Fig. 1). Each point represents a mean plasma concentration of three animals. Vertical bars represent the standard error of each mean.

Figure 1 exhibits an apparent trend of relative absorption rate in the decreasing order for the four injections tested: 75 mg/ml propylene glycol solution >50 mg/ml

[1] LS 8100, Beckman Instruments, Inc.

0022-3549/82/0400-0476$01.00/0

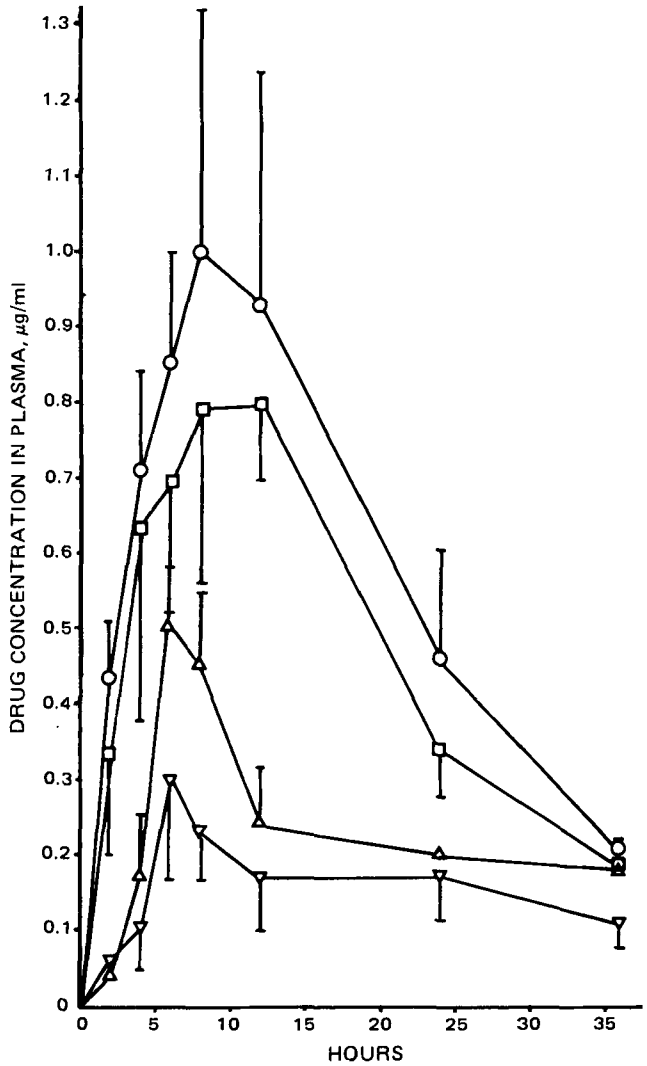

Figure 1—*Plasma concentration of I in heifers. Key: ○, 75 mg/ml propylene glycol solution; □, 50 mg/ml propylene glycol solution; △, 100 mg/ml propylene glycol–water (1:1) solution; and ▽, 100 mg/ml aqueous solution.*

propylene glycol solution >100 mg/ml propylene glycol–water (1:1) solution >100 mg/ml aqueous solution. The absorption rate difference between the two propylene glycol solutions revealed that concentration and/or injection volume had some effect on the subcutaneous absorption of I. Since the dose was kept constant, the injection volume varied inversely with the concentration. For a given increase in the injection volume, there exists a disproportionate ratio between increase in surface area and the increased volume. Therefore, from the passive diffusion standpoint, the smaller the injection volume, the faster the absorption. Atropine (6), sodium ion (7), sugars (8), testosterone (9), and aminoglycosides (10) were all found to be absorbed more rapidly when the compounds were administered in smaller injection volumes. This injection volume effect has been reviewed previously in review articles on intramuscular and subcutaneous injections (11, 12). The injection volume effect appears to be responsible for the rate difference between the absorption of I from the two propylene glycol solutions. However, the effect is ambiguous when the dose volume is relatively small. It was reported (4, 13, 14) that the intramuscular

Table I—Pharmacokinetic and Physicochemical Parameters of the Solutions Investigated

Solutions[a]	C_{max}, μg/ml	AUC, μg/ml hr	1/Viscosity,[b] cp^{-1}	Solubilities, mg/ml I	Solubilities, mg/ml Free Base
A	1.03 ± 0.30	21.29 ± 5.71	0.04	89.9	21.7
B	0.89 ± 0.19	17.10 ± 3.25	0.04	89.9	21.7
C	0.50 ± 0.14	8.60 ± 2.34	0.25	130.0	4.17
D	0.30 ± 0.08	5.61 ± 2.15	1.45	v. soluble	0.44

[a] A = 75 mg/ml propylene glycol solution of I; B = 50 mg/ml propylene glycol solution of I; C = 100 mg/ml propylene glycol-water (1:1) solution of I; D = 100 mg/ml aqueous solution of I. [b] From ref. 4.

absorption of isonicotinamide was independent of the injection volume which ranged from 5 to 20 μl. It was postulated that the effective absorption area might not vary in the case of small injection volume ranging from 5 to 20 μl. In yet another case, a reversed relationship between the injection volume and the absorption rate of I was observed in rabbits that were injected subcutaneously 0.5, 1.0, and 2.0 ml of a propylene glycol solution of I (15). The authors attributed this deviation from the result predicted by diffusion controlled absorption to the precipitation of I at the interface of the injected solution and surrounding tissue.

From the plasma concentration curves shown in Fig. 1, the following can be observed: the drug is absorbed faster from the propylene glycol solution than from the aqueous solution, the absorption rate of I from the propylene glycol–water solution is intermediate between those from the propylene glycol and the aqueous solution. These results at first may seem paradoxical to the previous finding (4) that propylene glycol, *via* its contribution to vehicle viscosity, inhibits intramuscular absorption. One could speculate that factors affecting intramuscular absorption might not be applicable to subcutaneous absorption. Nevertheless, the viscosity effect on subcutaneous absorption was shown to be operative for polyethylene glycol 400 solution of a prostaglandin (5). The paradox might be explained by the following analysis. Table I summarizes the maximum plasma concentration (C_{max}) and the area under the concentration–time curve (AUC) for the curves shown in Fig. 1. Also listed are solubilities of I and its free base in the respective vehicles. From Table I it appears that both C_{max} and AUC can be correlated to the free base solubility. Because the pKa and the aqueous solubility of I are low (3.4 and 0.44 mg/ml, respectively), it is likely that I is converted to its free base and precipitated to some degree at the injection site due to the infiltration of tissue fluid that has a pH of 6.0 (12). Consequently, the higher the free base solubility in the vehicle, the more available the drug for absorption. In the case of propylene glycol injection, the ionized drug concentration will decrease due to neutralization; however, the free base species would be maintained because of the relatively high solubility of the free base in propylene glycol. In the case of the aqueous injection, both the salt species and the free base species would decrease because of neutralization and precipitation. The change in drug solubility is apparently the predominant factor governing the absorption rate of I in the present study. Therefore, absorption of I by subcutaneous injection is enhanced, rather than inhibited, by propylene glycol.

(1) A. J. Spiegel and M. M. Noseworthy, *J. Pharm. Sci.*, **52,** 917 (1963).
(2) K. S. Lin, J. Anschel, and C. J. Swartz, *Bull. Parenter. Drug Assoc.*, **25,** 40 (1971).
(3) H. Kobayashi, Y. Miyoshi, K. Kitamura, Y. Yoshizaki, S. Muranishi, and H. Sezaki, *Chem. Pharm. Bull.*, **25,** 2862 (1977).
(4) K. Kakemi, H. Sezaki, K. Okumura, H. Kobayashi, and S. Furusawa, *ibid.*, **20,** 443 (1972).
(5) B. H. Vickery, G. I. McRae, J. S. Kent, and R. V. Tomlinson, *Prostaglandins Med.*, **5,** 93 (1980).
(6) H. Schiriftman and A. A. Kondritzer, *Am. J. Physiol.*, **191,** 591 (1957).
(7) G. F. Warner, E. L. Dobson, N. Pace, M. E. Johnston, and C. R. Finney, *Circulation*, **8,** 732 (1953).
(8) R. B. Sund and J. Schen, *Acta Pharmacol. Toxicol.*, **21,** 313 (1964).
(9) T. Tanaka, H. Kobayashi, K. Okumura, S. Muranishi, and H. Sezaki, *Chem. Pharm. Bull.*, **22,** 1275 (1974).
(10) M. Pfeffer and D. R. Van Harken, *J. Pharm. Sci.*, **70,** 449 (1981).
(11) B. E. Ballard, *ibid.*, **57,** 357 (1968).
(12) F. L. S. Tse and P. G. Welling, *J. Parenter. Drug Assoc.*, **34,** 409 (1980).
(13) K. Kakemi, H. Sezaki, K. Okumura, C. Takada, and S. Furusawa, *Chem. Pharm. Bull.*, **19,** 2058 (1971).
(14) K. Kakemi, H. Sezaki, K. Okumura, and S. Ashida, *ibid.*, **17,** 1332 (1969).
(15) J. S. Kent, R. V. Tomlinson, C. M. Ackley, and J. Hsu, *Drug Dev. Ind. Pharm.*, **7,** 261 (1981).

Cheng-Der Yu [x]
John S. Kent
Institute of Pharmaceutical Sciences
Syntex Research
Palo Alto, CA 94304

Received December 3, 1981.
Accepted for Publication December 30, 1981.
The authors thank Vickie L. Cain for her technical assistance and Dr. B. Poulsen for his support and helpful comments.

BOOKS

REVIEWS

Antitumor Agents Based on Natural Product Models. Edited by JOHN M. CASSADY and JOHN D. DOUROS. Academic, 111 Fifth Ave., New York, NY 10003. 1980. 500 pp. 15 × 23 cm.

This text is volume 16 of *Medicinal Chemistry, A Series of Monographs*. The emphasis of the book is on lead or novel antineoplastic agents, structure–activity relationships, modes of action, and toxicology of natural products. The choice of agents which is discussed in the monograph is rational and appropriate for the scope of the text. The book serves the purpose of assimilating diverse topics on natural product antineoplastic agents of clinical importance. In general, the text is well-written, concise and well-referenced, and includes pertinent structures, synthetic schemes, and biological data. The text is written with emphasis on the current development or status of a given group of agents and states scientific areas where further development is required.

The book is divided in the following contributions by individual authors:

Chapter 1, "The Development of New Antitumor Anthracyclines" (F. Arcamone), details the basic chemical modifications at the C-9, C-13, and C-14 of the amino sugar residue and of the chromophore of anthraquinone comparing the antitumor activity against HeLa cell, L-1210, P-388, and gross leukemia growth.

Chapter 2, "Trichothecanes" (T. W. Doyle and W. T. Bradner), discusses the history, mechanism of action, toxicity, metabolism, bioassay, cytotoxicity, and structure–activity relationships for antitumor activity in the P-388, L-1210, and B-16 tumor models.

Chapter 3, "Nucleosides" (M. Ohno), summarizes the structure–activity relationships of C- and N-pyrimidine nucleosides required to block the growth of tumors, bacteria, and viruses as evaluated by several investigators.

Chapter 4, "Mitomycins" (W. A. Remers), relates the history, chemical properties, mode of action, and structure–activity relationships for antibacterial and antitumor activity in the L-1210 and P-388 tumors, and the newly synthetic analogues of mitomycin.

Chapter 5, "Recent Progress in Bleomycin Studies" (H. Umezawa), deals with the chemistry and biosynthesis of bleomycin and phleomycin, including a revised structure of bleomycin, copper and iron complexes of bleomycin, the mechanism of action against squamous cell carcinomas, and other therapeutic uses of the agents.

Chapter 6, "Streptozocin" (P. F. Wiley), reviews the fermentation and isolation processes of streptozocin from bacterial cultures, its pharmacology, toxicology, carcinogenicity, mutagenicity, antibacterial, and antineoplastic modes of action, chemical studies, and the structure–activity relationships of several analogues.

Chapter 7, "Terpenoid Antitumor Agents" (J. M. Cassady and M. Suffness), correlates the structures, possible modes of action, and structure–activity relationships in the KB cytotoxicity screen of NCI of mono- and sesquiterpenes, diterpenes, bufadienolides, cardenolides, with anolides, cucurbitacins, and quassinoids.

Chapter 8, "Dimeric Catharanthus Alkaloids" (K. Gerzon), surveys the history, clinical observations, assay methods, mode of action, toxicity, polarity, and structure–activity relationships of vinblastine and vincristine, including a discussion of chemical modification of vinblastine.

Chapter 9, "Podophyllotoxins" (I. Jardine), discusses the history, clinical aspects, structures and chemical synthesis, and modes of action of podophyllotoxins, VM26, VP16-213, and steganacin against the P-815 mastocytoma and L-1210 leukemia cell growth.

Chapter 10, "Maytansinoids" (Y. Komoda and T. Kishi), reviews the isolation of natural and chemical synthesis of novel derivatives of maytansinoids and antitumor activity, toxicity, and effects on cellular growth and biochemical parameters.

Chapter 11, "Harringtonine and Related Cephalotaxine Esters" (C. R. Smith, Jr., K. L. Mikolajczak, and R. G. Powell), relates the characteristics, configuration, and antineoplastic activity of cephalotaxine and its esters. Total synthesis of cephalotaxine, chemical conversion to its naturally occurring esters, biosynthesis of ester analogues and structure–activity relationship against P-388 and L-1210 tumor growth are reviewed.

Chapter 12, "Camptothecin" (M. E. Wall and M. C. Wani), covers the naturally occurring, total and semisynthesized camptothecin analogues, antitumor activity, effects on RNA and DNA components of the cell, and structure–activity relationships.

Chapter 13, "Microbial Transformation as an Approach to Analogue Development" (J. P. Rosazza), offers a general discussion of the use of microorganisms to transform metabolic compounds to new, highly active antitumor agents. Examples used for transformation include bacterial and plant natural products and miscellaneous agents.

Chapter 14, "Miscellaneous Natural Products With Antitumor Activity" (M. Suffness and J. Douros), surveys a series of antitumor agents

0022-3549/82/0400-0478$01.00/0

(1) A. J. Spiegel and M. M. Noseworthy, *J. Pharm. Sci.*, **52,** 917 (1963).
(2) K. S. Lin, J. Anschel, and C. J. Swartz, *Bull. Parenter. Drug Assoc.*, **25,** 40 (1971).
(3) H. Kobayashi, Y. Miyoshi, K. Kitamura, Y. Yoshizaki, S. Muranishi, and H. Sezaki, *Chem. Pharm. Bull.*, **25,** 2862 (1977).
(4) K. Kakemi, H. Sezaki, K. Okumura, H. Kobayashi, and S. Furusawa, *ibid.*, **20,** 443 (1972).
(5) B. H. Vickery, G. I. McRae, J. S. Kent, and R. V. Tomlinson, *Prostaglandins Med.*, **5,** 93 (1980).
(6) H. Schiriftman and A. A. Kondritzer, *Am. J. Physiol.*, **191,** 591 (1957).
(7) G. F. Warner, E. L. Dobson, N. Pace, M. E. Johnston, and C. R. Finney, *Circulation*, **8,** 732 (1953).
(8) R. B. Sund and J. Schen, *Acta Pharmacol. Toxicol.*, **21,** 313 (1964).
(9) T. Tanaka, H. Kobayashi, K. Okumura, S. Muranishi, and H. Sezaki, *Chem. Pharm. Bull.*, **22,** 1275 (1974).
(10) M. Pfeffer and D. R. Van Harken, *J. Pharm. Sci.*, **70,** 449 (1981).
(11) B. E. Ballard, *ibid.*, **57,** 357 (1968).
(12) F. L. S. Tse and P. G. Welling, *J. Parenter. Drug Assoc.*, **34,** 409 (1980).
(13) K. Kakemi, H. Sezaki, K. Okumura, C. Takada, and S. Furusawa, *Chem. Pharm. Bull.*, **19,** 2058 (1971).
(14) K. Kakemi, H. Sezaki, K. Okumura, and S. Ashida, *ibid.*, **17,** 1332 (1969).
(15) J. S. Kent, R. V. Tomlinson, C. M. Ackley, and J. Hsu, *Drug Dev. Ind. Pharm.*, **7,** 261 (1981).

Cheng-Der Yu [x]
John S. Kent
Institute of Pharmaceutical Sciences
Syntex Research
Palo Alto, CA 94304

Received December 3, 1981.
Accepted for Publication December 30, 1981.
The authors thank Vickie L. Cain for her technical assistance and Dr. B. Poulsen for his support and helpful comments.

BOOKS

REVIEWS

Antitumor Agents Based on Natural Product Models. Edited by JOHN M. CASSADY and JOHN D. DOUROS. Academic, 111 Fifth Ave., New York, NY 10003. 1980. 500 pp. 15 × 23 cm.

This text is volume 16 of *Medicinal Chemistry, A Series of Monographs*. The emphasis of the book is on lead or novel antineoplastic agents, structure–activity relationships, modes of action, and toxicology of natural products. The choice of agents which is discussed in the monograph is rational and appropriate for the scope of the text. The book serves the purpose of assimilating diverse topics on natural product antineoplastic agents of clinical importance. In general, the text is well-written, concise and well-referenced, and includes pertinent structures, synthetic schemes, and biological data. The text is written with emphasis on the current development or status of a given group of agents and states scientific areas where further development is required.

The book is divided in the following contributions by individual authors:

Chapter 1, "The Development of New Antitumor Anthracyclines" (F. Arcamone), details the basic chemical modifications at the C-9, C-13, and C-14 of the amino sugar residue and of the chromophore of anthraquinone comparing the antitumor activity against HeLa cell, L-1210, P-388, and gross leukemia growth.

Chapter 2, "Trichothecanes" (T. W. Doyle and W. T. Bradner), discusses the history, mechanism of action, toxicity, metabolism, bioassay, cytotoxicity, and structure–activity relationships for antitumor activity in the P-388, L-1210, and B-16 tumor models.

Chapter 3, "Nucleosides" (M. Ohno), summarizes the structure–activity relationships of C- and N-pyrimidine nucleosides required to block the growth of tumors, bacteria, and viruses as evaluated by several investigators.

Chapter 4, "Mitomycins" (W. A. Remers), relates the history, chemical properties, mode of action, and structure–activity relationships for antibacterial and antitumor activity in the L-1210 and P-388 tumors, and the newly synthetic analogues of mitomycin.

Chapter 5, "Recent Progress in Bleomycin Studies" (H. Umezawa), deals with the chemistry and biosynthesis of bleomycin and phleomycin, including a revised structure of bleomycin, copper and iron complexes of bleomycin, the mechanism of action against squamous cell carcinomas, and other therapeutic uses of the agents.

Chapter 6, "Streptozocin" (P. F. Wiley), reviews the fermentation and isolation processes of streptozocin from bacterial cultures, its pharmacology, toxicology, carcinogenicity, mutagenicity, antibacterial, and antineoplastic modes of action, chemical studies, and the structure–activity relationships of several analogues.

Chapter 7, "Terpenoid Antitumor Agents" (J. M. Cassady and M. Suffness), correlates the structures, possible modes of action, and structure–activity relationships in the KB cytotoxicity screen of NCI of mono- and sesquiterpenes, diterpenes, bufadienolides, cardenolides, with anolides, cucurbitacins, and quassinoids.

Chapter 8, "Dimeric Catharanthus Alkaloids" (K. Gerzon), surveys the history, clinical observations, assay methods, mode of action, toxicity, polarity, and structure–activity relationships of vinblastine and vincristine, including a discussion of chemical modification of vinblastine.

Chapter 9, "Podophyllotoxins" (I. Jardine), discusses the history, clinical aspects, structures and chemical synthesis, and modes of action of podophyllotoxins, VM26, VP16-213, and steganacin against the P-815 mastocytoma and L-1210 leukemia cell growth.

Chapter 10, "Maytansinoids" (Y. Komoda and T. Kishi), reviews the isolation of natural and chemical synthesis of novel derivatives of maytansinoids and antitumor activity, toxicity, and effects on cellular growth and biochemical parameters.

Chapter 11, "Harringtonine and Related Cephalotaxine Esters" (C. R. Smith, Jr., K. L. Mikolajczak, and R. G. Powell), relates the characteristics, configuration, and antineoplastic activity of cephalotaxine and its esters. Total synthesis of cephalotaxine, chemical conversion to its naturally occurring esters, biosynthesis of ester analogues and structure–activity relationship against P-388 and L-1210 tumor growth are reviewed.

Chapter 12, "Camptothecin" (M. E. Wall and M. C. Wani), covers the naturally occurring, total and semisynthesized camptothecin analogues, antitumor activity, effects on RNA and DNA components of the cell, and structure–activity relationships.

Chapter 13, "Microbial Transformation as an Approach to Analogue Development" (J. P. Rosazza), offers a general discussion of the use of microorganisms to transform metabolic compounds to new, highly active antitumor agents. Examples used for transformation include bacterial and plant natural products and miscellaneous agents.

Chapter 14, "Miscellaneous Natural Products With Antitumor Activity" (M. Suffness and J. Douros), surveys a series of antitumor agents

0022-3549/82/0400-0478$01.00/0

from higher plants and microbial sources which were not covered elsewhere in the text but of sufficient scientific interest as possible new agents.

Reviewed by Iris H. Hall
Department of Medicinal Chemistry
School of Pharmacy
University of North Carolina
Chapel Hill, NC 27514

Terpenoids and Steroids, Vol. 10. Senior Reporter, J. R. HANSON. The Royal Society of Chemistry, Burlington House, London W1V 0BN, England. 1981. 284 pp. 15 × 22 cm. (Available from: Special Issues Sales, American Chemical Society, 1155 16th Street, N.W., Washington, DC 20036.)

This is the 10th volume on terpenoids and steroids in the valuable series first published 11 years ago. The aim of the series is to provide systematic, comprehensive, and critical reviews of progress in the major areas of chemical research. This volume reviews literature published between September 1978 and August 1979.

Volume 10 does not contain a subject index but is organized in a systematic manner that facilitates the location of information. There is also an extensive author index which is helpful to those following the research of a given individual. The book contains 1700 chemical structures and is documented with 1900 references, conveniently listed on the page of each chapter where first noted.

Part I, which covers the terpenoids, is divided into chapters that include sesquiterpenoids, diterpenoids, triterpenoids, and carotenoids and polyterpenoids. Chapters on monoterpenoids and the biosynthesis of terpenoids and steroids, unlike many of the earlier volumes, are not included. The chapter on monoterpenoids will be included in the next volume.

Part II, which covers the steroids, is divided into two chapters. The chapter on physical methods includes sections on structure and conformation, NMR spectroscopy, chiroptical phenomenon, mass spectrometry, miscellaneous physical properties, and analytical methods. The chapter on steroid reactions and partial syntheses contains sections devoted to each of these topics.

The first section is divided topically according to the more common functional groups and such important subjects as molecular rearrangements, functionalization of nonactivated positions, and photochemical reactions. The second section on partial syntheses, covers cholestane derivatives, vitamin D and its metabolites, pregnanes, androstanes and oestranes, cardenolides, heterocyclic steroids, and microbiological oxidations.

An unusual variety of terpenoid structures, particularly from insect and marine sources, has been included in this volume. The sharp increase in the use of high-field ^{1}H-NMR and ^{13}C-NMR is evident in this review.

The six reporters who prepared this volume are to be commended for maintaining the high standards set by the previous volumes in this series. Everyone interested in the chemistry of terpenoids and/or steroids should have access to this volume and the others in the series.

Reviewed by Norman J. Doorenbos
College of Science
Southern Illinois University
at Carbondale
Carbondale, IL 62901

Lexikon der Hilfsstoffe für Pharmazie, Kosmetik und angrenzende Gebiete. By HERBERT P. FIEDLER, Editio Cantor Aulendorf, D-7960 Aulendorf, West Germany, 2 Volumes, 1081 pp., 17 × 24 cm., 1981, Price: 245 DM.

In view of the scarcity of textbooks dealing exclusively with excipients, the revised and expanded edition of the Lexikon der Hilfsstoffe is a timely contribution to the reference libraries of pharmaceutical companies, regulatory agencies, and schools of pharmacy. Comparison of the contents with the original one-volume edition published in 1970 demonstrates the evolution of a broader and more critical attitude toward available technical information on excipients.

The author has provided a series of tables listing specific physical properties of excipients, types of surfactants used in pharmaceutical or cosmetic preparations, HLB values, MAC (maximum workplace concentration) values, colorants suitable for cosmetic preparations, and a table of the German and English titles of selected excipients together with their Merck Index and Chemical Abstracts Registry Numbers where appropriate.

The main body of the text lists excipients in alphabetical order with information on their physical, chemical, and biological properties. There is considerable variation in coverage between excipients, which reflects the author's judgment or the extent of information available to him. It is clear that Dr. Fiedler has made a special effort to make these volumes useful to English-speaking pharmaceutical scientists. However, the construction of some of the interminable German sentences may create impatience in readers with a limited knowledge of the language.

As far as this reviewer knows, no similarly detailed encyclopedia of excipients has appeared in the English language. Until this gap is properly filled, the *Lexikon der Hilfsstoffe* will remain a valuable source book for pharmaceutical scientists engaged in dosage form design, production, and control.

Reviewed by Jack Cooper
School of Pharmacy
University of California
San Francisco, CA 94143

USAN and the USP Dictionary of Drug Names 1982. United States Pharmacopeial Convention, 12601 Twinbrook Parkway, Rockville, MD 20852. 1981. 614 pp. 21 × 28 cm. Price $25.00 (Foreign: $40.00 AO rate, $27.00 surface rate).

The 1982 edition of *USAN and the USP Dictionary of Drug Names* has been updated in some subtle but important ways. The entry format and familiar orange cover are the same but the book itself is 104 pages longer than last year. There are 96 new adopted names in this edition, inclusive to June 15, 1981. Many International Nonproprietary Names and graphic formulas from the World Health Organization's listings have been added as well as the molecular weights of compounds where appropriate.

There are over 17,000 entries and 2043 adopted names in this issue. The three appendixes and five lists that appear in the back of the book are the same as last year.

USAN is the officially recognized source of drug names for the USP, the National Formulary, and the major source used by the FDA in referring to drug substances. Consequently, this book is an invaluable reference to those in the drug trade and health professionals.

Staff Review

Synthesis with Stable Isotopes of Carbon, Nitrogen, and Oxygen. By DONALD G. OTT. Wiley, 605 Third Ave., New York, NY 10016. 1981. 224 pp. 16 × 24 cm. Price $28.50.

This book is designed for chemists who are confronted with the need to prepare a compound with a stable isotope of carbon, nitrogen, or oxygen. It is intended to be useful for individuals actively involved in labeled compound synthesis as well as for chemists just entering the field.

Although compounds are presented in chapters according to functional groups, not all compounds appear in designated chapters. However, the text contains an index that lists all labeled compounds. The compounds are cited in the index as a product of synthetic procedures or as a reactant. Unfortunately, the index does not indicate information other than the compounds.

from higher plants and microbial sources which were not covered elsewhere in the text but of sufficient scientific interest as possible new agents.

Reviewed by Iris H. Hall
Department of Medicinal Chemistry
School of Pharmacy
University of North Carolina
Chapel Hill, NC 27514

Terpenoids and Steroids, Vol. 10. Senior Reporter, J. R. HANSON. The Royal Society of Chemistry, Burlington House, London W1V 0BN, England. 1981. 284 pp. 15 × 22 cm. (Available from: Special Issues Sales, American Chemical Society, 1155 16th Street, N.W., Washington, DC 20036.)

This is the 10th volume on terpenoids and steroids in the valuable series first published 11 years ago. The aim of the series is to provide systematic, comprehensive, and critical reviews of progress in the major areas of chemical research. This volume reviews literature published between September 1978 and August 1979.

Volume 10 does not contain a subject index but is organized in a systematic manner that facilitates the location of information. There is also an extensive author index which is helpful to those following the research of a given individual. The book contains 1700 chemical structures and is documented with 1900 references, conveniently listed on the page of each chapter where first noted.

Part I, which covers the terpenoids, is divided into chapters that include sesquiterpenoids, diterpenoids, triterpenoids, and carotenoids and polyterpenoids. Chapters on monoterpenoids and the biosynthesis of terpenoids and steroids, unlike many of the earlier volumes, are not included. The chapter on monoterpenoids will be included in the next volume.

Part II, which covers the steroids, is divided into two chapters. The chapter on physical methods includes sections on structure and conformation, NMR spectroscopy, chiroptical phenomenon, mass spectrometry, miscellaneous physical properties, and analytical methods. The chapter on steroid reactions and partial syntheses contains sections devoted to each of these topics.

The first section is divided topically according to the more common functional groups and such important subjects as molecular rearrangements, functionalization of nonactivated positions, and photochemical reactions. The second section on partial syntheses, covers cholestane derivatives, vitamin D and its metabolites, pregnanes, androstanes and oestranes, cardenolides, heterocyclic steroids, and microbiological oxidations.

An unusual variety of terpenoid structures, particularly from insect and marine sources, has been included in this volume. The sharp increase in the use of high-field ^{1}H-NMR and ^{13}C-NMR is evident in this review.

The six reporters who prepared this volume are to be commended for maintaining the high standards set by the previous volumes in this series. Everyone interested in the chemistry of terpenoids and/or steroids should have access to this volume and the others in the series.

Reviewed by Norman J. Doorenbos
College of Science
Southern Illinois University
at Carbondale
Carbondale, IL 62901

Lexikon der Hilfsstoffe für Pharmazie, Kosmetik und angrenzende Gebiete. By HERBERT P. FIEDLER, Editio Cantor Aulendorf, D-7960 Aulendorf, West Germany, 2 Volumes, 1081 pp., 17 × 24 cm., 1981, Price: 245 DM.

In view of the scarcity of textbooks dealing exclusively with excipients, the revised and expanded edition of the Lexikon der Hilfsstoffe is a timely contribution to the reference libraries of pharmaceutical companies, regulatory agencies, and schools of pharmacy. Comparison of the contents with the original one-volume edition published in 1970 demonstrates the evolution of a broader and more critical attitude toward available technical information on excipients.

The author has provided a series of tables listing specific physical properties of excipients, types of surfactants used in pharmaceutical or cosmetic preparations, HLB values, MAC (maximum workplace concentration) values, colorants suitable for cosmetic preparations, and a table of the German and English titles of selected excipients together with their Merck Index and Chemical Abstracts Registry Numbers where appropriate.

The main body of the text lists excipients in alphabetical order with information on their physical, chemical, and biological properties. There is considerable variation in coverage between excipients, which reflects the author's judgment or the extent of information available to him. It is clear that Dr. Fiedler has made a special effort to make these volumes useful to English-speaking pharmaceutical scientists. However, the construction of some of the interminable German sentences may create impatience in readers with a limited knowledge of the language.

As far as this reviewer knows, no similarly detailed encyclopedia of excipients has appeared in the English language. Until this gap is properly filled, the *Lexikon der Hilfsstoffe* will remain a valuable source book for pharmaceutical scientists engaged in dosage form design, production, and control.

Reviewed by Jack Cooper
School of Pharmacy
University of California
San Francisco, CA 94143

USAN and the USP Dictionary of Drug Names 1982. United States Pharmacopeial Convention, 12601 Twinbrook Parkway, Rockville, MD 20852. 1981. 614 pp. 21 × 28 cm. Price $25.00 (Foreign: $40.00 AO rate, $27.00 surface rate).

The 1982 edition of *USAN and the USP Dictionary of Drug Names* has been updated in some subtle but important ways. The entry format and familiar orange cover are the same but the book itself is 104 pages longer than last year. There are 96 new adopted names in this edition, inclusive to June 15, 1981. Many International Nonproprietary Names and graphic formulas from the World Health Organization's listings have been added as well as the molecular weights of compounds where appropriate.

There are over 17,000 entries and 2043 adopted names in this issue. The three appendixes and five lists that appear in the back of the book are the same as last year.

USAN is the officially recognized source of drug names for the USP, the National Formulary, and the major source used by the FDA in referring to drug substances. Consequently, this book is an invaluable reference to those in the drug trade and health professionals.

Staff Review

Synthesis with Stable Isotopes of Carbon, Nitrogen, and Oxygen. By DONALD G. OTT. Wiley, 605 Third Ave., New York, NY 10016. 1981. 224 pp. 16 × 24 cm. Price $28.50.

This book is designed for chemists who are confronted with the need to prepare a compound with a stable isotope of carbon, nitrogen, or oxygen. It is intended to be useful for individuals actively involved in labeled compound synthesis as well as for chemists just entering the field.

Although compounds are presented in chapters according to functional groups, not all compounds appear in designated chapters. However, the text contains an index that lists all labeled compounds. The compounds are cited in the index as a product of synthetic procedures or as a reactant. Unfortunately, the index does not indicate information other than the compounds.

from higher plants and microbial sources which were not covered elsewhere in the text but of sufficient scientific interest as possible new agents.

Reviewed by Iris H. Hall
Department of Medicinal Chemistry
School of Pharmacy
University of North Carolina
Chapel Hill, NC 27514

Terpenoids and Steroids, Vol. 10. Senior Reporter, J. R. HANSON. The Royal Society of Chemistry, Burlington House, London W1V 0BN, England. 1981. 284 pp. 15 × 22 cm. (Available from: Special Issues Sales, American Chemical Society, 1155 16th Street, N.W., Washington, DC 20036.)

This is the 10th volume on terpenoids and steroids in the valuable series first published 11 years ago. The aim of the series is to provide systematic, comprehensive, and critical reviews of progress in the major areas of chemical research. This volume reviews literature published between September 1978 and August 1979.

Volume 10 does not contain a subject index but is organized in a systematic manner that facilitates the location of information. There is also an extensive author index which is helpful to those following the research of a given individual. The book contains 1700 chemical structures and is documented with 1900 references, conveniently listed on the page of each chapter where first noted.

Part I, which covers the terpenoids, is divided into chapters that include sesquiterpenoids, diterpenoids, triterpenoids, and carotenoids and polyterpenoids. Chapters on monoterpenoids and the biosynthesis of terpenoids and steroids, unlike many of the earlier volumes, are not included. The chapter on monoterpenoids will be included in the next volume.

Part II, which covers the steroids, is divided into two chapters. The chapter on physical methods includes sections on structure and conformation, NMR spectroscopy, chiroptical phenomenon, mass spectrometry, miscellaneous physical properties, and analytical methods. The chapter on steroid reactions and partial syntheses contains sections devoted to each of these topics.

The first section is divided topically according to the more common functional groups and such important subjects as molecular rearrangements, functionalization of nonactivated positions, and photochemical reactions. The second section on partial syntheses, covers cholestane derivatives, vitamin D and its metabolites, pregnanes, androstanes and oestranes, cardenolides, heterocyclic steroids, and microbiological oxidations.

An unusual variety of terpenoid structures, particularly from insect and marine sources, has been included in this volume. The sharp increase in the use of high-field ^{1}H-NMR and ^{13}C-NMR is evident in this review.

The six reporters who prepared this volume are to be commended for maintaining the high standards set by the previous volumes in this series. Everyone interested in the chemistry of terpenoids and/or steroids should have access to this volume and the others in the series.

Reviewed by Norman J. Doorenbos
College of Science
Southern Illinois University
at Carbondale
Carbondale, IL 62901

Lexikon der Hilfsstoffe für Pharmazie, Kosmetik und angrenzende Gebiete. By HERBERT P. FIEDLER, Editio Cantor Aulendorf, D-7960 Aulendorf, West Germany, 2 Volumes, 1081 pp., 17 × 24 cm., 1981, Price: 245 DM.

In view of the scarcity of textbooks dealing exclusively with excipients, the revised and expanded edition of the Lexikon der Hilfsstoffe is a timely contribution to the reference libraries of pharmaceutical companies, regulatory agencies, and schools of pharmacy. Comparison of the contents with the original one-volume edition published in 1970 demonstrates the evolution of a broader and more critical attitude toward available technical information on excipients.

The author has provided a series of tables listing specific physical properties of excipients, types of surfactants used in pharmaceutical or cosmetic preparations, HLB values, MAC (maximum workplace concentration) values, colorants suitable for cosmetic preparations, and a table of the German and English titles of selected excipients together with their Merck Index and Chemical Abstracts Registry Numbers where appropriate.

The main body of the text lists excipients in alphabetical order with information on their physical, chemical, and biological properties. There is considerable variation in coverage between excipients, which reflects the author's judgment or the extent of information available to him. It is clear that Dr. Fiedler has made a special effort to make these volumes useful to English-speaking pharmaceutical scientists. However, the construction of some of the interminable German sentences may create impatience in readers with a limited knowledge of the language.

As far as this reviewer knows, no similarly detailed encyclopedia of excipients has appeared in the English language. Until this gap is properly filled, the *Lexikon der Hilfsstoffe* will remain a valuable source book for pharmaceutical scientists engaged in dosage form design, production, and control.

Reviewed by Jack Cooper
School of Pharmacy
University of California
San Francisco, CA 94143

USAN and the USP Dictionary of Drug Names 1982. United States Pharmacopeial Convention, 12601 Twinbrook Parkway, Rockville, MD 20852. 1981. 614 pp. 21 × 28 cm. Price $25.00 (Foreign: $40.00 AO rate, $27.00 surface rate).

The 1982 edition of *USAN and the USP Dictionary of Drug Names* has been updated in some subtle but important ways. The entry format and familiar orange cover are the same but the book itself is 104 pages longer than last year. There are 96 new adopted names in this edition, inclusive to June 15, 1981. Many International Nonproprietary Names and graphic formulas from the World Health Organization's listings have been added as well as the molecular weights of compounds where appropriate.

There are over 17,000 entries and 2043 adopted names in this issue. The three appendixes and five lists that appear in the back of the book are the same as last year.

USAN is the officially recognized source of drug names for the USP, the National Formulary, and the major source used by the FDA in referring to drug substances. Consequently, this book is an invaluable reference to those in the drug trade and health professionals.

Staff Review

Synthesis with Stable Isotopes of Carbon, Nitrogen, and Oxygen. By DONALD G. OTT. Wiley, 605 Third Ave., New York, NY 10016. 1981. 224 pp. 16 × 24 cm. Price $28.50.

This book is designed for chemists who are confronted with the need to prepare a compound with a stable isotope of carbon, nitrogen, or oxygen. It is intended to be useful for individuals actively involved in labeled compound synthesis as well as for chemists just entering the field.

Although compounds are presented in chapters according to functional groups, not all compounds appear in designated chapters. However, the text contains an index that lists all labeled compounds. The compounds are cited in the index as a product of synthetic procedures or as a reactant. Unfortunately, the index does not indicate information other than the compounds.

from higher plants and microbial sources which were not covered elsewhere in the text but of sufficient scientific interest as possible new agents.

Reviewed by Iris H. Hall
Department of Medicinal Chemistry
School of Pharmacy
University of North Carolina
Chapel Hill, NC 27514

Terpenoids and Steroids, Vol. 10. Senior Reporter, J. R. HANSON. The Royal Society of Chemistry, Burlington House, London W1V 0BN, England. 1981. 284 pp. 15 × 22 cm. (Available from: Special Issues Sales, American Chemical Society, 1155 16th Street, N.W., Washington, DC 20036.)

This is the 10th volume on terpenoids and steroids in the valuable series first published 11 years ago. The aim of the series is to provide systematic, comprehensive, and critical reviews of progress in the major areas of chemical research. This volume reviews literature published between September 1978 and August 1979.

Volume 10 does not contain a subject index but is organized in a systematic manner that facilitates the location of information. There is also an extensive author index which is helpful to those following the research of a given individual. The book contains 1700 chemical structures and is documented with 1900 references, conveniently listed on the page of each chapter where first noted.

Part I, which covers the terpenoids, is divided into chapters that include sesquiterpenoids, diterpenoids, triterpenoids, and carotenoids and polyterpenoids. Chapters on monoterpenoids and the biosynthesis of terpenoids and steroids, unlike many of the earlier volumes, are not included. The chapter on monoterpenoids will be included in the next volume.

Part II, which covers the steroids, is divided into two chapters. The chapter on physical methods includes sections on structure and conformation, NMR spectroscopy, chiroptical phenomenon, mass spectrometry, miscellaneous physical properties, and analytical methods. The chapter on steroid reactions and partial syntheses contains sections devoted to each of these topics.

The first section is divided topically according to the more common functional groups and such important subjects as molecular rearrangements, functionalization of nonactivated positions, and photochemical reactions. The second section on partial syntheses, covers cholestane derivatives, vitamin D and its metabolites, pregnanes, androstanes and oestranes, cardenolides, heterocyclic steroids, and microbiological oxidations.

An unusual variety of terpenoid structures, particularly from insect and marine sources, has been included in this volume. The sharp increase in the use of high-field ^{1}H-NMR and ^{13}C-NMR is evident in this review.

The six reporters who prepared this volume are to be commended for maintaining the high standards set by the previous volumes in this series. Everyone interested in the chemistry of terpenoids and/or steroids should have access to this volume and the others in the series.

Reviewed by Norman J. Doorenbos
College of Science
Southern Illinois University
at Carbondale
Carbondale, IL 62901

Lexikon der Hilfsstoffe für Pharmazie, Kosmetik und angrenzende Gebiete. By HERBERT P. FIEDLER, Editio Cantor Aulendorf, D-7960 Aulendorf, West Germany, 2 Volumes, 1081 pp., 17 × 24 cm., 1981, Price: 245 DM.

In view of the scarcity of textbooks dealing exclusively with excipients, the revised and expanded edition of the Lexikon der Hilfsstoffe is a timely contribution to the reference libraries of pharmaceutical companies, regulatory agencies, and schools of pharmacy. Comparison of the contents with the original one-volume edition published in 1970 demonstrates the evolution of a broader and more critical attitude toward available technical information on excipients.

The author has provided a series of tables listing specific physical properties of excipients, types of surfactants used in pharmaceutical or cosmetic preparations, HLB values, MAC (maximum workplace concentration) values, colorants suitable for cosmetic preparations, and a table of the German and English titles of selected excipients together with their Merck Index and Chemical Abstracts Registry Numbers where appropriate.

The main body of the text lists excipients in alphabetical order with information on their physical, chemical, and biological properties. There is considerable variation in coverage between excipients, which reflects the author's judgment or the extent of information available to him. It is clear that Dr. Fiedler has made a special effort to make these volumes useful to English-speaking pharmaceutical scientists. However, the construction of some of the interminable German sentences may create impatience in readers with a limited knowledge of the language.

As far as this reviewer knows, no similarly detailed encyclopedia of excipients has appeared in the English language. Until this gap is properly filled, the *Lexikon der Hilfsstoffe* will remain a valuable source book for pharmaceutical scientists engaged in dosage form design, production, and control.

Reviewed by Jack Cooper
School of Pharmacy
University of California
San Francisco, CA 94143

USAN and the USP Dictionary of Drug Names 1982. United States Pharmacopeial Convention, 12601 Twinbrook Parkway, Rockville, MD 20852. 1981. 614 pp. 21 × 28 cm. Price $25.00 (Foreign: $40.00 AO rate, $27.00 surface rate).

The 1982 edition of *USAN and the USP Dictionary of Drug Names* has been updated in some subtle but important ways. The entry format and familiar orange cover are the same but the book itself is 104 pages longer than last year. There are 96 new adopted names in this edition, inclusive to June 15, 1981. Many International Nonproprietary Names and graphic formulas from the World Health Organization's listings have been added as well as the molecular weights of compounds where appropriate.

There are over 17,000 entries and 2043 adopted names in this issue. The three appendixes and five lists that appear in the back of the book are the same as last year.

USAN is the officially recognized source of drug names for the USP, the National Formulary, and the major source used by the FDA in referring to drug substances. Consequently, this book is an invaluable reference to those in the drug trade and health professionals.

Staff Review

Synthesis with Stable Isotopes of Carbon, Nitrogen, and Oxygen. By DONALD G. OTT. Wiley, 605 Third Ave., New York, NY 10016. 1981. 224 pp. 16 × 24 cm. Price $28.50.

This book is designed for chemists who are confronted with the need to prepare a compound with a stable isotope of carbon, nitrogen, or oxygen. It is intended to be useful for individuals actively involved in labeled compound synthesis as well as for chemists just entering the field.

Although compounds are presented in chapters according to functional groups, not all compounds appear in designated chapters. However, the text contains an index that lists all labeled compounds. The compounds are cited in the index as a product of synthetic procedures or as a reactant. Unfortunately, the index does not indicate information other than the compounds.

from higher plants and microbial sources which were not covered elsewhere in the text but of sufficient scientific interest as possible new agents.

Reviewed by Iris H. Hall
Department of Medicinal Chemistry
School of Pharmacy
University of North Carolina
Chapel Hill, NC 27514

Terpenoids and Steroids, Vol. 10. Senior Reporter, J. R. HANSON. The Royal Society of Chemistry, Burlington House, London W1V 0BN, England. 1981. 284 pp. 15 × 22 cm. (Available from: Special Issues Sales, American Chemical Society, 1155 16th Street, N.W., Washington, DC 20036.)

This is the 10th volume on terpenoids and steroids in the valuable series first published 11 years ago. The aim of the series is to provide systematic, comprehensive, and critical reviews of progress in the major areas of chemical research. This volume reviews literature published between September 1978 and August 1979.

Volume 10 does not contain a subject index but is organized in a systematic manner that facilitates the location of information. There is also an extensive author index which is helpful to those following the research of a given individual. The book contains 1700 chemical structures and is documented with 1900 references, conveniently listed on the page of each chapter where first noted.

Part I, which covers the terpenoids, is divided into chapters that include sesquiterpenoids, diterpenoids, triterpenoids, and carotenoids and polyterpenoids. Chapters on monoterpenoids and the biosynthesis of terpenoids and steroids, unlike many of the earlier volumes, are not included. The chapter on monoterpenoids will be included in the next volume.

Part II, which covers the steroids, is divided into two chapters. The chapter on physical methods includes sections on structure and conformation, NMR spectroscopy, chiroptical phenomenon, mass spectrometry, miscellaneous physical properties, and analytical methods. The chapter on steroid reactions and partial syntheses contains sections devoted to each of these topics.

The first section is divided topically according to the more common functional groups and such important subjects as molecular rearrangements, functionalization of nonactivated positions, and photochemical reactions. The second section on partial syntheses, covers cholestane derivatives, vitamin D and its metabolites, pregnanes, androstanes and oestranes, cardenolides, heterocyclic steroids, and microbiological oxidations.

An unusual variety of terpenoid structures, particularly from insect and marine sources, has been included in this volume. The sharp increase in the use of high-field ^{1}H-NMR and ^{13}C-NMR is evident in this review.

The six reporters who prepared this volume are to be commended for maintaining the high standards set by the previous volumes in this series. Everyone interested in the chemistry of terpenoids and/or steroids should have access to this volume and the others in the series.

Reviewed by Norman J. Doorenbos
College of Science
Southern Illinois University
at Carbondale
Carbondale, IL 62901

Lexikon der Hilfsstoffe für Pharmazie, Kosmetik und angrenzende Gebiete. By HERBERT P. FIEDLER, Editio Cantor Aulendorf, D-7960 Aulendorf, West Germany, 2 Volumes, 1081 pp., 17 × 24 cm., 1981, Price: 245 DM.

In view of the scarcity of textbooks dealing exclusively with excipients, the revised and expanded edition of the Lexikon der Hilfsstoffe is a timely contribution to the reference libraries of pharmaceutical companies, regulatory agencies, and schools of pharmacy. Comparison of the contents with the original one-volume edition published in 1970 demonstrates the evolution of a broader and more critical attitude toward available technical information on excipients.

The author has provided a series of tables listing specific physical properties of excipients, types of surfactants used in pharmaceutical or cosmetic preparations, HLB values, MAC (maximum workplace concentration) values, colorants suitable for cosmetic preparations, and a table of the German and English titles of selected excipients together with their Merck Index and Chemical Abstracts Registry Numbers where appropriate.

The main body of the text lists excipients in alphabetical order with information on their physical, chemical, and biological properties. There is considerable variation in coverage between excipients, which reflects the author's judgment or the extent of information available to him. It is clear that Dr. Fiedler has made a special effort to make these volumes useful to English-speaking pharmaceutical scientists. However, the construction of some of the interminable German sentences may create impatience in readers with a limited knowledge of the language.

As far as this reviewer knows, no similarly detailed encyclopedia of excipients has appeared in the English language. Until this gap is properly filled, the *Lexikon der Hilfsstoffe* will remain a valuable source book for pharmaceutical scientists engaged in dosage form design, production, and control.

Reviewed by Jack Cooper
School of Pharmacy
University of California
San Francisco, CA 94143

USAN and the USP Dictionary of Drug Names 1982. United States Pharmacopeial Convention, 12601 Twinbrook Parkway, Rockville, MD 20852. 1981. 614 pp. 21 × 28 cm. Price $25.00 (Foreign: $40.00 AO rate, $27.00 surface rate).

The 1982 edition of *USAN and the USP Dictionary of Drug Names* has been updated in some subtle but important ways. The entry format and familiar orange cover are the same but the book itself is 104 pages longer than last year. There are 96 new adopted names in this edition, inclusive to June 15, 1981. Many International Nonproprietary Names and graphic formulas from the World Health Organization's listings have been added as well as the molecular weights of compounds where appropriate.

There are over 17,000 entries and 2043 adopted names in this issue. The three appendixes and five lists that appear in the back of the book are the same as last year.

USAN is the officially recognized source of drug names for the USP, the National Formulary, and the major source used by the FDA in referring to drug substances. Consequently, this book is an invaluable reference to those in the drug trade and health professionals.

Staff Review

Synthesis with Stable Isotopes of Carbon, Nitrogen, and Oxygen. By DONALD G. OTT. Wiley, 605 Third Ave., New York, NY 10016. 1981. 224 pp. 16 × 24 cm. Price $28.50.

This book is designed for chemists who are confronted with the need to prepare a compound with a stable isotope of carbon, nitrogen, or oxygen. It is intended to be useful for individuals actively involved in labeled compound synthesis as well as for chemists just entering the field.

Although compounds are presented in chapters according to functional groups, not all compounds appear in designated chapters. However, the text contains an index that lists all labeled compounds. The compounds are cited in the index as a product of synthetic procedures or as a reactant. Unfortunately, the index does not indicate information other than the compounds.

In many cases, the synthesis of a compound is provided in detail, but sometimes the reader is referred to a reference. References are used liberally throughout the text. The author indicates that the text does not contain all syntheses that have been developed for stable isotopes considered in the book, and states that the preparations presented represent types of reaction methods and techniques that may be applicable to many products other than those shown in the text. The efficient synthesis of key intermediates has been considered to be particularly important.

The text is concise, unique, and useful for individuals wishing to synthesize labeled compounds with stable isotopes and should be beneficial to all chemists involved in this area of research.

Reviewed by Stanley M. Shaw
Bionucleonics Department
Purdue University
West Lafayette, IN 47907

Anionic Polymeric Drugs. Edited by L. G. DONARUMA, R. M. OTTENBRITE, and O. VOGL. Wiley, 605 Third Ave. New York, NY 10016. 1980. 356 pp. 15×23 cm. Price $39.50.

This work is written as a first volume in a series to be published under the heading "Polymers in Biology and Medicine." The series is aimed at integrating knowledge in polymer sciences; it deals with endogenous polymers on one hand, and synthetic polymers used in biological and medical applications on the other.

The book is written by a number of experts, each contributing in their field. The work presents an overview of polymers as drugs, drug carriers, drug delivery systems, and as biopolymers in medicine. The structure and biological activity of polysaccharides and polycarboxylic acids are reviewed, with a discussion of the synthesis, characterization, and chelating properties of polycarboxylic acids.

An extensive review is provided of the divinyl ether–maleic anhydride copolymers (Pyran copolymer) and related structures. The discussion ranges from a captivating historical background through an in-depth discussion on a range of biological activities as they relate to structure, including the effects of polymers on the immune system. Subsequently the work expands on antiviral activity, effect on mixed-function oxidases, interferon induction, and antitumor activity.

The monograph represents a thorough and broad review of the chemistry, physics, charcterization, pharmacological, and physiological effects of polyanions with emphasis on the so-called Pyran polymers which have been studied most extensively. The editors have succeeded in bridging the gap between polymer science, biology, and medicine by providing a balanced mix that brings the reader up to date with the frontier of this fundamental research.

Reviewed by Felix Theeuwes
Vice President, Product
Research and Development
Alza Corporation
Palo Alto, CA 94304

Foreign Compound Metabolism in Mammals, Vol. 6. A Specialist Periodical Report. Senior Reporter D. E. HATHWAY. The Royal Society of Chemistry, Burlington House, London, W1V OBN, England, 1981. 390 pp. 13 × 22 cm. Price $138.00.

This book is the latest in a series of literature reviews on the titled subject which are compiled by Dr. Hathway and associates every two years. For the most part, the organization of the book follows the format introduced in the previous volume. With the exception of the first chapter on pharmacokinetics, the emphasis is on papers published during 1978 and 1979 pertaining to the biotransformation of xenobiotics. Although most of the book is devoted to drugs, there are chapters on "Industrial Chemicals and Miscellaneous Organic Compounds," "Agricultural Chemicals," and "Food Additives."

This series represents the closest thing available to a systematic, periodic review of both the conceptual and compound-oriented aspects of the drug metabolism literature. Although the reviewed literature is 2–3 years old, a search of the *Science Citation Index* for the cited references can bring anyone up to date in the areas of drug metabolism covered in a relatively short time. The material presented appears adequately indexed to allow this volume to be used for reference purposes. In contrast to the previous volume, an author index has been omitted. This is not a serious loss because most workers are more interested in following a particular subject or compound rather than an author (other than themselves). The table of contents is as sufficiently detailed as a subject index whereas the "Index of Compounds and Metabolites" at the back of the book lists specific compounds discussed.

Despite a few lapses found, *e.g.*, misspelling my name, eliminating three coauthors (reference 43 on p. 205) and misplacing reference 60 on p. 207, the authors appear to have succeeded in producing a valuable (and expensive) contribution to the practice of drug metabolism.

Reviewed by Morton A. Schwartz
Department of Biochemistry
and Drug Metabolism
Hoffmann–La Roche Inc.
Nutley, NJ 07110

Steroid Analysis by HPLC: Recent Applications (Chromatographic Science Series, Volume 16). Edited by MARIE P. KAUTSKY, Dekker, Inc., 270 Madison Avenue, New York, New York 10016, 1981. 397 pages bound and illustrated. 15 × 23 cm. $45 (Price is 15% higher outside the U.S. and Canada).

This book is divided into 11 major sections on: Bile acids, cardiac glycosides and related steroids, progestins, synthetic adrenocorticosteroids in pharmaceutical preparations and biological fluids, estrogens, D vitamins, determination of sterol intermediates in cholesterol biosynthesis, steroid hormones in adrenal and testicular cells, enzymatic steroid epimers, and analysis of natural and synthetic hormones in foods and feeds.

This volume is a collection of reviews by practicing chromatographers who describe their own work in detail and review in less detail work done by numerous others. Some 1980 references are cited but most are from 1979 or before. Recent reviews are included in the 654 references cited in the eleven sections. However, the editor states that the volume makes no attempt to include all of the recent applications of HPLC to steroid analysis.

The book is written for practicing analytical chemists, presenting laboratory tested approaches to problems in steroid separation and quantitation. Sufficient details are included to enable the analyst to quickly set up a system that would give satisfactory chromatography for routine analyses. This book would be a good source for information for any chromatographer who may be faced with an analysis in the steroid field for the first time. It could also be used for the purpose of reviewing any topic in the subject areas for developing new ideas, and for identifying key references. However, anyone using this book for the latter purpose should also supplement the information by surveying the current literature, since the publication rate of recent advances in the steroid area has been growing rapidly.

Reviewed by Robert E. Graham
Food and Drug Administration
Dallas District
Dallas, TX 75204

Food Chemicals Codex, Third Edition. Prepared by the Committee on Codex Specifications, Food and Nutrition Board, Division of Biological Sciences, Assembly of Life Sciences, National Research Council, National Academy of Sciences, 2101 Constitution Ave., N.W., Washington, D.C. 20418. 1981. 735 pp. Price $45.00.

The *Food Chemicals Codex* is the definitive source of information on food additives and processing aids. This new edition has been extensively revised and updated since the second edition, published in 1972. Over 800 food ingredients and processing materials are included in 776 monographs, 113 of which are new. A series of 400 IR spectra for many

In many cases, the synthesis of a compound is provided in detail, but sometimes the reader is referred to a reference. References are used liberally throughout the text. The author indicates that the text does not contain all syntheses that have been developed for stable isotopes considered in the book, and states that the preparations presented represent types of reaction methods and techniques that may be applicable to many products other than those shown in the text. The efficient synthesis of key intermediates has been considered to be particularly important.

The text is concise, unique, and useful for individuals wishing to synthesize labeled compounds with stable isotopes and should be beneficial to all chemists involved in this area of research.

Reviewed by Stanley M. Shaw
Bionucleonics Department
Purdue University
West Lafayette, IN 47907

Anionic Polymeric Drugs. Edited by L. G. DONARUMA, R. M. OTTENBRITE, and O. VOGL. Wiley, 605 Third Ave. New York, NY 10016. 1980. 356 pp. 15×23 cm. Price $39.50.

This work is written as a first volume in a series to be published under the heading "Polymers in Biology and Medicine." The series is aimed at integrating knowledge in polymer sciences; it deals with endogenous polymers on one hand, and synthetic polymers used in biological and medical applications on the other.

The book is written by a number of experts, each contributing in their field. The work presents an overview of polymers as drugs, drug carriers, drug delivery systems, and as biopolymers in medicine. The structure and biological activity of polysaccharides and polycarboxylic acids are reviewed, with a discussion of the synthesis, characterization, and chelating properties of polycarboxylic acids.

An extensive review is provided of the divinyl ether–maleic anhydride copolymers (Pyran copolymer) and related structures. The discussion ranges from a captivating historical background through an in-depth discussion on a range of biological activities as they relate to structure, including the effects of polymers on the immune system. Subsequently the work expands on antiviral activity, effect on mixed-function oxidases, interferon induction, and antitumor activity.

The monograph represents a thorough and broad review of the chemistry, physics, charcterization, pharmacological, and physiological effects of polyanions with emphasis on the so-called Pyran polymers which have been studied most extensively. The editors have succeeded in bridging the gap between polymer science, biology, and medicine by providing a balanced mix that brings the reader up to date with the frontier of this fundamental research.

Reviewed by Felix Theeuwes
Vice President, Product
Research and Development
Alza Corporation
Palo Alto, CA 94304

Foreign Compound Metabolism in Mammals, Vol. 6. A Specialist Periodical Report. Senior Reporter D. E. HATHWAY. The Royal Society of Chemistry, Burlington House, London, W1V OBN, England, 1981. 390 pp. 13 × 22 cm. Price $138.00.

This book is the latest in a series of literature reviews on the titled subject which are compiled by Dr. Hathway and associates every two years. For the most part, the organization of the book follows the format introduced in the previous volume. With the exception of the first chapter on pharmacokinetics, the emphasis is on papers published during 1978 and 1979 pertaining to the biotransformation of xenobiotics. Although most of the book is devoted to drugs, there are chapters on "Industrial Chemicals and Miscellaneous Organic Compounds," "Agricultural Chemicals," and "Food Additives."

This series represents the closest thing available to a systematic, periodic review of both the conceptual and compound-oriented aspects of the drug metabolism literature. Although the reviewed literature is 2–3 years old, a search of the *Science Citation Index* for the cited references can bring anyone up to date in the areas of drug metabolism covered in a relatively short time. The material presented appears adequately indexed to allow this volume to be used for reference purposes. In contrast to the previous volume, an author index has been omitted. This is not a serious loss because most workers are more interested in following a particular subject or compound rather than an author (other than themselves). The table of contents is as sufficiently detailed as a subject index whereas the "Index of Compounds and Metabolites" at the back of the book lists specific compounds discussed.

Despite a few lapses found, *e.g.*, misspelling my name, eliminating three coauthors (reference 43 on p. 205) and misplacing reference 60 on p. 207, the authors appear to have succeeded in producing a valuable (and expensive) contribution to the practice of drug metabolism.

Reviewed by Morton A. Schwartz
Department of Biochemistry
and Drug Metabolism
Hoffmann–La Roche Inc.
Nutley, NJ 07110

Steroid Analysis by HPLC: Recent Applications (Chromatographic Science Series, Volume 16). Edited by MARIE P. KAUTSKY, Dekker, Inc., 270 Madison Avenue, New York, New York 10016, 1981. 397 pages bound and illustrated. 15 × 23 cm. $45 (Price is 15% higher outside the U.S. and Canada).

This book is divided into 11 major sections on: Bile acids, cardiac glycosides and related steroids, progestins, synthetic adrenocorticosteroids in pharmaceutical preparations and biological fluids, estrogens, D vitamins, determination of sterol intermediates in cholesterol biosynthesis, steroid hormones in adrenal and testicular cells, enzymatic steroid epimers, and analysis of natural and synthetic hormones in foods and feeds.

This volume is a collection of reviews by practicing chromatographers who describe their own work in detail and review in less detail work done by numerous others. Some 1980 references are cited but most are from 1979 or before. Recent reviews are included in the 654 references cited in the eleven sections. However, the editor states that the volume makes no attempt to include all of the recent applications of HPLC to steroid analysis.

The book is written for practicing analytical chemists, presenting laboratory tested approaches to problems in steroid separation and quantitation. Sufficient details are included to enable the analyst to quickly set up a system that would give satisfactory chromatography for routine analyses. This book would be a good source for information for any chromatographer who may be faced with an analysis in the steroid field for the first time. It could also be used for the purpose of reviewing any topic in the subject areas for developing new ideas, and for identifying key references. However, anyone using this book for the latter purpose should also supplement the information by surveying the current literature, since the publication rate of recent advances in the steroid area has been growing rapidly.

Reviewed by Robert E. Graham
Food and Drug Administration
Dallas District
Dallas, TX 75204

Food Chemicals Codex, Third Edition. Prepared by the Committee on Codex Specifications, Food and Nutrition Board, Division of Biological Sciences, Assembly of Life Sciences, National Research Council, National Academy of Sciences, 2101 Constitution Ave., N.W., Washington, D.C. 20418. 1981. 735 pp. Price $45.00.

The *Food Chemicals Codex* is the definitive source of information on food additives and processing aids. This new edition has been extensively revised and updated since the second edition, published in 1972. Over 800 food ingredients and processing materials are included in 776 monographs, 113 of which are new. A series of 400 IR spectra for many

In many cases, the synthesis of a compound is provided in detail, but sometimes the reader is referred to a reference. References are used liberally throughout the text. The author indicates that the text does not contain all syntheses that have been developed for stable isotopes considered in the book, and states that the preparations presented represent types of reaction methods and techniques that may be applicable to many products other than those shown in the text. The efficient synthesis of key intermediates has been considered to be particularly important.

The text is concise, unique, and useful for individuals wishing to synthesize labeled compounds with stable isotopes and should be beneficial to all chemists involved in this area of research.

Reviewed by Stanley M. Shaw
Bionucleonics Department
Purdue University
West Lafayette, IN 47907

Anionic Polymeric Drugs. Edited by L. G. DONARUMA, R. M. OTTENBRITE, and O. VOGL. Wiley, 605 Third Ave. New York, NY 10016. 1980. 356 pp. 15×23 cm. Price $39.50.

This work is written as a first volume in a series to be published under the heading "Polymers in Biology and Medicine." The series is aimed at integrating knowledge in polymer sciences; it deals with endogenous polymers on one hand, and synthetic polymers used in biological and medical applications on the other.

The book is written by a number of experts, each contributing in their field. The work presents an overview of polymers as drugs, drug carriers, drug delivery systems, and as biopolymers in medicine. The structure and biological activity of polysaccharides and polycarboxylic acids are reviewed, with a discussion of the synthesis, characterization, and chelating properties of polycarboxylic acids.

An extensive review is provided of the divinyl ether–maleic anhydride copolymers (Pyran copolymer) and related structures. The discussion ranges from a captivating historical background through an in-depth discussion on a range of biological activities as they relate to structure, including the effects of polymers on the immune system. Subsequently the work expands on antiviral activity, effect on mixed-function oxidases, interferon induction, and antitumor activity.

The monograph represents a thorough and broad review of the chemistry, physics, charcterization, pharmacological, and physiological effects of polyanions with emphasis on the so-called Pyran polymers which have been studied most extensively. The editors have succeeded in bridging the gap between polymer science, biology, and medicine by providing a balanced mix that brings the reader up to date with the frontier of this fundamental research.

Reviewed by Felix Theeuwes
Vice President, Product
Research and Development
Alza Corporation
Palo Alto, CA 94304

Foreign Compound Metabolism in Mammals, Vol. 6. A Specialist Periodical Report. Senior Reporter D. E. HATHWAY. The Royal Society of Chemistry, Burlington House, London, W1V OBN, England, 1981. 390 pp. 13 × 22 cm. Price $138.00.

This book is the latest in a series of literature reviews on the titled subject which are compiled by Dr. Hathway and associates every two years. For the most part, the organization of the book follows the format introduced in the previous volume. With the exception of the first chapter on pharmacokinetics, the emphasis is on papers published during 1978 and 1979 pertaining to the biotransformation of xenobiotics. Although most of the book is devoted to drugs, there are chapters on "Industrial Chemicals and Miscellaneous Organic Compounds," "Agricultural Chemicals," and "Food Additives."

This series represents the closest thing available to a systematic, periodic review of both the conceptual and compound-oriented aspects of the drug metabolism literature. Although the reviewed literature is 2–3 years old, a search of the *Science Citation Index* for the cited references can bring anyone up to date in the areas of drug metabolism covered in a relatively short time. The material presented appears adequately indexed to allow this volume to be used for reference purposes. In contrast to the previous volume, an author index has been omitted. This is not a serious loss because most workers are more interested in following a particular subject or compound rather than an author (other than themselves). The table of contents is as sufficiently detailed as a subject index whereas the "Index of Compounds and Metabolites" at the back of the book lists specific compounds discussed.

Despite a few lapses found, *e.g.*, misspelling my name, eliminating three coauthors (reference 43 on p. 205) and misplacing reference 60 on p. 207, the authors appear to have succeeded in producing a valuable (and expensive) contribution to the practice of drug metabolism.

Reviewed by Morton A. Schwartz
Department of Biochemistry
and Drug Metabolism
Hoffmann–La Roche Inc.
Nutley, NJ 07110

Steroid Analysis by HPLC: Recent Applications (Chromatographic Science Series, Volume 16). Edited by MARIE P. KAUTSKY, Dekker, Inc., 270 Madison Avenue, New York, New York 10016, 1981. 397 pages bound and illustrated. 15 × 23 cm. $45 (Price is 15% higher outside the U.S. and Canada).

This book is divided into 11 major sections on: Bile acids, cardiac glycosides and related steroids, progestins, synthetic adrenocorticosteroids in pharmaceutical preparations and biological fluids, estrogens, D vitamins, determination of sterol intermediates in cholesterol biosynthesis, steroid hormones in adrenal and testicular cells, enzymatic steroid epimers, and analysis of natural and synthetic hormones in foods and feeds.

This volume is a collection of reviews by practicing chromatographers who describe their own work in detail and review in less detail work done by numerous others. Some 1980 references are cited but most are from 1979 or before. Recent reviews are included in the 654 references cited in the eleven sections. However, the editor states that the volume makes no attempt to include all of the recent applications of HPLC to steroid analysis.

The book is written for practicing analytical chemists, presenting laboratory tested approaches to problems in steroid separation and quantitation. Sufficient details are included to enable the analyst to quickly set up a system that would give satisfactory chromatography for routine analyses. This book would be a good source for information for any chromatographer who may be faced with an analysis in the steroid field for the first time. It could also be used for the purpose of reviewing any topic in the subject areas for developing new ideas, and for identifying key references. However, anyone using this book for the latter purpose should also supplement the information by surveying the current literature, since the publication rate of recent advances in the steroid area has been growing rapidly.

Reviewed by Robert E. Graham
Food and Drug Administration
Dallas District
Dallas, TX 75204

Food Chemicals Codex, Third Edition. Prepared by the Committee on Codex Specifications, Food and Nutrition Board, Division of Biological Sciences, Assembly of Life Sciences, National Research Council, National Academy of Sciences, 2101 Constitution Ave., N.W., Washington, D.C. 20418. 1981. 735 pp. Price $45.00.

The *Food Chemicals Codex* is the definitive source of information on food additives and processing aids. This new edition has been extensively revised and updated since the second edition, published in 1972. Over 800 food ingredients and processing materials are included in 776 monographs, 113 of which are new. A series of 400 IR spectra for many

In many cases, the synthesis of a compound is provided in detail, but sometimes the reader is referred to a reference. References are used liberally throughout the text. The author indicates that the text does not contain all syntheses that have been developed for stable isotopes considered in the book, and states that the preparations presented represent types of reaction methods and techniques that may be applicable to many products other than those shown in the text. The efficient synthesis of key intermediates has been considered to be particularly important.

The text is concise, unique, and useful for individuals wishing to synthesize labeled compounds with stable isotopes and should be beneficial to all chemists involved in this area of research.

Reviewed by Stanley M. Shaw
Bionucleonics Department
Purdue University
West Lafayette, IN 47907

Anionic Polymeric Drugs. Edited by L. G. DONARUMA, R. M. OTTENBRITE, and O. VOGL. Wiley, 605 Third Ave. New York, NY 10016. 1980. 356 pp. 15×23 cm. Price $39.50.

This work is written as a first volume in a series to be published under the heading "Polymers in Biology and Medicine." The series is aimed at integrating knowledge in polymer sciences; it deals with endogenous polymers on one hand, and synthetic polymers used in biological and medical applications on the other.

The book is written by a number of experts, each contributing in their field. The work presents an overview of polymers as drugs, drug carriers, drug delivery systems, and as biopolymers in medicine. The structure and biological activity of polysaccharides and polycarboxylic acids are reviewed, with a discussion of the synthesis, characterization, and chelating properties of polycarboxylic acids.

An extensive review is provided of the divinyl ether–maleic anhydride copolymers (Pyran copolymer) and related structures. The discussion ranges from a captivating historical background through an in-depth discussion on a range of biological activities as they relate to structure, including the effects of polymers on the immune system. Subsequently the work expands on antiviral activity, effect on mixed-function oxidases, interferon induction, and antitumor activity.

The monograph represents a thorough and broad review of the chemistry, physics, charcterization, pharmacological, and physiological effects of polyanions with emphasis on the so-called Pyran polymers which have been studied most extensively. The editors have succeeded in bridging the gap between polymer science, biology, and medicine by providing a balanced mix that brings the reader up to date with the frontier of this fundamental research.

Reviewed by Felix Theeuwes
Vice President, Product
Research and Development
Alza Corporation
Palo Alto, CA 94304

Foreign Compound Metabolism in Mammals, Vol. 6. A Specialist Periodical Report. Senior Reporter D. E. HATHWAY. The Royal Society of Chemistry, Burlington House, London, W1V OBN, England, 1981. 390 pp. 13 × 22 cm. Price $138.00.

This book is the latest in a series of literature reviews on the titled subject which are compiled by Dr. Hathway and associates every two years. For the most part, the organization of the book follows the format introduced in the previous volume. With the exception of the first chapter on pharmacokinetics, the emphasis is on papers published during 1978 and 1979 pertaining to the biotransformation of xenobiotics. Although most of the book is devoted to drugs, there are chapters on "Industrial Chemicals and Miscellaneous Organic Compounds," "Agricultural Chemicals," and "Food Additives."

This series represents the closest thing available to a systematic, periodic review of both the conceptual and compound-oriented aspects of the drug metabolism literature. Although the reviewed literature is 2–3 years old, a search of the *Science Citation Index* for the cited references can bring anyone up to date in the areas of drug metabolism covered in a relatively short time. The material presented appears adequately indexed to allow this volume to be used for reference purposes. In contrast to the previous volume, an author index has been omitted. This is not a serious loss because most workers are more interested in following a particular subject or compound rather than an author (other than themselves). The table of contents is as sufficiently detailed as a subject index whereas the "Index of Compounds and Metabolites" at the back of the book lists specific compounds discussed.

Despite a few lapses found, *e.g.*, misspelling my name, eliminating three coauthors (reference 43 on p. 205) and misplacing reference 60 on p. 207, the authors appear to have succeeded in producing a valuable (and expensive) contribution to the practice of drug metabolism.

Reviewed by Morton A. Schwartz
Department of Biochemistry
and Drug Metabolism
Hoffmann–La Roche Inc.
Nutley, NJ 07110

Steroid Analysis by HPLC: Recent Applications (Chromatographic Science Series, Volume 16). Edited by MARIE P. KAUTSKY, Dekker, Inc., 270 Madison Avenue, New York, New York 10016, 1981. 397 pages bound and illustrated. 15 × 23 cm. $45 (Price is 15% higher outside the U.S. and Canada).

This book is divided into 11 major sections on: Bile acids, cardiac glycosides and related steroids, progestins, synthetic adrenocorticosteroids in pharmaceutical preparations and biological fluids, estrogens, D vitamins, determination of sterol intermediates in cholesterol biosynthesis, steroid hormones in adrenal and testicular cells, enzymatic steroid epimers, and analysis of natural and synthetic hormones in foods and feeds.

This volume is a collection of reviews by practicing chromatographers who describe their own work in detail and review in less detail work done by numerous others. Some 1980 references are cited but most are from 1979 or before. Recent reviews are included in the 654 references cited in the eleven sections. However, the editor states that the volume makes no attempt to include all of the recent applications of HPLC to steroid analysis.

The book is written for practicing analytical chemists, presenting laboratory tested approaches to problems in steroid separation and quantitation. Sufficient details are included to enable the analyst to quickly set up a system that would give satisfactory chromatography for routine analyses. This book would be a good source for information for any chromatographer who may be faced with an analysis in the steroid field for the first time. It could also be used for the purpose of reviewing any topic in the subject areas for developing new ideas, and for identifying key references. However, anyone using this book for the latter purpose should also supplement the information by surveying the current literature, since the publication rate of recent advances in the steroid area has been growing rapidly.

Reviewed by Robert E. Graham
Food and Drug Administration
Dallas District
Dallas, TX 75204

Food Chemicals Codex, Third Edition. Prepared by the Committee on Codex Specifications, Food and Nutrition Board, Division of Biological Sciences, Assembly of Life Sciences, National Research Council, National Academy of Sciences, 2101 Constitution Ave., N.W., Washington, D.C. 20418. 1981. 735 pp. Price $45.00.

The *Food Chemicals Codex* is the definitive source of information on food additives and processing aids. This new edition has been extensively revised and updated since the second edition, published in 1972. Over 800 food ingredients and processing materials are included in 776 monographs, 113 of which are new. A series of 400 IR spectra for many

In many cases, the synthesis of a compound is provided in detail, but sometimes the reader is referred to a reference. References are used liberally throughout the text. The author indicates that the text does not contain all syntheses that have been developed for stable isotopes considered in the book, and states that the preparations presented represent types of reaction methods and techniques that may be applicable to many products other than those shown in the text. The efficient synthesis of key intermediates has been considered to be particularly important.

The text is concise, unique, and useful for individuals wishing to synthesize labeled compounds with stable isotopes and should be beneficial to all chemists involved in this area of research.

Reviewed by Stanley M. Shaw
Bionucleonics Department
Purdue University
West Lafayette, IN 47907

Anionic Polymeric Drugs. Edited by L. G. DONARUMA, R. M. OTTENBRITE, and O. VOGL. Wiley, 605 Third Ave. New York, NY 10016. 1980. 356 pp. 15×23 cm. Price $39.50.

This work is written as a first volume in a series to be published under the heading "Polymers in Biology and Medicine." The series is aimed at integrating knowledge in polymer sciences; it deals with endogenous polymers on one hand, and synthetic polymers used in biological and medical applications on the other.

The book is written by a number of experts, each contributing in their field. The work presents an overview of polymers as drugs, drug carriers, drug delivery systems, and as biopolymers in medicine. The structure and biological activity of polysaccharides and polycarboxylic acids are reviewed, with a discussion of the synthesis, characterization, and chelating properties of polycarboxylic acids.

An extensive review is provided of the divinyl ether–maleic anhydride copolymers (Pyran copolymer) and related structures. The discussion ranges from a captivating historical background through an in-depth discussion on a range of biological activities as they relate to structure, including the effects of polymers on the immune system. Subsequently the work expands on antiviral activity, effect on mixed-function oxidases, interferon induction, and antitumor activity.

The monograph represents a thorough and broad review of the chemistry, physics, charcterization, pharmacological, and physiological effects of polyanions with emphasis on the so-called Pyran polymers which have been studied most extensively. The editors have succeeded in bridging the gap between polymer science, biology, and medicine by providing a balanced mix that brings the reader up to date with the frontier of this fundamental research.

Reviewed by Felix Theeuwes
Vice President, Product
Research and Development
Alza Corporation
Palo Alto, CA 94304

Foreign Compound Metabolism in Mammals, Vol. 6. A Specialist Periodical Report. Senior Reporter D. E. HATHWAY. The Royal Society of Chemistry, Burlington House, London, W1V OBN, England, 1981. 390 pp. 13 × 22 cm. Price $138.00.

This book is the latest in a series of literature reviews on the titled subject which are compiled by Dr. Hathway and associates every two years. For the most part, the organization of the book follows the format introduced in the previous volume. With the exception of the first chapter on pharmacokinetics, the emphasis is on papers published during 1978 and 1979 pertaining to the biotransformation of xenobiotics. Although most of the book is devoted to drugs, there are chapters on "Industrial Chemicals and Miscellaneous Organic Compounds," "Agricultural Chemicals," and "Food Additives."

This series represents the closest thing available to a systematic, periodic review of both the conceptual and compound-oriented aspects of the drug metabolism literature. Although the reviewed literature is 2–3 years old, a search of the *Science Citation Index* for the cited references can bring anyone up to date in the areas of drug metabolism covered in a relatively short time. The material presented appears adequately indexed to allow this volume to be used for reference purposes. In contrast to the previous volume, an author index has been omitted. This is not a serious loss because most workers are more interested in following a particular subject or compound rather than an author (other than themselves). The table of contents is as sufficiently detailed as a subject index whereas the "Index of Compounds and Metabolites" at the back of the book lists specific compounds discussed.

Despite a few lapses found, *e.g.*, misspelling my name, eliminating three coauthors (reference 43 on p. 205) and misplacing reference 60 on p. 207, the authors appear to have succeeded in producing a valuable (and expensive) contribution to the practice of drug metabolism.

Reviewed by Morton A. Schwartz
Department of Biochemistry
and Drug Metabolism
Hoffmann–La Roche Inc.
Nutley, NJ 07110

Steroid Analysis by HPLC: Recent Applications (Chromatographic Science Series, Volume 16). Edited by MARIE P. KAUTSKY, Dekker, Inc., 270 Madison Avenue, New York, New York 10016, 1981. 397 pages bound and illustrated. 15 × 23 cm. $45 (Price is 15% higher outside the U.S. and Canada).

This book is divided into 11 major sections on: Bile acids, cardiac glycosides and related steroids, progestins, synthetic adrenocorticosteroids in pharmaceutical preparations and biological fluids, estrogens, D vitamins, determination of sterol intermediates in cholesterol biosynthesis, steroid hormones in adrenal and testicular cells, enzymatic steroid epimers, and analysis of natural and synthetic hormones in foods and feeds.

This volume is a collection of reviews by practicing chromatographers who describe their own work in detail and review in less detail work done by numerous others. Some 1980 references are cited but most are from 1979 or before. Recent reviews are included in the 654 references cited in the eleven sections. However, the editor states that the volume makes no attempt to include all of the recent applications of HPLC to steroid analysis.

The book is written for practicing analytical chemists, presenting laboratory tested approaches to problems in steroid separation and quantitation. Sufficient details are included to enable the analyst to quickly set up a system that would give satisfactory chromatography for routine analyses. This book would be a good source for information for any chromatographer who may be faced with an analysis in the steroid field for the first time. It could also be used for the purpose of reviewing any topic in the subject areas for developing new ideas, and for identifying key references. However, anyone using this book for the latter purpose should also supplement the information by surveying the current literature, since the publication rate of recent advances in the steroid area has been growing rapidly.

Reviewed by Robert E. Graham
Food and Drug Administration
Dallas District
Dallas, TX 75204

Food Chemicals Codex, Third Edition. Prepared by the Committee on Codex Specifications, Food and Nutrition Board, Division of Biological Sciences, Assembly of Life Sciences, National Research Council, National Academy of Sciences, 2101 Constitution Ave., N.W., Washington, D.C. 20418. 1981. 735 pp. Price $45.00.

The *Food Chemicals Codex* is the definitive source of information on food additives and processing aids. This new edition has been extensively revised and updated since the second edition, published in 1972. Over 800 food ingredients and processing materials are included in 776 monographs, 113 of which are new. A series of 400 IR spectra for many

essential oils and flavoring compounds is also new to this edition. Specifications for flavor aromatics and isolates are now given in clear tabular form.

In the area of policy, the new edition contains a set of guidelines for "good manufacturing practice" developed by the Committee on Codex Specifications.

Officially, the Codex is recognized by the Food and Drug Administration which adopted certain Codex specifications in 1971.

This book is essential to anyone working in the areas of food science and technology, quality control, and good research. More than 600 scientists from a variety of disciplines contributed to this work as well as many trade associations and professional societies.

Purchasers of this edition are entitled to receive three supplements to the Codex, included in the purchase price.

Staff Review

Textbook of Biopharmaceutic Analysis. By R. V. SMITH and J. T. STEWART. Lea & Febiger, 600 Washington Square, Philadelphia, PA 19106. 1981. 308 pp. 18 × 25 cm. Price $25.00 (Canada $30.00)

To better prepare the practitioner for anticipated new roles in the delivery of health care, pharmaceutical education has evolved from a product oriented emphasis to a clinically oriented one. This change has given rise to such courses as biopharmaceutics, clinical pharmacy, and clinically oriented clerkships and externships. In addition, it often has necessitated the restructuring of the traditional basic science courses in order to provide a more adequate background for the clinical sciences. This textbook treats those aspects of analytical chemistry, analytical microbiology and biochemistry, and drug assay that concern the development and application of procedures for the determination of drugs and their metabolites in the biological fluids. This volume appears to be the first attempt to provide such a body of knowledge in textbook form for utilization in the pharmacy curriculum.

This book is divided into three sections: "Defining the Problem," "The Separation Step," and "The Measurement Step." This sequence is based on the approach that one would presumably follow in developing a methodology for the determination of a drug or its metabolites in biological fluids. The first section presents relevant background material, covers the development of methods for determining trace levels of medicaments in biological fluids, and deals with the procurement and characterization of reference standards. While three sources of reference standards are mentioned, unfortunately, the United States Pharmacopeial Convention has been overlooked.

The second section reviews the major separation and purification techniques including liquid–solid extraction, liquid–liquid extraction, partition coefficient, ion-pairing procedures, and the major chromatographic methods, *i.e.*, TLC, GC, HPLC, gel permeation, and ion-exchange chromatography.

The third section covers techniques for measurement and encompasses 10 chapters. Separate chapters are devoted to the following topics: statistical treatment of data, treatment of chromatographic data, UV-visible absorption and emission spectrophotometry, fluorimetry and phosphorimetry, electroanalytical methods, radiochemical methods, immunoassay techniques (RIA, EMIT, HI, SLFIA, and spin immunoassay), microbiological assay methods, enzymatic analysis, and a very brief concluding chapter on the method of selecting the appropriate analytical procedure for a particular situation. An array of pertinent literature references is provided at the end of each chapter along with a series of learning objectives to assist the student in reviewing the chapter content. Additional recommended readings are presented for more advanced students.

This text is written in a lucid manner, is well-organized, and the information is presented in a logical format. While the content of this book may be presented as a separate course offering, the subject matter may be more appropriately covered as segments in those courses where the basic concepts are taught, or it may possibly be included as a component of one of the clinical science courses. This material is important and serves well as a bridge between the clinical sciences and the basic pharmaceutical sciences. It merits consideration in the pharmaceutical curriculum.

Reviewed by Martin I. Blake
University of Illinois
College of Pharmacy
Chicago, IL 60612

Pharmacognosy, 8th edition. VARRO E. TYLER, LYNN R. BRADY, and JAMES E. ROBBERS. Lea & Febiger, Philadelphia, PA 19106. 1981. 520 pp. 18 × 25 cm. Illustrated with Numerous chemical structures, figures and photographs. Price: $31.50 U.S., $37.75 Canada.

This modern pharmacognosy text is all-inclusive and deals with drugs of natural origin that make up close to 50% of all medicinals currently employed. It has been the standard textbook of pharmacognosy in the U.S. for a number of years, and is the only one which has been periodically updated. It provides a systematic and comprehensive review of plant and animal drugs in a biochemical classification system. Major chapter titles include, general introduction, carbohydrates and related compounds, glycosides and tannins, lipids, volatile oils, resins, steroids, alkaloids, peptide hormones, enzymes, vitamins, antibiotics, biologicals, allergens and allergenic preparations, poisonous plants, and a new section entitled, herbs and "health foods". Several obsolete drugs and references have been deleted and new materials added where appropriate. Many of the chemical structures have been redrawn to reflect appropriate steric configurations. New prescription products as examples of the various drugs have been added as required.

In general, the new edition has retained the flavor of the previous ones with much updating. The chapter on herbs and "health foods" is a welcome addition to a subject that has gained popularity in recent years. This chapter has wisely divided the literature references into two groups, *e.g.*, authoritative and advocacy literature. This will help the pharmacist and others who use it, to determine whether the references their patients use are good or bad since self medication with herbs and teas has become common. However, several excellent recent references on the hazards of herbal teas and ginsing tea analysis have been omitted, and should be included in the next edition. As a constructive criticism, more recent key journal articles and reviews also should be included in the chapter references. This edition is really top-heavy with text references. Since text references tend to be dated by publication time, this policy detracts from access to recent literature and the usefulness of the book. This text is a must for all pharmacists.

Reviewed by Ara Der Marderosian
Professor of Pharmacognosy
Philadelphia College of
Pharmacy and Science
Philadelphia, PA 19104

BOOK NOTICES

Abrege de Chimie Analytique. Tome I. Chimie des Solutions. By MICHAEL GUERNET and MICHEL HAMON. Masson 120, bd St-Germain 75280 Paris, Cedex 06, France. 1981. 238 pp. 19 × 21 cm.

Addendum to the Second Supplement to USP XX and to NF XV. The United States Pharmacopeial Convention, Inc., 20th & Northampton Street, Easton, PA 18042. 342 pp.

Aliphatic and Related Natural Product Chemistry. Vol. 2. (A Specialist Periodical Report). Senior Reporter: F. D. GUNSTONE. The Royal Society of Chemistry, Distribution Centre, Blackhorse Rd., Letchworth Herts., SG6 1HN, England. 1981. 265 pp. 13 × 22 cm. Price $104.00.

Alkaloid Chemistry. By MANFRED HESSE. Wiley, One Wiley Drive, Somerset, NJ 08873. 1981. 231 pp. 15 × 23 cm.

Biochemical Regulation of Blood Pressure. Edited by RICHARD L. SOFFER. Wiley, One Wiley Drive, Somerset, NJ 08873. 1981. 456 pp. 15 × 23 cm. Price. $49.50.

Biochemistry of Antimicrobial Action. 3rd ed. By T. J. FRANKLIN and G. A. SNOW. Methuen, Inc. 733 Third Avenue, New York, NY 10017. 1981. 217 pp. 15 × 24 cm. Price $35.00 (hardcover), $17.95 (paperback).

Biopharmazie. Theorie und Praxis der Pharmakokinetik. By HERAUSGEGEBEN von J. MEIER, H. RETTIG and H. HESS. George Thieme Verlag, Stuttgart, West Germany. 1981. 473 pp. 17 × 24 cm. (German).

Coca and Cocaine, Vol. 3, issues 2–3 of the Journal of Ethno-Pharmacology. Edited by L. RIVIER, J. G. BRUHN. Elsevier, P. O. Box 211, 1000 AE Amsterdam, The Netherlands. 1981. 379 pp. 16 × 24 cm.

essential oils and flavoring compounds is also new to this edition. Specifications for flavor aromatics and isolates are now given in clear tabular form.

In the area of policy, the new edition contains a set of guidelines for "good manufacturing practice" developed by the Committee on Codex Specifications.

Officially, the Codex is recognized by the Food and Drug Administration which adopted certain Codex specifications in 1971.

This book is essential to anyone working in the areas of food science and technology, quality control, and good research. More than 600 scientists from a variety of disciplines contributed to this work as well as many trade associations and professional societies.

Purchasers of this edition are entitled to receive three supplements to the Codex, included in the purchase price.

Staff Review

Textbook of Biopharmaceutic Analysis. By R. V. SMITH and J. T. STEWART. Lea & Febiger, 600 Washington Square, Philadelphia, PA 19106. 1981. 308 pp. 18 × 25 cm. Price $25.00 (Canada $30.00)

To better prepare the practitioner for anticipated new roles in the delivery of health care, pharmaceutical education has evolved from a product oriented emphasis to a clinically oriented one. This change has given rise to such courses as biopharmaceutics, clinical pharmacy, and clinically oriented clerkships and externships. In addition, it often has necessitated the restructuring of the traditional basic science courses in order to provide a more adequate background for the clinical sciences. This textbook treats those aspects of analytical chemistry, analytical microbiology and biochemistry, and drug assay that concern the development and application of procedures for the determination of drugs and their metabolites in the biological fluids. This volume appears to be the first attempt to provide such a body of knowledge in textbook form for utilization in the pharmacy curriculum.

This book is divided into three sections: "Defining the Problem," "The Separation Step," and "The Measurement Step." This sequence is based on the approach that one would presumably follow in developing a methodology for the determination of a drug or its metabolites in biological fluids. The first section presents relevant background material, covers the development of methods for determining trace levels of medicaments in biological fluids, and deals with the procurement and characterization of reference standards. While three sources of reference standards are mentioned, unfortunately, the United States Pharmacopeial Convention has been overlooked.

The second section reviews the major separation and purification techniques including liquid–solid extraction, liquid–liquid extraction, partition coefficient, ion-pairing procedures, and the major chromatographic methods, *i.e.*, TLC, GC, HPLC, gel permeation, and ion-exchange chromatography.

The third section covers techniques for measurement and encompasses 10 chapters. Separate chapters are devoted to the following topics: statistical treatment of data, treatment of chromatographic data, UV-visible absorption and emission spectrophotometry, fluorimetry and phosphorimetry, electroanalytical methods, radiochemical methods, immunoassay techniques (RIA, EMIT, HI, SLFIA, and spin immunoassay), microbiological assay methods, enzymatic analysis, and a very brief concluding chapter on the method of selecting the appropriate analytical procedure for a particular situation. An array of pertinent literature references is provided at the end of each chapter along with a series of learning objectives to assist the student in reviewing the chapter content. Additional recommended readings are presented for more advanced students.

This text is written in a lucid manner, is well-organized, and the information is presented in a logical format. While the content of this book may be presented as a separate course offering, the subject matter may be more appropriately covered as segments in those courses where the basic concepts are taught, or it may possibly be included as a component of one of the clinical science courses. This material is important and serves well as a bridge between the clinical sciences and the basic pharmaceutical sciences. It merits consideration in the pharmaceutical curriculum.

Reviewed by Martin I. Blake
University of Illinois
College of Pharmacy
Chicago, IL 60612

Pharmacognosy, 8th edition. VARRO E. TYLER, LYNN R. BRADY, and JAMES E. ROBBERS. Lea & Febiger, Philadelphia, PA 19106. 1981. 520 pp. 18 × 25 cm. Illustrated with Numerous chemical structures, figures and photographs. Price: $31.50 U.S., $37.75 Canada.

This modern pharmacognosy text is all-inclusive and deals with drugs of natural origin that make up close to 50% of all medicinals currently employed. It has been the standard textbook of pharmacognosy in the U.S. for a number of years, and is the only one which has been periodically updated. It provides a systematic and comprehensive review of plant and animal drugs in a biochemical classification system. Major chapter titles include, general introduction, carbohydrates and related compounds, glycosides and tannins, lipids, volatile oils, resins, steroids, alkaloids, peptide hormones, enzymes, vitamins, antibiotics, biologicals, allergens and allergenic preparations, poisonous plants, and a new section entitled, herbs and "health foods". Several obsolete drugs and references have been deleted and new materials added where appropriate. Many of the chemical structures have been redrawn to reflect appropriate steric configurations. New prescription products as examples of the various drugs have been added as required.

In general, the new edition has retained the flavor of the previous ones with much updating. The chapter on herbs and "health foods" is a welcome addition to a subject that has gained popularity in recent years. This chapter has wisely divided the literature references into two groups, *e.g.*, authoritative and advocacy literature. This will help the pharmacist and others who use it, to determine whether the references their patients use are good or bad since self medication with herbs and teas has become common. However, several excellent recent references on the hazards of herbal teas and ginsing tea analysis have been omitted, and should be included in the next edition. As a constructive criticism, more recent key journal articles and reviews also should be included in the chapter references. This edition is really top-heavy with text references. Since text references tend to be dated by publication time, this policy detracts from access to recent literature and the usefulness of the book. This text is a must for all pharmacists.

Reviewed by Ara Der Marderosian
Professor of Pharmacognosy
Philadelphia College of
Pharmacy and Science
Philadelphia, PA 19104

BOOK NOTICES

Abrege de Chimie Analytique. Tome I. Chimie des Solutions. By MICHAEL GUERNET and MICHEL HAMON. Masson 120, bd St-Germain 75280 Paris, Cedex 06, France. 1981. 238 pp. 19 × 21 cm.

Addendum to the Second Supplement to USP XX and to NF XV. The United States Pharmacopeial Convention, Inc., 20th & Northampton Street, Easton, PA 18042. 342 pp.

Aliphatic and Related Natural Product Chemistry. Vol. 2. (A Specialist Periodical Report). Senior Reporter: F. D. GUNSTONE. The Royal Society of Chemistry, Distribution Centre, Blackhorse Rd., Letchworth Herts., SG6 1HN, England. 1981. 265 pp. 13 × 22 cm. Price $104.00.

Alkaloid Chemistry. By MANFRED HESSE. Wiley, One Wiley Drive, Somerset, NJ 08873. 1981. 231 pp. 15 × 23 cm.

Biochemical Regulation of Blood Pressure. Edited by RICHARD L. SOFFER. Wiley, One Wiley Drive, Somerset, NJ 08873. 1981. 456 pp. 15 × 23 cm. Price. $49.50.

Biochemistry of Antimicrobial Action. 3rd ed. By T. J. FRANKLIN and G. A. SNOW. Methuen, Inc. 733 Third Avenue, New York, NY 10017. 1981. 217 pp. 15 × 24 cm. Price $35.00 (hardcover), $17.95 (paperback).

Biopharmazie. Theorie und Praxis der Pharmakokinetik. By HERAUSGEGEBEN von J. MEIER, H. RETTIG and H. HESS. George Thieme Verlag, Stuttgart, West Germany. 1981. 473 pp. 17 × 24 cm. (German).

Coca and Cocaine, Vol. 3, issues 2–3 of the Journal of Ethno-Pharmacology. Edited by L. RIVIER, J. G. BRUHN. Elsevier, P. O. Box 211, 1000 AE Amsterdam, The Netherlands. 1981. 379 pp. 16 × 24 cm.

essential oils and flavoring compounds is also new to this edition. Specifications for flavor aromatics and isolates are now given in clear tabular form.

In the area of policy, the new edition contains a set of guidelines for "good manufacturing practice" developed by the Committee on Codex Specifications.

Officially, the Codex is recognized by the Food and Drug Administration which adopted certain Codex specifications in 1971.

This book is essential to anyone working in the areas of food science and technology, quality control, and good research. More than 600 scientists from a variety of disciplines contributed to this work as well as many trade associations and professional societies.

Purchasers of this edition are entitled to receive three supplements to the Codex, included in the purchase price.

Staff Review

Textbook of Biopharmaceutic Analysis. By R. V. SMITH and J. T. STEWART. Lea & Febiger, 600 Washington Square, Philadelphia, PA 19106. 1981. 308 pp. 18 × 25 cm. Price $25.00 (Canada $30.00)

To better prepare the practitioner for anticipated new roles in the delivery of health care, pharmaceutical education has evolved from a product oriented emphasis to a clinically oriented one. This change has given rise to such courses as biopharmaceutics, clinical pharmacy, and clinically oriented clerkships and externships. In addition, it often has necessitated the restructuring of the traditional basic science courses in order to provide a more adequate background for the clinical sciences. This textbook treats those aspects of analytical chemistry, analytical microbiology and biochemistry, and drug assay that concern the development and application of procedures for the determination of drugs and their metabolites in the biological fluids. This volume appears to be the first attempt to provide such a body of knowledge in textbook form for utilization in the pharmacy curriculum.

This book is divided into three sections: "Defining the Problem," "The Separation Step," and "The Measurement Step." This sequence is based on the approach that one would presumably follow in developing a methodology for the determination of a drug or its metabolites in biological fluids. The first section presents relevant background material, covers the development of methods for determining trace levels of medicaments in biological fluids, and deals with the procurement and characterization of reference standards. While three sources of reference standards are mentioned, unfortunately, the United States Pharmacopeial Convention has been overlooked.

The second section reviews the major separation and purification techniques including liquid–solid extraction, liquid–liquid extraction, partition coefficient, ion-pairing procedures, and the major chromatographic methods, *i.e.*, TLC, GC, HPLC, gel permeation, and ion-exchange chromatography.

The third section covers techniques for measurement and encompasses 10 chapters. Separate chapters are devoted to the following topics: statistical treatment of data, treatment of chromatographic data, UV-visible absorption and emission spectrophotometry, fluorimetry and phosphorimetry, electroanalytical methods, radiochemical methods, immunoassay techniques (RIA, EMIT, HI, SLFIA, and spin immunoassay), microbiological assay methods, enzymatic analysis, and a very brief concluding chapter on the method of selecting the appropriate analytical procedure for a particular situation. An array of pertinent literature references is provided at the end of each chapter along with a series of learning objectives to assist the student in reviewing the chapter content. Additional recommended readings are presented for more advanced students.

This text is written in a lucid manner, is well-organized, and the information is presented in a logical format. While the content of this book may be presented as a separate course offering, the subject matter may be more appropriately covered as segments in those courses where the basic concepts are taught, or it may possibly be included as a component of one of the clinical science courses. This material is important and serves well as a bridge between the clinical sciences and the basic pharmaceutical sciences. It merits consideration in the pharmaceutical curriculum.

Reviewed by Martin I. Blake
University of Illinois
College of Pharmacy
Chicago, IL 60612

Pharmacognosy, 8th edition. VARRO E. TYLER, LYNN R. BRADY, and JAMES E. ROBBERS. Lea & Febiger, Philadelphia, PA 19106. 1981. 520 pp. 18 × 25 cm. Illustrated with Numerous chemical structures, figures and photographs. Price: $31.50 U.S., $37.75 Canada.

This modern pharmacognosy text is all-inclusive and deals with drugs of natural origin that make up close to 50% of all medicinals currently employed. It has been the standard textbook of pharmacognosy in the U.S. for a number of years, and is the only one which has been periodically updated. It provides a systematic and comprehensive review of plant and animal drugs in a biochemical classification system. Major chapter titles include, general introduction, carbohydrates and related compounds, glycosides and tannins, lipids, volatile oils, resins, steroids, alkaloids, peptide hormones, enzymes, vitamins, antibiotics, biologicals, allergens and allergenic preparations, poisonous plants, and a new section entitled, herbs and "health foods". Several obsolete drugs and references have been deleted and new materials added where appropriate. Many of the chemical structures have been redrawn to reflect appropriate steric configurations. New prescription products as examples of the various drugs have been added as required.

In general, the new edition has retained the flavor of the previous ones with much updating. The chapter on herbs and "health foods" is a welcome addition to a subject that has gained popularity in recent years. This chapter has wisely divided the literature references into two groups, *e.g.*, authoritative and advocacy literature. This will help the pharmacist and others who use it, to determine whether the references their patients use are good or bad since self medication with herbs and teas has become common. However, several excellent recent references on the hazards of herbal teas and ginsing tea analysis have been omitted, and should be included in the next edition. As a constructive criticism, more recent key journal articles and reviews also should be included in the chapter references. This edition is really top-heavy with text references. Since text references tend to be dated by publication time, this policy detracts from access to recent literature and the usefulness of the book. This text is a must for all pharmacists.

Reviewed by Ara Der Marderosian
Professor of Pharmacognosy
Philadelphia College of
Pharmacy and Science
Philadelphia, PA 19104

BOOK NOTICES

Abrege de Chimie Analytique. Tome I. Chimie des Solutions. By MICHAEL GUERNET and MICHEL HAMON. Masson 120, bd St-Germain 75280 Paris, Cedex 06, France. 1981. 238 pp. 19 × 21 cm.

Addendum to the Second Supplement to USP XX and to NF XV. The United States Pharmacopeial Convention, Inc., 20th & Northampton Street, Easton, PA 18042. 342 pp.

Aliphatic and Related Natural Product Chemistry. Vol. 2. (A Specialist Periodical Report). Senior Reporter: F. D. GUNSTONE. The Royal Society of Chemistry, Distribution Centre, Blackhorse Rd., Letchworth Herts., SG6 1HN, England. 1981. 265 pp. 13 × 22 cm. Price $104.00.

Alkaloid Chemistry. By MANFRED HESSE. Wiley, One Wiley Drive, Somerset, NJ 08873. 1981. 231 pp. 15 × 23 cm.

Biochemical Regulation of Blood Pressure. Edited by RICHARD L. SOFFER. Wiley, One Wiley Drive, Somerset, NJ 08873. 1981. 456 pp. 15 × 23 cm. Price. $49.50.

Biochemistry of Antimicrobial Action. 3rd ed. By T. J. FRANKLIN and G. A. SNOW. Methuen, Inc. 733 Third Avenue, New York, NY 10017. 1981. 217 pp. 15 × 24 cm. Price $35.00 (hardcover), $17.95 (paperback).

Biopharmazie. Theorie und Praxis der Pharmakokinetik. By HERAUSGEGEBEN von J. MEIER, H. RETTIG and H. HESS. George Thieme Verlag, Stuttgart, West Germany. 1981. 473 pp. 17 × 24 cm. (German).

Coca and Cocaine, Vol. 3, issues 2–3 of the Journal of Ethno-Pharmacology. Edited by L. RIVIER, J. G. BRUHN. Elsevier, P. O. Box 211, 1000 AE Amsterdam, The Netherlands. 1981. 379 pp. 16 × 24 cm.

essential oils and flavoring compounds is also new to this edition. Specifications for flavor aromatics and isolates are now given in clear tabular form.

In the area of policy, the new edition contains a set of guidelines for "good manufacturing practice" developed by the Committee on Codex Specifications.

Officially, the Codex is recognized by the Food and Drug Administration which adopted certain Codex specifications in 1971.

This book is essential to anyone working in the areas of food science and technology, quality control, and good research. More than 600 scientists from a variety of disciplines contributed to this work as well as many trade associations and professional societies.

Purchasers of this edition are entitled to receive three supplements to the Codex, included in the purchase price.

Staff Review

Textbook of Biopharmaceutic Analysis. By R. V. SMITH and J. T. STEWART. Lea & Febiger, 600 Washington Square, Philadelphia, PA 19106. 1981. 308 pp. 18 × 25 cm. Price $25.00 (Canada $30.00)

To better prepare the practitioner for anticipated new roles in the delivery of health care, pharmaceutical education has evolved from a product oriented emphasis to a clinically oriented one. This change has given rise to such courses as biopharmaceutics, clinical pharmacy, and clinically oriented clerkships and externships. In addition, it often has necessitated the restructuring of the traditional basic science courses in order to provide a more adequate background for the clinical sciences. This textbook treats those aspects of analytical chemistry, analytical microbiology and biochemistry, and drug assay that concern the development and application of procedures for the determination of drugs and their metabolites in the biological fluids. This volume appears to be the first attempt to provide such a body of knowledge in textbook form for utilization in the pharmacy curriculum.

This book is divided into three sections: "Defining the Problem," "The Separation Step," and "The Measurement Step." This sequence is based on the approach that one would presumably follow in developing a methodology for the determination of a drug or its metabolites in biological fluids. The first section presents relevant background material, covers the development of methods for determining trace levels of medicaments in biological fluids, and deals with the procurement and characterization of reference standards. While three sources of reference standards are mentioned, unfortunately, the United States Pharmacopeial Convention has been overlooked.

The second section reviews the major separation and purification techniques including liquid–solid extraction, liquid–liquid extraction, partition coefficient, ion-pairing procedures, and the major chromatographic methods, *i.e.*, TLC, GC, HPLC, gel permeation, and ion-exchange chromatography.

The third section covers techniques for measurement and encompasses 10 chapters. Separate chapters are devoted to the following topics: statistical treatment of data, treatment of chromatographic data, UV-visible absorption and emission spectrophotometry, fluorimetry and phosphorimetry, electroanalytical methods, radiochemical methods, immunoassay techniques (RIA, EMIT, HI, SLFIA, and spin immunoassay), microbiological assay methods, enzymatic analysis, and a very brief concluding chapter on the method of selecting the appropriate analytical procedure for a particular situation. An array of pertinent literature references is provided at the end of each chapter along with a series of learning objectives to assist the student in reviewing the chapter content. Additional recommended readings are presented for more advanced students.

This text is written in a lucid manner, is well-organized, and the information is presented in a logical format. While the content of this book may be presented as a separate course offering, the subject matter may be more appropriately covered as segments in those courses where the basic concepts are taught, or it may possibly be included as a component of one of the clinical science courses. This material is important and serves well as a bridge between the clinical sciences and the basic pharmaceutical sciences. It merits consideration in the pharmaceutical curriculum.

Reviewed by Martin I. Blake
University of Illinois
College of Pharmacy
Chicago, IL 60612

Pharmacognosy, 8th edition. VARRO E. TYLER, LYNN R. BRADY, and JAMES E. ROBBERS. Lea & Febiger, Philadelphia, PA 19106. 1981. 520 pp. 18 × 25 cm. Illustrated with Numerous chemical structures, figures and photographs. Price: $31.50 U.S., $37.75 Canada.

This modern pharmacognosy text is all-inclusive and deals with drugs of natural origin that make up close to 50% of all medicinals currently employed. It has been the standard textbook of pharmacognosy in the U.S. for a number of years, and is the only one which has been periodically updated. It provides a systematic and comprehensive review of plant and animal drugs in a biochemical classification system. Major chapter titles include, general introduction, carbohydrates and related compounds, glycosides and tannins, lipids, volatile oils, resins, steroids, alkaloids, peptide hormones, enzymes, vitamins, antibiotics, biologicals, allergens and allergenic preparations, poisonous plants, and a new section entitled, herbs and "health foods". Several obsolete drugs and references have been deleted and new materials added where appropriate. Many of the chemical structures have been redrawn to reflect appropriate steric configurations. New prescription products as examples of the various drugs have been added as required.

In general, the new edition has retained the flavor of the previous ones with much updating. The chapter on herbs and "health foods" is a welcome addition to a subject that has gained popularity in recent years. This chapter has wisely divided the literature references into two groups, *e.g.*, authoritative and advocacy literature. This will help the pharmacist and others who use it, to determine whether the references their patients use are good or bad since self medication with herbs and teas has become common. However, several excellent recent references on the hazards of herbal teas and ginsing tea analysis have been omitted, and should be included in the next edition. As a constructive criticism, more recent key journal articles and reviews also should be included in the chapter references. This edition is really top-heavy with text references. Since text references tend to be dated by publication time, this policy detracts from access to recent literature and the usefulness of the book. This text is a must for all pharmacists.

Reviewed by Ara Der Marderosian
Professor of Pharmacognosy
Philadelphia College of
Pharmacy and Science
Philadelphia, PA 19104

BOOK NOTICES

Abrege de Chimie Analytique. Tome I. Chimie des Solutions. By MICHAEL GUERNET and MICHEL HAMON. Masson 120, bd St-Germain 75280 Paris, Cedex 06, France. 1981. 238 pp. 19 × 21 cm.

Addendum to the Second Supplement to USP XX and to NF XV. The United States Pharmacopeial Convention, Inc., 20th & Northampton Street, Easton, PA 18042. 342 pp.

Aliphatic and Related Natural Product Chemistry. Vol. 2. (A Specialist Periodical Report). Senior Reporter: F. D. GUNSTONE. The Royal Society of Chemistry, Distribution Centre, Blackhorse Rd., Letchworth Herts., SG6 1HN, England. 1981. 265 pp. 13 × 22 cm. Price $104.00.

Alkaloid Chemistry. By MANFRED HESSE. Wiley, One Wiley Drive, Somerset, NJ 08873. 1981. 231 pp. 15 × 23 cm.

Biochemical Regulation of Blood Pressure. Edited by RICHARD L. SOFFER. Wiley, One Wiley Drive, Somerset, NJ 08873. 1981. 456 pp. 15 × 23 cm. Price. $49.50.

Biochemistry of Antimicrobial Action. 3rd ed. By T. J. FRANKLIN and G. A. SNOW. Methuen, Inc. 733 Third Avenue, New York, NY 10017. 1981. 217 pp. 15 × 24 cm. Price $35.00 (hardcover), $17.95 (paperback).

Biopharmazie. Theorie und Praxis der Pharmakokinetik. By HERAUSGEGEBEN von J. MEIER, H. RETTIG and H. HESS. George Thieme Verlag, Stuttgart, West Germany. 1981. 473 pp. 17 × 24 cm. (German).

Coca and Cocaine, Vol. 3, issues 2–3 of the Journal of Ethno-Pharmacology. Edited by L. RIVIER, J. G. BRUHN. Elsevier, P. O. Box 211, 1000 AE Amsterdam, The Netherlands. 1981. 379 pp. 16 × 24 cm.

Controlled Release of Pesticides and Pharmaceuticals. Edited by DANNY H. LEWIS. Plenum, 227 West 17th St., New York, NY 10011. 1981. 339 pp. 15 × 25 cm. Price $42.50.

Demographic Trends and Drug Abuse, 1980–1995. (NIDA Research Monograph 35, May 1981). Edited by LOUISE G. RICHARDS. National Institute of Drug Abuse, Division of Research, 5600 Fishers Lane, Rockville, MD 20857. 1981. 102 pp. 14 × 23 cm.

Hazards in the Chemical Laboratory. Edited by L. BRETHERICK. The Royal Society of Chemistry, Distribution Centre, Blackhorse Road, Letchworth, Herts., SG6 1HN, England. 1981. 567 pp. 15 × 21 cm. Price £15.00.

Le Rat de Laboratorie. 1-Reactif Biologique. By GUY JADOT. Masson, 120 Boulevard Saint-Germain 75280. Paris, Cedex 06, France. 1981. 115 pp. 13 × 21 cm.

Medicinal & Aromatic Plants Abstracts. Edited by S. NAGARAJAN and H. C. JAIN. Vol. 3. No. 1. pp. 1–116-2/81 ISSN:0250-4367. (Reporting Current World Literature). Including a bibliography on *Tylophora indica (Burm.f.)* Merrill. Publication & Information Directorate, CSIR Hillside Rd., New Delhi-110012. 115 pp. 17 × 24 cm.

Microbial Testers. Probing Carcinogenesis. Edited by I. CECIL FELKNER. Dekker, 270 Madison Ave., New York, NY 10016. 1981. 264 pp. 15 × 23 cm.

Neurotransmitter Receptors. Part 2. Biogenic Amines. (Receptors and Recognition. Series B Volume 10). Edited by H. I. YAMAMURA and S. J. ENNA. Methuen, Inc., 733 Third Ave., New York, NY 10017. 1981. 273 pp. 15 × 24 cm. Price $37.50.

Organisch-chemische Nomenklatur. Einfuhrung in die Grundlagen mit Regeln und Beispielen. By Von Dr. PHILIPP FRESENIUS, Karlsruhe. Wissenschaftliche Verlagsgesellschaft mbH Postfach 40, 7000 Stuttgart 1, West Germany. 1981. 139 pp. 15 × 23 cm. Price DM 28.

Pharmacology for the Anesthesiologist. By BIJAN K. BASAK. Technomic Publishing Co., Inc., 265 Post Rd. West, Westport, CT 06880. 1981. 209 pp. 15 × 23 cm. Price $22.50.

Pharmacy, Drugs and Medical Care. 3rd ed. By MICKEY C. SMITH and DAVID A. KNAPP. The Williams & Wilkins Co., P. O. Box 969, Easton, MD 21601. 1981. 330 pp. 15 × 23 cm. Price $19.95.

Pharmazeutisches Taschenbuch. By von HANS KAISER and von HERMANN J. ROTH. Wissenschaftliche Verlagsgesellschaft mbH, Postfach 40, D-7000 Stuttgart 1, West Germany. 1981. 675 pp. 12 × 17 cm. Price DM 74. (German).

Pills & the Public Purse. The Routes to National Drug Insurance. By MILTON SILVERMAN, PHILIP R. LEE, and MIA LYDECKER. University of California Press, 2223 Fulton St., Berkeley, CA 94720. 1981. 231 pp. 15 × 23 cm. Price $15.95.

Protective Groups in Organic Synthesis. By THEODORA W. GREENE. Wiley, One Wiley Drive, Somerset, NJ 08873. 1981. 349 pp. 15 × 23 cm. Price $37.50.

Psychotropic Drug Handbook. 3rd ed. By PAUL PERRY, BRUCE ALEXANDER, and BARRY L. LISKOW. Harvey Whitney Books, 4906 Cooper Rd., Cincinnati, Ohio 45242. 1981. 198 pp. 10 × 17 cm. Price $9.50.

Purinergic Receptors. Receptors and Recognition. Series B Vol. 12. Edited by G. BURNSTOCK. Methuen Inc., 733 Third Ave., New York, NY 10017. 1981. 365 pp. 15 × 23 cm. Price $49.95.

Reagents for Organic Synthesis. Vol. 9. By MARY FIESER, RICK L. DANHEISER, and WILLIAM R. ROUSH. Wiley, One Wiley Drive, Somerset, NJ 08873. 1981. 596 pp. 15 × 23 cm. Price $39.50.

Regulatory Toxicology and Pharmacology. Vol. 1, Number 1, June 1981. Edited by FREDERICK COULSTON, ALBERT C. KOLBYE, JR., and C. JELLEFF CARR. Academic Press, 111 Fifth Ave., New York, NY 10003. 1981. 112 pp. 17 × 25 cm.

The Total Synthesis of Natural Products. Vol. 4. Edited by JOHN APSIMON. Wiley, One Wiley Drive, Somerset, NJ 08873. 1981. 610 pp. 15 × 23 cm. Price $60.00.

A publication of the
American Pharmaceutical Association—
the National Professional Society
of Pharmacists

JOURNAL OF PHARMACEUTICAL SCIENCES

INDEX TO AUTHORS
INDEX TO SUBJECTS

VOLUME 71
JANUARY TO DECEMBER, 1982

Published monthly under the supervision of the Board of Trustees

An Updated Review of the "Drug Lag"

At the time this editorial is being written—and which, due to the lead-time necessitated by the *Journal's* production schedule, is long before our subscribers will have an opportunity to read it—the public press and broadcast media are filled with widely contradictory assessments as to whether the United States or the Soviet Union currently enjoys overall military superiority.

In many respects, this debate reminds us of a similar one in the health care field which has raged on with comparable intensity and, seemingly, for as lengthy a period of time. We refer to the so-called "drug lag"—a highly controversial subject which we have addressed in editorials on several previous occasions and most particularly in the April 1978 issue of this journal.

All sorts of data, statistics, and "evidence" are paraded out by those on each side of the question in an attempt to prove their claim that either (*a*) in this country, drugs are approved much more slowly than in other developed nations, with the result that the American public is deprived of significant public health benefits, or (*b*) there really is little, if any, difference in the speed of U.S. drug approvals when compared across the board with other major nations.

Furthermore, it cannot be claimed that the issue has suffered from lack of attention or study. Indeed, at least four separate analyses have either just been completed or are about to be so.

These include: (*a*) a study by the FDA's Office of Planning and Evaluation, which was released in mid-March 1982; (*b*) another study conducted at George Washington University under a contract from FDA's New Drug Evaluation Division, which also was released in mid-March 1982; (*c*) an analysis being conducted by the FDA Commissioner's Task Force on New Drug Review, which is soon to submit its report through Health and Human Services Secretary Richard S. Schweiker; and (*d*) the findings and recommendations of the Federal Drug Approval Process Commission, a body sponsored by the U.S. Congress and serving under the chairmanship of F. Gilbert McMahon of Tulane University. At the time of our writing, this latter body was circulating a "final draft" version of its recommendations, and the formal report itself was due to be released almost any day.

Hopefully, each of these studies in its own way will contribute to an understanding of the process and to improvements in its operation.

But even while these studies were still under way, we noted a number of new drug approvals that were announced with accompanying FDA statements that the approval was processed in some sort of expedited manner. Two of the most recent "fast-track" drug approvals included the antiviral herpes agent, acyclovir, which cleared FDA in less than 9 months, and the calcium channel blocker, verapamil, which completed all its FDA processing in just over a year from first filing.

These examples—and several similar ones—demonstrate that, given the right set of circumstances, FDA drug approval can be quite swift.

Finally, we were especially impressed with an FDA year-end report released in early January of this year, in which it was claimed that over twice as many new drug entities were approved during 1981 (27 in all) as compared with 1980 (12 in all). Furthermore, the FDA's statistics showed that the average period from submission of application to final approval for marketing of new chemical entities has dropped from 37.5 months in 1979 to 31.2 months in 1981. With respect to the "fast-track" drugs, the decline was even more dramatic: from 17 months in 1976–78 to just 10 months in the 1979–81 period.

Even the General Accounting Office—not known for handing out very many good "report cards"—issued a conclusion to an investigation it completed in late 1981, which stated that the FDA, since 1978, has "approved more drugs in less time than before, despite an increased workload."

All of this suggests to us that if truly there ever was a drug lag, it no longer exists—or is at least of manageable proportions and susceptible to administrative remedies within the regulatory agency. Consequently, new legislation or major changes in the pertinent existing regulations would now appear to be of doubtful value.

Indeed, legislative or regulatory tinkering could actually prove to be more disruptive than beneficial, insofar as expediting the judicious approval of new drugs. With those thoughts in mind, we personally would recommend that, for the immediate future anyway, Congress "cool it" with respect to amending the present drug approval provisions of the Federal Food, Drug, and Cosmetic Act.

—EDWARD G. FELDMANN
American Pharmaceutical Association
Washington, DC 20037

0022-3549/82/0500-0483$01.00/0

JOURNAL OF PHARMACEUTICAL SCIENCES

MAY 1982
VOLUME 71 NUMBER 5

RESEARCH ARTICLES

Kinetics and Mechanism of Hydroxy Group Acetylations Catalyzed by *N*-Methylimidazole

NIVEDITA K. PANDIT * **and KENNETH A. CONNORS** ˣ

Received July 6, 1981, from the *School of Pharmacy, University of Wisconsin, Madison, WI 53706.* Accepted for publication September 4, 1981. * Present address: Boehringer-Ingelheim, Ridgefield, CT 06877.

Abstract □ The kinetics of acetylation of alcohols by acetyl chloride and acetic anhydride, with *N*-methylimidazole as the catalyst, were studied in acetonitrile solution at 25°; some measurements were also made with 4-dimethylaminopyridine as the catalyst. The acetic anhydride–*N*-methylimidazole system proceeds entirely by a general base catalysis, whereas the acetyl chloride–*N*-methylimidazole system reacts entirely *via* a nucleophilic route, with the intermediate formation of the *N*-acylated catalyst. The reaction of this intermediate with the alcohol is general base catalyzed. The acetyl chloride–4-dimethylaminopyridine system also reacts *via* the nucleophilic route. In the acetic anhydride–4-dimethylaminopyridine system a small fraction of the intermediate was detected. The acetic anhydride–*N*-methylimidazole system was studied in *n*-propanol–acetonitrile solvent mixtures; no spectral evidence for intermediate formation was seen. However, the hydrolysis reaction in acetic anhydride–*N*-methylimidazole, studied over a wide range of water–acetonitrile mixtures, revealed a change in mechanism from general base in dry acetonitrile to a solely nucleophilic route at high water concentrations.

Keyphrases □ Acetylation—kinetics and mechanism, hydroxy groups catalyzed by *N*-Methylimidazole □ Kinetics—mechanism of hydroxy group acetylations, catalyzed by *N*-Methylimidazole □ *N*-Methylimidazole—kinetics and mechanism of hydroxy group acetylations, catalyst □ 4-Dimethylaminopyridine, acetylation catalyst.

Acetylations of hydroxy compounds are usually carried out with acetic anhydride or acetyl chloride as the acylating agent. Pyridine is commonly used as a catalyst. Several catalysts more powerful than pyridine are now available, most notably 4-dimethylaminopyridine, which was developed by Steglich and Höfle (1–3) as a catalyst for synthetic acetylations, and has since been applied to analytical acetylations (4–7). This study introduced *N*-methylimidazole as an analytical acylation catalyst (8–11). The relative catalytic effectiveness of pyridine–*N*-methylimidazole–4-dimethylaminopyridine is about $1:3 \times 10^2:1.7 \times 10^4$, respectively (12), in aprotic solvents.

Although the mechanisms of acyl transfer reactions have been well studied, most investigations have been of acyl transfer to water, that is, of the hydrolysis of carboxylic acid derivatives in aqueous solution. These kinetic and mechanistic results, therefore, may not be applicable to acylation reactions carried out in aprotic solvents. Because synthetic and analytical acylations usually employ nonaqueous media, it is important to understand the course of the reactions and the role of the catalyst in these systems, and several laboratories have described studies of the newer catalysts (particularly of 4-dimethylaminopyridine) in aprotic solvents. The mechanism of the catalysis is not well understood, and there is disagreement among the interpretations of reactivity data for these systems; these viewpoints are cited in the later discussion.

To achieve an understanding of the mode of catalysis by *N*-methylimidazole, the present study was designed to allow systematic kinetic measurements to be made over a wide range of conditions. The reaction systems are relatively simple but represent practical situations. Acetic anhydride and acetyl chloride are the two acylating agents studied. *N*-methylimidazole is the catalyst, though some observations were also made on 4-dimethylaminopyridine because of its importance; hence, four separate combinations of acylating agent and catalyst were studied. The acyl acceptor was an alcohol or water, and the solvent was acetonitrile, modified in some cases by the addition of alcohol or water.

EXPERIMENTAL

Materials—Acetyl chloride and acetic anhydride, analytical reagent grade[1], were used directly. *N*-Methylimidazole[2] was distilled at 10–12 mm Hg pressure; atmospheric bp 199°. 4-Dimethylaminopyridine[2] was recrystallized from *n*-hexane; mp 113°. The alcohols were of analytical reagent quality and were used directly; their purities were checked by gas chromatography.

[1] Mallinckrodt Chemical Co.
[2] Aldrich Chemical Co.

0022-3549/82/0500-0485$01.00/0

Acetonitrile, technical grade[2], was refluxed over phosphorus pentoxide for 1 hr, then distilled from phosphorus pentoxide at 80–81°. The water content of this product was ~0.003% as determined by visual Karl Fischer titration.

Kinetic Procedure—A typical kinetic run was carried out as follows: Solutions of appropriate concentrations of the acetylating agent, the catalyst, and the hydroxy compound were prepared in acetonitrile and equilibrated at 25 ± 0.1°. Acetonitrile (4.0 ml), 3.0 ml of the catalyst solution, and 1.0 ml of the acetylating agent solution were added to a 10-ml volumetric flask. The reaction was initiated by adding 2.0 ml of the solution of hydroxy compound. The well-mixed solution was transferred to a 1-cm spectrophotometer cell, and the absorbance was monitored at a selected wavelength as a function of time[3]. The absorbance at the completion of reaction (A_∞) was measured after the lapse of ~10 half-lives.

All measurements were made at 25.0 ± 0.1°.

RESULTS AND DISCUSSION

Kinetic Scheme—The design and interpretation of the kinetic experiments were based on the model represented by Scheme I:

$$AX + N \underset{k_{-1}}{\overset{k_1}{\rightleftharpoons}} I^+ + X^-$$

$$\downarrow k'_A[\mathrm{ROH}] \qquad \downarrow k'_I[\mathrm{ROH}]$$

$$AOR + HX \qquad AOR + NH^+$$

Scheme I

where AX is the acetyl compound (acetyl chloride or acetic anhydride), N is the catalyst (N-methylimidazole or 4-dimethylaminopyridine), I^+ is an intermediate acetylammonium ion, X^- is the counterion (chloride or acetate), and ROH is the acetyl acceptor (alcohol or water). Although a single general rate equation is too complex to be useful, several important cases arise from the operation of: (*a*) the ratio k_1/k_{-1}; (*b*) the detailed nature of k'_A and k'_I; (*c*) the relative magnitudes of k'_A and k'_I; (*d*) the relative concentrations of the reactants; (*e*) the method of observation; (*f*) the nature of ROH. The experiments were designed to evaluate the validity of Scheme I and to obtain estimates of the parameters. Scheme II outlines some of the possible cases:

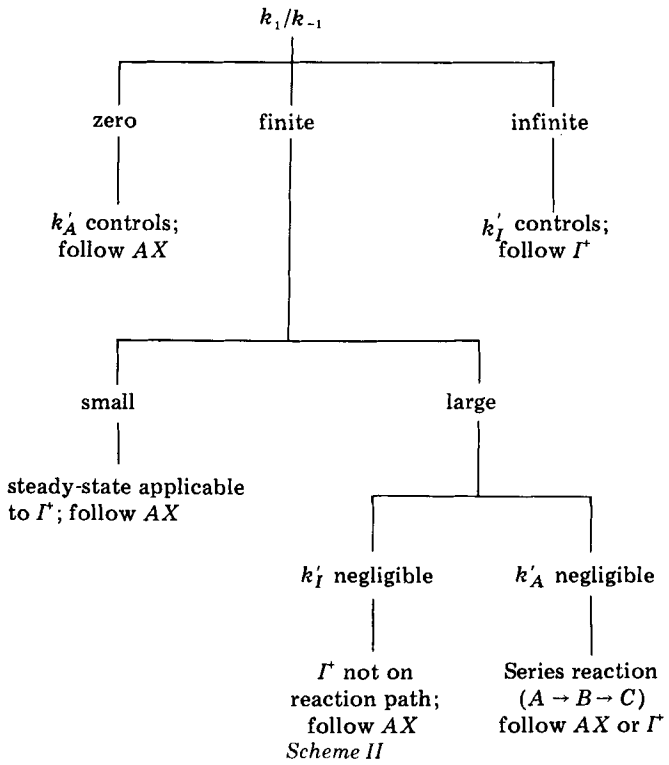

Scheme II

[3] Cary 14 and Cary 16 spectrophotometers, equipped with thermostatted cell compartments.

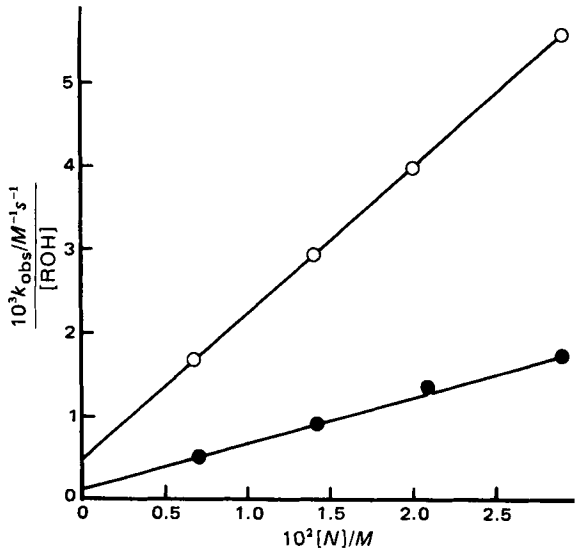

Figure 1—*Plot according to Eq. 3 for the acetylchloride–*N*-methylimidazole system. Key: (○), sec-butanol; (●), isopropanol.*

In this study the reactions were followed spectrophotometrically by monitoring the loss of AX or I^+ with time. The initial concentration of hydroxy compound usually was at least 50 times that of the acetylating agent, and in most cases good first-order behavior was observed, the apparent first-order rate constant k_{obs} being evaluated from a plot of log $(A_t - A_\infty)$ *versus* time. The precision of k_{obs} was ~2%. Deviations from first-order behavior are pointed out as appropriate.

Acetyl Chloride–*N*-Methylimidazole–Alcohols—When acetonitrile solutions of acetyl chloride and N-methylimidazole are mixed, the absorbance of the resulting solution is much greater than that calculated for the mixture of reactants. It is inferred that a very fast and quantitative formation of N-acetyl-N'-methylimidazolium ion occurs; this is the intermediate I^+ in Scheme I. At a given concentration of catalyst and varying concentrations of acetyl chloride, the same absorbance was produced as long as $[AX]_0 > [N]_0$ and *vice versa*, showing that the formation of I^+ was quantitative. The spectrum of the intermediate showed λ_{max} = 245 nm, log ϵ_{max} = 3.51. Since N-methylimidazole shows λ_{min} = 245 nm, log ϵ_{min} = 0.2, the reaction was followed at 245 nm, with initial condition $[AX]_0 < [N]_0$. In a typical reaction $[AX]_0 = 8 \times 10^{-4}$ M and $[\mathrm{ROH}]_0 = 0.5$ M.

This system therefore appears to be a case in which k_1/k_{-1} is essentially infinite (Scheme II), the observed reaction being (Scheme III):

$$I^+ + \mathrm{ROH} \xrightarrow{k'_I} \mathrm{ROAc} + NH^+$$

Scheme III

In Scheme III ROAc represents the acetylated alcohol.

It is anticipated that k'_I is given by Eq. 1, which is a testable assumption.

$$k'_I = k_I + k_{IN}[N] \qquad \text{(Eq. 1)}$$

The hypothetical rate equation is, therefore:

$$\frac{-d[I^+]}{dt} = (k_I + k_{IN}[N])[I^+][\mathrm{ROH}] \qquad \text{(Eq. 2)}$$

The experimental rate equation was found to be $-d[I^+]/dt = k_{obs}[I^+]$, the plots being linear over the course of the reactions. Therefore:

$$\frac{k_{obs}}{[\mathrm{ROH}]} = k_I + k_{IN}[N] \qquad \text{(Eq. 3)}$$

Table I—Rate Constants for the Acetyl Chloride–*N*-Methylimidazole System in Acetonitrile at 25° [a]

Alcohol	$10^3 k_I/M^{-1}s^{-1}$	$k_{IN}/M^{-2}s^{-2}$	$10^3 k_A/M^{-1}s^{-1}$
n-Propanol	0.16 (0.025)	0.50 (0.007)	4.61 (0.021)
n-Butanol	0.36 (0.026)	0.98 (0.006)	4.49 (0.032)
Isopropanol	0.15 (0.030)	0.053 (0.002)	1.49 (0.036)
sec-Butanol	0.49 (0.024)	0.17 (0.001)	3.32 (0.025)

[a] Standard deviation in parentheses, evaluated from the least-squares fit to the appropriate linear equation.

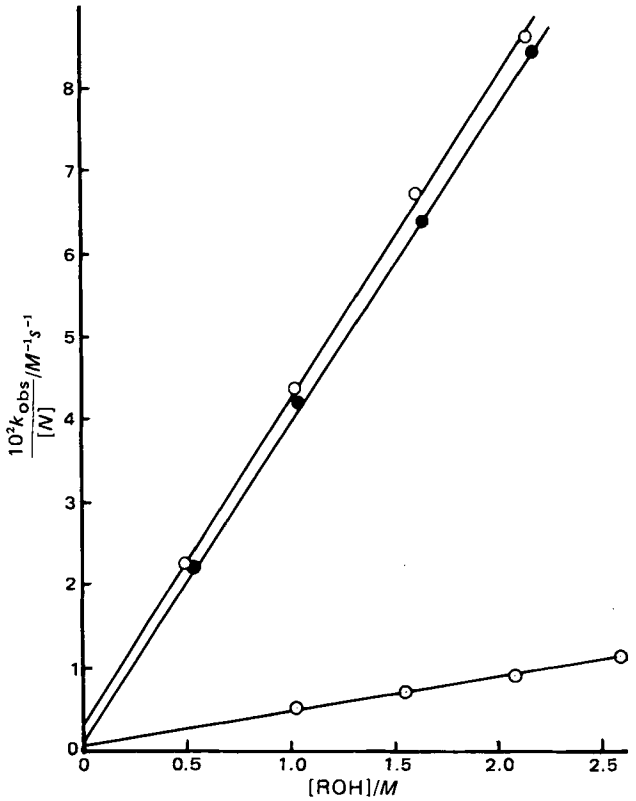

Figure 2—*Plot according to Eq. 9 for the acetic anhydride–*N*-methylimidazole system. Lines from top to bottom:* n-*propanol,* n-*butanol, isopropanol.*

Equation 3 suggests that a plot of $k_{obs}/[ROH]$ *versus* $[N]$ will be linear, where $[N]$ represents free *N*-methylimidazole. Since it was shown that conversion to the intermediate is quantitative, $[N]$ is given by:

$$[N] = [N]_0 - [AX]_0 \qquad \text{(Eq. 4)}$$

Moreover, $[N]$ should remain constant at this value throughout the course of the reaction, because each *N*-methylimidazole released from I^+ upon reaction with ROH accepts a proton, since it is the strongest base in the system.

Figure 1 shows a plot according to Eq. 3 for *sec*-butanol and isopropanol. Similar behavior was observed for *n*-propanol and *n*-butanol, and the resulting estimates of k_I and k_{IN} are listed in Table I.

To evaluate k'_A, the acetylation of these four alcohols by acetyl chloride was examined in the absence of *N*-methylimidazole. The first-order plots were linear for ~1 half-life, perhaps as a consequence of the proton release accompanying the acetylation. If k'_A is given by:

$$k'_A = k_A + k_{AN}[N] \qquad \text{(Eq. 5)}$$

evidently the rate equation in the absence of *N*-methylimidazole is $-d[AX]/dt = k_A[AX][ROH]$, or $k_{obs}/[ROH] = k_A$, where k_{obs} is evaluated from the initial linear portion of the plots. The k_A estimates obtained in this way are given in Table I.

It is evidently impossible to determine k_{AN} for this system, because acetyl chloride and *N*-methylimidazole cannot coexist in significant concentrations.

Acetic Anhydride–*N*-Methylimidazole–Alcohols—When acetonitrile solutions of acetic anhydride and *N*-methylimidazole are mixed, the resulting spectrum can be quantitatively accounted for as the sum of the spectra of these two solutes; thus, there is no spectral evidence for intermediate formation. Since the counterion should have little effect on the spectrum of the cation, and the intermediate in the acetyl chloride–*N*-methylimidazole system exhibited an intense absorption at 245 nm, it is inferred that in the present case k_1/k_{-1} is close to zero. The acetylating agent is acetic anhydride (λ_{max} = 240 nm, log ϵ_{max} = 2.0). The reaction was monitored at 245 nm, corresponding to a minimum in the spectrum of the catalyst. The apparent first-order plots were linear for at least 4 half-lives. The initial concentrations were: acetic anhydride, 0.02 *M*; alcohols, 0.5–2.6 *M*; *N*-methylimidazole, 0.011–0.11 *M*.

Table II—Rate Constants for the Acetic Anhydride–*N*-Methylimidazole System in Acetonitrile at 25° [a]

Alcohol	$10^3 k_1/M^{-1}s^{-1}$	$10^5 k_A/M^{-1}s^{-1}$	$10^2 k_{AN}/M^{-2}s^{-1}$
n-Propanol	0.70 (1.05)	2.4 (3.7)	4.03 (0.05)
n-Butanol	1.20 (1.42)	8.3 (10.2)	3.80 (0.06)
Isopropanol	0.007 (0.011)	0.15 (0.11)	0.413 (0.002)

[a] Standard deviation in parentheses.

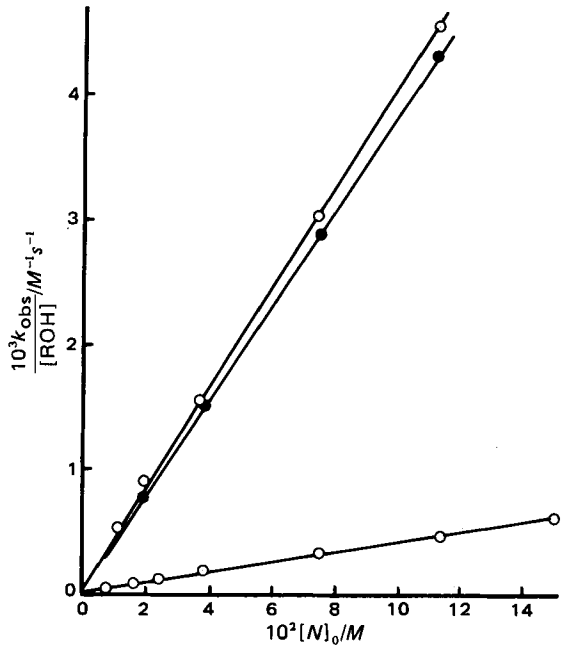

Figure 3—*Plot according to Eq. 10 for the acetic anhydride–*N*-methylimidazole system. Lines from top to bottom:* n-*propanol,* n-*butanol, isopropanol.*

Although the intermediate could not be detected spectrally, its possible presence is admitted in the rate equation for the loss of anhydride:

$$-\frac{d[AX]}{dt} = k_1[AX][N] + k'_A[AX][ROH] - k_{-1}[I^+][X^-] \qquad \text{(Eq. 6)}$$

The assumption is made that all of the H^+ produced in the acetylation is accepted by X^- (acetate); then $[X^-] = 0$, so Eq. 6 becomes:

$$-\frac{d[AX]}{dt} = k_1[AX][N] + k'_A[AX][ROH] \qquad \text{(Eq. 7)}$$

This assumption is justified in the later discussion. By hypothesis, $k'_A = k_A + k_{AN}[N]$. The experimental rate equation is $-d[AX]/dt = k_{obs}[AX]$, so:

$$k_{obs} = k_1[N] + k_A[ROH] + k_{AN}[ROH][N] \qquad \text{(Eq. 8)}$$

If in a series of experiments the catalyst concentration is held constant while the alcohol concentration is varied, the plotting form of Eq. 9 is used:

$$\frac{k_{obs}}{[N]} = k_1 + \left(\frac{k_A}{[N]} + k_{AN}\right)[ROH] \qquad \text{(Eq. 9)}$$

whereas, if [ROH] is kept constant and $[N]$ is varied, Eq. 10 can be used.

$$\frac{k_{obs}}{[ROH]} = k_A + \left(\frac{k_1}{[ROH]} + k_{AN}\right)[N] \qquad \text{(Eq. 10)}$$

Thus, from the slopes and intercepts of these two plots, the constants k_1, k_A, and k_{AN} can be evaluated.

Figure 2 is the plot according to Eq. 9, and Fig. 3 shows Eq. 10 plotted for three alcohols in the acetic anhydride–*N*-methylimidazole system. The rate constants estimated by this treatment are given in Table II; the k_1 and k_A values are not significantly different from zero.

This system was used to investigate the medium effect of the alcohol on the rate and mechanism. The reaction was studied in *n*-propanol–acetonitrile mixtures, with the results shown in Table III. Good first-order kinetics were observed, but at an alcohol concentration of 80%, sharp deviations from first-order kinetics were seen. The dependence of k_{obs}

Table III—Dependence of Rate Constant on Solvent Composition for the Acetic Anhydride–*N*-Methylimidazole System in *n*-Propanol–Acetonitrile Mixtures [a]

Concentration of *n*-Propanol		
Volume, %	Molarity	$10^3 k_{obs}/s^{-1}$
20	2.67	3.93
30	4.00	5.92
40	5.34	8.08
50	6.68	9.81
60	8.02	12.0
70	9.35	14.4

[a] $[AX]_0 = 2.95 \times 10^{-3}\ M$; $[N]_0 = 3.76 \times 10^{-2}\ M$; temp. = 25°.

upon [ROH] is linear, and no spectral evidence was seen for intermediate formation, indicating that there is no mechanism change over this range of solvent composition. The alcohol is functioning as a reactant, and has no kinetically significant medium effect over the range reported in Table III.

Acetic Anhydride–*N*-Methylimidazole–Water—In one stage of this study, the water was treated as an instance of a hydroxy compound, in relatively low concentration, undergoing acetylation in acetonitrile solution; another stage involved the hydrolysis in water–acetonitrile mixtures over a wide range of composition.

This system behaved dramatically differently from the corresponding anhydride–alcohol system, in that when water was present a strong UV absorption was observed, similar to that ascribed to intermediate formation in acetyl chloride solutions. At low water concentrations the initial absorbance was proportional to the water concentration. It is inferred that water alters the polarity of the medium, making the formation of the *N*-acetyl-*N'*-methylimidazolium intermediate possible. With this hypothesis the following kinetic treatment, based on Scheme I, describes the system. Since reaction may take place *via* both AX and I^+ (at a given water concentration both species may be present), and the change in absorbance may receive contributions from both routes, the rate $-d([AX] + [I^+])/dt = -d[AX]/dt - d[I^+]/dt$ is needed. From the kinetic scheme:

$$-\frac{d[AX]}{dt} = k_1[AX][N] + k'_A[AX][H_2O] - k_{-1}[I^+][X^-] \quad \text{(Eq. 11)}$$

$$-\frac{d[I^+]}{dt} = k_{-1}[I^+][X^-] + k'_I[I^+][H_2O] - k_1[AX][N] \quad \text{(Eq. 12)}$$

Therefore,

$$-\frac{d([AX] + [I^+])}{dt} = k'_A[AX][H_2O] + k'_I[I^+][H_2O] \quad \text{(Eq. 13)}$$

The concentrations $[AX]$ and $[I^+]$ are related by Eq. 14, where the nature of R′ is examined later:

$$[AX] = R'[I^+] \quad \text{(Eq. 14)}$$

Therefore, $-d[AX]/dt = -R'(d[I^+]/dt)$, or:

$$-\frac{d([AX] + [I^+])}{dt} = -(1 + R')\frac{d[I^+]}{dt} \quad \text{(Eq. 15)}$$

Substituting Eq. 14 into 13:

$$-\frac{d([AX] + [I^+])}{dt} = (k'_I + R'k'_A)[I^+][H_2O] \quad \text{(Eq. 16)}$$

Equations 15 and 16 are combined to give:

$$-\frac{d[I^+]}{dt} = \left(\frac{k'_I + R'k'_A}{1 + R'}\right)[I^+][H_2O] \quad \text{(Eq. 17)}$$

An alternative development in terms of AX yields:

$$-\frac{d[AX]}{dt} = \left(\frac{k'_I + R'k'_A}{1 + R'}\right)[AX][H_2O] \quad \text{(Eq. 18)}$$

It follows that:

$$-\frac{d([AX] + [I^+])}{dt} = \left(\frac{k'_I + R'k'_A}{1 + R'}\right)[H_2O]([AX] + [I^+]) \quad \text{(Eq. 19)}$$

If R′ is invariant with time, Eq. 19 has a first-order form, with the observed rate constant given by:

$$k_{obs} = \left(\frac{k'_I + R'k'_A}{1 + R'}\right)[H_2O] \quad \text{(Eq. 20)}$$

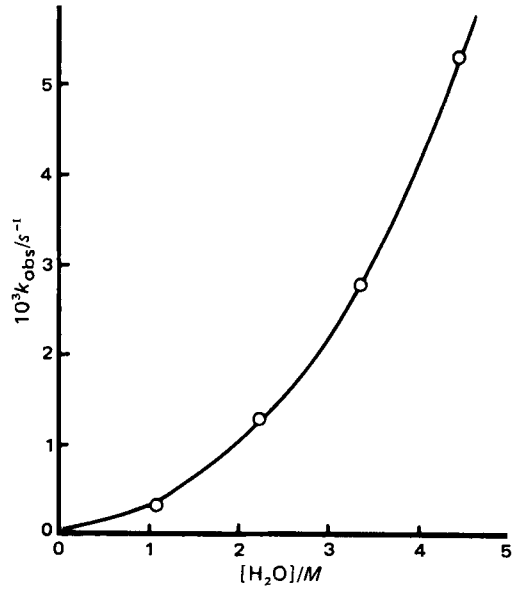

Figure 4—*Dependence of* k_{obs} *on water concentration in the acetic anhydride–*N*-methylimidazole system;* $[N]_0 = 1.5 \times 10^{-3}$ M.

It can be shown that Eq. 20 applies also when the total absorbance of the solution is followed.

The nature of R′ is now investigated. The concentrations $[AX]$ and $[I^+]$ might be controlled by the equilibrium relation:

$$K = \frac{k_1}{k_{-1}} = \frac{[I^+][X^-]}{[AX][N]} \quad \text{(Eq. 21)}$$

or $[AX] = R[I^+]$, where $R = [X^-]/K[N]$. Another possibility is that the steady-state approximation may be applied to $[I^+]$, giving:

$$[AX] = \left(\frac{k_{-1}[X^-] + k'_I[H_2O]}{k_1[N]}\right)[I^+] \quad \text{(Eq. 22)}$$

Comparison with Eq. 14 gives:

$$R' = \frac{[X^-]}{K[N]} + \frac{k'_I[H_2O]}{k_1[N]} \quad \text{(Eq. 23)}$$

The quantity R′ is therefore a function of water concentration through $[H_2O]$, k_1, and K, all of which increase as the water content of the medium increases. As $[H_2O]$ increases, R′ will approach zero and k_{obs} will approach $k'_I[H_2O]$. At very low $[H_2O]$, R′ will become large and k_{obs} will approach $k'_A[H_2O]$. Equations 22 and 23 include equilibrium control as a special case.

In general, R′ is also a function of time (at given water concentration), so first-order kinetics may not be observed when R′ is finite. This means that deviations from first-order kinetics are most likely to be observed at water concentrations where R′ is making a significant contribution to k_{obs}, that is, where both k'_A and k'_I are contributing.

Deviations from first-order kinetics were seen at water concentrations <20% v/v (4.45 *M*); above this concentration good first-order plots were obtained. Figures 4 and 5 show the dependence of k_{obs} on water concentration in the low and high water concentration regions. From the slope at high water concentration, k'_I is found to be $1.05 \times 10^{-3}\ M^{-1}\ s^{-1}$ (at $[N]_0 = 3.76 \times 10^{-4}\ M$). An estimate of the slope at $[H_2O] = 0$ gives $k'_A \approx 2 \times 10^{-4}\ M^{-1}\ s^{-1}$ ($[N]_0 = 1.50 \times 10^{-3}\ M$).

The dependence of k_{obs} on $[N]$ can be investigated by combining Eq. 20 with the detailed expressions for k'_A, k'_I, and R′, but the results are complex and difficult to interpret (13). The experimental observation is that k_{obs} shows positive curvature as a function of $[N]_0$ at low water concentration and negative curvature at high water concentration.

The linear portion of Fig. 5 suggests that R′ becomes negligible above ~5–10 *M* water; presumably above this value the medium is polar enough to support the extensive formation of the intermediate. Below 5–10 *M* water the reaction proceeds *via* both the anhydride and the intermediate.

The acetyl chloride–*N*-methylimidazole system was also studied in the presence of water, but very complicated kinetics were observed. This is thought to be a consequence of the unanticipated production of acetic anhydride in the system, which can occur in this way. Acetyl chloride hydrolyzes (*via* the intermediate) to give acetic acid, which transfers a proton to *N*-methylimidazole yielding acetate ion. At low water con-

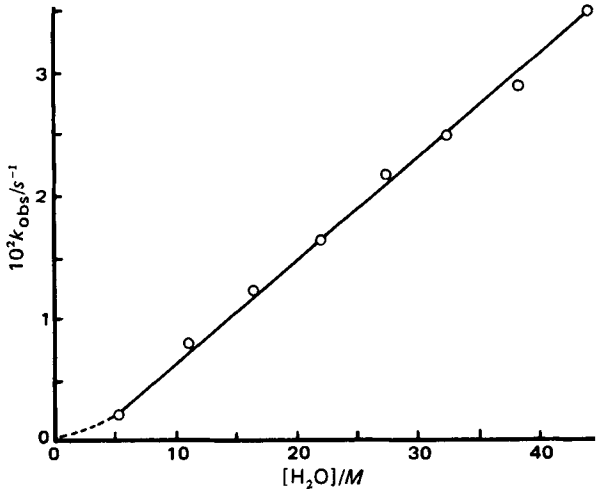

Figure 5—*Dependence of* k_{obs} *on water concentration for the acetic anhydride–N-methylimidazole systems;* $[N]_0 = 3.76 \times 10^{-4}$ M. *The dashed line represents the behavior seen in Fig. 4, but the two figures were obtained at different catalyst concentrations.*

centrations, acetate will react with the intermediate I^+ to generate acetic anhydride, according to Scheme I. Further study of this complex system did not seem warranted.

Catalysis by 4-Dimethylaminopyridine—A mixture of acetyl chloride and 4-dimethylaminopyridine in acetonitrile shows a rapid and quantitative conversion to the intermediate, with λ_{max} = 315 nm, log ϵ_{max} = 4.5. The acetylation of isopropanol was followed at 315 nm. The reactions did not exhibit good first-order kinetic behavior; the reason is unknown. By estimating rate constants from the initial stage of the reaction, data treatment according to the method described for the acetyl chloride–*N*-methylimidazole system yielded the approximate estimates $k_I = 6.4 \times 10^{-4}\ M^{-1}\ s^{-1}$ and $k_{IN} = 1.3\ M^{-2}\ s^{-1}$.

When acetonitrile solutions of acetic anhydride and 4-dimethylaminopyridine are mixed, a rapid but small absorbance increase is obtained at λ_{max} = 315 nm. This is attributed to intermediate formation. Using the molar absorptivity found in the acetyl chloride–dimethylaminopyridine system, it is estimated that 5–10% conversion to the intermediate occurs. The acetylation of isopropanol was studied, the loss of anhydride being followed. Deviations from first-order kinetics were observed, though the deviations were less pronounced than in the acetyl chloride system. Estimates of k_{obs} from the initial portions of the plots led to the estimates $k_A \simeq 0$ and $k_{AN} \simeq 0.5\ M^{-2}\ s^{-1}$. The estimate of k_{AN} may include a contribution from the k_{IN} route.

Mechanism of *N*-Methylimidazole Catalysis—This study has shown that catalysis of acetylations by *N*-methylimidazole can be accounted for in terms of Scheme IV. The intermediate I^+ is the *N*-acetyl-*N'*-methylimidazolium ion (I). The rate constants can be described as follows: k_A = the uncatalyzed reaction; k_{AN} = general base catalysis; k_I = the nucleophilic route; and k_{IN} = general base catalysis of the nucleophilic route.

When *AX* is acetyl chloride, k_1/k_{-1} is very large, the reaction occurs essentially only *via* the I^+ route. When *AX* is acetic anhydride, k_1/k_{-1}

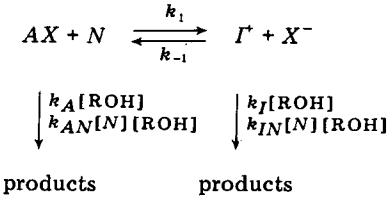

Scheme IV

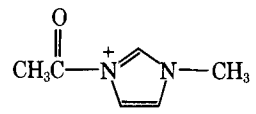

I

is zero, and the reaction occurs entirely *via* the *AX* route. The k_I and k_{IN} reactions are conjectured to occur as shown in Schemes V and VI, where *N* represents *N*-methylimidazole:

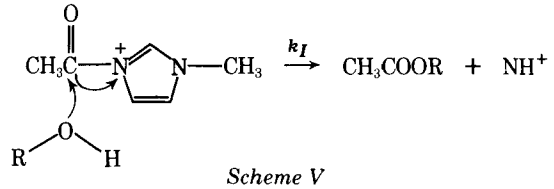

Scheme V

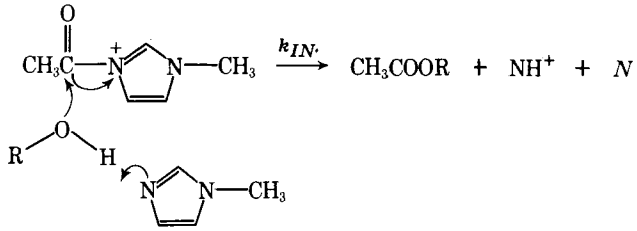

Scheme VI

The mechanisms for acetyl chloride and acetic anhydride are different because chloride is a better leaving group than acetate. When *N*-methylimidazole is replaced by the more powerful catalyst 4-dimethylaminopyridine, some intermediate formation is detected even in the acetic anhydride system. When water is added to the acetonitrile medium, intermediate formation occurs in the acetic anhydride–*N*-methylimidazole system, which constitutes a case in which the mechanism changes from the pure *AX* route (in dry acetonitrile) to the pure I^+ route (in acetonitrile containing $\geq$10 *M* water). This effect can be ascribed to the increase in the polarity in the medium, which will promote formation of the polar intermediate. The dielectric constant of acetonitrile is 36 and that of water is 78. In contrast, incorporation of *n*-propanol into acetonitrile led to no detectable intermediate formation. This is consistent with the view that alcohol–acetonitrile mixtures are not more polar than pure acetonitrile; the dielectric constant of *n*-propanol is 20.5. Besides the spectral and kinetic evidence described here, these mechanistic conclusions are supported by other results. *N*-acetyl-*N'*-methylimidazolium acetate could not be synthesized in acetonitrile, but in a previous report it was found that the chloride salt could be prepared (14). The rate of acetylation of isopropanol by acetic anhydride–*N*-methylimidazole has been investigated in a series of aprotic solvents, with a very small solvent effect being observed (15). This is consistent with the general base (k_{AN}) route but not with the formation of the polar intermediate. It may be noted that the third-order rate constants determined titrimetrically for acetic anhydride–*N*-methylimidazole acetylations in earlier work (8, 15) may now be identified as k_{AN} in Scheme IV.

Comparison of k_A and k_I for the acetyl chloride–*N*-methylimidazole system (Table I) shows that $k_A > k_I$ for each alcohol studied. This means that diversion through the unassisted nucleophilic route (k_I) actually inhibits the reaction relative to the uncatalyzed (k_A) process, possibly because of stabilization of the intermediate by electron delocalization as indicated in II. (Similar delocalization can occur in the 4-dimethylaminopyridine intermediate.)

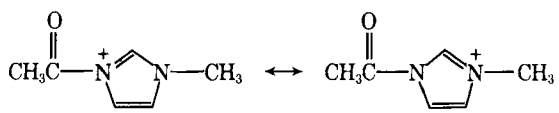

II

Table IV—Rate Constants for Acetylation of Isopropyl Alcohol in Acetonitrile at 25° [a]

	Acetyl Chloride				Acetic Anhydride			
	k_A	k_{AN}	k_I	k_{IN}	k_A	k_{AN}	k_I	k_{IN}
N-Methylimidazole	0.0015	—	0.00015	0.053	0	0.0041	—	—
4-Dimethylaminopyridine	—	—	0.00064	1.3	0	0.5	—	—

[a] Units of rate constants as in Tables I and II.

Although it has not been possible to measure both k_{AN} and k_{IN} for the same system, Table IV gathers rate constants that have been obtained for both acetylating agents and both catalysts with isopropanol. Analogy with the k_A/k_I ratio suggests that k_{AN} may be $>k_{IN}$, whereas Table IV indicates that $k_{IN} > k_{AN}$ (although these data are not for precisely the same system).

These observations may account for the puzzling report (3) that 1-ethynylcyclohexanol is acetylated faster by acetic anhydride than by acetyl chloride in the presence of 4-dimethylaminopyridine (in $CDCl_3$ solution). If the mechanisms are as described here, the intermediate is quantitatively formed from acetyl chloride, with the concomitant consumption of an equimolar amount of 4-dimethylaminopyridine; thus, the concentration of free catalyst is depleted and is very low under the conditions described. The reaction occurs by the k_I and k_{IN} routes. In the acetic anhydride system, on the other hand, no intermediate is formed, with the result that the catalyst concentration remains high, and the reaction proceeds *via* the k_{AN} route. Under the reported conditions (3), using the rate constants in Table IV, it is calculated that the rate in the anhydride system is greater than the rate in the acetyl chloride system.

Effect of the Solvent—The rates and mechanisms of acylation reactions can be affected by the reaction medium through the operation of several effects.

The Ratio k_1/k_{-1}—This ratio describes the formation of the polar final state ($I^+ + X^-$) from the less polar initial state ($AX + N$). An increase in solvent polarity should increase k_1/k_{-1}; this effect was seen in the system acetic anhydride–*N*-methylimidazole–water, in which k_1/k_{-1} changes from practically zero at low water concentration to very large in substantial water concentrations. The mechanism is changed as a consequence. In the intermediate range where k_1/k_{-1} is finite, both reaction routes are accessible and the kinetics are complex.

Since much prior kinetic study of acylation mechanisms has emphasized fully aqueous systems, the nucleophilic route has often been implicated for those reactions, as in the pyridine-catalyzed hydrolysis of acetic anhydride (16). As the present study shows, however, the extent of *N*-acylammonium intermediate formation can be very sensitive to the solvent.

The Rate Constants k_A, k_{AN}, k_I, *and* k_{IN}—These will be expected to respond to solvent polarity in accord with the postulate that increased solvent polarity will increase the rate if the transition state is more polar than the initial state and *vice versa*. For example, the k_{AN} route will involve some charge separation in the transition state, so k_{AN} may increase slightly as the solvent is made more polar.

The initial state for the k_I and k_{IN} routes is highly polar, being I^+ or the ion-pair I^+X^-. The effect of the solvent will depend upon the relative polarity of the transition state. Greater acylation rates in nonpolar solvents, in terms of a favored breakdown of the charged intermediate to neutral products, has been accounted for (17). This requires the following reaction (in the symbols of Scheme IV): $I^+X^- + ROH \rightarrow AOR + N + HX$. The proton transfer must also be part of (or take place prior to) the rate determining step. If the reaction is $I^+ + ROH \rightarrow AOR + NH^+$, the solvent effect should be modest. In interpreting a solvent effect in these terms, the concurrent behavior of k_1/k_{-1}, which may alter the route of the reaction, must be taken into account.

The Basicity of the Catalyst (N) *and the Counterion* (X^-)—Upon this property depend the proton-accepting abilities of these bases, the effectiveness of X^- as a leaving group, and the nucleophilicity of *N*. As the solvent is changed, the relative basicity of a pair of bases may change.

Acetonitrile is a weaker base than water, so acids are weaker in acetonitrile than in water (as measured by their acid dissociation constants). For carboxylic acids, the relationship between pKa in acetonitrile and water is (18):

$$\text{pKa (acetonitrile)} = \text{pKa (water)} + 4.4$$

whereas for the conjugate acids of amines it is:

$$\text{pKa (acetonitrile)} = 0.47\ \text{pKa (water)} + 2.2$$

The different behavior for acids RCOOH and RNH_3^+ is a consequence of the lower dielectric constant of acetonitrile and its poor anion-solvating capability. The base strengths of acetate and *N*-methylimidazole in acetonitrile, as calculated with these relationships, are:

Acetic acid: pKa (acetonitrile) = 9.15, pKa (water) = 4.75

N-Methylimidazole: pKa (acetonitrile) = 5.5, pKa (water) = 7.0

In water, *N*-methylimidazole is a stronger base than acetate, but in acetonitrile, acetate is the stronger base. This conclusion was used in the derivation of Eq. 7.

The possibility of nucleophilic catalysis is largely determined by the relative basicities of the leaving group (X^-) and the attacking nucleophile (*N*). If pKa (NH^+) > pKa (HX), then the nucleophile is a stronger base than the leaving group, and the nucleophilic route (*via* formation of the *N*-acylated nucleophile) is favored, whereas if pKa (HX) > pKa (NH^+) the nucleophilic route is not favored, and the direct general base route is more probable. As described previously, acetate is a much stronger base than is *N*-methylimidazole in acetonitrile, hence, formation of *N*-acetyl-*N'*-methylimidazolium acetate is not probable from acetic anhydride. The observation of reaction solely *via* the k_{AN} route is consistent with this description. In the acetyl chloride case, however, *N*-methylimidazole is a stronger base than chloride in acetonitrile [chloride is solvated in acetonitrile, whereas larger anions are not (19)], so the nucleophilic route predominates.

Since 4-dimethylaminopyridine is a stronger base than is *N*-methylimidazole, it would be expected to form the acyl intermediate to a greater extent (with a given AX). This behavior was observed: with acetic anhydride, *N*-methylimidazole gave no detectable intermediate, whereas 4-dimethylaminopyridine gave 5–10% conversion to the intermediate.

Molecular Aggregation—In solvents of low dielectric constant, ion-pairs and higher ionic aggregates can be detected. The reactivity of an ion-pair will in general differ from that of a dissociated ion, so ion-pair formation may have kinetic consequences. Acetonitrile is a solvent of moderate polarity, and ion-pairing will not be as extensive as in solvents of much lower dielectric constant. It has not been found necessary to invoke the ion-pair I^+X^- in the present kinetic treatment. Greater reactivity of acetic anhydride than of acetyl chloride (with 4-dimethylaminopyridine catalyst) in nonpolar solvents by postulating the I^+X^- ion-pair has been reported (3), the explanation being that the I^+Cl^- ion-pair is tightly bound and therefore less reactive than the more loosely bound I^+OAc^- ion-pair. An alternative explanation for these results was given previously.

A recent study (20) questioned whether the intermediate I^+ is on the reaction path in 4-dimethylaminopyridine-catalyzed acetylations, and proposed a mechanism in which the catalyst attacks a molecular complex of anhydride and alcohol formed in a pre-equilibrium, giving a solvated ion-pair. No kinetic evidence for this mechanism was presented. The presence of molecular complexes is very likely in these systems, hydrogen-bonded complexes of alcohols with H-bond acceptors being probable in nonpolar solvents. In highly aqueous systems, complex formation of the hydrophobic type can occur. The *N*-methylimidazole systems studied here did not require the mechanistic presence of complexes. It is possible that such species may be responsible for some of the anomalous kinetic behavior seen with 4-dimethylaminopyridine, but this was not investigated[4].

Unusual rate equations for the reaction of anilines with acetyl halides in the presence of *N*-methylimidazole, in nonpolar solvents has been reported (21). Rate terms included the quantities $[I^+X^-]^2$ and $[I^+X^-][AX]$. Such terms may arise because of the presence of ion-pairs and molecular complexes.

REFERENCES

(1) W. Steglich and G. Höfle, *Angew. Chem. Int. Ed.*, **8**, 981 (1969).

(2) G. Höfle and W. Steglich, *Synthesis*, **1972**, 620.

(3) G. Höfle, W. Steglich, and H. Vorbrüggen, *Angew. Chem. Int. Ed.*, **17**, 569 (1978).

(4) K. A. Connors and K. S. Albert, *J. Pharm. Sci.*, **62**, 845 (1973).

(5) E. L. Rowe and S. M. Machkovech, *ibid.*, **66**, 273 (1977).

(6) V. Fell and C. R. Lee, *J. Chromatogr.*, **121**, 41 (1976).

(7) F. de Fabrizio, *J. Pharm. Sci.*, **69**, 854 (1980).

(8) K. A. Connors and N. K. Pandit, *Anal. Chem.*, **50**, 1542 (1978).

(9) R. Wachowiak and K. A. Connors, *ibid.*, **51**, 27 (1979).

(10) S. L. Wellons, M. A. Carey, and D. K. Eider, *ibid.*, **52**, 1374 (1980).

(11) A. S. Bittner, L. E. Harris, and W. F. Campbell, *J. Agr. Food Chem.*, **28**, 1242 (1980).

(12) S.-F. Lin and K. A. Connors, *J. Pharm. Sci.*, **70**, 235 (1981).

(13) N. K. Pandit, Ph.D. thesis, University of Wisconsin, Madison, Wis., 1980.

[4] Side-reactions in this system may be responsible for the kinetic behavior. Several products of such reactions have been identified (3).

(14) A. O. Obaseki, M.S. thesis, University of Wisconsin, Madison, Wis., 1980.
(15) N. K. Pandit, A. O. Obaseki, and K. A. Connors, *Anal. Chem.*, **52**, 1678 (1980).
(16) A. R. Fersht and W. P. Jencks, *J. Am. Chem. Soc.*, **92**, 5432, 5442 (1970).
(17) A. Hassner, L. R. Krepski, and V. Alexanian, *Tetrahedron*, **34**, 2069 (1978).
(18) J. F. Coetzee and I. M. Kolthoff, *J. Am. Chem. Soc.*, **79**, 6110 (1957).
(19) M. K. Chantooni and I. M. Kolthoff, *ibid.*, **89**, 1582 (1967).
(20) E. Guibe-Jampel, G. Le Corre, and M. Wakselman, *Tetrahedron Lett.*, **1979**, 1157.
(21) S. A. Lapshin, V. A. Dadali, Y. S. Simanenko, and L. M. Litvinenko, *Zh. Org. Khim.*, **13**, 586 (1977).

ACKNOWLEDGMENTS

This work was supported by National Science Foundation Grant CHE 78-06603.

Metabolism of Tocainide in the Rat

RAMAN VENKATARAMANAN *, FRANK S. ABBOTT, and JAMES E. AXELSON ˣ

Received June 24, 1981, from the *Faculty of Pharmaceutical Sciences, University of British Columbia, Vancouver, B.C., Canada V6T IW5.* Accepted for publication August 28, 1981. * Present address: University of Pittsburgh, 3501 Terrace Street, Pittsburgh, PA 15261.

Abstract □ The metabolism of tocainide, an oral antiarrhythmic agent, was studied in male Wistar rats following oral administration of 15 mg/kg of tocainide hydrochloride. Qualitative and quantitative identification of the metabolites in urine was carried out by GC–mass spectrometry and electron capture detector gas chromatography. About 15–20% of the dose administered was excreted as intact drug in the urine. An additional 20% of the dose was present as acid hydrolysable conjugates. Enzymatic hydrolysis (β-glucuronidase) revealed half of the acid hydrolysable conjugates to be a glucuronide. The enzyme mediated hydrolysis was blocked by its specific inhibitor saccharo-1,4-lactone. *N*-acetyl tocainide, an oxidatively deaminated tocainide, an aldehyde adduct of tocainide, and a cyclic hydantoin derivative of tocainide were also identified as metabolites in the urine samples.

Keyphrases □ Tocainide—oral antiarrhythmic agent, study of metabolism, rats □ Metabolism—of tocainide, after oral administration in rats □ GC–mass spectrometry—determination of metabolism of tocainide, rats

Tocainide, 2-amino-2′,6′-propionoxylidide (I), a structural analog of lidocaine (II), is an experimental antiarrhythmic agent, presently undergoing clinical trials (1–4). In humans, tocainide is completely absorbed following oral administration (5), and most of the orally or intraperitoneally administered dose, up to 15 mg/kg, of tocainide is absorbed in rats (6). Kinetic studies carried out in rats revealed the presence of dose dependent elimination of tocainide ≥20 mg/kg (6). Identification of the pathways contributing to the nonlinearity was not possible previously due to the lack of information on the metabolism of tocainide in rats. The present report describes the metabolic fate of tocainide in male Wistar rats.

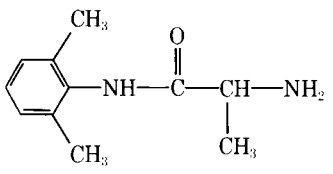

I

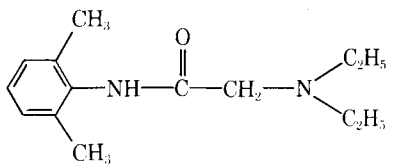

II

EXPERIMENTAL

Animal Experimentation—Adult male Wistar rats with an average weight of 200 g (190–210 g) were used in the present study (animals were obtained from the University of British Columbia animal care unit). The animals were maintained in 0.41- × 0.34- × 0.18-m metallic cages (6 rats/cage) in a controlled environment (24°) for at least 3 days prior to experimentation. Wooden shavings were used as bedding under elevated cages (18 cm from the bottom of the cages). The photoperiod was controlled to provide a dark cycle from 8 pm to 6 am and a light cycle from 6 am to 8 pm. The animals had access *ad libitum* to food (rat chow) and water during this period. The animals were fasted for 8–10 hours prior to and during the experiments; however, water was allowed *ad libitum*.

An aqueous solution of tocainide hydrochloride[1] or 3′,4′,5′-trideuterated tocainide hydrochloride was given orally (stomach tube) to animals under light ether anesthesia. Dosed animals were housed in separate stainless steel metabolic cages (24.5 × 17.5 × 18 cm) with facilities for collecting urine samples free of fecal contamination, into an amber-colored bottle. Twenty-four hours postdose, the sides of the cage and the collecting funnel were washed three times with distilled water to recover all excretory products. The urine samples were stored in the freezer until analyzed.

Analytical Methods—Measurement of intact tocainide in urine samples was carried out by using an electron capture detector gas chromatographic method previously reported (7).

The presence of conjugated tocainide in urine samples was determined by acidic and enzymatic hydrolysis. For the acid hydrolysis, 1 ml of urine was incubated with 1 ml of 1 *N* HCl in a sealed glass ampul for 1 hr at 100°. An aliquot of this solution was used for the analysis of tocainide.

Preliminary studies with enzymes from different sources suggested maximal hydrolysis of the conjugates to occur when bovine liver β-glucuronidase was used. The enzymatic hydrolysis involved the addition of 1 ml of 1 *M* acetate buffer (pH 5.0) and 0.2 ml of β-glucuronidase[2] to 1 ml of urine and incubation of the mixture at 37° for 24 hr. At the end of the incubation period the samples were analyzed for intact tocainide. Additional experiments were also carried out to determine the effect of saccharo-1,4-lactone[3], 0.1 m*M* final concentration, on the enzyme mediated hydrolysis of tocainide conjugates.

Multiple extraction of the urine samples (25–30 ml), without any pH adjustments or at pH 9.0 (ammonium hydroxide and ammonium carbonate) or at pH 9.0 and 12.0 using sodium hydroxide, was carried out

[1] Astra Pharmaceutical Products, Framingham, Mass.
[2] Glucurase, Sigma Chemical Co., St. Louis, Mo.
[3] Calbiochem, La Jolla, Calif.

0022-3549/82/0500-0491$01.00/0

(14) A. O. Obaseki, M.S. thesis, University of Wisconsin, Madison, Wis., 1980.
(15) N. K. Pandit, A. O. Obaseki, and K. A. Connors, *Anal. Chem.*, **52**, 1678 (1980).
(16) A. R. Fersht and W. P. Jencks, *J. Am. Chem. Soc.*, **92**, 5432, 5442 (1970).
(17) A. Hassner, L. R. Krepski, and V. Alexanian, *Tetrahedron*, **34**, 2069 (1978).
(18) J. F. Coetzee and I. M. Kolthoff, *J. Am. Chem. Soc.*, **79**, 6110 (1957).
(19) M. K. Chantooni and I. M. Kolthoff, *ibid.*, **89**, 1582 (1967).
(20) E. Guibe-Jampel, G. Le Corre, and M. Wakselman, *Tetrahedron Lett.*, **1979**, 1157.
(21) S. A. Lapshin, V. A. Dadali, Y. S. Simanenko, and L. M. Litvinenko, *Zh. Org. Khim.*, **13**, 586 (1977).

ACKNOWLEDGMENTS

This work was supported by National Science Foundation Grant CHE 78-06603.

Metabolism of Tocainide in the Rat

RAMAN VENKATARAMANAN *, FRANK S. ABBOTT, and JAMES E. AXELSON ˣ

Received June 24, 1981, from the *Faculty of Pharmaceutical Sciences, University of British Columbia, Vancouver, B.C., Canada V6T IW5.* Accepted for publication August 28, 1981. * Present address: University of Pittsburgh, 3501 Terrace Street, Pittsburgh, PA 15261.

Abstract □ The metabolism of tocainide, an oral antiarrhythmic agent, was studied in male Wistar rats following oral administration of 15 mg/kg of tocainide hydrochloride. Qualitative and quantitative identification of the metabolites in urine was carried out by GC–mass spectrometry and electron capture detector gas chromatography. About 15–20% of the dose administered was excreted as intact drug in the urine. An additional 20% of the dose was present as acid hydrolysable conjugates. Enzymatic hydrolysis (β-glucuronidase) revealed half of the acid hydrolysable conjugates to be a glucuronide. The enzyme mediated hydrolysis was blocked by its specific inhibitor saccharo-1,4-lactone. *N*-acetyl tocainide, an oxidatively deaminated tocainide, an aldehyde adduct of tocainide, and a cyclic hydantoin derivative of tocainide were also identified as metabolites in the urine samples.

Keyphrases □ Tocainide—oral antiarrhythmic agent, study of metabolism, rats □ Metabolism—of tocainide, after oral administration in rats □ GC–mass spectrometry—determination of metabolism of tocainide, rats

Tocainide, 2-amino-2′,6′-propionoxylidide (I), a structural analog of lidocaine (II), is an experimental antiarrhythmic agent, presently undergoing clinical trials (1–4). In humans, tocainide is completely absorbed following oral administration (5), and most of the orally or intraperitoneally administered dose, up to 15 mg/kg, of tocainide is absorbed in rats (6). Kinetic studies carried out in rats revealed the presence of dose dependent elimination of tocainide ≥20 mg/kg (6). Identification of the pathways contributing to the nonlinearity was not possible previously due to the lack of information on the metabolism of tocainide in rats. The present report describes the metabolic fate of tocainide in male Wistar rats.

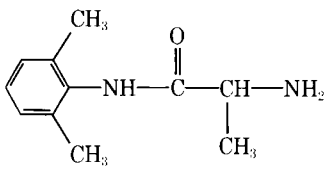

I

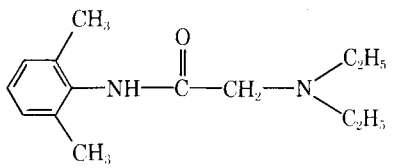

II

EXPERIMENTAL

Animal Experimentation—Adult male Wistar rats with an average weight of 200 g (190–210 g) were used in the present study (animals were obtained from the University of British Columbia animal care unit). The animals were maintained in 0.41- × 0.34- × 0.18-m metallic cages (6 rats/cage) in a controlled environment (24°) for at least 3 days prior to experimentation. Wooden shavings were used as bedding under elevated cages (18 cm from the bottom of the cages). The photoperiod was controlled to provide a dark cycle from 8 pm to 6 am and a light cycle from 6 am to 8 pm. The animals had access *ad libitum* to food (rat chow) and water during this period. The animals were fasted for 8–10 hours prior to and during the experiments; however, water was allowed *ad libitum*.

An aqueous solution of tocainide hydrochloride[1] or 3′,4′,5′-trideuterated tocainide hydrochloride was given orally (stomach tube) to animals under light ether anesthesia. Dosed animals were housed in separate stainless steel metabolic cages (24.5 × 17.5 × 18 cm) with facilities for collecting urine samples free of fecal contamination, into an amber-colored bottle. Twenty-four hours postdose, the sides of the cage and the collecting funnel were washed three times with distilled water to recover all excretory products. The urine samples were stored in the freezer until analyzed.

Analytical Methods—Measurement of intact tocainide in urine samples was carried out by using an electron capture detector gas chromatographic method previously reported (7).

The presence of conjugated tocainide in urine samples was determined by acidic and enzymatic hydrolysis. For the acid hydrolysis, 1 ml of urine was incubated with 1 ml of 1 *N* HCl in a sealed glass ampul for 1 hr at 100°. An aliquot of this solution was used for the analysis of tocainide.

Preliminary studies with enzymes from different sources suggested maximal hydrolysis of the conjugates to occur when bovine liver β-glucuronidase was used. The enzymatic hydrolysis involved the addition of 1 ml of 1 *M* acetate buffer (pH 5.0) and 0.2 ml of β-glucuronidase[2] to 1 ml of urine and incubation of the mixture at 37° for 24 hr. At the end of the incubation period the samples were analyzed for intact tocainide. Additional experiments were also carried out to determine the effect of saccharo-1,4-lactone[3], 0.1 m*M* final concentration, on the enzyme mediated hydrolysis of tocainide conjugates.

Multiple extraction of the urine samples (25–30 ml), without any pH adjustments or at pH 9.0 (ammonium hydroxide and ammonium carbonate) or at pH 9.0 and 12.0 using sodium hydroxide, was carried out

[1] Astra Pharmaceutical Products, Framingham, Mass.
[2] Glucurase, Sigma Chemical Co., St. Louis, Mo.
[3] Calbiochem, La Jolla, Calif.

0022-3549/82/0500-0491$01.00/0

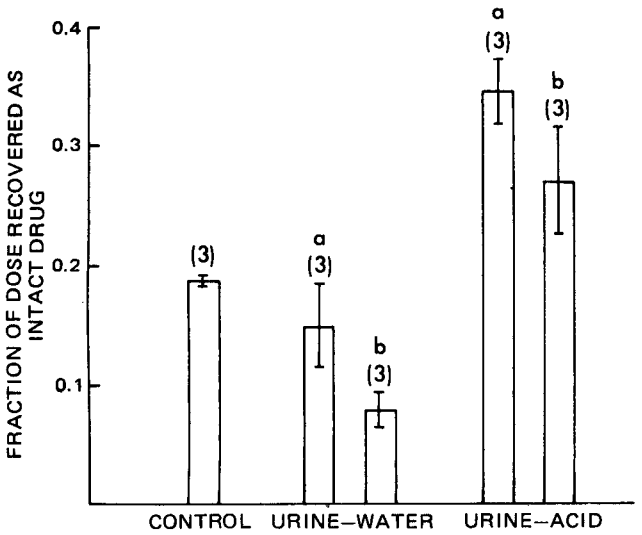

Figure 1—*Acid hydrolysis of tocainide conjugate in oven at 100°. Data presented as mean ± SD. The number in the parentheses refers to the number of experiments carried out.* a = *1-hr incubation time;* b = *2-hr incubation time.*

in a separatory funnel with an equal volume of methylene chloride[4]. In another experiment the urine samples (25 ml) were freeze-dried and the residue was dissolved in methanol (5 ml). The methanolic solution was then filtered and concentrated to ~1 ml under nitrogen at room temperature. Methylene chloride and methanolic extracts of urine were analyzed by GC–mass spectrometry[5] to determine the presence of other metabolites of tocainide. The GC component of the GC–mass spectrometric system was equipped with a 1.8-m × 2-mm i.d. coiled glass column packed with Silar 10 C[6] coated on ChromoSorb W–HP (100–120 mesh). The injection port temperature was 170° and the oven temperature was programmed from 100 to 250° at 10°/min. The temperature was held at 250° until the end of the analysis. Helium was used as a carrier gas at a flow rate of 30 ml/min. The temperature of the separator was 280°. The ionization energy was 70 eV and the accelerating voltage was 820 V. The mass spectrometer was operated in the scanning mode and the mass spectra were recorded continuously at 5-sec intervals during an entire run.

Methylation of the extracted samples was carried out by the addition of 100 μl of trimethylanilinium hydroxide[7] and subsequent incubation at 100° for ~10 min.

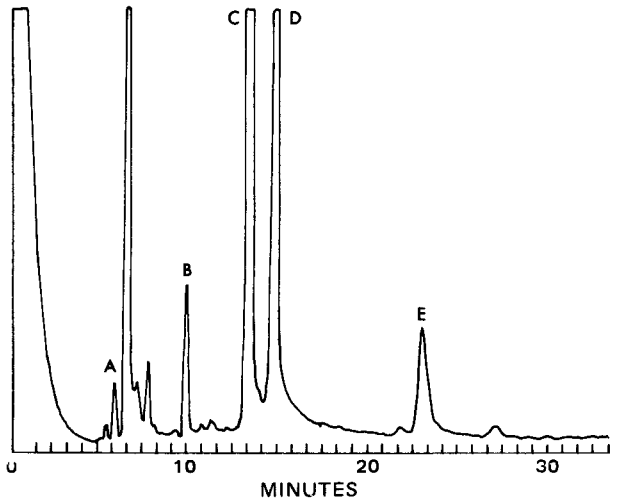

Figure 2—*GC–mass spectrometer total ion current trace of methylene chloride extract of urine sample using Silar 10-C column.*

[4] Caledon Laboratories, Ontario, Canada.
[5] Varian Mat III GC/MS with Data Base.
[6] Applied Science Laboratories, State College, Pa.
[7] Methelute, Pierce Chemical Co., Rockford, Ill.

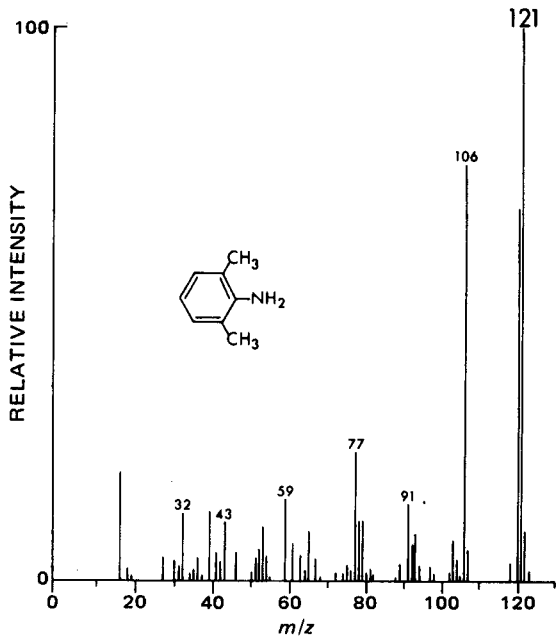

Figure 3—*Mass spectrum and the postulated structure of a metabolite of tocainide (III). This compound corresponds to peak A of Fig. 2.*

RESULTS

The results of the acid hydrolysis studies are summarized in Fig. 1. Incubation of the urine samples with hydrochloric acid liberated tocainide corresponding to >15% of the dose administered. Control experiments carried out in the absence of any acid revealed nearly a 20% loss of tocainide during the experimental process following 1 hr of hydrolysis. This would imply that the actual amount of tocainide present as conjugate would be >20% of the administered dose. Longer periods of incubation (2 hr) resulted in further reduction in the recovery of tocainide from the conjugates. This could be due to the breakdown of tocainide under the conditions of hydrolysis employed in this study.

Enzymatic hydrolysis (β-glucuronidase) of the urine, revealed the presence of nearly 7% of the dose administered as a glucuronide conjugate. The enzymatic hydrolysis mediated by β-glucuronidase was blocked by its specific inhibitor saccharo-1,4-lactone, thus confirming the conjugate to be a glucuronide. The percent of dose recovered as intact tocainide in untreated urine, β-glucuronidase treated urine, and urine treated with β-glucuronidase and saccharo-1,4-lactone were 17.5 ± 1.1 (n = 3), 24.0 ± 0.7 (n = 3), and 17.0–17.7 (n = 2).

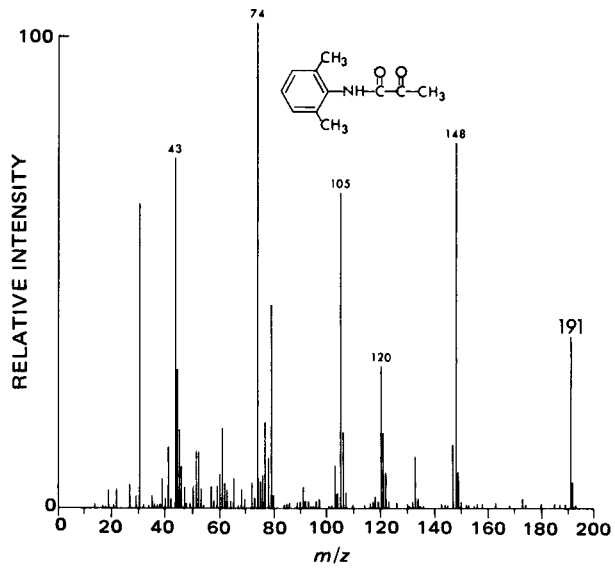

Figure 4—*Mass spectrum and the postulated structure of a metabolite of tocainide (IV). This compound corresponds to peak B of Fig. 2.*

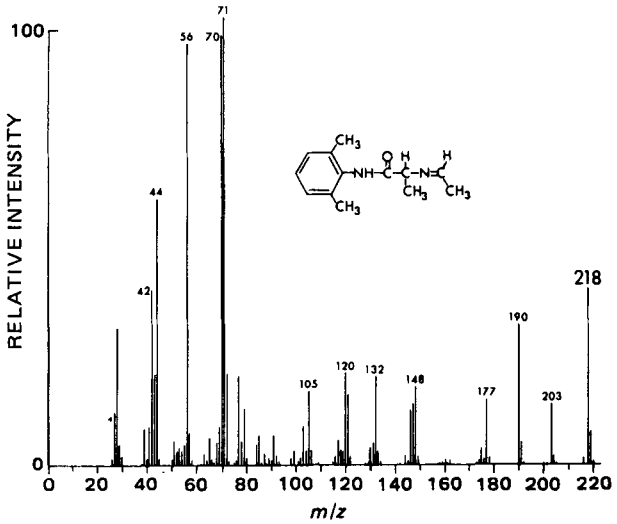

Figure 5—*Mass spectrum and the postulated structure of a metabolite of tocainide (V). This compound corresponds to peak C of Fig. 2.*

Other Metabolites of Tocainide—The chromatogram obtained following injection of the methylene chloride extract of tocainide onto a Silar 10 C column of the GC–mass spectrometer is shown in Fig. 2. Confirmation as to the origin of peaks A, B, C, D, and E were obtained from studies using trideuterated tocainide. The presence of molecular ions at *m/z* values of (M ± 3) following analysis of the urine of rats administered trideuterated tocainide pointed to tocainide as the source of these peaks. Since all three deuterium labels were present in all of these peaks, it was inferred that these peaks result from modification of the structure by metabolism at the side chain. The other peaks present in the chromatogram were from endogenous materials in the urine.

Peak A—Peak A appeared in the methylene chloride extract of urine samples at pH 9.0 as well as in the methanolic extract of the freeze-dried urine samples with a retention time of ~5 min. The mass spectrum and the postulated structure of the compound (III) are shown in Fig. 3. The molecular ion was at *m/z* 121 (124) and the base peak was at *m/z* 106 (109). The compound, however, seems to account for <5% of the dose administered.

Peak B—Peak B was present in the methylene chloride and the methanolic extract of the urine samples. The molecular ion at *m/z* 191 corresponds to a composition of $C_{11}H_{13}NO_2$ (Fig. 4). The presence of peaks at *m/z* 105, 120, and 148 suggested intactness of the carboxy-xylidide moiety of tocainide. The abundant peak at *m/z* 43 corresponded to C_2H_3O. This compound (IV) eluted at about 10 min in the chromatogram and was also present in small quantities in the urine samples.

Peak C—Peak C was present in the following extracts of rat urine: (*a*) direct extraction of urine with methylene chloride; (*b*) extracts of urine at pH 9.0 (ammonium carbonate and ammonium hydroxide) with

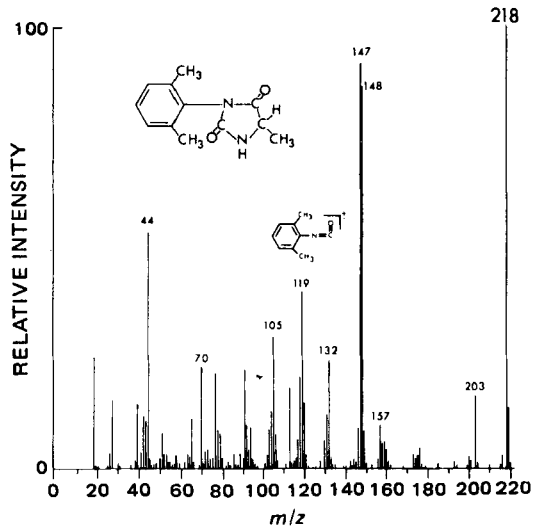

Figure 6—*Mass spectrum of the cyclic compound VI.*

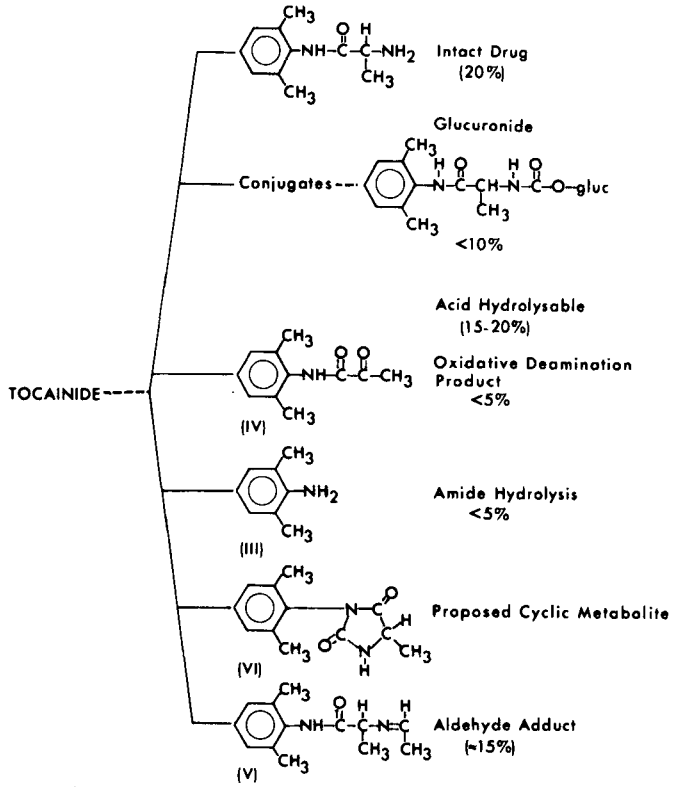

Scheme I—Proposed metabolic products of tocainide. The structures and the relative amounts of the proposed metabolites of tocainide. The percentage values are the percent of dose excreted as a particular metabolite.

methylene chloride; (*c*) extracts of acid hydrolyzed urine extracted with methylene chloride at pH 9.0 (ammonium carbonate and ammonium hydroxide); (*d*) methanolic extracts of freeze-dried urine.

When subjected to mass spectral analysis, this compound revealed a molecular ion at *m/z* 218 suggesting the addition of 26 mass units to the parent compound (Fig. 5). The presence of *m/z* 221 in studies using the trideuterated tocainide suggested that all three deuterium atoms are present in this compound. The persistence of the deuterium atoms in the aromatic ring was also evident from the presence of the following peaks: *m/z* 105 (108), 120 (123), 132 (135), 148 (151), 177 (180), 190 (193), and 203 (206). The presence of ions of the following composition: C_8H_9 (105), $C_8H_{10}N$ (120), $C_9H_{10}NO$ (148), $C_{11}H_{15}NO$ (177), and $C_{11}H_{14}N_2O$ (190) indicated the intactness of the major skeleton to tocainide. The peak at *m/z* 203 (M −15) suggested the presence of a methyl group as part of the structural modification. Ions of *m/z* 28 (C_2H_4), 42 (C_2H_4N), and 70 (C_4H_8N) in samples obtained following administration of tocainide or trideuterated tocainide indicated that these fragments must arise from the side chain. The fragmentation, thus observed, corresponds to an aldehyde adduct (V) of tocainide. The adduct appears to be one of the major metabolic pathways of tocainide in rats. Preliminary estimates show nearly 15% or more of the dose of tocainide to be eliminated *via* this metabolic pathway.

Peak D—Peak D in Fig. 2 corresponded to intact tocainide. Nearly 20% of the dose administered appeared in the urine as intact drug in the 24-hr period following drug administration.

Peak E—Direct extraction of the urine samples with methylene chloride or extraction, following adjustment of the urine pH to 9.0 with ammonium carbonate and ammonium hydroxide or sodium hydroxide, resulted in peak E which eluted at ~23 min.

The parent ion at *m/z* 218 (221) suggested this compound to be a product from tocainide with the addition of 26 mass units (Fig. 6). Ions of the composition C_8H_9 (105) and C_8H_9N (122) indicate the xylidine moiety of tocainide to be intact. The presence of a peak at *m/z* 119 (122) and not at 120 (123) indicates the xylidine nitrogen to be tertiary. The abundance of *m/z* at 147 (150) indicates that the carboxylidine moiety of tocainide is also intact but for the loss of one hydrogen atom, further suggesting that the amide nitrogen is tertiary and possibly part of a cyclic system. The presence of a methyl group is indicated by *m/z* at 203 (M −15). The compound could be methylated (implying the presence of a replaceable hydrogen) but failed to form any derivative with heptafluo-

robutyric anhydride[7]. The mass fragmentation pattern of this compound was identical with the fragmentation pattern of 3-(2,6-xylyl)-5-methyl hydantoin (VI)[1].

The relative amounts of VI in the methanolic extract was quite high as compared to the methylene chloride extract. This could be due to the generation of the cyclic compound from the glucuronide conjugate that was dissolved in methanol.

DISCUSSION

The metabolic products of tocainide are summarized in Scheme I. Following oral, intravenous, or intraperitoneal administration of tocainide (15 mg/kg) to rats, ~15–20% of the dose is excreted as intact drug over a 24-hr period (6). Nearly 44% of an oral dose was excreted as free tocainide in humans while an acid or β-glucuronidase hydrolyzable metabolite accounted for nearly 23% of the tocainide dose administered (8). A novel biotransformation pathway was put forth to explain the disposition of tocainide in humans (8). The proposed structure of this metabolite was tocainide carbamoyl O-β-D-glucuronide. During preliminary work in rats, the authors identified the presence of a similar conjugate of tocainide in rat urine. Acid hydrolysis (nonspecific) as well as enzyme (β-glucuronidase) hydrolysis (specific for glucuronide conjugate) of the urine samples were carried out to determine the nature of the conjugates.

Use of β-glucuronidase corresponding to 1000 U of enzyme resulted in maximal release of tocainide from its conjugates. Addition of trace quantities (10 μl) of chloroform as suggested previously (9) did not result in any increase in the yield of tocainide from the conjugates. Under the conditions of the enzymatic hydrolysis (24 hr at 37°), no detectable degradation of tocainide was observed. Enzymatic hydrolysis resulted in the liberation of tocainide, equivalent to ~7–10% of the dose administered. Addition of saccharo-1,4-lactone into the incubation medium prevented the enzyme mediated hydrolysis of the conjugate, thus indicating the conjugate to be a glucuronide.

Acid hydrolysis of the urine sample resulted in the liberation of tocainide corresponding to ~20% of the administered dose. Simultaneous experiments showed that there is a loss of nearly 20% of tocainide in the control samples (urine sample–distilled water instead of 1 *N* HCl). This suggested that one is probably underestimating the amount of acid hydrolysable conjugates by the method used, due to the degradation of tocainide at the pH and temperature used for acid hydrolysis. Further proof for this hypothesis came about from the stability studies of tocainide carried out at different temperatures and in the presence of acid of different strength. An increase in the strength of the acid (1 *N* to 12 *N*) as well as the time of incubation resulted in a progressive reduction in the amount of tocainide remaining in an aqueous solution of the drug at 100°. Consistent with this observation, incubation of the urine samples for a longer period of time (>2 hr) or with acids of higher normality (2 *N*, 6 *N*, or 12 *N*) provided decreased estimates of the conjugates present in urine. The use of higher temperatures (autoclaving of the urine sample with water for 35 min) also degraded tocainide, but to a greater extent than that seen at 100°.

During these experiments tocainide was observed to degrade at a faster rate in the presence of urine. To determine the possible role of urea in this degradation, tocainide was incubated with 8 *M* urea for 1 hr at 100°. At these higher concentrations of urea marked degradation of tocainide was observed. It is possible that the degradation of tocainide at higher temperature is to some extent related to the urea in the urine sample. Hence, it should be noted that the estimates of the acid hydrolysable conjugates carried out in the present study are only an approximation of the actual amount present in the urine.

Experiments carried out under optimal conditions for the enzymatic hydrolysis of the glucuronide conjugates of tocainide did not account for all of the conjugates observed following acid hydrolysis. It would appear that there are other conjugates of tocainide which also yield tocainide following acid hydrolysis. Acetylation is a known metabolic pathway for the elimination of primary amines (10). GC–mass spectrometric analysis has identified the presence of small quantities of *N*-acetyl derivative of tocainide in the rat urine. It is also possible that tocainide is eliminated by an as yet unidentified conjugation pathway.

Cleavage of the amide group (amide hydrolysis) has been shown to be a metabolic pathway for the elimination of a number of lidocaine analogs (11–14). In the present study, small quantities of 2,6-dimethylaniline were observed as a metabolite of tocainide (Fig. 3).

Condensation of a metabolite of lidocaine with acetaldehyde generates N^1-ethyl-2-methyl-N^3-(2,6-dimethylphenyl)-4-imidazolidinone (14). Such condensation reactions can occur under very mild reaction conditions (14). An aldehyde adduct of tocainide was observed in relatively large quantities (nearly 15% of the dose administered in the present study). The adduct was present in the methylene chloride and the ether extract of the urine samples.

A small quantity of oxidatively deaminated tocainide was also proposed to be present as a metabolite in rats (Fig. 4).

In addition to being formed from an unstable metabolite of tocainide, the cyclic compound was also present in small quantities in the urine sample as inferred by its presence in the methylene chloride extract of the urine sample at pH < 9.0 (15). The presence of a cyclic hydantoin metabolite of etidocaine in humans was reported previously (11). This hydantoin metabolite was a close structural analog of the cyclic metabolite observed in the present study.

Thus, the metabolic pathway shown in Scheme I accounts for nearly 60–70% of the dose of tocainide. Even though not identified in the present study, hydroxylation of the aromatic ring is a possible additional pathway of elimination of tocainide.

REFERENCES

(1) D. G. McDevitt, A. S. Nies, G. R. Wilkinson, R. F. Smith, R. L. Woosley, and J. A. Oates, *Clin. Pharmacol. Ther.*, **19,** 396 (1976).

(2) R. A. Winkle, P. J. Meffin, J. W. Fitzgerald, and D. C. Harrison, *Circulation*, **54,** 884 (1976).

(3) R. L. Woosley, D. G. McDevitt, A. S. Nies, R. F. Smith, G. R. Wilkinson, and J. A. Oates, *ibid.*, **56,** 980 (1977).

(4) P. J. Meffin, R. A. Winkle, T. F. Blaschke, J. Fitzgerald, and D. C. Harrison, *Clin. Pharmacol. Ther.*, **22,** 42 (1977).

(5) D. Lalka, M. B. Meyer, B. R. Duce, and A. T. Elvin, *ibid.*, **19,** 757 (1976).

(6) R. Venkataramanan and J. E. Axelson, *J. Pharmacol. Exp. Ther.*, **215,** 231 (1980).

(7) R. Venkataramanan and J. E. Axelson, *J. Pharm. Sci.*, **67,** 201 (1978).

(8) A. T. Elvin, *et al.*, *ibid.*, **69,** 47 (1980).

(9) L. G. Richards, M. C. Castle, and G. L. Lage, *Drug Metab. Dispos.*, **5,** 469 (1977).

(10) H. G. Mandel, in "Fundamentals of Drug Metabolism and Drug Disposition," B. N. La Du, H. G. Mandel, and E. L. Way, Eds., Williams & Wilkins, Baltimore, Md. 1971, p. 149.

(11) D. J. Morgan, M. P. Smyth, T. Thomas, and J. Vine, *Xenobiotica*, **7,** 365 (1977).

(12) J. Thomas, D. Morgan, and T. Vine, *ibid.*, **6,** 39 (1976).

(13) T. J. Goehl, J. B. Davenport, and M. J. Stanley, *ibid.*, **3,** 761 (1973).

(14) S. D. Nelson, G. D. Breck, and W. F. Trager, *J. Med. Chem.*, **16,** 1106 (1973).

(15) R. Venkataramanan and J. E. Axelson, *Xenobiotica*, **11,** 259 (1981).

ACKNOWLEDGMENTS

This work was supported by the British Columbia Heart Foundation (65-0566).

The authors are grateful to the Canadian Heart Foundation for the fellowship awarded to R. Venkataramanan and to Astra Pharmaceutical Products, Inc. for drug samples provided.

Studies on the Absorption of Practically Water-Insoluble Drugs following Injection V: Subcutaneous Absorption in Rats from Solutions in Water Immiscible Oils

KOICHIRO HIRANO ˣ, TERUHISA ICHIHASHI, and HIDEO YAMADA

Received March 2, 1981, from the *Shionogi Research Laboratories, Shionogi & Co., Ltd., Fukushima-ku, Osaka, 553, Japan.* Accepted for publication September 2, 1981.

Abstract □ To elucidate the kinetics and mechanisms of subcutaneous absorption of practically water-insoluble drugs in oily solutions, the absorption behaviors of select azo dyes and other prototype agents were investigated by a local clearance method in the dorsum in intact rats. The absorption of the drug components appeared to be first-order. The first-order rate constant (k) was inversely proportional to the cube root of the injection volume. In more limited studies, essentially the same behavior was observed in the rat abdomen, and the difference in k between the dorsal and abdominal injections was slight. The comparison of k of a given compound from different oily vehicles showed that k was governed predominantly by the distribution coefficient (K) between the oily vehicle and the aqueous subcutaneous medium and depended little on the viscosity of the vehicle. This distributioning relationship was shown through correlation of the rate constants with *in vitro* distribution coefficients. A plot of log k *versus* log K for all the compounds tested was linear with a slope of ~−0.7. This linear relationship allows adequate prediction of absorption rates of other drugs from oily vehicles. The observed subcutaneous absorption rates and behaviors are compared with previous results involving the intramuscular route.

Keyphrases □ Absorption, subcutaneous—from solutions in water immiscible oils, rats □ Water-insoluble drugs—subcutaneous absorption from solutions in water immiscible oils, rats □ Drug clearance—local clearance method following subcutaneous injection of practically water-insoluble drugs, drug absorption kinetics from oily solution, rats.

A previous study (1) investigated the intramuscular absorption characteristics of practically water-insoluble drugs in oily solutions in rats and considered the major factors governing the absorption kinetics. In parenteral drug administration, the subcutaneous route is as useful and important as the intramuscular route for early screening and preclinical testing of drugs in laboratory animals. The extensiveness of the subcutaneous tissue and its porosity and loose attachment allow injections of larger volumes than can be easily given intramuscularly. Thus, subcutaneous administration is applicable for dose–response experiments and multiple dosing experiments in small animals.

Since the publication of Schou's review (2) of drug absorption from subcutaneous connective tissue, there has been an increasing interest in quantitatively evaluating the subcutaneous absorption rate of drugs (3–6). However, very little work has been done on the absorption characteristics of marginally water-soluble drugs relative to highly water-soluble drugs in aqueous solution. The absorption rate and the resulting pharmacological responses of hydrophobic drugs are dependent primarily on the dosage form or physicochemical state of the preparation, and thus, it is very important to clarify the relationship of the kinetics of release of such drugs to the physical form in which they were administered.

The present study was undertaken to clarify the absorption mechanisms and kinetics attending subcutaneous injection of practically water-insoluble drugs in oily solutions and to compare them with intramuscular injection. Several azo compounds and testosterone were used as model drugs and a variety of water-immiscible oils were used as model vehicles. Subcutaneous absorption rates of these model drugs were measured in intact rats by a local clearance method first reported by Secher-Hansen *et al.* (3). Rates were compared across diverse experimental systems and conditions to evaluate the contribution of physicochemical factors to the kinetic process.

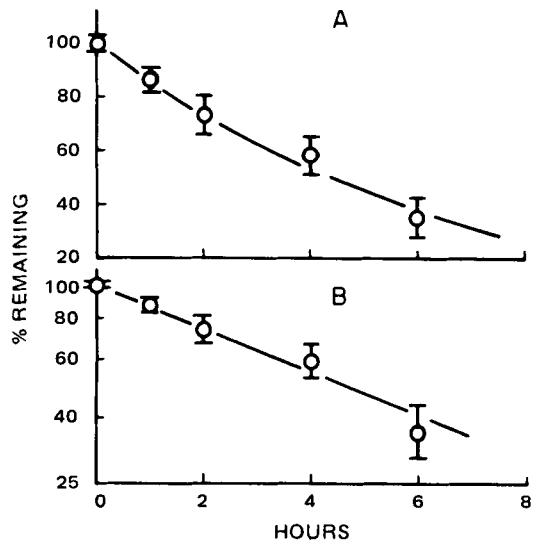

Figure 1—*Absorption time course of* p-*hydroxyazobenzene in sesame oil solution after subcutaneous injection into the intact rat. Initial drug concentration (C_0), 1 mg/ml; injection volume (V_0), 0.5 ml. Each data point represents the mean of four or five experiments and the vertical bar indicates the standard deviation.*

EXPERIMENTAL

Materials—Azo dyes (*p*-hydroxyazobenzene[1], *p*-aminoazobenzene[2], *o*-aminoazotoluene[3], 1-phenylazo-2-naphthylamine[2]), and testosterone[2] were selected as model compounds. These compounds are unionized under physiological conditions and are the same as used in a previous study (1). Sesame oil[4], medium-chain (C_8–C_{12}) triglycerides[5], isopropyl myristate[6], diethyl sebacate[6], and simethicone[7] were selected for their wide ranging viscosities and solubilizing powers. Other than simethicone, the oils were the same as used previously (1). All other chemicals used in this study were of analytical or reagent grade.

Preparation of Test Solutions—Test injection solutions for the absorption studies were prepared by dissolving the drugs in the oily media and then clarifying the media by passing the solutions through membrane filters (1). All test solutions of the azo dyes and testosterone were ascer-

[1] Eastman Kodak Co., New York.
[2] Tokyo Kasei Kogyo Co., Ltd., Japan.
[3] Ishizu Pharmaceutical Co., Ltd., Japan.
[4] Maruishi Pharmaceutical Co., Japan.
[5] Miglyol 812, Chemische Werke Witten, West Germany.
[6] Nikko Chemicals Co., Japan.
[7] KF 96 (20), Shinetsu Kagaku Kogyo Co., Japan.

0022-3549/82/0500-0495$01.00/0

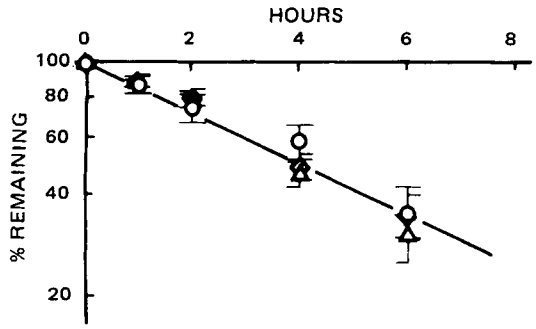

Figure 2—*Effect of initial concentration (C_0) on the subcutaneous absorption of* p-*hydroxyazobenzene in sesame oil (V_0 = 0.5 ml). Each data point represents the mean of at least three experiments and the vertical bar indicates the standard deviation. Key: (C_0) ⊖, 1 mg/ml; ⏃, 5 mg/ml; ◇, 20 mg/ml.*

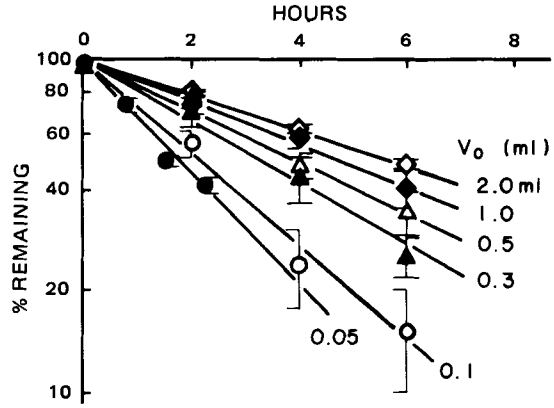

Figure 3—*Effect of injection volume (V_0) on the subcutaneous absorption of* p-*hydroxyazobenzene in sesame oil (20 mg/ml). Each data point represents the mean of at least three experiments and the vertical bar indicates the standard deviation.*

tained to be chemically and physically stable over the experimental period.

Procedure for Subcutaneous Absorption—Male Wistar albino rats (260–280 g) were used in all absorption experiments. Prior to an experiment, the hair in the center region (area, 5 × 5 cm^2) of the dorsum (or abdomen) of the rat was removed with an electric clipper[8]. With the rats under light anesthesia with ether, a given volume of test solution was injected into the subcutaneous space near the center of the shorn area using a calibrated syringe connected to a 0.50 × 25-mm needle[9] at an injection speed between 0.04 and 0.4 ml/sec. Immediately after withdrawal of the needle, a rapidly drying adhesive[10] was applied to the insertion site to prevent leakage. During an absorption experiment, each rat was housed in a cage and allowed freedom of movement and easy access to water and food. At various intervals postinjection, each rat was decapitated and bled, and the tissues around the injection site containing the oily depot were excised as completely as possible and then minced. Drug remaining at the injection site was extracted from the minced tissues with 20 ml of ethyl acetate, and the amount of drug was determined. Most of the test compounds recovered from the tissue were within the oily deposits and there appeared to be little drug recovered from the surrounding tissues. Decomposition and metabolism of the model compounds at the injection site were presumed to be negligible; thus, their clearance in the absorption experiments is mainly attributed to removal by blood and lymphatic flows. Three to five rats were used for each time interval in all the absorption experiments.

Measurement of Absolute Viscosity—The kinematic viscosity of each oily solvent was determined with a viscometer[11] and converted into the absolute viscosity using its density, which was measured with a calibrated flask[12]. These determinations were done at 37°.

Determination of the Distribution Coefficient—The distribution coefficient (K) of a model compound between an oily solvent and 0.9% (w/v) NaCl in water (saline) was determined by equilibrating an oily solution with saline and computing K from the equilibrium saline concentration and the initial concentration in the oil phase (1).

Analytical Method—In the absorption experiments extracts containing the azo dyes were adequately diluted with ethyl acetate and analyzed colorimetrically (1). Extracted testosterone was assayed by a gas chromatographic method (1). Three-milliliter samples were shaken with 0.6 g of Al_2O_3–silica gel (1:1) to remove interfering substances. The mixture was centrifuged for 5 min at 3000 rpm and 1 ml of the supernatant liquid was mixed with 0.1 ml of the internal standard (3β-acetoxy-5α-androstan) in ethyl acetate. Two microliters of these solutions was injected using the same instrument settings reported previously (1). For determination of the distribution coefficients, test compounds in saline equilibrated with oily solutions of known initial concentration were assayed by direct spectrophotometric methods (1).

RESULTS

Time Course of Drug Absorption and Effect of Initial Drug Concentration—It was reported (5) that benzyl alcohol, which is relatively hydrophobic, was absorbed from an aqueous medium in the rat subcutaneous region according to first-order kinetics. However, the kinetic process for subcutaneous absorption of practically water-insoluble drugs from oily solutions has not been explored.

The time course of subcutaneous absorption in a typical experiment is illustrated in Fig. 1, which shows the profile for *p*-hydroxyazobenzene absorbed from a sesame oil solution. The initial drug concentration (C_0) and the injection volume (V_0) are given in the legend. The fraction (percent) of *p*-hydroxyazobenzene remaining at the injection site was plotted against time on arithmetic and logarithmic scales. The linear relationship shown in Fig. 1B indicates this compound is absorbed according to first-order kinetics. To verify this, the effect of the initial drug concentration (C_0) on the absorption rate was examined. Figure 2 shows the absorption time courses of *p*-hydroxyazobenzene from solutions initially of 1, 5, and 20 mg/ml on a semilogarithmic scale. All three profiles are approximately linear with the same slope. Similar results were obtained with other compounds such as *p*-aminoazobenzene and *o*-aminoazotoluene. These findings suggest that subcutaneous absorption of practically water-insoluble and unionized drugs from oily solutions behaves as a first-order process.

Effect of Injection Volume—It has been noted that the injection volume of aqueous (7, 8) or oily (9) solutions might be an important factor influencing intramuscular absorption rates of drugs. A previous report (1) revealed the quantitative relationship between the absorption rate constant and the injection volume for intramuscular administration of practically water-insoluble drugs administered as oily solutions. However, for subcutaneous administration, the effect of the injection volume has not always been clear (10, 11).

Figure 3 compares the absorption time courses of *p*-hydroxyazobenzene injected in different volumes on a semilogarithmic scale. Each absorption profile is linear and the slopes decrease with increased injection volume. Figure 4 demonstrates the relation between the observed first-

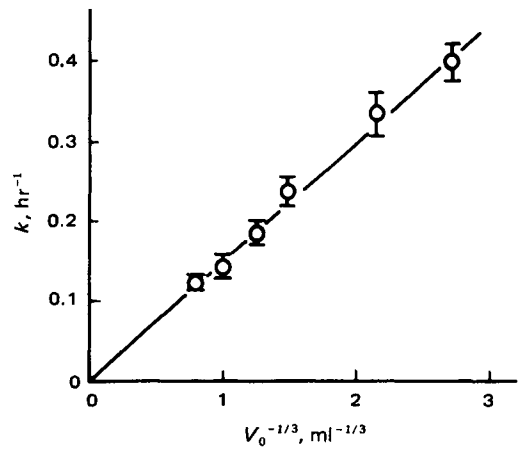

Figure 4—*Relationship between the first-order absorption rate constant (k) and injection volume (V_0). The values of* k *were estimated from the data shown in Fig. 3 by the least-squares method and are plotted together with their standard errors.*

[8] Thrive SNB-25, Daito Electric Mfg. Co., Japan.
[9] Terumo Co., Ltd., Japan.
[10] Aron Alpha, Toa Gousei Kagaku Co., Ltd., Japan.
[11] Ubbelohde, Kaburagi Kagaku Kikai Kogyo Co., Japan.
[12] Cassia, Shibota Kagaku Kikai Kogyo Co., Japan.

Table I—Values of Absolute Viscosity of Oil (η), Distribution Coefficient (K), and First-Order Absorption Rate Constant (k)

Oil	η(cps)	*p*-Hydroxyazobenzene		*p*-Aminoazobenzene		*o*-Aminoazotoluene	
		K[a]	k, hr^{-1} [b]	K[a]	k, hr^{-1} [b]	K[a]	k, hr^{-1} [b]
Simethicone	16.0	17	3.00 (0.41)	29	1.32 (0.17)	310	0.43 (0.04)
Isopropyl myristate–simethicone (1:9, v/v)	13.2	54	1.66 (0.12)	—	—	—	—
Isopropyl myristate–simethicone (2:8, v/v)	10.7	160	0.98 (0.08)	170	0.70 (0.06)	1700	0.21 (0.02)
Isopropyl myristate–simethicone (4:6, v/v)	7.6	510	0.30 (0.01)	550	0.34 (0.03)	5400	0.13 (0.02)
Sesame oil	35	1300	0.21 (0.01)	1200	0.12 (0.009)	13400	0.034 (0.004)
Isopropyl myristate	3.6	2900	0.13 (0.01)	1700	0.11 (0.008)	20000	0.023 (0.001)
Medium chain triglycerides	15	3500	0.084 (0.007)	2900	0.061 (0.003)	27000	0.017 (0.002)
Diethyl sebacate	3.9	15000	0.029 (0.003)	9900	0.030 (0.003)	75000	0.011 (0.001)

[a] Distribution coefficient; the ratio of the drug concentration in oil to that in 0.9% NaCl aqueous solution (saline) at equilibrium (37°). [b] Estimated by the least-squares method and given with the standard error (SE) in parentheses.

order absorption rate constant (k) and injection volume (V_0). It was evident from this figure that k was inversely proportional to the cube root of V_0.

Comparison of Absorption Rates between Dorsal and Abdominal Subcutaneous Injections—A significant difference in the absorption half-life of ^{131}I-labeled insulin injected subcutaneously into the human arm and thigh was noted (12). Given this difference, and considering the fact that subcutaneous drug injections to animals are not always limited to the dorsal site, the abdomen was selected as a second subcutaneous injection site to draw site-to-site comparisons. Drug absorption time courses from this site with different injection volumes were evaluated, and again first-order absorption rate constants were obtained from semilogarithmic plots. The values are compared in Fig. 5 with those obtained for the dorsal injections. The relationship between the rate constant of absorption and the volume of material injected found by dorsal subcutaneous injection also held for the subcutaneous abdominal injections. Remarkably, differences in the absorption rate constants between these two injection sites were negligible. These findings showed that, at least with these substances and under these experimental conditions, absorption behaviors of the two sites are virtually identical.

Comparison of Absorption Rates from Various Oily Solvents—Up to this point, sesame oil was used as the oily solvent since it is commonly used as a parenteral solvent. To clarify possible influences of the oily medium on absorption kinetics, the absorption time courses from different oily vehicles were evaluated. Figure 6 shows absorption time profiles of *p*-hydroxyazobenzene from six oily vehicles, diethyl sebacate, medium chain triglycerides[5], isopropyl myristate, sesame oil, and two isopropyl myristate–simethicone systems (40:60 and 20:80, v/v), all administered at the same volume. The semilogarithmic plots are linear but each has a different slope. Similar results were obtained for *p*-aminoazobenzene and *o*-aminoazotoluene. The first-order absorption rate constants obtained from these experiments are summarized in Table I along with the viscosities (η) of the oil solvents and the distribution coefficients (K, oily vehicle/saline). Clearly, the distribution coefficient is the predominant factor controlling the absorption rates from these oily vehicles.

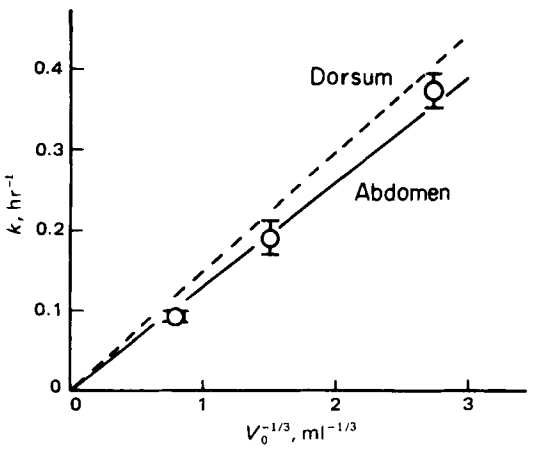

Figure 5—*Comparison of the subcutaneous absorption rate constants (k) of p-hydroxyazobenzene in sesame oil at various injection volumes (V_0) between injection sites on the dorsum and abdomen of rat (C_0, 5 mg/ml). The k values were estimated by the least-squares method and plotted together with their standard errors. Key: (—○—) abdomen; (- - -) dorsum (same as shown in Fig. 4).*

DISCUSSION

Shape of Depot and Drug Absorption Kinetics—It is observed that when a given volume of water-immiscible oil is injected subcutaneously, the major part of it is confined to the injection site by the connective tissues and possibly other surrounding tissues. Also the depot formed in such a manner tends to take the shape of a flattened oblate or prolate spheroid. These observations are similar to those described previously (13), where w/o emulsions containing radioactive substances were used to define the local distribution. The shape of the oily depot, which determines the surface area of the oily phase exposed to the body fluids, is thought to be a critical factor affecting drug absorption. The geometry of the oily depot may depend on the injection volume, the fluidity of the oily solution, hydrodynamic factors such as the injection speed, the available space at the injection site, and/or body movements. The deposit configuration is undoubtedly time-dependent. Visual observation confirmed geometrical change of the depots caused by spreading. These were initially abrupt but became very slight after a short time. Water-immiscible oils such as sesame oil apparently disappear much more slowly from the subcutaneous site than do the drug components they contain (14). A previous study (1) showed that sesame oil was also very slowly absorbed from the m. gastrocnemius of the rat during the first several hours after injection. Therefore, it seems reasonable to regard the surface area of the oily depot as a constant during the absorption process except for a short period immediately after injection. The state of the oily depots and the first-order absorption characteristic of the rate process strongly suggest that the absorption behavior of drugs in oily solutions deposited subcutaneously is very similar to that of the intramuscular route (1). Therefore, the kinetic treatment previously proposed for intramuscular absorption (1) seems equally applicable to the subcutaneous situation.

The kinetics of absorption from an intramuscular, oil deposit were developed for a physical model in which mass transfer was strictly controlled by diffusion through the interface of the depot with the tissue.

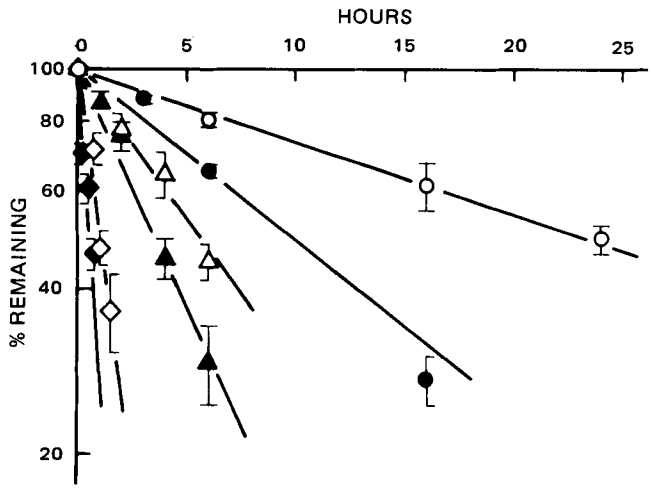

Figure 6—*Time courses of the subcutaneous absorption of p-hydroxyazobenzene from various oily vehicles (C_0, 0.5–5 mg/ml; V_0, 0.5 ml). Each data point represents the mean of at least three experiments and the vertical bar indicates the standard deviation. Key: (○) diethyl sebacate; (●) medium chain triglycerides; (△) isopropyl myristate; (▲) sesame oil; (◇) isopropyl myristate–simethicone (40:60, v/v); (◆) isopropyl myristate–simethicone (20:80, v/v).*

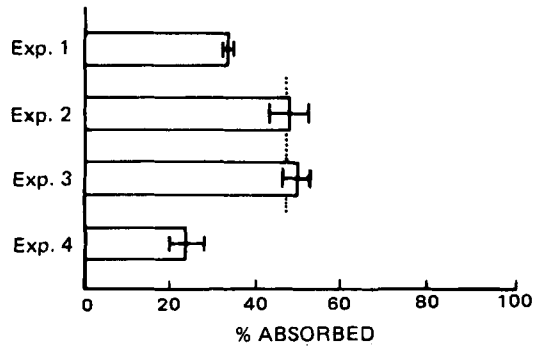

Figure 7—*Comparison of the subcutaneous absorption of* p-*aminoazobenzene among various injection methods at a constant dose. The dotted line shows the value for Exps. 2 and 3 predicted from the results of Exp. 1. Each data point shows the mean of at least four experiments. Key: Exp. 1, 4 mg/ml–0.5 ml; Exp. 2, 20 mg/ml–0.1 ml; Exp. 3, 4 mg/ml–0.1 ml, 5 injections at different points; Exp. 4, 4 mg/ml–0.5 ml (o/w emulsion).*

The interface was seen as a series barrier, possibly with significant diffusional resistances on each side of the interface, *i.e.*, in the boundary layer in the depot and in the tissue immediately in contact with the depot. Mass transfer coefficients (permeability coefficients) k_o and k_a describe the diffusive velocities in the depot's boundary and the tissue, respectively. It is implicit that the depot acts as a well-stirred phase everywhere except at its interface. It was also assumed in developing the model that: (*a*) over the full course of drug release the depot's interfaces and surface area remain essentially constant; (*b*) the distribution coefficient of a drug between the depot and the tissue fluids strictly governs the relative concentrations on each side of the interface; (*c*) the depot acts as a reservoir for the drug; (*d*) the body of the animal acts as a diffusional sink; and (*e*) there is no assimilation of the oily vehicle by the body over the course of drug release. With these assumptions the release process becomes a first-order depletion of a reservoir into a sink by means of diffusion across an oil–water boundary. The following equations were derived for the quasi-steady-state (period after establishment of the gradient across the boundary):

$$\ln (W/W_0) = -kt \qquad \text{(Eq. 1)}$$

and

$$k = \frac{k_o A}{V_0\left(1 + \frac{k_o}{k_a} K_i\right)} \qquad \text{(Eq. 2)}$$

where W_0 and W represent the dose and the remaining amount of the drug at any time t, respectively; V_0 and A are the injection volume and the surface area of the oily depot, respectively; k_o and k_a are the diffusive velocities of the drug in the oily and aqueous tissue boundaries, respectively; K_i is the distribution coefficient at the interface; and k is the first-order absorption rate constant (1). Equation 1 describes the expected first-order behavior, while Eq. 2 characterizes the rate constant for the series barrier situation.

Comparison of Absorption Rates among Various Injection Methods—Equation 2 contains the ratio, A/V_0, which describes the geometrical aspects of the absorption process. The dependency of drug-release rate on the injected volume centers around the interdependency of area and volume. When the shape of the injected mass is spherical or near spherical, the area–volume ratio is simply $3/r$ or three times the reciprocal radius of the equivalent sphere. This is directly proportional to the reciprocal cube root of the volume[13]. Therefore, for an injection acting as a near spherical (or spheroidal) mass, it is expected that the absorption rate constant of an incorporated drug will be proportional to the $V_0^{-1/3}$, a dependency on volume which was closely followed in the subcutaneous administrations as evidenced in Figs. 4 and 5.

[13] When the injected mass takes the shape of a spheroid or a near spheroid and retains the same shape (dimensions) for alterations in injection volume, the same cube root volume dependency can also be derived mathematically as follows:

Spheroid 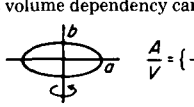

$$\frac{A}{V} = \left\{\frac{3}{2\beta}\left(\frac{3}{4\pi\beta}\right)^{-\frac{1}{3}}\left(1 + \frac{\beta^2}{2\sqrt{1-\beta^2}} \log \frac{1+\sqrt{1-\beta^2}}{1-\sqrt{1-\beta^2}}\right)\right\} V^{-\frac{1}{3}}$$

$(a > b,\ b/a = \beta)$

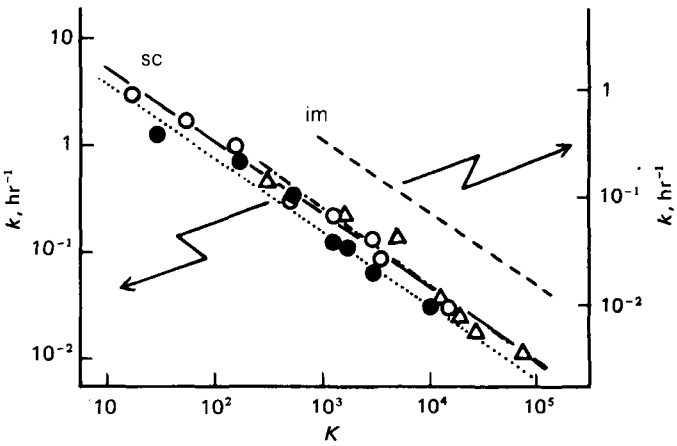

Figure 8—*Plots of* k versus K *on log–log scale for three model compounds. Key: (—○—) p-hydroxyazobenzene; (·····●·····) p-aminoazobenzene; (-·-▵-·-) o-aminoazotoluene; (sc) data for subcutaneous injection at* C_0 = *0.5–5 mg/ml and* V_0 = *0.5 ml; (im) data for intramuscular injection m. gastrocnemius) at* C_0 = *5 mg/ml and* V_0 = *0.05 ml reported previously (1).*

The preceding discussion indicates that the absorption rate constant is dependent on injection volume and not on the initial drug concentration. This means that the absorption rate can be manipulated by the injection method even if the drug, solvent, and dose are fixed. This was demonstrated experimentally using *p*-aminoazobenzene in sesame oil solution. Figure 7 shows the percentage of this drug absorbed 3 hr after injection of a fixed dose, 2 mg/rat, by four differing injection protocols. In Exp. 1 a single, 0.5-ml injection of solution containing 4 mg/ml was given; in Exp. 2 a single, 0.1-ml injection of solution containing 20 mg/ml was given; in Exp. 3 five injections were given at different sites, each with 0.1 ml of solution containing 4 mg/ml; and in Exp. 4 a single, 0.5-ml injection of an o/w emulsion [equal volumes of sesame oil containing 8 mg/ml of *p*-aminoazobenzene and saline containing 2% (w/v) polysorbate 80; emulsion particle diameter, 2–10 μm] was given. The theory was tested as follows. The first-order absorption rate constant (k_1) was determined in Exp. 1. Using this k_1 value, the value of the percentage absorbed for Exp. 2 can be estimated by the following equation derived from Eq. 1 and the cube root volume dependency:

$$\text{Percent absorbed} = 100\{1 - \exp[-k_1(V_1/V_2)^{1/3}t]\} \qquad \text{(Eq. 3)}$$

The dotted line in Fig. 7 shows the value estimated by substitution of the calculated value, 0.12 (hr^{-1}), for k_1, of 5 for V_1/V_2 (the actual injection volume ratio), and of 3 (hr) for t in Eq. 3. In Exp. 3 the absorption at each injection site will proceed independently and to the same extent; thus, the dotted line also shows the estimate for the third case as the injection volume at each injection point is equal to that in Exp. 2. The value calculated from the results of Exp. 1 agrees well with the observed values of Exps. 2 and 3. Accordingly, it is concluded that the reciprocal cube root volume dependency expressed in Eq. 3 will be generally applicable. These findings imply that faster absorption occurs when the injection volume per one site is minimized either by increasing the number of injections or by using more concentrated solutions.

Addition of surface-active agents and emulsifiers to injected oily solutions of drugs has been reported to enhance the absorption of the oily vehicle (9) or practically water-insoluble drugs contained therein (15). Recently, emulsion systems have been promoted as novel drug delivery systems for some anticancer agents (16). Figure 7 shows that the absorption of *p*-aminoazobenzene from the emulsion system (Exp. 4) would be slower than that from oily solution (Exp. 1). However, so many new variables are introduced when the administration system is changed to an emulsion that it is impossible to even qualitatively interpret this result.

Correlation among the Absorption Rate Constant, Viscosity, and the Distribution Coefficient—It was shown previously (17) that a certain correlation exists between the viscosity of vaccines (aluminum monostearate paraffin gels) injected subcutaneously into rabbits and guinea pigs and the degree of enhancement and prolongation of the antitoxin levels. However, as is evident from Table I, no distinguishable relationship was observed between the viscosity (η) of the vehicle and the absorption rate constant (k) under our experimental conditions (η, 3.6–35 cps). This difference is not surprising when it is realized that the

Table II—Predicted and Observed Subcutaneous Absorption Rate Constants (k) [a]

Test Compound	M.W.[b]	K[c]	k, hr^{-1} Predicted[d]	k, hr^{-1} Observed (SE)
Testosterone	288	1.30×10^2	0.79	0.64 (0.09)
1-Phenylazo-2-naphthylamine	247	3.82×10^5	0.0035	0.0053 (0.0003)

[a] Sesame oil solution; C_0, 2.5 mg/ml for testosterone and 5 mg/ml for 1-phenylazo-2-naphthylamine; V_0, 0.5 ml. [b] Molecular weight. [c] Distribution coefficient (sesame oil/saline) at 37°. [d] Calculated using the regression equation obtained from all sc data in Fig. 8: $\log k = -0.68 \log K + 1.33$

gelled systems of Coles *et al.* (17) could hardly act as well-stirred phases. Moreover, smaller mass transfer coefficients (k_o) due to the increased viscosity are expected to elevate the role in rate control played by the vehicle's boundary layer.

If the term $(k_o/k_a)K_i$ in Eq. 2 is $\ll 1$, Eq. 2 is approximated by:

$$k = Ak_o/V_0 \qquad \text{(Eq. 4)}$$

This equation signifies that diffusion in the oily phase is the rate limiting process in drug absorption as appears to be the case for the gels of Coles *et al.* (17). However, this relationship does not appear representative of the behavior of the present systems as k, according to Eq. 4, depends upon k_o, which in turn depends on viscosity of the oily vehicle, but not on K_i. On the other hand, when the term $(k_o/k_a)K_i$ is $\gg 1$, which seems very likely due to the large distribution coefficients (K_i) of the drugs between the phases considered here, Eq. 2 is approximated by:

$$k = Ak_a/(V_0K_i) \qquad \text{(Eq. 5)}$$

This equation signifies that k is independent of k_o; that is, independent of the viscosity of the oily vehicle and dependent on K_i. Given the partitioning dependency of the process (Table I), the present results seem to favor the relationship as written in Eq. 5 on two counts. Partitioning and diffusion across a tissue boundary also appear to control rates of intramuscular absorption (1).

Taking the logarithm of both sides of Eq. 5 gives:

$$\log k = \log (Ak_a/V_0) - \log K_i \qquad \text{(Eq. 6)}$$

The term $\log (Ak_a/V_0)$ in this equation is governed by the injection volume and the permeability of the drug in the connective tissues adjacent to the oily depot. According to Eq. 6, a plot of $\log k$ *versus* $\log K_i$ should give a single straight line with a slope of -1 for compounds having a similar tissue permeability as long as the injection volume is maintained constant. Figure 8 shows this plot for the three compounds presented in Table I, all of which have similar molecular weights. In this plot the *in vitro* bulk distribution coefficient (K, oily solvent/saline) is used instead of the *in vivo* distribution coefficient (K_i) which is not measurable. The plot indicates linear relationships over a wide range of K values for all three compounds. The regression equations ($x = \log K$, $y = \log k$) and their correlation coefficient (r) for the individual compounds are as follows: for *p*-hydroxyazobenzene, $y = -0.686x + 1.398$ ($r = -0.994$); for *p*-aminoazobenzene, $y = -0.689x + 1.256$ ($r = -0.982$); for *o*-aminoazotoluene, $y = -0.733x + 1.594$ ($r = -0.974$). From these separate results, the following experimental equation relating the rate constant to the *in vitro* distribution coefficient is evident:

$$\log k = \log (Ak_a/V_0) - \delta \log K \qquad \text{(Eq. 7)}$$

The resultant values for δ are of the order of -0.7, whereas perfect *in vivo–in vitro* distributioning correlation would yield a value of -1.0. This slight deviation might be attributable to fundamental, systematic differences in partitioning sensitivities between the *in vivo* and *in vitro* systems, to a not totally negligible diffusional resistance in the vehicle's boundary layer, which itself precludes exact adherence to Eq. 5, or to the coexistence of another absorption mechanism not accounted for in Eq. 2, *i.e.*, absorption of the drug as the result of assimilation of the injected medium by the body. In any case, the experimental equation can be put in the following, general phenomenological form:

$$k = \gamma/V_0{}^mK^\delta \qquad \text{(Eq. 8)}$$

where γ is a coefficient lumping together all intangible experimental parameters. This relationship seems to have practical value for the estimation of absorption rates of diverse drugs from diverse oily vehicles.

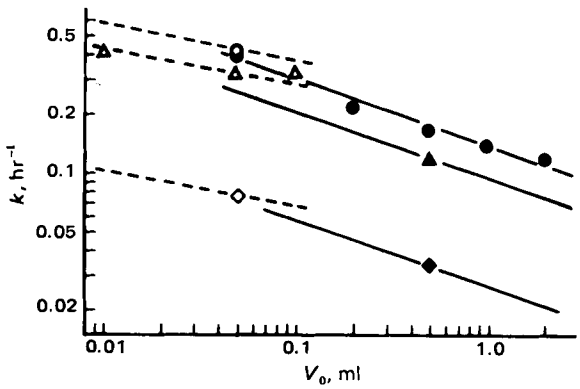

Figure 9—*Comparison of the absorption rate constants (k) at various injection volumes (V_0) between subcutaneous (dorsum) and intramuscular (m. gastrocnemius) injections in intact rats. The straight lines for subcutaneous injection of* p-aminoazobenzene *and* o-aminoazotoluene, *and those for intramuscular injection of* p-hydroxyazobenzene *and* o-aminoazotoluene *are depicted to pass through one data point with a slope of −0.33 and −0.14, respectively. The subcutaneous data are shown elsewhere in this paper and those for intramuscular injection are quoted from a previous work (1). Key: (—●—) (sc), (---○---) (im),* p-hydroxyazobenzene; *(—▲—) (sc), (---△---) (im),* p-aminoazobenzene; *(—◇—) (sc), (---◇---) (im),* o-aminoazotoluene.

Figure 8 also shows with a broken line the corresponding regression line for the intramuscular absorptions of the same three compounds (1). The parallelism of the regression lines suggests a strong similarity in distributioning behavior at the injection's interface between the subcutaneous and intramuscular routes.

Prediction of Absorption Rates of Other Drugs—Figure 8 shows the regression lines of three separate compounds to be essentially inseparable when the injection volume was fixed. Their composite regression equation is: $\log k = -0.68 \log K + 1.33$ ($r = -0.98$). It was anticipated through this colinearity that this relationship might provide a means of estimating absorption rate constants (k) of other drugs simply from the K values determined in the *in vitro* saline system. To examine this possibility, testosterone and 1-phenylazo-2-naphthylamine, compounds with molecular weights similar to the three compounds presented in Fig. 8, were selected as additional test substances. Absorption rate constants predicted from their respective K values and the above regression equation were compared with experimental values. The results appear in Table II. For these compounds, the predicted values agree well with the observed values. This satisfactory result suggests the absorption behaviors of other drugs may be similarly predicted.

Comparison of Absorption Rates between Subcutaneous and Intramuscular Routes in Rats—It was found (12) that no significant difference in the absorption rates of ^{131}I-labeled insulin[14] (insulin suspensions) from subcutaneous and intramuscular tissues exists at either the thigh or arm region in humans. No such comparison between sites exists for a drug presented in oily solution. In the present and a previous (1) report, the quantitative relationships between the absorption rate constant (k) and the injection volume (V_0) for subcutaneous and intramuscular routes has been elucidated in rats. By both routes the value of k was proportional to $V_0{}^m$. However, the experimental m values for subcutaneous (dorsum) and intramuscular (m. gastrocnemius) injections in intact rats are apparently different and are -0.33 and -0.14, respectively.

In Fig. 9, k values in intact rats obtained by the subcutaneous route (dorsum) for the three test compounds at various injection volumes (V_0) are compared with those by the intramuscular route (1). Although the data points available for direct comparison are few in this figure, it appears that the values by the two routes may be quantitatively compatible. If this is true, then a change in volume dependency (m) is apparent as the injected volume goes from the very small volumes given intramuscularly to the relatively large subcutaneous volumes.

REFERENCES

(1) K. Hirano, T. Ichihashi, and H. Yamada, *Chem. Pharm. Bull.*, **29**, 519 (1981).

(2) J. Schou, *Pharmacol. Rev.*, **13**, 441 (1961).

[14] Lente insulin, Squibb, Co.

(3) E. Secher-Hansen, H. Langgard, and J. Schou, *Acta Pharmacol. Toxicol.*, **25**, 162, 290 (1967).
(4) *Ibid.*, **26**, 9 (1968).
(5) B. E. Ballard and E. Menczel, *J. Pharm. Sci.*, **56**, 1476 (1967).
(6) R. H. Levy and M. Rowland, *J. Pharmacokinet. Biopharm.*, **2**, 313, 337 (1974).
(7) R. B. Sund and J. Shou, *Acta Pharmacol. Toxicol.*, **21**, 313 (1964).
(8) M. Pfeffer and D. R. Van Harken, *J. Pharm. Sci.*, **70**, 449 (1981).
(9) T. Tanaka, H. Kobayashi, K. Okumura, S. Muranishi, and H. Sezaki, *Chem. Pharm. Bull.*, **22**, 175 (1974).
(10) J. H. Leathem, *Proc. Soc. Exp. Biol. Med.*, **68**, 92 (1948).
(11) W. L. Honrath, A. Wolff, and A. Meli, *Steroids*, **2**, 425 (1963).
(12) J. J. Nora, W. D. Smith, and J. R. Cameron, *J. Pediatr.*, **64**, 547 (1964).
(13) E. A. Brown, T. G. Metcalf, and L. W. Slanety, *Ann. Allergy*, **19**, 1016 (1961).
(14) R. Deanesly and A. S. Parkes, *J. Physiol.*, **78**, 155 (1933).
(15) J. C. Bauernfeind and H. L. Newmark, *Bull. Parenter. Drug Assoc.*, **24**, 169 (1970).
(16) S. Muranishi, *Yakugaku Zasshi*, **100**, 687 (1980).
(17) C. L. J. Coles, K. R. Heath, M. L. Hilton, K. A. Lees, P. W. Muggleton, and C. A. Walton, *J. Pharm. Pharmacol.*, **17**, 87S (1965).

ACKNOWLEDGMENTS

The authors thank Mrs. J. Kagawa for her technical assistance and thank Prof. M. Nakagaki, Kyoto University, for his valuable comments on the manuscript.

Studies on the Absorption of Practically Water-Insoluble Drugs Following Injection VI: Subcutaneous Absorption from Aqueous Suspensions in Rats

KOICHIRO HIRANO ˣ and HIDEO YAMADA

Received April 8, 1981, from the *Shionogi Research Laboratories, Shionogi & Co., Ltd., Fukushima-ku, Osaka, 553, Japan.* Accepted for publication May 20, 1981.

Abstract □ The absorption characteristics and kinetics of practically water-insoluble drugs following subcutaneous injection of their aqueous suspensions were investigated in intact rats by the local clearance method and compared with those following intramuscular injection reported previously. The plot of the cube root of the residual fraction of the drug in the injection site *versus* time gave a good linear relationship under various experimental conditions. The absorption rate constant (j) increased with decreasing particle size. This increase was remarkable in the region of mean particle diameter <2–3 μm, while it was gradual or slight in the region above this. This phenomenon was explained by the fact that the *in vivo* spreading of particles of more than ~3 μm was still more limited by the network of the fibrous tissues. Between j and the initial drug concentration (C_0) or injection volume (V_0), the practically important relationship $j \propto C_0^g V_0^h$ ($g = -0.66$ and $h = -0.32$) could approximately be derived from the experimental results. Comparison of j values among various compounds with different solubility (C_s') in saline but with similar colloidal properties (particle size distribution and sedimentation volume) showed that a log j *versus* log C_s' plot gave a nearly straight line with a slope of ~0.5. All the results observed for the subcutaneous absorption were similar to those for intramuscular absorption and could reasonably be explained by the kinetic model proposed for intramuscular absorption.

Keyphrases □ Absorption, subcutaneous—from aqueous suspensions of practically water-insoluble drugs, rats □ Water-insoluble drugs—subcutaneous absorption from aqueous suspensions, rats □ Aqueous suspensions—subcutaneous absorption of practically water-insoluble drugs, rats

Although subcutaneous administration of aqueous suspensions is very popular for practically water-insoluble drugs in preclinical animal experiments, little has been studied on their absorption mechanisms and kinetics except for the particle-size effect on pharmacological responses (1). Previously investigated (2, 3) were the absorption behaviors of subcutaneously implanted solid drugs (sphere, disk, and cylindrical shapes) and the absorption kinetic process was clarified. The intramuscular absorption characteristics of practically water-insoluble drugs from aqueous suspension were investigated in detail, and a kinetic equation was proposed for the drug absorption, which was obtained empirically and was very useful (4).

In the present work, similar investigations for the subcutaneous route were done with the local clearance method in intact rats. The purpose of the present study was to clarify the relationship between the absorption rate and physicochemical properties (particle size, initial drug concentration, injection volume, drug solubility, *etc.*), to express this relationship in appropriate mathematical terms, and to compare the results with those for the intramuscular route reported previously (4).

The findings obtained in this study will offer a novel and useful guide for more detailed screening and preclinical testing in laboratory animals of new drugs under development.

EXPERIMENTAL

Materials—Azo dyes (*p*-aminoazobenzene, *p*-hydroxyazobenzene, *o*-aminoazotoluene, and 1-phenylazo-2-naphthylamine), sulfa drugs (N^1-acetylsulfamethoxazole and sulfamethoxazole), and a steroid (betamethasone dipropionate[1]) were used as models for practically water-insoluble drugs. These azo dyes and sulfa drugs were the same as those used in a previous study (4). Betamethasone dipropionate was of medicinal grade and its purity was ascertained to be satisfactory through elementary analysis, melting point measurement, and TLC. Methylcellulose[2] and polysorbate 80[3], used as dispersing agents for preparations, were the same as those reported previously (4). All other chemicals were of analytical or reagent grade.

To compare the spreading area of injected particles, the following standard particles of different sizes were also used: two polystyrene latexes (0.721 and 1.305 μm in mean diameter based on number size distribution)[4], polyvinyltoluene latex (2.956 μm)[4], spores (4.94 μm)[5], di-

[1] Schering Corp., Bloomfield, N.J.
[2] Metolose SM-15, Shinetsu Kagaku Kogyo Co., Ltd., Tokyo.
[3] Kao Atlas Co., Ltd., Tokyo.
[4] The Dow Chemical Co., Indianapolis, Ind.
[5] Coulter Electronics, Ltd., Dunstable.

0022-3549/82/0500-0500$01.00/0

(3) E. Secher-Hansen, H. Langgard, and J. Schou, *Acta Pharmacol. Toxicol.*, **25**, 162, 290 (1967).
(4) *Ibid.*, **26**, 9 (1968).
(5) B. E. Ballard and E. Menczel, *J. Pharm. Sci.*, **56**, 1476 (1967).
(6) R. H. Levy and M. Rowland, *J. Pharmacokinet. Biopharm.*, **2**, 313, 337 (1974).
(7) R. B. Sund and J. Shou, *Acta Pharmacol. Toxicol.*, **21**, 313 (1964).
(8) M. Pfeffer and D. R. Van Harken, *J. Pharm. Sci.*, **70**, 449 (1981).
(9) T. Tanaka, H. Kobayashi, K. Okumura, S. Muranishi, and H. Sezaki, *Chem. Pharm. Bull.*, **22**, 175 (1974).
(10) J. H. Leathem, *Proc. Soc. Exp. Biol. Med.*, **68**, 92 (1948).
(11) W. L. Honrath, A. Wolff, and A. Meli, *Steroids*, **2**, 425 (1963).
(12) J. J. Nora, W. D. Smith, and J. R. Cameron, *J. Pediatr.*, **64**, 547 (1964).
(13) E. A. Brown, T. G. Metcalf, and L. W. Slanety, *Ann. Allergy*, **19**, 1016 (1961).
(14) R. Deanesly and A. S. Parkes, *J. Physiol.*, **78**, 155 (1933).
(15) J. C. Bauernfeind and H. L. Newmark, *Bull. Parenter. Drug Assoc.*, **24**, 169 (1970).
(16) S. Muranishi, *Yakugaku Zasshi*, **100**, 687 (1980).
(17) C. L. J. Coles, K. R. Heath, M. L. Hilton, K. A. Lees, P. W. Muggleton, and C. A. Walton, *J. Pharm. Pharmacol.*, **17**, 87S (1965).

ACKNOWLEDGMENTS

The authors thank Mrs. J. Kagawa for her technical assistance and thank Prof. M. Nakagaki, Kyoto University, for his valuable comments on the manuscript.

Studies on the Absorption of Practically Water-Insoluble Drugs Following Injection VI: Subcutaneous Absorption from Aqueous Suspensions in Rats

KOICHIRO HIRANO ˣ and HIDEO YAMADA

Received April 8, 1981, from the *Shionogi Research Laboratories, Shionogi & Co., Ltd., Fukushima-ku, Osaka, 553, Japan.* Accepted for publication May 20, 1981.

Abstract □ The absorption characteristics and kinetics of practically water-insoluble drugs following subcutaneous injection of their aqueous suspensions were investigated in intact rats by the local clearance method and compared with those following intramuscular injection reported previously. The plot of the cube root of the residual fraction of the drug in the injection site *versus* time gave a good linear relationship under various experimental conditions. The absorption rate constant (j) increased with decreasing particle size. This increase was remarkable in the region of mean particle diameter <2–3 μm, while it was gradual or slight in the region above this. This phenomenon was explained by the fact that the *in vivo* spreading of particles of more than ~3 μm was still more limited by the network of the fibrous tissues. Between j and the initial drug concentration (C_0) or injection volume (V_0), the practically important relationship $j \propto C_0^g V_0^h$ ($g = -0.66$ and $h = -0.32$) could approximately be derived from the experimental results. Comparison of j values among various compounds with different solubility (C_s') in saline but with similar colloidal properties (particle size distribution and sedimentation volume) showed that a log j *versus* log C_s' plot gave a nearly straight line with a slope of ~0.5. All the results observed for the subcutaneous absorption were similar to those for intramuscular absorption and could reasonably be explained by the kinetic model proposed for intramuscular absorption.

Keyphrases □ Absorption, subcutaneous—from aqueous suspensions of practically water-insoluble drugs, rats □ Water-insoluble drugs—subcutaneous absorption from aqueous suspensions, rats □ Aqueous suspensions—subcutaneous absorption of practically water-insoluble drugs, rats

Although subcutaneous administration of aqueous suspensions is very popular for practically water-insoluble drugs in preclinical animal experiments, little has been studied on their absorption mechanisms and kinetics except for the particle-size effect on pharmacological responses (1). Previously investigated (2, 3) were the absorption behaviors of subcutaneously implanted solid drugs (sphere, disk, and cylindrical shapes) and the absorption kinetic process was clarified. The intramuscular absorption characteristics of practically water-insoluble drugs from aqueous suspension were investigated in detail, and a kinetic equation was proposed for the drug absorption, which was obtained empirically and was very useful (4).

In the present work, similar investigations for the subcutaneous route were done with the local clearance method in intact rats. The purpose of the present study was to clarify the relationship between the absorption rate and physicochemical properties (particle size, initial drug concentration, injection volume, drug solubility, *etc.*), to express this relationship in appropriate mathematical terms, and to compare the results with those for the intramuscular route reported previously (4).

The findings obtained in this study will offer a novel and useful guide for more detailed screening and preclinical testing in laboratory animals of new drugs under development.

EXPERIMENTAL

Materials—Azo dyes (*p*-aminoazobenzene, *p*-hydroxyazobenzene, *o*-aminoazotoluene, and 1-phenylazo-2-naphthylamine), sulfa drugs (N^1-acetylsulfamethoxazole and sulfamethoxazole), and a steroid (betamethasone dipropionate[1]) were used as models for practically water-insoluble drugs. These azo dyes and sulfa drugs were the same as those used in a previous study (4). Betamethasone dipropionate was of medicinal grade and its purity was ascertained to be satisfactory through elementary analysis, melting point measurement, and TLC. Methylcellulose[2] and polysorbate 80[3], used as dispersing agents for preparations, were the same as those reported previously (4). All other chemicals were of analytical or reagent grade.

To compare the spreading area of injected particles, the following standard particles of different sizes were also used: two polystyrene latexes (0.721 and 1.305 μm in mean diameter based on number size distribution)[4], polyvinyltoluene latex (2.956 μm)[4], spores (4.94 μm)[5], di-

[1] Schering Corp., Bloomfield, N.J.
[2] Metolose SM-15, Shinetsu Kagaku Kogyo Co., Ltd., Tokyo.
[3] Kao Atlas Co., Ltd., Tokyo.
[4] The Dow Chemical Co., Indianapolis, Ind.
[5] Coulter Electronics, Ltd., Dunstable.

0022-3549/82/0500-0500$01.00/0

Table I—Particle Size (D_{ss}), Distribution Constant (n), and Sedimentation Volume (V_{sed}) of Aqueous Suspensions of Test Compounds Prepared by the Controlled Preparation Method

Compound	D_{ss}, μm[a]	n[b]	V_{sed}, cm³/g
Sulfamethoxazole	4.0	2.9	1.7
N^1-Acetylsulfamethoxazole	3.5	2.6	1.7
p-Aminoazobenzene	4.2	2.7	2.0
p-Hydroxyazobenzene	3.6–4.1	2.5–2.7	2.8–3.1
o-Aminoazotoluene	3.9	2.7	2.4
1-Phenylazo-2-naphthylamine	4.0	2.5	2.2

[a] Mean particle diameter obtained from Rosin-Rammler plot. [b] This value (obtained from Rosin-Rammler plot) shows the degree of narrowness of particle size distribution. The larger the value, the narrower the particle size distribution.

vinylbenzene latex (8.99 μm)[4], and ragweed pollen (17.95 μm)[5]. These are nearly spherical and commonly used as size calibrators for particle size measurements.

Preparation of Test Suspensions—Unless otherwise mentioned, the vehicle composed of 0.5% (w/v) of methylcellulose, 0.005% of polysorbate 80, and 0.9% NaCl was used as a dispersion medium for the same reason mentioned previously (4). This vehicle was presaturated with the drug to be dispersed and filtered through a membrane filter[6], then used for making the various preparations. To regulate particle size, all test aqueous suspensions were prepared by fractionation techniques using natural or centrifugal sedimentation. The suspensions formulated according to the controlled preparation method in which they were intended to contain particles of ~4 μm in average diameter, described in the previous report (4), were used unless otherwise mentioned. Hereafter, these suspensions are referred to as controlled suspensions. Colloidal properties such as mean particle diameters (D_{ss}), distribution constants (n), and sedimentation volumes (V_{sed}) of the test suspensions prepared by this method appear in Table I. The suspensions other than the controlled ones were prepared by similar methods with appropriate modifications. After adjustment of the drug concentration in a test suspension, it was stored at 25° until use. The syringeability for all the suspensions was good in the same needle (25G × 2.54 cm)[7] and syringe used in the absorption experiment.

Procedure of Absorption Experiment—Male Wistar albino rats (250–290 g) were used in all absorption experiments. The subcutaneous region near the center of the dorsum of intact rat was selected as a model injection site and the same local clearance method described in the previous paper (5) was employed for the present investigations. Since almost all of the drug remaining in the injection site was undissolved and unchanged, the absorption experiment adopted was considered to be appropriate for understanding the true absorption phenomena from the systems of interest.

Measurement of Physicochemical Properties of Test Compounds and Suspensions—For the solubilities of model drugs in 0.9% (w/v) NaCl (saline) or in pH 7.25 phosphate buffer (0.067 *M* Na_2HPO_4–KH_2PO_4) isotonized with NaCl, previously obtained data (4) were used. The solubilities in 2% (w/v) bovine serum albumin[8] in pH 7.25 isotonic phosphate buffer were determined according to a method similar to that described in the previous paper (4). The density (ρ) of the model compound, and the sedimentation volume (V_{sed}) and particle size distribution (D_{ss} and n) of each test suspension were also measured by the methods described in the previous report (4).

Analytical Method—*Samples from Absorption Experiments*—The amounts of test compounds other than betamethasone dipropionate remaining in the injection site were determined colorimetrically as described previously (4). Betamethasone dipropionate was analyzed by the HPLC method under the following conditions: HPLC apparatus[9]; UV detector (254 nm); column[10], 25 cm × 2.1-mm ϕ; mobile phase, *n*-hexane–isopropyl ether–ethanol–H_2O (5:20:1.5:10, v/v, upper layer); flow rate (pressure), 0.43–0.46 ml/min (84 kg/cm²).

Samples from Other Experiments—The concentrations of model compounds other than betamethasone dipropionate in test suspensions were analyzed spectrophotometrically as described in the previous paper (4). For the analysis of betamethasone dipropionate, the optical density was read at 243 nm after dilution with ethanol–H_2O (1:1, v/v). The sample solutions (filtrate or supernate) for the determination of the solubilities of azo compounds in 2% bovine serum albumin solution were assayed by a colorimetric method similar to that reported previously (4). Those of sulfa drugs were assayed as follows: One milliliter of the sample solution was thoroughly mixed with 5 ml of pH 4.7 buffer [1 *N* HCl–1 *N* CH_3COONa, 3:7 (v/v)] and from this mixture the sulfa drug was extracted with 10 ml of ethyl acetate. A portion of this extract was freed of the solvent *in vacuo* then assayed colorimetrically after diazotization according to the method described in the previous paper (4).

[6] Millipore membrane filter HA., Millipore Corp., Bedford, Mass.
[7] Terumo Co., Ltd., Tokyo.
[8] Sigma Chemical Co., St. Louis, Mo.
[9] Dupont 830 LC,
[10] Zorbax SIL,

Table II—List of Data (C_0, V_0, and j for *p*-Hydroxyazobenzene Suspension[a]) Used for Estimation of Parameters g and h, and the Values Estimated[b]

C_0, mg/ml	V_0, ml	j, hr^{-1}	Comment
0.5	0.50	0.27	V_0: constant
1.0	0.50	0.14	
20.0	0.50	0.025	
50.0	0.50	0.015	
5.0	0.05	0.12	C_0: constant
5.0	0.10	0.10	
5.0	0.50	0.046	
5.0	2.00	0.032	
50.0	0.050	0.020	W_0: constant
25.0	0.10	0.027	
2.5	1.00	0.045	
1.25	2.00	0.11	

$g = -0.656$ (0.049), $h = -0.315$ (0.057)

[a] Controlled suspension. [b] The values g and h were estimated by multiple regression analysis and are given together with the standard errors in parentheses.

RESULTS AND DISCUSSION

State of the Depot and Drug Absorption Kinetics—Although the subcutaneous region is composed of networks of loosely cross-linked fibrous tissues, injected solutions form a pool (depot) with lateral spread (6, 7). This was also observed in experiments using aqueous suspensions of some dyes and uniform latexes. In addition, the suspension particles were confined to such networks and their spreading was not so extensive as that of the aqueous dispersion medium (vehicle) after injection. For example, even in the case of a 1-ml injection of 0.5% (w/v) of uniform latex of 0.7 μm in diameter (this size seems to be the approximate lower limit for common preparations) into the dorsal subcutaneous region of rats, the resulting lateral spreading area of the particles did not exceed ~30% of that of the aqueous vehicle. This spreading area became smaller with increasing particle size. These findings clearly indicated that the subcutaneously injected particles were loosely agglomerated at the injection site.

In common cases, a drug in aqueous suspension injected subcutaneously must first become dissolved in the tissue fluids surrounding the particle agglomerate, diffuse into the intercellular space (or intracellular region) of the connective tissues, and then permeate the vascular membranes until it enters the blood or lymph stream. The participation of direct absorption of the fine particles by phagocytosis or some other mechanisms can not be completely denied (8, 9). However, their contribution to the drug absorption may be much smaller than that of the above mentioned mechanism *via* the dissolution process except for exceedingly fine particles of water-insoluble drugs (10).

It was indicated previously (11) that the connective tissue ground substance formed a diffusion barrier to the subcutaneous absorption of carbohydrates with different molecular weights in aqueous solution. The relationship between the absorption rates of a variety of compounds subcutaneously implanted in rats and their physicochemical properties

Table III—Check of Experimentally Determined g and h Values Using Betamethasone Dipropionate Aqueous Suspensions

Experiment Number	C_0, mg/ml	V_0, ml	$j(i)/j(1)$ Calculated	$j(i)/j(1)$ Experimental
1[a]	2	0.05		
	2	0.50	0.48	0.49 (0.03)
2[b]	1	0.50		
	10	0.50	0.22	0.26 (0.03)

[a] Vehicle, 0.01% (w/v) polysorbate 80 + 0.01% (w/v) benzalkonium chloride + 0.38% (w/v) $NaH_2PO_4 \cdot 2H_2O$ + 1.79% (w/v) $Na_2HPO_4 \cdot 12H_2O$; D_{ss} (n), 7.1 μm (2.5). [b] Vehicle, 0.5% (w/v) methylcellulose SM-15 + 0.01% (w/v) polysorbate 80 + 0.9% (w/v) NaCl; D_{ss} (n), 2.5 μm (2.6).

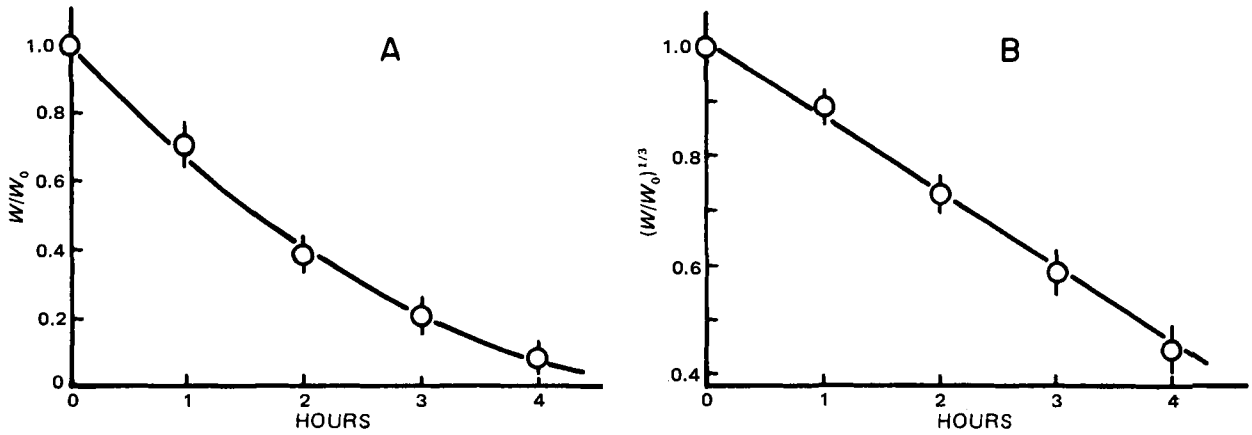

Figure 1—*Time course of* p-*hydroxyazobenzene absorption from subcutaneous injection site. Each point represents the mean of at least four experiments; vertical bar shows the standard deviation.* C_0 = *1 mg/ml;* V_0 = *0.5 ml.*

were studied (2). It was concluded that the absorption from this system was solution rate limited. Visual observations of present experimental systems supported this conclusion, since the tissue fluid colored by the dissolution of a dye was almost limited to the narrow region close to the surface of the particles or their agglomerate except for a short period immediately after injection.

On the basis of the above findings, it is assumed that the absorption is controlled by diffusion from the surface of the agglomerate. The process of this absorption seems to have a resemblance to that observed after intramuscular injection. Thus, the absorption model proposed for the intramuscular injection in a previous study (4) is expected to be applicable to the subcutaneous injection as well. From that model the following kinetic equations could be derived to describe the intramuscular absorption process (4). The fraction of the drug amount (W) remaining at the injection site to the dose (W_0) was given as a function of time (t):

$$(W/W_0)^{1/3} = 1 - jt \qquad \text{(Eq. 1)}$$

where j was defined as an absorption rate constant. This j could be related to the *in vivo* solubility (C_s), density of the drug crystal (ρ), *in vivo* dissolution rate constant (k), and the dose (W_0), using a correction parameter (ϵ) for the effective surface area of the particle agglomerate for the *in vivo* dissolution:

$$j = k\epsilon C_s \rho^{-2/3} W_0^{-1/3}/3 \qquad \text{(Eq. 2)}$$

In this equation the parameter ϵ was assumed to be an unknown function of the effective particle size (D), initial volume concentration (C_0/ρ) of the suspended drug, injection volume (V_0), and other factors (U) containing hydrodynamic factors (injection speed and pressure) and the histological and physiological factors in the injection site:

$$\epsilon = F(D, C_0/\rho, V_0, U) \qquad \text{(Eq. 3)}$$

The relationship between ϵ (or j) and C_0, V_0, or D was investigated experimentally (4).

In the present study, the above kinetic relationships proposed for the intramuscular absorption were checked to ascertain their applicability for the subcutaneous absorption and then developed to gain greater understanding of its phenomena.

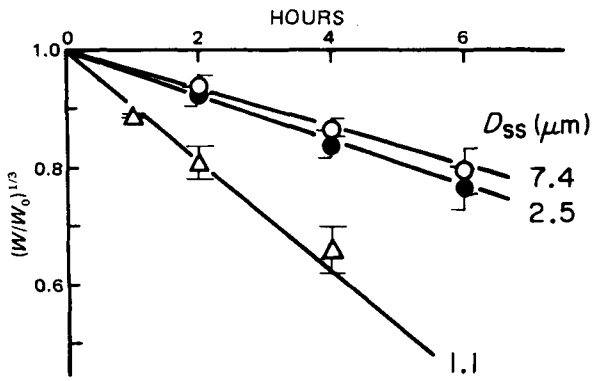

Figure 2—*Effect of particle size on subcutaneous absorption of* p-*hydroxyazobenzene. Each point represents the mean of at least three experiments; vertical bar indicates the standard deviation.* C_0 = *5 mg/ml;* V_0 = *0.5 ml.*

Time Course of Drug Absorption—First, the validity of Eq. 1 was checked experimentally. Figure 1 shows a plot of the residual fraction (W/W_0) or its cube root of the drug remaining in the injection site against time after dorsal subcutaneous administration of the controlled aqueous suspension of *p*-hydroxyazobenzene into intact rats. The initial drug concentration (C_0) and injection volume (V_0) are given in the legend. The cube root plot (B) gave a good linear relationship while the other (A) showed an upward curvature. This tendency was common throughout the following absorption experiments of different conditions, and the correlation coefficient obtained by the least-squares linear regression from the cube root plot was always larger than that from the linear plot. These results suggest that Eq. 1 is appropriate for describing the time course of the subcutaneous drug absorption from aqueous suspensions. In addition, the moderate magnitude of the standard deviations shown in Fig. 1 demonstrated that the other factors (U) in the parameter ϵ might be well-controlled under the experimental conditions in this study.

Effect of Particle Size on Absorption—The particle size of a suspension is an important factor for intramuscular (12–14) and subcutaneous absorption (1) as well as for absorptions from other routes (15). If the suspension particles are dispersed at the injection site too extensively to aggregate with each other, and, hence, the drug transport from the surface of each particle takes place independently, the particle size effect on the absorption may appear most strongly. In such a case, theoretically, $\epsilon = 6(W_0/\rho)^{1/3}/D$ for monodispersed spherical particles (diameter, D) and therefore is inversely proportional to the particle size (4). However, this is expected to be rare in practice because of the agglomerate formation in the injection site, except in an exceedingly dilute suspension with very fine particles. Thus, the relationship between the drug absorption

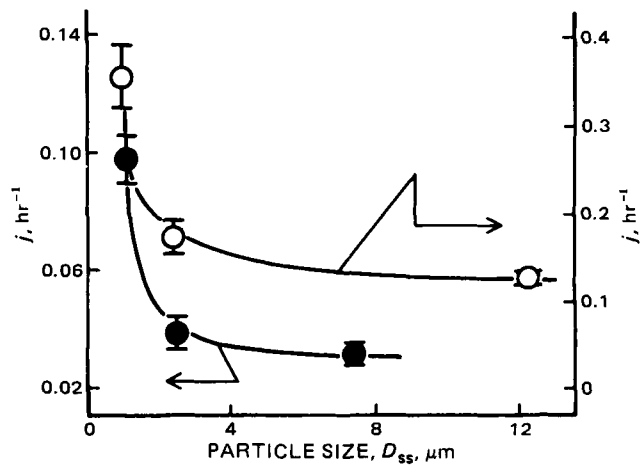

Figure 3—*Relation between absorption rate constant* (j) *and particle size* (D_{ss}). *The value of* j *was estimated by the least-squares method and is plotted with the standard error. Key:* —●—, *sc* (V_0 = *0.5 ml*); —○—, *im* (V_0 = *0.05 ml*); p-*hydroxyazobenzene concentration of both injections, 5 mg/ml.*

Table IV—Comparison of Subcutaneous Absorption Rate Constants (j) with *In Vitro* Solubilities (C_s' and C_s'') and Values of $MW^{-0.5}\rho^{-0.34}$

Compound	*In Vitro* Solubility C_s', mg/ml[a]	*In Vitro* Solubility C_s'', mg/ml[b]	$MW^{-0.5}\rho^{-0.34}$ [c]	j, hr^{-1} [d]
Sulfamethoxazole	5.7[e]	7.2	0.0549	0.374 (0.015)
N^1-Acetylsulfamethoxazole	0.076	<0.76	0.0522	0.168 (0.013)
p-Aminoazobenzene	0.049	0.41	0.0672	0.0652 (0.0037)
p-Hydroxyazobenzene	0.034	<0.69	0.0637	0.0420 (0.0035)
o-Aminoazotoluene	0.007	<0.14	0.0625	0.0193 (0.0016)
1-Phenylazo-2-naphthylamine	0.0003	0.076	0.0585	0.00241 (0.00014)

[a] Solubility in saline [0.9% (w/v) NaCl aqueous solution] at 37°. [b] Solubility in 2% (w/v) bovine serum albumin in pH 7.25 isotonic phosphate buffer at 37°. [c] MW, molecular weight; ρ, density. This term is defined in detail in the text. [d] Value estimated by the least-squares method from the data shown in Fig. 6; listed with the standard error in parentheses. [e] Solubility in pH 7.25 isotonic phosphate buffer at 37° (solubility in saline at 37°, 0.61 mg/ml). Solubilities of other test compounds in saline agreed well with those in the buffer.

rate and particle size seems to be very complicated. A previous study on the intramuscular absorption showed that the increase in the absorption rate constant (j) with decreasing mean particle diameter (D_{ss}) was remarkable in the region of D_{ss} smaller than 2–3 μm, while it was gradual or slight in the region above this (4).

Figure 2 compares subcutaneous absorption time profiles of *p*-hydroxyazobenzene from three preparations with different mean particle diameters (D_{ss}) but with similar distribution constants (n) and sedimentation volumes (V_{sed}): D_{ss} (n), 7.4 μm (2.5), 2.5 μm (2.8), and 1.1 μm (2.9); V_{sed}, 2.8–3.2 cm^3/g. The absorption rate constant (j) was obtained from the slope of each linear relationship in this figure and then plotted against D_{ss} in Fig. 3. For comparison, the results from similar experiments of the intramuscular route (m. gastrocnemius) are also shown. Figure 3 suggests that the relationship between j and D_{ss} for the subcutaneous route is qualitatively similar to that for the intramuscular route. The particles smaller than 2–3 μm in diameter seem to pass more easily through the network of the fibrous tissues accompanying the spreading of the dispersion medium during injection. This may cause a looser agglomeration of the particles and result in the abrupt change in j below this particle size.

Figure 4 shows the effect of particle size on the lateral spreading of the particle agglomerate. Here, six water-insoluble standard particles with different mean diameters ($\bar{D}$, obtained from the number size distribution curve) were used for comparison. The similarity of the form of this curve to those in Fig. 3 may support the above speculation. The participation of direct absorption mechanisms involving phagocytosis must be also considered but their contributions seem to be relatively small under the present experimental conditions. In any event, the tendency of the particle size effect appears to have a very important practical meaning.

Effect of Initial Drug Concentration and Injection Volume—If the injected particles form no agglomerate and the drug transport from each particle proceeds independently, and if this process is a rate-determining step, the absorption rate constant (j) does not depend on the dose and is inversely proportional to the particle size as mentioned previously. However, this was not the case for the subcutaneous injection of ordinary aqueous suspensions. The absorption rate constant (j), given by Eq. 2, is a function of the dose W_0 and the parameter ϵ. The term W_0 is the product of the initial drug concentration (C_0) and injection volume (V_0). The parameter ϵ is assumed to depend on C_0 and V_0, but their relationship is not known. Therefore, the quantitative relationship between j and C_0 or V_0 is also not clear.

To elucidate this relationship, the absorption time courses of the controlled suspensions of *p*-hydroxyazobenzene with different C_0 and V_0 were followed, then their absorption rate constants (j) were obtained from the same plot as Fig. 1B. In Fig. 5 j is plotted against C_0 at fixed V_0 (0.5 ml) or against V_0 at fixed C_0 (5 mg/ml) on a log–log scale. The linear relationships of both plots allow the following tentative and approximate representation:

$$j = fC_0^g V_0^h \qquad \text{(Eq. 4)}$$

where f is a constant that depends on the drug and its suspension preparation.

Thus, the experimental values of g and h were estimated by multiple regression analysis from 12 sets of data for the controlled suspensions of *p*-hydroxyazobenzene. The original data used for this estimation and resulting g and h values are summarized in Table II. Next, to ascertain the applicability of these experimental values ($g = -0.66$ and $h = -0.32$), additional examinations were done using aqueous suspensions of betamethasone dipropionate. Employing Eq. 4 and the g and h values determined above, the ratio of $j(i)$ at $C_0(i)$ and $V_0(i)$ to $j(1)$ at $C_0(1)$ and $V_0(1)$ for suspensions with the same drug and similar colloidal properties can be represented as:

$$j(i)/j(1) = [C_0(i)/C_0(1)]^{-0.66}\,[V_0(i)/V_0(1)]^{-0.32} \qquad \text{(Eq. 5)}$$

Table III compares the calculated and experimental ratios $j(i)/j(1)$ for the case where $C_0(i)/C_0(1) = 10$ or $V_0(i)/V_0(1) = 10$. These comparisons showed good mutual agreements, despite the fact that the vehicle and the colloidal properties of the suspensions tested here differed considerably from those of the controlled suspension of *p*-hydroxyazobenzene used for the estimation of g and h values. Therefore, Eq. 5, obtained ex-

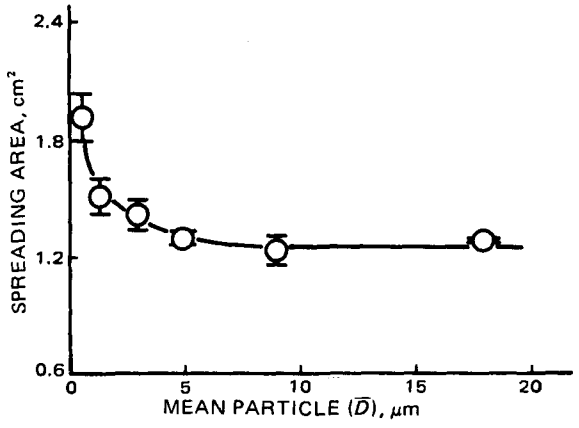

Figure 4—*Effect of particle size on the lateral spreading area of the particle agglomerate formed by subcutaneous injection of aqueous suspension. Each point represents the mean of three experiments; vertical bar indicates the standard deviation. These data were obtained using water-insoluble standard particles of various sizes under the following conditions:* C_0 *= 5 mg/ml;* V_0 *= 1.0 ml; measurement, 5 min after injection.*

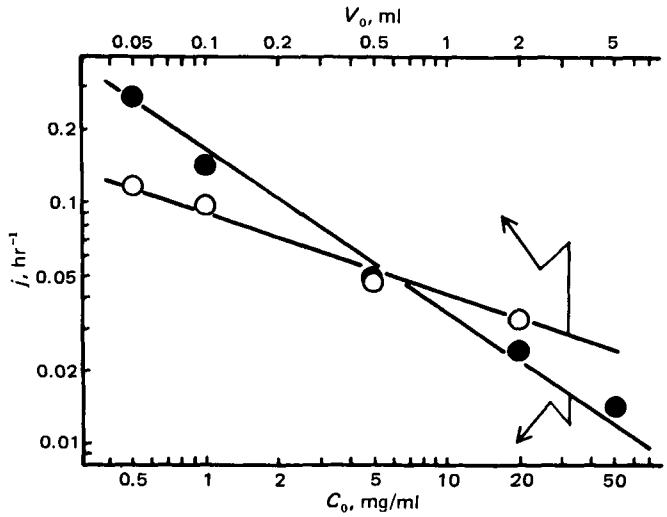

Figure 5—*Relation between absorption rate constant* (j) *and injection volume* (V_0) *or initial drug concentration* (C_0) *for the controlled suspension of* p*-hydroxyazobenzene. The value of* j *was estimated by the least-squares method. Key: —●—, constant* V_0 *(0.5 ml); —○—, constant* C_0 *(5 mg/ml).*

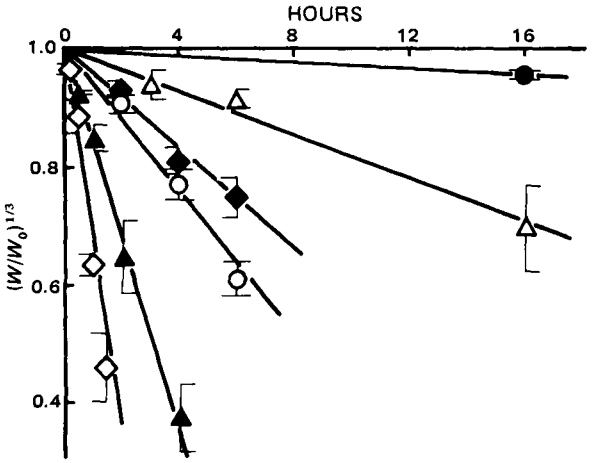

Figure 6—*Comparison of absorption rate among various compounds (controlled suspension). Each point represents the mean of three or four experiments; vertical bar indicates the standard deviation.* C_0 *= 5 mg/ml;* V_0 *= 0.5 ml. Key: —●—, 1-phenylazo-2-naphthylamine; —△—, o-aminoazotoluene; —◆—, p-hydroxyazobenzene; —○—, p-aminoazobenzene; —▲—,* N^1*-acetylsulfamethoxazole; —◇—, sulfamethoxazole.*

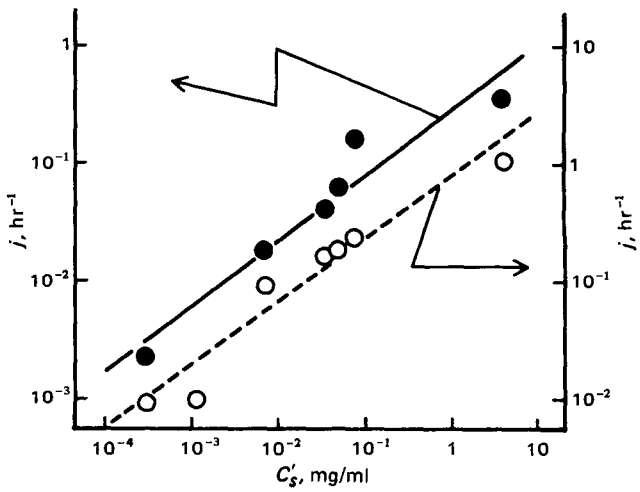

Figure 7—*Relationship between absorption rate constant* (j) *and in vitro solubility* (C_s'). *The value of* j *was estimated by the least-squares method from the data shown in Fig. 6. Key: —●—, sc* (C_0 *= 5 mg/ml;* V_0 *= 0.5 ml); —○—, im* (C_0 *= 5 mg/ml;* V_0 *= 0.05 ml), cited from a previous study (4).*

perimentally, is expected to be generally applicable for aqueous suspensions other than the model ones tested here.

Using the above results, the relationship between the parameter ϵ and C_0 or V_0 can be clarified empirically in the following manner:

$$j = fC_0^{-0.66}V_0^{-0.32} \quad \text{(Eq. 6)}$$

Employing the relationship $W_0 = C_0V_0$, Eq. 2 can be rewritten as:

$$j = kC_s\rho^{-2/3}\epsilon C_0^{-1/3}V_0^{-1/3}/3 \quad \text{(Eq. 7)}$$

From the equivalency of Eqs. 6 and 7, the parameter ϵ must satisfy the following relationship:

$$\epsilon = F(D, C_0/\rho, V_0, U) = \delta(C_0/\rho)^{-0.33}V_0^{0.01} \quad \text{(Eq. 8)}$$

where δ is a term that depends on the remaining factors D and U. Equation 8 means that the parameter ϵ depends little on the injection volume (V_0) but decreases by increasing initial drug concentration (C_0). This also implies that the degree of agglomeration may tend to increase with an increase in C_0. Substitution of Eq. 8 for ϵ in Eq. 7 yields:

$$j = (kC_s\delta/3)\rho^{-0.34}C_0^{-0.66}V_0^{-0.32} \quad \text{(Eq. 9)}$$

The above empirical equation obtained for the subcutaneous route demonstrates a great similarity to that for the intramuscular route, which was given by the following equation (4):

$$j_m = (k_mC_s\delta_m/3)\rho^{-0.45}C_0^{-0.55}V_0^{-0.32} \quad \text{(Eq. 10)}$$

It should be noted that the correlation between the absorption rate constant and injection volume is identical for the two routes.

Although Eqs. 9 and 10 are derived empirically, they should be very important and useful since they give relationships between the dose and absorption rate constant which have been unknown until now.

Comparison of Absorption Rate among Various Compounds—Equation 9 shows that the absorption rate constants (j) of different compounds depend upon the values of k, C_s, and ρ when the preparation-dependent parameters (δ) are the same. As defined previously, ρ, k, and C_s represent the density of the drug, the *in vivo* dissolution rate constant, and *in vivo* solubility in the injection site, respectively. Of these factors, only the value of ρ can be determined by an *in vitro* experiment; the other two (k and C_s) cannot be completely estimated from such an experiment. From a practical point of view, an attempt was made to clarify the quantitative relationship between j and the above three factors (or their first approximations).

Figure 6 compares the subcutaneous absorption time profiles of six test compounds. In this comparison, the controlled suspensions with similar colloidal properties (Table I) were used to minimize the variation in δ in Eq. 9. All the compounds gave good linear relationships with different slopes. Their observed absorption rate constants (j) are summarized in Table IV with their physicochemical factors such as *in vitro* solubilities in saline and 2% (w/v) bovine serum albumin (C_s' and C_s'', respectively).

As discussed previously, the absorption is inferred to be a diffusion-controlled process. Diffusion coefficients of compounds having low molecular weight (MW) are known to be inversely proportional to the square root of MW (16). The *in vivo* dissolution rate constant (k) in Eq. 9 is considered to be proportional to the diffusion coefficient, like that *in vitro* (2, 17). Therefore, Eq. 9 can be converted to

$$j = (\theta\delta/3)\mathrm{MW}^{-0.5}\rho^{-0.34}C_sC_0^{-0.66}V_0^{-0.32} \quad \text{(Eq. 11)}$$

where θ is a constant. Thus, the values of $\mathrm{MW}^{-0.5}\rho^{-0.34}$ for model drugs were calculated and are in Table IV as the correction term. However, these values were similar to each other for the compounds tested here. In contrast, the *in vitro* solubility was a more dominant factor and had a positive relation with the absorption rate constant.

Equation 11 means that the plot of j (or $j_{corr} = j\mathrm{MW}^{0.5}\rho^{0.34}$, if the correction for MW and ρ is necessary) against *in vivo* solubility (C_s) on a log–log scale gives a straight line with a slope of unity at the constant initial drug concentration (C_0) and injection volume (V_0). The closed circles in Fig. 7 show this plot using *in vitro* solubility (C_s') in Table IV instead of *in vivo* solubility (C_s). This gave a nearly straight line with a slope of 0.53 (regression equation, $\log j = 0.525 \log C_s' - 0.578$; correlation coefficient, $r = 0.956$). Using j_{corr} in place of j, a similar relationship was also obtained ($\log j_{corr} = 0.534 \log C_s' + 0.660$, $r = 0.953$).

In Fig. 7, similar data for the intramuscular administration (m. gastrocnemius), cited from a previous study (4), are also plotted with open circles. Remarkably, the slopes of these plots for the two routes were almost identical. This shows a strong similarity in the absorption mechanism between the two routes. The deviation of the slope from unity observed in Fig. 7 may be attributed mainly to a gradual increase in the ratio C_s/C_s' with decreasing C_s' caused by the relatively larger solubilization effect of the protein components in the body fluid for the drug having a smaller solubility. The comparison of C_s' and C_s'' in Table IV supports this explanation.

The good linear relationship between $\log j$ (or $\log j_{corr}$) and $\log C_s'$ mentioned previously is expected to be applicable for predicting the subcutaneous absorption rates of other compounds in the controlled suspensions from C_s'. For instance, the prediction (from the regression equation, $\log j_{corr} = 0.534 \log C_s' + 0.660$) for the test material, betamethasone dipropionate (MW = 504; $\rho = 1.23$ g/cm^3; $C_s' = 0.002$ mg/ml) gave a value of 0.007 hr^{-1} for j (at $C_0 = 5$ mg/ml and $V_0 = 0.5$ ml), which almost agreed with the experimental value of 0.0096 ($\pm$0.0011) hr^{-1} observed using the following controlled suspension: $D_{ss} = 4.3$ μm; $n = 2.6$. This satisfactory result suggests that similar prediction will be possible for other drugs.

Comparison of Absorption Rates between Subcutaneous and Intramuscular Routes—Hitherto, drug absorption kinetics and mechanisms from aqueous suspensions in the subcutaneous route have been clarified, and their strong similarity to those by the intramuscular route, discussed previously (4), have been pointed out. A direct comparison of absorption rates between the two routes seems to be usable but there has been little available data (18). Table V shows this com-

Table V—Comparison of Absorption Rate Constants (j) between Subcutaneous (sc) and Intramuscular (im) Routes [a]

Compound	j, hr^{-1}	
	sc[b]	im[c]
Sulfamethoxazole	0.78	1.10 ± 0.07
p-Aminoazobenzene	0.14	0.18 ± 0.01
p-Hydroxyazobenzene	0.090 (0.12 ± 0.02)[d]	0.17 ± 0.01
o-Aminoazotoluene	0.040	0.093 ± 0.005
1-Phenylazo-2-naphthylamine	0.0050	0.0093 ± 0.0006

[a] Controlled suspension. C_0, 5 mg/ml; V_0, 0.05 ml. [b] Estimated by extrapolation of data shown in Table IV using Eq. 5. [c] Experimental data (with standard error) cited from the previous report (4). [d] Experimental value (with standard error).

parison using five controlled suspensions. To compare at the same drug concentration (C_0) and injection volume (V_0), the values estimated by extrapolation of the data shown in Table IV using Eq. 5 were used for the absorption rate constants (j) in the subcutaneous route. This comparison shows that the absorption rate from the subcutaneous route is slower than that from the intramuscular route for all the test suspensions. A similar tendency was previously observed for injections of drug-oil solutions (5). The relationship between j and C_0 in the subcutaneous route differed slightly from that in the intramuscular route (Eqs. 9 and 10). Therefore, it should be noted that the difference in j shown in Table V may increase with increasing C_0.

REFERENCES

(1) V. G. Foglia, J. C. Penhos, and E. Montuori, *Endocrinology*, **57**, 559 (1955).

(2) B. E. Ballard and E. Nelson, *J. Pharmacol. Exp. Ther.*, **135**, 120 (1962).

(3) B. E. Ballard and E. Nelson, *J. Pharm. Sci.*, **51**, 915 (1962).

(4) K. Hirano, T. Ichihashi, and H. Yamada, *Chem. Pharm. Bull.*, **29**, 817 (1981).

(5) K. Hirano, T. Ichihashi, and H. Yamada, *J. Pharm. Sci.*, **71**, 495 (1982).

(6) E. A. Brown, T. G. Metcalf, and L. W. Slanetz, *Ann. Allergy*, **19**, 1016 (1961).

(7) F. L. Ashley, S. Braley, T. D. Rees, D. Goulian, and D. L. Ballantyne, Jr., *Plastic Reconstruc. Surg.*, **39**, 411 (1967).

(8) C. R. Beresford, L. Golberg, and J. P. Smith, *Br. J. Pharmacol.*, **12**, 107 (1957).

(9) T. D. Rees, D. L. Ballantyne, Jr., I. Seidman, and G. A. Hawthorne, *Plastic Reconstruc. Surg.*, **39**, 402 (1967).

(10) J. Lewin and F. Huidobro, *Acta Physiol. Lat. Am.*, **3**, 17 (1953).

(11) E. Secher-Hansen, H. L. Langgard, and J. Schou, *Acta Pharmacol. Toxicol.*, **26**, 9 (1968).

(12) F. H. Buckwalter and H. L. Dickison, *J. Am. Pharm. Assoc. Sci. Ed.*, **47**, 661 (1958).

(13) L. G. Miller and J. H. Fincher, *J. Pharm. Sci.*, **60**, 1733 (1971).

(14) N. Kitamori, S. Kawaziri, and T. Matsuzawa, "Abstracts of Papers," 93th Annual Meeting of Japan Pharmaceutical Society, Tokyo, April 1973, p. 266.

(15) J. H. Fincher, *J. Pharm. Sci.*, **57**, 1825 (1968).

(16) W. D. Stein, "The Movement of Molecules across Cell Membranes," Academic, New York, N.Y. 1967, p. 67.

(17) W. Nernst, *Z. Phys. Chem.*, **47**, 52 (1904).

(18) J. J. Nora, W. D. Smith, and J. R. Cameron, *J. Pediatr.*, **64**, 547 (1964).

ACKNOWLEDGMENTS

The authors thank Mrs. J. Kagawa for her technical assistance and Prof. M. Nakagaki, Kyoto University, for his valuable comments on the manuscript.

Dissolution and Bioavailability Studies of Whole and Halved Sustained-Release Theophylline Tablets

KEITH J. SIMONS **, EVELYN M. FRITH ‡, and F. ESTELLE R. SIMONS ‡

Received July 24, 1980, from the **Faculty of Pharmacy, and* ‡ *Section of Allergy and Clinical Immunology, Department of Pediatrics, Faculty of Medicine, University of Manitoba, Winnipeg, Manitoba, Canada, R3T 2N2.* Accepted for publication August 5, 1981.

Abstract □ In dissolution studies of whole and halved 100-mg sustained-release theophylline tablets, drug release from halved tablets was significantly higher. These differences were not reflected in the bioavailability studies. The area under the curve (AUC) mean absorption time and fraction-of-dose recovered in urine at 24 hr were not significantly different following the ingestion of whole or halved 100-mg tablets. The elimination rate constant, half-life, volume of distribution, plasma, and renal clearance values were consistent with values reported previously. Discrepancies were found in the 24-hr metabolite distribution as compared to literature values and may be accounted for by the age and health of the subjects and the frequency of dosing.

Keyphrases □ Dissolution—whole and halved sustained-release theophylline tablets □ Sustained-release system—dissolution of whole and halved theophylline tablets □ Bioavailability—whole and halved sustained-release theophylline tablets □ Theophylline—bioavailability and dissolution study of whole and halved sustained-release tablets

Breaking sustained-release theophylline tablets in half is commonly practiced to achieve more accurate milligrams per kilogram dosing in children. The extent to which this affects dissolution and bioavailability is unknown.

In this investigation, 100-mg sustained-release theophylline tablets[1] were used to study the effect of halving tablets on dissolution and bioavailability. No published information about the dissolution of these tablets was available. After oral administration of the 100-mg tablet, however, 90% of the dose was absorbed within 14 hr and almost 100% was absorbed by 28 hr (1). When 300-mg tablets were dissolved, 50% of the dose entered solution by 2 hr and > 90% of the dose entered solution by 6 hr (1).

EXPERIMENTAL

Dissolution—The official USP dissolution apparatus was used (2). Simulated gastric and intestinal fluids were used as dissolution media (2).

Simulated gastric fluid, USP (2), was prepared by dissolving 2 g of sodium chloride and 3.2 g of pepsin in 7 ml of HCl and diluting the solution to 1000 ml with distilled water. This test solution had a pH of 1.2.

Simulated intestinal fluid, USP (2), was prepared by dissolving 6.8 g

[1] Theo-Dur, Astra Pharmaceuticals Canada Ltd., Mississauga, Canada L4X 1M4.

0022-3549/82/0500-0505$01.00/0

Table V—Comparison of Absorption Rate Constants (j) between Subcutaneous (sc) and Intramuscular (im) Routes [a]

Compound	j, hr^{-1}	
	sc[b]	im[c]
Sulfamethoxazole	0.78	1.10 ± 0.07
p-Aminoazobenzene	0.14	0.18 ± 0.01
p-Hydroxyazobenzene	0.090 (0.12 ± 0.02)[d]	0.17 ± 0.01
o-Aminoazotoluene	0.040	0.093 ± 0.005
1-Phenylazo-2-naphthylamine	0.0050	0.0093 ± 0.0006

[a] Controlled suspension. C_0, 5 mg/ml; V_0, 0.05 ml. [b] Estimated by extrapolation of data shown in Table IV using Eq. 5. [c] Experimental data (with standard error) cited from the previous report (4). [d] Experimental value (with standard error).

parison using five controlled suspensions. To compare at the same drug concentration (C_0) and injection volume (V_0), the values estimated by extrapolation of the data shown in Table IV using Eq. 5 were used for the absorption rate constants (j) in the subcutaneous route. This comparison shows that the absorption rate from the subcutaneous route is slower than that from the intramuscular route for all the test suspensions. A similar tendency was previously observed for injections of drug-oil solutions (5). The relationship between j and C_0 in the subcutaneous route differed slightly from that in the intramuscular route (Eqs. 9 and 10). Therefore, it should be noted that the difference in j shown in Table V may increase with increasing C_0.

REFERENCES

(1) V. G. Foglia, J. C. Penhos, and E. Montuori, *Endocrinology*, **57**, 559 (1955).

(2) B. E. Ballard and E. Nelson, *J. Pharmacol. Exp. Ther.*, **135**, 120 (1962).

(3) B. E. Ballard and E. Nelson, *J. Pharm. Sci.*, **51**, 915 (1962).

(4) K. Hirano, T. Ichihashi, and H. Yamada, *Chem. Pharm. Bull.*, **29**, 817 (1981).

(5) K. Hirano, T. Ichihashi, and H. Yamada, *J. Pharm. Sci.*, **71**, 495 (1982).

(6) E. A. Brown, T. G. Metcalf, and L. W. Slanetz, *Ann. Allergy*, **19**, 1016 (1961).

(7) F. L. Ashley, S. Braley, T. D. Rees, D. Goulian, and D. L. Ballantyne, Jr., *Plastic Reconstruc. Surg.*, **39**, 411 (1967).

(8) C. R. Beresford, L. Golberg, and J. P. Smith, *Br. J. Pharmacol.*, **12**, 107 (1957).

(9) T. D. Rees, D. L. Ballantyne, Jr., I. Seidman, and G. A. Hawthorne, *Plastic Reconstruc. Surg.*, **39**, 402 (1967).

(10) J. Lewin and F. Huidobro, *Acta Physiol. Lat. Am.*, **3**, 17 (1953).

(11) E. Secher-Hansen, H. L. Langgard, and J. Schou, *Acta Pharmacol. Toxicol.*, **26**, 9 (1968).

(12) F. H. Buckwalter and H. L. Dickison, *J. Am. Pharm. Assoc. Sci. Ed.*, **47**, 661 (1958).

(13) L. G. Miller and J. H. Fincher, *J. Pharm. Sci.*, **60**, 1733 (1971).

(14) N. Kitamori, S. Kawaziri, and T. Matsuzawa, "Abstracts of Papers," 93th Annual Meeting of Japan Pharmaceutical Society, Tokyo, April 1973, p. 266.

(15) J. H. Fincher, *J. Pharm. Sci.*, **57**, 1825 (1968).

(16) W. D. Stein, "The Movement of Molecules across Cell Membranes," Academic, New York, N.Y. 1967, p. 67.

(17) W. Nernst, *Z. Phys. Chem.*, **47**, 52 (1904).

(18) J. J. Nora, W. D. Smith, and J. R. Cameron, *J. Pediatr.*, **64**, 547 (1964).

ACKNOWLEDGMENTS

The authors thank Mrs. J. Kagawa for her technical assistance and Prof. M. Nakagaki, Kyoto University, for his valuable comments on the manuscript.

Dissolution and Bioavailability Studies of Whole and Halved Sustained-Release Theophylline Tablets

KEITH J. SIMONS **, EVELYN M. FRITH ‡, and F. ESTELLE R. SIMONS ‡

Received July 24, 1980, from the **Faculty of Pharmacy, and* ‡ *Section of Allergy and Clinical Immunology, Department of Pediatrics, Faculty of Medicine, University of Manitoba, Winnipeg, Manitoba, Canada, R3T 2N2.* Accepted for publication August 5, 1981.

Abstract □ In dissolution studies of whole and halved 100-mg sustained-release theophylline tablets, drug release from halved tablets was significantly higher. These differences were not reflected in the bioavailability studies. The area under the curve (AUC) mean absorption time and fraction-of-dose recovered in urine at 24 hr were not significantly different following the ingestion of whole or halved 100-mg tablets. The elimination rate constant, half-life, volume of distribution, plasma, and renal clearance values were consistent with values reported previously. Discrepancies were found in the 24-hr metabolite distribution as compared to literature values and may be accounted for by the age and health of the subjects and the frequency of dosing.

Keyphrases □ Dissolution—whole and halved sustained-release theophylline tablets □ Sustained-release system—dissolution of whole and halved theophylline tablets □ Bioavailability—whole and halved sustained-release theophylline tablets □ Theophylline—bioavailability and dissolution study of whole and halved sustained-release tablets

Breaking sustained-release theophylline tablets in half is commonly practiced to achieve more accurate milligrams per kilogram dosing in children. The extent to which this affects dissolution and bioavailability is unknown.

In this investigation, 100-mg sustained-release theophylline tablets[1] were used to study the effect of halving tablets on dissolution and bioavailability. No published information about the dissolution of these tablets was available. After oral administration of the 100-mg tablet, however, 90% of the dose was absorbed within 14 hr and almost 100% was absorbed by 28 hr (1). When 300-mg tablets were dissolved, 50% of the dose entered solution by 2 hr and > 90% of the dose entered solution by 6 hr (1).

EXPERIMENTAL

Dissolution—The official USP dissolution apparatus was used (2). Simulated gastric and intestinal fluids were used as dissolution media (2).

Simulated gastric fluid, USP (2), was prepared by dissolving 2 g of sodium chloride and 3.2 g of pepsin in 7 ml of HCl and diluting the solution to 1000 ml with distilled water. This test solution had a pH of 1.2.

Simulated intestinal fluid, USP (2), was prepared by dissolving 6.8 g

[1] Theo-Dur, Astra Pharmaceuticals Canada Ltd., Mississauga, Canada L4X 1M4.

0022-3549/82/0500-0505$01.00/0

Table I—Percentage of Theophylline Dissolved of Total from 100-mg Sustained-Release Tablets

Time, hr	Gastric, 100 mg (0.5 tablet)	Gastric, 100 mg	Intestinal, 100 mg (0.5 tablet)	Intestinal, 100 mg
1	33.0 ± 3.2	21.2 ± 3.2	36.3 ± 4.5	29.1 ± 2.3
2	42.1 ± 3.7	29.6 ± 0.9	45.8 ± 7.2	37.2 ± 3.8
3	49.5 ± 4.2	34.0 ± 1.2	52.7 ± 7.4	43.1 ± 4.7
4	54.9 ± 4.3	39.4 ± 1.7	58.5 ± 7.8	47.2 ± 4.9
5	60.4 ± 4.5	43.5 ± 1.5	63.3 ± 8.2	52.3 ± 5.5
6	65.8 ± 4.7	46.1 ± 2.5	66.7 ± 8.6	56.0 ± 6.4
7			70.1 ± 7.2	61.0 ± 6.6
8			73.8 ± 8.5	64.5 ± 6.9
9			76.8 ± 7.6	67.7 ± 7.5
10			78.6 ± 6.5	72.0 ± 7.2
11			82.3 ± 8.4	75.2 ± 8.6
12			84.4 ± 6.7	78.4 ± 7.9
25			91.2 ± 3.5	95.1 ± 7.6

of potassium phosphate (KH_2PO_4) in 250 ml of distilled water. To this solution was added 190 ml of 0.2 *N* sodium hydroxide and 400 ml of distilled water. Ten grams of pancreatin were then added and the resulting solution adjusted to pH 7.5 ± 0.1 with 0.2 *N* sodium hydroxide. This solution was diluted to 1000 ml with distilled water.

The 100-mg sustained-release theophylline tablets, as whole or halved tablets, were tested up to six times in each dissolution medium. The tablet, or tablet halves, were placed in the gold-plated basket and immersed in 900 ml of dissolution medium at 37° in the dissolution apparatus. The basket was rotated at 100 ± 5 rpm. Samples were withdrawn at 1, 2, 3, 4, 5, and 6 hr in gastric fluid and at 1, 2, 3, 4, 5, 6, 7, 8, 9, 10, 11, 12, and 25 hr in intestinal fluid under sink conditions.

Bioavailability—Relative bioavailability studies were carried out in seven normal adult volunteers, four female and three male, on 2 study days, 1 week apart, after informed consent was obtained. Their mean age was 30 ± 7 yr (range: 21–39 yr) and their mean weight was 72 ± 21 kg (range: 54–100 kg). As determined by a comprehensive medical history they were in excellent health, were nonsmokers, and were not taking any medication at the time of the study. All volunteers had normal complete blood counts and normal screening tests for renal and hepatic function.

All subjects refrained from the ingestion of tea, coffee, chocolate, and cola for 48 hr before and during the 2 separate study days. On each study day, after an overnight fast with ingestion of no more than 480 ml of water, a heparin lock was inserted, a control blood sample was withdrawn, and a control urine specimen collected. Each subject received a mean 5.20 ± 0.24 mg/kg (range: 4.9–4.6 mg/kg) dose of theophylline to the nearest whole 100-mg sustained-release tablet. Tablets were administered whole or halved along with 120 ml of water. Subjects were assigned by random choice into Study Group 1 or Study Group 2. Study Group 1 received whole tablets the first week and halved tablets the second week. Study Group 2 received the halved tablets the first week and whole tablets the second week.

Blood samples were withdrawn at 0.25, 0.5, 0.75, 1.0, 1.25, 1.5, 2, 3, 4, 6, 8, 10, 12, 14, 18, and 24 hr. Serum was separated and frozen along with an aliquot of accurately measured pooled 24-hr urine until analysis for theophylline content could be performed. Subjects ate meals of uniform composition 4 and 8 hr after ingestion of the dose.

Assay Procedure—There are many methods for measuring theophylline concentrations and these have been adequately reviewed (3). Reversed-phase high-pressure liquid chromatography (HPLC) appears to be the method of choice and was used in this study[2]. Although direct injection methods are available for both theophylline (4–7) and its metabolites (8), the chromatograms obtained using these methods were not satisfactory. Since theophylline is bound to plasma proteins (9) some of these methods only measured unbound drug. The procedures developed and used were based on older methods (10) involving extraction.

Theophylline Extraction Procedure—To 50 μl of dissolution medium, urine, or serum in a 10 × 75-mm test tube was added 50 μl of aqueous solution of β-hydroxyethyltheophylline (15 μg/ml) as internal standard. A 25-μl aliquot of 20% trichloroacetic acid was added and the solution was vortexed and centrifuged. The supernate was transferred into a clean 13 × 100-mm test tube. After buffering with 300 μl of 2.5 *M* acetate buffer (pH 6.4) the solution was extracted with 2 ml of chloroform–isopropanol (20:1) by vortexing and centrifugation. The aqueous supernate was aspirated and the organic layer evaporated to dryness using low heat and a stream of dry nitrogen. The sample was redissolved in 50–100 μl of mobile phase and a 25 μl aliquot was injected directly onto the column. Theophylline concentration was calculated from a calibration curve of the peak height ratio of theophylline to the internal standard *versus* concentration.

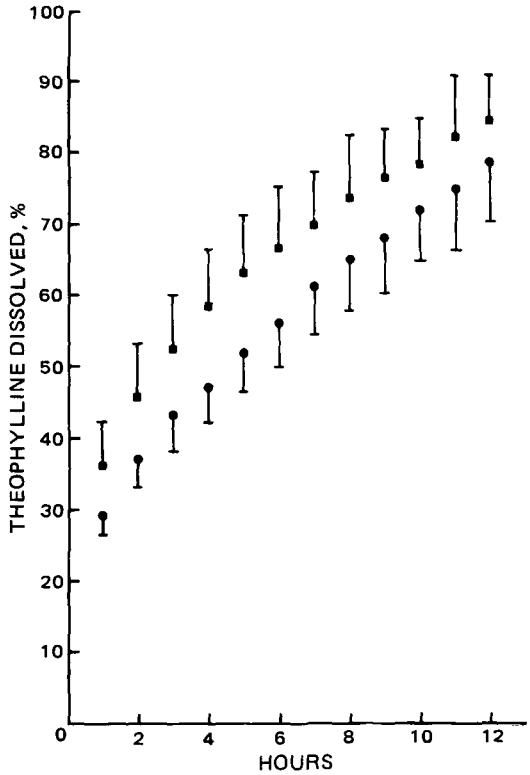

Figure 1—*Percent theophylline dissolved in simulated intestinal fluid* versus *time, from whole, (●) or halved (■) 100-mg sustained-release tablets.*

Theophylline Metabolite Extraction Procedure—To 200 μl of urine, test sample, or standards in solution in urine was added 50 μl of aqueous solution of theobromine (150 μg/ml). After buffering with 150 μl of 2.5 *M* acetate buffer (pH 6.4), the solution was extracted with 4 ml of chloroform–isopropanol (20:1) by vortexing and centrifugation.

The supernate was transferred to a clean test tube with a Pasteur pipet, and 50 μl was diluted with 200 μl filtered, distilled water to yield a final dilution of 1:10 of the urine sample. Exactly 25 μl of the diluted supernate was injected into the HPLC. The concentration of 1-methyluric acid was calculated from a calibration curve in which absolute peak heights *versus* concentration were plotted.

The organic layer from the sample was transferred to a clean, dry test tube and evaporated to dryness in a water bath at 60° with dry nitrogen. The sample was redissolved in 500 μl of mobile phase, and 25 μl was injected onto the chromatograph. The concentrations of 3-methylxanthine and 1,3-dimethyluric acid were calculated from calibration curves constructed by plotting the peak height ratios of the two metabolites to theobromine *versus* concentration of the metabolites.

HPLC Conditions—A 30-cm × 3.9-mm i.d. stainless steel column[3] was used in all assay procedures.

The mobile phase for theophylline was 9% acetonitrile in 0.01 *M* acetate buffer (pH 4.0). At a flow rate of 2 ml/min and an operating pressure of 1500–2000 psi, theophylline and β-hydroxyethyltheophylline had retention times of 4.9 and 6.2 min, respectively.

The mobile phase for 1-methyluric acid was 5% methanol in 0.05 *M* phosphate buffer (pH 4.75). At a flow rate of 2.0 ml/min the 1-methyluric acid had a retention time of 4.0 min.

The mobile phase for the other two theophylline metabolites was 11% methanol in 0.05 *M* phosphate buffer (pH 4.75). At a flow rate of 2 ml/min, 3-methylxanthine, 1,3-dimethyluric acid, and theobromine had retention times of 2.9, 4.2, and 5.1 min, respectively.

[2] The HPLC system consisted of a Model U6K injector, a Model 6000A high-pressure pump, and a Model 440 absorbance detector, all from Waters Associates, Milford, Mass. A 10 mv Omniscribe recorder from Houston Instrument, Austin, Tex. completed the system.

[3] μ Bondapak C_{18}, Waters Associates, Milford, MA 01757

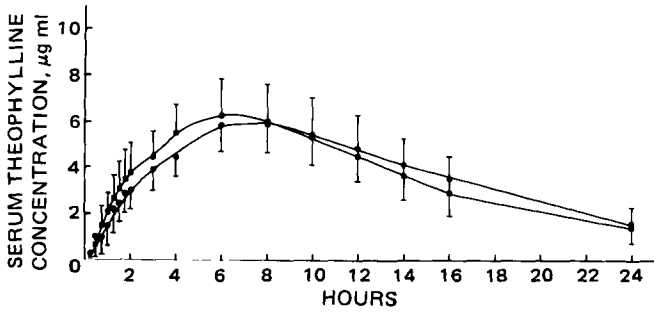

Figure 2—*Mean serum theophylline concentration* versus *time curves from seven normal volunteers who ingested a 5-mg/kg dose as whole (●) or halved (■) 100-mg sustained-release tablets.*

Data Analysis—The theophylline concentration *versus* time curve data from halved and whole 100-mg sustained-release tablets in simulated gastric and intestinal fluid were analyzed by plotting the cumulative percent dissolved *versus* time.

From each of the seven subjects who ingested a mean 5.2 mg/kg dose of theophylline as whole or halved 100-mg tablets, the log serum theophylline concentrations *versus* time curve was plotted. From the terminal linear portion of the curve, the first-order elimination rate constant (K_e) was calculated by:

$$\log Cp = \log Cp_0 - \frac{K_e}{2.303} t \qquad \text{(Eq. 1)}$$

where Cp is the serum theophylline concentration at any time t, and Cp_0 is the extrapolated serum theophylline concentration at zero time, *i.e.*, the y intercept. Elimination half-life values ($t_{1/2}$) were calculated by:

$$t_{1/2} = \frac{0.693}{K_e} \qquad \text{(Eq. 2)}$$

The fraction of the dose absorbed (f) at any time t was calculated by the formula:

$$f = \frac{(Xa)^t}{(Xa)^\infty} = \frac{Cp + K_e \int_0^t Cp\, dt}{K_e \int_0^\infty Cp\, dt} \qquad \text{(Eq. 3)}$$

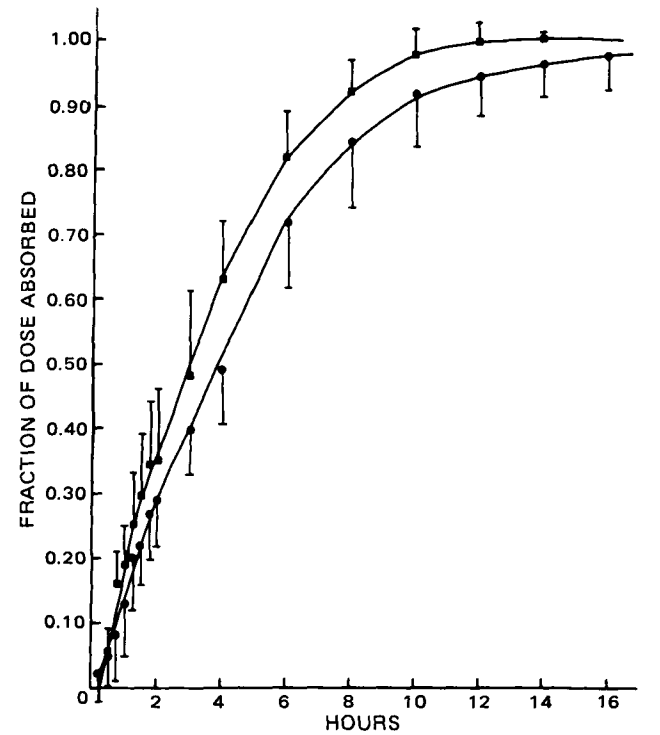

Figure 3—*Mean fractions of a 5-mg/kg dose of theophylline absorbed* versus *time in seven normal volunteers who ingested whole (●) or halved (■) 100-mg sustained-release tablets.*

Table II—Serum Theophylline Concentrations (μg/ml) at Each Sampling Time following the Ingestion of a 5-mg/kg Dose as Whole or Halved 100-mg Sustained-Release Tablets

Subjects	Time, hr 0	0.25	0.5	0.75	1.0	1.25	1.5	1.75	2	3	4	6	8	10	12	14	16	24
Whole Tablets																		
A	—	1.20	1.82	2.21	2.90	3.76	3.66	4.07	4.11	5.26	5.35	7.28	7.17	5.88	5.04	4.09	3.45	1.22
B	—	*tr*[a]	0.42	0.84	1.22	1.85	2.46	3.48	3.72	4.34	5.31	5.21	4.62	3.95	3.27	2.43	1.41	0.36
C	—	—	*tr*	0.90	1.21	1.73	1.87	2.33	2.39	2.81	3.25	4.61	4.03	3.40	2.49	1.76	1.16	*tr*
D	—	0.32	1.34	0.54	0.93	1.61	2.01	2.24	2.53	3.89	4.92	7.48	7.83	7.37	6.34	5.35	4.81	2.37
E	—	*tr*	*tr*	0.04	0.69	1.30	1.76	1.82	1.96	3.13	3.60	5.42	6.59	6.39	5.49	4.61	3.96	1.57
F	—	0.15	1.22	1.77	2.61	3.16	3.19	3.33	3.41	4.35	4.52	5.62	5.79	5.57	5.36	5.00	4.75	3.31
G	—	—	0.02	0.39	0.86	1.57	1.82	2.69	2.88	3.39	4.12	5.14	5.66	6.16	5.94	5.09	4.72	1.71
Mean ± *SD*		0.24 ± 0.12	0.86 ± 0.73	0.96 ± 0.77	1.49 ± 0.89	2.14 ± 0.93	2.40 ± 0.75	2.85 ± 0.80	3.00 ± 0.78	3.88 ± 0.85	4.44 ± 0.82	5.82 ± 1.11	5.96 ± 1.35	5.53 ± 1.40	4.85 ± 1.42	4.05 ± 1.41	3.47 ± 1.57	1.76 ± 1.01
Halved Tablets																		
A	—	*tr*	0.79	2.39	3.06	3.49	4.18	4.86	5.12	6.26	6.88	7.76	7.10	6.13	4.69	3.87	2.94	0.94
B	—	*tr*	0.67	2.02	2.25	2.53	2.91	3.78	3.46	4.49	4.90	5.43	4.52	3.54	2.73	1.70	1.08	0.05
C	—	*tr*	0.92	1.33	1.89	1.80	2.19	2.41	2.54	3.20	3.66	3.74	3.23	2.51	1.32	0.88	0.36	*tr*
D	*tr*	*tr*	0.27	0.79	1.53	2.84	3.49	3.62	3.85	5.41	6.47	8.21	7.85	7.18	5.92	4.75	3.87	1.93
E	—	*tr*	0.54	1.10	1.63	2.30	2.12	2.83	3.15	3.84	5.60	5.92	5.81	5.76	5.10	4.35	3.87	2.10
F	*tr*	*tr*	0.75	2.31	3.17	4.33	4.94	5.12	5.10	5.94	6.67	6.82	6.66	6.15	5.91	4.83	4.31	2.02
G	—	—	*tr*	0.20	0.86	1.21	1.36	1.76	1.40	1.80	4.31	5.85	6.16	6.18	5.46	5.05	4.03	1.65
Mean ± *SD*			0.66 ± 0.23	1.45 ± 0.82	2.06 ± 0.84	2.64 ± 1.04	3.03 ± 1.26	3.48 ± 1.24	3.52 ± 1.34	4.42 ± 1.60	5.50 ± 1.25	6.25 ± 1.51	5.90 ± 1.58	5.35 ± 1.67	4.45 ± 1.76	3.63 ± 1.66	2.92 ± 1.58	1.45 ± 0.80

[a] *tr* = Trace: indicates that theophylline was detected but the concentrations were too low to quantitate.

Table III—Fraction (f) of a 5-mg/kg Dose of Theophylline Absorbed at Each Sampling Time following Ingestion of Whole or Halved 100-mg Sustained-Release Tablets

Subject	Time, hr													
	0.25	0.5	0.75	1.0	1.25	1.5	1.75	2	3	4	6	8	10	12	14	16	24
								Whole Tablets									
A	0.10	0.15	0.19	0.25	0.33	0.33	0.37	0.38	0.51	0.57	0.84	0.95	0.97	1.00	1.00	1.02	1.00
B	0.0	0.04	0.07	0.11	0.17	0.23	0.32	0.36	0.47	0.62	0.77	0.87	0.94	0.99	1.01	0.98	1.00
C	0.0	0.0	0.10	0.14	0.21	0.23	0.29	0.31	0.40	0.50	0.79	0.88	0.94	0.94	0.94	0.92	0.94
D	0.03	0.12	0.05	0.08	0.14	0.18	0.20	0.23	0.37	0.49	0.79	0.92	0.99	0.99	0.99	1.01	1.00
E	0.0	0.0	0.0	0.06	0.12	0.17	0.18	0.19	0.32	0.40	0.64	0.86	0.96	0.99	1.00	1.02	1.00
F	0.01	0.10	0.15	0.22	0.28	0.28	0.30	0.31	0.42	0.46	0.62	0.71	0.77	0.82	0.86	0.91	1.00
G	0.0	0.0	0.03	0.07	0.13	0.15	0.23	0.25	0.31	0.40	0.57	0.70	0.84	0.93	0.96	1.01	1.00
Mean ± *SD*	0.02 ± 0.04	0.06 ± 0.06	0.08 ± 0.07	0.13 ± 0.08	0.20 ± 0.08	0.22 ± 0.06	0.27 ± 0.07	0.29 ± 0.07	0.40 ± 0.07	0.49 ± 0.08	0.72 ± 0.10	0.84 ± 0.10	0.92 ± 0.08	0.95 ± 0.06	0.97 ± 0.05	0.98 ± 0.05	
								Halved Tablets									
A	0.0	0.06	0.17	0.23	0.26	0.32	0.38	0.41	0.54	0.65	0.84	0.93	0.98	0.98	1.00	1.00	1.00
B	0.0	0.06	0.18	0.21	0.24	0.28	0.37	0.36	0.51	0.63	0.85	0.94	0.99	1.03	1.02	1.01	1.03
C	0.0	0.11	0.16	0.23	0.23	0.29	0.33	0.36	0.50	0.64	0.83	0.95	1.02	0.99	0.99	0.97	0.98
D	0.0	0.02	0.07	0.13	0.24	0.30	0.31	0.34	0.50	0.63	0.88	0.96	1.02	1.01	1.00	0.99	1.00
E	0.0	0.06	0.12	0.19	0.26	0.25	0.33	0.37	0.48	0.71	0.84	0.92	1.00	1.01	1.00	1.01	1.00
F	0.0	0.07	0.21	0.29	0.40	0.47	0.49	0.50	0.61	0.72	0.83	0.91	0.96	1.03	1.01	1.02	1.00
G	0.0	0.0	0.20	0.08	0.11	0.13	0.17	0.14	0.19	0.44	0.67	0.81	0.92	0.96	1.02	1.01	1.00
Mean ± *SD*	0.0	0.05 ± 0.04	0.16 ± 0.05	0.19 ± 0.07	0.25 ± 0.08	0.29 ± 0.10	0.34 ± 0.10	0.35 ± 0.11	0.48 ± 0.13	0.63 ± 0.09	0.82 ± 0.07	0.92 ± 0.05	0.98 ± 0.04	1.00 ± 0.03	1.01 ± 0.01		

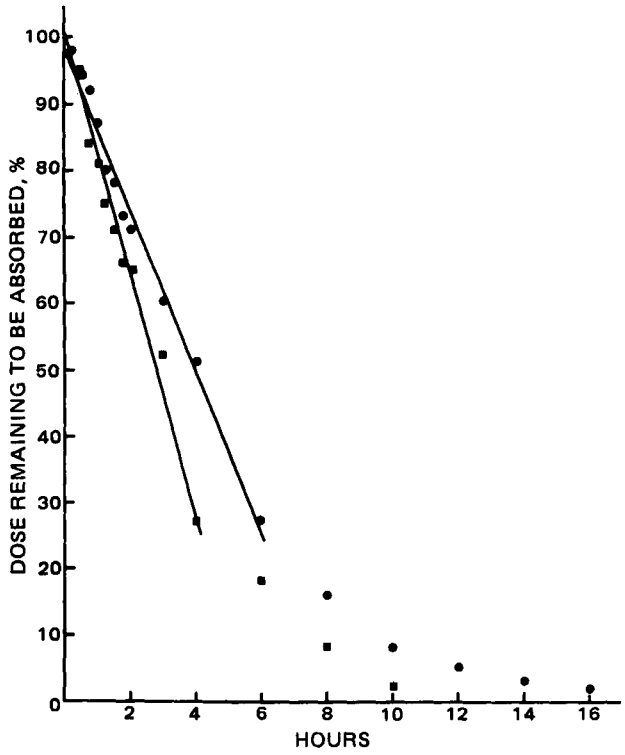

Figure 4—*Mean percentages of a 5-mg/kg dose of theophylline remaining to be absorbed* versus *time in seven normal volunteers who ingested whole (●) or halved (■) 100-mg sustained-release tablets.*

where $\int_0^t Cp\,dt$ and $\int_0^\infty Cp\,dt$ are the areas under the serum concentration *versus* time curves for time 0 to any time t and time 0 to infinity (*i.e.*, total amount absorbed), respectively. The areas $\int_0^t Cp\,dt$ and $\int_0^{t_n} Cp\,dt$ were calculated using the trapezoid method to time t_n. The area $t_n \int^\infty Cp\,dt$ was calculated using Eq. 4 and added to the area $\int_0^{t_n} Cp\,dt$ (11).

$$\int_{t_n}^{\infty} Cp\,dt = \frac{Cp_n}{K_e} \qquad \text{(Eq. 4)}$$

The mean absorption time (MAT) was calculated by (12):

$$\text{MAT} = \frac{\int_0^\infty Cpt\,dt}{\int_0^\infty Cp\,dt} - \frac{1}{K_e} \qquad \text{(Eq. 5)}$$

Plasma clearance (Cl) of theophylline was given by:

$$Cl = \frac{\text{dose}}{\int_0^\infty Cp\,dt} \qquad \text{(Eq. 6)}$$

where $\int_0^\infty Cp\,dt$ is the area under the serum concentration *versus* time curve for time zero to infinity as calculated in Eq. 3.

The apparent volume of distribution for theophylline (V_d) was calculated from:

$$V_d = \frac{Cl}{K_e} \qquad \text{(Eq. 7)}$$

The renal clearance of theophylline (Cl_R) was calculated by the formula:

$$Cl_R = f_e Cl \qquad \text{(Eq. 8)}$$

where f_e is the fraction of the total amount of the dose in 24 hr urine excreted as theophylline (11).

RESULTS

The mean cumulative percentage of theophylline dissolved from the whole and halved 100-mg sustained-release tablets at each sample time in simulated gastric and intestinal fluids is tabulated in Table I. The mean cumulative percent of theophylline dissolved from the whole and halved 100-mg tablets in intestinal fluid *versus* time is shown in Fig. 1.

Table IV—Theophylline Pharmacokinetics Parameters in Normal Volunteers following the Ingestion of a 5-mg/kg Dose as Whole or Halved 100-mg Sustained-Release Tablets

Subject	AUC, μg/ml/hr	MAT, hr	Elimination Values from Log Plot		Volume of Distribution, (V_d), l/kg	Plasma Clearance (Cl), ml/min/kg	Renal Clearance (Cl_R), ml/min/kg
			K_e, hr^{-1}	$t_{1/2}$, hr			
			Whole Tablets				
A	112.75	3.60	0.11	6.30	0.40	0.74	0.09
B	66.65	4.21	0.18	3.85	0.46	1.36	0.17
C	56.82	4.08	0.16	4.33	0.55	1.47	0.12
D	147.00	4.01	0.08	8.66	0.47	0.63	0.20
E	109.94	5.05	0.10	6.93	0.47	0.79	0.20
F	150.16	5.91	0.03	23.10	1.17	0.58	0.14
G	115.18	6.14	0.11	6.30	0.39	0.71	0.08
Mean ± *SD*	108.36 ± 35.35	4.71 ± 1.00	0.11 ± 0.05	8.50 ± 6.64	0.56 ± 0.27	0.90 ± 0.36	0.14 ± 0.05
			Halved Tablets				
A	109.26	3.37	0.13	5.33	0.35	0.76	0.07
B	59.23	3.86	0.20	3.47	0.46	1.54	0.12
C	39.64	3.35	0.23	3.01	0.55	2.10	0.21
D	136.99	3.29	0.09	7.70	0.45	0.68	0.21
E	128.47	3.44	0.07	9.90	0.58	0.67	0.22
F	139.91	2.64	0.09	7.70	0.42	0.63	0.12
G	111.14	5.28	0.10	6.93	0.44	0.74	0.12
Mean ± *SD*	103.52 ± 39.16	3.60 ± 0.82	0.13 ± 0.06	6.29 ± 2.48	0.46 ± 0.08	1.02 ± 0.57	0.15 ± 0.06

Serum theophylline concentrations from the seven subjects following the administration of a mean theophylline dose of 5.2 mg/kg theophylline as whole or halved 100-mg tablets are listed in Table II. The mean serum theophylline concentration *versus* time plots for the two doses are shown in Fig. 2.

The fractions of the dose of theophylline absorbed (f) at each time interval for each subject following the dose as whole and halved tablets are shown in Table III. The mean values following each dose *versus* time is shown in Fig. 3. The pharmacokinetic parameters, AUC, MAT, K_e, $t_{1/2}$, V_d, Cl_1, and Cl_R for each subject, following both doses, are listed in Table IV. The mean percentage of the dose to be absorbed following the ingestion of whole or halved 100-mg tablets *versus* time is given in Fig. 4. The amounts of the dose recovered in 24 hr in the urine as unchanged theophylline and the various metabolites are shown in Table V. In Table VI the metabolites and theophylline recovery is reported as percentages of theophylline equivalents of the 24-hr urine recovery.

DISCUSSION

The only reference to dissolution data in the literature was from the manufacturer as reported by one group of investigators (1). From the 300-mg sustained-release tablets, 50% of the dose was reported to be in solution by 2 hr and > 90% was in solution by 6 hr. No specifications were reported. In the present study, in gastric fluid, 46.1 ± 2.5 and 65.8 ± 4.7% of the dose was in solution at 6 hr from whole and halved 100-mg tablets, respectively (Table I). The stomach mean emptying time for enteric-coated tablets has been reported to be 3.61 ± 1.47 hr (13); therefore, dissolution studies in gastric fluid were stopped at 6 hr.

In intestinal fluid, 52.7 ± 7.8% of the dose was released in 3 hr by halved 100-mg tablets, and 52.3 ± 5.5% was released in 5 hr by whole 100-mg tablets. After 12 hr, 84.4 ± 6.7% of the dose was in solution from halved tablets and 78.4 ± 7.9% of the dose in 10 hr from whole tablets (Table I). With the paucity of information available in the literature (1), it was not possible to compare previously reported results with the results from the present study.

These sustained-release theophylline tablets are reported to release theophylline by a zero-order rate, *i.e.*, equivalent to an infusion; therefore, plots of percentage released *versus* time should be linear. It was possible to fit a straight line by linear regression ($r = 0.99$) to the terminal portion of the percentage released *versus* time curve. However, the lines did not pass through the origin (Fig. 1). From these data it would appear that the first portion of any dose is probably released by first-order diffusion.

Table V—Fraction of a 5-mg/kg Dose of Theophylline Excreted as Unchanged Drug or Metabolites in 24 hr following the Ingestion of Whole or Halved 100-mg Sustained-Release Tablets by Normal Volunteers

Subject	Theophylline and Metabolites, mg/24 hr				Total Xanthines [a]	Dose	Dose Recovered, %
	1-Methyluric Acid	3-Methylxanthine	1,3-Dimethyluric Acid	Theophylline			
				Whole Tablets			
A	71.28	41.33	193.08	38.34	330.94	500	66.19
B	61.85	36.08	102.72	27.89	228.20	300	76.07
C	64.32	39.46	131.15	19.34	246.44	300	82.15
D	30.56	21.39	52.11	47.36	148.84	300	49.33
E	36.32	23.09	67.26	40.66	163.58	400	40.90
F	50.13	31.72	115.12	64.27	254.13	300	84.71
G	56.08	34.52	204.25	36.76	317.04	500	63.41
							66.11 ± 16.47
				Halved Tablets			
A	70.45	39.20	233.53	32.29	358.75	500	71.75
B	51.89	36.39	187.72	22.30	285.36	300	95.12
C	62.36	37.28	102.38	21.53	218.02	300	72.67
D	43.05	22.75	46.67	48.36	158.78	300	52.93
E	30.05	15.56	44.81	43.87	131.77	400	32.94
F	56.30	33.28	114.16	47.82	244.65	300	81.55
G	44.22	25.33	158.68	41.00	269.23	500	51.55
							65.50 ± 20.97

[a] Calculated as theophylline equivalents on a molar basis.

Table VI—Fraction of the 24-hr Urine Content of a 5-mg/kg Dose of Theophylline Excreted as Unchanged Drug or Metabolites following the Ingestion of Whole or Halved 100-mg Sustained-Release Tablets by Normal Volunteers

Subject	Distribution of Theophylline Metabolites in 24 hr, %			
	1-Methyl-uric Acid	3-Methyl-xanthine	1,3-Dimethyl-uric Acid	Theo-phylline
	Whole Tablets			
A	21.42	13.71	53.29	11.59
B	26.95	15.81	45.01	12.22
C	25.95	17.57	48.62	7.84
D	20.42	15.78	31.99	31.82
E	22.08	15.49	37.57	24.86
F	19.62	13.70	41.39	25.29
G	17.59	11.95	58.86	11.60
Mean ± *SD*	22.00 ± 3.37	14.86 ± 1.85	45.25 ± 9.23	17.89 ± 9.22
	Halved Tablets			
A	19.53	11.99	59.48	9.00
B	18.08	14.00	60.11	7.82
C	28.44	18.77	42.91	9.88
D	26.96	15.66	26.86	30.46
E	22.68	12.96	31.07	33.29
F	22.89	14.93	42.64	19.55
G	17.06	10.79	56.25	15.91
Mean ± *SD*	22.23 ± 4.34	14.16 ± 2.63	45.62 ± 13.51	17.99 ± 10.38

A fraction of each dose in these tablets is contained in uncoated granules. As the tablets do not readily disintegrate, the availability of this portion of the dose by pore diffusion would account for the nonlinear 2–3 hr first-order release of drug. The remaining fraction of the dose is contained in coated pellets. As the tablet begins to disintegrate and the portion of the dose in these pellets is released, the rate of drug availability begins to approximate a zero-order infusion release. This ultimately causes the terminal portion of the curve to approach linearity as shown in Fig. 1. Fractions of the dose released from halved tablets were significantly higher than from whole tablets at all times ($p < 0.05$). This is probably due to the increased surface area exposed by breaking the tablets.

In this bioavailability study in normal subjects of whole and halved 100-mg sustained-release theophylline tablets, relative bioavailability was assessed by comparing the areas (time zero to infinity) under the serum concentration *versus* time curves (*AUC*) (Fig. 2). For halved 100-mg tablets, the *AUC* was 103.52 ± 39.16 μg/ml/hr and for whole tablets 108.36 ± 35.83 μg/ml/hr (Table IV). These were not significantly different ($p = 0.05$). In addition, although the mean serum theophylline concentrations following the ingestion of the halved tablets were numerically higher than the values obtained for the whole tablets up to 8 hr, none of the values were significantly different ($p = 0.05$) (Table II).

The fraction of the dose absorbed at any time (f) was calculated using Eq. 3. All subjects absorbed 50% of the dose from either whole or halved 100-mg sustained-release tablets in the 3–4 hr period (Table III, Fig. 3). Except for subject F, following the ingestion of the whole tablets, all other subjects absorbed 90–100% of the dose in the 8–12 hr period. This is consistent with previous reports (1).

The mean percentage of the dose remaining to be absorbed *versus* time is shown in Fig. 4. The initial portion of the graph is linear. These results can be used to confirm the results of dissolution data that there is apparent zero-order release of theophylline from these tablets. The terminal nonlinear portion of the curve is probably due to the fact that the fraction absorbed calculated using Eq. 3 is approaching the asymptote. Theophylline absorption is rapid and complete once the drug is in solution (14).

The mean absorption times (MAT) calculated from Eq. 5 are shown in Table IV. The average MAT of 3.60 ± 0.82 hr following ingestion of the halved tablet was not significantly different ($p = 0.05$) from the value of 4.71 ± 1.00 hr obtained from the whole tablets. In addition, these values are not significantly different ($p = 0.05$) from previously reported values (15) of 5.67 ± 1.40 and 4.20 ± 1.48 hr following the ingestion of whole and halved 300-mg sustained-release tablets, respectively.

The mean theophylline elimination half-life values in these seven subjects following ingestion of these 100-mg sustained-release tablets were 8.50 ± 6.64 hr for whole tablets and 6.29 ± 2.48 hr for halved tablets. These values are not significantly different ($p = 0.05$) and are comparable to literature values of 3.6–12.8 hr in normal, healthy adults (16). Subject F had an extremely long half-life of 23 hr (Table IV) following ingestion of the whole tablets.This is probably not the true half-life, but a value distorted by continued absorption from the sustained-release dosage form. The half-life in this subject following the halved tablet was 7.70 hr.

The apparent volume of distribution for theophylline following ingestion of whole 100-mg tablets was 0.56 ± 0.27 liter/kg. This was not significantly different ($p = 0.05$) from 0.46 ± 0.08 liter/kg obtained from the halved 100-mg tablets. Both values were comparable to those reported in the literature (16).

Total body clearance of theophylline was found to be 0.90 ± 0.36 and 1.02 ± 0.57 ml/min/kg following ingestion of whole and halved 100-mg sustained-release theophylline tablets, respectively. These clearances were not significantly different ($p = 0.05$) from each other or from values reported in the literature (16). Renal clearance of theophylline has been shown to be dependent upon the urine flow rate (17). However, the values found in this study of 0.14 ± 0.05 and 0.15 ± 0.06 ml/min/kg following the ingestion of whole and halved 100-mg tablets, respectively, were not significantly different ($p = 0.05$) from each other or from values previously reported in the literature (17, 18).

The quantities of theophylline and its metabolites, 1-methyluric acid, 3-methylxanthine, and 1,3-dimethyluric acid, recovered in 24-hr urine following ingestion of ~5-mg/kg dose as whole or halved 100-mg tablets are shown in Table V. The metabolite recovery values were converted to theophylline equivalents and reported along with theophylline as total xanthines. This permitted the calculation of the percentage of the dose recovered in the urine as unchanged drug and metabolites during the 24 hr period. Mean recoveries of 66.11 ± 16.47 and 65.50 ± 20.97% following ingestion of whole and halved tablets, respectively, were not significantly different ($p = 0.05$).

The distribution of the various metabolites following the whole or halved tablet doses (Table VI) were not significantly different ($p = 0.05$). This is not surprising since the other parameters such as *AUC*, MAT, K_e, $t_{1/2}$, V_d, Cl and Cl_R were not significantly affected by halving the tablets. However, when compared to other values in the literature, some differences were observed. In a study where 15 older patients were given sustained-release tablets (19), theophylline recovery was 7.7 ± 6.1%, whereas in the present study 17.89 ± 9.27% was found. The recovery of 3-methylxanthine (19) was 36.2 ± 7.3%, while only 14.86 ± 1.85% was recovered in this study. The recoveries of 16.5 ± 3.3% and 39.6 ± 4.5% for 1-methyluric acid and 1,3-dimethyluric acid, respectively (19), were not significantly different ($p = 0.05$) from the present study.

In the previously reported study (19), middle-aged to elderly patients were used, whereas the present study used healthy, young subjects. The older patients were at steady state and 116 ± 36% of the 24-hr dose was recovered in the urine. The younger subjects only received a single dose and only 66.11 ± 47% of the dose was recovered in the 24-hr urine. These differences may account for the discrepancies.

In summary the theophylline elimination parameters such as half-life ($t_{1/2}$), elimination rate constant (K_e), apparent volume of distribution (V_d), clearance (Cl), and renal clearance (Cl_R) were not significantly different from literature values obtained in similar subjects. The metabolite excretion pattern differed from that previously reported but the differences in subject age and in the dosage regimen may have accounted for these discrepancies. In conclusion, halving the sustained-release 100-mg theophylline tablets to achieve more accurate mg/kg doses should not affect drug therapy in patients.

REFERENCES

(1) M. Weinberger, L. Hendeles, and L. Bighley, *N. Engl. J. Med.*, **299**, 852 (1978).

(2) "The United States Pharmacopeia," 19th rev., Mack Publishing, Easton, Pa., 1975, pp. 651, 765.

(3) L. Hendeles, M. Weinberger, and G. Johnson, *Clin. Pharmacokinet.*, **3**, 294 (1978).

(4) J. W. Nelson, A. L. Cordry, G. C. Aron, and R. A. Bartell, *Clin. Chem.*, **23**, 124 (1977).

(5) J. J. Orcutt, P. P. Koyak Jr., S. A. Gillman, and L. H. Cummins, *ibid.*, **23** 599 (1977).

(6) G. W. Peng, M. A. F. Gadalla, and W. L. Chiou, *ibid.*, **24**, 357 (1978).

(7) B. R. Manno, J. E. Manno, and B. C. Hilman, *J. Anal. Toxicol.*, **3**, 81 (1979).

(8) R. K. Desiraju and E. T. Sugita, *J. Chromatogr. Sci.*, **15**, 563 (1977).
(9) K. J. Simons, F. E. R. Simons, C. J. Briggs, and L. Lo, *J. Pharm. Sci.*, **68**, 252 (1979).
(10) R. F. Adams, F. L. Vandemark, and G. J. Schmidt, *Clin. Chem.*, **22**, 1903, (1976).
(11) M. Gibaldi and D. Perrier, "*Pharmacokinetics*," Marcel Dekker, New York, N.Y., 1975, pp. 1–43.
(12) D. J. Cutler, *J. Pharm. Pharmacol.*, **30**, 476 (1978).
(13) J. G. Wagner, "Biopharmaceutics and Relevent Pharmacokinetics," Drug Intelligence Publications, Hamilton, Ill., 1971, pp. 98–147, 163–165.
(14) L. Hendeles, M. Weinberger, and L. Bighley, *Am. J. Hosp. Pharm.*, **34**, 525 (1977).
(15) P. O. Fagerström, *Eur. J. Resp. Dis. Suppl. 109*, **61**, 62 (1980).
(16). R. I. Ogilvie, *Clin. Pharmacokinet.*, **3**, 267 (1978).
(17) G. Levy and R. Koysooko, *J. Clin. Pharmacol.*, **16**, 329 (1976).
(18) J. W. Jenne, E. Wyze, F. S. Rood, and F. M. MacDonald, *Clin. Pharmacol. Ther.*, **13**, 349 (1972).
(19) J. W. Jenne, H. T. Nagasawa, and R. D. Thompson, *ibid.*, **19**, 375 (1976).

ACKNOWLEDGMENTS

Supported by the Children's Hospital of Winnipeg Research Foundation and by Astra Pharmaceuticals Canada Ltd., Mississauga, Canada.

The authors acknowledge the help of the late Dr. Sidney Riegelman, School of Pharmacy, University of California, San Francisco, for his invaluable help with the computer programming and data analysis, Dr. Roman Bilous, Faculty of Pharmacy, University of Manitoba, who provided the USP Dissolution Apparatus, and Dr. Ray Fynes, Astra Pharmaceuticals, Canada Ltd. for his support during the entire project.

Dr. F. Estelle R. Simons is a Queen Elizabeth II scientist.

Determination of Related Compounds in Aspirin by Liquid Chromatography

C. D. PFEIFFER and J. W. PANKEY ˣ

Received May 22, 1981, from the *Analytical Laboratories, The Dow Chemical Company, Midland, MI 48640.* Accepted for publication July 15, 1981.

Abstract □ A rapid liquid chromatographic procedure has been validated for the determination of salicylic acid, salsalate, acetylsalicylsalicylic acid, and acetylsalicylic anhydride in aspirin. Samples are dissolved in methylene chloride and analyzed directly by adsorption chromatography in a 7-min separation using an isocratic mobile phase. Recoveries averaged 99% over a 200–10,000 ppm concentration range with standard deviations of <4% for the four compounds of interest. Detection limits ranged from 5 to 36 ppm. Compared to a recently published reversed-phase liquid chromatographic procedure for analyzing aspirin, this method is twice as fast, more sensitive, and avoids the use of hydroxylic solvents which lead to degradation of aspirin and acetylsalicylic anhydride.

Keyphrases □ Aspirin—determination of salicylic acid and related compounds by liquid chromatography □ Liquid chromatography—determination of salicylic acid and related compounds in aspirin □ Salicylic acid—determination in aspirin by liquid chromatography, related compounds

Several recent papers (1–5) have discussed the possible immunological response to the presence of low levels of related compounds in aspirin. Methods, too numerous to discuss, employing gas chromatography, spectrophotometry, liquid chromatography, *etc.*, have been published describing the determination of salicylic acid (I), salsalate (II), acetylsalicylic anhydride (III), and acetylsalicylsalicylic acid (IV) in aspirin. Liquid chromatography (LC) appears to be the most useful approach with respect to specificity, speed, and sensitivity. Various LC methods have appeared in the literature employing adsorption, polar bonded phase, as well as reversed-phase column packings.

After considering the various LC methods, it appeared that the methods employing adsorption chromatography are most appropriate for the determination of related compounds in aspirin on a routine basis. Reversed-phase methods are not desirable because III and aspirin are not stable in the mixed aqueous–organic eluents used in that

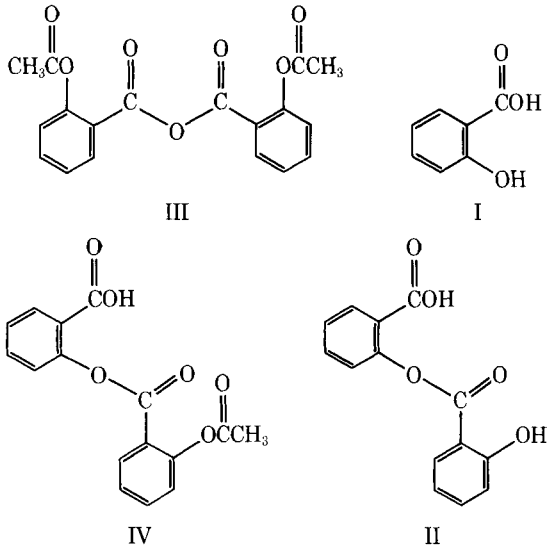

form of LC (5). In addition, the selectivity of the reversed-phase system is such that I elutes from the column immediately following aspirin and a poor detection limit is found for I because the larger aspirin peak tails into the peak for I. This difficulty can be avoided by using fluorescence detection (6) to selectively detect I, but this requires the use of dual detectors which increases the cost and complexity of the LC system.

Several normal-phase LC systems have been published for these analyses. A silica gel support containing perchloric acid as a stationary phase for the determination of I, III, and IV in aspirin has been used (7). In another study (8) a polar bonded phase[1] column has been used for the separation of II, III, IV, and other compounds. However,

[1] CYANO.

0022-3549/82/0500-0511$01.00/0

(8) R. K. Desiraju and E. T. Sugita, *J. Chromatogr. Sci.*, **15**, 563 (1977).
(9) K. J. Simons, F. E. R. Simons, C. J. Briggs, and L. Lo, *J. Pharm. Sci.*, **68**, 252 (1979).
(10) R. F. Adams, F. L. Vandemark, and G. J. Schmidt, *Clin. Chem.*, **22**, 1903, (1976).
(11) M. Gibaldi and D. Perrier, "*Pharmacokinetics*," Marcel Dekker, New York, N.Y., 1975, pp. 1–43.
(12) D. J. Cutler, *J. Pharm. Pharmacol.*, **30**, 476 (1978).
(13) J. G. Wagner, "Biopharmaceutics and Relevent Pharmacokinetics," Drug Intelligence Publications, Hamilton, Ill., 1971, pp. 98–147, 163–165.
(14) L. Hendeles, M. Weinberger, and L. Bighley, *Am. J. Hosp. Pharm.*, **34**, 525 (1977).
(15) P. O. Fagerström, *Eur. J. Resp. Dis. Suppl. 109*, **61**, 62 (1980).
(16). R. I. Ogilvie, *Clin. Pharmacokinet.*, **3**, 267 (1978).
(17) G. Levy and R. Koysooko, *J. Clin. Pharmacol.*, **16**, 329 (1976).
(18) J. W. Jenne, E. Wyze, F. S. Rood, and F. M. MacDonald, *Clin. Pharmacol. Ther.*, **13**, 349 (1972).
(19) J. W. Jenne, H. T. Nagasawa, and R. D. Thompson, *ibid.*, **19**, 375 (1976).

ACKNOWLEDGMENTS

Supported by the Children's Hospital of Winnipeg Research Foundation and by Astra Pharmaceuticals Canada Ltd., Mississauga, Canada.

The authors acknowledge the help of the late Dr. Sidney Riegelman, School of Pharmacy, University of California, San Francisco, for his invaluable help with the computer programming and data analysis, Dr. Roman Bilous, Faculty of Pharmacy, University of Manitoba, who provided the USP Dissolution Apparatus, and Dr. Ray Fynes, Astra Pharmaceuticals, Canada Ltd. for his support during the entire project.

Dr. F. Estelle R. Simons is a Queen Elizabeth II scientist.

Determination of Related Compounds in Aspirin by Liquid Chromatography

C. D. PFEIFFER and J. W. PANKEY ˣ

Received May 22, 1981, from the *Analytical Laboratories, The Dow Chemical Company, Midland, MI 48640.* Accepted for publication July 15, 1981.

Abstract □ A rapid liquid chromatographic procedure has been validated for the determination of salicylic acid, salsalate, acetylsalicylsalicylic acid, and acetylsalicylic anhydride in aspirin. Samples are dissolved in methylene chloride and analyzed directly by adsorption chromatography in a 7-min separation using an isocratic mobile phase. Recoveries averaged 99% over a 200–10,000 ppm concentration range with standard deviations of <4% for the four compounds of interest. Detection limits ranged from 5 to 36 ppm. Compared to a recently published reversed-phase liquid chromatographic procedure for analyzing aspirin, this method is twice as fast, more sensitive, and avoids the use of hydroxylic solvents which lead to degradation of aspirin and acetylsalicylic anhydride.

Keyphrases □ Aspirin—determination of salicylic acid and related compounds by liquid chromatography □ Liquid chromatography—determination of salicylic acid and related compounds in aspirin □ Salicylic acid—determination in aspirin by liquid chromatography, related compounds

Several recent papers (1–5) have discussed the possible immunological response to the presence of low levels of related compounds in aspirin. Methods, too numerous to discuss, employing gas chromatography, spectrophotometry, liquid chromatography, *etc.*, have been published describing the determination of salicylic acid (I), salsalate (II), acetylsalicylic anhydride (III), and acetylsalicylsalicylic acid (IV) in aspirin. Liquid chromatography (LC) appears to be the most useful approach with respect to specificity, speed, and sensitivity. Various LC methods have appeared in the literature employing adsorption, polar bonded phase, as well as reversed-phase column packings.

After considering the various LC methods, it appeared that the methods employing adsorption chromatography are most appropriate for the determination of related compounds in aspirin on a routine basis. Reversed-phase methods are not desirable because III and aspirin are not stable in the mixed aqueous–organic eluents used in that

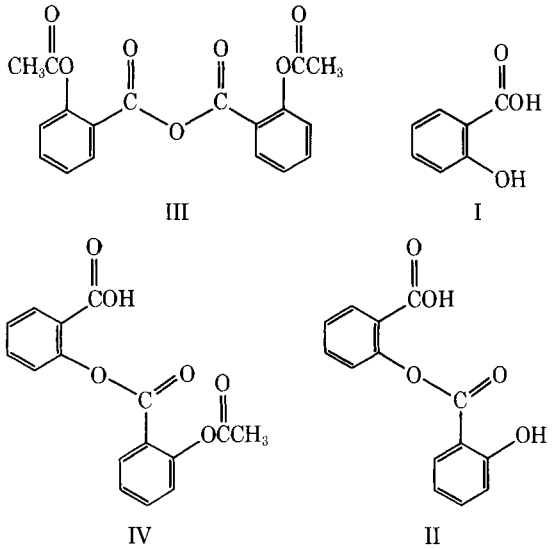

form of LC (5). In addition, the selectivity of the reversed-phase system is such that I elutes from the column immediately following aspirin and a poor detection limit is found for I because the larger aspirin peak tails into the peak for I. This difficulty can be avoided by using fluorescence detection (6) to selectively detect I, but this requires the use of dual detectors which increases the cost and complexity of the LC system.

Several normal-phase LC systems have been published for these analyses. A silica gel support containing perchloric acid as a stationary phase for the determination of I, III, and IV in aspirin has been used (7). In another study (8) a polar bonded phase[1] column has been used for the separation of II, III, IV, and other compounds. However,

[1] CYANO.

0022-3549/82/0500-0511$01.00/0

Table I—Recovery Data for Related Compounds

Level Spiked	Percent Recovery I	II	III	IV
10,000 ppm	100.9	96.8	95.9	98.3
10,000 ppm	98.7	95.1	96.1	98.7
5,000 ppm	100.0	96.6	95.5	98.8
5,000 ppm	101.0	97.5	96.2	96.8
1,000 ppm	98.8	98.2	95.2	98.8
1,000 ppm	96.6	98.5	97.7	98.4
500 ppm	103.1	101.1	98.2	98.2
500 ppm	100.0	102.1	96.6	96.3
200 ppm	93.8	99.5	90.2	94.1
200 ppm	104.2	106.4	106.3	98.3
200 ppm	108.4	105.9	101.0	108.4
Average	100.5	99.79	97.17	98.65
SD	3.87	3.72	3.98	3.53

the separation on silica gel described previously (9) appears to be the most practical for use on a routine basis, and modification of this approach was used in this current work.

EXPERIMENTAL

Reagents—Hexane, chloroform, and methylene chloride of distilled-in-glass quality were used[2,3]. Glacial acetic acid of reagent grade[4] and 2,2-dimethoxypropane (98%)[5] were used as purchased.

Standards—Salicylic acid[6], salsalate[7], and acetylsalicylic anhydride[8] were used as purchased. The acetylsalicylsalicylic acid was synthesized[9] and characterized utilizing spectroscopic and chromatographic techniques to confirm its identity and purity.

A standard solution containing I, II, III, and IV was accurately prepared by weight in methylene chloride with each component at ~800 μg/ml. This concentrated standard solution was accurately diluted to yield a standard at the ~40-μg/ml level, and was used to calibrate the LC system. It was observed that the standard solutions were somewhat unstable and, therefore, all standards were prepared fresh whenever the system was recalibrated.

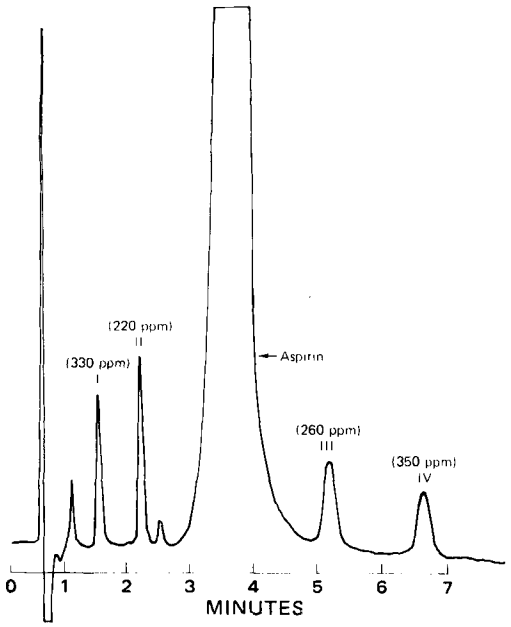

Figure 1—*Analysis of spiked aspirin. Column, 4.6 × 150 mm, Zorbax-SIL; flow rate, 3.0 ml/min; injection, 10 μl; detector, 0.016 aufs at 254 nm; mobile phase, hexane–chloroform–acetic acid (80:19:3).*

[2] Burdick and Jackson Laboratories, Inc., Muskegon, Mich.
[3] MCB Manufacturing Chemists, Inc., Cincinnati, Ohio.
[4] J. T. Baker Co., Phillipsburg, N.J.
[5] Aldrich Chemical Co., Milwaukee, Wis.
[6] United States Pharmacopeial Convention, Inc., Rockville, Md.
[7] Pfaltz & Bauer, Inc., Stamford, Conn.
[8] Tridom Chemical, Inc., Hauppauge, N.Y.
[9] Dow Chemical Co.

Apparatus—The liquid chromatograph was a modular system consisting of a pump[10], sample injection valve[11], and a single wavelength (254 nm) UV detector[12]. A computing integrator[13] was used for measuring peak areas and calculating results of analyses.

The microparticulate silica gel column[14] (4.6 × 150 mm) was purchased prepacked from the supplier. Prior to use, the column was activated using 2,2-dimethoxypropane (10). Ten column volumes of a solution consisting of methylene chloride–acetic acid–2,2-dimethoxypropane, 96:2:2 (v/v/v) were pumped through the column at a flow rate of 3.0 ml/min to condition and activate the packing. The column was then equilibrated by pumping mobile phase, hexane–chloroform–acetic acid, 80:19:3 (v/v/v), at a flow rate of 3.0 ml/min until a flat base line was obtained, ~15 min. The specific LC conditions used for the analysis were: mobile phase—hexane–chloroform–acetic acid, 80:19:3 (v/v/v); temperature ambient; detector wavelength, 254 nm, 0.016 aufs; injection, 10 μl.

Sample Preparation—Samples of aspirin crystals were dissolved in methylene chloride (20 mg/ml) and analyzed directly by LC. The sample solutions were injected as soon as dissolution had occurred because it was observed that aspirin hydrolyzed to I in methylene chloride solution. Therefore, artificially high results were obtained for I unless sample solutions were analyzed immediately.

Samples of aspirin tablets were finely ground and dissolved in methylene chloride (20 mg/ml). The resulting solutions were rapidly filtered[15] to remove insoluble materials, and the clear filtrate was immediately analyzed by LC. This entire dissolution–filtering operation was completed in less than 2 min to minimize formation of I.

RESULTS AND DISCUSSION

Validation—A typical chromatogram of a spiked aspirin sample is shown in Fig. 1. The linearity of the LC system was demonstrated by

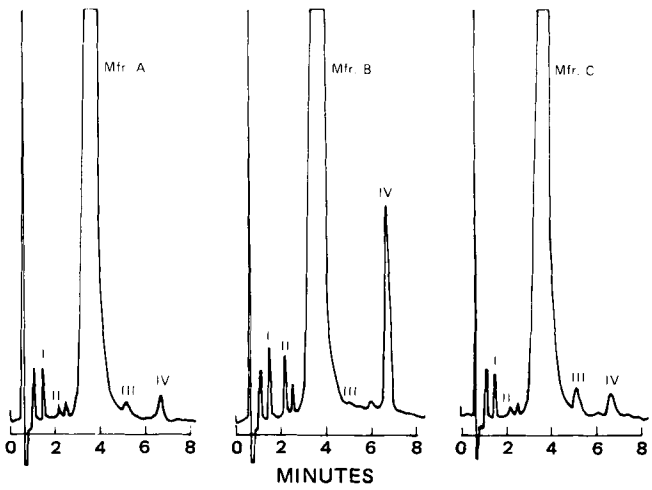

Figure 2—*Comparison of aspirin crystals. Same conditions as Fig. 1.*

[10] Model M-45, Waters Associates, Milford, Mass.
[11] Model 7125, Rheodyne, Inc., Berkeley, Calif.
[12] Model 1203, Laboratory Data Control, Riviera Beach, Fla.
[13] System I, Spectra Physics, Santa Clara, Calif.
[14] Zorbax SIL, 6μ, DuPont Co., Wilmington, Del.
[15] 0.45 μ Fluropore Filter, Sample Clarification Kit, Waters Associates, Milford, Mass.

Table II—Precision Study for Analysis of Aspirin

Component	Compound I	II	III	IV
Day 1	103[a]	195	758	1455
	105	188	750	1421
	101	179	702	1388
	103	179	701	1348
	99	181	722	1394
Day 2	112	171	678	1309
	101	173	695	1361
	103	179	699	1363
	98	177	706	1386
	106	179	701	1356
Average	103.1	180.1	711.2	1378.1
SD	3.98	6.93	13.86	40.6

[a] Measured in parts per million.

Table III—Detection Limits for Aspirin-Related Compounds

Compound	Peak Area, ppm	Peak Height, ppm
I	14	15
II	5	6
III	6	19
IV	11	36

chromatographing a series of standard solutions containing varying levels of the four compounds of interest. Plots of peak area against concentration yield straight lines going through the origin for up to the equivalent of 1% of each of the related compounds in the samples. The peak height response was also linear up to 1200 ppm at 0.016 aufs.

For the recovery study, a sample of aspirin was analyzed in triplicate using the external standard technique to determine the native levels of the related compounds. Recovery data were generated by spiking the control sample at levels in a 200–10,000 ppm range with the components of interest and analyzing those components by the external standard technique. The results were corrected for native levels of each component before calculating the recovery values. The results are summarized in Table I. The data demonstrated that relative standard deviations of 4% were obtained for the four compounds of interest.

Precision data were generated by analyzing a single sample of aspirin 5 times on each of two consecutive days. The results are summarized in Table II. The precision obtained would have been predicted from the recovery study, further demonstrating the validity of the method.

The detection limits of the method for the four components of interest for both peak area and peak height are summarized in Table III. The minimum detectable quantity was defined as a peak <2.5 times the short-term peak-to-peak baseline noise. The retention times for several other aspirin related compounds on this LC system are listed in Table IV. Chromatograms of typical bulk aspirin samples are shown in Fig. 2; results are summarized in Table V.

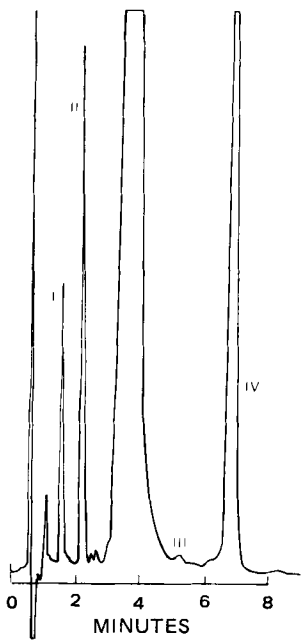

Figure 3—*Analysis of Aspirin Tablet. Same conditions as Fig. 1.*

Table IV—Retention Times of Aspirin-Related Compounds

Compound	Retention Time, min
Salicylic Acid	1.6
Salsalate	2.2
p-Acetoxybenzoic Acid	2.5
Acetylsalicylic Acid	3.6
Acetylsalicylic Anhydride	5.2
p-Hydroxyisophthalic Acid	6.3
Acetylsalicylsalicylic Acid	6.7
p-Acetoxyisophthalic Acid	13.0
p-Hydroxybenzoic Acid	15.5

Table V—Analysis of Bulk Aspirin

Manufacturer	I	II	III	IV
A	190[a]	16	81	230
B	260	100	*ND*[b]	2000
C	160	16	110	190

[a] Measured in parts per million. [b] Not detected at a detection limit of 6 ppm.

Table VI—Analysis of Aspirin Tablets

Brand	I	II	III	IV
A	640[a]	650	ND[b]	4300
B	440	650	ND	4800
C	240	*ND*[c]	ND	650
D	460	690	ND	4400
E	330	20	ND	530
F	540	700	ND	4500

[a] Measured in parts per million. [b] Not detected at a detection limit of 6 ppm. [c] Not detected at a detection limit of 5 ppm.

Mobile Phase—During this investigation, it was found that the aspirin separation was somewhat dependent on the particular brand of chloroform used. Various suppliers use different preservatives to inhibit degradation, and it was found in particular that ethanol used as a preservative had a significant effect on retention times.

The separation between III and aspirin is most critically affected. Using a ratio of hexane–chloroform–acetic acid of 80:19:3 (v/v/v), with a nonpolar hydrocarbon stabilizer in the chloroform, the relative retention of III to aspirin was 1.59. With 80:19:3 and 1% ethanol in the chloroform, the relative retention was 1.36. Thus, when ethanol is used as a preservative in chloroform, the relative amount of chloroform in the mobile phase should be reduced to adequately resolve III and aspirin.

Analysis of Tablets—While this method was developed and validated for the specific determination of related compounds in bulk aspirin, it is also applicable to the analysis of aspirin tablets. A complicating factor in the analysis of tablets is the presence of starch and other insoluble excipients in the sample matrix which must be removed prior to the LC separation. However, this was readily accomplished *via* filtration using the filter described previously. A small, 4.6 × 50-mm guard column packed with pellicular silica gel[16] was used to protect the analytical column when analyzing tablets.

The method was not formally validated for the analysis of tablets. However, the LC separation was evaluated for this application by analyzing six commercial brands of tablets. A typical chromatogram is shown in Fig. 3 and the results are summarized in Table VI. It is interesting to note that no III was detected in any of the samples analyzed. At this time, it is not known whether these particular brands were formulated from bulk aspirin not containing III, or if III is not stable in the starch matrix since the starch may contain up to 14% water.

CONCLUSIONS

A new, rapid method has been validated for the determination of related compounds in bulk aspirin. Recoveries averaged 99% with a standard deviation of <4% for the four compounds of interest over a 200–10,000 ppm concentration range. For a single determination, results may be expected to be <7.7% relative error at the 95% confidence level.

This method has three significant advantages compared to the re-

[16] Corasil II, Waters Associates, Milford, Mass.

versed-phase LC procedure recently published by the United States Food and Drug Administration (11, 12). In addition to being twice as fast, the selectivity of the adsorption LC system is such that I and II elute prior to aspirin, permitting a low limit of detection for I. The normal phase LC method avoids the use of hydroxylic solvents, which lead to degradation of aspirin and III preventing accurate determination of III by reversed-phase LC. This method uses an inexpensive fixed wavelength (254 nm) UV detector and has a lower limit of detection than any previously published normal phase LC procedure.

REFERENCES

(1) H. Bundgaard, *J. Pharm. Pharmacol.*, **26,** 18 (1974).

(2) A. L. DeWeck, *Int. Arch. Allergy Appl. Immunol.*, **41,** 393 (1971).

(3) H. Bundgaard and A. L. DeWeck, *ibid.*, **49,** 119 (1975).

(4) H. D. Schlumberger, *ibid.*, **48,** 467 (1975).

(5) J. C. Reepmeyer and R. D. Kirchhoefer, *J. Pharm. Sci.*, **68,** 1167 (1979).

(6) R. D. Kirchhoefer and W. E. Juhl, *ibid.*, **69,** 548 (1980).

(7) S. O. Jansson and I. Anderson, *Acta Pharm. Suec.*, **14,** 161 (1977).

(8) G. Chevalier, R. Rohrbach, C. Bollett, and M. Coude, *J. Chromatogr.*, **138,** 193 (1977).

(9) H. Bundgaard, *Arch. Pharm. Chemi Sci. Ed.*, **4,** 103 (1976).

(10) R. A. Bredeweg, L. D. Rothman, and C. D. Pfeiffer, *Anal. Chem.*, **51,** 2061 (1979).

(11) R. D. Kirchhoefer, R. C. Reepmeyer, and W. E. Juhl, *J. Pharm. Sci.*, **69,** 550 (1980).

(12) R. D. Kirchhoefer, *ibid.*, **69,** 1188 (1980).

Soft Drugs V: Thiazolidine-Type Derivatives of Progesterone and Testosterone

NICHOLAS BODOR *x and KENNETH B. SLOAN ‡

Received April 8, 1981, from the **Department of Medicinal Chemistry, College of Pharmacy, J. Hillis Miller Health Center, University of Florida, Gainesville, FL 32610* and the ‡*Inter$_x$ Research Corporation, Lawrence, KS 66044.* Accepted for publication August 5, 1981.

Abstract □ Progesterone and testosterone are natural soft drugs, but to be used as drugs, their fast and facile metabolism must be prevented and their delivery controlled. A prodrug–soft drug combination can serve this purpose. Thiazolidines of testosterone, testosterone 17-propionate and progesterone were synthesized from the reaction of cysteine alkyl esters, *N*-methylaminoethanethiol, and mercaptamine and their hydrochlorides with the appropriate steroids. The thiazolidines function as bioreversible derivatives of the parent steroids.

Keyphrases □ Soft drugs—thiazolidine-type derivatives of progesterone and testosterone □ Prodrugs—thiazolidine-type derivatives of progesterone and testosterone □ Progesterone—thiazolidine-type derivatives, prodrugs □ Testosterone—thiazolidine-type derivatives, prodrugs

Oral contraception is accomplished currently by products containing synthetic hormones, mostly as fixed combinations of synthetic estrogens and progestins (1). The contraceptive action of these products is mediated primarily by inhibition of ovulation through specific macromolecular receptors for each hormone. It is clear that if the natural hormones, *e.g.*, progesterone and estradiol, were delivered to the receptors, they would elicit the same contraceptive effect as the synthetic analogs. The advantage of this method is that the natural hormone might decrease or eliminate the side effects accompanying synthetic contraceptive agents. Some of these side effects are the result of oxidative metabolism (2), such as the one involving the 17α-ethinyl group in norethindrone (17β-hydroxy-19-nor-17α-pregn-4-en-20-yn-3-one) or norgestrel (13-ethyl-17β-hydroxy-18,19-dinor-17α-pregn-4-en-20-yn-3-one), which leads to destruction of cytochrome P-450 (3).

Natural hormones such as progesterone, estradiol, and testosterone are natural soft drugs (4, 5); that is, due to their efficient and nontoxic metabolic disposition, they will not cause unexpected toxicity at concentrations close to their natural levels. On the other hand, natural hormones administered as drugs suffer from low physiological availability because, as natural substances, the body has developed efficient mechanisms for their metabolism and excretion. For example, the α,β-unsaturated ketone and the 20-ketone in progesterone are reduced in the liver to give pregnane-3α,20-diol, which can then be conjugated and excreted (1). In addition, the natural hormones are virtually insoluble in water which precludes their efficient dissolution and absorption from most formulations. Thus, to utilize progesterone as a contraceptive drug component, solutions to the problems of slow dissolution (water solubility) and rapid metabolism must be found.

In the case of hydrocortisone (4), the preferred approach to solving the described problems is through chemical modification, *i.e.*, a prodrug. However, progesterone is a difficult candidate for such an approach because the only functional groups available for reversible modification are the 3- and 20-ketones. Therefore, an extension of the spirothiazolidine approach (4) seemed the most attractive, as thiazolidines are unique examples of a bioreversible steroidal ketone derivative. The spontaneous S_N1 cleavage of the thiazolidine (6) to a β-thioethylene imine is followed by hydrolysis of the imine [possibly through a hydration–disassociation mechanism (7)] to regenerate the parent carbonyl compound (4). In addition to their potential bioreversibility, thiazolidines were attractive as prodrugs because they could be prepared from cysteine. Consequently, the hydrolysis products (steroid and cysteine) of the prodrugs would not present any unusual metabolic burden to the body. The carboxylic group of cysteine could also be easily esterified, thus providing a convenient method for changing the lipophilicity/hydrophilicity of the derivatives. In addition to progesterone, testosterone thiazolidines were also investigated[1].

[1] Part 4 of this series (N. Bodor, K. B. Sloan, R. J. Little, S. H. Selk, and L. Caldwell, *Int. J. Pharm;* in press).

0022-3549/82/0500-0514$01.00/0

versed-phase LC procedure recently published by the United States Food and Drug Administration (11, 12). In addition to being twice as fast, the selectivity of the adsorption LC system is such that I and II elute prior to aspirin, permitting a low limit of detection for I. The normal phase LC method avoids the use of hydroxylic solvents, which lead to degradation of aspirin and III preventing accurate determination of III by reversed-phase LC. This method uses an inexpensive fixed wavelength (254 nm) UV detector and has a lower limit of detection than any previously published normal phase LC procedure.

REFERENCES

(1) H. Bundgaard, *J. Pharm. Pharmacol.*, **26,** 18 (1974).

(2) A. L. DeWeck, *Int. Arch. Allergy Appl. Immunol.*, **41,** 393 (1971).

(3) H. Bundgaard and A. L. DeWeck, *ibid.*, **49,** 119 (1975).

(4) H. D. Schlumberger, *ibid.*, **48,** 467 (1975).

(5) J. C. Reepmeyer and R. D. Kirchhoefer, *J. Pharm. Sci.*, **68,** 1167 (1979).

(6) R. D. Kirchhoefer and W. E. Juhl, *ibid.*, **69,** 548 (1980).

(7) S. O. Jansson and I. Anderson, *Acta Pharm. Suec.*, **14,** 161 (1977).

(8) G. Chevalier, R. Rohrbach, C. Bollett, and M. Coude, *J. Chromatogr.*, **138,** 193 (1977).

(9) H. Bundgaard, *Arch. Pharm. Chemi Sci. Ed.*, **4,** 103 (1976).

(10) R. A. Bredeweg, L. D. Rothman, and C. D. Pfeiffer, *Anal. Chem.*, **51,** 2061 (1979).

(11) R. D. Kirchhoefer, R. C. Reepmeyer, and W. E. Juhl, *J. Pharm. Sci.*, **69,** 550 (1980).

(12) R. D. Kirchhoefer, *ibid.*, **69,** 1188 (1980).

Soft Drugs V: Thiazolidine-Type Derivatives of Progesterone and Testosterone

NICHOLAS BODOR *x and KENNETH B. SLOAN ‡

Received April 8, 1981, from the **Department of Medicinal Chemistry, College of Pharmacy, J. Hillis Miller Health Center, University of Florida, Gainesville, FL 32610* and the ‡*Inter$_x$ Research Corporation, Lawrence, KS 66044.* Accepted for publication August 5, 1981.

Abstract □ Progesterone and testosterone are natural soft drugs, but to be used as drugs, their fast and facile metabolism must be prevented and their delivery controlled. A prodrug–soft drug combination can serve this purpose. Thiazolidines of testosterone, testosterone 17-propionate and progesterone were synthesized from the reaction of cysteine alkyl esters, *N*-methylaminoethanethiol, and mercaptamine and their hydrochlorides with the appropriate steroids. The thiazolidines function as bioreversible derivatives of the parent steroids.

Keyphrases □ Soft drugs—thiazolidine-type derivatives of progesterone and testosterone □ Prodrugs—thiazolidine-type derivatives of progesterone and testosterone □ Progesterone—thiazolidine-type derivatives, prodrugs □ Testosterone—thiazolidine-type derivatives, prodrugs

Oral contraception is accomplished currently by products containing synthetic hormones, mostly as fixed combinations of synthetic estrogens and progestins (1). The contraceptive action of these products is mediated primarily by inhibition of ovulation through specific macromolecular receptors for each hormone. It is clear that if the natural hormones, *e.g.*, progesterone and estradiol, were delivered to the receptors, they would elicit the same contraceptive effect as the synthetic analogs. The advantage of this method is that the natural hormone might decrease or eliminate the side effects accompanying synthetic contraceptive agents. Some of these side effects are the result of oxidative metabolism (2), such as the one involving the 17α-ethinyl group in norethindrone (17β-hydroxy-19-nor-17α-pregn-4-en-20-yn-3-one) or norgestrel (13-ethyl-17β-hydroxy-18,19-dinor-17α-pregn-4-en-20-yn-3-one), which leads to destruction of cytochrome P-450 (3).

Natural hormones such as progesterone, estradiol, and testosterone are natural soft drugs (4, 5); that is, due to their efficient and nontoxic metabolic disposition, they will not cause unexpected toxicity at concentrations close to their natural levels. On the other hand, natural hormones administered as drugs suffer from low physiological availability because, as natural substances, the body has developed efficient mechanisms for their metabolism and excretion. For example, the α,β-unsaturated ketone and the 20-ketone in progesterone are reduced in the liver to give pregnane-3α,20-diol, which can then be conjugated and excreted (1). In addition, the natural hormones are virtually insoluble in water which precludes their efficient dissolution and absorption from most formulations. Thus, to utilize progesterone as a contraceptive drug component, solutions to the problems of slow dissolution (water solubility) and rapid metabolism must be found.

In the case of hydrocortisone (4), the preferred approach to solving the described problems is through chemical modification, *i.e.*, a prodrug. However, progesterone is a difficult candidate for such an approach because the only functional groups available for reversible modification are the 3- and 20-ketones. Therefore, an extension of the spirothiazolidine approach (4) seemed the most attractive, as thiazolidines are unique examples of a bioreversible steroidal ketone derivative. The spontaneous S_N1 cleavage of the thiazolidine (6) to a β-thioethylene imine is followed by hydrolysis of the imine [possibly through a hydration–disassociation mechanism (7)] to regenerate the parent carbonyl compound (4). In addition to their potential bioreversibility, thiazolidines were attractive as prodrugs because they could be prepared from cysteine. Consequently, the hydrolysis products (steroid and cysteine) of the prodrugs would not present any unusual metabolic burden to the body. The carboxylic group of cysteine could also be easily esterified, thus providing a convenient method for changing the lipophilicity/hydrophilicity of the derivatives. In addition to progesterone, testosterone thiazolidines were also investigated[1].

[1] Part 4 of this series (N. Bodor, K. B. Sloan, R. J. Little, S. H. Selk, and L. Caldwell, *Int. J. Pharm;* in press).

0022-3549/82/0500-0514$01.00/0

EXPERIMENTAL[2]

Biological—*In vivo* animal tests used standard procedures for the Clauberg and seminal vesicle and ventral prostate weight tests.

Plasma Hydrolysis Studies of Thiazolidines—Whole blood was drawn from female beagles immediately before the hydrolysis study. The whole blood was treated with edetate disodium as an anticoagulant. The blood was centrifuged at 2000 rpm for 10 min. The plasma was removed from the red blood cells and filtered through a 0.2-μm methylcellulose membrane filter. Concentrated spiking solutions of the thiazolidines (Table I) were prepared in dimethylformamide. Small volumes of these solutions (20 μl/ml of plasma) were added to the plasma to give the appropriate concentrations. Methyl testosterone (0.020 mg/ml) was added as an internal standard for chromatography. The samples were mixed thoroughly and placed in a water bath at 37°, equipped with a shaking mechanism. Samples (5 μl) were withdrawn at ~12-hr intervals for injection onto the high-pressure liquid chromatograph. The mobile phase was tetrahydrofuran–methanol–water (1:1:2) at a 2.0-ml/min flow rate. The eluate was monitored at 254 nm for progesterone. The progesterone concentration was determined by comparison of the peak areas of the sample and standard solutions, and corrected using the internal standard. Hydrolysis rates were determined by the rate of appearance of progesterone. Straight lines were determined using a least-squares fit.

Pharmacokinetics of XI in Dogs—Female beagle dogs were used for the study which included a crossover experiment. The dogs were placed in separate stainless steel cages 24 hr prior to administration of the drug. Water was available at all times and normal feeding schedules were maintained. The dogs were dosed with 2.5 μCi of drug by intravenous injection in the front leg over a 30 sec period. The ^{14}C-labeled progesterone was 1 μCi/mg. The ^{14}C-labeled XI was 0.446 μCi/mg. All drugs were dissolved in 100 μl of benzyl alcohol. Blood samples (~4 ml) were drawn from the jugular vein of the dog using tubes containing edetate disodium as an anticoagulant preservative. Blood samples were taken at 5, 10, 15, 30, 45, 60, and 90 min, 2, 4, 6, 8, 12, 24, 32, and 48 hr, and at other appropriate times after injection. The blood (3.5 ml) was transferred to a tared 25-ml heavy duty centrifuge tube with a polytef-lined screw cap. The samples were weighed accurately before extraction. Extractions were performed by shaking for 10 min with 10 ml of 10% ethylene dichloride in ether (v/v) on a wrist-shaker, centrifuging for 15 min at 2000 rpm, and transferring the organic phase to new liquid scintillation vials. Samples were extracted twice and the organic phases from each extraction were combined. The organic solvent was evaporated to dryness in a 50° water bath under dry nitrogen stream. The extracts were dissolved in 15 ml of scintillation cocktail and mixed thoroughly. The samples were stored overnight at 4° prior to counting to reduce chemiluminescence.

Urine samples from each dog were collected at 24 and 48 hr after dosing. Both samples were frozen separately until all the studies were completed and all samples were prepared at once. The urine was thawed and the total volumes measured. A small amount of well mixed urine from each sample was centrifuged to remove particulate matter. One milliliter of each sample was quantitatively transferred to a liquid scintillation vial containing 0.5 ml of 0.5 *N* hydrochloric acid and mixed. Fifteen milliliters of scintillation cocktail was added to each vial and mixed. Samples were then counted.

Recovery experiments were conducted using radioactive labeled drugs at three blood levels for each of the three compounds in whole dog blood. Extraction efficiencies for each compound at each blood level were determined using 10% ethylene dichloride in ether as a solvent. For each compound, studies were conducted at blood levels of 0.001, 0.0001, and 0.00005 μCi/3 ml of blood. For each blood level, 18 ml of blood was transferred to a tared, heavy-duty centrifuge tube and weighed accurately. Each pool of blood was spiked at the appropriate concentration using either 30 or 60 μl of a spiking solution (methanol). The spiked blood was shaken for 30 min to reach equilibrium. Five replicate 3-ml samples were drawn from each pool and transferred to tared 25-ml heavy-duty centrifuge tubes equipped with polytef-lined screw caps and weighed accurately.

Each sample was extracted twice by shaking for 15 min on a wrist-shaker with 10 ml of 10% ethylene dichloride in ether, centrifuging for 10 min at 2200 rpm, and transferring the supernate to a liquid scintillation vial. Combined extracts were evaporated to dryness under a dry nitrogen stream at 55°. The residues were dissolved in 15 ml of scintillation cocktail. Samples were stored overnight at 4° to reduce chemiluminescence and then counted.

Distribution Studies in Rats—Approximately 1 μCi/mmole of progesterone, XI, and VIII*a* in 5 ml of benzyl alcohol were injected intravenously in the tail veins of six female rats (90–120 g). They were then placed in a clean metabolism cage and their urine and feces were collected.

Table I—Thiazolidines of Testosterone and Testosterone 17β-Propionate

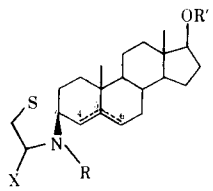

Compound	X	R	Δ	R′
I*a*	$CO_2C_2H_5$	H	5,6	COC_2H_5
I*b*	$CO_2C_2H_5$	H	4,5	COC_2H_5
II*a*	$CO_2C_2H_5$	H	5,6	H
II*b*	$CO_2C_2H_5$	H	4,5	H
III	$CO_2CH_2CH_2OH$	H	5,6	COC_2H_5
IV	$CO_2CH_2CH_2OH$	H	5,6	H
V	H	H	5,6	COC_2H_5
VI	H	H	5,6	H
VII	H	CH_3	5,6	H

Thiazolidines of Progesterone

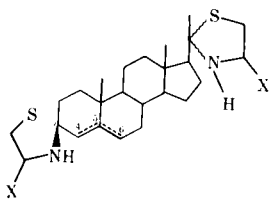

Compound	X	Δ
VIII*a*	$CO_2C_2H_5$	5,6
VIII*b*	$CO_2C_2H_5$	4,5
X	$CO_2C_4H_9$	4,5
XI	$CO_2C_6H_{13}$	4,5:5,6(1:1)
XII	$CO_2C_{10}H_{21}$	4,5

Thiazolidines of Progesterone

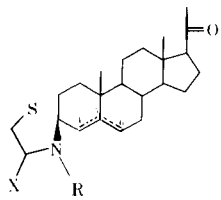

Compound	X	R	Δ
IX*a*	$CO_2C_2H_5$	H	5,6
IX*b*	$CO_2C_2H_5$	H	4,5
XIII	H	H	5,6
XIV	H	COH	5,6
XV	H	$COCH_3$	5,6
XVI	H	$COCH_2NHCO_2$-$CH_2C_6H_5$	5,6
XVII	H	CH_3	5,6

[2] Radiolabeled counting was performed on a Beckman LS-100C Scintillation Counter. TLC were run on Brinkman Polygram Sil G/UV 254. Melting points (uncorrected) were taken with a Thomas–Hoover capillary apparatus. NMR spectra were recorded on a Varian T-60 (^1H spectra) or on a Bruker WP-80 (^{13}C spectra) spectrophotometer. Infrared spectra were obtained on a Beckman Acculab 4 infrared spectrophotometer, while UV spectra were determined on a Carey Model 14 spectrophotometer. Optical rotations were obtained using a Perkin Elmer 141 polarimeter. HPLC analyses were run on a Waters 6000A solvent delivery system U6K universal injector and a 440 Dual Channel UV detector. Microanalyses were performed by Midwest Microlab, Ltd, Indianapolis, Ind. Progesterone, testosterone, testosterone propionate, cysteine methyl, and ethyl ester hydrochlorides were obtained from Sigma. 2-Aminoethanethiol hydrochloride was obtained from Aldrich, the scintillation cocktails were Aquasol or Biofluor from New England Nuclear, the protein solubilizer was Protosol from New England Nuclear, while all other reagents were obtained from Mallinckrodt unless otherwise specified. The cysteine glycerol, butyl, hexyl, and decyl esters were prepared according to Voullie (8) *et al.*, and the *N*-acyl-thiazolidines were prepared according to Sloan *et al.*[3] The hairless mice (SKH-hr-1) were obtained from the Temple University Skin and Cancer Hospital. *In vivo* animal tests were conducted at the National Institutes of Health.

[3] K. B. Sloan, N. Bodor, and J. Zupan, *Tetrahedron*, in press.

Sixty minutes after injection each rat was anesthetized with ether, and its blood was collected in a preweighed test tube containing 4 drops of 15% edetate disodium. Each rat was then sacrificed with more ether and dissected. The fat deposits, spleen, kidneys, ovaries, liver, lungs, heart, brain, intestinal walls, GI contents, and the tail were all removed and each one placed in a preweighed test tube.

After each organ (except the tail) was weighed, it was homogenized with a known amount of water in a glass tissue grinder. The tail was wrapped in aluminum foil, frozen in liquid nitrogen, shattered with a hammer, and mixed thoroughly with a known volume of water. The feces were diluted with water and mixed thoroughly. Samples (0.5 ml) of the homogenates or suspensions and 1.0 ml of a protein solubilizer–ethanol mixture were placed in liquid scintillation counting vials. The vials containing the samples were heated at 55° for 60 min, and if necessary, the samples were decolorized by heating with 0.1–0.5 ml of 30% hydrogen peroxide. After the samples were cooled, 15.0 ml of scintillation cocktail and 0.5 ml of 0.5 *N* HCl were added to the samples, and they were counted. A quenching curve was obtained using tissue samples, protein solubilizer, hydrogen peroxide, and scintillation cocktail. The urine from each rat was collected directly in a scintillation vial, and counted in 15.0 ml of scintillation cocktail.

Percutaneous Distribution in Mice—For the percutaneous delivery study, the thiazolidine VIII*a* and progesterone were dissolved in ethanol–isopropyl myristate (90:10) and applied to the backs of six hairless mice using a bandage to form an occlusive application. The mice were then placed in metabolism cages for 24 hr and then sacrificed. The bandages were then removed and the surface of the skins were washed three times with 5 ml of ethanol. The washes were combined with the patches and counted. An epidermal plug, 2 cm in diameter, was taken from each carcass from directly beneath where the patches (3 cm^2) had been with a leather punch. The epidermal plugs, the remainder of the carcasses, the urine, and feces were processed as described for the rat distribution study.

Reaction of Testosterone 17β-propionate with Cysteine Ethyl Ester Hydrochloride—To a mixture of testosterone 17β-propionate (1.0 g, 0.0029 mole) and cysteine ethyl ester hydrochloride (3.70 g, 0.02 mole) was added 10 ml of pyridine. The solution was allowed to sit at room temperature overnight under a nitrogen atmosphere in a tightly closed flask. The solution was then partitioned using methylene chloride–water (100:100) and the methylene chloride layer was separated, dried over sodium sulfate, and concentrated to give a solid residue. The residue was crystallized from 10 ml of hot ethanol to give 0.35 g (mp 144–147°, 26% yield) of 5-androstene-17β-propionyloxy-3-spiro-2′-(4′-ethoxycarbonyl-1′,3′-thiazolidine), I*a*: TLC (silica gel, ether) R_f 0.45; IR (KBr): 1735 cm^{-1} (s, C=O); ^{1}H-NMR ($CDCl_3$): δ 5.53–5.2 (m, 1, C*H*=C), 4.6 (t, *J* = 8 Hz, 1, C*H*O_2C), 4.21 (q, *J* = 7 Hz, 2, CH_3CH_2O), 4.2–3.8 (m, 1, O_2CC*H*N), 3.4–2.7 (m, 2, CH_2S), 1.29 (t, *J* = 7 Hz, 3, CH_3CH_2O), 1.01 (s, 3, CH_3—C), 0.8 (s, 3, CH_3—C), and 2.7–1.0 (m, 24, N*H*, CH_2 and C*H*); ^{13}C-NMR ($CDCl_3$): δ 174.7, 171.9 (CO_2), 140.7 (C-5), and 122.4 (C-6); $[\alpha]_D^{25}$ −55° (*C* = 0.55, ethanol).

Anal.—Calc. for $C_{27}H_{41}NO_4S$: C, 68.17; H, 8.69; N, 2.95. Found: C, 68.46; H, 8.78; N, 2.70.

The mother liquor was concentrated to 5 ml and allowed to crystallize further. This gave 0.51 g (mp 100–104°, 37% yield) of a mixture containing primarily 4-androstene-17β-propionyloxy-3-spiro-2′-(4′-ethoxycarbonyl-1′,3′-thiazolidine), I*b*, but with some I*a* (ratio ~9:1, I*b*:I*a*). TLC and IR were the same as for I*a*. The ^{1}H-NMR spectrum was the same except that the major (90%) C*H*=C absorption was a singlet as δ 5.3; ^{13}C-NMR ($CDCl_3$): δ 174.7, 171.9 (CO_2), 148.7 (C-5), and 123.0 (C-4); $[\alpha]_D^{25}$ = +10 (*C* = 0.49, ethanol).

Anal.—Calc. for $C_{27}H_{41}NO_4S$: C, 68.17; H, 8.69; N, 2.95. Found: C, 68.28; H, 8.79; N, 2.75.

Compounds II*a*, II*b*, III, and IV were prepared in a similar manner and had NMR and IR spectra consistent with the assigned structures.

5- and 4-Androstene-17β-ol-3-spiro-2′-(4′-ethoxycarboxyl-1′,3′-thiazolidine)—These are II*a* and II*b*, respectively.

II*a*: mp 136–140° from ethanol, 32% yield; $[\alpha]_D^{25}$ = −60° (*C* = 0.47, $CHCl_3$).

Anal.—Calc. for $C_{24}H_{37}NO_3S$: C, 68.69; H, 8.89; N, 3.34. Found: C, 68.58; H, 8.79; N, 3.18.

II*b*: An amorphous powder from water; $[\alpha]_D^{25}$ = +2° (*C* = 0.45, $CHCl_3$).

Anal.—Calc. for $C_{24}H_{37}NO_3S$: C, 68.69; H, 8.89; N, 3.34. Found: C, 67.87; H, 8.79; N, 3.54.

The 4-androstene-3-thiazolidine could be crystallized from 1 ml of ethanol to give a light yellow fibrous solid (0.28 g, mp 67–75°), which was identical in all respects with the crude product and gave a low carbon analysis also.

5-Androstene-17β-propionyloxy-3-spiro-2′-(4′-β-hydroxyethoxycarbonyl-1′,3′-thiazolidine)—III: mp 127–130° from ether; $[\alpha]_D^{25}$ = −49° (*C* = 0.5, $CHCl_3$).

Anal.—Calc. for $C_{27}H_{41}NO_5S$: C, 66.00; H, 8.34, N, 2.84; S, 6.52. Found: C, 65.90; H, 8.55; N, 2.68; S, 6.69.

5-Androstene-17β-ol-3-spiro-2′-(4′-β-hydroxyethoxycarbonyl-1′,3′-thiazolidine)—IV: mp 135–140° from ether.

Anal.—Calc. for $C_{24}H_{37}NO_4S$: C, 66.22; H, 8.50, N, 3.21; S, 7.36. Found: C, 66.16; H, 8.77; N, 3.39; S, 7.48.

Reaction of Progesterone with Cysteine Ethyl Ester Hydrochloride—Progesterone (1.0 g, 0.0032 mole) was mixed with increasing amounts of cysteine ethyl ester hydrochloride (0.65 g, 0.0035 mole, one equivalent; 1.30 g, 0.0070 mole, two equivalents; 2.60 g, 0.014 mole, four equivalents; 3.90 g, 0.021 mole, six equivalents) and dissolved in pyridine (10 ml) in four separate reactions. The reactants were kept at room temperature overnight under nitrogen in a tightly closed flask. Each reaction was then concentrated *in vacuo* (0.1 mm, 1 hr, 45°) to give a gummy solid which was suspended in 50 ml of ethylene dichloride. The ethylene dichloride suspensions were extracted with 10 ml of water, dried over sodium sulfate and concentrated *in vacuo* to give yellow solids which were analyzed by TLC and NMR spectroscopy. Only the reaction with six equivalents of cysteine ethyl ester hydrochloride appeared to give a homogeneous product. All of the reaction products were suspended in 25 ml of boiling ethanol and filtered. In the case of the reactions with four and six equivalents, there was a considerable amount of the ethanol insoluble material. The ethanol insoluble fraction from the reaction with four equivalents of cysteine ethyl ester hydrochloride was a mixture, but that from six equivalents was homogeneous and it was identified as 17β-(4″-ethoxycarbonyl-2″-methyl-1″,3″-thiazolidine-2″-yl)-5-androstene-3-spiro-2′-(4′-ethoxycarbonyl-1′,3′-thiazolidine)VIII*a* (1.2 g, mp 167–170°, 67% yield); IR (KBr): 1735 cm^{-1} (s, C=O); ^{1}H-NMR ($CDCl_3$): δ 5.6–5.2 (m, 1, C*H*=C), 4.20 (q, *J* = 7 Hz, 4, OCH_2CH_3), 4.1–3.65 (m, 2, O_2CC*H*—N), 3.5–2.6 (m, 4, CH_2—S), 1.57 (s, 3, CH_3—C(N)—S), 1.03 (s, 3, CH_3—C), 0.85 (s, 3, CH_3—C), 1.3 (t, *J* = 7 Hz, 6, CH_3CH_2O), 2.6–0.6 (m, 19, CH_2 and C*H*); ^{13}C-NMR ($CDCl_3$): δ 171.9 (CO_2), 140.6 (C-5) and 122.6 (C-4); $[\alpha]_D^{25}$ = −92° (*C* = 0.56, $CHCl_3$); TLC (silica gel, ether) R_f 0.42.

Anal.—Calc. for $C_{31}H_{48}N_2O_4S_2$: C, 64.54; H, 8.39; N, 4.86. Found: C, 64.61; H, 8.44; N, 4.63.

The crystals obtained from the 25-ml ethanol solutions contained mixtures except for the product from the reaction of progesterone with one equivalent of cysteine ethyl ester hydrochloride. Those crystals were identified as 5-pregnene-20-one-3-spiro-2′-(4′-ethoxycarbonyl-1′,3′-thiazolidine) (IX*a*) with about 10% of the 4-pregnene IX*b* as a contaminant (0.45 g, mp 127–134°, 33% yield); IR (KBr): 1735 and 1700 cm^{-1} (s) (C=O); ^{1}H-NMR ($CDCl_3$): δ 5.6–5.2 (m, 1, C*H*=C), 4.26 (q, *J* = 7 Hz, 2, CH_3CH_2O), 4.2–3.8 (m, 1, O_2CC*H*N), 3.6–2.8 (m, 2, CH_2S), 2.11 (s, 3, CH_3—C=O), 1.02 (s, 3, CH_3—C), 0.63 (s, 3, CH_3—C), 1.3 (t, *J* = 7 Hz, 3, CH_3CH_2O), 2.8–0.6 (m, 19, CH_2 and C*H*); ^{13}C-NMR ($CDCl_3$): δ 209.7 (C-20 = O), 171.9 (CO_2), 140.6 (C-5) and 122.5 (C-6); $[\alpha]_D^{25}$ = +11° (*C* = 0.58, $CHCl_3$); TLC (silica gel, ether) R_f 0.34.

Anal.—Calc. for $C_{26}H_{39}NO_3S$: C, 70.07; H, 8.82; N, 3.14. Found: C, 69.84; H, 8.80; N, 3.05.

In the case where six equivalents of cysteine ethyl ester hydrochloride was used, a precipitate formed after the reaction was allowed to run overnight. In a separate reaction, that precipitate was filtered to give VIII*a* (mp 164–170, 61% yield).

The following were prepared in a similar manner. Their NMR and IR spectra were consistent with the assigned structures.

17β-(4″-Butoxycarbonyl-2″-methyl-1″,3″-thiazolidine-2″-yl)-4-androstene-3-spiro-2′-(4′-butoxycarbonyl-1′,3′-thiazolidine)— mp 149–150°, from ethanol; $[\alpha]_D^{25}$ = −38° (*C* = 0.58, $CHCl_3$).

Anal.—Calc. for $C_{35}H_{50}N_2O_4S_2$: C, 66.42; H, 8.92; N, 4.43. Found: C, 66.90; H, 9.20; N, 4.30.

17β-(4″-Hexoxycarbonyl-2″-methyl - 1″,3″ - thiazolidine-2″-yl)-4- and 5-androstene-3-spiro-2′-(4′-hexoxycarbonyl-1′,3′-thiazolidine) (*XI*)—mp 113–115°, from ethanol; $[\alpha]_D^{25}$ = −25° (*C* = 0.51, $CHCl_3$).

Anal.—Calc. for $C_{39}H_{64}N_2O_4S_2$: C, 67.98; H, 9.36; N, 4.07. Found: C, 68.40; H, 9.48; N, 3.90.

17β-(4″-Decoxycarbonyl-2″-methyl-1″,3″-thiazolidine-2″-yl)-4-androstene-3-spiro-2′-(4′-decoxycarbonyl-1′,3′-thiazolidine) (*XII*) —mp 100–102°, from ethanol.

Anal.—Calc. for $C_{47}H_{80}N_2O_4S_2$: C, 70.45; H, 10.66; N, 3.50. Found: C, 70.62; H, 10.20; N, 3.40.

Preparation of 17β-(4″-Ethoxycarbonyl-2″-methyl-1″,3″-thiazolidine-2″-yl)-4-androstene-3-spiro-2′-(4′ - ethoxycarbonyl - 1′,3′-

Table II—Hydrolyses of Thiazolidines [a]

	$t_{1/2}$ [b], hr
Mono-thiazolidines	
IX*b*	22 h
IX*a*	77 h
XIII	16 h
Bis-thiazolidines	
VIII*b*	41 h
VIII*a*	106 h
XI	164 h

[a] Time for one-half the theoretical amount of progesterone to form. [b] Concentration of thiazolidines in plasma was 0.040 mg/ml.

thiazolidine) (VIII*b*)—Cysteine ethyl ester hydrochloride (11.2 g, 0.06 mole) was suspended in 40 ml of triethylamine with vigorous stirring for 1 hr at room temperature. The triethylamine hydrochloride was filtered and the filtrate was concentrated to give cysteine ethyl ester as an oil. The oil was dissolved in 30 ml of pyridine and allowed to react with 3.2 g (0.01 mole) of progesterone at room temperature for 3.5 days. The suspension that resulted was filtered and crystallized from ethyl acetate to give 2.7 g (mp 162–165°, 47% yield) of the desired product: IR (KBr): 1740 cm^{-1} (s, C=O); ^{1}H-NMR ($CDCl_3$): δ 5.23 (s, 1, C*H*=C), 4.2 (q, *J* = 7 Hz, 4, CH_3CH_2O), 4.2–3.6 (m, 2, O_2CCHN), 3.50–2.65 (m, 4, CH_2S), 1.55 (s, 3, CH_3—C(N)S), 1.3 (t, *J* = 7 Hz, 6, CH_3CH_2O), 1.03 (s, 3, CH_3—C), 0.85 (s, 3, CH_3—C), 2.6–0.6 (m, 19, CH_2 and C*H*); ^{13}C-NMR ($CDCl_3$): δ 171.9 and 172.0 (CO_2), 148.9 (C-5) and 122.9 (C-4); $[\alpha]_D^{25} = -24°$ (*C* = 0.63, $CHCl_3$).

Anal.—Calc. for $C_{31}H_{48}N_2O_4S_2$: C, 64.54; H, 8.39; N, 4.86. Found: C, 64.59; H, 8.46; N, 4.88.

Preparation of 4-Pregnene-20-one-3-spiro-2′-(4′-ethoxycarbonyl-1′,3′-thiazolidine) (IX*b*)—Compound VIII*a* (1.0 g) was heated in 25 ml of 80% acetic acid at 65° for 3.5 min then quickly neutralized with 400 ml of ice cold water containing 25 g of sodium bicarbonate. The suspension that resulted was filtered and dried to give 0.41 g of a white solid which was about 65% pure. The solid was crystallized from ethanol (7 ml) to give 0.22 g (mp 131–135°, 28% yield) of the desired product; IR (KBr): 1735 and 1700 cm^{-1} (s, C=O); ^{1}H-NMR ($CDCl_3$): δ 5.30 (s, 1, C*H*=C), 4.23 (q, *J* = 7 Hz, 2, CH_3CH_2O), 4.4–3.9 (m, 1, O_2CCHN), 3.6–2.8 (m, 2, CH_2S), 2.15 (s, 3, CH_3—C=O), 1.3 (t, 3, *J* = 7 Hz, CH_3CH_2O), 1.03 (s, 3, CH_3—C), 0.63 (s, 3, CH_3—C), 2.8–0.6 (m, 19, CH_2 and C*H*); ^{13}C-NMR ($CDCl_3$): δ 209.7 (C-20), 171.9 (CO_2), 148.7 (C-5), and 123.1 (C-6); $[\alpha]_D^{25}$ = +98° (*C* = 0.47, $CHCl_3$).

Anal.—Calc. for $C_{26}H_{39}NO_3S$: C, 70.07; H, 8.82; N, 3.14. Found: C, 70.00; H, 8.89; N, 2.55.

Preparation of 5-Andostrene-17β-ol-3-spiro-2′-(3′-methyl-1′,3′-thiazolidine) (VII)—*N*-Methylaminoethanethiol (1.3 g, 0.014 mole) was warmed to its melting point, 2.0 g (0.0069 mole) of testosterone was added, and the mixture was heated at ~130° for 40 min. The mixture was dissolved in methylene chloride (80 ml), and the solution was washed with water (40 ml), separated, dried over sodium sulfate, and concentrated to give an orange gum. The gum was extracted with 50 ml of refluxing cyclohexane. The cyclohexane was concentrated to 15 ml and cooled to give 0.67 g (mp 112–123°, 27% yield) of the desired thiazolidine: TLC (silica gel, ether) R_f 0.30; IR (KBr): 3400 cm^{-1} (m, OH); ^{1}H-NMR ($CDCl_3$): δ 5.5–5.3 (m, 1, C*H*=C), 3.67 (t, 1, *J* = 7 Hz, C*H*—OH), 3.5–3.17 (m, 2, CH_2—N), 3.17–3.77 (m, 2, CH_2—S), 2.37 (s, 3, CH_3—N), 1.05 (s, 3, CH_3—C), 0.78 (s, 3, CH_3—C), and 2.7–0.8 (m, 20, O*H*, CH_2— and C*H*); ^{13}C-NMR ($CDCl_3$): δ 140.6 (C-5) and 122.5 (C-6).

Anal.—Calc. for $C_{22}H_{35}NOS$: C, 73.07; H, 9.75; N, 3.87. Found: C, 73.19; H, 9.41; N, 3.88.

The filtrate was concentrated to 5 ml, the cyclohexane was decanted from some gum that precipitated, and the cyclohexane was concentrated to dryness to give an additional 0.80 g (32% yield) of the desired product as a foam which was identical with the crystalline material by TLC, NMR, and IR.

5-Pregnene-20-one-3-spiro-2′-(3′-methyl-1′,3′-thiazolidine) (XVII) was prepared in a similar manner (mp 149–151°, from hexane, 25% yield); IR (KBr): 1710 cm^{-1} (s, C=O); ^{1}H-NMR ($CDCl_3$): δ 5.5–5.2 (m, 1, C*H*=C), 2.8–3.5 (m, 4, CH_2—N), 2.33 (s, 3, CH_3—N), 2.13 (s, 3, CH_3CO), 1.03 (s, 3, CH_3—C), and 0.63 (s, 3, CH_3C).

Anal.—Calc. for $C_{24}H_{37}NOS$: C, 74.36; H, 9.62; N, 3.61. Found: C, 74.60; H, 9.80; H, 3.45.

Preparation of 5-Pregnene-20-one-3-spiro-2′-(1′,2′-thiazolidine) (XIII)—A mixture of 3.14 g (0.01 mole) of progesterone and 6.7 g (0.06 mole) of 2-aminoethanethiol hydrochloride was suspended in 20 ml of pyridine overnight at room temperature under a nitrogen atmosphere.

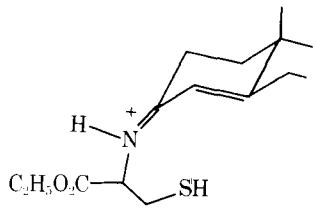

XVIII

The suspension was concentrated *in vacuo*. The residue that resulted was partitioned between methylene chloride–water (100:150 ml). The methylene chloride layer was dried over sodium sulfate, concentrated, and the residue triturated with 10 ml of warm methanol. Almost all of the residue went into solution. After the suspension had cooled, it was filtered to give 1.72 g (mp 127–136°, 46% yield) of the desired compound: TLC (silica gel, ether) R_f 0.20; IR (KBr): 3300 (w, N—H), and 1700 cm^{-1} (s, C=O); ^{1}H-NMR ($CDCl_3$): 5.5–5.2 (m, 1, C*H*=C), 3.6–2.9 (m, 4, SCH_2—CH_2—N), 2.11 (s, 3, CH_3C=O), 1.03 (s, 3, CH_3—C), 0.63 (s, 3, CH_3—C) and 2.9–0.6 (m, 21, CH_2, C*H* and N*H*); $[\alpha]_D^{25}$ = +104° (*C* = 0.51, $CHCl_3$).

Anal.—Calc. for $C_{23}H_{35}NOS$: C, 73.94; H, 9.44; N, 3.75. Found: C, 73.69; H, 9.80; N, 4.00.

Compounds V and VI were prepared in a similar manner. Their NMR and IR spectra were consistent with the assigned structures.

5-Androstene-17β-ol-3-spiro-2′-(1′,3′-thiazolidine) (VI)—TLC (silica gel, ether) R_f 0.24; $[\alpha]_D^{25}$ = +83° (*C* = 0.57, $CHCl_3$).

Anal.—Calc. for $C_{21}H_{33}NOS$: C, 72.57; H, 9.57; N, 4.03. Found: C, 72.56; H, 9.23; N, 4.03.

5-Androstene - 17β-propionyloxy-3-spiro-2′-(1′,3′-thiazolidine):V—mp 152–157° (from methanol, 71% yield); TLC (silica gel, ether) R_f 0.16; $[\alpha]_D^{25}$ = +69° (*C* = 0.52, $CHCl_3$).

Anal.—Calc. for $C_{24}H_{37}NO_2S$: C, 71.41; H, 9.24; N, 3.47. Found: C, 71.32; H, 9.38; N, 3.15.

Preparation of [4-^{14}C]-VIII*a* and XI—[4-^{14}C]Progesterone (100 mg, 100 μCi) was mixed with 1 g of cysteine ethyl or hexyl ester hydrochloride in 2 ml of pyridine. The systems were purged with nitrogen and then stirred overnight under nitrogen. The reaction mixtures were dissolved in 50 ml of ether and extracted with 25 ml of water. The water layers were extracted with an additional 50 ml of ether. The two ether layers were combined, dried over magnesium sulfate and evaporated. Methanol (10 ml) was added to each residue and after they were cooled the solutions gave 47 mg of VIII*a* from the reaction with the ethyl ester and 114 mg of XI from the reaction with hexyl ester. Both thiazolidines were analyzed by radiochromatograph and found to be homogeneous (VIII*a*, R_f = 0.8; XI, R_f = 0.7) using silica gel and ether.

RESULTS AND DISCUSSION

Chemistry—The synthesis and biological activity of the thiazolidines of hydrocortisone and hydrocortisone derivatives have been described recently (4). Similar reaction conditions were used in this study except for the preparation of the *N*-methylthiazolidines and the 4,5-double bond isomers of the mono- and dithiazolidines of progesterone, where special reaction conditions were necessary. As in the hydrocortisone series, the product from the reaction of cysteine with the steroids could not be isolated. However, as opposed to the hydrocortisone series where only one thiazolidine isomer was obtained from the reaction with the cysteine esters or an aminoethanethiol, testosterone and progesterone gave two series of thiazolidine isomers. The simplest case was the testosterone series. The reaction between testosterone 17β-propionate and cysteine ethyl ester hydrochloride gave two isomers, I*a* and I*b* (Table I) which were separated by fractional crystalization from ethanol. The elucidation of the structures of these isomers was reported recently[4], and it was shown that the isomers are the 4,5- and 5,6-double bond isomers as indicated by their optical rotations and ^{1}H- and ^{13}C-NMR spectra when compared with known 4,5- and 5,6-double bond isomers of 3-ethylene ketals and with each other. Although testosterone also gave two double bond isomers from its reaction with cysteine ethyl ester hydrochloride, only the 5,6-double bond isomer II*a* could be isolated in pure form.

Similar reactions of progesterone could be directed to give either the 5,6-double bond mono-3-thiazolidine IX*a* or di-3,20-thiazolidine VIII*a* by using either one or six equivalents, respectively, of cysteine ester hy-

[4] K. B. Sloan, N. Bodor, and R. J. Little, *Tetrahedron*, in press.

Table III—Total Radioactivity (Disintegrations per Minute) in Blood [a] after Intravenous Administration [b] to Dogs of 2.5 μCi of Progesterone [c] and XI [d]

Dog	Drug	Time, hr												
		0.08	0.16	0.25	0.5	0.75	1.0	1.5	2	4	6	8	12	24
1	Progesterone	1084	564	564	394	384	264	172	144	80	27	—	34	10
1	XI	85	16	0	0	11	3	6	20	13	10	0	7	0
2	Progesterone	1177	917	666	509	387	365	278	273	80	105	78	62	33
2	XI	156	58	49	57	68	43	57	60	55	29	—	50	27

[a] 4-ml sample. [b] In 100 μl of benzyl alcohol. [c] 8×10^{-6} mole. [d] 8.14×10^{-6} mole.

drochloride. No significant amounts of the 4,5-double bond isomers VIII*b* and IX*b* were observed in these crude reaction mixtures based on an analysis of the shape and position of the C*H*=C absorption in the ^{1}H-NMR spectra. Since the thiazolidines decomposed on TLC plates and during column chromatography, analysis of the ^{1}H-NMR spectra of the isomers was the only reliable means of qualitatively determining the extent of the reactions and ratio of isomers. On the other hand, when butyl, hexyl, or decyl cysteine ester hydrochlorides were used instead of the ethyl ester, mixtures of the double bond isomers were isolated, or the 4,5-double bond isomer was the predominant isomer in the mixture (X, XI, and XII, Table I).

The preparation of the 4,5-double bond isomer VIII*b* from the reaction of cysteine ethyl ester with progesterone was accomplished without an acid catalyst necessary for the 4,5 → 5,6 migration by using the free base rather than the hydrochloride of cysteine ethyl ester.

In the second case (IX*b*), the successful synthesis was based on the observation of the iminium ion XVIII (9) as an intermediate in the UV monitored hydrolyses of the 4,5-double bond thiazolidines (4). This suggested that generation of the iminium ion followed by quenching of the reaction with base would result in recyclization of the imine to the thiazolidine, without concomitant reisomerization of the double bond to the 5,6-position. Indeed, when VIII*a* was treated with aqueous acetic acid at 65° for 3.5 min, then with cold aqueous bicarbonate, a mixture of progesterone and IX*b* was obtained from which IX*b* was easily isolated by crystallization from ethanol.

The success of the partial hydrolysis reaction to generate IX*b* was based in part on the observation that the 20-ketone thiazolidine hydrolyzed faster than the 3-ketone thiazolidine. This was not surprising since in addition to suggesting that the thiazolidine of α,β-unsaturated steroidal ketones could not be isolated, a previous report (10) suggested that thiazolidines of 17- and 20-steroidal ketones could not be obtained from the base catalyzed reaction of cysteine with the steroid. Thus, it was expected that both ketones would be difficult to derivatize for progesterone. In addition, the formation of the iminium ion XVIII from the 5,6-double bond isomer VIII*a* obviously could not be instantaneous because the double bond had to isomerize to the 4,5-position. Hence, the reaction time of 3.5 min was not only essential to ensure the complete conversion of VIII*a* to XVIII, but it also allowed more time for the complete hydrolysis of the 20-ketone thiazolidine to take place.

Since the 4′-ethoxycarboxyl group is electron withdrawing, the 4′ unsubstituted thiazolidines were prepared in an attempt to improve the hydrophilicity of the thiazolidines by increasing the pKa of the amine group, thus increasing the concentration of the conjugate acid of the thiazolidine at any pH. Since the rate of hydrolysis of thiazolidines is directly related to the pKa of the amine group (11), a 4′-unsubstituted thiazolidine (*e.g.*, XIII) was expected to be more easily hydrolyzed than the 4′-alkoxycarbonyl thiazolidines (*e.g.*, IX*a*). However, it was also expected that if the 4′-position was left unsubstituted, and an alkyl group was introduced into the 3′-position of the thiazolidine, it would be as soluble as the 4′-unsubstituted thiazolidine, and would also be more stable (11).

The 4′-unsubstituted thiazolidine XIII was prepared from the reaction of progesterone with six equivalents of aminoethanethiol hydrochloride in pyridine. Only the monothiazolidine was obtained even when 12 equivalents of the aminoethanethiol was used. Inspection of the positions of the 18-CH_3 and 19-CH_3 absorptions in the NMR spectra of the crude reaction mixtures showed that XIII was the only product present, even before work-up. The 18-CH_3 absorption shifted from 40 to 38 to 51 Hz in going from progesterone to the 3-mono IX*a* to the 3,20-dithiazolidine VIII*a* while the 19-CH_3 absorption shifted from 71 to 62 Hz in going from progesterone to the mono-3-IX*a* and the di-3,20-thiazolidine VIII*a*. Thus, the position of the 18- and 19-CH_3 absorptions at 38 and 62 Hz and the 20-CH_3 at 127 Hz in the NMR spectrum of XIII indicated only mono-3-thiazolidine formation.

Use of the aminoethanethiol rather than the hydrochloride in the reaction did not result in the preferential formation of the 4,5-double bond isomer. In fact, it was difficult to determine that XIII was the 5,6-double bond isomer. Because of the large number of scans necessary to obtain the ^{13}C-NMR spectra, deuterochloroform samples of XIII decomposed significantly before a satisfactory spectrum could be obtained. The structure of XIII was established from its ^{1}H-NMR spectrum, which showed the broad multiplet expected for 5,6-double bond isomers[4], and from the ^{13}C-NMR spectrum of its *N*-acyl derivative (XV: 141.0, C-5; 121.7, C-6)[3]. Although it is conceivable that XIII was actually the 4,5-double bond isomer which then underwent isomerization upon acylation, none of the 4′-substituted or unsubstituted 4,5-double bond thiazolidine isomers gave any *N*-acylthiazolidine (only hydrolysis products)[3] suggesting that XIII was not the 4,5-double bond isomer. It was also possible that XIII was a mixture of the two isomers and that the 4,5-double bond isomer hydrolyzed and the 5,6-double bond isomer was acylated. This would explain the rather low yields of the *N*-acylthiazolidine from these reactions. However, the ^{1}H-NMR spectrum of XIII is consistent with the presence of only the 5,6-double bond isomer.

The testosterone and testosterone 17β-propionate 4′-unsubstituted thiazolidines were prepared in the same manner as the progesterone analogs. The structures of the testosterone and testosterone propionate derivatives were determined from their ^{1}H-NMR spectra and the ^{13}C-NMR spectra of their *N*-acyl derivatives[3].

Attempts to prepare the *N*-methyl thiazolidines of progesterone and testosterone using the conditions previously used to prepare the other thiazolidines[1,4] were unsuccessful. In addition, although azeotropic distillation using *p*-toluenesulfonic acid in benzene as a catalyst was partially successful, an acid catalyst failed to drive the reaction between the steroid and *N*-methylaminoethanethiol (12) to completion. Furthermore, it was impossible to separate the unreacted starting material from the thiazolidine by crystallization or chromatography since excessive decomposition of the thiazolidine occurred in both cases. Finally, it was discovered that the reaction could be driven to completion by heating a mixture of the steroid with *N*-methylaminoethanethiol (two equivalents) at about 130° for 30 or 40 min. The products could then be conveniently isolated by crystallization. As in the other 4′-unsubstituted case, the only isomer obtained was the 5,6-double bond isomer VII, determined by comparison of its ^{13}C-NMR spectrum (carbon absorptions at δ 140.6 and 122.5) with that of other 5,6-double bond isomers[4]. The ^{1}H-NMR spectrum of the crude reaction product was identical to that of the pure product.

The preparation of the *N*-acyl thiazolidines XIV, XV and XVI *via* direct acylation has been described separately[3]. Thiazolidines III, IV, X, XI, and XII were prepared by substituting the appropriate cysteine ester for cysteine ethyl hydrochloride in the usual reaction conditions.

Although the hydrolysis of thiazolidines in buffers has been carefully studied already (11), their hydrolysis in plasma has not been reported. Table II shows the hydrolysis rates of some selected thiazolidines. The rates were obtained by following the appearance of progesterone so the values are qualitative, especially when considering the dithiazolidines VIII*a*, VIII*b*, and XI, where two separate rates corresponding to the hydrolyses of the 3- and 20- thiazolidines are involved. However, the data does show that the 4,5-double bond isomers release progesterone 2.5 to 3.5 times faster than the 5,6-double bond isomers and the 4′-unsubsti-

Table IV—Excretion of Progesterone and Its Metabolites in Urine after Intravenous Administration of [4-^{14}C]Progesterone [a] and [4-^{14}C]-XI [b] to Dogs

Dog	Drug	μCi			
		0–24 hr	24–48 hr	Total μCi	(% Dose)
1	Progesterone	0.71	0.13	0.84	(34%)
1	XI	0.027	0.036	0.063	(2.5%)
2	Progesterone	0.84	0.015	0.85	(34%)
2	XI	0.033	0.038	0.071	(2.8%)

[a] 2.5 mg of 1 μCi/mg progesterone (2.5 μCi) 100 μl benzyl alcohol; 8×10^{-2} *M* progesterone. [b] 5.6 mg of 0.446 μCi/mg XI (2.5 μCi) in 100 μl benzyl alcohol; 8.14×10^{-2} *M* XI.

Table V—Distribution of [4-^{14}C]Progesterone, XI, and VIII in Rats [a] 1 hr after Intravenous Tail Administration [b]

Compound	Dose, mg/kg	Dosage Equivalents of Progesterone, mg/kg	Organ	% Dose/Organ Mean ± *SE*
Progesterone	0.98	0.98[c]	Liver	16.25 ± 1.33
			Lungs	0.50 ± 0.07
			Blood	2.91 ± 0.39
			Feces	35.15 ± 2.97
XI	2.21	1.01[c]	Liver	14.22 ± 1.13
			Lungs	79.22 ± 4.14
			Blood	3.55 ± 0.51
			Feces	0.24 ± 0.06
VIII*a*	1.96	1.07[c]	Liver	14.39 ± 1.38
			Lungs	60.73 ± 1.12
			Blood	2.07 ± 0.49
			Feces	2.39 ± 0.27
VIII*a*	0.135	0.074[c]	Liver	40.57 ± 1.56
			Lungs	22.15 ± 1.62
			Blood	18.56 ± 2.68
			Feces	16.18 ± 4.5
VIII*a*	0.143	0.078[d]	Liver	34.41 ± 2.14
			Lungs	20.20 ± 1.76
			Blood	5.49 ± 0.56
			Feces	5.69 ± 0.94

[a] $n = 6$. [b] 5 μl benzyl alcohol vehicle. [c] Activity of progesterone 1 μCi/mg. [d] Activity of progesterone 9.47 μCi/mg, $n = 4$.

tuted thiazolidine about 5 times faster than the 4′-ethoxycarbonyl thiazolidine.

The low solubility of the thiazolidines in water was very difficult to determine accurately. An approximate value was obtained by dissolving the thiazolidines in acetonitrile and adding the acetonitrile solution to a pH 7.4 buffer solution until turbidity was produced. The suspension was then filtered through a millipore 0.2-μm filter and the filtrates were decomposed with acid and analyzed by UV for progesterone. No measurable water solubility was observed for the 3,20-dithiazolidines using this technique. The mono-3-thiazolidine XIII was about as soluble as progesterone (5 mg/liter) and the mono-3-thiazolidine IX*b* was about one-third as soluble.

Biology—Preliminary pharmacokinetic studies on the thiazolidines were concerned with determining their bioavailability and their distribution. 4-^{14}C-Labeled VIII*a* and XI were synthesized for this purpose from [4-^{14}C]progesterone. Initially, XI was given intravenously as a benzyl alcohol solution (0.1 ml) to two female beagle dogs in a crossover study. The results are shown in Tables III and IV. Table III shows that the level of [4-^{14}C]steroid found in the dog's blood after administration of progesterone itself was usually at least one order of magnitude higher than that after administration of [4-^{14}C]-XI in the first few minutes after injection. Samples that were taken over several days after injection showed little consistent variation in the level of radiolabeled steroid from either progesterone or XI. Moreover, Table IV shows that the higher blood levels of [4-^{14}C]steroid obtained from progesterone compared to XI resulted in higher levels (about one order of magnitude) of excreted [4-^{14}C]steroid.

Obviously, the pattern of distribution of XI and its parent compound were very much different. Consequently, whole animal distribution studies were run to determine where the labeled steroid was going. Table V shows the distribution results in rats ($n = 6$) from intravenous tail injections of labeled progesterone VIII*a* and XI as benzyl alcohol solutions; benzyl alcohol was used as a vehicle to be consistent with the dog study. Only the data for the four major distribution sites are given in Table V, but the total recovery of labeled material was 66% for progesterone, 75% for VIII*a*, and 100% for XI.

Table VI—Androgenic Test [a]

Compound	Total Dose, mg	Seminal Vesicle Weight, mg	Ventral Prostate Weight, mg
Testosterone	16.0	14.0 ± 2.0	38.5 ± 2.5
	32.0	13.4 ± 1.2[b]	45.7 ± 2.0
	64.0	28.9 ± 3.2	67.1 ± 2.5
VII	4.0	8.2 ± 0.4	39.9 ± 1.9
	8.0	9.9 ± 0.6	45.7 ± 2.5
	16.0	15.8 ± 0.8	50.9 ± 3.4
Vehicle		6.4 ± 0.3	8.3 ± 0.5

[a] The compounds were given orally as a suspension in sesame oil daily for 10 days starting on day of castration using 10 rats/dose. [b] Unusually low value compared to data at same concentration in all other control experiments (17.0 ± 1.7 mg).

The finding of extremely high concentrations in the lung when the thiazolidines were injected is rather surprising. It did not seem to be an artifact and, if real, might have specific importance in site-specific drug delivery. The reason for the high concentration can be related to the fact that it was found that in a number of species (rabbit, rat, hamster); the mixed function oxygenase activity is at least one order of magnitude higher in the lung than in the liver (13). On the other hand, the importance of cysteine residue (14) in some slow reacting substance of anaphylaxis implies its more complex involvement in drug binding (through its —SH function) than originally believed.

None of the progesterone derivatives which were given orally or subcutaneously had even one-tenth the activity of a subcutaneous dose of progesterone in the Clauberg test. Although some of the testosterone thiazolidines had marginal activity in androgenic tests, their dose response curves were not parallel with those of the standard (*e.g.*, the parent steroid), so no estimation of their potency was possible. However, one derivative, VII, the *N*-methylthiazolidine of testosterone, was definitely more active than its parent steroid. The data for VII are presented in Table VI. It is representative of the data for the other thiazolidines in that it shows that the two dose response curves are not parallel.

Compound VIII*a* also was applied topically to hairless mice to see what effect the thiazolidine had on the residence time of the steroid in a biological membrane, as progesterone was found to show activity in controlling acne (15). Thus, a stronger binding pro-progesterone would have longer effect and reduced systemic activity. The results of the comparative percutaneous absorption and distribution of labeled steroid from doses of VIII*a* and progesterone are shown in Table VII. Those results show a remarkable tendency of the thiazolidine VIII*a* to increase the relative amount of labeled steroid in the skin. Whether this tendency is due to the greater lipophilicity of the thiazolidines or to the possible formation of disulfide bonds from the interaction of the ring-opened

Table VII—Dermal Delivery of Progesterone and VIII*a*

	Progesterone[a], % Dose Mean ± *SE*[c]	VIII*a*[b], % Dose Mean ± *SE*
Feces	16.65 ± 1.75	0.95 ± 0.13
Urine	7.00 ± 1.14	0.40 ± 0.09
Skin circle[d]	1.98 ± 0.10	4.52 ± 1.18
Intestine/fat	2.28 ± 0.47	0.09 ± 0.00
Liver	0.75 ± 0.06	0.08 ± 0.01
Blood	0.08 ± 0.02	0.28 ± 0.04
Kidney/spleen	0.06 ± 0.01	0.03 ± 0.01
Lung	0.04 ± 0.02	0.01 ± 0.00
Subtotal	28.74	6.36
Patch[e]	54.06 ± 1.6	83.46 ± 1.4
Total	82.80	89.82

[a] 75 μl of a solution of 0.9 mg in 675 μl in ethanol–isopropylmyristate (90:10). [b] 75 μl of a solution of 1.85 mg in 675 μl ethanol–isopropylmyristate (90:10). [c] $n = 6$. [d] 2-cm diameter plug of epidermis taken directly under the bandage patch (3 cm^2). [e] Includes the contents of an ethanolic wash of the skin circle after the bandage patch was removed.

thiazolidine with thiol groups in the skin cannot be determined at this time.

Thus, a series of thiazolidine derivatives of progesterone and testosterone were prepared and characterized. Except for VII the thiazolidines were found to be inactive or less active than their parent steroids in animal models. This lack of activity can be explained by the rapid distribution of the thiazolidines out of blood followed by a slow release of the parent, such that the biological concentration of steroid is always too low to be biologically effective.

REFERENCES

(1) R. Deghenghi and A. J. Manson, in "Medicinal Chemistry," 3rd ed., Wiley, New York, N.Y. 1970.

(2) E. C. Horning, J. P. Thenot, and E. D. Helton, *J. Toxicol. Environ. Health*, **4**, 341 (1978).

(3) P. R. Ortiz de Monellano, K. L. Kunze, G. S. Yost, and B. A. Milo, *Proc. Natl. Acad. Sci. USA*, **76**, 746 (1979).

(4) N. Bodor and K. B. Sloan, U.S. pat, 4,069,322 (Jan. 17, 1978) and 4,239,757 (Dec. 16, 1980).

(5) N. Bodor, J. J. Kaminski, and S. H. Selk, *J. Med. Chem.*, **23**, 469 (1980).

(6) W. M. Schubert and Y. Motoyana, *J. Am. Chem. Soc.*, **87**, 5507 (1965).

(7) R. T. Williams, "Detoxication Mechanisms," Chapman and Hall, London, England, 1959, p. 128.

(8) M. Voullie, M. Laurre, G. Maillard, P. Muller, and R. Zasui, French pat. 1,241,102; through *Chem. Abstr.*, **57**, 15235 (1962).

(9) J. L. Johnson, M. E. Herr, J. C. Babcock, A. E. Fonken, J. E. Stafford, and F. W. Heyl, *J. Am. Chem. Soc.*, **78**, 430 (1956).

(10) S. Lieberman, P. Brazeau, and L. Hariton, *ibid.*, **70**, 3094 (1948).

(11) R. Luhowy and F. Meneghini, *ibid.*, **101**, 420 (1979).

(12) E. D. Bergmann and A. Kaluszyner, *Recueil*, **78**, 289 (1959).

(13) G. E. R. Hook and J. R. Bend, *Life Sci.*, **18**, 279 (1976).

(14) R. C. Murphy, S. Hammarstrom, and B. Samuelsson, *Proc. Natl. Acad. Sci. USA*, **76**, 4276 (1979).

(15) J. Girard, A. Barbier, and C. Lafille, *Arch. Dermatol. Res.*, **269**, 281 (1980).

ACKNOWLEDGMENTS

Supported by National Institutes of Health Grant N01-HD-7-2833.

The authors thank Dr. Henry Gabelnick of the Center for Population Research, National Institutes of Health for many helpful discussions. They also acknowledge the synthetic contributions of Dr. Norman Kuo, Dr. Stefano Pogany, Dr. Jose Alexander, Roy J. Little, and Ken Knutson; the analytical assistance of Dr. Richard Shaffer and Janet Smith; and the biological testing performed by Sally H. Selk.

High-Performance Liquid Chromatographic Assay for Bumetanide in Plasma and Urine

DAVID E. SMITH

Received May 26, 1981, from the *University of Michigan, College of Pharmacy, Ann Arbor, MI 48109.* Accepted for publication August 20, 1981.

Abstract □ A new high-performance liquid chromatographic (HPLC) method was developed for the analysis of bumetanide in plasma and urine. A reversed-phase column was fitted to the instrument and fluorescent (excitation λ = 338 nm, emission λ = 433 nm) and UV (254 nm) detectors were utilized to monitor simultaneously bumetanide and the internal standard, acetophenone, respectively. The assay is rapid, sensitive, and specific. Plasma bumetanide concentrations can be detected as low as 5 ng/ml using a 0.20-ml sample. Time-consuming extraction and/or derivatization steps are not required. The only clean-up procedure involved is the precipitation of plasma proteins with acetonitrile.

Keyphrases □ Bumetanide—high-performance liquid chromatographic determination in plasma and urine □ High-performance liquid chromatography—determination of bumetanide in plasma and urine □ Diuretics—bumetanide, determination in plasma and urine by high-performance liquid chromatography

Bumetanide (3-*n*-butylamino-4-phenoxy-5-sulfamoylbenzoic acid) is a new, high-ceiling diuretic with a pharmacological action similar to furosemide (1–4). However, on a molecular weight basis, bumetanide is 40–60 times more potent (1–4). Studies describing the pharmacokinetics and disposition of bumetanide have been sparse due to the lack of a sensitive and specific assay method. Fluorimetric (1), GLC (5), radioactive (6, 7), radioimmune (8), and high-performance liquid chromatographic (HPLC) (9) assays currently are available for the determination of bumetanide in biological fluids. However, all of these methods have inherent disadvantages, including time-consuming extraction, derivatization, or incubation steps (1, 5–9), large sample requirements (1, 5–7, 9), poor sensitivity (1, 5), or lack of specificity (1, 8).

Therefore, a rapid, sensitive, and specific HPLC assay was developed, without requiring prior extraction and/or derivatization, for the measurement of bumetanide in plasma and urine. The analytical method is suitable for bioavailability and pharmacokinetic studies in dogs and human subjects.

EXPERIMENTAL

Chemicals—Bumetanide[1], acetophenone[2], acetic acid[3], and phosphoric acid[4] were used as received. The methanol[3], acetonitrile[5] (glass-distilled), and deionized water[6] were filtered and degassed prior to use.

Standard Solutions—Bumetanide (4.12 mg) was dissolved in 50% acetonitrile–distilled water to yield a stock solution of 41.2 μg/ml. This stock solution was diluted 20- (2.06 μg/ml) and 100-fold (0.412 μg/ml) to give the working standard solutions for urine and plasma, respectively. Acetophenone was diluted in 50% acetonitrile–distilled water to yield a 0.50 mg/ml stock solution for urine and a 0.25 mg/ml stock solution for plasma.

Instrumentation—Samples were analyzed using a high-performance liquid chromatograph[7] equipped with a U6-K universal injector[8], a flu-

[1] Hoffmann-La Roche, Nutley, N.J.
[2] Sigma Chemical Co., St. Louis, Mo.
[3] Baker Analyzed Reagent, J. T. Baker Chemical Co., Phillipsburg, N.J.
[4] Certified ACS, Fisher Scientific Co., Fair Lawn, N.J.
[5] MCB Manufacturing Chemists, Cincinnati, Ohio.
[6] Milli-Q Reagent-Grade Water System, Millipore Corp., Bedford, Mass.
[7] Model 6000A, Waters Associates, Milford, Mass.
[8] Model U6-K, Waters Associates, Milford, Mass.

0022-3549/82/0500-0520$01.00/0

thiazolidine with thiol groups in the skin cannot be determined at this time.

Thus, a series of thiazolidine derivatives of progesterone and testosterone were prepared and characterized. Except for VII the thiazolidines were found to be inactive or less active than their parent steroids in animal models. This lack of activity can be explained by the rapid distribution of the thiazolidines out of blood followed by a slow release of the parent, such that the biological concentration of steroid is always too low to be biologically effective.

REFERENCES

(1) R. Deghenghi and A. J. Manson, in "Medicinal Chemistry," 3rd ed., Wiley, New York, N.Y. 1970.

(2) E. C. Horning, J. P. Thenot, and E. D. Helton, *J. Toxicol. Environ. Health*, **4**, 341 (1978).

(3) P. R. Ortiz de Monellano, K. L. Kunze, G. S. Yost, and B. A. Milo, *Proc. Natl. Acad. Sci. USA*, **76**, 746 (1979).

(4) N. Bodor and K. B. Sloan, U.S. pat, 4,069,322 (Jan. 17, 1978) and 4,239,757 (Dec. 16, 1980).

(5) N. Bodor, J. J. Kaminski, and S. H. Selk, *J. Med. Chem.*, **23**, 469 (1980).

(6) W. M. Schubert and Y. Motoyana, *J. Am. Chem. Soc.*, **87**, 5507 (1965).

(7) R. T. Williams, "Detoxication Mechanisms," Chapman and Hall, London, England, 1959, p. 128.

(8) M. Voullie, M. Laurre, G. Maillard, P. Muller, and R. Zasui, French pat. 1,241,102; through *Chem. Abstr.*, **57**, 15235 (1962).

(9) J. L. Johnson, M. E. Herr, J. C. Babcock, A. E. Fonken, J. E. Stafford, and F. W. Heyl, *J. Am. Chem. Soc.*, **78**, 430 (1956).

(10) S. Lieberman, P. Brazeau, and L. Hariton, *ibid.*, **70**, 3094 (1948).

(11) R. Luhowy and F. Meneghini, *ibid.*, **101**, 420 (1979).

(12) E. D. Bergmann and A. Kaluszyner, *Recueil*, **78**, 289 (1959).

(13) G. E. R. Hook and J. R. Bend, *Life Sci.*, **18**, 279 (1976).

(14) R. C. Murphy, S. Hammarstrom, and B. Samuelsson, *Proc. Natl. Acad. Sci. USA*, **76**, 4276 (1979).

(15) J. Girard, A. Barbier, and C. Lafille, *Arch. Dermatol. Res.*, **269**, 281 (1980).

ACKNOWLEDGMENTS

Supported by National Institutes of Health Grant N01-HD-7-2833.

The authors thank Dr. Henry Gabelnick of the Center for Population Research, National Institutes of Health for many helpful discussions. They also acknowledge the synthetic contributions of Dr. Norman Kuo, Dr. Stefano Pogany, Dr. Jose Alexander, Roy J. Little, and Ken Knutson; the analytical assistance of Dr. Richard Shaffer and Janet Smith; and the biological testing performed by Sally H. Selk.

High-Performance Liquid Chromatographic Assay for Bumetanide in Plasma and Urine

DAVID E. SMITH

Received May 26, 1981, from the *University of Michigan, College of Pharmacy, Ann Arbor, MI 48109.* Accepted for publication August 20, 1981.

Abstract □ A new high-performance liquid chromatographic (HPLC) method was developed for the analysis of bumetanide in plasma and urine. A reversed-phase column was fitted to the instrument and fluorescent (excitation λ = 338 nm, emission λ = 433 nm) and UV (254 nm) detectors were utilized to monitor simultaneously bumetanide and the internal standard, acetophenone, respectively. The assay is rapid, sensitive, and specific. Plasma bumetanide concentrations can be detected as low as 5 ng/ml using a 0.20-ml sample. Time-consuming extraction and/or derivatization steps are not required. The only clean-up procedure involved is the precipitation of plasma proteins with acetonitrile.

Keyphrases □ Bumetanide—high-performance liquid chromatographic determination in plasma and urine □ High-performance liquid chromatography—determination of bumetanide in plasma and urine □ Diuretics—bumetanide, determination in plasma and urine by high-performance liquid chromatography

Bumetanide (3-*n*-butylamino-4-phenoxy-5-sulfamoylbenzoic acid) is a new, high-ceiling diuretic with a pharmacological action similar to furosemide (1–4). However, on a molecular weight basis, bumetanide is 40–60 times more potent (1–4). Studies describing the pharmacokinetics and disposition of bumetanide have been sparse due to the lack of a sensitive and specific assay method. Fluorimetric (1), GLC (5), radioactive (6, 7), radioimmune (8), and high-performance liquid chromatographic (HPLC) (9) assays currently are available for the determination of bumetanide in biological fluids. However, all of these methods have inherent disadvantages, including time-consuming extraction, derivatization, or incubation steps (1, 5–9), large sample requirements (1, 5–7, 9), poor sensitivity (1, 5), or lack of specificity (1, 8).

Therefore, a rapid, sensitive, and specific HPLC assay was developed, without requiring prior extraction and/or derivatization, for the measurement of bumetanide in plasma and urine. The analytical method is suitable for bioavailability and pharmacokinetic studies in dogs and human subjects.

EXPERIMENTAL

Chemicals—Bumetanide[1], acetophenone[2], acetic acid[3], and phosphoric acid[4] were used as received. The methanol[3], acetonitrile[5] (glass-distilled), and deionized water[6] were filtered and degassed prior to use.

Standard Solutions—Bumetanide (4.12 mg) was dissolved in 50% acetonitrile–distilled water to yield a stock solution of 41.2 μg/ml. This stock solution was diluted 20- (2.06 μg/ml) and 100-fold (0.412 μg/ml) to give the working standard solutions for urine and plasma, respectively. Acetophenone was diluted in 50% acetonitrile–distilled water to yield a 0.50 mg/ml stock solution for urine and a 0.25 mg/ml stock solution for plasma.

Instrumentation—Samples were analyzed using a high-performance liquid chromatograph[7] equipped with a U6-K universal injector[8], a flu-

[1] Hoffmann-La Roche, Nutley, N.J.
[2] Sigma Chemical Co., St. Louis, Mo.
[3] Baker Analyzed Reagent, J. T. Baker Chemical Co., Phillipsburg, N.J.
[4] Certified ACS, Fisher Scientific Co., Fair Lawn, N.J.
[5] MCB Manufacturing Chemists, Cincinnati, Ohio.
[6] Milli-Q Reagent-Grade Water System, Millipore Corp., Bedford, Mass.
[7] Model 6000A, Waters Associates, Milford, Mass.
[8] Model U6-K, Waters Associates, Milford, Mass.

0022-3549/82/0500-0520$01.00/0

Table I—Interday Variability of Slopes and Intercepts Derived from the Standard Curves of Bumetanide

Curve No.	Slope	Y-Intercept	r^2
	In Plasma[a]		
1	0.0235	0.0075	0.9998
2	0.0251	0.0237	0.9997
3	0.0249	0.0130	0.9997
4	0.0232	0.0082	0.9999
5	0.0234	0.0142	0.9997
Mean	0.0240	0.0133	0.9998
SD	0.0009	0.0065	0.0001
	In Urine[b]		
1	1.674	0.014	0.9997
2	1.804	0.022	0.9997
3	1.829	0.018	0.9993
4	1.626	0.011	0.9998
5	1.700	0.011	0.9999
Mean	1.727	0.015	0.9997
SD	0.087	0.005	0.0002

[a] Standard curves were constructed on five different days over a 12-day period. [b] 11-day period.

orescence spectrophotometer[9], and a variable wavelength UV absorbance detector[10]. A reversed-phase column[11] (25 cm × 4.6-mm i.d.) was fitted to the instrument and a dual-pen recorder[12] was used at a chart speed of 20 cm/hr. Fluorescent (excitation λ = 338 nm, emission λ = 433 nm) and UV (254 nm) detection were used to monitor simultaneously bumetanide and the internal standard, respectively.

Plasma Assay of Bumetanide—Bumetanide stock solution (0.412 μg/ml) was added in volumes of 0, 2.5, 5, 15, 30, 50, 75, and 100 μl to 0.20 ml of blank plasma to provide calibration standards of 0 (no bumetanide added), 5.2, 10.3, 30.9, 61.8, 103, 154, and 206 ng/ml. A 50-μl aliquot of the internal standard (0.25 mg/ml) was added to the mixture which was then shaken on a vortex mixer[13]. Precipitation of plasma proteins was accomplished by addition of 0.40 ml of acetonitrile. The mixture was shaken again on a vortex mixer and then sonicated[14] for ~2 min. After 10 min of centrifugation[15] (0.75 speed), the supernate was transferred to a clean test tube. An appropriate aliquot was then injected directly into the loop injector. Plasma samples were prepared in an identical manner except for the addition of bumetanide stock solution.

The mobile phase consisted of methanol–water–acetic acid (70:30:1), pumped isocratically at a flow rate of 1.5 ml/min, at ambient temperature.

Urine Assay of Bumetanide—Bumetanide stock solution (2.06 μg/ml) was added in volumes of 0, 2, 5, 15, 30, 50, 75, and 100 μl to 0.10 ml of blank urine and 0.10 ml distilled water to provide calibration standards of 0 (no bumetanide added), 0.0412, 0.103, 0.309, 0.618, 1.03, 1.54, and 2.06 μg/ml. A 50-μl aliquot of the internal standard (0.50 mg/ml)

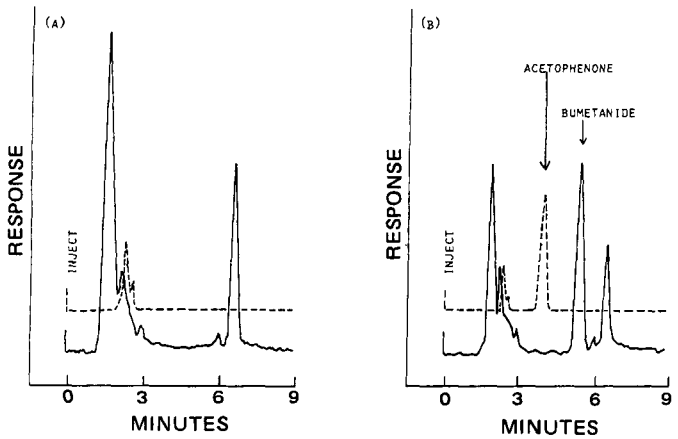

Figure 1—*Chromatograms for blank plasma (A) and for plasma spiked with bumetanide and the internal standard, acetophenone (B). Detection: fluorescence (——); UV (- - -).*

[9] Model 650-10S, Perkin-Elmer, Mountainview, Calif.
[10] Model 450, Waters Associates, Milford, Mass.
[11] Partisil-10 ODS-3, Anspec Co., Ann Arbor, Mich.
[12] Model 585, Linear, Irvine, Calif.
[13] Thermolyne Maxi-mix, VWR Scientific, Detroit, Mich.
[14] Bransonic Model 12, VWR Scientific, Detroit, Mich.
[15] Model HN-SII, VWR Scientific, Detroit, Mich.

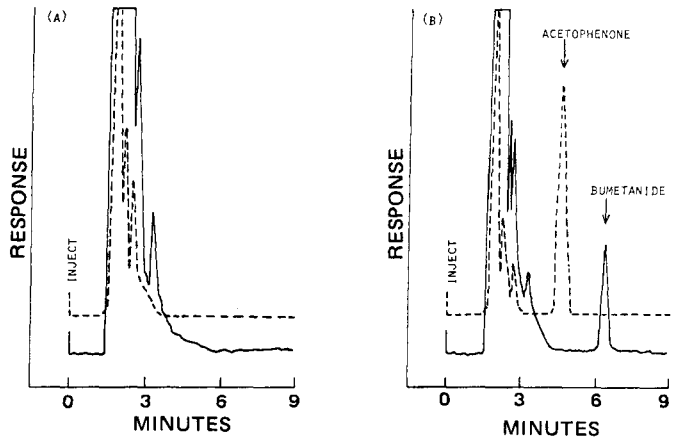

Figure 2—*Chromatograms for blank urine (A) and for urine spiked with bumetanide and the internal standard, acetophenone (B). Detection: fluorescence (——); UV (- - -).*

was added to the mixture which was then shaken on a vortex mixer. An appropriate volume was injected directly into the loop injector. Urine samples were prepared in an identical manner except for the addition of bumetanide stock solution.

The mobile phase consisted of 50% acetonitrile in 0.015 *M* phosphoric acid aqueous solution, pumped isocratically at a flow rate of 2.0 ml/min, at ambient temperature.

RESULTS AND DISCUSSION

Figure 1 shows a typical chromatogram for the analysis of bumetanide in plasma. Using the appropriate mobile phase, as described previously, the retention times for bumetanide and acetophenone were 5.5 and 4.0 min, respectively. A representative standard curve of the bumetanide–acetophenone peak height ratio over the bumetanide plasma concentration range 5.2–206 ng/ml resulted in the following linear least-squares regression equation: $Y = 0.0235X + 0.0075$; $r^2 = 0.9998$. With fluorescence detection, concentrations as low as 5 ng/ml were measured for bumetanide (peak to noise ratio ≥5) using 0.20-ml plasma samples.

Figure 2 shows a typical chromatogram for the analysis of bumetanide in urine. A different mobile phase than that used for the plasma assay was necessary for the analysis of bumetanide in urine, due to the presence

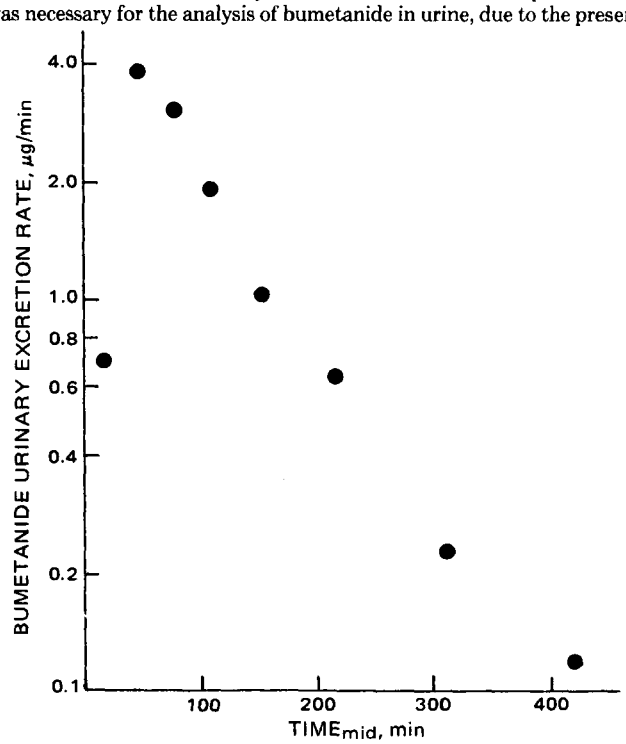

Figure 3—*Urinary excretion rate* versus *midpoint time plot of unchanged bumetanide after oral administration of 1.0 mg of bumetanide to a healthy volunteer.*

Table II—Intraday and Interday Variability of Bumetanide Concentration in Plasma Samples

Intraday[a]				Interday[b]			
Added, ng/ml		Measured, ng/ml	% Bias[c]	Added, ng/ml		Measured, ng/ml	% Bias[c]
5.2	Mean:	4.8	−7.7	5.2	Mean:	4.8	−7.7
	SD:	0.1			*SD*:	0.2	
	CV, %:	2.1			*CV*, %:	4.2	
61.8	Mean:	62.9	1.8	61.8	Mean:	62.2	0.6
	SD:	1.4			*SD*:	1.6	
	CV, %:	2.2			*CV*, %:	2.6	
154.0	Mean:	152.0	−1.3	154.0	Mean:	153.0	−0.6
	SD:	2.6			*SD*:	3.0	
	CV, %:	1.7			*CV*, %:	1.9	

[a] Mean values represent five different plasma samples. [b] Mean values represent plasma samples analyzed on 5 different days over a 12-day period. [c] % Bias = 100 × (measured concentration − added concentration)/added concentration.

Table III—Intraday and Interday Variability of Bumetanide Concentration in Urine Samples

Intraday[a]				Interday[b]			
Added, ng/ml		Measured, ng/ml	% Bias[c]	Added, ng/ml		Measured, ng/ml	% Bias[c]
41.2	Mean:	39.6	−3.9	41.2	Mean:	40.5	−1.7
	SD:	1.5			*SD*:	2.1	
	CV, %:	3.8			*CV*, %:	5.2	
618.0	Mean:	626.0	1.3	618.0	Mean:	632.0	2.3
	SD:	15.8			*SD*:	10.0	
	CV, %:	2.5			*CV*, %:	1.6	
1540.0	Mean:	1510.0	−1.9	1540.0	Mean:	1530.0	−0.6
	SD:	7.1			*SD*:	33.6	
	CV, %:	0.5			*CV*, %:	2.2	

[a] Mean values represent five different urine samples. [b] Mean values represent urine samples analyzed on 5 different days over an 11-day period. [c] % Bias = 100 × (measured concentration − added concentration)/added concentration.

Table IV—Recovery of Bumetanide from Plasma

Concentration, ng/ml	Peak Height Ratio, Plasma *versus* Water, %	
5.2		97.1
		96.6
		95.1
		93.0
		101.0
	Mean	96.6
	SD	3.0
61.8		
		96.4
		102.0
		95.8
		100.0
		97.3
	Mean	98.3
	SD	2.6
154		
		100.0
		99.3
		102.0
		101.0
		99.4
	Mean	100.0
	SD	1.0

of endogenous interference peaks. With the appropriate solvent system, as described previously, bumetanide and acetophenone had retention times in urine of 6.5 and 4.5 min, respectively. A representative standard curve of bumetanide–acetophenone peak height ratio over the bumetanide urine concentration range 0.0412–2.06 μg/ml resulted in the following linear least-squares regression equation: $Y = 1.674X + 0.014$; $r^2 = 0.9997$.

Both the plasma and urine assays were specific with respect to possible metabolite interference. Several metabolites of bumetanide (2′-alcohol, 3′-alcohol, 4′-alcohol, and 3′-acid), which have been reported recently in healthy volunteers (6), were obtained[1] and found to elute in the void volume prior to the elution of the compounds of interest (bumetanide and acetophenone). The desbutyl derivative was not available but should also elute in the void volume.

Standard curves of bumetanide in plasma (5.2–206 ng/ml) were constructed on 5 different days to determine the variability of the slopes and intercepts (Table I). The results show little day-to-day variability of slope and intercept as well as good linearity ($r^2 > 0.999$) over the plasma concentration range studied. The coefficient of variation for the slope was 3.8%. Standard curves of bumetanide in urine (0.0412–2.06 μg/ml) were also constructed (Table I). The coefficient of variation for the slope was 5.0% and all five curves showed good linearity ($r^2 > 0.999$) over the urine concentration range studied.

Table II shows the intra- and interday precision and accuracy for the plasma assay of bumetanide, assessed at three concentrations. The precision of the assay, as determined by the coefficient of variation, was ≤4.2% intraday as well as interday. In addition, the assay was quite accurate even at plasma concentrations as low as 5.2 ng/ml (bias = 7.7%). Other plasma concentrations had a bias ≤1.8%. A similar comparison was made for the urine assay of bumetanide as shown in Table III. The method was found to be precise (CV ≤5.2%) and accurate (bias ≤3.9%) intraday as well as interday.

The recovery of bumetanide from plasma proteins was assessed by comparing the bumetanide–acetophenone peak height ratio in plasma samples *versus* samples prepared in water. Five comparisons at three different concentrations were made. As shown in Table IV, the recovery of bumetanide from plasma was essentially complete at all concentrations.

Stability studies of plasma spiked with bumetanide (12.0, 50.0, and

Table V—Stability of Bumetanide in Plasma

Added Concentration, ng/ml	Measured Concentration/Added Concentration, % Days					
	0	1	3	8	21	31
12.0	96.7	100.0	—	104.0	108.0	97.5
50.0	104.0	98.4	97.6	99.6	96.2	95.0
140.0	102.0	99.3	97.1	99.3	100.0	101.0

140 ng/ml) were performed over a 31-day period (Table V). Plasma samples were stored in the freezer at −20° until the time of analysis. The results demonstrate that bumetanide can be stored frozen in plasma for at least 1 month without degradation.

Figure 3 shows a urinary excretion rate *versus* midpoint time plot of unchanged bumetanide after oral administration of 1.0 mg of bumetanide to a healthy volunteer. The biological half-life, as determined by linear regression using the last four data points from the log-linear terminal portion of the curve, was 84.5 min. The fraction of the oral dose excreted unchanged in the urine was 0.445. Both of these parameters are in agreement with values from other studies (5, 6–8, 10).

REFERENCES

(1) E. H. Østergaard, M. P. Magnussen, C. K. Nielsen, E. Eilertsen, and H.-H. Frey, *Arzneim.-Forsch.*, **22**, 66 (1972).

(2) M. J. Asbury, P. B. B. Gatenby, S. O'Sullivan, and E. Bourke, *Br. Med. J.*, **1**, 211 (1972).

(3) K. H. Olesen, B. Sigurd, E. Steiness, and A. Leth, *Acta Med. Scand.*, **193**, 119 (1973).

(4) D. L. Davies, A. F. Lant, N. R. Millard, A. J. Smith, J. W. Ward, and G. M. Wilson, *Clin. Pharmacol. Ther.*, **15**, 141 (1974).

(5) P. W. Feit, K. Roholt, and H. Sørensen, *J. Pharm. Sci.*, **62**, 375 (1973).

(6) S. C. Halladay, I. G. Sipes, and D. E. Carter, *Clin. Pharmacol. Ther.*, **22**, 179 (1977).

(7) P. J. Pentikäinen, P. J. Neuvonen, M. Kekki, and A. Penttilä, *J. Pharmacokinet. Biopharm.*, **8**, 219 (1980).

(8) W. R. Dixon, R. L. Young, A. Holazo, M. L. Jack, R. E. Weinfeld, K. Alexander, A. Liebman, and S. A. Kaplan, *J. Pharm. Sci.*, **65**, 701 (1976).

(9) L. A. Marcantonio and W. H. R. Auld, *J. Chromatogr.*, **183**, 118 (1980).

(10) P. J. Pentikäinen, A. Penttilä, P. J. Neuvonen, and G. Gothoni, *Br. J. Clin. Pharmacol.*, **4**, 39 (1977).

ACKNOWLEDGMENTS

The author thanks Hoffmann–La Roche, for graciously supplying bumetanide as well as the drug's reported metabolites.

Application of the Ammonia Gas-Sensing Electrode: Determination of Drugs Having a Carboxyamide Group by Decomposition with Acid

SHOICHIRO TAGAMI ˣ and MASAKO FUJITA

Received June 8, 1981, from the *Toyama Medical and Pharmaceutical University, Sugitani, Toyama, Japan.* Accepted for publication August 19, 1981.

Abstract □ A simple potentiometric method for the determination of drugs having a carboxyamide group is described. Ethenzamide, niacinamide, pyrazinamide, or salicylamide was refluxed with 20% HCl and the carboxyamide was hydrolyzed. The ammonia evolved at a pH >11 and was determined without separation from the decomposition solution using an ammonia gas-sensing electrode. A linear calibration plot was obtained with drugs in the range of 2×10^{-5}–1×10^{-2} *M*. This method was applied to the analysis of injection and powder-containing auxiliary compounds.

Keyphrases □ Ammonia gas-sensing electrode—analysis of drugs with a carboxyamide group by decomposition with acid □ Potentiometry—determination of ammonia using an ammonia gas-sensing electrode □ Carboxyamide groups—determination of carboxyamide moiety using ammonia gas-sensing electrode analysis

Methods for the determination of drugs having a carboxyamide group are based on the determination of ammonia liberated by refluxing the carboxyamide compounds in alkaline solution. The ammonia is distilled and determined by titration. The methods described in the United States (1), British (2), and Japanese (3) Pharmacopoeias are based on these principles. Spectrophotometric methods of analysis for the determination of carboxyamide having a pyridine ring are based on the König reaction (4) of pyridine derivatives with cyanogen bromide. These methods are sensitive and relatively free from interference; however, they have the disadvantage of using the extremely toxic cyanogen bromide. Polarographic and microbiological methods (5) have also been employed, but they are tedious and time consuming. The gas-permeable membrane electrode is advantageous because of its simplicity, accuracy of assay, and lower cost compared with the conventional methods. However, its applications to drug analysis have not been widely reported in the literature, although the analysis of *N*-unsubstituted carbamates and meprobamate has been studied (6).

This paper describes a potentiometric method for the determination of drugs having a carboxyamide group. Assay methods for ethenzamide (o-ethoxybenzamide), salicylamide, niacin (nicotinamide), and pyrazinamide were developed. The samples were refluxed with 20% HCl and the carboxyamide was hydrolyzed, liberating an equivalent amount of ammonium ion. After alkalinization, the ammonia was determined with an ammonia gas-sensing electrode.

EXPERIMENTAL

Apparatus—The ammonia gas-sensing electrode[1] consisted of an ammonia gas-permeable membrane, a pH glass-electrode, and a silver–silver chloride reference electrode. The potential measurement system consisted of a pH/mV meter[2] and recorder[3].

All measurements were carried out at 20° in an 80-ml cell equipped with a magnetic stirrer.

Reagents—Ethenzamide[4], salicylamide[4], and pyrazinamide[4] were purified twice by recrystallization from water and then dried *in vacuo* at room temperature for 5 hr. Niacinamide[5] was dried *in vacuo* at room temperature for 4 hr. Other chemicals used were reagent grade.

A stock solution of 0.1 *M* NH_4Cl was prepared for testing the ammonia response of the electrode, and 5 *M* NaOH was employed to adjust the pH of the solution to within the operating range of the electrode.

[1] Model 5002-05 T, Horiba, Co., Kyoto, Japan.
[2] Model F-7ss, Hitachi-Horiba Instruments, Horiba Co., Kyoto, Japan.
[3] Model EPR-22A, Toa-Denpa Co., Tokyo, Japan.
[4] Tokyo Kasei Co., Tokyo, Japan.
[5] Japanese Pharmacopoeia Reference Standard.

0022-3549/82/0500-0523$01.00/0

140 ng/ml) were performed over a 31-day period (Table V). Plasma samples were stored in the freezer at −20° until the time of analysis. The results demonstrate that bumetanide can be stored frozen in plasma for at least 1 month without degradation.

Figure 3 shows a urinary excretion rate *versus* midpoint time plot of unchanged bumetanide after oral administration of 1.0 mg of bumetanide to a healthy volunteer. The biological half-life, as determined by linear regression using the last four data points from the log-linear terminal portion of the curve, was 84.5 min. The fraction of the oral dose excreted unchanged in the urine was 0.445. Both of these parameters are in agreement with values from other studies (5, 6–8, 10).

REFERENCES

(1) E. H. Østergaard, M. P. Magnussen, C. K. Nielsen, E. Eilertsen, and H.-H. Frey, *Arzneim.-Forsch.*, **22**, 66 (1972).

(2) M. J. Asbury, P. B. B. Gatenby, S. O'Sullivan, and E. Bourke, *Br. Med. J.*, **1**, 211 (1972).

(3) K. H. Olesen, B. Sigurd, E. Steiness, and A. Leth, *Acta Med. Scand.*, **193**, 119 (1973).

(4) D. L. Davies, A. F. Lant, N. R. Millard, A. J. Smith, J. W. Ward, and G. M. Wilson, *Clin. Pharmacol. Ther.*, **15**, 141 (1974).

(5) P. W. Feit, K. Roholt, and H. Sørensen, *J. Pharm. Sci.*, **62**, 375 (1973).

(6) S. C. Halladay, I. G. Sipes, and D. E. Carter, *Clin. Pharmacol. Ther.*, **22**, 179 (1977).

(7) P. J. Pentikäinen, P. J. Neuvonen, M. Kekki, and A. Penttilä, *J. Pharmacokinet. Biopharm.*, **8**, 219 (1980).

(8) W. R. Dixon, R. L. Young, A. Holazo, M. L. Jack, R. E. Weinfeld, K. Alexander, A. Liebman, and S. A. Kaplan, *J. Pharm. Sci.*, **65**, 701 (1976).

(9) L. A. Marcantonio and W. H. R. Auld, *J. Chromatogr.*, **183**, 118 (1980).

(10) P. J. Pentikäinen, A. Penttilä, P. J. Neuvonen, and G. Gothoni, *Br. J. Clin. Pharmacol.*, **4**, 39 (1977).

ACKNOWLEDGMENTS

The author thanks Hoffmann–La Roche, for graciously supplying bumetanide as well as the drug's reported metabolites.

Application of the Ammonia Gas-Sensing Electrode: Determination of Drugs Having a Carboxyamide Group by Decomposition with Acid

SHOICHIRO TAGAMI ˣ and MASAKO FUJITA

Received June 8, 1981, from the *Toyama Medical and Pharmaceutical University, Sugitani, Toyama, Japan.* Accepted for publication August 19, 1981.

Abstract □ A simple potentiometric method for the determination of drugs having a carboxyamide group is described. Ethenzamide, niacinamide, pyrazinamide, or salicylamide was refluxed with 20% HCl and the carboxyamide was hydrolyzed. The ammonia evolved at a pH >11 and was determined without separation from the decomposition solution using an ammonia gas-sensing electrode. A linear calibration plot was obtained with drugs in the range of 2×10^{-5}–1×10^{-2} *M*. This method was applied to the analysis of injection and powder-containing auxiliary compounds.

Keyphrases □ Ammonia gas-sensing electrode—analysis of drugs with a carboxyamide group by decomposition with acid □ Potentiometry—determination of ammonia using an ammonia gas-sensing electrode □ Carboxyamide groups—determination of carboxyamide moiety using ammonia gas-sensing electrode analysis

Methods for the determination of drugs having a carboxyamide group are based on the determination of ammonia liberated by refluxing the carboxyamide compounds in alkaline solution. The ammonia is distilled and determined by titration. The methods described in the United States (1), British (2), and Japanese (3) Pharmacopoeias are based on these principles. Spectrophotometric methods of analysis for the determination of carboxyamide having a pyridine ring are based on the König reaction (4) of pyridine derivatives with cyanogen bromide. These methods are sensitive and relatively free from interference; however, they have the disadvantage of using the extremely toxic cyanogen bromide. Polarographic and microbiological methods (5) have also been employed, but they are tedious and time consuming. The gas-permeable membrane electrode is advantageous because of its simplicity, accuracy of assay, and lower cost compared with the conventional methods. However, its applications to drug analysis have not been widely reported in the literature, although the analysis of *N*-unsubstituted carbamates and meprobamate has been studied (6).

This paper describes a potentiometric method for the determination of drugs having a carboxyamide group. Assay methods for ethenzamide (o-ethoxybenzamide), salicylamide, niacin (nicotinamide), and pyrazinamide were developed. The samples were refluxed with 20% HCl and the carboxyamide was hydrolyzed, liberating an equivalent amount of ammonium ion. After alkalinization, the ammonia was determined with an ammonia gas-sensing electrode.

EXPERIMENTAL

Apparatus—The ammonia gas-sensing electrode[1] consisted of an ammonia gas-permeable membrane, a pH glass-electrode, and a silver–silver chloride reference electrode. The potential measurement system consisted of a pH/mV meter[2] and recorder[3].

All measurements were carried out at 20° in an 80-ml cell equipped with a magnetic stirrer.

Reagents—Ethenzamide[4], salicylamide[4], and pyrazinamide[4] were purified twice by recrystallization from water and then dried *in vacuo* at room temperature for 5 hr. Niacinamide[5] was dried *in vacuo* at room temperature for 4 hr. Other chemicals used were reagent grade.

A stock solution of 0.1 *M* NH_4Cl was prepared for testing the ammonia response of the electrode, and 5 *M* NaOH was employed to adjust the pH of the solution to within the operating range of the electrode.

[1] Model 5002-05 T, Horiba, Co., Kyoto, Japan.
[2] Model F-7ss, Hitachi-Horiba Instruments, Horiba Co., Kyoto, Japan.
[3] Model EPR-22A, Toa-Denpa Co., Tokyo, Japan.
[4] Tokyo Kasei Co., Tokyo, Japan.
[5] Japanese Pharmacopoeia Reference Standard.

0022-3549/82/0500-0523$01.00/0

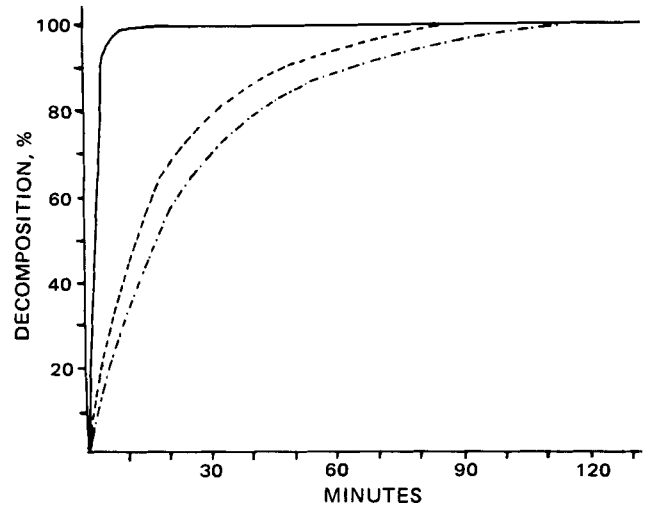

Figure 1—*Effect of 20% HCl concentration on drug decomposition. Key: —, pyrazinamide, niacinamide; - - -, ethenzamide; and — · —, Salicylamide.*

The internal filling solution supplied with the ammonia electrode was used.

An electrode storage solution of 0.01 *M* NH_4Cl for storage overnight or a weekend was prepared and the electrode tip was immersed in this solution. In 10^{-5}–10^{-4} *M* ammonia measurements, the use of the electrode immersed in 0.01 *M* NH_4Cl led to erroneous results because the gas-permeable membrane absorbed ammonium chloride and did not regenerate when washed with water. The electrode tip was therefore immersed in a buffer solution[6], pH 4, between measurements.

Standard Drug Solutions—A mixture of 307.78 mg (2.50×10^{-3} moles) of pyrazinamide and 50 ml of 20% HCl was placed in a 100- ml round-bottom flask and boiled gently in an oil bath for 20 min. The flask was then cooled, the solution poured into a 250-ml beaker, and diluted with ~150 ml of water. A drop of methyl orange was added and, while cooling the beaker continuously, the acid was carefully neutralized with 10 *N* NaOH solution until the indicator began to change color. Using a pH meter, the solution was adjusted to pH 6.5 with diluted sodium hydroxide solution, and the solution was poured into a 250-ml volumetric flask and diluted to full volume with water. The concentration of the final pyrazinamide solution was 1×10^{-2} *M*, corresponding to 1×10^{-2} *M* ammonia. Standard solutions for calibration were obtained by diluting this stock solution with water.

Other standard solutions of ethenzamide, salicylamide, and niacinamide were prepared in a similar manner as described previously according to the corresponding drug decomposition time shown in Fig. 1.

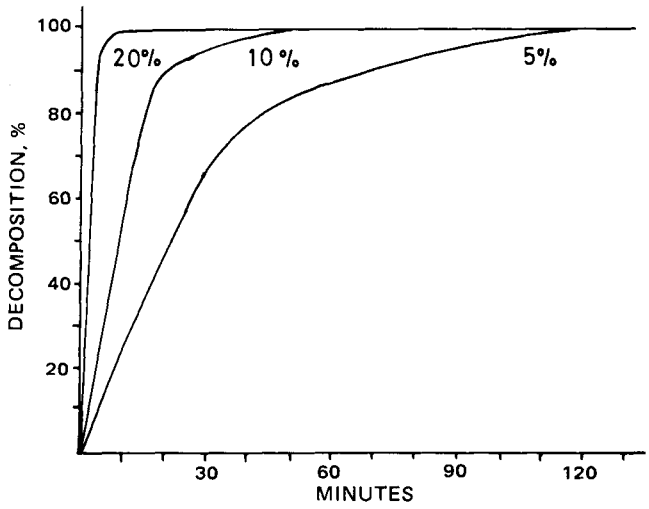

Figure 2—*Effect of various HCl concentrations on niacinamide decomposition.*

[6] Orion Research, Inc., Cambridge, U.K.

Table I—Determination of Drugs Having a Carboxyamide Group

Drug	Number	Taken, mg	Found, mg	Recovery, %
Ethenzamide	1	4.13	4.12	99.8
	2	4.13	4.16	100.7
	3	4.13	4.15	100.5
	4	41.30	41.21	99.8
	5	41.30	41.30	100.0
	6	41.30	41.34	100.1
			Mean	100.15
			± *SD*	0.37
Salicylamide	1	3.43	3.46	100.9
	2	3.43	3.44	100.3
	3	3.43	3.42	99.7
	4	34.28	34.08	99.4
	5	34.28	34.40	100.4
	6	34.28	34.60	100.9
			Mean	100.27
			± *SD*	0.62
Niacinamide	1	3.05	3.02	99.0
	2	3.05	3.07	100.7
	3	3.05	3.06	100.3
	4	30.53	30.72	100.6
	5	30.53	30.33	99.3
	6	30.53	30.41	99.60
			Mean	99.92
			± *SD*	0.71
Pyrazinamide	1	1.23	1.24	100.8
	2	1.23	1.22	99.2
	3	12.31	12.40	100.7
	4	12.31	12.34	100.2
	5	12.31	12.28	99.8
	6	12.31	12.39	100.6
			Mean	100.22
			± *SD*	0.62

Assay Procedure—A mixture of 123 mg (~1×10^{-3} mole) of pyrazinamide and 20 ml of 20% HCl was boiled for 20 min. The resultant solution was adjusted to pH 6.5, diluted to 100 ml in a volumetric flask, and then 20 ml of this solution was diluted to 100 ml with water. A 50-ml portion of the sample was transferred to an ~80-ml cell (3.5 × 9-cm), 1 ml of 5 *M* NaOH was added, and the mixture was incubated for 30 min at 20°. Finally, the ammonia electrode was immersed in the solution, and the potential measurements were carried out. The ammonia concentration in the sample solution was determined from the calibration curve.

Assay procedures of ethenzamide, salicylamide, and niacinamide were carried out in a similar manner. The ammonia concentration was determined from the calibration curve prepared from the corresponding standard drug solutions.

Because of the temperature dependence of the ammonia electrode, the sample solution was maintained at 20 ± 0.1° and stirred during the measurement. Since the potential may vary as a result of changes in the internal filling solution, the solution was replaced with fresh solution before subsequent use.

Assay of Niacinamide Injection—A mixture of 3 ml (equivalent to 150 mg of niacinamide) of the injection and 25 ml of 20% HCl was boiled for 30 min. The resultant solution was poured into a 250-ml volumetric flask and diluted to full volume with water. The ammonia concentration in the 50-ml portion of the sample was determined using an ammonia gas-sensing electrode.

Assay of 10% Niacinamide Powder—A portion of the powder (equivalent to ~153 mg of niacinamide) was accurately weighed out, and 25 ml of acetone was added. The solution was swirled for 5 min to extract the niacinamide and allowed to stand for ~3 min. The supernatant acetone solution was removed and 25 ml of acetone was added to the residue. The extraction procedure was carried out four times and the solution was finally filtered through a dry filter into a dry flask. The collected acetone fractions were evaporated to dryness. The residue was then refluxed for 30 min with 25 ml of 20% HCl. The same procedure as described previously was followed.

RESULTS AND DISCUSSION

The dissolved ammonia in the sample solution diffused through the hydrophobic gas-permeable membrane and dissolved in the internal filling solution. The resulting pH change was then measured.

A mixture of ethenzamide, salicylamide, niacinamide, or pyrazinamide,

Table II—Determination of Niacinamide Injection [a]

Number	Taken, mg	Found, mg	Recovery, %
1	30.00	32.36	107.8
2	30.00	32.20	107.3
3	30.00	32.34	107.8
4	30.00	32.14	107.1
5	30.00	32.35	107.8
6	30.00	32.23	107.4
		Mean	107.53
		± *SD*	0.31

[a] 50 mg in 1 ml.

Table III—Determination of 10% Niacinamide Powder

Number	Taken, mg	Found, mg	Recovery, %
1	30.94	35.79	115.7
2	30.62	35.63	116.4
3	30.61	35.55	116.1
4	30.94	35.87	116.0
5	30.68	35.63	116.1
6	30.72	35.53	115.8
		Mean	116.0
		± *SD*	0.24

and 20% HCl was boiled gently and the resultant ammonia in the decomposition solution was determined at various boiling times. In the case of ethenzamide and salicylamide, the electrode potentials reached a maximum at boiling times of 90 and 120 min, respectively. However, the electrode potentials of pyrazinamide and niacinamide reached a maximum at the same boiling times of 10 min. In the case of decomposition with 10 and 5% HCl, the electrode potentials of niacinamide reached a maximum at boiling times of 60 and 90 min, respectively (Figs. 1 and 2).

In the potential measurements, the level of ions in the decomposition solution (osmotic strength) is not equal to that of the internal filling solution. Water vapor as well as ammonia can move across the gas-permeable membrane, modifying the concentration of the internal filling solution. Since such changes lead to errors in potential measurements, standards and samples should have approximately the same level of ions in solution (7). Therefore, the standard solution of drug used the corresponding pure drug instead of ammonium chloride.

When the potential *versus* the logarithm of drug concentration was plotted, a linear calibration plot was obtained in the drug concentration range of 2×10^{-5}–1×10^{-2} *M*.

The amount of drug was determined in the pure drug powder. According to the Pharmaceopoeia, ethenzamide (8), salicylamide (9), and niacinamide (10, 11) determined on a dry weight basis should be over 98, 98, and 98.5% pure, respectively. Pyrazinamide (1) contains not less than 99% and not more than 101.0%. The recoveries of the drugs are given in Table I. The amounts of ethenzamide, salicylamide, niacinamide, and pyrazinamide can be determined with average errors of 0.15, 0.27, 0.08, and 0.22%, respectively.

The determination of commercially available niacinamide injection was carried out on six 3-ml samples (equivalent to ~150 mg niacinamide) of niacinamide injection, which is a sterile solution of niacinamide in water. A mixture of 3 ml of niacinamide injection and 25 ml of 20% HCl was boiled for 20 min and the potential measurements were carried out as described previously. According to the United States (10) and Japanese (11) Pharmacopoeias, niacinamide injection contains not less than 95% and not more than 110% of the labeled amount of $C_6H_6N_2O$. The recoveries of niacinamide injection are given in Table II. The mean recovery was 107.5 ± 0.31%. The accuracy of the proposed method was checked by the König method. The recoveries of niacinamide injection from four samples were 107.3, 106.4, 106.4, and 108.7%, respectively; the mean value was 107.2 ± 1.09%.

In determining other commercially available 10% niacinamide powders, a suitable extraction was sought. (Extraction of niacinamide is necessary to avoid interference from auxiliary compounds.) Niacinamide is very soluble in water (1 g in 1 ml) as are the auxiliary compounds; however, methanol does not dissolve the auxiliary compounds and separation of the extract from the powder is difficult. Niacinamide powder (10%) was extracted with acetone, since acetone does not inhibit the assay of pure niacinamide powder. After dissolution in acetone, the supernate was removed. The extraction was carried out four times and the extract filtered from the powder. The auxiliary compound was very hygroscopic, and it is thought that the niacinamide in the auxiliary compound was not homogeneous. Therefore, the recovery of the assay varied from 98 to >100%. The 10% niacinamide powder was mixed thoroughly in a mortar with a pestle and was dried *in vacuo* at room temperature for 24 hr (Table III). The mean recovery was 116.0 ± 0.24%. According to the Japanese Pharmacopoeia, niacinamide tablets contain not less than 95.0 and not more than 115.0% of the labeled amount of $C_6H_6N_2O$, but the description as a percentage of niacinamide powder is not noted. The accuracy of the proposed method was checked using the König method. The assay was performed on three samples of the 10% powder. The recoveries were 115.7, 118.5, and 115.3%, respectively, with a mean value of 116.5%.

CONCLUSIONS

In the Pharmacopoeial assay methods for ethenzamide, pyrazinamide, and salicylamide, the ammonia gas liberated by decomposition with sodium hydroxide is determined by acid titration (1, 8, 9). Using this method, the separation of the ammonia gas is difficult and tedious. The following procedures have been described previously for the analysis of niacinamide: (*a*) the sodium hydroxide decomposition method, (*b*) the nonaqueous titration method (12), (*c*) the colorimetric method for pure powder (10, 11), and the König method for injections. The sodium hydroxide decompositon method is identical to the method discussed. In the nonaqueous titration method, the normality factor is unstable. The colorimetric method is nonspecific, and the König method is adopted for the determination of injections in Japanese Pharmacopoeia IX (11) and USP XIX (13). The latter method is influenced by the experimental conditions (14, 15) and has the disadvantage of using extremely toxic cyanogen bromide. The present method using an ammonia gas-sensing electrode, beside being simple, has high specificity and precision.

REFERENCES

(1) "The United States Pharmacopoeia," 20th rev., Mack Publishing, Easton, Pa., 1980, p. 692.

(2) "The British Pharmacopoeia," University Printing House, Cambridge, U.K., 1973, p. 288.

(3) "The Japanese Pharmacopoeia," 9th rev., Hirokawa Publishing Co., Tokyo, Japan, 1976, p. 468.

(4) "Official Method of Analysis of the Association of Official Analytical Chemists," W. Horwity, Ed., 12th ed. Association of Official Analytical Chemists, Washington, D.C., 1975, p. 828.

(5) R. Strohencker and H. M. Henning, "Vitamin Assay Tested Methods," 1965, pp. 195, 201, and 207.

(6) S. Van-Vlasselaer and F. Cruke, *Ann. Pharm. Fr.*, **31**, 769 (1973).

(7) "Instruction Manual," Orion Research Inc., Cambridge, U.K., 1978, p. 23.

(8) "The Japanese Pharmacopoeia," 7th rev., Nankodo Publishing Co., Kyoto, Japan, 1965, p. 154.

(9) *Ibid.*, p. 508.

(10) "The United States Pharmacopeia," 20th rev., Mack Publishing, Easton, Pa., 1980, p. 548.

(11) "The Japanese Pharmacopoeia," 9th rev., Hirokawa Publishing Co., Tokyo, Japan, 1976, p. 436.

(12) *Ibid.*, 8th rev., Nankodo Publishing Co., Kyoto, 1973, p. 317.

(13) "The United States Pharmacopeia," 19th rev., Mack Publishing, Easton, Pa., 1975, p. 341.

(14) H. Makino, *Iyakuhin Kenkyu*, **3**, 175 (1972).

(15) I. Utsumi and M. Sameshima, *Yakugaku Kenkyu*, **29**, 980 (1957).

Liquid Membrane Phenomena in Haloperidol Action

S. B. BHISE, P. R. MARWADI, S. S. MATHUR, and R. C. SRIVASTAVA ˣ

Received May 27, 1981, from the *Birla Institute of Technology and Science, Pilani-333031, India.* Accepted for publication August 20, 1981.

Abstract □ Haloperidol, a surface-active neuroleptic drug, was shown to generate a liquid membrane on a supporting membrane. Transport of adrenalin, noradrenalin, dopamine, serotonin, histamine, glutamic acid, γ-aminobutyric acid, and sodium, potassium, and calcium ions through the haloperidol liquid membrane was studied. The data indicate that the phenomenon of a liquid membrane plays a significant role in the mechanism of action of haloperidol.

Keyphrases □ Liquid membrane phenomena—effect on haloperidol action □ Haloperidol—liquid membrane phenomena, effect on mechanism of action □ Surface-active drugs—haloperidol, effect of liquid membrane phenomena

A wide variety of biologically active agents have been shown to be surface active (1–4). This does not appear to be a coincidence. In a number of cases a definite correlation between surface activity and biological effects has been demonstrated (1, 3, 4). Most of the potent neuroleptics are known to behave like powerful surface-active agents (2) and the surface activities of neuroleptic drugs also correlate with their clinical potencies (1). Palm *et al.* (5) concluded that regardless of the chemical structure, mainly the surface activity of psychotropic drugs determines their potencies toward all kinds of membranes, especially that of catecholamine-storing particles. Surface-active agents have been shown (6–8) to generate liquid membranes which completely cover the interface at or above the critical micelle concentration of the surfactants when added to water or aqueous solutions. Therefore, it is likely that the liquid membrane phenomena may have an important role in the mechanism of action of such drugs, and deserves a systematic investigation. Haloperidol is a neuroleptic drug belonging to the class of butyrophenones and is known to be surface active in nature (2).

Haloperidol acts by modifying the permeabilities of catecholamines and a few neurotransmitter amino acids in biological cells (2). To date, this effect has been explained solely on the basis of specific drug interaction with the receptors. No serious attempt has been made to assess the contribution of the liquid membrane to the mechanism of its action. Experiments were designed to demonstrate the existence of a haloperidol liquid membrane at the interface. Data on the transport of endogenous amines, neurotransmitter amino acids, and sodium, potassium, and calcium ions through the haloperidol liquid membrane were obtained. A cellulose acetate membrane–water interface was chosen as a site for the formation of the liquid membrane. In this way, any active and specific interaction of the drug with the membrane that alters the permeabilities of relevant permeants was ruled out and only data on passive transport was obtained.

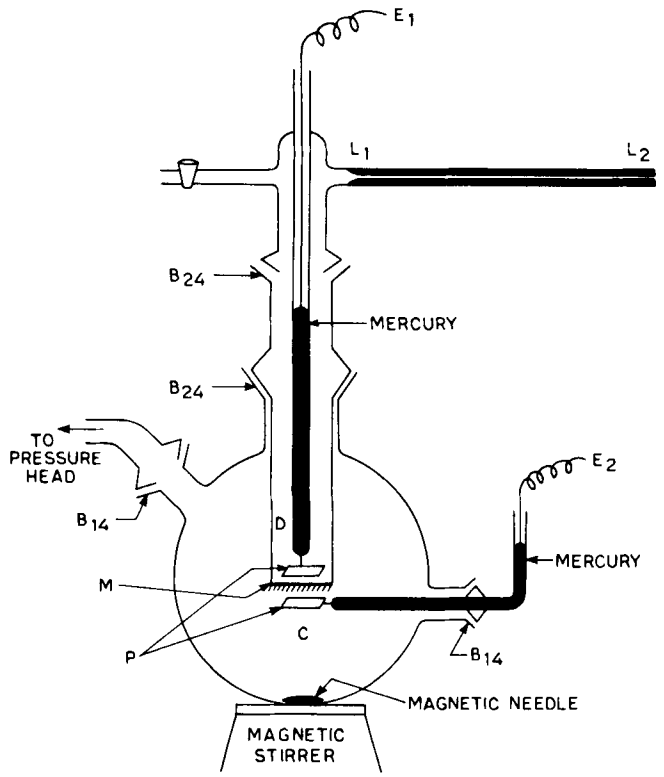

Figure 1—*The transport cell. Key: M, supporting membrane (cellulose acetate millipore filter); P, bright platinum electrodes; L_1L_2, 17-cm capillary tube with 1.33 × 10^{-1} cm diameter and E_1 and E_2, electrode terminals. Volume of Compartments C and D are 590 and 50 ml, respectively.*

EXPERIMENTAL

Materials—Haloperidol[1], dopamine chlorhydrate[2], adrenalin hydrogen tartrate[2], L-noradrenalin[3], serotonin creatinine sulfate[4], histamine acid phosphate[5], L-glutamic acid[5], γ-aminobutyric acid[5] (I), sodium chloride[6], potassium chloride[6], calcium chloride[6], and water glass-distilled over potassium permanganate were used.

Methods—The critical micelle concentration (CMC) of aqueous haloperidol was determined from the plots of surface tension *versus* concentration at 37 ± 0.1°. The surface tensions were measured using the method of capillary rise. The CMC value found for aqueous solutions of haloperidol, was 1.064 × 10^{-6} *M*. To prepare the aqueous solutions of haloperidol, the weight of drug necessary to attain the desired concentration was dissolved in ethanol and added with constant stirring to the aqueous phase. The stirring was continued for ~12 hr. In the aqueous solutions of haloperidol thus prepared, the final concentration of ethanol was never allowed to exceed 0.1% (v/v) because a control experiment showed that 0.1% (v/v) solution of ethanol in water did not lower the surface tension of water to any measurable extent.

The all-glass cell described earlier (8) was used for the transport studies (Fig. 1). The transport cell was separated into two compartments by a cellulose acetate millipore filter[7] which acted as a support for the liquid membrane.

For measurements of hydraulic permeability, aqueous haloperidol solutions of various concentrations ranging from 0 to 1.064 × 10^{-5} *M* were filled in Compartment C of the transport cell (Fig. 1), while Compartment D was filled with distilled water. The concentration range was selected

[1] B. P. Searle (India).
[2] Loba Chemie.
[3] Fluka A.G..
[4] Koch Light Laboratories Ltd.
[5] BDH.
[6] Analar grade.
[7] Sartorius, Cat. No. 11107 of thickness 1 × 10^{-4} m and area 5.373 × 10^{-5} m^2.

0022-3549/82/0500-0526$01.00/0

to get data on both the lower and higher sides of the CMC of haloperidol. Known pressures were applied on Compartment C by adjusting the pressure head and the resulting volume flux was measured by noting the rate of advancement of the liquid meniscus in capillary L_1L_2 with a cathetometer reading up to 0.001 cm and a stopwatch reading up to 0.1 sec. The magnitude of the applied pressures also was measured by noting the position of the pressure head, with a cathetometer reading up to 0.001 cm. During the volume flux measurements the solution in Compartment C was well stirred and electrodes E_1 and E_2 were short circuited so that the electro-osmotic back flow that developed due to streaming potentials did not interfere with the observations.

To measure permeability of endogenous amines, amino acids, and sodium, potassium, and calcium ions, two sets of experiments were performed. In the first set of experiments, Compartment C of the transport cell was filled with the respective permeants, prepared in 4.256×10^{-6} *M* aqueous solution of haloperidol and Compartment D was filled with distilled water. In the second set of experiments Compartment D was filled with 4.256×10^{-6} *M* solution of haloperidol and Compartment C was filled with aqueous solutions of the permeants. No haloperidol was used in the control experiments. The initial concentrations chosen for the endogenous amines, amino acids, and cations were comparable to their concentrations in the vicinity of nervous tissue. The condition of no net volume flux ($J_v = 0$) was attained by adjusting the pressure head attached to Compartment C of the transport cell so that the liquid meniscus in capillary L_1L_2 remained stationary. After a known period of time, the concentration of the permeant in the other compartment was measured. The amount of permeant gained by Compartment D divided by the time and the area of the membrane gave the value of solute flux (J_s). The value of solute permeability was estimated using the definition (9, 10):

$$\left(\frac{J_s}{\Delta\pi}\right)_{Ju=0} = \omega \qquad \text{(Eq. 1)}$$

where $\Delta\pi$ is the osmotic pressure difference. The value of $\Delta\pi$ used in the calculation of ω was the average of the $\Delta\pi$ values at the beginning ($t = 0$) and end of the experiment. During the permeability measurements, the solution in Compartment C was kept well stirred. All measurements were made at constant temperature by placing the transport cell (Fig. 1) in a thermostat set at 37 ± 0.1°.

Estimations—The amounts of the various permeants transported to Compartment D were estimated as follows:

Endogenous Amines—The amounts of the catecholamines, namely dopamine, noradrenalin, and adrenalin, were estimated fluorometrically at 325 nm (11). Though the fluorescence maximum of serotonin is reported to be 330 nm (12), it was measured at 325 nm since a quartz cell was used. Histamine was estimated by measuring the fluorophor derived from its reaction with *o*-phthalaldehyde[8] (11, 13) at 450 nm. A UV-visible–near IR spectrophotometer[9] with fluorescence attachment was used for fluorescence measurements.

Amino Acids—The amounts of glutamic acid and γ-aminobutyric acid were estimated by spectrophotometric[10] determination of their reaction products with ninhydrin[5] (14) at 570 nm.

Cations—The amounts of sodium, potassium, and calcium ions were determined using an atomic absorption spectrophotometer[11] using emission mode.

The estimations were carried out using the following lines: sodium, 589.6 nm; potassium, 766.5 nm; and calcium, 422.7 nm.

RESULTS AND DISCUSSION

Liquid Membrane Formation—From the hydraulic permeability data at various haloperidol concentrations (Fig. 2), it is obvious that the linear relationship is obeyed in all cases:

$$J_v = L\,\Delta P \qquad \text{(Eq. 2)}$$

where J_v represents the volume flux per unit area of the membrane, ΔP is the applied pressure difference, and L is the hydraulic conductivity coefficient. The values of L show (Table I) a progressive decrease as the haloperidol concentration is increased from 0 to its CMC value, *i.e.*, 1.064×10^{-6} *M*. When the haloperidol concentration is increased further, the value of L also decreases, but much less than the decrease observed up to the CMC value of haloperidol. This trend is in keeping with Kesting's

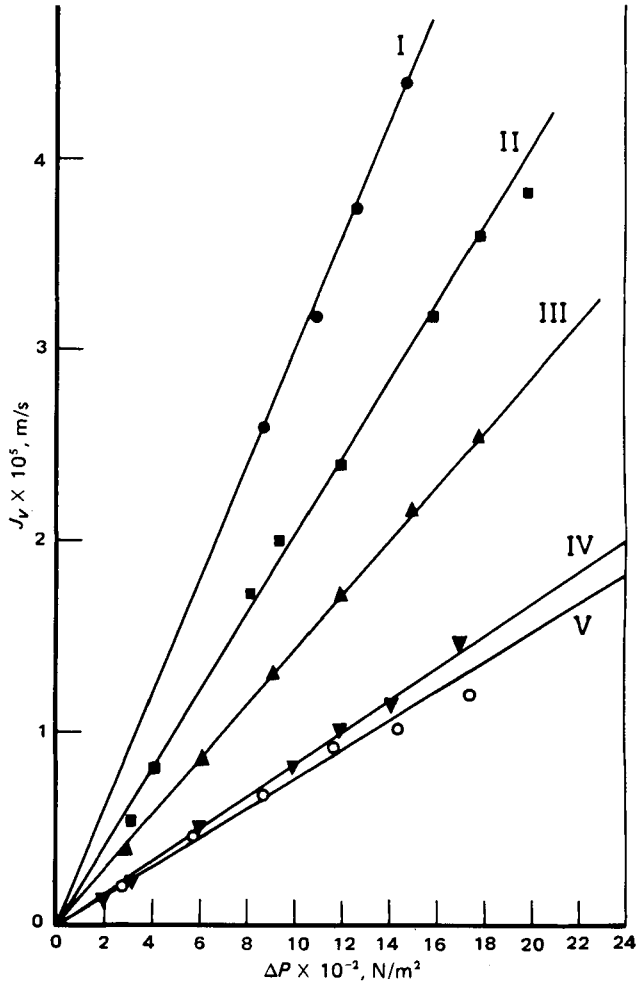

Figure 2—*Hydraulic permeability data. Curves I, II, III, IV, and V are for 0, 1.064×10^{-7}, 5.32×10^{-7}, 1.064×10^{-6}, and 1.064×10^{-5} M haloperidol concentrations, respectively.*

liquid membrane hypothesis (6–8), where the surfactant concentration is increased, the supporting membrane gets progressively covered with the surfactant layer liquid membrane. Then, at the CMC, the supporting membrane is completely covered with the liquid membrane. The decrease in the value of L beyond the CMC of haloperidol, could possibly be due to densing of the liquid membrane (6).

In light of the mosaic membrane model (15–17) analysis of the flow data (Fig. 2, Table I) supports the existence of the liquid membrane in series with the supporting membrane. At concentrations lower than the CMC, the supporting membrane is only partially covered with the liquid membrane. The equation for the volume flux of water for such a case can be written as:

$$J_v = \left[L^c\left(\frac{A^c}{A^c + A^s}\right) + L^s\left(\frac{A^s}{A^c + A^s}\right)\right]\Delta P \qquad \text{(Eq. 3)}$$

where A represents area of the membrane denoted by the superscripts, and superscripts c and s represent the bare supporting membrane and the supporting membrane covered with the liquid membrane, respectively. In the present case L^c represents the value of the hydraulic conductivity when no haloperidol was used, and L^s represents the value of the hydraulic conductivity when the haloperidol concentration equals its CMC. At half the CMC, the fraction of the total area covered with the liquid membrane will be halved and, therefore, the value of L should be equal to $(L^c + L^s/2)$. Similarly, for 0.1 CMC of haloperidol, the value of L should equal $(0.9\,L^c + 0.1\,L^s)$. The values of L were computed in this way, corresponding to the two haloperidol concentrations given in Table I. These values match the experimentally determined values well.

Solute Permeability in the Presence of Haloperidol—The value of ω for endogenous amines, amino acids, and cations are given in Table II. To make sure that the supporting membrane of the transport cell was completely covered with the haloperidol liquid membrane, the concentration of haloperidol chosen for the present study was 4.256×10^{-6} *M*, which is much higher than its critical micelle concentration. Haloperidol,

[8] Sigma Chemical Co.
[9] Varian Cary 17-D spectrophotometer.
[10] Bausch and Lomb Spectronic-20.
[11] Perkin Elmer, model 306.

Table I—Values of L at Various Haloperidol Concentrations

	Haloperidol Concentration × 10^7, M				
	0	1.064 (0.1 CMC)	5.320 (0.5 CMC)	10.64 (CMC)	106.4
$L^a \times 10^8$ (m^3/s N)	2.804 ± 0.4368	2.095 ± 0.1273	1.603 ± 0.2015	0.7993 ± 0.0692	0.7662 ± 0.0216
$L^b \times 10^8$ (m^3/s N)	—	2.6035 ± 0.3996	1.8017 ± 0.2510	—	—

[a] Experimental values. [b] Calculated values on the basis of mosaic model (Eq. 3).

being surface active, has both hydrophobic and hydrophilic parts in its structure. The orientation of its molecules will, therefore, be significant when it forms a liquid membrane. The hydrophobic ends of the haloperidol molecules would be preferentially oriented toward the hydrophobic supporting membrane and their hydrophilic ends will face outwards, away from the supporting membrane. When haloperidol is in compartment C of the transport cell (first set of experiments) the haloperidol liquid membrane will present a polar surface to the permeant present in the same compartment. In the second set of experiments, however, where haloperidol is in Compartment D of the transport cell and the aqueous solution of the permeant is in Compartment C, the haloperidol liquid membrane would present a hydrophobic surface to the permeant. Therefore, the orientation of haloperidol molecules with respect to approaching permeant would be different in the two sets of experiments.

The values of ω given in Table II indicate that when the hydrophobic surface of the haloperidol liquid membrane faces the approaching permeant (second experiment), a marked decrease in their permeability is observed. The haloperidol liquid membrane, thus, offers resistance to the transport of these permeants in this specific orientation. This reduction in the passive transport of biogenic amines, amino acids, and cations is likely to be accompanied by a reduction in their active transport. This occurs because the access of these permeants to the active carrier site of the biological membrane is likely to be effectively reduced due to the resistance of the haloperidol liquid membrane. The results also indicate that this specific orientation of haloperidol molecules with hydrophobic ends facing the catecholamines and amino acids, would be necessary for the liquid membrane to resist the flow of these species. In the first set of experiments, where haloperidol orients its hydrophilic ends toward the catecholamines or amino acids, the permeability of these substances is increased in the presence of haloperidol. This indicates that the orientation of haloperidol with its hydrophobic ends facing the permeants would be necessary even in biological cells.

In cells, haloperidol reduces the permeability of catecholamines (2). Despite the fact that the present experiments were carried out using a cellulose acetate membrane, the results are similar to those observed in biological cells. This indicates that the liquid membrane generated by haloperidol contributes to the resistance of the flow of catecholamines.

The haloperidol liquid membrane also resists the flow of glutamic acid and γ-aminobutyric acid (Table II). The antiemetic and antipsychotic actions of haloperidol are explained on the basis of reduced permeability of dopamine to biological cells, which is under the influence of the γ-aminobutyric acid–glutamic acid system (2). To investigate whether a similar trend is observed on nonspecific membranes, the dopamine permeability was measured in the presence of γ-aminobutyric acid. Interestingly, the present set of experiments also indicates that the presence

Table II—Solute Permeability ω of Endogenous Amines, Amino Acids, and Cations in Presence of 4.256×10^{-6} M Haloperidol.

	ω_1[a] × 10^{12} moles/s N	ω_2[b] × 10^{12} moles/s N	ω_3[c] × 10^{12} moles/s N	ω_4[d] × 10^{12} moles/s N
Dopamine	887.3	680.0	2607.0	274.4
Noradrenalin	75.8	65.9	294.3	
Adrenalin	50.7	undetectable	237.4	
Serotonin	193.7	94.5	348.1	
Histamine	48.8	109.1	318.8	
Glutamic acid	58.9	47.3	81.0	
γ-Aminobutyric acid	119.8	86.6	152.2	
Sodium (chloride)	172.9	53.4	70.7	
Potassium (chloride)	175.5	157.1	101.3	
Calcium (chloride)	119.2	111.7	106.8	

[a] ω_1: control value—when no haloperidol was used. [b] ω_2: haloperidol in Compartment D of the transport cell. [c] ω_3: haloperidol in Compartment C of the transport cell. [d] ω_4: in the presence of γ-aminobutyric acid and haloperidol.

hydrophobic

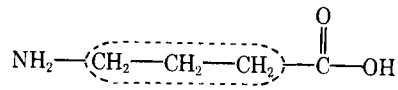

γ-aminobutyric acid

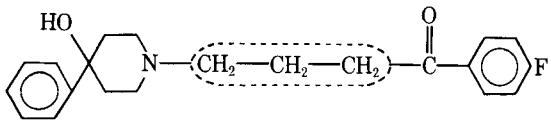

haloperidol

of γ-aminobutyric acid increases resistance to the transport of dopamine through haloperidol liquid membrane (Table II). This can be explained by a strengthening of the hydrophobic core of haloperidol liquid membrane by γ-aminobutyric acid, which is obvious from the similarity of the hydrophobic components of their structures.

It is tempting to suggest that increased passive resistance to the flow of dopamine in the presence of γ-aminobutyric acid, coupled with the resistance to the flow of glutamic acid by the haloperidol liquid membrane, is likely to contribute to the mechanism of action of haloperidol.

It was reported (18) that haloperidol is considerably more potent on a milligram basis than chlorpromazine *in vivo*. The formation of liquid membrane phenomena might explain this. Because haloperidol exhibits greater surface activity than chlorpromazine (1, 2), the former will form liquid membranes at a lesser concentration, making it pharmacologically effective even at a comparatively lower concentration.

The present study shows that haloperidol reduces the permeability of serotonin (Table II). This agrees with the observations reported on biological cells (19). The extrapyramidal effects of antipsychotic drugs like haloperidol reportedly are resistant to levodopa therapy (20). Since reduced concentration of serotonin in cerebrospinal fluid has also been linked with a defect of extrapyramidal function (21, 22), the reduced permeability of serotonin in the presence of antipsychotic drugs like haloperidol offers a clue to the causation of extrapyramidal symptoms.

The observation of increased permeability of histamine in the presence of haloperidol, and its biological implication, if any, remains to be explained.

The resistance offered by haloperidol liquid membrane to the flow of sodium, potassium, and calcium cations is probably due to hydrophilicity of the ions. Unlike the observation in the case of endogeneous amines and amino acids, even when the hydrophilic ends of haloperidol are facing the approaching cations, the permeability of these ions is reduced (Table II). This may be because the ions are more hydrophilic and experience more resistance to their flow. This observation may have some biological implications relative to nerve conduction.

REFERENCES

(1) P. Seeman and H. S. Bialy, *Biochem. Pharmacol.*, **12**, 1181 (1963).

(2) P. A. J. Janssen, *Int. J. Neuropsychiatry*, **S**, 10 (1967).

(3) P. Seeman, *Pharmacol. Rev.*, **24**, 583 (1972).

(4) A. Felmeister, *J. Pharm. Sci.*, **61**, 151 (1972).

(5) D. Palm, H. Grobecker, and I. J. Bak, in "Bayer Symposium—II. New Aspects of Storage and Release Mechanisms of Catecholamines," H. J. Shumann and G. Kroneberg, Eds., Springer-Verlag, Berlin, 1970, pp 188–198.

(6) R. E. Kesting, W. J. Subcasky, and J. D. Paton, *J. Colloid Interface Sci.*, **28**, 156 (1968).

(7) R. C. Srivastava and S. Yadav, *ibid.*, **69**, 280 (1979).
(8) R. C. Srivastava and R. P. S. Jakhar, *J. Phys. Chem.*, **85**, 1457 (1981).
(9) A. Katchalsky and P. F. Curran, "Nonequilibrium Thermodynamics in Biophysics," Harvard University Press, Cambridge, Mass., 1967, pp 113–116.
(10) A. Katchalsky and O. Kedem, *Biophys. J.*, **2**, 53 (1962).
(11) S. Udenfriend, "Fluorescence Assay in Biology and Medicine," vol. I, Academic, New York, N.Y., 1969, p. 140.
(12) R. L. Bowman, P. A. Caulfield, and S. Udenfriend, *Science*, **122**, 32 (1955).
(13) D. von Redlich and D. Glick, *Anal. Biochem.*, **10**, 459 (1965).
(14) S. Moore and W. H. Stein, *J. Biol. Chem.*, **21**, 907 (1954).
(15) K. S. Speigler and O. Kedem, *Desalination*, **1**, 311 (1966).
(16) T. K. Sherwood, P. L. T. Brain, and R. E. Fischer, *Ind. Eng., Chem. Fundam.*, **6**, 2 (1967).
(17) F. L. Harris, G. B. Humphreys, and K. S. Spiegler in "Membrane Separation Processes," Elsevier, Amsterdam, The Netherlands, 1966, pp 126.
(18) S. H. Snyder, *Am. J. Psychiatry*, **133**, 197 (1976).
(19) M. Grabowska, *Pol. J. Pharmacol.*, **28**, 253 (1976).
(20) R. Byck, in "Pharmacological Basis of Therapeutics," 5th ed., L. S. Goodman and A. Gilman, Eds., Macmillan, New York, N.Y., 1975, p. 172.
(21) O. Hornykiewicz, *Pharmacol. Rev.*, **18**, 925 (1966).
(22) T. N. Chase and D. L. Murphy, *Ann. Rev. Pharmacol.*, **13**, 188 (1973).

ACKNOWLEDGMENTS

The authors thank the Department of Science and Technology, Government of India, for supporting the investigation. They also thank Searle (India) Ltd. for the gift of haloperidol and for their active interest in the research work, and Dr. H. L. Kundu, Dean, Educational Hardware Division of the Institute for his kind cooperation.

High-Pressure Liquid Chromatographic Determination of Promethazine Plasma Levels in the Dog After Oral, Intramuscular, and Intravenous Dosage

RAJNI B. PATEL AND PETER G. WELLING ˣ

Received July 6, 1981, from the *School of Pharmacy, University of Wisconsin, Madison, WI 53706.* Accepted for publication August 27, 1981.

Abstract □ Plasma levels of promethazine were determined using a high-pressure liquid chromatographic procedure incorporating a fixed wavelength (254 nm) UV detector, following single 50-mg intravenous, intramuscular, and oral doses to two male dogs. Initial plasma promethazine concentrations following intravenous doses were 556 and 535 ng/ml in the two dogs. The subsequent decline in drug levels were satisfactorily described by a triexponential function. Peak promethazine levels of 76 and 64 ng/ml were obtained 0.5 hr following intramuscular doses. Peak levels for the oral doses were 10.6 and 11.0 ng/ml occurring 2 hr after dosing. The apparent biological half-life of promethazine, obtained from only 2–3 data points, varied from 8.5 to 27.7 hr. Areas under the promethazine plasma curves, compared to values obtained from intravenous doses between 0 and 24 hr, indicated that systemic availability of intact drug was 55–73% following intramuscular injection and 8.3–9.5% following oral administration.

Keyphrases □ High-pressure liquid chromatography—determination of promethazine plasma levels after oral, intramuscular, and intravenous dosage, dogs □ Promethazine—high-pressure liquid chromatographic determination of plasma levels after oral, intramuscular, and intravenous dosage, dogs □ Pharmacokinetics—high-pressure liquid chromatographic determination of promethazine plasma levels after oral, intramuscular, and intravenous dosage, dogs

Promethazine has been used extensively for the control of allergy and as a sedative and antiemetic; however, little information is available on its bioavailability from oral dosage forms or on its pharmacokinetics. This has been due to the absence of suitable methods for determining promethazine in body fluids.

Gas chromatographic procedures have been used to measure promethazine (1, 2) and other phenothiazines (3, 4), but these methods lack sensitivity and require extensive sample preparation before chromatography. Studies in this laboratory showed that unless promethazine is separated from its various metabolites prior to gas chromatography, spurious results may result from on-column reduction of oxidized metabolites to the parent compound (5).

High-pressure liquid chromatographic (HPLC) procedures for promethazine have been reported recently (6–8). Two of the procedures (6, 7) require either large samples or prior derivatization, while the other (8) requires the use of electrochemical detection. The lack of assays suitable for routine use is the major cause for the scarcity of information on the pharmacokinetics of promethazine in animals (2, 9) and humans (1, 10) in the literature.

The use of a specific and sensitive HPLC assay to measure plasma promethazine levels following single oral, intramuscular, and intravenous doses to male dogs is described. Preliminary details of the liquid chromatographic procedure and comparisons with a gas chromatographic assay have been described elsewhere (5).

EXPERIMENTAL

Assay for Promethazine in Plasma—To 2 ml of plasma were added 200 μl of a 0.56-μg/ml aqueous solution of chlorpromazine hydrochloride (equivalent to 0.5 μg/ml of chlorpromazine) as internal standard, 0.5 ml of 1.0 *N* sodium hydroxide, and 8 ml of methylene chloride. After shaking for 15 min at low speed on a horizontal shaker and centrifuging at 3000×*g* for 5 min, the upper aqueous phase was discarded by aspiration. The organic phase was transferred to a clean tube and evaporated to dryness under nitrogen at room temperature. The tube was rinsed with 1 ml of methylene chloride and was again evaporated to dryness. The residue was reconstituted in 60 μl of the chromatographic mobile phase by vortexing, centrifuged at 3000×*g* for 1 min, and 20 μl of the supernate was injected into the chromatograph.

The HPLC consisted of a solvent pump[1]; a fixed-volume (20 μl) injection valve[2]; a 10-μm particle size, reversed-phase octadecyl column[3]

[1] Model 110, Altex Scientific, Berkeley, Calif.
[2] Rheodyne sample injector.
[3] Lichrosorb C-18 reversed-phase column, Altex Scientific, Berkeley, Calif.

0022-3549/82/0500-0529$01.00/0

(7) R. C. Srivastava and S. Yadav, *ibid.*, **69**, 280 (1979).
(8) R. C. Srivastava and R. P. S. Jakhar, *J. Phys. Chem.*, **85**, 1457 (1981).
(9) A. Katchalsky and P. F. Curran, "Nonequilibrium Thermodynamics in Biophysics," Harvard University Press, Cambridge, Mass., 1967, pp 113–116.
(10) A. Katchalsky and O. Kedem, *Biophys. J.*, **2**, 53 (1962).
(11) S. Udenfriend, "Fluorescence Assay in Biology and Medicine," vol. I, Academic, New York, N.Y., 1969, p. 140.
(12) R. L. Bowman, P. A. Caulfield, and S. Udenfriend, *Science*, **122**, 32 (1955).
(13) D. von Redlich and D. Glick, *Anal. Biochem.*, **10**, 459 (1965).
(14) S. Moore and W. H. Stein, *J. Biol. Chem.*, **21**, 907 (1954).
(15) K. S. Speigler and O. Kedem, *Desalination*, **1**, 311 (1966).
(16) T. K. Sherwood, P. L. T. Brain, and R. E. Fischer, *Ind. Eng., Chem. Fundam.*, **6**, 2 (1967).
(17) F. L. Harris, G. B. Humphreys, and K. S. Spiegler in "Membrane Separation Processes," Elsevier, Amsterdam, The Netherlands, 1966, pp 126.
(18) S. H. Snyder, *Am. J. Psychiatry*, **133**, 197 (1976).
(19) M. Grabowska, *Pol. J. Pharmacol.*, **28**, 253 (1976).
(20) R. Byck, in "Pharmacological Basis of Therapeutics," 5th ed., L. S. Goodman and A. Gilman, Eds., Macmillan, New York, N.Y., 1975, p. 172.
(21) O. Hornykiewicz, *Pharmacol. Rev.*, **18**, 925 (1966).
(22) T. N. Chase and D. L. Murphy, *Ann. Rev. Pharmacol.*, **13**, 188 (1973).

ACKNOWLEDGMENTS

The authors thank the Department of Science and Technology, Government of India, for supporting the investigation. They also thank Searle (India) Ltd. for the gift of haloperidol and for their active interest in the research work, and Dr. H. L. Kundu, Dean, Educational Hardware Division of the Institute for his kind cooperation.

High-Pressure Liquid Chromatographic Determination of Promethazine Plasma Levels in the Dog After Oral, Intramuscular, and Intravenous Dosage

RAJNI B. PATEL AND PETER G. WELLING ˣ

Received July 6, 1981, from the *School of Pharmacy, University of Wisconsin, Madison, WI 53706.* Accepted for publication August 27, 1981.

Abstract □ Plasma levels of promethazine were determined using a high-pressure liquid chromatographic procedure incorporating a fixed wavelength (254 nm) UV detector, following single 50-mg intravenous, intramuscular, and oral doses to two male dogs. Initial plasma promethazine concentrations following intravenous doses were 556 and 535 ng/ml in the two dogs. The subsequent decline in drug levels were satisfactorily described by a triexponential function. Peak promethazine levels of 76 and 64 ng/ml were obtained 0.5 hr following intramuscular doses. Peak levels for the oral doses were 10.6 and 11.0 ng/ml occurring 2 hr after dosing. The apparent biological half-life of promethazine, obtained from only 2–3 data points, varied from 8.5 to 27.7 hr. Areas under the promethazine plasma curves, compared to values obtained from intravenous doses between 0 and 24 hr, indicated that systemic availability of intact drug was 55–73% following intramuscular injection and 8.3–9.5% following oral administration.

Keyphrases □ High-pressure liquid chromatography—determination of promethazine plasma levels after oral, intramuscular, and intravenous dosage, dogs □ Promethazine—high-pressure liquid chromatographic determination of plasma levels after oral, intramuscular, and intravenous dosage, dogs □ Pharmacokinetics—high-pressure liquid chromatographic determination of promethazine plasma levels after oral, intramuscular, and intravenous dosage, dogs

Promethazine has been used extensively for the control of allergy and as a sedative and antiemetic; however, little information is available on its bioavailability from oral dosage forms or on its pharmacokinetics. This has been due to the absence of suitable methods for determining promethazine in body fluids.

Gas chromatographic procedures have been used to measure promethazine (1, 2) and other phenothiazines (3, 4), but these methods lack sensitivity and require extensive sample preparation before chromatography. Studies in this laboratory showed that unless promethazine is separated from its various metabolites prior to gas chromatography, spurious results may result from on-column reduction of oxidized metabolites to the parent compound (5).

High-pressure liquid chromatographic (HPLC) procedures for promethazine have been reported recently (6–8). Two of the procedures (6, 7) require either large samples or prior derivatization, while the other (8) requires the use of electrochemical detection. The lack of assays suitable for routine use is the major cause for the scarcity of information on the pharmacokinetics of promethazine in animals (2, 9) and humans (1, 10) in the literature.

The use of a specific and sensitive HPLC assay to measure plasma promethazine levels following single oral, intramuscular, and intravenous doses to male dogs is described. Preliminary details of the liquid chromatographic procedure and comparisons with a gas chromatographic assay have been described elsewhere (5).

EXPERIMENTAL

Assay for Promethazine in Plasma—To 2 ml of plasma were added 200 μl of a 0.56-μg/ml aqueous solution of chlorpromazine hydrochloride (equivalent to 0.5 μg/ml of chlorpromazine) as internal standard, 0.5 ml of 1.0 *N* sodium hydroxide, and 8 ml of methylene chloride. After shaking for 15 min at low speed on a horizontal shaker and centrifuging at 3000×*g* for 5 min, the upper aqueous phase was discarded by aspiration. The organic phase was transferred to a clean tube and evaporated to dryness under nitrogen at room temperature. The tube was rinsed with 1 ml of methylene chloride and was again evaporated to dryness. The residue was reconstituted in 60 μl of the chromatographic mobile phase by vortexing, centrifuged at 3000×*g* for 1 min, and 20 μl of the supernate was injected into the chromatograph.

The HPLC consisted of a solvent pump[1]; a fixed-volume (20 μl) injection valve[2]; a 10-μm particle size, reversed-phase octadecyl column[3]

[1] Model 110, Altex Scientific, Berkeley, Calif.
[2] Rheodyne sample injector.
[3] Lichrosorb C-18 reversed-phase column, Altex Scientific, Berkeley, Calif.

0022-3549/82/0500-0529$01.00/0

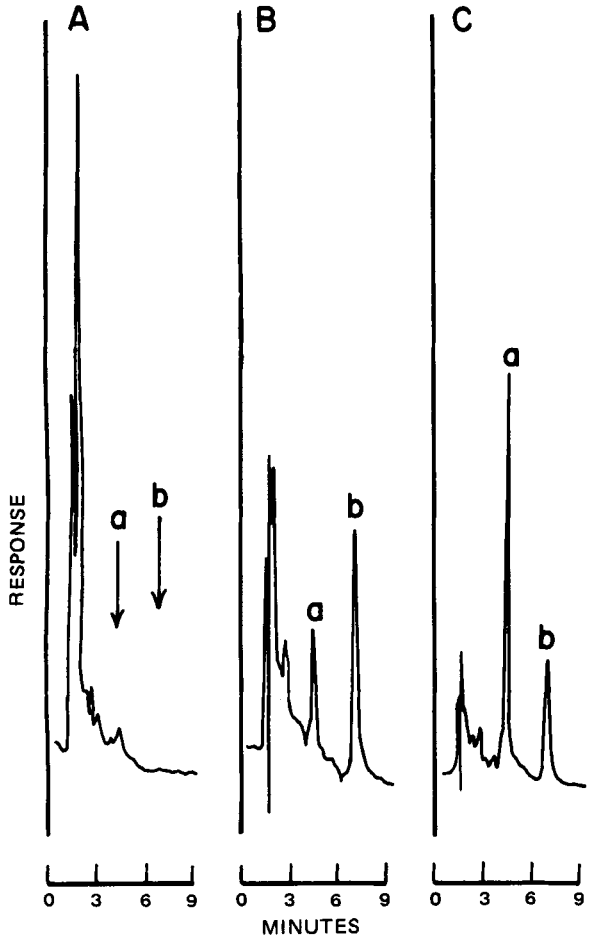

Figure 1—*Chromatograms obtained from (A) plasma containing no drugs; (B) a plasma sample obtained 12 hr following intramuscular injection, containing 9.1 ng/ml promethazine (a) and 50 ng/ml chlorpromazine (b); and (C) a plasma sample obtained 2 hr following intramuscular injection, containing 60 ng/ml promethazine (a) and 50 ng/ml chlorpromazine (b).*

(4.6 mm × 25 cm); a precolumn[4]; and a fixed wavelength (254 nm) detector[5]. Chromatograms were recorded on a chart recorder[6] with 10-mV input and 20-cm/hr chart speed. The mobile phase consisted of 42% acetonitrile and 3% *n*-nonylamine in 0.02 *M* phosphate buffer, pH 2.5. The flow rate was 2 ml/min at a pump pressure of 2.0×10^3 psi.

Dog Study—Two 3-year-old, mixed-breed, beagle-type dogs weighing 16 and 17 kg were fasted overnight before receiving 50-mg doses of promethazine orally[7], and by intramuscular[8] and intravenous[8] injection on three separate occasions at least 1 week apart. (Doses were administered at 8 am.)

During each experiment the dog was placed in a restraining sling, designed so that the dog could stand or rest comfortably but could not displace indwelling catheters which were placed into leg veins. To familiarize the dogs with this procedure, they were placed in the apparatus for 6 hr during each of the 3 days preceding the study.

Tablet doses (2 × 25 mg) were placed on the back of the dogs' tongues, so that the tablets were not fractured or chewed before being swallowed. This was immediately followed by 50 ml of water administered *via* an irrigating syringe[9]. Intramuscular doses were administered in 1 ml of physiological saline into a hind-leg thigh muscle. Intravenous doses were administered in 1 ml of physiological saline into a hind-leg vein over a 30-sec period.

Following the oral dose, blood samples (7–8 ml) were taken immediately before, at 30 min, and at 1, 2, 3, 4, 6, 8, 12, and 24 hr after dosing. An additional blood sample was drawn 15 min after the intramuscular dose, while additional samples were drawn at 5, 10, 15, and 45 min following the intravenous dose. During the initial 6-hr sampling period, blood samples were obtained *via* a vein infusion set[10] positioned in the front leg. The infusion set was kept patent by means of an intravenous drip (4 drops/min) of normal saline[11] containing 1 U/ml of sodium heparin[12]. At each sampling time 2 ml of residual fluid were withdrawn from the infusion set before drawing a 7–8-ml blood sample into a clean syringe[13]. The sets were removed after 6 hr and the dogs were released from the

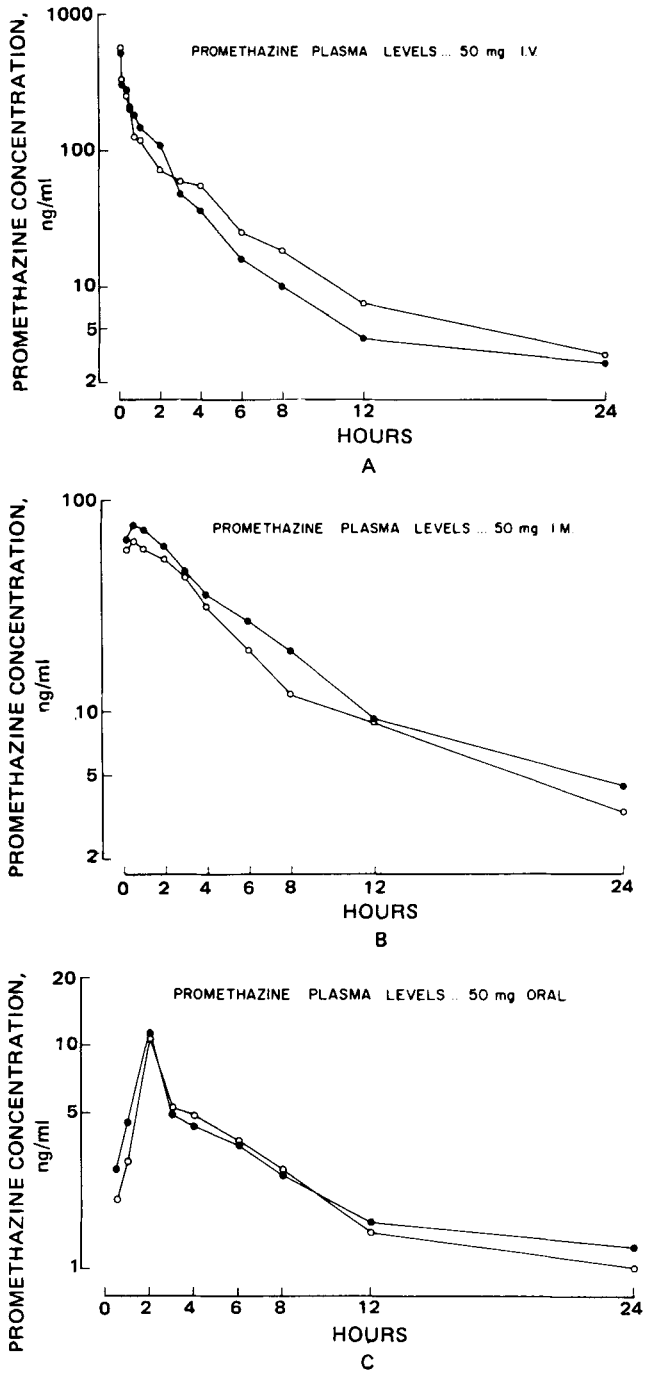

Figure 2—*Promethazine plasma levels in Dog 1 (○) and Dog 2 (●) following a single 50-mg (A) intravenous, (B) intramuscular, or (C) oral dose.*

[4] CO:PELL ODS, 30-38 m. Whatman Inc., Clifton, N.J.
[5] Model 153, Altex Scientific, Berkeley, Calif.
[6] Model 023, Perkin-Elmer Instrument Division, Norwalk, Conn.
[7] Phenergan, 25-mg tablets, Lot 1800131, Wyeth, Philadelphia, Pa.
[8] Promethazine Hydrochloride Injection, Lot 80B023, 50 mg/ml, Geneva Generics, Bloomfield, Col.
[9] Pharmaseal Labs., Glendale, Calif.
[10] Miniset, vein infusion set with winged adaptor, Travenol Laboratories, Deerfield, Ill.
[11] Sodium chloride 0.9% irrigating solution, USP, Travenol Laboratories, Deerfield, Ill.
[12] Panheprin, Lot 23795 AF, 1000 USP U ml^{-1}, Abbott Laboratories, North Chicago, Ill.
[13] B-D 10-cc syringe Luer Slip Tip, Becton, Dickinson and Co., Rutherford N.J.

Table I—Day-to-Day Reproducibility of the Assay for Promethazine in Plasma[a]

Concentration in Plasma, ng/ml	Found, ng/ml	Recovery, %	Coefficient of variation, %
1	1.1	110	10.8
2.5	2.54	102	8.4
5	5.21	104	6.8
10	10.2	102	5.7
25	24.7	99	5.9
50	47.6	95	5.3
75	71.8	96	1.8
100	103.0	103	2.1
150	149.6	100	2.0
200	196.6	98	4.5
250	252.3	101	2.3

[a] n = 10 for all concentrations.

Table II—Retention Times of Various Phenothiazines

Phenothiazine Compound	Retention Time, min
Promethazine-5-sulfoxide	2.4
Promethazine	4.5
Promazine	4.5
Chlorpromazine	7.2
Triflupromazine	9.0
Thioridazine	10.5

apparatus. Subsequent blood samples were obtained in heparinized tubes[14]. The samples were drawn immediately, and before the blood came into contact with the rubber tube stoppers, they were replaced by cork stoppers wrapped in aluminum foil. Plasma was separated from blood by centrifugation and stored at −20° until assayed. All samples were assayed within 2 weeks of collection.

Reagents—Human plasma for assay development was purchased[15]. Dog plasma for assay validation in this species was obtained from dogs in the School of Pharmacy animal care facility. Promethazine hydrochloride[16], promethazine-5-sulfoxide hydrochloride[16], and chlorpromazine hydrochloride[17], of reference standard quality; acetonitrile[18], methylene chloride[18], toluene[19], potassium phosphate monobasic[19], of analytical grade quality; and n-nonylamine (98%)[20] and hexamethyldisilazane[21], as supplied were used. All glassware was silanized with 5% hexamethyldisilazane in toluene prior to use.

RESULTS

Assay for Promethazine in Plasma—Typical chromatograms obtained from dog plasma containing no added compounds and from plasma containing promethazine and chlorpromazine (internal standard) are shown in Fig. 1. Retention times for promethazine and chlorpromazine were 4.5 and 7.0 min, respectively. Assay response was linear for promethazine concentrations between 1 and 250 ng/ml. The coefficient of variation in assay response was 11% for a promethazine concentration of 1 ng/ml, and was <10% for all other concentrations. The linear regression of the promethazine–chlorpromazine peak height ratios against promethazine concentrations from repeated determinations was $y = 0.013 + 0.053\,x$, $r = 0.999$, $n = 100$. The day-to-day reproducibility of the procedure, determined during the assay of actual plasma samples, is shown in Table I. The extraction efficiency for promethazine was 94.5 ± 5.6% (n = 5). Substituting dog plasma for human plasma did not affect the assay results.

The use of n-nonylamine in the liquid chromatographic mobile phase has the effect of reducing compound retention time and improving the peak shape on chromatograms (11). This modification improves assay sensitivity. Promethazine-5-sulfoxide, a major metabolite of promethazine, has a retention time of 2.5 min under the chromatographic conditions used, and any peak resulting from the presence of this metabolite was obscured by endogenous plasma components (5). The retention times of some phenothiazines in the system are shown in Table II.

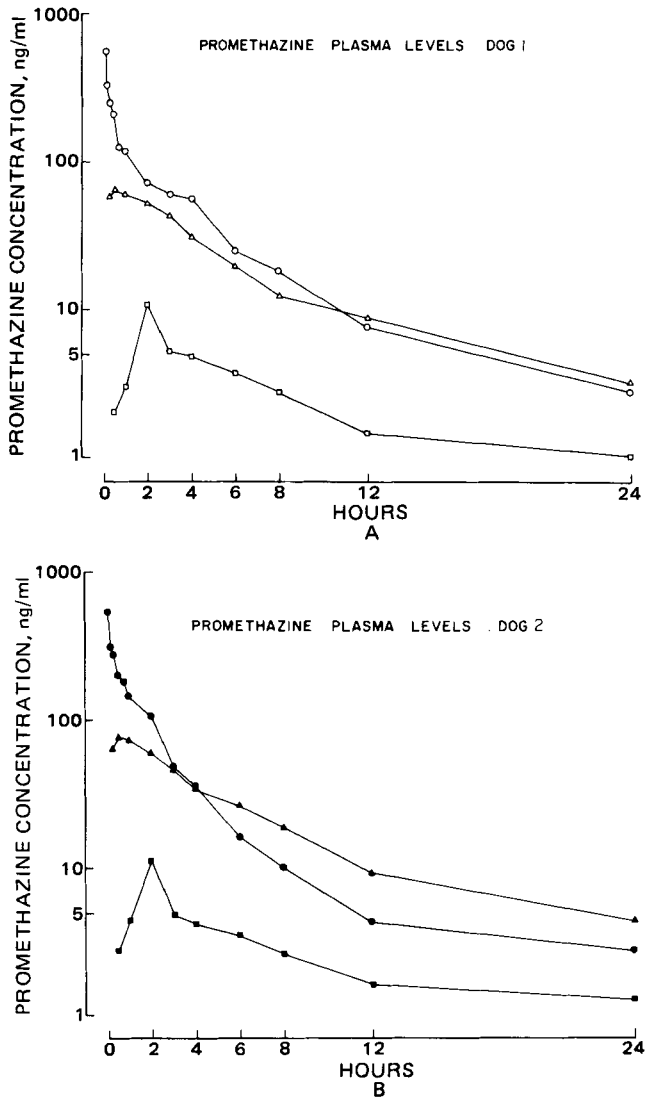

Figure 3—*Promethazine plasma levels following (A) single 50-mg intravenous (○), intramuscular (△), and oral (□) doses to Dog 1; and (B) single 50-mg intravenous (●), intramuscular (▲), and oral (■) doses to Dog 2.*

Pharmacokinetic Study in Dogs—Preliminary studies showed that the rubber stoppers, supplied with the evacuated glass tubes[14], reduce the apparent promethazine concentration by 25–30% compared with values obtained when aluminum-wrapped cork stoppers are used. Plasticizers in the rubber stoppers previously have been shown to displace chlorpromazine from plasma protein binding sites with subsequent redistribution of drug from plasma water into erythrocytes (12). Although it has not been shown that a similar phenomenon occurs with promethazine, the good assay results obtained with the aluminum cork stoppers justified their use.

The plasma promethazine profiles following single 50-mg oral, intramuscular, and intravenous doses of promethazine (hydrochloride) are shown in Fig. 2. The profiles obtained from the three dosage routes are combined for each dog for comparison in Fig. 3.

The promethazine plasma levels were similar in the two dogs. Concentrations of 556 and 535 ng/ml were obtained 5 min after the intravenous doses. Plasma levels declined rapidly at first and then more slowly to reach values of 3–4 ng/ml at 24 hr. The decline in plasma levels appeared to be triphasic in nature. Graphical analysis of the individual data sets in terms of a triexponential function gave rise to half-lives of 0.18, 1.9, and 8.3 hr and 0.14, 1.4, and 27.7 hr from the three exponents in Dogs 1 and 2, respectively. The coefficients of determination [$r^2 = (\Sigma obs^2 - \Sigma dev^2)/\Sigma obs^2$] between observed and predicted promethazine plasma concentrations using the triexponential function were 0.9996 and 0.9997.

[14] Green Stoppered Vacutainer, evacuated glass tubes coated with 143 U of sodium heparin, Becton-Dickinson, Rutherford, N.J.
[15] American Red Cross, Madison, Wis.
[16] Wyeth Laboratories, Inc., Philadelphia, Pa.
[17] Smith Kline & French Laboratories, Philadelphia, Pa.
[18] Burdick & Jackson, Muskegon, Mich.
[19] Fisher Scientific Co., Fair Lawn, N.J.
[20] Aldrich Chemical Co., Milwaukee, Wis.
[21] Pierce Chemical Co., Rockford, Ill.

Peak promethazine levels of 76 and 64 ng/ml were obtained at 0.5 hr following the intramuscular doses; levels declined rapidly and then at a slower rate after 8–12 hr. At 24 hr the levels from these were similar to those observed following intravenous injection. The terminal half-lives, which were calculated from 12- and 24-hr data points in one dog, and the 8–24-hr data points in the other, were 8.5 and 11.6 hr.

Two hours following the administration of oral doses, peak promethazine levels of 10.6 and 11.0 ng/ml were obtained. The subsequent decline in drug levels was again nonlinear, and the drug was barely detectable in plasma at 24 hr. The later times of peak promethazine levels after oral doses, compared to intramuscular doses, indicates that absorption is slower *via* the oral route.

The efficiency of drug absorption from intramuscular and oral doses can be calculated by comparison of areas under plasma curves resulting from the different doses. The trapezoidal areas under plasma curves for Dog 1 in a 24-hr period were 714, 391, and 59 ng hr/ml following intravenous, intramuscular, and oral doses, respectively. In Dog 2 the equivalent values were 650, 472, and 62 ng hr/ml. Since the same dosage was given by each route, the absorption efficiency of unchanged promethazine can be obtained by direct comparison of area values. Thus, compared with intravenous values, drug bioavailability was 55 and 73% after intramuscular doses, and after oral doses, 8.3 and 9.5%.

DISCUSSION

The assay for promethazine used in this study is suitable for routine laboratory use. Sample preparation is uncomplicated and compounds are measured using a fixed wavelength UV detector. The method is sufficiently sensitive and specific to monitor plasma promethazine levels in animals and humans during a 24-period following therapeutic doses (5).

The reduction in plasma promethazine levels observed when rubber stoppers were used in blood collection tubes is similar to that reported previously for chlorpromazine (12). Failure to account for this may give rise to considerable assay error. The present data do not establish, however, that the mechanism causing reduced promethazine levels is the same as that for chlorpromazine. As a result, protein-binding characteristics of promethazine and other phenothiazines under different situations are being examined.

The plasma promethazine levels obtained in the two dogs show that the pharmacokinetics of promethazine are complex, and its disposition in the body cannot be described in terms of a simple one- or two-compartment kinetic model. It cannot be determined from these data whether the apparent triphasic decline in plasma levels following intravenous doses is due to differential uptake of drug by deep and shallow tissue compartments or to concentration-dependent changes in drug binding to plasma proteins.

Comparison of the areas under plasma curves from the three dosage routes indicates that the overall bioavailability of intact promethazine is reduced somewhat after intramuscular injection compared to intravenous administration. This is not uncommon (13) and probably results from partial degradation of drug at the intramuscular injection site and from slow release of some drug from the site at later, postsampling times.

The marked reduction in promethazine plasma levels following oral doses, compared to intravenous and intramuscular doses, indicates inefficient absorption by this dosage route. The degree of reduction is greater than that previously reported in rabbits (9), where systemic drug availability was calculated to be 50%, but appears to be similar to that reported in a single human volunteer following 12.5-mg intravenous and oral doses (14).

Although extensive first-pass metabolism of oral promethazine has been inferred (10, 14), the data currently available from this and previous studies is insufficient to determine the relative contributions of limited absorption and first-pass metabolism to the poor systemic availability of oral promethazine.

As the availability of poorly absorbed drugs is likely to be more variable, and more easily influenced by other factors, than that of efficiently absorbed compounds, the results obtained in this study confirm that promethazine is a compound with potential bioequivalence problems (15). The data presented here and elsewhere (10, 14) indicate that the dog may be a suitable animal model for promethazine bioavailability studies.

REFERENCES

(1) G. Taylor, R. T. Calvert, and J. B. Houston, *Anal. Lett.*, **12,** 1435 (1979).

(2) C. J. Reddrop, W. Reiss, and T. F. Slater, *J. Chromatogr.*, **192,** 375 (1980).

(3) D. N. Bailey and J. J. Guba, *Clin. Chem.*, **28,** 1211 (1979).

(4) C. H. Ng and J. L. Crammer, *Br. J. Clin. Pharmacol.*, **4,** 173 (1977).

(5) R. B. Patel and P. G. Welling, *Clin. Chem*, **27,** 1780 (1981).

(6) G. J. DiGregorio and E. Ruch, *J. Pharm. Sci.*, **69,** 1457 (1980).

(7) J. E. Wallace, E. L. Shimek, Jr., S. C. Harris, and S. Stavchansky, *Clin. Chem.*, **27,** 253 (1981).

(8) J. E. Wallace, E. L. Shimek, S. Stavchansky, and S. C. Harris, *Anal. Chem.*, **53,** 960 (1981).

(9) G. Taylor and J. B. Houston, *J. Pharm. Pharmacol. (Suppl.)*, **31,** 40P (1979).

(10) J. Quinn and R. Calvert, *ibid.*, **28,** 59P (1976).

(11) N. H. C. Cooke, *Altex Chromatogram*, **3** (June), 1 (1980).

(12) K. K. Midha, J. C. K. Loo, and M. L. Rowe, *Res. Commun. Psychol. Psychiatry, Behav.*, **4,** 193 (1979).

(13) C. T. Viswanathan, H. E. Booker, and P. G. Welling, *J. Clin. Pharmacol.*, **18,** 100 (1978).

(14) J. B. Houston, *Pharm. Int.*, **2,** 37 (1981).

(15) *Fed. Regist.*, **42,** 1624 (1977).

ACKNOWLEDGMENTS

This research was supported by National Institutes of Health Grant GM 20327.

The authors gratefully acknowledge the excellent technical assistance of David S. Irwin.

Relative Bioavailability of Chlorthalidone in Humans: Adverse Influence of Polyethylene Glycol

ROGER L. WILLIAMS ˣ, CHERYL D. BLUME, EMIL T. LIN, NICHOLAS H. G. HOLFORD, and LESLIE Z. BENET

Received May 1, 1981, from the *Drug Studies Unit, the School of Pharmacy, University of California, San Francisco, CA 94143.* Accepted for publication August 27, 1981.

Abstract □ The bioavailability of two commercial preparations of chlorthalidone was studied in healthy male subjects. Reference solutions/suspensions for the two products were chlorthalidone dissolved in a solution of water–polyethylene glycol and a solution/suspension of chlorthalidone. Bioavailability of the chlorthalidone in water–polyethylene glycol solution was significantly reduced in comparison to one of the commercial preparations, and trends in the data suggested that it was less well absorbed than either the chlorthalidone in water solution/suspension or the other commercial preparation of chlorthalidone. These data, together with previous reports indicating that polyethylene glycol may retard the absorption of some drugs *in vitro*, suggest that this compound should not be used to aid dissolution of drug in a reference standard for bioavailability investigations.

Keyphrases □ Chlorthalidone—relative bioavailability in humans, adverse influence of polyethylene glycol □ Bioavailability—chlorthalidone in humans, adverse influence of polyethylene glycol □ Polyethylene glycol—adverse influence on relative bioavailability of chlorthalidone, humans

Chlorthalidone[1] [2-chloro-5-(1-hydroxy-3-oxo-1-isoindolinyl)benzene-sulfonamide] is a diuretic agent with a relatively long half-life (~45 hr), correspondingly long duration of effect, and a low incidence of adverse effects. Because it is now possible for several manufacturers to market the drug in the United States, studies will be performed to assess the bioequivalence of different formulations of chlorthalidone. Guidelines issued by the U.S. Food and Drug Administration (FDA) for the performance of these investigations recommend that bioequivalency studies of chlorthalidone be performed against a standard reference solution of chlorthalidone in at least 20 individuals in a two-way crossover design (1).

Because chlorthalidone is poorly soluble in water (12 mg/100 ml water at 20°) (2), FDA guidelines recommend a solution of chlorthalidone in polyethylene glycol (I) as the reference standard for bioavailability because polyethylene glycol aids the dissolution of the drug in water. Preliminary studies, however, have suggested that chlorthalidone in a water–polyethylene glycol solution is less well absorbed than a tablet formulation. To assess this possibility and to evaluate a generic preparation of chlorthalidone in accordance with FDA guidelines, a crossover investigation was designed to determine the relative bioavailability of different formulations of chlorthalidone.

EXPERIMENTAL

Clinical Study—The study was performed in the clinical facilities of the Drug Studies Unit, University of California, San Francisco. Subjects were healthy male volunteers between the ages of 21 and 40 and within 10% of standard weight for height and body frame size (3). Information about the study was given to each participant prior to entry and each subject signed a consent form indicating they were informed of the purpose and procedures of the study. The study lasted 12 weeks, during which the participants were administered a single dose of each of four preparations of chlorthalidone with a 3-week wash-out period between each dose.

Table I—Measurement of Blood Concentration–Time Curves in 12 Healthy Male Subjects After a Single 50-mg Dose of Chlorthalidone (Treatment A)

Parameter	Mean ± *SD*
T_{lag}, hr	0.513 ± 0.564
K_{abs}, hr^{-1}	0.168 ± 0.125
$T_{1/2_{abs}}$, hr	7.73
α, hr^{-1}	0.992 ± 0.623
$T_{1/2_\alpha}$, hr	0.929 ± 0.442
β, hr^{-1}	0.0181 ± 0.0082
$T_{1/2_\beta}$, hr	46.7 ± 22.2
V_1/F^a, l	14.4 ± 25.5
V_{dss}/F^a, l	11.0 ± 4.66
Vd_{area}/F^b	11.3 ± 4.05
Cl/F^a, liter/hr	0.184 ± 0.044
Cl/F^b, liter/hr	0.180 ± 0.046
Cl_{renal}, liter/hr	0.080 ± 0.018

[a] Calculated using computer fitted parameters. [b] Calculated using measured *AUC* values.

The following four formulations of chlorthalidone were administered as a single oral dose in the study: Two 25-mg chlorthalidone tablets[2] taken with 180 ml of water (Treatment A); chlorthalidone[3], two 25-mg tablets taken with 180 ml of water (Treatment B); chlorthalidone in water–polyethylene glycol solution, 50 mg/100 ml followed by an 80-ml water rinse of the dosing container (Treatment C); and chlorthalidone in solution/suspension, 50 mg/100 ml water, followed by an 80-ml water rinse of the dosing container (Treatment D). Chlorthalidone in solution or solution/suspension was prepared according to the following procedures. For treatment C, 10% water–polyethylene glycol 4000 solution was heated to 37° and added to chlorthalidone powder to give, after filtration, 50 mg of drug/100 ml of solution. Assay of solution, using the same assay as for blood, for Treatment C confirmed that the content of chlorthalidone was appropriate. For Treatment D, 50 mg of chlorthalidone was stirred in 100 ml of water prior to dosing.

Dose Administration—Twenty-two healthy males participated in the study. Twelve of the 22 subjects received all four formulations of chlorthalidone according to a balanced 4 × 4 Latin square design. Three subjects were assigned to each of four treatment sequences. An additional 10 subjects received only the formulation of chlorthalidone used in Treatment B and chlorthalidone in water–polyethylene glycol solution. Five of these subjects were randomly assigned to one of the two possible treatment sequences (product used in Treatment B followed by water–polyethylene glycol solution of drug) and five were assigned to the reverse procedure. Postexperiment analysis of the data indicated no sequence, period, or crossover effects in the 12 individuals receiving all four treatments. The data for Treatment B and for chlorthalidone in water–polyethylene glycol solution (Treatment C) from these 12 individuals were, therefore, combined with the data in the additional 10 subjects receiving these treatments to give 22 individuals who received both Treatments B and C. These data provided bioequivalency data for chlorthalidone tablets required by FDA for premarketing approval.

Dosing of chlorthalidone occurred at 8 am on a treatment day, followed by blood and urine collections for a period of 120 hr. Beginning with the 8 am dose, blood was collected at the following time periods: 0, 0.5, 1, 2, 3, 4, 6, 8, 12, 24, 48, 72, 96, and 120 hr. Urine was collected at the following time periods, beginning with the 8 am dose: 0–2, 2–4, 4–6, 6–8, 8–12,

[1] The drug is marketed as Hygroton by Ciba-Geigy in Europe and under license by USV Pharmaceuticals in the United States.

[2] U.S.V. Laboratories, lot No. 06009.

[3] Mylan Pharmaceuticals, lot No. E021M.

0022-3549/82/0500-0533$01.00/0

Table II—Variables Assessing Bioequivalence Between Four Formulations of Chlorthalidone in 12 Subjects

Variable	Treatment[a] A	Treatment[b] B	Treatment[c] C	Treatment[d] D	P^e	Newman-Keuls: B versus A	Newman-Keuls: B versus C	Newman-Keuls: C versus D
$AUC_{0-\infty}$, mg × hr/liter	293 ± 67[f]	336 ± 53	278 ± 71	305 ± 74	0.074			
Amount in $urine_{0-120\ hr}$, mg	18.3 ± 2.5	22.1 ± 5.6	16.6 ± 3.4	17.9 ± 3.2	0.019	0.05	0.05	0.05
Ka, hr^{-1}	0.168 ± 0.13	0.253 ± 0.17	0.162 ± 0.13	0.185 ± 0.10	0.420			
β, hr^{-1}	0.0181 ± 0.0082	0.020 ± 0.010	0.0173 ± 0.004	0.0156 ± 0.0052	0.520			
C_{peak}, mg/l	3.73 ± 0.93	4.62 ± 0.80	3.36 ± 0.74	3.93 ± 1.12	0.022		0.05	
T_{peak}, hr	13.8 ± 6.3	10.8 ± 5.0	12.1 ± 11.7	16.1 ± 12.3	0.517			

[a] Tablet[2]. [b] Tablet[3]. [c] Chlorthalidone in water and polyethylene glycol. [d] Chlorthalidone solution/suspension in water. [e] Analysis of variance. [f] Standard Deviation.

12–24, 24–48, 48–72, 72–96, and 96–120 hr. Aliquots of urine were taken after volume measurement and both blood and urine samples were stored at −20° until analysis. Subjects fasted overnight (10 hr) prior to dosing and continued fasting until a standard lunch was administered 4 hr after dosing. They were ambulatory during the study but did not engage in strenuous exertion.

Drug Analysis—Chlorthalidone concentrations in whole blood and urine were assayed with high-pressure liquid chromatography (HPLC). Whole blood assay was performed because chlorthalidone is known to concentrate in red blood cells, whereas the concentrations in plasma are low. The method of assay is summarized here; however, details of the method will be presented in a separate publication.

Whole blood (0.2 ml) was mixed with an equal volume of distilled water, sonicated for 5 min, and mixed with acetonitrile containing phentolamine hydrochloride (internal standard). After mixing and centrifugation, the supernate was transferred to a clean tube and evaporated under nitrogen until ~0.4 ml of the solution remained. A portion of this sample was injected into the loop injector of the high-pressure liquid chromatograph. Urine was handled as blood with the exceptions that the sonication and centrifugation steps were not included and the urine internal standard was pentobarbital sodium. Chromatography was performed on a high-performance liquid chromatograph[4] equipped with a variable wavelength spectrophotometric detector[5]. The UV detector was set at 210 nm for blood and 250 nm for urine samples. The lower limit of sensitivity of the assay in blood was 200 ng/ml with a coefficient of variation of 5.0% and 750 ng/ml in urine with a coefficient of variation of 6.6%.

Pharmacokinetic and Statistical Analysis—To obtain the absorption and elimination rate constants, the blood concentration–time data were fitted to a two-compartment body model with first-order input and lag time. Due to the prolonged peak time, the absorption half-time was assumed to be longer than that for the fast disposition constant, α. This is consistent with values obtained previously (4) following intravenous dosing. Weighting of each data point was performed by squaring the value of the reciprocal of the observation. Parameter estimates were obtained using a nonlinear least-square computer program (3). The area under the plasma concentration curve (AUC) for chlorthalidone in blood was calculated by trapezoidal rule to C_{peak} and log-trapezoidal rule thereafter. $AUC_{120\ hr-\infty}$ was estimated from the concentration of chlorthalidone in blood at 120 hr divided by the terminal rate constant of elimination obtained from the fitting procedure. This area was added to the $AUC_{0-120\ hr}$ to give $AUC_{0-\infty}$. C_{peak} and T_{peak} represent the points of the highest concentration of chlorthalidone observed in blood and the time this concentration occurred. As verification of the fitting procedure, chlorthalidone clearance/F was also calculated using the noncompartmental method of dividing dose by $AUC_{0-\infty}$, where F is the fraction of the oral dose available to the systemic circulation. Renal clearance was determined by dividing the amount of drug excreted into the urine at 120 hr by the $AUC_{0-120\ hr}$.

The following parameters were analyzed statistically: absorption and elimination rate constants, $AUC_{0-\infty}$, amount of drug excreted in the urine in 120 hr, and C_{peak} and T_{peak} (5). Significant differences between treatments were identified using the Newman-Keuls test.

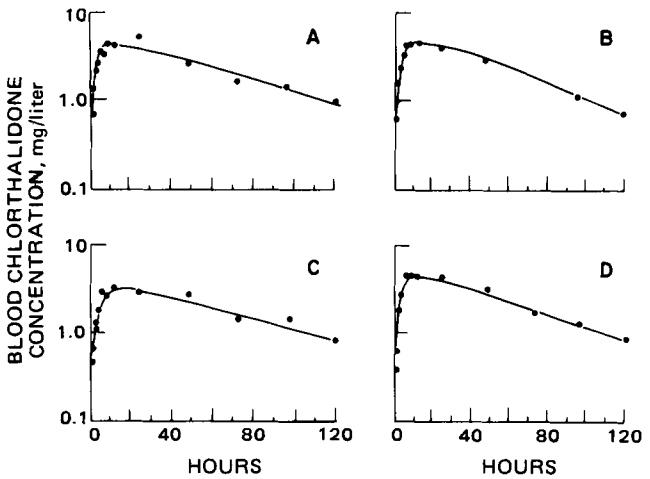

Figure 1—*Blood chlorthalidone concentration–time curves in a single individual (Subject 1) following administration of Treatment A, Treatment B, chlorthalidone in water/polyethylene glycol solution (Treatment C), and chlorthalidone in water solution/suspension (Treatment D).*

[4] Perkin-Elmer Series 3.
[5] Schoeffel, model SP 770.

RESULTS AND DISCUSSION

Representative blood concentration–time curves observed in a single individual (Subject 1) after each of the four treatments are shown in Fig. 1. Pharmacokinetic parameters derived from the curves in the 12 individuals receiving Treatment A are shown in Table I. Variables assessing bioequivalence in the 12 subjects who received all four treatments are shown in Table II and in the 22 subjects who received Treatments B and C in Table III. Table II also contains the results of the Newman-Keuls analysis that tested which of the four treatments differed. Table IV shows the comparison of values in all four preparations for the amount of drug excreted in the urine in 120 hr and the $AUC_{0-\infty}$. Because urine was collected for only approximately three half-lives of chlorthalidone, this measurement is probably less valuable in assessing chlorthalidone bioavailability than $AUC_{0-\infty}$.

The data in Table I correspond well with previous reports of chlorthalidone pharmacokinetics following an oral dose of the drug. Fleuren *et al.*, (4) reported a plasma clearance/F of 9.55 liter/hr for chlorthalidone (Treatment A) after a single dose of the drug. Using the Reiss *et al.* (6) value of 0.0138 for the plasma to blood ratio of chlorthalidone, this plasma clearance may be converted to a blood clearance of 0.132 liter/hr. This corresponds to the value of 0.184 liter/hr observed in this study for Treatment A, given the apparent variability in plasma to blood ratio of chlorthalidone over concentrations exhibited following clinical doses of the drug. This variability occurs as a consequence of saturable binding

Table III—Variables Assessing Bioequivalence Between Two Formulations of Chlorthalidone in 22 Subjects

Variable	Treatment B[a], mean ± SD	Treatment C[b], mean ± SD	P^c
$AUC_{0-\infty}$, mg/liter·hr	322 ± 60	272 ± 56	0.0023
Amount in $urine_{0-120\ hr}$, mg	20.2 ± 5.1	15.7 ± 3.3	0.0003
Ka, hr^{-1}	0.248 ± 0.20	0.134 ± 0.12	0.0315
β, hr^{-1}	0.0193 ± 0.0085	0.0168 ± 0.0045	0.2583
C_{peak}, mg/liter	4.03 ± 0.98	3.03 ± 0.69	0.0001
T_{peak}, hr	13.3 ± 8.9	18.2 ± 17.2	0.2134

[a] Tablet[3]. [b] Chlorthalidone in water and polyethylene glycol solution. [c] Analysis of variance.

Table IV—Comparison of $AUC_{0-\infty}$ and $Ae_{0-120\ hr}$ Values[a]: Ratio of Individual Values with Mean ± *SD*

Subject	$AUC_{0-\infty}$ Treatment A/C	$AUC_{0-\infty}$ Treatment B/C	$AUC_{0-\infty}$ Treatment D/C	$AUC_{0-\infty}$ Treatment B/A	Amount of Drug in $Urine_{0-120\ hr}$ Treatment A/C	Amount of Drug in $Urine_{0-120\ hr}$ Treatment B/C	Amount of Drug in $Urine_{0-120\ hr}$ Treatment D/C	Amount of Drug in $Urine_{0-120\ hr}$ Treatment B/A
1	0.97	1.23	1.00	1.26	1.45	1.43	1.43	0.98
2	1.04	0.94	0.93	0.90	0.74	1.56	1.01	2.11
3	1.56	1.09	1.53	0.70	1.37	1.49	1.61	1.08
4	1.51	1.57	1.18	1.04	1.19	1.42	1.48	1.19
5	0.89	0.79	1.13	0.89	1.67	2.23	1.96	1.34
6	1.46	0.97	1.62	0.66	1.30	1.07	1.32	0.83
7	1.16	1.36	1.05	1.17	0.86	1.08	0.84	1.24
8	1.27	1.60	1.08	1.25	0.80	0.90	0.82	1.12
9	1.11	1.43	0.86	1.28	1.49	1.55	1.32	1.04
10	0.97	1.87	1.23	1.92	1.28	1.14	1.68	0.90
11	0.97	1.10	1.06	1.13	1.41	1.71	1.22	1.22
12	1.31	1.32	0.99	1.01	1.04	0.83	0.63	0.80
13		0.95				1.02		
14		1.38				0.93		
15		1.13				1.23		
16		1.18				1.67		
17		1.09				1.32		
18		0.94				1.18		
19		1.40				1.34		
20		1.02				1.02		
21		0.88				1.24		
22		1.66				1.37		
Mean	1.19	1.22	1.14	1.10	1.22	1.31	1.28	1.15
SD	0.23	0.28	0.23	0.33	0.30	0.32	0.39	0.34

[a] Treatments A, B, and D compared with Treatment C; Treatment B compared with A.

of drug to erythrocytes (7). Fleuren *et al.* (4) reported a terminal half-life of 44.1 hr, whereas a value of 46.7 hr was obtained in this study. Although absolute bioavailability could not be assessed in this study, Fleuren and coworkers reported that the fraction of drug absorbed into the systemic circulation after an oral dose is ~0.60. Multiplying the clearance/*F* values by 0.60 yields a blood chlorthalidone clearance of ~0.110 liter/hr (1.84 ml/min). Slightly less than three-quarters of the chlorthalidone clearance is represented by renal elimination of unchanged drug, while the remainder presumably occurs as a result of hepatic biotransformation and biliary excretion. With a low distribution volume and a relatively long terminal half-life, chlorthalidone belongs to the category of drugs that are poorly extracted from the blood.

The data in Table III demonstrate a statistically significant difference between Treatments B and C for several parameters, apparently because of the larger number of individuals studied. From this study, Treatment B is absorbed more rapidly, attains a higher concentration of chlorthalidone in the blood, produces a greater $AUC_{0-\infty}$, and results in a greater amount of drug excreted in the urine by 120 hr in comparison with the drug in the water–polyethylene glycol solution. The data in this table also indicate that for $AUC_{0-\infty}$, Treatment B differs from Treatment C (as does Treatment A) according to the 75:75 rule (FDA), in which 75% of the individuals must demonstrate a test value within 75% of the value for the reference solution.

Previous investigations have suggested that polyethylene glycol can retard drug absorption. In 1966 it was demonstrated in two different *in vitro* systems that polyethylene glycol retarded the dissolution and absorption of phenobarbital (8). It was suggested that this effect probably occurred as a consequence of complexation of phenobarbital with polyethylene glycol. This particular phenomenon was observed only for phenobarbital, however, and not for pentobarbital, barbital, or barbituric acid. It was demonstrated more recently using the *in situ* rat gut technique, that both polyethylene glycol 4000 and 6000 retarded the rate of disappearance of salicylic acid from the gut (9). The clinical data in this report corroborate these *in vitro* observations on the potential influence of polyethylene glycol on drug dissolution and/or absorption.

Polyethylene glycol 4000 is one of several polyethylene glycols produced by reacting ethylene oxide with ethylene glycol or water; they bear the general formula of $H(CH_2CH_2)_nOH$. Used as demulcents, polyethylene glycols are found in water-soluble ointment bases, as ingredients of lotions and suppositories, and as tablet coatings. Although polyethylene glycol 4000 results in improved solubility of chlorthalidone in water, the data in this investigation, as well as previous reports (8, 9), indicate that it is not an appropriate constituent for use in chlorthalidone bioavailability studies. Its use in bioequivalency investigations for other drugs should probably be discouraged until it can be shown to be inert in the test system employed.

The data in Tables II and IV suggest also that Treatment B may be slightly more bioavailable than a water solution/suspension of chlorthalidone or the currently marketed preparation of the drug, Treatment A. Whatever differences exist between the treatments in this study, however, are not likely to be of clinical significance. These observations raise the following issue: As pharmaceutical technology advances, generic formulations of marketed drugs may be produced that are substantially more bioavailable than the innovators' products. In such circumstances, the FDA may be in the unenviable position of requesting that generic manufacturers either design a product with lower bioavailability characteristics or alter the drug content of their formulation. As an alternative, the FDA may ask the innovator to reformulate. Whatever the final decision, the results of this study emphasize the importance of including the innovator's formulation in assessing the bioequivalence of a generic product.

REFERENCES

(1) "Guidelines for *In Vivo* Bioavailability Studies for Chlorthalidone Diuretics," Food and Drug Administration, U.S. Department of Health and Human Services, Rockville, Md., 1979.

(2) "The Merck Index," 8th ed., P. G. Stecker, Ed., Merck, Rahway, N.J., 1968, p. 252.

(3) N. H. G. Holford, in "Public Procedures Notebook," H. M. Perry and J. J. Woods, Eds., Bolt, Beranek, and Newman, Cambridge, Mass., 1979.

(4) H. L. J. Fleuren, Th.A. Thien, C. P. W. Verwey-van Wissen, and J. M. van Rossum, *Eur. J. Clin. Pharmacol.*, **15,** 35 (1979).

(5) A. Bostrom, "Repeated Measures Analysis of Variance," Scientific Computing Services, University of California, San Francisco, Calif.

(6) W. Riess, U. C. Dubach, D. Burckhardt, W. Theobald, P. Vuillard, and M. Zimmerli, *Eur. J. Clin. Pharmacol.*, **12,** 375 (1977).

(7) H. L. J. M. Fleuren, Ph.D. thesis, University of Amsterdam, The Netherlands, 1979.

(8) P. Singh, J. K. Guillory, T. D. Sokoloski, L. Z. Benet, and V. N. Bhatia, *J. Pharm. Sci.*, **55,** 63 (1966).

(9) S. Stavchansky, A. Martin, and A. Loper, *Res. Commun. Chem. Pathol. Pharmacol.*, **24,** 77 (1979).

ACKNOWLEDGMENTS

Supported in part by U.S. Public Health Service Training Grant No. 07456 from the National Institute of General Medical Sciences and in part by a grant from Mylan Pharmaceuticals, Morgantown, W.Va.

GLC Method for Iminodibenzyl and Desipramine Impurities in Imipramine Hydrochloride and Its Formulated Products

DON W. THOMPSON

Received December 12, 1980, from the *Food and Drug Administration, Atlanta, GA 30309.* Accepted for publication August 26, 1981.

Abstract □ A GLC method is described for the determination of iminodibenzyl and desipramine impurities in imipramine hydrochloride and its formulated products. These impurities were extracted from an alkaline solution with a mixture of 30% methylene chloride in hexane for chromatography on a 3% OV-17 GLC column. Iminodibenzyl was determined using anthracene as an internal standard and desipramine was determined (after derivatization) using nortriptyline as an internal standard. Based on spiked excipient mixtures typically used to compound imipramine tablets, recoveries were 93–109% for iminodibenzyl and 93–107% for desipramine at 0.2–0.4% of the labeled claim of imipramine. Minimum detection levels were ~0.02% for each impurity, and procedural standards gave coefficients of variation of <1% for each impurity. The method was linear in the 0.05–0.5 μg range and typically gave correlation coefficients ≥0.999.

Keyphrases □ Imipramine—GLC method for determining iminodibenzyl and desipramine impurities, drug substance and formulated products □ GLC—determination of iminodibenzyl and desipramine impurities in imipramine and its formulated products □ Antidepressants—GLC determination of iminodibenzyl and desipramine impurities in imipramine and its formulated products □ Desipramine—as an impurity in imipramine, determined by GLC

A determination of the kinds and amounts of organic impurities in drugs and drug formulations is a measure of both product stability and good manufacturing practices. Impurities may be present as by-products of synthesis, inadequate purification after synthesis, or from decomposition due to improper storage and handling.

It would be highly impractical to analyze for all of the possible organic impurities that might be present in imipramine and its formulated products. The present study determined which imipramine impurities might be indicators of both product stability and good manufacturing practices and developed an analytical system capable of measuring one or more of these impurities.

Several investigators have reported analytical procedures for imipramine and its related compounds using techniques such as GLC (1–6), GC–mass spectrometry (7–10), TLC (11–15), HPLC (16–20), and spectrophotometric methods (21–24). However, these reports primarily applied to the analysis of imipramine and its biological metabolites rather than the analysis of impurities in the drug substance.

Other investigators have reported impurities in imipramine and its formulated products by TLC. Adank and Hammerschmidt (25) reported the presence of eight impurities in commercial imipramine drug substance with total impurities < 0.2% and no single entity > 0.05%. The presence of similar amounts and kinds of impurities in commercial clomipramine (a compound structurally related to imipramine) was also reported (26). McErlane *et al.* (27) performed a study on impurities in imipramine, desipramine, and their formulations. When 19 lots of imipramine tablets from seven manufacturers were tested, five impurities were detected. Two of the major impurities were iminodibenzyl and desipramine at levels of up to 0.3% of the labeled claim of the drug.

A recent study (28) reported relatively high levels of impurities in imipramine samples taken from a hospital pharmacy in Richmond, Virginia. Iminodibenzyl levels of up to 2.8% and desipramine levels of up to 3.2% by GC–mass spectrometry techniques were reported. These results appear high when compared with this and previous studies (25–27).

The present report describes a GLC procedure for the quantitative determination of two major imipramine impurities, iminodibenzyl and desipramine, which appear to be indicators of product stability and good manufacturing practices.

EXPERIMENTAL

Materials—Desipramine hydrochloride, nortriptyline hydrochloride, and iminodibenzyl were the respective USP or NF reference standards. Reagent grade anthracene[1] was used as received. All other reagents and solvents were analytical reagent grade.

Apparatus—Analyses were performed on a gas chromatograph[2] equipped with a flame ionization detector and a strip chart recorder[3]. Air and hydrogen flow rates were set to maximize the detector response. The amplifier sensitivity settings were generally 3–6 × 10^{-10} amps full scale.

Column—A 1.8-m (6 ft) × 2-mm glass column packed with 3% OV-17 on 100–120 mesh Gas Chrom Q was conditioned overnight at 260° with nitrogen flow. The column temperature was maintained at 190° for the iminodibenzyl determination and 240° for the desipramine determination. The injection port and detector temperatures were held at 250°. Nitrogen was used as the carrier gas at 40 ml/min.

Edetate Disodium Solution—Four grams of ACS edetate disodium was dissolved in 50 ml of 1.5 *N* NaOH.

Internal Standard Solution—Approximately 4 mg of USP nortriptyline hydrochloride reference standard and ~2.5 mg of reagent grade anthracene were dissolved in 60 ml of methylene chloride. This was diluted to 200 ml with hexane and mixed thoroughly.

Standard Preparation—Approximately 2.5 mg each of USP reference iminodibenzyl and desipramine standards (accurately weighed) were dissolved in methanol and diluted to volume in a 5-ml volumetric flask (prepare fresh daily). Aliquots (100, 200, and 300 μl) of the standard preparation were then transferred to separate 15-ml test tubes fitted with polytef-lined screw caps. Each was evaporated to dryness using a nitrogen stream and gentle heat.

Procedure—A portion of imipramine hydrochloride drug substance, tablets or injection, equivalent to ~50 mg of imipramine hydrochloride was accurately weighed and transferred to a 15-ml test tube with a polytef-lined screw cap. The internal standard solution (5 ml) and 5 ml of the edetate disodium solution were added (for the injection, substitute 2 ml of 10% NaOH plus 400 mg of edetate disodium). The solution was shaken vigorously for 5 min and centrifuged until the upper organic layer was clear. A 4–4.5 ml portion of the upper layer was transferred to a tapered 15-ml centrifuge tube and evaporated to 0.5–1 ml using nitrogen and gentle heat. To equilibrate the system, 1–2 μl of this sample extract was injected into the gas chromatograph three or more times prior to quantitation.

[1] Eastman Kodak Co., Rochester, N.Y.
[2] Perkin-Elmer Model 900.
[3] Perkin-Elmer Model 56.

0022-3549/82/0500-0536$01.00/0

Table I—Tabulation of Recoveries on Synthetic Tablet Formulations [a]

Manufacturer/ Number		μg, Iminodibenzyl Added per 50 mg Imipramine	%, Iminodibenzyl Recovered	μg, Desipramine Added per 50 mg Imipramine	%, Desipramine Recovered
I	1	100	102	100	93
	2	100	99	100	104
	3	150	104	150	94
	4	200	100	200	100
	5	200	104	200	104
II	1	150	102	150	102
	2	150	102	150	104
	3	150	97	150	104
	4	150	109	150	104
	5	150	101	150	105
III	1	100	94	100	104
	2	100	97	100	105
	3	150	98	150	107
	4	200	97	200	105
	5	200	98	200	107
IV	1	100	93	100	101
	2	100	98	100	102
	3	150	102	150	101
	4	200	99	200	102
	5	200	98	200	106
V	1	100	99	100	105
	2	100	102	100	100
	3	150	102	150	101
	4	200	99	200	103
	5	200	99	200	104
Mean			99.8		102.7
SD			3.4		3.4

[a] Excipient mixtures typically used to compound imipramine tablets.

The peak height ratios of iminodibenzyl to anthracene internal standard *versus* concentration for the calibration curve was plotted.

After the iminodibenzyl determination, 0.5 ml of methylene chloride and 5–7 drops of reagent grade acetic anhydride were added to the sample and standard extracts. This solution was mixed thoroughly and allowed to stand at room temperature for ~5 min. Then, 0.5 ml of methanol was added, mixed, and evaporated to dryness using a nitrogen stream and moderate heat (steam bath). The residue was dissolved in ~1 ml of 30% methylene chloride in hexane.

The GC column was maintained at 240° for the desipramine calibration curve, as previously described for iminodibenzyl, using peak height ratios of desipramine to nortriptyline internal standard.

RESULTS AND DISCUSSION

The TLC systems reported previously for imipramine and its impurities (25–27) showed good separations and adequate sensitivities for all the compounds when applied to an examination of imipramine drug substance and some commercial products. Eight impurities were detected at levels of ≤0.3% based on spot size and intensity. The predominant impurities were shown to be iminodibenzyl and desipramine. Additional examination of some commercial products by TLC, GLC, and GC–mass spectrometry in this laboratory did not reveal any impurities other than those reported previously.

Preliminary decomposition studies were conducted to determine the conditions necessary for the formation of iminodibenzyl and desipramine impurities in imipramine drug substance. Imipramine was heated at 100° in 0.1 *N* HCl for 3 hr with a current of air flowing over the surface. This treatment was followed by a 15-min exposure to long-wave UV light. TLC examination of the treated imipramine drug substance, compared to a nontreated sample, revealed a significant increase in both iminodibenzyl and desipramine content based on R_f values and spot intensity. The chromatogram of the treated sample was similar to that of a nontreated commercial imipramine tablet in that at least eight different known decomposition products were observed.

In another decomposition study, pure (by TLC) imipramine free base was exposed to normal laboratory fluorescent lighting and/or air for 72 hr on a silica gel TLC plate. At the end of this exposure period, the imipramine was extracted with methanol to be rechromatographed. The

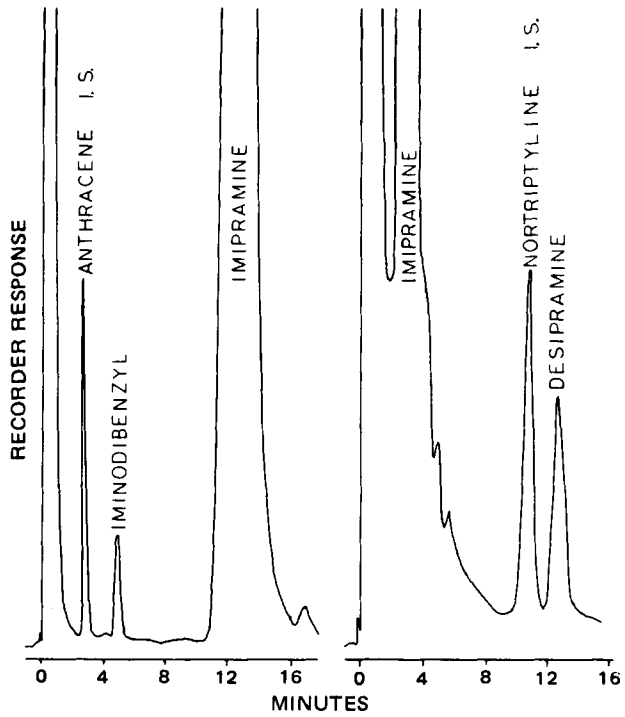

Figure 1—*Gas chromatogram of a commercial imipramine hydrochloride tablet extract at a column temperature of 190° prior to derivatization (left). The chromatogram on the right is the same extract at a column temperature of 240° after derivatization.*

imipramine exposed only to fluorescent light showed no discoloration and indicated only a trace of an impurity at the same R_f value as that of desipramine. The imipramine exposed to both the fluorescent lighting and air showed considerable discoloration and five additional spots on TLC. The predominant spots were those corresponding in R_f value to iminodibenzyl and desipramine. Although the presence of both iminodibenzyl and desipramine was confirmed by GC–mass spectrometry, the predominant compound present at the R_f value for iminodibenzyl had a molecular weight of 240 and is currently unidentified. Because chromatographically pure imipramine free base was used, it would appear that the unidentified compound is definitely related to imipramine. Interestingly, no compound with a molecular weight of 240 was detected in any of the commercial products examined in this study.

The decomposition studies indicated that there is a probability of some type of decomposition occurring in imipramine if adequate control of heat, light, air, and moisture is not used during commercial product formulation. In addition, iminodibenzyl and possibly desipramine may be present as part of these decomposition products.

The GLC procedure used offers comparable sensitivity to TLC (~0.02–0.04% impurities based on the labeled claim of imipramine) and considerable improvement over TLC in accuracy and precision. The method is linear in the 0.05–0.5 μg range and standard curves typically give correlation coefficients of ≥0.999. Procedural standards gave coefficients of variation of <1% for each impurity. The uncertainty of quantitation of impurities by TLC using spot size and intensity was estimated to be ±30%.

Two commercial tablet products were encountered which consistently gave low iminodibenzyl and desipramine recoveries. Further study revealed that calcium salts were present as high percentage excipients in the two products in question. Additional recovery studies using only iminodibenzyl and desipramine standards and the calcium salts revealed that calcium was indeed interfering with the assay. Several techniques such as multiple extractions, pH adjustments, and salting out were all used without success. Edetate disodium was finally added to complex the calcium and this provided successful assay results.

Excipient mixtures used to compound imipramine tablets from five different manufacturers were spiked with iminodibenzyl and desipramine at three concentration levels (Table I) and assayed in quintuplicate as a measure of precision and accuracy. Recoveries for iminodibenzyl ranged from 93 to 109% with a mean of 99.8% and a standard deviation of 3.4%. Recoveries for desipramine ranged from 93 to 107% with a mean of 102.7% and a standard deviation of 3.4%. A typical chromatogram of a com-

Table II—Impurities in Imipramine Tablets, Injection, and Drug Substance [a]

Brand	Product	Strength	Iminodibenzyl, %	Desipramine, %
A	a	50 mg	0.47	0.13
	a	25 mg	0.35	0.15
	a	10 mg	013	0.13
B	a	50 mg	0.05	0.05
	a	25 mg	0.05	0.09
	a	10 mg	0.18	0.13
C	a	50 mg	0.08	0.16
	a	25 mg	0.10	0.09
	a	10 mg	0.22	0.11
D	a	50 mg	0.04	0.11
	a	25 mg	0.07	0.09
E	a	50 mg	0.08	0.07
	a	25 mg	0.05	0.06
F	a	50 mg	0.08	0.06
	a	25 mg	0.04	0.05
	a	10 mg	0.07	0.09
G	a	50 mg	0.37	0.12
H	b	12.5 mg/ml	0.08	0.07
I	c	N/A	0.06	0.10
J	c	N/A	0.03	0.08

[a] Product a, tablet; product b, injection; and product c, drug substance.

mercial tablet extract shown in Fig. 1 demonstrates that adequate separation is achieved for all compounds. The increased retention time of the desipramine derivative is apparent from the relative locations of imipramine in each chromatogram.

The reactions of desipramine and nortriptyline with acetic anhydride to form their respective derivatives appear to be quantitative within 5 min based on the absence of underivatized desipramine and nortriptyline peaks in the gas chromatogram. Iminodibenzyl does not form the derivative under the conditions used in the method, nor with moderate heat (~100°).

No interfering GLC peaks were detected in any commercial products at the retention times of the anthracene and nortriptyline internal standards.

A tabulation of iminodibenzyl and desipramine levels found in some commercial products is shown in Table II. Wide variations in impurity levels were found for the various products and manufacturers. There are currently no USP limits for either iminodibenzyl or desipramine in tablets or injections and only a limit of 0.1% of iminodibenzyl in imipramine drug substance USP. Since imipramine USP was used in the manufacturing of the products studied, some decomposition must have occurred either in the manufacturing process or because of instability of the finished product. Interestingly, product C was found to contain more iminodibenzyl (0.37%) 3 years prior to its expiration date, whereas product A (50 mg) contained only a small amount of iminodibenzyl (0.08%) within 3 months of its expiration date.

REFERENCES

(1) H. J. Weder and M. H. Bickel, *J. Chromatogr.*, **37,** 181 (1968).

(2) G. Nyberg and E. Matensson, *ibid.*, **143,** 491 (1977).

(3) S. Dawling and R. A. Braithwaite, *ibid.*, **146,** 449 (1978).

(4) L. A. Gifford, P. Turner, and C. M. B. Pare, *ibid.*, **105,** 107 (1975).

(5) D. N. Bailey and P. I. Jatlow, *Clin. Chem.*, **22,** 1697 (1976).

(6) F. Dorrity, Jr., M. Linnoila, and R. L. Habig, *ibid.*, **23,** 1326 (1977).

(7) J. T. Biggs, W. H. Holland, S. Chang, P. P. Hipps, and W. R. Sherman, *J. Pharm. Sci.*, **65,** 261 (1976).

(8) R. G. Jenkins and R. O. Friedel, *ibid.*, **67,** 17 (1978).

(9) A. Frigerio, G. Belvedere, F. DeNadai, R. Fanelli, C. Pantarotto, E. Riva, and P. L. Morselli, *J. Chromatogr.*, **74,** 201 (1972).

(10) J. M. Wilson, L. J. Williamson, and V. A. Raisys, *Clin. Chem.*, **23,** 1017 (1977).

(11) M. Sheehan and P. Haythorn, *J. Chromatogr.*, **132,** 237 (1977).

(12) J. H. Speaker, *J. Chromatogr. Sci.*, **12,** 297 (1974).

(13) A. Viala, F. Gouezo, and C. Gola, *J. Chromatogr.*, **45,** 94 (1969).

(14) D. C. Fenimore, C. J. Meyer, C. M. Davis, F. Hsu, and A. Zlatkis, *ibid.*, **142,** 399 (1977).

(15) J. Christiansen and L. F. Gram, *J. Pharm. Pharmacol.*, **25,** 604 (1973).

(16) A. Nagy and E. Treiber, *ibid.*, **25,** 599 (1973).

(17) A. Bonora and P. A. Borea, *Experientia*, **34,** 1486 (1978).

(18) J. H. Knox and J. Jurand, *J. Chromatogr.*, **103,** 311 (1975).

(19) M. R. Detaevernier, L. Dryon, and D. L. Massart, *ibid.*, **128,** 204 (1976).

(20) J. H. M. Van Den Berg, H. J. J. M. DeRuwe, and R. S. Deelder, *ibid.*, **138,** 431 (1977).

(21) T. Sutfin and W. Jusko, *J. Pharm. Sci.*, **68,** 703 (1979).

(22) W. French, F. Matsui, and J. Truelove, *Can. J. Pharm. Sci.*, **3,** 33 (1968).

(23) S. Ahuja, C. Spitzer, and F. Brofazi, *J. Pharm. Sci.*, **57,** 1979 (1968).

(24) "The United States Pharmacopeia," 20th rev., United States Pharmacopeial Convention, Inc., Rockville, Md., 1980, p. 397.

(25) K. Adank and W. Hammerschmidt, *Chimia*, **18,** 361 (1964).

(26) K. Adank and T. Schmidt, *ibid.*, **23,** 299 (1969).

(27) K. M. McErlane, N. M. Curran, and E. G. Lovering, *J. Pharm. Sci.*, **66,** 1015 (1977).

(28) J. J. Saady, N. Narasimhachari, and R. O. Friedel, *Clin. Chem.*, **27,** 343 (1981).

ACKNOWLEDGMENTS

The provision of GC–mass spectrometry data by Mr. Perry S. Wilkes and technical assistance from Grayson R. Rogers of the U.S. Food and Drug Administration, and Dr. James T. Stewart of the University of Georgia, are appreciated.

Bioavailability, Pharmacokinetics, and Analgesic Activity of Ketamine in Humans

J. A. CLEMENTS *x, **W. S. NIMMO** ‡, **and I. S. GRANT** ‡§

Received May 14, 1981, from the *Heriot-Watt University, Department of Pharmacy, Edinburgh, EH1 2JH, Scotland, and the ‡Departments of Anaesthesia, Western Infirmary, Glasgow, G11 6NT, Scotland. Accepted for publication August 26, 1981. §Present address: Department of Anaesthesia, Ninewells Hospital, Dundee, Scotland.

Abstract □ The pharmacokinetics of ketamine in analgesic doses after intravenous, intramuscular, and oral administration was investigated in healthy volunteers. Plasma ketamine concentration–time curves were fitted by a two-compartment open model with a terminal half-life of 186 min. Absorption after intramuscular injection was rapid and the bioavailability was 93%. However, only 17% of an oral dose was absorbed because of extensive first-pass metabolism. Simultaneous measurements of the elevation of pain threshold in an ischemic exercise test showed a marked effect for 15–60 min after intramuscular injection, but little or no effect after the oral solution. Pain threshold elevation occurred at plasma ketamine concentrations above 160 ng/ml.

Keyphrases □ Ketamine—bioavailability, pharmacokinetics, and analgesic activity in humans, intravenous, intramuscular, and oral administration compared □ Pharmacokinetics—ketamine, intravenous, intramuscular, and oral dosage forms compared □ Anesthetics—ketamine, bioavailability, pharmacokinetics, and analgesic activity in humans

Ketamine [2-*o*-chlorophenyl-2-(methylamino)cyclohexanone] is an anesthetic induction agent which produces sleep rapidly after intravenous injection of 1–2 mg/kg (1). It may also be given by intramuscular injection (6–10 mg/kg) and this route is used extensively in children. The oral route has not been used, although a self-administration of 300 mg and loss of consciousness has been reported (2).

Wieber *et al.* (3) reported the pharmacokinetics of intravenous ketamine (2.5 mg/kg) in five patients to be in accordance with a two-compartment model with a mean terminal half-life of 2.52 hr. Idvall *et al.* (4) found the mean half-life in 31 patients to be 79 min after an intravenous infusion.

In lower doses, ketamine also has analgesic properties (5, 6) and has been used in post-operative pain relief (7–9), but the pharmacokinetics have not been reported.

This paper reports the pharmacokinetics of ketamine in healthy volunteers who received analgesic doses by intravenous and intramuscular injection and as an oral solution. Simultaneous measurements were made of the elevation of the pain threshold in an ischemic exercise test (10).

EXPERIMENTAL

Procedure—In the first study, ketamine hydrochloride[1] was administered by intravenous injection (0.25 or 0.125 mg of base/kg body weight) on separate occasions to five healthy, fasting adult volunteers [age: 33.8 ± 1.4 (*SE*) years; weight: 74.8 ± 2.1 kg]. On a third occasion, an injection of normal saline was given.

In the second study, normal saline or ketamine (0.5 mg/kg) was given to six healthy, fasting adult volunteers [age: 31.8 ± 2.0 (*SE*) years; weight: 70.7 ± 4.4 kg] by intramuscular injection or as an oral solution on separate occasions. On each occasion, the subject drank 50 ml of orange juice with or without ketamine in solution and simultaneously received an intramuscular injection of ketamine or normal saline into the triceps muscle of the dominant arm.

Each study was a crossover design, the order of administration was randomized, and the subject and the person recording pain scores were not aware of the nature of the administered solution. Samples of venous blood (8 ml) were removed from the dominant arm at 0 (blank), 3, 5, 10, 15, 20, 30, and 45 min and at 1, 2, 4, and 7 hr.

Pain Measurements—The method was a modification of the ischemic exercise test of Harrison and Bigelow (10) and was described previously (11). The test was carried out during a 30-min control period before, and at 0, 5, 10, 15, 20, 30, 40, 50, and 60 min (first study) or at 0, 15, 30, 45, 60, 75, 90, and 120 min (second study) after administration of ketamine or normal saline.

Elevation of pain threshold was indicated by a reduction of the "pain score" or an increase in the time to reach intolerable pain, or both, when compared with corresponding values in the subject on the same day during the control period.

Analysis of Blood Samples—Immediately after collection in heparinized tubes, plasma was separated and stored at −20° until as-

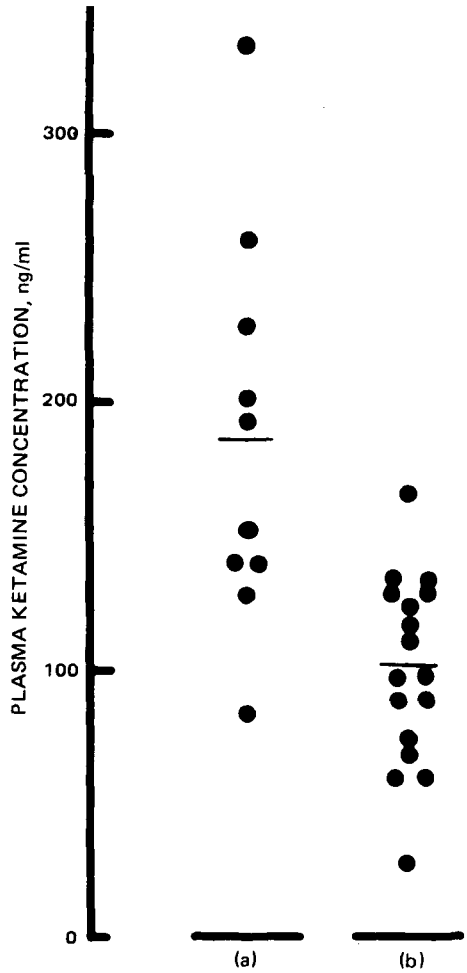

Figure 1—*Distribution of plasma ketamine concentration (ng/ml) that corresponds to pain scores after 75 to 105-sec ischemic exercise of (a) "none" or "mild" or (b) "moderate" or "severe," after intramuscular ketamine (0.5 mg/kg) in six subjects.*

[1] Ketalar, Parke-Davis & Co., Pontypool, U.K.

0022-3549/82/0500-0539$01.00/0

Table I—Absorption Rate Constants (K_a, min^{-1}) and Bioavailability (F) of Ketamine, 0.5 mg/kg, Given by Intramuscular Injection or as an Oral Solution

Subject	Intramuscular Injection[a]			Oral Solution		
	K_a'	K_a''	F_{area}	F_{area}	F (Eq. 1)	F (Eq. 2)
1	0.040	0.038	0.965	0.145	0.032	0.160
2	0.054	0.043	0.923	0.163	0.204	0.190
3	0.412	—	—	—	—	0.155
4	0.285	0.130	0.972	0.112	0.092	0.115
5	0.069	—	—	—	—	0.309
6	0.142	0.146	0.859	0.245	0.158	0.239
Mean	—	—	0.930	0.166	—	0.195
SE	—	—	0.026	0.028	—	0.028

[a] K_a' from nonlinear regression. K_a'' from method of Loo-Riegelman (22).

sayed. Plasma samples were analyzed in duplicate or triplicate for ketamine and norketamine (metabolite 1) as their heptafluorobutyryl derivatives on a gas chromatograph with electron-capture detection (12–14). Dehydronorketamine (metabolite 2) consistently gave two peaks on the chromatogram; this was observed previously by White *et al.* (15).

Pharmacokinetic Analysis—Plasma ketamine concentrations were fitted to a two-compartment model by nonlinear regression with a simplex algorithm (16, 17); individual data points were weighted as recommended by Ottaway (18).

Preliminary estimates of the apparent volume of the central compartment, the absorption rate constant (second study), and transfer microconstants were obtained using an analog computer. Goodness of fit criteria used were the run test and the number test on the signs of the residuals (19) and a test statistic for serial correlation between residuals (20). Both of these criteria indicated a satisfactory fit in all cases.

The bioavailability (F_{area}) was calculated from the ratio of the trapezoidal area (with correction for the area beyond the last data point and adjustment for dose) after intramuscular or oral administration to that after intravenous injection in the same subject. Apparent distribution volumes of the central compartment (V_1), at steady-state ($V_{d_{ss}}$), and during the terminal phase (V_{d_β}) and total body clearance values (TBC) (21), were not corrected for bioavailability. Estimates of the absorption rate constant were also obtained by the method of Loo and Riegelman (22).

The fraction of the dose lost by first-pass metabolism (F) was calculated from:

$$F = 1 - \frac{TBC}{Q_1} \qquad \text{(Eq. 1)}$$

where TBC is the clearance value for ketamine after intravenous injection and Q_1, the hepatic blood flow, was taken as 1.53 liters/min (23), and from:

$$F = \frac{Q_1}{Q_1 + X_0/(AUC)_{oral}} \qquad \text{(Eq. 2)}$$

where $(AUC)_{oral}$ is the area under the plasma ketamine concentration–time curve after oral administration of the dose X_0 (21).

The Student t test was used in tests of statistical significance.

RESULTS

Pharmacokinetics—Immediately after intravenous injection, plasma ketamine concentrations fell rapidly, and the data were fitted by a two-compartment open model with a mean terminal half-life of 186 ± 10 min. The concentration y (ng/ml) at time t(min) after injection was given by:

$$y = 82\exp(-0.044t) + 22\exp(-0.0039t)$$

after a 0.125 mg/kg dose (Eq. 3)

and by:

$$y = 108\exp(-0.039t) + 40\exp(-0.0038t)$$

after a 0.25 mg/kg dose (Eq. 4)

There were no significant differences in the values of α, β, apparent distribution volumes, or clearance for the two doses.

Ketamine was rapidly absorbed after intramuscular injection with apparent absorption half-times of 2–17 min. The estimated interval between the injection and the appearance of ketamine in the plasma (lag time) was less than 4 min and the bioavailability was 93% (Table I). Apparent peak concentrations (C_{max}) of between 100 and 425 ng/ml occurred at 5–30 min (t_{max}) after injection. Absorption rate constants calculated by the Loo–Riegelman method agreed well with those from nonlinear regression, except in one subject in whom absorption was very rapid. The mean (±SE) terminal plasma half-life (155 ± 12 min) did not differ significantly from that after intravenous injection (186 ± 10 min) and no difference was observed in the clearance values (23.2 and 19.1 ml/min/kg, respectively) (Table II).

After oral administration, ketamine absorption was incomplete, with only 16.6% of the dose reaching the systemic circulation. The lag time was between 4 and 13 min (mean 8.0 min). The mean apparent peak concentration of 44 ng/ml (range 15–80 ng/ml) was much lower than the value (243 ng/ml) after intramuscular injection (Table II). The fractions of the oral dose available to the systemic circulation, as calculated from Eq. 2, were in close agreement with observed values; however, the fractions predicted from clearance values after intravenous injection (Eq. 1) agreed well in only two of the four subjects (Table I).

Norketamine was found in measurable concentrations after each route of administration. After intravenous injections of 0.125 and 0.25 mg/kg, apparent peak concentrations of 15–30 ng/ml and 20–60 ng/ml, respectively, occurred at 15–60 min. Areas under the plasma norketamine concentration–time curves (corrected for dose) did not differ significantly. Although the mean peak norketamine concentration after oral admin-

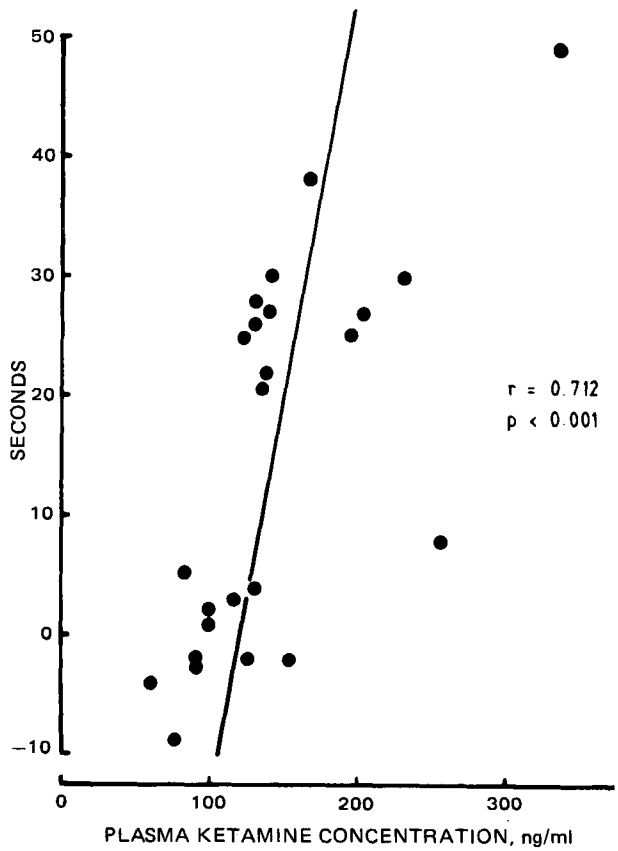

Figure 2—*Increase in time of ischemic exercise to intolerable pain (sec)* versus *plasma ketamine concentrations (ng/ml) after intramuscular injection of ketamine (0.5 mg/kg) in six subjects.*

Table II—Pharmacokinetic Values (Mean ± *SE*) for Ketamine and Norketamine in Fasting Volunteers after Intravenous Injection, Intramuscular Injection, or Oral Administration of Ketamine [a]

Pharmacokinetic Value	Administration Route, dose: Intravenous Injection, 0.25 mg/kg	Intramuscular Injection, 0.5 mg/kg	Oral Solution, 0.5 mg/kg
	Ketamine		
C_{max}, ng/ml	—	243 (49)	44 (10)
t_{max}, min	—	22 (4)	30 (5)
Half-life ($t_{1/2\beta}$), min	186 (8)	155 (12)	174 (50)
AUC[b], min ng/ml	27.5 (1.2)	23.6 (2.2)	4.8 (0.8)
TBC[c], ml/min kg	19.1 (1.1)	23.2 (2.7)	—
	Norketamine		
C_{max}, ng/ml	40 (6)	92 (10)	200 (44)
t_{max}, min	63 (23)	78 (14)	60 (13)
AUC, min ng/ml	35.4 (3.8)	31.3 (3.8)	36.7 (3.9)

[a] $N = 6$. [b] *AUC*, area under plasma concentration time curve, corrected to an administered dose of 0.5 mg/kg. [c] *TBC*, clearance value, not corrected for bioavailability.

istration was higher than after intramuscular injection, the areas were similar and neither differed significantly from that after intravenous injection (Table II).

Pain Measurements—In the control period, before administration of ketamine or normal saline, severe pain was observed after 75–105 sec of exercise and was reproducible in each individual on each occasion. The pain became intolerable after a further 7 sec (range 1–13 sec). The pain threshold was considered to have been raised when the pain was graded as "none" or "mild" at these times, or when the time to reach intolerable pain was significantly prolonged, or both.

After intravenous injection of ketamine, the pain threshold elevation lasted for less than 10 min after 0.25 mg/kg and less than 5 min after 0.125 mg/kg (14). At 15 and 30 min after intramuscular injection of ketamine, the period of ischemic exercise before pain became intolerable was significantly prolonged, by 24 and 21 sec, respectively. At later times, and also after injection of normal saline, the period was not prolonged (11).

Elevation of pain threshold after intramuscular injection occurred in all individuals for up to 1 hr; the corresponding plasma ketamine concentrations were between 85 and 330 ng/ml. Concentrations that corresponded to a pain score of "none" or "mild" after 75–105 sec of ischemic exercise were significantly higher (186 ± 23 ng/ml) than those when pain scores were "moderate" or "severe" (101 ± 8 ng/ml) (Fig. 1). There was a significant correlation between the plasma ketamine concentrations and the increase in time taken to reach intolerable pain (Fig. 2) in the hour after injection, but no significant correlation was found for norketamine concentrations.

After oral administration, pain thresholds were not markedly elevated, and subjects experienced moderate or severe pain after 75–105 sec of ischemic exercise. The mean increase in exercise time before intolerable pain was reached was not significant except at 30 min after administration when the increase (9 sec) reached significance ($0.05 > p > 0.025$). Plasma ketamine concentrations were between 17 and 65 ng/ml. Norketamine concentrations were higher, in the range 80–390 ng/ml. No significant correlations were observed between plasma ketamine or plasma norketamine concentrations and the increase in time to reach intolerable pain.

DISCUSSION

The pharmacokinetics of intravenous ketamine in the analgesic doses used in this study are similar to those previously reported for anesthetic doses (3). Plasma concentration–time data were adequately fitted by a two-compartment open model, and apparent distribution volumes, terminal plasma half-lives, and clearance values after analgesic doses (0.125 or 0.25 mg/kg) in volunteers did not differ significantly from those reported for anesthetic doses (2.5 mg/kg) in patients (14). Mean terminal plasma half-lives after anesthetic and analgesic doses were 151 and 186 min, respectively. Both times are much longer than the value (79 min) reported for patients at the end of an intravenous infusion (4). This difference is attributed to the relatively short sampling period (2–2.5 hr) used in the latter study, since early termination of sample leads to underestimation of the half-life (24). Analysis of data for this period after intravenous injection of ketamine gave an apparent half-life of 105 min.

The low plasma ketamine concentrations after oral administration could have been due to incomplete absorption from the GI tract or to extensive metabolism during the first-pass through the liver. The relatively high concentrations of the metabolite norketamine suggest that liver metabolism is largely responsible. Where the liver is the sole site of metabolism, the area under the curve of concentration of metabolite *versus* time is independent of route of administration (25). Since the area under the norketamine concentration–time curves after oral administration was similar to that after intravenous injection (after correction for dose), the low plasma ketamine concentrations can be attributed solely to the extensive first-pass metabolism. Also, the fraction of the oral dose reaching the systemic circulation, as calculated from Eq. 2 on the assumption that absorption from the gut lumen was complete, was in good agreement with F_{area}, the fraction calculated from area analysis.

Estimation of the fraction of an oral dose reaching system circulation from areas after intravenous injection, using Eq. 1, gave good agreement in two subjects but underestimated the values in two.

Since elevation of pain threshold was previously reported to be associated with plasma ketamine concentrations above 100–150 ng/ml (11, 14), the absence of any marked effect after oral administration may be explained by the low concentrations of ketamine as these did not exceed 80 ng/ml. Norketamine has been shown to have pharmacological activity, including analgesic properties, in the rat (15) but its effects in humans are not known. As high norketamine concentrations, up to 390 ng/ml, were found in some subjects after oral administration of ketamine, it is possible that this metabolite, either alone or in combination with ketamine, was responsible for the small increase in time taken to reach intolerable pain during ischemic exercise. However, no correlation was observed between the increase in time to reach intolerable pain and plasma norketamine concentration. The activity of other metabolites formed by hydroxylation of the cyclohexanone ring (Metabolites 3 and 4) is not known and these are not measured in the assay. In view of the extensive first-pass metabolism, oral administration of ketamine in a dose of 0.5 mg/kg is not satisfactory for producing analgesia.

After intramuscular injection, ketamine was rapidly and almost completely absorbed, and the fall in the terminal plasma concentrations represented the elimination phase, since the half-life did not differ from that observed after intravenous injection.

Intramuscular injection of ketamine produced a marked elevation of pain threshold for between 15 and 60 min. Using the criterion of a pain score of "none" or "mild," after 75 to 105 sec of ischemic exercise or an increase of 20 sec or more in the time to intolerable pain, it was found that elevation of pain occurred consistently at plasma ketamine concentrations exceeding 160 ng/ml, but not at concentrations below 80 ng/ml (Fig. 1). These data make it possible to design dosage regimens and may increase the usefulness of ketamine as an analgesic agent.

REFERENCES

(1) M. M. Ghoneim and K. Korttila, *Clin. Pharmacokinet.*, **2**, 344 (1977).

(2) M. Johnstone, *Anaesth. Intensive Care*, **1**, 70 (1972).

(3) J. Wieber, R. Gugler, J. H. Hengstmann, and H. J. Dengler, *Anaesthetist*, **24**, 260 (1975).

(4) J. Idvall, I. Ahlgren, K. F. Aronsen, and P. Stenberg, *Br. J. Anaesth.*, **51**, 1167 (1979).

(5) D. B. Caro, *Anaesthesia*, **29**, 227 (1974).

(6) R. D. Wilson, T. J. Herrin, and J. V. Richey, Report of 5th European Congress of Anaesthesiology, Paris, France, 1978, p. 56.

(7) Y. Ito and K. Ichyanagi, *Anaesthesia*, **29**, 222 (1974).

(8) L. Clausen, D. M. Sinclair, and C. H. Hasselt, *S. Afr. Med. J.*, **49**, 1437 (1975).

(9) T. R. Austin, *Br. Med. J.*, **2**, 943 (1976).

(10) I. B. Harrison and N. H. Bigelow, *Proc. Assoc. Res. Nerv. Ment. Dis.*, **23**, 154 (1943).

(11) I. S. Grant, W. S. Nimmo, and J. A. Clements, *Br. J. Anaesth.*, **53**, 805 (1981).

(12) T. Walle and H. Ehrsson, *Acta Pharm. Suec.*, **7**, 389 (1970).

(13) T. Chang and A. J. Glazko, *Anesthesiology*, **36**, 401 (1972).

(14) J. A. Clements and W. S. Nimmo, *Br. J. Anaesth.*, **53**, 27 (1981).

(15) P. F. White, R. R. Johnston, and C. R. Pudwill, *Anaesthesiology*, **42**, 179 (1975).

(16) J. A. Nelder and R. Mead, *Comput. J.*, **7**, 308 (1965).

(17) J. A. Clements and L. F. Prescott, *J. Pharm. Pharmacol.*, **28**, 707 (1976).

(18) J. H. Ottaway, *Biochem. J.*, **134**, 729 (1973).

(19) P. V. Pedersen, *J. Pharmacokinet. Biopharm.*, **5**, 513 (1977).
(20) J. Durbin and G. S. Watson, *Biometrika*, **37**, 409 (1950).
(21) M. Gibaldi and D. Perrier, "Drugs and the Pharmaceutical Sciences, Vol. 1, Pharmacokinetics," Marcel Dekker, New York, N.Y., 1979, pp. 232–252.
(22) J. C. K. Loo and S. Riegelman, *J. Pharm. Sci.*, **57**, 918 (1968).
(23) M. Rowland, *ibid.*, **61**, 70 (1972).
(24) M. Gibaldi and H. Weintraub, *ibid.*, **60**, 624 (1971).
(25) K. S. Pang and J. R. Gillette, *ibid.*, **67**, 703 (1978).

ACKNOWLEDGMENTS

The authors are grateful to the Scottish Hospital Endowments Research Trust for financial support.

Synthesis, Hydrolytic Reactivity, and Anticancer Evaluation of *N*- and *O*-Triorganosilylated Compounds as New Types of Potential Prodrugs

FANG-TING CHIU, YOUNG HWAN CHANG, GÜNAY ÖZKAN, GERALD ZON ×, KENNETH C. FICHTER *, and LAWRENCE R. PHILLIPS ‡

Received April 24, 1981, from the *Department of Chemistry, The Catholic University of America, Washington, DC 20064*, the **Mid-Atlantic Research Institute, Bethesda, MD 20014*, and the ‡*Bureau of Biologics, Food and Drug Administration, Bethesda, MD 20205.* Accepted for publication August 6, 1981.

Abstract □ *N*- and *O*-Triorganosilylated compounds related to various anticancer agents were synthesized for evaluation as potential anticancer prodrugs. ^{1}H-NMR and UV kinetic measurements of hydrolytic desilylation were used to correlate relative rates of structural unmasking with steric bulk about the silicon reaction center. The *tert*-butyldimethylsilyl ester of chlorambucil and a number of *O*-triorganosilylated carbamate derivatives of nor-nitrogen mustard showed significant activity against P-388 lymphocytic leukemia in mice.

Keyphrases □ Prodrugs—*N*- and *O*-triorganosilylated compounds, synthesis, potential anticancer prodrug □ Anticancer agents—synthesis of *N*- and *O*-triorganosilylated compounds, potential anticancer prodrugs □ Triorganosilylated compounds—synthesis and evaluation of potential anticancer prodrugs

In an earlier investigation of potential anticancer prodrugs (1), it was found that *O*-aryl-*N*,*N*-bis(2-chloroethyl)phosphorodiamidates are resistant toward chemical activation involving P-OAr hydrolysis and failed to provide evidence for *in vivo* formation of phosphoramide mustards, which are usually cytotoxic and may exhibit anticancer activity (2). The hydrolytic lability (3) of Si—N and Si—O bonds suggested that strategically triorganosilylated derivatives of known oncostatic agents might constitute a class of compounds which are, for kinetic reasons, more suitable candidates for anticancer prodrugs. The possibility of controlling drug unmasking rates (desilylation) by manipulating the nature of the silicon reaction center represents an interesting feature of these hypothetical compounds. The expected hydrolysis byproducts, namely triorganosilanols and disiloxanes, are generally nontoxic (4). Derivatization with a triorganosilyl group increases lipophilicity; consequently, triorganosilyl prodrugs might eventually prove to be useful against central nervous system cancers, which apparently require somewhat more lipophilic chemotherapeutic agents for effective penetration of the blood–brain barrier (5).

In view of the widespread interest in the design of anticancer prodrugs (6, 7) and the development of organosilicon compounds as medicinal agents (8), the aforementioned proposal is unique in that it encompasses both of these growing research areas. This report is the first of a series of exploratory investigations of hydrolytically labile *N*- and *O*-triorganosilyl prodrugs having potential anticancer activity. These studies include the synthesis of several new classes of nitrogen mustards, measurement of hydrolytic desilylation rates by a combination of ^{1}H-NMR and UV methods, examination of the hydrolysis mechanisms by Hammett-type kinetic studies and ^{18}O-labeling, and the comparison of screening results obtained with experimental cancers in mice.

EXPERIMENTAL

NMR refers to ^{1}H-NMR at 60 MHz, except as noted; chemical shifts refer to deuterochloroform and are relative to internal tetramethylsilane, unless specified otherwise. ^{31}P-NMR spectra were recorded at 40.25 MHz using a $\pi/2$ pulse (13 μsec) and a 2-sec repetition time. All organosilicon starting materials were commercially available and were checked for purity by NMR; if necessary, further purification was achieved by either conventional distillation or recrystallization. All handling and reactions of organosilicon compounds were performed under an atmosphere of dry nitrogen; all reagents and solvents were anhydrous. Satisfactory elemental analyses were not always possible, due to hydrolytic reactivity. However, each product was reliably characterized by NMR as well as IR (9–11) and/or mass spectroscopy. In all cases, NMR signal integrations established that product purity was >90%. Electron-impact mass spectra were scanned from samples introduced *via* a solids' direct probe inlet. The probe, when loaded with a sample and properly positioned with respect to the ion source, was heated at 100°/min from ambient temperature to a final temperature of 320°. The ion source temperature was 180°, the ionizing potential was 70 eV, and the ionizing current was 50 μA. Analytical thin-layer chromatography (TLC) employed 2.5 × 10-cm plates coated with a 250-μm layer of silica gel containing a fluorescent indicator; component visualization was achieved with iodine vapor and/or a short wavelength UV lamp. Column chromatography utilized 60–200 mesh silica gel, which was dried by heating at 150° for 24 hr and then cooling to room temperature under nitrogen.

All compounds having a bis(2-chloroethyl)amino functionality are potentially toxic and/or mutagenic and should be handled with extreme care.

***O,O*-Dimethyl-*N,N*-bis(2-chloroethyl)phosphoramidate (III)** —Lithium methoxide was prepared fresh by slowly adding a benzene solution (10 ml) of methanol (6.5 ml) to a mixture of benzene (10 ml) and sliced lithium wire (15 cm, 6.11 mmoles/cm) at 25°. After an additional 3 hr of stirring, a solution of I (12) (10.4 g, 40 mmoles) in benzene (40 ml)

0022-3549/82/0500-0542$01.00/0

(19) P. V. Pedersen, *J. Pharmacokinet. Biopharm.*, **5**, 513 (1977).
(20) J. Durbin and G. S. Watson, *Biometrika*, **37**, 409 (1950).
(21) M. Gibaldi and D. Perrier, "Drugs and the Pharmaceutical Sciences, Vol. 1, Pharmacokinetics," Marcel Dekker, New York, N.Y., 1979, pp. 232–252.
(22) J. C. K. Loo and S. Riegelman, *J. Pharm. Sci.*, **57**, 918 (1968).
(23) M. Rowland, *ibid.*, **61**, 70 (1972).
(24) M. Gibaldi and H. Weintraub, *ibid.*, **60**, 624 (1971).
(25) K. S. Pang and J. R. Gillette, *ibid.*, **67**, 703 (1978).

ACKNOWLEDGMENTS

The authors are grateful to the Scottish Hospital Endowments Research Trust for financial support.

Synthesis, Hydrolytic Reactivity, and Anticancer Evaluation of *N*- and *O*-Triorganosilylated Compounds as New Types of Potential Prodrugs

FANG-TING CHIU, YOUNG HWAN CHANG, GÜNAY ÖZKAN, GERALD ZON ×, KENNETH C. FICHTER *, and LAWRENCE R. PHILLIPS ‡

Received April 24, 1981, from the *Department of Chemistry, The Catholic University of America, Washington, DC 20064*, the **Mid-Atlantic Research Institute, Bethesda, MD 20014*, and the ‡*Bureau of Biologics, Food and Drug Administration, Bethesda, MD 20205.* Accepted for publication August 6, 1981.

Abstract □ *N*- and *O*-Triorganosilylated compounds related to various anticancer agents were synthesized for evaluation as potential anticancer prodrugs. ^{1}H-NMR and UV kinetic measurements of hydrolytic desilylation were used to correlate relative rates of structural unmasking with steric bulk about the silicon reaction center. The *tert*-butyldimethylsilyl ester of chlorambucil and a number of *O*-triorganosilylated carbamate derivatives of nor-nitrogen mustard showed significant activity against P-388 lymphocytic leukemia in mice.

Keyphrases □ Prodrugs—*N*- and *O*-triorganosilylated compounds, synthesis, potential anticancer prodrug □ Anticancer agents—synthesis of *N*- and *O*-triorganosilylated compounds, potential anticancer prodrugs □ Triorganosilylated compounds—synthesis and evaluation of potential anticancer prodrugs

In an earlier investigation of potential anticancer prodrugs (1), it was found that *O*-aryl-*N*,*N*-bis(2-chloroethyl)phosphorodiamidates are resistant toward chemical activation involving P-OAr hydrolysis and failed to provide evidence for *in vivo* formation of phosphoramide mustards, which are usually cytotoxic and may exhibit anticancer activity (2). The hydrolytic lability (3) of Si—N and Si—O bonds suggested that strategically triorganosilylated derivatives of known oncostatic agents might constitute a class of compounds which are, for kinetic reasons, more suitable candidates for anticancer prodrugs. The possibility of controlling drug unmasking rates (desilylation) by manipulating the nature of the silicon reaction center represents an interesting feature of these hypothetical compounds. The expected hydrolysis byproducts, namely triorganosilanols and disiloxanes, are generally nontoxic (4). Derivatization with a triorganosilyl group increases lipophilicity; consequently, triorganosilyl prodrugs might eventually prove to be useful against central nervous system cancers, which apparently require somewhat more lipophilic chemotherapeutic agents for effective penetration of the blood–brain barrier (5).

In view of the widespread interest in the design of anticancer prodrugs (6, 7) and the development of organosilicon compounds as medicinal agents (8), the aforementioned proposal is unique in that it encompasses both of these growing research areas. This report is the first of a series of exploratory investigations of hydrolytically labile *N*- and *O*-triorganosilyl prodrugs having potential anticancer activity. These studies include the synthesis of several new classes of nitrogen mustards, measurement of hydrolytic desilylation rates by a combination of ^{1}H-NMR and UV methods, examination of the hydrolysis mechanisms by Hammett-type kinetic studies and ^{18}O-labeling, and the comparison of screening results obtained with experimental cancers in mice.

EXPERIMENTAL

NMR refers to ^{1}H-NMR at 60 MHz, except as noted; chemical shifts refer to deuterochloroform and are relative to internal tetramethylsilane, unless specified otherwise. ^{31}P-NMR spectra were recorded at 40.25 MHz using a $\pi/2$ pulse (13 μsec) and a 2-sec repetition time. All organosilicon starting materials were commercially available and were checked for purity by NMR; if necessary, further purification was achieved by either conventional distillation or recrystallization. All handling and reactions of organosilicon compounds were performed under an atmosphere of dry nitrogen; all reagents and solvents were anhydrous. Satisfactory elemental analyses were not always possible, due to hydrolytic reactivity. However, each product was reliably characterized by NMR as well as IR (9–11) and/or mass spectroscopy. In all cases, NMR signal integrations established that product purity was >90%. Electron-impact mass spectra were scanned from samples introduced *via* a solids' direct probe inlet. The probe, when loaded with a sample and properly positioned with respect to the ion source, was heated at 100°/min from ambient temperature to a final temperature of 320°. The ion source temperature was 180°, the ionizing potential was 70 eV, and the ionizing current was 50 μA. Analytical thin-layer chromatography (TLC) employed 2.5 × 10-cm plates coated with a 250-μm layer of silica gel containing a fluorescent indicator; component visualization was achieved with iodine vapor and/or a short wavelength UV lamp. Column chromatography utilized 60–200 mesh silica gel, which was dried by heating at 150° for 24 hr and then cooling to room temperature under nitrogen.

All compounds having a bis(2-chloroethyl)amino functionality are potentially toxic and/or mutagenic and should be handled with extreme care.

***O,O*-Dimethyl-*N,N*-bis(2-chloroethyl)phosphoramidate (III)** —Lithium methoxide was prepared fresh by slowly adding a benzene solution (10 ml) of methanol (6.5 ml) to a mixture of benzene (10 ml) and sliced lithium wire (15 cm, 6.11 mmoles/cm) at 25°. After an additional 3 hr of stirring, a solution of I (12) (10.4 g, 40 mmoles) in benzene (40 ml)

0022-3549/82/0500-0542$01.00/0

was added over a 30-min period. 2,3,11,12-Dibenzo-1,4,7,10,13,16-hexaoxacyclooctadeca-2,11-diene (0.3 g) was added and stirring was continued overnight at 25°. After separation of lithium chloride by suction filtration and evaporation of solvent from the filtrate, the yellow residue was chromatographed on a column (40 × 4 cm) of dry silica gel using chloroform–methanol (24:1) as eluent; R_f = 0.60. Evaporation of solvent gave III as a pale yellow oil (75%) which was used without further purification. NMR: δ 3.82 (d, 6H, 2-CH_3) and 3.52 (m, 8H, 4-CH_2) ppm; mass spectrum: *m/z* 249 (M^+, 2-Cl).

***O,O*-Bis(trimethylsilyl)- *N,N*- bis(2-chloroethyl)phosphoramidate (IV)**—A mixture of III (0.26 g, 1 mmole), sodium iodide (0.45 g, 3 mmoles), and acetonitrile (5 ml) was treated dropwise with a solution of trimethylchlorosilane (0.35 g) in acetonitrile (3 ml) over 20 min. After 3 hr of continued stirring, followed by solvent evaporation, the residue was extracted with carbon tetrachloride (5 ml) to give IV (85%), which is extremely sensitive to atmospheric moisture and hydrolyzes to give hexamethyldisiloxane. NMR: δ 3.43 (m, 8H, 4-CH_2) and 0.28 [s, 18H, 2-Si(CH_3)$_3$] ppm.

***O,O*-Bis(*tert*-butyldimethylsilyl) -*N,N*- bis(2-chloroethyl)-phosphoramidate (V)**—Reaction of III and *tert*-butyldimethylchlorosilane in the presence of sodium iodide according to the identical procedure described for IV gave product V (56%) as a pale yellow oil. Attempts to decolorize this material by either preparative TLC or column chromatography on dry silica gel led to hydrolysis of the *tert*-butyldimethylsilyl groups, as evidenced by isolation of the corresponding triorganosilanol. NMR: δ 3.42 (m, 8H, 4-CH_2), 0.90 [s, 18H, 2-C(CH_3)$_3$], and 0.23 [s, 12H, 2-Si(CH_3)$_2$] ppm. For V (45 mg, 0.1 mmole) and tris[3-(heptafluoropropylhydroxymethylene)-*d*-camphorato]europium (156 mg, 0.13 mmole) in deuterochloroform (1 ml), the expected resonance doubling of enantiotopic groups (13) was observed and diastereotopic methyl groups in V were resolved: δ 2.37 [s, 9H, C(CH_3)$_3$], 2.09 [s, 9H, C(CH_3)$_3$], 1.97 (s, 3H, SiCH_3), 1.87 (s, 3H, SiCH_3), 1.52 (s, 3H, SiCH_3), and 1.35 (s, 3H, SiCH_3) ppm. IR (neat): 2950, 2900, and 2875 (C—H), 1366 [C(CH_3)$_3$], 1250 (P=O), and 1045 (Si—O) cm^{-1}.

***O,O*-Bis(diphenylmethylsilyl) -*N,N*- bis(2-chloroethyl)phosphoramidate (VI)**—Compound VI was synthesized (60%) from diphenylmethylchlorosilane and III by the same procedure described for IV. Purification of the crude product was achieved by rapid elution from dry silica gel using carbon tetrachloride eluent to remove 1,3-dimethyl-1,1,3,3-tetraphenyldisiloxane (R_f = 0.5, carbon tetrachloride) and then ether to collect VI (R_f = 0.85, ether) as a colorless oil. NMR: δ 7.44 (m, 20H, 4-C_6H_5), 3.15 (m, 8H, 4-CH_2), and 0.67 (s, 6H, 2-SiCH_3) ppm. For VI (0.1 *M*) and tris[3-(heptafluoropropylhydroxymethylene)-*d*-camphorato]europium (0.13 *M*) in deuterochloroform, the expected resonance doubling of enantiotopic groups was observed: δ 0.95 (s, 3H, SiCH_3) and 0.82 (s, 3H, SiCH_3) ppm. IR (neat): 3090, 3060, and 3035 (C_6H_5), 2950 (C—H), 1270 (P=O), 1050 (Si—O), and 760 and 700 (C_6H_5) cm^{-1}.

***O,O*-Bis(*tert*-butyldiphenylsilyl) -*N,N*- bis(2-chloroethyl)-phosphoramidate (VII)**—Reaction of *tert*-butyldiphenylchlorosilane and III in a manner identical to that described above for the preparation of IV was followed by column chromatography using dry silica gel, eluting first with carbon tetrachloride to remove *tert*-butyldiphenylsilanol (R_f = 0.3, carbon tetrachloride), and then with ether to remove VII (90%, R_f = 0.81, ether). NMR: δ 7.56 (m, 20H, 4-C_6H_5), 3.06 (m, 8H, 4-CH_2), and 1.14 [s, 18H, 2-C(CH_3)$_3$] ppm. For VII (0.1 *M*) and tris[3-(heptafluoropropylhydroxymethylene)-*d*-camphorato]europium (0.13 *M*) in deuterochloroform, the expected resonance doubling of enantiotopic groups was observed: δ 1.33 [s, 9H, C(CH_3)$_3$] and 0.95 [s, 9H, C(CH_3)$_3$] ppm. IR (neat): 3055 (C_6H_5), 2950 and 2850 (C—H), 1375 [C(CH_3)$_3$], 1255 (P=O), 1130 (Si—O), and 740 and 700 (C_6H_5) cm^{-1}.

***O* - Methyl -*N,N* - bis(2 - chloroethyl)phosphorodiamidate (VIII)**—A solution of methanol (1 ml, 24.7 mmoles) in benzene (5 ml) was added (20 min) to a stirred suspension of sliced lithium wire (3.6 cm, 22 mmoles) in benzene (5 ml) at 25°, and after 4 hr it appeared that all of the metal had reacted. The resultant suspension of lithium methoxide was added dropwise by syringe to a chilled mixture of I (5.2 g, 20 mmoles) and 2,3,11,12-dibenzo-1,4,7,10,13,16-hexaoxacyclooctadeca-2,11-diene (0.1 g) in benzene (30 ml). After 5 hr of stirring at 25°, lithium chloride was removed by suction filtration and the filtrate containing intermediate II was diluted with benzene (18 ml). Dry ammonia was bubbled through the stirred filtrate at 5° until precipitation of ammonium chloride was complete. After separation of the precipitate and removal of solvent *in vacuo*, the residue was chromatographed on a dry silica gel column (40 × 4 cm) using methanol–chloroform (5:95, 250 ml). The concentrated eluate was dissolved in benzene (8 ml) and diluted with low-boiling petroleum ether until turbid. Refrigeration afforded pure VIII (51%), mp 75–78°. NMR: δ 3.84 [d ^3J(PH) = 11 Hz, 3H, CH_3], 3.80–3.35 (m, 8H, 4-CH_2), and 3.00 (broad, 2H, NH_2) ppm. IR (mull): 3403 and 3268 (NH_2), 1362 (OCH_3), and 1218 (P=O) cm^{-1}.

Anal.—Calc. for $C_5H_{13}N_2O_2PCl_2$: C, 25.55; H, 5.58; N, 11.92. Found: C, 25.49; H, 5.64; N, 11.91.

***O*-(*tert*-Butyldimethylsilyl) -*N,N*- bis(2-chloroethyl)phosphorodiamidate (X)**—A stirred mixture of VIII (0.94 g, 4 mmoles), sodium iodide (0.9 g, 6 mmoles), 2,3,11,12-dibenzo-1,4,7,10,13,16-hexaoxacyclooctadeca-2,11-diene (0.15 g), and acetonitrile (15 ml) at 25° was treated dropwise (30 min) with a solution of *tert*-butyldimethylchlorosilane (1.1 g, 7 mmoles) in acetonitrile (10 ml). After 5 hr, solvent was removed *in vacuo* and the residue was extracted with carbon tetrachloride (15 ml). Removal of carbon tetrachloride *in vacuo* gave X as a viscous pale yellow oil (70%). Attempts to further purify X by flash chromatography on dry silica gel led to hydrolysis of the *tert*-butyldimethylsilyl group, as evidenced by isolation of the corresponding silanol. NMR: δ 3.56 (m, 8H, 4-CH_2), 3.40 (d, 2H, NH_2), 0.92 [s, 9H, C(CH_3)$_3$], and 0.25 [s, 6H, Si(CH_3)$_2$] ppm. IR (neat): 3350 (NH_2), 2980 and 2950 (C—H), 1351 [C(CH_3)$_3$], 1260 (P=O), and 1100 (Si—O) cm^{-1}.

***O*-Trimethylsilyl-*N,N*-bis(2 - chloroethyl)phosphorodiamidate (IX)**—The synthetic procedure was analogous to that described above for X, and yielded IX as a colorless oil (87%). Compound IX is extremely sensitive to atmospheric moisture and rapidly hydrolyzes to give hexamethyldisiloxane, which was identified in partially decomposed samples of IX by chemical shift comparisons with authentic material. NMR: δ 3.55 (m, 8H, 4-CH_2), 3.39 (d, 2H, NH_2), and 0.30 [s, 9H, Si(CH_3)$_3$] ppm. IR (neat): 3324 (NH_2), 2975, 2932, and 2872 (C—H), 1238 (P=O), and 1121 (Si—O) cm^{-1}.

***O*-(*tert*-Butyldiphenylsilyl) -*N,N*- bis(2-chloroethyl)phosphorodiamidate (XI)**—Reaction of VIII and *tert*-butyldiphenylchlorosilane in exactly the same manner as that described above for the synthesis of X afforded crude material, which was chromatographed on a column (40 × 2 cm) of dry silica gel using carbon tetrachloride (100 ml) to first remove *tert*-butyldiphenylsilanol (R_f = 0.3, carbon tetrachloride). Compound XI (65%) was then eluted with ether (150 ml); R_f = 0.78, ether. NMR: δ 7.57 (m, 10H, 2-C_6H_5), 3.49 (m, 8H, 4-CH_2), 3.29 (d, 2H, NH_2), and 1.12 [s, 9H, C(CH_3)$_3$] ppm. IR (neat): 3447 and 3278 (NH_2), 3094 and 3075 (C_6H_5), 2981 and 2895 (C—H), 1372 [C(CH_3)$_3$], 1230 (P=O), 1111 (Si—O), and 743 and 698 (C_6H_5) cm^{-1}.

Bis(2-chloroethyl)amine (nor-nitrogen mustard)—A stirred mixture of bis(2-chloroethyl)amine hydrochloride (35.7 g, 0.2 mole) in ice-water (100 ml) and ether (100 ml) was titrated rapidly with aqueous sodium hydroxide (1 *N*), using phenolphthalein indicator. The ether layer was separated and the aqueous layer was extracted quickly three times with ether (80 ml). The combined ether layer and washings were dried with magnesium sulfate (4 g) at 5° and then carefully concentrated on a rotary evaporator. Rapid Kugelrohr distillation of the residue gave (94%) bis(2-chloroethyl)amine[1] as a colorless oil, bp 46–50° (3 mm). NMR: δ 3.44 (t, 4H, 2-CH_2Cl), 2.77 (t, 4H, 2-NCH_2), and 1.82 (s, 1H, NH) ppm. IR (neat): 3348 (NH) cm^{-1}.

***N*-Trimethylsilyl-*N,N*-bis(2-chloroethyl)amine (XII)**—A solution of trimethylchlorosilane (30 ml, 125 mmoles) in ether (30 ml) was added dropwise (30 min) to a stirred solution of bis(2-chloroethyl)amine (7.1 g, 50 mmoles) and triethylamine (8.4 ml, 55 mmoles) in ether (150 ml) at 5°. After stirring for 15 hr at 25° and then removal of solvent *in vacuo*, triethylamine hydrochloride was separated by suction filtration. Fractional distillation of the filtrate gave (90%) XII as a colorless oil, bp 45–47° (1 mm). Compound XII decomposes relatively slowly at room temperature, but is extremely reactive toward hydrolysis of the trimethylsilyl group to give hexamethyldisiloxane. The presence of this disiloxane in partially hydrolyzed samples of XII is evidenced by chemical shift comparisons with authentic material. NMR δ 3.65 (m, 8H, 4-CH_2) and −0.06 [s, 9H, Si(CH_3)$_3$] ppm. IR (neat): 2980 and 2893 (C—H), 1262 (SiCH_3), and 980 (Si—N) cm^{-1}.

***N*-(*tert*-Butyldimethylsilyl) -*N,N*- bis(2-chloroethyl)amine (XIII)**—Bis(2-chloroethyl)amine (7.1 g, 50 mmoles), *tert*-butyldimethylchlorosilane (9.0 g, 60 mmoles), and triethylamine (9.2 ml) were refluxed in ether (150 ml) for 5 hr. After cooling, triethylamine hydrochloride was removed by suction filtration and fractional distillation of the filtrate led to isolation (83%) of XIII as a colorless oil, bp 58–60° (2 mm), which is best stored at low temperatures with complete exclusion of moisture. NMR: δ 3.95 (t, 4H, 2-CH_2Cl), 3.29 (t, 4H, 2-NCH_2), 1.20 [s, 9H, C(CH_3)$_3$], and 0.03 [s, 6H, Si(CH_3)$_2$] ppm. IR (neat): 2980, 2946, and 2863 (C—H), and 960 (Si—N) cm^{-1}.

[1] Bis(2-chloroethyl)amine undergoes rapid intramolecular alkylation in polar solvents such as water, but may be stored in ether at low temperatures for short periods of time.

Table I—Hydrolysis Kinetic Data [a]

Compound	Initial Concentration, *M*	pH[b]	Method[c]	k'[d], sec^{-1}	$\tau_{1/2}$[e], min
V	1.8×10^{-2}	7.4	NMR	3.00×10^{-3}	3.8
X	1.5×10^{-2}	7.4	NMR	4.02×10^{-4}	28.6
XV	2.3×10^{-2}	7.4	NMR	6.37×10^{-4}	18.1
	2.7×10^{-2}	6.4	UV (226 nm)	4.00×10^{-5}[f]	
	2.7×10^{-2}	7.4	UV (226 nm)	3.03×10^{-4}[f]	
	2.7×10^{-2}	8.4	UV (226 nm)	5.12×10^{-4}[f]	
XVI	2.3×10^{-2}	7.4	NMR	4.26×10^{-4}	27.0
	1.0×10^{-3}	7.4	UV (260 nm)	4.23×10^{-4}	27.2
XVII	1.0×10^{-3}	7.4	UV (260 nm)	3.37×10^{-4}	34.2
XVIII	2.1×10^{-2}	7.4	NMR	8.66×10^{-4}	13.3
	1.0×10^{-3}	7.4	UV (260 nm)	9.00×10^{-4}	12.8
XXVI	3.0×10^{-3}	6.4	NMR	—[g]	
	3.0×10^{-3}	7.4	NMR	1.07×10^{-4}	1.08
	3.0×10^{-3}	8.4	NMR	1.1×10^{-4}	1.14

[a] Compound V was studied in a dioxane–0.05 *M* lutidine buffer (pH 7.4) mixture (60:40), all other NMR studies were similarly carried out using a tromethamine buffer component. All UV studies refer to a dioxane–0.10 *M* tromethamine buffer mixture (50:50). In all cases the temperature was 27 ± 1°. [b] The indicated pH value refers to the aqueous buffer component prior to mixing with dioxane. [c] See text and Experimental section for details. [d] Pseudo first-order rate constant for desilylation, except as noted. [e] $\tau_{1/2} = \ln 2/k'$. [f] Refers to carbonate production following desilylation. [g] Not determined; the reaction was too fast to monitor by the NMR method.

***N*-Aryldimethylsilyl-*N*,*N*-bis(2-chloroethyl)amines**—The procedure described above for compound XII was applied to a series of aryldimethylchlorosilanes and afforded (80–90%) the following products, which were purified by fractional vacuum distillation and identified by NMR (CCl_4): *p*-methoxyphenyl (45–46°, 2 mm), δ 7.20 (broad s, 4H, C_6H_4), 3.60 (s, 3H, OCH_3), 3.50 (m, 8H, 4-CH_2), and 0.13 [s, 6H, $Si(CH_3)_2$]; *p*-tolyl (43–44°, 2 mm), δ 7.40 (broad s, 4H, C_6H_4), 3.60 (m, 8H, 4-CH_2), 2.50 (s, 3H, CH_3), and 0.13 [s, 6H, $Si(CH_3)_2$]; phenyl (40–42°, 2 mm), δ 7.30 (m, 5H, C_6H_5), 3.40 (m, 8H, 4-CH_2), and 0.08 [s, 6H, $Si(CH_3)_2$], *p*-fluorophenyl (41–43°, 2 mm), δ 7.30 (m, 4H, C_6H_4), 3.50 (m, 8H, 4-CH_2), and 0.07 [s, 6H, $Si(CH_3)_2$]; and *p*-chlorophenyl (45–46°, 2 mm), δ 7.40 (m, 4H, C_6H_4), 3.50 (m, 8H, 4-CH_2), and 0.06 [m, 6H, $Si(CH_3)_2$] ppm.

***O*-Trimethylsilyl-*N*,*N*-bis(2-chloroethyl)carbamate (XIV)**—A cold (−10°) solution of XII (2 g, 11 mmoles) in ether (10 ml) and pentane (35 ml) containing bis(2-chloroethyl)amine (0.16 g) as a required catalyst was reacted with anhydrous carbon dioxide gas for 4 hr. The progress of the reaction was monitored by IR with diminishing intensity of the Si—N absorption at 980 cm^{-1} and concomitant increase of the C=O absorption at 1748 cm^{-1} indicating the extent of product formation. Precipitated material was removed by suction filtration, and fractional distillation of the filtrate gave (90%) XIV as a colorless oil, bp 56–57° (1 mm). NMR: δ 3.30 (m, 8H 4-CH_2) and 0.03 [s, 9H, $Si(CH_3)_3$] ppm. IR (neat): 2970, 2933, and 2872 (C—H), 1748 (C=O), 1270 ($SiCH_3$), and 1160 (Si—O) cm^{-1}.

***O*-(*tert*-Butyldimethylsilyl)-*N*,*N*-bis(2-chloroethyl)carbamate (XV)**—Compound XV, bp 82–84° (2 mm), was prepared and isolated (65%) in a manner identical to that described above for XIV. Attempted distillation of XV at somewhat higher pressure and temperature (~100°) led to violent decomposition. NMR: δ 3.55 (broad s, 8H, 4-CH_2), 0.92 [s, 9H, $C(CH_3)_3$], and 0.22 [s, 6H, $Si(CH_3)_2$] ppm. IR (neat): 2981, 2950, and 2880 (C—H), 1750 (C=O), 1380 [$C(CH_3)_3$], 1258 ($SiCH_3$), and 1161 (Si—O) cm^{-1}.

***O*-(*tert*-Butyldiphenylsilyl)-*N*,*N*-bis(2-chloroethyl)carbamate (XVII)**—A solution of *tert*-butyldiphenylchlorosilane (27.5 g, 0.1 mole) in ether (30 ml) was added dropwise (30 min) to a cold (5°) solution of bis(2-chloroethyl)amine (12.6 g, 0.11 mole) and triethylamine (16.8 ml) in ether (270 ml). After 3 hr of stirring at 25°, the reaction mixture was cooled to −10° and (without filtration) anhydrous carbon dioxide was bubbled through it for 4 hr. Precipitated material was separated by suction filtration and ether was removed from the filtrate by fractional distillation. The residue obtained by further concentration *in vacuo* (25°, 0.1 mm, 18 hr) was extracted with benzene (25 ml), leaving undissolved material that was removed by suction filtration. Low-boiling petroleum ether was added to the filtrate until turbidity was apparent, and the solution was then stored in a freezer. Compound XVII was isolated either as an oil or a low-melting solid, mp 40–45°. NMR: δ 7.63 (m, 10H, 2-C_6H_5), 3.76 (m, 8H, 4-CH_2), and 1.22 [s, 9H, $C(CH_3)_3$] ppm. IR (neat): 3106 and 3071 (C_6H_5), 2993, 2951, and 2891 (C—H), 1715 (C=O), 1391 [$C(CH_3)_3$], 1255 ($SiCH_3$), 1121 (Si—O), and 744 and 702 (C_6H_5) cm^{-1}.

***O*-Diphenylmethylsilyl-*N*,*N*-(2-chloroethyl)carbamate(XVI)**—The same procedure described above for the synthesis of XVII gave (75%) XVI as a colorless oil, which was isolated upon cooling the benzene–petroleum ether solution of the crude product. NMR: δ 7.42 (m, 10H, 2-C_6H_5), 3.40 (t, 4H, 2-CH_2Cl), 2.70 (t, 4H, 2-NCH_2), and 0.45 (s, 3H, $SiCH_3$) ppm. IR (neat): 3092, 3075, and 3030 (C_6H_5), 1748 (C=O), 1254 ($SiCH_3$), 1122 (Si—O), and 732 and 698 (C_6H_5) cm^{-1}.

***O*-Tribenzylsilyl-*N*,*N*-bis(2-chloroethyl)carbamate XVIII**—Compound XVIII was synthesized according to essentially the same procedure as that described above for XVI, except that the reaction mixture was treated with gaseous carbon dioxide for 7 hr at −10°. Crystallization of the crude product from benzene–petroleum ether gave pale yellow crystals, mp 106–108°. NMR: δ 6.95 (m, 15H, 3-C_6H_5), 3.51 (m, 8H, 4-CH_2), and 2.00 (s, 6H, 3-$SiCH_2$) ppm. IR (mull): 3070 (C_6H_5), 1716 (C=O), 1155 (Si—O), and 722 and 685 (C_6H_5) cm^{-1}.

***O*-Triethoxysilyl-*N*,*N*-bis(2-chloroethyl)carbamate (XIX)**—The synthetic procedure described above for compound XVII yielded (75%) XIX as a colorless oil, which was isolated upon cooling the benzene–petroleum ether solution of the crude product. NMR: δ 4.06–3.55 (m, 14H, 2-NCH_2CH_2Cl and 3-OCH_2) and 1.25 (t, 9H, 3-CH_3) ppm. IR (neat): 2995 and 2896 (C—H), 1685 (C=O), and 1162 (Si—O) cm^{-1}.

***O*-Aryldimethylsilyl-*N*,*N*-bis(2-chloroethyl)carbamates**—The same procedure described above for compound XIV was applied to each member of the series of *N*-aryl-*N*,*N*-bis(2-chloroethyl)amines and afforded (50–80%) the following products, which were purified by fractional vacuum distillation and identified by NMR (CCl_4): *p*-methoxyphenyl (40–41°, 0.3 mm), δ 6.80 (m, 4H, C_6H_4), 3.80 (s, 3H, OCH_3), 3.30 (m, 8H, 4-CH_2), and 0.35 [s, 6H, $Si(CH_3)_2$]; *p*-tolyl (55–56°, 1 mm), δ 7.20 (broad s, 4H, C_6H_4), 3.20 (m, 8H, 4-CH_2), 2.30 (s, 3H, CH_3), and 0.32 [s, 6H, $Si(CH_3)_2$]; phenyl (53–54°, 1 mm), δ 7.30 (broad s, 5H, C_6H_5), 3.3 (m, 8H, 4-CH_2), and 0.30 [s, 6H, $Si(CH_3)_2$]; *p*-fluorophenyl (42–43°, 0.5 mm), δ 7.40 (m, 4H, C_6H_4), 3.2 (m, 8H, 4-CH_2), and 0.29 [s, 6H, $Si(CH_3)_2$]; *p*-chlorophenyl (50–51°, 0.5 mm), δ 7.50 (m, 4H, C_6H_4), 3.30 (m, 8H, 4-CH_2), and 0.28 [s, 6H, $Si(CH_3)_2$] ppm.

Bis-carbamoyldisiloxane (XX)—A stirred solution of bis(2-chloroethyl)amine (13.1 g, 0.12 mole) and triethylamine (17.6 ml) in ether (250 ml) at 5° was treated dropwise (1 hr) with a solution of 1,3-dichloro-1,1,3,3-tetramethyldisiloxane (10 ml, 0.052 mole) in ether (20 ml). After stirring for 2 hr at 25°, triethylamine hydrochloride was removed by suction filtration and the filtrate was reacted with gaseous anhydrous carbon dioxide for 6 hr at −10°. Further processing as described above for compound XVII led to isolation of XX as a pale yellow oil, which was isolated upon cooling the benzene–petroleum ether solution of crude product. NMR: δ 3.81 (broad s, 16H, 4-NCH_2CH_2Cl), 0.41 [broad s, 6H, 2-$Si(CH_3)_2$] and 0.23 [d, 6H, 2-$Si(CH_3)_2$] ppm. IR (neat): 2940 and 2885 (C—H), 1711 (C=O), 1269 ($SiCH_3$), and 1100 (Si—O) cm^{-1}.

***O*-(*tert*-Butyldimethylsilyl)-*N*-(2-chloroethyl)carbamate (XXI)**—A mixture of *tert*-butyldimethylsilanol (0.8 g, 6 mmoles) and 2-chloroethylisocyanate (3.6 g, 34 mmoles) was heated at 110° for 3 hr, after which time IR analysis indicated the absence of isocyanate starting material (2275 cm^{-1}) and the presence of product (1710 cm^{-1}). Volatiles were removed *in vacuo* (0.1 mm) at 25° and pentane (10 ml) soluble material was then extracted from the residue. Removal of pentane yielded (25%) crude XXI, mp 54–55°, which contained 20% isocyanate starting material and was used without further purification; compound XXI undergoes extensive fragmentation giving silanol and isocyanate when stored at 5° for 2–3 weeks. NMR: δ 5.16 (broad s, 1H, NH), 3.75–3.40 (m, 4H, NCH_2CH_2Cl), 1.03 [s, 9H, $C(CH_3)_3$], and 0.20 [s, 6H, $Si(CH_3)_2$]; integrations corrected for 20% $ClCH_2CH_2NCO$, δ 3.85 (s) ppm, mass spectrum: no M^+; base peak *m/z* 180 (M^+, −57), loss of $C(CH_3)_3$.

***O*-(*tert*-Butyldimethylsilyl)-*N*-{*p*-[*N'*,*N'*-bis(2-chloroethyl)-amino]}phenylcarbamate (XXII)**—A mixture of *p*-isocyanatophenyl mustard (1.09 g, 4.2 mmoles), *tert*-butyldimethylsilanol (0.39 g, 3

Table II—Screening Data for *In Vivo* Anticancer Activity against L-1210 Lymphoid Leukemia and P-388 Lymphocytic Leukemia in Mice

Compound	Vehicle[a]	Dose/Inj., mg/kg	Total Inj.	Treatment Schedule[b]	Screen[c]	max T/C, %[d]
V	A	750	1	1 × 1	L 1210	132
X	A	250	1	1 × 1	L 1210	138
XIII	B	18.75	3	4 × 3	P 388	171
	B	9.37	3	4 × 3	P 388	145
XIV	B	100	1	1 × 1	P 388	166
	B	100	1	1 × 1	P 388	137
XV	B	400	1	1 × 1	P 388	174
XVII	C	200	1	1 × 1	P 388	148
XVIII	D	50	3	4 × 3	P 388	214
	D	100	2	4 × 2	P 388	180
XX	C	25	9	1 × 9	P 388	165
	C	50	9	1 × 9	P 388	208
XXII	A	10	3	4 × 3	P 388	203
	A	10	3	4 × 3	P 388	158
	A	20	3	4 × 3	P 388	182
XXIII	B	200	1	1 × 1	P 388	159
XXVII	C	200	5	1 × 5	L 1210	131

[a] A = mixture of distilled water and polyoxyethylene sorbitan monooleate; B = hydroxypropylcellulose; C = mixture of saline and polyoxyethylene sorbitan monooleate; D = saline. Samples for injection were prepared immediately prior to use. [b] For example, 4 × 3 indicates a 4-day interval between treatments repeated three times; all injections were given ip. [c] For L-1210, the inoculum was 10^5 cells; for P-388, the inoculum was 10^6 cells. [d] Maximum T/C evaluation parameter which was obtained, where T/C % = (treated survivors/control survivors) × 100. A value of ≥125% indicates activity. In all cases, the max T/C % was obtained without drug-associated mortality.

mmoles), and toluene (15 ml) was refluxed until the isocyanate IR absorption (2268 cm^{-1}) was no longer detected (24 hr). Concentration *in vacuo* (0.1 mm) at 25° gave a pale yellow oil, which was extracted three times with low-boiling petroleum ether (45 ml). The combined petroleum ether extracts were concentrated to half-volume and then kept at −10° for 15 hr to afford (60%) product XXII, mp 58–60°. NMR (220 MHz): δ 7.40–6.50 (AA′BB′ q, 4H, C_6H_4), 3.64 (m, 8H, 4-CH_2), 0.85 [s, 9H, $C(CH_3)_3$], and 0.21 [s, 6H, $Si(CH_3)_2$] ppm. IR (neat melt): 3348 (NH), 3085 (C_6H_5), 2982 and 2880 (C—H), 1715 (C=O), 1260 ($SiCH_3$), 1120 (Si—O), and 837 (C_6H_4-*p*) cm^{-1}.

Anal.—Calc. for $C_{17}H_{28}N_2O_2SiCl_2$: C, 52.17; H, 7.16; N, 7.16. Found: C, 52.13; H, 7.12; N, 7.28.

***O*-(*tert*-Butyldimethylsilyl)chlorambucil (XXIII)**—A solution of chlorambucil[2] (0.92 g, 3 mmoles) in benzene (10 ml) was added dropwise (20 min) to a stirred suspension of sodium hydride (96 mg, 4 mmoles) in benzene (3 ml) at 25°. After continued stirring for 3 hr, a solution of *tert*-butyldimethylchlorosilane (0.76 g, 5 mmoles) in benzene (5 ml) was slowly added (20 min), and the mixture was refluxed for 3 hr. The reaction mixture was cooled to 25° and solid materials were removed by suction filtration. The filtrate was concentrated and further removal of volatile *in vacuo* (0.1 mm) at 25° yielded (77%) XXIII as a viscous pale yellow syrup. NMR (carbon tetrachloride): δ 6.65 (AA′BB′ q, 4H, C_6H_4), 3.56 (broad s, 8H, 2-NCH_2CH_2Cl), 2.75–1.65 (m, 6H, $CH_2CH_2CH_2$), 0.86 [s, 9H, $C(CH_3)_3$], and 0.15 [s, 6H, $Si(CH_3)_2$] ppm. IR (neat): 3030 (C_6H_4), 2975 and 2875 (C—H), 1722 (C=O), 1371 [$C(CH_3)_3$], 1200 ($SiCH_3$), 1155 (Si—O), and 832 (C_6H_4-*p*) cm^{-1}.

***O*-(*tert*-Butyldiphenylsilyl)chlorambucil (XXIV)**—Chlorambucil (0.92 g, 3 mmoles), sodium hydride (96 mg, 4 mmoles), and *tert*-butyldiphenylchlorosilane (0.83 g, 3 mmoles) were used to prepare XXIV in a manner identical to that described above for XXIII. The product was isolated (77%) as a viscous oil, which showed no evidence (NMR) of significant contamination by either the starting chlorosilane or its corresponding silanol. NMR: δ 7.90–7.15 (m, 10H, 2-C_6H_5), 7.15–6.35 (AA′BB′ q, 4H, C_6H_4), 3.55 (broad s, 8H, 2-NCH_2CH_2Cl), 2.75–1.40 (m, 6H, $CH_2CH_2CH_2$), and 1.13 [s, 9H, $C(CH_3)_3$] ppm.

***N*-(*tert*-Butyldimethylsilyl)cyclophosphamide (XXV)**—A solution of *tert*-butyldimethylchlorosilane (0.75 g, 5 mmoles) in ether (10 ml) was added slowly (30 min) to a stirred solution of anhydrous cyclophosphamide[3] (0.79 g, 3 mmoles) and triethylamine (0.5 ml) in ether (20 ml) at 5°. After continuous stirring for 24 hr at 25°, the reaction mixture was cooled to −78° and solid materials were collected at that temperature by suction filtration under a nitrogen atmosphere. The solids were immediately extracted with tetrahydrofuran, and this solvent was then removed on a rotary evaporator. The residue was chromatographed on a column (40 × 4 cm) of dry silica gel, using chloroform as the eluent, and the concentrated eluate gave XXV as low-melting crystals, mp 45–47°. NMR (220 MHz): δ 4.46–4.15 (m, 2H, OCH_2) 3.70 (t, 4H, 2-CH_2Cl), 3.45–3.20 (m, 6H, 3-NCH_2), 2.20–1.64 (m, 2H, $CH_2CH_2CH_2$), 1.09 [s, 9H, $C(CH_3)_3$], 0.37 (s, 3H, $SiCH_3$), and 0.22 (s, 3H, $SiCH_3$). The observation of resonance doubling for the $Si(CH_3)_2$ moiety is due to the chirality at phosphorus in XXV (diastereotopic CH_3 groups), and unambiguously establishes that the *tert*-butyldimethylsilyl group is bonded to the cyclophosphamide ring system. ^{31}P-NMR (deuterochloroform, 25% H_3PO_4 external reference): δ 13.82 *versus* 10.78 for cyclophosphamide ppm, mass spectrum: no M^+; *m/z* 317 (M^+, −57), loss of $C(CH_3)_3$, 2-Cl isotope cluster.

***O,O*-Bis(*tert*-butyldimethylsilyl)fluorouracil (XXVI)**—A stirred mixture of fluorouracil (1.30 g, 10 mmoles) and *tert*-butyldimethylchlorosilane (3.3 g, 22 mmoles) in benzene (20 ml) was brought to reflux, and a solution of triethylamine (3.4 ml, 22 mmoles) in benzene (8 ml) was then added dropwise over a 1-hr period. The mixture was refluxed for an additional 15 hr, and then cooled to 25° for separation of triethylamine hydrochloride and unreacted fluorouracil by suction filtration. Volatile materials were removed first on a rotary evaporator and then under high vacuum (0.1 mm) at 25° for 24 hr. The residual material was dissolved in ether (15 ml) decolorized with dry activated charcoal, and then reconcentrated to afford XXVI (67%) as a colorless oil, which crystallized upon standing at −10°, mp ~30°. Contamination of XXVI by fluorouracil was excluded by NMR and IR analyses, which showed no detectable absorptions due to the amido functionalities. Compound XXVI is extremely reactive toward moisture. NMR: δ 7.88 (d, 1H, vinylic H), 0.99 [two overlapping s, 18H, 2-$C(CH_3)_3$], 0.33 [s, 6H, $Si(CH_3)_2$], and 0.21 [s, 6H, $Si(CH_3)_2$] ppm.

***tert*-Butyldimethylsilylftorafur (XXVII)**—A stirred mixture of ftorafur (2 g, 9.8 mmoles) and *tert*-butyldimethylchlorosilane (3 g, 20 mmoles) in benzene (35 ml) was brought to reflux, and a solution of triethylamine (2 ml) in benzene (10 ml) was then added dropwise over a period of 1 hr. The mixture was further reacted and processed as described above for XXVI to afford (56%) product XXVII, mp 149–150°, which was recrystallized from carbon tetrachloride. NMR: δ 7.52 (d, $^3J_{FH}$ = 6 Hz, 1H, vinyl), 6.10 (m, 1H, methine), 4.50–3.80 (m, 2H, CH_2O), 2.70–1.85 (m, 4H, CH_2CH_2O), 0.95 [s, 9H, $SiC(CH_3)_3$], and 0.15 [s, 6H, $Si(CH_3)_2$] ppm.

***O*-Trimethylsilylbenzohydroxamic Acid (XXVIII)**[4]—A solution of benzohydroxamic acid (1.37 g, 10 mmoles), trimethylchlorosilane (1.27 ml, 10 mmoles), and triethylamine (1.5 ml, 10 mmoles) in tetrahydrofuran (15 ml) was stirred for 3 days at 25°, and triethylamine hydrochloride was then removed from the reaction mixture by suction filtration. After initial concentration of the filtrate on a rotary evaporator, the residue was kept under high vacuum (0.1 mm) for 2 days at 25°. The crude crystalline product (~100%), mp 96–99°, was used without further purification (25% starting material) due to its hydrolytic reactivity. For XXVIII, NMR: δ 8.00 (broad s, 1H, NH), 7.80–7.42 (m, 2H, *ortho* H), 7.40–7.18 (m, 3H, *meta* and *para* H), and 0.15 [s, 9H, $Si(CH_3)_3$].

***O*-(*tert*-Butyldimethylsilyl)benzohydroxamic Acid (XXIX)**—The synthetic procedure described above for compound XXVIII was applied

[2] Chlorambucil (NSC-3088) was obtained from the Drug Synthesis and Chemistry Branch of the National Cancer Institute.

[3] Cyclophosphamide monohydrate (NSC 26271) was obtained from the Drug Synthesis and Chemistry Branch of the National Cancer Institute. Water of hydration was removed *in vacuo* over phosphorus pentoxide (0.1 mm, 25°, ≥48 hr).

[4] For the preparation of *N,O*-bis(trimethylsilyl)benzohydroxamic acid and its *para*-substituted derivatives, see Ref. 14.

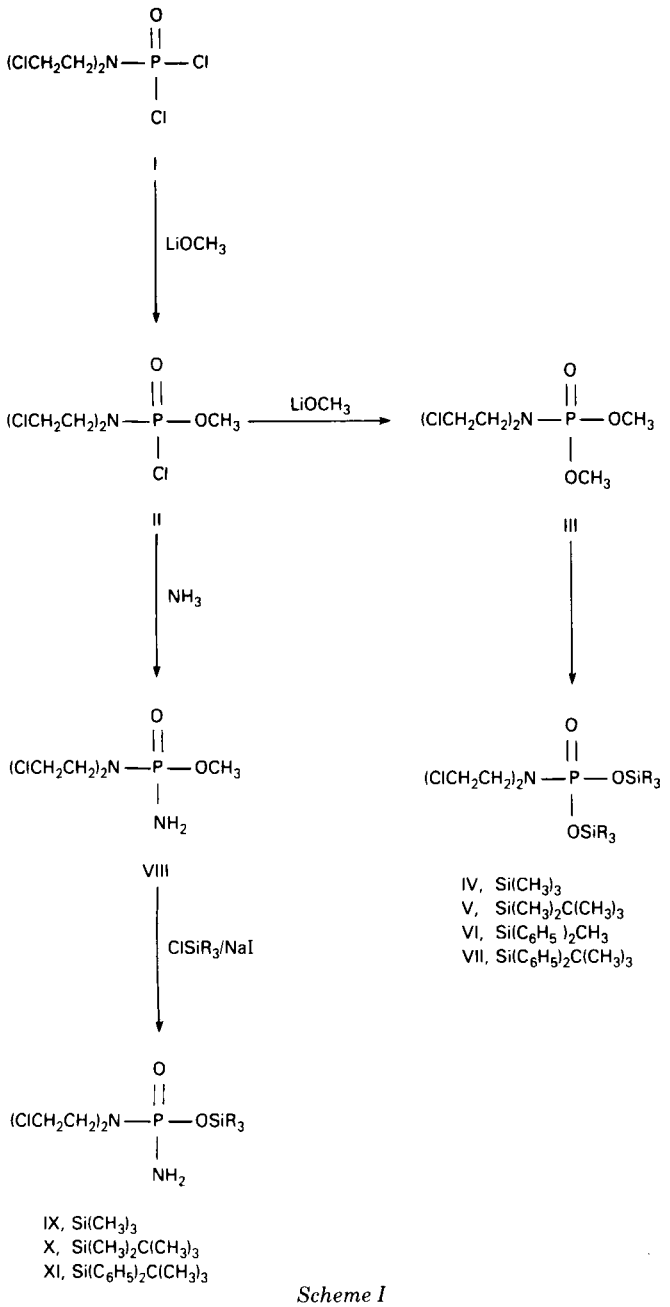

Scheme I

to the reaction of benzohydroxamic acid (1.37 g, 10 mmoles) with equimolar amounts of *tert*-butyldimethylchlorosilane and triethylamine. The resultant product (~100%), mp 127–129°, was found by NMR analysis to be free of detectable contamination by its bistriorganosilylated analog. NMR: δ 8.23 (broad s, 1H, NH), 8.00–7.67 (m, 2H, *ortho* H), 7.67–7.27 (m, 3H, *meta* and *para* H), 1.00 [s, 9H, $C(CH_3)_3$], and 0.25 [s, 6H, $Si(CH_3)_2$].

Anal.—Calc. for $C_{13}H_{21}NO_2Si$: C, 62.11; H, 8.42; N, 5.57. Found: C, 62.12; H, 8.37; N, 5.81.

***N,O*-Bis(*tert*-butyldimethylsilyl)hydroxyurea (XXX)**—A solution of *tert*-butyldimethylchlorosilane (3.8 g, 25 mmoles) in ether (15 ml) was added dropwise (50 min) to a stirred solution of hydroxyurea (1.52 g, 20 mmoles) and triethylamine (3.06 ml, 20 mmoles) in ether (25 ml) at 5°, and the mixture was stirred at 25° for 18 hr. Triethylamine hydrochloride was removed by suction filtration, and the filtrate was concentrated on a rotary evaporator. The residue was extracted with ether (25 ml) and XXX was then obtained (25%) as a microcrystalline solid (mp 92.5–110°) by removal of solvent *in vacuo* (18 hr, 0.1 mm, 20°). NMR: δ 5.80 (broad s, 1H, NHO), 5.30 (broad s, 1H, NH), 0.93 [s, 18H, 2-$C(CH_3)_3$], 0.25 [s, 6H, $OSi(CH_3)_2$], and 0.17 [s, 6H, $NSi(CH_3)_2$]. Mass spectrum: *m/z* 304 (M^+), <1%; 247 (M^+, −57), 36%, loss of $C(CH_3)_3$.

Prodrug Hydrolysis Kinetics by NMR—The compound (15–23 mmoles) to be studied was placed in an NMR tube and then dissolved in dioxane (0.60 ml). Either tromethamine or lutidine buffer (0.40 ml, 0.05 *M*, pH 7.4) was added, and after rapid mixing the spectral region from δ 0.7–0 was repeatedly recorded as a function of time using a fixed-sweep rate. Total peak height for starting material and the triorganosilanol hydrolysis product remained constant and was equated with the initial concentration of starting material, C_0. The decreasing peak height for starting material was equated with the concentration of starting material at time *t*, C_t. Linear least-squares fits of $\ln(C_0/C_t)$ *versus* *t* gave the pseudo first-order rate constants (*k'*) and half-life ($\tau_{1/2}$) values listed in Table I. The NMR probe temperature (27 ± 1°) was measured using the chemical shift difference between methyl and hydroxyl protons in methanol (15).

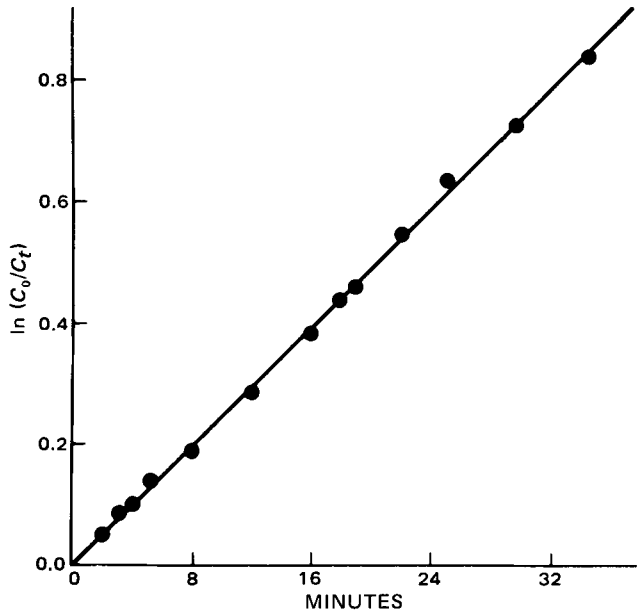

Figure 1—*Pseudo first-order kinetic plot for hydrolysis of X (1.5 × 10^{-2} M) in dioxane–0.05 M tromethamine buffer (pH 7.4) mixture (60:40) at 27°. Substrate concentration terms C_0 and C_t were determined by NMR (see text for details).*

Prodrug Hydrolysis Kinetics by UV—Stock solutions of each compound were prepared in dioxane at concentrations of 6.0 × 10^{-4}–5.4 × 10^{-2} *M*. An aliquot (1.5 ml) was rapidly mixed with an equal volume of tromethamine buffer (0.1 *M*, pH 7.4–8.4), and the reaction mixture was monitored continuously as a function of time *t*, using a fixed wave-

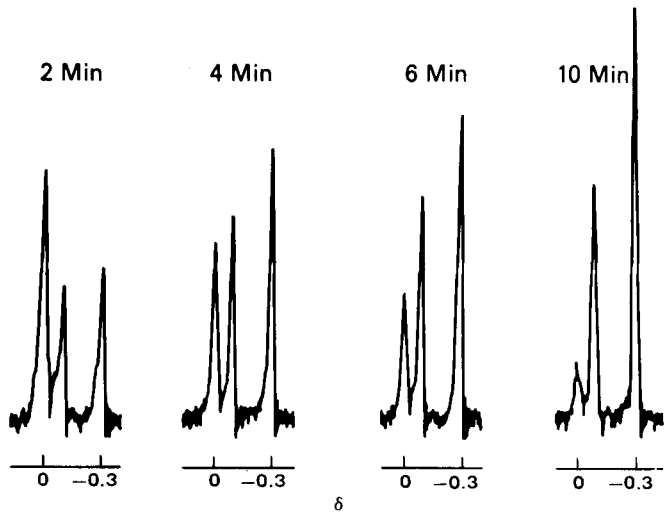

Figure 2—*Variation in the dimethylsilyl NMR (60 MHz) spectral region for V (1.8 × 10^{-2} M) as a function of time (min) in dioxane–0.05 M lutidine buffer (pH 7.4) mixture (60:40) at 27°. Chemical shifts are relative to V (0 δ); the absorption signal at −0.08 δ is assigned to the monoester derived from partial hydrolysis of V, while the* tert*-butyldimethylsilanol signal is at −0.30 δ.*

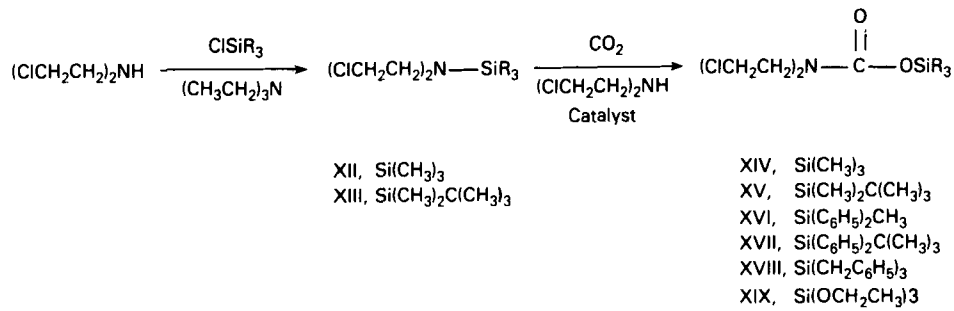

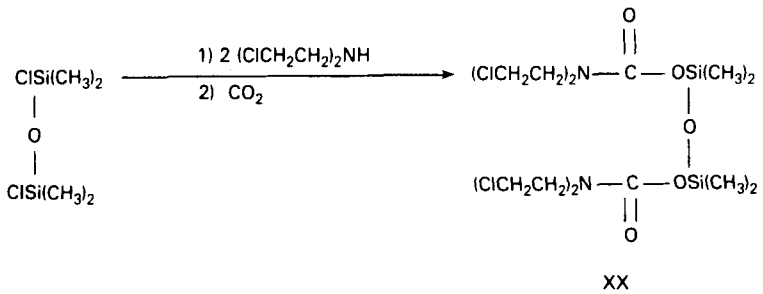

XX

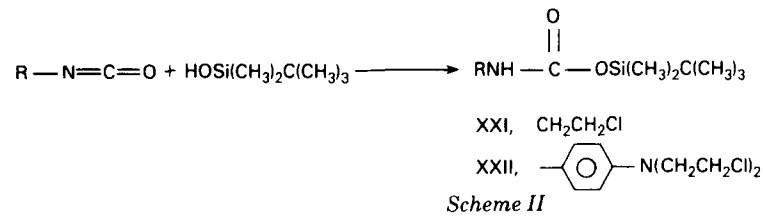

Scheme II

length (Table I) and a reference sample containing the dioxane–buffer mixture (50:50). The initial absorbance was equated with A_0 and the final absorbance after 4 hr was equated with A_∞. Linear least-squares fits of $\ln [(A_\infty - A_0)/(A_\infty - A)]$ *versus* t gave the pseudo first-order rate constants (k') and half-life ($\tau_{1/2}$) values listed in Table I. The temperature (27 ± 1°) of the UV samples after equilibration in the spectrophotometer was measured with a small thermometer.

NMR Kinetic Measurements with Aryldimethylsilyl Compounds—Each of the five *N*-aryldimethylsilyl-*N*,*N*-bis(2-chloroethyl)-amines (2.5×10^{-2} mmoles) was dissolved in deuterochloroform (0.5 ml) and was then reacted with a large excess of absolute ethanol (0.5 ml) using NMR to monitor the reaction rate at a spectrometer probe temperature of 27 ± 1°. The relative concentrations of each starting material and its corresponding ethoxysilane product were determined from dimethylsilyl absorption intensities at $\delta \sim 0.15$ and ~0.08, respectively, using scale-expansion, low RF-power, and a fast sweep rate. Linear least-squares fits of $\ln(C_0/C_t)$ *versus* t had an average slope-error of ± ~5%, and gave the following pseudo first-order rate constants: p-OCH_3, 1.14×10^{-3} sec^{-1} ($\tau_{1/2}$ 10.1 min); p-CH_3, 1.43×10^{-1} sec^{-1} ($\tau_{1/2}$ 8.1 min); p-H, 2.73×10^{-3} sec^{-1} ($\tau_{1/2}$ 4.2 min); p-F, 6.86×10^{-3} sec^{-1} ($\tau_{1/2}$ 1.7 min); and p-Cl, 1.04×10^{-2} sec^{-1} ($\tau_{1/2}$ 1.1 min). The previously described NMR method for

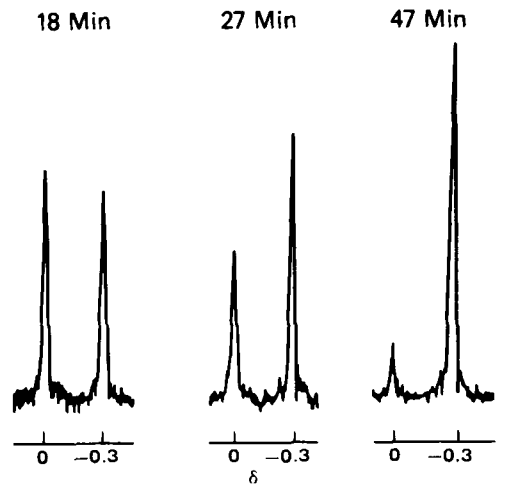

Figure 3—*Variation in the dimethylsilyl NMR (60 MHz) spectral region for XV (2.3×10^{-2} M) as a function of time (min) in dioxane–0.05 M tromethamine (pH 7.4) mixture (60:40) at 27°. The chemical shift of* tert*-butyldimethylsilanol (−0.30 δ) is relative to XV (0 δ).*

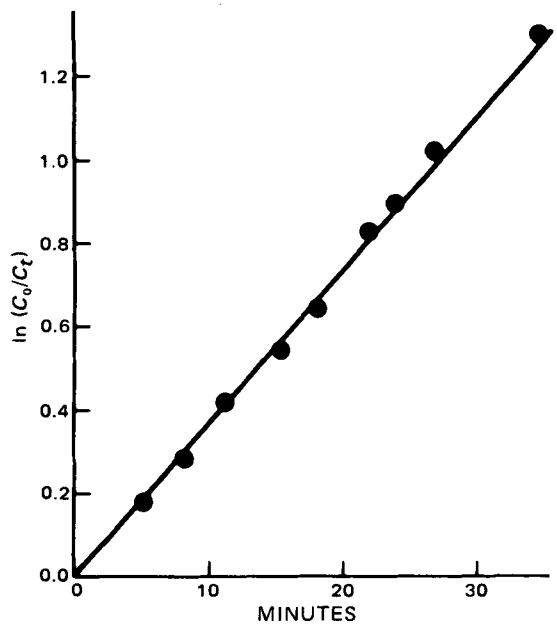

Figure 4—*Pseudo first-order kinetic plot for hydrolysis of XV (2.3×10^{-2} M) in dioxane–0.05 M tromethamine buffer (pH 7.4) mixture (60:40) at 27°. Substrate concentration terms C_0 and C_t were determined by NMR (see text and Fig. 3).*

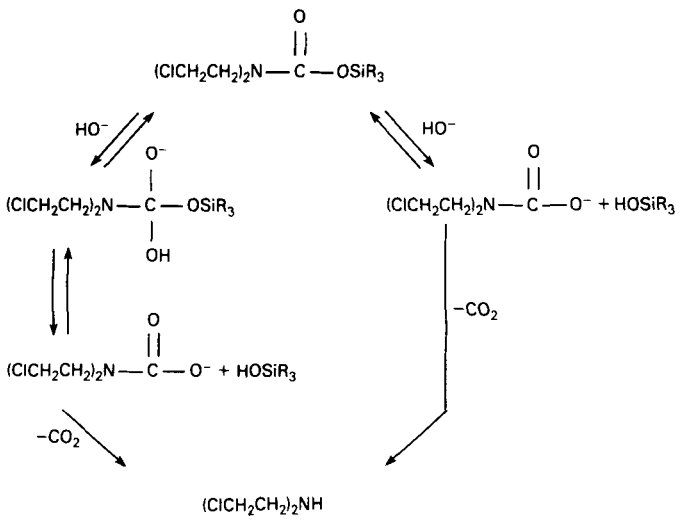

Scheme III

measurement of prodrug hydrolysis kinetics was applied to solutions containing each of the five *O*-aryldimethylsilyl-*N*,*N*-bis(2-chloroethyl)-carbamates (2.5×10^{-2} mmoles) in a mixture of dioxane (0.5 ml) and tromethamine buffer (0.5 ml, 0.05 *M*, pH 7.4). For these reactions at 27 ± 1°, linear least-squares fits (± ~5% average slope-error) gave the following pseudo first-order rate constants: *p*-OCH_3, 1.65×10^{-4} sec^{-1} ($\tau_{1/2}$ 70.0 min); *p*-CH_3, 1.69×10^{-4} sec^{-1} ($\tau_{1/2}$ 68.3 min); *p*-H, 3.87×10^{-4} sec^{-1} ($\tau_{1/2}$ 29.8 min); *p*-F, 1.17×10^{-3} sec^{-1} ($\tau_{1/2}$ 9.9 min); and *p*-Cl, 1.58×10^{-3} sec^{-1} ($\tau_{1/2}$ 7.3 min).

^{18}O-Labeling Studies—A freshly prepared sample of silanol-free XXI (10 mg) was dissolved in a magnetically stirred mixture of dioxane (0.4 ml), tromethamine buffer (0.2 ml of 0.2 *M*, pH 7.4), and ^{18}O-enriched water (0.2 ml, >95 g-atom % ^{18}O). After 3 hr at room temperature, the reaction mixture was extracted with fractionally distilled pentane (3 × 1 ml), and the extract was then analyzed by mass spectroscopy to determine the relative proportion of ^{16}O- and ^{18}O-containing *tert*-butyldimethylsilanol. The (M^+, −57) ions observed at *m/z* 75 and 77 arise from loss of *tert*-butyl and had a normalized intensity of 99.87 and 100.00%, respectively. When unlabeled silanol (5 mg) was extracted from a simulated reaction mixture containing normal water, the ion intensities at *m/z* 75 and 77 were 100.00 and 4.78%, respectively, whereas use of 50:50 v/v mixture of water and ^{18}O-labeled water (18 hr of contact time) led to extraction of silanol having ion intensities at *m/z* 75 and 77 equal to 100.00 and 14.94%, respectively.

Anticancer Screening—Selected compounds (Table II) were evaluated against L-1210 lymphoid leukemia and P-388 lymphocytic leukemia in either male or female mice. Pertinent details and the results of these tests are given in Table II.

RESULTS AND DISCUSSION

Syntheses—The methodology for constructing *O*-triorganosilyl derivatives of phosphoramide mustard was developed by first pursuing the synthesis of diester model compounds IV–VII (Scheme I). These materials were prepared by reaction of common precursor III with the corresponding triorganochlorosilane and sodium iodide in acetonitrile solvent (16). The same demethylation–silylation procedure was used to convert common precursor VIII into target compounds IX–XI. Proton NMR spectra of these products showed two-proton amido resonance signals and were devoid of detectable methoxy signals, indicating that *N*-silylation of the amide functionality (17, 18) is not a significant side reaction.

O-Triorganosilyl carbamate derivatives of nor-nitrogen mustard (XIV–XIX, Scheme II) were obtained by Breederveld's (19) reaction sequence, namely, *N*-silylation followed by insertion of carbon dioxide into the Si—N bond, which requires excess amine as a catalyst and presumably (19) involves triorganosilyl group-transfer from an *N*-triorganosilyl-*N*,*N*-bis(2-chloroethyl)amine to the carbamic acid derivative or nor-nitrogen mustard.

The *N*-triorganosilyl-*N*,*N*-bis(2-chloroethyl)amines can be isolated (*e.g.*, XII and XIII); however, they readily decompose and were usually converted *in situ* to the final carbamate product. Biscarbamoyldisiloxane XX was similarly prepared from 1,3-dichloro-1,1,3,3-tetramethyldisiloxane, while *tert*-butyldimethylsilyl carbamate XXI was obtained by direct addition of *tert*-butyldimethylsilanol to 2-chloroethyl isocyanate. The silanol–isocyanate addition reaction has not been reported previously, and has been shown[5] to be generally applicable to variously structured triorganosilanols and alkyl/aryl isocyanates. Accordingly, it was possible to convert *p*-isocyanatophenylmustard into carbamate derivative XXII by reaction with the appropriate silanol.

Tert-butyldimethylsilyl (XXIII) and *tert*-butyldiphenylsilyl (XXIV) esters of the anticancer drug chlorambucil (20) were prepared by direct *O*-silylation using the sodium salt of this carboxylic acid. The anticancer agents cyclophosphamide (21), fluorouracil (22), ftorafur (23), benzohydroxamic acid (24), and hydroxyurea (25) were also silylated by conventional methods and gave derivatives XXV–XXX, respectively. By analogy to structurally related systems (14, 17, 26, 27), the triorganosilyl groups in compounds XXV–XXX may undergo either positional exchange (between oxygen and nitrogen bonding sites) or rotational isomerization; however, these dynamic processes are not a central issue in the present study. On the other hand, it is worthwhile to note that ^1H-NMR spectra for XXV–XXX were consistent with the presence of a single (major) isomer. The connectivities used to represent compounds XXV–XXX are the best guess structures as opposed to definite assignments of bonding.

Hydrolysis Kinetics—Hydrolytic unmasking of the candidate triorganosilyl prodrugs was first examined by ^1H-NMR monitoring of the dimethylsilyl spectral region for the phosphoramide mustard derivative X, using an organic solvent (dioxane)–aqueous buffer mixture to achieve sufficient substrate solubility for these continuous-wave measurements. Gradually decreasing intensity for the dimethylsilyl absorption of X was accompanied by increasing signal intensity for the dimethylsilyl moiety in the hydrolysis byproduct, *tert*-butyldimethylsilanol (δ −0.30, relative to X). The sum of these two resonance signals, which remained constant, provides a relative measure of the initial concentration of X, C_0, while the diminishing signal intensity for X is a relative measure of substrate concentration at time *t*, C_t. For hydrolysis of X at pH 7.4[6], 27°, a least-squares fit of $\ln(C_0/C_t)$ *versus* *t* (Fig. 1) indicated a good linear correlation and gave the pseudo first-order rate constant (k') and half-life ($\tau_{1/2}$) listed in Table I.

Spectra (Fig. 2) obtained with diester V under analogous reaction conditions showed the conversion of starting material into *tert*-butyldimethylsilanol (δ −0.30, relative to V) and a monoester intermediate (δ −0.08, relative to V), which undergoes comparatively slow hydrolysis to afford the fully unmasked phosphoramidic mustard.[7] Kinetic analysis based on the decreasing signal intensity of V afforded the monodesilylation rate data given in Table I. Multiplication of the 3.8-min half-life for V by a correction factor of 2 gives a value which is ~four times less than the 28.6-min half-life for X. This relatively small difference in half-lives is presumably due to leaving group effects, since the steric bulk about the back-side tetrahedral face of silicon is virtually the same in each compound. Pro(phosphoramide mustards) IX and XI were similarly examined by NMR in an attempt to determine the influence of the triorganosilyl group on hydrolytic stability; however, compound IX was too reactive to study by this method, and the *tert*-butyl signals from XI and its silanol byproduct were extensively overlapped at 60 MHz.

Alkaline hydrolysis of *O*-triorganosilyl carbamic acid mustards can occur by initial attack of hydroxide ion at either the carbonyl carbon, as in *O*-alkyl carbamates (28), or at silicon to give the conjugate base of carbamic acid mustards (Scheme III), which would then undergo relatively rapid decarboxylation to release nor-nitrogen mustard. While both reaction pathways lead to formation of the same bis-alkylating agent, the silicon-attack route would appear to allow for greater control over the rate of nor-nitrogen mustard release. Differentiation between the two mechanistic possibilities was first approached by studying structure–reactivity relationships. Extension of the NMR kinetic method to hydrolysis of *O*-trimethylsilyl carbamate XIV was precluded by this compound's exceedingly short lifetime in aqueous media; however, production of triorganosilanol from compounds XV, XVI, and XVIII could be conveniently monitored from changes in the methylsilyl or silyl-bearing

[5] K. C. Fichter and G. Zon, unpublished results.

[6] This and related pH values refer to the aqueous buffer component used to prepare the mixed solvent system. The true pH of such mixtures is poorly defined. Since the purpose of the present kinetic measurements was to evaluate *relative* substrate reactivities, and roughly gauge the stabilities of these potential prodrugs for possible correlation with *in vivo* biological activity, no attempt was made to devise either a more refined pH measurement or a more realistic *in vitro* kinetic system.

[7] Lutidine buffer causes a solvent-induced chemical shift separation between the dimethylsilyl signals for V and the monoester intermediate. The signals were accidentally isochronous in the dioxane–tromethamine buffer mixture used for studying X.

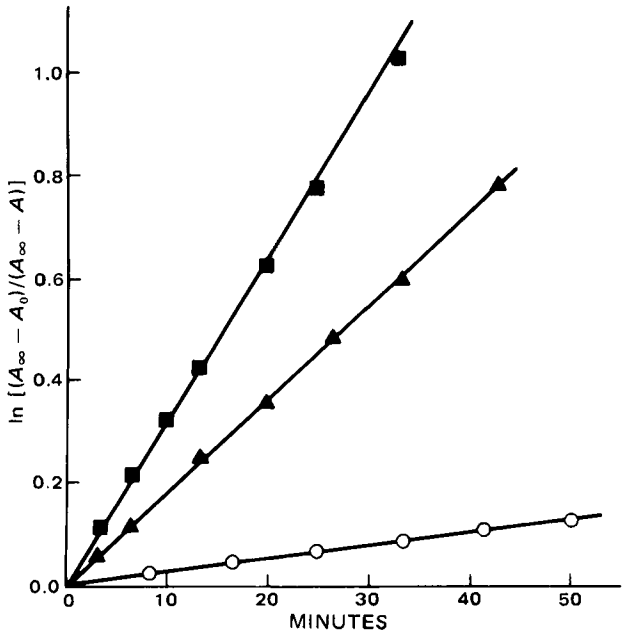

Figure 5—*Pseudo first-order kinetic plots for hydrolysis of XV (2.7 × 10^{-2} M) in 50:50 dioxane–0.10 M tromethamine buffer (pH 8.4, ■; pH 7.4, ▲; pH 6.4, ○) at 27°. The UV absorbance (A) values were measured at 226 nm (see text for details).*

methylene spectral region, as seen from representative spectra obtained with XV (Fig. 3). For each of these compounds, the signal for the triorganosilanol byproduct appeared at higher field (lower δ), relative to starting material, due to removal of the carbonyl group deshielding effect. In all cases, the formation of triorganosilanol obeyed a first-order rate law (*e.g.*, Fig. 4); however, the substrate half-life values (Table I) revealed only a twofold reactivity range for this series of SiR_3 groups: XVIII, 13.3 min; XV, 18.1 min; and XVI, 27.0 min.

Previous studies of the alkaline hydrolysis of carbamates have employed UV spectroscopy to measure reaction kinetics (28). When this method was applied to compound XV in mixtures of dioxane and tromethamine buffer at pH 6.4, 7.4, and 8.4 (27°), the absorbance (A) at 226 nm afforded linear plots of $\ln[(A_\infty - A_0)/(A_\infty - A)]$ *versus* t (Fig. 5), and the calculated rate constants (Table I) increased with elevated concentrations of hydroxide ion. The UV-derived rate constant for hydrolysis of XV at pH 7.4 (3.03×10^{-4} sec^{-1}) is about one-half the magnitude of the rate constant (6.37×10^{-4} sec^{-1}) for production of *tert*-butyldimethylsilanol from XV measured by NMR under the same reaction conditions. This difference can be accommodated by assuming the existence of carbamic acid mustard, since the absorbance at 226 nm is most likely due to carbonate ion which is formed by decarboxylation of this metastable intermediate (28).

Compounds XVI–XVIII have phenyl substituents that obscure the 226 nm UV region. Kinetic data (Table I) for hydrolysis of these silylated carbamates at pH 7.4 were thus obtained from absorbance changes measured at 260 nm, and correspond to the rate of triorganosilanol production rather than carbonate formation. This interpretation is supported by the fact that the UV- and NMR-derived half-lives for two of these compounds are essentially equivalent: XVI, 27.2 and 27.0 min, respectively; XVIII, 12.8 and 13.3 min, respectively.

It is enlightening to compare the relative rates of desilylation in the homologous series of carbamates represented by XV–XVIII. The order of increasing substrate stability ($\tau_{1/2}$) at pH 7.4 is XVIII (13.0 min[8]) <XV (18.1 min) <XVI (27.1 min[8]) <XVII (34.2 min), which parallels the approximate order of increasing steric bulk of the triorganosilyl group in each compound. This correlation of relative reactivity with substrate structure is consistent with a hydrolysis mechanism involving hydroxide ion attack at silicon (Scheme III); however, the ratios of rate constants cover a surprisingly small range of values: XV/XVIII = 0.72, XVI/XVIII = 0.48, and XVII/XVIII = 0.38. In view of the fact that steric hindrance to S_N2 attack at silicon can lead to a more pronounced deceleration of solvolysis rates[9], and that the rate of hydroxide attack at the carbonyl

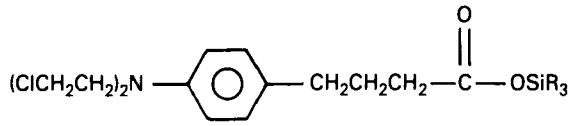

XXIII, $Si(CH_3)_2C(CH_3)_3$
XXIV, $Si(C_6H_5)_2C(CH_3)_3$

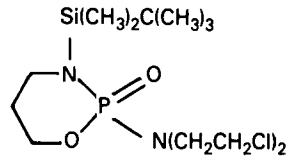

XXV

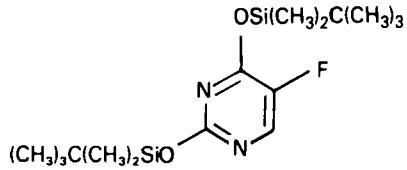

XXVI

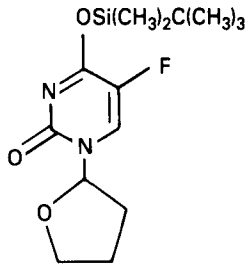

XXVII

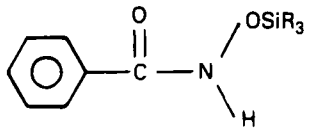

XXVIII, $Si(CH_3)_3$
XXIX, $Si(CH_3)_2C(CH_3)_3$

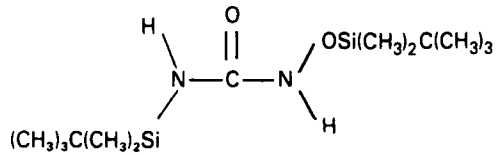

XXX

carbon in carbamates is also subject to steric retardation (28), the *O*-silyl carbamate hydrolysis mechanism was further probed by a Hammett-type kinetic study. Proton NMR measurements using a series of *para*-substituted *O*-aryldimethylsilyl carbamate derivatives of nor-nitrogen mustard afforded desilylation rate constants which correlated linearly with the σ^o substituent constant (Fig. 6) and indicated that the reaction constant, ρ, for dioxane–tromethamine buffer (pH 7.4) was equal to 2.39. The sign and magnitude of this ρ value indicate mechanistic similarity to the alkaline solvolysis of *para*-substituted aryldimethylsilanes (ρ = 1.94 for σ^o), which is known to occur by nucleophilic attack of hydroxide ion at silicon (30). Another line of evidence in support of S_N2 attack at silicon in the *O*-silyl carbamates derives from the approximately equal ρ value of 2.18 measured for ethanolysis of the corresponding series of *N*-aryldimethylsilylamines (Fig. 7), wherein silicon must be the reaction center.

The preceding mechanistic rationale can be justifiably countered by arguing that a ρ value of ~2 does not exclude the possibility of attack at

[8] Average value obtained from NMR and UV measurements.

[9] For example, triethylsilylacetate hydrolizes 38-times slower than trimethylsilyl acetate (29).

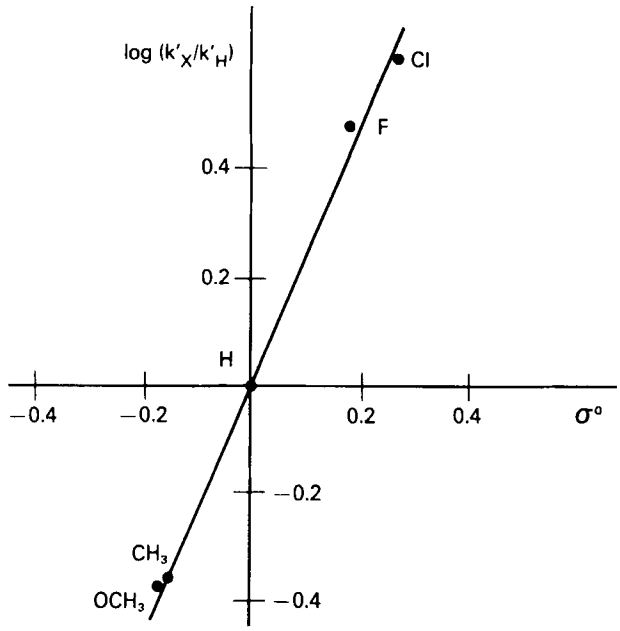

Figure 6—*NMR-derived Hammett plot (r = 0.996) for the hydrolysis of* para-*substituted* O-*aryldimethylsilyl-*N,N-*bis(2-chloroethyl)carbamates in 50:50 dioxane–0.05* M *tromethamine buffer (pH 7.4) at 27°; for details and the values of* k', *see* Experimental *section. The values used for* σ° *are as follows:* p-OCH_3, *−0.16 (30, 31);* p-CH_3, *−0.15 (30);* p-*H, 0.01;* p-*F, 0.17 (31);* p-*Cl, 0.27.*

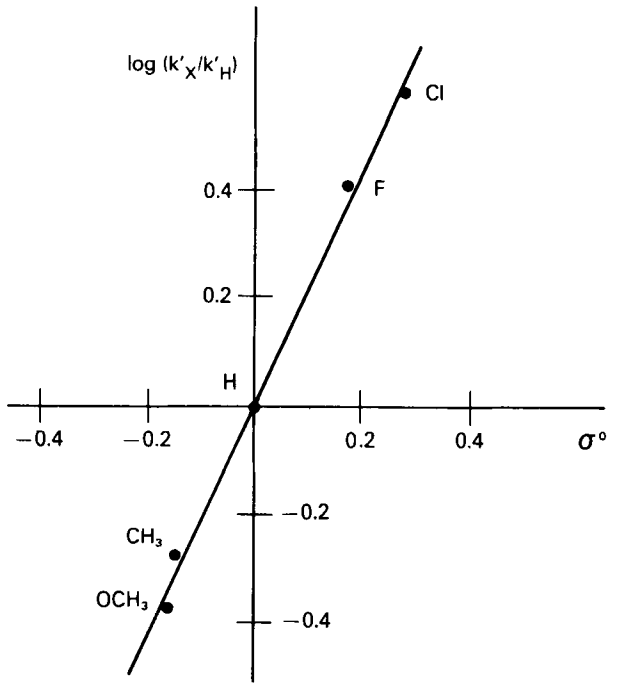

Figure 7—*NMR-derived Hammett plot (r = 0.997) for the solvolysis of* para-*substituted* N-*aryldimethylsilyl-*N,N-*bis(2-chloroethyl)amines in 50:50 ethanol–deuterochloroform at 27°; for details and the values of* k', *see* Experimental *section. The values used for* σ° *are given in the caption for Fig. 6.*

the carbamate carbonyl position, since electron-withdrawing aryl substituents would be expected to facilitate the formation of a negatively charged tetrahedral intermediate. The carbonyl-attack mechanism for hydrolysis of *O*-triorganosilyl carbamates was therefore ruled out by determining that reaction of model compound XXI in dioxane–tromethamine buffer (pH 7.4) containing a 50:50 mixture of water and ^{18}O-enriched water leads to formation of a 50:50 mixture of ^{16}O- and ^{18}O-containing silanols. Hydroxide ion attack at the carbonyl carbon in XXI cannot lead to complete incorporation of oxygen 18, as was observed, since the results of a control reaction (see Experimental) demonstrated that oxygen exchange in *tert*-butyldimethylsilanol is relatively slow (<10%) under the conditions used for hydrolysis, and a presolvolytic mechanism[10] gives an oxygen 18 content which cannot exceed ~17%. Granted that S_N2 attack at silicon also holds for analogs of XXI, the previously mentioned insensitivity to steric effects at the silicon reaction center in compounds XV–XVIII can only be speculated on. One possibility is a leveling effect which results from the fact that all of these SiR_3 moieties have relatively large R groups. An alternative explanation is that the well-known propensity for pentacoordination during nucleophilic substitution at silicon leads to either a late transition state or intermediate (32) wherein the rate of O—SiR_3 bond cleavage is primarily controlled by leaving group stability, which is a constant factor in structures XV–XVIII.

Extension of the kinetic studies to the hydrolysis of other triorganosilylated derivatives of anticancer agents focused upon evaluating the release rate of fluorouracil from compound XXVI, as there is widespread interest in developing new classes of *in vivo* precursors to fluorouracil (33–40), but apparently no available information on systems which utilize organosilicon chemistry. Proton NMR spectra obtained with compound XXVI in dioxane–tromethamine buffer (pH 7.4) revealed that the two dimethylsilyl singlets arising from the chemically nonequivalent silyl groups in XXVI decrease in intensity at the same rate, with concomitant appearance of the *tert*-butyldimethylsilanol signal. Evidently, a monosilylated intermediate is too short-lived to be detected by low-resolution NMR under these reaction conditions (Table I), which led to a half-life for XXVI of only 1.08 min. At a buffer pH of 6.4, these spectral changes were too fast to measure, while at pH 8.4 the half-life of XXVI was 1.14 min. The increase in reaction rate with decreasing pH suggests that hydrolysis in the pH range of 6.4–8.4 proceeds by hydrogen ion catalysis; *i.e.*, protonation at the N_1 and/or N_3 positions.

Anticancer Screening—Selected compounds were screened according to standard protocol (41) for either L-1210 or P-388 leukemias in either male or female mice. The hydrophobicity of these samples generally required the use of either hydroxypropylcellulose or aqueous polyoxyethylene sorbitan monooleate as the vehicle for intraperitoneal injections. For L-1210, the inoculum was 10^5 cells; for P-388, the inoculum was 10^6 cells. Mean survival time was used as the evaluation parameter: a test/control percentage (T/C%) ≥125 indicates activity. Compounds VI, VII, XI, XXV, and XXVI were inactive against the L-1210 lymphoid leukemia; compounds XVI, XXI, and XXVIII–XXX were inactive in the P-388 test system. Table II summarizes pertinent data for those compounds which exhibited activity. Since it was not possible to have the parent (nonsilylated) drugs tested in parallel with these active analogs, an evaluation of prodrug *versus* parent drug activities could only be made in a highly qualitative manner by comparisons with screening data which had been previously obtained with the parent drug against the same type of cancer using similar vehicles, dose/injection, and treatment schedules. A computer-assisted search was conducted[11], and it was found that reasonable comparisons could be made for phosphoramide mustard, nor-nitrogen mustard, and ftorafur, but not for *p*-aminophenyl mustard (XXII) and chlorambucil (XXIII). The 138% T/C obtained with X is much less than the 265% T/C value given by phosphoramide mustard at a single-dose injection of 200 mg/kg, whereas the 131% T/C determined for XXVII is essentially identical to the 130% T/C value exhibited by ftorafur under similar test conditions. Except for compound XVI, which was inactive, silylmustard XIII and *O*-silylcarbamates XIV–XVIII and XX covered a range of activities (T/C% ~150–200) roughly equal to that of the parent nor-nitrogen mustard (T/C% 210 at 37.5 mg/kg, 1 × 10), although the modality for treatment within this set of compounds was variable.

CONCLUSIONS

Kinetic measurements have demonstrated that triorganosilyl groups in *O*-silyl esters of phosphoramide mustard, *N*-silyl nor-nitrogen mustards, *O*-silylcarbamoyl nor-nitrogen mustards, and *O*-silylated fluorouracil can be used as hydrolytically labile moieties for the design of new classes of potential anticancer prodrugs. Relative hydrolysis rates, pH

[10] If it is assumed that C—OSi bond cleavage in a tetrahedral *O*-silyl carbamate ion is slow relative to proton shifts and SiR_3 migration between the three oxygen atoms in this intermediate, then a 50:50 mixture of water and ^{18}O-enriched water would scramble one ^{18}O-label among a total of six oxygens, and thus lead to ~17% incorporation at the C—OSi linkage prior to its fragmentation.

[11] NCI Automated Information Section of the Drug Evaluation Branch.

effects, Hammett studies, and ^{18}O-labeling data are all consistent with rate-limiting hydroxide ion attack at silicon in the *O*-silyl carbamates; however, increasing steric bulk about the silicon reaction center has a relatively small rate-retarding influence (<5-fold).

On the other hand, long-range electronic effects caused by *para* substituents in *O*-aryldimethylsilyl carbamates are substantial, as evidenced by a ρ value of 2.39 in dioxane–tromethamine buffer (pH 7.4).

Such electronic control may therefore be useful for fine-tuning the release of an active agent by a prodrug. Triorganosilylation of cyclophosphamide, fluorouracil, benzohydroxamic acid, and hydroxyurea obliterated the activity of these anticancer agents, whereas analogous alterations of phosphoramide mustard, nor-nitrogen mustard, *p*-aminophenylmustard, chlorambucil, and ftorafur led, in general, to retention of anticancer activity. The especially encouraging screening results obtained for *O*-tribenzylsilyl carbamate derivative XVIII have led to its recent selection by NCI for further evaluation in its tumor panel testing program. These screening results and studies of additional triorganosilylated anticancer prodrugs will be reported in the future.

REFERENCES

(1) F.-T. Chiu, F.-P. Tsui, and G. Zon, *J. Med Chem.*, **22,** 802 (1979).

(2) O. M. Friedman, A. Myles, and M. Colvin, in "Advances in Cancer Chemotherapy," Dekker, New York, N.Y., 1979, pp. 143–204.

(3) R. R. LeVier, M. L. Chandler, and S. R. Wendel, in "Biochemistry of Silicon and Related Problems," G. Bendz and I. Lindqvist, Eds., Plenum, New York, N.Y., 1978, pp. 479–480.

(4) *Ibid.*, pp. 485–510.

(5) G. W. Peng, V. E. Marquez, and J. S. Driscoll, *J. Med. Chem.*, **18,** 846 (1975).

(6) P. Workman and J. A. Double, *Biomedicine*, **28,** 255 (1978).

(7) T. A. Connors, *Chem. Ind.*, **1980,** 447.

(8) R. J. Fessenden and J. S. Fessenden, *Adv. Organometal. Chem.*, **18,** 275 (1980).

(9) D. Dolphin and A. E. Wick, "Tabulation of Infrared Spectral Data," Wiley-Interscience, New York, N.Y., 1977.

(10) H. Bürger, K. Burczyk, and O. Smrekar, *Monatsh. Chem.*, **100,** 766 (1969).

(11) C. J. Pouchert, "The Aldrich Library of Infrared Spectra," 2nd ed., Aldrich Chemical Co., Milwaukee, Wis., 1978.

(12) S. M. Ludeman and G. Zon, *J. Med. Chem.*, **18,** 1251 (1975).

(13) K. Mislow and M. Raban in "Topics in Stereochemistry," vol. 1, N. L. Allinger and E. L. Eliel, Eds., Wiley-Interscience, New York, N.Y., 1967, pp. 1–38.

(14) Y. H. Chang, F.-T. Chiu, and G. Zon, *J. Org. Chem.*, **46,** 342 (1981).

(15) A. L. Van Geet, *Anal. Chem.*, **42,** 679 (1970).

(16) T. Morita, Y. Okamoto, and H. Sakurai, *Tetrahedron Lett.*, **1978,** 2523.

(17) P. K. G. Hodgson, R. Katz, and G. Zon, *J. Organometal. Chem.*, **117,** C63 (1976).

(18) L. Riesel and C. Taeschner, *Z. Chem.*, **20,** 151 (1980).

(19) H. Breederveld, *Rec. Trav. Chim.*, **81,** 276 (1962).

(20) M. Ochoa, Jr., *Ann. N.Y. Acad. Sci.*, **163,** 921 (1969).

(21) D. L. Hill, "A Review of Cyclophosphamide," Charles C Thomas, Springfield, Ill., 1975.

(22) J. A. Montgomery and R. F. Struck, in "Progress in Drug Research," vol. 17, E. Jucker, Ed., Birkhäuser Verlag, Basel, Switzerland, 1973, pp. 328–332.

(23) J. L. Au, A. T. Wu, M. A. Friedman, and W. Sadée, *Cancer Treatment Rep.*, **63,** 343 (1979).

(24) B. van't Riet, G. L. Wampler, and H. L. Elford, *J. Med. Chem.*, **22,** 589 (1979).

(25) R. Moran and M. J. Straus, *Cancer Res.*, **39,** 1616 (1979).

(26) C. H. Yoder, W. C. Copenhafer, and B. DuBeshter, *J. Am. Chem. Soc.*, **96,** 4283 (1974).

(27) W. Walter and H. W. Lüke, *Angew. Chem. Intern. Ed. Engl.*, **14,** 427 (1975).

(28) I. Christenson, *Acta Chem. Scand.*, **18,** 904 (1964).

(29) R. H. Prince and R. E. Timms, *Inorg. Chim. Acta*, **2,** 260 (1968).

(30) J. Hetflejš, F. Mareš, and V. Chvalovský, *Coll. Czech. Chem. Commun.*, **30,** 1643 (1965).

(31) R. W. Taft, Jr., S. Ehrenson, I. C. Lewis, and R. E. Glick, *J. Am. Chem. Soc.*, **81,** 5352 (1959).

(32) L. H. Sommer and D. L. Bauman, *J. Am. Chem. Soc.*, **91,** 7045 (1969).

(33) G.-J. Koomen, F. Van Alewijk, D. Blok, and U. K. Pandit, *Heterocycles*, **12,** 1535 (1979).

(34) T. Kametani, K. Kigasawa, M. Hiiragi, K. Wakisaka, S. Haga, Y. Nagamatsu, H. Sugi, K. Fukawa, O. Irino, T. Yamamoto, N. Nishimura, A. Taguchi, T. Okada, and M. Nakayama, *J. Med. Chem.*, **23,** 1324 (1980).

(35) Kaken Chem. Co., Ltd., Japanese pat. 80 57,571; through *Chem. Abstr.*, **93,** 239450d (1980).

(36) O. Asano and F. Kato, Japanese pat. 78 124,275; through *Chem. Abstr.*, **90,** 121644e (1979).

(37) S. Ozaki, Y. Ike, and H. Mori, Japanese pat. 78 63,389; through *Chem. Abstr.*, **89,** 180032f (1978).

(38) M. Kurono, Y. Sakai, H. Yokohama, and S. Fujii, Japanese pat. 78 59,678; through *Chem. Abstr.*, **89,** 180034h (1978).

(39) M. Hori, Y. Tada, and A. Koda, Japanese pat. 79 14,982; through *Chem. Abstr.*, **91,** 39522a (1979).

(40) Kotobuki Seiyaku K. K., Belgian pat. 870,982; through *Chem. Abstr.*, **91,** 39526e (1979).

(41) Instruction 14 "Screening Data Summary Interpretation and Outline of Current Screen," Drug Evaluation Branch, Drug Research and Development, Division of Cancer Treatment, National Cancer Institute, Bethesda, MD, 1973, and subsequent insert pages which specify the most recent updating.

ACKNOWLEDGMENTS

Supported in part by National Institutes of Health Research Grants CA 18366 and CA 21345, PHS/DHHS, which were awarded to Gerald Zon.

All anticancer screening tests were carried out through the Drug Synthesis and Chemistry Branch (DSCB), Development Therapeutics Program, Division of Cancer Treatment, National Cancer Institute, and with the assistance of Dr. V. L. Narayanan, Chief, DSCB.

The authors thank Dr. Philip K. G. Hodgson for carrying out some early exploratory experiments, and Mr. Nathaniel H. Greenberg (NCI, Drug Evaluation Branch) and Mr. John F. Waters (NCI, Automated Information Section) for their assistance in obtaining comparative screening data.

Interaction of Povidone with Aromatic Compounds III: Thermodynamics of the Binding Equilibria and Interaction Forces in Buffer Solutions at Varying pH Values and Varying Dielectric Constant

J. A. PLAIZIER-VERCAMMEN ˣ **and R. E. DE NÈVE**

Received July 21, 1981 from the *Faculteit Geneeskunde en Farmacie, Vrije Universiteit Brussel, Laarbeeklaan, 103 B-1090 Brussels, Belgium.* Accepted for publication August 31, 1981.

Abstract □ The complex formation of a series of aromatic compounds with povidone was studied in buffer solutions and organic solvent mixtures by equilibrium dialysis. For all the ligand molecules studied, a linear relationship was found between r, the number of moles of bound ligand per mole of povidone, and the free ligand concentration. The binding constants and the free energies of binding ($-\Delta F$), were greater for compounds in the nonionic state and increased with the number of hydroxyl groups which were capable of forming hydrogen bonds. They decreased with temperature elevation. The thermodynamic data showed entropy gains during the binding process accompanied by small negative enthalpy values. The increased ability to form hydrogen bonds and the increase in ionization of the ligand molecule was reflected in more negative ΔH and decreasing ΔS values. (The thermodynamic values were interpreted on the basis of the "iceberg" concept of water structure.) From these entropy and enthalpy changes, hydrogen and hydrophobic bondings appeared to be the most important types of binding. In organic solvent mixtures, the association constants lowered with increasing ethanol or propylene glycol concentration; a line relationship between the free energy and the dielectric constant of the solvent mixtures was observed.

Keyphrases □ Povidone—interaction with aromatic compounds, thermodynamic considerations □ Complexation—evaluation of povidone–aromatic compound interaction, thermodynamic considerations □ Thermodynamics—interaction of povidone with aromatic compounds

Two types of binding appear to be important in the complexing of ligand molecules onto povidone. It was suggested (1) that hydrogen bonding plays a role, since substituted groups capable of hydrogen bonding enhanced complex formation. However, ligand molecules in the nonionic form, showed a greater tendency to form complexes than when in the ionic state (2–4), indicating the importance of hydrophobic binding. The thermodynamics of binding (5–10) and the thermodynamic properties of the interaction between povidone and small molecules have been reported previously (2, 4, 11–17).

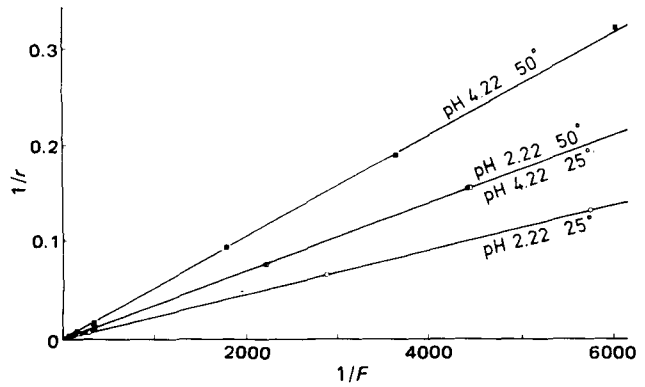

Figure 1—*Influence of temperature on complex formation of 4-hydroxysalicylic acid with povidone. The 4-hydroxysalicylic acid concentration was* 2.5×10^{-4}–2.00×10^{-2} M, *the povidone concentration was 6.00% (*8.57×10^{-5} M*).*

However, the influence of the dissociation of the ligand molecule on the thermodynamic constants has not been studied. To achieve more insight into the binding process, this study evaluated how the thermodynamic constants are affected by the degree of ionization of the ligand molecules and by the dielectric constant of the solvent.

EXPERIMENTAL

Materials—Povidone[1] (molecular weight 700,000) was used as the macromolecule.

The following ligand molecules were studied: benzoic acid[2], nicotinic acid[3] (niacin), isonicotinic acid[2] (isoniazid), salicylic acid[4], salicylamide[2], salicylic acid hydrazide[5], 4-hydroxysalicylic acid[6], 5-hydroxysalicylic acid[4] (gentisic acid), and 5-nitrosalicylic acid[6].

The following buffer solutions were used: hydrochloric acid–potassium chloride buffer (18), pH 1.30 and 1.93; McIllvaine buffers (19), pH 2.20–5.60; a phosphate buffer (18), pH 7.00; a boric acid–sodium tetraborate buffer (20), pH 7.20; and a boric acid–sodium hydroxide buffer (18), pH 9.20 with sodium chloride. The solutions were brought to the ionic strength given in Table I. Sodium chloride showed no tendency to complex with povidone (21). The pH of the solutions was always checked potentiometrically[7] and adjusted, if necessary.

To control the influence of the dielectric constant on complex formation, water–ethanol and water–propylene glycol mixtures were prepared in various proportions, providing a range of dielectric constants. The dielectric constants of the mixtures were measured with a meter[8] at 25.0 and 35.0°.

Equilibrium Dialysis—The ligand–macromolecule interactions were investigated using the method of equilibrium dialysis described previously (22–26).

Dialysis cells[9] similar to those described by Neuhoff (27) were used. The regenerated cellulose membranes were freed of soluble material by leaching in frequently refreshed water and were then immersed in the respective buffers. The two compartments of the dialysis cells were filled, one with solution, the other with the same ligand solution containing the macromolecule.

The cells were rotated at 5 rpm in a constant temperature bath until equilibrium was reached. The povidone-free compartment was analyzed for free ligand. Experiments were carried out at 25.0 and 50.0° with the buffer solutions, and at 25.0 and 35.0° with the ethanol–water and propylene glycol–water mixtures.

Spectrophotometric Analysis—The ligand molecules, with UV absorption bands between 224 and 320 nm, were spectrophotometrically[10] determined in the samples from the dialysis experiments.

RESULTS AND DISCUSSION

The polymer concentration, as well as the range of cosolute concentration, are indicated in Table I.

[1] Povidone (Kollidon K 90), BASF, Brussels, Belgium.
[2] UCB, Brussels, Belgium.
[3] BHD, Poole, England.
[4] Merck, Darmstadt, West Germany.
[5] Aldrich, Beerse, Belgium.
[6] Merck-Schuchardt, München, West Germany.
[7] Radiometer, Copenhagen, Denmark.
[8] Deka meter, DK 300 WTW.
[9] Kontron Diapack.
[10] Perkin-Elmer, model 124.

0022-3549/82/0500-0552$01.00/0

Table I—Association Constants, $nk = k_1$ (liter/mole) for Povidone–Cosolute Systems in Buffer Solutions at Varying pH

Ligand Molecule	pKa of Ligand	Ionic Strength	Ligand Concentration	Povidone Concentration, $M \times 10^5$	pH	$nk = k_1$ ($\times 10^{-3}$), liter/mole 25.0°	50.0°
Benzoic acid	4.2[a]	0.25	$1.00.10^{-4}$–$2.00.10^{-2}$	8.57	3.40[b]	7.8	8.5
Benzoic acid	4.2[a]	0.25	$1.00.10^{-4}$–$2.00.10^{-2}$	8.57	5.00[b]	2.5	2.0
Nicotinic acid	4.83[a]	0.32	$5.00.10^{-4}$–$1.00.10^{-2}$	7.14	5.60[b]	1.1	0.7
Isonicotinic acid	4.84[a]	0.32	$5.00.10^{-4}$–$1.00.10^{-2}$	7.14	5.60[b]	1.5	1.2
Salicylic acid	2.97[a]	0.15	$2.50.10^{-4}$–$1.00.10^{-2}$	8.57	2.20[b]	16.2	15.4
Salicylic acid	2.97[a]	0.15	$2.50.10^{-4}$–$1.00.10^{-2}$	8.57	3.80[b]	13.1	9.9
Salicylamide	8.20[c]	0.25	$2.50.10^{-4}$–$5.00.10^{-3}$	8.57	5.00[b]	9.3	8.9[d]
Salicylamide	8.20[c]	0.25	$2.50.10^{-4}$–$5.00.10^{-3}$	8.57	5.00[b]	9.3	8.5
Salicylamide	8.20[c]	0.15	$2.50.10^{-4}$–$1.00.10^{-2}$	8.57	7.20[e]	8.6	6.5
Salicylamide	8.20[c]	0.15	$2.50.10^{-4}$–$1.00.10^{-2}$	8.57	9.20[f]	2.1	1.4
Salicylic acid hydrazide	—	0.25	$1.00.10^{-4}$–$5.00.10^{-3}$	8.57	7.00[g]	9.0	7.7
4-OH-Salicylic acid	3.22[a]	0.25	$2.50.10^{-4}$–$2.00.10^{-2}$	8.57	2.22[b]	44.1	29.7
4-OH-Salicylic acid	3.22[a]	0.25	$2.50.10^{-4}$–$2.00.10^{-2}$	8.57	4.22[b]	28.5	17.5
5-OH-Salicylic acid	2.93[a]	0.25	$2.50.10^{-4}$–$1.00.10^{-2}$	7.14	1.93[h]	24.3	19.2
5-OH-Salicylic acid	2.93[a]	0.25	$2.50.10^{-4}$–$1.00.10^{-2}$	7.14	3.93[b]	18.4	10.8
5-NO_2-Salicylic acid	2.30[a]	0.15	$1.00.10^{-4}$–$2.00.10^{-3}$	7.14	1.30[h]	6.0	4.6
5-NO_2-Salicylic acid	2.30[a]	0.25	$1.00.10^{-4}$–$2.00.10^{-3}$	7.14	3.30[b]	10.8	8.5

[a] pKa of the carboxyl function. [b] McIllvaine buffer. [c] pKa of the hydroxyl function. [d] 40.0°. [e] Boric acid–sodium tetraborate buffer. [f] Boric acid–sodium hydroxide buffer. [g] Phosphate buffer. [h] Hydrochloric acid–potassium chloride buffer.

Preliminary experiments indicated that the binding constants were independent of povidone concentration. For the experiments carried out on the solvent mixtures, a Donnan correction (28) was taken into account.

Theory of Multiple Equilibria—The principles and concepts, fundamental to an understanding of macromolecular binding, have been reported (22–26, 29–30). If no interaction phenomena take place (25–26, 30–33), reversible binding can be described by the equation:

$$r = \frac{nkF}{1 + kF} \qquad \text{(Eq. 1)}$$

where r is the number of moles of cosolute bound per mole of polymer, n is the number of binding sites per mole of macromolecule, F is the molar concentration of free ligand at equilibrium, and k is the intrinsic binding constant (in liters per mole) for the cosolute on the binding sites.

The data were evaluated using a rearrangement of Eq. 1 in a double reciprocal plot, as suggested by Klotz (34):

$$\frac{1}{r} = \frac{1}{nkF} + \frac{1}{n} \qquad \text{(Eq. 2)}$$

The results could also be described by the Freundlich isotherm:

$$r = nkF^{1/m} \qquad \text{(Eq. 3)}$$

where $m = 1$.

Association Constants and Thermodynamics in Buffer Solutions—A characteristic set of results is shown in Fig. 1, where $1/r$ was plotted against $1/F$; the slope of this plot was $1/nk$, and the intercept on the ordinate was $1/n$. Straight lines nearly intersecting the origin were obtained; the other derivatives under investigation behaved similarly. From Eq. 1 it can be seen that this implies $kF \ll 1$, which is equivalent to Eq. 3 where $m = 1$. From Eq. 2, it is observed $1/n$ equals zero, or n is infinite, indicating a large number of adsorption sites. The fraction of the drug bound to povidone did not vary significantly with drug concentration and the binding process appeared nonsaturable.

The results were in accordance with other sources (2, 4, 14, 17, 35, 36) reporting on the complex formation between povidone and ligand molecules. It has been found (2, 14, 25) that the y-axis intercept values ($1/n$) are often determined with great uncertainty, implying it has no physical meaning. In this case, it is preferable to use the values of $nk = k_1$ (25) since it is a measure of the strength of the binding, while n only indicates the binding capacity.

The association constants, nk, deduced from the slopes for povidone–cosolute systems in buffer solutions at different temperatures, are listed in Table I. The thermodynamic functions could be compared with each other because parameters such as the nature of buffer ions and ionic strength had no influence on the binding tendency (1) and consequently, on the thermodynamic functions.

The association constants, for all the derivatives under investigation, were largest at 25.0°, except for benzoic acid in the undissociated form (pH 3.40) (Table I).

The increase in the number of hydroxyl functions substituted on the benzene ring involved higher association constants (4-hydroxysalicylic acid > salicylic acid > benzoic acid), suggesting the importance of hydrogen bonding.

However, the compounds generally interacted to a lesser degree in the ionic than in the nonionic state, suggesting the importance of the hydrophobicity of the substances in the binding process. An exception was 5-nitrosalicylic acid, which showed an increasing binding tendency at higher pH values.

From the association constants, $nk = k_1$ (see Table I) and its temperature dependence, thermodynamic functions for the binding of one mole of ligand with one mole of povidone could be obtained (Table II). For all the ligand molecules, the largest free energy ($-\Delta F$) values were obtained at 50.0° (Table II). From the thermodynamic data listed in Table II, it was clear that the binding process involved a gain in entropy ($+\Delta S$) and that the enthalpies varied from small positive values (benzoic acid, pH 3.40) to small negative values. The standard free energy of binding could be computed from the thermodynamic relation:

$$\Delta F^\circ = -RT \ln k_1 \qquad \text{(Eq. 4)}$$

where $k_1 = nk$, R is the gas constant, and T the absolute temperature.

Assuming no significant temperature dependence of enthalpy change occurring within the temperature range used, the standard enthalpy change ΔH° for the association of one mole of ligand with one mole of macromolecule was estimated from:

$$\ln \frac{nk_{T_1}}{nk_{T_2}} = \frac{-\Delta H^\circ}{R}\left(\frac{1}{T_1} - \frac{1}{T_2}\right) \qquad \text{(Eq. 5)}$$

Table II—Thermodynamic Data for the Binding of One Mole of Ligand by One Mole of Povidone in Buffer Solutions at Varying pH

Ligand Molecule	pH	ΔF_1°, kcal/mole 25.0°	ΔF_2°, kcal/mole 50.0°	ΔH°, kcal/mole	ΔS°, cal/mole degree
Benzoic acid	3.40[a]	−5.3	−5.8	+0.7	20.1
Benzoic acid	5.00[a]	−4.6	−4.9	−1.5	10.4
Nicotinic acid	5.60[a]	−4.2	−4.3	−3.0	4.0
Isonicotinic acid	5.60[a]	−4.4	−4.5	−2.1	7.5
Salicylic acid	2.20[a]	−5.7	−6.2	−0.4	18.0
Salicylic acid	3.80[a]	−4.3	−5.9	−2.1	11.8
Salicylamide	5.00[a]	−5.4	−5.7[b]	−0.5	16.5
Salicylamide	5.00[a]	−5.4	−5.8	−0.7	15.8
Salicylamide	7.20[c]	−5.4	−5.6	−2.1	10.9
Salicylamide	9.20[d]	−4.5	−4.6	−3.2	4.6
Salicylic acid hydrazide	7.00[e]	−5.4	−5.8	−0.9	15.0
4-Hydroxysalicylic acid	2.22[a]	−6.3	−6.6	−3.0	11.1
4-Hydroxysalicylic acid	4.22[a]	−6.1	−6.3	−3.8	7.8
5-Hydroxysalicylic acid	1.93[f]	−6.0	−6.3	−1.8	14.0
5-Hydroxysalicylic acid	3.93[a]	−5.8	−6.0	−4.9	5.8
5-Nitrosalicylic acid	1.30[f]	−5.2	−5.4	−1.9	10.9
5-Nitrosalicylic acid	3.30[a]	−5.5	−5.8	−1.8	12.4

[a] McIllvaine buffer. [b] 40.0°. [c] Boric acid–sodium tetraborate buffer. [d] Boric acid–sodium hydroxide buffer. [e] Phosphate buffer. [f] Hydrochloric acid–potassium chloride buffer.

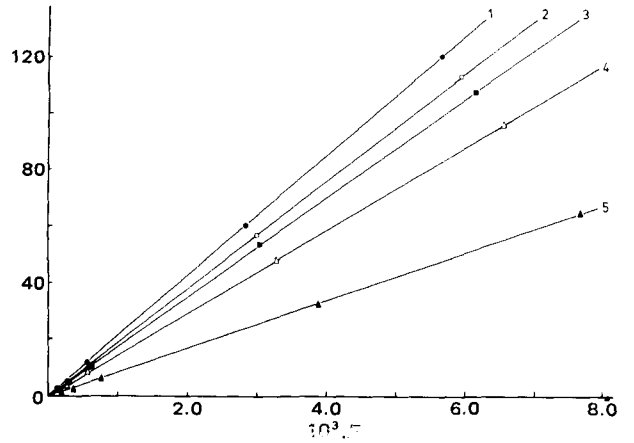

Figure 2—*Influence of solvent mixtures on complex formation. Complexing of 5-hydroxysalicylic acid with povidone. The 5-hydroxysalicylic acid concentration was 2.50 × 10⁻⁴–1.00 × 10⁻² M, the povidone concentration was 5.00% (7.14 × 10⁻⁵ M). Key: 1, water; 2, 5% (v/v) propylene glycol; 3, 10% propylene glycol; 4, 20% (v/v) propylene glycol; 5, 50% (v/v) propylene glycol.*

where T_1 and T_2 represent the absolute temperatures under investigation. The relationship:

$$\Delta F^\circ = \Delta H^\circ - T\Delta S^\circ \qquad \text{(Eq. 6)}$$

permitted calculation of the entropy of binding.

The thermodynamic functions calculated from $nk = k_1$ do not necessarily refer to a single site on the macromolecule. However, their values are useful in considering the nature of the binding, in comparing the binding of different ligand molecules by the same macromolecule, or in analyzing the effect of factors such as pH and ionic strength on the binding (25).

For the ligand molecules investigated, both ΔH° and ΔS° decreased while the degree of dissociation increased. An exception was 5-nitrosalicylic acid, where ΔH° and ΔS° increased with an increase in the degree of dissociation.

From the four types of binding, which could be considered in complex formation of ligands with povidone, *i.e.*, ion–dipole, dipole–dipole, hydrogen, and hydrophobic bonding, the latter appeared to play an important role. Indeed, if complex formation was only due to hydrogen bonding, both ΔH° and ΔS° should be negative (37). However, ΔS° showed a positive value which is characteristic of not only hydrophobic (5, 38–40), but also electrostatic bonding (5–6). Although the ligand molecules also were investigated as ions, this last type of bonding was unlikely to occur since povidone has no ionizable groups (41). The results ruled out the possibility of electrostatic bonding because of the positive influence of the dielectric constant (D) of the solution and the ionic strength (1) on the binding (5). On the other hand, positive enthalpies

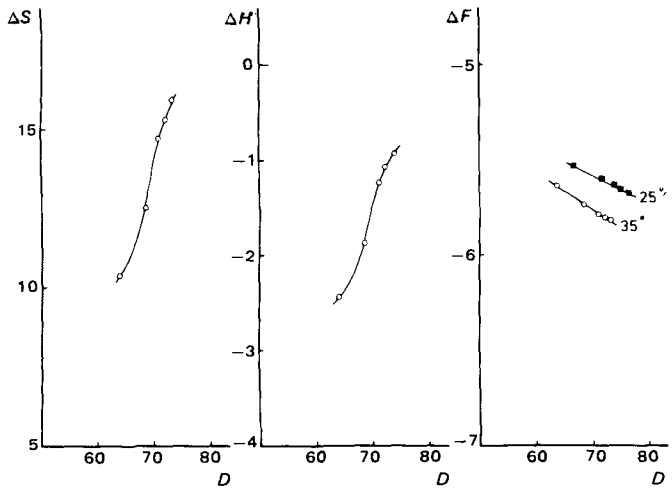

Figure 3—*Complex formation between salicylic acid and povidone. Change of free energy (ΔF°), enthalpy (ΔH°), and entropy (ΔS°) as a function of the ethanol concentration and dielectric constant.*

Table III—Thermodynamic Data (liter/mole) for Povidone–Cosolute Systems as a Function of Solvent Mixtures and Corresponding Dielectric Constant (Ligand Concentration: 2.50 × 10⁻⁴ *M*–1.00 × 10⁻² *M*)

Ligand	Solvent Mixtures, % (v/v)	Dielectric Constant		$nk = k_1$ (×10⁻³), liter/mole 25.0°	$nk = k_1$ (×10⁻³), liter/mole 35.0°
	Ethanol	25.0°	35.0°		
Salicylic acid	0.0	76.4	73.3	14.3	13.6
	2.5	75.2	72.1	13.8	13.0
	5.0	73.9	70.9	13.5	12.6
	10.0	71.5	68.6	12.8	11.6
	20.0	66.6	63.8	11.4	9.9
4-Hydroxy-salicylic acid	0.0	76.4	73.3	39.4	36.2
	2.5	75.2	72.1	37.9	33.9
	5.0	73.9	70.9	35.9	32.1
	10.0	71.5	68.6	33.9	28.9
	20.0	66.6	63.8	29.4	24.6
5-Hydroxy-salicylic acid	0.0	76.4	73.3	21.2	18.6
	2.5	75.2	72.1	20.5	18.0
	5.0	73.9	70.9	19.4	17.1
	10.0	71.5	68.6	18.0	16.0
	20.0	66.6	63.8	15.9	14.1
	Propylene glycol				
5-Nitrosalicylic acid	0.0	76.4	73.3	21.2	18.6
	5.0	74.1	71.1	19.1	16.8
	10.0	71.8	68.9	17.6	15.5
	20.0	67.2	64.5	14.7	12.9
	50.0	53.4	51.2	8.4	7.3

(9) and large positive entropies are characteristic of hydrophobic bondings. It is believed that entropy plays a dominant role in this process (38). From the results [*i.e.*, negative enthalpies (Table II) and the decrease of complex formation with increasing temperature] it could be deduced that the binding process was not only due to hydrophobic bondings (5, 42), but also to exothermic reactions, such as Van der Waals forces or hydrogen bondings.

Positive entropies are associated with many reactions involving the binding of ligand molecules onto povidone. They were generally attributed to the formation of hydrophobic bonds (2, 4, 11, 12, 15, 17) although hydrogen bonding cannot be overlooked (2, 12, 14, 15).

The results are interpreted on the basis of the "iceberg" concept (43) which assumes that hydrocarbon groups, present both in the polymer and in the aromatic cosolutes, are surrounded in aqueous solution with one or more layers of water molecules which are more highly ordered than the molecules in ordinary liquid water. Those layers are referred to as icebergs. In polar groups, such as carboxylic groups and anions, there will also be true hydration about the substituent group.

The entropy changes occurring during the binding process are solely due to the disordering of the icebergs that accompany both the polymer and the cosolute molecules (5). The complex formed will be accompanied by an iceberg which is less ordered compared to the icebergs of the two separate entities which results in a proportional gain in entropy. In studies concerning the interaction of povidone with aromatic compounds, it was calculated (12) that the net enthalpy change was associated with: (*a*) the heat needed to overcome any specific interactions (*i.e.*, true hydration) between water and the macromolecule and between water and the ligand molecule; (*b*) exothermic interaction between the dehydrated entities; and (*c*) exothermic interaction between the water and the bound system (*i.e.*, reformation of true hydration), and is essentially constant with a value of −5 kcal/mole. This value represented the interaction of the polar groups of the polymer with the π-electron system of the aromatic cosolutes (12). By subtracting this value from ΔH° in Table II, the net enthalpy changes associated with the disordering of the water molecules in the icebergs around the polymer and the cosolute can be computed before the binding and the reformation of hydrogen bonds in the icebergs around the complex. These positive enthalpies, and the entropy values are responsible for the hydrophobic bonds.

Ionic groups or substituents capable of hydrogen bond formation may also contribute to the enthalpy values of bonding. Furthermore, hydrogen bonds are able to weaken hydrophobic bonds (5). The results (Table II)

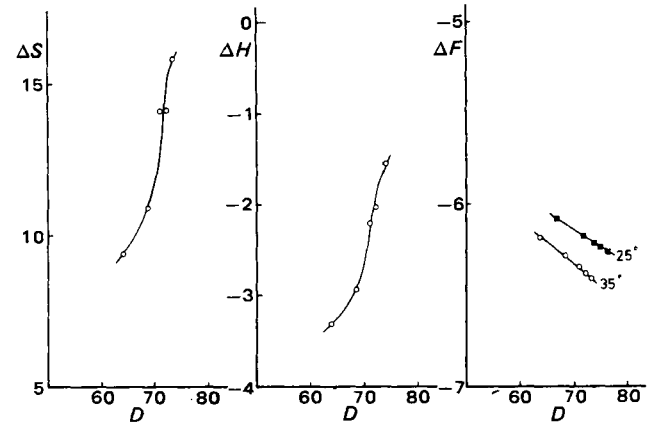

Figure 4—*Complex formation between 4-hydroxysalicylic acid and povidone. Change in free energy (ΔF°), enthalpy (ΔH°), and entropy (ΔS°) as a function of the ethanol concentration and the dielectric constant.*

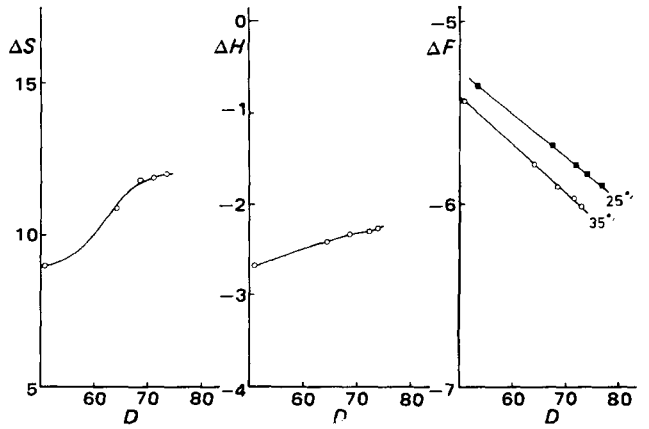

Figure 6—*Complex formation between 5-hydroxysalicylic acid and povidone. Change of free energy (ΔF°), enthalpy (ΔH°), and entropy (ΔS°) as a function of the propylene glycol concentration and dielectric constant.*

agreed with this iceberg concept in that the increase in the ability to form hydrogen bonds (from benzoic acid over salicylic acid to 4- and 5-hydroxysalicylic acid) and the increase in ionization of the ligand molecules is reflected in more negative enthalpy and decreasing entropy values. Therefore, hydrogen bonding was associated with higher binding constants while hydrophobic bonding was associated with the lower constants. One exception was 5-nitrosalicylic acid which, in the case of the bulky nitro group, steric hindrance would be a significant factor (2). The thermodynamic constants obtained for a series of aromatic compounds (12) can be interpreted similarly. From positive enthalpies and high positive entropy values for benzene, both thermodynamic constants diminish more and more with an increasing number of hydroxyl functions substituted on the benzene ring (more possibilities for hydrogen bonding) and are smallest for ionized ligand molecules. It is concluded that both types of bondings, hydrophobic and hydrogen, must play a role in the binding process.

Povidone contains hydrophilic (pyrrolidine ring) and hydrophobic (vinyl chain) groups. A molecular model of the povidone macromolecule shows that the pyrrolidine ring and the paraffin backbone are accessible for the ligand molecules (16). Therefore, it is assumed that the hydrophilic segment is responsible for hydrogen bonding, the paraffin backbone for hydrophobic bonding.

Thermodynamics in Solvent Mixtures—For three ligand molecules, isotherms were determined in a series of ethanol–water mixtures and for one ligand molecule in propylene glycol–water mixtures. A characteristic set of experimental data is shown in Fig. 2, where r is plotted as a function of the free ligand concentration F. In these solvent mixtures, the shape of the isotherms are the same as in the buffer solutions.

From the isotherms, the association constants were determined and summarized in Table III with the measured dielectric constants of the different solvent mixtures. With the aid of the association constants obtained at two temperatures, the thermodynamic functions were computed and represented as a function of the dielectric constants in Figs. 3–6.

From Table III it is noted that the association constants and therefore, the free energies ($-\Delta F$), diminish with increasing ethanol or propylene glycol concentration. For these same concentrations, the association constants are largest at 25.0°; for all the solvent mixtures, the reactions are exothermic ($\Delta H°$ negative), accompanied by high positive entropy values (Figs. 3–6). For the three ligand molecules under investigation, a linear relationship is found between the free energy ($-\Delta F$) and the dielectric constant of the solvent.

This relationship can be written as:

$$-\Delta F° = cst + k'D \qquad \text{(Eq. 7)}$$

or

$$\ln nk = cst + k'D \qquad \text{(Eq. 8)}$$

The shape of the $\Delta H°$ and $\Delta S°$ curves indicated that enthalpy and entropy are connected.

A decrease in bond formation with a decrease in dielectric constant is generally attributed to hydrophobic bonds (4, 5, 44, 45). However, the decrease in dielectric constant influenced the solubility of the ligand molecule; therefore, changes in the solubility of ligand are responsible for the change in the binding tendency.

The correlation between degree of binding, solubility, and dielectric constant of solvent mixtures is being investigated.

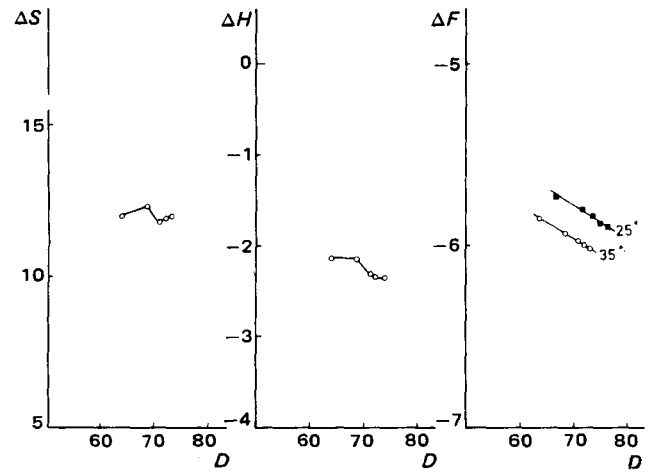

Figure 5—*Complex formation between 5-hydroxysalicylic acid and povidone. Change of free energy (ΔF°), enthalpy (ΔH°), and entropy (ΔS°) as a function of the ethanol concentration and dielectric constant.*

REFERENCES

(1) J. A. Plaizier and R. E. De Nève, *J. Pharm. Sci.*, **70,** 252 (1981).

(2) G. Jürgensen Eide and P. Speizer, *Acta Pharm. Suec.*, **4,** 185 (1967).

(3) W. Scholtan, *Arzneim.-Forsch.*, **14,** 469 (1964).

(4) R. Voight, H. H. Schultze, and S. Keipert, *Pharmazie*, **31,** 863 (1976).

(5) W. Kauzmann, *Adv. Protein Chem.*, **14,** 1 (1959).

(6) I. M. Klotz, *Ann. N.Y. Acad. Sci.*, **226,** 18 (1973).

(7) F. Karush, *J. Am. Chem. Soc.*, **72,** 2705 (1950).

(8) H. J. Weder and M. H. Bickel, *J. Pharm. Sci.*, **59,** 1563 (1970).

(9) D. C. Poland and H. A. Scheraga, *J. Phys. Chem.*, **69,** 2431 (1965).

(10) E. J. Cohn and J. T. Edsall, "Proteins, Amino Acids and Peptides," Reinhold, New York, N.Y., 1943.

(11) M. J. Cho, A. G. Mitchell, and M. Pernarowski, *J. Pharm. Sci.*, **60,** 720, (1971).

(12) P. Molyneux and H. P. Frank, *J. Am. Chem. Soc.*, **83,** 3169 (1961).

(13) E. Killmann, *Kolloid-Z. Z. Polym.*, **242,** 1119 (1970).

(14) W. Scholtan, *Makromol. Chem.*, **11,** 131 (1953).

(15) E. Ullmann, K. Thoma, and P. Mohrschulz, *Arch. Pharm.*, **302,** 756 (1969).

(16) H. P. Frank, S. Barkin, and F. R. Eirich, *J. Phys. Chem.*, **61**, 1375 (1957).
(17) S. Keipert, I. Korner, and R. Voight, *Pharmazie*, **31**, 790 (1976).
(18) "Tables Scientifiques," 6th ed., J. R. Geigy, Ed., Documenta Geigy, Basel, Switzerland, 1962.
(19) P. J. Elving, J. M. Markovitz, and I. Rosenthal, *Anal. Chem.*, **28**, 1179 (1956).
(20) J. H. Block, E. B. Roche, T. O. Soine, and Ch. O. Wilson, "Inorganic Medicinal and Pharmaceutical Chemistry," Lea & Febiger, Philadelphia, Pa., 1974.
(21) E. Killmann, *Kolloid-Z. Z. Polym.*, **242**, 1103 (1970).
(22) J. T. Edsall and J. Wyman, "Biophysical Chemistry," vol. 1, Academic, New York, N.Y., 1958.
(23) I. M. Klotz, in "The Proteins," vol. 1, part B, H. Neurath and K. Bailey, Eds., Academic, New York, N.Y., 1953.
(24) C. Tanford, "Physical Chemistry of Macromolecules," Wiley, New York, N.Y., 1966.
(25) R. M. Rosenberg and I. M. Klotz, in "A Laboratory Manual of Analytical Methods of Protein Chemistry," vol. 2, P. Alexander and R. J. Block, Eds., Pergamon, London, 1960.
(26) J. Steinhardt and J. A. Reynolds, "Multiple Equilibria in Proteins," Academic, New York, N.Y., 1969.
(27) V. Neuhoff and F. Kühl, *Arzneim.-Forsch.*, **19**, 1898 (1969).
(28) F. P. Donnan, *Chem. Rev.*, **1**, 73 (1924).
(29) I. M. Klotz, *Arch. Biochem.*, **9**, 109 (1946).
(30) I. M. Klotz and D. L. Hunston, *J. Biol. Chem.*, **250**, 3001 (1975).
(31) L. W. Nichol, G. D. Smith, and A. G. Ogston, *Biochim. Biophys. Acta*, **184**, 1 (1969).
(32) J. E. Fletcher and A. A. Spector, *Mol. Pharmacol.*, **13**, 387 (1977).
(33) F. Karush and M. Sonenberg, *J. Am. Chem. Soc.*, **71**, 1369 (1949).
(34) I. M. Klotz, F. M. Walker, and R. B. Pivan, *ibid.*, **68**, 1486 (1946).
(35) T. Higuchi and R. Kuramoto, *J. Am. Pharm. Assoc., Sci. Ed.*, **43**, 393 (1954).
(36) *Ibid.*, **43**, 398 (1954).
(37) K. Münzel, *Dtsch. Apoth. Ztg.*, **107**, 1312 (1967).
(38) M. Abu-Hamdiyyah, *J. Phys. Chem.*, **69**, 2720 (1965).
(39) C. K. Bahal and H. B. Kostenbauder, *J. Pharm. Sci.*, **53**, 1027 (1964).
(40) W. Scholtan, *Arzneim.-Forsch.*, **13**, 288, 347 (1963).
(41) L. May, M. Hines, L. Weintraub, J. Scudder, and S. Graff, *Surgery*, **35**, 191 (1954).
(42) C. B. Anfinsen, M. L. Anson, K. Bailey, and J. T. Edsall, "Advances in Protein Chemistry," vol. XIV, Academic, London, England, 1959.
(43) H. S. Frank and M. Evans, *J. Chem. Phys.*, **13**, 507 (1945).
(44) K. Nishida and H. Watanabe, *Kolloid-Z. Z. Polym.*, **244**, 346 (1971).
(45) S. Keipert, J. Becker, and R. Voight, *Pharmazie*, **32**, 280 (1977).

ACKNOWLEDGMENTS

Abstracted from a thesis submitted by J. A. Plaizier-Vercammen to the Vrije Universiteit Brussel, in partial fulfillment of the Doctor of Philosophy degree requirements.

The authors thank Mr. G. R. Bultinck for technical assistance.

Nitro- *para*- and *meta*-Substituted 2-Phenylindolizines as Potential Antimicrobial Agents

CLAUDIO L. K. LINS, JOHN H. BLOCK ˣ, and ROBERT F. DOERGE

Received May 20, 1980, from the *School of Pharmacy, Oregon State University, Corvallis, OR 97321.* Accepted for publication June 26, 1981.

Abstract □ Some *para*- and *meta*-substituted nitro-2-phenylindolizines were prepared and tested as potential antimicrobial agents. The syntheses were accomplished *via* the Chichibabin–Stepanow synthesis, using the properly substituted α-picoline and phenacyl bromides followed by direct nitration.

Keyphrases □ Antimicrobial activity—potential, nitro *para*- and *meta*-substituted 2-phenylindolizines □ 2-Phenylindolizines—potential antimicrobials, nitro *para*- and *meta*-substituted, synthesis □ Heterocycles—*para*- and *meta*-substituted 2-phenylindolizines, preparation, potential antimicrobials

Earlier reports (1–4) have generated considerable interest in the fundamental chemistry of the indolizine heterocyclic system (I). However, there have been few reports of the biological activity of indolizines (5–7), and no systematic study has been reported.

BACKGROUND

One report (8) considered 2-(4-fluoro-2-methylphenyl)indolizine and 2-(4-fluoro-2-methylphenyl)-7-methylindolizine as carcinogens, but failed to mention whether these compounds were actually tested for carcinogenic properties. 2-(4-Cyclohexylphenyl)indolizine was reported to be noncarcinogenic when painted on the skin of experimental animals (9).

Another report (10) considered 1-indolizinealanine to be a tryptophan antimetabolite. Preliminary tests (11) reported that indolizine-1-acetic acid, the structural analog of indole-3-acetic acid(heteroauxin), showed some auxinlike activity.

1-Diethylaminomethyl-3-methyl-2-phenylindolizine reportedly possessed central nervous system (CNS) depressant activity (12). No useful activity was found for some 1-aminoalkyl-2-phenylindolizines, which were screened for their effects on the CNS in mice and in cats (13). The compounds were stimulants at low doses, depressants at higher doses, and caused death by convulsions.

The 2,3-bis(*p*-methoxyphenyl)indolizines were reported to possess antiexudative activity (14). It was previously reported (15) that 2-(4-fluoro-3-methylphenyl)indolizine decreased the duration of paralysis caused by the drug zoxazolamine when tested in rats. No anti-inflammatory activity for 2-(*p*-methylphenyl)-1-phenylindolizine and 2-(*p*-bromophenyl)-1-(*p*-methoxyphenyl)indolizine was found (16) relative to the reference indoxole.

Rosseels *et al.* (17) found that 3-acetyl-2-alkyl-1-nicotinoylindolizines showed anti-inflammatory activities equivalent to acetylsalicylic acid, and 2-ethyl and 2-*n*-propyl-1-nicotinoylindolizines possessed analgesic activities greater than that of antipyrine.

Two earlier reports (18, 19) stated that N^1-substituted hydrazides of indolizine-2-carboxylic acid were more active than iproniazid in the inhibition of monoamine oxidase. Antonini *et al.* (20) also found that 3-(3-aminopropyl)-2-methylindolizine possessed antiserotonin antihis-

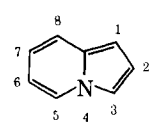

I

0022-3549/82/0500-0556$01.00/0

(16) H. P. Frank, S. Barkin, and F. R. Eirich, *J. Phys. Chem.*, **61**, 1375 (1957).
(17) S. Keipert, I. Korner, and R. Voight, *Pharmazie*, **31**, 790 (1976).
(18) "Tables Scientifiques," 6th ed., J. R. Geigy, Ed., Documenta Geigy, Basel, Switzerland, 1962.
(19) P. J. Elving, J. M. Markovitz, and I. Rosenthal, *Anal. Chem.*, **28**, 1179 (1956).
(20) J. H. Block, E. B. Roche, T. O. Soine, and Ch. O. Wilson, "Inorganic Medicinal and Pharmaceutical Chemistry," Lea & Febiger, Philadelphia, Pa., 1974.
(21) E. Killmann, *Kolloid-Z. Z. Polym.*, **242**, 1103 (1970).
(22) J. T. Edsall and J. Wyman, "Biophysical Chemistry," vol. 1, Academic, New York, N.Y., 1958.
(23) I. M. Klotz, in "The Proteins," vol. 1, part B, H. Neurath and K. Bailey, Eds., Academic, New York, N.Y., 1953.
(24) C. Tanford, "Physical Chemistry of Macromolecules," Wiley, New York, N.Y., 1966.
(25) R. M. Rosenberg and I. M. Klotz, in "A Laboratory Manual of Analytical Methods of Protein Chemistry," vol. 2, P. Alexander and R. J. Block, Eds., Pergamon, London, 1960.
(26) J. Steinhardt and J. A. Reynolds, "Multiple Equilibria in Proteins," Academic, New York, N.Y., 1969.
(27) V. Neuhoff and F. Kühl, *Arzneim.-Forsch.*, **19**, 1898 (1969).
(28) F. P. Donnan, *Chem. Rev.*, **1**, 73 (1924).
(29) I. M. Klotz, *Arch. Biochem.*, **9**, 109 (1946).
(30) I. M. Klotz and D. L. Hunston, *J. Biol. Chem.*, **250**, 3001 (1975).
(31) L. W. Nichol, G. D. Smith, and A. G. Ogston, *Biochim. Biophys. Acta*, **184**, 1 (1969).
(32) J. E. Fletcher and A. A. Spector, *Mol. Pharmacol.*, **13**, 387 (1977).
(33) F. Karush and M. Sonenberg, *J. Am. Chem. Soc.*, **71**, 1369 (1949).
(34) I. M. Klotz, F. M. Walker, and R. B. Pivan, *ibid.*, **68**, 1486 (1946).
(35) T. Higuchi and R. Kuramoto, *J. Am. Pharm. Assoc., Sci. Ed.*, **43**, 393 (1954).
(36) *Ibid.*, **43**, 398 (1954).
(37) K. Münzel, *Dtsch. Apoth. Ztg.*, **107**, 1312 (1967).
(38) M. Abu-Hamdiyyah, *J. Phys. Chem.*, **69**, 2720 (1965).
(39) C. K. Bahal and H. B. Kostenbauder, *J. Pharm. Sci.*, **53**, 1027 (1964).
(40) W. Scholtan, *Arzneim.-Forsch.*, **13**, 288, 347 (1963).
(41) L. May, M. Hines, L. Weintraub, J. Scudder, and S. Graff, *Surgery*, **35**, 191 (1954).
(42) C. B. Anfinsen, M. L. Anson, K. Bailey, and J. T. Edsall, "Advances in Protein Chemistry," vol. XIV, Academic, London, England, 1959.
(43) H. S. Frank and M. Evans, *J. Chem. Phys.*, **13**, 507 (1945).
(44) K. Nishida and H. Watanabe, *Kolloid-Z. Z. Polym.*, **244**, 346 (1971).
(45) S. Keipert, J. Becker, and R. Voight, *Pharmazie*, **32**, 280 (1977).

ACKNOWLEDGMENTS

Abstracted from a thesis submitted by J. A. Plaizier-Vercammen to the Vrije Universiteit Brussel, in partial fulfillment of the Doctor of Philosophy degree requirements.

The authors thank Mr. G. R. Bultinck for technical assistance.

Nitro- *para*- and *meta*-Substituted 2-Phenylindolizines as Potential Antimicrobial Agents

CLAUDIO L. K. LINS, JOHN H. BLOCK ˣ, and ROBERT F. DOERGE

Received May 20, 1980, from the *School of Pharmacy, Oregon State University, Corvallis, OR 97321.* Accepted for publication June 26, 1981.

Abstract □ Some *para*- and *meta*-substituted nitro-2-phenylindolizines were prepared and tested as potential antimicrobial agents. The syntheses were accomplished *via* the Chichibabin–Stepanow synthesis, using the properly substituted α-picoline and phenacyl bromides followed by direct nitration.

Keyphrases □ Antimicrobial activity—potential, nitro *para*- and *meta*-substituted 2-phenylindolizines □ 2-Phenylindolizines—potential antimicrobials, nitro *para*- and *meta*-substituted, synthesis □ Heterocycles—*para*- and *meta*-substituted 2-phenylindolizines, preparation, potential antimicrobials

Earlier reports (1–4) have generated considerable interest in the fundamental chemistry of the indolizine heterocyclic system (I). However, there have been few reports of the biological activity of indolizines (5–7), and no systematic study has been reported.

BACKGROUND

One report (8) considered 2-(4-fluoro-2-methylphenyl)indolizine and 2-(4-fluoro-2-methylphenyl)-7-methylindolizine as carcinogens, but failed to mention whether these compounds were actually tested for carcinogenic properties. 2-(4-Cyclohexylphenyl)indolizine was reported to be noncarcinogenic when painted on the skin of experimental animals (9).

Another report (10) considered 1-indolizinealanine to be a tryptophan antimetabolite. Preliminary tests (11) reported that indolizine-1-acetic acid, the structural analog of indole-3-acetic acid(heteroauxin), showed some auxinlike activity.

1-Diethylaminomethyl-3-methyl-2-phenylindolizine reportedly possessed central nervous system (CNS) depressant activity (12). No useful activity was found for some 1-aminoalkyl-2-phenylindolizines, which were screened for their effects on the CNS in mice and in cats (13). The compounds were stimulants at low doses, depressants at higher doses, and caused death by convulsions.

The 2,3-bis(*p*-methoxyphenyl)indolizines were reported to possess antiexudative activity (14). It was previously reported (15) that 2-(4-fluoro-3-methylphenyl)indolizine decreased the duration of paralysis caused by the drug zoxazolamine when tested in rats. No anti-inflammatory activity for 2-(*p*-methylphenyl)-1-phenylindolizine and 2-(*p*-bromophenyl)-1-(*p*-methoxyphenyl)indolizine was found (16) relative to the reference indoxole.

Rosseels *et al.* (17) found that 3-acetyl-2-alkyl-1-nicotinoylindolizines showed anti-inflammatory activities equivalent to acetylsalicylic acid, and 2-ethyl and 2-*n*-propyl-1-nicotinoylindolizines possessed analgesic activities greater than that of antipyrine.

Two earlier reports (18, 19) stated that N^1-substituted hydrazides of indolizine-2-carboxylic acid were more active than iproniazid in the inhibition of monoamine oxidase. Antonini *et al.* (20) also found that 3-(3-aminopropyl)-2-methylindolizine possessed antiserotonin antihis-

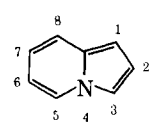

I

0022-3549/82/0500-0556$01.00/0

Table I—Indolizines

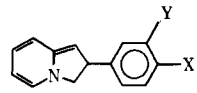

Compound Number	X	Y	Melting Point	Percent Yield	Formula	Analysis Calc.	Analysis Found
XI*a*	H	H	214–215°	80	$C_{14}H_{11}N$	—	—[a]
XI*b*	Br	H	253–254°	86	$C_{14}H_{10}NBr$	—	—[b]
XI*c*	H	Br	175–176°	81	$C_{14}H_{10}NBr$[c]	271.000	271.000
XI*d*	Cl	H	245–246°	88	$C_{14}H_{10}NCl$	—	—[b]
XI*e*	H	Cl	160–161°	96	$C_{14}H_{10}NCl$[c]	227.050	227.050
XI*f*	OCH_3	H	227–228°	28	$C_{15}H_{13}NO$	—	—[d]
XI*g*	H	OCH_3	125–126°	89	$C_{15}H_{13}NO$[c]	223.100	223.099
XI*h*	CH_3	H	215–216°	85	$C_{15}H_{13}N$	—	—[b]
XI*i*	H	CH_3	143–145°	60	$C_{15}H_{13}N$[c]	207.105	207.105

[a] Reference 36. [b] Reference 43. [c] Empirical formula confirmed by high resolution mass spectrometry[11]. [d] Reference 44.

tamine and antiacetylcholine properties with some CNS activity.

Some reports (21, 22) considered 2-alkyl-3- and 2-alkyl-1-(4-dialkylaminoalkoxybenzoyl)indolizine derivatives as antianginal agents. Other groups (23, 24) reported that 2- and 3-benzoylindolizine derivatives showed hemodynamic characteristics similar to those of amiodarone with noncompetitive antiadrenergic properties.

It was reported (25) that 2-[4-(2-indolizinyl)phenyl]propionitrile and propionic acid derivatives have analgesic, antipyretic, and anti-inflammatory activities. The indolizine analog of pindolol was found to have nonselective β-adrenergic blocking activity (26).

The chemotherapeutic effectiveness of numerous heterocyclic compounds containing a nitro moiety is well documented. Nitrofurazine (II) is used in urinary tract infections and is effective against both Gram-positive and Gram-negative organisms (27, 28). Metronidazole (III) is an effective trichomonacidal agent used in vaginal infections (29). Outside of the United States, ipronidazole (IV) and tinidazole (V) are used for their antimicrobial action (30, 31). Niridazole (VI) and the open-chain analog, nithiazide (VII), are known to have antibacterial activities (32, 33).

There is a need for the development of new antimicrobial agents because of resistance developed by the microbial organisms, toxic side effects, limited spectrum of activity, and inability to concentrate in desired tissues using the compounds now available. The antimicrobial properties of indolizines have not been studied. For this reason, a preliminary investigation of the antimicrobial action of substituted phenylindolizines with and without the nitro group was conducted.

RESULTS AND DISCUSSION

Preparation of Compounds—All the compounds prepared were *para*- and *meta*-substituted 2-phenylindolizines (Table I, compounds XI*a–i*). They were prepared from α-picoline (VIII) and phenacylbromides (IX) *via* the Chichibabin–Stepanow synthesis (34) (Scheme I). The α-picoline and phenacyl bromides were combined to form a pyridinium salt (X) (Table II, compounds Xa–i), which was cyclized in refluxing aqueous sodium bicarbonate to the corresponding indolizine (XI). The indolizines in solution were unstable in light, especially when in chloroform.

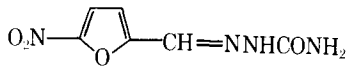

II

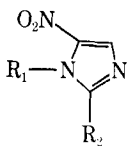

III: $R_1 = -CH_2CH_2OH$, $R_2 = -CH_3$
IV: $R_1 = -CH_3$, $R_2 = -CH(CH_3)_2$
V: $R_1 = -CH_2CH_2SO_2CH_2CH_3$, $R_2 = -CH_3$

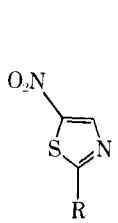

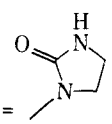

VI: R =
VII: R = $-NHCONHCH_2CH_3$

A mechanism for the Chichibabin–Stepanow synthesis was postulated earlier (35). Nitration of 2-phenylindolizine derivatives (XI) was accomplished with nitric acid (d = 1.4) in the presence of concentrated sulfuric acid at 0° (36). The mechanism by which 2-phenylindolizines are nitrated was recently discussed (37). The orientation of the nitro group appears to depend on the reagent and experimental conditions. Nitration of indolizines in a mixture of nitric and sulfuric acid occurs at the 1-position (36), but nitration in acetic anhydride occurs at the 3-position (38). Thus, in acetic anhydride, it is presumably the free indolizine which is nitrated at the position commonly susceptible to electrophilic attack. With nitric or sulfuric acid as the solvent, 1-nitration predominates because the attached species is a 3-protonated indolizine. UV studies show that indolizines are almost completely protonated at the 3-position (39).

The first step of the proposed mechanism (Scheme II) for the nitration of indolizines using a nitric and sulfuric acid mixture is protonated at the 3-position (XIV). Protonation blocks position 3 from further electrophilic attack. The second step is the nitronium ion attack at the 1-position, forming 1-nitroindolizinium cation (XV). In the presence of a base, proton removal occurs, yielding compound XVII. With excess nitronium ions,

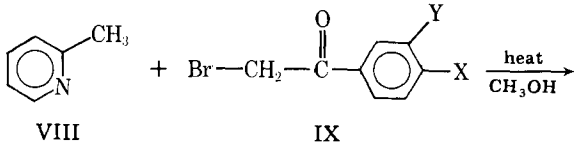

VIII IX

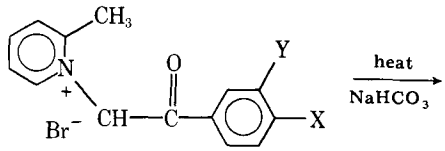

X

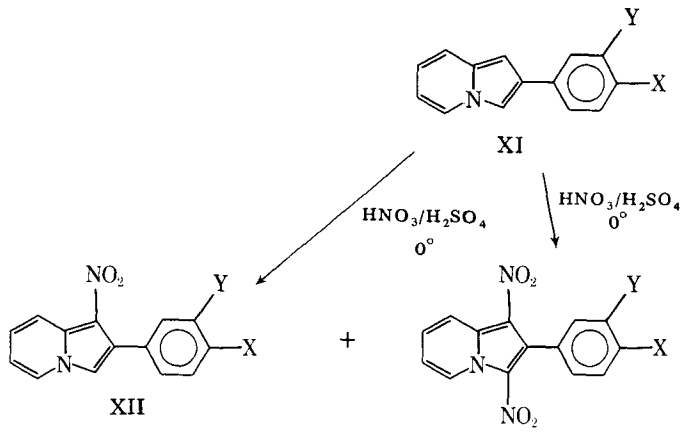

XII XIII

Scheme I—Synthesis of nitro-2-phenylindolizine.

Table II—Pyridinium Bromides

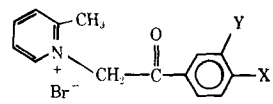

Compound Number	X	Y	Melting Point	Percent Yield	Formula
X*a*	H	H	215–216°	70	$C_{14}H_{14}BrNO$
X*b*	Br	H	185–186°	27	$C_{14}H_{13}Br_2NO$
X*c*	H	Br	250–251°	62	$C_{14}H_{13}Br_2NO$
X*d*	Cl	H	145–148°	33	$C_{14}H_{13}BrClNO$
X*e*	H	Cl	227–228°	58	$C_{14}H_{13}BrClNO$
X*f*	OCH_3	H	140–141°	84	$C_{15}H_{16}BrNO_2$
X*g*	H	OCH_3	185–186°	75	$C_{15}H_{16}BrNO_2$
X*h*	CH_3	H	183–185°	54	$C_{15}H_{16}BrNO$
X*i*	H	CH_3	195–197°	60	$C_{15}H_{16}BrNO$

further nitration can occur at position 3, forming 1,3-dinitroindolizinium cation (XVI). In a basic environment, proton removal occurs giving compound XVIII.

The nitro derivatives XI*j*, XVII*a–f*, and XVIII*a–f* used in this study were purified by alumina-column chromatography and preparative TLC. They rapidly turned green if not protected from air and sunlight. In some situations the reaction mixture contained both the 1-nitro (XII) and 1,3-dinitro indolizine (XIII); in others only the 1,3-dinitroindolizine (XIII) could be isolated. Because the compounds did not exhibit the desired biological activity, no attempt was made to improve yields.

Biological Results—Compounds XI*j*, XVII*a–f*, and XVIII*a–f* were evaluated *in vitro* for antibacterial activity against Gram-negative *Escherichia coli* and Gram-positive *Staphylococcus aureus* bacteria. A preliminary disk-agar diffusion test was done using nitrofurazone[1] and chloramphenicol[1] as standards. None of the test compounds exhibited any antimicrobial activity against the organisms tested. Negative results were also obtained when the indolizine was placed directly onto the test agar.

EXPERIMENTAL

Antimicrobial Evaluation—The bacteria used were Gram-negative *E. coli* and Gram-positive *S. aureus*[2]. Before antimicrobial testing, the compounds in solution were sterilized using a fritted-glass filtering disk[3] (40).

The disk-agar diffusion method following the Kirk–Bauer procedure (41) was used for preliminary testing. The basic concept is that the size of the zone of inhibition correlates with the antimicrobial activity of the agent being tested.

The standard procedure requires the use of a special agar for susceptibility testing of microorganisms[4] and a standard inoculum applied in a potency for each of the chemotherapeutic agents being tested.

The experimental disks[5] were placed in a methanol solution containing varying amounts of the indolizine and then were air dried and placed on the top of the agar. The pure compounds (5 mg) were also placed directly on the top of the agar. Disks previously soaked in methanol and then air dried were used as blanks.

Chemistry—Melting point values were determined using an open capillary melting point apparatus[6] and are uncorrected. The NMR spectrometer[7] was used with tetramethylsilane as an internal standard and deuterated chloroform as a solvent. IR[8] and UV[9] spectra were recorded on suitable double-beam spectrophotometers. Mass spectra were obtained with a single-focusing magnetic mass spectrophotometer equipped with a data recording system[10]. Elemental analyses were performed by high-resolution mass spectrometry[11].

Analytical TLC plates were precoated with silica gel[12]. The preparative TLC plates were coated with silica gel[13] (20 × 20 cm, 2 mm). The three methylene chloride–hexane developing systems used were A (1:3), B (1:1), and C (3:1). Spots were visualized with UV light at 254 nm. The purity of each compound was confirmed in each of the TLC systems and in a 40% acetonitrile high-pressure liquid chromatography (HPLC) system[14] using a persilated octadecylsilane column[15]. All compounds gave spectral data consistent with the proposed structure.

The necessary phenacyl bromides were prepared by bromination of the corresponding acetophenone in methanol (42).

Synthesis of *m*-Substituted 2-Phenylindolizines (Table I)—A typical synthesis will be described for 2-(*m*-methylphenyl)indolizine (XI*i*). 3′-Methylacetophenone (3.4 g, 0.025 mole) was diluted with 10 ml of anhydrous methanol in a 25-ml triple-necked flask. Bromine (4.0 g, 0.025 mole) diluted in 2.5 ml of anhydrous methanol was added dropwise for 10 min. If the reaction mixture became clear, more bromine was added until a dark red color persisted. After 30 min of stirring, the mixture was poured into a beaker containing chipped ice. The resulting crystals were washed several times with cold water. (When the substituted phenacyl

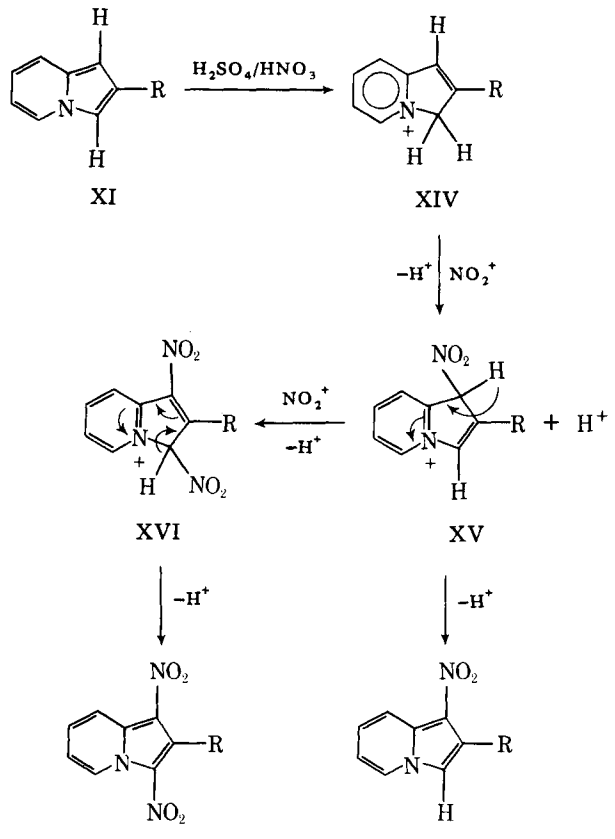

Scheme II—Mechanism of nitration for indolizines.

[1] Sensi-Disc, microbial susceptibility test discs, BBL, Cockeysville, Md.
[2] From a collection maintained by Oregon State University, Departments of Microbiology and Food Science and Technology.
[3] Pyrex brand chemical glass #774, UF Porosity, Corning Glass Works, Corning, N.Y.
[4] Mueller-Hinton agar, Difco Laboratories, Detroit, Mich.
[5] No. 740-E, Schleicher & Schuell, Keene, N.H.
[6] Thomas-Hoover.
[7] Varian Anaspect EM 360.
[8] Perkin-Elmer model 727.
[9] Beckman model DB-GT.
[10] System Industries 150.
[11] High resolution mass spectrometer CEC-21B-110. Instrument set at 70 eV. Analyses were done at the Department of Chemistry, University of Oregon, Eugene, Ore.
[12] Silica gel 60 F-254, EM reagents.
[13] Silica gel PF-254 + 366, EM reagents.
[14] Model ALC/GPC 201 liquid chromatograph, model M 6000A pump, model U-6K injector, Waters Associates, Milford, Mass.
[15] Corasil C_{18}, Waters Associates, Milford, Mass.

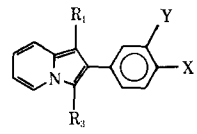

Table III—Nitroindolizines

Compound	X	Y	R_1	R_3	M.P.	Percent Yield	Formula	Analysis Calc.	Analysis Found
XVIII*a*	H	H	NO_2	NO_2	245–246°	14	$C_{14}H_9N_3O_4$	—	—[a]
XI*j*	NO_2	H	H	H	236–237°	50	$C_{14}H_{10}N_2O_2$	—	—[a]
XVII*a*	NO_2	H	NO_2	H	235–236°	3	$C_{14}H_9N_3O_4$	—	—[a]
XVII*b*	Br	H	NO_2	H	153–155°	3	$C_{14}H_9BrN_2O_2$[b]	315.985	315.985
XVIII*b*	Br	H	NO_2	NO_2	265–266°	15	$C_{14}H_8BrN_3O_4$[b]	360.970	360.972
XVII*c*	H	Br	NO_2	H	174–175°	14	$C_{14}H_9BrN_2O_2$[b]	315.985	315.982
XVIII*c*	Cl	H	NO_2	NO_2	215–216°	3	$C_{14}H_8ClN_3O_4$[b]	317.020	317.022
XVII*d*	H	Cl	NO_2	H	190–191°	18	$C_{14}H_9ClN_2O_2$[b]	272.035	272.033
XVIII*d*	OCH_3	H	NO_2	NO_2	268–269°	2	$C_{15}H_{11}N_3O_5$[b]	313.070	313.067
XVIII*e*	H	OCH_3	NO_2	NO_2	183–184°	17	$C_{15}H_{11}N_3O_5$[b]	313.070	313.070
XVII*e*	CH_3	H	NO_2	H	178–179°	5	$C_{15}H_{12}N_2O_2$[b]	252.090	252.088
XVIII*f*	CH_3	H	NO_2	NO_2	235–236°	12	$C_{15}H_{11}N_3O_4$[b]	297.075	297.075
XVII*f*	H	CH_3	NO_2	H	179–180°	5	$C_{15}H_{12}N_2O_2$[b]	252.090	252.090

[a] Reference 36. [b] Empirical formula confirmed by high resolution mass spectrometry[11].

bromide was a liquid it was washed in a separator.) The crystalline material was transferred to a 50-ml flask and α-picoline (2.25 g, 0.025 mole) in 25 ml of anhydrous methanol was added. The solution was refluxed for 30 min. A precipitate formed, which was filtered and washed with cold water and recrystallized from hot ethyl acetate or ether. The white crystalline solid was then placed in a 50-ml round-bottom flask containing sodium bicarbonate (2.10 g, 0.025 mole) in 25 ml of water. The mixture was refluxed for 10 min. The resulting yellow precipitate was filtered, washed with water, and recrystallized from ethyl acetate. Yields and analytical data are found in Table I.

Synthesis of Nitroindolizines (Table III)—*1,3-Dinitro-2-phenylindolizine* (*XVIII*a)—2-Phenylindolizine (XI*a*) (2.0 g, 10.4 mmoles) dissolved in 10 ml (0.155 mmole) of nitric acid (d = 1.4) was warmed according to Borrows *et al.* (36) to form green-orange crystals (mp 233–238°). The crystals were recrystallized from acetic acid to give 0.40 g (14%) of compound XI*a* as a dark yellow solid: mp 245–246°. Compound XI*a* appeared as one spot when analyzed by TLC (solvent system C, R_f 0.43). UV (CH_3OH): 220 (log 4.27), 252 (4.04), 300 (3.85), and 355 (4.25) nm; mass spectrum: *m/z* 283 (M+, 100%).

2-(p-Nitrophenyl)indolizine (*XI*j)—Nitric acid (d = 1.4; 0.35 ml, 5.43 mmoles) was added dropwise over a 5-min period to an ice-cold stirred solution of 0.50 g (2.59 mmoles) 2-phenylindolizine (XI*a*) in concentrated sulfuric acid (36). A yellow-brown precipitate (0.40 g) was formed and recrystallized first from acetonitrile, and then acetone–charcoal yielding 0.30 g (50%) 2-(*p*-nitrophenyl)indolizine (XI*b*); mp 236–237°, which appeared as one spot when analyzed by TLC (solvent system B, R_f 0.43). UV (CH_3OH): 240 (log 3.52), 300 (2.93), and 340 (3.15) nm; mass spectrum: *m/z* 238 (M+, 100%).

1-Nitro-2-(p-nitrophenyl)indolizine (*XVII*a)—Nitric acid (d = 1.4; 0.8 ml, 12.4 mmoles) was added dropwise over 5 min to an ice-cold stirred solution containing 2.0 g (8.40 mmoles) of 2-(*p*-nitrophenyl)indolizine (XI*j*) in 2.0 ml of concentrated sulfuric acid (36). A green–yellow precipitate was formed and recrystallized from acetonitrile and then from acetone with charcoal, yielding 0.07 g (3%) of XVII*a* as yellow needles (mp 235–236° dec.). Compound XVII*a* appeared as one spot when analyzed by TLC (solvent system C, R_f 0.43). UV (CH_3OH): 220 (log 4.50), and 275 (4.33) nm; mass spectrum: *m/z* 283 (M+, 100%).

1-Nitro-2-(p-bromophenyl)indolizine (*XVII*b) *and 1,3-Dinitro-2-p-bromophenyl)indolizine* (*XVIII*b)—Nitric acid (d = 1.4; 0.1 ml, 1.55 mmoles) was added dropwise over 5 min to an ice-cold stirred solution containing 0.35 g (1.29 mmoles) 2-(*p*-bromophenyl)indolizine (XI*b*) in 2.0 ml of concentrated sulfuric acid in a 50-ml round-bottom flask equipped with a magnetic stirring bar. The dark red solution was stirred for 38 min at 0°. The mixture was poured into a beaker containing 20 g of crushed ice and yielded 0.30 g of a dark green solid; mp 150–165°. The precipitate was placed in an alumina column, and compound XVIII*b* was eluted using a mixture of 1:1 hexane–methylene chloride as the eluant. The eluate was evaporated under vacuum and the residue was recrystallized from acetone, yielding 0.012 g (3%) of a dark yellow precipitate (mp 153–155° dec.). Compound XVII*b* appeared as one spot when analyzed by TLC (solvent system C, R_f 0.70). UV (CH_3OH): 214 (log 4.23), 260 (4.52), and 286 (4.32) nm; mass spectrum: *m/z* 316 (M+, 95%) and 318 (M + 2, 100%).

Changing the solvent to methylene chloride–hexane (3:1) caused the elution of compound XVIII*b*. The eluate was evaporated under vacuum and yielded 0.05 g (15%) of a light yellow precipitate (mp 265–266° dec.). Compound XVIII*b* appeared as one spot when analyzed by TLC (solvent system C, R_f 0.45). UV (CH_3OH): 210 (log 4.23) and 236 (4.50) nm; mass spectrum: *m/z* 361 (M+, 89%) and 363 (M + 2, 100%).

1-Nitro-2-(m-bromophenyl)indolizine (*XVII*c)—Nitric acid (d = 1.4; 0.175 ml, 2.72 mmoles) was added dropwise over 5 min to an ice-cold stirred solution of 0.75 g (2.76 mmoles) of 2-(*m*-bromophenyl)indolizine (XI*c*) in 10 ml of concentrated sulfuric acid in a 50-ml round-bottom flask equipped with a magnetic stirring bar. The light yellow solution was stirred for 38 min at 0°. The mixture was poured into a beaker containing 20 g of crushed ice and filtered under vacuum using a sintered-filter funnel with medium porosity. The red-yellow precipitate was recrystallized from acetonitrile and yielded 0.12 g (14%) yellow needles (mp 174–175° dec.). Compound XVII*c* appears as one spot when analyzed by TLC (solvent system C, R_f 0.73). UV (CH_3OH): 215 (log 4.30), 242 (4.48), and 295 (4.17) nm; mass spectrum: *m/z* 191 (100%), 316 (M+, 48%), and 318 (M + 2, 52%).

1,3-Dinitro-2-(p-chlorophenyl)indolizine (*XVIII*c)—Nitric acid (d = 1.4; 0.175 ml, 2.72 mmoles) was added dropwise over 10 min to an ice-cold stirred solution containing 0.65 g (2.86 mmoles) of 2-(*p*-chlorophenyl)indolizine (XI*d*) in 10 ml of concentrated sulfuric acid in a 50-ml round-bottom flask equipped with a magnetic stirring bar. The mixture turned light yellow immediately and turned dark red after the addition of the final 0.05 ml of nitric acid.

The solution was stirred for 38 min, keeping the temperature at 0°. The mixture was poured into a sintered-filter funnel containing 20 g of crushed ice. After washing the filter with cold water several times, 0.30 g of a green-yellow precipitate (mp 130–145°) was recovered. The solid was placed in an alumina column and eluted with a mixture of 3:1 methylene chloride–hexane. The eluate was evaporated under vacuum. The green-yellow precipitate was recrystallized from acetonitrile and yielded 0.030 g (3%) yellow crystals (mp 215–216° dec.). Compound XVIII*c* appeared as one spot when analyzed by TLC (solvent system C, R_f 0.43). UV (CH_3OH): 235 (log 4.37) nm; mass spectrum: *m/z* 272 (100%) and 317 (M+, 25.2%).

1-Nitro-2-(m-chlorophenyl)indolizine (*XVII*d)—Nitric acid (d = 1.4; 0.08 ml, 1.24 mmoles) was added dropwise over 5 min to an ice-cold stirred solution containing 0.30 g (1.32 mmoles) 2-(*m*-chlorophenyl)-indolizine (XI*e*) dissolved in 2.0 ml of concentrated sulfuric acid. The light yellow solution was stirred for 38 min at 0°. The mixture was poured in a beaker containing 20 g of crushed ice. A red precipitate formed at once. The suspension was adjusted to pH 10.5 by adding 20% KOH solution. A bright yellow precipitate (0.3 g, mp 150–165° dec.) was recovered. The precipitate was recrystallized from acetonitrile and yielded 0.07 g (18%) of yellow needles (mp 190–191° dec.). Compound XVII*d* appeared as one spot when analyzed by TLC (solvent system B, R_f 0.49). UV (CH_3OH): 215 (log 4.29), 242 (4.46), and 295 (4.15) nm; mass spectrum: *m/z* 227 (100%) and 272 (M+, 25%).

1,3-Dinitro-2-(p-methoxyphenyl)indolizine (*XVIII*d)—Nitric acid (d = 1.4; 0.1 ml, 1.55 mmoles) was added dropwise over 5 min to an ice-cold stirred solution containing 0.33 g (1.48 mmoles) of 2-(*p*-methoxyphenyl)indolizine (XI*f*) dissolved in 2.0 ml of concentrated sulfuric acid in a 50-ml round-bottom flask equipped with a magnetic stirring bar. The reddish-brown mixture was stirred for 38 min at 0°. The solution was poured into a beaker containing 20 g of crushed ice and basified to pH

10.5 by adding 20% KOH solution. A yellow precipitate (0.40 g, mp 160–165°) was recovered. The precipitate was placed in an alumina oxide column and eluted with a mixture of methylene chloride–hexane (3:1). The eluate was evaporated under vacuum apparatus and yielded 0.010 g (2.2%) yellow crystals (mp 268–269°). Compound XVIII*d* appeared as one spot when analyzed by TLC (solvent system C, R_f 0.43). UV (CH_3OH): 210 (log 3.43) and 234 (3.72) nm; mass spectrum: *m/z* 313 (M+, 100%).

1,3-Dinitro-2-(m-*methoxyphenyl*)*indolizine* (*XVIIIe*)—Nitric acid (*d* = 1.4; 0.1 ml, 1.55 mmoles) was added dropwise over 5 min to an ice-cold stirred solution containing 0.33 g (1.4 mmoles) 2-(*m*-methoxyphenyl)indolizine (XI*g*) dissolved in 2.0 ml of concentrated sulfuric acid in a 50-ml round-bottom flask equipped with a magnetic stirring bar. The orange-yellow solution was stirred for 38 min at 0°. The mixture was poured into a beaker containing 20 g of crushed ice and basified with 20% KOH solution until pH 10.5. The yellow precipitate (0.14 g, mp 130–145° dec.) was recrystallized from acetonitrile and yielded 0.08 g (17%) rust-red needles(mp 183–184° dec.). Compound XI*j* appeared as one spot when analyzed by TLC (solvent system C, R_f 0.66). UV (CH_3OH): 220 (log 4.25), 236 (4.39), 290 (4.07) nm; mass spectrum: *m/z* 69 (100%) and 314 (M+, 95.5%).

1-Nitro-2-(p-*methylphenyl*)*indolizine* (*XVIIe*) *and 1,3-Dinitro-2-*(p-*methylphenyl*)*indolizine* (*XVIIIf*)—Nitric acid (*d* = 1.4; 0.1 ml, 1.55 mmoles) was added dropwise over 5 min to an ice-cold stirring solution containing 0.30 g (1.44 mmoles) 2-(*p*-methylphenyl)indolizine (XI*h*) dissolved in 2.0 ml of concentrated sulfuric acid in a 50-ml round-bottom flask equipped with a magnetic stirring bar. The dark yellow solution was stirred for 38 min at 0°. The mixture was poured into a beaker containing 20 g of crushed ice and adjusted to pH 10.5 by adding 20% KOH solution. The yellow suspension was filtered using a sintered-glass funnel and the yellow precipitate was dried overnight in a vacuum desiccator (0.36 g, mp 130–145° dec.). The precipitate was recrystallized from acetonitrile and then acetone. A greenish-yellow precipitate (0.12 g, mp 160–195°) was recovered. The solid was purified in an alumina oxide column using 1:3 methylene chloride–hexane. The filtrate was evaporated under vacuum. TLC using solvent system C showed two spots: starting material XI*h* (R_f 0.80) and compound XVII*e* (R_f 0.67). The nitroindolizine XVII*e* was separated by preparative TLC with solvent system B. The yellow band (R_f 0.53) was scraped off the plate and extracted with acetone. Yellow crystals were recovered yielding 0.02 g (5%), mp 178–179° dec. UV (CH_3OH): 210 (log 4.08), 255 (4.56), and 280 (4.22) nm; mass spectrum: *m/z* 252 (M+, 100%).

Further elution of the column using 1:1 methylene chloride–hexane followed by a more polar 3:1 mixture yielded 0.05 g (12%) of a bright yellow compound (mp 235–236° dec.). Compound XVIII*f* appeared as one spot when analyzed by TLC (solvent system C, R_f 0.38). UV (CH_3OH): 235 (log 4.40) and 265 (4.04) nm; mass spectrum: *m/z* 297 (M+, 100%).

1-Nitro-2-(m-*methylphenyl*)*indolizine* (*XVIIf*)—Nitric acid (*d* = 1.4; 0.1 ml, 1.55 mmoles) was added dropwise over 5 min to an ice-cold stirred solution containing 0.30 g (1.44 mmoles) of 2-(*m*-methylphenyl)-indolizine (XI*i*) dissolved in 2.0 ml of concentrated sulfuric acid in a 50-ml round-bottom flask containing a magnetic stirring bar. The light yellow mixture was stirred for 38 min at 0° and poured into a beaker containing 20 g of crushed ice. The solution was adjusted to pH 10.5 by adding 20% KOH. The yellow suspension was filtered using a sintered-filter funnel. The yellow precipitate was dried overnight under vacuum. The compound (0.33 g, mp 100–125° dec.) was recrystallized from acetonitrile and then acetone, yielding 0.03 g (mp 160–165° dec.) greenish-yellow crystals. TLC using solvent system C showed two spots; one from the starting material, XI*i* (R_f 0.86) and the other from compound XVII*f* (R_f 0.69). The nitro derivative was purified by preparative TLC using solvent system B. The yellow band (R_f 0.66) was scraped off from the plate and placed in a Hirsch funnel. The silica gel was washed several times with acetone until all yellow color disappeared. The filtrate was concentrated under vacuum yielding 0.02 g (5%) sparkling yellow crystals (mp 179–180° dec.), which turned light green immediately on contact with air. UV (CH_3OH): 210 (log 4.07), 240 (4.39), 294 (4.06), and 350 (4.07); mass spectrum: *m/z* 252 (M+, 100%).

REFERENCES

(1) A. Galbraith, T. Small, and V. Boekelheide, *J. Org. Chem.*, **24,** 582 (1959).

(2) V. Boekelheide and H. Miller, *ibid.*, **26,** 431 (1961).

(3) V. Boekelheide and R. J. Windgassen, *J. Am. Chem. Soc.*, **81,** 1456 (1959).

(4) R. J. Windgassen, W. H. Saunders, and V. Boekelheide, *ibid.*, **81,** 1459 (1959).

(5) W. B. Harrell, Ph.D. thesis, Oregon State University, 1967, p. 31.

(6) W. B. Harrell and R. F. Doerge, *J. Pharm. Sci.*, **57,** 1989 (1968).

(7) W. B. Harrell, *ibid.*, **59,** 275 (1970).

(8) N. P. Buu-Hoi and N. D. Xuong, *J. Chem. Soc.*, **1953,** 386.

(9) N. P. Buu-Hoi, L. C. Bink, T. B. Loc, N. D. Xuong, and P. Jacquignon, *ibid.*, **1957,** 3126.

(10) J. A. Carbon and S. Brehm, *J. Org.Chem.*, **26,** 3376 (1961).

(11) M. Cardellini, S. Ottolino, and P. Tafaro, *Ann. Chim. (Rome)*, **58,** 1206 (1968); through *Chem. Abstr.*, **70,** 77753a (1969).

(12) W. B. Harrell and R. F. Doerge, *J. Pharm. Sci.*, **56,** 225 (1967).

(13) L. A. Walter and P. Margolis, *J. Med. Chem.*, **10,** 498 (1967).

(14) W. Engle, E. Seeger, H. Teufel, and A. Eckenfels, German pat. 1,922,191 (Nov. 12, 1970); through *Chem. Abstr.*, **74,** 1299w (1971).

(15) N. P. Buu-Hoi and D. P. Hien, *Biochem. Pharmacol.*, **17,** 1227 (1968).

(16) K. H. Kallay and R. F. Doerge, *J. Pharm. Sci.*, **61,** 949 (1972).

(17) G. Rosseels, H. Inion, J. R. Matteazzi, M. Peiren, M. Prost, M. Descamps, C. Tornay, M. Colot, and R. Charlier, *Eur. J. Med. Chem.-Chim. Ther.*, **10,** 579, (1975).

(18) M. Cardellini, F. Claudi, M. Grifantini, U. Gulini, and S. Martelli, *J. Pharm. Sci.*, **66,** 259 (1977).

(19) F. Claudi, M. Grifantini, U. Gulini, S. Martelli, and P. Natalini, *ibid.*, **66,** 1355 (1977).

(20) I. Antonini, M. Cardellini, F. Claudi, P. Franchetti, U. Gulini, G. D. Caro, and F. Venturi, *ibid.*, **66,** 1692 (1977).

(21) J. Gubin, G. Rosseels, M. Peiren, M. Prost, M. Descamps, S. Richards, J. Bauthier, and R. Charlier, *Eur. J. Med. Chem.-Chim.Ther.*, **12,** 345 (1977).

(22) J. Gubin and G. Rosseels, German Offen. 2,707,048 (Sept. 1, 1977); through *Chem. Abstr.*, **88,** 6719e (1978).

(23) R. H. Charlier, J. C. Richard, and J. A. Bauthier, *Arzneim.-Forsch.*, **27,** 1445 (1977).

(24) P. Olster and R. Charlier, *ibid.*, **28,** 2232 (1978).

(25) T. Muro, T. Nakao, and K. Ogawa, *Jpn. Kokai*, 7787, 193 (July 20, 1977); through *Chem. Abstr.*, **88,** 50648c (1978).

(26) D. Blondeau, H. Sliwa, and C. DeCeaurriz, *Eur. J. Med. Chem.-Chim. Ther.*, **13,** 576 (1978).

(27) M. C. Dodd and W. B. Stillman, *J. Pharmacol. Exp. Ther.*, **82,** 11 (1944).

(28) C. O. Wilson, O. Gisvold, and R. F. Doerge, "Textbook of Organic Medicinal and Pharmaceutical Chemistry," Lippincott, Philadelphia, Pa., 1977, p. 127.

(29) C. Cosar, L. Jolou, and M. Bonazet, *Ann. Inst. Pasteur*, **96,** 238 (1959).

(30) K. Buyler, H. L. Howes, J. E. Lynch, and D. K. Piric, *J. Med. Chem.*, **10,** 891 (1959).

(31) W. M. Miller, L. H. Howes, V. R. Kasupick, and A. R. English, *ibid.*, **13,** 849 (1970).

(32) C. R. Lambert, M. Wilhelm, H. Striebel, F. Kradolfer, and P. Schmidt, *Experentia*, **20,** 452 (1964).

(33) "The Merck Index," 9th ed., Merck and Co., Inc., Rahway, N.J., 1968.

(34) A. E. Chichibabin and E. H. Stepanow, *Chem. Ber.*, **62,** 1068 (1929).

(35) D. R. Bragg and G. D. Wibberly, *J. Chem. Soc.*, **1962,** 2627.

(36) E. T. Borrows, D. O. Holland, and J. Kenyon, *ibid.*, **2,** 1069 (1946).

(37) L. Greci and J. H. Ridd, *J. Chem. Soc. Perkin II*, **1979,** 312.

(38) J. A. Hickman and D. G. Wibberly, *J. Chem. Soc. Perkin I*, **1972,** 2954.

(39) W. L. Armarego, *J. Chem. Soc.*, **1964,** 4226.

(40) E. H. Morton, *J. Bacteriol.*, **47,** 379 (1943).

(41) A. Ballows, "Current Technique for Antibiotic Susceptibility Testing," C. C Thomas, Springfield, Ill., 1972, p. 6.

(42) M. Rebstock and E. L. Pfeifer, *J. Am. Chem. Soc.*, **74,** 3209 (1952).

(43) N. P. Buu-Hoi and H. Nguyen, *Rec. Trav. Chim. Pays-Bas*, **68,** 441, 1949.

(44) N. P. Buu-Hoi, P. Jacquignon, N. D. Xuong, and D. Lavit, *J. Org. Chem.*, **19,** 1370, 1954.

ACKNOWLEDGMENTS

Presented in part before the Medicinal Chemistry and Pharmacognosy

Section, Academy of Pharmaceutical Sciences, St. Louis, MO. meeting, March 1981.

Abstracted in part from the thesis submitted by C. L. K. Lins to Oregon State University in partial fulfillment of the Doctor of Philosophy degree requirements.

Supported by the Oregon State University Research Office from National Institutes of Health Biomedical Research Support Grant RR07079.

Synthesis and Bioevaluation of a Series of Alkyl Ethers of *p*-*N*,*N*-Bis(2-chloroethyl)aminophenol

J. W. WISE, J. E. WYNN ˣ, R. L. BEAMER, and C. T. BAUGUESS

Received July 6, 1981, from the *Department of Basic Pharmaceutical Sciences, College of Pharmacy, University of South Carolina, Columbia, SC 29208.* Accepted for publication September 4, 1981.

Abstract □ A series of even numbered normal alkyl ethers (C_2–C_{14}) of *p*-*N*,*N*-bis(2-chloroethyl)aminophenol were synthesized and evaluated as to acute toxicity in mice and effects on survival in L-1210 leukemic mice. All of the ether derivatives demonstrated significantly lower acute toxicity than the parent phenol mustard. Significant survival times (≥125%) were obtained with all compounds except the hexyl derivative. The decyl ether produced the greatest significant increase and the ethyl ether the lowest significant increase in mean survival time. Significant survival times were produced at four dosage levels for the butyl, decyl, and dodecyl derivatives, three dosage levels for the octyl and tetradecyl derivatives, and one dosage level for the ethyl derivative.

Keyphrases □ Alkyl ethers—synthesis of alkyl ethers *p*-*N*,*N*-bis(2-chloroethyl)aminophenol □ Bioevaluation—alkyl ethers of *p*-*N*,*N*-bis(2-chloroethyl)aminophenol, toxicity in HA/ICR mice □ Antitumor activity—alkyl ethers of *p*-*N*,*N*-bis(2-chloroethyl)aminophenol, survival in L-1210 leukemic mice

Phenol mustard, *p*-[*N*,*N*-bis(2-chloroethyl)amino]-phenol, has demonstrated a low therapeutic index (1). Less toxic derivatives of phenol mustard have resulted from the synthesis of various esters of the phenol (1–3).

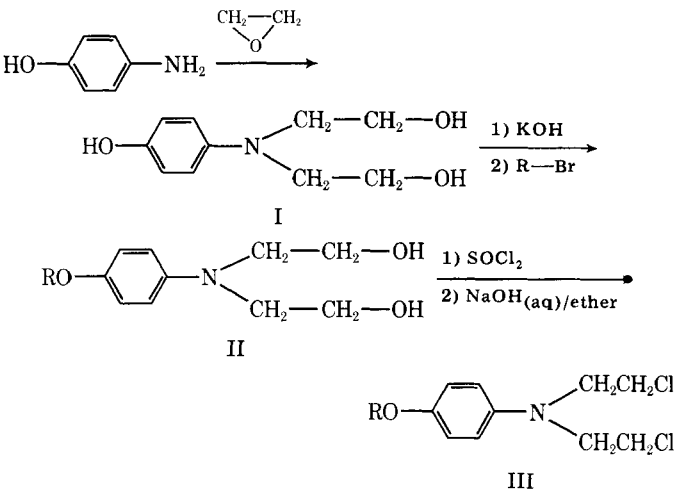

IIa, IIIa: R = CH_3—CH_2—
IIb, IIIb: R = CH_3—$(CH_2)_2$—CH_2—
IIc, IIIc: R = CH_3—$(CH_2)_4$—CH_2—
IId, IIId: R = CH_3—$(CH_2)_6$—CH_2—
IIe, IIIe: R = CH_3—$(CH_2)_8$—CH_2—
IIf, IIIf: R = CH_3—$(CH_2)_{10}$—CH_2—
IIg, IIIg: R = CH_3—$(CH_2)_{12}$—CH_2—

Scheme I

In an effort to develop latent derivatives of phenol mustard, a series of its substituted benzoate esters were studied (1). The results lent support to the hypothesis that hydrolysis of esters of *p*-[*N*,*N*-bis(2-chloroethyl)amino]-phenol to the free phenol mustard is a necessary step for antitumor activity (1). The effectiveness of aniline mustard, *N*,*N*-bis(2-chloroethyl)aniline, in the treatment of advanced plasma cell tumors has been demonstrated (4). The results indicated that aniline mustard was the optimally active compound in this system, and only those compounds that could be metabolized to a phenolic mustard demonstrated activity.

A series of alkyl ethers of phenol mustard should provide potentially latent nitrogen mustard derivatives with variable metabolic routes (5, 6). Such compounds would be expected to demonstrate antineoplastic activity with a reduction in host toxicity. In addition, lipophilicity would increase with the length of the alkyl chain. The specific objectives of this investigation were to: (*a*) synthesize a series of even-numbered, normal alkyl ethers (C_2–C_{14}) of *p*-[*N*,*N*-bis(2-chloroethyl)amino]phenol, (*b*) determine the acute toxicity as measured by the LD_{50} for each compound studied, and (*c*) determine the effect of each compound on the prolongation of life of L-1210 leukemic mice.

The compounds evaluated in this project were synthesized using Scheme I.

EXPERIMENTAL

Chemistry[1]—p-N,N-*Bis(2-hydroxyethyl)aminophenol* (*I*)—Twenty grams (0.18 mole) of *p*-aminophenol was added to a flask containing 200 ml of absolute methanol and equipped with a reflux condenser. The solution was stirred mechanically until dissolution occurred and then was cooled to 0°. Twenty grams (0.45 mole) of ethylene oxide was added to the cold reaction mixture. Stirring was continued and the reaction was allowed to reach room temperature. The resulting crystals were filtered and recrystallized from ethanol. The product had a melting point of 139.5–141° compared with the reported value of 140° (7).

[1] All IR spectral data were obtained from chloroform solutions of the derivatives on sodium chloride plates using a Beckman Model Acculab-4 spectrophotometer. Nuclear magnetic resonance spectra were obtained from deuterated chloroform solutions of the derivatives using a Hitachi-Perkin-Elmer model R-24 high resolution spectrometer with tetramethylsilane as the internal standard. The reported melting points were obtained using a Thomas Hoover capillary melting point apparatus and are uncorrected. The reported content of hydrogen, carbon, and nitrogen were obtained from analyses performed by Galbraith Laboratories, Knoxville, Tenn. All lyophilization was accomplished using a VirTis Model 10 freeze-dryer.

0022-3549/82/0500-0565$01.00/0

Section, Academy of Pharmaceutical Sciences, St. Louis, MO. meeting, March 1981.

Abstracted in part from the thesis submitted by C. L. K. Lins to Oregon State University in partial fulfillment of the Doctor of Philosophy degree requirements.

Supported by the Oregon State University Research Office from National Institutes of Health Biomedical Research Support Grant RR07079.

Synthesis and Bioevaluation of a Series of Alkyl Ethers of *p*-*N*,*N*-Bis(2-chloroethyl)aminophenol

J. W. WISE, J. E. WYNN ˣ, R. L. BEAMER, and C. T. BAUGUESS

Received July 6, 1981, from the *Department of Basic Pharmaceutical Sciences, College of Pharmacy, University of South Carolina, Columbia, SC 29208.* Accepted for publication September 4, 1981.

Abstract □ A series of even numbered normal alkyl ethers (C_2–C_{14}) of *p*-*N*,*N*-bis(2-chloroethyl)aminophenol were synthesized and evaluated as to acute toxicity in mice and effects on survival in L-1210 leukemic mice. All of the ether derivatives demonstrated significantly lower acute toxicity than the parent phenol mustard. Significant survival times (≥125%) were obtained with all compounds except the hexyl derivative. The decyl ether produced the greatest significant increase and the ethyl ether the lowest significant increase in mean survival time. Significant survival times were produced at four dosage levels for the butyl, decyl, and dodecyl derivatives, three dosage levels for the octyl and tetradecyl derivatives, and one dosage level for the ethyl derivative.

Keyphrases □ Alkyl ethers—synthesis of alkyl ethers *p*-*N*,*N*-bis(2-chloroethyl)aminophenol □ Bioevaluation—alkyl ethers of *p*-*N*,*N*-bis(2-chloroethyl)aminophenol, toxicity in HA/ICR mice □ Antitumor activity—alkyl ethers of *p*-*N*,*N*-bis(2-chloroethyl)aminophenol, survival in L-1210 leukemic mice

Phenol mustard, *p*-[*N*,*N*-bis(2-chloroethyl)amino]-phenol, has demonstrated a low therapeutic index (1). Less toxic derivatives of phenol mustard have resulted from the synthesis of various esters of the phenol (1–3).

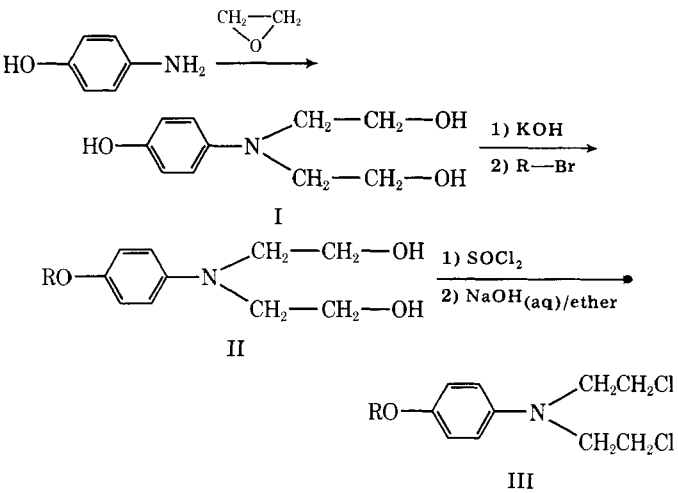

IIa, IIIa: R = CH_3—CH_2—
IIb, IIIb: R = CH_3—$(CH_2)_2$—CH_2—
IIc, IIIc: R = CH_3—$(CH_2)_4$—CH_2—
IId, IIId: R = CH_3—$(CH_2)_6$—CH_2—
IIe, IIIe: R = CH_3—$(CH_2)_8$—CH_2—
IIf, IIIf: R = CH_3—$(CH_2)_{10}$—CH_2—
IIg, IIIg: R = CH_3—$(CH_2)_{12}$—CH_2—

Scheme I

In an effort to develop latent derivatives of phenol mustard, a series of its substituted benzoate esters were studied (1). The results lent support to the hypothesis that hydrolysis of esters of *p*-[*N*,*N*-bis(2-chloroethyl)amino]-phenol to the free phenol mustard is a necessary step for antitumor activity (1). The effectiveness of aniline mustard, *N*,*N*-bis(2-chloroethyl)aniline, in the treatment of advanced plasma cell tumors has been demonstrated (4). The results indicated that aniline mustard was the optimally active compound in this system, and only those compounds that could be metabolized to a phenolic mustard demonstrated activity.

A series of alkyl ethers of phenol mustard should provide potentially latent nitrogen mustard derivatives with variable metabolic routes (5, 6). Such compounds would be expected to demonstrate antineoplastic activity with a reduction in host toxicity. In addition, lipophilicity would increase with the length of the alkyl chain. The specific objectives of this investigation were to: (*a*) synthesize a series of even-numbered, normal alkyl ethers (C_2–C_{14}) of *p*-[*N*,*N*-bis(2-chloroethyl)amino]phenol, (*b*) determine the acute toxicity as measured by the LD_{50} for each compound studied, and (*c*) determine the effect of each compound on the prolongation of life of L-1210 leukemic mice.

The compounds evaluated in this project were synthesized using Scheme I.

EXPERIMENTAL

Chemistry[1]—p-N,N-*Bis(2-hydroxyethyl)aminophenol* (*I*)—Twenty grams (0.18 mole) of *p*-aminophenol was added to a flask containing 200 ml of absolute methanol and equipped with a reflux condenser. The solution was stirred mechanically until dissolution occurred and then was cooled to 0°. Twenty grams (0.45 mole) of ethylene oxide was added to the cold reaction mixture. Stirring was continued and the reaction was allowed to reach room temperature. The resulting crystals were filtered and recrystallized from ethanol. The product had a melting point of 139.5–141° compared with the reported value of 140° (7).

[1] All IR spectral data were obtained from chloroform solutions of the derivatives on sodium chloride plates using a Beckman Model Acculab-4 spectrophotometer. Nuclear magnetic resonance spectra were obtained from deuterated chloroform solutions of the derivatives using a Hitachi-Perkin-Elmer model R-24 high resolution spectrometer with tetramethylsilane as the internal standard. The reported melting points were obtained using a Thomas Hoover capillary melting point apparatus and are uncorrected. The reported content of hydrogen, carbon, and nitrogen were obtained from analyses performed by Galbraith Laboratories, Knoxville, Tenn. All lyophilization was accomplished using a VirTis Model 10 freeze-dryer.

0022-3549/82/0500-0565$01.00/0

Table I—Physical Data and Elemental Analysis for the *p-N,N*-Bis(2-hydroxyethyl)aminophenyl Alkyl Ethers

Compound	R	Yield, %	Melting Point	Formula	Analysis, % Calc.	Found
II*a*	$CH_3—CH_2—$	82	34–35°	$C_{12}H_{19}NO_3$	C 64.00	63.83
					H 8.44	8.39
					N 6.22	6.33
II*b*	$CH_3—(CH_2)_2—CH_2—$	60.5	41–42°	$C_{14}H_{23}NO_3$	C 66.40	66.29
					H 9.09	9.23
					N 5.53	5.43
II*c*	$CH_3—(CH_2)_4—CH_2—$	75	43–44°	$C_{16}H_{27}NO_3$	C 68.33	68.39
					H 9.61	9.85
					N 4.98	4.74
II*d*	$CH_3—(CH_2)_6—CH_2—$	63	47.5–49°	$C_{18}H_{31}NO_3$	C 69.90	70.12
					H 10.03	10.14
					N 4.53	4.38
II*e*	$CH_3—(CH_2)_8—CH_2—$	69	49.5–51°	$C_{20}H_{35}NO_3$	C 71.22	71.00
					H 10.38	10.56
					N 4.15	4.03
II*f*	$CH_3—(CH_2)_{10}—CH_2—$	82	55–56.5°	$C_{22}H_{39}NO_3$	C 72.33	72.49
					H 10.68	10.82
					N 3.83	3.74
II*g*	$CH_3—(CH_2)_{12}—CH_2—$	45	58–59°	$C_{24}H_{43}NO_3$	C 73.28	73.02
					H 10.94	10.87
					N 3.56	3.22

Table II—Physical Data and Elemental Analysis for the *p-N,N*-Bis(2-chloroethyl)aminophenyl Alkyl Ethers

Compound	R	Yield, %	Melting Point	Formula	Analysis, % Calc.	Found
III*a*	$CH_3—CH_2—$	65	Oil	$C_{12}H_{17}Cl_2NO$	C 54.98	54.96
					H 6.49	6.29
					N 5.35	5.27
III*b*	$CH_3—(CH_2)_2—CH_2—$	53	Oil	$C_{14}H_{21}Cl_2NO$	C 57.95	58.14
					H 7.24	7.47
					N 4.83	4.81
III*c*	$CH_3—(CH_2)_4—CH_2—$	63	Oil	$C_{16}H_{25}Cl_2NO$	C 60.40	60.50
					H 7.86	7.80
					N 4.40	4.23
III*d*	$CH_3—(CH_2)_6—CH_2—$	49	Oil	$C_{18}H_{29}Cl_2NO$	C 62.45	62.44
					H 8.38	8.50
					N 4.05	3.99
III*e*	$CH_3—(CH_2)_8—CH_2—$	89	35.5–36.5°	$C_{20}H_{33}Cl_2NO$	C 64.19	64.29
					H 8.83	9.00
					N 3.74	3.62
III*f*	$CH_3—(CH_2)_{10}—CH_2—$	55	44–45°	$C_{22}H_{37}Cl_2NO$	C 65.69	65.54
					H 9.21	9.30
					N 3.48	3.39
III*g*	$CH_3—(CH_2)_{12}—CH_2—$	59	Oil	$C_{24}H_{41}Cl_2NO$	C 66.98	66.73
					H 9.53	9.79
					N 3.26	2.92

Synthesis of p-N,N-*Bis(2-hydroxyethyl)aminophenyl Alkyl Ethers* (*II a–g*)—Ten grams (0.05 mole) of I was dissolved in a reaction flask containing 300 ml of ethanol, 200 ml of water, and 7 g of KOH. This mixture was stirred and heated to reflux. An excess (0.15 mole) of the appropriate alkyl bromide (ethyl, butyl, hexyl, octyl, decyl, dodecyl, or tetradecyl) was introduced and reflux was continued for 24 hr. Excess solvent was removed *in vacuo* and the residue was mixed with ether. The ether solution was filtered to remove potassium bromide. The ethereal filtrate was extracted three times with 10% KOH solution to remove unreacted starting material. The ether layer was evaporated *in vacuo*. With the exception of the butyl, octyl, and tetradecyl derivatives, solid products suitable for analysis were obtained after cooling to 0°. The butyl and octyl derivatives were recrystallized from a methanol–water system, and lyophilized to yield analytically pure product. The tetradecyl derivative was purified by recrystallization from an acetone–water system. The new compounds were characterized by physical data (Table I) and IR and NMR spectra.

Synthesis of p-N,N-*Bis(2-chloroethyl)aminophenyl Alkyl Ethers* (*III* a–g)—Three-tenths of a mole of the appropriate derivative of II was dissolved in a minimum amount of chloroform. Five milliliters of absolute ethanol, then 1 ml of thionyl chloride, was added during continuous stirring. The reaction mixture was cooled to 0° on dry ice, 10 ml of thionyl chloride was added and the solution was allowed to reach room temperature. The mixture was concentrated *in vacuo* to remove solvent and excess thionyl chloride. Upon standing, solid products were obtained for the decyl and dodecyl derivatives. These products were recrystallized from an ethanol–water system and light-colored crystals were obtained. The ethyl, butyl, hexyl, and octyl derivatives were initially isolated as the hydrochloride salt. These products were converted to the free base by mixing with 10% NaOH and extracting with ether. Evaporation of the ether yielded oils suitable for analysis for the ethyl and hexyl derivatives. The butyl and octyl derivatives were recrystallized from an acetone–water system and lyophilized to yield analytical samples. The tetradecyl derivative was initially isolated as the free base and purified by recrystallization from an ethanol–water system. The ethyl, butyl, and octyl derivatives existed as black crystalline solids below 15° and as oils at room temperature. The hexyl derivative was an oil at 0° and room temperature. The tetradecyl derivative existed as a brown semi-solid below 15° and as an oil at room temperature. The final products were characterized by physical data (Table II) and IR and NMR spectra.

Biological Evaluation—*Test Animals*—DBA/2 mouse strain[2], BDF_1 mouse strain[2], HA/ICR mouse strain[3], and L-1210 leukemic mice (tumor source)[4] were used.

Instruments—The necessary equipment included an electronic cell counter[5], a channelizer[5], a dilutor[5], an *x-y* recorder[5], a hemocytometer[6], and a microscope[7].

Materials—Counting diluent[5], red blood cell-lysing reagent[5], crystal violet[8], Giemsa stain[9], isotonic diluting solution[10], trypan blue[11], and

[2] Jackson Laboratories.
[3] ARS/Sprague-Dawley.
[4] National Cancer Institute, National Institutes of Health, Bethesda, Md.
[5] Model ZB counter and accessories, Coulter Electronics.
[6] American Optical Co.
[7] Model RA, Carl Zeis, West Germany.
[8] Matheson, Coleman & Bell.
[9] Fisher Scientific Co.
[10] Microbiological Assoc.
[11] Allied Chemical Co.

Table III—Summary of the Bioevaluation Data for the *p*-*N*,*N*-Bis(2-chloroethyl)aminophenyl Alkyl Ethers

Compound Number (Derivative)	LD_{50}[a], μmoles/kg	Dose[a], mg/kg	Number of Animals	Mean Survival Day (±*SE*)	Control Mean Survival Day (±*SE*)	T/C, %[b]
III*a* (Ethyl)	1640	25	6	9.83 (0.31)	8.50 (0.34)	116
		50	6	10.00 (0.68)	8.50 (0.34)	118
		75	6	9.33 (0.42)	8.50 (0.34)	110
		100	6	10.67 (0.21)	8.50 (0.34)	126
		125	6	10.17 (0.17)	8.50 (0.34)	120
		150	6	9.33 (0.92)	8.50 (0.34)	110
		200	6	7.33 (0.67)	8.50 (0.34)	86
III*b* (Butyl)	714	25	6	9.50 (0.34)	9.00 (0.37)	106
		50	6	10.00 (0.63)	9.00 (0.37)	110
		75	5	11.40 (0.51)	9.00 (0.37)	127
		100	5	11.60 (0.87)	9.00 (0.37)	129
		125	6	12.50 (0.56)	9.00 (0.37)	139
		150	6	12.83 (0.54)	9.00 (0.37)	143
		200	6	6.50 (0.34)	9.00 (0.37)	72
III*c* (Hexyl)	1069	25	6	10.00 (0.52)	9.33 (0.21)	107
		50	6	10.00 (0.52)	9.33 (0.21)	107
		75	6	10.50 (0.43)	9.33 (0.21)	113
		100	6	10.17 (0.48)	9.33 (0.21)	109
		125	6	10.67 (0.42)	9.33 (0.21)	114
		150	6	9.33 (0.21)	9.33 (0.21)	100
		200	6	9.83 (0.31)	9.33 (0.21)	105
III*d* (Octyl)	>1156	25	5	9.20 (0.66)	7.83 (0.31)	118
		50	6	9.67 (0.33)	7.83 (0.31)	123
		75	6	9.83 (0.40)	7.83 (0.31)	126
		100	5	10.20 (0.37)	7.83 (0.31)	130
		125	6	12.33 (0.80)	9.00 (0.37)	137
		150	6	10.83 (0.79)	9.00 (0.37)	120
		200	6	10.00 (0.37)	9.00 (0.37)	111
III*e* (Decyl)	>1070	25	6	9.33 (0.42)	9.00 (0.37)	104
		50	6	10.33 (0.49)	9.00 (0.37)	115
		75	6	11.67 (0.61)	9.00 (0.37)	130
		100	6	13.17 (0.70)	9.00 (0.37)	146
		125	6	14.67 (0.61)	9.00 (0.37)	163
		150	6	14.50 (0.80)	9.00 (0.37)	161
		200	6	7.67 (0.33)	9.00 (0.37)	85
III*f* (Dodecyl)	>995	25	6	12.33 (0.42)	9.00 (0.37)	137
		50	5	12.60 (0.51)	9.00 (0.37)	140
		75	6	13.83 (0.48)	9.00 (0.37)	154
		100	6	12.33 (0.56)	9.00 (0.37)	137
		125	6	11.00 (0.58)	9.00 (0.37)	122
		150	6	9.67 (0.44)	9.00 (0.37)	107
		200	6	9.83 (0.31)	9.00 (0.37)	109
III*g* (Tetradecyl)	>1395	25	6	10.17 (0.31)	9.00 (0.37)	113
		50	5	10.40 (0.25)	9.00 (0.37)	116
		75	6	11.33 (0.33)	9.00 (0.37)	126
		100	5	12.20 (0.37)	9.00 (0.37)	136
		125	5	11.40 (0.51)	9.00 (0.37)	127
		150	6	11.00 (0.58)	9.00 (0.37)	122
		200	5	9.00 (0.37)	9.00 (0.37)	100

[a] Administered in propylene glycol. [b] The T/C% value represents the ratio of the sum of the number of days the animals in a treated group survived (T) to the sum of the number of days the animals in the control group survived (C) multiplied by 100.

Wright's stain[8] were obtained commercially. The ether derivatives of III were prepared in the laboratory, and their physical and analytical data are reported in Table III.

Pretoxicity Testings—Groups of two healthy (HA/ICR) male mice were injected intraperitoneally with 500[12], 100, 10, 1, or 0.1 mg of test drug/kg in propylene glycol to evaluate the dose range for the pharmacological screen and LD_{50} determination.

Pharmacological Screen and LD_{50} Evaluation—Five groups, each with six HA/ICR mice, were selected. A gross screen was conducted for acute toxicity, and results were recorded during the 3 hr following injection. The mice were observed and weighed every day for 21 days, and the mortalities were recorded daily. A linear regression and correlation coefficient program (8) and a graphic method (9) were applied to determine the LD_{50} for each drug test.

Transplantation Procedures—Sterile equipment was used under aseptic conditions. DBA/2 (6–9 week old) host mice bearing L-1210 leukemia for 6–7 days were the tumor donors, and were sacrificed under ether vapor, immersed in 0.1% benzalkonium chloride, and swabbed with 70% ethanol. A 10-ml hypodermic syringe equipped with a 20-gauge needle (flushed with heparin at 1000 USP U/ml) was inserted into the abdominal cavity of the mouse and aspirated to obtain the lymphoid leukemia L-1210 cells (10). The leukemia cells were placed in a container over ice. One drop of ascitic fluid was prepared for microscope examination. Cell morphology was determined by staining with Wright's or Giemsa stain to differentiate the leukocytes and lymphoblasts (11). Ascitic fluid containing at least 95% lymphoblasts or lymphocytes was used for transplantation in DBA/2 mice for tumor maintenance and in BDF_1 mice for antileukemic studies. Cell counts and viability were determined using an electronic counter and a hemocytometer, respectively, as described in a recent report (3). The inoculum contained 1×10^5 cells in 0.1 ml. A 1-ml tuberculin syringe equipped with a 25-gauge needle was used to inject 0.1 ml of diluted ascitic L-1210 cells into the DBA/2 or BDF_1 mice. All inoculations of L-1210 cells were made within 1 hr after cell removal from the host mouse to ensure a viable transplant.

In Vivo *Determination of Antileukemic Activities by Survival Times*—On Day 0, the tumor was implanted into BDF_1 male mice; the number of survivors was recorded daily during the test period. The doses used were below the LD_{10} value of each test drug to minimize drug toxicity (12). The test solutions were injected within 15 min after preparation at a dose volume not to exceed 0.01 ml/g of body weight. The test drug solutions were administered intraperitoneally to each test group on Days

[12] Compounds III*d*, III*e*, and III*f* were limited by solubility to an upper dosage of 400 mg/kg.

2 and 5. The experiment was evaluated on the day of death for the last animal in a test group or after 30 days (12).

RESULTS AND DISCUSSION

Chemistry—The starting material (I) was obtained in 90% yields using a modification of the condensation of ethylene oxide with *p*-aminophenol reported previously (7). The ether intermediates (II*a–g*) were then obtained by reacting I with the appropriate alkyl bromide. The conditions for the Williamson synthesis of *p*-nitrophenyl ethers (13) were modified to produce II*a–g*. Because I has a higher pKa than *p*-nitrophenol, more base and a more polar solvent system were used to enhance the formation of the phenolate nucleophile. The reaction proceeded *via* a S_N2 displacement of the bromide by the phenolate nucleophile (14).

The primary isolation and purification step was the formation of the potassium salt of unreacted I and subsequent extraction with ether. Theoretical yields for II*a–g* ranged from 45 to 82% (Table I). The alkyl ethers of I were stable, low-melting solids with solubility in a variety of organic solvents. The IR spectra of these intermediates exhibited characteristic —OH absorption as a broad band between 3600 and 3100 cm^{-1}. The sharp absorption at 1240 cm^{-1} confirmed the presence of the ether function. The aliphatic and aromatic C—H stretching frequencies appeared in the region of 3150–2850 cm^{-1}. The intensity of the aliphatic absorption varied with the size of the alkyl substituent. The aromatic ring stretching occurred at 1520 cm^{-1}. The NMR spectra of these compounds, using $CDCl_3$ as a solvent, contained four distinct absorption patterns. A triplet (2H) (quartet for the ethyl derivative, II*a*) centered at 3.9 ppm, was observed for the methylene group adjacent to the ether oxygen. The remaining methylene groups in the alkyl side chain appeared, in the range of 1.6 to 2.0 ppm, as a multiplet for II*b* and II*c* and as a sharp singlet for the remaining homologs. The terminal methyl group absorbed as a triplet (3H) in the region of 1.2–1.4 ppm. The ethylene bridge yielded two triplets integrating for four protons each. The triplet at 3.3 ppm was assigned to the $—CH_2—$ groups adjacent to the nitrogen and the triplet at 3.7 ppm was assigned to the $—CH_2—$group adjacent to the —OH group. The alcoholic proton absorption appeared as a singlet (2H) in the region of 4.0–4.3 ppm. The four aromatic protons appeared as a typical A_2B_2 multiplet centered in the region of 6.6–6.7 ppm. Analytical purity was determined by elemental analysis (Table I).

The final products (III*a–g*) were obtained using thionyl chloride as the chlorinating agent. The vigor of the reaction was controlled by cooling to <0° and allowing the reaction mixture to slowly reach room temperature. The generation of hydrochloride gas in this reaction led to the formation and isolation of the hydrochloride salts of the ethyl, butyl, hexyl, and octyl derivatives. The IR spectra of the hydrochloride salts contained a strong absorption at 2400 cm^{-1} and medium absorptions at 3620 and 3650 cm^{-1}, confirming the presence of a tertiary amine salt. The NMR spectra of the hydrochloride salts contained a singlet at 7.0 ppm (N—H) and the aromatic protons displayed an AA'BB' pattern which appeared as two doublets centered at 6.8 and 7.7 ppm. Following neutralization with base, the N—H absorptions disappeared from both the IR and NMR spectra and the NMR pattern for the aromatic protons merged into a typical A_2B_2 multiplet centered at 6.6 ppm.

All of the final products (III*a–g*) were isolated and characterized as their free bases in yields ranging from 49 to 89%. The hydrochloride salts were neutralized by extracting ether solutions of the salts with 10% NaOH. Compounds III*a* and III*c* were isolated as oils suitable for analysis following the evaporation of the ether solution. All other products were recrystallized to yield analytically pure oils or solids (Table II). (Compounds III*b* and III*d* were also lyophilized.) The final products (III*a–g*) demonstrated solubility in ether, chloroform, ethanol, and methanol and were nearly insoluble in water. Upon chlorination of the dihydroxy intermediates (II*a–g*), the broad free OH band on the IR spectra disappeared and absorptions characteristic of halogenated hydrocarbons appeared at 1220 and 750 cm^{-1}. The NMR spectra of the nitrogen mustard derivatives (III*a–g*) demonstrated the loss of 2—OH protons. In addition the eight ethylene protons appeared as a sharp singlet in the region of 3.6–3.9 ppm. Other absorptions in the NMR spectra of compounds III*a–g* appeared as described for their precursors (II*a–g*). The purity of the nitrogen mustard products (III*a–g*) was determined by elemental analysis (Table II).

Biological Evaluation—The LD_{50} values for compounds III*a–c* were obtained using probit analysis and linear regression (Table III) (8, 9). Determination of exact LD_{50} values for compounds III*d–g* was restricted by the limited solubility of those compounds in propylene glycol. The LD_{50} values for compounds III*d–g* presented in Table III represent the highest doses that could be administered in propylene glycol. No deaths occurred at those dose levels, therefore, the LD_{50} values are considerably higher. As anticipated, the ether derivatives of phenol mustard demonstrated much less toxicity than reported for phenol mustard or for its unhindered benzoate and fatty acid esters (1, 3). In this series the butyl derivative (III*b*) exhibited the highest toxicity, 714 μm/kg, compared to a 74.8–162.4 μm/kg[13] range for the phenol mustard (1). The remaining compounds, III*a* and III*c–g*, demonstrated LD_{50} values comparable to, or higher than, cyclophosphamide, 1078 μm/kg in HA/ICR mice, an effective antineoplastic agent that is less toxic than clinically useful nitrogen mustards (3).

Table IV—Summary: Optimum Dose and Survival Time for the *p*-*N*,*N*-bis(2-chloroethyl)aminophenyl Alkyl Ethers

Compound Number (Derivative)	Optimum Dose		T/C, %
	mg/kg	μmoles/kg	
III*a* (Ethyl)	100	382	126
III*b* (Butyl)	150	517	143
III*c* (Hexyl)	125	393	114
III*d* (Octyl)	125	361	137
III*e* (Decyl)	125	335	163
III*f* (Dodecyl)	75	187	154
III*g* (Tetradecyl)	100	233	136

The effect of compounds III*a–g* on the prolongation of life of L-1210 leukemic mice was determined. A comparison of the survival of treated groups (T) to untreated control groups (C) was performed. A calculated T/C ratio ≥125% implied that the drug treatment significantly increased the life span. Table III summarizes the T/C% survivals produced at each dose level for each compound, the number of animals used per dosage level, and the mean survival for each animal group. The doses producing optimum survival for each compound are summarized in Table IV.

The decyl derivative (III*e*) produced the highest mean survival time (T/C% values) in the series, 163% at a dose of 335 μm/kg (125 mg/kg) as illustrated in Table IV. The ethyl derivative (III*a*) demonstrated the lowest significant optimum T/C% values in this series, 126% at 382 μm/kg (100 mg/kg). This was the only dose level at which significant survival (≥125%) was obtained for the ethyl derivative (III*a*). The butyl (III*b*), decyl (III*e*), and dodecyl (III*f*) derivatives produced significant survival at four dosage levels each and the octyl (III*d*) and tetradecyl (III*g*) derivatives at three dosage levels. Only the hexyl derivative (III*c*) failed to produce a significant T/C% value at any of the dosage levels investigated.

The differences in the observed toxicities and T/C% survival times may possibly be attributed to differences in both the metabolism and lipophilic character of the compounds studied. The ethyl ether of *p*-nitrophenol has been shown to undergo *O*-dealkylation both at a rapid rate *in vitro* and to a great extent (78%) *in vivo* (5). Conjugation of the phenolic mustard resulting from the *O*-dealkylation of III*a* would result in enhanced elimination, lower toxicity, and reduced antineoplastic activity. The butyl ether of *p*-nitrophenol has been shown to undergo *O*-dealkylation at a much slower rate and to a lesser extent than the ethyl ether (5). The (ω-1)-hydroxylation pathway has been reported to be a primary metabolic route for the butyl ether of *p*-nitrophenol in rabbits (6). Longer chain alkyl ethers of *p*-nitrophenol undergo *O*-dealkylation at a negligible rate and to a lesser extent *in vivo* and the (ω-1)-hydroxylation pathway is probably most important in their metabolism (5, 6). The lower LD_{50} value and the activity observed against L-1210 mouse leukemia for the butyl derivative (III*b*) may be attributed to the role of these metabolic pathways, as well as the solubility of the parent compound and the (ω-1)-hydroxy metabolite. The observation of lower toxicity for the longer chain ether derivatives, hexyl (III*c*)–tetradecyl (III*g*), is consistent with the expectation of negligible *O*-dealkylation for any of them. For the octyl (III*d*)–tetradecyl (III*g*) derivatives, the lower toxicity, coupled with an increase in the lipid solubility of both the parent compounds and their (ω-1)-hydroxy metabolites, should contribute to the observed antileukemic activity.

The lack of a significant prolongation of life in leukemic mice, at any of the dosage levels evaluated for the hexyl derivative (III*c*), cannot be explained on the basis of expected metabolism nor by the anticipated solubility properties of the compound and its (ω-1)-hydroxy metabolite. The role played by a complex combination of these factors may be important and could serve as the basis for a future investigation. An additional possibility is that in an aqueous solution of these compounds, a freely rotating alkyl sidechain could fold back and assume a conformation that would allow interaction between the sidechain and the ring and/or

[13] Unpublished data from these laboratories.

the bis(2-chloroethyl)amino moiety. In an attempt to gain further insight into this consideration, stereomodels and atomic models were constructed for the final products (IIIa–g). From both model types it appeared that the hexyl side chain was the appropriate length to allow the terminal methyl group to sterically affect the nitrogen atom. The ethyl and butyl side chains were too short for such an interaction and side chains longer than hexyl appeared subject to repulsion by the chloroethyl groups, thus, reducing their steric interaction with the nitrogen atom. Such an interaction between the nitrogen atom and the hexyl side chain could sterically hinder the participation of the nitrogen atom in the formation of the aziridinium ion intermediate. Such an interaction could reduce the reactivity of the hexyl derivative (IIIc) which would in turn reduce its antileukemic effectiveness and contribute to its relatively low toxicity.

REFERENCES

(1) S. Vickers, P. Hebborn, J. F. Moran, and D. J. Triggle, *J. Med. Chem.*, **12**, 491 (1969).

(2) P. Hebborn and J. F. Danielli, *Biochem. Pharmacol.*, **1**, 19 (1958).

(3) C. T. Bauguess, Y. Y. Lee, J. W. Kosh, and J. E. Wynn, *J. Pharm. Sci.*, **70**, 46 (1981).

(4) T. A. Connors and M. E. Whisson, *Nature*, **210**, 866 (1966).

(5) R. E. McMahon, H. W. Culp, and J. Mills, *J. Med. Chem.*, **6**, 343 (1963).

(6) H. Tsukamoto, H. Yoshimura, and H. Tsuyi, *Chem. Pharm. Bull.*, **12**, 987 (1964).

(7) W. C. J. Ross and G. P. Warwick, *J. Chem. Soc.*, **1955**, 3110.

(8) "Manual No. 4022N" (model 1766), Monroe Calculator Co., Morristown, N.J., 1970.

(9) L. C. Miller and M. L. Tainter, *Proc. Soc. Exp. Biol. Med.*, **57**, 261 (1944).

(10) *Jax Notes*, No. 410, Jackson Mice Co., Bar Harbor, Me., 1972.

(11) A. Joseph, E. Morholt, and P. F. Brandwein, "A Sourcebook for the Biological Sciences," Harcourt, Brace & World, New York, N. Y., 1966, p. 117.

(12) B. J. Abbott, *Cancer Chemother. Rep., Part 3*, **3**, 2 (1972).

(13) A. Spiegel and H. Sabbath, *Chem. Ber.* **34**, 1937 (1905).

(14) R. Morrison and R. Boyd, "Organic Chemistry," Allyn and Bacon, Boston, Mass., 1966, p. 471.

Comparison of the Absorption, Excretion, and Metabolism of Suxibuzone and Phenylbutazone in Humans

YUKIHIRO YASUDA *x, TAKASHI SHINDO *, NARUO MITANI *, NAOBUMI ISHIDA *, FUMITOSHI OONO ‡, and TAKAMASA KAGEYAMA §

Received March 9, 1981, from the * *Research Laboratory, Taiho Pharmaceutical Co., Ltd., Kawauchi-cho, Tokushima, 771-01, Japan*, ‡ the *Second Department of Internal Medicine, School of Medicine, Kouchi University, Okatoyo-machi, Nangoku-shi, Kouchi, 781-51, Japan*, and the § *Department of Orthopedic Surgery, Sagamihara National Hospital, Kamitsuruma, Sagamihara-shi, 228, Japan.* Accepted for publication August 21, 1981.

Abstract □ The absorption, excretion, and metabolism of a single oral dose of suxibuzone, a new nonsteroidal anti-inflammatory agent, in healthy male volunteers were compared with those of phenylbutazone. After oral administration of either suxibuzone or phenylbutazone, phenylbutazone, oxyphenbutazone, and γ-hydroxyphenylbutazone were found in the plasma; phenylbutazone was the main metabolite of suxibuzone and phenylbutazone. In the urine, *p*-γ-dihydroxyphenylbutazone and several glucuronide conjugates also were found. Spectrometric and/or enzymatic analysis showed that these glucuronide conjugates were suxibuzone glucuronide, 4-hydroxymethylphenylbutazone glucuronide, 4-hydroxymethyloxyphenbutazone glucuronide, oxyphenbutazone glucuronide, and phenylbutazone glucuronides (two types: *O*-glucuronide and C-4-glucuroxide) after suxibuzone administration, and oxyphenbutazone glucuronide and phenylbutazone glucuronide after phenylbutazone administration. The conjugates specific to suxibuzone administration, suxibuzone glucuronide, 4-hydroxymethylphenylbutazone glucuronide, and 4-hydroxymethyloxyphenbutazone glucuronide, were excreted in the first 6 hr urine. These findings and the pharmacokinetics of these metabolites in the plasma and urine show that suxibuzone is a prodrug of phenylbutazone.

Keyphrases □ Suxibuzone—*in vivo* absorption, excretion, and metabolism compared to phenylbutazone, humans □ Phenylbutazone—*in vivo* absorption, excretion, and metabolism compared to suxibuzone, human □ Pharmacokinetics—suxibuzone and phenylbutazone, *in vivo* humans □ Anti-inflammatory agents—suxibuzone and phenylbutazone, *in vivo*, humans

Suxibuzone is a derivative of phenylbutazone, in which the proton at the C-4-position of the pyrazolidine ring is replaced by a β-carboxypropionyloxymethyl group. The outstanding feature of the drug is that it has extremely low ulcerogenicity (1, 2) although its anti-inflammatory, analgesic, and antipyretic properties are as strong as those of an equimolar dosage of phenylbutazone (3).

This feature of suxibuzone can be understood by comparing the biological fates of suxibuzone and phenylbutazone; however, there have been no studies on metabolism of suxibuzone in humans. Therefore, the present study compared the metabolic pathways and pharmacokinetics of suxibuzone and phenylbutazone in humans.

EXPERIMENTAL

Materials—Suxibuzone[1], phenylbutazone[1], oxyphenbutazone[1], and γ-hydroxyphenylbutazone[1] were used as received. 4-Hydroxymethylphenylbutazone[2] was synthesized and purified.

Chromatography—HPLC was performed using a μ-Bondapak C_{18} column (30 × 0.4-cm i.d.)[3], which was fitted with a 254-nm UV detector. For low-resolution liquid chromatography, a column (20 × 2.5 cm) packed with Amberlite XAD-2 resin (coarse grade 35–50 mesh)[4] or Dowex-1 resin (200–400 mesh)[5] was used.

GC was carried out under the following conditions: column 5% Silicon GE SE-30 on Chromosorb W AW-DMCS 60–80 mesh[6], 2 m × 3-mm i.d.; column temperature, 275°; nitrogen flow rate, 60 ml/min; and detector, flame ion detector.

TLC was carried out using commercial silica gel plates[7] with the following solvent systems (SS):

[1] S. A. Esteve Laboratory, Barcelona, Spain.
[2] Taiho Pharmaceutical Co., Research Laboratory, Tokushima, Japan.
[3] Waters Associates, Milford, Mass.
[4] Rohm and Haas Co.
[5] Dow Chemical Co.
[6] Shimadzu, Kyoto, Japan.
[7] Kieselgel 60 F_{254}, Precoated, 0.25-mm thick, Merck, West Germany.

0022-3549/82/0500-0565$01.00/0

the bis(2-chloroethyl)amino moiety. In an attempt to gain further insight into this consideration, stereomodels and atomic models were constructed for the final products (IIIa–g). From both model types it appeared that the hexyl side chain was the appropriate length to allow the terminal methyl group to sterically affect the nitrogen atom. The ethyl and butyl side chains were too short for such an interaction and side chains longer than hexyl appeared subject to repulsion by the chloroethyl groups, thus, reducing their steric interaction with the nitrogen atom. Such an interaction between the nitrogen atom and the hexyl side chain could sterically hinder the participation of the nitrogen atom in the formation of the aziridinium ion intermediate. Such an interaction could reduce the reactivity of the hexyl derivative (IIIc) which would in turn reduce its antileukemic effectiveness and contribute to its relatively low toxicity.

REFERENCES

(1) S. Vickers, P. Hebborn, J. F. Moran, and D. J. Triggle, *J. Med. Chem.*, **12**, 491 (1969).

(2) P. Hebborn and J. F. Danielli, *Biochem. Pharmacol.*, **1**, 19 (1958).

(3) C. T. Bauguess, Y. Y. Lee, J. W. Kosh, and J. E. Wynn, *J. Pharm. Sci.*, **70**, 46 (1981).

(4) T. A. Connors and M. E. Whisson, *Nature*, **210**, 866 (1966).

(5) R. E. McMahon, H. W. Culp, and J. Mills, *J. Med. Chem.*, **6**, 343 (1963).

(6) H. Tsukamoto, H. Yoshimura, and H. Tsuyi, *Chem. Pharm. Bull.*, **12**, 987 (1964).

(7) W. C. J. Ross and G. P. Warwick, *J. Chem. Soc.*, **1955**, 3110.

(8) "Manual No. 4022N" (model 1766), Monroe Calculator Co., Morristown, N.J., 1970.

(9) L. C. Miller and M. L. Tainter, *Proc. Soc. Exp. Biol. Med.*, **57**, 261 (1944).

(10) *Jax Notes*, No. 410, Jackson Mice Co., Bar Harbor, Me., 1972.

(11) A. Joseph, E. Morholt, and P. F. Brandwein, "A Sourcebook for the Biological Sciences," Harcourt, Brace & World, New York, N. Y., 1966, p. 117.

(12) B. J. Abbott, *Cancer Chemother. Rep., Part 3*, **3**, 2 (1972).

(13) A. Spiegel and H. Sabbath, *Chem. Ber.* **34**, 1937 (1905).

(14) R. Morrison and R. Boyd, "Organic Chemistry," Allyn and Bacon, Boston, Mass., 1966, p. 471.

Comparison of the Absorption, Excretion, and Metabolism of Suxibuzone and Phenylbutazone in Humans

YUKIHIRO YASUDA *x, TAKASHI SHINDO *, NARUO MITANI *, NAOBUMI ISHIDA *, FUMITOSHI OONO ‡, and TAKAMASA KAGEYAMA §

Received March 9, 1981, from the * *Research Laboratory, Taiho Pharmaceutical Co., Ltd., Kawauchi-cho, Tokushima, 771-01, Japan*, ‡ the *Second Department of Internal Medicine, School of Medicine, Kouchi University, Okatoyo-machi, Nangoku-shi, Kouchi, 781-51, Japan*, and the § *Department of Orthopedic Surgery, Sagamihara National Hospital, Kamitsuruma, Sagamihara-shi, 228, Japan.* Accepted for publication August 21, 1981.

Abstract □ The absorption, excretion, and metabolism of a single oral dose of suxibuzone, a new nonsteroidal anti-inflammatory agent, in healthy male volunteers were compared with those of phenylbutazone. After oral administration of either suxibuzone or phenylbutazone, phenylbutazone, oxyphenbutazone, and γ-hydroxyphenylbutazone were found in the plasma; phenylbutazone was the main metabolite of suxibuzone and phenylbutazone. In the urine, *p*-γ-dihydroxyphenylbutazone and several glucuronide conjugates also were found. Spectrometric and/or enzymatic analysis showed that these glucuronide conjugates were suxibuzone glucuronide, 4-hydroxymethylphenylbutazone glucuronide, 4-hydroxymethyloxyphenbutazone glucuronide, oxyphenbutazone glucuronide, and phenylbutazone glucuronides (two types: *O*-glucuronide and C-4-glucuroxide) after suxibuzone administration, and oxyphenbutazone glucuronide and phenylbutazone glucuronide after phenylbutazone administration. The conjugates specific to suxibuzone administration, suxibuzone glucuronide, 4-hydroxymethylphenylbutazone glucuronide, and 4-hydroxymethyloxyphenbutazone glucuronide, were excreted in the first 6 hr urine. These findings and the pharmacokinetics of these metabolites in the plasma and urine show that suxibuzone is a prodrug of phenylbutazone.

Keyphrases □ Suxibuzone—*in vivo* absorption, excretion, and metabolism compared to phenylbutazone, humans □ Phenylbutazone—*in vivo* absorption, excretion, and metabolism compared to suxibuzone, human □ Pharmacokinetics—suxibuzone and phenylbutazone, *in vivo* humans □ Anti-inflammatory agents—suxibuzone and phenylbutazone, *in vivo*, humans

Suxibuzone is a derivative of phenylbutazone, in which the proton at the C-4-position of the pyrazolidine ring is replaced by a β-carboxypropionyloxymethyl group. The outstanding feature of the drug is that it has extremely low ulcerogenicity (1, 2) although its anti-inflammatory, analgesic, and antipyretic properties are as strong as those of an equimolar dosage of phenylbutazone (3).

This feature of suxibuzone can be understood by comparing the biological fates of suxibuzone and phenylbutazone; however, there have been no studies on metabolism of suxibuzone in humans. Therefore, the present study compared the metabolic pathways and pharmacokinetics of suxibuzone and phenylbutazone in humans.

EXPERIMENTAL

Materials—Suxibuzone[1], phenylbutazone[1], oxyphenbutazone[1], and γ-hydroxyphenylbutazone[1] were used as received. 4-Hydroxymethylphenylbutazone[2] was synthesized and purified.

Chromatography—HPLC was performed using a μ-Bondapak C_{18} column (30 × 0.4-cm i.d.)[3], which was fitted with a 254-nm UV detector. For low-resolution liquid chromatography, a column (20 × 2.5 cm) packed with Amberlite XAD-2 resin (coarse grade 35–50 mesh)[4] or Dowex-1 resin (200–400 mesh)[5] was used.

GC was carried out under the following conditions: column 5% Silicon GE SE-30 on Chromosorb W AW-DMCS 60–80 mesh[6], 2 m × 3-mm i.d.; column temperature, 275°; nitrogen flow rate, 60 ml/min; and detector, flame ion detector.

TLC was carried out using commercial silica gel plates[7] with the following solvent systems (SS):

[1] S. A. Esteve Laboratory, Barcelona, Spain.
[2] Taiho Pharmaceutical Co., Research Laboratory, Tokushima, Japan.
[3] Waters Associates, Milford, Mass.
[4] Rohm and Haas Co.
[5] Dow Chemical Co.
[6] Shimadzu, Kyoto, Japan.
[7] Kieselgel 60 F_{254}, Precoated, 0.25-mm thick, Merck, West Germany.

0022-3549/82/0500-0565$01.00/0

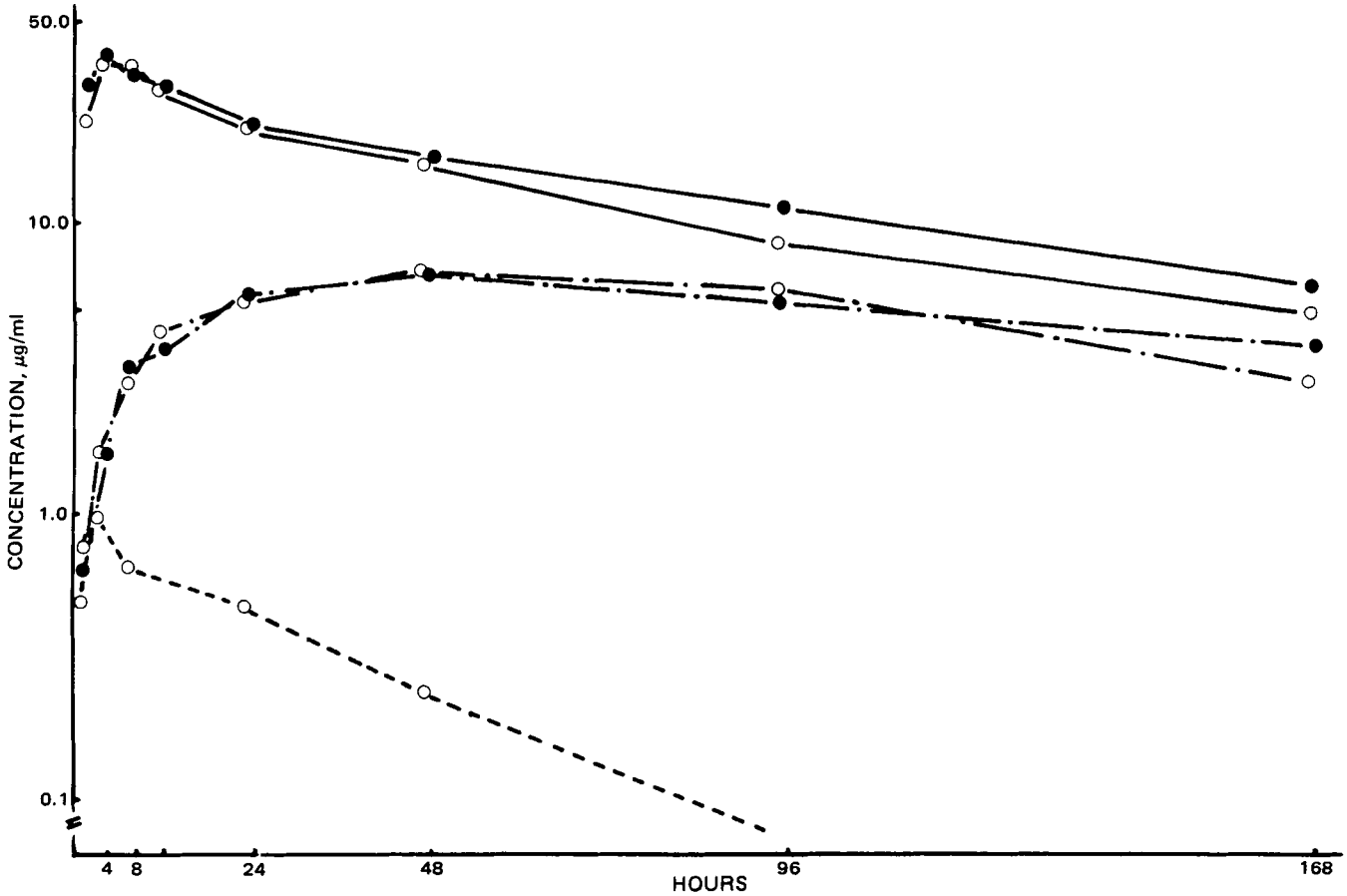

Figure 1—*Mean plasma concentration of phenylbutazone, oxyphenbutazone and γ-hydroxyphenylbutazone after oral administration of suxibuzone or phenylbutazone. Key: —, phenylbutazone; -·-, oxyphenbutazone; ---, γ-hydroxyphenylbutazone; ○, suxibuzone administration, ●, phenylbutazone administration.*

SS 1: chloroform–methanol–formic acid (100:50:5)
SS 2: ethyl acetate–butanone–formic acid–water (50:30:10:10)
SS 3: chloroform–methanol–formic acid (100:40:5)
SS 4: chloroform–methanol–formic acid (100:20:5)
SS 5: chloroform–methanol–acetone–formic acid (100:20:20:5)

Spectrometric Measurements—Direct inlet mass spectra were measured under the following conditions: ionizing energy, 75 eV; ionizing current, 200 μA; and acceleration voltage, 7 kV. GC–mass spectrometry was performed with a mass spectrometer under similar conditions, except that the ionizing energy was 24 eV and by GC under the conditions described above. Field desorption–mass spectrometry was carried out using a carbon emitter; acceleration voltage, 7 kV; and cathode voltage, −6 kV.

UV spectra were measured in methanol solution. NMR spectra were recorded in deuterated methanol with tetramethylsilane as internal standard.

Treatment of Subjects and Collection of Samples—Six male volunteers (weight, 54–68 kg; age, 27–35 years), who had had no other medication for at least 2 weeks before the experiments, were randomly divided into two groups and given a single 426-mg (3 capsules) oral dose of suxibuzone[8] or an equimolar amount, 300 mg (3 tablets), of phenylbutazone[9]. Four weeks after the first administration, the test was repeated on the two groups but interchanging the drug.

Blood was withdrawn at intervals during the first 7 days after drug administration and mixed with heparin to rapidly separate the plasma. Urine was collected quantitatively for the first 7 days, and feces were collected for the first 2 days. The excreta were kept frozen until analyzed.

Identification and Quantitative Analysis of Metabolites in Plasma—Plasma (6 ml) taken from blood of three volunteers 2 and 4 hr after drug administration was used for identification of metabolites. The sample was diluted with 9 ml of saline, adjusted to pH 2 with 2 *N* HCl, and extracted twice with 6 volumes of benzene–cyclohexane (1:1 v/v). The organic phase was divided into two portions, which were evaporated under nitrogen gas.

One residue was dissolved in a small amount of methanol and chromatographed on a reversed-phase column, using a mobile phase of a linear gradient of methanol in 0.05 *M* KH_2PO_4(0–100% methanol, 8%/min; flow rate, 2.0 ml/min) on a high-pressure liquid chromatograph[10] (4).

The other residue was dissolved in 100 μl of a freshly prepared solution of anhydrous chloroform and *N,O*-bis(trimethylsilyl)trifluoroacetamide[11] (I) (1:4 v/v) and stood for 1 hr at room temperature. The resulting trimethylsilylated derivatives were then analyzed by GC[12] and GC–mass spectrometry[13].

Plasma samples (2 ml) separated 2, 4, 8, 12, 24, 48, 96, and 168 hr after drug administration, were analyzed quantitatively by GC using tetraphenylethylene as an internal standard. The recoveries of suxibuzone, phenylbutazone, oxyphenbutazone, and γ-hydroxyphenylbutazone added to plasma at concentrations of 5–20 μg/ml were all more than 90%. The detection limits were 0.1 μg/ml for suxibuzone, and 0.05 μg/ml for other metabolites.

Identification of Free Metabolites in Urine—Samples of 5–10 ml of pooled urine were acidified and extracted with benzene–cyclohexane and the remaining aqueous phase was then extracted twice with 6 volumes of methylene chloride. The organic phases were then treated as described for plasma and the metabolites were identified by HPLC, GC, and GC–mass spectrometry.

Identification of Conjugated Metabolites in Urine—Pooled urine samples (500–1000 ml) were adjusted to pH 2 and extracted with benzene–cyclohexane to eliminate free metabolites. The aqueous phase was then saturated with sodium chloride and extracted twice with 6 volumes of ethyl acetate, and the organic layer was evaporated to dryness. The

[8] Lot 8D 77, Taiho Pharmaceutical Co.
[9] Butazolidin, Lot 1520 ATOH FF, Japan-Ciba-Geigy.
[10] Model LC-2, Shimadzu, Kyoto, Japan.
[11] Pierce Chemical Co.
[12] Model GC-4CM, Shimadzu, Kyoto, Japan.
[13] Model JMC-01SG-2 connected with a JGC-20K Gas Chromatography, JEOL, Tokyo, Japan.

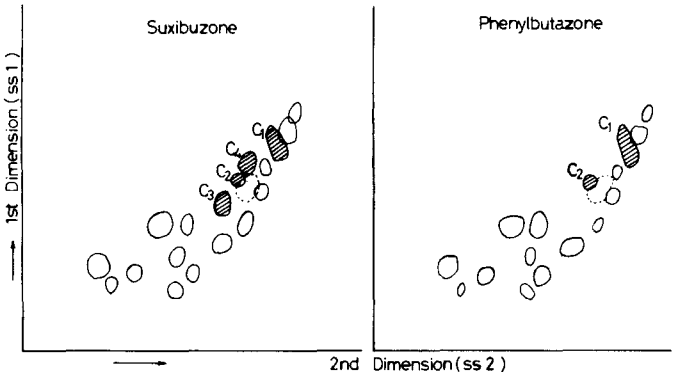

Figure 2—*Typical examples of thin-layer chromatograms of glucuronides in urine after suxibuzone or phenylbutazone administration.*

residue was dissolved in distilled water (containing 1% v/v methanol) and the glucuronide fraction was obtained by the method of Kamil *et al.* (5). The glucuronide fraction was analyzed by TLC on silica gel. Samples were spotted on the gel and developed in two dimensions with solvent systems SS 1 and SS 2. The material visualized by reaction with naphthoresorcinol (blue) or anisaldehyde (green-gray), which were not seen on chromatography of control urine, were scraped off, dissolved in 5 ml of 0.067 (1/15) *M* acetate buffer (pH 5.5), and incubated with 1000 U of β-glucuronidase[14] at 37° for 3 hr. The samples were then treated in a way similar to that described for identification of free metabolites.

The four kinds of glucuronides (II, III, IV, V) were isolated and identified as follows. The 0–6 hr urine samples from three volunteers were

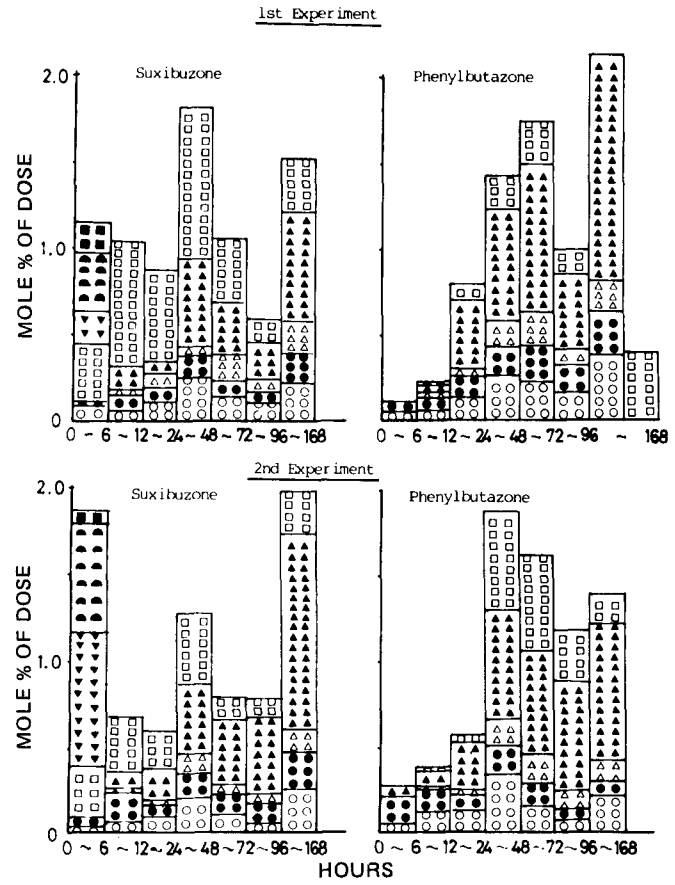

Figure 3—*Urinary excretion of unchanged drugs and their metabolites after oral administration of suxibuzone or phenylbutazone. Key:* ○, *phenylbutazone;* ●, *phenylbutazone glucuronide;* △, *oxyphenbutazone;* ▲, *oxyphenbutazone glucuronide;* □, *γ-hydroxyphenylbutazone;* ■, *suxibuzone glucuronide;* ◓, *4-hydroxymethylphenylbutazone glucuronide;* ▼, *4-hydroxymethyloxyphenbutazone glucuronide.*

[14] Type I, Bacterial, Sigma Chemical Co.

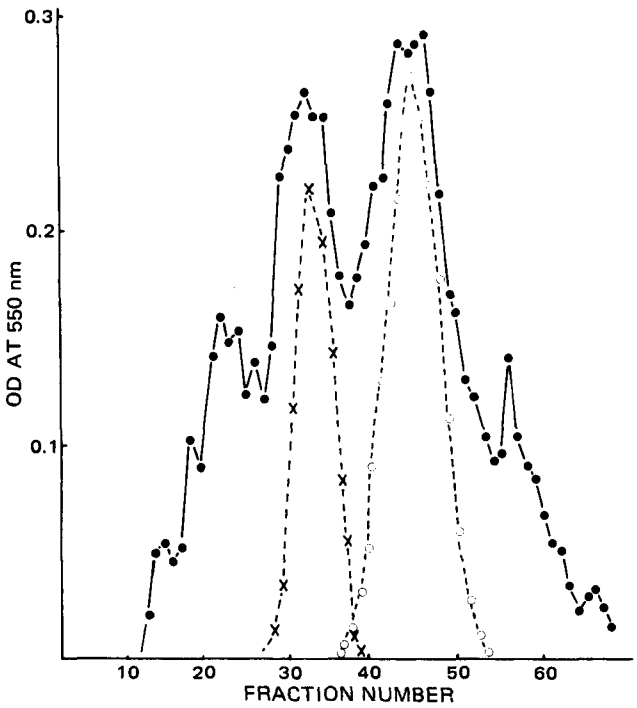

Figure 4—*Elution pattern of II and III on Dowex-1. Key:* ●, *orcinol reaction, OD at 550 nm;* X, *II;* ○, *III, TLC(SS 2), OD at 254 nm.*

combined and used for isolation of II and III; 12–24 hr urine samples were used for isolation of IV. In addition, bile from rats treated orally with phenylbutazone was used as a source of V to obtain a sufficient amount for spectrometric measurement. Each urine sample (1000 ml) was adjusted to pH 2 with concentrated HCl and extracted twice with 6 volumes of methylene chloride. The aqueous phase was applied to an Amberlite XAD-2 column, and the fraction eluted with 20–80% methanol was purified by the method of Kamil *et al.* (5). The glucuronide mixture thus obtained was separated on a Dowex-1 column with 60% methanol in 0.01 *N* HCl and by preparative TLC with SS 2.

The isolated glucuronides were then subjected to spectrometric measurements. For mass spectrometry, the glucuronides were converted to their methyl and methyl acetyl derivatives as follows. The glucuronide fraction was dissolved in a small amount of methanol (~500 μl), mixed with 5 volumes of ethereal diazomethane, and kept for 20 min at room temperature. The methylated glucuronides were dissolved in anhydrous pyridine (500 μl), mixed with an equal volume of anhydrous acetic acid, stood overnight, and then precipitated by adding distilled water.

Bile was collected by cannula from the bile duct of rats (male Wistar, 200–250 g) over a 24-hr period after receiving 200 mg/kg phenylbutazone by stomach tube. Fifty milliliters of the bile was diluted with 8 volumes of a saline solution. The aqueous phase remaining after extraction of free metabolites was saturated with sodium chloride and extracted twice with 6 volumes of ethyl acetate. The extract was evaporated under reduced pressure, and the residue was dissolved in a small amount of methanol and subjected to preparative TLC with SS 2. The fraction that released phenylbutazone on β-glucuronidase treatment was eluted with methanol and purified further with HPLC on a reversed-phase column using 40% methanol (flow rate, 1.0 ml/min) as a mobile phase. The samples obtained were characterized by UV[15], mass spectrometry, and NMR[16] spectra.

Quantitative Analysis of Metabolites in Urine—Samples (5 ml) of urine collected 0–6, 6–12, 12–24, 24–48, 48–72, 72–96, and 96–168 hr after drug administration were used to assay for metabolites. Each urine sample (pH 2) was extracted with 10 ml of 0.1 *M* phosphate buffer (pH 7.0). The aqueous phase was acidified and extracted twice with 20 ml of methylene chloride and the extracts were treated in the same way as plasma extracts. This procedure eliminated interfering peaks in the chromatogram.

For determination of the amounts of conjugated metabolites, the aqueous phase obtained after extraction with benzene–cyclohexane was used. The extracts with ethyl acetate were treated with a mixture of 3000

[15] Model 124, Hitachi, Tokyo, Japan.
[16] Model MH-400, Bruker.

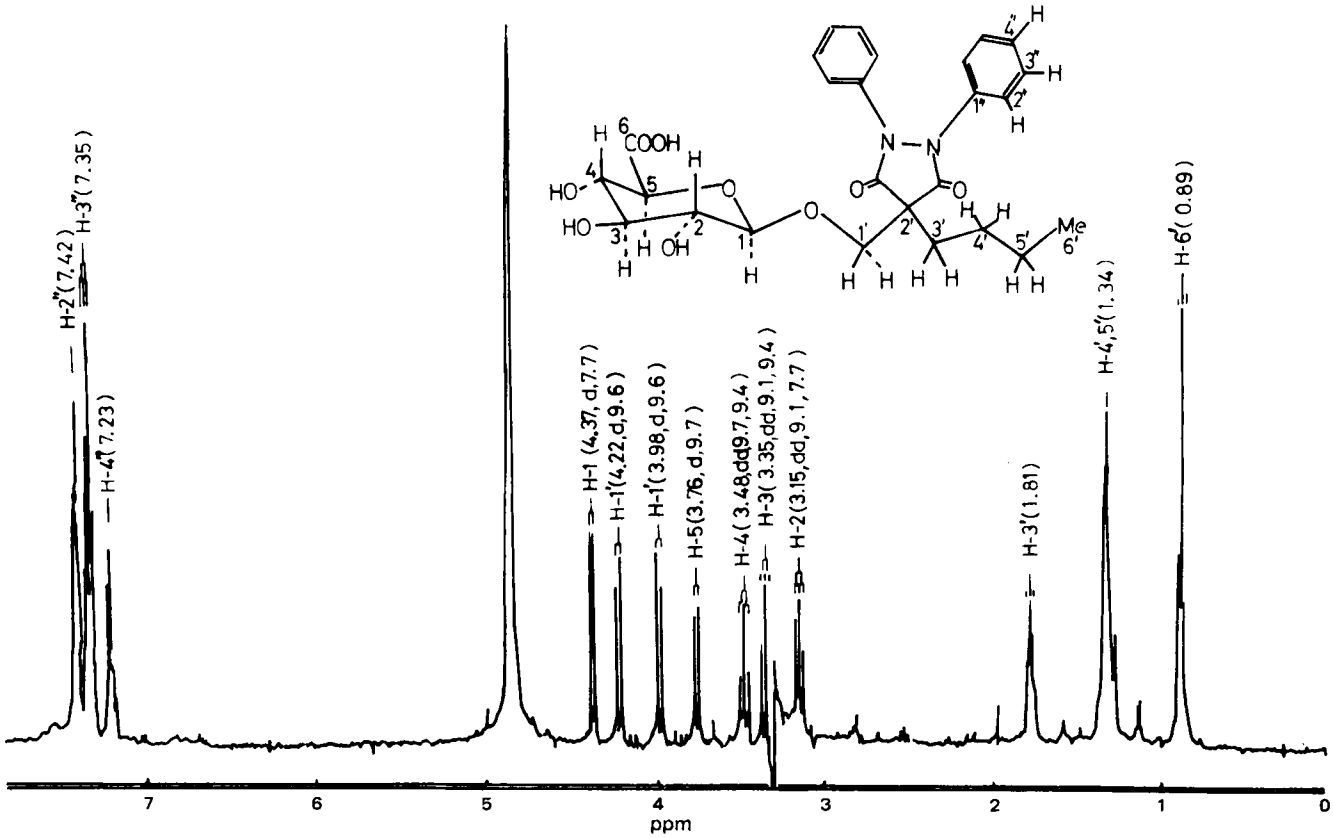

Figure 5—*NMR spectrum of II.*

U of β-glucuronidase and 10 U of sulfatase[17] in acetate buffer (pH 5.5) at 37° for 3 hr, and the concentrations of the respective aglycones released were determined by GC as described previously.

The recoveries of synthetic reference compounds in the range of 10–40 μg/ml by these extraction procedures were all >90%.

Quantitative Analysis of Suxibuzone and Phenylbutazone in Feces—The daily feces were homogenized with 3 volumes of water, adjusted to pH 2, and extracted with 5 volumes of benzene-cyclohexane. The concentrations of suxibuzone and phenylbutazone were determined by GC by procedures similar to those described for urine samples.

RESULTS

Identification of Metabolites in Plasma—The metabolites in plasma were first analyzed by HPLC. Three specific metabolites with retention times of 10.5, 10.0, and 9.4 min were observed in plasma after suxibuzone administration. These metabolites were identified as phenylbutazone, oxyphenbutazone, and γ-hydroxyphenylbutazone by comparing their retention times to those of authentic samples. No unchanged suxibuzone or 4-hydroxymethylphenylbutazone, a possible metabolite of suxibuzone, was detected. The plasma extract was also analyzed by GC and GC-mass spectrometry after trimethylsilylation of the metabolites. Three metabolites with retention times of 4.0, 7.9, and 6.8 min, corresponding to those of trimethylsilylated phenylbutazone, trimethylsilylated oxyphenbutazone, and trimethylsilylated γ-hydrophenylbutazone, respectively, were observed. These metabolites were confirmed further by GC-mass spectrometry. The trimethylsilylated derivatives had characteristic fragments at m/z 380(M^+), 337, 308, and 246 like trimethylsilylated phenylbutazone, at 468, (M^+), 425, 396, 334, and 246 like trimethylsilylated oxyphenbutazone, and at 468(M^+), 376, 351, 338, and 246 like trimethylsilylated γ-hydroxyphenylbutazone, respectively. No conjugates were detected in the residual aqueous phase of plasma remaining after extraction with benzene–cyclohexane. Thus, the main metabolites in human plasma after suxibuzone administration were confirmed to be phenylbutazone, oxyphenbutazone, and γ-hydroxyphenylbutazone. These metabolites were the same as those observed in plasma after phenylbutazone administration.

Quantitative Analysis of Metabolites in Plasma—The time courses of changes in the mean plasma phenylbutazone, oxyphenbutazone, and γ-hydroxyphenylbutazone concentrations after administration of suxibuzone and phenylbutazone are shown in Fig. 1. The plasma phenylbutazone concentration was higher than that of other metabolites after administration of either suxibuzone or phenylbutazone. The mean plasma phenylbutazone concentration reached a maximum of 35.96 and 38.51 μg/ml as soon as 4 hr after administration of suxibuzone and phenylbutazone, respectively, and then decreased slowly between 8 and 168 hr, corresponding to elimination half-lives of 61.8 ± 5.0 (*SE*) hr on suxibuzone administration and 72.3 ± 3.6 hr on phenylbutazone administration. These values are comparable to that of 70.9 ± 5 hr reported by Levi *et al.* (6).

Change in the plasma oxyphenbutazone concentration exhibited similar time courses after administration of suxibuzone and phenylbutazone; it reached a maximum of ~7 μg/ml after 48 hr and decreased to 3–4 μg/ml within 168 hr.

On the other hand, the time course of change in the plasma γ-hydroxyphenylbutazone concentration after suxibuzone and phenylbutazone administrations were somewhat different; namely, it remained <0.1 μg/ml for at least 168 hr after phenylbutazone administration, but reached a maximum of ~1 μg/ml at 4 hr after suxibuzone administration. The difference between its concentrations 2–24 hr after administration of phenylbutazone and suxibuzone was statistically significant ($p < 0.05$).

These results show that suxibuzone was rapidly decomposed to phenylbutazone and that the plasma levels of phenylbutazone and oxyphenbutazone after suxibuzone administration were as high as those after phenylbutazone administration.

Identification of Metabolites in Urine—As in plasma, phenylbutazone, oxyphenbutazone, and γ-hydroxyphenylbutazone were extracted from urine with benzene–cyclohexane. A metabolite extracted with methylene chloride and derivatized with I exhibited a specific peak with a retention time of 13.0 min on GC. This metabolite was determined as p-γ-dihydroxyphenylbutazone by GC–mass spectrometry. The mass spectrum of this trimethylsilylated derivative had characteristic fragment ions at m/z 556(M^+), 426, 334, 246, 181, 93, and 77, like those reported previously (7). No unchanged suxibuzone or 4-hydroxymethylphenylbutazone was detected in the urine and the specifically determined metabolites were the same as those found in the urine of subjects treated with phenylbutazone.

Enzymatic Identification of Conjugated Metabolites—An enzy-

[17] Type V, Sigma Chemical Co.

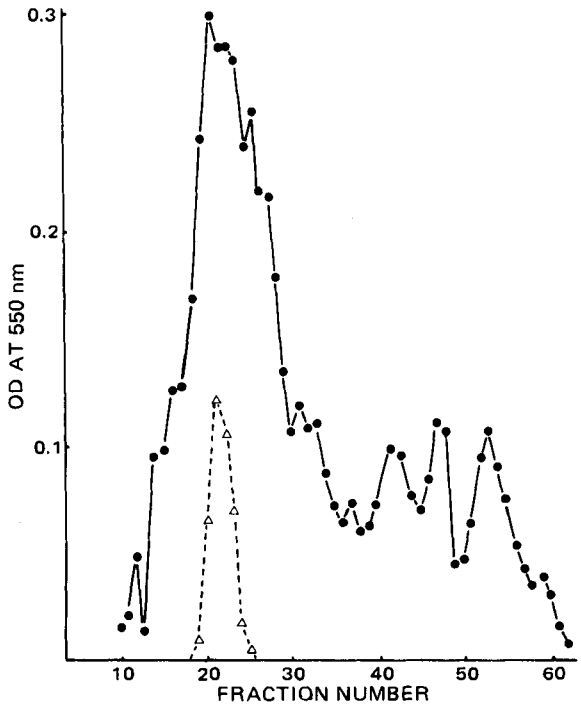

Figure 6—*Elution pattern of IV on Dowex-1. Key: ●, orcinol reaction, OD at 550 nm; △, IV, TLC(SS 2), OD at 254 nm.*

matic method was used to identify conjugated metabolites. The glucuronide mixture was separated by two-dimensional TLC, and the spots of material located by color reactions were analyzed by GC–mass spectrometry after hydrolysis with β-glucuronidase and derivatization with I. Typical thin layer chromatograms of glucuronides in urine after administration of suxibuzone and phenylbutazone are shown in Fig. 2. Analysis of each spot on the chromatogram after suxibuzone administration by GC showed that spot C_1 corresponded to trimethylsilylated phenylbutazone, spots C_2 and C_3 to trimethylsilylated oxyphenbutazone, and spot C_4 to trimethylsilylated suxibuzone and trimethylsilylated phenylbutazone, respectively. Chromatograms of urine samples after phenylbutazone administration gave spots C_1 and C_2 which corresponded to trimethylsilylated phenylbutazone and trimethylsilylated oxyphenbutazone, respectively. When the trimethylsilylated suxibuzone derivative of spot C_4 was analyzed by GC–mass spectrometry, the mass fragments coincided with those of the authentic compound; *m/z* 510(M^+), 485, 395, 380, 264, 183, 173, 105, 93, and 77. This confirms that spot C_4 contains suxibuzone glucuronide. Spots C_2 and C_3 both contained trimethylsilylated oxyphenbutazone. Spot C_3 was found only in the 0–6 hr urine sample after suxibuzone administration, whereas spot C_2 was observed after both suxibuzone and phenylbutazone and gradually became larger with increase in the plasma concentration and urinary excretion of oxyphenbutazone (Figs. 1 and 3). Hence, spot C_2 is considered to correspond to oxyphenbutazone glucuronide. Similarly, spot C_1 was expected to be phenylbutazone glucuronide (V) and the glucuronides (III,II) corresponding to spots C_3 and C_4 appeared only after suxibuzone administration.

Structures of Metabolites II and III—Compounds II and III were isolated on a preparative scale by the procedure shown in Fig. 4. Parts of both metabolites were converted to their methyl (II/1,III/1) and methyl acetyl (II/2,III/2) derivatives. The mass and NMR spectra (Fig. 5) show that II and III are 4-hydroxymethylphenylbutazone glucuronide and 4-hydroxymethyloxyphenbutazone glucuronide, respectively; *i.e.*, conjugates in which the oxymethyl residue at the C-4-position of the pyrazolidine ring is attached to glucuronic acid *via* an O—C bond. In the mass spectra of the methyl derivatives II/1 and III/1, the presence of glucuronyl residue was indicated by molecular ions at *m/z* 528 and 558, respectively, together with corresponding aglycone fragment ions at *m/z* 338 and 368. (Under the conditions used, III was dimethylated at the carboxyl group of glucuronic acid and at the hydroxyl group of one of the phenyl rings.) This was confirmed by the mass spectra of the methyl acetyl derivatives II/2 and III/2; namely, molecular ions were observed at *m/z* 654 and 684, respectively, indicating triacetylation at the three hydroxyl groups of glucuronic acid. The existence of an oxymethyl residue was deduced from subsequent fragmentation of *m/z* 338 to 308 (loss of $CH_2{=}O$) for II/1 and

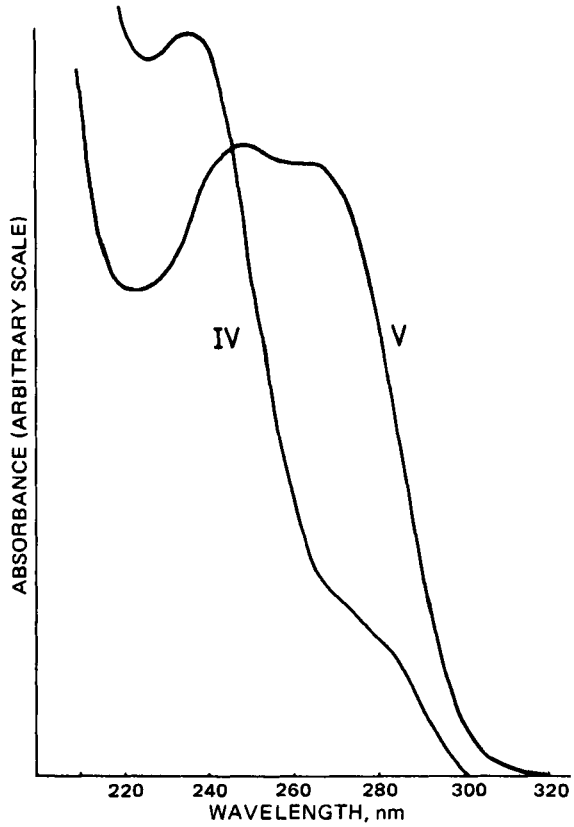

Figure 7—*UV spectra of IV and V.*

of *m/z* 368 to 338 for III/1. Furthermore, the ion set of *m/z* 338, 308, 264, and 183 observed for II/1 coincided with that of authentic 4-hydroxymethylphenylbutazone. The fragment ions at *m/z* 368, 338, 294, and 213 observed for III/1 were each shifted by *m/z* 30 relative to the corresponding fragment ions generated from 4-hydroxymethylphenylbutazone. This suggests the involvement of a methoxy groups in one of the phenyl rings (*e.g.*, $CH_3OC_6H_4N^+{=}NC_6H_5$ for the fragment ion at *m/z*

II

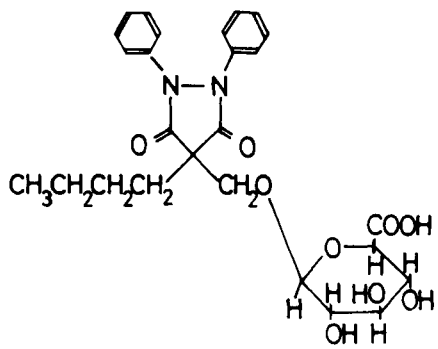

III

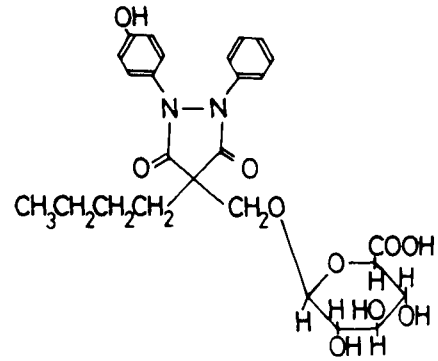

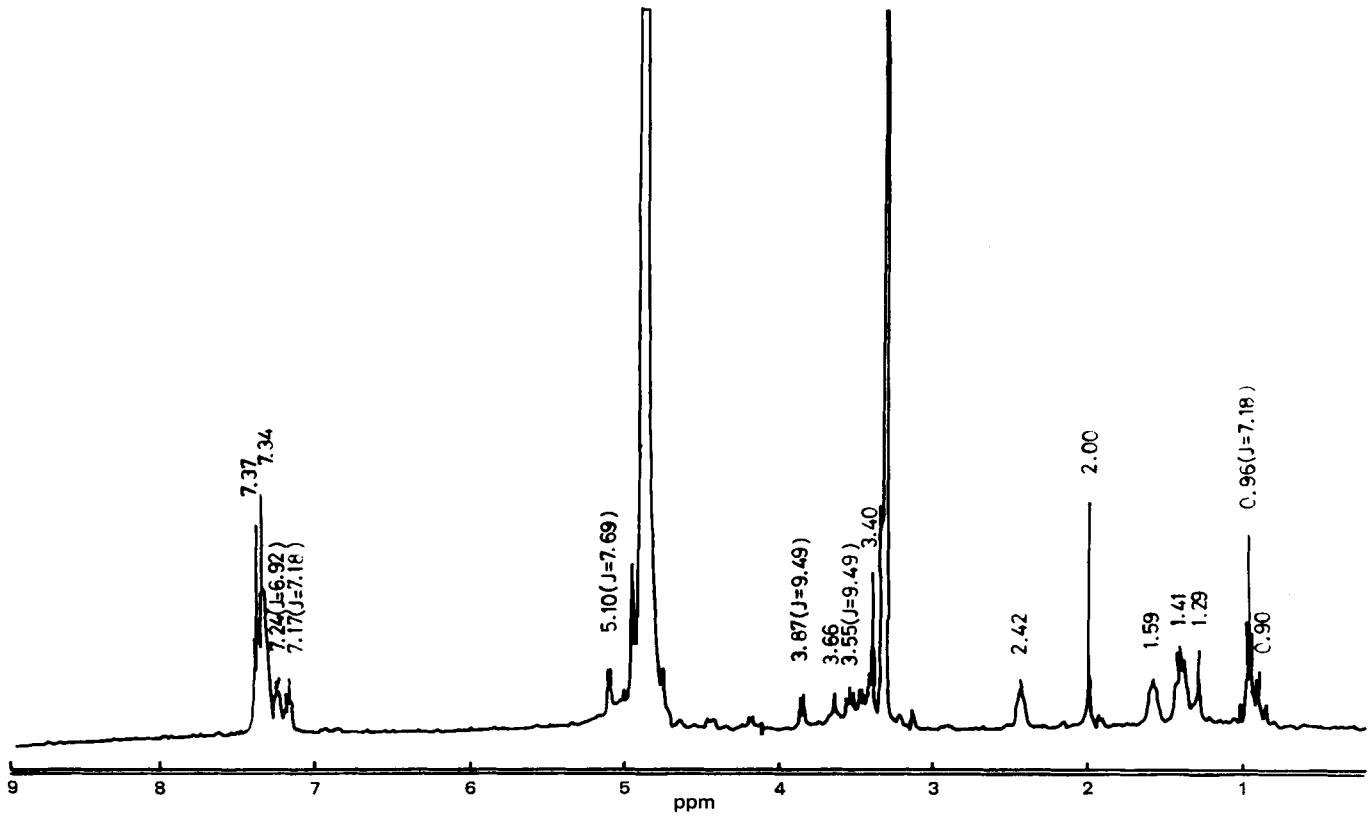

Figure 8—*NMR spectrum of V.*

213) and consequently suggests that the hydroxyl group in one of the phenyl rings is not attached to glucuronic acid. Confirmation of the assignments of the positions of glucuronidation in II and III were obtained from NMR spectra. The 400-MHz spectrum of II is shown in Fig. 5. Of significance for the assignment of glucuronidation at the oxygen of oxymethyl group is the appearance of an anomeric proton of glucuronic acid at δ4.37 ppm and of methylene protons of the oxymethyl group at δ4.22 and δ3.98 ppm, both of which are separated into a doublet with a geminal coupling constant of 9.6 Hz. The anomeric proton of glucuronic acid in III appeared at δ4.36 ppm, which is very close to that in II. The doublet signals (J = 9.0 Hz) of aromatic protons at δ6.72 and δ7.22 ppm established the existence of the hydroxyl group at the *para*-position of one of the phenyl rings in III. The proposed structures of II and III are shown.

The aglycones of 4-hydroxymethylphenylbutazone and 4-hydroxymethyloxyphenbutazone obtained by hydrolysis of II and III seemed to be converted to phenylbutazone (or trimethylsilylated phenylbutazone) and oxyphenbutazone (or trimethylsilylated oxyphenbutazone), respectively, during the process of hydrolysis with β-glucuronidase and/or trimethylsilylation with I under the conditions used. Hence, the spot C_4 was concluded to be that of a mixture of suxibuzone glucuronide and II, while spot C_3 was concluded to be that of III.

Structures of IV and V—The existence of C-4-phenylbutazone glucuronide in humans; *i.e.*, a conjugate in which the pyrazolidine ring is directly attached to glucuronic acid *via* a C—C bond and which is not hydrolyzed by β-glucuronidase, was demonstrated previously (8). On the other hand, the existence in humans and animals of a phenylbutazone glucuronide that can be hydrolyzed by β-glucuronidase (9, 10) was reported. Since there is little of this hydrolyzable phenylbutazone glucuronide in human urine, the structure of this compound(V) was first elucidated using bile of rats treated with phenylbutazone and then the identity of the material in rats and humans confirmed by TLC. C-4-phenylbutazone glucuronide (IV) was isolated from human urine.

The elution pattern of IV is shown in Fig. 6. Compound IV was identified as C-4-phenylbutazone glucuronide by mass spectrometry and UV studies (Fig. 7). The presence of glucuronic acid in the methyl ester of

Table I—Fecal Excretion of Suxibuzone and Phenylbutazone after Oral Administration

Subject Number		mole % of dose 0–24 hr	24–48 hr
	Suxibuzone Administration		
1	Suxibuzone	0.0	0.0
	Phenylbutazone	0.2	0.2
2	Suxibuzone	0.0	0.0
	Phenylbutazone	0.5	0.3
3	Suxibuzone	0.0	0.0
	Phenylbutazone	0.2	0.2
	Phenylbutazone Administration		
1	Phenylbutazone	0.2>	0.2>
2	Phenylbutazone	0.2>	0.2>
3	Phenylbutazone	0.4	0.5

IV

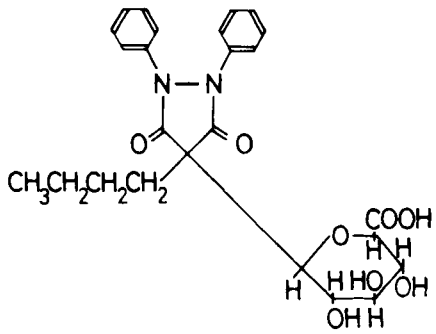

V

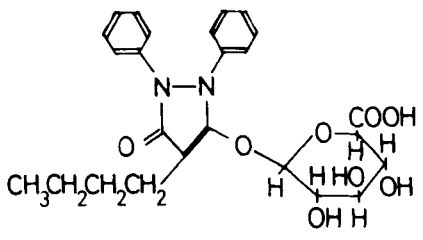

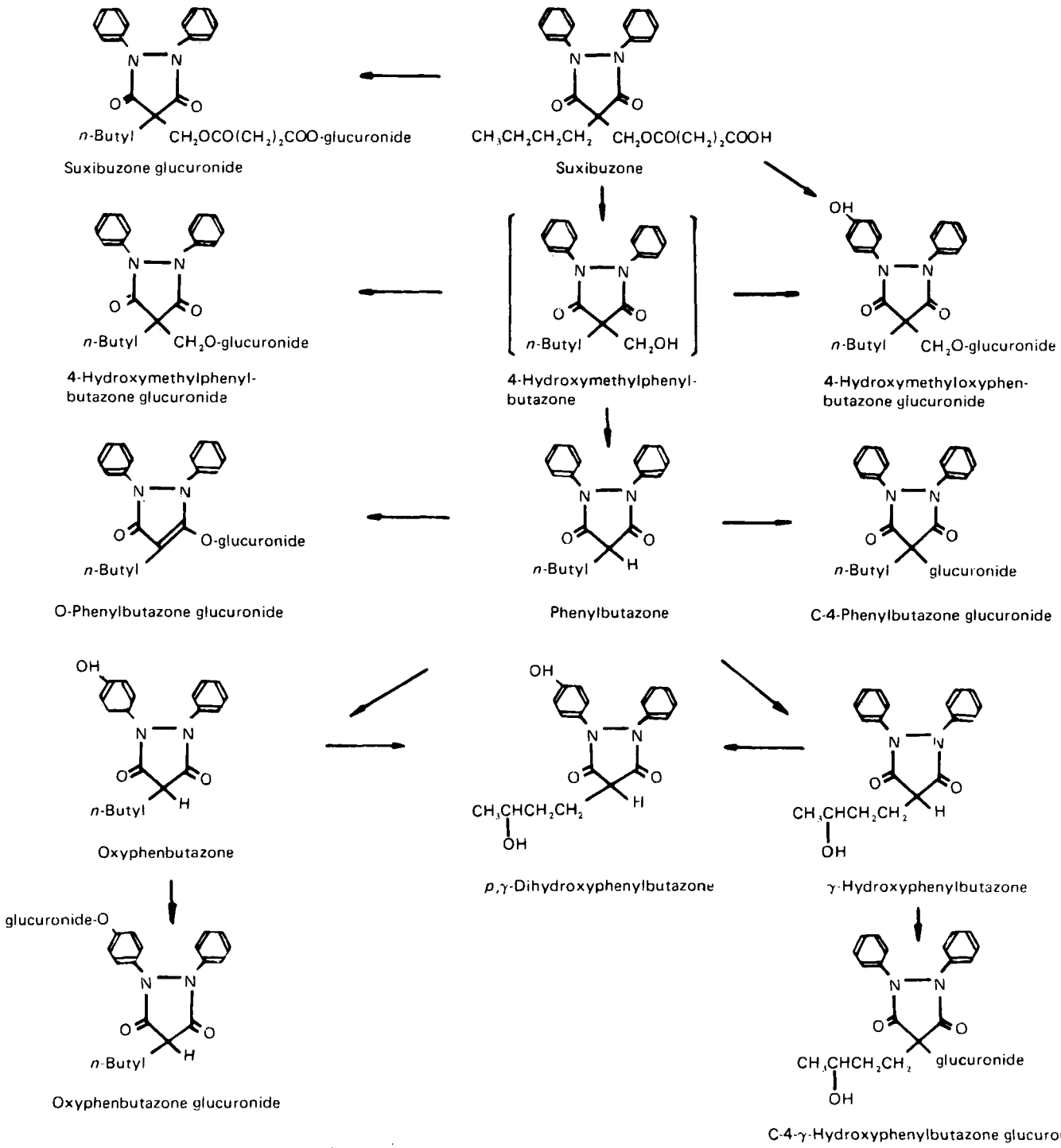

Scheme I—Metabolic pathway of suxibuzone in humans.

IV was evidenced by a molecular ion at m/z 498 and a corresponding aglycone fragment ion at m/z 308. The UV spectrum of IV revealed the presence of diphenyldioxopyrazolidine ring with an intact 1,3-dicarbonyl system exhibiting a UV absorbance maximum (λ_{max}) at 236 nm. These data coincide well with those reported previously (8).

Since V was labile under the conditions used for derivatization with diazomethane and with I, the molecular ion was detected by field desorption–mass spectrometry. The field desorption–mass spectrum of V showed two ion peaks of a molecular ion at m/z 484 and a fragment ion at m/z 308 corresponding to its aglycone. Positive evidence for an O—C attachment of glucuronic acid was obtained from the UV and NMR spectra of V (Figs. 7 and 8). The UV spectrum indicated the presence of an enolic dioxopyrazolidine ring exhibiting a UV absorption at λ_{max} = 250 and ~265 nm instead of at λ_{max} = 236 nm for IV with an intact 1,3-dicarbonyl system. The NMR spectrum established an O—C attachment of glucuronic acid more directly by exhibiting downfield shifts of an anomeric proton of the glucuronic acid at δ5.10 ppm (J = 7.69 Hz) and of allylic protons of the n-butyl side chain at δ2.42 ppm. From these results it was concluded that V is an O-phenylbutazone glucuronide. The proposed structures of IV and V are as shown.

When co-chromatographed by two-dimensional TLC with solvent systems SS 1 and SS 2, IV and V migrated together giving a single spot. Hence, spot C_1 in Fig. 2 is considered to contain both O-phenylbutazone glucuronide and IV. With solvent system SS 5, however, IV and V were separated by TLC exhibiting R_f values of 0.46 and 0.51, respectively. The methanol extracts of spot C_1 after suxibuzone or phenylbutazone administration were chromatographed with solvent system SS 5 using IV and V as reference compounds. The band corresponding to that of V was eluted with methanol and treated with β-glucuronidase and the release of phenylbutazone was confirmed by GC. The band corresponding to that of IV did not release phenylbutazone on β-glucuronidase treatment.

Quantitative Analysis of the Metabolites in Urine—Figure 3 shows

the molar percentages of doses of suxibuzone and phenylbutazone excreted as various metabolites in the urine in different times. (Since 4-hydroxymethylphenylbutazone was obtained by hydrolysis of its conjugate with β-glucuronidase and was observed as phenylbutazone on GC, the ratio of II to *O*-phenylbutazone glucuronide by TLC separation was determined first. The amount of each metabolite was then calculated from the ratio and the total amount observed as phenylbutazone. The amount of III and oxyphenbutazone glucuronide were determined by similar treatments.) As seen in Fig. 3, the composition of metabolites excreted in the first 6-hr urine samples after administration of suxibuzone and phenylbutazone were different. The 0–6 hr urine after suxibuzone administration mostly contained the metabolites specific to suxibuzone administration; namely, suxibuzone glucuronide, II, and III. The amounts of these metabolites excreted were 0.12% of the dose of suxibuzone for suxibuzone glucuronide, 0.45% for II, and 0.44% for III. The amounts of these metabolites were negligible in urine samples collected at later times after suxibuzone administration.

Only the urinary excretion of γ-hydroxyphenylbutazone differed after administrations of suxibuzone and phenylbutazone; those of phenylbutazone, oxyphenbutazone, and their conjugates were similar. The percentages of the urinary excretion of phenylbutazone and *O*-phenylbutazone glucuronide during 168 hr after drug administration were 0.93 and 0.79%, respectively, of the dose of suxibuzone, and 1.20 and 0.95%, respectively, of the dose of phenylbutazone. Similarly, in the 0–168 hr samples, oxyphenbutazone and its conjugate amounted to 0.49 and 2.73%, respectively, of the dose of suxibuzone, and 0.63 and 3.42%, respectively, of the dose of phenylbutazone. On the other hand, the excretion of γ-hydroxyphenylbutazone in the first 24-hr urine samples was 2.44% of the dose of suxibuzone. This was 15 times that after phenylbutazone administration and seems to reflect the concentrations in the plasma. At more than 24 hr after administration of suxibuzone and phenylbutazone, the excretions of γ-hydroxyphenylbutazone were similar.

The cumulative urinary excretion of the metabolites measured amounted to ~8% of the dose within 168 hr after administration of either suxibuzone or phenylbutazone.

Excretion in Feces—The fecal excretions of suxibuzone and phenylbutazone are summarized in Table I. The percentages of excreted phenylbutazone were <1% of the dose, after both suxibuzone and phenylbutazone administration. No unchanged suxibuzone was detected in the feces; therefore, the absorptions of both drugs appear to be complete.

DISCUSSION

On the basis of the present results on suxibuzone and phenylbutazone in humans and findings on phenylbutazone by other groups (7, 8, 11–15), a scheme for the biotransformation of suxibuzone is shown in Scheme 1.

Analysis of urinary metabolites elucidated possible pathways of biotransformation from suxibuzone to phenylbutazone. No unchanged suxibuzone was observed in the plasma, but the excretion of suxibuzone glucuronide in the urine suggests that part of the oral dose of suxibuzone is absorbed in an unchanged form and excreted as the glucuronide. Detection of II suggests that suxibuzone was hydrolyzed by esterases (9) to give 4-hydroxymethylphenylbutazone, which is considered to be labile and to decompose to phenylbutazone spontaneously unless otherwise conjugated with glucuronic acid at the oxymethyl side chain. The excretion of III indicates the existence of a pathway in which unchanged suxibuzone or an intermediary between suxibuzone and phenylbutazone (*e.g.*, 4-hydroxymethylphenylbutazone) undergoes oxidation at the *para*-position of one of the phenyl rings. Consequently, this means that part of the unchanged suxibuzone absorbed can yield oxyphenbutazone without being metabolized to phenylbutazone. If this type of pathway exists for producing γ-hydroxyphenylbutazone (*e.g. via* a 4-hydroxymethyl-γ-hydroxyphenylbutazone), it could explain the significantly higher plasma level of γ-hydroxyphenylbutazone during a 24-hr period after suxibuzone administration. [The higher plasma level of γ-hydroxyphenylbutazone after suxibuzone administration may contribute to the lower plasma level of uric acid than that after phenylbutazone administration (10), since γ-hydroxyphenylbutazone was reported to enhance the excretion of uric acid (16).] The excretions of these metabolites specific to suxibuzone in the first 6 hr urine may be the cause of the slightly (though not significantly) lower plasma level of phenylbutazone after suxibuzone administration.

Although V hydrolysed by β-glucuronidase in rat or human urine could not be detected previously (7, 8), a hydrolyzable *O*-phenylbutazone glucuronide was isolated, the existence of which has already been suggested (9, 10). Hence, phenylbutazone undergoes two different types of glucuronidation and is excreted in the urine.

Most ester-type drugs are considered to be hydrolyzed by esterases bound to the intestinal mucosa, so the form of the drug which enters the portal venous blood will be greatly affected by the activities of these esterases (17–19). This also seems to be the case for suxibuzone, judging from the rate of hydrolysis of suxibuzone determined using homogenates of intestine of various animals and from the metabolites detected in plasma and urine (9). For example, in dogs, in which the intestine have very low esterase activity, unchanged suxibuzone was detected in the plasma; but in rats, in which the intestine has high esterase activities, no suxibuzone was detected in the plasma and no suxibuzone glucuronide or II were found in the urine. In humans the esterase activity of the intestine is reported to be relatively high (18, 19), and no unchanged suxibuzone was detected in the plasma or feces. Moreover, the changes in concentration of metabolites in the plasma exhibited almost the same time courses after the administration of suxibuzone and phenylbutazone. These observations imply that most of the suxibuzone administered orally is hydrolyzed to phenylbutazone by intestinal esterases before transfer to the portal venous blood.

The results obtained in the present study indicate that suxibuzone is a prodrug of phenylbutazone in humans. The metabolic fate and pharmacokinetic properties of suxibuzone ensure that this drug is as effective as phenylbutazone. The reason why suxibuzone is less ulcerogenic than phenylbutazone is considered to be that suxibuzone remaining in GI tracts is not as harmful as phenylbutazone to GI mucosa, since the unchanged suxibuzone does not inhibit the function of mitochondria and prostaglandin synthetases (unpublished data).

REFERENCES

(1) H. Fujimura, K. Tsurumi, I. Morii, and T. Suzuki, *Pharmacometrics*, **14,** 379 (1977).

(2) Y. Shiokawa *et al.*, *Igaku No Ayumi*, **114,** 115 (1980).

(3) A. Kanda, J. Yamamoto, H. Murakami, K. Tajima, and H. Fujimura, *Pharmacometrics*, **19,** 33 (1980).

(4) T. Marunaka, T. Shibata, Y. Minami, Y. Umeno, and T. Shindo, *J. Pharm. Sci.*, **69,** 1258 (1980).

(5) I. A. Kamil, J. N. Smith, and R. T. Williams, *Biochem. J.*, **50,** 235 (1952).

(6) A. J. Levi, S. Sherlock, and D. Walke, *Lancet*, **15,** 1275 (1968).

(7) O. M. Bakke, G. M. Praffan, and D. S. Davis, *Xenobiotica*, **4,** 237 (1974).

(8) W. Dieterle, J. W. Faigle, F. Fruh, H. Mory, W. Theobald, W. Alt, and W. Richter, *Arzneim.-Forsch.*, **26,** 572 (1976).

(9) T. Shindo, Y. Yasuda, K. Taira, N. Mitani, A. Kanda, and A. Akazawa, *Yakugaku Zashi*, **99,** 1186 (1979).

(10) T. Kageyama, F. Oono, Y. Yasuda, T. Shindo, N. Mitani, A. Maruden, and A. Akazawa, *Jpn. J. Clin. Pharmacol. Ther.*, **10,** 525 (1979).

(11) J. W. Faigle and W. Dieterle, *J. Int. Med. Res., Suppl.* 2, **5,** 2 (1977).

(12) J. J. Burns, R. K. Rose, T. Chenkin, A. Goldman, A. Schubert, and B. B. Brodie, *J. Pharmacol. Exp. Ther.*, **109,** 346 (1953).

(13) J. J. Burns, R. K. Rose, S. Goodwin, J. Reichental, E. C. Horning, and B. B. Brodie, *ibid.*, **113,** 481 (1955).

(14) J. Wagner, H. Stierlin, and R. Pulver, "Abstracts VII," European Rheumatology Congress, Brighton, England, 1971.

(15) I. J. McGilveray, K. K. Midha, and N. Mousseau, *Pharmacologist*, **16,** 218 (1974).

(16) J. J. Burns, T. F. Yu, P. G. Dayton, A. B. Gutman, and B. B. Brodie, *Ann. N.Y. Acad. Sci.*, **86,** 253 (1960).

(17) K. Krisch, "The Enzyme," vol. V, 3rd ed., P. O. Boyer, Ed., Academic, New York, N.Y., 1971, p. 43.

(18) H. Shindo, K. Kawai, K. Fukuda, M. Matsumura, K. Tanaka, M. Tanaka, and T. Yokota, "Abstracts V," Symposium on Drug Metabolism and Action, Shizuoka, Japan, 1973.

(19) M. Inoue, M. Tsuboi, and M. Sugiura, *J. Pharmacol.*, **29,** 9 (1979).

ACKNOWLEDGMENTS

The authors thank Mr. I. Miura, Laboratories of Natural Products Chemistry, Otsuka Pharmaceutical Co., Ltd. for carrying out NMR experiments. They also thank Mr. Y. Minami for mass spectra and accurate mass determinations.

Oral Hydrocortisone Pharmacokinetics: A Comparison of Fluorescence and Ultraviolet High-Pressure Liquid Chromatographic Assays for Hydrocortisone in Plasma

ROGER D. TOOTHAKER *¶, GLORIA M. SUNDARESAN ‡, JOHN P. HUNT ‡, THOMAS J. GOEHL ‡, KEITH S. ROTENBERG ‡, VADLAMANI K. PRASAD ‡, WILLIAM A. CRAIG §, and PETER G. WELLING *x

Received March 30, 1981, from the *School of Pharmacy, University of Wisconsin, Madison, WI 53706, the ‡Division of Biopharmaceutics, United States Food and Drug Administration, Washington, DC 20204, and the §Veterans Administration Hospital, Madison, WI 53705. Accepted for publication September 2, 1981. ¶Present address: Department of Pharmaceutics, BG-20, School of Pharmacy, University of Washington, Seattle, WA 98195.

Abstract □ Three fasted, male subjects received single 10-, 30-, and 50-mg oral doses of hydrocortisone tablets on separate occasions. Endogenous hydrocortisone was suppressed by giving 2 mg of dexamethasone 9 hr prior to dosing. Plasma samples obtained serially for 8 hr after hydrocortisone dosing were assayed by reversed-phase high-pressure liquid chromatography (HPLC) with UV detection and by normal-phase HPLC with fluorescence detection of the dansylhydrazine derivative of hydrocortisone. The two assay methods yielded equivalent plasma hydrocortisone concentrations. Metabolite interference was absent in both assay methods. Drug concentrations in plasma from all three doses of hydrocortisone were described by one-compartment open-model kinetics, with first-order absorption and elimination, and an absorption lag time. Mean C_{max} values of 199, 393, and 419 ng/ml were obtained at 1.0, 1.0, and 1.7 hr following the 10-, 30-, and 50-mg doses, respectively. Hydrocortisone was cleared from plasma with an elimination half-life of ~1.5 hr. Within the dosage range studied, plasma levels of hydrocortisone were related, but not directly proportional, to dose size. This apparent lack of proportionality may be due to reduced drug availability or altered distribution with increasing dose.

Keyphrases □ High-pressure liquid chromatography—comparison of fluorescence and UV high-pressure liquid chromatographic assays for hydrocortisone in plasma, humans □ Hydrocortisone—comparison of fluorescence and UV high-pressure liquid chromatographic assays for hydrocortisone in plasma, humans □ Pharmacokinetics—comparison of fluorescence and UV high-pressure liquid chromatographic assays for hydrocortisone tablets in plasma, humans

A number of high-pressure liquid chromatographic (HPLC) assays for hydrocortisone in biological fluids have recently appeared in the literature. Most of these employ UV detection of underivatized hydrocortisone (1–7), while others are based on detection of a fluorescent hydrocortisone derivative (8, 9).

In this report two assay methods, one using normal phase HPLC with fluorescence detection of the dansyl derivative of hydrocortisone and the other using reversed-phase HPLC with UV detection of hydrocortisone, were compared by assaying plasma samples obtained during an 8-hr period from three healthy volunteers who had ingested hydrocortisone tablets. The plasma concentration *versus* time data permits preliminary description of the pharmacokinetics of exogenous hydrocortisone.

EXPERIMENTAL

Materials—Materials used in the HPLC–fluorescence assay have been described previously (8). For the HPLC–UV assay, chemical standards of hydrocortisone[1] and internal standard Δ^4-pregnene-17α, 20β,21-triol-3,11-dione[1] were analytical grade. Reagent grade methylene chloride[2] was distilled prior to use. All other solvents and chemicals were reagent grade and were used as supplied. Plasma for construction of standard curves was obtained from healthy volunteers between 7 and 9 am subsequent to administration of 2 mg of dexamethasone at 11 pm the previous day (10).

Subjects—Three male volunteers (22–45 years old) underwent complete physical examinations including blood and urine analyses after giving informed consent. Vital signs and laboratory values for all subjects were normal. The subjects weighed 64–75 kg, and their heights ranged from 178 to 180 cm.

Protocol—Subjects were instructed to take no drugs for at least 1 week before the study, and no drugs other than the required doses of dexamethasone and hydrocortisone during the study. No caffeine-containing beverages were permitted for 1 day before or during the plasma sampling period following each dose of hydrocortisone. Each hydrocortisone dose was administered after overnight fast, and no food was permitted until 4 hr postdose.

Each subject received 10-, 30-, and 50-mg doses of hydrocortisone at least 1 week apart according to a randomized design. Each hydrocortisone dose was given as 1 or more 10-mg tablets[3], which were swallowed whole.

At 11 pm on the day before hydrocortisone administration, subjects received 20 ml (2 mg) of dexamethasone elixir[4] with 180 ml of water orally. Hydrocortisone was administered at 8 am the following morning with 180 ml of water.

Heparinized blood samples (10 ml) were taken from a forearm vein immediately before and then at 0.25, 0.5, 1, 1.5, 2, 3, 4, 5, 6, 7, and 8 hr postdose Subjects were ambulatory during the sampling period. Plasma was obtained by centrifugation and divided into two portions. Both portions were frozen at −20°: one portion was packed in dry ice and sent by air freight to the Food and Drug Administration laboratories for fluorimetric analysis; the other was assayed in this laboratory by the HPLC–UV method.

Fluorimetric Assay—The fluorimetric HPLC assay of plasma samples was carried out using a previously described method (8).

UV Assay—The HPLC–UV assay used was a modified version of a previously described method (1). Plasma (1 ml) containing 200 ng internal standard, and 0.1 ml of 2 *N* aqueous sodium hydroxide was vortexed with 10 ml of methylene chloride for 1 min and then centrifuged for 15 min at 500×*g*. Plasma and the creamy interface were aspirated off, and the organic layer was transferred to a clean tube and evaporated to dryness at room temperature under nitrogen. The tube walls were rinsed with 1 ml of methylene chloride which was evaporated as described previously. The residue was reconstituted in 100 μl of the HPLC mobile phase (60% aqueous methanol) and a 20-μl aliquot was injected into the chromatograph. The liquid chromatograph consisted of a 2.1 × 70-mm precolumn[5] and a 4.6 × 250-mm reversed-phase analytical column[6], through which mobile phase, 60% aqueous methanol, was pumped at a rate of 1.0 ml/min. Column effluent was monitored at 254 nm with a fixed wavelength detector[7]. Elution times for hydrocortisone and internal standard were 10 and 8 min, respectively. Calibration was by the method of peak height ratios. For plasma samples that yielded hydrocortisone and internal standard peak height ratios of <0.1 (hydrocortisone concentrations <25 ng/ml), a second injection was performed and the peak height ratios

[1] Sigma Chemical Co., St. Louis, MO 63178.
[2] Aldrich Chemical Co., Milwaukee, WI 53233.
[3] Hydrocortisone 10-mg tablets, Lot V 2478, Merck Sharp and Dohme Labs., West Point, PA 19486.
[4] Decadron Elixir, Lot A 3240, Merck Sharp and Dohme Labs.
[5] CO:PELL ODS, 30–38 m, Whatman Inc., Clifton, NJ 07014.
[6] Lichrosorb C18, 10 m, Altex Scientific Inc., Berkeley, CA 94710.
[7] Model 440, Waters Associates, Milford, MA 01757.

0022-3549/82/0500-0573$01.00/0

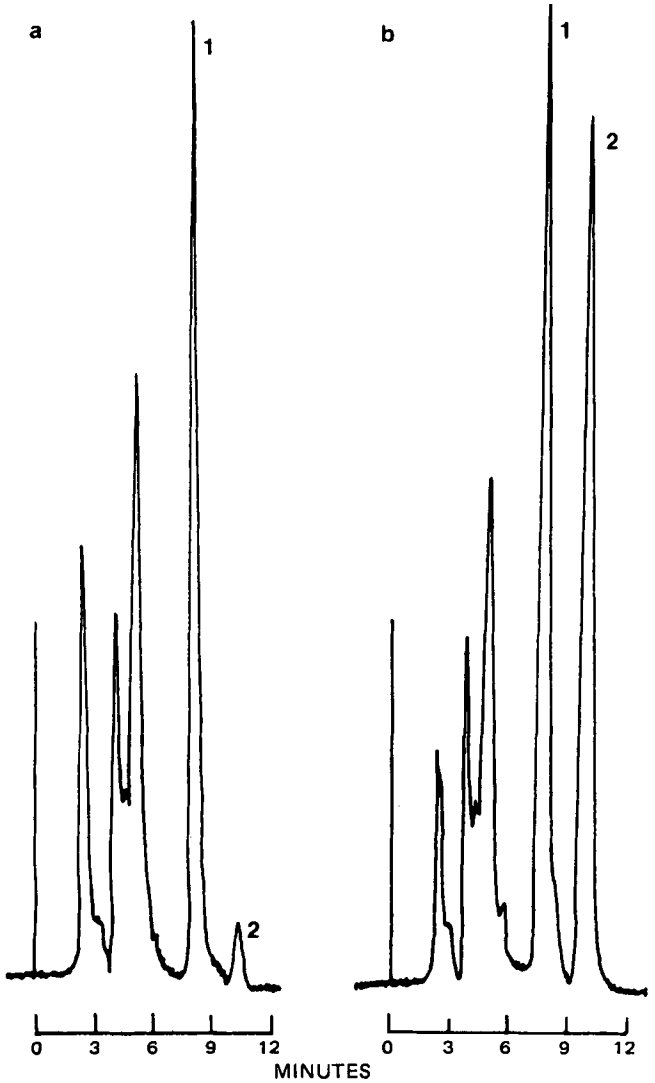

Figure 1—*Representative Chromatograms from HPLC–UV assay of hydrocortisone, peak 2, and internal standard, peak 1, extracted from human plasma.* a—*Dexamethasone—suppressed plasma containing 200 ng/ml internal standard and 11 ng/ml hydrocortisone (endogenous).* b—*Sample plasma containing 200 ng/ml internal standard and 149 ng/ml hydrocortisone (dosed + endogenous).*

obtained from the two injections were averaged. The endogenous hydrocortisone concentration in predose plasma was subtracted from all postdose values to obtain circulating levels of drug resulting from administered hydrocortisone. The assay was linearly sensitive to plasma hydrocortisone concentrations between 5 and 700 ng/ml. Coefficients of variation from multiple replicates ($n = 6$) were within 4% at the higher drug concentrations and within 8% at the lower drug concentrations. Assay recovery was 82 ± 2% for hydrocortisone and 83% for internal standard (single determination).

Pharmacokinetic and Statistical Analysis—Plasma hydrocortisone concentration data from all three doses were adequately described in terms of the one-compartment open pharmacokinetic model with first-order absorption and elimination and an absorption lag time. Thus, the hydrocortisone concentration C in plasma at any time t after dosing was shown by (11):

$$C = \frac{FD}{V}\left(\frac{k_a}{k_a - k_{el}}\right)\left[e^{-k_{el}(t-t_0)} - e^{-k_a(t-t_0)}\right] \qquad \text{(Eq. 1)}$$

where k_a and k_{el} are the first-order absorption and elimination rate constants, t_0 is the absorption lag time, F is the fraction of dose (D) absorbed, and V is the apparent distribution volume of drug in the body.

Equation parameters were obtained by nonlinear regression of individual hydrocortisone concentration data sets using the program NREG (12) on a digital computer[8].

[8] Univac Model 1100.

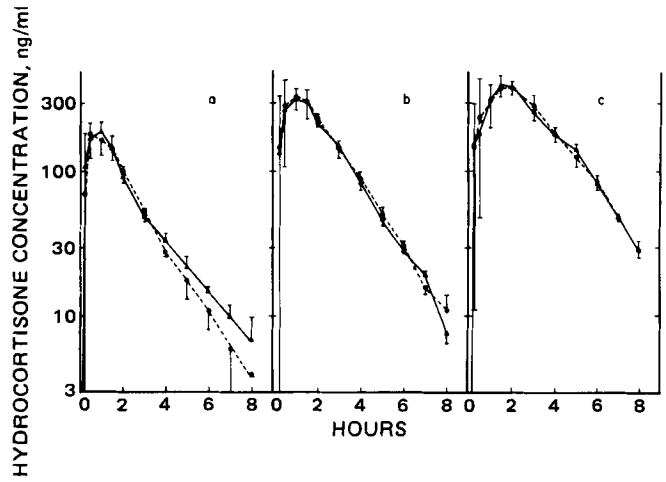

Figure 2—*Mean hydrocortisone plasma concentration* versus *time curves for three subjects (±1 SD) at dosages of* a, *10-mg;* b, *30-mg; and* c, *50-mg. Key:* ▲—▲, *UV;* ●---●, *fluorescence.*

Comparison of the hydrocortisone concentration values obtained by the two assay procedures was by paired t test. Pharmacokinetic parameters were analyzed for dose and assay effects by ANOVA. Factors shown to have a significant effect by ANOVA were further analyzed using Tukey's significant difference test (13).

RESULTS

Figure 1 shows two representative chromatograms from the HPLC–UV assay. Figure 1*a* illustrates the low level of endogenous hydrocortisone in suppressed plasma. The standard curve for hydrocortisone concentrations between 5 and 700 ng/ml in plasma was given by:

$$Y = -0.014\ (\pm 0.010) + 0.00497\ (\pm 0.00003)\ X \qquad \text{(Eq. 2)}$$

where $r = 0.999$ and $n = 6$.

Comparisons of the UV and Fluorescence Assays—Mean plasma hydrocortisone concentrations obtained using the two assay methods are shown in Fig. 2. Drug concentrations obtained by the different assays at each sampling time were compared by paired t test, and a significant difference between assays was obtained at only 2 of the 33 sampling times (11 sampling times at each dose level). The linear regression of the results obtained at all sampling times with the UV assay *versus* those obtained with the fluorescence assay is shown in Fig. 3. The regression had a slope

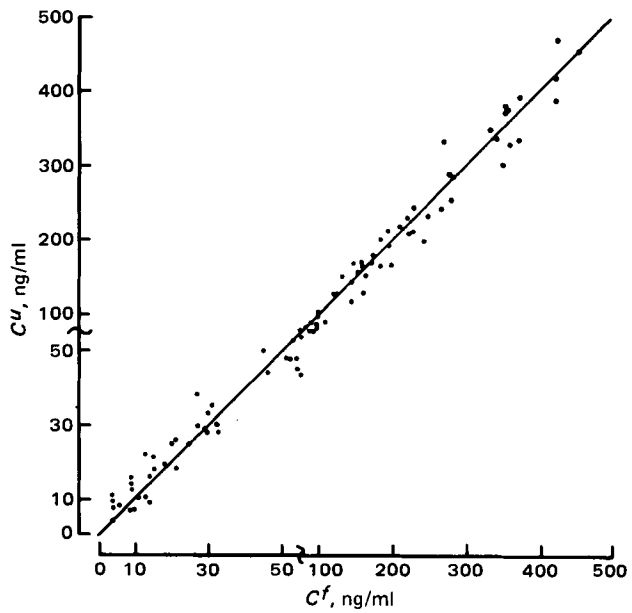

Figure 3—*Plasma hydrocortisone concentrations as obtained by UV detection* (C^u) versus *those obtained by fluorescence detection* (C^f). *Y = 0.992x + 1.59; n = 94, r = 0.987.*

Table I—Mean Values of Pharmacokinetic Parameters Obtained Following 10-, 30-, and 50-mg Oral Doses of Hydrocortisone, with Analysis by HPLC–UV Assay

Parameter	Value			Statistic
	10-mg dose	30-mg dose	50-mg dose	
k_a, hr^{-1}	7.7 ± 7.3[a]	7.7 ± 6.3	1.4 ± 0.5	AB > C[b]
t_0, hr	0.18 ± 0.07	0.26 ± 0.14	0.13 ± 0.23	B > A > C
k_{el}, hr^{-1}	0.47 ± 0.06	0.54 ± 0.04	0.43 ± 0.03	NSD[c]
$t_{1/2el}$, hr	1.50 ± 0.17	1.29 ± 0.09	1.62 ± 0.09	NSD
C_{max}[d], ng/ml	199 ± 29	393 ± 58	419 ± 45	CB > A
T_{max}[e], hr	1.0 ± 0.5	1.0 ± 0.5	1.7 ± 0.3	C > AB
C_{max}/D[f], 10^{-6}/ml	19.9 ± 2.9	13.1 ± 2.0	8.4 ± 0.9	A > B > C
F/V[g], 10^{-6}/ml	23.5 ± 3.6	17.0 ± 2.5	13.7 ± 1.5	A > B > C
AUC_{trap}[h], ng hr/ml	474 ± 48	958 ± 113	1559 ± 142	C > B > A
r^2[i]	0.98 ± 0.02	0.99 ± 0.02	0.99 ± 0.01	NSD

[a] Standard deviation (n = 3). [b] A = 10-mg dose, B = 30-mg dose, C = 50-mg dose. [c] No significant differences ($p > 0.05$). [d] Maximum observed concentration of hydrocortisone in plasma. [e] Time of observed C_{max}. [f] Maximum concentration of hydrocortisone in plasma divided by dose. [g] The fraction of the dose which is adsorbed, expressed as a concentration in the apparent distribution volume; obtained by dividing the function FD/V, from Eq. 1, by the dose. [h] Area under plasma hydrocortisone concentration profile calculated by trapezoidal rule with end correction. [i] Coefficient of determination from nonlinear regression analysis of plasma data using Eq. 1 [$r^2 = (\Sigma obs^2 - \Sigma dev^2)/\Sigma obs^2$].

of 0.99, an intercept that was not significantly different from zero, and a correlation coefficient of 0.987 ($p < 0.001$).

Pharmacokinetic Analysis—No statistical differences were observed in the values of any pharmacokinetic parameters resulting from the two assay methods. Therefore, only those values obtained using the HPLC–UV assay are presented in Table I.

The high coefficients of determination that resulted from analysis of individual data sets indicated that hydrocortisone plasma profiles following oral doses are adequately described by a one-compartment kinetic model. Following the 10- and 30-mg doses, hydrocortisone was absorbed rapidly and peak drug levels in plasma were obtained 1 hr postdose. Following the 50-mg dose, hydrocortisone was absorbed at a slower rate, yielding peak drug levels in plasma at ~1.7 hr. For all three dosages, description of the absorption phase of drug profiles was improved by incorporation of a lag time. After achieving peak values, drug levels declined with a mean half-life of 1.3–1.6 hr; this value was independent of dose size.

Although the maximum concentrations of hydrocortisone in plasma, and also the areas under the drug concentration *versus* time curves, increased with increasing drug doses, they were not dose-proportional. Both C_{max} and AUC_{trap} increased twofold when hydrocortisone dose was increased threefold from 10 to 30 mg. When the dose was further increased 1.6-fold to 50 mg, the value of AUC_{trap} increased in proportion to the dose, while C_{max} increased by a factor of 1.1. When the values of C_{max} and FD/V were normalized for dose, there was a progressive decrease in both of these values as the dose was increased from 10 to 50 mg.

DISCUSSION

HPLC assays for hydrocortisone in biological fluids have the advantage of greater compound specificity than previously used fluorescence (14, 15), competitive protein binding (16), enzyme immunoassay (17), and radioimmunoassay (18) procedures. HPLC assay with a fluorescence detector was claimed to be more sensitive than other analytical methods (8).

The results of this study show that an HPLC assay with UV detection, which requires no derivatization step, is equally specific and sensitive to the HPLC fluorescence assay. Both procedures are capable of measuring hydrocortisone concentrations in plasma following therapeutic doses, are free of interference from hydrocortisone metabolites and endogenous substances in plasma, and are also capable of measuring endogenous hydrocortisone levels following suppression by dexamethasone. The HPLC–UV assay is simpler and less time consuming than the HPLC fluorescence procedure and is therefore the method of choice.

The pharmacokinetic parameter values obtained in the clinical studies are largely in agreement with those published previously. While the elimination phase of plasma hydrocortisone levels was well defined, the short duration of the absorption phase, and also an apparent lag time, does not permit accurate description of this phase. Therefore, the use of first-order kinetics in the present interpretation does not preclude the possibility of alternative absorption mechanisms.

Mean elimination half-lives of hydrocortisone were 90, 77, and 97 min, respectively, following the 10-, 30-, and 50-mg doses. Previous studies using intravenous hydrocortisone have reported drug half-lives between 58 and 161 min (19–23). Circulating levels of hydrocortisone were quite variable at each dose level, which is consistent with previous observations (24, 25).

Additional studies are necessary to confirm the apparent lack of proportionality between circulating levels of hydrocortisone and the administered dose, although similar results to those obtained in this study were reported in subjects receiving oral cortisone acetate (26).

A number of possible factors might cause dose-nonproportionality in hydrocortisone plasma levels. Drug absorption efficiency may be reduced at higher doses due to limited tablet dissolution or to reduced transport across the GI epithelium. Hydrocortisone levels may also be influenced by changes in drug–protein binding. At low drug concentrations, hydrocortisone binds predominantly to the high affinity, low capacity protein transcortin (19, 27). At drug levels >200 ng/ml, binding sites on the transcortin molecule become saturated, and binding to the low affinity, high capacity binding sites of plasma albumin accounts for an increasing proportion of the bound drug. Due to the preponderance of low affinity binding at high drug levels, the percentage of circulating hydrocortisone in the bound form decreases. In the present study, hydrocortisone plasma concentrations >200 ng/ml were achieved with the 30- and 50-mg doses. Reduced overall binding of drug following the higher doses would permit a greater proportion of the drug to enter extravascular fluids, causing a reduction in plasma levels. The reduced binding of hydrocortisone to plasma proteins at high drug concentrations may also increase hepatic clearance during the first-pass, resulting in a smaller proportion of administered drug reaching the systemic circulation (28).

While circulating levels of endogenous hydrocortisone remain constant following dexamethasone suppression (10), further suppression of endogenous levels may result from the administered hydrocortisone by a feedback mechanism. However, suppressed endogenous hydrocortisone levels are low compared with the levels that resulted from administered compound, and further reduction in suppressed levels would not have noticeably affected the results.

Studies have been initiated to examine the dose-proportionality of hydrocortisone pharmacokinetics following parenteral doses.

REFERENCES

(1) N. R. Scott and P. F. Dixon, *J. Chromatogr.*, **164**, 29 (1979).

(2) J. O. Rose and W. J. Jusko, *ibid.*, **162**, 273 (1979).

(3) F. J. Frey, B. M. Frey, and L. Z. Benet, *Clin. Chem.*, **25**, 1944 (1979).

(4) J. H. M. VandenBerg, C. R. Mol, R. S. Deelder, and S. M. M. Thijssen, *Clin. Chim. Acta*, **78**, 165 (1977).

(5) D. C. Garg, J. W. Ayres, and J. G. Wagner, *Res. Commun. Chem. Pathol. Pharmacol.*, **18**, 137 (1977).

(6) G. E. Reardon, A. M. Caldarella, and E. Canalis, *Clin. Chem.*, **25**, 122 (1979).

(7) P. M. Kabra, L. Tsai, and L. J. Marton, *ibid.*, **25**, 1293 (1979).

(8) T. J. Goehl, G. M. Sundaresan, and V. K. Prasad, *J. Pharm. Sci.*, **68**, 1374 (1979).

(9) T. Kawasaki, M. Maeda, and A. Tsuji, *J. Chromatogr.*, **163**, 143 (1979).

(10) T. J. Goehl, G. M. Sundaresan, J. P. Hunt, V. K. Prasad, R. D. Toothaker, and P. G. Welling, *J. Pharm. Sci.*, **69**, 1409 (1980).

(11) J. G. Wagner, "Fundamentals of Clinical Pharmacokinetics," Drug Intelligence Publications, Hamilton, Ill., 1975, pp. 81.

(12) "MACC Nonlinear Regression Routines," Academic Computer Center, University of Wisconsin-Madison 53706, 1972.

(13) J. Neter and W. Wasserman, "Applied Linear Statistical Models," Richard D. Irwin, Homewood, Ill., 1974, pp. 474–477.
(14) G. Dower and F. Stahl, *Gen. Med. Monthly*, **10**, 443 (1965).
(15) D. Mattingly, *J. Clin. Pathol.*, **15**, 374 (1962).
(16) B. Murphy and C. Poltee, *J. Clin. Endocrinol.*, **24**, 919 (1964).
(17) Y. Kobayashi, T. Ogihara, K. Amitoni, F. Watanabe, T. Kiguchi, I. Ninomiya, and Y. Kumahara, *Steroids*, **32**, 137 (1978).
(18) J. Seth and L. M. Brown, *Clin. Chim. Acta*, **86**, 109 (1978).
(19) W. R. Beisel, V. C. Diraimondo, P. Y. Chao, J. M. Rosner, and P. H. Forsham, *Metabolism*, **13**, 942 (1964).
(20) J. Scheuer and P. K. Bondy, *J. Clin. Invest.*, **36**, 67 (1957).
(21) P. J. Fell, *Clin. Endocrinol.*, **1**, 65 (1972).
(22) P. L. Morselli, V. Marc, S. Garattini, and M. Zaccala, *Biochem. Pharmacol.*, **19**, 1643 (1970).
(23) R. E. Peterson, J. B. Wyngaarden, S. L. Guerra, B. B. Brodie, and J. J. Bunim, *J. Clin. Invest.*, **34**, 1779 (1955).
(24) D. Abelson and D. A. Borcherds, *J. Clin. Endocrinol.*, **19**, 219 (1959).
(25) H. Kehlet, C. Binder, and M. Blichert-Toft, *Clin. Endocrinol.*, **5**, 37 (1976).
(26) W. A. Colburn, A. R. DiSanto, S. S. Stubbs, R. E. Monovich, and K. E. DiSante, *J. Clin. Pharmacol.*, **20**, 428 (1980).
(27) W. J. Jusko, in "The Effect of Disease States on Drug Pharmacokinetics," L. Z. Benet, Ed., APhA, Washington, D.C., 1976, p. 115.
(28) A. A. Sandberg and W. R. Slaunwhite, Jr., *J. Clin. Invest.*, **42**, 51 (1963).

ACKNOWLEDGMENTS

Funds for this study were provided by U.S. Food and Drug Administration Contract 223-78-3006.

Acrylic Microspheres *In Vivo* V: Immunological Properties of Immobilized Asparaginase in Microparticles

PETER EDMAN and INGVAR SJÖHOLM ˣ

Received February 2, 1981, from the *Department of Pharmaceutical Biochemistry, Biomedical Center, University of Uppsala, Box 578, 751 23 Uppsala, Sweden.* Accepted for publication September 3, 1981.

Abstract □ L-Asparaginase was immobilized in microparticles of polyacrylamide. Such particles were then injected by intramuscular/subcutaneous, intraperitoneal, or intravenous routes into mice to investigate the immunological consequences of the immobilization. Entrapment of L-asparaginase in microparticles did not prevent the formation of antibodies in intensively treated animals. Intraperitoneal and intravenous injections of particles produced significantly higher antibody levels than soluble L-asparaginase. Antigen administered intramuscularly/subcutaneously in microparticles elicited, however, a weak immune response. Dependent on the route of administration, the particles may thus function as an adjuvant. A modified Arthus reaction in the foot pads of immunized mice indicated that antigenicity decreased when L-asparaginase was immobilized in microparticles. Injection of free L-asparaginase, intramuscularly/subcutaneously (2 × 20 IU) in the preimmunized mice produced no effects on the serum level of L-asparagine, whereas intramuscular/subcutaneous injection of L-asparaginase in microparticles produced a depression of the serum concentration. It is concluded that the intramuscular/subcutaneous injection of L-asparaginase in microparticles is the choice route of administration with respect to duration and the immunological reaction.

Keyphrases □ L-Asparaginase—immunological properties of immobilized L-asparaginase in microparticles □ Microparticles—immunological properties of immobilized L-asparaginase □ Immunological properties—of immobilized L-asparaginase in microparticles

Exogenous enzymes have been used increasingly in biological systems to test their usefulness in treating genetic disorders, *e.g.*, lysosomal storage diseases (1, 2), or for therapeutic purposes, *e.g.*, L-asparaginase to depress circulating L-asparagine in the treatment of acute lymphatic leukemia (3). These enzymes are often used in the immobilized or polymerized form in order to prolong their duration (4–6). However, the desired prolonged effect is seemingly in conflict with the efforts to decrease their immunological properties manifested by the production of antibodies and hypersensitivity reactions, which is enhanced when exposure to the exogenous protein is prolonged. Thus, enzymes in liposomes have been shown to be immunogenic[1]. The liposomes have even, in some instances, been shown to exert adjuvant effects (7). This effect may be due partly to leakage of enzyme molecules out of the liposomes or lysis of the liposomes, but the findings that the adjuvant properties are related to the composition of the liposomes (7, 8) suggest that the adjuvant effects are inherently connected with the liposomes themselves. Likewise, polymethylmethacrylate has been shown to increase the immunogenic properties of simultaneously administered influenza virons (9). The adjuvant effect is strongly correlated to the route of administration, with intravenous or intraperitoneal injections of the immobilized systems generally producing relatively higher antibody titers (7, 10).

The present study was undertaken to investigate the immunological consequences of the utilization of microparticles of polyacrylamide as carrier of exogenous proteins *in vivo*. The polymer itself is not immunogenic (11), but immobilized proteins are partly localized on the surface of the microparticles during the preparation as evidenced by their interaction with cellular surface structures (12) or affinity chromatography material (13). Even if the major portion of the immobilized protein is secluded inside the microparticles, the fraction on the surface should exert immunological properties. The aim was to find the optimal route for the administration of immobilized L-asparaginase.

EXPERIMENTAL

Materials—Aspartate aminotransferase[2] (83 IU/mg) isolated from porcine heart, and malic dehydrogenase[2] (2000 IU/ml) from pigeon breast

[1] In the present paper, the term immunogenic is used to describe the property of a macromolecular system to evoke an immunological response, *e.g.*, antibody production and T-cell stimulation, while the term antigenic is restricted to the property to react with the immunological effectors in a sensitized organism.
[2] Sigma Chemical Co.

0022-3549/82/0500-0576$01.00/0

(13) J. Neter and W. Wasserman, "Applied Linear Statistical Models," Richard D. Irwin, Homewood, Ill., 1974, pp. 474–477.
(14) G. Dower and F. Stahl, *Gen. Med. Monthly*, **10**, 443 (1965).
(15) D. Mattingly, *J. Clin. Pathol.*, **15**, 374 (1962).
(16) B. Murphy and C. Poltee, *J. Clin. Endocrinol.*, **24**, 919 (1964).
(17) Y. Kobayashi, T. Ogihara, K. Amitoni, F. Watanabe, T. Kiguchi, I. Ninomiya, and Y. Kumahara, *Steroids*, **32**, 137 (1978).
(18) J. Seth and L. M. Brown, *Clin. Chim. Acta*, **86**, 109 (1978).
(19) W. R. Beisel, V. C. Diraimondo, P. Y. Chao, J. M. Rosner, and P. H. Forsham, *Metabolism*, **13**, 942 (1964).
(20) J. Scheuer and P. K. Bondy, *J. Clin. Invest.*, **36**, 67 (1957).
(21) P. J. Fell, *Clin. Endocrinol.*, **1**, 65 (1972).
(22) P. L. Morselli, V. Marc, S. Garattini, and M. Zaccala, *Biochem. Pharmacol.*, **19**, 1643 (1970).
(23) R. E. Peterson, J. B. Wyngaarden, S. L. Guerra, B. B. Brodie, and J. J. Bunim, *J. Clin. Invest.*, **34**, 1779 (1955).
(24) D. Abelson and D. A. Borcherds, *J. Clin. Endocrinol.*, **19**, 219 (1959).
(25) H. Kehlet, C. Binder, and M. Blichert-Toft, *Clin. Endocrinol.*, **5**, 37 (1976).
(26) W. A. Colburn, A. R. DiSanto, S. S. Stubbs, R. E. Monovich, and K. E. DiSante, *J. Clin. Pharmacol.*, **20**, 428 (1980).
(27) W. J. Jusko, in "The Effect of Disease States on Drug Pharmacokinetics," L. Z. Benet, Ed., APhA, Washington, D.C., 1976, p. 115.
(28) A. A. Sandberg and W. R. Slaunwhite, Jr., *J. Clin. Invest.*, **42**, 51 (1963).

ACKNOWLEDGMENTS

Funds for this study were provided by U.S. Food and Drug Administration Contract 223-78-3006.

Acrylic Microspheres *In Vivo* V: Immunological Properties of Immobilized Asparaginase in Microparticles

PETER EDMAN and INGVAR SJÖHOLM ˣ

Received February 2, 1981, from the *Department of Pharmaceutical Biochemistry, Biomedical Center, University of Uppsala, Box 578, 751 23 Uppsala, Sweden.* Accepted for publication September 3, 1981.

Abstract □ L-Asparaginase was immobilized in microparticles of polyacrylamide. Such particles were then injected by intramuscular/subcutaneous, intraperitoneal, or intravenous routes into mice to investigate the immunological consequences of the immobilization. Entrapment of L-asparaginase in microparticles did not prevent the formation of antibodies in intensively treated animals. Intraperitoneal and intravenous injections of particles produced significantly higher antibody levels than soluble L-asparaginase. Antigen administered intramuscularly/subcutaneously in microparticles elicited, however, a weak immune response. Dependent on the route of administration, the particles may thus function as an adjuvant. A modified Arthus reaction in the foot pads of immunized mice indicated that antigenicity decreased when L-asparaginase was immobilized in microparticles. Injection of free L-asparaginase, intramuscularly/subcutaneously (2 × 20 IU) in the preimmunized mice produced no effects on the serum level of L-asparagine, whereas intramuscular/subcutaneous injection of L-asparaginase in microparticles produced a depression of the serum concentration. It is concluded that the intramuscular/subcutaneous injection of L-asparaginase in microparticles is the choice route of administration with respect to duration and the immunological reaction.

Keyphrases □ L-Asparaginase—immunological properties of immobilized L-asparaginase in microparticles □ Microparticles—immunological properties of immobilized L-asparaginase □ Immunological properties—of immobilized L-asparaginase in microparticles

Exogenous enzymes have been used increasingly in biological systems to test their usefulness in treating genetic disorders, *e.g.*, lysosomal storage diseases (1, 2), or for therapeutic purposes, *e.g.*, L-asparaginase to depress circulating L-asparagine in the treatment of acute lymphatic leukemia (3). These enzymes are often used in the immobilized or polymerized form in order to prolong their duration (4–6). However, the desired prolonged effect is seemingly in conflict with the efforts to decrease their immunological properties manifested by the production of antibodies and hypersensitivity reactions, which is enhanced when exposure to the exogenous protein is prolonged. Thus, enzymes in liposomes have been shown to be immunogenic[1]. The liposomes have even, in some instances, been shown to exert adjuvant effects (7). This effect may be due partly to leakage of enzyme molecules out of the liposomes or lysis of the liposomes, but the findings that the adjuvant properties are related to the composition of the liposomes (7, 8) suggest that the adjuvant effects are inherently connected with the liposomes themselves. Likewise, polymethylmethacrylate has been shown to increase the immunogenic properties of simultaneously administered influenza virons (9). The adjuvant effect is strongly correlated to the route of administration, with intravenous or intraperitoneal injections of the immobilized systems generally producing relatively higher antibody titers (7, 10).

The present study was undertaken to investigate the immunological consequences of the utilization of microparticles of polyacrylamide as carrier of exogenous proteins *in vivo*. The polymer itself is not immunogenic (11), but immobilized proteins are partly localized on the surface of the microparticles during the preparation as evidenced by their interaction with cellular surface structures (12) or affinity chromatography material (13). Even if the major portion of the immobilized protein is secluded inside the microparticles, the fraction on the surface should exert immunological properties. The aim was to find the optimal route for the administration of immobilized L-asparaginase.

EXPERIMENTAL

Materials—Aspartate aminotransferase[2] (83 IU/mg) isolated from porcine heart, and malic dehydrogenase[2] (2000 IU/ml) from pigeon breast

[1] In the present paper, the term immunogenic is used to describe the property of a macromolecular system to evoke an immunological response, *e.g.*, antibody production and T-cell stimulation, while the term antigenic is restricted to the property to react with the immunological effectors in a sensitized organism.
[2] Sigma Chemical Co.

0022-3549/82/0500-0576$01.00/0

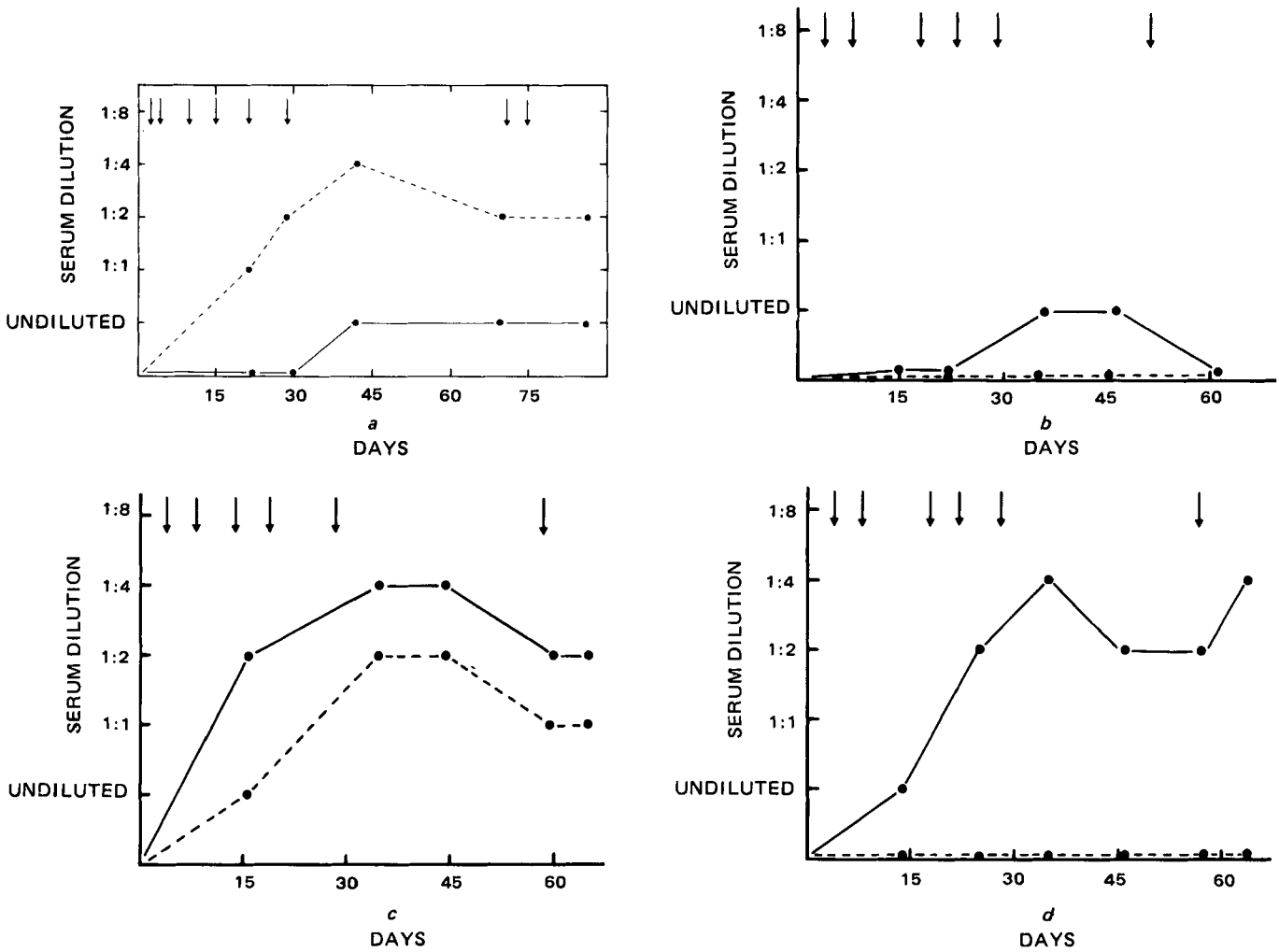

Figure 1—*Antibody response in mice after immunization with* L-*asparaginase in microparticles or in soluble form. 5 IU of* L-*asparaginase was administered on the days indicated by arrows at the top of the graphs. The antibody titer of the serum is measured by Ouchterlony double diffusion as described under* Materials and Methods. *(a)* L-*Asparaginase was given im/sc in microparticles (●—●) or in free form (●- - -●), with Freund's complete/incomplete adjuvant in the back of mice*[10]. *(b)* L-*Asparaginase was given im/sc in microparticles (●—●) or in free form (●- - -●), in 0.1 ml of physiological saline in the back of mice*[9]. *(c)* L-*Asparaginase was given ip in microparticles (●—●) or in free form (●- - -●) in physiological saline in mice*[10]. *(d)* L-*Asparaginase was given iv in microparticles (●—●) or in free form (●- - -●) in physiological saline in mice*[9].

muscle, were used without further purification. Acrylamide[3], *N,N'*-methylenebisacrylamide[3], *N,N',N',N'*-tetramethylethylenediamine[2], tromethamine[2], α-ketoglutaric acid[2], nadide[2] (NADH, reduced form), L-asparagine monohydrate[4], Nessler's reagent[2], and other chemicals were of analytical grade. L-Asparaginase[5] from *Escherichia coli* was used without further purification.

Preparation of Microparticles—Microparticles[6] (TC% = 8–25[7]) with immobilized L-asparaginase were prepared according to a reported method (5) by emulsion polymerization of acrylamide and bisacrylamide with L-asparaginase. In a typical example, the aqueous phase was composed of 5.0 ml of acrylamide (6% w/v) and *N,N'*-methylenebisacrylamide (2% w/v) in 0.005 *M* phosphate buffer, pH 7.4.

The protein was dissolved in the acrylic monomer solution. After the addition of 100 μl of ammonium peroxydisulfate (500 mg/ml in water) to the water phase, it was immediately homogenized with 200 ml of chloroform–toluene (1:4) containing a detergent[8], polyoxyethylene–polyoxypropylene (0.5 g), to produce a w/o emulsion. The polymerization was initiated by adding 1.0 ml of *N,N,N',N'*-tetramethylethylenediamine to the emulsion. The microparticles were isolated by centrifugation, washed several times with buffer, and after the last washing suspended in physiological saline. The mean diameter of the microparticles was ~0.25–0.30 μm.

[3] Eastman Kodak Co.
[4] Merck Co.
[5] Crasnitin was obtained as a gift from Bayer (Sverige) AB, Stockholm.
[6] U.S. pat. 4,061,966.
[7] The nomenclature suggested by Hjertén (1962) (14).
[8] Pluronics F-68, Ugine Kuhlman, Paris, France.

Assay of Native and Immobilized L-Asparaginase—L-Asparaginase activity was determined by direct nesslerization of the ammonia produced by its reaction with L-asparagine (5, 15). The absorbance was determined at 500 nm. Enzyme and substrate blanks were included in all assays. A standard curve was prepared with ammonium sulfate. One unit of activity is defined as the amount of enzyme catalyzing the formation of 1.0 μmole of ammonia/min at 37°.

Determination of L-Asparagine—Assay of serum of L-asparagine was performed according to a reported fluorometric method (16). Blood was taken from the tail vein or the orbital plexus of 4 to 5 mice and centrifuged at 4° for 15 min to obtain serum. The serum samples were pooled to obtain 60 μl of serum and carefully mixed with 150 μl of 5% trichloroacetic acid. After centrifugation at 4° for 10 min, the supernate was extracted three times with diethylether and the L-asparagine was analyzed.

Animals—Male mice[9,10] were used throughout. At the start of the experiments they weighed 20 g.

Immunization Procedures—Groups of 10 mice were injected with L-asparaginase (5 IU in microparticles or in soluble form) by different routes: intramuscular/subcutaneous, intraperitoneal, and intravenous. The enzyme was administered in physiological saline (intramuscular/subcutaneous, intraperitoneal, and intravenous) or in Freund's complete/incomplete adjuvant (intramuscular/subcutaneous). The animals received booster injections after 4, 8, 18, 22, 28, and 52 days. Blood samples were taken before the first injection and after 2, 4, 5, 8, and 10 weeks.

[9] NMRI-mice, Anticimex, Stockholm, Sweden.
[10] C3H-mice, Bomholtsgård, Denmark.

Table I—Arthus Reaction in Preimmunized Mice after Asparaginase Injections

Number of Mice	Immunization Procedure	Provoking Enzyme Preparation[a]	Mean Diameter ± *SD* of Left and Right Foot Pad[b], cm	Probability[c]	Mean Ratio ± *SD* of Foot Pad Thickness	Probability[c]
4	Soluble L-asparaginase im/sc[d]	Soluble Enzyme	0.36 ± 0.02 0.25 ± 0.01	<0.01	1.43 ± 0.17	<0.05
4	Soluble L-asparaginase im/sc[d]	Microparticles	0.37 ± 0.03 0.33 ± 0.01	>0.05	1.14 ± 0.10	
5	Microparticles im/sc[d]	Soluble Enzyme	0.37 ± 0.01 0.26 ± 0.01	<0.01	1.41 ± 0.08	<0.01
4	Microparticles im/sc[d]	Microparticles	0.37 ± 0.01 0.34 ± 0.01	>0.05	1.11 ± 0.06	
5	Soluble L-asparaginase ip	Soluble Enzyme	0.36 ± 0.01 0.26 ± 0.01	<0.01	1.39 ± 0.10	<0.01
5	Soluble L-asparaginase ip	Microparticles	0.33 ± 0.01 0.31 ± 0.01	>0.05	1.06 ± 0.06	
4	Microparticles ip	Soluble Enzyme	0.36 ± 0.01 0.23 ± 0.01	<0.01	1.58 ± 0.14	<0.01
3	Microparticles ip	Microparticles	0.33 ± 0.01 0.30 ± 0.01	>0.05	1.12 ± 0.03	

[a] Mice were challenged by injection into the left hind foot pad of either 10 μl of L-asparaginase (80 IU/ml) or 10 μl of immobilized L-asparaginase in microparticles (80 IU/ml, dry weight 23.1 mg/ml) and into the right food pad of 10 μl of physiological saline or 10 μl of microparticles not containing any enzyme (dry weight 23.1 mg/ml). [b] The thickness of the foot pads was measured 3 hr after provocation. [c] The significance of the difference was calculated by variance analysis. [d] These groups were previously injected with 50 IU L-asparaginase ip in microparticles or in soluble form.

The blood was collected from the tail vein or from the orbital plexus, pooled, and centrifuged at 4° to obtain serum. Each mouse received 35–45 IU of L-asparaginase during the study.

Antibody Determination—The antibody titer was assayed by double immunodiffusion in agar gel as described previously (17). The titer was determined by the highest dilution of serum which produced precipitation with the antigen (5 μg of L-asparaginase in 10 μl of physiological saline was placed in the center well).

Mice, pretreated with immobilized or native L-asparaginase by different routes of administration, were tested for the Arthus reaction (18). The enzyme, 10 μl containing 0.8 IU in soluble form or in microparticles (dry weight 0.23 mg), was injected into the left foot pad of the hind leg. The right foot pad, which served as control, was injected with the same volume, 10 μl, of microparticles not containing any enzyme, or with physiological saline.

Three hours later, and again at 24 and 48 hr, the thickness of both foot pads was measured with a micrometer gauge and the ratio between the two calculated.

Autoradiography—Whole body autoradiography was performed according to the method of Ullberg (19). ^{14}C-Labeled microparticles (4.1 mg; 400,000 dpm) were injected intramuscularly/subcutaneously in some mice with physiological saline in the back. After 2 months the animals were sacrificed with ether and frozen in hexane–solid carbon dioxide (−78°). The mice were embedded in a gel of carboxy-methylcellulose and cut into 20- or 60-μm sagittal sections with a microtome. The sections were cut at −15–20° and freeze-dried. The slices were pressed against photographic films which were exposed for up to 6 months.

RESULTS

Antibody Production in Mice after Treatment with L-Asparaginase in Microparticles—L-Asparaginase was immobilized in microparticles as described previously. The microparticles were injected in mice by different routes and the antibody titers obtained were followed up to ~2.5 months by double immunodiffusion tests. The results are shown in Figs. 1*a*–1*d* and compared with the response obtained after treatment with the same amounts of free, soluble enzyme given under identical conditions.

Immobilization of L-asparaginase in microparticles of polyacrylamide did not prevent the formation of specific antibodies in intensively treated animals. However, it is evident from Fig. 1*a* that the immune response after intramuscular/subcutaneous injection in Freund's adjuvant is weak and significantly weaker than after injection of soluble enzyme. A weak precipitin line was detectable only in undiluted serum. Any antibody production after intramuscular/subcutaneous injection of soluble enzyme in physiological saline is not detectable (Fig. 1*b*), presumably as a consequence of the short half-life of the enzyme.

Figures 1*c* and 1*d* demonstrate the adjuvant effect of the microparticles

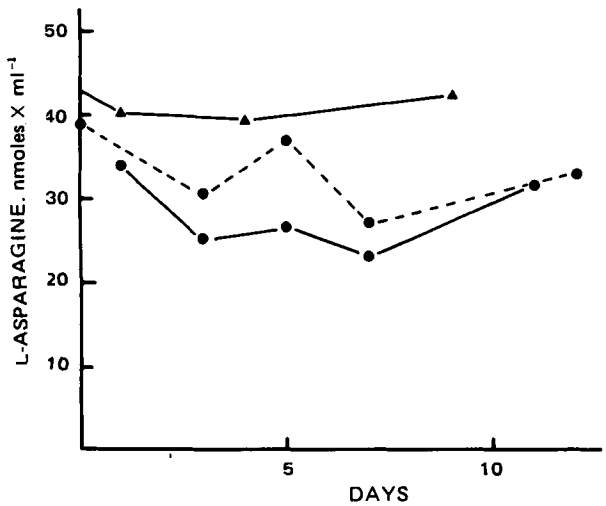

Figure 2—*L-Asparagine concentration in serum after a single ip injection of L-asparaginase (50 IU) in microparticles (●—●) or in free solution (●---●). Each point represents samples drawn from 4–5 mice[10]. The animals were preimmunized with L-asparaginase in microparticles injected im/sc in Freund's adjuvant. The normal L-asparagine concentration (▲—▲) was obtained from a control group given only physiological saline.*

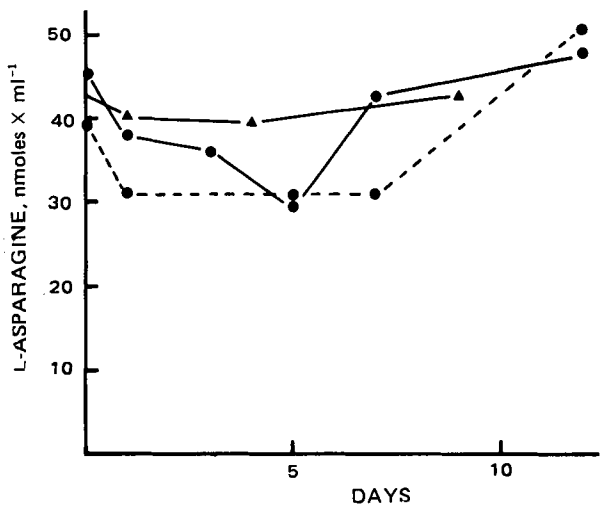

Figure 3—*L-Asparagine concentration in serum after a single ip injection of asparaginase (50 IU) in microparticles (●—●) or in soluble form (●---●). Each point represents serum samples drawn from 4–5 mice[10]. These animals were preimmunized with free L-asparaginase injected im/sc in Freund's adjuvant. The normal L-asparagine concentration (▲—▲) was obtained from a control group given only physiological saline.*

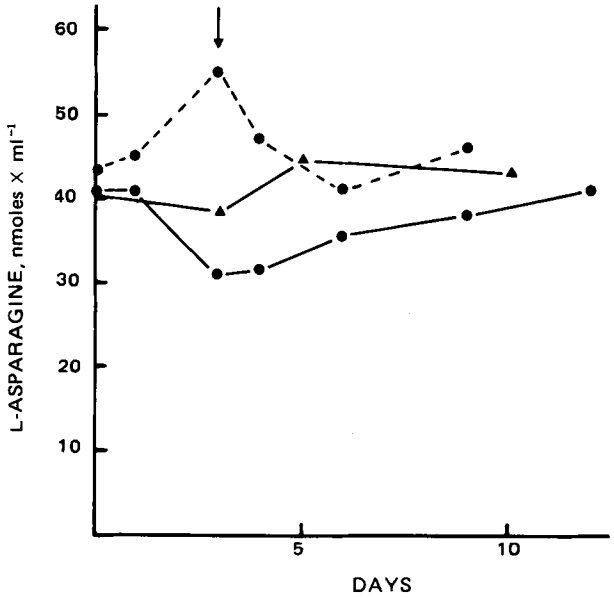

Figure 4—*L-Asparagine concentration in serum. Each point represents pooled samples from 4–5 mice[10] given im/sc 2 × 20 IU of* L*-asparaginase (with an interval of 3 days) in microparticles (●—●) or in free solution (●---●). The animals were preimmunized with* L*-asparaginase in microparticles injected ip. The arrow shows the time for the second injection of 20 IU* L*-asparaginase in microparticles or in free form. The normal* L*-asparagine concentration (▲—▲) was obtained from a control group given only physiological saline.*

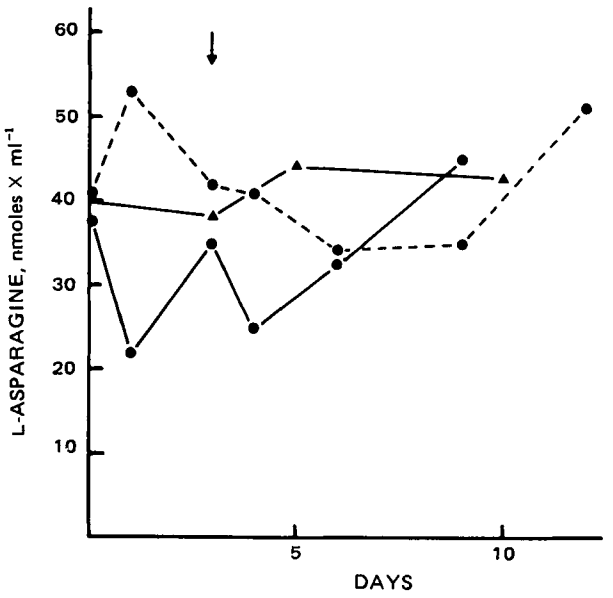

Figure 5—*L-Asparagine concentration in serum. Each point represents pooled serum from 4–5 mice[10] given im/sc 2 × 20 IU of asparaginase (with an interval of 3 days) immobilized in microparticles (●—●) or in free form (●---●). The animals were preimmunized with free* L*-asparaginase given ip. The arrow shows the time for the second injection of 20 IU* L*-asparaginase in microparticles or in free form. The normal* L*-asparagine concentration (▲—▲) was obtained from a control group given only physiological saline.*

administered as intraperitoneal and intravenous injections. After intraperitoneal injection of L-asparaginase in microparticles, a rapid and high production of specific antibodies was seen and in addition, high titers were obtained after intravenous injection. Intravenous injection of native L-asparaginase did not produce any antibodies which could be detected by immunodiffusion, while intraperitoneal injection was effective in producing high amounts of antibodies. The abdomen is drained by the lymphatic vessels, and it is obvious that the strong response is a consequence of the administration of the L-asparaginase close to the lymph nodes.

Studies with a Modified Arthus Test—Under standardized conditions the level of circulating specific antibodies can be estimated in different Arthus tests, in which an antigen–antibody complex mediated hypersensitivity reaction is provoked in different tissues.

Table I presents results from an Arthus reaction test in the foot pads of mice immunized in different standardized ways. The reaction is expressed as the ratio of the thickness of the foot pad injected with the sample (L-asparaginase in soluble or immobilized form) to that of the foot pad injected with empty microparticles or with physiological saline. Mice treated with L-asparaginase intraperitoneally and intramuscularly/subcutaneously were used for the Arthus reaction. Independent of the state of the antigen (immobilized or soluble) with which the mice were immunized, all mice gave an Arthus reaction 3 hr after injection when both native and immobilized L-asparaginase had been used. The swelling at the sites of injection were retracted after 24 hr. L-Asparaginase in the microparticles gave the same or smaller response (thickness of the left foot pads) than the same dose of soluble enzyme. However, the reaction was partly unspecific, in the sense that the microparticles themselves produced an increase in the size of the foot pads, which was significantly larger than that produced by physiological saline. In fact, the response given by the enzyme in microparticles was statistically not significantly larger than that given by the particles themselves. Consequently, the response measured as the ratio of the thickness of the two foot pads was significantly lower with the enzyme administered in microparticles than with soluble enzyme. This means that the antigenicity of the enzyme is decreased by immobilization in microparticles.

L-Asparaginase Effect in Preimmunized Mice—The capacity of differently immunized mice to neutralize and inhibit the effect of L-asparaginase administered in different ways has also been studied. Figures 2–5 show the results obtained from mice in which the serum concentration of L-asparagine was followed as a measure of the L-asparaginase activity and duration. Normally, intramuscular injection of 2 × 2.5 IU of L-asparaginase in microparticles or 5–10 IU injected intravenously depresses the L-asparagine to almost 0 values for 5–7 days, but in the preimmunized animals, considerably higher doses have to be used for any effects on the L-asparagine. Even 50 IU of the enzyme produced only a small and transient effect. Figure 2 illustrates the effects obtained after intraperitoneal injection of 50 IU of L-asparaginase in microparticles or in native form into mice previously treated with free L-asparaginase by the intramuscular/subcutaneous route. Only small effects on the serum level were obtained and no significant differences could be detected between free and immobilized enzyme. Similar results were obtained when the same amount of enzyme in microparticles or in soluble form was injected intraperitoneally into mice pretreated with microparticles given by the intramuscular/subcutaneous route (Fig. 3). A 10–20% reduction of the serum concentration of L-asparagine was achieved the day after injection, but the level was soon normalized.

The results shown in Fig. 4 illustrate the effect of enzyme in microparticles and native enzyme given intramuscularly/subcutaneously in two doses (2 × 20 IU, with an interval of three days) into mice previously treated with immobilized L-asparaginase in microparticles by the intraperitoneal route. Injection of free enzyme did not produce any depression of the serum level of L-asparagine, while some reduction of the serum concentration was achieved when the particles were given intramuscularly/subcutaneously.

Figure 5 shows the changes seen after intramuscular/subcutaneous injection of 2 × 20 IU of L-asparaginase in free or immobilized forms into mice previously treated with native L-asparaginase intraperitoneally. In this case, injection of immobilized enzyme produced lower levels the day after injection, but they were normalized again after 3 days. The same procedure was repeated after the second injection; low values (25–30 nmoles) were found the day after injection, which were normalized again after 2–3 days. Intramuscular injection of L-asparaginase in free solution did not affect the serum concentration of L-asparagine at all.

Whole Body Autoradiography after Intramuscular Subcutaneous Injection of Microparticles in Mice—Figure 6 shows the distribution of C^{14}-labeled microparticles 2 months after intramuscular/subcutaneous injection. The particles were encapsulated at the injection site, and no radioactivity could be detected in the liver or spleen.

DISCUSSION

The microparticle is a macroporous bead in which the immobilized macromolecules are partly entrapped, partly fixed in the polymer bundles forming the network (20). Consequently, a fraction of the immobilized molecules, and their antigenic determinants, will be exposed on the

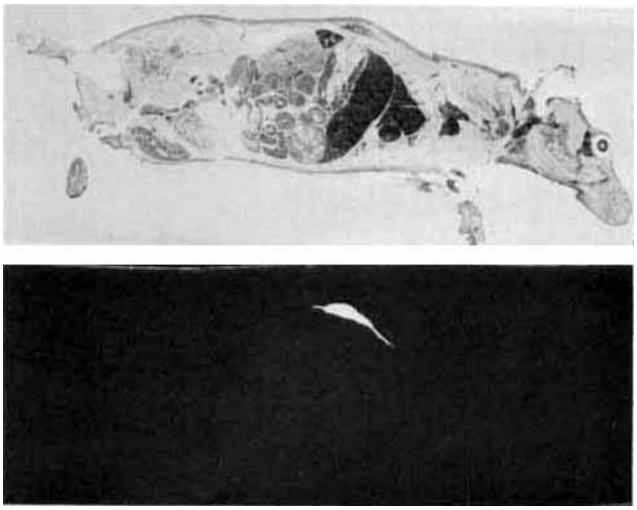

Figure 6—*Whole body autoradiogram of a mouse 2 months after im/sc injection of C^{14}-labeled microparticles (400,000 dpm in 4.1 mg). Bottom: Corresponding tissue section 20 μm.*

surface of the microparticles, and this fraction will be larger, the smaller the beads are. The polyacrylamide forming the microparticle is not immunogenic itself. Therefore, it is to be expected that the immunological response provoked by the immobilized proteins will be determined by the immunogenic properties of the exposed macromolecules and, providing the microparticle has no adjuvant effect, will be related to the size of the particles and will be smaller than that exerted by the native macromolecule administered under the same conditions. As shown, this hypothesis holds true when L-asparaginase is injected intramuscularly with Freunds adjuvant. As a result, soluble enzyme slowly diffuses out from the oil depot with a strong immunological response, which is amplified by the adjuvant. On the other hand, the microparticles stay at the site of injection, as shown by the autoradiogram, and are not reached by the immunocompetent cells to any significant degree. Consequently, there is a low immunological response. When the microparticles are given in saline, the response is quantitatively the same, while the soluble L-asparaginase is rapidly distributed and degraded with poor reaction as a result. The reaction in the two strains of mice used is the same in this respect.

After intraperitoneal administration of L-asparaginase in microparticles, high antibody production could be seen both in the diffusion test and in the modified Arthus reaction, which was stronger than with soluble enzyme. This is a surprising result, as it is known that the particles are rapidly cleared from the abdomen and the circulation and taken up by cells belonging to the reticuloendothelial system in bone marrow, liver, and spleen (21), and thereby are prevented from a primary reaction with the immune system. However, it is apparent that the rapid uptake in the macrophages triggers a secondary response mediated *via* some lymphocyte activating factor (LAF as found in ref. 22). In this sense the microparticles may function as an adjuvant, considerably improving the immunological response.

The distribution of the microparticles after intravenous injection is the same as after intraperitoneal injection, and the antibody production is consequently the same. However, the immune response after intravenous injection of free L-asparaginase is significantly impaired and no antibodies could be detected in the double immunodiffusion tests. The $t_{1/2}$ of the enzyme is short and the direct effect on the lymph system is not obtained in the same way as after intraperitoneal administration.

The modified Arthus test employed gives information not only about the antibody production in the mice, but also, in this modification, about the antigenicity of the L-asparaginase in soluble and in immobilized form. The antibody-mediated reaction on injection of different samples in the foot pads is estimated from the degree of the edema produced, when the sample is injected in one foot and the appropriate control in the other. It can be seen in Table 1 that the injections of microparticles with L-asparaginase produce a much smaller reaction than native enzyme, despite the fact that the unspecific reaction from the microparticles themselves is stronger than from physiological saline. Thus, it can be concluded that the antigenicity is decreased as a consequence of the immobilization in the microparticles.

Earlier studies have shown that the optimal way of administration of immobilized L-asparaginase is the intramuscular/subcutaneous route, when the duration of the effect on the L-asparagine level *in vivo* is considered. The present results also indicate that the intramuscular injection is the preferred way of administration as far as the immunological response is concerned, giving the smallest antibody production. In addition, the effect of L-asparaginase given in microparticles as intramuscular/subcutaneous injection in immunized animals is more pronounced than of intraperitoneal injection. Thus, 50 IU of L-asparaginase given intraperitoneally gave a slight decrease in the L-asparagine level, while an intramuscular/subcutaneous 2 × 20 IU dose slightly decreased the level for 5–7 days.

REFERENCES

(1) P. E. Belchetz, I. P. Braidman, J. C. W. Crawley, and G. Gregoriadis, *Lancet* **2,** 116 (1977).

(2) D. A. Tyrell, B. E. Ryman, B. R. Keeton, and V. Dubowitz, *Br. Med. J.* **2,** 88 (1976).

(3) H. F. Oettgen, L. J. Old, E. A. Boyse, H. A. Campbell, F. S. Philips, B. D. Clarkson, L. Tallal, R. D. Leeper, M. K. Schwartz, and J. H. Kim, *Cancer Res.*, **27,** 2619 (1967).

(4) T. M. S. Chang, *Nature*, **229,** 117 (1971).

(5) P. Edman and I. Sjöholm, *J. Pharmacol. Exp. Ther.*, **211,** 663 (1979).

(6) S. Updike, C. Prieve, and J. Magnuson, *Birth Defects. Orig. Artic. Ser.*, **9,** 77 (1973).

(7) A. C. Allison and G. Gregoriadis, *Nature*, **252,** 252 (1974).

(8) T. Yasuda, G. F. Dancey, and S. C. Kinsky, *Proc. Natl. Acad. Sci. USA*, **74,** 1234 (1977).

(9) J. Kreuter and P. P. Speiser, *Infect. Immun.*, **13,** 204 (1976).

(10) T. D. Heath, D. C. Edwards, and B. E. Ryman, *Biochem. Soc. Trans.*, **4,** 129 (1976).

(11) P. A. Drewes, A. O. Kamp, and J. W. Winkelman, *Experientia*, **34,** 316 (1978).

(12) I. Ljungstedt, B. Ekman, and I. Sjöholm, *Biochem. J.*, **170,** 161 (1978).

(13) B. Ekman and I. Sjöholm, *Nature*, **257,** 825 (1975).

(14) S. Hjertén, *Arch. Biochem. Biophys. Suppl.*, **1,** 147 (1962).

(15) T. O. Yellin and J. C. Wriston, Jr., *Biochemistry*, **5,** 1605 (1966).

(16) D. A. Cooney, R. A. Capizzi, and R. E. Handschumacher, *Cancer Res.*, **30,** 929 (1970).

(17) O. Ouchterlony, in "Handbook of Experimental Immunology," D. M. Weir, Ed., Blackwell Scientific, Oxford, England, 1967, p. 655.

18. G. Gregoriadis and A. C. Allison, *FEBS Lett.*, **45,** 71 (1974).

19. S. Ullberg, "Proceedings of the 2nd UN International Conference on the Peaceful Uses of Atomic Energy," vol. 24, 1958, p. 248.

(20) B. Ekman, C. Lofter, and I. Sjöholm, *Biochemistry*, **15,** 5115 (1976).

(21) I. Sjöholm and P. Edman, *J. Pharmacol. Exp. Ther.*, **211,** 656 (1979).

(22) I. Roitt, "Essential Immunology," 3rd ed., Blackwell Scientific, Oxford, England, 1977, p. 214.

ACKNOWLEDGMENTS

This work was supported by the Swedish Board for Technical Development (project no 78-3614) and the I.F. Foundation for Pharmaceutical Research, Stockholm.

The technical assistance of Miss Siv Larsson and Mrs. Linnéa Wallsten was appreciated.

High-Pressure Liquid Chromatographic Determination of Amitriptyline and Its Major Metabolites in Human Whole Blood

GABRIELLE A. SMITH ˣ, PIERRE SCHULZ, KATHLEEN M. GIACOMINI, and TERRENCE F. BLASCHKE

Received January 23, 1981, from the *Division of Clinical Pharmacology, Department of Medicine, Stanford University Medical Center, Stanford, CA, 94305.* Accepted for publication August 12, 1981

Abstract □ A sensitive, specific, high-pressure liquid chromatographic method using an internal standard was developed for the determination of amitriptyline and its major metabolites in whole blood. Analysis was carried out on a microparticulate silica column with a mobile phase consisting of acetonitrile–methanol–aqueous ammonium hydroxide (93:7:0.4). Linear calibration curves ranging to 250 ng/ml were obtained for all compounds using UV absorbance detection at 220 nm. The lower limit of detection was 2 ng/ml for amitriptyline and 10-hydroxyamitriptyline, and 6 and 16 ng/ml for nortriptyline and its 10-hydroxylated metabolite, respectively. Human whole blood samples collected after single intravenous and single oral doses can be analyzed using this procedure.

Keyphrases □ High-pressure liquid chromatography—determination of amitriptyline and its major metabolites in whole human blood □ Amitriptyline—high-pressure liquid chromatographic determination in whole human blood, major metabolites determined □ Metabolites—of amitriptyline, determination by high-pressure liquid chromatography

Amitriptyline, 10,11-dihydro-*N*,*N*-dimethyl-5*H*-dibenzo[*a*,*d*]cycloheptene-Δ^5,γ-propylamine (I) is a commonly used tricyclic antidepressant. It undergoes extensive metabolism in humans, the major pathways being *N*-demethylation and hydroxylation at the 10-position. The major metabolites of I, 10-hydroxyamitriptyline (II), nortriptyline (IV), and the *trans* (V) and *cis* (VI) isomers of 10-hydroxynortriptyline are shown in Fig. 1.

Various methods have been described for measuring I and its major metabolites in biological fluids, including radioimmunoassay (1), UV spectrometry (2), GC with flame ionization (2, 3) or nitrogen detection (3, 4), GC–mass spectrometry (5), and high-pressure liquid chromatography (HPLC) using UV absorbance detection (6, 7). Except for the procedure using mass spectrometry, no method has sufficient sensitivity to separate and quantitate I and its major metabolites in single-dose pharmacokinetic studies.

This paper describes a specific HPLC method for the measurement of I, II, IV, V, and VI in human whole blood. Detection is by UV absorbance and no derivitization is required prior to analysis. The sensitivity is sufficient to measure accurately the low drug and metabolite concentrations observed during single-dose pharmacokinetic studies in humans.

EXPERIMENTAL

Reagents and Materials—Propranolol hydrochloride[1] (internal standard) was obtained commercially and was used as the salt. Amitriptyline hydrochloride[2], [^{14}C]amitriptyline hydrochloride (specific activity 7.1×10^{-3} mCi/mg), nortriptyline hydrochloride[3], 10-hydroxyamitriptyline[2], and *cis*- and *trans*-10-hydroxynortriptyline[2] were used as provided. Acetonitrile and methanol were purchased as glass-distilled solvents[4]. The water used in extraction was glass-distilled. Aqueous ammonium hydroxide (58%)[5] was analytical reagent grade.

Standard Solutions—Methanolic solutions of amitriptyline hydrochloride, nortriptyline hydrochloride, and the hydroxylated metabolites were prepared at a concentration of 5 ng/μl. The concentration of the internal standard was 10 ng/μl, also in methanol. New solutions of amitriptyline hydrochloride and nortriptyline hydrochloride were made every 3 weeks; the remainder were freshly prepared every 6–8 weeks. All were stored at 4°, with no detectable decomposition during the storage period.

Sample Preparation—A 10-μl aliquot containing 100 ng of the internal standard was dispensed with a syringe[6] into a 15-ml culture tube fitted with a polytef-lined screw cap. One milliliter of hemolyzed whole blood, 1.0 ml of water, 100 μl of 5.0 *M* NaOH, and 6.0 ml of hexane–*n*-butanol (98:2) were added. The mixture was shaken[7] for 10 min followed by centrifugation at 2800 rpm for 5 min. The tube was then immersed in an acetone–dry ice bath until the aqueous phase was frozen. The organic phase was poured into a second tube with an elongated cone (capacity ~50 μl) at its base, and the still-frozen aqueous phase was quickly washed with another 1.0 ml of hexane–*n*-butanol which was then added to the extract. This combined extract was evaporated to dryness at 40° under vacuum on a vortex evaporator[8]. One-hundred microliters of the mobile phase used in the chromatography was added to the resulting residue. The tube was capped, vortexed for 30 sec, and centrifuged for 5 min. All of the mixture was drawn into a 100-μl syringe[6] and injected into the chromatograph.

Apparatus—The modular high-pressure liquid chromatograph consisted of a constant-flow pump[9], a valve-type injector[10], a variable

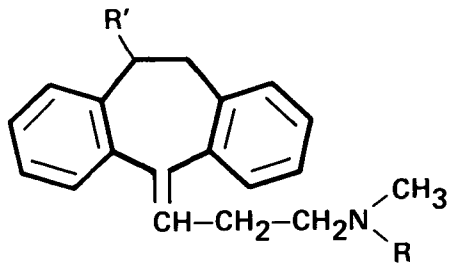

	R	R'
I	CH_3	H
II	CH_3	OH
IV	H	H
V,VI	H	OH

Figure 1—*Amitriptyline (I), 10-hydroxyamitriptyline (II), nortriptyline (IV) and* cis- *and* trans-*10-hydroxynortriptyline (V, VI, respectively).*

[1] Sigma Chemical Co., St. Louis, Mo..
[2] Merck, Sharp & Dohme Research Laboratories, Rahway, N.J.
[3] Eli Lilly and Co., Indianapolis, Ind.
[4] Burdick and Jackson Laboratories, Muskegon, Mich.
[5] Mallinckrodt Chemical Works, St. Louis, Mo.
[6] Hamilton Co., Reno, Nev.
[7] Labquake reciprocating shaker, Labindustries, Berkeley, Calif.
[8] Buchler Instruments (Div. of Searle Analytic Inc.), Fort Lee, N.J.
[9] Chromatography pump, model 6000A, Waters Associates, Milford, Mass.
[10] Sample injection valve, model U6K, Waters Associates, Milford, Mass.

0022-3549/82/0500-0581$01.00/0

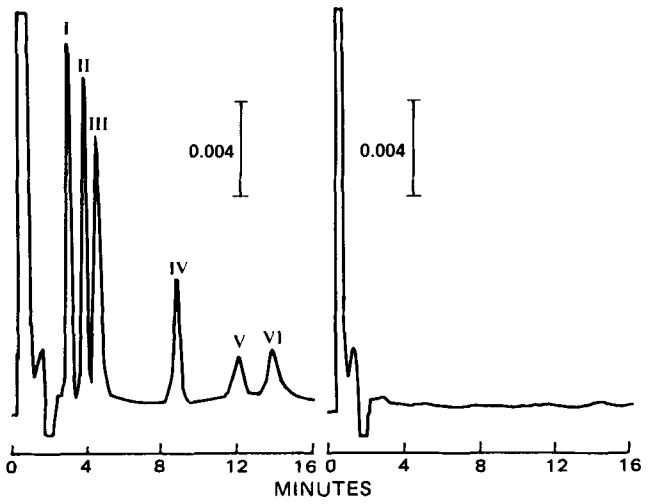

Figure 2—*Chromatograms of extracts from blank human whole blood (right) and blank blood spiked with 100 ng of I, II, III (internal standard), IV, V, and VI per milliter (left).*

wavelength absorbance detector[11] (set at 220 nm), and a strip-chart recorder[12] (0.5 cm/min). A stainless-steel column (250 mm × 2.0-mm i.d.) packed with 5-μm silica[13] was obtained commercially and fitted with a water-jacket[14].

Chromatographic Conditions—The mobile phase was acetonitrile–methanol–aqueous ammonium hydroxide (93:7:0.4). The flow rate was 1.5 ml/min with a column inlet pressure of 3100 psi. Column temperature was maintained at 22° by using a water-jacket connected to a constant temperature water bath. Overnight the flow rate was reduced to 0.1 ml/min.

Calibration—The assay was calibrated by analyzing 1.0-ml aliquots of blank hemolyzed whole blood to which 5–250 ng of I and II, 10–250 ng of IV, V, and VI, and 100 ng of the internal standard had been added. In each sample, the peak height ratio of each tricyclic component relative to the internal standard was calculated. These ratios were plotted against concentration to determine the linearity of the extraction and detector response for each species. In addition, each ratio was divided by the amount of the corresponding component in that sample to give a normalized peak height ratio. These normalized ratios were averaged, and the mean value for each tricyclic component was used to determine the amount present in unknown samples. The precision of the assay was estimated by calculating the coefficient of variation (*CV*) for each set of normalized peak height ratios.

To determine whether the method was valid for plasma samples as well as for whole blood, a calibration curve was prepared using duplicate 1.0-ml plasma aliquots spiked to 25, 100, and 250 ng/ml with each species. The linearity and precision of this assay were calculated as described.

Reproducibility—Aliquots (1 ml) of hemolyzed normal human whole blood were spiked with 25, 100, or 200 ng of each species and assayed in quintuplicate using the described method. Absolute peak heights were measured and the *CV* was calculated for each concentration.

To ascertain whether the assay would be useful if it were carried out from various blood volumes, the same procedure was used to determine the reproducibility of extraction from 0.5, 1.5, and 2.0 ml of whole blood spiked with 100 ng/ml of I and its metabolites. Each volume was assayed in quadruplicate. The rationale for this experiment was that clinically and in pharmacokinetic studies, concentrations of I and its metabolites in a particular blood sample may be lower or higher than those of the standards. To keep the concentrations within the range of the standards, it is necessary to use variable blood volumes.

Efficiency—The efficiency of extraction of I from hemolyzed whole blood into the organic phase was determined by spiking 1.0-ml aliquots of blood with ^{14}C-I, and determining the amounts of ^{14}C-I in the evaporated hexane–*n*-butanol extract by liquid scintillation counting. The extraction procedure was identical to that in the other parts of the study. Concentrations of 20, 50, 100, and 200 ng of ^{14}C-I/ml were extracted in duplicate. Results obtained as counts per minute were converted to disintegrations per minute using the external standard method. These values were compared with those obtained by adding the same amounts of labeled I directly to scintillation fluid, and the resulting ratios were expressed as the percent extraction.

Recovery—Aliquots (1 ml) of hemolyzed whole blood were spiked with known tricyclic quantities (50 and 200 ng/ml, five replicates for each concentration). After the samples were extracted and chromatographed as described, the peak heights for I and its metabolites were compared with the peak heights obtained when the same amount of each component in a standard solution was injected directly onto the column.

RESULTS

Chromatography—The retention times for I, its metabolites, and the internal standard are shown in Fig. 2. Occasional day-to-day adjustment of the methanol concentration (±0.1%) was necessary to obtain optimal separation between II and III. Column temperature was also a critical factor in maintaining this separation. Since room temperature fluctuated daily between 22 and 32°, the use of a column water-jacket maintained at 22° greatly improved baseline stability and peak resolution. In some samples from human subjects, a broad contaminant peak appeared between III and IV; careful manipulation of the methanol concentration was required to prevent it from eluting with one of the peaks of interest.

Calibration—A typical calibration curve relating peak height ratio to concentration was linear for all species over the concentration range studied. The *CV* for the estimation of I averaged 5.2%; corresponding values for the metabolites ranged from 3.6 to 10.2%. A standard curve was assayed with each set of unknowns. The limits of detection of an extracted standard, defined as five times the baseline noise, were 2 ng/ml for I and II, 6 ng/ml for IV, and 16 ng/ml for V and VI.

For the standards prepared in plasma, plots of concentration *versus* peak height ratio were linear with *CV* values of 1.8% for I, and 2.2–10.8% for the metabolites.

Reproducibility—Data showing the reproducibility of the assay are summarized in Table I. All species extracted consistently at three different concentrations from 1.0 ml of hemolyzed whole blood. The averaged normalized peak height values showed no trend with increasing concentration.

For any given sample size, extraction of all components was highly reproducible. There was a trend towards a lower percentage of extraction for all species with increasing sample size. This was probably due to a change in the volume ratio of aqueous to organic phase.

Efficiency and Recovery—Extraction efficiency was compared with overall recovery as described. For 20–200 ng/ml concentrations of ^{14}C-I, the amount of labeled drug partitioning into the organic phase varied from 96 to 100%. The total amount of I recovered from the assay procedure was 61% of an original 50 ng/ml concentration, and 53.5% for 200 ng/ml. Recovery of the metabolites was also consistent (46–69%).

DISCUSSION

Previously reported high-pressure liquid chromatographic assays for I have been unable to separate all of the metabolites of interest using a single procedure. As such, they were inadequate for studying the disposition of I in humans, since the metabolites are pharmacologically active, and are often present at concentrations comparable to those of the unchanged drug. To analyze blood samples from subjects participating in a single-dose pharmacokinetic study, it was necessary to develop a simple and rapid procedure which could resolve the parent drug from its demethylated and 10-hydroxylated metabolites. Since unchanged I was the major component of interest in the separation, a normal-phase chromatographic procedure was developed which would elute I first (as the most nonpolar species), giving maximum sensitivity for quantitation. It was possible, to separate I, II, IV, V, and VI in a total run time of 15 min by careful adjustment of the methanol concentration.

Propranolol was chosen as the internal standard, since it did not interfere chromatographically with any of these compounds. However, zymelidine, which eluted at 14 min under the described conditions, could have been used for samples in which VI was not present. Aqueous ammonium hydroxide was used at a low concentration in the mobile phase to decrease chemisorption on the silica column, which leads to peak tailing.

Although this paper describes chromatography on 5-μm packing material, acceptable peak resolution can be obtained using 10-μm silica with slight modifications of the chromatographic conditions. In this laboratory, a 250 × 2.0-mm i.d. column packed with 10-μm silica[15] was used for

[11] Model 450, Waters Associates, Milford, Mass.
[12] Model 9176, Varian Instruments, Palo Alto, Calif.
[13] MicroPak Si-5, Varian Instruments, Walnut Creek, Calif.
[14] Varian Instruments, Walnut Creek, Calif.
[15] MicroPak Si-10, Varian Instruments, Walnut Creek, Calif.

Table I—Reproducibility of Recovery of Amitriptyline and Metabolites from Spiked Hemolyzed Whole Blood

Compounds Added to Whole Blood	Normalized Peak Heights × 10^2[a]					
	25 ng[b]	100 ng[b]	200 ng[b]	0.5 ml[c]	1.5 ml[c]	2.0 ml[c]
I	1.69 ± 0.05	1.83 ± 0.06	1.73 ± 0.04	1.78 ± 0.06	1.57 ± 0.06	1.37 ± 0.08
II	1.53 ± 0.06	1.57 ± 0.06	1.53 ± 0.03	1.56 ± 0.05	1.47 ± 0.03	1.38 ± 0.06
IV	0.56 ± 0.06	0.61 ± 0.02	0.64 ± 0.01	0.65 ± 0.01	0.55 ± 0.03	0.48 ± 0.02
V	0.18 ± 0.02	0.15 ± 0.01	0.16 ± 0.004	0.18 ± 0.005	0.14 ± 0.004	0.13 ± 0.007
VI	0.21 ± 0.02	0.20 ± 0.01	0.23 ± 0.03	0.23 ± 0.005	0.19 ± 0.01	0.18 ± 0.01

[a] Mean ± *SD*, $n = 5$ for columns 1–3, $n = 4$ for columns 4–6. [b] Amount of I and metabolites added to 1.0 ml of blank, hemolyzed whole blood. [c] Volumes of blank, hemolyzed whole blood to which 100 ng of each component was added.

several months for quantitation of I and all of its metabolites. The use of a water-jacket to maintain column eqilibrium should not be necessary if laboratory ambient temperature fluctuates 3° or less daily.

Plasma samples can be analyzed satisfactorily using the same procedure as that followed for blood samples. As evidenced by the reproducibility of the normalized peak height values of I and the fact that there was no trend in these values with concentration, adsorption to glassware, if it occurred, did not present a problem with the calibration of the assay. This is in contrast to other extraction procedures where adsorption to glassware has resulted in erratic recoveries (7). Butanol was added to the extracting solvent to prevent emulsification and to improve extraction of the more polar metabolites and the internal standard. It is likely that this short-chain alcohol acts like isoamyl alcohol in decreasing adsorption of basic drugs to glass. When standard solutions were assayed, all methanol was evaporated off before the addition of whole blood, as it otherwise affected the cleanliness of the extract. Maximum recovery depended on careful attention to every step of the extraction, particularly the pooling of the organic phase, evaporation, and final vortexing.

Although the addition of bases to mobile phases used with silica columns is known to decrease column life (8), the low concentration of aqueous ammonium hydroxide used in this procedure caused little deterioration of the packing material. A greater problem arose from column contamination by sample extracts, resulting in broadening or even splitting of the peaks. This condition was rectified periodically by removing the top few millimeters of packing material and replacing it with glass microbeads. The use of a guard column packed with pellicular silica should circumvent this problem.

The present method offers several advantages over some previously published procedures. The extraction is simple and rapid, the chromatography is short (15 min), yet allows good separation of I and its known active metabolites. The sensitivity is good, which should allow pharmacokinetic studies to be carried out; the procedure can be applied to either whole blood or plasma. For high-clearance compounds such as I, whole blood measurements may be preferable, obviating the need for determining the red cell to plasma partition coefficient, which may be concentration-dependent.

REFERENCES

(1) J. W. Hubbard, K. K. Midha, J. K. Cooper, and C. Charette, *J. Pharm. Sci.*, **67**, 1571 (1978).

(2) H. E. Hamilton, J. E. Wallace, and K. Blum, *Anal. Chem.*, **47**, 1139 (1975).

(3) L. A. Gifford, P. Turner, and C. M. B. Pare, *J. Chromatogr.*, **105**, 107 (1975).

(4) J. Vasiliades and K. C. Bush, *Anal. Chem.*, **48**, 1708 (1976).

(5) W. A. Garland, R. R. Muccino, B. H. Min, J. Cupano, and W. E. Fann, *Clin. Pharmacol. Ther.*, **25**, 844 (1979).

(6) F. L. Vandemark, R. F. Adams, and G. J. Schmidt, *Clin. Chem.*, **24**, 87 (1978).

(7) H. F. Proless, H. J. Lohmann, and D. G. Miles, *ibid.*, **24**, 1948 (1978).

(8) A. Wehrli, J. C. Hildenbrand, H. P. Keller, R. Stampfli, and R. W. Frei, *J. Chromatogr.*, **149**, 199 (1978).

ACKNOWLEDGMENTS

Supported by a grant from the National Institute of Aging AG01340. Dr. Blaschke is a Burroughs Wellcome Scholar in Clinical Pharmacology, and recipient of a Research Career Development Award (GM00407) from the National Institutes of Health. Dr. Schulz was supported by the Fonds National Suisse de la Recherche, the Holderbank Foundation, and the Merck Foundation. Dr. Giacomini is supported by an NRSA (GM07344) from the National Institutes of Health.

The authors are grateful to Anthony Abang for technical assistance, and to Linda Halloran for preparation of the manuscript.

NOTES

Analysis of Conjugated Estrogens in a Vaginal Cream Formulation by Capillary Gas Chromatography

G. K. PILLAI and K. M. McERLANE ˣ

Received June 9, 1981, from the *Faculty of Pharmaceutical Sciences, University of British Columbia, Vancouver, British Columbia, V6T 1W5, Canada.* Accepted for publication August 26, 1981.

Abstract □ A capillary gas-chromatographic method is described for the quantitative analysis of nine equine estrogens in a vaginal cream formulation. The sodium sulfate ethers of the estrogens were selectively extracted from the formulation, subjected to enzyme hydrolysis, and derivatized to their oxime-trimethylsilyl esters. Resolution of the resulting derivatives was achieved on a short (15 m) capillary column, wall-coated with cyanopropylmethyl silicon stationary phase.

Keyphrases □ Estrogens—conjugated, analysis of a vaginal cream formulation by capillary gas chromatography □ GC—capillary, analysis of conjugated estrogens in a vaginal cream formulation □ Vaginal cream formulation—conjugated estrogens, analysis by capillary gas chromatography

The pharmaceutical product known as conjugated estrogens, is a mixture of nine or more equine estrogens isolated from the urine of pregnant mares (1). As their sodium sulfate salts, they have been used in tablet, injectable, and cream formulations for relieving symptoms associated with menopause. Application of the vaginal cream

Table I—Reproducibility of Recovery of Amitriptyline and Metabolites from Spiked Hemolyzed Whole Blood

Compounds Added to Whole Blood	Normalized Peak Heights × 10^2[a]					
	25 ng[b]	100 ng[b]	200 ng[b]	0.5 ml[c]	1.5 ml[c]	2.0 ml[c]
I	1.69 ± 0.05	1.83 ± 0.06	1.73 ± 0.04	1.78 ± 0.06	1.57 ± 0.06	1.37 ± 0.08
II	1.53 ± 0.06	1.57 ± 0.06	1.53 ± 0.03	1.56 ± 0.05	1.47 ± 0.03	1.38 ± 0.06
IV	0.56 ± 0.06	0.61 ± 0.02	0.64 ± 0.01	0.65 ± 0.01	0.55 ± 0.03	0.48 ± 0.02
V	0.18 ± 0.02	0.15 ± 0.01	0.16 ± 0.004	0.18 ± 0.005	0.14 ± 0.004	0.13 ± 0.007
VI	0.21 ± 0.02	0.20 ± 0.01	0.23 ± 0.03	0.23 ± 0.005	0.19 ± 0.01	0.18 ± 0.01

[a] Mean ± *SD*, $n = 5$ for columns 1–3, $n = 4$ for columns 4–6. [b] Amount of I and metabolites added to 1.0 ml of blank, hemolyzed whole blood. [c] Volumes of blank, hemolyzed whole blood to which 100 ng of each component was added.

several months for quantitation of I and all of its metabolites. The use of a water-jacket to maintain column eqilibrium should not be necessary if laboratory ambient temperature fluctuates 3° or less daily.

Plasma samples can be analyzed satisfactorily using the same procedure as that followed for blood samples. As evidenced by the reproducibility of the normalized peak height values of I and the fact that there was no trend in these values with concentration, adsorption to glassware, if it occurred, did not present a problem with the calibration of the assay. This is in contrast to other extraction procedures where adsorption to glassware has resulted in erratic recoveries (7). Butanol was added to the extracting solvent to prevent emulsification and to improve extraction of the more polar metabolites and the internal standard. It is likely that this short-chain alcohol acts like isoamyl alcohol in decreasing adsorption of basic drugs to glass. When standard solutions were assayed, all methanol was evaporated off before the addition of whole blood, as it otherwise affected the cleanliness of the extract. Maximum recovery depended on careful attention to every step of the extraction, particularly the pooling of the organic phase, evaporation, and final vortexing.

Although the addition of bases to mobile phases used with silica columns is known to decrease column life (8), the low concentration of aqueous ammonium hydroxide used in this procedure caused little deterioration of the packing material. A greater problem arose from column contamination by sample extracts, resulting in broadening or even splitting of the peaks. This condition was rectified periodically by removing the top few millimeters of packing material and replacing it with glass microbeads. The use of a guard column packed with pellicular silica should circumvent this problem.

The present method offers several advantages over some previously published procedures. The extraction is simple and rapid, the chromatography is short (15 min), yet allows good separation of I and its known active metabolites. The sensitivity is good, which should allow pharmacokinetic studies to be carried out; the procedure can be applied to either whole blood or plasma. For high-clearance compounds such as I, whole blood measurements may be preferable, obviating the need for determining the red cell to plasma partition coefficient, which may be concentration-dependent.

REFERENCES

(1) J. W. Hubbard, K. K. Midha, J. K. Cooper, and C. Charette, *J. Pharm. Sci.*, **67**, 1571 (1978).

(2) H. E. Hamilton, J. E. Wallace, and K. Blum, *Anal. Chem.*, **47**, 1139 (1975).

(3) L. A. Gifford, P. Turner, and C. M. B. Pare, *J. Chromatogr.*, **105**, 107 (1975).

(4) J. Vasiliades and K. C. Bush, *Anal. Chem.*, **48**, 1708 (1976).

(5) W. A. Garland, R. R. Muccino, B. H. Min, J. Cupano, and W. E. Fann, *Clin. Pharmacol. Ther.*, **25**, 844 (1979).

(6) F. L. Vandemark, R. F. Adams, and G. J. Schmidt, *Clin. Chem.*, **24**, 87 (1978).

(7) H. F. Proless, H. J. Lohmann, and D. G. Miles, *ibid.*, **24**, 1948 (1978).

(8) A. Wehrli, J. C. Hildenbrand, H. P. Keller, R. Stampfli, and R. W. Frei, *J. Chromatogr.*, **149**, 199 (1978).

ACKNOWLEDGMENTS

Supported by a grant from the National Institute of Aging AG01340. Dr. Blaschke is a Burroughs Wellcome Scholar in Clinical Pharmacology, and recipient of a Research Career Development Award (GM00407) from the National Institutes of Health. Dr. Schulz was supported by the Fonds National Suisse de la Recherche, the Holderbank Foundation, and the Merck Foundation. Dr. Giacomini is supported by an NRSA (GM07344) from the National Institutes of Health.

The authors are grateful to Anthony Abang for technical assistance, and to Linda Halloran for preparation of the manuscript.

NOTES

Analysis of Conjugated Estrogens in a Vaginal Cream Formulation by Capillary Gas Chromatography

G. K. PILLAI and K. M. McERLANE ˣ

Received June 9, 1981, from the *Faculty of Pharmaceutical Sciences, University of British Columbia, Vancouver, British Columbia, V6T 1W5, Canada.* Accepted for publication August 26, 1981.

Abstract □ A capillary gas-chromatographic method is described for the quantitative analysis of nine equine estrogens in a vaginal cream formulation. The sodium sulfate ethers of the estrogens were selectively extracted from the formulation, subjected to enzyme hydrolysis, and derivatized to their oxime-trimethylsilyl esters. Resolution of the resulting derivatives was achieved on a short (15 m) capillary column, wall-coated with cyanopropylmethyl silicon stationary phase.

Keyphrases □ Estrogens—conjugated, analysis of a vaginal cream formulation by capillary gas chromatography □ GC—capillary, analysis of conjugated estrogens in a vaginal cream formulation □ Vaginal cream formulation—conjugated estrogens, analysis by capillary gas chromatography

The pharmaceutical product known as conjugated estrogens, is a mixture of nine or more equine estrogens isolated from the urine of pregnant mares (1). As their sodium sulfate salts, they have been used in tablet, injectable, and cream formulations for relieving symptoms associated with menopause. Application of the vaginal cream

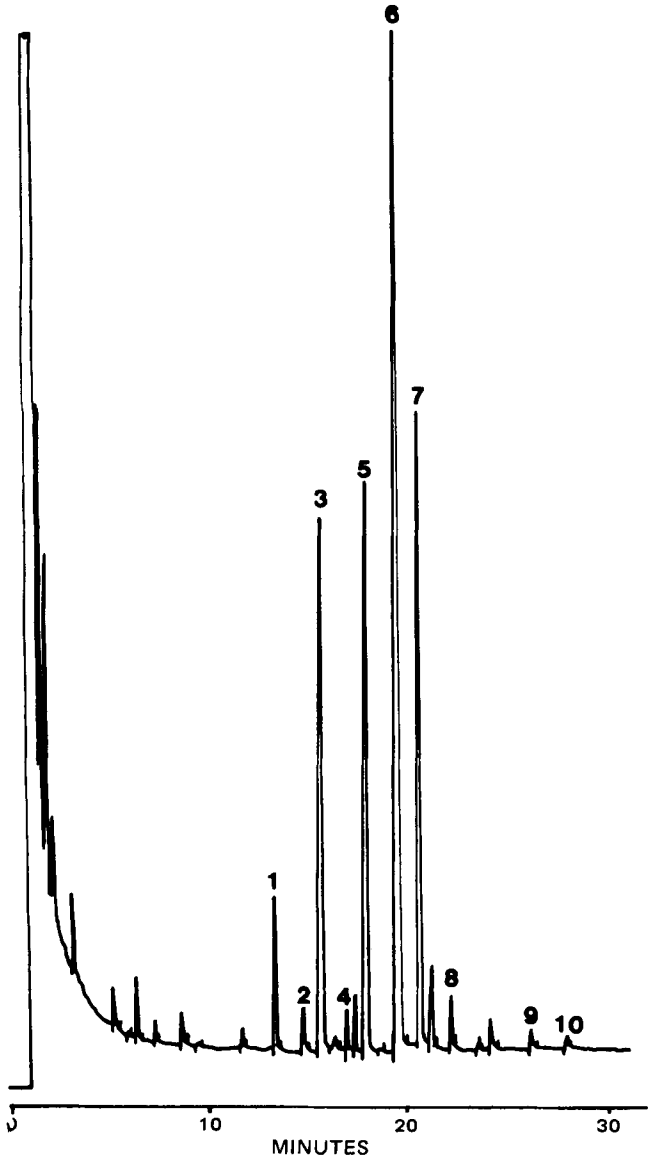

Figure 1—*Chromatogram of equine estrogens as their oxime–trimethylsilyl derivatives derived from a vaginal cream formulation. Key: 1, 17α-estradiol; 2, 17β-estradiol; 3, 17α-dihydroequilin; 4, 17β-dihydroequilin; 5, ethinyl estradiol (internal standard); 6, estrone; 7, equilin; 8, 17α-dihydroequilenin; 9, 17β-dihydroequilenin; and 10, equilenin.*

has been shown to produce a marked improvement in vaginal and vasomotor symptoms (2), and it has been noted that estradiol and estrone plasma levels significantly increased after a single dose. Since estrogens are readily absorbed into the bloodstream after local application, an accurate and selective method for quality assessment of the cream is as essential as one for the tablet and injectable formulations.

At the present time, the assay contained in the United States Pharmacopeia (3) is a colorimetric procedure that quantifies only the two major steroids, estrone and equilin. A gas chromatographic (GC) procedure is specified only for identification of the steroid mixture. Monographs in USP relate to the tablet formulation only. More selective packed column (4, 5) and capillary column (6) GC methods have been reported for the quantitative analysis of the individual steroids in conjugated estrogens. However, these methods have been suitable only for tablet and injectable formulations.

Table I—Analysis of Vaginal Cream Formulation [a]

Component	Potency[a]	Percentage
17α-Estradiol	0.0196	3.14
17β-Estradiol	0.0054	0.86
17α-Dihydroequilin	0.0941	15.07
17β-Dihydroequilin	0.0074	1.18
Estrone	0.3122	49.99
Equilin	0.1497	23.97
17α-Dihydroequilenin	0.0113	1.81
17β-Dihydroequilenin	0.0015	0.24
Equilenin	0.0233	3.73
Total	0.6245	99.92

[a] Expressed as milligrams of the sodium sulfate salts in each gram of cream (label claim: 0.625 mg/g). Average of two assays.

The quantitative method described herein is a modification of a capillary GC assay described previously (6) for tablet and injectable formulations.

EXPERIMENTAL

A capillary gas chromatograph[1] operated in the split mode was used with a flame ionization detector and a data terminal[2] for all measurements. A commercial 15 m × 0.25-mm borosilicate column[3], wall-coated with cyanopropylmethyl silicon liquid phase (Silar 10C), was used with a helium carrier gas flow of 0.8 ml/min through the column and a split vent flow of 40 ml/min. The column inlet pressure was 10 psi. The injector and detector temperatures were 250° and the oven was programmed from 170° for 7 min to 220° at 2.3°/min and was maintained at the upper temperature until elution of the last peak (equilenin).

Materials and Supplies—Methylene chloride, chloroform, acetic acid, sodium acetate, and sodium chloride were reagent grade quality. *N,O*-Bis(trimethylsilyl)trifluoroacetamide and pyridine were silylation grade[4]. Sulfatase enzyme[5], ethinyl estradiol[6], hydroxylamine hydrochloride[7], and equine estrogens[8] were used without further purification.

Sample Preparation—An accurately weighed sample of the vaginal cream, equivalent to ~1 mg of conjugated estrogens, was transferred directly into a 50-ml screw-capped centrifuge tube. Ten milliliters of a 10% solution of sodium chloride in water were added and the tube was shaken thoroughly. The suspended cream was washed twice with 25-ml portions of methylene chloride and the organic phase was discarded after centrifugation.

Nitrogen was bubbled through the aqueous phase to remove any residual methylene chloride until its odor was no longer apparent. To the aqueous extract was added 15 ml of acetate buffer (pH 5.2, 0.02 *M*), 2000 U of sulfatase enzyme, and the mixture was incubated for 30 min at 45°. Following hydrolysis of the sodium sulfate esters, a 0.2-ml aliquot of the internal standard, ethinyl estradiol (1.0 mg/ml), in chloroform was added and the mixture was shaken for 15 min on a rotary tube tumbler[9]. After centrifuging, the chloroform layer was separated and evaporated under a gentle nitrogen stream. The equine estrogens were then converted to their oxime–trimethylsilyl derivatives by the addition of 200 μl of hydroxylamine hydrochloride in pyridine (2.0%) and heating the solution in a screw-capped conical vial[10] for 30 min at 70°. After conversion of the keto-steroids to their oxime derivatives, the remaining hydroxy functions were silylated by the addition of 150 μl of *N,O*-bis(trimethylsilyl)trifluoroacetamide and further heating the vials for 10 min at 70°. A 2-μl aliquot was used for analysis.

RESULTS AND DISCUSSION

The chromatogram shown in Fig. 1 is representative of the steroid profile obtained from the analysis of a vaginal cream formulation. The identity of each steroid was established previously (6) by comparison with authentic equine estrogens. The resolution of the capillary column is sufficient to separate all the estrogen steroids along with the internal standard in ~28 min.

[1] Model 5830A, Hewlett-Packard, Avondale, Pa.
[2] Model 18850A, Hewlett-Packard, Avondale, Pa.
[3] Alltech Associates, Rockford, Ill.
[4] Pierce Chemical Co., Rockford, Ill.
[5] Type H-2, Sigma Chemical Co., St. Louis, Mo.
[6] Sigma Chemical Co., St. Louis, Mo.
[7] British Drug Houses, London, England.
[8] Ayerst Pharmaceuticals, Montreal, Quebec, Canada.
[9] RotoRack, Fisher Scientific Co. Ltd., Vancouver, B.C., Canada.
[10] Reacti-Vial, Pierce Chemical Co., Rockford, Ill.

The quantitation of each of the equine estrogens separated in this fashion was accomplished by using the relative response ratios of each estrogen as compared to the internal standard, ethinyl estradiol. For such determinations, the response ratio and linearity of response were determined by injection of six aliquots of each individual steroid at levels bracketing the anticipated quantity in the mixture with a constant amount of internal standard. For all such measurements, the correlation between peak area ratios and concentrations was 0.998 or better.

Extraction of the water soluble sodium sulfate salts of the equine estrogens required the addition of sodium chloride to suppress emulsion formation. The methylene chloride extraction effectively removed lipid soluble formulation excipients as evidenced by a chromatogram that was essentially devoid of extraneous peaks other than those of the equine estrogens. Subsequent hydrolysis of the sulfate conjugates with 2000 U of sulfatase enzyme had earlier been reported (5) as sufficient for hydrolysis of 1 mg of the conjugates, even in the presence of small amounts of phosphates.

The quantitative assay data obtained from the analysis of two aliquots of a vaginal cream formulation is given in Table I. The quantities of estrone and equilin are within the limits specified for conjugated estrogens in the United States Pharmacopeia (3). The total potency determined indicates that the product was 99.9% of labeled claim.

In summary, this method represents the first quantitative procedure for the total analysis of the steroid composition in an estrogen vaginal cream formulation.

REFERENCES

(1) R. Roman, C. A. Yates, J. F. Miller, and W. J. A. VandenHeuvel, *Can. J. Pharm. Sci.*, **10**, 8 (1974).

(2) R. N. Dickerson, R. Bressler, C. D. Christian, and H. W. Hermann, *Clin. Pharmacol. Ther.*, **26**, 502 (1979).

(3) "The United States Pharmacopeia," 20th rev., Mack Publishing, Easton, Pa., 1980.

(4) R. Johnson, R. Masserano, R. Haring, B. Kho, and G. Schilling, *J. Pharm. Sci.*, **64**, 1007 (1975).

(5) K. M. McErlane and N. M. Curran, *ibid.*, **66**, 523 (1977).

(6) G. K. Pillai and K. M. McErlane, *ibid.*, **70**, 1072 (1981).

ACKNOWLEDGMENTS

This research was supported by a grant from the Natural, Applied, and Health Sciences, University of British Columbia.

The authors would like to thank Ayerst Pharmaceuticals, Montreal, Canada for the generous gift of equine estrogens and formulations required.

Effect of Some Formulation Adjuncts on the Stability of Benzoyl Peroxide

V. DAS GUPTA

Received June 8, 1981, from the *University of Houston, College of Pharmacy, Department of Pharmaceutics, Houston, TX 77030.* Accepted for publication August 26, 1981.

Abstract □ The stability of benzoyl peroxide in polyethylene glycol ointment base and some liquid vehicles (acetone, ethanol, propylene glycol, and their mixtures) was studied. Some solutions also contained an additional ingredient (acetanilide, benzoic acid, chlorhydroxyquinoline, and hydroxyquinoline) as a possible stabilizer. Benzoyl peroxide decomposed very fast (first-order K value 0.028 day^{-1} at 24°) in polyethylene glycol ointment base. At 50°, the potency of benzoyl peroxide in polyethylene glycol ointment base decreased to <1% in 5 days. Decomposition in solutions is complex. Considering acetone as a standard vehicle, ethanol improved the stability of benzoyl peroxide and propylene glycol had an adverse effect on the stability. Of the stabilizers studied, only chlorhydroxyquinoline improved the stability.

Keyphrases □ Benzoyl peroxide—stability, effect of some formulation adjuncts □ Formulations—benzoyl peroxide, effect of some formulation adjuncts on stability □ Keratolytics—benzoyl peroxide, effects of some formulation adjuncts on stability

Benzoyl peroxide formulations are used extensively for the treatment of acne; however the literature on the stability of benzoyl peroxide is scarce. Gruber *et al.* (1) studied the stability of some commercial lotions containing I but the formulations' excipients were not reported. According to that report, benzoyl peroxide usually decomposes to benzoic acid and carbon dioxide.

The stability of benzoyl peroxide in pharmaceutical gels was reported by Bollinger *et al.* (2). These authors recommended the use of sodium hydroxide over triethanolamine as a neutralizing agent. Moreover, gels containing some acetone were reported to be very stable (even at higher temperature) *versus* ethanol which had an adverse effect on the stability of benzoyl peroxide. These studies used a selective titrimetric analysis method (3).

A stability-indicating assay method using high-pressure liquid chromatography (HPLC) was reported recently (4). The report questioned the accuracy of the titrimetric method (3) which is also official in the USP (5). The latest USP–NF edition (6) recommends the same titrimetric method of analysis for both hydrous benzoyl peroxide and its lotion.

The purpose of these investigations was to study the effect of some formulation adjuncts, polyethylene glycol ointment USP (7), some liquid vehicles, and some possible stabilizers, on the stability of benzoyl peroxide.

EXPERIMENTAL

Chemicals and Reagents—All the chemicals and reagents were either USP, NF, or ACS grade and were used without further purification. Benzoyl peroxide granules[1] and hydrous benzoyl peroxide granules[2] were used as received.

Apparatus—The HPLC[3] was equipped with a multiple wavelength detector[4], a recorder[5], and a digital integrator[6].

Column—A nonpolar column[7] (30 cm × 4-cm i.d.) was used.

Chromatographic Conditions—The mobile phase contained 60% (v/v) of acetonitrile and 0.8% (v/v) of glacial acetic acid in water. The flow rate was 2.5 ml/min and the temperature was ambient. The sensitivity was set at 0.04 (254 nm) and the chart speed was 30.5 cm/hr.

Preparation of Ointments for Stability Studies—A 2.0% (w/w)

[1] Aldrich Chemical Co., Milwaukee, Wis.

[2] Pennwalt Corp., Buffalo, N.Y.; generously supplied by Alcon Laboratories, Fort Worth, Texas.

[3] Model ALC 202 equipped with a U6K universal injector, Waters Associates, Milford, Mass.

[4] Spectroflow monitor SF770, Schoeffel Instrument Corp., Westwood, N.J.

[5] Omniscribe 5213-12, Houston Instruments, Austin, Texas.

[6] Autolab minigrator, Spectra-Physics, Santa Clara, Calif.

[7] μBondapak C_{18} (catalog no. 27324), Waters Assoc., Milford, Mass.

0022-3549/82/0500-0585$01.00/0

The quantitation of each of the equine estrogens separated in this fashion was accomplished by using the relative response ratios of each estrogen as compared to the internal standard, ethinyl estradiol. For such determinations, the response ratio and linearity of response were determined by injection of six aliquots of each individual steroid at levels bracketing the anticipated quantity in the mixture with a constant amount of internal standard. For all such measurements, the correlation between peak area ratios and concentrations was 0.998 or better.

Extraction of the water soluble sodium sulfate salts of the equine estrogens required the addition of sodium chloride to suppress emulsion formation. The methylene chloride extraction effectively removed lipid soluble formulation excipients as evidenced by a chromatogram that was essentially devoid of extraneous peaks other than those of the equine estrogens. Subsequent hydrolysis of the sulfate conjugates with 2000 U of sulfatase enzyme had earlier been reported (5) as sufficient for hydrolysis of 1 mg of the conjugates, even in the presence of small amounts of phosphates.

The quantitative assay data obtained from the analysis of two aliquots of a vaginal cream formulation is given in Table I. The quantities of estrone and equilin are within the limits specified for conjugated estrogens in the United States Pharmacopeia (3). The total potency determined indicates that the product was 99.9% of labeled claim.

In summary, this method represents the first quantitative procedure for the total analysis of the steroid composition in an estrogen vaginal cream formulation.

REFERENCES

(1) R. Roman, C. A. Yates, J. F. Miller, and W. J. A. VandenHeuvel, *Can. J. Pharm. Sci.*, **10**, 8 (1974).

(2) R. N. Dickerson, R. Bressler, C. D. Christian, and H. W. Hermann, *Clin. Pharmacol. Ther.*, **26**, 502 (1979).

(3) "The United States Pharmacopeia," 20th rev., Mack Publishing, Easton, Pa., 1980.

(4) R. Johnson, R. Masserano, R. Haring, B. Kho, and G. Schilling, *J. Pharm. Sci.*, **64**, 1007 (1975).

(5) K. M. McErlane and N. M. Curran, *ibid.*, **66**, 523 (1977).

(6) G. K. Pillai and K. M. McErlane, *ibid.*, **70**, 1072 (1981).

ACKNOWLEDGMENTS

This research was supported by a grant from the Natural, Applied, and Health Sciences, University of British Columbia.

The authors would like to thank Ayerst Pharmaceuticals, Montreal, Canada for the generous gift of equine estrogens and formulations required.

Effect of Some Formulation Adjuncts on the Stability of Benzoyl Peroxide

V. DAS GUPTA

Received June 8, 1981, from the *University of Houston, College of Pharmacy, Department of Pharmaceutics, Houston, TX 77030.* Accepted for publication August 26, 1981.

Abstract □ The stability of benzoyl peroxide in polyethylene glycol ointment base and some liquid vehicles (acetone, ethanol, propylene glycol, and their mixtures) was studied. Some solutions also contained an additional ingredient (acetanilide, benzoic acid, chlorhydroxyquinoline, and hydroxyquinoline) as a possible stabilizer. Benzoyl peroxide decomposed very fast (first-order K value 0.028 day^{-1} at 24°) in polyethylene glycol ointment base. At 50°, the potency of benzoyl peroxide in polyethylene glycol ointment base decreased to <1% in 5 days. Decomposition in solutions is complex. Considering acetone as a standard vehicle, ethanol improved the stability of benzoyl peroxide and propylene glycol had an adverse effect on the stability. Of the stabilizers studied, only chlorhydroxyquinoline improved the stability.

Keyphrases □ Benzoyl peroxide—stability, effect of some formulation adjuncts □ Formulations—benzoyl peroxide, effect of some formulation adjuncts on stability □ Keratolytics—benzoyl peroxide, effects of some formulation adjuncts on stability

Benzoyl peroxide formulations are used extensively for the treatment of acne; however the literature on the stability of benzoyl peroxide is scarce. Gruber *et al.* (1) studied the stability of some commercial lotions containing I but the formulations' excipients were not reported. According to that report, benzoyl peroxide usually decomposes to benzoic acid and carbon dioxide.

The stability of benzoyl peroxide in pharmaceutical gels was reported by Bollinger *et al.* (2). These authors recommended the use of sodium hydroxide over triethanolamine as a neutralizing agent. Moreover, gels containing some acetone were reported to be very stable (even at higher temperature) *versus* ethanol which had an adverse effect on the stability of benzoyl peroxide. These studies used a selective titrimetric analysis method (3).

A stability-indicating assay method using high-pressure liquid chromatography (HPLC) was reported recently (4). The report questioned the accuracy of the titrimetric method (3) which is also official in the USP (5). The latest USP–NF edition (6) recommends the same titrimetric method of analysis for both hydrous benzoyl peroxide and its lotion.

The purpose of these investigations was to study the effect of some formulation adjuncts, polyethylene glycol ointment USP (7), some liquid vehicles, and some possible stabilizers, on the stability of benzoyl peroxide.

EXPERIMENTAL

Chemicals and Reagents—All the chemicals and reagents were either USP, NF, or ACS grade and were used without further purification. Benzoyl peroxide granules[1] and hydrous benzoyl peroxide granules[2] were used as received.

Apparatus—The HPLC[3] was equipped with a multiple wavelength detector[4], a recorder[5], and a digital integrator[6].

Column—A nonpolar column[7] (30 cm × 4-cm i.d.) was used.

Chromatographic Conditions—The mobile phase contained 60% (v/v) of acetonitrile and 0.8% (v/v) of glacial acetic acid in water. The flow rate was 2.5 ml/min and the temperature was ambient. The sensitivity was set at 0.04 (254 nm) and the chart speed was 30.5 cm/hr.

Preparation of Ointments for Stability Studies—A 2.0% (w/w)

[1] Aldrich Chemical Co., Milwaukee, Wis.

[2] Pennwalt Corp., Buffalo, N.Y.; generously supplied by Alcon Laboratories, Fort Worth, Texas.

[3] Model ALC 202 equipped with a U6K universal injector, Waters Associates, Milford, Mass.

[4] Spectroflow monitor SF770, Schoeffel Instrument Corp., Westwood, N.J.

[5] Omniscribe 5213-12, Houston Instruments, Austin, Texas.

[6] Autolab minigrator, Spectra-Physics, Santa Clara, Calif.

[7] μBondapak C_{18} (catalog no. 27324), Waters Assoc., Milford, Mass.

0022-3549/82/0500-0585$01.00/0

Table I—Solutions Prepared For Stability Studies

Solution Number	Concentration of Benzoyl Peroxide	Vehicle, % v/v	Other Ingredient
1	0.1	Acetone	—
2	0.1	Acetone 75 Ethanol 25	—
3	0.1	Acetone 50 Ethanol 50	—
4	0.1	Acetone 25 Ethanol 75	—
5	0.1	Acetone 75 Propylene glycol 25	—
6	0.1	Acetone 50 Propylene glycol 50	—
7	0.1	Acetone 25 Propylene glycol 75	—
8	0.1	Acetone 50 Ethanol 50	0.01% of 8-hydroxyquinoline
9	0.1	Acetone 25 Propylene glycol 75	0.01% of 8-hydroxyquinoline
10	0.1	Acetone 25 Propylene glycol 75	0.01% of acetanilide
11	0.1	Acetone 25 Propylene glycol 75	0.01% of benzoic acid
12	1.0	Acetone 50 Propylene glycol 50	—
13	1.0	Acetone 50 Propylene glycol 50	0.1% of 8-hydroxyquinoline sulfate
14	1.0	Acetone 50 Propylene glycol 50	0.1% of 5-chloro-8-hydroxyquinoline

benzoyl peroxide ointment was prepared by mixing 612.0 mg of benzoyl peroxide granules with 6 ml of acetone and then incorporating this mixture with enough polyethylene glycol ointment USP (7) to make 30 g of ointment. Separate lots of ointments containing 0.01% (w/w) of acetanilide or benzoic acid in addition to 2% (w/w) of benzoyl peroxide were also prepared. After the initial assays, the ointments were divided into two portions and transferred to 30-g opal ointment jars[8]. One portion was stored at 50°; the other portion at room temperature (24°).

Preparation of Solutions for Stability Studies—Solutions containing 0.1% of benzoyl peroxide in various vehicles (acetone, ethanol, propylene glycol, or mixtures of two) were prepared using a simple solution method. Benzoyl peroxide granules were always dissolved in acetone. Some of the solutions also contained an additional ingredient (Table I). After the initial assays, the solutions were transferred to amber-colored, 120-ml glass bottles[8] and stored at 24°.

Another set of solutions containing 1.0% of benzoyl peroxide were prepared from hydrous benzoyl peroxide granules. The vehicle and additional ingredients added are listed in Table I. These solutions were also stored in amber-colored glass bottles at 24°.

Assay Procedure—The HPLC analysis used is similar to one reported previously (4). The internal standard was hydroxyprogesterone caproate. The stock solutions of benzoyl peroxide and the internal standard in methanol (1.0 mg/ml each) were prepared fresh daily. The standard solution was prepared by mixing 2.0 ml of the stock solution of benzoyl peroxide with 4.0 ml of the internal standard stock solution and then bringing the volume to 50.0 ml with methanol.

Preparation of Assay Solutions from Ointments—An appropriate quantity of the ointment containing 2.0 mg of benzoyl peroxide was weighed accurately and dissolved in 30 ml of methanol. A 4.0-ml portion of the internal standard stock solution was added and the mixture brought to volume (50.0 ml) with methanol.

[8] Brockway Glass Co., Brockway, Pa.

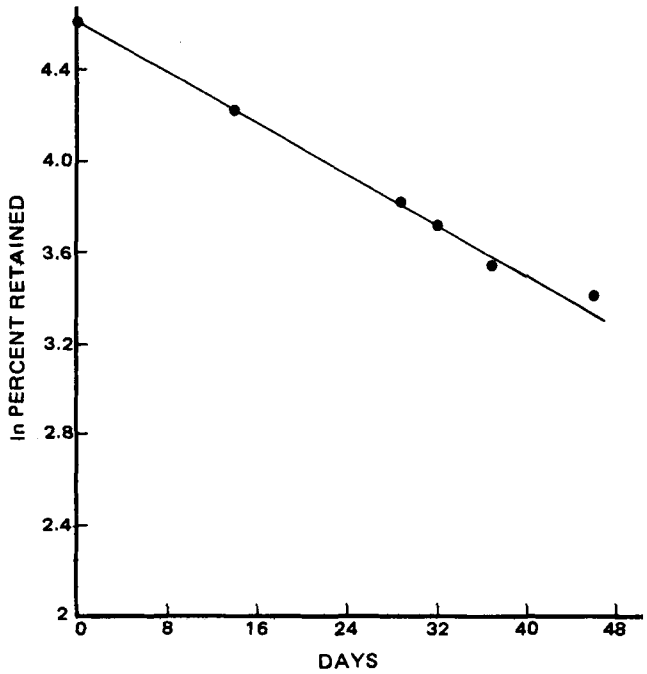

Figure 1—*First-order plot of decomposition (at 24°) of benzoyl peroxide in polyethylene glycol ointment base USP. The results of ointments containing an additional ingredient (acetanilide or benzoic acid) were similar.*

All the solutions studied were diluted with methanol to a concentration (based on the label claim) of 40.0 μg/ml of benzoyl peroxide. Before final dilution, enough of the internal standard stock solution was added to contain 80.0 μg/ml in the final solution.

Injections—A 20.0-μl aliquot of the assay solution was injected into the chromatograph at the conditions described. For comparison, an identical volume of the standard solution was injected after the assay eluted.

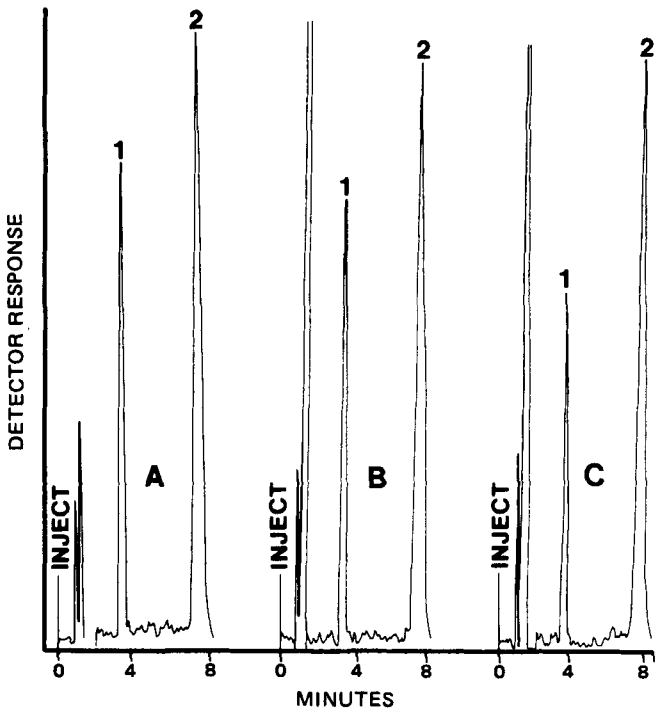

Figure 2—*Sample chromatograms. Peaks 1 and 2 are from benzoyl peroxide and hydroxyprogesterone caproate (internal standard), respectively. The long peak (out of scale) after injection in chromatograms B and C is from acetone. Chromatogram A is from a standard solution (see text) and B and C from 97-days-old solutions (Numbers 4 and 7, Table I), respectively.*

Table II—Assay Results of Solutions [a]

Solution Number[b]	Percent Retained					
	0 day	10 days	46 days	50 days	60 days	97 days
1	101.3	101.4	97.7	—	—	85.2
2	101.8	100.8	98.2	—	—	85.6
3	101.3	101.1	100.2	—	—	89.5
4	102.2	101.8	100.7	—	—	90.9
5	101.1	98.3	96.5	—	—	82.8
6	102.0	98.3	94.2	—	—	81.7
7	100.9	95.6	90.3	—	—	74.7
8	100.0	100.8	99.2	—	—	86.4
9	99.8	97.7	93.3	—	—	72.6
10	100.6	98.2	92.5	—	—	73.2
11	100.6	99.1	95.1	—	—	76.8
12	101.2	97.7	—	81.8	76.9	—
13	100.7	100.1	—	83.1[c]	78.3[c]	—
14	100.1	98.7	—	94.2[c]	87.1[c]	—

[a] For results of ointments stored at 24°, see Fig. 1. Almost all benzoyl peroxide decomposed in 5 days in ointments stored at 50°. [b] For composition of the solutions, see Table 1. [c] These solutions had discolored to light yellow due to oxidation of hydroxyquinoline/chlorhydroxyquinoline.

Calculations—Since the ratios of peak heights were directly related to concentrations, the results were calculated using the equation:

$$100 \times \frac{R_{pha}}{R_{phs}} = \text{percent of the label claim} \qquad \text{(Eq. 1)}$$

where R_{pha} is the ratio of the peak heights of benzoyl peroxide and hydroxyprogesterone caproate of the assay solution and R_{phs} is that of the standard solution.

After the initial assays, the ointments and solutions were reassayed after appropriate time intervals.

RESULTS AND DISCUSSION

The results (Fig. 1, and footnote *a* in Table II) indicate that benzoyl peroxide decomposes quickly when mixed with polyethylene glycol ointment base. The K value at room temperature was 0.028/day. It has been postulated (2) that OH groups in the vehicle had an adverse effect on the stability of benzoyl peroxide. At 50°, almost all of the benzoyl peroxide in polyethylene glycol ointment base decomposed in 5 days. The addition of acetanilide (a commonly used stabilizer for hydrogen peroxide) and benzoic acid (a major decomposition product of benzoyl peroxide) did not improve the stability of benzoyl peroxide. The lag period, which was prominent in solutions, almost disappeared in 2% (w/w) ointment of benzoyl peroxide in polyethylene glycol base.

After the lag period, the solutions decomposed slowly without following any particular order of reaction. However, the following observations might be made from the data (Table I, and Figs. 1 and 2):

1. Ethanol improves the stability of benzoyl peroxide when substituted for acetone (Solutions 3 and 4 *versus* 1, Table II).
2. Propylene glycol hastens the degradation when substituted for acetone (solutions 5–7 *versus* 1, Table II). An attempt to substitute glycerin for acetone (50% v/v) was unsuccessful. There was a problem preparing a single homogeneous phase.
3. The addition of acetanilide, benzoic acid, and hydroxyquinoline did not improve the stability (Solutions 9–11 *versus* 7, Table II). 8-Hydroxyquinoline (oxine) has been reported (8) to improve the stability of hydrogen peroxide in certain pharmaceutical gels.
4. Chlorhydroxyquinoline improved the stability of benzoyl peroxide (solution 14 *versus* 12–13, Table II). This is probably the reason why commercial formulations contain this compound (9).
5. The decomposition of benzoyl peroxide appears to be concentration dependent (solution 6 *versus* 12, Table II). Solution 12 was prepared from hydrous benzoyl peroxide (71%) *versus* Solution 6 which was prepared from benzoyl peroxide (98%). Another solution similar to 12 was prepared using benzoyl peroxide (98%) and this solution was slightly more stable than Solution 12. All commercial formulations are prepared from hydrous benzoyl peroxide to prevent explosion.

In brief, the decomposition of benzoyl peroxide is complex and susceptible to many factors, some of them still unknown. Furthermore, the benefits of adding stabilizer(s) are themselves controversial (2). It has been suggested (2) that addition of chelating agents (citric acid or edetate disodium) might have an adverse effect on the stability of benzoyl peroxide. Yet some commercial products (9) add these chelating agents to improve the stability.

The effect of small traces of impurities in benzoyl peroxide, the vehicles, and additives is still not well understood. The stability of benzoyl peroxide needs to be thoroughly investigated. Further work is in progress in this laboratory.

REFERENCES

(1) M. Gruber, R. Klein, and M. Foxx, *J. Pharm. Sci.*, **58,** 566 (1969).

(2) J. N. Bollinger, D. Lewis, and V. M. Mendez, *ibid.*, **66,** 718 (1977).

(3) R. E. Daly, J. J. Lomner, and L. Chafetz, *ibid.*, **64,** 1999 (1975).

(4) F. W. Burton, R. R. Gade, and W. L. McKenzie, *ibid.*, **68,** 280 (1979).

(5) "The United States Pharmacopeia," 19th rev., Mack Publishing, Easton, Pa., 1975, p. 51.

(6) "The USP-NF," 1980 ed., United States Pharmacopeial Convention, Rockville, Md., 1980, pp. 75–76.

(7) *Ibid.*, p. 1246.

(8) A. I. El Assasy, A. A. Elbary, and Y. H. Hanza, *Cosmet. Toilet.*, **91,** 54 (1976).

(9) "Physicians Desk Reference," 34th rev., Medical Economics, Oradell, N.J., 1980, p. 818.

ACKNOWLEDGMENTS

Supported in part by Alcon Laboratories, Inc., Fort Worth, TX 76101.

Common Ion Equilibria of Hydrochloride Salts and the Setschenow Equation

JOSEPH B. BOGARDUS

Received July 21, 1981, from the *College of Pharmacy, University of Kentucky, Lexington, KY 40506.* Accepted for publication September 3, 1981.

Abstract □ A simple equation was derived to describe the relationship between the aqueous solubility of sparingly soluble salts (S_0) and the empirical Setschenow salting-out constant (k): $k = 0.217/S_0$. This relationship and the Setschenow equation were found to be valid only at low concentrations of added salt. This equation agreed with recently published data when compared for the effect of the chloride ion on the solubility of a series of drug hydrochloride salts. The theoretical treatment also predicts the curvature which has been reported in literature Setschenow plots at higher salt concentrations. As the concentration of added salt increases, the apparent k value is not constant but is dependent on solubility and the rate of change of solubility with added salt concentration. It was concluded that the Setschenow treatment is generally inappropriate for description and analysis of common ion equilibria.

Keyphrases □ Hydrochloride salts—relationship of aqueous solubility and Setschenow constant □ Setschenow equation—relationship between solubility of hydrochloride salts □ Common ion equilibria—of hydrochloride salts and Setschenow equation

In several studies the empirical Setschenow equation has been used to describe the effect of the chloride ion on the solubility of drug hydrochloride salts (1–5). Although this equation was originally proposed to describe salting-out phenomena of nonelectrolytes (6), it appeared to adequately describe suppression of solubility by the common ion effect. In other investigations the principles of solubility product equilibrium were used for describing the solubility of drug salts (7, 8). The solubility product treatment was essential in studying the solubility of doxycycline hydrochloride since self-association to form a dimer dominated the aqueous solubility (8).

The present study was initiated to examine the relationship between the empirical Setschenow equation and rigorous solubility product equilibrium theory. The mathematical treatment shows that the apparent Setschenow salting-out constant (k) is not a physical chemical constant. It is related to solubility or the solubility product constant only at low concentrations of added salt. Due to these limitations and the difficulty in detecting self-association of drug, rigorous solubility product relationships should be used to describe common ion equilibria of hydrochloride salts.

THEORY

The solubility product constant (K_{sp}) for the hydrochloride salt of a weak base is defined as:

$$K_{sp} = S\,[Cl^-] \qquad \text{(Eq. 1)}$$

where S is the concentration of the protonated base and $[Cl^-]$ is the chloride ion concentration at equilibrium. The chloride ion concentration is expressed as the sum:

$$[Cl^-] = S + [NaCl] \qquad \text{(Eq. 2)}$$

where [NaCl] is the concentration of added salt (8).

When [NaCl] = 0, $S = S_0 = [Cl^-]$ and the solubility product constant is:

$$K_{sp} = S_0^2 \qquad \text{(Eq. 3)}$$

This equation is valid only when self-association of drug is negligible (8). The Setschenow equation can be written:

$$\log \frac{S_0}{S} = k[NaCl] \qquad \text{(Eq. 4)}$$

where k is the apparent salting-out constant. It is assumed that the salting-out behavior is due only to chloride ion, and specific cation effects are negligible. Literature data using ammonium or sodium chlorides indicate that this assumption is valid (4, 8). The salting-out constant is the slope of a plot of log S_0/S *versus* [NaCl]:

$$k = \frac{d \log \frac{S_0}{S}}{d\,[NaCl]} = \frac{-\frac{dS}{d\,[NaCl]}}{2.303\,S} \qquad \text{(Eq. 5)}$$

This equation indicates that the apparent salting-out constant depends on the solubility and the rate of change of solubility with added salt concentration. The limiting slope at low added salt concentration is:

$$\lim_{[NaCl]\to 0} k = \frac{-\lim_{[NaCl]\to 0}\left(\frac{dS}{d\,[NaCl]}\right)}{2.303\,S_0} \qquad \text{(Eq. 6)}$$

since, as [NaCl] → 0, $S \to S_0$.

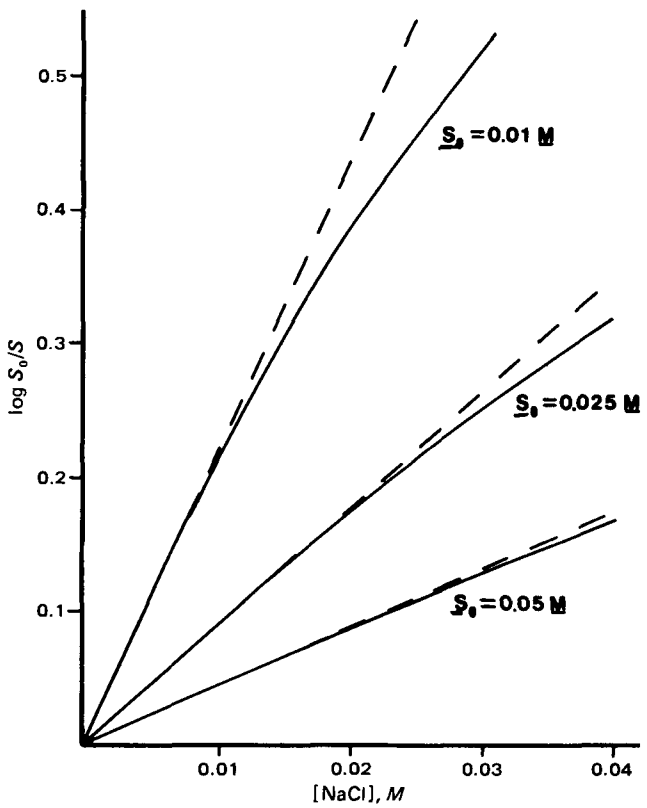

Figure 1—*Hypothetical Setschenow plots at three* S_0 *values according to Eqs. 3 and 7 (—). The initial slopes (- - -) were calculated using Eq. 10.*

0022-3549/82/0500-0588$01.00/0

Table I—Comparison of Experimental and Calculated Salting-out Constants

Hydrochloride Salt	25°		37°	
	k^a_{exp}	k^b_{calc}	k^a_{exp}	k^b_{calc}
Phenazopyridine	18.06	16.5	11.57	11.5
Cyproheptadine	21.18	20.9	14.80	13.7
Bromhexine	20.00	21.3	16.78	16.8
Trihexyphenidyl	8.24	12.6	5.66	5.8
Isoxsuprine	6.32	7.4	6.30	5.6
Chlortetracycline	9.60	9.7	6.52	8.9
Methacycline	8.24	5.7	6.36	4.9
Papaverine	5.09	2.3	3.60	1.8
Demeclocycline	3.73	3.1	2.68	2.4
Doxycycline	5.3[c]	1.8[b], 5.1[d]	—	—

[a] From Ref. 1 except as noted. [b] Calculated using Eq. 10. [c] Calculated from the data in Ref. 8. [d] Calculated using Eq. 12 and $K_{sp} = 1.8 \times 10^{-3}\ M^2$ (8).

From Eqs. 1 and 2 and the quadratic formula, the following expression for S is obtained:

$$S = \frac{-[\mathrm{NaCl}] \pm ([\mathrm{NaCl}]^2 + 4K_{sp})^{1/2}}{2} \qquad \text{(Eq. 7)}$$

The derivative with respect to [NaCl] is:

$$\frac{dS}{d\,[\mathrm{NaCl}]} = \frac{-1 \pm [\mathrm{NaCl}]([\mathrm{NaCl}]^2 + 4K_{sp})^{-1/2}}{2} \qquad \text{(Eq. 8)}$$

and the limit of this differential is:

$$\lim_{[\mathrm{NaCl}]\to 0} \left(\frac{dS}{d[\mathrm{NaCl}]}\right) = -1/2 \qquad \text{(Eq. 9)}$$

Therefore, from Eqs. 6 and 9, the limiting value of the salting-out constant has a simple relationship with solubility:

$$k_l = \lim_{[\mathrm{NaCl}]\to 0} k = \frac{1}{4.606\,S_0} = \frac{0.217}{S_0} \qquad \text{(Eq. 10)}$$

or in log form:

$$\log k_l = -\log S_0 - 0.664 \qquad \text{(Eq. 11)}$$

In the absence of self-association, S_0 and K_{sp} are related by Eq. 3, and the limiting value of the salting-out constant can also be written as:

$$k_l = \frac{0.217}{K_{sp}^{1/2}} \qquad \text{(Eq. 12)}$$

DISCUSSION

Figure 1 contains hypothetical Setschenow plots which were generated at solubilities of 0.01, 0.025, and 0.05 M using Eqs. 3 and 7. The range of S_0 and salt concentration were chosen to be similar to that reported previously (1) for several drug salts. At each concentration the lines show downward curvature with increasing salt concentration. With decreasing drug salt solubility the deviations from the initial slope based on Eq. 10 begin to appear at progressively lower concentrations of added salt. Curved Setschenow plots of this type were reported for the hydrochloride salts of phenazopyridine, cyproheptadine, and bromhexine (1). These compounds have solubilities of ~0.01 M, which is consistent with the theoretically generated data. More soluble drug salts, as expected, showed lower slopes and essentially linear relationships.

The experimental salting-out constants at 25 and 37° for several compounds are compared in Table I with values calculated from their solubilities. Good agreement was obtained in most cases with the largest differences appearing with the most soluble salts which have the smallest slopes. Papaverine was approximately two times more sensitive to salt than would be predicted from its solubility. The calculated and experimental values for methacycline differ by 30–40%.

The k_{exp} for doxycycline shows poor agreement with the value calculated from S_0 using Eq. 10. This is not unexpected, since doxycycline is known to form a dimer and higher order complexes in aqueous solution (8). These equilibria cause the apparent solubility product calculated from Eq. 3 ($13.1 \times 10^{-3}\ M^2$) to be larger than the limiting K_{sp} ($1.8 \times 10^{-3}\ M^2$), which was determined under conditions where self-association was negligible. Thus, the k_{calc} from Eq. 10 is incorrect because of the solubility-increasing effect of self-association. Calculations of k using the limiting K_{sp}, which is not influenced by self-association, provides a value similar to the experimental constant.

In view of the known self-association of doxycycline, it is surprising that k_{exp} is so similar to k_{calc}. This appears to be due to compensation of S_0 and dS/d[NaCl] in Eq. 5. The approximately three-fold higher solubility ($S_0/K_{sp}^{1/2}$) caused by self-association is compensated by a three-fold higher salting-out rate estimated from the slope of the plot of S *versus* [NaCl]. The added salt may be decreasing the stability of the associated species.

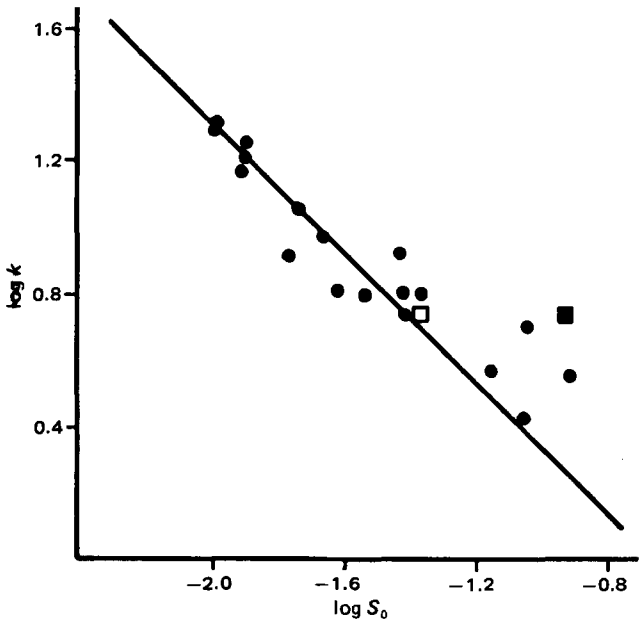

Figure 2—*Relationship between salting-out constant and solubility. Key: (—) Eq. 11; (●) 25 and 37°, data from (1), for the drugs in Table I; (■) observed data for doxycycline hydrochloride; (□) experimental* k *value and* S_0 *calculated from the limiting* K_{sp} *using Eq. 3.*

Since the initial slope is most important in a Setschenow plot, and this region is most susceptible to the effects of self-association, the use of this method may lead to erroneous results. A probable explanation for the poor agreement with papaverine and methacycline hydrochlorides is that the solubilities (S_0) are anomalously high due to self-association. This would be especially likely for methacycline, which is structurally similar to doxycycline. Based on the limited doxycycline data, self-association appears to have a stronger effect on solubility than it does on the apparent salting-out constant.

The solubility product constant is inversely proportional to the square of the salting-out constant (Eq. 12). A doubling in the slope of a Setschenow plot corresponds to a four-fold decrease in K_{sp}. Thus, K_{sp} is a more sensitive indicator of common ion effects than the salting-out constant. A major disadvantage of the use of Setschenow plots is that self-association of the drug cannot be detected. This is not a problem when the data are analyzed according to the principles of solubility product equilibrium since the apparent K_{sp}, calculated as the product of solubility and chloride concentrations, will not be constant (8).

The existence of a linear correlation between log k and log S_0 has been shown (1). More soluble drug salts were found to have smaller salting-out constants. These observations are theoretically predicted by Eq. 11. In Fig. 2 the salting-out constant and solubility of the drug salts in Table I are plotted according to Eq. 11. The experimental data show good agreement with the theoretical line of slope = −1.0. Points for doxycycline, papaverine, and methacycline lie above the line, which is consistent with the proposed self-association of these compounds.

Few of the drugs deviate negatively from the theoretically predicted relationship. Trihexyphenidyl at 25° and chlortetracycline at 37° are below the line, but at the other temperature these compounds show satisfactory agreement. These apparent deviations cannot be explained at present.

The results of this study indicate that the Setschenow treatment, originally proposed to describe salting-out of nonelectrolytes, is inappropriate for description of common ion equilibria of hydrochloride salts. Data analysis based on solubility product equilibrium theory is a more satisfactory approach.

REFERENCES

(1) S. Miyazaki, M. Oshiba, and T. Nadai, *J. Pharm. Sci.*, **70**, 594 (1981).

(2) S. Miyazaki, M. Oshiba, and T. Nadai, *Int. J. Pharm.*, **6**, 77 (1980).
(3) S. Miyazaki, H. Inoue, T. Nadai, T. Arita, and M. Nakano, *Chem. Pharm. Bull.*, **27**, 1441 (1979).
(4) S. Miyazaki, M. Nakano, and T. Arita, *ibid.*, **23**, 1197 (1975).
(5) S.-L. Lin, L. Lachman, C. J. Swartz, and C. F. Huebner, *J. Pharm. Sci.*, **61**, 1418 (1972).
(6) F. A. Long and W. F. McDevit, *Chem. Rev.*, **51**, 119 (1952).
(7) J. V. Swintosky, E. Rosen, R. E. Chamberlain, and J. R. Guarini, *J. Am. Pharm. Assoc., Sci. Ed.*, **45**, 34 (1956).
(8) J. B. Bogardus and R. K. Blackwood, Jr., *J. Pharm. Sci.*, **68**, 188 (1979).

ACKNOWLEDGMENTS

The author thanks Dr. Rima Bawarshi for comments and review of the manuscript.

High-Pressure Liquid Chromatographic Determination of Cimetidine in Plasma and Urine

G. W. MIHALY ˣ, S. COCKBAIN, D. B. JONES, R. G. HANSON, and R. A. SMALLWOOD

Received April 22, 1981, from the *Gastroenterology Unit, Department of Medicine, University of Melbourne, Austin Hospital, Heidelberg, 3084, Victoria, Australia.* Accepted for publication August 26, 1981.

Abstract □ An assay is described for the determination of the H_2-receptor antagonist, cimetidine, in human plasma and urine. Alkalinized plasma or urine was extracted with methylene chloride, the organic phase was evaporated, and the reconstituted residue was analysed by high-pressure liquid chromatography (HPLC) using a reversed-phase prepacked plastic column housed in a radial compression module. The metabolite, cimetidine sulfoxide, was identified but could not be quantitated due to interference from the solvent front. The sensitivity limit of the assay was 25 ng/ml. The assay was applied to the measurement of plasma and urine samples in a pilot pharmacokinetic study. Cimetidine was substantially absorbed and rapidly eliminated (plasma elimination half-life of 112–130 min). Plasma cimetidine concentrations could be measured to 12 hr after a 200-mg dose (iv or oral), but they were below the sensitivity of the assay by 24 hr. Urinary excretion of unmetabolized cimetidine accounted for 40–50% of the administered dose in the first 12 hr. This assay is simpler and more sensitive than those previously described, and it is suitable for the measurement of cimetidine in plasma and urine of subjects receiving doses appropriate for clinical use.

Keyphrases □ Cimetidine—high-pressure liquid chromatographic analysis in plasma and urine □ High-pressure liquid chromatography—analysis, cimetidine, human plasma and urine □ H_2-Receptor antagonists—cimetidine, high-pressure liquid chromatographic analysis in plasma and urine

The H_2-receptor antagonist, cimetidine, profoundly inhibits gastric acid secretion and is effective in the treatment of gastric and duodenal ulcers (1). Studies have shown that the degree of inhibition of gastric acid secretion is related to cimetidine plasma level measurements (2).

Chromatographic assays for the measurement of blood, plasma, and urine concentrations of cimetidine have been published. The sample treatment in these methods is complex and involves multiple extraction steps (3, 4). Moreover, samples are chromatographed on silica-based column packing which is likely to limit the column's efficiency and life under alkaline conditions. A simple micromethod for the estimation of plasma cimetidine has also been reported (5). This method exhibited low precision and sensitivity, as well as lengthy chromatography.

A more sensitive liquid chromatographic method for measuring cimetidine in plasma and urine, using a simple, single extraction step in sample treatment, is reported. Chromatography is rapid and conducted on a column system[1,2] which recently has become commercially available. These columns operate under conditions that produce greater column efficiency and allow longer column life. This method has been applied to a pilot study on a patient with a gastric ulcer, in which the influence of a 6-week course of cimetidine (1 g/day) on its own disposition and elimination is investigated.

EXPERIMENTAL

Instrumentation—A constant flow high-pressure liquid chromatograph[3] was used for all assays. This consisted of a solvent delivery system[4], a universal injector[5], and a variable wavelength UV absorbance detector[6] operating at 228 nm. The plastic column was obtained prepacked[1] (100 mm × 8-mm i.d.) and was housed in a radial compression module[2] which maintained external column pressure at ~2500 psi.

Reagents—Pure samples of cimetidine, cimetidine sulfoxide, and the internal standard, burimamide, were obtained[7]. The HPLC mobile phase contained UV grade acetonitrile[8], triethylamine[9], phosphoric acid[10], and glass-distilled water.

Calibration Standards—A pool of drug-free plasma was spiked with pure cimetidine to a concentration of 5000 ng/ml. By a series of quantitative double dilutions with additional drug-free plasma, standards of 2500, 1250, 625, and 312.5 ng/ml were prepared and stored at −20°. Similarly, drug-free urine was spiked with pure cimetidine to a concentration of 200 μg/ml and diluted to prepare standards of 100, 50, and 25 μg/ml. Calibration curves were prepared by plotting the relationship between the peak height ratios of cimetidine–burimamide and the cimetidine concentration in each sample.

Recoveries of cimetidine and burimamide from plasma or urine were estimated by comparing the peak height of cimetidine obtained after extraction, against that obtained when the same amount of cimetidine from an aqueous stock solution was chromatographed.

Extraction of Plasma—Burimamide (internal standard, 10 μg/ml, 200 μl), NaOH (2 *M*, 0.5 ml), and methylene chloride (20 ml) were added to 1.0 ml of plasma in a 30-ml glass tube. After vortex mixing (60 sec) and centrifugation (3000 rpm, 10 min), the organic layer was carefully transferred into a second tube and evaporated under a gentle stream of

[1] Rad Pak A, Waters Associates, Milford, Mass.
[2] RCM-100, Waters Associates, Milford, Mass.
[3] Waters Associates, Carlton, Melbourne, 3053, Australia.
[4] Waters Associates, Model 6000A.
[5] Waters Associates, Model U6K.
[6] Waters Associates, Model 450.
[7] Smith Kline and French Laboratories Ltd. Hertfordshire, England.
[8] Waters Associates, Carlton, Melbourne, 3053, Australia.
[9] BDH Laboratories, Port Fairy, 3284, Australia.
[10] Merck, Darmstadt, West Germany.

0022-3549/82/0500-0590$01.00/0

(2) S. Miyazaki, M. Oshiba, and T. Nadai, *Int. J. Pharm.*, **6**, 77 (1980).
(3) S. Miyazaki, H. Inoue, T. Nadai, T. Arita, and M. Nakano, *Chem. Pharm. Bull.*, **27**, 1441 (1979).
(4) S. Miyazaki, M. Nakano, and T. Arita, *ibid.*, **23**, 1197 (1975).
(5) S.-L. Lin, L. Lachman, C. J. Swartz, and C. F. Huebner, *J. Pharm. Sci.*, **61**, 1418 (1972).
(6) F. A. Long and W. F. McDevit, *Chem. Rev.*, **51**, 119 (1952).
(7) J. V. Swintosky, E. Rosen, R. E. Chamberlain, and J. R. Guarini, *J. Am. Pharm. Assoc., Sci. Ed.*, **45**, 34 (1956).
(8) J. B. Bogardus and R. K. Blackwood, Jr., *J. Pharm. Sci.*, **68**, 188 (1979).

ACKNOWLEDGMENTS

The author thanks Dr. Rima Bawarshi for comments and review of the manuscript.

High-Pressure Liquid Chromatographic Determination of Cimetidine in Plasma and Urine

G. W. MIHALY ˣ, S. COCKBAIN, D. B. JONES, R. G. HANSON, and R. A. SMALLWOOD

Received April 22, 1981, from the *Gastroenterology Unit, Department of Medicine, University of Melbourne, Austin Hospital, Heidelberg, 3084, Victoria, Australia.* Accepted for publication August 26, 1981.

Abstract □ An assay is described for the determination of the H_2-receptor antagonist, cimetidine, in human plasma and urine. Alkalinized plasma or urine was extracted with methylene chloride, the organic phase was evaporated, and the reconstituted residue was analysed by high-pressure liquid chromatography (HPLC) using a reversed-phase prepacked plastic column housed in a radial compression module. The metabolite, cimetidine sulfoxide, was identified but could not be quantitated due to interference from the solvent front. The sensitivity limit of the assay was 25 ng/ml. The assay was applied to the measurement of plasma and urine samples in a pilot pharmacokinetic study. Cimetidine was substantially absorbed and rapidly eliminated (plasma elimination half-life of 112–130 min). Plasma cimetidine concentrations could be measured to 12 hr after a 200-mg dose (iv or oral), but they were below the sensitivity of the assay by 24 hr. Urinary excretion of unmetabolized cimetidine accounted for 40–50% of the administered dose in the first 12 hr. This assay is simpler and more sensitive than those previously described, and it is suitable for the measurement of cimetidine in plasma and urine of subjects receiving doses appropriate for clinical use.

Keyphrases □ Cimetidine—high-pressure liquid chromatographic analysis in plasma and urine □ High-pressure liquid chromatography—analysis, cimetidine, human plasma and urine □ H_2-Receptor antagonists—cimetidine, high-pressure liquid chromatographic analysis in plasma and urine

The H_2-receptor antagonist, cimetidine, profoundly inhibits gastric acid secretion and is effective in the treatment of gastric and duodenal ulcers (1). Studies have shown that the degree of inhibition of gastric acid secretion is related to cimetidine plasma level measurements (2).

Chromatographic assays for the measurement of blood, plasma, and urine concentrations of cimetidine have been published. The sample treatment in these methods is complex and involves multiple extraction steps (3, 4). Moreover, samples are chromatographed on silica-based column packing which is likely to limit the column's efficiency and life under alkaline conditions. A simple micromethod for the estimation of plasma cimetidine has also been reported (5). This method exhibited low precision and sensitivity, as well as lengthy chromatography.

A more sensitive liquid chromatographic method for measuring cimetidine in plasma and urine, using a simple, single extraction step in sample treatment, is reported. Chromatography is rapid and conducted on a column system[1,2] which recently has become commercially available. These columns operate under conditions that produce greater column efficiency and allow longer column life. This method has been applied to a pilot study on a patient with a gastric ulcer, in which the influence of a 6-week course of cimetidine (1 g/day) on its own disposition and elimination is investigated.

EXPERIMENTAL

Instrumentation—A constant flow high-pressure liquid chromatograph[3] was used for all assays. This consisted of a solvent delivery system[4], a universal injector[5], and a variable wavelength UV absorbance detector[6] operating at 228 nm. The plastic column was obtained prepacked[1] (100 mm × 8-mm i.d.) and was housed in a radial compression module[2] which maintained external column pressure at ~2500 psi.

Reagents—Pure samples of cimetidine, cimetidine sulfoxide, and the internal standard, burimamide, were obtained[7]. The HPLC mobile phase contained UV grade acetonitrile[8], triethylamine[9], phosphoric acid[10], and glass-distilled water.

Calibration Standards—A pool of drug-free plasma was spiked with pure cimetidine to a concentration of 5000 ng/ml. By a series of quantitative double dilutions with additional drug-free plasma, standards of 2500, 1250, 625, and 312.5 ng/ml were prepared and stored at −20°. Similarly, drug-free urine was spiked with pure cimetidine to a concentration of 200 μg/ml and diluted to prepare standards of 100, 50, and 25 μg/ml. Calibration curves were prepared by plotting the relationship between the peak height ratios of cimetidine–burimamide and the cimetidine concentration in each sample.

Recoveries of cimetidine and burimamide from plasma or urine were estimated by comparing the peak height of cimetidine obtained after extraction, against that obtained when the same amount of cimetidine from an aqueous stock solution was chromatographed.

Extraction of Plasma—Burimamide (internal standard, 10 μg/ml, 200 μl), NaOH (2 *M*, 0.5 ml), and methylene chloride (20 ml) were added to 1.0 ml of plasma in a 30-ml glass tube. After vortex mixing (60 sec) and centrifugation (3000 rpm, 10 min), the organic layer was carefully transferred into a second tube and evaporated under a gentle stream of

[1] Rad Pak A, Waters Associates, Milford, Mass.
[2] RCM-100, Waters Associates, Milford, Mass.
[3] Waters Associates, Carlton, Melbourne, 3053, Australia.
[4] Waters Associates, Model 6000A.
[5] Waters Associates, Model U6K.
[6] Waters Associates, Model 450.
[7] Smith Kline and French Laboratories Ltd. Hertfordshire, England.
[8] Waters Associates, Carlton, Melbourne, 3053, Australia.
[9] BDH Laboratories, Port Fairy, 3284, Australia.
[10] Merck, Darmstadt, West Germany.

0022-3549/82/0500-0590$01.00/0

Table I—Pharmacokinetic Parameters and Cumulative Urinary Excretion Data for Cimetidine [a]

Pharmacokinetic Parameters	Study Number I	II	III	IV
Dose, mg	200	200	200	200
Route	iv	oral	oral	iv
$AUC_{0\to\infty}$, ng min/ml × 10^{-3}	350.2	308.0	315.8	487.3
$t_{1/2\beta}$, min	129.7	122.8	114.8	112.6
Cl_s, ml/min	563.6	563.6	406.8	406.8
Vd_β, liters	105.5	99.9	67.4	66.1
F, × 10^2	—	89.3	65.8	—
Cumulative percent of dose excreted in urine:				
4 hr	35.2	29.0	26.7	31.2
8 hr	46.8	37.4	36.0	36.0
12 hr	49.1	41.1	38.8	38.0
24 hr	50.1	44.4	40.4	38.8

[a] Studies I and II were undertaken before a 6-week course of cimetidine (1 g/day), while III and IV were undertaken immediately after the course of therapy. ($AUC_{0\to\infty}$ = area under the plasma concentration–time curve; $t_{1/2\beta}$ = terminal elimination phase half-life; Cl_s = systemic clearance; Vd_β = volume of distribution; F = bioavailability fraction.)

nitrogen at 45°. The residue was reconstituted in 100 μl of the chromatographic mobile phase and 40 μl was injected onto the liquid chromatograph.

Extraction of Urine—Burimamide (1 mg/ml, 25 μl), NaOH (2 *M*, 100 μl), and methylene chloride (5 ml) were added to 250 μl of urine in a 30-ml glass tube, and the sample was treated as described for the plasma. Only 20 μl of the reconstituted residue was injected onto the chromatograph.

Chromatography—The mobile phase was 1% triethylamine and 5% acetonitrile in water, adjusted to pH 3 with phosphoric acid (85% v/v). The flow rate was 3 ml/min at a back pressure of 1500 psi. The retention times of burimamide and cimetidine were 2.4 and 3.8 min, respectively. Under these conditions the peaks were resolved completely to baseline.

Patient Sampling—The effect of a course of cimetidine on drug disposition was assessed in a pilot study of a female patient with a gastric ulcer (age, 49 years; weight, 59 kg). The patient underwent intravenous and oral pharmacokinetic studies before and after a 6-week course of cimetidine. After an overnight fast, the patient received a 200-mg/15-ml dose *iv* of cimetidine over 5 min (Table I, Study I). Venous blood samples (10 ml) were withdrawn before the cimetidine dose and at intervals to 24 hr. Urine was also collected predose and over a 24-hr period. At 48 hr, after an overnight fast, a 200-mg tablet of cimetidine was administered with 150 ml of water (Table I, Study II). Blood and urine were again collected over a 24-hr period. The patient then began a 6-week course of cimetidine (200 mg three times daily and 400 mg at night). Twenty four hours after the final dose, the oral and intravenous pharmacokinetic studies were repeated (Table I, Studies III and IV). In all studies food was withheld for the first 3 hr. Thereafter a standard meal was supplied, and free access to water was allowed.

Calculations—Pharmacokinetic parameters were derived from the plasma cimetidine concentration *versus* time data, using the nonlinear least squares regression program, AUTOAN (6), and standard pharmacokinetic formula (7).

RESULTS AND DISCUSSION

Column effluent was monitored at 228 nm, since this corresponds to the wavelength of maximum UV absorbance of cimetidine. For the chromatographic separation of cimetidine, the radial compression column system offers several advantages over the stainless steel, packed reversed-phase columns. Chromatography is faster and more efficient, enhancing sensitivity. The columns are less expensive and more robust, and the use of an acidified mobile phase (pH 3) containing triethylamine gives longer column life.

Single step extraction with methylene chloride results in simple sample preparation. Figure 1 (A and B) shows the chromatograms of a blank predose plasma extract and a plasma extract obtained after a single oral dose of cimetidine. Plasma from the patient receiving cimetidine showed a distinct peak at 3.8 min, which represented 801 ng/ml of cimetidine. No peaks corresponding to the cimetidine sulfoxide metabolite were present. Figure 1(C) shows the chromatogram of 100 ng of each of the reference compounds, cimetidine sulfoxide, burimamide, and cimetidine, injected as an aqueous solution. There is satisfactory separation of cimetidine from both the internal standard and the sulfoxide metabolite.

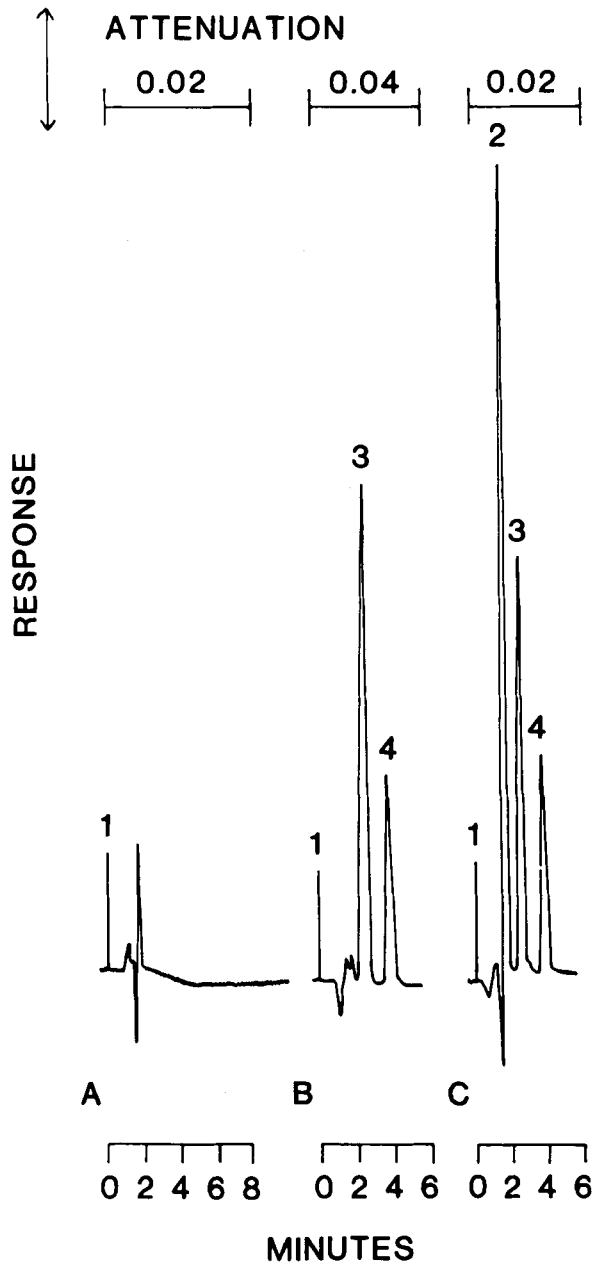

Figure 1—*High-pressure liquid chromatograms for a blank plasma extract (A); an extract of a plasma sample obtained from a patient who received a single dose of cimetidine (cimetidine concentration = 801 ng/ml) (B); and reference compounds showing the injection event (1), cimetidine sulfoxide (2), the internal standard, burimamide (3), and cimetidine (4), for which 100 ng of each compound was injected as a mixed solution in the mobile phase (C).*

In the chromatograms of some patients' plasma samples, a single broad peak eluted at 32 min. This peak was attributed to a cimetidine metabolite because it was absent from predose sample chromatograms. However, it could not be identified, since appropriate pure metabolite standards were unavailable.

Chromatograms of blank urine and a urine specimen collected after a single intravenous dose of cimetidine are shown in Fig. 2. Due to the much higher concentrations of cimetidine in urine, the detector attenuation was reduced. The late-eluting component seen in some plasma chromatograms was not seen in any urine chromatograms, suggesting that this presumed metabolite is not excreted in urine in significant amounts.

Cimetidine sulfoxide, which has been identified as a major metabolite of cimetidine (8), did not interfere with the assay. Although this metabolite appeared in the chromatogram of an aqueous stock solution at a retention time of 1.7 min (Fig. 1C), it was not possible to quantitate it due to interference from the solvent front.

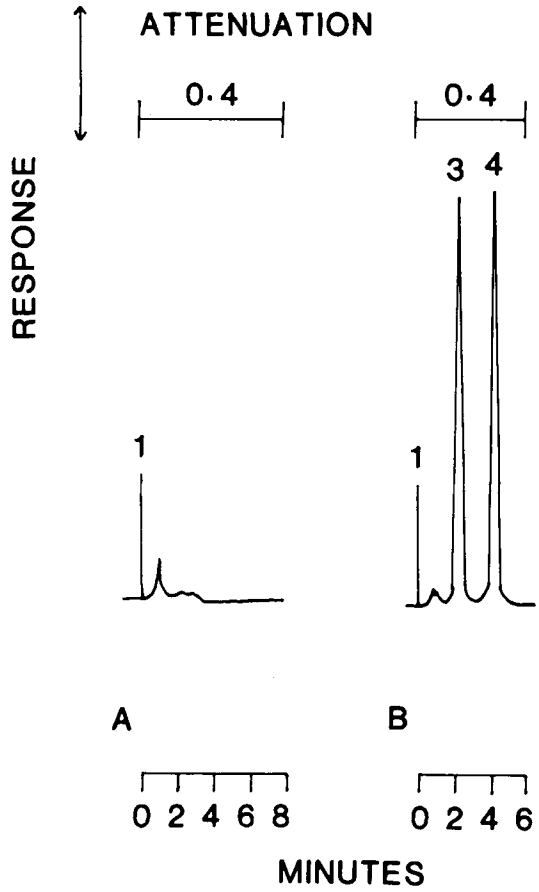

Figure 2—*High-pressure liquid chromatograms for a blank urine extract (A); and an extract of urine sample obtained from a patient who had received a single dose of cimetidine (cimetidine concentration = 156 μg/ml) (B). The peaks are the injection event (1); the internal standard, burimamide (3); and cimetidine (4).*

Methylene chloride was chosen as the extraction solvent because it gave optimal recovery of cimetidine with minimal extraction of endogenous components that might have interfered with quantitation. Analytical recoveries of cimetidine and burimamide were 60 and 31%, respectively. The limit of detection for both cimetidine and burimamide in plasma was 25 ng/ml, which gave peaks four times that of the baseline noise at the highest detector sensitivity. Ranitidine and oxmetidine, two other H_2-receptor antagonists under clinical evaluation, did not interfere with the assay.

The precision of the assay was assessed by replicate assays of aliquots of the same sample spiked with pure cimetidine. The coefficient of variation for same-day assays of plasma cimetidine levels was 4.6% at 1000 ng/ml (n = 6); for urine it was 0.4% at 55 μg/ml (n = 7). The coefficient of variation of day-to-day assays of plasma cimetidine levels over 4 weeks was 6.6% at 960 ng/ml (n = 9). The value for urine over the same period was 3% at 54 μg/ml (n = 5). The accuracy of cimetidine determination was not influenced by dried methylene chloride-extracted residue, stored for up to 5 days at 20°.

This method can be readily extended to the assay of burimamide, although this H_2-receptor antagonist is now only used in animal experiments. For burimamide assays, cimetidine is used as the internal standard. This approach has been successfully applied to the analysis of burimamide in samples obtained from animal studies.

The assay was applied to the measurement of plasma samples obtained from a pilot pharmacokinetic study. Figure 3 shows the semilogarithmic plot of plasma cimetidine concentrations following intravenous and oral doses, which were administered before (Table I, Studies I and II) and after (Table I, Studies III and IV) a 6-week course of cimetidine. The resultant pharmacokinetic and urinary excretion data for this patient are presented in Table I.

In all studies, plasma cimetidine could be estimated only to 12 hr, since by 24 hr, concentrations were below the sensitivity of the assay (25 ng/ml). The pharmacokinetic results agree with earlier studies (9, 10) and show that oral cimetidine is substantially absorbed and that both oral and intravenous cimetidine undergo rapid elimination. The urinary excretion

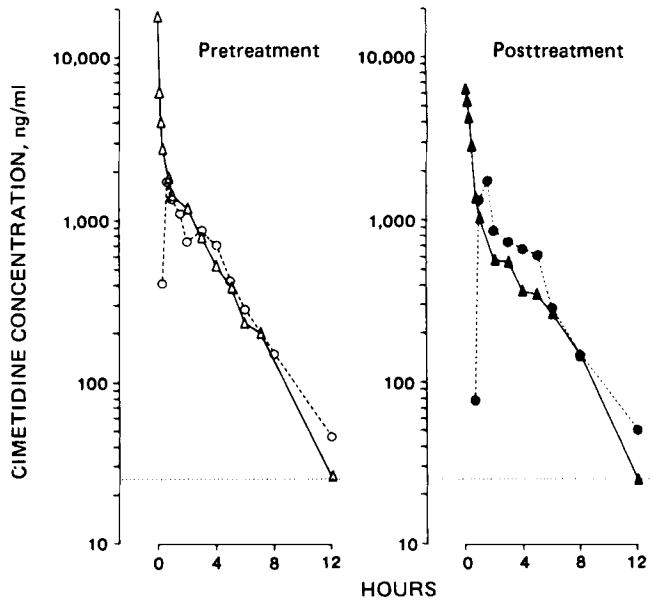

Figure 3—*Semilogarithmic plot of the mean plasma cimetidine concentration* versus *time following intravenous and oral administration of cimetidine to a patient before and after a 6-week course of treatment with cimetidine. Key: Pretreatment: (△) 200 mg, iv; (○) 200 mg, oral. Posttreatment: (▲) 200 mg, iv; (●) 200 mg, oral.*

data (Table I) confirm that renal clearance of unmetabolized drug is an important route of elimination. Approximately 40–50% of an administered dose is excreted unchanged in urine within the first 12 hr.

In contrast to an earlier study (10), the 6-week course of treatment in the patient appeared to alter the disposition of cimetidine (Table I). However, no firm conclusions can be drawn from this pilot study in one patient, and further studies are now under way.

Advantages of this assay over earlier published methods are increased precision and sensitivity (2–4-fold) resulting from improved chromatographic conditions. In addition, sample treatment has been kept simple. From the pilot pharmacokinetic study, it is apparent that the proposed method is sufficiently sensitive and specific for cimetidine quantitation in both plasma and urine, when clinically used doses are administered.

REFERENCES

(1) K. D. Bardhan, in, "Further Experience with H_2-Receptor Antagonists in Peptic Ulcer Disease and Progress in Histamine Research," A. Torsoli, P. E. Lucchelli, and R. W. Brimblecombe, Eds., Excerpta Medica, Amsterdam, 1980, p. 5.

(2) R. N. Brimblecombe and W. A. M. Duncan, in, "Cimetidine, Proceedings of the Second International Symposium on Histamine H_2-receptor Antagonists," W. L. Burland and M. A. Simkins, Eds. Excerpta Medica, Amsterdam (1977), p. 54.

(3) W. C. Randolph, V. L. Osborne, S. S. Walkenstein, and A. P. Intoccia, *J. Pharm. Sci.*, **66,** 1148 (1977).

(4) N. E. Larsen, *J. Chromatogr.*, **163,** 57 (1979).

(5) S. J. Soldin, D. R. Fingold, P. C. Fenje, and W. A. Mahon, *Ther. Drug. Monit.*, **1,** 371 (1979).

(6) J. G. Wagner, "Fundamentals of Clinical Pharmacokinetics," Drug Intelligence Publications, Hamilton, Ill., 1975, p. 434.

(7) M. Gilbaldi and D. Perrier, in, "Drugs and the Pharmaceutical Sciences," J. Swarbrick, Ed., vol. 1, Marcel Dekker, New York, N.Y., 1975, pp. 281, 293.

(8) D. C. Taylor, P. R. Creswell, and D. C. Bartlett, *Drug Metab. Disp.*, **6,** 21 (1978).

(9) S. S. Walkenstein, J. W. Dubb, W. C. Randolph, W. J. Westlake, R. M. Stote, and A. P. Intoccia, *Gastroenterology*, **74,** 360 (1978).

(10) G. Bodemar, B. Norlander, L. Fransson, and A. Walan, *Br. J. Clin. Pharmacol.*, **7,** 23 (1979).

ACKNOWLEDGMENTS

Supported by the National Health and Medical Research Council of Australia.

The authors thank Mrs. J. Anderson for technical assistance, Mrs. S. Evans for clerical help, and Smith, Kline and French Ltd. for samples of pure drugs.

Enhanced Rectal Bioavailability of Polypeptides Using Sodium 5-Methoxysalicylate as an Absorption Promoter

SUMIE YOSHIOKA *§, **LARRY CALDWELL** ‡, **and TAKERU HIGUCHI** *‡ x

Received June 24, 1981, from the *Department of Pharmaceutical Chemistry, University of Kansas, Lawrence, KS 66045, and the ‡INTERx Research Corporation, Lawrence, KS 66044. Accepted for publication October 16, 1981. §Present address: National Institute of Hygienic Sciences, 18-1, Kamiyoga 1-chome, Setagaya-ku, Tokyo 158, Japan.

Abstract □ The absorption-promoting effect of sodium 5-methoxysalicylate was studied in the rat with respect to rectal delivery of pentagastrin and gastrin. Rectal bioavailability was quantitated by direct comparison of pharmacological effect with intravenous dose response. Coadministration of the absorption adjuvant greatly enhanced the rectal bioavailability of the model polypeptides. Sodium 5-methoxysalicylate, therefore, is representative of a new type of absorption promoter which appears to facilitate rectal absorption of polypeptide drug entities.

Keyphrases □ Bioavailability—rectal, absorption of small polypeptides, rats □ Polypeptides—pentagastrin and gastrin, rectal bioavailability, rats □ Adjuvant—absorption effect of sodium 5-methoxysalicylate, rats

Parenteral injection has long been the only reliable method to administer polypeptide drugs. Successful oral dosage forms of biologically active polypeptides have traditionally been elusive (1). However, there has been some limited success using the rectal delivery route as an alternative to the parenteral route.

Surface-active agents have been shown to increase rectal absorption of water-soluble polypeptides such as insulin (2). More recently, enhanced rectal delivery of theophylline and lidocaine using sodium salicylate as an absorption promoter was reported (3, 4), and enhanced rectal delivery of insulin in rats using 5-methoxysalicylate as an absorption adjuvant has been demonstrated (5). The use of salicylates as rectal absorption adjuvants represents a divergence from the traditional surfactant-enhanced delivery of poorly absorbed drugs. Furthermore, nontoxic salt forms of salicylate appear to be less tissue damaging than surfactant-type absorption adjuvants (3, 6).

The present study was designed to evaluate the feasibility of rectal delivery of small polypeptides using 5-methoxysalicylate as an absorption promoter.

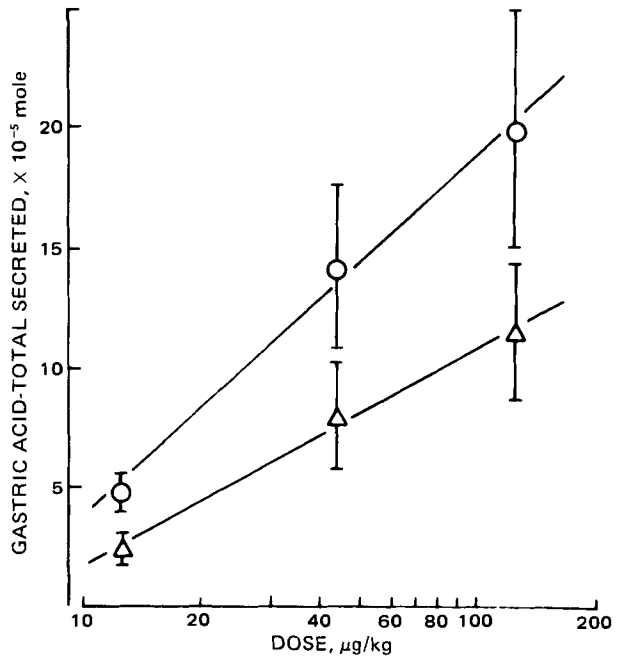

Figure 1—*Intravenous dose response of total gastric acid secretion following intravenous administration of gastrin (△) and pentagastrin (○) to anesthetized rats. The drug dosages were 12.5, 44.0, and 125 μg/kg. The error bars represent standard deviations with n=6.*

EXPERIMENTAL

Male Long-Evans rats, 230–290 g, were fasted 36 hr prior to experimentation. Rats were anesthetized with pentobarbital sodium (50 mg/kg ip) and surgically prepared for gastric perfusion according to the method of Ghosh and Schild (7). The stomachs were rinsed and ultimately perfused with 20 ml of physiological saline solution. The perfusion rate was 2 ml/min provided by a peristaltic pump. Perfusate and rat body temperature were held constant at 38° and the pH of the perfusate was held constant at 4.0[1] with 0.05 *N* NaOH as the titrant. Stomach acid output was continuously monitored by recording the amount of titrant required to maintain a constant pH with respect to time.

The target polypeptides for rectal delivery were pentagastrin[2] (5 residues) and gastrin[3] (17 residues). Aqueous polypeptide solutions were made up and adjusted to pH 8.0 using ammonium hydroxide and the ionic strength was adjusted to $\mu = 0.15$ with sodium chloride. Polypeptide concentration in these solutions was 250 μg/ml. Both pentagastrin and gastrin were administered intravenously (external jugular) to obtain dose–response curves.

Identical drug solutions were also administered rectally as microenema formulations (0.5 ml/kg) with or without the addition of 50 mg/ml of

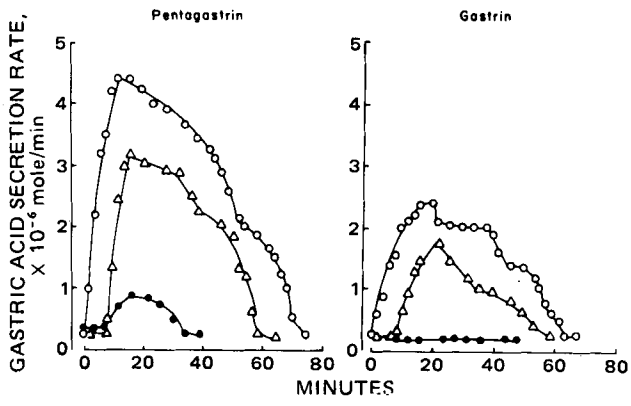

Figure 2—*Typical, single animal profiles of gastric acid secretion following administration of pentagastrin and gastrin to anesthetized rats. The solutions were administered: intravenous with 125 μg polypeptide/kg in saline (○); rectally with 125 μg polypeptide/kg in saline, pH 8.0 (●); and rectally with 125 μg polypeptide/kg rat and 25 mg 5-methoxysalicylate/kg rat in saline, pH 8.0 (△).*

[1] pH Stat, Radiometer, Copenhagen.
[2] Peptavalon, Ayerst Laboratories, Inc.
[3] Porcine intrail mucosa, Sigma. A mixture of gastrin I and gastrin II prepared through Sephadex stage as described by Gregory and Tracy (8).

0022-3549/82/0500-0593$01.00/0

Table I—Total Amount of Gastric Secretion Stimulated by Pentagastrin

Experiment No.	Gastric Acid Secreted, $\times 10^{-5}$ mole				
	Intravenous Administration			Microenema 125 μg/kg[a]	
	12.5[a]	44[a]	125[a]	No Adjuvant	Adjuvant[b]
1	3.3	10.0	22.6	2.9	21.4
2	4.8	9.1	15.9	0.6	12.5
3	6.0	14.0	19.2	2.3	10.6
4	5.5	15.9	29.6	1.0	11.3
5	4.2	17.0	18.0	0.2	10.4
6	5.0	18.8	13.5	2.7	10.3
Mean	4.8	14.1	19.8	1.6	12.9
SD	0.9	3.5	5.2	1.1	3.9
Pharmacologic effect Relative to Intravenous, %			100	8	65
Bioavailability[c], %			100 (defined)	6	33

[a] Dose of pentagastrin (μg/kg). [b] Sodium 5-methoxysalicylate (25 mg/kg). [c] Based on dose–response curve, effect *versus* log dose.

Table II—Total Amount of Gastric Secretion Stimulated by Gastrin

Experiment Number	Gastric Acid Secreted, $\times 10^{-5}$ mole				
	Intravenous Administration			Microenema, 125 μg/kg[a]	
	12.5[a]	44[a]	125[a]	No Adjuvant	Adjuvant[b]
1	3.8	6.4	7.6	0	4.6
2	2.8	5.6	14.1	0	1.6
3	1.7	11.3	8.9	0	7.3
4	2.1	8.6	14.6	0	4.6
5	1.4	9.5	10.4	0	4.4
6	2.4	5.3	12.2	0	6.9
Mean	2.4	7.8	11.3	0	4.9
SD	0.8	2.2	2.6		1.9
Pharmacologic effect Relative to intravenous, %			100	0.0	43
Bioavailability[c], %			100 (defined)	—	18

[a] Dose of gastrin (μg/kg). [b] Sodium 5-methoxysalicylate (25 mg/kg). [c] Based on dose response curve, effect *versus* log dose.

sodium 5-methoxysalicylate. After the addition of the sodium 5-methoxysalicylate as a potential absorption adjuvant, the microenema was readjusted to pH 8.0 before administration. As a separate control, a solution of 5-methoxysalicylate without the polypeptides was administered.

RESULTS AND DISCUSSION

Gastrin-like compounds were chosen for this study for several reasons. Gastric acid secretion is relatively easy to monitor in a test animal and at the same time is particularly sensitive to circulating hormone levels. The relationship between pharmacological response and the logarithm of the intravenous dose is relatively linear over a significant dosage range (Fig. 1)[4]. This allows for a reasonable bioavailability assessment of the rectally administered aqueous polypeptide solutions by comparing the pharmacological effect with the intravenous dose–response curve.

Figure 2 shows typical, single animal plots of gastric acid secretion rate after intravenous or rectal administration of both pentagastrin and gastrin at doses of 125 μg/kg. The area under the curve represents the total amount of gastric acid secretion in response to administration of either pentagastrin or gastrin in the presence or absence of adjuvant. The time course of the pharmacological response following intravenous administration did not decline in an apparent zero-order fashion and, therefore, may not directly represent the logarithm of the drug–plasma concentration. Nevertheless, the response profiles are similar regardless of administration route and should allow for a reasonable rectal bioavailability assessment based on the intravenous dose response.

Rectal administration of 125 μg/kg of pentagastrin resulted in only 6 ± 4% bioavailability relative to intravenous dose response (uncertainties are expressed as standard deviations) (Table I). The addition of 5 mg of sodium 5-methoxysalicylate to the microenema resulted in a bioavailability of 33 ± 10%, a five-fold increase in drug delivery to the active site. The rectal administration of 125 μg/kg of gastrin without the absorption adjuvant resulted in no detecetable response (Table II). However, the addition of the absorption adjuvant to the microenema resulted in 18 ± 7% drug delivery.

In a separate series of experiments, the concentration of absorption adjuvant in the microenema formulations was lowered from 5 to 1% (w/v). In these experiments the bioavailability of rectally administered gastrin was only 8%, suggesting a dose-response relationship between adjuvant concentration and the absorption promoting effect.

The microenema formulations containing 5% sodium 5-methoxysalicylate are hyperosmotic. In control experiments in which an osmolar equivalent of sodium chloride was substituted for the adjuvant, no enhancement of rectal absorption was seen due to an osmolarity effect. Additional control experiments in which 5-methoxysalicylate was administered rectally without the polypeptide hormone produced no change in stomach acid output. Thus, the observed improvement in rectal polypeptide delivery must be attributed to the adjuvant, which appears to effect a temporary change in the normal mucosal permeability of the rectal compartment.

From this study, it is apparent that sodium 5-methoxysalicylate is representative of a new type of absorption promoter which facilitates nonparenteral polypeptide drug delivery. As nonparenteral alternatives, rectal dosage forms such as microenemas and suppositories may offer a convenient means of expanding polypeptide drug therapy beyond the clinical setting.

[4] The response to higher dosage appears to be more variable than the response in the lower dosage range.

REFERENCES

(1) D. M. Matthews, *Physiol. Rev.*, **55**, 537 (1975).

(2) E. Touitou, M. Donbrow, and E. Azaz, *J. Pharm Pharmacol.*, **30**, 662 (1978).

(3) T. Nishihata, J. H. Rytting, and T. Higuchi, *J. Pharm. Sci.*, **69**, 744 (1980).

(4) *Ibid.*, **70**, 71 (1981).

(5) T. Nishihata, J. H. Rytting, T. Higuchi, and L. Caldwell, *J. Pharm. Pharmacol.*, **33**, 334 (1981).

(6) T. Nishihata, J. H. Rytting, L. Caldwell, S. Yoshioka, and T. Higuchi, "The Alfred Benzon Symposium 17," Munksgaard, Copenhagen, 1981.

(7) M. N. Ghosh and H. O. Schild, *Br. J. Pharmacol.*, **13**, 54 (1958).

(8) R. A. Gregory and H. J. Tracey, *Gut*, **5**, 103 (1964).

Decreases in Ciliary Beat Frequency Due to Intranasal Administration of Propranolol

H. J. M. van de DONK ˣ and F. W. H. M. MERKUS

Received May 28, 1981, from *The Department of Biopharmaceutics, Faculty of Pharmacy and Faculty of Medicine, Plantage Muidergracht 14, 1018 TV Amsterdam, The Netherlands.* Accepted for publication September 2, 1981.

Abstract □ Recently the intranasal application of 5% propranolol was proposed in order to prevent the extensive first-pass metabolism of this drug. The ciliary epithelium in the nose affects the removal of dust, allergens, and microorganisms. The decreasing effect of propranolol on the ciliary beat frequency of human adenoid tissue and chicken embryo tracheas was measured with a photoelectric registration device. After nasal application of 5% propranolol, the drop is diluted by the nasal mucus. It was found that even 0.1% propranolol had a deleterious effect on the cilia of chicken and human tissue. Ciliary movement was arrested irreversibly within 20 min.

Keyphrases □ Propranolol—decrease in ciliary beat frequency due to intranasal administration □ Intranasal administration—propranolol, decrease in ciliary beat frequency □ Ciliary movement—decrease due to intranasal administration of propranolol

The extensive use of nasal drops necessitated the investigation of the effects of nasal medication on the ciliary beat frequency. The nasal ciliary epithelium effects the removal of dust, allergens, and microorganisms that are precipitated after inhalation. This nasal clearance is a physiological defense mechanism which should not be disturbed. A method has been developed to investigate the influence of drugs on the ciliary beat frequency (1). With this method the ciliary beat frequency of chicken embryo tracheas is measured with a photoelectric registration device. The effects of preservatives (2) and nasal drops (3) have been investigated previously. A good correlation has been found between the ciliary beat frequency of ciliary epithelium of human adenoids and of chicken embryo tracheas (4). Recently, the intranasal application of propranolol has been suggested in order to prevent the first-pass effect of this drug after oral administration (5). As propranolol is used in chronic therapies, the effects of intranasal application on the ciliary beat frequency may be important. Therefore, the effect of propranolol on the ciliary beat frequency of chicken embryo tracheas and human adenoid tissue was investigated.

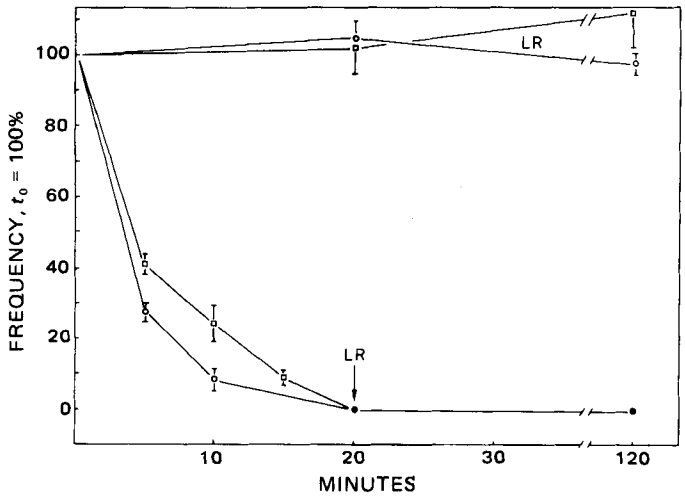

Figure 1—*Time* versus *ciliary beat frequency plot: effect of 0.1% propranolol hydrochloride on the cilia of human adenoids and chicken embryo tracheas. Locke-Ringer (LR) solution was used as a reference. Key: (□), human; (○), chicken; (●), Locke-Ringer.*

Table I—The Decreasing Effect of Propranolol on the Ciliary Beat Frequency of Chicken Embryo Tracheal Epithelium and Human Adenoid Epithelium

Compound	Frequency[a], % Time 2 min	10 min	20 min	Species
Propranolol hydrochloride, 1%	0	0	0	Chicken
Propranolol hydrochloride, 0.1%	70	8	0	Chicken
Propranolol hydrochloride, 0.1%	77	25	0	Human

[a] Frequency as a percentage of the initial frequency.

EXPERIMENTAL

The effects of a solution containing 1% propranolol hydrochloride[1], made isotonic with sodium chloride and of a 10-fold dilution of this solution in Locke-Ringer, were investigated. Both solutions were adjusted to pH 7.4. The effects on the ciliary beat frequency were assessed on six different tracheas for each concentration and for the reference (Locke-Ringer) and on pieces of six different human adenoids for the 10-fold dilution and the reference.

RESULTS

The effects of 1 and 0.1% propranolol are demonstrated in Table I. Frequencies are listed as a percentage of the frequency just before the start of the experiments. The solution containing 1% propranolol arrested ciliary movement of chicken embryo tracheas within 2 min. The 10-fold dilution arrested the ciliary movement of both human adenoids and chicken embryo tracheas within 20 min. This effect was irreversible: rinsing with Locke-Ringer solution after a 20-min contact with 0.1% propranolol did not restore ciliary movement within 2 hr.

The effects of 0.1% propranolol are shown in more detail in Fig. 1 with *SEM* values indicated by vertical bars.

DISCUSSION

The use of a nasal drop containing 5% propranolol has been suggested (5). This nasal drop is diluted by the nasal mucus after application, therefore, the investigation began with 1% propranolol which had a deleterious effect on ciliary movement of chicken embryo tracheas. Propranolol (0.1%) also irreversibly arrested the ciliary movement of chicken and human cilia within 20 min. It is not likely that the nasal drop will be diluted more than 50 times in 20 min, especially since it interferes with the nasal clearance.

For repeated intranasal administration of propranolol, its ciliotoxicity should be taken into account.

REFERENCES

(1) H. J. M. van de Donk, J. Zuidema, and F. W. H. M. Merkus, *Rhinology*, **18**, 93 (1980).

(2) H. J. M. van de Donk, I. P. Muller-Plantema, J. Zuidema, and F.

[1] Propranolol hydrochloride (B.P.) 0504001/4 PO 821A ICI

0022-3549/82/0500-0595$01.00/0

W. H. M. Merkus, *ibid.*, **18**, 119 (1980).
(3) H. J. M. van de Donk, J. Zuidema and F. W. H. M. Merkus, *ibid.*, **19**, 215 (1981).
(4) *Ibid.*, in press.
(5) A. Hussain, T. Foster, S. Hirai, T. Kashihara, R. Batenhorst, and M. Jones, *J. Pharm. Sci.*, **69**, 1240 (1980).

ACKNOWLEDGMENTS

The authors wish to thank Mrs. N. Verhoeven for her assistance in performing the experiments, Dr. N. van Proosdij (R. C. Hospital, Sittard) for supplying the human adenoids, and Mrs. B. Eckmann for secretarial work.

Influence of Ethylene Oxide Exposure on the Extraction of Indomethacin from Dimethicone Polymeric Rods

P. R. HURST ˣ, P. V. PEPLOW, and P. von DADELSZEN

Received June 30, 1981 from the *Department of Anatomy, University of Otago Medical School, Dunedin, New Zealand.* Accepted for publication September 2, 1981.

ABSTRACT □ Dimethicone polymeric rods were made to contain 0.3, 2.0, or 3.3% by weight of indomethacin. For each different loading of indomethacin, some of the rods were treated with ethylene oxide at 55° for 1 hr, while others were not exposed to the gas. Treated and untreated rods were sliced, placed in ethanol to extract the indomethacin, and the concentrations of indomethacin in the extracts determined by fluorometry and high-performance liquid chromatography (HPLC). After ethylene oxide treatment, the quantity of indomethacin in the extracts was significantly reduced in rods containing 0.3 and 2.0% indomethacin. For the rods containing 3.3% indomethacin, the recovery of the drug from treated rods was not significantly different from those not exposed.

Keyphrases □ Ethylene oxide—extraction of indomethacin from dimethicone polymeric rods □ Indomethacin—dimethicone polymeric rods, influence of ethylene oxide exposure □ Polymeric rods—dimethicone, ethylene oxide exposure on extraction of indomethacin □ Fluorometry—determination of influence of ethylene oxide exposure on the extraction of indomethacin from dimethicone polymeric rods □ High-performance liquid chromatography—determination of influence of ethylene oxide exposure on the extraction of indomethacin from dimethicone polymer rods

The development of simple systems or devices for drug delivery over extended periods has potentially wide usage, especially for delivery of compounds to selected sites in the body. In this regard, experiments have been performed with a system which can provide a sustained release of nonsteroidal anti-inflammatory drugs such as indomethacin or naproxen from dimethicone polymeric rods (1). In these and other studies (2, 3) the quantity of drug released *in vivo* is determined by measuring the residual amount of drug in the rods at various time periods and subtracting it from values from similar rods prepared in an identical manner but which were not placed in the body. The measurements are performed on ethanolic or methanolic extracts of the rods.

Before being fitted into the body, such rods must be sterilized. Since autoclaving and chemical methods (such as placing in aqueous ethanol) appear unsuitable for this system, ethylene oxide gas treatment has been used.

The present study indicates that by using this method of sterilization, there is a decrease in the percentage of indomethacin that can be extracted into ethanol from rods containing the drug at low concentrations (<3% w/w).

EXPERIMENTAL

Indomethacin[1] was recrystallized, dried, and either 0, 10, 60, or 100 mg was thoroughly mixed with 3 g of dimethicone[2]. Following the addition of catalyst (15 mg) the different mixtures were forced into vinyl tubing (french gauge 5, 1-mm i.d.)[3] and allowed to polymerize. Rods of 1-cm length were cut and weighed and either stored at room temperature or subjected to ethylene oxide exposure (1.2–1.4 g/liter) in a stainless steel sterilizer[4]. In this apparatus the gas was released from ampuls into a chamber initially evacuated to 150 mm Hg. Following exposure to the gas for 1 hr at 55°, the rods were aerated for at least 12 hr and left for 2 days at room temperature.

Rods containing indomethacin were weighed, cut into thin slices, and the drug extracted with ethanol (2 ml/day for 4 days). The amounts of indomethacin in the extracts were determined by fluorometry and HPLC with standard solutions of indomethacin prepared from the recrystallized compound. For the fluorometric analysis, samples were assayed in duplicate using a spectrophotofluorometer[5] with an excitation wavelength of 295 nm and an emission wavelength of 361 nm. Continuous scan recordings over an emission range of 300 to 450 nm (constant excitation wavelength of 295 nm) were also made of certain extracts of the gassed and nongassed rods. For HPLC, 10 μl samples were injected into a C18 μ Bondapak column[6] with a mobile phase of methanol–50 m*M* KH_2PO_4 (3:1), pH 6.72, and a flow rate of 2 ml/min. The UV absorbance at 230 nm of the column eluate was continuously recorded with a variable wavelength UV detector[6]. Heights of the peaks corresponding in position to the indomethacin standards were measured to determine the amounts of indomethacin in the extracts. These amounts, compared with those determined to be present initially on the basis of the quantity of indomethacin in the mixture and the weight of each rod, were used to calculate percentage recoveries.

RESULTS

For the rods not subjected to ethylene oxide exposure, over 90% of the incorporated indomethacin was recovered into ethanol when measurements on the extracts were made by fluorometry (Fig. 1). This was confirmed by HPLC of the extracts of rods made from the 60 and 100 mg/mixture. (The HPLC system used did not allow a reliable measurement of indomethacin in the extracts obtained from the 10 mg/mixture rods as the peaks assigned to indomethacin were not sufficiently large to be accurately quantitated.) Following ethylene oxide treatment, however, the recovery of indomethacin into alcohol was significantly reduced for

[1] Sigma Chemical Co., St. Louis, Mo.
[2] Silastic, 382 medical grade elastomer, Dow Corning Corp., Midland, Mich.
[3] Latex Products Pty.
[4] Victoria MK II, Medical Electronics Ltd, U.K.
[5] Aminco-Bowman, Model 768 G, American Instrument Co., Silver Spring, Md.
[6] Waters Associates, Milford, Mass.

0022-3549/82/0500-0596$01.00/0

W. H. M. Merkus, *ibid.*, **18**, 119 (1980).
(3) H. J. M. van de Donk, J. Zuidema and F. W. H. M. Merkus, *ibid.*, **19**, 215 (1981).
(4) *Ibid.*, in press.
(5) A. Hussain, T. Foster, S. Hirai, T. Kashihara, R. Batenhorst, and M. Jones, *J. Pharm. Sci.*, **69**, 1240 (1980).

ACKNOWLEDGMENTS

The authors wish to thank Mrs. N. Verhoeven for her assistance in performing the experiments, Dr. N. van Proosdij (R. C. Hospital, Sittard) for supplying the human adenoids, and Mrs. B. Eckmann for secretarial work.

Influence of Ethylene Oxide Exposure on the Extraction of Indomethacin from Dimethicone Polymeric Rods

P. R. HURST ˣ, P. V. PEPLOW, and P. von DADELSZEN

Received June 30, 1981 from the *Department of Anatomy, University of Otago Medical School, Dunedin, New Zealand.* Accepted for publication September 2, 1981.

ABSTRACT □ Dimethicone polymeric rods were made to contain 0.3, 2.0, or 3.3% by weight of indomethacin. For each different loading of indomethacin, some of the rods were treated with ethylene oxide at 55° for 1 hr, while others were not exposed to the gas. Treated and untreated rods were sliced, placed in ethanol to extract the indomethacin, and the concentrations of indomethacin in the extracts determined by fluorometry and high-performance liquid chromatography (HPLC). After ethylene oxide treatment, the quantity of indomethacin in the extracts was significantly reduced in rods containing 0.3 and 2.0% indomethacin. For the rods containing 3.3% indomethacin, the recovery of the drug from treated rods was not significantly different from those not exposed.

Keyphrases □ Ethylene oxide—extraction of indomethacin from dimethicone polymeric rods □ Indomethacin—dimethicone polymeric rods, influence of ethylene oxide exposure □ Polymeric rods—dimethicone, ethylene oxide exposure on extraction of indomethacin □ Fluorometry—determination of influence of ethylene oxide exposure on the extraction of indomethacin from dimethicone polymeric rods □ High-performance liquid chromatography—determination of influence of ethylene oxide exposure on the extraction of indomethacin from dimethicone polymer rods

The development of simple systems or devices for drug delivery over extended periods has potentially wide usage, especially for delivery of compounds to selected sites in the body. In this regard, experiments have been performed with a system which can provide a sustained release of nonsteroidal anti-inflammatory drugs such as indomethacin or naproxen from dimethicone polymeric rods (1). In these and other studies (2, 3) the quantity of drug released *in vivo* is determined by measuring the residual amount of drug in the rods at various time periods and subtracting it from values from similar rods prepared in an identical manner but which were not placed in the body. The measurements are performed on ethanolic or methanolic extracts of the rods.

Before being fitted into the body, such rods must be sterilized. Since autoclaving and chemical methods (such as placing in aqueous ethanol) appear unsuitable for this system, ethylene oxide gas treatment has been used.

The present study indicates that by using this method of sterilization, there is a decrease in the percentage of indomethacin that can be extracted into ethanol from rods containing the drug at low concentrations (<3% w/w).

EXPERIMENTAL

Indomethacin[1] was recrystallized, dried, and either 0, 10, 60, or 100 mg was thoroughly mixed with 3 g of dimethicone[2]. Following the addition of catalyst (15 mg) the different mixtures were forced into vinyl tubing (french gauge 5, 1-mm i.d.)[3] and allowed to polymerize. Rods of 1-cm length were cut and weighed and either stored at room temperature or subjected to ethylene oxide exposure (1.2–1.4 g/liter) in a stainless steel sterilizer[4]. In this apparatus the gas was released from ampuls into a chamber initially evacuated to 150 mm Hg. Following exposure to the gas for 1 hr at 55°, the rods were aerated for at least 12 hr and left for 2 days at room temperature.

Rods containing indomethacin were weighed, cut into thin slices, and the drug extracted with ethanol (2 ml/day for 4 days). The amounts of indomethacin in the extracts were determined by fluorometry and HPLC with standard solutions of indomethacin prepared from the recrystallized compound. For the fluorometric analysis, samples were assayed in duplicate using a spectrophotofluorometer[5] with an excitation wavelength of 295 nm and an emission wavelength of 361 nm. Continuous scan recordings over an emission range of 300 to 450 nm (constant excitation wavelength of 295 nm) were also made of certain extracts of the gassed and nongassed rods. For HPLC, 10 μl samples were injected into a C18 μ Bondapak column[6] with a mobile phase of methanol–50 m*M* KH_2PO_4 (3:1), pH 6.72, and a flow rate of 2 ml/min. The UV absorbance at 230 nm of the column eluate was continuously recorded with a variable wavelength UV detector[6]. Heights of the peaks corresponding in position to the indomethacin standards were measured to determine the amounts of indomethacin in the extracts. These amounts, compared with those determined to be present initially on the basis of the quantity of indomethacin in the mixture and the weight of each rod, were used to calculate percentage recoveries.

RESULTS

For the rods not subjected to ethylene oxide exposure, over 90% of the incorporated indomethacin was recovered into ethanol when measurements on the extracts were made by fluorometry (Fig. 1). This was confirmed by HPLC of the extracts of rods made from the 60 and 100 mg/mixture. (The HPLC system used did not allow a reliable measurement of indomethacin in the extracts obtained from the 10 mg/mixture rods as the peaks assigned to indomethacin were not sufficiently large to be accurately quantitated.) Following ethylene oxide treatment, however, the recovery of indomethacin into alcohol was significantly reduced for

[1] Sigma Chemical Co., St. Louis, Mo.
[2] Silastic, 382 medical grade elastomer, Dow Corning Corp., Midland, Mich.
[3] Latex Products Pty.
[4] Victoria MK II, Medical Electronics Ltd, U.K.
[5] Aminco-Bowman, Model 768 G, American Instrument Co., Silver Spring, Md.
[6] Waters Associates, Milford, Mass.

0022-3549/82/0500-0596$01.00/0

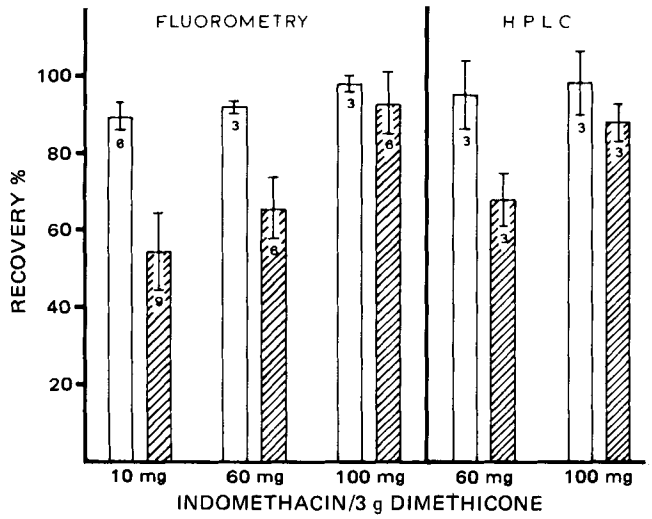

Figure 1—*Mean percentage recovery of indomethacin from dimethicone rods at different concentrations following ethylene oxide treatment (hatched bars). Standard deviations and the number of rods extracted in each group are shown. Results of gassed and ungassed rods at each indomethacin concentration were compared by t test analysis. This revealed no significant difference for the rods containing 100 mg of indomethacin/mixture. For the 60- and 10-mg/mixture groups, however, p values were <0.01 and <0.001, respectively.*

the 10 and 60 mg/mixture rods (Fig. 1). There was also a slight reduction in the recoveries for the 100 mg/mixture rods, but this difference was not significant, as determined by *t* test analysis, from the ungassed rods.

Continuous scan recording by the fluorometer showed no change in the shape of the curves obtained from the analysis of extracts of gassed rods, and no additional peaks were seen in the trace recordings of the HPLC analysis.

DISCUSSION

These results provide evidence that ethylene oxide treatment reduces the extraction into alcohol of a common nonsteroidal anti-inflammatory drug incorporated into a dimethicone delivery system. This effect was dependent upon the concentration of the drug, with the lower doses (10 and 60 mg/mixture) being most affected. For the rods made from 100 mg indomethacin/mixture, over 90% of the drug was recovered after gassing, indicating that rods made to contain the drug at this concentration would be suitable for studies of indomethacin release rates from dimethicone rods placed in the body. The similarity in profiles of the extracts from the gassed and nongassed rods (continuous fluorometric scan and HPLC tracings) suggest that no alteration in the qualitative composition of the extracts occurred. The reasons for the reduced recoveries of indomethacin at the two lowest concentrations were not investigated here. One possibility is that at low drug concentrations, a greater matrix volume would be unoccupied by the drug and is available to be taken up by the gas. This, in turn, might alter the diffusion properties of the matrix or chemically interfere with the drug, thereby reducing its extraction into alcohol.

It would be valuable to know if other nonsteroidal anti-inflammatory drugs, and those steroids that are currently being used in conjunction with dimethicone systems (4, 5, 6), are affected by ethylene oxide gassing.

REFERENCES

(1) P.V. Peplow and P. R. Hurst, *Prostaglandins Med.*, **6**, 29 (1981).

(2) L. H. Hoffman, G. B. Strong, G. R. Davenport, and J. C. Frölich, *J. Reprod. Fertil.*, **50**, 231 (1977).

(3) Y. W. Chien, S. E. Mares, J. Berg, S. Huber, H. J. Lambert, and K. F. King, *J. Pharm. Sci.*, **64**, 1776 (1975).

(4) C. G. Nilsson, P. Lähteenmäki, D. N. Robertson, and T. Luukkainen, *Acta. Endocrinol.*, **93**, 380 (1980).

(5) C.-G. Nilsson and T. Luukkainen, *Contraception*, **15**, 295 (1977).

(6) P. F. Wadsworth, R. Heywood, D. G. Allen, R. J. Sortwell, and R. M. Walton. *ibid.*, **20**, 177 (1979).

ACKNOWLEDGMENTS

This work was supported by the Medical Research Council of New Zealand.

The authors thank Mr. G. Elliot, Dunedin Public Hospital, for performing the ethylene oxide sterilization of the rods.

COMMUNICATIONS

Model-Independent Steady-State Volume of Distribution

Keyphrases □ Pharmacokinetics—evaluation of model-independent steady-state volume of distribution □ Drug disposition—first-order disposition rates, evaluation of model-independent steady-state volume of distribution □ Models, pharmacokinetic—methods to evaluate model-independent steady-state volume of distribution

To The Editor:

Recently, pharmacokinetic methods have been proposed to evaluate model-independent input and disposition parameters for drugs exhibiting first-order disposition rates (1–4). The use of these statistical moment parameters is appealing, not only because of the relatively simple calculations involved, but also because the parameters determined are independent of any modeling assumptions, which greatly facilitates cross-study comparison of drug disposition. For example, Benet and Sheiner (5) have compiled volume of distribution steady-state (Vd_{ss}) data for numerous drugs using statistical moment analysis. However, as proposed (4), the method is valid only for single dose instantaneous input data and will result in an overestimation of Vd_{ss} when applied to data obtained after infusion or multiple dose input. The purpose of this communication is to report a simple method to obtain Vd_{ss} values from multiple intravenous bolus and/or infusion data.

For a drug administered by bolus injection, a single distribution–elimination rate parameter, the mean residence time (MRT_{iv}), can be evaluated using statistical moment analysis (1). The MRT_{iv} describes the average time a drug molecule spends in the body and is determined

0022-3549/82/0500-0597$01.00/0

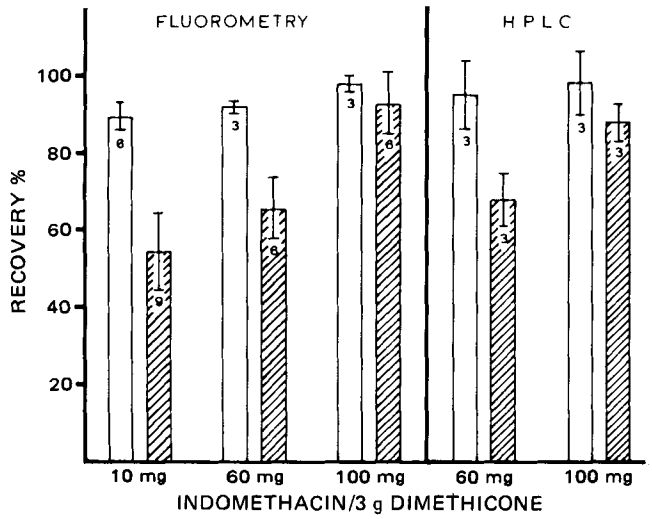

Figure 1—*Mean percentage recovery of indomethacin from dimethicone rods at different concentrations following ethylene oxide treatment (hatched bars). Standard deviations and the number of rods extracted in each group are shown. Results of gassed and ungassed rods at each indomethacin concentration were compared by t test analysis. This revealed no significant difference for the rods containing 100 mg of indomethacin/mixture. For the 60- and 10-mg/mixture groups, however, p values were <0.01 and <0.001, respectively.*

the 10 and 60 mg/mixture rods (Fig. 1). There was also a slight reduction in the recoveries for the 100 mg/mixture rods, but this difference was not significant, as determined by *t* test analysis, from the ungassed rods.

Continuous scan recording by the fluorometer showed no change in the shape of the curves obtained from the analysis of extracts of gassed rods, and no additional peaks were seen in the trace recordings of the HPLC analysis.

DISCUSSION

These results provide evidence that ethylene oxide treatment reduces the extraction into alcohol of a common nonsteroidal anti-inflammatory drug incorporated into a dimethicone delivery system. This effect was dependent upon the concentration of the drug, with the lower doses (10 and 60 mg/mixture) being most affected. For the rods made from 100 mg indomethacin/mixture, over 90% of the drug was recovered after gassing, indicating that rods made to contain the drug at this concentration would be suitable for studies of indomethacin release rates from dimethicone rods placed in the body. The similarity in profiles of the extracts from the gassed and nongassed rods (continuous fluorometric scan and HPLC tracings) suggest that no alteration in the qualitative composition of the extracts occurred. The reasons for the reduced recoveries of indomethacin at the two lowest concentrations were not investigated here. One possibility is that at low drug concentrations, a greater matrix volume would be unoccupied by the drug and is available to be taken up by the gas. This, in turn, might alter the diffusion properties of the matrix or chemically interfere with the drug, thereby reducing its extraction into alcohol.

It would be valuable to know if other nonsteroidal anti-inflammatory drugs, and those steroids that are currently being used in conjunction with dimethicone systems (4, 5, 6), are affected by ethylene oxide gassing.

REFERENCES

(1) P.V. Peplow and P. R. Hurst, *Prostaglandins Med.*, **6**, 29 (1981).

(2) L. H. Hoffman, G. B. Strong, G. R. Davenport, and J. C. Frölich, *J. Reprod. Fertil.*, **50**, 231 (1977).

(3) Y. W. Chien, S. E. Mares, J. Berg, S. Huber, H. J. Lambert, and K. F. King, *J. Pharm. Sci.*, **64**, 1776 (1975).

(4) C. G. Nilsson, P. Lähteenmäki, D. N. Robertson, and T. Luukkainen, *Acta. Endocrinol.*, **93**, 380 (1980).

(5) C.-G. Nilsson and T. Luukkainen, *Contraception*, **15**, 295 (1977).

(6) P. F. Wadsworth, R. Heywood, D. G. Allen, R. J. Sortwell, and R. M. Walton. *ibid.*, **20**, 177 (1979).

ACKNOWLEDGMENTS

This work was supported by the Medical Research Council of New Zealand.

The authors thank Mr. G. Elliot, Dunedin Public Hospital, for performing the ethylene oxide sterilization of the rods.

COMMUNICATIONS

Model-Independent Steady-State Volume of Distribution

Keyphrases □ Pharmacokinetics—evaluation of model-independent steady-state volume of distribution □ Drug disposition—first-order disposition rates, evaluation of model-independent steady-state volume of distribution □ Models, pharmacokinetic—methods to evaluate model-independent steady-state volume of distribution

To The Editor:

Recently, pharmacokinetic methods have been proposed to evaluate model-independent input and disposition parameters for drugs exhibiting first-order disposition rates (1–4). The use of these statistical moment parameters is appealing, not only because of the relatively simple calculations involved, but also because the parameters determined are independent of any modeling assumptions, which greatly facilitates cross-study comparison of drug disposition. For example, Benet and Sheiner (5) have compiled volume of distribution steady-state (Vd_{ss}) data for numerous drugs using statistical moment analysis. However, as proposed (4), the method is valid only for single dose instantaneous input data and will result in an overestimation of Vd_{ss} when applied to data obtained after infusion or multiple dose input. The purpose of this communication is to report a simple method to obtain Vd_{ss} values from multiple intravenous bolus and/or infusion data.

For a drug administered by bolus injection, a single distribution–elimination rate parameter, the mean residence time (MRT_{iv}), can be evaluated using statistical moment analysis (1). The MRT_{iv} describes the average time a drug molecule spends in the body and is determined

0022-3549/82/0500-0597$01.00/0

by dividing the area under the concentration multiplied by time–time curve [area under the moment curve ($AUMC$)] by the area under the concentration–time curve (AUC):

$$MRT_{iv} = \frac{AUMC_{iv}}{AUC_{iv}} \quad \text{(Eq. 1)}$$

As shown previously by Benet and Galeazzi (4), a model independent distribution volume (Vd_{ss}) may be determined from the dose (D), MRT_{iv}, and AUC_{iv} as follows:

$$Vd_{ss} = \frac{D(MRT_{iv})}{AUC_{iv}} = \frac{D(AUMC_{iv})}{(AUC_{iv})^2} \quad \text{(Eq. 2)}$$

If the same dose (D) is administered as an infusion over a time (t') or is divided into increments ($D_1, D_2, \ldots D_n$) and administered as a combination of infusions and/or boluses at different times ($T_1, T_2, \ldots T_n$), the area under the curve (AUC_{total}) will equal the AUC_{iv}; but the $AUMC_{total}$ will be greater than the $AUMC_{iv}$, resulting in an overestimation of Vd_{ss} if $AUMC_{total}$ is used in Eq. 2. For a case where the drug is administered as a single infusion rather than a bolus, the MRT_{total} and the $AUMC_{total}$ are easily corrected, since the infusion will increase the MRT_{iv} by $0.5t'$ (6), and:

$$AUMC_{iv} = AUMC_{total} - AUC_{iv}(0.5t') \quad \text{(Eq. 3)}$$

When multiple dosing occurs, the correction is somewhat more complex, since there is a delay (T) in the input of a fraction of the dose. Assuming there is no previous dosing, the delay time will increase the MRT_{iv} by T if administered as a bolus and by $0.5t' + T$ if administered as an infusion, and:

$$AUMC_{iv} = AUMC_{total} - AUC_{iv}(0.5t' + T) \quad \text{(Eq. 4)}$$

The general form for n bolus and/or infusion doses then becomes:

$$AUMC_{iv} = \sum_{i=1}^{n} AUMC_i - \sum_{i=1}^{n} AUC_i(0.5t_i' + T_i) \quad \text{(Eq. 5)}$$

where: $t_i' = 0$ for a bolus dose and $T_1 = 0$.

Dividing both sides of Eq. 5 by AUC_{iv} (the total AUC calculated), and recognizing the ratio of the individual AUC_i's to AUC_{iv} is the fraction of the total dose administered (F_i), one obtains:

$$MRT_{iv} = MRT_{total} - \sum_{i=1}^{n} F_i(0.5t_i' + T_i) \quad \text{(Eq. 6)}$$

Equation 6 may be used to correct total moment data for use in Eq. 2, even when a bolus is administered during an infusion. Although it is not valid if residual drug is present prior to characterization of the concentration–time curve, corrections for the residual drug are possible in certain instances. One may be tempted to correct for oral dosing by adding $1/K_a$ to the summation term in Eq. 6, but the fraction of the oral dose absorbed must be known as well as K_a. Finally, calculation of $AUMC_{total}$ and AUC_{total} are subject to extrapolation errors as described previously (3, 4), so it is advisable to obtain data which will allow excellent characterization of the terminal elimination rate constant after the last dose increment is administered, or to collect samples until the concentration of drug is essentially zero.

(1) K. Yamaoka, T. Nakagawa, and T. Uno, *J. Pharmacokinet. Biopharm.*, **6**, 547 (1978).

(2) D. J. Cutler, *J. Pharm. Pharmacol.*, **30**, 476 (1978).

(3) S. Riegelman and P. Collier, *J. Pharmacokinet. Biopharm.*, **8**, 509 (1980).

(4) L. Z. Benet and R. L. Galeazzi, *J. Pharm. Sci.*, **68**, 1071 (1979).

(5) L. Z. Benet and L. B. Sheiner, in "The Pharmacological Basis of Therapeutics," 6th ed. A. G. Gillman, L. S. Goodman, and A. Gillman, Eds., Macmillan, New York, N.Y., 1980, pp. 1675, 1737.

(6) W. J. Jusko, in "Applied Pharmacokinetics: Principles of Therapeutic Drug Monitoring," W. E. Evans, J. J. Schentag, and W. J. Jusko, Eds., Applied Therapeutics, Inc., San Francisco, Calif., 1980, p. 662.

Arthur B. Straughn
Department of Pharmaceutics
College of Pharmacy
University of Tennessee Center for the Health Sciences
Memphis, TN 38163

Received November 12, 1981.
Accepted for publication February 26, 1982.

Tampon Leachable Substances: Acute Toxicity

Keyphrases □ Tampons—leachable substances, acute toxicity □ Toxicity, acute—tampon leachable substances, intramuscular implantation in rabbits □ Inhibition of cell growth—acute toxicity of tampon leachable substances □ Dehydration—tissue response, acute toxicity of tampon leachable substances

To the Editor:

The use of tampons for the control of menstrual flow has been associated with the induction of vaginal ulcerations, mucosal changes, and toxic shock syndrome. The evidence for those clinical phenomena has been reviewed recently (1), emphasizing the role of dehydration and alteration of calcium levels in the vaginal tissue as important mechanisms in the induction of vaginal ulceration. Since we are not aware of any reports on the potential toxicity of leachable substances of tampons, two acute toxicity tests were performed on regular and superabsorbant tampons available commercially. The tests performed were: a tissue culture inhibition of cell growth test on aqueous extracts (23°) of whole tampons (Table I); and a 7-day intramuscular implantation test in rabbits using (*a*) the absorbant material of the tampons (excluding the casing and fibrous material), (*b*) partially hydrated absorbant material, and (*c*) fibrous material (excluding casing and absorbant material (Table II).

The decrease in the gross rating of the muscle implant of the partially hydrated tampon material as compared to the dry material implant was consistent with the generally accepted conclusion that dehydration is a major factor in the initiation of vaginal ulceration. Also, the soluble, leachable components of the tampons tested have a significant cellular toxicity at concentrations well below that which might be expected in vaginal secretions adjacent to a tampon. The tissue culture test covers a period of time (72 hr) of usual tampon usage, and several tampons are frequently used in that period. It should also be noted that there was a significant concentration-dependent response for both extracts and that the highest concentration tested was 50% with respect to the original extract.

0022-3549/82/0500-0598$01.00/0

by dividing the area under the concentration multiplied by time–time curve [area under the moment curve ($AUMC$)] by the area under the concentration–time curve (AUC):

$$MRT_{iv} = \frac{AUMC_{iv}}{AUC_{iv}} \quad \text{(Eq. 1)}$$

As shown previously by Benet and Galeazzi (4), a model independent distribution volume (Vd_{ss}) may be determined from the dose (D), MRT_{iv}, and AUC_{iv} as follows:

$$Vd_{ss} = \frac{D(MRT_{iv})}{AUC_{iv}} = \frac{D(AUMC_{iv})}{(AUC_{iv})^2} \quad \text{(Eq. 2)}$$

If the same dose (D) is administered as an infusion over a time (t') or is divided into increments ($D_1, D_2, \ldots D_n$) and administered as a combination of infusions and/or boluses at different times ($T_1, T_2, \ldots T_n$), the area under the curve (AUC_{total}) will equal the AUC_{iv}; but the $AUMC_{total}$ will be greater than the $AUMC_{iv}$, resulting in an overestimation of Vd_{ss} if $AUMC_{total}$ is used in Eq. 2. For a case where the drug is administered as a single infusion rather than a bolus, the MRT_{total} and the $AUMC_{total}$ are easily corrected, since the infusion will increase the MRT_{iv} by $0.5t'$ (6), and:

$$AUMC_{iv} = AUMC_{total} - AUC_{iv}(0.5t') \quad \text{(Eq. 3)}$$

When multiple dosing occurs, the correction is somewhat more complex, since there is a delay (T) in the input of a fraction of the dose. Assuming there is no previous dosing, the delay time will increase the MRT_{iv} by T if administered as a bolus and by $0.5t' + T$ if administered as an infusion, and:

$$AUMC_{iv} = AUMC_{total} - AUC_{iv}(0.5t' + T) \quad \text{(Eq. 4)}$$

The general form for n bolus and/or infusion doses then becomes:

$$AUMC_{iv} = \sum_{i=1}^{n} AUMC_i - \sum_{i=1}^{n} AUC_i(0.5t_i' + T_i) \quad \text{(Eq. 5)}$$

where: $t_i' = 0$ for a bolus dose and $T_1 = 0$.

Dividing both sides of Eq. 5 by AUC_{iv} (the total AUC calculated), and recognizing the ratio of the individual AUC_i's to AUC_{iv} is the fraction of the total dose administered (F_i), one obtains:

$$MRT_{iv} = MRT_{total} - \sum_{i=1}^{n} F_i(0.5t_i' + T_i) \quad \text{(Eq. 6)}$$

Equation 6 may be used to correct total moment data for use in Eq. 2, even when a bolus is administered during an infusion. Although it is not valid if residual drug is present prior to characterization of the concentration–time curve, corrections for the residual drug are possible in certain instances. One may be tempted to correct for oral dosing by adding $1/K_a$ to the summation term in Eq. 6, but the fraction of the oral dose absorbed must be known as well as K_a. Finally, calculation of $AUMC_{total}$ and AUC_{total} are subject to extrapolation errors as described previously (3, 4), so it is advisable to obtain data which will allow excellent characterization of the terminal elimination rate constant after the last dose increment is administered, or to collect samples until the concentration of drug is essentially zero.

(1) K. Yamaoka, T. Nakagawa, and T. Uno, *J. Pharmacokinet. Biopharm.*, **6**, 547 (1978).

(2) D. J. Cutler, *J. Pharm. Pharmacol.*, **30**, 476 (1978).

(3) S. Riegelman and P. Collier, *J. Pharmacokinet. Biopharm.*, **8**, 509 (1980).

(4) L. Z. Benet and R. L. Galeazzi, *J. Pharm. Sci.*, **68**, 1071 (1979).

(5) L. Z. Benet and L. B. Sheiner, in "The Pharmacological Basis of Therapeutics," 6th ed. A. G. Gillman, L. S. Goodman, and A. Gillman, Eds., Macmillan, New York, N.Y., 1980, pp. 1675, 1737.

(6) W. J. Jusko, in "Applied Pharmacokinetics: Principles of Therapeutic Drug Monitoring," W. E. Evans, J. J. Schentag, and W. J. Jusko, Eds., Applied Therapeutics, Inc., San Francisco, Calif., 1980, p. 662.

Arthur B. Straughn
Department of Pharmaceutics
College of Pharmacy
University of Tennessee Center for the Health Sciences
Memphis, TN 38163

Received November 12, 1981.
Accepted for publication February 26, 1982.

Tampon Leachable Substances: Acute Toxicity

Keyphrases □ Tampons—leachable substances, acute toxicity □ Toxicity, acute—tampon leachable substances, intramuscular implantation in rabbits □ Inhibition of cell growth—acute toxicity of tampon leachable substances □ Dehydration—tissue response, acute toxicity of tampon leachable substances

To the Editor:

The use of tampons for the control of menstrual flow has been associated with the induction of vaginal ulcerations, mucosal changes, and toxic shock syndrome. The evidence for those clinical phenomena has been reviewed recently (1), emphasizing the role of dehydration and alteration of calcium levels in the vaginal tissue as important mechanisms in the induction of vaginal ulceration. Since we are not aware of any reports on the potential toxicity of leachable substances of tampons, two acute toxicity tests were performed on regular and superabsorbant tampons available commercially. The tests performed were: a tissue culture inhibition of cell growth test on aqueous extracts (23°) of whole tampons (Table I); and a 7-day intramuscular implantation test in rabbits using (*a*) the absorbant material of the tampons (excluding the casing and fibrous material), (*b*) partially hydrated absorbant material, and (*c*) fibrous material (excluding casing and absorbant material (Table II).

The decrease in the gross rating of the muscle implant of the partially hydrated tampon material as compared to the dry material implant was consistent with the generally accepted conclusion that dehydration is a major factor in the initiation of vaginal ulceration. Also, the soluble, leachable components of the tampons tested have a significant cellular toxicity at concentrations well below that which might be expected in vaginal secretions adjacent to a tampon. The tissue culture test covers a period of time (72 hr) of usual tampon usage, and several tampons are frequently used in that period. It should also be noted that there was a significant concentration-dependent response for both extracts and that the highest concentration tested was 50% with respect to the original extract.

0022-3549/82/0500-0598$01.00/0

Table I—Inhibition of Cell Growth

Extract Concentration, %[a]	Inhibition of Cell Growth, % Regular[b]	Superabsorbant[c]
10	12	5
15	18	16
20	22	24
25	28	33
30	30	42
35	39	52
40	38	57
45	47	62
50	48	64

[a] Undiluted Extract = 100%. [b] Regular tampon: extracted with 95 ml of distilled water. [c] Superabsorbant tampon: extracted with 75 ml of distilled water.

Table II—Intramuscular Implantation: Tampon Material

Implanted Material	Gross Rating[a]	Histopathologic Rating[a]
Absorbant material[b]	3	4
Absorbant material[c]	3	4
Partially hydrated absorbant material	0	4
Fibrous material[b]	0	4
Fibrous material[c]	0	4

[a] Ratings: 0, equivalent to negative control; 3, marked positive response; 4, equivalent to positive control. [b] Regular tampon. [c] Superabsorbant tampon.

Muscle tissue reaction (necrotic and inflammatory) to the absorbant and fibrous materials of tampons were the most severe of any materials tested in this laboratory, actually exceeding the positive control response in some cases. The isolated fibrous material which has lower absorbancy than the absorbant material did not show a positive gross response but had a histopathologic rating equivalent to the absorbant material, suggesting that the response was not totally due to dehydration. Fibrous material has been reported to be present in biopsies of vaginal lesions (1). Although the rabbit muscle response can not be considered to be identical to the response of vaginal tissue, the presence of fibrous material in vaginal lesions indicates that tampon material comes into intimate contact with vaginal tissue. Tissue dehydration has been demonstrated to alter calcium levels of vaginal tissue, facilitates contact of tampon material with the tissue, and undoubtedly alters cellular response to leachable toxic components of tampons. The inhibition of cell growth reported in Table I was observed in normal liquid tissue culture medium where dehydration is not a factor. The effect of leachable, soluble components of tampons on cells partially impaired or altered by dehydration is not known. The potential for the exacerbation of the ulcerative process by leachable substances of tampons is apparent.

(1) E. G. Friedrich, *Clin. Obstet. Gynecol.*, **24**, 395 (1981).

John Autian[x]
E. O. Dillingham
W. H. Lawrence
J. E. Turner
Materials Science Toxicology Laboratories
The University of Tennessee Center for the Health Sciences
Memphis, TN 38163

Received October 6, 1981.
Accepted for publication January 28, 1982.

0022-3549/82/0500-0599$01.00/0

Simplified Method to Study Stability of Pharmaceutical Systems

Keyphrases □ Decomposition—determination of shelf-life using analytic methodologies □ Kinetics—decomposition, determination of shelf-life using analytic methodologies □ Stability—simplified method of study in pharmaceutical systems

To the Editor:

In a previous report (1), shelf-life, defined as the time for 10% decomposition at 25°, was estimated by a simplified method. The method involved carrying out a number of kinetic tests at different temperatures followed by linear regression of the logarithm of $t_{0.9}$ (the time required for the drug to decompose to 90% of its original value) on the reciprocal of absolute temperature. Simulated data were used initially to test the linearity of such plots. Since it had been reported previously (2) that it was not possible to distinguish between first-, zero-, and simple second-order kinetics when the decomposition was <10%, it was believed the plots of ln ($t_{0.9}$) *versus* $1/T$ would be linear.

In a subsequent criticism of a previous study (1), it was stated that the use of this Arrhenius approach for all orders of reaction was erroneous and that the slope of the line would be highly dependent on the initial concentration (3). For this reason, and because of analytical difficulties when decomposition is <10%, it was concluded that this method was of little use.

The problem arises because $t_{0.9}$ was defined with respect to the original concentration. It was tacitly assumed (1) that all test samples would have the same initial concentration, whereas it was implied (3) that this would not be the case necessarily.

The purpose of this communication is to point out that plots of $\ln(t_\alpha)$ (where t_α is the time to decompose from concentration C_1 to C_2) *versus* $1/T$ will be linear for all reaction orders irrespective of the α value chosen. If C_1 equals the initial concentration (C_0), and it is the same for all experiments, and C_2 is 90% of C_0, then $t_\alpha = t_{0.9}$.

Assuming the usual rate expression:

$$dC/dt = -kf(C) \qquad \text{(Eq. 1)}$$

where $f(C)$ is some function of concentration, then integrating between the limits t_2 and t_1 ($t_2 - t_1 = t_\alpha$):

$$g(C_2) - g(C_1) = -kt_\alpha \qquad \text{(Eq. 2)}$$

where $g(C)$ is the integrated form of $f(C)$. If a number of kinetic experiments are performed at different temperatures, each starting with approximately the same initial concentration, and C_1 and C_2 are chosen the same for all experiments, then $g(C_2) - g(C_1)$ is constant (G). Substituting this into Eq. 2, assuming the Arrhenius equation is applicable:

$$G = -k_a \exp[-E(1/T - 1/T_a)/R]t_\alpha \qquad \text{(Eq. 3)}$$

where k_a is the rate constant at the arbitrarily chosen temperature, T_a, and E is the activation energy. Rearranging and taking logarithms:

$$\ln(t_\alpha) = \ln(-G/k_a) + E(1/T - 1/T_a)/R \qquad \text{(Eq. 4)}$$

Thus a plot of $\ln(t_\alpha)$ *versus* $(1/T - 1/T_a)$ will be linear with slope E/R and intercept $\ln(-G/k_a)$. If C_1 is chosen

Table I—Inhibition of Cell Growth

Extract Concentration, %[a]	Inhibition of Cell Growth, % Regular[b]	Superabsorbant[c]
10	12	5
15	18	16
20	22	24
25	28	33
30	30	42
35	39	52
40	38	57
45	47	62
50	48	64

[a] Undiluted Extract = 100%. [b] Regular tampon: extracted with 95 ml of distilled water. [c] Superabsorbant tampon: extracted with 75 ml of distilled water.

Table II—Intramuscular Implantation: Tampon Material

Implanted Material	Gross Rating[a]	Histopathologic Rating[a]
Absorbant material[b]	3	4
Absorbant material[c]	3	4
Partially hydrated absorbant material	0	4
Fibrous material[b]	0	4
Fibrous material[c]	0	4

[a] Ratings: 0, equivalent to negative control; 3, marked positive response; 4, equivalent to positive control. [b] Regular tampon. [c] Superabsorbant tampon.

Muscle tissue reaction (necrotic and inflammatory) to the absorbant and fibrous materials of tampons were the most severe of any materials tested in this laboratory, actually exceeding the positive control response in some cases. The isolated fibrous material which has lower absorbancy than the absorbant material did not show a positive gross response but had a histopathologic rating equivalent to the absorbant material, suggesting that the response was not totally due to dehydration. Fibrous material has been reported to be present in biopsies of vaginal lesions (1). Although the rabbit muscle response can not be considered to be identical to the response of vaginal tissue, the presence of fibrous material in vaginal lesions indicates that tampon material comes into intimate contact with vaginal tissue. Tissue dehydration has been demonstrated to alter calcium levels of vaginal tissue, facilitates contact of tampon material with the tissue, and undoubtedly alters cellular response to leachable toxic components of tampons. The inhibition of cell growth reported in Table I was observed in normal liquid tissue culture medium where dehydration is not a factor. The effect of leachable, soluble components of tampons on cells partially impaired or altered by dehydration is not known. The potential for the exacerbation of the ulcerative process by leachable substances of tampons is apparent.

(1) E. G. Friedrich, *Clin. Obstet. Gynecol.*, **24**, 395 (1981).

John Autian[x]
E. O. Dillingham
W. H. Lawrence
J. E. Turner
Materials Science Toxicology Laboratories
The University of Tennessee Center for the Health Sciences
Memphis, TN 38163

Received October 6, 1981.
Accepted for publication January 28, 1982.

0022-3549/82/0500-0599$01.00/0

Simplified Method to Study Stability of Pharmaceutical Systems

Keyphrases □ Decomposition—determination of shelf-life using analytic methodologies □ Kinetics—decomposition, determination of shelf-life using analytic methodologies □ Stability—simplified method of study in pharmaceutical systems

To the Editor:

In a previous report (1), shelf-life, defined as the time for 10% decomposition at 25°, was estimated by a simplified method. The method involved carrying out a number of kinetic tests at different temperatures followed by linear regression of the logarithm of $t_{0.9}$ (the time required for the drug to decompose to 90% of its original value) on the reciprocal of absolute temperature. Simulated data were used initially to test the linearity of such plots. Since it had been reported previously (2) that it was not possible to distinguish between first-, zero-, and simple second-order kinetics when the decomposition was <10%, it was believed the plots of ln ($t_{0.9}$) *versus* $1/T$ would be linear.

In a subsequent criticism of a previous study (1), it was stated that the use of this Arrhenius approach for all orders of reaction was erroneous and that the slope of the line would be highly dependent on the initial concentration (3). For this reason, and because of analytical difficulties when decomposition is <10%, it was concluded that this method was of little use.

The problem arises because $t_{0.9}$ was defined with respect to the original concentration. It was tacitly assumed (1) that all test samples would have the same initial concentration, whereas it was implied (3) that this would not be the case necessarily.

The purpose of this communication is to point out that plots of $\ln(t_\alpha)$ (where t_α is the time to decompose from concentration C_1 to C_2) *versus* $1/T$ will be linear for all reaction orders irrespective of the α value chosen. If C_1 equals the initial concentration (C_0), and it is the same for all experiments, and C_2 is 90% of C_0, then $t_\alpha = t_{0.9}$.

Assuming the usual rate expression:

$$dC/dt = -kf(C) \qquad \text{(Eq. 1)}$$

where $f(C)$ is some function of concentration, then integrating between the limits t_2 and t_1 ($t_2 - t_1 = t_\alpha$):

$$g(C_2) - g(C_1) = -kt_\alpha \qquad \text{(Eq. 2)}$$

where $g(C)$ is the integrated form of $f(C)$. If a number of kinetic experiments are performed at different temperatures, each starting with approximately the same initial concentration, and C_1 and C_2 are chosen the same for all experiments, then $g(C_2) - g(C_1)$ is constant (G). Substituting this into Eq. 2, assuming the Arrhenius equation is applicable:

$$G = -k_a \exp[-E(1/T - 1/T_a)/R]t_\alpha \qquad \text{(Eq. 3)}$$

where k_a is the rate constant at the arbitrarily chosen temperature, T_a, and E is the activation energy. Rearranging and taking logarithms:

$$\ln(t_\alpha) = \ln(-G/k_a) + E(1/T - 1/T_a)/R \qquad \text{(Eq. 4)}$$

Thus a plot of $\ln(t_\alpha)$ *versus* $(1/T - 1/T_a)$ will be linear with slope E/R and intercept $\ln(-G/k_a)$. If C_1 is chosen

as the labeled concentration and C_2 = 90% of this, then $-G/k_a$ is the shelf-life at temperature T_a (assuming no overage in the product).

An advantage of this method is that the activation energy and shelf-life can be estimated without assuming a particular reaction order. An average value for E can be estimated by appropriately grouping data into sets with each set having a different α value, then solving them simultaneously by weighted nonlinear regression to estimate an average E across sets and a $-G/k_a$ for each set.

An analogous technique has been used in thermogravimetric analysis (4–6), in which a number of nonisothermal experiments were performed at different linear heating rates. The logarithm of the reaction rate at a selected percentage decomposition *versus* $1/T$ was plotted using this technique. The reaction rate at a specific fraction of decomposition was estimated by linear interpolation. In the method suggested previously, t_α can be estimated similarly by linear interpolation, by alternative methods (*e.g.*, cubic splines, polynomial regression), or by assuming knowledge of the functional relationship [$f(C)$] as was done previoulsy (1).

(1) A. K. Amirjahed, *J. Pharm. Sci.*, **66**, 785 (1977).
(2) N. G. Lordi and M. W. Scott, *ibid.*, **54**, 531 (1965).
(3) S. Baker and S. Niazi, *ibid.*, **67**, 141 (1978).
(4) H. C. Anderson, *J. Polym. Sci., Part C*, **6**, 175 (1964).
(5) H. L. Friedman, *ibid.*, **6**, 183 (1964).
(6) J. Leyko, M. Maciezowski, and R. Szuniewicz, *J. Thermal Anal.*, **17**, 263 (1979).

Ian G. Tucker
Pharmacy Department
University of Queensland
St. Lucia 4067
Australia

Received October 15, 1981.
Accepted for publication January 13, 1982.

Simplified Method to Study Stability of Pharmaceutical Systems: A Response

Keyphrases □ Decomposition—determination of shelf-life using analytic methodologies, response □ Kinetics—decomposition, determination of shelf-life using analytic methodologies, response □ Stability—simplified method of study in pharmaceutical systems, response

To the Editor:

The preceding paper (1) discusses my earlier criticism, based on pragmatic reasons, of the paper (2) published by Amirjahed (3). It was suggested by Amirjahed (3) that if only 10% decomposition of a product is monitored, it is possible to ascertain the shelf-life, while using less than sophisticated analytic methodologies such as may be available in small institutional settings. My criticism that the initial concentration of the sample is important is still valid regardless of how the kinetic equation is manipulated such as reported by Tucker (1):

$$\ln(t_\alpha) = \ln(-G/k_a) + E\,(1/T - 1/T_a)/R \qquad \text{(Eq. 1)}$$

where t_α is the time to decompose from concentration C_1 to C_2, and $-G/k_a$ becomes the shelf-life at temperature T_a for a 10% concentration change. However, the assumptions involved here are self-defeating. It assumes that all preparations have similar initial concentrations and that there is no overage in the product (1). It should be reiterated that a ±5% variation in the content is routinely acceptable. This alone will discard the calculations that require identical starting concentrations. Furthermore, obtaining sufficient data points during 10% decomposition of the product (which may have several excipients) is a difficult, but not impossible, task and requires sophisticated analytic technology. Together, these arguments make such exercises as reported by Amirjahed (3) and Tucker (1) of merely academic interest and could be misleading if their use is suggested in those instances where operators may not be fully aware of these pitfalls. I would highly recommend that the authors (1, 3) use these equations with actual data collected in the laboratory and show their validity. It is only when such studies are reported that the validity of the interesting concept reported by Amirjahed (3) can be ascertained.

(1) I. G. Tucker, *J. Pharm. Sci.*, **71**, 599 (1982).
(2) S. Bakar and S. Niazi, *ibid.*, **67**, 141 (1978).
(3) A. K. Amirjahed, *ibid.*, **66**, 785 (1977).

Sarfaraz Niazi
Department of Pharmacy
College of Pharmacy
University of Illinois at
the Medical Center
Chicago, IL 60612

Received October 30, 1981.
Accepted for publication January 13, 1982.

Use of Unbound Drug Concentration in Blood to Discriminate Between Two Models of Hepatic Drug Elimination

Keyphrases □ Plasma protein binding—effect on systemic unbound blood drug concentration of orally administered drug □ Hepatic drug clearance—discrimination between two models, venous equilibrium model, sinusoidal perfusion model

To the Editor:

Two well-defined models have been proposed to describe the hepatic elimination of drugs and other compounds. These models differ in their basic hypotheses and in some of their quantitative predictions, *e.g.*, concerning the influence of blood flow, protein binding, and drug metabolizing activity on extraction ratio and hepatic clearance.

Model 1 (the equilibrium or well-stirred model) assumes that the liver is a single, well-stirred compartment, and that the concentration of unbound drug in hepatic venous blood is in equilibrium with unbound drug throughout the liver (1). Model 2 (the sinusoidal perfusion or parallel tube model) assumes that at any point along the hepatic sinusoid, the concentration of drug in the liver cell will equal

0022-3549/82/0500-0600$01.00/0

as the labeled concentration and C_2 = 90% of this, then $-G/k_a$ is the shelf-life at temperature T_a (assuming no overage in the product).

An advantage of this method is that the activation energy and shelf-life can be estimated without assuming a particular reaction order. An average value for E can be estimated by appropriately grouping data into sets with each set having a different α value, then solving them simultaneously by weighted nonlinear regression to estimate an average E across sets and a $-G/k_a$ for each set.

An analogous technique has been used in thermogravimetric analysis (4–6), in which a number of nonisothermal experiments were performed at different linear heating rates. The logarithm of the reaction rate at a selected percentage decomposition *versus* $1/T$ was plotted using this technique. The reaction rate at a specific fraction of decomposition was estimated by linear interpolation. In the method suggested previously, t_α can be estimated similarly by linear interpolation, by alternative methods (*e.g.*, cubic splines, polynomial regression), or by assuming knowledge of the functional relationship [$f(C)$] as was done previoulsy (1).

(1) A. K. Amirjahed, *J. Pharm. Sci.*, **66**, 785 (1977).
(2) N. G. Lordi and M. W. Scott, *ibid.*, **54**, 531 (1965).
(3) S. Baker and S. Niazi, *ibid.*, **67**, 141 (1978).
(4) H. C. Anderson, *J. Polym. Sci., Part C*, **6**, 175 (1964).
(5) H. L. Friedman, *ibid.*, **6**, 183 (1964).
(6) J. Leyko, M. Maciezowski, and R. Szuniewicz, *J. Thermal Anal.*, **17**, 263 (1979).

Ian G. Tucker
Pharmacy Department
University of Queensland
St. Lucia 4067
Australia

Received October 15, 1981.
Accepted for publication January 13, 1982.

Simplified Method to Study Stability of Pharmaceutical Systems: A Response

Keyphrases □ Decomposition—determination of shelf-life using analytic methodologies, response □ Kinetics—decomposition, determination of shelf-life using analytic methodologies, response □ Stability—simplified method of study in pharmaceutical systems, response

To the Editor:

The preceding paper (1) discusses my earlier criticism, based on pragmatic reasons, of the paper (2) published by Amirjahed (3). It was suggested by Amirjahed (3) that if only 10% decomposition of a product is monitored, it is possible to ascertain the shelf-life, while using less than sophisticated analytic methodologies such as may be available in small institutional settings. My criticism that the initial concentration of the sample is important is still valid regardless of how the kinetic equation is manipulated such as reported by Tucker (1):

$$\ln(t_\alpha) = \ln(-G/k_a) + E\,(1/T - 1/T_a)/R \qquad \text{(Eq. 1)}$$

where t_α is the time to decompose from concentration C_1 to C_2, and $-G/k_a$ becomes the shelf-life at temperature T_a for a 10% concentration change. However, the assumptions involved here are self-defeating. It assumes that all preparations have similar initial concentrations and that there is no overage in the product (1). It should be reiterated that a ±5% variation in the content is routinely acceptable. This alone will discard the calculations that require identical starting concentrations. Furthermore, obtaining sufficient data points during 10% decomposition of the product (which may have several excipients) is a difficult, but not impossible, task and requires sophisticated analytic technology. Together, these arguments make such exercises as reported by Amirjahed (3) and Tucker (1) of merely academic interest and could be misleading if their use is suggested in those instances where operators may not be fully aware of these pitfalls. I would highly recommend that the authors (1, 3) use these equations with actual data collected in the laboratory and show their validity. It is only when such studies are reported that the validity of the interesting concept reported by Amirjahed (3) can be ascertained.

(1) I. G. Tucker, *J. Pharm. Sci.*, **71**, 599 (1982).
(2) S. Bakar and S. Niazi, *ibid.*, **67**, 141 (1978).
(3) A. K. Amirjahed, *ibid.*, **66**, 785 (1977).

Sarfaraz Niazi
Department of Pharmacy
College of Pharmacy
University of Illinois at
the Medical Center
Chicago, IL 60612

Received October 30, 1981.
Accepted for publication January 13, 1982.

Use of Unbound Drug Concentration in Blood to Discriminate Between Two Models of Hepatic Drug Elimination

Keyphrases □ Plasma protein binding—effect on systemic unbound blood drug concentration of orally administered drug □ Hepatic drug clearance—discrimination between two models, venous equilibrium model, sinusoidal perfusion model

To the Editor:

Two well-defined models have been proposed to describe the hepatic elimination of drugs and other compounds. These models differ in their basic hypotheses and in some of their quantitative predictions, *e.g.*, concerning the influence of blood flow, protein binding, and drug metabolizing activity on extraction ratio and hepatic clearance.

Model 1 (the equilibrium or well-stirred model) assumes that the liver is a single, well-stirred compartment, and that the concentration of unbound drug in hepatic venous blood is in equilibrium with unbound drug throughout the liver (1). Model 2 (the sinusoidal perfusion or parallel tube model) assumes that at any point along the hepatic sinusoid, the concentration of drug in the liver cell will equal

0022-3549/82/0500-0600$01.00/0

as the labeled concentration and C_2 = 90% of this, then $-G/k_a$ is the shelf-life at temperature T_a (assuming no overage in the product).

An advantage of this method is that the activation energy and shelf-life can be estimated without assuming a particular reaction order. An average value for E can be estimated by appropriately grouping data into sets with each set having a different α value, then solving them simultaneously by weighted nonlinear regression to estimate an average E across sets and a $-G/k_a$ for each set.

An analogous technique has been used in thermogravimetric analysis (4–6), in which a number of nonisothermal experiments were performed at different linear heating rates. The logarithm of the reaction rate at a selected percentage decomposition *versus* $1/T$ was plotted using this technique. The reaction rate at a specific fraction of decomposition was estimated by linear interpolation. In the method suggested previously, t_α can be estimated similarly by linear interpolation, by alternative methods (*e.g.*, cubic splines, polynomial regression), or by assuming knowledge of the functional relationship [$f(C)$] as was done previoulsy (1).

(1) A. K. Amirjahed, *J. Pharm. Sci.*, **66**, 785 (1977).
(2) N. G. Lordi and M. W. Scott, *ibid.*, **54**, 531 (1965).
(3) S. Baker and S. Niazi, *ibid.*, **67**, 141 (1978).
(4) H. C. Anderson, *J. Polym. Sci., Part C*, **6**, 175 (1964).
(5) H. L. Friedman, *ibid.*, **6**, 183 (1964).
(6) J. Leyko, M. Maciezowski, and R. Szuniewicz, *J. Thermal Anal.*, **17**, 263 (1979).

Ian G. Tucker
Pharmacy Department
University of Queensland
St. Lucia 4067
Australia

Received October 15, 1981.
Accepted for publication January 13, 1982.

Simplified Method to Study Stability of Pharmaceutical Systems: A Response

Keyphrases □ Decomposition—determination of shelf-life using analytic methodologies, response □ Kinetics—decomposition, determination of shelf-life using analytic methodologies, response □ Stability—simplified method of study in pharmaceutical systems, response

To the Editor:

The preceding paper (1) discusses my earlier criticism, based on pragmatic reasons, of the paper (2) published by Amirjahed (3). It was suggested by Amirjahed (3) that if only 10% decomposition of a product is monitored, it is possible to ascertain the shelf-life, while using less than sophisticated analytic methodologies such as may be available in small institutional settings. My criticism that the initial concentration of the sample is important is still valid regardless of how the kinetic equation is manipulated such as reported by Tucker (1):

$$\ln(t_\alpha) = \ln(-G/k_a) + E\,(1/T - 1/T_a)/R \qquad \text{(Eq. 1)}$$

where t_α is the time to decompose from concentration C_1 to C_2, and $-G/k_a$ becomes the shelf-life at temperature T_a for a 10% concentration change. However, the assumptions involved here are self-defeating. It assumes that all preparations have similar initial concentrations and that there is no overage in the product (1). It should be reiterated that a ±5% variation in the content is routinely acceptable. This alone will discard the calculations that require identical starting concentrations. Furthermore, obtaining sufficient data points during 10% decomposition of the product (which may have several excipients) is a difficult, but not impossible, task and requires sophisticated analytic technology. Together, these arguments make such exercises as reported by Amirjahed (3) and Tucker (1) of merely academic interest and could be misleading if their use is suggested in those instances where operators may not be fully aware of these pitfalls. I would highly recommend that the authors (1, 3) use these equations with actual data collected in the laboratory and show their validity. It is only when such studies are reported that the validity of the interesting concept reported by Amirjahed (3) can be ascertained.

(1) I. G. Tucker, *J. Pharm. Sci.*, **71**, 599 (1982).
(2) S. Bakar and S. Niazi, *ibid.*, **67**, 141 (1978).
(3) A. K. Amirjahed, *ibid.*, **66**, 785 (1977).

Sarfaraz Niazi
Department of Pharmacy
College of Pharmacy
University of Illinois at
the Medical Center
Chicago, IL 60612

Received October 30, 1981.
Accepted for publication January 13, 1982.

Use of Unbound Drug Concentration in Blood to Discriminate Between Two Models of Hepatic Drug Elimination

Keyphrases □ Plasma protein binding—effect on systemic unbound blood drug concentration of orally administered drug □ Hepatic drug clearance—discrimination between two models, venous equilibrium model, sinusoidal perfusion model

To the Editor:

Two well-defined models have been proposed to describe the hepatic elimination of drugs and other compounds. These models differ in their basic hypotheses and in some of their quantitative predictions, *e.g.*, concerning the influence of blood flow, protein binding, and drug metabolizing activity on extraction ratio and hepatic clearance.

Model 1 (the equilibrium or well-stirred model) assumes that the liver is a single, well-stirred compartment, and that the concentration of unbound drug in hepatic venous blood is in equilibrium with unbound drug throughout the liver (1). Model 2 (the sinusoidal perfusion or parallel tube model) assumes that at any point along the hepatic sinusoid, the concentration of drug in the liver cell will equal

0022-3549/82/0500-0600$01.00/0

that in the sinusoid but that this concentration will fall as blood traverses the sinusoid (2).

Determination of which of the two models is the more appropriate to describe hepatic drug elimination is at present in dispute (3, 4). One of the important practical applications of these models is the calculation of intrinsic hepatic drug clearance, which measures the ability of the liver to remove drug irreversibly from liver water; for many compounds it can be regarded as an index of the activity of the drug metabolizing enzymes (5). The method of calculating intrinsic hepatic clearance differs between the two models, so that the same pharmacokinetic data may lead to two quite different answers. This is particularly true of high-clearance drugs (5, 6). Clearly, there is a need for an accurate and unambiguous method of measurement of hepatic drug metabolizing function for these high-clearance drugs, which is applicable to the intact animal rather than only to isolated liver enzyme preparations.

An extensive theoretical comparison of the two models showed that the greatest discrepancies between the predictions of the two models occur when the following parameters:

1. availability
2. steady-state drug concentration in hepatic venous blood
3. area under the blood drug concentration–time curve following a single oral dose
4. steady-state drug concentration in blood following constant oral drug administration for a highly extracted drug are examined under perturbations of either hepatic blood flow or of the degree of binding within the blood (7).

However, to date there are few experimental data available, and the evidence that is available does not single out one model as being more appropriate. For example, studies with lidocaine (3) from one laboratory using the isolated perfused rat liver preparation support the venous equilibrium model, whereas similar studies with galactose (8) from a second laboratory support the sinusoidal perfusion model. So far, experiments designed to discriminate between the two models of hepatic drug elimination have only involved examination of the effect of hepatic blood flow on the steady-state output concentration of highly cleared drugs in the perfused rat liver preparation. This is because hepatic blood flow is easily monitored and controlled in this preparation.

As a result of a series of computer simulations we have performed, relating intrinsic clearance to various pharmacokinetic indexes, another discriminant between Models 1 and 2 has emerged. The equations relating the area under the blood drug concentration–time curve following a single oral dose with the determinants of hepatic drug elimination (7) are for the venous equilibrium model (model 1):

$$AUC_{po} = \frac{D_{po}}{fu_b\, CLu_{int}} \qquad \text{(Eq. 1)}$$

and for the sinusoidal perfusion model (model 2):

$$AUC_{po} = \frac{D_{po}\,(e^{-fu_b\, CLu_{int}/Q_H})}{Q_H(1 - e^{-fu_b\, CLu_{int}/Q_H})} \qquad \text{(Eq. 2)}$$

where:

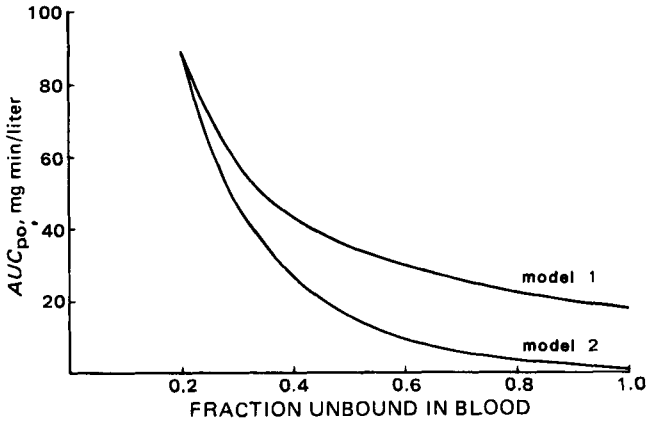

Figure 1—*Effect of fraction of unbound drug in blood on* AUC_{po} *for 200 mg of meperidine administered orally.*

D_{po} = dose administered by the oral route,
fu_b = fraction of unbound drug in blood,
CLu_{int} = intrinsic hepatic clearance of unbound drug, and
Q_H = hepatic blood flow.

From these equations, expressions can be derived which relate the area under the unbound blood drug concentration–time curve following a single oral dose ($AUCu_{po}$) with the determinants of hepatic drug elimination for model 1:

$$AUCu_{po} = fu_b\, AUC_{po} = \frac{D_{po}}{CLu_{int}} \qquad \text{(Eq. 3)}$$

and for model 2:

$$AUCu_{po} = fu_b\, AUC_{po} = \frac{fu_b\, D_{po}\,(e^{-fu_b\, CLu_{int}/Q_H})}{Q_H(1 - e^{-fu_b\, CLu_{int}/Q_H})} \qquad \text{(Eq. 4)}$$

Simulations of Eqs. 1–4 were performed for the drug meperidine and the following parameters were used:

Q_H = 1.5 liter/min
D_{po} = 200 mg
fu_b = 0.2
CLu_{int} = 11.25 liter/min (model 1)
CLu_{int} = 6.872 liter/min (model 2)

The systemic blood clearance of meperidine is ~0.9 liter/min (9), which corresponds to an hepatic extraction ratio of 0.6. Systemic blood clearance is a model-independent variable, whereas intrinsic clearance is model-dependent, *i.e.*, the value calculated depends on whether model 1 or 2 is invoked. Hence, two different values are given for intrinsic hepatic clearance of meperidine. Figure 1 shows the relationship between the fraction free in blood and AUC_{po}, according to Eqs. 1 and 2. The results are consistent with those described previously (7), in that a greater dependence of AUC_{po} on free fraction is predicted by model 2. Figure 2 shows the relationship between the fraction free in blood and area under the unbound blood drug concentration–time curve following a single oral dose, according to Eqs. 3 and 4. The $AUCu_{po}$ appears to be a much better discriminator between the two models than AUC_{po}, because $AUCu_{po}$ should be independent of free fraction in blood according to model 1 but not to model 2. These simulations present another and potentially more powerful method of discriminating between the two models using

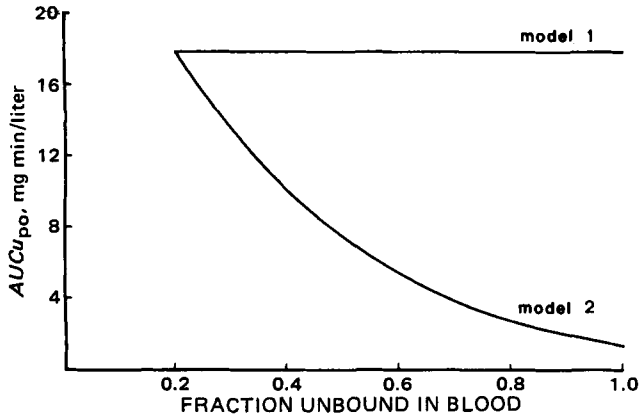

Figure 2—*Effect of fraction of unbound drug in blood on* AUC *of unbound drug concentration (*$AUCu_{po}$*) versus time for 200 mg of meperidine administered orally.*

the isolated perfused rat liver preparation. It is theoretically possible to vary the fraction of unbound drug in the perfusate by at least 10-fold for a highly bound drug, whereas the hepatic perfusion rate may only reasonably be varied by less than twofold (3). A preliminary investigation of the plasma protein binding of propranolol has been carried out using equilibrium dialysis. The results of this investigation show that it is possible to achieve a 10-fold variation of the fraction of unbound drug by varying the concentration of bovine serum albumin and α_1-acidglycoprotein in the perfusate[1].

The predictions of models 1 and 2 for the relationship between free fraction in blood and the steady-state unbound drug concentration in the reservoir of the isolated perfused rat liver preparation (Cu_{ss}) following constant-rate drug administration into the portal vein are analogous to those described for $AUCu_{po}$. The equations relating fraction of unbound drug in blood with Cu_{ss} can be derived from the equations presented by Pang and Rowland (7) and for model 1:

$$Cu_{ss} = \frac{R}{CLu_{int}} \qquad \text{(Eq. 5)}$$

and for model 2:

$$Cu_{ss} = \frac{fu_b\, Re^{(-fu_b\, CLu_{int}/Q_H)}}{Q_H[1 - e^{(-fu_b\, CLu_{int}/Q_H)}]} \qquad \text{(Eq. 6)}$$

where R is the infusion rate of drug into the portal vein.

Hence, the effect of changing free fraction of drug in perfusate on the steady-state unbound drug concentration in the reservoir following constant-rate drug administration into the portal vein in the isolated perfused rat liver preparation may also be used to discriminate between the two models.

(1) M. Rowland, L. Z. Benet, and G. G. Graham, *J. Pharmacokinet. Biopharm.*, **1**, 123 (1973).

(2) K. Winkler, S. Keiding, and N. Tygstrup, in "The Liver: Quantitative Aspects of Structure and Functions," G. Paumgartner and R. Presig, Eds. Karger, Basel, 1973, pp. 144–155.

(3) K. S. Pang, and M. Rowland, *J. Pharmacokinet. Biopharm.*, **5**, 655 (1977).

(4) L. Bass, *Gastroenterology*, **76**, 1504 (1979).

[1] D. B. Jones, D. J. Morgan, G. W. Mihaly, and R. A. Smallwood, Unpublished observations.

(5) A. S. Nies, D. G. Shand, and G. R. Wilkinson, *Clin. Pharmacokinet.*, **1**, 135 (1976).

(6) L. Bass and K. Winkler, *Clin. Exp. Pharmacol. Physiol.*, **7**, 339 (1980).

(7) K. S. Pang and M. Rowland, *J. Pharmacokinet. Biopharm.*, **5**, 625 (1977).

(8) S. Keiding and E. Chiarantini, *J. Pharmacol. Exp. Ther.*, **205**, 465 (1978).

(9) E. A. Neal, P. J. Meffin, P. B. Gregory, and T. F. Blaschke, *Gastroenterology*, **77**, 96 (1979).

Denis J. Morgan[x]
Kenneth Raymond
Victorian College of Pharmacy Ltd.
381 Royal Parade
Parkville
Victoria, Australia 3052

Received September 4, 1981.
Accepted for publication February 19, 1982.

Filter-Probe Extractor: A Tool for the Rapid Determination of Oil–Water Partition Coefficients

Keyphrases □ Filter-probe extractor—tool for rapid determination of oil–water partition coefficients □ Oil–water partition coefficients—rapid determination using filter-probe extractor □ Thermodynamics—filter-probe extractor use for rapid determination of oil–water partition coefficients

To the Editor:

The distribution of solutes between water and oil has been the subject of hundreds of studies since the end of the last century (1). The oil–water partition coefficient [or liquid–liquid distribution constant, as recommended (2) by IUPAC] is of use in separation science as it indicates the extent of extraction in a two-phase system. Also, since the partition coefficient is taken (3) as a measure of solute hydrophobicity, it is an often used parameter in, for example, preformulation and drug design (QSAR) studies. Partition coefficients have been determined by a large number of methods, including shake flask, counter-current distribution (4), and various automated methods including the AKUFVE (5) and SEGSPLIT (6) approaches.

Recently, we published a study (7) on the thermodynamics of solute oil–water partitioning, where use was made of a modification of a rapid solvent extraction method described by Cantwell and Mohammed (8) for photometric acid-base titrations in the presence of an immiscible solvent. Using various data manipulations, these workers have been able to demonstrate (9, 10) that their method provides ion-pair distribution coefficients and is of consequent use in drug analysis. Here we wish to communicate some of our experiences with a modified filter-probe for measuring oil–water partition coefficients of molecules of pharmaceutical interest, and to draw attention to the fact that the method has particular use for the examination of the effect of a large number of variables on the distribution process. It is emphasized that the apparatus here described is similar to, but not the same as, that developed by Cantwell and Mohammed.

0022-3549/82/0500-0602$01.00/0

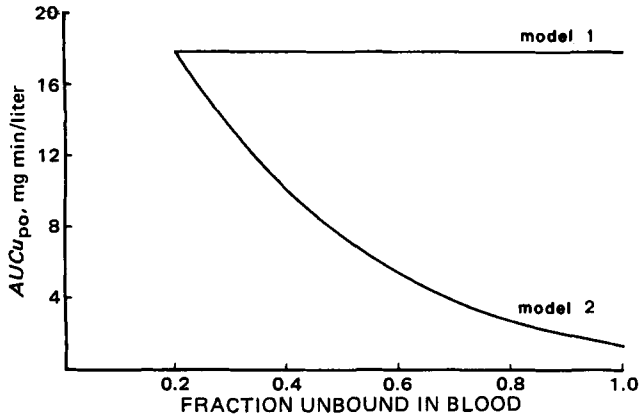

Figure 2—*Effect of fraction of unbound drug in blood on* AUC *of unbound drug concentration (*$AUCu_{po}$*) versus time for 200 mg of meperidine administered orally.*

the isolated perfused rat liver preparation. It is theoretically possible to vary the fraction of unbound drug in the perfusate by at least 10-fold for a highly bound drug, whereas the hepatic perfusion rate may only reasonably be varied by less than twofold (3). A preliminary investigation of the plasma protein binding of propranolol has been carried out using equilibrium dialysis. The results of this investigation show that it is possible to achieve a 10-fold variation of the fraction of unbound drug by varying the concentration of bovine serum albumin and α_1-acidglycoprotein in the perfusate[1].

The predictions of models 1 and 2 for the relationship between free fraction in blood and the steady-state unbound drug concentration in the reservoir of the isolated perfused rat liver preparation (Cu_{ss}) following constant-rate drug administration into the portal vein are analogous to those described for $AUCu_{po}$. The equations relating fraction of unbound drug in blood with Cu_{ss} can be derived from the equations presented by Pang and Rowland (7) and for model 1:

$$Cu_{ss} = \frac{R}{CLu_{int}} \qquad \text{(Eq. 5)}$$

and for model 2:

$$Cu_{ss} = \frac{fu_b\, Re^{(-fu_b\, CLu_{int}/Q_H)}}{Q_H[1 - e^{(-fu_b\, CLu_{int}/Q_H)}]} \qquad \text{(Eq. 6)}$$

where R is the infusion rate of drug into the portal vein.

Hence, the effect of changing free fraction of drug in perfusate on the steady-state unbound drug concentration in the reservoir following constant-rate drug administration into the portal vein in the isolated perfused rat liver preparation may also be used to discriminate between the two models.

(1) M. Rowland, L. Z. Benet, and G. G. Graham, *J. Pharmacokinet. Biopharm.*, **1**, 123 (1973).

(2) K. Winkler, S. Keiding, and N. Tygstrup, in "The Liver: Quantitative Aspects of Structure and Functions," G. Paumgartner and R. Presig, Eds. Karger, Basel, 1973, pp. 144–155.

(3) K. S. Pang, and M. Rowland, *J. Pharmacokinet. Biopharm.*, **5**, 655 (1977).

(4) L. Bass, *Gastroenterology*, **76**, 1504 (1979).

[1] D. B. Jones, D. J. Morgan, G. W. Mihaly, and R. A. Smallwood, Unpublished observations.

(5) A. S. Nies, D. G. Shand, and G. R. Wilkinson, *Clin. Pharmacokinet.*, **1**, 135 (1976).

(6) L. Bass and K. Winkler, *Clin. Exp. Pharmacol. Physiol.*, **7**, 339 (1980).

(7) K. S. Pang and M. Rowland, *J. Pharmacokinet. Biopharm.*, **5**, 625 (1977).

(8) S. Keiding and E. Chiarantini, *J. Pharmacol. Exp. Ther.*, **205**, 465 (1978).

(9) E. A. Neal, P. J. Meffin, P. B. Gregory, and T. F. Blaschke, *Gastroenterology*, **77**, 96 (1979).

Denis J. Morgan[x]
Kenneth Raymond
Victorian College of Pharmacy Ltd.
381 Royal Parade
Parkville
Victoria, Australia 3052

Received September 4, 1981.
Accepted for publication February 19, 1982.

Filter-Probe Extractor: A Tool for the Rapid Determination of Oil–Water Partition Coefficients

Keyphrases □ Filter-probe extractor—tool for rapid determination of oil–water partition coefficients □ Oil–water partition coefficients—rapid determination using filter-probe extractor □ Thermodynamics—filter-probe extractor use for rapid determination of oil–water partition coefficients

To the Editor:

The distribution of solutes between water and oil has been the subject of hundreds of studies since the end of the last century (1). The oil–water partition coefficient [or liquid–liquid distribution constant, as recommended (2) by IUPAC] is of use in separation science as it indicates the extent of extraction in a two-phase system. Also, since the partition coefficient is taken (3) as a measure of solute hydrophobicity, it is an often used parameter in, for example, preformulation and drug design (QSAR) studies. Partition coefficients have been determined by a large number of methods, including shake flask, counter-current distribution (4), and various automated methods including the AKUFVE (5) and SEGSPLIT (6) approaches.

Recently, we published a study (7) on the thermodynamics of solute oil–water partitioning, where use was made of a modification of a rapid solvent extraction method described by Cantwell and Mohammed (8) for photometric acid-base titrations in the presence of an immiscible solvent. Using various data manipulations, these workers have been able to demonstrate (9, 10) that their method provides ion-pair distribution coefficients and is of consequent use in drug analysis. Here we wish to communicate some of our experiences with a modified filter-probe for measuring oil–water partition coefficients of molecules of pharmaceutical interest, and to draw attention to the fact that the method has particular use for the examination of the effect of a large number of variables on the distribution process. It is emphasized that the apparatus here described is similar to, but not the same as, that developed by Cantwell and Mohammed.

0022-3549/82/0500-0602$01.00/0

The apparatus consists of an efficient mixing chamber (fitted with vortex spoilers and a well-sealed lid), one or two filter probes immersed in the mixed phases, and a pumping system that pumps the probed phase(s) through a spectrophotometric flow-through cell and back to the mixing chamber (see refs. 7 and 8 for schematics). The mixing chamber is thermostated and can have a volume from 50 to 1000 ml. Figure 1 gives the design of our modified filter probe, which is machined out of a stainless steel block. There is almost zero contact between the phases and the protective polytef spacer, compared to the polytef mesh (8) and wafer (10) that Cantwell and Mohammed place behind their filter material (to increase flow).

With our earlier experiments on the partitioning of hydrophobic drugs, it was found that using the latter configurations adsorption of drug onto the polytef was a problem. With the modified probe, postfiltration flow is improved by 20 radial channels (0.2-mm depth) cut into the surface of the cylindrical stainless steel block. Adsorption to polytef was such an early problem that all connecting tubing is now constructed of an HPLC-grade 1.0-mm bore stainless steel tube. In addition, HPLC pumps are used to effect flow, since these give no adsorption problems (unlike peristaltic pumps) and can be readily used with volatile solvents.

For our studies, a cellulose filter paper[1] was used for the probing of the aqueous phase and a polytef film[2] for probing of the oil. (Any hard cellulose filter paper should suffice for the hydrophilic filter probe.) We prefer to monitor the aqueous phase, and as a general procedure add only aqueous phase to the system, pump, adjust recorder baseline, add solute in a volume of the aqueous phase; after further equilibration (given by constant recorder reading), add a volume of oil, equilibrate, add an equal volume of oil, equilibrate, add a third equal volume of oil, and equilibrate. Since it takes between 0.5 and 15 min to reach equilibration (depending on pumping rates, phase volumes, and partition coefficient), one can very quickly determine from these experiments the effect of solute concentration on distribution. One can then go on to study the effect of various variables on the partitioning process; *e.g.*, temperature can be altered if the thermodynamics are to be studied, or a pH stat can be employed to obtain the pH–partition profile of a compound and hence determine the pKa.

Since the method is rapid, it can be used to determine the partition characteristics of relatively unstable compounds. Phase volume ratios of 1000:1 are possible, though the probed phase must have a volume greater than that of the pumping circuit. The range of partition coefficients that can be measured is $\sim +5.3$ to -5.3 log units, though this is dependent on the sensitivity of the analytical method. Generally, a pumping rate of between 1.0 and 1.5 ml/min is used: greater speeds result in overloading of the filter system.

There are three potential disadvantages to the procedure: One is evaporation of solute. This was found for benzene in our original experiments, and has since been described[3] as a problem common to all conventional methods for determining the partition coefficient of benzene, but which should be circumvented by the use of a closed system. The second, more serious problem, is that of adsorption. This has been circumvented in our system by employing stainless steel fittings and tubing and HPLC pumps, but it could still be a problem for some very polar compounds. Adsorption is very clearly seen in the step before addition of oil by a continuing fall in recorder reading, which is seen to be reversible during washing. Another problem encountered is the use of silicon-based filters as hydrophobic probes when cyclohexane and 2,2,4-trimethylpentane are used. Here it is found that after a short time the filters become permeable to the aqueous phase, due to a stripping of the filter material.

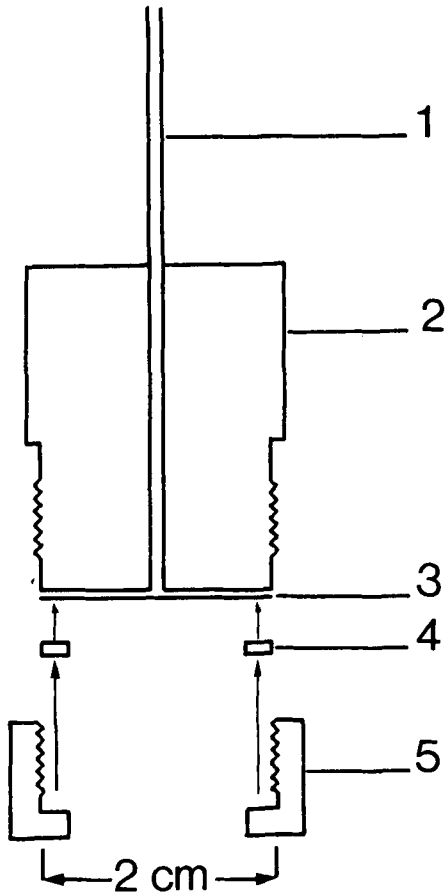

Figure 1—*Filter-probe extractor. 1, 1.0-mm bore stainless steel tube; 2, cylindrical stainless steel block; 3, filter material; 4, polytef o-ring spacer; and 5, screw-on stainless steel cap.*

To date, this modified filter probe system has been used in our laboratory for a number of studies including the aforementioned thermodynamics study and the determination of the partitioning of unstable compounds, peptides, and various hydrophilic and hydrophobic neutral drugs. Cyclohexane, 2,2,4-trimethylpentane, 1-octanol, and chloroform have all been successfully employed as oil phases. Table I illustrates the close agreement between partition coefficients determined by both conventional shakeflask and the described filter-probe methods (7). The filter probe system can be described as a simple and convenient tool for not only determining ion-pair equilibria (8–10), but also, as discussed here, both for "one-off" determination of solute oil–water partition coefficients, and

[1] 589/3 Blauband filter paper, Schleicher and Schüll
[2] Mitex LC 10-μm with 68% porosity, Millipore.
[3] C. Hansch, Pomona College, Calif., personal communication.

Table I—Comparison between Shake-Flask and Filter Probe Methods for Determining Partition Coefficients between Oil [a] and Water [b]

Solute	Log Partition Coefficients (Molar Scale) at 25° (*SD*)			
	Shake-Flask		Filter Probe	
o-Chloroaniline	0.983	(0.012)	0.978	(0.021)
p-Chloroaniline	0.462	(0.012)	0.462	(0.019)
Methyl Benzoate	1.77	(0.046)	1.78	(0.056)
p-Nitrotoluene	1.97	(0.030)	1.92	(0.060)
p-Cresol	−0.395	(0.025)	−0.379	(0.019)

[a] 2,2,4-Trimethylpentane.
[b] Phosphate buffer pH 7.

for the examination of various environmental variables on the partitioning process.

(1) C. Hansch and A. Leo, "Substituent Constants for Correlation Analysis in Chemistry and Biology," Wiley, New York, N.Y., 1979.
(2) *Pure Appl. Chem.*, **21**, 109 (1970).
(3) J. Iwasa, T. Fujita, and C. Hansch, *J. Med. Chem.*, **8**, 150 (1965).
(4) N. C. Saha, N. Bhattacharjee, N. G. Asak, and A. Lahiri, *J. Chem. Eng. Data*, **8**, 405 (1963).
(5) S. S. Davis and G. Elson, *J. Pharm. Pharmacol., Suppl.*, **26**, 90P (1974).
(6) J. F. M. Kinkel and E. Tomlinson, *Int. J. Pharm.*, **6**, 261 (1980).
(7) J. F. M. Kinkel, E. Tomlinson, and P. Smit, *ibid.*, **9**, 121 (1981).
(8) F. F. Cantwell and H. Y. Mohammed, *Anal. Chem.*, **51**, 218 (1979).
(9) H. Y. Mohammed and F. F. Cantwell, *ibid.*, **51**, 1006 (1979).
(10) *Ibid.*, **52**, 553 (1980).

E. Tomlinson
Subfaculty of Pharmacy
University of Amsterdam
Plantage Muidergracht 24
1018TV Amsterdam
The Netherlands

Received August 21, 1981.
Accepted for publication January 21, 1982.
The filter-probe extractor was machined by H. van Ijzendoorn, and J. F. M. Kinkel, H. Wijnne, and P. Smit were involved in using and developing the total procedure.

BOOKS

Applied Pharmacokinetics: Principles of Therapeutic Drug Monitoring. Edited by WILLIAM E. EVANS, JEROME J. SCHENTAG, and WILLIAM J. JUSKO. Applied Therapeutics, P.O. Box 31-747, San Francisco, CA 94131. 1980. 708 pp. 15 × 23 cm. Price $34.00.

As noted in the preface, this text is intended as a "source of the objective criteria and systematic approaches necessary for rational application of pharmacokinetics in clinical practice." The editors and authors have achieved that goal admirably. The text is primarily a compilation of information on specific drugs amenable to therapeutic monitoring and for which there is sufficient literature to permit a critical review. A particularly attractive approach is the inclusion of "counterpoint" discussions which accompany several chapters. These are intended to present another author's perspective when a consensus of opinion did not exist on that topic.

An introductory chapter is followed by a discussion (and a counterpoint presentation) of clinical pharmacokinetic consultation services and three chapters dealing with pharmacokinetics in renal and liver disease and in neonates. The remaining chapters are devoted to specific drugs and include: theophylline, aminoglycosides, cephalosporins, phenytoin, digoxin, lidocaine, procainamide, quinidine, propranolol, salicylates, methotrexate, tricyclic antidepressants, lithium, and heparin. Counterpoint discussions accompany the sections on theophylline, aminoglycosides, phenytoin, and lidocaine. The final chapter is concerned with guidelines for collection and the pharmacokinetic analysis of data.

Each chapter dealing with a specific drug contains the following major topics: introduction/background, absorption, distribution, elimination, concentration *versus* response and toxicity, clinical application of pharmacokinetic data, assay methods, and summary. Adhering to a common format enhances the readability of the text and permits the reader easy access to specific desired information. The chapters are concise, written well, and are replete with summary tables and figures. Each chapter has a substantial reference list and literature citations are current.

This book is unquestionably the best text of this type currently available. The editors by necessity have assumed a basic understanding in pharmacokinetics and as a result there are few expositions on fundamental principles and relatively few equations are employed. The reviewer believes this to be an advantage of the text.

A difficulty with publishing a compilation of this type is the fact that much of the material will become rapidly dated as a result of the literature explosion in the area of clinical pharmacokinetics. The editors are certainly aware of this and mention in the preface that this is the first edition. One presumes that others will follow. In subsequent revisions, the editors are encouraged to employ the approach for compiling clinical pharmacokinetic data as suggested by Sheiner *et al.* [*J. Pharmacokinet. Biopharm.*, **9**, 59 (1981)]. The text might also benefit from a table of symbols to be used uniformly throughout (and with common units, if possible).

The reviewer has no hesitation in recommending this text to pharmacy and medical practitioners who are involved in drug therapy and who are interested in improving theory. Pharmacy students in advanced courses, all Pharm.D. students, and clinical pharmacology fellows should consider this a most useful text.

Reviewed by Michael Mayersohn
College of Pharmacy
University of Arizona
Tucson, AZ 85721

0022-3549/82/0500-0604$01.00/0

Table I—Comparison between Shake-Flask and Filter Probe Methods for Determining Partition Coefficients between Oil [a] and Water [b]

Solute	Log Partition Coefficients (Molar Scale) at 25° (*SD*)			
	Shake-Flask		Filter Probe	
o-Chloroaniline	0.983	(0.012)	0.978	(0.021)
p-Chloroaniline	0.462	(0.012)	0.462	(0.019)
Methyl Benzoate	1.77	(0.046)	1.78	(0.056)
p-Nitrotoluene	1.97	(0.030)	1.92	(0.060)
p-Cresol	−0.395	(0.025)	−0.379	(0.019)

[a] 2,2,4-Trimethylpentane.
[b] Phosphate buffer pH 7.

for the examination of various environmental variables on the partitioning process.

(1) C. Hansch and A. Leo, "Substituent Constants for Correlation Analysis in Chemistry and Biology," Wiley, New York, N.Y., 1979.
(2) *Pure Appl. Chem.*, **21**, 109 (1970).
(3) J. Iwasa, T. Fujita, and C. Hansch, *J. Med. Chem.*, **8**, 150 (1965).
(4) N. C. Saha, N. Bhattacharjee, N. G. Asak, and A. Lahiri, *J. Chem. Eng. Data*, **8**, 405 (1963).
(5) S. S. Davis and G. Elson, *J. Pharm. Pharmacol., Suppl.*, **26**, 90P (1974).
(6) J. F. M. Kinkel and E. Tomlinson, *Int. J. Pharm.*, **6**, 261 (1980).
(7) J. F. M. Kinkel, E. Tomlinson, and P. Smit, *ibid.*, **9**, 121 (1981).
(8) F. F. Cantwell and H. Y. Mohammed, *Anal. Chem.*, **51**, 218 (1979).
(9) H. Y. Mohammed and F. F. Cantwell, *ibid.*, **51**, 1006 (1979).
(10) *Ibid.*, **52**, 553 (1980).

E. Tomlinson
Subfaculty of Pharmacy
University of Amsterdam
Plantage Muidergracht 24
1018TV Amsterdam
The Netherlands

Received August 21, 1981.
Accepted for publication January 21, 1982.
The filter-probe extractor was machined by H. van Ijzendoorn, and J. F. M. Kinkel, H. Wijnne, and P. Smit were involved in using and developing the total procedure.

BOOKS

Applied Pharmacokinetics: Principles of Therapeutic Drug Monitoring. Edited by WILLIAM E. EVANS, JEROME J. SCHENTAG, and WILLIAM J. JUSKO. Applied Therapeutics, P.O. Box 31-747, San Francisco, CA 94131. 1980. 708 pp. 15 × 23 cm. Price $34.00.

As noted in the preface, this text is intended as a "source of the objective criteria and systematic approaches necessary for rational application of pharmacokinetics in clinical practice." The editors and authors have achieved that goal admirably. The text is primarily a compilation of information on specific drugs amenable to therapeutic monitoring and for which there is sufficient literature to permit a critical review. A particularly attractive approach is the inclusion of "counterpoint" discussions which accompany several chapters. These are intended to present another author's perspective when a consensus of opinion did not exist on that topic.

An introductory chapter is followed by a discussion (and a counterpoint presentation) of clinical pharmacokinetic consultation services and three chapters dealing with pharmacokinetics in renal and liver disease and in neonates. The remaining chapters are devoted to specific drugs and include: theophylline, aminoglycosides, cephalosporins, phenytoin, digoxin, lidocaine, procainamide, quinidine, propranolol, salicylates, methotrexate, tricyclic antidepressants, lithium, and heparin. Counterpoint discussions accompany the sections on theophylline, aminoglycosides, phenytoin, and lidocaine. The final chapter is concerned with guidelines for collection and the pharmacokinetic analysis of data.

Each chapter dealing with a specific drug contains the following major topics: introduction/background, absorption, distribution, elimination, concentration *versus* response and toxicity, clinical application of pharmacokinetic data, assay methods, and summary. Adhering to a common format enhances the readability of the text and permits the reader easy access to specific desired information. The chapters are concise, written well, and are replete with summary tables and figures. Each chapter has a substantial reference list and literature citations are current.

This book is unquestionably the best text of this type currently available. The editors by necessity have assumed a basic understanding in pharmacokinetics and as a result there are few expositions on fundamental principles and relatively few equations are employed. The reviewer believes this to be an advantage of the text.

A difficulty with publishing a compilation of this type is the fact that much of the material will become rapidly dated as a result of the literature explosion in the area of clinical pharmacokinetics. The editors are certainly aware of this and mention in the preface that this is the first edition. One presumes that others will follow. In subsequent revisions, the editors are encouraged to employ the approach for compiling clinical pharmacokinetic data as suggested by Sheiner *et al.* [*J. Pharmacokinet. Biopharm.*, **9**, 59 (1981)]. The text might also benefit from a table of symbols to be used uniformly throughout (and with common units, if possible).

The reviewer has no hesitation in recommending this text to pharmacy and medical practitioners who are involved in drug therapy and who are interested in improving theory. Pharmacy students in advanced courses, all Pharm.D. students, and clinical pharmacology fellows should consider this a most useful text.

Reviewed by Michael Mayersohn
College of Pharmacy
University of Arizona
Tucson, AZ 85721

0022-3549/82/0500-0604$01.00/0

A publication of the
American Pharmaceutical Association—
the National Professional Society
of Pharmacists

JOURNAL OF PHARMACEUTICAL SCIENCES

INDEX TO AUTHORS
INDEX TO SUBJECTS

VOLUME 71
JANUARY TO DECEMBER, 1982

Published monthly under the supervision of the Board of Trustees

Training Pharmacists for Today—Not Yesterday

Approximately 10 years ago, the National Pharmaceutical Council and the Student American Pharmaceutical Association established a cooperative activity known as the Pharmaceutical Industry Summer Internship Program.

From its inception, the program has flourished; it has been well-supported by various major drug companies, and each year the number of student applicants has exceeded the total positions annually available. To date, about 1,000 students have had an opportunity to participate in the program.

In theory, the program sounded as if it would be a terrific learning experience. As described, the student would have a meaningful opportunity to add to that student's overall knowledge of pharmacy, with emphasis on its industrial aspects. Training would be offered within the industry setting which would supplement that received in traditional types of pharmacy practice.

But cynics had their doubts. All too often in the past, pharmacists have been taken in by the industry. Beneath the attractive surface glitter of other drug industry programs or projects, there have been too many instances of an ulterior motive.

Consequently, many pharmacy leaders suspected that the NPC-SAPhA Summer Internship Program would turn out in actuality to be either: (a) a clever way to get cheap help as laboratory glassware washers or for other routine "floor sweeper" type jobs; or (b) an ingenious scheme to "brainwash" selected student leaders regarding the industry's position on various pharmaceutically related policy matters or political issues.

But it didn't turn out that way at all! In fact, all the students, with whom we have talked after they participated in the program, have enthusiastically related how much they learned, how they were given exposure to a broad spectrum of industry operations, and how much immediate attention and instruction they received from the highly committed and well-qualified professionals who served as their preceptors.

The typical industry program is of about 12-weeks duration on a full-time basis; this is equivalent to about one-fourth of the one-year pharmacy internship required by most states. Generally, the internship is of a broad general nature, with the student spending the entire summer at a single drug company, but with rotating assignments in several different departments or divisions, such as quality control, marketing, manufacturing, formulation development, and so on. All those assigned any responsibility for the interns emphasize learning over productivity and, by training, they usually are pharmacists themselves.

The program did not turn out this well by pure accident. The NPC wisely drew up a document entitled "Guidelines for Pharmaceutical Industry Internships" which gives direction to each individual company in operating its respective program in a way that will provide reasonable uniformity and consistency from one firm to another. Furthermore, to its credit, the NPC has consistently shown good judgment in organizing and operating the program. For example, when initially established, considerable constructive input was provided by the SAPhA leadership, and ever since its inception, the entire program has been regularly monitored by a joint NPC-SAPhA committee.

In light of the beneficial nature of this internship learning experience, efforts have been made to get individual state boards of pharmacy to award credit for participation in such programs. This credit—to a maximum of 500 hours of the total 1,500 hours typically specified—would partially fulfill the experimental training requirements of state boards of pharmacy as one of the requisites for pharmacy licensure. To date, some 32 state boards of pharmacy either will allow, or will consider, various amounts of time in nontraditional practice experience as counting toward the total internship requirement.

Regrettably, however, the remaining states have refused to give credit for participation in either the NPC-SAPhA industry program, or for various other equally commendable, nontraditional practice experiences. The latter include the Veterans Administration Hospital Pharmacy Undergraduate Training Programs, the U.S. Public Health Service COSTEP Training Program, national or state pharmaceutical association internships, or a host of other programs conducted under the auspices of colleges, governmental agencies, or drug companies.

Both the SAPhA House of Delegates and the National Association of Boards of Pharmacy adopted resolutions at their 1981 Annual Meetings calling on individual state pharmacy boards to recognize and credit nontraditional practice experience. Recognition and credit would be conditioned upon a determination that a particular program met established criteria including preceptor orientation and written reports.

At its recently concluded 1982 Annual Meeting, the APhA House of Delegates considered the adoption of a similar policy position for the Association.

Hopefully, the 20 reluctant boards of pharmacy will give due consideration to this matter. Pharmacy today is not practiced as it was 50 years ago; as a result, it makes little sense that the only practice experience that will be accepted toward licensure should be exclusively oriented toward the way pharmacy was practiced in 1932 rather than in 1982.

—EDWARD G. FELDMANN
American Pharmaceutical Association
Washington, DC 20037

0022-3549/82/0600-0605$01.00/0

JOURNAL OF PHARMACEUTICAL SCIENCES

JUNE 1982
VOLUME 71 NUMBER 6

RESEARCH ARTICLES

Factors Influencing Axial and Radial Tensile Strengths of Tablets

PAUL J. JAROSZ * and EUGENE L. PARROTT ˣ

Received June 8, 1981, from the *Division of Pharmaceutics, College of Pharmacy, University of Iowa, Iowa City, IA 52242.* Accepted for publication October 13, 1981. *Present address: Ortho Pharmaceutical Corp., Raritan, NJ 08869.

Abstract □ The axial and radial tensile strengths of compressed tablets have been measured by a tensiometer. A comparison of these strengths is indicative of the bonding strength in two directions and may be related to the tendency toward capping. The influence of compressional force, concentration of binder, and time on the tensile strengths of several materials is presented.

Keyphrases □ Tensile strength—factors influencing axial and radial tensile strengths in tablets □ Tablets—factors influencing axial and radial tensile strengths □ Compressional force—factors influencing axial and radial tensile strengths of tablets

Tablets must possess sufficient strength to withstand mechanical handling and transport. Various types of tests (abrasion, bending, indentation hardness, diametral crushing) have been used to express strength (1); however, the data from these tests seldom can be correlated in a precise manner. Even the most common strength test of diametral crushing may cause failure of the tablet by more than one type of force (2, 3). If the test method is designed so that tablet failure is a result of the application of tensile strength only, strength may be expressed precisely in terms of kilograms per square centimeter (4–7).

Most pharmaceutical tablets are anisotropic and nonhomogeneous, with the values of their properties (*e.g.*, density and strength) varying in different directions. The purpose of this investigation was to measure the axial and radial tensile strengths of tablets as influenced by compressional force, concentration of binder, and aging.

EXPERIMENTAL

Preparation of Tablets—Powders to be granulated were blended in a planetary mixer[1]. The appropriate amount of granulating solution was added and mixed for 5 min. The mass was passed through an oscillating granulator[2], collected on drying trays, and dried overnight in a forced-air oven at ambient temperature. A 16/20-mesh size fraction of the dried granulation was separated by standard sieves. Directly compressible materials were separated by standard sieves into a 60/80-mesh size fraction. An appropriate weight of the material to produce tablets from 0.3 to 0.5 cm thick was compressed by means of 1.275-cm flat-faced punches and the die fitted to a hydraulic press[3] for 5 sec at the desired compressional force. The die wall was prelubricated with 5% magnesium stearate in acetone. At least 72 hr elapsed between tablet compression and measurement of tablet strength to allow for any stress relaxation. The weight and thickness of 10 tablets were determined.

Measurement of Radial Tensile Strength—The radial tensile strength of the tablet was measured by a diametral compression test. The tensiometer[4] was modified for compression by the use of a compression device used for calibration of the mercury manometer of the tensiometer. Steel bolt heads served as platens for the radial compression test. To ensure that the tablet failed in tension, a padding, consisting of three layers of manila computer cards 1 mm thick, was used (5, 6, 8). The length of each paper strip was sufficient to extend over the edge of the bolt head. The pad was replaced after ~200 tablets had been fractured. The tablet was strained at the rate of 0.299 cm/min. The maximum force for tablet failure resulting from tensile stress (3, 4) was determined, and the force–displacement profile was recorded. The maximum tensile failure force F_σ of 10 tablets was determined, and the average was used to calculate the radial tensile strength (σ_x) by the relationship:

$$\sigma_x = \frac{2F_\sigma}{\pi Dt} \qquad \text{(Eq. 1)}$$

where D is the diameter (1.275 cm) and t is the thickness of the tablet (9).

Measurement of Axial Tensile Strength—The tablet was linearly aligned and fixed between the machined heads of two 1.275 × 2.54-cm steel bolts by means of a cyanoacrylate resin adhesive[5]. The adhesive was cured at room temperature for at least 36 hr prior to testing. By use of a pair of adapters, the bolt–tablet–bolt assemblage was fitted horizontally into the tensiometer. The tablet was strained at the rate of 0.229 cm/min. The tensiometer allowed the recording of the stress component against the extension, proportional to the distance moved by the crosshead beam. The distance traveled by the crosshead beam was magnified 16 times and recorded on the drum chart paper. The value of the maximum force was recorded only if failure was due to tension stresses. Tablet failure occurred in the body of the tablet and not near the tablet–bolt interface. The av-

[1] KitchenAid, Hobart Corporation, Troy, Ohio.
[2] Type FGS, Erweka-Apparatebau, GmbH, Heusenstamm Kr., Offenbach Main, West Germany.
[3] Carver press, model C, Menomonee Falls, Wis.
[4] Hounsfield Tensiometer, Type W, Tensiometer Ltd., Croydon, England.
[5] Eastman 910 Adhesive, Eastman Kodak, Kingsport, Tenn.

0022-3549/82/0600-0607$01.00/0

Table I—Density of Materials and Granulations

Material	Density, g/cm³
Microcrystalline cellulose[a]	1.34
Benzoic Acid	1.36[b]
Dibasic calcium phosphate[c]–povidone[d] (1.0%)	2.45
Dibasic calcium phosphate[c]–povidone[d] (7.0%)	2.43
Dibasic calcium phosphate[e]–starch (1.2%)	2.13
Dibasic calcium phosphate[e]–starch (4.5%)	2.12
Heptane, normal	0.679
Hydrous lactose[f]–povidone (1.0%)	1.44
Hydrous lactose[f]–povidone (9.0%)	1.44
Hydrous lactose[f]–starch (1.9%)	1.46

[a] Avicel PH 102, FMC Corp., Marcus Hook, PA 19061. [b] S. Shah, Ph.D. Thesis, The University of Iowa, Iowa City, Ia., 1975. [c] Ruger Chemical Co., Inc. [d] Plasdone K 29–32, GAF Corp., New York, NY 10020. [e] Emcompress, Edward Mendell Co. [f] USP, Humko-Sheffield, Memphis, TN 38101.

erage maximum force of axial tensile failure of 10 tablets was used to calculate the axial tensile strength by the relationship (10):

$$\sigma_z = \frac{4F_a}{D^2} \qquad \text{(Eq. 2)}$$

Measurement of Density—The densities of the materials and granulations were determined by pycnometry using *n*-heptane at 25° and are given in Table I. The measured dimensions and weight of each cylindrical tablet were used to calculate the apparent density of the tablet. The relative density used in the Heckel plot is the quotient of the apparent density of the tablet and the density of the material. The values of porosity used in the Ryshkewitch relationship were calculated from the relationship:

$$\text{porosity} = (1 - \rho_{\text{apparent}}/\rho) \qquad \text{(Eq. 3)}$$

Conservation curves, rather than tables of the dimensions and calculations, are presented for each tablet.

RESULTS AND DISCUSSION

The consolidation of a powder to form a tablet proceeds through several stages during compression (11, 12). As a force is applied to a powder, interparticular rearrangement causes consolidation to the closest packing. Additional compressional force results in deformation of the particles by brittle fragmentation; plastic, nonrecoverable conformation changes; and/or elastic, recoverable conformation changes. Eventually, maximum consolidation is attained at which an increase in compressional force no longer reduces the relative volume of the tablet. It has been shown (13), in terms of density, that the distribution of compressional pressure within a tablet exists. It was previously demonstrated that the bond formation is greater in a region where, because of compressional pressure, distribution is more intense (14).

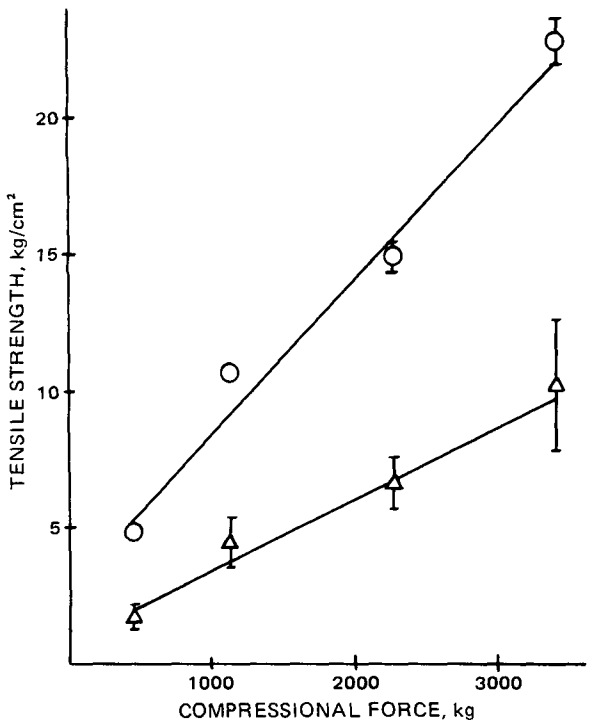

Figure 1—*The influence of compressional force on tensile strengths of tablets compressed of 60/80-mesh size dibasic calcium phosphate dihydrate*[6]. *Key: (△) axial; (○) radial.*

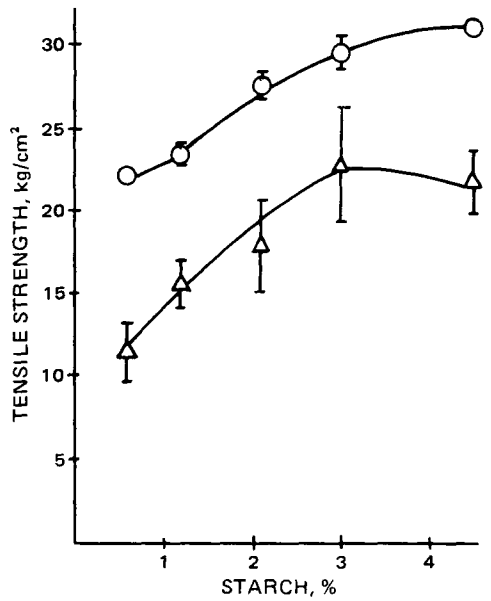

Figure 2—*The influence of starch on the tensile strengths of tablets of dibasic calcium phosphate dihydrate*[6] *compressed at 2268 kg. Key: (△) axial; (○) radial.*

For an isotropic, homogeneous tablet, the radial and axial tensile strengths should be equal. The distribution of compressional force, differences in density within a tablet, and the mixture of materials contribute to the nonhomogeneity of the tablet and to the nonuniformity of tensile strengths. To demonstrate this, the axial and radial tensile strengths were measured experimentally. Typical results for several materials are given in Table II in which there is a difference in the axial and radial tensile strengths for each material.

As shown in Table II, the variance of radial tensile strength is less than the variance of the axial tensile strength. The experimental conditions

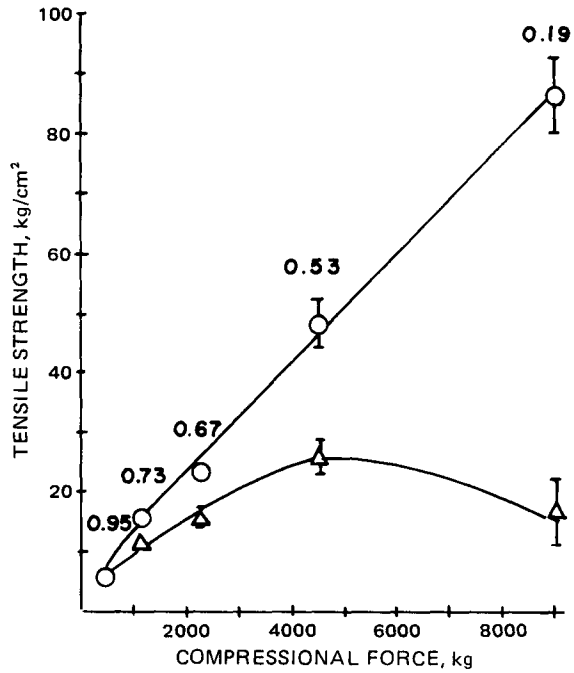

Figure 3—*The influence of compressional force on tensile strengths of tablets of dibasic calcium phosphate dihydrate*[6] *granulated with 1.2% starch. At each compressional force the value is given for* σ_z/σ_x. *Key: (△) axial; (○) radial.*

Table II—Strength Characteristics of 1.275-cm Diameter Cylindrical Tablets of Several Directly Compressible Materials

Material	Compressional Force, kg	Mean Force of Axial Tensile Failure, kg[d]	Axial Tensile Strength, σ_z, kg/cm^2	Mean Force of Radial Tensile Failure, kg[d]	Thickness, cm[d]	Radial Tensile Strength, σ_x, kg/cm^2	$\frac{\sigma_z}{\sigma_x}$
Dibasic calcium phosphate dihydrate[a]	454	2.2 (0.8)[e]	1.7 (0.4)[f]	4.6 (0.2)[e]	0.479 (0.005)[e]	4.8 (0.1)[f]	0.35
	1134	5.6 (1.6)	4.4 (0.9)	9.5 (0.4)	0.443 (0.004)	10.7 (0.3)	0.41
	2268	8.4 (1.6)	6.6 (0.9)	12.4 (0.6)	0.414 (0.001)	14.9 (0.5)	0.44
	3402	13.0 (4.2)	10.2 (2.4)	18.5 (0.9)	0.404 (0.003)	22.8 (0.8)	0.45
Lactose, anhydrous[b]	907	15.1 (3.0)	11.8 (1.6)	12.9 (0.5)	0.428 (0.001)	15.1 (0.4)	0.78
Microcrystalline cellulose[c]	454	19.6 (1.4)	15.4 (0.8)	28.4 (0.4)	0.429 (0.007)	33.0 (0.4)	0.47
Aspirin	1361	14.0 (1.9)	11.0 (1.1)	13.4 (0.6)	0.437 (0.002)	15.3 (0.5)	0.72
Benzoic acid	454	14.2 (1.4)	11.1 (0.7)	16.2 (1.0)	0.494 (0.012)	16.4 (0.7)	0.68
	1134	15.2 (1.2)	11.9 (0.6)	17.4 (0.6)	0.482 (0.013)	18.0 (0.4)	0.66
	3402	17.0 (3.0)	13.3 (1.6)	14.0 (1.2)	0.479 (0.008)	14.7 (0.9)	0.90

[a] Emcompress, Edward Mendell Co., Carmel, N.Y. [b] Lactose Direct Tabletting, Humko-Sheffield. [c] Avicel PH 102, FMC Corp. [d] Average of 10 tablets. [e] Standard deviation. [f] Confidence interval at 95% probability.

of the diametral compression (radial) test are specifically controlled to ensure tablet failure only because of tension stresses. The axial test has the disadvantage of requiring the adapter–bolt–tablet assemblage to be placed horizontally in the tensiometer. Bending stress due to the mass of the adapter and the torsion stress due to loading are present in each sample. These additional stresses add to the deviation in applied tension stress required to cause failure of the tablet. A similar set of experimental values using another apparatus has been reported (15).

The radial tensile strength is greater than the axial tensile strength with a brittle material (dibasic calcium phosphate dihydrate[6]). The difference may be a reflection of the number of clean particle bonds and of original particle bonds oriented in the axial and radial direction. In brittle fracture, clean surfaces are formed during compression, and two fresh, clean surfaces bond to form the strongest bond. A newly formed surface may bond to an original surface of another particle, whereas two original surfaces, which bond during compression, probably form the weakest bond.

When a brittle material is compressed along the vertical (axial) axis, the stress upon each particle does not necessarily compress the particle along the axial direction because of the random packing and alignment of the particles toward each other during the stages of compression; however, a greater potential exists for vertical stress on the particles during the relocation and fragmentation stages due to the movement of the punch. The overall result is that more clean surfaces are created when they are normal to the radial than to the axial direction. As the compressional force is increased, a brittle fracture results in a stronger, radial tensile strength than axial tensile strength (Fig. 1). The slope (0.00577, $r = 0.990$) of the radial tensile strength–force line is twice that of the slope (0.00275, $r = 0.993$) of the axial tensile strength–force line.

The Griffith fracture theory (16) proposes that failure results from the existence of flaws or cracks within the sample. If more bonds are formed in the radial direction, the potential for the presence of a flaw or crack is greater in the axial than the radial direction. This concept appears to be supported by the results shown in Fig. 1.

Influence of Compressional Force and Concentration of Binder—In tableting technology, a blend of pharmaceutical powders is commonly granulated with a granulating or binding solution. The incorporation of the binder increases the adhesiveness of the formulation. As shown in Fig. 2, the radial tensile strength of tablets compressed at 2268 kg of force from dibasic calcium phosphate dihydrate[6] granulated with starch paste is increased as the concentration of starch is increased. The axial tensile strength is increased to its greatest value at 3% starch and is not increased by an additional increase in the starch concentration.

The effect of compressional force on the tensile strength of tablets compressed from dibasic calcium phosphate dihydrate[6] with 1.2% starch is shown in Fig. 3. For the given concentration of binder, the axial tensile strength is increased to a maximum value at 4536 kg of force and is not increased at greater compressional forces.

The tensile strengths of tablets compressed from dibasic calcium

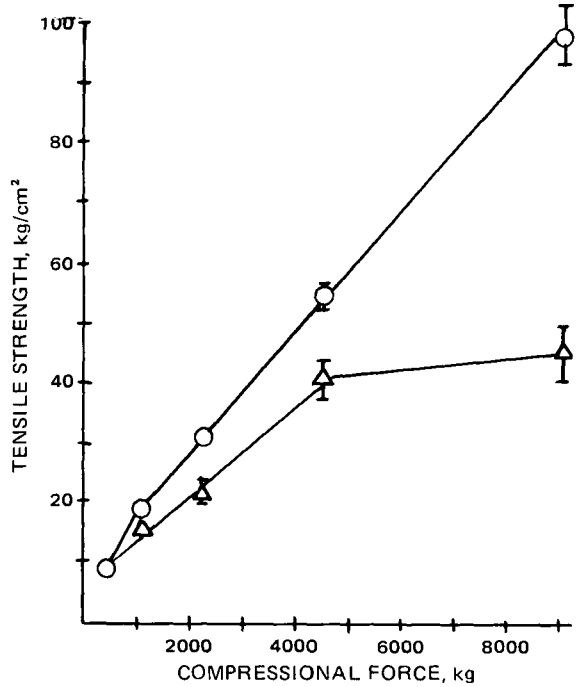

Figure 4—*The influence of compressional force on the tensile strengths of tablets compressed of dibasic calcium phosphate dihydrate[6] granulated with 4.5% starch. Key: (△) axial; (○) radial.*

[6] Emcompress, Edward Mendell Co., Carmel, N.Y.

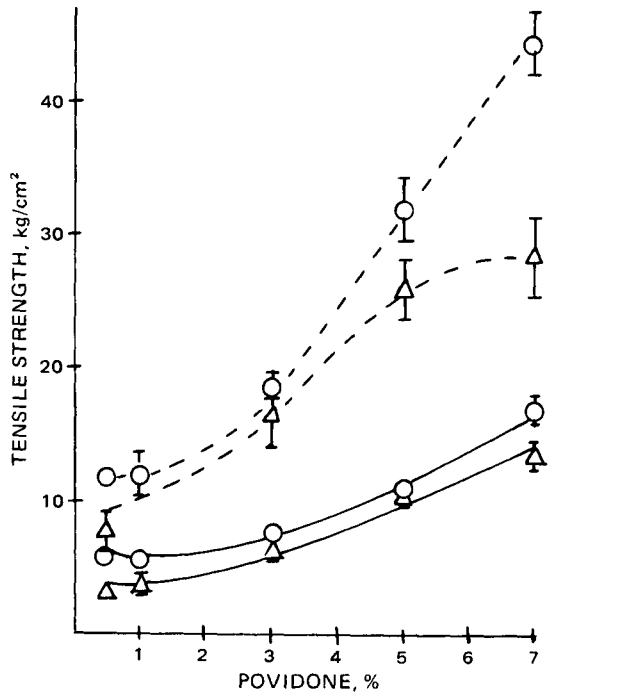

Figure 5—*The influence of povidone on the tensile strengths of tablets of dibasic calcium phosphate dihydrate[7] compressed at 2268 (——) and at 4536 kg (- - - -). Key: (△) axial; (○) radial.*

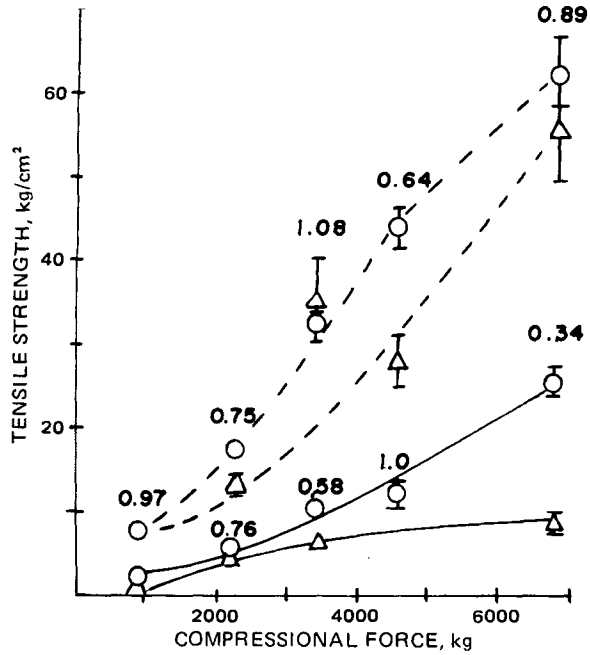

Figure 6—*The influence of compressional force on the tensile strengths of tablets of dicalcium phosphate dihydrate granulated with 1.0 (—) and with 7.0% (- - - -) povidone. At each compression force the value is given for σ_z/σ_x. Key: (△) axial; (○) radial.*

phosphate dihydrate[6] with 4.5% starch are shown in Fig. 4. The rate of increase of radial tensile strength with an increase in compressional force is essentially the same as that of the tablet containing 1.2% starch. The maximum axial tensile strength is attained at the same compressional force as for the tablet containing 1.2% starch, but there is no decrease in axial strength as the compressional force is increased further. This difference in the axial and radial tensile strength–force profiles indicates that consolidation is not uniform throughout the entire tablet mass.

Similarly, for tablets compressed at 2268 and 4536 kg of force from dibasic calcium phosphate dihydrate[7] granulated with povidone, the tensile strengths are increased as the concentration of povidone is increased (Fig. 5). The influence of compressional force on tensile strength of tablets of dibasic calcium phosphate dihydrate[7] and povidone is illustrated in Fig. 6. As the compressional force is increased, the slope of the radial tensile strength *versus* percent of binder increases more rapidly than the slope of the axial tensile strength. A maximum axial tensile strength is attained at 5–6% povidone when compressed at 4536 kg.

The influence of compressional force on the tensile strengths of tablets

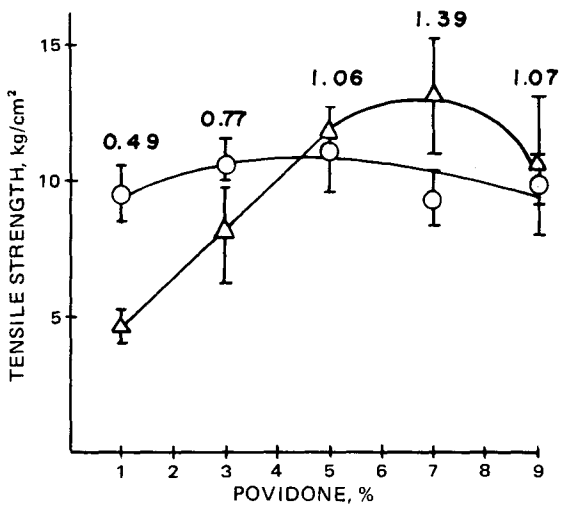

Figure 7—*The initial influence of povidone on the tensile strengths of tablets of hydrous lactose compressed at 1134 kg. At each compressional force the value is given for σ_z/σ_x. Key: (△) axial; (○) radial.*

[7] Ruger Chemical Co., Irvington, N.J.

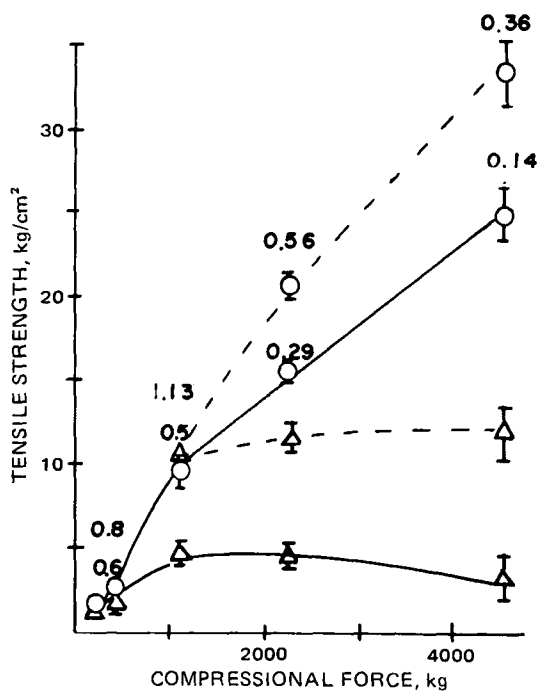

Figure 8—*The influence of compressional force on the tensile strengths of tablets of hydrous lactose granulated with 1 (—) and 9.0% (- - - -) povidone. At each compressional force the value is given for σ_z/σ_x. Key: (△) axial; (○) radial.*

of dibasic calcium phosphate dihydrate[7] granulated with 1.0 and 7.0% povidone is shown in Fig. 6. The strength of tablets compressed from dibasic calcium phosphate dihydrate[6] is increased only moderately with an increase in compressional force. At low concentrations of binder, the effect of compressional force on dibasic calcium phosphate dihydrate[7] is moderate, but at high concentrations, 7% of binder, the tensile strength is significantly increased with an increase in compressional force (Fig. 6).

The influence of povidone concentration on the tensile strength of hydrous lactose tablets compressed at 1134 kg of force is shown in Fig. 7. The concentration of povidone has little effect on the radial tensile strength. As the concentration of povidone is increased, the axial tensile strength is increased rapidly to values that exceed the radial tensile strength. Thus, povidone axially strengthens a tablet of hydrous lactose to a greater extent than a tablet of dibasic calcium phosphate dihydrate.

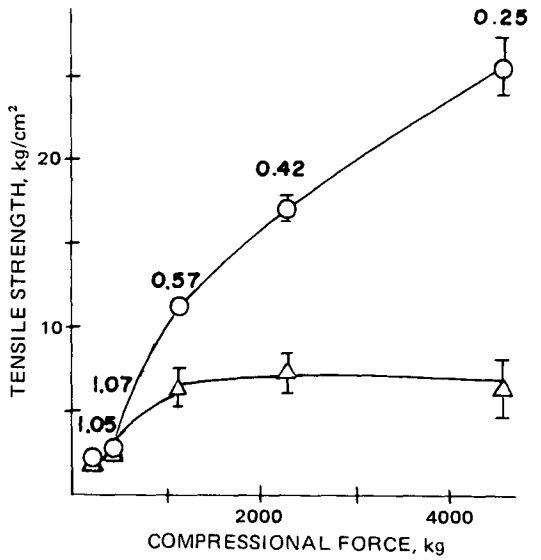

Figure 9—*The influence of compressional force on tensile strengths of tablets of hydrous lactose granulated with 1.9% starch. At each compressional force the value is given for σ_z/σ_x. Key: (△) axial; (○) radial.*

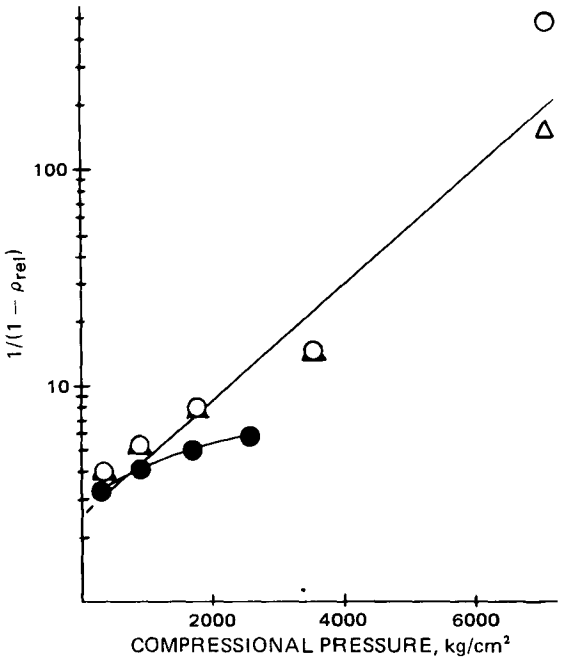

Figure 10—*Density–compressional pressure relationship according to Heckel plot. Key: (●) dibasic calcium phosphate dihydrate[6]; (○) with 1.2% starch; (△) with 4.5% starch.*

Since the granulating solvent was water, in which lactose is soluble, the lactose may have partially dissolved at the surface of the granules and upon drying formed bridges, which mechanically strengthened the tablet (17, 18).

The influence of compressional force on the tensile strengths of tablets composed of hydrous lactose with 1.0 and 9.0% povidone is shown in Fig. 8. There is a maximum axial tensile strength attained at a low concentration of binder with an observed tendency for capping at high compressional forces. Lactose behaves as a Mohr body (19) and is known to be prone to capping (20). A similar result is shown in Fig. 9 for tablets of hydrous lactose granulated with 1.9% starch.

Behavior of Material—Heckel (21, 22) characterized the behavior of materials during compression by the relationship:

$$\log \frac{1}{1-\rho_{rel}} = \frac{KP}{2.303} + A \qquad \text{(Eq. 4)}$$

where ρ_{rel} is the relative density, P is the compressional pressure, and K and A are constants. The slope (K) has been related to the reciprocal of the mean yield pressure, which is the minimum pressure required to cause

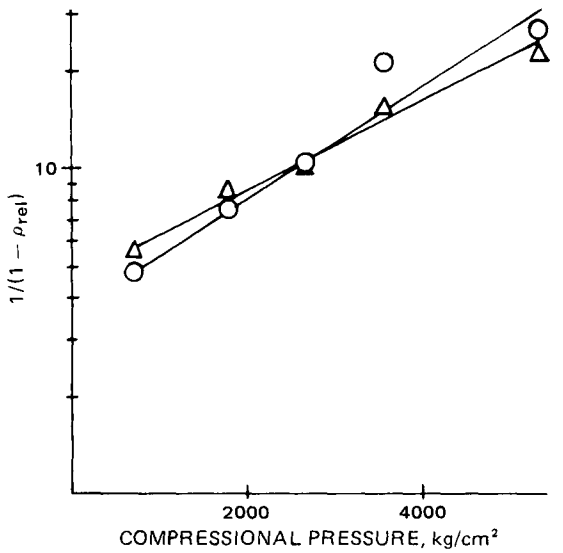

Figure 11—*Density–compressional pressure relationship according to Heckel plot for dibasic calcium phosphate dihydrate[7] granulated with povidone. Key: (△) 1.0% povidone; (○) 7.0% povidone.*

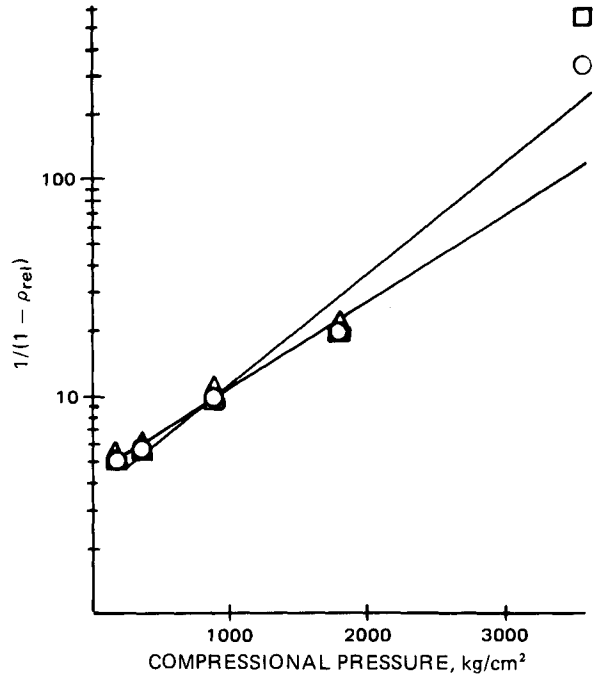

Figure 12—*Density–compressional pressure relationship according to Heckel plot of hydrous lactose granulated with povidone and starch. Key: (△) 1.0% povidone; (○) 9.0% povidone; (□) 1.9% starch.*

deformation of the material undergoing compression (23). The intercept of the curved portion of the curve at low pressure represents a value due to densification by particle rearrangement. The intercept obtained from the slope of the upper portion of the Heckel plot is a reflection of the densification obtained during consolidation. A large value of the slope indicates the onset of plastic deformation at relatively low pressures (24). A Heckel plot for tablets of dibasic calcium phosphate dihydrate[6] is shown in Fig. 10. The small value of the slope indicates consolidation of dibasic calcium phosphate dihydrate is not by plastic deformation but primarily by brittle fracture (25).

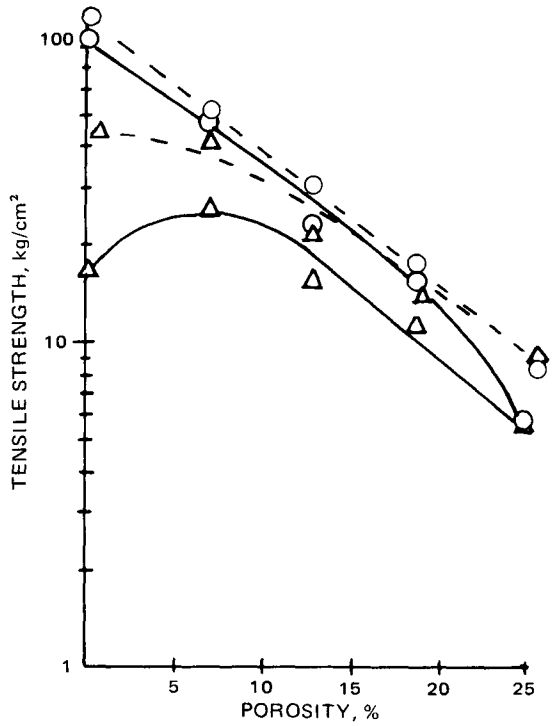

Figure 13—*Tensile strengths–porosity relationship of logarithmic form of the Ryshkewitch equation for dibasic calcium phosphate dihydrate[6] granulated with 1.2 (——) and 4.5% (- - - -) starch. Key: (△) axial; (○) radial.*

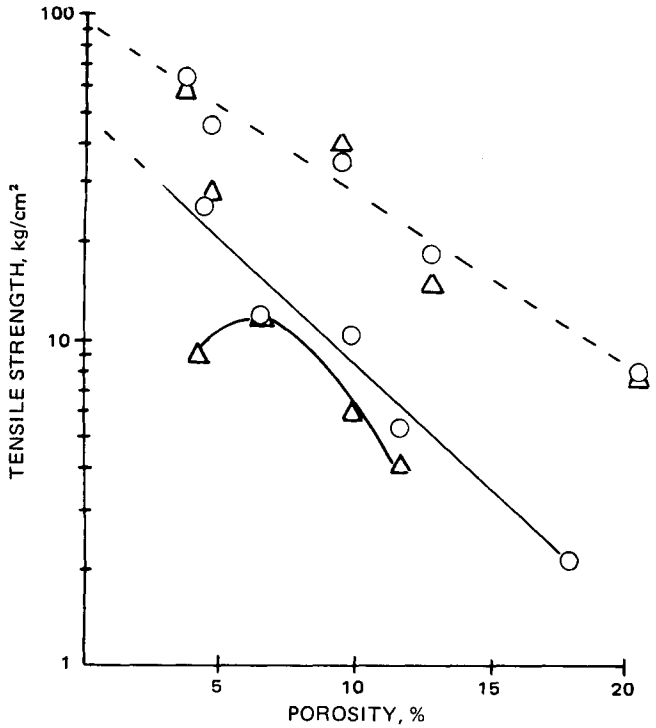

Figure 14—*Tensile strengths–porosity relationship of logarithmic form of Ryshkewitch equation for dibasic calcium phosphate dihydrate[7] granulated with 1.0 (—) and 7.0% (- - - -) povidone. Key: (△) axial; (○) radial.*

The effect of the addition of starch to dibasic calcium phosphate dihydrate[6] is shown in Fig. 10. The lower mean yield pressures (1442 and 1904 kg/cm^2 with 1.2 and 4.5% binder, respectively) for dibasic calcium phosphate[6] granulated with starch, than the mean yield pressure (4303 kg/cm^2) for dibasic calcium phosphate dihydrate indicate that the addition of starch confers some plastic property to the mass. The density–compressional pressure relationship of dibasic calcium phosphate dihydrate[7] granulated with povidone is plotted in Fig. 11. The lower mean yield pressure (2535 kg/cm^2) for dibasic calcium phosphate dihydrate[7] granulated with 7.0% povidone than the mean yield pressure (3282 kg/cm^2) with 1.0% povidone indicates the onset of plastic deformation with an increase in concentration of the binder.

The Heckel plots for lactose granulated with povidone and for lactose granulated with starch are shown in Fig. 12. The mean yield pressure is

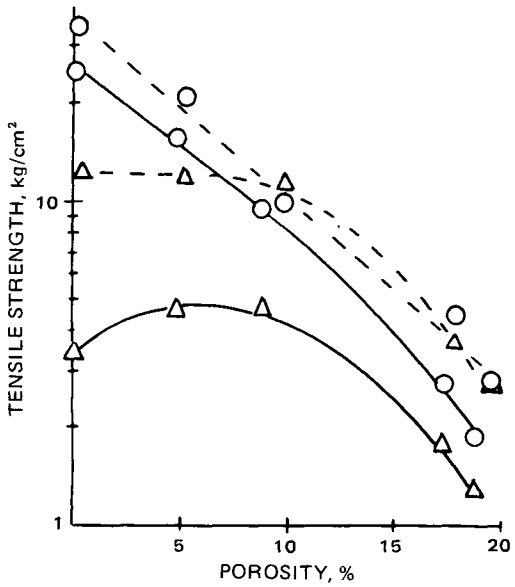

Figure 15—*Tensile strengths–porosity relationship of logarithmic form of the Ryshkewitch equation for hydrous lactose granulated with 1.0 (—) and 9% (- - - -) povidone. Key: (△) axial; (○) radial.*

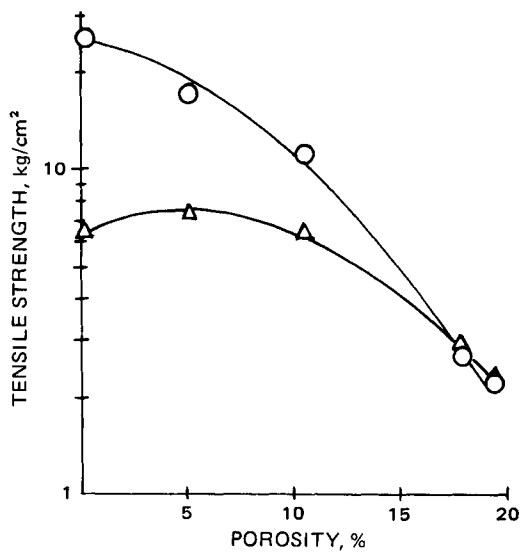

Figure 16—*Tensile strengths–porosity relationship of logarithmic form of Ryshkewitch equation for hydrous lactose granulated with 1.9% starch. Key: (△) axial; (○) radial.*

decreased as the concentration of plastically deformed povidone is increased. The addition of a plastic binder to an excipient tends to confer some plasticity to the excipient.

Ryshkewitch (26) observed that:

$$\log \sigma_x = \log \sigma_{max} - bp \qquad \text{(Eq. 5)}$$

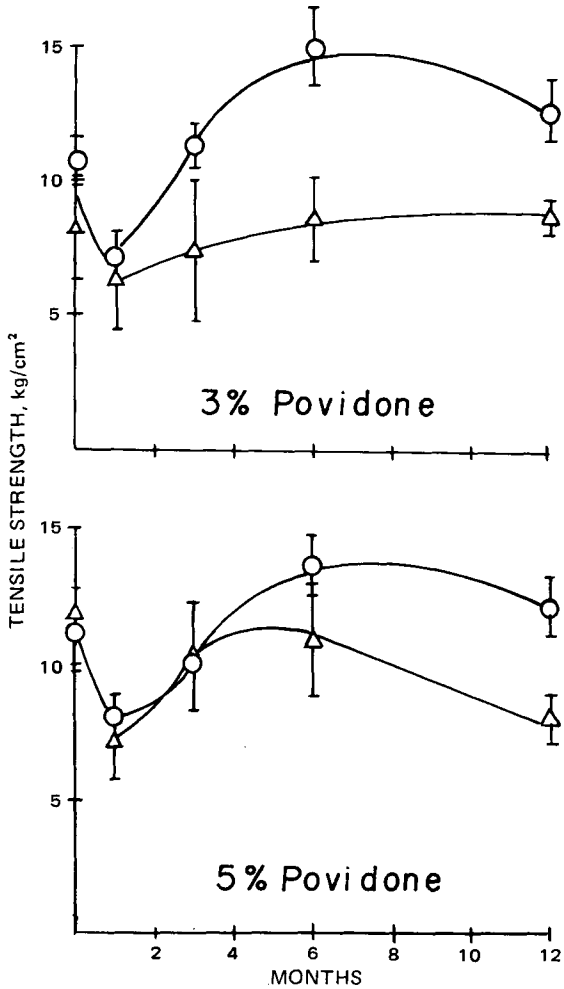

Figure 17—*The influence of time on the tensile strength of tablets of hydrous lactose granulated with 3 and 5% povidone. Key: (△) axial; (○) radial.*

Table III—Values of Constants b and σ_{max} of the Ryshkewitch Equation

	b	σ_{max}	r
Lactose granulated with 1.9% starch	5.7	31.8	0.981
Lactose granulated with 1.0% povidone[a]	5.5	27.4	0.996
Lactose granulated with 9.0% povidone	5.3	36.1	0.996
Dibasic calcium phosphate dihydrate[b] granulated with 1.0% povidone	7.6	48.2	0.979
Dibasic calcium phosphate dihydrate[b] granulated with 7.0% povidone	5.1	89.3	0.991
Dibasic calcium phosphate dihydrate[c] granulated with 1.2% starch	4.6	95.4	0.993
Dibasic calcium phosphate dihydrate[c]	4.1	106.6	0.999

[a] Regression of four points only. [b] Ruger Chemical Co. [c] Emcompress, Edward Mendell Co.

where σ_x is the radial tensile strength, σ_{max} is the theoretical radial tensile strength at zero void, b is a constant, and p is porosity.

In Fig. 13 the logarithms of tensile strengths are plotted against the porosity of tablets compressed from dibasic calcium phosphate dihydrate[6] granulated with 1.2 and 4.5% starch, and the increase in starch increases the radial tensile strength 47%, even though the porosity remains at 25%. The increase in starch increases the radial tensile strength only 12% as zero void is approached.

The Ryshkewitch relationship of tensile strength to the porosity of dibasic calcium phosphate dihydrate[7] granulated with 1.0 and 7.0% povidone is shown in Fig. 14. The maximum axial tensile strength occurs at 6–7% porosity, which is the same porosity as for dibasic calcium phosphate dihydrate[6,7] and starch.

Similarly, the Ryshkewitch relationships for hydrous lactose with 1.0 and 9.0% povidone are plotted in Fig. 15. A nine-fold increase in concentration of povidone causes a 58% increase in radial tensile strength near 20% porosity and only a 34% increase near zero void. The Ryshkewitch relationship for hydrous lactose with starch is shown in Fig. 16. Values for the constants of the Ryshkewitch equation are given in Table III.

It appears that the concentration of the binder has a greater influence in more porous tablets than in those approaching zero void. As compressional force is increased and the porosity of the tablet is decreased, the interparticular distances through which adhesive forces operate are shorter. Thus, the adhesive forces of the material are stronger at lower porosity, and a lesser amount of binder would be required to produce a tablet of the desired strength.

Index of Capping—The elastic property of a material is responsible for the capping or failure of a tablet perpendicular to its compressional axis. When the compressional force is removed, shear deformation occurs as the elastic material rebounds (27). Strains are magnified about regions of low density, and upon release of the force, there may be a mechanical failure.

Binders are added to materials having poor adhesive property to strengthen intergranular binding and, thus, reduce the tendency to cap. For elastic materials the elastic energy released, when the punch pressure is relieved, overcomes the bonds present between particles in that region and capping occurs. Binders are plastic materials, and under compression these materials undergo plastic deformation. The total energy of compression is dissipated throughout the entire material being compressed. A greater part of the total energy of compression is absorbed by the binder at greater concentrations, and less energy is stored elastically by the elastic deformation of the other materials of the formulation. Upon removal of the compressional force, there is less elastic recovery and a reduced tendency toward capping.

A weak axial tensile strength has been associated with capping (1, 10, 28). A comparison of Figs. 3 and 4 shows that the maximum axial tensile strength for a tablet of dibasic calcium phosphate dihydrate[6] containing 4.5% starch is reached at the same compressional force as for a tablet containing 1.2% starch, but there is no decrease in axial strength after reaching the maximum value for the tablet containing 4.5% starch. The slopes of the radial tensile strength–force curves are nearly identical. The difference in axial and radial tensile strengths indicates that the tablet is not as strongly bonded in the axial direction as in the radial direction. As the axial and radial tensile strengths are measures of bonding, it appears that the ratio σ_z/σ_x could be used as an index of capping. The ratio would be unity for a homogeneous tablet and would decrease toward zero as the homogeneity became progressively less.

The data presented in Fig. 6 for the tablets of dibasic calcium phosphate dihydrate[7] with 1.0 and 7.0% povidone support the statement that an increase in concentration of binder reduces capping. At the highest compressional force (6804 kg) the ratio σ_z/σ_x is 0.34 and 0.89 for 1.0 and 7.0% povidone, respectively. Capping does not occur as the dibasic calcium phosphate dihydrate is a brittle material, and fragmentation occurs and is the mode of consolidation.

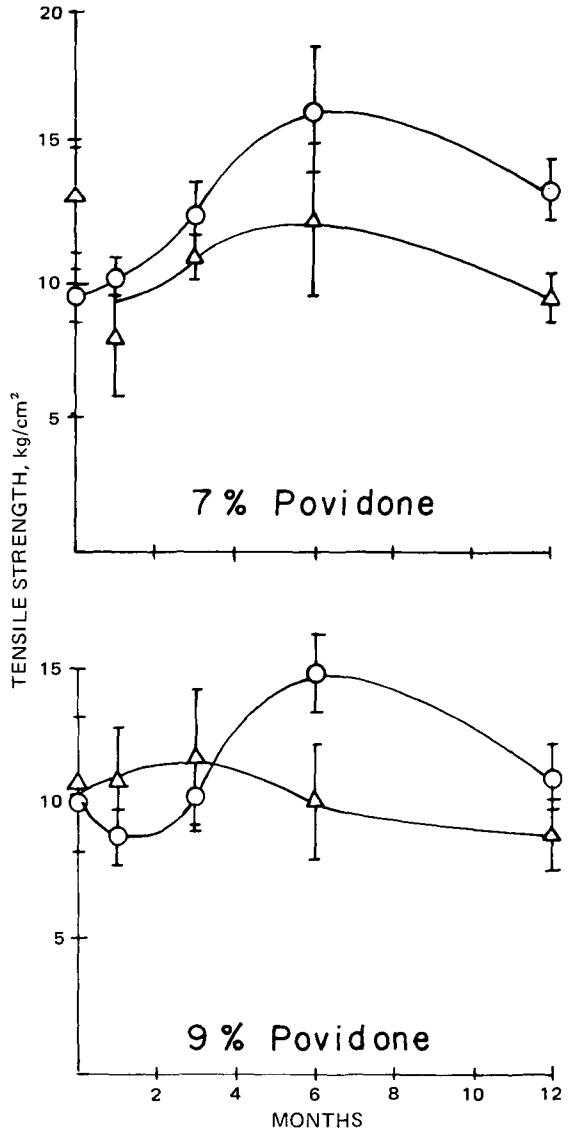

Figure 18—*The influence of time on the tensile strength of tablets of hydrous lactose granulated with 7 and 9% povidone. Key: (△) axial; (○) radial.*

With nonbrittle materials, considerable consolidation may be due to elastic bonding. As elastic rebound will occur when the compressional force is removed, the tablet will have a capping tendency. For such materials, a low value for σ_z/σ_x indicates that capping is likely. To properly evaluate the probability of capping, the mechanism of bonding or consolidation and the ratio of the axial and radial tensile strengths must be considered. Hydrous lactose with povidone attains a maximum axial tensile strength at a low concentration of binder with a tendency for capping at high compressional forces. At the highest compressional force (4536 kg) for hydrous lactose tablets, containing 1.0 and 9.0% povidone, the ratio σ_z/σ_x is 0.14 and 0.36, respectively.

Aging—Changes in strength of tablets have been reported to be a function of strain recovery (29), time (30), and loss of moisture (31, 32). Five formulations of tablets weighing 800 mg were prepared by compression at 1134 kg of force for hydrous lactose containing from 1.0 to 9.0% povidone. The tablets were stored in tightly closed glass containers at 43% relative humidity and ambient temperature. The axial and radial tensile strengths measured initially and at 1, 3, 6, and 12 months are shown in Fig. 17 for hydrous lactose with 3.0 and 5.0% povidone. Similar plots are shown in Fig. 18 for hydrous lactose tablets with 7.0 and 9.0% povidone. The implication is that the tensile strength did not change to a significant extent after 1 year in storage. A report (33) that the hardness

of hydrochlorothiazide tablets composed of lactose and povidone did not change after 1 year at room temperature supports this implication.

REFERENCES

(1) A. Ritter and H. Sucker, *Pharm. Tech.*, **4**, No. 9, 108 (1980).
(2) K. Ridgway, *Pharm. J.*, **205**, 709 (1970).
(3) W. C. Rudnick, A. R. Hunter, and F. C. Holden, *Mater. Res. Stand.*, **1**, 283 (1963).
(4) J. T. Fell and J. M. Newton, *J. Pharm. Sci.*, **59**, 688 (1970).
(5) P. J. F. Wright, *Mag. Concr. Res.*, **7**, 87 (1955).
(6) L. L. Simon, *Constructional Rev.*, **29**, 23 (1956).
(7) J. T. Fell and J. M. Newton, *J. Pharm. Pharmacol.*, **20**, 657 (1968).
(8) N. B. Mitchell, *Mater. Res. Stand.*, **1**, 780 (1961).
(9) M. M. Frocht, "Photoelasticity," Vol. 2, Wiley, New York, N.Y., 1948, p. 127.
(10) C. Nystrom, W. Alex, and K. Malmqvist, *Acta Pharm. Suec.*, **14**, 317 (1977).
(11) D. Train, *J. Pharm. Pharmacol.*, **8**, 74S (1956).
(12) E. L. Parrott, in "Pharmaceutical Dosage Forms: Tablets," Vol. 2, H. A. Lieberman and L. Lachman, Eds., Dekker, New York, N.Y., 1981.
(13) D. Train, *Trans, Inst. Chem. Engrs.*, **35**, 258 (1957).
(14) D. Train and J. A. Hersey, *Powder Metall.*, **6**, 20 (1960).
(15) E. Turba and H. Rumpf, *Chem. Eng. Tech.*, **36**, 230 (1964).
(16) A. A. Griffith, *Proc. 1st Int. Cong. Appl. Mech.*, **1924**, 55.
(17) W. O. Opakunle and M. S. Spring, *J. Pharm. Pharmacol.*, **28**, 915 (1976).
(18) K. T. Jaiyeoba and M. S. Spring, *ibid.*, **32**, 1 (1980).
(19) E. Shotton and B. A. Obiorah, *J. Pharm. Sci.*, **64**, 1213 (1975).
(20) N. L. Henderson and A. J. Bruneo, *ibid.*, **59**, 1336 (1970).
(21) R. W. Heckel, *Trans. Metall. Soc. AIME*, **221**, 671 (1961).
(22) R. W. Heckel, *ibid.*, **221**, 1001 (1961).
(23) R. York, *J. Pharm. Pharmacol.*, **30**, 6 (1978).
(24) P. York and N. Pilpel, *J. Pharm. Pharmacol.*, Suppl., **25**, 1P (1973).
(25) K. A. Khan and C. T. Rhodes, *J. Pharm. Sci.*, **64**, 444 (1975).
(26) E. Ryshkewitch, *J. Am. Ceramic Soc.*, **36**, 65 (1953).
(27) J. A. Seitz and G. M. Flessland, *J. Pharm. Sci.*, **54**, 1353 (1965).
(28) C. Nystron, K. Malmqvist, J. Mazur, W. Alex, and A. W. Holzer, *Acta Pharm. Suec.*, **15**, 226 (1978).
(29) M. E. Aulton, D. N. Travers, and P. J. P. White, *J. Pharm. Pharmacol.*, **25**, 79P (1973).
(30) R. P. Bhatia and N. G. Lordi, *J. Pharm. Sci.*, **68**, 896 (1979).
(31) Z. T. Chowhan and A. A. Amaro, *Drug. Dev. Ind. Pharm.*, **5**, 545 (1979).
(32) Z. T. Chowhan, *J. Pharm. Pharmacol.*, **32**, 10 (1980).
(33) A. S. Alam and E. L. Parrott, *J. Pharm. Sci.*, **60**, 263 (1971).

ACKNOWLEDGMENTS

Abstracted in part from a dissertation submitted by Paul J. Jarosz to the Graduate College, University of Iowa, in partial fulfillment of the Doctor of Philosophy degree requirements.

Determination of Octanol–Water Equivalent Partition Coefficients of Indolizine and Substituted 2-Phenylindolizines by Reversed-Phase High-Pressure Liquid Chromatography and Fragmentation Values

CLAUDIO L. K. LINS, JOHN H. BLOCK ˣ, ROBERT F. DOERGE, and GERARD J. BARNES

Received May 19, 1980, from the *School of Pharmacy, Oregon State University, Corvallis, OR 97331.* Accepted for publication July 27, 1981.

Abstract □ Octanol–water partition values were calculated using fragmentation values and measured rapidly by high-pressure liquid chromatography (HPLC) on bonded octadecylsilane supports. Log *P* for indolizine, π, and fragment (*f*) values for the indolizinyl substituents were determined using both methods. Good agreement was obtained for all three values.

Keyphrases □ Partition coefficient—indolizine and 2-phenylindolizines, determination by high-pressure liquid chromatography and fragmentation values □ Indolizine—substituted 2-phenylindolizines, partition coefficients determined by high-pressure liquid chromatography and fragmentation values □ High-pressure liquid chromatography—determination of partition coefficients of indolizine and 2-phenylindolizines □ Fragmentation values—determination of partition coefficients of indolizine and 2-phenylindolizine

There is considerable interest in partition coefficient determination in the area of rational drug design (1). The partition coefficient, log *P*, represents the distribution of a substance between an organic and aqueous phase. Several methods may be used to determine partition coefficients including the shake-flask method, liquid–liquid chromatography on liquid impregnated plate technique, and high-pressure liquid chromatography (HPLC).

No studies have been done on the log *P* of indolizines. Indolizine (I) is a 10π aromatic heterocyclic compound with the nitrogen at the bridge head position. It is nearly electrically neutral and weakly basic with a pKa value of 3.94 (2).

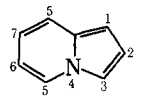

I

For the normal shake-flask method, octanol and water have been used previously as the biological lipid and aqueous phases, respectively, in partition determination (3). Due to the instability of the indolizine nucleus, measuring log *P* values of this compound by this technique has proven difficult. The shake-flask procedure (4) is a tedious, time-consuming process and subject to purity, stability, and mass-balance problems from the compounds being measured.

BACKGROUND

Liquid chromatography on paper or lipid-impregnated plates has been used as an alternative to octanol–water partition. Martin (5) derived Eq. 1 for thin-layer or paper chromatography (TLC):

0022-3549/82/0600-0614$01.00/0

of hydrochlorothiazide tablets composed of lactose and povidone did not change after 1 year at room temperature supports this implication.

REFERENCES

(1) A. Ritter and H. Sucker, *Pharm. Tech.*, **4**, No. 9, 108 (1980).
(2) K. Ridgway, *Pharm. J.*, **205**, 709 (1970).
(3) W. C. Rudnick, A. R. Hunter, and F. C. Holden, *Mater. Res. Stand.*, **1**, 283 (1963).
(4) J. T. Fell and J. M. Newton, *J. Pharm. Sci.*, **59**, 688 (1970).
(5) P. J. F. Wright, *Mag. Concr. Res.*, **7**, 87 (1955).
(6) L. L. Simon, *Constructional Rev.*, **29**, 23 (1956).
(7) J. T. Fell and J. M. Newton, *J. Pharm. Pharmacol.*, **20**, 657 (1968).
(8) N. B. Mitchell, *Mater. Res. Stand.*, **1**, 780 (1961).
(9) M. M. Frocht, "Photoelasticity," Vol. 2, Wiley, New York, N.Y., 1948, p. 127.
(10) C. Nystrom, W. Alex, and K. Malmqvist, *Acta Pharm. Suec.*, **14**, 317 (1977).
(11) D. Train, *J. Pharm. Pharmacol.*, **8**, 74S (1956).
(12) E. L. Parrott, in "Pharmaceutical Dosage Forms: Tablets," Vol. 2, H. A. Lieberman and L. Lachman, Eds., Dekker, New York, N.Y., 1981.
(13) D. Train, *Trans, Inst. Chem. Engrs.*, **35**, 258 (1957).
(14) D. Train and J. A. Hersey, *Powder Metall.*, **6**, 20 (1960).
(15) E. Turba and H. Rumpf, *Chem. Eng. Tech.*, **36**, 230 (1964).
(16) A. A. Griffith, *Proc. 1st Int. Cong. Appl. Mech.*, **1924**, 55.
(17) W. O. Opakunle and M. S. Spring, *J. Pharm. Pharmacol.*, **28**, 915 (1976).
(18) K. T. Jaiyeoba and M. S. Spring, *ibid.*, **32**, 1 (1980).
(19) E. Shotton and B. A. Obiorah, *J. Pharm. Sci.*, **64**, 1213 (1975).
(20) N. L. Henderson and A. J. Bruneo, *ibid.*, **59**, 1336 (1970).
(21) R. W. Heckel, *Trans. Metall. Soc. AIME*, **221**, 671 (1961).
(22) R. W. Heckel, *ibid.*, **221**, 1001 (1961).
(23) R. York, *J. Pharm. Pharmacol.*, **30**, 6 (1978).
(24) P. York and N. Pilpel, *J. Pharm. Pharmacol.*, Suppl., **25**, 1P (1973).
(25) K. A. Khan and C. T. Rhodes, *J. Pharm. Sci.*, **64**, 444 (1975).
(26) E. Ryshkewitch, *J. Am. Ceramic Soc.*, **36**, 65 (1953).
(27) J. A. Seitz and G. M. Flessland, *J. Pharm. Sci.*, **54**, 1353 (1965).
(28) C. Nystron, K. Malmqvist, J. Mazur, W. Alex, and A. W. Holzer, *Acta Pharm. Suec.*, **15**, 226 (1978).
(29) M. E. Aulton, D. N. Travers, and P. J. P. White, *J. Pharm. Pharmacol.*, **25**, 79P (1973).
(30) R. P. Bhatia and N. G. Lordi, *J. Pharm. Sci.*, **68**, 896 (1979).
(31) Z. T. Chowhan and A. A. Amaro, *Drug. Dev. Ind. Pharm.*, **5**, 545 (1979).
(32) Z. T. Chowhan, *J. Pharm. Pharmacol.*, **32**, 10 (1980).
(33) A. S. Alam and E. L. Parrott, *J. Pharm. Sci.*, **60**, 263 (1971).

ACKNOWLEDGMENTS

Abstracted in part from a dissertation submitted by Paul J. Jarosz to the Graduate College, University of Iowa, in partial fulfillment of the Doctor of Philosophy degree requirements.

Determination of Octanol–Water Equivalent Partition Coefficients of Indolizine and Substituted 2-Phenylindolizines by Reversed-Phase High-Pressure Liquid Chromatography and Fragmentation Values

CLAUDIO L. K. LINS, JOHN H. BLOCK ˣ, ROBERT F. DOERGE, and GERARD J. BARNES

Received May 19, 1980, from the *School of Pharmacy, Oregon State University, Corvallis, OR 97331.* Accepted for publication July 27, 1981.

Abstract □ Octanol–water partition values were calculated using fragmentation values and measured rapidly by high-pressure liquid chromatography (HPLC) on bonded octadecylsilane supports. Log *P* for indolizine, π, and fragment (*f*) values for the indolizinyl substituents were determined using both methods. Good agreement was obtained for all three values.

Keyphrases □ Partition coefficient—indolizine and 2-phenylindolizines, determination by high-pressure liquid chromatography and fragmentation values □ Indolizine—substituted 2-phenylindolizines, partition coefficients determined by high-pressure liquid chromatography and fragmentation values □ High-pressure liquid chromatography—determination of partition coefficients of indolizine and 2-phenylindolizines □ Fragmentation values—determination of partition coefficients of indolizine and 2-phenylindolizine

There is considerable interest in partition coefficient determination in the area of rational drug design (1). The partition coefficient, log *P*, represents the distribution of a substance between an organic and aqueous phase. Several methods may be used to determine partition coefficients including the shake-flask method, liquid–liquid chromatography on liquid impregnated plate technique, and high-pressure liquid chromatography (HPLC).

No studies have been done on the log *P* of indolizines. Indolizine (I) is a 10π aromatic heterocyclic compound with the nitrogen at the bridge head position. It is nearly electrically neutral and weakly basic with a pKa value of 3.94 (2).

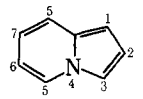

I

For the normal shake-flask method, octanol and water have been used previously as the biological lipid and aqueous phases, respectively, in partition determination (3). Due to the instability of the indolizine nucleus, measuring log *P* values of this compound by this technique has proven difficult. The shake-flask procedure (4) is a tedious, time-consuming process and subject to purity, stability, and mass-balance problems from the compounds being measured.

BACKGROUND

Liquid chromatography on paper or lipid-impregnated plates has been used as an alternative to octanol–water partition. Martin (5) derived Eq. 1 for thin-layer or paper chromatography (TLC):

0022-3549/82/0600-0614$01.00/0

Table I—Estimated Log *P* Values on HPLC Using Octanol-Saturated Water as Mobile Phase

Compounds	Log *k'*	Log *P*	
		Literature[a]	HPLC[b]
Anisole	0.518	2.08	2.08
p-Chloroacetophenone	0.711	2.35	2.29
p-Bromoacetophenone	0.884	2.43	2.48
Toluene	1.09	2.71	2.71
Chlorobenzene	1.24	2.84	2.87
Benzophenone	1.49	3.18	3.15
Indolizine (I)	0.894	—	2.49 ± 0.02[c]

[a] Reference 18. [b] Equation 3. [c] Standard error of the estimate from Eq. 3.

$$\log P = \log K + R_m \qquad \text{(Eq. 1)}$$

where K is a constant for the system, $R_m \approx \log [(1/R_f) - 1]$ where R_f has the usual meaning.

Reversed-phase HPLC has been used to measure the lipophilicity of several compounds. In HPLC, the capacity factor k' replaces R_m and is defined as:

$$k' = \frac{(t_r - t_0)}{t_0} = \frac{(V_r - V_0)}{V_0} = \frac{(d_r - d_0)}{d_0} \qquad \text{(Eq. 2)}$$

where:

t_r = retention time of the compound
t_0 = retention time of the solvent
V_r = retention volume of the compound
V_0 = retention volume of the solvent or dead volume
d_r = distance between the peak of the compound and peak of the solvent front
d_0 = distance between the point of injection and the peak of the solvent front.

Haggerty and Murrill (6) measured log *P* values for a family of nitrosoureas using a column packed with octadecylsilane bonded to silica[1] and eluted with 30% acetonitrile in pH 7.41 buffer solution. Another study (7) obtained good correlation between log *k'* and log *P* of some substituted phenol and aniline derivatives using bonded[2] columns with various mixtures of distilled water and acetone as the eluent. Exhaustive silylation of octadecylsilane reversed-phase columns were reported to give a better correlation between *k'* and log *P* than the untreated packing material (8). The rationale is that exhaustive silylation eliminates adsorption phenomena due to free SiOH sites.

The lipophilicities of 1,4-benzodiazepine derivatives were determined using oleyl alcohol supported on a porous silica[3] as an HPLC procedure and the results were compared with reversed-phase TLC techniques (9). Similar work was done (10) using 1-octanol supported on diatomaceous earth[4] with octanol-saturated water as the eluent.

Various HPLC techniques were compared (11) using three different columns: one reversed-phase[1], one unmodified absorption system[5], and one nonbonded porous silica[6] coated with 1-octanol or squalene. Several good correlations between log *k'* and log of biological activity were reported. Investigators using these techniques were warned to be careful in interpreting these correlations. Unger *et al.* (12) had near perfect agreement between shake-flask and reversed-phase HPLC procedures over a log *P* range of 3.5 units, using octanol-saturated pH 7.00 (0.01 *M*) phosphate buffer as the mobile phase, and silylated octadecyl-bonded silica[1] as the stationary phase.

The latter HPLC procedure (12) was used in the present study to determine the log *P* of unstable indolizine. Then, a modified HPLC method was developed to measure partition coefficients of 3.5 to 5.0. Using this method, the π and fragment values for the indolizinyl substituent were also determined.

EXPERIMENTAL

Solvents were analytical reagent quality, and the 1-octanol for chromatographic purposes was purified according to reported procedures (13). Standards were obtained from commercial sources. Indolizine and 2-phenylindolizines were synthesized by the Boekelheide (14) method and *via* the Chichibabin-Stepanow (15, 16) route, respectively.

[1] Corasil C18, Waters Associates, Milford, Mass.
[2] Porasil B, Waters Associates, Milford, Mass.
[3] Porasil C, Waters Associates, Milford, Mass.
[4] Hyflosupercel, Johns-Manville.
[5] Corasil II, Waters Associates, Milford, Mass.
[6] Porasil A, Waters Associates, Milford, Mass.

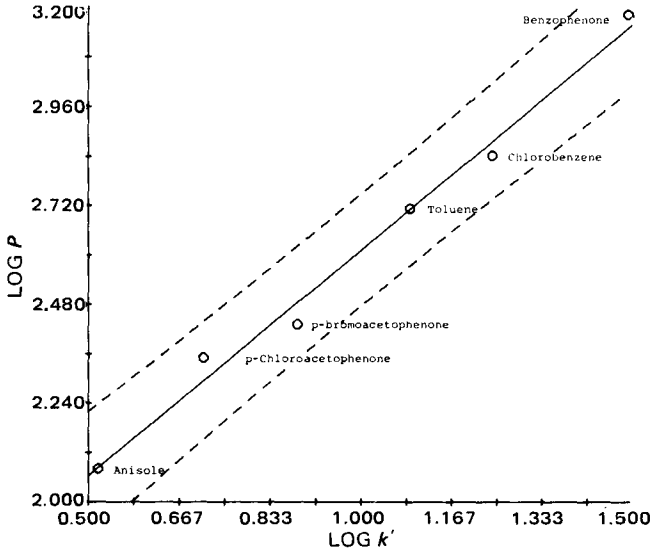

Figure 1—*Literature log* P *values* versus *log* k' *determined by octanol-coated octadecylsilyl-bonded support with octanol-saturated water as mobile phase. Key: (- - -) the 95% confidence limits of the predicted line; (○) standards are from Table I.*

Samples were dissolved in water-saturated octanol and/or a minimal amount of methanol. Sodium nitrate in octanol-saturated water was used as a suitable nonretained compound to define dead volume, V_0. Sample concentrations were adjusted so that the relative peak areas remained approximately constant.

The high-pressure liquid chromatograph[7] consisted of a pump[8] and injector[9]. A UV–visible spectrophotometer[10] with low dead volume flow cells was used as detector. Standards and indolizines were analyzed at 260 nm. Peaks were measured on a 25-cm dual pen recorder[11]. The column packing of silica particles (37–50 μm) with an octadecylsilane-bonded coating[1] was persilated by McCall's method (8). Stainless steel columns (2-mm i.d.) in lengths of 5, 10, 30, and 60 cm were packed using published "tap-fill" procedures (17), and then mounted onto the liquid chromatograph.

Two methods were used to determine log *P*. One system followed Unger's procedure (12). The second procedure was patterned after reported methods (6–8) using persilated octadecylsilane columns[1] with 40% (v/v) acetonitrile in water as the mobile phase to determine large log *P* values (range 3.5 to 5.0) of standards and 2-phenylindolizines. Samples were dissolved in acetonitrile and/or a minimal amount of methanol. For both procedures, all solutions containing solute were first filtered[12] to reduce contamination or column clogging. All experiments were performed at ambient temperature (25°).

Log *P* values for unknowns obtained from HPLC data were determined by calculation using regression analysis derived from literature log *P* values (18) *versus* their log *k'* obtained experimentally. Daily standards were run with excellent reproducibility. Statistical analyses were performed using a statistical package[13].

RESULTS AND DISCUSSION

Log *P* Determination of Indolizine by HPLC—Due to the instability of indolizine, its log *P* value was estimated using HPLC techniques. Compounds possessing physical properties similar to those of indolizine were selected. These reference compounds (the first six compounds in Table I) were electrically neutral and had partition coefficients close to the estimated value for indolizine (log *P* 2.45 calculated by the fragment method). These compounds were chromatographed on a silylated column[1] coated with octanol. The mobile phase was octanol-saturated water

[7] Model ALC/GPC 201 Liquid Chromatograph, Waters Associates, Milford, Mass.
[8] Model M6000A, Waters Associates, Milford, Mass.
[9] Model U-6K, Waters Associates, Milford, Mass.
[10] Varian Model 635.
[11] Soltec.
[12] Fritted Disc, 10–15μ, Pyrex.
[13] Oregon State University Statistical Interaction Programming System (SIPS).

Table II—Estimated Log *P* Values on HPLC Using 40% (v/v) Acetonitrile in Water

Compound	Log *k'*	Log *P*	
		Literature[a]	HPLC[b]
o-Dibromobenzene	0.580	3.64	3.60
m-Dibromobenzene	0.732	3.75	3.93
Dibenzofuran	0.748	4.12	3.96
Fluorene	0.857	4.18	4.21
Diphenylacetylene	1.10	4.78	4.76

[a] Reference 18. [b] Equation 4.

using a 10-cm column. A linear relationship between log *P* values and their log *k'* values (Fig. 1) is given by:

$$\log P = 1.516\ (\pm\ 0.059) + 1.094\ (\pm\ 0.057) \log k' \qquad \text{(Eq. 3)}$$

$$n = 6, s = 0.0453, r^2 = 0.9893, F_{1,4} = 370$$

The values in parentheses are the standard errors, *n* is the number of compounds, *s* is the standard error of the corrleation, r^2 is the coefficient of determination, and *F* is the overall significance parameter with the indicated degrees of freedom.

Unger *et al.* (12) showed that nitrogenous compounds capable of hydrogen bonding with nonsilated silanol sites deviated from the calculated regression line. Pyridine and certain substituted pyridines deviated the most. Quinoline did not deviate as much. Acridine, 2,6-lutidine, and *N,N*-dimethylaniline fit the regression model. It appears that as the pKa of an amine decreases and steric hindrance about the nitrogen increases the ability to adsorb onto an open silanol site decreases. Indolizine has a reported pKa of 3.94 (2), far lower than that for pyridine (5.19) or quinoline (4.90). Furthermore, protonation of indolizine occurs on carbons 1 and 3, not on the nitrogen atom (19). The ring nitrogen is sterically hindered. Finally, in some unreported earlier work[14] the use of shift reagents was investigated in an attempt to simplify the proton NMR spectrum of indolizines. No noticeable change in the chemical shifts of any of the protons was obtained, which is strong evidence of a very weakly basic and/or sterically hindered nitrogen (20). For these reasons, reference compounds containing nitrogen capable of hydrogen bonding to silanol sites on the HPLC column were omitted.

The log *k'* value for indolizine (0.894) was measured under the same conditions used for the standards (Table I) and a log *P* value of 2.49 was calculated using Eq. 3.

Determination of π Value of the Indolizinyl Moiety by HPLC—Because the 2-phenylindolizines are more stable than indolizine their log *P* determinations using the traditional shake-flask procedure (4) were attempted without success. These compounds degrade in solution with changes detectable in the UV spectrum within 1 hr. Undoubtedly agitation in the octanol–water system hastened this degradation. Thus, an HPLC procedure was devised.

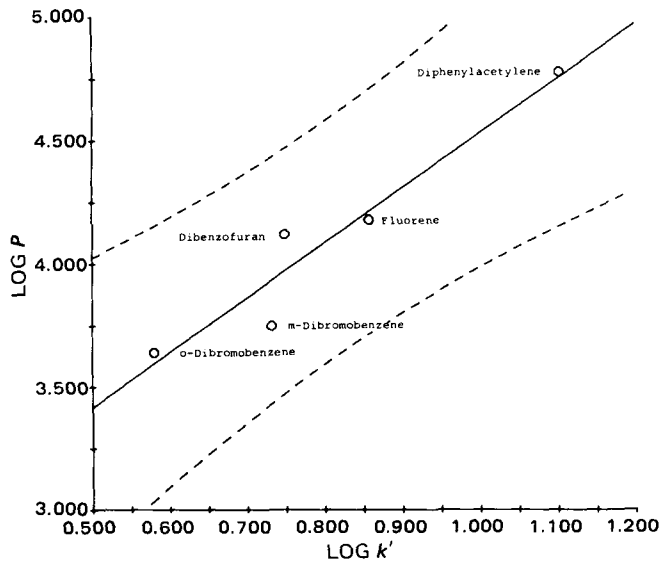

Figure 2—*Literature log* P *value* versus *log* k' *determined by 10-cm column*[1] *using 40% (v/v) acetonitrile in water as the mobile phase. Key: (- - -) the 95% confidence limits of the predicted line; (○) standards are from Table II.*

[14] J. H. Block, unpublished.

Table III—Estimated Log *P* on HPLC of 2-Phenylindolizines

Compound	X	Y	Log *k'*[a]	Log *P* HPLC[b]
II*a*	H	H	0.892	4.29 (±0.07)
II*b*	OCH_3	H	0.851	4.20 (±0.07)
II*c*	H	OCH_3	0.826	4.14 (±0.06)
II*d*	CH_3	H	1.19	4.96 (±0.16)
II*e*	H	CH_3	1.15	4.87 (±0.14)
II*f*	Cl	H	1.30	5.20 (±0.19)
II*g*	H	Cl	1.27	5.14 (±0.18)
II*h*	Br	H	1.40	5.43 (±0.23)
II*i*	H	Br	1.35	5.31 (±0.21)

[a] Values measured on a persilated column[1] (10 cm) using 40% (v/v) acetonitrile as the eluant. [b] Equation 4; numbers within the parentheses are the standard error of the estimate.

The octanol–water HPLC system is limited to compounds having a log *P* of 3.15 which is the log *P* of octanol itself (18). Any compound with a greater log *P* would, in theory, remain on the HPLC column indefinitely. Using either the π or fragment approach of calculating log *P* values, the log *P* values for the 2-phenyl substituted indolizines were estimated to be in the range of 4–5.

Selected standards (Table II) with known log *P* values (18) in this range were chromatographed using several different solvent systems. These consisted of a reversed-phase persilated column[1] with different column lengths and different concentrations of acetonitrile in water as the mobile phase. Columns[1] varied in length from 5 to 10 cm and the solvent system consisted of acetonitrile concentrations in the range of 35–50%. Good linear relationships (Fig. 2) were found in a system using 40% acetonitrile in a 10-cm column[1]. The results are displayed in Table II and represented by:

$$\log P = 2.300\ (\pm\ 0.2967) + 2.234\ (\pm\ 0.360) \log k' \qquad \text{(Eq. 4)}$$

$$n = 5, s = 0.1416, r^2 = 0.9251, F_{1,3} = 37.0$$

A variety of 2-phenylindolizine analogs with widely different lipophilicities were prepared (Table III). These compounds have different substituents in the *para* and *meta* positions on the 2-phenyl groups. These substituted 2-phenylindolizines were chromatographed under conditions identical to those in Table II. Their log *k'* values were used to calculate their log *P* values using Eq. 4 (Table III).

π Value Correlation from HPLC Data—An investigation was conducted to determine whether the retention times of substituted 2-phenylindolizines using a persilated column[1] were proportional to their Hansch π constants (17). The previously described mobile phase of 40% acetonitrile in water using a 10-cm column was used. An excellent linear relationship was found between the log *P* values of the 2-phenyl substituents and log *k'*. The results are represented by:

$$\text{Log } P_{\text{substituent}} = 0.696\ (\pm\ 0.027) + 1.674\ (\pm 0.072) \log k' \qquad \text{(Eq. 5)}$$

$$n = 9, s = 0.0452, r^2 = 0.9874, F_{1,7} = 548.2$$

There is no complete set of π values for substituted phenyl compounds. That is, there are π values for CH_3, CH_3O, Cl, Br, and C_6H_5, but not tolyl, anisyl, *etc.* Since π_H is defined as zero, the log *P* values of the intact molecule (toluene, anisole, *etc.*) were used as an estimate of π to obtain Eq. 5.

The $\pi_{\text{indolizinyl}}$ values were calculated by subtracting the log *P* of the complete molecule, which represents the substituent (21) from the log *P* of the substituted indolizine (Table IV):

$$\pi_{\text{indolizinyl}} = \log P_{\text{substituted indolizine}} - \log P_{\text{substituent}} \qquad \text{(Eq. 6)}$$

The calculated $\pi_{\text{indolizinyl}}$ values vary from 2.03 and 2.44 with a mean of 2.41, a standard error of ±0.045, and a coefficient of variation of 6.0%.

Examination of the $\pi_{\text{indolizinyl}}$ results in Table IV shows that they can be placed into two groups. Compounds II*a*–II*e* compose one group with a mean of 2.14 and II*f*–II*i* have a mean of 2.36. The latter group contains the halogens. Hansch and Leo[15] have found that halogen adds about 0.2 units to π and fragment values. Correcting for the halogen effect, the mean $\pi_{\text{indolizinyl}}$ value becomes 2.15 (±0.024) with a coefficient of variation of 3.4%.

[15] A. Leo and C. Hansch, personal communications.

Table IV—$\pi_{indolizinyl}$ and $f_{indolizinyl}$ Values Using HPLC, 2-Phenyl Substituent [a]

Compound	Log $P_{substituent}$ [b]	$\pi_{indolizinyl}$ [c]	$f_{substituent}$ [d]	$f_{indolizinyl}$ [e]
IIa	2.13	2.16	1.90	2.39
IIb	2.11	2.09	1.88	2.32
IIc	2.11	2.03	1.88	2.26
IId	2.69	2.26	2.46	2.49
IIe	2.69	2.17	2.46	2.39
IIf	2.84	2.36 (2.16)	2.61	2.59 (2.39)
IIg	2.84	2.30 (2.10)	2.61	2.53 (2.33)
IIh	2.99	2.44 (2.24)	2.76	2.67 (2.47)
IIi	2.99	2.32 (2.12)	2.76	2.55 (2.35)

[a] See Table II for log k' and log P results obtained by chromatography. [b] Reference 18. [c] Equation 6; values within the parentheses are corrected for the presence of a halogen. [d] Reference 21; obtained by subtracting f_H (0.23) from log P of the 2-phenyl substituent. [e] Equation 8; values within the parentheses are corrected for the presence of a halogen.

Log P of Indolizine Calculated by the Fragment Method—The log P of the indolizine nucleus can be also calculated by the fragment method using values from model systems (18).

For example, for the fused aromatic ring model, the aromatic carbon (f_{CH}) has a value of 0.35 and the bridgehead carbon next to a heteroatom (f_C^*) is 0.44. For the nitrogen, several values can be used depending on the specific location of the atom in the molecule. According to a previous report (21), the fragment constant for the nitrogen in a ring system such as indole or pyrrole (−0.67) lies between the values of the nitrogen attached to one aromatic ring (−1.03), and two aromatic rings (−0.03). The fragment value for N-phenyl pyrrole is −0.56. Indolizine (I) is a special case because the nitrogen is located at the bridgehead position of the molecule. The nitrogen in this system is more lipophilic than the usual heterocyclic nitrogen because the unshared electrons on the nitrogen resonate among all the atoms of the ring (22). The low pKa (3.94) and the fact that protonation occurs on carbons 1 and 3 is further evidence of the special nature of this nitrogen. For this reason, a fragment value of −0.44 was used as an approximation of the nitrogen constant for indolizine[15]. This value represents a nitrogen in an aromatic system attached to two aromatic rings. The addition of all these fragment values is illustrated below:

$$\log P = 7 f_{(CH)} + f_{(C)}^* + f\text{—}\underset{\phi}{\overset{|}{\underset{\phi}{N}}}\text{—}\phi \qquad \text{(Eq. 7)}$$

$$= 7\,(0.35) + (0.44) + (-0.44)$$

$$= 2.45$$

In a similar manner, the fragment substituents of 2-phenylindolizines were calculated by the fragment method (20) and listed in Table IV. Indolizinyl fragment values were calculated by subtracting fragment substituent values from log P values:

$$f_{indolizinyl} = \log P - f_{substituent} \qquad \text{(Eq. 8)}$$

The average indolizinyl fragment value is 2.47 with a sample standard error of ±0.044. The fragment values vary from 2.26 to 2.67 with a coefficient of variation of 5.4%.

As was done with the π determination, the fragment results in Table IV can be divided into two groups with the methyl and methoxy substituted compounds IIa–IIe in the first group and the halogen substituted compounds IIf–IIi in the second. The average fragment value for the nonhalogenated indolizines is 2.37 and for the halogenated indolizines is 2.59. Applying a correction of 0.2 for the halogenated compounds, the average decreases to 2.39. The average $f_{indolizinyl}$ for all 11 compounds then becomes 2.38(±0.024) with a coefficient of variation of 3.0%.

Both the fragment and π approach to calculating log P values assumes that partial partition coefficients are additive. They also assume that each substituent behaves independently in terms of any effect on lipophilicity; this is not true. To correct for interactions, the fragment approach uses correction terms or different fragment substituent values dependent on the type of parent molecule containing the substituent. Nevertheless, neither method differentiates between a *meta* and *para* substituent in terms of resonance *versus* inductive effects on lipophilicity. Furthermore, both approaches ignore any resonance or inductive effect that the indolizine ring might have on the phenyl ring.

In both the fragment and π approaches, the individual substituent values are derived from known compounds whose partition coefficients were obtained by the classical shake-flask procedures. There have been no reported studies on the partitioning behavior of indolizine. It is difficult to extrapolate this heteroaromatic to other heteroaromatic systems for the reasons already stated. Nevertheless, the results obtained for indolizine by the different methods described in this paper show good consistency and can be considered a measure of lipophilicity for future quantitative structure–activity relationship (QSAR) studies involving indolizine.

REFERENCES

(1) A. Leo, C. Hansch, and D. Elkins, *Chem. Rev.*, **71**, 525 (1971).

(2) W. F. Armarego, *J. Chem. Soc.*, **1964**, 4226.

(3) M. S. Tute, *Adv. Drug Res.*, **6**, 1 (1971).

(4) T. Fujita, J. Iwasa, and C. Hansch, *J. Am. Chem. Soc.*, **86**, 5175 (1964).

(5) A. J. P. Martin, *Biochem. Soc. Symp.*, **3**, 4 (1949).

(6) W. J. Haggerty, Jr. and E. A. Murrill, *Res./Dec.*, **25**, 30 (1974).

(7) R. M. Carlson, R. E. Carlson, and H. L. Kopperman, *J. Chromatogr.*, **107**, 219 (1975).

(8) J. McCall, *J. Med. Chem.*, **18**, 549 (1975).

(9) A. Hulshoff and J. H. Perrin, *J. Chromatogr.*, **129**, 263 (1976).

(10) M. S. Mirrlees, S. J. Moulton, C. T. Murphy, and P. J. Taylor, *J. Med. Chem.*, **19**, 615 (1976).

(11) D. Henry, J. H. Block, J. L. Anderson, and G. R. Carlson, *ibid.*, **19**, 619 (1976).

(12) S. H. Unger, J. R. Cook, and J. S. Hollenberg, *J. Pharm. Sci.*, **67**, 1364 (1978).

(13) W. P. Purcell, G. E. Bass, and J. M. Clayton, "Strategy of Drug Design," Wiley, New York, N.Y., 1973, p. 128.

(14) V. Boekelheide and R. J. Windgassen, Jr., *J. Am. Chem. Soc.*, **81**, 1456 (1959).

(15) A. E. Chichibabin and E. N. Stepanow, *Chem. Ber.*, **62**, 1068 (1929).

(16) C. L. K. Lins, J. H. Block, and R. F. Doerge, *J. Pharm. Sci.*, **71**, 556 (1982).

(17) L. R. Snyder and J. J. Kirkland, "Introduction to Modern Liquid Chromatography," Wiley, New York, N.Y., 1974, p. 189.

(18) Pomona College Medicinal Chemistry Project, Pomona College, Claremont, Calif., July 1978.

(19) M. P. Carmody, M. J. Cook, N. L. Dassanayake, A. R. Katritzky, P. Linda, and R. D. Tack, *Tetrahedron*, **32**, 1767 (1976).

(20) C. Beaute, Z. W. Wolkowski, and N. Thoai, *Tetrahedron Lett.*, **1971**, 817.

(21) C. Hansch and A. Leo, "Substituent Constants for Correlation Analysis in Chemistry and Biology," Wiley, New York, N.Y., 1979, pp. 18–43.

(22) E. T. Borrows and D. O. Holland, *Chem. Rev.*, **42**, 611 (1948).

ACKNOWLEDGMENTS

Presented in part before the Medicinal Chemistry and Pharmacognosy Section, APhA Academy of Pharmaceutical Sciencies, St. Louis meeting, March 31, 1981.

This paper constitutes a portion of C. L. K. Lins' Doctor of Philosophy degree requirements, Oregon State University, 1980.

This work was supported by the Oregon State University Research Office and from National Institutes of Health Biomedical Research Support Grant RR07079.

The authors thank Professors Corwin Hansch and Albert Leo for supplying a value for the halogen effect and an estimate for the fragment value for the indolizine nitrogen.

Quantitative Structure–Activity Relationships of Purines II: Prediction of Activity against Adenocarcinoma CA755 and Toxicity in Mice

ZOHAR NEIMAN and FRANK R. QUINN ˣ

Received June 11, 1981, from the *Laboratory of Medicinal Chemistry and Biology, Division of Cancer Treatment, National Cancer Institute, National Institutes of Health, Bethesda, MD 20205.* Accepted for publication September 16, 1981.

Abstract □ Quantitative structure–activity relationships (QSAR) were derived for a number of 2,6-mono- and disubstituted purines. The derived equations relate the anticancer activity in murine Adenocarcinoma CA755 to the molar refractivity of substituents at position 2 and electron-withdrawing effects of substituents at position 6. A QSAR was also derived for the acute toxicity (LD_{50}) of substituents at position 6. The results suggest that toxicity is relatively independent of the nature of the substituent.

Keyphrases □ Anticancer activity—of purines, prediction of activity against Adenocarcinoma CA755 and toxicity in mice □ Purines—anticancer activity, prediction of activity against Adenocarcinoma CA755 and toxicity in mice, structure–activity relationship □ Structure–activity relationships—of purines, prediction of activity against Adenocarcinoma CA755 and toxicity in mice

Purine (I) and purine nucleosides comprise a very important class of potential anticancer agents (1). Many hundreds of purine analogs have been synthesized (2) and tested for their anticancer properties. Of the purine bases, only mercaptopurine and thioguanine have found general usage in the clinical treatment of cancer (3).

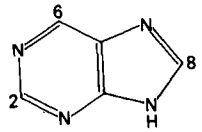

In a previous study (4) it was demonstrated that quantitative structure–activity relationships (QSAR) were possible with purines in spite of the fact that the purine ring system is not typically aromatic (5). In the present study quantitative structure–activity correlations were derived for the *in vivo* activity and toxicity of a number of 2- and 6-substituted purines against the murine solid tumor Adenocarcinoma 755(CA755).

It has been pointed out (6) that CA755 is a test system that is artificially sensitive to purines. Under the protocols for testing drugs against CA755 (7) many purines prove to be impressively carcinostatic and sometimes carcinolytic. However, these test conditions, in which the drug is administered 24 hr after tumor implantation, reflect treatment during early stages of the disease. It has been shown (6) that, if treatment is delayed until the disease is well-advanced, a situation more typical of that encountered in humans, these purines are not as effective. The principal value in using data from a sensitive system such as CA755 is that the effect of subtle structural changes on the activity may be easily discerned. The ultimate effectiveness of any analog against other animal or human tumors would still have to be determined.

EXPERIMENTAL

The substituted constants employed in this study included the hydrophobic parameter π and the Swain-Lupton field and resonance constants $\mathcal{F}$ and $\mathcal{R}$ (8). The molar refractivity (MR) was used as a measure of steric bulk (8). The physicochemical parameters which appear in the correlations are given in Table I. Substituent constants were taken from the recent literature (9). Values of π not available from the literature were calculated by the additive method (10); MR values were calculated from Vogel's bond refraction values (11).

It should be noted that the π values used in this study were determined in an aromatic system, *i.e.*, from benzene derivatives. Purine, on the other hand, is a nitrogen heterocycle and substituents on the purine ring may undergo various perturbations due to inter- and intramolecular associations with the ring nitrogens. It is quite possible that π values for purine substituents would differ considerably from those of their benzene analogs. The major deviations from standard π values would be expected for substituents at positions 2 and 8, both of which are adjacent to two-ring nitrogen atoms. The 6 position, on the other hand, may be similarly af-

Table I—Physicochemical Parameters

Substituent	π	$\mathcal{R}$	MR
Hydrogen	0	0	0.103
Methyl	0.56	−0.13	0.565
Cyano	−0.57	0.19	0.633
Chloro	0.71	−0.15	0.603
Bromo	0.86	−0.17	0.888
Iodo	1.12	−0.19	1.394
Methoxy	−0.02	−0.51	0.787
Ethoxy	0.38	−0.44	1.247
n-Propoxy	1.05	−0.45	1.706
Amino	−1.23	−0.68	0.542
Methylamino	−0.47	−0.74	1.033
Dimethylamino	0.18	−0.92	1.555
Trimethylammonium	−5.96	0	—
Benzamido	0.49	−0.27	3.464
Hydrazino	−0.88	−0.71	0.844
Hydroxylamino	−1.34	−0.40	0.722
Methylthio	0.61	—	1.382
Ethylthio	1.07	—	1.842
n-Propylthio	1.57	—	2.357
n-Butylthio	2.07	—	2.819
iso-Butylthio	2.16	—	2.819
sec-Butylthio	2.16	—	2.819
2′-Propynylthio	1.01	—	2.141
Cyanomethylthio	−0.23	—	1.869
Cyclopentylthio	2.25	—	2.994
Phenylthio	2.32	—	3.429
Thiocyanate	0.41	—	1.340
2-Imidazolinthio	0.63	—	2.741
1′-Methyl-4′-nitroimidazol-5′-ylthio	0.27	—	3.582
Benzylthio	2.57	—	3.793
3,4-Dimethylbenzylthio	3.57	—	4.680
o-Chlorobenzylthio	3.53	—	3.484
o-Fluorobenzylthio	2.96	—	3.780
o-Nitrobenzylthio	2.29	—	4.410
m-Chlorobenzylthio	3.28	—	4.234
p-Fluorobenzylthio	2.96	—	3.780
2′-Pyridylmethylthio	1.16	—	3.633
Methylsulfonyl	−1.63	0.22	1.349
Ethylsulfonyl	−1.13	—	1.814
n-Propylsulfonyl	−0.63	—	2.279
n-Butylsulfonyl	−0.13	—	2.743
Fluorosulfonyl	0.05	0.22	0.865
Sulfonamide	−1.82	0.19	1.228
N-Methylsulfonamide	−1.32	—	1.712
N-*n*-Propylsulfonamide	−0.32	—	2.643
N-iso-Butylsulfonamide	0.23	—	3.282
N′-3′-Methoxypropylsulfonamide	−0.34	—	3.285
N-2′-Ethoxyethylsulfonamide	−0.44	—	3.242
N-Benzylsulfonamide	0.19	—	4.053

0022-3549/82/0600-0618$01.00/0

Table II—Observed and Predicted CA755 Activity of Mono- and Disubstituted Purines

Number	Compound	log(1/C)[a] Observed	log(1/C)[a] Predicted	|Δlog(1/C)|
I	Purine	Inactive	4.18	—
II	6-Chloro	4.23	4.08	0.15
III	6-Bromo	4.50	4.06	0.44
IV	6-Iodo	4.52	4.03	0.49
V	6-Methoxy	3.00	3.65	0.65
VI	6-*n*-Propoxy	3.42	3.73	0.31
VII	6-Hydrazino	3.22	3.42	0.20
VIII	6-Trimethyl-ammonio	4.34	4.26	0.08
IX	6-Methylthio	4.51	4.04	0.47
X	6-Ethylthio	4.45	4.04	0.41
XI	6-Methylsulfonyl	4.04	4.52	0.48
XII	6-Sulfonamide	4.26	4.48	0.22
XIII	2-Methyl-6-amino	3.23	3.19	0.04
XIV	2-Chloro-6-methylamino	3.37	3.10	0.27
XV	2-Bromo-6-amino	2.56	3.04	0.48
XVI	2-Amino-6-chloro	4.05	3.82	0.23
XVII	2-Amino-6-bromo	3.91	3.80	0.11
XVIII	2-Amino-6-iodo	3.91	3.78	0.13
XIX	2-Amino-6-methyl-sulfonyl	4.04	4.26	0.22
XX	2-Dimethylamino-6-methylamino	3.12	2.65	0.47
XXI	2,6-Bishydrazino	2.77	3.02	0.25
XXII	2,6-Bis(methyl sulfonyl)	3.64	3.63	0.01
XXIII	2-Flurosulfonyl-6-chloro	3.18	3.67	0.49

[a] *C* is the concentration (moles/kg) which produced a tumor weight regression = 80%. [b] From Eq. 1.

fected but to a lesser extent since substituents are α to only one-ring nitrogen. This effect was tested by examining the π values of a number of 2-substituted pyridines in comparison with normal π values. Substituents were CN, Cl, Br, $COCH_3$, CH_3, C_2H_5, CH_3O, NH_2, $NHCOCH_3$ and NO_2. The following relationship was found:

$$\pi \text{ pyridines} = 0.38(\pm 0.17) + 0.49(\pm 0.22)\ \pi \text{ aromatics}$$

$$n = 10;\ r = 0.876;\ s = 0.227;\ F_{1,9} = 27.06\ (p < 0.001)$$

This relationship which was derived for some widely diverse substituents suggests that normal aromatic π values may be employed at position 6 with relative safety.

Antitumor data (Table II) were collected by the Drug Evaluation Branch, National Cancer Institute (NCI), according to the protocols (7) mentioned previously. A tumor fragment was implanted subcutaneously and treatment was initiated 24 hr later. The drug was administered daily for 11 consecutive days (QD1–11). On the twelfth day the animals were sacrificed and the tumor was excised and weighed. A compound is considered active in this system if it produces a tumor weight regression >58% (T/C ≤42%) compared to controls.

In the present study, a computer search was made of the NCI biological database for active 2-, 6-, and 8-substituted purines. 8-Substituted purines do not appear in the final correlation because there were too few active compounds to warrant their inclusion. Compounds containing SH or OH groups were excluded because these drugs exist as tautomers and no true substituent constants are available. Admittedly, this may narrow the conclusions somewhat. It has been shown, however, that one of the active forms of mercaptopurine and thioguanosine is the 6-methylthio derivative of each of those compounds obtained by *in vivo S*-methylation (12), and these analogs have been included in this study. Aminopurines, which have been shown to exist mainly in the NH_2 form (13), were included. Dose response plots were generated and the standard biological response was taken at T/C = 20%. C is the dose (moles/kg) that produces this response.

The toxicity correlation was restricted to 6-monosubstituted purines, since these comprise the major portion of purine bases tested by the NCI. The biological database was searched for those compounds for which a dose–response curve could be constructed and which showed reproducible toxicity. The LD_{50} (Table III), in moles/kg, was calculated by the probit method (14) from toxicity day (Day 11) survivors (15).

RESULTS AND DISCUSSION

Equation 1 was generated from the data in Tables I and II. The development of Eq. 1 is given in Table IV.

Table III—Observed and Predicted Toxicities of 6-Substituted Purines

Number	Substituent	log(1/LD_{50}) Observed	log(1/LD_{50}) Predicted[a]	|Δlog(1/LD_{50})|
I	Purine	Nontoxic	2.91	—
II	Chloro	2.73	2.91	0.18
III	Bromo	2.79	2.94	0.15
IV	Iodo	2.96	3.00	0.04
IX	Methylthio	3.16	3.07	0.09
X	Ethylthio	3.04	3.09	0.05
XXIX	Cyano	3.26	3.10	0.16
XXX	Ethoxy	3.24	3.08	0.16
XXXI	Amino	3.10	3.18	0.08
XXXII	Hydrazino	3.24	3.19	0.05
XXXIII	*n*-Propylthio	3.21	3.12	0.09
XXIV	*n*-Butylthio	3.06	3.14	0.08
XXXV	iso-Butylthio	3.15	3.12	0.03
XXXVI	*sec*-Butylthio	3.02	3.12	0.10
XXXVII	2′-Propynylthio	3.12	3.16	0.04
XXXVIII	Cyanomethylthio	3.35	3.29	0.06
XXXIX	Cyclopentylthio	3.23	3.14	0.09
XL	Phenylthio	3.32	3.22	0.10
XLI	2′-Imidazolinylthio	3.38	3.33	0.05
XLII	1′-Methyl-4′-nitro-imidazol-5′-ylthio[b]	3.60	3.55	0.05
XLIII	Benzylthio	3.13	3.25	0.12
XLIV	3′,4′-Dimethyl-benzylthio	3.20	3.28	0.08
LXV	*o*-Chlorobenzylthio	3.04	3.05	0.01
XLVI	*o*-Fluorobenzylthio	3.31	3.19	0.12
XLVII	*o*-Nitrobenzylthio	3.42	3.41	0.01
LXVIII	*m*-Chlorobenzylthio	3.22	3.23	0.01
L	*p*-Fluorobenzylthio	3.28	3.19	0.09
LI	2′-Pyridylmethylthio	3.38	3.43	0.05
LII	Ethylsulfonyl	3.30	3.41	0.11
LII	*n*-Propylsulfonyl	3.39	3.43	0.04
LIV	*n*-Butylsulfonyl	3.43	3.44	0.01
LV	*N*-Methylsulfon-amido	3.53	3.42	0.11
LVI	*N*-*n*-Propylsulfon-amido	3.43	3.45	0.02
LVII	*N*-iso-Butylsulfon-amido	3.58	3.50	0.08
LVIII	*N*-3′-Methoxypropyl-sulfonamido	3.48	3.58	0.10
LIX	*N*-2′-Ethoxyethyl-sulfonamido	3.57	3.59	0.02
LX	*N*-Benzylsulfonamido	3.58	3.65	0.07

[a] From Eq. 3. [b] Azathioprine.

$$\log(1/C) = 4.26(\pm 0.24) - 0.47(\pm 0.37)\ \text{MR}(2) + 1.18(\pm 0.55)\ \mathcal{R} \quad (6)$$

$$n = 22;\ r = 0.815;\ s = 0.372 \quad \text{(Eq. 1)}$$

Equation 1 relates the CA755 antitumor potency of 2,6-mono- and disubstituted purines to the molar refractivity of substituents at position 2 and the resonance constant $\mathcal{R}$ at position 6. The negative coefficient of the MR (2) term indicates that bulky substituents at position 2 are to be avoided for maximum potency in this tumor system. The larger positive coefficient of the $\mathcal{R}$ term suggests that potency in CA755 is predominantly influenced by the resonance effect of groups at position 6. Strong electron-withdrawing groups would be expected to increase potency. This is consistent with the observation that the 6-methylthio derivative ($\mathcal{R} = -0.11$) routinely produced complete tumor regression (T/C = 0%) at doses of 20 mg/kg. The 6-methoxy derivative ($\mathcal{R} = -0.51$), by comparison, requires ~10 times as much drug (250 mg/kg) to produce the same effect.

The 6-halo analogs (6-Cl, 6-Br, and 6-I) have about the same $\mathcal{R}$ values (−0.15, −0.17, and −0.19) as the 6-methylthio derivative and exhibit about the same potency as the latter. The 6-thiocyanate derivative ($\mathcal{R}$ = +0.19) was an outlier and was not included in Eq. 1. It was, however, one of the most potent compounds tested by the NCI, producing complete tumor regression at ~7 mg/kg. This analog may be, as suggested previously (16), a masked form of mercaptopurine, which may be produced by *in vivo* reduction.

The correlation coefficient of Eq. 1 is quite reasonable, considering the inherent variability in tumor weigh measurements. It accounts for ~66% of the variance in the biological data ($r^2 = 0.664$).

Equation 2, a toxicity correlation, was derived from the data in Tables I and III and includes only 6-thiopurines:

Table IV—Development of Equation 1

Intercept	MR (2)	$\mathcal{R}$ (6)	r	s	$F_{1,x}$	p	Equation
4.03	−0.72	—	0.560	0.519	$F_{1,21}$ = 9.16	<0.01	A
4.13	—	1.39	0.736	0.424	$F_{1,21}$ = 23.63	<0.001	B
4.26	−0.47	1.18	0.815	0.372	$F_{1,20}$ = 6.92[a]	<0.025	C

[a] This F value was obtained in comparison with Eq. B.

Table V—Development of Equation 3

Intercept	π(6)	MR (6)	r	s	$F_{1,x}$	p	Equation
3.30	−0.05	—	0.342	0.202	$F_{1,35}$ = 4.49	<0.05	A
3.04	—	0.08	0.452	0.192	$F_{1,35}$ = 8.73	<0.01	B
2.89	−0.15	0.19	0.908	0.092	$F_{1,34}$ = 116.06[a]	<0.001	C

[a] This F value of Eq. C is obtained in comparison with Eq. B.

$$\log(1/LD_{50}) = 2.95(\pm0.12) - 0.14(\pm0.02)\pi\ (6) + 0.17(\pm0.04)\text{MR}\ (6)$$
$$n = 29;\ r = 0.911;\ s = 0.076 \qquad \text{(Eq. 2)}$$

Equation 2 indicates that toxicity of 6-substituted thiopurines is influenced to about the same extent by the lipophilicity and bulkiness of groups at position 6. Toxicity would be expected to decrease with increasing lipophilicity. Bulky groups would be expected to increase the toxicity. To ensure that this was not a phenomenon peculiar to 6-thiopurines, seven additional compounds without sulfur bonds (II–IV, XXIX–XXXII) were included in the following:

$$\log(1/LD_{50}) = 2.89(\pm0.08) - 0.15(\pm0.03)\pi\ (6) + 0.19(\pm0.03)\ \text{MR}\ (6)$$
$$n = 36;\ r = 0.908;\ s = 0.092 \qquad \text{(Eq. 3)}$$

The development of Eq. 3 is given in Table V. Equation 3 is identical to Eq. 2 and appears to express a general structure–activity relationship for 6-substituted purines. In Eq. 3, the positive effect of increasing π (6) in order to decrease toxicity is offset by the toxicity-increasing effect of MR (6). This phenomenon has been observed in other systems[1], but the biochemical implications are not at all clear. There is some intercorrelation between MR (6) and π (6) (arc cos 0.38 = 68°) (17) as might be expected.

Equation 3 reflects the rather limited range of toxicities of 6-monosubstituted purines (Table III). Viewed together with Eq. 3, Eq. 1 suggests that, other things being equal, the development of more potent 6-substituted purines is not likely to result in a substantial increase in toxicity.

Few cancer QSAR studies have been published to date (18). This may be due both to the complexity of the problem and the nature of the data. Nevertheless, those studies that have been published show that cancer data will yield reasonable structure–activity correlations (15, 19, 20). In the present study, an attempt has been made to employ tumor weight inhibition data and standard physicochemical parameters in order to derive QSAR for an important class of antitumor agents. The correlations presented are reasonable and consistent with the data. The results suggest that other biological data obtained from the study of purines (enzyme inhibition data, *in vivo* survival data, *etc.*) may yield satisfactory correlations as well.

[1] Personal communication, C. Hansch, Seaver Chemistry Laboratory, Pomona College, Claremont, CA 91711.

REFERENCES

(1) J. A. Montgomery, in "Antineoplastic and Immunosuppressive Agents I," A. C. Sartorelli and D. G. Johns, Eds., Springer-Verlag, Berlin, 1974, chap. 5.

(2) J. H. Lister, "Purines," Wiley-Interscience, New York, N.Y., 1971, p. 9.

(3) W. H. Cone, in "Chemotherapy of Cancer," Lea & Febiger, Philadelphia, Pa., 1970, chap. 1.

(4) Z. Neiman and F. R. Quinn, *J. Pharm. Sci.*, **70,** 425 (1981).

(5) Z. Neiman, *Experientia*, **31,** 996 (1975).

(6) H. E. Skipper, J. A. Montgomery, J. R. Thompson, and F. M. Schabel, Jr., *Cancer Res.*, **19,** 425 (1958).

(7) R. I. Geran, N. H. Greenberg, M. M. MacDonald, A. M. Schumacher, and B. J. Abbott, *Cancer Chemother. Rep., Part 3*, **3,** 1 (1972).

(8) C. Hansch, A. Leo, S. H. Unger, K. H. Kim, D. Nikaitani, and E. J. Lien, *J. Med. Chem.*, **16,** 1207 (1973).

(9) C. Hansch and A. Leo, "Substituent Constants for Correlation Analysis in Chemistry and Biology," Wiley, New York, N.Y., 1979, Appendix I.

(10) *Ibid.*, Appendix II.

(11) A. I. Vogel, "A Text-Book of Practical Organic Chemistry," 3rd ed., Longman, London, 1970, p. 1036.

(12) L. S. Goodman and A. Gilman, in "The Pharmacological Basis of Therapeutics," 5th ed., Macmillan, New York, N.Y., 1975, p. 1279.

(13) J. H. Lister, "Purines," Wiley-Interscience, New York, N.Y., 1971, p. 8.

(14) A. J. Barr, J. H. Goodnight, J. P. Sall, and J. T. Helwig, "Statistical Analysis System," SAS Institute, Cary, N.C., 1979.

(15) F. R. Quinn, Z. Neiman, and J. Beisler, *J. Med. Chem.*, **24,** 636 (1981).

(16) T. Nagamachi, J. Fourrey, P. F. Torrence, J. A. Waters, and B. Witkop, *ibid.*, **17,** 403 (1974).

(17) S. H. Unger and C. Hansch, *ibid.*, **16,** 745 (1973).

(18) C. Hansch, *Farmaco, Ed. Sci.*, **34,** 89 (1979).

(19) C. Hansch, in "Correlation Analysis in Chemistry," N. B. Chapman and J. Shorter, Eds., Plenum, New York, N.Y., 1978, p. 426.

(20) F. R. Quinn and J. A. Beisler, *J. Med. Chem.*, **24,** 251 (1981).

Rectal Absorption of Nitroglycerin in the Rat: Avoidance of First-Pass Metabolism as a Function of Rectal Length Exposure

A. KAMIYA, H. OGATA*, and HO-LEUNG FUNG ˣ

Received June 8, 1981, from the *Department of Pharmaceutics, School of Pharmacy, State University of New York at Buffalo, Amherst, NY 14260.* Accepted for publication September 2, 1981. * Present address: National Institute of Hygienic Sciences, Tokyo, Japan.

Abstract □ Nitroglycerin administered orally undergoes substantial presystemic elimination. It was shown recently that first-pass hepatic metabolism of high clearance drugs can be substantially avoided *via* rectal administration. In applying this concept to nitroglycerin in rats, it was found that unrestricted rectal instillation of nitroglycerin (at 3.5-mg/kg dose) gave a mean ±*SD* bioavailability of 26.7 ± 7.0% (n = 6) compared to 1.8 ± 0.9% (n = 5) from oral dosing. This mode of dosing did not lead to complete avoidance of first-pass metabolism of nitroglycerin in rats. When the rectal exposure length to nitroglycerin was restricted to 3.5 cm from the anus, the mean ±*SD* bioavailability increased to 83.5 ± 74.5% (n = 14). However, the variability in bioavailability was extremely large. When the rectal exposure length was restricted to 2.0 cm from the anus (at 1.75-mg/kg dose), nitroglycerin bioavailability was estimated at 91.2 ± 30.4% (n = 6). The plasma nitroglycerin concentrations (>5 min) obtained after this mode of administration were similar to those achieved after intravenous dosing. The data showed that substantial avoidance of presystemic nitroglycerin metabolism can be achieved *via* rectal administration. This avoidance can be nearly complete if nitroglycerin is limited in exposure to only the lower rat rectum. It was also demonstrated that sustained (at least 24 hr) nitroglycerin delivery *via* the rat rectal route was feasible with an experimental osmotic minipump. This delivery system also produced nearly complete bioavailability for nitroglycerin in the rat.

Keyphrases □ Nitroglycerin—rectal absorption, avoidance of first-pass metabolism as a function of rectal length exposure, rats □ Absorption, rectal—nitroglycerin, avoidance of first-pass metabolism as a function of rectal length exposure, rats □ First-pass metabolism—avoidance as a function of rectal length exposure, nitroglycerin, rats

Nitroglycerin undergoes extensive and variable first-pass metabolism when administered orally in rats (1–3) and in humans (4). Recent studies showed that rectal administration of lidocaine, propranolol, and salicylamide in rats led to substantial avoidance of first-pass metabolism of these drugs (5–7). The possibility of similar improvement in bioavailability of nitroglycerin, another high-clearance drug, through the rectal route has been suggested (5). This hypothesis, however, has not been tested.

The studies reported here were designed, therefore, to determine the bioavailability of nitroglycerin after rectal administration in rats. Since drug spreading in the colon and rectum may lead to reduction of avoidance of first-pass metabolism (5), rectal dosing of nitroglycerin was carried out with three different lengths of rectal exposure to examine this effect. Finally, an experimental rectal delivery system was tested to explore whether sustained and complete absorption of nitroglycerin was feasible *via* the rectal route.

BACKGROUND

Since its introduction into clinical practice by Murrell (8) about 100 years ago, nitroglycerin has been the drug of choice for the acute relief and prophylaxis of angina pectoris. Interest in nitroglycerin has increased substantially in the past few years because new important clinical use for this drug has been documented. For example, nitroglycerin improved hemodynamics in patients with congestive heart failure (9), myocardial infarction (10), and unstable angina (11). Recently, this drug has been also used for the induction of hypotension during anesthesia and surgery (12). In spite of the long history of use and the increasing therapeutic scope of nitroglycerin, however, many basic aspects of the pharmacokinetics of this drug have not been investigated. The recent availability of sensitive analytical methods (13, 14) have made initiation of these studies (1–4) possible.

Oral sustained-release dosage forms of nitroglycerin are used clinically for prophylaxis of angina. The effectiveness of these dosage forms, and indeed the oral route itself, have been a subject of considerable debate in the literature (15). The pioneering work of Needleman *et al.* (1) showed that oral dosing of nitroglycerin in rats gave negligible blood concentrations of intact drug compared to those found for metabolites. Since human liver biopsy samples were shown to have an enzyme capacity similar to that found in rats, these authors concluded that there is no rational basis for oral nitroglycerin use. However, this suggestion had been refuted by clinical experience (16) and also by a well-conducted clinical study (17) which showed oral nitroglycerin to have significant benefits in controlling angina. Recent pharmacokinetic data (4, 18) also showed that intact nitroglycerin could be detected in plasma after oral admin-

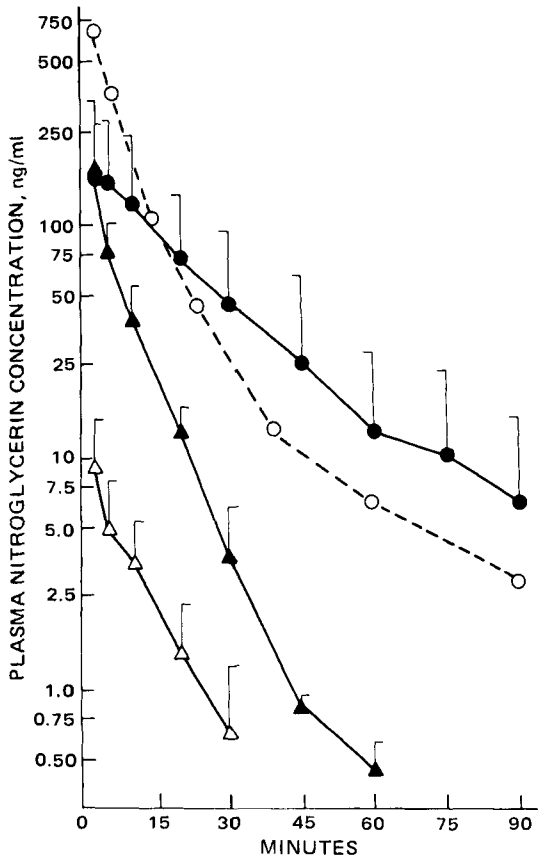

Figure 1—*Plasma nitroglycerin concentrations following different routes of administration at 3.50 mg/kg. Data represent mean ± SD of restricted rectal (3.5 cm) (●); unrestricted rectal (▲); and oral (△) administration. Plasma concentration curve after intravenous dosing (○) represents the predicted mean values calculated from a 1.75-mg/kg nitroglycerin dose*[8].

0022-3549/82/0600-0621$01.00/0

Table I—Bioavailability of Nitroglycerin following Different Routes of Administration

Route of Administration	Dose, mg/kg	Number of Animals	Peak Plasma Concentration[a], ng/ml	*AUC*[b], ng min/ml	Apparent Bioavailability[c], %
Oral	3.50	5	9 ± 5*	0.09 ± 0.04*	1.8 ± 0.9**
Unrestricted rectal	3.50	6	170 ± 58	1.28 ± 0.34	26.7 ± 7.0+
Restricted rectal (3.5 cm)	3.50	14	189 ± 181	4.02 ± 3.57	83.8 ± 74.5
Restricted rectal (2.0 cm)	1.75	6	129 ± 56	2.19 ± 0.73	91.2 ± 30.4

[a] Mean ± *SD*. [b] Area under plasma concentration *versus* time curve. [c] See *Experimental*. Symbols indicate significant difference from all other groups (*); from 100% and all other groups (**); and from 100% and restricted rectal (2.0 cm) dosing group (+).

istration of sustained-release capsules in humans. A report has appeared which suggests the bioavailability of a retard capsule to be ~20% of an equivalent dose of a sublingual tablet (4). In rats, the bioavailability of an oral nitroglycerin dose in aqueous solution was ~2% after a nitroglycerin dose of 7 mg/kg of body weight (2). Interanimal variability in oral bioavailability was also large. This variation has been found to be primarily due to the difference in the intrinsic activity of liver organic nitrate reductase in each individual animal (3). The composite evidence to date suggests, therefore, that although oral nitroglycerin may be bioavailable in part, first-pass metabolism (primarily hepatic in nature) is both extensive and variable.

A recent study has shown that the first-pass hepatic metabolism of lidocaine, another high clearance drug, could be avoided *via* rectal administration. This avoidance was partial in humans (5) but almost complete in rats (6). Nitroglycerin may exhibit a similar dependency. It was pointed out (7) that at least two sets of rectal veins (upper and lower) carry blood from the rat rectum: the upper rectal vein feeds into the portal vein, while the lower rectal vein empties into the inferior vena cava directly without first passing through the liver. Thus, drugs absorbed rectally and carried into the body *via* the upper rectal vein can be, in principle, subjected to first-pass elimination, while drug carried through the lower rectal vein is not. It is therefore anticipated that avoidance of first-pass metabolism may be dependent on the length of the rectum which is exposed to the drug solution. It is believed that there has not been any documentation of this phenomenon in the literature. Therefore, the bioavailability of rectally administered nitroglycerin as a function of rectal length exposure was examined to determine whether this hypothesis can be substantiated.

A major disadvantage of rectal delivery of drugs is that the bioavailability is highly variable. This variability may be caused by the difference in the time elapsed between rectal drug administration and bowel movement in individual subjects (19). If a rectal delivery device can be fabricated which produces ideal zero-order release at all times, then removal of the device for bowel movement and reinsertion of the same device (or for aesthetic reasons, a fresh one) afterwards will potentially allow the drug to be delivered at the same rate before and after bowel movement. For nitroglycerin, which has an extremely short half-life ($t_{1/2}$ = ~2–3 min) (2, 20, 21), zero-order delivery through the appropriate part of the rectum may also produce sustained plasma drug concentrations leading to potential prolongation of the therapeutic effects of the drug. The last part of this report deals with studies that explored the possibility of using an experimental osmotic pump system to produce sustained delivery and improved bioavailability of nitroglycerin in the rat.

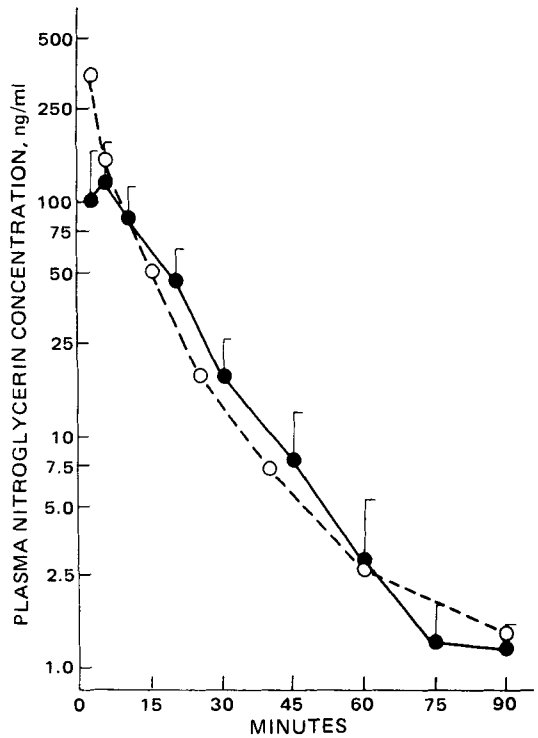

Figure 2—*Plasma nitroglycerin concentrations following restricted rectal (2.0 cm) administration at 1.75 mg/kg. Data represent mean ± SD after restricted rectal (2.0 cm) administration, (●); and mean after intravenous dosing*[8] (○).

EXPERIMENTAL

Materials—Nitroglycerin and isosorbide dinitrate solutions in hexane were prepared according to a previous report (14). A commercial 10% (w/w) nitroglycerin–lactose adsorbate[1] was used to prepare the aqueous and propylene glycol nitroglycerin solutions. To obtain the lactose-free nitroglycerin, an aqueous solution of the powder was extracted with ether, which was then evaporated under a gentle nitrogen stream. The resultant oil was dissolved in distilled water or propylene glycol to yield the appropriate concentration, which was then confirmed by gas chromatographic assay (14).

Animals—Male Sprague-Dawley rats[2] (300—360 g) were used. The right jugular vein was cannulated chronically (22). Animals were used after at least 16 hr of fasting prior to nitroglycerin administration and allowed free movement in a metabolic cage after dosing. Blood (~0.5 ml) was withdrawn *via* the jugular vein cannula at appropriate times.

Bolus Administration Studies—Nitroglycerin in normal saline solution (1.22 mg/ml) was used. For unrestricted rectal dosing, a septum plug[3] was affixed to the anus with glue[4]. Nitroglycerin was then injected into the rectum with a syringe through the septum. For restricted rectal

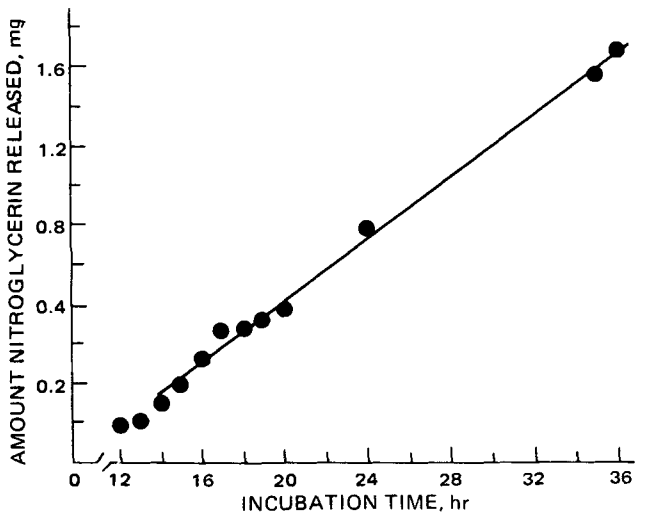

Figure 3—*A representative plot of* in vitro *nitroglycerin release from osmotic minipump.*

[1] Nitroglycerin 10% (w/w) in lactose, ICI America, Atlas Chemical Division, Wilmington, DE 19899.
[2] Blue Spruce Farms, Altamont, NY 12009.
[3] F-145 Septum plugs, 6.5-mm diameter, Alltech Associates, Arlington Heights, IL 60004.
[4] New Elmer's Wonder Bond, Borden, Inc., Columbus, OH 43215.

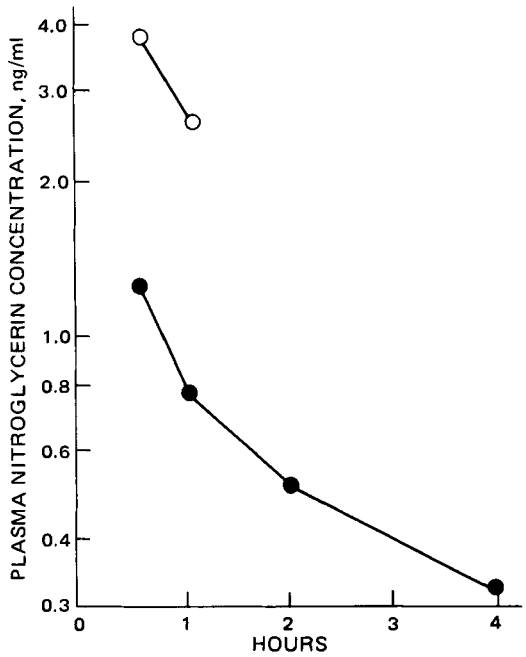

Figure 4—In vivo *nitroglycerin rectal delivery* via *osmotic minipump (upright placement). Different symbols indicate different animals. In the rat denoted by open circles, the plasma concentrations were indistinguishable from blank values at times beyond 1 hr.*

dosing, a device was constructed which connected two septum plugs at a fixed distance (either 2.0 or 3.5 cm) with a stainless steel wire. This device was inserted into the rectum from the anus while the animal was under slight ether anesthesia. The upper septum plug[5] was used to avoid upward spreading of nitroglycerin solution. The lower septum plug[3] was glued to the anus. Drug solution was injected into the rectum following the withdrawal of a volume of air from the rectum identical to that of the rectal drug solution. For oral administration, nitroglycerin solution was introduced by intubation to rats under slight ether anesthesia. Nitroglycerin doses were 3.50 mg/kg for unrestricted rectal dosing, restricted rectal dosing at 3.5-cm rectal length exposure, and oral dosing; and 1.75 mg/kg for restricted rectal dosing at 2.0-cm rectal length exposure. The lower dose was used in the last case because of limitations in the aqueous solubility of nitroglycerin and in the volume of dosing solution which could be injected at that specified rectal length exposure.

Sustained Rectal Delivery Studies—Osmotic pumps[6] were used as possible drug delivery systems for sustained rectal delivery of nitroglycerin. Nitroglycerin was dissolved in propylene glycol at 89.0 mg/ml. Each minipump was filled with ~0.25 ml of drug solution. The pump was placed at the bottom of a round-bottom flask in 200 ml of normal saline at 37°. The solution was stirred at 60 rpm and sampled from 12 to 36 hr (0.5 ml/sample) to determine the *in vitro* nitroglycerin release rate.

After this *in vitro* experiment, the minipump was washed with saline, blotted dry, and inserted into the rat. The osmotic pump was inserted into the rectum either in the upright (release hole pointing toward the intestine) or inverted position under slight ether anesthesia. For upright placement, the bottom of the osmotic pump was glued directly in place at the anus. For inverted placement, the neck plug of the pump was connected to a septum[3] by a stiff wire. This delivery system was inserted into the rectum and the septum was secured at the anus with glue. Blood samples were withdrawn up to 24 hr after insertion of these devices.

Assay of Nitroglycerin—After collection, blood samples were immediately transferred to chilled centrifuge tubes and centrifuged. Aliquots of plasma (0.2 ml) were mixed with 10 μl of 1 *N* silver nitrate and stored at −20° until assay. In the *in vitro* release experiment, 0.1-ml aliquots were assayed. The samples were extracted with hexane and nitroglycerin concentrations were determined by a previously reported gas chromatograph procedure (14) using isosorbide dinitrate as the internal standard.

The glue and septum plugs used were shown not to produce any interference in the assay of nitroglycerin. Sham experiments conducted using these devices showed also that the apparent clearance of nitroglycerin after intravenous injection was unaltered.

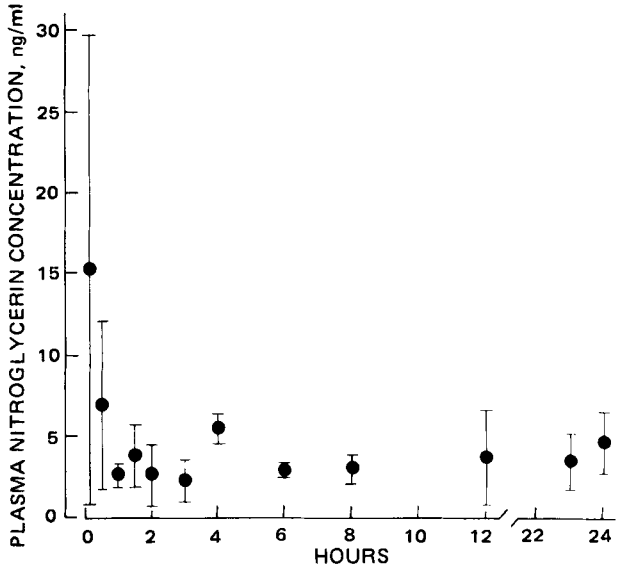

Figure 5—In vivo *nitroglycerin rectal delivery* via *osmotic minipump (inverted placement). Data represent mean* ± SD.

Calculation of Statistics—The area under the plasma concentration *versus* time curve (*AUC*) was computed using the spline method from a commercially available program with a desk top computer[7]. Residual area of *AUC* ($AUC_{t\to\infty}$) was estimated by C_t/k, where k was the first-order kinetic rate constant derived from linear least-square regression using the last three plasma concentrations of each experiment and C_t was the plasma nitroglycerin concentration at the last sampling time. The apparent bioavailability (F) after oral or rectal dosing was estimated by the traditional method of comparing the $AUC_{0\to\infty}$ to that of an equivalent intravenous dose. It is assumed here that the systemic clearance is independent of the route of administration. The apparent systemic clearance after intravenous bolus administration in rats has been found to be independent of dose from 0.15 to 2.5 mg/kg and has a value of 730 ± 241 ml/min/kg (mean ±*SD*, n = 26)[8].

Statistical analysis was performed using the unpaired t test and $p < 0.05$ was employed to establish statistical significance.

RESULTS AND DISCUSSION

Plasma nitroglycerin concentrations observed at various times after oral, rectal, and intravenous administration are shown in Fig. 1 (3.50-mg/kg dose) and Fig. 2 (1.75-mg/kg dose). Intravenous bolus doses of nitroglycerin at 3.50 mg/kg were found to be toxic to the animals, many of which exhibited immediate severe convulsions, presumably because of the extremely high initial concentrations. The intravenous curve shown in Fig. 1 was constructed, therefore, from the mean data of 1.75 mg/kg iv dose after correction for dose. It will be shown elsewhere[8] that the systemic intravenous nitroglycerin clearance in the rat is essentially concentration independent below its toxic dose.

Oral bioavailability of nitroglycerin at 3.50 mg/kg in aqueous solution was shown to be poor (Fig. 1). The apparent bioavailability was found to be ~2% at this dose (Table I), which agrees with data obtained previously at 7 mg/kg (2).

Three rectal lengths of exposure were used to determine the degree of avoidance of first-pass metabolism of nitroglycerin in the rat. In the first case, only one septum was affixed at the anus and the administered drug was allowed to spread unrestricted into the lower and upper intestines. In a preliminary experiment using a dye as a marker, it was noted that this mode of administration led to significant upward spreading of the rectal dose, presumably due to peristaltic movement of the GI tract. When nitroglycerin was given in this manner, the bioavailability was found to be 26.7 ± 7.0% (Table I) of a comparable intravenous dose. This bioavailability was ~15 times that of an oral dose, indicating that rectal dosing led to some avoidance of first-pass metabolism.

When the rectal dosing solution was restricted to a region no further than 3.5 cm from the anus, absorption of nitroglycerin was considerably improved but rather variable (Fig. 1). The terminal half-life obtained

[5] F-174 Septum, 9.0-mm diameter, Supelco, Inc., Bellefonte, PA 16823.
[6] ALZET Osmotic minipump, Model 2001, Alza, Palo Alto, CA 94304.
[7] Hewlett-Packard 9825A Calculator, Hewlett-Packard, Loveland, CO 80537.
[8] H.-L. Fung, G. A. Maier, H. Ogata, and A. Kamiya, unpublished data.

Table II—Individual Data on *In Vivo* Nitroglycerin Rectal Delivery *via* Osmotic Pump (Inverted Placement)

Rat	*In Vitro* Release Rate, μg/hr	Mean Plasma Nitroglycerin Concentration[a] (1 → 24 hr), ng/ml	Estimated[c] Mean *In Vivo* Release Rate, μg/hr
1	65.8	3.32 ± 2.14	48.0
2	38.7	3.46 ± 1.66	50.0
3	30.1	3.11 ± 1.41[b]	45.0
4	76.5	3.55 ± 1.76	51.3
Mean ± *SD*	52.8 ± 21.9	3.40 ± 1.72	48.6 ± 2.7

[a] Mean ± *SD*. [b] 1 → 4 hr only, rectal septum bitten off by animal. [c] $k_0 = C_{ss}Cl$.

after this mode of administration (16.5 ± 8.4 min, mean ± *SD*) appeared larger than, though not statistically different from, those observed after unrestricted rectal ($t_{1/2}$ = 10.1 ± 3.2 min) and intravenous administration (18.3 ± 6.1 min). Since the plasma clearance of nitroglycerin was shown to be independent of intravenous dose[8], it is unlikely that the systemic clearance of nitroglycerin has been altered with this mode of dosing. Any potential divergence in apparent plasma half-life in the present case might have arisen instead from differences in absorption rates among the treatments, since flip-flop kinetics might be operative after nonintravenous administration (2). Using these assumptions, the apparent bioavailability of nitroglycerin from this mode of rectal dosing (restricted, 3.5 cm) could be estimated as 83.8 ± 74.5% (Table I), which was ~3 times higher than that found in the case where the rectal solution was unrestricted.

Figure 2 shows the case in which the dose was restricted to the lowest 2.0 cm of the rectum. It is apparent that, except for the first time point, the rectal dose yielded similar plasma nitroglycerin concentrations compared to an equivalent intravenous dose. Indeed, the *AUC*'s calculated for these two routes of administration were not statistically different ($p > 0.05$). The bioavailability of this rectal mode of dosing was estimated at 91.2 ± 30.4% (Table I). The interanimal variability was noticeably smaller here than in the previous case where rectal exposure was set at 3.5 cm.

It is quite clear, then, that rectal administration of nitroglycerin in the rat leads to substantial avoidance of the first-pass metabolism of nitroglycerin. Consistent with anatomical prediction, this avoidance decreases when the rectal dose is exposed to the upper rectal area where drug can be adsorbed through the upper rectal veins and transported *via* the portal vein to the liver. It is believed that this is the first instance in which this suspected relationship of drug rectal length exposure to avoidance of first-pass metabolism has been clearly demonstrated.

A previous study has shown that instillation of lidocaine into the unrestricted rectum of rats led to near complete bioavailability of this drug (6). As far as can be determined, the present experimental procedure in the unrestricted rectum case was similar to that used by these authors, with the possibly important difference in the volume of rectal solution used. This study (6) used an instillation volume of 0.4 ml, whereas a volume of ~1.0 ml was used in the present study. The smaller volume used in the lidocaine study might permit less upward spreading of the dose, thus allowing more complete avoidance of first-pass metabolism. It is also possible that this apparent discrepancy may have arisen from the difference in the permeability and metabolic properties of the drugs themselves.

The osmotic minipump has been reported to produce sustained zero-order drug delivery *in vivo* (23). This particular experimental device was tested to explore whether rectal delivery of nitroglycerin can produce almost complete bioavailability as well as sustained plasma drug concentrations over a 24-hr period. When these minipumps were filled with a propylene glycol solution of nitroglycerin (an aqueous solution was impossible because of solubility limitations), the *in vitro* release was shown to be zero-order in nature (Fig. 3). Preliminary trials of these minipumps inserted into the animal in the upright position showed them to be ineffective in producing sustained plasma nitroglycerin concentrations (Fig. 4). Since zero-order delivery of drugs from the osmotic minipump depends, among other factors, on an unobstructed aperture in the pump itself, fecal materials which might have been deposited on the aperture could interfere with drug delivery. When the osmotic minipump was inverted so that the pump aperture now pointed toward the anus (which was sealed with a septum), the desired pharmacokinetic release profile was observed. Figure 5 shows the mean (±*SD*) plasma concentrations of nitroglycerin over 24 hr after insertion of the rectal osmotic minipumps in the inverted position in four rats. Although these pumps had been pre-equilibrated in saline at 37° for at least 36 hr (during which time the *in vitro* release rate was determined), an initial burst of nitroglycerin release was observed upon insertion of those devices. However, the plasma nitroglycerin concentrations from 1 to 24 hr after rectal pump insertion were quite stable (Fig. 5 and Table II).

It was noted that the *in vitro* drug release rate of the minipumps was quite variable. The reasons for this variability are not known presently. The *in vivo* release rate of each minipump could not be measured directly but could be approximated by the equation $k_0 = C_{ss}Cl$ where C_{ss} is the measured mean steady-state plasma nitroglycerin concentration in each animal and Cl is the systemic clearance of nitroglycerin (which averages 241 ml/min/300-g rat). Based on the mean values (Table II) the estimated *in vivo* release rates for the osmotic pumps appeared similar to the measured *in vitro* rates. This agreement suggests that near complete bioavailability can be achieved with this mode of rectal dosing. It would appear then that the experimental osmotic pump, when placed in the inverted position, can provide both sustained and complete delivery of nitroglycerin *via* the rectal route.

CONCLUSIONS

The present studies showed that rectal dosing of nitroglycerin in rats can lead to substantial avoidance of first-pass metabolism. If the nitroglycerin dose can be restricted to the lower rectum, this avoidance can be made complete. It has been shown that an experimental osmotic pump is capable of producing sustained and apparent zero-order release of nitroglycerin over a 24-hr period. Since the degree of avoidance of first-pass metabolism from rectal administration is somewhat less in humans when compared to the rat (5, 6), the applicability of the present findings to rectal absorption of nitroglycerin in humans has to be validated.

REFERENCES

(1) P. Needleman, S. Lang, and E. M. Johnson, Jr., *J. Pharmacol. Exp. Ther.*, **181,** 489 (1972).

(2) P. S. K. Yap and H.-L. Fung, *J. Pharm. Sci.*, **67,** 584 (1978).

(3) G. A. Maier, C. Arena, and H.-L. Fung, *Biochem. Pharmacol.*, **29,** 646 (1980).

(4) V. H. Maier-Lenz, L. Ringwelski, and A. Windorder, *Arzneim.-Forsch.*, **30,** 320 (1980).

(5) A. G. de Boer, D. D. Breimer, H. Mattie, J. Pronk, and J. M. Gubbens-Stibbe, *Clin. Pharmacol. Ther.*, **26,** 701 (1979).

(6) A. G. de Boer, D. D. Breimer, J. Pronk, and J. M. Gubbens-Stibbe, *J. Pharm. Sci.*, **69,** 804 (1980).

(7) A. G. de Boer and D. D. Breimer, in "Drug Absorption," L. F. Prescott and W. S. Nimmo, Eds., Adis Press, Balgowlah, Australia, 1981, pp. 61–72.

(8) W. Murrell, *Lancet*, **I,** 80, 113, 225, 642 (1879).

(9) E. Mikulic, J. A. Franciosa, and J. N. Cohn, *Circulation*, **52,** 477 (1975).

(10) P. W. Armstrong, D. C. Walker, J. R. Burton, and J. O. Parker, *ibid.*, **52,** 1118 (1975).

(11) P. B. Oliver, D. E. Plots, and R. G. Pluss, *N. Engl. J. Med.*, **288,** 745 (1973).

(12) H. A. Kaplan, R. W. Dunbar, and E. L. Jones, *Anesthesiology*, **45,** 14 (1976).

(13) M. T. Rosseel and M. G. Bogaert, *J. Pharm. Sci.*, **62,** 754 (1973).

(14) P. S. K. Yap, E. F. McNiff, and H.-L. Fung, *ibid.*, **67,** 582 (1978).

(15) J. C. Krantz, Jr., and C. D. Leake, *Am. J. Cardiol.*, **36,** 407 (1975).

(16) I. Hirshleifer, *Curr. Ther. Res.* **15,** 158 (1973).

(17) T. Winsor and H. J. Berger, *Am. Heart J.*, **90,** 611 (1975).

(18) H. P. Blumenthal, H.-L. Fung, E. F. McNiff, and S. K. Yap, *Br. J. Clin. Pharmacol.*, **4,** 241 (1977).

(19) M. M. Nowak, B. Grundhofer, and M. Gibaldi, *Pediatrics* **54,** 23 (1974).

(20) S. Lang, E. M. Johnson, Jr., and P. Needleman, *Biochem. Pharmacol.*, **21,** 422 (1972).

(21) R. L. Stein, J. K. O'Brien, C. Irwin, J. K. Townsend-Parchman, and F. E. Hunter, Jr., *ibid.*, **29,** 1807 (1980).

(22) J. R. Weeks and J. D. Davis, *J. Appl. Physiol.*, **19,** 540 (1964).

(23) H. A. J. Struyker-Boudier and J. F. Smits, *J. Pharm. Pharmacol.*, **30,** 576 (1978).

ACKNOWLEDGMENTS

Supported in part by NIH grants HL 22273 and GM 20852.

A GLC–Nitrogen Phosphorous Detector Assay for Trifluoperazine in Plasma

R. M. H. ROSCOE, J. K. COOPER, E. M. HAWES, and K. K. MIDHA ˣ

Received May 29, 1981, from the *College of Pharmacy, University of Saskatchewan, Saskatoon, Saskatchewan S7N 0W0, Canada.* Accepted for publication September 11, 1981.

Abstract □ A GLC–nitrogen phosphorous detector (NPD) method for the quantitative determination of trifluoperazine in plasma is described. It depends on an organic extraction of trifluoperazine and the internal standard prochlorperazine from basified plasma. Following the extraction, the organic solvent is evaporated to dryness and the residue is reconstituted in a small volume of methyl alcohol. GLC analysis of aliquots of the methanolic solution using a NPD permitted the determination of 0.5 ng/ml of trifluoperazine in plasma. Standard curves for trifluoperazine over a concentration range of 0.5 to 15 ng/ml of plasma were linear with an overall variation coefficient of 5.3%. In isolated samples obtained from a normal healthy volunteer, application of this method to plasma concentration determinations after oral administration of a 5-mg trifluoperazine tablet, is demonstrated and compared with the concentrations obtained by GLC–mass spectrometry and radioimmunoassay procedures.

Keyphrases □ Trifluoperazine—GLC–nitrogen phosphorous detector analysis in human plasma □ Prochlorperazine—GLC–nitrogen phosphorous detector analysis of trifluoperazine in human plasma □ GLC–Nitrogen phosphorous detector—analysis of prochlorperazine in human plasma

Since the introduction of the major tranquilizers in the early 1950's, the phenothiazines with the piperazine ring system have been widely used. Over the past 25 years, several publications (1–5) have been concerned with the quantitation of chlorpromazine in biological fluids; however, the analysis of piperazine containing phenothiazines has been more difficult. Being therapeutically more potent, these antipsychotic drugs are administered in much smaller doses than chlorpromazine. Like chlorpromazine, these agents undergo extensive metabolism leading to numerous metabolites, several of which are pharmacologically active. These drugs are also subject to extensive first-pass (gut wall and/or hepatic) biotransformation. Other properties of these drugs include large interindividual variations in plasma levels following identical doses to volunteers or patients, extensive binding to multiple sites, large volumes of distribution, and their extreme instability in all stages of handling during analysis (4–7). Published reports indicate that the plasma concentrations of these piperazinyl phenothiazines in patients are much lower than those encountered with chlorpromazine. Thus, sensitivity requirements for these drugs are more stringent than those for the assay of chlorpromazine (8–10).

The techniques which may have the sensitivity for the quantitation of chlorpromazine and other antipsychotics include GLC–nitrogen phosphorous detector (NPD), GLC–electron capture detector (ECD), GLC–mass spectrometry (MS), HPLC–UV, HPLC–spectrofluorometric detector (SPF), and other procedures such as radioimmuno- and radioreceptor assays. For the orally administered antipsychotic agent, trifluoperazine, only the radioimmunoassay and GLC–MS methods of Midha *et al.* (11, 12) have demonstrated the necessary sensitivity to follow plasma concentration–time profiles following the

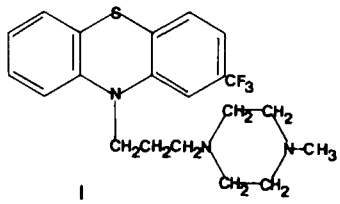

I

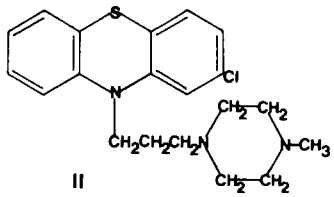

II

administration of single 5-mg doses of trifluoperazine in healthy human volunteers. These procedures are capable of quantitating plasma trifluoperazine concentrations in specimens collected as late as 24 hr postadministration of trifluoperazine.

A new GLC method for trifluoperazine (I) based on an organic extraction of basified plasma and quantitation using a more conventional NPD system with prochlorperazine (II) (the 7-chloro analog of trifluoperazine) as internal standard is described. Trifluoperazine in the concentration range 0.5–15 ng/ml of plasma can be quantitated in this method with an overall variation coefficient of 5.3%.

EXPERIMENTAL

Materials—Trifluoperazine dihydrochloride[1], *N*-desmethyltrifluoperazine dimaleate[1], trifluoperazine sulfoxide[1], 7-hydroxytrifluoperazine[1], and prochlorperazine dimaleate[2] were generously donated.

Heparinized evacuated tubes[3] were commercially obtained. All solvents used were HPLC grade, and all other chemicals were commercial analytical grade, used without further purification.

The assay was done in subdued light. Standard solutions of trifluoperazine, trifluoperazine metabolites, and prochlorperazine were prepared by dilution in ethanol and/or double distilled water. Appropriate dilutions of the standard solutions were made in outdated human plasma[4].

Plasma Level Study—A normal, healthy male volunteer (57 kg) fasted overnight was given a single 5-mg commercial trifluoperazine tablet orally[5]. Blood samples (10 ml) were withdrawn from the cubital vein into heparinized evacuated tubes, centrifuged, and separated plasma was stored at −4° for a maximum period of 7 days. During blood sample collection, care was taken to avoid contact of the blood with the rubber stopper of the evacuated tube.

Extraction of Trifluoperazine—One milliliter of aqueous internal

[1] Smith Kline and French Canada, Ltd., Mississauga, Ontario, Canada and Dr. A. A. Manian, National Institute of Mental Health, Rockville, Md.
[2] Rhône-Poulenc Pharma Inc., Montreal, Quebec, Canada.
[3] Venoject, Kimble-Terumo, Inc., Elkton, Md.
[4] Canadian Red Cross.
[5] Stelazine, Smith Kline and French Laboratories, Philadelphia, Pa.

0022-3549/82/0600-0625$01.00/0

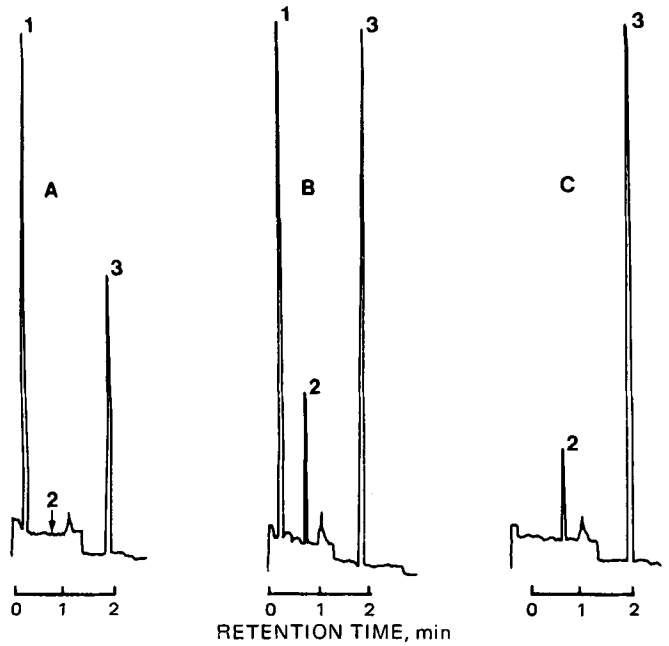

Figure 1—*GLC–NPD chromatogram of: (A), extracted blank human plasma; (B), extracted human plasma spiked with 2.5 ng/ml of trifluoperazine; (C), extracted plasma obtained from human volunteer 2.0 hr following the administration of 5 mg of trifluoperazine. (1, caffeine; 2, trifluoperazine; 3, prochlorperazine.)*

standard solution of prochlorperazine (100 ng/ml) and 0.5 ml of 10 *N* NaOH were added to a 2-ml plasma sample (spiked or from dosed volunteer) in a 10-ml polytef-lined screw-capped test tube. The sample was gently mixed[6] and 5 ml of *n*-pentane–isopropyl alcohol (50:1) was added. The tube was tightly capped and the drug and the internal standard were extracted from plasma by first mixing[7] for 15 min and then centrifuging[8] for 15 min at room temperature at 1720×*g*. Following centrifugation, ~4 ml of the upper organic layer was transferred with the aid of a disposable Pasteur pipet to a fresh tube, taking extreme care not to contact the organic–aqueous interface. The organic extract was evaporated[9] almost to dryness at 55°. The sides of the tube were washed down with ~1 ml of the extracting solvent and the contents re-evaporated[9] to dryness. The residue was then reconstituted in the same tube with 25 μl of methyl alcohol by mixing[6] and aliquots of 2–4 μl were injected into the gas chromatograph.

GLC—The gas chromatograph[10] was equipped with a nitrogen phosphorous detector. The column was a coiled glass tube[11], 1.8 m long × 2-mm i.d., packed with 3% phenyl methyl silicon[12] coated on acid-washed, dimethylchlorosilane-treated 100–120 mesh high-performance, flux-calcined diatomite support[13].

The column was conditioned at 335° for 12–24 hr with a low helium flow. For plasma analysis, the injection port, detector block, and column oven temperatures were 300, 300, and 310°, respectively. Helium was used as a carrier gas at a flow rate of 30 ml/min. Hydrogen and air flow rates and NPD bead voltages were optimized for maximum response at electrometer settings of 3 or 4.

Calculations—Peak height ratios were calculated by dividing the height of the peak due to trifluoperazine (0.89 min) by that of prochlorperazine, the internal standard (1.90 min). Calibration curves were constructed by plotting the spiked control plasma peak height ratios against the concentrations of trifluoperazine (nanograms per milliliter of plasma).

RESULTS AND DISCUSSION

Under the chromatographic conditions described previously, trifluoperazine and the internal standard prochlorperazine gave sharp and symmetrical peaks with retention times of 0.89 and 1.90 min, respectively. Figure 1A shows a typical chromatogram obtained by processing control blank plasma which contained 50 ng/ml of the internal standard, prochlorperazine. No extraneous peak at the retention time of trifluoperazine was observed. A chromatogram obtained when the method was applied to spiked human plasma containing 2.5 ng/ml of trifluoperazine and 50 ng/ml of the internal standard is shown in Fig. 1B. In the blank and spiked plasma (Fig. 1A, 1B) a sharp peak which had an identical retention time to caffeine was obtained. Caffeine was extracted in the procedure used, and because of the presence of four nitrogen atoms it gave a good response to the NPD.

Figure 1C shows a chromatogram of the plasma sample (2 ml) from blood withdrawn from a male volunteer (57 kg) at 2.0 hr after oral administration of a 5-mg commercial tablet. This sample was estimated to contain 1.45 ng/ml of trifluoperazine. There was no peak due to caffeine, since the subject was asked to withdraw from caffeine-containing beverages and food. A chromatographic analysis time of ~2 min was required for each sample.

The use of a mixed organic solvent system of *n*-pentane and isopropyl alcohol provided quantitative extraction of the drug and the internal standard in one step from basified plasma. The overall recoveries of trifluoperazine and prochlorperazine were of the order of 102.3 ± 3.6 and 90.7 ● 2.8%, respectively, as reported earlier (12). The use of isopropyl alcohol not only provides the necessary polarity needed for the quantitative extraction of the drug and the internal standard, it also retards the adsorption of these basic drugs onto the glass surface during extraction. It was also found useful to keep the concentration of the internal standard high, as the prochlorperazine competes with the drug for the adsorption sites on the glassware used for extraction. This type of observation has been made earlier with the structurally similar drug chlorpromazine (13), where it was found necessary to use very high concentrations of the internal standard mesoridazine.

The important metabolites of trifluoperazine, which are extracted under the conditions described previously, did not interfere in this procedure. These metabolites elute with retention times different from that of the drug and the internal standard. Figure 2 shows the chromatographic separation of these metabolites, *i.e.*, *N*-desmethyltrifluoperazine, 7-hydroxytrifluoperazine, and trifluoperazine sulfoxide, from trifluoperazine and the internal standard prochlorperazine. Trifluoperazine sulfone also did not interfere, as it was found to elute after the trifluoperazine sulfoxide.

After repeated injections into the gas chromatograph, an uneven response from the NPD was observed, which led to reduced sensitivity as well as the ratios of peak heights of the drug and the internal standard becoming irreproducible. This generally required readjustment of the NPD bead voltage or installation of a new bead.

An interesting problem of interference with respect to trifluoperazine was observed in the present GLC–NPD assay. If the plasma samples were prepared from blood collected in the heparinized brand of evacuated tubes[3], an interfering peak with nearly the same retention time as trifluoperazine was observed in the chromatograms. The interference, often observed as a double peak was small but significant. This was overcome by employing a different brand of evacuated tubes[14]. Some additional experimentation revealed that the interfering material was alkaline and aqueous soluble; however, positive chemical identification attempts by mass spectrometry were not successful. It should be noted that although the plasticizer effect (14) with trifluoperazine is not as significant as with other phenothiazines, care must be exercised during the collection of blood by evacuated tubes to see that the blood does not come in contact with the rubber stopper.

Table I—GLC–NPD Estimation of Trifluoperazine Added to Plasma[a]

Plasma Trifluoperazine, ng/ml	*n*	Average Peak/Height Ratio[b]	Coefficient of Variation, %
0.5	6	0.062	13.9
1.0	6	0.120	5.9
2.5	6	0.246	5.5
5.0	6	0.482	5.2
7.5	6	0.744	7.0
10.0	6	1.021	4.1
15.0	6	1.512	2.7

[a] Mean coefficient of variation = 5.3%, slope = 0.1003x ± 0.0035, and correlation = 0.9992. [b] Trifluoperazine–Prochlorperazine.

[6] Vortex Genie, Fisher Scientific Co., Edmonton, Alberta, Canada.
[7] Evapo-Mix, Fisher Scientific Co., Edmonton, Alberta, Canada.
[8] T-J6 Centrifuge, Beckman Instruments, Toronto, Ontario, Canada.
[9] Thermolyne Dri-Bath, Fisher Scientific Co., Edmonton, Alberta, Canada.
[10] Model 5840, Hewlett-Packard Canada Ltd., Edmonton, Alberta, Canada.
[11] Chromatographic Specialties, Brockville, Ontario, Canada.
[12] OV-17, Chromatographic Specialties, Brockville, Ontario, Canada.
[13] Gas Chrom Q, Chromatographic Specialties, Brockville, Ontario, Canada.
[14] Vacutainer, Becton Dickinson Co., Mississauga, Ontario, Canada.

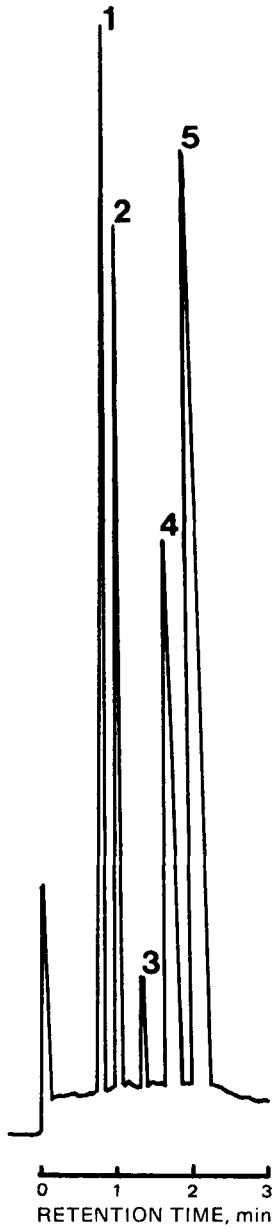

Figure 2—*GLC-NPD separation of trifluoperazine(1), N-desmethyltrifluoperazine (2), 7-hydroxytrifluoperazine (3), prochlorperazine (4), and trifluoperazine sulfoxide (5); OV-17 injector, 300°; oven, 310°; detector, 300°. Approximately 50 ng of each component on-column using nitrogen–phosphorous detection.*

The accuracy and precision of the GLC–NPD assay are demonstrated in Table I. Results are based on six determinations of each concentration of trifluoperazine, ranging from 0.5 to 15 ng/ml of plasma. The overall variation coefficient was 5.3%. The calibration curve obtained by plotting the peak height ratio of the trifluoperazine and prochlorperazine *versus* the concentration of trifluoperazine was linear over the 0.5–15.0-ng range of the drug/ml of plasma. A mean slope value of $0.1003x + 0.0035$ ($r^2 = 0.9996$) was obtained.

The application of the present method to plasma concentration determinations is shown in Table II, where the values obtained by the present method are given along with those obtained by GLC–MS and radioimmunoassay procedures. Because of the sensitivity limitations of the GLC–NPD assay, only concentrations around the peak times are shown from one volunteer. The GLC–NPD values compare well with the GLC–MS method; however, the radioimmunoassay gives values that are slightly higher than those obtained with the chemical methods. This is probably due to the cross-reactivity of the antiserum to the 7-hydroxy and *N*-desmethyl metabolites of trifluoperazine (11).

Table II—Comparison of Plasma Trifluoperazine Concentrations Determined by Three Different Methods

Subject Plasma Sample, hr	Trifluoperazine Plasma Concentration		
	GLC-NPD, ng/ml	Radioimmunoassay, ng/ml	GLC–MS, ng/ml
2.0	0.88	1.00	0.80
3.0	0.91	1.09	0.93
4.5	0.73	1.13	0.71

In conclusion, the described procedure is simple and specific for trifluoperazine. It may not have the sensitivity for single-dose pharmacokinetics and bioavailability studies for the drug, however, steady-state monitoring can be easily carried out. This procedure can also be easily adopted for the quantitative determination of prochlorperazine by using trifluoperazine as the internal standard. The other phenothiazine drugs which have been tested for plasma extraction and sensitivity are promazine, chlorpromazine, butaperazine, and promethazine. Thus, the described procedure has the potential for its applicability in the quantitative analysis of these drugs.

REFERENCES

(1) T. B. Cooper, *Clin. Pharmacokinet.*, **3**, 14 (1978).

(2) J. E. Fairbrother, *Pharm. J.*, **222**, 271 (1979).

(3) E. Usdin, *Crit. Rev. Clin. Lab. Sci.*, **2**, 347 (1971).

(4) K. K. Midha, J. K. Cooper, E. M. Hawes, J. W. Hubbard, R. M. H. Roscoe, H. U. Shetty, and P. K. F. Yeung, *Psychopharmacol. Bull.*, **17**, 15 (1981).

(5) K. K. Midha and R. Roscoe, "Therapeutic Drug Monitoring," A. Richens and V. Marks, Eds., Churchill Livingston, London, 1981.

(6) U. Breyer and G. Schmalzing, *Drug Metab. Dispos.*, **5**, 97 (1977).

(7) G. Schmalzing, *ibid.*, **5**, 104 (1977).

(8) R. Whelpton and S. H. Curry, *J. Pharm. Pharmacol.*, **28**, 869 (1976).

(9) D. H. Wiles and M. G. Gelder, *Br. J. Clin. Pharmacol.*, **8**, 565 (1979).

(10) J. C. K. Loo, K. K. Midha, and I. J. McGilveray, *Commun. Psychopharmacol.*, **4**, 121 (1980).

(11) K. K. Midha, J. W. Hubbard, J. K. Cooper, E. M. Hawes, S. Fournier, and P. K. F. Yeung, *Br. J. Clin. Pharmacol.*, **12**, 189 (1981).

(12) K. K. Midha, R. M. H. Roscoe, K. Hall, E. M. Hawes, J. K. Cooper, G. McKay, and H. U. Shetty, *Biomed. Mass Spectrom.*, in press.

(13) K. K. Midha, J. K. Cooper, I. J. McGilveray, A. G. Butterfield, and J. W. Hubbard, *J. Pharm. Sci.*, **70**, 1043 (1981).

(14) K. K. Midha, J. K. Cooper, Y. D. Lapierre, and J. W. Hubbard, *Can. Med. Assoc. J.*, **124**, 263 (1981).

ACKNOWLEDGMENTS

Presented in part at the Pharmaceutical Analysis and Control Section, APhA. Academy of Pharmaceutical Sciences, St. Louis Meeting, March 1981.

The authors gratefully acknowledge the Medical Research Council of Canada for the award of a Postdoctoral Fellowship to R. M. H. Roscoe and a Development Grant DG 222 to K. K. Midha.

Pectin–Gelatin Complex Coacervates I: Determinants of Microglobule Size, Morphology, and Recovery as Water-Dispersible Powders

JEAN N. McMULLEN *x, DAVID W. NEWTON ‡, and CHARLES H. BECKER §

Received March 9, 1981, from the **Faculty of Pharmacy, University of Montreal, Montreal, Canada H3C 3J7;* the ‡*Department of Pharmaceutics, College of Pharmacy, University of Nebraska Medical Center, Omaha NE 68105;* and the § *College of Pharmacy, University of Florida, Gainesville, FL 32610.* Accepted for publication September 3, 1981.

Abstract □ The pectin–gelatin complex coacervate system was evaluated and characterized. The effects of final pH, mixing pH, colloid ratio, and solution concentration were investigated. A recovery procedure yielding microglobules of a controlled and uniform size in dry powder form which were readily revertible in water to a polydispersed suspension was developed. The effect of various conditions and additives on the recovery morphology and size of the microglobules was evaluated.

Keyphrases □ Coacervate system—pectin–gelatin complex, final pH, mixing pH, colloid ratio, solution concentration □ Microglobules—pectin–gelatin, suspension in water, dry powder recovery system □ Pectin–gelatin system—microglobules, effects of final pH, mixing pH, colloid ratio, solution concentration

The complex ionic relations of the gelatin–acacia coacervate system have been established and reported previously (1–3) and have been used successfully in the microencapsulation of solids as well as liquids (4–10). Until recently (9), it was difficult to control the morphological characteristics of and recover a free-flowing powder of unagglomerated microglobules which were spontaneously dispersible in aqueous solutions. Therefore, it seemed desirable to develop a complex coacervate system from pectin and gelatin capable of yielding spherical globules of a uniform size that could be controlled for possible application as a pharmaceutical delivery system in parenteral or other products.

Although complex coacervation of the gelatin–pectin system was initially reported by Bungenberg de Jong (1) and employed as the basis of one patent in 1966 (11), the system has apparently received no further attention until this study. Studies of pectin–albumin (12) and pectin–polyethylenimine (13) have, however, been reported. This study was, therefore, undertaken to evaluate and characterize the fundamental complex ionic relations between the amphoteric protein, type A gelatin, and the low equivalent weight anionic colloid, pectin, with special emphasis on the effects of pH of coacervation (pH_c), mixing pH (pH_m), colloid ratio, and solution concentration on microglobule morphology, size, percent yield, and recovery technique yielding a free-flowing powder which was redispersible in water.

EXPERIMENTAL

Materials—Type A gelatin[1] and pectin, NF[2], were used in solutions containing 1% (w/w) benzyl alcohol for preservation. Formaldehyde solution, USP, glycerin, 99.6%, and isopropyl alcohol, 99%, were used in the recovery of microglobules in dry powder form. These and other reagents were of analytical reagent grade and were used as received.

Preparation and Recovery of Coacervates—Coacervates were prepared at 45° from 40.0-g batches stirred by means of a magnetic stirrer and polytef-coated bar at a speed sufficient to produce a vortex without entrainment of air bubbles. Stock pectin and gelatin solutions of the same weight concentration were prepared by dispersing the colloids in cold water, stirring for 30 min in a water bath at 45° and storing at 5° for no more than 24 hr before use. Appropriate weights of stock solutions of the same concentration were individually adjusted[3,4] to the mixing pH with 1.0 *N* NaOH at 45° to give the desired pectin to gelatin ratio. The gelatin solution was added to the pectin solution with stirring, and after 2 min the pH was lowered by fast addition of 0.5 *N* HCl to pH 5, then by slower addition of 0.5 *N* HCl until the desired pH_c was reached. The batch was stirred for 30 min then 5 ml of 37% (w/w) HCHO was added with stirring. After 30 min of stirring under ambient conditions, the batch was covered with paraffin film and allowed to stand for 15–20 hr. The batch was then

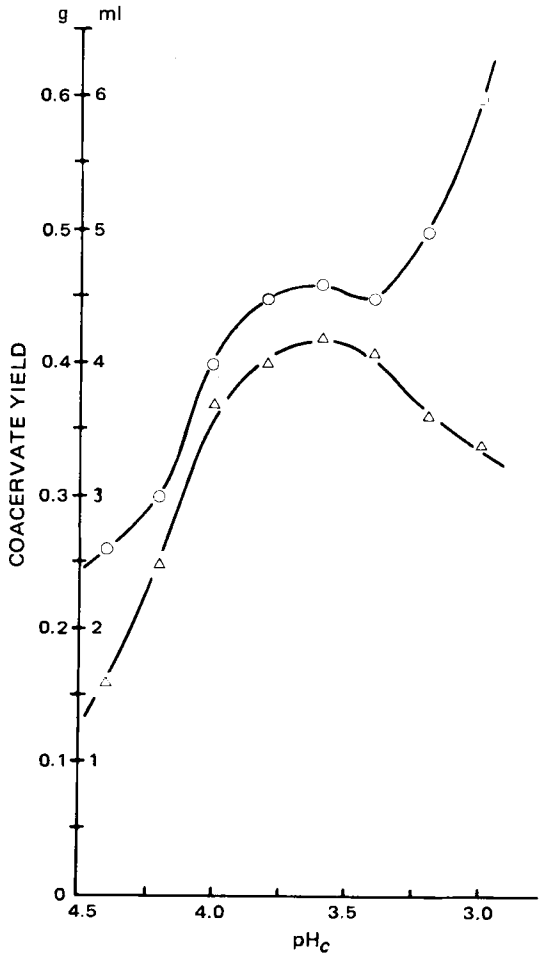

Figure 1—*Coacervate yields* versus pH_c *for isovolumetric (20 ml) 2% (w/w) gelatin and pectin solutions at* pH_m *9.0. Key:* O, *yield in milliliters after centrifugation at 2000 rpm for 60 min;* Δ, *yield of recovered dry microglobules, grams.*

[1] 275 Bloom, isoelectric point 8.6, Fisher Scientific Co., Fair Lawn, N.J.
[2] Sunkist Growers Inc., Ontario, Calif.
[3] Beckman Century SS-1 pH meter, Beckman Instruments, Fullerton, Calif.
[4] Miniature glass 476031 and calomel 476017 electrodes, Corning Scientific Products Co., Medfield, Mass.

0022-3549/82/0600-0628$01.00/0

Table I—Effect of pH_m on Diameter of Spherical Microglobules Produced from Isovolumetric Coacervates of 2% (w/w) Pectin (20 ml) and Gelatin (20 ml) Solutions Adjusted to pH_c 3.8 at 45°

pH_m	Diameter of Microglobules, ≤μm
3.80	0.5
5.85	1.1
6.51	1.4
6.98	2.0
8.06	3.9
9.01	5.4
9.49	7.3
10.04	10.0

stirred to resuspend any sedimented microglobules, and 40 g of the suspension was centrifuged at 1000–2000 rpm for 15–60 min, depending on microglobule size and morphology. The supernate was then decanted. The microglobules were resuspended in 5 ml of glycerin with a vortex mixer and 35 ml of isopropyl alcohol or other flocculating agent was slowly added while mixing. The flocculated microglobules were then filtered using a Buchner funnel and filter paper[5], washed with two 100-ml portions of isopropyl alcohol and dried for 15–20 hr in an oven at 36 ±1°.

Effect of Colloid Concentration—Pectin and gelatin solutions of 1.0, 1.5, 2.0, 2.5, and 3.0% (w/w) concentration were used. Batches were prepared by combining 20-g portions of each solution in order to give a colloid ratio of 1:1 (w/w). Coacervation was carried out for three pH_m values, 8.0, 9.0, and 10.0, over a pH_c range of 5.0–2.6, and evaluated for weight percent yield and microglobule morphology at 1000× under a microscope.

Effect of Colloid Ratio—Pectin to gelatin colloid ratios >1:1 were not studied because the average size of microglobules produced was <1 μm and, consequently, difficult to recover in dry form. The pectin–gelatin ratios studied, at a 2% (w/w) total colloid concentration, were 15, 25, 30, 33, 40, and 50% pectin fractions of total colloid. Coacervation was carried out according to the pH_m and pH_c conditions listed above. Microglobule morphology and weight percent yield were evaluated.

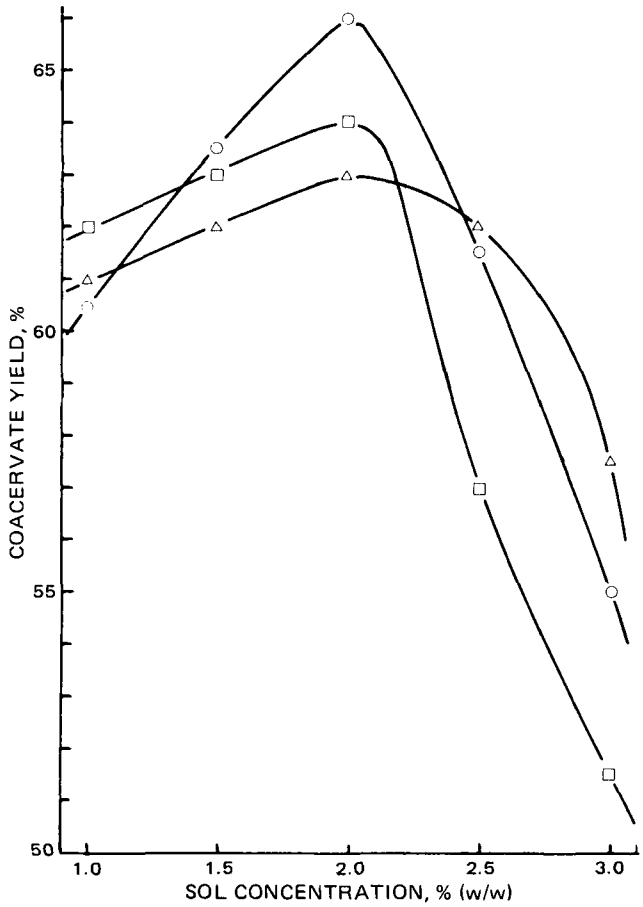

Figure 2—*Coacervate yield* versus *solution concentration for isogravimetric gelatin and pectin solutions adjusted to pH_m values of 8.0, 9.0, and 10.0 and coacervated to pH_c 3.5. Key: ○, pH_m = 8.0; □, pH_m = 9.0; △, pH_m = 10.0.*

[5] Whatman No. 3, Whatman, Inc., Clifton, N.J.

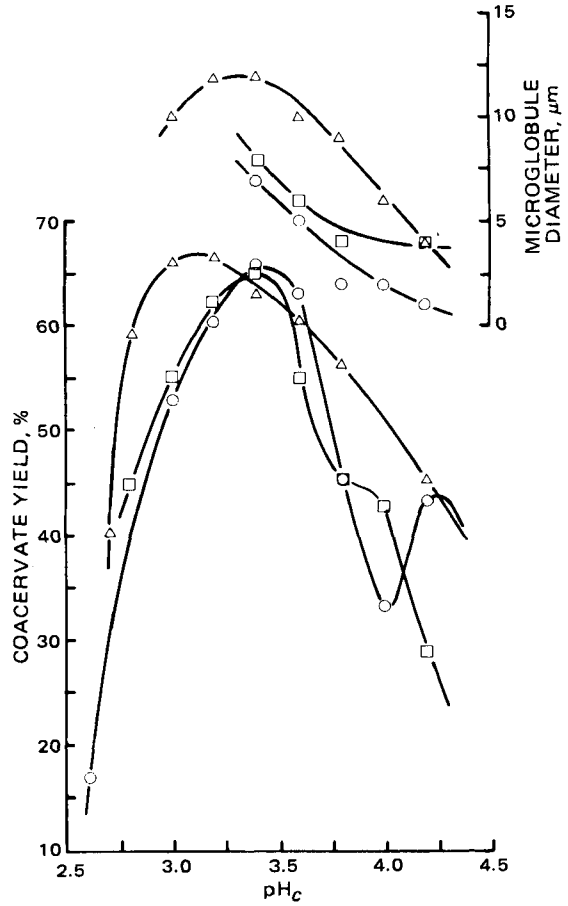

Figure 3—*Coacervate yield (left ordinate) and microglobule diameter (right ordinate)* versus *pH_c for isogravimetric (20 g) 2% (w/w) gelatin and pectin solutions adjusted to pH_m values of 8.0, 9.0, and 10.0. Key: ○, pH_m = 8.0; □, pH_m = 9.0; △, pH_m = 10.0.*

Effect of Additives on Recovery—Batches weighing 40.0 g were prepared from 2.0% (w/w) solutions to give a pectin–gelatin mixing ratio of 33:67%, and adjusted to a pH_m of 10.0 and pH_c of 4.5.

Glycerin volumes of 5, 10, 15, 20, 25, and 30 ml were slowly added to individual batches while mixing, with stirring at 45° after achieving pH_c 4.5.

Volumes of 37% (w/w) HCHO (adjusted to pH 5.0) of 2.5, 5.0, 7.5, 10.0, 12.5, and 15.0 ml were added to individual batches at 20° after achieving pH_c 4.5. The effect of formaldehyde treatment time was determined by adding 15 ml of 37% (w/w) HCHO and stirring for 1, 3, 7, 9, 12, 24, 36, and 54 hr.

Glycerin, propylene glycol, polyethylene glycol, 50% (v/v) isopropyl alcohol in distilled water, and distilled water were evaluated as redispersing media. Volumes of 5 ml of each were added to individual batches after centrifugation and decantation of the supernate.

The effect of various water miscible flocculating agents was determined by adding to individual batches 35 ml of isopropyl alcohol, 1-propanol, ethanol, methanol, and acetone.

All batches studied for the effect of additives on recovery were evaluated as to their dry product characteristics, such as coherence and friability, and redispersibility in distilled water.

RESULTS AND DISCUSSION

Until the effect of pH_m was elucidated, previously reported complex coacervation procedures, particularly for the gelatin–acacia system, were applied to the gelatin–pectin system with little success. Some results of this exploratory phase are summarized in Table I. As reported previously (14), mixing of isohydric solutions (pH 3–4) does not change the system pH significantly, a fact demonstrated in this study but also one that

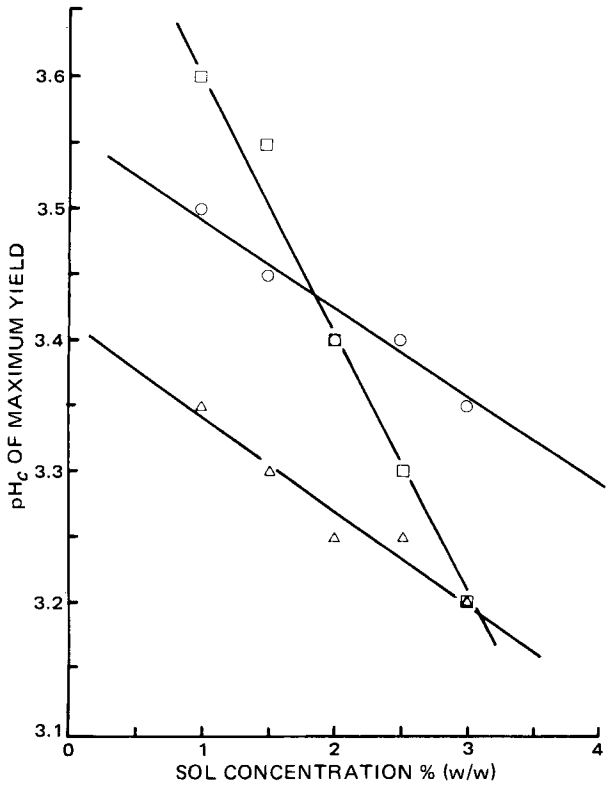

Figure 4—*pH_c of maximum microglobule yield* versus *total colloid concentration in pectin–gelatin (1:1) coacervates prepared from solutions adjusted to pH_m values of 8.0, 9.0, and 10.0. Key: ○, pH_m = 8.0; □, pH_m = 9.0; △ pH_m = 10.0.*

yielded such small globules as to be hardly resolvable under the microscope at 1000×. The method of Luzzi (4), mixing of isohydric (pH 6.5), isovolumetric solutions then adjusting the pH of the mixture with acid to the desired endpoint (pH 3.8), resulted in a marked increase in globule diameter to ~1 μm. The method of Newton (9), mixing of isovolumetric solutions, gelatin (pH 10) and pectin (pH 3.6), then adjusting the pH of the mixture with acid to the desired endpoint (pH 3.8), gave comparable results. These results suggested the possible involvement of the mixing pH in the control of microglobule size which was confirmed in a series of experiments where isohydric, isovolumetric solutions were adjusted to pH 7.0, 8.0, 9.0, 9.5, and 10.0 before mixing and coacervation to pH 3.8. The mean globule size increased from 2 to 10 μm as the mixing pH was increased from 7–10 (Table I).

Volume measurements of coacervate phases were impractical due to the noncoalescence of the globules into a continuous phase. A comparison of sediment volume of microglobules after centrifugation with yield based on dry weight as a function of pH_c is given in Fig. 1. The increasing sediment volume at pH_c <3.4 is attributed to a change in morphology from globular to elliptical particles having a lower packed density and greater hydration. Therefore, dry weight recovery was adopted to measure microglobule yields in all subsequent experiments.

Effect of Colloid Concentration—The results of studies to determine the effects of total colloid concentration on coacervate yield for solutions having equal concentrations of pectin and gelatin showed that maximum yield was obtained at a total colloid concentration of ~2% (w/w) for the mixing of isohydric, isogravimetric solutions coacervated to pH_c 3.5 (Fig. 2). The increasing efficiency of coacervation with increasing total colloid concentration up to a maximum of ~2.0% probably resulted from increased reactivity of the gelatin and pectin linear molecules as the forces of intramolecular aggregation limiting their movement were minimal. Above 2% (w/w) of total colloids, the decreasing efficiency of coacervation arises from an increasing salt or gegenion (*e.g.*, Na^+, Ca^{2+}, Cl^-) concentration which insulates the oppositely charged colloids, suppressing coacervation and increasing the mutual solubilities of the coacervate and equilibrium solution phases (14).

Figure 3 shows the relationship for the 2% colloid concentration between percent yield[6] and microglobule morphology as a function of pH_c

[6] Expressed as percent (w/w) of the total mass of pectin and gelatin in the coacervate system.

Table II—Effect of Glycerin on the Morphology and Powder Characteristics of Pectin–Gelatin Microglobules Recovered from Coacervate Systems Prepared from 2% (w/w) Pectin–Gelatin (33:67) at pH_m 10.0 and pH_c 4.5

Glycerin, % w/w[a]	Microglobule Characteristics: Morphology[b]	Microglobule Characteristics: Dimension, μm[c]	Recovered Product Characteristics[d]
0	S	11	C
13.5	S	14	C
25.7	S	12	C
31.9	S	13	C
49.1	E	22	F
56.1	E	20	F
72.4	E	21	F

[a] Percent by weight of coacervate system after achieving pH_c 4.5. [b] S—spheres; E—ellipsoids. [c] Maximum dimension of largest particle in field of view at 1000× magnification. [d] C, coarse powder; F, fine, light powder; both spontaneously revertible to individual units in aqueous suspension.

for pH_m values of 8.0, 9.0, and 10.0. Microglobule size increased as the pH_c decreased, until the maximum yield was reached, at which point the shape was transformed from spherical to ellipsoidal or amorphous.

The dependence of microglobule size on pH_c at fixed pH_m likely arises from the fact that as the pH_c is lowered, the relative ratio of pectin to gelatin increases in the coacervate. Furthermore, the more intense complex ionic relations of the pectin–gelatin *versus* the acacia–gelatin system would cause a greater coacervate reduction in the water content of the coacervate and a total coacervate colloid concentration >10%, a value reported for the gelatin–acacia system (15), thereby affecting droplet size and solubility[7].

As the system is adjusted to lower pH_c, the number of anionic charges on pectin decreases while the number of cationic charges increases on gelatin, resulting in more and more pectin being required for an equivalent union with gelatin. Therefore, at high pH_c values, the combination of both a high total colloid concentration and a low pectin–gelatin ratio in the coacervate resulted in stabilization of the coacervate drops as a result of a high viscosity and partial gelling of the microglobules precluding their coalescence. As the pH_c was lowered, the pectin–gelatin

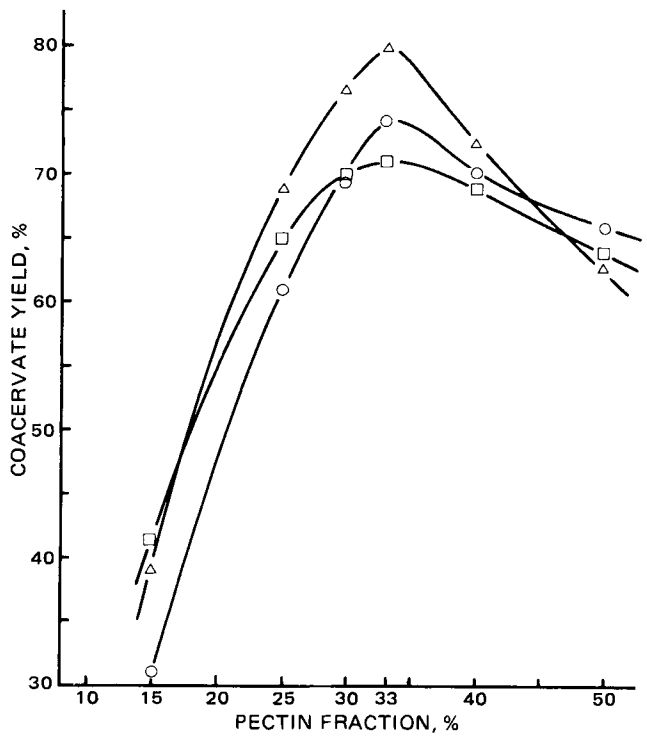

Figure 5—*Coacervate yield* versus *pectin–gelatin and pectin solutions adjusted to pH_m values of 8.0, 9.0, and 10.0 and coacervated to pH_c 3.5. Key: ○, pH_m = 8.0; □, pH_m = 9.0; △, pH_m = 10.0.*

[7] The lower the equivalent weight of anionic colloid the higher is its charge density and, thus, the stronger are its complex ionic relations with cationic gelatin. The equivalent weights of acacia and pectin (pectate) are 1200 and 200, respectively (1, 15).

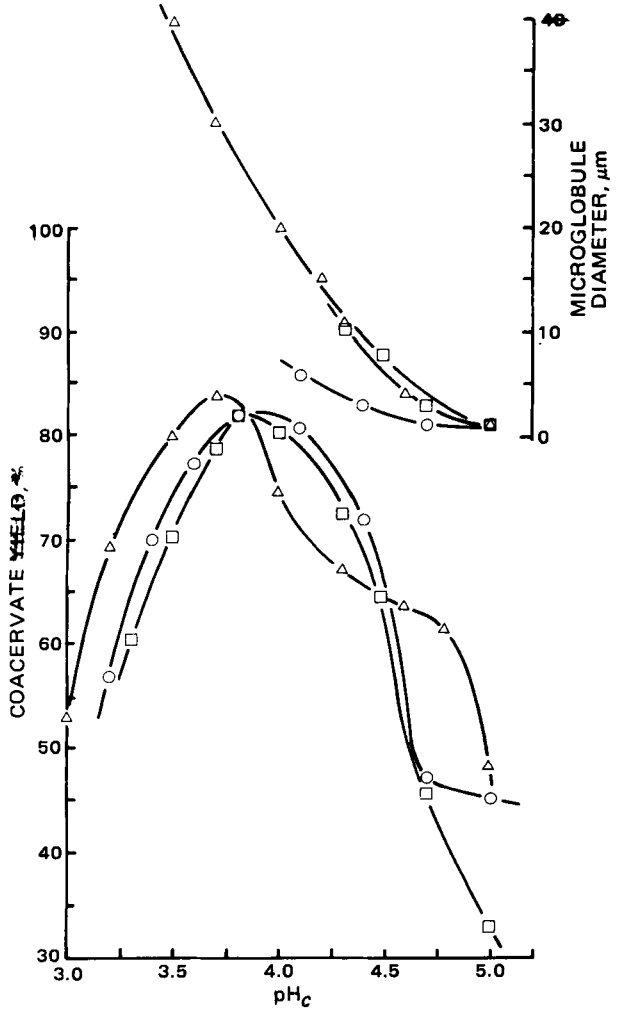

Figure 6—*Coacervate yield (left ordinate) and microglobule diameter (right ordinate)* versus *pH_c for coacervate systems prepared from a 33:67 gravimetric ratio of 2% (w/w) pectin and gelatin solutions, respectively, adjusted to pH_m values of 8.0, 9.0 and 10.0. Key: ○, pH_m = 8.0; □, pH_m = 9.0; △, pH_m = 10.0.*

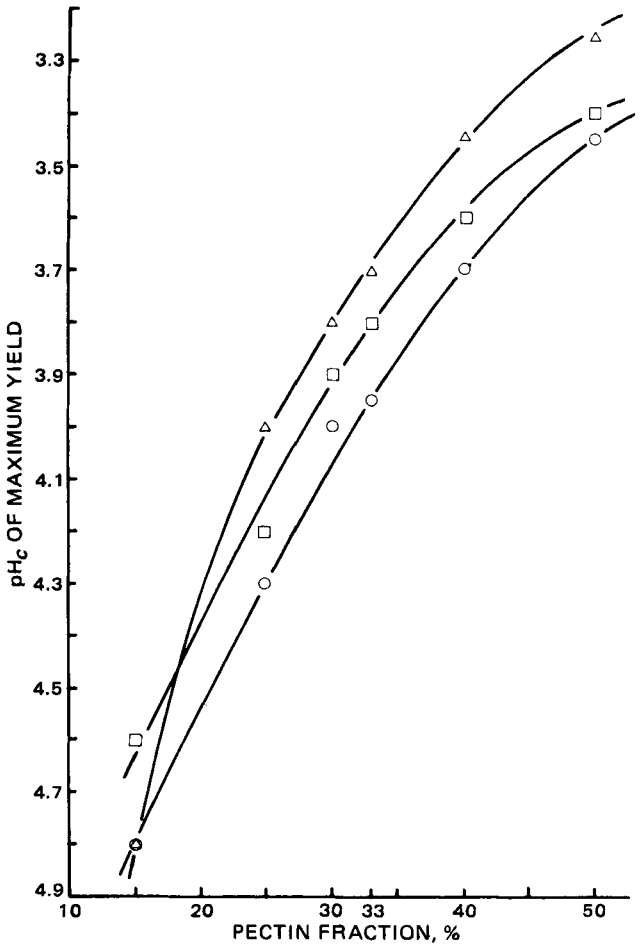

Figure 7—*pH_c of maximum yield* versus *pectin weight fraction of total colloid in coacervates prepared from 2% (w/w) gelatin and pectin solutions adjusted to pH_m values of 8.0, 9.0, and 10.0. Key: ○, pH_m = 8.0; □, pH_m = 9.0; △, pH_m = 10.0.*

ratio in the coacervate increased allowing microglobule growth to proceed further before an equilibrium sphere occurred at a higher equilibrium size.

Microglobule size increases with decreasing pH_c and with increasing pectin–gelatin ratio in the coacervate, probably as a result of increasing coacervate viscosity until the stabilizing forces become too weak to prevent deformation of the microglobules by the stirring forces. This results in ellipsoidal particles which cannot readily return to the spherical state because of their very viscous and gel-like state and finally amorphous particles as a result of agglomeration and partial coalescence of ellipsoidal particles. The microglobules are further stabilized from coalescing into a single phase by the anionic charge they acquire as they form above the optimum pH_c. As for the gelatin–acacia system (16), as the PH_c is lowered, the net charge on the microglobules remains negative because of the predominance of dissociated carboxylate groups on pectin and gelatin as opposed to cationic amino groups on gelatin.

The pronounced effect of pH_m on microglobule morphology is probably related to the pectin–gelatin ratio in the coacervate and the gegenion concentration. It has been reported that pectin molecules in solution exist in a high state of aggregation in solutions >0.1%, as a result of suppressed ionization of carboxyl groups (17). It was found through titration and pH *versus* viscosity studies of 2% solutions at 45° that some carboxyl groups are not readily ionizable until pH 7.5, above which such solutions show a sharp decrease in viscosity, which can be attributed to increased repulsive forces tending to further lower the degree of aggregation. Therefore at pH_m 8.0 in 2% (w/w) solutions, the reactivity of pectin with gelatin is limited by the higher degree in intramolecular aggregation as compared to that at higher pH_m, *i.e.*, 9.0 or 10.0. Subsequently, this results in a lower pectin–gelatin ratio at pH_c. As the pH_m is raised >8, deaggregation of pectin increases, permitting more pectin molecules to react with gelatin molecules and microglobules and higher yields.

Figure 4 indicates that as the solution concentration increases, the pH_c of maximum coacervation decreases; an observation also made previously (14) for gelatin–acacia coacervates. Again, as the concentration of solutions increases, so does that of the accompanying gegenions which suppress coacervation. Hence, pH_c must be lowered to increase the cationic charge on gelatin, while causing a smaller decrease in the anionic charges on both pectin and gelatin.

As expected, there was a linear relationship between the volume of 0.5 *N* HCl added and pH_c, verifying that the complex ionic relations between pectin and gelatin were stoichiometric and rapid (9, 18).

Effect of Colloid Ratio—On the basis of results obtained in studies of the optimum total colloid concentration to maximize microglobule yield, 2% (w/w) was used in evaluating the effect of varying pectin–gelatin ratios of 15:85, 25:75, 33:67, 40:60, and 50:50. Figure 5 indicates that the maximum yield was obtained at a colloid ratio of pectin–gelatin (33:67)

Table III—Flocculation Rates by Four Alcohols and Acetone of Coacervate Microglobules Prepared from 2% (w/w) Pectin–Gelatin (33:67) at pH_m 10.0 and pH_c 4.5

Flocculating Agent	Relative Flocculation Rate[a]	Product Characteristics[b]
1-Propanol	5	C, D
Isopropyl alcohol	4	C, D
Ethanol	3	G, N
Methanol	2	F, N
Acetone	1	F, N

[a] Rate increases from 5 to 1. [b] C, coarse powder; D, spontaneously dispersible to individual spheres in water; G, granular powder; N, not dispersible as individual spheres in water; F, fused filter cake mass.

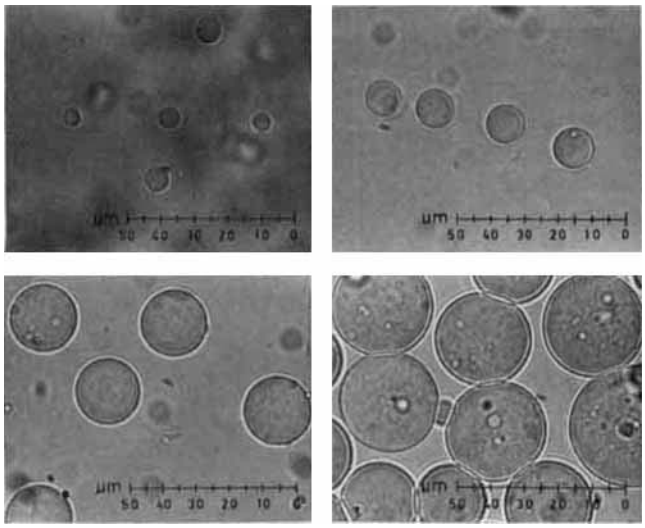

Figure 8—*Pectin–gelatin microglobules having nominal diameters of 5, 10, 20, and 30 μm.*

for the mixing of isohydric solutions coacervated to a pH_c of 3.5. The percent yields of microglobules ranged from ~70–80% of total colloids available, indicating a high reactivity in the complex coacervate system.

The fact that at a 15% pectin fraction the maximum yield was higher than expected is misleading because the microglobules or amorphous particles obtained were highly vacuolated, containing uncoacervated colloid-rich liquid, referred to as hollow spheres (19).

Figure 6 demonstrates the relationship for 2% (w/w) solutions between percent yield, microglobule diameter, and pH_c for pectin–gelatin colloid ratios of 33:67 at pH_m values of 8.0, 9.0, and 10.0. The microglobule diameter increased by ~3.3 μm/0.1 pH unit decrement, *i.e.*, from 20–40 μm as pH_c was lowered from 4.0 to 3.6 at pH_m 10.0. Microglobule diameter increased proportional to increasing pH_m and decreasing pH_c probably for the same reasons previously discussed. At $pH < pH_c$ of maximum yield, the globules became elliptical and amorphous.

Figure 7 shows that as the pectin fraction increased in coacervate systems of 2% (w/w) colloid concentration, the pH_c of maximum coacervation decreased from pH_m 8.0, 9.0, and 10.0.

Figure 8 shows typical microglobules having nominal diameters of 5, 10, 20, and 30 μm demonstrating control of microglobule size and the ability of spontaneously reverting to a polydisperse system like that of the gelatin–acacia microglobules in a figure from a study published previously (9).

Effect of Additives on Recovery—The effect of glycerin added to coacervate systems at 45° after achieving pH_c is shown in Table II. With the addition of ≥49% (w/w) glycerin, ellipsoidal particles were obtained, a possible result of partial dehydration of the pectin and gelatin molecules in the coacervate and of increased intramolecular association, resulting from the decreasing dielectric constant of the system. A similar result was found with gelatin–acacia coacervates where from 23 to 41% (v/v) of glycerin yielded nonvacuolated, spherical microglobules, but ≥44% (v/v) glycerin resulted in vacuolated ellipsoids (20). In the pectin–gelatin system, glycerin improved the fineness of the dry recovered powder, but had no apparent effect on the dispersibility of the microglobules in water.

The results of formaldehyde treatment of the microglobules showed that at least 10 ml of 37% HCHO, preferably 15 ml, per 40-g batch prepared from 2% (w/w) pectin–gelatin solutions (33:67) was required to obtain microglobules in dry powdered form spontaneously revertible to a dispersed suspension in water. This result was comparable to that for gelatin–acacia microglobules (9). A minimum formaldehyde treatment time of 9 hr was required to obtain redispersible microglobules prepared by the previously mentioned conditions.

Glycerin, propylene glycol, and polyethylene glycol were equally satisfactory as redispersing media for the formaldehyde treated, unflocculated, sedimented microglobules. Water and 50% (v/v) isopropyl alcohol yielded a finer dry powder, but the rate of filtration of the centrifuged sediments was unacceptably lengthened.

The flocculation rates of the microglobules, by 35-ml portions of four aliphatic alcohols and acetone added to the centrifuged sediments of microglobules (~3–4 ml, Fig. 1) resuspended in 5 ml of glycerin after preparation from 2% (w/w) pectin and gelatin solutions according to previously specified conditions, are described in Table III. Flocculation by only 1-propanol and isopropyl alcohol elicited microglobules spontaneously dispersible in aqueous suspension, whereas ethanol, methanol, and acetone resulted in filter cakes which were not revertible to suspensions of individual microglobules in water. Although these results corroborate those for gelatin–acacia (9) and gelatin (21) coacervate products, there is no readily discernible relationship, *e.g.*, with dielectric constant, ε[8]. The greater dehydration of pectin and some remaining hydrophilic groups on gelatin[9] by ethanol, methanol, and acetone, resulting from their stronger hydrogen bonding affinity for water, could explain the apparent intramolecular–intermolecular colloid aggregation and the failure of the microglobules to disperse as individual units upon suspension in water.

CONCLUSIONS

Based on these studies, it was possible to recover microglobules of controlled and uniform diameter from complex coacervates of pectin–gelatin by regulating the concentrations of pectin and gelatin solutions, pH_m, pH_c, and the pectin–gelatin ratio as well as certain additives. The spherical microglobules so obtained are spontaneously revertible to a dispersed system upon suspension of the powdered products in aqueous solutions.

REFERENCES

(1) H. G. B. de Jong, in "Colloid Science," vol. 2, H. R. Kruyt, Ed., Elsevier, New York, N.Y., 1949, pp. 186–193, 243–276, 338–450.

(2) A. B. Dhruv, T. E. Needham, Jr., and L. A. Luzzi, *Can. J. Pharm. Sci.*, **10**, 33 (1975).

(3) M. Glicksman and R. E. Sand, in "Industrial Gums," 2nd ed., R. L. Whistler, Ed., Academic, New York, N.Y., 1973, pp. 234–238.

(4) L. A. Luzzi and R. J. Gerraughty, *J. Pharm. Sci.*, **53**, 429 (1964).

(5) *Ibid.*, **56**, 634 (1967).

(6) *Ibid.*, **56**, 1174 (1967).

(7) S. Javidan, R. Hague, and R. G. Mrtek, *J. Pharm. Sci.*, **60**, 1825 (1971).

(8) P. L. Madan, L. A. Luzzi, and J. C. Price, *ibid.*, **61**, 1586 (1972).

(9) D. W. Newton, J. N. McMullen, and C. H. Becker, *ibid.*, **66**, 1327 (1977).

(10) H. Takenaka, Y. Kawashima, and S. Y. Lin, *ibid.*, **69**, 513 (1980).

(11) Ciba Ltd., French pat. 1,462,506 (1966); through *Chem. Abstr.*, **67**, 67587g (1967).

(12) A. P. Sal'chinkin and F. L. Movshovich, *Colloid J. (USSR)*, **6**, 15 (1940); through *Chem. Abstr.*, **36**, 29119 (1941).

(13) H. Deuel, J. Solms, and A. Denzler, *Mitt. Lebensm. Hyg.*, **45**, 73 (1954); through *Chem. Abstr.*, **48**, 9578b (1954).

(14) H. G. B. de Jong, in "Colloid Science," vol. 2, H. R. Kruyt, Ed., Elsevier, New York, N.Y., 1949, pp. 340–370.

(15) *Ibid.*, pp. 340–345, 362, 364, 368–370.

(16) *Ibid.*, pp. 322–326.

(17) H. S. Owens, H. Lotzkar, R. C. Merrill, and M. Peterson, *J. Am. Chem. Soc.*, **66**, 1178 (1944).

(18) H. Terayama, *J. Polym. Sci.*, **8**, 243 (1952).

(19) H. G. B. de Jong, in "Colloid Science," vol. 2, H. R. Kruyt, Ed., Elsevier, New York, N.Y., 1949, pp. 454–466.

(20) D. W. Newton, Ph.D. dissertation, University of Florida, Gainesville, Fla., 1976.

(21) J. R. Nixon, S. A. H. Khalil, and J. E. Carless, *J. Pharm. Pharmacol.*, **20**, 528 (1968).

(22) "Handbook of Chemistry and Physics," 56th ed., C. R. Weast, Ed., CRC, Cleveland, Ohio, 1975, p. E-56.

[8] The decreasing order of ε at 25° for the solvents is: methanol, 32.6; ethanol, 24.3; acetone, 20.7; 1-propanol, 20.1; isopropyl alcohol, 18.3 (22).

[9] Formaldehyde treatment renders the gelatin component partially insoluble by condensing with nonprotonated RNH_2, R'NHR, and RCONH groups, *i.e.*: $RNH_2 + R'NHR \xrightarrow{HCHO} RNHCH_2R'NHR + H_2O$, resulting in a more hydrophobic (less hydrogen bonding) product (23).

(23) H. L. Fraenkel-Conat, M. Cooper, and H. S. Olcott, *J. Am. Chem. Soc.*, **67**, 950 (1945).

ACKNOWLEDGMENTS

Abstracted in part from a dissertation presented by J. N. McMullen to the Graduate Council of the University of Florida in partial fulfillment of the Doctor of Philosophy degree requirements.

The authors thank Mrs. Ginette Simard and Mrs. Donna Earnshaw for their assistance in preparing this manuscript.

Pharmacokinetic Profile of Progabide, a New γ-Aminobutyric Acid-Mimetic Drug, in Rhesus Monkey

IKUO JOHNO, B. TERI LUDWICK, and RENÉ H. LEVY ˣ

Received March 30, 1981, from the *Departments of Pharmaceutics and Neurological Surgery, Schools of Pharmacy and Medicine, University of Washington, Seattle, WA. 98195.* Accepted for publication September 10, 1981.

Abstract □ The pharmacokinetic profile of progabide was investigated in five chronically catheterized male rhesus monkeys. The experimental design included single-dose intravenous bolus and oral administration at two dose levels (50 and 100 mg) and zero-order intravenous infusion for 7 days. Plasma samples were analyzed by electron-capture–GLC. Protein binding of the drug was determined by equilibrium dialysis (4°). A one-compartment open model with monoexponential decay was proposed to describe the pharmacokinetics. The mean parameters (±*SEM*) of the 50- and 100-mg iv bolus were: total body clearance, 2.09 (±0.15) and 1.53 (±0.18) liter/hr/kg; half-life, 0.656 (±0.054) and 0.789 (±0.079) hr; distribution volume, 1.97 (±0.08) and 1.79 (±0.21) liter/kg. Progabide was highly bound to plasma proteins and also to erythrocytes. The drug was rapidly absorbed (T_{max} < 1 hr at both doses). The mean bioavailability was attributed principally to a first-pass effect. In the constant rate infusion study, systemic clearance was larger than that of the single dose studies.

Keyphrases □ Progabide—pharmacokinetics in rhesus monkeys, plasma bioavailability □ Bioavailability—pharmacokinetics of progabide in plasma of rhesus monkeys □ Pharmacokinetics—bioavailability of progabide in plasma of rhesus monkeys □ Electron-capture–GLC—determination of progabide in rhesus monkey blood plasma, bioavailability, pharmacokinetics

Progabide[1] is a new γ-aminobutyric acid-mimetic drug with a broad spectrum of anticonvulsant activity (1–6). Progabide was designed to be a carrier of γ-aminobutyramide into the central nervous system where it would be broken down and release γ-aminobutyramide.

The present study was undertaken to characterize the pharmacokinetic behavior of progabide in the rhesus monkey in view of its efficacy testing in the chronic epileptic monkey model.

EXPERIMENTAL

Five healthy male rhesus monkeys (*Macaca mulatta*) (2.7–3.8 kg) were used in this study. The monkeys were maintained on fresh fruits and monkey chow and chaired for the duration of the study. Each monkey had two chronic catheters, one for drug administration (femoral vein) and one for blood sampling (jugular vein). The experimental design included single-dose and chronic administration studies. In the single-dose studies, each monkey received 50 or 100 mg of the drug intravenously and orally in a randomized fashion. The drug was dissolved in 100% polyethylene glycol 400[2] at concentrations of 25 and 50 mg/ml. Two milliliters of this solution was injected over 5 min through the femoral vein or administered by intranasal gastric intubation. Fourteen (50-mg dose) or 15 (100-mg dose) blood samples were collected over a 5–6-hr period. Ethylenediaminetetraacetic acid tripotassium salt was used as an anticoagulant, and the blood samples were stored in ice. They were centrifuged at 4° and the separated plasma was frozen immediately. The samples were kept frozen until assayed. Some blood samples were also frozen to determine the blood level of the drug and the total blood clearance in each monkey.

I

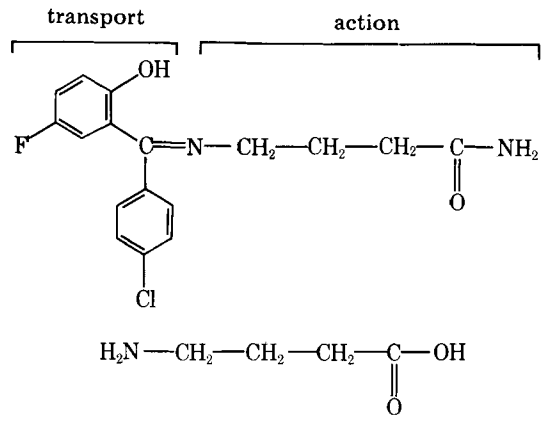

I

The chronic administration studies consisted of constant rate intravenous infusion for 7 days. The drug was dissolved in 80% polyethylene glycol 400 at a concentration of about 3 mg/ml (1.91–3.84 mg/ml), and the infusion rate was 1 ml/hr. Blood samples were collected during the accession to steady state (0–6 hr), on a daily basis during steady state, and during the post steady-state decay phase.

Protein binding of progabide was measured by equilibrium dialysis at 4° to minimize the degradation of drug in plasma. A volume of 0.7 ml of pooled monkey plasma, and an equal volume of isotonic phosphate buffer system (pH 7.4), were used. The dialyzing system consisting of plexiglass cells was rotated at a rate of 10 rev/min for 12 hr. The dialysis was carried out with spiked plasma samples with concentrations ranging from 0.4 to 34.6 μg/ml (determined postdialysis). The drug on both sides of the membrane was analyzed by electron-capture–GLC.

Progabide concentrations were determined by the method of Gillet and Dring[3] using a GLC equipped with electron-capture detector[4]. The column consisted of 3% OV-17 on Chromosorb W-HP (column length was 184.3 cm and 2-mm i.d.). Temperatures of detector, injection port, and oven were 300, 250, and 240°, respectively. An analog of progabide, [α-(chloro-4′-phenyl)chloro -5- hydroxy-2-benzylideneamino]-4-butyramide, was used as the internal standard.

Areas under intravenous and oral curves were calculated by the trapezoidal method (with extrapolation to infinite time). Systemic clearance was determined by dose–area ratio. Oral bioavailability was calculated by ratio of oral and intravenous areas.

[1] Synthélabo-L.E.R.S., Paris, France.
[2] J. T. Baker Chemical Co., Phillipsburg, NJ 08865.
[3] Unpublished method, 1978.
[4] Model 5710A, Hewlett-Packard, Palo Alto, CA 94304.

0022-3549/82/0600-0633$01.00/0

(23) H. L. Fraenkel-Conat, M. Cooper, and H. S. Olcott, *J. Am. Chem. Soc.*, **67**, 950 (1945).

ACKNOWLEDGMENTS

Abstracted in part from a dissertation presented by J. N. McMullen to the Graduate Council of the University of Florida in partial fulfillment of the Doctor of Philosophy degree requirements.

The authors thank Mrs. Ginette Simard and Mrs. Donna Earnshaw for their assistance in preparing this manuscript.

Pharmacokinetic Profile of Progabide, a New γ-Aminobutyric Acid-Mimetic Drug, in Rhesus Monkey

IKUO JOHNO, B. TERI LUDWICK, and RENÉ H. LEVY ˣ

Received March 30, 1981, from the *Departments of Pharmaceutics and Neurological Surgery, Schools of Pharmacy and Medicine, University of Washington, Seattle, WA. 98195.* Accepted for publication September 10, 1981.

Abstract □ The pharmacokinetic profile of progabide was investigated in five chronically catheterized male rhesus monkeys. The experimental design included single-dose intravenous bolus and oral administration at two dose levels (50 and 100 mg) and zero-order intravenous infusion for 7 days. Plasma samples were analyzed by electron-capture–GLC. Protein binding of the drug was determined by equilibrium dialysis (4°). A one-compartment open model with monoexponential decay was proposed to describe the pharmacokinetics. The mean parameters (±*SEM*) of the 50- and 100-mg iv bolus were: total body clearance, 2.09 (±0.15) and 1.53 (±0.18) liter/hr/kg; half-life, 0.656 (±0.054) and 0.789 (±0.079) hr; distribution volume, 1.97 (±0.08) and 1.79 (±0.21) liter/kg. Progabide was highly bound to plasma proteins and also to erythrocytes. The drug was rapidly absorbed (T_{max} < 1 hr at both doses). The mean bioavailability was attributed principally to a first-pass effect. In the constant rate infusion study, systemic clearance was larger than that of the single dose studies.

Keyphrases □ Progabide—pharmacokinetics in rhesus monkeys, plasma bioavailability □ Bioavailability—pharmacokinetics of progabide in plasma of rhesus monkeys □ Pharmacokinetics—bioavailability of progabide in plasma of rhesus monkeys □ Electron-capture–GLC—determination of progabide in rhesus monkey blood plasma, bioavailability, pharmacokinetics

Progabide[1] is a new γ-aminobutyric acid-mimetic drug with a broad spectrum of anticonvulsant activity (1–6). Progabide was designed to be a carrier of γ-aminobutyramide into the central nervous system where it would be broken down and release γ-aminobutyramide.

The present study was undertaken to characterize the pharmacokinetic behavior of progabide in the rhesus monkey in view of its efficacy testing in the chronic epileptic monkey model.

EXPERIMENTAL

Five healthy male rhesus monkeys (*Macaca mulatta*) (2.7–3.8 kg) were used in this study. The monkeys were maintained on fresh fruits and monkey chow and chaired for the duration of the study. Each monkey had two chronic catheters, one for drug administration (femoral vein) and one for blood sampling (jugular vein). The experimental design included single-dose and chronic administration studies. In the single-dose studies, each monkey received 50 or 100 mg of the drug intravenously and orally in a randomized fashion. The drug was dissolved in 100% polyethylene glycol 400[2] at concentrations of 25 and 50 mg/ml. Two milliliters of this solution was injected over 5 min through the femoral vein or administered by intranasal gastric intubation. Fourteen (50-mg dose) or 15 (100-mg dose) blood samples were collected over a 5–6-hr period. Ethylenediaminetetraacetic acid tripotassium salt was used as an anticoagulant, and the blood samples were stored in ice. They were centrifuged at 4° and the separated plasma was frozen immediately. The samples were kept frozen until assayed. Some blood samples were also frozen to determine the blood level of the drug and the total blood clearance in each monkey.

I

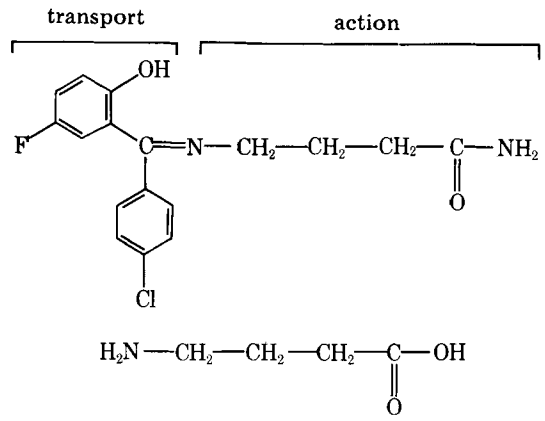

I

The chronic administration studies consisted of constant rate intravenous infusion for 7 days. The drug was dissolved in 80% polyethylene glycol 400 at a concentration of about 3 mg/ml (1.91–3.84 mg/ml), and the infusion rate was 1 ml/hr. Blood samples were collected during the accession to steady state (0–6 hr), on a daily basis during steady state, and during the post steady-state decay phase.

Protein binding of progabide was measured by equilibrium dialysis at 4° to minimize the degradation of drug in plasma. A volume of 0.7 ml of pooled monkey plasma, and an equal volume of isotonic phosphate buffer system (pH 7.4), were used. The dialyzing system consisting of plexiglass cells was rotated at a rate of 10 rev/min for 12 hr. The dialysis was carried out with spiked plasma samples with concentrations ranging from 0.4 to 34.6 μg/ml (determined postdialysis). The drug on both sides of the membrane was analyzed by electron-capture–GLC.

Progabide concentrations were determined by the method of Gillet and Dring[3] using a GLC equipped with electron-capture detector[4]. The column consisted of 3% OV-17 on Chromosorb W-HP (column length was 184.3 cm and 2-mm i.d.). Temperatures of detector, injection port, and oven were 300, 250, and 240°, respectively. An analog of progabide, [α-(chloro-4′-phenyl)chloro -5- hydroxy-2-benzylideneamino]-4-butyramide, was used as the internal standard.

Areas under intravenous and oral curves were calculated by the trapezoidal method (with extrapolation to infinite time). Systemic clearance was determined by dose–area ratio. Oral bioavailability was calculated by ratio of oral and intravenous areas.

[1] Synthélabo-L.E.R.S., Paris, France.
[2] J. T. Baker Chemical Co., Phillipsburg, NJ 08865.
[3] Unpublished method, 1978.
[4] Model 5710A, Hewlett-Packard, Palo Alto, CA 94304.

0022-3549/82/0600-0633$01.00/0

Table I—Pharmacokinetic Parameters of Progabide in the Monkey following Intravenous Bolus Administration at Two Doses [a]

Monkey Number	Body Weight[b], kg	Systemic Plasma Clearance, liter/hr/kg		Volume of Distribution, liter/kg		Half-Life, hr	
		50 mg	100 mg	50 mg	100 mg	50 mg	100 mg
564A	3.15	2.30	—	1.85	—	0.552	—
514A	3.47–3.77	1.96	1.70	1.81	1.47	0.643	0.556
706A	2.65–3.14	2.11	1.92	2.27	2.33	0.729	0.838
574A	3.10–3.80	1.60	1.09	1.95	1.42	0.822	0.901
020	3.50–3.53	2.50	1.40	1.96	1.92	0.532	0.860
Mean		2.09	1.53	1.97	1.79	0.656	0.789
(*SEM*)		(0.15)	(0.18)	(0.08)	(0.21)	(0.054)	(0.079)
Paired *t* test ($n = 4$)		NS		NS		NS	

[a] 50 and 100 mg. [b] The two values represent weights at beginning and end of experimentation period.

Table II—Pharmacokinetic Parameters of Progabide in the Monkey following Oral Administration at Two Doses [a]

Monkey Number	Half-Life, hr		Bioavailability, %	
	50 mg	100 mg	50 mg	100 mg
564A	0.615	—	29.1	—
514A	0.704	0.594	40.3	31.9
706A	0.821	1.02	69.3	87.0
574A	0.621	0.852	49.0	33.7
020	0.685	0.804	46.5	21.8
Mean	0.687	0.818	46.8	43.6
(±*SEM*)	(0.038)	(0.088)	(6.6)	(14.7)
Paired *t* test ($n = 4$)	NS		NS	

[a] 50 and 100 mg.

Table III—Protein Binding of Progabide in Monkey Plasma

Concentration, μg/ml	Free Fraction[a]
0.42	0.020 ± 0.005
0.75	0.030 ± 0.009
1.49	0.027 ± 0.0005
3.47	0.035 ± 0.003
8.91	0.051 ± 0.001
34.61	0.049 ± 0.003

[a] Values are the mean ±*SD* of three determinations.

RESULTS AND DISCUSSION

Single-Dose Intravenous Studies—Representative semilog plasma concentration–time curves obtained for the two intravenous bolus doses in monkeys 574A and 706A are shown in Figs. 1 and 2. The continuous lines were obtained by nonlinear least-squares fitting of experimental data points to a monoexponential equation. A summary of the pharmacokinetic parameters obtained from intravenous bolus administration is presented in Table I.

Progabide has a large systemic clearance, large distribution volume, and short biological half-life. The total body clearance at the 50- and 100-mg doses ranged from 1.60 to 2.50, and 1.09 to 1.92 liter/hr/kg, respectively. The distribution volume at the same doses ranged from 1.81 to 2.27 and 1.42 to 2.33 liter/kg, respectively. The apparent half-life at the 50-mg dose ranged from 0.53 to 0.82 hr and, at the 100-mg dose, from 0.56 to 0.90 hr. Although progabide clearance decreased with dose in all four monkeys, statistical comparison showed no significant difference ($p = 0.088$). There was also no apparent dose dependency in distribution volume or elimination half-life.

The progabide blood–plasma ratio was calculated in four monkeys and the mean value (±*SEM*) was 0.700 ± 0.019. Hematocrit was also measured in three monkeys with a mean of 36% yielding a mean red blood cell–plasma ratio of 0.17. If the free fractions found *in vitro* are applicable *in vivo*, it would suggest that progabide binds to erythrocytes.

Urinary excretion of unchanged drug was negligible during 24 hr. The large plasma clearance and low blood–plasma ratio of progabide suggest that progabide has a medium to high extraction ratio in rhesus monkeys (assuming all metabolism is hepatic and nonrenal elimination of progabide is negligible).

Single-Dose Oral Studies—Figures 3 and 4 show the plasma concentration–time profiles and bioavailability obtained following two single

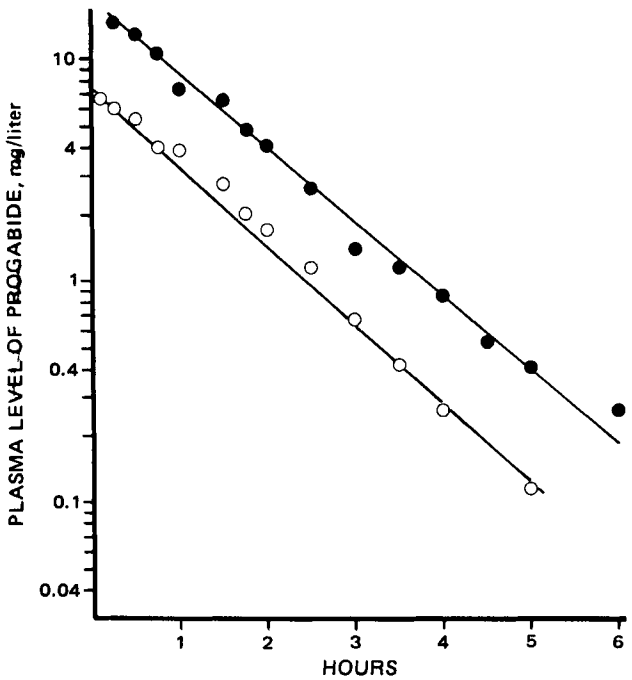

Figure 1—*Semilog plasma–time curve after intravenous bolus administration of progabide (50 mg, ○; 100 mg, ●) in monkey 574A.*

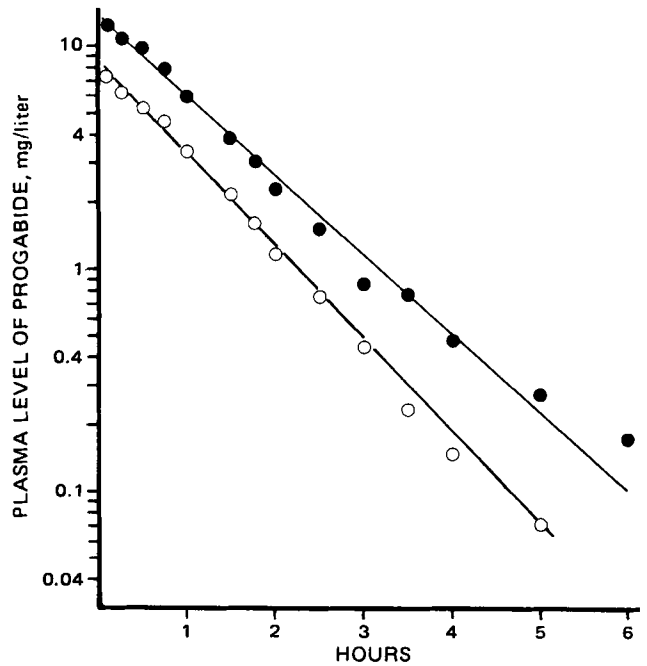

Figure 2—*Semilog plasma–time curve after intravenous bolus administration of progabide (50 mg, ○; 100 mg, ●) in monkey 706A.*

Table IV—Pharmacokinetic Parameters of Progabide Derived from Constant Rate Infusion Studies

Monkey Number	Infusion Rate, mg/hr	Steady-State Plasma Concentration, mg/liter	Systemic Plasma Clearance, liter/hr/kg	Postinfusion Half-Life, hr
514A	2.03	0.237	2.47	0.831
706A	1.92	0.314	2.31	1.028
574A	1.62	0.236	2.21	0.666
020	2.84	0.292	2.76	—
Mean	2.10	0.270	2.44[a]	0.842[b]
(±*SEM*)	(0.26)	(0.020)	(0.12)	(0.09)

[a] Using a two-way ANOVA, the levels of significance for the pairwise comparisons of infusion clearances to those of single dose studies were $p = 0.071$ for infusion *versus* 50-mg dose and $p = 0.0023$ for infusion *versus* 100-mg dose. [b] $p > 0.05$ when compared with single intravenous bolus studies using ANOVA.

oral and intravenous bolus doses in one monkey. Plasma half-life and bioavailability are tabulated in Table II. Progabide was absorbed rapidly and typically reached maximum plasma levels ~1 hr postdose. The bioavailability was between 29 and 69% with a mean (±*SEM*) of 46.8 (±6.6)% for the 50-mg dose and between 22 and 87% with a mean (±*SEM*) of 43.6 (±14.7)% for the 100-mg dose. There was no significant difference between the bioavailabilities of both doses ($p > 0.05$). The incomplete bioavailability is probably due to a first-pass effect and not to poor absorption. Based on a mean extraction ratio, the mean bioavailability was calculated to be 34%, which is in agreement with experimental findings. This calculation assumed complete metabolism in the liver with a hepatic blood flow of 13 liter/hr (7, 8).

Postabsorption half-lives ranged between 0.6 and 0.8 hr at the low dose, and between 0.6 and 1.0 hr at the high dose. These are in agreement with the corresponding intravenous data.

Protein Binding Studies—Protein binding of progabide was determined *in vitro* with plasma concentrations ranging from 0.4 to 34.6 μg/ml. Free fractions ranged between 0.020 and 0.051 (Table III) showing that progabide is highly bound to plasma proteins. Binding appeared concentration-dependent in this plasma level range.

Chronic Dosing Studies—A 7-day continuous zero-order infusion study was performed to test for the presence of any time dependency. A representative plasma concentration–time plot is shown in Fig. 5 and a summary of the pharmacokinetic parameters in four monkeys is given in Table IV. Steady state was achieved in a few hours as predicted from the single-dose studies. Steady-state plasma concentrations ranged between 0.24 and 0.31 mg/liter with infusion rates of 1.6–2.8 mg/hr. Systemic clearance values, ranging from 2.21 to 2.76 liter/hr/kg, were larger than those obtained in single-dose studies. These differences reached

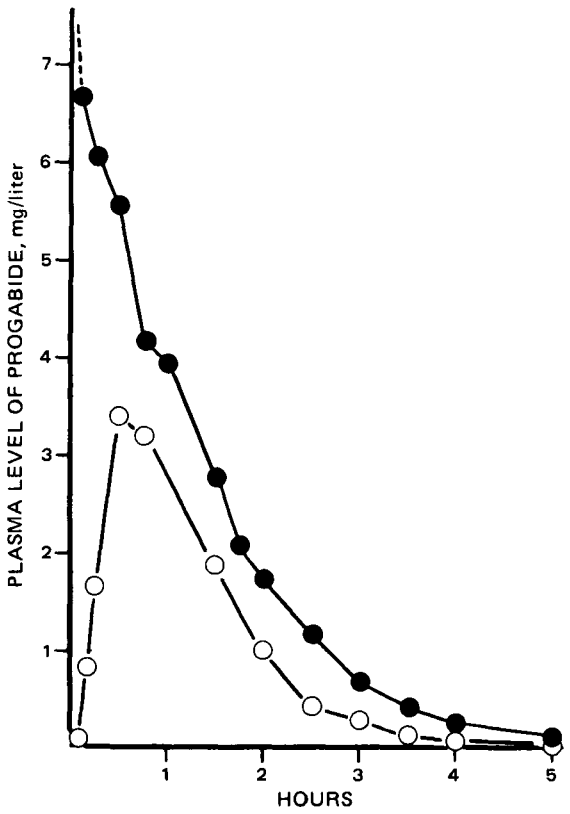

Figure 3—*Plasma concentration–time curve after the intravenous bolus (●) and oral (○) administration of 50 mg of progabide.*

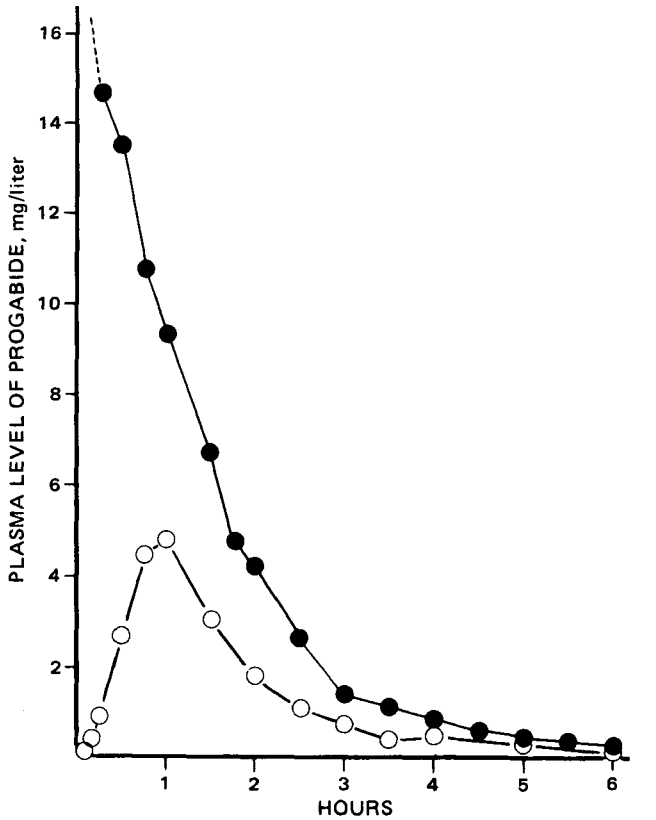

Figure 4—*Plasma concentration–time curve after the intravenous bolus (●) and oral (○) administration of 100 mg of progabide.*

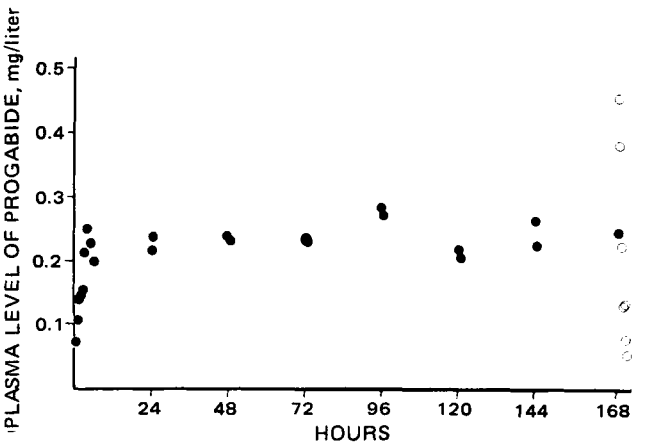

Figure 5—*Plasma concentration during (●) and after (○) the intravenous infusion of progabide in monkey 514A.*

significance for the comparison of the infusion values with the 100-mg dose. Post steady-state disappearance half-lives ranging from 0.67 to 1.03 hr were not different from the single-dose data, (the increase in the postinfusion plasma concentration seen in Fig. 5 was due to flushing of the catheter with saline at the time the infusion was stopped). No time-dependent change in clearance or half-life was exhibited over the 1-week period of the study.

In the rhesus monkey, progabide behaves as a medium extraction ratio drug with incomplete bioavailability and first-order disappearance kinetics. It exhibits nonlinearity in plasma binding *in vitro*. There was a tendency for systemic clearance to decrease within a two-fold dose range. Progabide exhibited no evidence of time dependency in clearance during chronic infusion.

REFERENCES

(1) K. G. Lloyd, S. Dreksler, and E. D. Bird, *Life Sci.*, **21**, 747 (1977).

(2) K. G. Lloyd, L. Shemen, and O. Hornykiewicz, *Brain Res.*, **127**, 269 (1977).

(3) K. G. Lloyd, P. Worms, H. Depoortere, and G. Bartholini, "GABA Neurotransmitters," Alfred Benzon, Symposium 12, Munksgaard, Copenhagen, Denmark, 1978, p. 308.

(4) G. Bartholini, B. Scatton, B. Zivkovic, and K. G. Lloyd, *Ibid.*, pp. 326.

(5) P. L. Morselli, L. Bossi, J. F. Henry, E. Zarifian, and G. Bartholini, *Brain Res. Bull., Suppl. 2*, **5**, 411 (1980).

(6) B. Scatton, B. Zivkovic, J. Dedik, P. Worms, H. Depoortere, K. Lloyd, and G. Bartholini, "Advances in Epileptology: XIth Epilepsy International Symposium," Raven, New York, N.Y., 1980, p. 445.

(7) R. P. Forsyth, A. S. Nies, F. Wyler, J. Heutze, and K. L. Melmon, *J. Appl. Physiol.*, **25**, 736 (1968).

(8) M. Rowland, *J. Pharm. Sci.*, **61**, 70 (1972).

ACKNOWLEDGMENTS

This study was supported by National Institutes of Health Contract No. NO1-NS-1-2282.

Determination of Ethinyl Estradiol in Solid Dosage Forms by High-Performance Liquid Chromatography

SUZANNE H. STRUSIAK, JOHN G. HOOGERHEIDE ˣ, and MAUREEN S. GARDNER

Received July 16, 1981, from the *Schering Corporation, Bloomfield, NJ 07003.* Accepted for publication September 17, 1981.

Abstract □ A rapid, reproducible high-performance liquid chromatographic system for the determination of ethinyl estradiol in solid dosage forms consisting of a reversed-phase column with a mobile phase of 0.05 *M* aqueous KH_2PO_4–methyl alcohol (2:3) and fluorescence detection has been developed. This stability-indicating method is applicable to tablets containing ethinyl estradiol alone or in combination with methyltestosterone and progesterones. The procedure has been used for the determination of ethinyl estradiol in single tablets, stability samples, and dissolution medium. Recovery of drug substance added to placebo was from 97.3 to 101.5% in stability and single-tablet assays, and 95.4 to 102.2% in dissolution assays. Reproducibility studies gave relative standard deviations of 0.4–2.2%.

Keyphrases □ Ethinyl estradiol—high-performance liquid chromatographic analysis, stability, content uniformity and dissolution assays □ High-performance liquid chromatography—analysis, ethinyl estradiol, fluorescence detection □ Estrogens—ethinyl estradiol, high-performance liquid chromatography, analysis of solid dosage forms

Ethinyl estradiol (I), a well known estrogen, is used in hormonal therapy, contraception, and certain cancer treatments. The steroid may be prescribed either alone, as in treatment of estrogen deficiency, or in combination with a progesterone in contraceptive formulations.

Current methods for the analysis of ethinyl estradiol include both wet chemical (1–4) and chromatographic methods. Among the latter are gas chromatography (GC) (5) and high-performance liquid chromatography (HPLC) with UV detection (6–10).

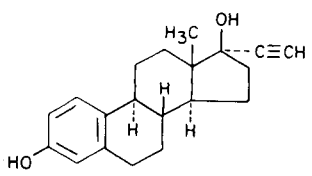

(I)

Determination of ethinyl estradiol by HPLC has been hampered by low sensitivity, as the administered dosages may be as low as 10 μg/tablet. To counter this lack of sensitivity, several investigators have proposed analyzing composite samples of up to 10 tablets (7, 8). While useful for stability assays, this approach is not suitable for either content uniformity or dissolution assays. Other investigators have increased detection sensitivity by using precolumn derivatization with dansyl chloride and fluorescence detection (11, 12). A much simpler approach is to use the native fluorescence of the phenolic ring of the steroid; this method has been used for normal phase HPLC of estrogens (13) and of ethinyl estradiol in cosmetics (14, 15).

A reversed-phase HPLC system with native fluorescence detection for the determination of ethinyl estradiol in solid dosage forms is described. The proposed method, which requires minimal sample preparation, is not only stability-indicating but also sensitive enough for use in content uniformity and dissolution assays.

EXPERIMENTAL

Materials—HPLC grade methyl alcohol[1], *o*-phenylphenol[2], and potassium phosphate monobasic crystals[2] (KH_2PO_4) were obtained from commercial sources. Ultrapure water was prepared by deionization, treatment for removal of organic compounds, and filtering[3].

Apparatus—The high-performance liquid chromatograph was equipped with a constant flow pump[4], an automatic injector[5], a fluores-

[1] Mallinckrodt, Inc., Paris, KY 40361.
[2] Matheson, Coleman and Bell, Cincinnati, OH 45212.
[3] Milli-Q Water Purification System, Millipore Corp., Bedford, MA 01730.
[4] Model M6000A Chromatography Pump, Waters Associates, Milford, MA 01757.
[5] WISP Model 710A Automatic Injector, Waters Associates, Milford, MA 01757.

0022-3549/82/0600-0636$01.00/0

significance for the comparison of the infusion values with the 100-mg dose. Post steady-state disappearance half-lives ranging from 0.67 to 1.03 hr were not different from the single-dose data, (the increase in the postinfusion plasma concentration seen in Fig. 5 was due to flushing of the catheter with saline at the time the infusion was stopped). No time-dependent change in clearance or half-life was exhibited over the 1-week period of the study.

In the rhesus monkey, progabide behaves as a medium extraction ratio drug with incomplete bioavailability and first-order disappearance kinetics. It exhibits nonlinearity in plasma binding *in vitro*. There was a tendency for systemic clearance to decrease within a two-fold dose range. Progabide exhibited no evidence of time dependency in clearance during chronic infusion.

REFERENCES

(1) K. G. Lloyd, S. Dreksler, and E. D. Bird, *Life Sci.*, **21**, 747 (1977).

(2) K. G. Lloyd, L. Shemen, and O. Hornykiewicz, *Brain Res.*, **127**, 269 (1977).

(3) K. G. Lloyd, P. Worms, H. Depoortere, and G. Bartholini, "GABA Neurotransmitters," Alfred Benzon, Symposium 12, Munksgaard, Copenhagen, Denmark, 1978, p. 308.

(4) G. Bartholini, B. Scatton, B. Zivkovic, and K. G. Lloyd, *Ibid.*, pp. 326.

(5) P. L. Morselli, L. Bossi, J. F. Henry, E. Zarifian, and G. Bartholini, *Brain Res. Bull., Suppl. 2*, **5**, 411 (1980).

(6) B. Scatton, B. Zivkovic, J. Dedik, P. Worms, H. Depoortere, K. Lloyd, and G. Bartholini, "Advances in Epileptology: XIth Epilepsy International Symposium," Raven, New York, N.Y., 1980, p. 445.

(7) R. P. Forsyth, A. S. Nies, F. Wyler, J. Heutze, and K. L. Melmon, *J. Appl. Physiol.*, **25**, 736 (1968).

(8) M. Rowland, *J. Pharm. Sci.*, **61**, 70 (1972).

ACKNOWLEDGMENTS

This study was supported by National Institutes of Health Contract No. NO1-NS-1-2282.

Determination of Ethinyl Estradiol in Solid Dosage Forms by High-Performance Liquid Chromatography

SUZANNE H. STRUSIAK, JOHN G. HOOGERHEIDE ˣ, and MAUREEN S. GARDNER

Received July 16, 1981, from the *Schering Corporation, Bloomfield, NJ 07003.* Accepted for publication September 17, 1981.

Abstract □ A rapid, reproducible high-performance liquid chromatographic system for the determination of ethinyl estradiol in solid dosage forms consisting of a reversed-phase column with a mobile phase of 0.05 *M* aqueous KH_2PO_4–methyl alcohol (2:3) and fluorescence detection has been developed. This stability-indicating method is applicable to tablets containing ethinyl estradiol alone or in combination with methyltestosterone and progesterones. The procedure has been used for the determination of ethinyl estradiol in single tablets, stability samples, and dissolution medium. Recovery of drug substance added to placebo was from 97.3 to 101.5% in stability and single-tablet assays, and 95.4 to 102.2% in dissolution assays. Reproducibility studies gave relative standard deviations of 0.4–2.2%.

Keyphrases □ Ethinyl estradiol—high-performance liquid chromatographic analysis, stability, content uniformity and dissolution assays □ High-performance liquid chromatography—analysis, ethinyl estradiol, fluorescence detection □ Estrogens—ethinyl estradiol, high-performance liquid chromatography, analysis of solid dosage forms

Ethinyl estradiol (I), a well known estrogen, is used in hormonal therapy, contraception, and certain cancer treatments. The steroid may be prescribed either alone, as in treatment of estrogen deficiency, or in combination with a progesterone in contraceptive formulations.

Current methods for the analysis of ethinyl estradiol include both wet chemical (1–4) and chromatographic methods. Among the latter are gas chromatography (GC) (5) and high-performance liquid chromatography (HPLC) with UV detection (6–10).

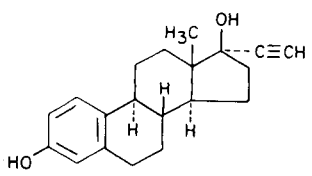

(I)

Determination of ethinyl estradiol by HPLC has been hampered by low sensitivity, as the administered dosages may be as low as 10 μg/tablet. To counter this lack of sensitivity, several investigators have proposed analyzing composite samples of up to 10 tablets (7, 8). While useful for stability assays, this approach is not suitable for either content uniformity or dissolution assays. Other investigators have increased detection sensitivity by using precolumn derivatization with dansyl chloride and fluorescence detection (11, 12). A much simpler approach is to use the native fluorescence of the phenolic ring of the steroid; this method has been used for normal phase HPLC of estrogens (13) and of ethinyl estradiol in cosmetics (14, 15).

A reversed-phase HPLC system with native fluorescence detection for the determination of ethinyl estradiol in solid dosage forms is described. The proposed method, which requires minimal sample preparation, is not only stability-indicating but also sensitive enough for use in content uniformity and dissolution assays.

EXPERIMENTAL

Materials—HPLC grade methyl alcohol[1], *o*-phenylphenol[2], and potassium phosphate monobasic crystals[2] (KH_2PO_4) were obtained from commercial sources. Ultrapure water was prepared by deionization, treatment for removal of organic compounds, and filtering[3].

Apparatus—The high-performance liquid chromatograph was equipped with a constant flow pump[4], an automatic injector[5], a fluores-

[1] Mallinckrodt, Inc., Paris, KY 40361.
[2] Matheson, Coleman and Bell, Cincinnati, OH 45212.
[3] Milli-Q Water Purification System, Millipore Corp., Bedford, MA 01730.
[4] Model M6000A Chromatography Pump, Waters Associates, Milford, MA 01757.
[5] WISP Model 710A Automatic Injector, Waters Associates, Milford, MA 01757.

0022-3549/82/0600-0636$01.00/0

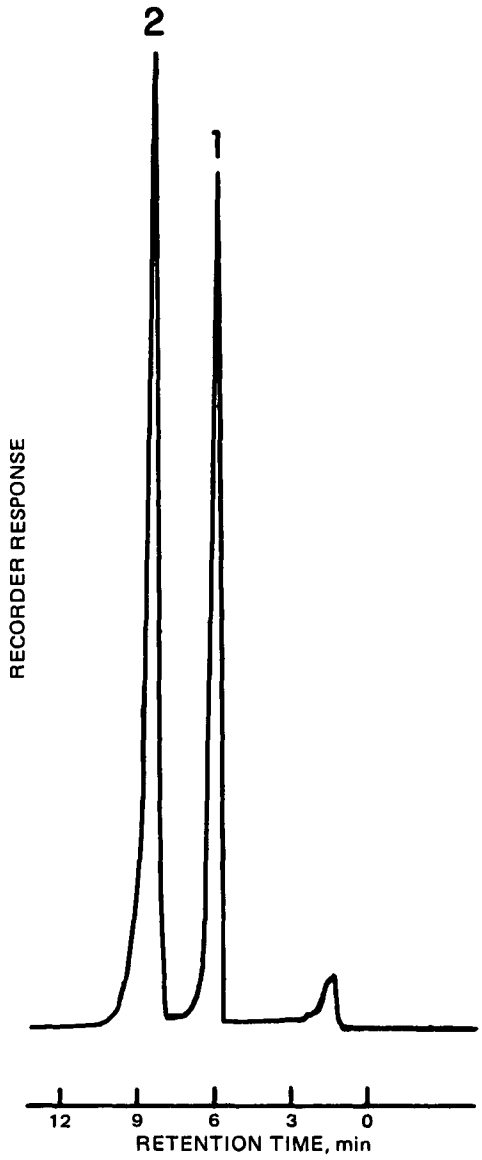

Figure 1—*High-performance liquid chromatogram of ethinyl estradiol and internal standard. Key: 1, o-phenylphenol; 2, ethinyl estradiol.*

cence detector (excitation at 280 nm, emission at 330 nm) containing a xenon lamp source[6], and a chart recorder[7]. The stainless steel column (25 cm × 4.6-mm i.d.) was packed with 10-μm, irregularly shaped, totally porous silica particles bonded with a C-8 hydrocarbon phase[8]. A 2.0-μm filter[9] was placed in-line before the column. A data acquisition system[10] was used for peak processing.

Chromatographic Conditions—The mobile phase was 0.05 *M* aqueous KH_2PO_4, filtered through a 0.45-μm filter[11]–methyl alcohol (2:3) and degassed for 20 min by using an ultrasonic water bath. The flow rate through the HPLC system was 2.0 ml/min. Helium was bubbled through the mobile phase constantly while the system was running.

Internal Standard Solution—A 0.1-mg/ml solution of *o*-phenylphenol was prepared in mobile phase. This solution was diluted to 1.0 μg/ml with mobile phase.

Standard Solution—Approximately 25 mg of ethinyl estradiol standard was accurately weighed, transferred to a 100-ml volumetric flask, and dissolved and diluted to 100 ml with methyl alcohol. This solution was diluted exactly 5:50 in methyl alcohol. A 2.00-ml aliquot of this solution and 5.00 ml of a 1.0-μg/ml internal standard solution were added to a 50-ml volumetric flask. Approximately 23 ml of methyl alcohol was added to the flask and diluted to volume with 0.05 *M* aqueous KH_2PO_4 to a final concentration of 1 μg/ml of ethinyl estradiol and 0.1 μg/ml of internal standard. A 50-μl aliquot was injected into the liquid chromatograph.

Determination of Ethinyl Estradiol in Solid Dosage Forms—Tablets containing 0.02 mg of ethinyl estradiol were assayed by adding single tablets to individual 50-ml centrifuge tubes containing 4.00 ml of aqueous 0.05 *M* KH_2PO_4. The sample was rotated for 15 min. A 2.00-ml aliquot of internal standard and 4 ml of methyl alcohol were added to the sample, which was again rotated for 15 min and centrifuged. The super-

[6] Model 650-10LC Fluorescence Detector, Perkin-Elmer Corp., Norwalk, CT 06856.

[7] Linear Model 485 Recorder, Linear Instruments Corp., Irvine, CA 92664.

[8] LiChrosorb RP8 Column, E. M. Laboratories, Inc., E. Merck, Elmsford, NY 10523.

[9] Model 7302 Column Inlet Filter, 2 μm, Rheodyne Incorporated, Cotati, CA 94928.

[10] PDP 11/34 minicomputer utilizing peak-112 Software, Digital Equipment Corp., Maynard, MA 01754.

[11] Millipore Filter, Type HA, Millipore Corp., Bedford, MA 01730.

Table I—Recovery of Ethinyl Estradiol Added to Tablet Placebos for Content Uniformity and Stability Assays

Formulation	Placebo, mg	Ethinyl Estradiol Added, mg	Ethinyl Estradiol Found, mg	Recovery, %
0.02 mg/tablet, placebo	181.0	0.0215	0.0216	100.5
	240.5		0.0216	100.5
	301.7		0.0213	99.1
	360.7		0.0213	99.1
	424.5		0.0213	99.1
0.02 mg/tablet, placebo[a]	230.5	0.0195	0.0195	100.0
	290.7		0.0198	101.5
	347.7		0.0194	99.5
	418.9		0.0194	99.5
0.05 mg/tablet, placebo	180.7	0.0538	0.0537	99.8
	241.5		0.0539	100.2
	300.2		0.0541	100.6
	361.0		0.0535	99.4
	421.1		0.0530	98.5
0.05 mg/tablet, placebo[a]	181.2	0.0488	0.0475	97.3
	242.0		0.0476	97.5
	307.3		0.0484	99.2
	360.7		0.0485	99.4
	422.3		0.0481	98.6
0.5 mg/tablet, placebo	121.1	0.538	0.545	101.3
	160.3		0.544	101.1
	201.2		0.545	101.3
	239.8		0.544	101.3
	280.3		0.540	100.4
0.5 mg/tablet, placebo[a]	120.6	0.516	0.520	100.8
	160.9		0.519	100.6
	200.8		0.512	99.2
	240.9		0.517	100.2
	280.8		0.513	99.4

[a] Heated 75°, 2 weeks.

Table II—Reproducibility of Ethinyl Estradiol Determinations for Content Uniformity and Stability Assays

Tablet Strength	Day	Assay, % Label			
0.02 mg/tablet		Lot a	Lot b	Lot c	Lot d[a]
	1	107.4	108.2	108.0	110.3
	2	108.6	110.2	109.9	107.7
	3	111.4	108.1	107.8	106.5
	4	108.1	—	—	106.1
$\bar{X}$		108.9	108.8	108.6	107.6
RSD, %		1.6	1.1	1.1	1.7
0.05 mg/tablet		Lot e	Lot f	Lot g	Lot h[a]
	1	109.0	105.4	105.3	108.1
	2	110.2	106.3	105.3	103.0
	3	108.2	104.5	106.5	105.6
	4	—	—	—	107.5
$\bar{X}$		109.1	105.4	105.7	106.0
RSD, %		0.9	0.8	0.7	2.2
0.5 mg/tablet		Lot i	Lot j	Lot k	Lot l[a]
	1	105.3	104.6	103.4	102.7
	2	105.7	105.8	101.5	103.3
	3	106.1	102.8	102.1	103.1
	4	—	—	—	99.4
$\bar{X}$		105.7	104.4	102.3	102.2
RSD, %		0.4	1.4	1.0	2.1

[a] Heated 75°, 2 weeks.

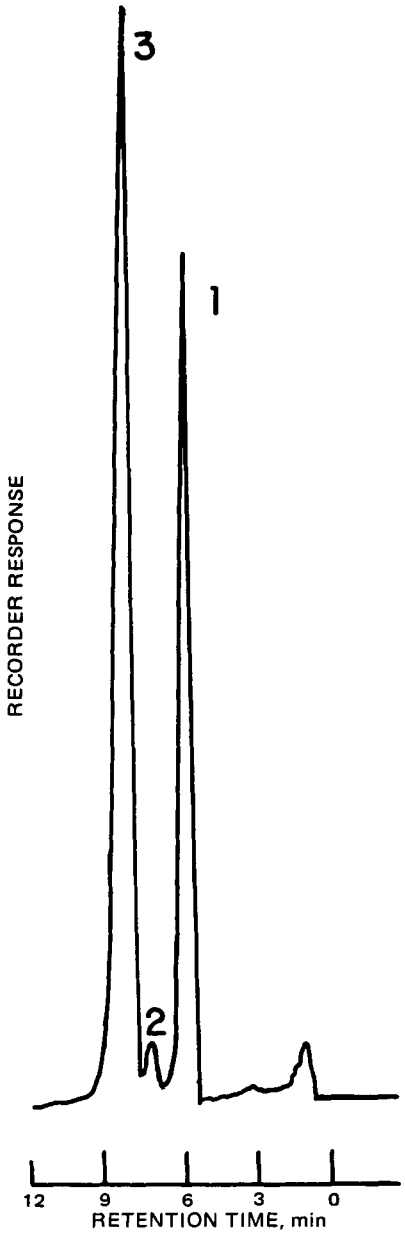

Figure 2—*High-performance liquid chromatogram of ethinyl estradiol tablet extract. Key: 1, o-phenylphenol; 2, butylparaben; 3, ethinyl estradiol.*

nate was transferred to a 25-ml volumetric flask. The samples were extracted two more times with ~5 ml of mobile phase and a 10-min rotation. The supernates were combined and a 50-μl aliquot injected into the liquid chromatograph. The ethinyl estradiol content was calculated as follows:

mg of ethinyl estradiol/tablet =

$$(R_{sam}/R_{std}) \times (W_{std}) \times (V_{sam}/V_o) \qquad \text{(Eq. 1)}$$

where:

R_{sam} = ratio of ethinyl estradiol to *o*-phenylphenol peak heights in the sample chromatogram;
R_{std} = peak height ratio in the standard chromatogram;
W_{std} = weight of ethinyl estradiol in the reference standard solution;
V_{sam} = total volume of sample solution;
V_o = total volume of *o*-phenylphenol in the sample solution.

This sample preparation allows for the determination of ethinyl estradiol in higher strength dosage forms. Tablets containing up to 0.5 mg of ethinyl estradiol may be assayed by adjusting extraction volumes and internal standard concentration to give final assay concentrations of 1 μg/ml of ethinyl estradiol and 0.1 μg/ml of internal standard.

Table III—Recovery of Ethinyl Estradiol Added to Formulation Placebos for Dissolution Assay

Formulation	Ethinyl estradiol Added, mg	Ethinyl estradiol Found, mg	Recovery, %
0.02 mg/tablet, 300-mg placebo	0.0102	0.0101	99.0
	0.0153	0.0154	100.7
	0.0205	0.0198	96.6
	0.0256	0.0258	100.8
0.05 mg/tablet, 300-mg placebo	0.0259	0.0248	95.7
	0.0388	0.0387	99.7
	0.0518	0.0508	98.1
	0.0647	0.0617	95.4
0.5 mg/tablet, 200-mg placebo	0.256	0.260	101.6
	0.384	0.380	99.0
	0.511	0.522	102.2
	0.639	0.610	95.5

Accelerated Degradation Studies—Accelerated degradation studies were conducted by heating the ethinyl estradiol drug substance at 178° for 16 hr as described previously (16), and heating the ethinyl estradiol tablets for 2 weeks at 75°.

Dissolution Assay Studies—A solution of 2 μg/ml of *o*-phenylphenol was prepared in methyl alcohol as the internal standard solution.

Approximately 25 mg of ethinyl estradiol standard was accurately weighed, transferred to a 50-ml volumetric flask, and dissolved and diluted to volume with methyl alcohol. This standard solution was diluted exactly 2:50 in methyl alcohol. A 1.00-ml aliquot of this solution and 1.00 ml of the 2 μg/ml internal standard were added to 900 ml of ultrapure water[3].

Determination of Ethinyl Estradiol in Dissolution Medium—Single tablets containing 0.02 mg of ethinyl estradiol were placed in 900 ml of ultrapure water[3] along with 1.00 ml of 2 μg/ml of the internal standard solution. Dissolution of the tablet was conducted at 37° for 1 hr. The samples and standards were then treated identically. The standard solutions and dissolution medium were filtered through a 1.2-μm filter[12], the filtrates equilibrated to room temperature, and the entire contents of each filtrate concentrated onto an activated C-18 cartridge[13] by using a vacuum to draw the solution through the cartridges. The cartridge was eluted with 20-ml 0.05 *M* aqueous KH_2PO_4–methyl alcohol (2:3) and a volume of 50 μl injected into the liquid chromatograph. The ethinyl estradiol content was calculated from Eq. 1.

This sample preparation also allows for the determination of higher levels of ethinyl estradiol in dissolution medium. Tablets containing up

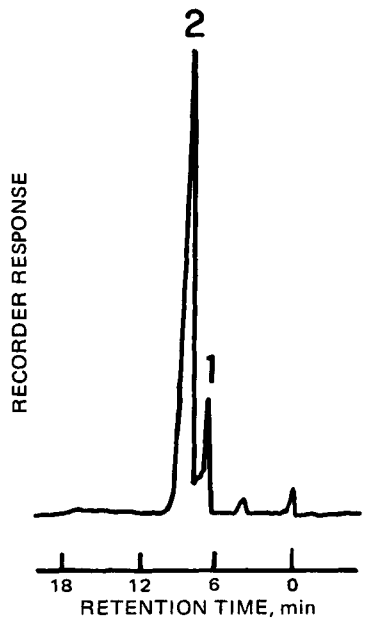

Figure 3—*High-performance liquid chromatogram of ethinyl estradiol drug substance subjected to accelerated degradation. Key: 1, unidentified decomposition product; 2, ethinyl estradiol.*

[12] Millipore Filter, Type RA, Millipore Corp., Bedford, MA 01730.
[13] Sep-Pak C-18 Cartridges, Waters Associates, Milford, MA 01757.

Table IV—Reproducibility of Ethinyl Estradiol Determinations in Dissolution Medium

Aliquot	Assay, mg recovered		
	Tablet, Strength A	Tablet, Strength B	Tablet, Strength C
1	0.0228	0.0492	0.363
2	0.0225	0.0502	0.360
3	0.0230	0.0508	0.357
4	0.0228	0.0491	0.355
5	0.0232	0.0495	0.372
6	0.0229	—	0.367
$\bar{X}$	0.0228	0.0498	0.362
RSD, %	1.0	1.6	1.8

to 0.5 mg of ethinyl estradiol were assayed by adjusting the internal standard concentration and dilutions to give approximate concentrations of 1 μg/ml of ethinyl estradiol and 0.1 μg/ml of the internal standard.

RESULTS AND DISCUSSION

Content Uniformity and Stability Assays—To develop a rapid, reproducible HPLC method for the determination of ethinyl estradiol, sample preparation was kept as simple as possible. In this method the tablet matrix is disintegrated by mixing with aqueous buffer, after which methyl alcohol is added to solubilize the drug substance; the final extracting solution has the same solvent composition as the mobile phase. Under these conditions, two extractions are sufficient to remove more than 99% of both active and internal standard from the tablet matrix; however, a third extraction was added to ensure quantitative recoveries.

To simplify the assay methods, ethinyl estradiol was detected by its native fluorescence rather than by precolumn fluorescence labeling. Both ethinyl estradiol and the internal standard, *o*-phenylphenol, have UV absorption maxima around 280 nm as well as from 200 to 220 nm. Excitation at either of these maxima produces broad ethinyl estradiol emission at 310 nm and *o*-phenylphenol emission at 340 and 420 nm. Adequate sensitivity and selectivity was maintained for these compounds by monitoring emission at 330 nm with a 20-nm spectral band width. While excitation can be done at either 220 or 280 nm, excitation at 220 nm leads to interferences of two types. First, more compounds absorb at 220 than at 280 nm, leading to a loss in detection specificity. Second, impurities in the mobile phase fluoresce to give a significant background. Large amounts of UV absorbing material, such as the methyltestosterone encountered in some formulations, absorb enough radiation to decrease the background, giving negative peaks which are potential chromatographic interferences. Both of the above detection interferences are of significantly lower magnitude when using excitation at 280 rather than 220 nm.

Due to the low levels of ethinyl estradiol and high detection sensitivity, care must be taken to avoid interferences due to fluorescent impurities. Glassware must be thoroughly cleaned and dried, avoiding any surfactants which could leave residues of fluorescing compounds on the glass. In the course of this work, it was also noted that spurious peaks arose from the use of latex dropper bulbs; particulate matter from the bulbs caused severe chromatographic interferences.

In the described method, ethinyl estradiol elutes with a retention time of 9 min and the internal standard elutes at 6 min (Fig. 1). Butylparaben, a tablet-coating excipient, chromatographs at 8 min and does not interfere with the assay. A sample chromatogram is shown in Fig. 2.

Ethinyl estradiol, when subjected to the extreme temperature conditions of 178° for 16 hr used in a previous study (16), degraded ~25%. The degradation products are separated from both ethinyl estradiol and the internal standard as shown in Fig. 3. A discussion of the degradation of ethinyl estradiol has been previously reported (16).

The linearity of the chromatographic system was demonstrated within the range of 0.61–1.42 μg/ml of ethinyl estradiol standard. Response *versus* concentration data gave a correlation coefficient of 0.9995 and an estimated relative standard deviation of linearity of 1.4%. Linearity of the sample preparation was tested over the range of 60–140% of the assay sample size for tablets containing 0.02 mg of ethinyl estradiol and yielded a correlation coefficient of 0.9999 and an estimated relative standard deviation of linearity of 0.64%. Linearity of the sample preparation was also demonstrated for high strength dosage forms of ethinyl estradiol tablets. The correlation coefficients obtained from these experiments were no less than 0.9994. No statistically significant bias was observed in any of the linearity experiments when extrapolated to zero sample size.

The accuracy of the content uniformity–stability method was demonstrated by the addition of ethinyl estradiol to varying amounts of placebo. As seen in Table I, recovery of ethinyl estradiol from the placebo is excellent, ranging from 97.3 to 101.5%.

The precision of the method was tested by performing replicate assays on several sample batches over a period of several days (Table II). The relative standard deviations of the assays were <2% for all normal batches, but increased slightly for heated samples.

Table V—Retention Times for Compounds Commonly Found in Combination with Ethinyl Estradiol

Compound	Relative Retention Time
Ethinyl Estradiol	1.00
Norethindrone	1.00
Norgestrel	1.49
Methyltestosterone	1.57
Norethindrone acetate	2.15
Ethynodiol diacetate	[a]

[a] No peak observed.

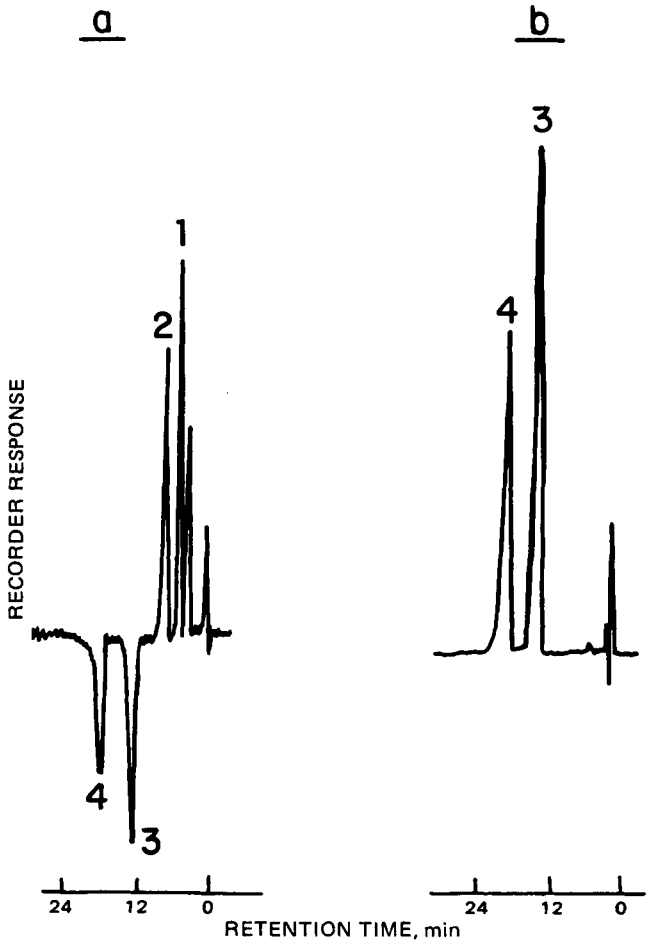

Figure 4—*High-performance liquid chromatogram of tablets containing both ethinyl estradiol and methyltestosterone, (a) fluorescence; (b) ultraviolet. Key: 1, o-phenylphenol; 2, ethinyl estradiol; 3, methyltestosterone; 4, progesterone (internal standard).*

Table VI—Reproducibility of Ethinyl Estradiol Determinations in the Presence of Methyltestosterone

Sample	Assay, % Label		
	Lot A[a]	Lot B[a]	Lot C[b]
1	109.9	108.0	103.7
2	112.1	105.3	104.6
3	109.9	105.0	—
$\bar{X}$	110.6	106.1	104.2
RSD, %	1.3	1.7	—

[a] 0.04 mg of ethinyl estradiol, 10 mg of methyltestosterone/tablet. [b] 0.02 mg of ethinyl estradiol, 5 mg of methyltestosterone/tablet.

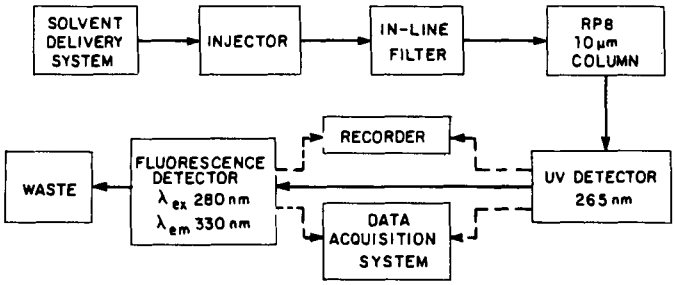

Scheme A—High-performance liquid chromatographic system for simultaneous determination of ethinyl estradiol and methyltestosterone.

Dissolution Assays—The medium chosen for the dissolution assays was ultrapure distilled water, from which ions and organic compounds had been removed[3]. Ultrapure water must be used to prevent concentration of any fluorescent impurities onto the cartridge[13].

Precision of ethinyl estradiol recovery from dissolution assay medium was demonstrated by preparing eight standard solutions as described previously and assaying these according to the HPLC method described. These eight standards produced a relative standard deviation of 2.1%.

Since relatively large volumes of liquid were passed through the cartridges[13], some breakthrough of ethinyl estradiol and internal standard was expected. Standard solutions were concentrated onto cartridges[13] series so that any breakthrough from one cartridge would be concentrated onto a second cartridge. The breakthrough observed was 5.7% for ethinyl estradiol and 6.6% for the internal standard. These losses were considered acceptable since both standard and sample solutions are concentrated onto the cartridges and lose equal amounts of material. The breakthrough percentage is constant over a wide range of sample size as demonstrated by recovery studies of ethinyl estradiol and internal standard from dissolution medium. Over the range of 10–500 ng/ml of ethinyl estradiol, peak height ratios were obtained with a relative standard deviation of 1.0%.

The accuracy of the method was demonstrated by the addition of varying amounts of ethinyl estradiol to a constant amount of placebo. The recovery of ethinyl estradiol for three different tablet strengths is seen in Table III. The recovery of ethinyl estradiol ranged from 95.4 to 102.2% with no statistically significant bias when extrapolated to zero sample size.

To avoid the differences of tablet-to-tablet variations, precision of the recovery of ethinyl estradiol from dissolution media was tested on single tablet equivalents of tablet grinds. The largest relative standard deviation observed is 1.8% (Table IV).

Separation of Ethinyl Estradiol from Other Drug Substances—This HPLC method is also applicable to the analysis of ethinyl estradiol in the presence of other drug substances. Various drug substances commonly found in combination with ethinyl estradiol were chromatographed by using the proposed HPLC system with UV detection at 220 nm. As the relative retention times in Table V indicate, norgestrel, methyltestosterone, and norethindrone acetate are all well separated from ethinyl estradiol; norethindrone coeluted with ethinyl estradiol and ethynodiol diacetate did not appear to elute from the column.

Assays for ethinyl estradiol were performed on tablets containing both ethinyl estradiol (0.04 mg/tablet) and methyltestosterone (10 mg/tablet). The chromatographic system for this analysis is given in Scheme A. The relative standard deviation of the determination of ethinyl estradiol in the presence of methyltestosterone was not greater than 1.9%, as shown in Table VI for replicate sample preparations. Figure 4 indicates that methyltestosterone causes no chromatographic interference in the assay for ethinyl estradiol.

REFERENCES

(1) "The United States Pharmacopeia," 20th rev., U.S. Pharmacopeial Convention, Rockville, Md., 1980, pp. 307–308.

(2) T. James, *J. Pharm. Sci.*, **61**, 1306 (1972).

(3) S. Hirai, A. Hussain, and S. Babhair, *ibid.*, **69**, 857 (1980).

(4) G. Ramana Rao, M. V. Sivaramakrishnan, and C. M. R. Srivastava, *Indian J. Pharm. Sci.*, **41**, 233 (1979).

(5) J. M. Talmage, M. H. Penner, and M. Geller, *J. Pharm. Sci.*, **54**, 1194 (1965).

(6) K. R. Bagon and E. W. Hammond, *Analyst*, **103**, 156 (1978).

(7) J. A. P. Gluck and E. Shek, *J. Chromatogr. Sci.*, **18**, 631 (1980).

(8) R. W. Roos, *J. Assoc. Off. Anal. Chem.*, **63**, 80 (1980).

(9) N. F. Swynnerton and J. B. Fischer, *J. Liq. Chrom.*, **3**, 1195 (1980).

(10) D. C. Tsilifonis and L. Chafetz, *J. Pharm. Sci.*, **69**, 1461 (1980).

(11) R. W. Roos, *ibid.*, **67**, 1735 (1978).

(12) G. J. Schmidt, F. L. Vandemark, and W. Slavin, *Anal. Biochem.*, **91**, 636 (1978).

(13) G. J. Krol, C. A. Mannan, R. E. Pickering, D. V. Amato, B. T. Kho, and A. Sonnenschein, *Anal. Chem.*, **49**, 1836 (1977).

(14) S. Ohnishi, A. Ogawa, and Y. Nishijima, *Bunseki Kagaku*, **28**, 82 (1979); through *Chem. Abstr.*, **90**, 192370y (1979).

(15) K. Kamata, R. Yamazoe, and H. Harada, *Eisei Kagaku*, **26**, 41 (1980); through *Chem. Abstr.*, **93**, 53730g (1980).

(16) M. L. Cotter, S. D. Levine, R. Mallory, and C. Shaw, *Tetrahedron Lett.*, **22**, 1939 (1978).

Use of Dipole Moment as a Parameter in Drug–Receptor Interaction and Quantitative Structure–Activity Relationship Studies

ERIC J. LIEN ˣ, ZONG-RU GUO, REN-LI LI, and CHING-TANG SU

Received June 11, 1981 from the *Section of Biomedicinal Chemistry, School of Pharmacy, University of Southern California, Los Angeles, CA 90033.* Accepted for publication July 31, 1981.

Abstract □ The theoretical basis for using dipole moment as a free-energy related parameter in studying drug–receptor interaction and quantitative structure–activity relationship (QSAR) is presented. Over 300 group dipole moments for aromatic substituents were compiled using the dipole moments of monosubstituted benzene derivatives. Examples in the literature of using dipole moment in QSAR studies are also presented.

Keyphrases □ Dipole moment—parameter in drug–receptor interaction and quantitative structure–activity relationships, list of 300 for aromatic substituents □ Quantitative structure–activity relationships—dipole moment as a parameter, 300 dipole moments listed for aromatic substituents □ Drug–receptor interaction—dipole moment as a parameter, list of 300 dipole moments for aromatic substituents

It is generally accepted that most interactions between drugs and receptors are physicochemical processes. When an equilibrium between a drug–receptor complex (DR), a free drug (D), and unoccupied receptor (R) is established, the reversible process can be expressed as:

$$D + R \underset{k_2}{\overset{k_1}{\rightleftharpoons}} DR \qquad \text{(Eq. 1)}$$

Under equilibrium conditions the following holds:

$$\log K = -\Delta G°/2.303RT \qquad \text{(Eq. 2)}$$

where $K = (k_1/k_2)$ is the association constant of the complex DR, $\Delta G°$ is the change in standard free energy during the formation of DR, T is the absolute temperature, and R is the gas constant.

The ability of each member of a series of drugs to bind to the receptor is dependent on the difference in the standard free energy change ($\Delta G°$) under the same condition. Factors contributing to this variation in $\Delta G°$ can be divided into three major categories: lipophilic, electronic, and steric.

THEORETICAL

Based on linear free-energy relationships, Hansch and Fujita (1, 2) developed a general model to quantitatively describe the relationships between biological activities and molecular structures:

$$\log (1/C) = -a\pi^2 + b\pi + \rho\sigma + dE_s + c \qquad \text{(Eq. 3)}$$

where $\log (1/C)$ is the negative logarithm of the concentration or dosage of a drug producing a standard biological response, π is the hydrophobic constant of the substituent, σ is the Hammett substituent, and E_s is the steric constant.

This model was later extended to include differences in degree of ionization, molecular size, and dipole moment, as well as branching (3–5):

$$\log \text{biological response} = -a(\log P)^2 + b \log P + c\,(\text{pKa} - \text{pH}) + d \log MW + e\,\mu + f\,\chi + g \qquad \text{(Eq. 4)}$$

where pKa − pH equals the log (undissociated/dissociated) for acids, μ is the dipole moment, and χ is the branching or other steric factors.

The electronic effects in drug–receptor interactions are represented by the electric dipole moment, μ.

All forces between atoms or drug molecules and receptors or biomacromolecules are electrostatic in origin. Several types of noncovalent interactions between drugs and receptors can be described as interactions between charges (long-range force), between charge and a dipole, and between dipoles (short-range forces).

The potential energy of interaction of two oppositely charged ions relative to the magnitudes of the charges q_1 and q_2 and the distance between them r, is given by Coulomb's law:

$$E = \frac{-q_1 q_2}{Dr} \qquad \text{(Eq. 5)}$$

where D is the dielectric constant through which the charges interact. The energy of interactions between charges and receptors is much larger than that of noncharged electronic effects, hydrophobic effects, and others. A charged species also has quite different transport properties than a noncharged species. Therefore, the ionic member in a series of compounds often does not fit the regression line obtained from the series of noncharged compounds and is usually excluded from the series in quantitative structure–activity relationship (QSAR) analysis.

The energy of interaction between an ion and a dipole is given by the following (6):

$$E = \frac{-N_a e\,\mu\cos\theta}{D(r^2 - d^2)} \qquad \text{(Eq. 6)}$$

where N_a is Avogadro's number, e is the magnitude of the charge, θ is the angle between the line joining the charge and the middle of the dipole and the line between the ends of the dipole, D is the dielectric constant, r is the distance between the charge and the middle of the dipole, and d is the length of the dipole. It is obvious from this equation that the extent to which an ion and a dipole interact is related to the dipole orientation.

The energy of interaction between two dipoles in the most favorable alignment is given by:

$$E = \frac{-2\mu_a\mu_b}{Dr^3} \qquad \text{(Eq. 7)}$$

where μ_a and μ_b stand for the dipole moments (6):

The average interaction for all orientations is given by:

$$E = \frac{-2\mu_a^2\mu_b^2}{3\,KTDr^6} \qquad \text{(Eq. 8)}$$

The energy of dipole-induced dipole interactions (Debye forces) is:

$$E = \frac{-\mu_a^2\alpha_b + \mu_b^2\alpha_a}{D^2r^6} \qquad \text{(Eq. 9)}$$

where α_a and α_b are the polarizabilities.

The dispersion interactions (London forces) are governed by:

$$E = \frac{-3\alpha_a\alpha_b[I_aI_b/(I_a + I_b)]}{2r^6} \qquad \text{(Eq. 10)}$$

where I_a and I_b stand for the ionization potentials.

Note that the dipole–dipole (Keesom) interactions are not only dependent on the orientation of the dipoles but also inversely proportional to the third power of distance (Eq. 7) or the sixth power of distance for all orientations (Eq. 8).

In QSAR studies it it assumed that the receptor remains unchanged; therefore, only the properties of the drug molecule need to be considered (μ_a, α_a, I_a, *etc.*).

In most of the published QSAR studies, the electronic parameters most commonly used are the Hammett σ constant and Taft polar constant σ^*. The Hammett σ constants result from the comparison of the pKa of a series of substituted benzoic acids to that of benzoic acid. They describe the magnitude of electronic effects of substituents on the reactive center attached to the benzene ring, *i.e.*, the dissociation constants of substituted

0022-3549/82/0600-0641$01.00/0

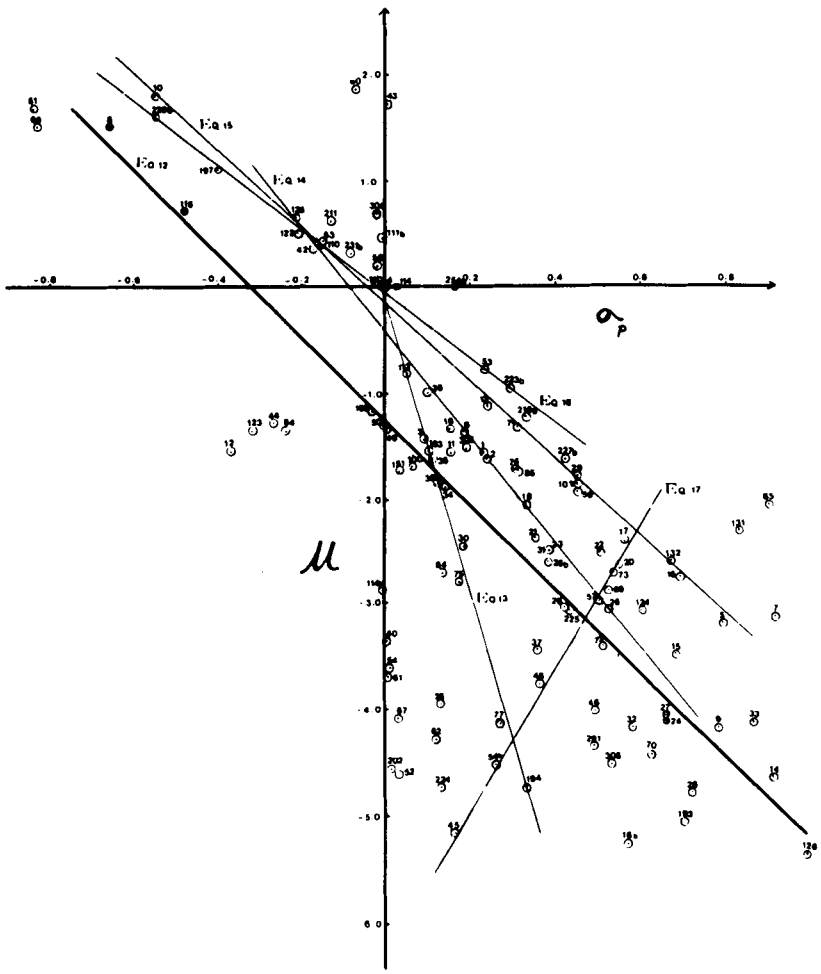

Figure 1—*A plot of* μ versus σ_p. *Note the scattering of the points, and the quite different slopes and intercepts for equations derived from various subsets.*

benzoic acids. In other words, σ constants are a measurement of substituent electronic effects on the reactivity of other parts of the same molecule. It is known that in using σ constants, the orientation and the rate or equilibrium of reactions can be predicted when aromatic compounds are substituted by various functional groups.

If interactions between drugs and receptors are controlled by the electronic nature of the substituents on the benzene ring, σ constants are suitable descriptors of electronic effects for QSAR analysis. However, not all the electronic effects of a series of drugs in drug–receptor complexes work by varying the electronic properties of another reactive center. Different substituents in a series of drugs may directly interact with receptors, *i.e.*, *via* charge–dipole, dipole–dipole, dipole–induced dipole, and induced dipole–induced dipole interactions between the substituent of a drug and a part of receptor. These interactions could affect the binding force of the drug with the receptor. Therefore, dipole moments, which are the quantitative measurements of separation of charge, should be useful in describing direct drug–receptor interactions through noncovalent bonding.

Group dipole moments of substituents are thermodynamically linear free-energy related functions. They are vectors with additive and constitutive properties. For congeneric series of compounds, dipole moments have been frequently found to correlate well with σ or other linear free-energy related parameters. For example, the dipole moments of substituted anilines have been correlated with the melting points, N–H stretching frequency in infrared spectra, as well as σ_p constants (7). Colinese *et al.*, also have found linear correlation between the dipole moments and $\nu_{(O-H)}$ of a series of 4′-substituted-4-hydroxyazobenzenes (8). It was also reported that for *N*-(4-substituted benzylidene)-4-hydroxyanilines that $\nu_{(O-H)}$ and $\mu_{(O-H)}$ are linearly related to Hammett's σ constant (9). A linear relationship between $\mu_{(O-H)}$ and the relative frequency shift ($\Delta\nu$) in dioxane has been used as an evidence of the dependence of $\mu_{(O-H)}$ on the strength of hydrogen bonding (9). Van Beek (10) also reported some linear relationships between dipole moments and σ constants in a few disubstituted benzene systems. Apparent correlation has also been reported between the N–H chemical shift and the dipole moment of lactams and thiolactams (11).

Despite successful correlation within limited series, the correlation between μ and σ may vary drastically or fail completely if noncongeneric groups are lumped together (Figs. 1 and 2).

Since Hammett's substituent constants (σ) are more readily available for a wide variety of substituents (12, 13) than dipole moments, the use of dipole moments in QSAR has only been reported by a few groups in spite of the direct relationship with interaction energy. The present report reviews the reported cases of QSAR using dipole moment as an independent electronic parameter, and compiles a table of group dipole moments for future use.

Method—More than 300 group dipole moments were collected (Appendix I), most of which were taken from McClellan's book (14). The magnitudes of the group dipole moments of substituents are equal to those of the corresponding monosubstituted benzene. The sign is taken by comparison of the electronegativities between the substituent and the aromatic carbon to which the group is connected. A negative sign stands for a negative end pointing away from the benzene ring.

A total of 114 substituent groups (for which both μ and σ are available) were analyzed to examine the interrelationship between μ and σ. Hammett's σ constants were taken from Hansch and Leo's book (13). All the regression lines were derived by computer[1] *via* the method of nonweighted least-squares fit.

RESULTS AND DISCUSSION

The overall correlations between Hammett σ constants and the group dipole moments of 114 substituents are shown in Eqs. 11 and 12:

$$\mu = -5.99\,\sigma_m - 0.53 \qquad \text{(Eq. 11)}$$
$$n = 114,\ r = 0.749,\ s = 1.279$$

[1] IBM 370/185 computer.

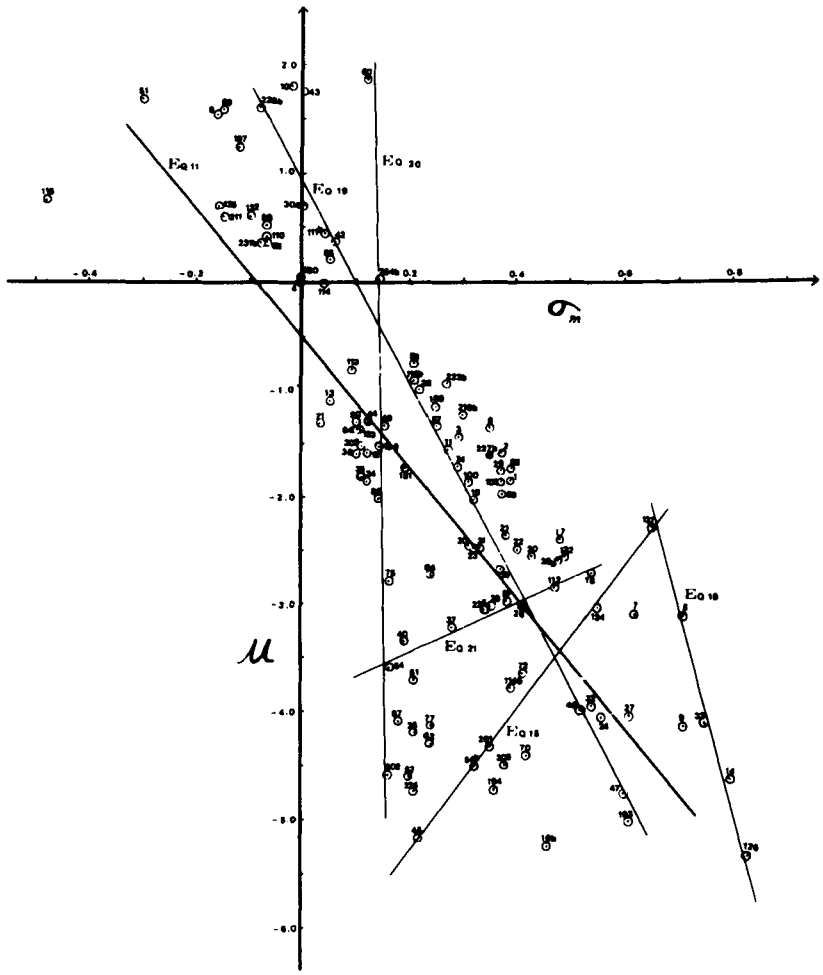

Figure 2—*A plot of* μ versus σ_m. *Note the scattering of the points, and the quite different slopes and intercepts for equations derived from various subsets.*

$$\mu = -3.65\,\sigma_p - 1.27$$
$$n = 114, r = 0.706, s = 1.367 \qquad \text{(Eq. 12)}$$

where μ is the group dipole moment of the substituent, and σ_m and σ_p are *meta*- and *para*-substituent constants, respectively.

Equations 11 and 12 indicate that the correlations between σ constants and dipole moments are not very good, and only 56 and 50%, respectively, ($r^2 \times 100$) of the variance in the data can be explained by these equations. In other words, about half of the variance in the data cannot be accounted for by these linear relationships. Comparison of Eqs. 11 and 12 shows that the correlation between σ_m and μ is better than that of σ_p and μ. This is probably due to the delocalization of π electrons between *para*-substituents and the benzene ring. The σ_m value is mainly a measure of inductive effect of the substituent and hence is more comparable to the group dipole moment.

The signs of the dipole moments of hydroxy and alkoxy groups are negative, *i.e.*, the oxygen atom is at the negative end of the dipoles in phenol and alkoxybenzene molecules. This can be explained in terms of the high electronegativity of oxygen in spite of the resonance effect in benzoic acid:

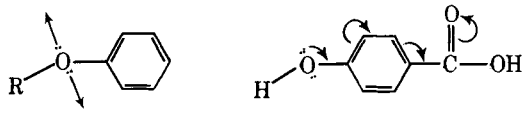

By dividing 11 substituents into subgroups graphically, there are quite different equations correlating dipole moments and σ constants as shown in Table I. In each subgroup no distinct structural relationship is found. The slopes range from −161 to +6.62, while the intercept ranges from +17.46 to −6.63.

Table I—Correlations Between Group Dipole Moment and σ Constants for Selected Subgroups from Table I, Showing Different Slopes and Intercepts [a]

	n	*r*	*SD*	*Equation*
$\mu = -6.82\,\sigma_p - 0.05$	13	0.965	0.459	(13)
$\mu = -4.83\,\sigma_p - 0.49$	15	0.999	0.079	(14)
$\mu = -3.68\,\sigma_p - 0.18$	14	0.999	0.065	(15)
$\mu = -2.99\,\sigma_p - 0.06$	10	0.999	0.036	(16)
$\mu = 6.42\,\sigma_p - 6.16$	8	0.995	0.097	(17)
$\mu = -16.52\,\sigma_m + 8.48$	5	0.994	0.147	(18)
$\mu = -8.57\,\sigma_m + 0.42$	14	0.954	0.603	(19)
$\mu = -161\,\sigma_m + 17.46$	8	0.910	0.909	(20)
$\mu = 2.20\,\sigma_m - 3.87$	9	0.946	0.099	(21)
$\mu = 6.62\,\sigma_m - 6.63$	5	0.999	0.041	(22)

[a] n = number of data points; r = correlation coefficient; and SD = standard deviation.

Although the application of dipole moment in QSAR is not as common as that of σ constants, in some cases it can play an important role in drug–receptor interactions. For example, Tute's results (15) on the inhibition of viral neuraminidase by 1-phenoxymethyl-3,4-dihydroquinolidines was reexamined. Using group dipole moment values instead of the components along the vertical axis μ_v, Eq. 23 was derived, which is slightly better than Tute's result using μ_v (Eq. 24):

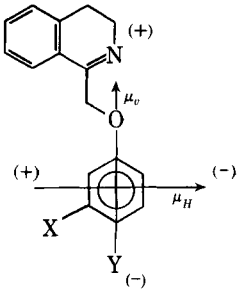

$$\log 1/C = 0.258\pi + 0.094\mu + 0.034\mu^2 + 2.596$$
$$n = 16, r = 0.956, s = 0.062 \qquad \text{(Eq. 23)}$$

Table II—Examples of the Application of Dipole Moment and Polarizability in QSAR [a]

Compounds	Biological Activity and Correlations Reported	Reference
1-Decylnipecotamides	Chlorinesterase inhibition. Inhibitory activity parallels the increase in dipole moment	16
Local anesthetics	Minimum blocking concentration (MBC) is a function of polarizability and ionization potential I_p $\log MBC = -a\alpha I_p + b$	17
Chloramphenicol analogs	Antimicrobial activity is a function of electronic polarization (P_e) $k_I = 2.76\,P_e - 6.55$ $n = 10, r = 0.991$	18
Cyclic ureas and thioureas	Respiratory stimulant activity is dependent on the dipole moment of three series of the compounds, while the acute lethal toxicity is a function of molecular weight	19
1-Decyl-3-carbamoylpiperidines	Butyrylcholinesterase $pI_{50} = -0.058\pi^2 + 0.923\pi - 0.456\mu + 5.589$ $n = 6, r^2 = 0.998$ (more data needed)	20
Anticonvulsants	Antielectroshock in mice $\log 1/C = 0.720 \log P - 0.396\mu + 3.144$ $n = 11, r = 0.967, SD = 0.189$	21
Sulfonamides	Antimicrobial activity measured as minimum inhibitory concentration (MIC) $\log 1/MIC = -0.11\ pKa + 0.041\mu^2 + 5.31$ $n = 10, r^2 = 0.91, SD = 0.18$	22
Nitroanilines	Sweetening potency $\log$ relative sweetness $= 1.31\pi - 1.08\sigma_0 + 0.45\mu^2 + 0.052(\alpha_R - \alpha_H) + 1.66$ $n = 9, r^2 = 0.976, SD = 0.149$ (too many parameters for too few data points)	22
Miscellaneous anticonvulsants	Antielectroshock activity $\log 1/C = -0.222(\log P)^2 + 1.153 \log P - 0.368\mu + 2.994$ $n = 18, r = 0.092, SD = 0.24$	23
Barbiturates, hydantoins, and imides	Antipentylenetetrazol seizures $\log 1/C = -0.123(\log P)^2 + 0.588 \log P - 0.597\mu + 0.825$ $n = 10, r = 0.99, SD = 0.12$	23
	Acute lethal toxicity $\log 1/C = -0.226(\log P)^2 + 0.800 \log P - 0.361\mu + 0.175$ $n = 10, r = 0.99, SD = 0.11$	2
Convulsants (lactams, thiolactams, ureas, and thioureas)	Acute lethal toxicity $\log 1/C = -0.364(\log P)^2 + 1.005 \log P + 0.247\mu + 1.298$ $n = 20, r = 0.89, SD = 0.24$	23
7-Substituted-1,4-benzodiazepinones	Antipentylenetetrazol seizures $\log 1/C = -0.301(\log P)^2 + 0.852 \log P - 0.629\mu + 4.139$ $n = 12, r = 0.915, SD = 0.227$	24
	Rotorod Ataxia log 1/C = 15.939 log Molecular Weight − 0.972 log P + 0.549μ − 33.187 $n = 16, r = 0.933, SD = 0.388$	24
Carbamates and aromatic compounds	Acetylcholinesterase inhibition $\log 1/K_d = -1.340 \log MR - 2.340\Sigma\pi + 2.404\Sigma\sigma - 0.478\,D + 0.338\mu + 4.818$ $n = 32, r = 0.945, SD = 0.594$	25
Quaternary ammonium compounds	Affinity for Acetylcholine Receptors $\log K = 0.784\pi_R - 0.353\,(\pi^{\oplus}_{-N\equiv})^2 - 0.171\,\pi^{\oplus}_{-N\equiv} + 0.736\mu_R + 2.309\,n_{OH} + 2.173$ $n = 128, r = 0.961, SD = 0.441$	26
N–$SCCl_3$ containing fungicides	Inhibition of spore germination *versus Stemphylium sarcinaeforme* $\log 1/C = -0.314\,(\log P)^2 + 2.385 \log P + 0.683\mu - 1.666$ $n = 14, r = 0.951, SD = 0.411$	27

[a] n = number of data points used in the regression, r = correlation coefficient, SD = standard deviation.

$$\log 1/C = 0.271\pi + 0.062\mu_v + 0.030\mu_v^2 + 2.552 \quad n = 16, r = 0.937, s = 0.074 \qquad \text{(Eq. 24)}$$

It seems that the substituent effect in the drug–receptor interaction depends more directly on the separation of charge μ than on the electronic distribution of the benzene ring (σ). Although the difference in the regressions obtained is small, this example illustrates the usefulness of the aromatic group dipole moment in QSAR.

Other examples of QSAR using dipole moment as an independent variable are shown in Table II. The examples presented and the theoretical relationships between dipole moment and intermolecular interaction energies with receptors, strongly suggest that dipole moment may be a parameter worth considering in QSAR, especially if σ or other electronic parameters fail to give meaningful correlation.

McFarland (22) has reported that in some cases μ^2 gives better correlation than μ; this may be due to the relatively narrow range of μ examined. When μ^2 is used, a wider range of values and a better correlation are obtained. Another report (28) found high degrees of intercorrelation between log molar refraction ($MR = P_e$) and log molar volume (MV), and between log molar refraction and log molecular mass (M):

$$\log MR = -0.290 + 0.981 \log MV \quad n = 213, r = 0.943, s = 0.086 \qquad \text{(Eq. 25)}$$

$$\log MR = -0.358 + 0.884 \log M \quad n = 213, r = 0.917, s = 0.104 \qquad \text{(Eq. 26)}$$

This is easily understandable from the following equations:

$$MR = \frac{n^2 - 1}{n^2 + 2}\frac{M}{d} \qquad \text{(Eq. 27)}$$

$$MV = \frac{M}{d} \qquad \text{(Eq. 28)}$$

The only substituent groups which will not fit Eqs. 27 and 28 are the ones with unusually high densities (d), such as heavy metals and polyhalogenated groups (28).

Furthermore, because of the interrelationship between MR (P_e) (29) and α, one would also expect similar relationship between α and M:

$$MR = P_e, P_e = (4/3)\pi N_a \alpha \qquad \text{(Eq. 29)}$$

where N_a is Avogadro's number.

It was recently reported (25) that charge-transfer effects of various carbamates and aromatic compounds can be separated into steric, electronic (μ and σ), and indicator variables (the number of lone pair electrons). They have also shown that the binding of these acetylcholinesterase inhibitors to the enzyme is well correlated with substituent constants like log MR, $\Sigma\pi$, $\Sigma\sigma$, and D (indicator variable, Table II).

The affinity constants of 128 quarternary ammonium compounds were correlated linearly with the hydrophobicity constant of the side chain (π_R), the dipole moment (μ_R), and the number of hydroxy group (n_{OH}). The dependence on the hydrophobicity constant of the quaternary ammonium head (π-$^{+}_{N\equiv}$) is parabolic (26).

The dipole moment of the heterocyclic ring bearing N-$SCCl_3$ group has also been shown to be important in determining the antifungal activity of these fungicides (27). This is true in the spore germination test against a single organism *S. sarcinaeforme* in QSAR as well as in a test using mixed organisms. In the latter case, discriminant analysis has indicated the important roles of both μ and log P (27).

It is hoped that the compilation of Table I will make it easier for medicinal chemists to use dipole moment as an independent electronic parameter in future QSAR work.

Appendix I—Aromatic Group Dipole Moments [a]

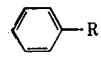

No.	Formula	R	μ_R (Debye)	WLN[b]	Solvent[c]	Temperature, °C
1	Br	—Br	−1.57	*E	cHx	20
2	Cl	—Cl	−1.59	*G	B	25
3	F	—F	−1.43	*F	B	30
4	H	—H	0.03	*H	L	25
5	$GeCl_3$	—$GeCl_3$	−3.15	*-GE-GGG	B	25
6	I	—I	−1.36	*I	B	30
7	NO	—NO	−3.09[d]	*NO	B	25
8	NH_2	—NH_2	1.53	*Z	B	25
9	NO_2	—NO_2	−4.13	*NW	B	25
10	N_2H_3	—$NHNH_2$	1.80	*MZ	D	25
11	N_3	—N=N=N	−1.56	*NNN	B	25
12	OH	—OH	−1.59	*Q	B	25
13	PH_2	—PH_2	−1.11	*PHH	Hx	20
14	SFO_2	—SO_2F	−4.59	*SWF	B	25
15	SF_5	—SF_5	−3.44	*SFFFFF	B	25
16	SH	—SH	−1.33	*SH	D	25
17	$SiCl_3$	—$SiCl_3$	−2.40	*-SI-GGG	B	25
18	SiF_3	—SiF_3	−2.72	*-SI-FFF	B	25
19	CCl_3	—CCl_3	−2.03	*XGGG	CCl_4	25
20	CF_3	—CF_3	−2.61	*XFFF	B	25
21	CF_3O	—OCF_3	−2.36	*OXFFF	B	25
22	CF_3S	—SCF_3	−2.50	*SXFFF	B	ns
23	CF_3Se	—$SeCF_3$	−2.48	*-SE-XFFF	B	ns
24	CN	—CN	−4.08	*CN	D	35
25	CNO	—N=C=O	−3.93	*NCO	B	20
26a	CNS	—SCN	−3.01	*SCN	B	25
26b	CNS	—NCS	−2.91	*NCS	B	20
27	CNSe	—SeCN	−4.01	*-SE-CN	B	25
28	CHO	—CHO	−3.02	*VH	B	25
29	CHO_2	—COOH	−1.30	*VQ	B	25
30	CHF_2O	—$OCHF_2$	−2.46	*OYFF	B	25
31	CHF_2S	—$SCHF_2$	−2.48	*SYFF	B	25
32	CHF_2OS	—$SOCHF_2$	−3.93	*SO&YFF	B	25
33	CHF_2O_2S	—SO_2CHF_2	−4.08	*SWYFF	B	25
34	CH_2Br	—CH_2Br	−1.87	*1E	B	25
35	CH_2Cl	—CH_2Cl	−1.83	*1G	B	20
36	CH_2I	—CH_2I	−1.60	*1I	CCl_4	25
37	CH_2NO	—$CONH_2$	−3.42	*VZ	B	25
38	CH_2NO	—CH=NOH(*trans*)	−0.87	*1UNQ-T	B	25
39	CH_2NO	—CH=NOH(*cis*)	−0.85	*1UNQ-C	B	25
40	CH_2NO	—NHCHO	−3.35	*MVH	CCl_4	ns
41	CH_2NO_2	—CH_2ONO	−2.10	*1ONO	ns	ns
42	CH_3	—CH_3	0.36	*1	B	25
43	CH_3O	—CH_2OH	1.73	*1Q	B	25
44	CH_3O	—OCH_3	−1.30	*O1	B	25
45	CH_3NS	—$NHCSNH_2$	−5.16	*MYZUS	D	25
46	CH_3OS	—$SOCH_3$	−3.98	*SO&1	B	20
47	CH_3O_2S	—SO_2CH_3	−4.75	*SW1	B	25
48	CH_3O_3S	—OSO_2CH_3	−3.77	*OSW1	B	25
49	CH_3S	—SCH_3	−1.34	*S1	B	ns
50	CH_3Se	—$SeCH_3$	−1.31	*-SE-1	ns	ns
51	CH_4N	—$NHCH_3$	1.69	*M1	B	25
52	CH_4NSO_2	—$NHSO_2CH_3$	−4.60	*MSW1	D	30
53	C_2H	—C≡CH	−0.77	*1UU1	B	25
54	C_2H_2N	—CH_2CN	−3.60	*1CN	D	25
55	$C_2H_2N_2O_2$		−6.63	*AT5NNVOJ	B	30
56	C_2H_3	—CH=CH_2	0.20	*1U1	B	25
57	C_2H_3O	—$COCH_3$	−2.90	*V1	B	25
58	$C_2H_3O_2$	—$OCOCH_3$	−1.72	*OV1	B	25
59	$C_2H_3O_2$	—$COOCH_3$	−1.92	*VO1	B	25
60	$C_2H_3O_2$	—CH_2COOH	1.86	*IVQ	D	25
61	C_2H_4NO	—$NHCOCH_3$	−3.65	*MV1	B	25
62	C_2H_4NS	—$NHCSCH_3$	−4.28	*MYUS	B	25
63	C_2H_5	—CH_2CH_3	0.39	*2	cHx	25
64	C_2H_5O	—OC_2H_5	−1.38	*O2	B	25
65	$C_2H_5O_2S$	—$SO_2C_2H_5$	−3.48	*SW2	B	25
66	$C_2H_5O_3S$	—$SO_3C_2H_5$	−4.99	*SW02	D	25
67	C_2H_5S	—CH_2SCH_3	1.46	*1S1	D	25
68	C_2H_5S	—SC_2H_5	−4.08	*S2	B	25
69	C_2H_6N	—$N(CH_3)_2$	1.61	*N1&1	B	25
70	C_2H_6OP	—$PO(CH_3)_2$	−4.39	*PO&1&1	B	20
71	C_2H_6P	—$P(CH_3)_2$	−1.31	*P1&1	B	20
72	C_3F_3	—C≡CCF_3	−3.38	*1UU1XFFF	B	ns
73	C_3F_7	—$CF(CF_3)_2$	−2.68	*XFXFFFXFFF	B	25
74	C_3HF_6O	—$C(OH)(CF_3)_2$	−1.71	*XQXFFFXFFF	L	25

continued

Appendix I—*Continued*

No.	Formula	R	μ_R (Debye)	WLN[b]	Solvent[c]	Temperature, °C
75	$C_3H_2F_3$	—CH=CHCF$_3$	−2.79	*1U1XFFF	B	ns
76	$C_3H_2F_3$	—C(CF$_3$)=CH$_2$	−2.25	*YU1&XFFF	B	20
77	C_3H_2N	—CH=CHCN(*trans*)	−4.12	*1U1CN -T	B	20
78	C_3H_2N	—CH=CHCN(*cis*)	−3.54	*1U1CN -C	B	20
79	C_3H_2NS		−1.21	*BT5N CSJ	CCl_4	20
80	C_3H_2NS		−1.33	*ET5N CSJ	CCl_4	20
81	C_3H_2NS		−1.89	*DT5N CSJ	CCl_4	20
82	$C_3H_2O_2$	—COCH$_2$CO—	−2.73	*V1V*	D	25
83	$C_3H_2O_2$	—OCOCH=CH—	−4.63	*OV1U1*	D	25
84	C_3H_3O	—CH=CHCHO	−2.71	*1U1VH	B	25
85	$C_3H_3O_2$	—CH=CHCOOH	−2.04	*1U1VQ	B	ns
86	$C_3H_3O_2$	—COCOCH$_3$	−2.44	*VV1	B	25
87	$C_3H_3N_2$		3.14	*AT5N CNJ	B	25
88	$C_3H_3N_2$		2.00	*AT5NNJ	B	25
89	$C_3H_3N_2$		2.26	*CT5MNJ	B	25
90	$C_3H_3N_2O$	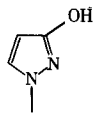	2.18	*AT5NNJ CQ	D	25
91	$C_3H_3N_2O$	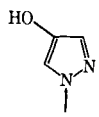	2.43	*AT5NNJ DQ	D	25
92	$C_3H_3N_2O$	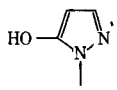	3.41	*AT5NNJ EQ	D	25
93	C_3H_3Se	—SeC≡CCH$_3$	−1.31	*-SE-1UU2	B	25
94	$C_3H_3O_2Se$	—SeCH=CHCOOH(*trans*)	−2.27	*SE-1U1VQ -T	B	25
95	$C_3H_3O_2Se$	—SeCH=CHCOOH(*cis*)	−1.69	*-SE-1U1VQ -C	B	25
96	C_3H_4	—CH=CHCH$_2$—	0.62	*1U2*	B	25
97	$C_3H_4O_2$	—CH$_2$CH$_2$COO—	−3.85	*2VO*	B	25
98	C_3H_5		0.51	*AL3TJ	B	25
99	C_3H_5O	—COC$_2$H$_5$	−2.90	*V2	B	30
100	$C_3H_5O_2$	—CH$_2$OCOCH$_3$	−1.68	*1OV1	L	25
101	$C_3H_5O_2$	—COOC$_2$H$_5$	−1.85	*VO2	B	25
102	$C_3H_5O_2$	—CH$_2$COOCH$_3$	−1.81	*1VO1	B	24
103	$C_3H_5O_2$	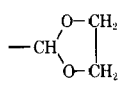	1.97[e]	*BT5O COTJ	B	20
104	C_3H_5OS	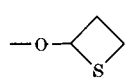	1.30	*O- CT4STJ	ns	ns
105	C_3H_5OS	—COSC$_2$H$_5$	−1.55	*VS2	B	25
106	C_3H_5OS	—CSOC$_2$H$_5$	−2.24	*YUS&O2	B	25
107	C_3H_6	—CH$_2$CH$_2$CH$_2$—	0.55	*3*	cHx	25
108	C_3H_6	—C(CH$_3$)=CH$_2$	0.77	*YU1	B	25
109	C_3H_6NO	—N(CH$_3$)COCH$_3$	−3.60	*N1&V1	B	25
110	C_3H_7	—CH(CH$_3$)$_2$	0.40	*Y	cHx	25
111	$C_3H_7O_2$	—CH(OCH$_3$)$_2$	1.06[e]	*Y01&01	B	20
112	C_4F_9	—(CF$_2$)$_3$CF$_3$	−2.86	*/XFF/4F	B	25
113	C_4H_3S		0.81	*BT5SJ	B	25

Appendix I—*Continued*

No.	Formula	R	μ_R (Debye)	WLN[b]	Solvent[c]	Temperature, °C
114a	C_4H_4	—(CH)$_4$—	0.00	*R A*B*	B	25
114b	C_4H_5O	—CH=CHCOCH$_3$	−2.89	*1U1V1	B	25
115	C_4H_8	—(CH$_2$)$_4$—	0.73	*4*	B	25
116	$C_4H_7O_2$	—CH$_2$OCOC$_2$H$_5$	−1.80	*1OV2	L	28
117	$C_4H_7O_2$	—CH$_2$COOC$_2$H$_5$	−1.85	*1VO$_2$	B	24
118	$C_4H_7O_2$	—COOCH(CH$_3$)$_2$	−1.82	*VOY	B	25
119	$C_4H_7O_2$	—CH$_2$CH$_2$OCOCH$_3$	−1.86	*2OV1	B	25
120	$C_4H_7O_2$	—CH=CHCOOCH$_3$	−2.13	*1U1VO1	B	30
121	$C_4H_7O_2$	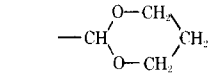	1.47[e]	*BT6O COTJ	B	20
122	C_4H_9	—C(CH$_3$)$_3$	0.52	*X	B	25
123	C_4H_9O	—O(CH$_2$)$_3$CH$_3$	−1.19	*O4	B	20
124	$C_4H_{10}O_3P$	—PO(OC$_2$H$_5$)$_2$	−3.04	*PO&O2&O2	CCl_4	25
125	$C_4H_{11}Si$	—CH$_2$Si(CH$_3$)$_3$	0.68	*1-SI-1&1&1	B	25
126	C_5N_3	—C(CN)=C(CN)$_2$	−5.30	*YCN&UYCN&CN	B	30
127	C_5H_3O	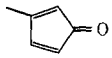	−4.10	* CL5VJ	B	30
128	C_5H_3OS	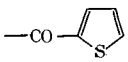	−3.45	*V- BT5SJ	B	25
129	$C_5H_3S_2$	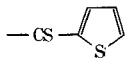	−3.15	*YUS- BT5SJ	B	ns
130	C_5H_4N		−1.94	* BT6NJ	B	25
131	C_5H_4N		−2.28	* CT6NJ	B	25
132	C_5H_4N		−2.57	* DT6NJ	B	25
133	C_5H_4NO	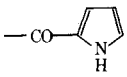	−1.64	*V- BT5MJ	B	25
134	C_5H_4NO	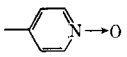	−4.52	* DT6NJ AO	ns	ns
135	C_5H_5NO	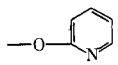	−1.96	*O- BT6NJ	B	20
136	C_5H_4NO	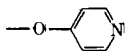	−2.46	*O- DT6NJ	B	20
137	$C_5H_4NO_3$	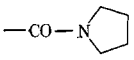	−4.10	*V- AT5NTJ	D	30
138	C_5H_5S		−1.10	* BT5SJ Cl	B	25
139	C_5H_5S	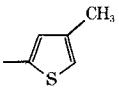	−0.88	* BT5SJ D1	B	25
140	C_5H_5S	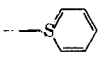	−0.79	* AT6SJ &5	B	30
141	$C_5H_6NO_2$	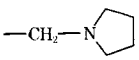	1.80	*1- AT5NTJ	D	25
142	$C_5H_6NO_2$	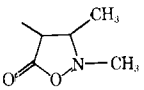	−5.65	* DT5NOVTJ A1 E1	B	ns
143	$C_5H_6NO_2$	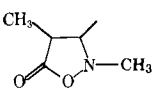	−5.70	* ET5NOVTJ A1 D1	B	ns

continued

Appendix I—*Continued*

No.	Formula	R	μ_R (Debye)	WLN[b]	Solvent[c]	Temperature, °C
144	$C_5H_6NO_2$	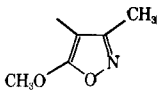	−2.32	* DT5NOJ CO1 E1	D	ns
145	$C_5H_6NO_2$	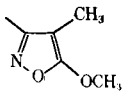	−2.83	* ET5NOJ CO1 D1	D	ns
146	$C_5H_7N_2O$	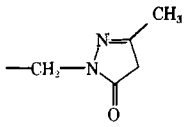	−3.10	*1- BT5NNV DHJ E1	D	25
147	$C_5H_7N_2O$	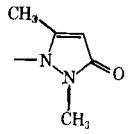	−5.47	* AT5NNVJ B1 E1	D	25
148	$C_5H_7N_2O$	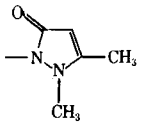	−5.47	* BT5NNVJ A1 E1	B	25
149	$C_5H_7N_2S$	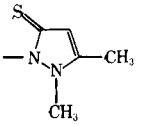	−7.60	* BT5NNYJ A1 CUS E1	D	25
150	$C_5H_7N_2S$	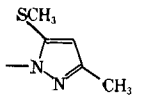	−2.80	* BT5NNJ CS1 E1	B	25
151	$C_5H_7O_2$	—CH=CHCOOC$_2$H$_5$	−1.73	*1U1VO2	L	26
152	C_5H_8NO	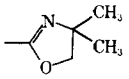	−1.11	* BT5N CO AUTJ E1 E1	B	25
153	C_5H_8NO		−3.96	* AT6NVTJ	B	25
154	$C_5H_8NO_3$	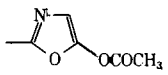	−2.95	* BT5N COJ DOV1	B	ns
155	$C_5H_8NO_4$	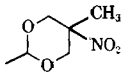	−4.47	* BT6O COTJ ENW E1	B	ns
156	$C_5H_{11}O_2$	—CH(OC$_2$H$_5$)$_2$	1.23[e]	*YO2 &O2	B	20
157	$C_6H_4N_2Br$	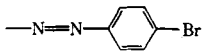	−1.47	*NUNR DE	B	25
158	C_6H_4BrO	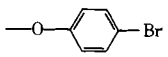	−1.59	*OR DE	B	20
159	C_6H_4BrO	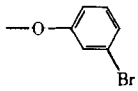	−1.78	*DR CE	B	20
160	C_6H_4BrO	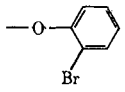	−2.20	*OR BE	B	20
161	$C_6H_4BrO_3S$	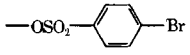	−3.82	*OSWR DE	B	25
162	$C_6H_4N_2Cl$	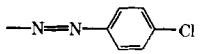	1.56	*NUNR DG	B	25
163	C_6H_4I	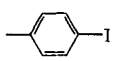	1.55	*R DI	B	25

Appendix I—*Continued*

No.	Formula	R	μ_R (Debye)	WLN[b]	Solvent[c]	Temperature, °C
164	C_6H_4IO	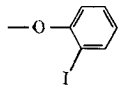	2.06	*OR BI	B	20
165	C_6H_4IO	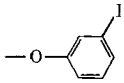	1.68	*OR CI	B	20
166	C_6H_4IO	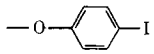	1.47	*OR DI	B	20
167	C_6H_4IS	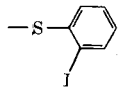	2.38	*SR BI	B	20
168	C_6H_4IS	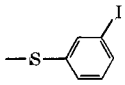	1.80	*SR CI	B	20
169	C_6H_4IS	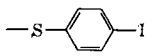	1.50	*SR DI	B	20
170	C_6H_4NO	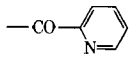	−2.95	*V- BT6NJ	B	25
171	C_6H_4NO	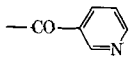	−3.01	*V- CT6NJ	B	25
172	C_6H_4NO	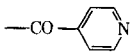	−3.06	*V- DT6NJ	B	25
173	$C_6H_4NO_2S$	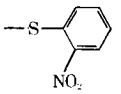	−5.22	*SR BNW	B	20
174	$C_6H_4NO_2S$	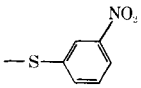	−4.04	*SR CNW	B	20
175	$C_6H_4NO_3$	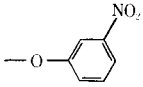	−4.04	*OR CNW	B	20
176	$C_6H_4NO_3$	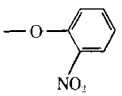	−4.60	*OR BNW	B	20
177	$C_6H_4NO_5S$	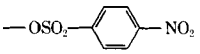	−4.72	*OSWR DNW	B	25
178	$C_6H_4NO_5S$	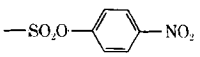	−2.76	*SWOR DNW	B	ns
179	$C_6H_4N_3O_4$	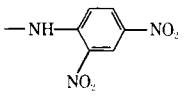	−6.36	*MR BNW DNW	B	ns
180	C_6H_5		0.00	*R	L	ns
181	C_6H_5NO	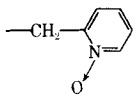	−4.13	*1- BT6NJ AO	B	25
182	C_6H_5NO	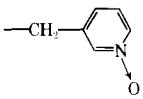	−4.61	*1- CT6NJ AO	B	25
183	C_6H_5NO	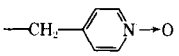	−4.63	*1- DT6NJ AO	D	25
184	$C_6H_5N_2$	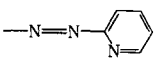	−1.36	*1UN- BT6NJ	B	25
185	$C_6H_5N_2$	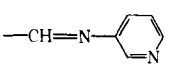	−2.98	*1UN- CT6NJ	B	25

continued

Appendix I—*Continued*

No.	Formula	R	μ_R (Debye)	WLN[b]	Solvent[c]	Temperature, °C
186	$C_6H_5N_2$	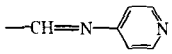	−4.16	*1UN- DT6NJ	B	25
187	$C_6H_5N_2O$	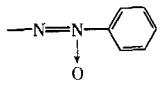	−1.73	*NUNO&R	B	25
188	$C_6H_5N_2O$	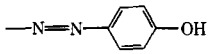	1.66	*NUNR DQ	B	25
189	C_6H_5O	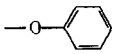	1.16	*OR	B	25
190	C_6H_5O	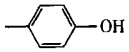	1.34	*R DQ	B	20
191	C_6H_5O		1.63	*R BQ	B	25
192	C_6H_5OS	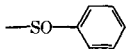	−4.07	*SO&R	B	25
193	$C_6H_5O_2S$	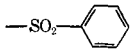	−5.05	*SWR	B	25
194	$C_6H_5O_3S$	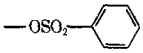	−4.72	*OSWR	B	25
195	C_6H_5S	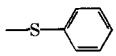	1.55[e]	*SR	B	25
196	$C_6H_5S_2$	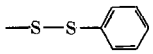	1.79	*SSR	B	25
197	C_6H_6N		1.11	*MR	B	25
198	C_6H_6N		1.45	*R BZ	B	25
199	C_6H_6N	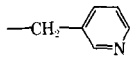	−2.18	*1- CT6NJ	B	25
200	C_6H_6N	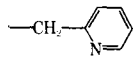	−1.89	*1- BT6NJ	B	25
201	C_6H_6N	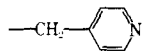	−2.65	*1- DT6NJ	B	25
202	$C_6H_6NO_2S$		−4.58	*MSWR	B	25
203	C_6H_6NS	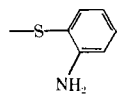	1.87	*SR BZ	B	20
204	C_6H_6NS	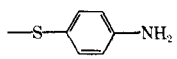	2.44	*SR DZ	B	20
205	$C_6H_6N_3$	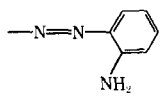	1.49	*NUNR BZ	B	20
206	$C_6H_6N_3$	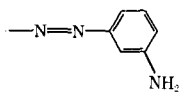	1.71	*NUNR CZ	B	20
207	$C_6H_6N_3$	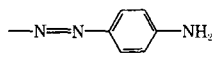	2.50	*NUNR DZ	B	20
208	$C_6H_9N_2O$	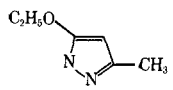	−2.65	* AT5NNJ C1 EO2	D	25
209	$C_6H_9N_2O$	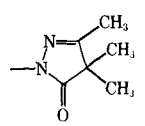	−2.83	* BT5NNV DHJ D1 D1 E1	D	25

Appendix I—*Continued*

No.	Formula	R	μ_R (Debye)	WLN[b]	Solvent[c]	Temperature, °C
210	$C_6H_9N_2S$	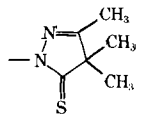	−3.16	* BT5NNY DHJ CUS D1 D1 E1	D	25
211	C_6H_{11}		0.62	*AL6TJ	B	30
212	$C_6H_{11}N_2$	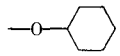	−1.55	*O- AL6TJ	B	20
213	$C_6H_{11}O$	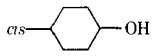	1.87	* AL6TJ DQ -C	B	25
214	$C_6H_{11}O$	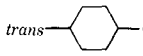	1.56	* AL6TJ DQ -T	B	25
215	$C_6H_{11}O_2$	$-CH_2CH_2OCOC_3H_7$	1.85	*2OV3	L	25
216	$C_6H_{11}O_2$	$-COOC_5H_{11}-n$	−1.99	*VO5	L	25
217	$C_6H_{11}N$	$-N(i-C_3H_7)_2$	1.53	*NY&&Y	B	25
218a	C_7H_4NO	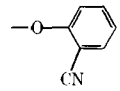	−4.88	*OR BCN	B	20
218b	C_7H_4NO	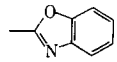	−1.22	* CT56 BN DOJ	B	25
219	C_7H_4NO	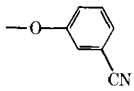	−4.01	*OR CCN	B	20
220	C_7H_4NO	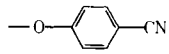	−4.23	*OR DCN	B	20
221	$C_7H_4NO_4$	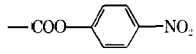	−4.43	*VOR DNW	B	40
222	C_7H_4NS	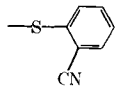	−5.04	*SR BCN	B	20
223a	C_7H_4NS	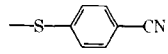	−4.14	*SR DCN	B	20
223b	C_7H_4NS	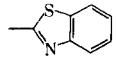	−0.94	* CT56 BN DSJ	B	20
224	$C_7H_5O_2$	$-OCOC_6H_5$	−1.90	*OVR	B	25
225	C_7H_5O	$-COC_6H_5$	−3.04	*VR	B	25
226	$C_7H_5O_3$	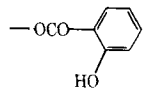	−1.92	*OVR BQ	B	25
227a	C_7H_6N	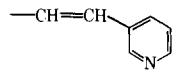	−2.90	*1U1- CT6NJ	B	25
227b	C_7H_6N	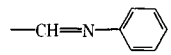	−1.61	*YUNR	B	25
228a	C_7H_6N	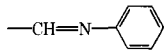	−2.70	*1U1- DT6NJ	B	25
228b	C_7H_6N	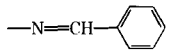	1.61	*NUYR	B	25
229	C_7H_6NO	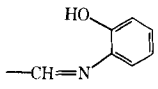	−2.73	*1UNR BQ	B	25
230	C_7H_6NO	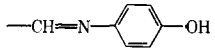	1.94	*NUCUNR DQ	B	25
231a	C_7H_6NO	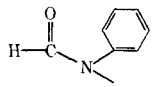	−3.44	*NR&VH	B	25
231b	C_7H_7	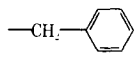	0.36	*1R	B	20

continued

Appendix I—*Continued*

No.	Formula	R	μ_R (Debye)	WLN[b]	Solvent[c]	Temperature, °C
232	C_7H_7BrNO	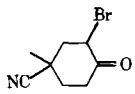	4.21	* DL6NTJ BE DCN	B	25
233	$C_7H_7N_2$	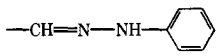	−2.03	*1UNMR	B	25
234	$C_7H_7N_2$	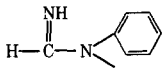	−2.20	*NR&YUM	D	25
235	$C_7H_7N_2O$	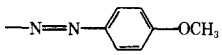	1.54	*NUNR DO1	B	20
236	C_7H_7O		1.38	*R BO1	B	35
237	$C_7H_7O_2$	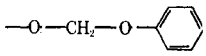	1.16	*O1OR	B	25
238	$C_7H_7O_3S$	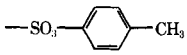	−5.29	*OSWR D1	B	ns
239	$C_7H_7S_2$	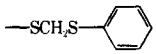	1.34	*S1SR	B	25
240	C_7H_8N	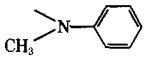	1.24	*N1&R	B	20
241	C_7H_8N	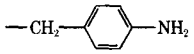	1.84	*1R DZ	B	ns
242	C_7H_8NO	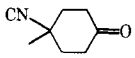	3.63	* DL6VTJ DCN	B	30
243	C_7H_8NO	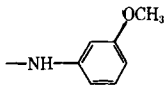	1.79	*MR C01	B	25
244	$C_7H_8NO_2S$	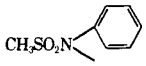	−4.41	*NR&SW1	D	30
245	$C_7H_8NO_3S$	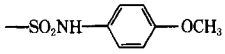	−5.08 −5.44	*SWMR DO1	B D	ns 25
246	$C_7H_8NO_3S$	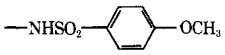	5.21 5.65	*MSWR DM1	B D	ns 25
247	$C_7H_8N_3$	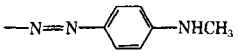	2.91	*NUNR DM1	B	20
248	C_7H_8P	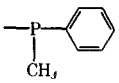	1.39	*P1&R	B	20
249	$C_7H_9N_2O$	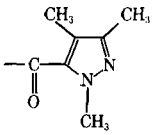	−2.80	*V- CT5NNJ B1 D1 E1	B	25
250	C_7H_9O	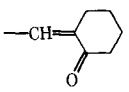	−3.23	*1U BL6VYTJ	B	25
251	$C_7H_{12}NO_2$	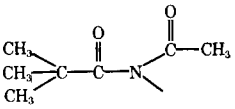	−3.59	*NV1&VX	B	20
252	$C_7H_{13}O_2$	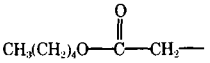	−2.13	*1VO5	B	25
253	$C_7H_{13}O_2$	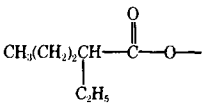	−2.05	*OVY2&3	B	25

Appendix I—*Continued*

No.	Formula	R	μ_R (Debye)	WLN[b]	Solvent[c]	Temperature, °C
254a	$C_7H_{13}O_2$	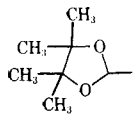	−1.70	*BT5O COTJ D1 D1 E1 E1	B	25
254b	C_8H_5	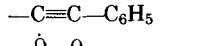	0.00	*1UU1R	CCl_4	25
255	$C_8H_5O_2$	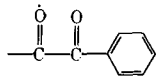	−3.71	*VVR	B	25
256	$C_8H_5O_3$	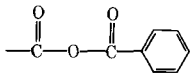	−3.30	*VOVR	B	25
257	C_8H_5Se	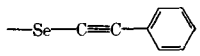	1.32	*-SE-1UU1R	B	25
258	C_8H_6Br	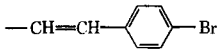	1.85	*1U1R DE	B	25
259	C_8H_6Cl	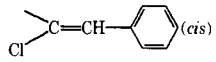	−1.68	*YGU1R -C	B	25
260	C_8H_6Cl	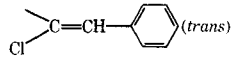	−1.29	*YGU1R -T	B	25
261	C_8H_6Cl	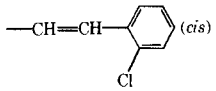	1.56	*1U1R BG -C	B	25
262	C_8H_6Cl	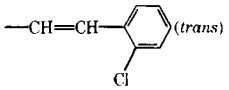	1.34	*1U1R BG -T	B	25
263	C_8H_6Cl	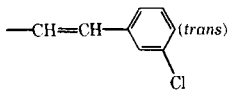	1.66	*1U1R CG -T	B	25
264	C_8H_6Cl	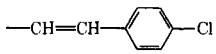	1.73	*1U1R DG	B	25
265	$C_8H_6Cl_3$	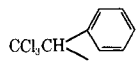	1.82	*YR&XGGG	B	17
266	C_8H_6F	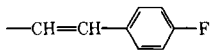	1.49	*1U1R DF	B	25
267	C_8H_6F	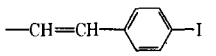	1.80	*1U1R DI	B	25
268	$C_8H_6NO_2$	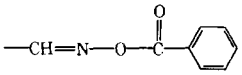	−3.32	*1UNOVR	B	25
269	$C_8H_6NO_2$	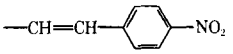	−4.74	*1U1R DNW	B	25
270	C_8H_7	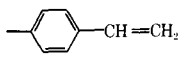	0.64	*R D1U1	B	ns
271	C_8H_7O	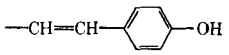	1.64	*1U1R DQ	B	25
272	C_8H_7O	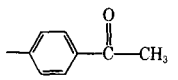	−3.11	*R DV1	B	20–60
273	$C_8H_7O_2$	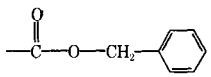	−2.06	*VO1R	B	30
274	$C_8H_7O_3$	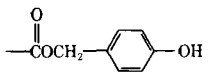	−2.56	*VO1R DQ	B	30
275	C_8H_7SSe	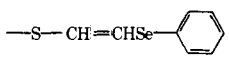	1.81	*S1U1-SE-R	B	25
276	C_8H_7Se	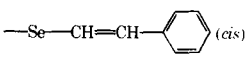	1.17	*-SE-1U1R -C	B	25

continued

Appendix I–*Continued*

No.	Formula	R	μ_R (Debye)	WLN[b]	Solvent[c]	Temperature, °C
277	C_8H_7Se	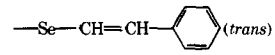	1.06	*-SE-1U1R -T	B	25
278	C_8H_8N	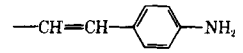	2.06	*1U1R DZ	B	25
279	C_8H_8N	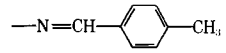	1.93	*NU1R D1	B	25
280	C_8H_8NO	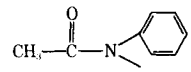	−3.61	*NR&V1	B	25
281	C_8H_8NO	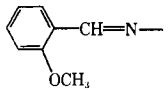	2.87	*NU1R BO1	B	25
282	$C_8H_8N_3O$	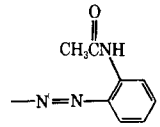	3.47	*NUNR BMV1	B	20
283	$C_8H_8N_3O$	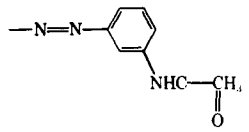	3.71	*NUNR CMV1	B	20
284	$C_8H_8N_3O$	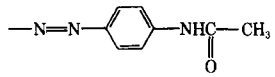	3.72	*NUNR DMV1	B	20
285	C_8H_9OS	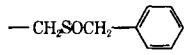	−3.76	*1SO&1R	B	25
286	$C_8H_9O_2$	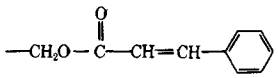	−2.27	*1OV1U1R	B	30
287	$C_8H_9O_2S$	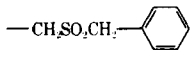	−4.25	*1SW1R	B	25
288	C_8H_9S	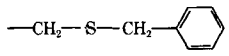	1.34	*1S1R	B	25
289a	$C_8H_9S_2$	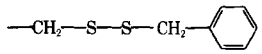	1.87	*1SS1R	B	25
289b	$C_8H_{10}NO_2S_2$	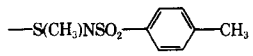	−7.46	*S1&UNSWR D1	B	20
290	$C_8H_{10}N_3$	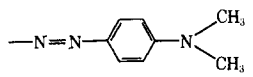	2.82	*NUNR DN1&1	B	20
291	$C_8H_{18}PO$	$PO(C_4H_9)_2$	−4.31	*PO&4&4	B	25
292	C_9H_7OS	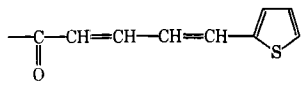	−3.25	*V1U2U1- BT5SJ	B	25
293	C_9H_7OS	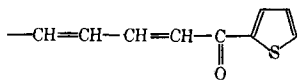	−3.50	*1U2U1V- BT5SJ	B	25
294	C_9H_7OS	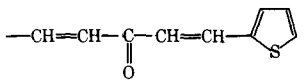	−3.21	*1U1V1U1- BT5SJ	B	25
295	$C_9H_7O_2$	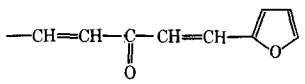	−3.29	*1U1V1U1-BT5OJ	B	25
296	$C_9H_7O_2$	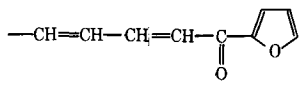	−3.27	*1U2U1V-BT5OJ	B	25
297	$C_9H_7O_4$	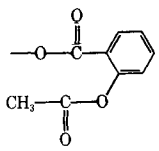	−2.54	*OVR BOV1	B	25

Appendix I—*Continued*

No.	Formula	R	μ_R (Debye)	WLN[b]	Solvent[c]	Temperature, °C
298	C_9H_9	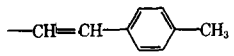	0.59	*1U1R D1	B	25
299	C_9H_9O	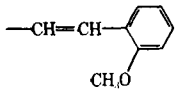	1.05	*1U1R DO1	B	25
300	C_9H_9O	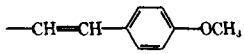	1.45 1.13	*1U1R DO1	B	25
301	$C_9H_9O_2$	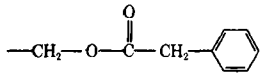	1.97	*1OV1R	B	24
302	$C_{10}H_{11}O_2$	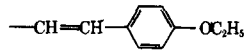	1.66	*1U1R DO2	B	25
303	$C_{10}H_{12}N$	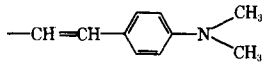	2.27	*1U1R DN1&1	B	25
304	$C_{12}H_{10}N$	$-N(C_6H_5)_2$	0.70	*NR&R	B	25
305	$C_{12}H_{10}P$	$-P(C_6H_5)_2$	−1.52	*PR&R	B	25
306	$C_{12}H_{10}PO$	$-PO(C_6H_5)_2$	−4.49	*PO&R&R	B	25

[a] Taken from Ref. 14 unless stated otherwise. [b] From E. G. Smith, "The Wiswesser Line—Formula Chemical Notation," McGraw-Hill, New York, N.Y., 1968. [c] Solvents: cHx = Cyclohexane, Hx = hexane, B = benzene, D = 1,4-dioxane, L = liquid state, ns = not stated. [d] V. I. Minkin, O. A. Osipov, and Y. A. Zhdanov "Dipole Moments in Organic Chemistry," English Translation by B. J. Hazzard, Plenum, New York, N.Y., 1970. [e] O. Exner, V. Jehlieka, and B. Uchytil, *Coll. Czech. Chem. Commun.*, **33**, 2862 (1968).

REFERENCES

(1) C. Hansch and T. Fujita, *J. Am. Chem. Soc.*, **86**, 1616 (1964).

(2) T. Fujita, J. Iwasa, and C. Hansch, *ibid.*, **86**, 5175 (1964).

(3) E. J. Lien, in "Medicinal Chemistry IV," Proceedings of the 4th International Symposium on Medicinal Chemistry, J. Mass, Ed., Elsevier, Amsterdam, The Netherlands 1974, pp. 319–342.

(4) E. J. Lien, in "Drug Design," vol. 5, E. J. Ariens, Ed., Academic, New York, N.Y., 1976, pp. 88–132.

(5) E. J. Lien, *Ann. Rev. Pharmacol. Toxicol.*, **21**, 31 (1981).

(6) B. Pullman and M. Weissbluth, "Molecular Biophysics," Academic, New York, N.Y., 1965, p. 153.

(7) K. C. Tseng, *Chem. J. (China)*, **32**, 136 (1964).

(8) D. C. Colinese, D. A. Ibbitson, and C. W. Stone, *J. Chem. Soc., B*, **1971**, 570.

(9) D. C. Colinese, *ibid.*, **1971**, 864.

(10) L. K. H. Van Beek, *Rec. Trav. Chim. Pays-Bas*, **76**, 729 (1957).

(11) E. J. Lien, J. T. Chou, and G. Gudauskas, *Spectrosc. Lett.*, **5**, 293 (1972).

(12) C. Hansch, A. Leo, S. H. Unger, K. H. Nikaitaini, and E. J. Lien, *J. Med. Chem.*, **16**, 1207 (1973).

(13) C. Hansch and A. Leo, "Substituent Constants for Correlation Analysis in Chemistry and Biology," Wiley, New York, N.Y., 1979.

(14) A. L. McClellan, "Tables of Experimental Dipole Moments," vol. 2, Rahara Enterprises, El Cerrito, 1974.

(15) M. S. Tute, *J. Med. Chem.*, **13**, 48 (1970).

(16) W. P. Purcell, J. G. Beasley, and R. P. Quintana, *Biochim. Biophys. Acta*, **88**, 235 (1964).

(17) D. Agin, L. Hersh, and D. Holtzman, *Proc. Natl. Acad. Sci. USA*, **53**, 592, (1965).

(18) A. Cammarata, *J. Med. Chem.*, **10**, 525 (1967).

(19) E. J. Lien and W. D. Kumler, *ibid.*, **11**, 214 (1968).

(20) J. M. Clayton and W. P. Purcell, *ibid.*, **12**, 1087 (1969).

(21) E. J. Lien, *ibid.*, **13**, 1189 (1970).

(22) J. W. McFarland, *Prog. Drug Res.*, **15**, 123 (1971).

(23) E. J. Lien, G. L. Tong, and L. L. Lien, *J. Pharm. Sci.*, **62**, 246 (1973).

(24) E. J. Lien, R. C. H. Liao, and H. G. Shinouda, *ibid.*, **68**, 463 (1979).

(25) C. T. Su and E. J. Lien, *Res. Commun. Chem. Pathol. Pharmacol.*, **29**, 403 (1980).

(26) E. J. Lien, E. J. Ariens, and A. J. Beld, *Eur. J. Pharmacol.*, **35**, 245 (1976).

(27) E. J. Lien and J. P. Li, *Acta Pharm. Jugosl.*, **30**, 15 (1980).

(28) C. D. Selassie, P. H. Wang, and E. J. Lien, *ibid.*, **30**, 135 (1980).

(29) E. J. Lien and L. Kennon, in "Remington's Pharmaceutical Sciences," 16th ed., A. Osol, Ed., Mack Publishing, Easton, Pa., 1980, pp. 160–181.

ACKNOWLEDGMENTS

This paper is dedicated to the late Warren D. Kumler for his pioneering work in electric dipole moments and acid–base dissociation constants.

The authors express their sincere thanks to Professor Corwin Hansch of Pomona College for his suggestions and encouragements, and to Dr. Albert Leo for his assistance in assigning the WLN to many of the groups listed.

Determination of Cyclobenzaprine in Tablets by High-Performance Liquid Chromatography

MAXINE L. HEINITZ

Received July 23, 1981, from the *Food and Drug Administration, Minneapolis, MN 55401.* Accepted for publication September 8, 1981.

Abstract □ A convenient high-performance liquid chromatographic method for the quantitative determination of cyclobenzaprine hydrochloride in tablets is described. Samples were dissolved in 0.05 *N* sulfuric acid and diluted with methanol. The cyclobenzaprine hydrochloride was chromatographed using an octylsilane column and the eluent acetonitrile–0.6% dibasic potassium phosphate aqueous buffer (pH 3.0) (75:25) at a flow rate of 1.5 ml/min. Naphazoline hydrochloride was used as an internal standard. The UV detector response at 254 nm was linear for cyclobenzaprine hydrochloride in the 0.005–0.03 mg/ml range under conditions of the analysis.

Keyphrases □ Cyclobenzaprine hydrochloride—determination in tablets by high-performance liquid chromatography □ High-performance liquid chromatography—determination of amount of cyclobenzaprine in tablets □ Naphazoline hydrochloride—internal standard in high-performance liquid chromatographic test for cyclobenzaprine hydrochloride in tablets

The pharmacopeial determination of the skeletal muscle relaxant cyclobenzaprine hydrochloride is tedious and time consuming. The procedure (1) consists of extraction of the chloride ion pair into methylene chloride, followed by back extraction into dilute sulfuric acid and quantitative measurement by UV spectrophotometry. As any degradation product would be expected to exhibit UV absorbance, the USP procedure will not be indicative of stability.

A number of procedures have been reported for the measurement of tricyclic antidepressant drugs in serum or in tablets by HPLC (2–11). Many of these methods use adsorption chromatography (2–6). Of those chromatographic systems utilizing reversed phases (7–11), the use of pentanesulfonic acid (10), sodium lauryl sulfate (11), or aliphatic amines (5) in the mobile phase was avoided. Premature deterioration of the column has been experienced in this laboratory when these reagents are used over an extended period of time. An eluent described previously (9) was adapted to the determination of cyclobenzaprine using an octyl-bonded silica column.

The procedure described was developed for the routine analysis of cyclobenzaprine hydrochloride in tablets. The method employs naphazoline hydrochloride as an internal standard and is readily adaptable to semi-automated analysis with equipment available in most laboratories.

EXPERIMENTAL

Chemicals—Cyclobenzaprine hydrochloride[1] raw material was assayed (100.5%) and its purity confirmed before use by the USP (1) monograph procedures. Naphazoline hydrochloride[2], amitriptyline hydrochloride[1], and desipramine hydrochloride[3] were used without further purification or analysis. All other reagents were commercial analytical reagent grade. Solvents[4] were glass distilled except for distilled water which was deionized and distilled.

Apparatus—The liquid chromatograph consisted of a pump and a fixed wavelength UV detector[5] (254 nm). Solutions were injected by an automated sample processor[6] set to inject 20 μl. The chromatograms were recorded and results calculated by a reporting integrator[7]. UV spectra were recorded on a recording spectrophotometer[8].

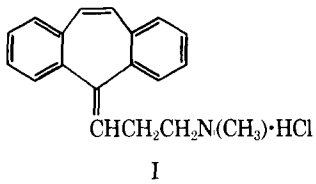

I

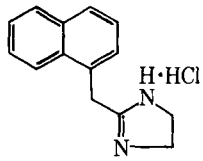

II

Chromatographic Conditions—The mobile phase consisted of acetonitrile–0.6% KH_2PO_4 aqueous buffer (pH 3.0) (75:25). A flow rate of 1.50 ml/min was maintained. Ambient temperature was used throughout these experiments. A 25 × 0.46-cm i.d. column containing an octyl-bonded phase on silica packing[9] was used. Following each day of use, the column was flushed with acetonitrile–water (75:25), followed by methanol at 1 ml/min and stored in methanol.

Reagents—The pH 3.0 buffer was prepared by dissolving 12 g of potassium phosphate, monobasic in 1800 ml and adjusting to pH 3.0 with phosphoric acid (1:3) using a calibrated pH meter and diluting to 2 liters. Naphazoline hydrochloride prepared as a 1-mg/ml solution in methanol was present as the internal standard at a final concentration of 0.05 mg/ml in the sample solution. The standard solution contained 0.01 mg/ml of cyclobenzaprine hydrochloride and 0.05 mg/ml of naphazoline hydrochloride.

Assay and Calculations—Twenty tablets[10] were accurately weighed and finely powdered to pass a 60-mesh sieve. The equivalent of 1 tablet mass was transferred to a 100-ml volumetric flask, 25 ml of 0.05 *N* sulfuric acid in water was added and the flask was shaken for 1 hr. Methanol was added to a volume of ~85 ml, the flask contents were swirled, and allowed to equilibrate to room temperature. (The mixing of these solvents resulted in a warm solution.) The flask was diluted to volume and mixed. A 10.0-ml aliquot of each sample and 5.00 ml of a 1 mg/ml internal standard were diluted with water to 100 ml, and an aliquot was filtered[11]. For individual tablet analyses, each tablet was dissolved and diluted as described previously.

Duplicate 20-μl aliquots of composite solutions and single 20-μl aliquots of individual tablet solutions were chromatographed. Measurement was by peak area ratio of sample and reference standard to the internal standard using an average of two standard injections. Calculations were done by the reporting integrator.

RESULTS AND DISCUSSION

A typical chromatogram of cyclobenzaprine in the presence of naphazoline is shown in Fig. 1. Linearity of response was demonstrated by chromatographing standard solutions. The graph of response to variation in the concentration over the 0.005–0.030 mg/ml range of cyclobenzaprine hydrochloride with a constant naphazoline hydrochloride concentration (0.050 mg/ml) was linear and passed through the origin.

To determine the precision of this method as compared to the official USP assay, six replicate composites from each of four different commercial lots of cyclobenzaprine tablets were assayed. The results are tabulated in Table I. The coefficient of variation averaged 1.57% by HPLC and 1.00% by the USP method. The devised procedure was con-

[1] Merck Sharp and Dohme, West Point, Pa.
[2] CIBA Pharmaceutical Co., Summit, N.J.
[3] Merrell National Laboratories, Cincinnati, Ohio.
[4] Methanol and acetonitrile were from Burdick and Jackson Laboratories, Muskegon, Mich.; methylene chloride was from Mallinckrodt, Saint Louis, Mo.
[5] Altex Model 322, Altex Scientific, Berkeley, Calif.
[6] Waters Intelligent Sample Processor (WISP) Model 710A, Waters Associates, Milford, Mass.
[7] HP3385A, Hewlett-Packard, Avondale, Pa.
[8] Cary 118, Varian Associates, Palo Alto, Calif.
[9] Zorbax C-8, DuPont Instruments, Wilmington, Del.
[10] Flexeril tablets, Merck Sharp and Dohme, West Point, Pa.
[11] Metricel GA-6 (0.45μ), Gelman Instrument Co., Ann Arbor, Mich.

0022-3549/82/0600-0656$01.00/0

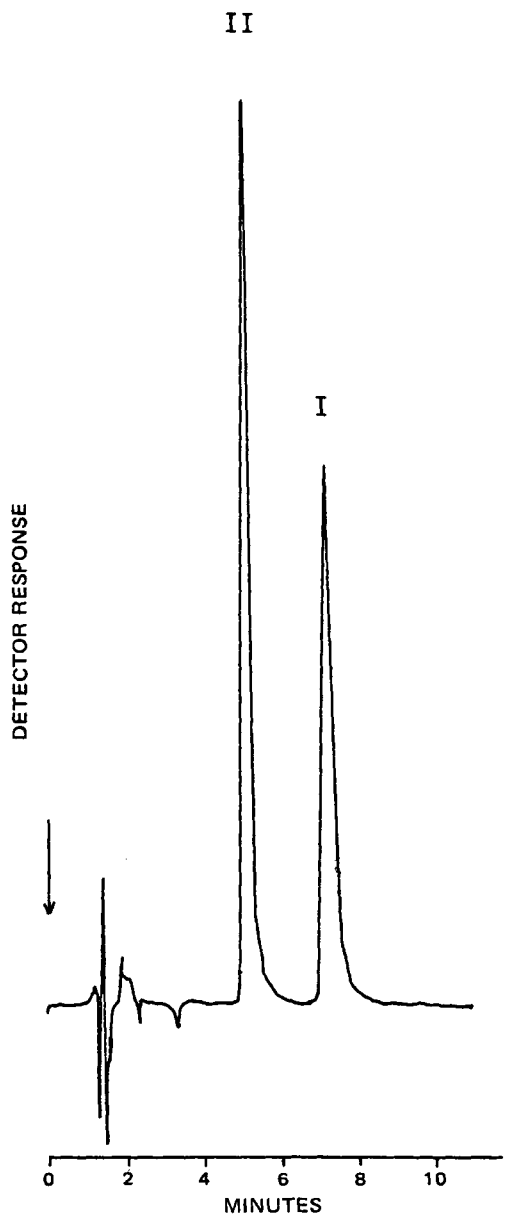

Figure 1—*Chromatogram of cyclobenzaprine hydrochloride tablet solution containing added naphazoline hydrochloride as internal standard. Key: (I) cyclobenzaprine; (II) naphazoline.*

sidered statistically acceptable. The results by liquid chromatography are slightly higher than those by the USP assay in three of four cases. Thirty tablets from each of the four lots were analyzed for content uniformity by the proposed HPLC method. The results are summarized in Table II.

During development of this assay a number of different variations of

Table I—Comparison of HPLC and USP Assay Results of Replicate Composite Preparations [a]

	Cyclobenzaprine Hydrochloride/Tablet, mg [b]			
	HPLC Method [c]		USP Method [d]	
	Mean	±*SD*	Mean	±*SD*
Sample 1	9.78	0.14	9.64	0.11
Sample 2	10.21	0.08	9.82	0.11
Sample 3	9.94	0.18	9.70	0.08
Sample 4	9.75	0.22	9.88	0.09

[a] Six replicate composites consisting of 20 tablets/composite were prepared from each of four commercial tablet lots. [b] Having a declaration of 10 mg of cyclobenzaprine hydrochloride/tablet. [c] Average of duplicate injections for each composite and standard solution. [d] The USP XX method for cyclobenzaprine hydrochloride tablets is extraction of the chloride ion pair into methylene chloride followed by back extraction into dilute sulfuric acid and quantitatively measured by UV spectrophotometry.

Table II—Results of 30 Individual Tablet Assays by HPLC [a]

Sample	Cyclobenzaprine Hydrochloride/Tablet, mg [b]			
	Range	Mean	±*SD*	*RSD*, %
1	9.29–10.09	9.73	0.26	2.67
2	9.68–10.44	10.00	0.22	2.20
3	9.56–10.12	9.84	0.18	1.83
4	8.72–10.17	9.69	0.34	3.51

[a] Thirty tablets from each sample were assayed. [b] Declaration of 10 mg of cyclobenzaprine hydrochloride/tablet.

Table III—Relationship of the Retention Time to the Phosphate Content in the Aqueous Portion of the Mobile Phase [a]

% KH_2PO_4 [b]	Retention Time, min		
	Cyclobenzaprine Hydrochloride	Amitriptyline Hydrochloride	Desipramine Hydrochloride
0.4	8.18	8.42	6.35
0.5	7.95	8.26	6.21
0.6	6.79	6.95	5.28

[a] The mobile phase consisted of acetonitrile–aqueous potassium phosphate pH 3.0 buffer (75:25); a 25 × 0.46-cm octyl-bonded phase on a silica column was used. [b] The phosphate content is expressed as the amount of monobasic potassium phosphate used to prepare the aqueous pH 3.0 buffer.

Table IV—Ultraviolet Absorption of Cyclobenzaprine Hydrochloride and Naphazoline Hydrochloride at Selected Wavelengths [a]

Compound	Wavelength, nm	$E^b \times 10^3$
Cyclobenzaprine hydrochloride	290	10.79 (max)
	254	10.26
Naphazoline hydrochloride	290	4.52 (sh)
	254	2.31

[a] Spectra recorded in water. [b] E = molar absorptivity.

the mobile phase were tried. The retention time of the cyclobenzaprine varied inversely with the acetonitrile content of the mobile phase. The proposed chromatographic system elutes cyclobenzaprine in ~7 min; but if the acetonitrile is reduced from 75:25 to 65:35, the retention time increases to 12 min. Substitution of methanol increases the retention time and magnifies the tailing.

The relationship of the phosphate content in the mobile phase to the retention time of cyclobenzaprine and two structurally related compounds is shown in Table III. As the concentration of phosphate decreases, the retention time increases.

Initially, only methanol was used to dissolve the tablet material. Choice of this solvent led to ~10% lower results by HPLC than by the USP procedure, even though measurement by UV spectrophotometry of the solution injected showed that the cyclobenzaprine was there at the expected level. Changing the solvent to water did not improve this disparity. When a small amount of acid was added to the solvent used to dissolve the tablet material, the HPLC results correlated well with those of the USP procedure. This problem may be caused by one of the tablet excipients. Examination of the chromatograms of solutions exhibiting low results did now show any evidence of band broadening. Some of the materials used in the tablet may be complexing with the cyclobenzaprine to either render the species immobile on the column, or in some other way interfere with the chromatography.

The use of a completely aqueous solvent for the tablet material was appealing because it would have eliminated the problem of heat formation on mixing the aqueous 0.05 *N* sulfuric acid with methanol. However, an entirely aqueous solvent, or acetonitrile and water, carry into solution most of the tablet excipients, which would then be injected on the column. By the use of methanol, many of the excipients can be removed by filtration prior to chromatography.

Naphazoline hydrochloride was selected for the internal standard for this study because it produced a symmetrical peak shape with good retention characteristics. The molecule possesses a large π-electron system with a good UV chromaphore.

The detector wavelength used throughout this study was 254 nm. More specificity would be gained by the use of the detector wavelength at 290 nm. The UV spectral parameters of cyclobenzaprine and naphazoline at these wavelengths are tabulated in Table IV. At 290 nm half the amount of naphazoline hydrochloride would give a detector response comparable to the response observed at 254 nm.

The HPLC assay procedure is rapid, precise, and specific for the analysis of cyclobenzaprine hydrochloride in tablets and represents a more convenient assay method than that of the USP.

REFERENCES

(1) "The United States Pharmacopeia," 20th rev., United States Pharmacopeial Convention, Rockville, Md., 1980, p. 185.

(2) J. H. Knox and J. Jurand, *J. Chromatogr.*, **103**, 311 (1975).

(3) I. D. Watson and M. J. Stewart, *ibid.*, **110**, 389 (1975).

(4) M. R. Detaevernier, L. Dryon, and D. L. Massart, *ibid.*, **128**, 204, (1976).

(5) J. H. M. Van den Berg, H. J. J. M. DeRuwe, R. S. Deelder, and T. A. Plomp, *ibid.*, **138**, 431 (1977).

(6) F. L. Vandemark, R. F. Adams, and G. J. Schmidt, *Clin. Chem.*, **24**, 87 (1978).

(7) J. R. Salmon and P. R. Wood, *Analyst*, **101**, 611 (1976).

(8) J. C. Kraack and P. Bijster, *J. Chromatogr.*, **143**, 499 (1977).

(9) R. R. Brodie, L. F. Chasseaud, and D. R. Hawkins, *ibid.*, **143**, 535 (1977).

(10) H. F. Proelss, H. J. Lohmann, and D. G. Miles, *Clin. Chem.*, **24**, 1948 (1978).

(11) D. Burke and H. Sokoloff, *J. Pharm. Sci.*, **69**, 138 (1980).

ACKNOWLEDGMENTS

The author gratefully acknowledges the assistance of William Potter, Laboratory Supervisor, who checked the calculations, made valuable comments, and provided the opportunity for this project. The author also thanks Richard D. Thompson for his technical advice and Keith Egli for proofreading the final manuscript and giving many helpful suggestions.

Derivatization of Chiral Amines with (*S*,*S*)-*N*-Trifluoroacetylproline Anhydride for GC Estimation of Enantiomeric Composition

JAMES D. ADAMS, Jr. *§ˣ, THOMAS F. WOOLF ‡, ANTHONY J. TREVOR *, LYALL R. WILLIAMS ‡, and NEAL CASTAGNOLI, Jr. ‡

Received June 8, 1981, from the * *Department of Pharmacology and the* ‡ *Department of Pharmaceutical Chemistry, University of California, San Francisco, CA 94143.* Accepted for publication September 16, 1981. § Present address: Department of Internal Medicine, Baylor College of Medicine, Texas Medical Center, Houston, TX 77030.

Abstract □ The reaction characteristics of (*S*,*S*)-*N*-trifluoroacetylproline anhydride were examined in an attempt to develop a quantitative GC assay of the enantiomers of the sterically hindered, chiral amine ketamine. With the aid of the individual enantiomers of ketamine and the corresponding synthetic *N*-trifluoroacetylprolyl amides, it was found that the derivatization reaction proceeds stereoselectively, in poor yield, and with some degree of racemization of the acylating reagent. The results indicate that care must be exercised when prolyl derivatizing reagents are chosen for assaying chiral amines.

Keyphrases □ (*S*,*S*)-*N*-Trifluoroacetylproline anhydride—derivatization of ketamine, GC estimation of enantiomeric composition □ GC analysis—detection of enantiomers of chiral amines with (*S*,*S*)-*N*-trifluoroacetylproline anhydride □ Enantiomers—derivatization of chiral amines with (*S*,*S*)-*N*-trifluoroacetylproline anhydride for GC estimation of enantiomeric composition

It is important to examine the extent to which chiral xenobiotics may undergo enantioselective metabolic transformations in an effort to characterize the effects which such processes may have on the pharmacological and toxicological properties of these substances (1, 2). In the case of chiral amines, quantitative estimations of enantiomeric composition have been achieved through GC analysis of the diastereomeric amides formed by derivatization with (*S*)-*N*-trifluoroacetylprolyl chloride [(*S*)-I] (3). Although commercially available as a solution in chloroform, this reagent is difficult to obtain in pure form and is susceptible to racemization (4). The corresponding imidazolide, compound (*S*)-II, is a relatively stable, crystalline solid (5). However, it was observed that this derivative reacts sluggishly with sterically hindered amines such as ketamine (III) (6). In an attempt to obtain a derivatizing reagent that can be prepared in crystalline form and that might react more readily with ketamine, the synthesis of (*S*,*S*)-*N*-trifluoroacetylproline anhydride [(*S*,*S*)-IV] was attempted. An attractive feature of (*S*,*S*)-IV is that inversion about one of the two chiral centers present in this molecule leads to the *meso*-diastereomeric species (*S*,*R*)-V which, in theory, should be separable from (*S*,*S*)-IV.

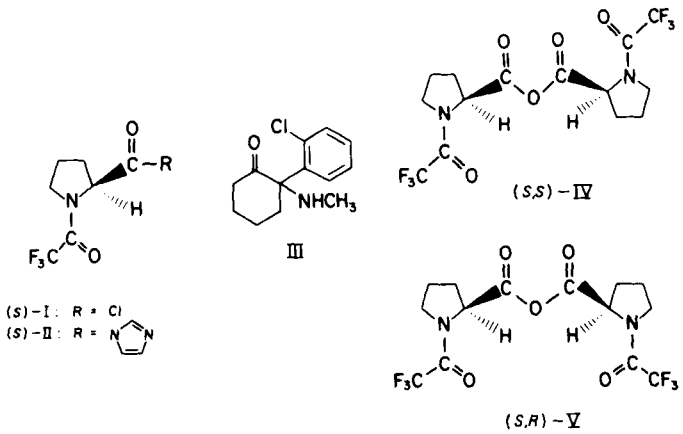

RESULTS AND DISCUSSION

The synthesis of (*S*,*S*)-IV from (*S*)-proline and trifluoroacetic anhydride was reported originally by Weygand (7). Attempts to repeat this synthesis initially led to the isolation of a species (mp 114–115°) which proved to be an isomer of the Weygand compound; longer reaction times however provided the Weygand compound (mp 138–140°). The electron impact mass spectra and NMR spectra of these products were essentially identical, which suggested that the two compounds were diastereomerically related. Since the high-melting isomer did not rotate plane polarized light, whereas the low-melting isomer was strongly levorotatory, the low-melting isomer was tentatively assigned the asymmetric structure (*S*,*S*)-IV and the Weygand compound the *meso*-structure, (*S*,*R*)-V.

Consistent with these assignments, reaction of (*S*,*S*)-IV with (*S*)-

0022-3549/82/0600-0658$01.00/0

The HPLC assay procedure is rapid, precise, and specific for the analysis of cyclobenzaprine hydrochloride in tablets and represents a more convenient assay method than that of the USP.

REFERENCES

(1) "The United States Pharmacopeia," 20th rev., United States Pharmacopeial Convention, Rockville, Md., 1980, p. 185.

(2) J. H. Knox and J. Jurand, *J. Chromatogr.*, **103**, 311 (1975).

(3) I. D. Watson and M. J. Stewart, *ibid.*, **110**, 389 (1975).

(4) M. R. Detaevernier, L. Dryon, and D. L. Massart, *ibid.*, **128**, 204, (1976).

(5) J. H. M. Van den Berg, H. J. J. M. DeRuwe, R. S. Deelder, and T. A. Plomp, *ibid.*, **138**, 431 (1977).

(6) F. L. Vandemark, R. F. Adams, and G. J. Schmidt, *Clin. Chem.*, **24**, 87 (1978).

(7) J. R. Salmon and P. R. Wood, *Analyst*, **101**, 611 (1976).

(8) J. C. Kraack and P. Bijster, *J. Chromatogr.*, **143**, 499 (1977).

(9) R. R. Brodie, L. F. Chasseaud, and D. R. Hawkins, *ibid.*, **143**, 535 (1977).

(10) H. F. Proelss, H. J. Lohmann, and D. G. Miles, *Clin. Chem.*, **24**, 1948 (1978).

(11) D. Burke and H. Sokoloff, *J. Pharm. Sci.*, **69**, 138 (1980).

ACKNOWLEDGMENTS

The author gratefully acknowledges the assistance of William Potter, Laboratory Supervisor, who checked the calculations, made valuable comments, and provided the opportunity for this project. The author also thanks Richard D. Thompson for his technical advice and Keith Egli for proofreading the final manuscript and giving many helpful suggestions.

Derivatization of Chiral Amines with (*S*,*S*)-*N*-Trifluoroacetylproline Anhydride for GC Estimation of Enantiomeric Composition

JAMES D. ADAMS, Jr. *§ˣ, THOMAS F. WOOLF ‡, ANTHONY J. TREVOR *, LYALL R. WILLIAMS ‡, and NEAL CASTAGNOLI, Jr. ‡

Received June 8, 1981, from the * *Department of Pharmacology and the* ‡ *Department of Pharmaceutical Chemistry, University of California, San Francisco, CA 94143.* Accepted for publication September 16, 1981. § Present address: Department of Internal Medicine, Baylor College of Medicine, Texas Medical Center, Houston, TX 77030.

Abstract □ The reaction characteristics of (*S*,*S*)-*N*-trifluoroacetylproline anhydride were examined in an attempt to develop a quantitative GC assay of the enantiomers of the sterically hindered, chiral amine ketamine. With the aid of the individual enantiomers of ketamine and the corresponding synthetic *N*-trifluoroacetylprolyl amides, it was found that the derivatization reaction proceeds stereoselectively, in poor yield, and with some degree of racemization of the acylating reagent. The results indicate that care must be exercised when prolyl derivatizing reagents are chosen for assaying chiral amines.

Keyphrases □ (*S*,*S*)-*N*-Trifluoroacetylproline anhydride—derivatization of ketamine, GC estimation of enantiomeric composition □ GC analysis—detection of enantiomers of chiral amines with (*S*,*S*)-*N*-trifluoroacetylproline anhydride □ Enantiomers—derivatization of chiral amines with (*S*,*S*)-*N*-trifluoroacetylproline anhydride for GC estimation of enantiomeric composition

It is important to examine the extent to which chiral xenobiotics may undergo enantioselective metabolic transformations in an effort to characterize the effects which such processes may have on the pharmacological and toxicological properties of these substances (1, 2). In the case of chiral amines, quantitative estimations of enantiomeric composition have been achieved through GC analysis of the diastereomeric amides formed by derivatization with (*S*)-*N*-trifluoroacetylprolyl chloride [(*S*)-I] (3). Although commercially available as a solution in chloroform, this reagent is difficult to obtain in pure form and is susceptible to racemization (4). The corresponding imidazolide, compound (*S*)-II, is a relatively stable, crystalline solid (5). However, it was observed that this derivative reacts sluggishly with sterically hindered amines such as ketamine (III) (6). In an attempt to obtain a derivatizing reagent that can be prepared in crystalline form and that might react more readily with ketamine, the synthesis of (*S*,*S*)-*N*-trifluoroacetylproline anhydride [(*S*,*S*)-IV] was attempted. An attractive feature of (*S*,*S*)-IV is that inversion about one of the two chiral centers present in this molecule leads to the *meso*-diastereomeric species (*S*,*R*)-V which, in theory, should be separable from (*S*,*S*)-IV.

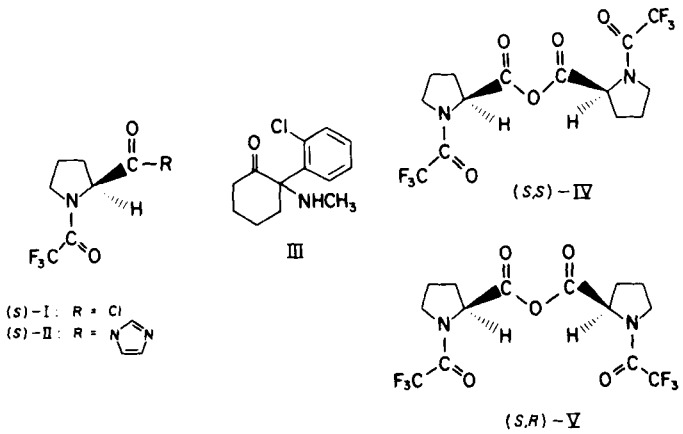

RESULTS AND DISCUSSION

The synthesis of (*S*,*S*)-IV from (*S*)-proline and trifluoroacetic anhydride was reported originally by Weygand (7). Attempts to repeat this synthesis initially led to the isolation of a species (mp 114–115°) which proved to be an isomer of the Weygand compound; longer reaction times however provided the Weygand compound (mp 138–140°). The electron impact mass spectra and NMR spectra of these products were essentially identical, which suggested that the two compounds were diastereomerically related. Since the high-melting isomer did not rotate plane polarized light, whereas the low-melting isomer was strongly levorotatory, the low-melting isomer was tentatively assigned the asymmetric structure (*S*,*S*)-IV and the Weygand compound the *meso*-structure, (*S*,*R*)-V.

Consistent with these assignments, reaction of (*S*,*S*)-IV with (*S*)-

0022-3549/82/0600-0658$01.00/0

α-methylbenzylamine [(S)-VI] yielded a product that displayed a single GC peak and that presumably corresponds to structure (S,S)-VII. Reaction of (S)-VI with (S,R)-V, on the other hand, yielded a product displaying two equally intense GC peaks corresponding to (S,S)-VII and (R,S)-VIII[1]. Additionally, reaction of (S,S)-IV with N-methylaniline (IX) yielded a levorotatory anilide [(S)-X], while the corresponding reaction with compound (S,R)-V yielded a racemic mixture of (S)-X and (R)-X.

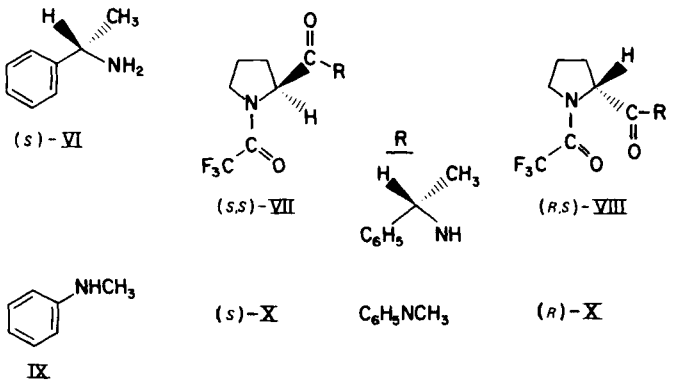

The experimental evidence described previously is sufficient to assign unambiguously the structure of the low-melting isomer. Parallel experimental results have led to the same conclusions (8). The data supporting the structure assignment of (S,R)-V, however, are also consistent with a racemic mixture of (S,S)-IV and (R,R)-IV. As has been reported with related systems, the ability to distinguish between such species is often not a trivial task (9). Therefore, the preparation of the racemate of IV was attempted by mixing equal amounts of (R,R)-IV [prepared from (R)-proline and trifluoroacetic anhydride] and (S,S)-IV. The product obtained after crystallization proved to be identical in every way to the high-melting isomer. The IR spectra of the presumed racemate and the high-melting isomer obtained from the Weygand procedure also were identical but were different from that of (S,S)-IV. Based on these results and the facile interchange which is reported to occur with mixtures of acetic anhydride and trifluoroacetic anhydride (10), it is possible that upon recrystallization, the racemic mixture of IV undergoes disproportionation to yield the thermodynamically more stable *meso*-isomer (S,R)-V.

The pathway leading to the formation of the *meso*-compound is likely to involve the oxazolinium intermediate (XI) (Scheme I). Recombination of the (R)-N-trifluoroacetylprolyl anion [(R)-XII] with (S)-XI leads to (S,R)-V. Compound (S,R)-V may also be formed from (S)-XII and (R)-XI. It seems reasonable to speculate that the formation of compound (S,R)-V from (S)-proline and trifluoroacetic anhydride also proceeds through XI, which may undergo inversion to (R)-XI through reversible tautomerism to the symmetric mesoionic species (XIII). A similar process has been proposed for the racemization of (S)-N-p-nitrobenzoylproline in the presence of acetic anhydride and a trace of acid (11).

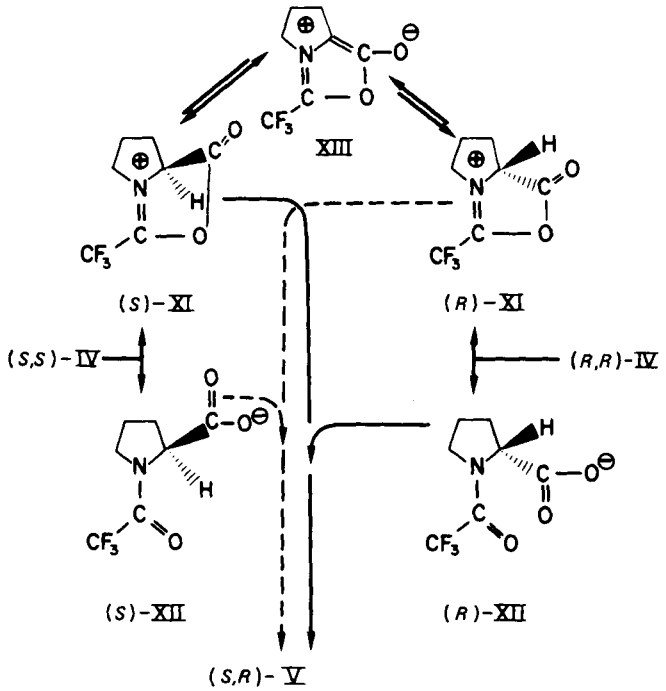

Scheme I

The utility of (S,S)-IV for the quantitative estimation of the enantiomeric composition of ketamine was examined next. GC analysis of the reaction product obtained between (S,S)-IV and racemic ketamine in the presence of triethylamine gave a pair of sharp peaks with baseline separation and mass spectra consistent with the expected amide structures (S,S)-XIV and (S,R)-XV[2]. With the aid of the pure ketamine enantiomers, the diastereomer with the shorter retention time was shown to be the (S)-N-trifluoroacetylprolyl amide of (S)-ketamine. Under a variety of reaction conditions, however, product formation appeared to favor the diastereomer having the longer retention time, *i.e.*, (S,R)-XV. For reasons to be discussed, reaction of racemic ketamine with (S,S)-IV also may yield significant amounts of the enantiomeric species (R,S)-XV.

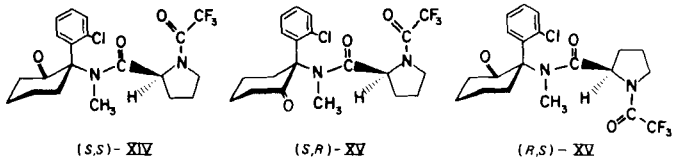

The two N-trifluoroacetylprolyl diastereomeric amides of (R)- and (S)-ketamine were obtained in analytically pure form from the reaction of (S)-N-trifluoroacetylprolyl chloride and individual ketamine enantiomers. Although the reaction with (R)-ketamine proceeded smoothly, attempts to prepare the corresponding amide of (S)-ketamine were accompanied by extensive inversion of the derivatizing reagent. The main product obtained in this reaction was the diastereomeric (R)-N-trifluoroacetylprolyl amide of (S)-ketamine, *i.e.*, (R,S)-XV. The N-trifluoroacetylproline recovered from the reaction mixture proved to be racemic, which indicates that racemization of the prolyl reagent during the reaction with (S)-ketamine is extensive.

GC analysis of the two diastereomers showed that the detector responses of these compounds were essentially identical. Consequently, the different peak heights observed in the analysis of racemic ketamine must be due to the stereoselective formation of the (S)-N-trifluoroacetylprolyl amide of (R)-ketamine and/or the (R)-N-trifluoroacetylprolyl amide of (S)-ketamine.

An additional frustration encountered in the attempts to develop a ketamine assay with (S,S)-IV was the low yields realized in these reactions. Based on peak heights found with the synthetic N-trifluoroacetylprolyl amides, the maximum combined yield of the two diastereomeric amides obtained upon reaction of racemic ketamine with (S,S)-IV was only 17% (Table I). The use of a large excess of the anhydride or introduction of additional anhydride during the course of the reaction did not influence the overall yield. Although somewhat better yields were obtained with (S)-I, the derivatization of ketamine with (S)-I was more stereoselective (Table I).

A pathway to account for these results would involve cleavage of the anhydride to the (S)-oxazolinium species [(S)-XI] and (S)-N-trifluoroacetylproline anion [(S)-XII]. Conversion of (S)-XI to XIII would deplete the acylating reagent and also generate 1 mole of acid. Although a 5:1 *M* ratio of triethylamine to ketamine was used, the large excess of (S,S)-IV could result in adequate acid production to protonate (and hence inactivate) the ketamine. The yellow color which developed during the course of the reaction is consistent with the report that XIII is yellow (12).

Analytical scale reactions with the individual isomers of ketamine again demonstrated the poor reactivity of (S)-ketamine with both (S,S)-IV and (S)-I (Table I). Extensive racemization occurred during these reactions. Since the chiral center of ketamine is tetrasubstituted, and therefore unlikely to racemize, the formation of the undesired diastereomer is attributed to inversion of the prolyl moiety. The reactions of (S,S)-IV and (S)-I with (R)-III proceeded in reasonable yields and were accompanied by only a limited amount of inversion (Table I). If it is assumed that the transition state energy for the formation of the prolyl

[1] For all such designations, the first symbol refers to the chirality of the N-trifluoroacetylprolyl moiety and the second symbol to the chirality of the amine.

[2] The absolute stereochemistry of ketamine-free base has been found to be R(+) and S(−). These data will be published in the near future.

Table I—GC Analysis of Ketamine following Derivatization with *N*-Trifluoroacetylpropyl Reagents[a]

Reactant	Reagent	Temperature (Time, hr)	Peak Areas[b] (*S,S*)-/(*R,S*)-XIV	Peak Areas[b] (*S,R*)-/(*R,S*)-XV	Yield, %[c]
(*R,S*)-III	(*S,S*)-IV	75° (2)	3	6	2
(*R,S*)-III	(*S,S*)-IV	75° (2)	3	8	2
(*R,S*)-III	(*S,S*)-IV	100° (1)	14	68	16
(*R,S*)-III	(*S,S*)-IV	100° (2)	21	63	17
(*R,S*)-III	(*S,S*)-IV	100° (4)	20	58	16
(*S*)-III	(*S,S*)-IV	75° (2)	2	0	1
(*S*)-III	(*S,S*)-IV	100° (2)	49	14	25
(*R*)-III	(*S,S*)-IV	75° (2)	0	6	3
(*R*)-III	(*S,S*)-IV	100° (2)	12	86	39
(*R,S*)-III	(*S*)-I	75° (2)	33	206	48
(*R,S*)-III	(*S*)-I	75° (4)	32	196	46
(*R,S*)-III	(*S*)-I	100° (1)	49	211	52
(*R,S*)-III	(*S*)-I	100° (2)	29	134	33
(*S*)-III	(*S*)-I	75° (2)	27	19	18
(*R*)-III	(*S*)-I	75° (2)	18	208	90

[a] The assays were performed according to the procedure described in the Experimental section. [b] Since (*S,S*)-IV and (*S*)-I are susceptible to inversion, the peak areas reported for reactions involving racemic ketamine represent the sum of the responses of the enantiomeric prolyl amides. [c] Yields were calculated on the basis of detector responses obtained with pure (*S,S*)-XIV and (*R,S*)-XV. Note that the individual enantiomers were run at one-half the concentration of racemic ketamine.

amide with (*S*)-ketamine is greater than with (*R*)-ketamine, the competing reaction pathway (Scheme I) leading to isomerization of (*S,S*)-IV and (*S*)-I would proceed to a greater extent in the reaction with (*S*)-ketamine than with (*R*)-ketamine. Once inversion has occurred, the energetically more favored reaction of (*S*)-ketamine with the (*R*)-prolyl reagent could occur preferentially.

The results obtained in this study clearly point to a number of difficulties with prolyl derivatizing reagents to which researchers should be alerted. Whenever possible, quantitative estimations based on GC analysis of reaction mixtures should be based on detector responses measured with the pure synthetic diastereomeric amides. Secondly, the possibility of stereoselective reactions with chiral amines and prolyl derivatizing reagents should be carefully evaluated. Finally, the stability of the derivatizing reagent with respect to racemization should be examined with the aid of the individual enantiomers of the amine. In the present study it has been found that the reaction of the anhydride reagent (*S,S*)-IV with ketamine proceeds stereoselectively, in poor yield, and is accompanied by inversion. Unfortunately, the corresponding reaction between the commercially available (*S*)-*N*-trifluoroacetylprolyl chloride suffers from similar limitations.

EXPERIMENTAL[3]

(*S,S*)-*N*-Trifluoroacetylproline Anhydride [(*S,S*)-IV]—Trifluoroacetic anhydride (84 g, 0.40 mole) was added dropwise with stirring under nitrogen and external cooling to an ice cold suspension of (*S*)-proline (23 g, 0.20 mole). After 3 hr, the volatile components were removed under vacuum and the residual yellow mass was recrystallized 3 times from ether to yield 22.9 g (0.06 mole, 57%) of white crystals, mp 114–115° [lit. (8) mp 114–115°]; NMR (deuterochloroform): 1.8–2.5 (m, 8H, CH_2), 3.79 (m, 4H, NCH_2), and 4.62 (t, J = 6.2 Hz, 2H, CH) ppm; IR (oil mull): 1822, 1760, 1690, 1460, 1380, 1360, 1350, 960, 940, 930, 910, 878, 840, 815, 795, and 768 cm^{-1}; electron impact mass spectrum (relative intensity): 404 (M^+, 0.4), 376 (0.5), 211 (1.4), 194 (44), 166 (100), 98 (9.8), 96 (35), and 69 (82); $[\alpha]_D^{22} = -98.6°$ (*C*, 0.7 mg/ml; benzene).

Anal.—Calc. for $C_{14}H_{14}N_2O_5F_6$: C, 41.60; H, 3.49; N, 6.93. Found: C, 41.53; H, 3.51; N, 6.83.

[3] Melting points were taken on a Thomas-Hoover apparatus and are uncorrected. IR spectra were obtained using a Beckman Aculab 2 spectrophotometer. NMR spectra were recorded on a Varian FT-80 instrument. Chemical shifts are reported in parts per million (ppm) relative to trimethylsilane. Chemical ionization mass spectra were taken on an Associated Electronics Inc. Model MS-902 double-focus mass spectrometer equipped with a direct inlet system and modified for chemical ionization. The electron impact mass spectra were recorded on a Hitachi model M-52 instrument. Specific rotation measurements were performed on a Perkin-Elmer 141 electronic polarimeter. GC analyses of the derivatized amines were recorded on a Hewlett-Packard 5700A machine equipped with a nickel electron capture detector. The column was a 3 m × 6-mm i.d. glass column packed with 3% SP 2250 coated on 100/120 mesh Supelcoport. Argon–methane carrier gas flow rate was 30 ml/min and the column temperature was 250°. Peak area integration was done automatically by a Hewlett-Packard 3380A integrating recorder. Microanalyses were performed by the Microanalytical Laboratory, University of California at Berkeley.

The corresponding reaction with (*R*)-proline provided the enantiomeric anhydride (*R,R*)-IV, in 36% yield: mp 114–115°; $[\alpha]_D^{22} = +106.5°$ (*C*, 0.7 mg/ml, benzene).

(*S,R*)-*N*-Trifluoroacetylproline Anhydride [(*S,R*)-V]—The reaction of (*S*)-proline (5.75 g, 0.05 mole) and trifluoroacetic anhydride (42.0 g, 0.20 mole) in 20 ml of methylene chloride at room temperature for 48 hr yielded 2.5 g (0.006 mole, 25%) of the *meso*-anhydride, (*S,R*)-V, which was recrystallized from ether: mp 139–140° [lit. (7) mp 138–140°]; NMR and electron impact mass spectrum were indistinguishable from (*S,S*)-IV; $[\alpha]_D^{22} = 0.0°$ (*C*, 0.66 mg/ml; benzene); IR (oil mull): 1822, 1760, 1690, 1465, 1380, 1368, 1355, 940, 930, 914, 874, 812, and 760 cm^{-1}.

Anal.—Calc. for $C_{14}H_{14}N_2O_5F_6$: C, 41.60; H, 3.49; N, 6.93. Found: C, 41.77; H, 3.62; N, 6.96.

(*S*)-*N*-(*N*-Trifluoroacetylprolyl)-*N*-methylaniline [(*S*)-X]—A mixture of (*S,S*)-IV (1.8 g, 4.5 mmoles) and *N*-methylaniline (5 g, 46.7 mmoles) was heated for 2 hr under nitrogen with stirring. The cooled reaction mixture was washed twice with 10 ml of hexane and the residual oil was subjected to a short path distillation under reduced pressure. The distillate was crystallized from chloroform to yield 0.6 g (2.0 mmoles, 22.4%) of a colorless solid: mp 136–138°; NMR (deuterochloroform): 1.5–2.3 (m, 4H, CH_2), 3.28 (s, 3H, CH_3), 3.76 (m, 2H, NCH_2), 4.43 (t, J = 6.3 Hz, 1H, CH), and 7.40 (m, 5H, phenylH) ppm; $[\alpha]_D^{22} = -102.9°$ (*C*, 0.7 mg/ml; benzene).

Anal.—Calc. for $C_{14}H_{15}N_2O_2F_3$: C, 56.00; H, 5.04; N, 9.33. Found: C, 55.65; H, 5.07; N, 9.28.

The same reaction carried out with (*S,R*)-V provided (*S,R*)-X in 17% overall yield: mp 102–104°; $[\alpha]_D^{22} = 0.0°$ (*C*, 0.7 mg/ml, benzene).

Anal.—Calc. for $C_{14}H_{15}N_2O_2F_3$: C, 56.00; H, 5.04; N, 9.33. Found: C, 56.05; H, 5.04; N, 9.31.

(*S,S*)-2-[*N*-(*N*-Trifluoroacetylprolyl)-*N*-methyl]amino-2-*o*-chlorophenylcyclohexanone [(*S*)-*N*-Trifluoroacetylprolyl Amide of (*S*)-Ketamine, (*S,S*)-XIV]—A solution of (*S*)-*N*-trifluoroacetylprolyl chloride (536 mg, 2.33 mmoles in 23 ml of methylene chloride) and (*S*)-III (13) (500 mg, 2.11 mmoles in 10 ml of toluene) was heated at 75° with stirring under nitrogen for 1.5 hr. After cooling, the reaction mixture was stirred with 30 ml of 0.2% NaOH, separated, and washed with 10 ml of 0.5% HCl. After drying with sodium sulfate, hexane was added and the resulting solution was cooled to 5° to produce 300 mg (0.7 mmole, 33.2%) of a solid: $[\alpha]_D^{22} = +41.6°$ (*C*, 0.77 mg/ml; benzene); mp 197–200°. The NMR, electron impact mass spectrum, and GC retention time of the product were identical to the corresponding values for (*S,R*)-XV and therefore, its structure is assigned as (*R,S*)-XV. Treatment of the mother liquor with an additional 5 ml of hexane caused the precipitation of a second solid (45 mg, 0.2 mmole) which proved to be racemic *N*-trifluoroacetylproline: mp 53–55°; $[\alpha]_D^{22} = 0.0°$ (*C*, 0.7 mg/ml; benzene); chemical ionization mass spectrum, 212 (MH^+).

Anal.—Calc. for $C_7H_8NO_3F_3$: C, 39.81; H, 3.79; N, 6.64. Found: C, 39.80; H, 3.88; N, 6.60.

The residue obtained from the mother liquor filtrate was chromatographed on 10 g of silica. Elution with benzene–ethanol (95:5) provided a solid, which after crystallization from toluene–hexane yielded 7 mg (0.016 mmole, 0.8%) of the desired amide (*S,S*)-XIV: mp 184–186°; chemical ionization mass spectrum (*m/z*, relative intensity): 433 and 431 (MH^+, 25, 100), 397 (10), 227 and 225 (50, 100), 211 and 209 (60, 100); GC retention time, 16.8 min.

Anal.—Calc. for $C_{20}H_{22}N_2O_3F_3Cl$: C, 55.75; H, 5.15; N, 6.50. Found: C, 55.56; H, 5.30; N, 6.46.

(*R*)-2-[*N*-(*N*-Trifluoroacetyl-(*S*)-prolyl)-*N*-methyl]amino-2-*o*-chlorophenylcyclohexanone [(*S*)-*N*-Trifluoroacetylprolyl Amide of (*R*)-Ketamine, (*S,R*)-XV]—(*S*)-*N*-Trifluoroacetylprolyl chloride and (*R*)-ketamine were allowed to react under the same conditions as described previously. After treatment with 0.2% NaOH, extraction with 0.5% HCl, and drying with sodium sulfate, addition of hexane and cooling led to the crystallization of 490 mg (1.14 mmoles, 54%) of (*S,R*)-XV: mp 200–202°; NMR (deuterochloroform): 1.5–2.6 (m, 11H, CH_2), 3.24 (s, 3H, NCH_3), 3.3–3.5 (q, 1H, CH), 3.7–3.9 (m, 2H, CH_2), 5.09 (t, 1H, CH), and 7.1–7.5 (m, 4H, phenylH) ppm; $[\alpha]_D^{22} = -41.2°$ (*C*, 0.68 mg/ml; benzene); chemical ionization mass spectrum was identical to (*S,S*)-XIV; GC retention time, 19.2 min.

Anal.—Calc. for $C_{20}H_{22}N_2O_3F_3Cl$: C, 55.75; H, 5.15; N, 6.50. Found: C, 55.70; H, 5.24; N, 6.32.

Amine Derivatization—Derivatizations of racemic ketamine and the individual enantiomers of ketamine for GC analysis were performed under similar conditions except that the concentration of racemic ketamine was twice that of the individual enantiomers. Reactions were carried out in 50 μl of toluene–methylene chloride–triethylamine (95:5:0.02) containing (*R,S*)-ketamine (1.68 m*M*) or the ketamine enantio-

mers (0.84 mM), and in each case a 30 M excess of (S,S)-IV or (S)-I. The reactions were performed in screw cap sealed, polytef-lined reaction vials which were heated to 75–100° for 1–4 hr in a block heater. At the end of the reaction, the mixtures were washed with 0.2% NaOH (50 μl) followed by 0.5% HCl (50 μl) and then dried over sodium sulfate. The solutions were carefully transferred with the aid of a Pasteur pipet to a second reaction vial and the solvent removed under a stream of dry nitrogen. The residues were dissolved in 100 μl of toluene, and 1 μl of the resulting solution was analyzed by GC. Retention times for (S,S)-XIV and (S,R)/(R,S)-XV were 16.8 and 19.2 min, respectively. Derivatization of (S)-α-methylbenzylamine with (S,S)-IV and (R,S)-V proceeded in a similar fashion. GC retention times for (S,S)-VII and (S,R)-VIII were 15.5 and 13.3 min, respectively, using the same conditions as for the ketamine analyses.

REFERENCES

(1) N. P. McGraw, P. S. Callery, and N. Castagnoli, Jr., *J. Med. Chem.*, **20**, 185 (1977).

(2) L. K. Low and N. Castagnoli, Jr., "Annual Reports in Medicinal Chemistry," vol. 13, F. H. Clarke, Ed., Academic, New York, N.Y., 1978, pp. 304–315.

(3) E. Gil-Av and D. Nurok, *Adv. Chromatogr.*, **16**, 99 (1978).

(4) I. Tomida and M. Matsuzaki, *Agr. Biol. Chem.*, **43**, 925 (1979).

(5) S. B. Matin, M. Rowland, and N. Castagnoli, Jr., *J. Pharm. Sci.*, **62**, 821 (1973).

(6) J. D. Adams, N. Castagnoli, and A. J. Trevor, *Proc. West. Pharmacol. Soc.*, **21**, 471 (1978).

(7) F. Weygand, P. Klinke, and I. Eigen, *Chem. Ber.*, **90**, 1896 (1957).

(8) I. Tomida and T. Kuwahara, *Agr. Biol. Chem.*, **42**, 1059 (1978).

(9) H. D. W. Hill, A. P. Zens, and J. Jacobus, *J. Am. Chem. Soc.*, **101**, 7090 (1979).

(10) S. Wolfe and P. M. Kazmaier, *Can. J. Chem.*, **57**, 2388 (1979).

(11) M. W. Williams and G. T. Young, *J. Chem. Soc.*, **4**, 3701 (1964).

(12) M. Goodman and K. C. Steubern, *J. Org. Chem.*, **27**, 3409 (1962).

(13) Bristol Myers Co., British pat. 1 330 878 (1973).

ACKNOWLEDGMENTS

This work was supported by National Institutes of Health training grants GM 23918-01 and GM 07175-04, and research grants GM 01791 and NS 17956.

Thomas Woolf is an AFPE H. A. B. Dunning Memorial Fellow.

In Vivo and *In Vitro* Studies with Sulfamate Sweeteners

GRAINNE McGLINCHEY, C. BERNADETTE COAKLEY, VIDA GESTAUTUS-TANSEY, JOHN GAULT *, and WILLIAM J. SPILLANE ˣ

Received August 28, 1981, from the *Chemistry Department, University College, Galway, Ireland.* Accepted for publication, September 28, 1981. *Present address: Regional Technical College, Sligo, Ireland.

Abstract □ The sweet compounds 2-methyl- and 3-methylcyclohexyl- and 2-cyclohexenylsulfamates were fed to Wistar albino rats. The urine (and feces in the case of 2-cyclohexenylsulfamate) was examined for possible amine, ketone, and alcohol metabolites. The total percent of metabolites formed was low and the hexenyl compound gave a particularly small quantity of metabolite. The results with these compounds are compared with those obtained from earlier *in vivo* studies with cyclamate and other sulfamates. In complementary *in vitro* studies, the four sweetest sulfamates, namely, cyclamate, cycloheptyl-, cyclooctyl-, and cyclopentylsulfamates were incubated with the cell-free extract of bacteria isolated from the feces of cyclamate fed rats. Some correlation was apparent between these *in vitro* experiments and previous *in vivo* studies. Preliminary mutagenicity testing (the Ames test) of some amines (corresponding to the sulfamates studied) has been carried out.

Keyphrases □ Sulfamate sweeteners—*in vivo* and *in vitro* studies of amine, ketone, and alcohol metabolites □ Metabolism—amine ketone, and alcohol metabolites of sulfamate sweeteners □ Cyclamates—*in vivo* and *in vitro* studies of amine, ketone, and alcohol metabolites

The controversial ban on the use of cyclohexylsulfamate (cyclamate) salts as nonnutritive sweeteners has provided a strong impetus for wide and varied toxicity studies of these compounds and their metabolites (1). Though at least some other sulfamates have a sweetness potency similar to the banned parent compound (2), and it has been suggested that certain of these sulfamates might be less readily metabolized than is cyclamate (3), nevertheless toxicological studies have been carried out on just a few such compounds (4). In the present work, *in vivo* animal feeding studies employed three other sweet sulfamates: 2- and 3-methylcyclohexyl- and 2-cyclohexenylsulfamates. In a complementary *in vitro* study, some of the sweetest known sulfamates have been incubated in cell-free extracts of the microorganisms responsible for the metabolism of cyclamate. Some work has been carried out on the mutagenicity of the amines to which these sulfamates give rise when metabolized.

EXPERIMENTAL

Reagents and Chemicals—The amines, ketones, and alcohols were commercially available and were used as obtained. The following compounds were synthesized by known literature methods: 2-methylcyclohexanol (5), cyclohexyl- (6), 2-methyl- (6), 3-methyl- (6), 2-cyclohexenyl- (7), *n*-octyl- (8), and phenyl- (9) sulfamates. Cyclopentyl-, cycloheptyl-, and cyclooctylsulfamates were previously prepared (4). All the synthesized sulfamates (as their sodium salts) gave a positive "sulfamate test" (2), satisfactory C, H, and N analysis, and the characteristic IR bands for sulfamates. 2-Cyclohexenylsulfamate gave an additional band in the 1640–1615 cm^{-1} region, which is characteristic of an ethylenic double bond.

***In Vivo* Experiments**—Female Wistar albino rats (200–257 g) were kept on solid food and water in rat metabolism cages[1]. The sodium salts of 2- and 3-methylcyclohexyl- and 2-cyclohexenylsulfamates were administered orally in water (~20 ml) at a level of 1.45 g/kg of body weight to groups of six rats (five in the case of 2-methylcyclohexylsulfamate). Prior to administration of the sulfamates, the rats were deprived of water for 24 hr. Prior to feeding, the urine of each rat was examined for metabolites by GLC. Similarly, the three sulfamates fed were screened for occluded amine, also by GLC. After administration of each sweet compound, the urine (and feces in the case of 2-cyclohexenylsulfamate) was collected for 3 days, bulked, and refrigerated for no more than 1 day when GLC analysis for the metabolites was carried out.

The urine and feces recovered from rats, fed 2-cyclohexenylsulfamate, was not analysed until the eighth day (instead of the customary fourth day), and accordingly, a study of the stabilities of 2-cyclohexenylamine and 2-cyclohexenone in urine and feces over a 7-day period was made.

[1] NKP, Kent, England.

0022-3549/82/0600-0661$01.00/0

mers (0.84 mM), and in each case a 30 M excess of (S,S)-IV or (S)-I. The reactions were performed in screw cap sealed, polytef-lined reaction vials which were heated to 75–100° for 1–4 hr in a block heater. At the end of the reaction, the mixtures were washed with 0.2% NaOH (50 μl) followed by 0.5% HCl (50 μl) and then dried over sodium sulfate. The solutions were carefully transferred with the aid of a Pasteur pipet to a second reaction vial and the solvent removed under a stream of dry nitrogen. The residues were dissolved in 100 μl of toluene, and 1 μl of the resulting solution was analyzed by GC. Retention times for (S,S)-XIV and (S,R)/(R,S)-XV were 16.8 and 19.2 min, respectively. Derivatization of (S)-α-methylbenzylamine with (S,S)-IV and (R,S)-V proceeded in a similar fashion. GC retention times for (S,S)-VII and (S,R)-VIII were 15.5 and 13.3 min, respectively, using the same conditions as for the ketamine analyses.

REFERENCES

(1) N. P. McGraw, P. S. Callery, and N. Castagnoli, Jr., *J. Med. Chem.*, **20**, 185 (1977).

(2) L. K. Low and N. Castagnoli, Jr., "Annual Reports in Medicinal Chemistry," vol. 13, F. H. Clarke, Ed., Academic, New York, N.Y., 1978, pp. 304–315.

(3) E. Gil-Av and D. Nurok, *Adv. Chromatogr.*, **16**, 99 (1978).

(4) I. Tomida and M. Matsuzaki, *Agr. Biol. Chem.*, **43**, 925 (1979).

(5) S. B. Matin, M. Rowland, and N. Castagnoli, Jr., *J. Pharm. Sci.*, **62**, 821 (1973).

(6) J. D. Adams, N. Castagnoli, and A. J. Trevor, *Proc. West. Pharmacol. Soc.*, **21**, 471 (1978).

(7) F. Weygand, P. Klinke, and I. Eigen, *Chem. Ber.*, **90**, 1896 (1957).

(8) I. Tomida and T. Kuwahara, *Agr. Biol. Chem.*, **42**, 1059 (1978).

(9) H. D. W. Hill, A. P. Zens, and J. Jacobus, *J. Am. Chem. Soc.*, **101**, 7090 (1979).

(10) S. Wolfe and P. M. Kazmaier, *Can. J. Chem.*, **57**, 2388 (1979).

(11) M. W. Williams and G. T. Young, *J. Chem. Soc.*, **4**, 3701 (1964).

(12) M. Goodman and K. C. Steubern, *J. Org. Chem.*, **27**, 3409 (1962).

(13) Bristol Myers Co., British pat. 1 330 878 (1973).

ACKNOWLEDGMENTS

This work was supported by National Institutes of Health training grants GM 23918-01 and GM 07175-04, and research grants GM 01791 and NS 17956.

Thomas Woolf is an AFPE H. A. B. Dunning Memorial Fellow.

In Vivo and *In Vitro* Studies with Sulfamate Sweeteners

GRAINNE McGLINCHEY, C. BERNADETTE COAKLEY, VIDA GESTAUTUS-TANSEY, JOHN GAULT *, and WILLIAM J. SPILLANE ˣ

Received August 28, 1981, from the *Chemistry Department, University College, Galway, Ireland.* Accepted for publication, September 28, 1981. *Present address: Regional Technical College, Sligo, Ireland.

Abstract □ The sweet compounds 2-methyl- and 3-methylcyclohexyl- and 2-cyclohexenylsulfamates were fed to Wistar albino rats. The urine (and feces in the case of 2-cyclohexenylsulfamate) was examined for possible amine, ketone, and alcohol metabolites. The total percent of metabolites formed was low and the hexenyl compound gave a particularly small quantity of metabolite. The results with these compounds are compared with those obtained from earlier *in vivo* studies with cyclamate and other sulfamates. In complementary *in vitro* studies, the four sweetest sulfamates, namely, cyclamate, cycloheptyl-, cyclooctyl-, and cyclopentylsulfamates were incubated with the cell-free extract of bacteria isolated from the feces of cyclamate fed rats. Some correlation was apparent between these *in vitro* experiments and previous *in vivo* studies. Preliminary mutagenicity testing (the Ames test) of some amines (corresponding to the sulfamates studied) has been carried out.

Keyphrases □ Sulfamate sweeteners—*in vivo* and *in vitro* studies of amine, ketone, and alcohol metabolites □ Metabolism—amine ketone, and alcohol metabolites of sulfamate sweeteners □ Cyclamates—*in vivo* and *in vitro* studies of amine, ketone, and alcohol metabolites

The controversial ban on the use of cyclohexylsulfamate (cyclamate) salts as nonnutritive sweeteners has provided a strong impetus for wide and varied toxicity studies of these compounds and their metabolites (1). Though at least some other sulfamates have a sweetness potency similar to the banned parent compound (2), and it has been suggested that certain of these sulfamates might be less readily metabolized than is cyclamate (3), nevertheless toxicological studies have been carried out on just a few such compounds (4). In the present work, *in vivo* animal feeding studies employed three other sweet sulfamates: 2- and 3-methylcyclohexyl- and 2-cyclohexenylsulfamates. In a complementary *in vitro* study, some of the sweetest known sulfamates have been incubated in cell-free extracts of the microorganisms responsible for the metabolism of cyclamate. Some work has been carried out on the mutagenicity of the amines to which these sulfamates give rise when metabolized.

EXPERIMENTAL

Reagents and Chemicals—The amines, ketones, and alcohols were commercially available and were used as obtained. The following compounds were synthesized by known literature methods: 2-methylcyclohexanol (5), cyclohexyl- (6), 2-methyl- (6), 3-methyl- (6), 2-cyclohexenyl- (7), *n*-octyl- (8), and phenyl- (9) sulfamates. Cyclopentyl-, cycloheptyl-, and cyclooctylsulfamates were previously prepared (4). All the synthesized sulfamates (as their sodium salts) gave a positive "sulfamate test" (2), satisfactory C, H, and N analysis, and the characteristic IR bands for sulfamates. 2-Cyclohexenylsulfamate gave an additional band in the 1640–1615 cm^{-1} region, which is characteristic of an ethylenic double bond.

***In Vivo* Experiments**—Female Wistar albino rats (200–257 g) were kept on solid food and water in rat metabolism cages[1]. The sodium salts of 2- and 3-methylcyclohexyl- and 2-cyclohexenylsulfamates were administered orally in water (~20 ml) at a level of 1.45 g/kg of body weight to groups of six rats (five in the case of 2-methylcyclohexylsulfamate). Prior to administration of the sulfamates, the rats were deprived of water for 24 hr. Prior to feeding, the urine of each rat was examined for metabolites by GLC. Similarly, the three sulfamates fed were screened for occluded amine, also by GLC. After administration of each sweet compound, the urine (and feces in the case of 2-cyclohexenylsulfamate) was collected for 3 days, bulked, and refrigerated for no more than 1 day when GLC analysis for the metabolites was carried out.

The urine and feces recovered from rats, fed 2-cyclohexenylsulfamate, was not analysed until the eighth day (instead of the customary fourth day), and accordingly, a study of the stabilities of 2-cyclohexenylamine and 2-cyclohexenone in urine and feces over a 7-day period was made.

[1] NKP, Kent, England.

0022-3549/82/0600-0661$01.00/0

Table I—Percent Recovery of 2-Methylcyclohexylamine, 2-Methylcyclohexanone, and 2-Methylcyclohexanol from Urine

Amine		Ketone		Alcohol	
μg	%	μg	%	μg	%
0.015	68.7	0.02	88.0	0.028	81.5
0.03	83.0	0.05	90.3	0.056	86.0
0.10	100.5	0.10	95.6	0.08	91.0
0.10	99.0	0.10	96.3	0.10	98.5
0.15	86.3	0.15	87.0	0.10	96.3
0.2	93.5	0.20	91.5	0.14	89.3
0.25	95.6	0.20	93.0	0.17	85.1
0.25	98.5	0.25	99.0	0.17	97.3
Mean	90.64		92.58		90.63
±*SE*	±8.41		±3.38		±5.15

The two metabolites were added individually to samples of rat urine and feces, and these samples were then refrigerated for 7 days, worked-up, and analyzed in the same manner as the actual samples from the feeding experiments.

General Work-Up Procedure, Standardization, and GLC Analysis—The details for other sulfamates have been reported previously (4). Analogous procedures and methods were employed for the three sulfamates. The GLC conditions were as follows. 2-Methylcyclohexylsulfamate metabolites: column temperature, 117°; gas flow rates, nitrogen, 60 ml/min, hydrogen, 60 ml/min, and overall (including air), 500 ml/min; retention times (min), 2-methylcyclohexylamine (4.5), 2-methylcyclohexanone (6.7), 2-methylcyclohexanol (10.1), and 4-methylcyclohexanol (internal standard) (12.6). 3-Methylcyclohexylsulfamate metabolites: column temperature and flow rates, as described previously; retention times (min), *n*-undecane (internal standard) (3.8), 3-methylcyclohexylamine (4.6), 3-methylcyclohexanone (7.2), and *cis*- and *trans*-3-methylcyclohexanols (10.5 and 11.7, respectively). 2-Cyclohexenylsulfamate metabolites: column temperature, 107°; gas flow rates were identical with those described previously; retention times (min), *n*-dodecane (internal standard) (11.0), 2-cyclohexenone (16.5), and 2-cyclohexenylamine (18.6). The lengthy retention times involved in the latter analysis could not be shortened on the column (4). This is because a rise in the temperature tended to cause the cyclohexenyl metabolite peaks to merge. The GLC conditions for analysis of the sulfamate metabolites used in the *in vitro* experiments have been described previously (4), except in the case of *n*-octyl- and phenylsulfamates. The following are the GLC conditions for the determination of the metabolites of these two sulfamates. *n*-Octylsulfamate metabolites: column temperature, 130°; nitrogen gas flow rate, 150 ml/min; retention times (min); *n*-octylamine (6.4), tridecane (internal standard) (9.6), and *n*-octanol (19.5). Phenylsulfamate metabolites: column temperature and nitrogen flow rate as for *n*-octylmetabolites; retention times (min), aniline (3.8), tridecane (internal standard) (9.6), and phenol (31.0).

***In Vitro* Experiments**—*Isolation of Organisms and Preparation of Cell-Free Extracts*—Wistar albino rats were fed cyclohexylsulfamate at the rate of 2 g/week for a 10-week period. The urine was tested for the presence of cyclamate metabolites, *i.e.*, cyclohexylamine, cyclohexanone, and cyclohexanol, using solvent extraction and identification by GLC (10). When a rat was consistently breaking down cyclamate to its metabolites, the feces were then used for the isolation of the microorganisms.

A nutrient broth agar containing 1% cyclohexylsulfamate was inoculated with a sample of fecal material, allowed to grow overnight, and transferred to a larger volume the following day. The bacteria were grown in a shaking incubator for 5 days after which they were harvested by centrifugation. The pellets were resuspended in a small volume of tromethamine-hydrochloride buffer, pH 7.2, and lysed by sonication.

Incubation Procedure and Analysis for Metabolites—Two milliliters of cell-free extract were incubated with 200 μmoles of test sulfamate in 2 ml of 0.1 *M* phosphate buffer, pH 6.8, for 2 hr at 50°. The reaction was stopped by adding 1 ml of 10 *N* NaOH followed by 4 ml of 20% sulfosalicylic acid.

The incubation mixture was extracted three times with 20-ml volumes of methylene chloride. The methylene chloride extracts were bulked and evaporated to dryness and the residue reconstituted with 1 ml of methylene chloride. Analysis for metabolites was then carried out using the procedure described previously. The incubation studies were carried out over a 2-hr period at 50°, pH 6.8, and were the conditions under which the enzymes present in the cell-free extract displayed maximum activity. The variations of enzyme activities with temperature, pH, and incubation time were determined in separate experiments.

Mutagenicity Testing—Amines were tested for their ability to cause base-pair substitution mutations using the mutant strain of *Salmonella typhimurium* TA 1535, according to the method described previously (11). Fifteen micrograms of the test substance contained in 0.1 ml of water was used in each case and 2-aminofluorene was used as a standard.

The mixed oxidase S-9 mixture was not used because the compounds under test were already presumed metabolites.

Table II—Percent Recovery of 3-Methylcyclohexylamine, 3-Methylcyclohexanone, and 3-Methylcyclohexanol from Urine

Amine		Ketone		Alcohol	
μg	%	μg	%	μg	%
0.05	73.5	0.01	105.7	0.05	75.6
0.15	85.6	0.02	78.6	0.15	89.1
0.25	105.3	0.03	79.8	0.25	93.0
0.25	96.5	0.10	98.6	0.40	98.0
0.45	103.0	0.10	102.5	0.40	89.1
0.70	98.4	0.20	97.8	0.60	103.5
1.20	99.0	0.30	95.4	0.80	98.2
Mean	94.47		94.06		92.36
±*SE*	±8.53		±8.49		±6.65

RESULTS AND DISCUSSION

In the present paper the three compounds, 2-methyl- and 3-methylcyclohexyl- and 2-cyclohexenylsulfamates, were administered as their sodium salts to rats. These studies extended previous studies in which sulfamates other than the "parent" sweet sulfamate, cyclohexylsulfamate (cyclamate), were fed to animals and the urine examined for breakdown products (4). Prior to administration of the three compounds in the present study, standard curves and percent recoveries of likely metabolites were determined using procedures established in earlier work (4). In Tables I–III, percent recoveries for metabolites of 2-methyl- and 3-methylcyclohexyl- and 2-cyclohexenylsulfamates are seen to be satisfactory. It should be noted that in general the quantities in micrograms used in the determination of the percent recoveries are in the same range as the amounts of metabolites found in the feeding experiments.

In other preliminary experiments, the sulfamates given to the animals were screened for small occluded amounts of metabolite(s) and the urine (feces in one instance) of the rats to be fed was screened for metabolites. Since it was not possible to examine the urine/feces of the rats that were fed 2-cyclohexenylsulfamate for 7 days after administering the sweetener, a study of the stabilities of 2-cyclohexenylamine and 2-cyclohexenone in urine/feces was made over a 7-day period. The stabilities of the two compounds, reported as percent survival, is excellent (Table IV). Samples of 2-cyclohexenols were not available but it appears unlikely that they were products of the metabolic cleavage of 2-cyclohexenylsulfamate.

The aim of the *in vivo* study was to examine the effect of introducing a substituent or double bond on metabolic breakdown of cyclohexylsulfamate. If metabolic breakdown was decreased, then the risks associated with cyclamate ingestion should be reduced. The first compound administered was 2-methylcyclohexylsulfamate. Table V shows that this compound was broken down by all rats to the metabolites 2-methylcyclohexylamine and/or 2-methylcyclohexanone. None of the rats in this group gave alcohol metabolites. In this work, as previously (4), the percent conversion to a particular metabolite is defined as the amount of metabolite found (milligrams) divided by the amount of sulfamate fed (milligrams) multiplied by a hundred times the ratio of the molecular weight of the sulfamate to that of the particular metabolite. In this instance, the mean percent conversions to amine and ketone are 0.00013 and 0.00067, respectively. In the case of the study with 3-methylcyclohexylsulfamate, the mean percent of 3-methylcyclohexylamine, 3-methylcyclohexanone, and 3-methylcyclohexanol formed were 0.014, 0.0002, and 0.0098, respectively (Table VI). After administration of 2-cyclohexenylsulfamate, only two rats in the group of six were found to be converters, and interestingly, these two rats gave amine only (mean percent, 0.00017) with no metabolites in their feces (Table VII). It was not possible to check positively for the presence of 2-cyclohexenols, since these compounds were not available. However, from experience it was felt that the retention time(s) of this alcohol(s) should be fairly close to that of the corresponding amine and ketone, but no traces were obtained in the vicinities of the peaks due to these metabolites, nor did any traces appear when the chromatograph was run 29 min, *i.e.*, 10 min after the appearance of the last peak.

Table VIII gives the mean percent and the percent total metabolites found in *in vivo* studies with the three sulfamates of the present study, five sulfamates previously administered to rats and, for comparison, some typical data for cyclohexylsulfamate.

Table III—Percent Recovery of 2-Cyclohexenylamine and 2-Cyclohexenone from Urine and Feces

Urine				Feces			
Amine		Ketone		Amine		Ketone	
μg	%	μg	%	μg	%	μg	%
1.5	101.7	2.0	97.9	1.5	76.2	2.00	60.5
4.0	139.0	3.0	73.1	4.0	93.9	5.00	68.5
6.0	99.3	4.0	103.0	6.0	99.2	7.5	71.3
6.0	105.2	6.0	86.5	7.0	93.7	8.5	86.2
7.0	98.3	10.0	104.2	8.0	106.4	9.5	105.3
8.0	100.8			8.0	97.6	10.0	85.4
Mean	107.4		92.94		94.5		79.5
±*SE*	±10.55		±10.5		±6.35		±12.77

Table IV—Stability of 2-Cyclohexenylamine and 2-Cyclohexenone in Urine and Feces over a 7-Day Period

Urine				Feces			
Amine		Ketone		Amine		Ketone	
Sample Added, μg	Survival, %	Sample Added, μg	Survival, %	Sample Added, μg	Survival, %	Sample Added, μg	Survival, %
5.8	99.0	7.2	83.5	5.8	92.5	7.2	71.5
5.8	96.5	7.2	90.2	5.8	86.4	7.2	85.2
5.8	90.3	7.2	104.3	5.8	98.2	7.2	87.2
Mean ± *SE*	95.3 ± 3.3		92.7 ± 7.8		92.4 ± 4.0		81.3 ± 6.5

Table V—Metabolism of 2-Methylcyclohexylsulfamate in Rats

	Metabolites						
	2-Methylcyclohexylamine		2-Methylcyclohexanone		2-Methylcyclohexanol		
Animal Number	mg	%	mg	%	mg	%	% Total Metabolites
1	0.0016	0.00012	0.00012	0.00009	None	0	0.00021
2	0.00049	0.00037	None	0	None	0	0.00037
3	None	0	0.0031	0.0024	None	0	0.00024
4	0.00013	0.0001	0.0005	0.00036	None	0	0.00046
5[a]	0.00007	0.00007	0.0004	0.00048	None	0	0.00055
Mean	0.00017	0.00013	0.00082	0.00067			0.00037
±*SE*	±0.00013	±0.00009	±0.0009	±0.00069			±0.00011

[a] Fed only 0.17 g instead of 0.26 g, based on 1.45 g/kg body weight.

Table VI—Metabolism of 3-Methylcyclohexylsulfamate in Rats

	Metabolites						
	3-Methylcyclohexylamine		3-Methylcyclohexanone		3-Methylcyclohexanol		
Animal Number	mg	%	mg	%	mg	%	% Total Metabolites
1[a]	0.013	0.014	None	0	0.026	0.028	0.042
2	0.01	0.008	None	0	None	0	0.008
3	0.062	0.03	None	0	0.049	0.027	0.057
4	0.066	0.03	None	0	None	0	0.030
5	None	0	0.00246	0.0012	0.008	0.004	0.0052
6	0.006	0.003	None	0	None	0	0.003
Mean	0.026	0.014	0.00041	0.0002	0.0138	0.0098	0.0242
±*SE*	±0.025	±0.011			±0.0158	±0.012	±0.0188

[a] Rat 1 received approximately half the amount of sulfamate.

Table VIII shows that the degree of metabolic cleavage by rats of various types of sulfamates is low, being generally <0.1%. Since the number of rats involved in each of the feeding studies was small, *i.e.*, five or six, any deductions made from the results in Table VIII regarding the relative stability of sulfamates would be tenuous. However, it seems that cyclooctylsulfamate, which gives rise to all three metabolites, is cleaved to a somewhat greater extent than the other sulfamates. On the other hand, the introduction of a double bond into the cyclohexyl system, *i.e.*, in 2-cyclohexenylsulfamate, appears to reduce metabolic breakdown considerably. This latter compound has a comparable level of sweetness to cyclamate (7). Interestingly, when the closely related and sweet 3-cyclohexenylsulfamate was administered intraduodenally for 2 weeks to rats at a dosage of 1 g/kg of body weight, no pathological changes in the main organs or tissues could be detected (7).

One of the sulfamates in Table VIII is not sweet; however, on the basis of a previous cursory examination, it was taken to be sweet (4). On careful examination it was classified as being bitter (13). Unterhalt and Böschemeyer (14), who first made this compound, also reported it as being nonsweet.

Complementary to the *in vivo* studies, a series of *in vitro* experiments have been carried out. In this study, the microorganisms responsible for the metabolism of cyclamate were isolated from the feces of rats fed cyclamate. A cell-free extract of these organisms was then incubated with the four sweetest known sulfamates and two standards to ascertain the extent to which these compounds were broken down to potentially toxic metabolites.

Earlier work (15) showed that dogs and humans fed on cyclamate

Table VII—Metabolism of 2-Cyclohexenylsulfamate in Rats

	Metabolites			
	2-Cyclohexenylamine		2-Cyclohexenone	
Animal Number	mg	%	mg	%
1	None	0	None	0
2	0.00047	0.00036	Trace	0
2[a]	Trace	0	Trace	0
3	None	0	None	0
4	0.00083	0.00068	Trace	0
4[a]	Trace	0	Trace	0
5	None	0	None	0
6	None	0	None	0
Mean	0.00022	0.00017[b]		
±*SE*	±0.00028	±0.00023		

[a] Results for feces. [b] The mean was obtained by dividing the summation of the percent of metabolite in the urine by 6.

Table VIII—Metabolism of Sulfamates in Rats

Cyclic Sulfamate	Percent Metabolites[a]			Total Metabolites, %	Reference
	Amine	Ketone	Alcohol		
Octyl	0.127	0.08	0.092	0.297	4
Heptyl	0.0514	0.0088	0.0034	0.064	2[b]
Hexyl[c]	0.0096	0.00095	0.004	0.0146	12
2-Methylhexyl	0.00013	0.00067	0	0.00037	This work
3-Methylhexyl	0.014	0.0002	0.0098	0.0242	This work
4-Methylhexyl	0.0073	0.0013	0	0.0085	4
2-Hexenyl	0.00017	0	0	0.00017	This work
Pentyl	0.057	0.016	0.0087	0.083	1[d]
Pentylmethyl	0.007	—[e]	0.007	0.0144	3[f]

[a] These percents were calculated by summing the percent metabolite for each rat, summing the totals, and dividing by the number of rats in each study. [b] Reference 2 in (4). [c] The figures for hexyl were obtained from data on six rats (2 groups of 3). The percent total metabolites represents the total for amine, ketone, and alcohol. In Ref. 12 the authors also detected "conjugated" cyclohexanol as a metabolite, so their total differs slightly. [d] Reference 1 in (4). [e] A ketone metabolite is not possible for this compound. [f] Reference 3 in (4).

produced large quantities of a metabolite, cyclohexylamine, in their urine. It was considered that this compound was the carcinogen, and it seemed likely that the conversion from cyclohexylsulfamate to cyclohexylamine was carried out by processing enzymes in the liver. Attempts to verify this *in vitro* study, however, met with little success (16).

The formation of cyclohexylamine and cyclohexanone from cyclamate by microorganisms isolated from guinea pig feces was demonstrated previously (17). This work was followed up by carrying out a partial purification of the enzyme involved, cyclohexylsulfamatase (18). The substrate specificity of the partially purified enzyme using several other sulfamates, which were generally not sweet, was also examined.

These studies subsequently partially purified and examined the properties of cyclohexylamine oxidase, which is the next enzyme in the metabolic sequence (19):

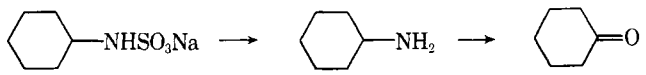

cyclohexylsulfamate cyclohexylamine cyclohexanone

Biochemical tests for Gram-negative enteric bacteria were first carried out on the bacteria whose cell-free extract carried out the sulfamatase function. These tests included indole production; hydrogen sulfide production; liquefaction of gelatin; cleavage of sugars, alcohols, and glucosides; and methyl red Voges Proskauer tests. The results of these tests indicated the presence of *Escherichia coli*, *Enterobacter hafniae*, and *Proteus mirabilis*. Pure cultures of these organisms were grown and cell-free extracts incubated with cyclohexylsulfamate, but it was found that greater activity was observed when a mixed culture was used.

A series of investigations was carried out to determine the optimum conditions for assay of enzyme activity. The variation in crude enzyme activity in relation to temperature, pH, and time of incubation was investigated and as a result, it was decided to adopt the incubation conditions as outlined previously: pH 6.8 for 2 hr at 50°.

Partial purification of the enzyme by ammonium sulfate fractionation (18) resulted in greatly reduced activity. Therefore, it was decided to conduct the studies using the crude enzyme extract. It has also been reported (18) that heat treatment of the crude enzyme extract (60° for 10 min) inactivates heat labile enzymes which are responsible for further degradation of cyclohexylamine, while leaving the heat stable sulfamatase unaffected. However, experience showed that the sulfamatase itself is largely inactivated by this procedure so it was not adopted. Consequently, the crude enzyme extract was used in the incubation studies.

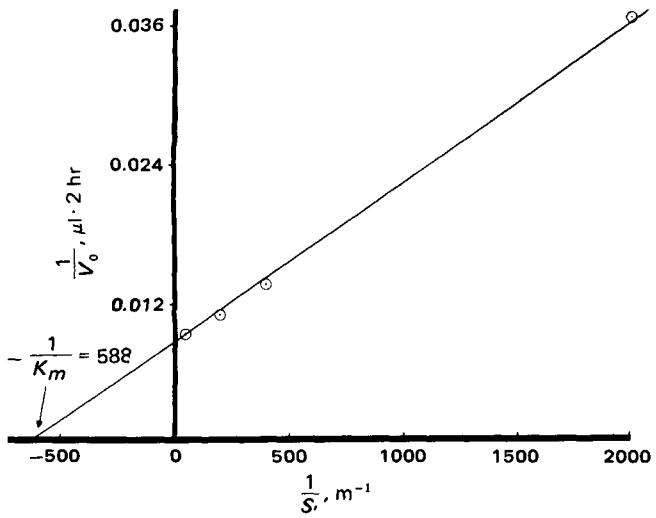

Figure 1—*Lineweaver-Burk plot for cyclohexylsulfamate.*

Table IX—Sulfamate Specificity of the Enzyme Extract and Mutagenicity (Ames Test) of the Corresponding Amines

N-Substituted Sulfamate	Relative Activity	Relative Sweetness[b]	Mutagenicity of Parent Amine[c]
Cyclohexyl	1[a]	1	0.02
Phenyl	5.3	—	—[d]
n-Octyl	6.4	—	—[d]
Cycloheptyl	0.52	0.83	—[d]
Cyclopentyl	0.50	0.24	0.006
Cyclooctyl	0	0.67	—[d]

[a] Total breakdown was 0.5%. [b] Data taken from Ref. 2; no values indicate not sweet. [c] Compared to standard 2-aminofluorene which is equal to one. [d] Zero or negligible.

In Table IX the results of incubation of various sulfamates with this enzyme extract are shown relative to cyclohexylsulfamate. The activities are computed as the sum of metabolites, *i.e.*, amine, alcohol, and ketone. Since it was found that *n*-octylsulfamate (which is not sweet) was the most labile substrate examined (18), this compound was included in the present study to assess the activity of the enzyme extract. As can be seen from Table IX, the enzyme extract was also highly active against this substrate, giving a relative activity of 6.4 as compared to cyclohexylsulfamate.

Phenylsulfamate was also included as another standard and it was found that it too was quite labile, in contrast to previous results, which indicated that the enzyme had only a very weak or uncertain activity on this substrate. It was confirmed that this breakdown was not due to impurities in the sulfamate and/or nonenzymatic hydrolysis. This was done by incubating the buffered substrate in the absence of the enzyme extract when no aniline or phenol was detected.

A variety of sulfamates was incubated previously (18), but apart from cyclohexylsulfamate, only two faintly sweet sulfamates, *n*-propyl- (2) and *ac*-tetrahydro-β-naphthyl (6) sulfamates, were included in the study. For the current incubation experiments, the four sweetest known sulfamates, cyclohexyl-, cycloheptyl-, cyclooctyl-, and cyclopentyl-, were incubated. Relative to cyclohexylsulfamate, all three had less activity. There was a partial correlation between the *in vivo* results in Table VIII for these four compounds and the *in vitro* results for the sulfamates in Table IX. Thus, in both types of experiments the heptyl- and pentyl-compounds were metabolized ~50% that of cyclohexylsulfamate. In the case of cyclooctylsulfamate, the results from the *in vivo* and *in vitro* studies contradict each other. The Michaelis constant (Km) for the enzyme with cyclohexylsulfamate was determined using a Lineweaver-Burk plot (Fig. 1) and was found to be 1.7×10^{-3} *M*. This indicates a three times greater affinity between enzyme and substrate than that reported previously (18).

In Table IX, preliminary studies on the mutagenicity of the amines of the sulfamates which were incubated are reported. The amines of all the sulfamates reported in Table IX show zero or negligible mutagenic activity [in the case of aniline this result was already established (20)]. The amines, isobutylamine and isoamylamine, both of whose sulfamates are moderately sweet (compared to cyclamate) (2), also show negligible mutagenicity, but *n*-butylamine, whose sulfamate is faintly sweet (2),

appeared to be mutagenic (60 revertants/15 μg). It should be stressed, however, that these are preliminary studies and would have to be confirmed using other tester strains of *Salmonella typhimurium*.

REFERENCES

(1) G. McGlinchey, Ph.D. thesis, National University of Ireland, 1980.

(2) G. A. Benson and W. J. Spillane, *J. Med. Chem.*, **19**, 869 (1976).

(3) W. J. Spillane, *J. Pharm. Sci.*, **62**, 1394 (1973).

(4) W. J. Spillane, G. A. Benson, and G. McGlinchey, *ibid.*, **68**, 372 (1979).

(5) "Organic Synthesis," coll. Vol. 2, A. H. Blatt, Ed., Wiley, New York, N.Y., 1966, p. 317.

(6) L. F. Audrieth and M. Sveda, *J. Org. Chem.*, **9**, 89 (1944).

(7) M. Avramoff and W. Taub, *Eur. J. Med. Chem.*, **13**, 81 (1978).

(8) C. Nofre and F. Pautet, *Bull. Soc. Chim. Fr.*, **1975**, 686.

(9) P. Baumgarten, *Chem. Ber.*, **59**, 1166 (1926).

(10) G. A. Benson and W. J. Spillane, *J. Chromatogr.*, **136**, 318 (1977).

(11) B. N. Ames, J. McCann, and E. Yamasaki, *Mutation Res.*, **31**, 347 (1975).

(12) A. Suenaga, S. Kojima, and H. Ichibagase, *ibid.*, **20**, 1357 (1972).

(13) W. J. Spillane and G. McGlinchey, *J. Pharm. Sci.*, **70**, 933 (1981).

(14) B. Unterhalt and L. Böschemeyer, *Z. Lebensm.-Unters.-Forsch.*, **145**, 93 (1971).

(15) S. Kojima and H. Ichibagase, *Chem. Pharm. Bull.*, **14**, 971 (1966).

(16) B. S. Drasar, A. G. Renwick, and R. T. Williams, *Biochem. J.* **129**, 881 (1972).

(17) M. Asahina, T. Niimura, T. Yamaha, and T. Takahashi, *Agr. Biol. Chem.*, **36**, 711 (1972).

(18) T. Niimura, T. Tokieda, and T. Yamaha, *J. Biochem. (Japan)*, **75**, 407 (1974).

(19) T. Tokieda, T. Niimura, F. Takamura, and T. Yamaha, *ibid.*, **81**, 851 (1977).

(20) J. McCann, E. Choi, E. Yamasaki, and B. N. Ames, *Proc. Natl. Acad. Sci. USA*, **72**, 5135 (1975).

ACKNOWLEDGMENTS

The authors thank the National Board for Science and Technology (Ireland) for a research grant, P. Considine (Galway) and E. Brady (Sligo) for their assistance with microbiological aspects of this work, and Professor B. Ames (Berkeley) for a sample of *Salmonella typhimurium* TA1535.

Plasma Levels of a Novel Antidysrhythmic Agent, Meobentine Sulfate, in Humans as Determined by Radioimmunoassay

JAMES T. WARREN *, GEOFFREY G. COKER ‡, RICHARD M. WELCH *, ARTHUR S. E. FOWLE ‡, and JOHN W. A. FINDLAY *x

Received July 27, 1981, from the * *Wellcome Research Laboratories, Research Triangle Park, NC 27709;* and the ‡ *Wellcome Research Laboratories, Beckenham, Kent BR3 3BS, U.K.* Accepted for publication September 21,1981.

Abstract □ A radioimmunoassay for the quantitation of meobentine sulfate, a novel antidysrhythmic and antifibrillatory agent in biological fluids, is described. Antisera were raised in rabbits in response to immunization with a conjugate of bovine serum albumin and a meobentine analog with a propionic acid sidechain *ortho* to the methoxyl group. These antisera have low affinities for *N*- and *O*-desmethylmeobentine metabolites, which show less than 5% cross-reaction in radioimmunoassay procedures employing either tritiated or radioiodinated radioligands. The radioimmunoassay using [^{125}I]meobentine was capable of detecting <0.4 ng/ml (40-pg mass) of meobentine. This assay was used to demonstrate the absorption of meobentine in humans after oral administration and also permitted studies of meobentine sulfate disposition in human plasma following two (2.5 and 5 mg/kg) oral doses. Mean peak meobentine concentrations in plasma occurred 3 hr postdose in both cases and were 230 and 451 ng/ml following the 2.5- and 5-mg/kg doses, respectively. The approximate mean terminal half-life after all treatments was 12 hr.

Keyphrases □ Meobentine sulfate—plasma levels in humans, radioimmunoassay □ Bioavailability—plasma levels of meobentine sulfate in humans determined by radioimmunoassay □ Radioimmunoassay—plasma levels of meobentine sulfate in humans

Meobentine sulfate [bis-(*N*-4-methoxybenzyl-*N'*-*N''*,dimethylguanidinium)sulfate] possesses marked antidysrhythmic properties against arrhythmias induced by ouabain and those induced by coronary artery ligation in dogs (1). It has been demonstrated that meobentine causes a significant incidence of spontaneous recovery from electrically induced fibrillation in the dog[1]. The electrophysiological properties of meobentine have been studied (2). Although very close in structure to the hypotensive agent, bethanidine (3), meobentine is not a neuronal blocking agent and thus, does not decrease blood pressure in animals when administered intravenously at effective antidysrhythmic doses (1). In this respect, meobentine also appears to be superior to the quaternary ammonium compound bretylium tosylate, which is indicated only for treatment of life-threatening ventricular arrhythmias (4) due to its severe hypotensive side effects.

The clinical safety and efficacy of meobentine sulfate when administered to humans by oral and parenteral routes are currently under study. Pharmacokinetic studies of meobentine in animals and humans, which are needed to facilitate the evaluation of meobentine in current clinical trials, require adequately sensitive and specific procedures for the determination of the drug in body fluids. Earlier gas and thin-layer chromatographic techniques lacked sensitivity, while administration and quantitation of radiolabeled meobentine is impractical for extensive pharmacokinetic studies in humans.

[1] W. Wastila *et al.*, submitted to *J. Pharm. Pharmacol.*

0022-3549/82/0600-0665$01.00/0

appeared to be mutagenic (60 revertants/15 μg). It should be stressed, however, that these are preliminary studies and would have to be confirmed using other tester strains of *Salmonella typhimurium*.

REFERENCES

(1) G. McGlinchey, Ph.D. thesis, National University of Ireland, 1980.

(2) G. A. Benson and W. J. Spillane, *J. Med. Chem.*, **19**, 869 (1976).

(3) W. J. Spillane, *J. Pharm. Sci.*, **62**, 1394 (1973).

(4) W. J. Spillane, G. A. Benson, and G. McGlinchey, *ibid.*, **68**, 372 (1979).

(5) "Organic Synthesis," coll. Vol. 2, A. H. Blatt, Ed., Wiley, New York, N.Y., 1966, p. 317.

(6) L. F. Audrieth and M. Sveda, *J. Org. Chem.*, **9**, 89 (1944).

(7) M. Avramoff and W. Taub, *Eur. J. Med. Chem.*, **13**, 81 (1978).

(8) C. Nofre and F. Pautet, *Bull. Soc. Chim. Fr.*, **1975**, 686.

(9) P. Baumgarten, *Chem. Ber.*, **59**, 1166 (1926).

(10) G. A. Benson and W. J. Spillane, *J. Chromatogr.*, **136**, 318 (1977).

(11) B. N. Ames, J. McCann, and E. Yamasaki, *Mutation Res.*, **31**, 347 (1975).

(12) A. Suenaga, S. Kojima, and H. Ichibagase, *ibid.*, **20**, 1357 (1972).

(13) W. J. Spillane and G. McGlinchey, *J. Pharm. Sci.*, **70**, 933 (1981).

(14) B. Unterhalt and L. Böschemeyer, *Z. Lebensm.-Unters.-Forsch.*, **145**, 93 (1971).

(15) S. Kojima and H. Ichibagase, *Chem. Pharm. Bull.*, **14**, 971 (1966).

(16) B. S. Drasar, A. G. Renwick, and R. T. Williams, *Biochem. J.* **129**, 881 (1972).

(17) M. Asahina, T. Niimura, T. Yamaha, and T. Takahashi, *Agr. Biol. Chem.*, **36**, 711 (1972).

(18) T. Niimura, T. Tokieda, and T. Yamaha, *J. Biochem. (Japan)*, **75**, 407 (1974).

(19) T. Tokieda, T. Niimura, F. Takamura, and T. Yamaha, *ibid.*, **81**, 851 (1977).

(20) J. McCann, E. Choi, E. Yamasaki, and B. N. Ames, *Proc. Natl. Acad. Sci. USA*, **72**, 5135 (1975).

ACKNOWLEDGMENTS

The authors thank the National Board for Science and Technology (Ireland) for a research grant, P. Considine (Galway) and E. Brady (Sligo) for their assistance with microbiological aspects of this work, and Professor B. Ames (Berkeley) for a sample of *Salmonella typhimurium* TA1535.

Plasma Levels of a Novel Antidysrhythmic Agent, Meobentine Sulfate, in Humans as Determined by Radioimmunoassay

JAMES T. WARREN *, GEOFFREY G. COKER ‡, RICHARD M. WELCH *, ARTHUR S. E. FOWLE ‡, and JOHN W. A. FINDLAY *x

Received July 27, 1981, from the * *Wellcome Research Laboratories, Research Triangle Park, NC 27709;* and the ‡ *Wellcome Research Laboratories, Beckenham, Kent BR3 3BS, U.K.* Accepted for publication September 21,1981.

Abstract □ A radioimmunoassay for the quantitation of meobentine sulfate, a novel antidysrhythmic and antifibrillatory agent in biological fluids, is described. Antisera were raised in rabbits in response to immunization with a conjugate of bovine serum albumin and a meobentine analog with a propionic acid sidechain *ortho* to the methoxyl group. These antisera have low affinities for *N*- and *O*-desmethylmeobentine metabolites, which show less than 5% cross-reaction in radioimmunoassay procedures employing either tritiated or radioiodinated radioligands. The radioimmunoassay using [^{125}I]meobentine was capable of detecting <0.4 ng/ml (40-pg mass) of meobentine. This assay was used to demonstrate the absorption of meobentine in humans after oral administration and also permitted studies of meobentine sulfate disposition in human plasma following two (2.5 and 5 mg/kg) oral doses. Mean peak meobentine concentrations in plasma occurred 3 hr postdose in both cases and were 230 and 451 ng/ml following the 2.5- and 5-mg/kg doses, respectively. The approximate mean terminal half-life after all treatments was 12 hr.

Keyphrases □ Meobentine sulfate—plasma levels in humans, radioimmunoassay □ Bioavailability—plasma levels of meobentine sulfate in humans determined by radioimmunoassay □ Radioimmunoassay—plasma levels of meobentine sulfate in humans

Meobentine sulfate [bis-(*N*-4-methoxybenzyl-*N'*-*N''*,dimethylguanidinium)sulfate] possesses marked antidysrhythmic properties against arrhythmias induced by ouabain and those induced by coronary artery ligation in dogs (1). It has been demonstrated that meobentine causes a significant incidence of spontaneous recovery from electrically induced fibrillation in the dog[1]. The electrophysiological properties of meobentine have been studied (2). Although very close in structure to the hypotensive agent, bethanidine (3), meobentine is not a neuronal blocking agent and thus, does not decrease blood pressure in animals when administered intravenously at effective antidysrhythmic doses (1). In this respect, meobentine also appears to be superior to the quaternary ammonium compound bretylium tosylate, which is indicated only for treatment of life-threatening ventricular arrhythmias (4) due to its severe hypotensive side effects.

The clinical safety and efficacy of meobentine sulfate when administered to humans by oral and parenteral routes are currently under study. Pharmacokinetic studies of meobentine in animals and humans, which are needed to facilitate the evaluation of meobentine in current clinical trials, require adequately sensitive and specific procedures for the determination of the drug in body fluids. Earlier gas and thin-layer chromatographic techniques lacked sensitivity, while administration and quantitation of radiolabeled meobentine is impractical for extensive pharmacokinetic studies in humans.

[1] W. Wastila *et al.*, submitted to *J. Pharm. Pharmacol.*

0022-3549/82/0600-0665$01.00/0

Radioimmunoassay methods have been applied increasingly to the quantitation of drugs (5, 6). This report describes the development of sensitive and specific radioimmunoassay procedures for meobentine, employing tritium or radioiodine ligands. The sensitivity limit for the procedure using the ^{125}I-labeled meobentine was <0.4 ng/ml (40-pg mass), while interference with desmethyl metabolites of the drug was minor. These analytical procedures were used to demonstrate the absorption of meobentine after oral administration to healthy subjects and to explore the relationship of plasma concentrations and relative oral bioavailability to the oral dose administered.

EXPERIMENTAL

Chemicals—Thin-layer chromatography (TLC) employed micropolyamide on a nylon support[2] or silica gel[3] on a glass support[4]. Radiochemical purities were determined by scanning thin-layer plates on a radiochromatogram scanner[5]. Bovine serum albumin[6] isobutyl chloroformate[6], Freund's complete adjuvant[7], [^{125}I]sodium iodide[8], and polyethylene glycol 6000[9] were obtained commercially. Methyl isothiocyanate, 4-hydroxybenzaldehyde, and 5% palladium on charcoal were obtained from a single supplier[10], as were chloramine-T and *N*-nitrosomethyl urea[11]. Beta-emitting radionuclides (^{3}H and ^{14}C) were quantitated in scintillation fluid[12] in a scintillation counter[13]. Gamma radiation was quantitated in a spectrometer[14]. *N*-Desmethylmeobentine was a gift[15], as also were guanethidine[16], clonidine[17], guanabenz[18], propranolol[19], isoproterenol[20], and procainamide[21].

Immunogen Preparation—*3-(5-Cyano-2-methoxyphenyl)-propionic Acid (II)*—A mixture of 10 g of 3-(5-bromo-2-methoxyphenyl)propionic acid (I) (7), cuprous cyanide (15 g), and pyridine (20 ml) was heated with stirring in a bath at 200° for 4 hr. The cooled material was triturated with water (150 ml) and filtered, and the solid mass of copper salts was extracted with warm dilute sodium hydroxide solution (2 × 100 ml). Acidification of the combined aqueous filtrates gave 7 g of the crude acid (II) mp 142–146°. Recrystallization from aqueous ethanol and then from benzene raised the mp to 147–148° (4.7 g).

Anal.—Calc. for $C_{11}H_{11}NO_3$: C, 64.39; H, 5.37; N, 6.83. Found: C, 63.53; H, 5.23; N, 6.32.

3-(5-Aminomethyl-2-methoxyphenyl)propionic Acid (III)—A mixture of 4.5 g of the cyano-acid (II) in ammonium hydroxide solution (35%; 30 ml) containing a nickel catalyst[22] (~2 g) was stirred under hydrogen at 10^7 N/m^2 and 100° for 4 hr. The mixture was filtered and the filtrate was evaporated to dryness. The resulting greenish solid was extracted with warm water (3 × 10 ml) and the extracts were freed from nickel salts by passage of H_2S followed by filtration. The amino acid (III), isolated by evaporation *in vacuo*, crystallized from aqueous ethanol in colorless platelets (2.5 g) mp 218–219° (dec).

Anal.—Calc. for $C_{11}H_{15}NO_3$: C, 63.2; H, 7.2; N, 6.7. Found: C, 63.09; H, 7.32; N, 6.78.

3-[2-Methoxy-5-(N′,N″-dimethylguanidinomethyl)phenyl]-propionic Acid (VI)—Methyl isothiocyanate (0.92 g) in ethanol (40 ml) was added to a solution of 2.4 g of the amino acid (III) in 1 *M* NaOH solution (12 ml). Sulfuric acid (0.5 *M*, 12 ml) was added 24 hr later, followed by acetone (100 ml). The solution was filtered from inorganic material and treated with methyl iodide (10 ml). After 1 hr the mixture was evaporated *in vacuo* and the residue was treated with 30% aqueous methylamine solution (40 ml). Gentle warming on a steam bath for 1 hr followed by evaporation to dryness yielded the product as a waxy solid. Recrystallization from isopropyl alcohol and then from water afforded colorless needles, mp 201–204° (0.9 g).

Anal.—Calc. for $C_{14}H_{21}N_3O_3$: C, 56.56; H, 7.80; N, 14.14; $1H_2O$, 6.06. Found: C, 56.23; H, 8.13; N, 13.87; loss at 100°/VAC 6.06.

3-[2-Methoxy-5-(N′,N″-dimethylguanidinomethyl)phenyl]propionic Acid Bovine Serum Albumin-Conjugate—A solution of the guanidino–propionic acid (VI) (0.05 g, 0.168 m*M*) in a warm, 20-ml mixture of dimethyl sulfoxide–dimethylformamide (2:1) was cooled to 0°. Triethylamine (0.035 liter, 0.252 m*M*) and isobutyl chloroformate (0.025 liter, 0.190 m*M*) were added and the solution was stirred for 1 hr at 0°. This cold (0°) solution of the mixed anhydride was added dropwise to a solution of bovine serum albumin (0.080 g, 0.065 m*M* ϵ-amino lysine residues) in 160 ml of a 0.1 *M* sodium bicarbonate solution at 0° and the mixture was stirred overnight at 4°. After filtering insoluble material, the solution was pressure dialysed through a membrane-containing filter unit[23] (50 psi, 2 liter H_2O), and finally lyophilized, yielding an amorphous powder (0.075 g).

Synthesis of Radiolabeled Compounds—*[^{3}H]bis(N-4-methoxybenzyl-N′,N″-dimethylguanidinium)sulfate*—This compound was prepared by a supplier under contract, using general tritium exchange procedures. The specific activity of this compound was estimated to be 0.8 Ci/m*M*.

Bis[N-(3-iodo-125-4-methoxybenzyl)-N′,N″-dimethylguanidinium]-sulfate (VIII).

N-4-Hydroxybenzyl-N′,N″-dimethylguanidinium iodide (VII)—Prepared as described previously (8).

Bis[N-(3-iodo-125,4-hydroxybenzyl)-N′,N″-dimethylguanidinium]sulfate (VIII)—To VII sulfate (2.7 μg, 11.2 n*M*) in phosphate buffer (70 μl, 0.5 *M*, pH 7.7) contained in a small test tube was added carrier-free [^{125}I]sodium iodide (1.12 n*M*, 2 mCi) in 20 μl of dilute sodium hydroxide followed by a freshly prepared solution of chloramine-T (47.25 μg, 0.168 μ*M*) in phosphate buffer (25 μl, 0.05 *M*, pH 7.7). After 1 min of agitation, a freshly prepared solution of sodium metabisulfite (0.64 mg, 3.36 μ*M*) in phosphate buffer (100 μl, 0.05 *M*, pH 7.7) was added to stop the reaction. The entire reaction mixture was then applied to the origin of a micropolyamide TLC plate (0.1 mm, 20 × 20 cm) and allowed to dry.

Bis[N-(3-iodo-125,4-methoxybenzyl)-N′,N″-dimethylguanidinium]-sulfate (IX)—To the origin of the TLC plate containing the iodinated phenolic guanidine VIII was repeatedly applied an ether solution of diazomethane prepared from *N*-nitrosomethyl urea (5 g) (9). The plate was then developed in the system H_2O–triethylamine (100:1) and then allowed to expose an X-ray film. Radioiodine-containing material remaining at the origin was eluted with methanol (3 × 5 ml) and the solution was stored at −80°. The specific activity of the material obtained (1 mCi) was estimated to be 179 Ci/m*M*. Radiochemical purity was established by TLC on silica gel in the system *n*-butanol–methanol–water–acetic acid (4:20:20:10) in which the R_f (0.6) of the iodinated product was identical to that of unlabeled meobentine sulfate.

Immunization Procedures—Male New Zealand white rabbits received a primary immunization of bovine serum albumin-drug conjugate (1 mg) in 0.9% saline (1 ml) emulsified with Freund's complete adjuvant (1 ml) as two intramuscular (vastus lateralis) and eight subcutaneous injections (along each side of the dorsal column) of 0.2 ml each. At intervals of 2, 4, and 6 weeks following the primary immunization, and at monthly intervals thereafter, booster immunizations of immunogen (0.5 mg) in saline (0.5 ml), emulsified with Freund's complete adjuvant (0.5 ml), were administered at multiple subcutaneous sites. Following the second and all subsequent booster immunizations, blood samples were collected from the central ear artery and the serum was separated and stored at −80°.

Clinical Studies—Six healthy subjects (three male and three female) each took 2.5 mg/kg of meobentine sulfate and then 5.0 mg/kg 1 week later. (One male subject did not complete the study at the higher dose.) The drug was administered in 100 ml of water. Plasma was sampled beforehand and at 0.25, 0.5, 0.75, 1, 1.5, 2, 3, 4, 6, 8, 24, 32, 48, and 56 hr afterwards. Samples were taken by collecting 5-ml venous blood into a lithium heparin tube which was immediately centrifuged. The separated plasma was then immediately removed and stored at −20° until assayed.

Radioimmunoassay Procedures—The assay buffer used throughout these studies was 0.05 *M* Na_2HPO_4, 0.15 *M* NaCl, and 0.01 *M* edetic acid,

[2] Schleicher and Schull, Inc., Keene, N.H.
[3] GF_{254}, E. Merck and Co., Elmsford, N.Y.
[4] E. Merck and Co., Elmsford, N.Y.
[5] Berthold LB2760, Beta Analytical Inc., Coraopolis, Pa.
[6] BSA, Cohn Fraction V, Sigma Chemical Co., St. Louis, Mo.
[7] Difco Labs, Detroit, Mich.
[8] Amersham Corp., Arlington Heights, Ill.
[9] Fisher Scientific Co., Raleigh, N.C.
[10] Aldrich Chemical Co., Milwaukee, Wis.
[11] Eastman Organic Chemicals, Rochester, N.Y.
[12] Aquasol-2, New England Nuclear Corp., Boston, Mass.
[13] Model 2650, Packard Instrument Co., Downer's Grove, Ill.
[14] Model 5260 Autogamma, Packard Instrument Co., Downer's Grove, Ill.
[15] Dr. F. Copp, Wellcome Research Labs, Beckenham, U.K.
[16] Ciba-Geigy, Inc., Summit, N.J.
[17] Boehringer-Ingelheim, Ingelheim, West Germany.
[18] Wyeth Labs, Inc., Radnor, Pa.
[19] Ayerst Labs, New York, N.Y.
[20] Winthrop Labs., New York, N.Y.
[21] E. R. Squibb and Sons, Princeton, N.J.
[22] Raney nickel.

[23] PM-10 filter unit, Amicon Corp., Danvers, Mass..

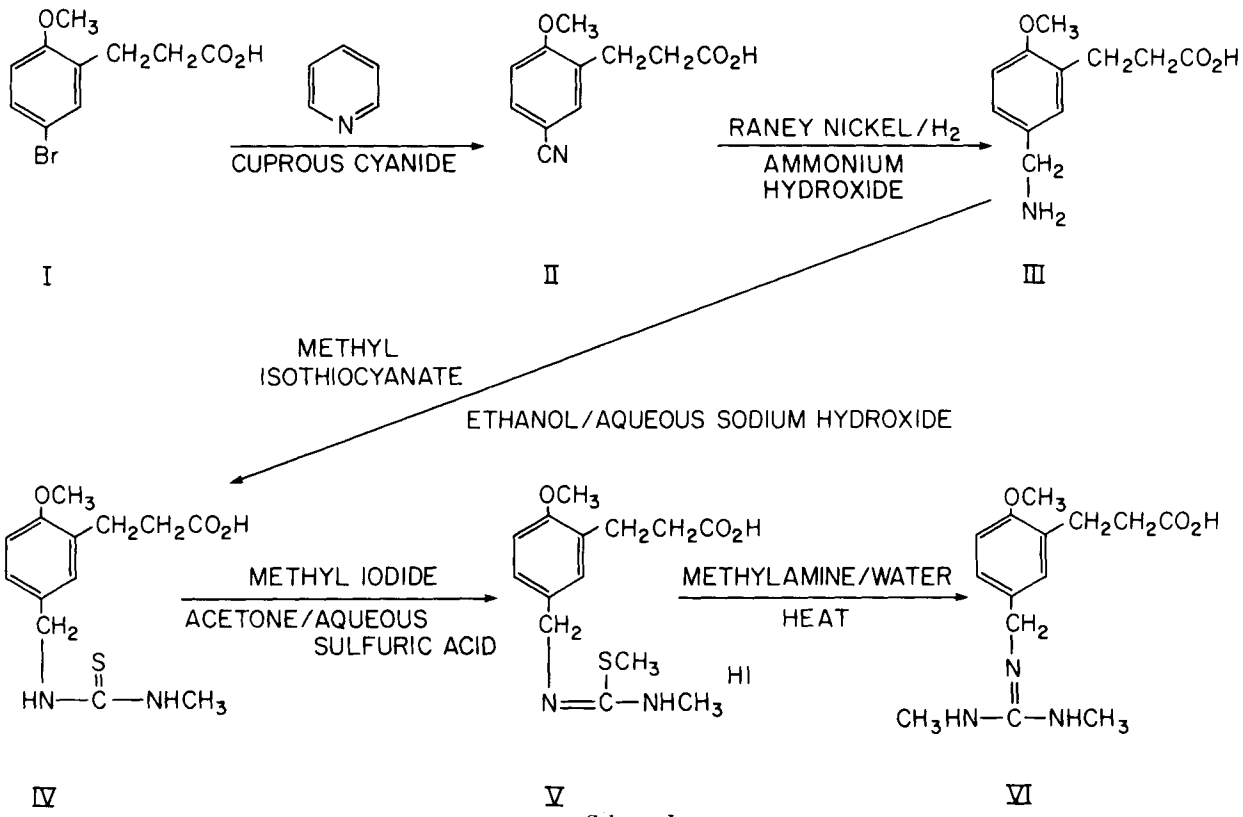

Scheme I

pH 7.0, containing 0.02% bovine serum albumin. Antibody-bound and free radioligand were separated by addition of polyethylene glycol 6000 at a concentration of 130 g/liter in assay buffer. After incubating with the polyethylene glycol 6000 for 30 min at 0°, the immunoglobulins were pelleted by centrifugation (4000×*g*) for 30 min at 4° and the supernate, containing free radioligand, was decanted. For assays employing the tritium label, the immunoglobulin pellet was redissolved in assay buffer (0.3 ml), scintillation fluid was added (3 ml), and the vials capped, mixed, and placed in specially prepared vials for liquid scintillation counting. For assays employing the radioiodine label, the tubes containing the immunoglobulin pellets were placed into a gamma counter. All assay points were established in duplicate. Raw scintillation counter data were automatically entered and stored in a computer file for later processing by computer program. All meobentine concentrations determined by radioimmunoassay are expressed as meobentine-free base, while doses administered are expressed as meobentine sulfate.

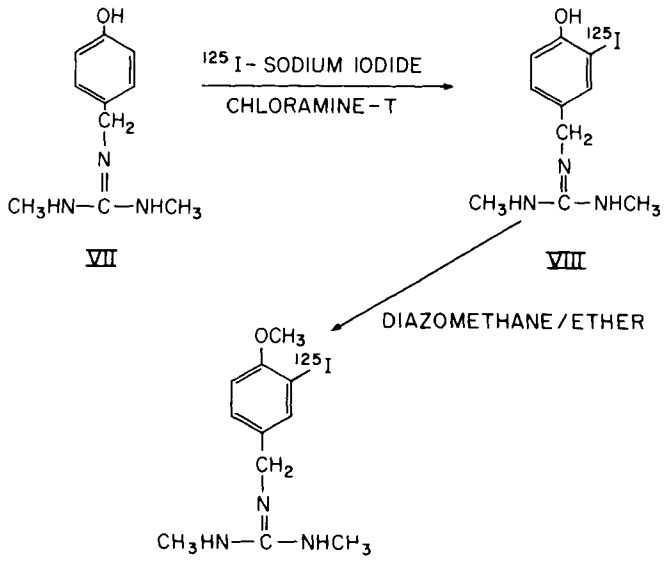

Scheme II

Antiserum Titrations—Varying dilutions of antiserum in assay buffer (0.5 ml) and normal blank plasma (0.1 ml; dog, rat, or human) were incubated with [^{3}H]meobentine (2 ng, 12,000 dpm) in buffer (0.5 ml) or [^{125}I]iodomeobentine (0.25 ng, 40,000 dpm) in buffer (0.5 ml) overnight at 4°. Background-binding tubes contained only radioligand and buffer. Aliquots of polyethylene glycol 6000 solution in assay buffer (1.1 ml) were added to the ice-cold incubation tubes, and the contents were vortex-mixed, incubated at 0° for 30 min, and centrifuged (4000×*g*, 30 min). After decanting the supernates, the immunoglobulin pellets were prepared for either liquid scintillation or gamma counting as described previously. The antiserum titer chosen for use in the radioimmunoassay was defined as that dilution which bound 40% of the total radioligand added.

Antisera Specificity—To determine the specificity of the antisera,

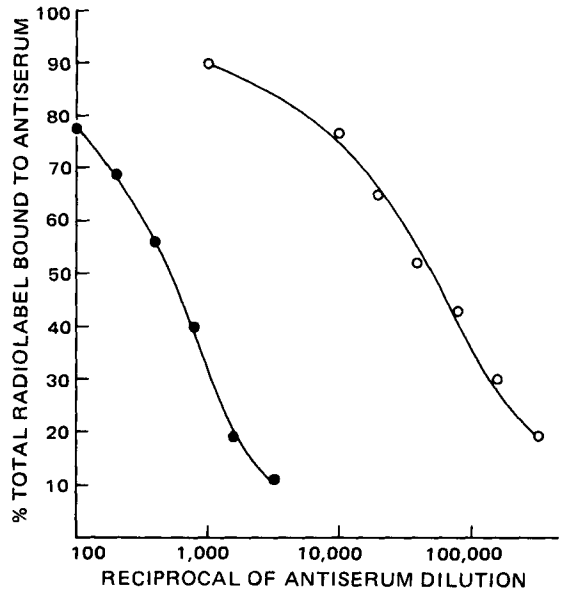

Figure 1—*Titration curves for meobentine antiserum used in the present experiments. Key:* ●, *[^{3}H]meobentine;* ○, *[^{125}I]iodomeobentine.*

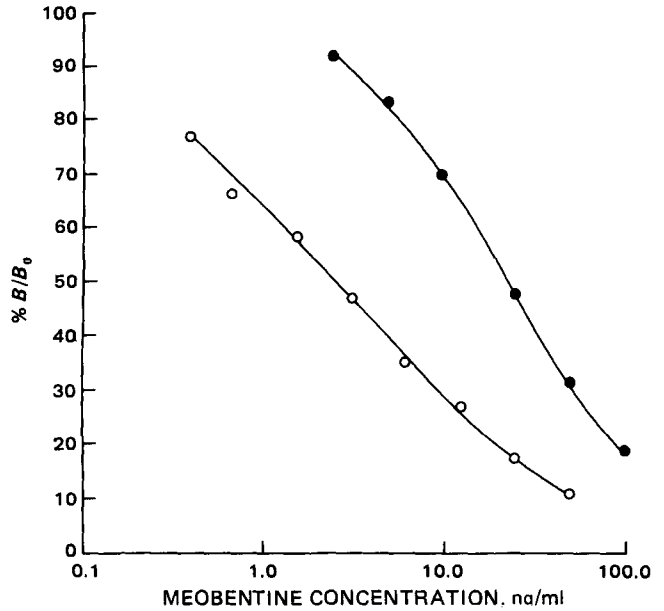

Figure 2—*Meobentine standard curves for tritium and radioiodine radioimmunoassays: mean of 8 curves in each case. Key: ●, [^{3}H]meobentine; ○, [^{125}I]iodomeobentine.*

the 0.1 ml of normal blank plasma added in the previously described procedure was replaced by 0.1 ml of increasing concentrations of meobentine, known metabolites, structurally related compounds, or various cardiovascular drugs in normal blank plasma. Incubation with radioligand and predetermined titer of antisera in assay buffer followed by isolation of the antibody-bound radioligand proceeded as described previously. Standard curves were expressed as percent B/B_0 *versus* log meobentine free base concentration, where B_0 represents the amount (cpm) of labeled meobentine (^{3}H or ^{125}I) bound in the absence of any unlabeled meobentine, and B is the amount bound in the presence of a given drug concentration (corrected for nonspecific binding). The cross-reactivity of each related compound was defined as the percentage ratio of the IC_{50} for meobentine to that of the compound studied, where IC_{50} is the concentration of each respective compound required to inhibit binding of radioligand to antiserum by 50% (10).

Radioimmunoassay of Unknown Plasma Samples—A series of meobentine standard solutions (2.5–250 ng/ml free base equivalents for ^{3}H-radioimmunoassay or 0.39–100 ng/ml for ^{125}I-radioimmunoassay) in normal blank plasma (0.1 ml) was incubated with [^{3}H]meobentine or [^{125}I]iodomeobentine and appropriately diluted antiserum as described previously. Spiked control samples of meobentine in blank plasma (0.1 ml) or unknown plasma samples appropriately diluted with normal blank plasma to enter the assay range were also incubated with radioligand and antiserum. Most unknown samples were assayed at two dilutions. Standard curves were linearized by a logit–log computer transformation of B/B_0 *versus* meobentine concentration data and unknown concentrations were determined by interpolation.

RESULTS

Immunogen Synthesis—A propionic acid analog (VI) of meobentine, with the acid chain attached to the phenyl ring *ortho* to the methoxyl group, was prepared from 3-(5-bromo-2-methoxyphenyl)propionic acid (I) by displacing bromine with cuprous cyanide to give the 5-cyano derivative (II) which was catalytically reduced to the benzylamine (III). The general method of Maxwell and Walton (8) was employed to convert the benzylamine derivative to IV, *via* the intermediates, IV and V. The synthetic scheme is shown in Scheme I. Elemental and spectral analysis established the identity of the hapten, which was coupled to bovine serum albumin by the mixed anhydride approach, described previously (11). No attempt to quantitate the extent of hapten incorporation to the immunogen was made.

Table I—Interassay Accuracy and Precision of Meobentine Radioimmunoassay Procedures

	Tritium Radioimmunoassay			
Spiked concentration[a]	3.0	15.0	30.0	150.0
Mean measured concentration	2.7	14.6	28.8	142.8
Coefficient of variation (n = 14)	11.1	5.5	5.2	6.0
	Radioiodine Radioimmunoassay			
Spiked concentration[a]	0.90	3.0	30.0	
Mean measured concentration	0.86	2.9	33.2	
Coefficient of variation (n = 15)	5.8	8.6	7.5	

[a] Concentration of meobentine sulfate (expressed as ng/ml free base equivalents) added to blank human plasma.

Table II—Cross-Reactivities of Related Compounds in Meobentine Radioimmunoassay Procedures

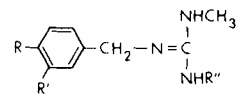

Compound	% Cross-Reactivity: Tritium Assay	% Cross-Reactivity: Radioiodine Assay
Meobentine (R = OCH_3, R′ = H, R″ = CH_3)	100 (IC_{50} = 22 ng/ml)	100 (IC_{50} = 2.2 ng/ml)
Hapten derivative (VI; R = OCH_3, R′ = $(CH_2)_2CO_2H$, R″ = CH_3)	116	340
O-Desmethylmeobentine (R = OH, R′ = H, R″ = CH_3)	4.7	2.3
N-Desmethylmeobentine (R = OCH_3, R′ = R″ = H)	2.4	3.4
Bethanidine (R = R′ = H, R″ = CH_3)	4.7	4.7
4-Methylbethanidine (R = R″ = CH_3, R′ = H)	NT[a]	41.0

Guanethidine, guanabenz, clonidine, bretylium, guanidine, 1,1-dimethylguanidine, *N*,*N*′-dimethylurea, *N*,*N*′-dimethylthiourea, procaine, procainamide, lidocaine, propranolol, isoproterenol, and morphine all showed <0.001% cross-reactivity.

NT—not tested.

Radioligand Syntheses—[^{3}*H*]*Meobentine*—This compound was obtained from meobentine by catalytic exchange of tritium for hydrogen with subsequent removal of labile tritium. The resulting, generally tritiated radioligand had a relatively low specific activity (0.8 Ci/m*M*). This feature limits the usefulness of the radioimmunoassay employing [^{3}H]-meobentine due to low sensitivity and lengthy scintillation counter times.

[^{125}*I*]*Iodomeobentine* (*IX*)—The need for a radioligand with much higher specific activity to enable the development of a more efficient and sensitive radioimmunoassay for meobentine necessitated the synthesis of a meobentine analog containing iodine 125 (Scheme II). An analog (and

Table III—Correlation of Plasma Meobentine Concentrations Determined by ^{3}H- and ^{125}I-Radioimmunoassays[a]

Sample	Meobentine Concentration (ng/ml): ^{3}H-Radioimmunoassay	^{125}I-Radioimmunoassay
Human	255	264
	514	485
	524	390
	512	530
	638	613
	254	238
	294	281
	411	370
	516	556
	475	495
Dog	9909	9341
	2772	2559
	1299	1215
	873	838
	618	538
	273	249
	353	315
	279	274
	256	264
	195	204
Rat	7837	7335
	3335	3478
	6799	6568
	3583	3470
	4097	3900

[a] Linear Regression Analysis Parameters: correlation coefficient = 0.999, slope = 0.949, y-intercept (^{3}H-radioimmunoassay) = 11.6 ng/ml.

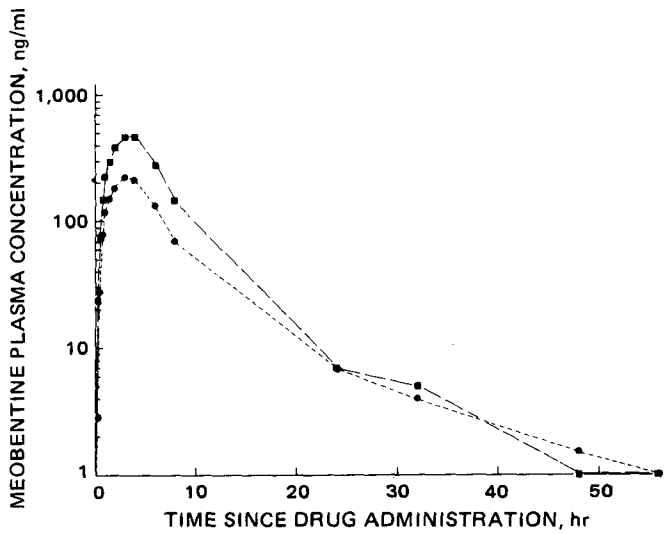

Figure 3—*Mean plasma meobentine concentrations (expressed as free base) following oral administration to normal human volunteers. Key: ●, 2.5 mg/kg (n = 6); ■, 5.0 mg/kg (n = 5).*

metabolite) of meobentine, VII, was synthesized from 4-hydroxybenzylamine (8). The phenol (VII) was *ortho*-iodinated with [^{125}I]sodium iodide by the method of Hunter and Greenwood (12). *In situ* methylation of the iodophenol with diazomethane followed by TLC purification afforded iodomeobentine of high specific activity.

Antisera Production—Two out of three rabbits immunized with the hapten produced useful antisera, detectable within 1 month and steadily increasing in titer with time. The highest titer elicited from the best rabbit was selected for further studies. Excess antibody bound > 90% of either radioligand and the working titers were 1/4000 and 1/100,000 for [^{3}H]-meobentine and [^{125}I]iodomeobentine, respectively (Fig. 1).

Assay Sensitivity and Precision—The sensitivity limit of the radioimmunoassay for meobentine sulfate employing a tritium or radioiodine label (defined as the concentration of unlabeled meobentine producing 10% inhibition of maximal [^{3}H]meobentine or [^{125}I]iodomeobentine binding) was 2.5 or 0.39 ng/ml, respectively. Typical mean standard curves for the two assay procedures are shown in Fig. 2; the coefficient of variation around each standard concentration point was <10%. Further confirmation of interassay precision was provided by the low coefficient of variation around means of assayed spiked plasma controls varying across the range of assay sensitivity (Table I).

Assay Specificity—Specificity data of this antiserum for meobentine, some known metabolites, and structurally related compounds are summarized in Table II for both tritiated and radioiodinated meobentine radioligands. Cross-reactivities with the two known metabolites, *O*-desmethyl and *N*-desmethylmeobentine, were low, being 2–5% in both assays. The desmethoxy analog, bethanidine, also showed relatively low cross-reactivity (5%) while the *para* methyl derivative, *N*-4-methylbenzyl-*N'*,*N''*-dimethylguanidine, was recognized much better by the antiserum, resulting in a higher (40%) cross-reactivity. As expected, the propionic acid hapten derivative (VI) used for the production of the immunizing conjugate was recognized by the antiserum more effectively than meobentine itself. A variety of other structurally related guanidines with (guanethidine, guanabenz, and clonidine) and without (guanidine and dimethylguanidine) substituents on the imino nitrogen atom showed little cross-reactivity. A number of drugs (procaine, procainamide, lidocaine, propranolol, isoproterenol, and morphine), which might be administered to patients concurrently with meobentine sulfate, had cross-reactivities of <0.001% in the radioimmunoassay.

Correlation of Tritiated and Radioiodinated Assay Methods—Since both assay methods were used in the analysis of different phases of the human disposition studies, it was imperative to demonstrate that analysis of given samples by both methods gave the same results. To this end, a number of plasma samples obtained from humans, dogs, and rats after meobentine treatment were analyzed by both methods. The results are shown in Table III. The slope and linear regression coefficient approach unity, indicating good agreement between results from tritiated and radioiodinated methods.

Disposition Studies in Humans—The radioimmunoassay employing [^{3}H]meobentine was used to assay plasma samples from humans who received two separate oral doses (2.5 and 5 mg/kg) of meobentine sulfate in water. Mean plasma levels of meobentine in these subjects are shown in Fig. 3. No detailed pharmacokinetic analysis was performed on these data, but some model-independent mean kinetic parameters are collated in Table IV. Mean observed maximum plasma concentrations were 239 and 451 ng/ml following 2.5 and 5.0-mg/kg doses, respectively (Table IV). The mean area under the plasma concentration–time curve (*AUC*) values increased ~1.8-fold on increasing the dose from 2.5 to 5 mg/kg. Thus, similar trends are evident in C_{max} and *AUC* values. The mean times to observed peak plasma concentration (T_{max}) were 3.3 and 3 hr after each of the 2.5 and 5-mg/kg doses, respectively. Meobentine half-life, as estimated from the limited number of points in the terminal disposition phase, ranged from 9 to 20 hr between individual subjects, while mean values following treatments were ~ 14 and 11 hr.

Table IV—Model-Independent Pharmacokinetic Parameters for Meobentine Sulfate (Mean ± *SD*)

Parameter	Oral Dose Administered	
	2.5 mg/kg (n = 6)	5.0 mg/kg (n = 5)
C_{max}, ng/ml	239.0 ± 68.4	451.0 ± 173.9
T_{max}, hr	3.3 ± 0.5	3.0 ± 0.7
AUC, hr ng/ml	1890 ± 526	3358 ± 1294
TBC/F, liter/hr[a]	78.6 ± 14.9	95.1 ± 29.6

[a] Total body clearance/fraction dose absorbed = dose/area under the curve (*AUC*).

DISCUSSION

Previous investigations have demonstrated the need for conjugation of drugs to macromolecules in order to render them immunogenic (5, 6, 13). In the present study, meobentine was coupled *via* a propionic acid sidechain to bovine serum albumin by a mixed anhydride procedure. Attachment of the 3-carbon bridge was *ortho* to the methoxyl group of meobentine, as shown in Scheme I. Antibodies formed in response to repeated immunization with this substance were used to develop two radioimmunoassay procedures for meobentine. One assay, employing a generally labeled [^{3}H]meobentine ligand, was precise and accurate and showed a sensitivity limit of 2.5 ng/ml (250 pg, actual mass). The use of [^{125}I]iodomeobentine (Scheme II), which had much greater specific activity, considerably increased efficiency and lowered sensitivity limits to <0.4 ng/ml (40 pg, actual mass) while retaining precision and accuracy (Fig. 2 and Table I). Plasma meobentine levels in the rat, dog, and humans following intravenous and oral administration, assayed by the two different procedures, agreed well (Table III). These radioimmunoassay procedures represent a significant advance in sensitivity and convenience over previously available methods for determination of meobentine in plasma. The sensitivity of the procedure using the iodinated radioligand, which is currently in use for analysis of meobentine disposition studies, exceeds that of analytical procedures reported for the related drugs, bethanidine (14) and bretylium (15, 16).

The ability of drug antisera to discern changes in molecular architecture normally is greatest for structural changes at sites distant from the site of attachment of the drug to macromolecular carrier in the immunizing conjugate. The applicability of this statement to the case of meobentine is not complete, as the data in Table II indicate. Thus, 4-methylbethanidine cross-reacts extensively, as expected for a relatively minor structural change close to the site of attachment of hapten to protein. However, the cross-reactivities of bethanidine (4.7%) and *O*-desmethylmeobentine (2.3–4.7%), which also involve relatively minor structural changes at the *para* position, are much lower. It is fortunate that the cross-reactivity of *O*-desmethylmeobentine is low, since this compound appears to be a major metabolite in the rat and dog (17), although the most likely circulating species, the *O*-glucuronide of *O*-desmethylmeobentine, would be expected to cross-react even less. *N*-Desmethylmeobentine, a lesser metabolite in the rat and dog (17), has lower cross-reactivity. The *O*-desmethoxy analog, bethanidine, while undergoing significant *N*-dealkylation in the rat and dog, has been reported to be excreted largely unchanged by humans (18). Bethanidine is not well recognized by the antiserum, while the 4-methyl analog binds strongly to the antibodies, indicating the sensitivity to changes in molecular charge localization and lipophilicity. A wide range of structurally similar guanidines and other cardiovascular drugs and potentially concurrently administered medications did not cross-react.

The applicability of the present radioimmunoassay techniques to pharmacokinetic studies is shown by the data in Fig. 3. Plasma levels 56 hr after a single oral dose could still be measured reliably by the [^{3}H]-meobentine assay, which was used for analysis of plasma samples in the

human studies described in this paper. The higher sensitivity and greater convenience of the [^{125}I]-based assay have resulted in its use in current meobentine studies. The plasma profile in the subjects studied indicated that meobentine kinetics are multicompartmental in nature with a long terminal half-life (11–14 hr). A long terminal half-life has also been seen with bethanidine (18) and bretylium (19) in humans. Mean peak meobentine plasma levels in the same group of volunteers essentially doubled from 239 to 451 ng/ml with an increase in dose from 2.5 to 5.0 mg/kg. Mean area under the curve also approximately doubled from 1890 to 3358 ng hr/ml over this dose range. These observations suggest linear kinetics for meobentine in the 2.5–5-mg/kg dose range. Clearance (TBC/F) did not change significantly with increasing dose. The extent of absorption and bioavailability of meobentine are currently under investigation in animals and humans. The related guanidine, bethanidine, has been reported to be well absorbed by humans (18).

Currently, these radioimmunoassay procedures are being applied to detailed studies of the disposition of meobentine sulfate in animals and humans. Studies of the absolute oral bioavailability and pharmacokinetics of meobentine sulfate will be presented elsewhere in the near future.

REFERENCES

(1) K. B. Touw, W. B. Wastila, F. C. Copp, and R. A. Maxwell, *Pharmacologist*, **19,** 173 (1977).

(2) C. Wang, C. James, and R. A. Maxwell, *ibid.*, **19,** 153 (1977).

(3) R. Wilson, C. Long, and W. S. Jagoe, *J. Ir. Med. Assoc.*, **56,** 9 (1965).

(4) J. Koch-Weser, *N. Engl. J. Med.*, **300,** 473 (1979).

(5) J. Landon and A. C. Moffat, *Analyst*, **101,** 225 (1976).

(6) V. P. Butler, *Pharmacol. Rev.*, **29,** 103 (1975).

(7) R. A. Barnes, E. R. Kraft, and L. Gordon, *J. Am. Chem. Soc.*, **71,** 3523 (1949).

(8) R. A. Maxwell and E. Walton, U.S. pat. 3,968,243 (1976).

(9) L. F. Fieser and M. Fieser, "Reagents for Organic Synthesis," vol. 1, Wiley, New York, N.Y., 1967, p. 192.

(10) G. E. Abraham, *J. Clin. Endocrinol. Metab.*, **29,** 866 (1969).

(11) R. Dixon, K. E. Fahrenholtz, W. Burger, and C. Perry, *Res. Commun. Chem. Pathol. Pharmacol.*, **16,** 121 (1977).

(12) W. M. Hunter and F. C. Greenwood, *Nature*, **194,** 495 (1962).

(13) B. F. Erlanger, *Pharmacol. Rev.*, **25,** 271 (1973).

(14) C. N. Corder, T. S. Klaniecki, R. H. McDonald, and C. Berlin, *J. Pharm. Sci.*, **64,** 785 (1975).

(15) C.-M. Lai, B. L. Kamath, J. E. Carter, P. Erhardt, Z. M. Look, and A. Yacobi, *ibid.*, **69,** 681 (1980).

(16) E. Patterson, P. Stetson, and B. R. Lucchesi, *J. Chromatogr.*, **181,** 33 (1980).

(17) J. T. Warren, R. M. Welch, and J. W. A. Findlay, *Pharmacologist*, **22,** 189 (1980).

(18) L. B. Turnbull, L. Teng, J. Newman, A. N. Chremos, and R. B. Bruce, *Drug Metab. Dispos.*, **4,** 269 (1976).

(19) J. L. Anderson, E. Patterson, J. G. Wagner, J. R. Stewart, M. L. Behm, and B. R. Lucchesi, *Clin. Pharmacol. Ther.*, **28,** 468 (1980).

(20) J. T. Warren, G. G. Coker, R. M. Welch, A. S. E. Fowle, and J. W. A. Findlay, *Pharmacologist*, **21,** 207 (1979).

ACKNOWLEDGMENTS

Presented in part, in preliminary form, at the ASPET Fall Meeting, Portland, Ore., August 1979 (20).

Automated Sampling of *In Vitro* Dissolution Medium: Effect of Sampling Probes on Dissolution Rate of Prednisone Tablets

THOMAS S. SAVAGE *x and CLYDE E. WELLS ‡

Received June 8, 1981, from the **Food and Drug Administration, Los Angeles, CA 90015*, and the ‡*National Center for Drug Analysis, St. Louis, MO 63101.* Accepted for publication September 18, 1981.

Abstract □ The effect of sampling probe size and location on the *in vitro* dissolution rate of prednisone tablets was examined. Using USP XX Apparatus 2 with an automated sampling system, dissolution rates were determined using two types of large filter-tipped probes and a small capillary probe. Each probe was tested at three locations within the kettle. The large probes caused hydrodynamic changes which, when compared with results obtained through manual sampling, resulted in significant changes in dissolution rates at each location. These changes were less evident when the capillary probe was used, with an insignificant difference between results of automated and manual sampling when the capillary probe was placed midway between the paddle shaft and the kettle wall.

Keyphrases □ Dissolution rates—effect of sampling probe size and location on dissolution rate of prednisone tablets □ Hydrodynamics—dissolution rates affected by sampling probe size and location, USP paddle method □ Prednisone—tablets in dissolution rate testing with effects of sampling probe size

Automated sampling and analysis of *in vitro* dissolution aliquots can be a useful, timesaving procedure. Several automated sampling systems are commercially available in which aliquots of the dissolution fluid, taken at specified times, travel into sample cups or into an automated analytical system. Results of such a system are not generally considered acceptable, however, unless they agree with those obtained by manual sampling.

A large number of dissolution testing variables have been identified (1). These need to be strictly controlled if reproducible results are to be obtained. Changes in any of these variables can have a significant effect on the dissolution rate of a dosage form. A previous study (2) showed that the dissolution rate is affected by the effects of various dissolution parameters on the hydrodynamics of the dissolution fluid. Another study (3) showed that the hydrodynamic disturbance caused by insertion of a relatively large object, such as a thermometer, into the dissolution fluid may cause a change in dissolution rate, and that the location of such an object can also have a significant effect.

With most automated sampling systems now in use, a relatively large filter-tipped probe is immersed in the dissolution fluid. The above studies imply that a large probe can affect the system hydrodynamics, and therefore the dissolution rate of some dosage forms, thereby causing results which differ from those obtained by manual sampling, and that a smaller probe may have less effect on the

0022-3549/82/0600-0670$01.00/0

human studies described in this paper. The higher sensitivity and greater convenience of the [^{125}I]-based assay have resulted in its use in current meobentine studies. The plasma profile in the subjects studied indicated that meobentine kinetics are multicompartmental in nature with a long terminal half-life (11–14 hr). A long terminal half-life has also been seen with bethanidine (18) and bretylium (19) in humans. Mean peak meobentine plasma levels in the same group of volunteers essentially doubled from 239 to 451 ng/ml with an increase in dose from 2.5 to 5.0 mg/kg. Mean area under the curve also approximately doubled from 1890 to 3358 ng hr/ml over this dose range. These observations suggest linear kinetics for meobentine in the 2.5–5-mg/kg dose range. Clearance (TBC/F) did not change significantly with increasing dose. The extent of absorption and bioavailability of meobentine are currently under investigation in animals and humans. The related guanidine, bethanidine, has been reported to be well absorbed by humans (18).

Currently, these radioimmunoassay procedures are being applied to detailed studies of the disposition of meobentine sulfate in animals and humans. Studies of the absolute oral bioavailability and pharmacokinetics of meobentine sulfate will be presented elsewhere in the near future.

REFERENCES

(1) K. B. Touw, W. B. Wastila, F. C. Copp, and R. A. Maxwell, *Pharmacologist*, **19,** 173 (1977).

(2) C. Wang, C. James, and R. A. Maxwell, *ibid.*, **19,** 153 (1977).

(3) R. Wilson, C. Long, and W. S. Jagoe, *J. Ir. Med. Assoc.*, **56,** 9 (1965).

(4) J. Koch-Weser, *N. Engl. J. Med.*, **300,** 473 (1979).

(5) J. Landon and A. C. Moffat, *Analyst*, **101,** 225 (1976).

(6) V. P. Butler, *Pharmacol. Rev.*, **29,** 103 (1975).

(7) R. A. Barnes, E. R. Kraft, and L. Gordon, *J. Am. Chem. Soc.*, **71,** 3523 (1949).

(8) R. A. Maxwell and E. Walton, U.S. pat. 3,968,243 (1976).

(9) L. F. Fieser and M. Fieser, "Reagents for Organic Synthesis," vol. 1, Wiley, New York, N.Y., 1967, p. 192.

(10) G. E. Abraham, *J. Clin. Endocrinol. Metab.*, **29,** 866 (1969).

(11) R. Dixon, K. E. Fahrenholtz, W. Burger, and C. Perry, *Res. Commun. Chem. Pathol. Pharmacol.*, **16,** 121 (1977).

(12) W. M. Hunter and F. C. Greenwood, *Nature*, **194,** 495 (1962).

(13) B. F. Erlanger, *Pharmacol. Rev.*, **25,** 271 (1973).

(14) C. N. Corder, T. S. Klaniecki, R. H. McDonald, and C. Berlin, *J. Pharm. Sci.*, **64,** 785 (1975).

(15) C.-M. Lai, B. L. Kamath, J. E. Carter, P. Erhardt, Z. M. Look, and A. Yacobi, *ibid.*, **69,** 681 (1980).

(16) E. Patterson, P. Stetson, and B. R. Lucchesi, *J. Chromatogr.*, **181,** 33 (1980).

(17) J. T. Warren, R. M. Welch, and J. W. A. Findlay, *Pharmacologist*, **22,** 189 (1980).

(18) L. B. Turnbull, L. Teng, J. Newman, A. N. Chremos, and R. B. Bruce, *Drug Metab. Dispos.*, **4,** 269 (1976).

(19) J. L. Anderson, E. Patterson, J. G. Wagner, J. R. Stewart, M. L. Behm, and B. R. Lucchesi, *Clin. Pharmacol. Ther.*, **28,** 468 (1980).

(20) J. T. Warren, G. G. Coker, R. M. Welch, A. S. E. Fowle, and J. W. A. Findlay, *Pharmacologist*, **21,** 207 (1979).

ACKNOWLEDGMENTS

Presented in part, in preliminary form, at the ASPET Fall Meeting, Portland, Ore., August 1979 (20).

Automated Sampling of *In Vitro* Dissolution Medium: Effect of Sampling Probes on Dissolution Rate of Prednisone Tablets

THOMAS S. SAVAGE *x and CLYDE E. WELLS ‡

Received June 8, 1981, from the **Food and Drug Administration, Los Angeles, CA 90015*, and the ‡*National Center for Drug Analysis, St. Louis, MO 63101.* Accepted for publication September 18, 1981.

Abstract □ The effect of sampling probe size and location on the *in vitro* dissolution rate of prednisone tablets was examined. Using USP XX Apparatus 2 with an automated sampling system, dissolution rates were determined using two types of large filter-tipped probes and a small capillary probe. Each probe was tested at three locations within the kettle. The large probes caused hydrodynamic changes which, when compared with results obtained through manual sampling, resulted in significant changes in dissolution rates at each location. These changes were less evident when the capillary probe was used, with an insignificant difference between results of automated and manual sampling when the capillary probe was placed midway between the paddle shaft and the kettle wall.

Keyphrases □ Dissolution rates—effect of sampling probe size and location on dissolution rate of prednisone tablets □ Hydrodynamics—dissolution rates affected by sampling probe size and location, USP paddle method □ Prednisone—tablets in dissolution rate testing with effects of sampling probe size

Automated sampling and analysis of *in vitro* dissolution aliquots can be a useful, timesaving procedure. Several automated sampling systems are commercially available in which aliquots of the dissolution fluid, taken at specified times, travel into sample cups or into an automated analytical system. Results of such a system are not generally considered acceptable, however, unless they agree with those obtained by manual sampling.

A large number of dissolution testing variables have been identified (1). These need to be strictly controlled if reproducible results are to be obtained. Changes in any of these variables can have a significant effect on the dissolution rate of a dosage form. A previous study (2) showed that the dissolution rate is affected by the effects of various dissolution parameters on the hydrodynamics of the dissolution fluid. Another study (3) showed that the hydrodynamic disturbance caused by insertion of a relatively large object, such as a thermometer, into the dissolution fluid may cause a change in dissolution rate, and that the location of such an object can also have a significant effect.

With most automated sampling systems now in use, a relatively large filter-tipped probe is immersed in the dissolution fluid. The above studies imply that a large probe can affect the system hydrodynamics, and therefore the dissolution rate of some dosage forms, thereby causing results which differ from those obtained by manual sampling, and that a smaller probe may have less effect on the

0022-3549/82/0600-0670$01.00/0

Table 1—Tape Program for Automated Dissolution Sampling System

Time, min	Peristaltic Valve Position	Function
0	1	Start
29:15	2	Sample
31:00	3	Wash
32:00	4	Standard
33:15	5	Empty Coil 1
34:30	6	Empty Coil 2
35:45	7	Empty Coil 3
37:00	8	Empty Coil 4
38:15	9	Empty Coil 5
39:30	10	Empty Coil 6
40:45	11	Wash
42:00	12	Stop

dissolution rate. A previous study (4) confirmed this implication by showing that manual aliquots taken while a large probe was suspended in the dissolution fluid gave higher results than those obtained when a small capillary probe or no probe was present.

In the work described in this paper, the effect of sampling probe size and probe location within the dissolution kettle were investigated by using an automated sampling system to collect aliquots through probes of several sizes and by comparing these results with those obtained by manual sampling.

EXPERIMENTAL

Principles—Dissolution testing was performed using the USP (5) method on a sample of 10-mg prednisone tablets which had been shown to be sensitive to changes in dissolution testing parameters[1]. Using an automated sampling system, samples were withdrawn at 30 min, sequentially diluted with water, and passed through a spectrophotometer flowcell, with absorbance measured at 242 nm. For comparison, manual samples were taken from separate dissolution runs, filtered, and determined spectrophotometrically.

The dissolution apparatus[2] was USP XX Apparatus 2 (6). Paddle rotation speed was maintained at 50 rpm with a gear plate. Temperature was maintained at 37.0 ± 0.5° using a heater-circulator[3] immersed in the water bath.

The automated sampling and analysis system[4] consisted of a multichannel peristaltic valve; plattered manifold for storage; and sequential analysis of sampled aliquots, tape programmer, peristaltic pump, spectrophotometer (set at 242 nm) with a 15-mm flowcell, and recorder. The apparatus was programmed according to Table I. This program allowed for sampling from each dissolution kettle at 30 min, with each aliquot being stored in a separate holding coil. A portion of standard solution was then introduced to the analytical system followed by sequential introduction of the contents of each sample storage coil. The schematic diagram in Fig. 1 shows the postsampling analytical system.

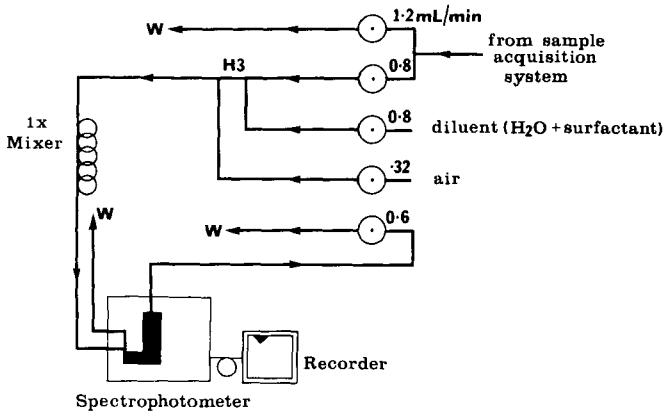

Figure 1—*Flow diagram for postsampling analytical system. All pump tubes are Tygon; all transmission tubing is trifluoroethylene, 1.0-mm i.d.; W indicates flow to waste reservoir.*

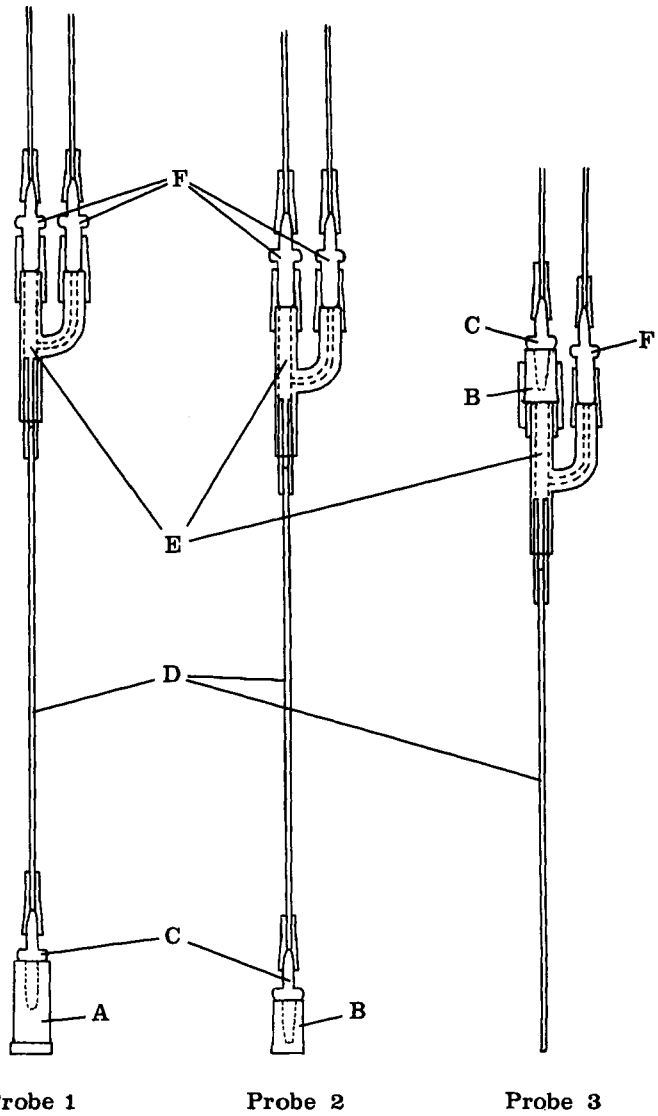

Figure 2—*Three types of probes used in automated sampling. Key: A, filter; B, filter; C, N7 nipple connector; D, glass capillary tube, size 0.8–1.10 × 100 mm; E, D1 "h"-connector; F, N5 nipple connector. Parts are connected to each other with sleeves of rubber tubing.*

The three types of sampling probes used with the automated sampling system are shown in Fig. 2. In Probes 1 and 2, commercially available filters[5,6] were attached to glass stalks connected to the "h"-connectors in the automated sampling system. The filters and stalks were suspended in the dissolution fluid throughout the dissolution run. In Probe 3, the glass stalk connected to the "h"-connector was extended into the dissolution fluid. The filter was attached "downstream" from the connector. Maximum immersed diameters for Probes 1, 2, and 3 were 8.0, 7.2, and 1.5 mm, respectively. Displacements of the immersed portions of the three probes were 1.1, 0.7, and 0.1 ml, respectively.

Manual sampling was performed using 50-ml syringes with 14-gauge needles. Aliquots were filtered through p 0.8-μm porosity membrane filters[7] and analyzed spectrophotometrically.

Reagents and Standards—Distilled water, deaerated by stirring under reduced pressure for 2 hr was used as the dissolution fluid.

[1] Cox, D. C., personal communication.
[2] Easi-Lift model 72-S, Hanson Research Co., Northridge, Calif.
[3] Braun Thermomix model 1441, VWR Scientific, Norwalk, Calif.
[4] Sample Acquisition System for Dissolution Rate Analysis (SASDRA) with Quality Control Manifold, Technicon Instruments Corp., Tarrytown, N.Y.
[5] No. 178-3985-P01 (Filter A), Technicon Instruments Corp., Tarrytown, N.Y.
[6] No. FT-6006 (Filter B), Centaur Chemical Co., Stamford, Conn.
[7] No. AAWP-02500, Millipore Corp., Bedford, Mass.

Table II—Results of Dissolution Testing of Prednisone Tablets, Percent of Label Declaration

Sampling System	Sampling Location A Mean	A SD	A N[a]	B Mean	B SD	B N	C Mean	C SD	C N
Manual	34.5	2.1	18	36.5	3.1	35	36.3	2.3	17
Automated, Probe 1	44.9	4.3	18	43.3	3.4	27	32.7	4.6	24
Automated, Probe 2		NT[b]		43.1	2.4	12		NT	
Automated, Probe 3	38.1	3.1	18	36.7	3.3	52	34.5	3.3	18

[a] Number of aliquots taken. [b] Not tested.

The diluent used in the automated analysis was prepared by adding 1 ml of surfactant[8] to 1 liter of water.

The standard stock solution was prepared by dissolving 25 mg of prednisone USP Reference Standard in 20 ml of ethyl alcohol and diluting to 500 ml with water. A working standard was prepared daily by diluting a 10-ml standard stock solution to 100 ml with water.

Procedure—Before the automated sampling system was used, all lines and coils were filled with their respective solutions, and the system was allowed to equilibrate by running in the "wash" position for ~30 min. To start the dissolution run, the peristaltic valve was set in Position 1, and the dissolution apparatus was turned on. With all paddles rotating and sampling probes in the proper positions within the kettle, tablets were dropped simultaneously into all kettles and the programmer was turned on. After the 30-min sample aliquot collection (with the peristaltic valve in Position 3), the probes were removed from the kettles and placed in a beaker of water until the end of the analysis.

Dissolution testing was performed with samples withdrawn either manually or by automation from one of the three positions shown in Fig. 3. Position A is 0–1 cm from the wall of the vessel, Position B is midway between the kettle wall and the paddle shaft, ±0.5 cm, and Position C is 0–1 cm from the paddle shaft. The vertical location of all three probe positions is midway between the surface of the dissolution fluid and the level of the top of the paddle blade. Position B is the generally accepted position for manual sampling (1).

RESULTS AND DISCUSSION

Accuracy and reproducibility of the automated system were tested by running the system with the probes immersed in standard solution concentration of 7.08 μg/ml, equivalent to 35.4% of the declared tablet content dissolved. Each set of sampling probes was tested in this manner, with two runs of 6 aliquots/run made for each probe. Recoveries were 102.6, 101.7, and 101.4%, with coefficients of variation of 0.408, 0.554, and 0.796 for Probes 1, 2, and 3, respectively. Linearity was tested by aspirating standard solutions of 1.6, 3.2, 4.8, 6.4, 7.8, and 9.6 μg/ml, equivalent to 8.0–48.0% of the declared tablet content dissolved, using each of the three types of sampling probes. The response was linear throughout this range for each type of probe.

Dissolution testing of prednisone tablets was performed, with aliquots taken from each of the three kettle locations. Sampling was done automatically, using the three automated sampling probes, and manually. Results are summarized in Table II.

Statistical comparisons of dissolution results using each of the automated sampling probes with results obtained by manual sampling indicated a significant effect of the size of the probe. When aliquots were taken from the generally recommended Position B, each of the larger probes (Probes 1 and 2) gave significantly higher results than those of manual sampling when the t criterion was used at the 1% level of significance. The difference between the results using the smaller Probe 3 and the manual results was insignificant. In Position A, automated sampling with all probes gave significantly higher results than manual sampling, although the results with the larger probes were much higher than with the smaller. A different hydrodynamic effect was seen, however, when automated sample probes were suspended in Position C. Automated results from this position were lower than those obtained by manual sampling, with the lowering effect being more pronounced with the larger probes.

By subjecting the manual sampling data for the three sampling positions to a two-way analysis of variance at the 2% level of significance, it was shown that there was no significant difference among the three mean percentages dissolved, thereby indicating that no significant horizontal concentration gradient existed within the kettle. The observed changes in dissolution rates obtained by automated sampling were, therefore, caused by interference by the sampling probes with the hydrodynamic flow within the kettle. The degree of interference was directly related to the size of the probe as well as to its location.

The hydrodynamic change caused by insertion of the large probes was confirmed by visual observation. The normal disintegration of the prednisone tablets within the dissolution kettle formed a regular cone-shaped pile of undissolved tablet material, with a small amount of material dispersed throughout the medium. Extension of the large Sampling Probe 1 into the medium at Position B caused an immediate shifting of the conical pile to one side, followed by the dispersal of considerably more tablet material throughout the medium. This dispersal would account for the higher dissolution results obtained. The effect was more pronounced when the probe was extended into Position A. With the large probe in Position C, the conical pile became taller and narrower, with an apparent decrease in the amount of dispersed material accounting for the lower dissolution results. The insertion of the capillary probe into any of the three positions caused little or no visible disturbance of the undissolved tablet material.

CONCLUSIONS

The large sampling probes provided with several commercially available automated dissolution sampling systems were shown to cause significant hydrodynamic disturbances, resulting in changes in the dissolution rate of a sample of prednisone tablets. The disturbances were reduced through the use of a small capillary probe. Probe location within the kettle was also shown to require careful control. While only one type of tablet was used in this study, the changes in dissolution hydrodynamics caused by the sampling probe could be expected to affect the dissolution

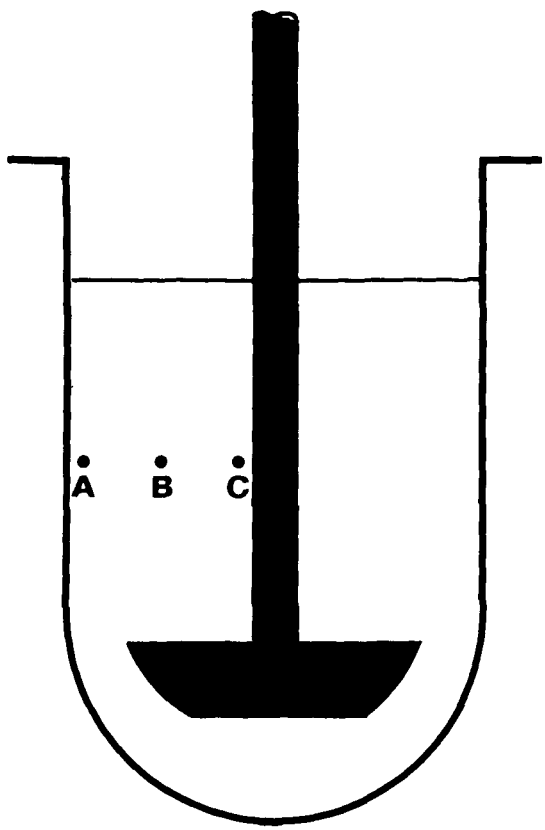

Figure 3—*Three probe locations used in dissolution sampling.*

[8] Brij-35, 30% aqueous solution, Fisher Scientific Co., Fair Lawn, N.J.

rate of other types of dosage forms. It is therefore recommended that the sampling probes used with automated sampling systems be made as small as possible, and that the horizontal sampling position be carefully maintained halfway between the paddle shaft and the kettle wall.

REFERENCES

(1) D. C. Cox, C. C. Douglas, W. B. Furman, R. D. Kirchhoefer, J. W. Myrick, and C. E. Wells, *Pharm. Technol.*, **2**, 40 (1978).

(2) F. L. Underwood and D. E. Cadwallader, *J. Pharm. Sci.*, **65**, 697 (1976).

(3) M. Lagas and C. F. Lerk, *Pharm. Weekbl.*, **113**, 1277 (1978).

(4) C. E. Wells, *J. Pharm. Sci.*, **70**, 232 (1981).

(5) "The United States Pharmacopeia," 20th rev., Mack Publishing Co., Easton, Pa., 1975, p. 655.

(6) *Ibid.*, p. 959.

Sequential Organ First-Pass Effects: Simple Methods for Constructing Compartmental Pharmacokinetic Models from Physiological Models of Drug Disposition by Several Organs

JAMES R. GILLETTE

Received April 22, 1981, from the *Laboratory of Chemical Pharmacology, National Heart, Lung, and Blood Institute, National Institutes of Health, Bethesda, MD 20205.* Accepted for publication September 22, 1981.

Abstract □ The relationships between organ clearances derived from physiological pharmacokinetic models and the first-order rate constants in compartmental pharmacokinetic models are frequently difficult to visualize when drugs are eliminated simultaneously by several organs. Two simple methods for showing these relationships are illustrated in this paper.

Keyphrases □ Pharmacokinetics—construction of compartmental models from physiological models of drug disposition, first-pass effects □ First-pass effects—construction of compartmental pharmacokinetic models from physiological models of drug disposition □ Compartmental models—construction of pharmacokinetic models from physiological models of drug disposition, first-pass effects

Changes in the blood concentrations of drugs after their oral administration are frequently fitted to a pharmacokinetic equation representing a three-compartment model in which it is assumed that all eliminating organs are within the central compartment. In such a model, a first-order rate constant (k_{31}) is frequently used to represent the absorption of a drug from the GI tract into a central compartment and first-order microconstants (k_{12}, k_{21}) are frequently used to represent the passage of the drug between the central and peripheral compartments. The elimination of the drug from the body is represented by a first-order microconstant (k_{10}) emanating solely from the central compartment. This model would be identical to that pictured in Fig. 1 except that k_{13}, k_{20}, and k_{30} would be zero.

Despite the simplicity of this model, it adequately describes the major events in the absorption and disposition of most drugs and, thus, has gained wide acceptance. But it is invalid in many situations, particularly those in which drugs are very rapidly cleared by enzymes in the GI mucosa, liver, and lung (the first-pass organs) and those situations in which the drug passes into the GI tract by reversible diffusion from mucosal blood into the lumen of the GI tract or by biliary excretion. Moreover, the model also fails to describe adequately the pharmacokinetics of metabolites that are rapidly cleared by various organs. In these situations it is necessary to consider physiological models.

Several years ago, Bischoff and Dedrick (1) developed a physiological approach in which Fick's Principle is applied to individual organs. In this approach, each organ comprises three homogeneous compartments: the blood, the interstitial fluid, and an intracellular compartment. Since a differential equation is required to express the rate of change in the amount of drug in these subcompartments of each organ, the number of equations required to describe changes in the disposition of the drug in the body at any given time can be quite large; frequently as many as 15–20 equations are used. It is possible to integrate a set of such equations by means of LaPlace transforms. Unfortunately, the pharmacokinetic constants obtained by integration of the simultaneous equations or from measurements of drug concentrations in blood are virtually impossible to interpret in physiological terms.

The present paper describes a general approach for developing pharmacokinetic models that combine some of the complexities that can occur during rapid simultaneous elimination of drugs by several organs with the simplicity of the linear three-compartment model. The approach is essentially intuitive and, thus, requires very little mathematical ability. It is illustrated by a model in which a drug is rapidly cleared by the GI mucosa, the liver, the lungs, and the kidneys.

THEORY

As in the three-compartment model, it is assumed that after rapid injection into the aorta, a drug is almost instantaneously distributed into a central compartment that includes most of the organs of elimination such as the kidneys, the GI mucosa, the liver, and the lungs. Thus, by the time the arterial concentration of the drug is estimated, the ratios of the intracellular concentrations of the drug in the organs included within the central compartment to the drug concentration in arterial blood have reached constant values. (This is usually estimated indirectly by measuring the drug concentration in systemic venous blood: draining a nonelimination organ such as an arm.) Under these quasi steady-state

0022-3549/82/0600-0673$01.00/0

rate of other types of dosage forms. It is therefore recommended that the sampling probes used with automated sampling systems be made as small as possible, and that the horizontal sampling position be carefully maintained halfway between the paddle shaft and the kettle wall.

REFERENCES

(1) D. C. Cox, C. C. Douglas, W. B. Furman, R. D. Kirchhoefer, J. W. Myrick, and C. E. Wells, *Pharm. Technol.*, **2**, 40 (1978).

(2) F. L. Underwood and D. E. Cadwallader, *J. Pharm. Sci.*, **65**, 697 (1976).

(3) M. Lagas and C. F. Lerk, *Pharm. Weekbl.*, **113**, 1277 (1978).

(4) C. E. Wells, *J. Pharm. Sci.*, **70**, 232 (1981).

(5) "The United States Pharmacopeia," 20th rev., Mack Publishing Co., Easton, Pa., 1975, p. 655.

(6) *Ibid.*, p. 959.

Sequential Organ First-Pass Effects: Simple Methods for Constructing Compartmental Pharmacokinetic Models from Physiological Models of Drug Disposition by Several Organs

JAMES R. GILLETTE

Received April 22, 1981, from the *Laboratory of Chemical Pharmacology, National Heart, Lung, and Blood Institute, National Institutes of Health, Bethesda, MD 20205.* Accepted for publication September 22, 1981.

Abstract □ The relationships between organ clearances derived from physiological pharmacokinetic models and the first-order rate constants in compartmental pharmacokinetic models are frequently difficult to visualize when drugs are eliminated simultaneously by several organs. Two simple methods for showing these relationships are illustrated in this paper.

Keyphrases □ Pharmacokinetics—construction of compartmental models from physiological models of drug disposition, first-pass effects □ First-pass effects—construction of compartmental pharmacokinetic models from physiological models of drug disposition □ Compartmental models—construction of pharmacokinetic models from physiological models of drug disposition, first-pass effects

Changes in the blood concentrations of drugs after their oral administration are frequently fitted to a pharmacokinetic equation representing a three-compartment model in which it is assumed that all eliminating organs are within the central compartment. In such a model, a first-order rate constant (k_{31}) is frequently used to represent the absorption of a drug from the GI tract into a central compartment and first-order microconstants (k_{12}, k_{21}) are frequently used to represent the passage of the drug between the central and peripheral compartments. The elimination of the drug from the body is represented by a first-order microconstant (k_{10}) emanating solely from the central compartment. This model would be identical to that pictured in Fig. 1 except that k_{13}, k_{20}, and k_{30} would be zero.

Despite the simplicity of this model, it adequately describes the major events in the absorption and disposition of most drugs and, thus, has gained wide acceptance. But it is invalid in many situations, particularly those in which drugs are very rapidly cleared by enzymes in the GI mucosa, liver, and lung (the first-pass organs) and those situations in which the drug passes into the GI tract by reversible diffusion from mucosal blood into the lumen of the GI tract or by biliary excretion. Moreover, the model also fails to describe adequately the pharmacokinetics of metabolites that are rapidly cleared by various organs. In these situations it is necessary to consider physiological models.

Several years ago, Bischoff and Dedrick (1) developed a physiological approach in which Fick's Principle is applied to individual organs. In this approach, each organ comprises three homogeneous compartments: the blood, the interstitial fluid, and an intracellular compartment. Since a differential equation is required to express the rate of change in the amount of drug in these subcompartments of each organ, the number of equations required to describe changes in the disposition of the drug in the body at any given time can be quite large; frequently as many as 15–20 equations are used. It is possible to integrate a set of such equations by means of LaPlace transforms. Unfortunately, the pharmacokinetic constants obtained by integration of the simultaneous equations or from measurements of drug concentrations in blood are virtually impossible to interpret in physiological terms.

The present paper describes a general approach for developing pharmacokinetic models that combine some of the complexities that can occur during rapid simultaneous elimination of drugs by several organs with the simplicity of the linear three-compartment model. The approach is essentially intuitive and, thus, requires very little mathematical ability. It is illustrated by a model in which a drug is rapidly cleared by the GI mucosa, the liver, the lungs, and the kidneys.

THEORY

As in the three-compartment model, it is assumed that after rapid injection into the aorta, a drug is almost instantaneously distributed into a central compartment that includes most of the organs of elimination such as the kidneys, the GI mucosa, the liver, and the lungs. Thus, by the time the arterial concentration of the drug is estimated, the ratios of the intracellular concentrations of the drug in the organs included within the central compartment to the drug concentration in arterial blood have reached constant values. (This is usually estimated indirectly by measuring the drug concentration in systemic venous blood: draining a nonelimination organ such as an arm.) Under these quasi steady-state

0022-3549/82/0600-0673$01.00/0

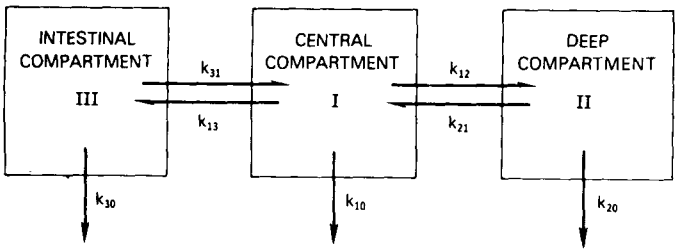

Figure 1—*Three-compartment pharmacokinetic model.*

conditions, virtually all of the drug entering a given organ in the central compartment leaves the organ by the venous blood and by excretion and metabolism; the rate of change in the amount of drug retained by the organ is negligible. When the drug is eliminated from the central compartment by a single organ, the rate of elimination under steady-state conditions may be described by the equivalent terms shown in Table I. In these terms Q_{organ} is the blood flow rate through the organ of elimination, C_{art} is the drug concentration in the arterial blood, and C_{out} is the drug concentration in the systemic blood leaving the organ. The organ availability of the drug (F_{organ}) equals C_{out}/C_{art} for that organ. As will be shown, it is also important to realize that Q_{organ}/C_{art} is the rate, expressed in amount per time, at which the drug enters the organ under steady-state conditions; *i.e.*, rate into organ. Moreover, F_{organ} may also be expressed as the rate out of organ/rate into organ. Thus, the clearance (Cl_{organ}) may be expressed by the equivalent terms shown in Table I.

When a drug is eliminated from the body by several organs, the total clearance from the central compartment is sometimes difficult to visualize. When all of the organs of elimination are perfused solely by arterial blood, the total clearances of elimination from the central compartment is the sum of the clearances of the individual organs. But some organs (notably the liver and the lungs) are perfused by venous blood as well as by arterial blood, and thus, the calculation of the total clearance of elimination from the central compartment depends on whether the drug is eliminated from the body by several organs in sequence. If the drug is eliminated by two or more organs in sequence, the total clearance of elimination from the central compartment contributed by organs is less than the sum of the individual organ clearances as calculated from the equation shown in Table I.

One approach that may be used to derive the equations for multiorgan clearances is to write the differential equations for the organs comprising the central compartment as in the Bischoff-Dedrick approach. The equations may then be set to zero, because the rate of change in the amount of drug present in the organs under the stated steady-state conditions is virtually negligible. The solution of the set of equations, however, is laborious and requires considerable mathematical skill. Moreover, the concept of organ clearances is lost, and the resulting equations are model dependent, in that each organ is assumed to be a well-stirred compartment (2).

For the present paper, two much simpler methods for the derivation of total clearance of elimination from the central compartment have been developed. In both methods a clearance term is defined as the rate of elimination of the drug divided by the concentration of the drug in a reference compartment, namely the systemic arterial blood.

In the first method, the partitioned blood flow method (Method A), the cardiac output is partitioned according to the arterial flow rates through the individual organs in the central compartment. One then visualizes the organs that a given blood supply must pass through before it reenters the systemic arterial circulation. For example, the blood serving the intestinal mucosa must also pass through the liver and the lung before it reenters the aorta (Fig. 2). Thus, in accordance with the rate equation in Table I, the rate of elimination of the drug from mucosal blood (G-1 flow) by the mucosa (G-1) may be written:

Table I—Equivalent Equations for the Rate and Clearance of Elimination of Drugs by Single Organs

(Rate of elimination) organ $= Q_{organ}(C_{art} - C_{out})$
$= Q_{organ}C_{art}[1 - (C_{out}/C_{in})] = Q_{organ}C_{art}(1 - F_{organ})$
= (Rate into organ)$(1 - F_{organ})$
$= Q_{organ}C_{art}E_{organ}$ = (Rate into organ) E_{organ}
$Cl_{organ} = Q_{organ}E_{organ}$
$= Q_{organ}(1 - F_{organ})$
= Rate of elimination by organ/C_{art}
= (Rate into organ) $(1 - F_{organ})/C_{art}$
= (Rate into organ) E_{organ}/C_{art}

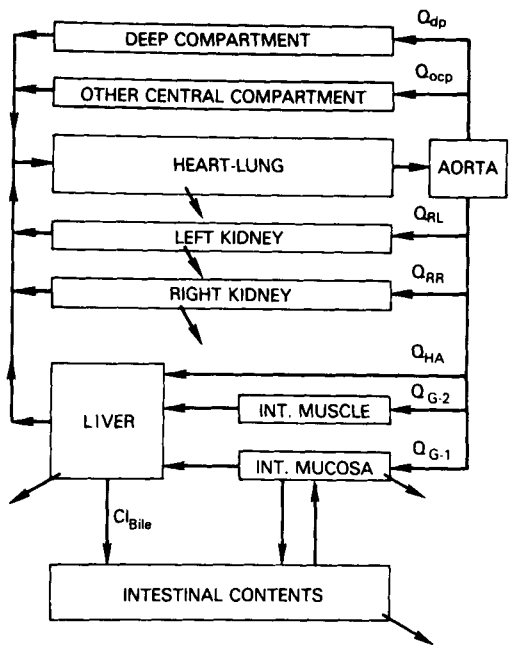

Figure 2—*A physiological pharmacokinetic model.*

rate of elimination from G-1 flow by G-1
$$= (\text{rate into } G\text{-}1 \textit{ via } G\text{-}1 \text{ flow})(1 - F_{G\text{-}1}) = C_{art}\,Q_{G\text{-}1}\,(1 - F_{G\text{-}1}) \quad \text{(Eq. 1)}$$

in which $F_{G\text{-}1}$ is the ratio of the rates at which the drug in amount per minute enters and leaves the capillary bed serving the intestinal mucosa.

The rate of elimination of the drug from the mucosal blood by the liver (H) depends on the concentration of the drug in blood leaving the mucosa and only indirectly on the concentration of the drug in the arteries. Thus:

rate of elimination from G-1 flow by H
$$= (\text{rate into } H \textit{ via } G\text{-}1 \text{ flow})(1 - F_H) = C_{art}Q_{G\text{-}1}F_{G\text{-}1}(1 - F_H) \quad \text{(Eq. 2)}$$

In Eq. 2, F_H is the ratio of the rates at which the drug leaves the liver by the hepatic vein (HV) and enters the liver by both the portal vein and the hepatic artery:

$$F_H = \frac{(Q_{G\text{-}1} + Q_{G\text{-}2} + Q_{HA})C_{HV}}{(Q_{G\text{-}1}F_{G\text{-}1} + Q_{G\text{-}2} + Q_{HA})C_{art}} \quad \text{(Eq. 3)}$$

In Eq. 3 $Q_{G\text{-}2}$ represents the portal venous flow of the blood that does not perfuse the mucosa. In rats this has been estimated to be ~75% of the total intestinal blood flow (3). In addition to intestinal blood, it also includes the gastric and splenic blood.

By the same reasoning, the rate of elimination of the drug in mucosal blood by the lung will depend on the hypothetical concentration that would have been present in the hepatic venous blood if the mucosal blood perfusing the mucosa were the only blood perfusing the liver. Thus:

rate of elimination from G-1 flow by L
$$= (\text{rate into } L \textit{ via } G\text{-}1 \text{ flow})\,(1 - F_L) = C_{art}Q_{G\text{-}1}F_{G\text{-}1}F_H\,(1 - F_L) \quad \text{(Eq. 4)}$$

In Eq. 4, F_L is the rate at which the drug leaves the lung by the pulmonary vein divided by the rate at which it enters the lung by the pulmonary artery. The total rate of elimination of the drug from the mucosal blood, $\text{rate}_{(G\text{-}1\text{ flow})}$ is the sum of the expressions given by Eqs. 1, 2, and 4:

$$\text{rate}_{(G\text{-}1\text{ flow})} = C_{art}Q_{G\text{-}1}(1 - F_{G\text{-}1}) + C_{art}Q_{G\text{-}1}F_{G\text{-}1}\,(1 - F_H) + C_{art}Q_{G\text{-}1}F_{G\text{-}1}F_H\,(1 - F_L) \quad \text{(Eq. 5)}$$

which on expansion and collection of terms becomes:

$$\text{rate}_{(G\text{-}1\text{ flow})} = C_{art}Q_{G\text{-}1}(1 - F_{G\text{-}1}F_HF_L) \quad \text{(Eq. 6)}$$

The mucosal blood clearance of the drug thus becomes:

$$Cl_{(G\text{-}1\text{ flow})} = \frac{\text{rate}_{(G\text{-}1\text{ flow})}}{C_{art}} = Q_{G\text{-}1}(1 - F_{G\text{-}1}F_HF_L) \quad \text{(Eq. 7)}$$

Table II—Poly Input Organ Clearances

Intestinal Mucosa
- metabolic: $Cl_{G\text{-}1(met)} = Q_{G\text{-}1}E_{G\text{-}1}f_{G\text{-}1(met)}$
- diffusion: $Cl_{G\text{-}1(dif)} = Q_{G\text{-}1}E_{G\text{-}1}f_{G\text{-}1(dif)}$
- since, $f_{G\text{-}1(met)} + f_{G\text{-}1(dif)} = 1$,
- total: $Cl_{G\text{-}1} = Q_{G\text{-}1}E_{G\text{-}1}$

Liver
- metabolic: $Cl_{pinH(met)} = (Q_{G\text{-}1}F_{G\text{-}1} + Q_{G\text{-}2} + Q_{HA})E_Hf_{H(met)}$
- biliary: $Cl_{pinH(biliary)} = (Q_{G\text{-}1}F_{G\text{-}1} + Q_{G\text{-}2} + Q_{HA})E_Hf_{H(biliary)}$
- since, $f_{H(met)} + f_{H(biliary)} = 1$,
- total: $Cl_{pinH} = (Q_{G\text{-}1}F_{G\text{-}1} + Q_{G\text{-}2} + Q_{HA})E_H$

Kidney
- left kidney: $Cl_{RL} = Q_{R1}E_{RR}$
- right kidney: $Cl_{RR} = Q_{RR}E_{RR}$
- total: $Cl_R = Q_{RL}E_{RL} + Q_{RR}E_{RR}$

Deep Compartment
- total: $Cl_{dp} = Q_{dp}E_{dp}$

Lung
- metabolism: $Cl_{pinL(met)} = [Q_{G\text{-}1}F_{G\text{-}1}F_H + (Q_{G\text{-}2} + Q_{HA})F_H + Q_{RL}F_{RL} + Q_{RR}F_{RR} + Q_{ocp} + Q_{dp}F_{dp}]E_Lf_{L(met)}$
- diffusion: $Cl_{pinL(dif)} = [Q_{G\text{-}1}F_{G\text{-}1}F_H + (Q_{G\text{-}2} + Q_{HA})F_H + Q_{RL}F_{RL} + Q_{RR}F_{RR} + Q_{ocp} + Q_{dp}F_{dp}]E_Lf_{L(dif)}$
- total: $Cl_{pinL} = [Q_{G\text{-}1}F_{G\text{-}1}F_H + (Q_{G\text{-}2} + Q_{HA})F_H + Q_{RL}F_{RL} + Q_{RR}F_{RR} + Q_{ocp} + Q_{dp}F_{dp}]E_L$

The partitioned blood flow clearance of drug from blood passing through several organs, thus, may be expressed as the partitioned blood flow rate times one minus the mathematical product of the drug availabilities of the organs through which the blood passes.

By similar reasoning, the clearance of the drug from the partitioned blood flow perfusing other organs may be written:

hepatic arterial blood clearance and G-2 arterial blood clearance

$$Cl_{(H\ flow)} + Cl_{(G\text{-}2\ flow)} = (Q_H + Q_{G\text{-}2})(1 - F_HF_L) \quad \text{(Eq. 8)}$$

left (RL) and right (RR) renal arterial blood clearances

$$Cl_{(RL\ flow)} = Q_{RL}(1 - F_{RL}F_L) \quad \text{(Eq. 9)}$$

$$Cl_{(RR\ flow)} = Q_{RR}(1 - F_{RR}F_L) \quad \text{(Eq. 10)}$$

Clearance from blood perfusing the nonelimination organs in the central compartment ($Cl_{ocp\ flow}$) and the deep compartment ($Cl_{dp\ flow}$) is:

$$Cl_{(ocp\ flow)} + Cl_{(dp\ flow)}F_{dp} = (Q_{ocp} + Q_{dp}F_{dp})(1 - F_L) \quad \text{(Eq. 11)}$$

In which F_{dp} is the fraction of the drug in blood perfusing the deep compartment tissues that does not enter the deep compartment, *i.e.*, $(1 - F_{dp})$ equals the rate of diffusion of the drug into the deep compartment divided by $Q_{dp}C_{art}$.

The total clearance of elimination of the drug from the central compartment (Cl_{10}) is, thus, the sum of the individual partitioned blood flow clearances:

$$Cl_{10} = Q_{G\text{-}1}(1 - F_{G\text{-}1}F_HF_L) + (Q_H + Q_{G\text{-}2})(1 - F_HF_L) + Q_{RL}(1 - F_{RL}F_L) + Q_{RR}(1 - F_{RR}F_L) + Q_{ocp}(1 - F_L) + Q_{dp}F_{dp}(1 - F_L) \quad \text{(Eq. 12)}$$

The rate constant of elimination from the central compartment is obtained from the relationship, $k_{10} = Cl_{10}/V_c$ in which V_c is the apparent volume of the central compartment.

Although the partitioned blood flow method (Method A) provides a simple, concise way of expressing Cl_{10}, it will fail when significant amounts of the drug are reabsorbed after the drug enters the lumen of the intestine either by biliary excretion or by passive diffusion from the blood across GI membranes. Method A also provides equations that are difficult to interpret when the various F_{organ} values approach 1.0 or when the investigator wishes to visualize the relative importance of the individual organs in clearing the drug from the body.

Method B was developed to overcome these difficulties. For this method, a general concept of clearance was envisioned, the poly input organ clearance or $Cl_{pin\ organ}$. In this concept, the rate of elimination of the drug by an organ is the difference in the rates at which the drug enters and leaves the organ *via* the blood under steady-state conditions. Thus, $Cl_{pin\ organ}$ may be expressed as:

$$Cl_{pin\ organ} = (\text{total rate in} - \text{total rate out})/C_{art}$$
$$= \text{total rate in}\ (1 - \text{total rate out/total rate in})/C_{art} \quad \text{(Eq. 13)}$$

The term (total rate out/total rate in), however, is the organ availability, F_{organ}. Thus:

$$Cl_{pin\ organ} = \frac{(\Sigma\ Q_iC_i)(1 - F_{organ})}{C_{art}} \quad \text{(Eq. 14)}$$

In turn, $1 - F_{organ}$ may be expressed as the extraction ratio of the drug by the organ, E_{organ}. Thus:

$$Cl_{pin\ organ} = \frac{(\Sigma\ Q_iC_i)E_{organ}}{C_{art}} \quad \text{(Eq. 15)}$$

However the C_i values may be expressed in terms of steady-state arterial concentration of the drug and the mathematical product (Π) of the individual availabilities of the organs through which the blood passes before it reaches the organ under consideration, *i.e.*, $\Pi\ F_{preorgan}$, where $F_{preorgan}$ is the F_{organ} of a given preorgan. Thus:

$$Cl_{pin\ organ} = \frac{C_{art}(\Sigma Q_i \Pi F_{preorgan})E_{organ}}{C_{art}} = (\Sigma Q_i \Pi F_{preorgan})E_{organ} \quad \text{(Eq. 16)}$$

From this general equation, equations may be written (Table II) for the poly input organ clearances in a system in which a drug is eliminated by the intestinal mucosa (both metabolically and by passive diffusion into the intestinal lumen), the liver (both metabolically and by biliary excretion), the lungs (both metabolically and by exhalation), and the kidneys (both metabolically and by excretion) (Fig. 2).

The model also includes an effective shunt in which it is recognized that only ~25% of the intestinal blood perfuses the intestinal mucosa (3); thus, $Q_{G\text{-}1}$ represents the intestinal blood that perfuses the mucosa and $Q_{G\text{-}2}$ represents the portion of the portal blood that has bypassed the mucosa. The equations in Table II also indicate how the poly input organ clearance by any given organ may be distributed between elimination by excretion or metabolism. The metabolic clearance by an organ may be expressed as a fraction, $f_{organ\ (met)}$, of the poly input organ total clearance. For example, the metabolic clearance by the mucosa is $Cl_{G\text{-}1\ (met)} = Cl_{G\text{-}1}f_{G\text{-}1\ (met)}$, in which $f_{G\text{-}1\ (met)}$ is the fraction of the total organ clearance due to metabolism. Similarly, the diffusional clearance may be written as $Cl_{G\text{-}1\ (dif)} = Cl_{G\text{-}1}f_{G\text{-}1\ (dif)}$, in which $f_{G\text{-}1\ (dif)}$ is the fraction of the total mucosal clearance due to diffusion. Thus, $f_{G\text{-}1\ (met)} + f_{G\text{-}1\ (dif)} = 1.0$. The equations may then be expanded to those shown in Table II.

The next step in the development of the compartmental model is to distribute the sequential organ clearances among the rate constants that emanate from the central pool. By *definition, any clearance by which* the drug irreversibly leaves the central compartment is a part of Cl_{10}. Thus, the investigator must decide whether a drug that leaves the central compartment by biliary excretion or passive diffusion across the intestinal mucosa into the intestinal lumen will be reabsorbed from the intestines. If the compound is not reabsorbed the clearances of these processes should be included in Cl_{10}. But if the drug is reabsorbed, the sum of the clearances of these processes equals Cl_{13}, the clearance for the passage of the drug into the GI tract. The investigator also must decide whether the drug that leaves the body by exhalation is reabsorbed. If the animal is in the open air, which contains negligible amounts of the drug, then the effective lung clearance by exhalation of the drug is part of Cl_{10}. But if the animal is placed into a closed chamber in which the drug vapor is at a significant concentration, the chamber becomes a pharmacokinetic compartment, which may be either closed or open. In this situation, the effective lung clearance by exhalation of the drug is not included in Cl_{10}, but is represented by a separate clearance. For the purpose of the present discussion, however, we will assume that the drug is reabsorbed from the GI tract and the animal is in the open air. With these assumptions, the components of Cl_{10}, Cl_{12}, and Cl_{13} are those shown in Table III.

The other microclearances for the three-compartment model may also be written, although some of them may not be immediately obvious. For example, the microclearance representing the passage of the drug from the deep compartment to the central compartment, Cl_{21}, may be visualized as a diffusional clearance, $Cl_{dp(dif)}$, but after leaving the deep compartment the drug must first pass through the lungs before it reenters the arterial circulation and, thus, Cl_{21} equals $Cl_{dp(dif)}F_L$. The drug that is removed by the lungs as it passes from the deep compartment into the arterial blood must also be accounted for. Thus, the microclearance, Cl_{20}, that represents an irreversible removal of the drug from the deep com-

Table III—Relationship between Various Microconstants of the Three-Compartment Model and the Poly Input Organ Clearance

Micro Clearance	Volume Times Microconstants	Components of Micro Clearances	Expanded Version of Micro Clearances
	Central Compartment to Gastrointestinal Tract		
Cl_{13}	V_1k_{13}	$Cl_{G\text{-}1(\text{dif})} + Cl_{\text{pin}H(\text{biliary})}$	$Q_{G\text{-}1}E_{G\text{-}1}f_{G\text{-}1(\text{dif})} + (Q_{G\text{-}1}F_{G\text{-}1} + Q_{G\text{-}2} + Q_{HA})E_Hf_{H(\text{biliary})}$
	Central Compartment to Deep Compartment		
Cl_{12}	V_1k_{12}	Cl_{dp}	$Q_{\text{dp}}E_{\text{dp}}$
	Central Compartment Irreversible Elimination		
Cl_{10}	V_1k_{10}	$Cl_{G\text{-}1(\text{met})} + Cl_{\text{pin}H(\text{met})} + Cl_{RL} + Cl_{RR} + Cl_{\text{pin}L}$	$Q_{G\text{-}1}E_{G\text{-}1}f_{G\text{-}1(\text{met})}$ $(Q_{G\text{-}1}F_{G\text{-}1} + Q_{G\text{-}2} + Q_{HA})E_Hf_{H(\text{met})}$ $Q_{RL}E_{RL} + Q_{RR}E_{RR}$ $[(Q_{G\text{-}1}F_{G\text{-}1} + Q_{G\text{-}2} + Q_{HA})F_H + Q_{RL}F_{RL}$ $+ Q_{RR}F_{RR} + Q_{\text{ocp}} + Q_{\text{dp}}F_{\text{dp}}]E_L$
	Deep Compartment to Central Compartment		
Cl_{21}	V_2k_{21}	$Cl_{\text{dp}(\text{dif})}F_L$	$Q_{\text{dp}}E_{\text{dp}}F_L$
	Deep Compartment Irreversible Elimination		
Cl_{20}	V_2k_{20}	$Cl_{\text{dp}(\text{met})} + Cl_{\text{dp}(\text{dif})}E_L$	$Cl_{\text{dp}(\text{met})} + Q_{\text{dp}}F_{\text{dp}}E_L$
	Gastrointestinal Tract to Central Compartment		
Cl_{31}	V_3k_{31}	—	$Cl_{g(\text{dif})}F_{G\text{-}1}F_HF_L$
	Gastrointestinal Tract Irreversible Elimination		
Cl_{30}	V_3k_{30}	—	$Cl_{g(\text{met})} + Cl_{g(\text{dif})}[E_{G\text{-}1}f_{G\text{-}1(\text{met})} + F_{G\text{-}1}E_Hf_{H(\text{met})} + F_{G\text{-}1}F_HE_L]$

partment will include not only the metabolism of the drug that takes place in the deep compartment, $Cl_{\text{dp}(\text{met})}$, but also the drug that is eliminated by the lungs as the drug passes from the deep compartment to the arterial circulation, $Cl_{\text{dp}(\text{dif})}E_L$. For this reason, a three-compartment model in which a drug is rapidly eliminated by the lungs theoretically should always include both Cl_{10} and Cl_{20}.

By a similar line of reasoning, a drug absorbed from the intestinal tract passes through the intestinal mucosa, the liver, and the lungs before it enters the arterial circulation; therefore, Cl_{31} must include not only the clearance of diffusion across the intestinal wall, $Cl_{g(\text{dif})}$, but also the availability of the drug as it passes through the various organs before it reaches the arterial circulation. Thus, Cl_{31} equals $Cl_{g(\text{dif})}F_{G\text{-}1}F_HF_L$. Moreover, Cl_{30} must include not only the drug that is eliminated in the feces or metabolized by intestinal flora, but also the metabolic clearance of the drug as it passes through the intestinal mucosa, the liver, and the lungs. Therefore, as shown in Table III:

$$Cl_{30} = Cl_{g(\text{met})} + Cl_{g(\text{dif})}[E_{G\text{-}1}f_{G\text{-}1(\text{met})} + F_{G\text{-}1}E_Hf_{H(\text{met})} + F_{G\text{-}1}F_HE_Lf_{L(\text{met})}] \quad \text{(Eq. 17)}$$

Thus, any compartmental model in which a drug is rapidly eliminated by the intestinal mucosa, the liver, or the lungs should theoretically always include Cl_{30} as well as Cl_{10}.

Once the microconstants have been written they may be incorporated into the equations derived for the appropriate compartmental models. The equations for the blood concentrations of a drug in the three-compartment model shown in Fig. 1 are given in the *Appendix*.

DISCUSSION

It is interesting that the intestinal mucosa and the liver are simultaneously a part of the intestinal compartment and the central compartment; and that the lung is simultaneously a part of the intestinal compartment, the central compartment, and the deep compartment. What the equations illustrate, however, is the artificiality of compartmental models when applied to complex physiological systems. Therefore, it is evident that the visualization of the body as a set of compartments is fraught with difficulties, not only because the volume of the various compartments is difficult to determine, but also because the clearances by which the drug is transferred from one compartment to another and eliminated from the body are difficult to visualize.

Both methods illustrated in this paper are based solely on the conservation of mass and the anatomy and function of the cardiovascular system. The investigator is at liberty to choose any model he or she wishes, to illustrate the effects of altering blood flow rates or reversible binding of drugs to blood components on the availabilities (F values) and extraction ratios (E values). Indeed, he or she may wish to choose different models for different organs. For example, the investigator may wish to use the well-stirred model (4) [in which $F = Q/(Q + f_B\,Cl^u_{\text{int}})$] and $E = f_B\,Cl^u_{\text{int}}/(Q + f_B\,Cl^u_{\text{int}})$ for the liver and the parallel tube model [in which $F = (\exp - f_B\,Cl^u_{\text{int}}/Q)$] and $E = 1 - [\exp - (f_B\,Cl^u_{\text{int}}/Q)]$ for the kidney (5), where Cl^u_{int} represents the free intrinsic clearance of the organ and f_B is the unbound fraction of drug in the blood.

With the principles for the partitioned blood clearances and the poly input organ clearances in mind, the investigator may construct other models. For example, a separate compartment to represent the gall bladder or blood shunts such as the portal vena cava may be introduced. Alternatively, the investigator may wish to simplify the model by setting the F values equal to one and the E values equal to zero when such simplifications seem warranted. Thus, the methods are not only simple, but also versatile.

With measurements of drug concentrations in blood alone, it is not possible to differentiate between the model described in Fig. 1 from the three-compartment model described by Gibaldi and Perrier (6) in which the drug is eliminated solely from a central compartment. The main purpose of the model described here is to provide the investigator with insights by which he or she may infer possible meanings of the individual microconstants of compartmental models and how changes in them might affect the pharmacokinetics of drugs. The use of these simplified physiological approaches should help investigators to understand the relationship between poly input first-pass effects in physiological systems and the pharmacokinetics as predicted by compartmental models. They also should clarify some of the problems that can arise in the interpretation of such models.

REFERENCES

(1) K. B. Bischoff and R. L. Dedrick, *J. Pharm. Sci.*, **57,** 1346 (1968).

(2) J. R. Gillette and K. S. Pang, *Clin. Pharmacol. Ther.*, **22,** 623 (1977).

(3) J. Svanick, *Acta Physiol. Scand. Suppl.*, **1973,** 385.

(4) M. Rowland, L. Z. Benet, and G. G. Graham, *J. Pharmacokinet. Biopharm.*, **1,** 123 (1973).

(5) K. S. Pang and M. Rowland, *ibid.*, **5,** 655 (1977).

(6) M. Gibaldi and D. Perrier, "Pharmacokinetics," Dekker, New York, N.Y., 1975, p. 89

APPENDIX

The solution of the three-compartment model shown in Fig. 1 by La-Place transforms gives the following equations for the drug concentration in blood:

Oral Administration:

$$C = \frac{\text{dose}}{V_1}\left[\frac{k_{31}(k_{20}+k_{21}-\gamma)}{(\alpha-\gamma)(\beta-\gamma)}e^{-\gamma t} + \frac{k_{31}(k_{20}+k_{21}-\alpha)}{(\gamma-\alpha)(\beta-\alpha)}e^{-\alpha t} + \frac{k_{31}(k_{20}+k_{21}-\gamma)}{(\gamma-\beta)(\alpha-\beta)}e^{-\beta t}\right]$$

Intravenous administration:

$$C = \frac{\text{dose } F_L}{V_1}\left[\frac{(k_{30}+k_{31}-\gamma)(k_{20}+k_{21}-\gamma)}{(\alpha-\gamma)(\beta-\gamma)}e^{-\gamma t} + \frac{(k_{30}+k_{31}-\alpha)(k_{20}+k_{21}-\alpha)}{(\gamma-\alpha)(\beta-\alpha)}e^{-\alpha t} + \frac{(k_{30}+k_{31}-\beta)(k_{20}+k_{21}-\beta)}{(\gamma-\beta)(\alpha-\beta)}e^{-\beta t}\right]$$

In these equations, γ, α, and β are the roots[1] of the transformed equation

$$0 = (s+\gamma)(s+\alpha)(s+\beta)$$
$$= (s+k_{30}+k_{31})(s+k_{10}+k_{12}+k_{13})(s+k_{20}+k_{21}) - k_{12}k_{21}(s+k_{30}+k_{31}) - k_{13}k_{31}(s+k_{20}+k_{21})$$

[1] When hypothetical values of the microconstants based on their physiological components are substituted into the transformed equation, the roots may be determined by iteration of synthetic division. Decreasing values of s (0 to $-\infty$) are iterated with a programmable calculator until all three values of s that satisfy the equation, $F(s) = 0$, are found. Unfortunately, the presence of k_{20} and k_{30} in the model precludes the calculation of the microconstants from actual data. In the three-compartment model of Gibaldi and Perrier (6), the elimination of a drug is represented solely by k_{10}. Thus, their method would overestimate the values of k_{31}, k_{21}, and k_{10} and would provide no adequate way of estimating k_{20} or k_{30}. However, simulations are still possible by substituting reasonable numerical values of the various microconstants into the equation.

Biological Effects of Nonalkaloid-Containing Fractions of *Erythroxylon coca*

ERNEST C. HARLAND, JAMES C. MURPHY ˣ, HALA ELSOHLY, DEBORAH GREUBEL, CARLTON E. TURNER, and E. S. WATSON

Received May 18, 1981, from the *Research Institute of Pharmaceutical Sciences, University of Mississippi, University, MS 38677.* Accepted for publication September 24, 1981.

Abstract □ Water soluble nonalkaloid fractions of *Erythroxylon coca* were screened in mice for their effects on oxygen utilization and central nervous system (CNS) activity. The fractions were screened in dogs for cardiovascular, blood glucose, and respiratory changes. No CNS effects were demonstrated in mice; however, there was a reduction in the oxygen utilization rate. Intravenous administration of the extract to dogs produced hyperglycemia, a reduction in heart rate, and a decrease in blood pressure. No substantial change in the respiratory rate and tidal or minute volumes were observed.

Keyphrases □ *Erythroxylon coca*—biological effects of nonalkaloid-containing fractions □ Nonalkaloids—fractions in *Erythroxylon coca*, effects □ Oxygen utilization rate—effects of *Erythroxylon coca* on oxygen utilization rate, mice, dogs □ CNS activity—effect of nonalkaloid-containing fractions of *Erythroxylon coca*

The plant *Erythroxylon coca* has been used in the cultures of many Latin American societies for medicinal, nutritional, and religious purposes for centuries (1). The pharmacological and possible psychological effects of coca have made its use by natives commonplace. It is reported to aid them in performing strenuous work and in coping with the harsh mountain environment. While cocaine is not the only biologically active compound in the coca plant, it is the principal alkaloid and the most studied of the active compounds. Alkaloid free fractions of the coca leaf extracts recently have been shown to reduce food consumption but do not show alterations in locomotor activity (2). Cocaine, at doses ranging from 3.45 to 27.6 mg/kg, produced dose-related increases in locomotor activity and decreases in food consumption (3).

It has been reported that chewing coca leaves causes the Latin American native to be more resistant to cold and fatigue and decreases the need for food and sleep (4, 5). Most of these effects have been considered to be related to cocaine, since cocaine has been shown to increase the heart rate and blood pressure and to elevate blood glucose levels (6).

The present study was undertaken to determine whether cocaine-free extracts would produce changes in oxygen utilization, blood glucose levels, respiration, and/or cardiovascular effects that could be related to the alleged enhancement of physical stamina in humans.

EXPERIMENTAL

Test Compounds—Coca leaves (*Erythroxylon coca*)[1] were obtained from Tingo Maria, Peru, and extracted as described previously (2). Briefly, the crude ethanol extract of coca leaves was partitioned between water (fraction A) and chloroform (fraction B). Fraction A was made cocaine free by dissolving in ammonium hydroxide solution and extracting 10 times with chloroform. Each chloroform fraction was subjected to GLC analysis. These fractions each showed the absence of cocaine peaks. Fraction A was further partitioned between butanol and water yielding two fractions: fraction C, the butanol phase; fraction D, the water phase. The fractions were dried on a rotary evaporator at 40°.

All test solutions were prepared in distilled water from dried fractions immediately prior to testing.

Test Animals—The mice were male ICR Swiss, weighing 26–30 g[2]. They were housed in shoe box caging on pelleted corncobs[3] with food[4] and water freely available. Food was withheld overnight prior to testing. The mice were maintained in an environment of 21 ± 1° and a 12 hr light–dark cycle.

[1] The plant material was obtained through Mr. Ing Alberto Trelles Barnett, Impresa Nacionale de la Coca, Lima, Peru, and through the United States Department of Justice and the United States State Department. It was identified as *Erythroxylon coca* by Dr. M. W. Quimby, Department of Pharmacognosy. Voucher specimens are stored in the drug plant herbarium at the School of Pharmacy, University of Mississippi, University, MS 38677.

[2] Harlan Industries, Cumberland, Ind.

[3] San-i-cel, Paxton Processing, Paxton, Ill.

[4] Purina Laboratory Chow 5001, Purina Mills, St. Louis, Mo.

0022-3549/82/0600-0677$01.00/0

$$C = \frac{\text{dose}}{V_1}\left[\frac{k_{31}(k_{20}+k_{21}-\gamma)}{(\alpha-\gamma)(\beta-\gamma)}e^{-\gamma t} + \frac{k_{31}(k_{20}+k_{21}-\alpha)}{(\gamma-\alpha)(\beta-\alpha)}e^{-\alpha t} + \frac{k_{31}(k_{20}+k_{21}-\gamma)}{(\gamma-\beta)(\alpha-\beta)}e^{-\beta t}\right]$$

Intravenous administration:

$$C = \frac{\text{dose } F_L}{V_1}\left[\frac{(k_{30}+k_{31}-\gamma)(k_{20}+k_{21}-\gamma)}{(\alpha-\gamma)(\beta-\gamma)}e^{-\gamma t} + \frac{(k_{30}+k_{31}-\alpha)(k_{20}+k_{21}-\alpha)}{(\gamma-\alpha)(\beta-\alpha)}e^{-\alpha t} + \frac{(k_{30}+k_{31}-\beta)(k_{20}+k_{21}-\beta)}{(\gamma-\beta)(\alpha-\beta)}e^{-\beta t}\right]$$

In these equations, γ, α, and β are the roots[1] of the transformed equation

$$0 = (s+\gamma)(s+\alpha)(s+\beta)$$
$$= (s+k_{30}+k_{31})(s+k_{10}+k_{12}+k_{13})(s+k_{20}+k_{21}) - k_{12}k_{21}(s+k_{30}+k_{31}) - k_{13}k_{31}(s+k_{20}+k_{21})$$

[1] When hypothetical values of the microconstants based on their physiological components are substituted into the transformed equation, the roots may be determined by iteration of synthetic division. Decreasing values of s (0 to $-\infty$) are iterated with a programmable calculator until all three values of s that satisfy the equation, $F(s) = 0$, are found. Unfortunately, the presence of k_{20} and k_{30} in the model precludes the calculation of the microconstants from actual data. In the three-compartment model of Gibaldi and Perrier (6), the elimination of a drug is represented solely by k_{10}. Thus, their method would overestimate the values of k_{31}, k_{21}, and k_{10} and would provide no adequate way of estimating k_{20} or k_{30}. However, simulations are still possible by substituting reasonable numerical values of the various microconstants into the equation.

Biological Effects of Nonalkaloid-Containing Fractions of *Erythroxylon coca*

ERNEST C. HARLAND, JAMES C. MURPHY ˣ, HALA ELSOHLY, DEBORAH GREUBEL, CARLTON E. TURNER, and E. S. WATSON

Received May 18, 1981, from the *Research Institute of Pharmaceutical Sciences, University of Mississippi, University, MS 38677.* Accepted for publication September 24, 1981.

Abstract □ Water soluble nonalkaloid fractions of *Erythroxylon coca* were screened in mice for their effects on oxygen utilization and central nervous system (CNS) activity. The fractions were screened in dogs for cardiovascular, blood glucose, and respiratory changes. No CNS effects were demonstrated in mice; however, there was a reduction in the oxygen utilization rate. Intravenous administration of the extract to dogs produced hyperglycemia, a reduction in heart rate, and a decrease in blood pressure. No substantial change in the respiratory rate and tidal or minute volumes were observed.

Keyphrases □ *Erythroxylon coca*—biological effects of nonalkaloid-containing fractions □ Nonalkaloids—fractions in *Erythroxylon coca*, effects □ Oxygen utilization rate—effects of *Erythroxylon coca* on oxygen utilization rate, mice, dogs □ CNS activity—effect of nonalkaloid-containing fractions of *Erythroxylon coca*

The plant *Erythroxylon coca* has been used in the cultures of many Latin American societies for medicinal, nutritional, and religious purposes for centuries (1). The pharmacological and possible psychological effects of coca have made its use by natives commonplace. It is reported to aid them in performing strenuous work and in coping with the harsh mountain environment. While cocaine is not the only biologically active compound in the coca plant, it is the principal alkaloid and the most studied of the active compounds. Alkaloid free fractions of the coca leaf extracts recently have been shown to reduce food consumption but do not show alterations in locomotor activity (2). Cocaine, at doses ranging from 3.45 to 27.6 mg/kg, produced dose-related increases in locomotor activity and decreases in food consumption (3).

It has been reported that chewing coca leaves causes the Latin American native to be more resistant to cold and fatigue and decreases the need for food and sleep (4, 5). Most of these effects have been considered to be related to cocaine, since cocaine has been shown to increase the heart rate and blood pressure and to elevate blood glucose levels (6).

The present study was undertaken to determine whether cocaine-free extracts would produce changes in oxygen utilization, blood glucose levels, respiration, and/or cardiovascular effects that could be related to the alleged enhancement of physical stamina in humans.

EXPERIMENTAL

Test Compounds—Coca leaves (*Erythroxylon coca*)[1] were obtained from Tingo Maria, Peru, and extracted as described previously (2). Briefly, the crude ethanol extract of coca leaves was partitioned between water (fraction A) and chloroform (fraction B). Fraction A was made cocaine free by dissolving in ammonium hydroxide solution and extracting 10 times with chloroform. Each chloroform fraction was subjected to GLC analysis. These fractions each showed the absence of cocaine peaks. Fraction A was further partitioned between butanol and water yielding two fractions: fraction C, the butanol phase; fraction D, the water phase. The fractions were dried on a rotary evaporator at 40°.

All test solutions were prepared in distilled water from dried fractions immediately prior to testing.

Test Animals—The mice were male ICR Swiss, weighing 26–30 g[2]. They were housed in shoe box caging on pelleted corncobs[3] with food[4] and water freely available. Food was withheld overnight prior to testing. The mice were maintained in an environment of 21 ± 1° and a 12 hr light–dark cycle.

[1] The plant material was obtained through Mr. Ing Alberto Trelles Barnett, Impresa Nacionale de la Coca, Lima, Peru, and through the United States Department of Justice and the United States State Department. It was identified as *Erythroxylon coca* by Dr. M. W. Quimby, Department of Pharmacognosy. Voucher specimens are stored in the drug plant herbarium at the School of Pharmacy, University of Mississippi, University, MS 38677.

[2] Harlan Industries, Cumberland, Ind.

[3] San-i-cel, Paxton Processing, Paxton, Ill.

[4] Purina Laboratory Chow 5001, Purina Mills, St. Louis, Mo.

0022-3549/82/0600-0677$01.00/0

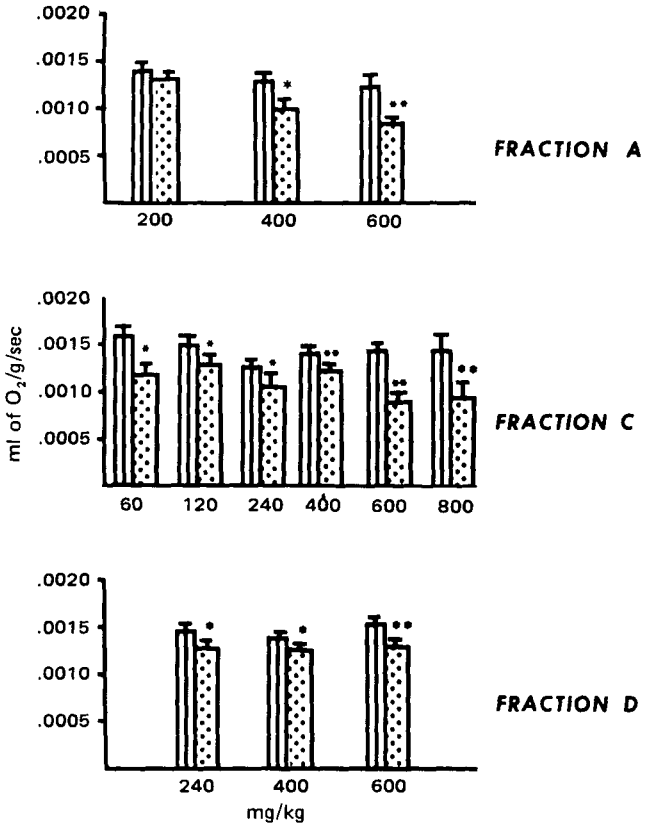

Figure 1—*Comparison of the effects of fractions A, C, and D on oxygen utilization in mice. Key: vertical bars represent* SEM (n = *12); (▥) vehicle; (∴) drug.* * p < *0.05.* ** p < *0.01.*

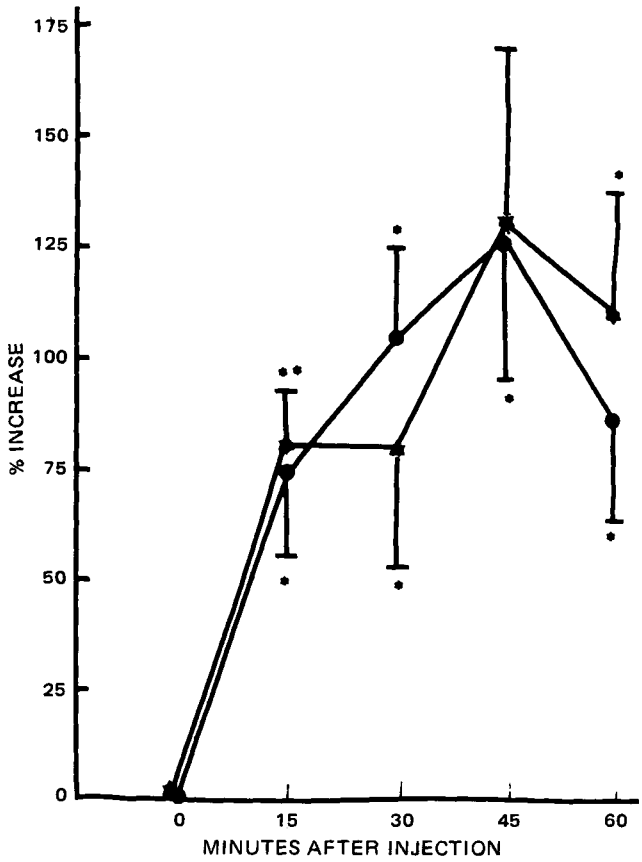

Figure 2—*Mean percent increases of plasma glucose levels in dogs following a single dose of 200 mg/kg, iv of fraction C (anesthetized* n = *4; conscious* n = *6). Key: vertical bar represents* SEM; *(★) anesthetized; (●) conscious.* * p < *0.05.* ** p < *0.01.*

The dogs[5] were conditioned, mongrel, adult males weighing 10–12.5 kg; vaccinated against distemper, hepatitis, and leptospirosis[6]; checked for internal parasites; and treated[7] as necessary. All dogs were free of heartworms and had two normal hemograms over the 3-week conditioning period.

Oxygen Utilization Screen—The oxygen utilization apparatus consisted of three widemouth 946 ml jars glued[8] to a 25 × 40 × 1.5-cm aluminum platform. Pelleted corncob bedding was placed in the bottom 2–3 cm of each jar to absorb urine. The platform and jars were placed in a constant temperature water bath[9] with water covering ~75% of the outer jar to maintain the temperature at 25°. This was done to minimize temperature change inside the jar during testing. A 4-cm piece of copper tubing (7-mm o.d.), fitted with a 3-way stopcock, was attached to the lid of the jar. This allowed the addition of air to the jar as well as attachment to a pressure transducer without breaking the jar's seal. A 7 × 7-cm nylon net bag filled with soda lime was suspended from the underside of the lid to absorb the carbon dioxide produced by the mouse. Ten mice were dosed intraperitoneally with either drug or vehicle. Five minutes after dosing, the mice were placed in the jar and the chamber was sealed. Twenty milliliters of air was added to the chamber and the resulting air pressure and the time required to return to baseline were recorded[10]. This allowed the determination of the amount of oxygen per gram per second utilized by the mouse using the following:

$$\text{ml } O_2/\text{g/sec} = \frac{20\ (\text{ml } O_2)}{\text{time (sec)} \times \text{wt of mouse (g)}} \qquad \text{(Eq. 1)}$$

Open Field Locomotor Screen—Locomotor activity was measured in an open field arena which consisted of 1 m^2 box with the floor marked off into 25 squares. The top was open and lighted by an overhead fluorescent lamp for better observation. Open field sessions were 5 min long and began 5 min following intraperitoneal injections. Treated and vehicle controls were run alternately to erase diurnal variation. Activity was measured by counting the number of squares the mouse entered during the test period. Statistical analysis was accomplished using the Mann-Whitney nonparametric test (7).

Respiratory and Cardiovascular Screen—The dogs used in the respiratory, cardiovascular, and blood glucose studies were anesthetized with pentobarbital (30 mg/kg). The femoral artery and vein were cannulated and a tracheotomy performed. Electrocardiograph[10] (ECG) (lead II), femoral arterial blood pressure[10], and respiratory parameters[11] (rate, tidal volume, minute volume, and oxygen uptake) were recorded. Arterial blood pO_2, pCO_2, and pH were measured at 15-min intervals[12].

Blood glucose levels[13] were determined at 15-min intervals on venous blood. Control parameters were recorded, then a single dose of fraction C was administered (200 mg/kg, iv). Blood pressure and heart rate were monitored constantly, while other samples and measurements were taken at 15-min intervals. Statistical evaluation of the data was performed using Student *t* test (8).

RESULTS AND DISCUSSION

In the partitioning of fraction A, ~26% of the starting material is removed in the butanol fraction. Five major and five minor constituents were detected in the butanol fraction by TLC.

The effects of fractions A, C, and D on the rate of oxygen utilization are shown in Fig. 1. Fraction A reduced the rate of oxygen utilization at doses ranging from 400 to 600 mg/kg, while fraction C reduced oxygen utilization at doses ranging from 60 to 800 mg/kg. Fraction D reduced the rate of oxygen utilization at 240 mg/kg, but lower doses were not tested. Partitioning fraction A between butanol and water successfully separated all other pharmacological activity into the butanol phase (fraction C).

Oxygen utilization rates are of interest since South American natives claim that chewing coca improves their ability to perform strenuous work, especially at high altitudes (1). Even though a decreased locomotor ac-

[5] Obtained from Memphis Animal Shelter, Memphis, Tenn.
[6] Decline-HL, Dellan Labs, Omaha, Neb.
[7] Telmintic, Pitman-Moore, Inc., Washington Crossing, N.J.
[8] Expoxe, Balkamp Ind., Indianapolis, Ind.
[9] Labline Instruments, Melrose Park, Ill.
[10] RM Dynograph, Beckman Instruments, Schiller Park, Ill.
[11] Collins Respirometer, Warren E. Collin, Inc., Braintree, Mass.
[12] Model 213 pH Blood Gas Analyzer, Instrumentation Laboratory, Lexington, Mass.
[13] Glucose Analyzer, Beckman Instruments, Schiller Park, Ill.

Table I—Effect of Fractions C and D on Open Field Activity in Mice

Compounmd	Dose	Counts/5 min ± *SEM*
Vehicle	0.5 ml	150.45 ± 12.0
Fraction C	200 mg/kg	117.8 ± 8.86[a]
	400 mg/kg	51.0 ± 9.25[b]
	600 mg/kg	42.1 ± 9.99[b]
Vehicle	0.5 ml	129.1 ± 16.1
Fraction D	200 mg/kg	138.2 ± 14.5
	400 mg/kg	175.20 ± 23.44
	600 mg/kg	179.60 ± 25.80

[a] $p < 0.05$. [b] $p < 0.001$.

tivity would decrease oxygen utilization, gross observation (9) of activity showed no difference between animals treated with fraction A and control animals. Additionally, fractions C and D produced a decrease in oxygen utilization (Fig. 1) while only fraction C produced a decrease in activity in the open field experiment (Table I). These data would indicate that the decrease in locomotor activity was not the only cause of decreased oxygen consumption.

A potent hyperglycemic effect was seen both in the anesthetized and conscious dogs treated with 200 mg/kg of fraction C. Blood glucose levels reached their peak 45 min after dosing and began to decline after 60 min (Fig. 2). This could explain a ready energy source which would improve the short-term ability to do work and alleviate hunger. The blood glucose levels begin to decline in 1 hr. This is the approximate length of time that chewing of coca leaves is reported to give stimulatory effects. The increased blood glucose is most likely due to a direct effect on glucose metabolism since no sugars remain in fraction C after extraction and separation. Therefore, it would seem that prolonged use of coca, by people on energy deficient diets, could lead to a rapid loss of the body's energy stores. However, histologically[14] no effect was observed on liver glycogen stores in mice 30 min postdose with 120 mg/kg of fraction C. These same mice showed significantly elevated blood glucose levels.

Since hard work or heavy exercise tends to increase cardiac output and mean arterial pressure, the sustained hypotensive effect and decrease in heart rate could be partially responsible for the enhanced work performance and endurance experienced by natives using coca.

Five minutes after injection of 200 mg/kg of fraction C, the heart rate of anesthetized dogs decreased from a mean of 200 to 125 bpm. The rate had not returned to baseline after a 60-min period (Fig. 3). Mean blood pressure dropped from 160 to 100 mm Hg concomitant with the initial fall in heart rate. Both systolic and diastolic pressures remained 20–30 mm Hg below baseline during the remainder of the test period (Fig. 4). There were no significant changes in oxygen uptake, tidal volume, minute volume, pO_2, pCO_2, or arterial blood pH; however, there was an initial increase in respiratory rate (panting). Electrocardiographic tracings

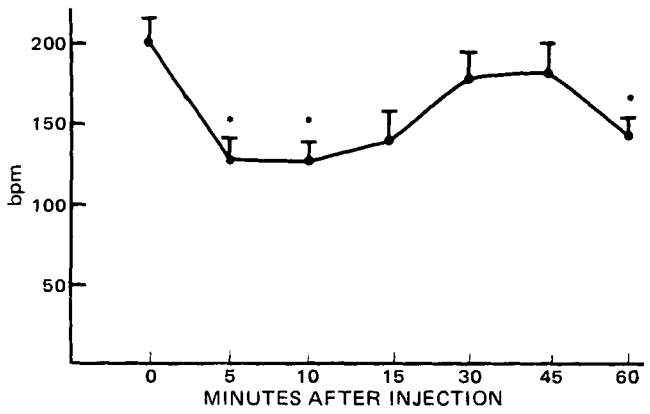

Figure 3—*Change in heart rate (beats per minute, bpm) of anesthetized dogs following a single dose of 200 mg/kg, iv of fraction C (n = 5). Vertical bar represents* SEM. * $p < 0.05$.

[14] Periodic acid schiff (Harleco) stain for glycogen, American Hospital Supply, Memphis, Tenn.

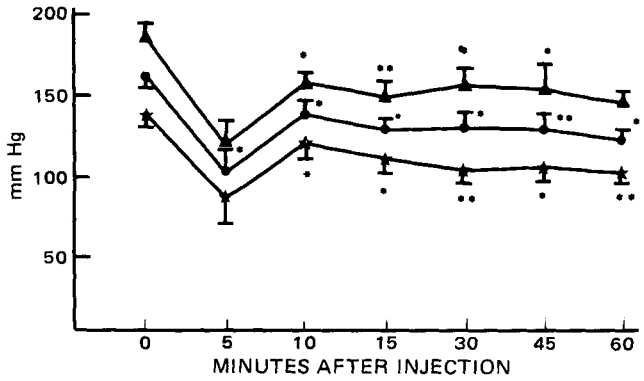

Figure 4—*Systolic, diastolic, and mean arterial blood pressure changes in anesthetized dogs following a single dose of 200 mg/kg, iv of fraction C (n = 5). Key: vertical bar represents* SEM; (▲), *systolic;* (★), *diastolic;* (●) *mean arterial.* * $p < 0.05$. ** $p < 0.01$.

frequently showed an inversion of the T wave, which returned to pretreatment polarity 20 min postinjection. Since pO_2 values remained stable during this period, the T wave inversion would not appear to be a hypoxic effect. No other ECG alterations were noted. No autonomic, CNS, hyperglycemic, or cardiovascular effects were obtained with fraction D.

A single 200-mg/kg dose, iv of fraction C given to conscious dogs produced a dramatic effect on the autonomic nervous system. Shallow, rapid panting and increased salivation, swallowing, and defecation began immediately after injection. Cyanosis and inactivity were produced and lasted ~1 hr postdose. These effects, exclusive of defecation, appeared to be masked in the anesthetized animals.

Vomiting, defecation, and inactivity are not problems reported by humans chewing the coca leaf. Chewing would slow intake of the drug and could modify most of the autonomic effects since the fraction would be absorbed over a longer period of time. It also appears that some compounds in the extract may be rapidly bound or metabolized since most effects return to normal levels within 10–30 min following a single injection. However, the increased blood glucose levels, lower blood pressure, and decreased heart rate remain, indicating that other compounds in the extract are longer acting.

The biological effects produced by noncocaine-containing coca fractions are not identical to those seen after cocaine administration. However, these data suggest that noncocaine-containing fractions may contribute to the beneficial effects seen in subjects chewing coca leaves.

REFERENCES

(1) E. Carroll, *Cocaine*, *NIDA Research Monograph*, **13**, 35–45 (1977).

(2) J. A. Bedford, H. N. ElSohly, G. L. Nail, M. C. Wilson, and C. E. Turner, *Pharmacol. Biochem. Behav.*, **14**, 725 (1981).

(3) J. A. Bedford, D. K. Lovell, C. E. Turner, M. A. ElSohly, and M. C. Wilson, *ibid.*, **13**, 403 (1980).

(4) C. Gutierriz-Noriega and V. Zapata-Ortiz, *Rueta Farmacol. Med. Exp.*, **1**, 1 (1948).

(5) M. F. Risemberg, *Rev. Med. Exp.*, **3**, 132 (1944).

(6) S. J. Mule', "Cocaine: Chemical, Social and Treatment Aspects," CRC Press, Cleveland, Ohio, 1976, p. 190.

(7) S. Siegal, "Nonparametric Statistics for the Behavioral Sciences," McGraw-Hill, New York, N.Y., 1956, p. 31.

(8) A. L. Edwards, "Experimental Design in Psychological Research," Holt, Rhinehart, and Winston, New York, N.Y., 1968, p. 81.

(9) M. W. Dunham, T. S. Miya, *J. Am. Pharm. Assoc., Sci. Ed.*, **46**, 208 (1957).

ACKNOWLEDGMENTS

This project was funded by the Research Institute of Pharmaceutical Sciences, University of Mississippi, University, Miss.

The authors thank Dr. I. W. Waters for his advice and assistance in the performance of this research.

Local Anesthetics: 2-*N*,*N*-Dialkylaminoacyl-2′-methyl (or 2′,6′-dimethyl)-4′-butylaminoanilides

WILLIAM O. FOYE ˣ, CHAUR-MING JAN, and BERTIL H. TAKMAN *

Received June 8, 1981, from the *Samuel M. Best Research Laboratory, Massachusetts College of Pharmacy and Allied Health Sciences, Boston, MA 02115;* and the **Astra Pharmaceutical Products, Inc., Worcester, MA 01606.* Accepted for publication September 29, 1981.

Abstract □ A series of tetracaine analogs based on the lidocaine structure, having a 2′-methyl-(or 2′,6′-dimethyl)-4′-butylaminoanilide moiety with α substitution on the dialkylaminoacyl function, has been synthesized. Local anesthetic activity was found with the *N*-butyl derivatives in both the 2′-methyl and 2′,6′-dimethyl series using both the method of rabbit cornea loss of reflex and spinal anesthesia in sheep. Duration of activity of the compounds was greater than that of lidocaine, but less than that of tetracaine, with comparable dosage levels.

Keyphrases □ Anesthetics—2-*N*,*N*- dialkylaminoacyl-2′-methyl (or 2′,6′-dimethyl)-4′-butylaminoanilides, local anesthetic, rabbits, sheep □ Tetracaine—synthesis of analogs from lidocaine structure □ Lidocaine—tetracaine synthesis

Tetracaine is employed as both an injectable and topical local anesthetic and remains in common use for spinal anesthesia (1). This compound, an ester, is fairly stable but suffers some loss of potency during autoclaving (2). To provide greater stability and possibly lower toxicity, a series of amide analogs based on the lidocaine structure has been synthesized. This series includes both 2-methyl and 2,6-dimethyl substituents in the aromatic ring, as well as alkyl groups on the α position of the aliphatic side chain, giving structures of Type 1:

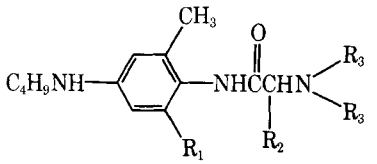

R_1 = H, CH_3
R_2 = H, CH_3, C_2H_5, C_3H_7, C_4H_9
R_3 = CH_3, C_2H_5

A few sterically hindered tetracaine analogs have been prepared previously: several 2-dialkylaminoethyl 4′-butylamino-2′,6′-dimethylbenzoates and two 2-*N*,*N*-dialkylaminoethyl-4′-butylamino-2′,6′-dimethylbenzamides (3). The latter compounds showed a long duration of activity but were appreciably toxic. No 2-*N*,*N*-dialkylaminoacyl-2′-methyl (or 2′,6′-dimethyl)-4′-butylaminoanilides, which comprise true lidocaine-type analogs of tetracaine, have been reported.

RESULTS AND DISCUSSION

Synthesis—The synthetic procedure followed is outlined in Scheme I. The starting material for the synthesis of the 2,6-dimethylanilides, 2,6-dimethyl-4-nitroaniline, was prepared by the method of Wepster (4), which involved the nitration of the *N*-tosyl derivative of 2,6-dimethylaniline. Attempts to nitrate *N*-chloroacetyl-2,6-dimethylanilide failed.

The preparation of some of the *N*-chloroacyl-2′-methyl-4′-nitroanilides was carried out using the procedure of Löfgren (5), using the reaction of chloroacyl chlorides with 2-methyl-4-nitroaniline. When this reaction was applied to 2,6-dimethyl-4-nitroaniline, no amide resulted. For the preparation of the *N*-haloacyl-2′,6′-dimethyl-4′-nitroanilides, or 2′-methyl derivatives where the acid halide was not commercially available,

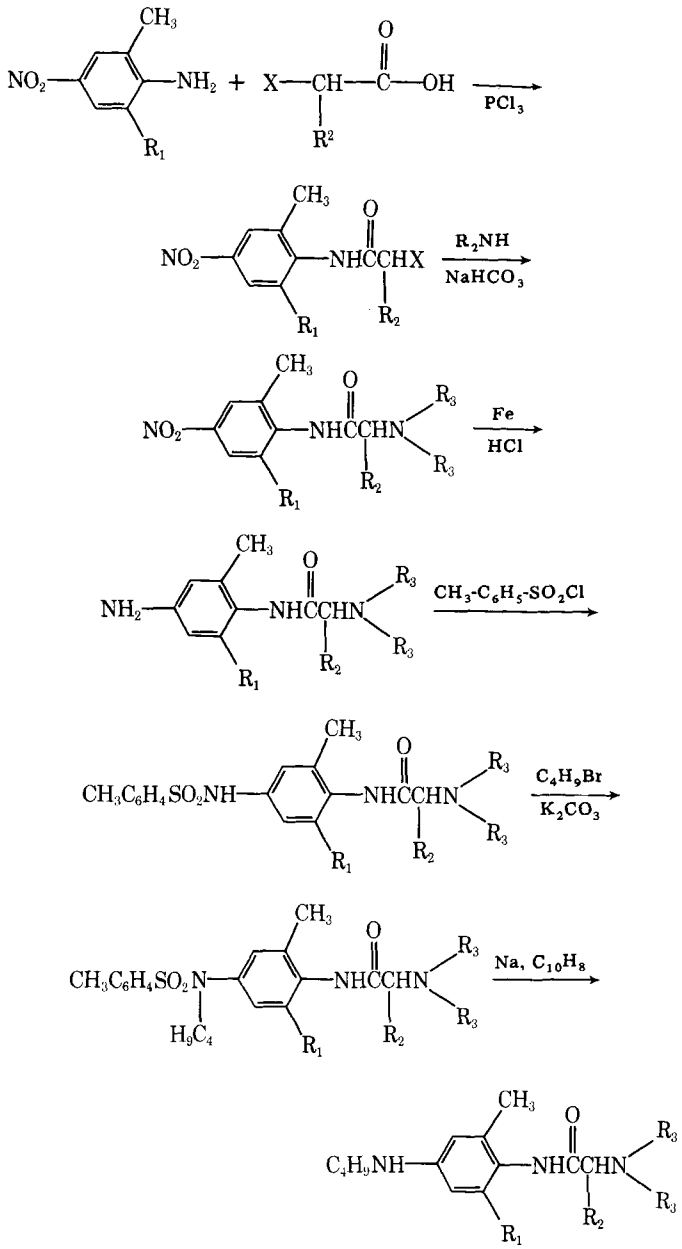

R_1 = H, CH_3
R_2 = H, CH_3, C_2H_5, C_3H_7, C_4H_9
R_3 = CH_3, C_2H_5

Scheme I

the method of Lemaire *et al.* (6) was successful. This involved the preparation of the acid chloride *in situ* with phosphorus trichloride.

The *N*,*N*-dialkylaminoacyl-2′-methyl (or 2′,6′-dimethyl)-4′-nitroanilides were obtained in conventional fashion from treatment of the α-haloacylanilides with dimethylamine hydrochloride in the presence of anhydrous sodium bicarbonate or from diethylamine. E_2 elimination was observed with the longer chain acyl functions. Physical constants of the haloacyl and dialkylaminoacyl derivatives are listed in Table I.

0022-3549/82/0600-0680$01.00/0

Table I—Physical Properties of 2-*N*,*N*-Dialkylaminoacyl-2′-methyl (or 2′,6′-dimethyl)-4′-nitroanilides

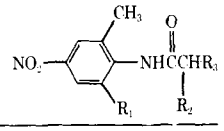

R_1	R_2	R_3	Yield, %	mp	Formula	IR, C=O cm^{-1}	Analysis, % Calc.	Found
H	H	Cl	74	121–122.5	$C_9H_9ClN_2O_3$	1675	C 47.28	47.28
							H 3.98	4.10
							N 12.25	12.20
							Cl 15.51	15.42
H	CH_3	Cl	70	115–116	$C_{10}H_{11}ClN_2O_3$	1670	C 49.50	49.67
							H 4.57	4.61
							N 11.54	11.49
							Cl 14.61	14.77
H	C_2H_5	Br	87	142–144	$C_{11}H_{13}BrN_2O_3$	1665	C 43.87	44.03
							H 4.35	4.49
							N 9.30	9.23
							Br 26.53	26.72
H	C_3H_7	Br	84	131.5–133	$C_{12}H_{15}BrN_2O_3$	1665	C 45.73	45.84
							H 4.80	4.96
							N 8.89	8.72
							Br 25.35	25.15
H	C_4H_9	Br	81	118–120	$C_{13}H_{17}BrN_2O_3$	1665	C 47.43	47.53
							H 5.21	5.28
							N 8.51	8.37
							Br 24.27	24.45
CH_3	H	Cl	77	234–236	$C_{10}H_{11}ClN_2O_3$	1660	C 49.50	49.60
							H 4.57	4.51
							N 11.54	11.44
							Cl 14.61	14.72
CH_3	CH_3	Cl	53	187–189	$C_{11}H_{13}ClN_2O_3$	1660	C 51.47	51.57
							H 5.10	5.18
							N 10.91	10.72
							Cl 13.81	14.01
CH_3	C_2H_5	Br	74	203–205	$C_{12}H_{15}BrN_2O_3$	1650	C 45.73	45.84
							H 4.80	5.09
							N 8.89	8.78
							Br 25.35	25.15
CH_3	C_3H_7	Br	73	181–183	$C_{13}H_{17}BrN_2O_3$	1650	C 47.43	47.57
							H 5.21	5.25
							N 8.51	8.35
							Br 24.27	24.35
CH_3	C_4H_9	Br	71	138–140	$C_{14}H_{19}BrN_2O_3$	1655	C 48.99	49.09
							H 5.58	5.67
							N 8.16	8.10
							Br 23.28	22.97
H	H	$N(CH_3)_2$	79	77–78	$C_{11}H_{15}N_3O_3$	1695	C 55.69	55.66
							H 6.37	6.38
							N 17.71	17.84
H	CH_3	$N(CH_3)_2$	87	81–82	$C_{12}H_{17}N_3O_3$	1700	C 57.36	57.43
							H 6.82	6.67
							N 16.72	16.84
H	C_2H_5	$N(CH_3)_2$	85	54.5–56	$C_{13}H_{19}N_3O_3$	1705	C 58.85	58.91
							H 7.22	7.25
							N 15.84	15.77
H	C_3H_7	$N(CH_3)_2$	86	85–86.5	$C_{14}H_{21}N_3O_3$	1700	C 60.20	60.22
							H 7.58	7.58
							N 15.04	14.99
H	C_4H_9	$N(CH_3)_2$	82	69–70	$C_{15}H_{23}N_3O_3$	1700	C 61.41	61.32
							H 7.90	7.72
							N 14.32	14.43
CH_3	H	$N(CH_3)_2$	87	91–93	$C_{12}H_{17}N_3O_3$	1670	C 57.36	57.36
							H 6.82	6.75
							N 16.72	16.67
CH_3	C_2H_5	$N(CH_3)_2$	80	125–127	$C_{14}H_{21}N_3O_3$	1655	C 60.20	60.18
							H 7.58	7.45
							N 15.04	15.01
CH_3	C_3H_7	$N(CH_3)_2$	82	106–108	$C_{15}H_{23}N_3O_3$	1650	C 61.41	61.60
							H 7.90	7.77
							N 14.32	14.27
CH_3	C_4H_9	$N(CH_3)_2$	75	95–96	$C_{16}H_{25}N_3O_3$	1650	C 62.52	62.25
							H 8.20	8.13
							N 13.67	13.56
H	H	$N(C_2H_5)_2$	93	73–74.5	$C_{13}H_{19}N_3O_3$	1700	C 58.85	58.93
							H 7.22	7.15
							N 15.84	15.90
H	CH_3	$N(C_2H_5)_2$	83	88–89	$C_{14}H_{21}N_3O_3$	1700	C 60.20	60.29
							H 7.58	7.49
							N 15.04	15.14
H	C_2H_5	$N(C_2H_5)_2$	80	69–70	$C_{15}H_{23}N_3O_3$	1710	C 61.41	61.42
							H 7.90	7.83
							N 14.32	14.18

Continued on next page

Table I—*Continued*

R_1	R_2	R_3	Yield, %	mp	Formula	IR, C=O cm^{-1}	Analysis, % Calc.	Found
H	C_3H_7	$N(C_2H_5)_2$	82	56–58	$C_{16}H_{25}N_3O_3$	1710	C 62.52	62.73
							H 8.20	8.05
							N 13.67	13.51
H	C_4H_9	$N(C_2H_5)_2$	79	52–53	$C_{17}H_{27}N_3O_3$	1705	C 63.53	63.61
							H 8.47	8.38
							N 13.07	13.13
CH_3	H	$N(C_2H_5)_2$	90	100–101	$C_{14}H_{21}N_3O_3$	1700	C 60.20	60.34
							H 7.58	7.80
							N 15.04	14.86
CH_3	C_2H_5	$N(C_2H_5)_2$	47	84–86	$C_{16}H_{25}N_3O_3$	1650	C 62.52	62.35
							H 8.20	8.15
							N 13.67	13.73
CH_3	C_3H_7	$N(C_2H_5)_2$	43	94–96	$C_{17}H_{27}N_3O_3$	1650	C 63.53	63.39
							H 8.47	8.41
							N 13.07	12.92
CH_3	C_4H_9	$N(C_2H_5)_2$	41	73–75	$C_{18}H_{29}N_3O_3$	1650	C 64.64	64.52
							H 8.71	8.68
							N 12.53	12.44

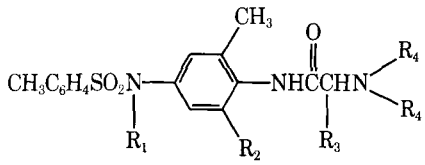

Table II—Physical Properties of 2-*N,N*-Dialkylaminoacyl-2′-methyl (or 2,′6′-Dimethyl-4′-(*p*-toluenesulfonamido)anilides

R_1	R_2	R_3	R_4	Yield, %	mp	Formula	IR, C=O cm^{-1}	Analysis, % Calc.	Found
H	H	H	CH_3	90	138–139	$C_{18}H_{23}N_3O_3S$	1660	C 59.81	59.76
								H 6.41	6.47
								N 11.62	11.50
								S 8.87	9.02
H	H	H	C_2H_5	95	119–121	$C_{20}H_{27}N_3O_3S$	1660	C 61.67	61.81
								H 6.99	7.06
								N 10.79	10.65
								S 8.23	8.31
H	H	CH_3	C_2H_5	85	67–68.5	$C_{21}H_{29}N_3O_3S$	1670	C 62.50	63.07
								H 7.24	7.44
								N 10.41	10.02
								S 7.95	7.70
H	H	C_2H_5	CH_3	82	128–130	$C_{20}H_{27}N_3O_3S$	1660	C 61.67	61.36
								H 6.99	6.96
								N 10.79	10.60
								S 8.23	8.37
H	H	C_2H_5	C_2H_5	78	54–57	$C_{22}H_{31}N_3O_3S$	1665	C 63.28	63.30
								H 7.48	7.61
								N 10.06	9.85
								S 7.68	7.64
H	H	C_3H_7	CH_3	87	81–84	$C_{21}H_{29}N_3O_3S$	1665	C 67.28	67.41
								H 7.27	7.32
								N 8.72	8.82
								S 6.65	6.68
H	H	C_4H_9	CH_3	69	80–84	$C_{22}H_{31}N_3O_3S$	1670	C 67.80	67.42
								H 7.47	7.62
								N 8.48	8.54
								S 6.45	6.47
H	CH_3	*H*	CH_3	79	195–197	$C_{19}H_{25}N_3O_3S$	1650	C 60.78	61.19
								H 6.71	6.61
								N 11.19	11.01
								S 8.54	8.20
H	CH_3	H	C_2H_5	64	160–162	$C_{21}H_{29}N_3O_3S$	1655	C 62.50	62.65
								H 7.24	7.18
								N 10.41	10.26
								S 7.95	7.95
H	CH_3	C_2H_5	CH_3	73	182–184	$C_{21}H_{29}N_3O_3S$	1655	C 62.50	62.28
								H 7.24	7.30
								N 10.41	10.00
								S 7.95	7.77
H	CH_3	C_2H_5	C_2H_5	81	174–177	$C_{23}H_{33}N_3O_3S$	1665	C 64.01	64.07
								H 7.71	7.60
								N 9.74	9.71
								S 7.43	7.39
H	CH_3	C_3H_7	CH_3	62	171–173	$C_{22}H_{31}N_3O_3S$	1650	C 63.28	63.16
								H 7.48	7.38
								N 10.06	9.95
								S 7.68	7.80

Table II—*Continued*

R_1	R_2	R_3	R_4	Yield, %	mp	Formula	IR, C=O cm^{-1}	Analysis, % Calc.	Found
H	CH_3	C_3H_7	C_2H_5	72	169–171	$C_{24}H_{35}N_3O_3S$	1660	C 64.69	64.71
								H 7.92	7.82
								N 9.43	9.26
								S 7.20	7.30
H	CH_3	C_4H_9	CH_3	81	70–75	$C_{23}H_{33}N_3O_3S$	1660	C 64.01	64.12
								H 7.71	7.73
								N 9.74	9.58
								S 7.43	7.16
H	CH_3	C_4H_9	C_2H_5	62	131–133	$C_{25}H_{37}N_3O_3S$	1660	C 65.33	65.41
								H 8.11	7.98
								N 9.14	9.12
								S 6.98	7.08
C_4H_9	H	H	CH_3	79	102–103	$C_{22}H_{31}N_3O_3S$	1690	C 63.28	63.33
								H 7.48	7.54
								N 10.06	10.02
								S 7.68	7.63
C_4H_9	H	H	C_2H_5	73	77–79	$C_{24}H_{35}N_3O_3S$	1700	C 64.69	64.85
								H 7.92	7.80
								N 9.43	9.28
								S 7.20	7.34
C_4H_9	H	CH_3	C_2H_5	63	110–111	$C_{25}H_{37}N_3O_3S$	1700	C 65.33	65.43
								H 8.11	8.06
								N 9.14	9.26
								S 6.98	7.09
C_4H_9	H	C_2H_5	CH_3	78	74–75	$C_{24}H_{35}N_3O_3S$	1695	C 64.69	64.58
								H 7.92	7.88
								N 9.43	9.32
								S 7.20	7.37
C_4H_9	H	C_2H_5	C_2H_5	80	62–68	$C_{26}H_{39}N_3O_3S$	1695	C 65.93	66.36
								H 8.30	8.42
								N 8.87	8.60
								S 6.77	6.68
C_4H_9	H	C_3H_7	CH_3	78	68–70	$C_{25}H_{37}N_3O_3S$	1695	C 65.33	65.30
								H 8.11	7.98
								N 9.14	9.07
								S 6.98	7.16
C_4H_9	H	C_4H_9	CH_3	75	55–57	$C_{26}H_{39}N_3O_3S$	1695	C 65.93	65.89
								H 8.30	8.44
								N 8.87	8.86
								S 6.77	6.74
C_4H_9	CH_3	H	C_2H_5	74	74–76	$C_{25}H_{37}N_3O_3S$	1690	C 65.33	65.34
								H 8.11	8.06
								N 9.14	9.00
								S 6.98	7.15
C_4H_9	CH_3	C_2H_5	C_2H_5	72	117.5–120	$C_{27}H_{41}N_3O_3S$	1650	C 66.49	66.65
								H 8.47	8.39
								N 8.62	8.56
								S 6.57	6.49
C_4H_9	CH_3	C_3H_7	CH_3	73	139–141	$C_{26}H_{39}N_3O_3S$	1650	C 65.93	65.89
								H 8.30	8.36
								N 8.87	8.88
								S 6.77	6.71
C_4H_9	CH_3	C_3H_7	C_2H_5	79	97–99	$C_{28}H_{43}N_3O_3S$	1650	C 67.03	67.02
								H 8.64	8.66
								N 8.37	8.28
								S 6.39	6.40
C_4H_9	CH_3	C_4H_9	CH_3	71	124–125	$C_{27}H_{41}N_3O_3S$	1650	C 66.49	66.42
								H 8.47	8.41
								N 8.62	8.58
								S 6.57	6.68

The reduction of the nitro group was done with iron and hydrochloric acid, according to the method of Clinton *et al.* (7), giving 85–95% yields of amine. The butylation of the 4-amino group was attempted by several procedures. Both direct alkylation with butyl bromide and reductive alkylation procedures using propionaldehyde and reducing agents gave mixtures of mono- and dibutylamino compounds. Monobutylation succeeded by using a modification of the method of Hendrickson and Bergeron (8), in which the amino group is first tosylated and then alkylated with butyl bromide. The alkylations generally required 5–10 days at room temperature. The regeneration of the amine from the *N*-butylsulfonamide was achieved in excellent yield by treatment with sodium naphthalene anion radical in 1,2-dimethoxyethane. The mechanism for this procedure is assumed to be the same as that proposed previously (9) for the sodium–liquid ammonia cleavage of toluenesulfonamides.

Physical constants of the 4′-*N*-tosyl intermediates prepared are listed in Table II, and of the 4′-amino and 4′-butylamino compounds are recorded in Table III.

Local Anesthetic Evaluation—Primary local anesthetic activity was measured by determining loss of reflex of the rabbit cornea (10), using lidocaine for comparison. With this method, both time of onset and duration of action may be determined; testing data are recorded in Table IV. Of the 4′-amino compounds which were not *N*-butylated, none showed significant activity by this procedure. Of the *N*-butyl derivatives, the 2′,6′-dimethyl compounds generally had a longer duration of action than the 2′-methyl substituted compounds. One 2′-methyl derivative, the α-butyl compound, had a comparable time for duration of activity, indicating that a greater extent of alkylation gave greater duration times. This was also the case among the 2′,6′-dimethyl derivatives, where the α-propyl and α-butyl compounds had the longest duration times. Times of onset of action were comparable in both series and were somewhat less than that of lidocaine. Duration times in both series were significantly greater than that for lidocaine.

Determination of the degree of spinal anesthesia in sheep, using the method of Lebeaux (11), was also done with four of the 2′,6′-dimethyl series, including one non-*N*-butyl derivative. Times of onset of activity as well as duration of anal block, digital block, and motor block were

Table III—Physical Properties of 2-*N,N*-Dialkylaminoacyl-2′-methyl (or 2,6′-Dimethyl)-4′-aminoanilides

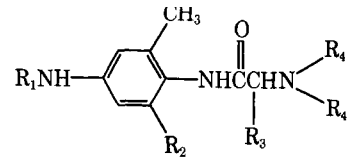

	R_1	R_2	R_3	R_4	%, Yield	mp	Formula	IR, C=O cm^{-1}	pKa	Analysis, % Calc.	Found
1	H	H	H	CH_3	95	100.5–102	$C_{11}H_{17}N_3O$	1650	7.39	C 63.74	63.77
										H 8.27	8.15
										N 20.27	20.29
2	H	H	H	C_2H_5	90	53–54	$C_{13}H_{21}N_3O$	1670	7.85	C 66.35	66.37
										H 8.99	8.89
										N 17.86	17.88
3	H	H	CH_3	CH_3	82	76–78	$C_{12}H_{19}N_3O$	1635	7.30	C 65.13	65.20
										H 8.65	8.61
										N 18.99	19.05
4	H	H	CH_3	C_2H_5	81	77–78	$C_{14}H_{23}N_3O$	1670	8.01	C 67.44	67.32
										H 9.30	9.31
										N 16.85	17.04
5	H	H	C_2H_5	CH_3	75	76–77	$C_{13}H_{21}N_3O$	1650	7.23	C 66.35	66.09
										H 8.99	8.81
										N 17.86	18.07
6	H	H	C_2H_5	C_2H_5	89	78–80	$C_{15}H_{25}N_3O$	1650	8.12	C 68.40	68.32
										H 9.57	9.58
										N 15.95	16.13
7	H	H	C_3H_7	CH_3	79	99–100	$C_{14}H_{23}N_3O$	1655	7.18	C 67.44	67.47
										H 9.30	9.36
										N 16.85	17.02
8	H	H	C_3H_7	C_2H_5	72	52–53	$C_{16}H_{27}N_3O$	1675	7.92	C 69.28	69.50
										H 9.81	9.83
										N 15.15	15.24
9	H	H	C_4H_9	CH_3	90	120–121	$C_{15}H_{25}N_3O$	1650	7.15	C 68.40	68.63
										H 9.57	9.63
										N 15.95	16.10
10	H	CH_3	H	CH_3	85	129–130	$C_{12}H_{19}N_3O$	1660	7.27	C 65.13	65.20
										H 8.65	8.55
										N 18.99	19.11
11	H	CH_3	H	C_2H_5	80	101–103	$C_{14}H_{23}N_3O$	1660	7.80	C 67.44	67.60
										H 9.30	9.39
										N 16.85	16.88
12	H	CH_3	C_2H_5	CH_3	69	139–141	$C_{14}H_{23}N_3O$	1650	7.15	C 67.44	67.15
										H 9.30	9.39
										N 16.85	16.54
13	H	CH_3	C_2H_5	C_2H_5	82	97–99	$C_{16}H_{27}N_3O$	1650	8.05	C 69.28	69.01
										H 9.81	9.84
										N 15.15	15.20
14	H	CH_3	C_3H_7	CH_3	70	179–181	$C_{15}H_{25}N_3O$	1650	7.20	C 68.40	68.28
										H 9.57	9.63
										N 15.95	15.97
15	H	CH_3	C_3H_7	C_2H_5	69	83–85	$C_{17}H_{29}N_3O$	1650	7.85	C 70.06	70.18
										H 10.03	10.10
										N 14.42	14.53
16	H	CH_3	C_4H_9	CH_3	82	183–185	$C_{16}H_{27}N_3O$	1650	7.01	C 69.28	69.29
										H 9.81	9.93
										N 15.15	15.23
17	H	CH_3	C_4H_9	C_2H_5	65	90–92	$C_{18}H_{31}N_3O$	1650	7.85	C 70.78	70.90
										H 10.23	10.24
										N 13.76	13.91
18	C_4H_9	H	H	CH_3	89	50–51	$C_{15}H_{25}N_3O$	1675	7.21	C 68.40	68.40
										H 9.57	9.47
										N 15.95	16.14
19	C_4H_9	H	H	C_2H_5	93	41–41.5	$C_{17}H_{29}N_3O$	1675	7.67	C 70.06	69.63
										H 10.03	9.99
										N 14.42	14.51
20	C_4H_9	H	CH_3	C_2H_5	79	134–136	$C_{18}H_{31}N_3O{\cdot}2HCl{\cdot}H_2O$	1690	8.20	C 54.49	54.41
										H 8.89	9.27
										N 10.59	9.98
										Cl 17.87	17.77
21	C_4H_9	H	C_2H_5	CH_3	84	55.5–57	$C_{17}H_{29}N_3O$	1660	7.25	C 70.06	69.88
										H 10.03	9.91
										N 14.42	14.31
22	C_4H_9	H	C_2H_5	C_2H_5	80	63–65	$C_{19}H_{33}N_3O$	1660	8.02	C 71.43	71.40
										H 10.41	10.47
										N 13.15	13.20
23	C_4H_9	H	C_3H_7	CH_3	85	48–49	$C_{18}H_{31}N_3O$	1665	7.25	C 70.78	70.83
										H 10.23	10.31
										N 13.76	13.81

Table II—*Continued*

	R_1	R_2	R_3	R_4	%, Yield	mp	Formula	IR, C=O cm^{-1}	pKa	Analysis, % Calc.	Found
24	C_4H_9	H	C_4H_9	CH_3	86	163–165	$C_{19}H_{33}N_3O$·HCl	1670	7.12	C 64.11	63.65
										H 9.63	9.66
										N 11.80	11.64
										Cl 9.96	10.11
25	C_4H_9	CH_3	H	C_2H_5	81	39–40	$C_{18}H_{31}N_3O$	1670	7.82	C 70.78	70.92
										H 10.23	10.14
										N 13.76	13.82
26	C_4H_9	CH_3	C_2H_5	C_2H_5	72	155–158	$C_{20}H_{35}N_3O$·2HCl·H_2O	1690	8.05	C 56.59	56.54
										H 9.26	9.62
										N 9.90	9.58
										Cl 16.70	16.45
27	C_4H_9	CH_3	C_3H_7	CH_3	90	45–47	$C_{19}H_{33}N_3O$	1660	7.18	C 71.43	71.51
										H 10.41	10.54
										N 13.15	13.20
28	C_4H_9	CH_3	C_3H_7	C_2H_5	71	176–178	$C_{21}H_{37}N_3O$·2HCl·0.7H_2O	1690	7.77	C 58.74	58.67
										H 9.46	9.32
										N 9.79	9.41
										Cl 15.69	15.82
29	C_4H_9	CH_3	C_4H_9	CH_3	79	204–206	$C_{20}H_{35}N_3O$·2HCl·0.5H_2O	1695	7.22	C 58.33	58.50
										H 9.28	9.05
										N 10.20	9.71
										Cl 16.36	16.15

measured and are listed in Table V. With this determination, the non-*N*-butyl derivative tested (number 13) showed activity somewhat greater in duration than that of lidocaine. The three *N*-butyl compounds tested showed greater duration of activity than 13, but were significantly less than that of tetracaine. It is concluded that this series of compounds has local anesthetic potency intermediate between that of lidocaine and tetracaine.

Ionization constants are listed in Table III for the 4′-amino derivatives. No correlation is evident between local anesthetic potency and pKa values. A previous attempt to find a correlation between ionization constants, oil–water partition coefficients, and local anesthetic activity failed to give statistically significant results (12), although some general trends were noted. Also, IR absorption frequencies for carbonyl absorption are listed in Table III. A previous study (13) revealed an optimum absorption frequency range for good anesthetic potency, but no optimum range for carbonyl absorption is evident for the durations of activity reported here. However, a definite effect of the α-substituent on increasing the wavelength at which carbonyl absorption occurs is apparent.

EXPERIMENTAL

Melting points were taken[1] and are uncorrected[2]. Infrared spectra were recorded on a spectrophotometer[3] using KBr pellets. TLC was carried out using silica gel plates, and the products were detected by exposure to iodine vapor or UV light. Organic reagents were supplied[4–6].

***N*-Haloacyl-2′-methyl (or 2′,6′-dimethyl)-4′-nitroanilides**—*Method 1*—Chloroacetyl chloride (14.91 g, 0.132 mole) was added rapidly to a solution of 18.26 g (0.12 mole) of 2-methyl-4-nitroaniline in 100 ml of glacial acetic acid at 15°. A solution of 45.2 g of sodium acetate trihydrate in 200 ml of water at 10° was added quickly. The mixture was shaken for 35 min, and the product was filtered, washed with 50% hydrochloric acid and water and dried. Recrystallization was generally done with ethanol and charcoal.

Method 2—A mixture of 15.22 g (0.1 mole) of 2-methyl-4-nitroaniline, 7 ml (0.084 mole) of phosphorus trichloride, and 0.105 mole of 2-bromocarboxylic acid in 250 ml of dry benzene was refluxed for 3 hr and filtered. The filtrate was evaporated, and the crude product was washed with 50% hydrochloric acid and water and dried. Recrystallization was done with aqueous ethanol and charcoal. Refluxing time for acylation of 2,6-dimethyl-4-nitroaniline was 24–48 hr.

Method 3—2,6-Dimethyl-4-nitroaniline (4) (15.0 g, 0.09 mole) and redistilled triethylamine (10.0 g, 0.1 mole) in 200 ml of anhydrous ether was cooled to 0–5°, and 14.12 g (0.125 mole) of chloroacetyl chloride was added dropwise with vigorous stirring and ice cooling for 1 hr. The mixture was shaken for 6 hr at room temperature and the ether was evaporated under reduced pressure. The crude product was washed with 50% hydrochloric acid and water, dried, and recrystallized from ethanol and charcoal.

2-*N,N*-Dimethylaminoacyl-2′-methyl (or 2′,6′-dimethyl)-4′-nitroanilides—Dimethylamine hydrochloride (16.15 g, 0.198 mole) and anhydrous sodium bicarbonate (16.63 g, 0.198 mole) in 300 ml of anhydrous benzene was stirred for 30 min, and chloroacetyl-2′-methyl-4′-nitroanilide (13.8 g, 0.066 mole) was added. The mixture was refluxed for 30 hr, cooled, and filtered. The benzene filtrate was extracted with four 80-ml portions of 1 *N* HCl, and the combined extracts were brought to pH 10 with 7 *N* NaOH solution. The precipitate was recrystallized from aqueous ethanol. When this method was applied to α-haloacyl 2,6-dimethyl-4-nitroanilines, the refluxing required 4–6 days.

For preparation of the *N,N*-diethyl derivatives, redistilled diethylamine was used.

2-*N,N*-Dialkylaminoacyl-2′-methyl (or 2′,6′-dimethyl)-4′-aminoanilides—To a stirred, boiling mixture of powdered iron (10.35 g, 0.185 mole), ethanol (85 ml), water (25 ml), and concentrated hydrochloric acid (1 ml) was added in 7.0-g portions (0.026 mole) of *N,N*-diethylaminoacetyl-2′-methyl-4′-nitroanilide. The heat source was removed during the addition. The mixture was stirred and boiled gently for 35 min, cautiously treated with 10.0 g of powdered sodium bicarbonate, stirred at boiling for 10 min, and filtered hot. The filter cake was washed with hot alcohol, and the alcohol was removed *in vacuo*. The residue was added to 15 ml of water and extracted three times with ethyl acetate. The extract was

Table IV—Local Anesthetic Activity: Method of Loss of Reflex by the Rabbit Cornea

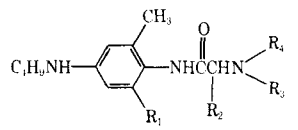

Number[a]	R_1	R_2	R_3	Onset, sec	Duration, min
18	H	H	CH_3	45	40
19	H	H	C_2H_5	25	65
20	H	CH_3	C_2H_5	40	50
21	H	C_2H_5	CH_3	30	35
22	H	C_2H_5	C_2H_5	55	40
23	H	C_3H_7	CH_3	15	55
24	H	C_4H_9	CH_3	30	90
25	CH_3	H	C_2H_5	30	65
26	CH_3	C_2H_5	C_2H_5	25	75
27	CH_3	C_3H_7	CH_3	35	100
28	CH_3	C_3H_7	C_2H_5	20	120
29	CH_3	C_4H_9	C_2H_5	65	105
Lidocaine				90–120	20–25

[a] 1% solutions, pH ~6.7, were tested.

[1] Mel-Temp apparatus.
[2] Microanalyses were done by Dr. F. B. Strauss, Oxford, England.
[3] Perkin-Elmer spectrophotometer Model 457A.
[4] Aldrich Chemical Co.
[5] Fisher Scientific Co.
[6] J. T. Baker Chemical Co.

Table V—Local Anesthetic Activity: Spinal Anesthesia in the Sheep

Number	%, Concentration	pH	Number of Animals	Onset (Anal), Min	Duration, min			Complete Recovery, Min
					Anal Block	Digital Block	Motor Block	
11	2.0	6.5	2	1–2	73	78	73[a]	178
25	0.25	6.0	2	3–5	25	18[a]	20[b]	60
	1.0	6.0	2	1.5	100	100	80	158
26	1.0	5.9	3	1	169	129	88[c]	320
27	1.0	5.3	2	1	180	142	36	>360[d]
Lidocaine	1.5	6.7	6	1	61 ± 16	51 ± 9	24 ± 7	95 ± 21
Tetracaine	0.5	6.25	6	1–1.5	302 ± 66	285 ± 46	208 ± 77	>360[d]
Glucose	5.0	6.2	4	—	0	0	0	—

[a] Frequency 75%. [b] Frequency 50%. [c] Frequency 67%. [d] Less than 24 hr.

dried ($MgSO_4$) and concentrated to a small volume. The syrupy residue was recrystallized from benzene–commercial hexane[7].

2-*N*,*N*-Dialkylaminoacyl-2′-methyl (or 2′,6′-dimethyl)-4′-(*p*-toluenesulfonamido)anilides—2-Dimethylaminoacetyl-2′-methyl-4′-aminoanilide (4.2 g, 0.021 mole) and redistilled pyridine (1.5 ml) in 40 ml of methylene chloride was cooled to 0°, and 4.46 g (0.023 mole) of *p*-toluenesulfonyl chloride was added slowly with stirring and ice-cooling during 30 min. The mixture was stirred for several hr at 0–5°, methylene chloride was removed *in vacuo*, and the residue was added to 80 ml of water. The pH was adjusted to 10 with dilute sodium hydroxide solution, the solution was extracted with ethyl acetate, and the extract was dried ($MgSO_4$). It was concentrated to a small volume, and the residue was recrystallized from benzene–commercial hexane[7].

2-*N*,*N*-Dialkylaminoacyl-2′-methyl (or 2′,6′-dimethyl)-4′-(*N*′-butyl-*p*-toluenesulfonamido)anilides—2-Dimethylaminoacetyl-2′-methyl-4′-(*p*-toluenesulfonamido)anilide (2.8 g, 0.0078 mole), anhydrous potassium carbonate (4.31 g, 0.031 mole), and redistilled *n*-butyl bromide (9.62 g, 0.0702 mole) in 70 ml of dry acetone was stirred at room temperature for 7 days. The mixture was filtered, and acetone was removed in a rotary evaporator. The residual syrup was crystallized from benzene–or ether–commercial hexane[7].

2-*N*,*N*-Dialkylaminoacyl-2′-methyl (or 2′,6′-dimethyl)-4′-butylaminoanilides—Naphthalene (4.64 g, 0.036 mole) in 30 ml of 1,2-dimethoxyethane was kept under nitrogen, and 0.83 g (0.036 mole) of sodium was added. After 5 min, 2.49 g (0.006 mole) of 2-dimethylaminoacetyl-2′-methyl-4′-(*N*′-butyl-*p*-toluenesulfonamido) anilide in 10 ml of 1,2-dimethoxyethane was added, and the solution was kept at room temperature under nitrogen for 80 min. Water was added to quench the reaction, and the solvent was removed in a rotary evaporator. The residue was added to 50 ml of water, the pH was brought to ~2, and the solution was extracted three times with ether. The aqueous solution was adjusted to pH 10 and extracted with ethyl acetate. The extract was dried ($MgSO_4$) and concentrated, and the residual syrup was crystallized from hexane.

Local Anesthetic Evaluation—Primary local anesthetic testing was done by measuring loss of reflex of the rabbit cornea according to Rose (10). Each compound was tested in sterile 1% aqueous solution, pH 6.7, using 1% lidocaine solution, containing no epinephrine, as standard. The test solution (3–4 drops) was applied to one eye of the rabbit, the other eye being treated with control solution, pH 6.7, containing no anesthetic. Using a soft cotton filament rolled to a fine point, the time at which loss of reflex on touching with the filament was recorded to indicate onset of action. The procedure was continued, and the time at which reflex activity returned was recorded for duration of action.

The extent of spinal anesthesia in the sheep was determined according to the procedure of Lebeaux (11). Sterile solutions (2 ml) of the test compounds at the concentrations indicated in Table V and containing glucose (50 mg/ml) were injected intrathecally between the L6 and S1 vertebra. Onset and duration times for sensory blocks from the anal and digital (hind limb) areas were recorded, and for motor block when the animals were able to stand. Frequency of block was 100% except where indicated. Lidocaine (1.5%) and tetracaine (0.5%) solutions were used as standards and glucose (5.0%) solution as control.

Ionization Constants—Determination of ionization constants was done according to the procedure of Albert and Serjeant (14) using a pH meter[8] with glass and calomel electrodes. Titrations of 0.001 *M* aqueous solutions of the compounds were made with 0.01 *N* KOH in 0.5-ml portions. Each titration yielded 10 pH values, giving 10 values for the pKa's, which were averaged. If pH values fell outside the 5–9 range, corrections were made for hydrogen or hydroxide ion concentrations.

REFERENCES

(1) B. H. Takman and H. J. Adams, in "Burger's Medicinal Chemistry," 4th ed., M. E. Wolff, Ed., Wiley, New York, N.Y., 1981, p. 661.

(2) T. D. Whittet, *Anesthesia*, **9**, 271 (1954).

(3) E. Honkanen, *Ann. Acad. Sci. Fenn.*, **99**, 80 (1960).

(4) B. M. Wepster, *Rec. Trav. Chim. Pays-Bas*, **73**, 809 (1954).

(5) N. Löfgren, *Ark. Kemi Mineral. Geol.*, **22A**, 1 (1946).

(6) H. Lemaire, C. H. Schramm, and A. Cahn, *J. Pharm. Sci.*, **50**, 831 (1961).

(7) R. O. Clinton, S. C. Laskowski, U. J. Salvador, and M. Wilson, *J. Am. Chem. Soc.*, **73**, 3674 (1951).

(8) J. B. Hendrickson and R. Bergeron, *Tetrahedron Lett.*, No. 5, 345 (1970).

(9) J. Kovacs and N. R. Ghatak, *J. Org. Chem.*, **31**, 119 (1966).

(10) C. L. Rose, *Anesth. Analg.*, **10**, 159 (1931).

(11) M. Lebeaux, *Lab. Animal Sci.*, **25**, 629 (1975).

(12) W. L. McKenzie and W. O. Foye, *J. Med. Chem.*, **15**, 291 (1972).

(13) W. O. Foye, H. B. Levine, and W. L. McKenzie, *ibid.*, **9**, 61 (1966).

(14) A. Albert and E. P. Serjeant, "The Determination of Ionization Constants," Chapman and Hall, London, England, 1971.

ACKNOWLEDGMENTS

Abstracted from a thesis submitted by C.-M. Jan to the Massachusetts College of Pharmacy and Allied Health Sciences in partial fulfillment of Doctor of Philosophy degree requirements.

Supported by funds from the John R. and Marie K. Sawyer Memorial Fund, Massachusetts College of Pharmacy and Allied Health Sciences.

[7] Skellysolve B.

[8] Beckman Research pH Meter.

Antitumor Agents LII: The Effects of Molephantinin on Nucleic Acid and Protein Synthesis of Ehrlich Ascites Cells

IRIS H. HALL ˣ, Y. F. LIOU, and K. H. LEE

Received June 19, 1981, from the *Division of Medicinal Chemistry, School of Pharmacy, The University of North Carolina, Chapel Hill, NC 27514.* Accepted for publication October 7, 1981.

Abstract □ Molephantinin, a germacranolide, has previously been shown to possess antineoplastic activity in rodents. The principle effect of molephantinin on Ehrlich ascites carcinoma cells was to depress DNA and protein synthesis both *in vivo* and *in vitro*. DNA synthesis was inhibited at the following sites: DNA polymerase, purine synthesis specifically at inosinic acid dehydrogenase and to a lesser degree at dihydrofolate reductase, pyrimidine synthesis at orotidine monophosphate decarboxylase, thymidine kinase, histone phosphorylation, and oxidative phosphorylation processes. The protein synthesis inhibition pattern resembled more an initiation inhibitor as opposed to an elongation inhibitor.

Keyphrases □ Molephantinin—effects on nucleic acid and protein synthesis of Ehrlich ascites cells □ Antitumor agents—effects of molephantinin on nucleic acid and protein synthesis of Ehrlich ascites cells □ DNA—synthesis, effects of molephantinin, Ehrlich ascites cells □ RNA—synthesis, effects of molephantinin, Ehrlich ascites cells □ Protein synthesis—effects of molephantinin, Ehrlich ascites cells

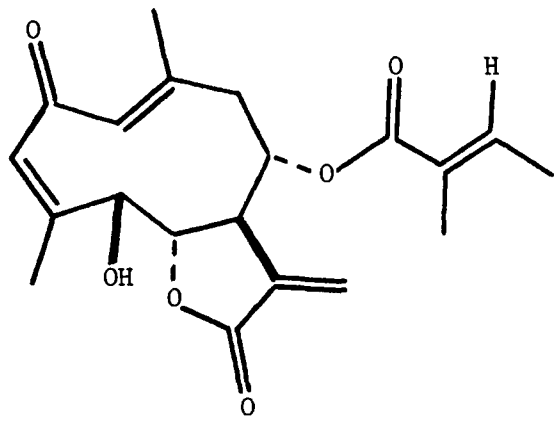

I

Molephantinin (I), a germacranolide, was originally isolated from the winter collection of *Elephantopus mollis*, a member of the herbal Compositae family. Subsequently, molephantinin was shown to be active against Walker 256 carcinosarcoma growth in rats at 2.5 mg/kg/day resulting in a T/C% = 397 (1, 2). Further studies demonstrated that the agent was also active against P-388 lymphocytic leukemia and Ehrlich ascites cell growth (3). *In vitro* DNA polymerase activity and oxidative phosphorylation processes were reported to be inhibited by molephantinin at a relatively high concentration (3). At this time a more detailed examination of the effects of molephantinin on Ehrlich ascites tumor cell metabolism is reported.

EXPERIMENTAL

In vitro incorporation of [^{3}H]thymidine, [^{3}H]uridine, or [^{3}H]leucine was determined using 10^6 Ehrlich ascites cells, 1 μCi of labeled precursor, minimum essential medium, and varying final concentrations of drug from 0.125–2.0 m*M* (4). The tubes were incubated at 37° for 60 min and inactivated by trichloroacetic acid. The insoluble acid, labeled DNA, was collected on glass filter discs[1], and RNA and protein were precipitated on nitrocellulose filters[2] by vacuum suction. Results are expressed as disintegrations per minute of incorporated precursor/hr/10^6 cells. For *in vitro* studies, cells were collected on Day 10 and the drug was incubated at 1.38 m*M*.

Ehrlich ascites cells (10^6) were injected intraperitoneally into CF_1 male mice (~22 g) on day 0. On Days 7, 8, and 9, molephantinin (12.5 mg/kg/day, ip in 0.05% polysorbate 80–water) was injected. Incorporation of thymidine into DNA was determined by the method of Chae *et al.* (5). One hour prior to the animal sacrifice on Day 10, 10 μCi, ip of [6-^{3}H]-thymidine (21.5 Ci/mmole) was injected. The DNA was isolated and the tritium content was determined in a toluene based scintillation fluid[3]. The DNA concentration was determined by the diphenylamine reaction using calf thymus DNA as a standard. Uridine incorporation into RNA was determined using 10 μCi of [5,6-^{3}H]uridine (22.4 Ci/mmole). RNA was extracted by the method of Wilson *et al.* (6). Using yeast RNA as a standard, the RNA content was assayed by the orcinol reaction. Leucine incorporation into protein was determined by the method of Sartorelli (7) using 10 μCi of [4,5-^{3}H]leucine (52.2 Ci/mmole). Extracted protein was determined by the Lowry procedure (8) using bovine albumin as a standard. *In vitro* and *in vivo* nuclear DNA polymerase activity was determined on isolated Ehrlich ascites cell nuclei (9). The incubation was that described by Sawada *et al.* (10) except that [methyl-^{3}H]deoxythymidine triphosphate (82.4 Ci/mmole) was used. The acid insoluble nucleic acid was collected on filters[1] and counted.

Nuclear RNA polymerase activities were determined on enzymes isolated from nuclei (9). Messenger, ribosomal, and transfer RNA polymerases were isolated using 0.3, 0.04, and 0.0 *M* concentrations of ammonium sulfate in magnesium chloride, respectively. The incubation medium was that of Anderson *et al.* (11) using [^{3}H]uridine triphosphate (23.2 Ci/mmole). The acid insoluble RNA was collected on nitrocellulose filters and counted.

Deoxythymidine as well as deoxythymidylate monophosphate and diphosphate kinase activities were measured spectrophotometrically at 340 nm at 20 min using reduced nadide (0.1 μmole) (12). [6-^{3}H]Thymidine (21.5 Ci/mmole) incorporation into the nucleotides was also measured using the reaction medium of Maley and Ochoa (12) and then plating the ether extracted reaction medium on polyethyleneiminecellulose plates. The plates were eluted with 0.5 *N* formic acid–0.6 *N* LiCl (1:1). After identifying R_f values consistent with the standards, thymidine, thymidylate monophosphate, thymidylate diphosphate, and thymidylate triphosphate, the areas on the plates were scraped and counted. Carbamyl phosphate synthetase activity was determined using the reaction medium of Kalman *et al.* (13) in the presence of ornithine and the enzyme ornithine transcarbamylase. Citrulline formed from ornithine was measured at 490 nm by the method of Archibald (14). Aspartate transcarbamylase activity was assayed using the incubation medium of Kalman *et al.* (13). The colorimetric determination of carbamyl aspartate was conducted by the procedure of Koritz and Cohen (15). Orotidine monophosphate decarboxylase activity was assayed by the method of Appel (16) using 0.1 μCi of [^{14}C]orotidine monophosphate (34.9 mCi/mmole). The [^{14}C]-carbon dioxide generated in 15 min was trapped in 1 *M* methanolic base[4] and counted. Thymidylate synthetase activity was determined using a

[1] Whatman GF/F.
[2] Millipore.
[3] Fisher Scintiverse.
[4] Hyamine Hydroxide, New England Nuclear.

0022-3549/82/0600-0687$01.00/0

Table I—The *In Vitro* Effects of Molephantinin at 1.38 m*M* Concentration on Ehrlich Ascites Cell Metabolism

Biochemical Parameter or Enzyme (n = 6)	% Control	
	Control x ± *SD*	Treated x ± *SD*
DNA polymerase	100 ± 14	55 ± 9[a]
Messenger RNA polymerase	100 ± 13	108 ± 11
Ribosomal RNA polymerase	100 ± 6	74 ± 7[a]
Transfer RNA polymerase	100 ± 10	128 ± 12[b]
Ribonucleotide reductase	100 ± 8	101 ± 15
[^{14}C]Formic acid incorporation into purines	100 ± 7	70 ± 9[a]
Phosphoribosyl pyrophosphate amido transferase	100 ± 11	77 ± 10[c]
Inosinic acid dehydrogenase	100 ± 6	43 ± 4[a]
Dihydrofolate reductase	100 ± 9	99 ± 12
Carbamyl phosphate synthetase	100 ± 10	104 ± 10
Aspartate transcarbamylase	100 ± 12	88 ± 9
Orotidine monophosphate decarboxylase	100 ± 9	20 ± 3[a]
Thymidylate synthetase	100 ± 13	92 ± 8
Thymidine kinase	100 ± 9	65 ± 6[a]
Thymidine monophosphate kinase	100 ± 8	18 ± 4[a]
Thymidine diphosphate kinase	100 ± 12	73 ± 7[b]
Oxidative Phosphorylation Processes Substrates:		
Succinate: State 4 respiration	100 ± 7	64 ± 9[a]
State 3 respiration	100 ± 4	75 ± 8[a]
α-Ketoglutarate: State 4 respiration	100 ± 5	69 ± 8[a]
State 3 respiration	100 ± 6	67 ± 9[a]

[a] $p \leq 0.001$. [b] $p \leq 0.005$. [c] $p \leq 0.010$.

Table II—The *In Vivo* Effects of Molephantinin at 12.5 mg/kg/day on Ehrlich Ascites Cell Metabolism

Biochemical Parameters or Enzymes (n = 6)	Control x ± *SD*	Treated x ± *SD*
[^{3}H]Thymidine incorporation into DNA	100 ± 8	19 ± 3[a]
[^{3}H]Uridine incorporation into RNA	100 ± 12	80 ± 12
[^{3}H]Leucine incorporation into protein	100 ± 13	56 ± 8[a]
DNA polymerase	100 ± 6	38 ± 4[a]
Messenger RNA polymerase	100 ± 12	90 ± 10
Ribosomal RNA polymerase	100 ± 8	70 ± 6[a]
Transfer RNA polymerase	100 ± 9	63 ± 4[a]
Ribonucleotide reductase	100 ± 8	90 ± 9
[^{14}C]Formic acid incorporation into purines	100 ± 12	19 ± 2[a]
Phosphoribosyl pyrophosphate amido transferase	100 ± 9	87 ± 5[b]
Inosinic acid dehydrogenase	100 ± 10	26 ± 7[a]
Dihydrofolate reductase	100 ± 12	67 ± 8[a]
Carbamyl phosphate synthetase	100 ± 10	96 ± 9
Aspartate transcarbamylase	100 ± 9	83 ± 8[a]
Orotidine monophosphate decarboxylase	100 ± 10	29 ± 3[a]
Thymidylate synthetase	100 ± 9	108 ± 10
Thymidine kinase	100 ± 9	63 ± 7[a]
Thymidine monophosphate kinase	100 ± 9	36 ± 6[a]
Thymidine diphosphate kinase	100 ± 7	84 ± 8[a]
[^{32}P]Phosphorylation of histones	100 ± 15	36 ± 8[a]
[^{32}P]Phosphorylation of nonhistones	100 ± 13	81 ± 11[b]
Cyclic adenosine monophosphate levels	100 ± 10	155 ± 14[a]
Number of tumor cells/per milliliter of ascites fluid	100 ± 6	24 ± 3[a]

[a] $p \leq 0.001$. [b] $p \leq 0.005$.

postmitochondrial supernate (9000×*g* for 10 min) and 5 μCi of [5-^{3}H]-deoxyuridine monophosphate (14 Ci/mmole) according to the method of Kampf *et al.* (17). [^{14}C]Formate incorporation into purines was determined by the method of Spassova *et al.* (18), using 0.5 μCi of [^{14}C]-formic acid (52.0 mCi/mmole). Purines were separated on silica gel TLC plates eluted with *n*-butanol–acetic acid–water (4:1:5). After identifying R_f values consistent with the standards, adenine and guanine, the plates were scraped and the radioactive content determined. Phosphoribosyl-1-pyrophosphate amidotransferase activity was determined on a supernatant fraction (600×*g* for 10 min) measuring the reduction of 0.6 μmole of nadide at 340 nm for 30 min (19). Inosinic acid dehydrogenase activity was determined spectrophotometrically at 340 nm for 30 min using a supernatant fraction (600×*g* for 10 min). The assay medium was that of Magasanik (20) which contained nadide. Dihydrofolate reductase activity was determined at 340 nm for 30 min as the oxidation of reduced nadide phosphate (21). Ribonucleotide reductase activity was determined by the method of Moore and Hurlbert (22) using [5-^{3}H]cytidine-5-diphosphate (25 Ci/mmole). Ribose and deoxyribose nucleotide were separated on polyethyleneiminecellulose plastic precoated plates eluted with 4% boric acid–4 *M* LiCl (4:3) and scraped at the R_f values consistent with the standard deoxycytidine diphosphate. *In vivo* phosphorylation of histones was determined by injecting 10 μCi of [γ^{32}P]adenosine triphosphate (30.0 Ci/mmole) into mice 1 hr prior to sacrifice. The nuclei were isolated (9), and the histone chromatin protein was extracted by the method of Raineri *et al.* (23). *In vitro* nonhistone protein phosphorylation, dependent on nuclear protein kinase, was determined using 2 n*M* of [γ-^{32}P]adenosine triphosphate (30.0 Ci/mmole) and isolated nuclei chromatin protein was collected on nitrocellulose filters (24). Cyclic 3′,5′-adenosine monophosphate levels were determined by the radioimmunoassay method of Gilman (25) using a commercial kit. An *in vitro* method was used to determine if the drug was an initiation or an elongation protein synthesis inhibitor by comparing with known standards, pyrocatechol violet and emetine, using 1 μCi of [^{3}H]leucine (52.2 Ci/mmole) incubated at 37° for 14 min. Aliquots of the reaction medium were spotted on filter paper[5], chemically extracted, and counted (4).

In vitro oxidative phosphorylation studies (26) were conducted on Ehrlich ascites cells using the substrates, α-ketoglutarate, or succinate. Basal oxygen consumption (State 4) was determined with an oxygen electrode connected to an oxygraph. The adenosine diphosphate was added to obtain State 3, or adenine diphosphate stimulated respiration. The number of microliters of oxygen consumed per hour per milligram of protein for States 3 and 4 was calculated. Protein was determined by the Lowry technique (8).

[5] Whatman No. 3.

Probable (p) significant differences were determined by the Student t test. Data are expressed in Tables I and II as percent of control with standard deviations; n is the number of animals per group.

RESULTS

The *in vitro* effects of molephantinin at 1.38 m*M* concentration are presented in Table I and the *in vivo* effects at 12.5 mg/kg/day are presented in Table II.

In vitro studies for the incorporation of labeled precursors into DNA, RNA, and protein revealed that all three were inhibited in the presence of molephantinin (Fig. 1). Thymidine incorporation into DNA was inhibited significantly with an $ID_{50} \cong 1.22$ m*M*. It may be noted that at the concentration that caused 50% inhibition of DNA synthesis, RNA synthesis was inhibited 30% and protein was inhibited 20% at 1.22 m*M*. The *in vivo* incorporation of thymidine incorporation into DNA was inhibited 81% after dosing for 3 days (Table II). The RNA synthesis was only inhibited 12%, whereas *in vivo* protein synthesis was inhibited 44% after 3 days dosing. The control value for thymidine incorporation was 107,533 dpm/mg of DNA, uridine incorporation was 51,192 dpm/mg of RNA, and leucine incorporation into protein was 19,181 dpm/mg of isolated protein.

Nuclear DNA polymerase activity for the control was 76,528 dpm/hr/mg of nucleoprotein which was suppressed *in vitro* 45% by drug presence (Table I) at 1.38 m*M*, and *in vivo* 62% (Table II) by 3-day administration of drug at 12.5 mg/kg/day. Messenger RNA polymerase activity for the control was 4867 dpm/hr/mg of protein, ribosomal RNA polymerase was 8751 dpm/hr/mg of protein, and transfer RNA polymerase activity was 10,792 dpm/mg of protein. Molephantinin caused little effect on messenger RNA polymerase activity either *in vitro* or after *in vivo* administration. However, ribosomal RNA polymerase activity was inhibited 26% *in vitro* in the presence of drug and 30% after *in vivo* administration of the drug. The transfer RNA polymerase activity was slightly elevated in both *in vitro* and *in vivo* studies.

Ribonucleotide reductase activity for the control was 153,791 dpm/mg of protein which was not affected by molephantinin administration. [^{14}C]Formate incorporation into purines for the control cells was 28,786 dpm/mg of protein which was suppressed 30% in the *in vitro* study and 81% after *in vivo* administration. Phosphoribosyl-pyrophosphate amido transferase activity for the control 10-day Ehrlich ascites cells was observed as an increase of 1.223 optical density unit/hr/mg of protein. *In vitro* presence of drug caused a 23% reduction while *in vivo* administration demonstrated only 13% reduction of enzyme activity. Inosinic acid dehydrogenase activity for the control was 0.358 optical density unit/hr/mg of protein. *In vitro* presence of drug caused 56% inhibition and *in*

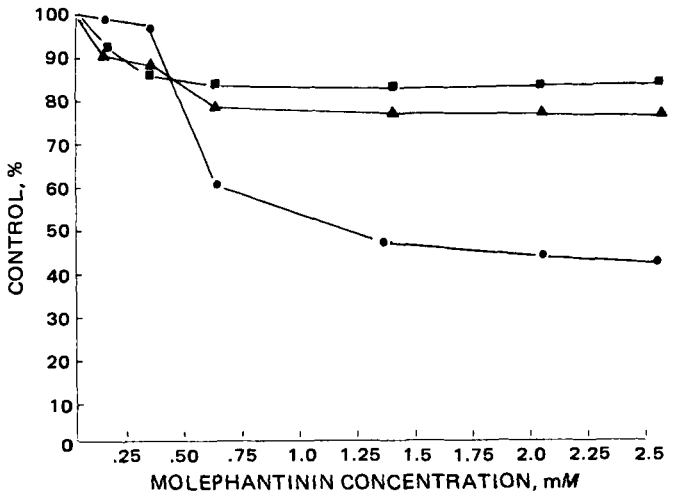

Figure 1—*The* in vitro *effects of molephantinin on nucleic acid and protein synthesis. Key:* ●, *[^{3}H]thymidine → DNA;* ▲, *[^{3}H]uridine → RNA;* ■, *[^{3}H]leucine → protein.*

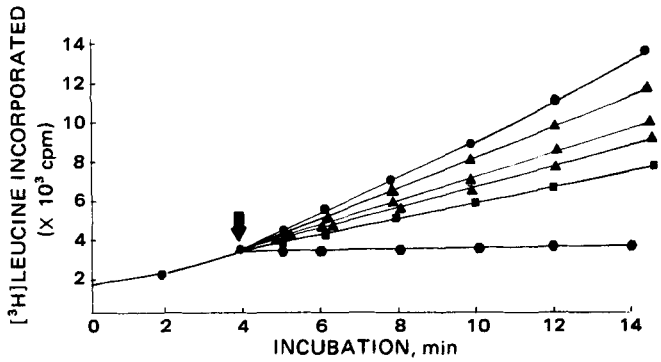

Figure 2—*Effect of pyrocatechol violet, emetine, and molephantinin on the protein synthesis of Ehrlich ascites homogenates using endogenous messenger RNA. Key:* ●, *control;* ▲, *molephantinin (10,100 and 1000 μM);* ■, *pyrocatechol violet (100 μM);* ●, *emetine (100 μM).*

vivo administration of drug resulted in 74% reduction of dehydrogenase activity. Dihydrofolate reductase activity for 10-day Ehrlich ascites cells was 0.514 optical density unit/hr/mg of protein which was unaffected by drug in the *in vitro* studies but was suppressed 33% by 3-day dosing.

Carbamyl phosphate synthetase activity for the control was 0.128 mg of carbamyl phosphate formed/hr/mg of protein. Aspartate carbamyl transferase activity for Day-10 Ehrlich ascites cells was 7.526 mg of carbamyl aspartate formed/hr/mg of protein. Neither of these enzymatic activities was suppressed significantly by molephantinin. Orotidine monophosphate decarboxylase activity for the control was 10,775 dpm of [^{14}C] carbon dioxide regenerated in 15 min/mg of protein. In the *in vitro* studies, there was an 80% reduction in the enzymatic activity, while in the *in vivo* studies there was a 71% reduction of the decarboxylase activity. Thymidylate synthetase activity for the control was 103,328 dpm/mg of protein which was not affected by molephantinin presence. Thymidine kinase activity for the control was 0.531 optical density unit/hr/mg of protein, which was reduced 35% in the *in vitro* studies and 37% in the *in vivo* studies. Thymidylate monophosphate kinase for the control was 0.305 optical density unit/hr/mg of protein which was suppressed 64% by the *in vitro* administration of molephantinin. Thymidylate diphosphate kinase activity in 10-day Ehrlich ascites cells was 0.238 optical density unit/hr/mg of protein which was reduced 16 and 27% in the *in vitro* and *in vivo* studies, respectively. The labeled nucleotide pool levels demonstrated a 54% reduction in the pool level of thymidylate diphosphate and a 58% reduction in thymidylate triphosphate level after 1-hr incubation with drug *in vitro*.

The basal respiration (State 4) of Day-10 Ehrlich ascites tumor cells with succinate as substrate was 5.273 μl of oxygen consumed/hr/mg of protein, while the adenosine diphosphate stimulate respiration (State 3) was 8.752 μl of oxygen consumed/hr/mg of protein. Molephantinin inhibited *in vitro* State 4 respiration by 36% and State 3 respiration by 25%. Using α-ketoglutarate as substrate resulted in a State 4 respiration of 3.569 μl of oxygen consumed/hr/mg of protein and in a State 3 respiration of 5.156 μl of oxygen consumed/hr/mg of protein. Molephantinin inhibited *in vitro* State 4 respiration 31% and State 3 respiration 33%.

Histone phosphorylation of chromatin protein for the control was at a rate of 3650 dpm/mg of isolated chromatin protein which was inhibited 64% by molephantinin administration for 3 days. Nonhistone chromatin phosphorylation for the control was 28,593 dpm/mg of chromatin protein isolation which was reduced 19% by molephantinin administration. Cyclic adenosine monophosphate levels for 10-day Ehrlich ascites cells was 3.65 pmole/10^6 cells. Drug administration for 3 days caused a 17% elevation of cyclic adenosine monophosphate levels of Ehrlich ascites cells. Molephantinin was shown to be a mild initiation inhibitor of protein synthesis (Fig. 2), which compared favorably to pyrocatechol violet, an initiation inhibitor, rather than to emetine, an elongation inhibitor.

DISCUSSION

Molephantinin administration at 12.5 mg/kg/day for 3 days significantly reduced DNA synthesis in Ehrlich ascites cells. The major sites of DNA synthesis inhibition appeared to occur at DNA polymerase, orotidine monophosphate decarboxylase, inosinic acid dehydrogenase, and thymidylate monophosphate kinase. These studies demonstrated that key enzymes in both the purine and pyrimidine pathways were markedly inhibited by molephantinin both *in vitro* and *in vivo*. The observed reduction in the level of either purine or pyrimidine nucleosides would account for the degree of reduction of labeled thymidine incorporation into DNA observed after administration of molephantinin. The germacronolides, eupaformosanin (27) and eupahyssopin (28), as well as the sesquiterpene lactones, helenalin and tenulin (29), have previously been shown to inhibit DNA polymerase activity, and thus, DNA synthesis in Ehrlich ascites cells. Eupaformosanin has been observed to reduce purine synthesis significantly (30). Supposedly, the moiety responsible for this inhibition is the O=CC=CH_2 system which exists both as an α-methylene-γ-lactone and as a C-8 ester side chain in molephantinin. The α-methylene-γ-lactone can undergo a rapid Michaelis-type addition with biological nucleophiles, *e.g.*, sulfhydryl, amino, and carboxyl group (29, 30), and has been shown to play a significant role in antineoplastic activity of sesquiterpene lactones.

Moderate reduction of other enzymes was observed after *in vivo* administration of molephantinin (*e.g.*, ribosomal RNA polymerase, dihydrofolate reductase, and thymidine kinase). *In vitro* administration of molephantinin resulted in a significant reduction in thymidylate diphosphate and triphosphate levels and an accumulation of thymidine. Inhibition of the phosphorylation of histone of the chromosomes was also observed. Inhibition of phosphorous 32 incorporation into histones has been demonstrated by eupaphyssopin, eupaformosanin, and helenalin (27–29). Supposedly, phosphorylation of histones helps to regulate cellular proliferation (31). Energy for this process is supplied by the mitochondrial oxidative phosphorylation process. As can be seen, molephantinin suppressed basal respiration and adenosine diphosphate stimulated respiration, thus reducing available energy sources. Preliminary studies have indicated molephantinin is an initiation inhibitor of protein synthesis in Ehrlich ascites cells. Formation of the initiation complex requires initiation factors which possess an exposed sulfhydryl group which may be alkylated by molephantinin's functional moieties. There appears to be a positive correlation between protein synthesis inhibitors and reduction of oxidative phosphorylation (32).

Molephantinin appears to be one of the more potent germacranolides and is more active than the sesquiterpene lactone, helenalin (27–29). Molephantinin has been shown to have a similar mode of action on the Ehrlich ascites cells as other germacranolides and sesquiterpene lactones.

REFERENCES

(1) K. H. Lee, H. C. Huang, and D. L. Harris, *J. Pharm. Sci.*, **64**, 1077 (1975).

(2) K. H. Lee, T. Ibuka, H. Furukawa, M. Kozuka, R. Y. Wu, I. H. Hall, and H. C. Huang, *ibid.*, **69**, 1050 (1980).

(3) I. H. Hall, K. H. Lee, C. O. Starnes, S. A. ElGebaly, T. Ibuka, Y. S. Wu, T. Kimura, and M. Haruna, *ibid.*, **67**, 1235 (1978).

(4) L. L. Liao, S. M. Kupchan, and S. B. Horwitz, *Mol. Pharmacol.*, **12**, 167 (1976).

(5) C. B., Chae, J. L. Irvin, and C. Piantadosi, *Proc. Am. Assoc. Cancer Res.*, **9**, 44 (1968).

(6) R. G. Wilson, R. H. Bodner, and G. E. MacHorter, *Biochim. Biophys. Acta.*, **378**, 260 (1975).

(7) A. C. Sartorelli, *Biochem. Biophys. Res. Commun.*, **27**, 26 (1967).
(8) O. H. Lowry, N. J. Rosenbough, A. L. Farr and R. J. Randall, *J. Biol. Chem.*, **193**, 265 (1951).
(9) W. C. Hymer and E. L. Kuff, *J. Histochem. Cytochem.*, **12**, 359 (1964).
(10) H. Sawada, K. Tatsumi, M. Sagada, S. Shirakawa, T. Nakumura, and G. Wakisaka, *Can. Res.*, **34**, 3341 (1974).
(11) K. M. Anderson, I. S. Mendelson, and G. Guzik, *Biochim. Biophys. Acta.*, **383**, 56 (1975).
(12) F. Maley and S. Ochoa, *J. Biol. Chem.*, **233**, 1538 (1958).
(13) S. M. Kalman, P. H. Duffield, and T. Brzozuski, *Am. Biol. Chem.*, **24**, 1871 (1966).
(14) R. M. Archibald, *J. Biol. Chem.*, **156**, 121 (1944).
(15) S. B. Koritz and P. P. Cohen, *J. Biol. Chem.*, **209**, 145 (1954).
(16) S. H. Appel, *J. Biol. Chem.*, **243**, 3929 (1968).
(17) A. Kampf, R. L. Barfknecht, P. J. Schaffer, S. Osaki, and M. P. Mertes, *J. Med. Chem.*, **19**, 903 (1976).
(18) M. K. Spassova, G. C. Russev, and E. V. Golovinsky, *Biochem. Pharmacol.*, **25**, 923 (1976).
(19) J. B. Wyngaarden and D. M. Ashton, *J. Biol. Chem.*, **234**, 1492 (1959).
(20) B. Magasanik, *Methods Enzymol.*, **6**, 106 (1963).
(21) Y. K. Ho, T. Kakala, and S. F. Zakrzewski, *Cancer Res.*, **32**, 1023 (1972).
(22) E. G. Moore and R. B. Hurlbert, *J. Biol. Chem.*, **241**, 4802 (1966).
(23) A. Raineri, R. C. Simsiman, R. K. Boutwell, *Cancer Res.*, **33**, 134 (1973).
(24) Y. M. Kish and L. J. Kleinsmith, *Methods Enzymol.*, **40**, 201 (1975).
(25) A. C. Gilman, *Proc. Natl. Acad. Sci. USA*, **67**, 305 (1970).
(26) I. H. Hall, K. H. Lee, C. O. Starnes, S. A. ElGebaly, T. Ibuka, Y. S. Wu, T. Kimura, and M. Haruna, *J. Pharm. Sci.*, **67**, 1235 (1978).
(27) I. H. Hall, K. H. Lee, W. L. Williams, Jr., T. Kimura, and T. Hirayama, *ibid.*, **69**, 294 (1980).
(28) I. H. Hall, K. H. Lee, S. A. ElGebaly, *ibid.*, **67**, 1232 (1978).
(29) I. H. Hall, K. H. Lee, E. C. Mar, C. O. Starnes, and T. G. Waddell, *J. Med. Chem.*, **20**, 333 (1977).
(30) K. H. Lee, I. H. Hall, E. C. Mar, C. O. Starnes, S. A. ElGebaly, T. G. Waddell, R. I. Hadnaft, C. G. Ruffner, and I. Widner, *Science*, **196**, 533 (1977).
(31) C. S. Rubin and O. M. Roseu, *Annu. Rev. Biochem.*, **44**, 81 (1975).
(32) S. B. Wilson and A. L. Moore, *Biochim. Biophys. Acta*, **292**, 603 (1973).

ACKNOWLEDGMENTS

Supported by American Cancer Society Grant CH-19 and National Cancer Institute Grant CA-26466.

The authors thank Larry Carpenter and Melba Gibson for their technical assistance on this project.

Herbal Remedies of the Maritime Indians: Sterols and Triterpenes of *Achillea millefolium* L. (Yarrow)

R. F. CHANDLER *x, S. N. HOOPER *, D. L. HOOPER ‡, W. D. JAMIESON §, C. G. FLINN §, and L. M. SAFE *¶

Received July 23, 1981, from the **College of Pharmacy and the* ‡*Department of Chemistry, Dalhousie University, Halifax, Nova Scotia, B3H 3J5*, and the §*Atlantic Research Laboratory, National Research Council, Halifax, Nova Scotia, B3H 3Z1.* Accepted for publication October 1, 1981. ¶ Present address: Department of Chemistry, University of Guelph, Guelph, Ontario, Canada N1G 2W1.

Abstract □ As part of ongoing studies of the medicinal aspects of Maritime flora, particularly the herbal remedies of the Micmac and Malecite Indians, the sterols and triterpenes of *Achillea millefolium* L. (Compositae), a widely used herbal remedy known commonly as yarrow, were determined. Using modern techniques, including nuclear magnetic resonance spectroscopy and combined GC–mass spectrometry, β-sitosterol was identified as the major sterol and α-amyrin as the major triterpene of this plant. The sterols stigmasterol, campesterol, and cholesterol and the triterpenes β-amyrin, taraxasterol, and pseudotaraxasterol were also identified. Successful therapeutic application of yarrow may be partly due to the presence of one or more of these compounds since many sterols and triterpenes exhibit a wide range of pharmacological activities. This is the first reported occurrence of cholesterol, campesterol, and the four triterpenes in yarrow.

Keyphrases □ *Achillea millefolium* L.—herbal remedies, extraction of triterpenes and sterols □ Triterpenes—extraction from *Achillea millefolium* L., herbal remedies, sterols □ Sterols—extraction from *Achillea millefolium* L., herbal remedies, triterpenes

Since the Trojan war (~1200 BC), *Achillea millefolium* L. has been used extensively by many cultures on different continents as a herbal remedy for various afflictions (1). While conducting studies on the medicinal aspects of the Maritime flora, particularly the herbal remedies of the Micmac and Malecite Indians (2, 3), it was observed that although *A. millefolium* (yarrow) had been widely used and extensively studied (1), very little had been reported regarding its sterols and triterpenes.

Some early articles and various screening papers have reported sterols, triterpenes (3–5), and saponins (6, 7) present in yarrow, although at least one paper stated that the plant contained no steroids (8). Only two authors have previously attempted to determine the nature of the sterols and triterpenes present in this plant. One of those authors documented the presence of stigmasterol and a sitosterol (9), while another reported the presence of β-sitosterol, its acetate, a phytol, and a diol (10).

Therefore, the examination of yarrow for the presence and nature of these compounds is described.

EXPERIMENTAL

Collection and Extraction—The aerial parts of *A. millefolium* were collected during the flowering stage from an open field near Scots Bay, Kings Co., Nova Scotia in September, 1979[1]. The plant material was dried in a forced-air oven at 60° and ground in a Wiley mill to a coarse powder (0.5 cm). This material (2.09 kg) was placed in a stainless steel tank and

[1] The plant material utilized in this investigation was identified as *Achillea millefolium* (L.) (Compositae) by Dr. M. J. Harvey, Department of Biology, Dalhousie University. Herbarium samples (Number 79-03) representing material collected for this investigation are available for inspection at the College of Pharmacy, Dalhousie University.

0022-3549/82/0600-0690$01.00/0

(7) A. C. Sartorelli, *Biochem. Biophys. Res. Commun.*, **27**, 26 (1967).
(8) O. H. Lowry, N. J. Rosenbough, A. L. Farr and R. J. Randall, *J. Biol. Chem.*, **193**, 265 (1951).
(9) W. C. Hymer and E. L. Kuff, *J. Histochem. Cytochem.*, **12**, 359 (1964).
(10) H. Sawada, K. Tatsumi, M. Sagada, S. Shirakawa, T. Nakumura, and G. Wakisaka, *Can. Res.*, **34**, 3341 (1974).
(11) K. M. Anderson, I. S. Mendelson, and G. Guzik, *Biochim. Biophys. Acta.*, **383**, 56 (1975).
(12) F. Maley and S. Ochoa, *J. Biol. Chem.*, **233**, 1538 (1958).
(13) S. M. Kalman, P. H. Duffield, and T. Brzozuski, *Am. Biol. Chem.*, **24**, 1871 (1966).
(14) R. M. Archibald, *J. Biol. Chem.*, **156**, 121 (1944).
(15) S. B. Koritz and P. P. Cohen, *J. Biol. Chem.*, **209**, 145 (1954).
(16) S. H. Appel, *J. Biol. Chem.*, **243**, 3929 (1968).
(17) A. Kampf, R. L. Barfknecht, P. J. Schaffer, S. Osaki, and M. P. Mertes, *J. Med. Chem.*, **19**, 903 (1976).
(18) M. K. Spassova, G. C. Russev, and E. V. Golovinsky, *Biochem. Pharmacol.*, **25**, 923 (1976).
(19) J. B. Wyngaarden and D. M. Ashton, *J. Biol. Chem.*, **234**, 1492 (1959).
(20) B. Magasanik, *Methods Enzymol.*, **6**, 106 (1963).
(21) Y. K. Ho, T. Kakala, and S. F. Zakrzewski, *Cancer Res.*, **32**, 1023 (1972).
(22) E. G. Moore and R. B. Hurlbert, *J. Biol. Chem.*, **241**, 4802 (1966).
(23) A. Raineri, R. C. Simsiman, R. K. Boutwell, *Cancer Res.*, **33**, 134 (1973).
(24) Y. M. Kish and L. J. Kleinsmith, *Methods Enzymol.*, **40**, 201 (1975).
(25) A. C. Gilman, *Proc. Natl. Acad. Sci. USA*, **67**, 305 (1970).
(26) I. H. Hall, K. H. Lee, C. O. Starnes, S. A. ElGebaly, T. Ibuka, Y. S. Wu, T. Kimura, and M. Haruna, *J. Pharm. Sci.*, **67**, 1235 (1978).
(27) I. H. Hall, K. H. Lee, W. L. Williams, Jr., T. Kimura, and T. Hirayama, *ibid.*, **69**, 294 (1980).
(28) I. H. Hall, K. H. Lee, S. A. ElGebaly, *ibid.*, **67**, 1232 (1978).
(29) I. H. Hall, K. H. Lee, E. C. Mar, C. O. Starnes, and T. G. Waddell, *J. Med. Chem.*, **20**, 333 (1977).
(30) K. H. Lee, I. H. Hall, E. C. Mar, C. O. Starnes, S. A. ElGebaly, T. G. Waddell, R. I. Hadnaft, C. G. Ruffner, and I. Widner, *Science*, **196**, 533 (1977).
(31) C. S. Rubin and O. M. Roseu, *Annu. Rev. Biochem.*, **44**, 81 (1975).
(32) S. B. Wilson and A. L. Moore, *Biochim. Biophys. Acta*, **292**, 603 (1973).

ACKNOWLEDGMENTS

Supported by American Cancer Society Grant CH-19 and National Cancer Institute Grant CA-26466.

The authors thank Larry Carpenter and Melba Gibson for their technical assistance on this project.

Herbal Remedies of the Maritime Indians: Sterols and Triterpenes of *Achillea millefolium* L. (Yarrow)

R. F. CHANDLER *x, S. N. HOOPER *, D. L. HOOPER ‡, W. D. JAMIESON §, C. G. FLINN §, and L. M. SAFE *¶

Received July 23, 1981, from the **College of Pharmacy and the* ‡*Department of Chemistry, Dalhousie University, Halifax, Nova Scotia, B3H 3J5*, and the §*Atlantic Research Laboratory, National Research Council, Halifax, Nova Scotia, B3H 3Z1.* Accepted for publication October 1, 1981. ¶ Present address: Department of Chemistry, University of Guelph, Guelph, Ontario, Canada N1G 2W1.

Abstract □ As part of ongoing studies of the medicinal aspects of Maritime flora, particularly the herbal remedies of the Micmac and Malecite Indians, the sterols and triterpenes of *Achillea millefolium* L. (Compositae), a widely used herbal remedy known commonly as yarrow, were determined. Using modern techniques, including nuclear magnetic resonance spectroscopy and combined GC–mass spectrometry, β-sitosterol was identified as the major sterol and α-amyrin as the major triterpene of this plant. The sterols stigmasterol, campesterol, and cholesterol and the triterpenes β-amyrin, taraxasterol, and pseudotaraxasterol were also identified. Successful therapeutic application of yarrow may be partly due to the presence of one or more of these compounds since many sterols and triterpenes exhibit a wide range of pharmacological activities. This is the first reported occurrence of cholesterol, campesterol, and the four triterpenes in yarrow.

Keyphrases □ *Achillea millefolium* L.—herbal remedies, extraction of triterpenes and sterols □ Triterpenes—extraction from *Achillea millefolium* L., herbal remedies, sterols □ Sterols—extraction from *Achillea millefolium* L., herbal remedies, triterpenes

Since the Trojan war (~1200 BC), *Achillea millefolium* L. has been used extensively by many cultures on different continents as a herbal remedy for various afflictions (1). While conducting studies on the medicinal aspects of the Maritime flora, particularly the herbal remedies of the Micmac and Malecite Indians (2, 3), it was observed that although *A. millefolium* (yarrow) had been widely used and extensively studied (1), very little had been reported regarding its sterols and triterpenes.

Some early articles and various screening papers have reported sterols, triterpenes (3–5), and saponins (6, 7) present in yarrow, although at least one paper stated that the plant contained no steroids (8). Only two authors have previously attempted to determine the nature of the sterols and triterpenes present in this plant. One of those authors documented the presence of stigmasterol and a sitosterol (9), while another reported the presence of β-sitosterol, its acetate, a phytol, and a diol (10).

Therefore, the examination of yarrow for the presence and nature of these compounds is described.

EXPERIMENTAL

Collection and Extraction—The aerial parts of *A. millefolium* were collected during the flowering stage from an open field near Scots Bay, Kings Co., Nova Scotia in September, 1979[1]. The plant material was dried in a forced-air oven at 60° and ground in a Wiley mill to a coarse powder (0.5 cm). This material (2.09 kg) was placed in a stainless steel tank and

[1] The plant material utilized in this investigation was identified as *Achillea millefolium* (L.) (Compositae) by Dr. M. J. Harvey, Department of Biology, Dalhousie University. Herbarium samples (Number 79-03) representing material collected for this investigation are available for inspection at the College of Pharmacy, Dalhousie University.

0022-3549/82/0600-0690$01.00/0

Table I—Nuclear Magnetic Resonance Assignments for Yarrow Triterpene Acetates

Group Assignment	α-Amyrin		β-Amyrin		Taraxasterol		ψ-Taraxasterol	
	Identity[a]	Shift[b]	Identity[a]	Shift[b]	Identity[a]	Shift[b]	Identity[a]	Shift[b]
CH_3—C	3H,s	0.81	6H,s	0.84	9H,s	0.85	3H,s	0.74
CH_3—C	9H,s	0.89	12H,s	0.89	3H,s	0.87	3H,s	0.85
CH_3—C	3H,s	0.93	—	—	3H,s	0.93	3H,s	0.86
CH_3—C	3H,s	1.00	6H,s	0.98	—	—	3H,s	0.88
CH_3—C	3H,s	1.02	—	—	3H,s	1.02	3H,s	0.95
CH_3—C	3H,s	1.08	—	—	—	—	3H,s	1.05
CH_3—C	—	—	—	—	3H,d[c]	1.02	3H,d[c]	1.04
CH_3—C=	—	—	—	—	—	—	3H,s	1.66
CH_2—CH=C	2H,m	1.90	2H,m	1.90	—	—	—	—
CH_3—CO	3H,s	2.06	3H,s	2.06	3H,s	2.05	3H,s	2.05
CH_3—CH	—	—	—	—	1H,m	2.10	1H,m	2.10
CH_2=C—CH	—	—	—	—	1H,m	2.40	—	—
CH—OAcetate	1H,t[d]	4.53	1H,t[d]	4.53	1H,t[d]	4.50	1H,q[e]	4.50
CH_2=C	—	—	—	—	2H,m	4.60	—	—
CH=C	1H,t[f]	5.14	1H,t[g]	5.18	—	—	1H,d[c]	5.27

[a] In deuterochloroform; number of hydrogens, multiplicity (d = doublet, m = multiplet, q = quartet, s = singlet, t = triplet), J = coupling constant. [b] δ, ppm. [c] J = 6 Hz. [e] J = 7, 11 Hz. [f] J = 3–4 Hz. [g] J = 6 Hz.

macerated in chloroform–methanol (1:1, v/v) for at least 24 hr; the extract was then drained from the tank. This process was repeated 3 times; the extracts were then combined and the solvent removed *in vacuo*, producing a dark green, waxy mass (78.8 g). This material was saponified following a published method (11). The nonsaponifiable portions were extracted with ether and the solvent was removed *in vacuo*, yielding an amber-colored residue (34.2 g).

Thin-Layer Chromatography—The nonsaponifiable portions were fractionated by preparative TLC using plates coated with silica gel[2] (11). Following visualization procedures, the sterols appeared as a red band ($R_f \simeq 0.25$) and the triterpenes as a red-brown band $R_f \simeq 0.40$). The material from these two bands was recovered by extracting the silica gel with ether and chloroform (12).

The triterpene band, converted to acetates (12), was further fractionated using silica gel[2] impregnated with silver nitrate (13). The visualization process, using 2′,7′-dichlorofluorescein (13), indicated that six bands were present; these were numbered according to increasing R_f. Following recovery from the silica gel with ether and chloroform, bands 3, 4, and 5 gave positive Liebermann-Burchard tests (14) for triterpenes. Bands 1, 2, and 6 produced negative tests and were not considered for further study.

Gas–Liquid Chromatography—The sterol fraction was analyzed using SE-30, OV-1, OV-17, and OV-225[3] columns[4], authentic reference standards, and cholestane as an internal standard (15). The triterpenes were similarly analyzed using SE-30, OV-17, and OV-225 columns and respective oven temperatures of 290, 275, and 250°. The acetates (12) of the taraxasterols and their dihydroderivatives were analyzed using OV-1 with an oven temperature of 275° and OV-17 and OV-225 columns.

Nuclear Magnetic Resonance Spectroscopy—All spectra were recorded in dilute solutions in deuterated solvents using tetramethylsilane as the internal reference[5,6].

Gas Chromatography–Mass Spectrometry—GC–mass spectrometry studies[7] were performed on a high-capacity 3% OV-1 flexible quartz capillary column[8] (25 m × 0.3-mm i.d.), which was directly interfaced to the source of the mass spectrometer. Electron impact mass spectra were determined at 70 eV and a source temperature of 260° (indicated). Source temperature was 230° (indicated) for the positive ion chemical ionization mass spectrometric studies. Methane was used as the ionizing gas at a source pressure of 0.02 torr (indicated), and helium was used as the carrier gas (2 ml/min).

Taraxasterol and pseudotaraxasterol acetates were also run on an OV-1 packed column[9] with an oven temperature of 290° and with helium as the carrier gas (35 ml/min).

Hydrogenation—Sufficient samples (2–3 mg) of taraxasterol acetate, pseudotaraxasterol acetate, and α-amyrin acetate fractions were dissolved in ethanol. Each was hydrogenated in a microhydrogenator[10] at room temperature and pressure using palladium–charcoal as the catalyst. After 3 hr, the reaction medium was filtered to remove the catalyst and reduced to dryness *in vacuo*.

Authentic Samples—Authentic samples of cholestane[11], β-sitosterol[11], stigmasterol[11], cholesterol[12], campesterol[13], α- and β-amyrin[14] were purchased; taraxasterol[15] and pseudotaraxasterol acetate[16] were gifts.

RESULTS AND DISCUSSION

Quantitative TLC indicated that sterols and triterpenes represented ~6 and 54%, respectively, of the nonsaponifiable materials in yarrow (11). GLC studies of the TLC fractions demonstrated that β-sitosterol was the major sterol present, representing ~75% of the sterols. Campesterol (10%), cholesterol (5%), stigmasterol (3%), and an unidentified sterol (6%) were also present. Sequential coinjection of the sterol fraction recovered from TLC with each of the authentic sterols produced single, symmetrical peaks, verifying the identity of these four sterols from yarrow.

Similar studies of the triterpene fraction using the SE-30 column indicated that there were four triterpenes in the material recovered from the TLC fractions. The OV-17 column presented a split peak, indicating the presence of at least five triterpenes. Complete separation, achieved on an OV-225 column, established that yarrow contained seven triterpenes. Comparison with authentic material verified that α-amyrin was the major triterpene present, representing ~42% of this fraction; β-amyrin (33%) and taraxasterol (18%) were also identified in this way. A fourth triterpene, tentatively identified as pseudotaraxasterol (4%), and three unidentified triterpenes accounted for the balance of this fraction (3%).

The triterpene fraction was acetylated (12) and subjected to argentation chromatography (13, 16, 17) to obtain sufficient amounts of pseudotaraxasterol to conduct instrumental and chemical analyses. Initially, six bands were obtained, although only bands 3, 4, and 5 produced positive Liebermann-Burchard tests (14) following elution from the silica gel. Bands 3, 4, and 5 were each subjected to further argentation chromatography. In this manner it was possible to obtain a few milligrams of α- and β-amyrin acetates from band 5, pseudotaraxasterol acetate from band 4, and taraxasterol acetate from band 3. Each of these samples was at least 80% pure, and nuclear magnetic resonance (NMR) (Table I) and GC–mass spectrometry (Tables II and III) data were collected for each.

The NMR spectra of α- and β-amyrin acetates and taraxasterol acetate in deuterochloroform and deuterobenzene were in keeping with similar compounds (18, 19).

The electron impact mass spectra of α- and β-amyrin acetate agreed

[2] Silica gel H, Brinkmann Instruments (Canada) Ltd., Toronto, Ontario, Canada, catalog number 7736.
[3] Three percent on 100–120 mesh Chromosorb W-HP.
[4] Chromatographic Specialties, Brockville, Ontario, Canada.
[5] Preliminary NMR spectra were recorded on Varian A-60, T-60, and CFT-20 spectrometers of Dalhousie University, Halifax.
[6] The 220 MHz NMR spectra were recorded on a Varian HR-220 spectrometer located at the Canadian 220 NMR Centre, Department of Medical Genetics, University of Toronto.
[7] Finnigan-MAT 4000 GC–MS quadrapole mass spectrometer coupled to an INCOS data system.
[8] Hewlett-Packard (Canada) Ltd., Mississauga, Ontario, Canada.
[9] Three percent on 100–120 mesh Gas Chrom. Q, 200 cm × 2 mm, Chromatographic Specialties, Brockville, Ontario, Canada.
[10] Supelco, Inc., Bellefonte, PA 16823.
[11] Sigma Chemical Co., St. Louis, Mo.
[12] Fisher Scientific Co., Montreal, Quebec, Canada.
[13] Applied Science, State College, Pa.
[14] Pfaltz and Bauer, Inc., Stamford, Conn.
[15] Professor T. R. Watson, Pharmacy Department, University of Sydney, Sydney, Australia.
[16] Dr. R. V. Madrigal, Northern Regional Research Laboratory, USDA, Peoria, Ill.

Table II—Relative Intensities in the Electron Impact Mass Spectra of Yarrow Triterpene Acetates

	Capillary Column					Packed Column	
m/z	α-Amyrin	β-Amyrin	Taraxasterol	Pseudo-taraxasterol	Dihydrotaraxasterol	Taraxasterol	Pseudo-taraxasterol
470[a]	—	—	—	—	0.3	—	—
468[a]	0.4	0.4	1.7	0.2	—	9.5	3.6
410	—	—	—	—	0.8	—	—
408	—	—	1.6	0.3	—	8.2	8.6
395	—	—	—	—	0.9	—	—
393	—	—	0.8	0.5	—	3.4	2.8
326	—	—	—	—	—	—	0.9
249	0.7	0.6	6.7	4.3	8.7	12	8.8
229	—	—	3.6	—	—	—	—
218	100	100	5.0	2.2	1.6	7.7	4.3
204	—	—	14	—	—	—	—
203	27	51	15	9.3	6.9	16	15
191	7.5	3.4	31	16	36	24	60
189	44	19	100	100	100	100	100
175	12	11	23	19	12	21	26
161	18	8.6	23	14	9.4	20	26
149	15	7.2	18	12	15	17	25
147	23	15	31	18	10	—	32
137	10	—	11	8.1	24	11	13
135	42	18	55	44	35	43	47
133	32	15	28	32	12	21	42
123	30	9.2	32	36	48	25	29
121	38	19	74	77	47	52	69
109	44	20	81	64	51	57	51
107	45	23	72	65	45	43	50

[a] Molecular ion (M+).

Table III—Relative Intensities in the Chemical Ionization Mass Spectra of Yarrow Triterpene Acetates[a]

m/z	α-Amyrin	β-Amyrin	Taraxasterol	Pseudotaraxasterol
468[b]	0.2	0.1	0.2	0.1
453	0.1	0.2	0.1	0.1
409	63	38	58	55
408	49	31	28	32
394	—	—	—	6.3
393	24	16	25	25
327	—	—	—	0.4
326	—	—	—	0.2
249	2.3	2.3	3.1	2.3
219	38	34	39	—
218	58	43	9.0	—
205	60	64	73	—
203	38	49	49	—
191	62	69	99	—
189	37	42	47	—
175	20	25	20	16
161	20	25	16	16
149	47	47	47	44
147	21	22	14	13
137	46	51	35	34
135	41	39	30	33
133	23	24	15	19
123	27	66	65	48
121	43	41	41	41
109	100	100	100	100
107	32	35	21	20

[a] Methane was the ionizing gas. [b] Molecular ion (M+).

with published data (13), while that of taraxasterol acetate was in keeping with predicted fragmentation patterns (20, 21). The positive chemical ionization mass spectra for these compounds differed only in the relative abundance of the fragment ions. All showed a base peak at *m/z* 109.

Direct comparison with authentic samples by GLC, NMR, and GC–mass spectrometry confirmed the identity of these three triterpene acetates.

The identification of pseudotaraxasterol (ψ-taraxasterol) was the most difficult and frustrating aspect of this research. Previous investigators also encountered this problem. As early as 1938 it was stated (22) that the material Power and Browning (23) had called homotaraxasterol was "a difficultly separable mixture of taraxasterol, ψ-taraxasterol, and possibly other unidentified substances."

The 220-MHz NMR spectrum provided valuable information that helped to identify this compound as pseudotaraxasterol. The spectrum of the acetate contained peaks for the acetate methyl group (2.05 ppm) and for the corresponding methine hydrogen (4.50 ppm) that were in keeping with the spectra described previously.

The spectrum also showed six methyl singlets present between 0.74 and 1.05 ppm. The three resonances that provided the most data, however, were those at 1.04, 1.66, and 5.27 ppm. The first was a three-proton doublet (J = 6 Hz), which corresponded to the features expected of a methyl group at a tertiary carbon. The signal at 1.66 ppm was not clearly defined, but contained a broad three-proton singlet corresponding to a vinylic methyl group. These groups normally appear in this region (1.63–1.80 ppm), and, although usually sharp and well defined (18), they may appear as a broad, less well defined peak at ~ 1.67 ppm (19). Irradiation experiments showed that a methine hydrogen coupled to the olefinic proton at 5.27 ppm also appeared at this resonance. This latter resonance was perhaps the most useful one in the entire spectrum. This one-proton signal appeared as a broad doublet (J = 6 Hz), the broadening presumably caused by additional coupling. The appearance of such a one-proton signal indicated that the other olefinic carbon was quaternary and either at a ring junction or bonded to a methyl group.

To determine the skeletal structure of the triterpene in question, a small amount was hydrogenated and the product was compared with those obtained by hydrogenating taraxasterol acetate and α-amyrin acetate. Of the limited number of compounds (Δ^5, Δ^9, Δ^{12}, Δ^{20}) that would produce the same product of catalytic hydrogenation as taraxasterol [$\Delta^{20(30)}$] and α-amyrin (Δ^{12}), only pseudotaraxasterol (Δ^{20}) fit the additional experimental facts presented by the NMR spectrum and by the mass spectrometry data to be discussed.

The GC–mass spectrometry data were obtained by both electron impact and methane positive chemical ionization. Although the diagnostic peak *m/z* 386 produced from cleavage of ring E (19) was absent in all spectra, a small peak at *m/z* 326 (386-acetic acid, 0.9%) occurred in the spectrum obtained by electron impact–mass spectrometry using a packed column and also at *m/z* 327 (0.4%) and 326 (0.2%) when positive chemical ionization–mass spectrometry and a capillary column were used. These peaks were not observed in the corresponding spectra of taraxasterol acetate. The hydrogenation experiment supplied further proof that the structure of pseudotaraxasterol was the correct assignment. Upon catalytic hydrogenation, both taraxasterol acetate and pseudotaraxasterol acetate produced a common product, dihydrotaraxasterol acetate. GC–mass spectrometry of these two products produced identical electron impact and positive chemical ionization spectra.

Conclusive proof of identity occurred when positive chemical ionization mass spectrometry and GLC on OV-17 and OV-225 columns showed that a sample of pseudotaraxasterol acetate[17] was identical to the pseudotaraxasterol acetate isolated from yarrow.

[17] A gift from Dr. R. V. Madrigal.

The second and smaller GLC peak obtained from the hydrogenation of taraxasterol acetate is believed to be the C-20 isomer (20α-methyl). This material produced a mass spectrum that was essentially identical to that of the other dihydrotaraxasterol acetate.

Thus, using modern instrumental techniques, four sterols and four triterpenes of yarrow were identified. β-Sitosterol was the major sterol and α-amyrin the major triterpene present. Other sterols identified were cholesterol, campesterol, and stigmasterol while the other triterpenes were β-amyrin, taraxasterol, and pseudotaraxasterol. Another study (24) found that pseudotaraxasterol occurred in *Tanacetum vulgare* L. (as did the other compounds) but it was not positively identified at that time due to sample size.

This study confirms that stigmasterol (9) and β-sitosterol (9, 10) are present in yarrow. It is also the first time that cholesterol, campesterol, α- and β-amyrin, taraxasterol, and pseudotaraxasterol have been reported in yarrow, although the presence of sterols and triterpenes have been previously noted (3–5, 10). No diols (10) were identified, although the possibility remains that they may have been the compounds observed with the longer relative retention time.

Much of the time and effort of this project was spent applying modern instrumental techniques to resolve a problem that has plagued chemists for over half a century—how to separate and identify taraxasterol and pseudotaraxasterol (22, 23).

REFERENCES

(1) R. F. Chandler, S. N. Hooper, and M. J. Harvey, *Econ. Bot.*, **36,** 203 (1982).

(2) R. F. Chandler, L. Freeman, and S. N. Hooper, *J. Ethnopharmacol.*, **1,** 49 (1979).

(3) R. F. Chandler and S. N. Hooper, *Can. J. Pharm. Sci.*, **14,** 103 (1979).

(4) Z. Kasprzyk and T. Kozierowska, *Bull. Acad. Pol. Sci. Ser. Sci. Biol.*, **14,** 645 (1966).

(5) R. L. McMurray, *Am. J. Pharm.*, **105,** 573 (1933).

(6) E. Wagner, *Seifensieder-Ztg.*, **68,** 35 (1941); through *Chem. Abstr.*, **35,** 3032–9.

(7) K. S. Tillyaev, K. K. Khalmatov, I. Primukhamedov, and M. A. Talipova, *Rastit. Resur.*, **9,** 58 (1973); through *Chem. Abstr.*, **78,** 121284q.

(8) M. E. Wall, C. S. Fenske, J. W. Garvin, J. J. Willaman, Q. Jones, B. G. Schubert, and H. S. Gentry, *J. Am. Pharm. Assoc., Sci. Ed.*, **48,** 695 (1959).

(9) O. Gisvold, *ibid.*, **24,** 1071 (1935).

(10) C. Ivanov and L. Yankov, *God. Vissh. Khimikotekhnol. Inst., Sofia*, **14,** 195, 223; **14,** 61, 73 (1967); through *Chem. Abstr.* **77,** 111471p, 111472q, 111473r, 111474s.

(11) "Method Ca 6b-53 The Official and Tentative Methods of the American Oil Chemists' Society," 3rd ed., American Oil Chemists' Society, Champaign, Ill., 1972.

(12) L. M. Safe, C. J. Wong, and R. F. Chandler, *J. Pharm. Sci.*, **63,** 464 (1974).

(13) R. V. Madrigal, R. D. Plattner, and C. R. Smith, Jr., *Lipids*, **10,** 208 (1975).

(14) H. H. S. Fong, in "Experiments in the Pharmaceutical Biological Sciences," M. H. Malone and J. L. McLaughlin, Eds., American Association of Colleges of Pharmacy, Stockton, Calif., 1973, pp. 43–51.

(15) S. N. Hooper and R. F. Chandler, *J. Pharm. Sci.*, **67,** 1157 (1978).

(16) H. E. Vroman and C. F Cohen, *J. Lipid Res.*, **8,** 150 (1967).

(17) L. J. Morris, *J. Lipid Res.*, **7,** 717 (1966).

(18) M. Shamma, R. E. Glick, and R. O. Mumma, *J. Org. Chem.*, **27,** 4512 (1962).

(19) N. S. Bhacca, and D. H. Williams, "Applications of NMR Spectroscopy in Organic Chemistry," Holden-Day, San Francisco, Calif., 1964, pp. 13–41; 77–89.

(20) H. Budzikiewicz, J. M. Wilson, and C. Djerassi, *J. Am. Chem. Soc.*, **85,** 3688 (1963).

(21) H. Budzikiewicz, C. Djerassi, and D. H. Williams, "Structure Elucidation of Natural Products by Mass Spectrometry, Vol II: Steroids, Terpenoids, Sugars, and Miscellaneous Classes," Holden-Day, San Francisco, Calif., 1964, p. 121.

(22) S. Burrows and J. C. E. Simpson, *J. Chem. Soc.*, **1938** 2042.

(23) F. B. Power and H. Browning, Jr., *ibid.*, **101,** 2411 (1912).

(24) R. F. Chandler, S. N. Hooper, D. L. Hooper, W. D. Jamieson, and E. Lewis, *Lipids*, **17,** 102 (1982).

ACKNOWLEDGMENTS

This work was supported by the Medical Research Council of Canada (MA-6448).

The authors thank Dr. M. J. Harvey, Associate Professor, Department of Biology, Dalhousie University, for his help in collecting and determining the plant material; Dr. A. A. Grey, Director, Canadian 220 MHz NMR Centre, Department of Medical Genetics, University of Toronto, for the NMR spectra and his valuable comments; Dr. T. R. Watson, Professor, Pharmacy Department, University of Syndey, Sydney, Australia, for the sample of taraxasterol; Dr. R. V. Madrigal, Northern Regional Research Laboratory, USDA, Peoria, Ill., for the sample of pseudotaraxasterol acetate; and Editorial Service, Faculty of Medicine, Dalhousie University for help in preparing this manuscript.

Mathematical Model for *In Vitro* Drug Release from Controlled Release Dosage Forms Applied to Propoxyphene Hydrochloride Pellets

FINN NORRING CHRISTENSEN *, FLEMMING YSSING HANSEN ‡, and HELLE BECHGAARD **

Received December 16, 1980, from the **Controlled Release Division, A/S Alfred Benzon, DK-1700 Copenhagen V, Denmark* and the ‡*Institute of Physical Chemistry, The Technical University of Denmark, DK-2800 Lyngby, Denmark.* Accepted for publication October 1, 1981.

Abstract □ The *in vitro* release of drugs from controlled-release dosage forms has been studied in terms of a diffusion model. The model has been applied to a pellet formulation containing propoxyphene hydrochloride. It is demonstrated that the model may be used to predict the drug release profile adequately, when the pellet size is changed and when the thickness of the coating is varied. The size distribution of pellets in an experiment may be too broad to justify a simulation with just one average pellet size. Therefore, the results for pellets of the same size are generalized to any size distribution of pellets in an experiment. This is only trivial if sink condition exists in the extraction medium, since under that condition, the release from each pellet type is independent of the releases from other pellet types. In that case, the total release may therefore be found as the sum of the individual releases. In the general case considered here, the releases are coupled.

Keyphrases □ Mathematical models—*in vitro* drug release from controlled-release dosage forms, propoxyphene hydrochloride pellets □ Propoxyphene hydrochloride pellets—mathematical model for *in vitro* drug release from controlled-release dosage forms □ Controlled-release dosage forms—mathematical model for *in vitro* drug release, propoxyphene hydrochloride pellets

In a recent paper (1) it was shown that a quasistationary diffusion description of the drug release from controlled release dosage forms formally leads to an expression of the same form as a Rosin-Rammler-Sperling-Weibull distribution when $\beta = 1$, (1–4). The advantage of the diffusion description is that it allows a prediction of the drug release as a function of pellet size and coat thickness once the diffusion coefficient for a given drug in the coat is known. In the present paper, the general solution to the diffusion description without the simplifying assumption about quasistationarity is considered.

THEORETICAL

It is assumed that pellets are spherical and consist of a core containing the drug and a coat which is the rate-limiting element in the release process (5). The radius of the core is b and the radius of the coated pellet is a giving a coat thickness of $(a - b)$.

In practice a dissolution test is done with a large number of pellets. If the pellets have a narrow size distribution, one may use the results for pellets of the given size. In the case of a broad size distribution, it is necessary to take that into account. In the present general solution to the diffusion description, both cases are discussed.

It is evident that the release profile, in general, may not be calculated as a superposition of the profiles from each pellet size since the increase of drug concentration in the extraction medium couples the releases from the pellets. Only in the case of zero concentration in the extraction medium (sink condition) no coupling is present, and a superposition of releases gives the total release.

It is important to note the simplifying assumptions inherent in this description. The initial phase, where dry pellets are introduced into an extraction medium, water penetrates the coat and dissolves the drug in the core, is not included in this description. This model may be applied from the time the drug in the core has been dissolved by the penetrating water. A time lag may be accounted for simply by shifting the zero point on the time axis, corresponding to the duration of the initial phase. Since there are no data available to calculate the initial phase kinetics, it is necessary to rely on experimental evidence for a reasonable assessment of time lag. It is a very important assumption that the pellets do not change dimensions (*e.g.*, due to swelling during the release period). In particular, if the pellet dimensions are determined from dry pellets, it is crucial to check that the dimensions are not changed after introduction into the extraction medium.

Assuming the drug concentration in the extraction medium is uniform at all times, due to effective stirring, the most general boundary condition to be considered is one where the drug concentration in the core gradually decreases as drug is released, while the drug concentration in the extraction medium gradually increases.

In the present paper, modifications of these boundary conditions are also considered. One modification is to assume sink conditions in the extraction medium and another is to assume a constant core concentration. From these examples it will be easy to see how to modify the calculation scheme in order to comply with other boundary conditions.

Pellets of Equal Size—As only radial diffusion is considered, the diffusion equation (6) for the coat is:

$$\frac{\partial[rC(rt)]}{\partial t} = D\frac{\partial^2[rC(rt)]}{\partial r^2} \qquad \text{(Eq. 1)}$$

where D is the diffusion coefficient for the particular drug in the coat, and $C(rt)$ is the drug concentration in the coat at distance r from the center at time t.

Equation 1 is solved with different boundary conditions and with the initial conditions:

$$C_e(t = 0) = 0 \qquad \text{(Eq. 2)}$$

$$C_c(t = 0) = C^0 \qquad \text{(Eq. 3)}$$

$$C(rt = 0) = 0 \qquad b < r < a \qquad \text{(Eq. 4)}$$

$$C(bt = 0) = \frac{C_c(t = 0)}{k_c} = \frac{C^0}{k_c} \text{ [see (Eq. 5)]}$$

where $C_e(t = 0)$ is the initial drug concentration in the extraction medium, and $C_c(t = 0)$ is the initial drug concentration in the core.

Variable Core and Extraction Medium Concentrations—The boundary conditions are sketched in Fig. 1 and may be expressed in the following way:

The Core-Coat Boundary—Assuming local equilibrium at the boundary at any time:

$$C_c(t) = k_c C(bt) \qquad \text{(Eq. 5)}$$

where k_c is the equilibrium constant. The continuity equation at the boundary may be written:

$$4\pi b^2 D\left[\frac{\partial C(rt)}{\partial r}\right]_{r=b} = \frac{4\pi b^3}{3}\frac{\partial C_c(t)}{\partial t} \qquad \text{(Eq. 6)}$$

and with Eq. 5:

$$\left[\frac{\partial C(rt)}{\partial r}\right]_{r=b} = \frac{bk_c}{3D}\frac{\partial C(bt)}{\partial t} \qquad \text{(Eq. 7)}$$

The Coat-Extraction Medium Boundary—The assumption of local equilibrium at the boundary gives:

$$C_e(t) = k_e C(at) \qquad \text{(Eq. 8)}$$

where k_e is the equilibrium constant. If there are n pellets of identical size, the continuity equation at the boundary may be written:

$$-n4\pi a^2 D\left[\frac{\partial C(rt)}{\partial r}\right]_{r=a} = V_e\frac{\partial C_e(t)}{\partial t} \qquad \text{(Eq. 9)}$$

0022-3549/82/0600-0694$01.00/0

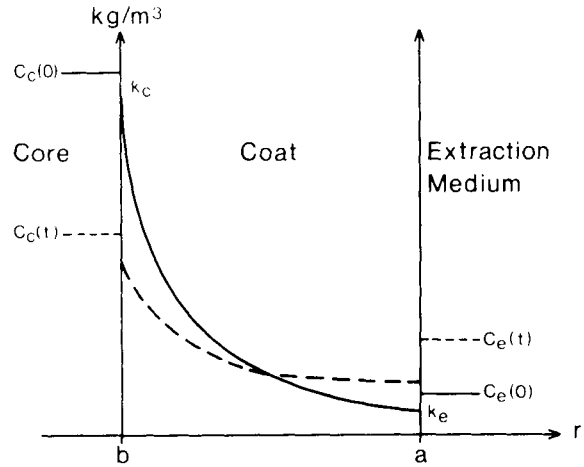

Figure 1—*A sketch of a segment of the core, coat, and extraction medium with boundary conditions corresponding to variable core and extraction medium concentrations. The stationary concentration profiles at time zero and at time* t *are shown. The concentration jumps at the boundaries are governed by the equilibrium constants* k_c *and* k_e.

where V_e is the volume of the extraction medium. Introduction of Eq. 8 into Eq. 9 gives:

$$\left[\frac{\partial C(rt)}{\partial r}\right]_{r=a} = -\frac{V_e k_e}{n4\pi a^2 D}\frac{\partial C(at)}{\partial t} \qquad \text{(Eq. 10)}$$

The time Laplace transform of Eq. 1 with Eq. 4 gives:

$$\frac{\partial^2 \tilde{C}(rs)}{\partial r^2} + \frac{2}{r}\frac{\partial \tilde{C}(rs)}{\partial r} - \frac{s}{D}\tilde{C}(rs) = 0 \qquad \text{(Eq. 11)}$$

where,

$$\tilde{C}(rs) = \int_0^\infty e^{-st} C(rt)\mathrm{d}t \qquad \text{(Eq. 12)}$$

is the Laplace transformed concentration. In the same way Eqs. 7 and 10 are Laplace transformed and give:

$$\left[\frac{\partial \tilde{C}(rs)}{\partial r}\right]_{r=b} = \frac{bk_c}{3D}[s\tilde{C}(bs)] - \frac{b}{3D}C^0 \qquad \text{(Eq. 13)}$$

and;

$$\left[\frac{\partial \tilde{C}(rs)}{\partial r}\right]_{r=a} = -\frac{V_e k_e}{n4\pi a^2 D}s\tilde{C}(as) \qquad \text{(Eq. 14)}$$

Equation 11 is a standard second-order differential equation with the solution

$$\tilde{C}(rs) = \frac{A}{r}\sinh\left(\sqrt{\frac{s}{D}}r\right) + \frac{B}{r}\cosh\left(\sqrt{\frac{s}{D}}r\right) \qquad \text{(Eq. 15)}$$

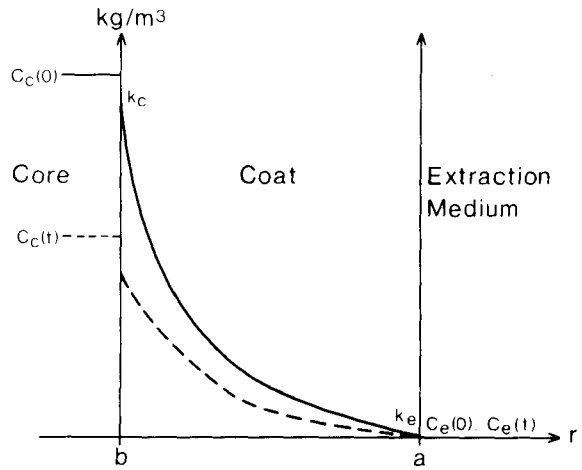

Figure 2—*A sketch of a segment of the core, coat, and extraction medium with boundary conditions corresponding to variable core conditions and sink conditions in the extraction medium. The stationary concentration profiles at time zero and time* t *are shown.*

The integration constants A and B are determined by inserting Eq. 15 into Eqs. 13 and 14. This gives the following system of equations, which in matrix form may be written:

$$\begin{bmatrix}\phi_1 & \phi_2\\ \phi_3 & \phi_4\end{bmatrix}\begin{bmatrix}A\\ B\end{bmatrix} = \begin{bmatrix}-\frac{C^0 b}{3}\\ 0\end{bmatrix} \qquad \text{(Eq. 16)}$$

where:

$$\phi_1 = b\sqrt{sD}\cosh\left(\sqrt{\frac{s}{D}}b\right) - D\sinh\left(\sqrt{\frac{s}{D}}b\right) - \frac{k_c s b^2}{3}\sinh\left(\sqrt{\frac{s}{D}}b\right) \qquad \text{(Eq. 17)}$$

$$\phi_2 = b\sqrt{sD}\sinh\left(\sqrt{\frac{s}{D}}b\right) - D\cosh\left(\sqrt{\frac{s}{D}}b\right) - \frac{k_c s b^2}{3}\cosh\left(\sqrt{\frac{s}{D}}b\right) \qquad \text{(Eq. 18)}$$

$$\phi_3 = a\sqrt{sD}\cosh\left(\sqrt{\frac{s}{D}}a\right) - D\sinh\left(\sqrt{\frac{s}{D}}a\right) + \frac{V_r k_e s a^2}{3}\sinh\left(\sqrt{\frac{s}{D}}a\right) \qquad \text{(Eq. 19)}$$

$$\phi_4 = a\sqrt{sD}\sinh\left(\sqrt{\frac{s}{D}}a\right) - D\cosh\left(\sqrt{\frac{s}{D}}a\right) + \frac{V_r k_e s a^2}{3}\cosh\left(\sqrt{\frac{s}{D}}a\right) \qquad \text{(Eq. 20)}$$

where the relative volume, $V_r = \dfrac{V_e}{\frac{n4\pi a^3}{3}}$

Equation 16 is solved for A and B, and after introduction of A and B in Eq. 15 is found:

$$\tilde{C}(rs) = \frac{-C^0 b^3\phi_4\sinh\left(\sqrt{\frac{s}{D}}r\right) + C^0 b^3\phi_3\cosh\left(\sqrt{\frac{s}{D}}r\right)}{3r(\phi_1\phi_4 - \phi_2\phi_3)} \qquad \text{(Eq. 21)}$$

By a reverse transformation of Eq. 21, $C(rt)$ can be found. This is done by residue calculation (7):

$$C(rt) = \sum_{l=1}^{\infty}\frac{C^0 b^3\left[(\phi_3)_{s_l}\cosh\left(\sqrt{\frac{s_l}{D}}r\right) - (\phi_4)_{s_l}\sinh\left(\sqrt{\frac{s_l}{D}}r\right)\right]e^{s_l t}}{3r\left(\frac{\partial}{\partial s}[\phi_1\phi_4 - \phi_2\phi_3]\right)_{s=s_l}} \qquad \text{(Eq. 22)}$$

Where s_l is the l'th pole of $\tilde{C}(rs)$ in Eq. 21. From Eq. 22 it is clear that $s_l \leq 0$, since $C(rt)$ is final. To find $C_e(t)$, Eq. 8 is used and we obtain from Eq. 22 after lengthy manipulations:

$$C_e(t) = \sum_{l=1}^{\infty}\frac{k_e C^0 b\sqrt{-\frac{s_l}{D}}e^{s_l t}}{N(s_l)} \qquad \text{(Eq. 23)}$$

where:

$$N(s_l) = \left[\sin\left(\sqrt{\frac{s_l}{D}}a\right)\cos\left(\sqrt{-\frac{s_l}{D}}b\right) - \sin\left(\sqrt{-\frac{s_l}{D}}a\right)\times\cos\left(\sqrt{-\frac{s_l}{D}}b\right)\right]\left\{\frac{k_c}{k_e} - \frac{3}{2k_e}\left[1 + \left(\frac{a}{b}\right)^2\right] + V_r\left(\frac{a}{b}\right)^2 - \frac{a^2 s_l}{D}\left[\frac{2}{3}V_r k_c + \frac{k_c}{2k_e}\left(1 - \frac{a}{b}\right) + \frac{V_r}{2}\left(\frac{a}{b} - 1\right)\right]\right\} + \left[\sin\left(\sqrt{-\frac{s_l}{D}}b\right)\sin\left(\sqrt{-\frac{s_l}{D}}a\right) + \cos\left(\sqrt{-\frac{s_l}{D}}a\right)\cos\left(\sqrt{-\frac{s_l}{D}}b\right)\right]a\sqrt{-\frac{s_l}{D}}\left[\frac{k_c}{2k_e}\left(2 + \frac{b}{a}\right) + \frac{V_r}{2}\left(2\frac{a}{b} + \left(\frac{a}{b}\right)^2\right) + \frac{V_r k_c s_l a^2}{6D}\left(1 - \frac{b}{a}\right)\right] \qquad \text{(Eq. 24)}$$

A convenient way of representing the results in Eq. 23 is to plot the release $R(t) = C_e(t)/C_e(t = \infty)$ as a function of time. It is evident that $R(t) \rightarrow 1$ for $t \rightarrow \infty$. The limiting value for $C_e(t)$ is given by the time independent term in Eq. 23, *i.e.*, one of the poles of $\bar{C}(rs)$ in Eq. 21 is zero. Indeed, it is clear from Eqs. 17–20 that $s = 0$ is a pole of $\bar{C}(rs)$. Let $s_1 = 0$, then Eq. 23 may be written:

$$R(t) = 1 + \sum_{l=2}^{\infty} \frac{k_e C^0 b \sqrt{-\frac{s_l}{D}}\, e^{s_l t}}{N(s_l) C_e(t = \infty)} \qquad \text{(Eq. 25a)}$$

where the concentration in the extraction medium at $t = \infty$ is found to be:

$$C_e(t = \infty) = \frac{C^0}{\frac{a^3}{b^3} V_r + \frac{k_c}{k_e} + \frac{1}{k_c}\left(\frac{a^3}{b^3} - 1\right)} \qquad \text{(Eq. 25b)}$$

Sink Condition in Extraction Medium–Variable Core Concentration—With the boundary conditions sketched in Fig. 2, Eq. 8 now changes to:

$$C(at) = 0 \qquad \text{(Eq. 26)}$$

The initial conditions (Eqs. 2–4) and the other boundary conditions (Eqs. 5 and 7) are unchanged. The integration constants A and B in Eq. 15 are now determined by introducing $\bar{C}(rs)$ into Eq. 13 and the Laplace transform of Eq. 26:

$$\bar{C}(as) = 0 \qquad \text{(Eq. 27)}$$

In analogy with Eq. 16, the following system of equations is obtained:

$$\begin{bmatrix} \phi_1 & \phi_2 \\ \phi_3' & \phi_4' \end{bmatrix} \begin{bmatrix} A \\ B \end{bmatrix} = \begin{bmatrix} -\frac{C^0 b^3}{3} \\ 0 \end{bmatrix} \qquad \text{(Eq. 28)}$$

where ϕ_1 and ϕ_2 are given in Eqs. 17 and 18 and

$$\phi_3' = \sinh\left(\sqrt{\frac{s}{D}}\, a\right) \qquad \text{(Eq. 29)}$$

$$\phi_4' = \cosh\left(\sqrt{\frac{s}{D}}\, a\right) \qquad \text{(Eq. 30)}$$

Equation 28 is solved for A and B, and it is found, as previously:

$$\bar{C}(rs) = \frac{-C^0 b^3 \phi_4' \sinh\left(\sqrt{\frac{s}{D}}\, r\right) + C^0 b^3 \phi_3' \cosh\left(\sqrt{\frac{s}{D}}\, r\right)}{3r(\phi_1 \phi_4' - \phi_2 \phi_3')} \qquad \text{(Eq. 31)}$$

where:

$$\phi_1 \phi_4' - \phi_2 \phi_3' =$$
$$\left[b\sqrt{sD} \cosh\left(\sqrt{\frac{s}{D}}\, b\right) - D \sinh\left(\sqrt{\frac{s}{D}}\, b\right) - \frac{k_c s b^2}{3} \sinh\left(\sqrt{\frac{s}{D}}\, b\right)\right] \cosh\left(\sqrt{\frac{s}{D}}\, a\right)$$
$$- \left[b\sqrt{sD} \sinh\left(\sqrt{\frac{s}{D}}\right) - D \cosh\left(\sqrt{\frac{s}{D}}\, b\right) - \frac{k_c s b^2}{3} \cosh\left(\sqrt{\frac{s}{D}}\, b\right)\right] \sinh\left(\sqrt{\frac{s}{D}}\, a\right) \qquad \text{(Eq. 32)}$$

By residue calculation (7) Eq. 31 is reversed and it is found that $C(rt)$:

$$C(rt) = \sum_{l=1}^{\infty} \frac{C^0 b^3 \left[(\phi_3')_{s=s_l} \cosh\left(\sqrt{\frac{s_l}{D}}\, r\right) - (\phi_4')_{s=s_l} \sinh\left(\sqrt{\frac{s_l}{D}}\, r\right)\right] e^{s_l t}}{3r\left[\frac{\partial}{\partial s}(\phi_1 \phi_4' - \phi_2 \phi_3')\right]_{s=s_l}} \qquad \text{(Eq. 33)}$$

where s_l is the l'th pole of $\bar{C}(rs)$ in Eq. 31. After lengthy manipulations the following is obtained:

$$C(rt) = \sum_{l=1}^{\infty} \frac{C^0 b}{r N'(s_l)} \left[\sin\left(\sqrt{-\frac{s_l}{D}}\, a\right) \times \cos\left(\sqrt{-\frac{s_l}{D}}\, r\right) - \cos\left(\sqrt{-\frac{s_l}{D}}\, a\right) \sin\left(\sqrt{-\frac{s_l}{D}}\, r\right)\right] e^{s_l t} \qquad \text{(Eq. 34)}$$

where:

$$N'(s_l) = \left[\frac{3}{2}\left(1 - \frac{a}{b}\right) - k_c\right] \left[\sin\left(\sqrt{-\frac{s_l}{D}}\, b\right) \times \cos\left(\sqrt{-\frac{s_l}{D}}\, a\right) - \sin\left(\sqrt{\frac{-s_l}{D}}\, a\right) \cos\left(\sqrt{-\frac{s_l}{D}}\, a\right)\right]$$
$$+ a\sqrt{-\frac{s_l}{D}} \left[\frac{k_c}{2}\left(1 - \frac{b}{a}\right) + \frac{3D}{2 s_l b^2}\right] \left[\sin\left(\sqrt{-\frac{s_l}{D}}\, a\right) \times \sin\left(\sqrt{-\frac{s_l}{D}}\, b\right) + \cos\left(\sqrt{-\frac{s_l}{D}}\, a\right) \cos\left(\sqrt{-\frac{s_l}{D}}\, b\right)\right] \qquad \text{(Eq. 35)}$$

It is clear from Eq. 34 that $C(at) = 0$ at any time t, in accordance with Eq. 26. The flux $dJ(t)/dt$ of drug into the extraction medium is given by:

$$\frac{dJ(t)}{dt} = -4\pi a^2 n D \left(\frac{\partial C(rt)}{\partial r}\right)_{r=a} \qquad \text{(Eq. 36)}$$

and the total amount of drug released at time t is given by:

$$\mathrm{M}(t) = -4\pi a^2 n D \int_0^t \left(\frac{\partial C(rt')}{\partial r}\right)_{r=a} dt' \qquad \text{(Eq. 37)}$$

From Eq. 34 it is found:

$$\left(\frac{\partial C(rt)}{\partial r}\right)_{r=a} = \sum_{l=1}^{\infty} -\frac{C^0 b}{a N'(s_l)} \sqrt{-\frac{s_l}{D}}\, e^{s_l t} \qquad \text{(Eq. 38)}$$

so

$$\mathrm{M}(t) = 4\pi a^2 n D \sum_{l=1}^{\infty} \frac{C^0 b}{a N'(s)} \sqrt{-\frac{1}{s_l D}} (e^{s_l t} - 1) \qquad \text{(Eq. 39)}$$

Divided by the total amount of drug, $M(t = \infty) = 4\pi b^3/3\, NC^0$ (neglecting the capacity of the coat) the release $R'(t)$ is obtained:

$$R'(t) = \frac{\mathrm{M}(t)}{\mathrm{M}(t = \infty)} = \frac{3aD}{b^2} \sum_{l=1}^{\infty} \frac{1}{N'(s_l)\sqrt{-s_l D}} (e^{s_l t} - 1) \qquad \text{(Eq. 40)}$$

Constant Core Concentration–Variable Extraction Medium Concentration—If the solubility of the drug in the core is low, the concentration of dissolved drug remains constant as long as there is undissolved drug in the core. The boundary conditions are sketched in Fig. 3, and Eq. 7 now changes to:

$$C_c(t) = C' = k_c C(bt) \qquad \text{(Eq. 41)}$$

The initial conditions and the other boundary conditions, Eqs. 8 and 10, are unchanged. The integration constants A and B in Eq. 15 are now determined by introducing $\bar{C}(rs)$ into Eq. 14 and the Laplace transform of Eq. 41:

$$\bar{C}(bs) = \frac{C'}{k_c s} \qquad \text{(Eq. 42)}$$

In analogy to Eqs. 16 and 28 the following set of equations is obtained:

$$\begin{bmatrix} \phi_1' & \phi_2' \\ \phi_3 & \phi_4 \end{bmatrix} \begin{bmatrix} A \\ B \end{bmatrix} = \begin{bmatrix} -\frac{C' b}{k_c s} \\ 0 \end{bmatrix} \qquad \text{(Eq. 43)}$$

where:

$$\phi_1' = \sinh\left(\sqrt{\frac{s}{D}}\, b\right) \qquad \text{(Eq. 44)}$$

$$\phi_2' = \cosh\left(\sqrt{\frac{s}{D}}\, b\right) \qquad \text{(Eq. 45)}$$

ϕ_3 and ϕ_4 are given by Eqs. 19 and 20, respectively. In analogy with the previous examples, it is now straightforward to derive an equation for the concentration:

$$C(rt) = \sum_{l=1}^{\infty} \frac{C' b e^{s_l t}}{k_c s r} \frac{\left[(\phi_4)_{s=s_l} \sinh\left(\sqrt{\frac{s_l}{D}}\, r\right) - (\phi_3)_{s=s_l} \cosh\left(\sqrt{\frac{s_l}{D}}\, r\right)\right]}{\left[\frac{\partial}{\partial s}(\phi_1' \phi_4 - \phi_2' \phi_3)\right]_{s=s_l}} \qquad \text{(Eq. 46)}$$

and with Eq. 8:

$$C_e(t) = \sum_{l=1}^{\infty} \frac{k_e C' b e^{s_l t}}{k_c s a} \frac{\left[(\phi_4)_{s=s_l} \sinh\left(\sqrt{\frac{s_l}{D}}\, a\right) - (\phi_3)_{s=s_l} \cosh\left(\sqrt{\frac{s_l}{D}}\, a\right)\right]}{\left[\frac{\partial}{\partial s}(\phi_1' \phi_4 - \phi_2' \phi_3)\right]_{s=s_l}} \qquad \text{(Eq. 47)}$$

At the moment when all undissolved drug has disappeared from the core, the concentration will be given by Eq. 23. Thus, the release profile will be given by two different expressions according to the conditions in the core.

Pellets of Different Size—*Variable Core and Extraction Medium Concentrations*—This is a generalization of the results derived for pellets of equal size to a situation where there is a distribution in the size of pellets used. Assuming that there are N different types of pellets involved, differing in size, coat material, *etc.*, for each of the N types of pellets there is an equation like Eq. 15. For the j'th type:

$$\tilde{C}_j(rs) = \frac{A_j}{r}\sinh\left(\sqrt{\frac{s}{D_j}}r\right) + \frac{B_j}{r}\cosh\left(\sqrt{\frac{s}{D_j}}r\right) \qquad \text{(Eq. 48)}$$

also allowing the diffusion coefficients D_j to be different. If the coating material is the same for all types of pellets $D_j = D$ for all j.

The boundary condition at the core-coat boundary is the same as in Eqs. 5 and 7 for each type of pellet, *i.e.*,

$$\left(\frac{\partial\tilde{C}_j(rs)}{\partial r}\right)_{r=b_j} = \frac{b_j k_{jc}}{3D_j}\left[s\tilde{C}_j(rs)\right] - \frac{b_j C_j^0}{3D_j} \qquad \text{(Eq. 49)}$$

The boundary condition at the coat-extraction medium boundary is:

$$V_e\left(\frac{\partial C_e(t)}{\partial t}\right) = \sum_{j=1}^{N} -4\pi a_j^2 n_j D_j\left(\frac{\partial C_j(rt)}{\partial r}\right)_{r=a_j} \qquad \text{(Eq. 50)}$$

with:

$$C_e(t) = k_{1e}C_1(a_1t) = \ldots = k_{je}C_j(a_jt) = \ldots = k_{Ne}C_N(a_Nt) \qquad \text{(Eq. 51)}$$

Time Laplace transformation of Eqs. 50 and 51 gives:

$$s\tilde{C}_e(s) = \sum_{j=1}^{N} -\frac{3}{a_j V_{rj}} D_j\left(\frac{\partial\tilde{C}_j(rs)}{\partial r}\right)_{r=a_j} \qquad \text{(Eq. 52)}$$

and:

$$\tilde{C}_e(s) = k_{1e}\tilde{C}_1(a_1s) = \ldots = k_{je}\tilde{C}_j(a_js) = \ldots = k_{Ne}\tilde{C}_N(a_Ns) \qquad \text{(Eq. 53)}$$

To determine the $2N$ integration constants, A_j and B_j, it is necessary to have $2N$ equations. The first N equations are obtained from Eq. 49 after introduction of $\tilde{C}_j(rs)$ from Eq. 48. The j'th equation has the form:

$$iA_j\left[\frac{1}{b_j}\sqrt{-\frac{s}{D_j}}\cos\left(\sqrt{-\frac{s}{D_j}}b_j\right) - \frac{1}{b_j^2}\sin\left(\sqrt{-\frac{s}{D_j}}b_j\right) - \frac{sk_{je}}{3D_j}\sin\left(\sqrt{-\frac{s}{D_j}}b_j\right)\right] + B_j\left[\frac{1}{b_j}\sqrt{-\frac{s}{D_j}}\sin\left(\sqrt{-\frac{s}{D_j}}b_j\right) - \frac{1}{b_j^2}\cos\left(\sqrt{-\frac{s}{D_j}}b_j\right) - \frac{sk_{jc}}{3D_j}\cos\left(\sqrt{-\frac{s}{D_j}}b_j\right)\right] = -\frac{b_jC_j^0}{3D_j} \qquad \text{(Eq. 54)}$$

The last N equations are obtained from Eqs. 52 and 53 after introduction of Eq. 48. The j'th equation has the form:

$$\sum_{l=1}^{N}\left\{iA_l\left[\sqrt{-\frac{s}{D_l}}\frac{1}{a_l}\cos\left(\sqrt{-\frac{s}{D_l}}a_l\right) - \frac{1}{a_l^2}\sin\left(\sqrt{-\frac{s}{D_l}}a_l\right) + \delta_{lj}\frac{V_{rj}k_{jl}s}{3D_j}\sin\left(\sqrt{-\frac{s}{D_j}}a_j\right)\right] + B_l\left[-\sqrt{-\frac{s}{D_l}}\frac{1}{a_l}\sin\left(\sqrt{-\frac{s}{D_l}}a_l\right) - \frac{1}{a_l^2}\cos\left(\sqrt{-\frac{s}{D_l}}a_l\right) + \delta_{jl}\frac{V_{rj}k_{jl}s}{3D_j}\cos\left(\sqrt{-\frac{s}{D_j}}a_j\right)\right]\right\} = 0 \qquad \text{(Eq. 55)}$$

The results in Eqs. 54 and 55 may conveniently be written in matrix form as

$$EF = G \qquad \text{(Eq. 56)}$$

where:

$$E = \begin{bmatrix} g_1 & 0 & 0 & \ldots & 0 \\ 0 & g_2 & 0 & \ldots & 0 \\ 0 & 0 & g_3 & \ldots & 0 \\ \vdots & \vdots & \vdots & & \vdots \\ 0 & 0 & 0 & \ldots & g_N \\ (c_1+l_1) & c_2 & c_3 & \ldots & c_N \\ c_1 & (c_2+l_2) & c_3 & \ldots & c_N \\ c_1 & c_2 & (c_3+l_3) & \ldots & c_N \\ \vdots & \vdots & \vdots & & \vdots \\ c_1 & c_2 & c_3 & \ldots & (c_N+l_N) \end{bmatrix} \begin{bmatrix} h_1 & 0 & 0 & \ldots & 0 \\ 0 & h_2 & 0 & \ldots & 0 \\ 0 & 0 & h_3 & \ldots & 0 \\ \vdots & \vdots & \vdots & & \vdots \\ 0 & 0 & 0 & \ldots & h_N \\ (d_1+f_1) & d_2 & d_3 & \ldots & d_N \\ d_1 & (d_2+f_2) & d_3 & \ldots & d_N \\ d_1 & d_2 & (d_3+f_3) & \ldots & d_N \\ \vdots & \vdots & \vdots & & \vdots \\ d_1 & d_2 & d_3 & \ldots & (d_N+f_N) \end{bmatrix} \qquad \text{(Eq. 57)}$$

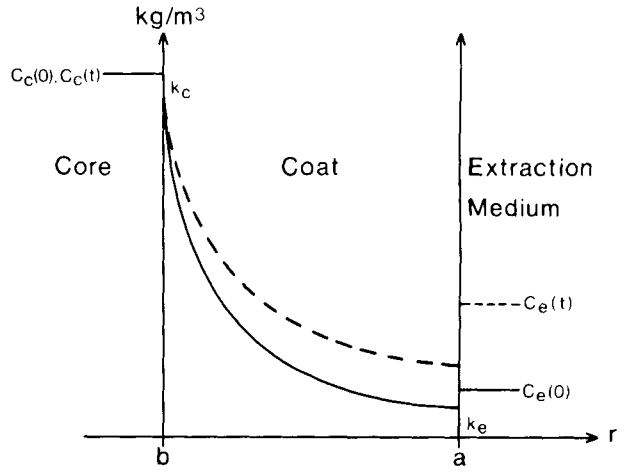

Figure 3—*A sketch of a segment of the core, coat, and extraction medium with boundary conditions corresponding to constant core concentration and variable extraction medium concentration. The stationary concentration profiles at time zero and time t are shown.*

and

$$F = \begin{bmatrix} iA_1 \\ iA_2 \\ \vdots \\ iA_N \\ B_1 \\ B_2 \\ \vdots \\ B_N \end{bmatrix} \quad \text{and} \quad G = \begin{bmatrix} -\frac{b_1C_1^0}{3D_1} \\ \vdots \\ -\frac{b_NC_N^0}{3D_N} \\ 0 \\ \vdots \\ 0 \end{bmatrix} \qquad \text{(Eq. 58)}$$

with:

$$g_i = \sqrt{-\frac{s}{D_i}}\frac{1}{b_i}\cos\left(\sqrt{-\frac{s}{D_i}}b_i\right) - \frac{1}{b_i^2} \times \sin\left(\sqrt{-\frac{s}{D_i}}b_i\right) - \frac{sk_{ic}}{3D_i}\sin\left(\sqrt{-\frac{s}{D_i}}b_i\right) \qquad \text{(Eq. 59)}$$

$$h_i = \sqrt{-\frac{s}{D_i}}\frac{1}{b_i}\sin\left(\sqrt{-\frac{s}{D_i}}b_i\right) - \frac{1}{b_i^2} \times \cos\left(\sqrt{-\frac{s}{D_i}}b_i\right) - \frac{sk_{ic}}{3D_i}\cos\left(\sqrt{-\frac{s}{D_i}}b_i\right) \qquad \text{(Eq. 60)}$$

$$c_i = \sqrt{-\frac{s}{D_i}}\frac{1}{a_i}\cos\left(\sqrt{-\frac{s}{D_i}}a_i\right) - \frac{1}{a_i^2}\sin\left(\sqrt{-\frac{s}{D_i}}a_i\right) \qquad \text{(Eq. 61)}$$

$$d_i = -\sqrt{-\frac{s}{D_i}}\frac{1}{a_i}\sin\left(\sqrt{-\frac{s}{D_i}}a_i\right) - \frac{1}{a_i^2}\cos\left(\sqrt{-\frac{s}{D_i}}a_i\right) \qquad \text{(Eq. 62)}$$

$$l_i = \frac{V_{ri}k_{ie}s}{3D_i}\sin\left(\sqrt{-\frac{s}{D_i}}a_i\right) \qquad \text{(Eq. 63)}$$

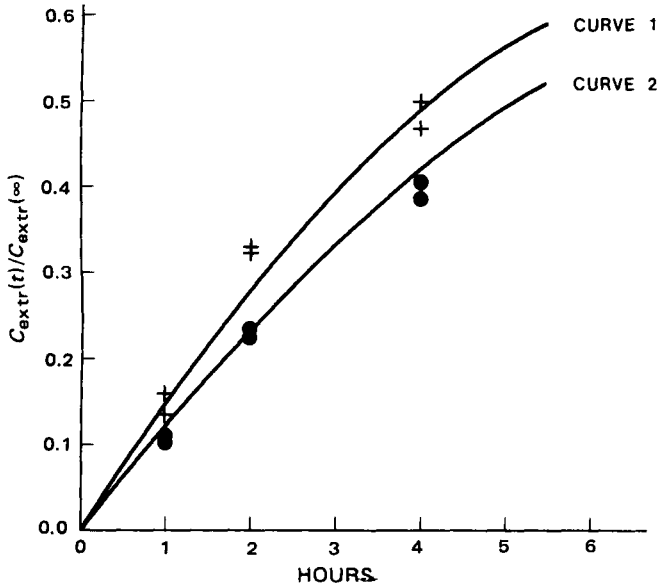

Figure 4—*Curve 1: Release profile calculated from Eq. 25 (or Eq. 56) when* a = *475 μm,* b = *459.2 μm,* V_{ri} = *75,* k_{ic} = k_{ie} = *1 to give the least-squares fit to experimental data. The diffusion coefficient is determined to be* $1.17 \times 10^{-13}\ m^2\ sec^{-1}$. *Curve 2: Predicted release profile of pellets when* a = *478.8 μm,* b = *459.2 μm,* V_{ri} = *75,* k_{ie} = k_{ic} = *1 and* D = $1.17 \times 10^{-9}\ cm^2\ sec^{-1}$.

$$f_i = \frac{V_{ri}k_{ie}s}{3D_i}\cos\left(\sqrt{-\frac{s}{D_i}}a_i\right) \qquad \text{(Eq. 64)}$$

Equation 56 is solved for iA_j and B_j (j = 1,N) and after introduction of iA_j, B_j into Eq. 49 for the j'th type of pellet, the following expression for $\bar{C}_j(rs)$ is found:

$$\bar{C}_j(rs) = \frac{\chi_j(rs)}{\psi_j(rs)} \qquad \text{(Eq. 65)}$$

where:

$$\chi_j(rs) = |E(j = G)|\sin\left(\sqrt{-\frac{s}{D_j}}r\right) + |E[(N + j) = G]| \times \cos\left(\sqrt{-\frac{s}{D_j}}r\right) \qquad \text{(Eq. 66)}$$

and:

$$\psi_j(rs) = r|E| \qquad \text{(Eq. 67)}$$

$|E|$ is the determinant of the E matrix (Eq. 57) and $|E(j = G)|$ is the determinant of the matrix obtained from E by replacing the j'th column with the vector G. Equation 65 may be reversed in the usual way by residue calculation:

$$C_j(rt) = \sum_{i=1}^{N}\frac{\chi_j(rs_i)e^{s_it}}{\left\{\frac{\partial}{\partial s}[\psi_j(rs)]\right\}_{s=s_i}} \qquad \text{(Eq. 68)}$$

where $\partial\psi/\partial s$ means a differentiation of the determinant $|E|$. This is done by replacing the elements in one row by the same elements differentiated with respect to s. In that way $2N$ new determinants are generated and they are all identical to the original determinant besides one row. Finally the $2N$ determinants are added giving the desired result. Therefore, it is necessary to know:

$$\frac{\partial g_i}{\partial s} = \left(\frac{1}{2D_i} - \frac{k_{ic}}{3D_i}\right)\sin\left(\sqrt{-\frac{s}{D_i}}b_i\right) + \frac{sk_{ic}b_i}{6D_i\sqrt{-sD_i}}\cos\left(\sqrt{-\frac{s}{D_i}}b_i\right) \qquad \text{(Eq. 69)}$$

$$\frac{\partial k_i}{\partial s} = \frac{1}{D_i}\left(\frac{1}{2} - \frac{k_{ic}}{3}\right)\cos\left(\sqrt{-\frac{s}{D_i}}b_i\right) - \frac{sk_{ic}b_i}{6D_i\sqrt{-sD_i}}\sin\left(\sqrt{-\frac{s}{D_i}}b_i\right) \qquad \text{(Eq. 70)}$$

$$\frac{\partial c_i}{\partial s} = \frac{1}{2D_i}\sin\left(\sqrt{-\frac{s}{D_i}}a_i\right) \qquad \text{(Eq. 71)}$$

$$\frac{\partial d_i}{\partial s} = \frac{1}{2D_i}\cos\left(\sqrt{-\frac{s}{D_i}}a_i\right) \qquad \text{(Eq. 72)}$$

$$\frac{\partial l_i}{\partial s} = \frac{V_{ri}k_{ie}}{3D_i}\left[\sin\left(\sqrt{-\frac{s}{D_i}}a_i\right) - \frac{a_i}{2}\sqrt{-\frac{s}{D_i}}\cos\left(\sqrt{-\frac{s}{D_i}}a_i\right)\right] \qquad \text{(Eq. 73)}$$

$$\frac{\partial f_i}{\partial s} = \frac{V_{ri}k_{ie}}{3D_i}\left[\frac{a_i}{2}\sqrt{-\frac{s}{D_i}}\sin\left(\sqrt{-\frac{s}{D_i}}a_i\right) + \cos\left(\sqrt{-\frac{s}{D_i}}a_i\right)\right] \qquad \text{(Eq. 74)}$$

These results can be programmed into a digital computer. The poles of $\bar{C}_j(rs)$ are found as the zero points of the determinant $|E|$, and once they are known, it is straightforward to use Eq. 68 for pellet type j and calculate $C_e(t)$ according to:

$$C_e(t) = k_{ie}C_j(a_jt) \qquad \text{(Eq. 75)}$$

Sink Condition in Extraction Medium–Variable Core Concentration—The boundary condition at the coat-extraction medium is:

$$C_i(a_it) = 0$$

for each type of pellet. That is, there is no coupling between the different types of pellets, which means that the release may be described as a superposition of the release from each type of pellet as given by Eq. 39, for example.

Other Boundary Conditions—It is fairly easy to adapt this calculation scheme to other relevant boundary conditions as discussed under Pellets of Equal Size.

RESULTS AND DISCUSSION

It has been shown that the general solution to the diffusion description of drug release from controlled-release solid dosage forms consisting of either one-size pellets or a broad-size distribution of pellets is straightforward and easy to handle in terms of matrix equations.

The poles s_n of $\bar{C}(rs)$ are found as the zero points of the determinant of the E matrix (Eqs. 56 and 65). The s_n has to be determined numerically, which may be done on computers. Once the poles have been found, either one of the concentrations $C_j(rt)$ and, thus, $C_e(t)$ may be calculated from Eqs. 68 and 75. It is noted that, due to Eq. 51, any one of the concentrations, $C_j(rt)$, may be used to calculate the extraction medium concentration, $C_e(t)$. Finally, it is noted that the one-size pellet case is included as a special case of the general treatment given previously, and in that case, Eq. 56 degenerates to Eq. 16.

As an illustration, the diffusion model has been applied to the prediction of the release profile of pellets with a known diffusion coefficient D and a coat thickness ($a - b$). Two experimental and calculated release profiles of propoxyphene hydrochloride pellets, coated with different amounts of a synthetic coat (5) are shown in Fig. 4. Curve 1 corresponds to pellets with a thin coat (8%) and Curve 2 to pellets with a thick coat (10%). Since the coating material is the same, it is assumed that the diffusion coefficients are identical in both cases which implies that the difference in release profiles is due to a different thickness of the coating. The diffusion model should be able to reproduce this difference if the model reflects essential features of the process. As the pellets had a narrow size distribution, only calculations for pellets of one size were used.

The dimensions of the pellets (a and b) were obtained from microscopy of a series of microtome sections of the pellets. It was found that b = 459.2 μm and a = 475.0 μm and 478.8 μm, respectively. Since there are only one-size pellets in the experiments, the results in Eq. 56 for N = 1 may be used. Adsorption phenomena were considered unimportant, and k_{ic} and k_{ie} were set equal to 1. The relative volume V_{ri} = 75. Equation 56 was then applied to fit data points for pellets with the thin coat (Curve 1) in order to obtain a value for the diffusion coefficient.

The experiments were conducted with the general boundary conditions with varying coat and extraction medium concentrations. It was possible to fit the data points with D = 420 $\mu m^2 h^{-1}$, ~ $1.17 \times 10^{-13}\ m^2\ sec^{-1}$ (Curve 1). Curve 2 was then calculated from Eq. 56 with the relevant b and a, and the predicted release profile is seen to be in good agreement with the experimental data. It is noted that the diffusion coefficient is somewhat different from the one reported earlier (1), where quasistationary conditions were imposed.

REFERENCES

(1) F. N. Christensen, F. Y. Hansen, and H. Bechgaard, *J. Pharm. Pharmacol.*, **32**, 580 (1980).

(2) J. A. Goldsmith, N. Randall, and S. D. Ross, *ibid.*, **30**, 347 (1978).

(3) R. Gurny, C. Revillard, and E. Doelker, *Pharm. Ind.*, **38**, 913 (1976).

(4) F. Langenbucher, *ibid.*, **38**, 472 (1976).

(5) A. M. Pedersen, U.S. Pat. 3,917,813 and 3,954,959 (1974).

(6) J. Crank, "The Mathematics of Diffusion," University Press, Oxford, 1956 corrected reprint 1964, p. 95.

(7) M. A. Lawrentjew and B. W. Schabat, "Methoden der Komplexen Funktionentheorie," VEB Deutscher Verlag der Wissenschaften, Berlin, 1967, p. 84–87.

APPENDIX

Variable	Units	
β	—	= parameter in the Rosin-Rammler-Sperling-Weibull distribution (See Ref. 1)
b	m	= radius of core
a	m	= radius of coated pellet
r	m	= radial distance from the center of a sphere
t	sec	= time
s	sec^{-1}	= frequency
s_i	sec^{-1}	= poles in Eq. 22
$C(rt)$	kg/m^3	= concentration of drug in coat at position r and at time t
$C_c(t)$	kg/m^3	= concentration of dissolved drug in the core at time t
$C_e(t)$	kg/m^3	= concentration of drug in extraction medium at time t
C^0	kg/m^3	= initial concentration of drug in core
$\bar{C}(rs)$	kgs/m^3	= time Laplace transform of $C(rt)$ at r
C'	kg/m^3	= constant core concentration in case of a sparingly soluble drug
D	m^2/sec	= diffusion coefficient of drug in coat
k_c	—	= distribution coefficient for drug between core and coat
k_e	—	= distribution coefficient for drug between extraction medium and coat
V_e	m^3	= volume of extraction medium
V_r	—	= the ratio of the volume of extraction medium to total volume of pellets
n	—	= number of pellets of identical size
$N(s_i)$	—	= denominator in Eq. 23 defined in Eq. 24
$M(t)$	kg	= total amount of drug released at time t
N	—	= number of different types of pellets in a sample
$J(t)$	$kg/sec\ m^2$	= flux of drug at time t

Stereoselective Disposition and Glucuronidation of Propranolol in Humans

BERNIE SILBER *[x], NICHOLAS H. G. HOLFORD, and SIDNEY RIEGELMAN [†]

Received August 10, 1981, from the *Departments of Pharmaceutical Chemistry and Pharmacy, School of Pharmacy, and Division of Clinical Pharmacology, Department of Medicine, School of Medicine, University of California, San Francisco, California.* Accepted for publication October 5, 1981.

[†] Deceased. * Present address: Department of Pharmaceutics, BG-20, School of Pharmacy, University of Washington, Seattle WA 98195.

Abstract □ Following oral dosing to steady state, the disposition of $S(-)$- and $R(+)$-propranolol and their corresponding glucuronide conjugates was studied in 4 healthy adults using doses from 40 to 320 mg/day of the racemate. Steady-state plasma concentrations of $S(-)$-propranolol and its corresponding glucuronide conjugate were greater than that for $R(+)$-propranolol and its corresponding conjugate. The average steady-state concentration of both enantiomers increased disproportionately to dose. There was a 52 ± 7 (mean ± *SD*) % decrease in the intrinsic clearance (Cl_{int}) of $S(-)$-propranolol and a 65 ± 22% decrease in the Cl_{int} of $R(+)$-propranolol over the dosing range studied. The terminal elimination half-lives of $S(-)$-propranolol and its glucuronide conjugate were longer than for the $R(+)$-enantiomer at all doses. The formation of glucuronide conjugates of $S(-)$- and $R(+)$-propranolol was best described by a saturable process in all subjects. Within individuals, the ratio of V'_{max}/K_m for the glucuronide conjugate of $S(-)$-propranolol was from 2.1- to 4.9-fold greater than for the conjugate of the $R(+)$-enantiomer. These studies demonstrate for the first time, that propranolol undergoes stereoselective disposition in humans.

Keyphrases □ Propranolol—$S(-)$- and $R(+)$-enantiomers and corresponding glucuronide conjugates, stereoselective disposition, humans □ Stereoselectivity—disposition of $S(-)$- and $R(+)$-propranolol, humans □ Glucuronide—conjugates of $S(-)$- and $R(+)$-propranolol in stereoselectivity disposition studies, humans

Propranolol [1-isopropylamino-3-(1-naphthoxy)-2-propanol] is a nonselective beta adrenergic blocking agent used clinically as a racemic mixture of the $S(-)$- and $R(+)$-enantiomers. Because $S(-)$-propranolol is about 100 times more potent as a beta blocker than the $R(+)$-enantiomer, $S(-)$-propranolol is believed to be largely responsible for the clinical effects of racemic drug (1).

Numerous investigators have described the absorption, distribution, metabolism, and elimination of propranolol in humans and animals. Pharmacokinetic studies in healthy volunteers and in patients have demonstrated up to 20-fold variation between individuals in plasma propranolol concentrations after oral doses (2–8). Age (9, 10); cigarette smoking (9, 11); concomitant drug intake (12);

0022-3549/82/0600-0699$01.00/0

REFERENCES

(1) F. N. Christensen, F. Y. Hansen, and H. Bechgaard, *J. Pharm. Pharmacol.*, **32**, 580 (1980).

(2) J. A. Goldsmith, N. Randall, and S. D. Ross, *ibid.*, **30**, 347 (1978).

(3) R. Gurny, C. Revillard, and E. Doelker, *Pharm. Ind.*, **38**, 913 (1976).

(4) F. Langenbucher, *ibid.*, **38**, 472 (1976).

(5) A. M. Pedersen, U.S. Pat. 3,917,813 and 3,954,959 (1974).

(6) J. Crank, "The Mathematics of Diffusion," University Press, Oxford, 1956 corrected reprint 1964, p. 95.

(7) M. A. Lawrentjew and B. W. Schabat, "Methoden der Komplexen Funktionentheorie," VEB Deutscher Verlag der Wissenschaften, Berlin, 1967, p. 84–87.

APPENDIX

Variable	Units	
β	—	= parameter in the Rosin-Rammler-Sperling-Weibull distribution (See Ref. 1)
b	m	= radius of core
a	m	= radius of coated pellet
r	m	= radial distance from the center of a sphere
t	sec	= time
s	sec^{-1}	= frequency
s_i	sec^{-1}	= poles in Eq. 22
$C(rt)$	kg/m^3	= concentration of drug in coat at position r and at time t
$C_c(t)$	kg/m^3	= concentration of dissolved drug in the core at time t
$C_e(t)$	kg/m^3	= concentration of drug in extraction medium at time t
C^0	kg/m^3	= initial concentration of drug in core
$\bar{C}(rs)$	kgs/m^3	= time Laplace transform of $C(rt)$ at r
C'	kg/m^3	= constant core concentration in case of a sparingly soluble drug
D	m^2/sec	= diffusion coefficient of drug in coat
k_c	—	= distribution coefficient for drug between core and coat
k_e	—	= distribution coefficient for drug between extraction medium and coat
V_e	m^3	= volume of extraction medium
V_r	—	= the ratio of the volume of extraction medium to total volume of pellets
n	—	= number of pellets of identical size
$N(s_i)$	—	= denominator in Eq. 23 defined in Eq. 24
$M(t)$	kg	= total amount of drug released at time t
N	—	= number of different types of pellets in a sample
$J(t)$	$kg/sec\ m^2$	= flux of drug at time t

Stereoselective Disposition and Glucuronidation of Propranolol in Humans

BERNIE SILBER *[x], NICHOLAS H. G. HOLFORD, and SIDNEY RIEGELMAN [†]

Received August 10, 1981, from the *Departments of Pharmaceutical Chemistry and Pharmacy, School of Pharmacy, and Division of Clinical Pharmacology, Department of Medicine, School of Medicine, University of California, San Francisco, California.* Accepted for publication October 5, 1981.

[†] Deceased. * Present address: Department of Pharmaceutics, BG-20, School of Pharmacy, University of Washington, Seattle WA 98195.

Abstract □ Following oral dosing to steady state, the disposition of $S(-)$- and $R(+)$-propranolol and their corresponding glucuronide conjugates was studied in 4 healthy adults using doses from 40 to 320 mg/day of the racemate. Steady-state plasma concentrations of $S(-)$-propranolol and its corresponding glucuronide conjugate were greater than that for $R(+)$-propranolol and its corresponding conjugate. The average steady-state concentration of both enantiomers increased disproportionately to dose. There was a 52 ± 7 (mean ± *SD*) % decrease in the intrinsic clearance (Cl_{int}) of $S(-)$-propranolol and a 65 ± 22% decrease in the Cl_{int} of $R(+)$-propranolol over the dosing range studied. The terminal elimination half-lives of $S(-)$-propranolol and its glucuronide conjugate were longer than for the $R(+)$-enantiomer at all doses. The formation of glucuronide conjugates of $S(-)$- and $R(+)$-propranolol was best described by a saturable process in all subjects. Within individuals, the ratio of V'_{max}/K_m for the glucuronide conjugate of $S(-)$-propranolol was from 2.1- to 4.9-fold greater than for the conjugate of the $R(+)$-enantiomer. These studies demonstrate for the first time, that propranolol undergoes stereoselective disposition in humans.

Keyphrases □ Propranolol—$S(-)$- and $R(+)$-enantiomers and corresponding glucuronide conjugates, stereoselective disposition, humans □ Stereoselectivity—disposition of $S(-)$- and $R(+)$-propranolol, humans □ Glucuronide—conjugates of $S(-)$- and $R(+)$-propranolol in stereoselectivity disposition studies, humans

Propranolol [1-isopropylamino-3-(1-naphthoxy)-2-propanol] is a nonselective beta adrenergic blocking agent used clinically as a racemic mixture of the $S(-)$- and $R(+)$-enantiomers. Because $S(-)$-propranolol is about 100 times more potent as a beta blocker than the $R(+)$-enantiomer, $S(-)$-propranolol is believed to be largely responsible for the clinical effects of racemic drug (1).

Numerous investigators have described the absorption, distribution, metabolism, and elimination of propranolol in humans and animals. Pharmacokinetic studies in healthy volunteers and in patients have demonstrated up to 20-fold variation between individuals in plasma propranolol concentrations after oral doses (2–8). Age (9, 10); cigarette smoking (9, 11); concomitant drug intake (12);

0022-3549/82/0600-0699$01.00/0

and renal (13), hepatic (14), and thyroid disease (15–17) have all been shown to affect the disposition of the drug. The disposition of propranolol in humans is highly dose dependent and this previously unrecognized observation may explain much of the apparent differences between individuals (18).

To date, pharmacokinetic studies involving propranolol have conclusions based on total [$S(-)$- plus $R(+)$-] propranolol concentrations. However, no information is available describing the pharmacokinetic behavior of each enantiomer measured simultaneously after administration of the racemate.

Racemic mixtures of drugs are commonly employed clinically. However, there may be large differences between enantiomers in their pharmacological activity, metabolism, and elimination. Warfarin enantiomers, for example, have significantly different anticoagulant properties, are metabolized differently, and have different rates of elimination (19–23).

Reports have indicated that the area under the plasma concentration–time curve (AUC) for $S(-)$-propranolol in the dog was 50% less than the AUC for the $R(+)$-enantiomer after administration of a single oral dose of the racemate (24, 25). Both groups found that the $S(-)$-enantiomer was more extensively glucuronidated and the AUC for the glucuronide conjugate of this enantiomer was over 3 times greater than the AUC for the glucuronide conjugate of $R(+)$-propranolol. However, no differences in the terminal elimination half-life of propranolol enantiomers or their glucuronide conjugates were observed.

The purpose of this study was to investigate, over a wide range of doses in humans, any differences in the disposition of $S(-)$- and $R(+)$-propranolol and formation of their corresponding glucuronide conjugates.

EXPERIMENTAL

Subjects were four healthy male volunteers. Informed consent was obtained and the protocol approved by the University of California, San Francisco, Committee on Human Research. All subjects had a medical history, physical examination, electrocardiogram (ECG), complete blood count with differential, urinalysis, and selected blood chemistries done. There was no evidence of renal or hepatic disease by medical history. Each subject had normal values of blood urea nitrogen, serum creatinine, urinalysis and urine culture, serum glutamic oxloacetic transaminase, lactic dehydrogenase, alkaline phosphatase, bilirubin, prothrombin time, and total serum proteins. All were nonsmokers and abstained from alcohol and marijuana and other medications until completion of the study. On each of 4 days/week that propranolol was taken, subjects were interviewed for side effects, had their pulse and blood pressure measured, and had a 1-min ECG rhythm strip taken.

All subjects were given 40, 80, 160, 240, and 320 mg/day of propranolol in divided doses every 6 hr for a total of 13 doses. No dietary restrictions were imposed, but food was withheld for at least 9 hr before and 3 hr after the 13th dose.

Blood samples were obtained at the end of the 8th, 9th, and 12th dosing intervals (trough concentrations) and at 0, 15, 30, 45, 60, and 90 min, and 2, 3, 4, 5, 6, 8, 10, and 12 hr following the 13th dose. Venous blood samples were obtained using an indwelling butterfly catheter whose patency was maintained by flushing with 1 ml of heparinized saline (10 U/ml) after obtaining each blood sample (26); these small doses of heparin do not affect the plasma protein binding or disposition of propranolol (27). After discarding 0.5 ml of blood, a 7-ml blood sample was collected in a sterile 12-ml disposable syringe. The blood sample was immediately transferred to a 16 × 150-mm polytef-lined screw cap test tube to which had been added 100 U of aqueous sodium heparin. After gentle mixing, blood samples were centrifuged at 2000 rpm (500×g) for 10 min. Plasma was transferred with a disposable Pasteur pipet to glass screw cap vials and stored at −20° until assay.

Assay for $S(-)$- and $R(+)$-Propranolol and Their Corresponding Glucuronide Conjugates—The concentrations of $S(-)$- and R(+)-propranolol and their corresponding glucuronide conjugates in plasma were measured in each subject after receiving doses of the racemate by a previously reported method (25). At each dosing rate, plasma concentrations were measured during the 13th dosing interval at steady state. Glucuronide concentrations were determined as the difference between enantiomer concentrations before and after enzymatic hydrolysis (25). One milliliter of plasma was extracted with ether after adding 0.4 ml of 0.2 N KOH by vortexing for 2 min and centrifuging at 2000 rpm (500×g) for 10 min. Ether extracts transferred to conical test tubes were evaporated to dryness under nitrogen. After adding 1 ml of methylene chloride, tubes were placed in a −78° bath. N-trifluoroacetyl-$S(-)$-prolyl chloride (0.3 ml) (the derivatizing agent) and 50 μl of triethylamine were added to the tubes, removed from the bath, and allowed to stand for 15 min. After adding 8 ml of 0.05N NaOH, vortexing for 2 min, and centrifuging at 2000 rpm (500×g) for 10 min, the upper layer was discarded and the lower layer evaporated to dryness under nitrogen after being transferred to culture test tubes. An aliquot of the residue, reconstituted with an equivolume mixture of acetonitrile and water, was injected onto the high-performance liquid chromatograph for analysis.

Data Analysis—The average steady-state concentration ($\overline{C}_{ss}$) of each enantiomer of propranolol and for each of their corresponding glucuronide conjugates during the 13th dosing interval was determined by:

$$\overline{C}_{ss} = \frac{AUC_0}{\tau} \qquad \text{(Eq. 1)}$$

where AUC_0 is the area under the plasma concentration–time curve after the oral dose, and τ is the dosing interval. The AUC of each propranolol enantiomer and for their corresponding glucuronide conjugates was calculated by the trapezoidal rule. The intrinsic clearance (Cl_{int}) of each propranolol enantiomer was calculated by the following (28):

$$Cl_{int} = \frac{D_0}{AUC_0} \qquad \text{(Eq. 2)}$$

where D_0 is the dose of each enantiomer; this is equal to one-half the total dose since the drug is administered as the racemate. This relationship assumes that the drug is totally absorbed and that all blood containing the drug passes through the liver before reaching the systemic circulation. The terminal elimination half-life of each propranolol enantiomer and their corresponding glucuronide conjugates was calculated by 0.693/terminal elimination rate constant (determined by least-squares regression utilizing at least four plasma concentration–time points in the log–linear region).

At steady state, the relationship between the formation of metabolite and its elimination is given by:

$$Cl_{f,M}\, C_{P_{ss}} = Cl_{el,M}\, C_{M_{ss}} \qquad \text{(Eq. 3)}$$

where $Cl_{f,M}$ is the formation clearance and $Cl_{el,M}$ is the elimination clearance for metabolite (M), and $C_{P_{ss}}$ and $C_{M_{ss}}$ are the concentrations of propranolol and metabolite, respectively. Rearrangement of Eq. 3 yields:

$$C_{M_{ss}} = Cl_{f,M}\frac{C_{P_{ss}}}{Cl_{el,M}} \qquad \text{(Eq. 4)}$$

for a first-order process and can be expressed as Eq. 5 for a saturable process:

$$C_{M_{ss}} = \frac{V_{max_M}}{K_{m_M} + C_{P_{ss}}}\frac{C_{P_{ss}}}{Cl_{el,M}} \qquad \text{(Eq. 5)}$$

where V_{max_M} and K_{m_M} are the Michaelis–Menten constants for a saturable metabolic process.

The formation clearance of each glucuronide conjugate (metabolite) can be estimated by substituting steady-state concentrations of propranolol enantiomers, their corresponding glucuronide conjugates, and the elimination clearance for each of the glucuronide conjugates into these equations.

Although the value of $Cl_{el,M}$ for the glucuronide conjugates is not known, in an earlier study (18) the renal clearance (Cl_r) for racemic (total) propranolol glucuronide ($Cl_{r,M}$) has been determined; previous investigators have shown that the clearance of propranolol glucuronide is primarily by the renal route (29). The $Cl_{r,M}$ for racemic propranolol glucuronide was independent of concentration in these same four subjects (18). Therefore, if it is assumed that the renal clearance is equal to the elimination clearance (*i.e.* $Cl_{r,M} = Cl_{el,M}$), then Eqs. 4 and 5 can be rewritten as Eqs. 6 and 7, respectively:

Table I—The Relationship Between the Intrinsic Clearance (Cl_{int}) of Propranolol Enantiomers and the Daily Dose of Racemic Propranolol

Week			3		4		5			
Dose, mg/day; racemate			160		240		320			Percent change in Cl_{int} from week 3 to week 5
Subject	Age, yr	Weight, kg	Cl_{int} of Propranolol Enantiomers (liters/min)[a] $S(-)$	$R(+)$	$S(-)$	$R(+)$	$S(-)$	$R(+)$		$S(-)$ / $R(+)$
MR	25	82	3.69	5.35	3.07	3.89	2.27	3.42		−48 / −46
TB	26	64	3.17	9.74	1.90	3.60	0.89	1.28		−62 / −87
AT	24	68	3.22	5.02	3.00	4.14	1.69	2.65		−48 / −47
TC	28	75	4.25	15.75	2.89	7.44	2.98	3.19		−51 / −80
									$x \pm SD$	-52 ± 7 / -65 ± 22

[a] The intrinsic clearance (Cl_{int}) was calculated according to Eq. 2.

$$C_{M_{ss}} = Cl_{f,M} \frac{C_{P_{ss}}}{Cl_{r,M}} \quad \text{(Eq. 6)}$$

$$C_{M_{ss}} = \frac{V_{max_M}}{K_{m_M} + C_{P_{ss}}} \frac{C_{P_{ss}}}{Cl_{r,M}} \quad \text{(Eq. 7)}$$

Because urinary excretion rate data is available for racemic propranolol glucuronide, the contribution by each glucuronide conjugate to the total renal clearance cannot be precisely estimated. However, the total renal clearance is the sum of the fractional contributions and can be defined by:

$$Cl_{r,M(-)} = \phi_{(-)}\, Cl_{r,M} \quad \text{(Eq. 8)}$$

for the glucuronide conjugate of $S(-)$-propranolol and by:

$$Cl_{r,M(+)} = \phi_{(+)}\, Cl_{r,M} \quad \text{(Eq. 9)}$$

for the glucuronide conjugate of $R(+)$-propranolol. The coefficient, ϕ, may be the same or different for each of the glucuronide conjugates. Therefore, for a saturable metabolic process, the Cl_f can be described by:

$$C_{M_{ss(-)}} = \frac{V_{max_{M(-)}}}{K_{m_{M(-)}} + C_{P_{ss(-)}}} \frac{C_{P_{ss(-)}}}{\phi_{(-)}\, Cl_{r,M}} \quad \text{(Eq. 10)}$$

for the glucuronide conjugate of $S(-)$-propranolol, and by:

$$C_{M_{ss(+)}} = \frac{V_{max_{M(+)}}}{K_{m_{M(+)}} + C_{P_{ss(+)}}} \frac{C_{P_{ss(+)}}}{\phi_{(+)}\, Cl_{r,M}} \quad \text{(Eq. 11)}$$

for the glucuronide conjugate of $R(+)$-propranolol.

To test the hypothesis that the formation of propranolol glucuronide is stereoselective, the predictions of six models were compared: Model 1, same V_{max} and K_m; Model 2, same V_{max}, different K_m; Model 3, different V_{max}, same K_m; Model 4, different V_{max} and K_m; Model 5, similar nonsaturable clearance; Model 6, different nonsaturable clearance.

Because ϕ appears in all equations of Cl_f, the value of V_{max} or Cl_f obtained for saturable or first-order processes, respectively, will have this coefficient incorporated into the estimate.

The formation clearance models listed above were specified (30). The parameters of the models listed previously were estimated by simultaneous unweighted nonlinear least-squares regression (31) of the $C_{M_{ss}}$ for each glucuronide conjugate *versus* the $C_{P_{ss}}$.

Discrimination between the models was made with the Schwarz criterion and Leonard test (32–34).

Mean values are reported with standard deviations; differences between means are evaluated by student's paired t test and are considered to be significant when $p < 0.05$ (35).

RESULTS

The dose-dependent elimination of propranolol and its major metabolites was previously reported in the same four individuals (18). Steady-state conditions were achieved in all subjects at each dosing rate. Steady-state trough concentrations of total [$S(-)$- and $R(+)$-] propranolol were attained at least by the ninth dose and only slight interday variation within subjects was observed.

Because concentrations of propranolol were near the sensitivity limit of the stereospecific assay with doses of 40 and 80 mg/day, enantiomer concentrations were not measured at these dosing rates. Concentrations of $S(-)$- and $R(+)$-propranolol, along with their corresponding glucuronide conjugates, were measured at dosing rates of 160, 240, and 320 mg/day.

Relationship Between the Intrinsic Clearance (Cl_{int}) of Propranolol Enantiomers and the Dosing Rate—The Cl_{int} of $S(-)$- and $R(+)$-propranolol at each dosing rate was determined according to Eq. 2. The Cl_{int} of $S(-)$-propranolol was always lower than the Cl_{int} of the $R(+)$-enantiomer (Table I). On the average, there was a 52 ± 7 (mean $\pm$ SD) % decrease in the Cl_{int} of $S(-)$-propranolol and a 65 ± 22% decrease in the Cl_{int} of $R(+)$-propranolol when the dose was increased from 160 to 320 mg/day.

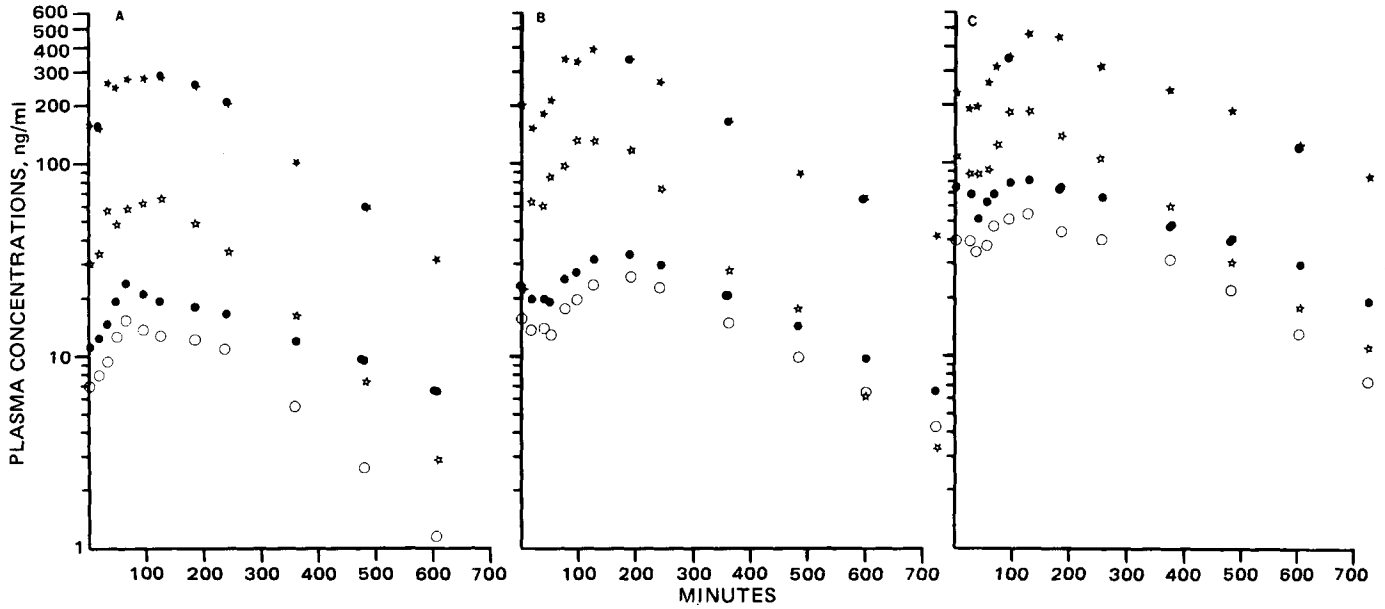

Figure 1—*Plasma concentrations of* S(−)-[●] *and* R(+)-[○] *propranolol and the glucuronide conjugates of* S(−)-[★] *and* R(+)-[*] *propranolol during the 13th dosing interval at steady state after: A, 160; B, 240; and C, 320 mg/day in subject AT. Similar results were seen in the three other subjects studied.*

Table II—Summary of Half-Lives, $t_{1/2}$, for Propranolol Enantiomers and Their Corresponding Glucuronide Conjugates

Dose, mg/day; racemic Subject	160		240		320	
	$t_{1/2}$, hr					
	Propranolol Enantiomer					
	$S(-)$	$R(+)$	$S(-)$	$R(+)$	$S(-)$	$R(+)$
MR	3.8	2.5	4.2	3.3	5.2	3.1
TB	3.5	2.7	4.7	3.2	8.3	5.0
AT	4.3	1.9	3.7	2.9	4.7	3.3
TC	4.5	3.1	4.5	4.2	5.0	3.3
$x \pm SD$	4.0 ± 0.5	2.6 ± 0.5[a]	4.3 ± 0.4	3.4 ± 0.6[a,b]	5.8 ± 1.7	3.7 ± 0.9[a]
	Glucuronide Conjugates of Propranolol Enantiomers					
Subject	$S(-)$	$R(+)$	$S(-)$	$R(+)$	$S(-)$	$R(+)$
MR	3.2	2.2	3.7	2.8	4.3	3.0
TB	2.9	2.2	3.6	3.3	7.3	4.6
AT	2.2	1.8	3.1	2.6	4.0	2.5
TC	2.7	1.8	3.6	3.8	4.3	3.5
$x \pm SD$	2.7 ± 0.4	2.0 ± 0.2[a]	3.5 ± 0.3[b]	3.1 ± 0.5[b]	4.5 ± 1.6	3.4 ± 0.9[a,b]

[a] $p < 0.05$ when compared with the value obtained for the $S(-)$-enantiomer at the same dosing rate. [b] $p < 0.05$ when compared with the value obtained for the same enantiomer at 160 mg/day.

Plasma Concentrations of $S(-)$- and $R(+)$-Propranolol and Their Corresponding Glucuronide Conjugates—Concentrations of $S(-)$-propranolol and its glucuronide conjugate were always greater than those for $R(+)$-propranolol and its glucuronide conjugate in all subjects at all dosing rates. Representative data obtained from subject AT is depicted in Fig. 1*A–C*.

The ratio of steady-state concentrations of $S(-)$- : $R(+)$-propranolol during the 13th dosing interval was 2.45 ± 1.12 at 160, 1.78 ± 0.60 at 240, and 1.51 ± 0.05 and 320 mg/day; and the ratio of the steady-state concentrations of the glucuronide conjugates of $S(-)$- : $R(+)$-propranolol was 4.74 ± 0.96 at 160, 3.64 ± 0.41 at 240, and 2.93 ± 0.17 at 320 mg/day.

There was a disproportionate increase in the $\bar{C}_{ss}$ of $S(-)$- and $R(+)$-propranolol in each subject as the daily dose was increased from 160 to 320 mg/day.

Terminal Elimination Half-Lives of Propranolol Enantiomers and Their Corresponding Glucuronide Conjugates—The half-life of $S(-)$-propranolol was 1.5-fold greater than for the $R(+)$-enantiomer at 160 mg/day ($p < 0.05$) and 1.6-fold greater at 320 mg/day ($p < 0.05$). In addition, the half-life of the glucuronide conjugate of $S(-)$-propranolol was 1.4-fold greater than for the conjugate of the $R(+)$-enantiomer at 160 mg/day ($p < 0.05$) and 1.3-fold greater at 320 mg/day ($p < 0.05$) (Table II). The half-life of both enantiomers and for their corresponding glucuronide conjugates increased with increasing dosing rate.

Estimation of the Formation Clearance (Cl_f) for Glucuronide Conjugates of $S(-)$- and $R(+)$-Propranolol—The Cl_f of glucuronide conjugates of $S(-)$- and $R(+)$-propranolol in all four subjects was best described by a saturable process. However, the model best explaining the data varied among the four subjects. The Cl_f for the glucuronide conjugate of $S(-)$-propranolol estimated by V'_{max}/K_m [$V_{max}/(\phi \cdot K_m)$] ranged from 496 to 1831 ml/min, whereas the Cl_f for the conjugate of $R(+)$-propranolol ranged from 202 to 477 ml/min. The summation of the individual Cl_fs for each individual determined in this investigation was compared with the value for the racemate Cl_f determined in the same individual (Table III).

DISCUSSION

A technique for the simultaneous determination of $S(-)$- and $R(+)$-propranolol along with their corresponding glucuronide conjugates after administration of the racemate was recently developed (25). Utilizing this technique, this investigation has shown that in healthy adults, the intrinsic clearance, plasma concentrations, elimination rate, and the formation clearance of glucuronide conjugates of propranolol enantiomers are substantially different.

The half-life of propranolol in humans after oral administration of the $R(+)$-enantiomer alone was reported to be shorter than after a dose of the racemate (36). In a previous report using a radioimmunoassay, the half-life of propranolol in rats after an intravenous dose of the $R(+)$-enantiomer was found to be shorter than after an intravenous dose of the racemate (37), whereas no difference was observed in mice when the same technique was employed (38).

These studies, however, do not predict the disposition of propranolol enantiomers after administration of the racemate, because $R(+)$-propranolol has no influence on liver blood flow, whereas racemic propranolol results in a decrease in liver blood flow. Because propranolol has a high extraction ratio and its clearance is blood flow limited, racemic propranolol would be expected to have a longer elimination half-life when compared with the half-life after $R(+)$-propranolol (39).

In a previous report (25), it was shown that in a patient with angina pectoris taking 200 mg of propranolol every 6 hr, the area under the plasma concentration–time curve for the $S(-)$-propranolol enantiomer was ~1.4 times greater than that for the $R(+)$-enantiomer. In the present investigation, concentrations of $S(-)$-propranolol were greater than those of $R(+)$-propranolol at each dosing rate (Fig. 1); these results confirm earlier findings but are in contrast to those observed in the dog (24, 25). In addition, the average steady-state concentration of each enantiomer increased disproportionately with doses from 160 to 320 mg/day. Similar to results observed in dogs, glucuronide concentrations of $S(-)$-propranolol were substantially greater than those for the glucuronide conjugate of the $R(+)$-enantiomer (24, 25).

The half-life of $S(-)$-propranolol and its glucuronide conjugate was greater than for the $R(+)$-enantiomer and its corresponding conjugate ($p < 0.05$) (Table II). In contrast, half-lives of propranolol enantiomers and their glucuronide conjugates were identical in the dog (24, 25).

Although the AUC for $S(-)$-propranolol was greater than that for the $R(+)$-enantiomer, it would be invalid to draw conclusions about the relative extent of bioavailability (F). Calculations of F for each enantiomer, based solely on AUCs after oral but not intravenous doses, must assume that the systemic clearances (Cl_s) of each enantiomer are identical. Although Cl_s, was not estimated, the intrinsic clearance of each enantiomer differed sharply and decreased with increasing dose (Table I).

In a previous report involving the same four individuals (18), it was shown that at steady state ~55% of an oral dose of propranolol could be accounted for by formation of three major metabolites: propranolol glucuronide, 4-hydroxypropranolol glucuronide, and α-naphthoxylactic acid. These metabolites are formed by different metabolic pathways and are eliminated by the kidneys in the urine (29). The formation of these metabolites was saturable in the dosage range studied.

The formation clearance (Cl_f) for the glucuronide conjugate of $S(-)$-propranolol (estimated by V'_{max}/K_m) was 2.1–4.9-fold greater than the Cl_f for the glucuronide conjugate of the $R(+)$-enantiomer in a given individual (Table III). However, when the sum of these individual Cl_fs was compared with the Cl_f for the racemate estimated from a previous investigation in the same individuals, a large disparity between estimates was observed. Because both V_{max} and ϕ for each glucuronide conjugate are unknown, it cannot be determined precisely whether the observed difference between $Cl_{f,T}$ and $Cl_{f,T'}$ (Table III) is due to a difference in V_{max}, ϕ, or both.

As previously mentioned, steady-state concentrations of $S(-)$-propranolol and its glucuronide conjugate were much higher than those for the $R(+)$-enantiomer and its conjugate in plasma. It is possible that other metabolites are being formed stereoselectively; at least some of these may be preferential for the $R(+)$-enantiomer. Although stereoselectivity in other metabolic pathways for propranolol has not been demonstrated in humans, a previous study (40) has recently shown that in the rat, $S(-)$-propranolol is preferentially hydroxylated to 4-hydroxypropranolol *in vivo* but not *in vitro*. 4-Hydroxypropranolol is equally active as a beta

Table III—Estimation of Formation Clearance for Glucuronide Conjugates of Propranolol

Subject	$Cl_{r,M}^{a}$, ml/min	Best Model[b]	Glucuronide Conjugate of $S(-)$-Propranolol: V'^{c}_{max}, nmole/min	K_m, nmole/ml	Cl_f $[V'_{max}/K_m]$, ml/min	Glucuronide Conjugate of $R(+)$-Propranolol: V'^{c}_{max}, nmole/min	K_m, nmole/ml	Cl_f $[V'_{max}/K_m]$, ml/min	$Cl_{f,T}^{d}$, ml/min	$Cl_{f,T'}^{e}$, ml/min
MR	79.4	4	344.8	0.37	931.9	10,632.5	38.15	278.7	1210.6	726.8
TB	55.6	3	178.4	0.36	495.6	72.6	0.36	201.7	697.3	723.5
AT	69.4	4	109.8	0.06	1830.0	67.6	0.18	375.6	2205.6	808.3
TC	97.2	3	142.5	0.14	1017.9	66.8	0.14	477.1	1495.0	923.7

[a] Renal clearance for racemic propranolol glucuronide; data from Silber *et al.* (18). [b] See data analysis section for description of models and selection criteria. [c] $V'_{max} = V_{max}/\phi$; see data analysis section for explanation. [d] $Cl_{f,T}$ represents the sum of the Cl_f for the glucuronide conjugates of $S(-)$- and $R(+)$-propranolol. [e] Estimated from V_{max}/K_m for racemic propranolol glucuronide; data from Silber *et al.* (18).

adrenergic blocking agent when compared with propranolol (41); presumably, the $S(-)$-enantiomer of 4-hydroxypropranolol is responsible for the beta blocking effects of a racemic mixture of $S(-)$- and $R(+)$-4-hydroxypropranolol.

Extensive deconjugation of propranolol glucuronide back to propranolol has been reported to occur in the dog (42). The occurrence of such a process in humans could be important since results from this study demonstrate that $S(-)$-propranolol is preferentially glucuronidated and that the resulting conjugate has a slower elimination rate when compared with the glucuronide conjugate for the $R(+)$-enantiomer (Table II). These findings may lend support to the theory proposed by Walle *et al.* (42) that propranolol glucuronide in humans serves as a storage pool or depot for the slow release of propranolol. This may be especially significant since deconjugation of propranolol glucuronide in humans should yield primarily $S(-)$-propranolol, the pharmacologically more active enantiomer. This presumes that the rate and extent of deconjugation, if it occurs, is equivalent for each glucuronide conjugate of propranolol.

The mechanism for the slower rate of elimination of the glucuronide conjugate of $S(-)$-propranolol cannot be explained by this investigation. Previous investigators have shown that the clearance of racemic propranolol glucuronide is primarily by the renal route (29). Further studies will need to establish whether the renal clearance of propranolol glucuronides are equivalent or different.

Because these results clearly demonstrate that the disposition and glucuronidation of $S(-)$- and $R(+)$-propranolol are not the same, and because they are essentially two distinct entities pharmacologically, future pharmacokinetic and pharmacodynamic studies involving propranolol should be focused on the pharmacologically more important $S(-)$-propranolol enantiomer rather than on total [$S(-)$- and $R(+)$-] concentrations of the drug.

REFERENCES

(1) A. M. Barrett and V. A. Cullum, *Br. J. Pharmacol.*, **34,** 43 (1968).

(2) W. A. Briggs, D. T. Lowenthal, W. J. Cirksena, W. E. Price, T. P. Gibson, and W. Flamenbaum, *Clin. Pharmacol. Ther.*, **18,** 606 (1975).

(3) C. A. Chidsey, P. Morselli, G. Bianchetti, A. Morganti, G. Leonetti, and A. Zanchetti, *Circulation*, **52,** 313 (1975).

(4) M. Esler, A. Zweifler, O. Randall, and V. DeQuattro, *Clin. Pharmacol. Ther.*, **22,** 299 (1977).

(5) A. Lehtonen, J. Kanto, and T. Kleimola, *Eur. J. Clin. Pharmacol.*, **11,** 155 (1977).

(6) M. Pine, L. Favrot, S. Smith, K. McDonald, and C. A. Chidsey, *Circulation*, **52,** 886 (1975).

(7) D. G. Shand, *Med. Clin. North Am.*, **58,** 1063 (1974).

(8) E. Vervolet, B. C. M. J. Takx-Kohlën, B. F. M. Pluym, and F. W. H. M. Merkus, *Clin. Pharmacol. Ther.*, **23,** 133 (1978).

(9) C. M. Castleden, C. M. Kay, and R. L. Parsons, *Br. J. Clin. Pharmacol.*, **2,** 303 (1975).

(10) C. M. Castleden and C. F. George, *ibid.*, **7,** 49 (1979).

(11) R. E. Vestal, A. J. J. Wood, R. A. Branch, D. G. Shand, and G. R. Wilkinson, *Clin. Pharmacol. Ther.*, **26,** 8 (1979).

(12) R. E. Vestal, D. M. Kornhauser, J. W. Hollifield, and D. G. Shand, *ibid.*, **25,** 19 (1979).

(13) G. Bianchetti, G. Grazini, and D. Branacaccio, *Clin. Pharmacokinet.*, **1,** 373 (1976).

(14) R. A. Branch and D. G. Shand, *ibid.*, **1,** 264 (1976).

(15) J. Feely and I. H. Stevenson, *Br. J. Clin. Pharmacol.*, **6,** 446 (1978).

(16) J. Feely, I. H. Stevenson, and J. Crooks, *Clin. Pharmacol. Ther.*, **28,** 40 (1980).

(17) J. G. Riddell, J. D. Neill, J. G. Kelly, and D. G. McDevitt, *ibid.*, **28,** 565 (1980).

(18) B. Silber, N. H. G. Holford, and S. Riegelman, APhA Academy of Pharmaceutical Sciences 29th National Meeting "Abstracts", **10,** 76 (1980).

(19) R. A. O'Reilly, *Clin. Pharmacol. Ther.*, **16,** 348 (1976).

(20) D. S. Hewick and J. McEwen, *J. Pharm. Pharmacol.*, **25,** 458 (1973).

(21) R. J. Lewis, W. F. Trager, K. K. Chan, A. Breckenridge, M. Orme, M. Rowland, and W. Schary, *J. Clin. Invest.*, **53,** 1607 (1974).

(22) T. A. Moreland and D. S. Hewick, *Biochem. Pharmacol.*, **24,** 1953 (1975).

(23) C. Hignite, J. Uetrecht, C. Tschanz, and D. Azarnoff, *Clin. Pharmacol. Ther.*, **28,** 99 (1980).

(24) T. Walle and U. K. Walle, *Res. Commun. Chem. Pathol. Pharmacol.*, **23,** 453 (1979).

(25) B. Silber and S. Riegelman, *J. Pharmacol. Exp. Ther.*, **215,** 643 (1980).

(26) N. H. G. Holford, S. Vozeh, P. Coates, J. R. Powell, J. F. Thiercelin, and R. Upton, *N. Engl. J. Med.*, **296,** 1300 (1977).

(27) B. Silber, M-W. Lo, and S. Riegelman, *Res. Commun. Chem. Pathol. Pharmacol.*, **27,** 419 (1980).

(28) K. S. Pang and M. Rowland, *J. Pharmacokinet. Biopharm.*, **5,** 625 (1977).

(29) W. J. Stone and T. Walle, *Clin. Pharmacol. Ther.*, **28,** 449 (1980).

(30) N. H. G. Holford, "MKMODEL—A Mathematical Modelling Tool, PROPHET Public Procedures Notebook," H. M. Perry, Ed., Bolt Beranek and Newman, Cambridge, Mass., 1982.

(31) G. Knott, *Comp. Prog. Biomed.*, **10,** 271 (1979).

(32) G. Schwarz, *Ann. Stat.*, **6,** 461 (1978).

(33) T. Leonard, "MRC Technical Report," University of Wisconsin, 1979.

(34) N. H. G. Holford, "MODELTEST—A Procedure for Selecting an Optimal Model, PROPHET Public Procedures Notebook," H. M. Perry, Ed., Bolt Beranek and Newman, Cambridge, Mass., 1982.

(35) J. H. Zar, "Biostatistical Analysis," Prentice-Hall, Englewood Cliffs, N.J., 1974, p. 121.

(36) C. F. George, T. Fenyvesi, M. E. Conolly, and C. T. Dollery, *Eur. J. Clin. Pharmacol.*, **4,** 74 (1972).

(37) K. Kawashima, A. Levy, and S. Spector, *J. Pharmacol. Exp. Ther.*, **196,** 517 (1976).

(38) A. Levy, S. H. Ngai, A. D. Finck, K. Kawashima, and S. Spector, *Eur. J. Pharmacol.*, **40,** 93 (1976).

(39) M. Rowland, L. Z. Benet, and G. G. Graham, *J. Pharmacokinet. Biopharm.*, **1,** 123 (1973).

(40) M. L. Powell, R. R. Wagoner, C.-S. Chen, and W. L. Nelson, *Res. Commun. Chem. Pathol. Pharmacol.*, **30,** 387 (1980).

(41) J. D. Fitzgerald and S. R. O'Donnell, *Br. J. Pharmacol.*, **45,** 207 (1972).

(42) T. Walle, E. C. Conradi, U. K. Walle, T. C. Fagan, and T. E. Gaffney, *Clin. Pharmacol. Ther.*, **26,** 686 (1979).

(43) W. F. Raub, *Fed. Proc. Fed. Am. Soc. Exp. Biol.*, **33,** 2390 (1976).

ACKNOWLEDGMENTS

Supported in part by a grant (GM-26556) from the National Institute of General Medical Sciences, National Institute of Health.

Data analysis and graphical examination of the results were performed on the PROPHET computer system, a specialized resource developed by the Chemical/Biological Information Handling Program of the National Institutes of Health (43).

We wish to thank Ms. Deborah J. Johnson and Mr. Richard Wagner for their able technical assistance during the course of this study and to Imperial Chemical Industries, Ltd. (Macclesfield, England) for their generous supplies of *S*(−)- and *R*(+)-propranolol hydrochloride.

NOTES

Sterility Testing of Fat Emulsions Using Membrane Filtration and Dimethyl Sulfoxide

A. M. PLACENCIA ˣ, G. S. OXBORROW, and J. W. DANIELSON

Received July 28, 1981, from the *Sterility Research Center, Minneapolis Center for Microbiological Investigations, Food and Drug Administration, Minneapolis, MN 55401.* Accepted for publication September 18, 1981.

Abstract □ A method was described for sterility testing of 10% fat emulsions, which consisted of solubilizing the emulsion in dimethyl sulfoxide and filtering the mixture using a polyester membrane. The procedure was rapid and avoided the problems of turbidity and plugging of the membrane filter encountered with other methods.

Keyphrases □ Dimethyl sulfoxide—sterility testing of 10% fat emulsions using membrane filtration □ Membrane filtration—sterility testing of 10% fat emulsions, dimethyl sulfoxide □ Fat emulsions—sterility testing using membrane filtration and dimethyl sulfoxide

Intravenous fat emulsions are used in peripheral and central vein infusions. Since bacterial contamination might be a problem with this kind of human drug product, a reliable method for sterility testing is necessary to ensure that possible contamination is detected.

The two basic methods for sterility testing (direct inoculation and membrane filtration) described in the USP XX (1) are not suitable to test this product. Direct inoculation of the product into growth media renders the media turbid and makes it impossible to observe microbial growth. To detect growth, various transfers must be made from the original inoculated media to fresh media, thus increasing the possibilities of contamination and extending the analysis time. Only small quantities of the product can be tested with this method. Membrane filtration of the product is difficult because the emulsified fat globules will not pass the commonly used membrane filters, and the filter pores become plugged. The present report describes a method for the sterility testing of fat emulsions in which membrane filtration is combined with the use of a solvent, dimethyl sulfoxide.

As part of the study, dimethyl sulfoxide was tested for bacteriostatic and fungistatic properties because of conflicting reports concerning its antimicrobial effects. It was shown (2) that 10% dimethyl sulfoxide protects and aids in the recovery of heat-shocked *Bacillus subtilis* spores. The high recovery of the bacteria has been linked to the capability of the compound to activate dormant spores (3, 4). At concentrations of 10, 20, and 30% in food transport systems, dimethyl sulfoxide acts as a cryoprotective agent and increases the survival of some bacteria (5). A solution of 10% dimethyl sulfoxide yielded a 100% recovery rate of *B. subtilis* phage after storage of the phage for 25 days at −20° (6). During freezing and thawing of *Aerobacter aerogenes* and red blood cells, 10–20% dimethyl sulfoxide increased the organisms' viability (7, 8). Dimethyl sulfoxide (100%) had no diffusible bacteriostatic activity when tested in disk agar diffusion sensitivity studies with various organisms (9). Normal growth of test organisms was obtained after 15-min exposure to 200,000 ppm (20%) dimethyl sulfoxide (10).

Dimethyl sulfoxide has been classified by other researchers as weakly antibacterial and antifungal (11). Bacterial growth was inhibited when 20% dimethyl sulfoxide was used in media (12, 13). Pottz *et al.* (14) found that 5–10% dimethyl sulfoxide was bacteriostatic and 20–80% bacteriocidal. Dimethyl sulfoxide (25%) was reported to inhibit the growth of bacteria isolated from leukemia and cancer patients (15). Dimethyl sulfoxide affects a wide range of bacteria and fungi in concentrations used in antimicrobial testing programs in the pharmaceutical industry (16).

The described method was designed to test the bacteriostatic and fungistatic capabilities of dimethyl sulfoxide to be used in the sterility testing of fat emulsions. Decimal reduction (D values) were determined using various test organisms.

EXPERIMENTAL

Dimethyl Sulfoxide Preparation—Dimethyl sulfoxide[1] was filter-sterilized using a polyester membrane[2] (0.2-μm pore size, 47-mm diameter) and stored in 25- and 50-ml amounts in sterile glass screw-capped tubes.

Sterility Testing of Fat Emulsions—Aliquots (100 ml) of a 10% intravenous fat emulsion[3] were aseptically transferred to sterile 38 × 200-mm glass screw-capped test tubes. To each tube, 25 ml of dimethyl sulfoxide was added. The mixture was vigorously stirred for 30 sec using a vortex mixer and then filtered through a 0.4-μm polyester membrane[2]. The membrane was rinsed with 100 ml of fluid D (1) and two 100-ml portions of fluid A (1), cut into two sections, transferred to fluid thioglycolate and soybean casein digest broth, and incubated as described in USP XX (1).

Bacteriostatic and Fungistatic Testing of Dimethyl Sulfoxide—Bacterial stock cultures containing <100 organisms/ml of the fol-

[1] Mallinckrodt Chemical Co., St. Louis, Mo.
[2] Nucleopore Corp., Pleasanton, Calif.
[3] Cutter Laboratories, Inc., Berkeley, Calif.

0022-3549/82/0600-0704$01.00/0

Data analysis and graphical examination of the results were performed on the PROPHET computer system, a specialized resource developed by the Chemical/Biological Information Handling Program of the National Institutes of Health (43).

We wish to thank Ms. Deborah J. Johnson and Mr. Richard Wagner for their able technical assistance during the course of this study and to Imperial Chemical Industries, Ltd. (Macclesfield, England) for their generous supplies of *S*(−)- and *R*(+)-propranolol hydrochloride.

NOTES

Sterility Testing of Fat Emulsions Using Membrane Filtration and Dimethyl Sulfoxide

A. M. PLACENCIA ˣ, G. S. OXBORROW, and J. W. DANIELSON

Received July 28, 1981, from the *Sterility Research Center, Minneapolis Center for Microbiological Investigations, Food and Drug Administration, Minneapolis, MN 55401.* Accepted for publication September 18, 1981.

Abstract □ A method was described for sterility testing of 10% fat emulsions, which consisted of solubilizing the emulsion in dimethyl sulfoxide and filtering the mixture using a polyester membrane. The procedure was rapid and avoided the problems of turbidity and plugging of the membrane filter encountered with other methods.

Keyphrases □ Dimethyl sulfoxide—sterility testing of 10% fat emulsions using membrane filtration □ Membrane filtration—sterility testing of 10% fat emulsions, dimethyl sulfoxide □ Fat emulsions—sterility testing using membrane filtration and dimethyl sulfoxide

Intravenous fat emulsions are used in peripheral and central vein infusions. Since bacterial contamination might be a problem with this kind of human drug product, a reliable method for sterility testing is necessary to ensure that possible contamination is detected.

The two basic methods for sterility testing (direct inoculation and membrane filtration) described in the USP XX (1) are not suitable to test this product. Direct inoculation of the product into growth media renders the media turbid and makes it impossible to observe microbial growth. To detect growth, various transfers must be made from the original inoculated media to fresh media, thus increasing the possibilities of contamination and extending the analysis time. Only small quantities of the product can be tested with this method. Membrane filtration of the product is difficult because the emulsified fat globules will not pass the commonly used membrane filters, and the filter pores become plugged. The present report describes a method for the sterility testing of fat emulsions in which membrane filtration is combined with the use of a solvent, dimethyl sulfoxide.

As part of the study, dimethyl sulfoxide was tested for bacteriostatic and fungistatic properties because of conflicting reports concerning its antimicrobial effects. It was shown (2) that 10% dimethyl sulfoxide protects and aids in the recovery of heat-shocked *Bacillus subtilis* spores. The high recovery of the bacteria has been linked to the capability of the compound to activate dormant spores (3, 4). At concentrations of 10, 20, and 30% in food transport systems, dimethyl sulfoxide acts as a cryoprotective agent and increases the survival of some bacteria (5). A solution of 10% dimethyl sulfoxide yielded a 100% recovery rate of *B. subtilis* phage after storage of the phage for 25 days at −20° (6). During freezing and thawing of *Aerobacter aerogenes* and red blood cells, 10–20% dimethyl sulfoxide increased the organisms' viability (7, 8). Dimethyl sulfoxide (100%) had no diffusible bacteriostatic activity when tested in disk agar diffusion sensitivity studies with various organisms (9). Normal growth of test organisms was obtained after 15-min exposure to 200,000 ppm (20%) dimethyl sulfoxide (10).

Dimethyl sulfoxide has been classified by other researchers as weakly antibacterial and antifungal (11). Bacterial growth was inhibited when 20% dimethyl sulfoxide was used in media (12, 13). Pottz *et al.* (14) found that 5–10% dimethyl sulfoxide was bacteriostatic and 20–80% bacteriocidal. Dimethyl sulfoxide (25%) was reported to inhibit the growth of bacteria isolated from leukemia and cancer patients (15). Dimethyl sulfoxide affects a wide range of bacteria and fungi in concentrations used in antimicrobial testing programs in the pharmaceutical industry (16).

The described method was designed to test the bacteriostatic and fungistatic capabilities of dimethyl sulfoxide to be used in the sterility testing of fat emulsions. Decimal reduction (D values) were determined using various test organisms.

EXPERIMENTAL

Dimethyl Sulfoxide Preparation—Dimethyl sulfoxide[1] was filter-sterilized using a polyester membrane[2] (0.2-μm pore size, 47-mm diameter) and stored in 25- and 50-ml amounts in sterile glass screw-capped tubes.

Sterility Testing of Fat Emulsions—Aliquots (100 ml) of a 10% intravenous fat emulsion[3] were aseptically transferred to sterile 38 × 200-mm glass screw-capped test tubes. To each tube, 25 ml of dimethyl sulfoxide was added. The mixture was vigorously stirred for 30 sec using a vortex mixer and then filtered through a 0.4-μm polyester membrane[2]. The membrane was rinsed with 100 ml of fluid D (1) and two 100-ml portions of fluid A (1), cut into two sections, transferred to fluid thioglycolate and soybean casein digest broth, and incubated as described in USP XX (1).

Bacteriostatic and Fungistatic Testing of Dimethyl Sulfoxide—Bacterial stock cultures containing <100 organisms/ml of the fol-

[1] Mallinckrodt Chemical Co., St. Louis, Mo.
[2] Nucleopore Corp., Pleasanton, Calif.
[3] Cutter Laboratories, Inc., Berkeley, Calif.

0022-3549/82/0600-0704$01.00/0

lowing ATCC test organisms were used to test dimethyl sulfoxide for bacterio- and fungistasis: *Bacillus subtilis* (6633), *Staphylococcus aureus* (6538), *Candida albicans* (10231), *Pseudomonas aeruginosa* (9027), *Clostridium perfringens* (11437), and *Aspergillus niger* (16404).

Six sets of four tubes each, containing 100 ml of fat emulsion[3], were prepared. Each tube was inoculated with 1 ml of a test organism suspension. Dimethyl sulfoxide (25 ml) was added to two tubes per set, and 50 ml to the remaining two tubes. All tubes were vigorously stirred for 30 sec using a vortex mixer. The mixtures were membrane-filtered using a 0.4-μm polyester membrane[2]. The membranes were washed with 200 ml of fluid A (1) and 100 ml of fluid D (1) and then cut into two sections. One section was transferred to fluid thioglycolate and the other to soybean casein digest broth. The fluid thioglycolate was incubated at 33 ± 2° and soybean casein digest broth at 23 ± 2°, both for 7 days (1).

D Value Determination—D values were determined using *B. subtilis* and *C. albicans*. *C. albicans* was used because the results of the bacteriostatic and fungistatic test showed that it was more sensitive to dimethyl sulfoxide at concentrations of 33%.

Spore stock suspensions containing ~10^9 *B. subtilis* organisms/ml of water were used for inoculum.

Cultures of *C. albicans* were grown in 13 × 100-mm trypticase soy agar slants at 37 ± 2° for 72 hr. The slants were washed with 2 ml of phosphate buffer to a final concentration of 10^9 organisms/ml.

Six 25-ml aliquots of a 10% fat emulsion were transferred to separate glass screw-capped test tubes. Three of the tubes were each inoculated with 0.1 ml of a spore stock suspension of *B. subtilis* and the other three tubes with *C. albicans*. The contents of the tubes were vigorously stirred using a vortex mixer, and 6.25 ml of dimethyl sulfoxide was added to each tube. The tubes were stirred as before, and 5-ml aliquots were taken at 0, 15, 30, 45, and 60 min. Each aliquot was filtered through a 0.4-μm polyester membrane. The membranes were washed with 100 ml of fluid A and transferred to 38 × 200-mm test tubes containing 100 ml of fluid A. The tubes were ultrasonicated for 6 min at 55 kHz and dilutions plated using trypticase soy agar. The plates were incubated at 35 ± 2° for 48 hr.

RESULTS

The results show that 20% dimethyl sulfoxide was not bacteriostatic or fungistatic to the test organisms used in this study. The growth rate of the sample was comparable to that of the control samples. A concentration of 33% dimethyl sulfoxide showed some fungistasis only against *C. albicans* after 7 days incubation at 23 ± 2°.

When 20% dimethyl sulfoxide was used, the D values of *B. subtilis* and *C. albicans* were >60 min.

The polyester membrane had good filtration rates, taking ~4 min to filter dimethyl sulfoxide and the emulsion. No problem was noted in the rinsing of the membrane with fluids A and D. Other membranes tested, such as acetate cellulose, pyroxylin, mixed esters of cellulose, and mixed cellulose acetate pyroxylin, were either dissolved by dimethyl sulfoxide or the pores were plugged by the fat emulsion.

In contrast to the direct inoculation of a product, the entire product could be analyzed in this membrane filtration method, with no problem of the media showing turbidity upon inoculation. The use of dimethyl sulfoxide as a solvent and of polyester membrane filters for the filtration of the product and rinsing fluids provided a rapid method of analysis. Since dimethyl sulfoxide showed no bacteriostasis or fungistasis and the analysis time was short, the probability of obtaining a better bacterial recovery is greatly increased by using the described method.

REFERENCES

(1) "The United States Pharmacopeia," 20th rev., U.S. Pharmacopeial Convention, Inc., Rockville, Md., 1980, pp. 873–882.

(2) L. B. Quesnel, B. L. Scott, and J. L. Taylor, in "Spore Research," J. Wolf, Ed., Academic, New York, N.Y., 1971, pp. 303–314.

(3) D. A. Cotter, J. W. Morin, and R. W. O'Connell, *Arch. Microbiol.*, **108**, 93 (1976).

(4) J. P. Widdowson, *Nature*, **214**, 812 (1967).

(5) A. W. Kotula, M. D. Pierson, B. S. Emswiler, and J. R. Guilfoyle, *Appl. Environ. Microbiol.*, **38**, 789 (1979).

(6) C. O. Yehle and R. H. Doi, *Can. J. Microbiol.*, **11**, 745 (1965).

(7) C. E. Huggins, *Transfusion*, **3**, 483 (1963).

(8) T. Nash, *Nature*, **4898**, 1113 (1963).

(9) G. S. Kalesperis, K. V. Prahlad, and D. L. Lynch, *Can. J. Microbiol.*, **21**, 213 (1975).

(10) V. L. Miller and A. C. Jerstad, *J. Med. Chem.*, **9**, 208 (1966).

(11) A. M. Kligman, *J. Am. Med. Assoc.*, **193**, 923 (1965).

(12) S. W. Jacob, M. Bischel, and R. J. Herschler, *Curr. Ther. Res.*, **6**, 134 (1964).

(13) D. C. Wood and J. Woo, *Ann. N.Y. Acad. Sci.*, **243**, 7 (1975).

(14) G. E. Pottz, J. H. Rampey, and F. J. Benjamin, *ibid.*, **141**, 261 (1967).

(15) F. B. Seibert, F. K. Farrelly, and C. C. Sheperd, *ibid.*, **141**, 175 (1967).

(16) H. Basch and H. H. Gadebusch, *Appl. Microbiol.*, **16**, 1953 (1968).

Tensile Strengths and Hardness of Tablets

PAUL J. JAROSZ * and EUGENE L. PARROTT ˣ

Received June 8, 1981, from the *Division of Pharmaceutics, College of Pharmacy, University of Iowa, Iowa City, IA 52242.* Accepted for publication October 13, 1981. *Present address: Ortho Pharmaceutical Corp., Raritan, NJ 08869.

Abstract □ The axial and radial tensile strengths were compared to the hardness of compressed tablets containing various concentrations of lubricants. Since radial tensile strength measurement considers the thickness of a tablet, and only tensile stress and axial tensile strength express the strength in the direction in which capping may occur, the tensile strengths characterize the strength of a tablet more completely than hardness.

Keyphrases □ Tensile strength—axial and radial tensile strengths compared to the hardness of compressed tablets □ Tablets—axial and radial tensile strengths compared to the hardness of compressed tablets

Although the strength of pharmaceutical tablets, which must be sufficient to withstand handling and shipment, may be expressed in a variety of ways, hardness (the force which, when applied diametrically to the tablet, causes fracture) has been the most common expression of strength. Studies of various hardness testers have shown the variations in fracture strength to be due to inaccuracies of instrumental scale values, zero errors, variations in the method of application of the load, physical dimensions, and shape of the tablet (1–4).

Although hardness has been a convenient and useful parameter for in-process control and quality assurance, it

0022-3549/82/0600-0705$01.00/0

lowing ATCC test organisms were used to test dimethyl sulfoxide for bacterio- and fungistasis: *Bacillus subtilis* (6633), *Staphylococcus aureus* (6538), *Candida albicans* (10231), *Pseudomonas aeruginosa* (9027), *Clostridium perfringens* (11437), and *Aspergillus niger* (16404).

Six sets of four tubes each, containing 100 ml of fat emulsion[3], were prepared. Each tube was inoculated with 1 ml of a test organism suspension. Dimethyl sulfoxide (25 ml) was added to two tubes per set, and 50 ml to the remaining two tubes. All tubes were vigorously stirred for 30 sec using a vortex mixer. The mixtures were membrane-filtered using a 0.4-μm polyester membrane[2]. The membranes were washed with 200 ml of fluid A (1) and 100 ml of fluid D (1) and then cut into two sections. One section was transferred to fluid thioglycolate and the other to soybean casein digest broth. The fluid thioglycolate was incubated at 33 ± 2° and soybean casein digest broth at 23 ± 2°, both for 7 days (1).

D Value Determination—D values were determined using *B. subtilis* and *C. albicans*. *C. albicans* was used because the results of the bacteriostatic and fungistatic test showed that it was more sensitive to dimethyl sulfoxide at concentrations of 33%.

Spore stock suspensions containing ~10^9 *B. subtilis* organisms/ml of water were used for inoculum.

Cultures of *C. albicans* were grown in 13 × 100-mm trypticase soy agar slants at 37 ± 2° for 72 hr. The slants were washed with 2 ml of phosphate buffer to a final concentration of 10^9 organisms/ml.

Six 25-ml aliquots of a 10% fat emulsion were transferred to separate glass screw-capped test tubes. Three of the tubes were each inoculated with 0.1 ml of a spore stock suspension of *B. subtilis* and the other three tubes with *C. albicans*. The contents of the tubes were vigorously stirred using a vortex mixer, and 6.25 ml of dimethyl sulfoxide was added to each tube. The tubes were stirred as before, and 5-ml aliquots were taken at 0, 15, 30, 45, and 60 min. Each aliquot was filtered through a 0.4-μm polyester membrane. The membranes were washed with 100 ml of fluid A and transferred to 38 × 200-mm test tubes containing 100 ml of fluid A. The tubes were ultrasonicated for 6 min at 55 kHz and dilutions plated using trypticase soy agar. The plates were incubated at 35 ± 2° for 48 hr.

RESULTS

The results show that 20% dimethyl sulfoxide was not bacteriostatic or fungistatic to the test organisms used in this study. The growth rate of the sample was comparable to that of the control samples. A concentration of 33% dimethyl sulfoxide showed some fungistasis only against *C. albicans* after 7 days incubation at 23 ± 2°.

When 20% dimethyl sulfoxide was used, the D values of *B. subtilis* and *C. albicans* were >60 min.

The polyester membrane had good filtration rates, taking ~4 min to filter dimethyl sulfoxide and the emulsion. No problem was noted in the rinsing of the membrane with fluids A and D. Other membranes tested, such as acetate cellulose, pyroxylin, mixed esters of cellulose, and mixed cellulose acetate pyroxylin, were either dissolved by dimethyl sulfoxide or the pores were plugged by the fat emulsion.

In contrast to the direct inoculation of a product, the entire product could be analyzed in this membrane filtration method, with no problem of the media showing turbidity upon inoculation. The use of dimethyl sulfoxide as a solvent and of polyester membrane filters for the filtration of the product and rinsing fluids provided a rapid method of analysis. Since dimethyl sulfoxide showed no bacteriostasis or fungistasis and the analysis time was short, the probability of obtaining a better bacterial recovery is greatly increased by using the described method.

REFERENCES

(1) "The United States Pharmacopeia," 20th rev., U.S. Pharmacopeial Convention, Inc., Rockville, Md., 1980, pp. 873–882.

(2) L. B. Quesnel, B. L. Scott, and J. L. Taylor, in "Spore Research," J. Wolf, Ed., Academic, New York, N.Y., 1971, pp. 303–314.

(3) D. A. Cotter, J. W. Morin, and R. W. O'Connell, *Arch. Microbiol.*, **108**, 93 (1976).

(4) J. P. Widdowson, *Nature*, **214**, 812 (1967).

(5) A. W. Kotula, M. D. Pierson, B. S. Emswiler, and J. R. Guilfoyle, *Appl. Environ. Microbiol.*, **38**, 789 (1979).

(6) C. O. Yehle and R. H. Doi, *Can. J. Microbiol.*, **11**, 745 (1965).

(7) C. E. Huggins, *Transfusion*, **3**, 483 (1963).

(8) T. Nash, *Nature*, **4898**, 1113 (1963).

(9) G. S. Kalesperis, K. V. Prahlad, and D. L. Lynch, *Can. J. Microbiol.*, **21**, 213 (1975).

(10) V. L. Miller and A. C. Jerstad, *J. Med. Chem.*, **9**, 208 (1966).

(11) A. M. Kligman, *J. Am. Med. Assoc.*, **193**, 923 (1965).

(12) S. W. Jacob, M. Bischel, and R. J. Herschler, *Curr. Ther. Res.*, **6**, 134 (1964).

(13) D. C. Wood and J. Woo, *Ann. N.Y. Acad. Sci.*, **243**, 7 (1975).

(14) G. E. Pottz, J. H. Rampey, and F. J. Benjamin, *ibid.*, **141**, 261 (1967).

(15) F. B. Seibert, F. K. Farrelly, and C. C. Sheperd, *ibid.*, **141**, 175 (1967).

(16) H. Basch and H. H. Gadebusch, *Appl. Microbiol.*, **16**, 1953 (1968).

Tensile Strengths and Hardness of Tablets

PAUL J. JAROSZ * and EUGENE L. PARROTT ˣ

Received June 8, 1981, from the *Division of Pharmaceutics, College of Pharmacy, University of Iowa, Iowa City, IA 52242.* Accepted for publication October 13, 1981. *Present address: Ortho Pharmaceutical Corp., Raritan, NJ 08869.

Abstract □ The axial and radial tensile strengths were compared to the hardness of compressed tablets containing various concentrations of lubricants. Since radial tensile strength measurement considers the thickness of a tablet, and only tensile stress and axial tensile strength express the strength in the direction in which capping may occur, the tensile strengths characterize the strength of a tablet more completely than hardness.

Keyphrases □ Tensile strength—axial and radial tensile strengths compared to the hardness of compressed tablets □ Tablets—axial and radial tensile strengths compared to the hardness of compressed tablets

Although the strength of pharmaceutical tablets, which must be sufficient to withstand handling and shipment, may be expressed in a variety of ways, hardness (the force which, when applied diametrically to the tablet, causes fracture) has been the most common expression of strength. Studies of various hardness testers have shown the variations in fracture strength to be due to inaccuracies of instrumental scale values, zero errors, variations in the method of application of the load, physical dimensions, and shape of the tablet (1–4).

Although hardness has been a convenient and useful parameter for in-process control and quality assurance, it

0022-3549/82/0600-0705$01.00/0

Table I—Hardness of Dibasic Calcium Phosphate Dihydrate with Various Concentrations of Magnesium Stearate Compressed at 1134 kg

	Magnesium Stearate, %						
	0.0	0.075	0.125	0.25	0.5	1.0	2.0
F_c, kp	9.4 N[a]	9.7 T[b]	9.7 N	9.9 T	8.4 N	8.1 T	9.6 N
	8.9 N	7.0 T	7.8 T	10.4 T	8.1 N	9.4 T	10.1 N
	9.4 N	9.3 N	9.6 N	9.7 T	8.5 T	8.9 N	10.6 T
	9.8 N	8.8 T	7.7 T	9.7 N	7.4 N	9.5 N	9.7 N
	8.9 T	7.3 T	9.0 N	9.4 N	8.4 N	9.4 N	9.5 N
	8.0 T	8.8 N	9.4 N	9.4 N	8.1 N	10.6 N	10.6 N
	9.9 T	7.5 N	9.4 N	8.5 T	8.7 N	8.9 T	9.8 N
	9.7 T	9.8 T	9.3 N	9.7 N	8.4 T	9.2 N	9.5 T
	8.7 T	10.2 T	8.9 N	9.9 N	8.9 N	9.6 N	9.4 N
	9.2 N	8.0 T	8.7 N	9.9 T		8.0 T	9.7 N
$\bar{X}$, kp	9.2	8.6	8.9	9.7	8.3	9.2	9.8
s, kp	0.6	1.1	0.7	0.5	0.4	0.8	0.4
CI[c]	0.4	0.8	0.5	0.3	0.3	0.6	0.3

[a] Nontension failure. [b] Tension failure. [c] Confidence interval at 95% probability.

is an empirical property. Tensile strength is a property of the compressed material, and it is a basic parameter which maintains consistency of property if the size of the tablet is changed (5). In an earlier report (6), the values of axial and radial tensile strengths were reported to present a directional appreciation of the strength of tablets. The purpose of the present report is to suggest that the evaluation of the axial and radial tensile strengths will characterize the strength of a tablet with more validity than hardness.

EXPERIMENTAL

The preparation of tablets and the method of measurement of the axial and radical tensile strengths of tablets by a tensiometer[1] have been reported previously (6). Tablet hardness was measured by diametral compression using a motor-driven hardness tester[2]. The maximum of the scale was 20 kp. Typical data are given in Table I. The mean hardness and the standard deviations plotted in the figures represent data for 10 tablets.

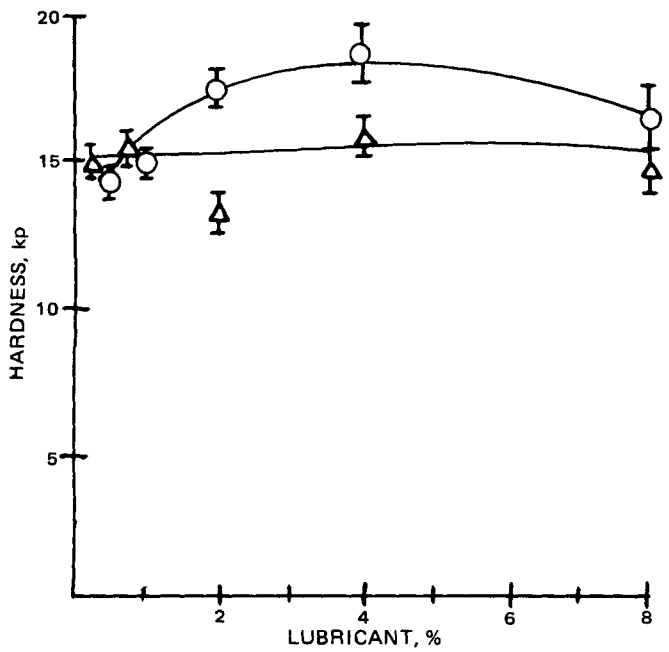

Figure 1—*The influence of the concentration of lubricant on the hardness of dibasic calcium phosphate dihydrate compressed at 2268 kg. Key: (○) hydrogenated vegetable oil; and (△) stearic acid.*

RESULTS AND DISCUSSION

Dibasic calcium phosphate dihydrate[3] and various concentrations of hydrogenated vegetable oil[4] and stearic acid were compressed at 2268 kg of force into flat-faced tablets with a 1.27-cm diameter. The hardness of the tablets was measured and plotted against the concentration of lubricant in Fig. 1. Based on the hardness values obtained by diametral compression, it is concluded that the addition of stearic acid to dibasic calcium phosphate dihydrate has no significant effect on the strength

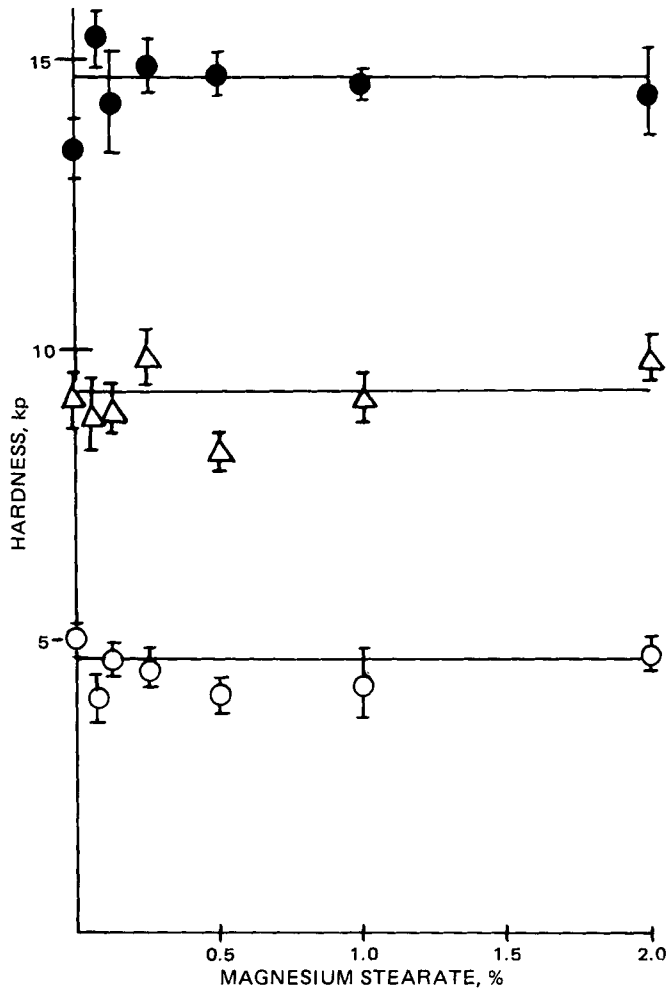

Figure 2—*The influence of the concentration of magnesium stearate on hardness of dibasic calcium phosphate dihydrate compressed at various forces. Key: (○) 454 kg; (△) 1134 kg; and (●) 2268 kg.*

[1] Hounsfield Tensiometer, Type W, Tensometer Ltd., Croydon, England.
[2] Schleuniger model 2E/205, Vector Corp., Marion, IA 52302.
[3] Encompress, Edward Mendell Co., Carmel, NY 10512.
[4] Lubritab, Edward Mendell Co., Carmel, NY 10512.

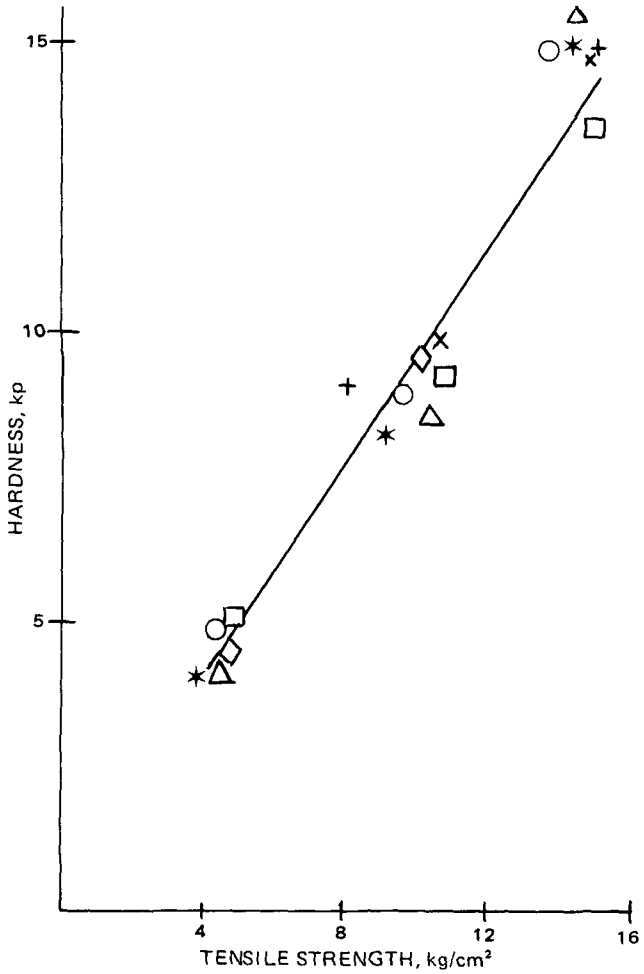

Figure 3—*The relationship of hardness and radial tensile strength for dibasic calcium phosphate dihydrate with various concentrations of magnesium stearate. Key: (□) 0%; (△) 0.075%; (○) 0.125%; (◇) 0.25%; (★) 0.5%; (+) 1.0%; and (×) 2.0%.*

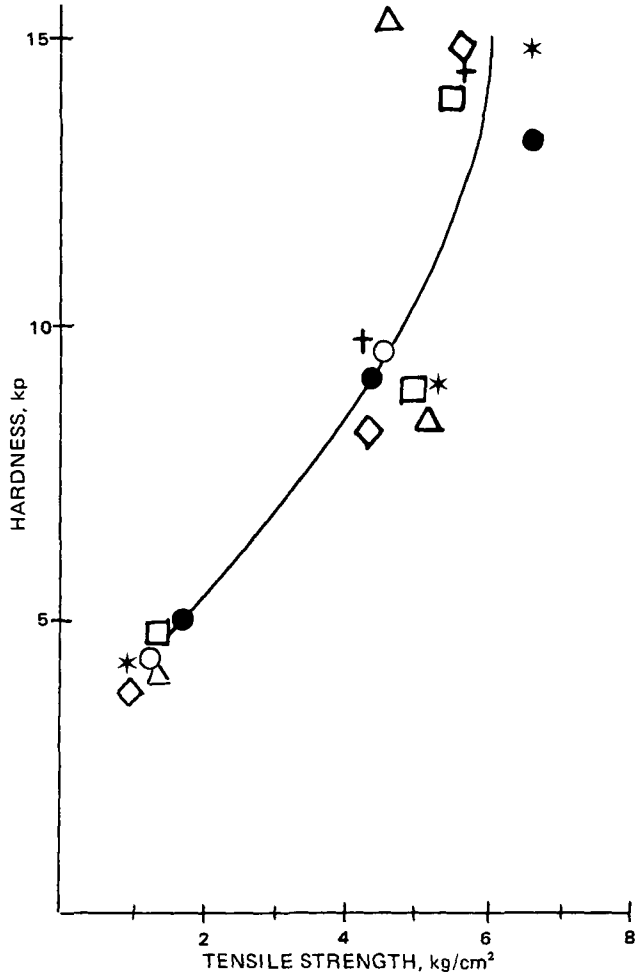

Figure 4—*The relationship of hardness and axial tensile strength for dibasic calcium phosphate dihydrate with various concentrations of magnesium stearate. Key: (●) 0%; (△) 0.075%; (□) 0.125%; (○) 0.25%; (◇) 0.5%; (★) 1.0%; and (+) 2.0%.*

of the tablet. For hydrogenated vegetable oil it appears that, as the concentration is increased to 4%, there is an increase in hardness as the concentration of lubricant is increased. A material that would lubricate and strengthen a tablet would be a useful excipient.

The wide variance in measurement may lead to erroneous conclusions. As illustrated in Fig. 1, for dibasic calcium phosphate dihydrate with hydrogenated vegetable oil, the variance in hardness may be a result of composite stresses (compressive, tensile, and shear) causing failure and minute differences in thickness of the tablets (5). In a tensile strength test, only tensile stress causes failure, and any difference in thickness is considered.

Dibasic calcium phosphate dihydrate and various concentrations of magnesium stearate were compressed at 454, 1134, and 2268 kg of force. The hardness of the tablets was measured and plotted against the concentration of lubricant in Fig. 2. Based on the hardness values obtained by diametral compression, it is concluded that the addition of magnesium stearate to dibasic calcium phosphate dihydrate has no significant effect on the strength of the tablet. As shown in Table I, the majority of the breakage was by a nontension failure. In the hardness tester, weaker tablets failed due to tensile stresses, and stronger tablets failed due to compressive stresses. For low values, the hardness is proportional to the radial tensile strength (Fig. 3).

The relationship of hardness to axial tensile strength is nonlinear as shown in Fig. 4. As the hardness is increased, at higher values of hardness, there is a progressive lessening of the rate of increase of axial tensile strength until a limiting axial tensile strength is attained. Thus, if the strength of a tablet as its hardness is considered, the axial tensile strength could be weak, and the tablet would be likely to laminate and cap under stress. If the axial tensile strength is measured, the strength in the axial direction and its implication in terms of capping are known. It appears that if both axial and radial tensile strengths are known, the strength of a tablet is basically characterized.

REFERENCES

(1) F. W. Goodhart, J. R. Draper, D. Dancz, and F. C. Ninger, *J. Pharm. Sci.*, **62**, 297 (1973).

(2) D. B. Brook and K. Marshall, *ibid.*, **57**, 481 (1968).

(3) F. W. Goodhart, J. R. Draper, M. J. Killeen, and F. C. Ninger, *ibid.*, **65**, 1072 (1976).

(4) W. A. Ritschel, F. S. Skinner, and R. Schlumpf, *Pharm. Acta Helv.*, **44**, 547 (1969).

(5) J. M. Newton, G. Rowley, J. T. Fell, D. G. Peacock, and K. Ridgway, *J. Pharm. Pharmacol.*, **23**, 195S (1971).

(6) P. J. Jarosz and E. L. Parrott, *J. Pharm. Sci.*, **71**, 607 (1982).

ACKNOWLEDGMENTS

Abstracted in part from a dissertation submitted by Paul J. Jarosz to the Graduate College, University of Iowa, in partial fulfillment of the Doctor of Philosophy degree requirements.

Structure–Activity Relationship Study of Anthraquinones: 1,4-Dihydroxy-5,8-bis[[2-(2-hydroxyethoxy)ethyl]amino]-9,10-anthracenedione, an Analog of an Established Antineoplastic Agent

ROBERT K. Y. ZEE-CHENG and C. C. CHENG

Received March 9, 1981, from the *Drug Development Laboratory, Mid-America Cancer Center, The University of Kansas Medical Center, Kansas City, KS 66103.* Accepted for publication July 20, 1981.

Abstract □ An oxygen analog of the antineoplastic anthraquinone, 1,4-dihydroxy-5,8-bis[[2-(2-hydroxyethyl)amino]ethyl]amino - 9,10 -anthracenedione, was synthesized. This compound, 1,4-dihydroxy-5,8-bis[[2-(2-hydroxyethoxy)ethyl]amino]-9,10-anthracenedione, was found to be inactive against P-388 lymphocytic leukemia. A comparative structure–activity study of these two anthraquinones in terms of previously postulated N—O—O triangulation hypothesis was discussed.

Keyphrases □ Antineoplastic agents—structure–activity relationship, 5,8-bis[[2-(2-hydroxyethoxy)ethyl]amino]-9,10-anthracenedione □ Structure–activity relationships—5,8-bis[[2-(2-hydroxyethoxy)ethyl]-amino]-9,10-anthracenedione □ Anthraquinones—antineoplastic agents, 5,8-bis[[2-(2-hydroxyethoxy)ethyl]amino] - 9,10-anthracenedione, structure–activity relationships

The importance of the nitrogen atom in the center of the side chain of 1,4-dihydroxy-5,8-bis[[2-(2-hydroxyethyl)-amino]ethyl]amino-9,10-anthracenedione (I), an outstanding antineoplastic drug, was noted previously (1, 2). Replacement of this critical nitrogen atom by other atoms, such as sulfur or carbon, resulted in compounds with no inhibitory action against leukemias P-388 or L-1210 in experimental animals (1). Based on the proposed N—O—O triangulation hypothesis (3), the structural and spatial relationship of this nitrogen atom to two oxygen atoms on the dihydroxyanthracenedione ring (I) has been correlated with that of the amino atom of daunosamine to the two oxygen functions on the aglycones of daunorubicin (II*a*) and doxorubicin (II*b*) (4, 5). The reported biological activity profile of these aminoanthraquinones and anthracycline antibiotics also has been found to be similar (5–7).

Interestingly, in recent publications, certain analogs of the anthracycline antibiotics, with the amino function of

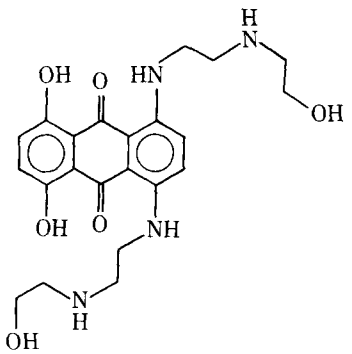

I

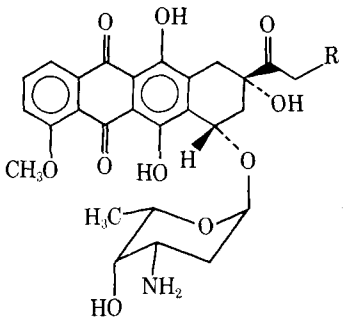

II*a*: R = H
II*b*: R = OH

the amino sugar moiety replaced by a hydroxyl or an acetoxyl group, possessed activity against P-388 or L-1210 leukemia.

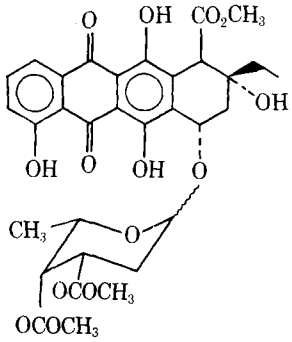

III

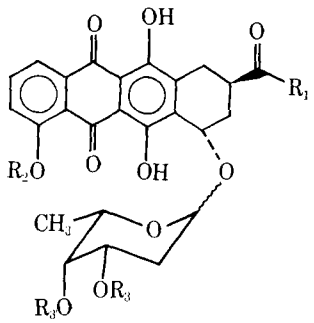

IV*a*: R_1 = H, R_2 = CH_3, R_3 = H
IV*b*: R_1 = H, R_2 = CH_3, R_3 = $COCH_3$
IV*c*: R_1 = OH, R_2 = CH_3, R_3 = H
IV*d*: R_1 = OH, R_2 = CH_3, R_3 = $COCH_3$
IV*e*: R_1 = H, R_2 = H, R_3 = H

0022-3549/82/0600-0708$01.00/0

These compounds include 2′-deoxy-di-*O*-acetyl-D-ribopyranosyl-ϵ-rhodomycinone (III) (8), 7-*O*-(2,6-dideoxy-α-L-*lyxo*-hexopyranosyl)daunomycinone (IV*a*), 3′-deamino-3′-hydroxydaunorubicin) and its diacetyl derivative (IV*b*) (9), the corresponding 3′-deamino-3′-hydroxydoxorubicin analog (IV*c*) and its diacetyl derivative (IV*d*) (10), and 2′-deoxy-L-fucopyranosylcarminomycinone (IV*e*) (11). However, the dosages required for activity are generally larger than those for the established antineoplastic agents I, II*a*, and II*b*. Activity displayed by these oxygenated analogs may not always be as potent. In addition, most other glycosides synthesized by these investigators failed to show activity against P-388 or L-1210 leukemia (8–11). Nevertheless, the information suggests that the significance of the nitrogen atom of compound I should be reexamined with respect to the corresponding oxygen atom. Consequently, 1,4-dihydroxy-5,8-bis[[2-(2-hydroxyethoxy)ethyl]amino] - 9,10-anthracenedione (VI) was synthesized.

EXPERIMENTAL

Compound VI was synthesized by placing 2.75 g (0.01 mole) of purified 5,8-dihydroxyleukoquinizarin (V) in a round-bottom flask equipped with a mechanical stirrer and a condenser. To this, 10.5 g (0.1 mole) of 2-(2-aminoethoxy)ethanol was added dropwise, with stirring. The mixture was heated with stirring under nitrogen at 60° in an oil bath for 2 hr, and allowed to stand at room temperature overnight. On the next day, the stirring rod (rinsed with 100 ml of ethanol which was added into the reaction mixture) was replaced by a glass sparge tube. Dry air was bubbled through the tube into the warm (50–60°) mixture for 4 hr, during which time the top of the condenser was connected to a water aspirator so that the entire system was under a slightly reduced pressure. The mixture was chilled and the separated solid product collected by filtration, washed successively with ethanol (10 ml), petroleum ether (20 ml), and diethyl ether (2 × 20 ml), and dried to give 3.66 g (82% yield) of VI. Recrystallization from a mixture of ethanol and petroleum ether (2:1) gave analytically pure VI as dark blue crystals, mp 156–157° (Scheme I). UV: λ_{max} (ethanol) 190 (log ϵ 4.23), 214 (4.35), 232 (4.48), 270 (4.07), 380 (3.69), 512 (3.52), 563 (3.86), 610 (4.31), and 662 (4.34) nm.

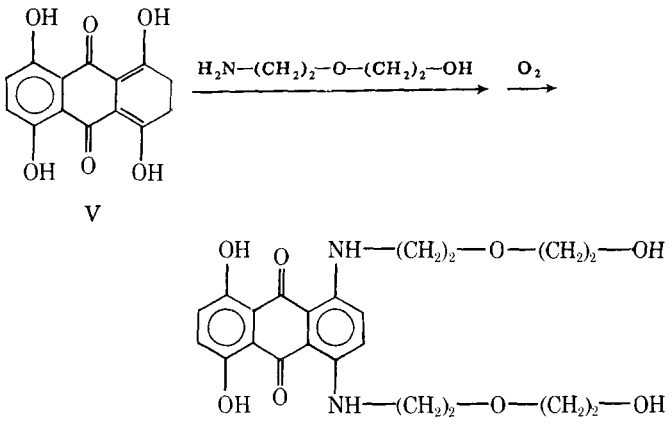

Scheme I

Anal.—Calc. for $C_{22}H_{26}N_2O_8$: C, 59.18; H, 5.87; N, 6.28. Found: C, 59.27; H, 6.03; N, 6.39.

RESULTS AND DISCUSSION

Although compound I has shown consistently outstanding antineoplastic activity in a number of experimental animal systems (1, 2, 5), compound VI was inactive against P-388 leukemia in the National Cancer Institute screening (T/C values at 200, 100, 50, and 25 mg/kg were 113, 110, 103, and 102%, respectively)[1]. This information, and the earlier negative test results of 1,4-dihydroxy-5,8-bis[(2-hydroxyethyl)amino]-9,10-anthracenedione (VII) against L-1210 leukemia (T/C values at 400, 200, and 100 mg/kg were 113, 110, and 103%, respectively), indicated that the oxygen atom (either in the form of —OH or —OR) cannot replace the particular nitrogen atom for antineoplastic activity in the aminoanthraquinone series.

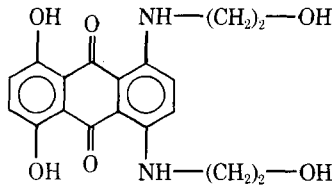

VII

The relevancy of this nitrogen atom to the originally proposed N—O—O triangulation pharmacophore (3) is also reaffirmed.

REFERENCES

(1) R. K. Y. Zee-Cheng and C. C. Cheng, *J. Med. Chem.*, **21**, 291 (1978).

(2) R. K. Johnson, R. K. Y. Zee-Cheng, W. W. Lee, E. M. Acton, D. W. Henry, and C. C. Cheng, *Cancer Treat. Rep.*, **63**, 425 (1979).

(3) K. Y. Zee-Cheng and C. C. Cheng, *J. Pharm. Sci.*, **59**, 1630 (1970).

(4) R. H. Adamson, *Cancer Chemother. Rep.*, **58**, 293 (1974).

(5) C. C. Cheng, G. Zbinden, and R. K. Y. Zee-Cheng, *J. Pharm. Sci.*, **68**, 393 (1979).

(6) B. F. Kimler, *Cancer. Res.*, **40**, 42 (1980).

(7) T. W. Plumbridge, V. Knight, K. L. Patel, and J. R. Brown, *J. Pharm. Pharmacol.*, **32**, 78 (1980).

(8) H. S. El Khadem, D. L. Swartz, and R. C. Cermak, *J. Med. Chem.*, **20**, 957 (1977).

(9) E. F. Fuchs, D. Horton, W. Weckerle, and E. Winter-Mihaly, *ibid.*, **22**, 406 (1979).

(10) D. Horton and W. R. Turner, *Carbohydr. Res.*, **77**, C8 (1979).

(11) H. S. El Khadem and D. L. Swartz, *J. Med. Chem.*, **24**, 112 (1981).

(12) R. I. Geran, N. H. Greenberg, N. M. MacDonald, A. M. Schumacker, and B. J. Abbott, *Cancer Chemother. Rep., Part 3*, **3**, 1 (1972).

ACKNOWLEDGMENTS

Supported by Research Grant R01-CA-28121, National Institutes of Health.

[1] For the general screening procedure, see Ref. 12. For the test data interpretation, see Instruction Booklet 14, "Screening Data Summary Interpretation and Outline of Current Screen," Drug Evaluation Branch, Division of Cancer Treatment, National Cancer Institute, Bethesda, MD 20014. In general, a minimum increase in survival of treated animals over controls resulting in a T/C ≥ 125% is necessary for a compound to be considered as active.

Gas Chromatographic Determination of Guanabenz in Biological Fluids by Electron-Capture Detection

JOHN A. KNOWLES ˣ, GRACE R. WHITE, CONSTANCE J. KICK, TAYLOR B. SPANGLER, and HANS W. RUELIUS

Received April 16, 1981, from the *Wyeth Laboratories, Inc., Philadelphia, PA 19101.* Accepted for publication September 17, 1981.

Abstract □ A sensitive gas chromatographic method for the determination of guanabenz [(2,6-dichlorobenzylidene)amino]guanidine in urine and plasma was developed. The method depends upon the acid hydrolysis of guanabenz to 2,6-dichlorobenzaldehyde, which has strong electron capturing properties and is volatile enough to be eluted from a gas chromatographic column. Concentrations as low as 0.1 ng of guanabenz/ml can be determined and recovery of the drug from urine and plasma samples is 81.8 ± 5.5% (*SD*). No interferences arising from plasma, urine, or reagents were encountered. Examples of the application of the method are given.

Keyphrases □ Guanabenz—gas chromatographic determination in biological fluids, electron-capture detection □ Electron-capture detection—gas chromatographic determination of guanabenz in biological fluids □ GC determination—guanabenz in biological fluids, electron-capture detection

Guanabenz, [(2,6-dichlorobenzylidene)amino]guanidine, (Scheme I) is a new agent which lowers blood pressure in hypertensive rats (1) and dogs (2), as well as in humans (3–5). When administered orally, the compound is subjected to extensive first-pass metabolism. Extensive metabolism and distribution into tissues resulted in very low concentrations of guanabenz in plasma when single oral doses, in the therapeutic range, were given to hypertensive patients (6). Thus, a highly sensitive method is required for the analysis of the drug in plasma, urine, and tissue samples derived from animal or clinical studies. Such a method, along with its application, is described in this report. Extraction of guanabenz from the sample, followed by acid hydrolysis to a volatile, strongly electron-capturing compound, led to a sensitivity of 0.1 ng/ml with an overall recovery of 81.8 ± 5.5%. No interferences stemming from reagent, urine, or plasma were observed.

EXPERIMENTAL

Materials—Sodium bicarbonate[1], sodium hydroxide[1], ether[1], toluene[1], and sulfuric acid[2] were all analytical reagent grade. The chromatographic standard, 2,6-dichlorobenzaldehyde[3], was recrystallized twice from absolute ethanol.

Extraction and Hydrolysis—The pH of a 1-ml aliquot of plasma or 0.5–3 ml urine (in a 12-ml screw-cap centrifuge tube) was adjusted to 10 by the addition of 2 ml of sodium bicarbonate–sodium hydroxide buffer (pH 10). Ether (5 ml) was added and the tube was sealed, shaken mechanically for 10 min, and then centrifuged for 5 min. Four milliliters of the ether layer was transferred to a clean centrifuge tube and the aqueous phase was re-extracted with an additional 3 ml of ether. After shaking and centrifuging the mixture, 3 ml of the ether layer was combined with the original 4 ml. The aqueous layer was discarded, and the ether extracts were shaken with 2 ml of 0.5 *N* sulfuric acid for 10 min, and centrifuged for 5 min. The ether phase was discarded by aspiration. Any residual ether was dispelled by placing the uncapped tube in a 60° water bath for 3 min prior to the addition of 2 ml of 12 *N* H_2SO_4. The tube was capped and placed in the 60° water bath. After 45 min, the tube was cooled in an ice bath, 0.1 ml of toluene was added, and the mixture was shaken for 10 min and centrifuged for 5 min. The aqueous phase was removed by a syringe aspirator, and after recentrifugation, 2–4 μl of the toluene solution was injected onto the gas chromatographic column.

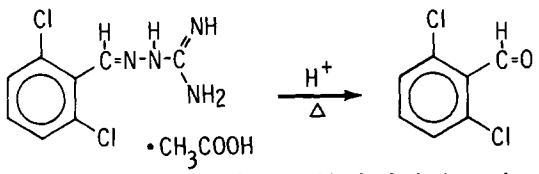

Scheme I—Structure of guanabenz and its hydrolysis product, 2,6-dichlorobenzaldehyde.

Chromatography—The procedure just described resulted in the acid hydrolysis of guanabenz to 2,6-dichlorobenzaldehyde which was quantitated by electron-capture gas chromatography[4]. The glass column was 6-mm o.d. (2-mm i.d.) × 3 m and packed with 1% neopentylglycol succinate on 60/80 mesh Chromosorb G AW-DMCS[5]. Its temperature was maintained at 200°, and the flow rate of the ultra-high pure helium[6] carrier gas was 20 ml/min. The flow rate of the purge gas (argon–methane, 95:5)[6] was 30 ml/min. The temperature of the injection port was 220° and that of the electron-capture detector was 320°.

Under these conditions, the retention time of 2,6-dichlorobenzaldehyde was 2.5 min (Fig. 1) and injection of a 4-μl aliquot resulting from the extraction and hydrolysis of a 0.2-ng/ml guanabenz standard gave a peak height of 14 mm.

A response curve to check detector linearity and recovery of guanabenz was determined daily by injecting 2–4-μl aliquots of solutions consisting of 2, 5, and 10 ng of 2,6-dichlorobenzaldehyde/ml of toluene into the chromatograph and plotting peak area *versus* concentration of the solution of the aldehyde.

A calibration curve of concentration of guanabenz *versus* detector response was determined daily by adding known amounts of guanabenz (0.1, 0.5, 1.0, 5.0, and 20.0 ng/ml) to control urine or plasma and then processing these standards in the same manner as unknown samples.

RESULTS AND DISCUSSION

Standard curves, constructed daily, were linear from 0.1 to 20 ng of guanabenz/ml, the range usually encountered in clinical studies. The minimal detection limit was 0.1 ng of guanabenz/ml. Recovery of the drug from aqueous solution, spiked human plasma, rhesus monkey plasma, and urine in the 0.1–20 ng/ml range was 81.8 ± 5.5% (*SD*; $n = 154$). This recovery was determined by use of the response curve for 2,6-dichlorobenzaldehyde.

No interfering chromatographic peaks were observed (Fig. 1) after acid hydrolysis of extracts obtained from control samples collected prior to dosing. Figure 2 presents the concentration–time curve of guanabenz in the plasma of a normotensive human subject following administration of a 24-mg oral dose of the drug.

The highly selective, sensitive, and accurate method, developed for the quantitation of guanabenz in biological fluids, depends on the hy-

[1] Mallinckrodt, St. Louis, Mo.
[2] Fisher Scientific Co., Fair Lawn, N.J.
[3] Aldrich Chemical Co., Milwaukee, Wis.
[4] Hewlett-Packard Model 7620, Avondale, Pa.
[5] Supelco, Inc. Bellefont, Pa.
[6] Matheson Gas Products, East Rutherford, N.J.

0022-3549/82/0600-0710$01.00/0

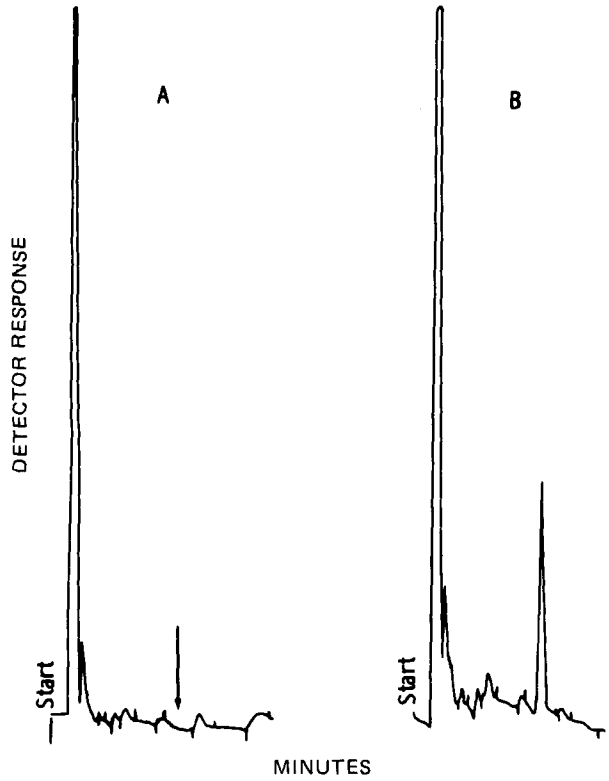

Figure 1—*(A) Gas chromatogram of a 0-hr plasma sample taken from a normotensive human subject. (B) Gas chromatogram of a plasma sample taken from the same human subject following oral administration of the drug.*

drolysis of the drug to 2,6-dichlorobenzaldehyde, a volatile compound which has strong electron-capturing properties. No 2,6-dichlorobenzaldehyde was found as a metabolite in plasma samples. If any were present, it would not interfere with the determination of guanabenz as it would be separated from the drug during the back extraction into dilute sulfuric acid.

This procedure is sensitive enough to enable concentrations as low as 0.1 ng/ml to be determined. This sensitivity permitted the determination of the very low drug concentrations in human plasma resulting from therapeutic doses and the calculation of pharmacokinetic parameters from these data (6). Furthermore, guanabenz was measured in rat brain (7) and in urine and plasma of rhesus monkeys (8).

An internal standard was not used in the procedure, because no compound could be found that would have extraction and hydrolysis characteristics similar to those of guanabenz when added to an unknown sample. The day-to-day variation of the method was <7%. No interferences from plasma, urine, or reagents were encountered. For standards containing 0.1 ng of guanabenz/ml, the recovery for 0.1 ng/ml was 82.6 ± 9.2% (*SD*); for 5 ng/ml, 81.6 ± 5.1%; and for 20 ng/ml, 81.1 ± 6.5%. These data, which were calculated from the detector response given by known amounts of 2,6-dichlorobenzaldehyde, demonstrate good recovery of the drug and high precision of the method.

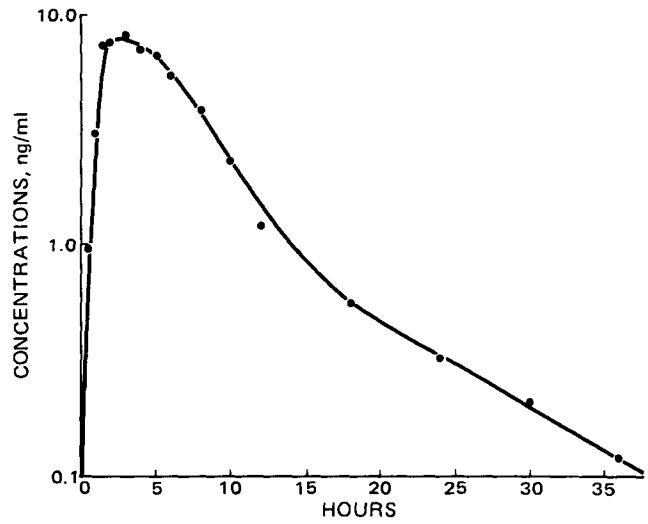

Figure 2—*Concentrations of guanabenz* versus *time in the plasma of a healthy subject after oral administration of 24 mg of guanabenz.*

REFERENCES

(1) T. Baum, D. K. Eckfield, N. Metz, J. L. Dinish, G. Rowles, R. Van Pelt, A. T. Shropshire, S. P. Fernandez, M. I. Gluckman, and W. F. Bruce, *Experientia* (Basel) **25,** 1066 (1969).

(2) R. K. Saini, A. P. Caputi, and E. Marmo, *Farmaco Ed. Prat.*, **28,** 359 (1973).

(3) R. S. Shah, B. R. Walker, S. K. Vanov, and R. H. Helfont, *Clin. Pharmacol. Ther.*, **19,** 732 (1976).

(4) F. G. McMahon, J. R. Ryan, A. K. Jain, R. Vargas, and S. K. Vanov, *ibid.*, **21,** 272 (1977).

(5) B. R. Walker, R. S. Shah, K. B. Ramanathan, S. K. Vanov, and R. H. Helfant, *ibid.*, **22,** 868 (1977).

(6) R. H. Meacham, M. Emmett, A. A. Kyriakopoulos, S. T. Chiang, H. W. Ruelius, B. R. Walker, R. G. Narins, and M. Goldberg, *ibid.*, **27,** 44 (1980).

(7) R. H. Meacham, H. W. Ruelius, C. J. Kick, J. R. Peters, S. M. Kocmund, S. F. Sisenwine, and R. L. Wendt, *J. Pharmacol. Exp. Ther.*, **214,** 594 (1980).

(8) R. H. Meacham, S. T. Chiang, C. J. Kick, S. F. Sisenwine, W. J. Jusko, and H. W. Ruelius, *Drug Metab. Dispos.*, **9,** 509 (1981).

The Measurement of Theophylline Metabolism in Hepatic Microsomes Using High-Performance Liquid Chromatography

THERESA C. HEMSWORTH and KENNETH W. RENTON ˣ

Received May 11, 1981 from the *Department of Pharmacology, Dalhousie University, Halifax, Nova Scotia, Canada B3H 4H7.* Accepted for publication September 11, 1981.

Abstract □ A method is described to measure the *in vitro* metabolism of theophylline by liver microsomes. The formation of 1-methyluric acid and 1,3-dimethyluric acid in incubation mixtures was determined by high-performance liquid chromatography. The formation of both metabolites was linear with time and the formation of 1-methyluric acid was blocked by allopurinol. This method will be useful in assessing potential drug interactions involving theophylline.

Keyphrases □ Theophylline—metabolism in hepatic microsomes, high-performance liquid chromatographic measurement □ Microsomes, hepatic—measurement of theophylline metabolism, high-performance liquid chromatography □ High-performance liquid chromatography—measurement of theophylline metabolism in hepatic microsomes □ Metabolism—theophylline in hepatic microsomes, high-performance liquid chromatography

Theophylline (1,3-dimethylxanthine) is a widely used antiasthmatic drug which is metabolized by hepatic microsomal enzymes (1). The use of theophylline can be problematic because of the narrow therapeutic range of serum concentrations and because of the large number of factors which can alter its metabolism and ultimate elimination (2). An *in vitro* system to study theophylline metabolism would be a useful technique to examine and define many of the factors which alter the elimination of this drug. Such a method for the study of radiolabeled theophylline has been described previously (3), but this technique was successful only with liver slices or with microsomes from animals previously induced with 3-methylcholanthrene. The present report discusses an improved method for the determination of theophylline metabolism in normal liver microsomes using high-performance liquid chromatography to quantitate the metabolites.

EXPERIMENTAL

Reagents and Chemicals—Theophylline[1], theobromine[1], 1,3-dimethyluric acid[1], 8-chlorotheophylline[1], and 1-methyluric acid[2] were used as received.

Chromatography—A liquid chromatograph[3] with reciprocating dual-piston constant flow rate pump and rotary valve injector[4] was equipped with a 20-μl loop, HPLC reversed-phase column[5], variable wavelength UV detector[6], and recorder[7]. The mobile phase contained 0.01 *M* sodium acetate–1% acetic acid–methanol (64:21:15, v/v/v). The solvent was degassed before use. Mobile phase flow rate was 0.4 ml/min.

Calibration Curves—Standard solutions which contained 0.10–10 μg/ml of 1-methyluric acid or 0.25–25 μg/ml of 1,3-dimethyluric acid and 100 μg/ml of 8-chlorotheophylline or 20 μg/ml of theobromine as internal standard were extracted and chromatographed in an identical manner to the incubation mixtures. Standard curves were linear throughout the range utilized.

Microsomal Biotransformation—Microsomes (3 mg of protein) were incubated in media (3) containing 50 m*M* tromethamine hydrochloride pH 7.5, 5 m*M* $MgCl_2$, 10 m*M* D-glucose-6-phosphate, 1 m*M* triphosphopyridine nucleotide, 10 U glucose-6-phosphate dehydrogenase, and 0.25 m*M* theophylline in a total volume of 3 ml. Incubations were carried out at 37° in a metabolic shaking water bath[8]. After 2 hr of incubation the mixture was placed on ice and 100 μg/ml of 8-chlorotheophylline was added. The incubation mixture was then extracted with 3 ml of chloroform–isopropanol (90:10, v/v) for 30 min to remove unmetabolized theophylline. The aqueous layer was dried in a stream of air and then reconstituted in a 100-μl HPLC mobile phase for chromatography using 295 nm for detection.

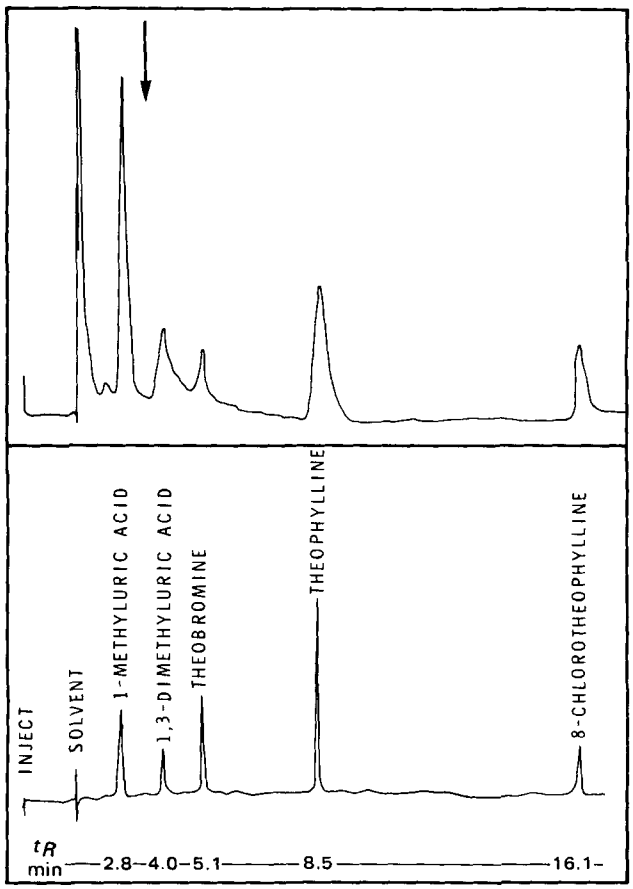

Figure 1—*HPLC for theophylline metabolites and internal standards. HPLC of extracted liver microsomes incubated with theophylline (upper). HPLC of 1-methyluric acid, 1,3-dimethyluric acid, theobromine, theophylline, and 8-chlorotheophylline standards (lower).*

[1] Sigma Chemical Co. St. Louis, Mo.
[2] Gift from Dr. J. Williams, University of Florida.
[3] Spectrophysics SP3500B.
[4] Rheodyne Model 7120.
[5] RP-8, 10 μm Brownlee Labs.
[6] Shoeffel UV variable wavelength detector.
[7] Fisher Recordall Series 5000.
[8] Dubnoff.

0022-3549/82/0600-0712$01.00/0

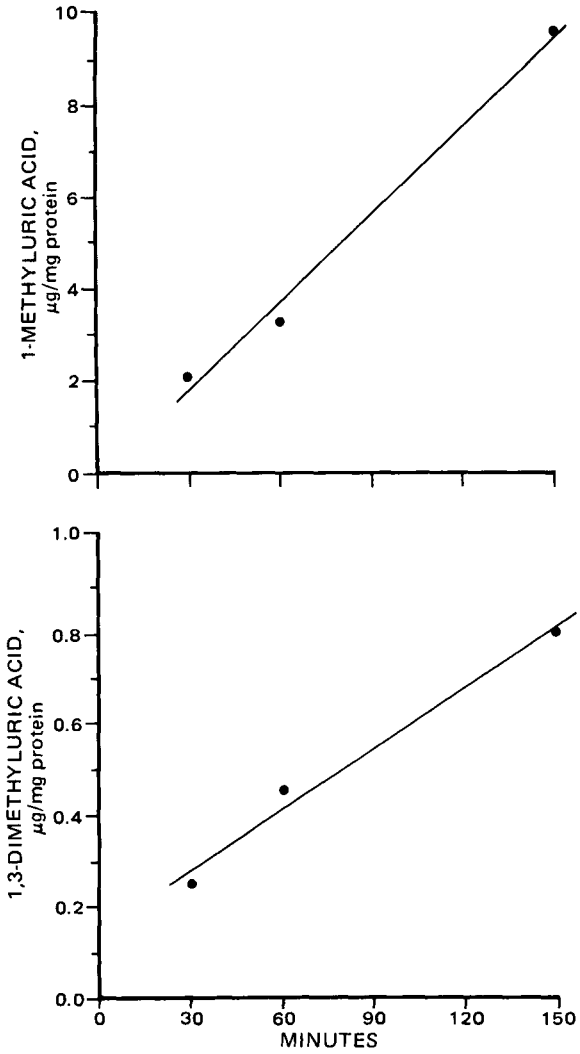

Figure 2—*Effect of increasing incubation time on production of 1-methyluric acid and 1,3-dimethyluric acid. The production of 1-methyluric acid (upper) and 1,3-dimethyluric acid (lower) from theophylline in microsomes prepared from rabbit liver were determined at 30, 60, and 150 min of incubation in a metabolic shaking water bath*[8].

Microsomes—Hepatic microsomes were prepared from rabbits using ultracentrifugation (4). Microsomal protein was determined by the method of Lowry using bovine serum albumin as a standard (5).

RESULTS AND DISCUSSION

A chromatogram of a hepatic microsomal incubation mixture demonstrated a clear separation of peaks for 1-methyluric acid, 1,3-dimethyluric acid, theophylline, theobromine, and 8-chlorotheophylline and is compared to a chromatogram of standards in Fig. 1. The production of 1-methyluric acid and 1,3-dimethyluric acid from theophylline by hepatic microsomes was determined to be linear for at least 150 min of incubation time (Fig. 2). A 2-hr incubation period was determined to give adequate amounts of metabolite for most experimental purposes. The amount of metabolites formed *in vitro* by rabbit liver microsomal enzyme metabolism of theophylline was 0.17 ± 0.04 μg of 1,3-dimethyluric acid/mg of protein/hr and 1.08 ± 0.58 μg of 1-methyluric acid/mg of protein/hr. Each value represents the mean ± standard error of microsomal preparations from four individual animals. The production of 3-methylxanthine from theophylline could not be detected in these incubation mixtures.

Table I—*In Vitro* Effect of Allopurinol[a] on *In Vitro* Theophylline Metabolism in Rabbits

	Control	Allopurinol[a]
1,3-Dimethyluric acid, μg/mg of protein/hr	0.04[b]	0.04
1-Methyluric acid, μg/ml of protein/hr	2.66	Not detectable

[a] 10^{-4} *M* allopurinol was added to microsomal incubation mixture. [b] Each value represents an individual incubation mixture using microsomes from the same control animal.

Allopurinol has been reported to decrease production of 1-methyluric acid from 1-methylxanthine (6, 7) by inhibiting xanthine oxidase. In this preparation, the addition of allopurinol (10^{-4} *M*) to the incubation mixture blocked production of 1-methyluric acid (minimum detectable limit 0.015 μg/mg of protein/hr) while not affecting production of 1,3-dimethyluric acid (Table I). This confirms that in this incubation system, 1-methyluric acid was being produced along the predicted metabolite route.

This method for the measurement of the metabolism of theophylline using an *in vitro* microsomal preparation does not require previous induction of hepatic microsomes and provides a rate of formation of specific major metabolites of theophylline. Use of this method can determine whether a change in theophylline elimination is due to specific changes in metabolite production and will also be useful in the investigation, assessment, and prediction of drug interactions involving alterations of theophylline metabolism.

REFERENCES

(1) J. F. Williams, S. Lowitt, and A. Szentivanyi, *Biochem. Pharmacol.*, **28**, 2935 (1979).

(2) R. I. Ogilvie, *Clin. Pharmacokinetics*, **3**, 267 (1978).

(3) S. Lohmann and R. Miech, *J. Pharm. Exp. Ther.*, **196**, 213 (1976).

(4) S. El Defrawry El Masry, G. M. Cohen, and G. J. Mannering, *Drug Metab. Dispos.*, **2**, 267 (1974).

(5) W. H. Lowry, N. J. Rosebrough, N. J. Farr, and R. J. Randall, *J. Biol. Chem.*, **193**, 265 (1951).

(6) S. Vozeh, R. A. Upton, S. Riegelman, and L. B. Scheiner, *N. Engl. J. Med.*, 298 (1978).

(7) J. J. Grygiel, L. M. Wing, J. Farkas, and D. Birkett, *Clin. Pharmacol. Ther.*, **26**, 660 (1979).

ACKNOWLEDGMENTS

Supported by the Medical Research Council of Canada.

Batch-Swirl Method for Detoxification of Isopropyl Myristate Used for Sterility Testing of Oils and Ointments: Membrane Selection

A. M. PLACENCIA ˣ, G. S. OXBORROW, and J. W. DANIELSON

Received July 23, 1981, from the *Minneapolis Center for Microbiological Investigations, Food and Drug Administration, Minneapolis, MN 55401.* Accepted for publication September 21, 1981.

Abstract □ A 1-hr batch-swirl method was developed for the preparation of isopropyl myristate to be used in the sterility testing of oils and ointments. The method is simpler and faster than that in *USP XX*. Flow rates of various membrane filters were tested. Cellulose acetate filters increased the filtration rate of oils and ointments and, thus, reduced the exposure time of possible microbial contaminants to the toxicity of isopropyl myristate.

Keyphrases □ Isopropryl myristate—batch-swirl method for detoxification, sterility testing of oils and ointments □ Microbial contamination—batch-swirl method for detoxification of isopropyl myristate used for sterility testing of oils and ointments □ Toxicity—batch-swirl method for detoxification of isopropyl myristate, sterility testing of oils and ointments

Problems are encountered when the *United States Pharmacopeia XX* (USP XX) method is used for the sterility testing of ointments and oils soluble in isopropyl myristate (1). Commercially prepared isopropyl myristate, which is used to dissolve the specimen, is toxic to microorganisms. It was found that the toxicity of isopropyl myristate is partially due to its pH variability, *i.e.*, the higher the pH of isopropyl myristate, the higher the decimal reduction (D value) of *Pseudomonas aeruginosa* (2, 3).

Heated isopropyl myristate has also been shown to be toxic to vegetative microorganisms during prolonged holding temperatures at 47° (3–5). Detoxification of isopropyl myristate by the USP method, which takes more than 8 hr to complete, makes the analysis time-consuming.

USP XX requires rinsing of the membrane with fluids A and D after a sample is filtered. However, after filtration of isopropyl myristate, the mixed cellulose acetate–pyroxylin membrane becomes hydrophobic and the water-based fluids, A and D, are difficult to filter.

Studies have indicated that the D value of *P. aeruginosa* is lower if the microorganisms are filtered through a 0.2-μm membrane rather than through a 0.45-μm membrane. The slower filtration rate of the 0.2-μm filter exposes the microorganisms to the isopropyl myristate for a longer time. Other authors have indicated that the use of the conventional membrane filtration technique may be the cause of low recovery rates of *P. aeruginosa* from oils or ointments (3, 6).

The present report describes a 1-hr batch-swirl method for the detoxification of isopropyl myristate and compares membrane filters used in the analysis of oils and ointments.

EXPERIMENTAL

Three methods for preparation of isopropyl myristate were compared:

Batch-Swirl Method—A 50-g amount of basic alumina (Brockman Activity 1, 80–200 mesh[1]) was weighed in a 1-liter glass beaker, and 500 ml of isopropyl myristate (detyl NF extra-isopropyl myristate NF[2]) was added. The beaker was covered with aluminum foil, and the mixture was swirled at high speed for 1 hr with a magnetic stirrer. The mixture was filter-sterilized through a 0.22-μm filter membrane (mixed cellulose acetate–pyroxylin, 47-mm diameter) and a disk prefilter[3]. Aliquots of 100 ml of filtrate were transferred to sterile 38 × 200-mm screw-capped glass test tubes for toxicity determinations.

USP XX Column-Filtered Method—Basic alumina was added to a 20 mm × 20-cm glass column to a height of 15 cm (54 g), 500 ml of isopropyl myristate was passed through the column, and the eluate was filter-sterilized as in the batch-swirl method.

Untreated Isopropyl Myristate—A 500-ml sample of isopropyl myristate obtained directly from the manufacturer was filter-sterilized as in previous methods.

pH Determination of Isopropyl Myristate—The pH of isopropyl myristate prepared for the three methods was determined after sterilization by the USP XX method, which uses the water rinse technique. A sample containing 100 ml of isopropyl myristate and 10 ml of double distilled water was transferred to a 250-ml container. The mixture was shaken vigorously for 1 hr by a mechanical shaker, then centrifuged for 20 min at 1800 rpm (529×*g*). The water layer was used to determine the pH.

Bacterial Culture Preparation—*Pseudomonas aeruginosa* (ATCC 10145) was used as a test microorganism because of its sensitivity to isopropyl myristate (4, 7). The culture was transferred to a trypticase soy agar slant and incubated for 24 hr at 35°. The slant was washed with sterile phosphate buffer and the final concentration of 10^9 organisms/ml was used as the stock solution for inoculation of isopropyl myristate.

D Value Determinations—Two test tubes, each containing 100 ml of isopropyl myristate, were prepared according to the previously described methods. A control tube of phosphate-buffered water was used to determine the initial bacterial concentration. Tubes were inoculated with 0.1 ml of stock culture solution, and all tubes were vigorously hand-shaken. One tube of isopropyl myristate from each preparation method was placed in a 47° water bath. Ten-milliliter samples were taken from each tube of isopropyl myristate at intervals of 10, 20, 30, 45, and 60 min and at 0-time from the buffered water control tube.

Aliquots were filtered through a 0.22-μm membrane[3], and membranes were transferred to 100 ml of fluid D before sonification for 6 min at 55 kHz. Dilutions were plated on trypticase soy agar and incubated at 35° for 48 hr.

Membrane Filter Evaluation—Time rates to filter the isopropyl myristate and the rinsing fluids, A and D, through various membranes (47-mm diameter, 0.2- and 0.45-μm pore sizes) were determined by placing the membrane in a membrane filtration assembly unit and filtering 100 ml of isopropyl myristate, followed by 200 ml of rinsing fluid D and 100 ml of fluid A.

[1] Fisher Scientific Co., Fair Lawn, N.J.
[2] Givaudan Corp., Clifton, N.J.
[3] Type AP 25 Millipore Corp., Bedford, Mass.

0022-3549/82/0600-0714$01.00/0

Table I—pH Levels of Isopropyl Myristate Prepared by Three Methods and Corresponding D Values of *Pseudomonas aeruginosa*

Method	pH	D Value, min: Room Temperature	D Value, min: 47°
USP XX Column-filtered			
A	6.7	>60.0	8.0
B	6.6	>60.0	9.3
Batch-Swirl			
A	6.7	>60.0	12.1
B	6.3	>60.0	11.6
Untreated			
A	4.0	11.4	<10.0
B	3.7	10.0	<10.0

Table II—Comparison of Flow Rates for Membrane Filters Used in the Filtration of Oils and Ointments

Membranes	Flow Rate, min[a]: Isopropyl Myristate 0.2 μm[b]	Isopropyl Myristate 0.45 μm[b]	Fluids A and D 0.2 μm[b]	Fluids A and D 0.45 μm[b]
Acetate Cellulose	2	1	3	1
Cellulose Nitrate	3	1	>120	20
Polyester	2	1	5	2
Mixed Esters of Cellulose	3	1	83	2
Polycarbonate	4	1	14	3
Mixed Cellulose Acetate–Pyroxylin	3	1	>120	19

[a] Approximate time. [b] Pore size of membrane.

RESULTS

The pH levels of the untreated isopropyl myristate, the USP XX column isopropyl myristate, and the batch-swirled isopropyl myristate are shown in Table I. The D values of *P. aeruginosa* obtained at room temperature and at 47°, which correspond to the three methods of preparation of isopropyl myristate, are also shown.

The approximate time required to filter isopropyl myristate and the rinsing fluids, A and D, through various membranes are given in Table II. The acetate cellulose membrane[4] and the polyester membrane[5] showed the fastest flow rates for the 0.2-μm membrane: 2 min for isopropyl myristate with both filters and 3 and 5 min, respectively, for rinsing fluids A and D. An oily film was noted on the polyester membrane after filtration of the isopropyl myristate and rinsing fluids A and D, regardless of pore size.

The flow rates of both the 0.2-μm mixed cellulose acetate–pyroxylin and the pyroxylin membranes exceeded 2 hr for the rinsing fluids. All of the 0.45-μm membranes had acceptable flow rates for isopropyl myristate. Flow rates for the rinsing fluids (pyroxylin, 20 min and cellulose acetate-pyroxylin, 19 min) were not acceptable.

DISCUSSION

The batch-swirl method for detoxification of isopropyl myristate used in the analysis of oils and ointments was simpler and faster than the USP XX method, *i.e.*, 1 hr *versus* 8 hr for the detoxification process. In the batch-swirl method, filter sterilization immediately followed the stirring, with no need for centrifugation. The pH of the isopropyl myristate prepared by the batch-swirl method met the requirements of the USP XX, and D values of the test organisms were comparable to those obtained by the USP XX method.

Use of cellulose acetate filters rather than 0.22- and 0.45-μm mixed cellulose acetate-pyroxylin membranes reduced the analysis time. Rapid filtration reduced the exposure time of microbial contaminants to the toxicity of isopropyl myristate and, thus, provided greater probability of their detection.

[4] Sartorius Filters, Inc., Hayward, Calif.
[5] Nucleopore, Pleasanton, Calif.

REFERENCES

(1) "The United States Pharmacopeia," 20th rev., U.S. Pharmacopeial Convention, Inc., Rockville, Md., 1980.

(2) F. W. Bowman, E. W. Knoll, M. White, and P. Mislivec, *J. Pharm. Sci.*, **61**, 532 (1972).

(3) K. Tsuji and J. H. Robertson, *Appl. Microbiol.*, **25**, 139 (1973).

(4) J. H. Robertson, *Bull. Parenter. Drug Assoc.*, 288 (1974).

(5) W. T. Sokolski and C. G. Chidester, *J. Pharm. Sci.*, **53**, 103 (1964).

(6) A. Hart and M. B. Ratansi, *J. Pharm. Pharmacol.*, **27**, 142 (1975).

(7) F. W. Bowman, in "Industrial Sterilization," G. B. Phillips and W. S. Miller, Eds., Duke University Press, Durham, N.C., 1972, p. 42.

Synthesis and Antitumor Testing of 3-Methenylthiochroman-4-one-1,1-dioxide

MARK H. HOLSHOUSER *x and LARRY J. LOEFFLER

Received July 6, 1981 from the *Division of Medicinal Chemistry, School of Pharmacy, The University of North Carolina, Chapel Hill, NC 27514.* Accepted for publication September 18, 1981.

* Present address: Department of Medicinal Chemistry, School of Pharmacy, Northeast Louisiana University, Monroe, LA 71209.

Abstract □ Treatment of thiochroman-4-one-1,1-dioxide (II) with paraformaldehyde and dimethylamine hydrochloride in isopropyl alcohol at reflux afforded directly in 89% yield the dimeric dihydropyran (IV), corresponding to the dimerization of the target compound 3-methenylthiochroman-4-one-1,1-dioxide (III). Neither the monomer III nor the expected Mannich base, 3-dimethylaminomethylthiochroman-4-one-1,1-dioxide, were isolated under conditions of the reaction. The monomer III could be prepared in 55% yield by sublimation of the dimer IV at 230–250°; however, redimerization slowly occurred at room temperature. The dimer IV was also prepared by the use of paraformaldehyde and *N*-methylanilinium trifluoroacetate. The monomer III was found to be marginally active at 10 mg/kg/day *versus* Ehrlich ascites tumor growth in mice.

Keyphrases □ Antitumor agents—3-methenylthiochroman-4-one-1,1-dioxide, synthesis, testing, dimerization, mice □ α-Methenyl carbonyl function—alkylating moiety in some antitumor agents, synthesis of 3-methenylthiochroman-4-one-1,1-dioxide

The presence of a ring system containing an α-methenyl carbonyl function is important as an alkylating moiety in some antitumor agents (1–5). So called quinone methides (1–3), α-methenyl derivatives of quinones, are thought to be active metabolic intermediates in alkylation mechanisms. In general, the stability of the α-methenyl carbonyl

0022-3549/82/0600-0715$01.00/0

Table I—pH Levels of Isopropyl Myristate Prepared by Three Methods and Corresponding D Values of *Pseudomonas aeruginosa*

Method	pH	D Value, min: Room Temperature	D Value, min: 47°
USP XX Column-filtered			
A	6.7	>60.0	8.0
B	6.6	>60.0	9.3
Batch-Swirl			
A	6.7	>60.0	12.1
B	6.3	>60.0	11.6
Untreated			
A	4.0	11.4	<10.0
B	3.7	10.0	<10.0

Table II—Comparison of Flow Rates for Membrane Filters Used in the Filtration of Oils and Ointments

Membranes	Flow Rate, min[a]: Isopropyl Myristate 0.2 μm[b]	Isopropyl Myristate 0.45 μm[b]	Fluids A and D 0.2 μm[b]	Fluids A and D 0.45 μm[b]
Acetate Cellulose	2	1	3	1
Cellulose Nitrate	3	1	>120	20
Polyester	2	1	5	2
Mixed Esters of Cellulose	3	1	83	2
Polycarbonate	4	1	14	3
Mixed Cellulose Acetate–Pyroxylin	3	1	>120	19

[a] Approximate time. [b] Pore size of membrane.

RESULTS

The pH levels of the untreated isopropyl myristate, the USP XX column isopropyl myristate, and the batch-swirled isopropyl myristate are shown in Table I. The D values of *P. aeruginosa* obtained at room temperature and at 47°, which correspond to the three methods of preparation of isopropyl myristate, are also shown.

The approximate time required to filter isopropyl myristate and the rinsing fluids, A and D, through various membranes are given in Table II. The acetate cellulose membrane[4] and the polyester membrane[5] showed the fastest flow rates for the 0.2-μm membrane: 2 min for isopropyl myristate with both filters and 3 and 5 min, respectively, for rinsing fluids A and D. An oily film was noted on the polyester membrane after filtration of the isopropyl myristate and rinsing fluids A and D, regardless of pore size.

The flow rates of both the 0.2-μm mixed cellulose acetate–pyroxylin and the pyroxylin membranes exceeded 2 hr for the rinsing fluids. All of the 0.45-μm membranes had acceptable flow rates for isopropyl myristate. Flow rates for the rinsing fluids (pyroxylin, 20 min and cellulose acetate-pyroxylin, 19 min) were not acceptable.

DISCUSSION

The batch-swirl method for detoxification of isopropyl myristate used in the analysis of oils and ointments was simpler and faster than the USP XX method, *i.e.*, 1 hr *versus* 8 hr for the detoxification process. In the batch-swirl method, filter sterilization immediately followed the stirring, with no need for centrifugation. The pH of the isopropyl myristate prepared by the batch-swirl method met the requirements of the USP XX, and D values of the test organisms were comparable to those obtained by the USP XX method.

Use of cellulose acetate filters rather than 0.22- and 0.45-μm mixed cellulose acetate-pyroxylin membranes reduced the analysis time. Rapid filtration reduced the exposure time of microbial contaminants to the toxicity of isopropyl myristate and, thus, provided greater probability of their detection.

[4] Sartorius Filters, Inc., Hayward, Calif.
[5] Nucleopore, Pleasanton, Calif.

REFERENCES

(1) "The United States Pharmacopeia," 20th rev., U.S. Pharmacopeial Convention, Inc., Rockville, Md., 1980.

(2) F. W. Bowman, E. W. Knoll, M. White, and P. Mislivec, *J. Pharm. Sci.*, **61**, 532 (1972).

(3) K. Tsuji and J. H. Robertson, *Appl. Microbiol.*, **25**, 139 (1973).

(4) J. H. Robertson, *Bull. Parenter. Drug Assoc.*, 288 (1974).

(5) W. T. Sokolski and C. G. Chidester, *J. Pharm. Sci.*, **53**, 103 (1964).

(6) A. Hart and M. B. Ratansi, *J. Pharm. Pharmacol.*, **27**, 142 (1975).

(7) F. W. Bowman, in "Industrial Sterilization," G. B. Phillips and W. S. Miller, Eds., Duke University Press, Durham, N.C., 1972, p. 42.

Synthesis and Antitumor Testing of 3-Methenylthiochroman-4-one-1,1-dioxide

MARK H. HOLSHOUSER *x and LARRY J. LOEFFLER

Received July 6, 1981 from the *Division of Medicinal Chemistry, School of Pharmacy, The University of North Carolina, Chapel Hill, NC 27514.* Accepted for publication September 18, 1981.

* Present address: Department of Medicinal Chemistry, School of Pharmacy, Northeast Louisiana University, Monroe, LA 71209.

Abstract □ Treatment of thiochroman-4-one-1,1-dioxide (II) with paraformaldehyde and dimethylamine hydrochloride in isopropyl alcohol at reflux afforded directly in 89% yield the dimeric dihydropyran (IV), corresponding to the dimerization of the target compound 3-methenylthiochroman-4-one-1,1-dioxide (III). Neither the monomer III nor the expected Mannich base, 3-dimethylaminomethylthiochroman-4-one-1,1-dioxide, were isolated under conditions of the reaction. The monomer III could be prepared in 55% yield by sublimation of the dimer IV at 230–250°; however, redimerization slowly occurred at room temperature. The dimer IV was also prepared by the use of paraformaldehyde and *N*-methylanilinium trifluoroacetate. The monomer III was found to be marginally active at 10 mg/kg/day *versus* Ehrlich ascites tumor growth in mice.

Keyphrases □ Antitumor agents—3-methenylthiochroman-4-one-1,1-dioxide, synthesis, testing, dimerization, mice □ α-Methenyl carbonyl function—alkylating moiety in some antitumor agents, synthesis of 3-methenylthiochroman-4-one-1,1-dioxide

The presence of a ring system containing an α-methenyl carbonyl function is important as an alkylating moiety in some antitumor agents (1–5). So called quinone methides (1–3), α-methenyl derivatives of quinones, are thought to be active metabolic intermediates in alkylation mechanisms. In general, the stability of the α-methenyl carbonyl

0022-3549/82/0600-0715$01.00/0

function is variable, depending on substitution (3). In working with novel compounds containing the thiochromone-1,1-dioxide (I) and thiochroman-4-one-1,1-dioxide (II) ring systems (6), it became desirable to synthesize the 3-methenyl derivative (III) (Scheme I), the sulfone analog of a naphthoquinone methide, as a potential antitumor agent of the alkylating type and a possible active metabolite of previously reported compounds (6). The synthesis, testing, and dimerization of III is the subject of this study.

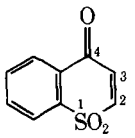

I

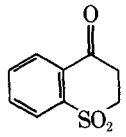

II

EXPERIMENTAL[1]

Sulfone Dimer (IV) (Method A)—Compound IV was formed by a modification of the method of Welch, *et al.* (7). A suspension of 7.76 g (39.6 mmoles) of II, 2.86 g (35.6 mmoles) of dimethylamine hydrochloride, 2.5 g (30 mmoles) of paraformaldehyde, and 0.72 ml of saturated hydrogen chloride–isopropyl alcohol solution in 25 ml of isopropyl alcohol was refluxed for 24 hr at 75°. At the end of this period a fine, white precipitate had formed. The suspension was cooled, filtered, and the solid washed with isopropyl alcohol and ether, then recrystallized from dimethylformamide. A white powder resulted with a melting point of 249–250° (yield 7.5 g, 89%).

Anal.—Calc. for $C_{20}H_{18}O_6S_2$: C, 57.39; H, 4.34. Found: C, 57.45; H, 4.22. IR: 1700 (C=O), 1300 (S=O, antisymmetrical), 1145 (S=O, symmetrical) cm^{-1}; NMR (acetone-d_6): δ 2.52 (s, 2, —C—CH_2—C—), 2.83 (s, 2, —OCH_2—), 4.10 (s, 2, 2′H), 4.39 [s, 2, 2 (II)], 7.57–8.30 (m, 8, 5–8H, 5′–8′H) ppm.

Sulfone Dimer IV (Method B)—Compound IV was also synthesized by a modification of the method of Gras (8). Paraformaldehyde (1.08 g, 12 mmoles), *N*-methylanilinium trifluoracetate (2.25 g, 10 mmoles), and (II) (1.96 g, 10 mmoles) were added to 12 ml of dioxane (dried over potassium hydroxide, then distilled from sodium metal). The mixture was refluxed for 2 hr under nitrogen, cooled, and 1.125 g (5 mmoles) of *N*-methylanilinium trifluoracetate, 0.54 g (6 mmoles) of paraformaldehyde, and 16 ml of dioxane were then added. The mixture was refluxed an additional 2 hr, allowed to cool, then extracted with chloroform, washed with a 2.5% sodium bicarbonate solution, dried over magnesium sulfate, and evaporated. The resulting white powder was dissolved in dimethyl sulfoxide and crystals formed as water was added. The product was collected and dried *in vacuo* at 100°, yielding 500 mg, 30%.

3-Methenylthiochroman-4-one-1,1-dioxide (III)—Compound IV, the dimer, (200 mg, 0.48 mmole) was placed in a sublimation apparatus and sublimed at 230–250° (1 mm Hg). On the condenser appeared a mixture of Compounds III and IV. Compound III could be purified by either repeated sublimation or column chromatography on silica gel eluted with chloroform, the monomer III eluting before the dimer IV. On immediate solvent evaporation and freezing in a desiccator, compound III remains relatively stable; yield: 110 mg (55%) observed mp 248–250°. TLC: silica gel, $CHCl_3$, R_f = 0.26. IR: 1699 (C=O), 1665 (C=C, conjugated), 1300 (S=O, antisymmetrical), 1145 (S=O, symmetrical) cm^{-1}; NMR ($CDCl_3$): δ 4.42 (s, 2,2H), 5.89 (d, 1, J = 1 Hz, =CH_2), 6.65 (d, 1, J = 1 Hz, =CH_2), 7.5–8.32 (m, 4, 5–8H) ppm.

***In Vivo* Ehrlich Ascites Screen**—All test compounds were homogenized in 0.05% polysorbate 80 and administered in doses ranging from 5 to 20 mg/kg/day ip. Tumor cells (2×10^6) were injected into CF_1 male mice (~25 g) on day 0 (n = 6). Test compounds were administered intraperitoneally on days 1–8. On day 9 the mice were sacrificed and peritoneal ascites cell volume and packed cell volume (ascites-crit) were determined by the method of Piantadosi *et al.* (9). Results of this screen are reported as percent inhibition calculated by the following:

$$\% \text{ inhibition} = 100 - \left[\frac{(\text{vol of treated})(\text{ascrit of treated})}{(\text{vol of control})(\text{ascrit of control})}\right] \times 100 \quad \text{(Eq. 1)}$$

6-Mercaptopurine was used as an internal standard. Six to eight mice were used per test compound, and >80% inhibition was considered significant.

RESULTS AND DISCUSSION

The classical synthetic approach to compound III involves Mannich base formation alpha to the carbonyl of II followed by base-catalyzed amine elimination. However, attempts to form the Mannich base (7) of II using dimethylamine hydrochloride and paraformaldehyde under acidic conditions (*i.e.*, the acid-catalyzed enol of II serving as a nucleophile) afforded an insoluble high-melting neutral product which was identified by NMR as the dihydropyran type dimer, IV (Scheme I). Compound IV resulted from the initially formed III, the desired product, which was formed either by spontaneous amine elimination (7) from the Mannich base or direct reaction with the hydroxycarbenium ion of protonated formaldehyde with no involvement of the amino species (10). Subsequently, a Diels-Alder type 1,4-addition of one molecule of III to the exomethylene group of another molecule of III occurred, forming the dihydropyran ring system of IV. High temperature was required to reverse the dimerization. Formation and subsequent isolation of III was accomplished by sublimation of IV at 230–250° (1 mm Hg), followed by rapid column chromatography of the material appearing on the condenser. Good yields of IV were obtained from II (89%), however, a poorer yield of III (55%) resulted in the reversal step. Furthermore, at room temperature and/or in the presence of solvent, III redimerized completely within 48 hr. The identical observed melting points for III and IV (248–250°) resulted from redimerization of III on slow heating, as indicated by TLC.

Specific reagents for preparing α-methenyl ketones provided an alternate method for the synthesis of III (8, 11, 12). Use of one of these agents, *N*-methylanilinium trifluoracetate (8) afforded IV as well. In anticipation of the same result, no other reagent was tried. It was of interest that this 3-exomethylene derivative of III is isolable in the thiochroman-4-one-1,1-dioxide series. This appeared not to be the case with the naphthoquinone methides previously generated, which required trapping (3). Isolability of such a reactive intermediate as III opens a route to the synthesis of a wide variety of novel 3-substituted thiochroman-4-one-1,1-dioxides *via* Michael, Diels-Alder, or 1,3-dipolar type reactions.

Freshly prepared and analyzed compound III, immediately tested at

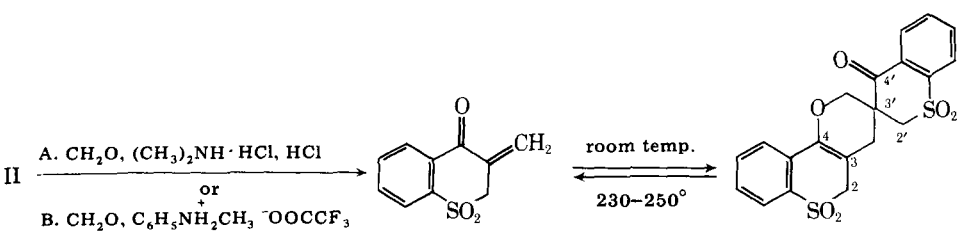

Scheme I

[1] All melting points were taken on a Thomas-Hoover capillary melting point apparatus and are uncorrected. TLC was performed on precoated plates (silica gel 60-F-254, EM reagents) with fluorescent backing. The plates were visualized by UV light. Elemental analyses were done by Atlantic Microlab, Atlanta, Ga., and agreed with theoretical values within ±0.4%.

Infrared spectra were obtained in NUJOL using a Perkin-Elmer Model 297 IR spectrophotometer. Photon NMR spectra were taken on a JEOLCO JNM-FX60 using tetramethylsilane as an internal standard. All IR and NMR spectra were completely consistent with assigned structures. Starting materials were used as received from suppliers unless otherwise indicated.

Table I—Effects of Test Compounds on Ehrlich Ascites Carcinoma[a] Growth

Compound	Dose, mg/kg/day ip	Survival at Day 9	Ascrit[b]	Ascites Volume, Mouse	Inhibition[c], %
0.05% Polysorbate 80		34/40	33.6 ± 8.7	1.8 ± 1.02	0.0
V[d]	5	8/8	22.0	2.45	57.1
	10	8/8	0.0	0.0	100.0
	20	8/8	35.7	0.88	81.8
III	10	8/8	43.8	0.15	80.0
IV	10	6/6	21.2	2.2	0.0
6-Mercaptopurine[e]	200	6/6	0.3	0.7	99.6

[a] 2×10^6 cells were injected intraperitoneally into 6 or 8 male CF_1 mice on day 0. The drug was administered from day 1 to 8. On day 9 the mice were sacrificed and the experiment was evaluated. [b] Packed cell volume as a percent. [c] Greater than 80% inhibition is required for significant activity. [d] Compound V is 3-chloromethylthiochromone-1,1-dioxide (6). [e] Sigma Chemical Co.

10 mg/kg/day in mice, *versus* Ehrlich ascites carcinoma tumor growth, was found to be only marginally active (80% inhibition of tumor growth) relative to many other compounds reported previously (6) (Table I). Several of these compounds, such as 3-chloromethylthiochromone-1,1-dioxide (V) (highly active in the test, giving 100% inhibition), could conceivably give rise to compound III *in vivo* by bioreduction and hydrogen chloride elimination (1, 3). The low activity observed with compound III may result from *in vivo* dimerization or other instability such as participation in Michael type reactions. The dimer (IV) was completely inactive in the antitumor test (Table I).

REFERENCES

(1) H. W. Moore, *Science*, **197**, 527 (1977).

(2) S. Omura, H. Tanaka, Y. Okada, and H. Marumo, *Chem. Commun.*, **1976**, 320.

(3) A. J. Lin, R. S. Pardini, L. A. Cosby, B. J. Lillis, C. W. Shansky, and A. C. Sartorelli, *J. Med. Chem.*, **16**, 1268 (1973).

(4) I. H. Hall, K. H. Lee, E. C. Mar, and C. O. Starnes, *ibid.*, **20**, 333 (1977).

(5) I. H. Hall, K. H. Lee, C. O. Starnes, S. A. El Gebaly, T. Ibuka, Y. S. Wu, T. Kimura, and M. Haruna, *J. Pharm. Sci.*, **67**, 1235 (1978).

(6) M. H. Holshouser, L. J. Loeffler, and I. H. Hall, *J. Med. Chem.*, **24**, 853 (1981).

(7) W. M. Welch, C. A. Harbert, R. Sarges, W. P. Stratten, and A. Weissman, *ibid.*, **20**, 699 (1977).

(8) T. L. Gras, *Tetrahedron Lett.*, **32**, 2955 (1978).

(9) C. Piantadosi, C. S. Kim, and J. L. Irvin, *J. Pharm. Sci.*, **58**, 921 (1969).

(10) E. Zeigler, *Monatsh. Chem.*, **18**, 334 (1947).

(11) A. Eschenmoser, *Angew. Chem. Int. Ed. Engl.*, **10**, 330 (1971).

(12) I. Paterson and I. Fleming, *Tetrahedron Lett.*, **33**, 993 (1979).

ACKNOWLEDGMENTS

The work was supported in part by a grant from the Research Council of the University of North Carolina at Chapel Hill.

During the course of this work, M. H. Holshouser was a Henry S. Wellcome Fellow, supported by the American Foundation for Pharmaceutical Education.

The authors wish to thank Dr. Iris H. Hall for her assistance in biological testing performed during this work.

Diazoketone and Chloromethylketone Analogs of Methotrexate as Potential Antitumor Agents

ALEEM GANGJEE *, THOMAS I. KALMAN, and THOMAS J. BARDOS ˣ

Received June 25, 1981, from the *Department of Medicinal Chemistry, School of Pharmacy, State University of New York at Buffalo, Buffalo, NY 14260.* Accepted for publication September 24, 1981. *Present address: Department of Pharmaceutical Chemistry and Pharmaceutics, School of Pharmacy, Duquesne University, Pittsburgh, PA 15282.

Abstract □ The synthesis of 4-amino-4-deoxy-N^{10}-methylpteroyl-(6-diazo-5-oxo)-L-norleucine and 4-amino-4-deoxy-N^{10}-methylpteroyl-(6-chloro-5-oxo)-L-norleucine, analogs of methotrexate in which the γ-carboxyl group is replaced by a diazoketone and a chloromethylketone, respectively, was carried out. The analogs inhibited the growth of leukemia L-1210 cells in culture by 50% at 4×10^{-7} *M* and 2×10^{-7} *M*, respectively, and were effective inhibitors of the synthesis of thymidylate in L-1210 cells *in vitro* ($I_{50} = 3 \times 10^{-6}$ *M*), exhibiting significant antifolate activity. The results demonstrated the feasibility of introducing chemically reactive groups at the γ-position of pteroyl glutamates with retention of biological activity. However, in the systems investigated thus far, there was no evidence of covalent bond formation due to these reactive groups at the active sites of the enzymes.

Keyphrases □ Methotrexate—diazoketone and chloromethylketone as potential antitumor agents □ Antitumor agents—potential, diazoketone and chloromethylketone analogs of methotrexate □ Analogs—diazoketone and chloromethylketone, of methotrexate, potential antitumor agents

Many structural analogs of the clinically useful antitumor agent methotrexate (4-amino-4-deoxy-N^{10}-methylpteroyl-L-glutamic acid, amethopterin) (1), modified at the carboxyl groups of its glutamic acid moiety, have been prepared in the past in attempts to alter the membrane transport properties and to improve the tissue distribution and selectivity of the drug, as well as to circumvent drug resistance. This class of methotrexate derivatives includes a variety of α- and γ-monoesters (2), diesters (3), amides (4), and peptides (4, 5) and also analogs in which the carboxyl groups are replaced by hydrogen (6–8), hydroxymethyl, or methyl (9) groups. As was observed for methotrexate analogs modified at other parts of the molecule (8, 10), with the possible exception of 10-deazaaminopterin

0022-3549/82/0600-0717$01.00/0

Table I—Effects of Test Compounds on Ehrlich Ascites Carcinoma[a] Growth

Compound	Dose, mg/kg/day ip	Survival at Day 9	Ascrit[b]	Ascites Volume, Mouse	Inhibition[c], %
0.05% Polysorbate 80		34/40	33.6 ± 8.7	1.8 ± 1.02	0.0
V[d]	5	8/8	22.0	2.45	57.1
	10	8/8	0.0	0.0	100.0
	20	8/8	35.7	0.88	81.8
III	10	8/8	43.8	0.15	80.0
IV	10	6/6	21.2	2.2	0.0
6-Mercaptopurine[e]	200	6/6	0.3	0.7	99.6

[a] 2×10^6 cells were injected intraperitoneally into 6 or 8 male CF_1 mice on day 0. The drug was administered from day 1 to 8. On day 9 the mice were sacrificed and the experiment was evaluated. [b] Packed cell volume as a percent. [c] Greater than 80% inhibition is required for significant activity. [d] Compound V is 3-chloromethylthiochromone-1,1-dioxide (6). [e] Sigma Chemical Co.

10 mg/kg/day in mice, *versus* Ehrlich ascites carcinoma tumor growth, was found to be only marginally active (80% inhibition of tumor growth) relative to many other compounds reported previously (6) (Table I). Several of these compounds, such as 3-chloromethylthiochromone-1,1-dioxide (V) (highly active in the test, giving 100% inhibition), could conceivably give rise to compound III *in vivo* by bioreduction and hydrogen chloride elimination (1, 3). The low activity observed with compound III may result from *in vivo* dimerization or other instability such as participation in Michael type reactions. The dimer (IV) was completely inactive in the antitumor test (Table I).

REFERENCES

(1) H. W. Moore, *Science*, **197**, 527 (1977).

(2) S. Omura, H. Tanaka, Y. Okada, and H. Marumo, *Chem. Commun.*, **1976**, 320.

(3) A. J. Lin, R. S. Pardini, L. A. Cosby, B. J. Lillis, C. W. Shansky, and A. C. Sartorelli, *J. Med. Chem.*, **16**, 1268 (1973).

(4) I. H. Hall, K. H. Lee, E. C. Mar, and C. O. Starnes, *ibid.*, **20**, 333 (1977).

(5) I. H. Hall, K. H. Lee, C. O. Starnes, S. A. El Gebaly, T. Ibuka, Y. S. Wu, T. Kimura, and M. Haruna, *J. Pharm. Sci.*, **67**, 1235 (1978).

(6) M. H. Holshouser, L. J. Loeffler, and I. H. Hall, *J. Med. Chem.*, **24**, 853 (1981).

(7) W. M. Welch, C. A. Harbert, R. Sarges, W. P. Stratten, and A. Weissman, *ibid.*, **20**, 699 (1977).

(8) T. L. Gras, *Tetrahedron Lett.*, **32**, 2955 (1978).

(9) C. Piantadosi, C. S. Kim, and J. L. Irvin, *J. Pharm. Sci.*, **58**, 921 (1969).

(10) E. Zeigler, *Monatsh. Chem.*, **18**, 334 (1947).

(11) A. Eschenmoser, *Angew. Chem. Int. Ed. Engl.*, **10**, 330 (1971).

(12) I. Paterson and I. Fleming, *Tetrahedron Lett.*, **33**, 993 (1979).

ACKNOWLEDGMENTS

The work was supported in part by a grant from the Research Council of the University of North Carolina at Chapel Hill.

During the course of this work, M. H. Holshouser was a Henry S. Wellcome Fellow, supported by the American Foundation for Pharmaceutical Education.

The authors wish to thank Dr. Iris H. Hall for her assistance in biological testing performed during this work.

Diazoketone and Chloromethylketone Analogs of Methotrexate as Potential Antitumor Agents

ALEEM GANGJEE *, THOMAS I. KALMAN, and THOMAS J. BARDOS ˣ

Received June 25, 1981, from the *Department of Medicinal Chemistry, School of Pharmacy, State University of New York at Buffalo, Buffalo, NY 14260.* Accepted for publication September 24, 1981. *Present address: Department of Pharmaceutical Chemistry and Pharmaceutics, School of Pharmacy, Duquesne University, Pittsburgh, PA 15282.

Abstract □ The synthesis of 4-amino-4-deoxy-N^{10}-methylpteroyl-(6-diazo-5-oxo)-L-norleucine and 4-amino-4-deoxy-N^{10}-methylpteroyl-(6-chloro-5-oxo)-L-norleucine, analogs of methotrexate in which the γ-carboxyl group is replaced by a diazoketone and a chloromethylketone, respectively, was carried out. The analogs inhibited the growth of leukemia L-1210 cells in culture by 50% at 4×10^{-7} *M* and 2×10^{-7} *M*, respectively, and were effective inhibitors of the synthesis of thymidylate in L-1210 cells *in vitro* ($I_{50} = 3 \times 10^{-6}$ *M*), exhibiting significant antifolate activity. The results demonstrated the feasibility of introducing chemically reactive groups at the γ-position of pteroyl glutamates with retention of biological activity. However, in the systems investigated thus far, there was no evidence of covalent bond formation due to these reactive groups at the active sites of the enzymes.

Keyphrases □ Methotrexate—diazoketone and chloromethylketone as potential antitumor agents □ Antitumor agents—potential, diazoketone and chloromethylketone analogs of methotrexate □ Analogs—diazoketone and chloromethylketone, of methotrexate, potential antitumor agents

Many structural analogs of the clinically useful antitumor agent methotrexate (4-amino-4-deoxy-N^{10}-methylpteroyl-L-glutamic acid, amethopterin) (1), modified at the carboxyl groups of its glutamic acid moiety, have been prepared in the past in attempts to alter the membrane transport properties and to improve the tissue distribution and selectivity of the drug, as well as to circumvent drug resistance. This class of methotrexate derivatives includes a variety of α- and γ-monoesters (2), diesters (3), amides (4), and peptides (4, 5) and also analogs in which the carboxyl groups are replaced by hydrogen (6–8), hydroxymethyl, or methyl (9) groups. As was observed for methotrexate analogs modified at other parts of the molecule (8, 10), with the possible exception of 10-deazaaminopterin

0022-3549/82/0600-0717$01.00/0

(10), none of these derivatives proved more effective than methotrexate. Modification at the α-position generally led to a marked decrease in biological activity including binding to the primary target dihydrofolate reductase, whereas substitution at the γ-carboxyl was better tolerated (4–10), with enzyme inhibitory activities approaching that of the parent drug.

The feasibility of introducing chemically reactive groups capable of covalent bond formation into the more permissive γ-position of pteroyl glutamates was explored. This type of modification may lead to the development of new active-site directed inhibitors (11) of folate metabolizing enzymes with potential antitumor activity. The replacements of the γ-carboxyl of methotrexate by a diazoketone and a chloromethylketone were chosen as prototypes of this modification. The diazoketone analog of glutamic acid, the antitumor antibiotic 6-diazo-5-oxo-L-norleucine (I) is a potent, irreversible inhibitor of glutamine amidotransferases (12). α-Haloketone analogs of various substrates are widely used for the affinity labeling of enzyme active sites (11–13).

In this report the synthesis and *in vitro* biological activities of the methotrexate analogs 4-amino-4-deoxy-N^{10}-methylpteroyl-(6-diazo-5-oxo)-L-norleucine (II) and 4-amino -4- deoxy-N^{10}-methylpteroyl-(6-chloro-5-oxo)-L-norleucine (III) are described. The results demonstrate that methotrexate can be substituted at the γ-position of its glutamate moiety with diazoketone and chloromethylketone functionalities, and that these modifications permit effective cellular uptake and expression of antifolate activity.

RESULTS AND DISCUSSION

Chemistry—The synthesis of the target compound (II) was accomplished by coupling 4-amino-4-deoxy-N^{10}-methylpteroic acid (14) (IV) with I using dicyclohexylcarbodiimide and 1-hydroxybenzotriazole *via* a modification of the peptide coupling procedure of Konig and Geiger (15, 16) (Scheme I). This coupling procedure, requiring milder conditions, was selected over the mixed anhydride method generally adopted for the coupling of IV with a variety of amino acid esters (6), mainly because of the known instability of I (17) to heat and pH extremes. Compound II displayed strong IR absorption bands at 2106 cm^{-1}, characteristic of the diazo moiety, and at 1633 and 1605 cm^{-1}, indicative of the ketone and amide, respectively. The NMR spectrum was consistent with the assigned structure; it included a singlet at 5.99 ppm associated with the methine proton of the diazoketone and a multiplet, strongly resembling a doublet, at 7.98 ppm assigned to the NH proton of the amide group.

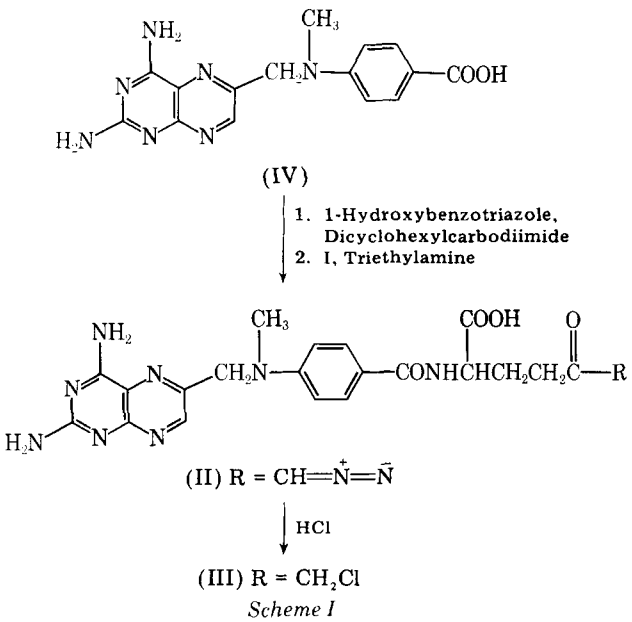

Scheme I

Treatment of II with dry hydrogen chloride afforded the hydrochloride salt of the chloromethylketone analog (III), illustrated in Scheme I. The IR spectrum of III included a strong band at 1725 cm^{-1}, characteristic of chloromethyl ketones, and at 1610 cm^{-1}, assigned to the amide. The NMR spectrum included a singlet at 4.48 ppm, assigned to the methylene protons of the chloromethylketone, in accordance with the assigned structure.

Biological Results—The growth of leukemia L-1210 cells in culture (18) was inhibited 50% by II and III at 4×10^{-7} *M* and 2×10^{-7} *M*, respectively. In L-1210 cells *in vitro*, both compounds showed the same antifolate activity as measured by the *in situ* thymidylate synthetase assay (19) ($I_{50} = 3 \times 10^{-6}$ *M*). The potency of II and III was within an order of magnitude of that of methotrexate. The activity in both assay systems may be attributed to methotrexate-like activity involving inhibition of intracellular dihydrofolate reductase.

In preliminary studies of the effects of II and III in isolated enzyme systems, the thymidylate synthetases of *Lactobacillus casei* (20) and human blast cells (21), dihydrofolate reductase of *L. casei* (22), and folylpolyglutamate synthetase of rat liver (23), no irreversible inactivation was demonstrated. In these systems methotrexate exerted reversible inhibitory activity, with the exception of folylpolyglutamate synthetase, for which methotrexate is a substrate (23). Using various experimental tumor and isolated enzyme systems in comparison with methotrexate, further studies of II and III are in progress.

The synthetic procedures described in this paper are currently being applied with appropriate modifications to the preparations of diazoketone and chloromethylketone analogs of folic acid and its derivatives.

EXPERIMENTAL[1]

4-Amino-4-deoxy-N^{10}-methylpteroyl- (6-diazo-5-oxo) -L-norleucine (II)—To a solution of 4-amino-4-deoxy-N^{10}-methylpteroic acid (IV) (14), (180 mg, 0.5 mmole) in 10 ml of dimethyl sulfoxide–tetrahydrofuran (1:1) cooled to 0° was added 1-hydroxybenzotriazole (67.2 mg, 0.5 mmole) and dicyclohexylcarbodiimide (102.5 mg, 0.5 mmole). The reaction mixture was stirred for 1 hr at 0° and 1 hr at room temperature. To this mixture, kept in the dark, was added a solution of 6-diazo-5-oxo-L-norleucine (86.2 mg, 0.5 mmole) in dimethyl sulfoxide (2 ml) and water (1.5 ml). The reaction coupling time was 3 hr, during which the pH of the reaction mixture was monitored and maintained at 7.9–8.0 by the addition of the required amount of a dilute solution of triethylamine–dimethyl sulfoxide–tetrahydrofuran (2:1:5). After 3 hr, the reaction mixture was cooled to −15° overnight and filtered. Tetrahydrofuran was removed from the filtrate by evaporation which was followed by filtration and evaporation of the filtrate *in vacuo* to dryness. The residue was stirred with *N,N*-dimethylformamide and filtered to afford a clear solution which was concentrated to half of its volume, cooled overnight (−15°), and filtered. The filtrate was evaporated to dryness and triturated with ethyl acetate; subsequent filtration followed by washing with tetrahydrofuran, water, and acetone afforded a yellow solid (II). The compound was homogeneous by TLC (silica gel, dimethylsulfoxide–H_2O, 1:1), yield 53% (71% based on unrecovered IV). IR (KBr): 2106 ($N^+{=}N^-$), 1633 ($COCHN_2$), 1605 (CONH) cm^{-1}; NMR (dimethyl sulfoxide-d_6): δ 3.22 (s, 3H, N—CH_3), 4.32 (m, 1H, α—CH), 4.79 (s, 2H, CH_2—N), 5.99 (s, 1H, $CH{=}N^+{=}N^-$), 6.67 (s, 2H, NH_2), 6.83 and 7.72 (2d, 4H, C_6H_4), 7.50 (broad s, 2H, NH_2), 7.98 (m, resembling a doublet, 1H, CONH), and 8.58 (s, 1H, C_7H) ppm.

Anal—Calc. for $C_{21}H_{22}N_{10} \cdot 0.5\ H_2O$: C, 51.74; H, 4.72; N, 28.75. Found: C, 52.04; H, 4.91; N, 27.71. (The low value for nitrogen is not unusual in the elemental analysis of diazo compounds.)

4-Amino-4-deoxy-N^{10}-methylpteroyl- (6-chloro-5-oxo) -L-norleucine hydrochloride (III). Compound II (115 mg, 0.24 mmole) was dissolved in dry *N,N*-dimethylformamide (6.5 ml) and cooled in an ice-water bath. Dry hydrogen chloride was bubbled into the cooled solution for 10 min. The deep brown solution was stirred for 1 hr at 4° and then poured into cold anhydrous diethyl ether (35 ml). The crude product was purified by repeated triturations with cold (4°) anhydrous diethyl ether, and finally with ether–ethanol mixture (10:1), to give a brown oil. Con-

[1] IR spectra were obtained using a Nicolet Model 7000 Fourier transform IR spectrometer on samples prepared in a potassium bromide pellet. NMR spectra were obtained using a Varian FT-80 instrument. Compounds were dissolved in dimethyl sulfoxide-d_6 from commercial sources with tetramethylsilane as the internal standard.

tinued treatment with several portions of cold anhydrous ether, followed by filtration in a dry box under nitrogen, gave III as a pale yellow solid, yield 98%. IR (KBr): 1725 ($COCH_2Cl$), 1610 (CONH) cm^{-1}; NMR (dimethyl sulfoxide-d_6): δ 3.26 (s, 3H, N—CH_3), 4.48 (s, 2H, CH_2Cl), 4.88 (broad s, 3H, CH_2 and α—CH), 6.83 and 7.75 (two d, 4H, C_6H_4), 7.95 (s, 2H, CONH), and 8.75 (s, 1H, C_7H) ppm. An analytical sample was obtained by drying over phosphorus pentoxide *in vacuo*.

Anal.—Calc. for $C_{21}H_{23}ClN_8O_4 \cdot HCl \cdot 4H_2O$: C, 42.36; H, 5.42; N, 18.82; Cl, 11.91. Found: C, 42.61; H, 5.47; N, 19.08; Cl, 11.73.

Cell Culture Studies—Growth inhibition of murine leukemia L-1210 cells in culture was determined as described previously (18). The cells were maintained in a medium[2] supplemented with 10% calf serum[3] and antibiotics (penicillin and streptomycin). The cultures were incubated at 37° for 40 hr. During this time, the density in the control cultures increased from 1.5×10^5 to $1.2–1.5 \times 10^6$ cell/ml. Cell viability was determined by the trypan blue dye exclusion technique.

Cellular Thymidylate Synthetase Assay—Studies of the inhibition of intracellular thymidylate synthesis were carried out using murine leukemia L-1210 cells suspended in modified Eagle's media (without folate). The L-1210 cell line was maintained by weekly passage of 10^5 cells into DBA/2HA mice and harvested 6 days after inoculation.

The cellular radioisotopic assay of thymidylate synthetase activity was performed as described previously (19) by measuring the extent of tritium released into water from [5-^{3}H]deoxyuridine[4] (specific activity 22 Ci/mmole). Radioactivity was determined by liquid scintillation counting techniques[5] using a counter and scintillation cocktail[6] with 30–35% counting efficiency.

ACKNOWLEDGMENTS

Presented in part at the 179th National Meeting of the American Chemical Society, Houston, TX, March 27, 1980.

This work was supported by Research Grants CA-06695 and CA-13604 and Training Grant 5-T32-CA-09166 from the National Cancer Institute, National Institutes of Health.

The authors thank Professor M. Bodanszky, Case Western Reserve University, for helpful suggestions, and the Developmental Therapeutics Program, Division of Cancer Treatment, National Cancer Institute for supplying samples of I and 2,4-diamino-6-hydroxymethylpteridine hydrobromide. The authors are grateful to Drs. J. J. McGuire and J. R. Bertino and Dr. Y. C. Cheng for the results with folylpolyglutamate synthetase and human thymidylate synthetase, respectively. The assistance of Mrs. K. Baranski and J. C. Yalowich in performing the cell culture assays is appreciated.

[2] RPMI 1640 medium.
[3] Dialyzed, GIBCO No. 644.
[4] Moravek Biochemicals.
[5] Packard Model 3255 TriCarb Counter.
[6] Fisher, Scinti Verse.

REFERENCES

(1) D. G. Johns and J. R. Bertino in "Cancer Medicine," J. R. Holland and E. Frei, III, Eds., Lea and Febiger, Philadelphia, Penn., 1973, p. 739.

(2) A. Rosowsky, G. P. Beardsley, W. D. Ensminger, H. Lazarus, and C.-S. Cheng, *J. Med. Chem.*, **21**, 380 (1978).

(3) A. Rosowsky, *ibid.*, **16**, 1190 (1973).

(4) J. R. Piper and J. A. Montgomery, in "Chemistry and Biology of Pteridines," R. L. Kisliuk and G. M. Brown, Eds., Elsevier-North Holland, New York, N.Y., 1979, p. 261.

(5) A. Rosowski and C.-S. Yu, *J. Med. Chem.*, **21**, 170 (1978).

(6) M. Chaykovsky, B. L. Brown, and E. J. Modest, *ibid.*, **18**, 909 (1975).

(7) D. C. Shuster, E. Tarnauceanu, D. Ionescu, V. Dobre, and I. Nicolescu-Duvaz, *ibid.*, **21**, 1162 (1978).

(8) J. A. Montgomery, J. R. Piper, R. D. Elliott, C. Temple, Jr., E. C. Roberts, and Y. F. Shealy, *ibid.*, **22**, 862 (1979).

(9) M. Chaykovsky, A. Rosowsky, and E. J. Modest, *J. Heterocycl. Chem.*, **10**, 425 (1973).

(10) F. M. Sirotnak, P. L. Chello, J. R. Piper, J. A. Montgomery, and J. I. DeGraw, in "Chemistry and Biology of Pteridines," R. L. Kisliuk and G. M. Brown, Eds., Elsevier-North Holland, New York, N.Y., 1979, p. 597.

(11) B. R. Baker, "Design of Active-Site Directed Irreversible Enzyme Inhibitors," Wiley, New York, N.Y., 1967.

(12) L. M. Pinkus, in "Methods of Enzymology," vol. 46, W. B. Jakoby and M. Wilcheck, Eds., Academic, New York, N.Y., 1977, p. 414.

(13) F. C. Hartman, *ibid.*, p. 130.

(14) J. R. Piper and J. A. Montgomery, *J. Org. Chem.*, **42**, 208 (1977).

(15) W. Konig and R. Geiger, *Chem. Ber.*, **103**, 788 (1970).

(16) W. Konig and R. Geiger, in "Chemistry and Biology of Peptides," J. Meienhofer, Ed., Ann Arbor Science, Ann Arbor, Mich., 1972, p. 343.

(17) H. W. Dion, S.A. Fusari, Z. L. Jakobowski, J. G. Zora, and Q. R. Bartz, *J. Am. Chem. Soc.*, **78**, 3075 (1956).

(18) M. Bobek, A. Bloch, P. Berkowitz, and T. J. Bardos, *J. Med. Chem.*, **20**, 458 (1977).

(19) T. I. Kalman and J. C. Yalowich in "Chemistry and Biology of Pteridines," R. L. Kisliuk and G. M. Brown, Eds., Elsevier-North Holland, New York, N.Y., 1979, p. 671.

(20) T. C. Crushberg, R. Leary, and R. L. Kisliuk, *J. Biol. Chem.*, **245**, 5293 (1968).

(21) B. J. Dolnick and Y. C. Cheng, *ibid.*, **252**, 7697 (1977).

(22) L. E. Gunderson, R. B. Dunlap, N. G. L. Harding, J. H. Freisheim, F. Ottig, and F. M. Huennekens, *Biochemistry*, **11**, 1018 (1972).

(23) J. J. McGuire, P. Hsieh, J. K. Coward, and J. R. Bertino, *J. Biol. Chem.*, **255**, 5776 (1980).

Paradoxical Increase in Aminoglycoside Body Clearance in Renal Disease When Volume of Distribution Increases

Keyphrases □ Pharmacokinetics—aminoglycosides in renal disease, clearance, volume of distribution □ Aminoglycosides—body clearance in renal disease with increased volume of distribution, pharmacokinetics □ Renal disease—aminoglycoside body clearance with increased volume of distribution, pharmacokinetics

To the Editor:

Recent studies in our laboratory on the disposition of gentamicin in dogs (1) and sheep (2) with glomerular disease indicated that gentamicin's volume of distribution (Vd) increased, while the glomerular filtration rate, as measured by endogenous creatinine clearance, decreased. A re-evaluation of these studies to include a comparison of renal clearance parameters demonstrates that body or systemic clearance of gentamicin (Cl_B) paradoxically increases in the face of a decreased glomerular filtration rate (Table I). The purpose of this communication is to explore the nature of this paradox and to assess its significance in predicting drug disposition from clinical estimates of the glomerular filtration rate.

Volume of distribution generally has been shown to remain constant or decrease in renal failure for drugs that are not extensively protein bound (4–6). Often the decrease in Vd is not physiological, but rather is dependent on the pharmacokinetic parameters used to estimate it. Thus, in a two-compartment open model, a decrease in elimination will result in a decrease in Vd_β, Vd_{area}, and Vd_B, but not Vc or Vd_{ss} which are estimates of the physiologic distribution space of the drug (7). Aminoglycoside antibiotics are not appreciably bound to serum proteins. They are distributed essentially in extracellular water, are eliminated unchanged by the kidney, and a decreased glomerular filtration rate decreases their elimination (8). However, Vd_{ss} and Vc of netilmicin (9, 10) and Vd calculated after constant intravenous infusion of gentamicin (11) increased in patients with a decreased glomerular filtration rate, as measured by creatinine and/or inulin clearance. This is similar to the situation seen in our laboratory in animals with glomerulonephropathy. The mechanism of increased Vd is not known and may be specifically related to the pathophysiology of acute glomerulonephropathy. This condition, which has been associated with sodium retention and concommitantly increased exchangeable body sodium (12), could cause fluid retention and thus an increased physiological Vd. Alternatively, the immunological events occurring at the glomerulus could release a vasoactive factor(s) which might increase tissue binding of drug. Since the etiologic diagnosis of the renal disease is often not reported in pharmacokinetic studies, some of the human patients in the studies cited may have had glomerular disease.

Clearance may be calculated from the following:

$$Cl_B = K_{el}Vc \qquad \text{(Eq. 1)}$$

$$Cl_B = \beta Vd_{area} \qquad \text{(Eq. 2)}$$

where K_{el} is the elimination rate constant, Vc is the volume of the central compartment, β is the overall elimination rate constant, and Vd_{area} is the volume of distribution calculated from the area; all are defined in terms of a two-compartment open pharmacokinetic model (7, 13, 14). Body clearance can also be calculated according to the following model-independent technique:

$$Cl_B = \frac{\text{Dose}}{AUC} \qquad \text{(Eq. 3)}$$

where AUC is the area under the plasma concentration *versus* time curve, and dose is the amount of absorbed drug unchanged in the body (13, 14). Incomplete collection of data points may result in spuriously low values for AUC due to low serum concentrations seen with the expanded Vd, the result being increased Cl_B.

An increase in Cl_B could reflect a physiological increase in drug clearance. Gentamicin Cl_B calculated using Eqs. 1 and 3 increased in animals with glomerulonephropathy (Table I). In the human studies cited (9, 11), the ratio of aminoglycoside clearance to the glomerular filtration rate (fractional urinary excretion) also increased with a decreasing glomerular filtration rate and increasing Vd. In one study (11), actual renal gentamicin clearance even exceeded the glomerular filtration rate in some patients. This finding is supported in a recent micropuncture study in rats (15), which demonstrated that expansion of extracellular fluid volume with saline or bicarbonate caused an increase in the fractional urinary excretion of gentamicin exceeding unity in some cases. Similar findings were also noted when furosemide was administered concurrently with gentamicin (16). In this study utilizing rabbits, gentamicin renal clearance exceeded the glomerular filtration rate, as determined by inulin clearance, when furosemide was coadministered. The authors attributed this to in-

Table I—Selected Pharmacokinetic Data [a] of Gentamicin Disposition in Dogs and Sheep with Normal or Decreased Renal Function Secondary to Glomerular Disease

Parameter	Units	Dogs [b]		Sheep [c]	
		Normal (n = 11)	Diseased (n = 4)	Normal (n = 6)	Diseased (n = 2)
GFR [d]	ml/min/kg	3.8 ± 0.9	1.9 ± 0.6	1.7 ± 0.3	0.5 ± 0.2
Cl_B	ml/min/kg	4.1 ± 0.6	5.3 ± 1.2	1.0 ± 0.2	1.4 ± 0.5
Vd_{ss}	liter/100 kg	34.1 ± 2.4	51.2 ± 2.5	24.5 ± 2.9	47.0 ± 7.4
Vc	liter/100 kg	19.2 ± 0.7	28.6 ± 4.2	11.3 ± 1.4	14.4 ± 1.8

[a] Mean ± *SD*. [b] Data revised and adapted from Riviere *et al.* (1) and Riviere and Coppoc (3) (two-compartment open pharmacokinetic model). [c] Data revised and adapted from Brown *et al.* (2) (three-compartment open pharmacokinetic model). [d] GFR = glomerular filtration rate (as determined by endogenous creatinine clearance).

0022-3549/82/0600-0720$01.00/0

creased gentamicin excretion by a renal tubular process, an event which was not present in the control animals studied. Finally, when water-deprived and hydrated rats were treated with gentamicin (17), the trend in changes seen in Cl_B and Vd with hydration were of similar nature to the animals with glomerulonephropathy. Extrapolation of these findings to the diseased animal is difficult due to the precisely defined experimental conditions of these studies. This is especially true in micropuncture experiments where small quantities of drug are involved. However, these data provide a physiologic basis for the pharmacokinetic changes detected in the dogs and sheep with acute glomerular disease.

It would appear that certain physiologic conditions and disease states associated with volume expansion and/or increased urine flow might lead to increased gentamicin clearance. This response may be modulated through a mechanism triggered by the abnormal fluid status. The increase in drug clearance may be a reflection of nephron heterogeneity (15) or a result of active tubular secretion, decreased proximal tubular reabsorption, or decreased nonionic back diffusion in the distal nephron (16, 18). Alternatively, glomerular disease may specifically increase the drug's ultrafilterability across the glomerular capillary membrane, normally restricted due to the Donnan Effect (18). This functional lesion would be expected to increase the fractional urinary excretion of gentamicin. Mechanistic studies have not been performed in diseased animals, and thus, further speculation is not warranted. This situation may not be seen in the chronic disease situation where individual nephrons have undergone compensatory hypertrophy. This chronic condition is pathophysiologically distinct and is clinically characterized by a different syndrome than is the acute disease process.

In view of these changes, one must be cautious in predicting Cl_B from the glomerular filtration rate, especially when an increased Vd is present, because these methods assume that this relationship does not change with the underlying disease process. However, certain disease conditions may uncouple this association of Cl_B to the glomerular filtration rate. Actual renal clearances of drug should be determined by measuring urinary drug excretion. Note that serum elimination half-life may remain relatively stable in the above situation because the increasing clearance will offset the increased volume of distribution. Dosage nomograms, which correlate elimination half-life or decreasing Cl_B with decreasing creatinine clearance, must be interpreted differently when Vd is known to have increased. Finally, additional studies relating drug disposition to specific pathophysiologic states of renal disease must be conducted to define the effects of various disease processes on drug clearance and volume of distribution, the two physiologic determinants of drug disposition.

(1) J. E. Riviere, G. L. Coppoc, E. J. Hinsman, and W. W. Carlton, *Antimicrob. Agents Chemother.*, **20,** 387 (1981).

(2) S. A. Brown, J. E. Riviere, and G. L. Coppoc, *Proc. Conf. Res. Workers Anim. Dis.*, **62,** 15A (1981).

(3) J. E. Riviere and G. L. Coppoc, *Am. J. Vet. Res.*, **42,** 1621 (1981).

(4) M. Gibaldi and D. Perrier, *J. Clin. Pharmacol.*, **12,** 201 (1972).

(5) V. Klotz, *Clin. Pharmacokinet.*, **1,** 104 (1976).

(6) M. Gibaldi, *Am. J. Med.*, **62,** 471 (1977).

(7) W. J. Jusko and M. Gibaldi, *J. Pharm. Sci.*, **61,** 1270 (1972).

(8) J. C. Pechere and R. Dugal, *Clin. Pharmacokinet.*, **4,** 170 (1979).

(9) P. G. Welling, A. Baumueller, C. C. Lau, and P. O. Nodsen, *Antimicrob. Agents Chemother.*, **12,** 328 (1977).

(10) J. C. Pechere, R. Dugal, and M. M. Pechere, *Clin. Pharmacokinet.*, **3,** 395 (1978).

(11) A. Gyselynck, A. Forrey, and R. Cutler, *J. Infect. Dis.*, **124** (Suppl), S70 (1971).

(12) R. J. Glassock and C. M. Bennett, in "Progress in Glomerulonephritis," P. Kincaid-Smith, A. J. F. d'Apice, and R. C. Atkins, Eds., John Wiley, New York, N.Y., 1979, p. 159.

(13) M. Gibaldi and D. Perrier, "Pharmacokinetics," Marcell Dekker, New York, N.Y., (1975).

(14) E. R. Garrett, *Int. J. Clin. Pharmacol.*, **16,** 155 (1978).

(15) H. O. Senekjian, T. F. Knight, and E. J. Weinman, *Kidney Int.*, **19,** 416 (1981).

(16) C. Carbon, A. Contrepois, A. Vigneron, and S. Lamotte-Barrillon, *J. Pharmacol. Exp. Ther.*, **213,** 600 (1980).

(17) J. LeCompte, L. Dumont, J. Hill, P. Du Souich, and J. Lelorier, *ibid.*, **218,** 231 (1981).

(18) E. Pastoriza-Munoz, D. Timmerman, S. Feldman, and G. J. Kalogomides, *ibid.*, **220** 604 (1982).

J. Edmond Riviere
Department of Veterinary
Physiology and Pharmacology
Purdue University
West Lafayette, IN 47960

Received November 20, 1981.
Accepted for publication March 30, 1982.
Discussions with Dr. Gordon L. Coppoc are gratefully acknowledged.
Present address: Laboratory of Pharmacology and Toxicology, School of Veterinary Medicine, North Carolina State University, Raleigh, NC 27606

Isosorbide Dinitrate: Pharmacokinetics after Intravenous Administration

Keyphrases □ Pharmacokinetics—intravenous administration of isosorbide dinitrate, bioavailability □ Bioavailability—pharmacokinetics of isosorbide dinitrate after intravenous administration □ Isosorbide dinitrate—pharmacokinetics after intravenous administration, bioavailability

To the Editor:

Isosorbide dinitrate is an organic nitrate found therapeutically useful in its sublingual and oral forms in various cardiovascular diseases such as angina pectoris (1) and congestive heart failure (2). Recently, Distante *et al.* (3) showed that an intravenous infusion of this drug (0.021–0.083 mg/min) was also effective in managing unstable angina. The availability of an intravenous dosage form of isosorbide dinitrate not only affords the opportunity to characterize the pharmacokinetics of this drug after this particular mode of therapy, it also allows the possibility to assess the bioavailability of this drug after other (*e.g.*, oral) routes of administration in patients. This latter subject has been of major controversy since Needleman *et al.* (4) made the assertion that oral nitrate therapy is irrational because of its complete first-pass metabolism.

A preliminary study has appeared which provided some initial information on this important issue. Taylor *et al.* (5) showed that in two normal, young subjects who received

0022-3549/82/0600-0721$01.00/0

creased gentamicin excretion by a renal tubular process, an event which was not present in the control animals studied. Finally, when water-deprived and hydrated rats were treated with gentamicin (17), the trend in changes seen in Cl_B and Vd with hydration were of similar nature to the animals with glomerulonephropathy. Extrapolation of these findings to the diseased animal is difficult due to the precisely defined experimental conditions of these studies. This is especially true in micropuncture experiments where small quantities of drug are involved. However, these data provide a physiologic basis for the pharmacokinetic changes detected in the dogs and sheep with acute glomerular disease.

It would appear that certain physiologic conditions and disease states associated with volume expansion and/or increased urine flow might lead to increased gentamicin clearance. This response may be modulated through a mechanism triggered by the abnormal fluid status. The increase in drug clearance may be a reflection of nephron heterogeneity (15) or a result of active tubular secretion, decreased proximal tubular reabsorption, or decreased nonionic back diffusion in the distal nephron (16, 18). Alternatively, glomerular disease may specifically increase the drug's ultrafilterability across the glomerular capillary membrane, normally restricted due to the Donnan Effect (18). This functional lesion would be expected to increase the fractional urinary excretion of gentamicin. Mechanistic studies have not been performed in diseased animals, and thus, further speculation is not warranted. This situation may not be seen in the chronic disease situation where individual nephrons have undergone compensatory hypertrophy. This chronic condition is pathophysiologically distinct and is clinically characterized by a different syndrome than is the acute disease process.

In view of these changes, one must be cautious in predicting Cl_B from the glomerular filtration rate, especially when an increased Vd is present, because these methods assume that this relationship does not change with the underlying disease process. However, certain disease conditions may uncouple this association of Cl_B to the glomerular filtration rate. Actual renal clearances of drug should be determined by measuring urinary drug excretion. Note that serum elimination half-life may remain relatively stable in the above situation because the increasing clearance will offset the increased volume of distribution. Dosage nomograms, which correlate elimination half-life or decreasing Cl_B with decreasing creatinine clearance, must be interpreted differently when Vd is known to have increased. Finally, additional studies relating drug disposition to specific pathophysiologic states of renal disease must be conducted to define the effects of various disease processes on drug clearance and volume of distribution, the two physiologic determinants of drug disposition.

(1) J. E. Riviere, G. L. Coppoc, E. J. Hinsman, and W. W. Carlton, *Antimicrob. Agents Chemother.*, **20,** 387 (1981).

(2) S. A. Brown, J. E. Riviere, and G. L. Coppoc, *Proc. Conf. Res. Workers Anim. Dis.*, **62,** 15A (1981).

(3) J. E. Riviere and G. L. Coppoc, *Am. J. Vet. Res.*, **42,** 1621 (1981).

(4) M. Gibaldi and D. Perrier, *J. Clin. Pharmacol.*, **12,** 201 (1972).

(5) V. Klotz, *Clin. Pharmacokinet.*, **1,** 104 (1976).

(6) M. Gibaldi, *Am. J. Med.*, **62,** 471 (1977).

(7) W. J. Jusko and M. Gibaldi, *J. Pharm. Sci.*, **61,** 1270 (1972).

(8) J. C. Pechere and R. Dugal, *Clin. Pharmacokinet.*, **4,** 170 (1979).

(9) P. G. Welling, A. Baumueller, C. C. Lau, and P. O. Nodsen, *Antimicrob. Agents Chemother.*, **12,** 328 (1977).

(10) J. C. Pechere, R. Dugal, and M. M. Pechere, *Clin. Pharmacokinet.*, **3,** 395 (1978).

(11) A. Gyselynck, A. Forrey, and R. Cutler, *J. Infect. Dis.*, **124** (Suppl), S70 (1971).

(12) R. J. Glassock and C. M. Bennett, in "Progress in Glomerulonephritis," P. Kincaid-Smith, A. J. F. d'Apice, and R. C. Atkins, Eds., John Wiley, New York, N.Y., 1979, p. 159.

(13) M. Gibaldi and D. Perrier, "Pharmacokinetics," Marcell Dekker, New York, N.Y., (1975).

(14) E. R. Garrett, *Int. J. Clin. Pharmacol.*, **16,** 155 (1978).

(15) H. O. Senekjian, T. F. Knight, and E. J. Weinman, *Kidney Int.*, **19,** 416 (1981).

(16) C. Carbon, A. Contrepois, A. Vigneron, and S. Lamotte-Barrillon, *J. Pharmacol. Exp. Ther.*, **213,** 600 (1980).

(17) J. LeCompte, L. Dumont, J. Hill, P. Du Souich, and J. Lelorier, *ibid.*, **218,** 231 (1981).

(18) E. Pastoriza-Munoz, D. Timmerman, S. Feldman, and G. J. Kalogomides, *ibid.*, **220** 604 (1982).

J. Edmond Riviere
Department of Veterinary
Physiology and Pharmacology
Purdue University
West Lafayette, IN 47960

Received November 20, 1981.
Accepted for publication March 30, 1982.
Discussions with Dr. Gordon L. Coppoc are gratefully acknowledged.
Present address: Laboratory of Pharmacology and Toxicology, School of Veterinary Medicine, North Carolina State University, Raleigh, NC 27606

Isosorbide Dinitrate: Pharmacokinetics after Intravenous Administration

Keyphrases □ Pharmacokinetics—intravenous administration of isosorbide dinitrate, bioavailability □ Bioavailability—pharmacokinetics of isosorbide dinitrate after intravenous administration □ Isosorbide dinitrate—pharmacokinetics after intravenous administration, bioavailability

To the Editor:

Isosorbide dinitrate is an organic nitrate found therapeutically useful in its sublingual and oral forms in various cardiovascular diseases such as angina pectoris (1) and congestive heart failure (2). Recently, Distante *et al.* (3) showed that an intravenous infusion of this drug (0.021–0.083 mg/min) was also effective in managing unstable angina. The availability of an intravenous dosage form of isosorbide dinitrate not only affords the opportunity to characterize the pharmacokinetics of this drug after this particular mode of therapy, it also allows the possibility to assess the bioavailability of this drug after other (*e.g.*, oral) routes of administration in patients. This latter subject has been of major controversy since Needleman *et al.* (4) made the assertion that oral nitrate therapy is irrational because of its complete first-pass metabolism.

A preliminary study has appeared which provided some initial information on this important issue. Taylor *et al.* (5) showed that in two normal, young subjects who received

0022-3549/82/0600-0721$01.00/0

intravenous isosorbide dinitrate, the plasma clearance was found to be 0.32 and 0.16 liter/min. Based on these values, these authors concluded that sublingual and oral administration of isosorbide dinitrate are only bioavailable to the extent of 6 and 3%, respectively. If these data can be confirmed in a larger group, they could represent an unusual example of very poor sublingual bioavailability of a small neutral compound given at a relatively low dose. Further, if shown applicable to patients, these data could also have wide-ranging implications regarding the clinical use as well as the regulatory policy of oral and sublingual dosage forms of isosorbide dinitrate. It follows then that there may be a necessity (and perhaps urgency) of further research in identifying the reasons for, and approaches in circumventing, the poor sublingual bioavailability of this drug.

We have expanded on the study of Taylor *et al.* (5) through an examination of the pharmacokinetics of isosorbide dinitrate in 11 cardiac patients after intravenous infusion at two different rates. These data were obtained as part of a comprehensive study which examined the pharmacokinetics of isosorbide dinitrate after intravenous, sublingual, oral, and percutaneous administration. Because the intravenous data are crucial in the strategic planning of further pharmaceutical research of this drug, we present here a preliminary report on this aspect for the interest of workers in this area.

Eleven angina patients were infused intravenously with an isosorbide dinitrate solution[1] which had been suitably diluted such that a total dose of 2 mg in 10 ml was delivered over 15 min (infusion rate = 0.133 mg/min). Two of these patients received isosorbide dinitrate again on another day at a slower infusion rate (0.083 mg/min), one for 1 hr and the other for a 2-hr duration. This latter infusion rate was identical to that used by Taylor *et al.* (5). The strength of the dosing solution, *via* an HPLC analysis developed in this laboratory[2], was determined to be at a mean of 94% of the theoretical value. The concentration of isosorbide dinitrate in the infusion solution emerging from the polyethylene infusion tubing was essentially identical both before and after the experiment, indicting that adsorptive loss to the infusion system was absent. Serial plasma samples were drawn, anticoagulated with sodium citrate, and frozen (−20°) until assayed for isosorbide dinitrate by GC–electron capture detection (6).

The terminal disapearance phase rate constant (β) was obtained by least-square regression of the last four concentration–time points. The area under the plasma concentration *versus* time curve from time zero to the last plasma sample collected (C_t) was determined by Lagrange integration (7). Total area under the curve (AUC) was estimated by addition of the residual area (~15%) which was calculated by dividing C_t by β. The systemic clearance (Cl_{iv}) was calculated by dividing the administered dose by AUC. The apparent volume of distribution (Vd_{area}) was then determined by dividing the systemic clearance by β (8).

Figure 1 shows the plasma concentration of isosorbide dinitrate after intravenous infusion in the patient population studied. Results from the short infusion (2 mg over 15 min) showed that steady-state concentrations were not

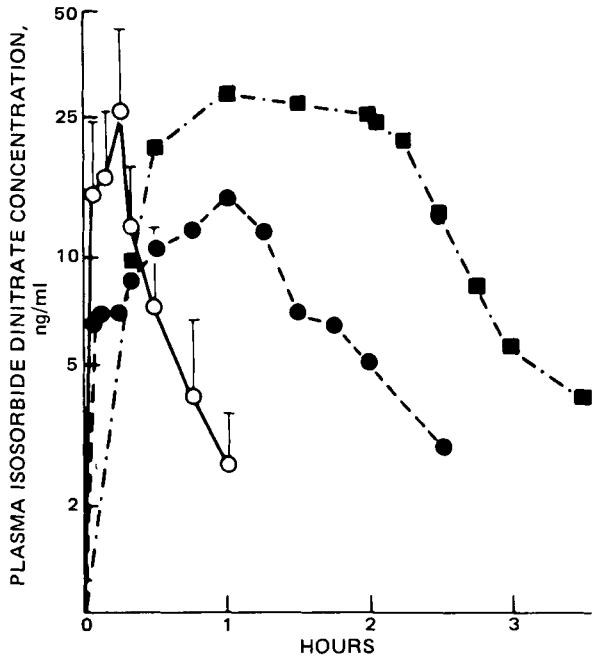

Figure 1—*Plasma isosorbide dinitrate concentrations observed after different rates and duration of intravenous infusion. Key: (○) 0.133 mg/min for 15 min, mean +SD, n = 11, (●) 0.083 mg/min for 1 hr, (■) 0.083 mg/min for 2 hr.*

achieved after this infusion regimen and that decline of plasma drug was apparently biexponential. Unfortunately, the initial rapid distributive phase observed after cessation of the infusion could not be quantitated due to insufficient sampling. The mean half-life of the terminal disappearance phase, however, was found to be 18 ± 7 min (± SD, n = 11), with a range of 10–30 min. The Cl_{iv} value was estimated at 3.4 ± 1.4 liter/min (mean ± SD, n = 11) with a range of 1.8–6.3 liter/min. The mean Vd_{area} (±SD) was estimated to be 101 ± 67 liters (range 46–241 liters). Infusion rate and duration did not appear to affect the pharmacokinetics of isosorbide dinitrate: in one patient, Cl_{iv} was estimated at 4.0 and 4.7 liter/min at infusion rates of 0.083 mg/min for 1 hr and 0.133 mg/min for 15 min, respectively; in a second patient, Cl_{iv} was 2.9 and 2.7 liter/min at infusion rates of 0.083 mg/min for 2 hr and 0.133 mg/min for 15 min, respectively.

If a prolonged elimination phase existed, but was undetected due to assay limitations, the Cl_{iv} values obtained here would be overestimated. However, in the patient infused for 2 hr at 0.083 mg/min, both the time to steady state, and concentration at steady state were consistent with the experimentally observed β and Cl_{iv} values, respectively. Regardless, a doubling of the terminal half-life for residual area calculation would only lead to a 7% decrease in Cl_{iv}. These observations suggest that the Cl_{iv} values obtained here are both internally consistent and reliable.

The clearance values observed in our patient population were, in general, at least 10-fold larger than those obtained by Taylor *et al.* (5) in two normal subjects. The reasons for this discordance are not known; however, a study is in progress which will reassess the validity of the low bioavailability estimates of sublingually and orally administered isosorbide dinitrate reported thus far, particularly to its applicability in cardiac patients.

[1] Isoket Ampullen, Pharma-Schwarz GmbH, 4019 Monheim, West Germany.

[2] H.-L. Fung and S. L. Chan, unpublished observation.

(1) T. Sweatman, G. Strauss, A. Selzer, and K. E. Cohn, *Am. J. Cardiol.*, **29**, 475 (1972).
(2) J. A. Franciosa, E. Mikulic, J. N. Cohn, E. Jose, and A. Fabie, *Circulation*, **50**, 1020 (1974).
(3) A. Distante, A. Maseri, S. Severi, A. Biagini, and S. Chierchia, *Am. J. Cardiol.*, **44**, 533 (1979).
(4) P. Needleman, S. Lang, and E. M. Johnson, *J. Pharmacol. Exp. Ther.*, **181**, 489 (1972).
(5) T. Taylor, L. F. Chasseaud, and E. Doyle, *Biopharm. Drug Dispos.*, **1**, 149 (1980).
(6) R. A. Morrison and H.-L. Fung, in "Abstracts", Vol. 10, No. 1, APhA Academy of Pharmaceutical Sciences, Washington, D.C., 1980, p. 126.
(7) K. C. Yeh and K. C. Kwan, *J. Pharmacokinet. Biopharm.*, **6**, 79 (1978).
(8) M. Gibaldi and D. Perrier, Eds., "Pharmacokinetics," Marcel Dekker, New York, N.Y., 1975.

R. A. Morrison
Ho-Leung Fung[x]
Department of Pharmaceutics
State University of New York at Buffalo
Amherst, NY 14260
D. Höhmann
T. Meinertz
E. Jähnchen
Pharmakologisches Institut
University of Mainz, West Germany

Received February 5, 1982.
Accepted for publication April 9, 1982.
Supported in part by NIH Grants HL 22273 and GM 20852 and by Pharma-Schwarz GmbH, West Germany.

Time-Dependent Kinetics VIII: Absence of Diurnal Oscillations in Valproic Acid Disposition Following Single Dose Administration to Rhesus Monkey

Keyphrases □ Valproic acid—time-dependent kinetics, absence of diurnal oscillations, disposition following single dose administration to rhesus monkey □ Kinetics, time-dependent—absence of diurnal oscillations in valproic acid disposition following single dose administration to rhesus monkey

To the Editor:

Valproic acid exhibits an unusual pharmacokinetic property in the rhesus monkey, namely, extensive diurnal oscillations in systematic clearance. An initial study in three normal rhesus monkeys showed that during constant rate intravenous infusion, steady-state levels increased at night with maxima 40–140% higher than the corresponding minima (1). In a subsequent study in four normal monkeys, where levels were monitored for 48 hr, it was found that the diurnal fluctuations in steady-state levels were reproducible in 2 consecutive days (2). Furthermore, after reversal of the 12-hr light–12-hr dark cycle, plasma concentrations tended to follow the phase shift with maxima during the reversed dark phase (actual day time) (2). In a later efficacy study in 12 epileptic monkeys, valproic acid was infused at a constat rate to achieve steady-state levels of 46, 97, and 147 μg/ml (3). The diurnal fluctuations in valproate levels were found at all three steady-state concentrations (4).

In each of the studies just described, the diurnal changes in valproate clearance were found under steady-state conditions. In the present study, the objective was to determine whether this phenomenon could be observed with an acute mode of administration. To this effect, valproate was administered at different times of day by intravenous boluses to a group of six rhesus monkeys. In addition, this design would allow a detection of diurnal effects in valproate distribution.

Six chair-adapted male rhesus monkeys (mean body weight 4.1 kg) with two chronic venous catheters (femoral for valproate bolus injection and jugular for blood sampling) were used in this study. Environmental conditions were maintained the same as those described previously (1, 2) (diurnal cycle: light period, 6 am–6 pm; dark period, 6 pm–6 am). Based on the findings of previous studies (valproate plasma levels remained stable or decreased during 10 am–6 pm, increased and reached a maximum during 6 pm–6 am, and tended to decline from 6 am–noon), the following times were selected for drug administration: 2 am, 8 am, 2 pm, and 8 pm. At these times of the day, valproate intravenous bolus injections were administered in a randomized fashion to six monkeys. At least 1 week of rest was allowed between any two injection times. From 2 to 4 replicate studies at each time period were conducted for each of the six monkeys.

At each time period, including replications, each monkey received 63.75 mg of valproic acid equivalent as sodium salt in 0.5 ml of sterile saline as an intravenous bolus injection. An additional 5 ml of saline was used to flush the line after bolus administration. Blood samples (2 ml) were collected in vacuum tubes containing edetic acid at 2, 20, 40, 60, and 100 min following drug administration. Plasma was separated and frozen until assay. Valproate was assayed by GLC using the procedure of Levy *et al.* (5).

The area under the plasma concentration–time curve (extrapolated to infinite time) was calculated by the trapezoidal rule and the systemic or total body clearance was computed from the dose–area relationship. The plasma valproate concentration time data were least-squares fitted to a monoexponential decay equation (BMDX-85), and the volume of distribution was calculated by the ratio of total body clearance and elimination rate constant. The null hypothesis of equal mean values for clearance, volume of distribution, and elimination rate constant among treatments was tested using a one-way ANOVA for repeated measures (BMDP2V). Then Tukey's method for multiple comparisons (6) was used to test for differences between particular pairs of treatments.

Mean plasma valproate concentration–time profiles at 2 am, 8 am, 2 pm, and 8 pm are shown in Fig. 1. Based on the findings of previous studies, which revealed the presence of circadian rhythms in steady-state valproate plasma levels (1–4), lower clearance values would be expected at 2 am and 8 pm than at 2 pm and 8 am. However, no significant difference in valproate clearance was observed between any of the four time periods. Volume of distribution and half-life also did not exhibit any time dependence ($p > 0.05$). Values of clearance, volume of distribu-

0022-3549/82/0600-0723$01.00/0

(1) T. Sweatman, G. Strauss, A. Selzer, and K. E. Cohn, *Am. J. Cardiol.*, **29**, 475 (1972).
(2) J. A. Franciosa, E. Mikulic, J. N. Cohn, E. Jose, and A. Fabie, *Circulation*, **50**, 1020 (1974).
(3) A. Distante, A. Maseri, S. Severi, A. Biagini, and S. Chierchia, *Am. J. Cardiol.*, **44**, 533 (1979).
(4) P. Needleman, S. Lang, and E. M. Johnson, *J. Pharmacol. Exp. Ther.*, **181**, 489 (1972).
(5) T. Taylor, L. F. Chasseaud, and E. Doyle, *Biopharm. Drug Dispos.*, **1**, 149 (1980).
(6) R. A. Morrison and H.-L. Fung, in "Abstracts", Vol. 10, No. 1, APhA Academy of Pharmaceutical Sciences, Washington, D.C., 1980, p. 126.
(7) K. C. Yeh and K. C. Kwan, *J. Pharmacokinet. Biopharm.*, **6**, 79 (1978).
(8) M. Gibaldi and D. Perrier, Eds., "Pharmacokinetics," Marcel Dekker, New York, N.Y., 1975.

R. A. Morrison
Ho-Leung Fung[x]
Department of Pharmaceutics
State University of New York at Buffalo
Amherst, NY 14260
D. Höhmann
T. Meinertz
E. Jähnchen
Pharmakologisches Institut
University of Mainz, West Germany

Received February 5, 1982.
Accepted for publication April 9, 1982.
Supported in part by NIH Grants HL 22273 and GM 20852 and by Pharma-Schwarz GmbH, West Germany.

Time-Dependent Kinetics VIII: Absence of Diurnal Oscillations in Valproic Acid Disposition Following Single Dose Administration to Rhesus Monkey

Keyphrases □ Valproic acid—time-dependent kinetics, absence of diurnal oscillations, disposition following single dose administration to rhesus monkey □ Kinetics, time-dependent—absence of diurnal oscillations in valproic acid disposition following single dose administration to rhesus monkey

To the Editor:

Valproic acid exhibits an unusual pharmacokinetic property in the rhesus monkey, namely, extensive diurnal oscillations in systematic clearance. An initial study in three normal rhesus monkeys showed that during constant rate intravenous infusion, steady-state levels increased at night with maxima 40–140% higher than the corresponding minima (1). In a subsequent study in four normal monkeys, where levels were monitored for 48 hr, it was found that the diurnal fluctuations in steady-state levels were reproducible in 2 consecutive days (2). Furthermore, after reversal of the 12-hr light–12-hr dark cycle, plasma concentrations tended to follow the phase shift with maxima during the reversed dark phase (actual day time) (2). In a later efficacy study in 12 epileptic monkeys, valproic acid was infused at a constat rate to achieve steady-state levels of 46, 97, and 147 μg/ml (3). The diurnal fluctuations in valproate levels were found at all three steady-state concentrations (4).

In each of the studies just described, the diurnal changes in valproate clearance were found under steady-state conditions. In the present study, the objective was to determine whether this phenomenon could be observed with an acute mode of administration. To this effect, valproate was administered at different times of day by intravenous boluses to a group of six rhesus monkeys. In addition, this design would allow a detection of diurnal effects in valproate distribution.

Six chair-adapted male rhesus monkeys (mean body weight 4.1 kg) with two chronic venous catheters (femoral for valproate bolus injection and jugular for blood sampling) were used in this study. Environmental conditions were maintained the same as those described previously (1, 2) (diurnal cycle: light period, 6 am–6 pm; dark period, 6 pm–6 am). Based on the findings of previous studies (valproate plasma levels remained stable or decreased during 10 am–6 pm, increased and reached a maximum during 6 pm–6 am, and tended to decline from 6 am–noon), the following times were selected for drug administration: 2 am, 8 am, 2 pm, and 8 pm. At these times of the day, valproate intravenous bolus injections were administered in a randomized fashion to six monkeys. At least 1 week of rest was allowed between any two injection times. From 2 to 4 replicate studies at each time period were conducted for each of the six monkeys.

At each time period, including replications, each monkey received 63.75 mg of valproic acid equivalent as sodium salt in 0.5 ml of sterile saline as an intravenous bolus injection. An additional 5 ml of saline was used to flush the line after bolus administration. Blood samples (2 ml) were collected in vacuum tubes containing edetic acid at 2, 20, 40, 60, and 100 min following drug administration. Plasma was separated and frozen until assay. Valproate was assayed by GLC using the procedure of Levy *et al.* (5).

The area under the plasma concentration–time curve (extrapolated to infinite time) was calculated by the trapezoidal rule and the systemic or total body clearance was computed from the dose–area relationship. The plasma valproate concentration time data were least-squares fitted to a monoexponential decay equation (BMDX-85), and the volume of distribution was calculated by the ratio of total body clearance and elimination rate constant. The null hypothesis of equal mean values for clearance, volume of distribution, and elimination rate constant among treatments was tested using a one-way ANOVA for repeated measures (BMDP2V). Then Tukey's method for multiple comparisons (6) was used to test for differences between particular pairs of treatments.

Mean plasma valproate concentration–time profiles at 2 am, 8 am, 2 pm, and 8 pm are shown in Fig. 1. Based on the findings of previous studies, which revealed the presence of circadian rhythms in steady-state valproate plasma levels (1–4), lower clearance values would be expected at 2 am and 8 pm than at 2 pm and 8 am. However, no significant difference in valproate clearance was observed between any of the four time periods. Volume of distribution and half-life also did not exhibit any time dependence ($p > 0.05$). Values of clearance, volume of distribu-

0022-3549/82/0600-0723$01.00/0

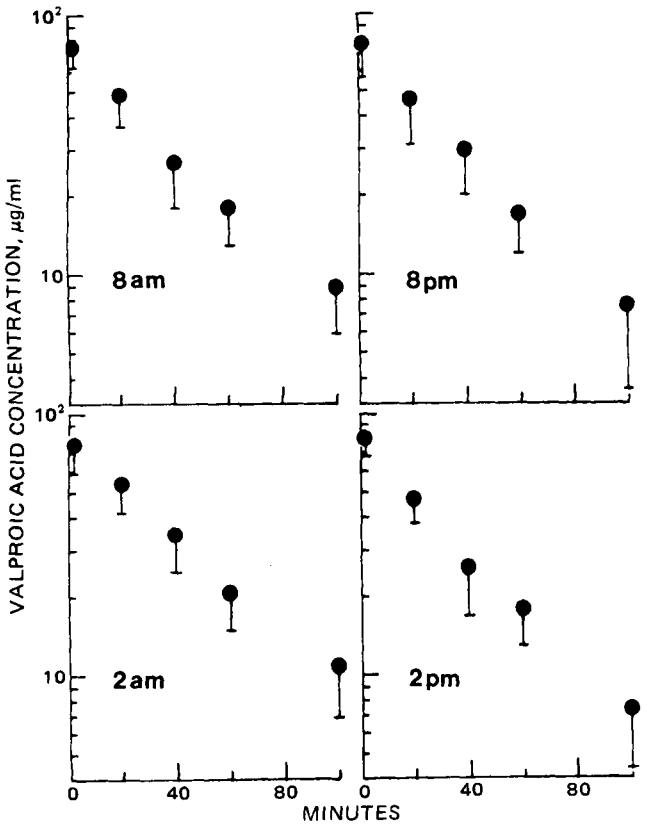

Figure 1—*Mean plasma valproate concentration–time profiles for six rhesus monkeys following four separate drug administrations by intravenous bolus injections.*

Table I—Pharmacokinetic Parameters Following Single Dose Administration of Valproic Acid to Rhesus Monkey

	2 am	8 am	2 pm	8 pm
Clearance, liter/hr^{-1} Mean (*SD*)	1.231 (0.369)	1.150 (0.267)	1.281 (0.390)	1.214 (0.264)
Volume of distribution, liter Mean (*SD*)	0.955 (0.263)	0.765 (0.080)	0.766 (.112)	0.795 (0.146)
Elimination Rate Constant, hour^{-1} Mean (*SD*)	1.312 (0.271)	1.517 (0.266)	1.636 (0.392)	1.573 (0.330)

tion, and half-life (Table I) are very similar to those found previously (1, 3, 7).

A consistent pattern of diurnal fluctuations in systemic clearance was previously found in three separate studies (1–4). The difference in experimental findings between those studies and the present one may be explained by the difference in the nature of the clearance obtained in both instances. In the former studies (1–4), valproate was administered by constant rate intravenous infusion and thus enabled the determination of an instantaneous systemic clearance at steady state. In the present study, however, valproate was administered by single bolus injection and resulted in the determination of an average clearance, a hybrid of the clearances operating during the elimination of the majority of the administered dose. Under steady-state conditions, differences in instantaneous clearance can be measured within a few hours and several (10–12) clearance determinations can be obtained in 24 hr. In contrast, the single dose approach revealed only four 2-hr hybrid samples of the diurnal evolution of drug clearance. Thus, in the case of valproic acid in the rhesus monkey, the single dose clearance represents an insensitive tool in the characterization of the time dependency in clearance.

Also, comparison of steady-state clearances between any two time points of the diurnal cycle involves only intraday variability in clearance. However, since each determination of single-dose clearance required several blood samples, any two clearance determinations (at the same time or at different times) were separated by at least a 1-week period. Appreciable interday variability was present. Table 1 shows that relative standard deviations of replicates at a given time of administration varied between 22 and 30%.

It may be argued that the particular group of six monkeys used in the present study does not exhibit the property of diurnal oscillations in steady-state clearance as was observed in previous studies (1–4). This possibility is eliminated by the fact that, in a later study (of diurnal fluctuations in cerebrospinal fluid valproate levels) four of the present six monkeys exhibited typical diurnal oscillations in steady-state plasma and cerebrospinal fluid levels (unpublished data). An alternative hypothesis to explain the findings of this study could be that chronic exposure to valproic acid is necessary to evoke a circadian rhythm in plasma concentration, *i.e.*, the constant presence of valproate *in vivo* would initiate an endogenous cycle in metabolism. This would be possible if, for example, chronic infusion (as opposed to bolus administration) of valproic acid was associated with depletion of cofactors necessary in the biotransformation of valproate. Such cofactors would then become rate-limiting and, if their synthesis or turnover rate was under diurnal control, valproate clearance would also exhibit a diurnal rhythm. In relation with this hypothesis, it is of interest to note that diurnal oscillations in steady-state levels have been observed with other drugs [ethosuximide (8), carbamazepine (9) and clonazepam (10)] in the rhesus monkey under the same experimental conditions. However, no studies of diurnal variation following single dose administration have been performed with these drugs. Therefore, several *in vivo* and *in vitro* metabolic studies will be necessary before the cofactor depletion hypothesis can be generalized.

(1) R. H. Levy, J. S. Lockard, I. H. Patel, and W. C. Congdon, *J. Pharm. Sci.*, **66**, 1154 (1977).

(2) J. S. Lockard, R. H. Levy, L. L. DuCharme, W. C. Congdon, and I. H. Patel, *Epilepsia*, **18**, 183 (1977).

(3) R. H. Levy, J. S. Lockard, I.H. Patel, and A. A. Lai, *ibid.*, **18**, 191 (1977).

(4) J. S. Lockard, R. H. Levy, W. C. Congdon, L. L. DuCharme, and I. H. Patel, *ibid.*, **18**, 205 (1977).

(5) R. H. Levy, L. Martis, and A. A. Lai, *Anal. Lett.*, **B11**, 257 (1978).

(6) D. G. Kleinbaum and L. C. Kupper, "*Applied Regression Analysis and Other Multivariate Methods*," Duxbury Press, Belmont, Calif., 1978, p. 264.

(7) A. A. Lai, R. H. Levy, and L. Martis, *Therapie*, **35**, 221 (1980).

(8) I. H. Patel, R. H. Levy, and J. S. Lockard, *J. Pharm. Sci.*, **66**, 650 (1977).

(9) J. S. Lockard, R. H. Levy, L. L. DuCharme, W. C. Congdon, and I. H. Patel, *Epilepsia*, **20**, 169 (1979).

(10) J. S. Lockard, R. H. Levy, W. C. Congdon, L. L. DuCharme, and L. D. Salonen, *ibid.*, **20**, 683 (1979).

R. H. Levy [x]
Departments of Pharmaceutics
and Neurological Surgery, BG-20
Schools of Pharmacy and Medicine
University of Washington
Seattle, WA 98195

C. T. Viswanathan
Biopharmaceutics Div., HFD522
Food and Drug Administration
5600 Fishers Lane
Rockville, MD 20857

J. S. Lockard
Department of Neurological Surgery
School of Medicine
University of Washington
Seattle, WA 98195

Received November 25, 1981.
Accepted for publication February 24, 1982.
Supported by National Institutes of Health Contract N01-NS-1-2282 and National Institutes of Health Grant NS-04053.

Centering Tool for Dissolution Vessels

Keyphrases □ Drug dissolution—testing, centering tool for dissolution vessels □ Centering tool—drug dissolution testing, for basket and paddle methods

To the Editor:

Proper alignment and standardization of equipment is essential to obtain reliable results in drug dissolution testing. The USP XX requires that the shaft in both the basket and paddle methods be positioned so that its axis is not >0.2 cm at any point from the vertical axis of the vessel (1). A centering tool for alignment of the shaft was previously described (2), and several centering tools are commercially available[1,2]. We have designed a centering tool which has been widely used in FDA laboratories and which we believe offers significant advantages over other designs.

The tool is machined from a block of plexiglass (Fig. 1). The sides of the tool are tapered at an angle of 30° from the axis so that the tool can be used with plastic or glass dissolution vessels or to align the base plates that support the dissolution vessels. The main slot is oversized to 10 mm to allow the tool to be used with 9.52-mm diameter shafts.

[1] Hanson Research Corp., Northbridge, CA 91324.
[2] Van-Kel Industries, Chatham, NJ 17928.

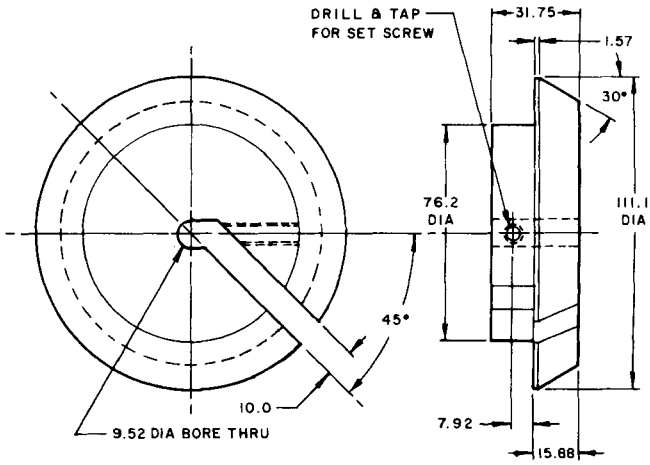

Figure 1—*Dissolution vessel centering tool. The material used was plexiglass and all measurements are in millimeters.*

The center portion of the slot is offset 45° from the main slot, so that the shaft can be accurately butted against the radius of the 9.50-mm center hole with a 6.35-mm screw. Securing the shaft against the center hole radius prevents the tool from accidental tipping when aligning the vessels. The final machining of the tapered edge is done with the device secured by its set screw to an arbor to ensure that the center hole and the tapered portion of the tool will be concentric.

While in use, the tool is slipped down the shaft into the mouth of the vessel, and the vessel is aligned with the tool after tightening the set screw. The design offers these advantages:

1. Locking the tool to the shaft prevents the alignment from changing while adjusting the kettle.
2. The circular design aligns the kettle's total circumference in one operation.
3. Dimension of the tool permits it to be used to align the base plate.

With proper use, most, if not all, of the centering tools previously described should be capable of aligning the shaft within USP specifications.

(1) "The United States Pharmacopeia," 20th rev. United States Pharmacopeial Convention, Rockville, Md., 1980, p. 959.
(2) D. C. Cox, C. C. Douglas, W. B. Furman, R. D. Kirchhoefer, J. W. Myrick, and C. E. Wells., *Pharm. Tech.*, **2**, 41 (1978).

Albert Serino
Chief, Facilities Services Section
Winchester Engineering & Analytical Center
Winchester, MA 01890

Received August 21, 1981.
Accepted for publication March 15, 1982.

R. H. Levy [x]
Departments of Pharmaceutics
and Neurological Surgery, BG-20
Schools of Pharmacy and Medicine
University of Washington
Seattle, WA 98195

C. T. Viswanathan
Biopharmaceutics Div., HFD522
Food and Drug Administration
5600 Fishers Lane
Rockville, MD 20857

J. S. Lockard
Department of Neurological Surgery
School of Medicine
University of Washington
Seattle, WA 98195

Received November 25, 1981.
Accepted for publication February 24, 1982.
Supported by National Institutes of Health Contract N01-NS-1-2282 and National Institutes of Health Grant NS-04053.

Centering Tool for Dissolution Vessels

Keyphrases □ Drug dissolution—testing, centering tool for dissolution vessels □ Centering tool—drug dissolution testing, for basket and paddle methods

To the Editor:

Proper alignment and standardization of equipment is essential to obtain reliable results in drug dissolution testing. The USP XX requires that the shaft in both the basket and paddle methods be positioned so that its axis is not >0.2 cm at any point from the vertical axis of the vessel (1). A centering tool for alignment of the shaft was previously described (2), and several centering tools are commercially available[1,2]. We have designed a centering tool which has been widely used in FDA laboratories and which we believe offers significant advantages over other designs.

The tool is machined from a block of plexiglass (Fig. 1). The sides of the tool are tapered at an angle of 30° from the axis so that the tool can be used with plastic or glass dissolution vessels or to align the base plates that support the dissolution vessels. The main slot is oversized to 10 mm to allow the tool to be used with 9.52-mm diameter shafts.

[1] Hanson Research Corp., Northbridge, CA 91324.
[2] Van-Kel Industries, Chatham, NJ 17928.

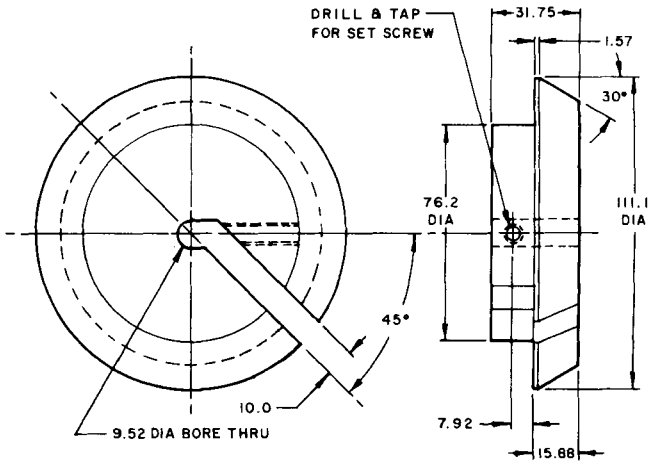

Figure 1—*Dissolution vessel centering tool. The material used was plexiglass and all measurements are in millimeters.*

The center portion of the slot is offset 45° from the main slot, so that the shaft can be accurately butted against the radius of the 9.50-mm center hole with a 6.35-mm screw. Securing the shaft against the center hole radius prevents the tool from accidental tipping when aligning the vessels. The final machining of the tapered edge is done with the device secured by its set screw to an arbor to ensure that the center hole and the tapered portion of the tool will be concentric.

While in use, the tool is slipped down the shaft into the mouth of the vessel, and the vessel is aligned with the tool after tightening the set screw. The design offers these advantages:

1. Locking the tool to the shaft prevents the alignment from changing while adjusting the kettle.
2. The circular design aligns the kettle's total circumference in one operation.
3. Dimension of the tool permits it to be used to align the base plate.

With proper use, most, if not all, of the centering tools previously described should be capable of aligning the shaft within USP specifications.

(1) "The United States Pharmacopeia," 20th rev. United States Pharmacopeial Convention, Rockville, Md., 1980, p. 959.
(2) D. C. Cox, C. C. Douglas, W. B. Furman, R. D. Kirchhoefer, J. W. Myrick, and C. E. Wells., *Pharm. Tech.*, **2**, 41 (1978).

Albert Serino
Chief, Facilities Services Section
Winchester Engineering & Analytical Center
Winchester, MA 01890

Received August 21, 1981.
Accepted for publication March 15, 1982.

REVIEWS

Concepts in Drug Metabolism (in Two Parts) Part B (Drug and Pharmaceutical Sciences, Vol. 10.) Edited by PETER JENNER and BERNARD TESTA. Dekker, 270 Madison Ave., New York, NY 10016. 1981. 627 pp. 15 × 23 cm. Price $65.00.

Concepts in Drug Metabolism is a two volume, multiauthored collection of essays on major topics in drug metabolism and allied fields. The various chapters reflect the state of knowledge from the viewpoint of each of the respective authors.

The contents of Part B are divided into nine chapters which deal with the following topics: The role of the endoplasmic reticulum in physiological and pathological situations; the hepatic cytochrome P-450 drug metabolizing systems; toxification and detoxification as a result of xenobiotic metabolism; enzyme induction and inhibition related to drug action and interactions; genetic aspects of drug metabolism; some evolutionary considerations regarding drug metabolism and toxicity; *in vivo* assessment of hepatic drug disposition; altered drug disposition in disease states; and is drug metabolism due to necessity, chance, mishap, or none of the above?

Since each chapter has been written by a different author, some overlapping has occurred. However, this demonstrates the relationship and interdependencies of the various topics. The reader will find that most of the chapters in Part B are more factual and less philosophical than some of the chapters found in Part A.

The chapters are well referenced and, although not being all inclusive, reflect a command of the most important research in each area. A drawback is that with few exceptions, Part B represents a review of the literature through 1978. The area of drug metabolism is a rapidly moving field, and many significant contributions have been made in the interval between the time the book was finished and the date of publication. This is a problem which is common to an active area of research.

Concepts in Drug Metabolism is intended for use by postgraduate students and research workers in the fields of biomedicinal chemistry, pharmacology, toxicology, and biochemistry. The two volume set makes an excellent text for a graduate level course in drug metabolism. Unfortunately, the cost of the books tends to prohibit purchase by students. The volume serves as a valuable guide in the area of drug metabolism; however, it is also an important source of new ideas since many of the chapters go beyond the basic facts, providing a conceptual, almost philosophical, approach to some of the topical areas.

Part B of *Concepts in Drug Metabolism* in conjunction with Part A provides an authoritative overview of basic topics and developments in drug metabolism and related areas. The two volume set is highly recommended for persons working in the general area of xenobiotic metabolism.

Reviewed by Sidney J. Stohs
University of Nebraska
College of Pharmacy
Lincoln NE 68508

Pharmaceutical Analysis: Modern Methods, Part A (Drugs and the Pharmaceutical Sciences Series, Vol. 11). Edited by JAMES W. MUNSON. Dekker, 270 Madison Ave., New York, NY 10016. 1981. 504 pp. 15.5 × 23.2 cm. Price $55.00 (Special Student Price $29.75).

As stated in the preface, this text is intended to "provide an intermediate level of coverage ... (it) is designed for the graduate student studying pharmaceutical analysis and for the researcher . . . who wishes to increase his personal awareness and understanding of modern techniques of pharmaceutical analysis."

The first three chapters offer a review of the theory, instrumentation, and applications to pharmaceutical analysis of gas chromatography (GC), pyrolysis GC, and GC–mass spectroscopy. The authors of each chapter have incorporated and harmonized theory and practice and have written three well-integrated chapters. The topics are covered at a depth suitable for a graduate course covering the GC aspects of pharmaceutical analysis.

The last three chapters deal with luminescence (fluorescence and phosphorescence) spectroscopy, liquid scintillation counting, and radioimmunoassays. The chapter authors have done an excellent job of presenting the underlying theory and applications of their individual topics: there is greater detail and breadth of coverage than is usually found in other textbooks devoted to pharmaceutical analysis. However, the interrelationship of these chapters with each other, or with the rest of the text, does not meet the high standard established in the first three chapters. In fact, if there is a fault with this text, it is in the organization and integration of the individual chapter topics with one another. For example, in terms of material, the logical arrangement would have been to incorporate the chapters on high-performance liquid chromatography and quantitative thin-layer chromatography, which are to be covered in Part B, with the chapters on GC found in this volume.

Nevertheless, the presentation and content of material in each chapter is excellent, and taken individually they are well-suited for graduate courses in pharmaceutical analysis. However, the ordering and arrangement of the topic chapters in both Part A and Part B make it ill-suited for courses that may be segregated into spectroscopic and separation techniques.

Reviewed by Wallace J. Murray
College of Pharmacy
University of Nebraska Medical Center
Omaha, NE 68105

REVIEWS

Concepts in Drug Metabolism (in Two Parts) Part B (Drug and Pharmaceutical Sciences, Vol. 10.) Edited by PETER JENNER and BERNARD TESTA. Dekker, 270 Madison Ave., New York, NY 10016. 1981. 627 pp. 15 × 23 cm. Price $65.00.

Concepts in Drug Metabolism is a two volume, multiauthored collection of essays on major topics in drug metabolism and allied fields. The various chapters reflect the state of knowledge from the viewpoint of each of the respective authors.

The contents of Part B are divided into nine chapters which deal with the following topics: The role of the endoplasmic reticulum in physiological and pathological situations; the hepatic cytochrome P-450 drug metabolizing systems; toxification and detoxification as a result of xenobiotic metabolism; enzyme induction and inhibition related to drug action and interactions; genetic aspects of drug metabolism; some evolutionary considerations regarding drug metabolism and toxicity; *in vivo* assessment of hepatic drug disposition; altered drug disposition in disease states; and is drug metabolism due to necessity, chance, mishap, or none of the above?

Since each chapter has been written by a different author, some overlapping has occurred. However, this demonstrates the relationship and interdependencies of the various topics. The reader will find that most of the chapters in Part B are more factual and less philosophical than some of the chapters found in Part A.

The chapters are well referenced and, although not being all inclusive, reflect a command of the most important research in each area. A drawback is that with few exceptions, Part B represents a review of the literature through 1978. The area of drug metabolism is a rapidly moving field, and many significant contributions have been made in the interval between the time the book was finished and the date of publication. This is a problem which is common to an active area of research.

Concepts in Drug Metabolism is intended for use by postgraduate students and research workers in the fields of biomedicinal chemistry, pharmacology, toxicology, and biochemistry. The two volume set makes an excellent text for a graduate level course in drug metabolism. Unfortunately, the cost of the books tends to prohibit purchase by students. The volume serves as a valuable guide in the area of drug metabolism; however, it is also an important source of new ideas since many of the chapters go beyond the basic facts, providing a conceptual, almost philosophical, approach to some of the topical areas.

Part B of *Concepts in Drug Metabolism* in conjunction with Part A provides an authoritative overview of basic topics and developments in drug metabolism and related areas. The two volume set is highly recommended for persons working in the general area of xenobiotic metabolism.

Reviewed by Sidney J. Stohs
University of Nebraska
College of Pharmacy
Lincoln NE 68508

Pharmaceutical Analysis: Modern Methods, Part A (Drugs and the Pharmaceutical Sciences Series, Vol. 11). Edited by JAMES W. MUNSON. Dekker, 270 Madison Ave., New York, NY 10016. 1981. 504 pp. 15.5 × 23.2 cm. Price $55.00 (Special Student Price $29.75).

As stated in the preface, this text is intended to "provide an intermediate level of coverage ... (it) is designed for the graduate student studying pharmaceutical analysis and for the researcher . . . who wishes to increase his personal awareness and understanding of modern techniques of pharmaceutical analysis."

The first three chapters offer a review of the theory, instrumentation, and applications to pharmaceutical analysis of gas chromatography (GC), pyrolysis GC, and GC–mass spectroscopy. The authors of each chapter have incorporated and harmonized theory and practice and have written three well-integrated chapters. The topics are covered at a depth suitable for a graduate course covering the GC aspects of pharmaceutical analysis.

The last three chapters deal with luminescence (fluorescence and phosphorescence) spectroscopy, liquid scintillation counting, and radioimmunoassays. The chapter authors have done an excellent job of presenting the underlying theory and applications of their individual topics: there is greater detail and breadth of coverage than is usually found in other textbooks devoted to pharmaceutical analysis. However, the interrelationship of these chapters with each other, or with the rest of the text, does not meet the high standard established in the first three chapters. In fact, if there is a fault with this text, it is in the organization and integration of the individual chapter topics with one another. For example, in terms of material, the logical arrangement would have been to incorporate the chapters on high-performance liquid chromatography and quantitative thin-layer chromatography, which are to be covered in Part B, with the chapters on GC found in this volume.

Nevertheless, the presentation and content of material in each chapter is excellent, and taken individually they are well-suited for graduate courses in pharmaceutical analysis. However, the ordering and arrangement of the topic chapters in both Part A and Part B make it ill-suited for courses that may be segregated into spectroscopic and separation techniques.

Reviewed by Wallace J. Murray
College of Pharmacy
University of Nebraska Medical Center
Omaha, NE 68105

A publication of the
American Pharmaceutical Association—
the National Professional Society
of Pharmacists

JOURNAL OF PHARMACEUTICAL SCIENCES

INDEX TO AUTHORS
INDEX TO SUBJECTS

VOLUME 71
JANUARY TO DECEMBER, 1982

Published monthly under the supervision of the Board of Trustees

Antibiotic Certification—An Anachronism

All too often it is human nature to continue to operate in a certain way or to do a certain thing, even though the reasons for performing that action have long ceased to exist. Moreover, in government and bureaucratic circles, the propensity for such behavior is all the more pronounced.

For these reasons, the Food and Drug Administration's current proposal to phase-out its antibiotic certification program comes as a refreshing change. Many of us on the Washington scene have become skeptics because we usually see "business as usual" from the federal government despite campaign promises to the contrary from politicians when they are running for office.

For those readers not familiar with the history of this certification program, a brief review would be appropriate.

When the first several antibiotic drugs initially were marketed in the 1940s, they were extremely crude concentrates of extracts obtained from microbial culture media. At that time, conventional chemical or instrumental methods of drug analysis were not applicable to them; in particular, those analytical procedures could not provide a true measure of the biological potency of the antibiotic test samples.

To meet this immediate problem, between 1945 and 1948, Congress passed legislation providing for the batch certification of the five antibiotics then available. The certification program was conducted by a laboratory within the Food and Drug Administration, and it used microbiological test procedures to measure growth inhibition of various organisms when tested against a relatively purified, standard reference sample of the crude antibiotic.

However, rapid advances in the manufacturing processes of production, synthesis, and purification soon made it possible to produce these antibiotics as essentially pure, homogeneous, crystalline substances with a degree of purity comparable to other fine chemicals.

In light of these modernized production procedures—along with the development of many new analytical techniques—it was not considered necessary to add to the certification program any of the dozens of newer antibiotics which subsequently came onto the market during the 1950s and very early 1960s. Indeed, because of these developments, by 1962 it was difficult to rationalize the continuation of the antibiotic certification program in any form, much less its wholesale expansion to cover all antibiotics as provided for in the 1962 Drug Amendments to the Federal Food, Drug, and Cosmetic Act.

Both APhA and the Pharmaceutical Manufacturers Association—as well as several other groups including the United States Pharmacopeia—testified in opposition to the antibiotic certification provision during 1959–1962 Congressional hearings conducted by Senator Kefauver and Representative Cellar. However, drug industry opposition suddenly evaporated, apparently as the result of a closed-door political compromise in which the industry agreed to accept antibiotic certification as a trade-off for having Congress not disturb the exclusivity of drug patents. At any rate, the bill passed by Congress and signed into law by President Kennedy in October 1962 included the section extending certification to all antibiotics.

Over the years, experience convincingly showed the antibiotic certification program to be a needless and costly exercise, because batch after batch was found to be well within compliance.

In light of this track record, in the late 1970s, the FDA began to exempt certain antibiotic dosage forms from the certification requirement. Then, in a somewhat surprise action, FDA Commissioner Arthur Hull Hayes, Jr., published a sweeping proposal in the Federal Register of May 7, 1982, calling for the elimination of the entire certification program for all antibiotic drugs. In essence, Dr. Hayes was saying that, rather than go through the lengthy and unnecessary process of a gradual phase-out, decisive action was clearly preferable. In our personal view, this action is both administratively logical and scientifically sound. Moreover, it will greatly minimize paperwork and procedural processing.

As an aside, one might properly wonder how the FDA is able to nullify or revoke a program enacted by Congress. It is because of the unique construction of the language used in the Act as it relates to the certification program. Specifically, FDA has the authority to grant exemptions from certification, and any antibiotic drugs so exempted no longer are subject to section 507 of the Act (the special category of antibiotic drugs), but are then automatically covered by section 505 of the Act (the so-called "new drugs" provision which covers drugs generally).

In concert with the FDA's proposed decertification action, the USP is actively preparing and promulgating revised monographs to ensure the continued existence of public standards of quality for these pharmaceutical products. Consequently, even in the absence of the FDA certification program, the combination of (*a*) compendial standards, (*b*) manufacturers' quality control testing, and (*c*) FDA market surveillance and enforcement will ensure the continued high quality of antibiotics in exactly the same manner as with all other pharmaceutical products (except for insulin and biologicals).

In a way, this FDA action makes such good sense that one is inclined simply to say, "fine," and then dismiss it from his or her mind. However, as noted in our opening paragraphs, society generally, and the government in particular, very rarely halts an activity or discards a procedure simply because it has become obsolete and outdated.

Consequently, we feel that Dr. Hayes, the FDA, and the Administration should be commended for this bold and decisive action.

—EDWARD G. FELDMANN
American Pharmaceutical Association
Washington, DC 20037

0022-3549/82/0700-0727$01.00/0

JOURNAL OF PHARMACEUTICAL SCIENCES

JULY 1982
VOLUME 71 NUMBER 7

RESEARCH ARTICLES

Kinetics and Mechanism of Hydrolysis of Labile Quaternary Ammonium Derivatives of Tertiary Amines

JOSEPH B. BOGARDUS * and TAKERU HIGUCHI ˣ

Received June 29, 1981, from the *Pharmaceutical Chemistry Department, School of Pharmacy, University of Kansas, Lawrence, KS 66044.* Accepted for publication October 22, 1981. *Present Address: College of Pharmacy, University of Kentucky, Lexington, KY 40506.

Abstract □ The kinetics and mechanism of hydrolysis of *N*-(4-hydroxy-3,5-dimethylbenzyl)pyridinium bromide and similar quaternary derivatives of niacinamide, *N*,*N*-dimethylaniline, and trimethylamine were investigated. pH–Rate profiles at 25° for formation of tertiary amine and 4-hydroxymethyl-2,6-dimethylphenol indicated that the zwitterionic quaternary phenoxide was the reactive species in alkaline solution. The apparent rate of hydrolysis was strongly inhibited by addition of small amounts of product tertiary amine, which is consistent with the presence of an intermediate in the reaction pathway. A mechanism was proposed for the hydrolysis and methanolysis of these compounds involving the reversible formation of the quinone methide, 4-methylene-2,6-dimethyl-2,5-cyclohexadien-1-one, followed by a trapping reaction with solvent or nucleophiles. Replacement of the phenolic hydrogen with methyl or acetyl groups greatly stabilized the molecule which is in agreement with the proposed mechanism. For the ester, the rate of amine release was limited by specific base catalyzed hydrolysis of the ester group. Compounds of this type may be useful in prodrug design for tertiary amines. The possibility of quinone methine intermediates in the degradation of structurally similar drugs, such as epinephrine, was discussed.

Keyphrases □ Hydrolysis—labile quaternary ammonium derivatives, tertiary amines □ Amines—tertiary, kinetics, mechanism of hydrolysis, labile quaternary ammonium derivatives □ Kinetics—labile quaternary ammonium derivatives, mechanism of hydrolysis, tertiary amines

In recent years a number of approaches have been investigated for preparation of prodrugs (1, 2). Tertiary amines are unusual in that derivatization forms quaternary ammonium compounds. Quaternary salts resulting from simple alkylation, however, are generally chemically stable and therefore are not useful as prodrugs. A class of labile quaternary ammonium salts of the following general type have been investigated previously (3–6):

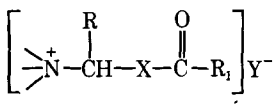

In this salt R and R_1 are hydrogen, alkyl, or aryl; X is oxygen or sulfur; and Y is a halogen. These compounds hydrolyze to form tertiary amine (>N—), aldehyde (RCHO), carboxylic acid (R_1COXH), and HY. Applications of this approach have included the preparation of soft quaternary germicides, anticholinergic agents, and antitumor agents.

In the present report, the kinetics and mechanism of hydrolysis of a different type of labile quaternary salt were studied. The general structure is:

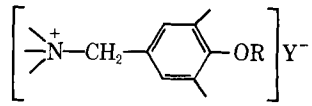

where R is H, CH_3, or CH_3CO and Y^- is Br^-. Simple tertiary amines were used as model compounds, although the results should be useful in the design of prodrugs. The 4-hydroxybenzyl structure of the quaternizing agent was chosen, since it is known to be a major factor in the instability of drugs such as epinephrine (7, 8). An unstable quinone methide was found to be an intermediate in the hydrolysis of the quaternary salts, and it is likely that the degradation of drugs such as epinephrine proceeds by an analogous mechanism.

EXPERIMENTAL

The following general sequence was used to prepare the quaternary salts *N*-(4-hydroxy-3,5-dimethylbenzyl)pyridinium bromide (I), *N*-(4-hydroxy-3,5-dimethylbenzyl)-3′-carbamoylpyridinium bromide (II), and *N*-(4-hydroxy-3,5-dimethylbenzyl)phenyldimethylammonium bromide (VIII): Formaldehyde and base were used to hydroxymethylate

0022-3549/82/0700-0729$01.00/0

2,6-dimethylphenol. The benzyl bromide was then prepared using hydrobromic acid–acetic acid. This compound was reacted with the corresponding tertiary amine to form the quaternary salt. Satisfactory elemental analyses were obtained on all stable compounds. NMR and IR spectra were run on commercial instruments[1,2]. Melting points were uncorrected.

4-Hydroxymethyl-2,6-dimethylphenol (III)—Equimolar amounts of 2,6-dimethylphenol[3], formaldehyde, and aqueous potassium hydroxide solution were reacted for 24 hr at 5° (9). The product precipitated upon neutralization and was recrystallized from chloroform, mp 101–102° [lit. (9) 105°]. UV (H_2O) 270, 220 nm max; IR (KBr): 3340 cm^{-1}; NMR [$(CD_3)_2SO$]: δ7.98 (s, 1H), 6.80 (s, 2H), 4.90 (s, 1H), and 2.17 (s, 6H) ppm.

4-Bromomethyl-2,6-dimethylphenol—A solution containing 0.5 g of III, 1 ml of 48% hydrobromic acid, and 10 ml of acetic acid was stirred for 0.5 hr at 6°. Cold chloroform (40 ml) and ice water (25 ml) were added, the organic layer was dried with calcium sulfate and rotary evaporated at room temperature. The unstable pink crystals could not be further characterized and were used immediately.

***N*-(4-hydroxy-3,5-dimethylbenzyl)pyridinium bromide (I)**—Immediately upon addition of pyridine to a solution of 4-bromomethyl-2,6-dimethylphenol in chloroform the quaternary compound precipitated, mp 190° dec. UV max (H_2O) 258 nm; IR (KBr): 3360 cm^{-1}; NMR [$(CD_3)_2SO$]: δ 9.25 (d, 2H), 8.35 (m, 4H), 7.24 (s, 2H), 5.77 (s, 2H), and 2.17 (s, 6H) ppm.

***N* - (4-hydroxy-3,5-dimethylbenzyl)-3′-carbamoylpyridinium bromide (II)**—The product precipitated from a solution of 1.6 g of niacinamide and 4-bromomethyl-2,6-dimethylphenol (prepared from 2 g of III) in 3 ml of dry dimethylformamide, mp 202°. NMR [$(CD_3)_2SO$]: δ 9.66 (s, 1H), 9.16 (m, 2H), 8.60 (s, 2H), 8.27 (t, 1H), 7.30 (s, 2H), 5.84 (s, 2H), 3.3 (s, 1H), and 2.22 (s, 6H) ppm.

***N* - (4-hydroxy-3,5-dimethylbenzyl)phenyldimethylammonium bromide (VIII)**—The procedure for I was followed with the substitution of *N*,*N*-dimethylaniline, mp 131–132°. IR (KBr): 3350 cm^{-1}; NMR [$(CD_3)_2SO$]: δ 7.67 (m, 5H), 6.50 (s, 2H), 4.84 (s, 2H), 3.50 (s, 7H), and 2.03 (s, 6H) ppm.

***N*-(4-acetoxy-3,5-dimethylbenzyl)pyridinium bromide (IV)**—A 0.5-g portion of I was acetylated with 1 ml of acetic anhydride in 3 ml of warm pyridine. The product crystallized upon cooling, mp 258°. UV max (H_2O) 258 nm; NMR [$(CD_3)_2SO$]: δ 9.25 (d, 2H), 8.33 (m, 3H), 7.33 (s, 2H), 5.80 (s, 2H), 2.33 (s, 3H), and 2.10 (s, 6H) ppm.

4-Dimethylaminomethyl-2,6-dimethylphenol—Mannich condensation of equimolar amounts of 2,6-dimethylphenol, formaldehyde, and dimethylamine in aqueous solution yielded the product (10). Recrystallization from benzene or ethanol—water gave long needles, mp 112° [lit. (10) 120–122°]. NMR (acetone-d_6): δ 6.83 (s, 2H), 3.22 (s, 2H), 2.19 (s, 6H), and 2.12 (s, 6H) ppm.

4-Hydroxy-3,5-dimethylbenzyltrimethylammonium Iodide (IX)—A literature procedure (10) for the reaction of 4-dimethylaminomethyl-2,6-dimethylphenol with methyl iodide in ether gave significant quantities of two byproducts (11). The water-soluble fraction containing IX and tetramethylammonium iodide was used. NMR (D_2O): δ 7.17 (s, 2H), 4.33 (s, 2H), [3.22 (s, $(CH_3)_4N^+$)], 3.07 (s, 9H), and 2.28 (s, 6H) ppm.

4-Hydroxymethyl-2,6-dimethylanisole—Two milliliters of dimethylsulfate was slowly added to 30 ml of a cold alkaline aqueous solution containing 1.0 g of III. The reaction mixture (two layers) was kept alkaline with 10% aqueous potassium hydroxide. After stirring 2 hr, the mixture was warmed gently and allowed to stand for 1 hr. The product was obtained as a yellow oil by ether extraction and solvent evaporation. NMR (CCl_4): δ 6.80 (s, 2H), 4.30 (s, 2H), 3.90 (s, 1H), 3.58 (s, 3H), and 2.17 (s, 6H) ppm.

4-Bromomethyl-2,6-dimethylanisole—A 0.5-g sample of 4-hydroxymethyl-2,6-dimethylanisole was converted to the bromide in 25 ml of 48% hydrobromic acid containing 1 ml of sulfuric acid. The product was extracted into 60 ml of chloroform, washed with 5% sodium bicarbonate solution, and dried with calcium sulfate. Evaporation of solvent gave a yellow oil. NMR (CCl_4): δ 6.91 (s, 2H), 4.28 (s, 2H), 3.65 (s, 3H), and 2.24 (s, 6H) ppm.

***N*-(4-methoxy-3,5-dimethylbenzyl)pyridinium bromide (VII)**—One milliliter of 4-bromomethyl-2,6-dimethylanisole was reacted with an equal volume of dry pyridine at 60°. Upon cooling, an oil separated which subsequently crystallized. Recrystallization from acetone afforded the pure product, mp 173–174°. UV max (H_2O) 257 nm; NMR (D_2O): δ 8.67 (m, 5H), 7.27 (s, 2H), 5.80 (s, 2H), 3.80 (s, 3H), and 2.34 (s, 6H) ppm.

Rate Studies—Reaction rates were measured in the thermostated cell compartment of a spectrophotometer[4]. Inorganic salts and nucleophiles were reagent grade and water was redistilled from an all-glass apparatus. Pseudo first-order rate constants were calculated[5] from the slopes of $\ln|A_\infty - A_t|$ *versus* time plots using the least-squares method. Correlation coefficients were consistently >0.998 and infinity values were taken after 10 half-lives. The pH of all solutions was measured[6] before and after the reactions and the change was <0.04. The reaction was initiated by injection of a concentrated stock solution into the buffer in the spectrophotometer cell. Wavelengths for the kinetic measurements were: I, 260 nm; II, 265 nm; IV, 250 and 285 nm; VIII, 250 nm; IX, 260 nm.

Reactions with half-lives <10 sec were followed using a stopped-flow spectrophotometer[7]. Transmittance–time data were converted to absorbance and then analyzed as before.

A high-performance liquid chromatograph (HPLC) with 254 nm detector was used[8]. The mobile phase consisting of pH 9.1, 5 m*M* borax buffer was pumped through the strong anion exchange column at 1.0 ml/min resulting in retention times of 3.5 (III) and 8.3 min (VI). Reaction solutions containing III and VI were extracted with 15 ml each of chloroform–ether–chloroform; the combined extracts were evaporated to dryness and reconstituted with 5 ml of methanol. The methanol solution was injected on the HPLC. The relative peak areas for III and VI were measured planimetrically. The aqueous phase from the extraction contained negligible amounts of the two compounds.

RESULTS

pH–Rate Profiles for Hydrolysis of I, II, and IV—In neutral to alkaline aqueous solutions, the quaternary ammonium salts of pyridine (I) and niacinamide (II) rapidly cleave to form the corresponding tertiary amine and III, as shown in Scheme I. The products were identified by UV, NMR, and TLC analyses. Repetitive UV scanning did not indicate the presence of an intermediate during the reaction. The rate was pH-de-

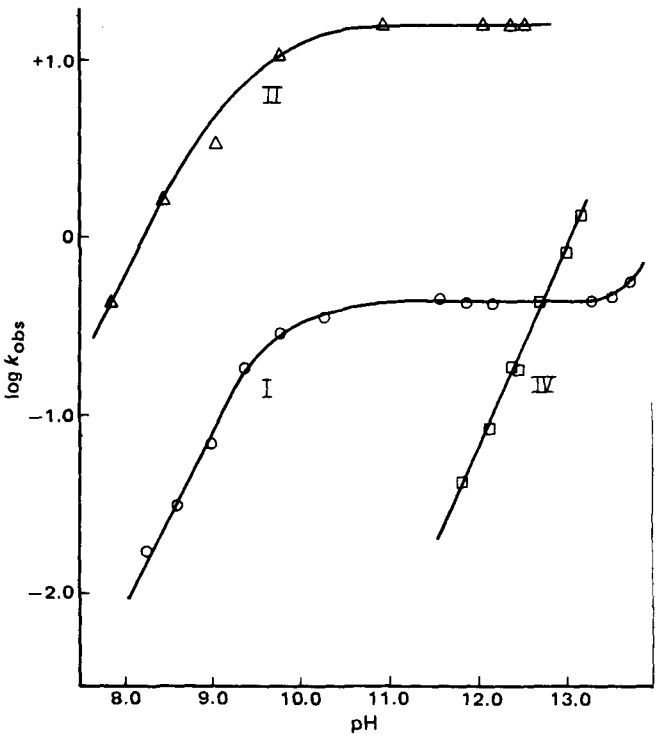

Figure 1—*Log* k_{obs}*–pH profiles for I, II, and IV at 25°,* $\mu = 1.0$ *(KCl). Parameters for the solid lines are: I,* (○) $k_{max} = 0.450\ min^{-1}$, $K_a' = 2.82 \times 10^{-10}$ *and* $k_{OH} = 0.250\ M^{-1}\ min^{-1}$; *II,* (△) $k_{max} = 15.6\ min^{-1}$ *and* $K_a' = 3.55 \times 10^{-10}$; *IV* (□) $k_{es} = 6.60\ M^{-1}\ min^{-1}$.

[1] Varian T-60.
[2] Beckman IR-33.
[3] Aldrich Chemical Co.
[4] Cary models 14, 15, or 16.
[5] Hewlett-Packard model 9810.
[6] Radiometer model 26.
[7] Durrum-Gibson.
[8] Dupont model 820.

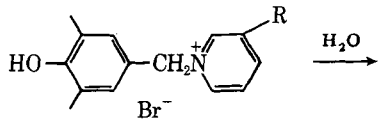

I: R = H
II: R = $CONH_2$

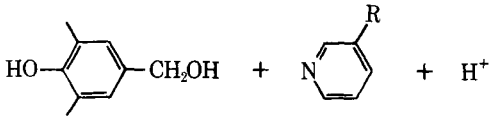

III

Scheme I

pendent and the spectrophotometrically determined log k_{obs}–pH profiles at 25° are shown in Fig. 1.

The reaction rates were increased by buffers and the buffer data are shown in Tables I and II. All data in Fig. 1 were extrapolated to zero buffer concentration. The lines for I and II in Fig. 1 were calculated according to:

$$k_{obs} = k_{max}\left(\frac{K_a'}{K_a' + a_H}\right) + k_{OH}K_w/a_H \qquad \text{(Eq. 1)}$$

where k_{obs} is the pseudo first-order rate constant at zero buffer concentration, k_{max} is the rate constant in the plateau region, K_a' is the dissociation constant of the reactant, k_{OH} is the apparent second-order rate constant for the effect of hydroxide on the conjugate base of I or II, K_w is the ion product of water, and a_H is the hydrogen ion activity. The rate of hydrolysis of II at high pH could not be accurately determined using the stopped-flow technique, and thus, k_{OH} could not be determined.

For the hydrolysis of I under conditions of pH < pK_a' and [I] $\simeq 10^{-4}$ *M*, the apparent rate constant became smaller during the reaction. This rate-retarding effect was due to the pyridine produced upon hydrolysis of I, according to the Law of Mass Action. The rate constants reported for this pH region were for the initial portion of the reaction where first-order conditions were well approximated or were obtained with more dilute solutions of I in longer path length UV cells. A study of this effect is reported in the next section.

Also shown in Fig. 1 is the effect of pH on the hydrolysis of IV, the acetate ester of I. As shown in Scheme II, this compound decomposed by consecutive kinetics:

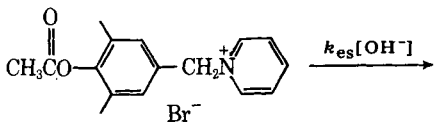

IV

$$CH_3COO^- + I \longrightarrow III + Pyridine$$

Scheme II

After hydrolysis of equal concentrations of I and IV at pH 12.5, the UV spectra of the products were identical. In the pH region studied, the rate of decomposition of I was three- to ten-fold faster than the hydrolysis of the ester. This allowed the rate constant for ester hydrolysis to be determined as the terminal slope of ln $|A_t - A_\infty|$ *versus* time plots.

The second-order rate constant for ester hydrolysis, k_{es}, was calculated from the slope of a plot of k_{obs} *versus* K_w/a_H according to:

$$k_{obs} = k_{es}K_w/a_H \qquad \text{(Eq. 2)}$$

Table I—Reaction Conditions and Buffer Data for the Hydrolysis of I[a]

pH	Buffer Species	Conc. Range, *M*	Number of Concs.	Number of k_{obs}
8.25	Borate	0.14–0.24	2	4
8.58	Borate	0.14–0.24	2	3
9.00	Borate	0.15–0.20	2	4
9.34	Carbonate	0.1–0.6	5	11
9.77	Carbonate	0.1–0.4	4	8
10.26	Carbonate	0.1–0.4	3	7
11.54–13.72	Hydroxide	—	—	—

[a] At 25°, μ = 1.0.

Table II—Reaction Conditions and Buffer Data for the Hydrolysis of II[a]

pH	Buffer Species	Conc. Range, *M*	Number of Concs.	Number of k_{obs}
7.85	Imidazole	0.05–1.0	4	8
8.45	Tromethamine	0.04–0.8	5	11
9.02	Borate	0.12–0.24	2	5
9.76	Carbonate	0.025–0.25	4	9
10.91	Butylamine	0.05–0.42	4	8
11.43	Phosphate	0.025–0.1	3	6
12.05–12.5	Hydroxide	—	—	—

[a] At 25°, μ = 1.0.

This reaction was first order in hydroxide ion, as indicated by the slope of 1.1 in Fig. 1. At pH 12.75 the rates of decomposition of I and IV were equal, *i.e.*, $k_{max} = k_{es}K_w/a_H$.

Effect of Added Pyridine on the Hydrolysis of I—In the pH-independent region for hydrolysis, addition of small amounts of pyridine at constant pH greatly decreased the observed rate constants. Figure 2 shows the kinetic effect of added pyridine at three pH values. The rate-retarding effect of pyridine decreased as pH increased, in the region where the hydrolysis reaction (Fig. 1) was strictly pH-independent. This mass law effect of pyridine was analogous to the common ion effect observed in many S_N1 reactions (12). A possible explanation for these data was a mechanism involving reversible dissociation of I to pyridine plus an intermediate (V). As shown in Scheme III, the intermediate can either react with pyridine to form starting material or with solvent irreversibly to form III:

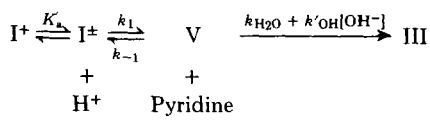

Scheme III

By applying the steady-state assumption to the intermediate, the rate law for loss of I may be expressed as shown in Eq. 3 where $[I]_T = [I^+] + [I^\pm]$ and [P] is the pyridine concentration:

$$\frac{-d[I]_T}{dt} = \frac{k_1(k_{H_2O} + k'_{OH}K_w/a_H)[I]_T}{k_{-1}[P] + k_{H_2O} + k'_{OH}K_w/a_H}\left(\frac{K_a'}{K_a' + a_H}\right) \qquad \text{(Eq. 3)}$$

The observed rate constant is defined as:

$$k_{obs} = \frac{k_1K_a'}{(K_a' + a_H)\left(1 + \left[\frac{k_{-1}[P]}{k_{H_2O} + k'_{OH}K_w/a_H}\right]\right)} \qquad \text{(Eq. 4)}$$

In the absence of added pyridine, $k_{-1}[P] \ll (k_{H_2O} + k'_{OH}K_w/a_H)$ and the rate constant is given by Eq. 1 with $k_{max} = k_1$ in the pH region where the k_{OH} term is negligible. Inversion and rearrangement of Eq. 4 gives:

$$\frac{1}{k_{obs}} = \left(\frac{k_{-1}[P]}{k_1(k_{H_2O} + k'_{OH}K_w/a_H)} + \frac{1}{k_1}\right)\left(1 + \frac{a_H}{K_a}\right) \qquad \text{(Eq. 5)}$$

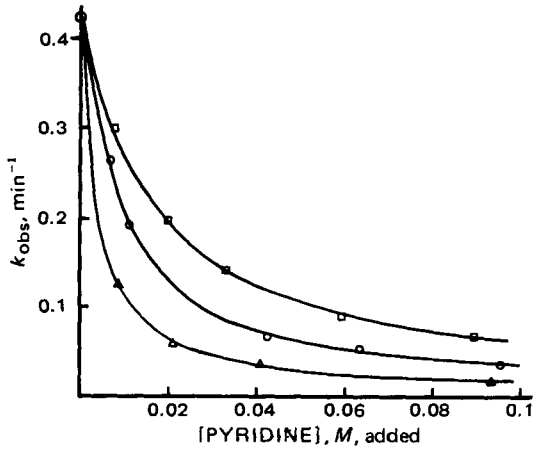

Figure 2—*Effect of added pyridine on the rate constant for hydrolysis of I at three pH values. Key:* (△) *pH 12.15,* (○) *pH 12.45,* (□) *pH 12.74.*

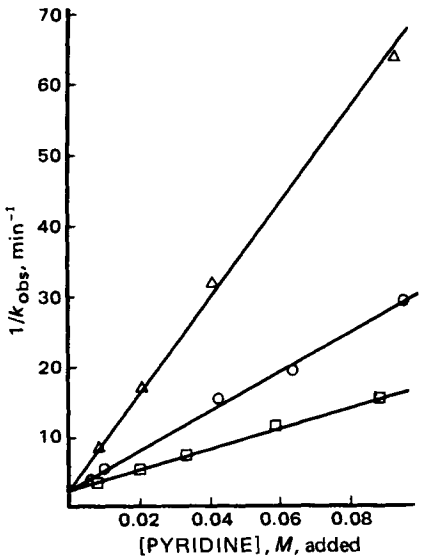

Figure 3—*Inverse rate constant for hydrolysis of I as a function of added pyridine concentration according to Eq. 5. Key:* (△) *pH 12.15,* (○) *pH 12.45,* (□) *pH 12.74.*

Equation 5 predicts a linear pH-dependent relationship between $1/k_{obs}$ and pyridine concentration, with slope = $k_{-1}/[k_1(k_{H_2O} + k'_{OH}K_w/a_H)]$ and intercept $1/k_1$. Figure 3 is an inverse plot according to Eq. 5 for the data in Fig. 2. Division of the intercept in Eq. 5 by the slope allows elimination of k_1 giving a hydroxide-dependent ratio, R:

$$R = \frac{k_{H_2O} + k'_{OH}K_w/a_H}{k_{-1}} \qquad \text{(Eq. 6)}$$

Figure 4 is a plot of R *versus* K_w/a_H with slope equal to $k'_{OH}/k_{-1} = 0.29$ and zero intercept. Thus, the reaction of the intermediate with water (k_{H_2O}) was negligible compared to k_{-1}. The slope of Fig. 3 indicates that the intermediate is 3.4-fold more reactive with pyridine than with hydroxide ion.

Effect of Added Substances on the Hydrolysis of I—The hydrolysis of I exhibited significant salt and solvent effects (Table III). The rate of hydrolysis at pH 12.8 decreased by one-half as ionic strength increased from 0.08 to 1.0. Identical rates of hydrolysis were obtained when potassium chloride–potassium iodide mixtures were used as electrolyte even though iodide is a stronger nucleophile in most displacement reactions. Addition of the polar nonelectrolytes, acetonitrile and dimethylformamide, at ~4 and 7% (v/v), respectively, strongly increased the observed rate at constant ionic strength.

Table IV contains apparent second-order rate constants and experimental conditions for the effect of several nucleophilic substances on the hydrolysis of I. A Brønsted plot of this data (log k_2^{app} *versus* pK'_a) showed a slope of ~0.1 indicating that the reaction was essentially insensitive to changes in basicity. The effect of imidazole was pH-dependent. As pH increased the apparent catalytic constant for imidazole decreased. In Fig. 5a, the apparent second-order rate constants for imidazole have been plotted against K_w/a_H. If the rate effect of imidazole anion was negligible compared to the neutral molecule, a description of the kinetic data gives:

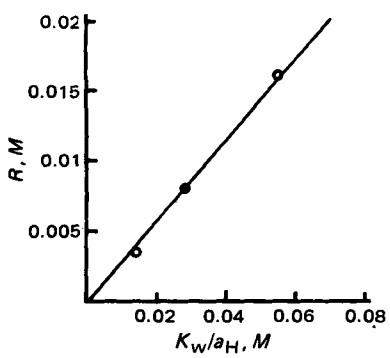

Figure 4—*Dependence of the ratio,* R, *on hydroxide ion concentration according to Eq. 6.*

Table III—Effect of Variations in Salt and Solvent Concentrations on the Hydrolysis of I

Conditions[a]	Ionic Strength	k_{obs}, min^{-1}	$\frac{k_{obs}}{k_{max}}$
0.92 *M* KCl	1.0	0.415	1
0.08 *M* KOH	0.08	0.800	1.9
0.4 *M* KI	1.0	0.414	1.0
0.8 *M* KI	1.0	0.410	0.99
1.15 *M* CH_3CN	1.0	0.611	1.5
1.02 *M* *N*,*N*-dimethylformamide	1.0	1.243	3.0

[a] All solutions contained 0.08 *M* KOH.

$$k_2^{app} = k_0\left[\frac{a_H}{K'_a + a_H}\right] \qquad \text{(Eq. 7)}$$

where k_0 is the second-order rate constant for the effect of neutral imidazole on the hydrolysis of I, and K'_a is the apparent dissociation constant for imidazole as an acid. Inversion and rearrangement gives:

$$\frac{1}{k_2^{app}} = \frac{1}{k_0} + \frac{K_w}{k_0K'_ba_H} \qquad \text{(Eq. 8)}$$

Equation 8 predicts a linear relationship between reciprocal rate constant and K_w/a_H as shown in Fig. 5b. The second-order rate constant for imidazole in Table IV was calculated from the intercept of Fig. 5b.

Upon hydrolysis of a concentrated solution of I in the presence of imidazole, *N*-(4-hydroxy-3,5-dimethylbenzyl) imidazole (VI) crystallized and was isolated as a product.

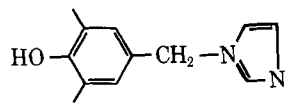

VI

The effect of added imidazole on the product composition for the hydrolysis of I at pH 12.70 was determined by HPLC. Figure 6 shows the effect of imidazole on the molar ratio of imidazole- and hydroxide-substituted products, $[VI]/[III]_\infty$, at the end of the reaction. The kinetic effect of added imidazole at pH 12.70, $k_2^{app} = 0.22\ M^{-1}\ min^{-1}$, can be interpolated from Fig. 5a. Therefore, the ratio of rate constants for the effects of imidazole and hydroxide at this pH was $k_2^{app}/k_{max} = 0.5\ M^{-1}$. Comparison of this value with the slope of Fig. 6, 14 M^{-1}, indicates that 28-fold more imidazole was appearing in the product than could be accounted for by the apparent second-order rate dependency.

The potent nucleophile cyanide ion had no effect on the rate of hydrolysis of I at pH 12.47 (Table IV). The low standard deviation for duplicate runs at each concentration of cyanide ion ($0.446 \pm 0.010\ min^{-1}$) indicated the absence of any effect other than that attributable to salt composition.

Stability of the *O*-methyl Quaternary Salts—No change in absorption spectrum was detectable when *N*-(4-methoxy-3,5-dimethylbenzyl)pyridinium bromide(VII) was dissolved in water, 1.0 *M* KOH, or 1.0 *M* NaCN and scanned with time over a 1-hr period. Replacement of the phenolic hydrogen by a methyl ether completely eliminated the instability of I in solution.

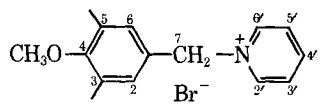

VII

When the NMR spectrum of VII in alkaline deuterium oxide (pD 13.1) was scanned over a 6-day period at room temperature, the benzylic protons (position 7) and the 2′ and 6′ protons of the pyridine ring were completely exchanged. Under these conditions, no decomposition of VII could be detected. Similar exchange has been reported for 1-methyl and 1-oxypyridinium ions (15). The analogous quaternary derivative of niacinamide was also stable in base but formed an apparent cyanide adduct with characteristic absorption maximum at 340 nm (16).

Hydrolysis of Aliphatic Quaternary Compounds—Analogous quaternary derivatives of *N*,*N*-dimethylaniline (VIII) and trimethylamine (IX) hydrolyzed similarly to I and II except that rate inhibition by the product amine was a more serious problem:

Table IV—Apparent Second-Order Rate Constants for the Effect of Nucleophiles on the Hydrolysis of I[a]

Species	pK'_a	k_2^{app}, M^{-1} min^{-1}	pH	Conc. Range, M
Iodide	—	0	12.75	0.4–0.8
Azide	4.0[b]	0.11[c]	12.75	(0.8)
Acetate	4.61[b]	0.168	12.61	0.08–0.94
Acetate	—	0.152	12.14	0.1–0.6
Methoxylamine	4.73[d]	0.23[c]	12.19	(0.4, 1.0)
Imidazole	7.21[b]	0.45[e]	—	0.05–1.0
Morpholine	8.87[b]	0.36	12.81	0.08–0.88
Cyanide	9.3[b]	0	12.47	0.1–0.8
Glycinate	9.76[b]	0.206	12.45	0.08–0.8
Glycinate	—	0.210	12.90	0.08–0.8
n-Butylamine	10.9[f]	0.68	12.88	0.07–0.7
Hydroxide	15.74	0.25	—	—

[a] At 25°, μ = 1.0. [b] Reference 13. [c] $(k_{obs} - k_0)/[N]$. [d] Reference 14. [e] pH independent. [f] pK'_a = pH − log[$\alpha_n/(1-\alpha_n)$], where α_n is the fraction of nonionized amine.

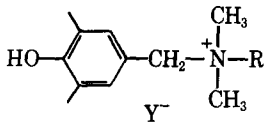

VIII: R = phenyl, Y = Br
IX: R = CH_3, Y = I

Initial rate data for VIII at neutral pH and the highest practicable dilution allowed estimation of k_{max} as shown in Table V. Stopped-flow measurements were not possible due to the instability of VIII in all solvents in which it was soluble. Hydrolysis of the trimethylammonium salt (IX) was studied using 10-cm UV cells in which first-order kinetics were obtained. Constant values of k_{max} were measured at pH 12.5 and 12.9.

Table V summarizes the hydrolysis data for I, II, VIII, and IX as a function of the pK'_a of the tertiary amine leaving group. When these data are plotted as log k_{max} *versus* pK'_a, heterocyclic and aliphatic ammonium compounds appear to fall on separate lines with slope ≃0.8, according to the limited data available. The aliphatic quaternary ammonium compounds are ~250 times more reactive than the pyridinium compounds. More data would be necessary to determine the existence of any possible structure–reactivity relationships.

Reactions in Methanol—The quaternary salts react in methanol to form amine and 4-methoxymethyl-2,6-dimethylphenol, which was identified by TLC comparison with a synthesized sample. In this solvent VIII exhibited unexpectedly high absorptivity, a different λ_{max} (285 nm), and a monoexponential decline in absorbance with $t_{1/2}$ = 17 sec. An identical rate constant and λ_{max} were reported previously (18) for the reaction of the quinone methide, 4-methylene-2,6-dimethyl-2,5-cyclohexadien-1-one (V), with methanol:

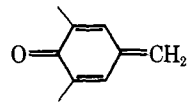

V

Apparently VIII completely dissociated to amine and V by the time the spectrophotometric data were obtained. The reaction of I and II was biexponential and showed a broad rise and fall in absorbance with time. An added complication was that the rates of both steps were sensitive to small amounts of water in the methanol. Due to this problem and the kinetic complexity of A ⇌ B → C systems, reactions in methanol were not studied further.

When the quaternary compounds were dissolved in polar aprotic solvents, *e.g.*, acetonitrile, dimethylformamide, or dimethyl sulfoxide, the dissociation equilibrium was again rapidly established. Since the reaction of V with these solvents was not possible, condensation reactions occurred to form dimeric products (19).

DISCUSSION

Mechanism of Hydrolysis—The intermediate in the aqueous reaction of these quaternary compounds was probably the quinone methide (V). A generalized form of Scheme III involving unimolecular dissociation of phenoxide zwitterion to V and tertiary amine, followed by trapping of the intermediate with solvent or nucleophiles, is consistent with the data. A kinetically indistinguishable pathway is possible, involving reaction of hydroxide with the protonated form of the quaternary compounds. If this mechanism were operative, compounds with the phenolic

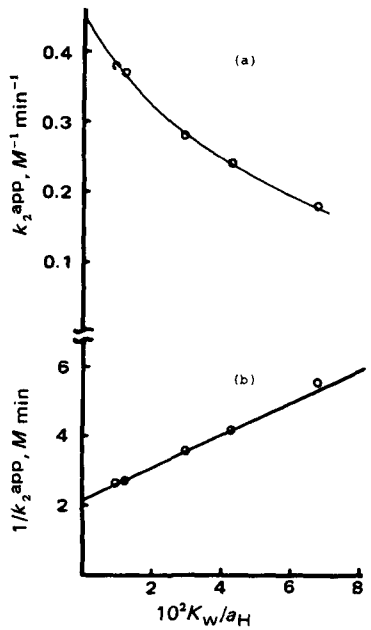

Figure 5—*Apparent rate constant for the effect of imidazole as a function of hydroxide ion concentration (a); data plotted according to Eq. 8 (b).*

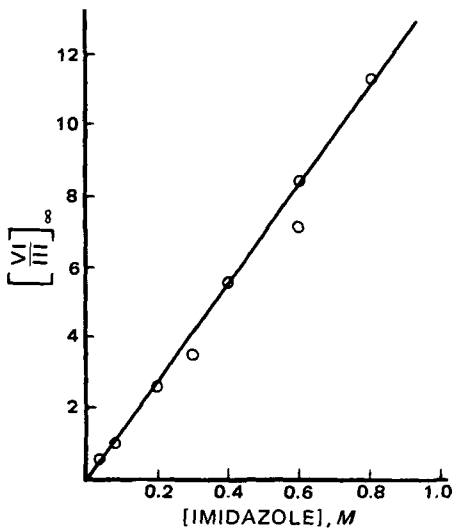

Figure 6—*Ratio of imidazole to hydroxide substitution in the product as a function of imidazole concentration for hydrolysis of I at pH 12.70, 25°, μ = 1.0 (KCl).*

Table V—Effect of Leaving Group Basicity on the Rates of Hydrolysis for I, II, VIII, and IX

Compound	pK'_a[a]	k_{max}, min^{-1}
I	5.52[b]	0.45
II	3.55[b]	15.6
VIII	5.15[c]	$10^3 \pm 10^1$
IX	9.75[c]	0.039

[a] pK'_a of the conjugate acid of the amine leaving group. [b] Reference 13. [c] Reference 17.

hydrogen replaced by a methyl group should exhibit comparable rates of hydrolysis to the phenolic derivatives. The complete stability of the methoxy compounds under conditions where their phenolic derivatives were quite unstable rules out a mechanism involving nucleophilic attack of hydroxide ion.

Although the proposed quinone methide intermediate (V) was too unstable in water to be observed spectrophotometrically, its presence was essential in explaining the kinetic data. Moreover, spectrophotometric detection of this compound upon methanolysis of the quaternary derivatives strongly suggested that the same intermediate occurred in water.

The mass law effect of added pyridine in the hydrolysis of I supports the proposed unimolecular mechanism. In the absence of added pyridine, the rate of reaction of V with solvent was faster than its reaction with pyridine. The rate-determining step under these conditions was the loss of reactant (k_1) and pH-independent kinetics were observed. Addition of small amounts of pyridine greatly increased the rate of reversion of V to starting material and caused the observed rate constant to exhibit an inverse dependence on pyridine concentration. The approximation that the rate of reaction of quinone methide with hydroxide was much faster than its reaction with pyridine was no longer valid. In this manner addition of pyridine transformed an apparently pH-independent reaction into one which was first-order in hydroxide.

The maximum rate of hydrolysis of the quaternary compounds of this study was quite sensitive to the structure and basicity of the tertiary amine leaving group (Table V). The rate increased with decreasing basicity of the leaving group for structurally similar compounds. Structural influence is demonstrated by the quaternary compounds of dimethylaniline and pyridine reacting at quite different rates, even though the amine leaving groups had similar pK'_a values. The large rate difference between the two structural classes is due to resonance stabilization of the pyridinium derivatives, as opposed to the instability of the aliphatic and aryl-aliphatic amines (20):

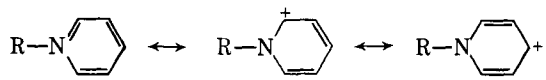

Charge delocalization of this type is not possible with salts of aliphatic or aryl-aliphatic amines.

Effect of Additives on the Rate of Hydrolysis—The effect of medium on reaction rates in solution is described by the Brønsted equation:

$$k = k_0 \frac{\gamma_A \gamma_B}{\gamma_\pm} \qquad \text{(Eq. 9)}$$

where k is the observed reaction rate constant, k_0 is the limiting value of the rate constant at zero concentrations of all solutes, and the γ's are the activity coefficients of the reactants and transition state (12). For the unimolecular reactions of the present report, this equation can be expressed as:

$$k = k_0 \frac{\gamma_z}{\gamma_\pm} \qquad \text{(Eq. 10)}$$

with γ_z defined as the activity coefficient of the zwitterionic reactant.

The hydrolysis of I involved a negative salt effect, *i.e.*, the compound was more stable as ionic strength increased. This phenomenon was due to stabilization of the zwitterionic reactant by added salt (a decrease in γ_z) more than the nonpolar transition state. Usually, a unimolecular reaction of an electrically neutral species is insensitive to variations in ionic strength (12). The highly polarized zwitterion of I, however, would be expected to be affected greatly by changes in ionic strength of the medium.

The addition of nonionic solutes at constant ionic strength caused a rate effect opposite to that of added salt. Acetonitrile or dimethylformamide stabilized the nonpolar transition state causing an increase in rate. This effect was exhibited more dramatically by the several thousand-fold increase in rate of decomposition in methanol compared to water. In addition, the reactant in methanol was presumably the nonionized phenol which was essentially unreactive in water.

The presence of several inorganic and organic nucleophilic species increased the rate of hydrolysis of I (Table IV). A Brønsted slope of ~0.1 was found for this data. Charged nucleophiles, *e.g.*, acetate, azide, imidazole anion, glycinate, and hydroxide, exhibited negative deviations compared to neutral substances of similar pK'_a values. The less polar amines, morpholine, and butylamine showed greater than first-order rate dependencies (11) while cyanide of similar basicity had no effect. These data suggest that the nucleophilic substances affect the activity coefficients rather than participating in a general acid–base or nucleophilic reaction with I.

The apparent Brønsted correlation of rate with basicity was probably a kinetic artifact arising from the effects of added solutes on the activity coefficients. The pH dependency of the effect of imidazole on the hydrolysis of I was in accord with this hypothesis. Imidazole anion is generally a much stronger nucleophile than the neutral form, although it was less effective in causing hydrolysis of I. This behavior is consistent with the expected effect of a charged species on the activity coefficients. The lack of kinetic dependency on cyanide ion is also in agreement with this hypothesis. Added sodium cyanide at constant ionic strength should have very little effect on the activity coefficient, although this compound is a strong nucleophile. The k_{OH} term observed in the hydrolysis of I was thought to be due to medium effects of hydroxide ion rather than a nucleophilic or base-catalyzed reaction.

Hydrolysis of the Ester (IV)—When the phenolic group of I was acetylated, the slow step in the overall rate of hydrolysis <pH 12.5 was the hydrolysis of the ester. The rapid hydrolysis of the quaternary compounds can, therefore, be moderated by the choice of a suitable ester function. The second-order rate constant for hydrolysis of IV is ~10-fold smaller than that for hydrolysis of phenyl acetate (13). This value is reasonable considering the rate-retarding steric and electronic effects of the two *ortho* methyl groups (21) and the accelerating effect of the ammonium group.

The results of this preliminary report indicate that quaternization and hydrolysis *via* quinone methides is a possible method for forming useful prodrug derivatives of tertiary amines. The simple amines studied represent a wide range of basicity and structure. Although actual drug molecules were not employed, the results are expected to be easily extrapolated to more complex molecules. Esterification yields a quaternary salt for which the release of the parent drug is controlled by ester hydrolysis. This is desirable since structure–reactivity relationships of esters are well known and the compounds should be substrates for enzymatic cleavage *in vivo*.

Possible Quinone Methide Intermediates in Drug Degradation—The abnormally high reactivity of drugs containing the *o*- or *p*-hydroxybenzyl alcohol structure has been recognized and studied previously (8). In a survey of reactions of several pharmaceuticals with bisulfite, an *o*- or *p*-hydroxyl or amino group was essential for reaction. *meta*-Substituted isomers as well as *o*- or *p*-methoxy derivatives were unreactive with sulfite under the experimental conditions. Substituted benzyl sulfonic acids were determined to be the products in several of the reactions. An explanation for these data would be reversible dehydration to form the quinone methide followed by a rapid reaction with bisulfite to form the sulfonate product.

The reaction of epinephrine with bisulfite also suggests the intermediacy of a quinone methide (7). Below pH 5 the rate of degradation was zero-order in bisulfite concentration indicating a unimolecular mechanism. Additional evidence for a quinone methide intermediate is the specific acid catalyzed racemization of epinephrine observed in the absence of bisulfite (22). The planar intermediate formed by dehydration could react with solvent to form optically inactive epinephrine.

REFERENCES

(1) T. Higuchi and V. Stella, Eds., "Pro-drugs as Novel Drug Delivery Systems," American Chemical Society, Washington, D.C., 1975.

(2) A. A. Sinkula and S. H. Yalkowsky, *J. Pharm. Sci.*, **64**, 181 (1975).

(3) N. Bodor, in "Design of Biopharmaceutical Properties through Prodrugs and Analogs," E. B. Roche, Ed., American Pharmaceutical Association, Washington, D.C., 1977, Chap. 7.

(4) N. Bodor, J. J. Kaminski, and S. Selk, *J. Med. Chem.*, **23**, 469 (1980).

(5) N. Bodor and J. J. Kaminski, *ibid.*, **23**, 566 (1980).
(6) N. Bodor, R. Woods, C. Raper, P. Kearney, and J. J. Kaminski, *ibid.*, **23**, 474 (1980).
(7) T. Higuchi and L. C. Schroeter, *J. Am. Chem. Soc.*, **82**, 1904 (1960).
(8) T. Higuchi and L. C. Schroeter, *J. Am. Pharm. Assoc., Sci. Ed.*, **48**, 535 (1959).
(9) K. Hultzsch, *Ber. Dtsch. Chem. Ges.*, **74**, 1533 (1941).
(10) P. D. Gardner, H. Sarrafizadeh Rafsanjani, and L. Rand, *J. Am. Chem. Soc.*, **81**, 3364 (1959).
(11) J. B. Bogardus, Ph.D. Thesis, University of Kansas, 1973.
(12) L. P. Hammett, "Physical Organic Chemistry," 2nd ed., McGraw-Hill, New York, N.Y., 1970.
(13) W. P. Jencks and M. Gilchrist, *J. Am. Chem. Soc.*, **90**, 2622 (1968).
(14) T. St. Pierre and W. P. Jencks, *J. Am. Chem. Soc.*, **90**, 3817 (1968).
(15) J. A. Zoltewicz, G. M. Kauffman, and C. L. Smith, *ibid.*, **90**, 5939 (1968).
(16) R. N. Lindquist and E. H. Cordes, *ibid.*, **90**, 1269 (1968).
(17) D. D. Perrin, "Dissociation Constants of Organic Bases in Aqueous Solutions," Butterworths, London, England, 1965.
(18) L. J. Filar and S. Winstein, *Tetrahedron Lett.*, **25**, 9 (1960).
(19) K. Fries and E. Brandes, *Justus Liebigs Ann. Chem.*, **542**, 48 (1939).
(20) M. H. Palmer, "The Structure and Reactions of Heterocyclic Compounds," Edward Arnold Publications, London, 1967, p. 23.
(21) N. A. Fischer, G. J. Leary, R. D. Topsom, and J. Vaughan, *J. Chem. Soc. (B)*, **1966**, 782.
(22) L. C. Schroeter and T. Higuchi, *J. Am. Pharm. Assoc., Sci. Ed.*, **47**, 426 (1958).

ACKNOWLEDGMENTS

Adapted in part from a dissertation submitted by J. B. Bogardus to the University of Kansas in partial fulfillment of the Doctor of Philosophy degree requirements.

This work was supported by a National Science Foundation Graduate Traineeship (J.B.B.).

Concentration-Dependent Disappearance of Fluorouracil from Peritoneal Fluid in the Rat: Experimental Observations and Distributed Modeling

JERRY M. COLLINS ˣ, ROBERT L. DEDRICK, MICHAEL F. FLESSNER, and ANTHONY M. GUARINO

Received February 12, 1981, from the *Biomedical Engineering and Instrumentation Branch, Division of Research Services and the Developmental Therapeutics Program, National Cancer Institute, National Institutes of Health, Bethesda, MD 20205.* Accepted for publication October 6, 1981.

Abstract □ The rate of disappearance of fluorouracil from peritoneal fluid has been experimentally measured and mathematically modeled. The experimental data were obtained following the instillation of 50 ml of dialysis fluid which contained an initial fluorouracil concentration ranging from 24 μM to 12 mM. The rate of disappearance was strongly dependent upon concentration. A distributed model has been formulated which incorporates concepts of diffusion with saturable metabolism and nonsaturable capillary uptake in the tissue surrounding the peritoneal fluid. This model successfully describes the experimental observations and also suggests that the effective penetration depth into tissue is highly dependent upon concentration.

Keyphrases □ Fluorouracil—concentration-dependent disappearance from peritoneal fluids, rats □ Pharmacokinetics—concentration-dependent disappearance of fluorouracil from peritoneal fluid, rats □ Peritoneal fluid—concentration-dependent disappearance of fluorouracil, rats

Although intraperitoneal injections are extensively used for the administration of drugs to rodents, there are few studies which examine the kinetic features of this route (1, 2). When drugs are administered in a small volume, it is usually assumed that absorption occurs through pathways which lead to the portal vein. For larger volumes, as used in peritoneal dialysis, nonportal pathways such as the ventral abdominal wall, diaphragm, and retroperitoneal tissues may have a significant role. Lymphatic uptake, although largely unexplored, is assumed to be quantitatively unimportant for substances with small molecular weights.

The rate of disappearance of drugs from peritoneal fluid is primarily a consequence of the concentration gradient established between peritoneal fluid and surrounding tissue. As drug molecules diffuse into this tissue, they can be carried away by capillary blood, metabolized by enzymes in the tissue, or be bound to tissue constituents. Removal by capillary blood is kinetically a first-order process, while metabolism and tissue uptake or binding are potentially saturable since these processes depend upon a finite number of sites.

The intraperitoneal administration of the pyrimidine analog, fluorouracil, is currently undergoing clinical evaluation for the treatment of several cancers which are initially confined to the abdomen (2, 3). Since the clinical range of intraperitoneal fluorouracil concentration is restricted by therapeutic considerations, a previously developed rat model was used for these peritoneal disappearance studies. The metabolism of fluorouracil is saturable (4), and at least some tissues surrounding the peritoneal cavity are sites for this metabolism (5). No tissue binding has been reported.

Data have been collected on the rate of peritoneal disappearance over a wide range of initial concentrations in order to observe metabolism in both linear and nonlinear regions. A distributed model has been formulated which incorporates concepts of diffusion with chemical reaction and capillary uptake in the surrounding tissue. The nonlinear partial differential equation was solved numerically with the appropriate initial and boundary conditions. The solution suggests that the effective penetration depth into the tissue and the rate of removal from the peritoneal cavity are concentration dependent.

0022-3549/82/0700-0735$01.00/0

(5) N. Bodor and J. J. Kaminski, *ibid.*, **23**, 566 (1980).
(6) N. Bodor, R. Woods, C. Raper, P. Kearney, and J. J. Kaminski, *ibid.*, **23**, 474 (1980).
(7) T. Higuchi and L. C. Schroeter, *J. Am. Chem. Soc.*, **82**, 1904 (1960).
(8) T. Higuchi and L. C. Schroeter, *J. Am. Pharm. Assoc., Sci. Ed.*, **48**, 535 (1959).
(9) K. Hultzsch, *Ber. Dtsch. Chem. Ges.*, **74**, 1533 (1941).
(10) P. D. Gardner, H. Sarrafizadeh Rafsanjani, and L. Rand, *J. Am. Chem. Soc.*, **81**, 3364 (1959).
(11) J. B. Bogardus, Ph.D. Thesis, University of Kansas, 1973.
(12) L. P. Hammett, "Physical Organic Chemistry," 2nd ed., McGraw-Hill, New York, N.Y., 1970.
(13) W. P. Jencks and M. Gilchrist, *J. Am. Chem. Soc.*, **90**, 2622 (1968).
(14) T. St. Pierre and W. P. Jencks, *J. Am. Chem. Soc.*, **90**, 3817 (1968).
(15) J. A. Zoltewicz, G. M. Kauffman, and C. L. Smith, *ibid.*, **90**, 5939 (1968).
(16) R. N. Lindquist and E. H. Cordes, *ibid.*, **90**, 1269 (1968).
(17) D. D. Perrin, "Dissociation Constants of Organic Bases in Aqueous Solutions," Butterworths, London, England, 1965.
(18) L. J. Filar and S. Winstein, *Tetrahedron Lett.*, **25**, 9 (1960).
(19) K. Fries and E. Brandes, *Justus Liebigs Ann. Chem.*, **542**, 48 (1939).
(20) M. H. Palmer, "The Structure and Reactions of Heterocyclic Compounds," Edward Arnold Publications, London, 1967, p. 23.
(21) N. A. Fischer, G. J. Leary, R. D. Topsom, and J. Vaughan, *J. Chem. Soc. (B)*, **1966**, 782.
(22) L. C. Schroeter and T. Higuchi, *J. Am. Pharm. Assoc., Sci. Ed.*, **47**, 426 (1958).

ACKNOWLEDGMENTS

Adapted in part from a dissertation submitted by J. B. Bogardus to the University of Kansas in partial fulfillment of the Doctor of Philosophy degree requirements.

This work was supported by a National Science Foundation Graduate Traineeship (J.B.B.).

Concentration-Dependent Disappearance of Fluorouracil from Peritoneal Fluid in the Rat: Experimental Observations and Distributed Modeling

JERRY M. COLLINS ˣ, ROBERT L. DEDRICK, MICHAEL F. FLESSNER, and ANTHONY M. GUARINO

Received February 12, 1981, from the *Biomedical Engineering and Instrumentation Branch, Division of Research Services and the Developmental Therapeutics Program, National Cancer Institute, National Institutes of Health, Bethesda, MD 20205.* Accepted for publication October 6, 1981.

Abstract □ The rate of disappearance of fluorouracil from peritoneal fluid has been experimentally measured and mathematically modeled. The experimental data were obtained following the instillation of 50 ml of dialysis fluid which contained an initial fluorouracil concentration ranging from 24 μM to 12 mM. The rate of disappearance was strongly dependent upon concentration. A distributed model has been formulated which incorporates concepts of diffusion with saturable metabolism and nonsaturable capillary uptake in the tissue surrounding the peritoneal fluid. This model successfully describes the experimental observations and also suggests that the effective penetration depth into tissue is highly dependent upon concentration.

Keyphrases □ Fluorouracil—concentration-dependent disappearance from peritoneal fluids, rats □ Pharmacokinetics—concentration-dependent disappearance of fluorouracil from peritoneal fluid, rats □ Peritoneal fluid—concentration-dependent disappearance of fluorouracil, rats

Although intraperitoneal injections are extensively used for the administration of drugs to rodents, there are few studies which examine the kinetic features of this route (1, 2). When drugs are administered in a small volume, it is usually assumed that absorption occurs through pathways which lead to the portal vein. For larger volumes, as used in peritoneal dialysis, nonportal pathways such as the ventral abdominal wall, diaphragm, and retroperitoneal tissues may have a significant role. Lymphatic uptake, although largely unexplored, is assumed to be quantitatively unimportant for substances with small molecular weights.

The rate of disappearance of drugs from peritoneal fluid is primarily a consequence of the concentration gradient established between peritoneal fluid and surrounding tissue. As drug molecules diffuse into this tissue, they can be carried away by capillary blood, metabolized by enzymes in the tissue, or be bound to tissue constituents. Removal by capillary blood is kinetically a first-order process, while metabolism and tissue uptake or binding are potentially saturable since these processes depend upon a finite number of sites.

The intraperitoneal administration of the pyrimidine analog, fluorouracil, is currently undergoing clinical evaluation for the treatment of several cancers which are initially confined to the abdomen (2, 3). Since the clinical range of intraperitoneal fluorouracil concentration is restricted by therapeutic considerations, a previously developed rat model was used for these peritoneal disappearance studies. The metabolism of fluorouracil is saturable (4), and at least some tissues surrounding the peritoneal cavity are sites for this metabolism (5). No tissue binding has been reported.

Data have been collected on the rate of peritoneal disappearance over a wide range of initial concentrations in order to observe metabolism in both linear and nonlinear regions. A distributed model has been formulated which incorporates concepts of diffusion with chemical reaction and capillary uptake in the surrounding tissue. The nonlinear partial differential equation was solved numerically with the appropriate initial and boundary conditions. The solution suggests that the effective penetration depth into the tissue and the rate of removal from the peritoneal cavity are concentration dependent.

0022-3549/82/0700-0735$01.00/0

EXPERIMENTAL

Separation of Fluorouracil from Its Metabolites—Fluorouracil is extensively metabolized by both anabolic and catabolic enzymes. The goal of this separation procedure was to isolate the parent compound, fluorouracil, but not necessarily to identify individual metabolites. A 10–25-μl sample of peritoneal fluid was applied to 250 μm of silica gel G TLC plates[1]. Each plate included a [^{14}C]fluorouracil[2] standard. The plates were developed for 10 cm by the upper phase of the solvent system of Koechlin *et al.* (6): ethyl acetate (60%, v/v), formic acid (5% v/v), and water (35%, v/v). Samples were counted in a liquid scintillation counter with automatic external standardization. In this system, 97% of [^{14}C]-fluorouracil radioactivity was located above R_f 0.45, while all metabolites were below R_f 0.45 ([^{14}C]floxuridine[2], 98%; [^{14}C]urea[3], 99%; [^{14}]fluoro-ureido-propionic acid, 99%). Since dihydrofluorouracil is unstable in this system, it was measured as fluoro-ureido-propionic acid or urea (6). [^{14}C]Fluoro-ureido-propionic acid was isolated by the procedure of Chauduri *et al.* (7) from the urine of rats given [^{14}C]fluorouracil. Urine was placed on anion exchange resin[4] (10 × 1 cm) and eluted with 50 ml of water, 80 ml of 0.05 *M* formic acid, 150 ml of 1.5 *M* formic acid, and finally 50 ml of 0.5 *M* HCl. [^{14}C]Fluoro-ureido-propionic acid was found in the third fraction. [^{14}C]Fluorouracil standard eluted in the second fraction, as validated by TLC.

Experimental Procedures—Female Sprague-Dawley rats[5] (220–240 g) were anesthetized with 50 mg/kg ip pentobarbital. Supplemental doses of 15 mg/kg im were given as required. Fluorouracil[2] was dissolved in peritoneal dialysis solution[6] (major components: 1.5% dextrose; 132 mEq Na; 3.5 mEq Ca; 1.5 mEq Mg; 99 mEq Cl; 35 mEq lactate), and the solution was warmed to 37°. [^{14}C]Fluorouracil was added to yield total fluorouracil concentrations ranging from 24 μM to 12 m*M*. Fifty milliliters of drug solution was injected into the peritoneal space through an 18-G needle. Periodic 100-μl samples were obtained by transcutaneous puncture with a 23-G needle. Rectal temperature was maintained at 37 ± 0.2° by means of a heat lamp and temperature controller[7].

Simulations—Although an analytical solution is not feasible for the model presented in the Appendix, Eqs. 1 and 2 can be integrated numerically, using Eqs. 3*a*, 3*b*, and 3*c* as initial and boundary conditions. The simulations presented in this paper were computed by means of the implicit form of the finite difference method, based on the algorithm of Carnahan *et al.* (8).

RESULTS

Measurements of fluorouracil disappearance from peritoneal fluid are plotted in Fig. 1. Initial fluorouracil concentrations in the peritoneal fluid ranged from 24 μM to 12 m*M*. There is a very strong dependence of disappearance rate on concentration. The rate of disappearance at low concentration is 10-fold greater than at high concentration.

The simulated disappearance curves shown in Fig. 1 were obtained by numerical integration of Eqs. 1–3 from Appendix I. The model parameters are discussed in Appendix II. The *a priori* parameters associated with the simulations in Fig. 1 provide an adequate representation of the data over the five orders of magnitude that drug concentration was measured. Although a statistical best fit was not attempted[8], an example of the ability of the distributed model to match more closely the experimental data is presented in Fig. 2. For these simulations, V_{max} was arbitrarily adjusted to 36 nmole/min/g and K_M to 5 μM, while the other parameters were unchanged.

Solution of Eqs. 1–3 also yields information about the concentration profile of drug in tissue. There are no experimental data for comparison, and these calculations are highly dependent on assumptions about model geometry. Nonetheless, there are some important predictions worthy of consideration. Figure 3 shows that the tissue concentration profile requires 15 min to become fully developed for an initial peritoneal concentration of 12 m*M*. In contrast, Fig. 4 shows that only 1 min is required for profile development when the initial peritoneal concentration is 24 μM. At high concentrations, >600 μm are needed for the tissue concentration to drop to 5% of the tissue fluid interfacial value, while <200 μm are required for the same percentage drop at low concentration. Also, there are qualitative differences in the shape of the profiles. At low concentrations, the fully developed profile is log-linear, since metabolism dominates and is essentially linear in this concentration range. At high concentration, the profile is convex downward as a result of changes in the extent of saturation of metabolism.

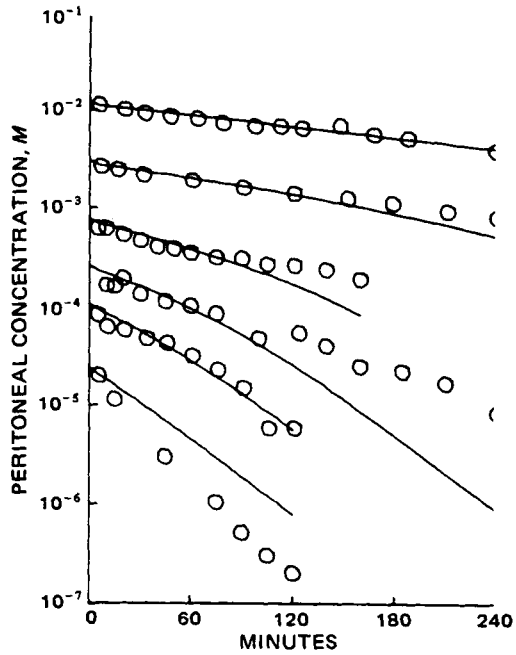

Figure 1—*Disappearance of fluorouracil from peritoneal fluid. Key: experimental data (O) plus simulations (—). Simulation parameters presented in Appendix II.*

DISCUSSION

The strong concentration-dependence of fluorouracil disappearance from peritoneal fluid is a novel observation and a challenge for pharmacokinetic modeling. It is likely that the peritoneal disappearance is

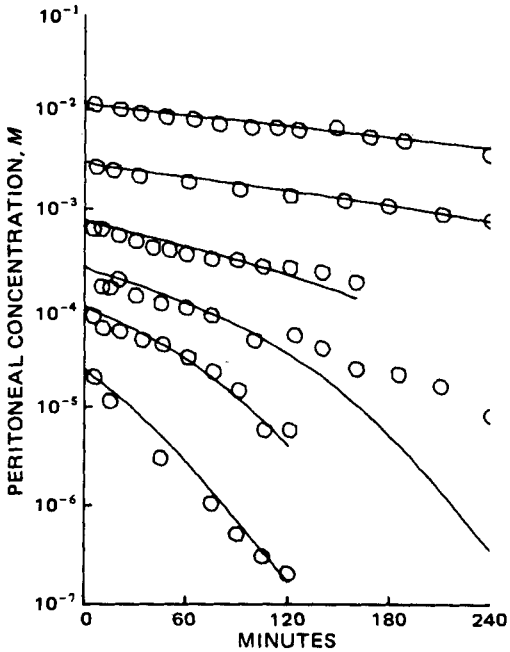

Figure 2—*Disappearance of fluorouracil from peritoneal fluid. Key: experimental data (O) plus simulations (—). Simulation parameters are the same as in Fig. 1, except that* K_M = 5 μM *and* V_{max} = 36 *nmole/min/g.*

[1] Analtech, Newark, Del.
[2] Obtained from the Developmental Therapeutics Program, National Cancer Institute.
[3] New England Nuclear, Boston, Mass.
[4] Dowex-1 anion exchange resin, BioRad, Richmond, Cal.
[5] Taconic Farms, Germantown, N.Y.
[6] Inpersol, Abbott Labs, North Chicago, Ill.
[7] Yellow Springs Instrument Co., Yellow Springs, Ohio.
[8] Such calculations would have limited usefulness in the absence of experimental data for tissue concentration profiles. These calculations would also be extremely expensive.

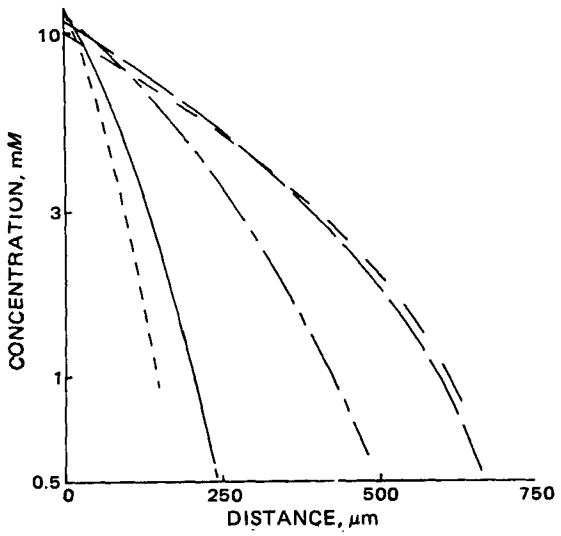

Figure 3—*Simulated time course for development of concentration profile in tissue. Initial concentration at interface is 12 m*M. *Key: (- - -) 30 seconds after dialysis fluid is added; (——) 1 min after; (— –) 5 min; (— —) 15 min; and (– – –) 30 min.*

a consequence of diffusion of drug into the surrounding tissue, where removal of fluorouracil by blood and metabolism by tissue enzymes are competing parallel processes. Although the drug is stable in peritoneal fluid itself, it is quite plausible that cells in the peritoneal membrane, and especially in the surrounding tissues, have sufficient enzyme capacity to account for the observed increase in fluorouracil disappearance at low concentrations. Both catabolic and anabolic enzymes for fluorouracil metabolism are widespread in body tissues, including abdominal organs (7, 9).

The selection of a modeling approach must be justified by the nature of the information obtained from the model. In the analysis of fluorouracil peritoneal disappearance data, there are two major items of interest: the depth to which the drug can penetrate into tissue and the relative role of removal by blood flow compared with metabolic elimination. Compartmental analysis is the major tool used in pharmacokinetic analysis. This approach consolidates areas of the body into regions in which the concentation is a function of time but not of anatomic position. Compartmental analysis cannot provide assistance for the two items outlined previously. Therefore, the next level of pharmacokinetic modeling has been utilized for the analysis of peritoneal uptake data, namely, direct consideration of positional variations in concentration.

Penetration distance is the crucial parameter for two major clinical questions which need to be answered regarding intraperitoneal therapy:

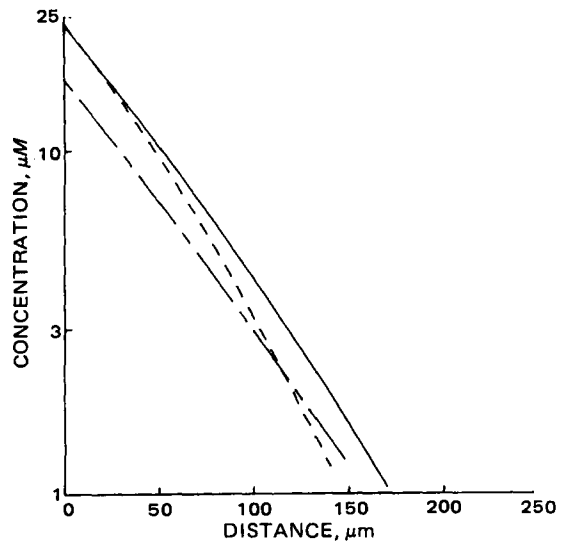

Figure 4—*Simulated time course for development of concentration profile in tissue. Initial concentration at interface is 24 μ*M. *Key: (- - -) 30 sec; (——) 1 min; (— –) 5 min after dialysis fluid is added.*

(a) How large a tumor will be exposed to drug levels which are in excess of those which can be achieved with systemic therapy. (b) Since GI mucosal cells are a major site for drug toxicity, what concentration can be administered safely, *i.e.*, does not cause penetration of high drug levels to these cells.

For comparative purposes, a penetration depth may be defined as the distance at which the tissue concentration has declined to some percentage of the interfacial concentration. As noted previously, the 5% penetration depth is a strong function of concentration: <200 μm for an interfacial concentration of 24 μM and >600 μm for 12 mM. Thus, not only are tissues exposed to higher concentrations as peritoneal fluid concentration is raised, but progressively deeper tissues are exposed. When referred to a typical cell diameter of 10 μm, these penetration distances are equivalent to a depth of 20–60 cells.

The second major question about peritoneal uptake concerns the relative roles for blood and metabolic removal. Fortunately, this question can be addressed without the specification of a particular geometry for tissue uptake. As long as the ratio of blood removal capacity to metabolic capacity is independent of position, some conclusions can be reached about their relative roles, regardless of the exact three-dimensional location of these processes in tissue. The dominant process is simply determined by a comparison of the removal terms in Eq. 2, $V_{max}/(K_M + C)$ *versus* PS/V. For the parameters given in Appendix II, the two removal processes are equally effective when C = 2.4 mM. At the highest concentration used in this study, 12 mM, blood flow removal is 5-fold greater than metabolic removal. However, as fluorouracil penetrates the tissue, its concentration is reduced until the dominant role is shifted to metabolism. In the linear range of metabolism ($K_M \ll C$) the rate of metabolism is 79 times as great as the rate of removal by flowing blood. The specific shape of the tissue concentration profile is dependent on model geometry, but the trends illustrated in Figs. 2 and 3 are generalized properties of distributed modeling.

Distributed models can be very useful in pharmacokinetics in special circumstances such as when there is a need for understanding the positional variation of concentration. Construction of distributed models requires information about kinetic properties as a function of position, and verification of distributed models requires experimental determination of concentration profiles in tissue. This combination of experimental data and distributed modeling is very rare. One excellent study describes the penetration of several anticancer drugs into brain tissue (10). However, there is no study in which a metabolized substance has been quantified. Indeed, the technology for exposing tissue to a rapidly metabolized drug and then quenching the metabolism and assaying for spatial variation in the concentration of the parent within ~200 μm probably does not exist.

Since the profile data are not available for fluorouracil, all quantitative aspects of the proposed model cannot be validated. The principal goal of this modeling effort has been to demonstrate the plausibility of a distributed model for the analysis of pharmacokinetic data. The model structure has been shown to be consistent with the peritoneal disappearance data, but no attempt has been made to choose the best model parameters based on statistical criteria. Despite its limitations, the distributed modeling process has given insight into the mechanisms of disappearance for fluorouracil and has suggested a strong dependence of penetration depth on peritoneal fluid concentration. Further experimental design could be guided by these results.

APPENDIX I

Distributed Model for Peritoneal Disappearance—The rate of disappearance of fluorouracil from peritoneal fluid can be governed by a variety of resistances to mass transport. The model which is described in this section is based on diffusion of fluorouracil through the extracellular space of peritoneal tissue. As will be discussed, there is no transcellular pathway, but intracellular drug is in equilibrium with extracellular concentration.

For a constant peritoneal fluid volume (V_{ip}), the rate of change of drug concentration in the peritoneal fluid (C_{ip}) depends on the diffusivity of the drug in surrounding tissue (D), the area available for transport (A), and the concentration gradient in the tissue at the tissue–fluid interface. The concentration in the surrounding tissue (C, extracellular or diffusible concentration) depends on both anatomic position and time. The diffusion problem has been represented by a one-dimensional model in which constant kinetic properties are assumed throughout the tissue; *i.e.*, diffusivity, capillary permeability (PS/V), maximum metabolic capacity (V_{max}), and half-saturating concentration (K_M). R is the ratio of intracellular to extracellular drug mass.

$$V_{ip}\frac{dC_{ip}}{dt} = -DA\left.\frac{\delta C(x,t)}{\delta x}\right|_{x=0} \quad \text{(Eq. 1)}$$

$$\frac{\delta C}{\delta t} = \frac{D}{R+1}\frac{\delta^2 C(x,t)}{\delta x^2} - \frac{1}{(R+1)}\frac{PS}{V}C(x,t) - \frac{1}{(R+1)}\frac{V_{max}C(x,t)}{K_M + C(x,t)} \quad \text{(Eq. 2)}$$

The term PS/V should be interpreted as effective capillary permeability, since tissue perfusion rate may also limit the rate of capillary removal. Metabolism is referred to extracellular fluorouracil concentration, since that was the basis in the hepatocyte parameter estimation (11).

Initially, the tissue concentration is zero throughout, and there is always some point ($x = x'$) where the gradient has vanished. As will be discussed, resistance to mass transfer posed by the peritoneal fluid is assumed to be negligible. Thus, the initial and boundary conditions are:

$$C_{ip}(0) = C(0,0) = C_0 \quad \text{(Eq. 3a)}$$

$$C(x,0) = 0 \quad \text{(Eq. 3b)}$$

$$\frac{\delta C(x',t)}{\delta x} = 0 \quad \text{(Eq. 3c)}$$

Resistance Within Peritoneal Fluid—The peritoneal fluid drug concentration, which is measured experimentally, is the bulk fluid concentration. The concentration at the interface between peritoneal fluid and tissue will be less than the bulk fluid concentration if the rate of drug transport in fluid is not much faster than the rate capacity of the tissue to take up drug. Resistance to drug transfer in the bulk fluid might be visualized as a stagnant layer adjacent to the tissue. Calculations for intraperitoneal fluorouracil based on stagnant layer thickness reported previously (12) suggest that this resistance is negligible at high concentrations and has a mild influence at low concentrations.

Diffusion Pathways—Drug diffusion through tissue may involve transcellular pathways in addition to extracellular movement. Several possibilities exist: (*a*) extracellular drug movement and very little, if any, intracellular uptake; (*b*) very rapid transcellular movement so that drug effectively moves through both pathways; and (*c*) moderate transcellular movement so that drug moves only extracellularly but equilibrates with intracellular space. The third option was selected based on a comparison of transfer rates through extracellular space, across cells, and across capillaries. A half-time for cellular uptake of fluorouracil of 40 sec or less can be calculated from reports for hepatoma cells (13), Ehrlich ascites cells (14), and L 1210 cells (15). Since the transcapillary exchange half-time of 140 sec, calculated from PS/V, is substantially slower, there is sufficient time for intracellular exchange and option (*a*) can be eliminated. The characteristic time (x^2/D) for extracellular diffusion is only 0.2 sec, based on a half-cell diffusion distance (5 μm) and a fluorouracil diffusivity of 1.2×10^{-6} cm^2/sec. Therefore, option (*b*) was eliminated since extracellular movement is very rapid compared to transcellular movement.

APPENDIX II

Parameter Selection—There are seven parameters in Eqs. 1 and 2. Since V_{ip} was experimentally set to 50 ml, six parameter values must be estimated:

1. Michaelis constant (K_M) was fixed at 30 μM. This value has been reported for fluorouracil metabolism in rat liver cells (11).
2. Maximum metabolic capacity per cubic centimeter of tissue (V_{max}) was fixed at 71 nmole/min/cm^3, a value which has been reported for rat liver tissue (11). Values of V_{max} or K_M for other tissues have not been reported.
3. Area of tissue available for flux (A) was set at 125 cm^2. If the measurements of Esperanca and Collins (16) of peritoneal surface area in human infants and adults are extrapolated using the 0.7 power of body weight to a 200-g rat, ~125 cm^2 is obtained.
4. Diffusivity (D) in tissue was estimated by the method of Schultz and Armstrong (12). First, aqueous diffusivity was estimated to be 10×10^{-6} cm^2/sec, based upon its molecular weight (17). Then the aqueous diffusivity was corrected for extracellular fluid fraction (0.3) and tortuosity (2.5) to yield a value of 1.2×10^{-6} cm^2/sec.
5. Capillary removal rate (PS/V) is the product of capillary permeability (P, cm/sec) and capillary surface per volume of tissue (S/V, cm^2/cm^3). Reported values of PS/V range from 0.004 sec^{-1} for the gastric wall of dogs for a hexose (18) to 7.6×10^{-4} sec^{-1} for glucose in muscle capillaries (19). Since 0.001 sec^{-1} is a reported value for tissue perfusion in rat muscle (20), the effective value for PS/V is limited by perfusion. A value of 5×10^{-4} sec^{-1} is consistent with these observations and provides reasonable agreement between the simulations and the data in the high-concentration concentration region where PS/V dominates.
6. The ratio (R) of intracellular to extracellular fluorouracil amount is calculated from the apparent distribution volume for fluorouracil and the extracellular fluid fraction of tissue. Based on a whole body distribution volume of 60% of body weight (4) and an extracellular fluid fraction of 0.3 (see item 4), an equal amount of drug is in the two spaces: $R = 1$.

REFERENCES

(1) G. Lukas, S. D. Brindle, and P. Greengard, *J. Pharmacol. Exp. Ther.*, **178**, 562 (1971).

(2) J. L. Speyer, P. H. Sugarbaker, J. M. Collins, R. L. Dedrick, R. W. Klecker, Jr., and C. E. Myers, *Cancer Res.*, **41**, 1916 (1981).

(3) J. L. Speyer, J. M. Collins, R. L. Dedrick, M. F. Brennan, A. R. Buckpitt, H. Londer, V. T. DeVita, Jr., and C. E. Myers, *ibid*, **40**, 567 (1980).

(4) J. M. Collins, R. L. Dedrick, F. G. King, J. L. Speyer, and C. E. Myers, *Clin. Pharmacol. Ther.*, **28**, 235 (1980).

(5) C. E. Myers, *Pharmacol. Rev.*, **33**, 1 (1981).

(6) B. A. Koechlin, F. Rubio, S. Palmer, T. Gabriel, and R. Duschinsky, *Biochem. Pharmacol.*, **15**, 435 (1966).

(7) N. K. Chaudhuri, K. L. Mukherjee, and C. Heidelberger, *Biochem. Pharmacol.*, **1**, 328 (1958).

(8) B. Carnahan, H. A. Luther, and J. O. Wilkes, "Applied Numerical Methods," Wiley, New York, N.Y., 1969, pp. 429–530.

(9) B. G. Gustavsson, A. Brandberg, C. G. Regardh, and O. E. Almersjo, *J. Pharmacokinet. Biopharm.*, **7**, 665 (1979).

(10) J. D. Fenstermacher, C. S. Patlak, and R. G. Blasberg, *Fed. Proc., Fed. Am. Soc. Exp. Biol.*, **33**, 2070 (1974).

(11) W. M. Williams and D. M. Kornhauser, *ibid.*, **38**, 259 (1979).

(12) J. S. Schultz and W. Armstrong, *J. Pharm. Sci.*, **67**, 696 (1978).

(13) R. M. Wohlhueter, R. S. McIvor, and P. G. Plagemann, *J. Cell. Physiol.*, **104**, 309 (1980).

(14) J. A. Jacquez, *Proc. Soc. Exp. Biol. Med.*, **109**, 133 (1962).

(15) D. Kessel and T. C. Hall, *Cancer Res.*, **29**, 1749 (1969).

(16) M. J. Esperanca and D. L. Collins, *J. Pediatric Surg.*, **1**, 162 (1966).

(17) N. A. Lassen and W. Perl, in "Tracer Kinetic Methods in Medical Physiology," Raven, New York, N.Y., 1979, p. 173.

(18) E. Renkin, *Circ. Res.*, **41**, 735 (1977).

(19) C. Crone and O. Christensen, in "Cardiovascular Physiology III," A. C. Guyton and D. B. Young, Eds., University Park Press, Baltimore, Md., 1979, Vol. 18, p. 172.

(20) K. B. Bischoff, R. L. Dedrick, D. S. Zaharko, and J. A. Longstreth, *J. Pharm. Sci.*, **60**, 1128 (1971).

Cardiac Stimulant Action of Constituents of *Aloe Saponaria*

AKIRA YAGI *x, SHOJI SHIBATA ‡, ITSUO NISHIOKA *, SHUICHI IWADARE ‡, and YUKISATO ISHIDA ‡

Received November 28, 1980, from the **Faculty of Pharmaceutical Sciences, Kyushu University, Maidashi, Higashi-ku, Fukuoka, Japan* and the ‡*School of Medicine, University of Hawaii, Honolulu, Hawaii.* Accepted for publication October 6, 1981.

Abstract □ A highly potent cardiotonic substance, calcium isocitrate, was isolated from *Aloe saponaria*, using solvent partition, nonionic porous resin, and gel permeation chromatographies. Cardiac stimulant activity of synthesized stereoisomers of calcium isocitrate was demonstrated in isolated guinea pig atria.

Keyphrases □ *Aloe Saponaria*—cardiac stimulation activity of various constituents, calcium isocitrate □ Calcium isocitrate—isolated from *Aloe saponaria*, cardiac stimulation of rabbit and rat, and guinea pig atria □ Stereoisomers—synthesis of calcium isocitrate stereoisomers, cardiac stimulation activity, rats, rabbits, guinea pigs

Aloe is a group of succulent plants native to dry areas, especially southern Africa. The leaves of *Aloe saponaria* have been used widely as folk medicine for various external and internal diseases such as burns, cuts, ulcers, and stomach disorders, *etc.* Aloin has been isolated from the plants as the major component (1) and is used as a purgative. While examining the antibacterial and antitumor activities of *Aloe* extracts (2), the cardioexcitatory effect of the extracts on the isolated atria was recently identified. The present experiments were undertaken to isolate the cardiotonic substances from *A. saponaria* and to evaluate their positive inotropic effects on isolated cardiac muscles.

EXPERIMENTAL

Materials[1]—Nonionic porous resin[2], anion exchange resin[3], dextran gel[4], dextran gel possessing both hydrophilic and lipophilic properties[5], and thin layer chromatography (TLC) aluminum sheets of silica gel[6] were purchased from suppliers. TLC was performed using butanol–ethanol–chloroform–28% ammonium hydroxide (4:5:2:8) and ethyl acetate–butanol–acetic acid–water (6:8:5:8) as solvent systems. Anisaldehyde–sulfuric acid and iodine were used as spraying reagents.

Chromatography—The flow rate for a column of resin[2] (4 × 6 cm) was ~20 ml/hr and for resin[3] (1.5 × 15 cm) was ~20 ml/hr. The gel filtration through dextran gel[4] (2.5 × 36 cm) and gel[5] (1.5 × 40 cm) was performed at room temperature at a flow rate of 21 ml/hr. The chromatography with silica gel[6] was performed through a column (2 × 22 cm).

Bioassay—Bioassay of compounds was performed on isolated atria of rat, rabbit, and guinea pig hearts. The atrium was separated from the rest of the heart and suspended in a 50-ml tissue bath containing Krebs-Ringer bicarbonate solution of the following composition (m*M*): sodium chloride, 120.3; potassium chloride, 4.8; calcium chloride, 1.2; magnesium sulfate, 1.3; potassium biphosphate, 1.2; sodium bicarbonate, 25.2; and glucose 5.5. The solution was continuously bubbled with a gas mixture of 95% oxygen and 5% carbon dioxide and maintained at 30°, pH 7.4. Tension was recorded isometrically through a force displacement transducer[7] and displayed on a polygraph[8]. In some experiments, spontaneously beating right atria were used; in other cases, the left atria were driven by an electrical stimulator[9] at a frequency of 1.0 Hz with square wave pulses of 5 msec at 100% above threshold voltage. The atria were allowed to equilibrate under 0.5-g tension for 60 min prior to beginning the experiment. The changes in contractile force and rate produced by the test agents are expressed as a percentage variation.

Extraction—The fresh leaves of *Aloe saponaria*[10] were harvested from the greenhouse of the herbal garden of Kyushu University. Fresh leaves (20 kg) were cut in half and colorless gelatinous pulp was separated carefully by scraping the green cortical layer which contained yellow phenolics. The homogenized pulp (6 kg) was extracted with distilled water, filtered, and the filtrate centrifuged at 10,000 rpm for 30 min. The supernate was dialyzed by dialysis membrane [11] against distilled water for 48 hr. The dialysate was flash evaporated at ≤50° to dryness (50 g).

Chromatography on Nonionic Porous Resin—The dialysate (4.4 g) suspended in methanol was chromatographed on a column of resin[2] (150 ml). After the methanolic eluate containing sugar moiety was excluded, the cardiac stimulant fraction was eluted with methanol–water (1:5) and water and evaporated to dryness.

Gel Permeation Chromatography—The crude extract dissolved in a small amount of water was reprecipitated by adding methanol to yield a colorless powder *A*. The colorless powder *A* (1 g) was chromatographed over dextran gel[4] (400 ml), using 3 ml of water as a solvent, and fractionated to fraction *A* (tube numbers 1–4) and Fraction *B* (tube numbers 5–10). Each fraction was flash evaporated to dryness and monitored by TLC. Fraction *B* (0.8 g) was further chromatographed over dextran gel[4] (400 ml), using 3 ml of water as a solvent, and fractionated to Fraction *C* (tube numbers 5–9, 0.3 g), and Fraction *D* (tube numbers 10–15, 0.2 g). Each fraction was flash evaporated to dryness and monitored by TLC.

Characterization of Compound I—Fraction *C* was reprecipitated from methanol to give a colorless powder, compound I, mp >290°, which had a strong absorption band due to carboxylate ion on IR spectrum, and presented a positive reaction to calcium ion (calcium oxalate). Compound I (1 g), dissolved in water (10 ml), was put on an anion exchange resin[3] column (20 ml) and eluted with water. The elution was continued until no residue was obtained in the flash evaporation. Then, 10% formic acid was passed through the column and the effluent was evaporated to dryness *in vacuo*. The residue (0.6 g) was chromatographed over dextran gel[5] using methanol as a solvent to give a colorless powder, compound I (free form). PMR (deuterium oxide) δ: 2.72(2H; d; d; J_{gem} = 16; J = 6, 10 Hz; —CH_2—CH_2—), 3.36(1H, m, —CH_2—CH—), 4.40(1H, d, J = 4 Hz, —CHOH—CH—). CMR (deuterium oxide) δ: 34.8(t, —CH_2—), 47.5(d, —CH—), 72.8(d, —CHOH—), 176.0, 179.0(s, COOH × 3). Compound I (free form, 40 mg) dissolved in methanol (10 ml) was methylated with diazomethane under ice cooling for 1 hr, and the reaction mixture was evaporated to dryness to yield a yellow oil (47 mg). The product was chromatographed over silica gel[7] using the solvent, ethyl acetate–chloroform (1:99), to give a colorless oil of the methyl ester (40 mg). $[\alpha]_D^{29}$ + 4.8°(*c*, 2.0 in chloroform). PMR (deuterochloroform) δ: 2.62(1H, d, d, J_{gem} = 18, J = 8 Hz, —CH_2—CH—), 2.90(1H, d, d, J_{gem} = 18, J = 8 Hz, —CH_2—CH—), 3.24(1H, d, J = 6 Hz, —CHOH—), 3.48(1H; sex; J = 8, 3 Hz; —CH—CH—CH_2—), 3.64, 3.66, 3.78($COOCH_3$ × 3), 4.32(1H; q; J = 6, 3 Hz; —CHOH—CH—). CMR (deuterium oxide) δ: 32.11(t, —CH_2—), 44.88(d, —CH—), 51.85, 52.15, 52.73(q, $COOCH_3$), 70.47(d,

[1] IR, PMR (tetramethylsilane as the internal standard), CMR (tetramethylsilane as the internal standard) and mass spectra were recorded using KOKEN DS-301, JEOL PS-100, JEOL FX-100, and JMS D-300, respectively. In the PMR descriptions, s = singlet, d = doublet, d,d = doublet of doublets, t = triplet, q = quartet, sex = sextet, and m = multiplet. Optical rotations were obtained on a JASCO DIP-4 and melting points were determined on a Yanagimoto melting point apparatus and are uncorrected.

[2] Amberlite XAD-2, Rohm and Hass Co. Ltd.

[3] Amberlite IRA-400 (OH^-), Rohm and Hass, Co. Ltd.

[4] Sephadex G-50, Pharmacia Fine Chemicals.

[5] Sephadex LH-20, Pharmacia Fine Chemicals.

[6] Merck 60.

[7] Grass model FT-03.

[8] Grass polygraph.

[9] Grass SD-5.

[10] A voucher specimen is available for inspection at Higashiyama Botanical Garden, Nagoya, Japan.

[11] Visking Co.

[12] Dowex 50W$_4$, Dow Chemical Co.

0022-3549/82/0700-0739$01.00/0

Table I—Positive Inotropic Effect of Fractions of *Aloe* Extracts on Isolated Atria

Fraction	Increase, % mean, (n = 2–3)	Concentration, mg/ml	Animal
Dialysate	35.8	0.5	rabbit
Nonionic porous resin[2]			
methanol–water (1:5)	550	1.0	rabbit
water	570	1.0	rabbit
Powder *A*	350	1.0	rat[b]
Fraction *A*[c]	220	1.0	rat
Fraction *C*[a,d]	243	3.0	rat
Fraction *D*[a,e]	88	3.0	rat
Isoproterenol	320	5×10^{-8} *M*	rabbit
Isoproterenol	250	5×10^{-8} *M*	rat

[a] Fraction *C* and *D* increased the heart rate 23.0–55.3%. [b] Tissues were beating spontaneously. Similar results were also observed on the electrically driven atria (1.0 Hz). [c] Fraction *A*: Mixture of calcium isocitrate, malate, succinate, *etc.* [d] Fraction *C*: Calcium isocitrate. [e] Fraction *D*: Calcium malate.

Table II—Positive Inotropic Effect of Various Synthesized Isocitrates on Guinea Pig Atria[a]

Compound[b]	Increase, %[c]	Concentration, mg/ml
(+)-Calcium isocitrate	30 ± 4	5×10^{-2}
	129 ± 16	10^{-1}
(±)-Calcium isocitrate	90 ± 8	5×10^{-2}
	171 ± 18	10^{-1}
(±)-Calcium alloisocitrate	115 ± 15	5×10^{-2}
	148 ± 8	10^{-1}
(+)-Calcium isocitrate[d]	132 ± 10	10^{-1}
Isoproterenol	330 ± 35	5×10^{-8} *M*

[a] Four atria from different animals were used for each experiment, mean ±*SE*. [b] All compounds caused no apparent change in heart rate. [c] Increase of norepinephrine, 10^{-6} mg/ml, 92%. [d] Isolated from *Aloe saponaria*.

—CHOH—), 170.9, 171.8, 172.9(s, $COOCH_3$). Mass spectrum *m/z*: 235($M^+ + 1$), 175($M^+ - 60$), 143($M^+ - 59, -32$), 115($M^+ - 60, -60$). The methyl ester was identified with methyl isocitrate (3, 4) by direct comparison (IR and TLC).

Characterization of Compound II—Fraction *D* (0.4 g) was reprecipitated from methanol to give a colorless powder, compound II, mp >290°, which had a strong absorption band due to a carboxylate ion on IR spectrum and presented a positive reaction to calcium ion (calcium oxalate). Compound II (1 g) dissolved in water (10 ml) was put on an anion exchange resin[3] column (20 ml) and eluted with water. The elution was continued until no residue was obtained in flash evaporation. Then, 10% formic acid was passed through the column and the effluent was evaporated to dryness *in vacuo*. The residue (170 mg) was chromatographed over dextran gel[5] (20 ml) using acetone as a solvent to give a colorless powder, compound II (free form, 50 mg) together with a small amount of Compound III and IV (free form). Compound II (free form) mp 101–102° (ethyl acetate), $[\alpha]_D^{20}$ −6.0° (*C*, 0.4 in acetone). IR (potassium bromide) cm^{-1}: 2800–2600 (hydroxyl), 1700 (carboxylic acid). PMR (deuteroacetone) δ: 2.74(2H; d; q, J_{gem} = 16 Hz; *J* = 8, 4 Hz; —CH_2—CH—), 4.50(1H; d; d; *J* = 8, 4 Hz; —CH—CH_2—), 7–8(3H, OH, COOH). Compound II (free form, 10 mg) dissolved in methanol (10 ml) was methylated with diazomethane under ice cooling for 1 hr, and the reaction product (12 mg) was chromatographed over silica gel[6] using the solvent, *n*-hexane–chloroform (1:1) to yield a colorless oil of methyl ester (10 mg). $[\alpha]_D^{21}$ −2.5° (*C*, 0.4 in chloroform). IR (liquid film) cm^{-1}: 3350 (hydroxyl), 1730(ester), 1440(methylene), 1100. PMR (deuterochloroform) δ: 2.66(1H, d, d, J_{gem} = 16, *J* = 5 Hz, —CH_2—), 3.25(1H, OH), 3.71, 3.81 ($COOCH_3$ × 2), 4.50(1H; d; d; *J* = 5, 5 Hz; —CHOH—CH_2—). CMR (deuterochloroform) δ: 38.38(—CH_2—), 51.91, 52.68($COOCH_3$ × 2), 67.09(CHOH), 170.56, 173.32(COOH × 2). Mass spectrum *m/z*: 163($M^+ + 1$), 103($M^+ - 59$). The methyl ester was identified with methyl malate by direct comparison (IR and TLC).

Characterization of Compound III—Compound III (free form) was obtained from Fraction *D*, which showed a positive reaction to calcium ion (calcium oxalate) by the following procedure for the isolation of Compound I (free form): mp 185° (acetone), IR (potassium bromide) cm^{-1}: 2800–2600(hydroxyl), 1700(carboxylic acid). PMR (deuteromethanol) δ: 2.56(2H, s, —CH_2—). CMR (deuteromethanol) δ: 29.77(—CH_2—), 175.78(COOH). Compound III (free form) was identified with succinic acid by direct comparison (IR and mixed melting point).

Characterization of Compound IV—Compound IV (free form) was obtained from the Fraction *D*, which showed a positive reaction to calcium ion (calcium oxalate) by the following procedure for the isolation of compound I (free form): mp 74–75° (ethyl acetate), $[\alpha]_D^{20}$ −6.8° (*C*, 6.6 in acetone), IR (potassium bromide) cm^{-1}: 2800–2600(hydroxyl), 1725(ester), 1440(methylene). PMR (deuterochloroform) δ: 2.86(2H; d; d; J_{gem} = 16; *J* = 8, 6 Hz; —CH_2—CH—), 2.80(3H, $COOCH_3$), 4.52(1H; q; *J* = 8, 6 Hz; —CH_2—CH—), 6.34(br, s, OH). CMR (deuteromethanol) δ: 38.32(—CH_2—), 52.80($COOCH_3$), 66.97(CHOH), 173.37($COOCH_3$), 174.60(COOH). Mass spectrum *m/z*: 149($M^+ - 17$), 103($M^+ - 45$), 89($M^+ - 59$). Based on the comparative study of CMR spectra the structure of compound IV (free form) was determined to be (−)-2-hydroxybutandiolic acid 4-methyl ester.

Syntheses of (±), (+) or (−)-Calcium Isocitrate and of (±)-Calcium Alloisocitrate—The following compounds were synthesized according to the literature (3):

(±)-*Isocitric Acid Lactone*—mp 156–158°[4] (ethyl acetate), PMR (deuterodimethyl sulfoxide) δ: 2.76(2H, d, *J* = 8 Hz), 3.70(1H; sex; *J* = 7.5, 8 Hz), 5.11(1H, d, *J* = 7.5 Hz), 10.5(2H, br).

(+)-*Isocitric Acid Lactone*—mp 152–153° (ethyl acetate), $[\alpha]_D^{26}$ +59.4° (*C*, 1.3 in water).

(−)-*Isocitric Acid Lactone*—mp 151–153° (ethyl acetate), $[\alpha]_D^{25}$ −53.0° (c, 1.1 in water).

(±)-*Alloisocitric Acid Lactone*—mp 155–157° (ethyl acetate), PMR (deuterodimethyl sulfoxide) δ: 2.75(2H, d, *J* = 7.5 Hz), 3.45(1H, m), 5.05(1H, d, *J* = 4.0 Hz), 9.70(2H, br).

(±)-Isocitric acid lactone (2.0 g) dissolved in 2 *N* NaOH (20 ml) was hydrolyzed at 90° for 3 hr and the reaction mixture was passed through cation exchange resin[12] (70 ml). Saturated calcium hydroxide solution was added to acidic eluate and the pH of the solution was made up to 9.0. After the filtration, the filtrate (200 ml) was concentrated to a 20 ml volume, and from the precipitate (±)-calcium isocitrate (2.78 g) was obtained. IR (potassium bromide) cm^{-1}: 3400, 1635, 1600, 1570, 1400, 1310, 1110, 1070. PMR (deuterium oxide–deuterium chloric acid) δ: 2.79(2H, d, *J* = 6.5 Hz), 3.46(1H, m), 4.50(1H, d, *J* = 3.9 Hz). Quantitative analysis of calcium ion for $(C_6H_5O_7)_2Ca_3 \cdot 5H_2O$: Calc. 20.43%. Found: 20.54%. In the same way as the formation of (±)-calcium isocitrate, (+),(−)-calcium isocitrate and (±)-calcium alloisocitrate were synthesized.

RESULTS AND DISCUSSION

Table I summarizes the cardiac stimulatory action (inotropic) of each fraction of *Aloe saponaria* extract after dialysis and chromatography using resin[2] and dextran gel[4]. The dialysate caused a positive inotropic action on isolated rabbit atria without any change in the diastolic tension. Pretreatment of atria with propranolol (10^{-6} *M*, a β-adrenoreceptor blocking agent) or phentolamine (10^{-6} *M*, an α-adrenoreceptor blocking agent) had no effect on the inotropic response to the dialysate. Thus, it is apparent that the cardiac stimulatory action of the dialysate and other extracts are not mediated through the stimulation of adrenergic receptors.

In the preliminary examinations on cellulose and silica gel chromatographs, using butanol–acetic acid–water (4:1:5) and butanol–ethanol–chloroform–28% ammonium hydroxide (4:5:2:8) as solvents, the inotropic substance in the dialysate was demonstrated to be a hydrophilic substance which is considerably stable for acid, alkaline, and heat treatments. Since the methanol eluate on resin[2] column chromatography failed to cause any inotropic effect, the fraction was completely excluded from active substances. Active components were obtained from the effluent of methanol–water (1:5) and water. Then, the gel filtration using dextran gel[4] was performed to give fractions of *A*, *C*, and *D*. From these fractions compounds I–IV were obtained. Each compound showed a single spot on TLC-2 and was determined to be a calcium salt of organic acid by the positive reaction to calcium ion. On the treatment with anion exchange resin[3], compound I or II provided an organic acid in the free form which did not cause any cardiac stimulation on the isolated rat atria. Thus, it is suggested that compounds I and II have cardiac stimulation action only in the form of calcium salts. The chemical and spectral examinations led to the conclusion that compounds I–IV are calcium salts of (+)-isocitric (3, 4), L-(−)-malic, succinic, and of (−)-2-hydroxybutandiolic acid 4-methyl ester, respectively. Calcium salts of the stereoisomers of isocitric acid were synthesized according to the literature (3) and the cardiotonic effect of these synthetic isomers and compound I on isolated atria were

carried out. As shown in Table II, calcium salts of (+), (±)-isocitric acid and (±)-alloisocitric acid caused a positive inotropic effect on isolated guinea pig atria to the same degree as compound I at a concentration of 10^{-4} g/ml, while no toxic effect such as arrhythmia was observed.

REFERENCES

(1) E. Leger, *Ann. Chim.*, **6**, 318 (1916).

(2) A. Yagi and I. Nishioka, The 2nd Symposium for Development and Application of Natural Products, 1978, Kyoto, Japan, p. 13.

(3) H. Katsura, *J. Chem. Soc. Jpn.*, **82**, 98 (1961).

(4) A. L. Patterson, C. K. Johnson, D. van der Helm, and J. A. Minkin, *J. Am. Chem. Soc.*, **84**, 309 (1962).

ACKNOWLEDGMENTS

The experiment was supported in part by a research grant from Banyu Pharmaceutical Co., Ltd.

The authors thank Mr. Y. Tanaka, Mr. I. Maetani, and Miss Y. Soeda for measurements of PMR, CMR, and mass spectra.

Antitumor Agents LIII: The Effects of Daphnoretin on Nucleic Acid and Protein Synthesis of Ehrlich Ascites Tumor Cells

I. H. HALL[x], K. TAGAHARA, and K. H. LEE

Received July 2, 1981, from the *Division of Medicinal Chemistry, School of Pharmacy, The University of North Carolina, Chapel Hill, NC 27514.* Accepted for publication October 7, 1981.

Abstract □ Daphnoretin, a dicoumaryl ether, has been shown to inhibit growth of Ehrlich ascites carcinoma cells. Dosing for three days at 6 mg/kg/day reduced the cell number per milliliter by 60%. *In vitro* DNA and protein synthesis studies demonstrated an $ID_{50} \cong 0.194$ m*M* and $ID_{50} \cong 0.340$ m*M*, respectively, for daphnoretin. Subsequently it has been shown that *in vivo* nucleic acid and protein synthesis were inhibited. Major sites in the DNA synthetic pathway inhibited significantly by daphnoretin were dihydrofolate reductase, orotidine monophosphate decarboxylase, thymidylate monophosphate kinase, and ribonucleotide reductase. Reduction of *in vitro* oxidative phosphorylation processes and acid hydrolytic enzymes were also inhibited in the presence of daphnoretin.

Keyphrases □ Daphnoretin—effects on nucleic acid and protein synthesis of Ehrlich ascites tumor cells, antitumor agent □ DNA—effects of daphnoretin, protein synthesis, Ehrlich ascites tumor cells □ Protein synthesis—effects of daphnoretin, DNA, Ehrlich ascites tumor cells □ Antitumor agents—the effects of daphnoretin on nucleic acid and protein synthesis of Ehrlich ascites tumor cells

Daphnoretin has been isolated from the whole plant of *Wikstroemia indica* C. A. Mey (Thymelaeaceae) (1), which is known as "Nan-Ling-Jao-Hua" or "Po-Lun" in Chinese folklore as a herbal remedy for the treatment of human syphilis, arthritis, whooping cough (2), and cancer (3). Daphnoretin was shown to have significant inhibitory activity *in vivo* against the Ehrlich ascites carcinoma growth in mice but did not demonstrate any activity against P-388 lymphocytic leukemia growth (4). A detailed examination of the effects of daphnoretin on nucleic acid and protein synthesis of Ehrlich ascites carcinoma cells is presented.

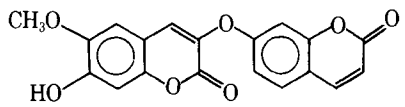

Daphnoretin

EXPERIMENTAL

CF_1 male mice (~30 g) were implanted with 2×10^6 Ehrlich ascites tumor cells intraperitoneally on day 0. Daphnoretin was suspended by homogenization in 0.05% polysorbate 80–water and 3–12 mg/kg ip was administered for 9 days to determine the inhibition of tumor growth. Mice were sacrificed on day 10, and the ascites fluid was collected from the peritoneal cavity. The volume and ascrit were determined for each animal and the inhibition of tumor growth was calculated (5). For the metabolic studies, mice were treated on days 7–9 with 6 mg/kg ip of daphnoretin. The animal was sacrificed on day 10 and the ascites fluid was harvested. The *in vitro* metabolic studies were performed at 0.340 m*M*.

In vitro incorporation of [^{3}H]thymidine, [^{3}H]uridine, or [^{3}H]leucine was determined using 10^6 Ehrlich ascites cells, 1 μCi labeled precursor, minimum essential medium, and varying final concentrations of drug from 0.035 to 0.35 m*M*. The tubes were incubated at 37° for 60 min and inactivated by trichloroacetic acid. The acid insoluble-labeled DNA was collected on glass filter discs[1], and RNA and protein were precipitated on nitrocellulose filters by vacuum suction (6). Results are expressed as disintegrations per minute of incorporated precursor per hour per 10^6 ascites cells.

For *in vivo* studies, incorporation of thymidine into DNA was determined by the method of Chae *et al.* (7). One hour prior to the animal sacrifice on day 10, 10 μCi of [6-^{3}H]thymidine (21.5 Ci/mmole, ip) were injected. The DNA was isolated and the tritium content was determined in a toluene based scintillation fluid[2]. The DNA concentration was determined by the diphenylamine reaction using calf thymus DNA as a standard. Uridine incorporation into RNA was determined using 10 μCi of [5,6-^{3}H]uridine (22.4 Ci/mmole). RNA was extracted by the method of Wilson *et al.* (8). Using yeast RNA as a standard, the RNA content was assayed by the orcinol reaction. Leucine incorporation into protein was determined by the method of Sartorelli (9) using 10 μCi of [4,5-^{3}H]leucine (52.2 Ci/mmole). Protein content was determined by the Lowry procedure using bovine serum albumin as a standard.

In vitro and *in vivo* nuclear DNA polymerase activity was determined on isolated Ehrlich ascites cell nuclei (10). The incubation was that described previously (11), except that [methyl-^{3}H]deoxythymidine triphosphate (82.4 Ci/mmole) was used. The acid insoluble nucleic acid was collected on filters and counted. Nuclear RNA polymerase activities were determined on enzymes isolated from nuclei. Messenger, ribosomal, and transfer RNA polymerase enzymes were isolated using 0.3, 0.04, and 0.0 *M* concentrations, respectively, of ammonium sulfate in magnesium chloride. The incubation medium was [^{3}H]uridine triphosphate (23.2 Ci/mmole) (12). The acid insoluble RNA was collected on nitrocellulose filters and counted.

Deoxythymidine, deoxythymidylate monophosphate, and diphosphate kinase activities were measured spectrophotometrically at 340 nm at 20

[1] GF/F glass filter discs.

[2] Fisher Scintiverse.

0022-3549/82/0700-0741$01.00/0

carried out. As shown in Table II, calcium salts of (+), (±)-isocitric acid and (±)-alloisocitric acid caused a positive inotropic effect on isolated guinea pig atria to the same degree as compound I at a concentration of 10^{-4} g/ml, while no toxic effect such as arrhythmia was observed.

REFERENCES

(1) E. Leger, *Ann. Chim.*, **6**, 318 (1916).

(2) A. Yagi and I. Nishioka, The 2nd Symposium for Development and Application of Natural Products, 1978, Kyoto, Japan, p. 13.

(3) H. Katsura, *J. Chem. Soc. Jpn.*, **82**, 98 (1961).

(4) A. L. Patterson, C. K. Johnson, D. van der Helm, and J. A. Minkin, *J. Am. Chem. Soc.*, **84**, 309 (1962).

ACKNOWLEDGMENTS

The experiment was supported in part by a research grant from Banyu Pharmaceutical Co., Ltd.

The authors thank Mr. Y. Tanaka, Mr. I. Maetani, and Miss Y. Soeda for measurements of PMR, CMR, and mass spectra.

Antitumor Agents LIII: The Effects of Daphnoretin on Nucleic Acid and Protein Synthesis of Ehrlich Ascites Tumor Cells

I. H. HALL[x], K. TAGAHARA, and K. H. LEE

Received July 2, 1981, from the *Division of Medicinal Chemistry, School of Pharmacy, The University of North Carolina, Chapel Hill, NC 27514.* Accepted for publication October 7, 1981.

Abstract □ Daphnoretin, a dicoumaryl ether, has been shown to inhibit growth of Ehrlich ascites carcinoma cells. Dosing for three days at 6 mg/kg/day reduced the cell number per milliliter by 60%. *In vitro* DNA and protein synthesis studies demonstrated an $ID_{50} \cong 0.194$ m*M* and $ID_{50} \cong 0.340$ m*M*, respectively, for daphnoretin. Subsequently it has been shown that *in vivo* nucleic acid and protein synthesis were inhibited. Major sites in the DNA synthetic pathway inhibited significantly by daphnoretin were dihydrofolate reductase, orotidine monophosphate decarboxylase, thymidylate monophosphate kinase, and ribonucleotide reductase. Reduction of *in vitro* oxidative phosphorylation processes and acid hydrolytic enzymes were also inhibited in the presence of daphnoretin.

Keyphrases □ Daphnoretin—effects on nucleic acid and protein synthesis of Ehrlich ascites tumor cells, antitumor agent □ DNA—effects of daphnoretin, protein synthesis, Ehrlich ascites tumor cells □ Protein synthesis—effects of daphnoretin, DNA, Ehrlich ascites tumor cells □ Antitumor agents—the effects of daphnoretin on nucleic acid and protein synthesis of Ehrlich ascites tumor cells

Daphnoretin has been isolated from the whole plant of *Wikstroemia indica* C. A. Mey (Thymelaeaceae) (1), which is known as "Nan-Ling-Jao-Hua" or "Po-Lun" in Chinese folklore as a herbal remedy for the treatment of human syphilis, arthritis, whooping cough (2), and cancer (3). Daphnoretin was shown to have significant inhibitory activity *in vivo* against the Ehrlich ascites carcinoma growth in mice but did not demonstrate any activity against P-388 lymphocytic leukemia growth (4). A detailed examination of the effects of daphnoretin on nucleic acid and protein synthesis of Ehrlich ascites carcinoma cells is presented.

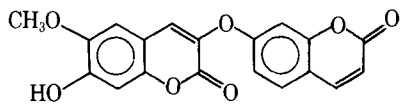

Daphnoretin

EXPERIMENTAL

CF_1 male mice (~30 g) were implanted with 2×10^6 Ehrlich ascites tumor cells intraperitoneally on day 0. Daphnoretin was suspended by homogenization in 0.05% polysorbate 80–water and 3–12 mg/kg ip was administered for 9 days to determine the inhibition of tumor growth. Mice were sacrificed on day 10, and the ascites fluid was collected from the peritoneal cavity. The volume and ascrit were determined for each animal and the inhibition of tumor growth was calculated (5). For the metabolic studies, mice were treated on days 7–9 with 6 mg/kg ip of daphnoretin. The animal was sacrificed on day 10 and the ascites fluid was harvested. The *in vitro* metabolic studies were performed at 0.340 m*M*.

In vitro incorporation of [^{3}H]thymidine, [^{3}H]uridine, or [^{3}H]leucine was determined using 10^6 Ehrlich ascites cells, 1 μCi labeled precursor, minimum essential medium, and varying final concentrations of drug from 0.035 to 0.35 m*M*. The tubes were incubated at 37° for 60 min and inactivated by trichloroacetic acid. The acid insoluble-labeled DNA was collected on glass filter discs[1], and RNA and protein were precipitated on nitrocellulose filters by vacuum suction (6). Results are expressed as disintegrations per minute of incorporated precursor per hour per 10^6 ascites cells.

For *in vivo* studies, incorporation of thymidine into DNA was determined by the method of Chae *et al.* (7). One hour prior to the animal sacrifice on day 10, 10 μCi of [6-^{3}H]thymidine (21.5 Ci/mmole, ip) were injected. The DNA was isolated and the tritium content was determined in a toluene based scintillation fluid[2]. The DNA concentration was determined by the diphenylamine reaction using calf thymus DNA as a standard. Uridine incorporation into RNA was determined using 10 μCi of [5,6-^{3}H]uridine (22.4 Ci/mmole). RNA was extracted by the method of Wilson *et al.* (8). Using yeast RNA as a standard, the RNA content was assayed by the orcinol reaction. Leucine incorporation into protein was determined by the method of Sartorelli (9) using 10 μCi of [4,5-^{3}H]leucine (52.2 Ci/mmole). Protein content was determined by the Lowry procedure using bovine serum albumin as a standard.

In vitro and *in vivo* nuclear DNA polymerase activity was determined on isolated Ehrlich ascites cell nuclei (10). The incubation was that described previously (11), except that [methyl-^{3}H]deoxythymidine triphosphate (82.4 Ci/mmole) was used. The acid insoluble nucleic acid was collected on filters and counted. Nuclear RNA polymerase activities were determined on enzymes isolated from nuclei. Messenger, ribosomal, and transfer RNA polymerase enzymes were isolated using 0.3, 0.04, and 0.0 *M* concentrations, respectively, of ammonium sulfate in magnesium chloride. The incubation medium was [^{3}H]uridine triphosphate (23.2 Ci/mmole) (12). The acid insoluble RNA was collected on nitrocellulose filters and counted.

Deoxythymidine, deoxythymidylate monophosphate, and diphosphate kinase activities were measured spectrophotometrically at 340 nm at 20

[1] GF/F glass filter discs.

[2] Fisher Scintiverse.

0022-3549/82/0700-0741$01.00/0

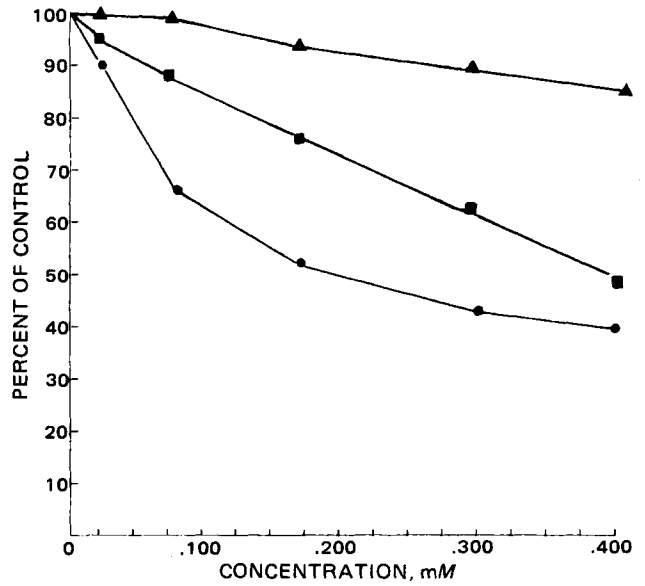

Figure 1—*The in vitro effects of daphnoretin on Ehrlich ascites nucleic acid and protein synthesis. Key: (●), [^{3}H]thymidine → DNA; (▲), [^{3}H]uridine → RNA; (■), [^{3}H]leucine → Protein.*

min using reduced nadide (0.1 μmole) (13). [6-^{3}H]Thymidine incorporation (21.5 Ci/mmole) into nucleotides was measured using the medium of Maley and Ochoa (13). The reaction medium was extracted with ether and the aqueous layer plated on polyethyleneiminecellulose plates and eluted with 0.5 *N* formic acid–0.6 *M* LiCl (1:1). Areas that correlated with the R_f values of thymidylate monophosphate, diphosphate, and triphosphate standards were scraped and counted.

Carbamyl phosphate synthetase activity was determined using the reaction medium of Kalman *et al.* (14) in the presence of ornithine and ornithine transcarbamylase. Citrulline formed from ornithine was measured at 490 nm by the method of Archibald (15). Aspartate transcarbamylase activity was assayed using the incubation medium of Kalman *et al.* (14). Colorimetric determination of carbamyl aspartate was conducted by the procedure of Koritz and Cohen (16). Orotidine monophosphate decarboxylase activity was assayed by the method of Appel (17) using 0.1 μCi of [^{14}C]orotidine monophosphate (34.9 mCi/mmole). The [^{14}C]carbon dioxide generated in 15 min was trapped in 1*M* KOH[3] and counted. Thymidylate synthetase activity was determined using a postmitochondrial supernate (9000×*g* for 10 min) and 5 μCi of [5-^{3}H]-deoxyuridine monophosphate (14 Ci/mmole) according to the method of Kampf *et al.* (18). [^{14}C]Formate incorporation into purines was determined by the method of Spassova *et al.* (19) using 0.5 μCi of [^{14}C]-formic acid (52.0 mCi/mmole). Purines were separated on silica gel TLC plates eluted with *n*-butanol–acetic acid–water (4:1:5).

After identifying R_f values consistent with the standards, adenine and guanine, the plates were scraped and the radioactive content determined. Phosphoribosyl-1-pyrophosphate amidotransferase activity was determined on a supernatant fraction (600×*g* for 10 min) measuring the reduction of 0.6 μmole of nadide at 340 nm for 30 min (20). Inosinic acid dehydrogenase activity was determined spectrophotometrically at 340 nm for 30 min using a supernatant fraction (600×*g* for 10 min). The assay medium was that of Magasanik, (21), which contained nadide. Dihydrofolate reductase activity was determined at 340 nm for 30 min as the oxidation of reduced nadide phosphate (22). Ribonucleotide reductase activity was determined by the method of Moore and Hurlbert (23) using [5-^{3}H]cytidine-5′-diphosphate (25 Ci/mmole). Ribose and deoxyribose nucleotide were separated on polyethyleneiminecellulose plastic precoated TLC plates eluted with 4% boric acid–4*M* LiCl (4:3) and scraped at the R_f values consistent with the standard deoxycytidine diphosphate.

In vivo phosphorylation of histones was determined by injecting 10 μCi of [γ-^{32}P]ATP (30.0 Ci/mmole) into mice 1 hr prior to sacrifice. The nuclei were isolated (10) and the histone chromatin protein was extracted by the method of Raineri *et al.* (24). *In vitro* nonhistone protein phosphorylation dependent on nuclear protein kinase was determined using 2.0 nmoles of [γ-^{32}P]ATP (30.0 Ci/mmole) and isolated nuclei chromatin protein was collected on nitrocellulose filters (25). Cyclic 3′,5′-adenosine monophosphate levels were determined by the radioimmunoassay method of Gilman (26) using a commercial kit.

In vitro oxidative phosphorylation studies (27) were conducted on Ehrlich ascites cells using the substrates, α-ketoglutarate or succinate. Basal oxygen consumption (State 4) was determined with an oxygen electrode connected to an oxygraph. The adenosine diphosphate was added to obtain State 3, or stimulated respiration. The number of microliters of oxygen consumed per hour per milligram of protein for States 3 and 4 were calculated. Deoxyribonuclease activity was measured at pH 5.0 by a modification of the de Duve method (28). Ribonuclease activity and acid cathepsin activity were determined at pH 5.0 by the method of Cho-Chung and Gullino (29). Protein content for the enzymatic assays was determined by the Lowry technique (30). UV studies between 210 and 340 nm for the binding of daphnoretin (20 μg/ml) to DNA (38 μg/ml) were performed in 0.1 *M* phosphate buffer, pH 7.2 (31) for 24 hr at room temperature.

[3] Hyamine hydroxide.

Table I—Antineoplastic Activity of Daphnoretin Against Ehrlich Ascites Tumor Growth

	N	Volume	Ascrit	Inhibition, %
Control	6	4.25	37.5	—
Daphnoretin				
3 mg/kg/day	6	0.08	59.5	97
6 mg/kg/day	6	0.16	35.0	96
12 mg/kg/day	6	0.45	36.2	90
6-Mercaptopurine	6	0.10	2.5	99

RESULTS

Daphnoretin successfully inhibited Ehrlich ascites growth at 3 mg/kg/day by 97%, at 6 mg/kg/day by 96%, and at 12 mg/kg/day by 90%. The normal number of Ehrlich ascites cells per milliliter on day 10 was 226 × 10^6. Daphnoretin treatment on days 7, 8, and 9 reduced the cell count by 60% (Table I).

Preliminary whole cell *in vitro* incorporation studies demonstrated that for DNA synthesis, the $ID_{50} \cong 0.194$ m*M* and for protein synthesis the $ID_{50} \cong 0.340$ m*M*. RNA synthesis was suppressed only marginally by daphnoretin *in vitro* demonstrating only 15% inhibition at 340 μmole (Fig. 1). Results from *in vitro* studies can be found in Table II, and results from *in vivo* studies can be found in Table III.

For the *in vivo* incorporation studies, the control values for 10-day Ehrlich ascites cells for thymidine incorporation into DNA were 107,533 dpm/mg of isolated DNA, 51,193 dpm/mg of isolated RNA for uridine incorporation, and 19,181 dpm/mg of isolated protein for leucine incorporation. After 3 days of dosing with daphnoretin at 6 mg/kg, DNA synthesis was reduced by 46%, RNA synthesis was suppressed by 42%, and protein synthesis was inhibited by 77%.

Nuclear DNA polymerase activity for the control was 76,528 dpm/hr/mg of nucleoprotein which was essentially unaffected by daphnoretin *in vitro* and was reduced by only 16% by *in vivo* administration of drug. Nuclear mRNA polymerase activity for the control was 4867 dpm/hr/mg of nucleoprotein, rRNA polymerase activity was 8751 dpm/hr/mg of protein, and tRNA polymerase activity was 10,792 dpm/mg of protein. Messenger RNA polymerase activity was suppressed by 10% *in vitro* and 17% *in vivo*, rRNA polymerase activity was elevated by 81% *in vitro* and 94% *in vivo*, and tRNA polymerase activity was reduced by 14% *in vitro* and 10% *in vivo*.

Ribonucleotide reductase activity for the control was 153,791 dpm/mg of protein which was suppressed by 31% *in vitro* and 39% *in vivo*. [^{14}C]-Formate incorporation into purines for the 10-day control was 28,786 dpm/mg of protein. Purine synthesis *in vitro* was inhibited by 32% and after drug administration for 3 days was suppressed by 30%. Phosphoribosyl pyrophosphate amidotransferase activity for the control was 0.544 optical density unit/hr/mg of protein. *In vitro* presence of drug resulted in a 39% reduction of enzymatic activity and *in vivo* administration of drug caused 31% suppression. Inosinic acid dehydrogenase activity for the control was 0.358 optical density unit/hr/mg of protein, reduced 19% by *in vivo* administration of drug. Dihydrofolate reductase activity for 10-day Ehrlich ascites cells was 0.514 optical density unit/hr/mg of protein which was inhibited by 53% *in vitro* and 59% *in vivo* by daphnoretin.

Carbamyl phosphate synthetase activity was 0.128 mg of carbamyl phosphate formed/hr/mg of protein for the control. Aspartate carbamyl transferase activity for 10-day Ehrlich ascites cells was 7.526 mg of car-

Table II—The *In Vitro* Effects of Daphnoretin at 340 μM Concentration on Ehrlich Ascites Cell Metabolism

Biochemical Parameter or Enzyme (n=6)	Percent Control: Control $\bar{x} \pm SD$	Percent Control: Treated $\bar{x} \pm SD$
DNA polymerase	100 ± 14	107 ± 9
mRNA polymerase	100 ± 13	90 ± 8
rRNA polymerase	100 ± 6	181 ± 10[a]
tRNA polymerase	100 ± 10	86 ± 7
Ribonucleotide reductase	100 ± 8	69 ± 4[a]
[^{14}C]Formic acid incorporation into purines	100 ± 7	68 ± 9[a]
Phosphoribosyl pyrophosphate amido transferase	100 ± 11	61 ± 6[a]
Inosinic acid dehydrogenase	100 ± 6	107 ± 7
Dihydrofolate reductase	100 ± 9	47 ± 7[a]
Carbamyl phosphate synthetase	100 ± 10	99 ± 8
Aspartate transcarbamylase	100 ± 12	100 ± 10
Orotidine monophosphate decarboxylase	100 ± 9	64 ± 5[a]
Thymidylate synthetase	100 ± 13	105 ± 7
Thymidine kinase	100 ± 9	75 ± 6[a]
Thymidylate monophosphate kinase	100 ± 8	26 ± 8[a]
Thymidylate diphosphate kinase	100 ± 10	83 ± 7
Acid deoxyribonuclease	100 ± 14	71 ± 13[a]
Acid ribonuclease	100 ± 19	73 ± 16
Acid cathepsin	100 ± 26	64 ± 22
[^{32}P]Phosphorylation of nonhistone proteins	100 ± 12	135 ± 8[a]
Oxidative phosphorylation processes		
Substrates:		
Succinate: State 4 respiration	100 ± 4	65 ± 6[a]
Succinate: State 3 respiration	100 ± 4	64 ± 4[a]
α-Ketoglutarate: State 4 respiration	100 ± 5	62 ± 7[a]
α-Ketoglutarate: State 3 respiration	100 ± 6	73 ± 5[a]

[a] $p \leq 0.001$.

bamyl aspartate formed/hr/mg of protein. Neither of these enzyme activities was affected by daphnoretin *in vitro* or *in vivo*. Orotidine monophosphate decarboxylase activity for the control was 10,775 dpm of $^{14}CO_2$ generated in 15 min/mg of protein. In the *in vitro* studies, decarboxylase activity was inhibited by 36%, and after drug administration *in vivo* the activity was reduced by 31%. Thymidylate synthetase activity for the control was 103,328 dpm/mg of protein which was unaffected by drug treatment. Thymidine kinase activity for the control was 0.531 optical density units/hr/mg of protein which was suppressed by 25% *in vitro* and 53% *in vivo*. Thymidylate monophosphate kinase activity for the control was 0.305 optical density units/hr/mg of protein inhibited by 74% *in vitro* and by 87% *in vivo*. Thymidylate diphosphate kinase activity for 10-day Ehrlich ascites cells was 0.238 optical density units/hr/mg of protein which was suppressed 17% *in vitro*, but daphnoretin had no effect *in vivo*. Thymidine incorporation studies into nucleotide showed that daphnoretin reduced the thymidylate monophosphate pools by 16%, thymidylate diphosphate pools by 53%, and thymidylate triphosphate levels by 45%. Deoxyribonuclease hydrolytic activity for day 10 Ehrlich ascites cells was 247 μg of DNA hydrolyzed/hr/mg of protein which was inhibited 29% *in vitro* by daphnoretin. Ribonuclease hydrolytic activity for control tumor cells was 43 μg of RNA hydrolyzed/hr/mg of protein which was suppressed 27% in the presence of drug. Cathepsin activity for the control was 869 μg of protein hydrolyzed/hr/mg of protein which was reduced 36% in the presence of daphnoretin.

The basal respiration (State 4) of day 10 Ehrlich ascites tumor cells with succinate as substrate was 5.273 μl of oxygen consumed/hr/mg of protein. Daphnoretin inhibited *in vitro* State 4 respiration 35% at 0.340 mM. Adenosine diphosphate stimulated (State 3) respiration was 8.752 μl of oxygen consumed/hr/mg of protein which was reduced 36% in the presence of daphnoretin. Using α-ketoglutarate as substrate resulted in

Table III—The *In Vivo* Effects of Daphnoretin at 6 mg/kg/day on Ehrlich Ascites Cell Metabolism

Biochemical Parameters or Enzymes (n=6)	Percent Control: Control 0.05% Polysorbate 80 $\bar{x} \pm SD$	Percent Control: Daphnoretin 6 mg/kg/day on Day 7, 8, and 9 $\bar{x} \pm SD$
[^{3}H]Thymidine incorporation into DNA	100 ± 8	63 ± 6[a]
[^{3}H]Uridine incorporation into RNA	100 ± 12	58 ± 4[a]
[^{3}H]Leucine incorporation into protein	100 ± 13	23 ± 3[a]
Number cells × 10^6/ml ascites fluid	100 ± 10	40 ± 6[a]
DNA polymerase	100 ± 6	84 ± 5[a]
mRNA polymerase	100 ± 12	83 ± 8[b]
rRNA polymerase	100 ± 8	194 ± 9[a]
tRNA polymerase	100 ± 9	90 ± 10[a]
Ribonucleotide reductase	100 ± 8	61 ± 7[a]
[^{14}C]Formic acid incorporation into purines	100 ± 12	70 ± 8[a]
Phosphoribosyl pyrophosphate amido transferase	100 ± 9	78 ± 3[a]
Inosinic acid dehydrogenase	100 ± 10	81 ± 9[a]
Dihydrofolate reductase	100 ± 12	41 ± 9[a]
Carbamyl phosphate synthetase	100 ± 10	104 ± 11
Aspartate transcarbamylase	100 ± 9	98 ± 8[a]
Orotidine monophosphate decarboxylase	100 ± 10	69 ± 7[a]
Thymidylate synthetase	100 ± 9	112 ± 11[a]
Thymidine kinase	100 ± 9	46 ± 8[a]
Thymidylate monophosphate kinase	100 ± 9	13 ± 4[a]
Thymidylate diphosphate kinase	100 ± 7	103 ± 9[a]
[^{32}P]Phosphorylation of histones	100 ± 15	64 ± 8[a]
[^{32}P]Phosphorylation of nonhistones	100 ± 13	206 ± 11[a]
Cyclic adenosine monophosphate levels	100 ± 10	117 ± 8

[a] $p \leq 0.001$. [b] $p \leq 0.005$.

a State 4 respiration of 3.569 μl of oxygen consumed/hr/mg of protein and in State 3 respiration of 5.156 μl of oxygen consumed/hr/mg of protein. In the presence of daphnoretin, State 4 respiration was reduced by 38% and State 3 was reduced by 27%. Histone phosphorylation of chromatin proteins for the control was at the rate of 3650 dpm/mg of isolated chromatin protein which was inhibited 36% after *in vivo* administration of daphnoretin. Nonhistone phosphorylation of chromatin proteins for the control was 28,593 dpm/mg of chromatin protein isolated, which was elevated 35% *in vitro* and 106% *in vivo*. Cyclic adenosine monophosphate levels for 10-day Ehrlich ascites cells was 3.65 pmoles/10^6 cells which was elevated 17% after daphnoretin administration for 3 days. The *in vitro* UV studies demonstrated that the spectrum of DNA and daphnoretin when present together caused a hyperchromic shift of DNA. However, there were no new peaks nor any shift to a higher wavelength, which probably suggests nonspecific binding of daphnoretin to DNA.

DISCUSSION

Daphnoretin significantly inhibited Ehrlich ascites tumor growth in CF_1 mice. DNA synthesis was inhibited at a low dose of daphnoretin, whereas protein synthesis was inhibited at a higher concentration. However, protein synthesis was inhibited to a greater degree than DNA synthesis after *in vivo* drug administration. The major enzymatic sites of inhibition by daphnoretin which could reduce DNA synthesis were thymidine kinase, thymidylate monophosphate kinase, ribonucleotide reductase, and dihydrofolate reductase. The reduction in enzymatic activity at any of these biochemical sites would be of sufficient magnitude to account for the degree of suppression of total DNA synthesis. Other minor sites of enzyme reduction are orotidine monophosphate decarboxylase, phosphoribosyl amidotransferase, and inosinic acid dehydrogenase as well as the incorporation of formic acid into purines and phosphorylation of histones. The magnitude of inhibition of the regulatory enzyme phosphoribosyl amido transferase of the purine pathway is of the same magnitude of reduction observed in the formate incorporation.

Daphnoretin also suppressed oxidative phosphorylation processes at 0.340 m*M*. Using the substrate succinate, which is a flavine adenine dinucleotide-linked dehydrogenase, daphnoretin suppressed basal and adenosine diphosphate stimulated respiration. The same was also true when using α-ketoglutarate, a nadide-linked dehydrogenase. Loss of energy from oxidative phosphorylation processes could account for the reduction of kinase activity of tumor cells since kinase reactions require ATP.

Daphnoretin reduced the catalytic enzyme activities responsible for the hydrolysis of nucleic acids and proteins. Elevation of the activities of these acid hydrolytic enzymes by the drug could account for the reduction of incorporation of radiolabeled precursors into nucleic acid or proteins. However, no elevation was observed with daphnoretin.

High cellular proliferation is associated with an increase in histone phosphorylation. As can be seen, daphnoretin reduced phosphorylation of chromatin histones (32). Although daphnoretin caused only a slight increase in cyclic adenosine monophosphate levels, elevated levels are associated with cessation of cellular division and reversal of tumor morphology to a normal state (33). A detailed study on the mechanism of protein synthesis inhibition has been reported (30).

REFERENCES

(1) K. H. Lee, K. Tagahara, H. Suzuki, R. Y. Wu, M. Haruna, I. H. Hall, and H. C. Huang, *J. Nat. Prod.*, **44**, 530 (1981).

(2) W. S. Kan, in "Pharmaceutical Botany," National Research Institute of Chinese Medicine, Taiwan, Republic of China, 1969, p. 391.

(3) A. Kato, Y. Hashimoto, and M. Kidokoro, *J. Nat. Prod.* **42**, 159 (1979).

(4) S. J. Torrance, J. J. Hoffmann, and J. R. Cole, *J. Pharm. Sci.*, **68**, 664 (1979).

(5) C. Piantadosi, C. S. Kim, and J. L. Irvin, *ibid.*, **58**, 821 (1969).

(6) L. L. Liao, S. M. Kupchan, and S. B. Horwitz, *Mol. Pharmacol.*, **12**, 167 (1976).

(7) C. B. Chae, J. L. Irvin, and C. Piantadosi, *Proc. Am. Assoc. Cancer Res.*, **9**, 44 (1968).

(8) R. G. Wilson, R. H. Bodner, and G. E. MacHorter, *Biochim. Biophys. Acta*, **378**, 260 (1975).

(9) A. C. Sartorelli, *Biochem. Biophys. Res. Commun.*, **27**, 26 (1967).

(10) W. C. Hymer and E. L. Kuft, *J. Histochem. Cytochem.*, **12**, 359 (1964).

(11) S. Shirakawa, T. Nakumura, and G. Wakisaka, *Can. Res.*, **34**, 3341 (1974).

(12) K. M. Anderson, I. S. Mendelson, and G. Guzik, *Biochim. Biophys. Acta.*, **383**, 56 (1975).

(13) F. Maley and S. Ochoa, *J. Biol. Chem.*, **233**, 1538 (1958).

(14) S. M. Kalman, P. H. Duffield, and T. Brzozuski, *J. Biol. Chem.*, **241**, 1871 (1966).

(15) R. M. Archibald, *J. Biol. Chem.*, **156**, 121 (1944).

(16) S. B. Koritz and P. P. Cohen, *ibid.*, **209**, 145 (1954).

(17) S. H. Appel, *ibid.*, **243**, 3929 (1968).

(18) A. Kampf, R. L. Barfknecht, P. J. Schaffer, S. Osaki, and M. P. Mertes, *J. Med. Chem.*, **19**, 903 (1976).

(19) M. K. Spassova, G. C. Russev, and E. V. Golovinsky, *Biochem. Pharmacol.*, **25**, 923 (1976).

(20) J. B. Wyngaarden and D. M. Ashton, *J. Biol. Chem.*, **234**, 1492 (1959).

(21) B. Magasanik, *Methods Enzymol.*, **6**, 106 (1963).

(22) M. K. Ho, T. Hakalo, and S. F. Zakrzwski, *Cancer Res.*, **32**, 1023 (1972).

(23) E. G. Moore and R. B. Hurlbert, *J. Biol. Chem.*, **241**, 4802 (1966).

(24) A. Raineri, R. C. Simsiman, and R. K. Boutwell, *Cancer Res.*, **33**, 134 (1973).

(25) Y. M. Kish and L. J. Kleinsmith, *Methods Enzymol.*, **40**, 201 (1975).

(26) A. C. Gilman, *Proc. Natl. Acad. Sci. USA*, **67**, 305 (1970).

(27) I. H. Hall, K. H. Lee, and S. A. ElGebaly, *J. Pharm. Sci.*, **67**, 552 (1978).

(28) I. H. Hall, K. S. Ishaq, and C. Piantadosi, *ibid.*, **63**, 625 (1974).

(29) Y. S. Cho-Chung and P. M. Gullino, *J. Biol. Chem.*, **248**, 4743 (1973).

(30) O. H. Lowry, N. J. Rosebrough, A. L. Farr, and R. J. Randall, *ibid.*, **193**, 265 (1951).

(31) K. H. Lee, I. H. Hall, E. C. Mar, C. O. Starnes, S. A. ElGebaly, T. G. Waddell, R. I. Hadgnaft, C. G. Ruffner, and I. Weidner, *Science* **196**, 533 (1977).

(32) C. S. Rubin and O. M. Roseu, *Ann. Rev. Biochem.*, **44**, 81 (1975).

(33) T. Posternak, *Ann. Rev. Pharmacol.*, **14**, 23 (1974).

ACKNOWLEDGMENTS

Supported by American Cancer Society Grant CH-19 and National Cancer Institute Grant CA-26466.

The authors thank Larry Carpenter, Mary Dorsey, Jerry McKee, and Melba Gibson for technical assistance on this project.

Antitumor Agents LIV: The Effects of Daphnoretin on *In Vitro* Protein Synthesis of Ehrlich Ascites Carcinoma Cells and Other Tissues

Y. F. LIOU, I. H. HALL ˣ, and K. H. LEE

Received July 2, 1981, from the *Division of Medicinal Chemistry, School of Pharmacy, University of North Carolina at Chapel Hill, Chapel Hill, NC 27514.* Accepted for publication October 7, 1981.

Abstract □ Daphnoretin has been shown to suppress Ehrlich ascites carcinoma growth in mice. One of the modes of action of the drug is to block protein synthesis; however, the inhibition of protein synthesis requires a higher concentration of drug than the inhibition of DNA synthesis. The inhibition of protein synthesis appears to occur during the elongation step with the drug preferentially binding to free ribosomes not engaged in active protein synthesis.

Keyphrases □ Daphnoretin—effects on *in vitro* protein synthesis of Ehrlich ascites carcinoma cells □ Antitumor agents—daphnoretin, effects on *in vitro* protein synthesis of Ehrlich ascites carcinoma cells □ Protein synthesis—effects of daphnoretin on *in vitro* protein synthesis of Ehrlich ascites carcinoma cells

Daphnoretin dicoumaryl ether, has been isolated from *Daphne mezereum* and *Wikstroemia indica* (Thymelaeaceae) (1–4). Daphnoretin, 3 to 12 mg/kg, has been demonstrated to significantly inhibit Ehrlich ascites carcinoma growth. Daphnoretin inhibited leucine incorporation into protein by 77% after administration of the drug at 6 mg/kg/day for 3 days. *In vitro* studies of leucine incorporation into protein of Ehrlich ascites cells demonstrated an $ID_{50} \cong 0.340$ m*M* (5). A more detailed study of the mechanism of protein synthesis inhibition is reported at this time.

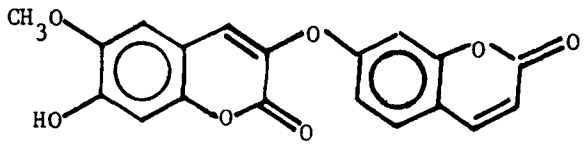

Daphnoretin

EXPERIMENTAL

The Ehrlich ascites tumor cell line was maintained in CF_1 male mice (~30 g). The tumor cells were harvested from mice on Day 10, which were inoculated on Day 0 with 2×10^6 Ehrlich ascites cells. The Ehrlich ascites lysates were prepared by an analogous method as outlined by Kruh *et al.* (6). The following were isolated from Ehrlich ascites lysates by literature techniques: runoff ribosomes (7), pH 5.0 enzymes (6), and uncharged transfer RNA (8). The Ehrlich ascites carcinoma initiation factors for protein synthesis were prepared as described by Majumdar *et al.* (9). The [^{3}H]methionyl tRNA was prepared from Ehrlich ascites cell tRNA according to the method of Takeishi *et al.* (10).

The effects of daphnoretin on endogenous protein synthesis of Ehrlich ascites cells (11) was carried out in a reaction medium (0.5 ml) containing 10 m*M* tromethamine (pH 7.6), 76 m*M* KCl, 1 m*M* ATP, 0.2 m*M* guanosine triphosphate, 15 m*M* creatine phosphate, 2 m*M* $MgCl_2$, 1 m*M* dithiothreitol, 0.1 m*M* of each of the 19 essential amino acids, 0.9 mg/ml of creatine phosphokinase, and 20 μCi of [^{3}H]leucine (56.6 Ci/mmole). An aliquot of the reaction mixture was incubated at 30°. After 5 min of incubation, test drugs or the standards, pyrocatechol violet or emetine, were added with a final concentration of 50, 100, and 500 μ*M*. At 1-min intervals, 50-μl aliquots were removed from the reaction tubes and spotted on filter papers[1], which were treated for 10 min in boiling 5% trichloroacetic acid, followed by 10 min in cold 5% trichloroacetic acid and washed with cold 5% trichloroacetic acid, ether–ethanol (1:1), and finally, ether. The filter papers were dried and counted in scintillation fluid[2].

The effects of daphnoretin, pyrocatechol violet, cycloheximide, and emetine on the ribosome profile and leucine incorporation (11) of Ehrlich ascites cell lysates were assayed using a reaction medium (500 μl) described previously. Following drug addition with a 100 μ*M* final concentration, the reaction was incubated for 4 min at 37°. The reaction was terminated by placing the tubes in ice and gradient buffer (1 ml of tromethamine, pH 7.6; 10 m*M* KCl; and 1.5 m*M* $MgCl_2$-$6H_2O$) was added. The mixture was layered over 36 ml of 10–25% linear sucrose gradient (11), prepared in gradient buffer, and centrifuged for 165 min at 25,000 rpm[3] at 4°. The absorbance profile at 260 nm was determined using a flow cell (light path of 0.2 cm) attached to a spectrophotometer[4]. Each gradient was fractionated into 1-ml aliquots. The protein was precipitated by trichloroacetic acid and counted.

The reaction medium for the polyuridine directed polyphenylalanine synthesis (12) contained 50 m*M* tromethamine (pH 7.6), 12.5 m*M* magnesium acetate, 80 m*M* KCl, 5 m*M* creatine phosphate, 0.05 mg/ml of creatine phosphokinase, 0.36 mg/ml of polyuridine[5] ($A_{280}/A_{260} = 0.34$), 0.5 μCi of [^{14}C]phenylalanine (536 mCi/mmole), 75 μg of uncharged Ehrlich ascites cell tRNA, 70 μg of Ehrlich ascites pH 5 enzyme preparation, and 0.9 A_{260} of Ehrlich ascites cell runoff ribosomes. Daphnoretin was present from 0.038–0.570 mmole final concentrations. Incubations were for 20 min at 30° after which a 35-μl aliquot was spotted on filter paper[1] and processed as indicated previously.

The reaction medium (200 μl) used to measure the formation of the 80S initiation complex and the methionyl puromycin reaction (13) contained 15 m*M* tromethamine (pH 7.6), 80 m*M* KCl, 1 m*M* ATP, 0.5 m*M* guanosine triphosphate, 20 m*M* creatine phosphate, 0.2 mg/ml of creatine phosphokinase, 3 m*M* magnesium acetate, 0.1 m*M* edetic acid, 1 m*M* dithiothreitol, 0.1 m*M* of each of the 19 essential amino acids, 3 mg of Ehrlich ascites cell lysates, 100 μg/ml of chlortetracycline[6], 3×10^5 cpm

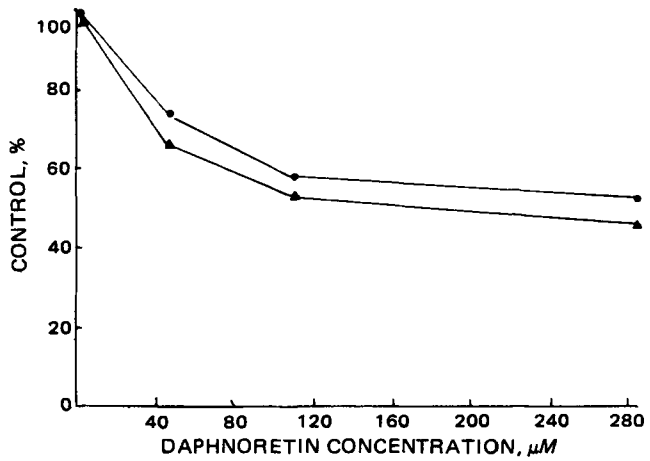

Figure 1—In vitro *effect of daphnoretin on whole cells of Ehrlich ascites protein synthesis. Key: (●), 60-min incubation; (▲), 90-min incubation.*

[1] Whatman No. 3.

[2] Scintiverse, Fisher Scientific Co.
[3] Beckman SW27 rotor.
[4] Gilford.
[5] Miles Laboratory, Inc.
[6] Sigma Chemical Co.

0022-3549/82/0700-0745$01.00/0

Table I—Effects of Daphnoretin on Ternary and 80S Complex Formation

	Concentration, μM	Complex Formation, pmoles	Control, %
Ternary Complex Formation			
Control		0.84	100
+ Aurintricarboxylic Acid	100	0.04	5
+ Emetine	100	0.74	89
+ Pyrocatechol Violet	100	0.10	12
+ Daphnoretin	280	0.78	94
+ Daphnoretin	560	0.76	90
80S Initiation Complex Formation			
Control	—	0.44	100
+ Aurintricarboxylic Acid	100	.05	11
+ Emetine	100	.44	100
+ Pyrocatechol Violet	100	.15	35
+ Daphnoretin	280	.42	96
+ Daphnoretin	560	.41	94

of methionine tRNA and 20 μg/ml of polyadenosine–uridine–guanosine and daphnoretin (560 μmole). The incubation was carried out at 23° and after 2 min, aliquots were withdrawn to analyze for the 80S complex formation. Puromycin (10 μg/ml) then was added to the reaction medium. The incubation was continued for another 6 min, and aliquots were withdrawn to analyze for the reaction of the 80S complex with puromycin. All aliquots (50 μl) were diluted to 250 μl of buffer (20 mM tromethamine, pH 7.6; 80 mM KCl; 3 mM magnesium acetate; 1 mM dithiothreitol; and 1 mM edetic acid), layered on 11.8 ml of 15–30% linear sucrose gradient and centrifuged for 3 hr at 36,000 rpm[7]. Fractions (0.4 ml) were collected and precipitated with 10% trichloroacetic acid on filter papers and counted.

The reaction mixtures (75 μl) for the ternary complex formation (14) contained 21.4 mM tromethamine (pH 8.0), 80 mM KCl, 0.26 mM guanosine triphosphate, 2.14 mM dithiothreitol, 10 μg of bovine serum albumin, 5 pmoles of Ehrlich ascites cell [^{3}H]methionyl-tRNA (met-tRNA$_f$) (1×10^4 cpm), 100 A_{260}/ml of crude Ehrlich ascites cell initiation factors, and 560 μM of drug or standards. The incubation was conducted for 5 min at 37° and terminated by the addition of 3 ml of cold buffer (21.4 mM tromethamine, pH 8.0, 80 mM KCl, 2.14 mM dithiothreitol). The samples were filtered through 0.45-μm nitrocellulose filters, washed twice in buffer, and counted.

The reaction mixture (75 μl) for the 80S initiation complex formation (14) contained, in addition to the components necessary for the ternary complex formation reaction, 1.9 mM magnesium acetate, 5 A_{260}/ml polyadenosine–uridine–guanosine and 100 A_{260}/ml of 80S Ehrlich ascites ribosomes. Incubations were conducted for 10 min at 37° and were then cooled to 4° and titrated to 5 mM with magnesium acetate. After 5 min at 4°, the samples were diluted with cold buffer (21.4 mM tromethamine, pH 8.0, 80 mM KCl, and 5 mM magnesium acetate and 2.14 mM dithiothreitol), and filtered as indicated for the ternary complex formation experiment.

Amino acid-tRNA activation steps were determined by the method of Moldave (15). The reaction medium contained 0.1 mM tromethamine (pH 7.4), 0.2 mM ATP, 0.3 mg/ml of pH 5 enzyme from Ehrlich ascites cells, and 2.5 μCi of [^{14}C]phenylalanine (536 mCi/mmole), [^{3}H]leucine (56.5 Ci/mmole) or [^{3}H]methionine (80.0 Ci/mmole) in a total volume of 1 ml. After incubation at 37° for 20 min, 2 ml of ice cold 10% trichloroacetic acid was added and the activated amino acid-tRNA were collected on nitrocellulose filters by suction.

P-388 lymphocytic leukemia cells and L-1210 lymphocytic lymphoma cells were obtained from DBA/2 male mice donors (~30 g). B-16 melanoma and Lewis lung tumor cells were obtained from C_{57}B1/6 male mice donors (~30 g). Antineoplastic tumor screens were conducted according to National Institutes of Health protocols (16). The Ehrlich ascites carcinoma tumor was maintained in CF_1 male mice.

Normal tissues (*i.e.*, liver, lung, brain, and kidney) were excised from CF_1 male mice (~30 g) and homogenized in 0.25 M sucrose and 0.001 M edetic acid.

[6-^{3}H]Thymidine (21.5 Ci/mmole) or [4,5-^{3}H]leucine (52.2 Ci/mmole) was incorporated *in vitro* into normal tissues and tumors using 1 μCi of labeled precursor and minimum essential medium with 10% fetal calf serum with drug concentrations varying from 0.042–0.340 mM. The tubes were incubated for 60 min at 37° (11). The acid insoluble DNA was collected on glass filter discs[8] and protein was collected on nitrocellulose filters by vacuum suction. Results are expressed as disintegrations per minute of incorporated precursors per hour per 10^6 cells or 10 mg of wet tissue.

[7] Beckman SW 40 rotor.

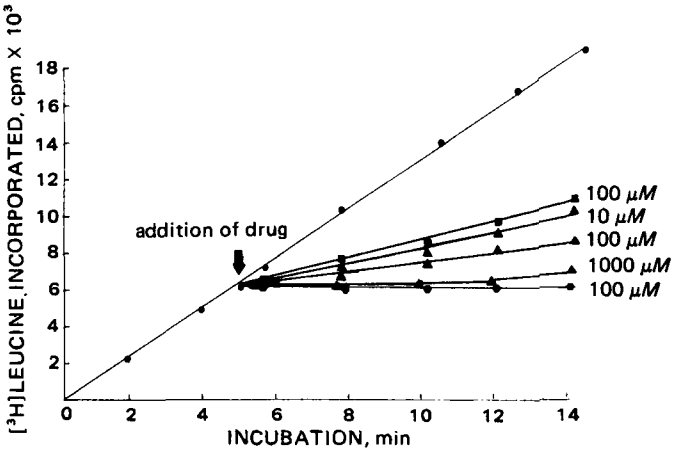

Figure 2—*Effect of pyrocatechol violet, emetine, and daphnoretin on the protein synthesis of Ehrlich ascites homogenates using endogenous messenger RNA. Key: (●) control; (■) pyrocatechol violet; (▲) daphnoretin; (●) emetine.*

RESULTS

The Ehrlich ascites whole-cell incubation studies demonstrated that daphnoretin, after 60 min of incubation, caused 50% inhibition at 240 μM and, after 90 min of incubation, 50% inhibition was achieved at 182 μM (Fig. 1). Twenty-eight percent suppression could be achieved at 560 μM concentration after 90-min incubation. The effect of daphnoretin on protein synthesis was compared to known inhibitors of protein synthesis (pyrocatechol violet is an initiation inhibitor that allows completion of the ongoing round of protein synthesis and causes accumulation of free 80S ribosomes, whereas emetine and cycloheximide are elongation inhibitors which freeze the ribosomes of the mRNA). When daphnoretin (50–500 μM) is added to the Ehrlich ascites lysate actively engaged in protein synthesis, there is a slight lag before inhibition of protein synthesis is effected (Fig. 2). Pyrocatechol violet demonstrated an even longer lag time, whereas emetine caused immediate inhibition of protein synthesis. The effect of daphnoretin, pyrocatechol violet, and cycloheximide on the ribosome profile and leucine incorporation can be seen in Fig. 3. Emetine induces the breakdown of the 80S polysome similar to the control, whereas pyrocatechol violet and daphnoretin allow the accumulation of the 80S ribosomal peak. Daphnoretin at 100 μM after 4-min incubation of lysate caused the release of radioactive peptides from the ribosomes similar to pyrocatechol violet. The results suggest that daphnoretin allows completion of the ongoing chain elongation steps and then causes the release of polypeptides from polyribosomes before it inhibits protein synthesis.

The effect of daphnoretin on the initiation steps of protein synthesis was examined using a fractionated Ehrlich ascites system. Table I shows daphnoretin had little or no effect on either the ternary complex[9] or the 80S initiation complex formation[10]. These studies indicated that daphnoretin was not an initiation inhibitor.

Further studies were performed to determine if daphnoretin was an elongation inhibitor. As can be easily seen in Fig. 4, daphnoretin inhibits polyuridine directed polyphenylalanine synthesis of purified runoff ribosomes from Ehrlich ascites tumor cells. Polyuridine-directed polyphenylalanine synthesis does not require the normal initiation and termination reactions; thus, agents that block this step are exclusively elongation type inhibitors.

In an additional study, the formation of the 80S initiation complex[10] and peptide bond formation was examined by treating Ehrlich ascites lysates with the elongation inhibitor, chlortetracycline, which specifically inhibits binding of the aminoacyl tRNA to the ribosome A site but does not inhibit the peptidyl transferase reaction. Thus, when [^{3}H]methionine-tRNA (met-tRNA$_f$) is added to the system, most of the radioactivity

[8] GF/F.
[9] eIF·GTP[^{3}H]methionyl-tRNA.
[10] 80S·adenosine–uridine–guanosine·eIF·GTP[^{3}H]methionyl-transfer RNA.

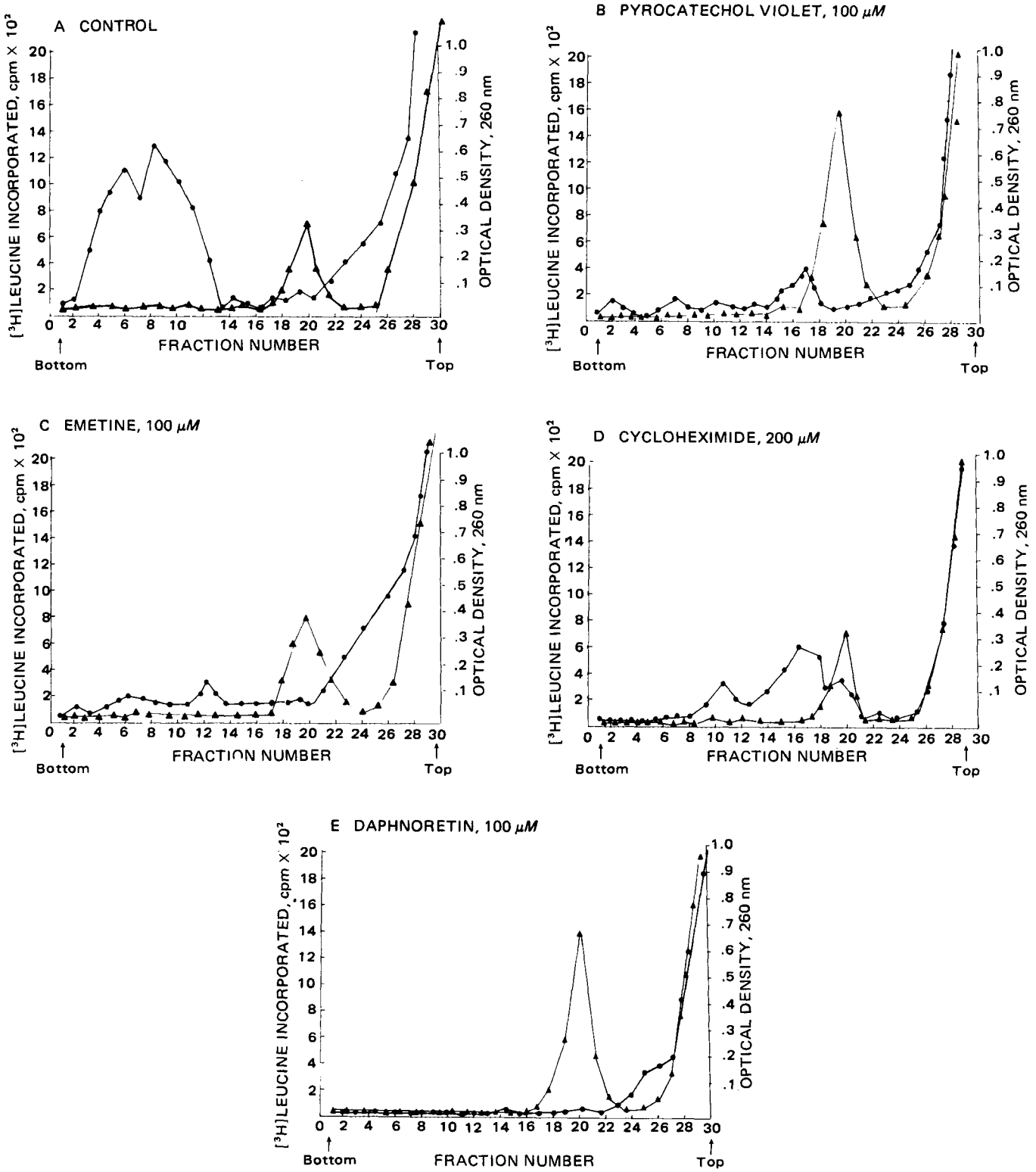

Figure 3—*Fate of nascent protein of protein synthesis in Ehrlich ascites tumor lysate. Key: (●) leucine incorporated; (▲) ribosomal profile.*

is found associated with the 80S initiation complex. Addition of polyadenosine–uridine–guanosine to the chlortetracycline-treated lysate allows formation of an 80S initiation complex (Fig. 5A), which then reacts with puromycin followed by the puromycin-induced release of [^{3}H]-methionine from the 80S complex (Fig. 5B). Daphnoretin (560 μ*M*) does not appear to inhibit the formation of the 80S initiation complex but did inhibit puromycin release of methionine, indicating that daphnoretin inhibits peptide bond formation in Ehrlich ascites ribosomes. Examination (Table II) of the formation of aminoacyl tRNA with phenylalanine, leucine, or methionine indicated that daphnoretin had no effect on the activation of amino acids for incorporation into polypeptides.

Examination of the *in vitro* leucine incorporation into protein for normal tissues of CF_1 male mice demonstrated that daphnoretin at 0.042–0.340 m*M* had no effect on protein synthesis by brain, kidney, or lung but suppressed *in vitro* protein synthesis by liver at low doses (Table III). Concentrations at 0.044 m*M* daphnoretin caused 53% inhibition, at 0.085 m*M* 34% inhibition, 0.177 m*M* 23% inhibition, and 0.340 m*M* 16% inhibition of leucine incorporation into liver proteins. Furthermore, daphnoretin did not suppress the protein synthesis of P-388 lymphocytic leukemia cells, L-1210 lymphocytic lymphomas, B-16

Table II—Effects of Daphnoretin on Amino Acid tRNA Activation in Ehrlich Ascites Cells

Inhibitor	Concentration, μM	Amino Acid Transfer RNA Formation, pmoles	Control, %
[^{14}C]Phenylalanine tRNA			
Control		0.209	100
+ Daphnoretin	10.2	0.205	98
+ Daphnoretin	102	0.201	96
+ Daphnoretin	1020	0.200	95
[^{3}H]Leucyl tRNA			
Control		0.893	100
+ Daphnoretin	10.2	0.848	95
+ Daphnoretin	102	0.830	93
+ Daphnoretin	1020	0.795	89
[^{3}H]Methionyl tRNA			
Control		0.757	100
+ Daphnoretin	10.2	0.741	98
+ Daphnoretin	102	0.719	95
+ Daphnoretin	1020	0.696	92

Table III—*In Vitro* Protein Synthesis of Normal Tissues

CF_1 Male Mouse (n = 6)	Control	Daphnoretin Concentration Control, %		
		0.044 μM	0.088 μM	0.177 μM
Liver (12,202 dpm/hr/10 mg)	100 ± 8	47 ± 4[a]	66 ± 6[a]	77 ± 9[a]
Kidney (8751 dpm/hr/10 mg)	100 ± 6	112 ± 8[b]	116 ± 6[a]	135 ± 7[a]
Lung (6564 dpm/hr/10 mg)	100 ± 5	113 ± 7[a]	129 ± 8[a]	124 ± 5[a]
Brain (6757 dpm/hr/10 mg)	100 ± 6	156 ± 9[a]	146 ± 8[a]	189 ± 6[a]

[a] $p \leq 0.001$. [b] $p \leq 0.010$.

melanoma and Lewis lung carcinoma as it did Ehrlich ascites carcinoma. Concomitantly, daphnoretin did not possess any antitumor activity in the P-388, L-1210, B-16, or Lewis screen.

Daphnoretin inhibited thymidine incorporation into nucleic acid resulting in an $ID_{50} \cong 0.194$ mM. However, daphnoretin did not suppress *in vitro* DNA synthesis in P-388, L-1210, B-16, and Lewis lung tumor cells. Similarly, daphnoretin had no effect on the *in vitro* thymidine incorporation with DNA of CF_1 mouse liver, lung, kidney, or brain.

DISCUSSION

Daphnoretin has been shown to be an elongation inhibitor of protein synthesis which allows the completion of ongoing polypeptide synthesis and releases the 80S ribosome. These observations suggest that daphnoretin binds to free ribosomes rather than the polyribosomes actively engaged in protein synthesis and similarly to other elongation inhibitors *e.g.* bruceantin, brusatol (17), T-2-toxin (18), verucarin (19), harring-

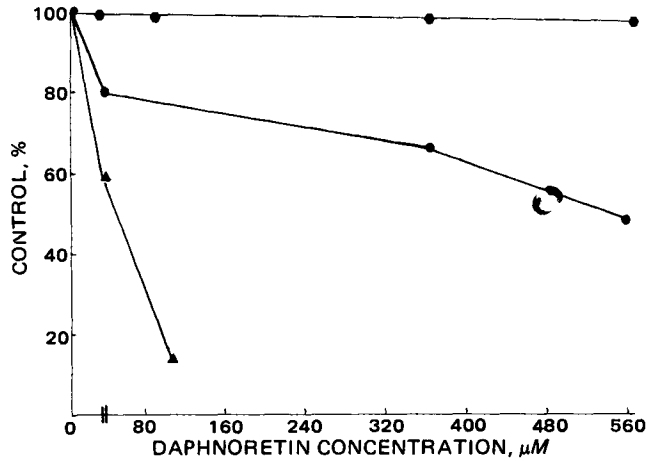

Figure 4—*Effect of daphnoretin on polyuridine-directed poly[^{14}C]-phenylalanine synthesis in Ehrlich ascites tumor cell system. Key: (●) control; (●) daphnoretin; (▲) emetine.*

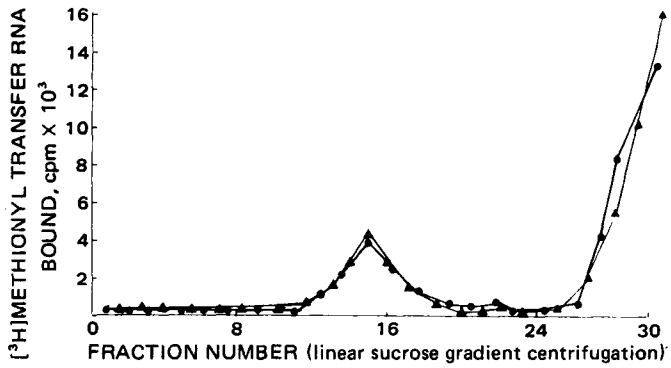

Figure 5A—*The formation of the 80S initiation complex of Ehrlich ascites tumor lysate system. Key: (●) control; (▲) daphnoretin (560 μM).*

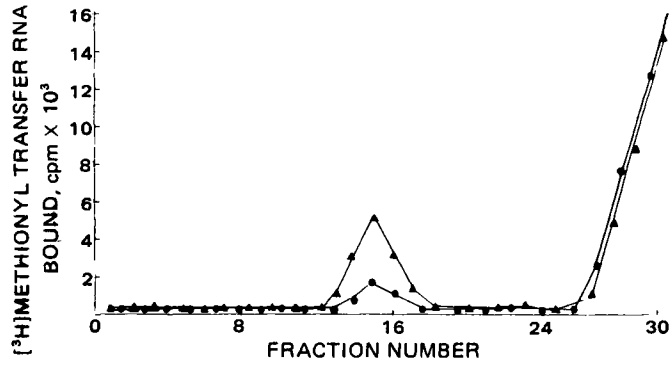

Figure 5B—*The formation of the methionyl puromycin reaction of Ehrlich ascites tumor lysate system. Key: (●) control and puromycin; (▲) daphnoretin (560 μM) and puromycin.*

tonine (20), and fusarenon-X (13). One explanation for this is that peptidyl tRNA or methionyl tRNA lowers affinity binding of drug to ribosome (21). Daphnoretin effectively blocked peptidyl transferase activity of the elongation process. The magnitude of inhibition of protein synthesis is of a sufficient degree to account for the cessation of cell growth. It has been reported previously that daphnoretin suppresses DNA synthesis with an $ID_{50} \cong 0.194$ mM (5). The present studies show that daphnoretin only suppresses protein and DNA synthesis in the Ehrlich ascites carcinoma cells, the only tumor screen in which daphnoretin demonstrated antineoplastic activity at 3–12 mg/kg/day. Protein and DNA synthesis of whole cells was not suppressed in normal mouse tissue, *e.g.*, brain, kidney, and lung; but there was a moderate reduction of protein synthesis in the liver. Daphnoretin was isolated from *Wikstroemia indica* C. A. Mey (Thymelaeaceae), which has been used as a herbal remedy to treat human cancer, arthritis, syphilis, and whooping cough (22, 23). This study of the mode of action of daphnoretin may explain some of the pharmacological properties of the plant.

REFERENCES

(1) K. H. Lee, K. Tagahara, H. Suzuki, R. Y. Wu, M. Haruna, I. H. Hall, H.-C. Huang, K. Ito, T. Iida, and J.-S. Lai, *J. Nat. Prod.*, **44**, 530 (1981).

(2) T. Tschesche, U. Schacht, and G. Legler, *Ann. Chem.*, **662**, 113 (1963).

(3) A. Kato, Y. Hashimoto, and M. Kidokoro, *J. Nat. Prod.*, **42**, 159 (1979).

(4) S. J. Torrance, J. J. Hoffman, and J. R. Cole, *J. Pharm. Sci.*, **68**, 664 (1979).

(5) I. H. Hall and K. H. Lee, *J. Pharm. Sci.*, **71**, 741 (1982).

(6) J. Kruh, L. Grossman, and K. Moldave, *Methods Enzymol*, **XIIb**, 732 (1968).

(7) M. H. Schreier and T. Staehelin, *J. Mol. Biol.*, **73**, 329 (1973).

(8) J. M. Ravel, R. D. Mosteller, and B. Hardesty, *Proc. Natl. Acad. Sci. USA*, **56**, 701 (1966).

(9) A. Majumdar, S. Reynolds, and N. K. Gupta, *Biochem. Biophys. Res. Commun.*, **67**, 689 (1975).

(10) K. Takeishi, T. Ukita, and S. Nishimura, *J. Biol. Chem.*, **243**, 5761 (1968).

(11) L. L. Liao, S. M. Kupchan, and S. B. Horwitz, *Mol. Pharmacol.*, **12**, 167 (1976).

(12) J. Jimenez, L. Sanchez, and D. Vasquez, *Biochim. Biophys. Acta*, **383**, 4271 (1975).

(13) J. Carter and M. Cannon, *Eur. J. Biochem.*, **84**, 103 (1978).

(14) S. H. Reynolds, A. Majumdar, A. Das Gupta, S. Palmieri, and N. K. Gupta, *Arch. Biochem. Biophys.*, **184**, 324 (1977).

(15) K. Moldave, *Methods Enzymol.*, **6**, 757 (1963).

(16) R. I. Geran, N. H. Greenberg, M. M. MacDonald, A. M. Schumacher, and B. J. Abbott, *Cancer Chemother. Rep.*, **3**, 9 (1972).

(17) I. H. Hall, Y. F. Liou, M. Okano, and K. H. Lee, *J. Pharm. Sci.*, **71**, 345 (1982).

(18) M. Cannon, A. Jimenez, and D. Vasquez, *Biochem. J.*, **160**, 137 (1976).

(19) E. Cundliffe, M. Cannon, and J. Davis, *Proc. Natl. Acad. Sci. USA*, **71**, 30 (1974).

(20) M. Fresno, A. Jimenez, and D. Vasquez, *Eur. J. Biochem.*, **72**, 323 (1977).

(21) M. Fresno, A. Gonzales, D. Vasquez, and A. Jimenez, *Biochem. Biophys. Acta*, **518**, 104 (1978).

(22) W. S. Kan, "Pharmaceutical Botany," National Research Institute of Chinese Medicine, Taiwan, Republic of China, 1969, p. 391.

(23) M. Sugi and Y. Nagashio, in "Cancer Therapy in Modern China," K. Kondo, Ed., Shizen Sha, Japan, 1977, p. 256.

ACKNOWLEDGMENTS

Supported by American Cancer Society Grant CH-19 (K. H. Lee and I. H. Hall) and National Cancer Institute Grant CA-17625 (in part) (K. H. Lee).

Square Root of Time Dependence of Matrix Formulations with Low Drug Content

HATEM FESSI, J.-P. MARTY, F. PUISIEUX, and J. T. CARSTENSEN *x

Received July 30, 1980 from the *Faculté de Pharmacie, Université de Paris-Sud, Châtenay-Malabry, 92290 France* and the **School of Pharmacy, University of Wisconsin, Madison, WI 53706.* Accepted for publication September 25, 1981.

Abstract □ One of the conditions of derivation of the Higuchi square root law is that $A/\epsilon > S/2$ where A is drug content per cubic centimeter of matrix tablet, ϵ is the porosity, and S is the solubility of the drug in the dissolution medium. In actuality, A/ϵ should be larger than S. It is shown in this work that a similar square root equation can be derived when $A/\epsilon < S$. Experimental data are presented supporting the equation $Q = A(Dt)^{1/2}$, where Q is the amount of drug released per square centimeter at time t and D is the diffusion coefficient.

Keyphrases □ Matrix formulations—square root of time dependence, with low drug content □ Dissolution—square root of time dependence of matrix formulations with low drug content □ Release rate—square root of time dependence of matrix formulations with low drug content

Many sustained-release products are designed around the principle of imbedding the drug in a porous matrix. Liquid will penetrate and dissolve the drug, which will then diffuse out into the exterior liquid (Fig. 1). In general, for the purpose of derivation, a slab is considered which has a unit cross-section, is infinite to the left (Fig. 1), has a porosity ϵ', contains A grams of drug (of density ρ) per cubic centimeter of matrix, and allows penetration and diffusion through the unit surface only. At time t a depth of h is penetrated.

BACKGROUND

Higuchi (1, 2) was the first to derive the following expression for the amount of material released (Q) through the unit surface. He cautions that "the equation would be essentially valid for systems in which A is greater than the solubility S or ϵS by a factor of three or four. Of course,

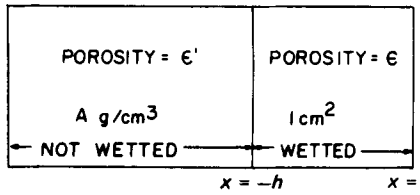

Figure 1—*Schematic of penetration of liquid into a solid matrix. The distance is denoted* x *(cm) and is zero at the surface and* −h *at the border of penetration.*

0022-3549/82/0700-0749$01.00/0

tonine (20), and fusarenon-X (13). One explanation for this is that peptidyl tRNA or methionyl tRNA lowers affinity binding of drug to ribosome (21). Daphnoretin effectively blocked peptidyl transferase activity of the elongation process. The magnitude of inhibition of protein synthesis is of a sufficient degree to account for the cessation of cell growth. It has been reported previously that daphnoretin suppresses DNA synthesis with an $ID_{50} \cong 0.194$ mM (5). The present studies show that daphnoretin only suppresses protein and DNA synthesis in the Ehrlich ascites carcinoma cells, the only tumor screen in which daphnoretin demonstrated antineoplastic activity at 3–12 mg/kg/day. Protein and DNA synthesis of whole cells was not suppressed in normal mouse tissue, *e.g.*, brain, kidney, and lung; but there was a moderate reduction of protein synthesis in the liver. Daphnoretin was isolated from *Wikstroemia indica* C. A. Mey (Thymelaeaceae), which has been used as a herbal remedy to treat human cancer, arthritis, syphilis, and whooping cough (22, 23). This study of the mode of action of daphnoretin may explain some of the pharmacological properties of the plant.

REFERENCES

(1) K. H. Lee, K. Tagahara, H. Suzuki, R. Y. Wu, M. Haruna, I. H. Hall, H.-C. Huang, K. Ito, T. Iida, and J.-S. Lai, *J. Nat. Prod.*, **44**, 530 (1981).

(2) T. Tschesche, U. Schacht, and G. Legler, *Ann. Chem.*, **662**, 113 (1963).

(3) A. Kato, Y. Hashimoto, and M. Kidokoro, *J. Nat. Prod.*, **42**, 159 (1979).

(4) S. J. Torrance, J. J. Hoffman, and J. R. Cole, *J. Pharm. Sci.*, **68**, 664 (1979).

(5) I. H. Hall and K. H. Lee, *J. Pharm. Sci.*, **71**, 741 (1982).

(6) J. Kruh, L. Grossman, and K. Moldave, *Methods Enzymol*, **XIIb**, 732 (1968).

(7) M. H. Schreier and T. Staehelin, *J. Mol. Biol.*, **73**, 329 (1973).

(8) J. M. Ravel, R. D. Mosteller, and B. Hardesty, *Proc. Natl. Acad. Sci. USA*, **56**, 701 (1966).

(9) A. Majumdar, S. Reynolds, and N. K. Gupta, *Biochem. Biophys. Res. Commun.*, **67**, 689 (1975).

(10) K. Takeishi, T. Ukita, and S. Nishimura, *J. Biol. Chem.*, **243**, 5761 (1968).

(11) L. L. Liao, S. M. Kupchan, and S. B. Horwitz, *Mol. Pharmacol.*, **12**, 167 (1976).

(12) J. Jimenez, L. Sanchez, and D. Vasquez, *Biochim. Biophys. Acta*, **383**, 4271 (1975).

(13) J. Carter and M. Cannon, *Eur. J. Biochem.*, **84**, 103 (1978).

(14) S. H. Reynolds, A. Majumdar, A. Das Gupta, S. Palmieri, and N. K. Gupta, *Arch. Biochem. Biophys.*, **184**, 324 (1977).

(15) K. Moldave, *Methods Enzymol.*, **6**, 757 (1963).

(16) R. I. Geran, N. H. Greenberg, M. M. MacDonald, A. M. Schumacher, and B. J. Abbott, *Cancer Chemother. Rep.*, **3**, 9 (1972).

(17) I. H. Hall, Y. F. Liou, M. Okano, and K. H. Lee, *J. Pharm. Sci.*, **71**, 345 (1982).

(18) M. Cannon, A. Jimenez, and D. Vasquez, *Biochem. J.*, **160**, 137 (1976).

(19) E. Cundliffe, M. Cannon, and J. Davis, *Proc. Natl. Acad. Sci. USA*, **71**, 30 (1974).

(20) M. Fresno, A. Jimenez, and D. Vasquez, *Eur. J. Biochem.*, **72**, 323 (1977).

(21) M. Fresno, A. Gonzales, D. Vasquez, and A. Jimenez, *Biochem. Biophys. Acta*, **518**, 104 (1978).

(22) W. S. Kan, "Pharmaceutical Botany," National Research Institute of Chinese Medicine, Taiwan, Republic of China, 1969, p. 391.

(23) M. Sugi and Y. Nagashio, in "Cancer Therapy in Modern China," K. Kondo, Ed., Shizen Sha, Japan, 1977, p. 256.

ACKNOWLEDGMENTS

Supported by American Cancer Society Grant CH-19 (K. H. Lee and I. H. Hall) and National Cancer Institute Grant CA-17625 (in part) (K. H. Lee).

Square Root of Time Dependence of Matrix Formulations with Low Drug Content

HATEM FESSI, J.-P. MARTY, F. PUISIEUX, and J. T. CARSTENSEN *x

Received July 30, 1980 from the *Faculté de Pharmacie, Université de Paris-Sud, Châtenay-Malabry, 92290 France* and the **School of Pharmacy, University of Wisconsin, Madison, WI 53706.* Accepted for publication September 25, 1981.

Abstract □ One of the conditions of derivation of the Higuchi square root law is that $A/\epsilon > S/2$ where A is drug content per cubic centimeter of matrix tablet, ϵ is the porosity, and S is the solubility of the drug in the dissolution medium. In actuality, A/ϵ should be larger than S. It is shown in this work that a similar square root equation can be derived when $A/\epsilon < S$. Experimental data are presented supporting the equation $Q = A(Dt)^{1/2}$, where Q is the amount of drug released per square centimeter at time t and D is the diffusion coefficient.

Keyphrases □ Matrix formulations—square root of time dependence, with low drug content □ Dissolution—square root of time dependence of matrix formulations with low drug content □ Release rate—square root of time dependence of matrix formulations with low drug content

Many sustained-release products are designed around the principle of imbedding the drug in a porous matrix. Liquid will penetrate and dissolve the drug, which will then diffuse out into the exterior liquid (Fig. 1). In general, for the purpose of derivation, a slab is considered which has a unit cross-section, is infinite to the left (Fig. 1), has a porosity ϵ', contains A grams of drug (of density ρ) per cubic centimeter of matrix, and allows penetration and diffusion through the unit surface only. At time t a depth of h is penetrated.

BACKGROUND

Higuchi (1, 2) was the first to derive the following expression for the amount of material released (Q) through the unit surface. He cautions that "the equation would be essentially valid for systems in which A is greater than the solubility S or ϵS by a factor of three or four. Of course,

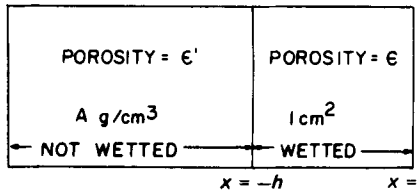

Figure 1—*Schematic of penetration of liquid into a solid matrix. The distance is denoted* x *(cm) and is zero at the surface and* −h *at the border of penetration.*

0022-3549/82/0700-0749$01.00/0

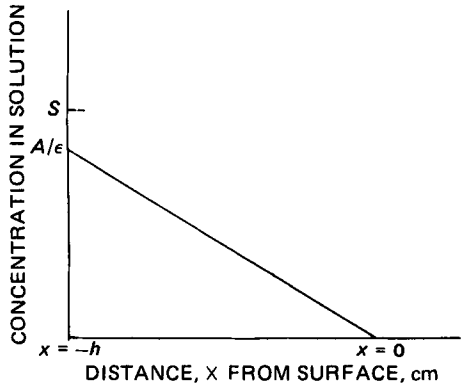

Figure 2—*Assumed concentration profile in the penetrating liquid for the situation in Fig. 1.*

if $A < S$ or ϵS, the drug would no longer be present as a solid and a different equation would apply."

$$Q = [2DS\epsilon(A - 0.5S\epsilon)]^{1/2}t^{1/2} \quad \text{(Eq. 1)}$$

The tortuosity term has been omitted since it does not apply in the following; ϵ is the porosity of the part of the matrix already penetrated by liquid, and S is the solubility (in gram per cubic centimeter) of the drug in the penetrating liquid. The point that A should be greater than S by a factor of three or four has been emphasized previously (3–5). In cases where the above is not the case, *ie.*, when

$$S > A/\epsilon \quad \text{(Eq. 2)}$$

derivations are nevertheless possible. The following sequence follows closely that described previously (1, 2, 5), and the following assumptions are made:

(*a*) sink conditions exist (*i.e.*, $C \sim O$) in the exterior liquid, where C is concentration of drug;

(*b*) the concentration gradient in the liquid in the penetrated space is linear;

(*c*) the diffusion coefficient is concentration independent;

(*d*) the drug content, A, is less than $S\epsilon$;

(*e*) the rate of dissolution is governed by the liquid penetration rate, not the dissolution rate.

The case where both dissolution and penetration rates play a part has been treated elsewhere (6, 7). Because of (*d*) and (*e*), the drug will, in fact, dissolve immediately when reached by liquid and form an unsaturated solution of concentration A/ϵ ($<S$). It is emphasized here that ϵ is the actual porosity in the penetrated space, *i.e.*, the original porosity, ϵ', and that created by dissolution of drug, A/ρ (presuming that an ideal solution forms). In the following, ϵ will be referred to as actual and ϵ' as measured porosity. It follows that:

$$\epsilon = \epsilon' + (A/\rho) \quad \text{(Eq. 3)}$$

The concentration profile shown in Fig. 2 will therefore apply. The

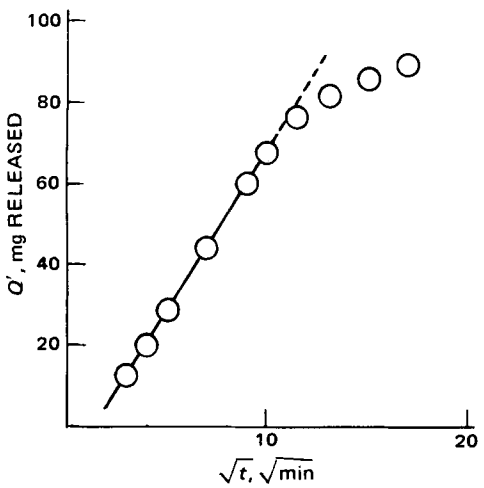

Figure 3—*Release data for Formula II, Table I.*

Table I—Compositions of Formulations Tested

	Formulation Number[a]			
	I	II	III	IV
Diphenhydramine HCl[b]	5	10	15	20
Polyvinyl acetate–polyvinyl chloride copolymer	50	50	50	50
Povidone	1.5	1.5	1.5	1.5
Magnesium stearate	3	3	3	3
Calcium phosphate, tribasic	←a sufficient quantity to 500 mg→			

[a] Percent by weight.
[b] The measured porosities of the formulations were 0.17, 0.16, 0.16, 0.17, and 0.13, respectively, giving drug concentrations on a volume basis of 0.067, 0.142, 0.200, and 0.260, respectively.

amount dissolved at time t is Q grams per square centimeter of surface and is given by:

$$Q = Ah - 0.5(A/\epsilon)h\epsilon = 0.5Ah \quad \text{(Eq. 4)}$$

Ah is the amount present in the matrix in the h-cm thick layer before dissolution started. After penetration to a depth of h, there are ϵ cubic centimeters of liquid per cubic centimeter of matrix and the average concentration is $0.5(A/\epsilon)$, so that the total amount not liberated to the exterior liquid is $h\epsilon(0.5A/\epsilon) = hA/2$.

Differentiation of Eq. 4 with respect to time gives:

$$dQ/dt = (A/2)dh/dt \quad \text{(Eq. 5)}$$

The diffusion of the drug takes place *via* Fick's law:

$$\text{Flux} = -D \times \text{Gradient} \quad \text{(Eq. 6)}$$

The flux is the amount of material passing through a unit cross-section per unit of time (dt). The cross-sectional area available for liquid is ϵ in square centimeters, and the amount of material passing through it is dQ/dt, so that the left hand side of Eq. 6 may be written:

$$\text{Flux} = (1/\epsilon)(dQ/dt) \quad \text{(Eq. 7)}$$

The gradient (dC/dx) is assumed to be constant [condition (*b*)] and drops from $C = A/\epsilon$ at $x = -h$ (Fig. 2) to zero at $x = 0$ [condition (*a*)]. Hence the gradient term in the right hand side of Eq. 6 is:

$$\text{Gradient} = dC/dx = [0 - (A/\epsilon)]/h = -A/(h\epsilon) \quad \text{(Eq. 8)}$$

so that inserting Eqs. 7 and 8 in Eq. 6 gives:

$$(1/\epsilon)dQ/dt = -D\{-[A/(h\epsilon)]\}$$

or

$$dQ/dt = DA/h \quad \text{(Eq. 9)}$$

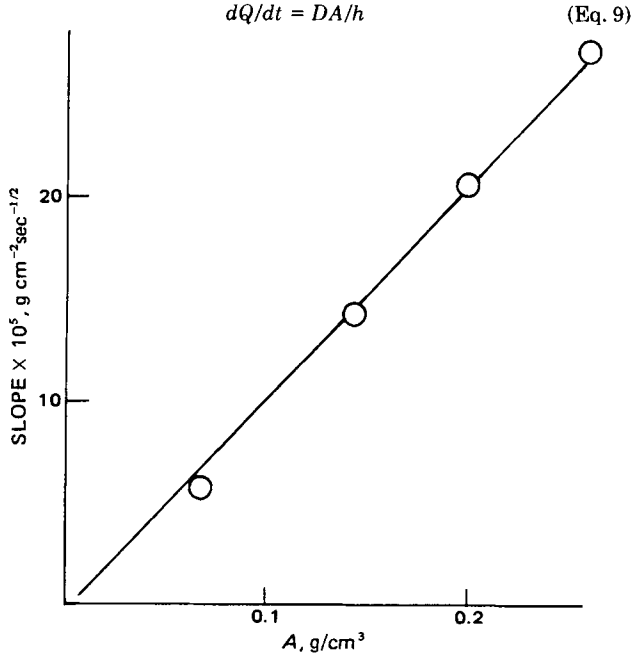

Figure 4—*Slopes of data as shown in Fig. 3 (divided by surface area) as a function of* A, *the drug content (Eq. 13) (data from Table III).*

Table II—Release Rate Data from Matrix Tablets of Four Drug Substances, Using Formula IV from Table I

Compound	S, g/cm³	Tablet Area, cm²	Tablet Volume, cm³	A, g/cm³	Experimental Porosity, ϵ'	Slope, mg min$^{-0.5}$	Adjusted Slope, $10^5 Q$, g cm^{-2} sec$^{-0.5}$	$10^{10} Q^2/S$
Diphenhydramine HCl	0.83	3.54	0.384	0.26	0.13	7.58	27.6	918
Acetaminophen	0.02	3.58	0.4	0.25	0.21	3.60	13	8450
Dyphylline[a]	0.17	3.48	0.37	0.27	0.16	5.26	19.5	2237
Theophylline	0.010	3.48	0.37	0.27	0.16	2.56	9.4	8836

Compound	Density, g/cm³	$\epsilon' + (A/\rho)$	A/ϵ	Molecular Weight
Diphenhydramine HCl	1.20	0.35	0.74	255
Acetaminophen	1.28	0.40	0.63	151
Dyphylline	1.18	0.39	0.69	254
Theophylline	1.28	0.37	0.73	180

[a] 7-(2,3-dihydroxypropyl)-1,3-dimethylxanthine, $C_{10}H_{14}N_4O_4$.

Combining Eqs. 4 and 9 yields:

$$(A/2)dh/dt = AD/h \qquad \text{(Eq. 10)}$$

or

$$hdh = 2Ddt \qquad \text{(Eq. 11)}$$

which integrates (with the initial condition that $h = 0$ at $t = 0$) to:

$$h^2 = 4Dt \qquad \text{(Eq. 12)}$$

Inserting Eq. 12 into Eq. 4 gives:

$$Q = A(Dt)^{0.5} \qquad \text{(Eq. 13)}$$

Equation 13 predicts that Q, the amount released per square centimeter of tablet surface, is proportional to the square root of time, and that the slope of such a plot is independent of porosity and solubility and is directly proportional to the drug content (per cubic centimeter) of the matrix.

As mentioned earlier, the case of (*d*), *i.e.*, of Eq. 2, is the exception rather than the rule. Only one case was reported in literature with drug concentrations where A may approach a low value close to S (8). These data fit fairly well to Eq. 13, but are difficult to analyze, because due to the lack of porosity data, the independence of Eq. 13 of the porosity cannot be tested in that specific case.

EXPERIMENTAL

Matrix tablets of the composition shown in Table I were produced as described in earlier publications (9–11). The matrix is sufficiently insoluble to consider it as completely insoluble (albeit the 1.5% povidone does dissolve to some extent).

Four drugs were tested (Table II) that have solubilities above and below the solubilities dictated by the Higuchi equation (Eqs. 1 and 2). The solubilities were tested by equilibrating excess of drug substance with water at 37 ± 0.2° in a rotating bottle in a waterbath. The concentrations in the supernate were determined spectrophotometrically at the peaks of the respective adsorption spectra. Densities were determined pycnometrically.

The tablets made were produced at various, controlled compression forces on an instrumented single punch machine (11). The porosities were measured using a mercury intrusion porosimeter[1]. The surface areas and volumes of the tablets were obtained from their dimensions. The dissolution rates were determined using a flow cell as described previously (6, 7, 9).

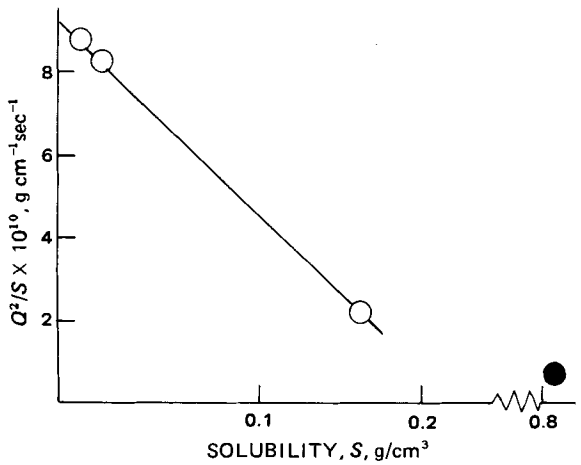

Figure 5—*Data from Table II plotted according to Eq. 18.*

RESULTS AND DISCUSSION

Figure 3 shows an example of dissolution of diphenhydramine hydrochloride from formulas as shown in Table I. It is seen that the amount released is linear in the square root of time up to the critical time (9, 10) when the tablet is completely penetrated by liquid. There is also a slight lag time, also explained in previous publications (9, 10). Slopes from four concentrations of drug are shown in Table III. The data in the last column are obtained by converting the slopes from plots like Fig. 3 to g sec^{-1} cm^{-2}, by multiplying by $10^{-3}/\sqrt{60}$ and dividing by the surface area of the tablet. This latter, in the case cited, is 3.54 cm², as it is in most of the tablets in question. An exception to this is the data leading to the Heckel plot mentioned at a later point[2]. Data of the type in Table III are plotted in Fig. 4, where the specific release rates (in grams per square centimeter sec$^{-0.5}$) are plotted as a function of A. According to Eq. 13 this should be a straight proportionality, which is borne out by the graph. The least squares fit line is:

$$y = 1.13 \times 10^{-3}x - 2 \times 10^{-6} \qquad \text{(Eq. 14)}$$

where $y = Qt^{-0.5}$ (g cm^{-2} sec$^{-1/2}$) and $x = A$ (g cm^{-3}). The intercept does not differ significantly from zero ($p = 0.001$) as predicted by Eq. 13. If this latter case is correct, then the slope of the plot in Fig. 4 should equal $D^{0.5}$, *i.e.*, $D^{0.5} = 1.13 \times 10^{-3}$ cm sec$^{-0.5}$ or $D \cong 10^{-6}$ cm² sec^{-1}, which is

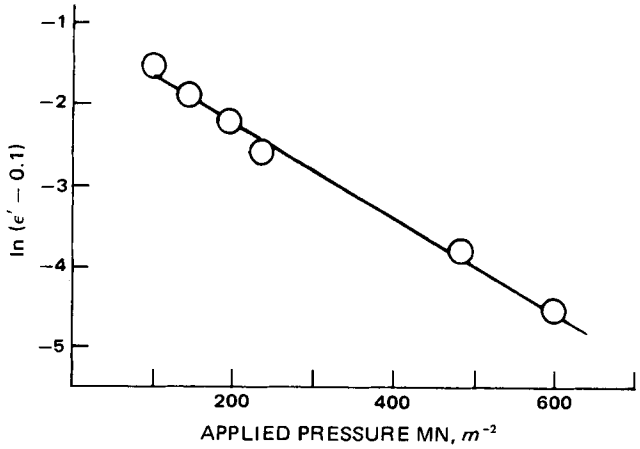

Figure 6—*Data from Table IV plotted as a Heckel function.*

[1] J. T. Carstensen and M. A. Zoglio, *J. Pharm Sci.*, Submitted for publication.
[2] The low porosity points in Table IV have slightly larger surface areas per tablet, due to a larger thickness.

Table III—Data for Diphenhydramine HCl Square Root Dissolution Rate Constants in a Series of Compositions[a]

Tablet Volume, cm^3	Drug, g/500-mg Tablet	A, g/cm^3	ϵ' Experimental	$\epsilon = \epsilon' + (A/\rho)$	Slope $\times 10^5$, $g\ cm^{-2}\ sec^{-1/2}$
0.375	0.025	0.067	0.173	0.23	5.82
0.351	0.050	0.142	0.163	0.28	14.4
0.375	0.075	0.20	0.164	0.33	20.8
0.384	0.100	0.26	0.13	0.38	27.6

[a] Porosity has been kept constant.

Table IV—Release Data of Diphenhydramine HCl as a Function of Porosity

Compression Force, MPa	$Q \times 10^5$ $g\ cm^{-2}\ sec^{-0.5}$	ϵ'	ϵ	$\ln(\epsilon' - 0.1)$
98	43	0.302	0.48	−1.600
147	39	0.260	0.45	−1.900
196	27	0.207	0.42	−2.235
234	25	0.169	0.39	−2.674
490	24	0.123	0.35	−3.772
588	24.3	0.111	0.34	−4.510

the right order of magnitude. The formulations listed in Table I all adhere to the inequality in Eq. 2, and they demonstrate the utility of the modification of the Higuchi equation in low concentration regions.

To further test the correctness of the developments described, it is noted that Eq. 1 may be written:

$$Q^2 = aS - bS^2 \qquad \text{(Eq. 15)}$$

where

$$a = 2D\epsilon A \qquad \text{(Eq. 16)}$$

and

$$b = D\epsilon^2 \qquad \text{(Eq. 17)}$$

This solubility dependence of the Higuchi equation has been checked and verified with three drug substances, the latter three listed in Table II. It is noted from the table that the A-values have been kept constant. If D is the same for the three substances, then a plot of Q^2/S *versus* S should give a straight line:

$$Q^2/S = a - bS \qquad \text{(Eq. 18)}$$

The slope and intercept should give the same value for D. It should be noted that according to the Stokes-Einstein equation:

$$D = kT/(6\pi\eta r) \qquad \text{(Eq. 19)}$$

where η is viscosity, k is Boltzmann's constant, T is absolute temperature, and r is the molecular radius. The value r should be proportional (roughly) to the cube root of the molar volume, so that the D-values should vary at the most by a factor of $(254/151)^{1/3} = 1.19$, *i.e.*, ~20%. It is assumed that the D-values of the three compounds are identical.

The data from the last three entries in Table II have been plotted according to Eq. 18, and are shown in Fig. 5; it can be seen that a straight line ensues. The least-squares fit equation is

$$10^{10}Q^2/S = -42{,}000\,S + 9300 \qquad \text{(Eq. 20)}$$

Hence, from the slope:

$$b = D\epsilon^2 = 0.42 \times 10^{-5} \qquad \text{(Eq. 21)}$$

so that setting $\epsilon = 0.38$ (Table III) gives $D = 3 \times 10^{-5}\ cm^2/sec$. From the intercept:

$$a = 9.3 \times 10^{-7} = 2D\epsilon A \qquad \text{(Eq. 22)}$$

so that setting $\epsilon = 0.38$ (Table III) gives $D = 10^{-5}\ cm^2/sec$. This demonstrates that substances adhering to the Higuchi requirements, in the system tested and using the test methods described, adhere to the Higuchi equation and give reasonable parameter values.

From the point of view of the present study, the most important point is that diphenhydramine has a Q^2/S value out of line with the remaining compounds.

An important difference between Eqs. 1 and 13 is that the latter is independent of the porosity, ϵ. This point is difficult to investigate, as shown below. Preparations were made at different preparative porosities, ϵ'. This was accomplished by varying the applied compression force at which the tablets were made.

The data are tabulated in Table IV. The force *versus* porosity data are consistent as demonstrated in the Heckel plot in Fig. 6. Of the preparations, the three made at the low pressures disintegrated, and hence, from a point of view of release, do not fall into the described models. The last three entries in Table IV, however, show that Q is not drastically a function of ϵ: Q is 24–25 $g\ cm^{-2}\ sec^{-0.5}$ over a range of initial porosity values of $\epsilon' = 0.11$–0.17 (*i.e.*, a 60% spread). However, due to the A-contribution to the porosity ϵ, the overall porosity, is 0.34–0.39, which is only at best a 20% variation. It would appear that a 20% variation in actual porosity, ϵ, causes a change of <4% in the slope (Q) of the square root plot, so that the effect of ϵ is small. Experimentally, it would have been desirable to have a wider spread of ϵ-values, but the disintegration is a problem at the lower end and the A-values a problem at the upper end.

It has been shown that when $A < S\epsilon$ the release rate for a matrix should be $Q = AD^{0.5}t^{0.5}$. Release plots of drug in situations where $A < S\epsilon$ have been shown to follow a square root law with slopes that are proportional to A. The proportionality constant gives a reasonable value of D ($2 \times 10^{-6}\ cm^2/sec$). Evidence is presented that the proportionality constant is independent of solubility, S, and porosity, ϵ.

REFERENCES

(1) T. Higuchi, *J. Pharm. Sci.*, **50**, 874 (1961).

(2) *Ibid.*, **52**, 1145 (1963).

(3) S. J. Desai, P. Singh, A. P. Simonelli, and W. Higuchi, *ibid.*, **55**, 1224 (1966).

(4) V. H. Lee and J. R. Robinson, in "Sustained Release Drug Delivery Systems," J. R. Robinson, Ed., Marcel Decker, New York, N.Y., 1979, p. 142.

(5) J. T. Carstensen, "Pharmaceutics of Solids and Solid Dosage Forms," J. Wiley, New York, N.Y., 1977, p. 173.

(6) M. Bamba, F. Puisieux, J.-P. Marty, and J. T. Carstensen, *Int. J. Pharm.*, **2**, 307 (1979).

(7) M. Bamba, F. Puisieux, J.-P. Marty, and J. T. Carstensen, *ibid.*, **3**, 87 (1979).

(8) I. Ellö, A. Grünwald-Fischer, and V. Hortobagyi, *Dan. Tidsskr. Farm.*, **42**, 185 (1968).

(9) H. Fessi, J.-P. Marty, F. Puisieux, and J. T. Carstensen, *Int. J. Pharm.*, **1**, 265 (1978).

(10) H. Fessi, F. Puisieux, J.-P Marty, and J. T. Carstensen, *Pharm. Acta Helv.*, **55**, 261 (1980).

(11) J. T. Carstensen, J.-P. Marty, F. Puisieux, and H. Fessi, *J. Pharm. Sci.*, **70**, 222 (1981).

Microencapsulation III: Preparation of Invertase Microcapsules

P. RAMBOURG, J. LÉVY, and M.-C. LÉVY ˣ

Received July 15, 1981, from the *Laboratoire de Pharmacie Galénique, E.R.A. au C.N.R.S. n°319, Faculté de Pharmacie, 51, rue Cognacq-Jay, F51096 REIMS Cédex, France.* Accepted for publication October 5, 1981.

Abstract □ Invertase was incorporated into polyamide microcapsules. The following parameters were studied: pH of the aqueous phase during interfacial polymerization; duration of the polymerization; surfactant concentration; stirring rate; improvements in the isolation procedure; effect of lyophilization. The inactivation of the encapsulated enzyme by pepsin was shown to be related to the acidic incubation medium and prompted incorporation of protective proteins in the microcapsules. This process allowed relative protection of the enzyme. In a second set of experiments, an emulsification–reticulation method was developed, which encapsulated invertase in a cross-linked protein. Various proteins and bifunctional acylating agents were tested. Microcapsules of immobilized invertase were prepared through cross-linking of the enzyme protein itself.

Keyphrases □ Microencapsulation—preparation of invertase microcapsules □ Invertase—preparation of microcapsules □ Emulsification–reticulation—preparation of invertase microcapsules

Invertase (β-D-fructofuranoside-fructohydrolase[1]) is lacking in the intestinal mucosa of some patients with constitutional intolerance to sucrose (1–4).

Accumulation of sucrose in the lumen prompts intense diarrhea, amplified further by microbial fermentation. The palliative treatment consists of adding large doses (~1 g) of yeast invertase to the food. As the excessive amount of the supplemented enzyme is probably related to its partial hydrolysis in the digestive tract, it was decided to microencapsulate invertase. Invertase microencapsulation with a 40% retention of enzymatic activity was recently reported (5).

This report deals with the preparation of such microcapsules through two different procedures (6–8). While in the well-known interfacial polymerization procedure (9), the capsule wall is made of an interfacially prepared polyamide, in the emulsion–reticulation procedure, it is made up of an interfacially prepared cross-linked protein. This second technique was progressively devised, and is reported herein.

Although much research has been devoted to the cross-linking of proteins, only a few authors have used this reaction in the preparation of microcapsules: Chang (9, 10), and more recently Miyawaki (11), reported on the chemical interactions between a protein and the acylating agent used in interfacial polymerization. Apparently, only Chang (12) attempted preparation of microcapsules walled in cross-linked proteins. However, he encountered serious difficulties in obtaining stable preparations.

In the cross-linking experiments, the aim was no longer to prepare therapeutically useful invertase microcapsules, but rather to test the feasability and limits of the method, with invertase used as a tracer.

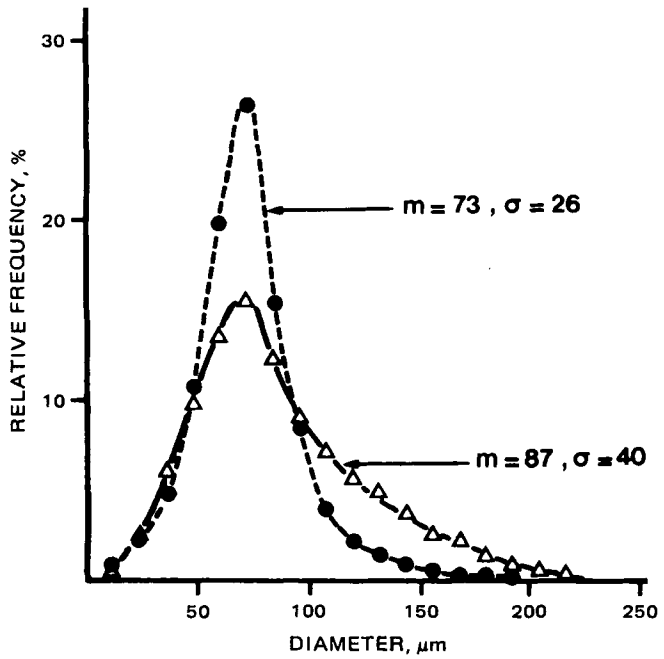

Figure 1—*Effect of the surfactant concentration on the size of microcapsules. Key: (●), sorbitan trioleate, 2%; (△), sorbitan trioleate, 1%.*

[1] E.C. No. 3.2.1.2.6.

EXPERIMENTAL

Reagents—Invertase from baker's yeast[2], exhibiting 34 U of activity/mg was used as a suspension (5%, w/v) in distilled water.

A buffer was adjusted to pH 9.8 by adding hydrochloric acid to a 0.45 *M* solution of Na_2CO_3. It was used to prepare a 6.67 g% (w/v) solution of alcalisoluble casein[3] and a 1.2 *M* solution of 1,6-hexamethylenediamine[4] (13.95%, w/v).

The organic solvent was a chloroform–cyclohexane mixture (1:4, v/v), which was used to prepare solutions of sebacoylchloride[4] (1:250, v/v), terephthaloylchloride[4] (0.04 *M* and 0.12 *M*), succinyl chloride[5] (0.04 *M*), toluene diisocyanate[6] (0.14 *M*), and piperazine[6] (1.2 *M*).

The surfactants were sorbitan trioleate[7] (1% solution v/v in the organic solvent) and polysorbate[7] (50% solution v/v in distilled water).

The dye for the permeability studies was erioglaucine A[8].

The proteolytic enzymes used were pepsin[9], pancreatin[10], and pronase[11].

Materials—Stirring was performed with a motor[12] and a 3-bladed screw (each blade was 16 mm long). An homogenizer[13] was used in one experiment. Lyophilization was performed with a freeze dryer[14].

Evaluation of Enzymatic Activity—A qualitative test was made using reactive strips[15]. Quantitative determinations were performed through the automated method of Goldstein and Lampen (13). The ac-

[2] Grade V, Sigma Chemical Co.
[3] Merck Darmstadt.
[4] Aldrich Chemical Co.
[5] Fluka.
[6] Eastman Kodak.
[7] Seppic Montanoir.
[8] Bleu Patenté 5, Prolabo.
[9] From porcine stomach mucosa, Sigma Chemical Co.
[10] From porcine pancreas, Sigma Chemical Co.
[11] Calbiochem.
[12] Heidolph: stirring motor type RZRII—adaptation system type RK6.
[13] Potter's homogenizer, Braun.
[14] Leybold.
[15] Clinistix, Ames.

0022-3549/82/0700-0753$01.00/0

Table I—Effect of the Polymerization pH on the Enzymatic Activity of Invertase Microcapsules

pH		
Buffer	Aqueous Phase	Enzymatic Activity, U/mg
9.8	10.8	19.5
8.4	9.8	6.8
7.2	8.8	6.5

Table II—Effect of the Polymerization Duration on the Enzymatic Activity of Invertase Microcapsules

Duration of the Polymerization Step, min	Enzymatic Activity, U/mg
2	17.4
3	19.5
5	19.5
10	13
20	11.5

tivity of the microcapsules was calculated relative to 1 mg of invertase used in each experiment.

Microencapsulation Procedures—A standard emulsion–polymerization procedure is as follows: In a 100-ml beaker cooled in an ice bath, the casein solution (1.5 ml), the invertase suspension (1 ml, *i.e.*, 50 mg of invertase), the hexamethylene diamine solution (0.5 ml), and the 1% solution of sorbitan trioleate (15 ml) were mixed. The stirrer was set at 650 rpm, and the sebacoyl chloride solution (15 ml) was added.

After a 3-min agitation, the suspension was diluted with the organic solvent (30 ml) and centrifuged (350×*g*, 30 sec).

The sediment was dispersed in 40 ml of the polysorbate solution and then transferred to a 500-ml beaker. Dispersion of the microcapsules was achieved by stirring with a glass rod (30 sec) and then by mechanical stirring (650 rpm, 2 min). Water (120 ml) was added, the suspension was agitated (300 rpm, 3 min), and then diluted further with 300 ml of water. A prolonged sedimentation then allowed isolation of the microcapsules, which were again suspended in distilled water.

Variations were introduced in the pH of the aqueous phase, in the duration of the polymerization steps, surfactant concentration, stirring rate, method of isolation of microcapsules, nature of the polyamide, and nature of the protective protein.

In the emulsion–reticulation experiments, no diamine was used in the emulsification step, while a protein (100–800 mg) was reacted with a bifunctional reagent. Cross-linking of invertase itself was performed with terephthaloylchloride with no diamine and no protein added.

Membrane Permeability Test—The typical emulsion–polymerization procedure was performed with 3 mg of erioglaucine A (MW 1159) added during the emulsification step. Blue microcapsules were obtained and one could microscopically observe their progressive discoloration through washing with water.

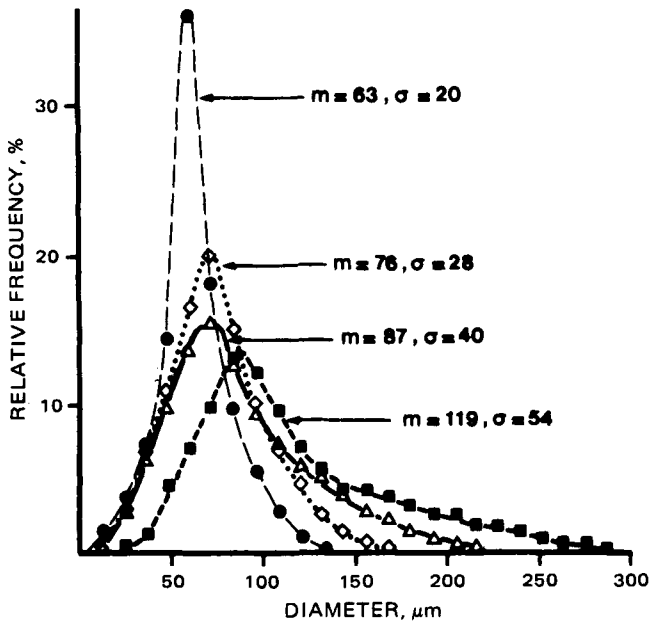

Figure 2—*Effect of the stirring rate on the size of microcapsules. Key: (■), 450 rpm; (△), 650 rpm; (◊), 900 rpm; (●), 1200 rpm.*

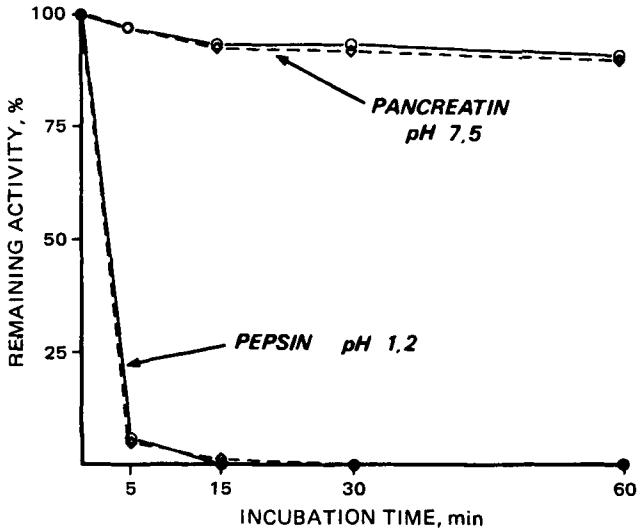

Figure 3—*Effect of proteases on the enzymatic activity of free and encapsulated invertase. Key: (○), free invertase; (◊), encapsulated invertase.*

RESULTS AND DISCUSSION

Interfacial Polymerization—When prepared through the standard procedure, the microcapsules were spherical, with their sizes ranging from 50 to 150 μm. A thin membrane, including insoluble particles of invertase, was to be seen. The permeability test was positive. When washed with water, the capsules became clear; the blue color passed into the surrounding liquid. Their enzymatic activity was 19.5 U/mg used in their preparation, *i.e.*, 57% of the activity (34 U) of free invertase.

Crushing of the microcapsules with an homogenizer[13] resulted only in a slight increase of activity: 22.2 U, *i.e.*, 61% of the activity (36.4 U) of crushed, free invertase. It was then concluded that invertase was lost or inactivated (to an extent of ~40%) during the microencapsulation process.

Lowering the pH of the aqueous phase during polymerization resulted in a loss of activity (Table I). Although the diamine solution increased the pH value, a rather basic medium was necessary for membrane formation.

The optimal duration of the polymerization step was shown (Table II) to be 3–5 min. Shorter time gave unstable capsules; longer time yielded thick membranes and eventually denatured the enzyme. With no surfactant used, no microcapsules were formed.

Increasing the concentration of the surfactant solution from 1 to 2%

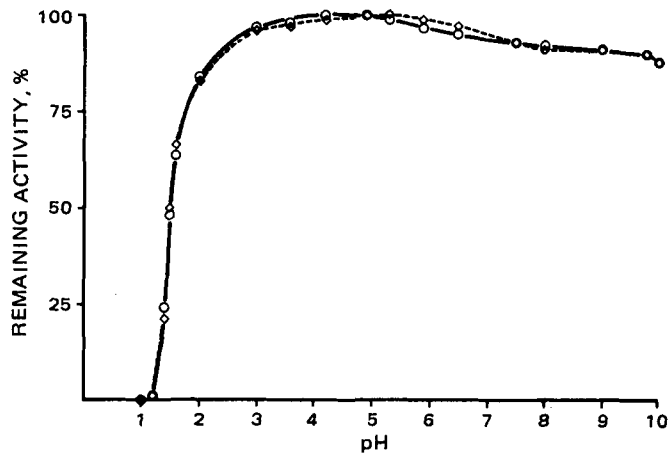

Figure 4—*Remaining activity of invertase (free and microencapsulated) after a 15-min incubation at different pH values. Key: (○), free invertase; (◊), microencapsulated invertase.*

Table III—Activity (U/mg, percent *versus* Free Invertase) of the Microcapsules Prepared from Various Diamines and Bifunctional Agents[a]

Bifunctional Agent	Diamine	Hexamethylene Diamine, 70 mg, 1.2 *M*	Piperazine, 52 mg, 1.2 *M*
Sebacoyl chloride	(67 mg): 0.018 *M*	26 U (76%)	—
Terephthaloyl chloride	(120 mg): 0.04 *M*	11.5 U (34%)	25.3 U (74%)
	(375 mg): 0.12 *M*	21 U (62%)	—
Toluene diisocyanate	(375 mg): 0.14 *M*	27 U (79%)	25.3 U (74%)

[a] Quantities in milligrams of the reagents used for 50 ml of invertase.

Table IV—Enzymatic Activity of Invertase Microcapsules after Incubation in Protease-Containing Media

Polymer	Initial Activity, U/mg (Percent *versus* Free Invertase)	Remaining Activity After Incubation, U/mg (Percent Initial Activity)						
		Pepsin, pH 1.4			Pancreatin, pH 7.5		Pronase, pH 8	
		5 min	15 min	30 min	5 min	30 min	5 min	30 min
None: free invertase	34(100)	15.5(48)	8(25)	2(6)	33.3(98)	31.7(93)	33.4(98)	31.4(92)
Hexamethylene diamine–Sebacoyl chloride	26(76)	12.9(50)	6.8(26)	1.8(7)	24.9(96)	25(96)	26.5(102)	26(100)
Hexamethylene diamine–Terephthaloylchloride, 120 mg	11.5(34)	9.2(80)	6.3(55)	2.6(23)	13.3(121)	18.2(166)	15.1(137)	19.2(175)
Hexamethylene diamine–Terephthaloylchloride, 375 mg	21(62)	15.8(75)	8.2(39)	2.7(13)	23.6(112)	25(119)	24(114)	25.3(120)
Hexamethylene diamine–Toluene diisocyanate	27(79)	12.4(46)	6.2(23)	1.6(6)	26.5(98)	26.5(98)	26.8(99)	27(100)

(Fig. 1) had little effect on the average size (87–73 μm) but resulted in a more homogeneous repartition of the diameters. With a 5% solution, however, the membranes were altered and a large amount of invertase escaped microencapsulation.

When the stirring speed was raised from 450 to 1200 rpm, the size of the capsules decreased regularly, while the distribution of their diameter became more and more homogeneous (Fig. 2). Simultaneously, the enzymatic activity rose to a maximum of 21.3 U/mg (63% retention).

Stirring became more efficient when the 3-bladed screw was replaced by a 5-bladed screw (each blade was 20 mm long, 9 mm wide).

The separation and washing of the microcapsules from the reaction medium is the most time-consuming step in the process. Several attempts were unsuccessful (replacement of polysorbate by other surfactants and washing with organic solvents: ethanol, dioxane, and acetone inactivated the enzyme). Another technique afforded an improvement. The sediment from the first centrifugation was suspended in a mixture of glycerin–polysorbate (3:1, v/v, 5–10 ml) and 50 ml of distilled water was added. After agitation and centrifugation (350×*g*, 5 min) the sediment was washed several times with water.

After lyophilization, observation of the dried microcapsules (optical *versus* electron scattering microscopy) showed the integrity of the membranes; they rehydrated instantaneously with no modification of the shape. When held at +4° for 50 days, the aqueous suspension lost 15% of its initial activity, while the lyophilizate completely retained the enzymatic activity.

Evaluation of the Protection of the Enzyme—The protecting effect of the microcapsule wall was evaluated toward proteolytic enzymes. Figure 3 shows that no noticeable differences were observed regarding the protection of the free *versus* microencapsulated invertase toward pancreatin and pepsin. The same result was obtained with pronase since the activity curve was similar to the curve established with pancreatin.

This unsatisfying result was readily explained when the activity of invertase was tested after a short incubation time at different pH values, with no other enzyme added (Fig. 4).

In agreement with literature data (14), invertase (either free or microencapsulated) was irreversibly denatured by standing in acidic medium <pH 3.

Changes in the nature of the wall were studied according to Table III.

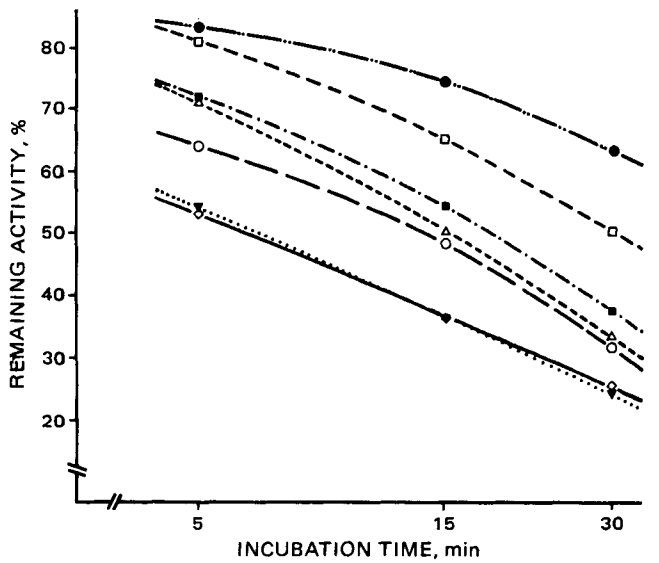

Figure 5—*Remaining activity of different invertase microcapsules after incubation at pH 1.5. Key: (●), hexamethylene diamine, terephthaloylchloride, 120 mg; (□), hexamethylene diamine, terephthaloylchloride, 375 mg; (■), hexamethylene diamine, toluene diisocyanate; (△), hexamethylene diamine, sebacoylchloride; (○), free invertase; (◊), piperazine, terephthaloylchloride; (▼), piperazine, toluene diisocyanate.*

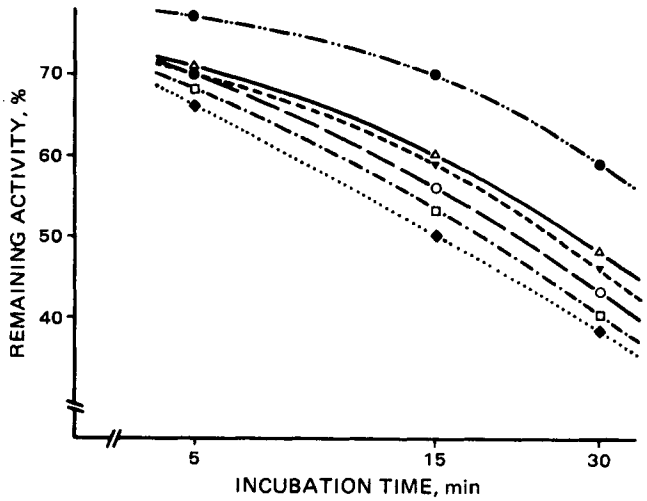

Figure 6—*Remaining activity of invertase microcapsules with nylon 6-10 membrane after incubation at pH 1.55. Protective effect of added proteins. Key: (●), gelatin; (△), casein, 100 mg; (▼), hemoglobin, 100 mg; (○), free invertase; (□), ovalbumin, 100 mg; (♦), albumin, 100 mg.*

Table V—Properties of Invertase Microcapsules with Nylon 6-10 Membranes Containing Different Proteins

Batch Number	Associated Protein (Weight)	Mean Diameter, μm	Invertase Activity, U/mg (% *versus* Free Invertase)	Effect of Incubation at pH 1.55 on the Invertase Activity, U/mg (% Initial Activity) 5 min	15 min	30 min
0	Free Invertase	—	34(100)	23.8(70)	19(56)	14.6(43)
1	Casein (100 mg)	50	26(76)	18.5(71)	15.6(60)	12.5(48)
2	Casein (50 mg)	45	25.7(75)	17.2(67)	13.6(53)	11.1(43)
3	Casein (200 mg)	60	23.2(68)	17.2(74)	14.2(61)	11.1(48)
4	Protamin (100 mg)	—	—[a]	—[a]	—[a]	—[a]
5	Albumin (100 mg)	50	25.3(74)	16.7(66)	12.7(50)	9.6(38)
6	Ovalbumin (100 mg)	50	26.3(77)	17.9(68)	13.9(53)	10.5(40)
7	Gelatin (100 mg)	40	20.4(60)	15.7(77)	14.3(70)	12(59)
8	Hemoglobin (50 mg)	50	21.1(62)	13.7(65)	10.3(49)	7.8(37)
9	Hemoglobin (100 mg)	45	20.8(61)	14.6(70)	12.3(59)	9.6(46)
10	Hemoglobin (200 mg)	50	21.6(64)	15.6(72)	13.2(61)	10.4(48)
11	Hemoglobin (400 mg)	65	19.9(59)	13.7(69)	11.1(56)	9.6(48)

[a] Isolation of microcapsules very difficult.

Table VI—Feasability of Microcapsules with Cross-Linked Protein Membrane

Protein–Acylating Agent		Feasability of Microcapsules
Casein–Sebacoyl chloride		Very unstable microcapsules
Casein–Terephthaloylchloride		Unstable but isolable
Albumin–Sebacoyl chloride		No microcapsules (after 3 min)
Albumin–Terephthaloylchloride	Albumin = 200 mg	Unstable but isolable
	Albumin = 400 mg	Stable microcapsules
Ovalbumin–Sebacoylchloride		No microcapsules (after 3 min)
Ovalbumin–Terephthaloylchloride	Ovalbumin = 200 mg	Unstable but isolable
	Ovalbumin = 400 mg	Stable microcapsules
Gelatin–Terephthaloylchloride		Unstable but isolable
Gelatin–Toluene diisocyanate		Stable microcapsules
Gelatin–Hexamethylene diisocyanate		Unstable but isolable
Gelatin–Succinyldichloride		Immediate coagulation after addition of succinyldichloride
Hemoglobin–Sebacoyl chloride		Stable microcapsules
Hemoglobin–Terephthaloylchloride	Hemoglobin = 400 mg	Very unstable microcapsules
	Hemoglobin = 600 mg	Stable microcapsules
Hemoglobin–Succinyldichloride		Stable microcapsules
Hemoglobin–Hexamethylene diisocyanate		Very unstable microcapsules

Stirring was effected by means of a 5-bladed screw at a speed of 1200 rpm.

The surfactant solution was 2% sorbitan trioleate. Isolation and washing of the microcapsules were performed through the glycerin–polysorbate method.

Formation of the microcapsules was satisfactory in every case except for the polymerization of piperazine with 0.04 *M* terephthaloylchloride. The mean size was 50 μm.

According to the improvements in the process, the activity of the microcapsules made from hexamethylene diamine and sebacoyl chloride reached 26 U/mg.

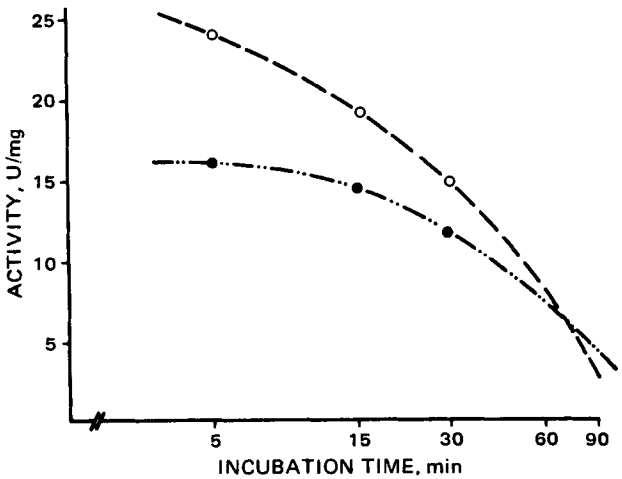

Figure 7—*Invertase microcapsules containing gelatin (nylon 6–10 membrane). Remaining activity after incubation at pH 1.55 as compared with free invertase. Key: (○), microcapsules with gelatin; (●), free invertase.*

These microcapsules were incubated at pH 1.5 for 5–30 min. The results of the activity measurements are plotted in Fig. 5: no radical improvement in the protection of invertase could be noticed. Moreover, the capsules made from hexamethylene diamine and terephthaloylchloride were destroyed by pancreatin, while an increase in the invertase activity was observed (Table IV).

Table VII—Microcapsules with Cross-Linked Protein Membrane: Mean Particle Size

Batch Number	Protein and Acylating Agent Nature and Weight, mg	Mean Diameter, μm
14	Casein, 200–Terephthaloylchloride, 375	50–100
15	Albumin, 400–Terephthaloylchloride, 750	40–80
16	Albumin, 600–Terephthaloylchloride, 750	40–70
17	Ovalbumin, 200–Terephthaloylchloride, 375	50–90
18	Ovalbumin, 400–Terephthaloylchloride, 375	20–100
19	Gelatin, 100–Terephthaloylchloride, 375	40–70
20	Gelatin, 100–Toluene diisocyanate, 750	20–40
21	Hemoglobin, 600–Terephthaloylchloride, 375	70–100
22	Hemoglobin, 800–Terephthaloylchloride, 375	120–150
23	Hemoglobin, 400–Sebacoyl chloride, 670	30–70
24	Hemoglobin, 600–Sebacoyl chloride, 670	40–80
25	Hemoglobin, 400–Succinyldichloride, 100	10–45

Table VIII—Microcapsules with Cross-Linked Protein Membrane: Effect of an Acidic Medium

Batch Number	Protein and Acylating Agent; Nature and Weight, mg	Activity, U/mg (Percent of Activity of Invertase Used)	Remaining Activity after Incubation at pH 1.5, U/mg (Percent of Initial Activity) 5 min	15 min	30 min
	Free Invertase	34(100)	21.6(64)	16.3(48)	10.5(31)
1	Nylon 6-10	26(76)	18.5(71)	13(50)	8.5(33)
14	Casein, 200–Terephthaloylchloride, 375	25(74)	14.5(58)	10(40)	6(24)
15	Albumin, 400–Terephthaloylchloride, 750	30(88)	21.6(72)	16.5(55)	11.4(38)
16	Albumin, 600–Terephthaloylchloride, 750	32(94)	24.3(76)	18.6(58)	12.8(40)
17	Ovalbumin, 200–Terephthaloylchloride, 375	26(76)	16.3(61)	11.5(44)	6.2(24)
18	Ovalbumin, 400–Terephthaloylchloride, 375	29.5(87)	15.1(51)	10(34)	5.3(18)
19	Gelatin, 100–Terephthaloylchloride, 375	10.4(31)	3.6(34)	2.7(26)	1.8(17)
20	Gelatin, 100–Toluene diisocyanate, 750	15(44)	6.6(44)	4.4(29)	3(20)
21	Hemoglobin, 600–Terephthaloylchloride, 375	32(94)	28.8(90)	23.4(73)	15.7(49)
22	Hemoglobin, 800–Terephthaloylchloride, 375	30(88)	27.6(92)	23.7(79)	18.9(63)
23	Hemoglobin, 400–Sebacoyl chloride, 670	32(94)	24(75)	18.6(58)	14.1(44)
24	Hemoglobin, 600–Sebacoyl chloride, 670	33(97)	27.7(84)	20.8(63)	15.5(47)
25	Hemoglobin, 400–Sucinyldichloride, 100	26(76)	21(81)	17.9(69)	15(58)

Table IX—Microcapsules of Cross-Linked Invertase (Terephthaloylchloride) Enzymatic Activity

Invertase, mg	Terephthaloylchloride, mg	Activity U/mg	% Activity of the Invertase Used	Total Activity, U Calculated	Measured	Difference
100	375	7.5	22	3400	750	−2650
200	375	16.3	48	6,800	3250	−3550
400	375	25.2	74	13,600	10,050	−3550

Changes in the Nature of the Protective Protein—To protect the microencapsulated invertase from the effect of lower pH values, changes were introduced in the nature and concentration of the accompanying protein (*i.e.*, alcalisoluble casein in the standard procedure). The following proteins were checked: protamine[16], human serum albumin, egg albumin, gelatin, human hemoglobin. These proteins were incorporated as 4% (w/v) solutions in the buffer, pH 9.8. The membrane was made from hexamethylene diamine and sebacoyl chloride (nylon 6-10) as before.

Protamine failed to give well-constituted microcapsules, as a reaction between protamine and the diacylchloride occurred. This observation prompted the development of the reticulation method. The results of successive assays are summarized in Table V.

The initial activity of all microcapsules prepared was in the 20–26 U/mg range. The slight decrease of activity observed with the higher concentrations in proteins may be due to a slowing down of the diffusion rate inside the capsules.

Figure 6 plots for six assays the effect of incubation at pH 1.55 on the enzymatic activity as a percentage of the initial activity of each batch. The good performance of gelatin is better illustrated in Fig. 7, where the invertase activity is now plotted as a percentage of the activity of the invertase used in the preparation. The slopes of the curves indicate that after ~1 hr, the microcapsules retain more enzymatic activity than does an equal amount of free invertase. However, only 6 U/mg (18% of activity) is still available.

Emulsification–Reticulation Procedure—While protamine actually afforded well-defined capsules, this protein rapidly was shown not to be an ideal material. With sebacoyl chloride (whatever the protamine concentration), the reticulation period necessary for gaining solid capsules had to be raised to 30 min. However, the membranes were very thin and vanished in water after 24 hr at +4°. With terephthaloylchloride, the results were somewhat better but the initial activity was low: with 200 mg of protamine and 750 mg of terephthaloylchloride (batch 12), it was 8.5 U (25%); with 400 mg of protamine (batch 13) it was 11 U (32%).

Using other cross-linked proteins gave better results. Table VI reports

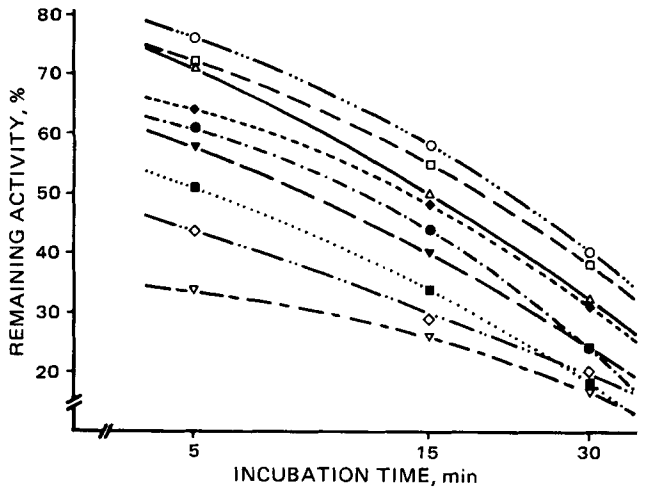

Figure 8—*Invertase microcapsules with cross-linked protein membrane: remaining activity after incubation at pH 1.5. Key: (○), batch 16 (Albumin, 600 mg–Terephthaloylchloride, 750 mg); (□), batch 15 (Albumin, 400 mg–Terephthaloylchloride, 750 mg); (△), batch 1 (Nylon 6-10); (♦), free invertase; (●), batch 17 (ovalbumin, 200 mg–terephthaloylchloride, 375 mg); (▼), batch 14 (casein, 200 mg–terephthaloylchloride, 375 mg); (■), batch 18 (ovalbumin, 400 mg–terephthaloylchloride, 375 mg); (◇), batch 20 (gelatin, 100 mg–toluene diisocyanate, 750 mg); (▽), batch 19 (gelatin, 100 mg–terephthaloylchloride, 375 mg).*

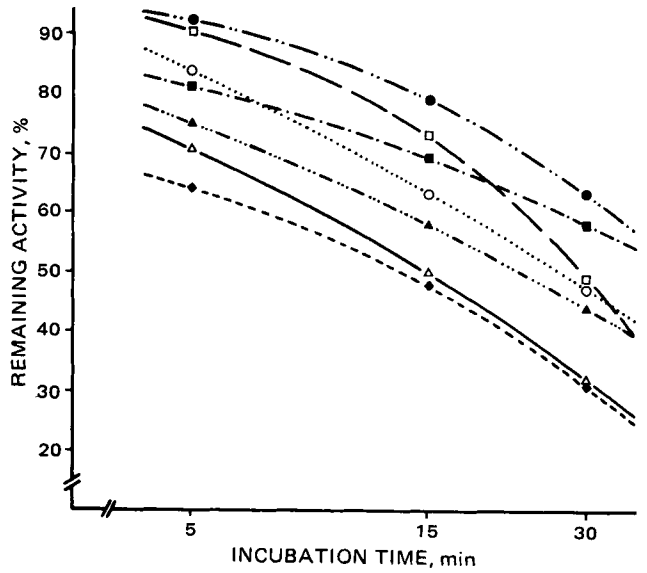

Figure 9—*Invertase microcapsules with cross-linked hemoglobin membrane: remaining activity after incubation at pH 1.5. Key: (●), batch 22 (hemoglobin, 800 mg–terephthaloylchloride, 375 mg); (□), batch 21 (hemoglobin, 600 mg–terephthaloylchloride, 375 mg); (○), batch 24 (hemoglobin, 600 mg–sebacoylchloride, 670 mg); (■), batch 25 (hemoglobin, 400 mg–succinyldichloride, 100 mg); (▲), batch 23 (hemoglobin, 400 mg–sebacoylchloride, 670 mg); (△), batch 1 (Nylon 6-10); (♦), free invertase.*

[16] Choay.

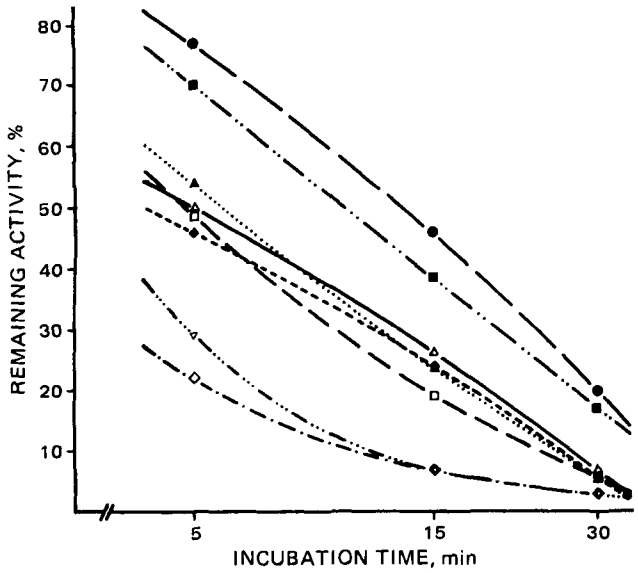

Figure 10—*Invertase microcapsules with acylated protein membrane: remaining activity after incubation with pepsin at pH 1.4. Key: (●), batch 25 (hemoglobin, 400 mg–succinyldichloride, 100 mg); (■), batch 22 (hemoglobin, 800 mg–terephthaloylchloride, 375 mg); (▲), batch 16 (albumin, 600 mg—terephthaloylchloride, 750 mg); (□), batch 17 (ovalbumin, 200 mg—terephthaloylchloride, 375 mg); (△), batch 1 (nylon 6-10); (♦), free invertase; (▽), batch 14 (casein, 200 mg–terephthaloylchloride, 375 mg); (◇), batch 20 (gelatin, 100 mg–toluene diisocyanate, 750 mg).*

on the feasability of various microcapsules while Tables VII and VIII summarize the results on batches 14–25.

The high retention of activity obtained with hemoglobin (94–97%), serum albumin (88–94%), and egg albumin (87%) is of interest.

Batches 15 and 16 (Fig. 8), and especially the microcapsules prepared from hemoglobin (batches 21–25, Fig. 9), were more resistant than the free enzyme toward inactivation caused by standing at pH 1.5.

The membrane was digested by the proteases. The microcapsules were destroyed within 5 (hemoglobin)–15 min (ovalbumin) in pepsin, pancreatin, or pronase. However, in some cases, and especially with hemoglobin (Fig. 10), a significant retention of activity was observed, even after the membrane was no longer visible.

Immobilized Invertase—An attempt was made to acylate invertase with no protein added. The reticulation agent was terephthaloylchloride. The amount of invertase admixed to 375 mg of terephthaloylchloride (2.5% solution (w/v) in the organic solvent) varied from 50 to 400 mg.

Though somewhat unstable, spherical microcapsules were obtained. Washing and transfer to water were only possible with the 100–400-mg capsules. The membranes did not survive a 3–4 day stay in water at +4°.

When evaluated immediately after the preparation, the enzymatic activity was as reported in Table IX. The loss of activity due to acylation tends to be a constant value. Terephthaloylchloride (375 mg) stoichiometrically combines with invertase so as to inhibit 3550 U of activity.

While invertase encapsulated in nylon membranes was irreversibly denatured by incubation in acidic medium, incorporation of various proteins in the capsules allowed relative protection. However, an interaction between the proteins and the bifunctional acylating agent was suspected and prompted the preparation of invertase encapsulated in cross-linked proteins. Invertase itself could be used both as the contents and as the cross-linked membrane. Application of this microencapsulation process to various proteins and polyhydroxylated substrates is under current investigation.

REFERENCES

(1) A. Dahlquist, *J. Clin. Invest.*, **41**, 463 (1962).

(2) H. A. Weijers, J. H. Kamer, D. H. A. Mossel, and W. R. Dicke, *Lancet* 296 (1960).

(3) C. Collombel and J. Cotte, *Pediatrie* 88 (1972).

(4) G. Schapira and J. C. Dreyfus, in "Pathologie moléculaire—Biologie moléculaire 2," Masson, Paris, 1975, p. 213.

(5) D. B. Johnson, M. L. O'Connor, T. J. Hackett, and M. Kierstan, *Biochem. Soc. Trans.*, **7**, 1, 21 (1979).

(6) P. Rambourg, J. Lévy, F. Puisieux, and M.-C. Lévy, Microencapsulation I, 2nd Int. Cong. Pharm. Technol., Paris, 1980, III, p. 5.

(7) M.-C. Lévy, P. Rambourg and J. Lévy, Microencapsulation II, 2nd Int. Cong. Pharm. Technol., Paris, 1980, III, p. 15.

(8) P. Rambourg, "Sur la microencapsulation de l'invertase et de l'hémoglobine: de la polymérisation interfaciale au procédé d'émulsion-réticulation." Thèse Doctorat 3ème cycle Université Paris-Sud—U.E.R. Chimie Thérapeutique 1980.

(9) T. M. S. Chang, *Science*, **146**, 524 (1964).

(10) T. M. S. Chang, F. C. MacIntosh, and S. G. Mason, *Can. J. Physiol. Pharmacol.*, **44**, 115 (1966).

(11) O. Miyawaki, K. Nakamura, and T. Yano, *Agric. Biol. Chem.*, **43**, 5, 1133 (1979).

(12) T. M. S. Chang, "Artificial Cells," Charles C Thomas, Springfield, Ill., 1972.

(13) A. Goldstein and J. O. Lampen, in "Methods in Enzymology," Academic, New York, N.Y., 1977, p. 504.

(14) K. Myrback, in "The Enzymes," 2nd ed., Vol. 4, P. Boyer, M. Lardy, and K. Myrback, Eds., Academic, New York, N.Y., 1960, p. 379.

Microencapsulation IV: Cross-Linked Hemoglobin Microcapsules

M.-C. LÉVY *x, P. RAMBOURG *, J. LÉVY *, and G. POTRON ‡

Received July 15, 1981, from the **Laboratoire de Pharmacie Galénique, E.R.A. au C.N.R.S. n° 319, Faculté de Pharmacie, 51, rue Cognacq-Jay, F 51096 REIMS Cédex, France.* and the *‡Laboratoire d'Hématologie, Centre Hospitalier Universitaire, Place Alexis Carrel, F 51092 REIMS Cédex, France.* Accepted for publication October 5, 1981.

Abstract □ Hemoglobin microcapsules were prepared through cross-linking of hemoglobin itself with various acyldichlorides. Variations in the reticulation conditions were performed in order to ameliorate the oxygen dissociation curve, the mean diameter, and the possibility for the microcapsules to be lyophilized. With terephthaloylchloride, as the cross-linking agent, incorporation of inositol hexaphosphate and glucose, followed by stabilization through glutaraldehyde and using a high stirring speed, allowed preparation of stable hemoglobin microcapsules, 5 μm in diameter, which suffered rapid lysis by proteases. They were able to ensure oxygen transfer: the dissociation curve was sigmoidal with a p50 = 13 mm Hg. They retained these properties after lyophilization followed by rehydration.

Keyphrases □ Hemoglobin—preparation of cross-linked microcapsules □ Microencapsulation—preparation of cross-linked hemoglobin microcapsules □ Cross-linking—proteins, microencapsulation of hemoglobin

Human hemoglobin has been subjected to microencapsulation by several authors: Chang (1–4) was the first to prepare hemoglobin microcapsules through interfacial polymerization or coacervation processes. However, the membrane made of nylon, polystyrene, collodion, or silicon rubber (dimethicone membrane[1]) failed to be biodegradable.

More recently, Kondo (5–8) used polyphthaloyl-L-lysine as the wall-constituting polymer and the microcapsules could be digested by proteolytic enzymes.

Vigneron (9, 10) obtained similar results through interfacial polymerization between sebacoyl chloride and hexamethylene diamine with L-lysine admixed.

On the other hand, whereas cross-linking of hemoglobin by various reagents [dialdehydes (11, 12), carbodiimides (13), diepoxides, diisocyanates (14), and unsaturated sulfones (14, 15)] has been extensively studied, application of the procedure to clinical problems has been restricted to the preparation of hemoglobin, modified in order to increase its life-span when used as a blood replacement fluid.

In continuation of microencapsulation experiments through cross-linking of proteins (16–18), this paper deals with the application of this concept to hemoglobin.

EXPERIMENTAL

Reagents—Human hemoglobin was used. Red blood cells were collected from citrated human blood by centrifugation and washed with isotonic sodium chloride solution. After centrifugation, the red cells were subjected to hemolysis. Stromas were eliminated by successive filtration through membranes with porosities of 3 μm then 0.2 μm. The hemoglobin solution (6%, w/v) was added to glucose (2%, w/v) and then lyophilized.

Several buffers were prepared with pH's ranging from 9.8 (0.45 *M* Na_2CO_3; HCl to pH 9.8); [0.5 *M* bis(2-hydroxyethyl)amino-tris(hydroxymethyl) methane(I)[2]; HCl to pH 9.8] to 10.5 (0.45 *M* Na_2CO_3; HCl to pH 10.5); and 11.5 (0.45 *M* Na_2CO_3; HCl to pH 11.5), (2 *M* Na_2CO_3; HCl to pH 11.5).

The organic solvent was chloroform–cyclohexane (1:4, v/v). It was used to prepare solutions of terephthaloylchloride[3] (2.5 and 5 g%, w/v), sebacoyl chloride[3] (2.25 and 4.5 g%, w/v), and succinylchloride[4] (0.25, 0.50, and 1 g%, w/v).

An etheral solution of 12% glutaraldehyde (v/v) was prepared from a 25% aqueous solution[3] (v/v) through extraction with diethyl ether from a sodium chloride-saturated solution.

The surfactants were sorbitan trioleate[5] [2, 5, and 10% solutions (v/v) in the organic solvent] sorbitan monolaurate[5] [5 and 10% solutions (v/v) in the organic solvent], lecithin from soybean[6] [1, 2, 3, and 5% solutions (w/v) in the organic solvent]. Polysorbate[5] was used for the transfer of microcapsules, as a 1:3 mixture (v/v) with glycerin.

The other reagents were inositol hexaphosphate[2], sodium chloride solution 0.9 g% (w/v), and buffered sodium chloride solution, pH 7.3.

Macromolecular solutions (plasma substitutes) were used for resistance assays (dextran[7], modified gelatin[8,9]).

Materials—A stirrer[10], fitted with a 5-bladed screw (maximal speed: 1800 rpm) was first used and later replaced by an homogenizer[11], fitted with a metallic double blade (maximal speed: 23,000 rpm).

The oxygen dissociation curves were recorded with an analyzer[12].

Procedures—The hemoglobin lyophilisate (1.4 g, corresponding to 0.35 g of glucose and 1.05 g of hemoglobin) was dissolved in the buffer (3 ml) and emulsified with 15 ml of 2% surfactant solution (1200 rpm) at 0°.

The acylchloride solution (15 ml) was added and stirred for 3 min. The organic solvent (30 ml) was then mixed into the suspension. After centrifugation (350×*g*, 30 sec), the sediment was resuspended in the glycerin–surfactant mixture (5–10 ml) to which 50 ml of 0.9% aqueous NaCl was then added. The suspension was centrifuged (350×*g*, 5 min) and the sediment washed twice in 0.9% NaCl. Finally, the hemoglobin microcapsules were suspended in 30 ml of buffered sodium chloride solution.

After freezing at −30°, the suspension was easily lyophilized to yield a light brownish powder.

Modifications in the Reticulation Conditions—*Buffer*—Several 0.45 *M* Na_2CO_3 buffers (pH increasing from 9.8 to 11.5) were used during the polymerization step. Other attempts were made with a 2 *M* Na_2CO_3 buffer (pH 11.5) and with a I buffer[2], pH 9.8.

Acylating Agent—Several acyldichlorides were used as acylating agents at different concentrations: terephthaloylchloride, sebacoyl chloride, succinyldichloride, and a dialdehyde:glutaric dialdehyde.

Surfactant—Sorbitan trioleate, sorbitan monolaurate, and soybean lecithin were checked at different concentrations during the polymerization step.

Stirring—Variations of stirring conditions were made by replacement of the stirrer[10] by an homogenizer[11].

Temperature—Microcapsules were prepared at 20, 0, and −10°. Use of a nitrogen atmosphere was attempted to avoid oxidation of hemoglobin.

Further Treatment of the Microcapsules—Before lyophilization

[1] Silastic.

[2] Sigma.
[3] Aldrich.
[4] Fluka.
[5] Seppic Montanoir.
[6] Metabio.
[7] Rheomacrodex, Egic.
[8] Plasmagel, Roger Bellon.
[9] Haemaccel, Hoechst.
[10] Heidolph stirrer—stirring motor type RZRII—Adaptation system type RK6.
[11] Virtis 23 homogenizer, Bioblock.
[12] Hem-O-Scan analyzer, Aminco.

0022-3549/82/0700-0759$01.00/0

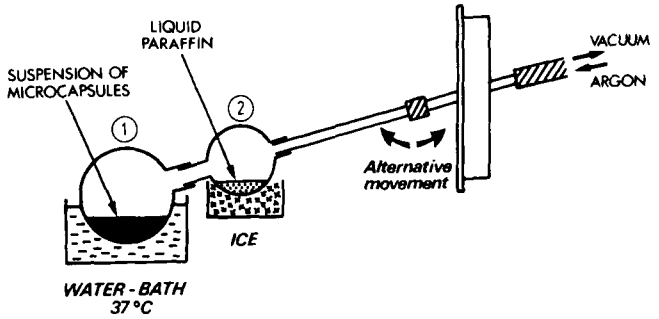

Figure 1—*Scheme of the apparatus used for deoxygenation of microencapsulated hemoglobin.*

glucose was added to the microcapsule suspension, as a hemoglobin protector (19).

Stabilization with Glutaraldehyde—To strengthen the cross-linked wall, microcapsules were prepared according to the following process: Microcapsules were obtained from hemoglobin and terephthaloylchloride at 0° in a pH 9.8 buffer with 5% sorbitan monolaurate (stirring speed: 1800 rpm). The capsules were centrifuged, resuspended in 60 ml of 0.9% NaCl solution, and 0.4 ml of a 25% aqueous glutaraldehyde solution was added. After a 3-min reaction, the capsules were isolated as before.

Incorporation of Inositol hexaphosphate—Inositol hexaphosphate is known to lower the oxygen affinity of hemoglobin (20, 21). Therefore, it was added to the hemoglobin microcapsules, either through incubation (20 hr, 4°) of the microcapsules in the phosphate solution (external phase) or during the preparation of the microcapsules (internal phase).

Assays—*Centrifugation*—Microcapsules were centrifuged for 60 min at 100,000×*g* (4°).

Resistance of Microcapsules to Ultrasound—Evaluation followed a 15-min treatment at 45 kHz.

Resistance to Freezing–Defreezing Cycles—Freezing at −30° followed by melting at 20° was repeated 4 times.

Aging—Suspensions of capsules in water or in 0.9 g% NaCl solution were stored at +4°.

Resistance to Macromolecular Solutions—Microcapsules were suspended in different macromolecular plasma substitutes at 37°.

Degradability Effect of Proteases—Microcapsules were incubated at 37° in different media containing proteases: pepsin (0.32 g %, w/v) in a hydrochloric acid solution (pH 2); pancreatin (1 g %, w/v) in a KH_2PO_4–NaOH buffer (pH 7.5); pronase 4×10^{-3} g % (w/v) in a $Na_2B_4O_7$–KH_2PO_4 buffer (pH 8) with $Ca(CH_3COO)_2$ (0.176 g %, w/v).

Oxygen Transfer Properties—Permeability toward oxygen was studied by using the apparatus depicted in Fig. 1.

A suspension of microcapsules of suitable concentration was prepared in a phosphate buffer (pH 7.5). Flask 1 contained the suspension and was heated to 37°. Flask 2 contained liquid petrolatum[13] and was cooled in an ice bath. The apparatus was continuously agitated and evacuated to 10^{-1}–10^{-2} T, after which argon was introduced. After several cycles, the apparatus was placed in an upright position so as to cover the deoxygenated suspension with liquid petrolatum. The microcapsule suspension was then transfered into the measurement cell of a spectrometer through a syringe containing liquid petrolatum so as to avoid any contact with air.

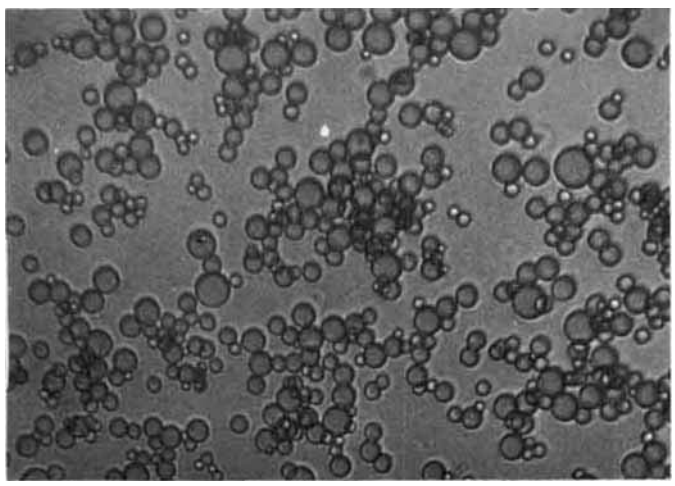

Figure 2—*Photomicrograph of hemoglobin microcapsules with cross-linked hemoglobin membrane (terephthaloylchloride).*

[13] Nujol.

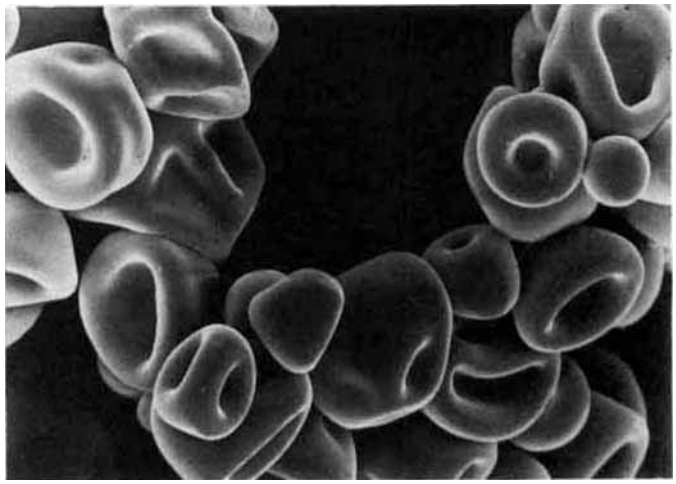

Figure 3—*Scanning electron micrograph of hemoglobin microcapsules with cross-linked hemoglobin membrane (terephthaloylchloride).*

After recording of the initial spectrum of the microcapsules, progressive reoxygenation was performed by bubbling air through the suspension with a syringe (0.5 ml in 15 sec) while the spectra were successively measured.

The saturation curve was recorded by plotting the percentage of oxyhemoglobin *versus* the partial pressure of oxygen.

RESULTS AND DISCUSSION

The initial typical procedure gave reddish spherical microcapsules. Their size was ~60 μm (σ = 23 μm) (Fig. 2).

A scanning electron micrograph of the dehydrated microcapsules is presented in Fig. 3.

Hemoglobin was chemically modified by terephthaloylchloride, which was indicated by examination of the film, isolated at the interface of an aqueous solution of hemoglobin and an organic solution of terephthaloylchloride. The IR spectrum of the film showed significant differences from that of hemoglobin in the fingerprint area (700–1500 nm).

After a 60-min centrifugation at 100,000×*g* (4°), the microcapsules were found mainly unaltered. However, the supernate was slightly colored, indicative of some hemoglobin leak. The microcapsules resisted a 15-min treatment by ultrasound at 45 kHz. Four freezing–defreezing cycles did not affect the microcapsules. Rehydration of the lyophilized microcapsules regenerated their spherical shape; however, a large amount of hemoglobin (20–25% of the total amount of hemoglobin used) was oxidized to methemoglobin during the process. Suspending the capsules in water resulted in turgescence, diffusion of hemoglobin, and, finally, lysis of the membrane. In 0.9% NaCl solution, hemoglobin also slowly diffused into the medium. After suspension in macromolecular solutions, optical microscopic observation showed the membrane to be collapsed, especially in the case of the larger capsules. The original spherical shape was regenerated through resuspension in an isotonic aqueous medium.

Table I—Hemoglobin Microcapsules with a Cross-Linked Hemoglobin Wall (Terephthaloylchloride): Influence of Nature and Concentration of the Lipophilic Surfactant [a]

Surfactant	Concentration, %	Mean diameter, μm	σ, μm
Sorbitan trioleate	2	40.8	18.9
	5	32.6	13.9
	10	23.4	10.8
Sorbitan monolaurate	5	24.9	8
	10	27.4	11.5
Soybean lecithin	1	27	10.2
	2	30.6	12.5
	3	30.2	12.5
	5	26.9	13

[a] Stirring speed: 1600 rpm.

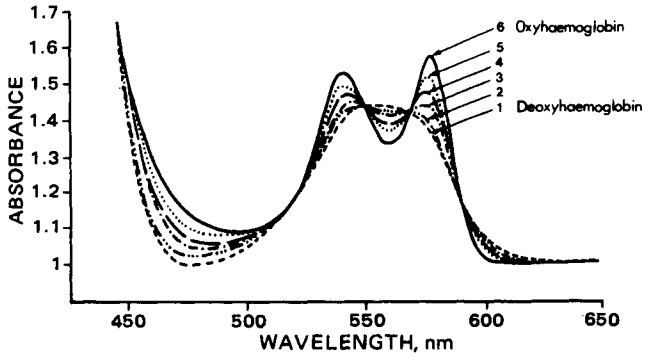

Figure 4a—*Visible absorption spectra of hemoglobin microcapsules: progressive reoxygenation of deoxyhemoglobin (curve 1) to oxyhemoglobin (curve 6).*

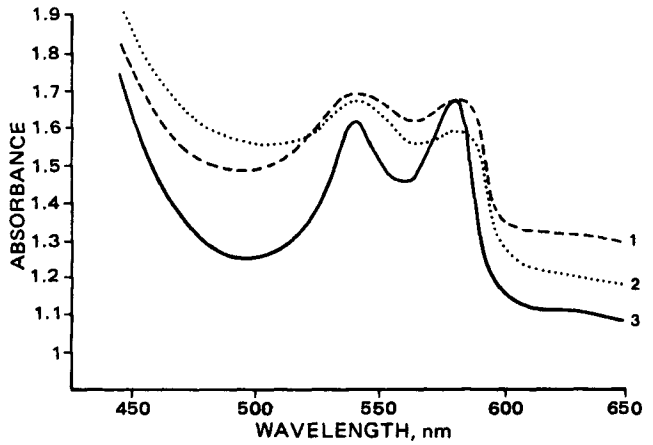

Figure 4b—*Absorption spectra of hemoglobin microcapsules, influence of the cross-linking reagent. Key: curve 1, terephthaloylchloride; curve 2, sebacoyl chloride; curve 3, glutaraldehyde.*

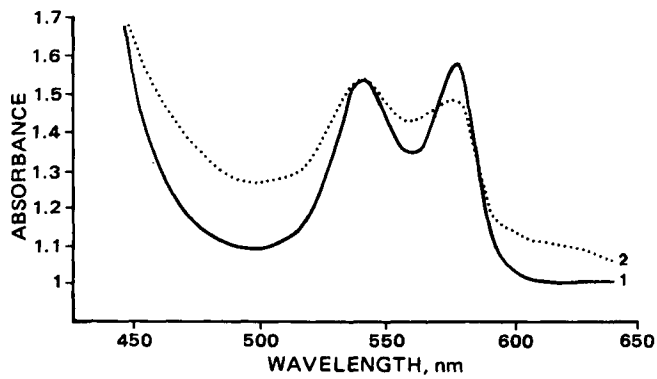

Figure 4c—*Absorption spectra of lyophilized hemoglobin microcapsules (terephthaloylchloride as cross-linking agent). Key: curve 1, glucose added prior to lyophilization; curve 2, without glucose.*

The microcapsules were destroyed after a 2-min incubation in pepsin or pronase, 1-min in pancreatin.

The electronic spectrum of the deoxygenated capsules (Fig. 4a) was characteristic of deoxyhemoglobin and gradually changed to the spectrum of oxyhemoglobin upon oxygenation.

The oxygen dissociation curve (curve 1, Fig. 5a) was not sigmoidal and differed from that of a hemoglobin solution (curve 3) or of normal human blood (curve 4). The p50 was only 6 mm Hg.

The initial procedure then allowed preparation of relatively stable hemoglobin microcapsules, the membranes of which were resistant, biodegradable, and permeable to oxygen.

However, the mean diameter was far too large, presence of methemoglobin had to be avoided, the lyophilization process needed improvements, and the oxygen affinity had to be reduced.

The following results were gained upon modifications of the procedure: Attempts to raise the pH of the 0.45 *M* Na_2CO_3 buffer from 9.8 to 11.5,

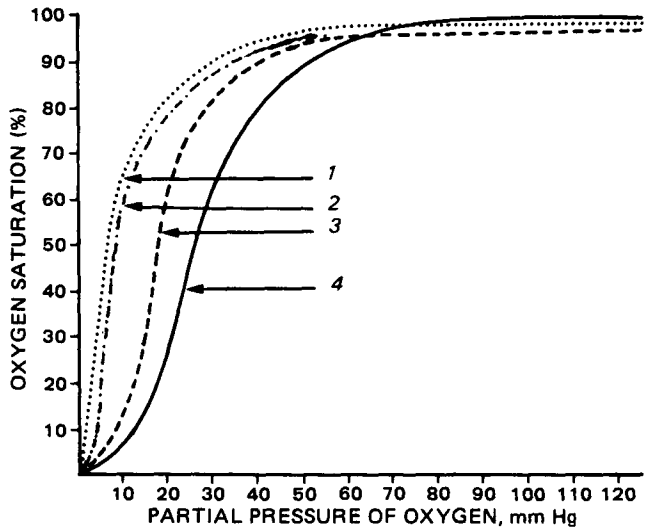

Figure 5a—*Oxygen dissociation curves. Key: curve 1, hemoglobin microcapsules with terephthaloylchloride as cross-linking agent; curve 2, hemoglobin microcapsules with glutaraldehyde as cross-linking agent; curve 3, hemoglobin solution; curve 4, normal human blood.*

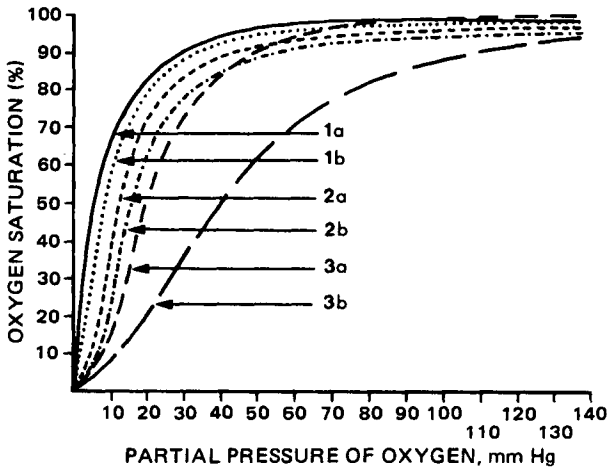

Figure 5b—*Oxygen dissociation curves of hemoglobin microcapsules without subsequent treatment and after stabilization with glutaraldehyde: effect of adding inositol hexaphosphate. Key: 1a, untreated microcapsules (p50 = 6 mm Hg); 1b, untreated microcapsules with inositol hexaphosphate added to the external phase (p50 = 8 mm Hg); 2a, stabilized microcapsules (p50 = 11 mm Hg); 2b, stabilized microcapsules with inositol hexaphosphate incorporated in the internal phase (p50 = 13 mm Hg); 3a, hemoglobin solution (p50 = 18 mm Hg); 3b, hemoglobin solution + inositol hexaphosphate (p50 = 39 mm Hg).*

as well as increasing the molarity to 2 *M* were not useful. However, replacing the sodium carbonate buffer by a 0.5 *M* I buffer, pH 9.8, gave good results. Increasing the concentration of terephthaloylchloride provided partial denaturation of hemoglobin. Sebacoyl chloride and succinylchloride gave poor results: the membranes were tiny and hemoglobin diffused into water, while the absorption spectrum was strongly altered (Fig. 4b, curves 1 and 2). On the contrary, glutaraldehyde yielded nice microcapsules which suffered practically no diffusion of hemoglobin. The absorption spectrum (Fig. 4b, curve 3) was unaltered and the p50 was 7 mm Hg. The oxygen dissociation curve was slightly sigmoidal (Fig. 5a). The microcapsules could be easily lyophilized. They were destroyed within 2 min in pepsin (pH 2) and only 2–3 hr in pancreatin (pH 7.5).

From the various surfactants checked (Table I), 5% sorbitan monolaurate seemed to give the best results regarding the average size and the distribution of diameters. Soybean lecithin also gave interesting results. Variation in the nature and concentration of surfactant did not affect the absorption spectrum nor the affinity curve.

The stirrer[10] used previously allowed only a maximum speed of 1800 rpm, but the use of the homogenizer[11] (metallic double blade) drastically improved the size of capsules (Table II). While graduation 100 of the

Table II—Hemoglobin Microcapsules with a Cross-Linked Hemoglobin Wall (Terephthaloylchloride): Influence of Stirring Conditions

Stirrer	Speed	Surfactant Compound	Surfactant Concentration, %	Mean diameter, μm	σ, μm
Stirrer[a]	1800 rpm	Sorbitan trioleate	10	18.7	8.6
		Soybean lecithin	1	20.6	7.7
		Sorbitan monolaurate	5	19.2	6.5
Homogenizer[b]	Graduation 10	Sorbitan monolaurate	5	9.8	4.9
	Graduation 40	Sorbitan monolaurate	5	4.9	1.2

[a] Heidolph stirrer-stirring motor type RZRII-Adaptation System type RK6. [b] Virtis 23 homogenizer, Bioblock.

apparatus corresponds to a maximum speed of 23,000 rpm, graduation 40 yielded capsules with a 4.9-μm diameter (σ = 1.2).

With microcapsules prepared at 20°, hemoglobin was altered. At −10°, hemoglobin rapidly diffused from the microcapsules. Again, the best results were gained at 0°. An attempt was made to prepare the microcapsules from deoxyhemoglobin under nitrogen. No improvement in the qualities of the capsules (p50 = 6 mm Hg) could be observed. Adding an amount of glucose equal to the weight of hemoglobin used prevented alteration of the hemoglobin during lyophilization (Fig. 4c).

When the capsules prepared from hemoglobin and terephthaloylchloride were further stabilized with glutaraldehyde they became very resistant. They resisted ultracentrifugation (100,000×g, 60 min, + 4°), freezing, melting cycles, and lyophilization. They were, however, rendered less deformable than previously and showed greater resistance to proteases (pepsin, 2 min; pancreatin, 30 min; pronase 2–3 hr). Diffusion of hemoglobin out of the wall was much slower. Interestingly, their p50 was now 11 mm Hg and the curve became slightly sigmoidal in shape (Fig. 5b).

Incorporation of inositol hexaphosphate induced modifications of the oxygen dissociation curves (Fig. 5b).

With standard microcapsules [not stabilized with glutaraldehyde (p50 = 6 mm Hg)], inositol hexaphosphate was only efficient when added in the external phase (p50 = 8 mm Hg). This result was probably due to inositol hexaphosphate being washed out during the isolation step of microcapsules.

On the contrary, with glutaraldehyde-stabilized capsules (p50 = 11 mm Hg), inositol hexaphosphate was not efficient when added to external phase (p50 unchanged = 11 mm Hg), but raised the p50 to 13 mm when in the internal phase. These last two results show that inositol hexaphosphate did not diffuse through glutaraldehyde-stabilized membranes.

The hemoglobin microcapsules prepared through the emulsion–reticulation method present interesting properties: one could actually obtain stable and biodegradable microcapsules with a 5-μm diameter, with a membrane permeable to oxygen but not to hemoglobin and inositol hexaphosphate, with a sigmoidal saturation curve (p50 = 13 mm Hg), and which could be lyophilized. Complementary work is necessary to evaluate their rheological and biological properties.

REFERENCES

(1) T. M. S. Chang, *Science*, **146**, 524 (1964).

(2) T. M. S. Chang, *Trans. Am. Soc. Artif. Intern. Organs*, **12**, 13 (1966).

(3) T. M. S. Chang, F. C. MacIntosh, and S. G. Mason, *Can. J. Physiol. Pharmacol.*, **44**, 115 (1966).

(4) T. M. S. Chang, *Science*, **3**, 62 (1967).

(5) M. Arakawa, T. Kondo, and B. Tamamushi, *Biorheology*, **12**, 57 (1975).

(6) M. Arakawa and T. Kondo, *Can. J. Physiol. Pharmacol.*, **55**, 6, 1378 (1977).

(7) T. Kondo, M. Arakawa, and B. Tamamushi, in "Microencapsulation," J. R. Nixon, Ed., Drugs and the Pharmaceutical Sciences, Dekker, New York, Basel, 1976, Vol. 3, p. 63.

(8) W. Sekiguchi and A. Kondo, *J. Jpn. Soc. Blood Transf.*, **13**, 153 (1966).

(9) C. Vigneron, M. Ndong Nkoume, and P. Labrude, 1st Int. Cong. Pharm. Technol. Paris, Vol. 4, 63 (1977).

(10) M. Ndong Nkoume, B. Teisseire, P. Labrude, and C. Vigneron, 2nd Int. Cong. Pharm. Technol. Paris, Vol. 4, 1 (1980).

(11) K. Bonhard, in "Forschungsergebnisse der Transfusions medizin und Immun haematologie," M. Matthes and V. Nagel, Eds., Berlin Medicus, 1976, Vol. 3, p. 547.

(12) J. W. Payne, *Biochem. J.*, **135**, 867 (1973).

(13) W. Mok, D. E. Chen, and A. Mazur, *Fed. Proc. Fed. Am. Soc. Exp. Biol.*, **34**, 1458 (1975).

(14) K. C. Morris, P. Bonsen, and M. B. Laver, U.S. Patent 4,061,736 (1977).

(15) P. Labrude, F. Bonneaux, E. Dellacherie, J. Neel, and C. Vigneron, *Ann. Pharm. Fr.*, **37**, 7, 291 (1979).

(16) P. Rambourg, J. Lévy, F. Puisieux, and M.-C. Lévy, 2nd Int. Cong. Pharm. Technol., Paris, Vol. 3, 5, 1980.

(17) M.-C. Lévy, P. Rambourg, and J. Lévy, 2nd Int. Cong. Pharm. Technol. Paris, Vol. 3, 15, 1980.

(18) P. Rambourg, J. Lévy, and M.-C. Lévy, *J. Pharm. Sci.*, **71**, 753 (1982).

(19) P. Labrude, C. Vigneron, and C. Streiff, *J. Pharm. Belg.*, **31**, 2, 191 (1976).

(20) K. Gersonde and C. Nicolau, *Blut*, **39**, 1 (1979).

(21) Q. H. Gibson and R. D. Gray, *Biochem. Biophys. Res. Commun.*, **41**, 2, 415 (1970).

Operation of Long-Range Substituent Effects in Rigid Opiates: Protonated and Unprotonated Oxymorphone

STEPHEN D. DARLING *, **VERA M. KOLB** ‡x, **GRETCHEN S. MANDEL** §, and **NEIL S. MANDEL** §

Received January 19, 1981, from the * *Department of Chemistry, The University of Akron, Akron, OH 44325;* the ‡ *Department of Chemistry and Biochemistry, Southern Illinois University, Carbondale, IL 62901;* and the § *Medical College of Wisconsin, Veterans Administration Medical Center, Wood, WI 53193.* Accepted for publication October 6, 1981.

Abstract □ The structure of protonated oxymorphone (amine salt) was determined by an X-ray crystallographic study. Significant differences were found with the previously determined structure of unprotonated oxymorphone (free base). Upon protonation on nitrogen, an elongation of the N—C bond occurred, accompanied by subtle changes in bond lengths and angles distant from the site of protonation. These changes in geometry are interpreted as a reflection of long-range substituent effects.

Keyphrases □ Oxymorphone—protonated and unprotonated, operation of long-range effects in rigid opiates □ Opiates—operation of long-range substituent effects, protonated and unprotonated oxymorphone □ Crystallography, X-ray—determination of structure of protonated and unprotonated oxymorphone

The existence of long-range substituent effects in morphines was proposed in 1979 (1). The anomalous variations in the pKa values of variously substituted morphines (2) were interpreted as the evidence for the existence of these effects. Additional evidence was sought to support the existence of these effects in morphines, including the X-ray evidence which is expected to show that a substituent introduced in the morphine molecule causes changes in bond lengths and angles, not only locally but throughout the entire molecule (1), and the voltammetric evidence, which is expected to demonstrate that the electron transfer from the lone electron pair of the nitrogen of morphines is affected by remote substitution. The data on voltammetric behavior of morphines recently published (3) may constitute the latter evidence[1]. The authors report here the X-ray evidence.

Early X-ray crystallographic studies of morphines were performed on morphine (4) and codeine (5) with the objective of determining their molecular structure and absolute stereochemistry, respectively. More recently, refined structures of morphine (6) and some of its pharmacologically important derivatives, such as naloxone (7) and oxymorphone (8), have been obtained. The latter studies responded to the needs of medicinal chemists who attempted to explain the pharmacological effects of morphine agonists and antagonists in terms of the geometric (9,10) and stereoelectronic (11–18) features of these molecules. After the publication of the refined structures of morphine (6) and naloxone (7), medicinal and quantum chemists started using these structures as an approximation of the structures of other morphine derivatives whose X-ray structures had not been determined (11–13, 15–17). Such approximations were widely used and did not stimulate additional X-ray work in the morphine field.

The approximate geometries were derived from the known geometries using three assumptions: (*a*) The geometry of a morphine does not change upon protonation of nitrogen (12, 15). Thus, the X-ray structure of morphine amine salt was used in place of the structure of the corresponding free base (12). (*b*) In morphines that differ only in the substituent on nitrogen, the geometry of *N*-nor moieties is the same (12, 13, 15–17). For example, the geometry of the *N*-nor moiety of nalorphone was assumed to be the same as that of morphine (12); in the same way, the geometries of the *N*-nor moieties of oxymorphone (13, 16, 17), nalmexone, naltrexone, and nalbuphine (16, 17) were derived from the geometry of naloxone. (*c*) Introduction of the substituent at C-2 and at the phenolic and alcoholic oxygens of morphine does not change its basic geometry (11). Therefore, skeletal structures of 2-amino morphine, codeine, heroin, and 6-acetyl morphine were assumed to be the same (11).

Justification of assumption *a* seems to be difficult when considering the IR data of amines and their salts, which suggests longer N—C bonds in protonated amines (19–21). The validity of these assumptions is challenged by the existence of long-range substituent effects in morphines (1): the introduction of a substituent in a rigid molecule like morphine is likely to cause distortions of bond angles and torsional angles, not only locally, but throughout the entire molecule. The geometry changes caused by long-range substituent effects are typically very small. However, it has been demonstrated recently that even very small differences in geometry significantly influence the results of quantum chemical calculations of oxymorphone (18). These results suggest that the use of exact (X-ray) structures of morphines is preferred to the use of approximate (slightly inaccurate) structures for quantum chemical studies of morphines.

The objective of this study was to test experimentally

Table I—Crystal Data

Crystal Parameter	Experimental or Calculated Value of Parameter
Molecular formula	$C_{17}H_{19}NO_4 \cdot HCl \cdot H_2O \cdot C_2H_6O$
Molecular weight	401.89
Crystal system	orthorhombic
Space group	$P2_12_12_1$
a	10.586 (4) Å
b	18.671 (5) Å
c	9.361 (3) Å
V_c [a]	1850.21 Å^3
Z [b]	4
D_c [c]	1.443 g cm^{-3}
D_o [d]	1.343 g cm^{-3}
$F(000)$ [e]	856
μ [f]	2.5 cm^{-1}
λ(molybdenum K_α) [g]	0.71069 Å

[a] Calculated volume of the unit cell. [b] Number of asymmetric units in the cell. [c] Calculated density. [d] Observed density. [e] $F(000)$ is equal to the total number of electrons in the cell. [f] Linear absorption coefficients. [g] X-ray wavelength of molybdenum K_α line.

[1] Presented at the International Conference on Conformational Analysis, Durham, N.H., June 1981.

0022-3549/82/0700-0763$01.00/0

Table II—Positional Parameters × 10^4 [a]

Atom[b]	x	y	z	B_{equiv}[c]
C1	5274 (4)	1407 (2)	7072 (4)	3.54 (18)
C2	5009 (4)	1048 (2)	5854 (5)	3.60 (18)
C3	4430 (4)	1377 (2)	4740 (4)	3.28 (16)
C4	4090 (4)	2080 (2)	4910 (4)	3.03 (16)
C5	3886 (4)	3235 (2)	4427 (4)	3.27 (18)
C6	5191 (4)	3421 (2)	3869 (4)	3.55 (19)
C7	5934 (4)	3948 (2)	4691 (5)	3.88 (18)
C8	6045 (4)	3699 (2)	6192 (5)	3.68 (19)
C9	4809 (4)	3345 (2)	8339 (4)	3.00 (17)
C10	5304 (4)	2580 (2)	8439 (4)	3.51 (18)
C11	4956 (4)	2120 (2)	7230 (4)	3.13 (17)
C12	4336 (4)	2422 (2)	6143 (4)	2.89 (16)
C13	3862 (4)	3186 (2)	6024 (4)	2.83 (16)
C14	4769 (4)	3659 (2)	6862 (4)	2.83 (17)
C15	2529 (4)	3236 (2)	6617 (4)	3.38 (18)
C16	2499 (4)	3042 (2)	8152 (4)	3.77 (19)
C17	3439 (5)	3261 (2)	10464 (5)	4.45 (21)
N1	3500 (3)	3432 (2)	8944 (3)	3.12 (14)
O1	4221 (3)	1046 (2)	3488 (3)	4.15 (14)
O2	3559 (3)	2529 (1)	3936 (3)	3.39 (12)
O3	5613 (3)	3128 (2)	2857 (3)	4.76 (15)
O4	4284 (3)	4355 (1)	7096 (3)	3.29 (12)
CL1	2013 (1)	4846 (1)	9700 (1)	4.62 (5)
OW1	713 (3)	5075 (2)	6825 (4)	4.91 (15)
OS1	3127 (4)	1514 (2)	896 (4)	6.12 (18)
CS1	3303 (7)	841 (3)	336 (7)	6.92 (32)
CS2	2526 (7)	731 (4)	−886 (8)	8.24 (38)

[a] Numbers in parentheses are the estimated standard deviations (*SD*) of the last digits. [b] Atom labeling is shown in Fig. 1. $S = CH_3CH_2OH$. $W = H_2O$. [c] B_{equiv} is defined in Ref. 27.

Table III—Anisotropic Thermal Parameters × 10^3 [a,b]

Atom	U_{11}	U_{22}	U_{33}	U_{12}	U_{13}	U_{23}
C1	53 (3)	38 (2)	44 (2)	4 (2)	−2 (2)	4 (2)
C2	46 (3)	37 (2)	54 (2)	5 (2)	2 (2)	1 (2)
C3	43 (2)	36 (2)	46 (2)	−3 (2)	5 (2)	−6 (2)
C4	33 (2)	42 (2)	40 (2)	0 (2)	0 (2)	0 (2)
C5	51 (3)	37 (2)	36 (2)	8 (2)	−8 (2)	−2 (2)
C6	51 (3)	42 (2)	43 (2)	15 (2)	1 (2)	11 (2)
C7	47 (3)	46 (2)	54 (2)	−2 (2)	6 (2)	8 (2)
C8	47 (3)	42 (2)	51 (2)	−4 (2)	−2 (2)	0 (2)
C9	39 (3)	35 (2)	40 (2)	1 (2)	−6 (2)	−1 (2)
C10	51 (3)	42 (2)	41 (2)	8 (2)	−9 (2)	2 (2)
C11	40 (2)	39 (2)	40 (2)	5 (2)	2 (2)	2 (2)
C12	39 (2)	29 (2)	41 (2)	3 (2)	3 (2)	0 (2)
C13	35 (2)	33 (2)	40 (2)	2 (2)	−3 (2)	0 (2)
C14	34 (2)	34 (2)	40 (2)	0 (2)	−2 (2)	−1 (2)
C15	34 (3)	44 (2)	50 (2)	4 (2)	−5 (2)	−1 (2)
C16	50 (3)	48 (2)	45 (2)	−3 (2)	4 (2)	−5 (2)
C17	67 (3)	57 (3)	46 (2)	2 (2)	0 (2)	7 (2)
N1	46 (2)	35 (2)	37 (2)	−2 (2)	1 (2)	0 (1)
O1	60 (2)	49 (2)	49 (2)	6 (2)	−8 (2)	−14 (1)
O2	49 (2)	38 (1)	42 (1)	5 (1)	−9 (1)	−2 (1)
O3	71 (2)	61 (2)	48 (2)	11 (2)	16 (2)	−1 (2)
O4	51 (2)	31 (1)	43 (1)	4 (1)	−3 (1)	1 (1)
CL1	63 (1)	60 (1)	52 (1)	18 (1)	−1 (1)	−14 (1)
OW1	66 (2)	59 (2)	61 (2)	−3 (2)	−3 (2)	−8 (2)
OS1	109 (3)	55 (2)	68 (2)	20 (2)	−9 (2)	0 (2)
CS1	116 (5)	68 (3)	79 (4)	26 (4)	−7 (4)	−6 (3)
CS2	114 (6)	98 (5)	101 (4)	23 (4)	−7 (5)	−28 (4)

[a] The anisotropic temperature factor has the form: $\exp -2\pi(U_{11}h^2a^{*2} + \ldots + 2U_{12}hka^*b^* + \ldots)$. [b] Numbers in parentheses are the estimated *SD* of the last digit.

the validity of assumption *a*: to establish, by an X-ray crystallographic study, whether protonation of nitrogens influences the geometry of morphines. The results of this study would also test the validity of the long-range substituent concept in morphines. Since the X-ray structure of an unprotonated morphine derivative, oxymorphone, has already been reported (8), the protonated oxymorphone (amine salt) was chosen as the subject of the X-ray structure determination.

EXPERIMENTAL

A single crystal of oxymorphone hydrochloride[2] (4,5α-epoxy-3,14-dihydroxy-17-methylmorphinan-6-one hydrochloride), suitable for X-ray analysis, was grown from 95% ethanol after slow evaporation. The size of the crystal used for data collection measured ~0.25 × 0.3 × 0.4 mm. The crystals were clear, colorless prisms.

Weissenberg and precision photographs showed the crystal to be orthorhombic and have systematic extinctions HOO:H=2*n* OKO:K=2*n* OOL:L=2*n* indicating space group $P2_12_12_1$ (number 19). The density was measured by flotation in a mixture of toluene and bromotrichloromethane. The crystal was mounted on a $P2_1$ automatic diffractometer[3] equipped with an incident beam graphite-crystal monochromator. All measurements were made at 25(±2)° using molybdenum K_α radiation. The unit-cell constants and the orientation matrix to be used in data collection were obtained from a least-square refinement of 15 centered general reflections. Crystal data are listed in Table I.

Data Collection—The diffraction data were collected by the θ–2θ scan technique at room temperature with graphite monochromated molybdenum K_α radiation. The scan rate varied from 2 to 10°/min, dependent on the intensity of diffraction maxima (scan width was based on $\Delta\theta = 1.00 + 0.15 \tan\theta$). A decay of ~50% was noted for the three standard reflections ($\bar{4},\bar{2},2;\bar{2},1,2;0,\bar{1},4$) monitored for every 50 reflections over the period of collection.

A total of 2172 reflections was collected, comprising the quadrant of reciprocal space where *h*, *k*, and *l* are each nonnegative. Of the 2172 reflections collected, 1710 were classified as observed for $|F_o|^2 > 3\sigma(|F_o|^2)$, where $|F_o|$ is the observed structure factor amplitude corrected for Lorentz and polarization effects.

Structure Determination and Refinement—The diffractometer data were reduced and corrected for decay using a program from the CRYSP programs (22). The structure was solved by direct methods using the MULTAN 74 program (23). The probable phase set, as determined by statistics and based on three origin and three starting reflections, produced an *E*-map containing 19 of the 27 heavy atoms in the structure. The remaining atoms were located in difference Fourier maps using the program set CRYM (24).

Full matrix least-square refinement on the heavy atom positions minimizing the quantity $\Sigma\omega(F_o^2 - F_c^2)^2$, where $\omega = 1/\sigma^2(F_o^2)$, was followed by the calculation of all hydrogen atom positions except for the hydroxyl hydrogen atoms and methyl hydrogen atoms which were located in difference Fourier maps. At this point, two cycles of isotropic full matrix least-squares resulted in an *R* value, $[= \Sigma(||F_o| - |F_c||)/\Sigma|F_o|]$

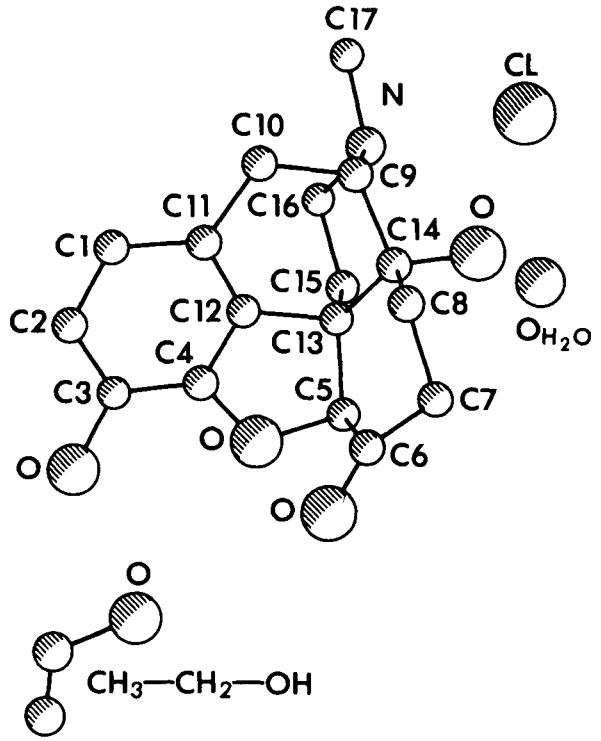

Figure 1—*Oxymorphone·HCl·H_2O·C_2H_5OH*

[2] Endo Laboratories, Inc.
[3] Syntex.

Table IV—Positional Parameters × 10^3 and Isotropic Thermal Parameters for the Hydrogen Atoms

Atom	x	y	z	B_{iso}
H1	573	117	780	4.54
H2	518	54	581	4.60
H5	333	359	409	4.27
H7A	554	440	467	4.88
H7B	677	399	430	4.88
H8A	654	402	672	4.68
H8B	641	323	620	4.68
H9	554	358	885	4.00
H10A	494	238	927	4.51
H10B	618	260	851	4.51
H15A	201	291	611	4.38
H15B	223	371	651	4.38
H16A	262	254	825	4.77
H16B	169	317	853	4.77
H17A	420	349	1074	5.45
H17B	262	345	1071	5.45
H17C	394	287	1068	5.45
NH	331	394	876	4.12
HO4	385	451	639	4.29
OWHA	91	499	761	5.91
OWHB	121	489	663	5.91
HS1A	314	49	102	7.92
HS1B	420	80	5	7.92
HS2A	268	28	−131	9.24
HS2B	274	110	−161	9.24
HS2C	168	79	−64	9.24
HOS1	385	159	127	7.12
HO1	464	71	342	5.15

0.112. Further full matrix least-square analysis of 245 variables—coordinates and anisotropic temperature factors for 27 heavy atoms, a secondary extinction parameter (25) and a scale factor—led to a final R value of 0.068 and a goodness-of-fit [$= \Sigma\omega(F_o^2 - F_c^2)^2/M - S)^{1/2}$] for $M = 2172$ reflections and $S = 245$ parameters of 9.7. (In this analysis the coordinates and isotropic temperature factors for 27 hydrogen atoms were held constant). The ωR value [$= [\Sigma\omega(F_o^2 - F_c^2)^2/\Sigma\omega F_o^4]^{1/2}$] was 0.117 and the R factor for the 3σ data set was 0.056. The estimated standard deviations were computed from the inverse matrix of the last full matrix, least-squares cycle. All shifts in parameters were less than their estimated standard deviations in the final refinement cycle. The scattering factors and anomalous dispersion terms for chlorine were taken from a published source[4], the scattering factors for hydrogen were taken from Stewart *et al.* (26).

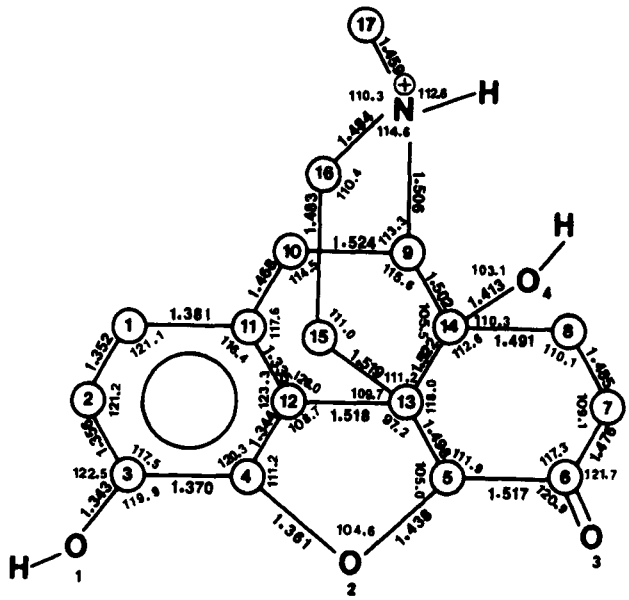

Figure 2—*Bond lengths and bond angles in protonated oxymorphone (oxymorphone·HCl·H_2O·C_2H_5OH). The estimated standard deviations are 0.005–0.006 Å for C—C, C—O, and C—N bonds, and 0.3–0.4° for C—C—(C,O,N) angles.*

[4] The International Tables for X-ray Crystallography (1962).

Table V—Interatomic Distances [Å] [a]

Bond	a [b]	b [c]	a − b	σ	(a−b)/σ [d]
C1—C2	1.352 (6)	1.406 (5)	−0.054	0.008	6.9
C2—C3	1.356 (6)	1.378 (5)	−0.022	0.008	2.8
C3—C4	1.370 (5)	1.376 (4)	−0.006	0.006	0.9
C4—C12	1.344 (5)	1.380 (4)	−0.036	0.006	5.6
C11—C12	1.335 (5)	1.375 (5)	−0.040	0.007	5.6
C1—C11	1.381 (6)	1.381 (4)	0		
C12—C13	1.518 (5)	1.493 (4)	0.025	0.006	3.9
C13—C5	1.498 (5)	1.547 (4)	−0.049	0.006	7.7
C5—C6	1.517 (6)	1.522 (4)	−0.005	0.007	0.7
C4—O2	1.361 (4)	1.392 (4)	−0.031	0.006	5.5
C5—O2	1.438 (5)	1.475 (3)	−0.037	0.006	6.4
C3—O1	1.343 (5)	1.375 (3)	−0.032	0.006	5.5
C6—C7	1.476 (6)	1.501 (4)	−0.025	0.007	3.5
C7—C8	1.485 (6)	1.522 (5)	−0.037	0.008	4.7
C8—C14	1.491 (6)	1.515 (4)	−0.024	0.007	3.3
C14—C13	1.522 (5)	1.548 (4)	−0.026	0.006	4.1
C14—C9	1.502 (5)	1.548 (5)	−0.046	0.007	6.5
C9—C10	1.524 (5)	1.545 (5)	−0.021	0.007	2.9
C10—C11	1.468 (5)	1.520 (5)	−0.052	0.007	7.3
C13—C15	1.519 (6)	1.539 (4)	−0.020	0.007	2.8
C15—C16	1.483 (6)	1.520 (4)	−0.037	0.007	5.1
C16—N	1.484 (5)	1.467 (4)	0.017	0.006	2.6
N—C17	1.459 (5)	1.464 (4)	−0.005	0.006	0.8
C14—O4	1.413 (4)	1.427 (4)	−0.014	0.006	2.5
C6—O3	1.182 (5)	1.221 (4)	−0.039	0.006	6.1
N—C9	1.506 (5)	1.474 (4)	0.032	0.006	5.0

[a] Numbers in parentheses are the estimated *SD* of the last digit. [b] Oxymorphone·HCl·H_2O·C_2H_5OH. [c] Oxymorphone·H_2O (8). [d] If $(a - b)/\sigma \geq 5$, the difference in bond lengths, $a - b$, is significant.

Table VI—Bond Angles [a]

Angle	a [b]	b [c]	a − b	σ	(a − b) /σ [d]
C4—C12—C13	108.7 (3)	109.2 (3)	−0.5	0.4	1.2
C4—C12—C11	123.3 (4)	122.9 (3)	0.4	0.5	0.8
C4—C3—C2	117.5 (4)	117.1 (3)	0.4	0.5	0.8
C4—C3—O1	119.9 (4)	119.3 (3)	0.6	0.5	0.8
C3—C2—C1	121.2 (4)	121.5 (3)	−0.3	0.5	0.6
C3—C4—C12	120.3 (4)	121.0 (3)	−0.7	0.5	1.4
O1—C3—C2	122.5 (3)	123.6 (3)	−1.1	0.4	2.6
C2—C1—C11	121.1 (4)	121.1 (2)	0		
C1—C11—C12	116.4 (4)	116.3 (3)	0.1	0.5	0.2
C1—C11—C10	125.8 (4)	126.6 (3)	−0.8	0.5	1.6
C11—C12—C13	128.0 (3)	127.9 (3)	0.1	0.4	0.2
C11—C10—C9	114.5 (3)	114.4 (3)	0.1	0.4	0.2
C12—C4—O2	111.2 (3)	111.6 (3)	−0.4	0.4	0.9
C12—C13—C15	109.7 (3)	109.3 (2)	0.4	0.4	1.1
C12—C13—C14	107.4 (3)	108.6 (3)	−1.2	0.4	2.9
C12—C11—C10	117.6 (4)	117.0 (3)	0.6	0.5	1.2
C12—C13—C5	97.2 (3)	98.3 (2)	−1.1	0.4	3.1
C10—C9—C14	115.6 (3)	114.2 (2)	1.4	0.4	3.9
C10—C9—N	113.3 (3)	116.0 (3)	−2.7	0.4	6.4
C9—C14—C13	105.5 (3)	105.5 (2)	0		
C9—N—C16	114.6 (3)	113.7 (2)	0.9	0.4	2.5
C9—N—C17	112.6 (3)	114.0 (3)	−1.4	0.4	4.1
C9—C14—C8	112.4 (3)	113.9 (3)	−1.5	0.4	3.6
C9—C14—O4	103.1 (3)	108.8 (2)	−5.7	0.4	15.8
C14—C13—C5	118.0 (3)	117.4 (2)	0.6	0.4	1.7
C14—C13—C15	111.2 (3)	109.5 (2)	1.7	0.4	4.7
C14—C8—C7	110.1 (4)	111.1 (3)	−1.0	0.5	2.0
O4—C14—C8	110.3 (3)	107.0 (3)	3.3	0.4	7.9
O4—C14—C13	112.5 (3)	110.7 (3)	1.8	0.4	4.3
C13—C14—C8	112.6 (3)	111.0 (2)	1.6	0.4	4.4
C13—C15—C16	111.0 (3)	111.3 (3)	−0.3	0.4	0.7
C13—C5—C6	111.9 (3)	113.7 (2)	−1.8	0.4	5.0
C13—C5—O2	105.0 (3)	104.5 (2)	0.5	0.4	1.4
C5—C6—C7	117.3 (4)	117.1 (2)	0.2	0.4	0.4
C5—O2—C4	104.6 (3)	104.0 (2)	0.6	0.4	1.7
C5—C6—O3	120.9 (4)	120.6 (3)	0.3	0.5	0.6
C5—C13—C15	112.1 (3)	112.9 (2)	−0.8	0.4	2.2
C6—C7—C8	109.1 (3)	111.0 (3)	−1.9	0.4	4.5
C6—C5—O2	108.6 (3)	108.6 (2)	0		
O3—C6—C7	121.7 (3)	122.3 (3)	−0.6	0.4	1.4
C15—C16—N	110.4 (3)	110.4 (2)	0		
C14—C9—N	106.1 (3)	105.5 (3)	0.6	0.4	1.4
C16—N—C17	110.3 (3)	109.7 (3)	0.6	0.4	1.4

[a] Numbers in parentheses are the estimated *SD* of the last digit. [b] Oxymorphone ·HCl·H_2O·C_2H_5OH. [c] Oxymorphone ·H_2O (8). [d] If $(a - b)/\sigma \geq 5$, the difference in bond angles, $a - b$, is significant.

Table VII—Torsional Angles [a]

Torsional Angle	a [b]	b [c]	a − b	σ	a − b /σ [d]
Ring A					
C1—C2—C3—C4	1.9 (6)	0.6 (5)	1.3	0.8	1.6
C2—C3—C4—C12	0.3 (6)	−3.6 (4)	−3.9	0.7	5.6
C3—C4—C12—C11	2.8 (6)	6.0 (5)	−3.2	0.8	4.0
C4—C12—C11—C1	−4.1 (6)	−4.9 (5)	0.8	0.8	1.0
C12—C11—C1—C2	2.4 (6)	1.8 (4)	0.6	0.7	0.9
C11—C1—C2—C3	0.5 (6)	0.3 (5)	0.2	0.8	0.3
Ring B					
C4—O2—C5—C13	−35.1 (4)	−32.7 (3)	−2.4	0.5	4.8
O2—C5—C13—C12	34.3 (4)	33.8 (3)	0.5	0.5	1.0
C5—C13—C12—C14	−23.2 (4)	−23.8 (3)	0.6	0.5	1.2
C13—C12—C4—O2	3.0 (4)	4.8 (3)	−1.8	0.5	3.6
C12—C4—O2—C5	20.0 (4)	18.0 (3)	2.0	0.5	4.0
Ring C					
C9—C10—C11—C12	4.7 (5)	9.1 (4)	−4.4	0.6	7.3
C10—C11—C12—C13	−4.2 (6)	−8.5 (5)	4.3	0.8	5.4
C11—C12—C13—C14	31.4 (5)	34.0 (4)	−2.6	0.6	4.3
C12—C13—C14—C9	−55.3 (4)	−56.2 (3)	0.9	0.5	1.8
C13—C14—C9—C11	61.9 (4)	61.9 (3)	0		
C14—C9—C10—C11	−35.6 (5)	−37.8 (4)	2.2	0.6	3.7
Ring D					
C5—C6—C7—C8	55.6 (5)	50.1 (4)	5.5	0.6	9.2
C6—C7—C8—C14	−62.6 (4)	−60.6 (4)	−2.0	0.6	3.3
C7—C8—C14—C13	55.8 (4)	56.5 (4)	−0.7	0.6	1.2
C8—C14—C13—C5	−40.8 (5)	−42.7 (4)	1.9	0.6	3.2
C14—C13—C5—C6	30.8 (5)	31.5 (4)	−0.7	0.6	1.2
C13—C5—C6—C7	−38.9 (5)	−35.2 (4)	−3.7	0.6	6.2
Ring E					
C9—C14—C13—C15	64.8 (4)	63.0 (3)	1.8	0.5	3.6
C14—C13—C15—C16	−57.0 (4)	−55.0 (3)	−2.0	0.5	4.0
C13—C15—C16—N	48.8 (4)	50.0 (3)	−1.2	0.5	2.4
C15—C16—N—C9	−53.8 (4)	−57.6 (3)	3.8	0.5	7.6
C16—N—C9—C14	62.5 (4)	66.4 (3)	−3.9	0.5	7.8
N—C9—C14—C13	−64.5 (4)	−66.7 (3)	2.2	0.5	4.4

[a] Numbers in parentheses are the estimated *SD* of the last digit. [b] Oxymorphone ·HCl·H_2O·C_2H_5OH. [c] Oxymorphone ·H_2O (8). [d] If (a − b)/σ ≥ 5, the difference in torsional angles, a − b, is significant.

Detailed information about the crystal structure of oxymorphone·HCl·H_2O·C_2H_5OH is given in Tables I–VII: crystal data (Table I), coordinates and B_{equiv} for nonhydrogen atoms (Table II), anisotropic thermal parameters (Table III), positional parameters and B_{iso} for hydrogen atoms (Table IV), interatomic distances (Table V), bond angles (Table VI), and torsional angles (Table VII).

The molecular structure of oxymorphone·HCl·H_2O·C_2H_5OH is depicted in Fig. 1, with bond lengths and bond angles shown in Fig. 2. For the purpose of comparison, the geometry of unprotonated oxymorphone (8) is also shown (Fig. 3).

RESULTS AND DISCUSSION

Inspection of Figs. 2 and 3 and Table V reveals some significant[5] differences in bond lengths of protonated and unprotonated oxymorphone. Thus, the N—C-9 is longer by 0.032 (6) Å in protonated oxymorphone (Scheme II) than in the unprotonated analog (Scheme III). The elongation of the N—C bond upon protonation is not unexpected in light of the IR data of amines and their salts[6] and is consistent with the previously described elongation of the N—C bonds of cyclazocine upon protonation (28).

Several C—C bonds are considerably shorter (0.036–0.054 Å) in the protonated than in the unprotonated molecule: C-1–C-2, C-10–C-11, C-5–C-13, C-9–C-14, C-11–C-12, and C-4–C-12. Significant differences in several C—O bonds are also observed. Comparison of bond angles for protonated and unprotonated oxymorphone (Table VI) reveals several small but significant differences of up to ~6 degrees. Similarly, several torsional angles of these two molecules differ for up to ~6 degrees (Table VII).

Observed changes in bond lengths, angles, and torsional angles distant from the site of protonation are interpreted as a reflection of long-range substituent effects in oxymorphone (1). Protonation leads to a formal positive electric charge on nitrogen, which can be transmitted further throughout the molecule *via* long-range inductive and electrostatic field effects (1). The elongation of the N—C bond upon protonation may introduce a local strain and conformational distortion which may be transmitted through the entire molecule by a slight flexing of bond and torsional angles (conformational transmission effect); in this way, the strain is shared by the whole structure (1).

While long-range effects are expected to influence the geometry of the entire molecule, the exact location and magnitude of the geometric changes are difficult to predict; observed changes therefore appear to be erratic. For this reason, extrapolation of the geometric changes observed here, upon protonation of oxymorphone to predictions of geometries of other morphine derivatives, is extremely difficult.

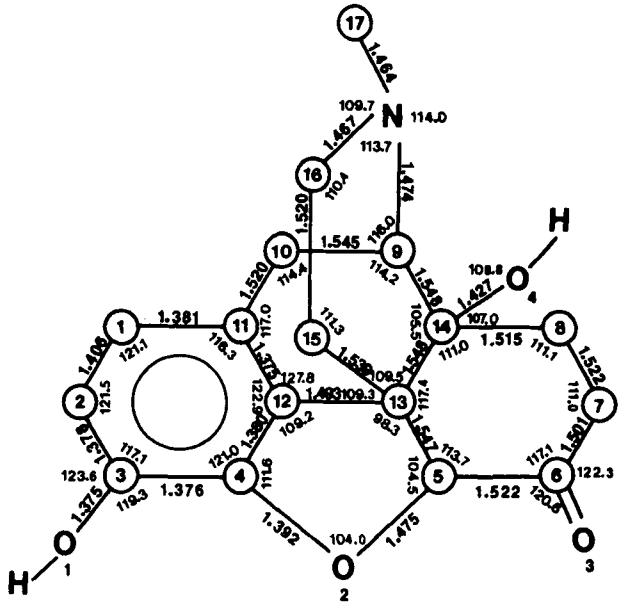

Figure 3—*Bond lengths and bond angles in unprotonated oxymorphone (oxymorphone·H_2O) (8). The estimated standard deviations are 0.004–0.005 Å for C—C, C—O, and C—N bonds, and 0.2–0.3° for C—C—(C,O,N) angles.*

REFERENCES

(1) V. M. Kolb, *J. Pharm. Sci.*, **68**, 1250 (1979).

(2) J. J. Kaufman, N. M. Semo, and W. S. Koski, *J. Med. Chem.*, **18**, 647 (1975).

(3) P. Surman, *Arch. Pharm.*, **312**, 734 (1979).

(4) M. Mackay and D. C. Hodgkin, *J. Chem. Soc.*, **1955**, 3261.

(5) G. Kartha, F. R. Ahmed, and W. H. Barnes, *Acta Crystallogr.*, **15**, 326 (1962).

(6) L. Gylbert, *ibid.*, *Sect.* **B29**, 1630 (1973).

(7) I. L. Karle, *ibid.*, *Sect.* **B30**, 1682 (1974).

(8) R. J. Sime, M. Dobler, and R. L. Sime, *ibid.*, *Sect.* **B32**, 2937 (1976).

(9) A. H. Beckett and A. F. Casy, *Progr. Med. Chem.*, **4**, 171 (1965).

(10) F. A. Gorin and G. R. Marshall, *Proc. Natl. Acad. Sci. USA*, **74**, 5179 (1977).

(11) G. H. Loew, D. Berkowitz, H. Weinstein, and S. Srebrenik, in "Molecular and Quantum Pharmacology," E. Bergmann and B. Pullman, Eds., D. Reidel Publ., Dodrecht, The Netherlands, 1974, pp. 355–389.

(12) H. E. Popkie, W. S. Koski, and J. J. Kaufman, *J. Am. Chem. Soc.*, **98**, 1342 (1976).

(13) G. Loew, H. Weinstein, and D. Berkowitz in "Environmental Effects on Molecular Structure and Properties," B. Pullman, Ed., D. Reidel Publ., Dodrecht, The Netherlands, 1976, pp. 239–258.

(14) B. V. Cheney, D. J. Duchamp, and R. E. Cristoffersen in "QuaSAR: Quantitative Structure Activity Relationships of Analgesics, Narcotic Antagonists, and Hallucinogens," NIDA Research Monograph 22, G. Barnett, M. Trsic, and R. Willette, Eds., U.S. Government Printing Office, Washington, D.C., 1978, pp. 218–249.

(15) J. J. Kaufman, *ibid.*, pp. 250–277.

[5] Significant differences are those which are >5σ. $\sigma = (\sigma_a^2 + \sigma_b^2)^{1/2}$, where σ_a and σ_b are standard deviations of the property measured (bond lengths, bond angles, *etc.*) of protonated and unprotonated oxymorphone.

[6] The N—H stretching frequencies of protonated amines (amine salts) are lower than those of their respective free bases (19–21). Since the frequency is directly related to the square root of the force constant of the bond (29), the lower frequency indicates a weaker and probably longer bond.

(16) G. H. Loew, D. S. Berkowitz, and S. K. Burt, *ibid.*, pp. 278–316.
(17) G. H. Loew and D. S. Berkowitz, *J. Med. Chem.*, **21**, 101 (1978).
(18) S. Scheiner and V. M. Kolb, *Proc. Natl. Acad. Sci. USA*, **77**, 5602 (1980).
(19) L. J. Bellamy, "The Infra-red Spectra of Complex Molecules," Wiley, New York, N.Y., 1966, pp. 246–260.
(20) D. J. Pasto and C. R. Johnson, "Organic Structure Determination," Prentice-Hall, Englewood Cliffs, N.J., 1969, pp. 110–122.
(21) R. M. Silverstein, G. C. Bassler, and T. C. Morrill, "Spectrometric Identification of Organic Compounds," Wiley, New York, N.Y., 1974, p. 76.
(22) G. S. Mandel and N. S. Mandel, *American Crystallography*, Association Abstract Series, 2, 6:77, Honolulu, Hawaii (1979).
(23) P. Main, M. M. Woolfson, and G. Germain, *MULTAN*, University of York Printing Unit, York, England, Version 1974.
(24) D. J. Duchamp, *Program and Abstracts*, American Crystallography Association Meeting, Bozeman, Montana (1964).
(25) A. C. Larson, *Acta Crystallogr.*, **23**, 664 (1967).
(26) R. F. Stewart, E. R. Davidson, and W. T. Simpson, *J. Chem. Phys.*, **42**, 3175 (1965).
(27) W. C. Hamilton, *Acta Crystallogr.*, **12**, 609 (1959).
(28) I. L. Karle, R. D. Gilardi, A. V. Fratini, and J. Karle, *Acta Crystallogr., Sect.* **B25**, 1469 (1969).
(29) R. M. Silverstein, G. C. Bassler, and T. C. Morrill, "Spectrometric Identification of Organic Compounds," Wiley, New York, N.Y., 1974, pp. 107–110.

ACKNOWLEDGMENTS

Presented at the Tenth Northeast Regional Meeting of the American Chemical Society, Potsdam, N.Y., June 1980 (Abstract 39).

This work was supported in part by grants from University Research Foundation, La Jolla, California, to V. M. Kolb, and from the Medical Research Service of the Veterans Administration, the Arthritis Foundation, and Kroc Foundation for Medical Research to N. S. Mandel.

The authors thank Professor Cal Y. Meyers for pointing out IR data of amines and their salts, which suggest longer N—C bonds in protonated amines. V. M. Kolb is grateful to Dr. Alan A. Rubin, Endo Laboratory, Inc., for generously donating the oxymorphone. A generous allocation of computer time from the Academic Computing Center of University of Akron is gratefully acknowledged.

Inquiries concerning the X-ray structure determination of oxymorphone should be addressed to Stephen D. Darling.

Medicated Tampons: Intravaginal Sustained Administration of Metronidazole and *In Vitro–In Vivo* Relationships

Y. W. CHIEN *x, J. OPPERMANN ‡, B. NICOLOVA ‡, and H. J. LAMBERT ‡

Received February 27, 1981, from **Rutgers—The State University, College of Pharmacy, Piscataway, NJ 08854* and ‡*Searle Laboratories, G. D. Searle & Co., Skokie, IL 60077.* Accepted for publication September 29, 1981.

Abstract □ The technical feasibility of utilizing tampons as a drug delivery system for prolonged intravaginal drug administrations was studied. Several commercially available brands of tampons were examined. The methodology for the incorporation of various doses of metronidazole, an antitrichomonas agent, in tampons was described. The sustained-release profile of metronidazole from these medicated tampons was characterized. Intravaginal administration of metronidazole *via* the medicated tampons was investigated in rhesus monkeys and human volunteers, and *in vitro–in vivo* correlations were established. The biopharmaceutics of intravaginal absorption of metronidazole *via* medicated tampons was analyzed in comparison with a vaginal solution formulation.

Keyphrases □ Metronidazole—intravaginal sustained administration in medicated tampons, *in vitro–in vivo* relationships □ Tampons—intravaginal sustained administration of metronidazole, *in vitro–in vivo* relationships □ Intravaginal administration—sustained metronidazole in tampons, *in vitro–in vivo* relationships

Tampons are made of cotton and/or cellulose and are commonly used for intravaginal insertion to absorb menstrual discharge (1). Numerous brands of vaginal tampons are commercially available. Their characteristics of high fluid absorbability and retention have been recommended for the absorption of extensive vaginal discharge in trichomonas-infected women.

Metronidazole[1] has been shown to be an effective antiprotozoal agent with a broad spectrum of activity against anaerobes (2–6). It is selectively absorbed by and produces cytotoxicity in anaerobes (6–8). Its efficacy in the treatment of *Trichomonas vaginalis* has been well documented (9). The idea of developing a medicated tampon to combine the therapeutic efficacy of metronidazole and the high fluid absorbability of tampon for trichomonas-infected women is thus generated.

Additionally, a high incidence of toxic shock syndrome was recently reported in menstruating women who used tampons, especially one brand[2] (10). Continuing epidemiological and microbiological studies at the Center for Disease Control have firmly related the pathogenesis of toxic shock syndrome to the infection of *Staphylococcus aureus* isolated from the vaginas of patients who suffered from toxic shock syndrome (98 *versus* 7% in the unmatched controls). On the other hand, no *S. aureus* could be recovered from the unused tampons, including those from tampon boxes used by the patients (10). The incidence of toxic shock syndrome further suggests the need to develop a medicated tampon, which administers an antistaphylococcal agent in the vagina in a controlled manner for a prolonged period of time, to protect the user from *S. aureus* infection.

The objective of this investigation is to evaluate the technical feasibility of using the tampon as an intravaginal drug delivery system. In this report, the methodology for

[1] Flagyl (SC-10295), Searle Laboratories, Division of G. D. Searle & Co., Skokie, IL 60077.

[2] Rely tampons.

0022-3549/82/0700-0767$01.00/0

(16) G. H. Loew, D. S. Berkowitz, and S. K. Burt, *ibid.*, pp. 278–316.
(17) G. H. Loew and D. S. Berkowitz, *J. Med. Chem.*, **21**, 101 (1978).
(18) S. Scheiner and V. M. Kolb, *Proc. Natl. Acad. Sci. USA*, **77**, 5602 (1980).
(19) L. J. Bellamy, "The Infra-red Spectra of Complex Molecules," Wiley, New York, N.Y., 1966, pp. 246–260.
(20) D. J. Pasto and C. R. Johnson, "Organic Structure Determination," Prentice-Hall, Englewood Cliffs, N.J., 1969, pp. 110–122.
(21) R. M. Silverstein, G. C. Bassler, and T. C. Morrill, "Spectrometric Identification of Organic Compounds," Wiley, New York, N.Y., 1974, p. 76.
(22) G. S. Mandel and N. S. Mandel, *American Crystallography*, Association Abstract Series, 2, 6:77, Honolulu, Hawaii (1979).
(23) P. Main, M. M. Woolfson, and G. Germain, *MULTAN*, University of York Printing Unit, York, England, Version 1974.
(24) D. J. Duchamp, *Program and Abstracts*, American Crystallography Association Meeting, Bozeman, Montana (1964).
(25) A. C. Larson, *Acta Crystallogr.*, **23**, 664 (1967).
(26) R. F. Stewart, E. R. Davidson, and W. T. Simpson, *J. Chem. Phys.*, **42**, 3175 (1965).
(27) W. C. Hamilton, *Acta Crystallogr.*, **12**, 609 (1959).
(28) I. L. Karle, R. D. Gilardi, A. V. Fratini, and J. Karle, *Acta Crystallogr., Sect.* **B25**, 1469 (1969).
(29) R. M. Silverstein, G. C. Bassler, and T. C. Morrill, "Spectrometric Identification of Organic Compounds," Wiley, New York, N.Y., 1974, pp. 107–110.

ACKNOWLEDGMENTS

Presented at the Tenth Northeast Regional Meeting of the American Chemical Society, Potsdam, N.Y., June 1980 (Abstract 39).

This work was supported in part by grants from University Research Foundation, La Jolla, California, to V. M. Kolb, and from the Medical Research Service of the Veterans Administration, the Arthritis Foundation, and Kroc Foundation for Medical Research to N. S. Mandel.

The authors thank Professor Cal Y. Meyers for pointing out IR data of amines and their salts, which suggest longer N—C bonds in protonated amines. V. M. Kolb is grateful to Dr. Alan A. Rubin, Endo Laboratory, Inc., for generously donating the oxymorphone. A generous allocation of computer time from the Academic Computing Center of University of Akron is gratefully acknowledged.

Inquiries concerning the X-ray structure determination of oxymorphone should be addressed to Stephen D. Darling.

Medicated Tampons: Intravaginal Sustained Administration of Metronidazole and *In Vitro–In Vivo* Relationships

Y. W. CHIEN *x, J. OPPERMANN ‡, B. NICOLOVA ‡, and H. J. LAMBERT ‡

Received February 27, 1981, from **Rutgers—The State University, College of Pharmacy, Piscataway, NJ 08854* and ‡*Searle Laboratories, G. D. Searle & Co., Skokie, IL 60077.* Accepted for publication September 29, 1981.

Abstract □ The technical feasibility of utilizing tampons as a drug delivery system for prolonged intravaginal drug administrations was studied. Several commercially available brands of tampons were examined. The methodology for the incorporation of various doses of metronidazole, an antitrichomonas agent, in tampons was described. The sustained-release profile of metronidazole from these medicated tampons was characterized. Intravaginal administration of metronidazole *via* the medicated tampons was investigated in rhesus monkeys and human volunteers, and *in vitro–in vivo* correlations were established. The biopharmaceutics of intravaginal absorption of metronidazole *via* medicated tampons was analyzed in comparison with a vaginal solution formulation.

Keyphrases □ Metronidazole—intravaginal sustained administration in medicated tampons, *in vitro–in vivo* relationships □ Tampons—intravaginal sustained administration of metronidazole, *in vitro–in vivo* relationships □ Intravaginal administration—sustained metronidazole in tampons, *in vitro–in vivo* relationships

Tampons are made of cotton and/or cellulose and are commonly used for intravaginal insertion to absorb menstrual discharge (1). Numerous brands of vaginal tampons are commercially available. Their characteristics of high fluid absorbability and retention have been recommended for the absorption of extensive vaginal discharge in trichomonas-infected women.

Metronidazole[1] has been shown to be an effective antiprotozoal agent with a broad spectrum of activity against anaerobes (2–6). It is selectively absorbed by and produces cytotoxicity in anaerobes (6–8). Its efficacy in the treatment of *Trichomonas vaginalis* has been well documented (9). The idea of developing a medicated tampon to combine the therapeutic efficacy of metronidazole and the high fluid absorbability of tampon for trichomonas-infected women is thus generated.

Additionally, a high incidence of toxic shock syndrome was recently reported in menstruating women who used tampons, especially one brand[2] (10). Continuing epidemiological and microbiological studies at the Center for Disease Control have firmly related the pathogenesis of toxic shock syndrome to the infection of *Staphylococcus aureus* isolated from the vaginas of patients who suffered from toxic shock syndrome (98 *versus* 7% in the unmatched controls). On the other hand, no *S. aureus* could be recovered from the unused tampons, including those from tampon boxes used by the patients (10). The incidence of toxic shock syndrome further suggests the need to develop a medicated tampon, which administers an antistaphylococcal agent in the vagina in a controlled manner for a prolonged period of time, to protect the user from *S. aureus* infection.

The objective of this investigation is to evaluate the technical feasibility of using the tampon as an intravaginal drug delivery system. In this report, the methodology for

[1] Flagyl (SC-10295), Searle Laboratories, Division of G. D. Searle & Co., Skokie, IL 60077.

[2] Rely tampons.

0022-3549/82/0700-0767$01.00/0

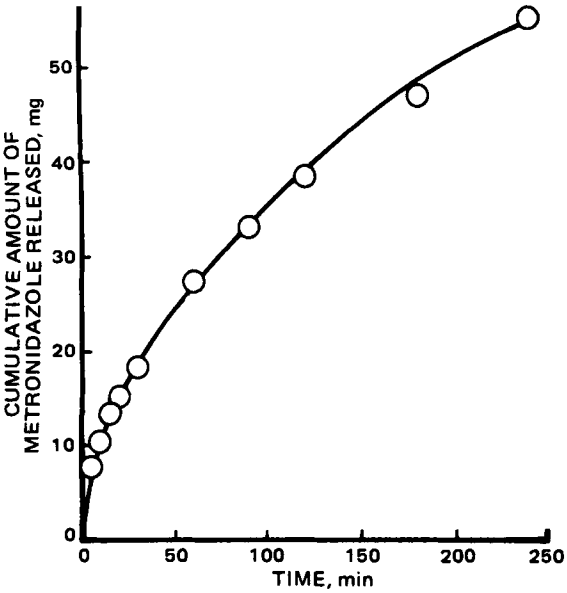

Figure 1—*Time course for the release of metronidazole from medicated Tampon I (A = 20.25 mg/cm³) into 200 ml of simulated vaginal fluid (pH 4.5) at 37° for 4 hr.*

the incorporation of various doses of metronidazole in several well-known brands of tampon is described, and the sustained-release profile of metronidazole from these medicated tampons is characterized. Sustained intravaginal administration of metronidazole *via* the tampon was also examined in both rhesus monkeys and human volunteers. *In vitro–in vivo* correlations were established and the biopharmaceutics of intravaginal absorption of metronidazole was also analyzed.

EXPERIMENTAL

Materials—Both metronidazole[1] and various commercial brands[3–5] of tampon (I–IV) were used as obtained. All the reagents or solvents used were analytical reagent grade.

Impregnation of Tampons with Metronidazole—Impregnation of tampons with metronidazole was achieved by preparing a concentrated metronidazole solution in acetone–methanol combinations and placing an aliquot of this solution onto the tip of the tampons. The solution was allowed to diffuse throughout the tampon body and the solvent was then evaporated under controlled conditions. This process was repeated until the desired amount of metronidazole was impregnated.

***In Vitro* Elution Studies of Medicated Tampons**—A polyethylene tube (6-cm length; 1.6-cm o.d.; 1.5-cm i.d.) with 20 evenly distributed openings (2.5 mm in diameter) was fabricated as the tampon holder for *in vitro* drug elution studies to simulate the constriction produced by the vaginal wall on the tampon *in situ*. All *in vitro* elution studies of medicated tampons were conducted under sink conditions in 200 ml of simulated vaginal fluid (0.026 *M* citric acid and 0.024 *M* sodium citrate in distilled water at pH 4.5) in a 250-ml reagent bottle thermostated at 37° in a waterbath (with a shaking rate of 80 oscillations/min). A 1-ml aliquot was withdrawn at each scheduled interval for up to 4 hr. After appropriate dilution, the concentration of metronidazole in the simulated vaginal fluid was determined spectrophotometrically[6] at its λ_{max} value of 316 nm. Several long-term (*e.g.*, 24 hr) drug elution studies were also carried out to ensure that 100% release of the impregnated metronidazole could be achieved from various brands of tampons.

Intravaginal Release Studies of Medicated Tampons—Five female, mid-cycle rhesus monkeys, weighing 4.7–6.5 kg, were used for crossover intravaginal release studies. Each monkey was tranquilized with 3 mg im of phencyclidine hydrochloride[7]. After tranquilizing, the animal was placed on its stomach on a V-board with the legs hanging freely over the end. The vagina was then sufficiently distended with a speculum to permit the easy insertion of a medicated tampon (1.5 cm in length). After insertion, each animal was placed in a primate chair[8] until the tampon was removed. The tampon was removed at 2, 4, 8, 16.5, or 25.5 hr after insertion by gently pulling on the string (which is attached to the tampon). The residual amount of metronidazole in each tampon was then analyzed spectrophotometrically following a 4-hr extraction with 40 ml of methanol.

Table I—*In Vitro* Release of Metronidazole from Various Brands of Tampon

Brands[a]	Surface Area, cm^2	Volume of Liquid Retained[b], ml/tampon	$Q/t^{1/2}$ [c], $\mu g/cm^2/min^{1/2}$
I	22.93	32.2	79.4
II	21.34	35.5	76.9
III	27.26	30.0	37.4
IV	28.99	24.0	51.6

[a] Each tampon was impregnated with 60 mg of metronidazole. [b] Volume of simulated vaginal fluid absorbed by 10-min soaking of tampon at room temperature. [c] *In vitro* release profile determined in simulated vaginal fluid at 37°.

Pharmacokinetics of Intravaginal Absorption—*[^{14}C]Metronidazole*—[^{14}C]Metronidazole, 1-(2[U-^{14}C]hydroxyethyl)-2-methyl-5-nitroimidazole[9], with a radiochemical purity >98% was used. The labeled drug was diluted with unlabeled metronidazole to yield a specific activity of 1.13 μCi/mg.

[^{14}C]Metronidazole-Tampon—Following the method described earlier, Tampon I was impregnated with 48.3 μCi (42.75 mg) of [^{14}C]-metronidazole.

Intravaginal Absorption of [^{14}C]Metronidazole from Medicated Tampons—One rhesus monkey was selected from the group that was used in the earlier intravaginal release studies. The animal was tranquilized and the [^{14}C]metronidazole-impregnated tampon was inserted in the manner as described previously. A urinary catheter[10] and a venous catheter[11] were also inserted. The patency of the venous catheter was maintained with a slow infusion of saline. The animal was secured in a

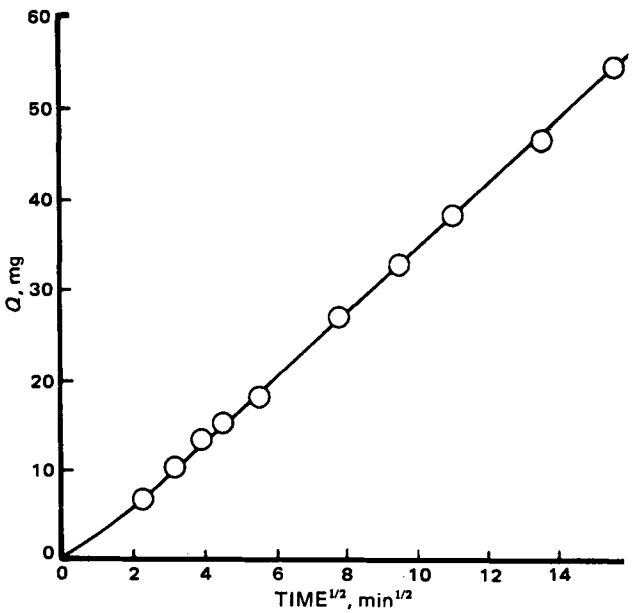

Figure 2—*Linear relationship between the cumulative amount of metronidazole (Q) released from medicated Tampon I and the square root of time ($t^{1/2}$) as defined in Eq. 1. The data from Fig. 1 were plotted.* $Q/t^{1/2} = 79.4\ \mu g/cm^2/min^{1/2}$.

[3] Tampax menstrual tampons (I), Tampax Inc., Palmer, MA 01069.
[4] Kotex tampons, (II), Kimberly-Clark Corp., Neenah, WI 54956.
[5] Playtex self-adjusting tampons (III) and Playtex self-adjusting tampons with deodorant (Playtex-D) (IV), International Playtex Co., Division Rapid-American Corp., Dover, DE 19901.
[6] Coleman Model 124D Spectrophotometer, Perkin-Elmer, Scientific Products, McGaw Park, IL 60085.
[7] Sernylan, Bio-Centric Laboratories, Inc., St. Joseph, MO 64502.
[8] XPL-515-SASR, Plas Laboratories, Scientific Div., Plastics Manufacturing and Supply Inc., Lansing, MI 48906.
[9] Amersham Corp., Arlington Heights, IL 60005.
[10] Bardex Foley Catheter, 10 French.
[11] B-D Longdwel, 20 gauge, with 2-inch catheter needle.

Table II—Apparent Diffusivities of Metronidazole and Porosity–Tortuosity Ratio in Various Brands of Tampons

Brands	$(D_m C_s)^{1/2}$ [a], $mg^{1/2}/cm^{1/2}/min^{1/2}$	$D_m \times 10^6$, cm^2/sec	ϵ/θ [b]
I	28.0×10^{-3}	1.03	0.213
II	29.5×10^{-3}	1.14	0.236
III	24.6×10^{-3}	0.79	0.164
IV	33.5×10^{-3}	1.47	0.304

[a] Slope of the linear $Q/t^{1/2}$ *versus* $(2A - C_s)^{1/2}$ plots, where C_s = 12.7 mg/ml. [b] The ratio of porosity over tortuosity as calculated from Eq. 3 using a D value of 4.84×10^{-6} cm^2/sec, which was determined polarographically from the following relationship: $D = [(i_d)/0.605nCm^{2/3}t^{1/2}]^2$. *p*-Nitrophenol ($D = 9.18 \times 10^{-6}$ cm^2/sec) was run simultaneously as reference.

primate chair[8] until the tampon was removed and then transferred to a metabolism cage for continuous urine collections. Two milliliters of blood were collected at 3, 6, 8, 24, 26, 28, 30, 72, 96, and 120 hr. Urine was collected at 24, 48, 72, 96, and 120 hr.

Intravaginal Absorption of [^{14}C]*Metronidazole in Solution*—Three female rhesus monkeys, weighing 4.5–5.0 kg, were tranquilized with 1 mg/kg of phencyclidine hydrochloride[7]. After tranquilizing, catheters were placed in the saphenous vein[11] and urinary bladder[10]. A slow infusion of saline was initiated to maintain patency of the saphenous vein catheter. The animals were then placed on their backs on a V-board with the legs in a vertical (lithotomy) position and the pelvic area was supported and slightly elevated. A solution of 1 mg/kg of [^{14}C]metronidazole in 0.5 ml of distilled water was then quantitatively instilled into the vagina with a micropipet.

The animals were maintained in a tranquilized state by periodic administration of phencyclidine hydrochloride (1 mg/kg/90 min) for the first 5 hr after drug administration. Then, the animals were transferred to primate chairs[8] and remained there until 24 hr after drug administration. At this time the catheters were removed, the vaginal vault was thoroughly rinsed with 50 ml of saline, and the animals were transferred to metabolism cages for continuing urine and plasma collection.

Radioactivity Measurements—Aliquots (100–500 μl) of plasma, urine, or tampon extracts were added to 4 ml of water in scintillation vials. Ten milliliters of liquid scintillation solution[12] was added and the mixture was agitated to form a gel. Each sample was then assayed for carbon 14 content by liquid scintillation spectrometry[13].

RESULTS AND DISCUSSION

***In Vitro* Release Studies of Medicated Tampons**—The release profile of metronidazole from a medicated tampon in simulated vaginal fluid (pH 4.5) under a sink condition is shown in Fig. 1. Mechanistic analyses of this nonlinear drug release profile suggested that the release of metronidazole from tampons is under a matrix-controlled process and follows the same Q *versus* $t^{1/2}$ release pattern as demonstrated earlier in the release of norgestomet from hydrogel-type drug delivery device (11). The linear Q–$t^{1/2}$ relationship observed can be defined mathematically by:

$$Q = [D_m(2A - C_s)C_s t]^{1/2} \quad \text{(Eq. 1)}$$

where Q is the cumulative amount of metronidazole released from a unit surface area of a tampon; D_m is the effective diffusivity of metronidazole in the tampon matrix; A is the initial amount of metronidazole impregnated per unit volume of tampon; C_s is the solubility of metronidazole in the simulated vaginal fluid; and t is the time. As demonstrated in Fig. 2 a Q *versus* $t^{1/2}$ linearity was followed. The slope of this linearity is thus defined as:

$$Q/t^{1/2} = [D_m(2A - C_s)C_s]^{1/2} \quad \text{(Eq. 2)}$$

The $Q/t^{1/2}$ profiles for various brands of tampons are compared in Table I. It is noted that Tampons I and II released metronidazole at very much the same magntiude of $Q/t^{1/2}$, which was slightly more than twice the value of $Q/t^{1/2}$ for Tampon III; and the *in vitro* release of metronidazole from Tampon IV (Tampon III with deodorant) was observed to be 40%

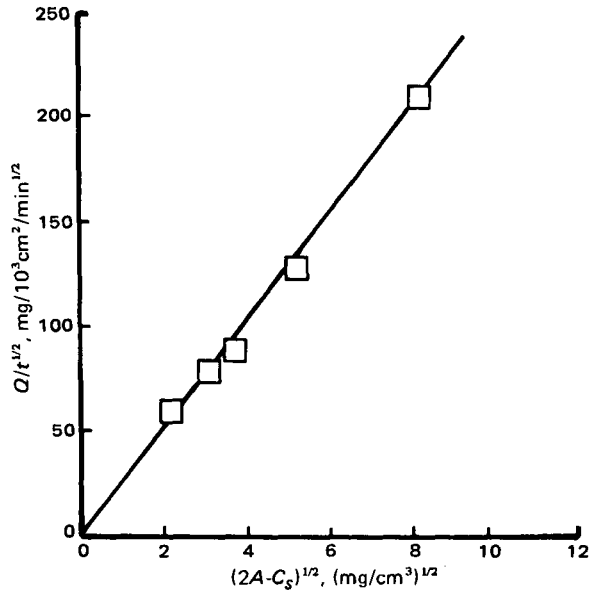

Figure 3—*Linear relationship between the values of* $Q/t^{1/2}$ *and* $(2A - C_s)^{1/2}$ *as defined in Eq. 2.*

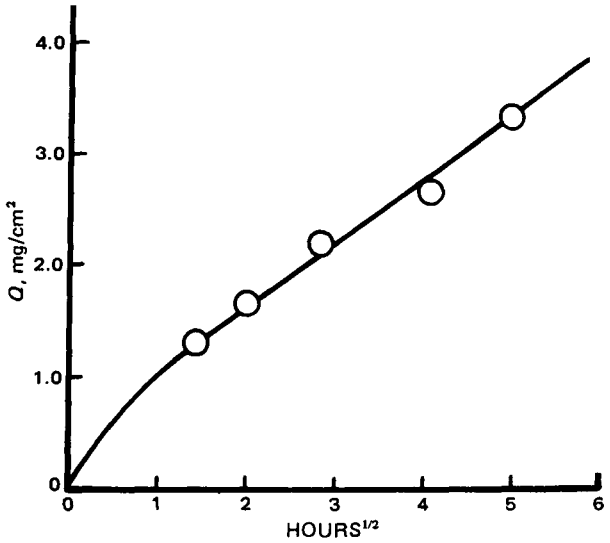

Figure 4—*Intravaginal release of metronidazole from Tampon I (A = 20.25 mg/cm^3) in five rhesus monkeys for up to 25 hr.* $Q/t^{1/2}$ *= 74.9 μg/cm^2/min$^{1/2}$.*

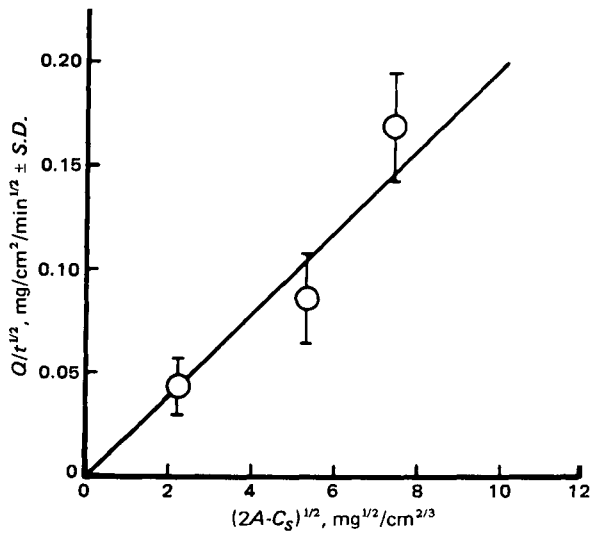

Figure 5—*Linear dependency of the intravaginal* $Q/t^{1/2}$ *data determined in rhesus monkeys on the* $(2A - C_s)^{1/2}$ *values of metronidazole in Tampon I.*

[12] PCS liquid scintillation solution, Amersham/Searle Corp., Arlington Heights, Ill.

[13] Mark II Spectrometer, Searle Analytic Inc., Des Plaines, Ill.

Table III—*In Vitro*—*In Vivo* Correlation on the Sustained Release of Metronidazole from Tampons

Types	Release Conditions	$Q/t^{1/2}$, $\mu g/cm^2/min^{1/2}$
I[a]	*In vitro* elution	79.4
	Monkey vagina	74.9
III[b]	*In vitro* elution	37.4
	Human vagina	45.9

[a] A = 20.25 mg/cm^3. [b] A = 6.59 mg/cm^3.

faster than Tampon III. No correlation could be estalished between the values of $Q/t^{1/2}$ and the extent of liquid retention of the tampons.

The effect of the dose of metronidazole initially impregnated in a tampon on the sustained-release profile of metronidazole was also studied. Equation 2 suggests that the magnitude of $Q/t^{1/2}$ values should increase as the drug content (A) in the tampon increases. A dose level ranging from 60 to 360 mg/tampon was investigated. As suggested by Eq. 2, the results confirmed that $Q/t^{1/2}$ values show a linear dependency on the square root of $(2A - C_s)$ values (Fig. 3). These data indicate that the dosage administered intravaginally to a subject can be controlled by incorporating an appropriate amount of metronidazole in the tampon.

The slope of this linear $Q/t^{1/2}$ *versus* $(2A - C_s)^{1/2}$ relationship is defined by $(D_m C_s)^{1/2}$. If the aqueous solubility (C_s) of metronidazole is known or predetermined, the effective diffusivity (D_m) of metronidazole in a tampon matrix can be calculated. A D_m value ranging from 0.79 to 1.47 × 10^{-6} cm^2/sec was determined (Table II). Using the relationship:

$$D_m = D\frac{\epsilon}{\theta} \qquad \text{(Eq. 3)}$$

and the solution diffusivity (D) which was determined independently by dc polarography (12), the ratio of porosity (ϵ) over tortuosity (θ) can be estimated (Table II). It appears that the value of ϵ/θ varies from one brand of tampon to another (ranging from 0.164 to 0.304). The higher values of D_m and ϵ/θ for Tampon IV than for Tampon III are, apparently, due to the addition of deodorant in Tampon IV. The pretreatment by a fragrance (as the deodorant) with an o/w-type surfactant, such as polysorbate 20, should result in the enhancement of wettability of the tampon cotton and/or the reduction of drug–cotton interaction, leading to a higher porosity-tortuosity (ϵ/θ) ratio and, hence, a greater diffusivity (D_m) in the tampon matrix. It is also noticed that a lower liquid retention was obtained for Tampon IV than for Tampon III (Table I).

Intravaginal Release Studies of Medicated Tampons in Rhesus Monkeys—The intravaginal release profile of metronidazole from medicated tampons in rhesus monkeys is illustrated in Fig. 4. As expected from Eq. 1, the results indicated that the intravaginal release profile of

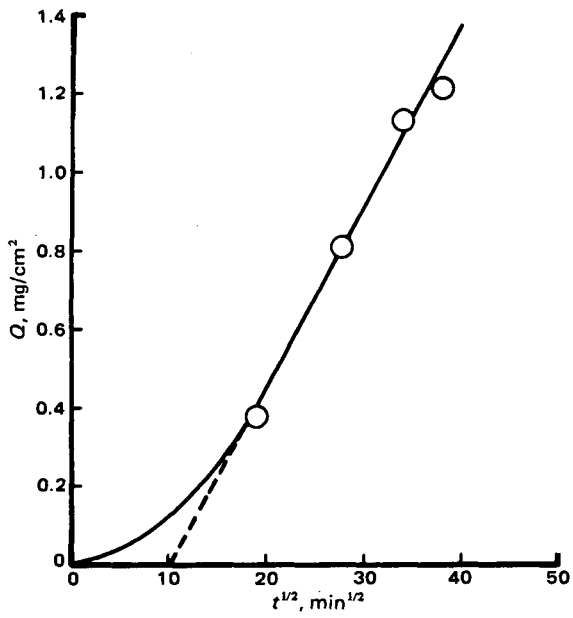

Figure 6—*Intravaginal release of metronidazole from Tampon III (A = 6.59 mg/cm^3) in a human volunteer for up to 24 hr. Q/t$^{1/2}$ = 45.9 μg/cm^2/min$^{1/2}$.*

Table IV—Effect of the Days in Menstrual Cycles on the Sustained Release of Metronidazole [a]

Days[b]	$Q/t^{1/2}$, mg/min$^{1/2}$	
	8 pm → 8 am	8 am → 8 pm
1	0.301	0.595
7	0.215	0.452
14	0.366	0.647
21	0.344	0.444

[a] For each 12-hr insertion, each volunteer receives one tampon (III) impregnated with 60 mg of metronidazole. [b] Days after the termination of menstruation.

metronidazole also follows the linear Q *versus* $t^{1/2}$ relationship. A $Q/t^{1/2}$ value of 74.9 μg/cm^2/min$^{1/2}$ was calculated. This intravaginal release rate of metronidazole (74.9 μg/cm^2/min$^{1/2}$) was found to be very close to the *in vitro* release rate (79.4 μg/cm^2/min$^{1/2}$) determined in the 4-hr drug elution studies (Fig. 2 and Table III).

Tampon I was also impregnated with 3 dosage levels of metronidazole and examined in rhesus monkeys to test the applicability of Eq. 2 to the *in vivo* condition. Results (Fig. 5) were in agreement with the *in vitro* observations (Fig. 3). Assuming that metronidazole has a solubility (C_s) in vaginal secretions similar to that in the simulated vaginal fluid (12.7 mg/ml), the effective diffusivity (D_m) can be calculated from the slope of $Q/t^{1/2}$ *versus* $(2A - C_s)^{1/2}$ plot. A value of 7.21 × 10^{-7} cm^2/sec is the result. It is only slightly lower than the value of 10.3 × 10^{-7} cm^2/sec determined in *in vitro* studies (Table II).

Intravaginal Release Studies of Medicated Tampons in Human Volunteers—The intravaginal release profile of metronidazole from medicated tampons in human volunteers is illustrated in Fig. 6. In this study, Tampon III was medicated and tested in one volunteer for a duration from 6 hr up to 24 hr. An intravaginal release rate of 45.9 μg/cm^2/min$^{1/2}$ was achieved. This release rate was found to be only slightly higher than the 37.4 μg/cm^2/min$^{1/2}$ measured in the 4-hr *in vitro* elution study (Table III).

Considering the cyclic variation in vaginal physiology, the effect of physiological phases in a menstrual cycle on the intravaginal release of metronidazole from medicated tampons was examined in one volunteer. The data in Table IV suggest that the intravaginal release rate of metronidazole first decreases right after menstruation and then increases toward the middle of the cycle just prior to ovulation. This behavior is very similar to the cyclic pattern observed in rhesus monkeys on the intravaginal absorption of hydrophilic and hydrophobic n-alkanols (13).

A higher rate of intravaginal release was also consistently observed in those medicated tampons inserted in daytime (8 am–8 pm) as compared to those inserted at night (8 pm–8 am). The observation may be related to the higher physical activity shown in the daytime, which may give a greater secretion of vaginal fluid.

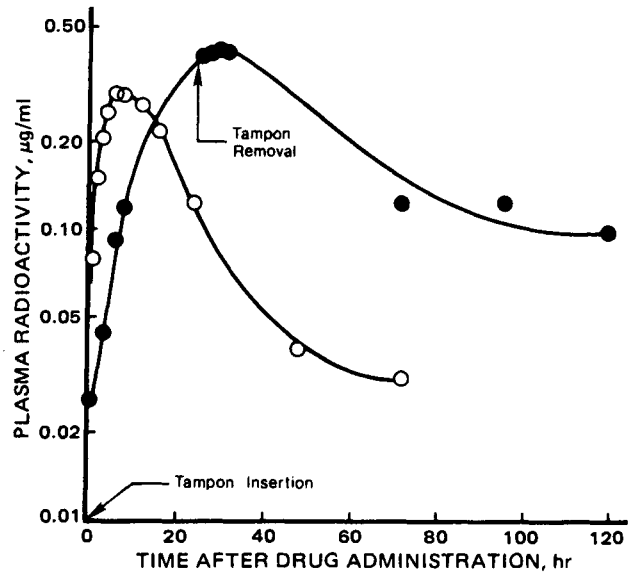

Figure 7—*Comparative plasma profiles of total radioactivity in rhesus monkeys administered with [^{14}C]metronidazole in solution dose (○; 5 mg; n = 3) and via medicated Tampon III (●; 42.75 mg; n = 1), where n is the number of subjects tested. The tampon was inserted for 25 hr while solution was administered for 24 hr.*

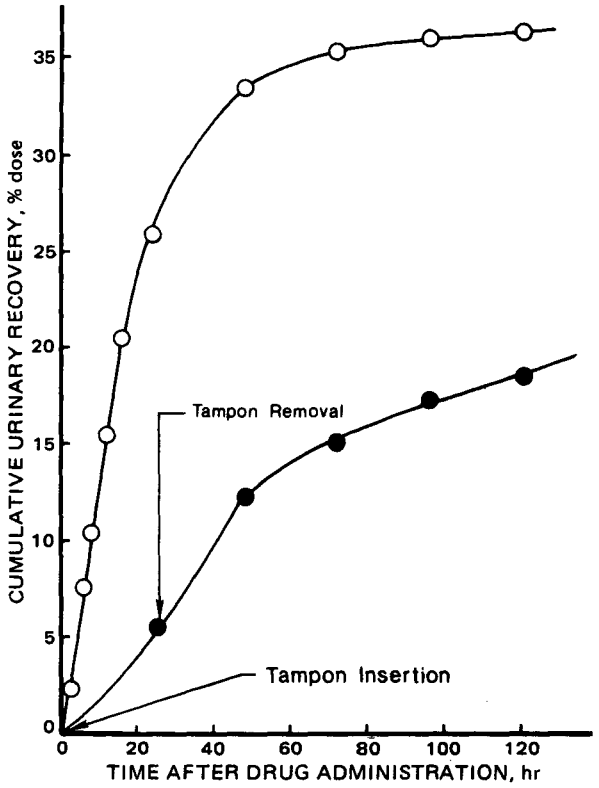

Figure 8—*Cumulative urinary recovery of total radioactivity (percent of the applied dose) after the intravaginal administrations of [^{14}C]-metronidazole in rhesus monkeys through solution dose (○) and medicated Tampon III (●). Conditions are the same as in Fig. 7.*

***In Vitro–In Vivo* Correlations**—The correlations between the *in vitro* data and intravaginal release profiles, as shown in Table III, are very encouraging. The results suggest that the 24-hr intravaginal release of metronidazole from medicated tampons in both rhesus monkeys and human volunteers can be predicted from the 4-hr *in vitro* drug elution study.

Comparative Plasma Profiles of Metronidazole—To study the comparative systemic bioavailability by intravaginal drug administration *via* medicated tampon and solution formulation, one unit of Tampon III was medicated with 48.3 μCi (42.75 mg) of [^{14}C]metronidazole and then inserted into the monkey vagina for 25 hr. Analysis of the ethanol extract of the removed tampon (by double 50-ml extractions) indicated that 10.4 mg of [^{14}C]metronidazole still remained in the tampon. Complete combustion of the extracted tampon to [^{14}C]carbon dioxide and water further demonstrated that an additional 1.2% (0.51 mg) of the original radioactivity was present in the tampon[14]. These results suggest that altogether, 74.5% (31.84 mg) of the [^{14}C]metronidazole incorporated into the tampon was released in the rhesus monkey during the 25-hr insertion period. This result is in agreement with the data obtained from similar experiments conducted with unlabeled metronidazole utilizing a UV spectrophotometric assay technique.

The plasma profile of total radioactivity following the 25-hr intravaginal administration of [^{14}C]metronidazole in the rhesus monkey *via* medicated tampon is compared with that following the intravaginal administration of [^{14}C]metronidazole in a solution formulation for 24 hr (Fig. 7). Results show that the peak plasma carbon 14 concentration occurs at 6 hr during administration of the solution dose, whereas after the vaginal tampon medication the peak is reached at a much later time (30 hr after insertion or 5 hr after tampon removal). These observations suggest a delayed intravaginal uptake of metronidazole by the sustained release mechanism of the medicated tampon as compared to the drug administration in solution dose. On the other hand, 5 hr after the removal of the tampon, the plasma radioactivity eliminates at basically the same rate as that following solution administration. These results suggest that the use of tampons as the intravaginal drug delivery device does not change the elimination kinetics of metronidazole from the body.

Comparing the areas under the plasma carbon 14 concentration curves (0–120 hr, corrected for the difference in the doses applied), it was estimated that the systemic bioavailability of metronidazole administered by the medicated tampon is only 27.2% of the solution dose. The low relative systemic bioavailability (27.2%) may occur if the majority of metronidazole released from the medicated tampon remains in the vaginal tract to exert a localized therapeutic activity. This possibility is confirmed by the observation that the peak plasma carbon 14 concentration is reached at 5 hr after removal of the medicated tampons (Fig. 7).

Comparative Urine Excretion Profiles of Metronidazole—Figure 8 compares the rate and extent of the urinary excretion of radioactivity after intravaginal administration of [^{14}C]metronidazole in solution formulation (5 mg) and medicated tampon (42.75 mg) to rhesus monkeys. Apparently, the rate and extent of urinary recovery of the radioactivity were significantly reduced when [^{14}C]metronidazole was administered *via* the medicated tampon. The observed reduction in the rate of urinary recovery is in agreement with the result observed in the plasma profiles (Fig. 7). This could well be the outcome of the sustained release of metronidazole from the medicated tampon, which prolongs the uptake of drug by the vagina.

Only 18.5% of the released dose was recovered in the urine during the 5-day observation period. [The majority (13%) was excreted in the 4-day period following removal of the tampon.] This is considerably lower than the 36.3% recovered from the solution dose during the same period (Fig. 8). By comparison with the vaginal absorption of the solution dose, it is estimated that the medicated tampon produces a relative systemic bioavailability of 51%, which is almost twice the value (27.2%) calculated from the plasma data (Fig. 7). This difference suggests that metronidazole molecules administered by sustained release medicated tampon may become more locally available *via*, possibly, binding to the vaginal wall. The bound metronidazole is then excreted *via* the perieum venous plexus, which drains the vaginal tissue and rectum, flows into the pudentum vein, and ultimately into the vena cava, resulting in a lower systemic bioavailability (13).

[14] Sample Oxidizer, Packard Model 306, Packard Instruments Corp., Lincolnwood, Ill.

REFERENCES

(1) F. Sadik, *J. Am. Pharm. Assoc.*, **NS 12,** 565 (1972).

(2) R. F. Jennison, P. Stenton, and L. Watt, *J. Clin. Pathol.*, **14,** 431 (1961).

(3) P. E. Thompson, *Arch. Invest. Med.*, **1,** 165 (1970).

(4) P. I. Long, *J. Am. Med. Assoc.*, **223,** 1378 (1972).

(5) F. P. Tally, V. L. Sutter, and S. M. Finegold, *Calif. Med.*, **117,** 22 (1972).

(6) D. I. Edwards, M. Dye, and H. Carne, *J. Gen. Microbiol.*, **76,** 135 (1973).

(7) R.M. J. Ings, J. A. McFadzean, and W. E. Ormerod, *Biochem. Pharmacol.*, **23,** 1421 (1974).

(8) M. Muller and D. G. Lindmark, *Antimicrob. Agents Chemother.*, **9,** 696 (1976).

(9) A. J. Pereyra and J. D. Lansing, *J. Obstet. Gynecol.*, **24,** 499 (1964).

(10) Center for Disease Control, *Morbidity & Mortality Report*, **29,** 441 (1980).

(11) Y. W. Chien and E. P. K. Lau, *J. Pharm. Sci.*, **65,** 488 (1976).

(12) Y. W. Chien, Ph.D. thesis, The Ohio State University, Columbus, Ohio, 1972.

(13) G. L. Flynn, N. F. H. Ho, S. Hwang, E. Owada, A. Molokhia, C. R. Behl, W. I. Higuchi, T. Yotsuyanagi, Y. Shah, and J. Park, in "Controlled Release Polymeric Formulations," D. R. Paul and F. W. Harris, Eds., American Chemical Society, Washington, D.C., 1976, p. 87.

ACKNOWLEDGMENTS

The authors wish to thank Ms. D. Jefferson for her technical assistance.

Synthesis and Bioevaluation of a Series of Fatty Acid Esters of *p*-[*N*,*N*-Bis(2-chloroethyl)amino]phenol

J. E. WYNN ˣ, M. L. CALDWELL, J. R. ROBINSON, R. L. BEAMER, and C. T. BAUGUESS

Received July 31, 1981, from the *Department of Basic Pharmaceutial Sciences, College of Pharmacy, University of South Carolina, Columbia, SC 29208.* Accepted for publication October 6, 1981.

Abstract □ A series of even numbered fatty acid esters (C_2–C_{18}) of *p*-[*N*,*N*-bis(2-chloroethyl)amino]phenol were synthesized and evaluated as to acute toxicity as well as effectiveness against L-1210 mouse leukemia. The acetate through the decanoate derivatives demonstrated toxicity between 2 and 3 times that of phenol mustard in HA/ICR mice. The less soluble laurate, myristate, palmitate, and stearate derivatives were less toxic. Significant survival times in the leukemia studies (T/C% ≥ 125) were observed for all compounds except the acetate and hexanoate derivatives. The myristate derivative produced the greatest significant increase in survival time, 162%. The palmitate and stearate derivatives produced significant survival at five and four dosage levels, respectively. The butyrate and laurate derivatives produced significant survival at three dosage levels and the octanoate, decanoate, and myristate at two dosage levels.

Keyphrases □ Fatty acid esters—synthesis of fatty acids of *p*-[*N*,*N*-bis(2-chloroethyl)amino]phenol, toxicity, effectiveness against L-1210 mouse leukemia □ *p*-[*N*,*N*-Bis(2-chloroethyl)amino]phenol—synthesis of fatty acid esters for toxicity and effectiveness against L-1210 mouse leukemia □ Bioevaluation—synthesis of fatty acid esters of *p*-[*N*,*N*-bis(2-chloroethyl)amino]phenol, toxicity, effectiveness against L-1210 mouse leukemia

Efforts to develop latent forms of phenol mustard, *p*-[*N*,*N*-bis(2-chloroethyl)amino]phenol, have resulted in the synthesis of various esters of the phenol (1–3), as well as its ether derivatives (4). A previous study (2) on a series of substituted benzoate esters of phenol mustard suggested that the toxicity of those esters was related to their hydrolysis to the phenolic mustard. They also suggested that antitumor activity in Walker 256 tumor paralleled hydrolysis of the esters to phenol mustard. A retrospective QSAR study on a number of derivatives of aniline mustard has been performed (5). That study supports the concept that, in general, antitumor activity parallels hydrolysis to phenol mustard, as well as toxicity. That evaluation of the aforementioned series of benzoate esters of phenol mustard suggests that the hydrolyzed form of the ester is not the principle antitumor agent.

An earlier report from this laboratory compared the antileukemic activity of the acetate, hexanoate, and decanoate esters of phenol mustard (3). Those results indicated a decrease in toxicity and an increase in antileukemic activity was associated with an increase in the length of the fatty acid side chain. In light of these results, it was felt that an expanded series of fatty acid esters would provide additional information with respect to the effect of chain length on toxicity and antileukemic activity. The specific objectives of this report were to: (*a*) synthesize a series of even numbered fatty acid esters (C_2–C_{18}) of *p*-[*N*,*N*-bis(2-chloroethyl)amino]phenol, (*b*) determine the acute toxicity as measured by the LD_{50} for each compound studied, and (*c*) determine the effect of each compound on the prolongation of life of L-1210 leukemic mice.

The compounds evaluated in this project were synthesized using either Method A or Method B as shown in Scheme I.

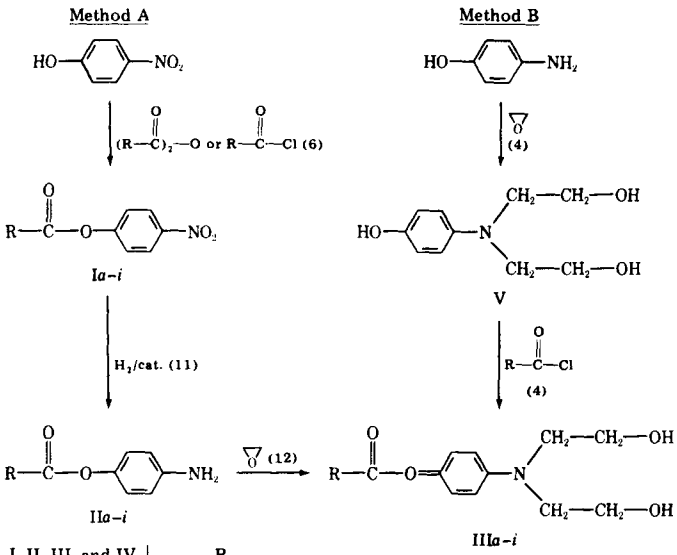

I, II, III, and IV	R
a	CH_3—
b	CH_3—$(CH_2)_2$—
c	CH_3—$(CH_2)_4$—
d	CH_3—$(CH_2)_6$—
e	CH_3—$(CH_2)_8$—
f	CH_3—$(CH_2)_{10}$—
g	CH_3—$(CH_2)_{12}$—
h	CH_3—$(CH_2)_{14}$—
i	CH_3—$(CH_2)_{16}$—

Scheme I

EXPERIMENTAL

Synthesis of the Fatty Acid Esters of *p*-[*N*,*N*-Bis(2-hydroxyethyl)amino]phenol (IIIa–*i*), Method A—*Step I: Synthesis of the p-Nitrophenyl Esters (Ia–i).*—Ninety milliliters of 1,4-dioxane, 10 ml of pyridine, and 13.9 g (0.1 mole) of *p*-nitrophenol were stirred at room temperature until solution of the *p*-nitrophenol was complete. Then, 0.1 mole of either acetic or butyric anhydride, or the appropriate acid chloride for all other derivatives, was added slowly with stirring. The reaction mixture was stirred at room temperature in a glass-stoppered flask for ~2 hr. The volume of the reaction mixture was then reduced ~50% *in vacuo*. The products separated as a solid with the exception of the butyrate, hexanoate, and octanoate derivatives which were oils. The products were removed by filtration or by use of a separatory funnel and washed 3–5 times with a 5% sodium carbonate solution. After drying in a vacuum desiccator, the solid products were recrystallized from absolute ethanol. The oily products were dried *in vacuo* for 30–60 min and the pure products were characterized by physical data (Table I) and IR spectra and NMR spectra[1].

[1] All IR spectra were obtained using potassium bromide pellets or neat on sodium chloride plates using a Beckman Model IR-20A Spectrophotometer. NMR spectra were obtained from solutions of the derivatives in deuterated chloroform using a Hitachi–Perkin-Elmer Model R-24 high resolution spectrometer with tetramethylsilane as the internal standard. The elemental analyses reported were performed by either Galbraith Laboratories, Knoxville, Tenn. or Atlantic Microlab, Inc., Atlanta, Ga. Melting points reported were obtained using a Thomas Hoover capillary melting point apparatus and are uncorrected. All hydrogenation reactions were carried out in a Parr Low-Pressure Hydrogenation Apparatus.

0022-3549/82/0700-0772$01.00/0

Table I—Physical Data and Elemental Analysis for the Fatty Acid Esters of *p*-Nitrophenol (I*a–i*) and *p*-Aminophenol (II*a–i*)

Compound Number	mp or bp		Yield, %	Molecular Formula	Calculated, %			Found, %		
	Observed	Lit. Value, (9, 10)			C	H	N	C	H	N
I*a*	76.5°–77°	79°	56	$C_8H_7NO_4$	[b]					
I*b*	185°/760mm[a]	134°/0.8	52	$C_{10}H_{11}NO_4$	[b]					
I*c*	160°/1mm[a]	155°/0.8mm	50	$C_{12}H_{15}NO_4$	[b]					
I*d*	183°/760mm[a]	164°/0.3mm	71	$C_{14}H_{19}NO_4$	[b]					
I*e*	32°–34°	31°	57	$C_{16}H_{23}NO_4$	[b]					
I*f*	44°–45°	44.5°–45°	85	$C_{18}H_{27}NO_4$	[b]					
I*g*	53°–54°	54.5°–55°	83	$C_{20}H_{31}NO_4$	[b]					
I*h*	61.5–63°	62°–64°	61	$C_{22}H_{35}NO_4$	[b]					
I*i*	66.5°–67.5°	66.5°–67°	65	$C_{24}H_{39}NO_4$	[b]					
II*a*	70°–71°	70°–72°	43	$C_8H_9NO_2$	[b]					
II*b*	57°–59°		93	$C_{10}H_{13}NO_2$	67.4	7.26	7.82	66.95	7.17	7.82
II*c*	210°/760mm[a]		48	$C_{12}H_{17}NO_2$	69.56	8.21	6.76	69.36	8.17	6.65
II*d*	35°–36°		87	$C_{14}H_{21}NO_2$	71.48	8.93	5.95	[c]		
II*e*	39°–40°		29	$C_{16}H_{25}NO_2$	73.00	9.50	5.32	73.14	9.62	5.23
II*f*	46°–47°		55	$C_{18}H_{29}NO_2$	74.23	9.96	4.81	74.16	10.02	4.73
II*g*	59°–60°		76	$C_{20}H_{33}NO_2$	75.24	10.35	4.39	75.05	10.18	4.39
II*h*	73°–74.5°		73	$C_{22}H_{37}NO_2$	76.08	10.66	4.03	75.89	10.49	4.00
II*i*	79°–80°		75	$C_{24}H_{41}NO_2$	76.80	10.93	3.73	76.65	11.02	3.69

[a] Temperature/pressure at which fractions used for analysis and subsequent reaction were collected. [b] Characterized using comparative melting or boiling points, IR and NMR spectra. [c] An acceptable elemental analysis could not be obtained, but acceptable products were obtained in the subsequent reaction, Step III, Method A.

Step II: Reduction of the p-*Nitrophenyl Esters*—A solution containing 0.02 mole of the appropriate *p*-nitrophenol ester in 150 ml of absolute ethanol was placed in a reaction bottle. Sixty milligrams (0.0002 mole) of platinum oxide was added and the mixture was shaken under pressure with hydrogen until a pressure drop representing 0.06 mole of hydrogen uptake (4.92 psi) was observed. The catalyst was removed by filtration and the filtrate concentrated *in vacuo*. The product separated from the concentrated solution after cooling to 0°. Recrystallization from absolute ethanol yielded solid derivatives with the exception of the hexanoate ester which was an oil. The pure *p*-aminophenyl esters (II*a–i*) were characterized by physical data (Table I) and IR and NMR spectra.

Step III: Condensation of the p-*Aminophenyl Esters with Ethylene Oxide*—The *p*-[*N,N*-bis(2-hydroxyethyl)amino]phenyl esters (III*a–g*) were formed by dissolving 0.0005 mole of the appropriate *p*-aminophenyl ester in a minimum amount of absolute methanol using a 500-ml round-bottomed reaction flask. Two grams (0.05 mole) of cold ethylene oxide were added to 20 ml of methanol at 0°. The cold ethylene oxide–methanol mixture was added with continuous stirring to the methanol solution of the *p*-aminophenyl ester. The reaction flask was packed in dry ice and allowed to reach room temperature. The methanol and excess ethylene oxide were removed *in vacuo*. The solid products were recrystallized from absolute ethanol. The butyrate and hexanoate derivatives were isolated as semisolids, which gave crystalline solids when recrystallized from acetone–water. Acceptable products were not obtained for the palmitate nor the stearate derivatives (III*h* and III*i*). The pure derivatives were characterized by physical data (Table II) and IR and NMR spectra.

Synthesis of the Fatty Acid Esters of *p*-[*N,N*-Bis(2-hydroxyethyl)amino]phenol (III*a–i*), Method B—The *p*-[*N,N*-bis(2-hydroxyethyl)amino]phenol (V) was prepared using a procedure reported earlier (4). Absolute ethanol (250 ml); powdered KOH (2.8 g); (V) (9.5 g, 0.05 mole); and 0.05 mole of either myristoyl chloride, palmitoyl chloride, or stearoyl chloride were added to a glass 500-ml round bottomed flask, equipped with a magnetic stirrer and a glass stopper. The flask was stoppered and the solution was allowed to stir overnight. The resulting product was removed by filtration, the filtrate reduced *in vacuo*, and the residue dissolved in 100 ml of acetone. To the acetone solution was added 50 ml of water and the suspension was allowed to cool at 5° overnight. The crystals were filtered from the acetone–water solution and combined with the original product. Recrystallization from acetone–water gave analytically pure products (III*g–i*) which were characterized by physical data (Table II) and IR and NMR spectra.

Synthesis of the Fatty Acid Esters of *p*-[*N,N*-Bis(2-chloroethyl)amino]phenol (IV*a–i*)—A solution of 10 ml of chloroform, 0.3 ml of absolute ethanol, and 0.5 ml of thionyl chloride was stirred in a 100-ml round bottomed flask until room temperature was reached. To this solution 0.005–0.01 mole of the appropriate derivative of III was added slowly as the solution was stirred. The reaction flask was fitted with a condensor and a drying tube and packed in dry ice after solution was complete. An additional 1.5 ml of thionyl chloride was added to the cold solution. The reaction mixture was allowed to reach ambient temperature

Table II—Physical Data and Elemental Analysis for the Fatty Acid Esters of *p*-[*N,N*-Bis(2-hydroxyethyl)amino]phenol (III*a–i*) and of *p*-[*N,N*-Bis(2-chloroethyl)amino]phenol (IV*a–i*)

Compound Number	mp	Method	Yield, %	Molecular Formula	Calculated, %			Found, %		
					C	H	N	C	H	N
III*a*	74.5°–76°[a]	A	52	$C_{12}H_{17}NO_4$	60.25	7.11	5.85	60.20	7.18	5.76
III*b*	71.5°–72°	A	48	$C_{14}H_{21}NO_4$	62.92	7.86	5.24	63.06	7.75	5.34
III*c*	52°–53°	A	46	$C_{16}H_{25}NO_4$	65.08	8.47	4.75	64.95	8.51	4.69
III*d*	63°–65°	A	74	$C_{18}H_{29}NO_4$	66.87	8.98	4.33	66.75	8.86	4.41
III*e*	66°–69°	A	25	$C_{20}H_{33}NO_4$	68.38	9.40	3.99	68.52	9.36	4.04
III*f*	73°–76°	A	44	$C_{22}H_{37}NO_4$	69.60	9.76	3.69	69.50	9.57	3.48
III*g*	80°–83°	B	74	$C_{24}H_{41}NO_4$	70.76	10.07	3.44	70.91	10.15	3.47
III*h*	83°–86°	B	86	$C_{26}H_{45}NO_4$	71.72	10.34	3.22	71.52	10.44	3.20
III*i*	88–90°	B	71	$C_{28}H_{49}NO_4$	72.57	10.58	3.02	72.62	10.34	3.06
IV*a*	Oil[b]		32	$C_{12}H_{15}NO_2Cl_2$[c]	50.53	5.61	4.93	50.62	5.61	4.93
IV*b*	50°–52°		42	$C_{14}H_{19}NO_2Cl_2$	55.26	6.25	4.61	55.61	6.52	4.42
IV*c*	40.5°–41°		40	$C_{16}H_{23}NO_2Cl_2$	57.83	6.93	4.22	58.02	6.85	4.12
IV*d*	Oil		33	$C_{18}H_{27}NO_2Cl_2$	60.00	7.50	3.88	59.79	7.51	3.61
IV*e*	Semisolid		22	$C_{20}H_{31}O_2Cl_2$	61.86	7.99	3.61	61.81	8.01	3.47
IV*f*	40°–42°		53	$C_{22}H_{35}NO_2Cl_2$	63.46	8.41	3.37	63.10	8.38	3.54
IV*g*	41°–42.5°		55	$C_{24}H_{39}NO_2Cl_2$	64.86	8.78	3.15	65.06	8.58	3.32
IV*h*	43°–44°		62	$C_{26}H_{43}NO_2Cl_2$	66.10	9.11	2.97	66.40	9.16	2.98
IV*i*	46°–49°		57	$C_{28}H_{47}NO_2Cl_2$	67.20	9.40	2.80	67.11	9.46	2.80

[a] Literature value 82.5°(1). [b] Consistent with literature observation (1). [c] Calculated for the acetate mustard (IV*a*) with one-half mole of water.

and stirred for 24 hr. The mixture was concentrated *in vacuo*. An ether solution of the residue was washed with 5% sodium carbonate or sodium bicarbonate solutions and the ether removed *in vacuo*. The acetate, hexanoate, decanoate, and laurate derivatives were obtained in pure form from absolute ethanol. The acetate (IV*a*) was an oil, the decanoate (IV*e*) a semisolid, and the hexanoate (IV*c*) and laurate (IV*f*) were light brown solids. The butyrate mustard separated from ethyl acetate as a light-brown solid. The octanoate (IV*d*) was isolated as a dark oil from acetone. The myristate (IV*g*), palmitate (IV*h*), and stearate (IV*i*) derivatives were obtained from acetone–water (80:20) as light brown to off-white solids. All pure products were characterized by IR and NMR spectra. Physical data and elemental analysis are given in Table II for all final products.

Biological Evaluation—*Test Animals*—DBA/2 mouse strain[2], BDF_1 mouse strain[2], HA/ICR mouse strain[3], and L-1210 leukemic mice (tumor source)[4] were used.

Instruments—The necessary equipment included an electronic cell counter[5], a channelizer[5], a dilutor[5], an x-y recorder[5], a hemocytometer[6], and a microscope[7].

Materials—Counting diluent[5], red blood cell-lysing reagent[5], crystal violet[8], Giemsa stain[9], isotonic diluting solution[10], trypan blue[11], and Wright's stain[8] were obtained commercially. The ester derivatives of *p*-[*N*,*N*-bis(2-chloroethyl)amino]phenol were prepared as described in this report, and their physical and analytical data are reported in Table II.

Pharmacological Screen and LD_{50} Evaluation—Five groups of six (HA/ICR) mice each were selected. A gross screen was conducted for acute toxicity, and results were recorded during the 3 hr following injection. The mice were observed and weighed every day for 21 days, and the mortalities were recorded daily. A linear regression and correlation coefficient program (6) and a graphic method (7) were applied to determine the LD_{50} for each drug tested.

Transplantation Procedures and *In Vivo* Determination of Antileukemic Activity Survival Times—Using the procedures described earlier for a series of ethers of phenol mustard (4), the transplantation procedures and *in vivo* determination of antileukemic activity by survival times were conducted. The palmitate (IV*h*) and stearate (IV*i*) derivatives were poorly soluble in propylene glycol; therefore, an equal mixture of polyethylene glycol 400, propylene glycol, and ethanol was used for these two derivatives. This solvent mixture allowed the evaluation of higher dosage levels of IV*h* and IV*i* in the survival studies.

RESULTS AND DISCUSSION

The synthesis of the even numbered fatty acid esters of *p*-[*N*,*N*-bis(2-hydroxyethyl)amino]phenol (III*a–i*) was accomplished *via* either Method A or Method B (Scheme I). The initial synthetic approach (Method A) consisted of an uncomplicated sequence of routine organic synthetic reactions. Using Method A, all of the *p*-nitro intermediates (I*a–i*), all of the *p*-amino intermediates (II*a–i*), and the acetate through the laurate diol intermediates (III*a–f*) were obtained in satisfactory yields. The condensation of ethylene oxide with the *p*-aminophenyl palmitate or stearate led to the isolation of the corresponding *p*-[*N*-(2-hydroxyethyl)amino]phenyl ester. The *p*-aminophenyl myristate gave very poor yields of the diol (≤12%) in addition to the monohydroxy ethyl derivative, when condensed with ethylene oxide. Method B provided an alternate route to intermediates III*g–i*, giving good yields of quality products. Compounds IV*a–i* were obtained following the reaction of thionyl chloride with the diol precursors. Not all of the final products were isolated as crystalline solids but an acceptable elemental analysis was obtained for each compound.

The use of Method A to obtain III*a–f* involved three synthetic steps. Step I, the esterification of *p*-nitrophenol, followed a modification of a procedure reported previously (8) in the synthesis of fatty acid esters of acetaminophen. The replacement of pyridine as a solvent with a mixture of dioxane (90 ml) and pyridine (10 ml) simplified the isolation of the ester products. The yields of the esters (I*a–i*) ranged from 50 to 85% and the observed melting points or boiling points (Table I) were consistent with reported values (9, 10). Step II, the reduction of I*a–i* to II*a–i*, employed the procedure described by Adams and Cohen (11) for the reduction of an aromatic nitro group in the presence of an ester. Yields for Step II ranged from 29 to 93%. The condensation of ethylene oxide with the *p*-aminophenyl esters (II*a–i*), Step III, followed the procedure described by Rao and Price (12) with elimination of the reflux step. This had no effect on the yields, which ranged from 25 to 74% for compounds III*a–f*.

Method B employed a modification of the method described by Wise, *et al.* (4) in the synthesis of a series of alkyl ethers of V. When the myristoyl, palmitoyl, or stearoyl chlorides were added to an alcoholic solution containing the potassium phenolate of Compound V, a quality product was isolated in final yields of 71 to 86% for III*g–i*.

The final nitrogen mustard products (IV*a–i*) were prepared by the method of Benitez *et al.* (13). Although the procedure was conducted at low temperature, tarry crude products were always obtained initially and final yields were relatively low (22–62%). The use of another chlorinating agent, *e.g.*, phosphorus oxychloride or phosphorus pentachloride, proved less satisfactory than thionyl chloride.

Physical data for I*a–i* and II*a–i*, as well as the elemental analyses for II*a–i*, are presented in Table I. The *p*-aminophenyl octanoate failed to yield satisfactory elemental analysis but provided acceptable products from Step III. The physical data and elemental analyses for III*a–i* and the IV*a–i* are shown in Table II. Within each series of compounds there was observed a decrease in the melting points as the chain length of the acid increased to C_6 or C_8, then the melting points increased through the stearate derivative. An exception was noted in the acetate mustard (IV*a*) which was isolated as an oil containing an average of one-half mole of water of hydration. The remainder of the final products (IV*b–i*) followed this melting point trend.

All intermediates and final products were characterized by their IR and NMR spectra. Within each homologous series there were observed the expected characteristic IR and NMR absorptions. The effect of increasing the alkyl chain length produced the only notable spectral differences between members of the same series. The IR spectra of the I*a–i* contained the following characteristic absorptions: aromatic and aliphatic C—H stretching bands between 3100 and 2900 cm^{-1}, a carbonyl absorption band at 1750 cm^{-1}, and an absorption at 875 cm^{-1}, indicating the presence of the nitro group. The C—H stretching bands and the carbonyl band were present in this region for each series of compounds. Reduction of the I*a–i* to II*a–i* resulted in the loss of the nitro group absorption and the appearance of the N—H stretching absorption at ~3400 cm^{-1}. This distinct absorption changed to a broad band in the region of 3400–3200 cm^{-1}, when the II*a–i* were condensed with ethylene oxide, indicating the presence of III*a–i*.

Compounds IV*a–i* were distinguished from the corresponding *p*-bis(2-hydroxyethyl)amino compounds by the absence of the broad —OH band in the IR spectrum. In addition, the final products contained absorption in the region of 650 cm^{-1} that is characteristic for the C—Cl bond. The presence of water was indicated in the acetate mustard by the observation of a broad band from 3500 to 3300 cm^{-1}. Only slight shifts in the carbonyl absorption were observed between the different series of compounds.

The NMR spectra of each series of compounds contained characteristic absorptions for the alkyl side chain. The observed chemical shift values for the alkyl pattern did not demonstrate much difference from one series of compounds to the next. In each series the methyl group of the acetate derivatives appeared as a 3-proton singlet at 2.55. In the butyrate, through the stearate derivatives in each series, the pattern consisted of the following absorptions: 2.45–2.55 δ (t, 2H) for the methylene alpha to the carbonyl; a triplet (3H) centered in the range of 0.85–1.05δ for the terminal methyl group; and a multiplet (which appeared as a singlet for the higher members of each series) centered in the range of 1.5–2.1δ for the remainder of the alkyl chain. The aromatic protons of I*a–i* displayed an AA′XX′ pattern which appeared as two doublets (2H each) centered at 7.25 and 8.2δ. Reduction of I*a–i* to II*a–i* changed the aromatic proton absorption from the AA′XX′ pattern to an AA′BB′ pattern which exhibited two doublets (2H each) centered at 6.5 and 7.0δ. This pattern, which appeared to be a quartet, was essentially the same for the remaining series of compounds (III*a–i* and IV*a–i*). The esters II*a–i* also displayed a singlet at 3.52δ for the two amino protons which disappeared from the spectra of II*a–g* following the condensation with ethylene oxide.

The NH_2 absorption was replaced by the absorption characteristic for the *p*-[*N*,*N*-bis(2-hydroxyethyl)amino] moiety, which in this series includes two triplets (4H each) centered around 3.5 and 3.7δ and the two alcoholic protons, which appeared as a singlet between 3.0 and 4.2δ. The NMR spectra of the products isolated from the condensation with the

[2] Jackson Laboratories.
[3] ARS/Sprague–Dawley.
[4] National Cancer Institute, National Institutes of Health, Bethesda, Md.
[5] Model ZB Counter and accessories, Coulter Electronics.
[6] American Optical Co.
[7] Model RA, Carl Zeis, West Germany.
[8] Matheson, Coleman & Bell.
[9] Fisher Scientific Co.
[10] Microbiological Associates.
[11] Allied Chemical Co.

Table III—Summary of the Bioevaluation Data for the Fatty Acid Esters of *p*-[*N*,*N*-Bis(2-chloroethyl)amino]phenol

Compound Number (Derivative)	LD_{50}[a], μmoles/kg	Dose, mg/kg	Number of Animals	Mean Survival Day (±*SE*) Test Group	Mean Survival Day (±*SE*) Control Group	T/C %[b]
IV*a*,[c]		2.25	6			95
(Acetate)	50.8	2.03	6			106
		1.50	6			115
		1.00	6			108
		0.50	6			102
IV*b*,		75	6	4.0(0.37)	9.33(0.33)	44
(Butyrate)	<82.2	50	5	5.6(0.68)	9.33(0.33)	62
		25	6	10.5(0.56)	9.33(0.33)	113
		10	6	11.83(0.54)	9.33(0.33)	127
		5	6	12.17(0.75)	9.33(0.33)	130
		2	5	12.40(0.68)	9.33(0.33)	133
IV*c*,[c]		2.50	6			98
(Hexanoate)	53.3	2.02	6			112
		1.00	6			117
		0.50	6			113
IV*d*,		25	6	9.83(0.79)	8.60(0.40)	114
(Octanoate)	73.1	10	6	10.33(0.88)	8.60(0.40)	120
		5	5	12.20(0.37)	8.60(0.40)	142
		2	4	11.25(0.48)	8.60(0.40)	131
IV*e*,[c]		2.05	6			112
(Decanoate)	55.4	1.82	6			150
		1.50	6			131
		1.00	6			123
		0.50	6			110
IV*f*,		75	6	9.00(1.21)	9.33(0.42)	97
(Laurate)	>240	50	6	12.00(0.86)	8.8 (0.20)	136
		25	6	11.83(0.87)	8.8 (0.20)	134
		10	6	12.67(1.05)	8.8 (0.20)	144
		5	6	11.33(0.61)	9.33(0.42)	122
IV$_g$		100	6	7.00(1.10)	9.40(0.60)	75
(Myristate)	>225	50	6	13.33(1.31)	9.40(0.60)	142
		25	6	11.50(0.50)	9.40(0.60)	122
		10	6	11.83(0.87)	9.40(0.60)	162
		5	5	11.20(0.49)	9.40(0.60)	119
IV*h*		150	6	12.33(0.76)	8.7 (0.48)	142
(Palmitate)	>211.9	100	5	13.2(0.80)	8.7 (0.48)	152
		75	6	12.83(0.79)	8.7 (0.48)	148
		50	6	12.67(0.49)	9.5 (0.50)	133
		25	6	12.5(1.48)	9.5 (0.50)	132
		10	6	10.33(0.49)	9.5 (0.50)	109
IV*i*,	>200	200	6	13.33(0.67)	9.25(0.48)	144
(Stearate)		150	6	13.00(0.73)	9.25(0.48)	141
		100	6	12.00(0.77)	9.25(0.48)	130
		50	6	12.33(0.61)	9.50(0.56)	130
		25	6	11.67(0.56)	9.50(0.56)	123
		10	6	10.83(0.70)	9.50(0.56)	114
		5	6	10.33(0.49)	9.50(0.56)	109

[a] Administered in propylene glycol. [b] The T/C% represents the ratio of the sum of the number of days the animals in a treated group survived (T) to the sum of the number of days the animals in the control group survived (C) multiplied by 100. [c] A summary of data reported earlier.

p-aminophenyl palmitate and stearate esters, and one of the products from the *p*-aminophenyl myristate ester, indicated that only 1 mole of ethylene oxide had condensed with the amine. These spectra contained one amino proton and the ethylene triplets integrated for only two protons each. The NMR spectra of the final products (IV*a–i*) demonstrated a loss of the two alcoholic protons present in III*a–i*. In addition, the eight ethylene protons appeared as a sharp singlet in the region of 3.5–3.8δ. The aromatic protons and the alkyl side chain absorptions appeared as described previously. The presence of one-half mole of water of hydration in the acetate mustard (IV*a*) was verified by NMR, as well as IR and elemental analysis.

Biological Evaluation—The LD_{50} values for compounds IV*a* and IV*c–e* were determined using probit analysis and linear regression and are presented in μmoles/kg in Table III (6, 7). The data for the butyrate mustard (IV*b*) indicates that its LD_{50} is <25 mg/kg (82.2 μmoles/kg). Determination of exact LD_{50} values for compounds IV*f–i* was restricted by their limited solubility in propylene glycol. The 100 mg/kg dosage level was the highest that could be administered for those compounds in propylene glycol. Only a few isolated deaths occurred in the LD_{50} studies for IV*f* and IV*g*, and no deaths occurred at any dosage levels for IV*h* and IV*i*. The results of the LD_{50} study indicate that IV*b* and IV*d* have a toxicity slightly less than, but comparable to, IV*a*, IV*c*, and IV*e* reported earlier (3). All of these fatty acid ester derivatives (IV*a–i*) appear to be less toxic than the unhindered benzoate esters of a previous report (2).

The acetate through the decanoate mustards (IV*a–e*) demonstrates acute toxicities comparable to, or greater than, that observed for the parent phenolic mustard, *p*-[*N*,*N*-bis(2-chloroethyl)amino]phenol, 74.8 (2)–162.4 μmoles/kg in HA/ICR mice[12]. Compounds IV*a–e* are 2–3 times more toxic than the phenolic mustard when LD_{50} values in HA/ICR mice are compared. These esters are more lipophilic in nature and should be more readily absorbed and distributed in the biologic system than the phenolic mustard. This enhanced distribution, coupled with the possible ester hydrolysis to the free phenol, may account for these observations. The lower toxicities observed for compounds IV*f–i* may be related in part to their lower aqueous solubility. All of Compounds IV*a–i* appear to be much more toxic than the comparable series of even numbered ethers (C_2–C_{14}) of phenolic mustard (LD_{50} range 714–>1395 μmoles/kg) recently reported (4).

The effect of compounds IV*a–i* on the prolongation of life of L-1210 leukemic mice was determined. A comparison of the survival of treated groups (T) to untreated control groups (C) was performed. A calculated T/C ratio ≥125% implied that the drug treatment significantly increased the life span. Table III summarizes the T/C% survivals produced at each dosage level for each compound, the number of animals used per dosage level, and the mean survival for each animal group. The doses producing optimum survival for each compound are summarized in Table IV.

Compound IV*g* produced the highest mean survival time (T/C%) in this series, 162% at a dose of 10 mg/kg (22.5 μmoles/kg). Compounds IV*d*, IV*e*, and IV*g* produced significant survival at two dosage levels and compounds IV*b* and IV*f* at three dosage levels each. Compounds IV*h* and

[12] Unpublished data from these laboratories.

Table IV—Summary: Optimum Dose and Survival Time for the Fatty Acid Esters of *p*-[*N*,*N*-bis(2-chloroethyl)amino]phenol

Compound Number (Derivative)	Optimum Dose		T/C%
	mg/kg	μmoles/kg	
IV*a* (Acetate)	1.5	5.4	115
IV*b* (Butyrate)	2.0	6.6	133
IV*c* (Hexanoate)	1.0	3.0	117
IV*d* (Octanoate)	5.0	13.9	142
IV*e* (Decanoate)	1.82	4.7	150
IV*f* (Laurate)	10.0	24.0	144
IV*g* (Myristate)	10.0	22.5	162
IV*h* (Palmitate)	100.0	211.9	152
IV*i* (Stearate)	200.0	400.0	144

IV*i* produced significant survival at five and four dosage levels, respectively. Compounds IV*a* and IV*c* failed to produce significant T/C% survival at any of the dosage levels investigated.

The enzymatic hydrolysis rates for a series of fatty acid esters of acetaminophen have been determined by Bauguess *et al.* (8). Those results indicate the near complete and rapid hydrolysis of the acetate and butyrate esters and a decrease in the rate of hydrolysis for the hexanoate ester which was more rapidly hydrolyzed than the octanoate ester. The rate and completeness of hydrolysis declined from the decanoate through the myristate esters, and only limited hydrolysis could be obtained for the palmitate and stearate esters of acetaminophen. This work by Bauguess, coupled with the suggestion by Hansch *et al.* (5) that the antitumor activity for esters of phenolic mustard is due primarily to the intact ester rather than the hydrolysis product, phenol mustard, provides some insight into the biologic results reported in this paper.

Compounds IV*h* and IV*i* demonstrated low toxicity in the survival studies as well as the toxicity studies. The results for these two compounds are consistent with the expectation of a slow and limited enzymatic hydrolysis rate *in vivo*. The high doses for these compounds required the use of a different solvent mixture due to their limited solubility in propylene glycol. It is feasible that their poor solubility and hydrolysis properties resulted in a continuous and prolonged absorption from the injection site, thus providing significant survival over a greater range of doses. Both IV*f* and IV*g* demonstrated toxicity at the highest respective doses used in the survival study. These two compounds produced significant survival at the medium dosage levels, while activity dropped off at the lowest dose level (5 mg/kg). The toxicity at the higher dosage levels is consistent with an expected increase in hydrolysis of these two compounds, as well as indicating toxicity differences between the leukemic test mice (BDF_1 strain) and the HA/ICR strain used in the LD_{50} determinations. The optimum survival dose level for both IV*f* and IV*g* of 10 mg/kg was much less than IV*h* and IV*i* but was greater than the lower members of the series, IV*a–e*. Optimum survival was observed at lower dosage levels for IV*c*, IV*d*, and IV*e* (Table IV). This observation is consistent with the higher toxicity observed for these compounds, as well as the expected increase in enzymatic hydrolysis when compared to compounds IV*f–i*.

Compound IV*b* produced optimum survival at a slightly higher dose than IV*c* (6.6 *versus* 3.0 μmoles/kg). If the intact ester derivative of phenolic mustard is the active antileukemic molecule, then a higher dose would be required for IV*b* to achieve optimum activity in order to compensate for its anticipated rapid hydrolysis.

Compound IV*a* produced optimum survival at a dose comparable to the optimum dose of IV*b*. The failure of IV*a* to produce significant survival at any dose level suggests that an effective level of IV*a* could not be sustained long enough to be effective against the leukemia, probably due to very rapid hydrolysis *in vivo*. Compound IV*c* also failed to significantly prolong the life of leukemic mice. This observation cannot be related to the expected hydrolysis within the series. However, in the alkyl ether series studied earlier, the *n*-hexyl derivative produced similar survival results in leukemic mice (4).

The possibility that the 6-carbon ether derivative is of appropriate length to interact with the nitrogen atom when in dilute solution, has been suggested. A similar interaction could occur between the terminal methyl of the hexanoate side chain and the nitrogen atom of the mustard moiety. Such an interaction could sterically hinder the participation of the nitrogen atom in the formation of the aziridinium ion intermediate, thus reducing the reactivity of IV*c*. This in turn could reduce its antileukemic effectiveness.

REFERENCES

(1) W. C. J. Ross, G. P. Warwick, and J. J. Roberts, *J. Chem. Soc.* **1955,** 3110.

(2) S. Vickers, P. Hebborn, J. F. Moran, and D. J. Triggle, *J. Med. Chem.*, **12,** 491 (1969).

(3) C. T. Bauguess, Y. Y. Lee, J. W. Kosh, and J. E. Wynn, *J. Pharm. Sci.*, **70,** 46 (1981).

(4) J. W. Wise, J. E. Wynn, R. L. Beamer, and C. T. Bauguess, *J. Pharm. Sci.*, in press.

(5) A. Panthananickal, C. Hansch, and A. Leo, *J. Med. Chem.*, **21,** 16 (1978).

(6) Manual No. 4022N, model 1766, Monroe Calculator Co., Morristown, N.J., 1970.

(7) L. C. Miller and M. L. Tainter, *Proc. Soc. Exp. Biol. Med.*, **57,** 261 (1944).

(8) C.T. Bauguess, F. Sadik, J. H. Fincher, and C. W. Hartman, *J. Pharm. Sci.*, **64,** 117 (1975).

(9) H. Zahn and F. Schade, *Chem. Ber.*, **96,** 1747 (1963).

(10) S. Kreisky, *Acta. Chem. Scand.*, **11,** 913 (1957).

(11) R. Adams and F. L. Cohen, in "Organic Synthesis," Vol. I, H. Gilman and A. H. Blatt, Eds., Wiley, New York, N.Y., 1961, p. 240.

(12) G. V. Rao and C. Price, *J. Med. Chem.*, **27,** 205 (1962).

(13) A. Benitez, L. O. Ross, and L. Goodman, *J. Am. Chem. Soc.*, **82,** 4585 (1960).

ACKNOWLEDGMENTS

This work was supported in part by an institution grant to the University of South Carolina, PHI-IN-107, through the American Cancer Society, provided for the purpose of funding cancer related research.

High-Performance Liquid Chromatographic Analysis of Digoxin Formulations

BELACHEW DESTA and K. M. McERLANE ˣ

Received June 9, 1981, from the *Faculty of Pharmaceutical Sciences, University of British Columbia, Vancouver, BC, Canada V6T 1W5.* Accepted for publication October 2, 1981.

Abstract □ A rapid, selective, and simple high-performance liquid chromatographic (HPLC) assay for digoxin formulations is described. The method utilizes a conventional octadecyl bonded phase column with detection at 220 nm. The analytical procedure has been applied for the quantitation of digoxin in tablets, elixir, and injectable formulations with a resulting relative standard deviation of 1.45, 1.70, and 1.80%, respectively. The method is sufficiently sensitive to monitor content uniformity of individual tablets. Potential impurities or degradation products are resolved from the digoxin peak in a total chromatographic time of <15 min.

Keyphrases □ High-performance liquid chromatography—analysis of digoxin formulations □ Digoxin—high-performance liquid chromatographic analysis, assay of tablet, injectable, and elixir formulations □ Formulations—high-performance liquid chromatographic analysis of digoxin formulations: tablets, elixir, and injectable

Digoxin is a cardioactive glycoside isolated from the leaves of *Digitalis lanata* and is the most frequently used drug in the treatment of congestive heart failure. Its low dosage and narrow therapeutic safety margin require assurance of potency and content uniformity of dosage forms, particularly in tablet formulations. The potential for the presence of degradation products or impurities introduces an additional requirement of assay specificity.

Previous methods for the analysis of digoxin as its drug substance and in formulations have largely been colorimetric (1–7), fluorometric (8–13), or chromatographic. The latter methods have included paper (14, 15), thin-layer (16–18), column (19, 20), gas-liquid (21–25), and high-performance liquid chromatographic (HPLC) methods (26–32). Colorimetric methods are largely nonselective and lack high sensitivity. Fluorometric methods, although more selective and certainly more sensitive, lack specificity, since the acidic fluorogenic reaction required would lead to an identical fluorescent species for digoxin and its potential impurities. GC methods require the preparation of a sufficiently volatile derivative. However, the derivitization procedures cause hydrolysis of the digitoxose sugar residues and, thus, would be inappropriate for the determination of the intact digoxin moiety in the presence of its degradation products. The utilization of HPLC for the determination of digoxin provides a distinct advantage since the digitalis glycoside does not require pretreatment to facilitate chromatographic manipulation. HPLC has been used by several investigators (30, 31) for the quantitative measurement of digoxin drug substance and its degradation products. The methods, although providing an indication of the hydrolysis rate of digoxin drug substance in aqueous media, were not applied to dosage forms.

Therefore, it would appear that there is a need for a method of analysis of digoxin in its dosage forms that is reliable and accurate as well as sufficiently sensitive to facilitate single-tablet assay. Such a method is described in this paper.

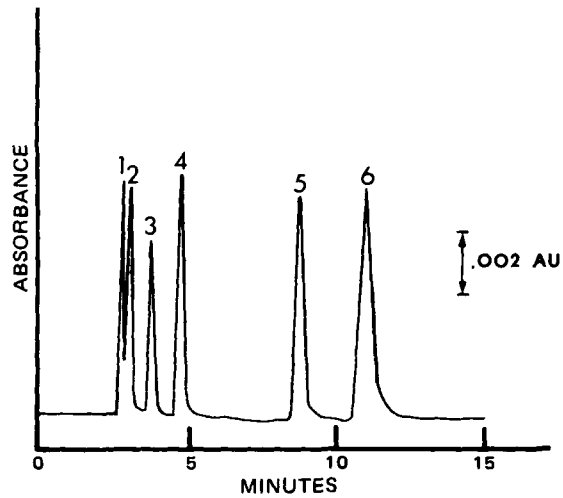

Figure 1—*HPLC of a synthetic mixture of digitalis glycosides. Sequence of elution: 1, digoxigenin; 2, digoxigenin monodigitoxoside; 3, digoxigenin bisdigitoxoside; 4, digoxin; 5, 17α-ethynylestradiol internal standard; 6, gitoxin. Mobile Phase: water–methanol–isopropanol–methylene chloride (47:40:9:4), flow rate: 1.2 ml/min.*

EXPERIMENTAL

Apparatus—A high-performance liquid chromatograph[1] equipped with dual pumps[2], a 20-μl injector[3], and a dynamically stirred mixing chamber[4] were used throughout with a variable wavelength detector[5] and an electronic data processor[6]. All analyses were performed on a 4.6 mm × 250-mm column[7] packed with 5-μm bonded octadecylsilane (C_{18} phase).

Materials—Water, methanol, isopropanol, and methylene chloride were of HPLC grade[8]. Digoxin[9] and 17α-ethynylestradiol[10] were used without further purification.

Preparation of Internal Standard Solutions—An accurately weighed quantity, equivalent to 100 mg of 17α-ethynylestradiol, was dissolved in 100 ml of methanol.

Preparation of Standard Solutions of Digoxin—A stock solution was prepared by dissolving an accurately weighed quantity, equivalent to 20 mg of digoxin, in 80 ml of boiling methanol, cooling the flask to room temperature, and bringing the final volume to 100 ml with methanol. Six aliquots equivalent to 0.1, 0.2, 0.4, 1.0, 2.0, and 2.5 mg of digoxin were added to 100-ml volumetric flasks. A 2.5-ml aliquot of the internal standard was added to each flask, followed by an amount of methanol required to bring the volume to 35 ml. The flasks were then brought to volume with distilled water and thoroughly mixed. Three injections of each of the six standard solutions containing digoxin and 17α-ethynylestradiol were used to establish linearity and response ratios.

Sample Preparation—Not less than 30 tablets were weighed and

[1] Model 322, Beckman Instruments, Inc. Toronto, Ontario, Canada.
[2] Model 100A, Beckman Instruments, Inc.
[3] Model 210, Beckman Instruments, Inc.
[4] Model 400, Beckman Instruments, Inc.
[5] Model 100-10, Hitachi Ltd., Tokyo, Japan.
[6] Model C-RIA, Shimadzu Corp., Kyoto, Japan.
[7] Ultrasphere, Beckman Instruments, Inc.
[8] Fisher Scientific, Vancouver, B.C., Canada.
[9] Boehringer Mannheim Corp., Mannheim, G.F.R.
[10] Sigma Chemical Co., St. Louis, Mo.

0022-3549/82/0700-0777$01.00/0

Table I—Results of the Analysis of Composite Samples of Digoxin Tablets by HPLC and the USP Method

	Percent of Label Claim							
	Brand A				Brand B		Brand C	
	0.125 mg		0.25 mg		0.25 mg		0.25 mg	
Number	HPLC Method	USP Method	HPLC Method	USP Method	HPLC Method	USP Method	HPLC Method	USP Method
1	98.0	103.0	94.0	105.6	98.8	101.4	101.6	97.7
2	101.2	96.1	96.8	96.2	97.2	98.8	100.0	102.7
3	99.2	94.9	95.2	98.4	98.0	103.0	104.8	103.2
4	101.2	—	95.2	—	97.6	—	98.4	—
Mean	99.9	98.0	95.3	100.1	97.9	101.0	101.2	101.2

triturated to a fine powder. An accurately weighed quantity, equivalent to 1.25 mg of digoxin, was transferred to a 100-ml volumetric flask. Ten milliliters of distilled water was added and the flask was swirled for 2–3 min. Exactly 32.5 ml of methanol was added and the mixture was mechanically shaken for 15 min. The suspension was filtered using filter paper[11], and the residue was washed with three 5-ml portions of distilled water. The combined filtrate and washings were collected in a 100-ml volumetric flask containing a 2.5-ml aliquot of the internal standard solution, and the flask was brought to volume with distilled water and thoroughly mixed. A 20-μl sample, containing 12.5 ng/μl of digoxin and 25 ng/μl of the internal standard, was injected into the liquid chromatograph.

Single Tablet Assay—One tablet was placed in a 100-ml volumetric flask and treated in the same manner as the tablet composite assay.

Injectable Formulation Assay—The contents of 20 ampules were bulked and a 2-ml aliquot was transferred to a 10-ml volumetric flask (in the case of the 0.05 mg/ml injection) or to a 50-ml volumetric flask (in the case of the 0.25 mg/ml injection). Aliquots of 0.25 ml and 1.25 ml of internal standard solution were added to the 10- and 50-ml volumetric flasks, respectively. A volume of 0.25 ml (0.25 mg) of the internal standard solution was added to the 10-ml volumetric flask, and 1.25 ml (1.25 mg) of the internal standard solution was added to the 50-ml volumetric flask. A volume of methanol equivalent to 2.8 and 14.0 ml, was added to the 10- and 50-ml volumetric flasks, respectively. The theoretical final concentration of digoxin and the internal standard were 10 and 25 ng/μl, respectively.

Elixir—A 20-ml aliquot of the elixir was transferred to a 100-ml volumetric flask, followed by 2.5 ml of the internal standard solution and 20 ml of methanol. The flask was brought to volume with distilled water and thoroughly mixed. The theoretical final concentration of digoxin and the internal standard were 10 and 25 ng/μl, respectively.

Precision of Tablet Assay—A total of 40 digoxin tablets were weighed and triturated to a fine powder. Six aliquots, equivalent to 1.25 mg of digoxin, were weighed into six volumetric flasks and treated as described under tablet assay. Three injections were made for each sample.

Recovery of Digoxin from Tablets—Six aliquots of digoxin tablets were prepared as described previously. To each aliquot an accurately weighed[12] quantity of digoxin reference standard[9], equivalent to 0.625 mg, was added, and the samples were treated as described under tablet assay. Three injections were made for each sample.

HPLC Conditions for Tablet and Injectable Formulation Assays—The mobile phase consisted of water–methanol–isopropanol–methylene chloride (47:40:9:4) and was pumped at a flow rate of 1.2 ml/min. The UV detector was set at 220 nm.

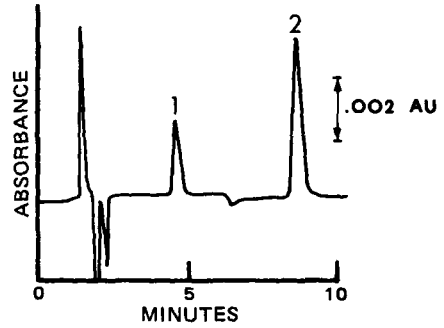

Figure 2—*HPLC of a digoxin tablet formulation. Sequence of elution: 1, digoxin; 2, 17α-ethynyl estradiol. Mobile Phase: refer to Fig. 1.*

[11] Number 1, Whatman Paper, W. and R. Balston Ltd., Eng.
[12] Cahn Electrobalance, Ventron Instruments Corp., Paramount, Calif.

HPLC Conditions for Elixir Formulation Assay—The mobile phase consisted of water–methanol–isopropanol–methylene chloride (51:42:5:2). All other conditions were identical to those described for tablet and injectable formulation assay.

RESULTS AND DISCUSSION

A chromatogram of a standard mixture of digoxin and its potential degradation products, digoxigenin, digoxigenin monodigitoxoside, digoxigenin bisdigitoxoside, as well as a common impurity, gitoxin, and the internal standard, ethynylestradiol, is given in Fig. 1. From this chromatogram it can be ascertained that the common potential impurities would not interfere with the assay of digoxin (Peak 4). In addition, common tablet excipients such as starch, lactose, methylcellulose, and stearate lubricants were subjected to the extraction procedure for the tablet assay and were found to be noninterfering.

The presence of a relatively small amount of methylene chloride in the mobile phase contributes to absorption of radiant energy at 220 nm and therefore raises the baseline. However, the presence of a considerably large amount of water minimizes the absorbance effect of methylene chloride. The problem of miscibility of the two solvents is resolved by the presence of methanol and isopropanol. Moreover, since there is sufficient differential absorbance contributed by digoxin, it has been consistently shown that no problem arises from the presence of methylene chloride. A description of the evolution of the mobile phase has been given (33) where the HPLC separation of a number of cardiac glycosides has been reported using different proportions of the four solvents (water–methanol–isopropanol–methylene chloride).

Calibration curves were constructed, and the relative response ratios of digoxin to the internal standard, 17α-ethynylestradiol, was found to be 1.426 for the analysis of digoxin tablets and injection, and 1.386 for the analysis of digoxin elixir. The relative standard deviation was 2% (n = 6) in both cases. Calibrations were performed for each batch of solvent systems prepared on a daily basis.

The chromatogram depicted in Fig. 2 is representative of a composite assay of a tablet containing 0.25 mg of digoxin. The initial baseline disturbance and the small negative peak at ~6.5 min are due to a solvent effect from the sample injection.

The recovery data for the extraction of digoxin from tablets (0.25 mg) was determined by adding an amount of digoxin reference standard equivalent to half of the amount of digoxin contained in the tablet sample. Analysis of six such samples resulted in recovery values of 99.7, 101.3, 96.8, 102.6, 95.2, and 103.4% of the total quantity expected. The mean and relative standard deviation were found to be 99.8 and 3.2%, respectively, with a 95% confidence limit of (±) 3.4. The precision of the assay was

Table II—Results of HPLC Single-Tablet Assay of Digoxin Tablets

	Percent of Label Claim[a]	
Number	0.125 mg	0.25 mg
1	90.0	92.8
2	91.4	96.4
3	105.8	92.6
4	102.4	106.0
5	93.9	102.0
6	96.8	94.8
7	94.6	98.6
8	96.8	96.9
9	101.2	93.2
10	98.4	92.8
Mean ($\bar{x}$)	97.1	96.6
RSD[b], %	5.1	4.6

[a] Brand A. [b] Relative standard deviation.

Table III—Results of the Analysis of Digoxin Injection and Elixir Formulations by HPLC and the USP Method

	Percent of Label Claim					
	Injection				Elixir	
	0.05 mg/ml		0.25 mg/ml		0.05 mg/ml	
Number	HPLC Method	USP Method	HPLC Method	USP Method	HPLC Method	USP Method
1	102.5	103.2	98.4	101.2	100.5	101.6
2	98.5	101.2	102.4	101.9	98.6	97.4
3	97.5	99.6	99.2	102.7	97.4	98.2
4	99.0	—	98.9	—	101.2	—
5	100.0	—	97.6	—	—	—
6	99.0	—	98.4	—	—	—
Mean ($\bar{x}$)	99.4	101.3	99.1	101.9	99.4	99.1
RSD[a], %	1.7	1.8	1.6	0.8	1.8	2.2

[a] Relative standard deviation.

independently determined on six aliquots of the same tablet lot. The values for the percentage of label claim were: 98.0, 99.4, 98.2, 98.0, 101.4, and 100.5% with a mean value of 99.2% and a relative standard deviation of 1.45%. Therefore, it can be observed from the above data that the assay has satisfactory accuracy and precision.

The application of the HPLC assay to three commercial sources of digoxin tablet formulations provided the data given in Table I. Four aliquots of each of the four tablet lots were independently assayed, and it can be observed that all lots were well within the USP limits of 92–108% (7). The same four lots were assayed by the USP colorimetric method for digoxin tablets and the results are also given in Table I. The respective mean assay values for the four lots compare favorably; however, a significant time benefit of the HPLC assay was noted. The time taken for the total assay of four aliquots of a single tablet lot using the USP method was ~4.5 hr, while the HPLC assay required only 45 min.

The USP monograph for content uniformity of tablets is a long colorimetric procedure requiring repetition of the tablet assay for each of 10 tablets. Consequently, the HPLC procedure developed was applied to a single-tablet assay of 10 randomly selected tablets from two tablet strengths obtained from the same manufacturer. As shown in Table II, the individual assay results for a 0.125-mg tablet fell within 90.0–105.8% and for a 0.25-mg tablet, 92.6–106.0%. The general requirement for content uniformity of tablets in the USP specifies that the potency of all 10 tablets must fall within 85–115% of the label claim. Hence the tablets selected in this determination met the pharmacopeial requirements. The assay time for the HPLC method was significantly shorter.

The analysis of digoxin injection indicated that the peaks due to digoxin and the internal standard are free from interference from formulation excipients. The chromatogram was essentially identical to that shown for a tablet formulation (Fig. 2). The assay results (Table III) for two strengths of injectable formulation obtained from the same manufacturer provided a mean potency of 99.4 and 99.1% with a respective relative standard deviation of 1.7 and 1.6%. The mean potency of the HPLC assay compares favorably with that obtained for the same formulations using the USP assay (Table II).

Due to the presence of excipients in the elixir formulation, the relative composition of mobile phase for this assay was modified slightly. The chromatogram depicted in Fig. 3 is representative of the analysis of a single elixir formulation. Peaks 1–4 and 6 were due to pharmaceutical excipients. Peak 4 was determined to be methylparaben, the remaining excipients, however, were not identified. The assay results obtained from 4 aliquots of this formulation are given in Table III and indicate a mean potency of 99.4%, with a relative standard deviation of 1.8%. The assay results for the elixir formulation as obtained by the USP method (Table III) compare favorably with those obtained from the HPLC assay method. It is significant that the analysis of both the injectable and elixir formulations was achieved by simple dilution of the formulation. The USP, on the other hand, requires a prior solvent extraction for the analysis of the elixir.

In comparison with the long, labor-intensive requirements for the assay of tablet, injectable,and elixir formulations as outlined in the USP, the HPLC method described herein provides a significant advantage in terms of selectivity, simplicity, convenience, and time of analysis.

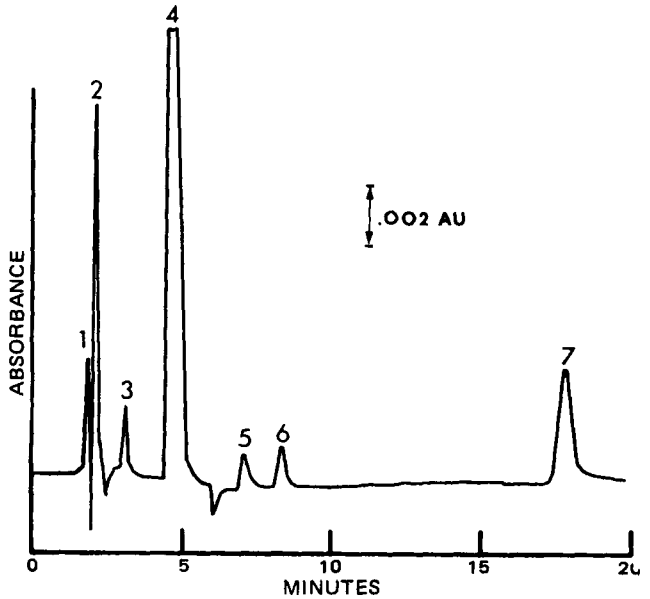

Figure 3—*HPLC of a digoxin elixir formulation. Sequence of elution: 1–3, unknown; 4, methylparaben; 5, digoxin; 6, unknown; 7, 17 α-ethynylestradiol. Mobile Phase: Water–methanol–isopropanol–methylene chloride (51:42:5:2) flow rate: 1.2 ml/min.*

REFERENCES

(1) Ph. Lafon, *C. R., Hebd. Seances Acad. Sci.*, **100,** 1463 (1885).

(2) H. Beljet, *Schweiz. Apoth. Ztg.*, **56,** 71, 84 (1918).

(3) M. Pesez, *Ann. Pharm. Fr.*, **10,** 104 (1952).

(4) D. H. E. Tattje, *J. Pharm. Pharmacol.*, **9,** 29 (1957).

(5) P. Mesnard and G. Devaux, *C. R. Hebd. Seances Acad. Sci.*, **253,** 497 (1961).

(6) J. W. Myrick, *J. Pharm. Sci.*, **58,** 1018 (1969).

(7) "United States Pharmacopeia," 20th rev., U.S. Pharmacopeial Convention, Rockville, Md., 1980.

(8) K. B. Jensen, *Acta. Pharmacol. Toxicol.*, **9,** 66 (1953).

(9) D. Wells, B. Katzung, and F. H. Meyers, *J. Pharm. Pharmacol.*, **13,** 389 (1961).

(10) I. M. Jakovljevic, *Anal. Chem.*, **35,** 1513 (1963).

(11) A. J. Khoury, in "Automation in Analytical Chemistry," Technicon Symposium, 1966, Vol. I, Technicon Symposia Medad, Inc., White Plains, N.Y., 1967, pp. 192–195.

(12) L. F. Cullen, D. L. Packman, and G. J. Papariello, *J. Pharm. Sci.*, **59,** 697 (1970).

(13) L. Nyberg, K. E. Andersson, and A. Bertler, *Pharm. Suecica*, **11,** 459 (1974).

(14) H. Pötter, *Pharmazie.*, **18,** 554 (1963).

(15) G. Rabitzsch and S. Jungling, *J. Chromatogr.*, **41,** 96 (1969).

(16) W. Hauser, Th. Kartnig, and G. Verdino, *Scientia Pharm.*, **36,** 237 (1968).

(17) H. Pötter and H. Bärisch, *Pharmazie*, **27,** 315 (1972).

(18) F. J. Evans, P. A. Flemons, C. F. Duignan, and P. S. Cowley, *J. Chromatogr.*, **88,** 341 (1974).

(19) A. Stoll, E. Angliker, F. Barfuss, W. Kussmaul, and J. Renz, *Helv. Chim. Acta.*, **34,** 1460 (1951).

(20) F. Kaiser, *Arch. der Pharmazie.*, **299,** 263 (1966).

(21) R. W. Jelliffe and D. H. Blankenhorn, *J. Chromatogr.*, **12,** 268 (1963).

(22) L. Tan, *ibid.*, **45**, 68 (1969).
(23) E. Watson, P. Tramell, and S. M. Kalman, *ibid.*, **69**, 157 (1972).
(24) W. E. Wilson, S. A. Johnson, W. H. Perkins, and J. E. Ripley, *Anal. Chem.*, **39**, 40 (1967).
(25) A. H. Kibbe and O. E. Araujo, *J. Pharm. Sci.*, **62**, 1703 (1973).
(26) M. C. Castle, *J. Chromatogr.*, **115**, 437 (1975).
(27) W. Lindner and R. W. Frei, *ibid.*, **117**, 81 (1976).
(28) F. Nachtmann, H. Spitzy, and R. W. Frei, *ibid.*, **122**, 293 (1976).
(29) F. Erni and R. W. Frei, *ibid.*, **130**, 169 (1977).
(30) L. A. Sternson and R. D. Shaffer, *J. Pharm. Sci.*, **67**, 327 (1978).
(31) T. Sonobe, S. Hasumi, T. Yoshino, Y. Kobayashi, H. Kawata, and T. Nagai, *ibid.*, **69**, 410 (1980).
(32) Y. Fujii, H. Fukuda, Y. Saito, and M. Yamazaki, *J. Chromatogr.*, **202**, 139 (1980).
(33) B. Desta and K. M. McErlane, *J. Chromatogr.*, in press.

ACKNOWLEDGMENTS

This study was funded by a grant from the British Columbia Health Care Research Foundation.
Belachew Desta was supported by a fellowship from the World Health Organization.
The authors gratefully acknowledge all assistance.

Formation of Hydrotalcite in Mixtures of Aluminum Hydroxycarbonate and Magnesium Hydroxide Gels

ROGER K. VANDERLAAN *, JOE L. WHITE ‡, and STANLEY L. HEM *x

Received June 12, 1981, from the *School of Pharmacy and Pharmacal Sciences*, **Departments of Industrial and Physical Pharmacy, and* ‡*Agronomy Department, Purdue University, West Lafayette, IN 47907.* Accepted for publication October 13, 1981.

Abstract □ IR and X-ray analysis demonstrate that hydrotalcite forms during the aging of aluminum hydroxycarbonate gel and magnesium hydroxide gel mixtures. The formation of hydrotalcite produces a change in the pH-stat titrigram and a sharp increase in the pH of the mixture. Hydrotalcite was noted earlier in mixtures having a high molar ratio of magnesium to aluminum, a high total gel concentration, a high initial pH, or in mixtures stored at elevated temperatures. The addition of sorbitol to the mixtures substantially delayed the appearance of hydrotalcite. Nonacid-reactive hydrotalcite formed when mixtures of chloride-containing aluminum hydroxide gel and magnesium hydroxide gel were aged.

Keyphrases □ Hydrotalcite—formation, mixtures of aluminum hydroxycarbonate and magnesium hydroxide gels, IR and X-ray analysis □ Mixtures—formation of hydrotalcite in mixtures of aluminum hydroxycarbonate and magnesium hydroxide gels □ Gels—aluminum hydroxycarbonate and magnesium hydroxide gels, mixtures, formation of hydrotalcite

It has been reported recently that amorphous aluminum hydroxycarbonate gel forms a coating on magnesium hydroxide particles due to electrostatic attraction (1). This interaction was detected because the rate of acid neutralization of mixtures of aluminum hydroxycarbonate gel and magnesium hydroxide gel was slower than expected, based on individual rates of acid neutralization. The interaction occurred immediately and an additive rate of acid neutralization only occurred when the gels were separately added to the reaction vessel. As the mixtures aged, the rate of acid neutralization decreased further, suggesting that the amorphous aluminum hydroxycarbonate coating was becoming more ordered as the amorphous to crystalline phase transition occurred.

It was noticed, however, that the rate of acid neutralization in some aged mixtures was greater than the initial rate of acid neutralization. Thus, a further reaction appeared to be occurring during the aging of mixtures of aluminum hydroxycarbonate and magnesium hydroxide gels. This interaction is the focus of this study.

EXPERIMENTAL

Magnesium hydroxide gel[1] was obtained commercially as a paste containing the equivalent of 21% (w/w) MgO. Aluminum hydroxycarbonate gel was prepared as described previously (2) by the addition of 0.47 *M* $AlCl_3 \cdot 6H_2O$ to 0.53 *M* $NaHCO_3$ and 0.23 *M* Na_2CO_3 to a final pH of 6.5. Chloride-containing aluminum hydroxide gel was prepared as described previously (2) by the addition of 13% (v/v) strong ammonia solution to 0.29 *M* $AlCl_3 \cdot 6H_2O$ to a final pH of 7.0.

Aluminum and magnesium content were determined by chelatometric titration (3).

Mixtures of aluminum hydroxycarbonate gel or chloride-containing aluminum hydroxide gel and magnesium hydroxide gel were prepared on a weight basis. For example, a 200-g mixture containing a total of 0.6 mmole of metal/g in a magnesium–aluminum molar ratio of 5:1 was prepared by weighing magnesium hydroxide gel and aluminum hydroxycarbonate gel or chloride-containing aluminum hydroxide gel containing 100 mmoles of magnesium and 20 mmoles of aluminum, respectively. A solution containing an excipient was added when necessary. The final weight was adjusted to 200 g with double-distilled water and the mixture was stirred mechanically until uniform. The mixtures were aged in widemouth polyethylene bottles.

The acid neutralization reaction was monitored by an automated[2] pH-stat titrator at pH 3.0, 25° using a sample size which would theoretically neutralize 2.25 mEq (4).

X-ray diffractograms were obtained using air-dried samples in McCreery mounts (5). Diffractograms were recorded from 6 to 40° (2 θ) under the following conditions[3]: CuK_α radiation, 30 kV, 28 mamp, 2°/min.

IR[4] spectra were recorded using potassium bromide disks containing 0.8–2.0 mg of air-dried sample and 300 mg of KBr.

RESULTS AND DISCUSSION

The rate of acid neutralization of a mixture of aluminum hydroxycarbonate gel and magnesium hydroxide containing 0.6 mmole of metal/g in a magnesium–aluminum molar ratio of 5:1 decreased during the first 31 days of aging at 25° (Fig. 1A). A slight decrease in the total acid reac-

[1] HydroMagma, Merck & Co., Rahway, N.J.
[2] PHM 26, TTT II, ABU 12 (2.5 ml), TTA 3, SBR 2, Radiometer, Copenhagen, Denmark.
[3] Siemens AG Kristalloflex 4 generator, Type F diffractometer, Karlsrule, West Germany.
[4] Model 180, Perkin-Elmer Co., Norwalk, Conn.

0022-3549/82/0700-0780$01.00/0

(22) L. Tan, *ibid.*, **45**, 68 (1969).
(23) E. Watson, P. Tramell, and S. M. Kalman, *ibid.*, **69**, 157 (1972).
(24) W. E. Wilson, S. A. Johnson, W. H. Perkins, and J. E. Ripley, *Anal. Chem.*, **39**, 40 (1967).
(25) A. H. Kibbe and O. E. Araujo, *J. Pharm. Sci.*, **62**, 1703 (1973).
(26) M. C. Castle, *J. Chromatogr.*, **115**, 437 (1975).
(27) W. Lindner and R. W. Frei, *ibid.*, **117**, 81 (1976).
(28) F. Nachtmann, H. Spitzy, and R. W. Frei, *ibid.*, **122**, 293 (1976).
(29) F. Erni and R. W. Frei, *ibid.*, **130**, 169 (1977).
(30) L. A. Sternson and R. D. Shaffer, *J. Pharm. Sci.*, **67**, 327 (1978).
(31) T. Sonobe, S. Hasumi, T. Yoshino, Y. Kobayashi, H. Kawata, and T. Nagai, *ibid.*, **69**, 410 (1980).
(32) Y. Fujii, H. Fukuda, Y. Saito, and M. Yamazaki, *J. Chromatogr.*, **202**, 139 (1980).
(33) B. Desta and K. M. McErlane, *J. Chromatogr.*, in press.

ACKNOWLEDGMENTS

This study was funded by a grant from the British Columbia Health Care Research Foundation.
Belachew Desta was supported by a fellowship from the World Health Organization.
The authors gratefully acknowledge all assistance.

Formation of Hydrotalcite in Mixtures of Aluminum Hydroxycarbonate and Magnesium Hydroxide Gels

ROGER K. VANDERLAAN *, JOE L. WHITE ‡, and STANLEY L. HEM *x

Received June 12, 1981, from the *School of Pharmacy and Pharmacal Sciences*, **Departments of Industrial and Physical Pharmacy, and* ‡*Agronomy Department, Purdue University, West Lafayette, IN 47907.* Accepted for publication October 13, 1981.

Abstract □ IR and X-ray analysis demonstrate that hydrotalcite forms during the aging of aluminum hydroxycarbonate gel and magnesium hydroxide gel mixtures. The formation of hydrotalcite produces a change in the pH-stat titrigram and a sharp increase in the pH of the mixture. Hydrotalcite was noted earlier in mixtures having a high molar ratio of magnesium to aluminum, a high total gel concentration, a high initial pH, or in mixtures stored at elevated temperatures. The addition of sorbitol to the mixtures substantially delayed the appearance of hydrotalcite. Nonacid-reactive hydrotalcite formed when mixtures of chloride-containing aluminum hydroxide gel and magnesium hydroxide gel were aged.

Keyphrases □ Hydrotalcite—formation, mixtures of aluminum hydroxycarbonate and magnesium hydroxide gels, IR and X-ray analysis □ Mixtures—formation of hydrotalcite in mixtures of aluminum hydroxycarbonate and magnesium hydroxide gels □ Gels—aluminum hydroxycarbonate and magnesium hydroxide gels, mixtures, formation of hydrotalcite

It has been reported recently that amorphous aluminum hydroxycarbonate gel forms a coating on magnesium hydroxide particles due to electrostatic attraction (1). This interaction was detected because the rate of acid neutralization of mixtures of aluminum hydroxycarbonate gel and magnesium hydroxide gel was slower than expected, based on individual rates of acid neutralization. The interaction occurred immediately and an additive rate of acid neutralization only occurred when the gels were separately added to the reaction vessel. As the mixtures aged, the rate of acid neutralization decreased further, suggesting that the amorphous aluminum hydroxycarbonate coating was becoming more ordered as the amorphous to crystalline phase transition occurred.

It was noticed, however, that the rate of acid neutralization in some aged mixtures was greater than the initial rate of acid neutralization. Thus, a further reaction appeared to be occurring during the aging of mixtures of aluminum hydroxycarbonate and magnesium hydroxide gels. This interaction is the focus of this study.

EXPERIMENTAL

Magnesium hydroxide gel[1] was obtained commercially as a paste containing the equivalent of 21% (w/w) MgO. Aluminum hydroxycarbonate gel was prepared as described previously (2) by the addition of 0.47 *M* $AlCl_3 \cdot 6H_2O$ to 0.53 *M* $NaHCO_3$ and 0.23 *M* Na_2CO_3 to a final pH of 6.5. Chloride-containing aluminum hydroxide gel was prepared as described previously (2) by the addition of 13% (v/v) strong ammonia solution to 0.29 *M* $AlCl_3 \cdot 6H_2O$ to a final pH of 7.0.

Aluminum and magnesium content were determined by chelatometric titration (3).

Mixtures of aluminum hydroxycarbonate gel or chloride-containing aluminum hydroxide gel and magnesium hydroxide gel were prepared on a weight basis. For example, a 200-g mixture containing a total of 0.6 mmole of metal/g in a magnesium–aluminum molar ratio of 5:1 was prepared by weighing magnesium hydroxide gel and aluminum hydroxycarbonate gel or chloride-containing aluminum hydroxide gel containing 100 mmoles of magnesium and 20 mmoles of aluminum, respectively. A solution containing an excipient was added when necessary. The final weight was adjusted to 200 g with double-distilled water and the mixture was stirred mechanically until uniform. The mixtures were aged in widemouth polyethylene bottles.

The acid neutralization reaction was monitored by an automated[2] pH-stat titrator at pH 3.0, 25° using a sample size which would theoretically neutralize 2.25 mEq (4).

X-ray diffractograms were obtained using air-dried samples in McCreery mounts (5). Diffractograms were recorded from 6 to 40° (2 θ) under the following conditions[3]: CuK_α radiation, 30 kV, 28 mamp, 2°/min.

IR[4] spectra were recorded using potassium bromide disks containing 0.8–2.0 mg of air-dried sample and 300 mg of KBr.

RESULTS AND DISCUSSION

The rate of acid neutralization of a mixture of aluminum hydroxycarbonate gel and magnesium hydroxide containing 0.6 mmole of metal/g in a magnesium–aluminum molar ratio of 5:1 decreased during the first 31 days of aging at 25° (Fig. 1A). A slight decrease in the total acid reac-

[1] HydroMagma, Merck & Co., Rahway, N.J.
[2] PHM 26, TTT II, ABU 12 (2.5 ml), TTA 3, SBR 2, Radiometer, Copenhagen, Denmark.
[3] Siemens AG Kristalloflex 4 generator, Type F diffractometer, Karlsrule, West Germany.
[4] Model 180, Perkin-Elmer Co., Norwalk, Conn.

0022-3549/82/0700-0780$01.00/0

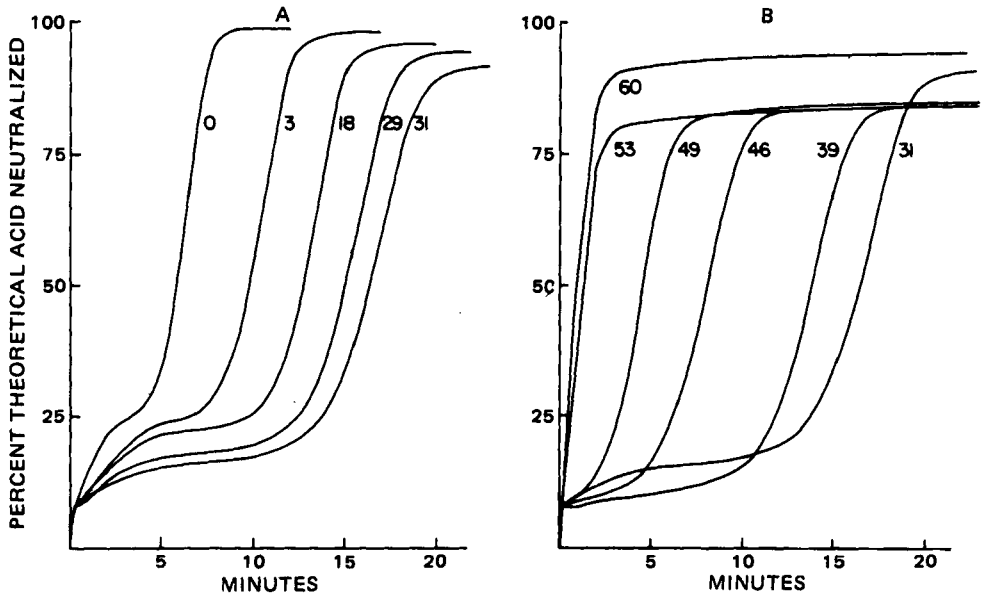

Figure 1—*pH-stat titrigram of a magnesium–aluminum molar ratio (5:1) of an aluminum hydroxycarbonate gel–magnesium hydroxide gel mixture containing 0.6 mmole of metal/g during aging at 25°. Each titrigram is labeled with the age of the mixture in days.*

tivity was also noted. After 31 days, a major reversal occurred in the rate of acid neutralization, *i.e.*, the rate of acid neutralization progressively increased until the mixture reacted in a rapid, single-phase reaction (Fig. 1B). With the establishment of a single, highly reactive phase, the total acid reactivity increased to the theoretical value. The acid reactivity of the mixture was monitored for 375 days at 25° but no further significant changes in the pH-stat titrigrams were observed.

Corresponding to the period of a decreasing rate of acid neutralization observed in Fig. 1A, the pH of the mixture (Fig. 2) decreased slightly during the initial aging period, which is consistent with the polymerization of aluminum hydroxide by the formation of double hydroxide bridges (6). After 37 days, the mixture exhibited a drastic change in pH, rising to pH 11.3 after 80 days at 25°. The pH remained at 11.3 until the study was terminated at 500 days.

The hydroxyl-stretching region of the IR spectrum of the freshly prepared mixture is shown in Fig. 3, Curve A. The broad absorption band between 3000 and 3700 cm^{-1} is characteristic of amorphous aluminum hydroxycarbonate gel with hydroxide groups in a continuum of environments, indicative of a highly disordered state (7). The sharp peak at 3698 cm^{-1} is indicative of the rigid environment of the brucite structure of magnesium hydroxide gel (8). After 48 days (Fig. 3, Curve B), the absorption band at 3698 cm^{-1} showed a dramatic decrease, signaling a reduction in the amount of magnesium present as brucite in the mixture. The decrease in the peak at 3698 cm^{-1} continued as the mixture aged, but the position of the brucite peak remained constant (Fig. 3, Curve C). The maximum absorption of the diffuse hydroxyl-stretching band shifted toward higher energy absorption.

Figure 4 shows the region of carbonate absorption in the IR spectrum of the mixture. The large initial split (Fig. 4, Curve A) in the carbonate peaks at 1406 and 1540 cm^{-1} is a result of coordination of carbonate to aluminum in the aluminum hydroxycarbonate gel (9). The shoulder at 1640 cm^{-1} is due in large part to free water adsorbed by the aluminum hydroxycarbonate. The region of carbonate absorption became less well defined after 48 days (Fig. 4, Curve B) while the splitting of the carbonate peaks increased slightly. A major structural change occurred by Day 61 as the peak at 1406 cm^{-1} was reduced to a shoulder and the peak at 1540 cm^{-1} was almost completely replaced by a single strong absorbance at 1463 cm^{-1} with a well-defined shoulder at 1448 cm^{-1}. This shift indicates

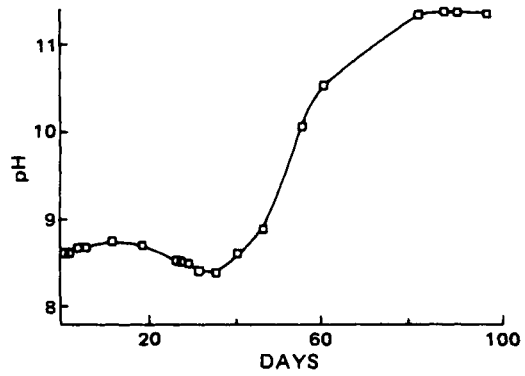

Figure 2—*pH of a magnesium–aluminum molar ratio (5:1) of an aluminum hydroxycarbonate gel–magnesium hydroxide gel mixture containing 0.6 mmole of metal/g during aging at 25°.*

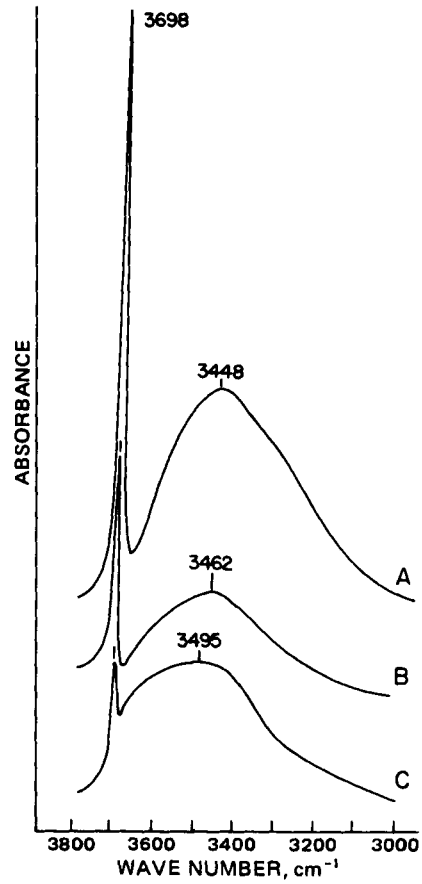

Figure 3—*Hydroxyl-stretching region of the IR spectrum of a magnesium–aluminum molar ratio (5:1) of an aluminum hydroxycarbonate gel–magnesium hydroxide gel mixture containing 0.6 mmole of metal/g during aging at 25°. Key: (A) initial; (B) 48 days; (C) 61 days.*

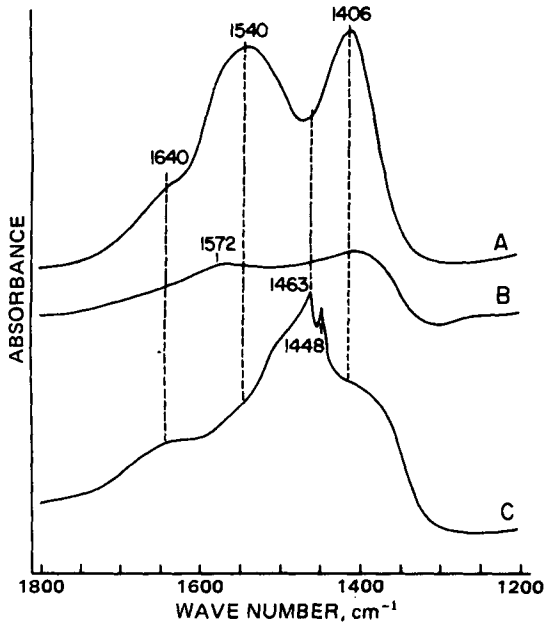

Figure 4—*Carbonate absorption region of the IR spectrum of a magnesium–aluminum molar ratio (5:1) of an aluminum hydroxycarbonate gel–magnesium hydroxide gel mixture containing 0.6 mmole of metal/g during aging at 25°. Key: (A) initial; (B) 48 days; (C) 61 days.*

that the carbonate ion is no longer strongly associated with aluminum but is in a less perturbed state. The peak of 1448 cm^{-1} is characteristic of a symmetrical carbonate anion as in sodium carbonate (10). The strong peak at 1463 cm^{-1} may result from the carbonate anion regaining its symmetrical character but being in a slightly different environment compared to sodium carbonate.

Figure 5 shows the 800–1200 cm^{-1} region of the IR spectrum during aging of the mixture at 25°. In the fresh mixture, the broad shoulder at 957 cm^{-1} indicates the disordered hydroxyl environment in the aluminum hydroxycarbonate gel. The peaks at 846 and 1094 cm^{-1} are present only when there is distortion of the carbonate ion, while the peak which appears at 878 cm^{-1} after 48 days is characteristic of unperturbed carbonate ion as found in sodium carbonate (11). The disappearance of the peak at 1094 cm^{-1} and the appearance of the free carbonate band at 878 cm^{-1} suggest that structural changes occurred in the mixture which resulted in a drastic change in environment for the carbonate ion.

X-ray diffractograms of the mixture during aging also suggest that structural changes occurred (Fig. 6). The initial X-ray diffractogram (Table I) had peaks at interplanar spacings of 4.74, 2.369, 1.794, 1.569, and 1.491 Å which corresponded to the peaks for brucite. In addition, there was a diffuse band between 15 and 35° (2 θ) which was attributed to disordered, amorphous aluminum hydroxycarbonate. After 48 days (Fig. 6, Curve B), the brucite peaks had diminished in intensity but remained sharp. In the case of both X-ray and IR observations, the peaks

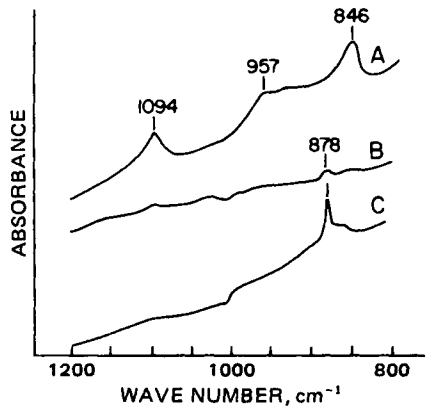

Figure 5—*Hydroxyl-bending region of the IR spectrum of a magnesium–aluminum molar ratio (5:1) of an aluminum hydroxycarbonate gel–magnesium hydroxide gel mixture containing 0.6 mmole of metal/g during aging at 25°. Key: (A) initial; (B) 48 days; (C) 61 days.*

Table I—X-ray Spacings of a Magnesium–Aluminum Molar Ratio (5:1) of Aluminum Hydroxycarbonate Gel–Magnesium Hydroxide Gel Mixture [a]

Age	Mixture, dÅ	Brucite[b], dÅ(I/I_0)	Hydrotalcite[c], dÅ (I/I_0)
Initial	4.74	4.77 (90)	7.84 (100)
	2.369	2.365 (100)	3.90 (60)
	1.794	1.794 (55)	2.60 (40)
	1.569	1.573 (35)	2.33 (25)
	1.491	1.494 (18)	
61 days	7.82		7.84
	4.72	4.77	
	3.91		3.90
	2.576		2.60
	2.354	2.365	
	2.33–2.30		2.33
		1.794	
		1.573	
		1.494	

[a] During aging at 25°, compared to reference brucite and hydrotalcite. [b] "Selected Powder Diffraction Data for Minerals," Joint Committee on Powder Diffraction Standards, Swarthmore, Pa., 1974, File 7-239. [c] *Ibid*, File 22-700.

corresponding to brucite decreased in intensity while maintaining a high degree of sharpness. This indicated a decrease in the total amount of brucite in the mixture but a high degree of crystallinity in the remaining brucite. The brucite peaks did not shift in location, even after 510 days, suggesting that the structure of the remaining brucite was not altered.

After 61 days, the peaks corresponding to brucite had decreased substantially and a new set of moderately sharp peaks appeared (Fig. 6, Curve C). After checking the mineralogical literature, the new peaks were indexed to be virtually identical to those of hydrotalcite, a magnesium aluminum hydroxycarbonate (Table I). The structure of hydrotalcite (Fig. 7) is unique, as it is composed of two layers of brucite in which aluminum replaces some magnesium. The positive charge on the brucite layer which results from the substitution is balanced by carbonate, hydroxyl, and other anions which are sandwiched between the substituted brucite layers (12–19).

The changes in the rate of acid neutralization, pH, IR spectrum, and X-ray diffraction of the magnesium–aluminum (5:1) mixture are consistent with the formation of hydrotalcite. The pH-stat titrigram after

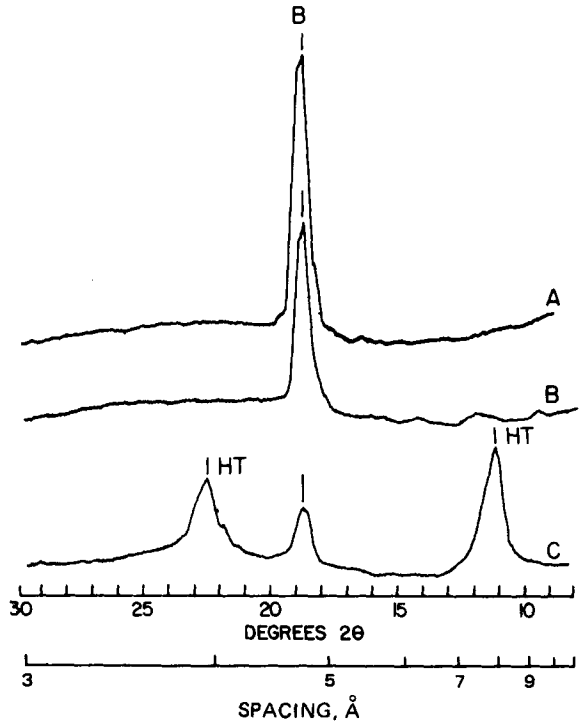

Figure 6—*X-ray diffractogram in the 3–9 Å region of a magnesium–aluminum molar ratio (5:1) of an aluminum hydroxycarbonate gel–magnesium hydroxide gel mixture containing 0.6 mmole of metal/g during aging at 25°. B and HT indicates the peaks corresponding to brucite and hydrotalcite, respectively. Key: (A) initial; (B) 48 days; (C) 61 days.*

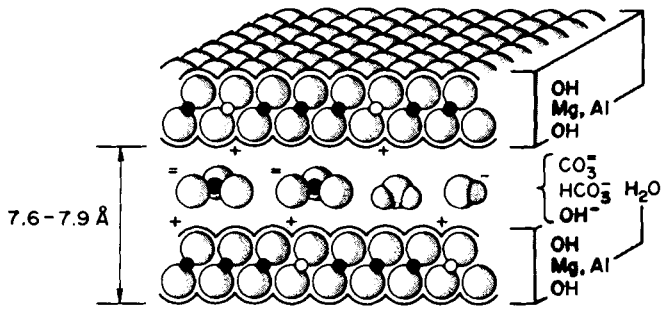

Figure 7—*Schematic representation of hydrotalcite (from ref. 8).*

60 days at 25° showed the same rapid, one-phase reaction as is characteristic of magneisum hydroxide. The reaction rate of hydrotalcite would be expected to be similar to magnesium hydroxide as both minerals are based upon the brucite crystal lattice.

The initial pH of the mixture, 8.7, was intermediate between pH 10.35 for the magnesium hydroxide gel, and pH 6.5 for the aluminum hydroxycarbonate gel. The rise in pH associated with the formation of hydrotalcite may be attributed to the presence of carbonate in the interlayer space of hydrotalcite. Carbonate ion neutralizes the positive charge of the substituted brucite layer more efficiently than hydroxyls and will, therefore, displace hydroxyls which cause the bulk pH to rise.

The formation of hydrotalcite in the mixtures was first noted in the IR spectrum by the decrease in the intensity of the brucite peak. The change in the carbonate band from a highly perturbed state, due to coordination to aluminum in aluminum hydroxycarbonate to a virtually unperturbed state (as would occur if carbonate functioned as a counterion between the substituted brucite layers), is consistent with the formation of hydrotalcite during aging of the mixtures. The X-ray diffractograms showed evidence of hydrotalcite at 61 days. Prior to this time, some decrease in the intensity of the brucite peaks was noted, but a sharp decrease in the intensity of the brucite peak occurred with the formation of hydrotalcite. Since the appearance of hydrotalcite in the mixture is sudden rather than gradual, and since no further significant changes were noted, it appears that some threshold condition must be reached after which the rapid formation of hydrotalcite can occur.

The magnesium to aluminum ratio in mixtures of aluminum hydroxycarbonate gel and magnesium hydroxide gel substantially affects the length of time before hydrotalcite is formed in the mixtures. A series of mixtures was prepared where each contained 0.6 mmole of metal/g but the magnesium–aluminum molar ratio was 5:1, 2:1, 1:1, 1:2, and 1:5. X-ray diffraction showed that hydrotalcite formed in the magnesium–aluminum mixture (5:1) after ~30–40 days of aging at 25°. Hydrotalcite was detected in the magnesium–aluminum mixture (2:1) after 200 days. The magnesium–aluminum mixtures (1:1 and 1:2) showed the presence of hydrotalcite before 516 days, while the magnesium–aluminum mixture (1:5) remained free of hydrotalcite through 516 days. Thus, the higher the molar ratio of magnesium to aluminum, the sooner hydrotalcite was formed. This may be due to the higher pH of the mixtures which contain a higher magnesium–aluminum ratio. The solubility of aluminum hydroxycarbonate increases in alkaline medium, thus facilitating the conversion to hydrotalcite.

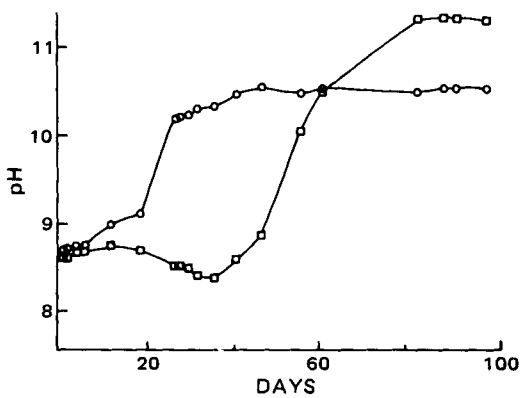

Figure 8—*pH of a magnesium–aluminum molar ratio (5:1) of an aluminum hydroxycarbonate gel–magnesium hydroxide gel mixture during aging at 25°. Key: (□) 0.6 mmole of metal/g; (○) 1.2 mmole of metal/g.*

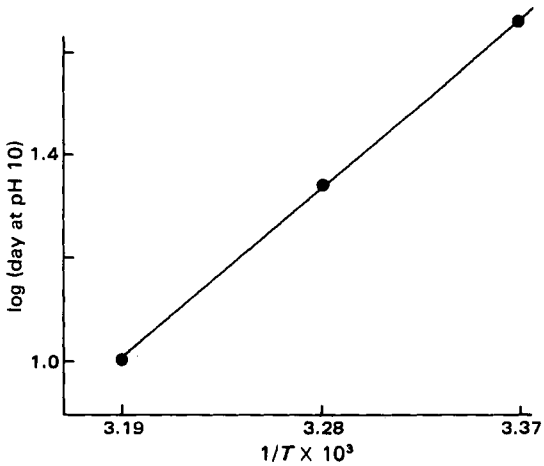

Figure 9—*Relationship of aging temperature to time for pH to increase to 10 for a magnesium–aluminum molar ratio (5:1) of an aluminum hydroxycarbonate gel–magnesium hydroxide gel mixture containing 0.6 mmole of metal/g.*

Hydrotalcite also appeared more rapidly as the concentration of the mixture was increased. As seen in Fig. 8, the pH of a magnesium–aluminum mixture (5:1) at 1.2 mmoles of metal/g rose sharply after ~20 days at 25°, while the pH of a magnesium–aluminum mixture (5:1) containing 0.6 mmole of metal/g increased after ~40 days at 25°. X-ray diffractograms and changes in the pH-stat titrigrams confirmed that hydrotalcite had formed in these mixtures. The formation of hydrotalcite would be expected to occur sooner in concentrated mixtures if, as suggested earlier, some threshold condition must be reached to initiate its formation.

Higher aging temperatures promoted more rapid formation of hydrotalcite, probably due to increased solubility at higher temperatures. Figure 9 is an Arrhenius-type plot of the log of the time for magnesium–aluminum mixture (5:1) containing 0.6 mmole of metal/g to reach pH 10 *versus* the reciprocal of the aging temperature (T). A linear relationship exists with a heat of activation of ~8.6 kcal/mole.

To observe the effect of initial suspension pH, a magnesium–aluminum mixture (5:1) containing 0.6 mmole of metal/g was divided into six portions. One portion served as the control, while three portions were brought to either pH 9.5, 10.0, or 10.5 with sodium hydroxide. One portion was brought to pH 10 with sodium carbonate to determine if the carbonate anion played a role in initiating the formation of hydrotalcite. The pH of the final portion was not altered, but a small amount of a similar mixture in which hydrotalcite had formed was added to serve as a seed. As seen in Table II, the time required for the pH to rise, indicating hydrotalcite formation, is inversely related to the initial pH of the mixture. The pH of the samples, which had been adjusted to pH 10.5 and 10.0, increased within 1 day, while the sample at pH 9.5 showed evidence of the formation of hydrotalcite within 10 days. The main factor appears to be pH rather than the reagent used to adjust the pH as similar results were obtained when either sodium hydroxide or sodium carbonate was used to adjust the pH. The increased solubility of aluminum hydroxycarbonate at higher pH conditions is believed to be responsible for the pH effect. Seeding the mixture with hydrotalcite had no effect as the pH profile of the seeded sample was similar to the control.

Table II—pH of Magnesium–Aluminum [a] at Different Initial pH

Day	Control	Initial pH Adjusted with NaOH			Initial pH Adjusted with Na_2CO_3	Seeded
		9.5	10.0	10.5	10.0	
0	8.75	9.50	10.00	10.50	10.00	8.75
1	8.47	9.53	10.48	11.36	10.37	8.44
10	8.34	11.09	10.50	11.63	11.02	8.32
18	8.34	—	—	—	—	8.45
21	8.34	—	—	—	—	8.74
24	8.71	—	—	—	—	8.74
28	8.81	—	—	—	—	9.66
30	9.58	—	—	—	—	9.97
34	10.11	—	—	—	—	10.20
41	10.41	—	—	—	—	—
167	11.27	11.81	12.03	12.34	11.51	11.51

[a] Magnesium–aluminum mixtures (5:1) containing 0.6 mmole of metal/g.

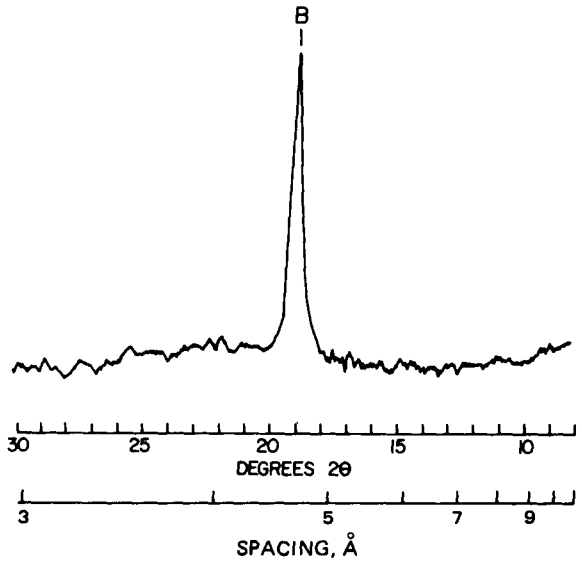

Figure 10—*X-ray diffractogram in the 3–9 Å region of a magnesium–aluminum molar ratio (2:1) of an aluminum hydroxycarbonate gel–magnesium hydroxide gel mixture containing 0.6 mmole of metal/g and 2% sorbitol after aging for 616 days at 25°. B indicates the peak corresponding to brucite.*

Two experiments were performed to determine if any excipients would act to stabilize the mixture by controlling the formation of hydrotalcite. A magnesium–aluminum mixture (2:1) containing 0.6 mmole of metal/g was divided into four portions. One portion served as the control, while the other three portions contained either 2% sorbitol, 0.5% simethicone, or 1% polysorbate 80. Hydrotalcite was found in the control and the mixtures containing simethicone or polysorbate 80 at approximately the same time, *i.e.*, after 200 days at 25°. As seen in Fig. 10, the X-ray diffractograms of the sample containing 2% sorbitol showed a very sharp brucite peak and no evidence of hydrotalcite after aging for 616 days at 25°.

Various other excipients were compounded with magnesium–aluminum mixtures (5:1) containing 0.9 mmole of metal/g. The mixtures were aged at 32° and the time required to reach pH 10 was recorded. As seen in Table III, all but two of the mixtures reached a pH of at least 10 within 18 days. Five control samples were included in the experiment to give an indication of the variability in the time required for hydrotalcite to form. The average time for the pH of the control to reach 10 was 12.6 days with 1.5 *SD*. Only the higher concentration of sodium citrate (0.5%) and 2% sorbitol were able to prevent the formation of hydrotalcite during the 52 days of the experiment. Sorbitol is known to hydrogen bond with aluminum hydroxycarbonate gel, while citrate anion is a chelating agent for aluminum. Figure 11 compares the pH-stat titrigrams of selected samples. Initial titrigrams of all samples except the sodium citrate-containing samples were identical. Mixtures containing sodium citrate exhibited

Table III—Effect of Selected Excipients on the Formation of Hydrotalcite in Magnesium–Aluminum Mixtures [a]

Excipient	Concentration, %	Time to Reach pH 10, days
Control	—	11
Control	—	12
Control	—	12
Control	—	13
Control	—	15
Amaranth	0.1	13
Bentonite	0.1	12
Disodium Edetate	0.1	16
Aminoacetic Acid	0.1	18
Methylparaben / Propylparaben	0.18 / 0.02	11
Napthol Yellow S	0.1	16
Sodium Citrate	0.1	15
Sodium Citrate	0.5	[b]
Sodium Saccharin	0.01	13
Sorbitol	2.0	[b]

[a] Magnesium–aluminum mixtures (5:1) containing 0.9 mmole of metal at 32°.
[b] pH did not rise above 10 for at least 52 days.

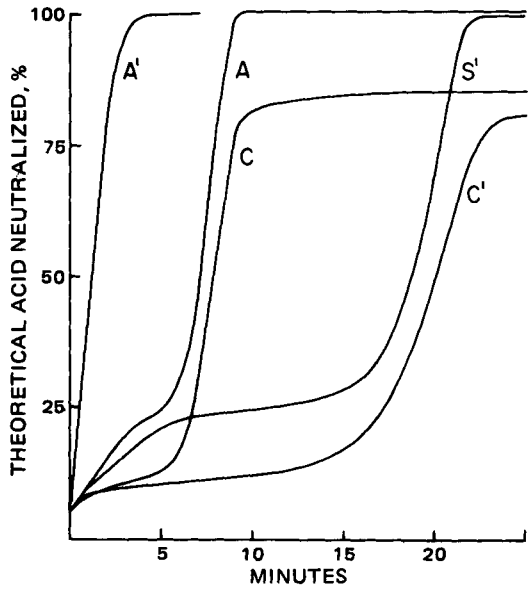

Figure 11—*pH-stat titrigram of magnesium–aluminum molar ratio (5:1) of an aluminum hydroxycarbonate gel–magnesium hydroxide gel mixture containing 0.9 mmole of metal/g containing various excipients. Key: (A) initial for all mixtures except sodium citrate-containing mixtures; (C) initial for 0.5% sodium citrate-containing mixture; (S^1) 2% sorbitol-containing mixture aged at 32° for 52 days; (C^1) 0.5% sodium citrate-containing mixture aged at 32° for 52 days; (A^1) all mixtures except sorbitol- and sodium citrate-containing mixtures aged at 32° for 52 days.*

a decrease in both rate and extent of acid reactivity in the region of aluminum hydroxycarbonate gel neutralization which was directly related to the concentration of sodium citrate, while the magnesium hydroxide portion of the pH stat titrigram was unaffected (1).

After 52 days at 32°, the pH-stat titrigram of the control and all the mixtures, except those containing 2% sorbital or 0.5% sodium citrate, consisted of a single, highly-reactive phase which is characteristic of the formation of hydrotalcite. The rate of acid neutralization of the sorbitol-containing mixture had decreased but the sample was completely reactive. The sodium citrate-containing sample exhibited both a decreased rate and extent of acid neutralization. Both sorbitol and sodium citrate substantially delayed the formation of hydrotalcite, although the use of citrate anion is not recommended due to its deleterious effect on acid neutralization.

The observations of the factors affecting the formation of hydrotalcite in mixtures of aluminum hydroxycarbonate gel and magnesium hydroxide gel support a previous conclusion (20) that the formation of hy-

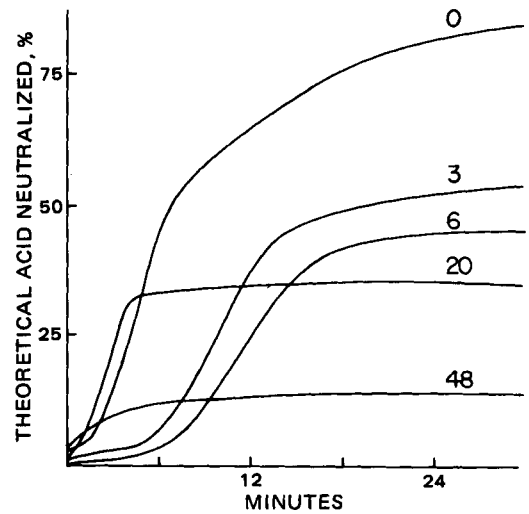

Figure 12—*pH-stat titrigram of magnesium–aluminum molar ratio (1:1) of a chloride-containing aluminum hydroxide gel–magnesium hydroxide gel mixture containing 0.6 mmole of metal/g during aging at 25°. Each titrigram is labeled with the age of the mixture in days.*

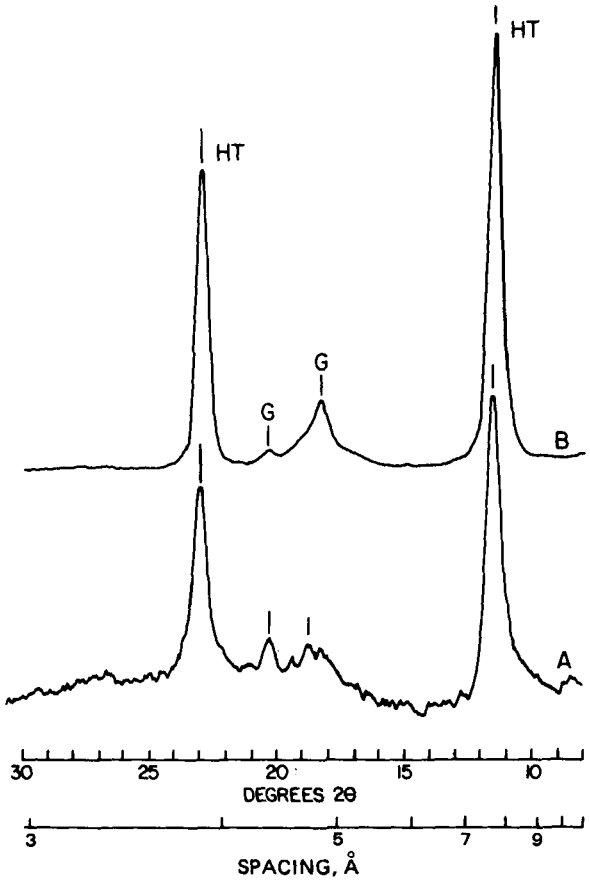

Figure 13—*X-ray diffractogram in the 3–9 Å region of a magnesium–aluminum molar ratio (1:1) of a chloride-containing aluminum hydroxide gel–magnesium hydroxide gel mixture containing 0.6 mmole of metal/g during aging at 25°. HT and G indicate the peaks corresponding to hydrotalcite and gibbsite, respectively. Key: (A) 69 days; (B) 173 days.*

drotalcite is a solution phenomena of the following type:

$$Na^+Al(OH)_4^- + 2[(MgOH)^+Cl^-] \rightarrow [AlMg_2(OH)_6]^+Cl^- + NaCl \quad \text{(Eq. 1)}$$

This conclusion was based on the observation that hydrotalcite formed when separate dialysis sacks containing aluminum hydroxide and magnesium carbonate were suspended in water at 60° for 3–6 months (21). Hydrotalcite (~90%) was found in the sack which initially contained aluminum hydroxide, ~10% was found in the dialysis medium, and virtually none was present in the sack which initially contained magnesium carbonate. Hydrotalcite had been precipitated previously (22) from a solution equimolar in aluminum chloride and magnesium chloride at pH 10 in the presence of 4 *N* Na_2CO_3.

The following sequence of reactions are hypothesized to occur when hydrotalcite forms during the aging of mixtures of aluminum hydroxycarbonate gel and magnesium hydroxide gel. At pH 8–9 magnesium hydroxide will have a relatively high tendency to donate hydroxyls:

$$Mg(OH)_2 \rightarrow MgOH^+ + OH^- \quad \text{(Eq. 2)}$$

Under these conditions aluminum hydroxide will tend to gain hydroxyls to form aluminate:

$$Al(OH)_3 + OH^- \rightarrow Al(OH)_4^- \quad \text{(Eq. 3)}$$

At first the pH of the mixture remains relatively constant due to the balance of Eqs. 2 and 3. After a period of time, the aluminum hydroxide is no longer able to readily assimilate hydroxyls and the suspension pH begins to rise due to the continued dissolution of magnesium hydroxide. The formation of hydrotalcite occurs by the same mechanism as proposed previously (20), *i.e.*, the coalesence of the products of Eqs. 2 and 3 as shown by Eq. 1. This mechanism is consistent with the sudden appearance of hydrotalcite in mixtures and also with the effect of magnesium–aluminum ratio, concentration, pH, and temperature observed in this study.

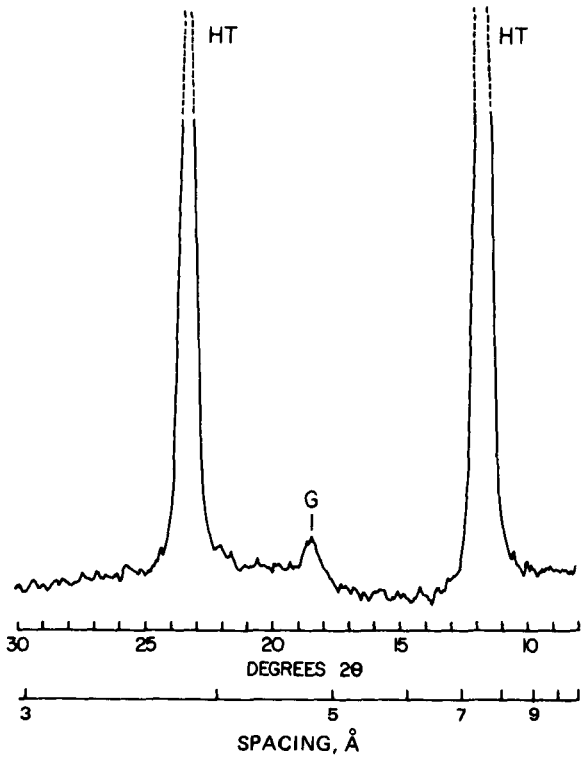

Figure 14—*X-ray diffractogram in the 3–9 Å region of the nonacid-reactive component of a magnesium–aluminum molar ratio (1:1) of a chloride-containing aluminum hydroxide gel and magnesium hydroxide gel containing 0.6 mmole of metal/g after aging for 173 days at 25°. HT and G indicate the peaks corresponding to hydrotalcite and gibbsite, respectively.*

A nonacid-reactive form of hydrotalcite is produced when a mixture of a chloride-containing aluminum hydroxide gel and magnesium hydroxide is aged at 25°. Compared to an aluminum hydroxycarbonate gel, a chloride-containing aluminum hydroxide gel shows a more rapid decrease in the rate of acid neutralization, and the total amount of acid neutralized at pH 3 also decreases (4). The pH of a mixture containing 0.6 mmole of metal/g in a magnesium–aluminum molar ratio of 1:1 increased from 6.6 to 8.5 after 8 days at 25°. The pH-stat titrigram also showed a change in shape at this same time (Fig. 12). However, in contrast to mixtures containing aluminum hydroxycarbonate gel, (Fig. 1) the total amount of acid neutralized decreased to ~15% of the theoretical yield after aging for 48 days. Well-crystallized hydrotalcite peaks were evident in the X-ray diffractograms after 69 days at 25° (Fig. 13, Curve A). No magnesium hydroxide peaks were present in the X-ray diffractogram, but peaks at 4.82 and 4.34 Å indicated the presence of gibbsite, a crystalline polymorph of aluminum hydroxide. An X-ray diffractogram of the mixture after 173 days at 25° (Fig. 13, Curve B) showed a further increase in the crystallinity of hydrotalcite.

The sharp peaks suggested a larger crystallite size for the hydrotalcite formed in the chloride-containing aluminum hydroxide gel and magnesium hydroxide gel mixtures than formed in the aluminum hydroxycarbonate gel and magnesium hydroxide gel mixtures. After 118 days at 25°, the unreactive fraction from the pH-stat test was collected and washed. An X-ray diffractogram (Fig. 14) shows that the nonacid reactive component is chiefly highly crystalline hydrotalcite. Thus, a nonacid-reactive aluminum hydroxide gel quickly gave rise to a nonacid-reactive form of hydrotalcite.

The formation of hydrotalcite during the aging of mixtures of aluminum hydroxide gel and magnesium hydroxide gel is important because the *United States Pharmacopeia* recognizes two mixtures of aluminum hydroxide gel and magnesium hydroxide gel, as well as magaldrate (23) which is a form of hydrotalcite having sulfate as the principal interlayer anion. Alumina and magnesia oral suspension (3) may contain a magnesium–aluminum molar ratio of between 0.4 and 0.8 and a total metal content of between 0.8 and 1.2 mmoles of metal/g. Magnesia and alumina oral suspension (24) may contain a magnesium–aluminum molar ratio of between 1.4 and 2.4 and a total metal content of between 0.9 and 1.2 mmoles of metal/g. These mixtures are within the range of magnesium–

aluminum and total metal concentration of the mixtures in which hydrotalcite was found to form on aging.

The present monographs for these mixtures do not contain any tests which would detect the presence of hydrotalcite, nor do they require the inclusion of sorbitol in the mixtures. Thus, there is the possibility of the formation of hydrotalcite during the aging of official aluminum hydroxide gel and magnesium hydroxide gel mixtures.

REFERENCES

(1) R. K. Vanderlaan, J. L. White, and S. L. Hem, *J. Pharm. Sci.*, **68,** 1498 (1979).

(2) S. L. Hem, E. J. Russo, S. M. Bahal, and R. S. Levi, *ibid.*, **59,** 317 (1970).

(3) "The United States Pharmacopeia," 20th rev., United States Pharmacopeial Convention, Inc., Rockville, Md., 1980, p. 23.

(4) N. J. Kerkhof, R. K. Vanderlaan, J. L. White, and S. L. Hem, *J. Pharm. Sci.*, **66,** 1528 (1977).

(5) H. P. Klug and L. E. Alexander, "X-Ray Diffraction Procedures for Polycrystalline and Amorphous Materials," Wiley, New York, N.Y., 1954, p. 300.

(6) S. L. Nail, J. L. White, and S. L. Hem, *J. Pharm. Sci.*, **65,** 1188 (1976).

(7) *Ibid.*, **65,** 231 (1976).

(8) C. J. Serna, J. L. White, and S. L. Hem, *ibid.*, **67,** 324 (1978).

(9) J. L. White and S. L. Hem, *ibid.*, **64,** 468 (1975).

(10) C. J. Serna, J. L. White, and S. L. Hem, *Soil Sci. Soc. Am. J.*, **41,** 1009 (1977).

(11) K. Nakamoto, "Infrared Spectra of Inorganic and Coordination Compounds," Wiley, New York, N.Y., 1963, p. 159.

(12) L. Ingram and H. F. W. Taylor, *Mineral. Mag.*, **36,** 465 (1967).

(13) R. Allmann, *Acta Crystallogr., Sect. B*, **24,** 972 (1968).

(14) R. Allmann and H. H. Lohse, *N. Jb. Miner. Mh.*, 161 (1966); through *Chem. Abst.*, **66,** 23112 g (1967).

(15) R. Allmann and H. P. Jepson, *N. Jb. Miner. Mh.*, 544 (1966); through *Chem. Abst.*, **72,** 60153 y (1970).

(16) R. Allmann, *N. Jb. Miner. Mh.*, 552 (1966); through *Chem. Abst.*, **72,** 60156 b (1970).

(17) R. Allmann, *Chimia*, **24,** 99 (1979); through *Chem. Abst.*, **73,** 8203 w (1970).

(18) R. Allmann, *Fortschr. Mineral.*, **48,** 24 (1971); through *Chem. Abst.*, **75,** 144866 h (1971).

(19) F. A. Mumpton, H. W. Jaffe, and C. S. Thompson, *Am. Mineral.*, **50,** 1893 (1965).

(20) H. Besson, S. Caillere, and S. Henin, *Clay Miner.*, **12,** 239 (1977).

(21) H. Besson, S. Caillere, and S. Henin, *C.R. Acad. Sci.*, **277,** 1273 (1973).

(22) M. M. Mortland and M. C. Gastuche, *ibid.*, **255,** 2131 (1962).

(23) "The United States Pharmacopeia," 20th rev. United States Pharmacopeial Convention, Inc., Rockville, Md., 1980, p. 457.

(24) *Ibid.*, p. 458.

ACKNOWLEDGMENTS

Supported in part by an American Foundation for Pharmaceutical Education Fellowship to R. K. Vanderlaan.

This report is Journal Paper 9007, Purdue University Agricultural Experimental Station, West Lafayette, Ind.

Toxicity of Polyalkylcyanoacrylate Nanoparticles I: Free Nanoparticles

B. KANTE *, P. COUVREUR *x, G. DUBOIS-KRACK ‡, C. DE MEESTER ‡, P. GUIOT §, M. ROLAND *, M. MERCIER ‡, and P. SPEISER ¶

Received May 21, 1981 from the **Laboratoire de Pharmacie Galénique and the* ‡*Laboratoire de Chimie Médicale, Toxicologie, et Bromatologie, Université Catholique de Louvain, 1200 Bruxelles, Belgium;* the §*Laboratoire de Chimie Physiologique, Université Catholique de Louvain et International Institute of Cellular and Molecular Pathology, 1200 Bruxelles, Belgium;* and the ¶*School of Pharmacy, Federal Institute of Technology, Zürich, Switzerland.* Accepted for publication October 7, 1981.

Abstract □ The present report describes preliminary results concerning the acute toxicity of placebo polyalkylcyanoacrylate nanoparticles used as drug carrier. It was demonstrated that nanoparticles induced cellular damage only at relatively high concentrations in the cell culture medium. The absence of mutagenicity was shown for both nanoparticles and their degradation products, and the LD_{50} for polybutyl- and polyisobutylcyanoacrylate nanoparticles was also determined.

Keyphrases □ Polyalkylcyanoacrylate—toxicity of nanoparticles □ Nanoparticles—polyalkylcyanoacrylate toxicity □ Toxicity—polyalkylcyanoacrylate nanoparticles □ Drug carrier systems—nanoparticles, toxicity of polyalkylcyanoacrylate

Previous studies have demonstrated the interest of polyalkylcyanoacrylate nanoparticles as a drug carrier (1, 2). The main advantage of these particles is their degradability at a rate depending on the length of the alkyl chain (3). These ultrafine particles (diameter of ~0.2 μm) are able to efficiently adsorb a variety of drugs in a stable and reproducible way (4). It has been shown previously that the binding of cytostatic drugs to nanoparticles modifies their distribution pattern in rat tissues and generally increases the tissue capture of these drugs (5, 6).

Recently, preliminary results of experimental chemotherapy were published (7) using actinomycin D-loaded polymethylcyanoacrylate nanoparticles against the growth of a transplantable soft sarcoma tissue of the rat. The results indicated that the use of polymethylcyanoacrylate nanoparticles as a drug carrier increased the anticancer activity of actinomycin towards subcutaneous sarcoma. Furthermore, these particles could be of interest in the field of long-acting insulin therapy (8).

However, it was important to have information about the toxicity of the carrier to determine if these results did not prohibit the use of nanoparticles in human medicine. The present report describes preliminary results concerning the acute toxicity of nondrug-bound nanoparticles towards cells in culture and the determination of the LD_{50} of the carrier.

EXPERIMENTAL

Polyalkylcyanoacrylate Nanoparticles Preparation—Polymethyl-, polybutyl-, and polyisobutylcyanoacrylate nanoparticles were prepared following previous methods (1, 6), slightly modified. To an

0022-3549/82/0700-0786$01.00/0

aluminum and total metal concentration of the mixtures in which hydrotalcite was found to form on aging.

The present monographs for these mixtures do not contain any tests which would detect the presence of hydrotalcite, nor do they require the inclusion of sorbitol in the mixtures. Thus, there is the possibility of the formation of hydrotalcite during the aging of official aluminum hydroxide gel and magnesium hydroxide gel mixtures.

REFERENCES

(1) R. K. Vanderlaan, J. L. White, and S. L. Hem, *J. Pharm. Sci.*, **68,** 1498 (1979).

(2) S. L. Hem, E. J. Russo, S. M. Bahal, and R. S. Levi, *ibid.*, **59,** 317 (1970).

(3) "The United States Pharmacopeia," 20th rev., United States Pharmacopeial Convention, Inc., Rockville, Md., 1980, p. 23.

(4) N. J. Kerkhof, R. K. Vanderlaan, J. L. White, and S. L. Hem, *J. Pharm. Sci.*, **66,** 1528 (1977).

(5) H. P. Klug and L. E. Alexander, "X-Ray Diffraction Procedures for Polycrystalline and Amorphous Materials," Wiley, New York, N.Y., 1954, p. 300.

(6) S. L. Nail, J. L. White, and S. L. Hem, *J. Pharm. Sci.*, **65,** 1188 (1976).

(7) *Ibid.*, **65,** 231 (1976).

(8) C. J. Serna, J. L. White, and S. L. Hem, *ibid.*, **67,** 324 (1978).

(9) J. L. White and S. L. Hem, *ibid.*, **64,** 468 (1975).

(10) C. J. Serna, J. L. White, and S. L. Hem, *Soil Sci. Soc. Am. J.*, **41,** 1009 (1977).

(11) K. Nakamoto, "Infrared Spectra of Inorganic and Coordination Compounds," Wiley, New York, N.Y., 1963, p. 159.

(12) L. Ingram and H. F. W. Taylor, *Mineral. Mag.*, **36,** 465 (1967).

(13) R. Allmann, *Acta Crystallogr., Sect. B*, **24,** 972 (1968).

(14) R. Allmann and H. H. Lohse, *N. Jb. Miner. Mh.*, 161 (1966); through *Chem. Abst.*, **66,** 23112 g (1967).

(15) R. Allmann and H. P. Jepson, *N. Jb. Miner. Mh.*, 544 (1966); through *Chem. Abst.*, **72,** 60153 y (1970).

(16) R. Allmann, *N. Jb. Miner. Mh.*, 552 (1966); through *Chem. Abst.*, **72,** 60156 b (1970).

(17) R. Allmann, *Chimia*, **24,** 99 (1979); through *Chem. Abst.*, **73,** 8203 w (1970).

(18) R. Allmann, *Fortschr. Mineral.*, **48,** 24 (1971); through *Chem. Abst.*, **75,** 144866 h (1971).

(19) F. A. Mumpton, H. W. Jaffe, and C. S. Thompson, *Am. Mineral.*, **50,** 1893 (1965).

(20) H. Besson, S. Caillere, and S. Henin, *Clay Miner.*, **12,** 239 (1977).

(21) H. Besson, S. Caillere, and S. Henin, *C.R. Acad. Sci.*, **277,** 1273 (1973).

(22) M. M. Mortland and M. C. Gastuche, *ibid.*, **255,** 2131 (1962).

(23) "The United States Pharmacopeia," 20th rev. United States Pharmacopeial Convention, Inc., Rockville, Md., 1980, p. 457.

(24) *Ibid.*, p. 458.

ACKNOWLEDGMENTS

Supported in part by an American Foundation for Pharmaceutical Education Fellowship to R. K. Vanderlaan.

This report is Journal Paper 9007, Purdue University Agricultural Experimental Station, West Lafayette, Ind.

Toxicity of Polyalkylcyanoacrylate Nanoparticles I: Free Nanoparticles

B. KANTE *, P. COUVREUR *x, G. DUBOIS-KRACK ‡, C. DE MEESTER ‡, P. GUIOT §, M. ROLAND *, M. MERCIER ‡, and P. SPEISER ¶

Received May 21, 1981 from the **Laboratoire de Pharmacie Galénique and the* ‡*Laboratoire de Chimie Médicale, Toxicologie, et Bromatologie, Université Catholique de Louvain, 1200 Bruxelles, Belgium;* the §*Laboratoire de Chimie Physiologique, Université Catholique de Louvain et International Institute of Cellular and Molecular Pathology, 1200 Bruxelles, Belgium;* and the ¶*School of Pharmacy, Federal Institute of Technology, Zürich, Switzerland.* Accepted for publication October 7, 1981.

Abstract □ The present report describes preliminary results concerning the acute toxicity of placebo polyalkylcyanoacrylate nanoparticles used as drug carrier. It was demonstrated that nanoparticles induced cellular damage only at relatively high concentrations in the cell culture medium. The absence of mutagenicity was shown for both nanoparticles and their degradation products, and the LD_{50} for polybutyl- and polyisobutylcyanoacrylate nanoparticles was also determined.

Keyphrases □ Polyalkylcyanoacrylate—toxicity of nanoparticles □ Nanoparticles—polyalkylcyanoacrylate toxicity □ Toxicity—polyalkylcyanoacrylate nanoparticles □ Drug carrier systems—nanoparticles, toxicity of polyalkylcyanoacrylate

Previous studies have demonstrated the interest of polyalkylcyanoacrylate nanoparticles as a drug carrier (1, 2). The main advantage of these particles is their degradability at a rate depending on the length of the alkyl chain (3). These ultrafine particles (diameter of ~0.2 μm) are able to efficiently adsorb a variety of drugs in a stable and reproducible way (4). It has been shown previously that the binding of cytostatic drugs to nanoparticles modifies their distribution pattern in rat tissues and generally increases the tissue capture of these drugs (5, 6).

Recently, preliminary results of experimental chemotherapy were published (7) using actinomycin D-loaded polymethylcyanoacrylate nanoparticles against the growth of a transplantable soft sarcoma tissue of the rat. The results indicated that the use of polymethylcyanoacrylate nanoparticles as a drug carrier increased the anticancer activity of actinomycin towards subcutaneous sarcoma. Furthermore, these particles could be of interest in the field of long-acting insulin therapy (8).

However, it was important to have information about the toxicity of the carrier to determine if these results did not prohibit the use of nanoparticles in human medicine. The present report describes preliminary results concerning the acute toxicity of nondrug-bound nanoparticles towards cells in culture and the determination of the LD_{50} of the carrier.

EXPERIMENTAL

Polyalkylcyanoacrylate Nanoparticles Preparation—Polymethyl-, polybutyl-, and polyisobutylcyanoacrylate nanoparticles were prepared following previous methods (1, 6), slightly modified. To an

0022-3549/82/0700-0786$01.00/0

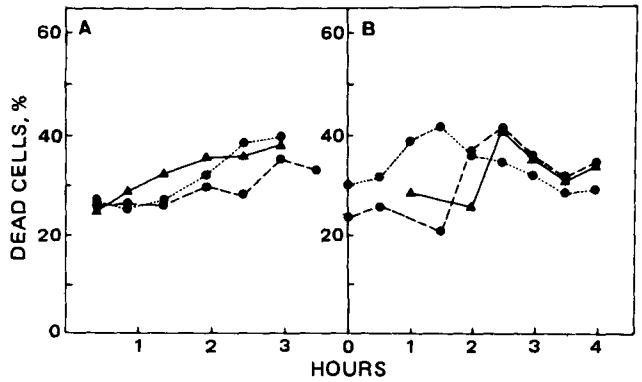

Figure 1—*Hepatocyte mortality after incubation with 0.5% of polybutylcyanoacrylate nanoparticles (- - - -) and 0.5% of nanoparticles polymerization medium (— • —) compared to controls (—). (A) Dye exclusion test (erythrosin B). (B) Lactic dehydrogenase leakage is expressed as a ratio of the lactic dehydrogenase activity in the medium compared to the total lactic dehydrogenase activity (medium and cells).*

aqueous solution (10 ml) of 0.01 *M* HCl containing 0.2% of a polysaccharide[1] and 0.8% of a polyoxyethylene–polyoxypropylene surfactant[2], butyl-[3], or isobutylcyanoacrylate[4] monomer (165 μl) was added under mechanical stirring. Polymethylcyanoacrylate nanoparticles were prepared in the same manner by adding the methylic monomer[3] (165 μl) to 10 ml of 0.01 *M* HCl containing 0.5% of polysorbate 20. After polymerization (at least 2 hr), each nanoparticle suspension was buffered at pH 7 using 100 μl of a molar solution of NaOH and 900 μl of a phosphate buffer[5]; NaCl (83 mg) was then added. No filtration was carried out before using, except in the case of the LD_{50} assays, where nanoparticles were filtered through a sintered glass filter (pore size 9–15 μm).

Scanning electron microscopy[6] showed mostly spherical particles with a diameter of ~0.2 μm for the polymethylcyanoacrylate preparations and of ~0.4 μm for the polyisobutyl- and polybutylcyanoacrylate preparations.

Cell Toxicity Procedures Using Placebo Nanoparticles—Hepatocytes were isolated using an *in situ* enzymatic perfusion method in the rat liver (9). Isolated cells were then incubated at 37° in a Waymouth medium supplemented with 10% newborn calf serum (10). Polybutylcyanoacrylate nanoparticles or their polymerization milieu were then added to obtain final concentrations of 0.5 and 1%, which corresponded,

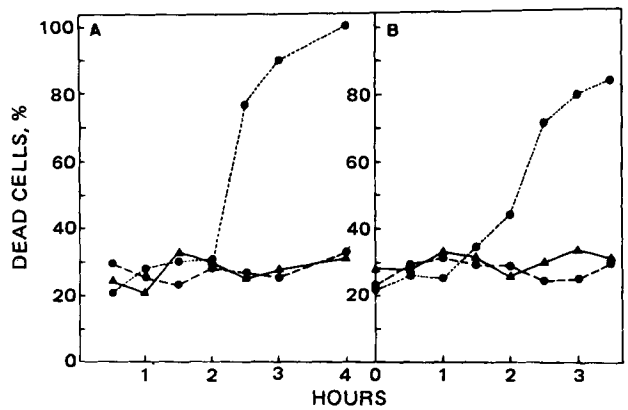

Figure 2—*Hepatocyte mortality after incubation with 1% of polybutylcyanoacrylate nanoparticles (- - - -) and 1% of nanoparticles polymerization medium (— • —) compared to controls (—). (A) Dye exclusion test (erythrosin B). (B) Lactic dehydrogenase leakage is expressed as a ratio of the lactic dehydrogenase activity in the medium compared to the total lactic dehydrogenase activity (medium and cells).*

[1] Dextran 70, Fison Laboratories, S.K.-RIT, Belgium.
[2] Pluronic L 63 Marles-Kuhlmann-Wyandotte, Paris, France.
[3] Loctite, Dublin, Ireland.
[4] Bucrylat Ethicon GmbH, Norderstedt, Germany.
[5] Phosphate buffer pH 7, USP XIX.
[6] Scanning Electron Microscope, Mini S.E.M. International Scientific Instruments, München, West Germany.

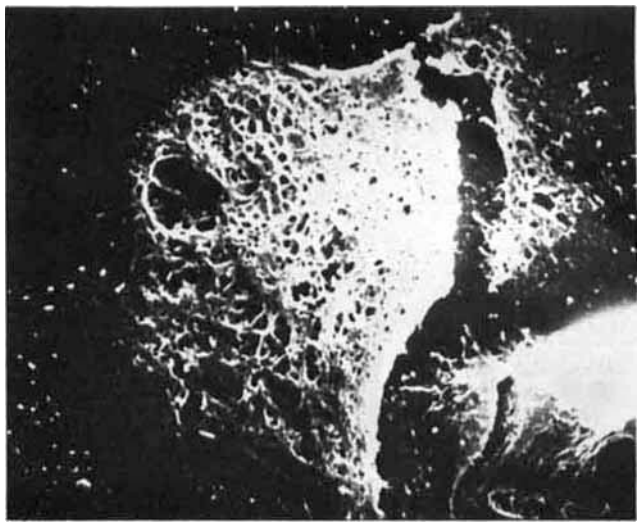

Figure 3—*Scanning electron microscopic appearance of a mouse peritoneal macrophage incubated 1 hr with polymethylcyanoacrylate nanoparticles at a concentration of 1% in the culture medium. The cell membrane appears to be completely perforated.*

respectively, to 7.5 and 15 mg of nanoparticles in 100 ml of the incubation medium, assuming the density of the polymer was equal to one.

Membrane integrity of the incubated cells was regularly controlled using both the 0.36% erythrosin B exclusion test and the leakage of lactic dehydrogenase, a cytosolic enzyme.

Macrophages were obtained after washing the peritoneal cavity of C 57 black mice three times with a medium[7] containing 0.1 mg/ml of streptomycin and 0.06 mg/ml of penicillin G. The liquid was incubated in plastic petri dishes containing a small glass coverslip. After 2 hr of incubation, the nonadhering cells were washed off with phosphate buffer solution, and the remaining macrophages were then further incubated at 37° in the culture medium[7] (containing 20% calf serum) in a 10% CO_2/90% air atmosphere incubator[8]. Nanoparticles were then added at a concentration of 1% in the culture medium. After 1 hr of incubation, nonadhering nanoparticles were washed off with phosphate buffer solution medium. Fresh medium was added to wash the macrophage monolayer culture. The macrophages were then fixed in glutaraldehyde (2.5% by volume in 0.1 *M* cacodylate buffer, pH 7.4) for 15 min at 37°, washed three times with cacodylate buffer, treated 1 hr at 4° with OsO_4 (1% w/v in 0.17 *M*

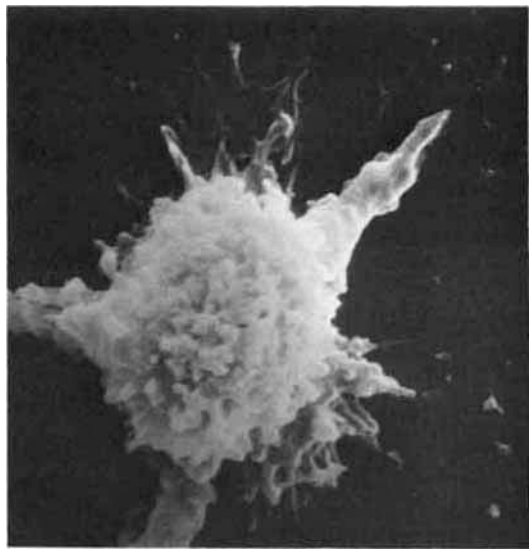

Figure 4—*Scanning electron microscopic appearance of a mouse peritoneal macrophage incubated 1 hr with polyisobutylcyanoacrylate nanoparticles at a concentration of 1% in the culture medium. The macrophage seems to be normal.*

[7] Eagle Dulbecco.
[8] Automatic CO_2 Controller type 3171, Forma Scientific, Marietta, Ohio.

Table I—Bacterial Toxicity Test

Salmonella typhimurium Strains	Bacterial Survival[a] × 10^7/Plate						
		Methyl Product,			Butyl Product,		
	Controls	150 μg	300 μg	1500 μg	150 μg	300 μg	1500 μg
TA 1530	129	116	112	3	150	140	135
TA 1535	101	84	74	0	111	75	67
TA 1538	90	105	70	0	107	78	68
TA 100	91	81	65	5	109	73	69
TA 98	83	77	68	3	104	73	72

[a] Number of survivals after incubation of the strains with polymethyl- and polybutylcyanoacrylate nanoparticles on nutrient agar plates.

Table II—Ames Mutagenicity Test with Nanoparticles Without Metabolic Activation

Salmonella typhimurium Strains	Histidine Revertants[a]/Plate						
		Methyl Product,			Butyl Product,		
	Spontaneous	30 μg	60 μg	150 μg	30 μg	60 μg	150 μg
TA 1530	23	19	13	19	17	17	12
TA 1535	6	10	9	12	9	14	12
TA 1538	25	14	37	15	17	9	16
TA 100	122	171	151	127	113	158	160
TA 98	44	10	14	22	23	24	23

[a] Number of revertants after incubation of the strains with polymethyl- and polybutylcyanoacrylate nanoparticles.

Table III—Ames Mutagenicity Test Involving Metabolic Activation with Nanoparticles

Salmonella typhimurium Strains	Histidine Revertants[a]/Plate						
		Methyl Product,			Butyl Product,		
	Spontaneous	15 μg	30 μg	150 μg	15 μg	30 μg	150 μg
TA 1530	9	8	9	5	5	11	9
TA 1535	11	7	8	10	7	9	11
TA 1538	15	8	11	8	9	11	9
TA 100	180	125	135	123	149	174	169
TA 98	14	12	13	10	13		19

[a] Number of revertants after metabolic activation and incubation with polymethyl- and polybutylcyanoacrylate nanoparticles.

Table IV—Ames Mutagenicity Test with the Degradation Products of Nanoparticles Without Metabolic Activation

Salmonella typhimurium Strains	Histidine Revertants[a]/Plate						
		Methyl Product,			Butyl Product,		
	Spontaneous	15 μg	30 μg	150 μg	15 μg	30 μg	150 μg
TA 1530	14	22	14	16	17	17	20
TA 1535	15	10	7	12	11	12	11
TA 1538	13	12	7	8	9	5	20
TA 100	145	122	137	131	168	141	138
TA 98	13	24	22	16	10	19	28

[a] Number of revertants after incubation of the strains with polymethyl- and polybutylcyanoacrylate nanoparticle degradation products.

barbital acetate buffer, pH 7.4) and washed with barbital acetate buffer.

Finally, the macrophages were washed five times with double distilled water, frozen in liquid nitrogen, and dried by lyophilization for 3 hr. The glass coverslips with the dried macrophages were then attached to metal disks and coated with a thin film of gold in a vacuum evaporator[9]. The specimens were then stored at room temperature until examination under a scanning electron microscope.

Mutagenicity Tests—Mutagenicity tests were performed on polybutyl- and polymethylcyanoacrylate nanoparticles using the *Salmonella typhimurium* method (11). This test was performed with and without metabolic activation[10] on both intact and degraded nanoparticles. A preliminary toxicity test was carried out to determine the maximum noninhibitory doses of nanoparticles.

Determination of Nanoparticle Histotoxicity—A total of 14 male mice[11] (20 g) were injected subcutaneously with 0.2 ml of a polyisobutylcyanoacrylate suspension containing 3 mg of nanoparticles. After 24 hr, six mice were sacrificed under carbon dioxide atmosphere, the skin was turned inside out and macroscopically examined according to a previously described method (12).

Three days later, the remaining animals were rechallenged with the same dose of nanoparticles and were divided into two groups of four mice. The first group was sacrificed 48 hr after the second injection, while the second group received a third injection and was sacrificed 2 days later. All these mice were treated as mentioned previously. Control mice, which received no injection, were treated in the same manner.

Determination of Nanoparticle LD_{50}—Six groups of 10 male NMRI mice (20 g) were treated with nanoparticles by injection in the tail vein. Each group received one of the following doses in a single injection, respectively: 12.5, 17.5, 22.5, 27.5, 32.5, and 40 ml/kg of polybutyl- or polyisobutylcyanoacrylate nanoparticles suspension. Both suspensions contained 9.2 mg of nanoparticles/ml. The same volumes of the polymerization milieu were injected into different groups of mice and the LD_{50} of this milieu was then determined.

RESULTS AND DISCUSSION

Toxicity of Polybutylcyanoacrylate Nanoparticles on Isolated Hepatocytes—At a concentration of 0.5% in the culture medium, neither polybutylcyanoacrylate nanoparticles nor nanoparticle polymerization medium modified the cellular integrity of the hepatocytes; in fact the lactic dehydrogenase leakage and the dye exclusion capacity of the cells remained comparable to the untreated hepatocytes (Fig. 1). In the case of the 1% final concentration, the polybutylcyanoacrylate nanoparticles greatly affected the integrity of the hepatocytes; the polymerization medium, on the other hand, exerted no effect (Fig. 2).

A cytotoxic effect appeared between 0.5 and 1% and seemed to proceed

[9] P-S1 Diode Sputter Coater, International Scientific Instruments, München, West Germany.

[10] Addition of cofactors supplemented liver "S_9" from Arochlor 1254 pretreated rats (11): 50 μl of "S_9" per plate.

[11] NMRI mice, Animal House of U.C.L., Louvain-en-Woluwe, Belgium.

Table V—Ames Mutagenicity Test Involving Metabolic Activation with the Degradation Products of Nanoparticles

Salmonella typhimurium Strains	Histidine Revertants[a]/Plate						
		Methyl Product,			Butyl Product,		
	Spontaneous	15 μg	30 μg	150 μg	15 μg	30 μg	150 μg
TA 1530	10	11	17	9	9	11	16
TA 1535	10	12	12	13	15	7	12
TA 1538	28	36		29	27		29
TA 100	178	137		120	170		133
TA 98	46	47	39	40	39	35	44

[a] Number of revertants after metabolic activation and incubation with polymethyl- and polybutylcyanoacrylate nanoparticle degradation products.

from the polymer itself rather than from the surfactants present in the nanoparticle polymerization medium. However, the 1% dose corresponded to a high ratio ($\sim 2 \times 10^4$) of particles per hepatocyte.

Scanning Electron Microscopy Studies with Macrophages—This microscopic study was performed to determine the exact morphological cell changes resulting from nanoparticle ingestion. Macrophages were used because of their high phagocytic capacity. It is known that toxicity of the polymer seems to be dependent on the biodegradation half-life which is prolonged with increasing alkylchain length (13). For this reason, it was decided to test polymethyl- and polyisobutylcyanoacrylate nanoparticles.

Scanning electron micrographs revealed marked morphological membrane modifications after incubation of the macrophages for 1 hr in the presence of polymethylcyanoacrylate nanoparticles at a 1% concentration in the culture medium (Fig. 3). The cell membrane appeared to be completely perforated. After incubation of the macrophages with polyisobutylcyanoacrylate nanoparticles under the same experimental conditions (1 hr at a concentration of 1%), no signs of toxicity were observed, and the morphological appearance of the macrophages under the scanning electron microscope seemed to be normal as compared with control (Fig. 4).

Mutagenicity Tests—Table I shows the bacterial survival of the *S. typhimurium* strains after incubation with nanoparticles on nutrient agar plates seeded with $2-7 \times 10^7$ viable cells. Polymethylcyanoacrylate induced an appreciable toxic effect when it was used at the dose of 1500 μg/plate. A slight inhibitory effect was observed with polybutyl- and polymethylcyanoacrylate nanoparticles at a concentration of 300 μg/plate. No toxicity was noted at the 150-μg dose. This dose was then considered the maximum noninhibitory level for the two types of polymer. The results of the Ames test, performed with different doses of nanoparticles and degradation products, are presented in Tables II–V. The assays were made either with or without metabolic activation. No mutagenic effect was observed using both nanoparticles and their degradation products. In all tests carried out, the number of induced revertants as compared with spontaneous revertants was not significantly increased. Furthermore, no dose–response effect was obtained. Although the Ames test was performed only with the polymethyl- and the polybutyl product, from the data obtained, it can be inferred that polyethyl- and polyisobutylcyanoacrylate nanoparticles are unlikely to be mutagenic. Indeed, in a mutagenic assay, the observed effect is closely dependent upon the chemical nature of the product tested, and polyalkylcyanoacrylates are very similar in their chemical structure.

In the Ames test, as in any mutagenicity assay, the observed mutations are related to only a very small part of the genome. Therefore, a negative result does not necessarily mean that the product under study is not mutagenic for humans (14); however, the Ames method is reliable in detecting carcinogens (15, 16). Moreover, cyanoacrylate polymers have been used in surgery for a long time, and until now, no carcinogenic action has been observed with these products (17, 18).

Nanoparticle Histotoxicity and LD_{50}—Twenty four hours after subcutaneous injection of 3 mg of polyisobutylcyanoacrylate nanoparticles, neither necrosis nor tissue irritation was visible. Furthermore, 48 hr after multiple treatments (2 or 3 injections) no hypersensitivity reaction nor granulomatous response was observed. Figure 5 shows the cumulative mortality of the mice after intravenous administration of different nanoparticle suspension volumes (milliliters per kilogram). Brought again to dry polymer weight per kilogram, the LD_{50} was determined to be 196 and 230 mg/kg for polyisobutylcyanoacrylate and polybutylcyanoacrylate nanoparticles, respectively. It should be noted, however, that the polymerization medium alone is not free of toxicity (LD_{50} = 33.4 ml/kg).

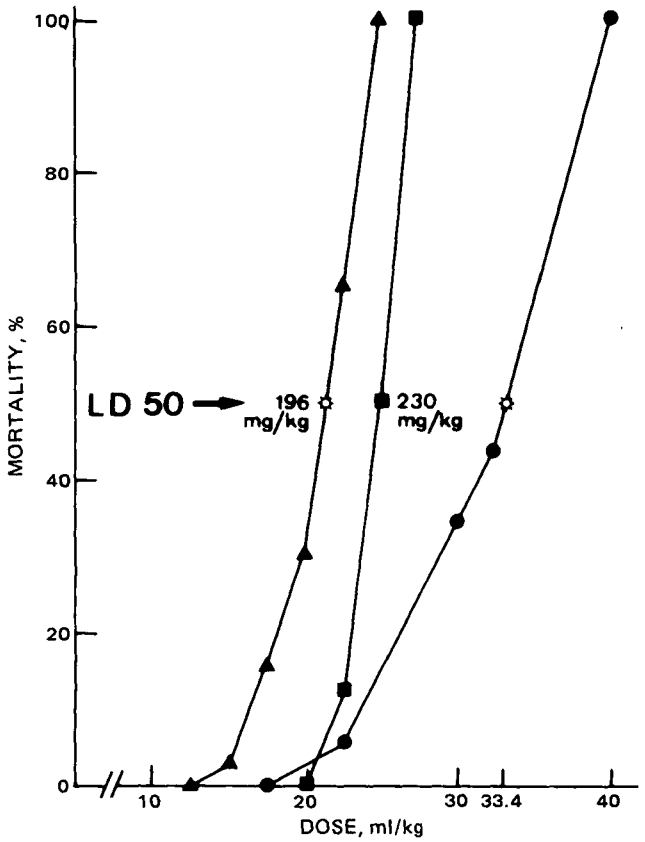

Figure 5—*Cumulative mortality of mice after intravenous administration of various nanoparticle suspension volumes. Key: (▲) polyisobutylcyanoacrylate nanoparticle; (■) polybutylcyanoacrylate nanoparticle; (●) nanoparticles polymerization medium.*

CONCLUSIONS

These first toxicological data obtained at the cellular and whole body animal levels did not demonstrate any acute toxicity susceptible to hinder the use of polyalkylcyanoacrylate nanoparticles in human medicine. Indeed, they induced cellular damage only at a relatively high concentration in the culture medium (1%). This toxicity is probably due to the presence of nanoparticle degradation products in the cytoplasm following their phagocytosis. This consideration could explain the lesser toxicity of the isobutyl product, which is more slowly biodegradable than the methyl derivative. Moreover, LD_{50} values are reasonable, and because of the presence of surfactants in the polymerization medium, it could be possible to reduce considerably the acute toxicity of the particles by washing off the surfactants and eventual remaining monomers. Finally, the absence of histotoxicity and mutagenicity for both nanoparticles and their degradation products are encouraging. These results will be completed by subacute and chronic toxicological studies and we will examine the possibility of decreasing the toxicity of an anticancer agent by its adsorption on polyisobutylcyanoacrylate nanoparticles.

REFERENCES

(1) P. Couvreur, B. Kante, M. Roland, P. Guiot, P. Baudhuin, and P. Speiser, *J. Pharm. Pharmacol.*, **31**, 331 (1979).

(2) P. Couvreur, B. Kante, and M. Roland, *Pharm. Acta Helv.*, **53**, 341 (1978).

(3) P. Couvreur, B. Kante, M. Roland, and P. Speiser, *J. Pharm. Sci.*, **68**, 1521 (1979).

(4) P. Couvreur, B. Kante, and M. Roland, *J. Pharm. Belg.*, **35**, 51 (1980).
(5) P. Couvreur, B. Kante, V. Lenaerts, V. Scailteur, M. Roland, and P. Speiser, *J. Pharm. Sci.*, **69**, 199 (1980).
(6) B. Kante, P. Couvreur, V. Lenaerts, P. Guiot, M. Roland, P. Baudhuin, and P. Speiser, *Int. J. Pharm.*, **7**, 45 (1980).
(7) F. Brasseur, P. Couvreur, B. Kante, L. Deckers-Passau, M. Roland, C. Deckers, and P. Speiser, *Eur. J. Cancer*, **16**, 1441 (1980).
(8) P. Couvreur, V. Lenaerts, B. Kante, M. Roland, and P. Speiser, *Acta Pharm. Technol.*, **26**, 220 (1980).
(9) G. Krack, O. Gravier, M. Roberfroid, and M. Mercier, *Biochim. Biophys. Acta*, **632**, 619 (1980).
(10) G. Krack, F. Goethals, D. Deboyser, and M. Roberfroid, *Toxicology*, **18**, 213 (1980).
(11) B. N. Ames, J. McCann, and E. Yamasaki, *Mutat. Res.*, **31**, 347 (1975).
(12) J. A. Rondelet and P. Froment, *Ann. Pharm. Franç.*, **27**, 63 (1968).
(13) R. M. Rice, A. F. Hegyeli, S. J. Gourlay, C. W. R. Wade, J. G. Dillon, H. Jaffe, and R. K. Kulkarni, *J. Biomed. Mat. Res.*, **12**, 43 (1978).
(14) B. N. Ames, W. E. Durston, E. Yamasaki, and F. D. Lee, *Proc. Nat. Acad. Sci. USA*, **70**, 2281 (1973).
(15) B. N. Ames, F. D. Lee, and W. E. Durston, *ibid*, **70**, 782 (1973).
(16) B. N. Ames, H. O. Kammen, and E. Yamasaki, *ibid.*, **72**, 3423 (1975).
(17) J. A. Collins, C. Pani, M. Seidenstein, G. Brandes, and F. Leonard, *Surgery*, **65**, 256 (1969).
(18) D. K. Ousterhout, W. T. Tumbusch, P. M. Margetis, and F. Leonard, *Br. J. Plast. Surg.*, **24**, 23 (1971).

ACKNOWLEDGMENTS

This work was supported by S.A. SOPAR Company (Belgium).
The authors thank Dr. D. N. Sainsbury (Loctite, Ireland) for the generous gift of the monomers. The assistance of Mrs. Duhamel and Mr. Pels was greatly appreciated.

Toxicity of Polyalkylcyanoacrylate Nanoparticles II: Doxorubicin-Loaded Nanoparticles

P. COUVREUR *x, B. KANTE *, L. GRISLAIN *, M. ROLAND *, and P. SPEISER ‡

Received May 21, 1981, from the * *Laboratoire de Pharmacie Galénique, Université Catholique de Louvain, 1200 Bruxelles, Belgium* and the ‡ *School of Pharmacy, Federal Institute of Technology, Zürich, Switzerland.* Accepted for publication October 7, 1981.

Abstract □ The possibility of significantly reducing toxicity of an anticancer drug such as doxorubicin by fixing it on polyisobutylcyanoacrylate nanoparticles was studied. It was shown that, when the drug was adsorbed on nanoparticles, significant reduction of both mortality and weight loss of mice were recorded under various administration schedules. Furthermore, cardiotoxicity was decreased due to the poor uptake by the myocardium.

Keyphrases □ Polyalkylcyanoacrylate—toxicity of doxorubicin-loaded nanoparticles □ Doxorubicin—toxicity of polyalkylcyanoacrylate nanoparticles □ Toxicity—doxorubicin-loaded polyalkylcyanoacrylate nanoparticles □ Drug carrier systems—toxicity of doxorubicin-loaded polyalkylcyanoacrylate nanoparticles

The first toxicological data concerning the polyalkylcyanoacrylate nanoparticles did not demonstrate any distinct toxicity susceptible to hinder their use in human medicine (1). The aim of the present investigation was to reduce considerably the toxicity of an anticancer drug such as doxorubicin by fixing it on nanoparticles. The idea of using doxorubicin in association with a macromolecular carrier such as DNA, to minimize the detrimental effect of this anticancer drug on normal cells, has been previously investigated (2, 3).

Doxorubicin, an anthracycline antibiotic, has produced encouraging results in the treatment of neoplastic diseases (4). However, it is toxic, with its most severe side effects involving the heart (acute and chronic cardiomyopathy), bone marrow, and intestine (5, 6). For these reasons, and because doxorubicin is highly adsorbed on nanoparticles, this cytostatic drug was chosen as the experimental model.

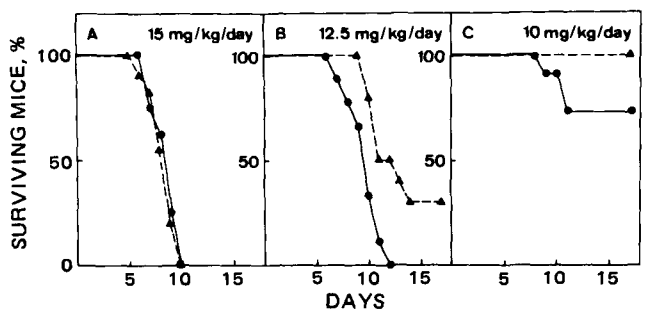

Figure 1—*Percent of surviving mice after intravenous administration on 3 consecutive days of various doses of free (●) and nanoparticle-bound doxorubicin (▲).*

EXPERIMENTAL

Polyalkylcyanoacrylate Nanoparticle Preparation—After dissolution of doxorubicin[1] (10 mg) in 10 ml of aqueous solution containing 100 mg of a polysaccharide[2], 50 mg of citric acid, and 1 mg of calcium chloride, 100 μl of isobutylcyanoacrylate monomer was dispersed under mechanical stirring.

After polymerization (3 hr), the resulting milky suspension was brought to isotonicity with 72 mg of sodium chloride. The size of the particles obtained was then estimated by measuring light scattering, arising from a laser source[3].

Measurement of Doxorubicin Linked to Nanoparticles—A 10-ml nanoparticle suspension was centrifuged[4] at 20,000 rpm for 1 hr. Sediment was then separated and dissolved in 10 ml of dioxane containing 20% water.

The content of doxorubicin was determined in both supernate and sediment by fluorimetric[5] dosage. For this purpose, 200-μl samples were diluted to 10 ml by water (for the supernate) or by dioxane (for the sediment) and measurements were performed using reference solutions of doxorubicin.

[1] Adriablastina, Montedison Farmaceutica Benelux, Bruxelles, Belgium.
[2] Dextran 70, Fison Laboratories, S.K.-RIT, Belgium.
[3] Nano-Sizer, Coulter Electronics, Harpenden, England.
[4] Beckman Centrifuge, model J-21C, Beckman Instruments, Palo Alto, Calif.
[5] Vitatron Fluorimeter, type U.F.D., Vitatron, Holland.

0022-3549/82/0700-0790$01.00/0

(4) P. Couvreur, B. Kante, and M. Roland, *J. Pharm. Belg.*, **35**, 51 (1980).
(5) P. Couvreur, B. Kante, V. Lenaerts, V. Scailteur, M. Roland, and P. Speiser, *J. Pharm. Sci.*, **69**, 199 (1980).
(6) B. Kante, P. Couvreur, V. Lenaerts, P. Guiot, M. Roland, P. Baudhuin, and P. Speiser, *Int. J. Pharm.*, **7**, 45 (1980).
(7) F. Brasseur, P. Couvreur, B. Kante, L. Deckers-Passau, M. Roland, C. Deckers, and P. Speiser, *Eur. J. Cancer*, **16**, 1441 (1980).
(8) P. Couvreur, V. Lenaerts, B. Kante, M. Roland, and P. Speiser, *Acta Pharm. Technol.*, **26**, 220 (1980).
(9) G. Krack, O. Gravier, M. Roberfroid, and M. Mercier, *Biochim. Biophys. Acta*, **632**, 619 (1980).
(10) G. Krack, F. Goethals, D. Deboyser, and M. Roberfroid, *Toxicology*, **18**, 213 (1980).
(11) B. N. Ames, J. McCann, and E. Yamasaki, *Mutat. Res.*, **31**, 347 (1975).
(12) J. A. Rondelet and P. Froment, *Ann. Pharm. Franç.*, **27**, 63 (1968).
(13) R. M. Rice, A. F. Hegyeli, S. J. Gourlay, C. W. R. Wade, J. G. Dillon, H. Jaffe, and R. K. Kulkarni, *J. Biomed. Mat. Res.*, **12**, 43 (1978).
(14) B. N. Ames, W. E. Durston, E. Yamasaki, and F. D. Lee, *Proc. Nat. Acad. Sci. USA*, **70**, 2281 (1973).
(15) B. N. Ames, F. D. Lee, and W. E. Durston, *ibid*, **70**, 782 (1973).
(16) B. N. Ames, H. O. Kammen, and E. Yamasaki, *ibid.*, **72**, 3423 (1975).
(17) J. A. Collins, C. Pani, M. Seidenstein, G. Brandes, and F. Leonard, *Surgery*, **65**, 256 (1969).
(18) D. K. Ousterhout, W. T. Tumbusch, P. M. Margetis, and F. Leonard, *Br. J. Plast. Surg.*, **24**, 23 (1971).

ACKNOWLEDGMENTS

This work was supported by S.A. SOPAR Company (Belgium).
The authors thank Dr. D. N. Sainsbury (Loctite, Ireland) for the generous gift of the monomers. The assistance of Mrs. Duhamel and Mr. Pels was greatly appreciated.

Toxicity of Polyalkylcyanoacrylate Nanoparticles II: Doxorubicin-Loaded Nanoparticles

P. COUVREUR *x, B. KANTE *, L. GRISLAIN *, M. ROLAND *, and P. SPEISER ‡

Received May 21, 1981, from the * *Laboratoire de Pharmacie Galénique, Université Catholique de Louvain, 1200 Bruxelles, Belgium* and the ‡ *School of Pharmacy, Federal Institute of Technology, Zürich, Switzerland.* Accepted for publication October 7, 1981.

Abstract □ The possibility of significantly reducing toxicity of an anticancer drug such as doxorubicin by fixing it on polyisobutylcyanoacrylate nanoparticles was studied. It was shown that, when the drug was adsorbed on nanoparticles, significant reduction of both mortality and weight loss of mice were recorded under various administration schedules. Furthermore, cardiotoxicity was decreased due to the poor uptake by the myocardium.

Keyphrases □ Polyalkylcyanoacrylate—toxicity of doxorubicin-loaded nanoparticles □ Doxorubicin—toxicity of polyalkylcyanoacrylate nanoparticles □ Toxicity—doxorubicin-loaded polyalkylcyanoacrylate nanoparticles □ Drug carrier systems—toxicity of doxorubicin-loaded polyalkylcyanoacrylate nanoparticles

The first toxicological data concerning the polyalkylcyanoacrylate nanoparticles did not demonstrate any distinct toxicity susceptible to hinder their use in human medicine (1). The aim of the present investigation was to reduce considerably the toxicity of an anticancer drug such as doxorubicin by fixing it on nanoparticles. The idea of using doxorubicin in association with a macromolecular carrier such as DNA, to minimize the detrimental effect of this anticancer drug on normal cells, has been previously investigated (2, 3).

Doxorubicin, an anthracycline antibiotic, has produced encouraging results in the treatment of neoplastic diseases (4). However, it is toxic, with its most severe side effects involving the heart (acute and chronic cardiomyopathy), bone marrow, and intestine (5, 6). For these reasons, and because doxorubicin is highly adsorbed on nanoparticles, this cytostatic drug was chosen as the experimental model.

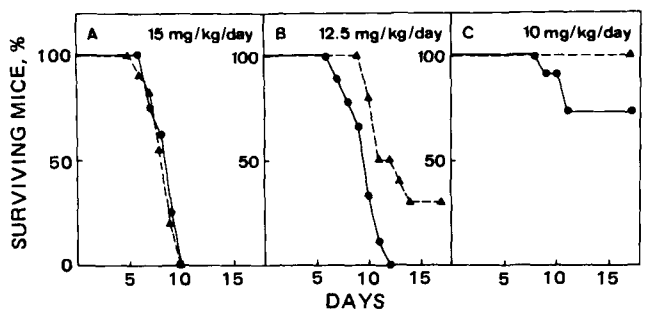

Figure 1—*Percent of surviving mice after intravenous administration on 3 consecutive days of various doses of free (●) and nanoparticle-bound doxorubicin (▲).*

EXPERIMENTAL

Polyalkylcyanoacrylate Nanoparticle Preparation—After dissolution of doxorubicin[1] (10 mg) in 10 ml of aqueous solution containing 100 mg of a polysaccharide[2], 50 mg of citric acid, and 1 mg of calcium chloride, 100 μl of isobutylcyanoacrylate monomer was dispersed under mechanical stirring.

After polymerization (3 hr), the resulting milky suspension was brought to isotonicity with 72 mg of sodium chloride. The size of the particles obtained was then estimated by measuring light scattering, arising from a laser source[3].

Measurement of Doxorubicin Linked to Nanoparticles—A 10-ml nanoparticle suspension was centrifuged[4] at 20,000 rpm for 1 hr. Sediment was then separated and dissolved in 10 ml of dioxane containing 20% water.

The content of doxorubicin was determined in both supernate and sediment by fluorimetric[5] dosage. For this purpose, 200-μl samples were diluted to 10 ml by water (for the supernate) or by dioxane (for the sediment) and measurements were performed using reference solutions of doxorubicin.

[1] Adriablastina, Montedison Farmaceutica Benelux, Bruxelles, Belgium.
[2] Dextran 70, Fison Laboratories, S.K.-RIT, Belgium.
[3] Nano-Sizer, Coulter Electronics, Harpenden, England.
[4] Beckman Centrifuge, model J-21C, Beckman Instruments, Palo Alto, Calif.
[5] Vitatron Fluorimeter, type U.F.D., Vitatron, Holland.

0022-3549/82/0700-0790$01.00/0

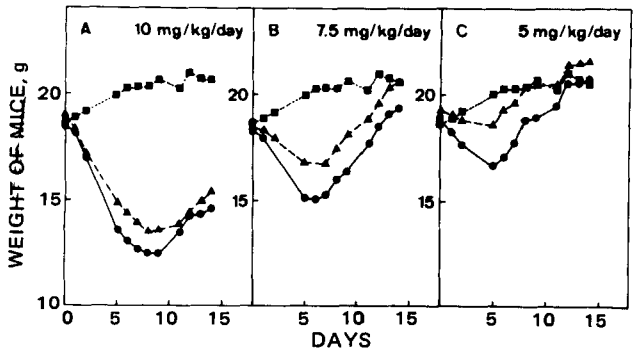

Figure 2—*Comparative loss of weight of the mice after intravenous administration on 3 consecutive days of various doses of free (●) and nanoparticle-bound doxorubicin (▲); (■) represents the weight of control mice.*

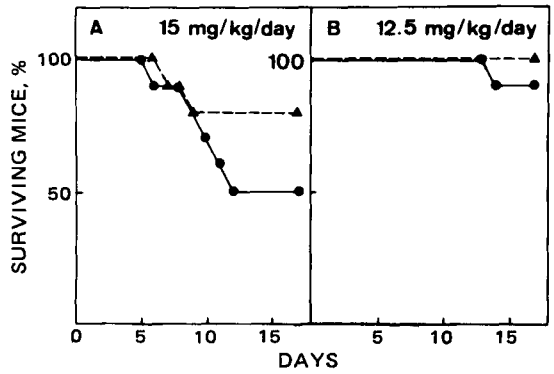

Figure 3—*Percent of surviving mice after intravenous administration on 2 consecutive days of various doses of free (●) and nanoparticle-bound doxorubicin (▲).*

Toxicity Studies—Toxicity of free and nanoparticle bound doxorubicin was determined using female mice[6]. Bound and free drug were given intravenously using various dosages for 5, 3, or 2 consecutive days of administration. During 5 consecutive days, 3, 4, 5, 6, and 8 mg/kg were given; 5, 7.5, 10, 12.5, and 15 mg/kg were given during 3 consecutive days; and 12.5 and 15 mg/kg during 2 consecutive days, respectively.

If the density of the polymer was assumed to be one, the cumulative dose of injected nanoparticles varied between 150 and 450 mg/kg of body weight.

An average of at least 10 mice were used per drug form in each dose series. The lethality was recorded 30 days after administration of the drug, and the weight of the mice was controlled daily.

Tape Sectioning Technique—After ether anesthesia, mice were killed by immersion in liquid nitrogen and embedded in a solution of carboxymethylcellulose. Sagittal sections measuring between 15 and 40

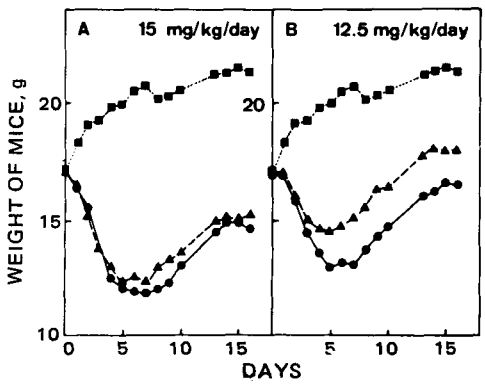

Figure 4—*Comparative loss of weight of the mice after intravenous administration on 2 consecutive days of various doses of free (●) and nanoparticle-bound doxorubicin (▲); (■) represents the weight of control mice.*

[6] NMRI mice, Animal House K.U.L., Heverlee, Belgium.

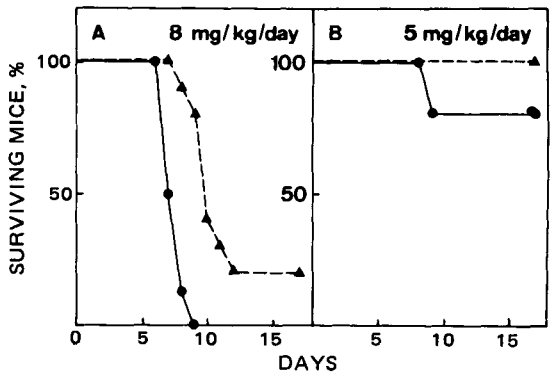

Figure 5—*Percent of surviving mice after intravenous administration on 5 consecutive days of various doses of free (●) and nanoparticle-bound doxorubicin (▲).*

μm were cut through the animals according to a previously described technique of tape-sectioning (7).

Fluorescence Technique—After drying, the sections were examined with an optic microscope[7] under UV light. A yellow filter[8] was used for the examination of doxorubicin fluorescence. Registration on film was taken on a daylight color film[9]. The exposure times were automatically determined using a photoelectric cell incorporated in the camera[10].

RESULTS AND DISCUSSION

The fluorimetric dosage showed that 94% of the doxorubicin employed was fixed by the nanoparticles. That corresponded to 94 mg of drug/g of polymer (confirmed by preliminary, unpublished data obtained by HPLC dosage).

Figure 1 shows the mortality, 15 days after injection, of either free or bound doxorubicin at doses of 15, 12.5, and 10 mg/kg/day. No mortality was recorded when free or bound doxorubicin was given at a dose less than or equal to 7.5 mg/kg/day. Except for a dose of 15 mg/kg/day, which appeared highly toxic in both forms tested (confirming that doxorubicin fixed to nanoparticles remained active), the mortality noted for nanoparticle-treated groups was always less than that recorded for the free drug injected groups. For example, after 12 days at the 12.5-mg/kg/day dose, a 100% mortality rate was observed in the free doxorubicin group, as compared to the 50% mortality rate in the nanoparticle-injected group (Fig. 1B).

These results were completed by controlling the weight of the treated animals (Fig. 2). At the doses of 10, 7.5, and 5 mg/kg/day, the loss of weight in the free doxorubicin group was significantly higher than that noted in the nanoparticles group ($p \geq 0.975$). At the dose of 5 mg/kg/day, the weight loss in the free doxorubicin group was twofold higher than for the groups injected with the bound drug (Fig. 2A). The mortality observed

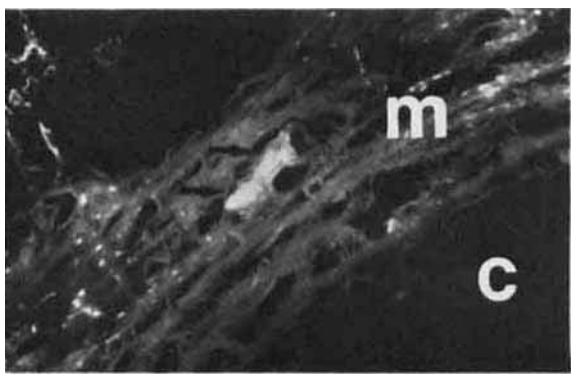

Figure 6—*Detail of a whole body fluorogram showing the heart of a mouse sacrificed 3 hr after the last of three injections of 10 mg/kg of free doxorubicin. There is a high accumulation of doxorubicin in the muscular fibers of the heart (→) (m = muscular myocardic fibers; c = myocardic cavity).*

[7] Fluorescent Microscope, Model Dialux 20, Leitz, Wetzlar, Germany.
[8] I_2 513-418, Leitz, Wetzlar, Germany.
[9] Kodak 400 ASA, Brussel, Belgium.
[10] Leitz Vario Orthomat System, Leitz, Wetzlar, Germany.

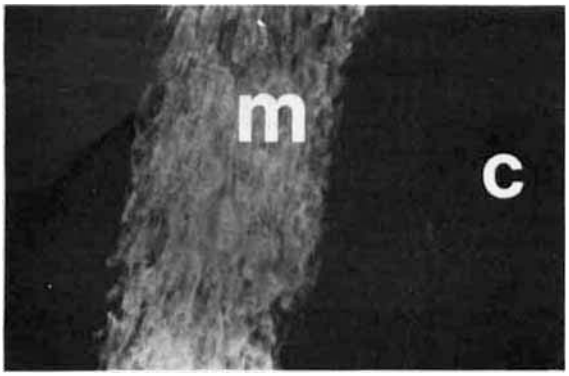

Figure 7—*Whole body fluorogram showing the heart of a mouse sacrificed 3 hr after the last of three injections of 10 mg/kg of doxorubicin bound to nanoparticles. In comparison with Fig. 6, no fluorescence appears in the myocardium (m = muscular myocardic fibers; c = myocardic cavity).*

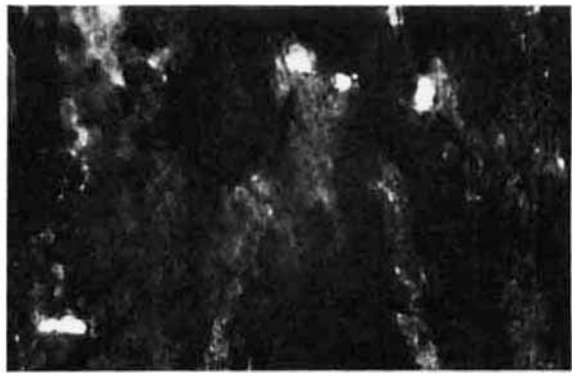

Figure 8—*Detail of whole body fluorogram of a mouse sacrificed 3 hr after the last of three injections of 10 mg/kg of doxorubicin bound to nanoparticles. Inversely to Fig. 6, fluorescence is retained in the lung (→).*

was primarily related to the intestinal toxicity of doxorubicin; the same mechanism was also responsible for the observed weight loss.

Therefore, at a dose of 10 mg/kg/day, the weight difference between mice treated with free doxorubicin and those treated with the bound drug was likely to be underestimated (Fig. 2C). No dead mice were recorded in the latter group, whereas significant mortality was noted in the former group. Dead mice were deleted from the weight loss charts.

When the administration schedules of both free and bound doxorubicin were limited to two successive injections of 12.5 and 15 mg/kg/day similar results were obtained. When the drug was linked to nanoparticles, significant differences in both mortality (Fig. 3) and weight loss (Fig. 4) were again observed. However, at the dose of 15 mg/kg/day, the weight loss difference (Fig. 3B) between the two experimental groups was underestimated for the same reasons mentioned previously.

Figure 5 shows the variance in time of the survival rate of the animals after five consecutive injections of 5 and 8 mg/kg/day of both free and bound doxorubicin, respectively. Three hours after the last of three daily injections of 10 mg/kg of body weight of both free and bound doxorubicin, mice were killed and sectioned. After drying, the sections were examined under a fluorescent microscope to determine which organs presented an orange-red fluorescence due to the presence of doxorubicin. Because a side effect of doxorubicin involved the heart, the investigations concentrated on the cardiac tissue. Figure 6 shows a high amount of cytostatic behavior in the cardiac muscle when free drug was injected into the animal. By contrast, no fluorescence was found in the myocardium after administration of the same dose of doxorubicin bound to the nanoparticles (Fig. 7). Examination of other organs confirmed the high uptake capacity of the nanoparticle adsorbed doxorubicin by the lung (Fig. 8) and liver, while the free drug seemed to show less fluorescence in these tissues. It appears that nanoparticle bound doxorubicin has a preferential distribution for organs such as the liver and lung, with significantly less distribution in the heart.

CONCLUSIONS

These results show a significant decrease of doxorubicin's toxicity when fixed to nanoparticles. This decrease corresponds to both a diminution in weight loss and to a higher survival rate in mice after administration of bound doxorubicin for various doses and administration schedules. In addition, the absence of doxorubicin fluorescence in the cardiac muscle when the drug was adsorbed on the nanoparticles can be of interest, considering the important cardiotoxicity of the drug. However, these observations were made on a limited number of animals and should be completed with a larger number of specimens injected under various administration schedules, dose, and time before sacrifice. It should be noted that the use of polyalkylcyanoacrylate nanoparticles as the drug carrier can reduce considerably the inherent toxicity and side effects of a cytotoxic drug and could be useful in cancer chemotherapy.

REFERENCES

(1) B. Kante, P. Couvreur, P. Guiot, G. Dubois-Crack, M. Roland, M. Mercier, and P. Speiser, *J. Pharm. Sci.*, **71**, 786 (1982).

(2) A. Trouet, D. Deprez-De Campeneere, M. De Smedt-Malengreaux, and G. Atassi, *Eur. J. Cancer*, **10**, 405 (1974).

(3) A. Trouet, D. Deprez-De Campeneere, and C. De Duve, *Nature New Biol.*, **239**, 110 (1972).

(4) J. Bernard, M. Weil, and C. Jacquillat, *Ann. Rev. Med.*, **25**, 39 (1974).

(5) D. Von Hoff, M. Rozencweig, M. Layard, M. Slavik, and F. Muggia, *Am. J. Med.*, **62**, 200 (1977).

(6) E. Lefrak, J. Pitha, S. Rosenheim, and J. Gottlieb, *Cancer*, **32**, 203 (1973).

(7) S. Ullberg, *Acta Radiol. Suppl.*, **118**, 1 (1954).

ACKNOWLEDGMENTS

This work was supported by S. A. SOPAR Company and by IRSIA (Institut pour l'Encouragement de la Recherche Scientifique dans l'Industrie et l'Agriculture).

The authors thank Professor Trouet, Dr. Tulkens and Dr. Deprez-De Campeneere for helpful discussions and valuable comments. The authors also thank Dr. D. N. Sainsbury (Loctite, Ireland) for the generous gift of the monomers. The excellent technical assistance of Mr. Bulckens and Mrs. Duhamel was greatly appreciated.

Theorems on the Apparent Volume of Distribution of a Linear System

D. P. VAUGHAN

Received April 10, 1981, from the *Department of Pharmaceutics, Faculty of Pharmaceutical Sciences, Sunderland Polytechnic, Sunderland, Tyne and Wear SR1 3SD, U.K.* Accepted for publication October 8, 1981.

Abstract □ If the concentration of drug in one compartment of a linear N-compartment system, without sinks and loss only from the sampled compartment is sampled, then the total apparent volume of distribution can be determined without knowledge of the topology of the system. This apparent volume is identical to the apparent volume of the corresponding closed system.

Keyphrases □ Volume of distribution—apparent, theorems of a linear system □ Linear system—theorems on the apparent volume of distribution □ Theorems—apparent volume of distribution of a linear system

Oppenheimer and others have derived a noncompartmental drug distribution volume (1). This volume is the ratio of the first statistical moment of the blood drug concentration–time function observed after a unit intravenous drug dose to the integral of the function on $(0,\infty)$. Benet and Galeazzi have re-presented Oppenheimer's derivation (2). In both these texts the derivation is not strictly analytical and relies mainly on unsubstantiated statements. However, this expression for a distribution volume has previously been derived, for an N-compartmental system, in a strict analytical fashion by Bright (3).

Bright's derivation is based on the following assumptions:

(*a*) irreversible drug loss from the compartmental system occurs only from the sampled compartment;

(*b*) the eigenvalues of the coefficient matrix are all real and distinct;

(*c*) if Compartment j is connected to Compartment i (i and $j \in 1,2,\ldots N, i \neq j$) by a rate constant, $k_{ji} > 0$, then compartment i is connected to compartment j by a rate constant $k_{ij} > 0$;

(*d*) $k_{ij} = k_{ji}$.

Conditions *c* and *d* define the coefficient matrix of the N-compartmental system as a symmetric matrix which directly implies condition *b*. Conditions *b* and *c*, but not necessarily condition *d*, are obviously realizable for mammillary and caternary compartmental systems (4, 5). However, condition *b* specifically excludes any compartmental system whose matrix has repeated real eigenvalues or has pairs of complex conjugate eigenvalues. Condition *c* excludes systems with nonreversible cycles involving three or more compartments, regardless of the validity of condition *b*.

Compartment systems, that are based on physiological considerations and include specific compartments for the arterial and venous blood, must contain nonreversible drug circulation cycles involving three or more compartments. Consequently, previous derivations (3) are not applicable to such systems.

In the present report, a relationship between the volume of distribution of a compartmental system and the first moment of the sampled function is derived. This derivation does not require conditions on the eigenvalues of the system, the topology of the system, or the intercompartmental rate constants.

THEORY

Consider an arbitrary set of N interconnected compartments in which it is possible for material in Compartment j to reach all other Compartments $i, i \neq j$. Such a system of compartments does not contain any sinks, disjointed sets of compartments, or subsystems (6). For such a system:

$$\begin{pmatrix} \dot{X}_1 \\ \dot{X}_2 \\ \dot{X}_3 \\ \vdots \\ \dot{X}_n \end{pmatrix} = \begin{pmatrix} -E_1 & k_{21} & k_{31} & \cdots & k_{N1} \\ k_{12} & -E_2 & k_{32} & & k_{N2} \\ k_{13} & k_{23} & -E_3 & & k_{N3} \\ \vdots & \vdots & \vdots & & \vdots \\ k_{1N} & k_{2N} & k_{3N} & & k_{N4} \end{pmatrix} \begin{pmatrix} X_1 \\ X_2 \\ X_3 \\ X_4 \end{pmatrix} \equiv \dot{\boldsymbol{X}} = \boldsymbol{AX} \quad \text{(Eq. 1)}$$

where $X_j (j \in 1,2,\ldots N)$ is the amount of drug in compartment j, and $\dot{X}_j$ is the first derivative with respect to time of X_j. Intercompartmental rate constants, k_{ji} and k_{ij}, are for drug transport from Compartment j to Compartment i and from Compartment i to Compartment j, respectively (j and $i \in 1,2,\ldots N, i \neq j$). Both k_{ij} and k_{ji} are ≥ 0. If a particular k_{ij} is zero, the status of k_{ji} cannot be inferred.

The E_j's are defined as:

$$E_j = k_{jo} + \sum_{\substack{i=1 \\ j \neq i}}^{N} k_{ji} \qquad (j \in 1,2,\ldots N) \quad \text{(Eq. 2)}$$

where $k_{jo} (k_{jo} \geq 0)$ is the rate constant for irreversible drug loss from the system *via* Compartment j.

The coefficient matrix $\boldsymbol{A}$ is a dominant diagonal matrix and, since the compartmental system does not contain any sinks or disjointed subsystems, matrix $\boldsymbol{A}$ cannot be reduced to a matrix of the form:

$$\begin{pmatrix} \boldsymbol{P} & \boldsymbol{O} \\ \boldsymbol{U} & \boldsymbol{Q} \end{pmatrix}$$

by some permutation of the rows and columns where $\boldsymbol{P}$ and $\boldsymbol{Q}$ are square matrixes and $\boldsymbol{O}$ consists of zero elements. These row column permutations are equivalent to a renumbering of the compartmental system (6).

Matrix $\boldsymbol{A}$ is irreducible and theorems have been given (7) for irreducible dominant diagonal matrixes of the form specified by matrix $\boldsymbol{A}$; thus, the determinant of matrix $\boldsymbol{A}$ is bound by $|\boldsymbol{A}| \neq 0$ if at least one $k_{jo} \geq 0$, and $|\boldsymbol{A}| = 0$ if all the $k_{jo} = 0$ for $j \in 1,2,\ldots N$.

A special form of matrix $\boldsymbol{A}$ is one in which only one k_{jo} is greater than zero. Considering such a system, and without loss of generality, let $k_{10} > 0$ and $k_{jo} = 0 (j \in 2,3,\ldots N)$. In this case:

$$|\boldsymbol{A}| = -\left(k_{10} + \sum_{j=2}^{N} k_{1j}\right) |\boldsymbol{M}_{11}| + \sum_{j=2}^{N} (-1)^{(j-1)} k_{j1} |\boldsymbol{M}_{1j}| \neq 0 \quad \text{(Eq. 3)}$$

where $\boldsymbol{M}_{11}$ is the principle minor of matrix $\boldsymbol{A}$ obtained by deleting Row 1 and Column 1, and the $\boldsymbol{M}_{1j}$'s are the minors of $\boldsymbol{A}$ obtained by deleting Row 1 and Column $j (j \in 2,3,\ldots N)$.

The minors, $\boldsymbol{M}_{11}$ and $\boldsymbol{M}_{1j}$ are independent of k_{10}. By setting $k_{10} = 0$ in Eq. 3 and utilizing Taussky's theorem, it follows that:

$$-\sum_{j=2}^{N} k_{1j} |\boldsymbol{M}_{11}| + \sum_{j=2}^{N} (-1)^{(j-1)} k_{j1} |\boldsymbol{M}_{1j}| = 0$$

consequently, Eq. 3 becomes:

$$|\boldsymbol{A}| = -k_{10} |\boldsymbol{M}_{11}| \quad \text{(Eq. 4)}$$

Volume of Distribution—Consider a closed irreducible compart-

0022-3549/82/0700-0793$01.00/0

mental system (*i.e.*, $k_{jo} = 0$ for all $j, j\epsilon 1,2,\ldots N$) with a unit drug impulse input, δD, into a particular compartment. Assume the drug concentration–time function, $\hat{C}(t)$, in Compartment 1 is observed. Since the system is closed, the amount of drug in the compartmental system at any time t is D. Also, since the system is irreducible and closed, the system will eventually achieve a state of drug concentration equilibrium. Consequently, the equilibrium drug concentration, $\hat{C}(\infty)$, in Compartment 1 is governed by $\hat{C}(\infty) > 0$. The volume of distribution of the closed system, V, may be defined as the scalar that maps the equilibrium concentration in the sampled compartment to the known amount of drug in the system, where $V = D/\hat{C}(\infty)$.

If the equilibrium concentration in all compartments of the closed system were identical, then V would define the exact volume of the system. However, since the latter condition cannot be assumed to hold for an arbitrarily closed compartmental system, the derived volume must be regarded as an apparent distribution volume. In general, $\hat{C}(\infty)$ will not be constant for all observation points. Consequently, the numerical value of V depends on which particular compartment is sampled.

The apparent volume of an open irreducible compartmental system is the same as the corresponding closed system. When the topology and intercompartmental rate constants of an open system are known, the distribution volume can be calculated readily. However, an analytical method for calculating V, which does not require specified topology or intercompartmental rate constants, would be useful since the calculated V would be model independent.

Theorem 1—For an irreducible compartmental system with irreversible drug loss from one compartment only and sampling from the same compartment, the first moment, $\bar{t}$, of the sample concentration–time function, $C(t)$, after an impulse input, δD, into the sample compartment is related to the apparent volume of distribution, V, of the corresponding closed compartmental system by:

$$\frac{D\bar{t}}{\int_0^\infty C(t)dt} = V$$

where $\bar{t} = \int_0^\infty tC(t)dt / \int_0^\infty C(t)dt$.

Proof—To establish a proof, expressions for $\bar{t}/\int_0^\infty C(t)dt$ of an open compartmental system with sampling and loss from one compartment and the concentration at $t = \infty$ in the corresponding closed system, $\hat{C}(\infty)$, are required. These expressions are derived first and then used to establish the theorem.

Open System—For an impulse input, δD, into Compartment 1, the initial conditions are $X_1(+0) = D$ and $X_j(+0) = 0$ for $j\epsilon 2,3,\ldots N$. With these initial conditions, the Laplace transform $x_1(s)$ of $X_1(t)$ can be expressed by standard methods as:

$$x_1(s) = \frac{D|s\boldsymbol{I} - \boldsymbol{M}_{11}|}{|s\boldsymbol{I} - \boldsymbol{A}|} = \frac{D(s^{N-1} + a_1 s^{N-2} \ldots a_{N-2}s + (-1)^{N-1}|\boldsymbol{M}_{11}|)}{(s^N + b_1 s^{N-1} \ldots b_{N-1}s + (-1)^N|\boldsymbol{A}|)} \quad \text{(Eq. 5)}$$

where b_j and a_j are $(-1)^j$ times the sum of the determinants of all the j-squared principle minors of matrix $\boldsymbol{A}, j\epsilon 1,2,\ldots N-1$, and matrix $\boldsymbol{M}_{11}$, respectively.

Since $\boldsymbol{A}$ and $\boldsymbol{M}_{11}$ are matrixes with real elements, the coefficients a_j and b_j are real. Both $\boldsymbol{A}$ and $\boldsymbol{M}_{11}$ are dominant diagonal matrixes and by the application of Gerschgorins root location theorem (8) both $\boldsymbol{A}$ and $\boldsymbol{M}_{11}$ have eigenvalues with negative real parts. Consequently, the polynomials $|s\boldsymbol{I} - \boldsymbol{A}|$ and $|s\boldsymbol{I} - \boldsymbol{M}_{11}|$ have coefficients that are all of the same sign (9). Since the diagonal elements of $\boldsymbol{A}$ and $\boldsymbol{M}_{11}$ are negative, the coefficients a_1 and b_1 are positive, consequently, $a_j > 0$ and $b_j > 0$ for all $j(j\epsilon 1,2,\ldots N-1)$ and $(-1)^N|\boldsymbol{A}| > 0$ as is $(-1)^{N-1}|\boldsymbol{M}_{11}|$.

By standard Laplace transform theory:

$$-\frac{dx_1(s)}{ds} = \int_0^\infty tX_1(t)dt = \lim_{ts\to 0} \frac{D[b_{N-1}(-1)^{N-1}|\boldsymbol{M}_{11}| - a_{N-2}(-1)^N|\boldsymbol{A}|]}{|\boldsymbol{A}|^2} \quad \text{(Eq. 6)}$$

which on substitution of Eq. 4 into Eq. 6 gives:

$$\int_0^\infty tX_1(t)dt = \frac{D(b_{N-1} - a_{N-2}k_{10})}{(-1)^{N-1}|\boldsymbol{M}_{11}|(k_{10})^2} \quad \text{(Eq. 7)}$$

Also, by standard Laplace transform theory:

$$\lim_{ts\to 0} \frac{x_1(s)}{} = \int_0^\infty X_1(t)dt = \frac{(-1)^{N-1}|\boldsymbol{M}_{11}|D}{(-1)^N|\boldsymbol{A}|} \equiv \frac{D}{k_{10}} \quad \text{(Eq. 8)}$$

The latter identity in Eq. 8 follows from Eq. 4. The limits in Eqs. 6 and 8 are guaranteed by the fact that $X_j, j\epsilon 1,2,\ldots N$, are nonnegative bounded functions such that $X_j(\infty) = 0$(10). The $X_j(t)$ functions are nonnegative since the off diagonal elements of A are ≥ 0 (11), and $X_j(\infty) = 0$ because the eigenvalues of A have negative real parts. Combining Eqs. 7 and 8 and substituting $X_1(t) = V_1C(t)$, where V_1 is the volume of Compartment 1, then:

$$\frac{D\int_0^\infty C(t)dt}{\left(\int_0^\infty C(t)dt\right)^2} = \frac{(b_{N-1} - a_{N-2}k_{10})}{(-1)^{N-1}|\boldsymbol{M}_{11}|}V_1 \quad \text{(Eq. 9)}$$

Closed System—In the arbitrary open system, $k_{10} > 0$ and $k_{jo} = 0$ for $j\epsilon 2,\ldots N$; consequently, the corresponding closed system is obtained by setting $k_{10} = 0$ in $\boldsymbol{A}$. Let the closed system matrix be $\hat{\boldsymbol{A}}$ and let $\hat{\boldsymbol{M}}_{11}$ be the matrix obtained by deleting Row one and Column one from $\hat{\boldsymbol{A}}$; $\hat{\boldsymbol{M}}_{11} = \boldsymbol{M}_{11}$ and from Eq. 4, $|\hat{\boldsymbol{A}}| = 0$. Let $\hat{X}_1(t)$ represent the mass–time function of drug in Compartment 1 after an impulse input, δD, into Compartment 1.

By standard Laplace transform theory:

$$\lim_{ts\to 0} \frac{s\hat{x}_1(s)}{} = X_1(\infty) = \lim_{s\to 0} \frac{ts|s\boldsymbol{I} - \boldsymbol{M}_{11}|}{|s\boldsymbol{I} - \hat{\boldsymbol{A}}|} = \lim_{s\to 0} t\,\frac{Ds(s^{N-1} + a_1 s^{N-2} \ldots a_{N-2}s + (-1)^{N-1}|\boldsymbol{M}_{11}|}{(s^N + \hat{b}_1 s^{N-1} \ldots \hat{b}_{N-1}s + (-1)^N|\hat{\boldsymbol{A}}|)} = \frac{(-1)^{N-1}|\boldsymbol{M}_{11}|D}{\hat{b}_{N-1}} \quad \text{(Eq. 10)}$$

where $\hat{b}_j$ is $(-1)^j$ times the sum of the determinants of all the j-squared principle minors of $\hat{\boldsymbol{A}}$.

Since the volume of distribution, V, is defined by $V = D/\hat{C}(\infty)$, and $V_1\hat{C}(\infty) = \hat{X}_1(\infty)$, then from Eq. 10:

$$V = \frac{\hat{b}_{N-1}}{(-1)^{N-1}|\boldsymbol{M}_{11}|}V_1 \quad \text{(Eq. 11)}$$

The equivalence of Eqs. 9 and 11 is necessary and sufficient for Theorem 1 to hold. Consequently, if:

$$\hat{b}_{N-1} = (b_{N-1} - a_{N-2}k_{10}) \quad \text{(Eq. 12)}$$

then Theorem 1 is established. The latter identity, Eq. 12, can be proved as follows: The coefficients b_{N-1}, $\hat{b}_{N-1}$, and a_{N-2} are given as:

$$b_{N-1} = (-1)^{N-1}\sum_{j=1}^{N}|\hat{\boldsymbol{M}}_{jj}|$$

$$\hat{b}_{N-1} = (-1)^{N-1}\sum_{j=1}^{N}|\hat{\boldsymbol{M}}_{jj}| \quad \text{(Eq. 13)}$$

$$a_{N-2} = (-1)^{N-2}\sum_{j=1}^{N-1}|\hat{\boldsymbol{M}}_{jj}| \quad \text{(Eq. 14)}$$

where M_{jj} and $\hat{M}_{jj}$ are the $(N-1)$ squared principle minors of the N-squared matrixes $\boldsymbol{A}$ and $\hat{\boldsymbol{A}}$, respectively, and the $\overline{M}_{jj}$'s are the $(N-2)$ squared principle minors of the $(N-1)$ squared matrix $\boldsymbol{M}_{11}$. The coefficient b_{N-1} can be expressed as:

$$b_{N-1} = (-1)^{N-1}\left[|\boldsymbol{M}_{11}| + \sum_{j=1}^{N-1}|\boldsymbol{P}_j|\right] \quad \text{(Eq. 15)}$$

where:

$$|\boldsymbol{P}_j| = \begin{vmatrix} -E_1 & \boldsymbol{r}_{j+1} \\ \boldsymbol{c}_{j+1} & \hat{\boldsymbol{M}}_{jj} \end{vmatrix}$$

and where $\boldsymbol{r}_{j+1}(j\epsilon 1,2,\ldots N-1)$ is the row of $N-2$ elements obtained from $(k_{21},k_{31},\ldots k_{N1})$ by striking out the element $k_{j+1,1}$ and $\boldsymbol{c}_{j+1}$ is the column of $N-2$ elements obtained from $(k_{12},k_{13},\ldots k_{1N})^T$ by striking out the element $k_{1,j+1}$. Expanding the determinants $|\boldsymbol{P}_j|(j\epsilon 1,2,\ldots N-1)$ by their first rows, then:

$$b_{N-1} = (-1)^{N-1}\left[|\boldsymbol{M}_{11}| - \left(k_{10} + \sum_{i=2}^{N}k_{1i}\right)\sum_{j=1}^{N-1}|\overline{\boldsymbol{M}}_{jj}| + \sum_{j=1}^{N-1}|Z_j|\right] \quad \text{(Eq. 16)}$$

where $|Z_j|$ is the summation of determinants associated with the expansion of $|\boldsymbol{P}_j|$ along $\boldsymbol{r}_{j+1}$. Since the elimination constant k_{10} does not occur in any $\boldsymbol{r}_{j+1}$ or any $\overline{\boldsymbol{M}}_{jj}$, the determinants $|Z_j|$ are independent of k_{10}. Since $\boldsymbol{M}_{11}$ is also independent of k_{10}, then $\hat{b}_{N-1}$ is directly obtainable from b_{N-1} by setting $k_{10} = 0$ in Eq. 16, thus:

$$\delta_{N-1} = (-1)^{N-1}\left[|\boldsymbol{M}_{11}| - \left[\sum_{i=2}^{N} k_{1i}\right]\sum_{j=1}^{N-1}|\overline{\boldsymbol{M}}_{jj}| + \sum_{j=1}^{N-1}|Z_j|\right] \quad \text{(Eq. 17)}$$

Substitution of Eqs. 16 and 17 into Eq. 12 establishes the identity expressed in Eq. 12 and thus complete the proof of Theorem 1.

Theorem 2—For a known nonnegative and finite drug input function, $\mathrm{In}(t)$, into Compartment 1 of an open irreducible compartmental system, with sample and loss from Compartment 1 only, the volume of distribution of the corresponding closed system, V, is given by:

$$V \equiv \frac{\int_0^\infty tC(t)dt}{\left(\int_0^\infty C(t)dt\right)^2} = \left[\frac{\int_0^\infty t\overline{R}(t)dt}{\int_0^\infty \overline{R}(t)dt} - \frac{\int_0^\infty t\mathrm{In}(t)dt}{\int_0^\infty \mathrm{In}(t)dt}\right]\frac{\int_0^\infty \mathrm{In}(t)dt}{\int_0^\infty \overline{R}(t)dt} \quad \text{(Eq. 18)}$$

where $\overline{R}(t)$ is the observed drug concentration–time function produced by the input function $\mathrm{In}(t)$, and $C(t)$ is the concentration–time function produced by a unit impulse input into Compartment 1. Both $\overline{R}(t)$ and $C(t)$ are observed in Compartment 1.

Proof—By application of standard linear system theory the mass of drug, $R(t)$, in Compartment 1 is:

$$R(t) = \int_0^t \mathrm{In}(\tau)X_1(t-\tau)d\tau \quad \text{(Eq. 19)}$$

where $X_1(t)$ is the mass–time function in Compartment 1 that would result from a unit impulse input into Compartment 1.

By the standard Laplace transform theory:

$$\int_0^\infty tR(t)dt = \frac{dR(s)}{ds} = \operatorname*{Lim}_{ts\to 0} \operatorname*{Lim}_{s\to 0} t\left[-\frac{d\mathrm{In}(s)}{ds}x_1(s) - \frac{dx_1(s)}{ds}\mathrm{In}(s)\right] \quad \text{(Eq. 20)}$$

Since $\mathrm{In}(t)$ is a nonnegative function with $\mathrm{In}(\infty) = 0$ the limit of $\mathrm{In}(s)$ as $s \to 0$ is $\int_0^\infty \mathrm{In}(t)dt$ and the limit of $-d\mathrm{In}(s)/ds$ as $s \to 0$ is $\int_0^\infty t\,\mathrm{In}(t)dt$. Also, since $X_1(t)$ is nonnegative and integrable on $(0,\infty)$ the limit of $x_1(s)$ as $s \to 0$ is $\int_0^\infty X_1(t)dt$, and the limit of $-dx_1(s)/ds$ is $\int_0^\infty tX_1(t)dt$. Applying a known theorem on the limits of products of Laplace transforms (10):

$$\int_0^\infty tR(t)dt = \int_0^\infty t\mathrm{In}(t)dt\int_0^\infty X_1(t)dt + \int_0^\infty tX_1(t)dt\int_0^\infty \mathrm{In}(t)dt \quad \text{(Eq. 21)}$$

Also, applying the known theorem on limits (10) to Eq. 19:

$$\int_0^\infty R(t)dt = \int_0^\infty \mathrm{In}(t)dt\int_0^\infty X_1(t)dt \quad \text{(Eq. 22)}$$

An expression for $\int_0^\infty tX_1(t)dt/\int_0^\infty X_1(t)dt$ is obtainable by a rearranging Eq. 21 and dividing by Eq. 22, which on dividing by $\int_0^\infty X_1(t)dt$ and utilizing Eq. 22 gives:

$$\frac{\int_0^\infty tX_1(t)dt}{\left(\int_0^\infty X_1(t)\right)^2} = \left(\frac{\int_0^\infty tR(t)dt}{\int_0^\infty R(t)dt} - \frac{\int_0^\infty t\mathrm{In}(t)dt}{\int_0^\infty \mathrm{In}(t)dt}\right)\frac{\int_0^\infty \mathrm{In}(t)dt}{\int_0^\infty R(t)dt} \quad \text{(Eq. 23)}$$

Substituting $V_1C(t) = X_1(t)$ and $V_1\overline{R}(t) = R(t)$ into Eq. 23 gives Eq. 18 and completes the proof of Theorem 2.

DISCUSSION

Theorems 1 and 2 state model-independent methods for calculating a drug distribution volume. The expressions are model independent in the sense that no knowledge of the topology of the compartmental system is required. Since no constraints on the topology are applied, then no constraints on either the eigenvalues of the coefficient matrix or on intercompartmental rate constants are applied. Additionally, it is not necessary to specify some functional form (*e.g.*, a summation of exponentials) to apply the equations. However, it is assumed in the derivation that irreversible drug loss from the system occurs only from the sampled compartment. The proofs of Theorems 1 and 2 are strictly analytical and have the advantage of being mainly algebraic. No concepts of clearance or equilibrium elimination are required.

The derived volume is clearly related to the apparent volume of the corresponding closed system.

Although the terms compartments are used in the derivation, their use should not be interpreted literally as circumscribable regions of space where physical translocation of matter takes place. The term is merely a convenience. Matrix $\boldsymbol{A}$ is simply an operator for a stable linear system, and the conditions of nonnegative off-diagonal elements in $\boldsymbol{A}$ are necessary if observations in the system are to be nonnegative functions. Also, the negative diagonal elements are necessary for stability. Consequently, the derivation could have followed equally well the line of considering a stable linear system which would also have yielded Eq. 1 but where the elements of Matrix $\boldsymbol{A}$ would have no meaning in relation to compartmental analysis. These latter concepts have been discussed previously (11).

To apply Theorem 1, it is not necessary to assume any functional form to describe the $C(t)$ data. The numerical values of the required integrals can be obtained by standard numerical methods (2). For Theorem 2, it is necessary to know the functional form of the input function. For example, the input function may be a step input of magnitude k and of duration τ. In this case $\int_0^\infty \mathrm{In}(t)dt = k\tau$ and $\int_0^\infty t\ \mathrm{In}(t)\ dt = k\tau^2/2$. The numerical values of the other integrals in Theorem 2 are obtainable by standard numerical methods.

REFERENCES

(1) J. H. Oppenheimer, H. L. Schwartz, and M. I. Surks, *J. Endocrinol. Metab.*, **41**, 319 (1975).

(2) L. Z. Benet, and M. Galeazzi, *J. Pharm. Sci.*, **68**, 1071 (1979).

(3) P. B. Bright, *Bull. Math. Biol.*, **35**, 69 (1973).

(4) J. Z. Hearon, *Bull. Math. Biophys.*, **15**, 121 (1953).

(5) D. P. Vaughan, and M. Dennis, *J. Pharmacokinet. Biopharm.*, **7**, 511 (1979).

(6) C. D. Thron, *Bull. Math. Biophys.*, **34**, 277 (1972).

(7) O. Taussky, *Am. Math. Monthly.*, **56**, 672 (1949).

(8) S. Gerschgorin, *Izv. Akad. Nauk. SSSR. Ser. Fiz-Mat*, **6**, 749 (1931).

(9) A. M. Krall, "Stability Techniques for Continuous Linear Systems," Chap. 5, Thomas Nelson & Sons, London, 1968.

(10) D. P. Vaughan, *J. Pharmacokinet. Biopharm.*, **5**, 271 (1977).

(11) R. Bellman, "Introduction to Matrix Analysis," Chap. 13, McGraw-Hill, New York, N.Y., 1960.

Synthesis and Hypoglycemic Activity of Benzamidophenyl-alkanoic Acid Derivates: New Inhibitors of Gluconeogenesis

ERICH RAPP and HORST P. O. WOLF ˣ

Received July 21, 1981, from the *Research Laboratories of Byk Gulden Lomberg Pharmaceuticals, D-7750 Konstanz, Federal Republic of Germany.* Accepted for publication October 13, 1981.

Abstract: □ A series of ω-[2-(*N*-alkylbenzamido)-phenyl]-alkanoic acids was synthesized and tested for its effects on blood glucose concentration in fasted rats and on gluconeogenesis from lactate and pyruvate in isolated perfused rat livers. The compounds led to a dose-dependent and reversible inhibition of gluconeogenesis, with 4-[2-(*N*-methyl-3-trifluoromethylbenzamido)-phenyl]-butanoic acid leading to a 50% inhibition at 0.02 m*M*. The compounds lowered blood glucose in fasted rats. No correlation between hypoglycemic effect and inhibition of gluconeogenesis could be detected, however.

Keyphrases □ Benzamidophenyl-alkanoic acid—derivatives, synthesis, hypoglycemic activity □ Gluconeogenesis—inhibited by synthesized benzamidophenyl-alkanoic acid derivatives □ Hypoglycemic activity—benzamidophenyl-alkanoic acid derivatives, new inhibitors of gluconeogenesis

Numerous substances have been reported to lower blood glucose levels by inhibiting gluconeogenesis in mammalian liver; various sites of inhibition have been discussed (1). So far, only biguanides have been used as therapeutic agents in the treatment of diabetes.

Recently, clanobutin [4-[4-chloro-*N*-(4-methoxyphenyl)-benzamido]butanoic acid, (I)[1]] (2) was found to be an inhibitor of gluconeogenesis from the precursors lactate and pyruvate (3). This led to the synthesis of a series of structurally related compounds in order to find more potent inhibitors of gluconeogenesis as potential hypoglycemic drugs.

In variation of structure I, the alkanoic acid chain was attached to the aromatic ring *ortho* to the amide nitrogen, which was kept substituted with a methyl or ethyl group. Chain length and substitution pattern were modified (Table I).

EXPERIMENTAL

Chemistry—*3-[2-(N-Methyl-4-chlorobenzamido)-phenyl]propionic Acid (IIb)*—*N*-Methyldihydrocarbostyril (III*b*) 4.84 g (30 mmoles) and 5.6 g (100 mmoles) of potassium hydroxide were dissolved in 20 ml of ethylene glycol monoethyl ether. While stirring, the mixture was refluxed for 3 hr. After cooling to room temperature, the solution was diluted with 200 ml of water and extracted with two portions of ether. The pH of the aqueous phase was brought to 8–8.5 by addition of 2 *N* HCl. A solution of 5.25 g (30 mmoles) of 4-chlorobenzoylchloride (IV*b*) in 50 ml of ether was added slowly, while the pH of the aqueous phase was held at 7.5–8.5 with 1 *N* NaOH. The aqueous layer was separated and washed with ether twice. The resulting acid was precipitated with 2 *N* HCl, washed with water, and dried. Recrystallization from ethyl acetate yielded 6.2 g of II*b*, mp 156–158° (66%). Compounds II*d*, *e*, *g*, *h*, *k*, and *m–u* were synthesized by the same procedure.

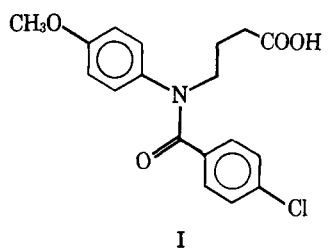

I

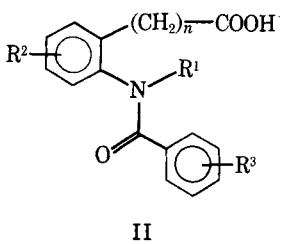

II

4-[2-(N-Methylbenzamido)phenyl]butanoic Acid (IIh)—2-Aza-2-methyl-benzo[*c*]-cycloheptanone (III*h*) [14.0 g (80 mmoles)], 17.9 g (320 mmoles) of potassium hydroxide, and 50 ml of ethylene glycol monoethyl ether were brought together in a glass pressure vessel and heated to 150° for 6 hr. After cooling to room temperature, the contents were diluted with 200 ml of water and adjusted to pH 9 with glacial acetic acid. After stirring 33.6 g (400 mmoles) of sodium bicarbonate into this solution, 11.8 g (80 mmoles) of benzoyl chloride in 20 ml of ether was added dropwise within 2 hr. Dilution with 800 ml of water was followed by extraction with ether. The aqueous phase was acidified with 2 *N* HCl and extracted three times with ethylene chloride. The organic fractions were collected and concentrated; the residue was recrystallized from ethyl acetate–petroleum ether (1:1) to give 19.6 g of II*h*, mp 102–103° (80%). Compounds II*a*, *b*, *c*, *f*, *i*, *j*, and *l* were prepared according to this method.

6-[2-(N-Methyl-3-trifluoromethylbenzamido)-phenyl]caproic Acid (IIu)—Oxalyl chloride [13.0 g (102 mmoles)] and one drop of dimethyl formamide were given to 12.5 g (34 mmoles) of 4-[2-(*N*-methyl-3-trifluoromethylbenzamido)-phenyl]butanoic acid (III*l*) in 40 ml of toluene. The mixture was stirred for 1.5 hr and then evaporated *in vacuo*. The residue was taken up in 50 ml of dry dioxane and added dropwise to 1.32 g (35 mmoles) of sodium borohydride in 20 ml of dioxane. The mixture was heated to 100° for 4 hr, then cooled to room temperature. Acidifying with 2 *N* HCl and dilution with 20 ml of water was followed by extraction of the product with two portions of ether. Evaporation left an oily residue (10.9 g), which was dissolved in 20 ml of pyridine and 10 ml of toluene and added to a solution of 11.8 g (61.7 mmoles) of *p*-toluenesulfonyl chloride in 40 ml of toluene; stirring at 40° was continued for 20 hr. After filtration, the solution was first washed with 2 *N* HCl and saturated sodium chloride solution, then dried and concentrated *in vacuo*. The tosylate was obtained as a viscous oil, was dissolved in 40 ml of ethanol, and added dropwise to a solution of 2.6 g (14.3 mmoles) of sodium diethyl malonate in 30 ml of ethanol. Refluxing for 24 hr was followed by removing ethanol. The residue, after extractive workup, yielded 4.1 g of a light brown oil. This was treated with potassium hydroxide in methanol–toluene (1:1) at room temperature (stirring for 30 hr). Workup led to 2.0 g of the free substituted malonic acid, which was decarboxylated by heating to 160° for 2.5 hr. After recrystallization from ether, 0.8 g of II*u*, mp 103–104° (2%) was obtained.

Pharmacology—*Hypoglycemic Activity* —Groups of 6–12 male Sprague-Dawley rats[2] (160–200 g) were fasted overnight. Using an oral tube, the substances were administered as aqueous, neutral solutions (10 ml/kg of body weight), with control rats receiving the same volume of 0.9% NaCl. The dosage range was 0.36–1.67 mmoles/kg of body weight. Blood samples were obtained prior to and at 2, 4, and 6 hr after administration by puncturing the retroorbital plexus. Blood glucose was measured by standard enzymatic procedure[3]. The results were expressed as relative change in comparison to the control group on log-transformed intraindividual ratios of treatment *versus* pretreatment. An effective dose, ED_{50} (25%) ± *SD*, was calculated from dose–response relationships by linear or nonlinear regression techniques. An ED_{50} of 25% indicated that 50% of the group showed at least a 25% decrease of blood glucose compared with controls. Intergroup comparison of change due to treatment was performed by ANOVA and subsequent Scheffé-contrasts or pairwise Student-Welch tests (Table I).

[1] Byk Gulden Lomberg, Pharmaceuticals, D-7750 Konstanz, Federal Republic of Germany. Synthesis see (2).

[2] Ivanovas 50; Ivanovas, Kisslegg, West Germany.

[3] Hexokinase/glucose-6-phosphate dehydrogenase (HK/G6PDH method).

0022-3549/82/0700-0796$01.00/0

Table I—Structure of Title Compounds: Effect on Blood Glucose

	R^1	R^2	R^3	n	Yield, %	m.p.[b]	Molecular Formula	Decrease of Blood Glucose[c], %	Analysis			
IIa[a]	$-CH_3$	—H	—H	2	39	122–124	$C_{17}H_{17}NO_3$	12[d,f]	calc. C 72.07	H 6.05	N 4.94	
									found C 72.15	H 6.07	N 4.90	
IIb	$-CH_3$	—H	4-Cl	2	66	156–158	$C_{17}H_{16}ClNO_3$	11	calc. C 64.25	H 5.08	N 4.41	Cl 11.16
									found C 64.00	H 5.14	N 4.18	Cl 11.35
IIc	$-CH_3$	—H	3,4-Cl_2	2	31	149–150	$C_{17}H_{15}Cl_2NO_3$	10	calc. C 57.97	H 4.29	N 3.98	Cl 20.13
									found C 57.99	H 4.36	N 3.91	Cl 20.17
IId	$-CH_3$	5-Cl	3,4-Cl_2	2	47	159–161	$C_{17}H_{14}Cl_3NO_3$	15[d,e]	calc. C 52.81	H 3.65	N 3.62	Cl 27.51
									found C 53.01	H 3.74	N 3.58	Cl 27.61
IIe	$-CH_3$	5-Cl	3-CF_3	2	55	124–126	$C_{18}H_{15}ClF_3NO_3$	15[d]	calc. C 56.04	H 3.92	N 3.63	Cl 9.19
									found C 55.81	H 3.81	N 3.86	Cl 9.33
IIf	$-C_2H_5$	5-CH_3	3,4-Cl_2	2	22	141–143	$C_{19}H_{19}Cl_2NO_3$	13[d]	calc. C 60.00	H 5.04	N 3.68	Cl 18.65
									found C 60.08	H 5.14	N 3.79	Cl 18.64
IIg	$-CH_3$	—H	2-phenyl	3	30	154–155	$C_{24}H_{23}NO_3$	8	calc. C 77.19	H 6.21	N 3.75	
									found C 77.06	H 6.23	N 3.52	
IIh	$-CH_3$	—H	—H	3	80	102–103	$C_{18}H_{19}NO_3$	9[d]	calc. C 72.71	H 6.44	N 4.71	
									found C 72.85	H 6.44	N 4.61	
IIi	$-CH_3$	—H	4-Cl	3	51	123–124	$C_{18}H_{18}ClNO_3$	20[d,f]	calc. C 65.16	H 5.47	N 4.22	Cl 10.69
									found C 65.05	H 5.52	N 4.23	Cl 10.67
IIj	$-CH_3$	—H	3,4-Cl_2	3	61	120–121	$C_{18}H_{17}Cl_2NO_3$	19[d,f]	calc. C 59.03	H 4.68	N 3.82	Cl 19.36
									found C 59.09	H 4.58	N 3.81	Cl 19.58
IIk	$-CH_3$	—H	2,4-Cl_2	3	12	102–103	$C_{18}H_{17}Cl_2NO_3$	17[d,e]	calc. C 59.03	H 4.68	N 3.82	Cl 19.36
									found C 58.98	H 4.73	N 3.73	Cl 19.28
IIl	$-CH_3$	—H	3-CF_3	3	30	84–85	$C_{19}H_{18}F_3NO_3$	20[d,f]	calc. C 62.46	H 4.97	N 3.83	F 15.60
									found C 62.36	H 4.92	N 3.89	F 15.40
IIm	$-CH_3$	—H	2,6-Cl_2	3	20	161–163	$C_{18}H_{17}Cl_2NO_3$	3	calc. C 59.03	H 4.68	N 3.82	Cl 19.36
									found C 58.90	H 4.73	N 4.06	Cl 19.38
IIn	$-CH_3$	6-OCH_3	4-Cl	3	66	121–122	$C_{19}H_{20}ClNO_4$	14[d,e]	calc. C 63.07	H 5.57	N 3.87	Cl 9.80
									found C 62.84	H 5.65	N 3.84	Cl 9.81
IIo	$-CH_3$	4-OCH_3	4-Cl	3	31	107–108	$C_{19}H_{20}ClNO_4$	15[d,e]	calc. C 63.07	H 5.57	N 3.87	Cl 9.80
									found C 63.07	H 5.44	N 3.79	Cl 9.63
IIp	$-CH_3$	4-OCH_3	2,4-Cl_2	3	38	90–91	$C_{19}H_{19}Cl_2NO_4$	12[d,e]	calc. C 57.59	H 4.83	N 3.54	Cl 17.89
									found C 57.77	H 4.91	N 3.44	Cl 17.98
IIq	$-CH_3$	5-OCH_3	3,4-Cl_2	3	39	87–88	$C_{19}H_{19}Cl_2NO_4$	21[d,f]	calc. C 57.59	H 4.83	N 3.54	Cl 17.89
									found C 57.41	H 4.98	N 3.51	Cl 17.61
IIr	$-CH_3$	—H	4-Cl	4	44	117–118	$C_{19}H_{20}ClNO_3$	9[d]	calc. C 65.99	H 5.83	N 4.05	Cl 10.25
									found C 65.85	H 5.73	N 4.01	Cl 10.34
IIs	$-CH_3$	—H	3-CF_3	4	50	81–83	$C_{20}H_{20}F_3NO_3$	21[d,f]	calc. C 63.32	H 5.31	N 3.69	
									found C 63.44	H 5.06	N 3.84	
IIt	$-CH_3$	—H	3,4-Cl_2	4	30	86–87	$C_{19}H_{19}Cl_2NO_3$	5	calc. C 60.01	H 5.04	N 3.68	Cl 18.65
									found C 60.21	H 5.16	N 3.74	Cl 18.26
IIu	$-CH_3$	—H	3-CF_3	5	2	103–104	$C_{21}H_{22}F_3NO_3$	4	calc. C 64.11	H 5.64	N 3.56	
									found C 64.24	H 5.90	N 3.58	

[a] All reported compounds show NMR spectra in accordance with expected structures. [b] Melting points are not corrected. [c] Percent decrease of blood glucose compared with controls after oral administration of 0.06 mmole/kg; the values represent the maximum decrease within 6 hr after administration, 6 rats/group. [d] Statistical tests: ANOVA and subsequent Scheffé-contrasts or pairwise Student-Welch tests with $p < 0.05$, two-sided. [e] $p < 0.01$, two-sided. [f] $p < 0.001$, two-sided.

Liver Perfusion—The isolated livers of rats fasted overnight were perfused in a nonrecirculating system (4). Krebs-Henseleit bicarbonate buffer (pH 7.4), saturated with an oxygen–carbon dioxide mixture (95:5) and containing L(+)-lactate[4] (1.6 m*M*) and pyruvate[5] (0.2 m*M*), was used for perfusion. The livers were perfused for 2 hr; the test substances were infused from 32–80 min using three different, increasing concentrations at 16-min intervals.

Analytical Method and Determination of K_i—Samples of the liver perfusion effluent were collected at 1-min intervals and analyzed for glucose. For each experiment, the values observed at 32, 48, 64, 80, and 96 min were obtained by averaging five neighboring values. The slight linear decline found in control experiments was taken into account by using the values at 32 and 96 min as a basis for linear interpolation. The concentration producing a 50% decrease in glucose due to inhibition of gluconeogenesis (K_i) was calculated from these data by linear or log–linear correlation.

Acute Toxicity—Five female mice[6] (22–26 g) were used for every group. The animals received water *ad libitum;* food was reduced to 50 g/kg of body weight 18 hr prior to administration. The test compounds were administered orally. LD_{50} values were calculated according to a previous study (5).

Synthesis—The title compounds were synthesized as follows: According to the known procedures, benzolactams (III) with varying ring size were prepared from substituted anilines (*via* internal Friedel-Crafts alkylation) (6), tetralones, and benzosuberones (*via* Beckmann or Schmidt rearrangement) (7, 8); the resulting lactams were *N*-alkylated to III with dimethyl- or diethylsulfate either directly or by use of phase-transfer catalysis (9). Benzolactams (III) were then hydrolyzed by refluxing with potassium hydroxide in ethylene glycol monoethyl ether; in some cases, glass pressure vessels were used for even higher reaction temperatures. Acylation of the amino group with substituted benzoyl chlorides (IV) and acidic workup led to compounds IIa–*t*. One

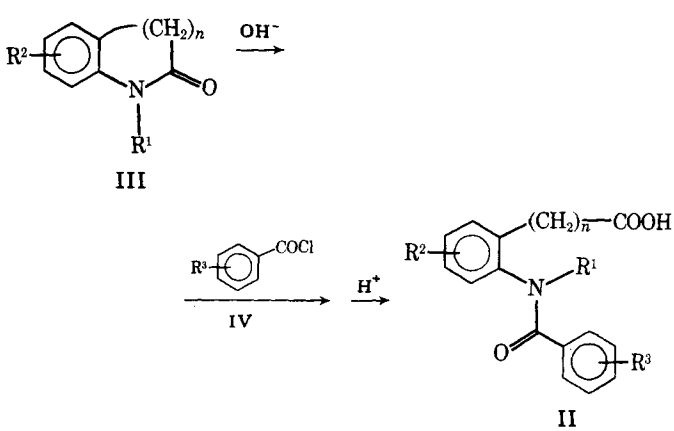

Scheme I

[4] K. Roth OHG, Karlsruhe, West Germany.
[5] Boehringer GmbH, Mannheim, West Germany.
[6] NMRI strain.

Table II—Biological Data and Toxicity

	Blood Glucose Decrease ED_{50} (25%) ± *SD* (*n*),[a] mmole/kg	Inhibition of Gluconeogenesis in Isolated Perfused Rat Liver, K_i ± *SD*, m*M*	Toxicity LD_{50} (oral) Mice, mmole/kg
II*a*	1.38 ± 0.13 (180)	0.68 ± 0.15	5.3
II*b*	>1.57 (29)	0.18	—
II*c*	>1.70 (60)	0.06	3.1
II*d*	not feasible (30)	0.03	—
II*e*	not feasible (60)	0.11	>2.6
II*f*	—	0.08	—
II*h*	1.51 ± 0.15 (180)	0.15 ± 0.05	>5.1
II*i*	0.99 ± 0.18 (180)	0.18 ± 0.03	3.9
II*j*	1.26 ± 0.17 (120)	0.05 ± 0.01	2.1
II*k*	1.66 ± 0.01 (60)	0.06	>2.7
II*l*	not feasible (60)	0.02	—
II*n*	not feasible	0.04	—
II*q*	not feasible	0.08	—
II*t*	not feasible	0.05	—
Buformin[a]	1.00 ± 0.40 (60)	>1.00	2.46

[a] *N* = number of animals tested. [b] 1-butylbiguanide hydrochloride.

further example, II*u*, was prepared by extension of the alkyl chain *via* malonic ester synthesis (Scheme I).

RESULTS AND DISCUSSION

Compounds II*a–u* were tested for their ability to lower blood glucose levels in fasted rats and to inhibit gluconeogenesis from lactate and pyruvate in the model isolated perfused liver of fasted rats.

The decrease of blood glucose after a single oral dose of 0.6 mmole/kg in overnight fasted rats was determined. Table I shows the maximum value within 6 hr after administration.

For a number of compounds, dose–response relationships were studied by calculating ED_{50} (25%) values from the corresponding data (dosage range 0.36–1.67 mmoles/kg). A dose–response relationship could not be found in all cases, *i.e.*, the ED_{50} value was not feasible (Table II).

The inhibition of gluconeogenesis from L(+)-lactate (1.6 m*M*) and pyruvate (0.2 m*M*) in the liver perfusion experiment is expressed by the inhibition constant K_i, *i.e.*, the concentration producing a 50% inhibition (Table II).

Acute toxicity data were determined for selected compounds (Table II).

The *in vivo* glucose lowering effects of the reported compounds were found to be in the same order of magnitude as the 1-butylbiguanide hydrochloride[7]. The butanoic acid derivatives (II*i* and *j*) showed the lowest ED_{50} (25%) values: 0.99 and 1.26 mmoles/kg.

Effective inhibitions of gluconeogenesis, however, were demonstrated by most members of the group, the best of which are II*d*, *j*, *l*, *n*, and *t* ($K_i \leq 0.05$ m*M*). Inhibition was fully reversible without delay upon terminating the infusion of the inhibitor substance. This coincides with results obtained on I (3). In comparison, 1-butylbiguanide hydrochloride fails to show a substantial effect upon gluconeogenesis in this model up to 1.0 m*M*.

Neither structure–activity relationships within the group II*a–u* nor any correlation between hypoglycemic activity and K_i values could be found.

Unsubstituted ω-phenylalkanoic acids have been reported to inhibit glucose synthesis from various precursors (10). 4-Phenylbutanoic acid effects a 60% inhibition at 4 m*M*. Structurally closely related to II are some 2-benzamidophenylacetic and -propionic acids, which were found to possess anti-inflammatory and analgesic activity (11).

Other inhibitors reported within the last 10 years include cyclopropanecarboxylic acid (12), phenelzine (13), tryptophan metabolites (14), 3-mercaptopicolinic acid (15), and aminopyrine (4), all effective in the range of 0.1–0.5 m*M*; 0.6 m*M* is reported for 2-bromooctanoate (16), 0.5–1.0 m*M* for pent-4-enoic acid (17), 2 m*M* for phenylpyruvate (18), and 5 m*M* for butylmalonate (19).

CONCLUSION

The data presented in Tables I and II indicate that some of the substituted ω-(2-benzamidophenyl)alkanoic acids of type II lower the blood glucose level *in vivo* significantly, while a larger group of compounds inhibit gluconeogenesis *in vitro*. Although no obvious correlation seems to exist between the two groups, a few substituted butanoic acids are effective in both models, especially II*j*, which, in addition to interesting ED_{50} and K_i values, possesses the lowest toxicity of the compounds measured. The inhibition constants of II*d*, *l*, and *n*, relatively nontoxic substances, belong to the lowest K_i values reported.

REFERENCES

(1) K. Klemm, W. Krastinat, and U. Krüger, *Drug Res.*, **29(I)** 1 (1979).

(2) M. S. A. Sherratt and L. Hue, *Biochem. Soc. Trans.*, **7**, 99 (1979).

(3) H. P. O. Wolf, J. Schlepper, V. Steinijans, and R. Scholz, *Biochem. Pharmacol.*, **29**, 1649 (1980).

(4) R. Scholz, W. Hansen, and R. G. Thurman, *Eur. J. Biochem.*, **38**, 64 (1973).

(5) J. T. Lichtfield, Jr. and F. W. Wilcoxon, *J. Pharmacol. Exp. Ther.*, **96**, 99 (1949).

(6) F. Mayer, L. van Zütphen, and H. Philipps, *Chem. Ber.*, **60**, 858 (1927).

(7) F. Möller in "Methoden der Organ. Chemie," E. Müller, Ed., Thieme-Verlag, Stuttgart, 1957, vol. XI, part 1, p. 892.

(8) M. Tomita, S. Minami, and S. Uyeo, *J. Chem. Soc. C*, **1969**, 183.

(9) R. Brehme, *Synthesis*, **1976**, 113.

(10) L. G. DeGaldeano, R. Bressler, and K. Brendel, *J. Biol. Chem.*, **248**, 2514 (1973).

(11) D. J. Drain, M. J. Daly, B. Davy, M. Horlington, J. G. B. Howes, J. M. Scruton, and R. A. Selway, *J. Pharm. Pharmacol.*, **22**, 684 (1970).

(12) J. J. Bahl, K. Brendel, and R. Bressler, *Fed. Proc. Fed. Am. Soc. Exp. Biol.*, **38**, 113, 149 (1979).

(13) R. Haeckel and M. Oellerich, *Eur. J. Clin. Invest.*, **7**, 393 (1977).

(14) S. A. Smith, K. F. R. Elliott, and C. Pogson, *Biochem. Pharmacol.*, **28**, 2145 (1979).

(15) M. N. Goodman, *Biochem. J.*, **150**, 137 (1975).

(16) B. M. Raaka and J. M. Lowenstein, *J. Biol. Chem.*, **254**, 3303 (1979).

(17) N. B. Rudermann, C. J. Toews, C. Lowy, I. Vreeland, and E. Shafrir, *Am. J. Physiol.*, **219**, 51 (1970).

(18) I. J. Arinze and M. S. Patel, *Biochemistry*, **12**, 4473 (1973).

(19) J. R. Williamson, J. Anderson, and E. T. Browning, *J. Biol. Chem.*, **245**, 1717 (1970).

ACKNOWLEDGMENTS

The authors gratefully acknowledge the expert technical assistance of F. Deppermann, M. Eisele, P. Lamm, and H. Merkel; and thank Dr. H. Müller for performing the toxicity studies.

[7] Batch no. 2036, Società Italiana Medicinali Scandicci, Italy.

Synthesis of ω-(4-Aminophenylsulfonamido)alkyl Disulfides and Thiosulfates and their Activity against Dihydropteroate Synthetase from Sulfanilamide-Resistant *Neisseria gonorrhoeae*

WILLIAM O. FOYE ˣ, JOEL M. KAUFFMAN *, and WICHAI SUTTIMOOL ‡

Received June 24, 1981, from the *Samuel M. Best Research Laboratory, Massachusetts College of Pharmacy and Allied Health Sciences, Boston, MA 02115.* Accepted for publication October 19, 1981. Present address: *Department of Chemistry, Philadelphia College of Pharmacy and Science, Philadelphia, PA 19104 and the ‡Department of Biochemistry, Chulalongkorn University, Bangkok, Thailand.

Abstract □ A series of ω-(4-aminophenylsulfonamido)alkyl disulfides and ω-(4-aminophenylsulfonamido)alkanethiosulfates was synthesized from the reaction of *p*-acetamidobenzenesulfanilyl chloride and either the aminoalkyl disulfide dihydrobromide or the aminoalkyl bromide hydrobromide followed by sodium thiosulfate. Several of the compounds showed inhibitory activity against dihydropteroate synthetase isolated from a sulfanilamide-resistant strain of *Neisseria gonorrhoeae* of the same order of activity as that of sulfanilamide. An increase in the hydrophobic nature of the sulfanilamide structure did not increase inhibitory activity against this enzyme.

Keyphrases □ ω-(4-Aminophenylsulfonamido)alkyl—disulfides and thiosulfates, synthesis, activity against dihydropteroate synthetase, sulfanilamide-resistant *Neisseria gonorrhoeae* □ *Neisseria gonorrhoeae*—synthesis of ω-(4-aminophenylsulfonamido)alkyl disulfides and thiosulfates, activity against dihydropteroate synthetase, sulfanilamide-resistant □ Dihydropteroate synthetase—synthesis of ω-(4-aminophenylsulfonamido)alkyl disulfides and thiosulfates, sulfanilamide-resistant *Neisseria gonorrhoeae*

The development of bacterial resistance to many of the antibiotics and synthetic antibacterials has reopened the search for synthetic antibacterials, particularly for use against resistant strains of bacteria. The inclusion of a reactive function in the sulfonamide molecule that might lead to an irreversible inhibitor of dihydropteroate synthetase appeared to offer a plausible approach to an agent of this type. The active site of dihydropteroate synthetase is not well defined, but it may be considered, like most enzymes, to contain disulfide bonds between juxtaposed cysteine residues. This provides an accessory receptor site which should bind with functional groups reactive toward disulfides. Accordingly, a series of *N*-sulfonamidoalkyl disulfides and thiosulfates (I) has been synthesized for testing against a drug-resistant organism. A sulfanilamide-resistant strain of *Neisseria gonorrhoeae* was available for this purpose (1). It has been shown (2) that carboxyl groups in the side chains of N_1-substituted sulfanilamides showed relatively high affinities toward a dihydropteroate synthesizing system of *Escherichia coli*, probably by interacting with an accessory area of the enzyme.

It is possible that a sulfonamido disulfide, previously

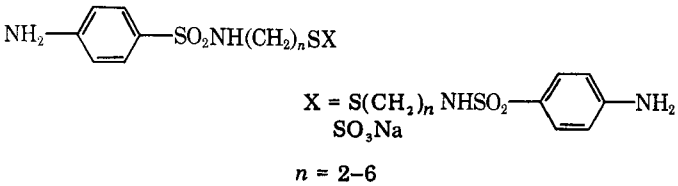

I

prepared in this laboratory, may have reacted with such an accessory receptor site. Bis[4-(4-acetamidobenzenesulfonamido)phenyl] disulfide was described as curative in mice infected with *Plasmodium berghei* (3). It was considered at the time that this molecule might be acting as a binding agent to DNA, but other related nonsulfonamido containing disulfides with good DNA binding potential showed no antimalarial activity (4).

Previously, other examples of molecules containing both sulfonamide and disulfide functions have been reported: several 4-aminobenzenesulfonamidoaryl disulfides (5) and two 4-aminobenzenesulfonamidoalkyl disulfides, where the alkyl function had two and three methylene units (6). Both series showed some antibacterial properties. No 4-aminobenzenesulfonamidoalkane thiosulfates have been reported as antibacterials.

RESULTS AND DISCUSSION

Chemistry—The synthesis of the 4-aminobenzenesulfonamidoalkyl disulfides is outlined in Scheme I. Reaction of polymethylene dibromides with potassium phthalimide gave the known ω-bromalkylphthalimides, which were separated from byproduct diphthalimides by recrystallization from hexane. Treatment of the bromoalkylphthalimides with sodium thiosulfate gave intermediate thiosulfates which were oxidized *in situ* with iodine to give the disulfides. Although the literature recommends addition of solid iodine (7) for this conversion, a solution of the stoichiometric amount of iodine in methanol was found superior for these compounds.

Removal of the phthaloyl groups by hydrazinolysis failed, but the use of hydrobromic acid, mixed with acetic (8) or propionic acid was successful in giving the aminoalkyl disulfide hydrobromides (II).

Sulfonamide formation from *N*-acetylsulfanilyl chloride and amines generally is catalyzed with aqueous sodium hydroxide or carbonate or anhydrous pyridine. Because of the alkali-sensitive disulfide function, these catalysts were unsuitable; the use of sodium bicarbonate gave the desired products. All of the acetamidobenzenesulfonamidoalkyl disulfides (III) were difficult to purify; washing with an aqueous solution of ethanol and acetic acid generally provided good yields of reasonably pure material.

Deacetylation was carried out in a boiling mixture of hydrochloric acid–water–glycol (1:1:2) for 10 min; prolonged heating cleaved the sulfonamide as well. Since the dihydrochlorides of the higher homologs (n = 4–6) were insoluble in hot water, the free amines (IV) were isolated by the action of ammonia on dilute solutions of the dihydrochlorides in hot methanol. With the n = 3 homolog, the free base actually separated from the acid reaction mixture. All of the disulfides had similar IR spectra showing N—H stretching frequencies at 3345–3440 and 3255–3370 cm^{-1}, and S—O stretching at 1322–1406 and 1138–1152 cm^{-1}.

The preparation of the 4-aminobenzenesulfonamidoalkane thiosulfates is outlined in Scheme II. Although the *N*-acetyl derivative of the sulfonamidoethane thiosulfate is known (9), only free amino sulfonamides have shown antifolate activity. Since either acid or basic hydrolysis of the acetyls would decompose the thiosulfate function, the free amino thiosulfates were prepared from the 4-aminobenzenesulfonamidoalkyl

0022-3549/82/0700-0799$01.00/0

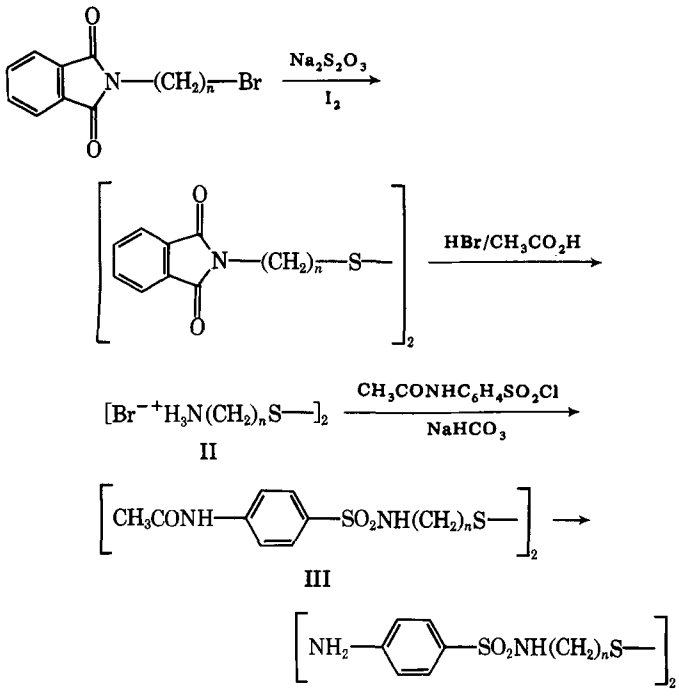

n = 2–6

Scheme I

bromides on reaction with sodium thiosulfate. The intermediate amine hydrochloride, where n = 3, was surprisingly insoluble in water. Conversion to the free base gave a water-soluble sodium salt of the desired thiosulfate.

Since the disulfides proved in general to be too insoluble for enzyme inhibition tests, a carboxyl group was introduced for water solubilization by preparing the bis(4-aminobenzenesulfonamido) derivative (V) of L-cystine (10). The melting point of the product (192–194°) agreed with that reported previously (193–194°) (10).

Inhibition of Dihydropteroate Synthetase—Determination of ID_{50} concentrations was carried out for sulfanilamide, sodium *p*-aminobenzenesulfonamidoethane (and -propane) thiosulfate, *N,N'*-bis(sulfanilyl)-L-cystine and *p*-aminobenzenesulfonamidopropyl bromide. The enzyme preparation used was an extract of a sulfanilamide-resistant strain of *N. gonorrhoeae* (1). Results are recorded in Table I.

Results of the inhibition study show that sulfanilamide itself showed the greatest inhibitory activity, although the ID_{50} values for the synthesized compounds fall within the same order of activity. It is possible that the additional bulk of the alkyl functions on the sulfonamide nitrogen reduces the binding ability of the compounds. If this were the case, it would be expected that the disulfide, with a nonlinear carboxyl group, would show the least inhibition. If the inhibition depended on a greater degree of hydrophobicity, then the bromoethyl derivative should have shown a greater inhibitory effect. It is apparent from the results, however, that a disulfide link with enzyme mercapto did not take place.

Since there was very little difference in inhibitory properties between the homologous thiosulfates, and the more hydrophobic bromoethyl derivative had even less activity, it is apparent that additional hydrophobic functions play no significant role in the binding at the receptor site. This finding agrees with a previous report (11) where it was found that inhibition of this enzyme by N_1-phenylsulfonamides was not improved by greater hydrophobicity.

Table I—Inhibition of Dihydropteroate Synthetase

Compound	Concentration range, m*M*	ID_{50}, μM
Sulfanilamide	0–0.6	59
Sodium 4-aminobenzenesulfonamidoethanethiosulfate	0–1.2	106
Sodium 4-aminobenzenesulfonamidopropanethiosulfate	0–1.2	108
N,N'-Bis(sulfanilyl)-L-cystine	0–1.2	160
4-Aminobenzenesulfonamidopropyl bromide	0–1.2	250

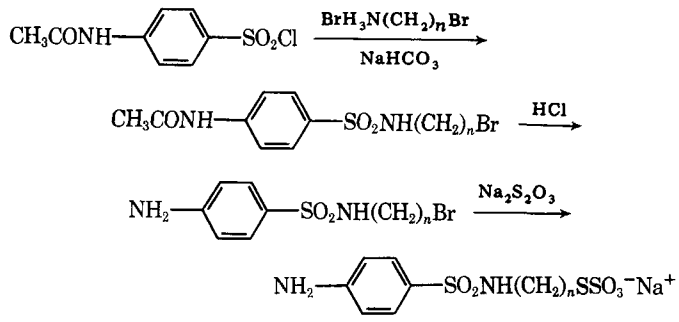

n = 2,3

Scheme II

EXPERIMENTAL[1]

α-Bromoalkyl-ω-phthalimides—These compounds were prepared esssentially by the method of Klayman *et al.* (12). The crude products were recrystallized from ethyl alcohol, dried, recrystallized from hexane, and cooled at 25° for several hours and then cooled at 3°. Yields of 48–66% were obtained from material which melted at literature values (12).

Bis(ω-Phthalimidoalkyl) Disulfides—The procedure is a modification of that of Dirscherl and Weingarten (7). To a heated solution of water (75 ml), methanol (75 ml), and α-bromoalkyl-ω-phthalimide (0.08 mole) was added 0.08 mole of sodium thiosulfate pentahydrate with stirring. After 1 hr at reflux temperature, the mixture was treated with 10.15 g (0.04 mole) of iodine in 60 ml of methanol during 45 min, followed by 10 min of refluxing. The two-phase system was stirred and cooled; the resulting solid was ground in a mortar, slurried with 150 ml of water for 1 hr, filtered, and dried. Yields of 89–95% were obtained from material whose melting points agreed with literature values (7, 8).

ω,ω'-Dithioalkanamine Dihydrobromides (II)—A mixture of 0.04 mole of the appropriate bis(ω-phthalimidoalkyl) disulfide, 22 ml of 48% hydrobromic acid, and either 22 ml of acetic acid (for n = 3, 4) or 22 ml of propionic acid (for n = 5, 6) was refluxed for 24 hr. The hot orange liquid was poured into 50 ml of water and kept overnight at 25°. Phthalic acid was removed by filtration, and the filtrates were freed from acids by rotary evaporation. The residue was slurried with 40 ml of water and 0.3 g of activated charcoal and filtered, and the filtrate was slurried with 25 ml of water and evaporated to dryness. The residue was dissolved in 50–100 ml of hot ethyl alcohol, cooled to 25°, and treated with 50–200 ml of ether. The isolated solid was washed with ether and dried. Physical constants of products are listed in Table II.

ω-(4-Acetamidophenylsulfonamido)alkyl Disulfides (III)—Purified *N*-acetylsulfanilyl chloride (mp 144–149°) (17.53 g, 0.075 mole) was dissolved in 150 ml of acetone, and a solution of 0.035 mole of the appropriate ω,ω'-dithioalkanamine dihydrobromide in 50 ml of water was added with ice cooling the mixture. A solution of 13.45 g (0.16 mole) of sodium bicarbonate in 170 ml of water was added dropwise with stirring below 10° during 40 min. The resulting mixture was heated at 50° for 20 hr, cooled in an ice bath, filtered, and washed with water. The solid was slurried with a solution of 200 ml of water, 100 ml of ethyl alcohol, and 10 ml of acetic acid for 4 hr and filtered. The product was dried over sodium hydroxide at 25°/0.4–1.0 torr for 16–24 hr. Physical constants of products are listed in Table II.

ω-(4-Aminophenylsulfonamido)alkyl Disulfides (IV)—With magnetic stirring, 0.004 mole of the preceding diacetyl derivative, 5 ml of HCl, 5 ml of water, and 10 ml of ethylene glycol were refluxed for 10 min. A thick precipitate of the dihydrochloride was generally obtained, 40 ml of water was added, and the solid was filtered and dried at 25°/0.5–1.5 T for 18 hr over sodium hydroxide. The solid was dissolved in 250 ml of boiling methanol, treated with 0.3 g of activated carbon, and diluted with 10 ml of 4 *N* ammonium hydroxide and 200 ml of water to precipitate the free base. It was filtered and dried as before. Physical constants of products are listed in Table II.

[1] Melting points were determined in capillaries with a Mel-Temp block and needed no correction. IR spectra were taken in KBr pellets using a Perkin-Elmer 457 grating spectrophotometer. Elemental analyses were done by Dr. F. B. Strauss, Oxford, England or by Instranal Laboratory, Rensselaer, N.Y. TLC was carried out using silica gel plates and exposure to iodine vapor. Organic reagents were supplied by Aldrich Chemical Co. or by Eastman Organic Chemicals. [7-^{14}C]*p*-Aminobenzoic acid (>95% radiochemical purity) was obtained from New England Nuclear Corp., Boston, Mass. Measurement of enzyme inhibition was done with a Packard Liquid Scintillation Spectrometer, model 3320. Frozen cells of sulfanilamide-resistant *Neisseria gonorrhoeae* strain 7134 were supplied by Johnna Ho, Harvard University School of Public Health.

Table II—Physical Constants of the Disulfides

Compound	n	Melting point	Yield, %	Formula	Analysis, % Calculated	Found
II	3	230–232[a]	86			
II	4	248–249[b]	87			
II	5	256–258 dec.	82	$C_{10}H_{24}N_2S_2 \cdot 2HBr$	Br 40.13	39.80
II	6	243–245 dec.	78	$C_{12}H_{28}N_2S_2 \cdot 2HBr$	Br 37.49	37.39
III	2	190–192[c,d]	92			
III	3	154–158 dec[e]	77			
III	4	145–149	68	$C_{24}H_{34}N_4O_6S_4$	C 47.81	47.95
					H 5.68	5.68
					N 9.30	9.21
III	5	130–131	81	$C_{26}H_{38}N_4O_6S_4$	C 49.50	49.48
					H 6.07	5.89
					N 8.88	8.30
III	6	123–125	72	$C_{28}H_{42}N_4O_6S_4$	C 51.03	51.13
					H 6.43	6.28
					N 8.50	8.47
IV	2	130–131[f]	92			
IV	3	152–153[g]	96			
IV	4	176–177	91	$C_{20}H_{30}N_4O_4S_4$	C 46.31	46.45
					H 5.83	5.71
					N 10.80	10.51
IV	5	166–167	87	$C_{22}H_{34}N_4O_4S_4$	C 48.32	48.50
					H 6.27	6.09
					N 10.25	10.20
IV	6	164–165.5		$C_{24}H_{38}N_4O_4S_4$	C 50.14	50.59
					H 6.66	6.42
					N 9.75	9.79
					S 22.31	22.30
V		192–194[h]	62	$C_{18}H_{22}N_4O_8S_4$		

[a] Lit. (6) mp 232°. [b] Lit. (7) mp 240°. [c] Commercially available 2,2′-dithiobisethanamine dihydrochloride was used as reagent instead of the hydrobromide. [d] Lit. (6) mp 194–196.5°. [e] Lit. (6) mp 162–163°. [f] Lit. (6) mp 129°. [g] Lit. (6) mp 154.5–155.5°. [h] Lit. (10) mp 193–194°.

2-(4-Acetamidophenylsulfonamido)ethyl Bromide—This was prepared from *N*-acetylsulfanilyl chloride and 2-bromoethylamine hydrobromide[2] by the same general procedure used for the ω-(4-acetamidophenylsulfonamido)alkyl disulfides. The crude product was slurried with aqueous sodium bicarbonate, filtered, and dried to give a 77% yield of material melting at 168–169° [lit. (13) mp 168–169°].

2-(4-Aminophenylsulfonamido)ethyl Bromide—The previous compound (9.63 g, 0.03 mole), 10 ml of 38% HCl, and 10 ml of 95% ethyl alcohol were refluxed for 30 min and diluted with 125 ml of water. The solution was decolorized with activated carbon and neutralized with sodium bicarbonate; the free base was filtered, slurried with 100 ml of water, filtered, and dried at 25°/0.8 torr for 20 hr to give an 84% yield of tan solid, mp 87.5–88.5° [lit. (14) mp 90–91°].

Sodium 2-(4-Aminophenylsulfonamido)ethanethiosulfate—A mixture of 5.97 g (0.024 mole) of sodium thiosulfate pentahydrate, 6.72 g (0.024 mole) of the previous product, 25 ml of methanol, and 25 ml of water was refluxed for 30 min and cooled to 25°. Solvent was removed by rotary evaporation, and the resulting solid was dried further by evaporation of 2 × 25 ml of absolute ethanol. The residue was shaken with 15 ml of dimethylformamide, cooled overnight, and the insoluble sodium bromide was removed. The filtrate was diluted with 50 ml of acetone, filtered after several hours, and the residue was dried at 20°/0.3 torr for 16 hr to give 8.81 g of crude solid, mp 178–182°. Recrystallization from 95% ethyl alcohol at −20° gave a 44% yield of colorless solid, mp 207.5–209°(dec), which gave a negative test for halogen.

Anal.—Calc. for $C_8H_{11}N_2NaO_5S_3$: C, 28.73; H, 3.32; N, 8.38; S, 28.77. Found: C, 28.76; H, 3.17; N, 8.39; S, 28.39.

3-(4-Acetamidophenylsulfonamido)propyl Bromide—This compound was prepared by the same method used for 2-(4-acetamidophenylsulfonamido)ethyl bromide, from *N*-acetylsulfanilyl chloride and 3-bromopropylamine (8). After heating, the solution was decolorized with activated carbon, diluted with 200 ml of water, and cooled to 3° before filtration to give a crude product that was recrystallized from 50% ethyl alcohol to give a 64% yield of tan prisms, mp 104–105.5°.

Anal.—Calc. for $C_{11}H_{15}BrN_2O_3S$: C, 39.41; H, 4.51; Br, 23.84. Found: C, 39.61; H, 4.20; Br, 24.10.

3-(4-Aminophenylsulfonamido)propyl Bromide—The previous compound (16.00 g, 0.048 mole), 20 ml of 38% HCl, and 20 ml of 95% ethyl alcohol were refluxed for 30 min, and the solid mass was transferred to a beaker with 100 ml each of water and 95% ethyl alcohol. After being heated, the solution was decolorized with activated carbon, cooled to 25°, and neutralized with sodium bicarbonate. The free base was filtered, slurried with 100 ml of water, and dried at 23°/0.2 torr for 16 hr to give 9.45 g (68%) of shiny, white prisms, mp 106–106.2°.

Anal.—Calc. for $C_9H_{13}BrN_2O_2S$: C, 36.86; H, 4.47; Br, 27.26; S, 10.94. Found: C, 37.05; H, 4.43; Br, 27.54; S, 10.75.

Sodium 3-(4-Aminophenylsulfonamido)propanethiosulfate—A mixture of 1.29 g (0.0052 mole) of sodium thiosulfate pentahydrate, 1.52 g (0.0052 mole) of the previous product, 5 ml of methanol, and 5 ml of water was refluxed for 25 min, cooled, and freed of solvent by rotary evaporation. After further evaporation with 5 ml of absolute ethanol, the remaining gum was leached with 20 ml of 97.5% ethyl alcohol and cooled overnight. The solid sodium bromide was removed, and the filtrate was diluted with 30 ml of 1-propanol and cooled to −20° to give 0.9 g of white solid, which was recrystallized from 18 ml of 95% ethyl alcohol at −20° to give 0.6 g (33%) of white prisms, mp 212.5–213.5°.

Anal.—Calc. for $C_9H_{13}N_2NaO_5S_3$: C, 31.02; H, 3.78; N, 8.04. Found: C, 31.29; H, 3.64; N, 8.05.

Determination of Enzyme Inhibition—ID_{50} values for the inhibition of dihydropteroate synthesis using a cell-free extract of dihydropteroate synthetase from *N. gonorrhoeae* (1) were determined for the test compounds using six inhibitor concentrations in duplicate experiments. The ID_{50} value was taken from the plot of the percent inhibition against the logarithm of the inhibitor concentration.

Solutions of the test compounds were made to contain the following components in a 200-μl volume: tris(hydroxymethyl)aminomethane hydrochloric acid buffer (140 m*M*, pH 5.8), dihydropteridine pyrophosphate (7 μ*M*) (15), [7-^{14}C]*p*-aminobenzoic acid (15 μ*M*), magnesium chloride hexahydrate (5 m*M*), 2-mercaptoethanol (0.1 *M*), test compound (0–1.2 m*M*), and enzyme (0.14 mg of protein). The reaction mixture without dihydropteridine pyrophosphate served as blank. After the mixture was incubated at 37° for 20 min, the reaction was stopped by the addition of 2-mercaptoethanol (20 μl). The amount of labeled dihydropteroate was measured as follows.

A portion (100 μl) of the reaction mixture was spotted on 3-mm chromatographic paper[3] (22.86 × 29.21 cm). The chromatogram was developed in descending fashion by immersing the lower margin of the paper in potassium phosphate buffer (0.1 *M*, pH 7.0) inside a chamber at room temperature. After the solvent front had moved 15 cm from the origin, the paper was removed and dried. Neither the labeled dihydropteroate nor the labeled pteroate moved under these conditions, whereas unreacted [7-^{14}C]*p*-aminobenzoic acid migrated with an R_f of 0.78. An area (3 × 3 cm) of the paper around the origin was cut into small pieces and put into a counting vial containing 10 ml of scintillation fluid consisting

[2] Aldrich Chemical Co.

[3] Whatman.

of the following in a volume of 1 liter: naphthalene (150 g), 2,5-diphenyloxazole (8 g), 1,4-bis(4-methyl-5-phenyl-oxazol-2-yl)benzene (0.6 g), ethylene glycol (20 ml), 2-ethoxyethanol (100 ml), and toluene to make 1 liter. The radioactivity was measured in the liquid scintillation counter with an 18% gain setting. Each vial was counted twice, and the data represent the average of two counts. Results are shown in Table I.

REFERENCES

(1) R. I. Ho, L. Corman, S. A. Morse, and M. S. Artenstein, *Antimicrob. Agents Chemother.*, **5**, 388 (1974).

(2) H. H. W. Thijssen, *J. Med. Chem.*, **20**, 233 (1977).

(3) W. O. Foye and J. P. Speranza, *J. Pharm. Sci.*, **59**, 259 (1970).

(4) W. O. Foye, J. J. Lanzillo, Y. H. Lowe, and J. M. Kauffman, *ibid.*, **64**, 211 (1975).

(5) S. Minakami and M. Kono, Japan Pat. 2425 (1967).

(6) R. Lehmann and E. Grivsky, *Bull. Soc. Chim. Belg.*, **55**, 52 (1946).

(7) W. Dirscherl and F. W. Weingarten, *Justus Liebigs Ann. Chem.* **574**, 131 (1951).

(8) A. Schöberl, M. Kawohl, and G. Hansen, *ibid.*, **614**, 83 (1958).

(9) W. O. Foye, Y.-L. Lai-Chen, and B. R. Patel, *J. Pharm. Sci.*, **70**, 49 (1981).

(10) F. Irreverre and M. X. Sullivan, *J. Am. Chem. Soc.*, **64**, 1488 (1942).

(11) G. H. Miller, P. H. Doukas, and J. K. Seydel, *J. Med. Chem.*, **15**, 700 (1972).

(12) D. L. Klayman, M. M. Grenan, and D. P. Jacobus, *ibid.*, **12**, 510 (1967).

(13) A. A. Goldberg and W. Kelly, *J. Chem. Soc.*, **1948**, 1919.

(14) E. L. Jackson, *J. Am. Chem. Soc.*, **72**, 395 (1950).

(15) R. I. Ho, L. Corman, and W. O. Foye, *J. Pharm. Sci.*, **63**, 1474 (1974).

ACKNOWLEDGMENTS

Abstracted in part from a thesis submitted by W. Suttimool to the Massachusetts College of Pharmacy and Allied Health Sciences in partial fulfillment of Doctor of Philosophy degree requirements.

Supported by funds from the John R. and Marie K. Sawyer Memorial Fund, Massachusetts College of Pharmacy and Allied Health Sciences.

Optical Purity Determination by NMR: Use of Chiral Lanthanide Shift Reagents and a Base Line Technique

G. H. DEWAR *x, J. K. KWAKYE *§, R. T. PARFITT *‡, and R. SIBSON ‡

Received June 10, 1981, from the **School of Pharmacy and Pharmacology* and ‡*School of Mathematics, University of Bath, Claverton Down, Bath, England BA2 7AY.* Accepted for publication October 6, 1981.

§ Present address: Faculty of Pharmacy, University of Science and Technology, Kumasi, Ghana, West Africa.

Abstract □ A method for optical purity determination of a range of chiral drug molecules by NMR spectroscopy is reported. This technique involves the use of optically active lanthanide shift reagents and a newly developed base line analysis. Its applicability was demonstrated for a variety of drugs including nonsteroidal antiinflammatory agents and some adrenergic agents. It is established that successful application of the method depends on a constant shift reagent to sample molar ratio, constant instrumental conditions for all solutions, and the use of a calibration curve derived from solutions containing the same total concentration of the two enantiomers. For the examples cited, the correlation coefficient is not <0.97, and a mathematical treatment is included which supports the basis of the method.

Keyphrases □ Optical purity determination—by NMR spectroscopy, use of chiral lanthanide shift reagents and a base line technique □ Chiral lanthanide shift reagents—determination of optical purity by NMR spectroscopy, base line technique □ NMR spectroscopy—determination of optical purity, use of chiral lanthanide shift reagents and a base line technique

The application of NMR spectroscopy to the quantitative analysis of pharmaceuticals has become widespread (1, 2) since the publication of Hollis (3) on the determination of aspirin, phenacetin, and caffeine mixtures. Provided that careful consideration is given to solvent, internal standard, and instrumental conditions (including spinning sidebands and carbon 13 satellites), mixtures, often of some complexity, can be analyzed with a high degree of accuracy. Optical purity determination is another aspect of the analysis of any drug presented in a resolved form (enantiomer) or the racemate of a particular diastereoisomer. Apart from polarimetry, which has been extensively employed despite its drawbacks, optical purity determination has been achieved by chromatographic methods such as GLC (4, 5) and HPLC (6, 7), isotope dilution (8), kinetic resolution (9), and NMR. Even before the discovery of chiral lanthanide shift reagents, the NMR method was used for optical purity measurement either by diastereoisomer formation (10, 11) or the application of chiral solvents (12, 13). Since the publication of Whitesides and Lewis (14) on the relatively large frequency differences between corresponding resonances of enan-

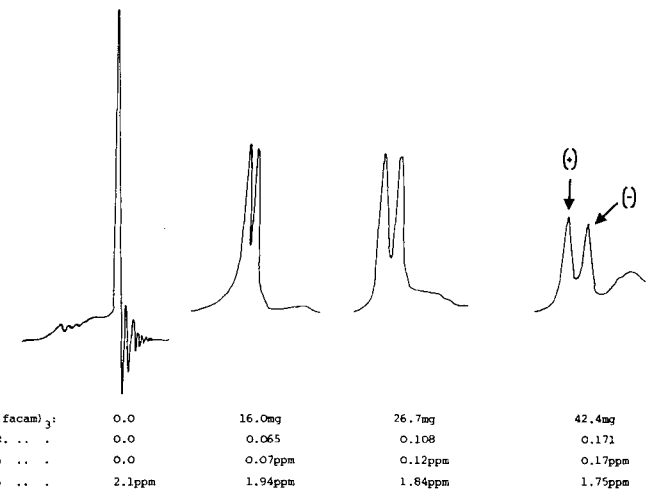

Figure 1—*Resonance of N—CH_3 of (±)-ephedrine in deuterated benzene on incremental addition of III.*

0022-3549/82/0700-0802$01.00/0

of the following in a volume of 1 liter: naphthalene (150 g), 2,5-diphenyloxazole (8 g), 1,4-bis(4-methyl-5-phenyl-oxazol-2-yl)benzene (0.6 g), ethylene glycol (20 ml), 2-ethoxyethanol (100 ml), and toluene to make 1 liter. The radioactivity was measured in the liquid scintillation counter with an 18% gain setting. Each vial was counted twice, and the data represent the average of two counts. Results are shown in Table I.

REFERENCES

(1) R. I. Ho, L. Corman, S. A. Morse, and M. S. Artenstein, *Antimicrob. Agents Chemother.*, **5**, 388 (1974).

(2) H. H. W. Thijssen, *J. Med. Chem.*, **20**, 233 (1977).

(3) W. O. Foye and J. P. Speranza, *J. Pharm. Sci.*, **59**, 259 (1970).

(4) W. O. Foye, J. J. Lanzillo, Y. H. Lowe, and J. M. Kauffman, *ibid.*, **64**, 211 (1975).

(5) S. Minakami and M. Kono, Japan Pat. 2425 (1967).

(6) R. Lehmann and E. Grivsky, *Bull. Soc. Chim. Belg.*, **55**, 52 (1946).

(7) W. Dirscherl and F. W. Weingarten, *Justus Liebigs Ann. Chem.* **574**, 131 (1951).

(8) A. Schöberl, M. Kawohl, and G. Hansen, *ibid.*, **614**, 83 (1958).

(9) W. O. Foye, Y.-L. Lai-Chen, and B. R. Patel, *J. Pharm. Sci.*, **70**, 49 (1981).

(10) F. Irreverre and M. X. Sullivan, *J. Am. Chem. Soc.*, **64**, 1488 (1942).

(11) G. H. Miller, P. H. Doukas, and J. K. Seydel, *J. Med. Chem.*, **15**, 700 (1972).

(12) D. L. Klayman, M. M. Grenan, and D. P. Jacobus, *ibid.*, **12**, 510 (1967).

(13) A. A. Goldberg and W. Kelly, *J. Chem. Soc.*, **1948**, 1919.

(14) E. L. Jackson, *J. Am. Chem. Soc.*, **72**, 395 (1950).

(15) R. I. Ho, L. Corman, and W. O. Foye, *J. Pharm. Sci.*, **63**, 1474 (1974).

ACKNOWLEDGMENTS

Abstracted in part from a thesis submitted by W. Suttimool to the Massachusetts College of Pharmacy and Allied Health Sciences in partial fulfillment of Doctor of Philosophy degree requirements.

Supported by funds from the John R. and Marie K. Sawyer Memorial Fund, Massachusetts College of Pharmacy and Allied Health Sciences.

Optical Purity Determination by NMR: Use of Chiral Lanthanide Shift Reagents and a Base Line Technique

G. H. DEWAR *x, J. K. KWAKYE *§, R. T. PARFITT *‡, and R. SIBSON ‡

Received June 10, 1981, from the **School of Pharmacy and Pharmacology* and ‡*School of Mathematics, University of Bath, Claverton Down, Bath, England BA2 7AY.* Accepted for publication October 6, 1981.

§ Present address: Faculty of Pharmacy, University of Science and Technology, Kumasi, Ghana, West Africa.

Abstract □ A method for optical purity determination of a range of chiral drug molecules by NMR spectroscopy is reported. This technique involves the use of optically active lanthanide shift reagents and a newly developed base line analysis. Its applicability was demonstrated for a variety of drugs including nonsteroidal antiinflammatory agents and some adrenergic agents. It is established that successful application of the method depends on a constant shift reagent to sample molar ratio, constant instrumental conditions for all solutions, and the use of a calibration curve derived from solutions containing the same total concentration of the two enantiomers. For the examples cited, the correlation coefficient is not <0.97, and a mathematical treatment is included which supports the basis of the method.

Keyphrases □ Optical purity determination—by NMR spectroscopy, use of chiral lanthanide shift reagents and a base line technique □ Chiral lanthanide shift reagents—determination of optical purity by NMR spectroscopy, base line technique □ NMR spectroscopy—determination of optical purity, use of chiral lanthanide shift reagents and a base line technique

The application of NMR spectroscopy to the quantitative analysis of pharmaceuticals has become widespread (1, 2) since the publication of Hollis (3) on the determination of aspirin, phenacetin, and caffeine mixtures. Provided that careful consideration is given to solvent, internal standard, and instrumental conditions (including spinning sidebands and carbon 13 satellites), mixtures, often of some complexity, can be analyzed with a high degree of accuracy. Optical purity determination is another aspect of the analysis of any drug presented in a resolved form (enantiomer) or the racemate of a particular diastereoisomer. Apart from polarimetry, which has been extensively employed despite its drawbacks, optical purity determination has been achieved by chromatographic methods such as GLC (4, 5) and HPLC (6, 7), isotope dilution (8), kinetic resolution (9), and NMR. Even before the discovery of chiral lanthanide shift reagents, the NMR method was used for optical purity measurement either by diastereoisomer formation (10, 11) or the application of chiral solvents (12, 13). Since the publication of Whitesides and Lewis (14) on the relatively large frequency differences between corresponding resonances of enan-

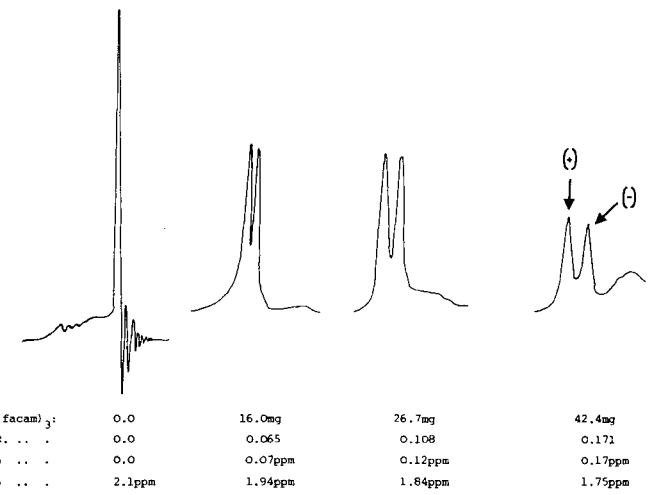

Figure 1—*Resonance of N—CH_3 of (±)-ephedrine in deuterated benzene on incremental addition of III.*

0022-3549/82/0700-0802$01.00/0

Table I—Lanthanide Induced Shift for Quantitatively Useful Groups of (±)-Ephedrine[a]

	Molar Ratio	Lanthanide Induced Shift, ppm[b] C—CH_3 δ	C—CH_3 Δv	N—CH_3 δ	N—CH_3 Δv	CH—N[c] δ	CH—N[c] Δv	O—CH δ	O—CH Δv	Aromatic H[d] δ	Aromatic H[d] Δv
(A)[e]	0.000	0.74	0.00	2.10	0.00	2.54	0.00	4.71	0.00	—	—
	0.060	0.04	0.70	0.84	1.26	1.68	0.86	3.85	0.86	—	—
	0.093	−0.27	1.01	0.74	1.36	1.23	1.31	3.35	1.36	—	—
	0.136	−0.64	1.38	0.67	1.43	0.67	1.87	2.78	1.93	—	—
(B)[f]	0.000	0.67	0.00	2.05	0.00	—	—	4.68	0.00	7.15	0.00
	0.045	0.90	0.23	1.97	−0.08	—	—	4.57	−0.11	7.00	−0.15
	0.096	1.02	0.35	1.88	−0.17	—	—	4.52	−0.16	6.85	−0.30
	0.136	1.11	0.44	1.81	−0.24	—	—	4.47	−0.21	6.75	−0.40
	0.182	1.20	0.53	1.72	−0.33	—	—	4.46	−0.22	6.63	−0.52
	0.240	1.39	0.72	1.56	−0.49	—	—	4.47	−0.21	6.47	−0.68
	0.292	1.53	0.86	1.40	−0.60	—	—	4.75	0.07	6.30	−0.85

[a] Concentration of 0.45 *M* in deuterated benzene. [b] Lanthanide induced shifts of I are routinely downfield, II upfield. Negative values of Δv indicate a shift effect uncharacteristic of the lanthanide agent (*e.g.*, upfield for I). [c] The C—*H*—N resonances were broad and featureless. [d] Average results for the aromatic protons. [e] Data for varying shift reagent II–drug molar ratio. [f] Data for varying shift reagent I–drug molar ratio.

Table II—Shift Data for (+)- and (−)-Ephedrine[a] in the Presence of Chiral Lanthanide Shift Reagents at Different Molar Ratios

	Molar Ratio	(−)-isomer δ	(−)-isomer Δv	(+)-isomer δ	(+)-isomer Δv	ΔΔv
(A)[b]	0.00	0.74	0.00	0.74	0.00	0.00
	0.076	0.05	0.69	0.18	0.56	0.13
	0.119	−0.34	1.08	−0.16	0.90	0.18
	0.153	−0.59	1.33	−0.35	1.09	0.24
	0.182	−0.86	1.60	−0.57	1.31	0.29
	0.212	−1.19	1.93	−0.86	1.60	0.33
(B)[c]	0.00	2.10	0.00	2.10	0.00	0.00
	0.065	1.91	0.19	1.98	0.12	0.07
	0.090	1.84	0.26	1.93	0.17	0.09
	0.108	1.77	0.33	1.89	0.21	0.12
	0.120	1.75	0.35	1.88	0.22	0.13
	0.172	1.64	0.46	1.81	0.29	0.17

[a] Concentration of 0.40 *M* in deuterated benzene. [b] Data for C—CH_3 signal at varying IV–drug molar ratios. [c] Data for N—CH_3 signal at varying III–drug molar ratios.

tiomeric amines in the presence of 3-(*tert*-butylhydroxymethylene)-*d*-camphorato europium, much attention has been given to the use of the method in routine optical purity determination (15). The problem with this approach is the difficulty in achieving complete separation of corresponding resonances of the enantiomers before serious line broadening occurs. The purpose of this report is to describe a method of optical purity determination which does not require complete separation of resonance indicative of each enantiomer in a mixture.

EXPERIMENTAL[1]

Materials—Hydrochloride or sulfate salts of (±)-, (+)-, and (−)-ephedrine[2] and (−)-ephedrine base[2] were used, as well as (±)-, (+)-, and (−)-propranolol hydrochloride[3]; (±)-, *S*(+)-, and *R*(−)-albuterol sulfate[4]; (±)-, (+)-, and (−)-ibuprofen[5]; (±)-, (+)-, and (−)-naproxen[6]; (±)- and (+)-ketoprofen[7]; and (±)- and (−)-fenoprofen calcium[8].

The lanthanide shift reagents tris(6,6,7,7,8,8,8-heptafluoro-2,2-dimethyl-3,5-octanedionato)europium (I)[9], tris(6,6,7,7,8,8,8-heptafluoro-2,2-dimethyl-3,5-octanedionato)praseodymium (II)[9], tris[3-(trifluoromethylhydroxymethylene)-*d*-camphorato], europium (111) derivative (III)[9], and tris[3-(trifluoromethylhydroxymethylene)-*d*-camphorato], praseodymium (111) derivative (IV)[9] were stored over phosphorus pentoxide in a desiccator.

NMR: Determination of Lanthanide Induced Shifts[10]—A solution (~0.2–0.4 *M*) of the racemic compound in the appropriate solvent (0.7 ml) was prepared and the NMR spectrum recorded. Compound I or II in quantities of 10–20 mg was added incrementally and the spectrum recorded after each addition.

Optical Purity Determination[10]—Different quantities of (+)- and (−)-isomers, or alternatively the racemate and either pure isomer or suitable derivatives, were mixed to give differing optical purities, but approximately the same final concentration of total drug when dissolved in the appropriate solvent (0.7 ml). The quantity of chiral lanthanide shift reagent necessary to give the desired shift reagent: drug molar ratio was added (see text and Tables II, III, and V–VIII for explanation and data) and the NMR spectrum of the various solutions recorded under identical instrumental conditions.

Derivatives[11]—*Ketoprofen Methyl Ester*—(±)-Ketoprofen (50 mg) in a mixture of methanol (20 ml) and concentrated hydrochloric acid (1 ml) was refluxed for 1 hr. Evaporation to dryness *in vacuo* gave an oil sufficiently pure for use in subsequent NMR analyses. IR (ν_{max}): 1740, 1690, 1590, and 1500 cm^{-1}; NMR ($CDCl_3$): δ 1.40 (3H, d, C—CH_3), 3.60 (3H, s, $COOCH_3$), 3.62 (1H, q, CH—CH_3), and 7.20–7.90 (9H, m, Ar—*H*) ppm.

Fenoprofen Methyl Ester—(±)-Fenoprofen calcium salt (0.5 g) was dissolved in warm methanol (40 ml), and concentrated hydrochloric acid (1 ml) was added. Concentration of the solution *in vacuo* and extraction with ether (3 × 15 ml) gave the ester as an oil. IR (ν_{max}): 1735, 1590, and 1500 cm^{-1}; NMR ($CDCl_3$): δ 1.48 (3H, d, CH—CH_3), 3.61 (3H, s,

[1] All NMR spectra were recorded on a Perkin-Elmer R12B instrument operating at 60 MHZ with a probe temperature of 37 ± 1°. Unless otherwise stated, tetramethylsilane was employed as internal standard. Abbreviations used in the experimental section to describe resonance appearance are as follows: s, singlet; d, doublet; dd, double doublet; q, quartet; m, multiplet. Solvents were dried over molecular sieve type 4A. IR spectra, obtained as liquid films or as potassium chloride discs (for solids), were recorded on a Pye Unicam SP200 instrument. Low resolution mass spectra were obtained from an automatic electron impact mass spectrometer 12 instrument at 70 eV.

[2] Lake and Cruickshank, Buckhaven, Fife, Scotland.

[3] ICI Limited, Alderley Park, Macclesfield, Cheshire, U.K.

[4] Allen and Hanbury Ltd., Bethnal Green, London, U.K.

[5] Boots Company Ltd., Nottingham, U.K.

[6] Syntex Laboratories, Inc., Calif.

[7] May and Baker Limited, Dagenham, Essex, U.K.

[8] Lilly Research Center, Basingstoke, U.K.

[9] Aldrich Chemical Co. Ltd., Gillingham, Kent, U.K.

[10] Ephedrine and propranolol proton salts were converted to the corresponding free amine by basifying an aqueous solution of the salt with 5 *M* NaOH. Ether or chloroform extraction was performed rapidly in the usual way. Final drying of samples was achieved *in vacuo* at 50°.

[11] The corresponding derivatives of optically pure material were similarly prepared.

Table III—Application of the Base Line Technique to Ephedrine [a] of Varying Optical Purity

Optical Purity[b], %	Separation[c], mm	$\left(1 - \frac{\text{optical purity}}{100}\right)$
0.0	4.70	1.00
25.6	3.80	0.74
47.3	2.71	0.53
76.0	1.48	0.24

[a] Ephedrine concentration of 0.30 *M* and shift reagent IV–drug molar ratio of 0.216 in deuterated benzene. [b] An optical purity of 0.00 refers to the racemate. The difference between the percentage of the two isomers in a mixture is the percent optical purity. Thus, a sample containing 99% (+)- and 1% (−)-isomer is 98% optically pure. If the percent optical purity is X, then that isomer enriched in the mixture has a percentage given by (X + 100)/2. [c] Using C—CH_3 signal at δ −1.0–−1.5 ppm.

$COOCH_3$), 3.62 (1H, q, CH—CH_3), and 6.72–7.53 (9H, m, Ar—*H*) ppm.

Albuterol Tri(trimethylsilyl)ether (*V*)—(±)-Albuterol (60 mg) was

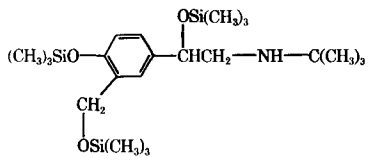

V

heated with *N,N*-bis-trimethylsilyltrifluoroacetamide (VI; 0.4 ml) at 130° for 15 min. The excess of VI and trifluoroacetamide were removed *in vacuo* at 50° to leave V as an oil. IR (ν_{max}): 3000, 1620, and 1508 cm^{-1}; NMR [$CDCl_3$; most shielded $(CH_3)_3Si$ 9H singlet resonance taken as δO]: δ 0.11 [9H, s, $(CH_3)_3Si$], 0.25 [9H, s, $(CH_3)_3Si$], 1.05 [9H, s, $—C(CH_3)_3$], 2.41–2.76 (3H, m, N*H* + CH_2N—, deuterated water reduces to 2H), 4.61–4.76 (3H, m, O—CH_2Ar + $ArCH$—), and 6.60–7.47 (3H, m, Ar—*H*) ppm. Distillation of the oil gave a fraction, bp 140–142°/0.8 mm Hg, of analytical purity; mass spectrum: *m/z* (%), 457 (2), 442 (5.7), 370 (34), 368 (98), 192 (3.4), 148 (18), and 147 (100).

Anal.—Calc. for $C_{22}H_{45}NO_3Si_3$: C, 58.3; H, 9.9; N, 3.1; Si, 18.5. Found[12]: C, 57.9; H, 9.9; N, 3.7; Si, 18.0.

***N*-Acetylpropranolol**—Freshly distilled acetic anhydride (0.3 ml) was added to (±)-propranolol (0.85 g) in tetrahydrofuran (5 ml) and the mixture stirred for 15 hr. The solvent was removed *in vacuo* and the residue dissolved in chloroform (20 ml). The organic layer was washed with 0.1 *M* HCl (10 ml), 0.1 *M* NaOH (10 ml), and then evaporated in the usual way. The residual oil crystallized from petroleum ether (40–60)–ether (1:3) as colorless needles of (±)-*N*-acetylpropranolol. Recrystallization from the same solvent mixture gave a sample (0.45 g; 46%) mp 104°[13], suitable for analysis. IR (ν_{max}): 2950, 1690, 1603, and 1470 cm^{-1}; NMR ($CDCl_3$): δ 1.11–1.42 (6H, overlapping dd, $—CH(CH_3)_2$) 2.07 (3H, s, $COCH_3$), 3.41–4.27 (7H, m, $ArOCH_2$ + $CH(OH)$ + CH_2NCO + $CONCH$), and 6.73–8.34 (7H, m, Ar—*H*) ppm.

RESULTS AND DISCUSSION

It was routine practice in this work to study the influence of the nonchiral shift reagents of I and II[9] on the NMR resonances of racemic molecules, before attempting to use the much more expensive chiral shift reagents, III and IV. Table I shows the lanthanide induced shift for 0.45 *M* (±)-ephedrine in deuterated benzene at varying II–ephedrine and I–ephedrine ratios. By this means it was possible to demonstrate the susceptibility of quantitatively important groups such as C—CH_3 and N—CH_3, which show sharp lines, to the shifting influence of the lanthanide agents. The absence of serious line broadening of the various

[12] Elemental analyses were performed by Butterworth Laboratories Ltd., Teddington, Middlesex, U.K.

[13] Melting points, which are uncorrected, were obtained on a Gallenkamp melting point apparatus Number 889339, supplied by Gallenkamp, Birmingham, U.K.

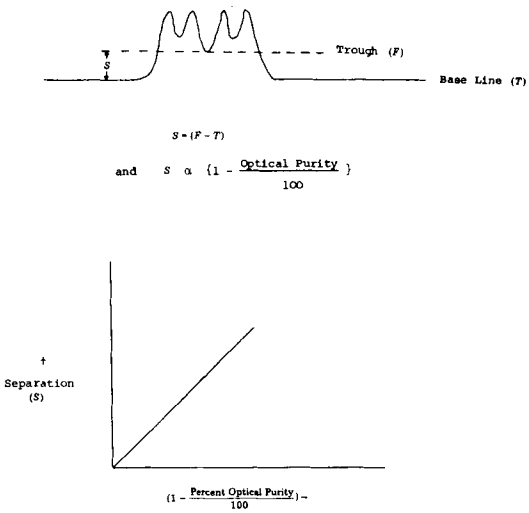

Figure 2—*The base line technique.*

resonances of (±)-ephedrine even at I–drug molar ratio of 0.292, was also observed. A plot of lanthanide induced shift (ppm) against lanthanide agent–ephedrine molar ratio for both nonchiral shift agents yields a linear standard curve for the important C—CH_3 and N—CH_3 groups in the concentration range studied (Table I). The magnitude of observed shifts for N—CH_3 and C—CH_3 in ephedrine, particularly with agent II, indicated their potential use in experiments with chiral lanthanide compounds.

Table II gives data for shifts and differential shifts of the (+)- and (−)-isomers of ephedrine in deuterated benzene in the presence of IV and III. The change in spectral appearance in the δ 1.75–2.10 (N—CH_3) region for 0.4 *M* (±)-ephedrine in deuterated benzene by addition of increasing quantities of III is shown in Fig. 1. Thus, the complexation of the optically active shift reagent with (+)- and (−)-ephedrine gives diastereoisomeric species with slightly different chemical shifts for corresponding groups within the drug molecule. In this case, the relatively large ΔΔv value of 0.33 for the overlapping C—CH_3 doublets at a molar ratio of 0.212 IV–drug, even though line broadening was slightly greater than with III, made IV the shift reagent of choice. It has been observed that for ephedrine, studied under the conditions shown in Table III and in the examples subsequently cited, the distance between the true base line (*T*, Fig. 2) and the trough between the overlapping resonances associated with corresponding groups in the two isomers (*F*, Fig. 2) is proportional to (1 − percent optical purity/100). The distance (*F* − *T*) is *S*, the separation. The principles of this base line technique are outlined, as applied to the analysis of the overlapping C—CH_3 doublets of ephedrine, in Fig. 2. An appropriate calibration curve then allows a sample of unknown optical purity to be determined.

The successful application of the method depends on three important factors:

1. The use of solutions containing a constant shift reagent–drug molar ratio once that ratio has been selected.
2. Determination under constant instrumental conditions for all solutions.
3. The use of a standard total concentration of the two isomers in the

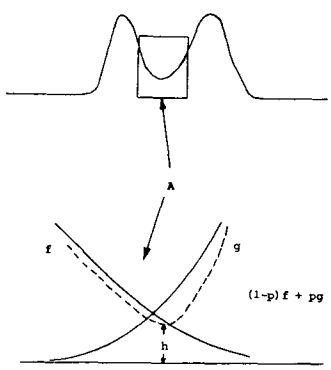

Figure 3—*Mathematical analysis of the overlapping portion of curves similar to the response appearance obtained in the base line technique.*

Table IV—Effect of Dilution with Deuterated Benzene on Lanthanide Induced Shift of (±)-Ephedrine in the Same Solvent

	Volume of deuterated benzene added, ml	C—CH_3		N—CH_3		O—CH	
		δ	Δν	δ	Δν	δ	Δν
(A)[b]	Original[a]	0.90	0.00	1.84	0.00	4.41	0.00
	0.1	1.00	0.10	1.93	0.09	4.53	0.12
	0.2	1.04	1.14	1.96	0.12	4.61	0.20
	0.3	1.05	0.15	1.98	0.14	4.63	0.22
	0.4	1.05	0.15	1.98	0.14	4.67	0.26
(B)[c]	Original[a]	1.13	0.00	1.75	0.00	4.37	0.00
	0.1	1.23	0.10	1.79	0.04	4.52	0.15
	0.2	1.34	0.21	1.89	0.14	4.68	0.31
	0.3	1.42	0.29	1.92	0.17	4.80	0.43
	0.4	1.47	0.34	1.95	0.20	4.89	0.52
	0.5	1.52	0.39	1.97	0.22	4.97	0.60

[a] 0.7-ml volume. [b] Data for compound I–drug molar ratio of 0.106. [c] Data for compound I–drug molar ratio of 0.212.

mixture for the calibration curve. In practice the concentration need not be the same for all solutions studied, provided that appropriate conversion to the standard concentration is effected for purposes of calibration.

It is considered that the relaxation phenomena associated with corresponding groups in such a diastereoisomeric complex need not necessarily be identical, and consequently, a mathematical analysis has been applied to similar overlapping curves. This is presented to support the basis of the method (Fig. 3):

In the region of the minimum (A), suppose that the left hand curve is $f(x)$, the right hand curve is $g(x)$; when it is assumed that $f' < 0, g' > 0$, $f'' > 0, g'' > 0$, and f, g such that for all relevant p, $(1 - p)f + pg$ has a minimum.

Suppose the minimum is at z, with a minimal value, h. The consequence of perturbing p to $(p + \delta p)$ is then considered. Write $\phi(x)$ for $(1 - p)f(x) + pg(x)$. Thus, z is governed by $\phi'(z) = 0$. Therefore:

$$(1 - p)f'(z) + pg'(z) = 0 \qquad \text{(Eq. 1)}$$

Thus, to find δz:

$$(1 - p - \delta p)f'(z + \delta z) + (p + \delta p)g'(z + \delta z) = 0 \qquad \text{(Eq. 2)}$$

where:

$$\phi'(z + \delta z) + \delta p[g'(z + \delta z) - f'(z + \delta z)] = 0 \qquad \text{(Eq. 3)}$$

And on expanding and using $\phi'(z) = 0$

$$\phi''(z)\delta z + 0(\delta z^2) + \delta p[g'(z) - f'(z) + 0(\delta z)] = 0 \qquad \text{(Eq. 4)}$$

Table V—Shift Data for (+)- and (−)-*N*-Acetylpropranolol[a] Using Reagent III

Molar Ratio	(+)-isomer δ	(+)-isomer Δν	(−)-isomer δ	(−)-isomer Δν	ΔΔ[b], ppm
0.000	2.10	0.00	2.10	0.00	0.00
0.183	3.07	0.97	2.92	0.82	0.15
0.276	3.64	1.54	3.42	1.32	0.22
0.367	4.15	2.05	3.87	1.77	0.28
0.521	4.70	2.60	4.39	2.29	0.31

[a] Concentration of 0.25 M acetylated drug in carbon tetrachloride, using $COCH_3$ signal. [b] Using the same shift reagent, the ΔΔν values in deuterated benzene and deuterated chloroform at ~0.5 molar ratios were 0.15 and 0.02 ppm, respectively.

Table VI—Application of the Base Line Technique to *N*-Acetylpropranolol[a] of Varying Optical Purity

Optical Purity, %	S[b], mm	$\left(1 - \frac{\text{optical purity}}{100}\right)$
0.0	4.90	1.00
24.9	3.90	0.75
50.4	2.80	0.50
75.4	1.40	0.25
100.0	0.20	0.00

[a] Concentration of 0.248 M in carbon tetrachloride, using agent III–acetylated drug molar ratio of 0.40. [b] Resonance of $COCH_3$ at δ3.9–4.2 ppm employed in the analysis.

where:

$$\delta z = \frac{-[g'(z) - f'(z)]}{\phi''(z)}\delta p + 0(\delta p^2) \qquad \text{(Eq. 5)}$$

Therefore:

$$h + \delta h = (1 - p - \delta p)f(z + \delta z) + (p + \delta p)g(z + \delta z)$$
$$= \phi(z + \delta z) + \delta p[g(z + \delta z) - f(z + \delta z)] \qquad \text{(Eq. 6)}$$

and:

$$\delta h = \phi'(z)\delta z + \tfrac{1}{2}\phi''(z)\delta z^2 + 0(\delta z^3) + \delta p\{[g(z) - f(z)] + [g'(z) - f'(z)]\,\delta z + 0(\delta z^2)\}$$
$$= \{\phi'(z)\delta z + [g(z) - f(z)]\delta p\} + \tfrac{1}{2}\phi''(z)\delta z^2 + [g'(z) - f'(z)]\delta p\delta z + 0(\delta p\delta z^2\delta z^3)\}$$
$$= [g(z) - f(z)\delta p] + \left\{\tfrac{1}{2}\phi''(z)\frac{[g'(z) - f'(z)]^2}{\phi''(z)^2} + [g'(z) - f'(z)]\frac{-g'(z) - f'(z)]}{\phi''(z)}\right\}\delta p^2 + 0(\delta p^3)$$
$$= [g(z) - f(z)]\delta p - \tfrac{1}{2}\frac{[g'(z) - f'(z)]^2}{\phi''(z)}(\delta p)^2 + 0(\delta p^3)$$

[note that $\phi'(z) = 0$] (Eq. 7)

Thus, δh is approximately linearly related to δp, with coefficient $g(z) - f(z)$, but the quadratic term does not vanish, and indeed the coefficient:

$$-\frac{[g'(z) - f'(z)]^2}{\phi''(z)}$$

need not even be particularly small; it is known that $g' < 0$ and $f' < 0$.

Results for the application of the base line technique to ephedrine of varying optical purity are shown in Table III and the corresponding calibration plot[S *versus* (optical purity/100)] yields a standard linear curve.

In accordance with previous work (16), the lanthanide induced shift produced by nonchiral and chiral shift reagents was found to be altered by dilution of prepared samples with more solvent. For a fixed shift reagent–ephedrine molar ratio, incremental addition of deuterated benzene caused a downfield shift proportional to the amount of solvent added.

Table VII—Application of the Base Line Technique to V[a]

Optical Purity, %	S[b], mm	$\left(1 - \frac{\text{optical purity}}{100}\right)$
0.0	7.00	1.00
25.0	5.20	0.75
50.0	3.70	0.50
75.3	1.80	0.25
100.0	0.15	0.00

[a] Concentration of 0.188 M in carbon tetrachloride employing III–derivatized drug molar ratio of 1.20. [b] ΔΔν (ppm) values of 7.8, 4.8, and 6.5 were obtained at III–drug derivative molar ratios of 1.20 in carbon tetrachloride, deuterated chloroform, and deuterated benzene, respectively. The analytical peak was that for $ArCH_2OSi\leqslant$ in all three cases, but least line broadening occurred in carbon tetrachloride.

Table VIII—Application of the Base Line Technique to Various Nonsteroidal Anti-inflammatory Agents or Their Derivatives

	Optical Purity, %	S, cm	$\left(1 - \frac{\text{optical purity}}{100}\right)$
Ibuprofen[a]	0.0	0.59	1.00
	23.7	0.44	0.76
	47.6	0.29	0.52
	75.0	0.15	0.25
	100.0	0.00	0.00
Naproxen[b]	0.0	1.61	1.00
	24.4	1.39	0.76
	49.0	1.05	0.51
	70.1	0.79	0.30
	100.0	0.40	0.00
Ketoprofen methyl ester[c]	0.0	0.90	1.00
	20.0	0.72	0.80
	45.0	0.48	0.55
	70.0	0.27	0.30
	78.0	0.19	0.22
Fenoprofen methyl ester[d]	0.0	1.80	1.00
	20.0	1.45	0.80
	55.0	0.86	0.45
	80.0	0.46	0.20

[a] Concentration of drug used was 0.23 *M* in carbon tetrachloride, using III–drug molar ratio of 0.366. The analytical peak was $ArCHCH_3$ in the region δ3.14–3.52 ppm. [b] Drug concentration was 0.29 *M* in deuterated chloroform–carbon tetrachloride (3:4), using III–drug molar ratio of 0.355. The analytical peak was at δ1.80–2.60 ppm ($ArCHCH_3$). [c] Drug derivative concentration was 0.30 *M* in carbon tetrachloride, using III–ester molar ratio of 0.406. The analytical peak was $ArCHCH_3$ in the region δ1.90–2.15. [d] Concentration of derivatized drug was 0.215 *M* in carbon tetrachloride using III–ester molar ratio of 0.919. The analytical peak was the $COOCH_3$ resonance in the δ5.20–5.30 region.

Higher molar ratios produced greater downfield shifts. Table IV shows results for two different molar ratios, using I as shift reagent, on successive addition of 0.1 ml volumes of deuterated benzene to a mixture prepared in 0.7 ml of the same solvent.

Data obtained on application of the base line technique to *N*-acetylpropranolol, compound V, ibuprofen, naproxen, ketoprofen methyl ester, and fenoprofen methyl ester are presented in Tables V–VIII and the corresponding calibration curves, when plotted, are linear. Appropriate derivatization was required in those cases of poor solubility of the parent drug in the solvents available, or where the number of points of complexation with the shift reagent was large, with consequent line broadening.

If authentic, optically pure samples of a drug are available, this method offers a useful means of routine optical purity determination up to ~90% optical purity. The susceptibility of a molecule to pseudocontact shifting influences of a lathanide agent can be quickly established using a nonchiral compound, and the appropriate shift reagent–drug molar ratio necessary in a given case found from incremental addition of the shift reagent (Table II).

It has also been observed that, in certain cases, the peak height difference (δh) of overlapping resonances from corresponding groups of optical isomers in the presence of a chiral shift reagent bears a linear relationship to optical purity up to levels of ~50%. However, there was little success in establishing optical purity at levels >50%. The instrumental and other conditions necessary for successful application of the base line technique similarly apply to the peak height difference method.

REFERENCES

(1) A. F. Casy, "PMR Spectroscopy in Biological and Medicinal Chemistry," Academic, London and New York, 1971, pp 1–51.

(2) F. Kasler, "Quantitative Analysis by NMR Spectroscopy," Academic, London and New York, 1973.

(3) D. P. Hollis, *Anal. Chem.*, **35,** 1682 (1963).

(4) J. P. Guette and A. Horeau, *Tetrahedron Lett.*, **1965,** 3049.

(5) E. Gil-Av, B. Feibush, and R. C. Sigler, *ibid.*, **1966,** 1009.

(6) W. H. Pirkle and D. L. Sikkenga, *J. Chromatogr.*, **123,** 400 (1976).

(7) S. Husain, P. Kunzelmann, and H. Schildnecht, *ibid.*, **135,** 367 (1977).

(8) J. A. Bersen and D. A. Ben-Efraim, *J. Am. Chem. Soc.*, **81,** 4083, (1959).

(9) A. Horeau, *ibid.*, **86,** 3171, (1964).

(10) M. Raban and K. Mislow, *Tetrahedron Lett.*, **1965,** 4249.

(11) *Ibid.*, **1966,** 3961.

(12) W. H. Pirkle and S. D. Beare, *J. Am. Chem. Soc.*, **91,** 5150 (1969).

(13) W. H. Pirkle, R. L. Muntz, and I. C. Paul, *ibid.*, **93,** 2817, (1971).

(14) G. M. Whitesides and D. W. Lewis, *ibid.*, **92,** 6979 (1970).

(15) P. Reisberg, I. A. Brenner, and J. I. Bodin, *J. Pharm. Sci.*, **65,** 592 (1976).

(16) L. Tomic, Z. Magerski, M. Tomic, and D. E. Sunko, *Chem. Commun.*, **1971,** 717.

Liposome Dialysis for Improved Size Distributions

MARK E. BOSWORTH, C. ANTHONY HUNT ˣ, and DOUGLAS PRATT

Received May 22, 1981 from the *School of Pharmacy, University of California, San Francisco, CA 94143.* Accepted for publication October 13, 1981.

Abstract □ A technique is described which allows reproducible preparation of liposomes with improved size–frequency distributions. The recent procedure of extrusion of crude liposome dispersions through controlled-pore polycarbonate membranes is used to control the upper limit of liposome diameter. Subsequent dialysis, using the same type of membrane, can remove the majority of liposomes smaller than a predetermined size. The pattern of dialysis of a liposome preparation is a function of the size–frequency distribution (as well as the membrane pore size) and can be used to approximate the distribution and/or used to monitor the reproducibility of liposome preparations.

Keyphrases □ Liposomes—dialysis for improved size–frequency distribution □ Polycarbonate membranes—dialysis of liposomes, size–frequency distribution □ Dialysis—liposomes, improved size–frequency distribution □ Distribution—size–frequency, liposome dialysis

It is recognized that liposome properties, both as model membranes and drug carrier systems, are dependent on their size (1–4). The differences in the plasma time course and tissue distribution seen between large multilamellar and small unilamellar vesicles are now well established (5), and even different size classes of large multilamellar vesicles can have significantly different pharmacokinetics (6). Unfortunately, the size distribution of the original multilamellar preparation previously described (7) is very heterogeneous and poorly reproducible. The use of this

0022-3549/82/0700-0806$01.00/0

Table VIII—Application of the Base Line Technique to Various Nonsteroidal Anti-inflammatory Agents or Their Derivatives

	Optical Purity, %	S, cm	$\left(1 - \frac{\text{optical purity}}{100}\right)$
Ibuprofen[a]	0.0	0.59	1.00
	23.7	0.44	0.76
	47.6	0.29	0.52
	75.0	0.15	0.25
	100.0	0.00	0.00
Naproxen[b]	0.0	1.61	1.00
	24.4	1.39	0.76
	49.0	1.05	0.51
	70.1	0.79	0.30
	100.0	0.40	0.00
Ketoprofen methyl ester[c]	0.0	0.90	1.00
	20.0	0.72	0.80
	45.0	0.48	0.55
	70.0	0.27	0.30
	78.0	0.19	0.22
Fenoprofen methyl ester[d]	0.0	1.80	1.00
	20.0	1.45	0.80
	55.0	0.86	0.45
	80.0	0.46	0.20

[a] Concentration of drug used was 0.23 *M* in carbon tetrachloride, using III–drug molar ratio of 0.366. The analytical peak was $ArCHCH_3$ in the region δ3.14–3.52 ppm. [b] Drug concentration was 0.29 *M* in deuterated chloroform–carbon tetrachloride (3:4), using III–drug molar ratio of 0.355. The analytical peak was at δ1.80–2.60 ppm ($ArCHCH_3$). [c] Drug derivative concentration was 0.30 *M* in carbon tetrachloride, using III–ester molar ratio of 0.406. The analytical peak was $ArCHCH_3$ in the region δ1.90–2.15. [d] Concentration of derivatized drug was 0.215 *M* in carbon tetrachloride using III–ester molar ratio of 0.919. The analytical peak was the $COOCH_3$ resonance in the δ5.20–5.30 region.

Higher molar ratios produced greater downfield shifts. Table IV shows results for two different molar ratios, using I as shift reagent, on successive addition of 0.1 ml volumes of deuterated benzene to a mixture prepared in 0.7 ml of the same solvent.

Data obtained on application of the base line technique to *N*-acetylpropranolol, compound V, ibuprofen, naproxen, ketoprofen methyl ester, and fenoprofen methyl ester are presented in Tables V–VIII and the corresponding calibration curves, when plotted, are linear. Appropriate derivatization was required in those cases of poor solubility of the parent drug in the solvents available, or where the number of points of complexation with the shift reagent was large, with consequent line broadening.

If authentic, optically pure samples of a drug are available, this method offers a useful means of routine optical purity determination up to ~90% optical purity. The susceptibility of a molecule to pseudocontact shifting influences of a lathanide agent can be quickly established using a nonchiral compound, and the appropriate shift reagent–drug molar ratio necessary in a given case found from incremental addition of the shift reagent (Table II).

It has also been observed that, in certain cases, the peak height difference (δh) of overlapping resonances from corresponding groups of optical isomers in the presence of a chiral shift reagent bears a linear relationship to optical purity up to levels of ~50%. However, there was little success in establishing optical purity at levels >50%. The instrumental and other conditions necessary for successful application of the base line technique similarly apply to the peak height difference method.

REFERENCES

(1) A. F. Casy, "PMR Spectroscopy in Biological and Medicinal Chemistry," Academic, London and New York, 1971, pp 1–51.

(2) F. Kasler, "Quantitative Analysis by NMR Spectroscopy," Academic, London and New York, 1973.

(3) D. P. Hollis, *Anal. Chem.*, **35,** 1682 (1963).

(4) J. P. Guette and A. Horeau, *Tetrahedron Lett.*, **1965,** 3049.

(5) E. Gil-Av, B. Feibush, and R. C. Sigler, *ibid.*, **1966,** 1009.

(6) W. H. Pirkle and D. L. Sikkenga, *J. Chromatogr.*, **123,** 400 (1976).

(7) S. Husain, P. Kunzelmann, and H. Schildnecht, *ibid.*, **135,** 367 (1977).

(8) J. A. Bersen and D. A. Ben-Efraim, *J. Am. Chem. Soc.*, **81,** 4083, (1959).

(9) A. Horeau, *ibid.*, **86,** 3171, (1964).

(10) M. Raban and K. Mislow, *Tetrahedron Lett.*, **1965,** 4249.

(11) *Ibid.*, **1966,** 3961.

(12) W. H. Pirkle and S. D. Beare, *J. Am. Chem. Soc.*, **91,** 5150 (1969).

(13) W. H. Pirkle, R. L. Muntz, and I. C. Paul, *ibid.*, **93,** 2817, (1971).

(14) G. M. Whitesides and D. W. Lewis, *ibid.*, **92,** 6979 (1970).

(15) P. Reisberg, I. A. Brenner, and J. I. Bodin, *J. Pharm. Sci.*, **65,** 592 (1976).

(16) L. Tomic, Z. Magerski, M. Tomic, and D. E. Sunko, *Chem. Commun.*, **1971,** 717.

Liposome Dialysis for Improved Size Distributions

MARK E. BOSWORTH, C. ANTHONY HUNT ˣ, and DOUGLAS PRATT

Received May 22, 1981 from the *School of Pharmacy, University of California, San Francisco, CA 94143.* Accepted for publication October 13, 1981.

Abstract □ A technique is described which allows reproducible preparation of liposomes with improved size–frequency distributions. The recent procedure of extrusion of crude liposome dispersions through controlled-pore polycarbonate membranes is used to control the upper limit of liposome diameter. Subsequent dialysis, using the same type of membrane, can remove the majority of liposomes smaller than a predetermined size. The pattern of dialysis of a liposome preparation is a function of the size–frequency distribution (as well as the membrane pore size) and can be used to approximate the distribution and/or used to monitor the reproducibility of liposome preparations.

Keyphrases □ Liposomes—dialysis for improved size–frequency distribution □ Polycarbonate membranes—dialysis of liposomes, size–frequency distribution □ Dialysis—liposomes, improved size–frequency distribution □ Distribution—size–frequency, liposome dialysis

It is recognized that liposome properties, both as model membranes and drug carrier systems, are dependent on their size (1–4). The differences in the plasma time course and tissue distribution seen between large multilamellar and small unilamellar vesicles are now well established (5), and even different size classes of large multilamellar vesicles can have significantly different pharmacokinetics (6). Unfortunately, the size distribution of the original multilamellar preparation previously described (7) is very heterogeneous and poorly reproducible. The use of this

0022-3549/82/0700-0806$01.00/0

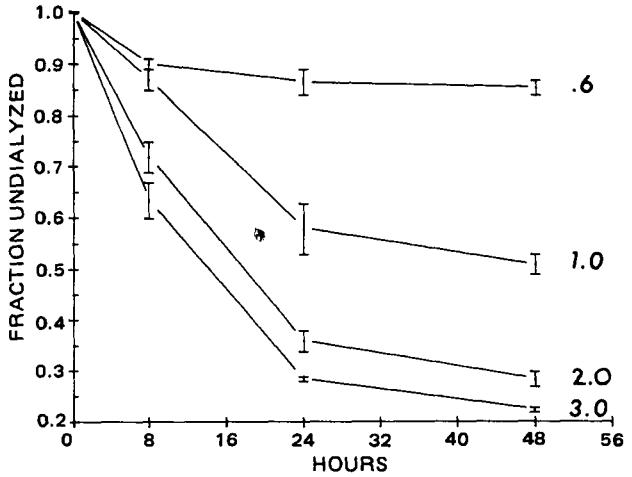

Figure 1—*The fraction of liposomes remaining in the dialysis cells is plotted* versus *time for a suspension [10 μmoles (total lipid)/ml] of mechanically dispersed liposomes dialyzed against either a 0.6-, 1.0-, 2.0-, or 3.0-μm pore-size membrane. Liposomes were quantified by measuring [^{14}C]cholesterol included in the membrane. The vertical bars give the range for duplicate runs using one preparation.*

preparation for *in vivo* tissue distribution studies may mask some differential effects of size. Indeed, complex blood level time courses have been attributed by some investigators to the heterogeneous size distribution of the administered liposomes (4).

Several procedures have attempted to improve the size distribution or encapsulation efficiency of the liposome preparation: sonication and centrifugation (8, 9), detergent dialysis (10–12), injection methods (13–15), French pressure cell (16, 17), reversed-phase evaporation (18), and others (19–21). All suffer from at least one of three faults: (*a*) the resulting size range is too wide or unpredictable; (*b*) the method produces liposomes in only one size range; or (*c*) there are restrictions on composition or specific solutes. However, a significant improvement in size distribution can be obtained by extrusion of a heterogeneous population through straight bore pore polycarbonate membranes of defined pore size (22, 23); this technique defines the upper size limit for the population but does not

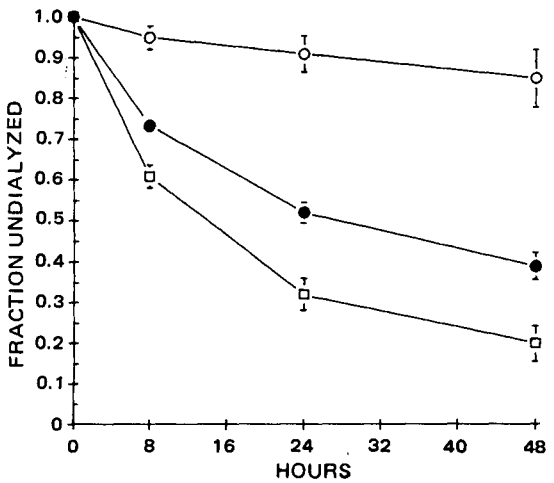

Figure 2—*The fraction of liposomes remaining in the dialysis cells is plotted* versus *time for a suspension [10 μmoles (total lipid)/ml] of small unilamellar French press liposomes dialyzed against either a 0.05 (○), 0.1 (●), or 0.2 (□) μm pore-size membrane. Liposomes were quantified as described in Fig. 1. The values are the means ± 1 SD for four preparations.*

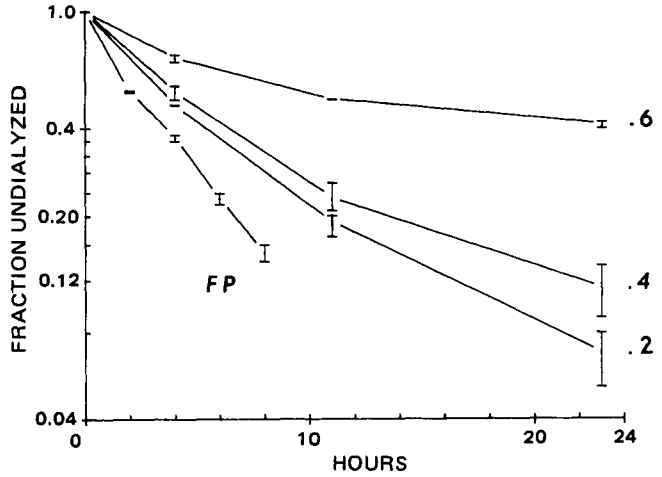

Figure 3—*The fraction of liposomes remaining in the dialysis cells is plotted* versus *time for four different batches of liposomes dialyzed against a 0.8-μm membrane. Liposome concentration and quantitation were as described in Fig. 1. The three upper curves are for liposomes prepared by two extrusions (see text) of mechanically dispersed liposomes through 0.6-, 0.4-, and 0.2-μm membranes. The lower curve is for French press liposomes. The vertical bars give the range for two preparations.*

affect the lower half of the distribution (control of the smaller size may be critical if liposome pharmacokinetics depend in part on the surface area or number of injected liposomes). In this report an improvement on the extrusion technique is described in which the extruded liposomes are subsequently dialyzed with the same type membrane with the object of removing a fraction of the smaller liposomes, thus narrowing the size distribution from its lower end.

EXPERIMENTAL

Chemicals—Purified egg yolk phosphatidylcholine (I), sodium dipalmitoyl phosphatidate (II), cholesterol (III), and α-tocopherol (IV) were chromatographic grade[1], as were sucrose [U-^{14}C] and cholesterol [4-^{14}C][2]. A universal scintillation reagent[3] was used. All other chemicals were

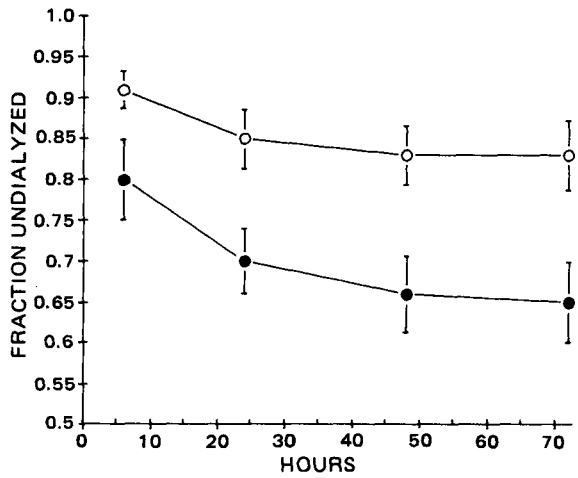

Figure 4—*The undialyzed fraction is plotted* versus *time for 1.0-μm extruded liposomes previously dialyzed against a 0.8-μm membrane. These values are for the previously described liposomes following 20 hr of dialysis against a 0.05-μm membrane (○) (essentially no dialysis of small liposomes), or following 20 hr of dialysis against a 0.8-μm membrane (●). Liposome concentration and quantitation were as described in Fig. 1. The values are the means ± 1 SD for nine preparations.*

[1] Sigma Chemical Co., St. Louis, Mo.
[2] New England Nuclear, Boston, Mass.
[3] PCS, Packard Instrument Co., Inc., Downer's Grove, Ill.

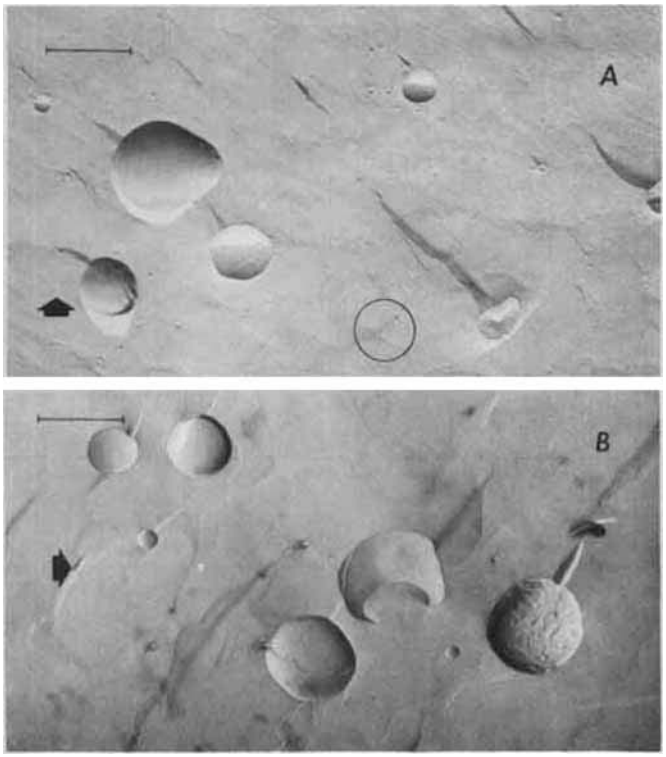

Figure 5—*Freeze-fracture electron micrographs of a mixture of liposomes before (A) and after (B) dialysis. The lipid in the original mixture (A) was from two sources: 70% consisted of a preparation of 1.0-μm extruded liposomes, the larger liposomes (Fig. 6), and 30% consisted of French press liposomes, the smaller liposomes (Fig. 2). Preparation is described in the text, and the mixture is described in Table I; in this mixture liposomes ≤80 nm in diameter account for ~99% of the total number (Fig. 8), ~58% of the total surface area (Fig. 9) and only 7% of the total liposome volume. Frame B shows the same mixture after 21 hr of dialysis against a 1.0-μm membrane; most of the small liposomes were removed. The bar in the upper left of each frame shows 1.0 μm. Within the circle in frame A are five of the small French press liposomes ranging in diameter from 16 to 57 nm.*

analytical reagent grade or better. The buffer, phosphate-buffered saline, contained 92 m*M* NaCl, 23 m*M* dibasic sodium phosphate, and 11 m*M* monobasic sodium phosphate. Prior to use, phosphatidic acid was obtained by chloroform extraction of an aqueous 0.4 *N* HCl solution of sodium phosphatidate containing 20% methanol.

Preparation of Liposomes—Multilamellar liposomes were prepared essentially as previously described (6, 22) and were composed of I–II–III–IV in the molar ratios 4:1:4.5:0.05 or 4:1:1:0.05. The α-tocopherol was added to retard autoxidation and improve stability (24). The lipids were dissolved in chloroform, mixed in a round-bottom flask, and subsequently evaporated to dryness under vacuum. An aliquot of buffer was added to the dried lipid; the mixture was then agitated by hand (at 20° after nitrogen purging) until all lipid was suspended, giving a final concentration of 10 μmoles of lipid/ml. In most cases a small amount of [^{14}C]cholesterol, as a liposomal membrane marker, was included with the other lipids. In other cases, 5 m*M* [^{14}C]sucrose, as an aqueous space marker, was included in the buffer used to disperse the lipids. This hand dispersal system results in the heterogeneous multilamellar population designated as being mechanically dispersed. The 1.0-μm extruded liposomes were prepared by placing the crude mechanically dispersed preparation in a 25-mm stirred ultrafiltration cell[4] fitted with a 1.0-μm pore-size polycarbonate membrane[5] and extruding it with positive nitrogen pressure at 10 ml/min. These liposomes could then be sequentially extruded through 0.8-, 0.6-, 0.4-, and 0.2-μm pore-size membranes to further reduce the size.

In selected cases the suspension was extruded twice through each membrane. The liposome size type was then designated by the smallest membrane size through which the suspension was extruded. The lipid recovery at each extrusion step was 100%, except at or below the 0.2-μm level; the extrusion was always done twice through the final membrane.

French press liposomes were prepared as previously described (16). A multilamellar liposome preparation was placed in a French pressure cell[6] and extruded three times at room temperature (flow rate ~15 ml/min) at 20,000 psi. The French press liposomes were then centrifuged at low speed to remove rubber particles sheared from the cells' O-rings during the extrusion.

Liposomes were dialyzed against the selected polycarbonate membrane as follows: 1 ml (or larger) dialysis cells (actual capacity 1.3 ml/side) were fitted with 25-mm membranes, and 1.0 ml of liposome suspension was placed in the sample chamber and 1.0 ml of buffer was placed in the second compartment. The cells were shaken at 5° on a horizontal shaker at 1.5–2 cycles/sec with a 5-cm amplitude. The dialysate side was replaced frequently with fresh buffer so as to maintain sink conditions. The total counts per minute of carbon on the sample side was monitored with time using scintillation-counting techniques. In the case where [^{14}C]sucrose was used as the liposomal marker, the nonentrapped sucrose was removed prior to the polycarbonate membrane dialysis by overnight dialysis *versus* excess buffer at 5° in a dialysis bag with a molecular weight cutoff of 10,000.

Electron Microscopy of Liposomes—For electron microscopy, ali-

Table I—Measured Liposome Diameter (μm) for Four Batches of Liposomes [a]

Liposome Type	Number Counted	Corrected mean Diameter	Liposome Diameter, Mean Surface Area[f]	Liposome Diameter, Mean Volume[g]
1.0 μm Undialyzed[b]	979	0.156	0.23	0.31
1.0 μm Dialyzed[c]	195	0.30	0.40	0.50
1.0 + FP Undialyzed[d]	9923	0.033	0.040	0.076
1.0 + FP Dialyzed[e]	1066	0.047	0.105	0.213

[a] Diameters were measured on freeze-fracture electron micrographs as described in the text; the frequencies were then corrected (25) to eliminate the freeze-fracture artifacts. [b] Mechanically dispersed liposomes extruded through 1.0-μm membrane (Fig. 6). [c] 1.0-μm extruded liposomes dialyzed against a 0.8-μm membrane (Fig. 6). [d] The mixture of 1.0-μm extruded and French press (FP) liposomes described in Fig. 8. [e] The dialyzed mixture of 1.0-μm extruded and French press liposomes described in Fig. 8. [f] The corrected diameter of each liposome was used to calculate its surface area; the average surface area of the sample was then calculated and these values are the diameters of the liposome having this average area. [g] The volume of each liposome was calculated from its corrected diameter; the average volume of the sample was then calculated and these values are the diameters of the liposome having this average volume.

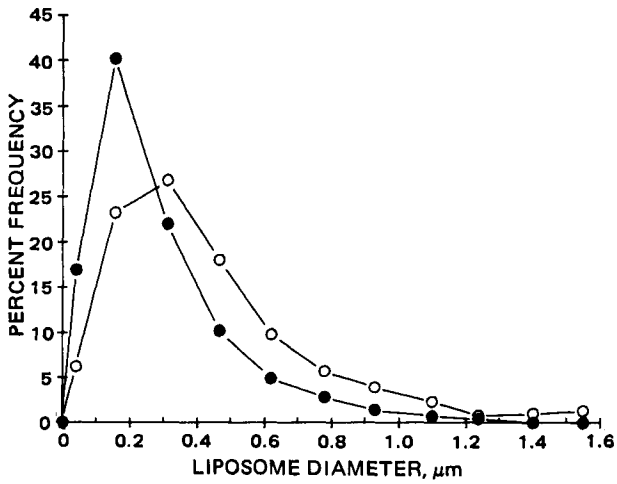

Figure 6—*The corrected percent of liposomes within equal diameter ranges is plotted* versus *the midpoint of the size range for 1.0-μm extruded liposomes before (●) and after (○) dialysis for 20 hr against a 0.8-μm membrane. The observed frequencies in each size range were corrected using the Wicksell method (25); the original data before applying the correction procedure is shown in Fig. 7.*

[4] Millipore Corp., Bedford, Mass.
[5] Nucleapore, Pleasanton, Calif.
[6] Aminco, Silver Spring, Md.

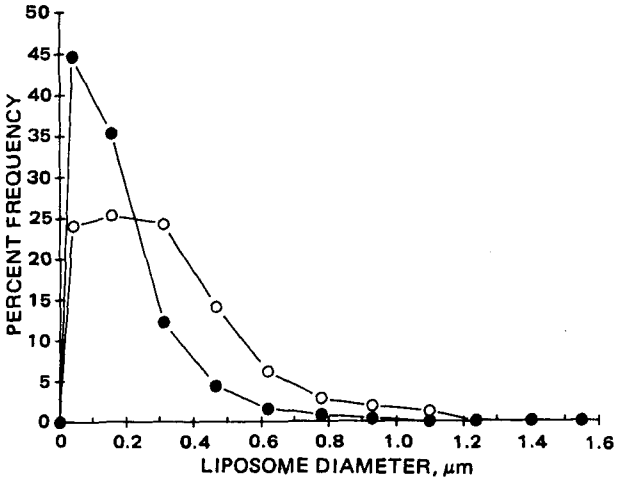

Figure 7—*The observed percent of liposomes within equal diameter ranges, as measured on the electron micrographs, is plotted* versus *the midpoint of the size range for 1.0-μm extruded liposomes before (●) and after (○) dialysis for 20 hr against a 0.8-μm membrane. The corrected data are shown in Fig. 6.*

quots of the liposome suspensions were diluted twofold with a 25% (v/v) solution of glycerin in buffer and kept at room temperature for 2 hr. The samples were then quickly frozen in liquid freon at ~−155° and stored at −190° in liquid nitrogen. Stored samples were transferred to the specimen stage of a freeze-fracture device[7], fractured at −115°, and then platinum-carbon coated. The replicas then were cleaned in dilute (1%) hypochlorite solution overnight, and rinsed for 10 min in several successive distilled water baths. A final 30-sec acetone rinse removed any remaining lipid. Replicas were then transferred to flamed 200-mesh grids and viewed at 80 kV. Magnification was determined using a carbon calibration grid.

RESULTS

Dialysis of Liposomes—Figure 1 shows results when mechanically dispersed liposomes were dialyzed against several different pore-size membranes. The initial rate and extent of dialysis increases with increasing pore size. The results suggest that the majority of liposomes are between 0.6 and 3.0 μm in diameter. When the French press liposomes, averaging 28 nm in diameter, were dialyzed against 0.05-, 0.1-, and 0.2-μm pore-size membranes (Fig. 2), the half-life of dialysis increased, as the ratio of the pore size to mean liposome diameter increased.

Figure 3 shows the results of a study in which 0.6, 0.4, and 0.2 μm extruded and French press liposomes were dialyzed against 0.8-μm membranes. There is a clear trend of more rapid and extensive dialysis as the liposome size decreases relative to membrane pore size. A first-order dialysis was seen only for the French press liposomes, where the membrane pore size is significantly larger than the largest liposomes in the suspension. Figure 4 shows the combined results of three separate studies in which 1.0-μm extruded liposomes were made and treated as follows: half of the batch was dialyzed for 20 hr against 0.8-μm membranes, the other half against 0.05-μm membranes. Both subbatches were subsequently dialyzed a second time against 0.8-μm membranes for 72 hr. There is a significant difference in dialysis patterns because a fraction of the smaller liposomes dialyzed across the 0.8-μm membrane, whereas no significant dialysis across the 0.05-μm membrane was detected. Aliquots of both subbatches, taken after the first dialysis step, were used to construct size frequency distributions.

The effects of dialysis on a heterogeneous population, consisting of 1.0-μm extruded liposomes and French press liposomes (70 and 30%, respectively, of the total lipid), pictured in Fig. 5, were dramatic. This mixture was selected to represent a worse-case example (it is similar in size composition to those resulting from sonication of mechanically dispersed liposomes for short periods of time). A sample of this heterogeneous batch was saved and the rest was dialyzed for 21 hr using 1.0-μm membranes. Electron microscopy was then done on the dialyzed and undialyzed samples

Control Studies—The effect of the dialysis system on liposome stability was assessed as follows: aliquots of 0.8-μm extruded liposomes of either the I–II–III–IV = 4:1:1:0.05 or 4:1:4.5:0.01 composition, containing [^{14}C]sucrose, were dialyzed against 0.05-μm membranes following the same procedures used in other studies; these two compositions (differing in cholesterol content) were chosen as medium- and low-permeability liposomes (1). It was previously established that these same liposome types, when labeled with [^{14}C]cholesterol, would not dialyze across 0.05-μm membranes, so the appearance of [^{14}C]sucrose on the dialysate side would be evidence of liposome instability. After 24 hr a maximum of 3% had leaked from the more permeable liposomes, whereas no leakage was detected from the less permeable liposomes. For the case where the label did dialyze, it was important to know if the liposomes dialyzed across intact. To answer this question, 0.4-μm extruded liposomes of the I–II–III–IV = 4:1:4.5:0.05 composition containing [^{14}C]sucrose were dialyzed to equilibrium against 3.0-μm membranes (the size distribution of these liposomes is such that all are small enough to dialyze). Samples of the dialysate side were chromatographed on a sepharose gel column[8], and all of the radioactivity appeared in the void volume, indicating that the liposomes had dialyzed across intact.

The rate and extent of liposome dialysis was found to be a function of several system variables. The dialyses were concentration-dependent; that is, with all other variables held constant (*e.g.*, liposome size, mem-

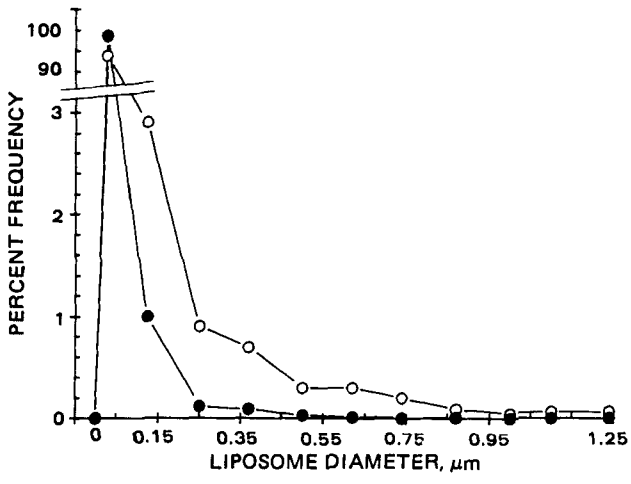

Figure 8—*The corrected percent of liposomes within equal diameter ranges is plotted* versus *the midpoint of the range for the liposome preparation consisting of a 1.0-μm-extruded (70% of total lipid) and French press liposomes (30% of total lipid) before (●) and after (○) dialysis for 20 hr against a 1.0-μm membrane. The original frequencies (not shown) were corrected to the observed frequencies using the Wicksell method (25).*

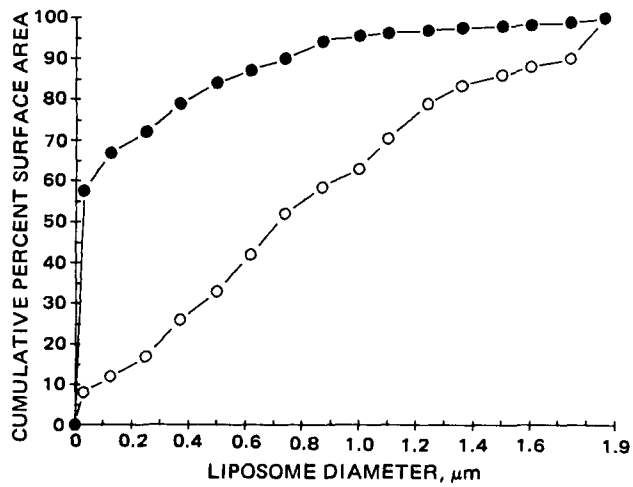

Figure 9—*The cumulative percent of total surface area (calculated from the corrected frequency data) for the two liposome populations shown in Fig. 8 is plotted* versus *the midpoint of the diameter range before (●) and after (○) dialysis.*

[7] Balzers, Berkhansted, U.K.

[8] G-50-80 Pharmacia Fine Chemical, Sweden.

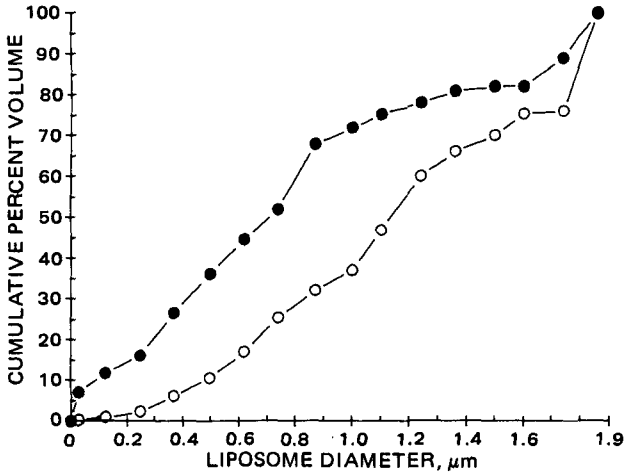

Figure 10—*The cumulative percent of the total volume (calculated from the corrected frequency data) for the two liposome populations shown in Fig. 8 is plotted* versus *the midpoint of the diameter range before (●) and after (○) dialysis.*

brane size), samples with higher lipid concentration dialyzed more slowly than more dilute samples. The agitation rate and the cell fill-volume were important. Three different modes of agitation rates (*i.e.*, motionless, gentle test tube inverter, and the horizontal shaker described previously) gave dialysis rates that covered a sixfold range. It was necessary to leave a small head space of air (~300 μl) when filling the cells, so that the dialyzing solution had the opportunity to agitate sufficiently. When these variables were held constant, the dialyses were reproducible.

Electron Microscopy and Liposome Sizing—Size–frequency distributions are obtained directly from diameter measurements on freeze-fracture electron micrographs. Figure 5 shows the mixture of 1-μm extruded and French press liposomes. A large number of small liposomes (Fig. 5A) were seen before dialysis, but were rare after dialysis (Fig. 5B).

Size distributions were constructed by assigning each liposome (on the photomicrograph) to size categories of 1-mm width (*e.g.*, 1–2 mm, 2–3 mm, *etc.*). Diameters of liposomes with oblong shape were calculated by averaging the values for their long and short axes. Diameter measurements were made for the above mixture from 8070× micrographs, except for the smallest liposomes, which were measured on 26,090× blow-ups of regions on the same 8070× micrographs. The ratio of smaller to larger liposomes found on each blowup was assumed to hold constant on the small scale micrograph. On the 26,090× micrographs all liposomes with diameters 0–3.3 mm were counted and measured; on the 8070× micrographs all liposomes >1.0 mm were counted and measured. After all liposomes had been counted and measured, the appropriate scaling correction was made to yield actual diameters. The total number of liposome profiles measured and counted in each experiment is shown in Table I.

There are certain inherent biases in the previously described method of sizing. A given fracture plane may not make an equatorial cut through a specific liposome, and it is more probable that a large liposome will be cut than a smaller one; this has the effect of making the apparent average diameter larger than the actual average diameter. The magnitude of the overall bias depends on factors such as the population range and the shape of the actual distribution. These biases are correctable using the mathematical approach developed by Wicksell (25), and the cumulative surface area or cumulative total liposome volume was plotted *versus* diameter and their parameters tabulated in Table I.

The corrected and uncorrected frequency plots for dialyzed (*i.e.*, those remaining after dialysis) and undialyzed 1.0-μm extruded liposomes are shown in Figs. 6 and 7. It can be seen that the correction procedure shifts the size distribution to smaller sizes. Nevertheless, there is a clear upward shift in average size for the dialyzed liposomes, with a doubling in average corrected diameter (from 0.156 to 0.3 μm, Table I). The corrected cumulative surface area and volume curves, not shown, also exhibit dramatic shifts toward larger diameters, which is reflected in the changes in the diameters of the liposomes with the average surface area and volume (Table I).

The data in Figs. 8–10 for the mixture of 1-μm extruded and French press liposomes illustrates an extreme case but serves as an example for a number of points. The corrected frequency *versus* size curve before

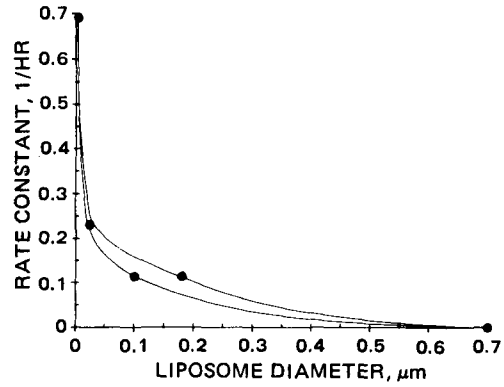

Figure 11—*The apparent first-order rate constant for various size liposomes against a 0.8-μm membrane is plotted* versus *their diameter. From left to right: (a) the rate constant for [^{14}C]inulin, assumed to be the upper limit for rate constants under the conditions used; (b) French press liposomes; (c) 0.2-μm extruded liposomes having an average diameter of 0.1 μm; (d) 0.2-μm extruded liposomes having an average diameter of 0.18 μm; (e) 0.7-μm extruded liposomes assuming negligible dialysis. The curves are arbitrary and drawn to approximate the actual underlying relationship.*

dialysis (Fig. 8) shows that ~99% of the liposomes are in the smallest size class, although French press liposomes comprised only 30% of the liposomal lipid; this class accounted for 58% of the total surface area, but only 7% of total liposome volume. Following dialysis the number of liposomes in the smallest size class decreased dramatically, but still accounted for ~95% of the total number (liposome dialysis was not limited to this size class; liposomes in the next few larger classes also dialyzed but to a lesser extent). Although dialysis of this mixture did not greatly increase the average diameter of the liposomes (Table I), it did produce a large increase in the diameter of the lipsomes with the average surface area and the average volume (Table I).

All differences noted between dialyzed and undialyzed preparations were significant; in the case where the fewest number of liposomes was measured (n = 195, Table I), the difference between mean diameters for the uncorrected dialyzed and undialyzed distributions was significant at the p <0.01 level (1-tailed t test using frequency *versus* log diameter distributions). For the corrected distributions (Fig. 5A) the level of significance between mean diameters before and after dialysis was greater.

Dialysis Simulations—The dialysis data for the French press liposomes (Fig. 2) indicates that when the preparation is homogeneous, dialysis is first order. Thus, the dialysis of a heterogeneous population may be simulated by a sum of first-order processes (or exponentials), one for each narrow size class as given by:

$$N_T = \sum_{i=1}^{n} N_{0,i}e^{-k_i t} + M \qquad \text{(Eq. 1)}$$

where N_T is the total number of liposomes remaining in the dialysis cell at time t, $N_{0,i}$ is the number in the ith narrow size class (*e.g.*, Fig. 5), k_i is the apparent first-order rate constant for dialysis of the ith class across a specific membrane, and M is the number of liposomes which cannot dialyze across that pore-size membrane. When a dialysis cleanup is complete, or after some time t, when dialysis is terminated, the fraction of liposomes in each size class will be:

$$N_{t,i}/N_T, N_{t,2}/N_T \ldots N/N_T \qquad \text{(Eq. 2)}$$

where

$$N_{t,i} = N_{0,i}e^{-k_i t} \qquad \text{(Eq. 3)}$$

Thus, if estimates of k_i can be obtained and the predialysis size–frequency distribution is known or can be approximated, the postdialysis size–frequency distribution can be determined. (If size–frequency distributions are not available, demonstrating the reproducibility of the dialysis pattern should ensure reproducibility of the final size–frequency distribution.) For example, the relationship between dialysis rate constant and diameter for the 0.8-μm membrane system described previously can be approximated (see Fig. 11). The maximum value of k_i is set equal to that obtained for a solution of [^{14}C]inulin. A rate constant of zero is assigned to liposomes >0.7-μm diameter, which were shown not to dialyze to any significant extent in this system over a 24-hr period. Additional rate constants are shown for French press liposomes of known mean diameter

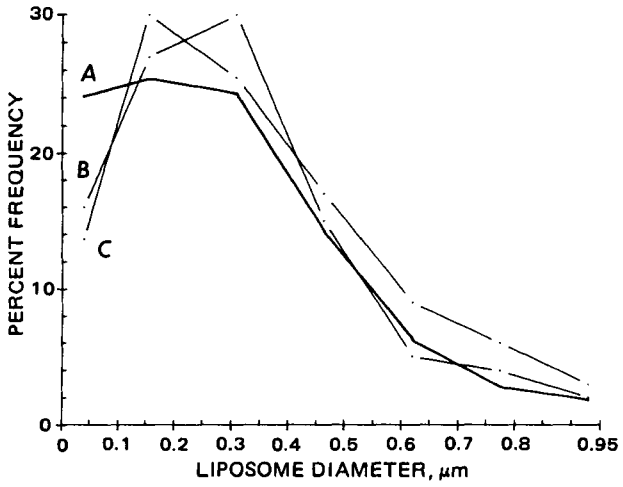

Figure 12—*Frequency, as percent of total, is plotted* versus *diameter. Curve* A *is replotted from Fig. 6 and is for 1.0-μm extruded liposomes following dialysis. Curves* B *and* C *are estimates of curve* A *calculated using Eq. 3, the undialyzed data in Fig. 6, and apparent dialysis rate constants interpolated from Fig. 10 as described in the text.*

and 0.2-μm extruded liposomes with mean diameters of 0.1 and 0.18 μm.

No attempt was made to fit the data in Fig. 11 to any specific function, rather the points were connected by two arbitrary curves to approximate the actual underlying pattern. Two sets of approximate rate constants were interpolated from this curve for the medium size of the seven smallest size categories used for construction of Fig. 6. Values of $N_{0,i}$ and M, obtained from the predialysis data in Fig. 6, along with seven estimates of k_i taken from each of the two curves in Fig. 11, were substituted into Eq. 1 to calculate the postdialysis in size–frequency distribution. The solid curve in Fig. 12 is the actual postdialysis size–frequency distribution. The broken curves are the two estimated size–frequency distributions and are reasonable given the limitations of both the method of calculation and the dialysis system: (*a*) the pores are not uniform in diameter; the manufacturer states that maximum pore size is 0—20% of the rated pore size; (*b*) pore size itself has a size–frequency distribution; (*c*) the technique for estimating the dialysis rate constants is crude; (*d*) the potential exists for large liposomes to block pores, thus reducing the effective dialysis rate constant for each size class.

DISCUSSION

A prerequisite for understanding the *in vivo* properties of liposomes is the availability of techniques to reproducibly prepare liposomes with defined size properties. With the exception of small unilamellar liposomes produced by prolonged sonication or carefully prepared French press liposomes, it is difficult to compare results between or within laboratories because the number, average size, size–frequency pattern, or surface area of the liposome dose rarely is known.

Because each liposome preparation has a characteristic dialysis profile for a given membrane and set of dialysis conditions (Figs. 1–4), dialysis data can be used as a means to compare the similarity of preparations and as a measure of their reproducibility. From the data presented (Figs. 1–4), the relative reproducibility of these preparations can be compared. Although the described technique is unsophisticated and simple, it does allow one to narrow the size–frequency distribution of any liposome batch while improving the reproducibility of preparation. Membrane extrusion under controlled conditions allows one to define and control the upper limit of liposome size anywhere between ~0.1 and 3.0 μm in diameter. This dialysis procedure allows control of the lower end of the size–frequency distributions.

Other techniques can be used to minimize the fraction of smaller liposomes in a preparation, but each has limitations. Separation of larger from smaller liposomes by centrifugation poorly discriminates between adjacent size classes and is further limited because liposomes of the same diameter may have different densities (*i.e.*, number of lamellae) and *vice versa*. Separation by filtration is possible in some cases when there is minimal interaction between liposomes and membranes (fiber types), but even at low pressure, some extrusion (22) occurs for all fluid-phase liposomes with the membranes used here. Filtration is more reliable when the process is carried out at a temperature below the phase transition temperature of the liposomal lipids (26, 27). Gel exclusion chromatography can be successfully used to obtain relatively narrow size distributions of small liposomes between ~20 and 80 nm in diameter and can also be used to control the lower end of the size–frequency distribution of larger liposomes when the adsorption of liposomal lipid onto the column can be minimized (this depends on liposome composition and column). Sedimentation field flow fractionation (28) is specifically designed for separation and analysis of particles in the liposome size range but is not designed for large-scale preparation; as the technique becomes more widely available it will, however, provide a technique to characterize the size–frequency distribution of liposome suspensions.

Control of liposome size may be critical when liposomes are designed for use as *in vivo* drug carriers. When *in vivo* fate is being followed using an aqueous space or liposomal membrane marker, the pharmacokinetic pattern seen will be a function primarily of the larger liposomes (Fig. 10), *i.e.*, the volume adjusted average size (29). Yet, the actual mechanisms governing liposome disposition are expected to be a function of the number of liposomes used and/or their total surface area, as well as diameter, when composition is held constant.

A combination of extrusion followed by dialysis, both using controlled-pored membranes, allows reproducible preparation of liposomes having a variety of definable size–frequency distributions. Subsequent use of dialysis rates can be used to obtain information about the size–frequency distribution and may be useful as a quality control technique.

REFERENCES

(1) F. Szoka and D. Papahadjopoulos, *Annu. Rev. Biophys. Bioeng.*, **9,** 467 (1980).

(2) A. D. Bangham, M. W. Hill, and N. G. A. Miller, *Methods Membr. Biol.*, **1,** 1 (1974).

(3) H. K. Kimelberg and E. Mayhew, *CRC Crit. Rev. Toxicol.*, **6,** 25 (1978).

(4) R. L. Juliano and D. Stamp, *Biochim. Biophys. Res. Commun.*, **63,** 651 (1975).

(5) H. K. Kimelberg, T. F. Tracy, Jr., S. M. Biddlecome, and R. S. Bourke, *Cancer Res.*, **36,** 2949 (1976).

(6) C. A. Hunt, Y. M. Rustum, E. Mayhew, and D. Papahadjopoulos, *Drug Metab. Dispos.*, **7,** 124 (1979).

(7) A. D. Bangham, M. M. Standish, and J. C. Watkins, *J. Mol. Biol.*, **13,** 238 (1965).

(8) C. Huang, *Biochemistry*, **8,** 344 (1969).

(9) Y. Barenholz, D. Gibbes, B. J. Litman, J. Goll, T. E. Thompson, and F. D. Carlson, *ibid.*, **16,** 2806 (1977).

(10) V. Rhoden and S. M. Goldin, *ibid.*, **18,** 4173 (1979).

(11) H. G. Enoch and P. Strittmatter, *Proc. Natl. Acad. Sci. USA*, **76,** 145 (1979).

(12) M. H. Milsmann, R. A. Schwendener, and H. G. Weder, *Biochim. Biophys. Acta*, **512,** 147 (1978).

(13) D. Deamer and A. D. Bangham, *ibid.*, **443,** 629 (1976).

(14) S. Batzri and E. D. Korn, *ibid.*, **298,** 1015 (1973).

(15) J. M. H. Kremer, M. W. J. Esker, C. Pathmamanoharan, and P. H. Weirsema, *Biochemistry*, **16,** 3932 (1977).

(16) Y. Barenholz, S. Amselem, and D. Lichtenberg, *FEBS Lett.*, **99,** 210 (1979).

(17) R. J. Hamilton, J. Goerke, L. S. S. Guo, M. C. Williams, and R. J. Havel, *J. Lipid Res.*, **21,** 981 (1980).

(18) F. Szoka, Jr. and D. Papahadjopoulos, *Proc. Natl. Acad. Sci. USA*, **75,** 4194 (1978).

(19) J. P. Reeves and R. M. Dowben, *J. Cell. Physiol.*, **73,** 49 (1969).

(20) D. Papahadjopoulos, W. J. Vail, K. Jacobson, and G. Poste, *Biochim. Biophys. Acta*, **394,** 483 (1975).

(21) W. R. Hargreaves and D. W. Deamer, *Biochemistry*, **17,** 3759 (1978).

(22) F. Olson, C. A. Hunt, F. C. Szoka, W. J. Vail, and D. Papahadjopoulos, *Biochim. Biophys. Acta*, **557,** 9 (1979).

(23) F. Szoka, F. Olson, T. Heath, W. Vail, E. Mayhew, E. Papahadjopoulos, and D. Papahadjopoulos, *ibid.*, **601,** 559 (1980).

(24) C. A. Hunt and S. Tsang, *Int. J. Pharm.*, **8,** 101 (1981).

(25) S. D. Wicksell, *Biometrika*, **17,** 84 (1925).

(26) A. M. Brendzel and I. F. Miller, *Biochim. Biophys. Acta*, **596,** 129 (1980).

(27) A. M. Brendzel and I. F. Miller, *ibid.*, **601,** 260 (1980).

(28) J. J. Kirkland, W. W. Yau, W. A. Doerner, and J. W. Grant, *Anal. Chem.*, **52**, 1944 (1980).
(29) C. Pidgeon and C. A. Hunt, *J. Pharm. Sci.*, **70**, 173 (1981).

ACKNOWLEDGMENTS

Abstracted in part from a dissertation submitted by M. E. Bosworth to the University of California in partial fulfillment of the Doctor of Philosophy degree requirements.

Supported by NIH Grants GM-24612, GM-26691, DAMD 17-79C-9045 from the U.S. Army Medical Research and Development Command and a University of California Regents Fellowship. Calculations were made using the PROPHET computer system of the Chemical/Biological Information Handling Program, NIH.

The authors thank Eileen Williams for manuscript preparation, and members of the Drug Delivery Research Group for helpful discussions.

Disposition of Quinidine in the Rabbit

THEODOR W. GUENTERT *, JIN-DING HUANG, and SVEIN ØIE ˣ

Received June 18, 1981, from the *Department of Pharmacy, School of Pharmacy, University of California, San Francisco, CA 94143.* Accepted for publication October 15, 1981. *Present address: Pharmazeutisches Institut, Universität Basel, Totengässlein 3, CH-4051 Basel, Switzerland.

Abstract □ Quinidine shows two-compartment characteristics in rabbits with a terminal half-life of 67 min for total drug and 58 min for unbound drug. Statistically, the values are not significantly different from each other ($p > 0.05$). The clearances for total and unbound drug are 52 and 464 ml/min/kg, respectively, and the total and unbound apparent volumes of distribution at steady state are 4.2 and 27.3 liters/kg, respectively. The unbound clearance and unbound apparent volume of distribution were inversely related to the unbound fraction of quinidine in plasma. The total clearance and apparent volume of distribution showed no relationship to the binding. Approximately 0.5% of the dose was excreted as unchanged quinidine. Six identifiable metabolites were found in the urine, accounting for ~14% of the dose. Two unknown metabolites were also observed in the urine. With the exception of 2′-quinidinone, these metabolites were formed in the rate-limiting step in the metabolite kinetics. The quinidine unbound fraction ranged from 0.06 to 0.23 in the eight rabbits studied. The binding of the metabolites was less pronounced, and only 3-hydroxyquinidine showed a significant correlation with quinidine binding.

Keyphrases □ Quinidine—disposition in rabbits, metabolites, binding □ Metabolites—binding, quinidine disposition, rabbits □ Binding—quinidine disposition, metabolites, rabbits □ Pharmacokinetics—disposition of quinidine, rabbits

Very little information exists regarding quinidine disposition in the rabbit, especially when unbound quinidine and metabolite concentrations are considered. The rabbit is, however, an attractive animal model for quinidine studies because it allows for sampling of sufficiently large blood volumes to determine both total and unbound concentrations; blood and urine sampling is simple; and if drug responses are desired, the response, measured as EKG changes, can be readily obtained (1).

As part of a long-term study of the disposition and response interrelationship between binding of quinidine to plasma proteins the pharmacokinetic picture of quinidine was evaluated in the rabbit.

EXPERIMENTAL

Quinidine Administration—Eight male New Zealand white rabbits (2.0–3.3 kg) were injected with 5.2 mg/kg of quinidine base as the gluconate salt[1] dissolved in 1 ml of saline into an ear vein over 2 min. Blood samples of 3-ml volume were obtained from the marginal vein in the other ear before the injections and again at 4, 8, 20, 40, 60, 90, 120, 150, 195, and 240 min after the injections. The blood was heparinized[2] to a final concentration of 5 U/ml. The blood was centrifuged and the plasma was stored at −20° until assayed. In addition, a 300-μl whole blood aliquot from the 4- and 150-min sampling time was also stored frozen until assayed. The red blood cells from the samples obtained at 20 min and at later time points were suspended in an equal volume of 6% dextran 75 in isotonic saline and reinfused within 10 min of sampling.

The urethra of each animal was cannulated with a catheter[3]. To ensure complete urine collection over the 4-hr study period, the bladder was rinsed twice with normal saline at the end of the study. The total urine collected was stored frozen until assayed.

Hepatic Blood Flow Determination—The hepatic blood flow was estimated in the individual animals 20–40 min after the end of the quinidine experiment by determining the indocyanine green blood clearance. Indocyanine green[4] (1 mg/kg) was infused over 30 sec into a marginal ear vein. Blood was collected from the marginal ear vein in the other ear by continuous withdrawal at a speed of 0.36 ml/min over a 12-min period, starting at the time of indocyanine green infusion.

The indocyanine green concentration in plasma of the withdrawn blood (C_{ICG}) was determined spectrophotometrically at 800 nm. Because the half-life of indocyanine green is 1 min and it does not enter the red blood

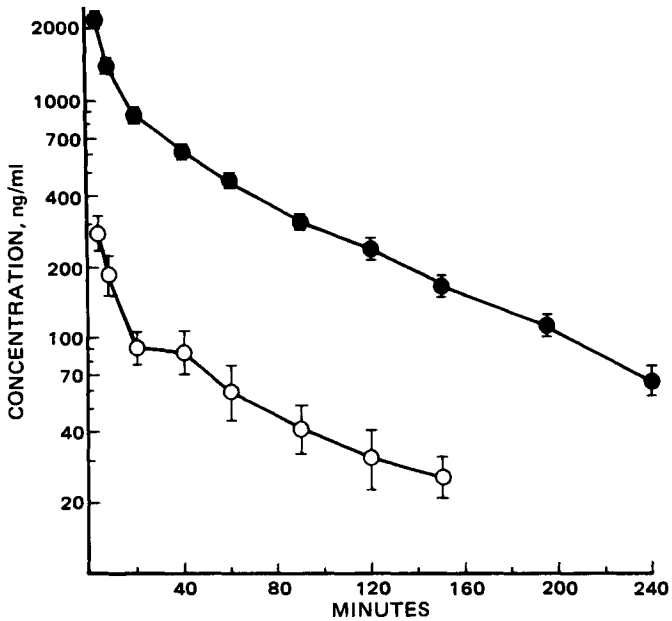

Figure 1—*Log-average plasma concentrations of total (●) and unbound (○) quinidine in eight rabbits after a 5.2-mg/kg intravenous injection.*

[1] Quinidine gluconate injection, USP, 80 mg/ml; Lilly, Indianapolis, Ind.
[2] Sodium heparin injection, USP, 1000 U/ml, Lilly, Indianapolis, Ind.
[3] French Foley Catheter #8, D. R. Bard, Ind., Murray Hill, N.J.
[4] Hynson, Westcott, & Dunning, Inc., Baltimore, Md.

0022-3549/82/0700-0812$01.00/0

(28) J. J. Kirkland, W. W. Yau, W. A. Doerner, and J. W. Grant, *Anal. Chem.*, **52**, 1944 (1980).
(29) C. Pidgeon and C. A. Hunt, *J. Pharm. Sci.*, **70**, 173 (1981).

ACKNOWLEDGMENTS

Abstracted in part from a dissertation submitted by M. E. Bosworth to the University of California in partial fulfillment of the Doctor of Philosophy degree requirements.

Supported by NIH Grants GM-24612, GM-26691, DAMD 17-79C-9045 from the U.S. Army Medical Research and Development Command and a University of California Regents Fellowship. Calculations were made using the PROPHET computer system of the Chemical/Biological Information Handling Program, NIH.

The authors thank Eileen Williams for manuscript preparation, and members of the Drug Delivery Research Group for helpful discussions.

Disposition of Quinidine in the Rabbit

THEODOR W. GUENTERT *, JIN-DING HUANG, and SVEIN ØIE ˣ

Received June 18, 1981, from the *Department of Pharmacy, School of Pharmacy, University of California, San Francisco, CA 94143.* Accepted for publication October 15, 1981. *Present address: Pharmazeutisches Institut, Universität Basel, Totengässlein 3, CH-4051 Basel, Switzerland.

Abstract □ Quinidine shows two-compartment characteristics in rabbits with a terminal half-life of 67 min for total drug and 58 min for unbound drug. Statistically, the values are not significantly different from each other ($p > 0.05$). The clearances for total and unbound drug are 52 and 464 ml/min/kg, respectively, and the total and unbound apparent volumes of distribution at steady state are 4.2 and 27.3 liters/kg, respectively. The unbound clearance and unbound apparent volume of distribution were inversely related to the unbound fraction of quinidine in plasma. The total clearance and apparent volume of distribution showed no relationship to the binding. Approximately 0.5% of the dose was excreted as unchanged quinidine. Six identifiable metabolites were found in the urine, accounting for ~14% of the dose. Two unknown metabolites were also observed in the urine. With the exception of 2′-quinidinone, these metabolites were formed in the rate-limiting step in the metabolite kinetics. The quinidine unbound fraction ranged from 0.06 to 0.23 in the eight rabbits studied. The binding of the metabolites was less pronounced, and only 3-hydroxyquinidine showed a significant correlation with quinidine binding.

Keyphrases □ Quinidine—disposition in rabbits, metabolites, binding □ Metabolites—binding, quinidine disposition, rabbits □ Binding—quinidine disposition, metabolites, rabbits □ Pharmacokinetics—disposition of quinidine, rabbits

Very little information exists regarding quinidine disposition in the rabbit, especially when unbound quinidine and metabolite concentrations are considered. The rabbit is, however, an attractive animal model for quinidine studies because it allows for sampling of sufficiently large blood volumes to determine both total and unbound concentrations; blood and urine sampling is simple; and if drug responses are desired, the response, measured as EKG changes, can be readily obtained (1).

As part of a long-term study of the disposition and response interrelationship between binding of quinidine to plasma proteins the pharmacokinetic picture of quinidine was evaluated in the rabbit.

EXPERIMENTAL

Quinidine Administration—Eight male New Zealand white rabbits (2.0–3.3 kg) were injected with 5.2 mg/kg of quinidine base as the gluconate salt[1] dissolved in 1 ml of saline into an ear vein over 2 min. Blood samples of 3-ml volume were obtained from the marginal vein in the other ear before the injections and again at 4, 8, 20, 40, 60, 90, 120, 150, 195, and 240 min after the injections. The blood was heparinized[2] to a final concentration of 5 U/ml. The blood was centrifuged and the plasma was stored at −20° until assayed. In addition, a 300-μl whole blood aliquot from the 4- and 150-min sampling time was also stored frozen until assayed. The red blood cells from the samples obtained at 20 min and at later time points were suspended in an equal volume of 6% dextran 75 in isotonic saline and reinfused within 10 min of sampling.

The urethra of each animal was cannulated with a catheter[3]. To ensure complete urine collection over the 4-hr study period, the bladder was rinsed twice with normal saline at the end of the study. The total urine collected was stored frozen until assayed.

Hepatic Blood Flow Determination—The hepatic blood flow was estimated in the individual animals 20–40 min after the end of the quinidine experiment by determining the indocyanine green blood clearance. Indocyanine green[4] (1 mg/kg) was infused over 30 sec into a marginal ear vein. Blood was collected from the marginal ear vein in the other ear by continuous withdrawal at a speed of 0.36 ml/min over a 12-min period, starting at the time of indocyanine green infusion.

The indocyanine green concentration in plasma of the withdrawn blood (C_{ICG}) was determined spectrophotometrically at 800 nm. Because the half-life of indocyanine green is 1 min and it does not enter the red blood

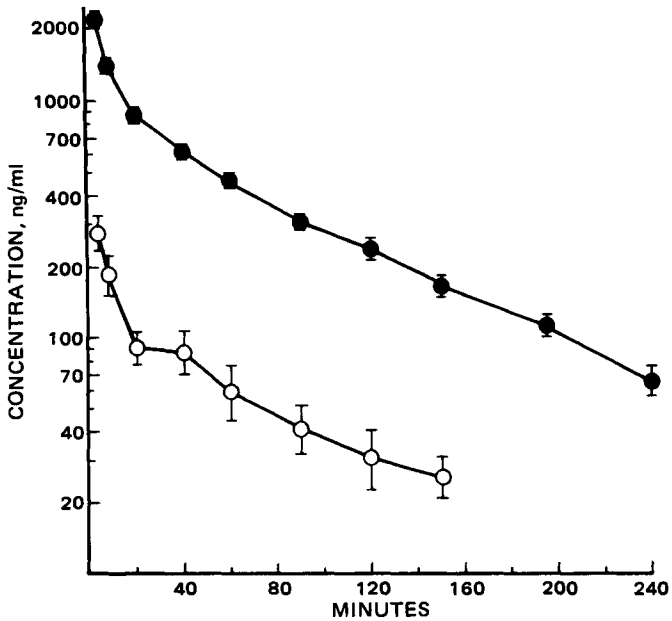

Figure 1—*Log-average plasma concentrations of total (●) and unbound (○) quinidine in eight rabbits after a 5.2-mg/kg intravenous injection.*

[1] Quinidine gluconate injection, USP, 80 mg/ml; Lilly, Indianapolis, Ind.
[2] Sodium heparin injection, USP, 1000 U/ml, Lilly, Indianapolis, Ind.
[3] French Foley Catheter #8, D. R. Bard, Ind., Murray Hill, N.J.
[4] Hynson, Westcott, & Dunning, Inc., Baltimore, Md.

0022-3549/82/0700-0812$01.00/0

Table I—Pharmacokinetic Parameters of Quinidine in Rabbits

Rabbit Number	Unbound Fraction	Clearance, ml/min/kg		Renal Clearance, ml/min/kg		Volume of distribution steady state, liter/kg		$t_{1/2,\alpha}$[a], min		$t_{1/2,\beta}$[a], min	
		Total	Unbound	Total	Unbound	Total	Unbound	Total	Unbound	Total	Unbound
1	0.06	51	797	0.3	4.3	2.8	31.3	1.6	2.3	50	34
2	0.19	53	277	0.5	2.7	4.5	21.4	9.9	3.3	77	76
3	0.15	44	295	0.5	3.1	4.5	24.2	11.4	4.3	90	71
4	0.18	47	254	[b]	[b]	4.0	22.7	3.1	0.7	64	81
5	0.06	51	922	0.05	0.9	3.4	48.4	3.7	2.5	60	45
6	0.16	64	401	0.04	0.3	5.0	28.0	6.0	4.7	65	59
7	0.23	48	211	[b]	[b]	4.0	12.6	4.7	2.3	70	54
8	0.11	58	554	0.3	2.4	5.0	28.8	6.2	4.8	61	45
Mean	0.14	52	464	0.3	2.3	4.2	27.3	5.8	3.1	67	58
SD	0.06	6	268	0.2	1.5	0.8	10.3	3.4	1.4	12	17

[a] $t_{1/2,\alpha}$ = fast disposition half-life; $t_{1/2,\beta}$ = terminal half-life. [b] Incomplete urine collection.

cells, the blood clearance of indocyanine green (Cl_{ICG}) can be determined by:

$$Cl_{ICG} = \frac{\text{Amount infused}}{C_{ICG}\,\tau\,(1-H)}$$

where τ is the time of withdrawal and H is the hematocrit value.

Protein Binding—Protein binding was determined in each plasma sample using an equilibrium dialysis technique (2): A 700-μl volume of freshly obtained plasma and of Krebs–Ringer bicarbonate buffer (pH 7.4) (3) was placed into the two half-cells of a 1-ml dialysis cell[5], separated by a dialysis membrane[6] (average pore radius 24 Å). The membrane was pretreated by soaking in water (10 min), ethanol (15 min), and buffer (120 min) before use. The cells were equilibrated in a shaker bath[7] at 37° for 6 hr ± 20 min. The plasma and buffer were then removed and assayed immediately, or frozen until assayed for quinidine and metabolite content.

Plasma Protein Concentration—The total plasma protein concentration was determined before the injection of quinidine and again 30 min after concluding the study. Plasma (100 μl) was mixed with 5 ml of biuret reagent[8], and the absorbance at 540 nm was determined within 1 hr. An aqueous solution containing 80 g/liter of total protein was used as a standard[9].

Quinidine Assays—Quinidine and quinidine metabolites in plasma, whole blood, or buffer from equilibrium dialysis were determined using a specific reversed-phase high-pressure liquid chromatographic method. A 100-μl sample to be analyzed was mixed with 200 μl of a methanolic solution containing 170 ng/ml of dihydroquinidine internal standard (quinidine-free). Plasma and blood samples were centrifuged in a microhematocrit centrifuge[10] at 12,000×*g* for 2 min. A 20-μl aliquot of the sample was then injected into a C-18 μBondapak column of 30-cm length and 3.9-mm bore[11], connected to an HPLC pump[12]. Methanol–water–phosphoric acid 85% (27:72.95:0.05, v/v/v) was used as the mobile phase at a flow rate of 1.0 ml/min. Detection was achieved using a fluorescence detector[13] with excitation at 245 nm and emission at 440 nm (cutoff filter). Correction of dihydroquinidine contamination in the injection contributing to the internal standard peak was made from injection of the samples prepared as described previously, without addition of the internal standard. All samples were analyzed within 1 week of collection. However, the frozen samples have been found to be stable for up to 12 months without change in analyzed concentration.

Quinidine and quinidine metabolites in urine were assayed by a method described by Guentert *et al.* (4): Urine (200 μl) or 500 μl of urine hydrolysate was mixed with 150 μl of aqueous solution of 34 μg/ml pronetalol (internal standard), and 1.5 ml of 1 *M* borate buffer (pH 9.4). The mixture was extracted into 10 ml of methylene chloride–isopropanol (4:1, v/v). The organic phase was removed and extracted with 1 ml of 0.1 *N* sulfuric acid. The aqueous phase was then alkalinized with 1.5 ml of 1 *M* borate buffer (pH 9.4) and extracted with 8 ml of methylene chloride–isopropanol (4:1, v/v). The organic layer was evaporated to dryness and the residue reconsitituted in 200 μl of eluent. A 50-μl aliquot was injected

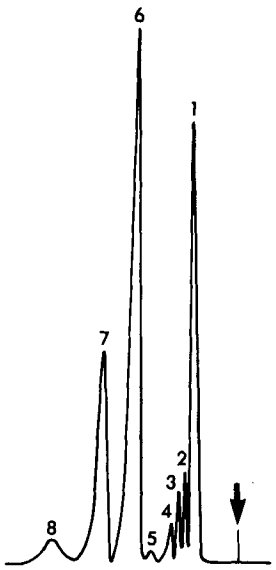

Figure 2—*Chromatogram obtained from plasma of rabbit no. 5 after a quinidine dose of 5.2 mg/kg. The arrow indicates time of injection. 1, quinidine-10,11-dihydrodiol; 2, 3-hydroxyquinidine; 3, 6-desmethylquinidine; 4, unknown metabolite; 5, quinidine-N-oxide; 6, quinidine; 7, dihydroquinidine (used as internal standard); 8, 2′quinidinone.*

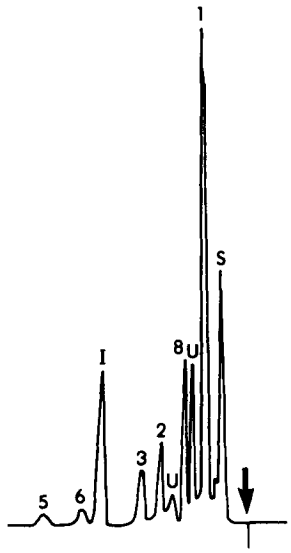

Figure 3—*Chromatogram obtained from the urine of rabbit No. 1 after a quinidine dose of 5.2 mg/kg. Identifications of peak numbers, (Fig. 2). 1, Pronetalol (internal standard); U, unknown metabolites.*

[5] Technilab Instruments, Inc., Pequannacock, N.J.
[6] VWR Scientific, Inc., San Francisco, Calif.
[7] Braun Melsungen AG, Germany.
[8] Sigma Chemical Co., St. Louis, Mo.
[9] Protein standard solution, Sigma Chemical Co.. St. Louis, Mo.
[10] IEC Model MB, Needham Heights, Md.
[11] Waters Associates, Inc., Milford, Mass.
[12] Altex Scientific model 110, Berkeley, Calif.
[13] Schoeffel Inst. Corp., model GM 970.

Table II—Rate Constants for the Various Metabolites, Min^{-1}

Rabbit Number	Peak 1 Quinidine-10,11-dihydrodiol		Peak 2 3-Hydroxyquinidine		Peak 3 6′-Desmethylquinidine		Peak 4 Unknown		Peak 5 Quinidine-*N*-oxide		Peak 8 2′-Quinidinone	
	Fast	Slow	Fast	Slow	Fast	Slow	Fast	Slow	Fast	Slow	Fast	Slow
1	0.142	0.010	[a]	[a]	[a]	[a]	0.606	0.009	0.104	0.011	0.020	0.004
2	0.024	0.011	0.098	0.007	[b]	[b]	0.140	0.006	[a]	[a]	0.012	0.0012
3	0.048	0.006	0.130	0.005	[b]	[b]	0.162	0.004	[a]	[a]	[a]	[a]
4	0.019	0.014	[a]	[a]	[a]	[a]	0.053	0.009	[a]	[a]	[a]	[a]
5	0.036	0.014	0.026	0.026	0.061	0.012	0.075	0.010	0.198	0.011	0.013	0.0002
6	0.039	0.010	0.104	0.009	[b]	[b]	0.103	0.008	0.290	0.008	0.024	0.0001
7	0.017	0.014	0.059	0.011	[b]	[b]	0.111	0.009	[a]	[a]	[a]	[a]
8	0.052	0.008	0.119	0.009	[b]	[b]	0.081	0.007	[a]	[a]	[a]	[a]
Mean	0.047	0.011	0.089	0.013	0.061	0.012	0.166	0.008	0.197	0.010	0.017	0.0014
SD	0.040	0.003	0.039	0.009	—	—	0.181	0.002	0.093	0.002	0.006	0.0018
n	8	8	6	6	1	1	8	8	3	3	4	4

[a] Not detected. [b] Only trace concentration was detected.

onto a μBondapak-phenyl column[11]. The mobile phase was acetonitrile–tetrahydrofuran–0.05 *M* phosphate buffer (pH 4.75) (15:6:79, v/v/v). The eluent was monitored using a variable wavelength detector[14] set at 230 nm. Quantitation of the compounds was achieved by using standard curves of quinidine and metabolites (5–8). The unknown metabolites were assumed to have identical spectroscopic behavior to quinidine. All standards were made from spiked blank plasma or urine samples and treated as described previously.

Hydrolysis of Urine—Urine (200 μl) was adjusted to pH 5.0 by addition of acetic acid. One milliliter of β-glucuronidase[8] (5000 Fishman U/ml) was added to the urine and incubated at 37° for 12 hr. The hydrolysate was analyzed for quinidine and metabolites as described previously. This method was at several instances compared to results obtained by hydrolysis with 0.1 ml of sulfatase[8] (2970 U/ml), containing 92,000 Fishman U/ml β-glucuronidase activity, and with incubation of 1 ml of denaturated β-glucuronidase (denatured by heating over steam bath for 5 min). Furthermore, the results were also compared to results from urine that had been refluxed with 2 *N* HCl at 100° for 1 hr. As the other two modes of hydrolysis did not give different results from β-glucuronidase, only the β-glucuronidase hydrolysis results are reported here. Incubation with denatured β-glucuronidase gave no significant alteration of the original urine concentration of quinidine and its metabolites. Standards made from spiked urine were treated identically to that described previously.

Pharmacokinetic Analysis—An open two-compartment model with a short-term, zero-order input was found suitable to describe the observed total and unbound quindine plasma concentration with time in all animals studied.

The metabolite concentrations could adequately be described by an apparent one-compartment model with a first-order rate of formation. The values of the rate constants were obtained using a fitting procedure (9) available through a computer system (10). Plasma concentrations were weighted by their inverse value squared. The clearance was determined using the dose and area under the plasma concentration–time curve, and the apparent volume of distribution at steady state was obtained by the area under the moment curve as described previously (11).

RESULTS

The log-averaged plasma concentrations of total and unbound quinidine in the eight animals as a function of time are given in Fig. 1. The various pharmacokinetic parameters for total and unchanged drug are given in Table I.

From three to six metabolites could be detected in plasma of the different rabbits. Only in rabbit No. 5 could six different metabolites be distinguished (Fig. 2). Five of these metabolites represent known metabolites [quinidine-10,11-dihydrodiol (8), 3-hydroxyquinidine (5, 12), 6′-desmethylquinidine (7), quinidine-*N*-oxide (6), 2′-quinidinone (13)]. Metabolite number 4 is unknown. Rate constants for the various metabolites are given in Table II.

Urine was found to contain at least eight metabolites of quinidine, of which five could be associated with known metabolic products (5–8, 12, 13). In Fig. 3 a chromatogram from urine of rabbit No. 1 is presented. Metabolite number 1, quinidine-10,11-dihydrodiol, appears to have a shoulder on many of the chromatograms, possibly indicative of the two diastereoisomers of this compound. In addition to the metabolites shown, the 6′-desmethylquinidine peak substantially increased upon hydrolysis of urine with β-glucuronidase, indicative of a 6′-desmethylquinidine conjugate (probably a glucuronide).

The fraction of the dose recovered as unchanged quinidine in urine ranged between 0.001 and 0.010. The fraction of the dose recovered as known quinidine metabolites, including the 6′-desmethylquinidine conjugate, ranged between 0.110 and 0.202 for the six rabbits where the urine collection was complete (Table III).

The blood to plasma ratio of quinidine in the rabbits was 1.05 ± 0.08, which is not statistically significantly different from 1.

The indocyanine green clearance, indicative of liver blood flow, was found to be 58 ± 12 ml/mg/kg.

The unbound fraction of quinidine in plasma varied between 0.06 and 0.23 in the eight rabbits (Table I). Of the known quinidine metabolites, only quinidine-10,11-dihydrodiol and 3-hydroxyquinidine could be evaluated for their binding to plasma protein. The unbound fraction in the eight rabbits varied between 0.26 and 0.46, with an average value of 0.34 and a *SD* of 0.06 for quinidine-10,11-dihydrodiol. In six of the rabbits, where 3-hydroxyquinidine was detected, the unbound fraction for this metabolite ranged between 0.16 and 0.32, with an average value of 0.25 and a *SD* of 0.06. The unknown metabolite (4), showed negligible binding, with an average ±*SD* of 0.74 ± 0.09. Of these metabolites, only 3-hydroxyquinidine showed a statistically significant correlation with the binding of quinidine ($r^2 = 0.84$, $p < 0.01$).

DISCUSSION

The disposition of both total and unbound quinidine in the rabbit can be described by a two-compartment model. Statistically, the fast disposition half-lives for total and unbound drug were not significantly different from each other and were found to be 5.8 and 3.1 min, respectively, indicating fast distribution. The slow disposition half-life for total drug at 67 min was not significantly different from that reported for unbound drug, 58 min ($0.10 > p > 0.05$). However, in two of the animals, No. 1 and 8, the terminal slope and half-life for total drug was significantly different from that of the unbound drug. This suggests that the rate constants of total and unbound drug for individual animals cannot be assumed to be interchangeable, even though the average population values show no differences. The observed half-life is much longer than the average half-life of 29 min previously reported in rabbits (1). However, these studies were carried out for only 50 min after an intravenous injection and for 60 min after the termination of an infusion over 90 min. This short collection time and the use of Cramer and Isaksson's assay method for quinidine (14), which has been shown to be nonspecific for quinidine (15), could be contributing factors to this discrepancy. Ueda and Nichols (16) found a slow disposition half-life for total drug that was much longer than that of this study. In a 3-hr study they observed a terminal half-life of 132 min, almost twice the value in this study. Except for using much larger and presumably older animals than those in this study, no significant differences in the experimental protocol can be found to explain this difference. Similarly, Ueda and Nichols also reported a much smaller clearance of quinidine than that reported in this study (16.8 ml/min/kg *versus* 52 ml/min/kg).

The fraction of quinidine excreted unchanged in the urine is very low (Table III). Provided the extrarenal clearance is predominantly hepatic, quinidine shows a high extraction ratio in the rabbit liver. The metabolic clearance of quinidine (52 ml/min/kg) approaches the value of hepatic blood flow (58 ml/min/kg). According to theoretical considerations, the total drug clearance of quinidine in this case should be independent of

[14] Hitachi Model 110-30, Altex Scientific, Berkeley, Calif.

Table III—Fraction of Administered Dose of Quinidine Recovered in the Urine of Rabbits after 4 Hr

Rabbit Number	Quinidine	Quinidine 10,11-dihydrodiol	2′-Quinidinone	3-Hydroxyquinidine	6-Desmethylquinidine	6-Desmethylquinidine conjugate	Quinidine-*N*-oxide	Unknown[a] metabolites
1	0.005	0.064	0.005	0.002	0.003	0.030	0.001	0.007
2	0.009	0.077	0.012	0.005	0.005	0.039	0.002	0.010
3	0.010	0.114	0.014	0.006	0.007	0.050	0.001	0.009
4	[b]	[b]	[b]	[b]	[b]	[b]	[b]	[b]
5	0.001	0.084	0.009	0.003	0.004	0.015	[c]	0.012
6	0.001	0.076	0.008	0.003	0.005	0.022	0.002	0.007
7	[b]	[b]	[b]	[b]	[b]	[b]	[b]	[b]
8	0.004	0.082	0.008	0.008	0.005	0.028	0.001	0.011
Mean	0.005	0.083	0.009	0.005	0.005	0.031	0.001	0.009
SD	0.004	0.017	0.003	0.002	0.001	0.012	0.001	0.002

[a] The sum of the two unknown metabolites (Fig. 3), assuming the metabolites have the same extractability and spectral characteristics as quinidine. [b] Incomplete urine collection. [c] Not detected.

the unbound fraction, and the unbound clearance inversely related to the unbound fraction (17). In accordance with this principle, the total clearance showed no statistically significant correlation with the unbound fraction ($p > 0.70$). The unbound clearance was strongly correlated with the inverse of the unbound fraction of quinidine in plasma ($p < 0.001$). These data confirm and support the previous observation in rabbits where the binding was altered by a bleeding procedure (18).

The apparent steady-state volume of distribution for total drug in this study, 4.2 liters/kg, was similar to the value calculated from the study of Ueda and Nichols (16). It showed no correlation with the unbound fraction in plasma ($p > 0.20$). The unbound apparent steady-state volume of distribution, however, showed a negative correlation with the unbound fraction ($p < 0.005$). This is the opposite to what could theoretically be expected for a compound with a large apparent volume of distribution (19) and is indicative of a correlation between tissue and plasma protein binding in individual animals.

Using the assay method described, the total recovery of the six identifiable metabolites and quinidine in the urine accounts for only 14% of the administered dose. Other primary or secondary metabolites must, therefore, account for the elimination of quinidine. However, only one conjugate of quinidine metabolites could be identified *via* enzymatic or acid hydrolysis of the urine.

Based on the fast elimination of unchanged quinidine in the rabbit, urine was collected for only 4 hr in this study. The terminal half-life of five of the metabolites in plasma was ~1 hr, suggesting that most of these compounds were eliminated in the collection period. The terminal half-lives of these metabolites are similar to that of quinidine, indicating that their formation is the rate-limiting step in their pharmacokinetic profile.

Accumulation of these metabolites after multiple doses will, therefore, only occur to a small degree. The sixth metabolite, 2′-quinidinone, exhibited a much slower elimination, with an apparent terminal half-life of 8 hr. The urinary recovery of this metabolite, with a study period of only 4 hr, therefore, was seriously underestimated and could possibly contribute to the overall low recovery of quinidine and metabolites in the urine. Because the observed half-life is greater than the study period, there is also little confidence in the estimated value of the half-life.

The protein binding of quinidine is variable; an unbound fraction varying from 0.06 to 0.23 was observed. Although two of the eight animals showed a statistically significant positive correlation between concentration and unbound fraction of quinidine in plasma, there was no difference in the terminal half-life between the total and unbound drug, suggesting that concentration-dependent binding is not a general phenomenon.

Because quinidine metabolites reportedly contribute to the pharmacologic activity (20), it may be of importance to note that all the metabolites for which protein binding was measured exhibited a lower binding than the parent compound. Of these metabolites for which binding could be evaluated, 3-hydroxyquinidine was the only one to show a statistically significant correlation with quinidine binding. This might suggest a common binding site and possible mutual displacement at high concentration.

REFERENCES

(1) V. E. Isaacs and R. D. Schoenwald, *J. Pharm Sci.*, **63,** 1119 (1974).

(2) T. W. Guentert and S. Øie, *ibid.*, **71,** 325 (1982).

(3) W. W. Umbreit, R. H. Burris, and J. F. Stauffer, "Manometric Techniques and Tissue Metabolism," Burgess, Minneapolis, Minn., 1951, p. 149.

(4) T. W. Guentert, A. Rakhit, R. A. Upton, and S. Riegelman, *J. Chromatogr.*, **183,** 514 (1980).

(5) F. I. Carroll, A. Philip, and M. C. Coleman, *Tetrahedron Lett.*, **21,** 1757 (1976).

(6) T. W. Guentert, P. E. Coates, and S. Riegelman, *APhA Acad. Pharm. Sci. Abstract*, **8,** 137 (1978).

(7) D. E. Drayer, D. T. Lowenthal, K.-M. Restivo, A. Schwartz, C. E. Cook, and M. M. Reidenberg, *Clin. Pharmacol. Ther.*, **24,** 31 (1978).

(8) S. E. Barrow, A. A. Taylor, E. C. Horning, and M. G. Horning, *J. Chromatogr.*, **181,** 219 (1980).

(9) N. Holford, in "Public Procedures Notebook," H. M. Perry and J. J. Wood, Eds., Bolt, Beraned, and Newman, Cambridge, Mass., 1979, p. 8.

(10) P. A. Castleman, C. H. Russell, F. N. Webb, C. A. Hollister, J. R. Siegel, S. R. Zdonik, and D. M. Fram, *Natl. Comput. Conf. Exposition Proc.*, **43,** 475 (1974).

(11) L. Z. Benet and R. L. Galeazzi, *J. Pharm. Sci.*, **68,** 1071 (1979).

(12) F. I. Carroll, D. Smith, and M. E. Wall, *J. Med. Chem.*, **17,** 985 (1974).

(13) K. H. Palmer, B. Martin, B. Baggett, and M. E. Wall, *Biochem. Pharmacol.*, **18,** 1845 (1969).

(14) G. Cramer and B. Isaksson, *Scand. J. Clin. Lab. Invest.*, **15,** 553 (1963).

(15) T. W. Guentert, P. E. Coates, R. A. Upton, D. L. Combo, and S. Riegelman, *J. Chromatogr.*, **162,** 59 (1979).

(16) C. T. Ueda and J. G. Nichols, *J. Pharm. Sci.*, **69,** 1400 (1980).

(17) G. R. Wilkinson and D. G. Shand, *Clin. Pharmacol. Ther.*, **18,** 377 (1975).

(18) T. W. Guentert and S. Øie, *J. Pharmacol. Exp. Ther.*, **215,** 165 (1980).

(19) S. Øie and T. N. Tozer, *J. Pharm. Sci.*, **68,** 1203 (1979).

(20) N. H. G. Holford, P. E. Coates, T. W. Guentert, S. Riegelman, and L. B. Sheiner, *Br. J. Clin. Pharmacol.*, **11,** 187 (1981).

Simultaneous Determination of Corticosterone, Hydrocortisone, and Dexamethasone in Dog Plasma Using High Performance Liquid Chromatography

M. ALVINERIE ˣ and P. L. TOUTAIN

Received May 22, 1981, from the *Station de Pharmacologie-Toxicologie, 180 chemin de Tournefeuille, 31300 Toulouse, France.* Accepted for publication October 13, 1981.

Abstract □ A sensitive, specific and reproducible high-performance liquid chromatographic procedure, using the normal phase and radial compression system, is described for the simultaneous determination of corticosterone, hydrocortisone, and dexamethasone in plasma, with prednisolone as the internal standard. Samples were extracted with methylene chloride and chromatographed on a microparticulate silica gel column using a radial compression system with UV detection at 254 nm. The assay has been applied in pharmacokinetic studies, and a typical plasma concentration–time profile for the three corticosteroids (all with 2 ng/ml sensitivity) is presented for dogs receiving dexamethasone.

Keyphrases □ Corticosterone—high-performance liquid chromatographic determination in dog plasma □ Hydrocortisone—high-performance liquid chromatographic determination in dog plasma □ Dexamethasone—high-performance liquid chromatographic determination in dog plasma □ High-performance liquid chromatography—determination of hydrocortisone, corticosterone, and dexamethasone in dog plasma □ Pharmacokinetics—high-performance liquid chromatographic determination of corticosteroids

Many methods for the determination of corticosteroids in plasma have been described, but many of them lack specificity or are too time-consuming for routine use.

Fluorometric techniques (1, 2) measure different steroids that fluoresce with varying intensity, but overestimate the true amounts of hydrocortisone and corticosterone. Analysis using GC (3) is complicated, because steroids with a C_{17} hydroxyacetone side chain undergo thermal degradation at the temperature employed. The assay of corticosteroids by GC would also seem to require the prior formation of a stable derivative. In competitive protein binding methods, the unknown and radiolabeled hydrocortisone compete for a hydrocortisone-binding protein such as transcortin (4–6). However, endogeneous substances with significant cross reactivity confound the assay performance. Radioimmunoassay is a competitive protein binding technique using an antibody to hydrocortisone as the binding protein. If the antibody is specific and binds hydrocortisone with high affinity, a sensitive assay can be made, although separation of hydrocortisone and corticosterone is crucial to obtaining a good specificity (7, 8). All these procedures are time-consuming and difficult to automate for use in a routine pharmacokinetic study.

The recent emergence of commercial high-pressure liquid chromatographic (HPLC) equipment (coupled with a sensitive UV detector), having the advantages of simple preliminary treatment of the sample, has attracted the attention of workers studying the analysis of corticosteroids in plasma.

Separation of corticosteroids by HPLC in humans has been documented by several authors (9, 10). However, in the dog, levels of endogeneous corticoids are lower than in humans, and techniques already described are not sensitive enough to be applied in this species.

The purpose of the present study was to report the use of a new radial compression system to determine simultaneously the plasma levels of endogenous and synthetic corticoids with a sensitivity level of ~2 ng/ml.

EXPERIMENTAL

Apparatus—The apparatus used in the extraction procedure was constant shaker[1] and a refrigerated centrifuge[2]. A constant volume high pressure liquid chromatograph[3] was equipped with a single wavelength 254 nm detector[4]. The column (10 × 0.8-cm i.d.) was packed with a 10-μm nominal normal phase[5] and was included in a radial compression system[6].

Reagents—Hydrocortisone, corticosterone, dexamethasone, and prednisolone reference standards[7] were used as received. Methylene chloride[8] and acetic acid[8] (analytical grade solvents) were used without further purification.

Mobile Phase—The mobile phase was prepared by mixing exact volumes of methylene chloride, methanol, and glacial acetic acid. The solution was strained and the gas removed. The ratio of methylene chloride, methanol, and acetic acid was 96:4:0.4 (v/v/v).

Operating Conditions—The UV detector was fixed at 254 nm, with a sensitivity of 0.005 aufs. A constant flow rate of 1.5 ml/min was maintained. The radial compression pressure was 1500 psi, and the inlet pressure was 200 psi. Chart speed was 0.5 cm/min.

Preparation of Standard Solutions—Each steroid was dissolved in methanol at a concentration of 1 mg/ml. The operating standard mixture was prepared by a 1:100 dilution in the elution solvent. Prednisolone was used as an internal standard at a concentration range of 1 mg/ml in methanol; a working solution was prepared by a 1:10 dilution in the same solvent.

Extraction Procedure—One milliliter of plasma sample, 1 ml of 0.1 *N* NaOH, and 10 ml of methylene chloride were added to a 30-ml tube[9]. The tubes were shaken for 10 min and centrifuged at 8400×*g* for 10 min at 4°. The methylene chloride layer was aspirated and evaporated at 40° under a nitrogen gas stream to prevent oxidation. The residue was dissolved in 100 μl of elution solvent and then injected into the column.

Calibration and Reproducibility—Pooled plasma of the dog was spiked with corticosterone and hydrocortisone (10–100 ng/ml) and with dexamethasone (10–1000 ng/ml). A constant amount of 100 ng of prednisolone as the internal standard was added to each sample (10 μl of a solution containing 10 μg/ml). Pooled plasma was extracted and was performed as outlined previously.

Calibration curves were constructed by calculating the ratio of the peak height of each compound to that of the internal standard, plotting the ratio against the amount of compound added to the sample. Peak heights of hydrocortisone and corticosterone were corrected for blank plasma response representing an endogenous serum component. The corrected peak height was used as the response.

Least-squares linear regression analysis was used to determine the slope, *y* intercept, and correlation coefficients.

The response of the HPLC system was linear in the concentration range

[1] Evapomix, Buchler Int. Fort Lee, N. J.
[2] J. 21, Beckman.
[3] Model M 45, Waters Associates, Milford, MA 01757.
[4] Model M 440, Waters Associates, Milford, MA 01757.
[5] Radialpack B, Waters Associates, Milford, MA 01757.
[6] Module RCM 100, Waters Associates, Milford, MA 01757.
[7] Sigma Chemical Co., St. Louis, MO 63178.
[8] Merck, Darmstardt, D 6100, West Germany.
[9] Corex.

0022-3549/82/0700-0816$01.00/0

Table I—Retention Times and Capacity Factor of Selected Glucocorticoids

Compound	Capacity Factor (K′)	Retention Time, min
Corticosterone	1.3	4.0
Dexamethasone	2	5.0
Hydrocortisone	2.5	6.0
Prednisolone	3.3	7.5

of 10–100 ng/ml for corticosterone and hydrocortisone and 10–100 ng for dexamethasone.

The analytical recovery of the compounds was measured by comparing the chromatographic peak heights from the analysis of biological samples, spiked with 100 ng of each compound and the peak height resulting from a direct injection of methanol standards.

Recovery of all compounds from plasma was 80–85% when ~85–90% of the methylene chloride layer was available for evaporation.

Assay precision was determined with successive sampling of pooled dog plasma. Ten successive samplings gave coefficients of variation <5% for all compounds: 3.39 for corticosterone, 4.90 for hydrocortisone, and 1.92 for dexamethasone.

Calculations—The concentration of corticosterone, hydrocortisone, and dexamethasone in the sample was determined from the following expression:

$$C_p: \frac{R}{a} + b \qquad \text{(Eq. 1)}$$

where C_p is the concentration of the substance in plasma (ng/ml), R is the peak height ratio (drug:internal standard), a is the slope of the calibration curve, and b is the y intercept.

Retention Time and Selectivity (Table I)—Normal-phase liquid chromatography using radial compression showed a high selectivity in the separation of corticosteroids. A good separation of the four compounds was obtained in 8 min.

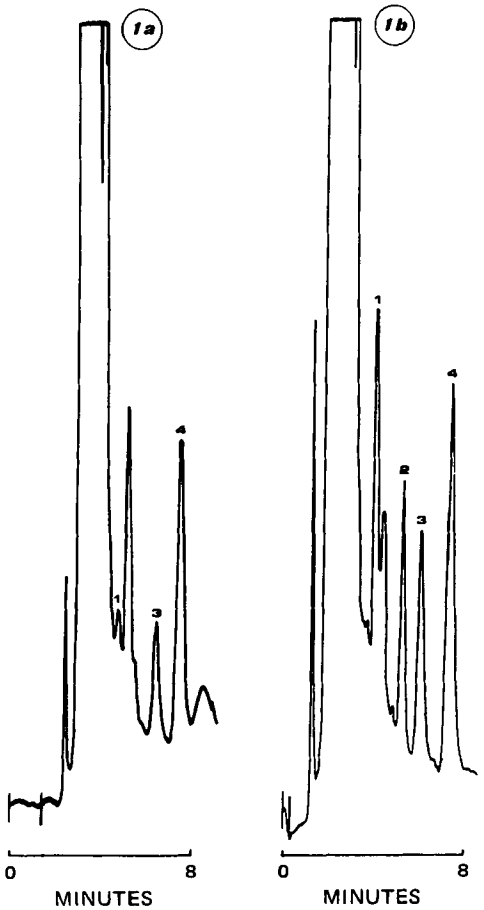

Figure 1—*Chromatogram of extracted blank dog plasma containing only internal standard (1a); chromatogram of extracted dog serum spiked with hydrocortisone, corticosterone, and dexamethasone (1b). 1, Corticosterone; 2, dexamethasone; 3, hydrocortisone; 4, prednisolone.*

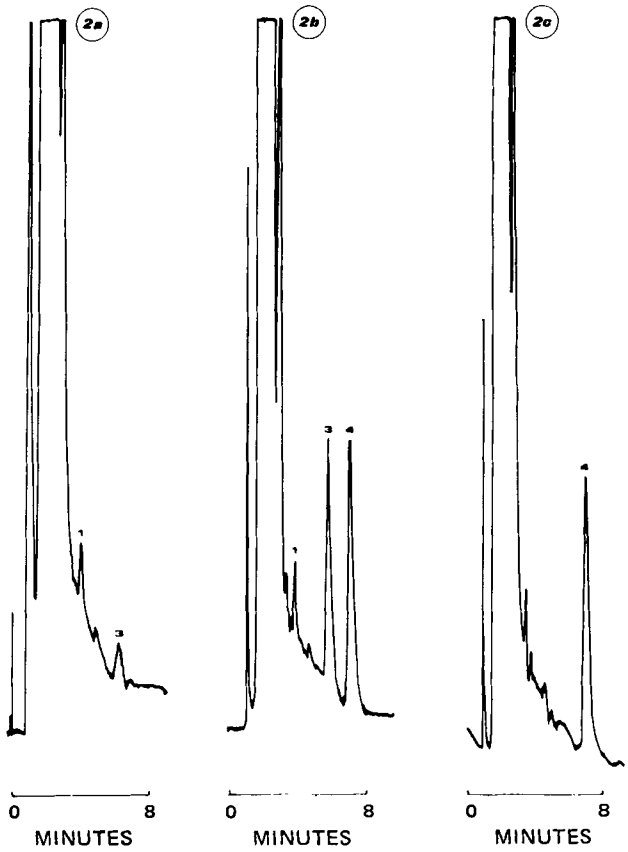

Figure 2—*Chromatogram of a plasma sample taken from a dog before the administration of corticotropin (2a); chromatogram of plasma 2 hr after the dose of corticotropin (2b); and chromatogram of extracted plasma after the injection of dexamethasone (2c). 1, Corticosterone; 3, hydrocortisone; 4 prednisolone.*

Drug Disposition Study—To test the ability of this method to detect endogenous corticosteroids, corticotropin[10] was administered intramuscularly (20 IU) into two dogs (11–12 kg; 4–5 years of age). To prove that exogenous corticoid could be detected, dexamethasone[11] was injected intravenously (1 mg/kg). Blood was withdrawn *via* the jugular vein at 15 and 30 min and 1, 2, 4, 8, and 24 hr after the treatment and placed in tubes containing 10 U of heparin. The plasma was separated immediately and stored at −20° until analysis.

RESULTS AND DISCUSSION

A chromatogram of a blank dog plasma extract and a chromatogram of plasma spiked with 40 ng of hydrocortisone, corticosterone, and dexamethasone are shown in Fig. 1. These chromatograms illustrate the response of the chromatographic system to 40 ng of corticosteroids/ml of plasma and to 100 ng of prednisolone which was used as the internal standard.

Figure 2*a* illustrates the chromatogram of a plasma sample taken from a dog before the administration of corticotropin. In addition, Fig. 2*b* illustrates the steroid concentration 2 hr after the dose of corticotropin; hydrocortisone concentrations were much greater in contrast to the small increase in corticosterone.

Figure 2*c* shows the effect of an injection of dexamethasone 12 hr postadministration. This chromatogram indicates that dexamethasone suppressed plasma corticosterone and hydrocortisone so that concentrations were no longer detectable. At this time, concentrations of dexamethasone were not detected.

Figure 3 presents a typical plasma concentration–time profile of dexamethasone after intravenous administration and the simultaneous evolution of the endogenous corticosteroids.

The simultaneous determination of corticosterone, hydrocortisone, dexamethasone, and prednisolone by this HPLC method proves to be

[10] ACTH-Choay, Choay, Paris, France.
[11] Azium, Unilabo, Levallois-Perret, France.

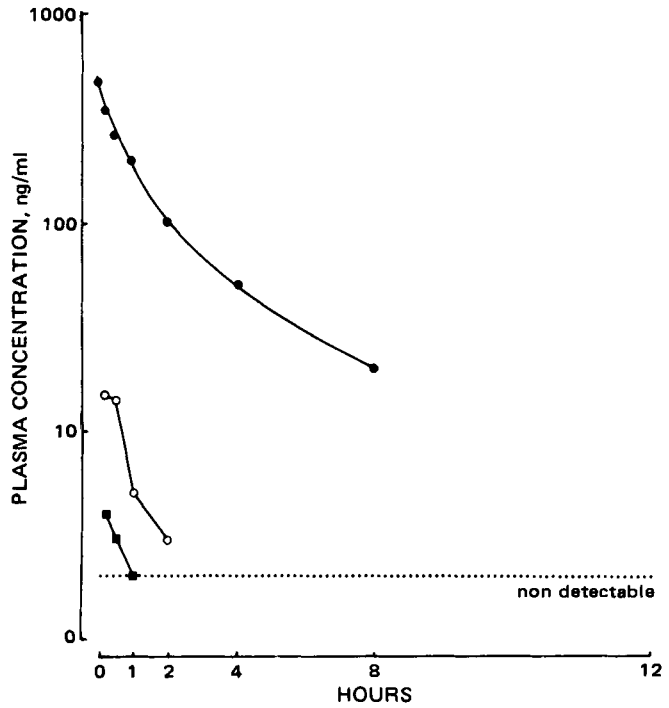

Figure 3—*Plasma concentration–time curve in the dog given a 1 mg/kg iv dose of dexamethasone. Key: (●), dexamethasone; (○), hydrocortisone; (■), corticosterone.*

efficient, precise, sensitive, and selective. It also allows the examination of the effects of dexamethasone on circulating hydrocortisone and corticosterone concentrations.

The selectivity of the extraction procedure and chromatographic system is demonstrated by the chromatogram from the blank plasma (Fig. 1*a*). Analysis of the figure indicates that there is no significant interference from endogenous compounds. It should be noted that one source of interference was encountered when the methylene chloride layer was recovered by filtration on phase-separating paper. One large interfering peak eluted at a retention time of 5 min and was labeled as an endogenous biological sample.

This chromatographic procedure differs from those previously described (11–19), as a new radial compression separation system was used. In this system a strong radial compression is applied to a soft column, thus diminishing the dead volume and the formation of preferential ways inside the column. This results in higher efficacy, with a lower pressure and increased flow rate. Moreover, it is possible to attain the same separation in 2 min with a flow rate of 6 ml/min and with only a 10% decrease in response.

Responses were considered significant when the signal to noise ratio was >1.5. In such conditions, using a detector sensitivity of 0.005 aufs, levels as low as 2 ng/ml, giving 0.5-cm peaks, could be quantitated.

In conclusion, the described method offers a simple, rapid, and reliable determination of corticosteroids for use in pharmacokinetic studies.

REFERENCES

(1) F. W. Funck and L. Sicha, *Med. Exp.*, **7**, 1 (1962).

(2) B. Favre and J. P. Moatti, *Ann. Rech. Vét.*, **8**, 111 (1977).

(3) W. L. Gardiner and E. C. Corning, *Biochim. Biophys. Acta*, **115**, 524 (1965).

(4) A. W. Meikle, L. G. Lagerquist, and F. H. Tyler, *Steroids*, **23**, 193 (1973).

(5) M. Hichens and A. F. Hogans, *Clin. Chem.*, **20**, 266 (1974).

(6) M. C. Dumasia, D. I. Chapman, M. S. Moss, and C. O'Connor, *J. Biochem.*, **133**, 401 (1973).

(7) S. W. Schalm, W. H. J. Summerskill, and V. L. M. Go, *Mayo Clinic. Proc.*, **51**, 761 (1976).

(8) D. C. Anderson, B. R. Hopper, B. L. Lasley, and S. S. Yen, *Steroids*, **28**, 179 (1976).

(9) W. Wortmann, C. Schnabel, and J. C. Touchstone, *J. Chromatogr.*, **84**, 396 (1973).

(10) J. Q. Rose and W. J. Jusko, *ibid.*, **162**, 273 (1979).

(11) J. C. K. Loo, A. G. Butterfield, F. Moffat, and N. Jordan, *ibid.*, **143**, 275 (1977).

(12) J. C. K. Loo and N. Jordan, *ibid.*, **143**, 314 (1977).

(13) S. E. Tsuei and J. J. Ashley, *ibid.*, **145**, 213 (1978).

(14) M. D. Smith, *ibid.*, **164**, 129 (1979).

(15) M. D. Smith and D. J. Hoffman, *ibid.*, **168**, 163 (1979).

(16) G. Cavina, G. Moretti, R. Alimenti, and B. Gallinella, *ibid.*, **175**, 12 (1979).

(17) M. Schoneshoffer and H. J. Dulce, *ibid.*, **164**, 17 (1979).

(18) N. R. Scott and P. F. Dixon, *ibid.*, **164**, 17 (1979).

(19) M. C. Petersen, R. L. Nation, and J. L. Ashley, *ibid.*, **183**, 131 (1980).

NOTES

Rapid Enzymatic Preparation of [^{14}C]D-Leucine from [^{14}C]DL-Leucine

GEORGE A. DIGENIS ˣ, RENSUKE GOTO, JAMES E. CHANEY, and OSAMU TAMEMASA

Received July 6, 1981, from the *Division of Medicinal Chemistry and Pharmacognosy, College of Pharmacy, University of Kentucky, Lexington, KY 40506.* Accepted for publication September 25, 1981.

Abstract □ A rapid enzymatic method for the preparation of [1-^{14}C]D-leucine is described. [1-^{14}C]D-Leucine was obtained from [1-^{14}C]DL-leucine by oxidative deamination of the L-isomer using immobilized L-amino acid oxidase. The total preparation (including ion exchange purification) was accomplished in 40 min with an 83% yield. The methodology is applicable to the production of [1-^{11}C]D-leucine, a potential imaging agent for tumor localization.

Keyphrases □ [^{14}C]D-leucine—rapid enzymatic preparation for tumor localization □ Enzymatic preparation—D-leucine isomers, [^{11}C]D-leucine production for tumor localization

Amino acids labeled with gamma-emitting radionuclides (carbon 11 or nitrogen 13) have been investigated for tumor localization, pancreatic scanning, and the study of normal physiological processes. Several ^{13}N-labeled L-amino acids have been synthesized enzymatically and their tissue distribution and pancreatic uptake studied in animals

0022-3549/82/0700-0818$01.00/0

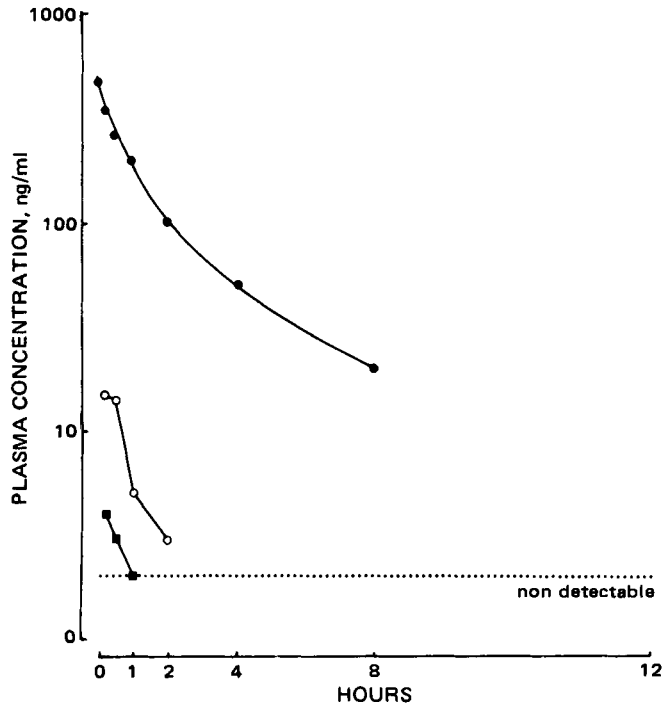

Figure 3—*Plasma concentration–time curve in the dog given a 1 mg/kg iv dose of dexamethasone. Key: (●), dexamethasone; (○), hydrocortisone; (■), corticosterone.*

efficient, precise, sensitive, and selective. It also allows the examination of the effects of dexamethasone on circulating hydrocortisone and corticosterone concentrations.

The selectivity of the extraction procedure and chromatographic system is demonstrated by the chromatogram from the blank plasma (Fig. 1*a*). Analysis of the figure indicates that there is no significant interference from endogenous compounds. It should be noted that one source of interference was encountered when the methylene chloride layer was recovered by filtration on phase-separating paper. One large interfering peak eluted at a retention time of 5 min and was labeled as an endogenous biological sample.

This chromatographic procedure differs from those previously described (11–19), as a new radial compression separation system was used. In this system a strong radial compression is applied to a soft column, thus diminishing the dead volume and the formation of preferential ways inside the column. This results in higher efficacy, with a lower pressure and increased flow rate. Moreover, it is possible to attain the same separation in 2 min with a flow rate of 6 ml/min and with only a 10% decrease in response.

Responses were considered significant when the signal to noise ratio was >1.5. In such conditions, using a detector sensitivity of 0.005 aufs, levels as low as 2 ng/ml, giving 0.5-cm peaks, could be quantitated.

In conclusion, the described method offers a simple, rapid, and reliable determination of corticosteroids for use in pharmacokinetic studies.

REFERENCES

(1) F. W. Funck and L. Sicha, *Med. Exp.*, **7**, 1 (1962).

(2) B. Favre and J. P. Moatti, *Ann. Rech. Vét.*, **8**, 111 (1977).

(3) W. L. Gardiner and E. C. Corning, *Biochim. Biophys. Acta*, **115**, 524 (1965).

(4) A. W. Meikle, L. G. Lagerquist, and F. H. Tyler, *Steroids*, **23**, 193 (1973).

(5) M. Hichens and A. F. Hogans, *Clin. Chem.*, **20**, 266 (1974).

(6) M. C. Dumasia, D. I. Chapman, M. S. Moss, and C. O'Connor, *J. Biochem.*, **133**, 401 (1973).

(7) S. W. Schalm, W. H. J. Summerskill, and V. L. M. Go, *Mayo Clinic. Proc.*, **51**, 761 (1976).

(8) D. C. Anderson, B. R. Hopper, B. L. Lasley, and S. S. Yen, *Steroids*, **28**, 179 (1976).

(9) W. Wortmann, C. Schnabel, and J. C. Touchstone, *J. Chromatogr.*, **84**, 396 (1973).

(10) J. Q. Rose and W. J. Jusko, *ibid.*, **162**, 273 (1979).

(11) J. C. K. Loo, A. G. Butterfield, F. Moffat, and N. Jordan, *ibid.*, **143**, 275 (1977).

(12) J. C. K. Loo and N. Jordan, *ibid.*, **143**, 314 (1977).

(13) S. E. Tsuei and J. J. Ashley, *ibid.*, **145**, 213 (1978).

(14) M. D. Smith, *ibid.*, **164**, 129 (1979).

(15) M. D. Smith and D. J. Hoffman, *ibid.*, **168**, 163 (1979).

(16) G. Cavina, G. Moretti, R. Alimenti, and B. Gallinella, *ibid.*, **175**, 12 (1979).

(17) M. Schoneshoffer and H. J. Dulce, *ibid.*, **164**, 17 (1979).

(18) N. R. Scott and P. F. Dixon, *ibid.*, **164**, 17 (1979).

(19) M. C. Petersen, R. L. Nation, and J. L. Ashley, *ibid.*, **183**, 131 (1980).

NOTES

Rapid Enzymatic Preparation of [^{14}C]D-Leucine from [^{14}C]DL-Leucine

GEORGE A. DIGENIS ˣ, RENSUKE GOTO, JAMES E. CHANEY, and OSAMU TAMEMASA

Received July 6, 1981, from the *Division of Medicinal Chemistry and Pharmacognosy, College of Pharmacy, University of Kentucky, Lexington, KY 40506.* Accepted for publication September 25, 1981.

Abstract □ A rapid enzymatic method for the preparation of [1-^{14}C]D-leucine is described. [1-^{14}C]D-Leucine was obtained from [1-^{14}C]DL-leucine by oxidative deamination of the L-isomer using immobilized L-amino acid oxidase. The total preparation (including ion exchange purification) was accomplished in 40 min with an 83% yield. The methodology is applicable to the production of [1-^{11}C]D-leucine, a potential imaging agent for tumor localization.

Keyphrases □ [^{14}C]D-leucine—rapid enzymatic preparation for tumor localization □ Enzymatic preparation—D-leucine isomers, [^{11}C]D-leucine production for tumor localization

Amino acids labeled with gamma-emitting radionuclides (carbon 11 or nitrogen 13) have been investigated for tumor localization, pancreatic scanning, and the study of normal physiological processes. Several ^{13}N-labeled L-amino acids have been synthesized enzymatically and their tissue distribution and pancreatic uptake studied in animals

0022-3549/82/0700-0818$01.00/0

(1–3). Transplanted tumors in rats have been detected by external scintigraphy using [^{11}C]carboxyl-labeled 1-aminocyclopentanecarboxylic acid (4). A modified synthesis[1] has been successfully utilized for the production of [^{11}C]carboxyl-labeled amino acids (5, 6). On the basis of data obtained from animal experiments and studies with humans it has been suggested that [^{11}C]carboxyl-labeled DL-tryptophan (7, 8) and DL-valine (9), when used in conjunction with positron computerized transaxial tomography, have significant potential as clinical pancreas-imaging agents.

Recent studies suggest that optically active isomers of ^{11}C-labeled amino acids would be biologically more interesting than the racemic amino acids. For example, it has been previously demonstrated (10) that ^{14}C-labeled D-isomers of some amino acids showed greater affinity for tumors in mice than did the L-isomers. More specifically, ^{14}C-labeled D-leucine has been shown to exhibit a preferential incorporation into tumor cells of nude mice bearing human colon and thyroid cancer[2].

The present report describes the methodology for the rapid preparation of D-leucine which makes possible the availability of this amino acid in its ^{11}C-labeled form as a potential diagnostic reagent for tumors.

EXPERIMENTAL

Immobilization of L-Amino Acid Oxidase—Snake venom L-amino acid oxidase[3] (50 mg) was dissolved in 30 ml of 0.1 *M* sodium pyrophosphate buffer, pH 8.3. Cyanogen bromide-activated sepharose-4B beads[3] (2.5 g) were washed and swollen by treating with 400 ml of 1×10^{-3} *N* HCl. The beads were recovered by filtration using a coarse sintered glass funnel and were immediately added to the buffered enzyme solution in a 50-ml round-bottom flask. The mixture was stoppered and gently mixed with a wrist action shaker at 4–5° for 30 hr. After immobilization, the beads were washed several times on a coarse sintered glass funnel using 0.1 *M* sodium pyrophosphate, pH 8.3, to remove the soluble enzyme. Subsequently, the immobilized enzyme was alternately washed twice with 0.1 *M* pyrophosphate buffer (pH 8.3) and 0.1 *M* acetate buffer (pH 5.6) and finally twice more with 0.1 *M* pyrophosphate buffer (pH 8.3). The resulting L-amino acid oxidase on sepharose-4B was stored at 5–7° in 50–100 ml of 0.1 *M* pyrophosphate buffer at pH 8.3.

Preparation of [1-^{14}C]D-Leucine—[1-^{14}C]DL-Leucine[4] (1.25 μCi) (specific activity: 59 mCi/mmole; concentration: 50 μCi/ml) and 2.5 g sepharose-immobilized L-amino acid oxidase were added to a 50-ml solution of 1×10^{-3} *M* DL-leucine[3] in 0.1 *M* sodium phosphate buffer (pH 8.3). The preparation was described previously. The resulting mixture was gently agitated on a gyratory shaker bath at 37° for 10 min with concomitant passage of oxygen through the reaction mixture at the rate of 0.5 liters/min using a gas dispersion tube.

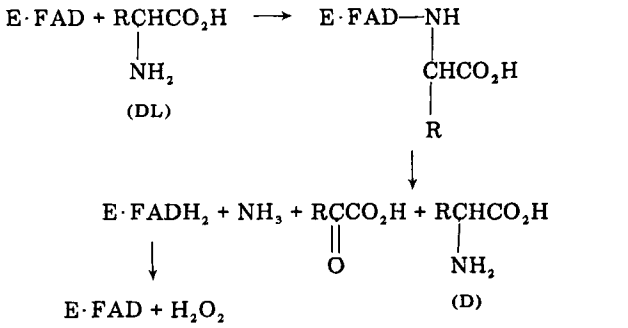

Scheme I—*Resolution of DL-leucine by oxidative deamination. FAD = flavin adenine dinucleotide, E = immobilized L-amino acid oxidase (L-AAO), and R = $CH_2CH(CH_3)_2$.*

The immobilized enzyme was removed from the reaction mixture by use of a sintered glass filter funnel and an aspirator vacuum. The filtrate was acidified with 1 ml of concentrated HCl and added to a cation exchange column (10 × 15 mm)[5]. The column was washed with two 50-ml portions of distilled water. (Insignificant amounts of radioactivity were found in the second wash.) The total radioactivity in these washings was 0.54 μCi. To recover the D-leucine the cation exchange column was eluted with 100 ml of 0.2 *N* NaOH which resulted in 0.52 μCi of radioactivity. The pH of the eluted [1-^{14}C]D-leucine solution was adjusted to 7.0, the resulting solution was concentrated to 1 ml, and an aliquot was applied to a silica gel TLC plate[6] (20 × 20 cm).

After two-dimensional chromatography [butanol[7]–acetic acid[8]–water (4:1:2) followed by phenol[9]–water, (75:25)] the plate was monitored by autoradiography[10]. The respective R_f values were 0.55 and 0.74. The position of the radioactive spot corresponded to the colored spot obtained prior to X-ray film exposure upon spraying with ninhydrin[3]. This spot corresponded to that of authentic leucine.

Optical Rotary Dispersion Spectropolarimetric Determination of the Production of D-Leucine—A solution of nonradioactive DL-leucine (1×10^{-3} *M*) was incubated with immobilized L-amino acid oxidase as described previously. The pH of the amino acid solution in 100 ml of 0.2 *N* NaOH recovered from the cation exchange column was adjusted to 7.0 and taken to dryness at 40° using a rotary evaporator. The residue was reconstituted into a 15-ml aqueous HCl solution (final pH 1.0). The optical rotary dispersion curve was determined in a 5-cm cell using an optical rotary dispersion spectropolarimeter[11]. The optical rotary dispersion spectrum was scanned in the wavelength region of 300 nm to 200 nm at a sensitivity setting of 350 millidegrees. The maximum absorbance was found at 224 nm. For comparison of the optical rotary dispersion spectrum to that of authentic D-leucine[3], a 0.25 m*M* solution of D-leucine in 0.2 *N* NaOH was prepared, dried, and reconstituted as for the previous solution. Also, a solution of D-leucine (0.5 m*M*) in 50 ml of 0.1*M* sodium pyrophosphate buffer was subsequently treated as the enzymatically produced D-leucine except for the enzyme exposure and the optical rotary dispersion was run.

Keto Acid Assay—The enzyme reaction was carried out as described previously using nonradioactive DL-leucine. 2,4-Dinitrophenylhydrazine[12] (0.5 ml, 0.1%) dissolved in 2 *N* HCl was added to vials containing 0.5 ml of the 50-ml filtrate. The mixtures were allowed to stand at 25° for 10 min, followed by the addition of 5 ml of 1.25 *N* NaOH. The optical densities at 440 nm using a spectrophotometer[13] were determined. A standard calibration curve was plotted and found to be linear at concentrations of keto acid (4-methyl-2-oxopentanoic acid[14]) ranging from 0.0625×10^{-3} *M* to 0.5×10^{-3} *M*.

RESULTS AND DISCUSSION

Resolution of [1-^{14}C]DL-leucine was accomplished by oxidative deamination as outlined in Scheme I. [1-^{14}C]D-Leucine was obtained from [1-^{14}C]DL-leucine by destruction of the L-isomer by the action of sepharose-immobilized L-amino acid oxidase at pH 8.3. When the reaction was complete (10 min) the mixture was acidified and passed through a cation exchange column to remove the keto acid. The column was washed with water until the eluate was practically free of radioactivity. Of the original activity in the starting [^{14}C]DL-leucine, 43% was found in these washings in the form of 4-methyl-2-oxopentanoic acid. This 43% recovery represents a yield of 86% for the keto acid. The [1-^{14}C]D-leucine was eluted from the column with 0.2 *N* NaOH in an 83.2% yield (41.6% of original radioactivity). These yields are an average of five experiments. An additional 11% of the unaccounted radioactivity (15%) was recovered by washing the enzyme two times with 50 ml of water. Two-dimensional TLC of the leucine recovered from the cation exchange column revealed that the product was pure and it chromatographed identically to authentic leucine as determined by spraying the plate with ninhydrin and finding that the ninhydrin positive spot coincided with the position of

[1] Bucherer-Strecker.
[2] O. Tamemasa, R. Goto, A. Takeda, and S. Maruo, manuscript in preparation.
[3] Sigma Chemical Co., St. Louis, Mo.
[4] Amersham Corporation, Arlington Heights, Ill.
[5] The resin (AG 50 W-X2, 50–100 mesh) and column were obtained from Bio-Rad Laboratories, Richmond, Calif.
[6] Quantum Industries, Fairfield, N.J.
[7] Aldrich Chemical Co., Milwaukee, Wis.
[8] Fisher Scientific Co., Cincinnati, Oh.
[9] Mallinckrodt Chemical Works, St. Louis, Mo.
[10] Packard Model 7201 Radiochromatogram Scanner, Packard Instrument Co., Downers Grove, Ill.
[11] JASCO Model UV-5.
[12] Eastman Chemical Co., Rochester, N.Y.
[13] Cary Model 118, Varian Associates, Instrument Division, Palo Alto, Calif.
[14] Tridem-Fluka, Inc., Hauppauge, N.Y.

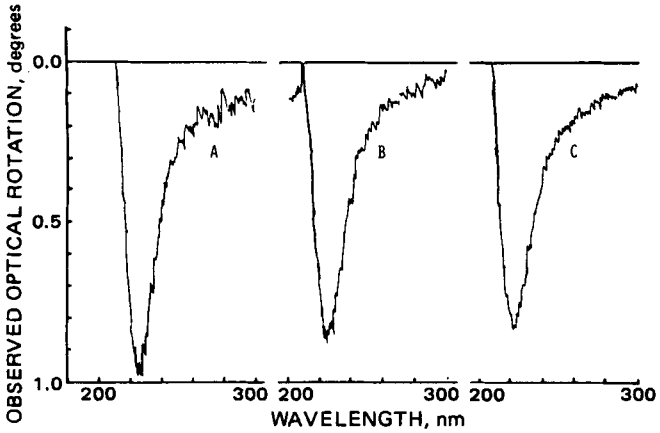

Figure 1—*Optical rotary dispersion curves for authentic D-leucine (A), authentic D-leucine recovered from cation exchange column (B), and enzymatically produced D-leucine after purification by cation exchange column chromatography (C).*

the radioactivity detected by autoradiography. The total resolution time including the ion exchange purification step was 40 min.

A nonradioactive resolution was analysed by optical rotary dispersion polarimetry in the range of 300–200 nm (Fig. 1). The optical rotary dispersion curve (Curve C) of the resolved D-leucine gave an optical rotation at 224 nm practically identical to that (Curve B) obtained by starting with half the amount of authentic D-leucine relative to the weight of DL-leucine used in the resolution and submitting it to the same ion exchange and reconstitution treatment applied to the resolved product.

The oxidative deamination of L-leucine in DL-leucine to the corresponding 4-methyl-2-oxopentanoic acid also was confirmed in the developmental work using nonradioactive DL-leucine by reacting aliquots of the reaction mixture with 2,4-dinitrophenylhydrazine yielding the 2,4-dinitrophenylhydrazone derivative which was monitored colorimetrically (440 nm) against standard 2,4-dinitrophenylhydrazone solutions. The keto acid yield was 84%. It was shown in this keto acid assay that the amino acid does not interfere with the analysis for the keto acid, making it unnecessary to separate the keto acid from the D-leucine.

Advantages of the oxidative deamination method for resolution are that it requires simple materials, is easily adaptable to hot cell conditions, and produces each of the enantiomers depending on the amino acid oxidase used.

REFERENCES

(1) M. B. Cohen, L. Spolter, N. S. MacDonald, and B. Cassen, *J. Nucl. Med.*, **13**, 422 (1972).

(2) N. Lembares, R. Dinwoodie, I. Gloria, P. Harper, and K. Lathrop, *ibid.*, **13**, 786 (1972).

(3) L. Spolter, M. B. Cohen, N. MacDonald, C. C. Chang, J. Takahashi, H. Neely, G. Hugh, S. Meyers, and D. Bobinet, *ibid.*, **15**, 535 (1974).

(4) R. L. Hayes, L. C. Washburn, B. W. Wieland, T. T. Sun, R. R. Turtle, and T. A. Butler, *ibid.*, **17**, 748 (1976).

(5) L. C. Washburn, T. T. Sun, B. L. Byrd, R. L. Hayes, T. A. Butler, and A. P. Callahan, *Radiopharm II (2nd Int. Symp.)*, 767 (1979).

(6) R. L. Hayes, L. C. Washburn, B. W. Wieland, T. T. Sun, and J. B. Anon, *Int. J. Appl. Radiat. Isot.*, **29**, 186 (1978).

(7) L. C. Washburn, B. W. Wieland, T. T. Sun, R. L. Hayes, and T. A. Butler, *J. Nucl. Med.*, **19**, 77 (1978).

(8) L. C. Washburn, T. T. Sun, B. L. Byrd, R. L. Hayes, and T. A. Butler, *ibid.*, **20**, 857 (1979).

(9) K. F. Hubner, G. A. Andrews, E. Buonocore, R. L. Hayes, L. C. Washburn, I. R. Collman, and W. D. Gibbs, *ibid.*, **20**, 507 (1979).

(10) O. Tamemasa, R. Goto, and T. Suzuki, *Gann*, **69**, 517 (1978).

ACKNOWLEDGMENTS

Financial support for this research was supplied by Grant No. 1 ROM GM 27962-01 from the National Institute of General Medical Sciences.

The authors thank Dr. Earl Rees of the Department of Medicine, College of Medicine for the use of and assistance in the operation of the JASCO-ORD/UV-5 spectropolarimeter used in the optical activity determinations.

Correction of Perfusate Concentration for Sample Removal

WILLIAM L. HAYTON ˣ and TINA CHEN

Received August 17, 1981, from the *College of Pharmacy, Washington State University, Pullman, WA 99164-6510.* Accepted for publication October 13, 1981.

Abstract □ Repeated sampling of a drug solution that is recirculated through a perfused body increases the rate of drug disappearance from the perfusate. When the volume of the drug solution (V_T) is maintained constant by addition of drug-free perfusate after sampling, the measured drug concentration (C_i) can be corrected for drug removed in previous samples by using the equation $C_i' = C_i V_T C_{i-1}'/(V_T - V_S)C_{i-1}$, where C_i' is the corrected drug concentration in the ith sample, V_S is the volume of the sample, and $C_1' = C_1$. An error in any particular C_i is not transmitted to a subsequent C_i' value. The method can be used when the time interval between samples and when V_S vary from sample to sample, but return of the drug from the perfused body to the perfusate after sampling may cause C_i' to be overestimated.

Keyphrases □ Perfusates—correction of perfusate concentration for sample removal □ Drug concentration—correction of perfusate concentration for sample removal □ Correction methods—perfusate concentrations for sample removal

Several experimental techniques involve the perfusion of a tissue, an organ, or an entire organism with a drug solution (perfusate); *e.g.*, muscle (1), kidney (2), placenta (3), liver (4), intestine (5), and fish (6). Samples of the perfusate are periodically removed for determination of drug concentration. One experimental approach involves sampling the perfusate after it is passed once through the perfused body. An alternative approach is to recirculate the perfusate, usually by pumping it from a reservoir, through the perfused body, and back to the reservoir. Using the once-through approach, correction for sampling is unnecessary. When samples are removed repeatedly from recirculated perfusate, however, the concentration of drug is reduced, as a result of sample removal, in all samples but the first. Sample removal thereby biases the concentration–time relationship and confounds a kinetic analysis of the data.

If the ratio of the total sample volume to the perfusate volume is small, the bias is small and may be ignored. This ratio can be reduced by reducing the sample volume, reducing the number of samples, or increasing the volume

0022-3549/82/0700-0820$01.00/0

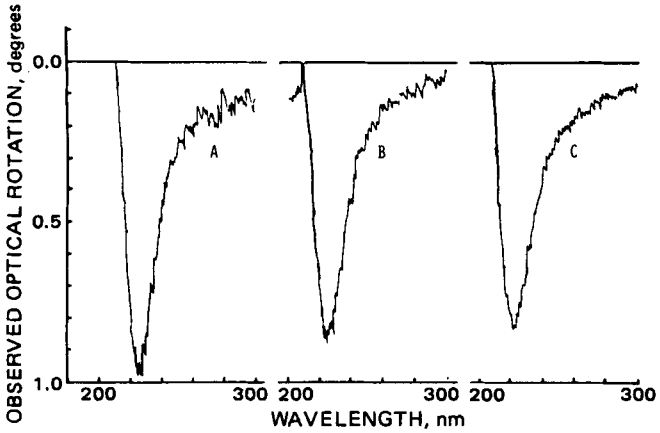

Figure 1—*Optical rotary dispersion curves for authentic D-leucine (A), authentic D-leucine recovered from cation exchange column (B), and enzymatically produced D-leucine after purification by cation exchange column chromatography (C).*

the radioactivity detected by autoradiography. The total resolution time including the ion exchange purification step was 40 min.

A nonradioactive resolution was analysed by optical rotary dispersion polarimetry in the range of 300–200 nm (Fig. 1). The optical rotary dispersion curve (Curve C) of the resolved D-leucine gave an optical rotation at 224 nm practically identical to that (Curve B) obtained by starting with half the amount of authentic D-leucine relative to the weight of DL-leucine used in the resolution and submitting it to the same ion exchange and reconstitution treatment applied to the resolved product.

The oxidative deamination of L-leucine in DL-leucine to the corresponding 4-methyl-2-oxopentanoic acid also was confirmed in the developmental work using nonradioactive DL-leucine by reacting aliquots of the reaction mixture with 2,4-dinitrophenylhydrazine yielding the 2,4-dinitrophenylhydrazone derivative which was monitored colorimetrically (440 nm) against standard 2,4-dinitrophenylhydrazone solutions. The keto acid yield was 84%. It was shown in this keto acid assay that the amino acid does not interfere with the analysis for the keto acid, making it unnecessary to separate the keto acid from the D-leucine.

Advantages of the oxidative deamination method for resolution are that it requires simple materials, is easily adaptable to hot cell conditions, and produces each of the enantiomers depending on the amino acid oxidase used.

REFERENCES

(1) M. B. Cohen, L. Spolter, N. S. MacDonald, and B. Cassen, *J. Nucl. Med.*, **13**, 422 (1972).

(2) N. Lembares, R. Dinwoodie, I. Gloria, P. Harper, and K. Lathrop, *ibid.*, **13**, 786 (1972).

(3) L. Spolter, M. B. Cohen, N. MacDonald, C. C. Chang, J. Takahashi, H. Neely, G. Hugh, S. Meyers, and D. Bobinet, *ibid.*, **15**, 535 (1974).

(4) R. L. Hayes, L. C. Washburn, B. W. Wieland, T. T. Sun, R. R. Turtle, and T. A. Butler, *ibid.*, **17**, 748 (1976).

(5) L. C. Washburn, T. T. Sun, B. L. Byrd, R. L. Hayes, T. A. Butler, and A. P. Callahan, *Radiopharm II (2nd Int. Symp.)*, 767 (1979).

(6) R. L. Hayes, L. C. Washburn, B. W. Wieland, T. T. Sun, and J. B. Anon, *Int. J. Appl. Radiat. Isot.*, **29**, 186 (1978).

(7) L. C. Washburn, B. W. Wieland, T. T. Sun, R. L. Hayes, and T. A. Butler, *J. Nucl. Med.*, **19**, 77 (1978).

(8) L. C. Washburn, T. T. Sun, B. L. Byrd, R. L. Hayes, and T. A. Butler, *ibid.*, **20**, 857 (1979).

(9) K. F. Hubner, G. A. Andrews, E. Buonocore, R. L. Hayes, L. C. Washburn, I. R. Collman, and W. D. Gibbs, *ibid.*, **20**, 507 (1979).

(10) O. Tamemasa, R. Goto, and T. Suzuki, *Gann*, **69**, 517 (1978).

ACKNOWLEDGMENTS

Financial support for this research was supplied by Grant No. 1 ROM GM 27962-01 from the National Institute of General Medical Sciences.

The authors thank Dr. Earl Rees of the Department of Medicine, College of Medicine for the use of and assistance in the operation of the JASCO-ORD/UV-5 spectropolarimeter used in the optical activity determinations.

Correction of Perfusate Concentration for Sample Removal

WILLIAM L. HAYTON ˣ and TINA CHEN

Received August 17, 1981, from the *College of Pharmacy, Washington State University, Pullman, WA 99164-6510.* Accepted for publication October 13, 1981.

Abstract □ Repeated sampling of a drug solution that is recirculated through a perfused body increases the rate of drug disappearance from the perfusate. When the volume of the drug solution (V_T) is maintained constant by addition of drug-free perfusate after sampling, the measured drug concentration (C_i) can be corrected for drug removed in previous samples by using the equation $C_i' = C_i V_T C_{i-1}'/(V_T - V_S)C_{i-1}$, where C_i' is the corrected drug concentration in the ith sample, V_S is the volume of the sample, and $C_1' = C_1$. An error in any particular C_i is not transmitted to a subsequent C_i' value. The method can be used when the time interval between samples and when V_S vary from sample to sample, but return of the drug from the perfused body to the perfusate after sampling may cause C_i' to be overestimated.

Keyphrases □ Perfusates—correction of perfusate concentration for sample removal □ Drug concentration—correction of perfusate concentration for sample removal □ Correction methods—perfusate concentrations for sample removal

Several experimental techniques involve the perfusion of a tissue, an organ, or an entire organism with a drug solution (perfusate); *e.g.*, muscle (1), kidney (2), placenta (3), liver (4), intestine (5), and fish (6). Samples of the perfusate are periodically removed for determination of drug concentration. One experimental approach involves sampling the perfusate after it is passed once through the perfused body. An alternative approach is to recirculate the perfusate, usually by pumping it from a reservoir, through the perfused body, and back to the reservoir. Using the once-through approach, correction for sampling is unnecessary. When samples are removed repeatedly from recirculated perfusate, however, the concentration of drug is reduced, as a result of sample removal, in all samples but the first. Sample removal thereby biases the concentration–time relationship and confounds a kinetic analysis of the data.

If the ratio of the total sample volume to the perfusate volume is small, the bias is small and may be ignored. This ratio can be reduced by reducing the sample volume, reducing the number of samples, or increasing the volume

0022-3549/82/0700-0820$01.00/0

of the perfusate. Reduction of the sample volume is limited by the sensitivity of the drug assay. Reducing the number of samples and increasing the perfusate volume are not good strategies as either one tends to obscure the kinetic behavior of the drug. In most cases the optimum approach is to remove a relatively large number of samples and to maintain the volume of the perfusate in the reservoir as small as is conveniently possible. To do this, the sampling-induced bias in the concentration–time data must be removed.

Two techniques for correction of perfusate concentration for sample removal have been described (4, 7). Both techniques require the assumption of a particular kinetic model before the correction can be made. The present report describes a relatively simple technique for correction of measured concentrations for previously removed samples. The correction is exact if no back transfer of drug occurs from the body to the perfusate after sampling. In many cases when back transfer does occur, the method introduces an acceptable error and may still be used.

EXPERIMENTAL

The perfusion system was the perfused body, an external reservoir, and a pump that recirculated perfusate between the reservoir and perfused body. Samples of perfusate were removed periodically from the reservoir and the concentration of drug in each perfusate sample was determined. The volume of the perfusate was maintained constant by addition of drug-free perfusate to the reservoir after a sample was removed. Because the sampling process removes drug from the perfusate, the concentration of drug in the sampled perfusate declined more rapidly than it would have if sampling had not occurred. If the perfused body eliminated drug from the perfusate by a zero-order process, the measured drug concentration would be corrected by adding the total amount of drug removed in previous samples divided by the volume of the perfusate.

Usually, however, the drug elimination rate is proportional to the drug concentration in the perfusate. In this case it is not correct to add the amount removed in samples to subsequently determined concentrations, since part of the drug removed as a sample would have been consumed if the sample had not been removed. The problem then is to determine how much of the drug that was removed in each sample to add to each subsequently measured concentration.

Assume that the drug concentration in the perfusate declines exponentially, and let C_i represent the measured drug concentration in the ith sample. The concentration of drug in the reservoir after removal of the first sample and addition of drug-free perfusate would be $C_1(V_T - V_S)/V_T$, where V_T and V_S are the volumes of the perfusate and the sample, respectively. The measured concentration of drug in the perfusate at the time that the second sample was removed can be corrected for drug removed in the first sample as follows:

$$C'_2 = C_2 V_T/(V_T - V_S) \qquad \text{(Eq. 1)}$$

C'_2 is the corrected drug concentration, *i.e.*, the concentration that would have been measured if the first sample had not been removed. In making the correction, it was assumed that the concentration of drug in the sample declined at the same rate as did the concentration of drug in the perfusate between the first and second samples. The measured concentration in the third sample can be corrected for drug removed in the first two samples:

$$C'_3 = C_3\left(\frac{V_T}{V_T - V_S}\right)\left(\frac{C'_2}{C_2}\right) \qquad \text{(Eq. 2)}$$

The term $V_T/(V_T - V_S)$ corrects for drug removed in the second sample, and the term C'_2/C_2 corrects for drug removed in the first sample. Correction of the fourth and subsequent samples is similar to the correction for the third sample:

$$C'_n = C_n\left(\frac{V_T}{V_T - V_S}\right)\left(\frac{C'_{n-1}}{C_{n-1}}\right) \qquad \text{(Eq. 3)}$$

RESULTS AND DISCUSSION

The validity of the method was explored by using it to correct calculated drug concentrations, assuming some probable cases for drug disappearance kinetics. The proposed method was exact when drug was eliminated monoexponentially from the perfusate by apparent first-order kinetics. The method permits flexibility in that the time interval between samples and the volume of each sample can be varied from sample to sample. In addition, an error in the concentration determined for a particular sample is not transmitted by the method to subsequent samples. When the drug concentration was assumed to decline according to a biexponential equation, the correction was also exact. However, a biexponential concentration–time relationship usually indicates that drug distributes between the perfused body and the perfusate. Simulations using the model described previously (7), a two-compartment model with drug distribution between perfusate and perfused body followed by drug elimination from the perfused body, showed that the method is not exact when drug returns from the perfused body as a result of an instantaneous decrease in the drug concentration in the perfusate. The corrected concentration in the sampled perfusate was higher than the corresponding concentration in unsampled perfusate from the third to the final sample. The percentage error increased with the sample number, and it depended on the amount of drug that returned to the perfusate after sampling, compared to the amount of drug in the perfusate. The error in the final corrected concentration increased with the number of samples, the sample volume, the apparent volume of distribution of the perfused body relative to the volume of perfusate, and as drug clearance from the perfused body increased relative to the reversible clearance between the perfusate and the perfused body. If the method is used when a distributive phase in the perfusate concentration–time data is apparent, simulation with the model described previously (7) is recommended to select a sampling regimen that does not introduce unacceptable error. In some cases the correction method described previously (7) may be required.

REFERENCES

(1) E. M. Renkin, *Am. J. Physiol.*, **183,** 125 (1955).

(2) I. Bekersky, L. Fishman, S. A. Kaplan, and W. A. Colburn, *J. Pharmacol. Exp. Ther.*, **212,** 309 (1980).

(3) I. Kihlström and J. E. Kihlström, *Biol. Neonate*, **39,** 150 (1981).

(4) R. Nagashima, G. Levy, and E. S. Sarcione, *J. Pharm. Sci.*, **57,** 1881 (1968).

(5) A. Tsuji, E. Nakashima, I. Kagami, and T. Yamana, *ibid.*, **70,** 772 (1981).

(6) C. M. Wood, B. R. McMahon, and D. G. McDonald, *Am. J. Physiol.*, **234,** R201 (1978).

(7) C. J. Timmer and H. P. Wijnand, *J. Pharmacokinet. Biopharm.*, **5,** 335 (1977).

ACKNOWLEDGMENTS

Supported in part by Grant GM 27924 from the National Institute of General Medical Sciences.

Thiazides IV: Comparison of Dissolution with Bioavailability of Chlorothiazide Tablets

VINOD P. SHAH [x], **PATRICK KNIGHT, VADLAMANI K. PRASAD, and BERNARD E. CABANA**

Received Jan 26, 1981, from the *Division of Biopharmaceutics, Bureau of Drugs, Food and Drug Administration, Washington, DC 20204.* Accepted for publication October 6, 1981.

Abstract □ Based on the initial dissolution rate profiles in water, a slow-dissolving, an intermediate-dissolving, and a fast-dissolving chlorothiazide 250-mg tablet were selected for the bioavailability and bioequivalence study. In addition, two marketed 500-mg chlorothiazide tablets were studied. The three 250-mg tablets were bioequivalent, as were the two 500-mg tablets. Therefore, the dissolution test conditions were modified to associate *in vitro* dissolution with *in vivo* performance of the product. Based on these results, it was concluded that a dissolution of 75% in 60 min by paddle method at 75 rpm in pH 7.4 phosphate buffer can be used as a quality assurance test for 250- and 500-mg chlorothiazide tablets.

Keyphrases □ Thiazides—dissolution–bioavailability comparison, chlorothiazide tablets □ Bioavailability—comparison to dissolution, thiazides, chlorothiazide tablets □ Dissolution—comparison to bioavailability, thiazides, chlorothiazide tablets □ Chlorothiazide—tablets, bioavailability–dissolution comparison, thiazides

A drug product such as a tablet or capsule consists of the active ingredient, the drug itself, and the inactive ingredients such as fillers, binding agents, lubricants, and other substances which, along with the process factors, influence the products' dissolution and its performance. The dissolution test has emerged as the single most important *in vitro* test for ensuring the quality of the solid oral dosage forms (tablets and capsules) and in many instances predicts the bioavailability of the product. In instances where the dissolution test results have been correlated with *in vivo* performance of the product, *in vitro* dissolution test criteria are used as part of bioequivalence requirements by the Food and Drug Administration. In the absence of *in vivo*-correlated *in vitro* results, the dissolution test can be used to ensure the characteristic of the batch.

The steps necessary to arrive at a meaningful correlation between *in vitro* dissolution and *in vivo* performance of a product include: (*a*) a dissolution survey of marketed multisource drug products by a method, (*b*) selection of drug products with a wide range of dissolution profiles for bioavailability study, (*c*) determination of apparent *in vitro–in vivo* correlation, and (*d*) refinement (if necessary) of the dissolution tests to reflect *in vivo* product performance and optimize the *in vitro–in vivo* correlation.

An *in vitro* dissolution test is reported for marketed chlorothiazide tablets which is associated with *in vivo* performance, and which could be utilized as a quality assurance test.

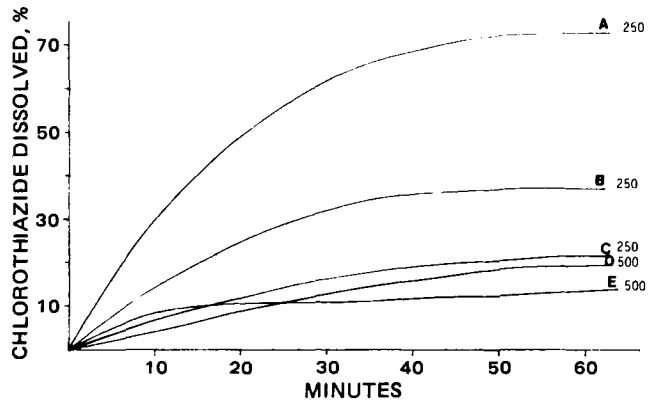

Figure 1—*Dissolution profiles of 250- and 500-mg chlorothiazide tablets in water by USP paddle method at 50 rpm.*

EXPERIMENTAL

Materials—The chlorothiazide tablets for the study were obtained directly from the manufacturers. The following products were used: 250 mg A, 250 mg B, 250 mg C, 500 mg D and 500 mg E[1].

***In Vitro* Dissolution Test**—The dissolution test was carried out by the procedure described in USP XX using the compendial Method II (paddle method) (1). Agitation speeds of 50, 75, and 100 rpm were used. The dissolution medium was distilled water, pH 7.4 or pH 8.0 phosphate buffer at 37 ± 0.2°.

***In Vivo* Tests**—The *in vivo* tests were carried out in 12 normal, healthy volunteers using a complete crossover Latin-square design. The urine samples were collected at intervals over a 72-hr period and were analyzed by a specific and sensitive HPLC method. The details of the study and the results are described elsewhere (2, 3).

RESULTS AND DISCUSSION

At present there is no dissolution test requirement for chlorothiazide 250- and 500-mg tablets in the compendia. The survey of dissolution profiles of marketed 250- and 500-mg tablets was carried out using a paddle method (USP XX, Method II) in water at 50 rpm. Several lots of the innovator's product were screened. The results of the survey (Table I, Fig. 1) suggest a wide variation in dissolution profiles under the test conditions. For 250-mg tablets, the dissolution varied from 15 to 81% in 30 min and from 21 to 88% in 60 min. Based on these results, three products with a wide range in dissolution profiles—slow dissolving product C, intermediate dissolving product B, and fast dissolving product A—were selected for the bioavailability–bioequivalence study. There are only two approved 500-mg chlorothiazide tablets on the market, and both showed very poor dissolution profiles. They were also used in the bioavailability–bioequivalence study.

The bioavailability–bioequivalence study was carried out in 12 healthy volunteers in a crossover fashion using 250-mg A, B, and C products. In another crossover study with 12 volunteers, 500-mg D and E products were used. The urine samples were collected at intervals over a 72-hr period and analyzed by a specific and sensitive HPLC method. The cumulative amount of drug excreted in 72 hr was calculated and used as a measure of the bioavailability of the product (Table II). The details of the *in vivo* studies are described elsewhere (2, 3).

From a 250-mg tablet, a mean of 42, 52, and 45 mg of chlorothiazide was recovered in 72 hr from C, B, and A tablets, respectively (Table II). The total amount of drug excreted in 72 hr was not significantly different between tablets. All products were bioequivalent.

In vitro dissolution results by the paddle method at 50 rpm in water could not be correlated with *in vivo* results because all the products showed approximately the same amount of drug elimination (absorption) in 72 hr and were bioequivalent. This suggests that the preliminary dis-

[1] 250 mg A: 250-mg chlorothiazide tablets from Danbury, batch no. 15069; 250 mg C: 250-mg chlorothiazide tablets from Merck, Sharp & Dohme, batch no. V1502; 250 mg B: 250-mg chlorothiazide tablets from Mylan, batch no. 066B; 500 mg E: 500-mg chlorothiazide tablets from Merck, Sharp & Dohme, batch no. 2762; and 500-mg D: 500-mg chlorothiazide tablets from Mylan, batch no. 054B.

0022-3549/82/0700-0822$01.00/0

Table I—Dissolution of Chlorothiazide Tablets by Paddle Method Under Different Conditions [a]

Product	Water		pH 7.4 Phosphate Buffer						pH 8 Phosphate Buffer			
	50 rpm		50 rpm		75 rpm		100 rpm		50 rpm		100 rpm	
	30 min	60 min	30 min	60 min	30 min	60 min	30 min	60 min	30 min	60 min	30 min	60 min
250 mg C	16	22	27	35	73	91	92	98	32	48	108	111
	(3.4)[b]	(3.7)	(2.7)	(2.6)	(3.8)	(2.2)	(3.0)	(1.5)	(7.5)	(7.0)	(3.8)	(3.2)
250 mg B	32	37	37	55	71	82	73	83	51	76	76	86
	(5.5)	(6.6)	(2.5)	(2.4)	(2.1)	(2.6)	(2.3)	(2.5)	(5.7)	(9.0)	(1.3)	(1.1)
250 mg A	62	73	67	73	94	97	99	99	*NS*	*NS*	100	100
	(3.9)	(4.4)	(2.3)	(2.1)	(3.4)	(3.3)	(2.9)	(2.9)			(3.8)	(3.2)
500 mg E	11	14	26	34	79	96	95	98	31	41	103	105
	(4.2)	(4.8)	(2.1)	(4.6)	(4.0)	(3.1)	(2.6)	(1.4)	(3.6)	(4.1)	(3.6)	(2.6)
500 mg D	13	20	20	32	56	78	79	94	24	43	97	110
	(0.8)	(2.6)	(3.3)	(4.0)	(7.2)	(4.2)	(4.4)	(2.5)	(2.1)	(5.6)	(3.1)	(2.0)

[a] Data represents mean dissolution of six tablets. [b] The standard deviation is given in parenthesis.

solution method for chlorothiazide tablets in water was overly discriminative. Therefore, this *in vitro* dissolution test was modified in order to arrive at a meaningful *in vitro* test.

Two types of *in vivo–in vitro* relationships are possible. The first type of relationship is where different *in vitro* dissolution results can be correlated with differences in observed *in vivo* parameters such as *AUC*, *Ae*, C_{max}, *etc.* The second type of relationship is where all products tested are bioequivalent, and *in vitro* dissolution data is associated with a minimum dissolution rate. In the case of chlorothiazide, where all three 250-mg products tested are bioequivalent (*i.e.*, no difference in amount of chlorothiazide recovered from urine in 72 hr), an attempt was made to obtain the latter type of *in vitro–in vivo* relationship. From the latter type of *in vitro–in vivo* relationship, and in the absence of any bioinequivalent product, the *in vitro* dissolution method will at least serve as a quality assurance test. Since several formulations made by different manufacturers were used in this study, one can be reasonably assured that a new product meeting this *in vitro* test will be bioequivalent with existing products.

Using USP Method II, the dissolution of 250-mg chlorothiazide tablets was carried out in pH 7.4 and 8.0 phosphate buffer at 50, 75, and 100 rpm (Table I). The dissolution results at 50 rpm were found to be slow and highly discriminative, whereas the agitation at 100 rpm was found to be so drastic and indiscriminative that it may not differentiate between the currently marketed bioequivalent products and a possible poorly bioavailable future generic product. The agitation at 75 rpm in pH 7.4 phosphate buffer was found to be appropriate and reasonable for all bioequivalent 250-mg products. Using pH 7.4 phosphate buffer medium and 75 rpm agitation, a dissolution of 70–94% in 30 min and 82–97% in 60 min was observed (Table II).

There are only two approved 500-mg chlorothiazide tablets on the market, and both showed poor dissolution in water at 50 rpm (Table I).

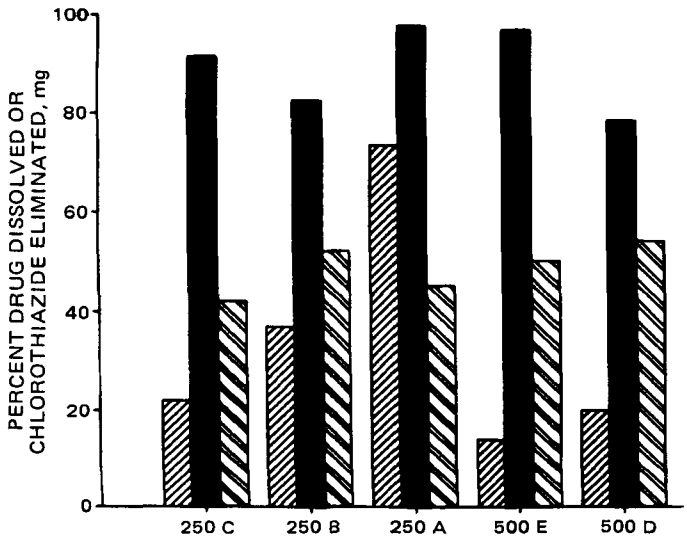

Figure 2—In vitro *dissolution (percent dissolved in 60 min) and* in vivo *cumulative elimination (milligrams in 72 hr) for 250- and 500-mg chlorothiazide tablets. Key: (▨) percent dissolved in water; (■) % dissolved in pH 7.4 phosphate buffer; and (▧) chlorothiazide eliminated in urine.*

Table II—Relationship Between *In Vitro–In Vivo* Parameters for Chlorothiazide Tablets

Product	*In Vitro* Dissolution Data[a]				*In Vivo* Cumulative[b] Excretion Data, mg mean ± *SD*	
	Water		pH 7.4 buffer			
	20 min	60 min	30 min	60 min		
250 mg C	16	22	73	91	42	15
250 mg B	32	37	71	82	52	25
250 mg A	62	73	94	97	45	19
500 mg E	11	14	79	96	50	13
500 mg D	13	20	56	78	54	15

[a] *In vitro* dissolution data obtained by paddle method in water at 50 rpm and pH 7.4 phosphate buffer at 75 rpm. [b] Represents mean cumulative excretion in 12 subjects.

Both products showed the same extent of absorption and elimination, and were bioequivalent. The dissolution of these two 500-mg products was studied under various test conditions. A dissolution of 56–79% in 30 min and 78–96% in 60 min was achieved by the paddle method at 75 rpm in pH 7.4 phosphate buffer.

As seen in Table II, approximately the same amount of drug was eliminated in urine in 72 hr from both 250- and 500-mg chlorothiazide tablets. There is no statistical difference in the bioavailability of these two products in normal healthy volunteers. The implications of this bioavailability finding are discussed separately (2–4). Both 250- and 500-mg tablets achieved approximately the same percent of dissolution in pH 7.4 phosphate buffer by the paddle method at 75 rpm. Figure 2 shows the relationship between *in vivo* and *in vitro* data. For comparison, *in vitro* dissolution data in water are also included. The figure clearly shows that the amount of drug eliminated in urine and the amount of drug dissolved in phosphate buffer are nearly the same in all five formulations studied.

In order to evaluate the appropriateness of the dissolution method and the acceptance limits as a routine quality control test, additional batches of chlorothiazide tablets were tested. These products[2] represented four manufacturers and were different from those that were used in the bioequivalency study. The results showed that all products dissolved >75% in 60 min, thus suggesting that these products would be bioequivalent.

A dissolution test which will ensure the quality of chlorothiazide tablets has been established. The product should dissolve not less than 75% in 60 min when the dissolution test is carried out by USP paddle method in 900 ml of pH 7.4 phosphate buffer at 37° and agitation of 75 rpm. On the basis of these findings, it is reasonable to expect that a product meeting such a dissolution criterion will be bioequivalent to the marketed product.

REFERENCES

(1) United States Pharmacopeia, XX, United States Pharmacopeial

[2] Bolar's 250-mg chlorothiazide tablet, batch no. 15319, 83% dissolution; Mylan's 250-mg chlorothiazide tablet, batch no. B027A, 77% dissolution; Danbury's 250-mg chlorothiazide tablet, batch no. 112935, 100% dissolution; and Merck, Sharp & Dohme's 500-mg chlorothiazide tablet, batch no. V1911, 83% dissolution.

Convention, Inc., Rockville, Md., 1980, p. 959.
(2) V. P. Shah, J. Lee, J. Hunt, V. K., Prasad, B. E. Cabana, and T. Foster, *Curr. Ther. Res.*, **29**, 802 (1981).
(3) P. Welling, D. M. Walter, R. B. Patel, W. A. Porter, J. L. Amidon, T. S. Foster, V. P. Shah, J. Hunt, and V. K. Prasad, *ibid.*, **29**, 815 (1981).
(4) V. P. Shah, J. Lee, J. Hunt, V. K. Prasad, B. E. Cabana, and T. Foster, *ibid.*, **29**, 823 (1981).

Effect of Skin Binding on Percutaneous Transport of Benzocaine from Aqueous Suspensions and Solutions

U. G. DALVI * and J. L. ZATZ ˣ

Received March 27, 1981, from the *Rutgers College of Pharmacy, Piscataway, NJ 08854.* Accepted for publication October 7, 1981.
* Present Address: E. R. Squibb & Sons, Inc., New Brunswick, NJ 08903.

Abstract □ Various aqueous suspensions of benzocaine containing nonionic surfactants exhibited the same rate of *in vitro* penetration through hairless mouse skin. Saturated solutions yielded a lower rate of benzocaine penetration due to depletion of drug from the donor portion of the diffusion cell. Extensive skin binding was responsible.

Keyphrases □ Benzocaine—effect of skin binding on percutaneous transport from aqueous suspensions and solutions □ Skin binding—effect on percutaneous transport of benzocaine from aqueous suspensions and solutions □ Percutaneous transport—effect of skin binding, of benzocaine from aqueous suspensions and solutions

The effect of surfactants on drug penetration through skin is an important aspect of formulation of topical drug products. The influence of these additives depends on the rate-limiting step in penetration, so that the type of preparation and conditions of application to the skin are important considerations. Penetration from aqueous solutions containing a fixed benzocaine concentration depended on the extent of benzocaine solubilization by surfactant included in the formula (1). Penetration flux was directly proportional to the unbound benzocaine concentration. A series of surfactant solutions saturated with benzocaine had the same rate of benzocaine penetration. No alteration of membrane permeability was found. This work was extended to aqueous gel suspensions to determine the rate limiting step in penetration and the influence of nonionic surfactants in these systems. The suspensions were similar to those utilized in previous studies of benzocaine release (2, 3).

EXPERIMENTAL

Materials and apparatus used for the *in vitro* penetration experiments were reported previously (1). Surfactants used in the formulations were commercially available polyoxyethylene nonylphenols[1]. The membrane was whole hairless mouse skin. The receptor solution (normal saline containing 0.25% chlorobutanol) was maintained at 37° and stirred at 500 rpm. The donor compartment was not stirred. Further details concerning experimental procedure appeared previously (1). All donor systems were studied in triplicate.

All the suspensions were prepared on a w/v basis. Accurately measured surfactant stock solution was transferred to a wide mouth glass jar containing a magnetic stirring bar. To that solution, the required amount of benzocaine was added and stirring was continued for ~15 min until all lumps were broken. A preweighed quantity of gelling agent was sprinkled on the top and stirring was continued for ~3 hr to yield a smooth homogeneous suspension. A control suspension without the drug was prepared for every formulation. All the suspensions were analyzed for benzocaine content and were stored at 30° until needed.

[1] Igepal CO series, GAF Corp., N.Y.

RESULTS AND DISCUSSION

Details of the suspension formulations are listed in Table I. In the case of all the formulations studied, when the cumulative amount of benzocaine in the receptor compartment was plotted against time, a linear relationship with a small lag time was observed. A typical plot is shown in Fig. 1. The gradual rise in penetration rate (Fig. 1) until steady state was achieved is typical of membrane controlled diffusion. When transport through the vehicle is rate limiting, the flux is initially high and then gradually decreases with time. A second indication that diffusion across the stratum corneum was the slow step in benzocaine transport is high flux values obtained from the suspension formulations, which will be discussed.

The flux values were calculated for all formulations (Table I). ANOVA showed that drug concentration, gelling agent, and surfactant concentration had no statistically significant effect on flux. No influence of the surfactants on skin membrane integrity was evident.

These results are similar to those with saturated benzocaine solutions (1). However, there is a surprising difference in the magnitude of the penetration values when saturated solutions are compared to suspensions. Mean benzocaine flux from saturated solutions was ~60 $\mu g\ hr^{-1}\ cm^{-2}$ (1), whereas the average flux for suspensions was 101 $\mu g\ hr^{-1}\ cm^{-2}$. This difference was unexpected since the free benzocaine concentration, which provides the driving force for diffusion, should have been the same in both types of preparation.

In penetration experiments, the amount of drug transported during the course of an experiment is usually small enough to justify the assumption that the donor concentration is constant. In conducting experiments on benzocaine solutions, there had been no reason to question the validity of this basic assumption. However, in view of the difference in benzocaine flux from saturated solutions as compared to suspensions, it was hypothesized that depletion of drug from the donor must have been taking place in the solution systems during the course of the penetration experiments.

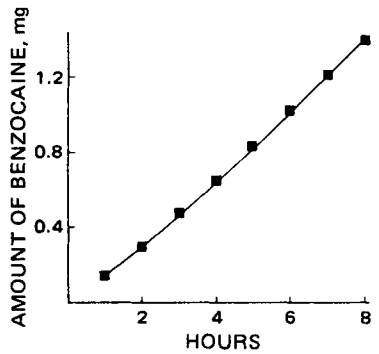

Figure 1—*Penetration of benzocaine through hairless mouse skin from a 5% suspension containing 0.0227 M polyoxyethylene (15) nonylphenol.*

0022-3549/82/0700-0824$01.00/0

Convention, Inc., Rockville, Md., 1980, p. 959.
(2) V. P. Shah, J. Lee, J. Hunt, V. K., Prasad, B. E. Cabana, and T. Foster, *Curr. Ther. Res.*, **29**, 802 (1981).
(3) P. Welling, D. M. Walter, R. B. Patel, W. A. Porter, J. L. Amidon, T. S. Foster, V. P. Shah, J. Hunt, and V. K. Prasad, *ibid.*, **29**, 815 (1981).
(4) V. P. Shah, J. Lee, J. Hunt, V. K. Prasad, B. E. Cabana, and T. Foster, *ibid.*, **29**, 823 (1981).

Effect of Skin Binding on Percutaneous Transport of Benzocaine from Aqueous Suspensions and Solutions

U. G. DALVI * and J. L. ZATZ ˣ

Received March 27, 1981, from the *Rutgers College of Pharmacy, Piscataway, NJ 08854.* Accepted for publication October 7, 1981.
* Present Address: E. R. Squibb & Sons, Inc., New Brunswick, NJ 08903.

Abstract □ Various aqueous suspensions of benzocaine containing nonionic surfactants exhibited the same rate of *in vitro* penetration through hairless mouse skin. Saturated solutions yielded a lower rate of benzocaine penetration due to depletion of drug from the donor portion of the diffusion cell. Extensive skin binding was responsible.

Keyphrases □ Benzocaine—effect of skin binding on percutaneous transport from aqueous suspensions and solutions □ Skin binding—effect on percutaneous transport of benzocaine from aqueous suspensions and solutions □ Percutaneous transport—effect of skin binding, of benzocaine from aqueous suspensions and solutions

The effect of surfactants on drug penetration through skin is an important aspect of formulation of topical drug products. The influence of these additives depends on the rate-limiting step in penetration, so that the type of preparation and conditions of application to the skin are important considerations. Penetration from aqueous solutions containing a fixed benzocaine concentration depended on the extent of benzocaine solubilization by surfactant included in the formula (1). Penetration flux was directly proportional to the unbound benzocaine concentration. A series of surfactant solutions saturated with benzocaine had the same rate of benzocaine penetration. No alteration of membrane permeability was found. This work was extended to aqueous gel suspensions to determine the rate limiting step in penetration and the influence of nonionic surfactants in these systems. The suspensions were similar to those utilized in previous studies of benzocaine release (2, 3).

EXPERIMENTAL

Materials and apparatus used for the *in vitro* penetration experiments were reported previously (1). Surfactants used in the formulations were commercially available polyoxyethylene nonylphenols[1]. The membrane was whole hairless mouse skin. The receptor solution (normal saline containing 0.25% chlorobutanol) was maintained at 37° and stirred at 500 rpm. The donor compartment was not stirred. Further details concerning experimental procedure appeared previously (1). All donor systems were studied in triplicate.

All the suspensions were prepared on a w/v basis. Accurately measured surfactant stock solution was transferred to a wide mouth glass jar containing a magnetic stirring bar. To that solution, the required amount of benzocaine was added and stirring was continued for ~15 min until all lumps were broken. A preweighed quantity of gelling agent was sprinkled on the top and stirring was continued for ~3 hr to yield a smooth homogeneous suspension. A control suspension without the drug was prepared for every formulation. All the suspensions were analyzed for benzocaine content and were stored at 30° until needed.

[1] Igepal CO series, GAF Corp., N.Y.

RESULTS AND DISCUSSION

Details of the suspension formulations are listed in Table I. In the case of all the formulations studied, when the cumulative amount of benzocaine in the receptor compartment was plotted against time, a linear relationship with a small lag time was observed. A typical plot is shown in Fig. 1. The gradual rise in penetration rate (Fig. 1) until steady state was achieved is typical of membrane controlled diffusion. When transport through the vehicle is rate limiting, the flux is initially high and then gradually decreases with time. A second indication that diffusion across the stratum corneum was the slow step in benzocaine transport is high flux values obtained from the suspension formulations, which will be discussed.

The flux values were calculated for all formulations (Table I). ANOVA showed that drug concentration, gelling agent, and surfactant concentration had no statistically significant effect on flux. No influence of the surfactants on skin membrane integrity was evident.

These results are similar to those with saturated benzocaine solutions (1). However, there is a surprising difference in the magnitude of the penetration values when saturated solutions are compared to suspensions. Mean benzocaine flux from saturated solutions was ~60 $\mu g\ hr^{-1}\ cm^{-2}$ (1), whereas the average flux for suspensions was 101 $\mu g\ hr^{-1}\ cm^{-2}$. This difference was unexpected since the free benzocaine concentration, which provides the driving force for diffusion, should have been the same in both types of preparation.

In penetration experiments, the amount of drug transported during the course of an experiment is usually small enough to justify the assumption that the donor concentration is constant. In conducting experiments on benzocaine solutions, there had been no reason to question the validity of this basic assumption. However, in view of the difference in benzocaine flux from saturated solutions as compared to suspensions, it was hypothesized that depletion of drug from the donor must have been taking place in the solution systems during the course of the penetration experiments.

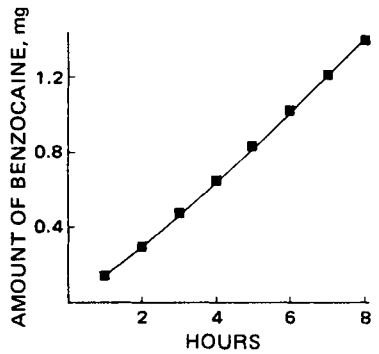

Figure 1—*Penetration of benzocaine through hairless mouse skin from a 5% suspension containing 0.0227 M polyoxyethylene (15) nonylphenol.*

0022-3549/82/0700-0824$01.00/0

Table I—Skin Penetration of Benzocaine from Aqueous Suspensions

Formulation	Benzocaine Concentration, % w/v	Gelling Agent, % w/v: Hydroxypropyl Cellulose	Gelling Agent, % w/v: Xanthan Gum	Surfactant Concentration $M \times 10^3$: $n = 50$	Surfactant Concentration $M \times 10^3$: $n = 15$	Flux ± *SD*, mg hr^{-1} $cm^{-2} \times 10^3$
A	1	2	—	—	22.7	97.3 ± 6.5
B	5	2	—	—	22.7	109.8 ± 4.3
C	10	2	—	—	22.7	98.6 ± 8.1
D	1	—	0.4	—	22.7	88.9 ± 7.3
E	5	—	0.4	—	22.7	97.3 ± 8.7
F	5	—	0.4	22.7	—	108.6 ± 6.3
G	5	—	0.4	—	2.27	107.8 ± 6.2

To test this hypothesis, a set of skin penetration experiments was conducted using a saturated aqueous benzocaine solution as donor, and at regular intervals the donor and receptor solutions were sampled and analyzed for benzocaine content. Figure 2 shows the results of these experiments. From the start, drug concentration in the donor dropped rapidly. The rate of drug transport to the receptor under sink conditions dropped during the 24-hr period for which data were collected. However, for the first 8–10 hr, the usual time allotted to previous experiments, the penetration rate was pseudo zero-order.

Assuming that the drug is distributed between donor, receptor, and skin at any given time, the donor and receptor were analyzed and the amount of benzocaine present in skin as a function of time was calculated by difference. Results are plotted in Fig. 2. There was significant uptake of benzocaine by the membrane. At the end of 24 hr, the skin contained 1.2 mg of benzocaine, while only 0.65 mg of benzocaine was left in the donor compartment.

To confirm the fact that a significant amount of benzocaine was actually retained in the skin, a new set of experiments was performed. A saturated aqueous solution was placed on hairless mouse skin and left undisturbed for 24 hr. At the end of 24 hr, the donor and receptor solutions were completely removed from the diffusion cell and analyzed for benzocaine content. The amount of benzocaine retained in the skin was estimated as the difference between the original quantity in the donor and that found in the analyses. The donor solution was then replaced by distilled water and the experiment was continued with regular withdrawal and replacement of receptor solution. The results are plotted in Fig. 3. Benzocaine release continued for the duration of the experiment (144 hr). Approximately 70% of the benzocaine estimated to be in the skin was removed during this period. These data confirm that a significant quantity of benzocaine was bound by the skin.

The mineral oil–water partition coefficient of benzocaine is ~0.9. Based on the relative volumes of the skin and donor compartments, the apparent skin–donor partition coefficient is many times higher than this value. Apparently, proteinaceous material in the skin is responsible for benzocaine uptake. Although no data on protein binding of benzocaine was found, other anilide local anesthetics such as lidocaine, mepivacaine, and bupivacaine are bound by proteins (4). Investigation of skin binding of drugs has not been extensive. *In vitro* binding of testosterone and benzyl alcohol to human dermis was reported previously (5, 6).

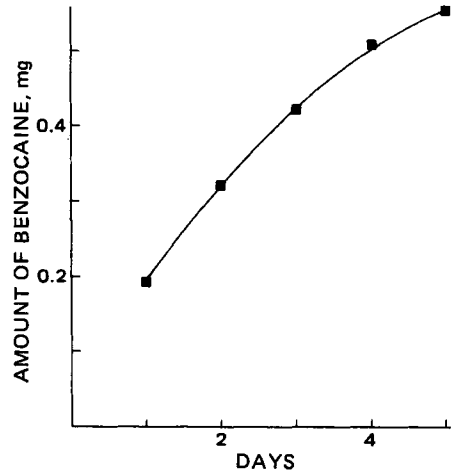

Figure 3—*Benzocaine release from the skin after complete withdrawal of donor solution.*

A dual sorption model was used (7) to explain the sorption and skin penetration behavior of aqueous scopolamine solutions. The same model is in qualitative agreement with the findings on benzocaine transport through hairless mouse skin. A significant portion of the benzocaine that enters the stratum corneum is immobilized there without contributing to the flux. This material, together with the benzocaine that partitions in the membrane and diffuses into the receptor, causes loss of benzocaine from the donor. If the donor is a suspension, the solid particles act as a reservoir to replenish lost benzocaine and maintain a constant concentration. Sorbed benzocaine equilibrates with nonimmobilized drug, the system eventually reaches diffusional steady state and the sorption of benzocaine by the membrane has no effect on the penetration flux. However, with benzocaine solutions, drug that is lost from the donor by penetration and sorption is not replaced and the driving force for penetration is reduced. The result is a decrease in the apparent steady-state

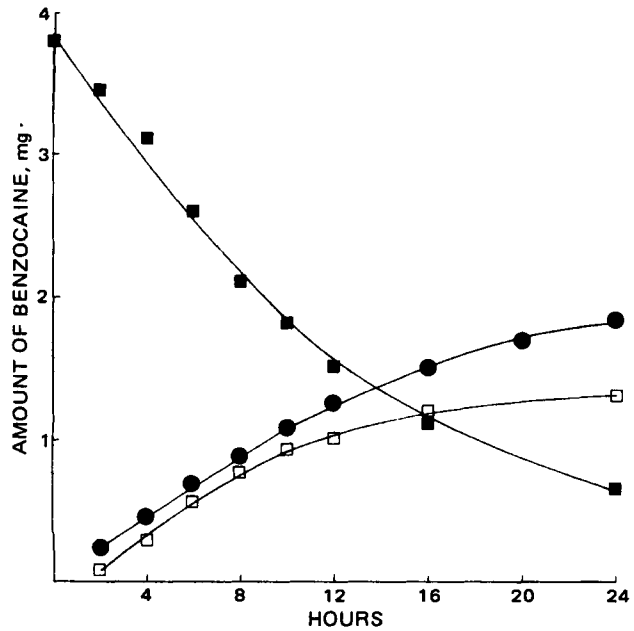

Figure 2—*Skin penetration of benzocaine from saturated aqueous solution. Key: (■) donor; (●) receptor; (□) skin.*

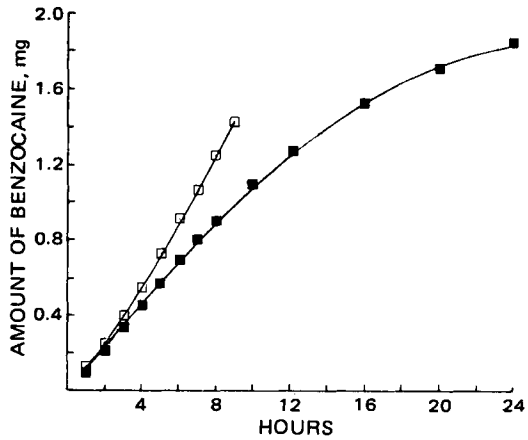

Figure 4—*Skin penetration of benzocaine from saturated aqueous solution. Key: (■) saturated solution; (□) saturated solution with 1 mg/ml of excess drug.*

flux value, in comparison to suspensions, as well as a continuing reduction in flux with time.

As a final test of this explanation, and to ensure that the surfactant used in the suspension formulations did not influence the results, experiments were performed using a saturated solution of benzocaine in water to which excess benzocaine (1 mg/ml) was added.

The results are plotted in Fig. 4 for the penetration profiles with and without excess drug in donor. It is evident that the slopes for the two curves are different. The flux for the donor with excess drug (100×10^{-3} mg hr^{-1} cm^{-2}) was very close to the values obtained for the suspension systems (Table I).

REFERENCES

(1) U. G. Dalvi and J. L. Zatz, *J. Soc. Cosmet. Chem.*, **32,** 87 (1981).

(2) F. Bottari, G. Di Colo, E. Nannipieri, M. F. Saettone, and M. F. Serafini, *J. Pharm. Sci.*, **66,** 926 (1977).

(3) G. Di Colo, V. Carelli, B. Giannaccini, M. F. Serafini, and F. Bottari, *ibid.*, **69,** 387 (1980).

(4) G. D. Tucker, R. N. Boyes, P. O. Bridenbough, and D. C. Moore, *Anesthesiology*, **33,** 287 (1970).

(5) E. Menczel and H. I. Maibach, *J. Invest. Dermatol.*, **54,** 386 (1970).

(6) E. Menczel and H. I. Maibach, *Acta Derm. Venereol.*, **52,** 38 (1972).

(7) S. K. Chandrasekaran, A. S. Michaels, P. S. Campbell, and J. E. Shaw, *AIChE J.*, **22,** 828 (1976).

ACKNOWLEDGMENTS

U. G. Dalvi is grateful for fellowship support provided by the Society of Cosmetic Chemists.

Degradation of Melphalan in Aqueous Solutions—Influence of Human Albumin Binding

HANS EHRSSON ˣ **and ULLA LÖNROTH**

Received April 28, 1981, from the *Karolinska Apoteket, S-104 01 Stockholm, Sweden.* Accepted for publication September 28, 1981.

Abstract □ The protein binding and degradation rate of melphalan in human albumin solutions and plasma have been investigated. In plasma, melphalan is bound 69.0 ± 3.4% (25°, melphalan concentration 25 μg/ml). The stability of melphalan when bound to albumin is about three times higher ($k = 3.07 \times 10^{-2} \pm 0.48 \times 10^{-2}$ hr^{-1}) than unbound in solution ($k = 1.14 \times 10^{-1} \pm 0.01$ hr^{-1}).

Keyphrases □ Melphalan—degradation studies in aqueous solutions, influence of human albumin binding □ Binding—human albumin to melphalan, degradation of melphalan in aqueous solutions □ Albumin, human—influence in binding with melphalan, degradation in aqueous solutions

Melphalan, an alkylating agent of the nitrogen mustard type, can be bound to plasma proteins as a result of a chemical reaction with the protein molecules as well as by a process of reversible adsorption (1). At least 60% of melphalan was bound to serum proteins (26°) as studied by an equilibrium dialysis technique (2). However, the quantitative determinations were performed using an unselective technique, and it is unclear to what extent the results are affected by a codetermination of degradation products of melphalan formed during the dialysis procedure. Melphalan (30%) was observed previously to be undialyzable in human plasma (4°), the quantitative determinations being performed by high-performance liquid chromatography (1). In the present study the reversible protein binding of melphalan in albumin solutions and human plasma has been determined by a modified ultrafiltration technique (3). Since the binding of melphalan to albumin might have a profound effect on its stability *in vivo* (4), the rate constants for the degradation of protein-bound and free melphalan have been evaluated.

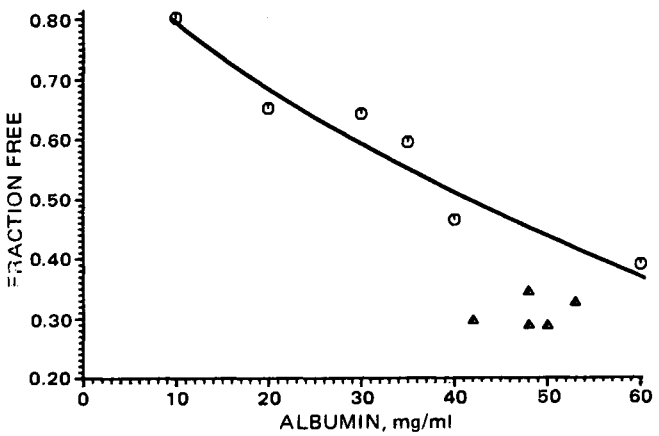

Figure 1—*Influence of albumin concentration on fraction free melphalan (25°; melphalan concentration: 25 μg/ml). The fraction free melphalan is a mean of four determinations. Key: (○) albumin solutions; (▲) plasma samples.*

EXPERIMENTAL

Degradation Studies—Melphalan[1], dissolved in 0.1 *M* HCl, was diluted 100 times with a solution of human albumin[2] in isotonic phosphate buffer pH 7.35 (NaCl concentration 0.095 *M*) or plasma[3] to a final melphalan concentration of 25 μg/ml. The mixture was incubated at 25.0 ± 0.1° and at appropriate times aliquots were analyzed by liquid chromatography.

Protein-Binding Studies—The protein binding was determined using a modified ultrafiltration technique (3). The studies were carried out at 25 ± 2° using albumin or plasma solutions containing 25 μg/ml of melphalan, unless otherwise stated. The degradation of melphalan in the ultrafiltrate was minimized by collecting it in albumin solutions containing the same concentration of albumin as the solution inside the dialysis tubing. No binding of melphalan to the dialysis membrane could be observed as studied by ultrafiltration of melphalan dissolved in isotonic phosphate buffer pH 7.35.

Quantitative Analysis—The quantitative determinations of melphalan were performed by liquid chromatography according to previous

[1] Sigma Chemical Co., St. Louis, Mo.

[2] Human albumin, essentially fatty acid free, Sigma Chemical Co. (A 1887), St. Louis, Mo.

[3] Blood was obtained from drug-free volunteers and collected in tubes containing heparin. The plasma was separated by centrifugation and stored at −20° until used.

0022-3549/82/0700-0826$01.00/0

flux value, in comparison to suspensions, as well as a continuing reduction in flux with time.

As a final test of this explanation, and to ensure that the surfactant used in the suspension formulations did not influence the results, experiments were performed using a saturated solution of benzocaine in water to which excess benzocaine (1 mg/ml) was added.

The results are plotted in Fig. 4 for the penetration profiles with and without excess drug in donor. It is evident that the slopes for the two curves are different. The flux for the donor with excess drug (100×10^{-3} mg hr^{-1} cm^{-2}) was very close to the values obtained for the suspension systems (Table I).

REFERENCES

(1) U. G. Dalvi and J. L. Zatz, *J. Soc. Cosmet. Chem.*, **32,** 87 (1981).

(2) F. Bottari, G. Di Colo, E. Nannipieri, M. F. Saettone, and M. F. Serafini, *J. Pharm. Sci.*, **66,** 926 (1977).

(3) G. Di Colo, V. Carelli, B. Giannaccini, M. F. Serafini, and F. Bottari, *ibid.*, **69,** 387 (1980).

(4) G. D. Tucker, R. N. Boyes, P. O. Bridenbough, and D. C. Moore, *Anesthesiology*, **33,** 287 (1970).

(5) E. Menczel and H. I. Maibach, *J. Invest. Dermatol.*, **54,** 386 (1970).

(6) E. Menczel and H. I. Maibach, *Acta Derm. Venereol.*, **52,** 38 (1972).

(7) S. K. Chandrasekaran, A. S. Michaels, P. S. Campbell, and J. E. Shaw, *AIChE J.*, **22,** 828 (1976).

ACKNOWLEDGMENTS

U. G. Dalvi is grateful for fellowship support provided by the Society of Cosmetic Chemists.

Degradation of Melphalan in Aqueous Solutions—Influence of Human Albumin Binding

HANS EHRSSON ˣ **and ULLA LÖNROTH**

Received April 28, 1981, from the *Karolinska Apoteket, S-104 01 Stockholm, Sweden.* Accepted for publication September 28, 1981.

Abstract □ The protein binding and degradation rate of melphalan in human albumin solutions and plasma have been investigated. In plasma, melphalan is bound 69.0 ± 3.4% (25°, melphalan concentration 25 μg/ml). The stability of melphalan when bound to albumin is about three times higher ($k = 3.07 \times 10^{-2} \pm 0.48 \times 10^{-2}$ hr^{-1}) than unbound in solution ($k = 1.14 \times 10^{-1} \pm 0.01$ hr^{-1}).

Keyphrases □ Melphalan—degradation studies in aqueous solutions, influence of human albumin binding □ Binding—human albumin to melphalan, degradation of melphalan in aqueous solutions □ Albumin, human—influence in binding with melphalan, degradation in aqueous solutions

Melphalan, an alkylating agent of the nitrogen mustard type, can be bound to plasma proteins as a result of a chemical reaction with the protein molecules as well as by a process of reversible adsorption (1). At least 60% of melphalan was bound to serum proteins (26°) as studied by an equilibrium dialysis technique (2). However, the quantitative determinations were performed using an unselective technique, and it is unclear to what extent the results are affected by a codetermination of degradation products of melphalan formed during the dialysis procedure. Melphalan (30%) was observed previously to be undialyzable in human plasma (4°), the quantitative determinations being performed by high-performance liquid chromatography (1). In the present study the reversible protein binding of melphalan in albumin solutions and human plasma has been determined by a modified ultrafiltration technique (3). Since the binding of melphalan to albumin might have a profound effect on its stability *in vivo* (4), the rate constants for the degradation of protein-bound and free melphalan have been evaluated.

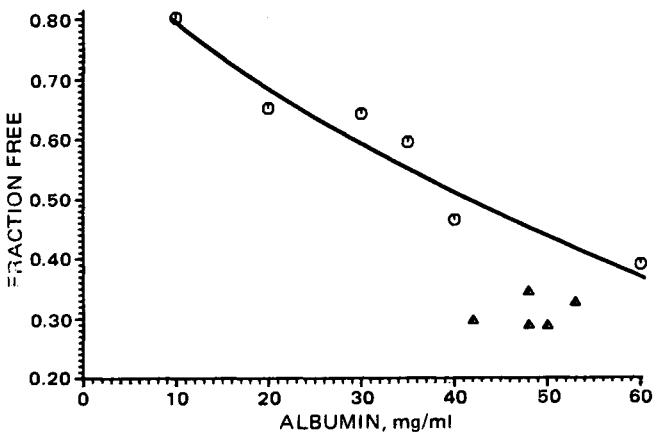

Figure 1—*Influence of albumin concentration on fraction free melphalan (25°; melphalan concentration: 25 μg/ml). The fraction free melphalan is a mean of four determinations. Key: (○) albumin solutions; (▲) plasma samples.*

EXPERIMENTAL

Degradation Studies—Melphalan[1], dissolved in 0.1 *M* HCl, was diluted 100 times with a solution of human albumin[2] in isotonic phosphate buffer pH 7.35 (NaCl concentration 0.095 *M*) or plasma[3] to a final melphalan concentration of 25 μg/ml. The mixture was incubated at 25.0 ± 0.1° and at appropriate times aliquots were analyzed by liquid chromatography.

Protein-Binding Studies—The protein binding was determined using a modified ultrafiltration technique (3). The studies were carried out at 25 ± 2° using albumin or plasma solutions containing 25 μg/ml of melphalan, unless otherwise stated. The degradation of melphalan in the ultrafiltrate was minimized by collecting it in albumin solutions containing the same concentration of albumin as the solution inside the dialysis tubing. No binding of melphalan to the dialysis membrane could be observed as studied by ultrafiltration of melphalan dissolved in isotonic phosphate buffer pH 7.35.

Quantitative Analysis—The quantitative determinations of melphalan were performed by liquid chromatography according to previous

[1] Sigma Chemical Co., St. Louis, Mo.

[2] Human albumin, essentially fatty acid free, Sigma Chemical Co. (A 1887), St. Louis, Mo.

[3] Blood was obtained from drug-free volunteers and collected in tubes containing heparin. The plasma was separated by centrifugation and stored at −20° until used.

0022-3549/82/0700-0826$01.00/0

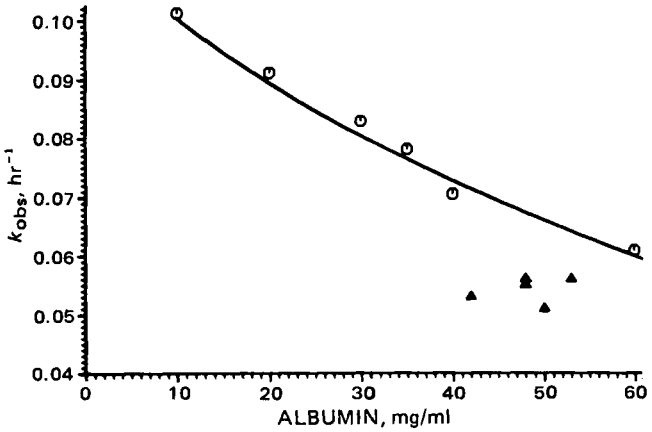

Figure 2—*Degradation rate of melphalan-influence of albumin concentration (25°; melphalan concentration: 25 μg/ml). Key: (○) albumin solutions; (▲) plasma samples.*

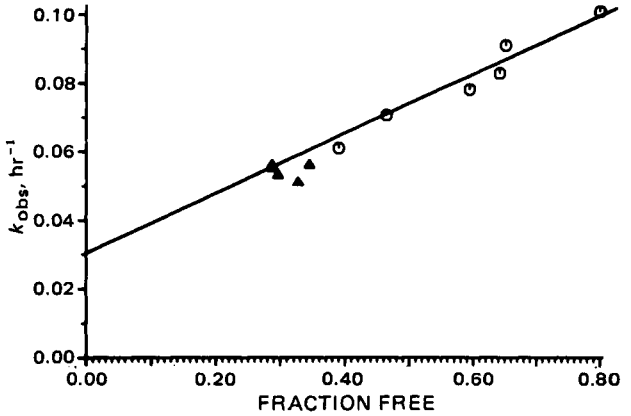

Figure 3—*Degradation rate* versus *fraction free melphalan (25°). Key: (○) albumin solutions; (▲) plasma samples.*

principles (1), using the same equipment as described previously (3). The results were evaluated using a standard curve prepared by adding known amounts of melphalan to albumin solutions and plasma.

RESULTS AND DISCUSSION

The protein binding of melphalan (25 μg/ml) was 69.0 ± 3.4% in plasma obtained from five donors, the mean albumin concentration being 48 mg/ml. No significant change in the degree of protein binding was observed in the concentration range 5–50 μg/ml of melphalan. The protein binding in albumin solutions was lower than in plasma containing comparable albumin concentrations (Fig. 1). The protein binding was 53.5 ± 1.7% at an albumin concentration of 40 mg/ml.

The influence of albumin concentration on the pseudo first-order rate constant for the degradation of melphalan is given in Fig. 2. The half-life for the degradation of melphalan is 9.88 ± 0.24 hr ($n = 10$, $r = 0.998$) at an albumin concentration of 40 mg/ml. The stability in plasma obtained from five donors is higher ($t_{1/2} = 12.80 \pm 0.52$ hr) than in albumin solutions containing comparable albumin concentrations.

The rate constant for the degradation of melphalan in albumin solutions (k_{obs}) can be expressed by (3):

$$k_{obs} = k_1 + f_{free}(k_2 - k_1)$$

where k_1 and k_2 are pseudo first-order rate constants for the degradation of protein-bound and free melphalan, respectively, and f_{free} is the fraction of free melphalan in solution. A plot of k_{obs} *versus* f_{free} in albumin solutions and plasma is given in Fig. 3. The fraction free melphalan in the albumin solutions was changed by the use of different albumin concentrations (10–60 mg/ml) at a constant ligand concentration (25 μg/ml). Evaluation of the rate constants by linear regression analysis using the data obtained in albumin solutions gave $k_1 = 3.07 \times 10^{-2} \pm 0.48 \times 10^{-2}$ hr^{-1} and $k_2 = 1.15 \times 10^{-1} \pm 0.09 \times 10^{-1}$ hr^{-1} ($r = 0.916$, $n = 24$). The rate constant for free melphalan obtained from the plot is in good agreement with the value obtained from degradation studies in albumin-free isotonic phosphate buffer pH 7.35 ($k_{obs} = 1.14 \times 10^{-1} \pm 0.01 \times 10^{-1}$ hr^{-1}, $n = 14$, $r = 0.999$). Thus, the stability of melphalan bound to albumin is about three times higher than unbound in solution.

Since the degradation rate of nitrogen mustards is increased markedly with increasing dielectric constant of the solvent (5), it can be concluded that the nitrogen mustard group of melphalan when bound to albumin is in a chemical environment with solvating properties different from those in pure aqueous solution. It has been shown previously (3) that the nitrogen mustard drug, chlorambucil, was efficiently protected from degradation when bound to albumin, the rate constant for the bound form being ~100 times lower than for chlorambucil being free in solution. This indicates that melphalan is bound to albumin in a different way than chlorambucil. Furthermore, it can be observed (Fig. 3) that the data obtained for melphalan in plasma fall on the line obtained from studies in pure albumin solutions. The increased stability for melphalan observed in plasma must, therefore, be due to a more excessive binding to albumin or to other plasma ligand(s) which bind the nitrogen mustard group in a similar way as albumin.

REFERENCES

(1) S. Y. Chang, D. S. Alberts, D. Farquhar, L. R. Melnick, P. D. Walson, and S. E. Salmon, *J. Pharm. Sci.*, **67**, 682 (1978).

(2) M. Chirigos and J. A. R. Mead, *Anal. Biochem.*, **7**, 259 (1964).

(3) H. Ehrsson, U. Lönroth, I. Wallin, M. Ehrnebo, and S. O. Nilsson, *J. Pharm. Pharmacol.*, **33**, 313 (1981).

(4) D. S. Alberts, S. Y. Chang, H. S. G. Chen, T. E. Moon, T. L. Evans, R. L. Furner, K. Himmelstein, and J. F. Gross, *Clin Pharmacol. Ther.*, **26**, 73 (1979).

(5) W. R. Owen and P. J. Stewart, *J. Pharm. Sci.*, **68**, 992 (1979).

HPLC Analysis of Indomethacin and Its Impurities in Capsule and Suppository Formulations

E. KWONG, G. K. PILLAI, and K. M. McERLANE ˣ

Received June 30, 1981, from the *Faculty of Pharmaceutical Sciences, The University of British Columbia, Vancouver, BC, V6T 1W5, Canada.* Accepted for publication October 5, 1981.

Abstract □ Indomethacin and its impurities in suppository and capsule formulations were quantitatively determined by HPLC using a reversed-phase, octadecyl column and a mobile phase of methanol–water–acetonitrile–acetic acid (55:35:10:1). Analysis of the suppository formulations provided a mean potency for indomethacin of 103.8%. The same formulation was found to contain 4-chlorobenzoic acid (0.02%), 5-methoxy-2-methyl-3-indoleacetic acid (0.07%), 4-chlorobenzoic acid-α-monoglyceride (0.39%), and indomethacin-α-monoglyceride (0.9%) as impurities. The latter two impurities were a result of the interaction of indomethacin and 4-chlorobenzoic acid with glycerin used in the suppository base. Capsule formulations were likewise assayed with an average potency of 99.9 and 101.5% for 25- and 50-mg dosage forms, respectively. Only one of the two capsule formulations examined contained detectable quantities of 4-chlorobenzoic acid (0.05%).

Keyphrases □ Indomethacin—HPLC analysis, impurities in capsule and suppository formulations □ HPLC—indomethacin, impurities in capsule and suppository formulations □ Formulations—indomethacin, impurities in capsule and suppositories, HPLC analysis

Indomethacin is an anti-inflammatory and analgesic agent used in the treatment of rheumatoid arthritis, gout, degenerative joint disease, and other inflammatory conditions that do not respond to salicylates. Indomethacin may be synthesized by several routes (1–5), but these are generally modifications of the original method (1). The USP XX (6) contains monographs for the drug substance and capsule formulations, and the BP 1973 (7) includes monographs for these, as well as suppository formulations. The official pharmacopeias do not specify tests for impurities, and the hydrolytic, titrimetric assay procedure would not be indicative of purity if substances with structural similarities were present.

It has been reported that indomethacin is subject to hydrolysis in basic solutions (8) and in the presence of polysorbates (9). However, in only one instance has the presence of impurities in untreated capsule and suppository formulations been noted (10). Previous HPLC assay methods reported for the analysis of indomethacin in plasma (11) or capsule formulations (12) were not concerned with the detection or determination of impurities. The present method offers a rapid and simple HPLC procedure for the simultaneous quantitation of indomethacin and its major impurities in capsule and suppository formulations.

EXPERIMENTAL

Materials—All indomethacin (I) capsule and suppository formulations were obtained directly from the manufacturer[1]. Testosterone[2], 4-chlorobenzoic acid[3] (II), 5-methoxy-2-methyl-3-indoleacetic acid[4] (III), glycerin[5], and I drug substance[2] were used without further purification.

Methanol, water, and acetonitrile were HPLC quality[6], and acetic acid[7] and ether[8] were reagent grade. TLC plates[9] were precoated with silica gel G-25 UV (254) (20 × 20 cm, 0.25 mm). Solvents used for TLC were reagent grade[8].

HPLC System—An isocratic HPLC[10] equipped with a single piston pump[11], 20-μl loop injector[12], fixed wavelength detector[13] (254 nm), electronic data system printer/plotter[14], and a 5-μ reversed-phase (C-18) column (4.6 mm × 25 cm)[15] were used throughout. The mobile phase consisted of methanol–water–acetonitrile–acetic acid (55:35:10:1) and was pumped at 1 ml/min.

Synthesis of 4-Chlorobenzoic acid-α-monoglyceride (IV)—In a

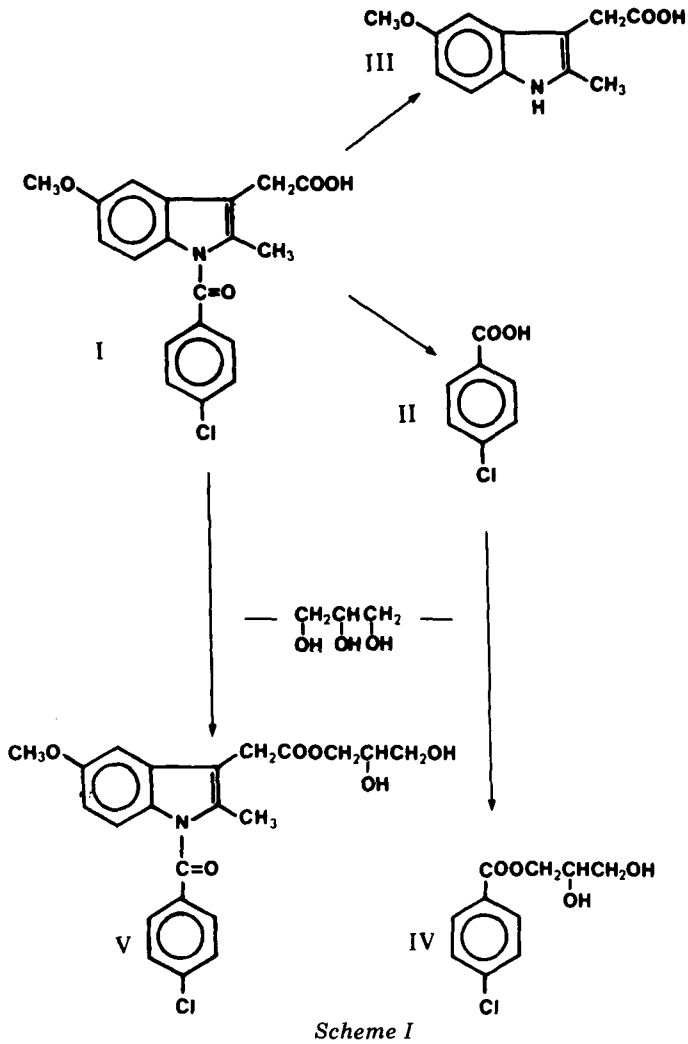

Scheme I

[1] Merck Sharp & Dohme, Kirkland, Quebec, Canada.
[2] Sigma Chemical Co., St. Louis, Mo.
[3] ICN Pharmaceuticals, Inc., Plainview, N.Y.
[4] Aldrich Chemical Co., Milwaukee, Wis.
[5] J. T. Baker Chemical Co., Phillipsburg, N.J.
[6] Fisher Scientific Co. Ltd., Vancouver, B.C., Canada.
[7] Canadian Industries Ltd., Vancouver, B.C., Canada.
[8] Caledon, Georgetown, Ontario, Canada.
[9] Machercy-Nagel and Co., Distributed by Brinkmann Instruments Inc., Westbury, N.Y.
[10] Altex Scientific Inc., Berkeley, Calif.
[11] Model 110A, Altex Scientific, Inc.
[12] Model 7125, Rheodyne Inc., Berkeley, Calif.
[13] Model 153, Altex Scientific Inc.
[14] Model C-R1A, Shimadzu Corp., Kyoto, Japan.
[15] Ultrasphere, Altex Scientific Inc.

0022-3549/82/0700-0828$01.00/0

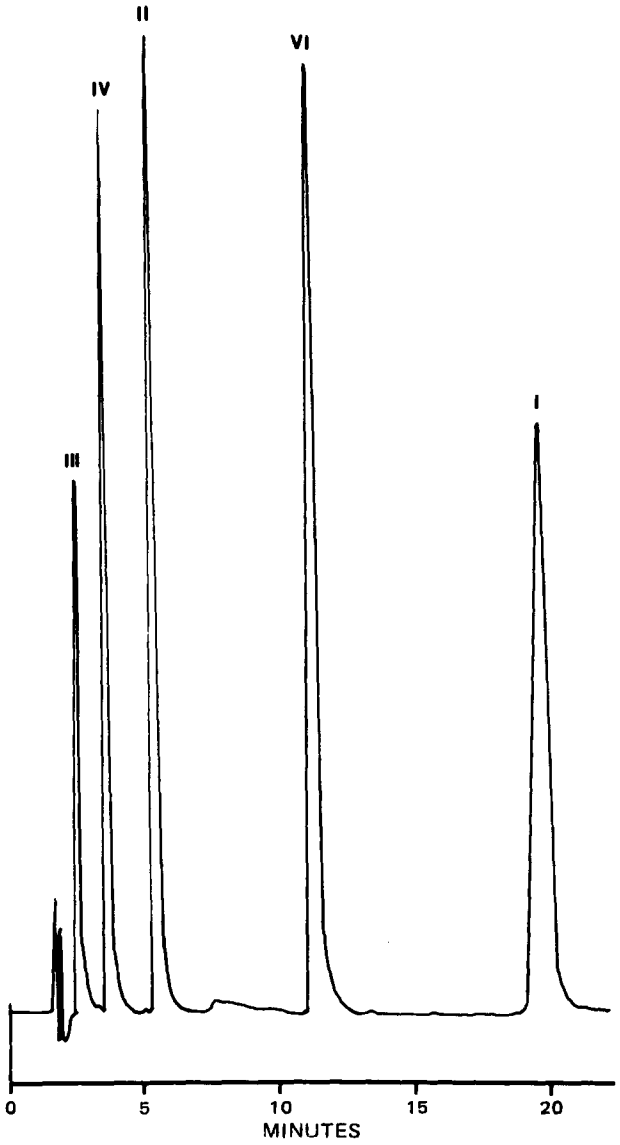

Figure 1—*HPLC of synthetic mixture of indomethacin and its impurities. Peaks: (I) indomethacin; (II) 4-chlorobenzoic acid; (III) 5-methoxy-2-methyl-3-indoleacetic acid; (IV) 4-chlorobenzoic acid-α-monoglyceride; (VI) the internal standard, testosterone.*

50-ml screw-capped culture tube, 1 g of II was heated with 30 ml of glycerin at 60° for 96 hr. During this period II went into solution. The glycerin solution was dissolved in water (50 ml) and extracted with three 50-ml portions of ether. The combined ether extracts were evaporated under vacuum and the residue was dissolved in a minimum volume of ether, diluted with petroleum ether (bp 60–80°)[5] and left at 4° until crystals separated. The crystalline material was recrystallized from ether–petroleum ether to a constant melting point (88–89°). The product was analyzed by HPLC to determine the absence of starting material or other impurities, and its structure was confirmed by PMR, IR, and mass spectrometric analysis. The compound exhibited identical characteristics to that reported earlier (10).

Table I—Slope of the Calibration Curves for Indomethacin and its Impurities Determined at 254 nm

Compound	Slope	Intercept	Correlation Coefficient[a]
Indomethacin (I)	1.05	0.17	0.999
4-Chlorobenzoic Acid (II)	1.008	0.0	0.999
5-Methoxy-2-methyl-3-indoleacetic acid (III)	0.380	−0.008	0.999
4-Chlorobenzoic acid-α-monoglyceride (IV)	0.834	−0.003	0.996

[a] $n = 4$.

Table II—Recovery of Indomethacin from Capsule and Suppository Formulations

Form and Dosage	Drug Weight in Formulation, mg	Amount of Drug Added, mg	Recovery mg	Recovery (%)
Suppository, 100 mg	50.06	20.12	69.52	99.1
Capsule, 50 mg	49.15	21.58	68.81	98.1
Capsule, 25 mg	25.08	15.20	40.10	99.6

Isolation and Identification of Indomethacin-α-monoglyceride (V)—A 100-mg suppository was crushed, suspended in 5 ml of water, and extracted with three 50-ml portions of ether. The combined ether extracts were evaporated under vacuum, the residue was taken up in 4 ml of ether, and applied in a narrow band to four TLC plates precoated with silica gel G-25 UV. The plates were eluted with ether–acetic acid (100:1) for a distance of 15 cm. The major impurity band corresponding to V (R_f 0.25) was removed from the four plates and extracted from the silica gel with 100 ml of chloroform. The subsequent identity of this material was confirmed by PMR, IR, and mass spectrometric analysis and was identical to that reported earlier (10).

Standard Solutions—Stock solutions of I (175 mg/50 ml), II (0.5 mg/100 ml), III (1 mg/100 ml), and IV (2 mg/25 ml) were prepared in methanol. Two working solutions of the internal standard, testosterone, were prepared in ether (50 mg/50 ml) and methanol (50 mg/50 ml).

Determination of Linearity and Calibration Curves—*Impurities*—To four 10-ml screw-capped culture tubes were added 0.25, 0.50, 1.0, and 1.5 ml of each of the stock solutions of II, III, and IV, along with 1 ml of the internal standard in methanol. The volume of each tube was brought to 10 ml with methanol and 20 μl was used for analysis of each sample.

Indomethacin—To four 10-ml screw-capped culture tubes were added 0.5, 1, 2, 3, 4, and 8 ml of the stock solutions of I, along with 1 ml of the internal standard in methanol. The volume of each tube was brought to 10 ml with methanol, and 20 μl was used for analysis of each sample.

Extraction of Capsule and Suppository Formulations—*Capsules*—The contents of four capsules (25- or 50-mg dose) were removed, weighed, and combined. Two aliquots equivalent to 50 mg of I were transferred to two 50-ml screw-capped culture tubes. A 3-ml aliquot of the internal standard in ether was added to each tube along with 15 ml of water and 25 ml of ether. The tubes were tightly capped and tumbled for 20 min. The ether layer was removed, dried, and evaporated under a stream of clean, dry nitrogen. The residue was dissolved in 30 ml of methanol and 20 μl was used for analysis.

Suppositories—Four suppositories (100 mg of I/dose) were weighed and crushed. Five aliquots equivalent to 50 mg were placed in five 50-ml screw-capped culture tubes and treated as described previously.

Recovery of Indomethacin from Formulations—An amount of I, equivalent to half the amount of I contained in a suppository formulation (~50 mg), was placed in a screw-capped tube. An aliquot of 3 ml of the internal standard in ether, 15 ml of water, and 25 ml of ether were added, and the mixture was treated as described previously. A similar recovery experiment was conducted on capsule formulations.

RESULTS AND DISCUSSION

A previous publication (10) reported the degradation of indomethacin and its interaction with glycerin used in a suppository base (Scheme I). To more precisely analyze indomethacin and its impurities, an HPLC

Table III—Quantitation of Indomethacin and its Impurities in Capsule and Suppository Formulations

Compound	Dosage Forms[a], % 100-mg[b] Suppository	50-mg[c] Capsule	25-mg[c] Capsule
Indomethacin (I)	103.800 ± 2.160	101.50	99.85
4-Chlorobenzoic Acid (II)	0.020 ± 0.002	0.05	None
5-Methoxy-2-methyl-3-indole-acetic acid (III)	0.070 ± 0.007		
4-Chlorobenzoic acid-α-monoglyceride (IV)	0.390 ± 0.023		
Indomethacin-α-mono-glyceride (V)	0.919 ± 0.067		

[a] All dosage forms were obtained from the same manufacturer. [b] Values are the mean of five determinations and are presented as the percentage based on labeled claim of indomethacin (±SD). [c] Values for capsules were taken from the average of two determinations.

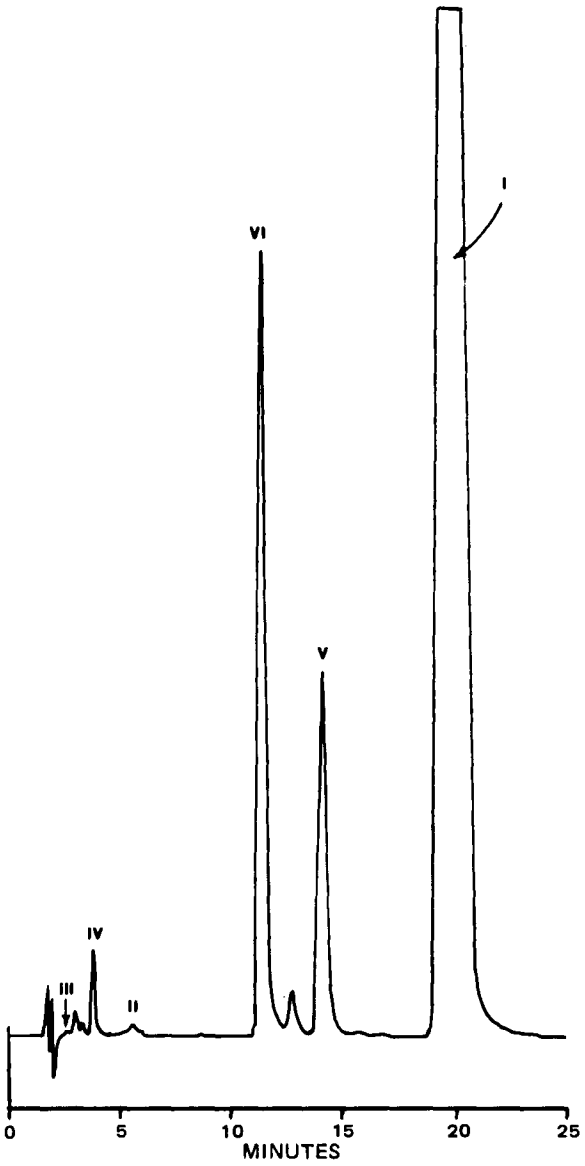

Figure 2—*HPLC of extract of indomethacin suppository formulation. Peaks: (I) indomethacin; (II) 4-chlorobenzoic acid; (III) 5-methoxy-2-methyl-3-indoleacetic acid; (IV) 4-chlorobenzoic acid-α-monoglyceride; (V) indomethacin-α-monoglyceride; (VI) the internal standard, testosterone.*

method was investigated. The chromatogram shown in Fig. 1 was obtained for a standard mixture of I and its impurities II–IV. Impurity V could not be included in this chromatogram due to lack of sufficient quantities of pure material. Calibration curves for I and the impurities II–IV were determined by dissolution in methanol containing the internal standard, testosterone. It was not possible to isolate a sufficiently pure crystalline form of V; therefore, the response factor for this impurity was equated to that of I. This was considered sufficiently accurate, as little difference in the UV absorptivity at 254 nm would be expected for these two compounds, due to the identical nature of the basic chromophore portion of both molecules. To establish the reliability of the calibration curves determined by dissolution in methanol, a single mixture of I and the impurities II–IV were likewise partitioned between the water–ether mixture used to extract the formulations. The recoveries of the drug and impurities from the aqueous phase into ether were quantitative. The response factors and correlation coefficients for I–IV are given in Table I.

The extraction of I from capsule and suppository formulations was determined by analysis of an aliquot of the formulation to which a quantity of indomethacin, equivalent to half of the theoretical amount of indomethacin, was added. The extraction efficiencies thus determined are summarized in Table II. The apparent high recovery indicates that the formulation excipients do not interfere with such a simple, single extraction.

The results obtained for the analysis of I and its impurities II–V in both capsule and suppository formulations are given in Table III. A representative chromatogram for a suppository formulation is shown in Fig. 2. Impurities II–V account for a total of 1.4% of the amount of indomethacin in the suppository formulation, while only small quantities of 4-chlorobenzoic acid were detected in one of the two capsule formulations.

Examination of the chromatogram of a suppository formulation (Fig. 2) reveals an impurity at 12.5 min following the internal standard. Several attempts to isolate and identify this material were unsuccessful. No attempt was made to isolate the minor components appearing between impurities III and IV. However, the remaining impurities II–V were confirmed by comparison of their retention times with authentic samples.

All formulations analyzed by the HPLC procedure described fall within the limits specified for capsule and suppository formulations in the USP (6) and BP (7). The presence of impurities, particularly in the suppository formulations represents a distinct example of the interaction of a drug with an excipient, glycerin. Although the amount of the α-monoglyceride impurities were less than 1.4% of the amount of indomethacin, these levels could be increased several-fold by holding the suppository at its melting point. Since all formulations were obtained fresh from the manufacturers, the rate of this reaction under normal storage conditions could not be determined, and accelerated stability studies were not considered due to the relatively low softening temperature of the suppository base.

REFERENCES

(1) T. Y. Shen, *et al.*, *J. Am. Chem. Soc.*, **85**, 488 (1963).

(2) T. Y. Shen, U.S. pat. 3,161,654 (1964).

(3) T. Y. Shen, Belgian pat. 649,169 (1964); through *Chem. Abstr.*, **64**, 6622 (1966).

(4) H. Yamamoto, V. Nakamura, and T. Kabayashi, Japanese pat., 7,036,745 (1970); through *Chem. Abstr.*, **75**, 5692 (1971).

(5) D. Bertazzoni, B. Bortoletti, and T. Perlotte, *Boll. Chim. Farm.*, **109**, 60 (1970); through *Chem. Abstr.*, **73**, 14610t (1970).

(6) "The United States Pharmacopeia XX," U.S. Pharmacopeial Convention, Rockville, Md., 1980.

(7) "British Pharmacopeia 1973," Her Majesty's Stationary Office, London, England 1973.

(8) B. R. Hajratwala and J. E. Dawson, *J. Pharm. Sci.*, **66**, 27 (1977).

(9) H. Krasowska, *Int. J. Pharm.*, **4**, 89 (1979).

(10) N. M. Curran, E. G. Lovering, K. M. McErlane, and J. R. Watson, *J. Pharm. Sci.*, **69**, 187 (1980).

(11) G. G. Skellern and E. G. Salole, *J. Chromatogr.*, **114**, 483 (1975).

(12) F. M. Plakogeannis, A. Ali, and S. Kazmi, *Drug. Dev. Ind. Pharm.*, **7**, 215 (1981).

Correlation of Antitumor Activity and Electron Deficiency of Nitrofuranylhydrazone Compounds

ROBERT A. NEWMAN ˣ, MICHAEL J. STRAUSS, and RICHARD RENFROW

Received June 12, 1981, from the *Vermont Regional Cancer Center and Departments of Pharmacology and Chemistry, University of Vermont, Burlington, VT 05405.* Accepted for publication October 22, 1981.

Abstract □ Phenylhydrazone derivatives of 5-nitro-2-furaldehyde were tested for antitumor activity against L-1210 murine leukemia *in vitro*. A substantial increase in antitumor activity was observed in these series of compounds as the electron deficiency of the six-membered aromatic ring was increased. A possible mechanism of action involving drug reduction as well as antibacterial and antitumor efficacy is discussed.

Keyphrases □ Nitrofuranylhydrazones—correlation, antitumor activity, electron deficiency □ Electron deficiency—correlation of antitumor activity, nitrofuranylhydrazone compounds □ Antitumor activity—electron deficiency, nitrofuranylhydrazone compounds

Nitrofuran compounds exhibit a wide range of useful pharmacologic activity. Nitrofurazone, for example, is a broad spectrum topical antibacterial agent used primarily in the treatment of mixed infections of wounds and diseases of the skin. Nitrofurantoin, a chemically related compound, is a urinary tract antiseptic quite active against many strains of common urinary pathogens. In addition to their current use as antibiotics, nitrofuran compounds have in the past been considered useful against selected neoplasias. *cis*-Dichlorodiammine platinum and bleomycin are currently considered two of the drugs of choice for the treatment of testicular carcinomas (1). However, the use of nitrofurazone and nitrofurantoin in testicular tumor therapy has been reported frequently during the past three decades (2–6).

Although there are a few reports of structure–activity relationships for nitrofurans as antitumor agents (7–10), this area has not been fully explored. This is especially true for simple phenylhydrazone derivatives of 5-nitro-2-furaldehyde. There still exists, therefore, potential for the development of new drugs in this class for the treatment of testicular or other tumor types.

The most thorough synthetic and pharmacologic studies on new types of antineoplastic nitrofuran derivatives are those of Ujiie and Miura *et al.* (7, 8, 10). These authors have prepared a series of compounds like Compounds I, II, and III, and have screened these in a variety of experimental tumor systems. Certain derivatives of Compounds I and II were found to completely cure Ehrlich ascites carcinoma in mice. The compounds are relatively nontoxic and doses of up to 1000 mg/kg did not cause any drug-related deaths. Moderate antitumor activity was also seen with Schiff base derivatives like Compound III.

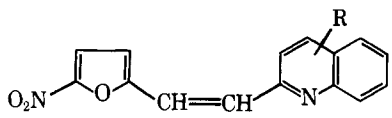

I

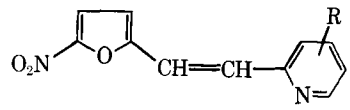

II

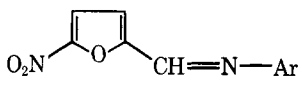

III

The present study describes the *in vitro* antitumor activity of a new series of phenylhydrazone derivatives of 5-nitro-2-furaldehyde. An examination was made of the correlation of electron withdrawing potential of each compound as a contributing factor to the possible mechanism of antibacterial and antitumor activity of this series of drugs.

EXPERIMENTAL

Cell Culture—Mouse leukemic L-1210 cells[1] were maintained in medium containing 10% fetal calf serum[2]. Stock cultures of cells were diluted with the medium to give final concentrations of 5×10^5 cells/ml. The compounds were dissolved in dimethyl sulfoxide and diluted to a concentration 500 times greater than the experimental level desired, so the 10 μl of the compound solution could be added to 5 ml of the inoculated growth medium. No precipitation occurred during this addition. This amount of compound in solution yielded a final dimethyl sulfoxide concentration of 0.2%, which itself had no effect on cell growth.

Each ID_{50} experiment (i.e., the determination of that dose which results in 50% inhibition of L-1210 growth) was run four times. Cell cultures were incubated at 37° in a 95% O_2–5% CO_2 humidified atmosphere and were counted after 96 hr. All cell counts were done by diluting the cell culture 1:40 and then counting with an electronic cell counter. The concentration of cells in the control tubes of L-1210 after 96 hr was ~2.5×10^6/ml.

Hydrazone Syntheses—The hydrazones were prepared from commercially available hydrazines and 5-nitrofurancarboxaldehyde by heating an ethanolic solution of these precursors containing a small portion of glacial acetic acid. The hydrazones that precipitated were recrystallized from ethanol and all had satisfactory elemental analyses. Elemental analyses and melting point data are listed in Table I.

RESULTS AND DISCUSSION

The series of nitrofuranylhydrazones like Compound IV clearly show a substantial and significant increase in antitumor activity as the electron deficiency of the six-membered aromatic ring increases.

The *in vitro* L-1210 screening data for the various compounds, the sum of σ values for the six-membered ring substituents, as well as pertinent ^{1}H-NMR shifts, are represented in Table II.

The metabolic reaction first occurring with most nitrofurans in animals involves reduction of the furanyl nitro group to a hydroxylamine (12). This is followed by further reduction to the amine and finally ring opening and fragmentation (13). Hydrolysis of the azomethine linkage can also

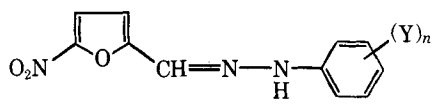

IV

[1] Sloan Kettering Institute, Rye, N.Y.
[2] McCoy's 5a, Grand Island Biological Co., Grand Island, N.Y.

0022-3549/82/0700-0831$01.00/0

Table I—Elemental Analysis and Melting Point Data of Nitrofuranylhydrazone Compounds

Compound	Formula	Theoretical, %	Found, %	Melting Point
IV*a*[a]	$C_{12}H_{11}N_3O_4$			same as lit. (11)
IV*b*	$C_{11}H_9N_5O_7$	C 57.14	56.90	
		H 3.92	3.88	181–185 dec.
		N 18.17	18.05	
IV*c*[a]	$C_{11}H_8N_3O_3Cl$			same as lit. (11)
IV*d*	$C_{12}H_9N_3O_5SF_2$	C 41.74	41.71	
		H 2.63	2.73	237–239 dec.
		N 12.17	12.05	
IV*e*[a]	$C_{11}H_8N_4O_5$			same as lit. (11)
IV*f*	$C_{11}H_8N_4O_5$	C 47.83	48.04	
		H 2.92	2.94	220–223 dec.
		N 20.28	20.15	
IV*g*	$C_{10}H_7N_5O_5$	C 43.33	43.32	
		H 2.55	2.60	238–241 dec.
		N 25.26	25.26	
IV*h*	$C_{11}H_7N_5O_7$	C 41.13	41.18	
		H 2.20	2.17	269–270 dec.
		N 21.80	21.60	
IV*i*	$C_{10}H_6N_6O_7$	C 37.28	37.54	
		H 1.88	2.02	242–245 dec.
		N 26.08	25.38	

occur, followed by oxidation to 5-nitrofuroic acid. The latter is found in the urine of experimental animals (14).

It should be noted that nitrofurans are reduced in a number of bacterial enzyme systems, and a number of researchers have advanced the theory that in accepting electrons, the nitrofurans interfere with the oxidation–reduction linked metabolism of the organism. It has been suggested that nitrofurazone interferes with normal metabolism by virtue of its capacity to be reduced (15). In addition, previous authors have concluded from a study of nitrofurans, nitrothiophenes, nitrobenzenes, and related compounds, that ease of reducibility plays a major role in the antibacterial effectiveness of heterocyclic nitro compounds (16). These authors also proposed a relationship between the redox potential developed by the organism in culture and that required by the inhibitory nitrofuran, implying that interference with microbial reproduction was associated with formation of a reduction product (hydroxylamine) from the nitro compound (17). Other workers have measured these reduction potentials and confirmed these proposals (18).

It is reasonable to assume that the well-known antibacterial activity of nitrofuranyl hydrazones and the *in vitro* antitumor activity observed against mouse leukemia L-1210 may have similarities with regard to their mechanisms of action. The dramatic increase in cytotoxicity with increasing electron deficiency of the pi system in IV*i*, (see Table II) suggests that biological activity may well be associated with a reductive process. The furanyl nitro group in IV*i* should be much more readily reduced than that in IV*a*. The relationship between L-1210 cytotoxicity and electron deficiency can qualitatively be seen by examining measures of the latter, *i.e.*, the summation of the σ_p and σ_0 values for the six-membered ring substituents, and/or the methine ^1H chemical shifts (Table II). Surprisingly, the antibacterial activity of IV*i*, one of the more active compounds against L-1210, was negligible against 18 Gram-positive and Gram-negative organisms compared with nitrofurazone and nitrofurantoin. It possessed somewhat better activity against two staphylococci (64 μg/ml minimal inhibitory concentration) but not as much activity as nitrofurazone (8 μg/ml) or nitrofurantoin (16–32 μg/ml). In contrast, the cytotoxicity of IV*i* is still very high against both HeLa cells and P-388 cells. The differential activity of IV*i* in the antineoplastic and antibacterial screens could result from an inability of the compound to penetrate the bacterial cell wall. The compound is extremely insoluble and is completely inactive in an *in vivo* L-1210 screen.

Perhaps the most surprising result of this report is that 5-nitrofurancarboxaldehyde is more cytotoxic than any of the hydrazones studied (Table II). This introduces the interesting possibility that hydrazone activity may, in part, result from hydrolytic cleavage to the parent aldehyde. The variation in hydrazone cytotoxicity may, in fact, be partially related to the variable rates of hydrolytic cleavage.

Table II—Antitumor Activity and Electron Deficiency Determinations of Nitrofuranylhydrazone Compounds

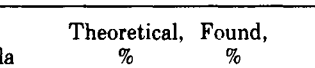

R = Ar-(Y)n		L-1210 ID_{50}, μg/ml	$\Sigma\sigma$[a]	δ ppm[b] CH=N
IV*a*	*p*-OCH_3	>10	−.27	7.7
IV*b*	*p*-H	3	0	7.7
IV*c*	*p*-Cl	5	+.23	7.8
IV*d*	*p*-SO_2CHF_2	4	+.73	7.8
IV*e*	*p*-NO_2	3	+.78	7.9
IV*f*	*o*-NO_2	1.8	+.97	8.6
IV*g*	2-aza-6-nitro	1.0	+1.43	8.5
IV*h*	2,4-dinitro	0.8	+1.75	8.6
IV*i*	2-aza-4,6-dinitro	0.5	+2.21	9.1
5-nitrofurancarboxaldehyde		0.1	—	

[a] Substituent constants (σ) were obtained from Ref. 19. In calculating the sums ($\Sigma\sigma$), the assumption was made that $\sigma ortho = \sigma para$. [b] NMR spectra were obtained in dimethyl sulfoxide d_6 solution with tetramethylsilane as an internal reference. They were recorded on a JEOL MH-100 NMR spectrometer.

Toxicological studies of many nitroheterocycles have revealed a substantial mutagenic and carcinogenic liability. Since mutagenic and antibacterial modes of action are probably intimately related at the molecular level, it is unlikely that important nonmutagenic antibacterial nitroheterocycles will be found. Because most antineoplastic agents have substantial carcinogenic acitivity, a liability of this type associated with an antineoplastic nitrofuran is not severe, and the potential use of such compounds in cancer chemotherapy should not be overlooked.

REFERENCES

(1) L. Einhorn, S. Williams, S. Turner, M. Troner, and F. A. Greco, *Cancer Res.*, **22,** 463 (1981).

(2) C. E. Friedgood, A. L. Danza, and A. Boccabella, *Cancer Res.*, **12,** 262 (1952).

(3) M. J. Szezokowski, A. L. Daywitt, and H. Elrick, *J. Am. Med. Assoc.*, **167,** 1066 (1958).

(4) E. Haltiwanger, *J. Urol.*, **86,** 125 (1961).

(5) J. F. Richardson and G. A. LeBlanc, *ibid.*, **93,** 717 (1965).

(6) A. R. MacKenzie, *Cancer*, **19,** 1369 (1966).

(7) T. Ujiie, *Chem. Pharm. Bull.*, **14,** 461 (1966).

(8) K. Miura and O. Ikuki, *ibid.*, **13,** 525 (1965).

(9) H. Katae, H. Iwana, Y. Takase, and M. Shimizu, *Arzneimittelforsch*, **17,** 1030 (1967).

(10) K. Miura, I. Masao, T. Oohashi, Y. Igarashi, and I. Okadi, *Chem. Pharm. Bull.*, **13,** 529 (1965).

(11) J. G. Pecca, J. Dobrecky, and S. M. Albonico, *J. Pharm. Sci.*, **60,** 650 (1971).

(12) A. H. Beckett and A. E. Robinson, *J. Med. Pharm. Chem.*, **1,** 135 (1959).

(13) A. M. Tennent and W. H. Ray, *Fed. Proc. Fed. Am. Soc. Exp. Biol.*, **22,** 367 (1963).

(14) J. Olivard, S. Valenti, and J. A. Buzard, *J. Med. Pharm. Chem.*, **5,** 24 (1962).

(15) D. C. Cramer, *J. Bacteriol.*, **54,** 119 (1947).

(16) O. Dann and E. F. Moller, *Chem. Ber.*, **80,** 23 (1947).

(17) O. Dann and E. F. Moller, *ibid.*, **82,** 76 (1949).

(18) T. Sasaki, *Pharm. Bull.*, **2,** 104 (1954).

(19) H. H. Jaffe, *Chem. Revs.* **53,** 191 (1953).

ACKNOWLEDGMENTS

The authors wish to thank Dr. J. Denton at Lerderle Laboratories for antibacterial screening data, and Dr. John McCormack, University of Vermont, Department of Pharmacology, for obtaining data on L-1210 screen.

Edetate Disodium-Mediated Chloramphenicol Resistance in *Pseudomonas cepacia*

P. A. NIELSEN ˣ and JO-ANN CLOSE

Received March 18, 1981, from the *Microbiology Section, Vick Divisions Research & Development, Richardson-Vicks, Inc., Mt. Vernon, NY 10553.* Accepted for publication October 16, 1981

Abstract □ The presence of edetate disodium decreased the susceptibility of a particular strain of *Pseudomonas cepacia* to chloramphenicol. The mechanism of this edetate disodium effect, which may be unique to this strain, remains obscure. Tests showed no enzymatic destruction by the microorganism of the chloramphenicol nor any chemical complexation of the antibiotic by the salt. The possibility does exist that edetate disodium alters the cell envelope or cytoplasmic membrane so as to block the transport of chloramphenicol to its site of action within the cell. This possibility is now under investigation.

Keyphrases □ Edetate disodium—mediated chloramphenicol resistance in *Pseudomonas cepacia* □ *Pseudomonas cepacia*—edetate disodium-mediated resistance □ Chloramphenicol—edetate disodium-mediated resistance in *Pseudomonas cepacia*

A house isolate (Strain 2487[1]) of *Pseudomonas cepacia* lost its normal susceptibility to chloramphenicol in the presence of edetate disodium. This was considered unusual since edetate disodium has been shown to reverse antibiotic resistance in some species of *Pseudomonas* (1), and chloramphenicol is one of the few antibiotics effective against *P. cepacia*. This report presents the results of an investigation of this phenomenon.

EXPERIMENTAL

Cultures of Strain 2487 and, for comparison, other house isolates or strains[2] were maintained on agar slants[3], incubated at 35°, and subcultured weekly. The desired concentration of sterile-filtered edetate disodium[4] was added to assay plates, either under aseptic conditions or just prior to autoclaving the media. The plates were seeded by swabbing over the agar surface in three planes 10^{-2} dilutions of cultures of the organisms as grown for 24 hr in broth[5] at 35°. Susceptibility determinations were done with disks[6] impregnated, respectively, with chloramphenicol (30 μg), colistin (10 μg), sulfisoxazole (50 μg), gentamicin (10 μg), and polymyxin B (50 μg), and applied to the surfaces of the seeded agar. These plates, in turn, were incubated for 24–48 hr at 35°, the longer period being necessary in some instances because high concentrations (0.1%) of edetate disodium slowed the growth of *P. cepacia*.

RESULTS AND DISCUSSION

The effect of edetate disodium on the activity against Strain 2487 of various antibiotics was mixed (Table I): Susceptibility to gentamicin was increased; susceptibility to chloramphenicol was decreased; and the activity of the other three agents was not altered.

The observed degree of resistance of Strain 2487 to chloramphenicol was related directly to the concentration of the salt. A linear response was obtained over a range of 0.0–0.1% of edetate disodium in the assay medium. This suggested the possibility that edetate disodium triggers the release of a substance from *P. cepacia* cells which destroys chloramphenicol or modifies the antibiotic to render it ineffective against the organism.

Accordingly, an experiment was carried out following the procedure of Miyamura (2) to determine whether edetate disodium promoted the release of a cell wall-bound enzyme such as chloramphenicol acetyltransferase which would inactivate the antibiotic, as is known to occur in other organisms (3).

Results (Table II) indicate there is present in *P. cepacia* no enzymatic inactivating mechanism for chloramphenicol. Apparently, this is not so in the case of *P. aeruginosa*; ~25–50% of the chloramphenicol was lost in the cultures of this species. This suggests, as previously reported (4), some uptake or destruction of the antibiotic.

Another possibility, that edetate disodium chelates chloramphenicol to make it unavailable to act upon *P. cepacia*, does not seem likely. In fact, additional sensitivity tests showed that edetate disodium actually enhanced the action of the antibiotic against *P. aeruginosa* and *Escherichia coli* (Table III). The data in Table III further suggest that this phenomenon may not be a uniform characteristic in *P. cepacia*. Strain 25416[2] failed to grow in the presence of edetate disodium, while another wild strain (Strain C) was essentially resistant to chloramphenicol.

In the apparent absence of enzymatic destruction or chemical complexation of chloramphenicol, the actual mechanism of the edetate disodium effect remains obscure. The possibility exists that edetate disodium chemically alters the cell envelope or cytoplasmic membrane so that transport of chloramphenicol to its point of action within the cell is blocked. More direct evidence might be obtained with the use of labeled chloramphenicol, and this is a subject for further investigation.

Table I—Sensitivity Pattern of *P. cepacia*[a]

Antibiotic	Agar[b]	Agar[b], +0.1% Edetate Disodium
Chloramphenicol	Susceptible	Resistant
Colistin	Resistant	Resistant
Sufisoxazole	Susceptible	Susceptible
Gentamicin	Resistant	Susceptible
Polymyxin B	Resistant	Resistant

[a] Vick Strain 2487. [b] Eugon agar, Becton Dickinson and Co.

Table II—Recovery of Chloramphenicol Following Incubation

Organism	Chloramphenicol, μg/ml	Recovery, %
P. cepacia[a]	25.0	100.0
P. cepacia[a], with medium containing 0.1% edetate disodium	24.5	98.0
P. aeruginosa[b]	18.5	74.0
P. aeruginosa[c]	14.5	58.0
Medium Control	23.0	92.0
Medium plus Edetate Disodium Control	23.5	94.0

[a] Vick Strain 2487. [b] Ps 28. [c] ATCC 15442.

Table III—Effect of Edetate Disodium on Chloramphenicol Susceptibility Pattern of Gram-negative Bacteria

	Chloramphenicol	
Organism	Agar[a], mm	Agar[a] +0.1% Edetate Disodium, mm
P. cepacia[b]	12.0[c]	0.0
P. cepacia[d]	18.0	8.6
P. cepacia[e]	5.4	No growth
P. cepacia[f]	<1.0	0.0
P. aeruginosa[g]	2.0	12.1
E. coli[h]	16.6	31.5

[a] Eugon agar, Becton Dickinson and Co. [b] Vick Strain 2487. [c] Diameter of inhibition zone surrounding disk. [d] American Type Culture Collection (ATCC) 17759. [e] ATCC 25416. [f] Vick Strain C. [g] ATCC 9027. [h] ATCC 8739.

[1] Richardson-Vicks, Inc.
[2] American Type Culture Collection (ATCC).
[3] Eugon Agar slants, Becton Dickinson and Co.
[4] Sequestrene, Ciba-Geigy Corp.
[5] Eugon broth, Becton Dickinson and Co.
[6] Bacto-Sensitivity Discs, Difco Labs.

0022-3549/82/0700-0833$01.00/0

REFERENCES

(1) R. Weiser, A. W. Asscher, and J. Wimpenny, *Nature (London)*, **219**, 1365 (1968).

(2) S. Miyamura, *J. Pharm. Sci.*, **53**, 604 (1964).

(3) W. V. Shaw, *Trans. Assoc. Am. Physicians*, **84**, 190 (1971).

(4) J. M. Ingram and M. Moustafa-Hassan, *Can. J. Microbiol.*, **21**, 1185 (1975).

ACKNOWLEDGMENTS

Mr. B. C. Tillery, Manager of R&D Publications, provided editorial assistance in the preparation of this manuscript.

Detection of Phytonadione in Vegetable Oil

DAVID EMLYN HUGHES

Received March 3, 1981, from the *Analytical Chemistry Division, Norwich-Eaton Pharmaceuticals, Box 191, Norwich, NY 13815.* Accepted for publication October 13, 1981.

Abstract □ A simple detection test for phytonadione (vitamin K_1) in vegetable oil is presented. A saturated sodium ethoxide solution was used to saponify vegetable oil and react with the freed phytonadione to form a blue compound. The specificity and mechanism of the colored compound formation is discussed.

Keyphrases □ Phytonadione—detection in vegetable oil □ Vegetable oil—detection of phytonadione □ Vitamins—detection of phytonadione in vegetable oil

Although many methods are available in the literature for the determination of phytonadione in standard solutions, pharmaceuticals, and infant formulas, no simple detection procedure for phytonadione determination in oil has been reported. Detection of phytonadione in oil is of use since vegetable oil solutions of phytonadione are used in the manufacture of multivitamin preparations and elemental diets (1, 2). The present report discusses the chemical (noninstrumental) detection of phytonadione in vegetable oil and aspects of the specificity and mechanism of the reaction.

Reviews for the determination of phytonadione by gas chromatography (3), fluorometric analysis (4), and thin-layer and paper chromatography (5) are available. Circular TLC (6), thin layer silica gel impregnated with silver nitrate or paraffin (7), and more recently UV derivatization (8) and electrochemical detection (9) have been employed for phytonadione analyses. Any of the described phytonadione determinations can be used if the phytonadione is contained in hexane, petroleum ether, acetone, or ethanol standard or sample solutions. Few determinations of phytonadione in vegetable oil samples have, however, been reported.

Phytonadione in vegetable oil presents complex sample-handling problems. The lipophilic nature of phytonadione prevents easy extraction and its alkaline sensitivity prohibits saponification of the vegetable oil without destroying the vitamin (10, 11). Phytonadione is photosensitive (12). Determination of phytonadione in vegetable oil has only been accomplished after time-consuming and complex sample preparation such as reduction by Raney's nickel catalyst (13) or enzymatic hydrolysis (11), conditions not desirable for a simple detection procedure.

Quality control laboratories, and others with similar time and financial limitations, may not find the time-consuming and complex methods presented thus far satisfactory for the detection (presence or absence) of phytonadione. In nonlipid media, some simple chemical detection tests have been reported. Phytonadione may be detected visually in ethanolic solution by reaction with sodium diethyldithiocarbamate (15), or 2,4-dinitrophenylhydrazine (16). No color tests have been reported for phytonadione in vegetable oil solutions.

A procedure has been developed in which detection of phytonadione in vegetable oil is based on the blue complex formed by sodium ethoxide. The procedure differs from that described previously (14) insofar as a saturated (3.4 *N*) sodium ethoxide solution saponifies the lipid medium. The sensitivity of the test is increased by the white background provided by saponification of the vegetable oil. The saponification results in the extraction of some solvent-dissociated phytonadione, which then reacts with sodium ethoxide.

EXPERIMENTAL

Reagents—All chemicals were analytical reagent grade and were used without further purification.

Procedure—One milliliter of a safflower oil solution of phytonadione was added to 1 ml of a saturated (3.4 *N*) solution of sodium hydroxide in ethanol. After the saponification process, a solid blue mass remained. Standards (in ethanol) and samples ranged in concentration from 50–5000 μg phytonadione/ml. In samples containing ≥500 μg/ml, an intensely blue-colored solution was formed almost immediately. The color then faded to gray or brown over a 10-min period. A blank of safflower oil treated with the alkaline alcoholic solution yielded a white soap. Cotton and peanut oil samples yielded identical results. Ascorbyl palmitate and polysorbate 80 did not interfere. The procedure was then applied to 1,4-naphthoquinone, menadione, and the bromination product of phytonadione.

The standards and samples were then tested with sodium diethyldithiocarbamate and 2,4-dinitrophenylhydrazine reagents using the reported procedures (15, 16).

RESULTS AND DISCUSSION

The standard solutions reacted with sodium ethoxide, sodium diethyldithiocarbamate, and 2,4-dinitrophenylhydrazine to form the colors reported in the literature. The sensitivity was found to be satisfactory to repetitively detect (6 trials) 50-μg/ml phytonadione/ml standard with sodium ethoxide and 10-μg/ml standard with sodium diethyldithiocarbamate. The 2,4-dinitrophenylhydrazine was formed an average of 50% of the trials at the 100-μg/ml level. No further investigation of this procedure was attempted. Neither the sodium ethoxide nor diethyldithiocarbamate procedure detected phytonadione in samples.

Detection of phytonadione in vegetable oil then was attempted by

0022-3549/82/0700-0834$01.00/0

REFERENCES

(1) R. Weiser, A. W. Asscher, and J. Wimpenny, *Nature (London)*, **219**, 1365 (1968).

(2) S. Miyamura, *J. Pharm. Sci.*, **53**, 604 (1964).

(3) W. V. Shaw, *Trans. Assoc. Am. Physicians*, **84**, 190 (1971).

(4) J. M. Ingram and M. Moustafa-Hassan, *Can. J. Microbiol.*, **21**, 1185 (1975).

ACKNOWLEDGMENTS

Mr. B. C. Tillery, Manager of R&D Publications, provided editorial assistance in the preparation of this manuscript.

Detection of Phytonadione in Vegetable Oil

DAVID EMLYN HUGHES

Received March 3, 1981, from the *Analytical Chemistry Division, Norwich-Eaton Pharmaceuticals, Box 191, Norwich, NY 13815.* Accepted for publication October 13, 1981.

Abstract □ A simple detection test for phytonadione (vitamin K_1) in vegetable oil is presented. A saturated sodium ethoxide solution was used to saponify vegetable oil and react with the freed phytonadione to form a blue compound. The specificity and mechanism of the colored compound formation is discussed.

Keyphrases □ Phytonadione—detection in vegetable oil □ Vegetable oil—detection of phytonadione □ Vitamins—detection of phytonadione in vegetable oil

Although many methods are available in the literature for the determination of phytonadione in standard solutions, pharmaceuticals, and infant formulas, no simple detection procedure for phytonadione determination in oil has been reported. Detection of phytonadione in oil is of use since vegetable oil solutions of phytonadione are used in the manufacture of multivitamin preparations and elemental diets (1, 2). The present report discusses the chemical (noninstrumental) detection of phytonadione in vegetable oil and aspects of the specificity and mechanism of the reaction.

Reviews for the determination of phytonadione by gas chromatography (3), fluorometric analysis (4), and thin-layer and paper chromatography (5) are available. Circular TLC (6), thin layer silica gel impregnated with silver nitrate or paraffin (7), and more recently UV derivatization (8) and electrochemical detection (9) have been employed for phytonadione analyses. Any of the described phytonadione determinations can be used if the phytonadione is contained in hexane, petroleum ether, acetone, or ethanol standard or sample solutions. Few determinations of phytonadione in vegetable oil samples have, however, been reported.

Phytonadione in vegetable oil presents complex sample-handling problems. The lipophilic nature of phytonadione prevents easy extraction and its alkaline sensitivity prohibits saponification of the vegetable oil without destroying the vitamin (10, 11). Phytonadione is photosensitive (12). Determination of phytonadione in vegetable oil has only been accomplished after time-consuming and complex sample preparation such as reduction by Raney's nickel catalyst (13) or enzymatic hydrolysis (11), conditions not desirable for a simple detection procedure.

Quality control laboratories, and others with similar time and financial limitations, may not find the time-consuming and complex methods presented thus far satisfactory for the detection (presence or absence) of phytonadione. In nonlipid media, some simple chemical detection tests have been reported. Phytonadione may be detected visually in ethanolic solution by reaction with sodium diethyldithiocarbamate (15), or 2,4-dinitrophenylhydrazine (16). No color tests have been reported for phytonadione in vegetable oil solutions.

A procedure has been developed in which detection of phytonadione in vegetable oil is based on the blue complex formed by sodium ethoxide. The procedure differs from that described previously (14) insofar as a saturated (3.4 *N*) sodium ethoxide solution saponifies the lipid medium. The sensitivity of the test is increased by the white background provided by saponification of the vegetable oil. The saponification results in the extraction of some solvent-dissociated phytonadione, which then reacts with sodium ethoxide.

EXPERIMENTAL

Reagents—All chemicals were analytical reagent grade and were used without further purification.

Procedure—One milliliter of a safflower oil solution of phytonadione was added to 1 ml of a saturated (3.4 *N*) solution of sodium hydroxide in ethanol. After the saponification process, a solid blue mass remained. Standards (in ethanol) and samples ranged in concentration from 50–5000 μg phytonadione/ml. In samples containing ≥500 μg/ml, an intensely blue-colored solution was formed almost immediately. The color then faded to gray or brown over a 10-min period. A blank of safflower oil treated with the alkaline alcoholic solution yielded a white soap. Cotton and peanut oil samples yielded identical results. Ascorbyl palmitate and polysorbate 80 did not interfere. The procedure was then applied to 1,4-naphthoquinone, menadione, and the bromination product of phytonadione.

The standards and samples were then tested with sodium diethyldithiocarbamate and 2,4-dinitrophenylhydrazine reagents using the reported procedures (15, 16).

RESULTS AND DISCUSSION

The standard solutions reacted with sodium ethoxide, sodium diethyldithiocarbamate, and 2,4-dinitrophenylhydrazine to form the colors reported in the literature. The sensitivity was found to be satisfactory to repetitively detect (6 trials) 50-μg/ml phytonadione/ml standard with sodium ethoxide and 10-μg/ml standard with sodium diethyldithiocarbamate. The 2,4-dinitrophenylhydrazine was formed an average of 50% of the trials at the 100-μg/ml level. No further investigation of this procedure was attempted. Neither the sodium ethoxide nor diethyldithiocarbamate procedure detected phytonadione in samples.

Detection of phytonadione in vegetable oil then was attempted by

0022-3549/82/0700-0834$01.00/0

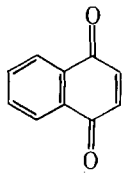

I

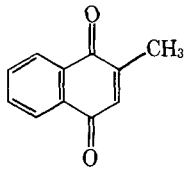

II

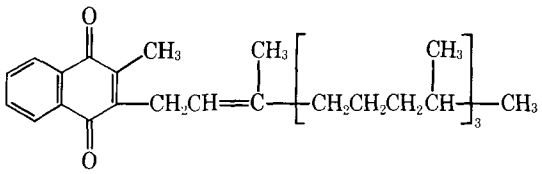

III

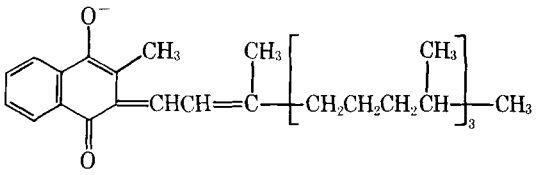

IV

saponification of the oil with sodium hydroxide. Potassium hydroxide did not consistently saponify the vegetable oil at room temperature. In the absence of degradation or dissolution in the saponified matrix or remaining lipid material, reaction with sodium ethoxide or sodium diethyldithiocarbamate should be possible. The sodium diethyldithiocarbamate color test was negative on all sample solutions. The limit of detectability was found to be 50 ppm for the sodium ethoxide color reaction. Of the reactions mentioned, only the sodium ethoxide reaction gave a positive test in vegetable oil, and then, only when the vegetable oil was saponified.

The specificity of the reaction of phytonadione with sodium ethoxide has not been reported. Some confusion concerning even the family of compounds that react to form a blue complex in dilute sodium ethoxide appears in the literature. It was noted (17), in part, that phytonadione dissolved in petroleum ether yielded a positive (blue) test with dilute sodium ethoxide, whereas the vitamin dissolved in oil gave a negative test. It was speculated that phytonadione was less stable in petroleum ether than in oil and that a reaction with an unspecified degradation product of phytonadione was actually responsible for the blue color. The selectivity of the reaction towards phytonadione analogs, therefore, has not been specified. It also is not clear whether the reaction occurs with a parent species or a degraded species.

In an attempt to examine the selectivity of the ethoxide reaction, 1,4-naphthoquinone (I) was subjected to the detection test. The absence of blue color indicated the 1,4-naphthoquinone nucleus was not sufficient for reaction. Menadione (vitamin K_3, II) did not give a positive test. Since phytonadione (III) differs only from menadione by a phytyl group, the phytyl group was found essential for the blue complex formation. Bromination of the double bond originating on the β-carbon of the phytyl group of phytonadione yielded a product that did not form a blue complex. The blue complex formed in the reaction with phytonadione was soluble in water, and it eluted before phytonadione on a reversed-phase LC column. The polar species formed was consistent with the structure of IV. The structure predicts that vitamin K_2 (which contains a polyprenyl group in place of the phytyl group) would form the same extended conjugation system. The vitamin K_2 family of compounds yield blue colors with ethoxide (16, 17). The shift from yellow (in phytonadione) to blue (IV) is consistent with increasing the conjugation of 1,4-naphthoquinone to the phytyl side chain to form an extended π or quasi-π system (18).

A previous report (17) has been cited (15, 16) as evidence that the reaction between phytonadione and ethoxide ion may actually be a reaction with a degradation product of phytonadione. It now appears that the reason ethoxide reacted with petroleum ether samples, but not with vegetable oil samples, may have been due to the lipophilic nature of phytonadione and solution conditions conducive to the formation of IV rather than with the selectivity of the reaction.

A simple detection method for phytonadione in vegetable oil has been developed in which an alkaline ethanolic solution simultaneously transforms the vitamin into a blue compound (consistent with IV) which can be easily visualized on a background of white, saponified vegetable oil. The reaction in standard ethanol solutions and vegetable oil samples is sensitive to phytonadione and vitamin K_2. The test is postulated to be specific to 1,4-naphthoquinones containing alkyl side chains with β-carbon double bonds which may form extended conjugation systems. The selectivity was found to be identical in ethanol standards and vegetable oil samples.

REFERENCES

(1) T. Takebe, K. Nakano, and R. Machida, *Japan* 77 50,251 (Cl. A61 K9/08), 23 Dec. 1977. Appl. 68.92,009, 17 Dec. 1968; through *Chem. Abst. Jpn.*, **88**, 177222s (1978).

(2) A. Osol, "Remington's Pharmaceutical Sciences," Mack Publishing, Easton, Pa., 1975, p. 951.

(3) A. J. Sheppard, A. R. Prosser, and W. D. Hubbard, *J. Am. Oil Chem. Soc.*, **49**, 619 (1972).

(4) A. T. R. Williams, *Lab. Equip. Dig.*, **14**(3), 67 (1976).

(5) H. Mayer and O. Isler, "The Vitamins," Vol. III, Academic, New York, N.Y., 1971, p. 418.

(6) M. H. Hashmi, F. Rafique Chughtai, and M. I. D. Chughtai, *Mikrochim. Acta*, **1**, 53 (1969).

(7) J. T. Matsehiner and J. M. Amelotti, *J. Lipid Res.*, **9**, 176 (1968).

(8) J. C. Vire and G. J. Patriarcho, *J. Pharm. Belg.*, **31**(2), 139 (1976).

(9) J. C. Vire and G. J. Patriarcho, *Analusis*, **6**(4), 155 (1978).

(10) O. Isler, *Angew. Chem.*, **71**, 7 (1959).

(11) S. A. Barnett, L. W. Frick, and H. M. Baine, *Anal. Chem.*, **52**, 610 (1980).

(12) J. P. Green and H. Dam, *Acta Chem. Scand.*, **8**, 1341 (1954).

(13) N. R. Trenner and F. A. Bacher, *J. Biol. Chem.*, **137**, 745 (1941).

(14) H. Dam, A. Geiger, J. Glavind, P. Karrer, W. Karrer, E. Rothschild, and H. Salomon, *Helv. Chim. Acta*, **22**, 310 (1939).

(15) F. Irreverre and M. X. Sullivan, *Science*, **94**, 497 (1941).

(16) A. Novelli, *ibid.*, **93**, 358 (1941).

(17) E. Fernholz and S. Ansbacher, *J. Am. Chem. Soc.*, **61**, 1613 (1939).

(18) C. N. R. Rao, "Ultraviolet and Visible Spectroscopy," Plenum, New York, N.Y. 1967, p. 174.

ACKNOWLEDGMENTS

The author thanks Robert J. Alaimo for valuable technical assistance.

The Direct Analysis of Tetracycline in Urine by Circular Dichroism Spectropolarimetry

JOHN M. BOWEN and NEIL PURDIE ˣ

Received August 4, 1981, from the *Chemistry Department, Oklahoma State University, Stillwater, OK 74078.* Accepted for publication October 23, 1981.

Abstract □ A method is described for the direct analysis of tetracycline in human urine using circular dichroism spectropolarimetry. The general applicability of the method to other drugs is discussed.

Keyphrases □ Circular dichroism—spectropolarimetry, tetracycline analysis in urine □ Tetracycline—analysis in urine, circular dichroism spectropolarimetry □ Spectropolarimetry—tetracycline analysis in urine, circular dichroism

Circular dichroism is the effect caused by the simultaneous absorption and rotation of an incident beam of plane polarized light measured as a function of wavelength (1). Ordinarily the technique is used in the study of electronic transition polarizations and in the investigation of molecular conformations or configurations (2).

In previous work its analytical potential was demonstrated in the qualitative analysis (3, 4) and quantitative determination of drugs of abuse, such as opiates (5), L-cocaine (6), and lysergide (7). The analyses were made directly on confiscated solid samples of forensic interest, meaning no prior sample preparation or separation was performed, nor was it necessary.

This report describes the preliminary results from the first application of circular dichroic spectropolarimetry to the direct analysis of drugs in biological fluids, namely tetracycline in human urine.

EXPERIMENTAL

An analytical standard sample of tetracycline hydrochloride was obtained[1]. Urine samples were taken from 10 volunteers who were known not to be on a program of administering drugs, legal or illegal. One volunteer was maintaining an established program of a 1.0-g daily dosage of tetracycline[2] using 500-mg capsules.

Circular dichroic spectra were taken on a spectropolarimeter[3] over the 240–360-nm wavelength range. Measurements were made on freshly collected specimens which had been diluted 50 times with distilled water. The pH of the solution was not controlled. Samples were placed in a 1-cm cell and measurements were made against a distilled water blank.

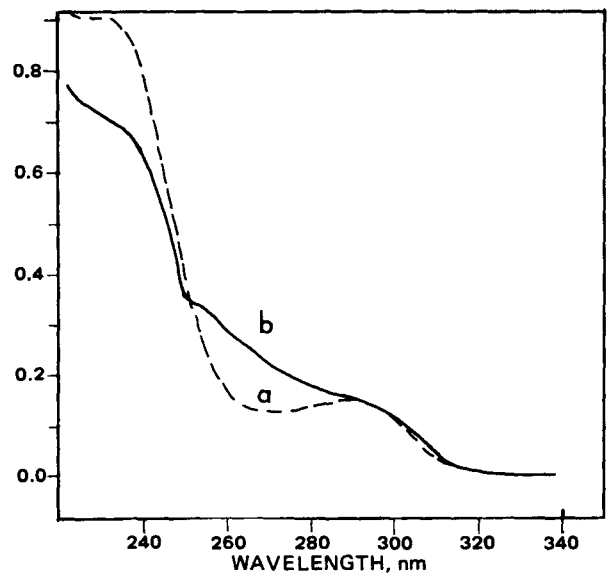

Figure 1—*UV absorption spectra of (a) urine (50 times dilution) and (b) urine with tetracycline (50 times dilution).*

RESULTS

The UV absorption spectra of urine with and without tetracycline from the prescribed volunteers are shown in Fig. 1. The principal difference in absorption, ~270 nm, is insufficient to quantitate with any degree of certainty. Even qualitative identification is speculative. Circular dichroic spectra of the same specimens are shown in Fig. 2. Samples had been diluted 50 times to prepare these solutions. The observed circular dichroic spectrum for urine shows small deviations from the baseline: negative at ~310 nm and positive at ~280 nm. Tetracycline in urine shows a large positive Cotton band at 295 nm and two smaller negative bands at 323 and 270 nm, respectively. Superimposed on the urine spectra of Fig. 2 is the spectrum for a 2.0×10^{-5} *M* or 8.9 μg/ml aqueous tetracycline solution. Positive qualitative identification is elementary.

The quantitativeness of circular dichroic spectropolarimetry in analysis can be demonstrated from a linear plot of experimental ellipticity, Ψ, at 295 nm *versus* molar concentration of standard tetracycline[1] in water. The slope of the calibration curve is the molar ellipticity coefficient $[\theta]_{295}$ and is calculated to be equal to +540. Using this value in the analysis of the urine samples, the concentration of dissolved tetracycline was calculated to be 2.4×10^{-5} *M* after dilution by 50 times, or 11 μg/ml in the excreted specimen.

With the present instrument, the limit of detection was found to be ~1.8 μg/ml for tetracycline.

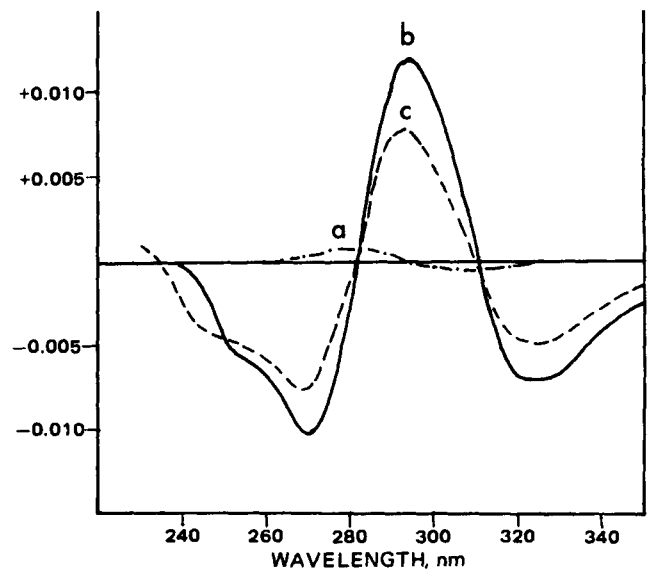

Figure 2—*Circular dichroic spectra of (a) urine (50 times dilution), (b) urine with tetracycline (50 times dilution), and (c) 2×10^{-5} M aqueous solution of tetracycline.*

[1] From the Drug Enforcement Administration *via* the Oklahoma State Bureau of Investigation.

[2] Panmycin, Upjohn Chemical Co.

[3] Cary 61, Varian Instruments, Inc.

0022-3549/82/0700-0836$01.00/0

DISCUSSION

Circular dichroic spectropolarimetry is a modified form of UV absorption spectrophotometry applicable to compounds which are both optically active and absorb light (2). All of the accepted procedures for UV absorption apply equally well to circular dichroism, and the data obey the simple Beer's Law dependence. Adjusting instrument parameters is not a problem as it is with GC, high-pressure liquid chromatography, or mass spectrometry (8) which reduces the routine analysis time. The time is reduced even further where separation is not a prerequisite to identification.

The detection limit for tetracycline in urine is 1.8 μg/ml. This value easily could be improved with a more modern instrument equipped with computer data handling accessories. A lower limit of detection is also possible if tetracycline is first separated from other species which absorb in the UV because of an improved signal–noise ratio. Based upon known $[\theta]$ values for other drugs such as morphine (5), codeine (5), cocaine (6), and lysergide (7), and comparing these to the value for tetracycline, calculations show that these drugs also can be quantitated, but only at overdose levels with the spectropolarimeter[3].

In general terms the most difficult analytical problem will arise when a mixture of optically active drugs are present (7); then separation will again be necessary. Dissolved sugars or proteins and glucuronide derivatives of extracted metabolites do not absorb for the most part, and they are not interfering.

REFERENCES

(1) J. B. Lambert, H. F. Shurvell, L. Verbit, R. G. Cooks, and G. H. Stout, "Organic Structural Analysis," Macmillan, New York, N.Y., 1976.

(2) S. F. Mason, *Q. Rev. Chem. Soc.*, **51**, 287 (1961).

(3) J. M. Bowen and N. Purdie, *Anal. Chem.*, **52**, 573 (1980).

(4) J. M. Bowen, T. A. Crone, A. O. Hermann, and N. Purdie, *ibid.*, **52**, 2436 (1980).

(5) T. A. Crone and N. Purdie, *ibid.*, **53**, 17 (1981).

(6) J. M. Bowen and N. Purdie, *ibid.*, **53**, 2237 (1981).

(7) J. M. Bowen, T. A. Crone, V. L. Head, H. A. McMorrow, R. K. Kennedy, and N. Purdie, *J. Forensic Sci.*, **26**, 664 (1981).

(8) A. B. Clark and M. D. Miller, *ibid.*, **23**, 21 (1978).

ACKNOWLEDGMENTS

This work was supported by NSF-CHE-7909388.

The authors thank Mr. Don Flynt of The Oklahoma State Bureau of Investigation for supplying the standard sample of tetracycline hydrochloride.

Tick Repellents I: Ethylene Glycol Acetamides

W. A. SKINNER ˣ, U. ROSENTRETER *, and T. ELWARD

Received July 7, 1981, from the *Life Sciences Division, SRI International, Menlo Park, California 94025.* Accepted for publication September 25, 1981. * Present address: Bayer AG, Postfach 101709, 5600 Wuppteral, West Germany.

Abstract □ Acetamides derived from ethylene glycol were synthesized and evaluated as repellents for the brown dog tick *Rhipicephalus sanguineus*. Several of these compounds showed repellency equal to the standard repellents, *N,N*-diethyl-*m*-toluamide and butopyranoxyl.

Keyphrases □ Tick repellents—ethylene glycol acetamides, synthesized □ Acetamides—ethylene glycol, synthesized, tick repellents □ Ethylene glycol—synthesized acetamides, tick repellents

A previous study of insect repellents showed that alkyl triethylene glycol monoethers had good mosquito repellency, being superior to *N,N*-diethyl-*m*-toluamide in certain tests against *Aedes aegypti* mosquitoes (1). Amides in general are known to be repellent to mosquitoes and other insects, the most widely used amide repellent being *N,N*-diethyl-*m*-toluamide.

During World War II, an extensive repellent screening program took place at the USDA Laboratories in Orlando, Florida. Compounds were screened for repellency both to yellow fever and malaria mosquitoes, and against fleas and ticks (2, 3). The ticks used for that program were the lone star tick, and about one thousand compounds were evaluated as tick repellents.

Since that time, major emphasis has been on mosquito repellents, largely supported by the U.S. Army Medical Research and Development Command. However, recently more emphasis has developed with regard to other militarily important insects: sand flies and ticks.

A previous study (3) evaluated a series of amides against ticks (*Amblyomma americanum*) and found that the di-*n*-butyl toluamides were best. Another study (4) found that certain amides and esters were effective against hard and soft ticks (*Ixodes persulcatus* P. Sch., *Dermacentor pecitus* Herm., *D. marginatus* Salz., *Hyalomma asiaticum* P. Sch., and *Alectorobius tholozan papillipas* Birula). Evaluated were butylacetanilide, tetrahydroquinoline, a mixture of ethyleneoxide–carbon dioxide (1:9)[1], dibutyl adipate, dimethyl phthalate, *N,N*-diethyl-*m*-toluamide benzimide, isoamyl acetamide, and benzoyl piperidine.

In the present study, a combination of the amide function with the ethylene glycol moiety were examined for repellent activity against ticks.

EXPERIMENTAL[2]

2-(Hydroxyethyoxy)acetamides—2-(2-Hydroxyethoxy) - *N*, *N* - diisopropylacetamide was prepared as follows: Sodium (1.4 g, 0.006 mole) was dissolved in 13 ml (0.24 mole) of ethylene glycol. After cooling to room temperature, 12 g (0.0676 mole) of *N,N*-diisopropyl-chloroacetamide (prepared from chloroacetylchloride and diisopropylamine) was added. The mixture was stirred at 90° for 1 hr. The ethylene glycol was distilled under reduced pressure and the residue taken up in ether, filtered to remove the sodium chloride, evaporated *in vacuo*, and distilled[3] to give 10.6 g of product, 125° air bath temperature/0.8 mm Hg.

2,2′-Ethylenedioxy-bis(*N,N* - dialkylacetamides)—2,2′- Ethylenedioxy-bis(*N,N*-diisopropylacetamide) was prepared as follows: A 150-ml three-necked flask was fitted with a stirrer, a reflux condenser, and a dropping funnel. Sodium (0.78 g, 0.034 mole) was suspended by vigorous stirring in 20 ml of boiling xylene. Ethylene glycol (1.05 g, 0.017 mole) was dropped slowly into the sodium suspension at reflux temperature, the suspension stirred and refluxed for an additional 7 hr, and then 6 g (0.034 mole) of *N,N*-diisopropyl-chloroacetamide in 15 ml of xylene was dropped into the stirred suspension at reflux temperature during 1 hr. The reaction mixture was refluxed and stirred for an additional hour.

[1] Carboxide.

[2] Elemental analyses were performed by the Microanalytical Laboratory, Department of Chemistry, Stanford University, Stanford, Calif.

[3] Distilled with a Kugelrohr.

0022-3549/82/0700-0837$01.00/0

DISCUSSION

Circular dichroic spectropolarimetry is a modified form of UV absorption spectrophotometry applicable to compounds which are both optically active and absorb light (2). All of the accepted procedures for UV absorption apply equally well to circular dichroism, and the data obey the simple Beer's Law dependence. Adjusting instrument parameters is not a problem as it is with GC, high-pressure liquid chromatography, or mass spectrometry (8) which reduces the routine analysis time. The time is reduced even further where separation is not a prerequisite to identification.

The detection limit for tetracycline in urine is 1.8 μg/ml. This value easily could be improved with a more modern instrument equipped with computer data handling accessories. A lower limit of detection is also possible if tetracycline is first separated from other species which absorb in the UV because of an improved signal–noise ratio. Based upon known $[\theta]$ values for other drugs such as morphine (5), codeine (5), cocaine (6), and lysergide (7), and comparing these to the value for tetracycline, calculations show that these drugs also can be quantitated, but only at overdose levels with the spectropolarimeter[3].

In general terms the most difficult analytical problem will arise when a mixture of optically active drugs are present (7); then separation will again be necessary. Dissolved sugars or proteins and glucuronide derivatives of extracted metabolites do not absorb for the most part, and they are not interfering.

REFERENCES

(1) J. B. Lambert, H. F. Shurvell, L. Verbit, R. G. Cooks, and G. H. Stout, "Organic Structural Analysis," Macmillan, New York, N.Y., 1976.

(2) S. F. Mason, *Q. Rev. Chem. Soc.*, **51**, 287 (1961).

(3) J. M. Bowen and N. Purdie, *Anal. Chem.*, **52**, 573 (1980).

(4) J. M. Bowen, T. A. Crone, A. O. Hermann, and N. Purdie, *ibid.*, **52**, 2436 (1980).

(5) T. A. Crone and N. Purdie, *ibid.*, **53**, 17 (1981).

(6) J. M. Bowen and N. Purdie, *ibid.*, **53**, 2237 (1981).

(7) J. M. Bowen, T. A. Crone, V. L. Head, H. A. McMorrow, R. K. Kennedy, and N. Purdie, *J. Forensic Sci.*, **26**, 664 (1981).

(8) A. B. Clark and M. D. Miller, *ibid.*, **23**, 21 (1978).

ACKNOWLEDGMENTS

This work was supported by NSF-CHE-7909388.

The authors thank Mr. Don Flynt of The Oklahoma State Bureau of Investigation for supplying the standard sample of tetracycline hydrochloride.

Tick Repellents I: Ethylene Glycol Acetamides

W. A. SKINNER ˣ, U. ROSENTRETER *, and T. ELWARD

Received July 7, 1981, from the *Life Sciences Division, SRI International, Menlo Park, California 94025.* Accepted for publication September 25, 1981. * Present address: Bayer AG, Postfach 101709, 5600 Wuppteral, West Germany.

Abstract □ Acetamides derived from ethylene glycol were synthesized and evaluated as repellents for the brown dog tick *Rhipicephalus sanguineus*. Several of these compounds showed repellency equal to the standard repellents, *N,N*-diethyl-*m*-toluamide and butopyranoxyl.

Keyphrases □ Tick repellents—ethylene glycol acetamides, synthesized □ Acetamides—ethylene glycol, synthesized, tick repellents □ Ethylene glycol—synthesized acetamides, tick repellents

A previous study of insect repellents showed that alkyl triethylene glycol monoethers had good mosquito repellency, being superior to *N,N*-diethyl-*m*-toluamide in certain tests against *Aedes aegypti* mosquitoes (1). Amides in general are known to be repellent to mosquitoes and other insects, the most widely used amide repellent being *N,N*-diethyl-*m*-toluamide.

During World War II, an extensive repellent screening program took place at the USDA Laboratories in Orlando, Florida. Compounds were screened for repellency both to yellow fever and malaria mosquitoes, and against fleas and ticks (2, 3). The ticks used for that program were the lone star tick, and about one thousand compounds were evaluated as tick repellents.

Since that time, major emphasis has been on mosquito repellents, largely supported by the U.S. Army Medical Research and Development Command. However, recently more emphasis has developed with regard to other militarily important insects: sand flies and ticks.

A previous study (3) evaluated a series of amides against ticks (*Amblyomma americanum*) and found that the di-*n*-butyl toluamides were best. Another study (4) found that certain amides and esters were effective against hard and soft ticks (*Ixodes persulcatus* P. Sch., *Dermacentor pecitus* Herm., *D. marginatus* Salz., *Hyalomma asiaticum* P. Sch., and *Alectorobius tholozan papillipas* Birula). Evaluated were butylacetanilide, tetrahydroquinoline, a mixture of ethyleneoxide–carbon dioxide (1:9)[1], dibutyl adipate, dimethyl phthalate, *N,N*-diethyl-*m*-toluamide benzimide, isoamyl acetamide, and benzoyl piperidine.

In the present study, a combination of the amide function with the ethylene glycol moiety were examined for repellent activity against ticks.

EXPERIMENTAL[2]

2-(Hydroxyethyoxy)acetamides—2-(2-Hydroxyethoxy) - *N*, *N* - diisopropylacetamide was prepared as follows: Sodium (1.4 g, 0.006 mole) was dissolved in 13 ml (0.24 mole) of ethylene glycol. After cooling to room temperature, 12 g (0.0676 mole) of *N,N*-diisopropyl-chloroacetamide (prepared from chloroacetylchloride and diisopropylamine) was added. The mixture was stirred at 90° for 1 hr. The ethylene glycol was distilled under reduced pressure and the residue taken up in ether, filtered to remove the sodium chloride, evaporated *in vacuo*, and distilled[3] to give 10.6 g of product, 125° air bath temperature/0.8 mm Hg.

2,2′-Ethylenedioxy-bis(*N,N* - dialkylacetamides)—2,2′- Ethylenedioxy-bis(*N,N*-diisopropylacetamide) was prepared as follows: A 150-ml three-necked flask was fitted with a stirrer, a reflux condenser, and a dropping funnel. Sodium (0.78 g, 0.034 mole) was suspended by vigorous stirring in 20 ml of boiling xylene. Ethylene glycol (1.05 g, 0.017 mole) was dropped slowly into the sodium suspension at reflux temperature, the suspension stirred and refluxed for an additional 7 hr, and then 6 g (0.034 mole) of *N,N*-diisopropyl-chloroacetamide in 15 ml of xylene was dropped into the stirred suspension at reflux temperature during 1 hr. The reaction mixture was refluxed and stirred for an additional hour.

[1] Carboxide.

[2] Elemental analyses were performed by the Microanalytical Laboratory, Department of Chemistry, Stanford University, Stanford, Calif.

[3] Distilled with a Kugelrohr.

0022-3549/82/0700-0837$01.00/0

Table I—2-(2-Hydroxyethoxy)acetamides [a]

Compound	R	Boiling point, 0.5 mm Hg	Yield, %	IR, cm^{-1}	Formula	Calc.	Found
I-1	C_2H_5, C_2H_5	135°	46	OH, 3400 Amide, 1650	$C_8H_{17}NO_3$	C 54.84 H 9.78 N 7.99	54.80 9.99 7.80
I-2	CH_3, H	136° mp 47	47	OH, 3300 Amide I, 1650 Amide II, 1550	$C_5H_{11}NO_3$	C 45.10 H 8.33 N 10.52	44.95 8.08 10.27
I-3	$CH(CH_3)_2$, $CH(CH_3)_2$	130°	86	OH, 3300 Amide, 1650	$C_{10}H_{21}NO_3$	C 59.09 H 10.41 N 6.89	58.97 10.55 6.70
I-4	Cyclohexyl, Cyclohexyl	170° mp 65	77	OH, 3300 Amide, 1650	$C_{16}H_{29}NO_3$	C 67.81 H 10.31 N 4.94	67.87 10.67 4.76

[a] $HO—CH_2CH_2OCH_2CONR_2$.

Table II—2,2′-Ethylenedioxy-bis-(*N,N*-dialkylacetamides) [a]

Compound	R	Boiling point, 0.5 mm Hg	Yield, %	IR, cm^{-1}	Formula	Calc.	Found
II-1	C_2H_5	160°	42	Amide, 1650	$C_{14}H_{28}N_2O_4$	C 58.31 H 9.79 N 9.71	58.44 9.91 9.79
II-2	$CH(CH_3)_2$	160°	56	Amide, 1650	$C_{18}H_{36}N_2O_4$	C 62.76 H 10.53 N 8.13	62.81 10.61 7.81

[a] $R_2N—COCH_2OCH_2CH_2OCH_2CONR_2$.

Table III—*N,N*-Dialkyl-2(2-alkyloxyethoxy)acetamides [a]

Compound	R	R′	Boiling Point, 0.5 mm Hg	Yield, %	IR, cm^{-1}	Formula	Calc.	Found
III-1	C_2H_5	C_8H_{17}	135°	55	Amide, 1650	$C_{16}H_{35}NO_3$	C 66.86 H 11.57 N 4.87	67.04 11.72 4.87
III-2	C_2H_5	C_6H_{13}	118°	59	Amide, 1650	$C_{14}H_{31}NO_3$	C 64.83 H 11.72 N 5.40	64.84 10.98 5.38
III-3	Cyclo- hexyl	CH_3	142°	95	Amide, 1650	$C_{17}H_{33}NO_3$	C 68.65 H 10.51 N 4.71	68.68 10.49 4.84
III-4	C_2H_5	$C_2H_5OCH_2CH_2$	120°	45	Amide, 1650	$C_{12}H_{27}NO_4$	C 58.27 H 10.19 N 5.66	58.34 9.99 5.61
III-5	C_2H_5	C_4H_9	104°	50	Amide, 1650	$C_{12}H_{27}NO_3$	C 62.30 H 10.89 N 6.05	62.35 10.93 5.96
III-6	$CH(CH_3)_2$	C_4H_9	112°	62	Amide, 1650	$C_{14}H_{31}NO_3$	C 64.83 H 11.27 N 5.40	64.77 11.26 5.32

[a] R′—O—$CH_2CH_2OCH_2CONR_2$.

Table IV—*N,N,N′,N′*-Tetraalkyl-2,2′-oxydiacetamides [a]

Compound	R	Boiling point, 0.5 mm Hg	Yield, %	IR, cm^{-1}	Formula	Calc.	Found
IV-1	C_2H_5	145°	91	Amide, 1650	$C_{12}H_{24}N_2O_3$	C 58.99 H 9.90 N 11.47	59.00 10.04 11.29
IV-2	C_3H_7	155°	91	Amide, 1650	$C_{16}H_{32}N_2O_3$	C 63.96 H 10.74 N 9.32	64.17 10.90 9.40
IV-3	C_4H_9	175°	96	Amide, 1650	$C_{20}H_{40}N_2O_3$	C 67.37 H 11.31 N 7.86	67.61 11.48 7.80

[a] $R_2NCOCH_2OCH_2CONR_2$.

After cooling to room temperature and filtering off the sodium chloride, the xylene was removed under reduced pressure. The residue was distilled with a spin evaporator to give 3.3 g of product, 160° air bath temperature/0.8 mm Hg.

***N,N*-Dialkyl-2(2-alkyloxyethoxy)acetamides**—*N,N*-Diethyl-2-(2-hexyloxyethoxy)acetamide was prepared by dropping 2-hexyloxyethanol (6 g, 0.041 mole) into a stirred suspension of 0.945 g (0.041 mole) of sodium in 20 ml of xylene. After refluxing for 1 hr, 6.14 g (0.041 mole) of *N,N*-diethylchloroacetamide was dropped into the alcoholate suspension. After refluxing for an additional 3 hr, the xylene was removed under reduced pressure. The residue was distilled with a spin evaporator to give 7.4 g of liquid, 125° air bath temperature/0.8 mm Hg. A second distillation gave 6.3 g of pure product, bp 134°/1.1 mm Hg.

***N,N,N′,N′*-Tetraalkyl-2,2′-oxydiacetamides**—*N,N,N′,N′*-Tetrapropyl-2,2′-oxydiacetamide was prepared by dropping diglycoloyl chloride (15 g, 0.0877 mole) in 10 ml of methylene chloride into a stirred

Table V—Tick Repellency Mean Percent Repellency at Test Level, mg/cm² [a]

Compound	1.0	0.66	0.44	0.29
I-1	15	—	—	—
I-2	17	—	—	—
I-3	40	—	—	—
I-4	30	—	—	—
II-1	—	—	5	—
II-2	45	—	15	—
III-1	85	40	10	—
III-2	90	30	—	—
III-3	100	75	45	5
III-4	13	—	—	—
III-5	50	20	—	—
III-6	100	45	15	—
IV-1	15	—	—	—
IV-2	40	—	—	—
IV-3	45	—	—	—
N,*N*-Diethyl-*m*-toluamide	80	58	30	17
Butopyranoxyl	95	—	30	—
Solvent Control	15	—	—	—
Nontreated Control	12	—	—	—

[a] Average of three separate tests.

solution of 48 ml (0.35 mole) of dipropylamine in 100 ml of methylene chloride at −40° during 30 min. The mixture was stirred at room temperature for an additional 10 hr. The methylene chloride was evaporated and the residue taken up in 300 ml of ether and filtered to remove the hydrochloride salt of the dipropylamine. The filtrate was extracted with concentrated potassium hydroxide solution. After drying with anhydrous magnesium sulfate and removal of ether *in vacuo*, the residue was distilled with a spin evaporator to yield 24 g of product, 165° air bath temperature/1.0 mm Hg.

Biological Testing—*Rhipicephalus sanguineus*, the brown dog tick, was the test arthropod. The assay was designed to take advantage of the natural inclination of unfed ticks to climb upward.

Test materials were weighed, dissolved in 95% ethanol, and 0.15 ml of the solution was applied to a disk. The disks were cut from filter paper[4] and were 2.9 cm in diameter. One disk was used per compound per treatment level. Treated disks were kept under a hood and allowed to dry for 24 hr before use.

Disks were then inserted in drilled-out vial caps so that the treated sides faced down when the caps were placed on the test chamber. The test chamber was a polystyrene vial (25 × 52 mm) with an untreated disk glued on the drilled out bottom. Fifteen holes were punched in both disks on the chamber with a 23-gauge needle.

Twenty unfed adult brown dog ticks (10 male and 10 female) sorted 24 hr before use, were placed in each test chamber. The chambers were held with the treated end upright under a hood and were slightly elevated on tongue depressors. After four hours, when the ticks had ceased wandering, the chamber was observed and the number of ticks that settled on the treated surface were counted. The results were expressed in the percentage of ticks repelled from the treated surface. The maximum test level was 1.0 mg/cm² and the dose increments were 0.18 log intervals. Nontreated, standard-treated, and solvent-treated disks were included in each test.

The minimum concentration for the standard *N*,*N*-diethyl-*m*-toluamide that gave consistent significant (>80%) repellency was found to be 1.0 mg/cm². Test materials active at levels lower than 1.0 mg/cm² were considered to be more repellent than *N*,*N*-diethyl-*m*-toluamide.

[4] Number 3 Whatman.

RESULTS AND DISCUSSION

For this study, it was necessary to develop a suitable tick repellency assay, and the brown dog tick, *R. sanguineus*, was chosen as the test species. A common behavior of ticks is to crawl upward and this was taken advantage of in the assay used. The apparatus used consisted of a plastic vial with a filter paper impregnated with the test substance in the top. A measurement was made of the number of ticks climbing upward after a set period of time, with varying concentrations of the test chemical on the filter paper.

Chemical data on the compounds synthesized are presented in Tables I–IV.

Repellency data are presented in Table V. With the tick assay used here, *N*,*N*-diethyl-*m*-toluamide and butopyranoxyl both exhibited good repellency at 1 mg/cm² concentration. Since it was the purpose of this study to determine whether these new compounds were better repellents than these standards, they were tested initially at 1-mg/cm² concentration except for Compound II-1.

Compounds described in Table I having a free hydroxy group were poor repellents, as were the compounds from Table II. The volatility of the bis-compounds in Table II probably was too low (bp = 160°/0.5 mm Hg). Also, two of the compounds in Table I were solids.

Compounds from Table III were more repellent, some of them being equivalent to *N*,*N*-diethyl-*m*-toluamide and butopyranoxyl at 1 mg/cm² concentrations. Compound III-3 seems the best of all, with a repellency of 45% at 0.44-mg/cm² concentration, compared to 30% for *N*,*N*-diethyl-*m*-toluamide and butopyranoxyl at that concentration.

Compounds described in Table IV were not very repellent, probably due to their higher boiling points and reduced volatility.

REFERENCES

(1) H. Johnson, J. DeGraw, J. Engstrom, W. A. Skinner, V. H. Brown, D. Skidmore, and H. I. Maibach, *J. Pharm. Sci.*, **64**, 693 (1975).

(2) USDA Agricultural Handbook No. 69, May 1954, compiled by W. V. King.

(3) S. I. Gertler, H. K. Gouck, and I. H. Gilbert, *J. Econ. Entomol.*, **55**, 451 (1962).

(4) V. P. Dremova and S. N. Smirnova, *Int. Pest Control*, **3**, 10 (1970).

ACKNOWLEDGMENTS

Supported in part by the U.S. Army Medical Research and Development Command Contract DADA 17-70-C-D112 and by SRI International's Institute Research and Development Program.

Surgical Catheterization of Hepatic-Portal and Peripheral Circulations and Maintenance in Pharmacokinetic Studies

JAY L. RHEINGOLD [§*], **PAUL PREISSLER** [‡], **PAUL SMITH** [‡], **and PAUL K. WILKINSON** [*¶x]

Received March 30, 1981, from the *School of Pharmacy, University of Connecticut, Storrs, CT 06268 and the ‡Center for Laboratory Animal Care, University of Connecticut Health Center, Farmington, CT 06032. Accepted for publication October 7, 1981. §Present address: American Cyanamid Co., Lederle Laboratories, Pearl River, NY 10965; ¶E. Merck & Co., Rahway, NJ 07065.

Abstract □ A surgical procedure for the chronic catheterization of mongrel dogs was presented with a detailed account of the use and maintenance of these catheters. The methodology allowed for a direct determination of the capacity of the liver to the intact animal to metabolize drugs. The technique permitted the investigator to study the oxidation of drugs by the liver in a specific concentration range and assessment of the first-pass effect of the liver when many drugs are administered *via* the oral route. The dogs were prepared and used in the drug pharmacokinetic studies for periods up to 24 days.

Keyphrases □ Catheterization—hepatic-portal, peripheral circulations, maintenance, pharmacokinetics □ Pharmacokinetics—maintenance of surgical catheterization, hepatic-portal peripheral circulations □ Metabolism—determination of liver capacity in intact dogs, pharmacokinetics, surgical catheterization of hepatic-portal and peripheral circulations and maintenance

Previous investigators (1–17) have reported that following either oral or intravenous administration of ethyl alcohol to humans or animals, there were differences in alcohol distribution in the vascular system. Most authors (1–13) concluded that arterio–venous equilibrium, as defined by zero arterial–venous concentration differences, was attained rapidly in humans. However, previous (14) and more recent studies (15–17) reported distributional trends not seen in the previous work. These results showed, by interpolation, that at only one point in time were equal arterial and venous concentrations attained, and that this time varied with each subject. Increased assay sensitivity and/or longer sampling time perhaps holds the key to the variance in observations.

This methodology permits the direct determination of the capacity of the liver in the intact animal to metabolize drugs. By infusing the liver directly, the blood alcohol concentration entering the liver can be controlled and the oxidation of ethanol in the liver of an intact animal in a specific concentration range under *in vivo* testing conditions can be studied. This technique is useful in assessing the first-pass effect on the liver, observed when many drugs are administered *via* the oral route.

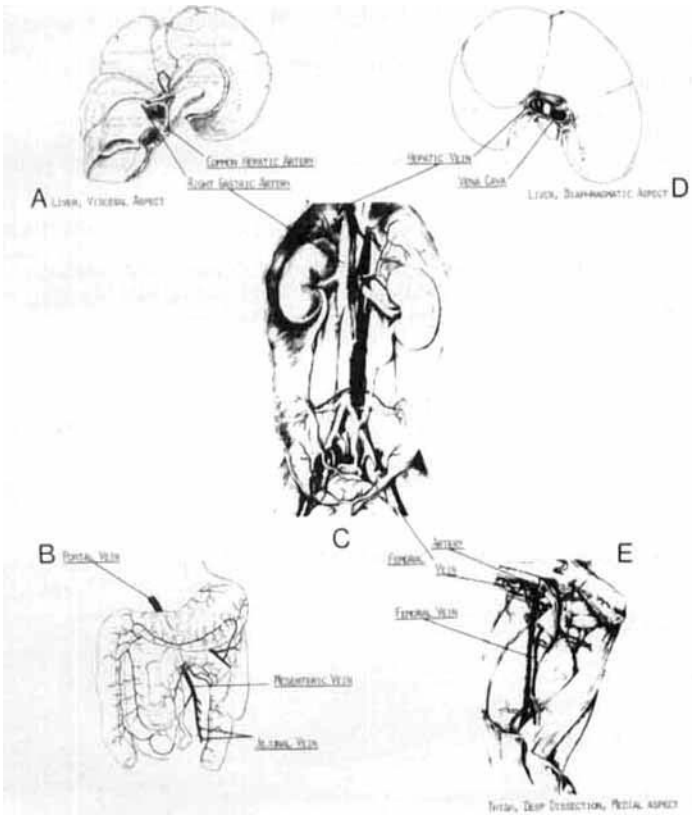

Figure 1—*Diagramatic representation of catheter placements. (Figures from Ref. 18.)*

EXPERIMENTAL

Criteria for Dog Selection—Healthy, full-grown male mongrel dogs (15–31 kg) were selected. The following initial laboratory check-up was performed on each of the dogs: complete blood count (red blood cell count), white blood cell count, differential, hemoglobin, hematocrit, mean corpuscular volume, mean corpuscular hemoglobin, mean corpuscular hemoglobin concentration, red blood cell morphology, sedimentation rate, fecal flotation rate (coccidiosis), creatinine clearance, SGOT, Knott's Test (heartworm), and Brucellosis Screen[1]. Dogs were wormed and vaccinated against rabies[2] and distemper[3].

Dogs selected for the study were quarantined for 1 month and maintained on an adequate diet of regular canine laboratory chow[4]. Prior to their release from quarantine, a similar laboratory check-up, as just described, was performed on each dog to detect any clinical changes and to determine the fitness of each dog for surgery.

Surgical Procedure—Indwelling venous catheters were secured surgically in the hepatic artery, portal vein, hepatic vein, and the femoral artery. An additional catheter was implanted within the saphenous vein.

Prior to surgery, the dogs were fasted (including water) for 6 hr. An enema[5] was administered to each dog 60 min prior to surgery. Acepromazine maleate[6] (0.55–1.10 mg/kg of body weight) was administered intramuscularly as a preanesthetic and/or tranquilizer, and an intravenous injection of sodium pentothal[7] was administered (22 mg/kg of body weight) for induction of anesthesia prior to intubation. With sedation, a 10-mm endotracheal tube[8] was fitted in the dog's throat to facilitate the administration of the anesthetic, methoxyflurane (2,2-dichloro-1,1-difluoroethyl methyl ether[9]) during surgery. A catheter[10] (20 gauge,

[1] Pitman-Moore, Inc., Washington Crossing, N.J.
[2] Trimune Rabies Vaccine, Rolynn Laboratories, Lenexa, Kan.
[3] Delcine HL, Dellen Laboratories, Omaha, Neb.
[4] Ralston Purina Co., St. Louis, Mo.
[5] C. B. Fleet Co., Murray Hill, N.J.
[6] Ayerst Laboratories, Rouses Point, N.Y.
[7] Abbott Laboratories, North Chicago, Ill.
[8] Portex, Hythe, Kent, England.
[9] Metofane, Pitman-Moore, Washington Crossing, N.J.
[10] Jelco Laboratories, Raritan, N.J.

0022-3549/82/0700-0840$01.00/0

15 mm) was inserted in the cephalic vein so that 5% dextrose in Ringer's Irrigation Solution[11] could be infused by intravenous drip during the entire surgical procedure (3–4 hr) and for 1 hr postoperation to prevent fluid loss through dehydration.

Aseptic technique was observed at all times within the surgical bay. Anesthetic intake, temperature, pulse, heart rate, respiratory rate, fluid intake, as well as urine and blood loss were monitored throughout the surgical procedure.

The dog was placed on its back and a catheter[12] was introduced into the urinary bladder. A 12-cm vertical abdominal midline incision was made. Skin, fascia, and muscle were spread laterally until the liver and the greater omentum were exposed. Capillary bleeding was arrested by electrocautery. The liver was deep red in color, firm in consistency, and friable.

Implantation of the first catheter into the hepatic artery required location of the right gastric artery. The right gastric artery leaves the common hepatic artery at nearly a right angle, runs into the lesser omentum at the pylorus, and continues to the lesser curvature of the stomach. The point at which the right gastric artery leaves the common hepatic artery was exposed, and the connective tissue surrounding it and on its surface was removed (Fig. 1A). A 1-mm longitudinal incision was made, and a 60-cm venous catheter[13] was fitted in the artery and advanced into the common hepatic artery. It was secured in the artery by suturing with nonabsorbable silk (000)[14] using a square knot stitch. The catheter was flushed using a 10-U heparin sodium/ml[15] solution *via* a 3-ml plastic syringe[16] attached to the sampling barrel of the catheter, and testing for patency by drawing back until bright red arterial blood appeared in the syringe. The catheter was kept patent by the maintenance of the 10-U heparin sodium/ml solution within the catheter throughout the surgical period. A similar procedure was followed for maintaining patency with the implantation of the three other catheters.

Following the insertion of the hepatic artery catheter, an indwelling catheter was placed in the portal vein. A 90-cm catheter[17] was advanced cranially into the portal vein through one of the mesenteric veins.

A mesenteric vein was isolated by the separation of connective tissue from its surface. With isolation, a 1-mm longitudinal cut was made and the catheter inserted and secured with nonabsorbable surgical silk (000), flushed, and kept patent (Fig. 1B).

With the hepatic artery and portal vein secured and patent, the peritoneum, fascia, and muscle were sutured by a horizontal mattress stitch using surgical chromic gut[18] leaving the skin to be sutured later. The two catheters were set aside for further placement.

A 6-cm cutdown was then made on the left pelvic limb, exposing the femoral artery and femoral vein. A 90-cm indwelling venous catheter was implanted into one of the numerous branches of the femoral vein and fed into the postcava with eventual placement in the hepatic sinus. This served as a site for sampling hepatic vein blood alcohol concentrations. The catheter was flushed and kept patent with heparin.

Nonabsorbable surgical silk (000) was again used for securing the catheter. To ensure proper placement, the distance from the femoral vein to the hepatic sinus was measured and marked on the catheter. When the catheter was secured with the silk, its position within the hepatic sinus was verified by feeling for its tip within the sinus through the wall of the vena cava (Figs. 1C and D). In addition, when the study was complete, a necropsy was performed on each dog revealing the proper position of all catheters.

A fourth catheter was then placed in one of the many branches of the femoral artery. A 1-mm longitudinal cut was made and the indwelling catheter fitted within the femoral artery and secured using nonabsorbable surgical silk (000) (Fig. 1E) and maintained with heparin.

The femoral fascia was sutured with surgical chromic gut and the catheters passed between the medial femoral fascia and the skin to the location of two abdominal catheters. This was done by using a sterile 10-mm endotracheal tube. The tube was inserted between the fascia and the skin after they had been separated by blunt forceps. The syringes were removed from the barrel of each catheter and the catheters advanced through the tube. Once the passage was complete and the endotracheal tube removed over the exposed ends of the catheters, heparin solution was again flushed through each of the catheters.

[11] Travenol Laboratories, Deerfield, Ill.
[12] Model No. 1730, C.R. Bard, Inc., Murray Hill, N.J.
[13] Style No. 1914, C. R. Bard, Inc., Murray Hill, N.J.
[14] Ethicon, Summerville, N.J.
[15] Organon, Inc., North Orange, N.J.
[16] Becton, Dickenson and Co., Rutherford, N.J.
[17] Style No. 1936, C. R. Bard, Inc., Murray Hill, N.J.
[18] Deknatel, Queens Village, N.Y.

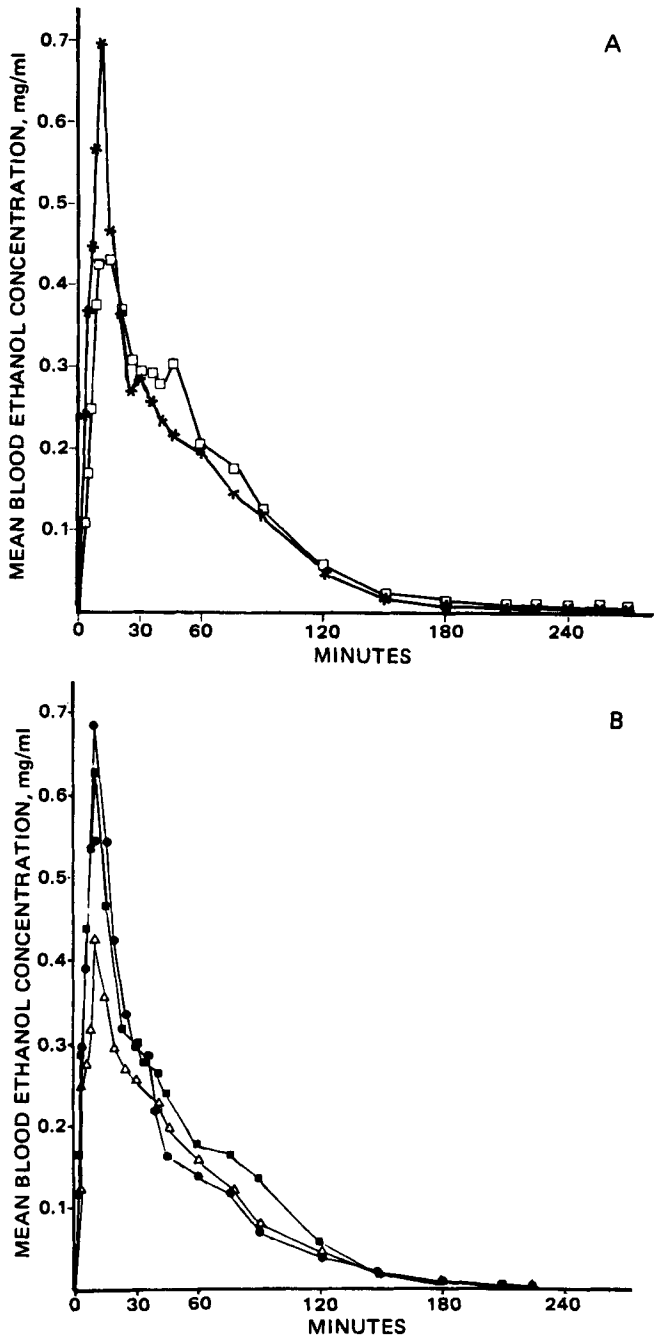

Figure 2—*Typical results of study conducted following surgery. Mean blood–ethyl alcohol concentrations following the 10-min intravenous infusion of 0.26 g/kg of ethyl alcohol* via *the cephalic vein to three dogs. Key: A: (✱) femoral artery; (□) femoral vein; B: (■) hepatic artery, (△) hepatic vein, (●) portal vein.*

The four catheters were placed under the skin to a location behind the dog's neck. This was accomplished by laterally separating (by blunt forceps) the skin and fascia so that the endotracheal tube could be placed between the tissues. A 2-cm incision was made in the dog's skin for the exit of the catheters from the tube. After the tube was positioned, the syringes were removed from the previously labeled catheter barrels and the catheters advanced through the tube. The tube was then removed and a polytef 3-way stopcock[19] was attached to the barrel of each catheter. Each catheter was checked for patency, flushed with 3-ml of the 10-U heparin sodium/ml solution, and the attached stopcock closed off.

The skin at the midline incision and the femoral triangle was then closed using surgical silk (000)[20]. Penicillin G benzathine and penicillin

[19] Model No. K-75, Pharmaseal, Inc., Toa Alta, P.R.
[20] Davis & Geck, Division of American Cyanamid Co., Stamford, Conn.

G procaine[21] (20,000 U/kg, respectively) was administered intravenously to prevent infection.

Following the surgical implantation, there was a need to protect the externalized vascular catheters from the trauma of biting and rubbing. A dog jacket[22], made of durable nylon net, afforded maximal protection and allowed the wound to heal. The jacket was adjustable, so as to fit a range of sizes, and contained two pockets, one on either side of the dog, enabling the housing and protection of the indwelling venous catheters. Clove oil was used as a chewing deterrent. Clove oil was found to be effective and long lasting without ill-effects. In addition, routing the catheters under the skin and through the dermis into an area covered by the jacket's pockets failed to attract the dog's attention and a deterrent from biting was accomplished and proved effective.

Postsurgical Procedure—The dogs were allowed to stabilize postsurgically for a period of 2–3 days. It was found that the heavier dogs required a shorter recovery time. They were permitted their normal diet *ad libitum*. Prior to each animal study the dogs were fasted and water withheld overnight. The four catheters were checked for patency and flushed daily with a 100-U heparin sodium/ml solution in physiological saline.

RESULTS AND DISCUSSION

The experimental design (19, 20), for which the above surgical procedure was developed, entailed the administration of several different doses of ethyl alcohol (8–10% v/v solutions in saline) *via* either the hepatic artery indwelling catheter or a 20-cm catheter[23] inserted at the time of each study into a cephalic vein. Studies were conducted at 2- or 3-day intervals to allow a sufficient wash-out period for the ethyl alcohol. Figures 2A and B show typical results from one such study in which 0.26 g of ethyl alcohol/kg of body weight was administered over 10 min *via* the cephalic vein. Blood samples from all four surgically placed catheters and a fifth catheter (20 cm) inserted at the time of study in the saphenous vein (a branch of the femoral vein) could be collected within a 15–20-sec time period. Thus, simultaneous blood collection at several locations in the vascular system is possible. Simultaneous sampling is essential in order to obtain accurate concentration gradients with time across the liver and within the peripheral circulation. Using the above surgical techniques, mongrel dogs were maintained with patent catheters up to 24 days (postsurgery). The catheters were patent at this time and could have been maintained longer. In this length of time, numerous studies could be conducted.

While the surgical procedure described was for a specific study with ethyl alcohol, it has utility for the study of any drug suspected of liver first-pass metabolism. With appropriate maintenance the catheters could remain patent for extended periods with minimal discomfort to the dog.

[21] Longocil, Fort Dodge Laboratories, Fort Dodge, Ia.
[22] Alice King Chatham Medical Arts, Los Angeles, Calif.
[23] Style No. 1617 C. R. Bard, Inc., Murray Hill, N.J.

REFERENCES

(1) J. W. Dundee, *Anesth. Analg. (Cleveland)*, **49**, 467 (1970).

(2) J. W. Dundee, M. Issac, and J. Taggart, *Q. J. Stud. Alcohol*, **32**, 741 (1971).

(3) J. G. Gostomzyk, *Des Anaesthesist*, **20**, 165 (1971).

(4) J. G. Gostomzyk, B. Dilger, and K. Dilger, *Z. Klin. Chem. Klin. Biochem.*, **7**, 162 (1969).

(5) E. K. Marshall, Jr. and W. F. Fritz, *J. Pharmacol. Exp. Ther.*, **109**, 431 (1953).

(6) H. W. Haggard and L. A. Greenberg, *J. Pharmacol. Exp. Ther.*, **52**, 150 (1934).

(7) R. N. Harger, H. R. Hulpieu, and V. V. Cole, *Fed. Proc. Fed. Am. Soc. Exp. Biol.* **4**, 123 (1945).

(8) R. B. Forney, H. R. Hulpieu, and R. N. Harger, *J. Pharmacol. Exp. Ther.*, **98**, 8 (1950).

(9) R. N. Harger, R. B. Forney, and R. S. Baker, *Q. J. Stud. Alchol*, **17**, 1 (1956).

(10) N. E. McCallum and J. G. Scroggie, *Med. J. Aust.*, **47**, 1031 (1960).

(11) R. B. Forney, F. W. Hughes, R. N. Harger, and A. B. Richards, *Q. J. Stud. Alcohol*, **25**, 205 (1964).

(12) R. B. Forney, Abstracts, APhA Academy of Pharmaceutical Sciences, San Francisco, Calif., **1**, pp. 28, 29 (1971).

(13) R. N. Harger, "Proceedings of the Third International Conference on Alcohol and Road Traffic," London, England 1963, pp. 212–218.

(14) J. P. Payne, D. W. Hill, and N. W. King, *Br. Med. J.*, **1**, 196 (1966).

(15) A. J. Sedman, Ph.D. Thesis, The University of Michigan, 1974.

(16) A. J. Sedman, P. K. Wilkinson, and J. G. Wagner, *J. Forensic Sci.*, **21**, 315 (1976).

(17) J. L. Rheingold, P. Priessler, P. Smith, and P. K. Wilkinson, Abstracts, APhA Academy of Pharmaceutical Sciences, 8(2), 78 (1978).

(18) M. E. Miller, G. C. Christensen, and H. E. Evans, "Anatomy of the Dog," W. B. Saunders, Philadelphia, Pa., 1968, p. 702.

(19) P. K. Wilkinson and J. L. Rheingold, *J. Pharmacokinet. Biopharm.*, **9**, 261 (1981).

(20) J. L. Rheingold, R. E. Lindstrom, and P. K. Wilkinson, *J. Pharmacokinet. Biopharm.*, **9**, 279 (1981).

ACKNOWLEDGMENTS

Work supported in part by the University of Connecticut Research Foundation Grant No. 302.

Paul K. Wilkinson would like to thank Dr. Gerald Hankes, DVM, Small Animal Clinic, School of Veterinary Medicine, Auburn University, Auburn, Ala. for his patience and expertise during the early development of this study; to Abbott Laboratories, North Chicago, Ill., where he was Summer Visiting Professor for photographic services; and to the University of Connecticut Health Sciences Center, Center for Laboratory Animal Care, Farmington, Conn., where the surgery was performed.

Conformation of Some Disubstituted 9-Acridanones

J. BARBE *x, A.-M. GALY *, R. FAURE ‡, A. MAHAMOUD ‡, and J.-P. GALY ‡

Received February 26, 1981, from the **Service de Chimie minérale, Faculté de Pharmacie, 27 Boulevard Jean-Moulin, 13385 Marseille Cedex 5, France*, and the ‡*Service de Chimie organique physique, Faculté des Sciences, rue Henri-Poincaré, 13397 Marseille Cedex 4, France.* Accepted for publication October 27, 1981.

Abstract □ Experimental dipole moments of some disubstituted 9-acridanones were compared to the vectorially and theoretically calculated values using CNDO/2 method. Results supported the existence of a presumed folding of these compounds with the prevalence of a quasi-equatorial conformation.

Keyphrases □ Acridanones—disubstituted, dipole moments, conformation as solutes, □ Conformations—disubstituted acridanones as solutes, dipole moments □ Dipole moments—acridanones, disubstituted, conformation as solutes

The special position of acridanone compounds has frequently been mentioned. Their structure has to be situated between those of acridine and acridane (1), since the former is aromatic while the latter is equivalent to a bridged diphenylamine structure. Acridanone derivatives were identified as metabolites of the acridinic drugs (2–4) as well as metabolites of some dibenzoazepine-like antiepileptic drugs such as carbamazepine (5–7).

These molecular transformations can modify the biological response if it stems from electronic distribution, and they can also induce side effects due to the new geometrical structures which could eventually carry out stereospecific actions.

Crystallographic data presently are the sole source of information about the acridanones structure (8). Because of this, it becomes worthwhile to define the conformation of acridanones as solutes and molecules isolated theoretically.

In this report the dipole moments of some disubstituted 9-acridanones were measured. They were calculated either by means of incremental vectorial addition or by the CNDO/2 method. Calculations and experimental results were compared to portray the molecular structure of the compounds studied.

EXPERIMENTAL

Materials—The following compounds were studied: 1,10-dimethyl-9-acridanone (I); 2,10-dimethyl-9-acridanone (II); 4,10-dimethyl-9-acridanone (III); 1-methyl-10-benzyl-9-acridanone (IV); 2-methyl-10-benzyl-9-acridanone (V); 2-methoxy-10-methyl-9-acridanone (VI); 2-methoxy-10-benzyl-9-acridanone (VII); 4-nitro-10-methyl-9-acridanone (VIII).

These compounds were prepared using phase transfer catalysis according to the process previously worked out with other acridine (9) or acridanone (10) derivatives. The purity of the samples studied was checked by HPLC[1].

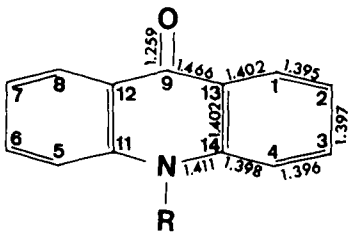

Figure 1—*Molecular geometry of the disubstituted acridanones studied.*

Methods—The dipole moments of the compounds as solutes in anhydrous benzene were measured at 25.00 ± 0.05°. The permittivity[2] and refractive index[3] of the solutions were extrapolated to infinite dilution according to previous reports (11, 12). The quantity $(\epsilon_{12} - n_{12}^2) - (\epsilon_1 - n_1^2)$ was plotted *versus* the molar concentrations, C, of the solute. The slope of the curve at $C = 0$ was then used to calculate the dipole moment, μ:

$$\mu^2 = \frac{9kT}{4\pi N} \frac{3}{(\epsilon_1 + 2)(n_1^2 + 2)} \frac{(\epsilon_{12} - n_{12}^2) - (\epsilon_1 - n_1^2)}{C} \qquad \text{(Eq. 1)}$$

where k is the Boltzmann's constant, N is Avogadro's number, T is the absolute temperature, and ϵ_i and n_i are the permittivities and refraction indexes, respectively, of the solutes (Index 1) and of the solutions (Index 12).

RESULTS AND DISCUSSION

Experimental dipole moments and the theoretical moments, calculated using vectorial incremental addition, are given in Table I. For these calculations, the following molecular increments were used: anisole, 1.25 D; diphenylamine, 1.08 D; nitrobenzene, 3.98 D; toluene, 0.40 D (13); and 4-pyridone, 5.30 D (14).

Molecules were examined as being planar. Nitrogen hybridization was successively considered as sp^2 and sp^3, and in each case a possible conjugation of the nitrogen lone-pair was taken into account. It must be kept in mind that conjugation modifies the value of dipolar increments because of the alteration of the electronic density at the level concerned. The values used are those previously given (15).

The molecules were assumed to be folded, which occurs along a fictitious N—O axis. Calculations were performed for different values of the angle, α, between each benzo ring of the heterocycle. The folding involves two limit-conformers known as R extra (quasi-axial) or R intra (quasi-equatorial) in accordance with the spatial orientation of the N—R bond. The conjugation concerns only the intra structure, because of the electronic hindrances in the extra structure. Four limit structures also were studied in the methoxy substituent: in structures M-1 or M-2, the methyl group is in the benzo plane, while in structures M-3 or M-4 it is out of the

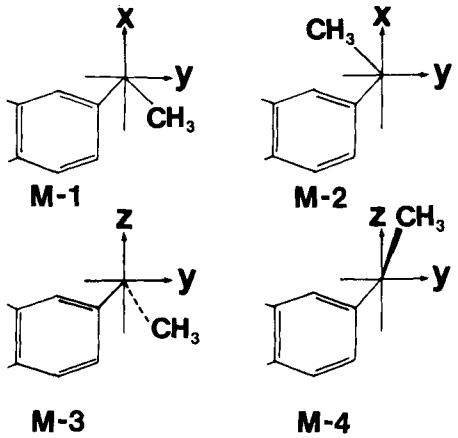

[1] Pump, M 6000 A, Waters Associates; column, 25-cm μBondapack C-18 Waters Associates; detector, variable wavelength UV spectrometer Cecil CE 212. Detection was operated at 254 nm. The mobile phase flow rate (methanol RP) was 3 ml/min^{-1}, *i.e.*, ~2000 psi.

[2] W.T.W. DM 01 dipolmeter with a DFL 1 cell.

[3] O.P.L. Abbe-type refractometer.

0022-3549/82/0700-0843$01.00/0

Table I—Experimental and Calculated Dipole Moments [a]

Compounds	μ exp.	μ lit.	μ CNDO/2	μ Vectorial Calculation [b]								
				Planar Structure		Folded Structure						
						R intra				R extra			
				N sp²	N sp³	α = 170°	160°	150°	140°	170°	160°	150°	140°
N-methyl acridanone	5.20	5.38(13) 3.50(13)	5.05	5.90	5.57	5.85	6.09	6.32	6.48				
					4.82	4.99	5.19	5.44	5.65	4.70	4.63	4.62	4.68
I	4.85		4.69	5.50	5.19	5.47	5.72	5.98	6.15				
					4.43	4.61	4.82	5.10	5.34	4.30	4.24	4.26	4.35
II	5.37		4.90	5.71	5.32	5.68	5.94	6.21	6.40				
					4.64	4.82	5.05	5.33	5.59	4.52	4.43	4.42	4.48
III	5.34		4.95	6.30	5.97	6.22	6.45	6.67	6.81				
					5.22	5.38	5.56	5.76	5.97	5.10	5.02	4.99	5.03
IV B-1	5.28			5.38	4.89	5.25	5.51	5.78	5.96				
					4.11	4.42	4.62	4.89	5.13	3.93	3.84	3.88	4.03
IV B-2	5.28			5.38	5.34	5.25	5.58	5.93	6.03				
					4.61	4.37	4.64	5.16	5.24	4.53	4.55	4.63	4.76
V B-1	5.32		5.14	5.52	5.10	5.46	5.73	6.01	6.21				
					4.32	4.63	4.84	5.13	5.38	4.14	4.03	4.04	4.15
V B-2	5.32		5.14	5.52	5.54	5.44	5.79	6.16	6.27				
					4.82	4.59	4.90	5.30	5.48	4.73	4.74	4.79	4.87
VI M-1	4.66		4.44	7.15	6.81	7.05	7.24	7.43	7.54				
					6.06	6.22	6.36	6.54	6.68	5.95	5.85	5.79	5.78
VI M-2	4.66		4.44	5.49	5.23	5.51	5.71	5.94	6.09				
					4.51	4.67	4.84	5.09	5.29	4.37	4.28	4.27	4.34
VI M-3	4.66		4.44	6.33	5.88	6.65	6.95	7.26	7.44				
					5.23	5.77	6.07	6.40	6.63	5.30	5.40	5.52	5.65
VI M-4	4.66		4.44	6.33	6.26	5.95	6.02	6.06	6.07				
					5.44	5.19	5.16	5.17	5.19	5.14	4.83	4.54	4.36
VI M-5	4.66		4.44		6.23	6.41	6.56	6.70	6.78				
					5.56	5.62	5.70	5.81	5.91	5.49	5.30	5.14	5.06
VII B-1, M-1	4.60		4.44	7.02	6.50	6.86	7.06	7.27	7.40				
					5.74	6.05	6.19	6.38	6.52	5.58	5.45	5.40	5.43
VII B-1, M-2	4.60		4.44	5.41	4.94	5.30	5.51	5.75	5.91				
					4.18	4.48	4.64	4.89	5.09	4.01	3.90	3.91	4.04
VII B-1, M-3	4.60		4.44	6.34	5.53	6.40	6.72	7.05	7.24				
					4.87	5.53	5.83	6.17	6.42	4.91	5.00	5.16	5.34
VII B-1, M-4	4.60		4.44	6.20	6.01	5.82	5.88	5.95	5.96				
					5.17	5.09	5.05	5.06	5.07	4.80	4.45	4.14	3.99
VII B-1, M-5	4.60		4.44	6.53	5.90	6.25	6.41	6.57	6.66				
					5.21	5.50	5.57	5.68	5.78	5.15	4.91	4.74	4.69
VII B-2, M-1	4.60		4.44		7.13	6.79	7.06	7.34	7.36				
					6.41	5.95	6.17	6.45	6.51	6.16	6.15	6.14	6.18
VII B-2, M-2	4.60		4.44		5.54	5.29	5.57	5.89	5.96				
					4.81	4.44	4.70	5.05	5.18	4.58	4.59	4.63	4.73
VII B-2, M-3	4.60		4.44		6.23	6.46	6.84	7.23	7.31				
					5.61	5.57	5.95	6.38	6.53	5.57	5.74	5.90	6.05
VII B-2, M-4	4.60		4.44		6.54	5.66	5.79	5.93	5.86				
					5.73	4.87	4.93	5.04	4.99	5.27	5.08	4.86	4.73
VII B-2, M-5	4.60		4.44		6.58	6.13	6.55	6.58	6.58				
					5.92	5.32	5.48	5.69	5.72	5.66	5.56	5.47	5.44
VIII	2.55		0.72 [c] 10.06 [d]	1.91		2.40	2.91	3.48	3.92				
						1.54	2.17	2.90	3.51	0.74	1.12	1.85	2.54

[a] In Debye units, D. [b] For each compound, there are the dipole moments calculated with (first line) and without (second line) conjugation. [c] Nitrogen dioxide and benzo plane are perpendicular. [d] Nitrogen dioxide and benzo ring-carriers are in the same plane.

benzo plane. Free rotation M-5 was also studied for this group. Conversely, free rotation was inconceivable for the benzyl substituent. So, only structure B-1 or B-2 was considered.

The molecular geometry was used for the CNDO/2 calculations (Fig. 1). Substituents are located along the bisector axis.

Bond length and angles are those drawn from the literature (16). Calculations were performed for a planar structure only. Dipole moments are given in Table I while bond indexes of some compounds are collated in Table II. These indexes can be compared to those corresponding to acridine derivatives (17). Average values of bond indexes in each case are summarized in Fig. 2. Comparison shows that the aromatic character of benzo rings is greater in acridanones than in acridines, unlike the aromatic character of the central ring which is lower in acridanones than in acridines. Consequently, the acridanone heterocycle can be assumed to be folded. Moreover, this statement agrees with the result of the comparison between experimental dipole moments and the vectorially calculated ones. There is also an agreement with UV spectra (18).

But, added to this, according to the latter comparison, a particular orientation of the methyl group of the methoxy substituent is involved: lone pairs of the extracyclic oxygen should be conjugated with the π cloud of the ring-carrier. Similarly, the most probable structure for the benzyl substituent seems to be the previously noted structure, B-1. This is in close agreement with the NMR spectra[4] presented in Table III. Indeed, structure B-1 is consistent with the deshielding of the benzylic protons, CH_2, ($5.52 < \delta < 5.57$ ppm) referring to those of the $\varphi—CH_2—NR_2$ like compounds ($3.30 < \delta < 3.96$ ppm) (19).

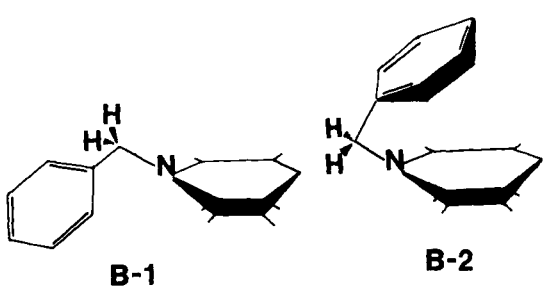

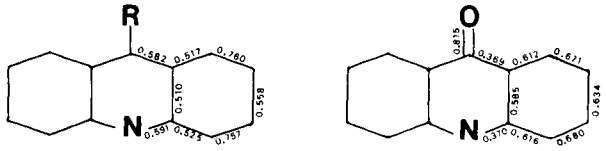

Figure 2—*Acridines and acridanones: diagrams with the averaged π bond indexes.*

[4] Varian XL 100 Spectrometer.

Table II—Bond Indexes of Some Compounds Studied

Bonds	Compounds					
	I	II	III	V	VI	VII
C_1—C_2	0.6616	0.6710	0.6849	0.6709	0.6692	0.6692
C_2—C_3	0.6499	0.6293	0.6441	0.6293	0.6256	0.6256
C_3—C_4	0.6758	0.6846	0.6695	0.6845	0.6849	0.6849
C_4—C_{14}	0.6190	0.6186	0.6037	0.6180	0.6187	0.6181
C_{14}—N_{10}	0.3784	0.3690	0.3769.	0.3713	0.3621	0.3643
N_{10}—C_{11}	0.3747	0.3767	0.3767	0.3791	0.3784	0.3808
C_{11}—C_5	0.6184	0.6179	0.6178	0.6045	0.6173	0.6040
C_5—C_6	0.6819	0.6822	0.6825	0.6890	0.6826	0.6894
C_6—C_7	0.6423	0.6418	0.6415	0.6347	0.6413	0.6342
C_7—C_8	0.6851	0.6855	0.6858	0.6908	0.6860	0.6913
C_8—C_{12}	0.6152	0.6144	0.6141	0.6076	0.6138	0.6069
C_{12}—C_{11}	0.5842	0.5831	0.5832	0.5874	0.5826	0.5868
C_{12}—C_9	0.3668	0.3683	0.3686	0.3697	0.3691	0.3705
C_9—O	0.8090	0.8168	0.8165	0.8163	0.8172	0.8166
C_9—C_{13}	0.3832	0.3667	0.3671	0.3668	0.3659	0.3660
C_{13}—C_{14}	0.5800	0.5832	0.5879	0.5828	0.5877	0.5873
C_{13}—C_1	0.5954	0.6182	0.6119	0.6182	0.6139	0.6140

Table III—Chemical Shifts and Assignment of Protons [a]

Compounds	Aromatics	—CH_2—	2-OCH_3	N—CH_3	φ-CH_3
I	8.5–7.0(m, 7H)			3.90(s, 3H)	3.10 (s, 3H)
II	8.0–7.2(m, 7H)			3.80(s, 3H)	2.45(s, 3H)
III	8.5–7.2(m, 7H)			3.85(s, 3H)	2.70(s, 3H)
IV	8.5–6.9(m, 12H)	5.45(s, 2H)			3.00(s, 3H)
V	8.6–7.1(m, 12H)	5.55(s, 2H)			2.45(s, 3H)
VI	8.7–7.2(m, 7H)		3.95(s, 3H)	3.85(s, 3H)	
VII	8.5–7.2(m, 12H)	5.55(s, 2H)	3.90(s, 3H)		
VIII	8.7–7.1(m, 7H)			3.60(s, 3H)	

[a] Solvent, dimethyl sulfoxide; internal standard, tetramethylsilane; temperature, ambient; multiplicity: m, multiplet; s, singlet.

No information is available, however, about the nitro group from the vectorial pattern, because of the supposed free rotation of this substituent. But, inclination of the latter upon the ring-carrier plane is close to 70°, according to the CNDO/2 calculations.

The agreement found between quantum mechanics calculations and incremental vectorial addition must be emphasized. Similar results were previously noted with some other acridine derivatives (17).

As for acridanones, they are presumably slightly folded, the angle of folding being close to 170°. Moreover, the prevailing structure should be the intrastructure.

REFERENCES

(1) J. M. F. Gagan, in "The Chemistry of Heterocyclic Compounds," Vol. 9, The Acridines, R. M. Acheson Ed., 2nd ed., Wiley, New York, N.Y., 1973, p. 141.

(2) H. Otaka and Y. Hashimoto, *Nippon Univ. J. Med.*, **2**, 1 (1960).

(3) H. Otaka, K. Kono, and R. Ito, *ibid.*, **3**, 235 (1961).

(4) H. Otaka, I. Ikeda, and R. Ito, *ibid.*, **3**, 245 (1961).

(5) S. Goenechea, G. Eckhardt, and H. D. Dersen, *Fresenius Z. Anal. Chem.*, **279**, 113 (1976).

(6) K. H. Beyer and O. Bredenstein, *Dtsch. Apoth. Ztg.*, **117**, 1713 (1977).

(7) K. H. Beyer and A. Wagemann, *Arzneim.-Forsch.*, **28**, 246 (1978).

(8) V. E. Zavodnik and L. A. Chetkina, *Tezisy Dokl. Vses Soveshch. Org. Kristallochim.*, **1**, 76 (1974).

(9) J. P. Galy, J. Elguero, E. J. Vincent, A. M. Galy, and J. Barbe, *Heterocycles*, **14**, 311 (1980).

(10) J. P. Galy, J. Elguero, E. J. Vincent, A. M. Galy, and J. Barbe, *Synthesis*, 944 (1979).

(11) E. A. Guggenheim, *Trans. Faraday Soc.*, **45**, 714 (1949).

(12) J. W. Smith, *ibid.*, **46**, 394 (1950).

(13) A. L. McClellan, "Tables of Experimental Dipole Moments," Vol. 1, Freeman, San Francisco, Calif., 1963.

(14) A. Albert and J. N. Phillips, *J. Chem. Soc.*, **1956**, 1294.

(15) C. Levayer, A. M. Galy, and J. Barbe, *J. Pharm. Sci.*, **69**, 116 (1980).

(16) M. Bodor, M. J. S. Dewar, and A. J. Hargel, *J. Am. Chem. Soc.*, **92**, 2929 (1970).

(17) A. M. Galy, J. P. Galy, R. Faure, and J. Barbe, *Eur. J. Med. Chem.*, **15**, 179 (1980).

(18) A. M. Galy, J. Barbe, J. P. Galy, and J. P. Lanza, *Il Farmaco, Ed. Sci.*, **36**, 38 (1981).

(19) N. F. Chamberlain, "The Practice of NMR Spectroscopy," Plenum, New York, N.Y., 1974.

Cattle and Sheep Skin Permeability: A Comparison of Frozen and Reconstituted Skin with that of Fresh Skin

Keyphrases □ Permeability—cattle and sheep skin, comparison of frozen and reconstituted skin with fresh skin □ Skin—permeability in cattle and sheep, comparison of frozen and reconstituted skin with fresh skin □ Topical drug delivery—cattle and sheep skin permeability, comparison of frozen and reconstituted skin with fresh skin

To the Editor:

It is known that freezing and reconstituting (*i.e.*, thawing) excised human skin does not significantly change the barrier properties it presents to the passive diffusion of drug molecules (1). This knowledge has led to substantial advances in the development of topical drug delivery systems for humans, because potentially useful systems can be identified from the results of *in vitro* screens using frozen and reconstituted human skin (2).

This communication presents data to establish that freezing and reconstituting cattle and sheep skin does not significantly alter their permeability.

It has previously been established (3) that the outer 1 mm of frozen and reconstituted cattle skin (*i.e.*, the stratum corneum, the viable epidermis, the papillary region of the dermis, and a portion of the reticular region of the dermis) acts as an homogeneous barrier to diffusing levamisole molecules. A corollary to this finding is that, for skin samples with thicknesses up to 1 mm, the product of the permeability constant (k_p in centimeters per minute) and the skin thickness (r in centimeters) (*i.e.*, k_pr) is a constant. A similar relationship has been observed for penetration of levamisole through the skins of Merino sheep (4).

To establish the relative permeabilities of fresh and reconstituted cattle and sheep skins, the following experiments were conducted.

Skin was harvested from an 8–9-month Shorthorn-Hereford cross calf in early spring and from a 12–18-month Merino cross ewe in mid-winter. The sheep was shorn and then finely clipped[1] and the calf finely clipped[1] immediately before skin samples were removed with a dermatome[2] set at 1.1 mm.

The permeability of fresh skin and skin that had been stored at −30° for 5–7 days and then thawed to levamisole from a 0.85% solution in an aqueous pH 8.9 buffer was determined using methods identical to those described previously (3).

Values of k_pr for levamisole penetrating through fresh and reconstituted skins are given in Table I.

There was no significant difference (at the 1 or 5% levels) between the values of k_pr for fresh and reconstituted cattle or sheep skin.

Table I—Permeability of Cattle and Sheep Skins to Levamisole[a]

Animal	Skin Thickness, cm	$10^6 k_pr$, $cm^2\ min^{-1}$
	Fresh	
Sheep	0.055	6.0
	0.066	7.7
	0.070	10.7
	0.071	9.2
	Frozen	
Sheep	0.077	7.2
	0.077	6.5
	0.077	8.4
	Fresh	
Calf	0.069	27.7
	0.071	26.8
	0.076	30.9
	0.092	33.7
	0.093	31.7
	Frozen	
Calf	0.065	26.5
	0.069	25.6
	0.071	29.3
	0.082	29.5
	0.086	30.2
	0.091	33.4

[a] From a 0.85% solution in an aqueous pH 8.9 buffer and water-bath temperature of 37°.

Although no relationship has been established between *in vitro* and *in vivo* permeability for cattle and sheep skins, it seems unlikely that live skin, with its blood supply and sweat and sebum secretions, would be appreciably less permeable than excised skin, unless the latter was damaged by the receptor solution.

Consequently, it is concluded that screens for cattle and sheep skin permeability that employ reconstituted skin (5–7) and utilize normal saline as a receptor phase have the potential to provide useful information to developers of veterinary topical dosage forms.

(1) R. B. Stoughton, in "Progress in the Biological Sciences in Relation to Dermatology," vol. 2, A. Rook and R. H. Champion, Eds., Cambridge University Press, Cambridge, England, 1964.
(2) R. J. Scheuplein, *J. Invest. Dermatol.*, **67**, 31 (1976).
(3) I. H. Pitman and S. J. Rostas, *J. Pharm. Sci.*, **71**, 427 (1982).
(4) I. H. Pitman, S. J. Rostas, and L. M. Downes, in press.
(5) I. H. Pitman, S. J. Rostas, and L. M. Downes, in press.
(6) I. H. Pitman and S. J. Rostas, *J. Pharm. Sci.*, **70**, 1181 (1981).
(7) L. M. Ponting and I. H. Pitman, *Aust. J. Pharm. Sci.*, **8**, 15 (1979).

Ian H. Pitman ˣ
Leanne M. Downes
School of Pharmaceutics
Victorian College of Pharmacy
Melbourne, 3052, Australia

Received October 13, 1981.
Accepted for publication April 8, 1982.
Supported by a grant from the Wool Research Trust Fund—Australian Wool Corporation.
The authors thank Mr. Ian Ray for technical assistance and I.C.I. Australia Ltd. for supplying animal skins.

[1] Andis R400 Oster A5 Clippers.
[2] Brown Electro Dermatome, model 902.

0022-3549/82/0700-0846$01.00/0

A publication of the
American Pharmaceutical Association—
the National Professional Society
of Pharmacists

JOURNAL OF PHARMACEUTICAL SCIENCES

INDEX TO AUTHORS
INDEX TO SUBJECTS

VOLUME 71
JANUARY TO DECEMBER, 1982

Published monthly under the supervision of the Board of Trustees

The NIH and Political Pressures

The National Institutes of Health have been in the news even more than usual in recent months. This has been due to a number of factors, including the vacancy in the office of the Director of the overall NIH, the long search for a new director, and the protracted formal approval and appointment process relating to Dr. James B. Wyngaarden once he had been selected. The news interest also has been due to the present vacancy of five of the individual Institute directorships and a sixth that will open up in the next few weeks.

Such "power vacuums" are natural stimuli for gossip and news media speculation—especially when they occur in the political hot-bed that is Washington, D.C.

But lately, the NIH has also been frequently in the news for another reason; namely, the current Congressional efforts to cut federal spending and to reduce the budgetary deficit. Without quoting statistics, it can be simply said that the NIH has not escaped major surgery with respect to its budgetary requests and perceived monetary needs.

All of this serves to remind us of the strong advocacy on the part of many pharmaceutical scientists about 10 to 15 years ago for the creation of a new, separate Institute to be devoted specifically to the pharmaceutical sciences. Presumably, such a new body would concentrate its research efforts and its extramural research funding on such subjects as improved drug delivery systems, pharmacokinetics, bioavailability, and related matters. However, the proposal never "caught fire," and eventually it fell by the wayside.

In retrospect, that may have been fortunate, although no one felt so at the time.

When the separate Institute proposal was first made and championed, federal support for health research generally and for the NIH in particular was flowing like the proverbial waters of Niagara. Today, however, the climate has changed dramatically.

The overall NIH budget and the budgets of the individual Institutes are presently undergoing fierce assaults. The only reason that deeply severe, or perhaps even mortal, fiscal surgery has not occurred is due to the strong support of powerful friends in Congress. When an influential Congressional Committee Chairman takes on a self-appointed and self-assumed role as protector and advocate of one or another of the respective Institutes, it can be safely predicted that the body will fare reasonably well.

And with the various pet diseases of individual Congressional leaders, it is not surprising that the Cancer Institute, or the Heart Institute, or the Aging Institute, or whichever, has managed to avoid wholesale cut-backs. Right or wrong, a fact of life in Washington is that no project, program, cause, or activity will go far or last very long unless it is the beneficiary of a strong lobbying force and potent Congressional allies.

Given the reality that any National Institute of Pharmaceutical Sciences could not begin to command such political support, its budget would immediately become fair game in the fiscal maneuvering. In turn, such ax-wielding would mean that pharmaceutical research and pharmaceutical scientists would take the brunt of eliminated research projects and terminations in employment.

Moreover, given the hindsight of historical experience, it is probably unfortunate that the present individual Institutes were ever created. Less interagency rivalry, less duplication of administrative management, less petty jockeying for resources and publicity, and less wastage in many other areas, would have resulted if there were only a single "National Institute of Health." Experience has shown that independence and strong individual identity among these multiple components are not always conducive to the most efficient and effective operation of our nation's major health research program.

—EDWARD G. FELDMANN
American Pharmaceutical Association
Washington, DC 20037

0022-3549/82/0800-0847$01.00/0

JOURNAL OF PHARMACEUTICAL SCIENCES

AUGUST 1982
VOLUME 71 NUMBER 8

RESEARCH ARTICLES

Extended Hildebrand Solubility Approach and the Log Linear Solubility Equation

A. MARTIN *x, P. L. WU *, A. ADJEI *, R. E. LINDSTROM ‡, and P. H. ELWORTHY §

Received July 30, 1981, from the **Drug Dynamics Institute, College of Pharmacy, University of Texas, Austin, TX 78712;* ‡*School of Pharmacy, University of Connecticut, Storrs, CT 06268;* and the §*Department of Pharmacy, The University of Manchester, Manchester M139PL, England.* Accepted for publication November 10, 1981.

Abstract □ The log linear solubility equation, $\log S = \log S_w + \sigma f$, was studied in relationship to the extended Hildebrand solubility approach. It is shown that the log linear form may be derived beginning with the extended Hildebrand approach. The log linear expression gives a good linear fit for semipolar drugs in a number of water–cosolvent mixtures. It is particularly successful when the solubility parameter, δ_1, of the cosolvent is 3 or more solubility parameter units larger than the solubility parameter, δ_2, of the drug. When the cosolvent tends to solvate the drug strongly, the log linear function may even hold where the solubility parameters of the drug and cosolvent are similar. It appears, however, not to be applicable to nonpolar cosolvent systems. An interfacial model for the solubility of drugs in polar mixed solvents is based on σ, a parameter that also figures prominently in the log linear solubility equation. When used to describe mixed solvent systems, the interfacial model applies in the region of the solubility profile (solubility *versus* solvent composition) where the log linear relationships hold. The extended Hildebrand solubility approach is applicable over a wide range of cosolvent composition in mixed systems from nonpolar organic solvents to water.

Keyphrases □ Solubility—extended Hildebrand approach, log linear equation □ Hildebrand equation—extended solubility approach, log linear solubility □ Log linear solubility equation—relationship to the extended Hildebrand solubility approach

Yalkowsky *et al.* (1), introduced a log linear equation:

$$\log S = \log S_w + \sigma f \qquad \text{(Eq. 1)}$$

which describes the solubility of some drugs in binary aqueous systems, where S is the solute solubility in moles per liter in a solvent consisting of water and a nonaqueous cosolvent, S_w is the drug's solubility in water, f is the volume fraction of the cosolvent, and σ is a parameter representing the solubilizing power of the cosolvent for the drug and depends on the polarity of the drug and the cosolvent. Equation 1 was found to be applicable to systems where the polarity of the drug was significantly less than either of the solvents in the binary mixture.

A study (2) on the solubility of *p*-aminoacetophenone in propylene glycol–water mixtures, found it necessary to expand Eq. 1 into a fifth degree polynomial of f to account for nonlinearity across the range of cosolvent (propylene glycol) composition. The linear dependence of logarithmic solubility on volume fraction of the cosolvent (Eq. 1) applied when the Hildebrand solubility parameters of both solvent components were much larger than the solubility parameter of the drug.

THEORETICAL

In the present report, it is shown that the linear relationship of Eq. 1 may be considered in terms of the extended Hildebrand solubility approach (3–5); a model in which the solubility parameter of the solute may be larger or smaller than that of either solvent or lie between the solubility parameters of the two solvents. When the range of solubility parameters of the solvent pair approaches the solubility parameter of the solute, the curve may bow sufficiently that a log linear expression of X_2 on f no longer fits the data satisfactorily. A quadratic or higher polynomial of f must then be used as required by the extended Hildebrand method.

The following derivation shows the relationship of the log linear equation to the extended Hildebrand solubility approach. For the solubility of a drug in pure water:

$$\log X_w = \log X^i - \log \alpha_w \qquad \text{(Eq. 2)}$$

where X_w and X^i are the mole fraction solubility in water and the ideal solubility of the solute, respectively. Log α_w is the logarithm of the solute activity coefficient in water. A general expression for the solubility of a drug in a binary mixture, consisting of water and an organic cosolvent, is:

$$\log X_2 = \log X^i - \log \alpha_2 \qquad \text{(Eq. 3)}$$

where X_2 and α_2 are the mole fraction solubility and activity coefficient, respectively, for the solute in the solvent mixture. Subtracting Eq. 2 from Eq. 3 results in:

$$\log X_2 = \log X_w + \log \alpha_w - \log \alpha_2 \qquad \text{(Eq. 4)}$$

0022-3549/82/0800-0849$01.00/0

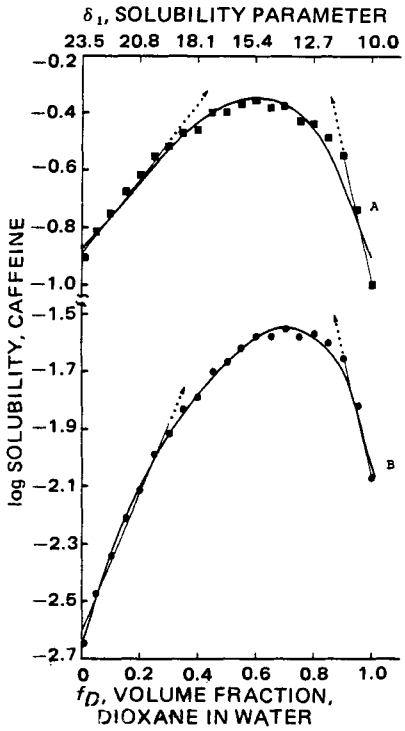

Figure 1—*Solubility of caffeine in dioxane–water mixtures at 25°. The curves were calculated using the extended Hildebrand solubility approach (4, 5). Key:(■) log molarity, Curve A; (●) log mole fraction, Curve B.*

The logarithmic solubility of a drug in water and the drug's log α_w are constants at a definite temperature. For caffeine in water at 25° (4), log $X_w = -2.64111$ and log $\alpha_w = 1.4764$; therefore, log $X^i = -1.1647$.

According to the extended Hildebrand approach (3–5), the activity coefficient of the drug in a mixed solvent is expressed as:

$$\log \alpha_2 = A(\delta_1^2 + \delta_2^2 - 2W) \qquad \text{(Eq. 5)}$$

where δ_1^2 and δ_2^2 are the cohesive energy densities of the solvent and solute, respectively, and W is the interaction energy density of solute and solvent. The term A is obtained from regular solution theory (6):

$$A = \frac{V_2\phi_1^2}{2.303RT} \qquad \text{(Eq. 6)}$$

where V_2 is the solute's liquid molar volume, ϕ_1 is the volume fraction of the pure or binary solvent (total volume fraction of the two solvents in the solution), R is the molar gas constant, and T is the absolute temperature.

Either W or log α_2/A may be regressed in a polynomial on δ_1 to obtain calculated values of log α_2 and mole fraction solubility, X_2 (Eq. 3). Log α_2/A_{calc} may also be obtained by a regression of log α_2/A on f_i, where f_i is the volume fraction of either solvent in a binary mixture (4), for example, water or its cosolvent. For dioxane, D, as the cosolvent:

$$\log \alpha_2/A_{calc} = C_0 + C_1 f_D + C_2 f_D^2 + C_3 f_D^3 + \ldots + C_n f_D^n \qquad \text{(Eq. 7)}$$

For caffeine in dioxane and water at 25°, the extended Hildebrand equation may be expressed as a fourth degree power series in conformity with Eqs. 4 and 7:

$$\log X_{2_{calc}} = \log X_w + \log \alpha_w - C_0A - C_1Af_D - C_2Af_D^2 - C_3Af_D^3 - C_4Af_D^4 \qquad \text{(Eq. 8)}$$

where C_0 is a constant of regression. C_1, C_2, C_3, and C_4 are the coefficients resulting from the regression analysis and remain constant over the range of binary solvent composition for a particular drug at a definite temperature. The value of A varies, although slightly, between 0.093 and 0.103 across the composition of water and dioxane in the caffeine system at 25°.

EXPERIMENTAL

The solubility data in mixed solvents employed in this paper were reported previously (4, 7–9). The drug was brought to equilibrium with the mixed solvent in a constant temperature shaker bath and the drug concentration was determined by spectrophotometric or other convenient analytic procedures. Densities were determined in glass pycnometers under controlled conditions. By obtaining the density of each solution, it was possible to express solubilities in units of molar, molal, or mole fraction concentration.

For calculations involving the extended Hildebrand solubility approach, regression analysis was conducted[1] using multiple linear regression programs (10).

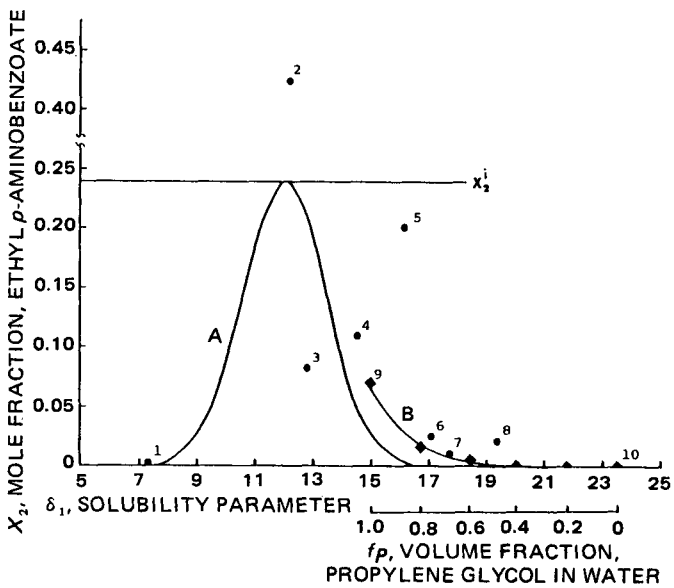

Figure 2—*Mole fraction of ethyl* p*-aminobenzoate in pure and binary solvents (9). A, regular solution curve at 25°; B, extended Hildebrand curve for ethyl* p*-aminobenzoate in propylene glycol–water mixture at 37°;* $X^i = 0.2404$ *at 25°. Key: (●) solubility in individual solvents at 25°; 1, hexane; 2, dimethylformamide; 3, ethanol; 4, methanol; 5, methylformamide; 6, ethylene glycol; 7, glycerin; 8, formamide; 9, propylene glycol (37°); 10, water(37°); (◆) solubility in propylene glycol–water mixtures at 37°, use of Eq. 18b.*

RESULTS AND DISCUSSION

Caffeine in Water–Dioxane Mixtures—Introducing the coefficients of regression analysis into Eq. 8 for caffeine in a mixed solvent system of water and dioxane (4), one obtains:

$$\log X_{2_{calc}} = \log X_w + \log \alpha_w - 14.6274A + 38.4195Af_D - 109.6076Af_D^2 + 114.3535Af_D^3 - 49.3831Af_D^4 \qquad \text{(Eq. 9)}$$

Equation 9 may be simplified by truncating it after the first term in f_D to yield:

$$\log X_{2_{calc}} = \log X_w + (\log \alpha_w - 14.6274A) + 38.4195Af_D \qquad \text{(Eq. 10)}$$

or in general:

$$\log X_{2_{calc}} = \log X_w + (\log \alpha_w - C_0A) + C_1Af_D \qquad \text{(Eq. 11)}$$

The quantity in parentheses is sufficiently small to be neglected since log α_w is equal to 1.4764 and $C_0A \cong 14.627 \times 0.1 = 1.4627$. If the regression procedure yielded log α_2/A with perfect accuracy, C_0 would exactly equal (log α_w)/A. This can be seen by setting f_D equal to zero in Eq. 11, for then the solvent obviously is water, and log α_2/A = log $\alpha_w/A = C_0$. With the quantity within the parentheses, Eq. 11, equal to zero, one arrives at an equation, expressed in mole fraction:

$$\log X_{2_{calc}} = \log X_w + \sigma f_D \qquad \text{(Eq. 12)}$$

analogous to Eq. 1, the log linear expression which, however, has usually been expressed in concentration units of moles per liters or grams per cubic centimeter. The coefficient, $C_1A = 38.4195A$ in Eq. 9, has been obtained by polynomial regression and is equal to σ in Eq. 1 when concentrations are expressed in mole fraction.

One form of the extended Hildebrand expression, Eq. 8, when carried

[1] University of Texas Cyber System.

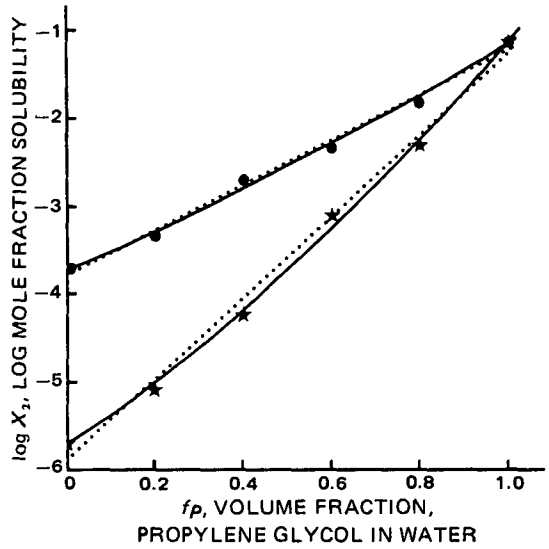

Figure 3—*Log mole fraction solubility of ethyl* p*-aminobenzoate (●) and hexyl* p*-aminobenzoate (★) in propylene glycol–water mixtures at 37° (9). Key: (——) from quadratic equations and (·····) from linear regression line.*

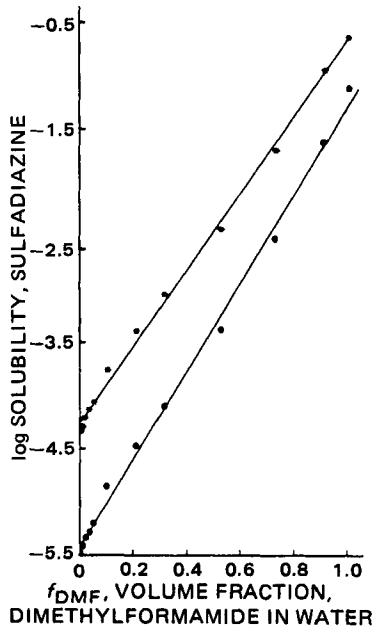

Figure 4—*Log solubility of sulfadiazine in dimethylformamide–water mixtures at 20° (7). Key: (●) log mole fraction (lower curve); (✱) log w/w; linear regression line (upper curve).*

to the fourth power in f_D, has been shown to reproduce the solubilities of caffeine in dioxane and water within <12% error and for most data points <4% error, a value within the range of experimental accuracy (4)[2].

In Fig. 1, log solubility of caffeine is plotted both in units of moles per liter and mole fraction *versus* volume fraction of the cosolvent, dioxane, as abscissa. Also marked along the horizontal axis (top of Fig. 1) are the solubility parameter values, δ_1, of the mixed solvents, consisting of water and dioxane.

In dealing with caffeine data in earlier reports (4, 5), various polynomial expressions were used. A cubic expression was not as satisfactory as the quartic equation; a quadratic expression yielded poor results; and an equation truncated to the linear term, σf_D, Eq. 12, would be unacceptable as a fit over most of the curve from dioxane (δ_1 = 10.01) to water (δ_1 = 23.45). As observed in Fig. 1, a linear fit is adequate from 0–30% cosolvent composition, although a straight line cannot reproduce exactly the slight curvature of the line. Both the upper and lower curves appear to be parabolic in form, but the curvature is so slight in the 0 to 30% region of dioxane concentration that the data points are adequately fit by a linear function. The intercept is the log solubility in water on a molar (Curve A) or mole fraction (Curve B) scale. In conformity with the criterion for linearity stated earlier, *i.e.*, δ_1 considerably larger than δ_2, the lowest value of δ_1 is 18.4, well above δ_2 = 13.8 of caffeine. It should be noted that the cosolvent of water in this case was not the pure solvent, dioxane, but rather a mixture of 30% dioxane–70% water. Using a log linear equation beyond 30 or 40% as seen in Fig. 1 would not produce meaningful results. Extrapolation into the region of the dashed lines in the direction of the arrows would produce erroneous values of solubility. Accordingly, the log linear technique, although often useful, should be used with caution over a wide range of solvent compositions. A little more effort is required to apply the extended Hildebrand solubility approach, but it usually can be made to reproduce solubility in mixed solvent systems with considerable fidelity across the entire range of binary solvent composition.

Although parts of the curve (0–30% dioxane in Fig. 1) may appear to be approximately linear, log solubility is ordinarily not a linear function of f (except where a strongly solvating cosolvent is present as seen later), and is better fitted with a power series in f or δ_1 rather than with a straight line.

In a manner similar to that discussed above, a 10% water in dioxane mixture could be taken as the cosolvent of dioxane in the region at the far right side of Fig. 1. At this low water concentration side of the figure, segments that are almost linear are observed in Curves A and B. Here, log solubilities *versus* volume fraction of water in the mixture produce linear functions only over a range of 10% water (δ_1 = 10–11.3). The curves begin to bow markedly at 10% water in dioxane because the solvent δ_1 is approaching the δ_2 value, 13.8, of the solute. According to regular solution theory, the solubility of a compound reaches a peak at a solvent composition where $\delta_1 = \delta_2$. The solubility curve approaches a maximum and then begins to decrease across this region and is greatly curved, as seen in the figure.

Results with theophylline, thebromine, and caffeine in other solvent mixtures have been reported (5). They show similar trends described here for caffeine in mixtures of water and dioxane.

The previous example of a log linear approach in relation to the extended Hildebrand model involved a solute with a solubility parameter, 13.8, between that of water, δ_1 = 23.45 and the cosolvent, dioxane, δ_1 = 10.01. By taking this broad view of the subject, one is able to observe more clearly the regions where a log linear equation is applicable and why it fails when the solubility parameter of the mixed solvent approaches the solubility parameter of the solute.

Alkyl *p*-Aminobenzoates in Water–Propylene Glycol Mixtures—The log linear equation, Eq. 1, was originally introduced by Yalkowsky *et al.* (1), to explain the exponential increase in solubility of poorly water soluble compounds upon the addition of an organic cosolvent to water. They found a number of examples from their own work and the literature in which the solubility data was fit by Eq. 1[3]. Unlike the case of caffeine in water and dioxane, Eq. 1 applies particularly well where the solubility parameter of the solute is 3 or 4 units below that of the organic component of the aqueous solvent. The solubility of *n*-alkyl *p*-aminobenzoates in propylene glycol–water mixtures and in several pure solvents has been investigated (9). Figure 2 was prepared using data on the solubility of ethyl *p*-aminobenzoate in binary as well as individual solvents. Mole fraction solubility is plotted against the solvent solubility parameter in Fig. 2 as done in studies involving the extended Hildebrand approach (3–5). The regular solution line is plotted in Fig. 2 to show the curve on which the experimental points would fall if these polar solute–solvent systems followed regular solution behavior at 25°. The regular solution line is calculated using the expression:

$$-\log X_2 = -\log X^i + A(\delta_1 - \delta_2)^2 \qquad \text{(Eq. 13)}$$

where all terms have been defined in earlier equations. The regular solution solubility reaches a peak value at a solubility parameter equal to that of the solute [δ_2 = 12.05 (cal/cm^3)$^{1/2}$]; the mole fraction solubility at this point has the ideal value, X^i = 0.2404, for ethyl *p*-aminobenzoate at 25°. At 37° it is 0.3236 ($-\log X^i_{37°}$ = 0.4900).

It is observed that solutions of ethyl *p*-aminobenzoate in the individual solvents are not regular solutions since they do not lie on the bell-shaped regular solution curve in Fig. 2. The solubility in most of the solvents falls below the ideal solubility line, $X^i_{25°}$ = 0.2404, and this indicates that ethyl

[2] In Ref. 4 the volume fraction of water was referred to as ϕ_w. It was used in place of f_D and this led to a polynomial expression different from Eq. 9, but both expressions result in the same calculated solubilities.

[3] A recent report (11) states that a number of semipolar drugs exhibit parabolic rather than linear log solubility *versus* cosolvent composition curves.

Table I—Regression Equations for Drugs in Binary Solvents Using the Log Linear and The Extended Hildebrand Approaches [a]

Mixture	Regression Equation	Log Linear and Log Quadratic Approach: Log mole Fraction of Solute *versus* Volume Fraction of Cosolvent	Extended Hildebrand Solubility Approach: Log α_2/A *versus* Solubility Parameter of Solvent
Ethyl *p*-aminobenzoate in propylene glycol–water $n = 6$, ${}^{a}F_{(1,4,0.05)} = 7.71$ ${}^{b}F_{(1,3,0.05)} = 10.1$ ${}^{c}F_{(2,3,0.05)} = 9.55$	Linear	$\log X_2 = -3.7861\ (\pm 0.0585) + 2.5359\ (\pm 0.0965)\ f$ $R^2 = 0.9942, s = 0.0808, F = 690^{a}$ (Eq. 14*a*)	$\frac{\log \alpha_2}{A} = -32.0622\ (\pm 1.5389) + 2.7418\ (\pm 0.0792)\ \delta_1$ $R^2 = 0.9967, s = 0.5603, F = 1199^{a}$ (Eq. 18*a*)
	Quadratic	$\log X_2 = -3.7319\ (\pm 0.0667) + 2.1296\ (\pm 0.3136)\ f + 0.4062\ (\pm 0.3010)\ f^2$ $R^2 = 0.9964, s = 0.0736$, overall $F = 417^{c}$ for f term, $F = 46.1^{b}$ for f^2 term, $F = 1.8^{b}$ (Eq. 14*b*)	$\frac{\log \alpha_2}{A} = -37.7097\ (\pm 13.0647) + 3.3430\ (\pm 1.3817)\ \delta_1 - 0.0156\ (\pm 0.0359)\ \delta_1{}^2$ $R^2 = 0.9969, s = 0.6274$, overall $F = 478^{c}$ for δ_1 term, $F = 5.9^{b}$ for δ_1^2 term, $F = 0.2^{b}$ (Eq. 18*b*)
Sulfadiazine in dimethylformamide–water $n = 14$, ${}^{d}F_{(1,12,0.04)} = 4.75$ ${}^{e}F_{(1,11,0.05)} = 4.84$ ${}^{f}F_{(2,11,0.05)} = 3.98$	Linear	$\log X_2 = -5.419\ (\pm 0.0234) + 4.2132\ (\pm 0.0483)\ f$ $R^2 = 0.9984, s = 0.0644, F = 7620^{d}$ (Eq. 15*a*)	$\frac{\log \alpha_2}{A} = -48.1326\ (\pm 1.4470) + 3.0574\ (\pm 0.0721)\ \delta_1$ $R^2 = 0.9934, s = 1.1105, F = 1796^{d}$ (Eq. 19*a*)
	Quadratic	$\log X_2 = -5.4279\ (\pm 0.0275) + 4.3429\ (\pm 0.2057)\ f - 0.1438\ (\pm 0.2213)\ f^2$ $R^2 = 0.9985, s = 0.0661$, overall $F = 3627^{f}$ for f term, $F = 446^{e}$ for f^2 term, $F = 0.4^{e}$ (Eq. 15*b*)	$\frac{\log \alpha_2}{A} = -67.1701\ (\pm 7.8444) + 5.2625\ (\pm 0.8997)\ \delta_1 - 0.0603\ (\pm 0.0245)\ \delta_1{}^2$ $R^2 = 0.9957, s = 0.9320$, overall $F = 1278^{f}$ for δ_1 term, $F = 34.2^{e}$ for δ_1^2 term, $F = 6.0^{e}$ (Eq. 19*b*)
Methylparaben in formamide–water $n = 10$, ${}^{g}F_{(1,8,0.05)} = 5.32$ ${}^{h}F_{(1,7,0.05)} = 5.59$ ${}^{i}F_{(2,7,0.05)} = 4.74$	Linear	$\log X_2 = -3.5757\ (\pm 0.0128) + 2.7342\ (\pm 0.0615)\ f$ $R^2 = 0.9960, s = 0.0230, F = 1979^{g}$ (Eq. 16*a*)	$\frac{\log \alpha_2}{A} = -145.0176\ (\pm 3.8840) + 7.4243\ (\pm 0.1706)\ \delta_1$ $R^2 = 0.9958, s = 0.2583, F = 1893^{g}$ (Eq. 20*a*)
	Quadratic	$\log X_2 = -3.6009\ (\pm 0.0086) + 3.2824\ (\pm 0.1213)\ f - 1.5847\ (\pm 0.3379)\ f^2$ $R^2 = 0.9990, s = 0.0121$, overall $F = 3599^{i}$ for f term, $F = 733^{h}$ for f^2 term, $F = 22^{h}$ (Eq. 16*b*)	$\frac{\log \alpha_2}{A} = 439.6364\ (\pm 105.2084) - 43.9957\ (\pm 9.2520)\ \delta_1 + 1.1301\ (\pm 0.2033)\ \delta_1{}^2$ $R^2 = 0.9992, s = 0.1187$, overall $F = 4498^{i}$ for δ_1 term, $F = 22.6^{h}$ for δ_1^2 term, $F = 30.9^{h}$ (Eq. 20*b*)
Methylparaben in dimethylformamide–water $n = 10$, ${}^{j}F_{(1,9,0.05)} = 5.32$ ${}^{k}F_{(1,7,0.05)} = 5.59$ ${}^{l}F_{(2,7,0.05)} = 4.74$	Linear	$\log X_2 = -3.607\ (\pm 0.0192) + 5.2419\ (\pm 0.0621)\ f$ $R^2 = 0.9989, s = 0.0326, F = 7123^{j}$ (Eq. 17*a*)	$\frac{\log \alpha_2}{A} = -89.4833\ (\pm 1.1243) + 5.0712\ (\pm 0.0546)\ \delta_1$ $R^2 = 0.9991, s = 0.3247, F = 8623^{j}$ (Eq. 21*a*)
	Quadratic	$\log X_2 = -3.5917\ (\pm 0.0245) + 5.0020\ (\pm 0.2457)\ f + 0.4927\ (\pm 0.4882)\ f^2$ $R^2 = 0.9995, s = 0.0326$, overall $F = 3570^{l}$ for f term, $F = 415^{k}$ for f^2 term, $F = 1.0^{k}$ (Eq. 17*b*)	$\frac{\log \alpha_2}{A} = -121.4289\ (\pm 12.3283) + 8.1844\ (\pm 1.1922)\ \delta_1 - 0.0752\ (\pm 0.0290)\ \delta_1{}^2$ $R^2 = 0.9995, s = 0.2477$, overall $F = 7412^{l}$ for δ_1 term, $F = 46.6^{k}$ for δ_1^2 term, $F = 6.7^{k}$ (Eq. 21*b*)

[a] The statistical parameters with each regression equation are n, the number of solvent mixtures used; R^2, the squared multiple correlation coefficient; s, the standard deviation of the sample; F, the Fisher F ratio, and the tabular value of F with degrees of freedom k and n-k-l at the 95% level. The value, k, is the number of independent variables in the equation. The F values in Column 1 are tabular Fisher ratios. ${}^{a}F$ values in Columns 3 and 4 are to be compared with the tabular ${}^{a}F$ value; likewise for ${}^{b}F, \ldots, {}^{e}F$.

Table II—Mole Fraction Solubilities of Ethyl *p*-Aminobenzoate at 37° in Propylene Glycol–Water Mixtures [a]

Propylene Glycol, %	δ_1 [b]	A [c]	Log α_2	$\frac{\text{Log } \alpha_2}{A}$	$X_{2_{obs}} \times 10^4$	$X_{2_{calc}} \times 10^4$ Linear Eq. 18*a*	$X_{2_{calc}} \times 10^4$, Quadratic Eq. 18*b*
0	23.45	0.1013	3.244	32.020	1.845	1.757	1.810
20	21.74	0.1011	2.839	28.080	4.688	5.278	5.218
40	20.07	0.1002	2.230	22.255	19.055	16.175	15.679
60	18.37	0.0990	1.847	18.657	46.026	49.870	48.389
80	16.68	0.0949	1.338	14.099	148.59	163.16	161.73
100	14.99	0.0775	0.671	8.658	690.24	645.06	661.48

[a] Reference 9; solubilities, $X_{2_{calc}}$, obtained with the extended Hildebrand solubility approach, Eqs. 18*a* and *b*; $-\log X_2^1 = 0.49000$, $\delta_2 = 12.05$, $V_2 = 144$. [b] Solvent solubility parameter, $(cal/cm^3)^{1/2}$. [c] Equation 6.

p-aminobenzoate is not highly solvated. By contrast, ethyl *p*-aminobenzoate associates strongly with *N*,*N*-dimethylformamide (Point 2 in Fig. 2), producing a solubility ($X_2 = 0.4260$) above the ideal solubility line. The point for ethyl *p*-aminobenzoate in propylene glycol at 37° (Point 9) lies slightly to the right of the regular solution curve which was drawn for solutions at 25°.

The discussion of the solubility parameter of the compound ($\delta_2 = 12.05$) and the regular solution line is also important for the treatment to follow. However, the current report is a study dealing with mixed solvent systems and attention is drawn to the propylene glycol–water mixtures in Fig. 2. One observes that the data points for the solubility of ethyl *p*-aminobenzoate in mixtures of water and propylene glycol (at 37°) lie alongside the 25° regular solution line. On this scale, solubility in water (Point 10) and in 20% propylene glycol (bottom scale) are imperceptible. The points rise to reasonable solubility values for 30–100% propylene glycol solutions. The line passing through the points in Fig. 2 was calculated using the extended Hildebrand solubility approach, Eq. 18a of Table I:

$$\log \alpha_2/A = -37.7097 + 3.3430\delta_1 - 0.0156\delta_1^2$$

Multiplying both sides by A and adding $-\log X^i$ yields:

$$-\log X_{2_{calc}} = 0.4900 + A(-37.7097 + 3.3430\delta_1 - 0.0156\delta_1^2) \quad \text{(Eq. 22)}$$

from which $X_{2_{calc}}$ is obtained.

Since the solubility parameter of propylene glycol ($\delta_1 = 15$) is sufficiently different from that of ethyl *p*-aminobenzoate ($\delta_2 = 12$), the curve in Fig. 2 may be transformed into a linear form by use of the log linear approach. Figure 3 shows the plots for two esters, ethyl and hexyl *p*-aminobenzoate, in propylene glycol–water mixtures at 37° (9).

The linear least-square line through the data is represented in Table I by Eq. 14*a*, and the linear form is compared with a quadratic expression, Eq. 14*b* for the ethyl ester. Although the coefficient of determination is higher for the quadratic, $R^2 = 0.9964$, than for the linear form, $R^2 = 0.9942$, the Fisher F ratio conversely is greater for the linear (690) than for the quadratic (417) expression. Furthermore, the partial F values for introducing f and then f^2 show that f^2 is not significant when its F value, 1.8, is compared with the table value, 10.1, at the 95% level. The log linear fit is, therefore, considered to be satisfactory.

In Table I (Eqs. 18*a* and *b*), the extended Hildebrand solubility approach is shown for a regression of log α_2/A on δ_1 in both linear and quadratic form for the ethyl ester. Again, the F value is significantly larger for the linear than the quadratic, and the partial F values suggest that the quadratic is not as satisfactory as the linear equation. Although the statistical analysis of the hexyl *p*-aminobenzoate in propylene glycol–water mixtures is not included here, the same conclusion was reached in the case of this ester. The comparison of X_2, observed, with X_2, calculated, for the ethyl ester using both the linear and quadratic forms, Eqs. 18*a* and *b*, is found in Table II. These results show the quadratic equation to yield slightly better solubility predictions. But the curves in Fig. 3 for the ethyl and hexyl esters of *p*-aminobenzoate show that differences between the linear and quadratic approaches are insignificant. Since only six data points are available, further statistical testing would not be fruitful.

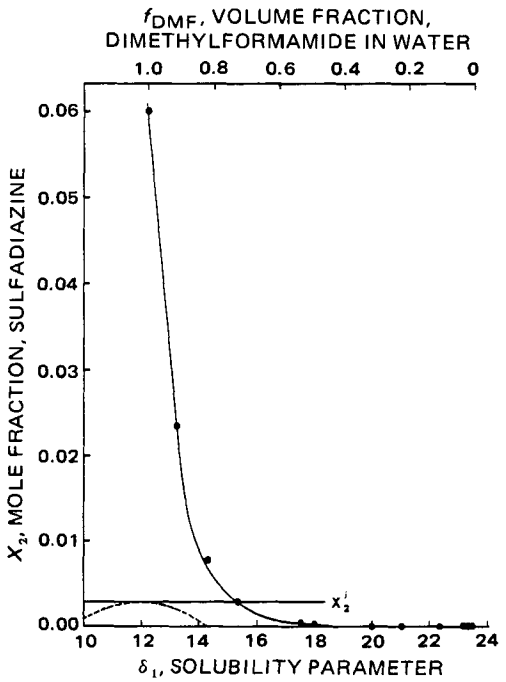

Figure 5—*Mole fraction solubility of sulfadiazine ($X_2^i = 0.0030$) in dimethylformamide–water mixtures at 20° (7). Key: (●) experimental solubility; (---) regular solution curve, Eq. 13; (—) extended Hildebrand line, Eq. 23 (cubic expression).*

Sulfadiazine in Water–Dimethylformamide Mixtures—The solubility of sulfadiazine in mixtures of water ($\delta_1 = 23.45$) and dimethylformamide ($\delta_1 = 12.14$) at 20° has been measured previously (7). The solubility parameter of sulfadiazine is 11.9, as calculated by the Fedors method (12). Yalkowsky *et al.* (1), referred to this study as one which should lend itself to a log linear analysis. The mole fraction solubility and grams of solute per gram of solution at different composition of cosolvent are shown in Fig. 4.

Although the solubility parameter of dimethylformamide is close to that of sulfadiazine, the points do not curve away from linearity as 100% dimethylformamide is approached. Similar results have been found with sulfonamides in dimethylacetamide. Dialkylamides strongly solvate the sulfonamides, and in a series of solvent mixtures, one of which is a dimethylamide, the curve rises to a sharply pointed apex rather than a rounded maximum. This phenomenon may account for the good fit provided by an exponential solubility curve, *i.e.*, a linear fit (Eq. 15*a*, Table I) on a plot of log solubility *versus* volume fraction. Mole fraction solubility is plotted against the solubility parameter, δ_1, of dimethylformamide–water mixtures in Fig. 5, in contrast to the log mole fraction plot of sulfadiazine in Fig. 4. In addition to δ_1, the volume fraction of dimethylformamide (f_{DMF}), in the water–cosolvent mixture is indicated on the horizontal axis (top line of Fig. 5). The extended Hildebrand solubility approach, Eq. 23, was used to plot a curve through the experimental points. The Hildebrand regular solution line, calculated with Eq. 13, is included in the figure to indicate its relationship to the experimental points and the extended Hildebrand line. The regular solution curve is flat rather than peaked as in Fig. 2 because of the scales used in the horizontal and vertical axes. The ideal mole fraction solubility, $X^i = 0.0030$, which corresponds to peak solubility on the regular solution line, is observed to be about one twentieth of the actual solubility of sulfadiazine in dimethylformamide at 20°. The regular solution line does not reproduce the solubility of sulfadiazine in water–dimethylformamide mixtures; whereas the extended Hildebrand solubility equation fits the experimental points well. The regression equation best employed for this purpose is a cubic expression:

$$\log \alpha_2/A_{calc} = -206.441 + 29.7528\delta_1 - 1.45599\delta_1^2 + 0.0258317\delta_1^3 \quad \text{(Eq. 23)}$$

where $n = 14$, $R^2 = 0.9998$, $s = 0.1998$, $F = 18609$, and $F_{(3,10,0.05)} = 3.71$. The linear and quadratic forms, Eq. 19*a* and *b* in Table I, are adequate

Table III—Solubility of Sulfadiazine in Water–Dimethylformamide Mixtures at 20° [a]

f_{DMF}	δ_1 (cal/cm^3)$^{1/2}$	V_1, cm^3/mole	A, cm^3/cal	log α_2	(log $\alpha_{2_{calc}}$)/A [b]	$X_{2_{obs}} \times 10^4$	$X^c_{2_{calc}} \times 10^4$	Residuals, %
0	23.45	18.05	0.12448	2.96185	23.71491	0.0327	0.0334	−2.1
0.005	23.39	18.36	0.12448	2.92739	23.47131	0.0354	0.0359	−1.4
0.01	23.33	18.67	0.12448	2.89891	23.23027	0.0378	0.0384	−1.6
0.02	23.21	19.30	0.12448	2.83592	22.75577	0.0437	0.0440	−0.7
0.03	23.09	19.92	0.12448	2.77743	22.29114	0.0500	0.0503	−0.6
0.05	22.86	21.17	0.12448	2.66751	21.42721	0.0644	0.0644	−0.0
0.10	22.26	24.29	0.12447	2.35255	19.32585	0.1330	0.1177	11.5
0.20	21.07	30.54	0.12444	1.95135	15.69879	0.3350	0.3333	0.5
0.30	19.88	36.81	0.12440	1.57822	12.57256	0.7910	0.8173	−3.3
0.50	17.49	49.32	0.12415	0.86574	6.75256	4.080	4.346	−6.5
0.70	15.18	61.44	0.12252	0.00805	0.05759	29.40	29.468	−0.2
0.78	14.32	65.98	0.11971	−0.41290	−3.09509	77.50	70.293	9.3
0.89	13.18	71.93	0.11182	−0.88909	−8.08018	232.0	239.84	−3.4
1.00	12.14	77.40	0.09609	−1.30320	−13.60746	602.0	608.05	−1.0

[a] Reference 7; back-calculated solubilities $X_{2_{calc}}$ obtained with the extended Hildebrand solubility approach; δ_2 = 11.9 (cal/cm^3)$^{1/2}$; V_2 = 167 cm^3/mole, log X^i_2 = −2.5236. [b] Equation 23, (cubic expression). [c] (log $\alpha_{2_{calc}}$)/A (above) × A (Column 4 above) = log $\alpha_{2_{calc}}$, then log $\alpha_{2_{calc}}$ + 2.5236 = log X_2.

for this purpose but the cubic equation (Eq. 23) is better, as indicated by its R^2, s, and F values. The δ_1 values for the solvent mixtures and the A values are found in Table III together with a comparison of actual solubilities, $X_{2_{obs}}$, and calculated values using the cubic expression, Eq. 23, together with Eq. 3 where log X^i = −2.5236 for sulfadiazine at 20°.

The statistical analyses presented in Table I indicate that the log linear equation (Eq. 19a) provides a satisfactory fit of the data across the range of solvent mixtures from water to pure dimethylformamide. Figure 4 also shows that the linear fit is quite adequate. Therefore, the log linear expression is suitable for sulfadiazine in dimethylformamide–water as well as for ethyl and hexyl p-aminobenzoate in propylene glycol–water mixtures. However, the curve in Fig. 5, where X_2 is plotted against δ_1 (or f_{DMF}), is best fit by a third degree power series (Eq. 23). The residuals (Table III) are surprisingly small when the data is fit with this cubic equation.

Log Linear Equation and Solubilizing Power, σ—In addition to expressing log solubility *versus* volume fraction, Eq. 1, in molar terms (1), Yalkowsky *et al.* (13) used mole fraction concentration:

$$\log X_2 = \log X_w + \sigma f \qquad \text{(Eq. 24)}$$

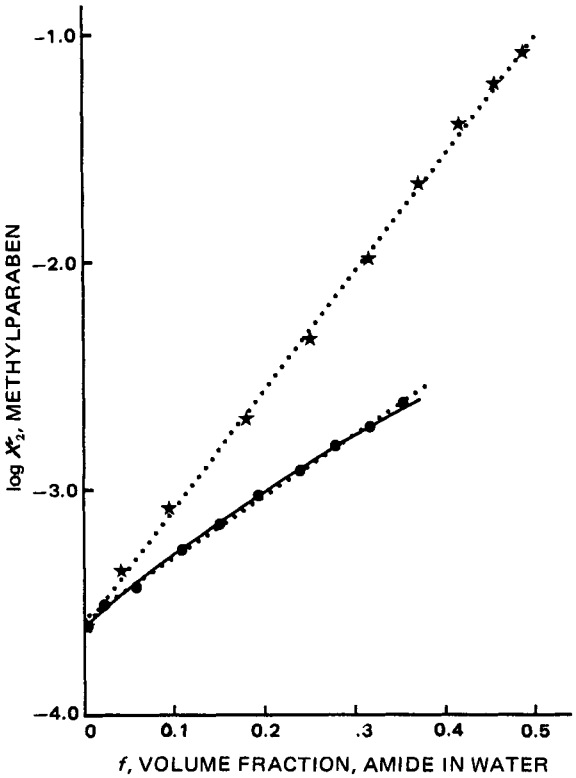

Figure 6—*Log mole fraction solubility of methylparaben in formamide–water (●) and dimethylformamide–water (★) at 25° (8). Key: (—) from Eq. 16b (quadratic); (·····) from Eqs. 16a and 17a using linear regression.*

X_2 is the mole fraction solubility of the solute at a volume fraction f of the cosolvent, X_w is the mole fraction solubility of the solute in water, and σ is a measure of the solubilizing power of the cosolvent for the drug (13). The term σ, which is the slope of the lines represented by Eq. 24, was defined for mixed solvent systems (12) as:

$$\sigma = \frac{C(\gamma_w - \gamma_c)\text{HYSA}}{2.303kT} \qquad \text{(Eq. 25)}$$

where γ_w and γ_c are macroscopic interfacial tensions between a model hydrophobic substance, tetradecane, and water, and between tetradecane and the pure cosolvent, respectively; C is a correction term for the macroscopic surface tensions, accounting for the small radius of curvature at the solute–solvent molecular surface; HYSA is the hydrophobic surface area of the semipolar solute as calculated by a computer program originally written by Hermann (14); k is the Boltzmann constant; and T is the absolute temperature. The value for C should remain relatively constant for various solute-mixed solvent systems, and the value was found to vary within a relatively narrow range, 0.52–0.56, for several systems (13). According to Eq. 25, the value of σ should not change for various compositions of water and cosolvent in a binary solvent mixture, σ being the constant slope of a linear expression, Eq. 24.

According to this interfacial model, it should be possible to calculate solubilities of drugs in polar solvent mixtures using either the linear form of the extended Hildebrand solubility approach:

$$\log X_2 = \log X^i - C_0A + \sigma f \qquad \text{(Eq. 26)}$$

or the log linear expression, Eq. 24, where $\sigma = C_1A$ is defined by Eq. 25.

The interfacial model was tested (8) by determining the solubility of methylparaben (δ_2 = 11) in aqueous systems containing various concentrations of the cosolvents, formamide, methylformamide, and dimethylformamide. Contrary to the requirements of Eq. 25, the σ values were observed to vary in formamide–water from 2.77 to 4.46. For a number of other amide–water cosolvent systems, values for σ varied from 3.40 for acetamide to 6.43 for dimethylpropionamide.

Figure 6 shows the log mole fraction solubility of methylparaben in formamide–water and dimethylformamide–water cosolvent systems. The curve with formamide as the cosolvent is not linear but rather parabolic, and it is well fit by a quadratic expression, Eq. 16b, Table I, of the form:

$$\log X_2 = \log X_w + \sigma f + C_2f^2 \qquad \text{(Eq. 27)}$$

The regression leading to Eq. 16b gives a log mole fraction solubility of methylparaben in water of −3.6009, whereas the experimental value is −3.6091. This is an error of 1.9% in predicting the experimental solubility, X_w = 0.000246, in water, a close estimation using a quadratic expression.

The need for a quadratic equation accounts for a previous inability (8) to obtain a constant value for σ over this range (f = 0.0–0.35) of formamide compositions. Despite the fact that a linear fit of the points produced a regression line with an R^2 of 0.996, visual observation of the curve indicated that σ (Eq. 24) would not be constant over this composition. One would not predict, however, that σ would vary as much as actually found (2.8–4.5). Despite this variability, it is interesting to calculate an average σ, leaving C as an adjustable parameter as suggested previously (13).

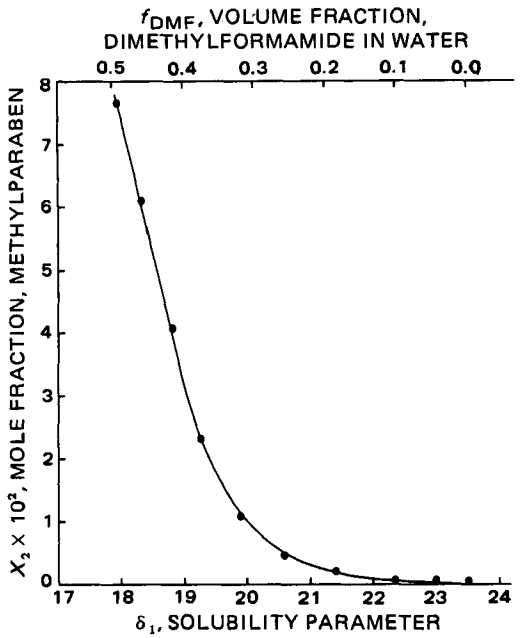

Figure 7—*Mole fraction solubility of methylparaben in dimethylformamide–water at 25° (8). Key: (●) experimental solubility; (—) back calculation curve, Eq. 21b, extended Hildebrand approach.*

The average value of σ in the formamide–water system, obtained from a least-squares linear fit of the curve in Fig. 6 is 2.734 (Eq. 16*a*). Referring to Eq. 25, $\gamma_w = 51.9$ for water–tetradecane and $\gamma_c = 31.2$ for formamide–tetradecane. The hydrophobic surface area of methylparaben is $130A^2$ or 130×10^{-16} cm^2. At 25°, $T = 298.15$°K and the Boltzmann constant equals 1.38×10^{-16} erg molecule^{-1} degree^{-1}. Using Eq. 25, one gets:

$$2.734 = \frac{C(51.9 \text{ erg/cm}^2 - 31.2 \text{ erg/cm}^2)\ 130 \times 10^{-16} \text{ cm}^2}{(2.303)\ (1.38 \times 10^{-16} \text{ erg/molecule deg})\ (298.15 \text{ deg})}$$

$$C \approx 0.9627 \cong 1.0$$

Yalkowsky *et al.*, accepted C values as large as 1.0, but not ordinarily for this kind of system. Considering the approximations, however, this is an acceptable fit.

In Fig. 6, one observes that for methylparaben in dimethylformamide–water, a plot of log X_2 *versus* volume fraction, $f = 0.0$ to $f = 0.5$, of the cosolvent appears to be linear. Here, the R^2 for linear and quadratic functions (Table I, Eqs. 17*a* and *b*) differ little. The partial F values show that the quadratic term is unnecessary. The volume fraction of dimethylformamide has been carried only to $f = 0.5$ in previous work (8) as observed in Fig. 6. However, the line probably becomes markedly curved at higher volume fractions of cosolvent, and Eqs. 17*a* and *b* can no longer be used here. This can be observed by setting $f = 1.0$, *i.e.*, 100% methylformamide, in Eqs. 17*a* and *b*, resulting in X_2 values greater than unity, which is not possible. Therefore the solubility of methylparaben in dimethylformamide–water can be considered log linear only to $f = 0.5$.

Both the linear and quadratic equations (Eqs. 17*a* and *b*, respectively) have a constant, equivalent to log X_w, of ~−3.60 (−3.607 for linear and −3.592 for quadratic) or $X_w = 0.000251$. The slope of the line, identified as σ, is ~5.2 (5.24 for linear and 5.0 for quadratic). Using Eq. 25 to calculate C, with γ_c for dimethylformamide–tetradecane equal to 4.6, one obtains at 25° in the range of $f = 0.0$–0.5:

$$5.2 = \frac{C(51.9 - 4.6)130 \times 10^{-16}}{(2.303)(1.38 \times 10^{-16})(298.15)}$$

$$C = (5.2/6.49) = 0.80$$

Although C is ordinarily considered to have a value of ~0.35–0.55, a value of 0.8 is not unreasonable.

The solubility equation suggested by Yalkowsky *et al.* (13):

$$\log S = \log S_w + \frac{C(\gamma_w - \gamma_c)\text{HYSA}}{2.303kT} \times f \qquad \text{(Eq. 28)}$$

should therefore provide a satisfactory approach for calculating the solubility of relatively hydrophobic drugs in water–cosolvent systems. The interfacial treatment is predicated on this log linear relationship between drug solubility and cosolvent volume fraction. If, however, the solubility parameter of the solute is similar to that of the cosolvent or is between the δ_1 value of the cosolvent and water, the points on the parabolic curve may be in a region of significant curvature; then the log linear equation and the interfacial model, involving σ, will not apply. On the other hand, the extended Hildebrand solubility approach handles drugs in polar and nonpolar solvent systems, whether the drug's solubility parameter is greater than, less than, or lies between the solubility parameters of a solvent pair, such as water and dimethylformamide. The following example demonstrates the use of the linear form of the extended Hildebrand solubility approach.

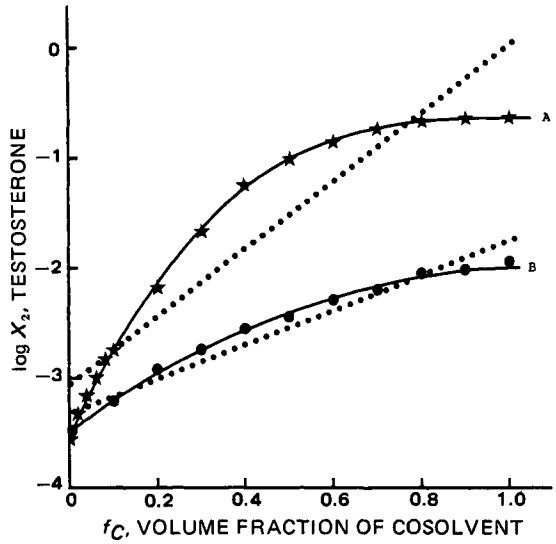

Figure 8—*Log mole fraction solubility of testosterone in chloroform–cyclohexane (★); and in isopropyl myristate–cyclohexane (●) at 25°. Key: (·····) linear regression line; (—) regression lines, (A) cubic, (B) quadratic.*

The solubility X_2 of methylparaben in dimethylformamide–water mixtures $\delta_1 = 18$ ($f = 0.5$) to $\delta_1 = 23.5$ ($f = 0.0$), from previous works (8) is shown in Fig. 7. The extended Hildebrand equation used to obtain the calculated line for these data may be linear, Eq. 21*a*, or quadratic, Eq. 21*b* of Table I. The statistical parameters show these equations to be equivalent. The A values range from 0.058 in pure dimethylformamide to 0.087 in water. The $-\log X^i = 1.0051$. At a volume fraction of dimethylformamide of 0.37, $\delta_1 = 19.28$ and $A = 0.0777$. Equation 21*a* yields log $\alpha_2/A = 8.2894$ and Eq. 21*b* gives log $\alpha_2/A = 8.4131$ for this mixture. When multiplied by A, the results from Eq. 21*a* gives log $\alpha_2 = 0.6441$. This value is added to $-\log X^i$ to obtain 1.6492. Changing the sign and taking the antilog results in $X_{\text{methylparaben}} = 0.0224$. The observed value is 0.0221. The percent error in the back calculation is thus 1.5%.

Nonpolar Cosolvent Systems—In contrast to water–cosolvent systems, it is interesting to consider nonpolar solvent mixtures having solubility parameters lower than the solubility parameters of the solute. An investigation to be published (15) involves a study of the solubility of testosterone ($\delta_2 = 10.9$) and testosterone propionate ($\delta_2 = 9.5$) in cyclohexane ($\delta_1 = 8.2$) with cosolvents such as chloroform ($\delta_1 = 9.1$), ethyl oleate ($\delta_1 = 8.6$), and isopropyl myristate ($\delta_1 = 8.9$). It was found that the log linear relationship did not hold in these systems. Even chloroform, which strongly solvates the steroidal solutes, did not produce a log linear plot. As observed in Fig. 8, the lines are markedly curved when plotted as log X_2 against the volume fraction of the cosolvent. Least-square straight lines are included, but statistical analysis is not needed to show that the experimental data yield nonlinear curves.

A report on benzoic acid in various proportions of hexane and ethyl acetate (16) was also studied for possible log linear characteristics. The solubility parameter of benzoic acid, 11.5, is greater than either hexane, 7.3, or ethyl acetate, 8.9. A plot of log X_2 *versus* volume fraction of the cosolvent, ethyl acetate, in the solvent mixture showed considerable curvature. The line was well fitted by a quadratic equation of the extended Hildebrand approach but not by the log linear form.

Ternary Solvent Systems—In recent work (17), the solubility of four sulfonamides has been determined in a ternary solvent consisting of dimethylacetamide ($\delta_1 = 11.1$), glycerin ($\delta_1 = 17.7$), and water ($\delta_1 = 23.5$). Two compounds of lower solubility in dimethylacetamide, namely sulfadiazine ($\delta_2 = 13.2$) and sulfisomidine ($\delta_2 = 12.6$), produced nearly

straight lines when log X_2 was plotted against the solubility parameter of the ternary solvent[4]. Two compounds of generally greater solubility, sulfathiazole (δ_2 = 13.1) and sulfamethoxazole (δ_2 = 11.6), produced highly curved lines which require quadratic or higher power series equations to fit the points. The solubility parameters of the drug molecules in these systems fall between the δ_1 values of the highly polar solvents, glycerin and water, and the strongly solvating aprotic solvent, dimethylacetamide. The curves show no peaks, but rather rise to a maximum mole fraction solubility in pure dimethylacetamide.

CONCLUSIONS

It may be concluded that the log linear solubility relationship, *i.e.*, log solubility *versus* volume fraction of cosolvent (Eq. 1) as introduced by Yalkowsky *et al.* (1), gives a good linear fit for semipolar drugs in a number of water–cosolvent mixtures, particularly when the solubility parameter of the solute is ~3 solubility parameter units lower than that of the cosolvent of a water–cosolvent mixture. When the cosolvent, such as dimethylformamide, is a strong solvating agent for the solute, sulfadiazine, a straight line function may persist up to 100% cosolvent even though the solubility parameters of drug and cosolvent are quite similar (<2 or 3 δ units apart).

For a system, caffeine, in an ordinary solvent pair, such as water and dioxane, or for theophylline in a moderately solvating mixture, such as water and polyethylene glycol 400 (5), the solubility parameter of the drug lies between the values of water and the cosolvent. Then, the log linear expression may be applied only over a limited range of solvent mixtures on either side of the solubility parameter of the solute. For example, the plot of log solubility *versus* volume fraction in a caffeine solution in water and dioxane was shown to be linear in dioxane from 0 to 30% and nearly linear in water from perhaps 0 to 10%. The log linear expression could not reproduce the solubility data for caffeine over the central range from 30 to 90% dioxane where the curve rises to an apex then falls as the solvent composition approaches pure dioxane.

In some systems, which might be predicted to follow the log linear relationship, a straight line function is not satisfactory but a higher order function, such as a quadratic or cubic in δ_1 or volume fraction provides a fit to the experimental data points. Systems of nonpolar solvents, *e.g.*, cyclohexane, in conjunction with cosolvents such as chloroform, isopropyl myristate, and ethyl acetate have not been found, in limited studies, to yield log linear relationships. These solutions, like more polar ones, are satisfactorily reproduced by use of quadratic, cubic, or quartic equations employed in the extended Hildebrand solubility approach. Ternary solvent systems, both polar and nonpolar, are under study.

It was found possible to derive the log linear equation from the extended Hildebrand solubility approach, thus providing a quasitheoretical foundation for the log linear equation based on solubility parameters.

[4] Volume fraction is not appropriate as the independent variable in a ternary solvent system, but solubility parameter of the solvent mixture may be used instead.

REFERENCES

(1) S. H. Yalkowsky, G. L. Flynn, and G. L. Amidon, *J. Pharm. Sci.*, **61**, 983 (1972).

(2) S. H. Yalkowsky and G. L. Flynn, *ibid.*, **63**, 1276 (1974).

(3) A. Martin, J. Newburger, and A. Adjei, *ibid.*, **69**, 487 (1980).

(4) A. Adjei, J. Newburger, and A. Martin, *ibid.*, **69**, 659 (1980).

(5) A. Martin, A. N. Paruta, and A. Adjei, *ibid.*, **70**, 1115 (1981).

(6) J. H. Hildebrand and R. L. Scott, "The Solubility of Nonelectrolytes," 3rd ed., Dover, New York, N.Y., 1964.

(7) P. H. Elworthy and H. E. C. Worthington, *J. Pharm. Pharmacol.*, **20**, 830 (1968).

(8) R. E. Lindstrom, *J. Pharm. Sci.*, **68**, 1141 (1979).

(9) S. H. Yalkowsky, G. L. Amidon, G. Zografi, and G. L. Flynn, *ibid.*, **64**, 48 (1975).

(10) N. H. Nie, C. H. Hull, J. G. Jenkins, K. Steinbrenner, and D. H. Bent, SPSS, Statistical Package for the Social Sciences, 2nd ed., McGraw-Hill, New York, N.Y., 1975.

(11) S. H. Yalkowsky and T. J. Rosemann, in "Techniques of Solubilization of Drugs," chap. 3, S. H. Yalkowsky, Ed., Dekker, New York, N.Y., 1981.

(12) R. F. Fedors, *Polymer. Eng. Sci.*, **14**, 147 (1974).

(13) S. H. Yalkowsky, S. C. Valvani, and G. L. Amidon, *J. Pharm. Sci.*, **65**, 1488 (1976).

(14) R. B. Hermann, *J. Phys. Chem.*, **76**, 2754 (1972).

(15) A. Martin, P. L. Wu, A. Adjei, M. Mehdizadeh, K. C. James, and C. Metzler, *J. Pharm. Sci.*, in press.

(16) M. J. Chertkoff and A. Martin, *J. Am. Pharm. Assoc., Sci. Ed.*, **49**, 444 (1960).

(17) S. T. Valesquez-Leon, Thesis, University of Texas, May, 1981.

ACKNOWLEDGMENTS

Support for the study was obtained in part from the professorship provided to A. Martin by Coulter R. Sublett.

The authors thank Alan Beerbower Energy Center, University of California at San Diego, for advice and assistance.

Effects of 3-Chloromethylthiochromone-1,1-dioxide on Nucleic Acid, Protein, and Aerobic and Anaerobic Metabolism of Ehrlich Ascites Tumor Cells

MARK H. HOLSHOUSER *, LARRY J. LOEFFLER, and IRIS H. HALL ˣ

Received April 22, 1981, from the *Division of Medicinal Chemistry, School of Pharmacy, University of North Carolina at Chapel Hill, Chapel Hill, NC 27514.* Accepted for publication October 6, 1981. *Present address: Division of Medicinal Chemistry, School of Pharmacy, Northeast Louisiana University, Monroe, LA 71209.

Abstract □ 3-Chloromethylthiochromone-1,1-dioxide was observed to be a potent inhibitor of Ehrlich ascites carcinoma growth and a moderate inhibitor of P-388 lymphocytic leukemia growth at 10 mg/kg/day. Preliminary *in vitro* studies showed that the agents significantly inhibited RNA and DNA synthesis in Ehrlich ascites cells. *In vivo* studies after dosing on Days 6, 7, and 8 demonstrated the same reductions in nucleic acid synthesis and a moderate reduction in protein synthesis. The primary site of nucleic acid synthesis, which was blocked by 3-chloromethylthiochromone, was at orotidine monophosphate decarboxylase in the primidine pathway. Other enzymes, in anaerobic and aerobic glycolysis, which were blocked include hexokinase, phosphofructokinase, succinic and α-ketoglutarate dehydrogenases, as well as States 3 and 4 of oxidative phosphorylation.

Keyphrases □ 3-Chloromethylthiochromone-1,1-dioxide—effect on nucleic acid, protein, aerobic and anaerobic metabolism of Ehrlich ascites tumor cells □ Metabolism—aerobic and anaerobic, effects of 3-chloromethylthiochromone-1,1-dioxide on nucleic acid, protein, Ehrlich ascites tumor cells □ RNA—effects of 3-chloromethylthiochromone-1,1-dioxide, Ehrlich ascites tumor cells □ DNA—effects of 3-chloromethylthiochromone-1,1-dioxide, Ehrlich ascites tumor cells

The antitumor activity of compounds containing the 1,4-naphthoquinone ring system has been reported previously. For example, dichloroallylawsone is currently in clinical trials in the United States (1–8). An investigation of sulfone analogs of naphthoquinones was undertaken recently (9), resulting in a series of substituted thiochromones and thiochroman-4-ones and their 1,1-dioxides. The synthesis and physical characteristics were reported previously (9). Certain of these agents were found to be active against the growth of Ehrlich ascites carcinoma and moderately active against P-388 lymphocytic leukemia growth in mice (9). The most potent compound, 3-chloromethylthiochromone-1,1-dioxide (I), afforded 100%

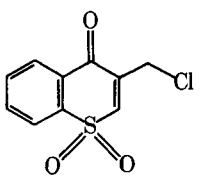

I

Scheme I

inhibition of Ehrlich ascites growth at 10-mg/kg/day dose ip (9). Previously, it has been postulated that certain 1,4-naphthoquinones require bioactivation by reduction of the quinone and subsequent displacement of a leaving group to form the potential alkylating agent (10). However, replacement of one of the naphthoquinone carbonyls with a sulfone group would alter the electronic character as well as the reduction potential of the molecules. The mechanism of action on cellular metabolism of the sulfone analogs may be different from the naphthoquinone; thus, a study of the effects of I on Ehrlich ascites cell metabolism was undertaken and those results are reported.

EXPERIMENTAL

Male CF_1 mice (~30 g) were implanted intraperitoneally on day 0 with 2×10^6 Ehrlich ascites tumor cells. For the anticarcinoma screens, animals were dosed intraperitoneally with compounds from Days 1 to 9. Animals were sacrificed on day 10; the volume of ascites fluid and the packed cell volume (ascitocrit) were determined (11). For the P-388 lymphocytic leukemia screen, BDF_1 male mice (~25 g) were implanted with 10^6 P-388 cells on Day 0. Test compounds were administered from Day 1 to 9 intraperitoneally. The day of death was recorded for both control and treated mice (12).

The metabolic *in vivo* studies were performed after inoculating CF_1 mice (~25 g) with 2×10^6 Ehrlich ascites tumor cells on Day 0. On Days 6, 7, and 8, a 10 mg/kg dose ip of I was administered. On Day 9, the mice were sacrificed and the ascites fluid was removed for *in vivo* biochemical assay. The number of tumor cells per milliliter and the 0.4% trypan blue uptake were determined with a hemocytometer. *In vitro* studies were conducted on Day-9 ascites cells with the drug present at 0.036–0.36 m*M* concentrations.

In vivo incorporation of thymidine into DNA was determined by the method of Chae *et al.* (13). One hour prior to the animal sacrifice on Day 9, 10 μCi of [6-^{3}H]thymidine[1] (24.7 Ci/mmole) was injected intraperitoneally. The DNA was isolated and the tritium content was determined in toluene–octoxynol (2:1), 0.4% of 2,5-diphenyloxazole, and 0.01% of 1,4-bis[2-(5-oxazolyl)]benzene scintillation fluid, and corrected for quenching. The DNA concentration was determined by the diphenylamine reaction using calf thymus DNA as a standard (13).

In vivo uridine incorporation of Ehrlich ascites cells into RNA was determined using 10 μCi of [5,6-^{3}H]uridine (24 Ci/mmole) injected into the animal 1 hr prior to sacrifice. The method of Wilson *et al.* (14) was used to extract RNA. Using yeast RNA as a standard, the RNA was quantitated by the orcinol reaction (14). *In vivo* leucine incorporation into protein was determined by the method of Sartorelli (15) using 10 μCi of [4,5-^{3}H]leucine (24.7 Ci/mmole) injected into the animal 1 hr prior to sacrifice. Extracted protein was determined by the Lowry (16) procedure using bovine albumin as the standard.

In vitro incorporation of [^{3}H]thymidine, [^{3}H]uridine, and [^{3}H]leucine[1] was determined using 10^6 Ehrlich ascites day-9 cells, 1 μCi of labeled precursor, 650 μl of minimum essential medium, and 100 ml of drug (0.36 m*M*) (17). The tubes were incubated at 37° for 60 min and inactivated by trichloroacetic acid. The acid insoluble labeled DNA was filtered on glass filter disks[2] and RNA and protein were filtered on nitrocellulose filters[3] by vacuum suction. Results were expressed as disintegrations per minute of incorporated precursor per hour per 10^6 cells.

In vivo nuclear DNA polymerase activity was determined on isolated Ehrlich ascites nuclei (18) after 3 days of dosing. The incubation medium was that of Sawada *et al.* (19) except that [^{3}H]deoxythymidine triphosphate (14 Ci/mmole) was used. The insoluble nucleic acids were collected on glass fiber filters[2] and counted.

In vivo nuclear RNA polymerase activities of Ehrlich ascites cells were determined with isolated nuclei (18). Messenger, ribosomal, and transfer RNA polymerases were isolated by using different concentrations of

[1] All isotopes were purchased from New England Nuclear and substrates and cofactors were purchased from Sigma or Calbiochem.
[2] Whatman GF/F.
[3] HA 0.45 μm, Millipore Corp.

0022-3549/82/0800-0857$01.00/0

Table I—Incorporation of Radiolabeled Precursors into Ehrlich Ascites Cells *In Vitro* During 1-hr Incubation with 3-Chloromethylthiochromone-1,1-dioxide

	Control	Control, %
[^{3}H]Thymidine Incorporation into DNA	100 ± 2[a]	17 ± 2[d]
[^{3}H]Uridine Incorporation into RNA	100 ± 5[b]	22 ± 4[d]
[^{3}H]Leucine Incorporation into Protein	100 ± 9[c]	88 ± 10

[a] 21,052 dpm/mg of DNA. [b] 37,651 dpm/mg of RNA. [c] 18,264 dpm/mg of protein. [d] $p \leq 0.001$.

ammonium sulfate in magnesium chloride (20). The incubation medium was that of Anderson *et al.* (20, 21) using [^{3}H]uridine triphosphate (23.2 Ci/mmole). Insoluble RNA was collected on nitrocellulose filters[3] and counted.

In vivo deoxythymidine and deoxythymidylate monophosphate and diphosphate kinase activities of Ehrlich ascites cells were measured spectrophotometrically at 340 nm for 20 min using 0.1 μmole of reduced nicotinamide adenine dinucleotide (22).

In vivo carbamyl phosphate synthetase activity of Ehrlich ascites cells was determined, using the reaction medium of Kalman *et al.* (23), in the presence of ornithine and ornithine transcarbamylase. Citrulline, formed from ornithine, was measured at 490 nm by the method of Archibald (24). *In vivo* aspartate transcarbamylase activity was assayed using the incubation medium of Kalman *et al.* (23). Colorimetric determination of carbamyl aspartate was carried out by the procedure of Koritz and Cohen (25). *In vivo* orotidine monophosphate decarboxylase activity was assayed by the method of Appel (26) using 0.1 μCi of [^{14}C]orotidine monophosphate (34.9 mCi/mmole). The [^{14}C]carbon dioxide generated in 15 min was trapped in potassium hydroxide[4] and counted. *In vitro* studies of orotidine monophosphate decarboxylase activity were conducted over the range of 0.036–0.36 mmole concentration of drug for 15 min. *In vivo* thymidylate synthetase activity of Ehrlich ascites cells was determined using a postmitochondrial (9000×*g* for 10 min) supernate and 5 μCi of [5-^{3}H]deoxyuridine monophosphate (11 Ci/mmole) according to the method of Kampf *et al.* (27). [^{14}C]Formate incorporation into purine of Ehrlich ascites cells was determined by the method of Spassova *et al.* (28) using 0.5 μCi of [^{14}C]formic acid (4.95 mCi/mmole). Purine was separated on silica gel TLC plates eluted with *n*-butanol–acetic acid–water (4:1:5). After identifying R_f values consistent with the standards, adenine and guanine, the plates were scraped and the radioactive content determined. Phosphoribosyl-1-pyrophosphate amidotransferase activity of Ehrlich ascites cells was determined on a supernate at 600×*g* for 10 min, measuring the reduction of 0.6 μmole of oxidized nicotinamide adenine dinucleotide at 340 nm for 30 min (29).

In vivo inosinic acid dehydrogenase activity of Ehrlich ascites cells was determined spectrophotometrically at 340 nm for 30 min using a supernatant fraction (600×*g* for 10 min). The assay medium was that of Magasanik (30) which contained nicotinamide adenine dinucleotide. *In vivo* dihydrofolate reductase activity of Ehrlich ascites cells was determined at 340 nm for 30 min as the oxidation of reduced nicotinamide adenine dinucleotide phosphate (31).

In vivo ribonucleotide reductase activity of Ehrlich ascites cells was determined by the method of Moore and Hurlbert (32) using [5-^{3}H]cytidine-5′-diphosphate (25 Ci/mmole). Ribose and deoxyribose nucleotides were separated on polyethyleneiminecellulose F plastic precoated TLC plates eluted with 4% boric acid–4 *M* LiCl (4:3) and scraped at the R_f values consistent with the standard deoxycytidine diphosphate.

In vivo phosphorylation of histones of Ehrlich ascites cells was determined by injecting 10 μCi of [γ-^{32}P]ATP (18.8 Ci/mmole) into mice 1 hr prior to sacrifice. The nuclei were isolated (17) and the histone chromatin proteins were extracted by the method of Raineri *et al.* (33). *In vivo* nonhistone protein phosphorylation dependent on nuclear protein kinase was determined using 2 nmoles of [γ-^{32}P]adenosine triphosphate (27 Ci/mmole) and isolated nuclei chromatin protein was collected on nitrocellulose filters (34). *In vivo* cyclic 3′,5′-adenosine monophosphate levels of Ehrlich ascites cells were determined by the radioimmunoassay method of Steiner *et al.* (35) using a commercial kit[5].

In vivo deoxyribonuclease (36), ribonuclease, and cathepsin (37) lysosomal enzymatic activities of Ehrlich ascites cells were determined using DNA, RNA, and azocasein as substrates, respectively. Bound acid hydrolytic enzymes were released using the detergent, octoxynol-100[6], pretreatment. Both free and total enzyme activities were observed by measuring nucleotides and aromatic peptide fragments which were determined at 260 and 280 nm, respectively. UV binding studies (38) were conducted *in vitro* with drug (0.36 m*M*) and DNA (35 μg/ml) in phosphate buffer, pH 7.2, over the 200–340 nm range for 24 hr at room temperature.

Table II—*In Vivo* Effects of 3-Chloromethylthiochromone-1,1-dioxide on Nucleic Acid and Protein Metabolism of Ehrlich Ascites Cells[a]

Parameter	Control, % Control	Control, % Treated
[^{3}H]Thymidine incorporation into DNA	100 ± 16	23 ± 15[b]
[^{3}H]Uridine incorporation into RNA	100 ± 9	23 ± 5[b]
[^{3}H]Leucine incorporation into protein	100 ± 13	50 ± 5[b]
Number of cells per milliliter of ascites fluid	100 ± 9	28 ± 8[b]
DNA polymerase	100 ± 10	94 ± 14
Messenger RNA polymerase	100 ± 13	93 ± 10
Ribosomal RNA polymerase	100 ± 6	91 ± 22
Transfer RNA polymerase	100 ± 14	125 ± 17
Thymidine kinase	100 ± 3	94 ± 10
Thymidylate monophosphate kinase	100 ± 8	103 ± 6
Thymidylate diphosphate kinase	100 ± 12	84 ± 5
Carbamyl phosphate synthetase	100 ± 7	145 ± 15[b]
Aspartate transcarbamylase	100 ± 9	116 ± 5
Orotidine monophosphate decarboxylase	100 ± 9	25 ± 4[b]
Thymidylate synthetase	100 ± 10	104 ± 11
[^{14}C]Formate incorporation into purine	100 ± 9	91 ± 7
Phosphoribosyl pyrophosphate amidotransferase	100 ± 8	93 ± 7
Inosinic acid dehydrogenase	100 ± 16	137 ± 6
Dihydrofolate reductase	100 ± 17	119 ± 33
Ribonucleotide reductase	100 ± 12	99 ± 10
Phosphorylation of histone proteins	100 ± 18	82 ± 3
Phosphorylation of nonhistone proteins	100 ± 10	183 ± 15[b]
Cyclic adenosine monophosphate levels	100 ± 6	148 ± 8[b]
Deoxyribonuclease	100 ± 11	118 ± 3
Ribonuclease	100 ± 4	109 ± 3
Cathepsin	100 ± 19	97± 13

[a] $n = 6$. [b] $p \leq 0.001$.

An *in vitro* method (39) was used to determine if the drug was an initiation or an elongation protein synthesis inhibitor of Ehrlich ascites cells by comparison with the standards, pyrocatechol violet and emetine, using 1 μCi of [^{3}H]leucine (24.7 Ci/mmole). The reaction medium was spotted on filter paper disks[7], which were treated for 10 min in boiling 5% trichloroacetic, for 10 min in cold 5% trichloroacetic; and washed with cold 5% trichloroacetic acid, ether–ethanol (1:1) ether; and counted (32).

In vitro and *in vivo* oxidative phosphorylation studies (40) were conducted on Ehrlich ascites cells and the liver homogenates[8] of tumor-bearing mice with the substrates, α-ketoglutarate or succinate. Basal oxygen consumption (State 4) was determined with an oxygen electrode connected to an oxygraph. Adenosine diphosphate was then added to obtain State 3 or stimulated respiration. The number of microlites of oxygen per hour per milligram of protein for States 3 and 4 were calculated. The following glycolytic and Krebs cycle enzymatic activities were determined spectrophotometrically: hexokinase (41), phosphofructokinase (42), lactic dehydrogenase (43), succinic dehydrogenase (44), α-ketoglutarate dehydrogenase, and malic dehydrogenase (45). To be consistent in the expression of data for the spectral enzyme studies, a unit of enzyme activity is defined as that quantity of activity giving a change in absorbance of 0.001/min under the condition of the assay. Protein for the enzymatic assay was determined by the Lowry technique (16).

Probable (p) significant differences were determined by Student's t test. Data are expressed in Tables I–VI as percent of the control with standard deviation (n equals the number of animals per group).

RESULTS

Compound I was shown to have 100% inhibition of Ehrlich ascites tumor growth at a 10 mg/kg ip dose. Doses of 20 and 30 mg/kg were found to be less active, *i.e.*, 25 and 18% inhibition, respectively. In the P-388 lymphocytic leukemia screen, I at 10 mg/kg/day intraperitoneally was marginally active at T/C% = 130 (Table VII). After dosing with the agent on days 6, 7, and 8, the cell count per milliliter of Ehrlich ascites fluid was reduced from 226 × 10^6 to 63 × 10^6. The *in vitro* incorporation studies

[4] Hyamine Hydroxide, New England Nuclear.
[5] Becton Dickinson radioimmunoassay kit, Iodine 125.
[6] Research Products International Corp.
[7] Whatman number 3.
[8] Homogenates (10%) in 0.25 *M* sucrose + 0.001 *M* ethylenediaminetetraacetic acid.

Table III—The *In Vitro* Effects of 3-Chloromethylthiochromone-1,1-dioxide on Orotidine Monophosphate Decarboxylase Activity in Ehrlich Ascites Cells

Control Treated *in vitro* concentration, m*M*	Control, %
	100 ± 8[a]
.036	86 ± 7
.090	84 ± 5
.180	68 ± 7
.360	44 ± 6

[a] $p \leq 0.001$.

(Table I) demonstrated, using 10^6 cells collected from 9-day Ehrlich ascites animals, that thymidine incorporation into DNA was reduced 83%, and uridine incorporation into RNA was reduced 78%. The *in vivo* thymidine incorporation into DNA for the control was 95,970 dpm/mg, which was reduced 77% by drug administration for 3 days. *In vivo* uridine incorporation into RNA for the untreated animals was 198,200 dpm/mg of RNA, which was reduced 77% by drug therapy. *In vivo* leucine incorporation into protein for the control was 37,946 dpm/mg of protein, which was reduced 50% in the treated animals.

The DNA and RNA polymerase activities were not altered by drug administration. The control values were 45,734 dpm/mg of nuclear protein for DNA polymerase, 6434 dpm/mg for mRNA polymerase, 7340 dpm/mg for rRNA polymerase, and 8254 dpm/mg of nuclear protein for tRNA polymerase. The activity for thymidine kinase was 8.90 enzyme units/mg of protein, thymidine monophosphate kinase was 8.65 enzyme units/mg of protein, and thymidine diphosphate kinase activity was 5.60 enzyme units/mg of protein. Drug treatment did not alter the activities of the kinases except for the diphosphate which was inhibited by 16%. Carbamyl phosphate synthetase activity for the control resulted in the formation of 0.117 mg of citrulline formed/hr/mg of protein, and aspartate transcarbamylase activity resulted in 0.81 mg of carbamyl aspartate formed per hour per milligram of protein. Drug administration resulted in an increase of 45% in carbamyl phosphate synthetase and 16% in aspartate transcarbamylase activities.

In vivo orotidylic monophosphate decarboxylase activity for the control was 26,298 dpm of [^{14}C]carbon dioxide produced/hr/mg of protein, which was reduced 75% by 3 days of drug treatment. *In vitro* orotidylic monophosphate decarboxylase activity was reduced significantly: 56%, by 0.36 m*M* concentration of drug (Table V). *In vivo* thymidylate synthetase activity for normal animals was 103,308 dpm of [^{3}H]thymidine formed hr/mg of protein, which was unchanged by drug therapy. *In vivo* [^{14}C]-formate incorporation into purines for the control was 10,788 dpm of purines/hr/mg of protein. *In vivo* phosphoribosyl pyrophosphate amidotransferase activity for normal cells was 376 enzyme units/mg of protein. *In vivo* inosinic monophosphate dehydrogenase activity resulted in 2.06 enzyme units/mg of protein. Drug treatment resulted in no change in amidotransferase activity but caused a 37% increase in the dehydrogenase activity.

In vivo dihydrofolate reductase activity was 8.56 enzyme units/mg of protein, which was increased 19% by drug treatment. *In vivo* ribonucleotide reductase activity was 155,065 dpm of [^{3}H]deoxycytidine diphosphate formed/hr/mg of protein. This was unaffected by drug treatment. *In vivo* histone phosphorylation for the control was 2954 dpm of [γ-^{32}P]incorporated into histones/hr/mg of nuclear protein, inhibited 18% by drug administration. Nonhistone phosphorylation resulted in 9807 dpm of [γ-^{32}P]incorporated into protein/hr/mg of chromatin protein, elevated 83% by drug therapy. *In vivo* cyclic adenosine monophosphate levels for the control were 3.6 pmole/10^6 cells elevated by 48% after drug administration.

The UV studies with I and DNA demonstrated an elevation of UV peaks at 222 and 240 nm, and a hyperchromic shift at 260 nm, indicating possible binding between the drug and nucleic acids. The effects on glycolytic and Krebs cycle enzymatic activities of I were dramatic. Hexokinase activity for untreated 9-day Ehrlich ascites cells was 195 enzyme units/mg of protein, which was inhibited 84% by drug administration (Table IV). Phosphofructokinase activity was determined for the control as 176 enzyme units/mg of protein, which was reduced 54% by the drug. Malic dehydrogenase activity for the control was 80 enzyme units/mg of protein and lactic dehydrogenase activity was 623 enzyme units/mg of protein. Treatment with I had little effect on these two dehydrogenase activities, causing 14 and 9% inhibition, respectively. Succinic dehydrogenase activity for the control was 69 enzyme units/mg of protein which was reduced 52% by drug treatment. α-Ketoglutarate dehydrogenase activity was measured as 1.68 enzyme units/mg of protein for the control cells, which was reduced 76% by drug therapy for 3 days.

Table IV—*In Vivo* Effects of 3-Chloromethylthiochromone-1,1-dioxide on Glycolytic and Krebs Cycle Enzyme Activities of Ehrlich Ascites Cells of CF_1 Mice [a]

Parameter	Control	Treated
Hexokinase	100 ± 9	14 ± 1[b]
Phosphofructokinase	100 ± 3	46 ± 3[b]
Lactic dehydrogenase	100 ± 9	91 ± 20
Malic dehydrogenase	100 ± 20	86 ± 19
Succinic dehydrogenase	100 ± 16	48 ± 3[b]
α-Ketoglutarate dehydrogenase	100 ± 11	24 ± 7[b]

[a] $n = 6$. [b] $p \leq 0.001$.

Table V—*In Vitro* Effects of 3-Chloromethylthiochromone-1,1-dioxide on Oxidative Phosphorylation Processes of 9-Day Ehrlich Ascites Cells [a]

Parameter	Control, % Control	Control, % Treated
Succinate —state 4	100 ± 7[b]	70 ± 7[f]
—state 3	100 ± 4[c]	59 ± 5[f]
α-Ketoglutarate—state 4	100 ± 5[d]	57 ± 10[f]
—state 3	100 ± 11[e]	49 ± 7[f]

[a] $n = 6$. [b] 5.27 μl O_2 consumed/hr/mg protein. [c] 8.73 μl O_2 consumed/hr/mg protein. [d] 3.57 μl O_2 consumed/hr/mg protein. [e] 5.16 μl O_2 consumed/hr/mg protein. [f] $p \leq 0.001$.

Both basal and adenosine diphosphate-stimulated respiration rates were reduced 75% by drug therapy *in vivo*, whereas *in vitro* studies at 0.36 m*M* concentration of drug demonstrated 30 and 41% inhibition, respectively, using succinate as substrate (Tables V and VI). The basal- and adenosine diphosphate-stimulated respiration rates using α-ketoglutarate as substrate were inhibited 82 and 86%, respectively. In the *in vitro* studies with α-ketoglutarate as substrate, I demonstrated 43 and 51% inhibition for States 4 and 3, respectively. The *in vivo* effects of the drug on liver respiration rates of tumor-bearing mice were not as severe as those observed in the tumor cells, and only minimal changes were observed (Table VI).

Figure 1 demonstrates that I, when incubated with endogenous mRNA and essential amino acids, follows a pattern of inhibition of protein synthesis, which resembles the initiation inhibitor, pyrocatechol violet, as opposed to the elongation inhibitor, emetine. The degree of inhibition of protein synthesis was relatively moderate.

DISCUSSION

A series of potential bioreductive alkylating agents have been synthesized (7, 8), specifically α-substituted naphthoquinones, quinoline-5,8-quinones, and naphthazarines which contain halomethyl, acetoxymethyl, carbamoylmethyl, and carbophenoxymethyl groups alpha to a carbonyl group as the alkylating moieties. A number of these agents were observed to be active in the sarcoma 180 and adenocarcinoma 755 ascites screens. A rough correlation between antitumor activity in the sarcoma 180 screen and polarographic reduction potential ($E_{1/2}$) of the quinone moiety was demonstrated. Those compounds that possessed the most negative half-wave reduction potential, *i.e.*, those compounds that were difficult to reduce, demonstrated the highest activity against sarcoma 180 tumor growth. Lin *et al.* (7, 8) suggested that those quinone deriva-

Table VI—*In Vivo* Effects of 3-Chloromethylthiochromone-1,1-dioxide on Oxidative Phosphorylation of CF_1 Mice [a]

Parameter	Control, % Control	Control, % Treated
Ehrlich Ascites Cells		
Succinate—state 4	100 ± 3	15 ± 3[b]
—state 3	100 ± 4	15 ± 2[b]
α-Ketoglutarate—state 4	100 ± 5	18 ± 7[b]
—state 3	100 ● 11	14 ± 2[b]
Liver from Tumor-Bearing Mice		
Succinate—state 4	100 ± 14	99 ± 9
—state 3	100 ± 6	86 ± 13
α-Ketoglutarate—state 4	100 ± 8	104 ± 17
—state 3	100 ± 12	120 ± 10[c]

[a] $n = 6$. [b] $p \leq 0.001$. [c] $p \leq 0.005$.

Table VII—The Antineoplastic Activity of 3-Chloromethylthiochromone-1,1-dioxide in the Ehrlich Ascites and P-388 Lymphocytic Leukemia Screens

Compound	Ehrlich Ascites Tumor Screen (CF_1 Male Mice) Dose, mg/kg	Survival After 9 Days	Ascrit	Ascites Volume	Inhibition, %[a]
Control (0.05% polysorbate 80–H_2O)	—	8/8	33.6 ± 8.7	1.8 ± 1.02	—
3-Chloromethylthiochromone-1,1-dioxide	5	8/8	22.0	2.45	57.1
	10	8/8	0.0	0.0	100.0
	20	8/8	35.7	0.88	75.1
	30	8/8	11.3	2.02	81.8
Mercaptopurine (standard)		6/6	3.0	0.1	99

Compound[b]	P-388 Lymphocytic Leukemia (BDF_1 Male Mice) Dose, mg/kg	Average Days Survived	T/C %[c]
Control (0.05% polysorbate-80/H_2O)	—	9.5	100
3-Chloromethylthiochromone-1,1-dioxide	10	12.4	130
	15	9.8	103
	30	2.9	toxic
Fluorouracil (standard)	25	17.6	186

[a] Greater than 80% inhibition is required for significant activity. [b] $n = 6$. [c] T/C % > 125 is required for significant activity.

tives, when reduced, suffered loss of a leaving group to form a quinone methide, a potential alkylating agent which could alkylate bionucleophiles. It was shown that such an active species could be trapped *in vitro* by an amine function or be allowed to dimerize.

The 3-substituted thiochromone-1,1-dioxides were synthesized as novel analogs of naphthoquinones. Isosteric replacement of one carbonyl with a sulfone group alters the electronic character and ease of reduction. However, preliminary experiments indicated that no apparent correlation existed between half-wave reduction potential and antineoplastic activity in the Ehrlich ascites screen. The thiochromone-1,1-dioxides may be acting as direct alkylating agents *via* a Michael-type addition or a carbamoylation reaction with some biological nucleophile or a direct displacement of the leaving group. For example, high reactivity of I with a variety of alcohols and amines would support this view.

In the naphthoquinone class, lapachol and dichloroallylawsone are the most potent antineoplastic agents (5). Lapachol is currently marketed in Brazil and dichloroallylawsone[9] [2-(3,3-dichloroallyl)-3-hydroxy-1-4-naphthoquinone] is in clinical trials in the United States (15). Bennett *et al.* (46) observed, in cultured L-1210 lymphoid leukemia cells, that dichloroallylawsone interfered with L-1210 cell respiration and inhibited pyrimidine biosynthesis at the dihydro-orotate dehydrogenase step. Thus, it is interesting to observe that the major effect of I is on basal (State 4) and adenosine diphosphate-stimulated (State 3) respiration in Ehrlich ascites cells. Drastic reduction in respiration of Ehrlich ascites cells was observed with succinate as substrate, which requires a flavin adenine nucleotide linked dehydrogenase, as well as α-ketoglutarate, which requires a nicotinamide adenine dinucleotide linked dehydrogenase, both *in vivo* and *in vitro*.

No effects were demonstrated on the respiration of livers of tumor-bearing mice, indicating that the drug has some tissue specificity. However, when the Krebs cycle dehydrogenase activities of Ehrlich ascites cells were measured, it was observed that both succinic dehydrogenase and α-ketoglutarate dehydrogenase activities were inhibited by this agent. Furthermore, activities of the regulatory enzymes of anaerobic glycolysis, hexokinase and phosphofructokinase, were also reduced significantly by I. These studies would indicate that after drug treatment, there existed a reduction in energy available from mitochondrial oxidative phosphorylation, as well as glycolytic substrate phosphorylation, for the synthetic process of rapidly proliferating tumor cells.

Initial studies indicated that I was a moderate inhibitor of protein

[9] NSC 126771.

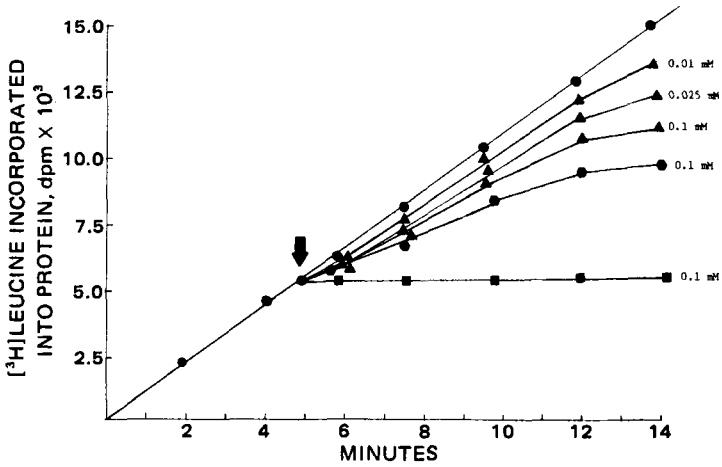

Figure 1—*Effect of 3-chloromethylthiochromone-1,1-dioxide on the initiation and elongation of protein molecular synthesis. Key: (●), control; (▲), drug, 0.01 mM, 0.025 mM, 0.1 mM; (●), pyrocatechol violet, 0.1 mM; (■), emetine, 0.1 mM; ↓, addition of drug.*

synthesis, probably blocking the initiation process of translation. Moderate elevation of cyclic adenosine monophosphate levels of the Ehrlich ascites cells was also observed after drug therapy. Elevated levels are linked with reversal of tumor morphology to a more normal state, reduction of cell proliferation, and enhanced cellular differentiation (47–49).

The inhibition of DNA and RNA synthesis appears to be caused by a lack of pyrimidine due to the fact that I blocks orotidine monophosphate decarboxylase activity, depleting uridylate monophosphate for the conversion to thymidylate monophosphate and cytidylate monophosphate. The decarboxylase enzyme was inhibited both *in vivo* and *in vitro* and is the same site of pyrimidine synthesis inhibition, which has been implicated for the standard clinical antineoplastic agent, azauridine-5′-phosphate (50).

Thus, this sulfone analog of 1,4-naphthoquinones has similar effects on tumor cell metabolism, *i.e.*, inhibition of pyrimidine synthesis and oxidative phosphorylation, as those reported for 1,4-naphthoquinones (46) despite the fact that the sulfone analog does not have the same electronic characteristics or reduction capability as the 1,4-naphthoquinones. Compound I does not suppress the oxidative phosphorylation process exclusively, but its effects are extended to the actual dehydrogenase and kinase enzymes which regulate anaerobic and aerobic glycolysis, indicating that the agent is not simply blocking the electron transport system by acting as an electron acceptor as would be expected for a quinone.

REFERENCES

(1) J. S. Driscoll, G. F. Hazard, Jr., H. B. Wood, Jr., and A. Goldin, *Cancer Chemother. Rep.*, **4**, 1 (1974).

(2) U. Sankawa, Y. Ebizuka, T. Miyazaki, Y. Isomura, H. Otsuka, S. Shubata, M. Inomata, and F. Fukuoka, *Chem. Pharm. Bull.*, **25**, 2392 (1977).

(3) T. H. Porter, G. S. Tsai, T. Kishi, H. Kishi, and K. Folkers, *Acta Pharm. Suec.*, **15**, 97 (1978).

(4) S. M. Tiffany, D. G. Graham, F. S. Vogel, M. W. Cass, and P. W. Jeffs, *Cancer Res.*, **38**, 3230 (1978).

(5) M. da Consolacao, F. Linardi, M. M. de Oliveria, and M. R. P. Sampaio, *J. Med. Chem.*, **18**, 1159 (1975).

(6) E. M. McKelvey, M. Lomedico, K. Lu, M. Chadwick, and T. L. Loo, *Clin. Pharmacol. Ther.*, **25**, 586 (1979).

(7) A. J. Lin, R. S. Pardini, L. A. Cosby, B. J. Lillis, C. W. Shansky, and A. C. Sartorelli, *J. Med. Chem.*, **16**, 1268 (1973).

(8) A. J. Lin, B. J. Lillis, and A. C. Sartorelli, *ibid.*, **18**, 917 (1975).

(9) M. H. Holshouser, L. J. Loeffler, and I. H. Hall, *ibid.*, **24**, 853 (1981).

(10) A. J. Lin and A. C. Sartorelli, *J. Org. Chem.*, **38**, 813 (1973).

(11) C. Piantadosi, C. S. Kim, and J. L. Irvin, *J. Pharm. Sci.*, **58**, 921 (1969).

(12) R. I. Geran, N. H. Greenberg, M. M. MacDonald, A. Schumacher, and B. Abbott, *Cancer Chemother. Rep., Part 3*, (2)**3**, 9 (1972).

(13) C. B. Chae, A. Williams, H. Krasny, J. L. Irvin, and C. Piantadosi,

Cancer Res., **30**, 2652 (1970).
(14) R. G. Wilson, R. H. Bodner, and G. E. MacHorter, *Biochim. Biophys. Acta*, **378**, 260 (1975).
(15) A. C. Sartorelli, *Biochem. Biophys. Res. Commun.*, **27**, 26 (1967).
(16) O. H. Lowry, N. J. Rosebrough, A. L. Farr, and R. J. Randall, *J. Biol. Chem.*, **193**, 265 (1951).
(17) I. H. Hall, K. H. Lee, S. A. ElGebaly, Y. Imakura, and R. Y. Wu, *J. Pharm. Sci.*, **68**, 883 (1979).
(18) W. C. Hymer and E. L. Kuff, *J. Histochem. Cytochem.*, **12**, 359 (1964).
(19) H. Sawada, K. Tatsumi, M. Sasada, S. Shirakawa, T. Nakumura, and G. Wakisaka, *Cancer Res.*, **34**, 3341 (1974).
(20) I. H. Hall, G. L. Carlson, G. S. Abernethy, and C. Piantadosi, *J. Med. Chem.*, **17**, 1253 (1974).
(21) K. M. Anderson, I. S. Mendelson, and G. Guzik, *Biochim. Biophys. Acta*, **383**, 56 (1975).
(22) F. Maley and S. Ochoa, *J. Biol. Chem.*, **233**, 1538 (1958).
(23) S. M. Kalman, P. H. Duffield, and T. Brzozouski, *J. Biol. Chem.*, **241**, 1871 (1966).
(24) R. M. Archibald, *J. Biol. Chem.*, **156**, 121 (1944).
(25) S. B. Koritz and P. P. Cohen, *ibid.*, **209**, 145 (1954).
(26) S. H. Appel, *ibid.*, **243**, 3929 (1968).
(27) A. Kampf, R. L. Barfknecht, P. J. Schaffer, S. Osaki, and M. P. Mertes, *J. Med. Chem.*, **19**, 903 (1976).
(28) M. K. Spassova, G. C. Russell, and E. V. Golovinsky, *Biochem. Pharmacol.*, **25**, 923 (1976).
(29) J. B. Wyngaarden and D. M. Ashton, *J. Biol. Chem.*, **234**, 1492 (1959).
(30) B. Magasanik, *Methods Enzymol.*, **6**, 106 (1963).
(31) M. K. Ho, T. Hakalo, and S. F. Zakrzewski, *Cancer Res.*, **32**, 1023 (1972).
(32) E. G. Moore and R. B. Hurlbert, *J. Biol. Chem.*, **241**, 4802 (1966).
(33) A. Raineri, R. C. Simsiman, and R. K. Boutwell, *Cancer Res.*, **33**, 134 (1973).
(34) Y. M. Kish and L. J. Kleinsmith, *Methods Enzymol.*, **40**, 201 (1975).
(35) A. L. Steiner, D. M. Kipnis, R. Utiger, and C. Parker, *Proc. Natl. Acad. Sci., USA*, **64**, 367 (1969).
(36) I. H. Hall, K. S. Ishaq, and C. Piantadosi, *J. Pharm. Sci.*, **63**, 625 (1974).
(37) Y. S. Cho-Chung and P. M. Gullino, *J. Biol. Chem.*, **248**, 4743 (1973).
(38) I. H. Hall, K. H. Lee, E. C. Mar, and C. O. Starnes, *J. Med. Chem.*, **20**, 333 (1977).
(39) L. L. Liao, S. M. Kupchan, and S. B. Horwitz, *Mol. Pharmacol.*, **12**, 167 (1976).
(40) I. H. Hall, K. H. Lee, C. O. Starnes, S. A. ElGebaly, T. Ibuka, Y. S. Wu, T. Kimura, and M. Haruna, *J. Pharm. Sci.*, **67**, 1235 (1978).
(41) D. G. Walker and J. J. Parry, *Methods Enzymol.*, **9**, 381 (1966).
(42) T. E. Masour, *ibid.*, **9**, 430 (1966).
(43) M. K. Schwartz and O. Bodansky, *ibid.*, **9**, 294 (1966).
(44) D. V. DerVartanian and C. Veerger, *Biochim. Biophys. Acta*, **92**, 233 (1964).
(45) S. Ochoa, A. H. Mehler, and A. Kornberg, *J. Biol. Chem.*, **174**, 979 (1948).
(46) L. L. Bennett, D. Smithers, L. M. Rose, D. J. Adamson, and H. J. Thomas, *Cancer Res.*, **39**, 4868 (1979).
(47) V. Stefanovich, *Res. Commun. Chem. Pathol. Pharmacol.*, **7**, 573 (1974).
(48) T. Posternak, *Annu. Rev. Pharmacol.*, **14**, 23 (1974).
(49) Y. S. Cho-Chung and P. M. Gullino, *Science*, **183**, 87 (1974).
(50) W. B. Pratt and R. W. Ruddon, "The Anticancer Drugs," Oxford University Press, New York, N.Y., 1979, p. 124.

An *In Vitro* Model for the Study of Antibacterial Dosage Regimen Design

ROGER D. TOOTHAKER *§, **PETER G. WELLING** *x, and **WILLIAM A. CRAIG** ‡

Received August 7, 1981, from the *School of Pharmacy, University of Wisconsin, Madison, WI 53706 and the ‡Veterans Administration Hospital, Madison, WI 53705. Accepted for publication November 16, 1981. §Present address: School of Pharmacy, University of Washington, Seattle, WA 98195.

Abstract □ A model was developed that is capable of simulating antibacterial agent concentration *versus* time profiles commonly observed following intravenous and intramuscular bolus injections, intravenous infusions, and oral doses, administered as single or multiple doses. The model consisted of two physical compartments separated by a membrane of a commercial hemodialyzer. The 1.08 m^2 membrane surface area allowed rapid transmembrane passage of drugs and other small molecules, while membrane pore size prevented bacterial passage. These characteristics allowed bacteria in one of the two compartments of the model to be exposed to time-variant drug concentrations without affecting the number or concentration of bacteria. The model was used to study the effects of a multiple intravenous bolus dosage regimen of ampicillin on *Escherichia coli* ATCC 12407.

Keyphrases □ Penicillin—*in vitro* model for the study of antibacterial dosage regimen design □ Models—*in vitro*, study of antibacterial dosage regimen design □ Antibacterials—*in vitro* model, study of dosage regimen design

The antibacterial agent concentration profiles to which bacteria are exposed *in vivo* vary with the method of drug administration. Continuous intravenous infusion yields constant plasma and tissue drug concentrations once steady state is achieved, while the short elimination half-life of most antimicrobial agents results in rapid decreases in plasma and interstitial fluid drug concentrations (1) following bolus intravenous, intramuscular, or oral doses.

Considerable progress has been made during the past 15 years in determining the mechanism of action of β-lactam antibiotics (2, 3). However, the relative therapeutic effectiveness of intermittent and continuous dosage regimens for these compounds is uncertain (4, 5). Attempted correlations of therapeutic effectiveness with various pharmacokinetic parameters, such as maximum plasma concentration (6), the time period during which drug levels exceed the minimum inhibitory concentration (7), area under the plasma level curve (8), intensity factor (9), and the degree of serum protein binding (10), have been difficult due to the many interactions between the drug, bacteria, infection site, and host. Information ob-

0022-3549/82/0800-0861$01.00/0

Cancer Res., **30**, 2652 (1970).
(14) R. G. Wilson, R. H. Bodner, and G. E. MacHorter, *Biochim. Biophys. Acta*, **378**, 260 (1975).
(15) A. C. Sartorelli, *Biochem. Biophys. Res. Commun.*, **27**, 26 (1967).
(16) O. H. Lowry, N. J. Rosebrough, A. L. Farr, and R. J. Randall, *J. Biol. Chem.*, **193**, 265 (1951).
(17) I. H. Hall, K. H. Lee, S. A. ElGebaly, Y. Imakura, and R. Y. Wu, *J. Pharm. Sci.*, **68**, 883 (1979).
(18) W. C. Hymer and E. L. Kuff, *J. Histochem. Cytochem.*, **12**, 359 (1964).
(19) H. Sawada, K. Tatsumi, M. Sasada, S. Shirakawa, T. Nakumura, and G. Wakisaka, *Cancer Res.*, **34**, 3341 (1974).
(20) I. H. Hall, G. L. Carlson, G. S. Abernethy, and C. Piantadosi, *J. Med. Chem.*, **17**, 1253 (1974).
(21) K. M. Anderson, I. S. Mendelson, and G. Guzik, *Biochim. Biophys. Acta*, **383**, 56 (1975).
(22) F. Maley and S. Ochoa, *J. Biol. Chem.*, **233**, 1538 (1958).
(23) S. M. Kalman, P. H. Duffield, and T. Brzozouski, *J. Biol. Chem.*, **241**, 1871 (1966).
(24) R. M. Archibald, *J. Biol. Chem.*, **156**, 121 (1944).
(25) S. B. Koritz and P. P. Cohen, *ibid.*, **209**, 145 (1954).
(26) S. H. Appel, *ibid.*, **243**, 3929 (1968).
(27) A. Kampf, R. L. Barfknecht, P. J. Schaffer, S. Osaki, and M. P. Mertes, *J. Med. Chem.*, **19**, 903 (1976).
(28) M. K. Spassova, G. C. Russell, and E. V. Golovinsky, *Biochem. Pharmacol.*, **25**, 923 (1976).
(29) J. B. Wyngaarden and D. M. Ashton, *J. Biol. Chem.*, **234**, 1492 (1959).
(30) B. Magasanik, *Methods Enzymol.*, **6**, 106 (1963).
(31) M. K. Ho, T. Hakalo, and S. F. Zakrzewski, *Cancer Res.*, **32**, 1023 (1972).
(32) E. G. Moore and R. B. Hurlbert, *J. Biol. Chem.*, **241**, 4802 (1966).
(33) A. Raineri, R. C. Simsiman, and R. K. Boutwell, *Cancer Res.*, **33**, 134 (1973).
(34) Y. M. Kish and L. J. Kleinsmith, *Methods Enzymol.*, **40**, 201 (1975).
(35) A. L. Steiner, D. M. Kipnis, R. Utiger, and C. Parker, *Proc. Natl. Acad. Sci., USA*, **64**, 367 (1969).
(36) I. H. Hall, K. S. Ishaq, and C. Piantadosi, *J. Pharm. Sci.*, **63**, 625 (1974).
(37) Y. S. Cho-Chung and P. M. Gullino, *J. Biol. Chem.*, **248**, 4743 (1973).
(38) I. H. Hall, K. H. Lee, E. C. Mar, and C. O. Starnes, *J. Med. Chem.*, **20**, 333 (1977).
(39) L. L. Liao, S. M. Kupchan, and S. B. Horwitz, *Mol. Pharmacol.*, **12**, 167 (1976).
(40) I. H. Hall, K. H. Lee, C. O. Starnes, S. A. ElGebaly, T. Ibuka, Y. S. Wu, T. Kimura, and M. Haruna, *J. Pharm. Sci.*, **67**, 1235 (1978).
(41) D. G. Walker and J. J. Parry, *Methods Enzymol.*, **9**, 381 (1966).
(42) T. E. Masour, *ibid.*, **9**, 430 (1966).
(43) M. K. Schwartz and O. Bodansky, *ibid.*, **9**, 294 (1966).
(44) D. V. DerVartanian and C. Veerger, *Biochim. Biophys. Acta*, **92**, 233 (1964).
(45) S. Ochoa, A. H. Mehler, and A. Kornberg, *J. Biol. Chem.*, **174**, 979 (1948).
(46) L. L. Bennett, D. Smithers, L. M. Rose, D. J. Adamson, and H. J. Thomas, *Cancer Res.*, **39**, 4868 (1979).
(47) V. Stefanovich, *Res. Commun. Chem. Pathol. Pharmacol.*, **7**, 573 (1974).
(48) T. Posternak, *Annu. Rev. Pharmacol.*, **14**, 23 (1974).
(49) Y. S. Cho-Chung and P. M. Gullino, *Science*, **183**, 87 (1974).
(50) W. B. Pratt and R. W. Ruddon, "The Anticancer Drugs," Oxford University Press, New York, N.Y., 1979, p. 124.

An *In Vitro* Model for the Study of Antibacterial Dosage Regimen Design

ROGER D. TOOTHAKER *§, **PETER G. WELLING** *x, and **WILLIAM A. CRAIG** ‡

Received August 7, 1981, from the *School of Pharmacy, University of Wisconsin, Madison, WI 53706 and the ‡Veterans Administration Hospital, Madison, WI 53705. Accepted for publication November 16, 1981. §Present address: School of Pharmacy, University of Washington, Seattle, WA 98195.

Abstract □ A model was developed that is capable of simulating antibacterial agent concentration *versus* time profiles commonly observed following intravenous and intramuscular bolus injections, intravenous infusions, and oral doses, administered as single or multiple doses. The model consisted of two physical compartments separated by a membrane of a commercial hemodialyzer. The 1.08 m^2 membrane surface area allowed rapid transmembrane passage of drugs and other small molecules, while membrane pore size prevented bacterial passage. These characteristics allowed bacteria in one of the two compartments of the model to be exposed to time-variant drug concentrations without affecting the number or concentration of bacteria. The model was used to study the effects of a multiple intravenous bolus dosage regimen of ampicillin on *Escherichia coli* ATCC 12407.

Keyphrases □ Penicillin—*in vitro* model for the study of antibacterial dosage regimen design □ Models—*in vitro*, study of antibacterial dosage regimen design □ Antibacterials—*in vitro* model, study of dosage regimen design

The antibacterial agent concentration profiles to which bacteria are exposed *in vivo* vary with the method of drug administration. Continuous intravenous infusion yields constant plasma and tissue drug concentrations once steady state is achieved, while the short elimination half-life of most antimicrobial agents results in rapid decreases in plasma and interstitial fluid drug concentrations (1) following bolus intravenous, intramuscular, or oral doses.

Considerable progress has been made during the past 15 years in determining the mechanism of action of β-lactam antibiotics (2, 3). However, the relative therapeutic effectiveness of intermittent and continuous dosage regimens for these compounds is uncertain (4, 5). Attempted correlations of therapeutic effectiveness with various pharmacokinetic parameters, such as maximum plasma concentration (6), the time period during which drug levels exceed the minimum inhibitory concentration (7), area under the plasma level curve (8), intensity factor (9), and the degree of serum protein binding (10), have been difficult due to the many interactions between the drug, bacteria, infection site, and host. Information ob-

0022-3549/82/0800-0861$01.00/0

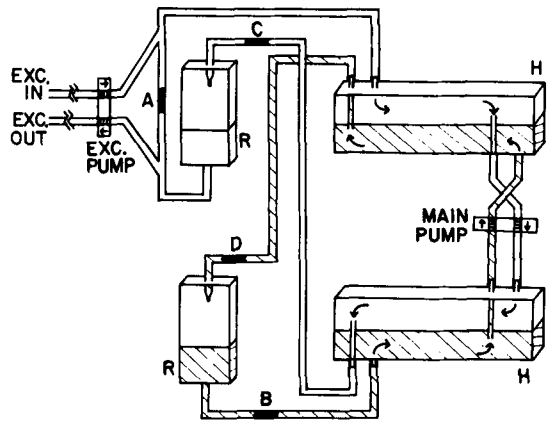

Figure 1—*Schematic diagram of model showing sampling ports (A,B,C,D), hemodialysis units (H), reservoirs (R), tubing, main pump, and exchange pump. Arrows indicate direction of broth flow.*

tained from *in vitro* studies of bactericidal kinetics at constant drug concentrations is not directly applicable to the situation *in vivo* where drug concentrations may undergo rapid changes. The importance of phenomena such as the postantibiotic effect in multiple dose antibiotic regimens has also been difficult to assess in animal models and clinical situations due to uncontrollable factors (11).

The present report describes the theory, characterization, and testing of an *in vitro* model which can be used to monitor the antibacterial effect of simulated plasma drug concentration profiles from constant intravenous infusions or from single or multiple intravenous bolus, intramuscular, or oral doses.

EXPERIMENTAL

Drugs—Solutions of anhydrous ampicillin powder[1] in Mueller-Hinton broth[2] were prepared immediately prior to use. Drug concentration was monitored by the inclusion of a trace amount of [^{14}C]penicillin G potassium[3] (16.22 mCi/mmole) in a broth solution of the unlabeled drug. Scintillation counts were obtained on 0.1-ml broth samples in 4.0 ml of a scintillation solution[4].

Bacteria—An overnight culture of *Escherichia coli*, ATCC 12407[5], in Mueller-Hinton broth was serially diluted in broth to ~10^2 colony-forming units/ml (cfu/ml) and allowed to grow to 10^8 cfu/ml. A 1.0-ml aliquot of this solution was used to inoculate the model. Bacterial growth was monitored in 16 × 125-mm glass tubes using optical density measurements obtained spectrophotometrically at 500 nm[6]. Optical density was linearly related to bacterial concentrations between 6×10^5 and 4×10^8 cfu/ml. The minimum inhibitory concentration for ampicillin against the test organism was obtained by the broth dilution method (12) with an initial inoculum size of 5×10^4 cfu/ml and incubation at 37° for 18 hr.

Viable Cell Assay—Viable cell counts were obtained by performing six consecutive serial dilutions of a 0.1-ml broth sample in 0.9 ml of 0.9% sodium chloride solution at 10°. Nutrient agar[2] plates were divided into eight sectors and streaked with duplicative 10-μl aliquots of each dilution. Visual inspection of the number of colonies formed in each sector after incubation at 37° for 12 hr gave the number of colony-forming units per milliliter in the original sample. Colony recounts following an additional 12 hr of incubation failed to show an increase in colony numbers.

Model Description—The model consisted of a closed loop of 0.95-mm i.d. tubing[7] on each side of the membrane of a hemodialyzer[8] (Fig. 1).

[1] Wyeth Laboratories, Philadelphia, Pa.
[2] Difco Laboratories, Detroit, Mich.
[3] Radiochemical Centre, Amersham, England.
[4] Aquasol, New England Nuclear, Boston, Mass.
[5] American Type Culture Collection, Rockville, Md.
[6] Spectronic 88, Bausch and Lomb, Rochester, N.Y.
[7] Tygon tubing.
[8] Gambro-Lundia Minor hemodialyzer, Gambro-Lundia, Lund, Sweden.

Table I—Kinetic Data for Ampicillin in the Experiment [a]

Dose	Time, Above MIC[b], hr	Time, Below MIC, hr	$t_{1/2}$, min	V_{TOT}, ml	C_0[c] MIC	AUC[d], μg min/ml, Above MIC	AUC[d], μg min/ml, $t^{0 \to 6\ hr}$
1	2.6	3.4	75	823	4.12	167	389
2	2.6	3.4	78	824	4.11	172	399
3	2.8	3.2	83	857	3.95	171	407

[a] Data presented in Fig. 5. The three ampicillin doses were administered at 6-hr intervals. [b] Minimum inhibitory concentration. [c] Ratio of drug concentration immediately after injection to the minimum inhibitory concentration for *E. coli*, ATCC 12407. [d] Area under ampicillin concentration *versus* time curve that is above the minimum inhibitory concentration and the area under the total curve during the 6 hr following each dose (minimum inhibitory concentration = 0.9 μg/ml).

Each dialyzer contained a 17-μm thick membrane[9] of 0.54-m^2 surface area. Two dialyzers were connected in series in order to increase membrane surface area and to decrease ultrafiltration of fluid across the membrane. The tubing was gas sterilized, and the model was assembled aseptically and filled with Mueller-Hinton broth. The broth was synchronously pumped through both tubing loops using a dual channel peristaltic pump[10] (main pump) in opposing flows past the membrane. The total volume of broth in the system was ~800 ml (Table I). A 1-liter glass infusion reservoir on each side of the system permitted pressure equalization and allowed the broth volume on each side of the model to be monitored. Access into the closed system was by syringe through injection sleeves from the arterial infusion sets[11]. A broth exchange loop, EXC. IN and EXC. OUT in Fig. 1, was connected to a tubing loop on one side of the model to allow aseptic introduction of fresh broth and removal of a mixture of broth and drug using a dual channel peristaltic pump[10] (exchange pump). The entire system was maintained at 37° in a 0.9-m^3 incubator[12].

Model Theory—The side of the model containing the broth exchange loop was designated the drug compartment; the other side was designated the bacterial compartment. Bacteria in the bacterial compartment could not penetrate the dialysis membrane and, thus, could not enter the drug compartment. Drug introduced into either compartment could rapidly equilibrate across the membrane due to the large membrane surface area, and could be removed from the system through the broth exchange loop on the drug compartment side of the model.

Simulated intravenous infusion concentration profiles in the bacterial compartment were obtained by injecting drug as a bolus into the drug compartment with the broth exchange loop closed (Fig. 2A). Drug concentration in the bacterial compartment C_{Ba} at time t is described as:

$$C_{Ba} = \frac{D}{V_{TOT}}[1 - e^{(k_{12}+k_{21})t}] \qquad \text{(Eq. 1)}$$

where D is the administered dose, V_{TOT} is the total volume of broth in the system, and k_{12} and k_{21} are first-order rate constants for drug movement across the dialysis membrane. Once drug equilibration in the model is achieved, the steady-state drug concentration is given by:

$$C_{Ba}^{ss} = D/V_{TOT} \qquad \text{(Eq. 2)}$$

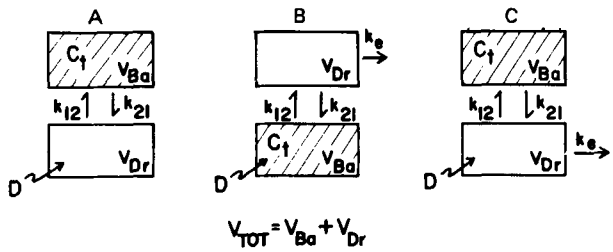

Figure 2—*Schematic representations of drug kinetics in the model during (A) intravenous infusion, (B) intravenous bolus injection, and (C) intramuscular or oral dosage simulations.* V_{Dr} *and* V_{Ba} *are the drug and bacterial compartment volumes, respectively.* C_t *is the concentration of drug in the volume* V_{Ba} *at time t, described in the text as* C_{Ba}. *Other symbols are described in text.*

[9] Cuprophan membrane.
[10] Model 1210, Harvard Apparatus, Millis, Mass.
[11] Travenol Laboratories, Deerfield, Ill.
[12] National Appliance, Hollywood, Fla.

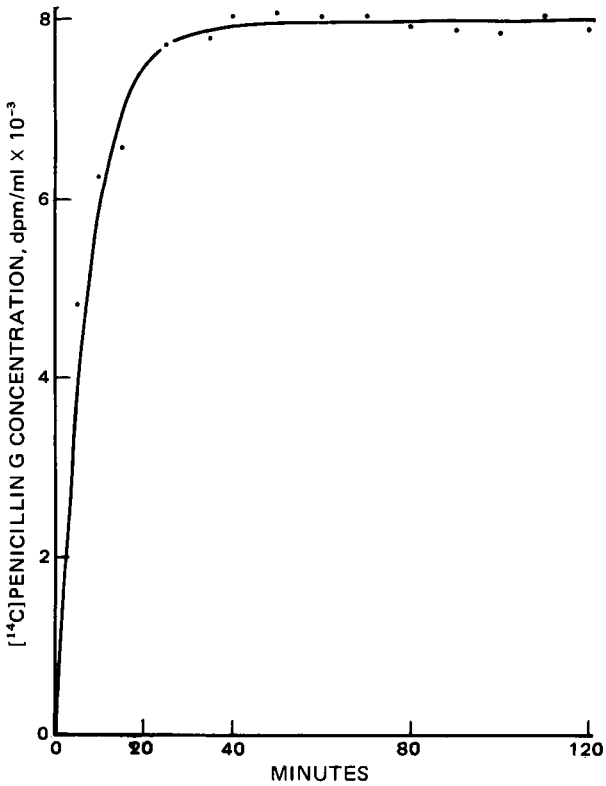

Figure 3—*Intravenous infusion simulation in the model showing experimentally determined drug concentration* versus *time data points.*

The desired C^{ss} value in the bacterial compartment of the model was obtained by selecting the proper dose for the total system volume according to Eq. 2. The time taken for drug levels in the bacterial compartment to reach C^{ss}_{Ba} is a function of the rate of drug passage across the membrane.

Intravenous bolus simulations were achieved by bolus drug injection into the bacterial compartment with the broth exchange loop functioning. The exchange pump speed controlled the rate of drug removal from the model (Fig. 2B). The bacterial compartment drug concentration is described by:

$$C_{Ba} = Ae^{-\alpha t} + Be^{-\beta t} \quad \text{(Eq. 3)}$$

where

$$A = \frac{D(k_{21} + k_e - \alpha)}{V_{Ba}(\beta - \alpha)} \quad \text{(Eq. 4)}$$

$$B = \frac{D(k_{21} + k_e - \beta)}{V_{Ba}(\alpha - \beta)} \quad \text{(Eq. 5)}$$

and

$$\begin{pmatrix}\alpha\\ \beta\end{pmatrix} = \frac{1}{2}\left[(k_{12} + k_{21} + k_e) \pm \sqrt{(k_{12} + k_{21} + k_e)^2 - 4k_{21}k_e}\right] \quad \text{(Eq. 6)}$$

As drug removal by the broth exchange loop was a first-order process, and passage of drug across the membrane was fast compared to drug elimination, a plot of the decrease in the logarithm of the drug concentration with time was linear.

Oral and intramuscular dosage simulations were obtained by injecting a drug bolus into the drug compartment with the broth exchange loop functioning. The membrane passage controlled the rate at which drug concentration increased in the bacterial compartment, while the rate of drug elimination was controlled by the exchange pump rate (Fig. 2C). Equation 7 describes the bacterial compartment drug concentration profile:

$$C_{Ba} = \frac{Dk_{12}}{V_{Ba}(\alpha - \beta)}\left[e^{-\beta t} - e^{-\alpha t}\right] \quad \text{(Eq. 7)}$$

The elimination rates for the intravenous bolus, intramuscular, and oral dose simulations are controlled by the exchange pump speed according to:

$$t_{1/2} = \frac{0.693V_{TOT}}{Q} \quad \text{(Eq. 8)}$$

where Q is the broth exchange loop flow rate.

Use of the Model to Examine the Antibacterial Effect of Ampicillin—The antibacterial effect of a multiple intravenous bolus dosage regimen of ampicillin on *E. coli*, ATCC 12407, was examined. A 1-ml inoculum of 1×10^8 cfu/ml of *E. coli*, which was in logarithmic growth phase, was injected into the bacterial compartment. Logarithmic bacterial growth in the model was monitored by means of optical density. When the bacterial concentration reached 5×10^6 cfu/ml, the first of three 3-mg ampicillin doses was administered as a 1-ml bolus into the bacterial compartment with the broth exchange loop functioning. Similar doses of ampicillin were given at 6 and 12 hr after the initial dose. Drug and viable bacteria concentrations were monitored every 0.5 hr for 18 hr following the first ampicillin dose. The serial dilutions in the bacterial assay served to dilute ampicillin in samples to noninterfering levels.

RESULTS

The kinetics of penicillin G disposition in the model were examined by injecting 0.5 ml of a mixture of 11.2 μg/ml of [^{14}C]penicillin G potassium and 962 μg/ml of unlabeled penicillin G potassium into the system. With the main pump flow rate set at 120 ml/min, circulation time for drug in the model was found to be <3 min. A 0.5-min drug equilibration half-time across the membrane was calculated from an intravenous infusion dose. Observed C^{ss} values under these conditions indicated that the drug did not bind to a significant degree to the dialysis membrane.

Drug concentration profiles in the bacterial compartment during intravenous infusion and oral dosage simulations are shown in Figs. 3 and 4. Multiple bolus intravenous injection simulations are shown in Fig. 5. The residual plot for the absorption phase of the oral simulation was linear, indicating that the approach to steady-state drug concentration in the bacterial compartment can be represented by a first-order process. The absorption and elimination half-lives for the oral dose simulations were ~5 and 53 min, respectively.

The possible effect of changes in the exchange pump flow rate on

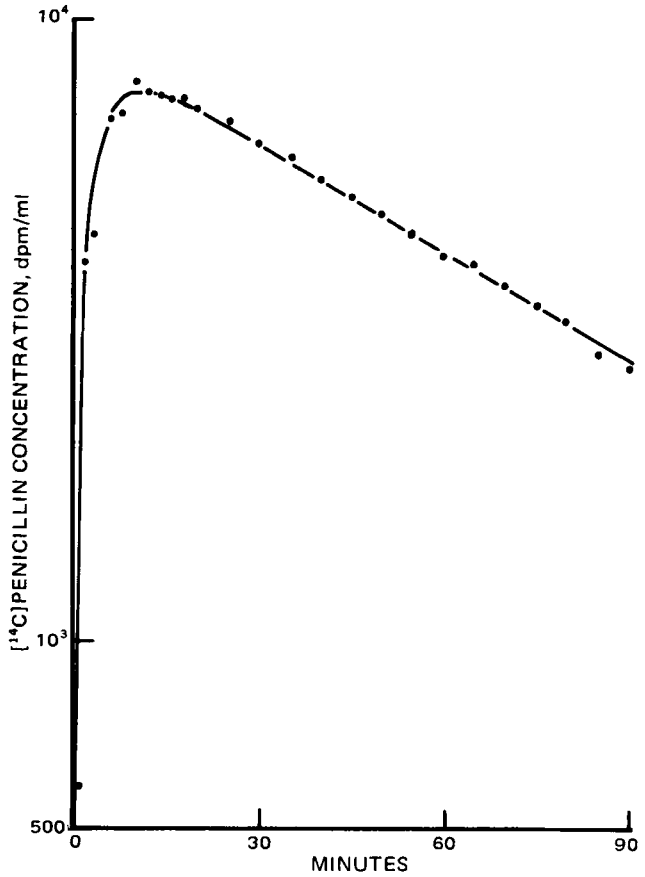

Figure 4—*Intramuscular injection or oral dosage simulation in the model showing experimentally determined bacterial compartment drug concentration* versus *time data points.*

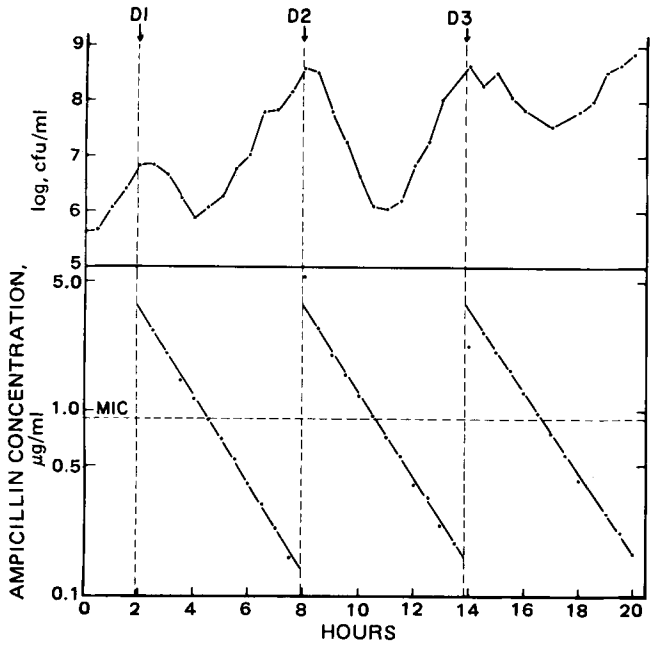

Figure 5—*Plots of the logarithm of the number of colony-forming units per milliliter (cfu/ml) and the log of the drug concentration* versus *time following three (D1,D2,D3) simulated intravenous bolus injections of ampicillin against* E. coli, *ATCC 12407. The minimum inhibitory concentration (0.9 μg/ml) is indicated as a horizontal dotted line.*

bacterial growth in the absence of drug was determined by varying the pump flow rates to yield simulated drug half-lives of infinity (exchange loop closed), 75, and 37 min. The tests were performed on different days using different bacterial inocula. The slopes ($\pm SD$), obtained by linear regression, for the logarithmic bacterial growth curves were 0.72 (±0.05) for $t_{1/2} = \infty$, 0.75 (± 0.02) for $t_{1/2} = 75$ min, and 0.78 (±0.01) for $t_{1/2} = 37$ min. These values were not significantly different from each other and show that bacterial growth rates were unaffected by broth exchange rates within the range of values studied.

The results of the repeated dose intravenous bolus simulation, using ampicillin against *E. coli*, ATCC 12407, are shown in Fig. 5. Pertinent data are presented in Table I. Bacterial kill occurred following each dose of antibiotic, and regrowth resumed shortly after antibiotic levels had fallen below the minimum inhibitory concentration. The time that elapsed between dosing and observed bactericidal effect tended to decrease slightly, but the maximum kill rate and the absolute amount of bacterial kill appeared also to differ with succeeding doses.

DISCUSSION

Antimicrobial therapy is generally administered on an empirical basis and optimization of effect through accurate dosage regimen design has not been accomplished in most cases.

It is difficult to establish accurate relationships between drug kinetics and antibacterial effects *in vivo* because of the contribution of many, often uncontrollable, factors such as tissue penetration, development of bacterial resistance, variable binding of drug to plasma proteins, and interactions of drugs with other substances. Failure to generate useful data in clinical situations, or by the use of animal models, has given rise to an increasing interest in the development of *in vitro* systems which may simulate in an idealistic manner the *in vivo*, clinical situation. While it is recognized that such systems exclude many of the variables that exist *in vivo*, they are nonetheless justified in that they attempt to establish relationships between changing drug concentrations and antibacterial effect in a controlled situation.

Some *in vitro* studies have examined the kinetics of antimicrobial effects using constant drug concentrations (13, 14). However, the results obtained in these studies do not apply to many clinical situations in which drug levels are constantly changing.

Other models have been designed to simulate varying drug levels with respect to time (15–19). In most of these systems, the addition of fresh broth in order to change the concentration of antibiotic results in simultaneous dilution of the organism (15, 16, 18, 19). In some models there is less than optimal control of the drug concentration *versus* time profiles.

The described model has advantages over previous systems in that the addition of fresh growth medium in order to dilute the concentration of antibiotic does not dilute the bacteria, and also the closed, continuously recycling system provides considerable flexibility for the simulation of a variety of single and repeated dosage regimens.

The rapid rate of drug equilibration across the dialyzer membranes observed with the present system can be altered by varying the membrane surface area. This would have the effect of altering the drug absorption rate in oral or intramuscular dose simulations and changing the time for steady-state drug levels to be achieved in the bacterial compartment during infusion simulations.

Tracer quantities of [^{14}C]penicillin G were used in this study to monitor both penicillin G and ampicillin levels, characterize the model, and provide preliminary data on dosage simulation. It is recognized that circulating total radioactivity does not necessarily represent microbiologically active drug, and the preliminary concentration effect relationships described in Fig. 5 must be interpreted in this light. However, the good agreement between drug concentrations relative to the minimum inhibitory concentration and the antibacterial effect serves to illustrate the usefulness of the model for this type of study. To characterize accurately the concentration–effect relationship of any chemically or bacteriologically unstable compound, it will be necessary to measure the concentration of active drug.

Various improvements to the described model are possible and are being investigated. For example, with appropriate engineering, the overall size of the system and the membrane surface area may be reduced to permit greater ease in handling without loss of model flexibility. However, the present model is suitable to study drug antibacterial activity under a variety of dosing conditions. The data in Fig. 5 were generated with the bacteria in logarithmic growth at the time of drug administration. With appropriate adjustment of experimental conditions, drug activity can be determined against bacteria in either logarithmic or stationary growth phases.

REFERENCES

(1) M. G. Bergeron, D. Beauchamp, A. Poirier, and A. Bastille, *Rev. Infect. Dis.*, **3**, 84 (1981).

(2) A. Tomasz, *ibid.*, **1**, 434 (1979).

(3) B. G. Spratt, *Sci. Prog. (Oxford)*, **65**, 101 (1978).

(4) F. Nordbring, *Scand. J. Infect. Dis., Suppl.*, **14**, 21 (1978).

(5) C. M. Kunin, *Rev. Infect. Dis.*, **3**, 4 (1981).

(6) J. Klastersky, D. Daneau, G. Swings, and D. Weerts, *J. Infect. Dis.*, **129**, 187 (1974).

(7) H. Eagle, R. Fleishman, and M. Levy, *N. Engl. J. Med.*, **248**, 481 (1953).

(8) H. W. Jaffe, A. L. Schroeter, G. H. Reynolds, A. A. Zaidi, J. E. Martin, and J. D. Thayer, *Antimicrob. Agents Chemother.*, **15**, 587 (1979).

(9) G. E. Schumacher, *J. Clin. Pharmacol.*, **15**, 656 (1975).

(10) R. Wise, A. P. Gillett, B. Cadge, S. R. Durham, and S. Baker, *J. Infect. Dis.*, **142**, 77 (1980).

(11) R. W. Bundtzen, A. U. Gerber, D. L. Cohn and W. A. Craig, *Rev. Infect. Dis.*, **3**, 28 (1981).

(12) J. A. Washington, in "Laboratory Procedures in Clinical Microbiology," 1st ed., Little, Brown, Boston, Mass., 1974, pp. 303–304.

(13) E. R. Garrett, *Scand. J. Infect. Dis., Suppl.*, **14**, 54 (1978).

(14) H. Mattie, *Rev. Infect. Dis.*, **3**, 19 (1981).

(15) A. Sanfilippo and G. Schioppacassi, *Chemotherapy*, **18**, 297 (1973).

(16) S. Grasso, G. Meinardi, I. De Carneri, and V. Tomassia, *Antimicrob. Agents Chemother.*, **13**, 570 (1978).

(17) M. J. S. Al-Asadi, D. Greenwood, and F. O'Grady, *ibid.*, **16**, 77 (1979).

(18) M. Nishida, T. Murakawa, T. Kamimura, and N. Okada, *ibid.*, **14**, 6 (1978).

(19) T. Murakawa, H. Sakamoto, T. Hirose, and M. Nishida, *ibid.*, **18**, 377 (1980).

Enhanced Rectal Absorption of Theophylline, Lidocaine, Cefmetazole, and Levodopa by Several Adjuvants

TOSHIAKI NISHIHATA, J. HOWARD RYTTING ˣ, and TAKERU HIGUCHI

Received December 18, 1980, from the *Pharmaceutical Chemistry Department, The University of Kansas, Lawrence, KS 66045.* Accepted for publication October 25, 1981.

Abstract □ Ten potential adjuvants for rectal absorption which are structurally similar to salicylate have been examined using an *in situ* perfusion of the rat rectum technique as well as an *in vivo* absorption method from microenemas. All of the adjuvants studied readily disappeared from the perfusate at pH 4.5; however, several were not absorbed well at pH 7.4. Only those that were lost rapidly from the perfusate at pH 7.4 were effective in enhancing the disappearance of the drugs (theophylline, lidocaine, cefmetazole, and levodopa) at either a pH of 4.5 or 7.4. The compounds that were effective in promoting the disappearance of drugs from the rectal perfusate all had hydroxy and carboxy groups. Those substances lacking a hydroxy group were not effective. The binding of these potential adjuvants and salicylates to rat rectum tissue was studied by equilibrium dialysis. Those adjuvants with relatively high binding to rat rectal tissue were better absorbed themselves and promoted the disappearance of drugs more than those substances exhibiting little binding. Thus, adjuvant binding to some feature of the rectal membrane appears to be important in the enhanced absorption of drugs from the rectum under the conditions of this study.

Keyphrases □ Absorption, rectal—enhanced rectal absorption of theophylline, lidocaine, cefmetazole, and levodopa by several adjuvants □ Theophylline—enhanced rectal absorption by several adjuvants □ Lidocaine—enhanced rectal absorption by several adjuvants □ Cefmetazole—enhanced rectal absorption by several adjuvants □ Levodopa—enhanced rectal absorption by several adjuvants

In other papers (1–3), salicylate has been shown to significantly improve the absorption of theophylline, lidocaine, cefmetazole, and levodopa from the rectum, particularly in their ionic forms. The present report describes the effects of several other compounds which are structurally similar to salicylate on the rectal absorption of these drugs. These potential adjuvants include the sodium salts of benzoic acid, *o*-anisic acid, *p*-anisic acid, 3-methoxysalicylic acid, 5-methoxysalicylic acid, 2,4-dihydroxybenzoic acid, 2,5-dihydroxybenzoic acid, 3,5-dihydroxybenzoic acid, 2,4-dimethoxybenzoic acid, and homovanillic acid. The drugs chosen for this study represent several different classes: theophylline is a neutral substance, lidocaine is a base, cefmetazole is an acid, and levodopa exists as a zwitterion in solution.

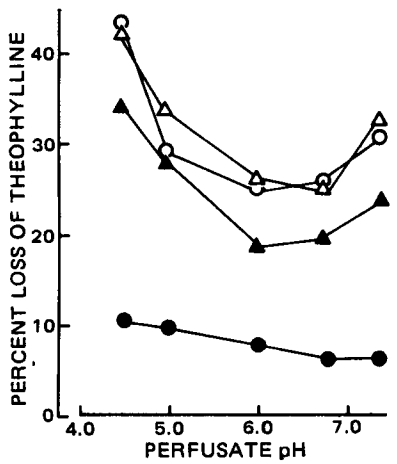

Figure 1—*The percent loss of theophylline from a perfusate of the rat rectum after 1 hr as a function of pH in the presence of 0.5% sodium homovanillate (○); sodium 5-methoxysalicylate (△); sodium 2,4-dihydroxybenzoate (▲); without an adjuvant (●).*

EXPERIMENTAL

Materials—Theophylline[1], sodium cefmetazole[2], and levodopa[2] were used as obtained from the manufacturer. Salicylic acid[3], benzoic acid[3], *o*-anisic acid[3], *p*-anisic acid[3], 3-methoxysalicylic acid[3], 5-methoxysalicylic acid[3], 2,4-dihydroxybenzoic acid[3], 2,5-dihydroxybenzoic acid[3], 3,5-dihydroxybenzoic acid[3], 2,4-dimethoxybenzoic acid[3], and homovanillic acid[3] were converted to the sodium salt by reacting the acid form with either sodium bicarbonate in water followed by recrystallization from ethanol or by reacting the acid with sodium ethoxide in anhydrous ethanol while bubbling nitrogen through the solution. Lidocaine[1] was converted to the hydrochloride salt by mixing with an equimolar solution of hydrochloric acid and evaporating to dryness without heat.

Animals—Sprague-Dawley male rates (200–300 g) were fasted for 16 hr prior to the experiments. During the experiment, the rats were kept on a 38° surface and were anesthetized with pentobarbital (60 mg/kg).

The *in situ* perfusion studies using the rat rectum and the *in vivo* absorption studies were carried out as described previously (2) with an ionic strength of 0.75. The pH of the perfusate was maintained constant by either the addition of 0.1 *N* NaOH or 0.1 *N* HCl, as needed. The analysis of theophylline, lidocaine, cefmetazole, and levodopa were performed by HPLC as described previously (2, 3). The analyses of the adjuvants used in the present study were done using HPLC with a reversed-phase column, 25 cm in length, a flow rate of 1.0 ml/min, and detection at 254 nm. The mobile phases consisted of mixtures of 0.1 *M* acetate buffer–methanol with ratios: 30:70 for benzoate, 2,4-dimethoxybenzoate, *o*-anisate, and *p*-anisate; 60:40 for homovanillate; 3-methoxysalicylate, and 5-methoxysalicylate; and 20:80 for 2,4-dihydroxybenzoate, 2,5-dihy-

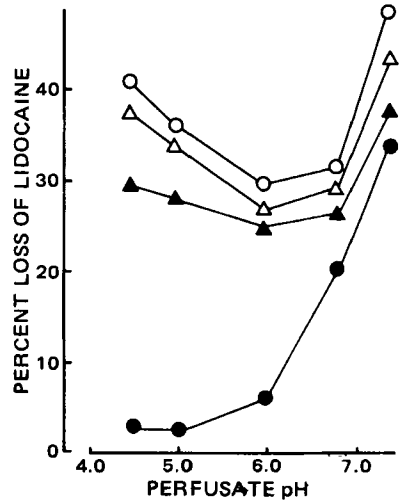

Figure 2—*The percent loss of lidocaine from a perfusate of the rat rectum after 1 hr as a function of pH in the presence of 0.5% sodium homovanillate (○); sodium 5-methoxysalicylate (△); sodium 2,4-dihydroxybenzoate (▲); without an adjuvant (●).*

[1] Sigma Chemical Co.
[2] Sankyo.
[3] Aldrich Chemical Co.

0022-3549/82/0800-0865$01.00/0

Table I—The Percent Loss of Drug and Adjuvant from Perfusate after 60 min at pH 4.5 [a]

Adjuvant	Theophylline	Lidocaine	Levodopa	Cefmetazole	Adjuvant[b]	Adjuvant[c]
—	10.3 ± 1.2	2.8 ± 0.9	2.4 ± 0.3	19.1 ± 2.8		
Benzoate	8.6 ± 1.2	—	2.3 ± 0.9	16.5 ± 5.2	40.6 ± 2.9	38.3 ± 3.2
o-Anisate	9.2 ± 0.7	—	3.5 ± 0.9	17.7 ± 3.9	36.3 ± 4.8	37.2 ± 5.6
p-Anisate	8.9 ± 0.7	—	2.1 ± 1.1	19.2 ± 1.9	40.2 ± 5.3	39.4 ± 2.8
3-Methoxysalicylate	34.5 ± 2.9[d]	40.6 ± 4.2[d]	28.4 ± 3.3[d]	39.6 ± 3.2[d]	30.3 ± 2.3	31.2 ± 3.5
5-Methoxysalicylate	42.6 ± 6.2[d]	37.5 ± 8.7[d]	30.4 ± 3.8[d]	51.6 ± 3.8[d]	32.5 ± 5.6	31.8 ± 4.3
2,4-Dihydroxybenzoate	34.3 ± 7.2[d]	29.5 ± 7.8[d]	22.5 ± 6.2[d]	39.6 ± 4.3[d]	29.8 ± 7.2	27.2 ± 2.5
2,5-Dihydroxybenzoate	29.8 ± 4.0[d]	34.7 ± 4.1[d]	23.8 ± 5.3[d]	32.6 ± 3.9[d]	26.3 ± 4.3	24.6 ± 3.2
3,5-Dihydroxybenzoate	25.2 ± 9.0[d]	24.9 ± 3.4[d]	18.6 ± 3.1[d]	28.4 ± 2.5[d]	20.5 ± 2.8	19.5 ± 3.2
2,4-Dimethoxybenzoate	7.9 ± 2.3	—	1.9 ± 0.8	15.7 ± 4.1	27.4 ± 4.8	27.7 ± 2.8
Homovanilate	43.5 ± 5.8[d]	40.8 ± 6.9[d]	28.5 ± 7.4[d]	43.5 ± 8.1[d]	30.5 ± 4.4	28.8 ± 2.6

[a] The uncertainties represent standard deviations. [b] Initial concentration of adjuvant was 0.5%. [c] Initial concentration of adjuvant was 2%. [d] $p < 0.001$ when compared to no adjuvant using a standard t test ($n \geq 4$).

Table II—The Percent Loss of Drug and Adjuvant from Perfusate after 60 min at pH 7.4 [a]

Adjuvant	Theophylline	Lidocaine	Levodopa	Cefmetazole	Adjuvant[b]	Adjuvant[c]
—	6.1 ± 0.8	33.5 ± 7.8	3.2 ± 1.1	2.6 ± 1.8		
Benzoate	5.2 ± 1.1		2.9 ± 0.9	3.1 ± 1.2	2.2 ± 1.5	
o-Anisate	4.1 ± 1.7		3.5 ± 0.7	2.8 ± 0.8	3.7 ± 1.5	
p-Anisate	6.1 ± 2.4		3.4 ± 1.7	3.5 ± 1.6	2.9 ± 1.3	
3-Methoxysalicylate	30.8 ± 5.3[d]		23.6 ± 3.5[d]	31.4 ± 4.3[d]	23.6 ± 4.2	14.1 ± 2.8
5-Methoxysalicylate	32.8 ± 9.3	43.5 ± 9.2	25.8 ± 4.3[d]	37.1 ± 7.7[d]	24.3 ± 6.2	14.7 ± 3.2
2,4-Dihydroxybenzoate	23.8 ± 7.1	37.8 ± 9.3	21.5 ± 6.3[d]	24.9 ± 6.7	18.4 ± 7.3	8.7 ± 2.8
2,5-Dihydroxybenzoate						
3,5-Dihydroxybenzoate	17.8 ± 2.1[d]		18.6 ± 3.1[d]	18.3 ± 1.8[d]	10.5 ± 4.8	6.1 ± 1.6
2,4-Dimethoxybenzoate	6.8 ± 1.9		5.2 ± 3.1	2.9 ± 1.8	6.4 ± 2.8	
Homovanilate	30.7 ± 5.2	48.3 ± 8.4	23.8 ± 6.2[d]	31.8 ± 8.6[d]	21.5 ± 3.8	11.8 ± 2.8

[a] The uncertainties represent standard deviations. [b] Initial adjuvant concentration was 0.5%. [c] Initial adjuvant concentration was 2%. [d] $p < 0.001$ when compared to no adjuvant using a standard t test.

droxybenzoate, and 3,5-dihydroxybenzoate. The absolute bioavailabilities were determined as described previously (2).

Binding Study of Adjuvants to Rat Rectal Tissue—The binding of various adjuvants with rat rectal tissue was studied using an equilibrium dialysis method. Dialysis tubing containing 1.4 mg of adjuvant and 200 mg of rectal tissue in 2.0 ml of 0.0667 *M* phosphate buffer at pH 7.4 was suspended in a 10-ml test tube containing 5 ml of the 0.0667 *M* phosphate buffer used earlier. After equilibration for 48 hr at 4°, the concentration of adjuvant in the outside solution was measured. The percent binding of adjuvant to 200 mg of rectal tissue was calculated from the following relationship:

$$\text{Percent Binding} = \{[T - (CV)]/T\}100 \qquad \text{(Eq. 1)}$$

where T, C, and V represent the total amount of adjuvant, the concentration of adjuvant in the outer solution, and the total volume of buffer (7.0 ml), respectively. The amount of adjuvant that is not bound is equal to CV.

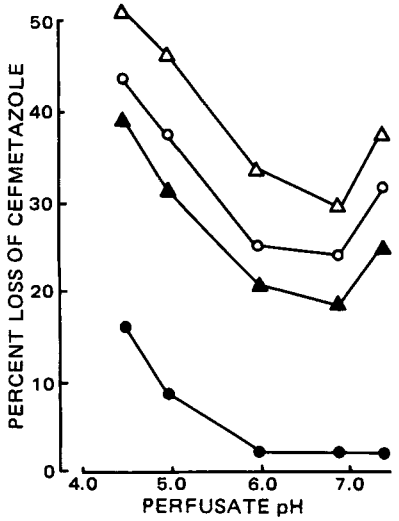

Figure 3—*The percent loss of cefmetazole from a perfusate of the rat rectum after 1 hr as a function of pH in the presence of 0.5% sodium homovanillate (○); sodium 5-methoxysalicylate (△); sodium 2,4-dihydroxybenzoate (▲); without an adjuvant (●).*

RESULTS AND DISCUSSION

Effect of Adjuvants on Drug Disappearance from Perfusate—Ten compounds have been studied regarding their effectiveness in enhancing the loss of theophylline, lidocaine, cefmetazole, and levodopa from a perfusing solution in the rat rectum. The pH profiles of the effects of three of the most potent absorption promoters, *i.e.*, homovanillate, 5-methoxysalicylate, and 3,5-dihydroxybenzoate, on the disappearance of theophylline, lidocaine, cefmetazole, and levodopa from the perfusate after 1 hr are shown in Figs. 1–4.

The disappearance of each of the drugs from the perfusing solution was significantly facilitated by the presence of each of these three adjuvants. The enhancement of loss from the perfusate was particularly evident at pH values >7.4 and <5.0. As shown in Fig. 5, the loss of adjuvant from the perfusate paralleled the extent of disappearance of the drugs studied. Similar results were observed using sodium salicylate as an adjuvant (2). Furthermore, as shown in Fig. 6, the disappearance of these three adjuvants was not affected by the presence or absence of the four drugs studied in the perfusate. This indicates that the enhancement of drug absorption by these adjuvants is not due to the formation of a complex with the drugs.

The effects of the 10 adjuvants studied on the disappearance of theophylline, lidocaine, cefmetazole, and levodopa from a rectal perfusate are summarized in Tables I and II for pH 4.5 and 7.4, respectively. The

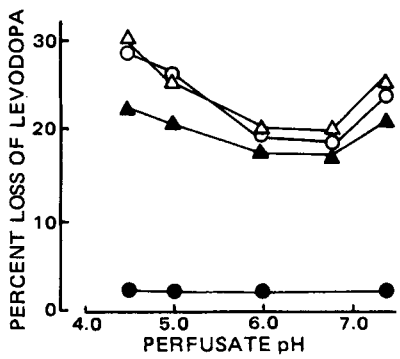

Figure 4—*The percent loss of levodopa from a perfusate of the rat rectum after 1 hr as a function of pH in the presence of 0.5% sodium homovanillate (○); sodium 5-methoxysalicylate (△); sodium 2,4-dihydroxybenzoate (▲); without an adjuvant (●).*

Table III—Absolute Bioavailabilities of a 15-mg/kg Dose of Theophylline and Cefmetazole [a]

Dose of 5-Methoxysalicylate, mg/kg	Bioavailability, % Theophylline	*n*	Cefmetazole	*n*
0	32.5 ± 12.4	4	7.8 ± 1.3	4
10	83.5 ± 9.2	1	18.5	1
15	128.4 ± 32.5	4	38.3 ± 4.2	4
30			48.6 ± 7.2	4
50			76.8	1
Dose of Sodium Homovanillate				
0	32.5 ± 2.4	4	7.8 ± 1.3	4
7.5	69.5 ± 14.8	4		
15	119.7 ± 28.5	4	21.8	1
30			34.7 ± 5.4	4
50			51.2 ± 8.4	4

[a] After rectal administration as a microenema in the presence of 5-methoxysalicylate and homovanillate.

extent of the disappearance of the adjuvants themselves is also shown.

All of the adjuvants studied readily disappeared from the perfusate at pH 4.5. However, at pH 7.4 the disappearance of all the adjuvants was somewhat lower and very low for benzoate, *o*- and *p*-anisate, and 2,4-dimethoxybenzoate. Those adjuvants that were not well absorbed at pH 7.4 did not significantly enhance the disappearance of the drugs at pH 4.5 or 7.4. However, those compounds, which readily disappeared from the perfusate at pH 7.4, facilitated the loss of drugs from the perfusates at pH 4.5 and 7.4.

The disappearance of the adjuvants from the perfusate as reflected by the percent lost after 1 hr did not depend on the initial concentration at pH 4.5. However, the loss of adjuvant at pH 7.4 did depend on the initial concentration with a greater percent loss occurring at the lower concentrations, as shown in the last two columns of Table II.

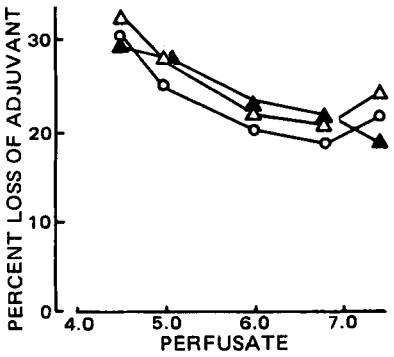

Figure 5—*The percent loss of sodium homovanillate (○), 5-methoxysalicylate (△) and 2,4-dihydroxybenzoate (▲) from a perfusate of the rat rectum after 1 hr as a function of pH. Initial concentration is 0.5%.*

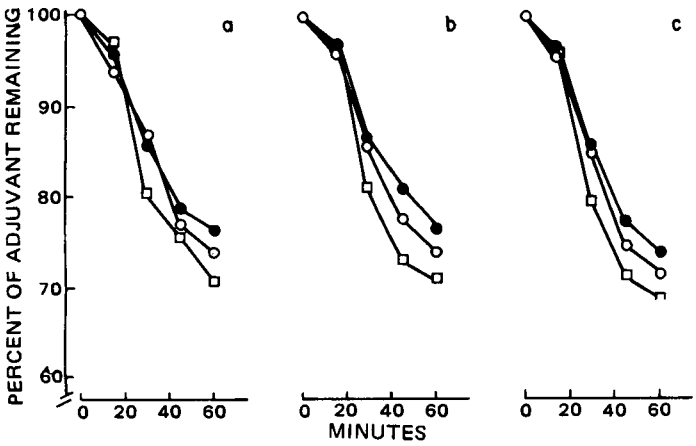

Figure 6—*Percent of homovanillate (●), 5-methoxysalicylate (○), and 2,4-dihydroxybenzoate (□) remaining in the perfusate as a function of time in the presence of (a) theophylline, (b) cefmetazole, or (c) in the absence of drug.*

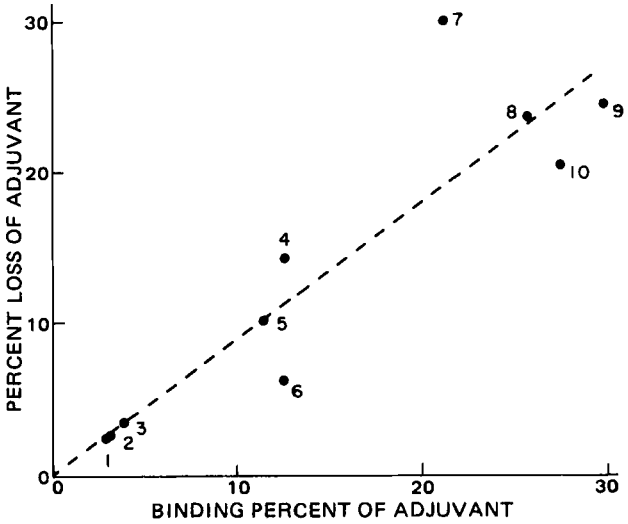

Figure 7—*Percent loss of adjuvant from perfusate at 60 min* versus *the percent binding of adjuvant to rat rectal tissue. Key: 1, benzoate; 2, p-anisate; 3, o-anisate; 4, 2,4-dihydroxybenzoate; 5, 3,5-dihydroxybenzoate; 6, 2,5-dihydroxybenzoate; 7, salicylate; 8, 3-methoxysalicylate; 9, 5-methoxysalicylate; 10, homovanillate.*

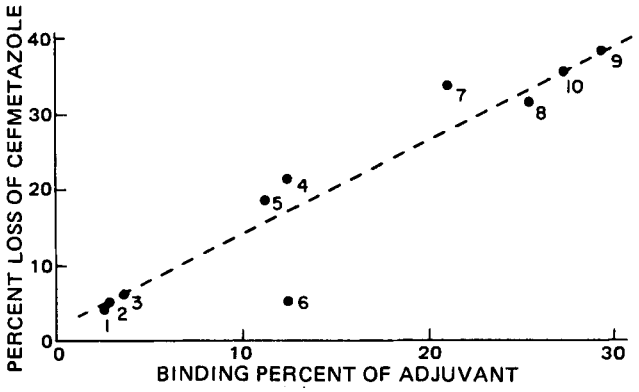

Figure 8—*Percent loss of cefmetazole from perfusate at 60 min* versus *the percent binding of adjuvant to rat rectal tissue. Key: 1, benzoate; 2, p-anisate; 3, o-anisate; 4, 2,4-dihydroxybenzoate; 5, 3,5-dihydroxybenzoate; 6, 2,5-dihydroxybenzoate; 7, salicylate; 8, 3-methoxysalicylate; 9, 5-methoxysalicylate; 10, homovanillate.*

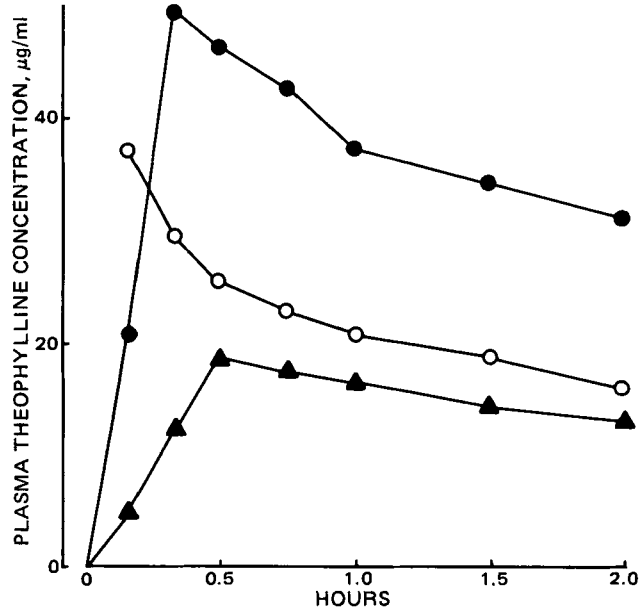

Figure 9—*Theophylline concentration (μg/ml) from an intravenous injection of 10 mg/kg (○) and from a microenema containing 15 mg/kg of theophylline (▲,●) and 15 mg/kg of sodium homovanillate (●).*

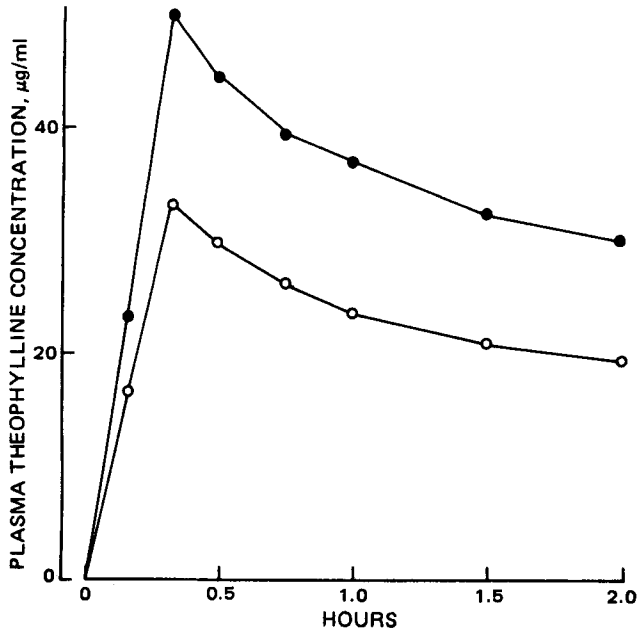

Figure 10—*Plasma theophylline concentration (μg/ml) from a microenema containing 15 mg/kg of theophylline and either 7.5 mg/kg (○) or 15 mg/kg (●) of 5-methoxysalicylate.*

The compounds that were effective in promoting the disappearance of drugs from the rectal perfusate all have hydroxy and carboxy groups. Benzoate, *o*- and *p*-anisate, and 3,5-dimethoxybenzoate do not have hydroxy groups, did not facilitate the disappearance of drugs from the perfusate, and did not disappear from the perfusate themselves at pH 7.4. It appears that for those substances which are chemically similar to salicylate, the presence of both the hydroxy and carboxy groups is important.

Binding of Adjuvants with Rat Rectum Tissue—The facts that those compounds which act as adjuvants for rectal absorption, both in this study and previous studies, disappear from the rectal perfusate even in their ionic form and that disappearance at pH 7.4 depends on their initial concentrations suggests that their potentiating effect may depend on their binding to some feature of the rat rectal tissue. Therefore, a binding study of these potential adjuvants and salicylate with rat rectal tissue was conducted at 4° using equilibrium dialysis.

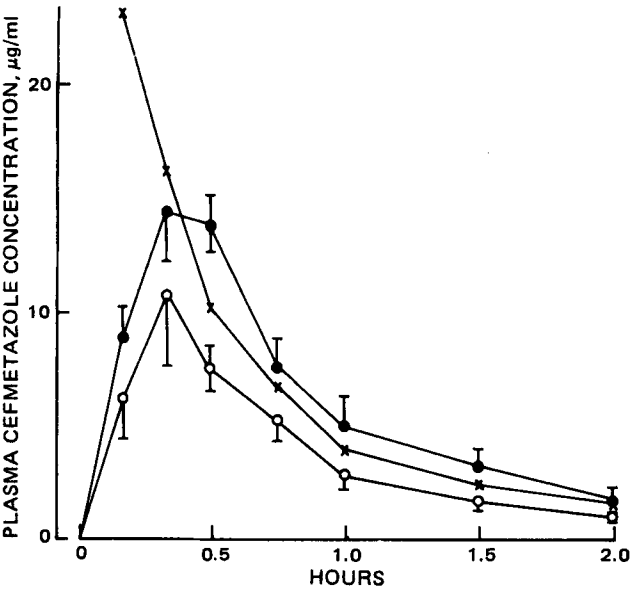

Figure 11—*Plasma cefmetazole concentration (μg/ml) in the rat from an intravenous injection of 10 mg/kg (x) and from a microenema containing 30 mg/kg of cefmetazole (○,●) and 30 mg/kg (○) or 50 mg/kg (●) of sodium homovanillate.*

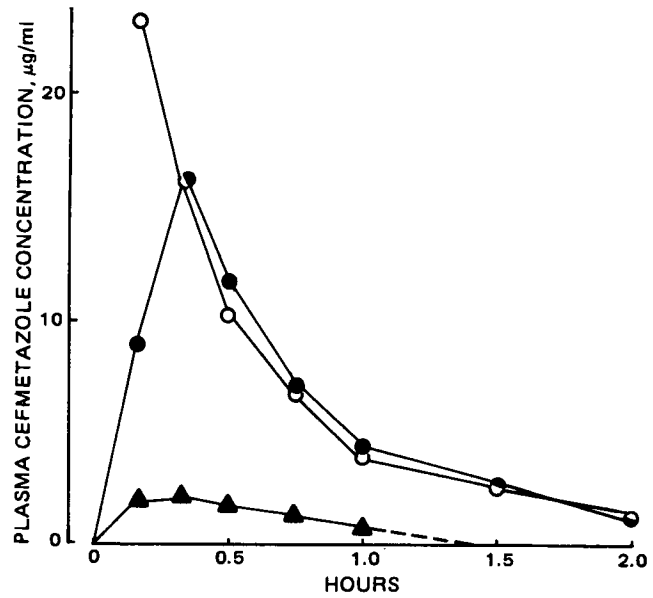

Figure 12—*Plasma cefmetazole concentration (μg/ml) in the rat from an intravenous injection of 10 mg/kg (○) and from a microenema containing 30 mg/kg cefmetazole (▲,●) and 30 mg/kg (●) of 5-methoxysalicylate or no adjuvant (▲).*

The relationship between the percent loss of adjuvant from perfusate at pH 7.4 and the extent of binding of the adjuvant with fat rectal tissue at the same pH is shown in Fig. 7. Figure 8 compares the percent loss of cefmetazole after a 1-hr perfusion in the presence of adjuvant with the percent of binding of the adjuvant. These data show a good correlation between the amount of adjuvant and drug lost and the binding of the adjuvant to rectal tissue. Those adjuvants with relatively high binding to the rectal tissue disappeared to a greater extent and promoted the disappearance of drugs more than those with little binding.

Thus, it appears that binding to some feature of the rectal membrane is necessary for facilitated rectal absorption of drugs and may suggest some type of active transport.

Effects of Adjuvants on Plasma Levels—The effect of homovanillate and 5-methoxysalicylate on the absorption of theophylline and cefmetazole after rectal administration as a microenema at pH 7.4 as reflected in plasma levels of the drug are shown in Figs. 9–12. In each case the absorption was rapid and facilitated by the presence of either homovanillate or 5-methoxysalicylate in the microenema solution and depended on the concentration of the adjuvant. Absolute bioavailabilities of theophylline and cefmetazole as a function of the concentration of homovanillate and 5-methoxysalicylate are shown in Table III.

REFERENCES

(1) T. Nishihata, J. H. Rytting, and T. Higuchi, *J. Pharm. Sci.*, **69**, 744 (1980).

(2) *Ibid.*, **70**, 71 (1981).

(3) *Ibid.*, **71**, 869, 1982.

ACKNOWLEDGMENTS

Supported in part by a grant from INTERx Research Corp., Lawrence, Kan. and R. P. Scherer, North American, Detroit, Mich.

Effect of Salicylate on the Rectal Absorption of Lidocaine, Levodopa, and Cefmetazole in Rats

TOSHIAKI NISHIHATA, J. HOWARD RYTTING[x], and TAKERU HIGUCHI

Received October 27, 1980, from the *Pharmaceutical Chemistry Department, The University of Kansas, Lawrence, KS 66045.* Accepted for publication November 3, 1981.

Abstract □ Salicylic acid and sodium salicylate have been found to enhance the absorption of lidocaine, levodopa, and cefmetazole after rectal administration to rats. These drugs represent a base (lidocaine), an acid (cefmetazole), and a substance (levodopa) which exists as a zwitterion in solution. The rectal absorption of each type of drug, as well as theophylline, a neutral compound, was enhanced by salicylate, particularly at pH values where the substances exist primarily in their ionic form. A requirement for the observed enhancement is that salicylate be present in the rectal membrane. The loss of drug from the perfusing solution was greater from solutions having an ionic strength of 0.75 than from those with $\mu = 0.15$.

Keyphrases □ Absorption, rectal—effect of salicylate on rectal absorption of lidocaine, levodopa, and cefmetazole, rats □ Salicylate—effect on rectal absorption of lidocaine, levodopa, and cefmetazole, rats □ Lidocaine—effect of salicylate on rectal absorption, rats □ Levodopa—effect of salicylate on rectal absorption, rats □ Cefmetazole—effect of salicylate on rectal absorption, rats

It has been reported (1, 2) that salicylate markedly enhanced the rectal absorption of theophylline. It was suggested that the effect of salicylate depends on its presence in the rectal membrane. It was also observed that the changes in absorption required the presence of salicylate in the formulation and that the mechanism of enhancement is different from that of surfactants.

The present report describes the extension of the use of salicylate to enhance the absorption of lidocaine, levodopa, and cefmetazole after rectal administration to rats. The drugs selected represent four different chemical classes: theophylline is a neutral substance, lidocaine is a basic material, cefmetazole is acidic, and levodopa exists as a zwitterion in solution. Furthermore, each of these drugs exhibits some difficulties in its administration and absorption. For example, it has been reported (3) that levodopa given rectally resulted in no rise in blood levodopa concentrations and no clinical benefit after rectal administration to parkinsonian patients. The purpose of this study was to examine to what extent the effects of salicylate are general and the extent rectal absorption enhancement depends on the specific drugs used. In addition, studies involving intravenous administration of salicylate were included to provide additional information about the mechanism of enhancement.

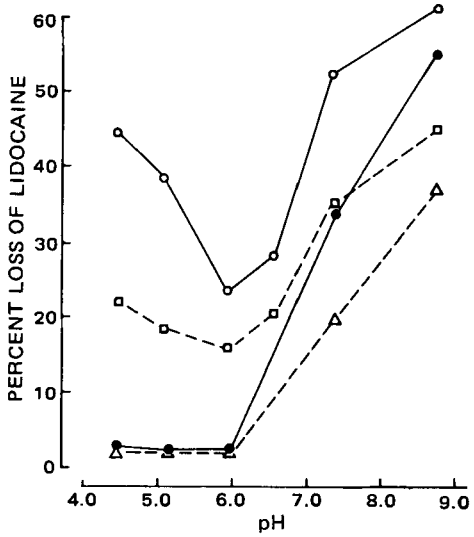

Figure 1—*Effect of pH, ionic strength, and salicylate on the disappearance of lidocaine hydrochloride from a perfusate in the rat rectum after 1 hr. The initial lidocaine hydrochloride concentration was 500 μg/ml, and the sodium salicylate concentration was 0.5 (○ and □) or 0% (● and △). The ionic strength was 0.75 (—) or 0.15 (- - -).*

EXPERIMENTAL

Materials—Sodium salicylate[1], lidocaine[2], sodium cefmetazole[3], and levodopa[3] were used as obtained from the manufacturers.

Animals—Sprague-Dawley male rats (200–300 g) were used in this study and were fasted for 16 hr prior to the experiment. During the experiment, the rats were kept on a 38° surface and were anesthetized with pentobarbital (60 mg/kg).

The *in situ* perfusion of the rat rectum and the *in vivo* absorption studies were carried out as described previously (1, 2) with the following modifications: The pH of the perfusate was maintained constant by either the addition of 0.1 *N* NaOH or 0.1 *N* HCl as needed. Some experiments were also carried out at an ionic strength of 0.15 and 0.75 using sodium chloride to obtain the desired ionic strength. The *in vivo* absorption studies involved administering 0.3 ml of the drug solution into a 2-cm section of the rectum which was isolated by ligation with thread.

Intravenous Infusion Studies—To maintain constant plasma salicylate concentrations, an intravenous infusion method was used for some experiments. After the rats were anesthetized with pentobarbital, a sodium salicylate solution (300 mg/ml), adjusted to pH 7.4 with 0.0114 *M* phosphate buffer, was infused into the leg vein of the rat through a polyethylene canula at a flow rate of 0.05 ml/min during the first 10 min and then at a flow rate of 0.02 ml/min for another 60 min. Beginning 10 min after starting the infusion of the salicylate solution, blood samples

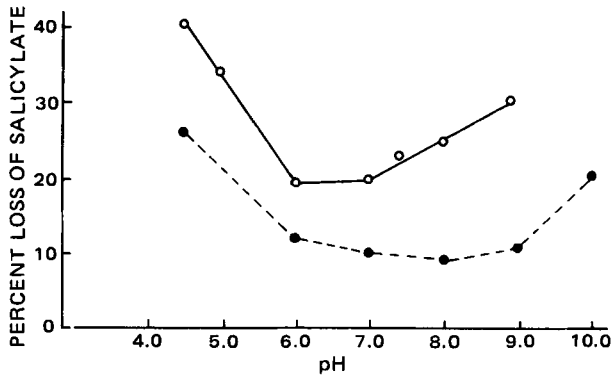

Figure 2—*The percent loss of salicylate from a perfusate as a function of pH having an initial concentration of 0.5% and ionic strength of 0.75 (○) and 0.15 (●).*

[1] Aldrich Chemical Co., 99+%.
[2] Sigma Chemical Co.
[3] Sankyo.

0022-3549/82/0800-0869$01.00/0

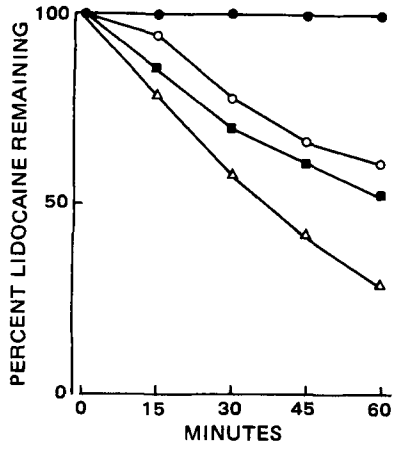

Figure 3—*The percent of lidocaine hydrochloride remaining in perfusate at pH 4.5 and an ionic strength of 0.75 with an initial lidocaine hydrochloride concentration of 500 μg/ml and sodium salicylate concentrations of 0 (●), 0.3 (○), 0.5 (■), and 1% (△).*

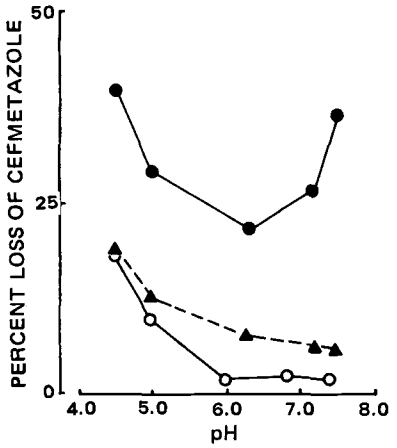

Figure 4—*Effect of pH and salicylate on the disappearance of cefmetazole from a perfusate in the rat rectum after 1 hr. The initial cefmetazole concentration was 200 μg/ml (○, ▲, and ●) and the sodium salicylate concentration was 0.5% (● and ▲). The ionic strength was 0.75 (○ and ●) and 0.15 (▲).*

were taken from the jugular vein at regular intervals to measure the concentration of salicylate in the plasma.

Assay Methods—Salicylate, theophylline, lidocaine, and levodopa were assayed by HPLC as described previously (2). For lidocaine a strong cation exchange column of 25-cm length was used. The mobile phase was 0.1 *M* acetate buffer at pH 3.0. The flow rate was 1 ml/min and a UV detector at 220 nm was used. For levodopa a reversed-phase column with a water–methanol mixture (95:5) as mobile phase was employed. The system was monitored at 254 nm.

The salicylate in the plasma was extracted with ether at a pH <2.0 after deproteinization with a 3.0% trichloroacetic acid solution. Following centrifugation, the ether layer was evaporated and the sediment was dissolved in methanol.

The lidocaine in the plasma was extracted with ether at pH 9.0 after deproteinization with a 3.0% trichloroacetic acid solution. Following centrifugation, the ether layer was evaporated and the sediment was dissolved in methanol.

Table I—Absolute Bioavailability of Cefmetazole as a Function of Initial Salicylate Concentration

Salicylate Dose, mg/kg	Bioavailability, %
0	—
5	22.8 ± 6.5[a]
10	34.5 ± 9.2
15	52.5 ± 7.3
25	91.4 ± 12.3
40	98.6 ± 15.7

[a] Uncertainties are expressed as standard deviations ($n \geq 4$).

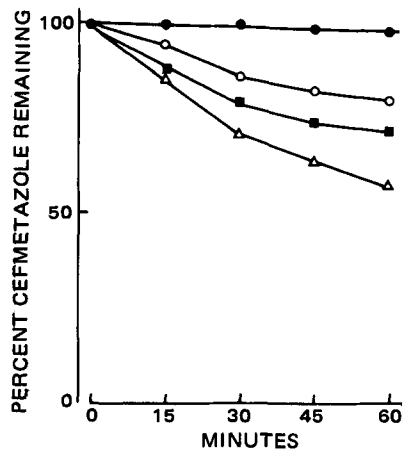

Figure 5—*The percent of cefmetazole remaining in perfusate at a pH of 7.4 and an ionic strength of 0.75 with an initial cefmetazole concentration of 200 μg/ml and sodium salicylate concentrations of 0 (●), 0.3 (○), 0.5 (■), and 1% (△).*

The levodopa in the plasma was extracted with acetone (5 times the sample volume). Following centrifugation, the supernate was evaporated and the sediment was dissolved in water.

Cefmetazole was also assayed by liquid chromatography using a high resolution reversed-phase column and an ion-pairing technique. The mobile phase consisted of a mixture of 77.5% (v/v) 0.025 *M* citrate buffer at pH 5.0 containing 0.005 *M* tetrabutylammonium (ion-pairing agent) and 22.5% (v/v) acetonitrile. The column effluent was monitored by UV absorption at 254 nm and peak height measurements were used for quantitation. The column was maintained at room temperature.

One-milliliter cefmetazole plasma samples were mixed with 0.1 ml of 0.01 *M* phosphoric acid and 0.6 ml of acetonitrile for 20–30 sec and then centrifuged at ~2000 rpm for 5 min. The supernate was then evaporated to dryness under nitrogen and the residue dissolved in 0.1 ml of water just prior to assay. Blank plasma samples containing drug concentrations up to 30 μg/ml were also measured to establish a calibration curve.

RESULTS AND DISCUSSION

Drug Disappearance from Perfusate—The pH profile of the effect of salicylate on the disappearance of lidocaine from a perfusate in the rat rectum is shown in Fig. 1. At pH values >6 and in the absence of salicylate, lidocaine disappeared readily from the perfusate and the presence of salicylate enhanced absorption only moderately. However, lidocaine loss was very small from acidic solutions in the absence of salicylate. At pH values <6, the presence of salicylate markedly enhanced the loss of lidocaine from perfusate solutions.

It is also apparent from Fig. 1 that the loss of lidocaine from the perfusate is greater with an ionic strength of 0.75 than at 0.15 using sodium chloride to adjust the ionic strength. As shown in Fig. 2, the loss of sali-

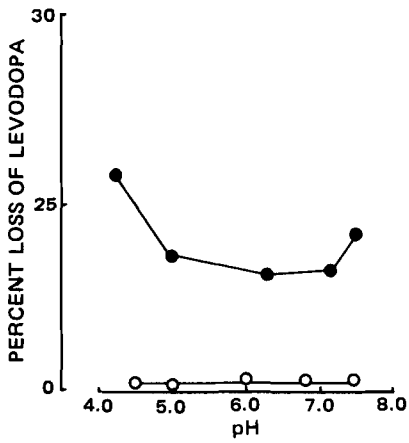

Figure 6—*Effect of pH and salicylate on the disappearance of levodopa from a perfusate in the rat rectum after 1 hr. The initial levodopa concentration was 200 μg/ml (○ and ●) and the sodium salicylate concentration was 0.5% (●).*

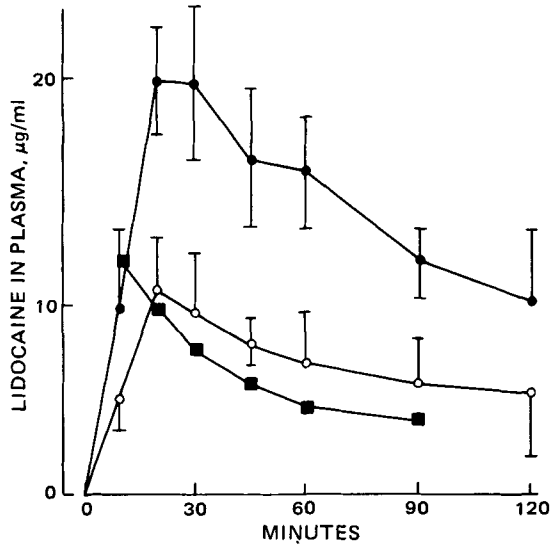

Figure 7—*Concentration of lidocaine in the plasma as a function of time after rectal administration of a microenema at pH 4.5 and a lidocaine hydrochloride dose of 60 mg/kg (● and ○) and sodium salicylate doses of 7.5 (○) and 15 mg/kg (●). Uncertainties are expressed as standard deviations by the error bars with* n = 6. *Lidocaine hydrochloride was also given intravenously (■) with a dose of 20 mg/kg.*

cylate is also greater at $\mu = 0.75$ than 0.15 from the perfusate at all pH values studied.

It appears that lidocaine is well absorbed from the rat rectum in the nonionic form which would predominate at basic pH values, but is not well absorbed from acidic solutions in which lidocaine exists as the protonated species. The presence of salicylate in the perfusate significantly increases the absorption of the water soluble form which is not absorbed effectively in the absence of salicylate.

As shown in Fig. 3, increasing the initial concentration of salicylate results in more rapid loss of lidocaine from the perfusate at pH 4.5. However, as reported previously (2), the disappearance rate constant of salicylate from the perfusate does not depend on the initial concentration of salicylate in the perfusate at a pH of 4.5, indicating that the disappearance of lidocaine from perfusate at a pH of 4.5 may depend on the amount of salicylate in the rectal membrane.

The loss of cefmetazole from perfusate in the rat rectum in the absence of salicylate was small as illustrated in Figs. 4 and 5. The addition of salicylate to the perfusate facilitated the disappearance of cefmetazole at all pH values. Again, the greatest enhancement was found at pH values at which the drug existed in the ionized state and at the higher ionic strength ($\mu = 0.75$). In fact, the effect of ionic strength is more pronounced for cefmetazole than for lidocaine. Furthermore, it was again observed that increasing concentrations of salicylate resulted in a more rapid disappearance of cefmetazole from the perfusing solution.

The presence of salicylate in the perfusate also promoted the disappearance of levodopa which was not absorbed significantly in the absence of salicylate at any pH (Fig. 6). The greatest enhancement occurred at

Table II—The Effect of Salicylate Given Intravenously on the Loss of Cefmetazole and Theophylline from Perfusate [a]

Minutes	Plasma Salicylate Concentration, mg/ml	Percent Remaining in Perfusate	Percent Remaining with no Salicylate (intravenous)
Cefmetazole			
0	1.99 ± 0.35	100	100
15	2.15 ± 0.28	100	100
30	2.28 ± 0.43	98.4 ± 0.5	99.5 ± 0.2
45	2.12 ± 0.30	97.6 ± 0.9	98.3 ± 0.8
60	2.03 ± 0.18	95.8 ± 1.2	96.2 ± 1.9
Theophylline			
0	2.13 ± 0.30	100	100
15	2.38 ± 0.43	100	100
30	2.45 ± 0.26	99.1 ± 0.3	99.2 ± 1.0
45	2.08 ± 0.25	97.8 ± 1.1	97.3 ± 0.8
60	2.21 ± 0.31	95.8 ± 1.1	95.4 ± 2.1

[a] Uncertainties are expressed as standard deviations ($n \geq 4$).

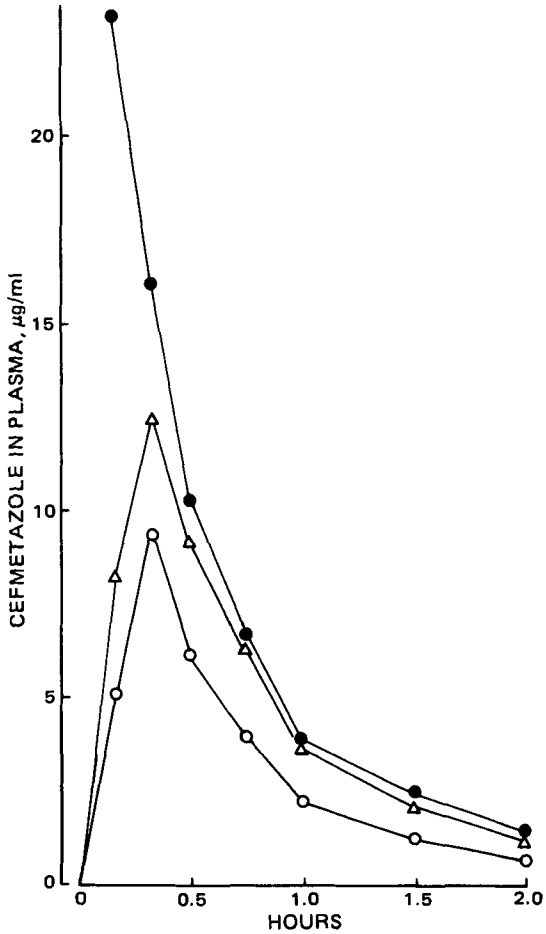

Figure 8—*Concentration of cefmetazole in the plasma as a function of time following rectal administration of a microenema at pH 7.4 and a cefmetazole dose of 15 mg/kg and 25 (○) or 40 mg (△) of sodium salicylate. Cefmetazole (10 mg/kg) was also given intravenously (●).*

pH values <5 and >7. Loss of levodopa was also more rapid with increasing concentrations of salicylate in the perfusate.

It was previously reported (1, 2) that salicylate itself was well absorbed at pH values <5 and >7.4. Thus, the disappearance rates of lidocaine, cefmetazole, and levodopa appear to depend on the effective disappearance of salicylate.

Plasma Levels Obtained from Microenemas—Lidocaine was administered as a solution at pH 4.5 because the perfusate studies indicated that it was absorbed at pH 7.4 in the absence of salicylate. Cefmetazole and levodopa were administered in solutions having pH values of 7.4.

As shown in Fig. 7, the plasma levels of lidocaine increased rapidly after rectal administration in the presence of salicylate. However, in the absence of salicylate, no lidocaine was found in the plasma. The detection limit for lidocaine was 2.5 μg/ml. Figure 6 also indicates that a higher dose of salicylate resulted in a higher blood level of lidocaine. As reported earlier (2), upon addition of salicylate at doses >15 mg/kg, the absolute bioavailability of lidocaine was nearly 100%.

Salicylate also markedly increased the blood levels of cefmetazole as illustrated in Fig. 8. Without the presence of salicylate, no cefmetazole was detected in the plasma. The minimum assay sensitivity was 0.1 μg/ml; however, in the presence of salicylate in solution, the plasma cefmetazole levels increased rapidly with maximum levels being reached 30 min after rectal administration. The absolute bioavailability as a function of salicylate concentration is shown in Table I.

As shown in Fig. 9, similar results were obtained for levodopa. In the absence of salicylate, levodopa was not found in the plasma. The sensitivity of the assay was 0.25 μg/ml. The absolute bioavailability of levodopa was ~75% in the presence of 15 mg of salicylate/kg.

These results indicate that salicylate may facilitate the rectal absorption of many types of drug substances, particularly in their ionic form.

Requirement of Salicylate in the Rectal Membrane—The disappearance of drug from the rectum appears to depend on the concurrent

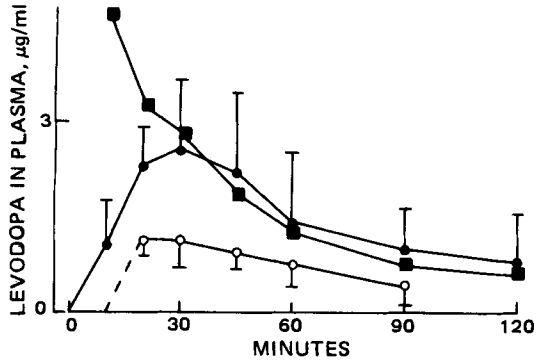

Figure 9—*Concentrations of levodopa in the plasma as a function of time following rectal administration of a microenema at pH 7.4 and a levodopa dose of 15 (● and ○), 7.5 (○), and 15 mg/kg (●) of sodium salicylate. Levodopa (10 mg/kg) was also given intravenously (■).*

rise in the plasma salicylate concentration after the simultaneous rectal administration of both salicylate and drug as shown in Fig. 10 for cefmetazole and levodopa. To examine the effect of salicylate levels independent of rectal absorption, the effect of salicylate given intravenously on the rectal absorption of cefmetazole and theophylline was studied. In this study, sodium salicylate was given by an intravenous infusion to maintain a relatively high plasma salicylate concentration of ~2 mg/ml. As shown in Table II and Fig. 10, salicylate in the plasma alone did not affect the loss of cefmetazole or theophylline from the solution perfusing the rat rectum. Furthermore, no salicylate was found in the perfusate, indicating that little if any salicylate was present in the rectal membranes after intraveous infusion of salicylate. Although salicylate is readily absorbed from the rectum to the plasma, the reverse does not occur under these conditions. It also appears that salicylate does not promote rectal drug absorption except when it is present in the rectal tissue. This is supported by the observation (2) that the enhancement of theophylline absorption from the rectum by salicylate was eliminated by washing the rectum with a buffer solution after pretreatment with salicylate. This is in contrast to the effect of sodium lauryl sulfate which continued after washing the rectum following pretreatment with sodium lauryl sulfate.

It appears that salicylate interacts with some feature of the rectal membrane facilitating the transport of drug substances from the rectum

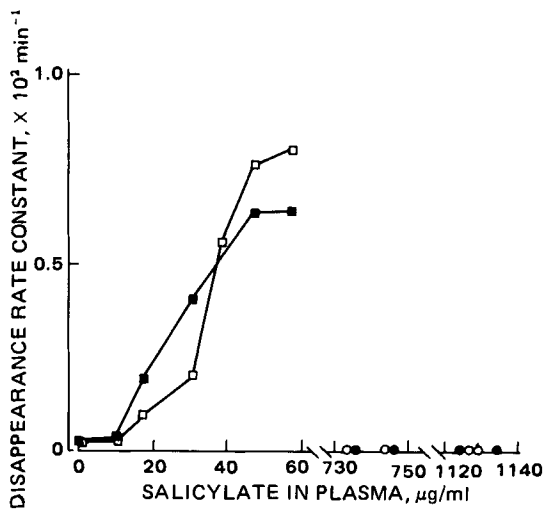

Figure 10—*Disappearance rate constant (× 10^2 min^{-1}) of cefmetazole (■) and levodopa (□) from perfusate as a function of salicylate concentration in the plasma following rectal administration. High plasma concentrations of salicylate following intravenous salicylate administration did not result in significant disappearance of cefmetazole (●) or levodopa (○).*

to the general circulation. Studies are continuing on the mechanism of this action.

REFERENCES

(1) T. Nishihata, J. H. Rytting, and T. Higuchi, *J. Pharm. Sci.*, **69**, 744 (1980).

(2) *Ibid.*, **70**, 71 (1981).

(3) T. Eisler, N. Eng, C. Plotkin, and D. B. Calne, *Neurology*, **31**, 215 (1981).

ACKNOWLEDGMENTS

Supported in part by a grant from INTER$_x$ Research Corporation, Lawrence, Kan. and R. P. Scherer, North America, Detroit, Mich.

Analysis of Iodochlorhydroxyquin in Cream Formulations and Bulk Drugs by High-Performance Liquid Chromatography

E. J. KUBIAK and J. W. MUNSON ˣ

Received June 6, 1981, from the *Quality Control Division, The Upjohn Company, Kalamazoo, MI 49001.* Accepted for publication October 23, 1981.

Abstract □ A high-performance liquid chromatographic method for the analysis of iodochlorhydroxyquin in creams and as bulk drugs has been developed. Iodochlorhydroxyquin was acetylated in the 8-position by reaction with acetic anhydride in pyridine. The resulting ester was mixed with the internal standard and chromatographed on a microparticulate silica column. Recovery was quantitative and the method was shown to be applicable to cream formulations from several manufacturers.

Keyphrases □ Iodochlorhydroxyquin—analysis in cream formulations and bulk drugs, high-performance liquid chromatography □ High-performance liquid chromatography—iodochlorhydroxyquin, analysis in cream formulations and bulk drugs □ Cream formulations—analysis of iodochlorhydroxyquin and bulk drugs by high-performance liquid chromatography

Iodochlorhydroxyquin (5-chloro-7-iodo-8-hydroxyquinoline) (I) has antifungal and antibacterial activities and is used in the treatment of inflamed skin conditions such as eczema, athlete's foot, and other fungal infections. Its use is generally limited to topical applications and is commercially available in lotion, cream, and ointment formulations. It is frequently formulated in combination with the corticosteroid, hydrocortisone. Monographs for

0022-3549/82/0800-0872$01.00/0

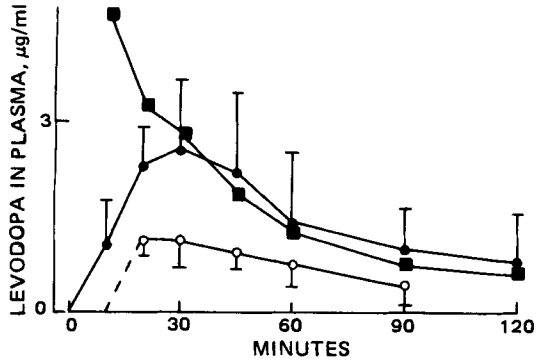

Figure 9—*Concentrations of levodopa in the plasma as a function of time following rectal administration of a microenema at pH 7.4 and a levodopa dose of 15 (● and ○), 7.5 (○), and 15 mg/kg (●) of sodium salicylate. Levodopa (10 mg/kg) was also given intravenously (■).*

rise in the plasma salicylate concentration after the simultaneous rectal administration of both salicylate and drug as shown in Fig. 10 for cefmetazole and levodopa. To examine the effect of salicylate levels independent of rectal absorption, the effect of salicylate given intravenously on the rectal absorption of cefmetazole and theophylline was studied. In this study, sodium salicylate was given by an intravenous infusion to maintain a relatively high plasma salicylate concentration of ~2 mg/ml. As shown in Table II and Fig. 10, salicylate in the plasma alone did not affect the loss of cefmetazole or theophylline from the solution perfusing the rat rectum. Furthermore, no salicylate was found in the perfusate, indicating that little if any salicylate was present in the rectal membranes after intraveous infusion of salicylate. Although salicylate is readily absorbed from the rectum to the plasma, the reverse does not occur under these conditions. It also appears that salicylate does not promote rectal drug absorption except when it is present in the rectal tissue. This is supported by the observation (2) that the enhancement of theophylline absorption from the rectum by salicylate was eliminated by washing the rectum with a buffer solution after pretreatment with salicylate. This is in contrast to the effect of sodium lauryl sulfate which continued after washing the rectum following pretreatment with sodium lauryl sulfate.

It appears that salicylate interacts with some feature of the rectal membrane facilitating the transport of drug substances from the rectum

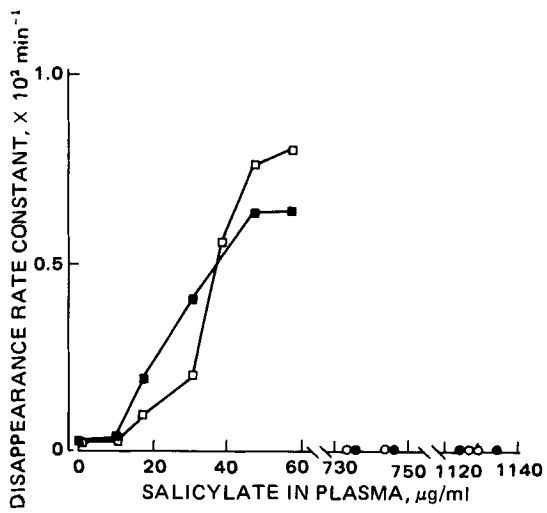

Figure 10—*Disappearance rate constant (× 10^2 min^{-1}) of cefmetazole (■) and levodopa (□) from perfusate as a function of salicylate concentration in the plasma following rectal administration. High plasma concentrations of salicylate following intravenous salicylate administration did not result in significant disappearance of cefmetazole (●) or levodopa (○).*

to the general circulation. Studies are continuing on the mechanism of this action.

REFERENCES

(1) T. Nishihata, J. H. Rytting, and T. Higuchi, *J. Pharm. Sci.*, **69**, 744 (1980).

(2) *Ibid.*, **70**, 71 (1981).

(3) T. Eisler, N. Eng, C. Plotkin, and D. B. Calne, *Neurology*, **31**, 215 (1981).

ACKNOWLEDGMENTS

Supported in part by a grant from INTER$_x$ Research Corporation, Lawrence, Kan. and R. P. Scherer, North America, Detroit, Mich.

Analysis of Iodochlorhydroxyquin in Cream Formulations and Bulk Drugs by High-Performance Liquid Chromatography

E. J. KUBIAK and J. W. MUNSON ˣ

Received June 6, 1981, from the *Quality Control Division, The Upjohn Company, Kalamazoo, MI 49001.* Accepted for publication October 23, 1981.

Abstract □ A high-performance liquid chromatographic method for the analysis of iodochlorhydroxyquin in creams and as bulk drugs has been developed. Iodochlorhydroxyquin was acetylated in the 8-position by reaction with acetic anhydride in pyridine. The resulting ester was mixed with the internal standard and chromatographed on a microparticulate silica column. Recovery was quantitative and the method was shown to be applicable to cream formulations from several manufacturers.

Keyphrases □ Iodochlorhydroxyquin—analysis in cream formulations and bulk drugs, high-performance liquid chromatography □ High-performance liquid chromatography—iodochlorhydroxyquin, analysis in cream formulations and bulk drugs □ Cream formulations—analysis of iodochlorhydroxyquin and bulk drugs by high-performance liquid chromatography

Iodochlorhydroxyquin (5-chloro-7-iodo-8-hydroxyquinoline) (I) has antifungal and antibacterial activities and is used in the treatment of inflamed skin conditions such as eczema, athlete's foot, and other fungal infections. Its use is generally limited to topical applications and is commercially available in lotion, cream, and ointment formulations. It is frequently formulated in combination with the corticosteroid, hydrocortisone. Monographs for

0022-3549/82/0800-0872$01.00/0

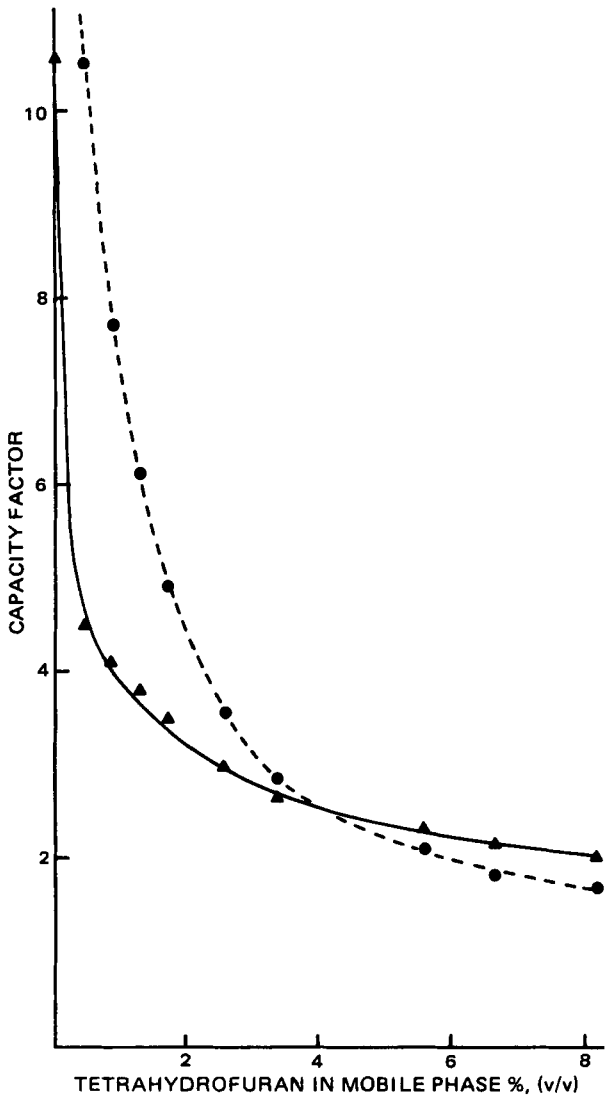

Figure 1—*Effect of tetrahydrofuran on the capacity factor of iodochlorhydroxyquin-8-acetate ester and the internal standard. Key: (●) testosterone acetate; (▲) iodochlorhydroxyquin acetate ester.*

I as bulk drug, cream, ointment, compound powder, and tablets appear in USP XX.

The USP XX assay for I in cream formulations involves extraction of the drug into carbon disulfide and quantitation by IR spectroscopy. The sample preparation in this assay is cumbersome in that it requires multiple extractions and one back-extraction step. Also, the use of quantitation by IR spectroscopy limits the extent to which the assay can be automated.

In this study a chromatographic method was developed with high specificity and an experimentally simple sample preparation. An approach utilizing acetylation of the 8-hydroxy group of I and normal-phase high-performance liquid chromatography (HPLC) was found to satisfy these conditions.

BACKGROUND

The analysis of I in dosage forms and biological samples has been accomplished by TLC, GC, and HPLC. Compound I has been analyzed using silica gel plates with a methanol–methoxyethanol–hydrochloric acid (88:10:2) developing solvent (1). Three unidimensional developments of the plate were required to completely isolate I from frequently encountered impurities. The following compounds were observed as impurities in samples of I: 5,7-dichloro-8-hydroxyquinoline (II); 5,7-diiodo-8-hydroxyquinoline (III); 5-chloro-8-hydroxyquinoline (IV); and 8-hydroxyquinoline (V). In a previous study (2), I was reacted with *N*-trimethylsilylimidazole to form the silyl ether in the 8-position. Silylated I and related compounds were separated and quantitated by GC using a methylsilicone column. The silyl ether was formed by reacting I with *N*-methyl-*N*-silyltrifluoroacetamide, and I was analyzed in several dosage forms by GC (3).

Table I—Relative Retention Times and Relative Responses for Related Compounds

Compound	Relative Retention[a]	Relative Response[b]
5-chloro-7-iodo-8-hydroxyquinoline (I)	1.00	1.00
5,7-dichloro-8-hydroxyquinoline (II)	1.08	0.07
5,7-diiodo-8-hydroxyquinoline (III)	0.94	0.64
5-chloro-8-hydroxyquinoline (IV)	1.45	0.04
8-hydroxyquinoline (V)	Not Detected	

[a] All compounds chromatographed as the 8-acetate ester. [b] Peak height response at 254 nm.

Extractive alkylation has also been used as a derivatizing procedure for I prior to GC analysis. Compound I is extracted into methylene chloride using tetraalkylammonium salts as ion pairing agents. Methyl iodide in the methylene chloride solution then reacts with I to form the 8-methyl ether which is then analyzed by GC. Tetrapentyl- and tetrahexylammonium hydroxide have been used as ion-pairing reagents (4). To avoid problems associated with the hydroxide portion of the ion-pairing reagent, tetrabutylammonium hydrogen sulfate has been employed as the pairing ion in the analysis of I in urine and plasma (5). Acetate ester formation has been used in the GC analysis of I in serum, urine, and milk (6). Compound I is extracted into pyridine–benzene (1:9) and then derivatized with acetic anhydride.

Iodochlorhydroxyquin has also been analyzed in urine by HPLC (7). This method used an anionic exchange resin and gradient elution to achieve satisfactory chromatography.

EXPERIMENTAL

Materials—Testosterone acetate[1], iodochlorhydroxyquin[2], 5,7-diiodo-8-hydroxyquinoline[3], 5,7-dichloro-8-hydroxyquinoline[3], 5-chloro-8-hydroxyquinoline[3], and 8-hydroxyquinoline[3] were used as received. Pyridine[4], glacial acetic acid[4], and acetic anhydride[4] were analytical reagent grade. Butyl chloride[5] and tetrahydrofuran[5] were distilled in glass. Water used in preparation of the mobile phase was deionized.

Mobile Phase—All mobile phases were prepared by mixing water-saturated butyl chloride with butyl chloride at a ratio of 1:1 and then adding the appropriate amounts of tetrahydrofuran and glacial acetic acid. The mobile phase used for analysis of I was butyl chloride–water-saturated butyl chloride–tetrahydrofuran–glacial acetic acid(55:55:3:2). All mobile phases were filtered before use.

Instrumentation—The HPLC system has been described previously (8). The column used contained microparticulate silica[6] (10 μm, 30 cm × 4 mm).

Quantitative Procedure for I in Creams—An accurately weighed quantity of cream equivalent to 30 mg of I was transferred to a 100-ml volumetric flask. Tetrahydrofuran (~70 ml) was added, shaken vigorously until the sample was completely dissolved, and tetrahydrofuran was added to volume. A standard preparation was prepared by dissolving an accurately weighed quantity of I (~30 mg) in 100.0 ml of tetrahydrofuran. The standard and sample preparations (5.0 ml) were transferred into suitable vials. Two milliliters of a pyridine–acetic anhydride mixture (1:1) were added to the sample and each vial was heated for 15 min at 60°. After the samples returned to ambient temperature, 15.0 ml of the internal standard solution, prepared by dissolving 450 mg of testosterone acetate in 60 ml of tetrahydrofuran and then diluting to 1000 ml with butyl chloride, was added and mixed thoroughly. A 3-ml portion of each sample

[1] Steraloids, Inc., Wilton, N.H.
[2] Ciba-Geigy, Summit, N.J.
[3] Aldrich Chemical Co., Milwaukee, Wis.
[4] Mallinckrodt, St. Louis, Mo.
[5] Burdick and Jackson Laboratories, Muskegon, Mich.
[6] μ-Porasil, Waters Associates, Milford, Mass.

Table II—Recovery of I Added to Placebo Formulation

Added, mg/g	Found, mg/g	Recovery, %
22.46	22.98	102.3
26.20	26.54	101.3
29.94	30.16	100.7
33.68	34.00	101.0
37.42	37.46	100.1

Table III—Analysis of I in Cream Formulations

Manufacturer	mg I/g[a]
A	30.6, 30.2
B	30.1, 30.1
	29.8, 29.7
	30.4, 30.3
C	30.5, 29.9
	29.9, 28.8
	30.0, 29.7
	30.2, 30.1
	30.0, 29.6
D	29.9, 30.0
	31.3, 30.7

[a] Duplicate assays. Each pair of results represents a different lot. Label quantity was 30 mg/g (3%).

was transferred to a second vial and evaporated to dryness under a gentle nitrogen flow at 40°. Residue was reconstituted in ~15 ml of mobile phase. (Gentle warming and/or vigorous shaking may be necessary to ensure reconstitution.) Aliquots of the final solution were chromatographed and quantitated using peak height or peak area ratios.

Quantitative Procedure for I Bulk Drug—An accurately weighed quantity of I (~30 mg) was transferred to a 100-ml volumetric flask. The same procedure was followed as with cream.

RESULTS AND DISCUSSION

Initial attempts to develop a direct liquid chromatographic assay for I were unsuccessful. Using silica columns, the retention times were excessive. Using reversed-phase chromatography (octadecylsilane, 10 μm), reasonable elution times were obtained but the peaks exhibited unacceptable tailing in most cases. The observed behavior suggested that I was binding strongly to silanol groups on both types of column packings. To avoid this problem, the approach of acetylating the highly polar 8-hydroxy group was undertaken. The resulting 8-acetate ester was much less polar and could be chromatographed easily using a silica column and a modified butyl chloride mobile phase.

The derivatization reaction (Scheme I) is rapid under the chosen conditions. It was determined experimentally that one-half the amount of acetylating reagent (pyridine–acetic anhydride mixture) called for in the procedure would give quantitative conversion to the ester in 15 min at 60°. It was also found that the reaction gives essentially 100% recovery in 5 min at 60°. The amount of acetylating reagent and the length of reaction time used in the final analytical procedure, therefore, represent excess quantities.

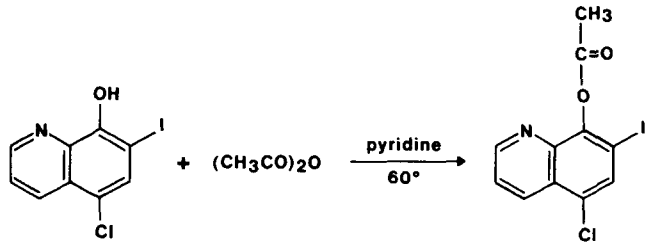

Scheme I

The effects of tetrahydrofuran and acetic acid on the capacity factors for the 8-acetate ester of I and testosterone acetate were studied by varying the amounts added to the mobile phase. The amount of butyl chloride in the mobile phase was kept constant; however, the ratios changed slightly. The effects of varying the amount of acetic acid were minimal. However, small changes in the tetrahydrofuran concentrations caused dramatic shifts in the capacity factors for both compounds as shown in Fig. 1. Therefore, the concentration of tetrahydrofuran must be carefully controlled to obtain reproducible results.

To evaluate the specificity of the chromatographic system, several related compounds were derivatized by acetylation and examined for chromatographic retention and response. Of the compounds tested (Table I), 5,7-diiodo-8-hydroxyquinoline (III) showed the greatest potential for interference. Figure 2 showed the chromatographic tracings

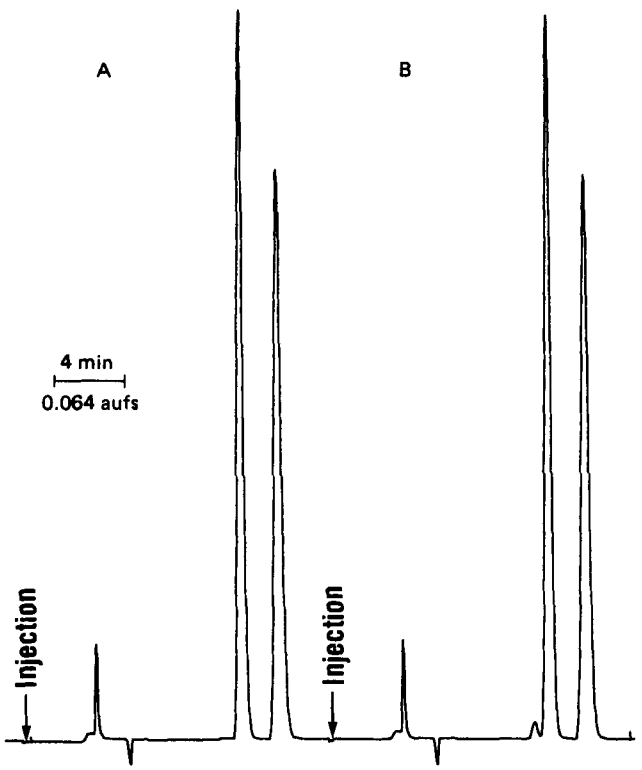

Figure 2—*Chromatographic tracings of a standard preparation before (A) and after (B) adding 3% 5,7-diiodo-8-hydroxyquinoline prior to derivatization step.*

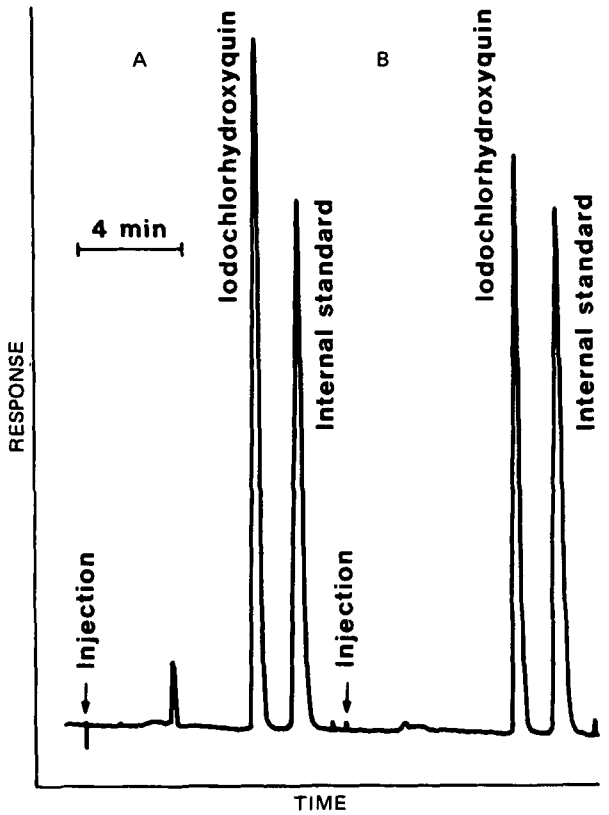

Figure 3—*Typical chromatographic tracings of sample preparation (A) and standard preparation (B). See text for details.*

Table IV—Analysis of Iodochlorhydroxyquin Bulk Drug

Lot	Purity, %	
	Peak Area Calc.	Peak Height Calc.
A	98.9, 98.3	99.4, 98.9
B	99.2, 99.9	99.5, 99.1
C	97.4, 98.7	98.9, 99.4
D	98.5, 98.4	98.3, 98.9
E	99.9, 99.4	99.2, 98.7
F	98.3, 98.9	98.2, 99.2

of a standard preparation before and after the addition of III in an amount equivalent to 3% of I. Baseline resolution was achieved and recovery of III was quantitative over the range of 1.5–5.0% expressed on the basis of I. While 5,7-dichloro-8-hydroxyquinoline elutes near the peak for I, its relative response at 254 nm is very low and should not interfere at low concentrations. Furthermore, no changes in assay results for I were observed with samples spiked with as much as 6% of III.

Typical chromatographic tracings for standard and sample preparations are shown in Fig. 3. No interferences were observed from formulation excipients, even though no sample clean-up steps were employed. No late eluting peaks were observed over an 8-hr period.

Placebo samples with added I were analyzed by this method to determine recovery efficiency. The recovery data (Table II) indicate that the procedure is quantitative for I over the range of 22–37 mg/g. This range corresponds roughly to 75–125% of label for the typical 3% cream formulations (30 mg/g). Replicate analysis of a single lot (n = 8) at 30 mg/g gave a 1.1% *RSD*. Results from the analyses of several lots of cream formulations from five manufacturers are shown in Table III. Good agreement with label content was observed in all cases.

A slightly modified procedure was used to analyze samples of bulk drug. Five samples of I (18–43 mg) were analyzed according to this procedure. The weight of I found was plotted against the weight of I added. The resulting linear regression equation had a slope of 1.00, an intercept of −0.02, and a correlation coefficient of 0.999. One lot of bulk drug was analyzed 10 times to determine the precision of the bulk drug assay. Using peak area ratios as the basis for calculation, the average value was 99.12% purity with a 1.1% *RSD*. Using peak height ratios, the mean was 99.21% purity with a 0.6% *RSD*. Six additional lots of iodochlorhydroxyquin bulk drug were analyzed in duplicate. The results of these assays are shown in Table IV.

REFERENCES

(1) R. O. Valle, D. Jimenez, G. S. Lopez, and J. Schroeder, *J. Chromatogr. Sci.*, **16**, 162 (1978).

(2) M. P. Gruber, R. W. Klein, M. E. Foxx, and J. Campisi, *J. Pharm. Sci.*, **61**, 1147 (1972).

(3) V. Hartmann and W. Herrman, *Pharm. Ind.*, **36**, 203 (1974).

(4) P. H. Degen, W. Schneider, P. Vuillard, U. P. Geiger, and W. Riess, *J. Chromatogr.*, **117**, 407 (1976).

(5) P. Hartvig and C. Fagerlund, *ibid.*, **140**, 170 (1977).

(6) C. Chen, K. Samejima, and Z. Tamura, *Chem. Pharm. Bull.*, **24**, 97 (1976).

(7) C. Chen, K. Hayakawa, T. Imanari, and Z. Tamura, *Chem. Pharm. Sci.*, **69**, 152 (1980).

(8) E. J. Kubiak and J. W. Munson, *J. Pharm. Sci.*, **69**, 152 (1980).

Distribution of Bile Salts Between 1-Octanol and Aqueous Buffer

MADHU VADNERE and SIEGFRIED LINDENBAUM ˣ

Received June 15, 1981, from the *Department of Pharmaceutical Chemistry, The University of Kansas, Lawrence, KS 66045.* Accepted for publication October 13, 1981.

Abstract □ The distribution of four bile salts: sodium cholate (I), sodium deoxycholate (II), sodium chenodeoxycholate (III), and sodium ursodeoxycholate (IV), between aqueous buffer and 1-octanol has been measured as a function of temperature between 25 and 55° and as a function of bile salt concentration at concentrations <0.1 mole/liter in the aqueous phase. The distribution isotherms obtained have been explained on the basis of reversible association in the aqueous phase. The treatment assumes that the bile acid exists as a monomer in the organic phase, which is verified by vapor pressure osmometry. A graphical method has been employed to estimate the association constants in the aqueous phase for the various equilibria encountered. An aggregation number of four for IV and 12 for I, II, and III has been estimated. From the results, thermodynamic functions associated with the transfer of each of the bile salts from water to octanol and those associated with association processes in the aqueous phase were calculated. These results are consistent with previous findings that the premicellar association of bile salts occurs by hydrophobic interaction. The thermodynamics of transfer of bile salts revealed an unfavorable enthalpic and favorable entropic contribution for all four bile salts. However, for IV, which is an epimer of III, both enthalpic and entropic contributions are reduced, compared to III, suggesting a pronounced effect of stereochemical orientation on hydrophobic interaction.

Keyphrases □ Partition coefficient—distribution of bile salts between 1-octanol and aqueous buffer □ Thermodynamics—distribution of bile salts between 1-octanol and aqueous buffer □ Surfactants—distribution of bile salts between 1-octanol and aqueous buffer

Bile salts are biological detergents which play an important role in the dissolution or dispersion of cholesterol and other lipids in the body (1, 2). The solubility of cholesterol in the sodium cholate–water and the sodium cholate–lecithin–water system was studied (3). It was shown (4) that bile salts were capable of solubilizing a large number of poorly water soluble organic and inorganic compounds. The solubilization of various steroidal hormones in bile salt solutions was investigated (5–7). It was demonstrated (8, 9) that the solubilities and dissolution rates of several unrelated poorly water-soluble drugs were

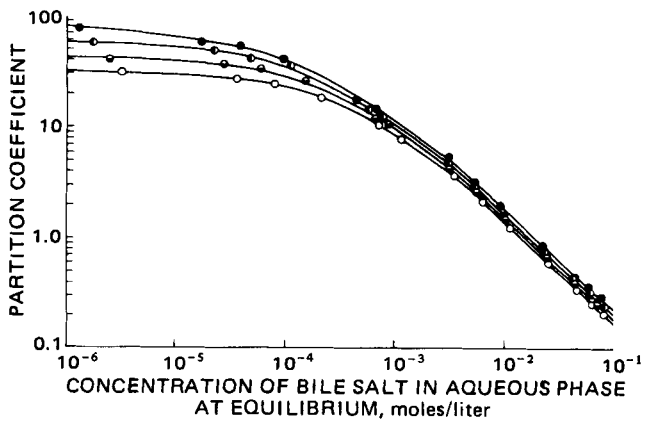

Figure 1—*Distribution isotherms for sodium deoxycholate at 25° (○), 35° (◒), 45° (◐), and 55° (●) between 1-octanol and 0.02 M trometh-amine buffer (pH 8). The solid line is calculated according to Eqs. 15a and b.*

0022-3549/82/0800-0875$01.00/0

Table IV—Analysis of Iodochlorhydroxyquin Bulk Drug

Lot	Purity, %	
	Peak Area Calc.	Peak Height Calc.
A	98.9, 98.3	99.4, 98.9
B	99.2, 99.9	99.5, 99.1
C	97.4, 98.7	98.9, 99.4
D	98.5, 98.4	98.3, 98.9
E	99.9, 99.4	99.2, 98.7
F	98.3, 98.9	98.2, 99.2

of a standard preparation before and after the addition of III in an amount equivalent to 3% of I. Baseline resolution was achieved and recovery of III was quantitative over the range of 1.5–5.0% expressed on the basis of I. While 5,7-dichloro-8-hydroxyquinoline elutes near the peak for I, its relative response at 254 nm is very low and should not interfere at low concentrations. Furthermore, no changes in assay results for I were observed with samples spiked with as much as 6% of III.

Typical chromatographic tracings for standard and sample preparations are shown in Fig. 3. No interferences were observed from formulation excipients, even though no sample clean-up steps were employed. No late eluting peaks were observed over an 8-hr period.

Placebo samples with added I were analyzed by this method to determine recovery efficiency. The recovery data (Table II) indicate that the procedure is quantitative for I over the range of 22–37 mg/g. This range corresponds roughly to 75–125% of label for the typical 3% cream formulations (30 mg/g). Replicate analysis of a single lot (n = 8) at 30 mg/g gave a 1.1% *RSD*. Results from the analyses of several lots of cream formulations from five manufacturers are shown in Table III. Good agreement with label content was observed in all cases.

A slightly modified procedure was used to analyze samples of bulk drug. Five samples of I (18–43 mg) were analyzed according to this procedure. The weight of I found was plotted against the weight of I added. The resulting linear regression equation had a slope of 1.00, an intercept of −0.02, and a correlation coefficient of 0.999. One lot of bulk drug was analyzed 10 times to determine the precision of the bulk drug assay. Using peak area ratios as the basis for calculation, the average value was 99.12% purity with a 1.1% *RSD*. Using peak height ratios, the mean was 99.21% purity with a 0.6% *RSD*. Six additional lots of iodochlorhydroxyquin bulk drug were analyzed in duplicate. The results of these assays are shown in Table IV.

REFERENCES

(1) R. O. Valle, D. Jimenez, G. S. Lopez, and J. Schroeder, *J. Chromatogr. Sci.*, **16**, 162 (1978).

(2) M. P. Gruber, R. W. Klein, M. E. Foxx, and J. Campisi, *J. Pharm. Sci.*, **61**, 1147 (1972).

(3) V. Hartmann and W. Herrman, *Pharm. Ind.*, **36**, 203 (1974).

(4) P. H. Degen, W. Schneider, P. Vuillard, U. P. Geiger, and W. Riess, *J. Chromatogr.*, **117**, 407 (1976).

(5) P. Hartvig and C. Fagerlund, *ibid.*, **140**, 170 (1977).

(6) C. Chen, K. Samejima, and Z. Tamura, *Chem. Pharm. Bull.*, **24**, 97 (1976).

(7) C. Chen, K. Hayakawa, T. Imanari, and Z. Tamura, *Chem. Pharm. Sci.*, **69**, 152 (1980).

(8) E. J. Kubiak and J. W. Munson, *J. Pharm. Sci.*, **69**, 152 (1980).

Distribution of Bile Salts Between 1-Octanol and Aqueous Buffer

MADHU VADNERE and SIEGFRIED LINDENBAUM ˣ

Received June 15, 1981, from the *Department of Pharmaceutical Chemistry, The University of Kansas, Lawrence, KS 66045.* Accepted for publication October 13, 1981.

Abstract □ The distribution of four bile salts: sodium cholate (I), sodium deoxycholate (II), sodium chenodeoxycholate (III), and sodium ursodeoxycholate (IV), between aqueous buffer and 1-octanol has been measured as a function of temperature between 25 and 55° and as a function of bile salt concentration at concentrations <0.1 mole/liter in the aqueous phase. The distribution isotherms obtained have been explained on the basis of reversible association in the aqueous phase. The treatment assumes that the bile acid exists as a monomer in the organic phase, which is verified by vapor pressure osmometry. A graphical method has been employed to estimate the association constants in the aqueous phase for the various equilibria encountered. An aggregation number of four for IV and 12 for I, II, and III has been estimated. From the results, thermodynamic functions associated with the transfer of each of the bile salts from water to octanol and those associated with association processes in the aqueous phase were calculated. These results are consistent with previous findings that the premicellar association of bile salts occurs by hydrophobic interaction. The thermodynamics of transfer of bile salts revealed an unfavorable enthalpic and favorable entropic contribution for all four bile salts. However, for IV, which is an epimer of III, both enthalpic and entropic contributions are reduced, compared to III, suggesting a pronounced effect of stereochemical orientation on hydrophobic interaction.

Keyphrases □ Partition coefficient—distribution of bile salts between 1-octanol and aqueous buffer □ Thermodynamics—distribution of bile salts between 1-octanol and aqueous buffer □ Surfactants—distribution of bile salts between 1-octanol and aqueous buffer

Bile salts are biological detergents which play an important role in the dissolution or dispersion of cholesterol and other lipids in the body (1, 2). The solubility of cholesterol in the sodium cholate–water and the sodium cholate–lecithin–water system was studied (3). It was shown (4) that bile salts were capable of solubilizing a large number of poorly water soluble organic and inorganic compounds. The solubilization of various steroidal hormones in bile salt solutions was investigated (5–7). It was demonstrated (8, 9) that the solubilities and dissolution rates of several unrelated poorly water-soluble drugs were

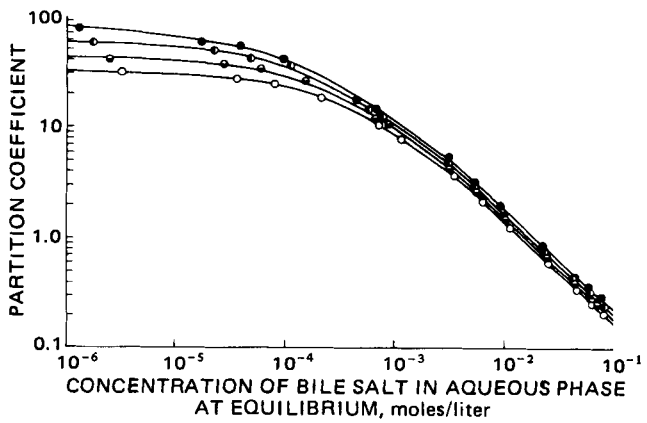

Figure 1—*Distribution isotherms for sodium deoxycholate at 25° (○), 35° (◒), 45° (◐), and 55° (●) between 1-octanol and 0.02 M trometh-amine buffer (pH 8). The solid line is calculated according to Eqs. 15a and b.*

0022-3549/82/0800-0875$01.00/0

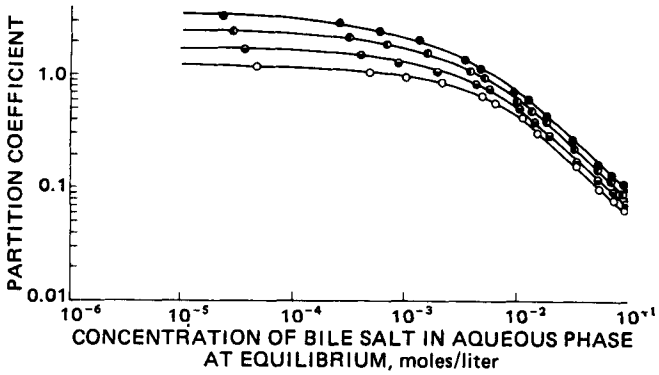

Figure 2—*Distribution isotherms for sodium cholate at 25° (○), 35° (◒), 45° (◐), and 55° (●) between 1-octanol and 0.02 M tromethamine buffer (pH 8). The solid line is calculated according to Eqs. 15a and b.*

increased by the presence of bile salts. Recently, it was reported (10) that the solubility of diazepam increased in bile salt solutions. This ability of bile salts to dissolve water-insoluble material has been attributed to the presence of micelles (2). A knowledge of factors that govern the micellization, therefore, is of great importance in understanding the role of these biological surfactants in the dissolution of poorly water-soluble substances.

As a part of the program to study the aggregation pattern of bile salts in aqueous solution, the partition method offered an interesting tool. The partition method has been used (11–13) to determine the critical micelle concentration of the quaternary ammonium salts. The distribution of four bile salts[1]: sodium cholate (I), sodium deoxycholate (II), sodium deoxychenocholate (III), and sodium ursodeoxycholate (IV) between 1-octanol and aqueous buffer was measured, and the results of these studies have been used to give information on the state of aggregation of bile salts in aqueous solution and the thermodynamics of the transfer process.

EXPERIMENTAL

Materials—The sources of bile acids and their purification are given elsewhere (14). [2,4-^{3}H]Cholic acid in ethanol[2], specific activity 1 mCi/6.7 × 10^{-4} mmoles; [^{3}H,(G)]deoxycholic acid in ethanol[2], specific activity 4 Ci/mmole; and [11,12(H)-^{3}H]chenodeoxycholic acid[3] in toluene–ethanol, specific activity 10.4 Ci/mmole were used without further purification. A sample of [^{14}C(G)]ursodeoxycholic acid[4] was purified by TLC (purity >99%). Benzil[5] was recrystallized several times from methanol, giving a melting point of 95.0 ± 0.5°. 1-Octanol[6] was used as obtained. The water was double deionized. The same liquid scintillation cocktail[7] was used for both aqueous and organic samples.

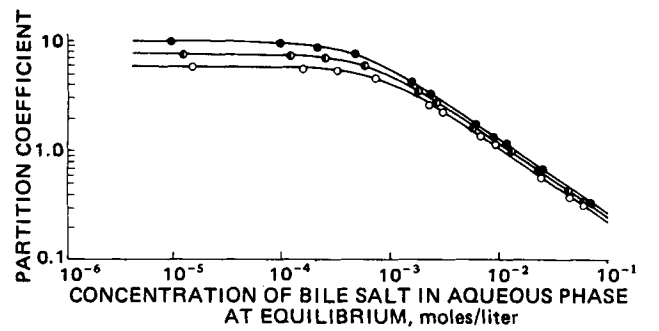

Figure 3—*Distribution isotherms for sodium ursodeoxycholate at 25° (○), 40° (◐), and 55° (●) between 1-octanol and 0.02 M tromethamine buffer (pH 8). The solid line is calculated according to Eqs. 15a and b.*

[1] These compounds exist largely as the free acids in 1-octanol.
[2] New England Nuclear Corp., Boston, Mass.; radiochemical purity was guaranteed to be >98%.
[3] Amersham, Arlington Heights, Ill.; purity >98%.

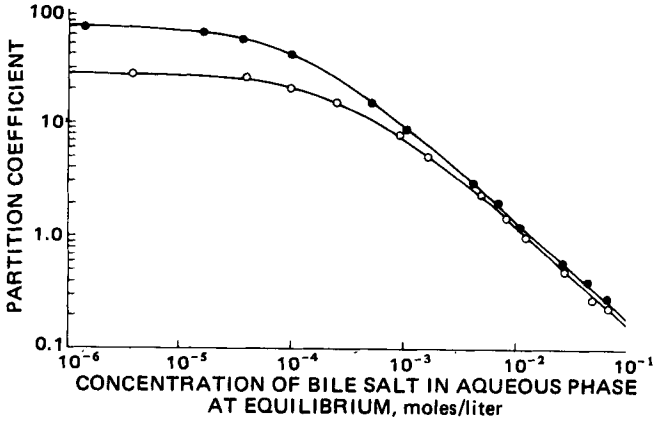

Figure 4—*Distribution isotherms for sodium chenodeoxycholate at 25° (○) and 55° (◐) between 1-octanol and 0.02 M tromethamine buffer (pH 8). The solid line is calculated according to Eqs. 15a and b.*

Partition Coefficient Measurements—The aqueous phase was 0.02 *M* tromethamine buffer (pH 8) and the organic phase was 1-octanol. To minimize volume changes due to mutual solubility, the aqueous and organic phases were presaturated with each other. The aqueous solutions of various concentrations of bile salt were prepared by dilution using a stock solution. ^{3}H-Labeled bile salt was incorporated for analytical determination.

Vials containing 4 ml of octanol and 4 ml of aqueous phase with various amounts of bile salt were shaken for 12 hr in a thermostated water bath. The temperature of the water bath was controlled to ±0.4°. Two samples of 1 ml each from both phases were withdrawn for analysis while keeping the vials thermostated. Scintillation cocktail[7] (10 ml) was added to each sample and mixed thoroughly. Count rates were measured on a liquid scintillation system[8]. The mass balance in the two phases was accounted for within ±2%. The maximum estimated error in the partition coefficient measurements was within ±5%.

Vapor Pressure Osmometry—Vapor pressure osmometry was used to determine the state of association of the bile acids in the organic phase. In this method (15), a steady-state temperature difference between a reference solution and a test solution and the pure solvent was determined. Thermistors were employed as temperature sensors and their electric resistance measured with an osmometer[9]. A solid-state null detector[10] was substituted to improve stability and sensitivity, and the temperature was controlled with a proportional thermistor temperature controller.

HYPOTHETICAL EQUILIBRIA

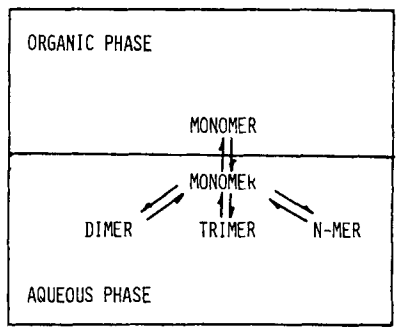

Scheme I

[4] Received from A. F. Hofmann, University of California, San Francisco, Calif.
[5] Eastman Kodak Co., Rochester, N.Y.
[6] Fisher Scientific Co., Pittsburgh, Pa.
[7] Aquasol, New England Nuclear Corp., Boston, Mass.
[8] Model LS 7500, Beckman Instruments, Southfield, Mich.
[9] Wheatstone bridge, Mechrolab Model 301 Vapor Pressure Osmometer.
[10] Keithley, 150B Microvolt Ammeter.

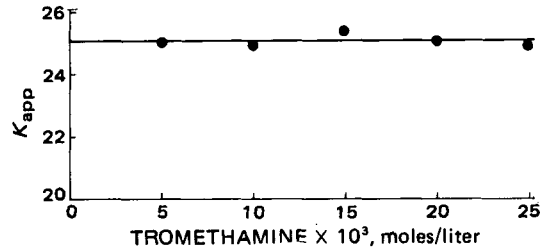

Figure 5—*Effect of concentration of tromethamine buffer on partition coefficient of sodium chenodeoxycholate at 25°, organic phase: 1-octanol, aqueous phase: 0.02 M tromethamine buffer (pH 8).*

RESULTS AND DISCUSSION

The experimental results for the partition of the sodium salts of the bile acids between 0.02 *M* tromethamine buffer (pH 8) and 1-octanol are summarized in Figs. 1–4. Here the partition coefficient, defined as the ratio of the bile salt concentration in the organic phase to the concentration of bile salt in the aqueous phase, is plotted as a function of the equilibrium bile salt concentration (moles/liter) in the aqueous phase. It can be shown that if a solute exhibits ideal behavior in each of two liquids in contact, and in equilibrium, then the partition coefficient is constant, independent of the concentration. It can be seen from Figs. 1–4 that the partition coefficient of all four bile salts studied varies with the concentration. At higher concentrations of bile salt much more solute is found in the aqueous phase than would be expected from a consideration of the partition behavior at lower concentrations.

A sharp break at the critical micelle concentration (CMC) in a plot of C_{org} *versus* C_{aq} was observed (11–13) for quaternary ammonium compounds. A phase separation model for the quaternary ammonium compounds based on the partition behavior was proposed. Unlike quaternary ammonium compounds, bile salts do not exhibit a sharp break in the C_{org} *versus* C_{aq} plot; instead the change in the slope is gradual. This behavior can be explained on the basis of the reversible association of bile salts in the aqueous phase.

Theoretical Considerations—The following treatment of the experimental data can be made by assuming that, although the bile salt present in the aqueous phase is composed of monomers and aggregates of bile salt, only monomeric bile salt is distributed between the two solvents. The hypothetical equilibria involved are presented in Scheme I.

It is conceivable that the monomeric form is partitioned as one or more of three species: free acid; sodium–bile salt ion pair; and tromethamine–bile salt ion pair.

Figure 5 shows the independence of partition coefficient on the tromethamine buffer concentration, indicating that bile salt is not partitioned as tromethamine–bile salt ion pair at pH 8. Figure 6 shows the effect of sodium ion concentration at pH 8 and 9.2. It is evident that at higher pH values, where the bile acid exists mostly in the ionized form, there is a linear dependence of the partition coefficient on the sodium ion concentration; whereas, at pH 8 there is virtually no sodium ion concentration dependence indicating negligible partitioning of bile salt

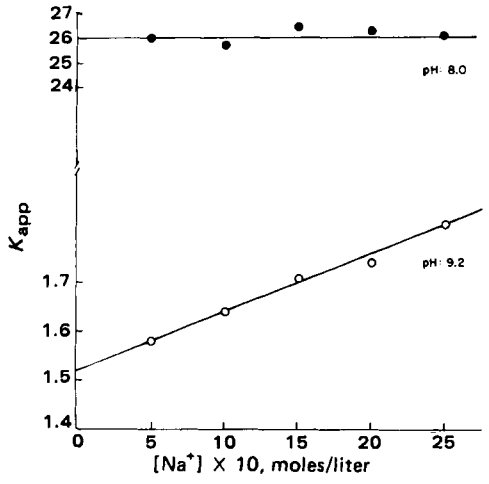

Figure 6—*Effect of sodium ion concentration on partition coefficient of sodium chenodeoxycholate at pH 8.0 (●) and pH 9.2 (○), 25°; organic phase: 1-octanol, aqueous phase: 0.02 M tromethamine buffer.*

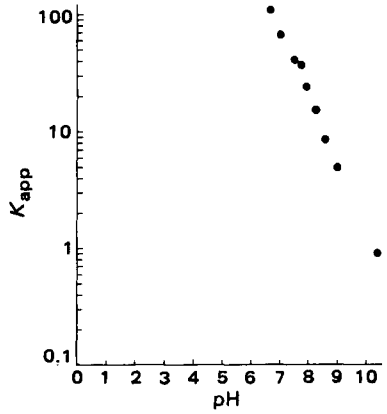

Figure 7—*Effect of hydrogen ion concentration on partition coefficient of sodium chenodeoxycholate at 25°; organic phase: 1-octanol, aqueous phase: 0.02 M tromethamine buffer.*

as the sodium salt ion pair compared to free acid. The marked dependence of partition coefficient on hydrogen ion concentration is seen in Fig. 7.

The concentration in the aqueous phase may be written as[11]:

$$[C]_{aq} = [\text{Monomer}] + 2[\text{Dimer}] + 3[\text{Trimer}] + \ldots \quad \text{(Eq. 1)}$$

where, $[C]_{aq}$ represents the total equilibrium molar concentration of bile salt in the aqueous phase.

Assuming that the association equilibria follow the mass law, the equilibria in the aqueous layer can be described in terms of association constants. Thus:

$$2\ \text{Monomer} \overset{K'_2}{\rightleftharpoons} \text{Dimer}$$

$$3\ \text{Monomer} \overset{K'_3}{\rightleftharpoons} \text{Trimer}$$

Therefore, Eq. 1 may be written as:

$$[C]_{aq} = [M]_{aq} + 2K'_2[M]^2_{aq} + 3K'_3[M]^3_{aq} + \ldots \quad \text{(Eq. 2)}$$

where, $[M]_{aq}$ is the monomer concentration in the aqueous phase. The concentration in the organic phase can be described by the following relationship:

$$[C]_{org} = K\frac{[H^+]}{[H^+] + K_a}[M]_{aq} \quad \text{(Eq. 3)}$$

where K is the intrinsic or true partition coefficient of the acid form, and K_a is the dissociation constant of the bile acid. Let:

$$K\frac{[H^+]}{[H^+] + K_a} = K^0_{app} \quad \text{(Eq. 4)}$$

where K^0_{app} is the apparent partition coefficient at a given pH in the infinitely dilute solution. Then Eq. 3 may be written as:

$$[C]_{org} = K^0_{app}[M]_{aq} \quad \text{(Eq. 5)}$$

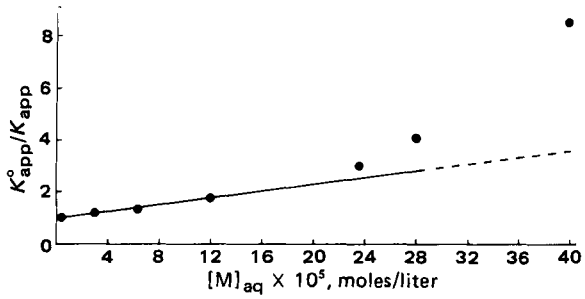

Figure 8—*A plot testing the possible occurrence of dimers in aqueous solutions of sodium deoxycholate at 25° according to Eq. 7.*

[11] The different forms identified as monomer, dimer, trimer, *etc.*, may consist of the free acids, charged anions, or mixtures of the two.

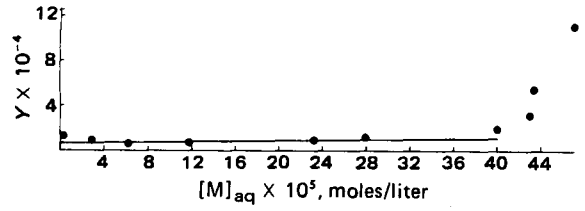

Figure 9—*A plot testing the possible occurrence of dimers and trimers in aqueous solutions of sodium deoxycholate at 25° according to Eq. 10.*

from Eqs. 2 and 5 the following can be written:

$$\frac{[C]_{aq}}{[C]_{org}} = \frac{1 + 2K'_2[M]_{aq} + 3K'_3[M]^2_{aq} + \ldots}{K^0_{app}}$$

or:

$$\frac{K^0_{app}}{K_{app}} = 1 + 2K'_2[M]_{aq} + 3K'_3[M]^2_{aq} + \ldots \quad \text{(Eq. 6)}$$

where $K_{app} = [C]_{org}/[C]_{aq}$ is the partition coefficient at the same given pH but at some finite concentration.

Proposed Testing of Assumptions—Since reversible associations of the type discussed are markedly dependent on the concentration of associating solute, it would be expected that in relatively dilute solutions, dimerization would be the primary equilibrium.

As the concentration of bile acid is increased, the tendency to form higher aggregates would be expected to be more pronounced. With this consideration, a simple test of the proposed relationship can be made.

If, at lower concentration of bile salt, the formation of dimers is the primary equilibrium, then to a first approximation, Eq. 6 can be reduced to:

$$K^0_{app}/K_{app} = 1 + 2K'_2[M]_{aq} \quad \text{(Eq. 7)}$$

From Eqs. 3 and 4, $[M]_{aq}$ can be obtained:

$$\frac{[C]_{org}}{K^0_{app}} = [M]_{aq} \quad \text{(Eq. 8)}$$

Figure 8 summarizes the results obtained when Eq. 7 was tested. The straight line relationship expressed by Eq. 7 is found to exist at lower concentration of II. The curvature apparent at higher concentration is due to the formation of higher polymeric species. The same trend is found for all four bile salts studied.

The proposition that higher polymeric species are found at higher concentration can be tested in a similar manner, for if the bile acid found in the aqueous phase is primarily present as monomer, dimer, and trimer, then Eq. 6 can be approximated by:

$$K^0_{app}/K_{app} = 1 + 2K'_2[M]_{aq} + 3K'_3[M]^2_{aq} \quad \text{(Eq. 9)}$$

or:

$$\frac{(K^0_{app}/K_{app}) - 1}{[M]_{aq}} = Y = 2K'_2 + 3K'_3[M]_{aq} \quad \text{(Eq. 10)}$$

The linearity expressed by this equation is tested in Fig. 9. Here, Y is plotted as a function of monomeric bile salt concentration in the aqueous phase. The expected intercept $2K'_2$ agrees within 5% with the value obtained from Fig. 8. A slope of 2.17×10^7 with correlation coefficient of 0.86 is obtained for this relationship.

By assuming that dimerization and tetramerization are the important equilibria, Eq. 6 may be reduced to:

$$K^0_{app}/K_{app} = 1 + 2K'_2[M]_{aq} + 4K'_4[M]^3_{aq} \quad \text{(Eq. 11)}$$

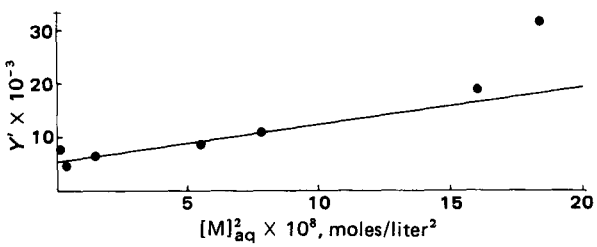

Figure 10—*A plot testing the possible occurrence of dimers and tetramers in aqueous solutions of sodium deoxycholate at 25° according to Eq. 12.*

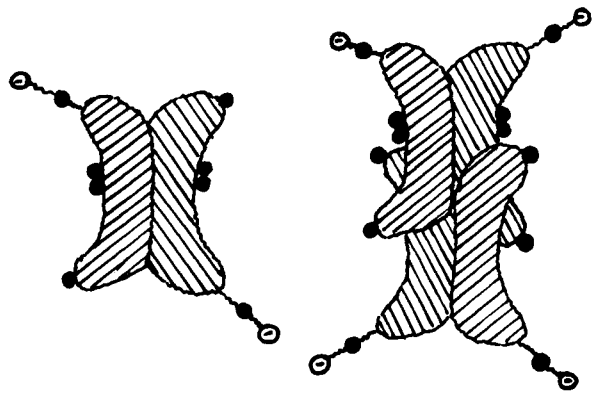

Figure 11—*Longitudual sections of dimers and tetramers; (●) OH groups; (⊖) negatively charged ionic group of bile salt.*

or:

$$\frac{(K^0_{app}/K_{app}) - 1}{[M]_{aq}} = 2K'_2 + 4K'_4[M]^2_{aq} \quad \text{(Eq. 12)}$$

Figure 10 illustrates a plot of this relationship. The theoretically expected straight line relationship is found to exist, with a correlation coefficient of 0.97. The linear relationship for 1-2-3 and 1-2-4 model extends over to the same concentration range with a somewhat better correlation for the latter one, however. Therefore, a monomer–dimer–tetramer species was considered to be prominent in this region. However, the existence of the trimer cannot be ruled out. A preponderance of tetramer over trimer is expected since a pair of dimers can come together with back-to-back hydrophobic interaction to form a tetramer with wide separation of charges (Fig. 11) (16), whereas in the trimer, charges would be expected to be closer, thus rendering it relatively less stable.

A curvature at higher concentration once again indicates that aggregates greater than tetramer are very likely. If it is assumed that, at higher concentration only monomer, dimer, tetramer, and 'n'mer are predominant species, then Eq. 2 reduces to:

$$[C]_{aq} = [M]_{aq} + 2K'_2[M]^2_{aq} + 4K'_4[M]^4_{aq} + nK'_n[M]^n_{aq} \quad \text{(Eq. 13)}$$

Rearranging and taking logs:

$$\log Y'' = \log nK'_n + n \log [M]_{aq} \quad \text{(Eq. 14)}$$

where:

$$Y'' = [C]_{aq} - [M]_{aq} - 2K'_2[M]^2_{aq} - 4K'_4[M]^4_{aq}$$

Thus, a plot of log Y'' *versus* log $[M]_{aq}$ should yield a straight line with slope equal to n, the aggregation number. The linearity of this double log

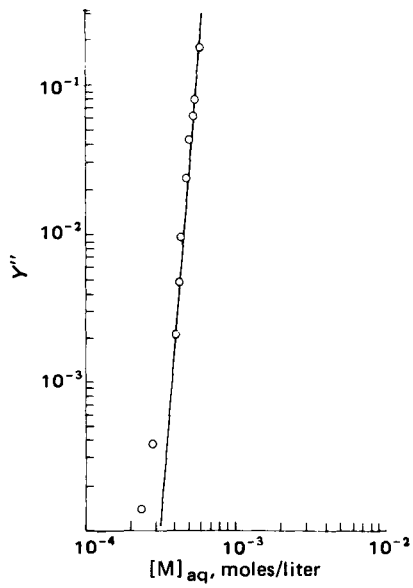

Figure 12—*A plot testing the possible occurrence of dimers, tetramers, and n-mers in aqueous solutions of sodium deoxycholate at 25° according to Eq. 14.*

Table I—Association Constants

Bile Salt (Aggregate Number)	Temp	log K'_2, M/liter^{-1}	log K'_4, M/liter^{-3}	log K'_{12}, M/liter^{-11}
Cholate	25°	2.20	4.00	25.70
(12)	35°	2.39	4.46	26.61
	45°	2.57	4.80	27.48
	55°	2.74	5.30	28.26
Deoxycholate	25°	3.48	10.30	36.78
(12)	35°	3.60	10.54	37.92
	45°	3.72	10.78	39.04
	55°	3.88	11.04	40.08
Ursodeoxycholate	25°	2.35	8.15	—
(4)	40°	2.51	8.45	—
	55°	2.65	8.78	—
Chenodeoxycholate	25°	3.43	10.30	36.78
(12)	55°	3.85	11.60	40.78

plot is tested in Fig. 12. The aggregation number and all the association constants are summarized in Table I. The aggregation number of 12 for II obtained in this study is in close agreement with the value 13 reported previously (17). However, the association constant value, log K'_{13} = 27.4, differs from log K'_{12} = 36.78, obtained in the present study. This discrepancy may be due to the octanol dissolved in the aqueous phase in this study.

It is recognized that the distribution of water and octanol in the equilibrium phases might change with the concentration of bile salt, in which case K^0_{app} would no longer be constant. In this treatment, it is assumed for the sake of simplicity that the composition of the equilibrium phases is unchanged by the presence of bile salt. This assumption may have a small effect on the values of the association constants derived in the treatment.

The partition isotherms were generated using the following:

$$K_{app} = [C]_{org}/[C]_{aq} \qquad \text{(Eq. 15}a\text{)}$$

and:

$$[C]_{aq} = \left(\frac{[C]_{org}}{K^0_{app}}\right) + 2K'_2\left(\frac{[C]_{org}}{K^0_{app}}\right)^2 + 4K'_4\left(\frac{[C]_{org}}{K^0_{app}}\right)^4 + 12K'_{12}\left(\frac{[C]_{org}}{K^0_{app}}\right)^{12} \qquad \text{(Eq. 15}b\text{)}$$

and association constants from Table I. Figures 1–4 show that there is good agreement between the calculated and experimental values.

On the basis of the preceding discussion, it is also possible to calculate the distribution of bile salt/acid in its various forms in aqueous solution. The results of such calculations are illustrated in Fig. 13. Here, the concentration of bile salt as a particular species has been plotted as a function of total concentration of bile salt in solution. The concentration of bile salt as monomers and dimers reaches a plateau, whereas dodecamer is seen to increase as the concentration of total bile salt in the system increases.

All the association constants, K'_2, K'_4, K'_{12}, follow a Van't Hoff type relationship which is seen in Fig. 14. From the slope of these lines it is possible to estimate ΔH^0 for association. The results of such calculations are listed in Table II. These results are in agreement with the expectations that hydrophobic interactions lead to a positive enthalpy change (18).

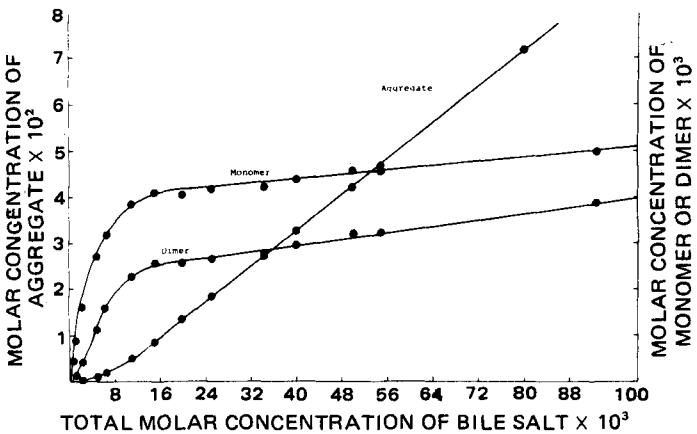

Figure 13—*A plot showing the distribution of sodium cholate among its various forms in aqueous solution at 25°.*

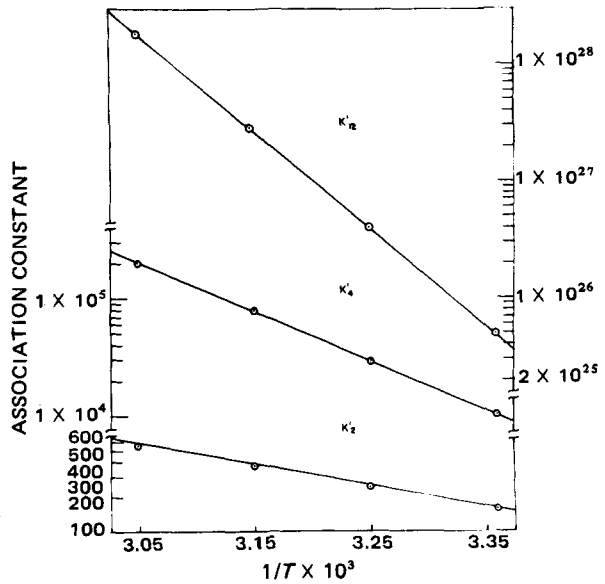

Figure 14—*A plot showing Van't Hoff type relationship for the association constants of sodium cholate.*

Figure 15 shows plots of log K^0_{app} *versus* $1/T$ for all the bile salts studied. If the activity coefficients in the two phases are assumed to be unity in very dilute solution, then from the slope of the plot log K^0_{app} *versus* $1/T$, estimates of ΔH^0 can be obtained. Also by using:

$$-\Delta G^0 = RT \ln K^0_{app}$$

and

$$\Delta G^0 = H^0 - T\Delta S^0$$

all of the thermodynamic functions for the transfer process can be obtained. Table III lists these thermodynamic transfer functions.

The values for the enthalpy of transfer of bile salt from the aqueous to the organic phase are all positive (unfavorable) (Table III). Positive values for ΔH^0 of transfer of hydrocarbon and aliphatic alcohols are also obtained (18). Positive values of ΔH^0 for this process are expected on the basis of the hydrophobic properties of these solutes. In aqueous solution the water molecules in the vicinity of these nonpolar molecules or moieties are more strongly hydrogen bonded so that a region of higher local order exists than in pure water. In partitioning out of the aqueous phase, the normal hydrogen bonded structure resumes, accompanied by a decrease in the amount of hydrogen bonding and a less ordered state. These processes are accompanied by an increase in enthalpy (the energy required to break hydrogen bonds) and an increase in entropy as expected for a loss in order. The data show that the entropy gain is greater for the more hydrophobic molecules. The dihydroxy bile salts, II and III, show a larger entropy change than I: the more polar tri-hydroxy bile salt. The data for IV demonstrate that it is not only the number of hydroxyl groups on the molecule that determine its hydrophobic character, but the orientation is also important. In IV, the —OH groups are no longer all in the α configuration, the —OH group in the 7 position is oriented toward the back of the molecule so that there is no longer a clearly hydrophobic side to the structure. As a consequence, even though it is a dihydroxy bile salt, IV shows a smaller positive change in entropy for the aqueous–organic transfer process than either of the other dihydroxy salts (II and III) or even the trihydroxy salt (I). Even for IV, however, hydrophobic forces appear to predominate since positive values of ΔH^0 and ΔS^0 are still obtained for the transfer process.

One of the assumptions in the foregoing model was that the bile acids do not associate in octanol. This was verified by using vapor pressure osmometry.

Table II—ΔH^0 for Association Process [a]

Bile salt	ΔH^0_{dimer}	$\Delta H^0_{tetramer}$	$\Delta H^0_{dodecamer}$
Cholate	4.0	4.8	3.2
Deoxycholate	3.0	2.8	4.0
Ursodeoxycholate	2.2	2.3	—
Chenodeoxycholate	3.1	4.8	4.9

[a] Kilocalories per mole of bile salt in the aggregate.

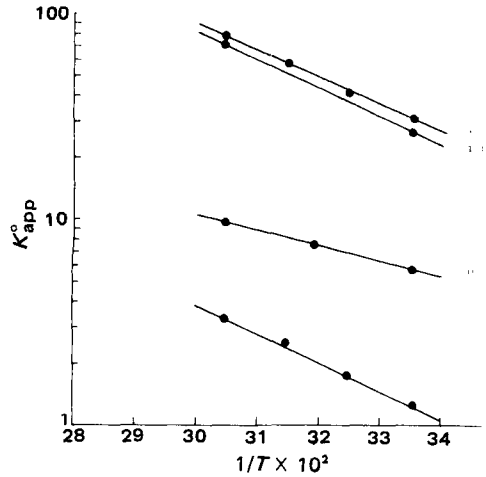

Figure 15—*A plot showing Van't Hoff type relationship for the* K^0_{app}, *sodium deoxycholate (II), sodium cholate (I), sodium ursodeoxycholate (IV), and sodium chenodeoxycholate (III).*

The osmolality of the test solution ($m_x\phi_x$), the reference solution ($m_r\phi_r$) and the measured resistance ratio ($\Delta R_x/\Delta R_r$) are related by:

$$\frac{m_x\phi_x}{m_r\phi_r} = \frac{\Delta R_x}{\Delta R_r}$$

where m is the molality, ϕ is the osmotic coefficient, ΔR is the change in resistance, and x and r refer to test and reference solutions, respectively.

If a nonassociating solute such as benzil is used as a reference, then the deviation of the ratio (ϕ_x/ϕ_r) from unity is related to the extent of association.

Table IV shows the ratio (ϕ_x/ϕ_r) for cholic and deoxycholic acids at 25°. It is seen that the ratio is ~0.8 and above in all cases, suggesting that under the conditions of the partition studies, the bile acid exists mainly as the monomer in the organic phase. It is likely that there is some association in the organic phase. However, for simplicity of calculation, this was assumed to be zero. This approximation may have an effect on the magnitude of the association constants.

Bile Acid–Octanol Complex—Figure 16 shows the effect of varying the ratio of octanol to isooctane in the organic phase, and it can be seen that octanol complexes with bile acid. A quantitative treatment may be obtained by considering that each mole of bile acid $(BA)_{aq}$ complexes with n moles of octanol (X) to give a complex $(BA\ X_n)_{org}$. Thus:

$$(BA)_{aq} + n\ X \overset{K_{eq}}{\rightleftharpoons} (BA\ X_n)_{org} \qquad \text{(Eq. 16)}$$

Accordingly:

$$K_{eq} = \frac{[(BA\ X_n)_{org}]}{[(BA)_{aq}][X]^n} \qquad \text{(Eq. 17)}$$

From Eqs. 15*a* and 17 it follows:

$$\log K_{app} = \log K_{eq} + n \log [M] \qquad \text{(Eq. 18)}$$

Table III—Thermodynamic Transfer Functions

Bile Salt	K^0_{app} 25°	ΔG^0 25°	ΔH^0 Kcal/mole	$T\Delta S^0$
Deoxycholate	32.0	−2.05	+6.0	8.05
Chenodeoxycholate	27.0	−1.95	+6.1	8.05
Ursodeoxycholate	5.8	−1.04	+3.4	4.44
Cholate	1.2	−0.11	+6.3	6.41

Table IV—ϕ_x/ϕ_r Ratio at 25°

Concentration of Bile Acid in Octanol	$\phi_c{}^a/\phi_b{}^b$	$\phi_{dc}{}^c/\phi_b$
0.005 *M*	0.83	0.87
0.010 *M*	0.81	0.83
0.020 *M*	0.76	0.80

[a] cholic acid. [b] benzil. [c] deoxycholic acid.

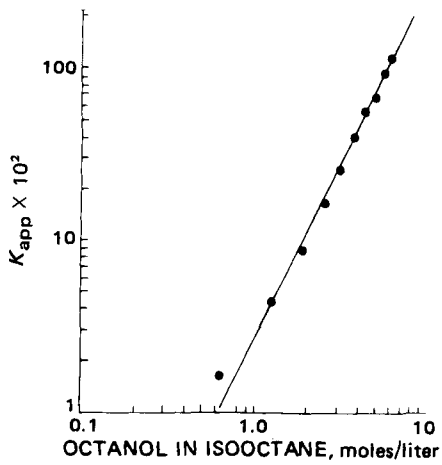

Figure 16—*A plot testing the possible complexation of sodium cholate with octanol according to Eq. 18.*

The linearity predicted in this double log plot is realized in Fig. 16. Binding numbers of 2, 1.7, and 1.8 are found for I, II, and III, respectively, suggesting that each mole of bile acid is solvated or complexed by 2 moles of octanol.

Since the solvation is the same in the organic phase for all bile acids studied, the differences in the free energy of partitioning results entirely from the differences in their interactions with water. The solvation of bile acids by octanol provides further support for the finding that bile acids are monomeric in the organic phase. There is evidence which suggests (19, 20) that in nonhydrogen bonding solvents, bile acids and their esters tend to form dimers and higher aggregates. Studies to determine the nature of the aggregates in nonhydrogen bonding solvents are presented in the following report (21).

REFERENCES

(1) P. H. Elsworthy, A. T. Florence, and C. B. Macfarlane, "Solubilization by Surface Active Agents," Chapman and Hall, London, 1968.

(2) A. F. Hofman and D. M. Small, *Annu. Rev. Med.*, **18,** 333 (1967).

(3) M. C. Bourges, D. M. Small, and D. G. Dervivchian, *Biochim. Biophys. Acta*, **144,** 189 (1967).

(4) F. Verzer, *Nutr. Abstr. Rev.*, **2,** 441 (1933).

(5) P. Ekwall and L. Sjoblom, *Acta. Chem. Scand.*, **3,** 1179 (1949).

(6) P. Ekwall and L. Sjoblom, *Acta Endocrinol.*, **4,** 179 (1950).

(7) P. Ekwall, T. Lundsten, and L. Sjoblom, *Acta Chem. Scand.*, **5,** 1383 (1951).

(8) T. R. Bates, M. Gibaldi, and J. L. Kanig, *Nature (London)*, **210,** 1331 (1966).

(9) T. R. Bates, M. Gibaldi, and J. L. Kanig, *J. Pharm. Sci.*, **55,** 191 (1966).

(10) M. Rosoff and A. T. M. Serajuddin, *Int. J. Pharm.*, **6,** 137 (1980).

(11) J. Czapkiewicz, B. Czapkiewicz Tutaj, and D. Struck, *Polish J. Chem.*, **52,** 2203 (1978).

(12) J. Czapkiewicz and B. Czapkiewicz Tutaj, *J. Colloid Interface Sci.*, **62,** (1977).

(13) B. Czapkiewicz Tutaj and J. Czapkiewicz, *Rocz. Chem. II*, **49,** 1353 (1975).

(14) M. Vadnere, R. Natarajan, and S. Lindenbaum, *J. Phys. Chem.*, **84,** 1900 (1980).

(15) P. Carpenter and S. Lindenbaum, *J. Solution Chem.*, **8,** 347 (1979).

(16) D. M. Small, in "The Bile Acid"—Chemistry: Vol. 1, P. P. Nair and D. Kritchevsky, Eds. Plenum, New York-London, 1971.

(17) S. Makino, J. A. Reynolds, and C. Tanford, *J. Biol. Chem.*, **248,** 4826 (1973).

(18) C. Tanford, "The Hydrophobic Effect," 2nd ed., Wiley, New York, N.Y., 1980.

(19) N. A. Mazer, G. B. Benedek, and M. C. Carey, *Biochemistry*, **19,** 601 (1979).

(20) R. O. Zimmerer and S. Lindenbaum, *J. Pharm. Sci.*, **68,** 581 (1979).

(21) M. Vadnere and S. Lindenbaum, *ibid.*, **71**, 875 (1982).

ACKNOWLEDGMENTS

This work was supported by grants from the National Institutes of Health (AM-18084) and the General Research Fund of the University of Kansas.

The authors thank the Tokyo Tanabe Co., Ltd. for providing the ursodeoxycholic acid used in this work.

Association of Deoxycholic Acid in Organic Solvents

MADHU VADNERE and SIEGFRIED LINDENBAUM[x]

Received August 27, 1981, from the *Department of Pharmaceutical Chemistry, The University of Kansas, Lawrence, KS 66045.* Accepted for publication October 27, 1981.

Abstract □ The distribution of deoxycholic acid (I) between aqueous buffer and an organic phase consisting of isooctane–1-octanol (70:30, v/v) (System A) or isooctane–chloroform (80:20, v/v) (System B) was studied. The distribution isotherms suggested that I associates strongly in the organic Systems A and B unlike in pure 1-octanol. Therefore, a previous model, describing distribution of bile salts between 1-octanol and aqueous buffer, was modified to include association of I in the organic phases to describe distribution behavior. The treatment suggested that I exists as monomer and dimer in System A with a dimerization constant of 820 M^{-1}. A model consisting of monomer–tetramer–hexamer in the organic phase best describes the data for System B. The data support the view that association in the organic phase is due to hydrogen bonding between bile acid molecules.

Keyphrases □ Deoxycholic acid—association in organic solvents □ Bile salts—association of deoxycholic acid in organic solvents □ Partition coefficient—association of deoxycholic acid in organic solvents

In the preceding paper (1), the distribution behavior of bile salts between aqueous buffer and 1-octanol was reported. By vapor pressure osmometry data, it was shown that bile acids exist primarily as monomers in 1-octanol[1]. A recent paper (2) reported strong association of bile acid esters in nonaqueous solvents such as carbon tetrachloride and chloroform using vapor pressure osmometry. The association in carbon tetrachloride is much stronger than in chloroform. The relatively low association in chloroform was attributed to the hydrogen bonding ability of chloroform. This probably also explains the monomeric state of bile acids in 1-octanol. If this were true, then modifying the hydrogen bonding solvent (*e.g.*, 1-octanol or chloroform) by addition of a nonhydrogen bonding nonpolar solvent like isooctane should result in an increased association of bile acid in such organic systems. In the present report the state of association of deoxycholic acid (I) is examined in two such modified solvent systems: isooctane–1-octanol (70:30) (System A) and isooctane–chloroform (80:20) (System B) using the distribution behavior of I between the organic phase and aqueous buffer. Partition equilibria were used to study the association of solutes in the organic phase on the basis of the previously determined association pattern in the aqueous phase.

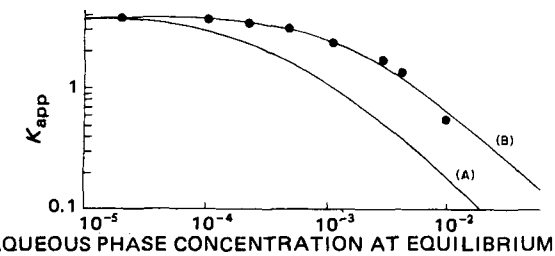

Figure 1—*Distribution isotherm for sodium deoxycholate at 25°. Curve A is based on the model in Scheme IA. Curve B is calculated on the basis of the model in Scheme IB. Key: (●) experimental data.*

[1] It was found that bile salts exist primarily in the acidic form in 1-octanol and in the anionic form in the aqueous phase under the experimental conditions of this investigation.

EXPERIMENTAL

Materials—The purity of sodium deoxycholate[2] (>99%) was confirmed by TLC and titration with perchloric acid in glacial acetic acid [^{3}H,(G)]deoxycholic acid in ethanol, specific activity 4 Ci/mmole[3], radiochemical purity 98%; 1-octanol[4]; 2,2,4-trimethylpentane (isooctane)[5] were used as obtained. The same scintillation cocktail[6] was used for both aqueous and organic samples.

Experimental details of partition coefficient measurements are given in the preceding paper (1).

RESULTS AND DISCUSSION

The experimental results obtained for the partition of I between 0.02 *M* tromethamine buffer (pH 8) and two mixed organic phases are summarized in Figs. 1 and 2. Here, the partition coefficient defined as the ratio of the bile salt (and acid) concentration in the organic phase to the concentration of bile salt (and acid) in the aqueous phase, is plotted as a function of the equilibrium total bile salt and acid concentration (moles/liter) in the aqueous phase.

The nature of the distribution isotherm obtained for System A is similar to one obtained for 1-octanol in the previous study (1). The distribution of I between 1-octanol and aqueous buffer was explained on the basis of reversible association of I in the aqueous phase and no association in the organic phase as shown in Scheme IA. In the present case, since

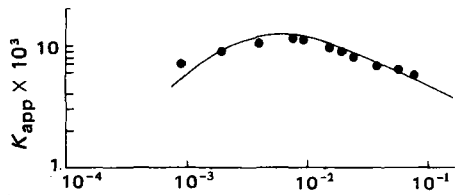

Figure 2—*Distribution isotherm for sodium deoxycholate at 25°. Organic phase isooctane–octanol (80:20, v/v). Aqueous phase 0.02 M tromethamine buffer (pH 8.0). Solid line represents distribution isotherm calculated on the basis of the 1-4-6 association model in organic phase. Key: (●) experimental data.*

[2] Calbiochem, LaJolla, Calif.
[3] New England Nuclear, Boston, Mass.
[4] Fisher Scientific Co., Pittsburgh, Pa.
[5] Eastman Kodak Co., Rochester, N.Y.
[6] Aquasol, New England Nuclear, Boston, Mass.

0022-3549/82/0800-0881$01.00/0

(21) M. Vadnere and S. Lindenbaum, *ibid.*, **71**, 875 (1982).

ACKNOWLEDGMENTS

This work was supported by grants from the National Institutes of Health (AM-18084) and the General Research Fund of the University of Kansas.

The authors thank the Tokyo Tanabe Co., Ltd. for providing the ursodeoxycholic acid used in this work.

Association of Deoxycholic Acid in Organic Solvents

MADHU VADNERE and SIEGFRIED LINDENBAUM[x]

Received August 27, 1981, from the *Department of Pharmaceutical Chemistry, The University of Kansas, Lawrence, KS 66045.* Accepted for publication October 27, 1981.

Abstract □ The distribution of deoxycholic acid (I) between aqueous buffer and an organic phase consisting of isooctane–1-octanol (70:30, v/v) (System A) or isooctane–chloroform (80:20, v/v) (System B) was studied. The distribution isotherms suggested that I associates strongly in the organic Systems A and B unlike in pure 1-octanol. Therefore, a previous model, describing distribution of bile salts between 1-octanol and aqueous buffer, was modified to include association of I in the organic phases to describe distribution behavior. The treatment suggested that I exists as monomer and dimer in System A with a dimerization constant of 820 M^{-1}. A model consisting of monomer–tetramer–hexamer in the organic phase best describes the data for System B. The data support the view that association in the organic phase is due to hydrogen bonding between bile acid molecules.

Keyphrases □ Deoxycholic acid—association in organic solvents □ Bile salts—association of deoxycholic acid in organic solvents □ Partition coefficient—association of deoxycholic acid in organic solvents

In the preceding paper (1), the distribution behavior of bile salts between aqueous buffer and 1-octanol was reported. By vapor pressure osmometry data, it was shown that bile acids exist primarily as monomers in 1-octanol[1]. A recent paper (2) reported strong association of bile acid esters in nonaqueous solvents such as carbon tetrachloride and chloroform using vapor pressure osmometry. The association in carbon tetrachloride is much stronger than in chloroform. The relatively low association in chloroform was attributed to the hydrogen bonding ability of chloroform. This probably also explains the monomeric state of bile acids in 1-octanol. If this were true, then modifying the hydrogen bonding solvent (*e.g.*, 1-octanol or chloroform) by addition of a nonhydrogen bonding nonpolar solvent like isooctane should result in an increased association of bile acid in such organic systems. In the present report the state of association of deoxycholic acid (I) is examined in two such modified solvent systems: isooctane–1-octanol (70:30) (System A) and isooctane–chloroform (80:20) (System B) using the distribution behavior of I between the organic phase and aqueous buffer. Partition equilibria were used to study the association of solutes in the organic phase on the basis of the previously determined association pattern in the aqueous phase.

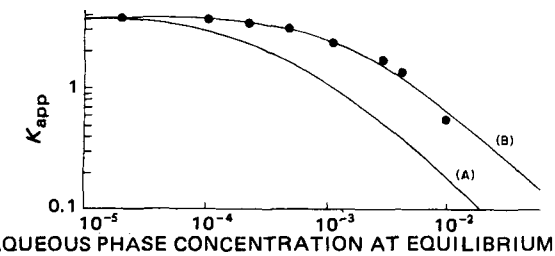

Figure 1—*Distribution isotherm for sodium deoxycholate at 25°. Curve A is based on the model in Scheme IA. Curve B is calculated on the basis of the model in Scheme IB. Key: (●) experimental data.*

[1] It was found that bile salts exist primarily in the acidic form in 1-octanol and in the anionic form in the aqueous phase under the experimental conditions of this investigation.

EXPERIMENTAL

Materials—The purity of sodium deoxycholate[2] (>99%) was confirmed by TLC and titration with perchloric acid in glacial acetic acid [^{3}H,(G)]deoxycholic acid in ethanol, specific activity 4 Ci/mmole[3], radiochemical purity 98%; 1-octanol[4]; 2,2,4-trimethylpentane (isooctane)[5] were used as obtained. The same scintillation cocktail[6] was used for both aqueous and organic samples.

Experimental details of partition coefficient measurements are given in the preceding paper (1).

RESULTS AND DISCUSSION

The experimental results obtained for the partition of I between 0.02 *M* tromethamine buffer (pH 8) and two mixed organic phases are summarized in Figs. 1 and 2. Here, the partition coefficient defined as the ratio of the bile salt (and acid) concentration in the organic phase to the concentration of bile salt (and acid) in the aqueous phase, is plotted as a function of the equilibrium total bile salt and acid concentration (moles/liter) in the aqueous phase.

The nature of the distribution isotherm obtained for System A is similar to one obtained for 1-octanol in the previous study (1). The distribution of I between 1-octanol and aqueous buffer was explained on the basis of reversible association of I in the aqueous phase and no association in the organic phase as shown in Scheme IA. In the present case, since

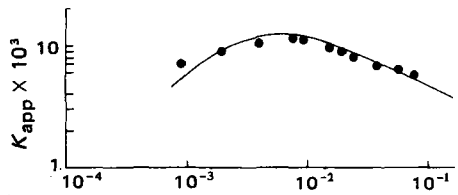

Figure 2—*Distribution isotherm for sodium deoxycholate at 25°. Organic phase isooctane–octanol (80:20, v/v). Aqueous phase 0.02 M tromethamine buffer (pH 8.0). Solid line represents distribution isotherm calculated on the basis of the 1-4-6 association model in organic phase. Key: (●) experimental data.*

[2] Calbiochem, LaJolla, Calif.
[3] New England Nuclear, Boston, Mass.
[4] Fisher Scientific Co., Pittsburgh, Pa.
[5] Eastman Kodak Co., Rochester, N.Y.
[6] Aquasol, New England Nuclear, Boston, Mass.

0022-3549/82/0800-0881$01.00/0

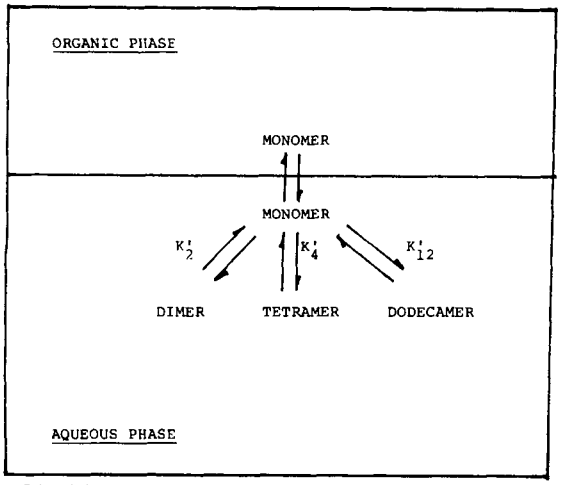

Scheme IA—The possible equilibria involved in the partitioning of bile salts between 1-octanol and aqueous solution.

the aqueous phase is not changed[7], association constants obtained previously are expected to remain constant and should describe the total concentration of I in the aqueous phase according to:

$$[C]_{aq} = [M]_{aq} + 2K'_2[M]^2_{aq} + 4K'_4[M]^4_{aq} + 12K'_{12}[M]^{12}_{aq} \quad \text{(Eq. 1)}$$

where, $[C]_{aq}$ is the total concentration of bile salt in the aqueous phase in moles per liter, $[M]_{aq}$ is the monomer concentration of bile salt in the aqueous phase[8] in moles per liter, and K'_2, K'_4, and K'_{12} represent association constants in the aqueous phase where subscripts refer to association numbers.

If the assumption that I does not associate in the organic solvent is true for System A, then the model shown in Scheme IA with the above association constants should describe the distribution isotherm. Calculations based on this model generated Curve A in Fig. 1. It is apparent from Fig. 1 that experimental points have significant positive deviation from Curve A. This positive deviation of partition coefficients from expected values based on the previous model suggests that there is much more solute in the organic phase than expected by assuming only monomers. This may be explained by considering reversible association of solute in the organic phase as shown in Scheme IB. This model assumes that only the monomer is transported from one phase to another, and higher aggregates are formed by the association of monomers in both phases. Thus, it can be shown that the concentration of bile salt and acid in the organic phase may be written as:

$$[C]_{org} = [M]_{org} + 2K_2[M]^2_{org} + 3K_3[M]^3_{org} + \ldots \quad \text{(Eq. 2)}$$

where, $[C]_{org}$ is the total concentration of I in the organic phase in moles per liter, $[M]_{org}$ is the monomer concentration of I in the organic phase

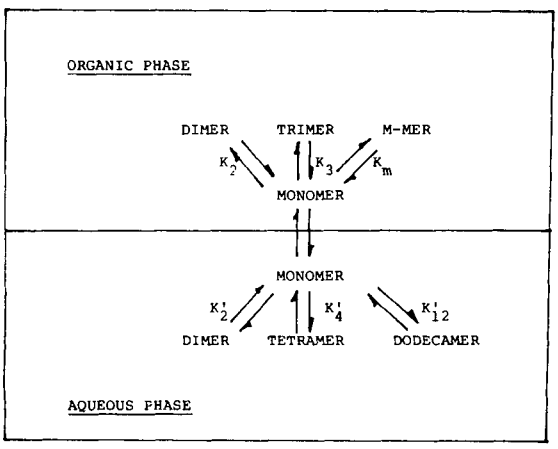

Scheme IB—The possible equilibria involved in the partitioning of bile salts between aqueous solution and Solvent Systems A or B.

[7] This assumes that the two organic phases either do not modify the aqueous phase or modify it to the same extent.

[8] This may be acid, anion, or a mixture of both.

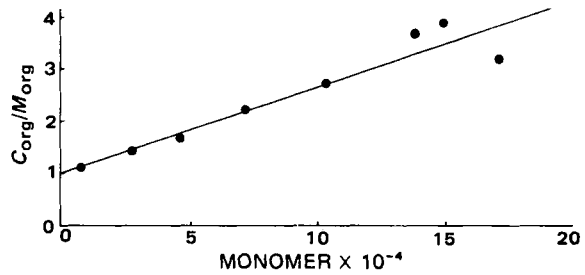

Figure 3—*A plot testing the possible occurrence of dimers in organic phase System A according to Eq. 6.*

in moles per liter, and K_2, K_3 . . . are association constants for I in the organic phase. Also:

$$K_{app} = [C]_{org}/[C]_{aq} \quad \text{(Eq. 3)}$$

$$K^0_{app} = [M]_{org}/[M]_{aq} = \lim_{c \to 0} K_{app} \quad \text{(Eq. 4)}$$

where, K_{app} is the apparent partition coefficient at any given concentration, and K^0_{app} is the apparent partition coefficient at infinite dilution.

By using carrier-free radiolabeled samples, K^0_{app} was obtained at concentration $<10^{-10}$ *M*. From Eq. 1 $[M]_{aq}$ was computed where $[C]_{aq}$ was known experimentally and aqueous association constants were used from previous studies (1). Using this computed value of $[M]_{aq}$ in Eq. 4, $[M]_{org}$ was calculated.

If the monomer and dimer are the primary species in the organic system, then Eq. 2 reduces to:

$$[C]_{org} = [M]_{org} + 2K_2[M]^2_{org} \quad \text{(Eq. 5)}$$

Rearranging gives:

$$([C]_{org}/[M]_{org}) = 1 + 2K_2[M]_{org} \quad \text{(Eq. 6)}$$

Thus, a plot of $([C]_{org}/[M]_{org})$ *versus* $[M]_{org}$ should give a straight line with unit intercept and slope = $2K_2$. This relationship can be seen in Fig. 3 for System A. It gives the estimate of $K_2 = 820\ M^{-1}$. Using this value of K_2 and Eqs. 1, 3, and 5, the distribution isotherm was generated as shown by Curve B in Fig. 1. It is seen that the curve calculated on the basis of the proposed model is in close agreement with the experimental data.

The distribution isotherm for System B exhibits a maximum (Fig. 2). This may be anticipated if the association in the organic phase is stronger than that in the aqueous phase until the CMC (critical micelle concentration) in the aqueous phase (CMC_{aq}) is reached. Under this circumstance the partition coefficient will increase until the CMC_{aq} is reached, the association in the aqueous phase being greater, the partition coefficient would be expected to decrease. Thus, a maximum in the isotherm may occur approximately in the concentration region corresponding to the CMC_{aq}. The value of the CMC thus estimated from this study is $\sim 7 \times 10^{-3}$ *M*, which compares reasonably well with literature values of 5–6 $\times 10^{-3}$ *M* (3–6).

A monomer–dimer treatment similar to the one used for System A did not yield a straight line relationship for System B. Instead, a positive

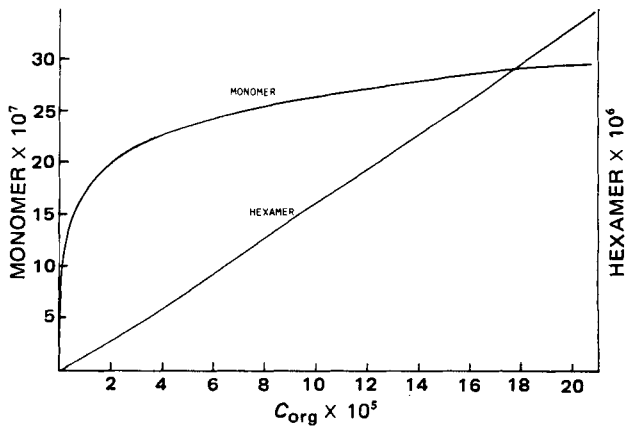

Figure 4—*A plot showing the distribution of deoxycholic acid among its various forms in Solvent System B.*

deviation was observed suggesting that higher aggregates exist in System B. The data for the system, therefore, were treated by a nonlinear least-squares fit to Eq. 2. The best fit was obtained for the monomer–tetramer–hexamer model in the organic phase. The estimated association constants were $K'_4 = 9.96 \times 10^2\ M^{-3}$, $K'_6 = 4.79 \times 10^{28}\ M^{-5}$. The distribution isotherm based on these constants is in good agreement with the experimental data (Fig. 2). Figure 4 shows the distribution of deoxycholic acid among its various forms in Solvent System B.

In studies with the methylester of deoxycholic acid (2), it was found that the methylester exists as monomers and dimers in chloroform ($K_2 \approx 14.0\ M^{-1}$) and monomers and tetramers in carbon tetrachloride ($K_4 \approx 2.8 \times 10^5\ M^{-3}$). Although no report was found in the literature for comparison with the present observations, a qualitative comparison can be made with the data derived previously (2). In pure octanol, hydrogen bonding interactions between solvent molecules and the hydroxyl and carboxyl groups of the bile acid are considerable. Consequently, this interaction precludes any appreciable self association of steroidal monomers. Solvent System A is a solvent of low polarity. Octanol is, therefore, expected to self associate to a significant extent in this solvent system (7). Thus, there is likely to be only weak interaction between 1-octanol and bile acid molecules. This leads to self association of solute molecules either between hydroxyl groups, carboxylic acid groups, or both. It was found in the preceding study (1) that under the condition of the experiment it is the free acid form that is partitioned in the organic phase. An acid form, because of its relatively more polar nature compared to the ester form, is expected to associate more strongly.

Even higher aggregation is expected, therefore, in Solvent System B, since this solvent is even less polar than Solvent System I. The organic phase has been rendered less polar, by increasing the isooctane concentration and by substituting 1-octanol (dielectric constant 10.34) with chloroform (dielectric constant 4.81).

These results have important significance in terms of mixed micelles of bile salts with lecithin (8). In a low dielectric inert medium such as the interior of a lecithin bilayer or liposome, pairwise association of bile salt molecules hydrogen-bonded to each other through their hydroxyl and/or carboxylic acid groups is plausible. Such a mixed disk model for bile salt lecithin micelles in which hydrogen bonded bile salt anion pairs are found within the interior of the micelle has been proposed previously (9). It cannot be decided on the basis of the present or previous (9) work whether the associated species are bile salt anions or free acid molecules. Molecular models suggest that the hydroxyl groups on the trihydroxy bile acids and dihydroxy bile acids can align to form hydrogen bonded pairs. It was suggested (10) that this hydrogen-bonded pairing occurs in aqueous solvents. However, it has been shown (1, 11) that in aqueous solution, bile salts are associated by hydrophobic forces. The previous hydrogen-bonded pairing model (10) appears to be the most likely structure in a low dielectric, nonhydrogen-bonded medium. The partition of bile salts from an aqueous to a lipid membrane phase would thus involve an inversion from hydrophobic back-to-back association in the aqueous phase, to hydrogen-bonded association in the lipid phase.

REFERENCES

(1) M. Vadnere and S. Lindenbaum, *J. Pharm. Sci.*, **71**, 875 (1981).

(2) J. Robeson, B. W. Foster, S. N. Rosenthal, E. T. Adams, Jr., and E. J. Fendler, *J. Phys. Chem.*, **85**, 1254 (1981).

(3) P. Ekwall, K. Fontell, and A. Sten, *Proceedings of the International Congress of Surface Activity*, London, 1957, p. 357.

(4) P. DeMoerlosse and R. Ruyssen, *J. Pharm. Belg.*, **14**, 95 (1959).

(5) H. Miyake, T. Murakoshi, and T. Histsugu, *Fukuoka-Igaku Zasshi*, **53**, 659 (1962).

(6) M. Vadnere and S. Lindenbaum, *Int. J. Pharm.*, in press.

(7) B. D. Anderson, "Specific Interactions in Nonaqueous Systems," Ph.D. Thesis, The University of Kansas, 1978.

(8) R. O. Zimmerer and S. Lindenbaum, *J. Pharm.Sci.*, **68**, 581 (1979).

(9) N. A. Mazer, G. B. Benedek, and M. C. Carey, *Biochemistry*, **9**, 601 (1980).

(10) D. G. Oakenfull and L. R. Fisher, *J. Phys. Chem.*, **82**, 2443 (1978).

(11) M. Vadnere, R. Natarajan, and S. Lindenbaum, *J. Phys. Chem.*, **84**, 1900 (1980).

ACKNOWLEDGMENTS

This work was supported by a grant from the National Institutes of Health (AM-18084).

Serum Prolactin Level Increase in Normal Subjects Following Administration of Perphenazine Oral Dosage Forms: Possible Application to Bioavailability Testing

RANDALL J. ERB ˣ and WILLIAM P. STOLTMAN

Received August 21, 1981, from the *Pharmadynamics Research, Inc., West Lafayette, IN 47906.* Accepted for publication November 3, 1981.

Abstract □ Two pilot studies were performed to determine if oral phenothiazine products could generate a significant increase in serum levels of the hormone prolactin. The two studies employed three and four healthy normal male subjects, respectively. In the first study the subjects received a screening dose, a placebo, one 8-mg perphenazine tablet, and two 8-mg perphenazine tablets. In the second study, the subjects were dosed with two 10-mg amitriptyline tablets, one 10-mg amitriptyline tablet with one combination tablet containing 10 mg of amitriptyline and 4 mg of perphenazine, and two combination tablets, each containing 10 mg of amitriptyline and 4 mg of perphenazine. In both cases the drug treatments produced a significant rise in the serum prolactin levels *versus* a placebo or control. This increase was defined as a prolactin response. The possible utility of this response in bioavailability testing is discussed.

Keyphrases □ Prolactin—serum prolactin level increase following administration of perphenazine oral dosage forms, application to bioavailability testing □ Bioavailability—application to testing, serum prolactin level increase following administration of perphenazine □ Perphenazine—oral dosage forms, serum prolactin level increase following administration, application to bioavailability testing

An adequate methodology for determining the bioavailability and bioequivalence of phenothiazine dosage forms has been sought for some time. The phenothiazines are a vital psychopharmaceutic tool in combating mental and emotional illnesses. In addition, these drugs are produced and marketed in a very large number of dosage

0022-3549/82/0800-0883$01.00/0

deviation was observed suggesting that higher aggregates exist in System B. The data for the system, therefore, were treated by a nonlinear least-squares fit to Eq. 2. The best fit was obtained for the monomer–tetramer–hexamer model in the organic phase. The estimated association constants were $K'_4 = 9.96 \times 10^2\ M^{-3}$, $K'_6 = 4.79 \times 10^{28}\ M^{-5}$. The distribution isotherm based on these constants is in good agreement with the experimental data (Fig. 2). Figure 4 shows the distribution of deoxycholic acid among its various forms in Solvent System B.

In studies with the methylester of deoxycholic acid (2), it was found that the methylester exists as monomers and dimers in chloroform ($K_2 \approx 14.0\ M^{-1}$) and monomers and tetramers in carbon tetrachloride ($K_4 \approx 2.8 \times 10^5\ M^{-3}$). Although no report was found in the literature for comparison with the present observations, a qualitative comparison can be made with the data derived previously (2). In pure octanol, hydrogen bonding interactions between solvent molecules and the hydroxyl and carboxyl groups of the bile acid are considerable. Consequently, this interaction precludes any appreciable self association of steroidal monomers. Solvent System A is a solvent of low polarity. Octanol is, therefore, expected to self associate to a significant extent in this solvent system (7). Thus, there is likely to be only weak interaction between 1-octanol and bile acid molecules. This leads to self association of solute molecules either between hydroxyl groups, carboxylic acid groups, or both. It was found in the preceding study (1) that under the condition of the experiment it is the free acid form that is partitioned in the organic phase. An acid form, because of its relatively more polar nature compared to the ester form, is expected to associate more strongly.

Even higher aggregation is expected, therefore, in Solvent System B, since this solvent is even less polar than Solvent System I. The organic phase has been rendered less polar, by increasing the isooctane concentration and by substituting 1-octanol (dielectric constant 10.34) with chloroform (dielectric constant 4.81).

These results have important significance in terms of mixed micelles of bile salts with lecithin (8). In a low dielectric inert medium such as the interior of a lecithin bilayer or liposome, pairwise association of bile salt molecules hydrogen-bonded to each other through their hydroxyl and/or carboxylic acid groups is plausible. Such a mixed disk model for bile salt lecithin micelles in which hydrogen bonded bile salt anion pairs are found within the interior of the micelle has been proposed previously (9). It cannot be decided on the basis of the present or previous (9) work whether the associated species are bile salt anions or free acid molecules. Molecular models suggest that the hydroxyl groups on the trihydroxy bile acids and dihydroxy bile acids can align to form hydrogen bonded pairs. It was suggested (10) that this hydrogen-bonded pairing occurs in aqueous solvents. However, it has been shown (1, 11) that in aqueous solution, bile salts are associated by hydrophobic forces. The previous hydrogen-bonded pairing model (10) appears to be the most likely structure in a low dielectric, nonhydrogen-bonded medium. The partition of bile salts from an aqueous to a lipid membrane phase would thus involve an inversion from hydrophobic back-to-back association in the aqueous phase, to hydrogen-bonded association in the lipid phase.

REFERENCES

(1) M. Vadnere and S. Lindenbaum, *J. Pharm. Sci.*, **71**, 875 (1981).

(2) J. Robeson, B. W. Foster, S. N. Rosenthal, E. T. Adams, Jr., and E. J. Fendler, *J. Phys. Chem.*, **85**, 1254 (1981).

(3) P. Ekwall, K. Fontell, and A. Sten, *Proceedings of the International Congress of Surface Activity*, London, 1957, p. 357.

(4) P. DeMoerlosse and R. Ruyssen, *J. Pharm. Belg.*, **14**, 95 (1959).

(5) H. Miyake, T. Murakoshi, and T. Histsugu, *Fukuoka-Igaku Zasshi*, **53**, 659 (1962).

(6) M. Vadnere and S. Lindenbaum, *Int. J. Pharm.*, in press.

(7) B. D. Anderson, "Specific Interactions in Nonaqueous Systems," Ph.D. Thesis, The University of Kansas, 1978.

(8) R. O. Zimmerer and S. Lindenbaum, *J. Pharm.Sci.*, **68**, 581 (1979).

(9) N. A. Mazer, G. B. Benedek, and M. C. Carey, *Biochemistry*, **9**, 601 (1980).

(10) D. G. Oakenfull and L. R. Fisher, *J. Phys. Chem.*, **82**, 2443 (1978).

(11) M. Vadnere, R. Natarajan, and S. Lindenbaum, *J. Phys. Chem.*, **84**, 1900 (1980).

ACKNOWLEDGMENTS

This work was supported by a grant from the National Institutes of Health (AM-18084).

Serum Prolactin Level Increase in Normal Subjects Following Administration of Perphenazine Oral Dosage Forms: Possible Application to Bioavailability Testing

RANDALL J. ERB ˣ and WILLIAM P. STOLTMAN

Received August 21, 1981, from the *Pharmadynamics Research, Inc., West Lafayette, IN 47906.* Accepted for publication November 3, 1981.

Abstract □ Two pilot studies were performed to determine if oral phenothiazine products could generate a significant increase in serum levels of the hormone prolactin. The two studies employed three and four healthy normal male subjects, respectively. In the first study the subjects received a screening dose, a placebo, one 8-mg perphenazine tablet, and two 8-mg perphenazine tablets. In the second study, the subjects were dosed with two 10-mg amitriptyline tablets, one 10-mg amitriptyline tablet with one combination tablet containing 10 mg of amitriptyline and 4 mg of perphenazine, and two combination tablets, each containing 10 mg of amitriptyline and 4 mg of perphenazine. In both cases the drug treatments produced a significant rise in the serum prolactin levels *versus* a placebo or control. This increase was defined as a prolactin response. The possible utility of this response in bioavailability testing is discussed.

Keyphrases □ Prolactin—serum prolactin level increase following administration of perphenazine oral dosage forms, application to bioavailability testing □ Bioavailability—application to testing, serum prolactin level increase following administration of perphenazine □ Perphenazine—oral dosage forms, serum prolactin level increase following administration, application to bioavailability testing

An adequate methodology for determining the bioavailability and bioequivalence of phenothiazine dosage forms has been sought for some time. The phenothiazines are a vital psychopharmaceutic tool in combating mental and emotional illnesses. In addition, these drugs are produced and marketed in a very large number of dosage

0022-3549/82/0800-0883$01.00/0

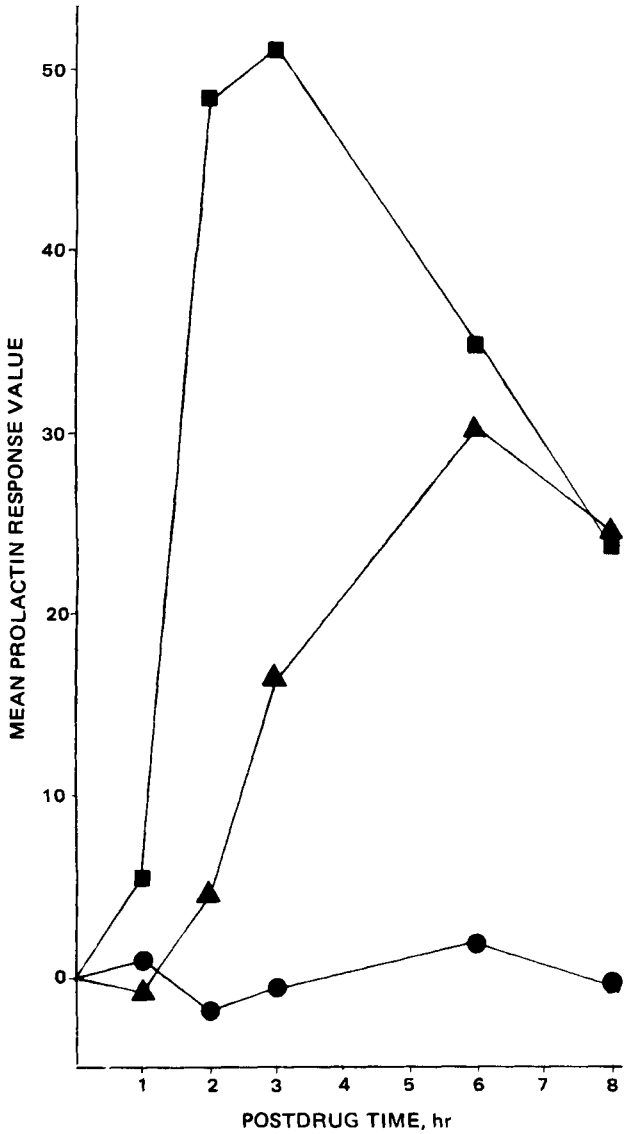

Figure 1—*The mean prolactin response* versus *time over an 8-hr postdrug period for three healthy, normal male subjects dosed with a placebo capsule (●); an 8-mg perphenazine tablet (▲); two 8-mg perphenazine tablets (■).*

forms. Also, several of the most frequently prescribed phenothiazines recently have lost patent protection or shall lose this protection in the near future. Hence, an adequate testing methodology for the phenothiazines is of critical importance. The present report presents data that should lead to the establishment of a meaningful, reliable, reproducible methodology of phenothiazine bioavailability and bioequivalence evaluations.

Traditionally, methods of assessing the major tranquilizers have centered around detection of the parent drug and metabolites in plasma by chemical assay. This approach has been based on the assumption that detectable plasma drug levels are adequately reflective of drug concentrations at critical sites in the central nervous system. There has been work published that suggests that this assumption may be incorrect (1, 2).

The mechanism of action of the phenothiazines has received considerable attention. There is much evidence that the phenothiazines act through a blockade of dopaminergic and noradrenergic receptors (3–9). Blockade of dopaminergic receptors with phenothiazines has been positively

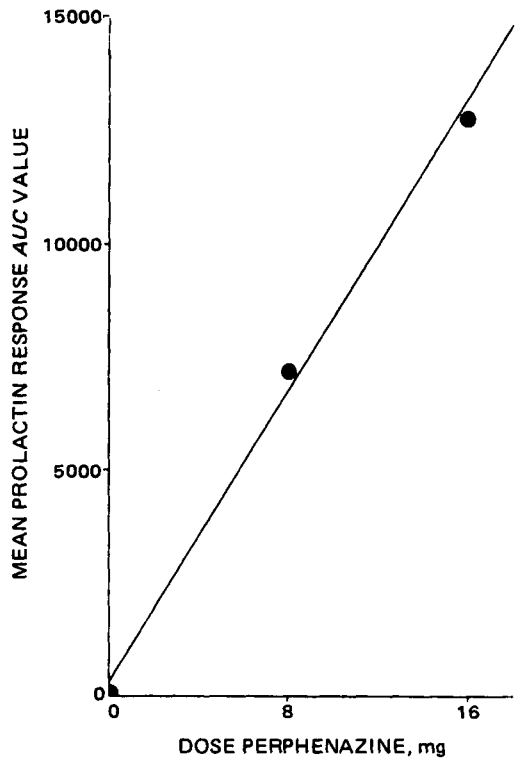

Figure 2—*The mean 60–480 min* AUC's *for the prolactin response for three healthy normal male subjects dosed with a placebo, one 8-mg perphenazine tablet, and two 8-mg perphenazine tablets* ($y = a_1x + a_0$; $y = 792.94x + 374.17$; $r^2 = 0.996$).

correlated with the antipsychotic effect of the phenothiazines (10–14).

Dopaminergic neurons also tonically inhibit the release of prolactin from the pituitary gland (15, 16). Intramuscular and intravenous administration of various phenothiazine products has generated a reproducible, dose-dependent response: an increase in serum prolactin level (17, 18). This increase has been attributed to the blockade of dopaminergic neurons (19). The change in plasma prolactin concentration to these neuroleptic agents correlates with their clinically observed antischizophrenic potency (13).

The present study was initiated to determine whether oral phenothiazine dosage forms also generate a prolactin response, and to preliminarily assess this response as a bioavailability/bioequivalence test procedure for phenothiazine dosage forms.

The results indicated that the oral phenothiazine doses dependably generated a prolactin response that was significantly greater than a placebo generated response. The method has much potential for bioavailability testing.

EXPERIMENTAL

Two studies were conducted to investigate changes in serum prolactin levels after administration of several oral phenothiazine dosage forms.

The first study investigated the changes in serum prolactin after the administration of tablet perphenazine to healthy normal subjects.

Subjects—Males (18–35 years of age) were employed as experimental subjects. All were classified as healthy and normal on the basis of the following: interview, physical examination, electrocardiograph, exercise stress test, chest X-ray, intraocular pressure measurement, microscopic urinalysis, hematology, and blood chemistry. Hematology included the following: red blood cell count, hemoglobin, hematocrit, mean corpuscular volume, mean corpuscular hemoglobin, and white blood cell count with differential. Blood chemistry included the following: triglycerides, serum

Table I—Prolactin Blood Level (ng/ml), Prolactin Response Values [a], and *AUC* Values [b]

Postdrug Time	Subject 1 Blood Level	Subject 1 Prolactin Response	Subject 2 Blood Level	Subject 2 Prolactin Response	Subject 3 Blood Level	Subject 3 Prolactin Response
			Placebo			
0	*ND*[c]		21.8		9.9	
60	11.5	2.6	11.0	0.3	10.7	0.6
120	7.4	−1.5	8.3	−2.4	10.5	−1.7
180	5.8	−3.1	11.6	0.9	12.8	−0.4
300	9.5	0.6	14.6	3.9	11.9	1.5
480	10.4	1.5	8.1	−2.6	13.2	0.1
60–480 *AUC*		12		306		135
			8-mg Perphenazine Tablet			
0	16.5		20.1		7.0	
60	9.4	0.5	10.3	−0.4	5.0	−2.2
120	14.8	5.9	15.4	4.7	13.3	4.0
180	32.5	23.6	23.3	12.6	14.4	12.9
300	42.1	33.2	40.5	29.8	31.0	27.4
480	43.6	34.7	29.5	18.8	18.5	20.1
60–480 *AUC*		10611		7554		7188
			Two 8-mg Perphenazine Tablets			
0	23.0		15.8		7.3	
60	15.1	6.2	16.6	5.9	9.9	3.9
120	72.3	63.4	53.0	42.3	19.8	37.9
180	74.5	65.6	57.8	47.1	32.1	44.3
300	47.5	38.6	46.5	35.8	28.4	30.3
480	44.0	35.1	27.4	16.7	19.6	19.9
60–480 *AUC*		19029		14004		12806

[a] Prolactin response = [prolactin in sample for subject] − [subject's mean placebo prolactin over 60–480-min postdrug]. [b] *AUC*'s (60–480 min) for three healthy male subject's dose with a placebo, one 8-mg perphenazine tablet, and two 8-mg perphenazine tablets. [c] No data.

Table II—ANOVA for Postdrug *AUC* Values [a]

Analysis of Variance for Dependent Variable 1

Source	Error Term	*F*	Sum of Squares	Degrees of Freedom	Mean Square	Expected Mean Square	
(1) Mean	*S*	11.0292	4.0517664E + 08	1	4.0517664E + 08	9.000(1)	3.000(3)
(2) *D*	*DS*	10.0762	2.4186097E + 08	2	1.2073047E + 08	3.000(2)	1.000(4)
(3) *S*			7.3480106E + 07	2	3.6740053E + 07	3.000(3)	
(4) *DS*			4.8006148E + 07	4	1.2001537E + 07	1.000(4)	

Estimates of Variance Components
(1) 4.0731379E + 07
(2) 3.6309650E + 07
(3) 1.2246694E + 07
(4) 1.2001531E + 07
Mean 11729.25000

Cell Means

D =	(1) Placebo	(2) One 8-mg perphenazine	(3) Two 8-mg perphenazine
	135.00000	7188.00000	12806.00000

S =	(1)	(2)	(3)	(4)
	7804.00000	7288.00000	2957.00000	

Cell Deviations

X(0.) − X(. .)			
D =	(1)	(2)	(3)
	−6574.66667	478.33333	6096.33333

X(S.) − X(. .)			
S =	(1)	(2)	(3)
	3174.33333	578.33333	−3752.66667

[a] 60–480 min for three healthy normal male subjects dosed with a placebo, 8 mg, and 16 mg of perphenazine.

glutamic oxalacetic transaminase, serum glutamic-pyruvic transaminase, phosphorus, alkaline phosphatase, uric acid, albumin, blood urea nitrogen, chloride, potassium, lactic dehydrogenase, calcium, bilirubin, total protein, glucose, sodium, albumin–globulin ratio, and creatinine. Each test value had to fall within the acceptable limits for the test for the subject to be accepted in the study. Each subject also signed an informed consent form prior to first participation in the study. Subjects abstained from any drug or drug product for the entire study. Each subject agreed to abstain from alcohol for 48 hr prior to each experiment. Subjects were not permitted tobacco for 12 hr prior to each experiment. Also, subjects were not to take anything orally, except water, for 10 hr prior to each experiment.

The subjects reported to the facility once a week for 4 consecutive weeks. They arrived at the facility at ~8 am. Each subject was briefly examined. The oral temperature, pulse, respiration, and blood pressure of each subject was determined and recorded. The predrug blood sample then was drawn.

Doses and Experimental Design—All three subjects received the doses in the same order. The doses were as follows: (*a*) one milligram of perphenazine as a liquid concentrate[1], (*b*) one 8-mg perphenazine tablet[2], (*c*) one placebo capsule, (*d*) two 8-mg perphenazine tablets. The first dose was used as a screening dose to prevent any hypersensitive individuals from receiving a larger dose. The perphenazine concentrate was administered mixed in ~175 ml of orange juice. No blood samples were taken from the subjects before or after the administration of this screening dose. The subjects were observed for any reaction that might constitute evidence of an allergic or hypersensitive response to the perphenazine. All of the subjects received all of the doses.

Blood Samples—Blood samples were obtained periodically from the volunteers during each of the other three experiments. Prior to each dose administration, a predrug blood sample was obtained. Five postdrug samples were obtained during each experiment at 1, 2, 3, 6, and 8 hr postdose.

Each blood sample was obtained from a vein in the antecubital space

[1] Trilafon concentrate, 16 mg/5 ml, Schering Corp., Kenilworth, NJ 07033.
[2] Trilafon tablets, 8 mg, Schering Corp., Kenilworth, NJ 07033.

Table III—Prolactin Blood Level (ng/ml), Prolactin Response [a], and *AUC* Values [b]

Postdrug Time	Subject 1 Blood Level	Subject 1 Response Value	Subject 2 Blood Level	Subject 2 Response Value	Subject 3 Blood Level	Subject 3 Response Value	Subject 4 Blood Level	Subject 4 Response Value
			Two 10-mg Amitriptyline Tablets					
0	41.7		29.7		15.2		23.5	
0[c]	19.9		14.3		13.2		16.3	
60	14.5	−5.40	11.9	−2.40	10.5	−2.70	14.6	−1.70
120	17.8	−2.10	10.7	−3.63	9.9	−3.30	32.9	16.60
180	10.6	−9.30	10.9	4.80	8.5	−4.70	30.2	13.90
300	18.6	−1.30	24.7	10.40	12.4	−.30	16.9	.60
480	37.0	17.10	33.6	19.30	29.3	16.10	22.8	6.50
0–480 AUC		57.0		3351.0		546.0		2820.0
			One 10-mg amitriptyline tablet and one combination tablet (10 mg amitriptyline, 4 mg perphenazine)					
0	35.4		12.9		16.1		23.5	
0[c]	23.9		9.4		14.3		15.0	
60	17.7	−6.20	8.0	−1.40	11.1	−3.20	13.1	−1.90
120	41.3	17.40	7.0	−2.40	20.2	5.90	49.4	34.40
180	58.3	34.40	25.8	16.40	80.6	66.30	65.3	50.30
300	88.6	64.70	22.3	12.90	79.9	65.60	43.5	28.50
480	50.0	26.10	47.8	38.40	86.5	72.20	39.2	24.20
0–480 AUC		15822.0		6639.0		22467.0		12930.0
			Two combination tablets (10 mg amitriptyline, 4 mg perphenazine each)					
0	37.6		10.4		19.4		22.7	
0[c]	30.6		8.5		14.1		15.1	
60	19.4	−11.20	8.5	0	9.4	−4.70	16.1	1.00
120	72.6	42.00	15.9	7.40	15.6	1.50	80.6	65.50
180	106.2	75.60	26.6	18.10	83.6	69.50	94.8	79.70
300	73.7	43.10	33.1	24.00	101.4	87.30	75.5	60.40
480	75.3	44.70	36.1	27.60	85.1	71.00	48.8	32.90
0–480 AUC		19140.0		8247.0		25549.0		23184.0

[a] Prolactin response = [prolactin in sample] − [predrug prolactin sample]. [b] *AUC* values (60–480 min) for four healthy male subjects given two 10-mg amitriptyline tablets, one 10-mg amitriptyline tablet, one 10-mg amitriptyline and 4-mg perphenazine combination tablet, and two combination tablets. [c] Sample used for prolactin response calculation.

using a 21-gauge thin-wall needle[3] inserted into a 10-ml plain, silicone-coated vacuum blood collection tube[4], 16 × 100 mm. Each sample tube was placed upright in a rack for ~15 min then centrifuged[5] for ~15 min at 3250 rpm. The serum was filtered[6] and transferred to a storage tube[7]. The storage tubes were sealed, placed in a rack, and stored in an upright position in a freezer at −15°.

Assay—The samples were assayed for their prolactin level using a prolactin radioimmunoassay[8] that had a sensitivity of ±2–3 ng/ml of prolactin/sample. The samples were prepared for assay[9] and the prolactin concentration was determined in a gamma well scintillation counter[10].

Calculations and Data Analysis—Several calculations were made once the serum prolactin was determined for each blood sample. First, the mean placebo prolactin concentration over time (60–480 min) for each of the three subjects was determined. Normally, data 0–480 min would have been analyzed. After the blood samples were analyzed it was discovered that the predrug prolactin levels were somewhat elevated. This was attributed to predrug anxiety; therefore, for this study, the predrug (zero) reading was ignored. Data analysis started with the 60-min sample. The second study employed two predrug samples. The prolactin level decreased in every case for the second sample verifying the earlier observation. The appropriate subject placebo mean value was subtracted from each serum prolactin concentration. The resulting value was defined as the prolactin response for each sample. The area under the prolactin response curve (*AUC*) was calculated for the 60–480-min postdrug period. These *AUC* data were used in a statistical analysis of the experiments.

Statistical Analysis—An ANOVA was performed on the prolactin response *AUC*'s. Pairwise comparisons were made between the treatments employing a least significant difference analysis. Using a method described previously (20), an adequate sample size estimate was calculated for future bioequivalence studies. This estimate was set to determine a sample size large enough to detect a difference of 20% between *AUC*'s, with $\alpha = 0.05$ and $\beta = 0.20$. Also calculated were the best-fitting regression line values for the mean *AUC*'s, and the r^2 value, which expressed the amount of variation in one variable, which could be attributed to the second variable.

A second study was conducted, with several differences in procedures. First, four subjects were employed instead of three. The criteria and methods used to select subjects were not changed.

Second, different dose treatments were selected for study. Again, each subject received the doses in the same order: (*a*) two 10-mg amitriptyline tablets[10], (*b*) one 10-mg amitriptyline tablet and one combination tablet containing 10 mg of amitriptyline and 4 mg of perphenazine[11], (*c*) two tablets each containing 10 mg of amitriptyline and 4 mg of perphenazine.

This dosing provided for a constant level (20 mg) of amitriptyline with increasing doses (0, 4, and 8 mg) of perphenazine.

Third, the prolactin response was defined differently. The prolactin response was defined as the serum prolactin concentration for any sampling time minus the serum prolactin concentration from the second predrug sample.

The data were treated in a manner similar to the data obtained from the first study, but with 0–480 min *AUC*'s being calculated.

RESULTS AND DISCUSSION

The serum prolactin levels, prolactin response values, and the 60–480 min *AUC*'s for the first experiment are presented in Table I. Examination of this table reveals that for each subject the *AUC* value for each experiment increased with the size of the perphenazine dose. The *F* value for the treatment variable was significant in the ANOVA. The least significant difference results indicated that a significantly larger prolactin response ($p < 0.05$) was generated by both the perphenazine dosage forms *versus* the prolactin response produced by the placebo (Table II). There was not a significant difference between the prolactin responses produced by the two perphenazine dosage forms. Given the small sample size, this was not surprising. The mean prolactin response values for the three doses are illustrated in Fig. 1. Despite the lack of a statistically significant

[3] Venoject multisample needles, 21 gauge × 3.81 cm (thin wall), Kimble-Terumo, Inc., Elkton, MD 21921.

[4] Venoject K-T-200 plain, silicon-coated vacuum blood collection tubes, 16 × 100 mm, 10 ml, Elkton, MD 21921.

[5] Spinnette C1370-1 centrifuge, Damon/IEC Division, Needham Heights, MA 02194.

[6] Filter Sampler, Blood Serum Filter, Standard Model, 16 mm × 10.16 cm, Glasrock Products, Inc., Fairburn, GA 30213.

[7] Frozen Serum Transport Containers, Biomedical Laboratories, Inc., Burlington, NC 27215.

[8] Prolactin RIA Diagnostic Kit, Abbott Laboratories, Diagnostics Division, North Chicago, IL 60064.

[9] Tracor 1285 Automatic Gamma System, Tracor Instruments, Austin, TX 78721.

[10] Elavil tablets, 10 mg, Merck Sharp & Dohme, West Point, PA 19486.

[11] Triavil tablets 4–10 mg, Merck Sharp & Dohme, West Point, PA 19486.

Table IV—ANOVA for Postdrug *AUC* Values [a]

Analysis of Variance for Dependent Variable 1

Source	Error Term	*F*	Sum of Squares	Degrees of Freedom	Mean Square	Expected Mean Square	
(1) Mean	*S*	30.9393	1.6509037E + 09	1	1.6509037E + 09	12.000(1)	3.000(3)
(2) *D*	*DS*	12.6304	6.4598068E + 08	2	3.2299034E + 08	4.000(2)	1.000(4)
(3) *S*			1.6007820E + 08	3	5.3359401E + 07	3.000(3)	
(4) *DS*			1.5343418E + 08	6	2.5572363E + 07	1.000(4)	

Estimates of Variance Components

(1) 1.3312869E + 08
(2) 7.4354495E + 07
(3) 1.7786467E + 07
(4) 2.5572363E + 07
\Mean 11729.25000

Cell Means

D =	(1)	(2)	(3)	(4)
	1693.50000	14464.50000	19029.75000	
S =	(1)	(2)	(3)	(4)
	11673.0000	6079.0000	16187.0000	12970.0000

Cell Deviations

X(0.)	− X(. .)			
D =	(1)	(2)	(3)	
	−10035.7500	2735.2500	7300.5000	
X(S.)	− X(. .)			
S =	(1)	(2)	(3)	(4)
	−56.2500	−5650.2500	4457.7500	1240.7500

[a] Analysis of variance for the 0–480 min postdrug *AUC* values for four healthy normal male subjects dosed with (*a*) two 10-mg amitriptyline tablets, (*b*) one 10-mg amitriptyline tablet and one combination tablet containing 10 mg of amitriptyline and 4 mg of perphenazine, and (*c*) two combination tablets, a dose of 20 mg of amitriptyline and 8 mg of perphenazine.

difference between the prolactin responses to the 8- and 16-mg perphenazine doses, the figure demonstrates that an increase in the prolactin response accompanied each increase in the perphenazine dosage level. The best fitting linear regression equation and the mean 60–480-min *AUC*'s are assembled in the dose–effect curve (Fig. 2). More than 99% of the prolactin response (variation) can be explained by the changes in the dose of perphenazine (*i.e.*, $r^2 \geq 0.99$). The subject sample size estimate (20) calculated using these data was 24.

Tables III and IV contain the data and the statistical analysis for the second pilot study using amitriptyline tablets and amitriptyline–perphenazine combination tablets. Again, each increase in the dose level of perphenazine was accompanied by an increase in the size of the 0–480-min *AUC*. Also, the *AUC*'s for both perphenazine treatments were significantly larger than the *AUC*'s calculated for the experiments where amitriptyline alone was given. Figure 3 portrays the mean prolactin response values over time for the three dose treatments. Figure 4 illustrates the mean 0–480 dose–effect curve minute *AUC* values for the three doses. Also, the best fitting linear regression equation is listed. A 93% variation in the *AUC* values can be accounted for by the changes in the perphenazine dosage levels. The subject sample size estimate calculated using these data was 30.

The results of these two studies support the findings of previous investigations demonstrating increased serum prolactin following the administration of various phenothiazine dosage forms. The present studies, however, employed oral phenothiazine dosage forms, in contrast with the parenteral dosage forms used earlier. This is an important addition, since the solid oral dosage forms are generally the least bioavailable but most heavily used in treatment. The present studies demonstrated that these oral dosage forms generated a statistically significant prolactin response.

It can be assumed that the mechanism by which the perphenazine generated the increase in serum prolactin is the same as proposed earlier, *i.e.*, a blockade of the dopaminergic pathways tonically inhibiting prolactin release. In this regard, less concern need be given to the active *versus* inactive metabolites of the drug. If a product of the metabolic breakdown of perphenazine also blockades the prolactin inhibitory pathway, it should also exert an antipsychotic action and contribute to the overall clinical effect.

Meaningful comparisons between the two studies are difficult to make. On the average, the 60–480 postdose *AUC*'s for the amitriptyline–perphenazine study were larger. Amitriptyline, however, should not have a significant effect on dopaminergic pathways (21). A *t* test was performed between the placebo *AUC*'s and the *AUC*'s calculated from the amitriptyline tablet dose treatment experiments. No significant difference was found between these data sets. Hence, the presence of the amitriptyline appears not to add to or detract from the prolactin response produced by the perphenazine, despite possible effect on noradrenergic sites.

The data obtained in these studies have implications for screening and bioavailability testing of phenothiazine products. Certainly any potential

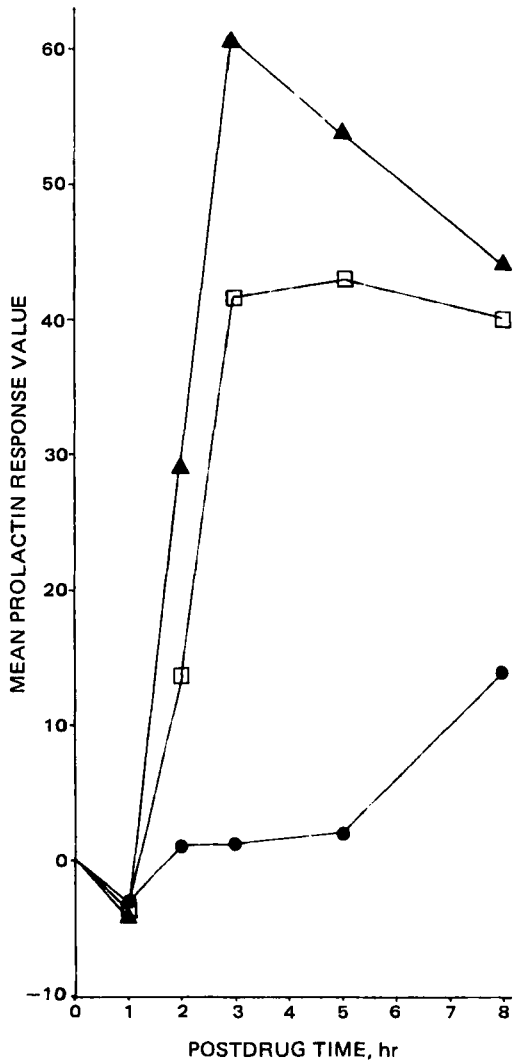

Figure 3—*The mean prolactin response* versus *time over an 8-hr postdrug period for four healthy, normal male subjects dosed with two 10-mg amitriptyline tablets (●); one 10-mg amitriptyline tablet and one 10-mg amitriptyline–4-mg perphenazine combination tablet (□); two combination 10-mg amitriptyline–4-mg perphenazine tablets (▲).*

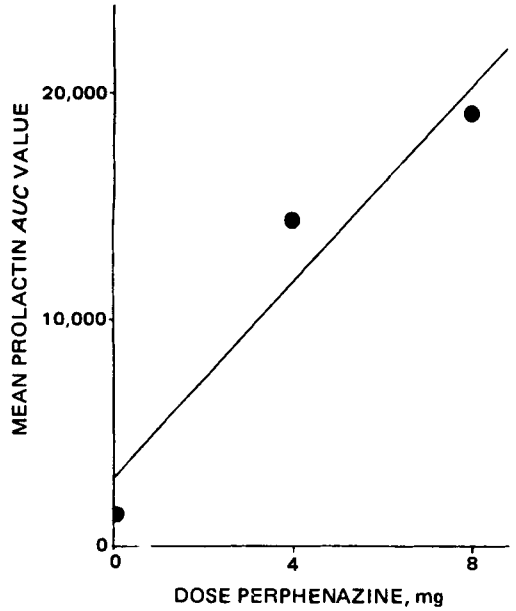

Figure 4—*The mean 60–480 min* AUC's *for the prolactin response for four healthy, normal male subjects dosed with two 10-mg amitriptyline tablets (0 mg of perphenazine); one 10-mg amitriptyline tablet and one combination tablet (4-mg perphenazine and 20-mg amitriptyline); and two combination tablets (total of 8-mg perphenazine and 20-mg amitriptyline) (*$y = a_1x + a_0$; $y = 2167.03x + 3061.13$; $r^2 = 0.931$*).*

phenothiazine product could be screened using the prolactin response. The prolactin response methodology is simpler, more economical, and more sensible; it reflects the proposed clinical effect at a site contiguous with the central nervous system. Therefore, expanded studies of this type, employing a larger subject sample size, could provide the basis for a bioavailability and bioequivalence testing methodology for all phenothiazine dosage forms. These studies could compare the prolactin response to a given product *versus* a placebo and a standard, or one standard product *versus* another, presumably equivalent, product. Some further quantification of the response will be necessary prior to applications of this methodology. It is the prolactin response, not prolactin blood levels, *per se*, that is dose-dependent for the phenothiazines, since intra- and intersubject variability in baseline serum prolactin levels are considerable. The prolactin response, however, is both reproducible and consistent.

REFERENCES

(1) F. A. Wiesel, G. Alfredsson, V. Likwornik, and G. Sedvall, *Life Sci.*, **16,** 1145 (1975).

(2) R. Ohman, M. Larsson, I. M. Nilsson, J. Engel, and A. Carlsson, *Naunyn-Schmiedebergs Arch. Pharmakol. Exp. Pathol.*, **299,** 105 (1977).

(3) H. Nyback and G. Sedvall, *J. Pharmacol. Exp. Ther.*, **162,** 294, 1968.

(4) J. M. van Rossum, *Arch. Int. Pharmacodyn.*, **160,** 492 (1966).

(5) A. Carlsson and M. Lindavist, *Acta Pharmacol. Toxicol.*, **20,** 140 (1963).

(6) J. W. Kebabian, G. L. Petzold, and P. Greengard, *Proc. Natl. Acad. Sci. USA*, **69,** 2145, 1972.

(7) B. S. Bunney, J. R. Walters, R. H. Roth, and G. K. Aghajanian, *J. Pharmacol. Exp. Ther.*, **185,** 560 (1973).

(8) P. Seeman, J. Chou-Wong, J. Tedesco, and K. Wong, *Proc. Natl. Acad. Sci. USA*, **72,** 4376 (1975).

(9) I. Creese, D. R. Burt, and S. H. Snyder, *Life Sci.*, **17,** 993 (1975).

(10) S. H. Snyder, S. P. Banerjee, H. I. Yamamura, and D. Greenberg, *Science*, **184,** 1243 (1974).

(11) A. Carlsson, *Biol. Psychiatry*, **13,** 3 (1978).

(12) G. Langer and E. J. Sachar, *Psychoneuroendocrinology*, **2,** 373 (1977).

(13) G. Langer, E. J. Sachar, P. H. Gruen, and F. S. Halpern, *Nature (London)*, **266,** 639 (1977).

(14) G. Sedvall and V. E. Grimm, in "Psychotropic Drugs: Plasma Concentrations and Clinical Response," G. D. Burrows and T. R. Norman, Eds., Dekker, New York, N.Y., 1981, pp. 331–360.

(15) A. G. Frantz, *Progr. Brain Res.*, **39,** 311 (1973).

(16) R. M. MacLead, in "Frontiers of Neuroendocrinology," L. Martini and W. F. Canog, Eds., Raven, New York, N.Y., 1976, p. 169.

(17) G. Langer, E. J. Sachar, and P. H. Gruen, *Psychopharmacol. Bull.*, **14,** 8 (1978).

(18) A. G. Frantz, D. L. Kleinberg, and G. L. Noel, *Recent Prog. Horm. Res.*, **28,** 527 (1972).

(19) G. Langer, E. J. Sachar, F. S. Halpern, P. H. Gruen, and M. Solomon, *J. Clin. Endocrinol. Metab.*, **45,** 996 (1977).

(20) V. L. Anderson and R. A. McLean, "Design of Experiments," Dekker, New York, N.Y., 1974, pp. 4–6.

(21) R. Byck, in "The Pharmacological Basis of Therapeutics," 5th ed., L. S. Goodman and A. Gilman, Eds., Macmillan New York, N.Y., 1975, p. 176.

Determination of Mianserin and Metabolites in Plasma by Liquid Chromatography with Electrochemical Detection

RAYMOND F. SUCKOW *x, THOMAS B. COOPER *, FREDERIC M. QUITKIN ‡, and JONATHAN W. STEWART ‡

Received July 21, 1981, from the **Analytical Psychopharmacology Laboratory, Rockland Research Institute, Orangeburg, NY 10962* and the ‡ *Depression Evaluation Service, New York State Psychiatric Institute, New York, NY.* Accepted for publication October 20, 1981.

Abstract □ A procedure for the determination of mianserin, desmethylmianserin, and 8-hydroxymianserin in plasma at therapeutic concentrations by liquid chromatography with electrochemical detection is described. Following a multiple-step extraction from alkaline plasma into methyl-*tert*-butyl ether, the reconstituted extract was injected onto a reversed-phase trimethylsilyl-packed column and eluted with an acetate–acetonitrile mobile phase containing an ion-paired reagent. The method provides an absolute recovery of 71–76% and a day-to-day precision of 5.4–9.1% for each compound at 25 ng/ml. The minimum quantifiable level for all three compounds was 5 ng/ml (*RSD* > 11%), and the detector response was linear up to 500 ng/ml. Fixed-dose steady-state plasma level data for 34 patients are reported.

Keyphrases □ Mianserin—determination in plasma, liquid chromatography, electrochemical detection, metabolites □ Liquid chromatography—determination of mianserin in plasma, electrochemical detection, metabolites □ Electrochemical detection—determination of mianserin in plasma by liquid chromatography, metabolites

High-pressure liquid chromatography (HPLC) with electrochemical detection is becoming an increasingly popular and useful combination for the quantitation of a wide variety of biologically important compounds (1). The sensitivity and selectivity of this detector makes it an important alternative tool to UV and fluorescence detection in biological science. The use of reversed-phase columns and ion-pairing reagents facilitate the examination of metabolite profiles in that rapid and efficient separation can be achieved in relatively short time periods. A method was recently described using ion-pair reversed-phase electrochemical detection for the determination of imipramine as well as its metabolites in plasma (2).

Mianserin hydrochloride (1,2,3,4,10,14b-hexahydro-2-methyldibenzo[*c*,*f*]pyrazino[1,2-*a*]azepine monohydrochloride) is a new tetracyclic antidepressant currently undergoing clinical evaluation in the United States. The chemical structures of this compound and known pharmacologically active metabolites are shown in Structure I. The pharmacology and therapeutic efficacy of mianserin in depressive illness have been reviewed (3) and the identification of its major urinary metabolites in various species including humans have been reported (4). The determination of mianserin in biofluids has been performed using GC with nitrogen detection (5) and by mass fragmentography (6). Neither assay included the simultaneous determinations of the metabolites found in plasma. To date HPLC has only been used for sample clean-up prior to mass fragmentography (7) and not for quantitation of mianserin.

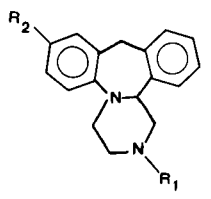

	R_1	R_2
MIANSERIN	CH_3	H
DESMETHYLMIANSERIN	H	H
8-HYDROXYMIANSERIN	CH_3	OH

In the present report, a liquid chromatographic method using electrochemical detection is described, which simultaneously quantitates mianserin, desmethylmianserin, and 8-hydroxymianserin in plasma. In addition, results of actual patient samples are reported.

EXPERIMENTAL

Apparatus—Chromatography was performed by a dual piston solvent delivery pump[1] connected to an automatic sampler[2]. Separations were achieved with either a 15-cm × 4.6-mm i.d. trimethylsilyl 5-μm particle size column[3] or a 25-cm × 4.6-mm i.d. octadecylsilyl 10-μm particle size column[4]. The detector system consisted of a thin-layer flow-through electrochemical cell[5] with glassy carbon as the working and auxiliary electrodes and a silver–silver chloride reference electrode. The potential and current response was monitored by an amperometric controller[6] and

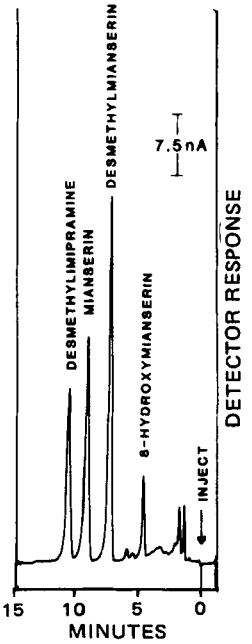

Figure 1—*Sample chromatogram of a 1-ml spiked plasma extract containing 25 ng of 8-hydroxymianserin and 100 ng each of mianserin and desmethylmianserin. One-half (50 μl) of the reconstituted extract was injected.*

[1] Model 6000A, Waters Associates, Milford, Mass.
[2] Wisp 710B, Waters Associates, Milford, Mass.
[3] LC-1, Supelco, Bellafonte, Pa.
[4] Partisil-10 ODS-3, Whatman Inc., Clifton, N.J.
[5] TL-5A, Bioanalytical Systems Inc., West Lafayette, Ind.
[6] Metrohm model E-611 V/A Detector, Brinkman Instruments, Inc., Westbury, N.Y.

0022-3549/82/0800-0889$01.00/0

Table I—Summary of the Linear Regression Data for the Standard Curve [a]

Compound	Slope ±*SD*, ng/ml	*x* Intercept ±*SD*, ng/ml	Correlation coefficient ±*SD*	Standard error of the estimate ±*SD*
Mianserin	76.28 ± 1.52	−0.41 ± 1.74	0.9999 ± 0.0001	1.93 ± 0.90
Desmethylmianserin	47.96 ± 1.29	0.99 ± 2.68	0.9999 ± 0.0002	1.72 ± 1.27
8-Hydroxymianserin	44.78 ± 4.16	4.10 ± 1.09	0.9986 ± 0.0012	1.50 ± 0.62

[a] Data computed from five consecutive standard curves.

recorder[7] and interfaced with a laboratory data acquisition system[8]. Aluminum column temperature control blocks were devised to fit columns of either size, and the temperature was controlled by a circulating water bath[9].

Reagents—Acetic acid[10], sodium acetate[10], sodium carbonate[10], and sodium bicarbonate[10] were all analytical reagent grade. Sodium heptane sulfonate[11] was used as received. Acetonitrile-UV[12] and methyl-*tert*-butyl ether[12] were used without further purification. Distilled water was passed through a water purification system[13] before use.

Standards—One milligram (free base) per milliliter of stock solution of mianserin hydrochloride[14], desmethylmianserin maleate[14], 8-hydroxymianserin maleate[14], and desmethylimipramine hydrochloride[15] were prepared in 0.1 *N* HCl. A stock solution of 1 mg/ml of 2-hydroxyimipramine[16] was prepared in methanol. For spiking plasma, the mianserin and desmethylmianserin stock solutions were diluted with 0.01 *N* HCl to give a working solution of 2 ng/μl of each. The stock solution of 8-hydroxymianserin was diluted with 0.1 *N* HCl to give working solutions of 1 ng/μl and 0.1 ng/μl. Desmethylimipramine was diluted with 0.01 *N* HCl to 2 ng/μl and 2-hydroxyimipramine was diluted with 0.1 *N* HCl to give 1 ng/μl to provide working solutions for the internal standard.

Standard curves were prepared containing five levels of spiked samples: 25, 50, 100, 200, and 400 ng/ml of mianserin and desmethylmianserin and 5, 10, 25, 50, and 100 ng/ml of 8-hydroxymianserin. Each set of standards included a blank.

Extraction—Internal standard, desmethylimipramine (25 μl, 50 ng), and 1.0 ml of 0.6 *M* carbonate buffer (pH 9.7) were added to 1.0 ml of plasma standard or unknown sample in specially washed glassware[17]. Eight milliliters of methyl-*tert*-butyl ether was added and the mixture was shaken for 15 min and centrifuged at 1500×*g* for 10 min. The organic layer was then transferred to a 15-ml tapered centrifuge tube containing 1.2 ml of 0.1 *N* HCl. After mixing for 10 min and centrifuging at 1500×*g* for 10 min, the organic layer was aspirated, the aqueous portion transferred to a 3-ml tapered glass-stoppered minicentrifuge tube, and neutralized with 0.5 ml of 0.6 *M* carbonate buffer (pH 9.7). Methyl-*tert*-butyl ether (0.5 ml) was added and the tube was stoppered, shaken, and centrifuged for 5 min at 1500×*g*. The lower aqueous layer was discarded and the organic layer transferred to a small glass vial[18].

The vial was placed within a 4-ml vial assembly (containing the adapter spring) and placed in a vacuum centrifuge[19]. The ether was evaporated under vacuum at 45°. The extract was then reconstituted with 100 μl of mobile phase, capped, and mixed.

Chromatographic Conditions—The mobile phase consisted of 0.1 *M* acetate buffer (pH 4.2)–acetonitrile (67:33) with 0.005 *M* sodium heptane sulfonate. The mixture was filtered and degassed prior to use.

[7] Houston Omniscribe model B5217 B-2, Houston Instruments, Austin, Tex.
[8] PDP 11/34 "Peak II" System, Digital Equipment Co., Maynard, Mass.
[9] Model FE, Haake Co., Saddlebrook, N.J.
[10] Fisher Scientific Co., Fairlawn, N.J.
[11] Eastman Kodak Co., Rochester, N.Y.
[12] Burdick and Jackson Laboratories, Muskegon, Mich.
[13] Milli-Q, Millipore Corp., Bedford, Mass.
[14] Organon, Inc., West Orange, N.J.
[15] USV Pharmaceutical Corp., Tuckahoe, N.Y.
[16] A gift from Dr. A. A. Manian, National Institute of Mental Health, Rockville, Md.
[17] All glassware (including disposable pipets) were soaked in detergent, washed, and then immersed in dichromate cleaning solution for 16–24 hr. The thoroughly rinsed glassware was neutralized with dilute ammonium hydroxide solution, thoroughly rinsed again with deionized double distilled water, and dried overnight at 160°.
[18] Limited Volume Insert, Waters Associates, Milford, Mass.
[19] Model SVC-100M Speed Vac Concentrator, Savant Instruments, Inc., Hicksville, N.Y.

Table II—Reproducibilty of Assays for Mianserin, Desmethylmianserin, and 8-Hydroxymianserin

Within Run [a] Concentration in Plasma, ng/ml	*RSD*,% Mianserin	Desmethylmianserin	8-Hydroxymianserin
100	3.3	2.9	7.2
50	6.9	5.9	8.5
10	4.7	4.3	11.8
5	8.1	10.4	8.2
Day-to-day [b]			
25	6.6	5.4	9.1

[a] $n = 6$. [b] $n = 5$.

Table III—Recovery of Mianserin, Desmethylmianserin, and 8-Hydroxymianserin from 1 ml of Plasma [a]

Compound	Recovery, %	*SD*, %	*RSD*, %
Mianserin, 50 ng	76	4.9	5.4
Desmethylmianserin, 50 ng	71	4.9	7.0
8-Hydroxymianserin, 25 ng	72	2.5	3.4

[a] $n = 6$.

The flow rate was 1.5 ml/min and temperature set at 30° resulting in an inlet pressure of ~1000 psi. The effluent was monitored through the detector cell at a potential of +1.05 V *versus* silver–silver chloride reference electrode.

Quantitation—All determinations were performed by calculating the peak height and/or area ratios of each compound to the internal standard. A linear regression analysis for each of the standard curves was performed by a computer program resulting in the calculation of slope, *x* intercept, correlation coefficient, and standard error.

RESULTS AND DISCUSSION

Mianserin, desmethylmianserin, and 8-hydroxymianserin were separated in a single chromatogram within 12 min. A typical chromatogram of spiked plasma is shown in Fig. 1. A blank plasma extract showed no endogenous interfering peaks (Fig. 2).

The absolute sensitivity (S/N ~3) of this method was checked by injecting a standard solution containing 1 ng of all three compounds. In practical terms the minimum quantifiable levels were 5 ng/ml of plasma. The electrochemical detector cell with glassy carbon as the working and auxilliary electrodes opposite each other permitted a linear detector response over a range from 5 to at least 500 ng. A summary of the data for the regression curves appears in Table I.

The precision of this method was determined by spiking six 1.0-ml aliquots of drug-free plasma with various levels of drug and metabolites. After the addition of 50 ng of internal standard, the sample was processed as described. The percent relative standard deviation for various levels are reported in Table II.

The absolute recovery was checked by preparing a solution of 50 ng of mianserin and desmethylmianserin, and 25 ng of 8-hydroxymianserin. The internal standard was added to each solution and the sample injected into the chromatograph. One milliliter of plasma was added to each of

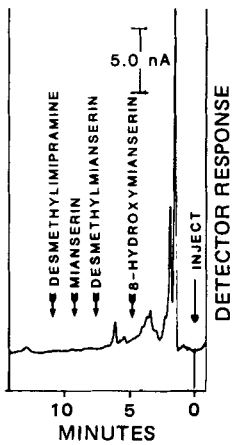

Figure 2—*Sample chromatogram of a 1-ml blank sample extract. The entire reconstituted extract (100 μl) was injected.*

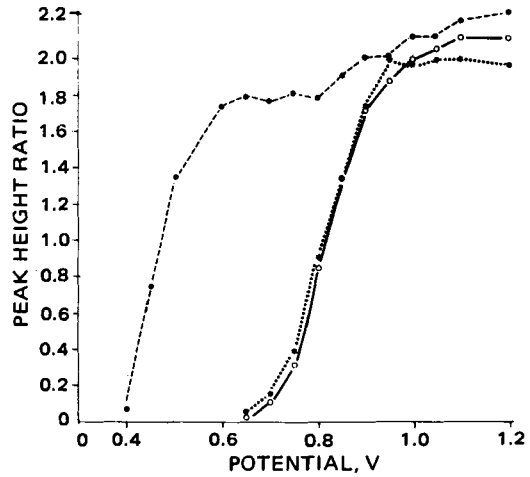

Figure 3—*A plot of the peak height ratio* (i.e., *detector response*) *against the oxidation potential* (versus *silver–silver chloride reference electrode*) *under the same chromatographic conditions described in the text:* (--●--) *8-hydroxymianserin,* (···*···) *desmethylmianserin,* (—o—) *mianserin.*

the same number of aliquots and processed routinely except for the internal standard. When the final extract was dried down, the internal standard was added (50 ng) with mobile phase and injected. The difference between the ratios of standards to internal standard in the processed samples *versus* direct injection samples gave a measure of the overall recovery (Table III).

The determination of the optimum oxidation potential for these compounds was done by injecting a standard solution of these compounds in methanol into the chromatograph at various potentials. A fixed wavelength UV detector[20] at 254 nm connected in series preceding the electrochemical cell, was used as an internal standard.

The ratios of the peak heights from the electrochemical and UV detectors were plotted against the various potentials. Figure 3 shows that the 8-hydroxymianserin undergoes oxidation at a more negative potential than either mianserin or its desmethyl metabolite. The lower oxidation potential of this metabolite is due to the presence of the ring hydroxyl group. A possible mechanism of electrochemical oxidation of hydroxylated derivatives could be explained by the formation of a quinone imine (8). Similar current–potential curves were observed with imipramine,

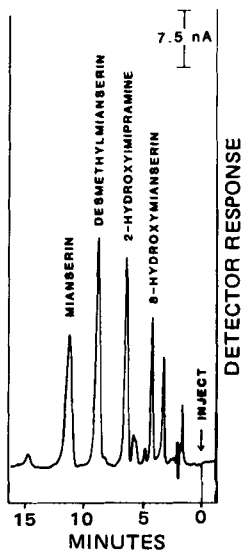

Figure 4—*Sample chromatogram of a 1-ml spiked plasma extract containing 50 ng each of mianserin and desmethylmianserin and 25 ng of 8-hydroxymianserin with 50 ng of 2-hydroxyimipramine as the internal standard. The column was octadecylsilane and the mobile phase was 0.1* M *acetate buffer (pH 4.2)–acetonitrile (65:35) with 0.005* M *heptane sulfonate. The flow rate was 1.3 ml/min.*

[20] Model 440, Waters Associates, Milford, Mass.

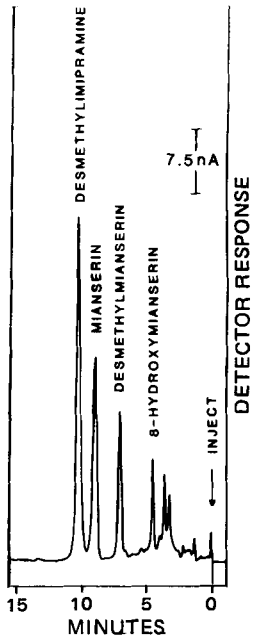

Figure 5—*Sample chromatogram of 1 ml of plasma sample from a patient receiving 120 mg/day of mianserin. Seventy percent reconstituted extract was injected. The plasma levels were calculated to be 13 ng of 8-hydroxymianserin, 21 ng of desmethylmianserin, and 45 ng of mianserin.*

desmethylimipramine, and their 2-hydroxy metabolites under similar experimental conditions (2). A mechanism of electrochemical oxidation of imipramine and chemically related dibenzazepines was recently described by a two-step three-electron ECE process[21] (9). Mianserin and its metabolites, which contain the dibenzazepine nucleus, may undergo similar mechanisms. The optimum potential found for electrochemical detection of mianserin and metabolites was +1.05 V *versus* silver–silver chloride which was compatible with that found previously for the internal standard, desmethylimipramine.

Interfering peaks from other pharmacologic agents, that may be administered concomitantly with this antidepressant, appeared from chlorpromazine and its metabolites and the hydroxylated metabolites of loxapine. Other low dose phenothiazine major tranquilizers such as fluphenazine, perphenazine, and haloperidol are generally found in much lower quantities in plasma and are not detected or elute beyond 12 min. Some commonly used benzodiazepines (flurazepam, chlordiazepoxide, and diazepam) are frequently administered anxiolytic and hypnotic adjuvants. These compounds, as well as their metabolites, would interfere

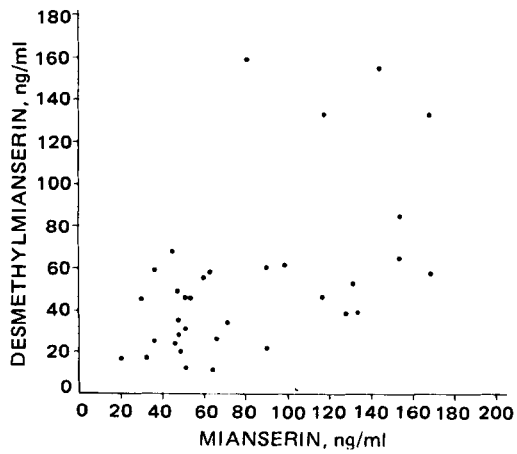

Figure 6—*Relationship between steady-state plasma mianserin and desmethylmianserin level in 34 patients on a fixed dose of 150 mg/day* (r = *0.54*).

[21] An electron-transfer step followed by a chemical reaction and a second electron-transfer step.

if a UV detector (at 254 nm) was used. However none of these drugs or metabolites were electrochemically responsive under the described conditions. A knowledge of the patient drug profile can be very helpful in the identification of interfering peaks.

The multistep extraction procedure used in this method was developed for the recovery of mianserin and its desmethylated and 8-hydroxy metabolites from plasma. A relatively clean chromatogram resulted with no endogenous interfering peaks but with an acceptable recovery of all compounds. Ether may be used in place of methyl-*tert*-butyl ether with a similar rate of recovery. However, it was found that methyl-*tert*-butyl ether required no prior distillation, was less likely to form peroxides, and was easier to handle in the laboratory. Mianserin and desmethylmianserin may also be extracted from plasma by either increasing the plasma pH to 12 and/or using a more nonpolar solvent such as *n*-heptane with 1.5% isoamyl alcohol thus eliminating the 8-hydroxymianserin from the assay. The other major metabolite found in human urine was mianserin-*N*-oxide. This metabolite may be present in plasma but is not extracted from a basic plasma medium.

This method was suitable for automatic sample processing. The use of the automatic injector was compatible with the electrochemical detector and the data acquisition systems. The primary concern in automating this system was the stability of the baseline with respect to drift. It was found that at a detector attenuation of 30 nA full scale or higher, the baseline remained virtually drift-free during a typical 6–8-hr run. In addition, there was no evidence of electrode contamination due to the possible oxidation products forming at the electrode during continuous operation.

If necessary, chromatography can be performed with an octadecylsilyl reversed-phase column with only a minor modification in mobile phase and a change in internal standard. However, several interfering endogenous plasma peaks were present in some samples, which may prove troublesome when low levels of drug are encountered. A spiked plasma sample using this column appears in Fig. 4.

Plasma samples from 34 different patients on a 150-mg/day fixed dose were analyzed for mianserin, desmethylmianserin and its 8-hydroxy metabolite. A representative chromatogram of a patient plasma sample appears in Fig. 5. The mean mianserin plasma level was found to be 81 ng/ml with a range of 20–169 ng/ml. The mean desmethyl metabolite was found to be 53 ng/ml with a range of 11–150 ng/ml. Of these samples, only four had measurable levels (5 ng/ml) of the 8-hydroxy metabolite and the remainder had traces (<5 ng) or none detected. Two patients receiving <150 mg/day (one 120 mg/day, and another 90 mg/day) were found to have 12 and 13 ng/ml of the 8-hydroxy metabolite, respectively. There was no apparent correlation between the plasma level of the nonconjugated 8-hydroxymianserin and the plasma levels of mianserin or desmethylmianserin. Figure 6 demonstrates the relatively weak correlation between mianserin and its desmethyl metabolite.

In three studies, where patients received 60 mg/day of mianserin, steady-state blood levels of mianserin were found in a 6–120-ng/ml range (10), 4–98 ng/ml (mean 36 ng/ml) (6), and a mean of 50 ng/ml (11). The presence of a significant amount of 8-hydroxymianserin as well as the parent compound has been reported (4), although desmethylmianserin could not be detected in the urine of two female volunteers. This was in contrast to earlier findings and rather unusual.

This method provides a means for the simultaneous determination of mianserin, desmethylmianserin, and 8-hydroxymianserin in plasma. The procedure is reliable and sensitive enough for routine plasma monitoring and single dose pharmacokinetic studies. In the single-dose studies, larger volumes of plasma (~3 ml) will be required to determine time points late in the pharmacokinetic curve.

REFERENCES

(1) P. T. Kissinger, C. S. Bruntlett, and R. E. Shoup, *Life Sci.*, **28,** 455 (1981).

(2) R. F. Suckow and T. B. Cooper, *J. Pharm. Sci.*, **70,** 257 (1981).

(3) R. N. Brogden, R. C. Heel, T. M. Speight, and G. S. Avery, *Drugs*, **16,** 273 (1978).

(4) G. D. DeJongh, H. M. vanden Wildenberg, H. Nieuwenhuyse, and F. vander Veen, *Drug Metab. Dispos.*, **9,** 48 (1981).

(5) J. Vink and H. J. M. Van Hal, *J. Chromatogr.*, **181,** 25 (1980).

(6) J. J. DeRidder, P. C. J. Koppens, and H. J. M. Van Hal, *ibid.*, **143,** 289 (1977).

(7) *Ibid.*, **143,** 281 (1977).

(8) M. Neptune, R. L. McCreery, and A. A. Manian, *J. Med. Chem.*, **22,** 196 (1979).

(9) S. N. Frank and A. J. Bard, *J. Electrochem. Soc.*, **122,** 898 (1975).

(10) J. Vink, H. J. M. Van Hal, and B. Delver, *J. Chromatogr.*, **181,** 115 (1980).

(11) S. Montgomery, R. McAuley, and D. B. Montgomery, *Br. J. Clin. Pharmacol.*, **5,** 71S (1978).

ACKNOWLEDGMENTS

Supported in part by Public Health Services Grant RR05651-10 from the Department of Health and Human Services.

2-^{14}C-1-Allyl-3,5-diethyl-6-chlorouracil I: Synthesis, Absorption in Human Skin, Excretion, Distribution, and Metabolism in Rats and Rabbits

RAVINDER KAUL ˣ, BERND HEMPEL, and GEBHARD KIEFER

Received August 10, 1981, from the *Research Laboratories, Pharmaceuticals Robugen GmbH, Postfach 266, D-7300 Esslingen, West Germany.* Accepted for publication November 3, 1981.

Abstract □ With ^{14}C-potassium cyanate as the starting material, 2-^{14}C-1-allyl-3,5-diethyl-6-chlorouracil was synthesized for *in vitro* and *in vivo* absorption studies in human skin and for metabolic studies in rats and rabbits. The radioactivity in the horny layer, epidermis, and dermis of the human skin was determined after different intervals of time, and the radioactivity excreted in the urine was measured by collecting samples for 5 days from a patient and also under occlusion conditions. Almost 90% of the radioactivity remained on the surface and ~6.28% penetrated and was systemically absorbed. Over a 5-day period, a total of 3.25% was excreted. Almost 3% was systemically absorbed and cumulated in the system. After intraperitoneal application in male and female rats, most of the radioactivity was excreted in the feces and urine, with female rats excreting more in the urine than male rats. The radioactivity rose in the organs in the first 3 hr and then decreased. At the end of 144 hr, no appreciable radioactivity could be found in the organs and tissues, except in the carcass where the cumulation was maximum (1%). After intravenous injection in rabbits, most of the radioactivity (80%) was excreted in the urine and only 4% in the feces. At the end of 96 hr, ~3% was cumulated in the body. The drug was quantitatively metabolized in both rats and rabbits: Metabolite 1 (70–85%), Metabolite 2 (10–15%), Metabolite 3 (5–10%), and Metabolite 4 (0.3%).

Keyphrases □ 2-^{14}C - 1 - Allyl-3,5-diethyl-6-chlorouracil—synthesis, absorption in human skin, excretion, distribution and metabolism, rats, rabbits □ Excretion—2-^{14}C-1-allyl-3,5-diethyl-6-chlorouracil, synthesis, absorption in human skin, distribution and metabolism, rats, rabbits □ Metabolism—2-^{14}C-1-allyl-3,5-diethyl-6-chlorouracil, synthesis, absorption in human skin, excretion, distribution, rats, rabbits □ Absorption—2-^{14}C-1-allyl-3,5-diethyl-6-chlorouracil, synthesis, human skin, excretion, distribution, metabolism, rats, rabbits

1-Allyl-3,5-diethyl-6-chlorouracil[1] (V) has shown promising therapeutic activity against herpes simplex and vaccinia virus (1, 2). It is used for the external treatment of herpes and other viral infections of the skin and mucous membranes. Its absorption in human skin and excretion, distribution, and metabolism in rats and rabbits were studied using ^{14}C-V.

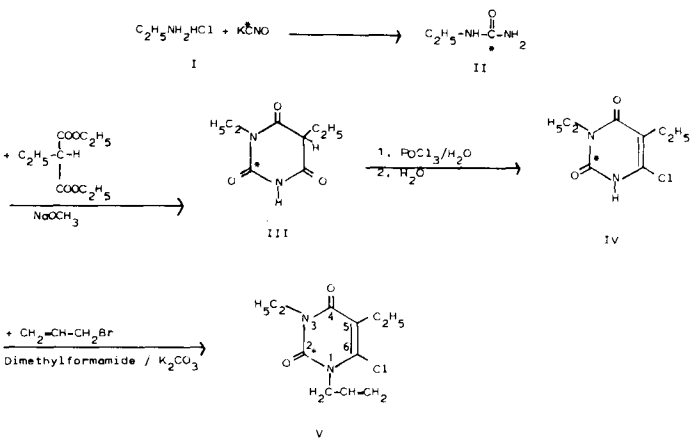

Scheme I

[1] Acluracil, Robugen GmbH, 7300 Esslingen/Neckar, West Germany.

EXPERIMENTAL[2]

Synthesis—For absorption studies in human skin and for metabolism studies, ^{14}C-V, specific activity 0.073 mCi/mmole was synthesized (Scheme I). The starting material was ^{14}C-potassium cyanate[3], specific activity 0.082 mCi/mmole.

^{14}C-N-Ethylurea (II)—A solution of ^{14}C-potassium cyanate (1.0 g, 12.33 mmoles) in 2 ml of water was added to ethylaminehydrochloride (I) (0.95 g, 11.77 mmoles) in water (1 ml) at 80° with constant stirring. The water was completely removed and the residue dried to give 1.72 g of ^{14}C-II (90.0% yield), mp 91–92° [lit. (3) mp 90–93°].

2-^{14}C-3,5-Diethylbarbituric Acid (III)—Diethyl ethylmalonate (2.17 g, 11.72 mmoles) was added dropwise to 5 ml of a 30% methanolic sodium methoxide solution. The reaction mixture was refluxed for 30 min with constant stirring. The methanolic solution (3 ml) of ^{14}C-II (1.72 g, 19.52 mmoles) was then added. The reaction mixture was refluxed for 5 hr at 100° with constant stirring under anhydrous conditions. After cooling, the solvent was evaporated to dryness and the residue was dissolved in 10 ml of hot water. The solution was acidified to pH 1–2 with 2.2 ml of concentrated hydrochloric acid and extracted with chloroform (5 × 15 ml). The solvent was removed and the residue crystallized from ether to give 2.16 g of 2-^{14}C-III (47.6% yield), mp 92–93° [lit. (4) mp 93–94°].

2-^{14}C-3,5-Diethyl-6-chlorouracil (IV)—Phosphorus oxychloride (2 ml) was added dropwise to a mixture of III (2.16 g, 11.73 mmoles) and water (0.1 ml). The reaction temperature was slowly raised to 100° with constant stirring, and after heating for 90 min it was cooled. The remaining phosphoryl chloride was decomposed carefully with 6 ml of water. The cooled mixture was stirred for 1 hr and allowed to stand in the refrigerator overnight. The white crystalline precipitate was filtered off, washed with ice cold water, and dried to give 1.23 g of 2-^{14}C-IV (52.1% yield), mp 168° [lit. (5) mp 167–169°].

2-^{14}C-1-Allyl-3,5-diethyl-6-chlorouracil (V)—Potassium carbonate (2.235 g), allyl bromide (0.68 ml), and dimethylformamide (12.5 ml) were added to 2-^{14}C-IV (1.23 g, 6.07 mmoles) under anhydrous conditions. The mixture was refluxed with stirring for 2 hr at 90–100° and filtered. The residue was washed with chloroform and the filtrate concentrated. The oily liquid was distilled *in vacuo* (bp 119–120°/0.1 mm) to give 1.17 g of 2-^{14}C-V (79.5% yield), specific activity 0.073 mCi/mmole [lit. (5) bp 118–120°/0.1 mm]. ^{1}H-NMR and mass spectra obtained were consistent with structure V. Radiochemical purity was checked by radioscanning of the TLC plates.

Radioactivity Measurements—The radioactive zones on TLC plates were located with a thin-layer scanner[4]. The radioassay in the solution was carried out in a two-canal liquid scintillation counter[5], using a scintillation solution of 1000 ml of dioxane, 180 g of naphthalene, 8 g of 2,5-diphenyloxazole, and 0.1 g of 1,4-bis[2-(4-methyl-5-phenyl-oxazolyl)] benzene. The external standardization technique was employed.

Application—*Human Skin*—A 0.4% solution of ^{14}C-V was made in water using 3% of a solubilizing agent[6]. For *in vitro* studies, 20 μl = 4.9 mg was applied on an area of 7 cm^2. For *in vivo* studies, 50 μl = 4.9 mg of a 0.1% solution of ^{14}C-V was applied on an area of 28 cm^2.

Rats and Rabbits—A 0.15% solution of ^{14}C-V was made in sterile water with 3% of a solubilizing agent[6]. Male and female Wistar rats (200–220 g) were given 7.5 mg/kg body weight of ^{14}C-V solution by intraperitoneal injection. The animals were kept in metabolic cages which enabled the collection of feces and urine separately. They were given free access to

[2] Melting points were taken on a Tottoli (Büchi, Switzerland) apparatus and are uncorrected.

[3] New England Nuclear Corp., Boston, Mass.

[4] Dr. Rudolf Berthold Co., Wildbad, West Germany.

[5] Tri-Carb model 3950, Packard Instrument Co., La Grange, Ill.

[6] Cremophor RH 40, BASF, Ludwigshafen, West Germany.

0022-3549/82/0800-0893$01.00/0

Table I—Relative and Absolute Concentrations in Various Tissues After Application *In Vitro* of 2-^{14}C-V [a]

Penetration time, min	Tissue	Quantity Applied, %	Tissue under 1 cm^2 of Surface, μg/cm^2	Respective Tissue, mg/ml	mmole[b]	Rejection, %
100	Horny layer	10.06	111.5	55.72	229.6	
	Epidermis	0.36	3.98	0.249	1.026	88.54
	Dermis	0.90	10.00	0.0965	0.381	
300	Horny layer	7.35	84.4	40.70	167.7	
	Epidermis	0.97	10.8	0.672	2.77	87.52
	Dermis	3.10	34.4	0.318	1.31	
1000	Horny layer	5.40	59.8	29.92	123.3	
	Epidermis	1.31	14.5	0.904	3.73	84.64
	Dermis	7.97	88.2	0.817	3.36	

[a] Application of 7.75 mg of 2-^{14}C-V/7 cm^2 of human skin. [b] Millimole per liter tissue.

Table II—Relative and Absolute Concentrations in Various Tissues or Urine After *In Vivo* Application of 2-^{14}C-V [a]

Penetration time, min	Tissue or Urine	Quantity Applied, %	Tissue under 1 cm^2 of Surface, μg/cm^2	Respective Tissue, mg/ml	mmole[b]	Rejection, %
100	Horny layer	12.97	22.69	11.35	46.74	
	Epidermis	0.93	1.63	0.102	0.42	83.11
	Dermis	1.94	3.39	0.031	0.13	
1000	Horny layer	13.54	23.70	11.85	48.83	
	Epidermis	0.78	1.36	0.085	0.35	75.10
	Dermis	1.69	2.95	0.027	0.11	
	Urine 5 days	3.24 total				
1000 under occlusion	Urine 5 days	9.375 total				78.23

[a] Application of 4.9 mg of 2-^{14}C-V/28 cm^2 of human skin. [b] Millimole per liter tissue.

Table III—Elimination of Radioactivity in Feces and Urine of Male and Female Rats After Intraperitoneal Administration of 2-^{14}C-V [a]

Sample	Hours	Average Percent of Applied Dose ±*SD* Male	Female
Feces	8	14.4 ± 4.3	10.2 ± 3.8
	16	30.7 ± 5.6	24.7 ± 5.2
	24	4.9 ± 2.2	2.9 ± 1.8
	48	5.1 ± 1.4	5.8 ± 1.6
	72	9.7 ± 1.9	8.6 ± 1.7
	96	1.2 ± 0.9	0.3 ± 0.1
	120	0.1 ± 0.03	0.3 ± 0.08
	144	0.04 ± 0.01	0.1 ± 0.08
	Total	66.1 ± 0.58	52.9 ± 1.1
Urine	8	3.6 ± 1.5	7.3 ± 1.8
	16	16.4 ± 2.4	21.3 ± 2.8
	24	2.0 ± 0.9	6.8 ± 1.7
	48	2.1 ± 0.8	2.3 ± 0.6
	72	2.4 ± 1.2	3.6 ± 1.4
	96	1.9 ± 0.8	1.8 ± 0.8
	120	0.1 ± 0.05	0.6 ± 0.1
	144	0.01 ± 0.005	0.1 ± 0.03
	Total	28.5 ± 0.09	43.8 ± 0.1

[a] Average of six animals; administration of 7.5 mg of 2-^{14}C-V.

Table IV—Elimination of Radioactivity in Feces and Urine of Male Rabbits After Intravenous Administration of 2-^{14}C-V [a]

Sample	Hours	Average Percent of Applied Dose ±*SD*
Feces	24	3.6 ± 1.4
	48	0.5 ± 0.1
	72	0.2 ± 0.1
	96	0.1 ± 0.07
	Total	4.4 ± 0.1
Urine	24	80.1 ± 6.8
	48	6.1 ± 2.6
	72	1.5 ± 0.8
	96	0.6 ± 0.2
	Total	88.3 ± 2.4

[a] Average of 3 animals; administration of 15.0 mg of 2-^{14}C-V.

food[7] and water and were kept at 22° and 55% humidity. The feces and urine were collected daily over a period of 144 hr. For studying the distribution, the rats were killed at different time intervals and all organs and tissues were removed separately. All samples were frozen at −20° and taken out before use. New Zealand male rabbits (2 kg each) were given a dose of 15 mg/kg body weight by intravenous injection into the ear vein. Feces and urine were collected daily over a 96-hr period. At the end of this period they were killed and organs and tissues removed and frozen.

Preparation of the Skin—In Vitro *Investigation*—The subcutaneous fat was carefully removed from skin mammary ablations shortly after surgery. Three different specimens of appropriate size were obtained. For each penetration period one specimen was used. The skin was gently cleaned and subcutaneous fat was removed. An area of 7 cm^2 was marked out. The solution of ^{14}C-V was applied for 90 sec by gently rubbing with a glass spatula. Subsequently, the specimen was stretched in a draft-free penetration chamber according to published procedures (6, 7). The subcutaneous side was in contact with gently agitated saline. The glass chamber was kept at a constant temperature of 32° for the indicated time period (penetration time).

In Vivo *Investigations*—Two patients were included in this study. A solution of ^{14}C-V was applied gently to a 28-cm^2 area of healthy skin, and the treated area was protected against unintentional abrasion by a wire cage under free access of air.

Processing of the Skin and Urine—In Vitro—After 100-, 300-, and 1000-min penetration time, the surplus of ^{14}C-V on the surface was removed gently with dry cotton. The specimens were then fastened on a rubber stopper and the horny layer removed by repeated stripping with adhesive tape[8] until a polished shining layer was visible, indicating that all horny skin was removed. Each of the ~20 strips was placed in a separate vial. After removal of the horny layer, a 28-mm^2 sample was punched out and cut horizontally on a freeze microtome[9]. The 16 slices of 10-μm thickness first-sectioned represented the epidermis. The remaining part representing the dermis was cut into 40-μm slices. Thus, ~70 samples were obtained in each experiment with one penetration time and were counted separately. Each sample was placed in a scintillation glass and 0.3 ml of 0.5 *N* NaOH was added. The closed glasses were kept

[7] Altromin, Altromin, Lage/Lippe, West Germany.

[8] Tesafilm, Beiersdorf, Hamburg, West Germany.

[9] Jung, Heidelberg, West Germany.

Table V—Tissue Distribution of Radioactivity in Male and Female Rats [a] at Different Time Intervals After Intraperitoneal Administration of 2-^{14}C-V

Specimen	Sex	Average Percent of Applied Dose, hr										
		1	3	5	8	16	24	48	72	96	120	144
Blood	Male	1.82	1.13	1.23	1.05	0.40	0.60	0.56	0.40	0.65	0.28	0.17
	Female	3.06	3.22	0.42	1.01	0.65	0.98	0.90	1.48	0.27	0.19	0.10
Liver	Male	1.94	1.66	1.47	1.32	0.38	0.31	0.02	0.28	0.08	0.06	0.08
	Female	2.53	3.61	1.43	0.86	0.27	0.71	0.40	0.33	0.18	0.04	0.21
Testes/ovary	Male	0.32	1.26	0.47	0.15	0.04	0.10	0.40	0.96	0.04	0.04	0.10
	Female	0.58	0.25	0.23	0.21	0.01	0.03	0.35	0.33	0.28	0.08	0.08
Kidneys	Male	1.04	0.63	0.65	1.05	0.18	0.21	0.22	0.41	0.08	0.12	0.06
	Female	0.79	0.94	0.53	0.38	0.01	0.24	0.45	0.25	0.07	0.18	0.05
Gut	Male	13.93	13.28	7.79	5.27	0.39	0.73	0.05	0.32	0.05	0.04	0.06
	Female	11.27	6.30	5.75	10.15	1.09	2.26	0.61	0.51	0.18	0.26	0.07
Spleen	Male	0.23	0.24	0.38	0.07	0.02	0.07	0.38	0.44	0.19	0.01	0.02
	Female	0.05	0.24	0.56	0.06	0.12	0.07	0.24	0.23	0.10	0.03	0.10
Stomach plus duodenum	Male	1.54	1.16	0.40	0.74	0.08	0.04	0.12	0.12	0.11	0.20	0.01
	Female	0.27	0.17	0.,34	0.21	0.12	0.12	0.25	0.54	0.11	0.16	0.01
Heart	Male	0.94	0.31	0.45	0.04	0.08	0.03	0.76	0.20	0.09	0.08	0.08
	Female	0.10	0.30	0.10	0.03	0.02	0.07	0.23	0.53	0.14	0.14	0.11
Lungs	Male	0.71	0.37	0.18	0.37	0.36	0.04	0.36	0.36	0.21	0.10	0.08
	Female	0.25	0.34	0.28	0.20	0.07	0.08	0.23	0.42	0.08	0.15	0.17
Brain	Male	0.71	1.08	0.68	0.14	0.08	0.11	0.07	0.18	0.38	0.04	0.04
	Female	1.20	0.15	0.09	0.03	0.04	0.05	0.29	0.15	0.11	0.06	0.12
Abdominal fat	Male	1.03	0.41	0.90	0.71	0.09	0.10	0.44	0.22	0.04	0.40	0.04
	Female	7.15	8.80	0.54	1.34	0.24	0.52	0.37	0.18	0.07	0.60	0.06
Muscles	Male	3.30	2.71	3.40	1.76	0.51	2.01	1.10	0.99	0.37	0.18	0.18
	Female	3.10	1.86	2.30	2.31	0.68	3.24	1.40	1.29	0.16	0.17	0.21
Subcutaneous fat	Male	1.39	0.32	0.85	0.89	0.03	0.29	0.43	0.07	0.04	0.10	0.05
	Female	1.02	6.31	0.93	0.22	0.11	0.34	0.34	0.36	0.04	0.10	0.06
Contents of gut	Male	45.97	60.81	65.48	61.14	13.49	3.82	0.70	0.56	0.45	1.12	0.10
	Female	45.26	47.96	59.32	47.43	5.84	2.57	1.27	1.32	0.41	1.14	0.05
Carcass	Male	20.25	9.84	11.55	14.37	6.27	5.71	2.60	3.42	1.67	1.08	1.02
	Female	19.52	14.96	20.86	13.38	17.99	9.16	5.15	5.48	2.64	0.92	1.21

[a] Average of six animals; administration of 7.5 mg of 2-^{14}C-V.

Table VI—Tissue Distribution of the Radioactivity in Male Rabbits [a] 96 hr After Intravenous Administration of 2-^{14}C-V

Specimen	Average Percent Applied Dose
Bones	1.88
Carcass	1.18
Muscles	0.09
Liver	0.07
Intestinal content	0.40
Heart	0.01
Kidney	0.03
Lungs	0.03
Brain	0.01
Blood	0.04
Total	3.73

[a] Average of three animals; administration of 15.0 mg of 2-^{14}C-V.

for 6 hr in an incubator at 75°. Scintillation solution then was added to each sample and the radioactivity measured.

In Vivo—Two penetration times (100 and 1000 min) were selected. The surplus ^{14}C-V was removed and the horny layer sampled as indicated above. A specimen of 28 mm^2 was punched out from the excised area and sliced in the same manner as described for *in vitro* experiments. By day urine was sampled over a 4-hr period and during the night over an 8-hr period; each volume was measured. Samples of 0.3 ml were taken and after addition of hyamine, added directly to the scintillation cocktail.

Penetration Under Occlusion—In a third patient, the pathological skin condition was simulated by occlusion technique, which causes hydration of the horny layer and thus facilitates the penetration. The horny skin was completely removed and 50 μl/28 cm^2 of 0.10% ^{14}C-V was applied and covered with occlusive film[10] for 1000 min, which helped the maximum penetration.

Calculation for Absorption in Human Skin—Subsequent calculations of disintegrations per minute of the percentage of the applied quantity and absolute quantities per layer of skin were performed using a computer program. Absolute quantities are given in micrograms within the respective layer calculated for a 1-cm^2 surface, in micrograms per milliliter of volume of the layer, and in millimoles (calculated on the basis of 1 liter of skin volume). The following tissue thicknesses were taken in calculation: horny layer, 20 μm; epidermis, 160 μm; and dermis, 1.5 mm.

Animal Sample Preparation—*Feces, Organs, and Tissues*—For qualitative and quantitative determination of the radioactivity, the feces samples were dried at 60°, powdered, homogenized[11], and extracted with methanol in a soxhlet apparatus for 48 hr. The organs and tissues were cut into fine pieces and extracted with methanol for 72 hr according to procedures described previously (8, 9). An aliquot (0.1 ml) of the samples was taken up for required measurements.

Urine—An aliquot (0.1–0.2 ml) was mixed directly into the scintillation solution and measured for radioactivity (10).

Chromatography—Analytical TLC was performed on 20 × 5-cm (0.25 mm) silica gel plates[12]. Solvent systems were (v/v): (*a*) petroleum ether–ethyl acetate (8:2); (*b*) petroleum ether–ethyl acetate (5:5); (*c*) cyclohexane–acetone (7:3); (*d*) chloroform–ether (6:4).

Gas Chromatography—Analytical GLC determinations were performed on a gas chromatograph[13] equipped with a flame-ionization detector. The chromatographic column was glass tubing (1.5 m × 0.4-mm i.d.) packed with 3% SE-30 on 100–120 mesh Varaport 30. The operating conditions were: injection port temperature, 230°; oven temperature, 200°; detector temperature, 250°; nitrogen (carrier gas) flow rate, 20 ml/min.

Enzymatic Hydrolysis of the Urine—The rabbit urine was adjusted to pH 7 with acetic acid and then extracted with ether for 96 hr in a liquid–liquid extractor, removing ~90% of the radioactivity (Extract A). The rest of the radioactivity could not be removed with organic solvents and was probably due to conjugates. The urine after ether extraction was concentrated to half of its volume and adjusted to pH 5.5 with concentrated acetic acid. It was diluted to half of its volume with acetate buffer. The enzymatic hydrolysis was done with 0.01 ml of β-glucuronidase and arylsulfatase[14]/ml of urine at 37° for 72 hr and extracted with ether for 96 hr (Extract B).

RESULTS AND DISCUSSION

Absorption in Human Skin—*In Vitro*—Table I shows that most of the applied ^{14}C-V (85–90%) remained on the skin surface or was washed

[10] Leukoflex, Beiersdorf, Hamburg, West Germany.

[11] Waring Blender, Bosch, Stuttgart, West Germany.
[12] Silica gel HF_{254}, E. Merck AG, Darmstadt, West Germany.
[13] Aerograph 1740, Varian.
[14] Glusulase, Boehringer, Mannheim, West Germany.

Table VII—TLC R_f Values of the Metabolites of V

	Solvent	R_f Metabolite 1	Metabolite 2	Metabolite 3	V
(*a*)	Petroleum ether–ethyl acetate (8:2)	*S*[a]	*S*	*S*	0.45
(*b*)	Petroleum ether–ethyl acetate (5:5)	0.38	0.63	0.71	0.85
(*c*)	Cyclohexane–acetone (7:3)	0.16	0.43	0.59	0.75
(*d*)	Chloroform–ether (6:4)	0.30	0.70	0.78	*F*[b]

[a] Start. [b] Front.

Table VIII—Ratio in Percent of Various Metabolites of V in Feces [a] and Urine [b] of Male and Female Rats

Sample	Sex	Percent Metabolite 1	Metabolite 2	Metabolite 3
Feces	Male	68	20	12
	Female	65	22	13
Urine	Male	85	10	5
	Female	88	8	4

[a] The feces of various time intervals were mixed together. [b] The urine of various time intervals were pooled together.

in the penetration chamber. Over a 1000-min period, however, ~8% penetrated into the dermis, which acted as a further transport system in the body. The absolute quantity within the respective layers calculated for a 1-cm^2 surface area showed the accumulation of the radioactivity in the dermis, the thickest tissue. The absolute values calculated with an equal tissue volume, however, showed a surprisingly higher molar concentration after a 1000-min period in all tissues. The rejection rate included the percentage of the radioactivity in the saline of the penetration chamber and on the surface of the skin which was wiped off with cotton.

In Vivo—The results are shown in Table II. Here also it is evident that most of the ^{14}C-V remained on the skin surface. The concentration in the horny layers was somewhat higher than *in vitro* studies; in the epidermis it was almost the same. However, the concentration in the dermis *in vivo* was much less than *in vitro* after a penetration time of 1000 min. This is because the circulation system does not play a role *in vitro*, and the drug accumulated in the excised skin. The difference (6.28%) between these *in vivo* and *in vitro* dermal concentrations after a penetration time of 1000 min could be considered as resorption of the drug through the circulatory system. It was more clear when the absolute concentration *in vitro* and *in vivo* was compared. The fact that ^{14}C-V was systemically absorbed in the system was also confirmed by the excretion of the radioactivity in the urine. Over a 5-day period, 3.24% of the activity was excreted after which it was negligible or had completely stopped showing that at least 3% of ^{14}C-V accumulated in the body. The difference between 100- and 1000-min studies showed that a steady state of penetration (*i.e.*, equilibrium between the passage of the substance from the horny skin and its further transport in the circulatory system) relatively soon had reached a standstill; probably it required <100 min. Because of the importance of absorption and excretion of ^{14}C-V, occlusion conditions were employed in a third patient to allow maximum penetration for a period of 1000 min. Similarly, 9.4% of the radioactivity (Table II) could be detected in the urine.

Animal Excretion—*Rats*—Table III shows the excretion of the radioactivity in feces and urine of male and female rats up to 144 hr. A total of 66.1% of the activity was excreted by the male rats in the feces and 28.5% in the urine. On the other hand, the female rats excreted ~52.9% in the feces and 43.8% in the urine. These different excretion rates in the feces and urine could be due to different physiological conditions in both sexes and the female rats excreted a greater quantity of urine than male rats. However, both male and female rats excreted >95% of the radioactivity (male 94.6%, female 96.7%) in the feces and the urine.

Rabbits—Table IV shows the excretion of the radioactivity in the feces and urine of male rabbits up to 96 hr. Most of the radioactivity (88.1% in urine and 3.6% in feces) was excreted after 24 hr. Excretion was slow and at the end of 96 hr, a total of 93% of the activity was excreted in the feces and the urine. This showed that in both rats and rabbits, the kidneys are one of the main elimination organs in the excretion of V and its metabolites.

Animal Distributions—*Rats*—Table V gives the values for male and female rats as percentages of applied dose. The radioactivity increased in all organs and tissues in the first 3 hr and then decreased. In blood the fall of the activity was slow and remained at a constant level between 16 and 72 hr. This was in agreement with urine where maximum excretion took place between these periods. This shows that metabolism of ^{14}C-V was complete after 16 hr and the maximum blood concentration was reached. However, some differences in values in male and female rats were recorded, showing the different metabolism rates in the two sexes. In the kidneys, the main organ of excretion, the radioactivity rose and decreased during various time intervals which can be explained due to throwback mechanisms. In all organs and tissues, however, the radioactivity decreased smoothly, except for a slight rise between 48 and 72 hr, which was due to redistribution phenomenon of these organs. In the liver, the main organ of biotransformation, no concentration of the radioactivity was observed after 5 hr. The high concentration of the activity in the intestine was due to feces that contained high activity and was subsequently excreted. This was further confirmed by contents of the intestinal tract which contained high activity and was ultimately excreted with feces. This shows that the liver plays an important part in the biotransformation and the activity in the feces originated mainly from the activity *via* the bile. At the end of 144 hr, <0.1% of the activity was found in all the organs and tissues of both male and female rats, except in the carcass, where values between 1.02 and 1.21% were recorded. In the carcass of both male and female rats, high radioactivity was accumulated even after 1 hr of application of ^{14}C-V and then decreased.

Rabbits—Table VI gives the values in the organs and tissues at the end of 96 hr. Except in the bones and carcass, very little activity could be found in the other organs and tissues. A total of 3.7% was found in the body after 96 hr.

Metabolism—*Rats*—The feces and the urine of rats showed on the TLC scanner Metabolites 1, 2, and 3 but no unchanged ^{14}C-V. Table VII gives the R_f values of the metabolites compared with ^{14}C-V.

The ratio of these metabolites in feces and urine of both male and female rats is given in Table VIII. Metabolite 1 is the major metabolite in the feces and urine of both male and female rats. The GLC investigations of the prepurified feces and urine showed the presence of another metabolite, 4, in 0.2% concentration. In the increasing order of their retention time in GLC, the metabolites were classified as follows: Metabolite 4 > Metabolite 1 > Metabolite 2 > Metabolite 3.

Rabbits—The combined rabbit urine after extraction with ether (Extract A) showed the presence of Metabolites 1, 2, and 3 in the ratio of 8.5:1.0:0.5. GLC showed the presence of Metabolite 4 in 0.3% concentration. The urine of the rabbits after enzymatic hydrolysis (Extract B) gave Metabolite 1 in 3% yield which showed that it occurred partially as a conjugate. Because of less radioactivity in the feces and many impurities, it could not be investigated properly.

REFERENCES

(1) K. K. Gauri and H. Kohlhage, *Chemotherapy*, **14**, 158 (1969).

(2) K. K. Gauri and B. Rohde, *Klin. Wochenschr.*, **47**, 375 (1969).

(3) R. Biltz and H. Jeltsch, *Ber. Dtsch. Chem. Ges.*, **56**, 1919 (1923).

(4) M. Boetius, B. Marchand, and G. Dietz, *J. Prakt. Chem.*, **7**, 135 (1958).

(5) K. K. Gauri, Patent Robugen, DP No P 1620 182 (1966).

(6) A. Zesch and H. Schaefer, *Arzneim.-Forsch./Drug Res.*, **26**, 1365 (1976).

(7) H. Schaefer, A. Zesch, and G. Stüttgen, *Arch. Dermatol. Res.*, **258**, 241 (1977).

(8) G. Ludwig, J. Weiss, and F. Korte, *Life Sci.*, **3**, 123 (1964).

(9) F. Korte and W. Kochen, *Med. Pharmacol. Exp.*, **15**, 404 (1966).

(10) R. Kaul, W. Klein, and F. Korte, *Tetrahedron*, **26**, 331 (1970).

2-^{14}C-1-Allyl-3,5-diethyl-6-chlorouracil II: Isolation and Structures of the Major Sulfur-Free and Three Minor Sulfur-Containing Metabolites and Mechanism of Biotransformation

RAVINDER KAUL ˣ, BERND HEMPEL, and GEBHARD KIEFER

Received August 10, 1981, from the *Research Laboratories, Pharmaceuticals Robugen GmbH, Postfach 266, D-7300 Esslingen, West Germany.* Accepted for publication November 3, 1981.

Abstract □ The metabolites of 1-allyl-3,5-diethyl-6-chlorouracil in rabbit urine were isolated by preparative thick-layer, liquid-column, and gas chromatography. With the aid of mass and ^{1}H-NMR spectra, and by comparison with an authentic sample, the major metabolite, 1, was identified as 6,8-diethyl-2-hydroxymethyl-tetrahydrooxazolo-[3,2-*c*]-pyrimidine-5,7(4H,6H)-dione, Metabolite 2 as 1-allyl-3-ethyl-5-(1-hydroxyethyl)-6-methylthiouracil, Metabolite 3 as 1-allyl-3,5-diethyl-6-methylthiouracil, and Metabolite 4 as 6,8-diethyl-2-hydroxymethyl-tetrahydrothiazolo-[3,2-*c*]pyrimidine-5,7(4H,6H)-dione. The mechanism of the formation of sulfur-containing metabolites is discussed, and a new metabolic pathway for the formation of methylthio compounds is proposed.

Keyphrases □ 2-^{14}C-1-Allyl-3,5-diethyl-6-chlorouracil—isolation and structures of the sulfur-free and sulfur-containing metabolites, mechanism of biotransformation □ Metabolites—2-^{14}C-1-allyl-3,5-diethyl-6-chlorouracil, isolation and structures of the major sulfur-free and sulfur-containing, mechanism of biotransformation □ Biotransformation—2-^{14}C-1-allyl-6-chlorouracil, isolation and structures, sulfur-free and sulfur-containing metabolites, mechanism □ Sulfur—2-^{14}C-1-allyl-3,5-diethyl-6-chlorouracil metabolites, isolation and structures, mechanism of biotransformation

1-Allyl-3,5-diethyl-6-chlorouracil[1] (I) has shown promising therapeutic activity against herpes simplex and vaccinia virus (1, 2) and is used for the external treatment of herpes and other viral infections of the skin and mucous membranes. Its absorption in human skin and excretion, distribution, and metabolism in rats and rabbits using ^{14}C-I were reported previously (3). The isolation and structure determination of the major and three minor metabolites are reported in this study.

EXPERIMENTAL[2]

Application—For the isolation of the metabolites, four male rabbits, each 2–2.5 kg, were kept in metabolism cages. Each rabbit was given 5 mg of ^{14}C-I daily [specific activity 0.073 mCi/mmole (3)] mixed in the food over a period of 3 months. They were given dry food[3] and water and kept under normal laboratory conditions. The urine samples were collected daily and frozen to avoid any decomposition.

Radioactivity Measurements—The radioactive zones on TLC plates were located with a thin-layer scanner[4]. The radioassay in the solution was carried out in a two-canal scintillation counter[5], using a scintillation solution of 1000 ml of dioxane, 180 g of naphthalene, 8 g of 2,5-diphenyl-oxazole, and 0.1 g of 1,4-bis[2-(4-methyl-5-phenyl-oxazolyl)] benzene. The external standardization technique was employed. An aliquot (0.1 ml) of the sample solution was directly mixed into the scintillation solution and measured for radioactivity.

Chromatography—Analytical TLC was performed on 20 × 5-cm (0.25 mm) silica gel plates[6]. The solvent system was petroleum ether–ethyl acetate (1:1, v/v). Preparative TLC was performed on 20 × 20-cm (2 mm) silica gel plates with the described solvent system. Column chromatography was carried out on 0.05–0.2-mm silica gel with increasing proportions of ethyl acetate in petroleum ether.

Gas Chromatography—Analytical GLC determinations were performed on a gas chromatograph[7] equipped with a flame-ionization detector. The chromatographic column was glass tubing (1.5 m × 0.4-mm i.d.) packed with 3% SE-30 on 100–120 mesh Varaport 30. The operating conditions were: injection port temperature, 230°; oven temperature, 200°; detector temperature, 250°; and nitrogen (carrier gas) flow rate, 20 ml/min.

Preparative gas chromatography was performed on a gas chromatograph[8] with a flame-ionization detector. The chromatographic column was aluminum tubing (4 m × 6-mm i.d.) packed with 3% SE-30 on 100–120 mesh Varaport 30. The operating conditions were: detector/injector temperature, 225°; exit tip temperature, 200°; column oven temperature, 200°, isotherm; split 1:14; and nitrogen (carrier gas) flow rate, 350 ml/min.

Metabolite Isolation—The urine was adjusted to pH 7 and extracted in a liquid–liquid extractor with ether for 96 hr yielding ~90% of the radioactivity (Extract A), which on TLC showed Metabolites 1, 2, and 3 in the ratio 8.5:1.0:0.5 (3). GLC also showed Metabolite 4 (0.3%) but no unchanged I. For the isolation of the metabolites, Extract A was first purified to remove major impurities. It was applied on preparative TLC plates in a linear form and developed in the solvent system. The silica gel beyond the start line was removed, extracted with methanol in a soxhlet apparatus, solvent removed, and concentrated nearly to 5 ml. The process was repeated again. Purified Extract A (30 μCi or 100 mg of total metabolites) was concentrated to dryness and taken up in petroleum ether. It was loaded on a glass column (80 × 3 cm), filled with silica gel and eluted with increasing proportions of ethyl acetate in petroleum ether using an automatic fraction collector. Eight hundred 20-ml fractions were collected. A radioassay was carried out with each fraction. The loaded radioactivity was recovered fully. The following eluates were pooled together and concentrated after analysis in GLC:

100–150 (25% ethyl acetate in petroleum ether)—Metabolite 3
151–250 (30% ethyl acetate in petroleum ether)—Metabolite 2
450–650 (65% ethyl acetate in petroleum ether)—Metabolite 1
651–800 (70% ethyl acetate in petroleum ether)—Metabolite 4

The concentrated eluate of Metabolite 1 was brown-colored. It was loaded on a silica gel column and eluted with 60% ethyl acetate in petroleum ether. The solvent was removed and the residue was twice crystallized from methanol to yield 45 mg of Metabolite 1, mp 163–164°. Metabolites 2–4 could not be further purified by column chromatography. GLC showed the presence of a number of impurities. The substance was therefore purified by preparative GLC, to yield 20 mg of Metabolite 2 and 8 mg of Metabolite 3. Attempts to isolate and purify Metabolite 4 failed due to the minimal amount.

Synthesis—*Metabolite 1 (6,8-Diethyl-2-hydroxymethyl-tetrahydrooxazolo-[3,2-c]pyrimidine-5,7(4H,6H)-dione)* — 6,8-Diethyl-2-bromomethyl-tetrahydrooxazolo[3,2-*c*]pyrimidine-5,7(4H,6H)dione (1.5 g, 5 mmoles), prepared according to the literature method (4), was dissolved in 10 ml of dimethylformamide and heated under reflux for 10 hr with silver acetate (20 mmoles), which was obtained by heating 2.8 g of silver carbonate and 20 ml of acetic acid. After cooling, the insoluble

[1] Acluracil, Robugen GmbH, 7300 Esslingen/Neckar, West Germany.
[2] Melting points were taken on a Tottoli (Büchi, Switzerland) apparatus and are uncorrected. Mass spectra were measured at an ionizing potential of 70 eV with a CH-7 Varian MAT spectrometer using a direct evaporator inlet system or by combination with a gas chromatograph. ^{1}H-NMR were recorded on a Varian HA-100 or Bruker XL-90 spectrometer using deuterochloroform, deuterobenzene, or carbon tetrachloride as the solvent and trimethylsilane as the internal standard.
[3] Altromin, Altromin, Lage/Lippe, West Germany.
[4] Dr. Rudolf Berthold Co., Wildbad, West Germany.
[5] Tri-Carb model 3950, Packard Instrument Co., La Grange, Ill.
[6] Silica gel HF_{254}, E. Merck AG, Darmstadt, West Germany.
[7] Aerograph 1740, Varian.
[8] Aerograph 712, Varian.

0022-3549/82/0800-0897$01.00/0

material was filtered off and the solvent evaporated. The residue was dissolved in chloroform and washed with a saturated solution of sodium bicarbonate followed by water. The organic layer was dried over sodium sulfate and filtered through active charcoal and the solvent was removed *in vacuo*. The residue was dissolved in methanol (10 ml). A solution of 0.6 g of sodium hydroxide in 3 ml of water was added and the reaction mixture kept for 16 hr at room temperature. The solvent was removed *in vacuo* and the residue dissolved in methanol–water (1:1) and loaded on an ion-exchange resin[9] (H^+) column and eluted with methanol–water (1:1). The eluates were pooled together and evaporated *in vacuo* and the residue crystallized from ethyl acetate–petroleum ether mixture to give Metabolite 1, mp 162.5–163.5°, in a 40% yield.

Anal.—Calc. for $C_{11}H_{16}N_2O_4$: C, 55.01; H, 6.71; N, 11.65. Found: C, 55.52; H, 6.28; N, 11.08.

Metabolite 3 (1-Allyl-3,5-diethyl-6-methylthiouracil)—Methyl mercaptan (10 g, 0.2 mole) in methanol was added to 50 ml of a 30% methanolic sodium methoxide solution. Compound I (36.4 g, 0.15 mole) was added with stirring. The reaction mixture was refluxed with stirring for 24 hr and poured into water. It was extracted with chloroform, the solvent evaporated, and the residue distilled *in vacuo* to give Metabolite 3, bp 109°/0.02 mm, in 36% yield.

Anal.—Calc. for $C_{12}H_{18}N_2O_2S$: C, 56.67; H, 7.13; N, 11.01; S, 12.61. Found: C, 56.70; H, 7.35; N, 11.31; S, 12.52.

Metabolite 4 (6,8-Diethyl-2-hydroxymethyl-tetrahydrothiazolo-[3,2-c]pyrimidine-5,7(4H,6H)-dione) — 1-(2′,3′-Epoxypropyl)-3,5-diethyl-6-chlorouracil (2.6 g, 10 mmoles), prepared according to the described method (5), was dissolved in dry dimethyl sulfoxide (20 ml) and sodium hydrogen sulfide (1.1 g, 20 mmoles) was added. The reaction mixture was then concentrated *in vacuo* and the residue poured into water. After it was extracted twice with methylene chloride, the organic layer was dried over sodium sulfate. The solvent was removed and the milky viscous liquid was purified by column chromatography using silica gel (0.05–2 mm) with methylene chloride as elution solvent to give Metabolite 4, mp 83°, in 40% yield.

Anal.—Calc. for $C_{11}H_{16}N_2O_3S$: C, 51.54; H, 6.25; N, 10.93; S, 12.54. Found: C, 50.86; H, 6.55; N, 10.44; S, 12.12.

RESULTS AND DISCUSSION

Mass and ^{1}H-NMR Spectrum of I—In the ^{1}H-NMR spectrum of I, both methyl groups appeared as triplets at δ 1.08 and 1.20 ppm. The methylene group at N-3 appeared as a quartet at δ 3.93, and the methylene group at N-1 appeared as a doublet at δ 4.65 ppm. In the allylic protons of

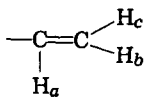

H_a appeared at δ 5.94 ppm as a multiplet, H_b at δ 5.22 ppm as a doublet, and H_c at δ 5.17 ppm as a doublet (J_{ab} = 12 Hz, J_{ac} = 17 Hz).

In the mass spectrum, the intensity ratio of the signals at *m/z* 242/244, 227/229, 201/203, 171/173, and 156/158 showed the presence of chlorine. The loss of ethyl isocyanate, C_2H_5CNO (242 → 171 or 227 → 156) supported by metastable peaks m* in the final sequence is characteristic of uracil and barbituric acid derivatives in a retro-Diels-Alder fragmentation (6–8). The fragmentation of I can be formulated according to Scheme I.

Structure of Metabolite 1—In the mass spectrum of the metabolite, the major fragmentation is formulated according to Scheme II, the formula of each fragment being established by high resolution mass spectrometry. Direct correlation between the fragments is demonstrated by the appearance of the metastable peaks m*. The mass spectrum of the metabolite showed the absence of chlorine in the molecule. First, the β-methyl group at C-8 was cleaved off the molecular ion leaving a highly stabilized cation. Next, the substituent at N-4 was removed: the expulsion of C_3H_4O showed one oxygen having been incorporated into the allylic side chain, while the other oxygen was bonded to the pyrimidine ring system. The loss of ethyl isocyanate (C_2H_5CNO) in the final sequence was similar to that of I. In the ^{1}H-NMR spectrum ($CDCl_3$), a signal appeared at δ 2.80 ppm (1 H) which, being exchangeable with deuterium oxide and also rather susceptible in position and line shape to both temperature and concentration, must be attributed to an hydroxide group. Since it was split into a triplet (J = 6.0 Hz), the metabolite must

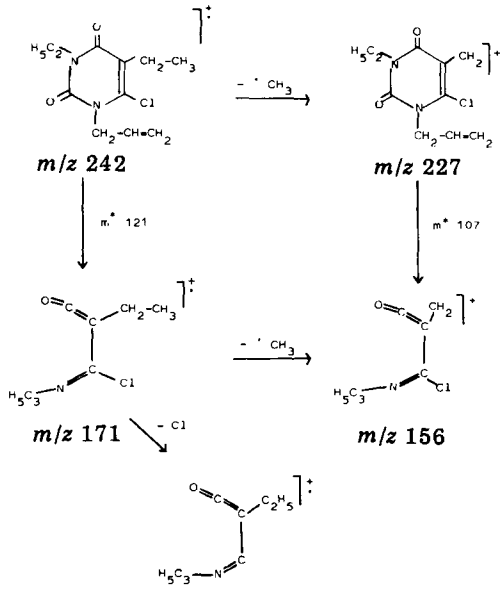

Scheme I

contain a —CH_2OH moiety. The lone C-2 proton appeared at the lowest field, split into seven lines (not a heptuplet). The methylene proton at both C-3 and exocyclic carbon were nonequivalent, however, rendering the spectrum unsusceptible to first-order analysis. The theoretical spectra for Metabolite 1 and for closely related compounds prepared by independent synthesis were calculated and fitted to the experimental data within ±0.01 Hz. Table I lists the data thus obtained which confirm the heterobicyclic structure for the metabolite. In each case, the less shielded C-3 protons were assigned to H^A by virtue of the larger coupling to H^C (J *cis* > J *trans* for five-membered ring) (9). Spectral analysis of all compounds listed in Table I additionally was complicated by the N—CH_2 quartet being superimposed upon the partial spectra of H^A, H^B, and $H^{D,E}$. By changing the solvent from $CDCl_3$ to C_6D_6, however, all protons situated on the fused five-membered ring appeared better shielded by 0.8–1.3 ppm, while signals of the N-6 and C-8 substituent protons were shifted slightly to lower field. Apparently, the benzene molecules orient themselves in a manner known from other amide spectra (10): farthest away from the negative end of the N—C—O dipole, thus, placing substituents at N-4 and C-9 directly within the diamagnetic shielding cone due to arene ring current. If spectra accumulation was possible, the rather low solubility of these compounds in benzene (<5 × 10^{-2} mole/liter) was more than offset by the well separated partial spectra[10]. These data establish Metabolite 1 as 6,8-diethyl-2-hydroxymethyl-tetrahydrooxazolo-[3,2-c]pyrimidine-5,7(4H,6H)-dione. The metabolite structure was confirmed by its independent synthesis; the synthetic Metabolite 1 mass spectrum and ^{1}H-NMR, GLC, and TLC data were identical with those of the isolated product.

Structure of Metabolite 3—The mass spectrum of Metabolite 3 showed the absence of chlorine in the molecule. The methyl group was also cleaved off here (254 → 239) and in a retro-Diels-Alder reaction supported by metastable peaks, the loss of ethyl isocyanate (239 → 168) subsequently took place. In this respect, the fragmentation was similar

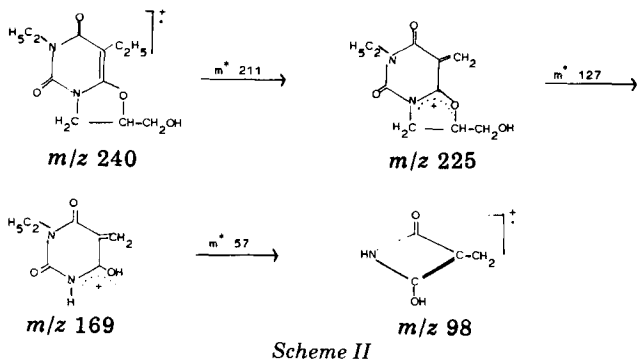

Scheme II

[9] Dowex 50 W × 4, Dow Chemical Co., Midland, Mich.

[10] In nitrobenzene-d_5 the effect is lost completely.

Table I—^{1}H-NMR Data of Tetrahydrooxazolo[3,2-*c*]pyrimidine-5,7(4H,6H)-dione Derivatives[a]

X	R^1	R^2	Solvent	H^{C}[b]	H^{A}	H^{B}	H^{D},H^{E}	J_{ac}	J_{bc}	$J_{dc,ec}$	J_{ab}	R^1		R^2	
Br	C_2H_5	C_2H_5	$CDCl_3$ (0.1 *M*)	5.124	4.277	4.061	3.639[c]	8.36	6.05	5.25	−10.90	CH_2	3.962	CH_2	2.354
												CH_3	1.213	CH_3	1.072
			C_6D_6 (0.01 *M*)	3.794	3.265	3.207	2.470	8.44	6.17	5.29	−10.75	CH_2	4.070	CH_2	~2.51
												CH_3	1.259	CH_3	1.23
Br	H	C_6H_5	$CDCl_3$ (0.003 *M*)	5.222	4.341	4.151	3.679[c]	8.55	6.12	4.84	−10.86	N—H	~7.88	C_6H_5	multi-plet
OCH_3	C_2H_5	C_2H_5	$CDCl_3$ (0.1 *M*)	4.981	4.156	4.016	3.687	8.64	6.69	3.70	−10.45	CH_2	3.959	CH_2	2.356
							3.645			4.49		CH_3	1.208	CH_3	1.064
			C_6D_6 (0.1 *M*)	3.890	3.276	3.264	2.781	8.72	6.63	3.84	−10.30	CH_2	4.074	CH_2	2.558
							2.665			4.37		CH_3	1.247	CH_3	1.247
OH^{Fd}	C_2H_5	C_2H_5	$CDCl_3$ (0.1 *M*)	4.982	4.173	4.100	4.030	8.59	6.94	3.35	−10.51	CH_2	3.951	CH_2	2.314
							3.831			3.71		CH_3	1.204	CH_3	1.051
			C_6D_6 (0.005 *M*)	3.678	3.165	3.337	2.956	8.71	6.82	3.51	−10.32	CH_2	4.092	CH_2	2.540
							2.714			4.02		CH_3	1.267	CH_3	1.255

[a] δ (ppm) relative to tetramethylsilane as internal standard; *J* (Hz); 30°. All spectra were measured at 90 MHz by Pulse-Fourier-Transform technique (8k interferogram, dwell time 560 or 840 μsec); number of scans varied between 1000 and 20,000, depending on concentration. [b] Values of δ and *J* given for H^A–H^F were obtained from theoretical spectra calculated with programs ITRCL1 and ITRCL2 (NICOLET users society) on a NICOLET BNC-12. [c] Spectra show some evidence of H^D,H^E-nonequivalence. [d] $\delta_{OH}F$ 2.797 ppm, J_{df} = 5.48 Hz, J_{ef} = 6.52 Hz.

to that of I, as also the fragment at *m/z* 136 appeared in both the spectra. The intensity of ions at m + 2 with 5.1% relative intensity and the loss of 47 mass units showed the presence of an SCH_3 group. The fragmentation of Metabolite 3 can be formulated according to Scheme III. In the ^{1}H-NMR spectrum ($CDCl_3$), near the signals of unchanged allyl and alkyl groups, a singlet appeared at δ 2.44 (3 protons) showing the presence of an SCH_3 group. These data establish Metabolite 3 as 1-allyl-3,5-diethyl-6-methylthiouracil, which was further confirmed by an independent synthesis. The synthetic Metabolite 3 mass spectrum, ^{1}H-NMR, GLC, and TLC data were identical with those of the isolated product.

Structure of Metabolite 2—In the mass spectrum the intensity ratio of the ions at *m/z* 272/270 and 257/255 with 6.5% relative intensity showed the presence of sulfur. The fragmentation pattern of Metabolite 2 (Scheme IV) was identical with I and Metabolite 3. The behavior of certain ions showed the presence of a hydroxyethyl group. The methyl group at C-5 was knocked off (270 → 255) and then a water molecule was eliminated (255 → 237), and in a retro-Diels-Alder reaction, the ion at *m/z* 166 was formed. By loss of a hydroxyethyl group, the ion at *m/z* 225 was formed and subsequently by retro-Diels-Alder reaction the ion at *m/z* 154 also formed. The loss of an allyl group with 41 mass units was also similar to the fragmentation of I and Metabolite 3. ^{1}H-NMR showed the protons of allylic and *N*-ethyl groups. The singlet at δ 2.43 ppm (3 protons) was assigned to an SCH_3— group. A doublet at δ 1.55 ppm (3 protons) was assigned to an hydroxide group. Due to nonavailability of the synthetic product, a comparison could not be made but these data confirm the Metabolite 2 as 1-allyl-3-ethyl-5-(1-hydroxyethyl)-6-methylthiouracil.

Structure of Metabolite 4—As Metabolite 4 could not be isolated, its structure, 6,8-diethyl-2-hydroxymethyl-tetrahydrothiazolo-[3,2-*c*]-pyrimidine-5,7(4H,6H)-dione, was based on mass spectra obtained by

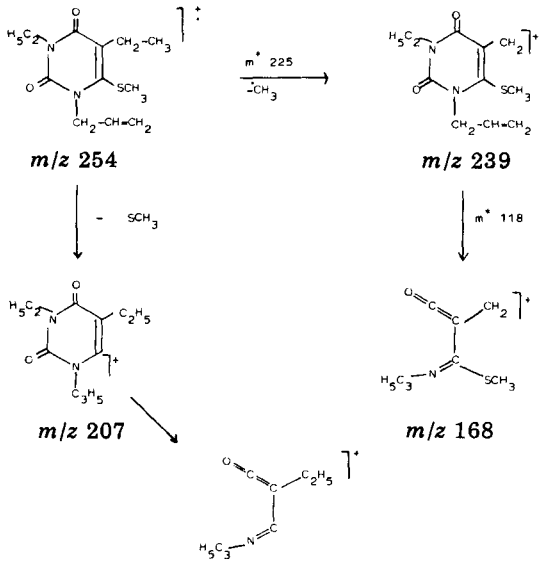

Scheme III

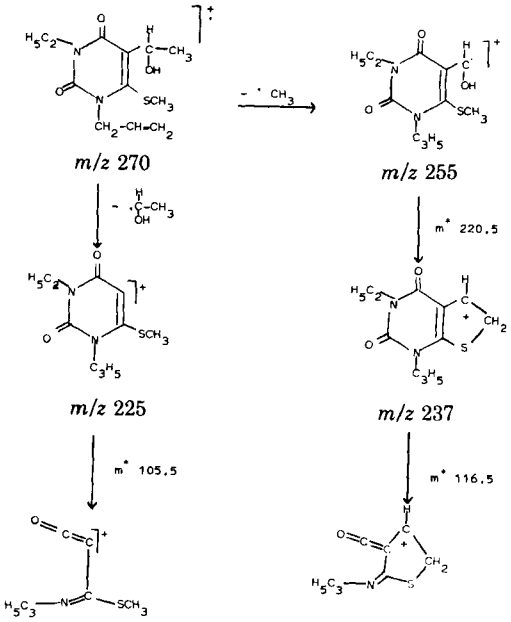

Scheme IV

the combination of GLC–mass spectrometry. In the mass spectrum of the metabolite, the metastable peaks establish the following major fragmentation:

$$m/z\ 256 \xrightarrow{m^*\ 227} m/z\ 241 \xrightarrow{m^*\ 120} m/z\ 170$$

The intensity of the ions at m + 2 with 5.1% relative intensity showed the presence of sulfur. First, the β-methyl group at C-8 was cleaved off the molecular ion (256 → 241) leaving a highly stabilized cation. The loss of ethyl isocyanate (241 → 170) by a retro-Diels-Alder fragmentation sup-

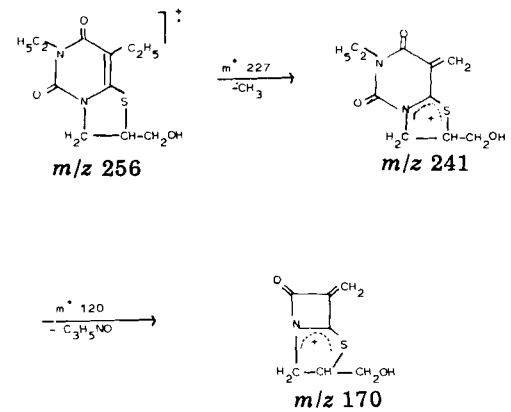

Scheme V

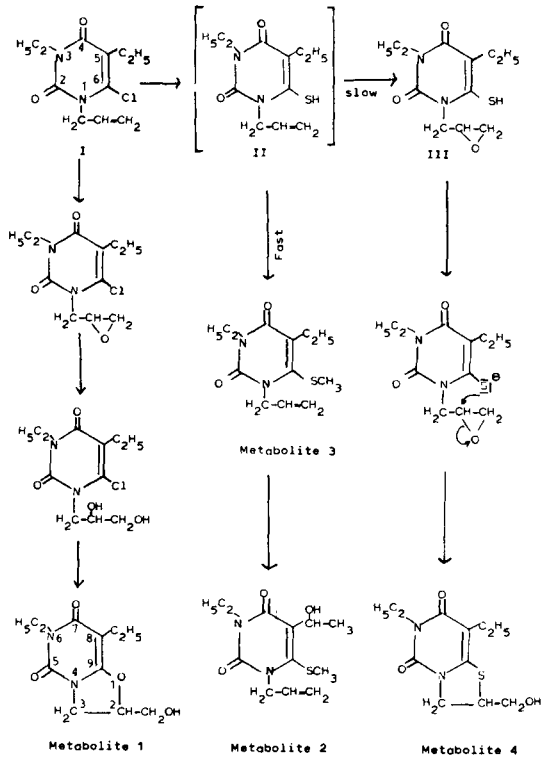

Scheme VI

ported by a metastable peak in the final sequence is characteristic of uracil and barbituric acid derivatives. The structure of the metabolite was confirmed by its independent synthesis. The synthetic Metabolite 4 showed the fragmentation pattern as shown in Scheme V, the molecular formula of each fragment was established by high resolution mass spectrometry. The mass spectrum of Metabolite 4 was identical in all respects with the synthetic product, and thus established its structure as 6,8-diethyl - 2 - hydroxymethyl-tetrahydrothiazolo-[3,2-*c*]pyrimidine-5,7-(4H,6H)-dione.

Mechanism of Biotransformation—*Metabolite 1*—In the formation of Metabolite 1, the first step is epoxidation of the allylic double bond of I followed by hydrolysis to propane-2,3-diol as described for analogous compounds (11). Subsequently, the β-hydroxy group substitutes the heterocyclic chlorine, thus forming the fused bicyclic Metabolite I *via* an intramolecular S_N reaction.

Metabolites 2–4—Recently, the formation of sulfur-containing metabolites from sulfur-free drugs has developed increasing interest. The methylthio (—SCH_3) metabolites have been reported in a number of drugs (12–18). The origin and the mechanism of formation of these methylthio metabolites is not known so far. Two pathways have been proposed: direct attachment of a methylthio group and transformation of mercapturic acids or glutathione conjugates (19, 20). Metabolite 4, due to its unique structure, supports the mechanism of the formation of methylthio metabolites *via* the formation of an intermediate thiol (—SH). A bicyclic sulfur-containing barbituric acid derivative of this type as a product of biochemical degradation has not yet been reported in the literature. A new metabolic pathway for the formation of this sulfur-containing Metabolite 4 and for the methylthio metabolites, 2 and 3, is proposed according to Scheme VI. In the formation of Metabolite 4, the first step is the substitution of chlorine by a thiol group forming an intermediate compound (II). This reaction may be enzymatic. The epoxidation of the double bond takes place giving Compound III. Subsequently, the sulfur atom attacks the β-carbon atom of the epoxide ring thus forming the fused bicyclic Metabolite 4 *via* an intramolecular S_N-reaction. The formation of methylthio Metabolites 2 and 3 may take place through this intermediate (II), as the enzymatic methylation of the thiols is reported *in vitro* and *in vivo* (21). It seems that the methylation of the intermediate (II) is a fast preferential reaction, therefore, larger amounts of Metabolites 2 and 3 are formed. The epoxidation of II is a slow specific reaction. The epoxide (III) is unstable. It has a pronounced tendency to ring closure leading to the stable Metabolite 4.

REFERENCES

(1) K. K. Gauri and H. Kohlhage, *Chemotherapy*, **14,** 158 (1969).

(2) K. K. Gauri and B. Rohde, *Klin. Wochenschr.*, **47,** 375 (1969).

(3) R. Kaul, B. Hempel, and G. Kiefer, *J. Pharm. Sci.*, **71,** 893 (1982).

(4) E. E. Smissman and J. W. Ayres, *J. Org. Chem.*, **36,** 2407 (1971).

(5) G. Kiefer, R. Kaul, K. Keppeler, and B. Hempel, *Arch. Pharmaz.*, **315,** 444 (1982).

(6) T. Nishiwaki, *Tetrahedron*, **22,** 3117 (1966).

(7) J. M. Rice, G. O. Dudek, and M. Barber, *J. Am. Chem. Soc.*, **87,** 4569 (1965).

(8) R. F. Skinner, E. G. Gallaher, and D. B. Predmore, *Anal. Chem.*, **45,** 574 (1973).

(9) L. E. Erickson, *J. Am. Chem. Soc.*, **87,** 1867 (1965).

(10) J. V. Hatton and R. E. Richards, *Mol. Phys.*, **5,** 139 (1962).

(11) D. J. Harvey, L. Glazener, C. Stratton, D. B. Johnson, R. M. Hill, E. C. Horning, and M. G. Horning, *Res. Commun. Chem. Pathol. and Pharmacol.*, **4,** 247 (1972).

(12) K. Kamei, M. Matsuda, and A. Momose, *Chem. Pharm. Bull.*, **23,** 683 (1975).

(13) A. Focella, P. Hesling, and S. Teitel, *Can. J. Chem.*, **50,** 2025 (1972).

(14) D. H. Chatfield and W. H. Hunter, *Biochem. J.*, **134,** 879 (1973).

(15) T. Ou, K. Tatsumi, and H. Yoshimura, *Biochem. Biophys. Res. Commun.*, **75,** 401 (1977).

(16) B. Stock and G. Spiteller, *Arzneim.-Forsch./Drug Res.*, **27,** 982 (1977).

(17) W. G. Stillwell, *Pharmacologist*, **19,** 169 (1977).

(18) M. Tateishi and H. Shimizu, *Xenobiotica*, **6,** 431 (1976).

(19) Z. H. Israili, P. G. Dayton, and J. R. Kiechel, *Drug Metab. Dispos.*, **5,** 411 (1978).

(20) P. Jenner and B. Testa, *Xenobiotica*, **8,** 1 (1978).

(21) M. Tateishi, S. Suzuki, and H. Shimizu, *J. Biol. Chem.*, **253,** 8854 (1978).

Study of the Metabolic Conversion of Imipramine and Desipramine to *N*-Nitrosodesipramine by Bacteria Using a Nitrogen-Selective GC Analysis

JOHN K. BAKER *x, ALICE M. CLARK ‡, and CHARLES D. HUFFORD ‡

Received September 9, 1981, from the **Department of Medicinal Chemistry and the* ‡*Department of Pharmacognosy, School of Pharmacy, University of Mississippi, University, MS 38677.* Accepted for publication November 12, 1981.

Abstract □ A GC method using dual nitrogen selective and flame ionization detectors was developed for the determination of *N*-nitrosodesipramine using *N*-butyryldesipramine as the internal standard. The precision of the method was found to be ±5.0% and the accuracy was ±4.9%. The method could be used to detect 10 ng/ml of *N*-nitrosodesipramine in bacterial cultures. When desipramine and sodium nitrite were incubated with aerobic or anaerobic bacteria, the nitrosamine level was found to be 10–300 times higher than the controls. When imipramine and potassium nitrate were incubated with a mixed anaerobic culture, the level of *N*-nitrosodesipramine was found to be 4.5 times higher than the control.

Keyphrases □ Imipramine—metabolic conversion to *N*-nitrosodesipramine by bacteria, nitrogen-selective GC, desipramine □ *N*-nitrosodesipramine—metabolic conversion of imipramine and desipramine by bacteria, nitrogen-selective GC □ Desipramine—metabolic conversion to *N*-nitrosodesipramine by bacteria, nitrogen-selective GC, imipramine □ Metabolic conversion—imipramine and desipramine to *N*-nitrosodesipramine by bacteria, nitrogen-selective GC

Previous studies have shown that secondary amines can be converted to carcinogenic *N*-nitroso amines when incubated with bacteria found in the intestine or bladder (1–4). It has also been demonstrated that bacteria can convert trimethylamine to dimethylamine and produce *N*-nitrosodimethylamine (3, 5). Though the conversion of these simple amines to *N*-nitroso compounds may have an impact on public health, the level of exposure to these compounds would be fairly low. The exposure to maintenance drugs such as desipramine and imipramine would be considerably higher, however, and these drugs might be converted to the *N*-nitroso derivatives in the intestine or bladder by bacteria. Recent studies in these laboratories with fungi have shown that these microorganisms *N*-demethylate imipramine in yields of 2–11% depending on the organism studied (6). Work presently in progress with aerobic and anaerobic bacteria has shown that many of the organisms give a 1–3% conversion from imipramine to desipramine. The objective of the present study was to develop an analytical method for *N*-nitrosodesipramine suitable for complex matrixes and to determine if either desipramine or imipramine would be converted to the nitrosamine in the presence of the bacteria.

EXPERIMENTAL

Synthesis of *N*-Nitrosodesipramine—Though there are references to *N*-nitrosodesipramine in the literature (7, 8), no synthetic information has been given nor have any of the spectral properties of the alleged compound been reported.

In the present study, 200 mg of the desipramine hydrochloride (0.66 mmole) was dissolved in 10 ml of water, made basic with 4 drops of concentrated ammonium hydroxide, then extracted with 15 ml of methylene chloride. The extract was dried with anhydrous sodium sulfate, then the extract was added to a solution containing 115 mg of nitrosonium tetrafluoroborate (0.66 mmole $NOBF_4$) in 5 ml of methylene chloride at room temperature. Over a 15-min period, 100 mg of pyridine in 2 ml of methylene chloride was added to the well-stirred suspension. After 1.5 hr the mixture was washed with 10 ml of 2 *N* HCl, 15 ml of 10% Na_2CO_3, then dried with anhydrous sodium sulfate. The solvent was evaporated to give 165 mg (85% yield) of the nitrosamine as a thick oil (IR: 1445 cm^{-1}, N=O). The mass spectrum of the nitrosamine obtained using the solid probe showed a fairly intense molecular ion at 295 (12%) and a peak at 265 characteristic of the loss of the nitrosyl group. The nitrosamine was also observed to produce peaks at 193 (100%), 208 (96%), 220 (50%), and 234 (32%) which were similar to those observed for the fragmentation of desipramine. The mass spectrum obtained by the GC mode (Fig. 1) was observed to be essentially the same.

Synthesis of *N*-Butyryldesipramine—Using 15 ml of toluene as the solvent, 200 mg of desipramine hydrochloride (0.55 mmole), 200 mg of butyric anhydride (1.3 mmoles), and 200 mg of pyridine were heated on a steam bath for 1 hr. The mixture was washed with 20 ml of aqueous 10% Na_2CO_3, the toluene layer was dried, then the solvent was evaporated under vacuum to give a 270-mg residue. The IR spectrum of this material indicated that the desired product was contaminated with a small amount of butyric anhydride. The residue was then sonicated with 10% Na_2CO_3 for 30 min, then extracted with methylene chloride, dried with anhydrous sodium sulfate, and evaporated to give 230 mg (95%) of the final product as an oil; IR (thin film): 2950, 1637, 1483, 1227, and 750 cm^{-1}; mass spectrum (GC mode): 336 (M^+, 7%), 234 (9%), 222 (13%), 208 (100%), 193 (45%), and 142 (89%).

Determination of *N*-Nitrosodesipramine—Sulfamic acid (30 mg) was added to a 10.0-ml sample of the bacterial culture to remove residual nitrite. Then, 20.0 μg of *N*-nitrosodesipramine (internal standard) in ethyl acetate was added, and the sample was extracted with 5 ml of isooctane. The isooctane layer was transferred to a conical evaporation tube[1],

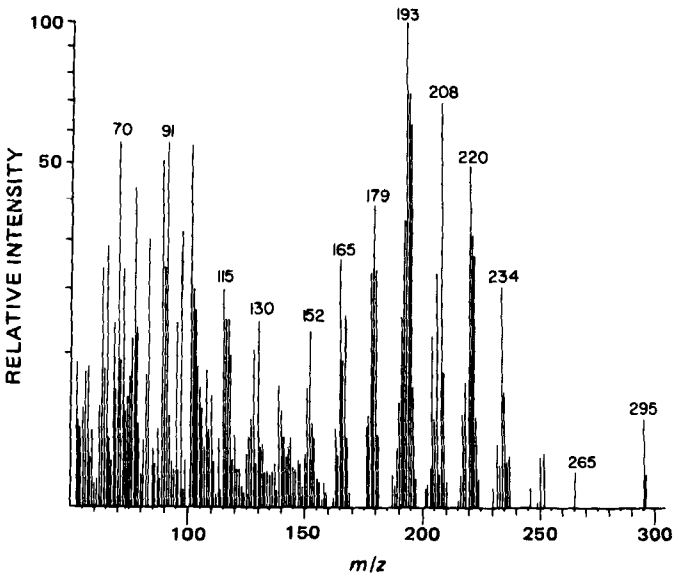

Figure 1—*Electron impact mass spectrum of N-nitrosodesipramine. The spectrum was obtained using the GC mode of operation with background correction with a sample of the nitrosamine obtained by synthesis.*

[1] Brinkmann 48 Place Concentrator, Brinkmann Instruments, Des Plaines, Ill.

0022-3549/82/0800-0901$01.00/0

Table I—Recovery of *N*-Nitrosodesipramine and *N*-Butyryldesipramine

Sample Medium	Extraction Recovery	
	N-Nitroso-desipramine, %[a]	Internal Standard, %[b]
Water	103.6	105.2
	96.6	101.4
	101.4	102.3
Mean ± *SD*	100.5 ± 3.6	103.0 ± 2.0
Sterilized Bacterial Culture	81.4	73.5
	96.3	90.9
	86.7	83.3
	93.0	94.3
Mean ± *SD*	89.4 ± 6.6	85.5 ± 9.2

[a] The sample was spiked with 1.0 μg/ml of *N*-nitrosodesipramine and the percent recovery was determined by comparison to the peak height obtained for 10 μg/50 μl of the nitrosamine in ethyl acetate. [b] The sample was spiked with 2.0 μg/ml of the internal standard and the percent recovery was determined by comparison to the peak height obtained for 20 μg/50 μl of the internal standard in ethyl acetate.

then evaporated at 80° under a stream of nitrogen. When the samples were almost dry, the walls of the evaporation tubes were washed down with 500 μl of methanol, then the samples were evaporated to dryness. The residue was taken up in 50 μl of ethyl acetate and 1.0 μl was used for the GC analysis.

The GC analysis[2] was conducted using dual nitrogen selective and flame ionization detectors with a dual pen recorder. The column (2 mm × 183 cm) was operated at 260° with helium as the carrier gas (30 ml/min) and with a packing of 3.0% methyl–phenyl silicone polymer[3] on a 110–120 mesh silanized support[4]. The carrier gas coming from the column was split equally between the flame ionization detector (H_2 = 19 ml/min) and rubidium bead nitrogen selective detector (H_2 = 2.3 ml/min), and each detector received 300 ml/min of air. Using these conditions, the retention time for *N*-nitrosodesipramine was 9.2 min and 14.9 min for *N*-butyryldesipramine. The nitrogen detector response index of the nitrosamine (response index = 0.155) was measured relative to caffeine as described previously (9).

In the analysis of the bacterial cultures, the presence of the nitrosamine was ascertained through the use of the retention times of the components

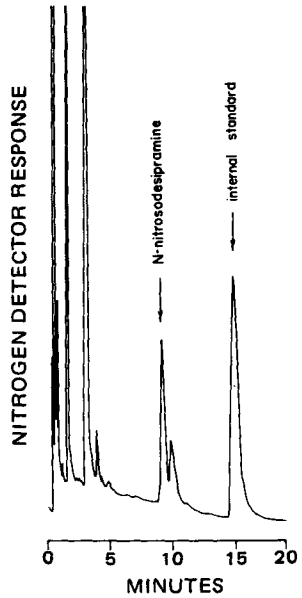

Figure 2—*Nitrogen-selective GC of bacterial cultures. The chromatogram was obtained from the extract of a culture of* Enterobacter aerogenes *containing desipramine and sodium nitrite. Though a dual flame ionization detector–nitrogen detector system was used for all samples, the flame ionization detector response has been omitted from the figure for simplicity.*

[2] Model 900, Perkin-Elmer Inc., Norwalk, Conn.
[3] OV-17, Analabs Inc., North Haven, Conn.
[4] Anachrom ABS, Analabs Inc., North Haven, Conn.

Table II—Accuracy and Precision of the Analytical Method

Bacterial Culture	*N*-Nitrosodesipramine, μg/ml[a]
1	1.108
2	1.060
3	1.042
4	0.987
Mean ± *SD*	1.049 ± 0.050

[a] A full-term Stage II culture not containing any drug or nitrite was sterilized, then spiked with 1.0 μg/ml of the nitrosamine. A 10-ml sample was then taken for analysis.

and the response index (9) of each component. Electron impact mass spectra[5] of the GC peaks were used as a secondary means of peak identification for some of the samples. Quantitations were based on the nitrogen-selective detector peak heights of the nitrosamine relative to the internal standard (*N*-butyryldesipramine). The method was calibrated using a simple solution containing a known quantity of the nitrosamine and the internal standard.

Incubation of Bacterial Cultures—Aerobic bacteria were grown according to a two-stage fermentation procedure using a defined medium (10) supplemented with either 25 m*M* $NaNO_2$ or 25 m*M* KNO_3. The Stage II cultures were incubated (37°, 250 rpm) with either 100 μg/ml of desipramine hydrochloride or 100 μg/ml of imipramine hydrochloride for 48 hr.

The anaerobic bacteria used in the study were isolated as pure cultures from the intestinal contents of a naive male Wistar rat. Mixed cultures of anaerobic bacteria from the large intestine and small intestine were also used.

Stage I cultures of the anaerobes were grown (24 hr, 37°) in 10 ml of the defined medium supplemented with either 25 m*M* $NaNO_2$ or 25 m*M* KNO_3 using an anaerobic chamber[6] for the culture tubes. Then 0.5 ml of the Stage I culture was transferred to the Stage II tubes containing 10 ml of the defined medium and 25 m*M* $NaNO_2$ or KNO_3 and 100 μg/ml of desipramine hydrochloride or imipramine hydrochloride. The Stage II cultures were incubated for 48 hr (37°) in fresh anaerobic chambers.

Control studies were conducted in which the defined sterile medium containing 25 m*M* $NaNO_2$ and 100 μg/ml of desipramine hydrochloride was adjusted to pH 5.0, 6.0, 7.0, and 8.0, then incubated with the same method for the Stage II aerobic cultures or the Stage II anaerobic cultures.

RESULTS AND DISCUSSION

Initial attempts to prepare *N*-nitrosodesipramine using desipramine, aqueous sodium nitrite, and hydrochloric acid (pH ≅ 3 maintained) were not successful. Even after 24 hr, the reaction mixture did not show significant amounts of the nitrosamine, but a large amount of another product that gave a GC–mass spectrum [*m/z* 240 (M^+, 100%), 193 (74%), 179 (15%), 167 (25%), and 83 (79%)] that would be consistent with a *C*-nitro derivative of iminodibenzyl. Due to a lack of pure reference standards of the four possible isomers of nitroiminodibenzyl, no attempts were made to establish the identity of the product.

Recently, it has been shown that nitrosonium tetrafluoroborate with pyridine can be used to produce nitrosamines of much higher purity (11). In particular, it was anticipated that the reagent would avoid the acidic conditions that are associated with *C*-nitrosation of aniline-like compounds. Indeed, it was found that this reagent gave an 85% yield of a high-purity product in 1.5 hr at room temperature. The mass spectrum of the product (Fig. 1) showed a molecular ion (295), a loss of the *N*-nitrosyl fragment (265), and the loss of the iminodibenzyl fragment (194) which would be characteristic of the *N*-nitroso compound as compared to the *C*-nitroso compound. The IR spectrum of the product was also characteristic of a nitrosamine.

In selecting an internal standard for the analysis of *N*-nitrosodesipramine, it was desirable to use a compound that was extremely lipophilic, like the nitrosamine and that had the same acid–base properties as the nitrosamine. The acetyl, propionyl, and butyryl amide derivatives of desipramine were investigated as potential internal standards and they were found to have retention times of 12.0, 13.0, and 14.9 min on the same GC system that gave a retention time of 9.3 min for the nitrosamine. Preliminary studies with bacterial cultures, to which no internal standard had been added, showed that cultures often produced small GC peaks

[5] Finnigan model 3221-F200 with INCOS data system, Sunnyvale, Calif.
[6] Gas Pak, Baltimore Biological Laboratories, Cockeysville, Md.

Table III—*N*-Nitrosodesipramine Formed in Aerobic Bacterial Cultures

Aerobe	Media Additives	*N*-Nitrosodesipramine, μg/ml	Final pH of Culture
Enterobacter aerogenes-13048[a]	100 μg/ml desipramine + 25 m*M* $NaNO_2$	3.36	5.6
Escherichia coli-27165	100 μg/ml desipramine + 25 m*M* $NaNO_2$	0.35	7.4
Klebsiella pneumoniae-27889	100 μg/ml desipramine + 25 m*M* $NaNO_2$	2.31	6.0
Proteus mirabilus[b]	100 μg/ml desipramine + 25 m*M* $NaNO_2$	2.46	5.8
Proteus vulgaris-27973	100 μg/ml desipramine + 25 m*M* $NaNO_2$	1.66	5.8
SI-1[c]	100 μg/ml desipramine + 25 m*M* $NaNO_2$	0.13	7.8
SI-2[c]	100 μg/ml desipramine + 25 m*M* $NaNO_2$	0.077	7.8
SI-3[c]	100 μg/ml desipramine + 25 m*M* $NaNO_2$	0.067	7.8
Control (pH 5)[d]	100 μg/ml desipramine + 25 m*M* $NaNO_2$	0.010	5.0
Control (pH 6)[d]	100 μg/ml desipramine + 25 m*M* $NaNO_2$	ND	6.0
Control (pH 7)[d]	100 μg/ml desipramine + 25 m*M* $NaNO_2$	0.019	7.0
Control (pH 8)[d]	100 μg/ml desipramine + 25 m*M* $NaNO_2$	0.010	8.0
Mixed SI[e]	100 μg/ml imipramine + 25 m*M* KNO_3	ND[f]	8.3
Mixed LI[g]	100 μg/ml imipramine + 25 m*M* KNO_3	ND	5.6
Control[h]	100 μg/ml imipramine + 25 m*M* KNO_3	ND	7.8

[a] All numbers refer to the American Type Culture Collection, Rockville, Md. [b] This culture was isolated from the large intestine of a naive Wistar rat and identified using a commercial culture identification system[7]. [c] Pure culture isolate from Wistar rat small intestines. [d] Sterile defined media adjusted to the indicated pH. [e] Mixed culture obtained from Wistar rat small intestines. [f] Below detection limit of ≅0.010 μg/ml. [g] Mixed culture obtained from Wistar rat large intestine. [h] Sterile defined media.

Table IV—*N*-Nitrosodesipramine Formed in Anaerobic Bacterial Cultures

Anaerobic	Media Additives	*N*-Nitrosodesipramine, μg/ml	Final pH of Culture
SI-B1[a]	100 μg/ml desipramine + 25 m*M* $NaNO_2$	0.56	7.2
SI-B5[a]	100 μg/ml desipramine + 25 m*M* $NaNO_2$	0.40	7.1
SI-B6[a]	100 μg/ml desipramine + 25 m*M* $NaNO_2$	0.63	6.6
LI-B2[b]	100 μg/ml desipramine + 25 m*M* $NaNO_2$	3.37	5.3
Control (pH 5.0)[c]	100 μg/ml desipramine + 25 m*M* $NaNO_2$	0.012	5.0
Control (pH 6.0)	100 μg/ml desipramine + 25 m*M* $NaNO_2$	0.029	6.0
Control (pH 7.0)	100 μg/ml desipramine + 25 m*M* $NaNO_2$	0.014	7.0
Control (pH 8.0)	100 μg/ml desipramine + 25 m*M* $NaNO_2$	0.005	8.0
Mixed SI[d]	100 μg/ml imipramine + 25 m*M* KNO_3	0.028	5.6
Mixed LI[e]	100 μg/ml imipramine + 25 m*M* KNO_3	0.165	6.1
Control[f]	100 μg/ml imipramine + 25 m*M* KNO_3	0.037	7.9

[a] Pure culture isolated from Wistar rat small intestines. [b] Pure culture isolated from Wistar rat large intestine. [c] Sterile defined media adjusted to the indicated pH. [d] Mixed culture obtained from Wistar rat small intestines. [e] Mixed culture obtained from Wistar rat large intestine. [f] Sterile defined media at the normal pH of the buffer system.

at 10.1 and 11.0 min that would have caused some minor problems if the acetyl or propionyl amides had been used as the internal standard.

Though isooctane is too nonpolar to be ideal for the extraction of most drugs, this property proved to be critical in obtaining extracts that gave high-quality chromatograms. Solvents such as methylene chloride were found to give good recoveries of the nitrosamine, but the chromatograms gave an off-scale response for the nitrogen-selective detector for the first 3–4 min and several large peaks that eluted after the nitrosamine. When isooctane was used for the extraction, high-quality chromatograms were obtained for the bacterial cultures (Fig. 2) and quantitative recoveries of the nitrosamine and the internal standard were obtained from aqueous model systems (Table I). A bacterial culture not containing any drug or *N*-nitrosodesipramine was harvested at the end of the Stage II fermentation, then the culture was sterilized and spiked with the nitrosamine and internal standard. Though the recoveries from this matrix were not quantitative (Table I), the recoveries were very high, and the recoveries of the nitrosamine and the internal standard were the same.

When a set of four sterilized bacterial cultures was spiked with a known quantity of the nitrosamine and then analyzed with the internal standard method, it was found that the average value for the determination was 4.9% higher than the true value (Table II), however, this error was within the ±5.0% variance for the method. Using the sample sizes as described in the experimental section, the detection limit was ~0.010 μg/ml. This detection limit was not due to signal–noise limitations, but because of the presence of a peak on the shoulder of the nitrosamine that was detectable at only these very low levels.

The analysis of the aerobic bacterial cultures (Table III) showed that the amount of desipramine converted to *N*-nitrosodesipramine was 10–300 times higher in the cultures than in the controls. The identity of the nitrosamine in each of the cultures was verified by a comparison of the retention time and nitrogen detector response index (9) of the unknown and the reference standard. The GC–mass spectra of some of the extracts were examined and found to be identical to the reference standard (Fig. 1).

The chemical *N*-nitrosation of simple secondary amines increases as the pH decreases, and the rate reaches a maximum at pH 3 for most aliphatic amines. Though a buffer system was used with the bacterial cultures, the pH of several of the cultures dropped during the fermentation. However, when desipramine and sodium nitrite were incubated under identical conditions in sterile media, only trace quantities of the nitrosamine was formed even at the lower pH range (Table III). After a consideration of all of these factors, the production of the nitrosamine in the cultures of *Enterobacter aerogenes*, *Klebsiella pneumoniae*, *Proteus mirabilus*, and *Proteus vulgaris* was considerably above the control values and above that which would be expected of any simple chemical model.

Preliminary studies with imipramine, potassium nitrate, and mixed aerobic cultures (Table III) indicated that *N*-nitrosodesipramine was not formed. Though a wide variety of aerobes have been previously demonstrated to convert nitrate to nitrite (4, 12), this conversion was not monitored in the present study. Thus, the absence of the nitrosamine could be the result of a low conversion of nitrate to nitrite or a result of a slow rate of *N*-demethylation.

Of the anaerobic cultures (Table IV), isolate LI-B2 was found to produce considerably higher levels of *N*-nitrosodesipramine than the control incubations. The isolates obtained from the small intestines produced nitrosamine levels above the control values, but the concentration was nearly an order of magnitude lower than for the large intestine isolate.

A mixed culture of large intestine anaerobes (Table IV) was found to produce a concentration of *N*-nitrosodesipramine 4.5 times higher than the control incubation of imipramine and potassium nitrate alone. Though the concentration of the nitrosamine formed in the mixed culture seemed low, it was 500–1000 times greater than the simple nitrosamines commonly found in food samples (13) or human feces (14).

CONCLUSIONS

The analytical method developed for the determination of *N*-nitrosodesipramine in bacterial cultures was found to give accurate and precise (±5.0%) results with good sensitivity (0.01 μg/ml). Using the nitrogen detector response index as an additional identification aid, the nitrosamine was easily quantitated in the complex bacterial culture matrix.

[7] API 20E System, Analytab Products, Plainview, N.Y.

Several of the aerobic and anaerobic cultures were found to give high levels of *N*-nitrosodesipramine when incubated with desipramine and sodium nitrite. Though it cannot be stated that the transformation was an entirely enzymatic reaction, the yield of the nitrosamine was far higher than could be obtained by the acid catalyzed reaction between nitrite and desipramine.

Preliminary studies with mixed anaerobic cultures with imipramine and nitrate showed that the nitrosamine was formed more rapidly than the control, but the yield was very low. Additional studies with pure cultures will be needed to determine if the low yield was due to a low rate of *N*-demethylation.

REFERENCES

(1) G. M. Hawksworth and M. J. Hill, *Br. J. Cancer*, **25**, 520 (1971).

(2) D. L. Collins-Thompson, N. P. Sen, B. Aris, and L. Schwinghamer, *Can. J. Microbiol.*, **18**, 1968 (1972).

(3) A. Ayanaba and M. Alexander, *Appl. Microbiol.*, **25**, 862 (1973).

(4) P. J. Coloe and N. J. Hayward, *J. Med. Microbiol.*, **9**, 211 (1976).

(5) A. Ayanaba, W. Verstraete, and M. Alexander, *J. Natl. Cancer Inst.*, **50**, 811 (1973).

(6) C. D. Hufford, G. A. Capiton, A. M. Clark, and J. K. Baker, *J. Pharm. Sci.*, **70**, 151 (1981).

(7) G. S. Rao and G. Krishna, *ibid.*, **64**, 1579 (1975).

(8) G. Scheunig and D. Ziebarth, *Pharmazie*, **33**, 722 (1978).

(9) J. K. Baker, *Anal. Chem.*, **49**, 906 (1977).

(10) G. Hawksworth and M. J. Hill, *Br. J. Cancer*, **29**, 353 (1974).

(11) H. T. Nagasawa, P. S. Fraser, and D. L. Yuzon, *J. Med. Chem.*, **16**, 538 (1973).

(12) V. J. Sander, *Hoppe-Seyler's Z. Physiol. Chem.*, **349**, 429 (1968).

(13) T. A. Gough, K. S. Webb, and R. F. Coleman, *Nature (London)*, **272**, 161 (1978).

(14) T. Wang, T. Kakizoe, P. Dion, R. Furrer, A. J. Varghese, and W. R. Bruce, *Nature (London)*, **276**, 180 (1978).

ACKNOWLEDGMENTS

Supported in part by the Research Institute of Pharmaceutical Sciences, School of Pharmacy, University of Mississippi.

The authors are grateful for the sample of desipramine hydrochloride provided by Merrell-National Laboratories. They also thank Mrs. Karen Varner for technical assistance.

Blood Level Studies of All-*trans*- and 13-*cis*-Retinoic Acids in Rats Using Different Formulations

R. S. SHELLEY, H. W. JUN ˣ, J. C. PRICE, and D. E. CADWALLADER

Received July 31, 1981, from the *Department of Pharmaceutics, School of Pharmacy, University of Georgia, Athens, GA 30602.* Accepted for publication November 12, 1981.

Abstract □ Studies to determine the bioavailability of all-*trans*-retinoic acid from a microencapsulated product were carried out using rats as test animals. The microcapsules were tableted in rat food and individual rats given a tablet containing the equivalent of 10 mg of all-*trans*-retinoic acid. Comparisons were made with bioavailability data obtained after intravenous and oral administrations of a solution and a suspension. The elimination of all-*trans*-retinoic acid following intravenous administration of 1- to 5-mg doses occurred by dose-dependent kinetics. The half-lives for the terminal linear portion of the elimination phase after the plateau level were 0.78, 0.74, and 0.93 hr for the 1-, 2.5-, and 5-mg doses, respectively. Based on the doses administered and the relative area under the serum level curves, the all-*trans*-retinoic acid microcapsules were found to be ~34% as bioavailable as the solution dosage form and the microfine suspension 93% as bioavailable. The bioavailability of all-*trans*-retinoic acid in oral solution was ~40% of the intravenous dose. For comparison, rats were also dosed intravenously with 13-*cis*-retinoic acid, and this compound was found not to follow dose-dependent kinetics at similar dosage levels used for all-*trans*-retinoic acid.

Keyphrases □ Bioavailability—Blood level studies of all-*trans*- and 13-*cis*-retinoic acids using different formulations, rats □ Microencapsulation—blood level studies of all-*trans*- and 13-*cis*-retinoic acids using different microencapsulated formulations, rats □ Blood level studies—all-*trans*- and 13-*cis*-retinoic acids using different formulations, rats □ Retinoic acids, all-*trans*- and 13-*cis*- —blood level studies using different formulations, rats

A number of retinoids have been shown to prevent or inhibit the growth of epithelial tumors. The use of these compounds for chemoprevention of tumors has been reviewed previously (1, 2). Although a long-term study with a synthetic retinoid was reported (3), most studies have been relatively short term with manual dosing of the retinoids. For long-term efficacy studies, a more economical and less troublesome mode of drug administration is through the diet of the test animals. However, simple mixing of retinoids with feed is precluded because of the unstable nature of the compounds toward air, light, and moisture. Earlier studies with vitamin A compounds have shown that these chemicals can be protected from environmental hazards by microencapsulation (4, 5).

Requirements of a microcapsule product are that first it must be readily miscible with the feed of the test animals, and second, it must be soluble or digestible in the GI tracts of the animals so that the retinoid is biologically available. In the present study, all-*trans*-retinoic acid was microencapsulated, and the bioavailability of the compound from the finished product was determined and compared with intravenously and orally administered retinoid using rats as test animals. Also, for comparison, rats were dosed intravenously with 13-*cis*-retinoic acid.

EXPERIMENTAL

Chemicals—All-*trans*-retinoic acid[1], 13-*cis*-retinoic acid[2], and all-*trans*-retinol acetate[3] were used as received. All other chemicals and reagents were the highest grade commercially available.

Microcapsules—All-*trans*-retinoic acid was encapsulated in gelatin–dextrose microcapsules by a process similar to that reported for the encapsulation of vitamin A derivatives (6) using a three-phase suspension

[1] Eastman-Kodak, Rochester, N.Y.
[2] Hoffmann-LaRoche, Nutley, N.J.
[3] Sigma Chemical Co., St. Louis, Mo.

0022-3549/82/0800-0904$01.00/0

Several of the aerobic and anaerobic cultures were found to give high levels of *N*-nitrosodesipramine when incubated with desipramine and sodium nitrite. Though it cannot be stated that the transformation was an entirely enzymatic reaction, the yield of the nitrosamine was far higher than could be obtained by the acid catalyzed reaction between nitrite and desipramine.

Preliminary studies with mixed anaerobic cultures with imipramine and nitrate showed that the nitrosamine was formed more rapidly than the control, but the yield was very low. Additional studies with pure cultures will be needed to determine if the low yield was due to a low rate of *N*-demethylation.

REFERENCES

(1) G. M. Hawksworth and M. J. Hill, *Br. J. Cancer*, **25**, 520 (1971).

(2) D. L. Collins-Thompson, N. P. Sen, B. Aris, and L. Schwinghamer, *Can. J. Microbiol.*, **18**, 1968 (1972).

(3) A. Ayanaba and M. Alexander, *Appl. Microbiol.*, **25**, 862 (1973).

(4) P. J. Coloe and N. J. Hayward, *J. Med. Microbiol.*, **9**, 211 (1976).

(5) A. Ayanaba, W. Verstraete, and M. Alexander, *J. Natl. Cancer Inst.*, **50**, 811 (1973).

(6) C. D. Hufford, G. A. Capiton, A. M. Clark, and J. K. Baker, *J. Pharm. Sci.*, **70**, 151 (1981).

(7) G. S. Rao and G. Krishna, *ibid.*, **64**, 1579 (1975).

(8) G. Scheunig and D. Ziebarth, *Pharmazie*, **33**, 722 (1978).

(9) J. K. Baker, *Anal. Chem.*, **49**, 906 (1977).

(10) G. Hawksworth and M. J. Hill, *Br. J. Cancer*, **29**, 353 (1974).

(11) H. T. Nagasawa, P. S. Fraser, and D. L. Yuzon, *J. Med. Chem.*, **16**, 538 (1973).

(12) V. J. Sander, *Hoppe-Seyler's Z. Physiol. Chem.*, **349**, 429 (1968).

(13) T. A. Gough, K. S. Webb, and R. F. Coleman, *Nature (London)*, **272**, 161 (1978).

(14) T. Wang, T. Kakizoe, P. Dion, R. Furrer, A. J. Varghese, and W. R. Bruce, *Nature (London)*, **276**, 180 (1978).

ACKNOWLEDGMENTS

Supported in part by the Research Institute of Pharmaceutical Sciences, School of Pharmacy, University of Mississippi.

The authors are grateful for the sample of desipramine hydrochloride provided by Merrell-National Laboratories. They also thank Mrs. Karen Varner for technical assistance.

Blood Level Studies of All-*trans*- and 13-*cis*-Retinoic Acids in Rats Using Different Formulations

R. S. SHELLEY, H. W. JUN ˣ, J. C. PRICE, and D. E. CADWALLADER

Received July 31, 1981, from the *Department of Pharmaceutics, School of Pharmacy, University of Georgia, Athens, GA 30602.* Accepted for publication November 12, 1981.

Abstract □ Studies to determine the bioavailability of all-*trans*-retinoic acid from a microencapsulated product were carried out using rats as test animals. The microcapsules were tableted in rat food and individual rats given a tablet containing the equivalent of 10 mg of all-*trans*-retinoic acid. Comparisons were made with bioavailability data obtained after intravenous and oral administrations of a solution and a suspension. The elimination of all-*trans*-retinoic acid following intravenous administration of 1- to 5-mg doses occurred by dose-dependent kinetics. The half-lives for the terminal linear portion of the elimination phase after the plateau level were 0.78, 0.74, and 0.93 hr for the 1-, 2.5-, and 5-mg doses, respectively. Based on the doses administered and the relative area under the serum level curves, the all-*trans*-retinoic acid microcapsules were found to be ~34% as bioavailable as the solution dosage form and the microfine suspension 93% as bioavailable. The bioavailability of all-*trans*-retinoic acid in oral solution was ~40% of the intravenous dose. For comparison, rats were also dosed intravenously with 13-*cis*-retinoic acid, and this compound was found not to follow dose-dependent kinetics at similar dosage levels used for all-*trans*-retinoic acid.

Keyphrases □ Bioavailability—Blood level studies of all-*trans*- and 13-*cis*-retinoic acids using different formulations, rats □ Microencapsulation—blood level studies of all-*trans*- and 13-*cis*-retinoic acids using different microencapsulated formulations, rats □ Blood level studies—all-*trans*- and 13-*cis*-retinoic acids using different formulations, rats □ Retinoic acids, all-*trans*- and 13-*cis*- —blood level studies using different formulations, rats

A number of retinoids have been shown to prevent or inhibit the growth of epithelial tumors. The use of these compounds for chemoprevention of tumors has been reviewed previously (1, 2). Although a long-term study with a synthetic retinoid was reported (3), most studies have been relatively short term with manual dosing of the retinoids. For long-term efficacy studies, a more economical and less troublesome mode of drug administration is through the diet of the test animals. However, simple mixing of retinoids with feed is precluded because of the unstable nature of the compounds toward air, light, and moisture. Earlier studies with vitamin A compounds have shown that these chemicals can be protected from environmental hazards by microencapsulation (4, 5).

Requirements of a microcapsule product are that first it must be readily miscible with the feed of the test animals, and second, it must be soluble or digestible in the GI tracts of the animals so that the retinoid is biologically available. In the present study, all-*trans*-retinoic acid was microencapsulated, and the bioavailability of the compound from the finished product was determined and compared with intravenously and orally administered retinoid using rats as test animals. Also, for comparison, rats were dosed intravenously with 13-*cis*-retinoic acid.

EXPERIMENTAL

Chemicals—All-*trans*-retinoic acid[1], 13-*cis*-retinoic acid[2], and all-*trans*-retinol acetate[3] were used as received. All other chemicals and reagents were the highest grade commercially available.

Microcapsules—All-*trans*-retinoic acid was encapsulated in gelatin–dextrose microcapsules by a process similar to that reported for the encapsulation of vitamin A derivatives (6) using a three-phase suspension

[1] Eastman-Kodak, Rochester, N.Y.
[2] Hoffmann-LaRoche, Nutley, N.J.
[3] Sigma Chemical Co., St. Louis, Mo.

0022-3549/82/0800-0904$01.00/0

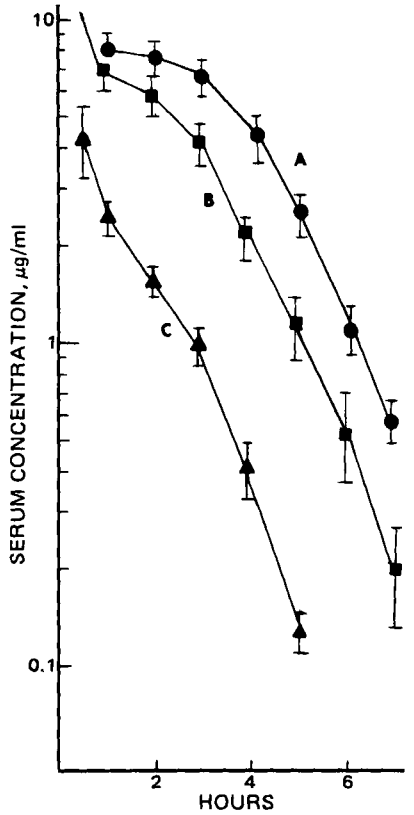

Figure 1—*Average serum concentrations of all-*trans*-retinoic acid following rapid intravenous administration in saline solution. Key: (▲) 1.0-mg dose, six rats; (■) 2.5-mg dose, six rats; (●) 5.0-mg dose, five rats.*

method. Gelatin was chosen as the major encapsulating material because it offers adequate bioavailability and good stability under various storage conditions (5, 7). The geometric mean diameter of the microcapsules was 0.19 mm with a geometric standard deviation of 1.81. The microcapsules were stored at −10° until needed for testing.

The microcapsules were assayed to determine content uniformity and stability using spectrophotometric analysis[4] after dissolution of the microcapsules in water at 65° and extraction with chloroform. The all-*trans*-retinoic acid content determined by assay of 12 samples (50 mg) of microcapsules from a homogenized mixture was found to be 2.83 ± 0.05 mg with a coefficient of variation of 1.77% indicating good uniformity of the formulation. The concentration of all-*trans*-retinoic acid in the microcapsules was 6.03% of the total weight.

Animal Dosing—Adult Sprague-Dawley rats (~360 g) were used. All dosed rats were fasted ~24 hr prior to dosing with retinoid. Water was available *ad libitum*. Orally dosed rats received 5- to 10-mg doses of all-*trans*-retinoic acid. Rats given intravenous injections were dosed with 1–5 mg of either all-*trans*-retinoic acid or 13-*cis*-retinoic acid. Oral and intravenous dosing was staggered ~5–10 min so that blood samples could be collected from each of the rats at approximately the same time intervals after dosing.

Oral doses of all-*trans*-retinoic acid were given in 0.5 ml of 0.3% NaOH–0.9% saline solution and in microfine suspension (<3-μm particles) *via* gastric intubation to lightly anesthetized rats. Intravenous injections for both all-*trans*- and 13-*cis*-retinoic acids were given in a 0.3% NaOH–0.9% saline solution and injected into the tail vein of lightly anesthetized rats.

All-*trans*-retinoic acid microcapsules were fed to fasted rats in the following manner. Ground-up rat food–microcystalline cellulose (2:1) was mixed with all-*trans*-retinoic acid microcapsules and tableted by compression into 12.5-mm disks at 2724 kg for 20 sec. Each tablet contained the equivalent of 10 mg of all-*trans*-retinoic acid. Ten rats were put in individual cages, and each rat was given one food tablet containing the all-*trans*-retinoic acid. Six or more of the rats consumed the tablets completely within 10 min.

Serum Collection—Multiple blood samples were collected from each rat using a modification of a previous method (8). Blood samples of 250–300 μl were collected under reduced pressure from an incision made at the distal end of the tail of unanesthetized rats and collected in serum separation tubes. Immediately following centrifugation, the serum samples were transferred to 15-ml screw-capped test tubes and stored at −10° where they remained for 20–60 hr before they were assayed. Because of the small amount of blood collected per sample, eight or nine blood samples could be taken from each rat over the time-course of 7–10 hr.

[4] Cary 118 Varian Instruments, Palo Alto, Calif.

Table I—Bioavailability Data for All-*trans*-Retinoic Acid Following Oral (5 and 10 mg) and Intravenous (1 mg) Doses

Formulation	*AUC*[a], μg hr/ml	Relative Availability to Oral Solution	Relative Availability to Intravenous Dose
Intravenous Solution, 1 mg	34.7 ± 4[b]	—	100
Oral Solution[c], 5 mg	13.74 ± 1.6	100	39.6
Microfine Suspension[d], 5 mg	12.8 ± 1.4	93	36.9
Microcapsules[e] tableted in rat food, 10 mg	4.6 ± 6[b]	33.5	13.3

[a] Corrected for the body weight. [b] Adjusted to 5 mg by dose ratios. [c] Average 9 rats. [d] Average 11 rats. [e] Average 12 rats.

Serum Assay—Serum samples were assayed by a reversed-phase high-pressure liquid chromatographic method reported previously (9).

A standard curve was obtained by comparing the peak height ratio of all-*trans*-retinoic acid or 13-*cis*-retinoic acid to all-*trans*-retinol acetate and the spiked serum all-*trans*-retinoic acid or 13-*cis*-retinoic acid concentration. Unknown serum sample concentrations were calculated by comparing the peak height ratios of the samples to the processed standards. The lower working limit for the assay was 100 ng/ml of serum

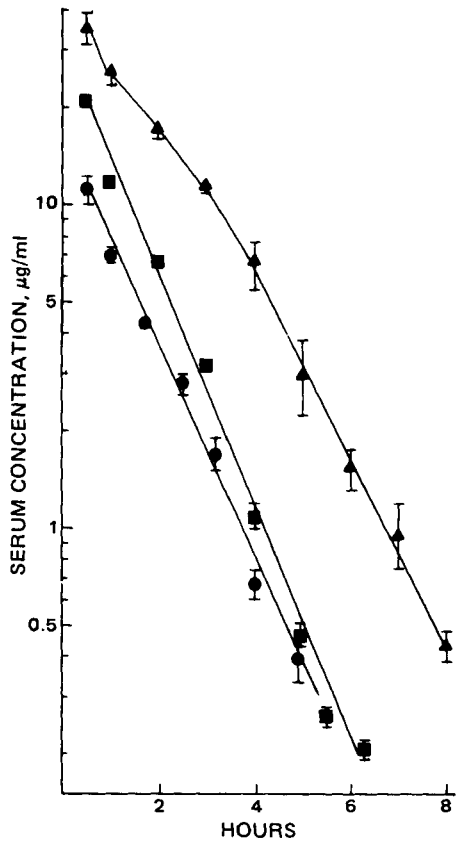

Figure 2—*Average serum concentrations of 13-*cis*-retinoic acid following rapid intravenous administration in saline solution. Key: (●) 1.25-mg dose, eight rats; (■) 2.5-mg dose, six rats; (▲) 5.0-mg dose, eight rats.*

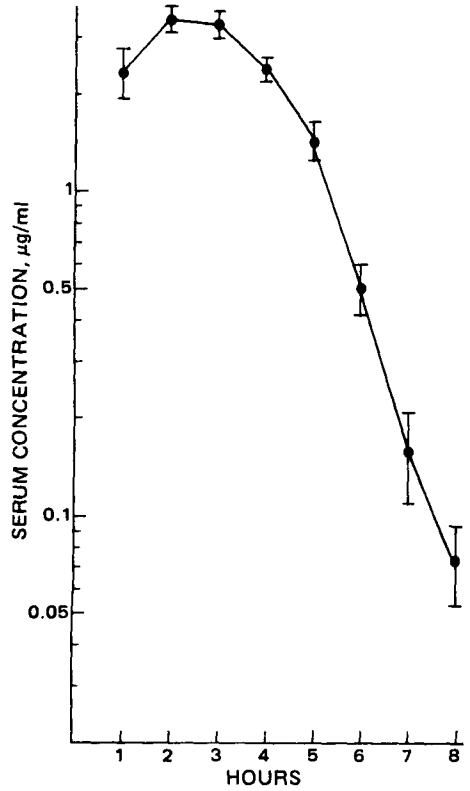

Figure 3—*Average serum concentrations of all-*trans*-retinoic acid following a 5.0-mg oral dose in saline solution to nine rats.*

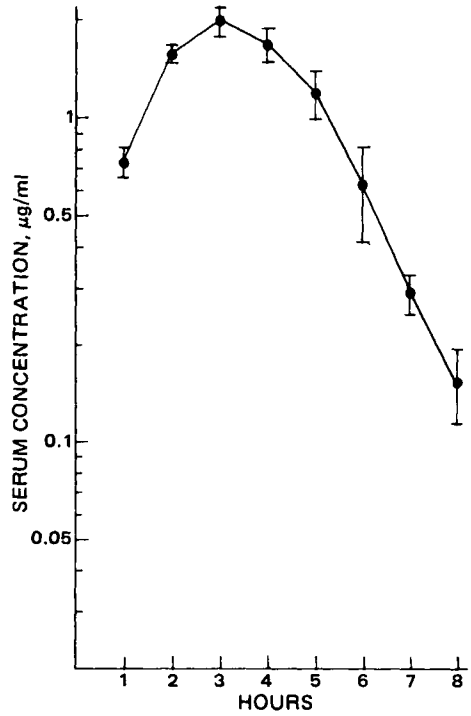

Figure 4—*Average serum concentrations of all-*trans*-retinoic acid following a 10-mg oral dose of encapsulated drug in animal food to 12 rats.*

and the recovery of all-*trans*-retinoic acid and 13-*cis*-retinoic acid was 102.9 ± 5.6 and 91.7 ± 5%, respectively. The areas under the serum level *versus* time curves were determined by the trapezoidal rule. The elimination half-lives were determined from the slope of the elimination curves by using a linear regression program with a programmable calculator.

RESULTS AND DISCUSSION

Serum levels *versus* time profiles following a 1-, 2.5-, and 5-mg iv dose of all-*trans*-retinoic acid were shown in Fig. 1. Serum concentrations showed a rapid decline immediately after injection as the retinoid was distributed into tissues. However, serum levels rapidly reached a plateau and remained stable for several hours before returning to the linear elimination phase. Increasing the dose of all-*trans*-retinoic acid to 2.5 and 5 mg, respectively, resulted in a more pronounced and longer plateau (Figs. 1A and 1B), indicating a possible saturation of elimination pathways at higher doses. The time required for the serum levels to return to the linear elimination phase after the plateau began was ~94, 135, and 190 min for the 1-, 2.5-, and 5-mg doses, respectively. The half-life for the linear elimination phase after the plateau was 0.78, 0.74, and 0.93 hr for the 1-, 2.5-, and 5-mg doses, respectively, and these values were not significantly different ($p > 0.05$).

Recently, after observing nonlinear declining of serum levels of all-*trans*-retinoic acid in the rat, several potential causes for the nonlinear kinetics were investigated (10). Dose-dependent elimination due to the saturation of biliary excretion was ruled out since the same nonlinear behavior in rats with biliary fistulas was observed. It was found that interrupting the enterohepatic recirculation system had no effect on the nonlinear elimination phenomenon. Also discovered was a greater conversion of all-*trans*-retinoic acid to all-*trans*-retinoyl-β-glucuronide, supposedly a minor metabolite, as the intravenous dose was increased. Both results indicated that the dose-dependent elimination was due to saturation of major metabolic pathways instead of saturation of biliary excretion. However, at the present time there is some disagreement as to what the major metabolic pathways might be in the biotransformation of all-*trans*-retinoic acid in rats (11–13).

For comparison, 13-*cis*-retinoic acid was intravenously administered in rats in 1.25-, 2.5-, and 5-mg doses and the results obtained summarized in Fig. 2. The saturation phenomenon was completely absent at lower doses and only a brief nonlinear phase was observed at the 5-mg dosage level. Also, the half-lives of the linear elimination phase were slightly longer than those of all-*trans*-retinoic acid, averaging 0.8–0.9 hr. Similar results were observed (14) when the disposition of all-*trans*- and 13-*cis*-retinoic acids in mice was studied. A plateau phenomenon was found in the serum level *versus* time curve following an intravenous injection of all-*trans*-retinoic acid but not for 13-*cis*-retinoic acid. Since dose-dependent kinetics were observed with all-*trans*-retinoic acid but not with 13-*cis*-retinoic acid, these results would indicate that the metabolic enzymes for these chemicals are probably different. However, currently there is little data available as to the enzymatic reactions of 13-*cis*-retinoic acid in rats.

Since the intravenous dose of all-*trans*-retinoic acid produced dose-dependent kinetics, it was not possible to accurately determine the area under the curve (*AUC*). However, an approximate *AUC* was obtained by using the trapezoidal rule and found to be 6.94 ± 0.8 μg hr/ml for the 1-mg iv dose. After adjusting and comparing the 1-mg dose to the 5-mg dose, the oral solution dosage form was found to be only 40% as bioavailable as the intravenous dose. The low bioavailability of the oral solution could be the result of either a first-pass effect occurring or from the inaccuracy of the *AUC* calculation due to the dose-dependent kinetics. For these reasons, all-*trans*-retinoic acid in oral solution was used as a standard for bioavailability comparisons to the other formulations.

Shown in Fig. 3 are the average serum levels after dosing nine rats orally with saline solutions containing 5 mg of all-*trans*-retinoic acid. Peak serum levels occurred after 2.5 hr with an elimination half-life of 0.69 hr and an *AUC* of 13.74 ± 1.6 μg hr/ml. Average peak serum level was 3.2 μg/ml. Results after oral administration of microcapsules in laboratory animal feed are shown in Fig. 4. The curve represents data averaged from 12 rats each dosed with the equivalent of 10 mg of all-*trans*-retinoic acid. Peak serum concentration occurred at ~3 hr and the *AUC* was 9.21 ± 1.2 μg hr/ml with an elimination half-life of 1.02 hr.

Figure 5 shows the average serum levels achieved when 11 rats were dosed orally with the microfine suspension dosage form. A 5-mg dose was administered which resulted in an average peak serum level time of 3 hr and an *AUC* of 12.8 ± 1.4 μg hr/ml with an elimination half-life of 0.65 hr.

Based on the doses administered and the relative area under the serum level curves (Table I), the all-*trans*-retinoic acid microcapsules were ~34% as bioavailable as the solution dosage form, and the microfine suspension was 93% bioavailable. The low bioavailability of the microcapsules is possible because all-*trans*-retinoic acid was not completely released from the microcapsules in the digestive tract of the rat. The half-life of the elimination phase was 1.5 times greater than that of the solution, indicating that absorption was probably still occurring after the

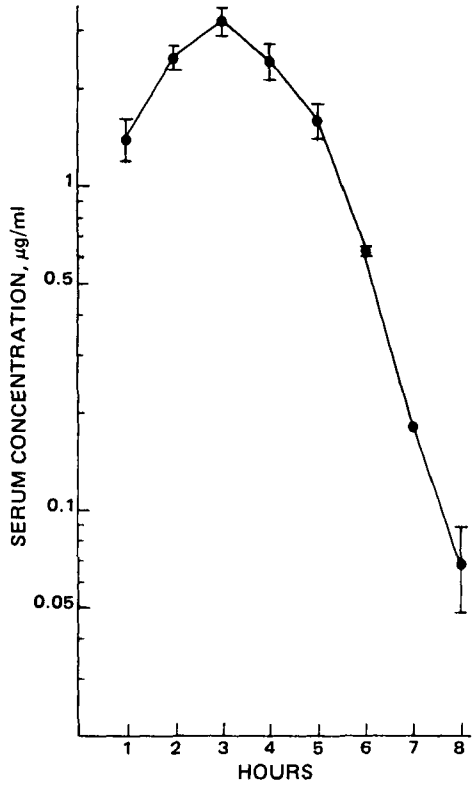

Figure 5—*Average serum concentrations of all-*trans*-retinoic acid following a 5.0-mg dose of a microfine suspension to 11 rats.*

peak concentration thus producing the slowly declining serum concentrations. Another possible cause of the slow release of the chemical from the microcapsules was interaction with the rat food in which the microcapsules were tableted. In a preliminary study, it was found that all-*trans*-retinoic acid crystals tableted in rat food were only 73% bioavailable as the solution, possibly indicating that the rat food in which the crystals were tableted was interfering with absorption.

The microfine suspension was formulated as a possible alternative to microencapsulation. It has the advantage of a greater bioavailability, but the disadvantages of being a less stable formulation and less readily miscible with the rat food as compared to the solid microcapsules. The primary purpose of microencapsulation was to stabilize the retinoids for feeding to rats in their laboratory diets for long-term testing of the compounds for chemo-prevention of tumors.

All-*trans*-retinoic acid was successfully microencapsulated and the bioavailability of the encapsulated and liquid dosage forms compared. Although the microcapsules were only 34% bioavailable as the solution dosage form, this is a good compromise because of the increased stability and ease of handling. Also, all-*trans*-retinoic acid was found to follow dose-dependent kinetics at the doses studied; whereas, 13-*cis*-retinoic acid did not follow dose-dependent kinetics when given at the same dosage levels as the all-*trans*-retinoic acid.

REFERENCES

(1) W. Bollage, *Int. Z. Vitaminforsch*, **40**, 299 (1970).

(2) M. B. Sporn, N. Dunlop, D. Newton, and J. Smith, *Fed. Proc. Fed. Am. Soc. Exp. Biol.*, **35**, 1332 (1976).

(3) C. D. Port, M. B. Sporn, and D. G. Kaufman, *Proc. Am. Assoc. Cancer Res.*, **16**, 21, (1975).

(4) J. T. Carstensen, *J. Pharm. Sci.*, **53**, 839 (1964).

(5) E. M. Olsen, J. D. Harvey, D. C. Hill, and H. D. Branion, *Poultry Sci.*, **38**, 929 (1959).

(6) E. J. Goett, E. E. MacDonough, and C. J. Salivar (Chas. Pfizer and Co.), U.S. Patent 2, 643, 209 (1953).

(7) J. T. Carstensen, E. S. Aron, D. C. Spera, and J. J. Vance, *J. Pharm. Sci.*, **55**, 561 (1966).

(8) S. T. Nerenberg and P. Zedler, *J. Lab. Clin. Med.*, **85**, 523 (1975).

(9) R. S. Shelley, J. C. Price, H. Won Jun, D. E. Cadwallader, and A. C. Capomacchia, *J. Pharm. Sci.*, **71**, 262 (1982).

(10) B. N. Swanson, C. A. Frolik, D. W. Zaharevitz, P. P. Roller, and M. B. Sporn, *Biochem. Pharmacol.*, **30**, 107 (1981).

(11) A. B. Roberts and H. F. DeLuca, *Biochem. J.*, **102**, 600 (1967).

(12) R. Hanni, F. Bigler, W. Meister, and G. Englert, *Helv. Chim. Acta*, **59**, 2221 (1976).

(13) A. B. Roberts and C. A. Frolik, *Fed. Proc. Fed. Am. Soc. Exp. Biol.*, **38**, 2524 (1979).

(14) C. Wang, S. Campbell, R. L. Furner, and D. L. Hill, *Drug Metab. Dispos.*, **8**, 8 (1980).

ACKNOWLEDGMENTS

Supported by Contract NO1 CP 85663 from the National Cancer Institute, National Institutes of Health, Bethesda, Md.

Tack Behavior of Coating Solutions I

S. K. CHOPRA * and R. TAWASHI ˣ

Received June 8, 1981, from the *Faculty of Pharmacy, University of Montreal, Montreal, Quebec, Canada H3C 3J7*, and the **Schering Canada, Inc., Pointe Claire, Quebec, Canada, H9R 1B4.* Accepted for publication November 3, 1981.

Abstract □ The tackiness of various tablet coating solutions was determined using a parallel plate technique with a tensile testing machine in conjunction with an oscilloscope where the separation force was displayed as a function of time. Measurements were made at various rates of separation on liquid films of constant thickness. Results showed that the force required to split a liquid film increases with an increase in rate of separation, and that tackiness increases with an increase in viscosity. The relation between tack and viscosity was not linear, and a modified Stefan equation was proposed.

Keyphrases □ Tablet coating solutions—tack behavior, viscosity □ Viscosity—tack behavior of tablet coating solutions □ Tackiness—tack behavior of tablet coating solutions

The effect of coating formulations and coating process variables on the appearance of a coated tablet has been the subject of various investigations (1–3). Much effort has been devoted to the study of the theory of adhesion of film-forming materials to the surface of a tablet (4–6). However, very little is known about the tackiness of coating solutions and its effect on the coating process. Studies on the evaluation of coating formulations have made some reference to the problem of tackiness of hydroxypropyl cellulose solutions during the coating process (7). However,

0022-3549/82/0800-0907$01.00/0

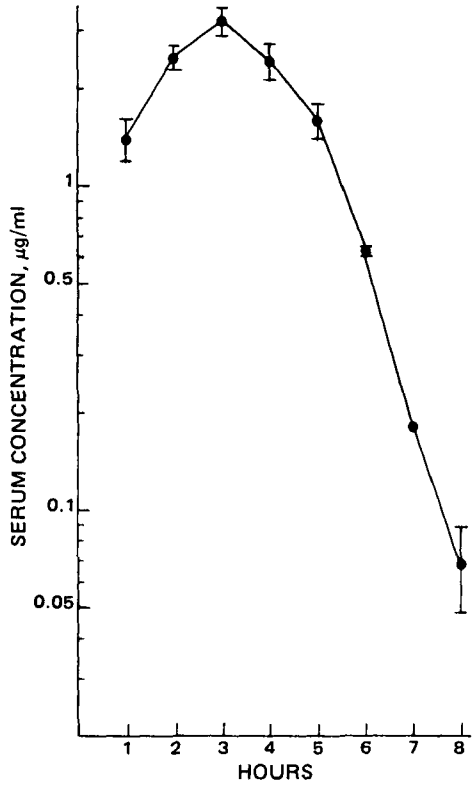

Figure 5—*Average serum concentrations of all-*trans*-retinoic acid following a 5.0-mg dose of a microfine suspension to 11 rats.*

peak concentration thus producing the slowly declining serum concentrations. Another possible cause of the slow release of the chemical from the microcapsules was interaction with the rat food in which the microcapsules were tableted. In a preliminary study, it was found that all-*trans*-retinoic acid crystals tableted in rat food were only 73% bioavailable as the solution, possibly indicating that the rat food in which the crystals were tableted was interfering with absorption.

The microfine suspension was formulated as a possible alternative to microencapsulation. It has the advantage of a greater bioavailability, but the disadvantages of being a less stable formulation and less readily miscible with the rat food as compared to the solid microcapsules. The primary purpose of microencapsulation was to stabilize the retinoids for feeding to rats in their laboratory diets for long-term testing of the compounds for chemo-prevention of tumors.

All-*trans*-retinoic acid was successfully microencapsulated and the bioavailability of the encapsulated and liquid dosage forms compared. Although the microcapsules were only 34% bioavailable as the solution dosage form, this is a good compromise because of the increased stability and ease of handling. Also, all-*trans*-retinoic acid was found to follow dose-dependent kinetics at the doses studied; whereas, 13-*cis*-retinoic acid did not follow dose-dependent kinetics when given at the same dosage levels as the all-*trans*-retinoic acid.

REFERENCES

(1) W. Bollage, *Int. Z. Vitaminforsch*, **40**, 299 (1970).

(2) M. B. Sporn, N. Dunlop, D. Newton, and J. Smith, *Fed. Proc. Fed. Am. Soc. Exp. Biol.*, **35**, 1332 (1976).

(3) C. D. Port, M. B. Sporn, and D. G. Kaufman, *Proc. Am. Assoc. Cancer Res.*, **16**, 21, (1975).

(4) J. T. Carstensen, *J. Pharm. Sci.*, **53**, 839 (1964).

(5) E. M. Olsen, J. D. Harvey, D. C. Hill, and H. D. Branion, *Poultry Sci.*, **38**, 929 (1959).

(6) E. J. Goett, E. E. MacDonough, and C. J. Salivar (Chas. Pfizer and Co.), U.S. Patent 2, 643, 209 (1953).

(7) J. T. Carstensen, E. S. Aron, D. C. Spera, and J. J. Vance, *J. Pharm. Sci.*, **55**, 561 (1966).

(8) S. T. Nerenberg and P. Zedler, *J. Lab. Clin. Med.*, **85**, 523 (1975).

(9) R. S. Shelley, J. C. Price, H. Won Jun, D. E. Cadwallader, and A. C. Capomacchia, *J. Pharm. Sci.*, **71**, 262 (1982).

(10) B. N. Swanson, C. A. Frolik, D. W. Zaharevitz, P. P. Roller, and M. B. Sporn, *Biochem. Pharmacol.*, **30**, 107 (1981).

(11) A. B. Roberts and H. F. DeLuca, *Biochem. J.*, **102**, 600 (1967).

(12) R. Hanni, F. Bigler, W. Meister, and G. Englert, *Helv. Chim. Acta*, **59**, 2221 (1976).

(13) A. B. Roberts and C. A. Frolik, *Fed. Proc. Fed. Am. Soc. Exp. Biol.*, **38**, 2524 (1979).

(14) C. Wang, S. Campbell, R. L. Furner, and D. L. Hill, *Drug Metab. Dispos.*, **8**, 8 (1980).

ACKNOWLEDGMENTS

Supported by Contract NO1 CP 85663 from the National Cancer Institute, National Institutes of Health, Bethesda, Md.

Tack Behavior of Coating Solutions I

S. K. CHOPRA * and R. TAWASHI ˣ

Received June 8, 1981, from the *Faculty of Pharmacy, University of Montreal, Montreal, Quebec, Canada H3C 3J7*, and the **Schering Canada, Inc., Pointe Claire, Quebec, Canada, H9R 1B4.* Accepted for publication November 3, 1981.

Abstract □ The tackiness of various tablet coating solutions was determined using a parallel plate technique with a tensile testing machine in conjunction with an oscilloscope where the separation force was displayed as a function of time. Measurements were made at various rates of separation on liquid films of constant thickness. Results showed that the force required to split a liquid film increases with an increase in rate of separation, and that tackiness increases with an increase in viscosity. The relation between tack and viscosity was not linear, and a modified Stefan equation was proposed.

Keyphrases □ Tablet coating solutions—tack behavior, viscosity □ Viscosity—tack behavior of tablet coating solutions □ Tackiness—tack behavior of tablet coating solutions

The effect of coating formulations and coating process variables on the appearance of a coated tablet has been the subject of various investigations (1–3). Much effort has been devoted to the study of the theory of adhesion of film-forming materials to the surface of a tablet (4–6). However, very little is known about the tackiness of coating solutions and its effect on the coating process. Studies on the evaluation of coating formulations have made some reference to the problem of tackiness of hydroxypropyl cellulose solutions during the coating process (7). However,

0022-3549/82/0800-0907$01.00/0

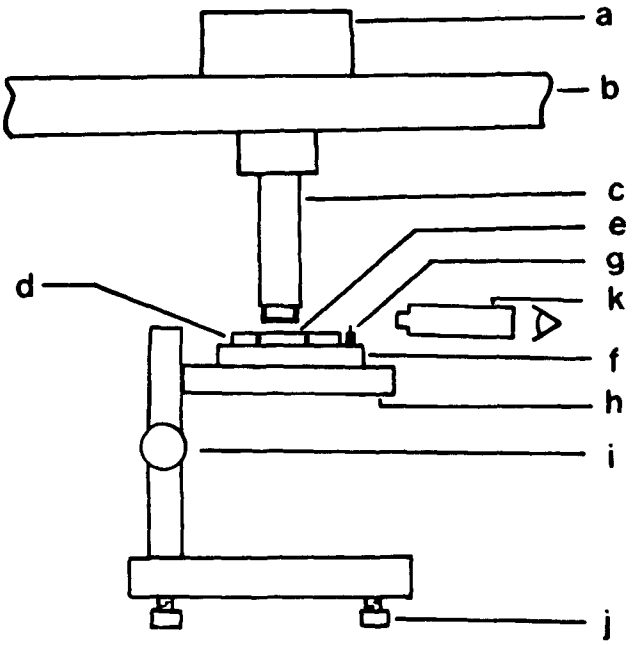

Figure 1—*Schematic diagram of tack measuring assembly in conjunction with a tensile tester. Key: a, load cell 500- or 5000-g capacity; b, crosshead bar; c, stainless steel probe, r = 0.5642; d, stainless steel ring; e, circular space; f, stainless steel plate; g, pin; h, vertically moving stage; i, knob for moving stage; j, leveling screws; k, telemicroscope.*

to our knowledge, no systematic, quantitative study on the tackiness of tablet coating solutions has been reported.

The objective of this study was to assess the tackiness of some polymer solutions used in tablet coating. Knowledge about the tacky behavior of coating formulations is a prerequisite for solving some of the technical problems encountered in tablet coating.

BACKGROUND

Tack is defined as the impulse per unit area (ft) necessary to separate two planes, initially in contact, through an intervening liquid (8). The basic expression for the separation of two flat circular plates in a viscous Newtonian liquid was given by Stefan (9) as follows:

$$F = \frac{3\pi\eta r^4}{4t}\left(\frac{1}{h_1^2} - \frac{1}{h_2^2}\right) \quad \text{(Eq. 1)}$$

Where F is the force (dynes) of separation, η is the viscosity (poise) of the liquid, r is the radius (centimeters) of the plates, h_1 and h_2 are the initial and final thicknesses (centimeters) of the liquid film, and t is the time (seconds) required for separation. The force of separation per square centimeter (f) is equal to $F/\pi r^2$, where πr^2 is the surface area of the plates. Therefore, tack can be expressed as:

$$ft = \frac{3\eta r^2}{4}\left(\frac{1}{h_1^2} - \frac{1}{h_2^2}\right) \quad \text{(Eq. 2)}$$

If the final thickness $h_2 \gg h_1$, then:

$$ft = \frac{3\eta r^2}{4h_1^2} \quad \text{(Eq. 3)}$$

The validity of the relation described by Eq. 3 has been questioned by various investigators because the experimental confirmation of the proposed equality was not satisfactory. Some of the experiments on tack appear to be inadequately designed due to the lack of suitable instrumentation. The deviation of other experimental results from Eq. 3 has been attributed to a variety of factors such as the effect of high rates of separation (10), onset of cavitation and formation of multiple filaments (11, 12), flow properties of highly viscous materials (13), surface roughness, and wettability of the solid surfaces (14).

Based on these considerations, studies were designed to evaluate and quantitate the various physicochemical parameters influencing the tackiness of tablet coating solutions.

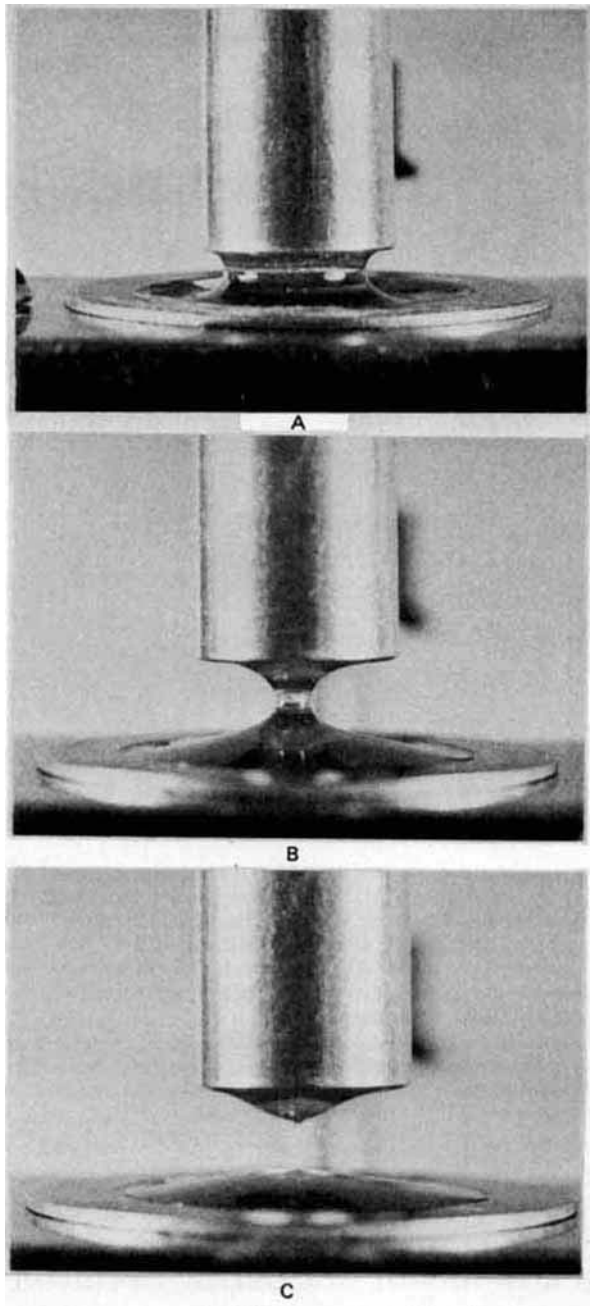

Figure 2—*Sequence of liquid film separation. Key: A, column formation; B, necking-down; C, final separation.*

EXPERIMENTAL

Materials—Polymers used in this study were hydroxypropyl methylcellulose[1] (5 cps), hydroxypropyl methylcellulose (15 cps), hydroxypropyl methylcellulose[1] (50 cps), hydroxypropyl cellulose[2], and povidone[3]. Solvents used for making coating solutions were distilled water, ethanol[4] (95%), and methylene chloride[5]. Newtonian liquids used were glycerin[6] (97%) and white mineral oil[7].

Measurement of Viscosity—All measurements were made on a rotational cup and bob viscometer[8] in conjunction with a strip chart recorder[9]. Temperature was held constant at 25° for aqueous test solutions

[1] Methocel E Premium (USP), The Dow Chemical Co., Midland, MI 48640.
[2] Klucel LF, Hercules Inc., Wilmington, DE 19899.
[3] Polyvinylpyrrolidone, plasdone K 29–32, GAF Corp., Linden, NJ.
[4] Les Alcools de Commerce Limitée, Ville St. Laurent, Quebec, Canada H4T 1N3.
[5] The Dow Chemical Co., Midland, MI 48640.
[6] Emery Industries Ltd., Toronto, Ontario, Canada.
[7] Bate Chemicals, Roydon Road, Montreal, Quebec, Canada.
[8] Rotovisco, Brinkmann Instruments, Inc., Westbury, NY 11590.
[9] Honeywell Electronik 194 Recorder, Honeywell Ltd., 6277 St. Jacques W., Montreal, Quebec, Canada.

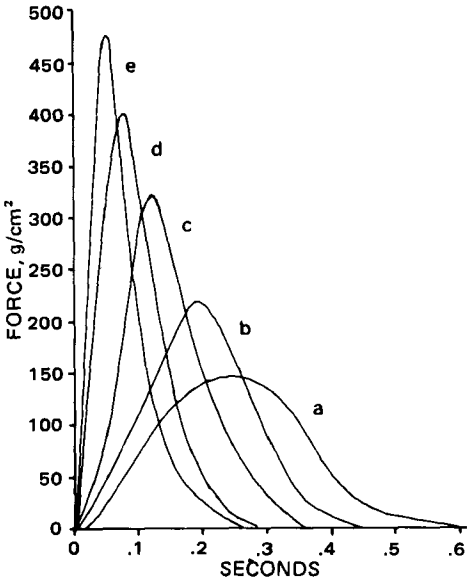

Figure 3—*Force–time oscillograms at various rates of separation for 10% (w/w) aqueous solution of hydroxypropyl methylcellulose (5 cps). Key: a, 8.33 × 10^{-3} cm/sec; b, 1.66 × 10^{-2} cm/sec; c, 3.33 × 10^{-2} cm/sec; d, 8.33 × 10^{-2} cm/sec; e, 1.66 × 10^{-1} cm/sec.*

and at 15° for polymer solutions in organic solvents. The cup and bob geometry was varied according to the viscosity of the sample.

Tack Measurement Assembly—Tack measurements were made using a tensile testing machine[10]. A schematic diagram of the assembly used is shown in Fig. 1.

The probe (Fig. 1c) and plate (Fig. 1f) are of stainless steel, type 302. The end of the probe was machined and lapped. The working area of the probe and plate were polished using techniques similar to that described previously (14).

The horizontal position of the bottom plate (Fig. 1f) was checked using a spirit level. Prior to the measurement of tack, it was ascertained that the probe was perfectly parallel to the plate.

Measurement of Film Thickness—The bottom plate (Fig. 1f) was brought into contact with the probe by raising the vertically moving stage (Fig. 1h). The pointed end of the pin (Fig. 1g) was then aligned with the crosshair line of the ocular micrometer attached to the telemicroscope[11] to mark the zero clearance between the probe and the plate.

The bottom plate was then lowered and the circular space (Fig. 1e) within the ring (Fig. 1d) was filled with ~0.5 ml of the test liquid. Utmost care was taken to avoid the introduction of air into the liquid during this transfer.

The bottom plate was then brought closer to the probe leaving a desired gap and any excess liquid was squeezed out. The difference in number of divisions between the new position and the zero position of the pointed end of the pin was used to calculate the film thickness of the liquid.

The resistance to necking-down takes place under the probe and not around it; therefore, the size of the reservoir is not of serious importance. The amount of the liquid should not be so small that the reservoir is

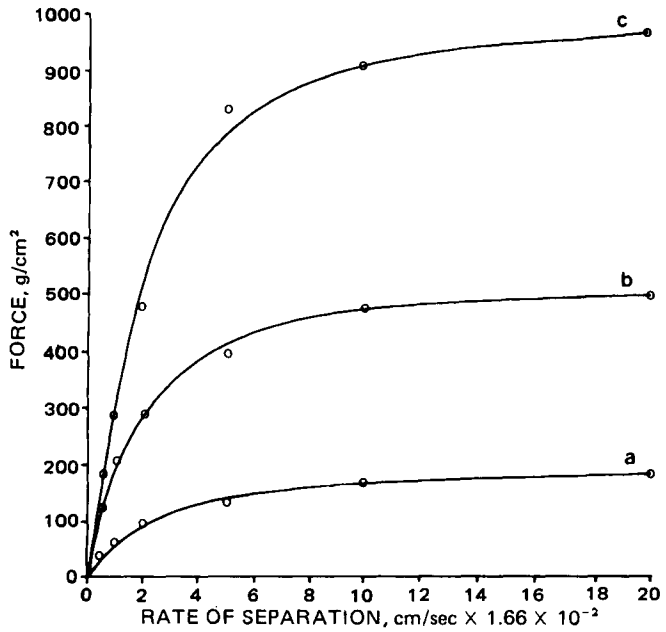

Figure 4—*Dependence of peak force on rates of separation for aqueous solutions of hydroxypropyl methylcellulose (5 cps). Key: a, 5% (w/w); b, 10% (w/w); c, 15% (w/w).*

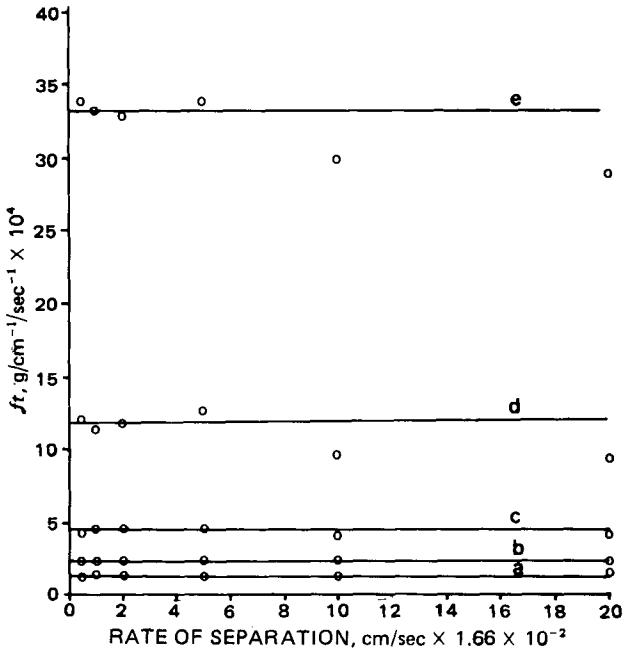

Figure 5—*Dependence of tack on rates of separation for aqueous solutions of hydroxypropyl methylcellulose (5 cps). Key: a, 5% (w/w), η = 0.29 poise; b, 7.5% (w/w), η = 0.8 poise; c, 10% (w/w), η = 2.44 poise; d, 15% (w/w), η = 9.5 poise; e, 20% (w/w), η = 41 poise.*

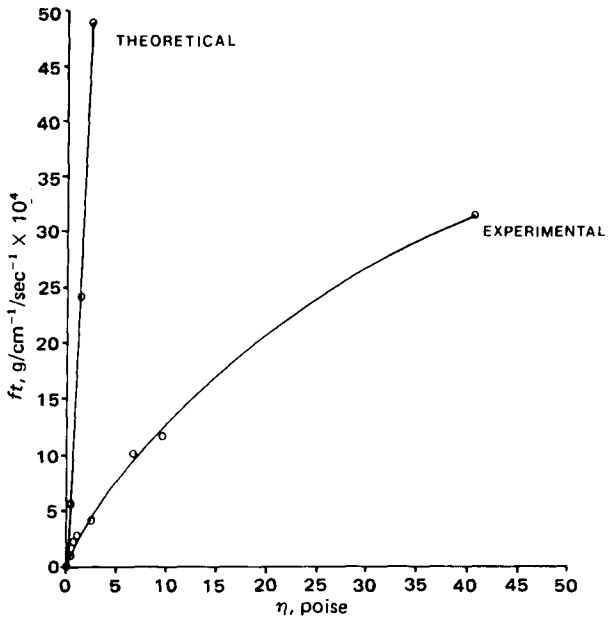

Figure 6—*Experimental and theoretical tack* versus *viscosity of aqueous solutions of hydroxypropyl methylcellulose (5 cps).*

[10] Instron Tensile Tester model 1130, Instron, Canada, Burlington, Ontario, Canada.

[11] Telemicroscope, model M101T, Gaertner Scientific Corp., Chicago, Ill.

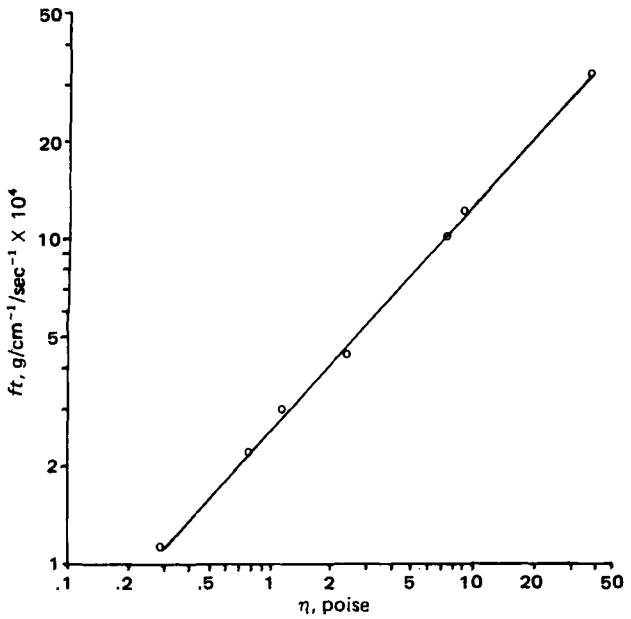

Figure 7—*Logarithmic relationship (tack versus viscosity) of experimental data shown in Fig. 6.*

completely used up at the very start of the necking-down process. When the volume of the test liquid is properly adjusted, a variation in volume of as much as 50% does not affect the tack measurement.

Measurement of Tack—After adjustment of the thickness of the test liquid, the crosshead bar (Fig. 1b) was allowed to move upwards at a specified speed. The test liquid first formed a column, necked-down, and then finally separated. The separation process was photographed and is shown in Fig. 2.

The events were recorded on a storage type oscilloscope[12] where the separation force (F) was displayed as a function of time. The measurements were made at 25° for aqueous test solutions and at 15° for polymer solutions prepared in organic solvents.

A minimum of six measurements were taken for every test solution at each separation rate. The test solution was changed if the presence of air bubbles was noticed.

RESULTS AND DISCUSSION

Effect of Rate of Separation on Force of Splitting Liquid Film—Figure 3 shows the force–time oscillograms obtained for a 10% aqueous solution of hydroxypropyl methylcellulose (5 cps) at various rates of separation. The traces show that as the time of separation decreases, the peak force increases.

The relation between peak force and the rate of separation for 5, 10, and 15% (w/w) aqueous solutions of hydroxypropyl methylcellulose (5 cps) is shown in Fig. 4. These plots demonstrate that the force required to split a liquid film increases with an increase in the rate of separation. The plots obtained are not linear and results are consistent with the experimental data presented in the study of tackiness of inks by Strasburger (15). Nevertheless, that author tried to fit the experimental data points to a theoretical straight line based on a modified Stefan equation derived previously (12):

$$F = \frac{3}{2}\pi\eta u\frac{r^4}{h_2{}^3} \qquad \text{(Eq. 4)}$$

where u is the rate of separation.

Effect of Rate of Separation on Tack—The plots of rate of separation *versus* tack of aqueous solutions of hydroxypropyl methylcellulose (5 cps) for concentrations ranging from 5 to 20% are shown in Fig. 5. The tack was calculated by dividing the area under the curves of the force–time oscillograms by the surface area of the probe.

Figure 5 illustrates that the tack is independent of the rate of separation for 5, 7.5, and 10% (w/w) aqueous solutions of hydroxypropyl methylcellulose (5 cps) solutions. These results are in agreement with Eq. 3. The tack values of 15 and 20% (w/w) solutions for rates of separation, $\geq 1.677 \times 10^{-1}$ cm/sec, fell below the average tack values obtained at lower rates of separation.

[12] Model 5113 with 5B12N time base and two 5A26 dual differential amplifiers, Tektronix, Inc., Beaverton, Ore.

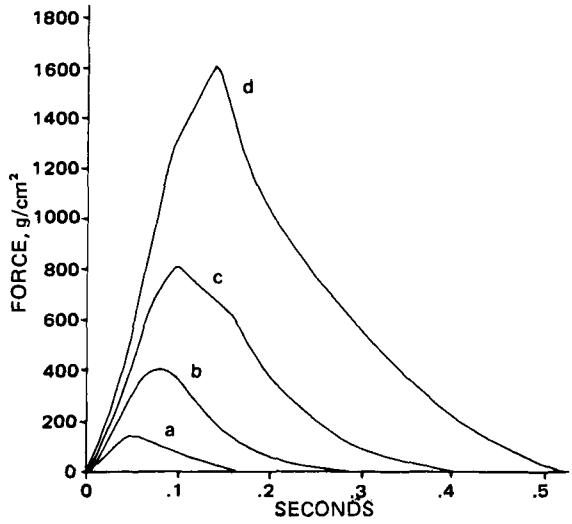

Figure 8—*Force–time oscillograms at rate of separation of 8.33×10^{-2} cm/sec for aqueous solutions of hydroxypropyl methylcellulose (5 cps). Key: a, η = 0.29 poise; b, η = 2.44 poise; c, η = 9.5 poise; d, η = 41 poise.*

A similar behavior was also noticed for pure liquids such as glycerin and liquid paraffin, where the tack values at the rate of separation of 3.33×10^{-1} cm/sec are lower than those obtained at a lower rate of separation (Table I). Thus, for a liquid of given viscosity, there is an upper limit of the rate of separation beyond which the equation described by Stefan is not applicable.

The reason for obtaining low tack values at higher rates of separation may be due to viscoelastic effects (9, 16). When the probe is pulled away from the plate, the liquid flows towards the axis of the plate at the rate governed by h_1, t, and η. When stress is applied slowly, *i.e.*, when t is long, the liquid responds by flow. If t is too short, the mechanism of rupture of the liquid film is quite different from that envisaged by Stefan. The liquid gets no chance to flow and the elastic forces become more important for the breakdown of the film. Under such circumstances, the tack values obtained are lower than that predicted by Eq. 3.

Effect of Viscosity on Tack—The relation between tack and viscosity is shown in Fig. 6. The theoretical ft was calculated by substituting the values of r, h, and η in Eq. 3. The experimental curve was plotted using the average of tack values obtained at various rates of separation for a number of solutions of hydroxypropyl methylcellulose (5 cps) in varying concentrations and hence viscosities.

Figure 6 shows that the experimental curve falls below the theoretical curve and also deviates from linearity as the viscosity of the test solution increases. The same experimental data plotted on a log–log scale is shown in Fig. 7 with a correlation coefficient of 0.9994, indicating the validity of the relationship $ft = k\,\eta^c$; k and c are constants with respective values of 24,862 and 0.6737. The value of k depends on the instrumental factor, k' and $3r^2/4h_1{}^2$. The value of k' was found to be 1.215×10^{-1}. The equation for the experimental conditions described then becomes:

$$ft = \frac{3}{4}r^2 k'\eta^{0.67}\frac{1}{h_1{}^2} \qquad \text{(Eq. 5)}$$

To confirm the relationship described in Eq. 5, aqueous solutions of three different molecular weight grades of hydroxypropyl methylcellu-

Table I—Tack Values of Glycerin and Liquid Paraffin at Various Rates of Separation [a]

Rate of Separation, cm/sec	ft (g/cm^{-1}/sec^{-1}) Liquid Paraffin (η = 1.20 poise)	ft (g/cm^{-1}/sec^{-1}) Glycerin, 97% (η = 5.17 poise)
8.33×10^{-3}	2.99×10^4	7.57×10^4
1.66×10^{-2}	2.83×10^4	7.32×10^4
3.33×10^{-2}	2.81×10^4	7.44×10^4
8.33×10^{-2}	2.99×10^4	7.47×10^4
1.66×10^{-1}	3.03×10^4	6.38×10^4
3.33×10^{-1}	2.45×10^4	5.98×10^4

[a] h_1 = 0.00108 cm.

Table II—Predicted and Experimental Tack Values of Various Polymer Solutions

Polymer	Concentrations, % (w/w)	Solvent	Viscosity, poise	ft ($g/cm^{-1}/sec^{-1} \times 10^4$) Predicted	Experimental
Hydroxypropyl methylcellulose (15 cps)	5	Water	1.26	2.90	2.91
	8	Water	8.4	10.34	10.9
Hydroxypropyl methylcellulose (50 cps)	3	Water	1.19	2.80	2.74
	5	Water	7.45	9.55	9.70
Hydroxypropyl cellulose	5	Water	0.85	2.23	2.01
	10	Water	9.54	11.27	11.4
Povidone	30	Water	.93	2.37	2.44
	43.5	Water	5.97	8.23	7.95
Hydroxypropyl methylcellulose (5 cps)	5	Ethanol–Methylene Chloride (50:50, w/w)	0.41	1.37	1.41
Hydroxypropyl methylcellulose (5 cps)	5	Ethanol–Methylene Chloride (75:25, w/w)	0.95	2.4	2.51
Hydroxypropyl methylcellulose (5 cps)	5	Ethanol–Water (50:50, w/w)	0.68	1.92	2.01
Hydroxypropyl methylcellulose (5 cps)	5	Ethanol–Water (75:25, w/w)	0.84	2.21	2.13

lose, a single grade of hydroxypropyl cellulose and of povidone, all in varying concentrations, were prepared. Solutions of hydroxypropyl methylcellulose (5 cps) were also prepared in mixtures of varying proportions of ethanol and methylene chloride, and ethanol and water.

The viscosities and the corresponding tack values of the above solutions were determined and the results are presented in Table II. This table illustrates that the experimental tack values, within a margin of error of ±5%, match the predicted tack values calculated using Eq. 5.

In the present study, the experimental tack values obtained for various coating solutions were lower than those predicted by Stefan's equation. Also, the relationship obtained between tack and viscosity was not linear. The low experimental tack values obtained in Fig. 6 could be attributed to the instrumental factors such as the surface roughness of the probe and plate. The nonlinearity of the relationship between the tackiness and viscosity cannot be attributed to the experimental conditions, as these were kept constant throughout the study.

One of the factors that can influence the values of tack is the initial lag in force. This is due to the finite time of acceleration of the crosshead bar before it attains a constant speed. The force–time oscillograms in Fig. 8 were obtained at the same rate of separation. The shape of the traces obtained for lower viscosity solutions (Fig. 8, Curves a and b) are different than those for higher viscosity solutions (Fig. 8, Curves c and d). This suggests that the mode of liquid film separation is different for the higher viscosity solutions. It has been suggested (9) that when the ratio η/t increases to a point where the flow pattern of the liquid towards the axis of the plate is not uniform, the resulting ft is a fraction of that calculated by Eq. 3. This may account for the nonlinearity between tack and viscosity.

Tack Effects in Tablet Coating—The fact that a force is required to separate two objects joined by a thin liquid film (Fig. 4) could explain the phenomenon of picking and sticking in the pan-coating process.

At any given moment during the process of pan coating, a thin film of coating solution is present between two tablets, or between a tablet and the wall of a coating pan. When the pan is allowed to rotate, the tablets are carried upwards by the combined effects of centrifugal and frictional forces until gravity overcomes the effects and the tablets cascade down. The force exerted by these moving tablets splits the liquid film before the complete evaporation of solvent occurs.

If the force required to split the liquid film is greater than the forces of adhesion between the polymer film and the tablets, then picking may occur. The picking here is defined as the transference of portions of polymer film from the weakly adhered parts of one tablet to another or to the wall of a coating pan. However, if the force exerted by the moving tablets is not sufficient to split the liquid film present between the wet tablets, then sticking may occur.

The fact that the resistance of the liquid film to splitting increases with the rate of separation may further explain why the picking is more pronounced in a larger pan than in a smaller one. In the larger coating pan, the tablets cascade down at higher velocity than in a small coating pan, and therefore, the stress exerted on the polymer film during the separation of wet tablets will be higher in the former than in the latter.

In the tablet coating process, coating solutions when applied are dilute solutions of high polymers. As the polymer solution dries during the coating process, the concentration of the polymer increases from ~5% to nearly 100%. Consequently, the flow behavior of the polymer solution changes from Newtonian to non-Newtonian and finally to an elastic solid. The tacky behavior of these solutions during the coating process is a target for future investigation.

REFERENCES

(1) D. S. Mody, M. W. Scott, and H. A. Liebermann, *J. Pharm. Sci.*, **53**, 949 (1964).

(2) J. F. Pickard and J. E. Rees, *Manuf. Chem. Aerosol News*, **45**, 19 (1974).

(3) P. A. Tuerck and D. E. McVean, *J. Pharm. Sci.*, **62**, 1534 (1973).

(4) J. A. Wood and S. W. Harder, *Can. J. Pharm. Sci.*, **5**, 18 (1970).

(5) R. C. Rowe and D. G. Fisher, *J. Pharm. Pharmacol.*, **28**, 886, 1976.

(6) E. L. Parrott and R. M. Fung, *J. Pharm. Sci.*, **69**, 439 (1980).

(7) N. O. Lindberg and E. Jonsson, *Acta Pharm. Suecica*, **9**, 589 (1972).

(8) I. Skeist, "Handbook of Adhesives," 2nd ed., Reinhold Publishing, Chapman & Hall, London, 1963, pp. 46–79.

(9) J. J. Bikerman, "The Science of Adhesive Joints," 2nd ed., Academic, New York, N.Y., 1968, pp. 91–119.

(10) F. A. Askew, *Paint Technol.*, **9**, 217 (1944).

(11) L. H. Sjohdahl, *Am. Ink Maker*, **29**, 31 (1951).

(12) W. H. Banks and C. C. Mill, *J. Colloid Sci.*, **8**, 137 (1953).

(13) F. R. Eirich "Rheology, Theory and Applications," vol. 3, 2nd ed., Academic, New York, N.Y., 1960, pp. 167–187.

(14) J. J. Bikerman, *Trans. Soc. Rheol.*, **1**, 3 (1957).

(15) H. Strasburger, *J. Colloid. Sci.*, **13**, 218 (1958).

(16) R. A. Erb and R. S. Hanson, *Trans. Soc. Rheol.*, **4**, 91 (1960).

ACKNOWLEDGMENTS

The authors thank Merck Frosst Laboratories for financial assistance and Mr. J. F. Millar for valuable suggestions.

Stereochemical Studies of Demethylated Ketamine Enantiomers

SUK CHANG HONG and JOHN N. DAVISSON ˣ

Received July 13, 1981, from the *Division of Medicinal Chemistry and Pharmaceutics, College of Pharmacy and Health Sciences, Northeast Louisiana University, Monroe, LA 71209.* Accepted for publication November 3, 1981.

Abstract □ The enantiomorphs of norketamine, 2-(*o*-chlorophenyl)-2-aminocyclohexanone, were synthesized and screened for biological activity. Resolution was achieved by fractional crystallization of the tartrate salts. Stereochemical purity was determined using standard GC or GC–MS analysis. Preliminary pharmacological evaluations revealed that intraperitoneally injected dextrorotatory norketamine caused a greater duration of loss of righting reflex in mice than the levorotatory isomer.

Keyphrases □ Ketamine—stereochemical studies of demethylated ketamine enantiomers □ Enantiomers—stereochemical studies of demethylated ketamine enantiomers □ Stereochemistry—studies of demethylated ketamine enantiomers

Ketamine, 2-(*o*-chlorophenyl)-2-(methylamino)cyclohexanone (I), is rapidly and extensively metabolized (1, 2). The parent compound is demethylated to norketamine (II), which is believed to undergo further oxidation and conjugation reactions. Numerous investigations concerning the pharmacological properties and metabolism of ketamine have been conducted during the past several years (1–5). More recently, the pharmacological actions of the enantiomers of ketamine also have been evaluated (3, 6). Human studies have resulted in the suggestion that dextrorotatory ketamine hydrochloride may be more acceptable as an anesthetic agent when compared to the racemic or levorotatory drug (6). Additionally, levorotatory ketamine hydrochloride was shown to cause significantly higher incidences of unusual dreaming and posthypnotic phenomena than the dextrorotatory isomer. Norketamine resulting from the administration of levorotatory ketamine hydrochloride showed higher plasma levels than that derived from the dextrorotatory enantiomer, especially in the postanesthetic period. Animal experiments have revealed similar patterns of pharmacological activities for the ketamine enantiomers. Stereochemical differences in metabolism and the possibility of certain metabolites having prolonged biological half-lives have been offered as possible explanations for posthypnotic phenomena (3).

Pharmacological data have been reported for racemic norketamine, but no information is available for the purified enantiomers (5). As part of an investigation to determine stereochemical and pharmacological relationships between enantiomers of ketamine and those of metabolites, the synthesis, resolution, and preliminary pharmacological studies of enantiomerically purified norketamine have been completed and are described in this report.

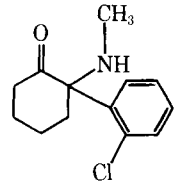

I

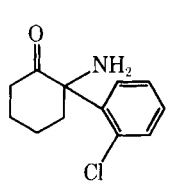

II

EXPERIMENTAL

Instrumentation—Melting points are reported as corrected values[1]. UV[2] and IR[3] spectra were recorded with double-beam spectrometers. NMR[4] spectra were recorded on a 60-MHz apparatus with tetramethylsilane as an internal reference. Optical rotation was measured with an automatic polarimeter[5]. GLC[6] conditions were as follows: glass column, 1.8 m × 2-mm i.d. packed with 3% SP2300 or 3% SP2401 on 100/120 mesh Supelcoport; carrier gas was nitrogen at 30 ml/min; the injector, column, and detector temperatures were 250, 210, and 275°, respectively. GC–MS[7] conditions were as follows: glass column, 1.8 m × 2-mm i.d. packed with 3% SP2300 or 3% SP2401 on 100/120 mesh Supelcoport; carrier gas was helium at 30 ml/min; injector, column, and source temperatures were 270, 230, and 225°, respectively. Ionization was at 75 eV.

Synthesis of Norketamine (II)—1-Bromocyclopentyl(o-chlorophenyl)ketone (III), 50 g (0.18 mole) (7, 8) was placed in a 500-ml round bottom flask containing 300 ml of 28% ammonium hydroxide solution which had been saturated with anhydrous ammonia. The mixture was agitated vigorously for 7 days at room temperature using a mechanical shaker. The dark brown bottom layer was separated, dissolved in 500 ml of cyclohexane–petroleum ether (5:1) solution, and placed in a refrigerator. After 2 days, 24 g (60% yield) of a white solid (mp 90.5–91.5°) was obtained. The IR spectrum revealed strong combined NH—OH stretching at 3225 cm^{-1} and C=N absorption at 1645 cm^{-1} consistent with the iminoalcohol intermediate (7). Without further purification, an isopropyl alcohol solution (200 ml) of 20 g (0.09 mole) of this solid was refluxed for 5 days. Crude norketamine was obtained by evaporation of the solvent under reduced pressure. The residue was dissolved in absolute ether and saturated with dry hydrogen chloride gas. The solid was filtered and dissolved in 50 ml of distilled water. The solution was neutralized with 10% sodium carbonate–ammonium hydroxide solution (1:1) and extracted with methylene chloride (3 × 200 ml). Evaporation of the solvent left a tan oily product (16 g) whose spectral data were identical to those of an analytical reference sample of racemic norketamine[8].

Resolution of Norketamine—A 20-g solution (0.09 mole) of racemic norketamine in 50 ml of methanol was mixed with a methanol solution (200 ml) of (+)-tartaric acid (15.1 g, 0.1 mole). The mixture was stirred overnight at room temperature and filtered. The solvent was evaporated at reduced pressure. The resulting crude solid was washed with 400 ml of 2-butanone and then dissolved in 5.4 liters of refluxing acetone. Fine needle-like crystals (7.5 g) were collected after storing the solution for 2 days at room temperature. The filtrate was saved for later isolation of the other enantiomer.

The bitartrate salt was recrystallized three additional times from acetone resulting in 4.8 g of fine needle-like crystals (mp 181–182°). The free base was obtained with 0.5 *N* NaOH solution and converted into the hydrochloride or bisuccinate salt using standard procedures. The hydrochloride salt was recrystallized from ethanol yielding a fine white solid, mp 175–177°; $[\alpha]_D^{25}$ −96.4° (*C* = 1.0, water). The bisuccinate salt was recrystallized from acetone yielding white platelets, mp 139–140°; $[\alpha]_D^{25}$ −66.2° (*C* = 1.0, water).

Anal.—Calc. for $C_{16}H_{20}ClNO_7$: C, 51.41; H, 5.39; N, 3.75; Cl, 9.48 O, 29.97. Found: C, 51.41; H, 5.39; N, 3.72; Cl, 9.43 O, 30.05. The combined filtrates remaining from the above procedures were evaporated to dryness. The remaining solid was dissolved in water, neutralized with 0.5 *N* NaOH, and extracted with methylene chloride. Following evaporation

[1] Thomas-Hoover Capillary Melting Point Apparatus.
[2] Perkin-Elmer Coleman model 124.
[3] Perkin-Elmer 710A Grating IR Spectrometer.
[4] Hitachi Perkin-Elmer NMR Spectrometer, model R-24A.
[5] Perkin-Elmer model 241.
[6] Hewlett Packard 402 High Efficiency Gas Chromatograph.
[7] DuPont Instruments Dimaspec 321 gas chromatograph-mass spectrometer interfaced with a DuPont Instruments 320 data system.
[8] Parke-Davis/Warner Lambert Co.

0022-3549/82/0800-0912$01.00/0

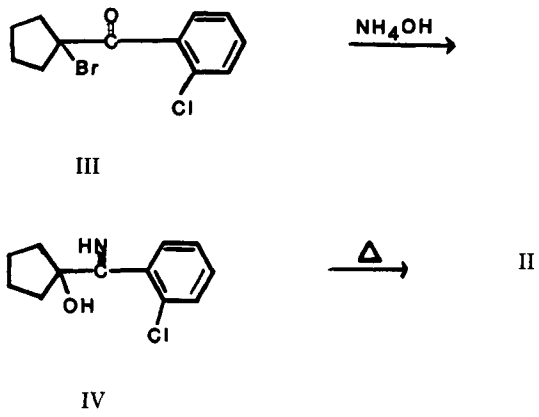

Scheme I—*Synthesis of norketamine.*

of the solvent, the residue was treated with (−)-tartaric acid in the same manner as described for (+)-tartaric acid. The resulting hydrochloride salt was recrystallized from ethanol yielding a fine white solid, mp 176–178°; $[\alpha]_D^{25}$ +95.0° (*C* = 1.0, *water*). The bisuccinate salt (mp 138–140°) was recrystallized from acetone; $[\alpha]_D^{25}$ +66.3° (*C* = 1.0, water).

Anal.—Calc. for $C_{16}H_{20}ClNO_7$: C, 51.41; H, 5.39; N, 3.75; Cl, 9.48 O, 29.97. Found: C, 51.43; H, 5.42; N, 3.73; Cl, 9.45 O, 30.05.

Determination of Stereochemical Purity—(+)-Norketamine bisuccinate, 2 mg (5.3 μmoles), was basified with 0.1 *N* NaOH and extracted with 3.0 ml of methylene chloride. The methylene chloride solution was separated and dried over anhydrous sodium sulfate. A 2-ml aliquot of this solution was mixed with 10 μl of a 0.5-*M* methylene chloride solution of (−)-α-methoxy-α-trifluoromethylphenylacetyl chloride (V) (9). The mixture was heated to 60° for 2 hr, cooled to room temperature and washed with 3 ml of 0.5 *N* HCl, 3 ml of 0.5 *N* NaOH, and 5 ml of distilled water. After drying over anhydrous sodium sulfate, the methylene chloride was evaporated under nitrogen, and the residue was dissolved in 25 μl of methanol. This solution (1–2 μl) was used for GLC and GC–MS analysis. (−)-Norketamine bisuccinate and racemic norketamine bisuccinate were derivatized in the same manner.

Animal Experiments—Male Swiss-Webster mice (25–32 g), provided with rodent laboratory chow[9] and water *ad libitum*, were housed in wire meshed cages (16 × 18 × 24 cm) suspended above indirect bedding. The temperature was maintained at 20–24° and the photoperiod was controlled to provide light from 6 am to 6 pm. Drugs were dissolved in distilled water and all injections were made intraperitoneally. Judgment of loss of righting reflex was made on an all-or-none basis after termination of drug injection. Mice that lost righting reflex were then placed on their backs in individual plastic cages and observed. Righting reflex was judged to be regained when an animal turned to a prone position

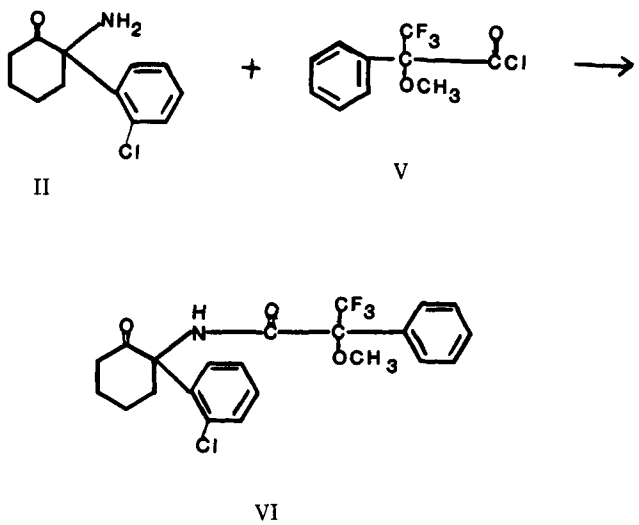

Scheme II—*Synthesis of the α-methoxy-α-trifluoromethylphenylacetamide analog of norketamine.*

[9] Purina.

Table 1—Effect of Norketamine Enantiomers upon the Duration of Loss of Righting Reflex in Mice

Compound	Dose[a], mg/kg	No. of Animals	Duration of Loss of Righting Reflex[b], min
(+)	100	8	6.8 ± 0.8
(−)	100	8	No Loss
(+)	200	14	46.1 ± 7.1[c]
(−)	200	14	25.2 ± 2.2[c]

[a] Animals received norketamine intraperitoneally and were observed for duration of loss of righting reflex. [b] Values represent the mean ± *SEM*. [c] $p < 0.01$ according to Student *t* test.

twice within a 10-sec period. All animal experiments were performed between 1 and 6 pm.

RESULTS AND DISCUSSION

The synthesis of norketamine was accomplished by utilizing an aminoketone synthesis introduced previously (7, 8) (Scheme I). The product was obtained directly from the thermal rearrangement of the intermediate Schiff base (IV) in a two-step sequence. This was accomplished in refluxing solvents ranging from methanol (bp 65°) to naphthalane[10] (bp 190°). Lower boiling alcohols produced greater yields with less decomposition than higher boiling solvents. In these studies refluxing IV in isopropyl alcohol resulted in an 80% yield of product after 5 days. Spectral data (IR, NMR) were consistent with the structure of norketamine, and the GLC retention time and mass spectrum were identical to those of an analytical reference sample.

Resolution of norketamine proved to be tedious. Formation of the diastereomeric bitartrate salts and subsequent recrystallization from acetone was found to be the most efficient method of resolution attempted. One major drawback was the large volumes of acetone needed to accomplish the purification.

Progress of the resolution was followed either by measuring optical activity or by GLC analysis. For the latter, diastereomers, formed by reacting the enantiomers with (−)-α-methoxy-α-trifluoromethylphen-

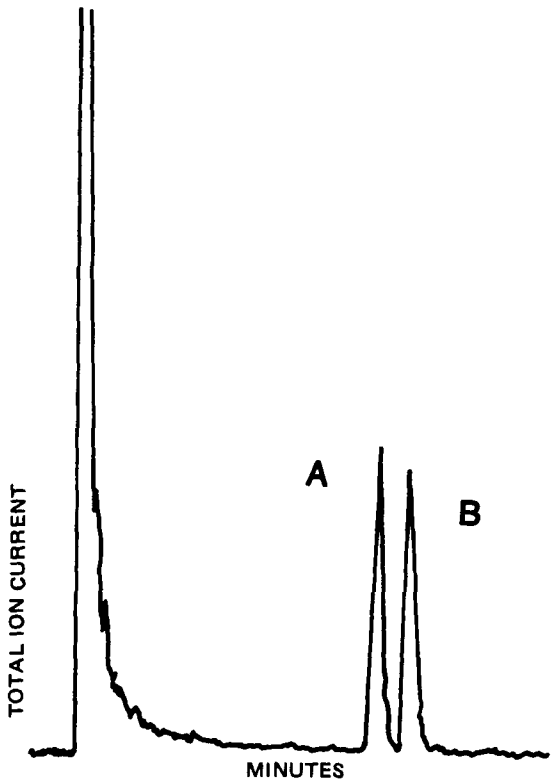

Figure 1—*Reconstructed gas chromatogram of the (−)-α-methoxy-α-trifluoromethylphenylacetamide analogs of (+)-norketamine (A) and (−)-norketamine (B).*

[10] Decalin.

ylacetyl chloride, were chromatographed over 3% SP2401 (9) (Scheme II). Using this system good separation of diastereomers was achieved (Fig. 1). Retention times of derivatized (+)-norketamine and (−)-norketamine were 13.5 and 14.9 min, respectively. These compounds failed to show a parent ion (m/z = 439) using electron impact mass spectroscopy, but when subjected to chemical ionization conditions, both displayed significant M + 1 ions. Fragmentation patterns also were consistent with the structures. When purified enantiomers were derivatized and subjected individually to GLC analysis, no contamination from the other stereoisomer could be detected, indicating that the resolution procedure had resulted in highly stereochemically pure norketamine.

The enantiomers were converted into either hydrochloride or bisuccinate salts. The former proved to be quite hygroscopic making the bisuccinate salts more convenient for subsequent studies. The signs of optical rotation were the same for both salts. The free bases were not highly purified to permit accurate measurements of their optical rotations, but using partially purified samples, it was determined that the signs of rotation for the free bases and the salts were the same. This observation is in contrast to reported optical rotations of ketamine (10). The free bases and hydrochloride salts for this compound show opposite signs of rotation.

Initial pharmacological evaluation revealed that intraperitoneally injected dextrorotatory norketamine bisuccinate caused a greater duration of loss of righting reflex in mice than the levorotatory isomer (Table I). At doses of 100 mg/kg (calculated on free base content) the levorotatory isomer failed to induce loss of righting reflex, whereas this same dose appeared to be near the ED_{50} value for the dextrorotatory form. At 200 mg/kg all animals lost righting reflex with the dextrorotatory compound, producing a significantly greater duration of loss (Table I). These preliminary studies also suggested that levorotatory norketamine bisuccinate may cause greater amounts of central excitation than the dextrorotatory form. This is based on the observation that animals receiving the levorotatory drug appeared to show greater amounts of spontaneous locomotor activity than those receiving the dextrorotatory isomer.

Similar actions as to loss of righting reflex and central excitation have been reported for the ketamine enantiomers (3). Also, it has been shown that racemic norketamine and ketamine are qualitatively similar with regard to central nervous system depressant effects and posthypnotic excitation (5). Because of the these findings, it is tempting to speculate that the levorotatory salts of ketamine and norketamine have identical stereochemical configurations; the same being true for the dextrorotatory forms. However, additional studies will be needed to establish the exact stereochemical relationships between these compounds as well as the pharmacological significance of the norketamine enantiomers.

REFERENCES

(1) T. Chang, W. A. Dill, and A. J. Glazko, *Fed. Proc. Fed. Am. Soc. Exp. Biol.*, **24**, 268 (1965).

(2) M. L. Cohen and A. J. Trevor, *Anesthesiology*, **39**, 370 (1973).

(3) M. P. Marietta, W. L. Way, N. Castagnoli, Jr., and A. J. Trevor, *J. Pharmacol. Exp. Ther.*, **202**, 157 (1977).

(4) D. A. McCathy, G. Chen, D. H. Kaump, and C. Ensor, *J. New Drugs*, **5**, 21 (1965).

(5) M. L. Cohen and A. J. Trevor, *J. Pharmacol. Exp. Ther.*, **189**, 351 (1974).

(6) P. F. White, J. Ham, W. Way, and A. J. Trevor, *Anesthesiology*, **52**, 231 (1980).

(7) C. L. Stevens, A. Thuillier, K. G. Taylor, F. A. Daniher, J. P. Dickerson, H. T. Hanson, N. A. Nielsin, N. A. Tikotkar, and R. M. Weier, *J. Org. Chem.*, **31**, 2601 (1966).

(8) C. L. Stevens, A. Thuillier, and F. A. Daniher, *ibid.*, **30**, 2962 (1965).

(9) J. Gal, *J. Pharm. Sci.*, **66**, 169 (1977).

(10) P. Newman, "Optical Resolution Procedures for Chemical Compounds," Optical Resolution Information Center, Manhattan College, Riverdale, N.Y., 1978, pp. 252–253.

Preparations of Solid Particulates of Theophylline–Ethylenediamine Complex by a Spray-Drying Technique

H. TAKENAKA *, Y. KAWASHIMA *ˣ, S. Y. LIN *, and Y. ANDO ‡

Received May 27, 1981, from the **Gifu College of Pharmacy, Mitahora, Gifu 502, Japan* and the ‡*Ichimaru Company, Matsuhora, Takatomi, Gifu 502-21, Japan.* Accepted for publication November 3, 1981.

Abstract □ Aqueous solutions of ethylenediamine and theophylline were spray dried to obtain solid particulates of theophylline–ethylenediamine complex to improve solubility of theophylline. Packing and flow properties of the spray-dried products were much improved when compared with those of original theophylline particles, due to their spherical shapes which were confirmed by a scanning electron microscope. The solubility of theophylline in the resultant products was found to be three to five times higher than that of original theophylline. The solubilities of the products decreased with increasing drying temperature and rotation speed of the atomizer, which was interpreted in terms of the contents of ethylenediamine in the products. The products were confirmed to be a mixture of aminophylline, α-aminophylline, and theophylline by X-ray analysis and NMR spectroscopy. The logarithm of the relative intensity of the X-ray diffraction peak of α-aminophylline to that of theophylline decreased linearly with drying temperature and rotation speed of the atomizer. Thermal decomposition of the spray-dried products involved liberations of crystal water at 100° and ethylenediamine between 110 and 127°. Liberation of ethylenediamine occurred *via* three steps for aminophylline, but with different steps for the spray-dried products.

Keyphrases □ Complexation—theophylline–ethylenediamine, preparations, spray-drying technique, solid particulates □ Theophylline—complexation with ethylenediamine, preparations, solid particulates, spray-drying technique □ Ethylenediamine—complexation with theophylline, preparations, solid particulates, spray-drying technique

The spray-drying technique has been accepted as a favorable method for drying a variety of heat-sensitive materials, such as foods, pharmaceuticals, enzymes, *etc.* The preparation of particulate solids from liquid droplets by chemical reaction during drying is one of the recent uses of this technique. Microcapsules of barbituric acid and phenobarbital with a tensioactive precondensate of the hexamethylolmelamine type, which form macromolecules under the influence of heat, have been prepared previously (1, 2). An ammonium sulfate sphere has been produced by the reaction of a single drop of phosphoric acid with gaseous ammonia (3).

The objective of the present study was to prepare solid particulates of the theophylline–ethylenediamine complex (*e.g.*, aminophylline) by a spray-drying technique. The manufacturing method of aminophylline referred to in the

0022-3549/82/0800-0914$01.00/0

ylacetyl chloride, were chromatographed over 3% SP2401 (9) (Scheme II). Using this system good separation of diastereomers was achieved (Fig. 1). Retention times of derivatized (+)-norketamine and (−)-norketamine were 13.5 and 14.9 min, respectively. These compounds failed to show a parent ion (m/z = 439) using electron impact mass spectroscopy, but when subjected to chemical ionization conditions, both displayed significant M + 1 ions. Fragmentation patterns also were consistent with the structures. When purified enantiomers were derivatized and subjected individually to GLC analysis, no contamination from the other stereoisomer could be detected, indicating that the resolution procedure had resulted in highly stereochemically pure norketamine.

The enantiomers were converted into either hydrochloride or bisuccinate salts. The former proved to be quite hygroscopic making the bisuccinate salts more convenient for subsequent studies. The signs of optical rotation were the same for both salts. The free bases were not highly purified to permit accurate measurements of their optical rotations, but using partially purified samples, it was determined that the signs of rotation for the free bases and the salts were the same. This observation is in contrast to reported optical rotations of ketamine (10). The free bases and hydrochloride salts for this compound show opposite signs of rotation.

Initial pharmacological evaluation revealed that intraperitoneally injected dextrorotatory norketamine bisuccinate caused a greater duration of loss of righting reflex in mice than the levorotatory isomer (Table I). At doses of 100 mg/kg (calculated on free base content) the levorotatory isomer failed to induce loss of righting reflex, whereas this same dose appeared to be near the ED_{50} value for the dextrorotatory form. At 200 mg/kg all animals lost righting reflex with the dextrorotatory compound, producing a significantly greater duration of loss (Table I). These preliminary studies also suggested that levorotatory norketamine bisuccinate may cause greater amounts of central excitation than the dextrorotatory form. This is based on the observation that animals receiving the levorotatory drug appeared to show greater amounts of spontaneous locomotor activity than those receiving the dextrorotatory isomer.

Similar actions as to loss of righting reflex and central excitation have been reported for the ketamine enantiomers (3). Also, it has been shown that racemic norketamine and ketamine are qualitatively similar with regard to central nervous system depressant effects and posthypnotic excitation (5). Because of the these findings, it is tempting to speculate that the levorotatory salts of ketamine and norketamine have identical stereochemical configurations; the same being true for the dextrorotatory forms. However, additional studies will be needed to establish the exact stereochemical relationships between these compounds as well as the pharmacological significance of the norketamine enantiomers.

REFERENCES

(1) T. Chang, W. A. Dill, and A. J. Glazko, *Fed. Proc. Fed. Am. Soc. Exp. Biol.*, **24**, 268 (1965).

(2) M. L. Cohen and A. J. Trevor, *Anesthesiology*, **39**, 370 (1973).

(3) M. P. Marietta, W. L. Way, N. Castagnoli, Jr., and A. J. Trevor, *J. Pharmacol. Exp. Ther.*, **202**, 157 (1977).

(4) D. A. McCathy, G. Chen, D. H. Kaump, and C. Ensor, *J. New Drugs*, **5**, 21 (1965).

(5) M. L. Cohen and A. J. Trevor, *J. Pharmacol. Exp. Ther.*, **189**, 351 (1974).

(6) P. F. White, J. Ham, W. Way, and A. J. Trevor, *Anesthesiology*, **52**, 231 (1980).

(7) C. L. Stevens, A. Thuillier, K. G. Taylor, F. A. Daniher, J. P. Dickerson, H. T. Hanson, N. A. Nielsin, N. A. Tikotkar, and R. M. Weier, *J. Org. Chem.*, **31**, 2601 (1966).

(8) C. L. Stevens, A. Thuillier, and F. A. Daniher, *ibid.*, **30**, 2962 (1965).

(9) J. Gal, *J. Pharm. Sci.*, **66**, 169 (1977).

(10) P. Newman, "Optical Resolution Procedures for Chemical Compounds," Optical Resolution Information Center, Manhattan College, Riverdale, N.Y., 1978, pp. 252–253.

Preparations of Solid Particulates of Theophylline–Ethylenediamine Complex by a Spray-Drying Technique

H. TAKENAKA *, Y. KAWASHIMA *ˣ, S. Y. LIN *, and Y. ANDO ‡

Received May 27, 1981, from the **Gifu College of Pharmacy, Mitahora, Gifu 502, Japan* and the ‡*Ichimaru Company, Matsuhora, Takatomi, Gifu 502-21, Japan.* Accepted for publication November 3, 1981.

Abstract □ Aqueous solutions of ethylenediamine and theophylline were spray dried to obtain solid particulates of theophylline–ethylenediamine complex to improve solubility of theophylline. Packing and flow properties of the spray-dried products were much improved when compared with those of original theophylline particles, due to their spherical shapes which were confirmed by a scanning electron microscope. The solubility of theophylline in the resultant products was found to be three to five times higher than that of original theophylline. The solubilities of the products decreased with increasing drying temperature and rotation speed of the atomizer, which was interpreted in terms of the contents of ethylenediamine in the products. The products were confirmed to be a mixture of aminophylline, α-aminophylline, and theophylline by X-ray analysis and NMR spectroscopy. The logarithm of the relative intensity of the X-ray diffraction peak of α-aminophylline to that of theophylline decreased linearly with drying temperature and rotation speed of the atomizer. Thermal decomposition of the spray-dried products involved liberations of crystal water at 100° and ethylenediamine between 110 and 127°. Liberation of ethylenediamine occurred *via* three steps for aminophylline, but with different steps for the spray-dried products.

Keyphrases □ Complexation—theophylline–ethylenediamine, preparations, spray-drying technique, solid particulates □ Theophylline—complexation with ethylenediamine, preparations, solid particulates, spray-drying technique □ Ethylenediamine—complexation with theophylline, preparations, solid particulates, spray-drying technique

The spray-drying technique has been accepted as a favorable method for drying a variety of heat-sensitive materials, such as foods, pharmaceuticals, enzymes, *etc.* The preparation of particulate solids from liquid droplets by chemical reaction during drying is one of the recent uses of this technique. Microcapsules of barbituric acid and phenobarbital with a tensioactive precondensate of the hexamethylolmelamine type, which form macromolecules under the influence of heat, have been prepared previously (1, 2). An ammonium sulfate sphere has been produced by the reaction of a single drop of phosphoric acid with gaseous ammonia (3).

The objective of the present study was to prepare solid particulates of the theophylline–ethylenediamine complex (*e.g.*, aminophylline) by a spray-drying technique. The manufacturing method of aminophylline referred to in the

0022-3549/82/0800-0914$01.00/0

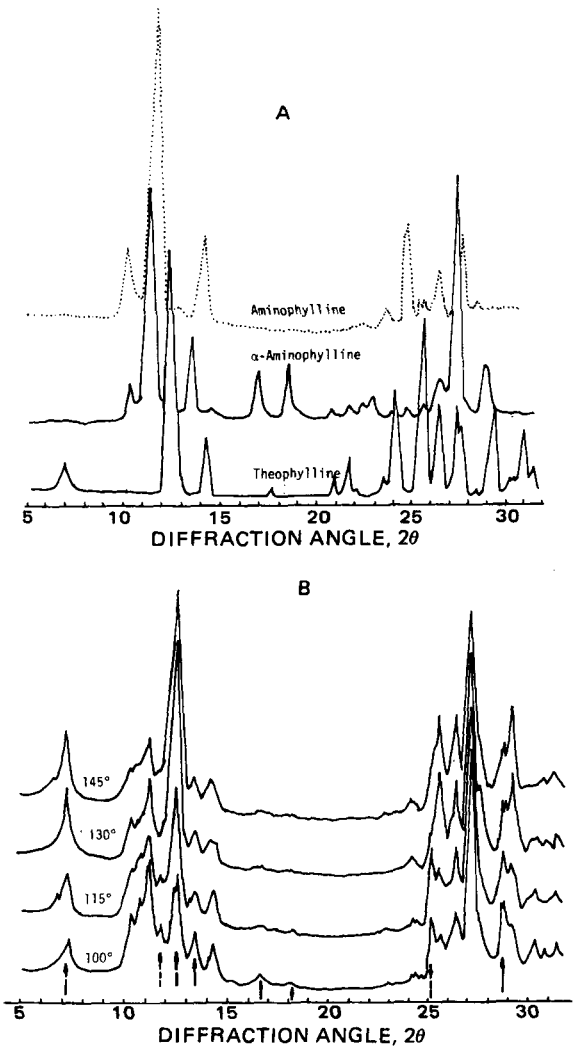

Figure 1—*(A) X-ray diffraction patterns of references; (B) the spray-dried products prepared at various spray-drying temperatures.*

Japanese Pharmacopeia (JP) involves a multistage process including reaction, filtration, drying, *etc.* In addition, the reaction takes several hours. The process of the present study offers the advantage of reducing the preparation steps, which can save time and cost. Another objective was to investigate the spray-drying conditions affecting the composition of the products. Thermal decomposition of spray-dried products by thermal analysis was also investigated.

EXPERIMENTAL

Materials—Theophylline[1] and ethylenediamine[1] used were chemical reagent grade. Aminophylline[1] (JP) and another theophylline–ethylenediamine complex, α-aminophylline, were used as a reference for identifying the spray-dried products. α-Aminophylline was produced by a method (JP) modified previously (4). Ethylenediamine purified by distillation (11.47 ml) was dissolved in 100 ml of absolute alcohol. Theophylline (30.82 g) was stirred into the resulting solutions. After agitation for several hours, the resultant precipitates were filtered and dried at 5–7° immediately after filtration without washing. The X-ray diffraction pattern of the products, *i.e.*, α-aminophylline, was different from that of aminophylline (JP) as shown in Fig. 1A. α-Aminophylline contained 13.9% ethylenediamine, 85.9% theophylline, and 0.2% water, which suggested the composition of α-aminophylline with 2 moles of theophylline, 1 mole of ethylenediamine, and small amounts of water.

[1] Nakarai Chemical LTD, Japan.

Table I—Micromeritic Properties of Spray-Dried Products

Drying Temperature	Rotation Speed of Atomizer, rpm	Dg[a], μm	σ,g[b]	ρ,g/cm³[c]	Solubility of Theophylline, mg/ml[d]
100	20,000	13.0	1.31	1.31	43.0
115	20,000	10.1	1.57	1.32	40.0
130	20,000	11.5	1.38	1.30	30.7
145	20,000	12.0	1.41	1.31	29.6
115	10,000	14.2	1.48	1.37	40.4
115	20,000[e]	10.1	1.57	1.32	40.0
115	40,000	9.8	1.34	1.39	29.0

[a] Geometric mean diameter. [b] Geometric standard deviation. [c] Particle density, the particle density of aminophylline is 1.43. [d] The solubilities of theophylline and aminophylline (JP) in water are 8.74 and 49.4 mg/ml, respectively, at 30°. [e] The parameters (*a*,*b*) in Eq. 1 of spray-dried products, original theophylline, and spray-dried theophylline are (0.16, 0.064), (0.23, 0.062), and (0.31, 0.036), respectively.

Spray-Drying Technique—Theophylline (53.5 g) and ethylenediamine (23.0 ml) were dissolved in 500 ml of water. The solutions were atomized in a drying chamber by a centrifugal wheel atomizer at rotations of 10,000, 20,000, or 40,000 rpm. The drying chamber was maintained at 100, 115, 130, or 145 ± 5°. The dried products were collected by a cyclone. As a reference, 500 ml of aqueous suspensions containing 53.5 g of theophylline was spray dried at 115° with an atomizer rotation speed of 20,000 rpm.

Measurement of Micromeritic Properties—The sizes of the spray-dried products were measured by a photographic counting method using a particle size analyzer[2]. The packing properties of the products were investigated by a tapping method. The true densities of the products were measured with a helium–air comparison pycnometer[3]. The surface topographs of the products coated with gold were investigated by a scanning electron microscope[4]. The solubilities of the products were measured in water at 30°.

Measurement of Physicochemical Properties—The contents of ethylenediamine and theophylline in the products were measured by a neutralization titration method with 0.1 *N* HCl and spectrophotometrically at 270 nm, respectively. Water contents were measured by the Karl Fischer method[5]. To analyze the crystalline form of the products, X-ray diffraction patterns were obtained by an X-ray diffractometer[6]. Thermal decomposition of the products was examined using a differential scanning calorimeter[7] with heating rate at 10°/min. Thermal analysis of the products treated with heating at 110 or 120° for 30 min was also carried out in a muffle to investigate the process of the thermal decomposition. NMR spectra of ethylenediamine, aminophylline, α-aminophylline, theophylline, and the spray-dried products were obtained in dimethyl sulfoxide using an NMR spectrometer[8].

RESULTS AND DISCUSSION

Micromeritic Properties of Spray-Dried Products—Size distribution of the spray-dried products was described in log-normal form. The geometric mean diameters of the products varied from 9.8 to 14.2 μm, and were independent of the drying temperature, but dependent on the rotation speed of the atomizer. The sizes of products decreased with an increase of the rotation speed, since the diameters of the spray droplets were reduced by enhancing the rotation speed. The geometric standard deviations of diameters of the products were 1.31–1.57 (Table I).

The scanning electron photographs of the original and the spray-dried theophylline and spray-dried products with ethylenediamine are exhibited in Fig. 2. The surface of the spray-dried theophylline was rough compared with that of the original crystal. A number of small spherical-sized products, which adhered to the crystals, yielded from the atomized solution of theophylline, are shown in Fig. 2B. Spray-dried products prepared from the formulation containing ethylenediamine yielded spheres covered with thin flake crusts, as shown in Figs. 2C and D. Loose internal texture of the products could be predicted from the characteristic surface topography. This was confirmed by the lower particle densities of the spray-dried products than original theophylline and aminophylline (JP) as tabulated in Table I.

[2] Karl Zeiss TGZ-3.
[3] Model 1302, Micromeritics Instrument Co.
[4] Nihon Denshi, JMS-SI, Japan.
[5] Kyoto Electronics Manufacturing Co., Japan.
[6] Nihon Denshi, JDX, Japan.
[7] Rigaku CN 80852, Japan.
[8] R-20B, Hitachi, High Resolution NMR Spectrometer, Japan.

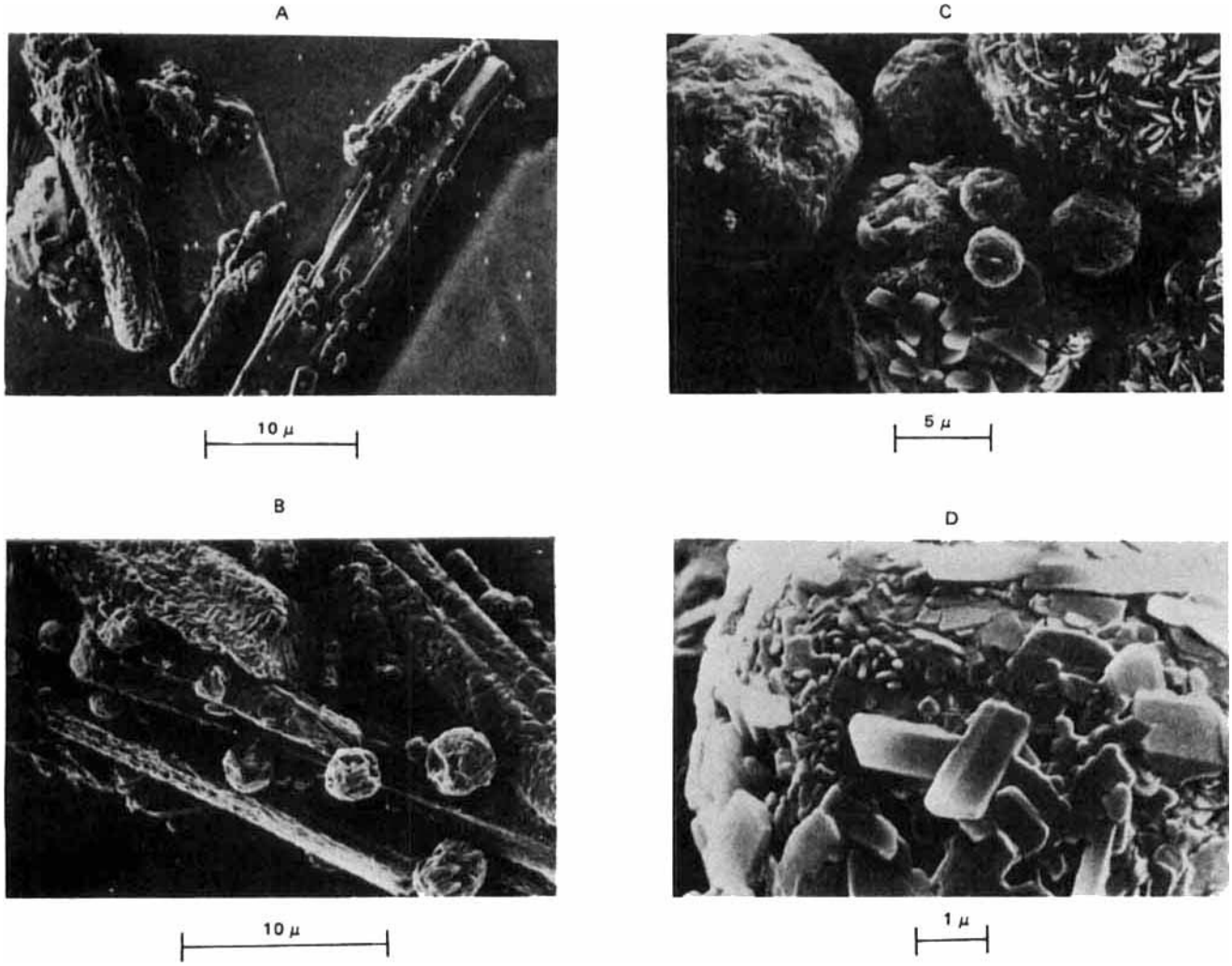

Figure 2—*Scanning electron microscopic photographs of spray-dried products. Key: (A) original theophylline; (B) spray-dried theophylline; (C) and (D) spray-dried products prepared at 115°, 20,000 rpm with the formulation containing ethylenediamine (20 ml) and theophylline (53.5 g).*

Packing and flow properties of the spray-dried products were much improved compared with those of original theophylline particles due to their spherical shapes. The packing process by tapping was described by the Kawakita equations (5, 6):

$$n/C = 1/ab + n/a \quad \text{(Eq. 1)}$$

$$C = (V_0 - V_n)/V_0 \quad \text{(Eq. 2)}$$

where a and b are constants representing the proportion of consolidation at the closest packing attained and packing velocity index, respectively, n is the number of taps, V_0 is the volume of powder in a measuring cylinder at the loosest packing, and V_n is the volume after the nth tapping. Parameter a in Eq. 1 for the spray-dried products was found to be smaller than that of original theophylline (Table I), which indicated that packing properties of the spray-dried products were improved.

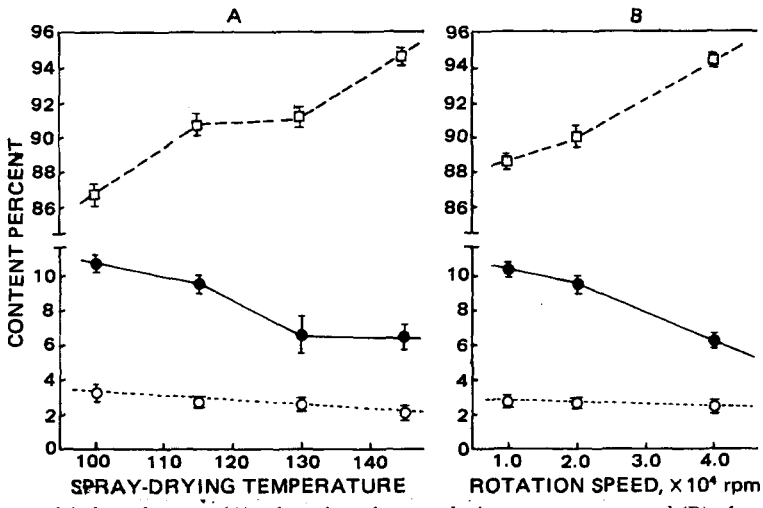

Figure 3—*Composition of the spray-dried products as (A) a function of spray-drying temperature and (B) of rotation speed of the atomizer. Key: (□) theophylline; (●) ethylenediamine; and (○) water.*

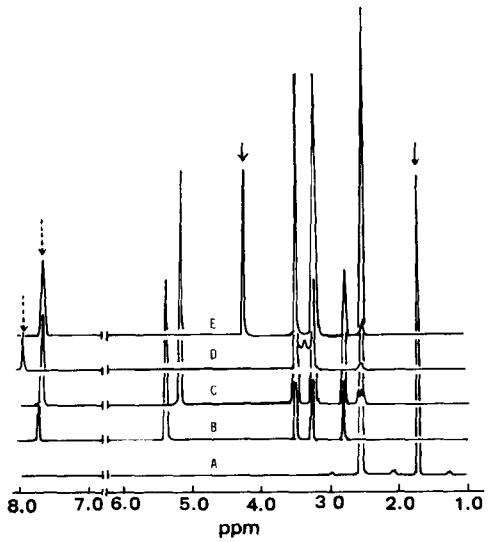

Figure 4—*NMR spectra of (A) ethylenediamine, (B) aminophylline, (C) α-aminophylline, (D) theophylline, and (E) the spray-dried products prepared at 115°, 20,000 rpm with the formulation containing ethylenediamine (20 ml) and theophylline (53.5 g). Key: (→) amino group protons of ethylenediamine; (- - -→) proton at position 8 of theophylline.*

The solubility of the spray-dried products with ethylenediamine was found to be three to five times higher than that of original theophylline, but lower than that of aminophylline (JP). However, no improvement in the solubility of the spray-dried theophylline without ethylenediamine was found. The solubilities of the products with ethylenediamine decreased with increase of both the drying temperature and the rotation speed of the atomizer. This finding could be interpreted in terms of the contents of ethylenediamine in the products, which decreased with an increase in the drying temperature and the rotation speed of the atomizer.

Physicochemical Properties of the Spray-Dried Products—The contents of theophylline in the products increased with increasing temperature of the drying chamber, whereas ethylenediamine contained in the products decreased with the temperature, as shown in Fig. 3. The ethylenediamine content in the products dropped sharply by raising the drying temperature higher than the boiling point of ethylenediamine (117°) but >6% ethylenediamine still remained. This finding suggested that ethylenediamine contained in the products did not exist as a free form adsorbed on the surface of the products but as a chemically bonded form, which resulted in preventing evaporation of ethylenediamine. This speculation was proven by NMR spectra of the spray-dried products in Fig. 4, which almost coincided with those of aminophylline and α-aminophylline. The signal of amino group protons of ethylenediamine in the product shifted to lower field (chemical shift, δ = 4.3 ppm) compared with that of ethylenediamine (δ = 1.7 ppm), which might be due to intermolecular hydrogen bondings. The hydrogen bondings might be attained by the interaction between the hydrogens of NH_3^+ of ethylenediamine formed by a proton migration from =NH of theophylline, and C=O at position 6 and $=N^-$ of theophylline (4, 7). The signal of the proton at position 8 of aminophylline and the spray-dried products shifted to a higher field compared with that of theophylline, as shown in Fig. 4, which support the migration of a proton from =NH of theophylline to NH_2 of ethylenediamine. Water content of the products decreased gradually with increased temperature.

Theophylline contents in the products increased with increased rotation speed of the atomizer, while the contents of ethylenediamine and water decreased with rotation speed (Fig. 3). An increase in the rotation speed of the atomizer reduced the diameters of resultant spray droplets by which evaporation speed was accelerated (Table I); therefore, this action was equivalent to raising drying temperature.

The X-ray diffraction patterns of the products prepared at various drying temperatures are exhibited in Fig. 1B. In the pattern of the spray-dried products, the characteristic peaks of theophylline appeared at 7.2 and 12.5°, of aminophylline at 11.8 and 25.2°, and of α-aminophylline at 11.2, 13.5, 16.7, 18.1, and 28.8°. These were confirmed by the references in Fig. 1A. The described X-ray diffraction analysis suggested that the spray-dried products were a mixture of these three compounds. The X-ray diffraction pattern varied with the drying temperature. The

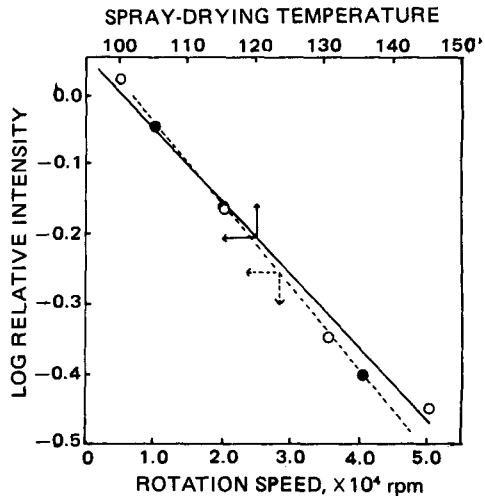

Figure 5—*Relative intensities of X-ray diffraction peak of α-aminophylline to theophylline as a function of spray-drying temperature (○) and of rotation speed of the atomizer (●).*

intensities of characteristic diffraction peaks of aminophylline at 25.2° and of α-aminophylline at 11.2, 16.7, and 18.1° decreased with the increasing drying temperature, whereas those of theophylline at 7.2, 12.5, and 29.3° increased strongly (Figs. 1A and B).

This relation can be described quantitatively in Fig. 5. The relative intensities (*RI*) of α-aminophylline to theophylline defined by Eq. 3 are plotted against drying temperature on a semilogarithmic graph:

$$RI = \frac{I(11.2°) - I(20.0°)}{I(12.5°) - I(20.0°)} \qquad \text{(Eq. 3)}$$

where I(11.2°) and I(12.5°) are the relative intensities of diffraction peaks of α-aminophylline and theophylline to that of sodium chloride at 31.7° used as an internal standard material, respectively, and I(20.0°) is the relative intensity of the base line to that of sodium chloride. The logarithm of the relative intensity correlated improportionately to the drying temperature. A similar correlation was found between the rotation speed of the atomizer and the logarithm of the relative intensity (Fig. 5).

Thermal Decomposition of the Spray-Dried Products—Differential scanning calorimetry and thermogravimetric thermograms of the references of aminophylline, α-aminophylline, and theophylline are exhibited in Fig. 6A by solid and dotted lines, respectively. On the differential scanning calorimetric curve of aminophylline, endothermic peaks at 100–103, 110, 120, 127, and 271° appeared. The endothermic peak at 100° was caused by releasing water, where the weight loss (4%) detected by thermogravimetric analysis corresponded to 1 mole of water. The endothermic peaks which appeared in the 110–127° range might have been caused by liberation of ethylenediamine, since the thermogravimetric curve revealed the weight loss corresponding to 1 mole of ethylenediamine. These findings indicate that ethylenediamine of aminophylline may be liberated by heating *via* three stages. The endothermic peak at 271° corresponds to the melting point of theophylline. The differential scanning calorimetric thermogram of α-aminophylline revealed two endothermic peaks at 116 and 271°. No endothermic peak at 100° caused by releasing water appeared on the thermogram, which was predicted by the Karl Fischer analysis described in the experimental section. The decomposition of α-aminophylline was completed up to 125°, at which point the weight loss reached 12%, equivalent to ~1 mole of ethylenediamine.

The differential scanning calorimetric thermograms of the spray-dried products are displayed as a function of drying temperature and of rotation speed of atomizer in Figs. 6B and C, respectively. On the differential scanning calorimetric curve of the product prepared at the relatively low drying temperature (*e.g.*, 100°), endothermic peaks appeared at 100, 116, and 271°. Liberation of ethylenediamine from the product was assumed to occur at 116°, because the endothermic peaks at 100 and 271° correspond to the releasing point of water and the melting point of theophylline, respectively. When the drying temperature was increased, the endothermic peak at 116° became weak, while another peak appeared at 127°, as seen on the thermogram of the products prepared at 115°. This finding indicates that the bond strength of ethylenediamine with theophylline in the products was affected by the drying temperature employed for spray drying. The latter peak became intense, whereas the former

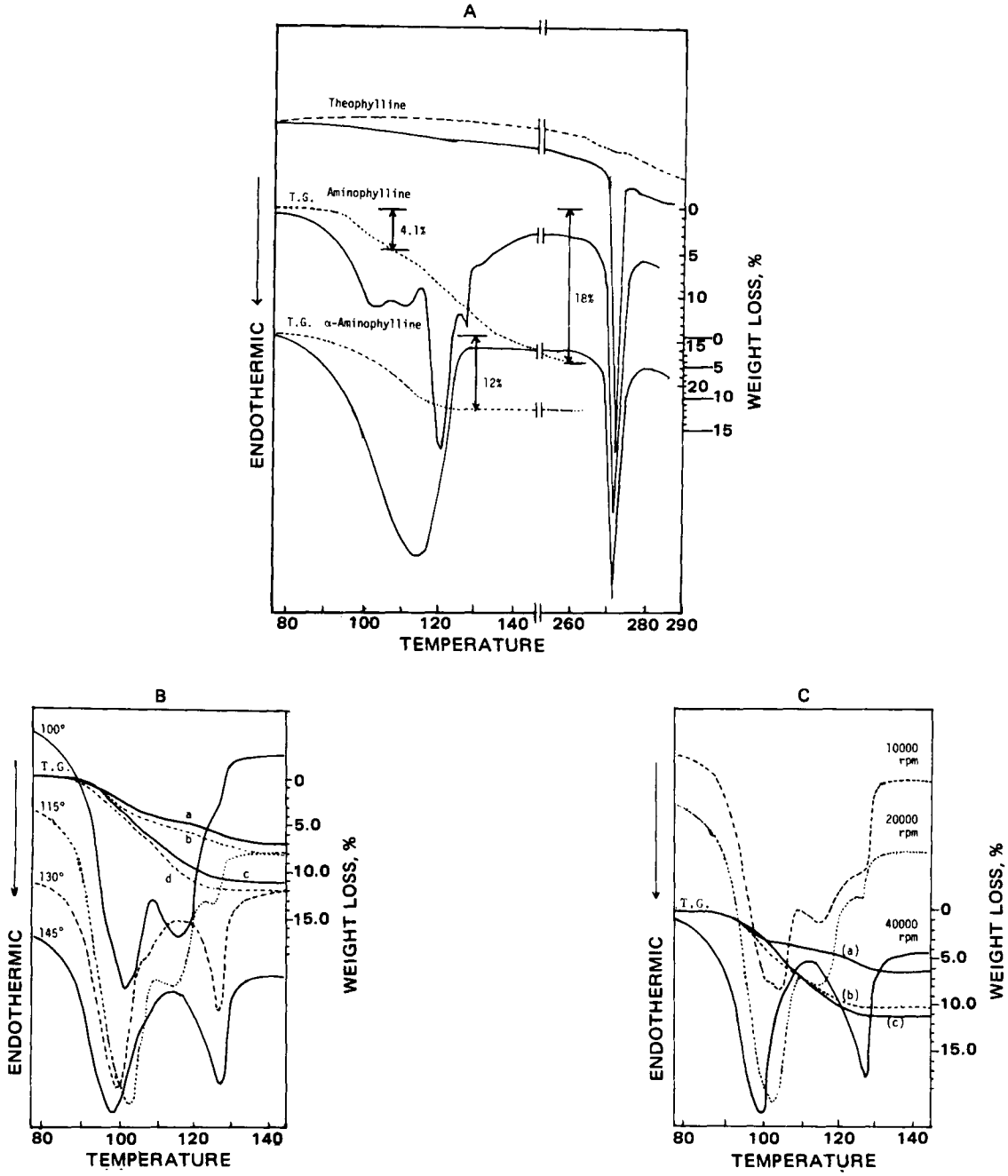

Figure 6—*Differential scanning calorimetric and thermogravimetric thermograms of (A) references; (B) the spray-dried products prepared at various spray-drying temperatures; and (C) rotation speed of the atomizer. Key: thermogravimetric curves in (B): (a) 145°; (b) 130°; (c) 115°; (d) 100°; thermogravimetric curves in (C): (a) 40,000 rpm; (b) 20,000 rpm; (c) 10,000 rpm.*

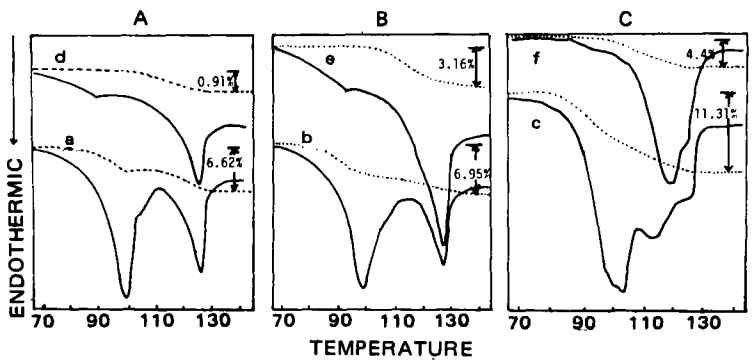

Figure 7—*Changes in differential scanning calorimetric and thermogravimetric thermograms of the spray-dried products by heat treatment. Key: spray-drying condition, a, b, c; (drying temperature, rotation speed of atomizer) and heat-treatment condition, d, e, f; (temperature, time) (A): a (115°, 40,000 rpm); (B): b (145°, 20,000 rpm); (C): c (115°, 10,000 rpm); d (120°, 30 min); e (120°, 30 min); f (110°, 30 min).*

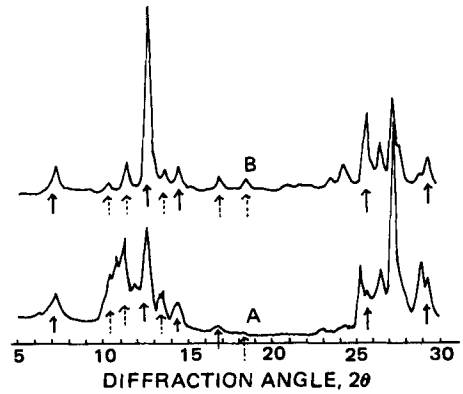

Figure 8—*Changes in X-ray diffraction patterns of the spray-dried products caused by heat-treatment. Key: (A) spray-dried products prepared at 115°, 10,000 rpm; (B) products treated at 110°, 30 min; (→) theophylline; (- - -→) α-aminophylline.*

peak disappeared when the drying temperature was >130°. The weight loss indicated by thermogravimetric curves in Fig. 6B corresponded approximately to the contents of water and ethylenediamine contained in the products as indicated in Fig. 3. The weight loss detected by thermogravimetric analysis decreased with an increase in the drying temperature as shown in Fig. 6B, as predicted from the findings in Fig. 3.

The changes in differential scanning calorimetry and thermogravimetric thermograms, with the rotation speed of the atomizer, are displayed in Fig. 6C. The thermal behaviors of the product prepared with high (low) rotational speed of the atomizer resembled those of the products prepared at high (low) drying temperature. As expected, the weight loss which appeared on the thermogravimetric curve decreased with increasing rotation speed of the atomizer.

Differential scanning calorimetric and thermogravimetric thermograms of the products treated with heating were compared with those of the products prior to the treatment in Fig. 7. After treatment by heating, the endothermic peak at 100° for water releasing disappeared from the thermogram. No weight loss on the thermogravimetric curve at 100° also indicated that the products treated by heating contained no crystalline water. However, an endothermic peak at 127° of the products prepared by spray drying at high temperature or with high rotation speed of the atomizer still remained even after heat treatment at 120°. The products prepared at low drying temperature or at low atomizing speed revealed an endothermic peak at 120° on the thermograph after heat treatment at 110°. The weight loss detected at 127 or 120° by thermogravimetric analysis suggested that some ethylenediamine still remained in the products even after heat treatment.

The X-ray diffraction pattern of the products treated with heating revealed characteristic peaks of theophylline and α-aminophylline at 7.2, 12.5, 14.2, 25.7, 29.3° and 10.2, 11.2, 13.5, 16.7, 18.1°, respectively. The peaks for theophylline strengthened, but no diffraction peaks for aminophylline appeared on the pattern in Fig. 8. These findings proved that the endothermic peak at 116 or 127°, that appeared on the thermogram of the spray-dried products, was caused by the liberation of ethylenediamine contained in a theophylline–ethylenediamine complex.

REFERENCES

(1) P. Speiser, H. P. Merkle, and L. Schibler, *Ger. Offen.*, **2**, 233, 428 (1973).

(2) C. Voellmy, P. Speiser, and M. Soliva, *J. Pharm. Sci.*, **66**, 631 (1977).

(3) Y. A. K. Abdul-Rahmn and E. J. Crosby, *Chem. Eng. Sci.*, **28**, 1273 (1973).

(4) J. Nishijo and F. Takenaka, *Yakugaku Zasshi*, **99**, 824 (1979).

(5) K. Kawakita and K. H. Ludde, *Powder Technol.*, **4**, 61, (1970/71).

(6) H. Takenaka, Y. Kawashima, and S. Y. Lin, *J. Pharm. Sci.*, **69**, 1388 (1980).

(7) T. Okano, K. Aita, and K. Ikeda, *Chem. Pharm. Bull.*, **15**, 1621 (1967).

ACKNOWLEDGMENTS

The authors thank Prof. A. Otsuka, Meijyo University, Nagoya, Japan, for use of the X-ray diffractometer and the differential scanning calorimeter.

Bioavailability of Regular and Controlled-Release Chlorpheniramine Products

J. A. KOTZAN *, J. J. VALLNER *x, J. T. STEWART *, W. J. BROWN *, C. T. VISWANATHAN ‡, T. E. NEEDHAM §, S. V. DIGHE ‡, and R. MALINOWSKI ‡

Received May 8, 1979, from the **Biological Availability Group Studies Laboratory, School of Pharmacy, University of Georgia, Athens, GA 30602*, the ‡*Food and Drug Administration, Rockville, MD*, and the §*Baxter Travenol Laboratories, Morton Grove, Ill.* Accepted for publication November 3, 1981.

Abstract □ The bioavailability of chlorpheniramine regular-release *versus* controlled-release products was compared using 15 human subjects. The dosage forms evaluated were an 8-mg barrier coated-bead capsule, an 8-mg repeat action tablet, two 4-mg tablets, and 4- and 8-mg syrups. Single doses of each product were administered orally in a 5-way crossover study, plasma samples were collected at specific time intervals, and chlorpheniramine levels assayed by HPLC. Pharmacokinetic analysis was based on a two-compartment open model. The average plasma elimination half-life of chlorpheniramine was calculated to be ~18.3 hr. The controlled-release products gave a higher C_{max} than the 4-mg syrup, but <two 4-mg tablets. The controlled-release products also extended the time necessary to attain peak drug levels compared to the 4- and 8-mg syrups. The area under the curve (*AUC*) data for the controlled-release products was not equivalent to equal amounts of the regular-release products. The study indicated that while the controlled-release chlorpheniramine products were successful in prolonging the time course of absorption, this was at the expense of incomplete bioavailability of the drug.

Keyphrases □ Chlorpheniramine—bioavailability of regular and controlled-release products □ Bioavailability—regular and controlled-release chlorpheniramine products □ Controlled-release products—bioavailability of chlorpheniramine

Chlorpheniramine maleate is commonly used in the treatment of various allergic conditions. The different dosage forms of chlorpheniramine maleate marketed include regular- (or immediate) release and controlled- (or sustained) release products.

Little comparative information is currently available

0022-3549/82/0800-0919$01.00/0

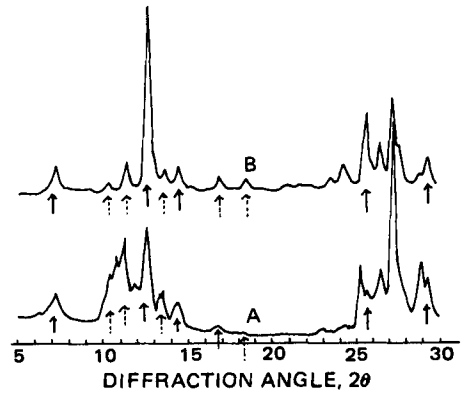

Figure 8—*Changes in X-ray diffraction patterns of the spray-dried products caused by heat-treatment. Key: (A) spray-dried products prepared at 115°, 10,000 rpm; (B) products treated at 110°, 30 min; (→) theophylline; (- - -→) α-aminophylline.*

peak disappeared when the drying temperature was >130°. The weight loss indicated by thermogravimetric curves in Fig. 6B corresponded approximately to the contents of water and ethylenediamine contained in the products as indicated in Fig. 3. The weight loss detected by thermogravimetric analysis decreased with an increase in the drying temperature as shown in Fig. 6B, as predicted from the findings in Fig. 3.

The changes in differential scanning calorimetry and thermogravimetric thermograms, with the rotation speed of the atomizer, are displayed in Fig. 6C. The thermal behaviors of the product prepared with high (low) rotational speed of the atomizer resembled those of the products prepared at high (low) drying temperature. As expected, the weight loss which appeared on the thermogravimetric curve decreased with increasing rotation speed of the atomizer.

Differential scanning calorimetric and thermogravimetric thermograms of the products treated with heating were compared with those of the products prior to the treatment in Fig. 7. After treatment by heating, the endothermic peak at 100° for water releasing disappeared from the thermogram. No weight loss on the thermogravimetric curve at 100° also indicated that the products treated by heating contained no crystalline water. However, an endothermic peak at 127° of the products prepared by spray drying at high temperature or with high rotation speed of the atomizer still remained even after heat treatment at 120°. The products prepared at low drying temperature or at low atomizing speed revealed an endothermic peak at 120° on the thermograph after heat treatment at 110°. The weight loss detected at 127 or 120° by thermogravimetric analysis suggested that some ethylenediamine still remained in the products even after heat treatment.

The X-ray diffraction pattern of the products treated with heating revealed characteristic peaks of theophylline and α-aminophylline at 7.2, 12.5, 14.2, 25.7, 29.3° and 10.2, 11.2, 13.5, 16.7, 18.1°, respectively. The peaks for theophylline strengthened, but no diffraction peaks for aminophylline appeared on the pattern in Fig. 8. These findings proved that the endothermic peak at 116 or 127°, that appeared on the thermogram of the spray-dried products, was caused by the liberation of ethylenediamine contained in a theophylline–ethylenediamine complex.

REFERENCES

(1) P. Speiser, H. P. Merkle, and L. Schibler, *Ger. Offen.*, **2**, 233, 428 (1973).

(2) C. Voellmy, P. Speiser, and M. Soliva, *J. Pharm. Sci.*, **66**, 631 (1977).

(3) Y. A. K. Abdul-Rahmn and E. J. Crosby, *Chem. Eng. Sci.*, **28**, 1273 (1973).

(4) J. Nishijo and F. Takenaka, *Yakugaku Zasshi*, **99**, 824 (1979).

(5) K. Kawakita and K. H. Ludde, *Powder Technol.*, **4**, 61, (1970/71).

(6) H. Takenaka, Y. Kawashima, and S. Y. Lin, *J. Pharm. Sci.*, **69**, 1388 (1980).

(7) T. Okano, K. Aita, and K. Ikeda, *Chem. Pharm. Bull.*, **15**, 1621 (1967).

ACKNOWLEDGMENTS

The authors thank Prof. A. Otsuka, Meijyo University, Nagoya, Japan, for use of the X-ray diffractometer and the differential scanning calorimeter.

Bioavailability of Regular and Controlled-Release Chlorpheniramine Products

J. A. KOTZAN *, J. J. VALLNER *x, J. T. STEWART *, W. J. BROWN *, C. T. VISWANATHAN ‡, T. E. NEEDHAM §, S. V. DIGHE ‡, and R. MALINOWSKI ‡

Received May 8, 1979, from the **Biological Availability Group Studies Laboratory, School of Pharmacy, University of Georgia, Athens, GA 30602*, the ‡*Food and Drug Administration, Rockville, MD*, and the §*Baxter Travenol Laboratories, Morton Grove, Ill.* Accepted for publication November 3, 1981.

Abstract □ The bioavailability of chlorpheniramine regular-release *versus* controlled-release products was compared using 15 human subjects. The dosage forms evaluated were an 8-mg barrier coated-bead capsule, an 8-mg repeat action tablet, two 4-mg tablets, and 4- and 8-mg syrups. Single doses of each product were administered orally in a 5-way crossover study, plasma samples were collected at specific time intervals, and chlorpheniramine levels assayed by HPLC. Pharmacokinetic analysis was based on a two-compartment open model. The average plasma elimination half-life of chlorpheniramine was calculated to be ~18.3 hr. The controlled-release products gave a higher C_{max} than the 4-mg syrup, but <two 4-mg tablets. The controlled-release products also extended the time necessary to attain peak drug levels compared to the 4- and 8-mg syrups. The area under the curve (*AUC*) data for the controlled-release products was not equivalent to equal amounts of the regular-release products. The study indicated that while the controlled-release chlorpheniramine products were successful in prolonging the time course of absorption, this was at the expense of incomplete bioavailability of the drug.

Keyphrases □ Chlorpheniramine—bioavailability of regular and controlled-release products □ Bioavailability—regular and controlled-release chlorpheniramine products □ Controlled-release products—bioavailability of chlorpheniramine

Chlorpheniramine maleate is commonly used in the treatment of various allergic conditions. The different dosage forms of chlorpheniramine maleate marketed include regular- (or immediate) release and controlled- (or sustained) release products.

Little comparative information is currently available

0022-3549/82/0800-0919$01.00/0

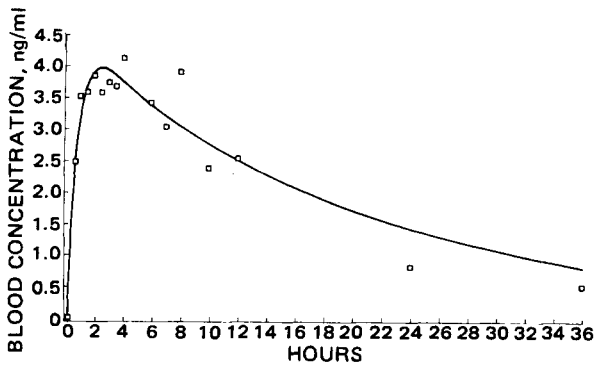

Figure 1—*A comparison of computer predicted (—)* versus *observed (□) chlorpheniramine plasma concentrations* versus *time following administration of the 4-mg syrup.*

concerning the bioavailability of regular-release *versus* controlled-release products or on comparisons among the various controlled-release products themselves. It is generally assumed that the controlled-release products prepared by different methods are bioequivalent. Chlorpheniramine maleate is commercially available as a coated slow-release bead, a repeat-action tablet, a single-dose tablet, and a syrup. *In vivo* comparison of these different dosage forms as well as differently designed products is not currently available.

The present study compares two different controlled-release products of chlorpheniramine maleate to equivalent doses of immediate-release tablets and an equivalent dose and single dose of the drug in solution. In addition, the study provides information regarding the bioequivalency of two sustained-release products formulated by different methods.

EXPERIMENTAL

Subjects—Fifteen healthy male volunteers [18–27 years old (mean 21), 66–80 kg (mean 74), and within ±10% of ideal weight for their height and age (1)] were selected for the study. All subjects were shown by medical examination to be in good physical condition with normal blood and urine chemistry. Informed consent was obtained from all subjects. Each volunteer was instructed to refrain from taking any medication for 1 week prior to and during the study.

The subjects fasted for 8 hr prior to the drug administration. Each subject received 200 ml of water at the time of dosing and at ~1.5 hr postdose. The same low-fat meal was provided for all subjects 3 hr after administration of the dose. A second meal was given to all subjects ~10 hr after initial drug administration. Throughout the study the subjects were ambulatory and proceeded with their normal daily routine. The dose was administered and blood samples (5 ml) were collected immediately before dosing and at 0.3, 0.7, 1, 1.5, 2, 2.5, 3, 3.5, 4, 6, 7, 8, 10, 12, 24, 36, 48, 72, 96, and 144 hr. Samples were drawn from a forearm vein into heparinized vacuum tubes using indwelling needles from 0 to 4 hr and by venipuncture thereafter. The plasma was separated and frozen until assayed.

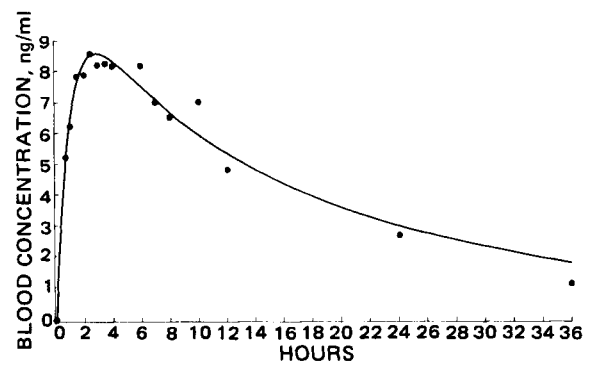

Figure 2—*A comparison of computer predicted (—)* versus *observed (●) chlorpheniramine plasma concentrations* versus *time following administration of the 8-mg syrup.*

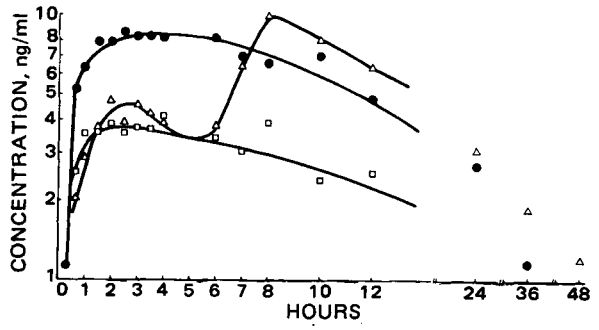

Figure 3—*A comparison of mean plasma concentration–time profiles for the 4- and 8-mg syrups of chlorpheniramine to the 4-mg tablet, administered at 0 and 6 hr. Key: 4-mg syrup (□), 8-mg syrup (●), 4-mg tablet (△).*

Study Design—The drugs as listed in the table below were administered using a five-way crossover design with all subjects receiving each dose.

	Strength	Dose
Drug 1[1]	4 mg	4 mg (0, 6 hr)
Drug 2[2]	8 mg	8 mg
Drug 3[3]	2 mg/5 ml	4 mg
Drug 4[4]	8 mg	8 mg
Drug 5[3]	2 mg/5 ml	8 mg

The subjects were formed into five groups of three subjects each, such that the total body weights of the five groups were essentially the same. The following scheme was used with 2 weeks between each study period:

	Study Period				
	1	2	3	4	5
Group A (Subjects 1–3)	Drug 1	Drug 2	Drug 3	Drug 4	Drug 5
Group B (Subjects 4–6)	Drug 2	Drug 5	Drug 4	Drug 3	Drug 1
Group C (Subjects 7–9)	Drug 3	Drug 1	Drug 5	Drug 2	Drug 4
Group D (Subjects 10–12)	Drug 4	Drug 3	Drug 1	Drug 5	Drug 2
Group E (Subjects 13–15)	Drug 5	Drug 4	Drug 2	Drug 1	Drug 3

Analysis—The HPLC analyses were performed on a liquid chromatograph[5]. The column contained a packing material consisting of an octadecylsilane material bonded to a microparticulate silica gel[6] (<10 μm) for reversed-phase chromatography. The mobile phase consisted of 1:4 acetonitrile–0.075 *M* monobasic ammonium phosphate whose pH was adjusted to 2.6 with concentrated phosphoric acid. The flow rate was set at 1.0 ml/min, the peaks were monitored at 254 nm, and the recorder sensitivity was set at 0.005 aufs.

Stock solutions of chlorpheniramine base (1.5 μg/ml) and brompheniramine base (2.5 μg/ml) were prepared by dissolving equivalent amounts of chlorpheniramine maleate and brompheniramine maleate in distilled water.

Plasma chlorpheniramine levels were determined by a modification of the HPLC procedure reported previously (2). To 1.5 ml of plasma in a 15-ml centrifuge tube were added 75 μl of brompheniramine (internal standard) and 1 ml of 5% aqueous potassium hydroxide. Ether (3 ml) was then added followed by shaking (15 min) and centrifugation (3000 rpm, 15 min). The aqueous layer was then frozen with the aid of a dry ice–acetone bath and the ether decanted into a clean 15-ml centrifuge tube. To this was added 0.1 ml of 0.5% phosphoric acid, the mixture shaken for 10 min, centrifuged, and refrozen. The ether layer was discarded, and the remaining aqueous portion was placed under a nitrogen stream for 5 min

[1] Chlortrimeton Tablets, Lot #7TW30P56540, Schering Corp., Kenilworth, NJ 07033.

[2] Chlortrimeton Repetabs, Lot #6CC15 and #56411, Schering Corp., Kenilworth, NJ 07033.

[3] Chlortrimeton Syrup, Lot #7ATN501, Schering Corp., Kenilworth, NJ 07033.

[4] Teldrin Spansules, Lot #27S72, Smith, Kline and French Laboratories, Philadelphia, PA 19101.

[5] Waters Associates liquid chromatograph equipped with an M-6000 pump, a U6K injector, and a model 440 UV absorbance detector, Milford, Mass.

[6] μ-Bondapak C_{18}, Waters Associates, Milford, Mass.

Table I—Average Plasma Concentrations[a] at each Sampling Time of Chlorpheniramine (ng/ml) from Five Different Administrations

Time, hr	Syrup, 8 mg	Drug 2, 8 mg	Drug 4, 8 mg	Tablet, 4 mg	Syrup, 4 mg
0.7	5.2 ± 4.3	1.6 ± 2.4	0.6 ± 1.1	2.0 ± 2.2	2.5 ± 2.1
1	6.3 ± 3.8	2.1 ± 2.0	0.7 ± 0.7	2.9 ± 2.5	3.5 ± 2.0
1.5	7.8 ± 3.4	2.6 ± 1.5	1.2 ± 1.3	3.8 ± 2.9	3.6 ± 1.6
2	7.9 ± 2.5	3.2 ± 2.0	1.7 ± 1.6	4.8 ± 2.4	3.9 ± 1.8
2.5	8.6 ± 3.1	2.7 ± 1.0	2.4 ± 2.4	3.9 ± 3.2	3.6 ± 1.1
3	8.2 ± 1.8	3.3 ± 1.1	2.8 ± 2.0	4.6 ± 2.4	3.8 ± 1.3
3.5	8.3 ± 2.2	3.2 ± 1.7	4.2 ± 1.9	4.3 ± 2.6	3.7 ± 2.5
4	8.2 ± 3.2	3.9 ± 1.7	4.6 ± 2.4	3.9 ± 2.4	4.1 ± 1.8
6	8.2 ± 3.3	6.1 ± 2.8	6.1 ± 2.6	3.8 ± 2.3	3.4 ± 1.0
7	7.0 ± 1.9	6.5 ± 1.8	5.2 ± 2.0	6.4 ± 4.1	3.1 ± 0.9
8	6.5 ± 1.4	7.3 ± 4.1	6.4 ± 3.3	10.0 ± 4.9	3.9 ± 1.8
10	7.0 ± 3.5	6.1 ± 4.1	5.1 ± 2.7	8.1 ± 3.2	2.4 ± 1.0
12	4.8 ± 2.9	4.9 ± 2.0	4.0 ± 2.5	6.4 ± 2.4	2.5 ± 1.0
24	2.7 ± 1.7	2.1 ± 0.9	1.8 ± 1.0	3.1 ± 2.0	0.8 ± 0.6
36	1.2 ± 1.0	1.0 ± 0.9	1.4 ± 1.0	1.9 ± 1.2	0.5 ± 0.5

[a] Mean of 15 values ± *SD*.

Table II—Mean Pharmacokinetic Parameters[a] Across Individual Subjects for Chlorpheniramine Maleate Dosage Forms

Parameter	Syrup, 8 mg	Drug 2, 8 mg	Drug 4, 8 mg	Tablet[c], 4 mg	Syrup, 4 mg
$t_{1/2}$, hr	17.3 ± 4.4	17.6 ± 4.4	21.2 ± 7.4	20.8 ± 4.4	14.6 ± 3.4
FD/V_c, ng/ml[b]	6.3 ± 2.4	4.9 ± 1.7	3.8 ± 1.7	5.4 ± 2.0	3.1 ± 1.0
Time of peak concentration, hr	3.8 ± 2.7	7.6 ± 2.3	6.1 ± 1.3	6.1 ± 2.3	3.4 ± 2.5
Peak concentration, ng/ml	11.3 ± 2.9	9.7 ± 3.9	7.5 ± 3.2	11.0 ± 4.1	5.9 ± 2.3
$AUC_{0\to\infty}$[d]	156.3 ± 60.7	119.2 ± 33.7	113.0 ± 46.2	169.6 ± 85.6	65.4 ± 21.8

[a] Mean of 15 values ± *SD*. [b] Fraction of the dose absorbed expressed as concentration in its distribution volume in the body calculated from $FD/V_c\beta = AUC_{0\to\infty}$. [c] Administered twice as single 4-mg doses at 0- and 6- hr intervals. [d] Obtained by trapezoidal rule technique. The last measured plasma concentration was divided by the least squares slope value for the β phase, indicating log–trapezoidal extrapolation to zero concentration (*i.e.*, $AUC_{0\to\infty}$).

to rid of residual ether. A 60- to 80-μl portion of the aqueous phase was then injected into the liquid chromatograph.

Calibration curves were constructed by adding 3.5-, 5.0-, 10-, and 20-μl quantities of the chlorpheniramine stock solution into individual 15-ml centrifuge tubes containing 1.5 ml of blank human plasma to give the equivalent of 3.5, 5.0, 10.0, and 20.0 ng of chlorpheniramine/ml. To each tube was then added 75 μl of brompheniramine stock solution (internal standard) and each tube assayed according to the procedure described above.

Ratios of chlorpheniramine peak heights to those of the internal standard (*D/IS*) were calculated for each chromatogram. Regression analysis of these data at the various concentrations of chlorpheniramine gave typical results: slope, 0.0403; intercept, 0.0212; and correlation coefficient, 0.9967 (n = 16). The standard error of estimate of $Y(D/IS)$ on X (chlorpheniramine concentration) was ±0.0122. The minimum detectable quantity of chlorpheniramine that can be measured using the procedure is 1 ng/ml (S/N = 2). The slope and intercept data from regression analysis for chlorpheniramine were then used to solve for drug concentration in the human plasma samples: D/IS = (slope X concentration) + intercept.

Interassay reproducibility of chlorpheniramine determined by the assay of spiked plasma samples containing 3.5, 5.0, 10.0, and 20.0 ng/ml gave percent relative standard deviations (*RSD*) of 9.7, 7.9, 5.4, and 5.0%, respectively (n = 10). Interassay reproducibility of the drug at the 2.5-ng/ml level was 15% (n = 10). Linearity of the calibration curve <2.5 ng/ml was assumed using the linear regression calculation for the standard curve data. Interassay accuracy data at the 3.5-, 5.0-, 10.0-, and 20.0-ng/ml levels gave the following typical results (n = 3): 6.6, 4.4, 0.7, and 0.15%, respectively.

Pharmacokinetic Analysis—Individual curves following administration of syrup dosage forms, that is, immediately available drug not having to undergo disintegration or dissolution, were graphed and the data analyzed *via* NLIN[7] or SAS[8]. Both one- and two-compartment open models with first-order absorption and elimination were examined. Although both models are indistinguishable if one only looks at the residual sum of squares of the model fit, the two-compartment model gives better results (Figs. 1 and 2).

All pharmacokinetic parameters reported here are the results of using the above computer program and the two-compartment model. For a particular dosage form, plasma half-lives for each subject were calculated from least-square fits of the terminal slope of the log plasma chlorpheniramine concentration *versus* time curve. The individual subject half-life data was then used to calculate the mean plasma half-life for the particular dosage form. The *AUC* data were calculated by computer using the trapezoidal rule technique. The last measured plasma concentration

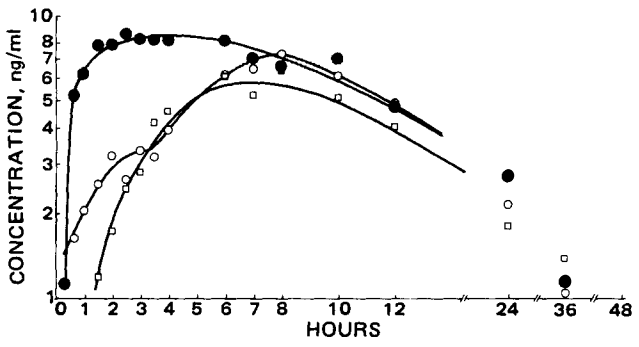

Figure 4—*A comparison of mean plasma concentration–time profiles for the 8-mg chlorpheniramine dosage forms studied (i.e., the immediately available syrup, the repeat action formulation, and the coated slow-release bead). Key: 8-mg syrup (●), Drug 2 (○), Drug 4 (□).*

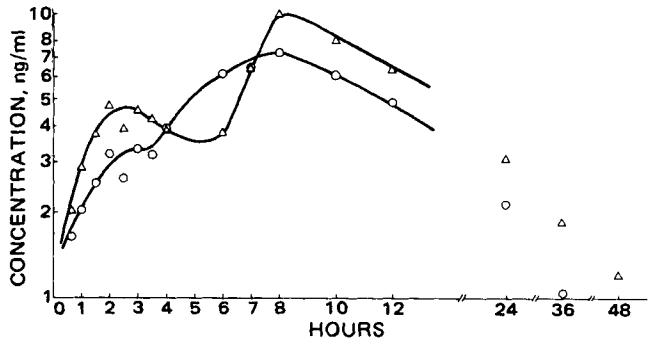

Figure 5—*A comparison of mean plasma concentration–time profiles for the repeat action chlorpheniramine formulation to two single 4-mg tablets, administered at 0 and 6 hr. Key: 4-mg tablet (△), Drug 2 (○).*

[7] A modified Gauss-Newton method for fitting nonlinear regression function by least squares. See Ref. 3 for details.

[8] Statistical Analysis System, SAS Institute, Inc., 1979 Users Guide.

Table III—Duncan's Multiple Range Tests of Pharmacokinetic Parameters

Dosage Form	Mean	Grouping[a]			F	$PR > F$
Peak Concentration (C_{max})						
8-mg Syrup	11.3 ng	A			8.70	0.0001
2 × 4-mg Tablets	11.0 ng	A				
Drug 2	9.7 ng	A				
Drug 4	7.5 ng		B			
4-mg Syrup	5.9 ng		B			
Time to Peak (t_{pk})						
Drug 2	7.6 hr	A			9.22	0.0001
2 × 4-mg Tablets	6.1 hr	A				
Drug 4	6.1 hr	A				
8-mg Syrup	3.9 hr		B			
4-mg Syrup	3.4 hr		B			
$t_{1/2}$						
Drug 4	21.2 hr	A			4.48	0.0033
2 × 4-mg Tablets	20.8 hr	A				
Drug 2	17.6 hr	A	B			
8-mg Syrup	17.3 hr	A	B			
4-mg Syrup	14.6 hr		B			
$AUC_{0\to\infty}$						
2 × 4-mg Tablets	169.6	A			11.89	0.0001
8-mg Syrup	156.3	A				
Drug 2	119.2		B			
Drug 4	113.0		B			
4-mg Syrup	65.4			C		
FD/V_c						
8-mg Syrup	6.34	A			11.42	0.0001
2 × 4-mg Tablets	5.42	A	B			
Drug 2	4.92		B			
Drug 4	3.83			C		
4-mg Syrup	3.14			C		

[a] Members of the same group are statistically similar at the $\alpha = 0.05$ level of significance.

was divided by the least-squares slope value for the β-phase, indicating log-trapezoidal extrapolation to zero concentration (*i.e.*, $AUC_{0\to\infty}$). Other bioavailability parameters were calculated following the usual methods (4).

RESULTS AND DISCUSSION

In examining controlled-release dosage forms, consideration of drug plasma levels is integral to ensuring that such dosage forms adhere to the release characteristics claimed. The barrier-coated bead product (Drug 4) is designed such that, "a therapeutic dose of antihistamine is released promptly and the remaining medication, released gradually, sustains the effect for a prolonged period" (5). The chlorpheniramine repeat action tablet (Drug 2) contains 8 mg of drug such that the "dosage is divided equally between an outer layer for rapid absorption and an inner core protected by special timed barrier for release 3–6 hr after ingestion" (6). In this study, three additional doses were administered: the 4- and 8-mg syrups to provide a comparison of plasma levels (if these quantities of drug were immediately released from an oral dose) and 4-mg tablet given at 0 and 6 hr to provide comparative repeat action plasma concentrations of two single doses.

The equation for an open two-compartment model with first-order absorption is (7):

$$C = Le^{-\alpha t} + Me^{-\beta t} + Ne^{-k_a t} \qquad \text{(Eq. 1)}$$

Using this equation, parameters fitting the model were derived for 4- and 8-mg syrups:

4-mg Syrup: $C = 2.8e^{-0.61t} + 4.4e^{-0.047t} - 7.2e^{-1.03t}$ residual sums of square = 1.87;

8-mg Syrup: $C = 4.0e^{-0.13t} + 7.3e^{-0.040t} - 11.3e^{-0.98t}$ residual sums of square = 2.66.

Only the data from the 4- and 8-mg syrups have been applied to the model since the other dosage forms or administrations were of a controlled form and, thus, not theoretically able to be fit to such a model. It should be noted that the one-compartment model was also examined. The criteria for choosing the two-compartment model to describe the data include lower sum of square, more valid plasma elimination half-life [considering recent literature information of 20–30 hr (8–11)], and curvature of the blood level–time curve data after C_{max}.

Figures 1 and 2 show plots of mean plasma chlorpheniramine levels *versus* time following oral administration of 4- and 8-mg syrups, respectively. The smooth curve in each figure is a computer prediction using the mathematical models derived for the respective syrups. Both figures show that a reasonable prediction of the data results when using the two-compartment model.

Table I shows the average plasma chlorpheniramine levels and standard deviation for each of the five different doses (dosage forms) as a function of time. Due to drug already in solution, the plasma levels for the two syrup treatments were detectable at 0.7 hr. The remaining dosage forms could only be detected 1 hr after administration. None of the five different doses were analytically detectable at 0.3 hr or >36 hr in plasma.

Figure 3 illustrates a plasma level–time profile for the 4- and 8-mg syrups and the 4-mg tablet (administered at 0 and 6 hr). The similarity of the blood levels of drug for the two 4-mg doses can be seen up to the 7-hr sample when the second 4-mg tablet, administered at 6 hr, began to show an increased chlorpheniramine concentration.

Plasma level profiles for the 8-mg syrup, Drug 4, and Drug 2 are shown in Fig. 4. It can be seen that Drug 4 and Drug 2 produce plasma levels which are essentially equivalent, while the peak level of the 8-mg syrup is definitely higher than the other two dosage forms. The similarity in plasma level profiles of Drug 2 and the two single administered 4-mg tablets is illustrated in Fig. 5.

The mean pharmacokinetic parameters for the various dosage forms of chlorpheniramine are shown in Table II. The average plasma elimination half-life ranges from 14.6 hr for the 4-mg syrup to 21.2 hr for Drug 4. An ANOVA of the $t_{1/2}$ of the five dosage forms of drug in each of the 15 subjects produced a calculated F value of 4.48 which, when compared to the $F_{0.99}$ (4, 56) of 3.65, indicates a significant difference in the half-life. The plasma elimination $t_{1/2}$ of the 4-mg syrup was significantly lower than Drug 4 and two 4-mg dosage forms as measured by the Duncan's Multiple Range Test (12). It is believed that the difference is attributable to the intersubject variability and the relatively low terminal phase levels of the 4-mg syrup which approached the limits of the assay sensitivity. The ~18.3-hr average half-life for all dosage forms studied is longer than that found previously (2), but is comparable to the reported 20–30 hr data (8–11).

The mean fraction of dose absorbed expressed as concentration in the distribution volume of the body (FD/V_c) ranged from 3.1 ng/ml after the 4-mg syrup to 6.3 ng/ml following the 8-mg syrup (Table II). As can be seen in Table III, three different categories of degrees of absorption are present with respect to the 8-mg syrup as the reference standard. The two 4-mg tablets are grouped with the 8-mg syrup, while the repeat action tablets and the two 4-mg tablets are members of both the reference standard and the second group. The coated slow-release beads and the 4-mg syrup dosage forms formed the last groups demonstrating significantly less absorption than the reference 8-mg syrup dosage form.

The peak concentration (C_{max}) of chlorpheniramine varied widely among the five different doses. However, the level of peak concentration increased as expected in the order of the 4-mg syrup, Drug 4, Drug 2, tablets, and 8-mg syrup. The calculated F value of 8.70, when compared to the $F_{0.99}$ (4, 56) of 3.65, showed that there is a significant difference between the highest plasma concentrations reached for each dose. In Table III, a Duncan's Multiple Range Test of these data indicates that the peak concentration produced by the 8-mg syrup is different from those peak concentrations found for Drug 4 and the 4-mg syrup in all 15 subjects. This shows that the controlled-release Drug 4 dosage form was apparently not releasing a large quantity of its dose immediately.

An ANOVA of the time to peak concentration produced a calculated F of 9.22, which is significantly different when compared to $F_{.99}$ (4, 56) of 3.65. Tables II and III show that the average t_{pk} of the 4- and 8-mg syrups are statistically similar. The t_{pk} of Drug 4 (6.1 hr) is not significantly different from Drug 2 (7.6 hr), even though the release mechanisms are not the same. Dissolution studies of these two dosage forms, currently underway in these laboratories, should provide additional drug release information.

An examination of the plasma half-life multiple range data reveals that Drug 2 and the 8-mg syrup displayed half-lives which could be considered in either the high or low groups (Table III). However, Drug 4 clearly had a statistically longer plasma half-life when compared to that of the 4- and 8-mg syrups. Of the four pharmacokinetic parameters evaluated, the plasma half-life measures displayed the lowest F value among the five dosage forms. It follows that the plasma half-life was the single parameter which displayed overlap between the dosage form groups. Thus, the sustained-release dosage forms have the least impact on the plasma half-lives of the chlorpheniramine blood levels when compared to their impact on peak time, peak height, and AUC.

There is a strong relationship between the type of chlorpheniramine dosage form and the AUC data from 0 hr to infinity. The AUC parameter

Table IV—*AUC* and *AUC* Ratios for Chlorpheniramine Dosage Forms

Subject	$AUC_{0-\infty}$ hr, μg hr/ml					*AUC* Ratios			
	A 4-mg Syrup	B 8-mg Syrup	C 2 × 4-mg Tablet	D Drug 4	E Drug 2	A/B	C/B	D/B	E/B
1	73.6	49.8	36.5	80.1	84.7	1.48	0.73	1.61	1.70
2	43.8	178.7	102.8	92.4	89.9	0.25	0.58	0.52	0.50
3	52.2	147.9	78.8	92.4	143.9	0.35	0.53	0.62	0.97
4	90.5	187.2	194.8	115.4	134.0	0.48	1.04	0.62	0.72
5	85.2	138.7	147.8	108.4	82.2	0.61	1.07	0.78	0.59
6	70.8	158.6	152.2	100.6	106.1	0.45	0.96	0.63	0.67
7	57.9	267.2	312.1	91.2	179.4	0.22	1.17	0.34	0.67
8	71.5	256.4	350.6	142.9	148.8	0.28	1.37	0.56	0.58
9	58.7	143.3	214.7	127.2	111.7	0.41	1.50	0.89	0.78
10	64.7	135.2	223.9	199.5	98.4	0.54	1.66	1.48	0.73
11	61.7	119.5	129.4	61.9	103.6	0.52	1.08	0.52	0.87
12	23.8	237.6	72.5	36.5	61.4	0.10	0.31	0.15	0.26
13	117.9	130.1	200.6	190.4	153.9	0.91	1.54	1.46	1.18
14	50.3	97.8	146.9	84.9	129.9	0.51	1.50	0.87	1.33
15	59.5	96.9	179.6	171.5	159.3	0.61	1.85	1.77	1.64
Mean	65.5	156.3	169.6	113.0	119.2	0.51[a]	1.13	0.85	0.88
CV, %	33	39	50	41	28	65	40	58	47
Percent of *AUC* ratios within limit of 0.75–1.25[b]			—	—	—	47%	33%	20%	27%

[a] 75/75 test for A/B would be 0.38–0.63 based on the 0.75–1.25 range. [b] See Ref. 13.

was the only pharmacokinetic measure which was separated into three distinct subgroups without any overlap. As expected, the 4-mg syrup delivered the least amount of drug over the duration of the blood sampling. This is because the amount of actual drug present is one-half the amount in all other administrations, and with the small dose administered, the blood levels of drug at early and late sampling times could not be determined by the analytical method. The *AUC* computed for a 4-mg tablet (by using the data from 0 to 6 hr and extrapolating to infinity) compared well with recent published data (11). The sustained dosage forms of Drugs 4 and 2 were not able to deliver the quantity of drug delivered by two of the 4-mg tablets or the single dose of 8-mg syrup. The sustained dosage forms comprised the intermediate Group B (Table III).

Table IV presents individual *AUC* data along with ratios of the individual *AUC* data per 8-mg syrup *AUC*. The mean *AUC* ratios for each dose and dosage form were approximately that of the predicted values. On an individual basis, however, the results show considerable deviation from the mean. Using these data, only a few individuals would pass the 75/75 test (13) because of the large intra- and intersubject variation.

Are the controlled-release dosage forms of chlorpheniramine successful? The most successful controlled-release dosage form should increase to the same peak concentration and at the same rate, when compared to the immediate release (noncontrolled) drug product. The dosage form should also increase the time the drug remains at the peak concentration and, in addition, have about twice the area under the blood level–time curve (assuming that the controlled-release dosage form contains twice the amount of drug contained in a normal, single oral dose). With these criteria, examination of Figs. 3–5 and Tables I–III would indicate that neither the coated slow-release bead product nor the tablet within a tablet product meet all of these conditions. Both of the controlled-release dosage forms give a higher peak concentration than the single 4-mg syrup, but both provided less drug concentration at the C_{max} than two 4-mg tablets. As expected, the time the peak levels occurred was extended over the immediately available syrups and was about the same time as the two 4-mg tablets. The *AUC* of the controlled-release formulations was not equivalent to the same amounts of noncontrolled release products, nor were they equal to two times the *AUC* of the 4-mg syrup (realizing the difficulties involved in obtaining an exact *AUC* for this small dose). Neither the coated bead nor tablet within a tablet was completely successful; however, more valid conclusions can be made following data reduction of a recently completed multiple-dose study of these same dosage forms.

REFERENCES

(1) K. Dien and C. Lentners, Eds., "Scientific Tables," 7th ed., Geigy Pharmaceuticals, Ardsley, N.Y., 1970, p. 712.

(2) N. K. Athanikar, G. W. Peng, R. L. Nation, S. M. Huang, and W. L. Chiou, *J. Chromatogr.*, **162**, 367 (1979).

(3) H. O. Hartley, *Technometrics*, **3**(2), 269 (1961).

(4) M. Gibaldi and D. Perrier, "Pharmacokinetics," Marcel Dekker, New York, N.Y., 1975, pp. 129–173.

(5) "Prescribing Information for Teldrin Spansule Capsules," Smith, Kline and French, Philadelphia, Pa., 1972, p. 1.

(6) "Product Information for Chlor-Trimeton Repetabs Tablets," Schering, Kenilworth, N.J., 1975, p. 1.

(7) M. Gibaldi and D. Perrier, "Pharmacokinetics," Marcel Dekker, New York, N.Y., 1975, p. 83.

(8) W. L. Chiou, N. K. Athanikar, and S. Huang, *N. Engl. J. Med.*, **300**, 501 (1979).

(9) J. J. Vallner, T. E. Needham, W. Chan, and C. T. Viswanathan, *Curr. Ther. Res.*, **26**, 449 (1979).

(10) E. A. Peets, M. Jackson, and S. Symchowicz, *J. Pharmacol. Exp. Ther.*, **180**, 464 (1972).

(11) A. Yacobi, R. G. Stoll, G. C. Chao, J. E. Carter, D. M. Baske, B. L. Kamath, A. H. Amann, and C. M. Lai, *J. Pharm. Sci.*, **69**, 1077 (1980).

(12) D. B. Duncan and M. Walser, *Biometrics*, **22**, 26 (1966).

(13) E. Purich in "Drug Absorption and Disposition: Statistical Considerations," K. S. Albert, Ed., American Pharmaceutical Association, Washington, D.C., (1980), p. 123.

ACKNOWLEDGMENTS

Supported by USPHS-FDA—Contract No. 223-77-3012.

Quantification of the Effect of Excipients on Bioavailability by Means of Response Surfaces I: Amoxicillin in Fat Matrix

MATÍAS LLABRÉS, JOSÉ L. VILA ˣ, and RAMÓN MARTÍNEZ-PACHECO

Received April 11, 1980, from the *Departamento de Farmacia Galénica, Facultad de Farmacia, Universidad de Santiago de Compostela, Spain.* Accepted for publication November 17, 1981.

Abstract □ A study was carried out to determine the effect of a fat excipient on the bioavailability of amoxicillin tablets. Three formulations with a fat excipient content of 10, 20, and 30%, respectively, were administered to 15 healthy volunteers according to a Latin-square design. The excretion curves were characterized with the help of two parameters, namely, the quantity of drug excreted between 0–2 and 0–12 hr postadministration, respectively. The effect of the fat excipient content was quantified with the use of polynomials whose corresponding orders were given by the ANOVA. In the case of both parameters, a quadratic response to the fat excipient content was found. At the same time, a dissolution study was carried out using a previously established method. Here, the parameters used to characterize the dissolution curves were the quantities of dissolved drug in 30 and 180 min, respectively. Again, a quadratic response to the fat excipient content was observed in the case of both parameters.

Keyphrases □ Amoxicillin—quantification of the effect of excipients on bioavailability by means of response surfaces, fat matrix □ Bioavailability—quantification of the effect of excipients by means of response surfaces, amoxicillin in fat matrix □ Excipients—quantification of the effect on bioavailability by means of response surfaces, amoxicillin in fat matrix

The quantification of the effect that certain excipients and technological procedures have on drug bioavailability is an interesting aspect of the field of pharmaceutical technology. Most of the investigations carried out with human subjects have used commercial formulations, that is, formulations whose composition and elaboration process are unknown (1–3). Therefore, only the bioequivalence or bioinequivalence of these formulations can be established. *In vitro* studies of drug release and drug dissolution, although more numerous, have failed to reflect the biopharmaceutical or clinical consequences of drug–technological factor interaction (4, 5).

BACKGROUND

Bioequivalence studies are usually based on the general linear model of ANOVA. This model, when applied to a three-way crossover design (formulation, subject, and period), takes the following form:

$$y_{ijk} = \mu + F_k + S_i + W_j + e_{ijk} \qquad \text{(Eq. 1)}$$

where y_{ijk} denotes the observation on the ith subject with the kth formulation on the jth period; μ represents the general mean; F_k, S_i, and W_j represent the effects produced by subject, formulation, and period, respectively; and e_{ijk} is the error associated with observation y_{ijk} and is assumed to have normal distribution with the mean zero and variance constant for all observations, σ^2. If this study were not confined only to establishing the bioequivalence or bioinequivalence between two formulations, but extended to include the quantification of the effects of excipients and technological factors on bioavailability, then the term F_k would have to be subdivided to meet these new demands. For example, if the study were to englobe factors A and B, and if the effect of each of these factors and of their mutual interaction were desired, then the term F_k would have to be replaced by the term:

$$A_m + B_n + AB_{mn} \qquad \text{(Eq. 2)}$$

where A_m represents the effect of factor A at level m, B_n the effect of factor B at level n, and AB_{mn} the effect of their interaction. Thus, the ANOVA could indicate the way in which these factors modify bioavailability and help establish not only the optimum formulation but also the *in vivo–in vitro* correlations.

Table I—Percent Composition and Mean Weight [a] of Formulations A, B, and C

Formulation	Amoxicillin Trihydrate	Fat, %	Talc, %	Mean Weight
A	85%	10	5	514
B	75%	20	5	582
C	65%	30	5	672

[a] Mean weight in kilograms.

The object of this study, which comprises three separate studies, is to quantify the effects which two excipients (a synthetic fat and a silica colloid) have on the bioavailability of amoxicillin tablets. Quantification was obtained by means of response surfaces expressed as low-order polynomials, a technique used to quantify the effects of excipients on some physicochemical properties of different dosage forms (6, 7). At the same time, a study was carried out to determine the effect of the above excipients on the dissolution rate of amoxicillin in formulations tested *in vivo*. Finally, the correlation between both series of data was also studied.

The present report studies the effect of a synthetic fat excipient at three equally spaced levels.

EXPERIMENTAL

Assayed Formulations and Analytical Method—Three formulations of amoxicillin trihydrate[1] tablets, containing 375 mg of anhydrous amoxicillin, were manufactured and studied. The percent composition of the three formulations, A, B, and C, is shown in Table I. The three formulations differed only in their synthetic fat[2] (mono-, di-, tripalmitate estearate of glycerin) content. In each case the hardness was 4 kg on the hardness tester scale[3].

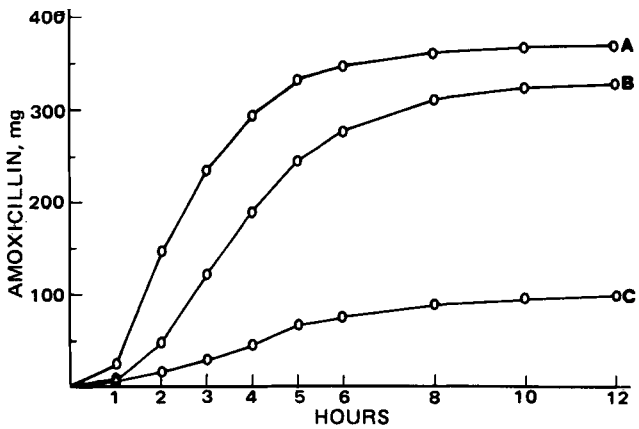

Figure 1—*Cumulative curves for the urinary excretion of unchanged amoxicillin.*

[1] Antibióticos S. A., lot A30H-106. Potency 859 μg/mg.
[2] Precirol, Gattefossé.
[3] Monsanto hardness tester.

0022-3549/82/0800-0924$01.00/0

Table II—Mean Values and Variances [a] for the *In Vivo* Parameters Employed

Formulation	E_2	E_{12}
A	143.4 (4129.2)	369.8 (4248.7)
B	45.8 (1433.4)	329.8 (14349.2)
C	17.4 (136.9)	102.4 (2416.3)

[a] Variances in parentheses.

The *in vivo* and *in vitro* samples were assayed by means of a spectrophotometric method which was specific for intact drug (8).

Clinical Protocol—Urine analysis of the unchanged drug was carried out in 15 healthy volunteers of both sexes, whose ages ranged from 20 to 32. The subjects, tested for renal insufficiency, gave a negative response. A written consent was obtained from each subject. Subjects were divided at random into three equal groups. A Latin-square 3 × 3 design with five replicates was used, and the washing period between successive administrations was 5 days. Immediately before a standard breakfast, the fasted subjects were given two tablets equivalent to 750 mg of anhydrous amoxicillin. Urine samples were collected 1, 2, 3, 4, 5, 6, 8, 10, and 12 hr postadministration.

Pharmacokinetic Analysis—The effect of fat content on the quantity of drug absorbed and on the absorption rate were the two parameters used to characterize the urinary excretion curves. These parameters can be characterized by E_{12} the total quantity of drug, expressed in milligrams, excreted in the 12 hr following administration; and E_2 the quantity of drug, expressed in milligrams, excreted in the first 2 hr postadministration (during which time the maximum urinary excretion rate of the free drug was observed).

Characterization of the formulations by means of pharmacokinetic parameters was ruled out for two reasons. First, the absorption processes observed in Formulations B and C were too complex; second, to avoid the introduction of estimation error, which would have been confused with the experimental error and would have entailed the use of nonparametric tests and, consequently, the loss of information about the assay in question.

Dissolution Rate Studies—Dissolution rate studies were carried out using the apparatus described previously (9). This apparatus was the flowthrough type without an accumulating reservoir. To calculate the quantity of dissolved drug at different times, the method proposed previously (10) was used. The following conditions were employed: angle agitation, 180; intensity of agitation, 6 oscillations/min; dissolution cell volume, 47.5 ml; flow rate, 1 ml/min. Enzyme-free juices, gastric and enteric, were the dissolution media employed. Three dissolution tests were carried out on each formulation using a tablet in each test, although the results refer to a 750-mg dose. The following parameters were employed to characterize the dissolution curves obtained: D_{180} was the quantity of drug, in milligrams, dissolved in 180 min, and D_{30} was the quantity of drug, in milligrams, dissolved in 30 min.

Statistical Analysis—Prior to the establishment of the ANOVA for the Latin-square design, the model was submitted to an additive test and to a variance homogeneity test in order to confirm its validity. Tukey's test (11) confirmed the additivity of the model. Nevertheless, Cochran's test (12) confirmed the existence of heterogeneous variances among the treatments for the two parameters under study. Therefore, the use of the three-way ANOVA in the Latin square lacked validity on account of power deficiency. To overcome this problem, and because the logarithmic transformation of data failed to stabilize the variances, the generalization of Scheffé's test proposed by Brown and Forsythe (13) was used. Although the latter test is a one-way ANOVA, in the presence of heterogeneous variances, it is a valid solution. According to Brown and Forsythe, the modification of Scheffé's probability is:

$$P_r\{(H - O)^2/(\sum Z_i^2 S_i^2/n_i) < (g - 1) F_{1-\alpha,g-1,f}\} \geq 1 - \alpha \quad \text{(Eq. 3)}$$

where $H = \Sigma Z_i \overline{X}_i$ is an estimation of $O = Z_i \mu_i$, f is defined by:

$$\frac{1}{f} = \sum \frac{C_i^2}{(n_i - 1)} \text{ and } C_i = \frac{(\sum Z_{ik}^2)\, S_i^2/n_i}{\sum_i \left(\sum_k Z_{ik}^2\right) S_i^2/n_i} \quad \text{(Eq. 4)}$$

where $\overline{X}_i$ is the mean of the treatments, S_i^2 is the variance, and g is the number of treatments.

For the *in vitro* parameters chosen, the corresponding one-way ANOVA was employed.

The study of response surfaces was achieved by subdividing the sum of squares for the term treatments of the ANOVA by means of a series of orthogonal polynomials which are defined by the number of factors studied as well as by the number of their levels (14). Therefore, such a study presupposes the use of an adequate experimental design. The subdivision in this study is achieved by means of the following polynomials (Z):

Treatments	Z_1	Z_2
T_1	−1	1
T_2	0	−2
T_3	1	1
Component	Linear	Quadratic

which subdivide the sum of squares for treatments in linear and quadratic responses. The levels of the factors studied must be equally spaced; if not, it would be impossible to carry out the orthogonal comparisons offered.

Once the type of response has been inferred, a polynomial function with the correspondent degree is adjusted to mean values by means of the least-square method.

RESULTS AND DISCUSSION

A quantitative study of bioavailability requires a grasp of two basic concepts. First, the concept of bioavailability includes the quantity of drug absorbed and the rate of absorption (15). Second, bioavailability is a random variable and, therefore, its interval (*i.e.*, a parameter which can measure interindividual variability) has to be estimated. The choice of the E_{12} parameter is clearcut, since it reflects the total quantity of drug absorbed, as the half-life of amoxicillin in ~1 hr. The E_2 parameter is mainly controlled by the rate of absorption, while depending to a certain degree on the total quantity of drug absorbed. There are two reasons for studying the variability of these parameters in the light of their respective variances: from a statistical point of view, variance gives a good idea of the interval; and variance homogeneity is a prequisite for the study of the ANOVA. Therefore, there is a combination of statistical and biopharmaceutical criteria.

Table III—Results of ANOVA for E_{12} [a]

i	H_i	$V(H)$	$g-1$	f	F	A	Results
1	−267.41	444.34	2	21	3.47	55.53	Significant linear response
2	−187.49	4270.80	2	21	3.47	172.16	Significant quadratic response
3	−39.96	1239.86	2	21	3.47	92.76	No significant contrast A *versus* B
4	−267.41	444.34	2	21	3.47	55.53	Significant contrast A *versus* C
5	−227.45	1117.71	2	21	3.47	88.07	Significant contrast B *versus* C

[a] $\alpha = 0.05$. The minimum value necessary for rejecting the null hypothesis is $A = \sqrt{(g-1)FV(H_i)}$ (Ref. 13).

Table IV—Results of ANOVA for E_2 [a]

i	H_i	$V(H)$	$g-1$	f	F	A	Results
1	−125.96	284.41	2	21	3.47	44.03	Significant linear response
2	69.26	666.67	2	21	3.47	68.02	Significant quadratic response
3	−97.61	370.85	2	21	3.47	50.73	Significant contrast A *versus* B
4	−125.96	284.41	2	21	3.47	44.03	Significant contrast A *versus* C
5	−28.35	104.69	2	21	3.47	26.95	Significant contrast B *versus* C

[a] $\alpha = 0.05$ (see Table III).

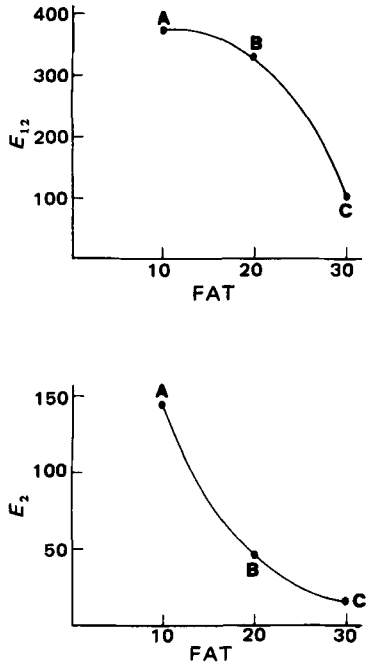

Figure 2—*Response curves for* E_{12} *and* E_2 *in function of fat content.*

Figure 1 shows the mean urine excretion accumulative curves of the three formulations studied. The mean values and the variances of the respective parameters are shown in Table II. The respective ANOVA results appear in Tables III and IV. The contrasts between pairs of formulations and the orthogonal contrasts used to study the influence of the excipient must be distinguished. From the contrasts between formulations, it can be inferred that A and B are bioequivalent using the mean value of the E_{12} parameter, the total quantity absorbed, but not so using the E_2 parameter, the rate of absorption. On the other hand, and in the case of both parameters, the variability of Formulation B is statistically greater than that of Formulation A. This means that Formulation B not only is absorbed more slowly but also its variability is much greater, two reasons for considering them to be bioinequivalent. Formulation C shows much lower values for both parameters.

With respect to the influence of the synthetic fat content on bioavailability, the ANOVA results imply a quadratic response for both parameters. Therefore, the following second-degree polynomials indicate a quantitative relationship between bioavailability and synthetic fat content in those formulations whose fat content lies within the limits of this study:

$$E_{12} = 222.320 + 24.138\,x - 0.938\,x^2 \qquad \text{(Eq. 5)}$$

$$E_2 = 310.280 - 20.150\,x + 0.346\,x^2 \qquad \text{(Eq. 6)}$$

in which x is the fat content expressed in percent. These polynomials are shown in Fig. 2. It can be seen that when the fat content is increased from 10 to 20%, there are no observable changes of importance, at first, in the mean quantity of drug absorbed; nevertheless, there is a marked decrease

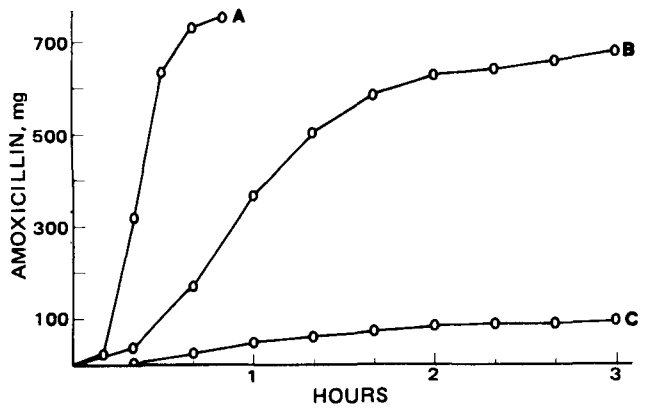

Figure 3—*Cumulative dissolution curves.*

Table V—Mean values of Three Dissolution Tests for the Chosen *In vitro* Parameters

Formulation	D_{30}	D_{180}
A	577.8	750.6
B	71.3	681.0
C	16.5	91.9

Table VI—Results of ANOVA for D_{180}

Source of Variation	Sum of Squares	Degrees of Freedom	F	α
Treatments	780,319.56	2	4013.14	<0.01
Linear	645,818.92	1	6642.83	<0.01
Quadratic	134,500.64	1	1383.46	<0.01
Residual	583.32	6		
Total	780,902.88	8		

Table VII—Results of ANOVA for D_{30}

Source of Variation	Sum of Squares	Degrees of Freedom	F	α
Treatments	632,495.56	2	176.25	<0.01
Linear	548,208.96	1	352.50	<0.01
Quadratic	84,286.60	1	46.97	<0.01
Residual	10,765.79	6		
Total	643,261.35	8		

in the rate of absorption. It can also be seen that when the fat content is increased from 20 to 30%, there are noticeable decreases in both E_2 and E_{12}. However, it can be seen that the variation coefficients obtained with the data listed in Table II increase when the fat content increases. In the case of the E_{12} parameter, these are 18, 36, and 48% for Formulations A, B, and C, respectively.

The use of these second-degree polynomials obtained from the mean values might lead to certain criticism. The ANOVA only indicates the existence of a statistically significant deviation in the linear relationship between the parameters and the synthetic fat content. This does not mean that the second-degree polynomial is the optimum function or that there is some physical–chemical basis for justifying its use. The fact is that it is the simplest linear function application to the statistical model used. With respect to the utility of these functions for determining the type of effect produced by the excipient, this depends on whether the function used can be said to be equivalent to the hypothetical function

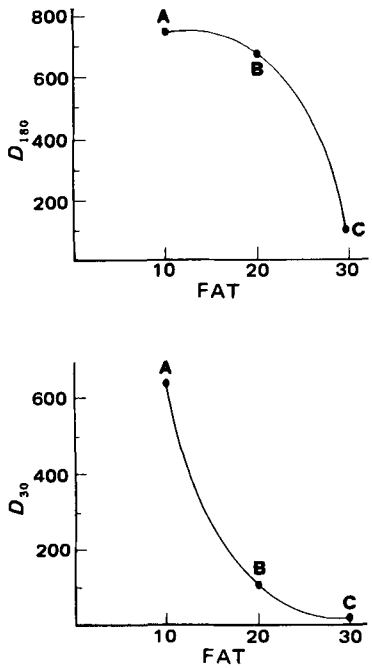

Figure 4—*Response curves for* D_{180} *and* D_{30} *in function of fat content.*

derived from those physical-chemical properties responsible for the modification involved and for the interaction between the dosage form and the physiological surroundings where drug release and drug absorption takes place. The best way to avoid any possible discrepancy between real behavior and that inferred from the ANOVA is to carefully choose the interval and the number of levels necessary for the study. The cost of the *in vivo* experiment necessarily limits the number of levels studied.

The dissolution accumulative curves obtained are shown in Fig. 3, while the mean values of the chosen parameters, D_{30} and D_{180}, are listed in Table V. A quadratic response for both parameters, with respect to the fat content, can be inferred from the one-way ANOVAs shown in Tables VI and VII. The polynomials, after least-squares adjustment, were:

$$D_{180} = 300.090 + 70.924\,x - 2.593\,x^2 \qquad \text{(Eq. 7)}$$

$$D_{30} = 1549.010 - 112.343\,x + 2.053\,x^2 \qquad \text{(Eq. 8)}$$

They are shown in Fig. 4. It is worth noting that this excipient exercises the same influence *in vitro* as it does *in vivo*.

Bioequivalence studies carried out on formulations whose composition is defined by an appropriate experimental design afford the opportunity of studying the effect of the different excipients on bioavailability; that is, the effect of these excipients on the quantity of drug absorbed and on the rate of absorption. The effect the excipients have on interindividual variability must also be considered. As has been pointed out previously (16, 17), it is not sufficient just to accept the null hypothesis for the parameters employed as an indication of bioequivalence between two formulations; the variability must also be similar.

REFERENCES

(1) M. C. Meyer, R. E. Dann, P. L. Whyatt, and G. W. A. Slywka, *J. Pharmacokinet. Biopharm.*, **2**, 287 (1974).

(2) A. V. Tembo, M. R. Hallmark, E. Sakmar, H. G. Bachmann, D. J. Weiller, and J. G. Wagner, *ibid.*, **5**, 257 (1977).

(3) K. S. Albert, S. W. Brown Jr., K. A. DeSante, A. R. DiSanto, R. D. Stewart, and T. T. Chen, *J. Pharm. Sci.*, **68**, 1312 (1979).

(4) E. Marlowe and R. F. Shangraw, *ibid.*, **56**, 498 (1967).

(5) T. A. Iranloye and E. L. Parrott, *ibid.*, **67**, 535 (1978).

(6) J. B. Schwartz, J. R. Flamholz, and R. H. Press, *ibid.*, **62**, 1165 (1973).

(7) J. M. Newton and F. N. Razzo, *J. Pharm. Pharmacol.*, **29**, 294 (1977).

(8) J. W. Smith, G. E. de Grey, and V. Patel, *Analyst*, **92**, 247 (1967).

(9) M. Llabrés, Tesis Doctoral, Santiago de Compostela (1975).

(10) M. Llabrés, R. Martínez-Pacheco, and J. L. Vila, *Il Farmaco Ed. Prat.*, **33**, 111 (1978).

(11) J. W. Tukey, *Biometrics*, **11**, 111 (1955).

(12) W. G. Cochran, *ibid.*, **3**, 22 (1947).

(13) M. B. Brown and A. B. Forsythe, *ibid.*, **30**, 719 (1974).

(14) W. G. Cochran and G. M. Cox. "Experimental Design," 2nd ed. Wiley, New York, N.Y., 1957 pp. 61–70.

(15) J. G. Wagner. "Fundamentals of Clinical Pharmacokinetics," Drug Intelligence Publications, Hamilton, Ill., 1975.

(16) W. J. Westlake, *J. Pharm. Sci.*, **62**, 1579 (1973).

(17) W. H. Barr, in "Dosage Form Design and Bioavailability," J. Swarbrick, Ed., Lea & Febiger, Philadelphia, Pa., 1973, pp. 31–75.

Quantification of the Effect of Excipients on Bioavailability by Means of Response Surfaces II: Amoxicillin in Fat–Silica Matrix

MATÍAS LLABRÉS, JOSÉ L. VILA ˣ, and RAMÓN MARTÍNEZ-PACHECO

Received April 11, 1980, from the *Departamento de Farmacia Galénica, Facultad de Farmacia, Universidad de Santiago de Compostela, Spain.* Accepted for publication November 17, 1981.

Abstract □ This report studies the bioavailability of amoxicillin in different fat–silica matrixes. A urinary excretion study was carried out on four formulations containing fat and silica excipients. The formulations were administered to 24 healthy volunteers according to a Latin-square design. The following percent proportions of fat–silica were used: 15:3.75, 15:7.50, 30:3.75, and 30:7.50. The urinary excretion curves were characterized using the quantity of unchanged drug excreted between 0–2 and 0–12 hr postadministration, respectively as parameters. The ANOVA results showed that both excipients had an additive effect on the quantity of drug excreted between 0 and 2 hr, whereas the effect on the quantity of drug excreted between 0 and 12 hr was also one of interaction between both excipients. Quantification of the ANOVA results in terms of excipient content was conducted by means of the adequate linear functions. At the same time, a dissolution study was carried out using the quantity of drug dissolved in 30 and 180 min as parameters. The behavior was similar to that encountered for the *in vivo* parameters.

Keyphrases □ Amoxicillin—effect of excipients on bioavailability by means of response surfaces, fat–silica matrix □ Bioavailability—effect of excipients by means of response surfaces, amoxicillin in fat–silica matrix □ Excipients—effect on bioavailability by means of response surfaces, amoxicillin in fat–silica matrix

The aim of the present study is to determine the effect which the combination of two excipients, a synthetic fat[1] and a silica colloid[2], has on the bioavailability of amoxicillin tablets.

EXPERIMENTAL

Assayed Formulations—Four formulations of amoxicillin trihydrate[3] tablets were manufacturerd and studied. Formulations, D, E, F, and G, contained 375 mg of anhydrous amoxicillin, and their percent composition is shown in Table I. Hardness, in each case, was 5 kg on the hardness tester scale[4].

Clinical Protocol—The urinary excretion of unchanged drug was studied in 24 healthy volunteers whose ages ranged from 20 to 30 years and who showed no evidence of renal insufficiency. The subjects were randomly divided into four equal groups. A Latin-square 4 × 4 design with 6 replicates was used, and the washing period was 5 days. Immediately before a standard breakfast, fasted subjects were given two tablets equivalent to 750 mg of anhydrous amoxicillin. Urine samples were collected at 1, 2, 3, 4, 5, 6, 8, 10, and 12 hr postadministration.

Pharmacokinetic Analysis—Characterization of the urinary excretion curves was achieved by means of the parameters mentioned in the previous report (1).

Dissolution Rate Studies—The apparatus and methodology used were both described in the previous report (1).

Statistical Analysis—Heterogeneous variances for the treatments

[1] Precirol, Gattefossè.

[2] Aerosil, Degussa.

[3] Antibióticos S.A. lot A30H-106, potency 859 μg/mg.

[4] Monsanto hardness tester.

0022-3549/82/0800-0927$01.00/0

derived from those physical-chemical properties responsible for the modification involved and for the interaction between the dosage form and the physiological surroundings where drug release and drug absorption takes place. The best way to avoid any possible discrepancy between real behavior and that inferred from the ANOVA is to carefully choose the interval and the number of levels necessary for the study. The cost of the *in vivo* experiment necessarily limits the number of levels studied.

The dissolution accumulative curves obtained are shown in Fig. 3, while the mean values of the chosen parameters, D_{30} and D_{180}, are listed in Table V. A quadratic response for both parameters, with respect to the fat content, can be inferred from the one-way ANOVAs shown in Tables VI and VII. The polynomials, after least-squares adjustment, were:

$$D_{180} = 300.090 + 70.924\,x - 2.593\,x^2 \qquad \text{(Eq. 7)}$$

$$D_{30} = 1549.010 - 112.343\,x + 2.053\,x^2 \qquad \text{(Eq. 8)}$$

They are shown in Fig. 4. It is worth noting that this excipient exercises the same influence *in vitro* as it does *in vivo*.

Bioequivalence studies carried out on formulations whose composition is defined by an appropriate experimental design afford the opportunity of studying the effect of the different excipients on bioavailability; that is, the effect of these excipients on the quantity of drug absorbed and on the rate of absorption. The effect the excipients have on interindividual variability must also be considered. As has been pointed out previously (16, 17), it is not sufficient just to accept the null hypothesis for the parameters employed as an indication of bioequivalence between two formulations; the variability must also be similar.

REFERENCES

(1) M. C. Meyer, R. E. Dann, P. L. Whyatt, and G. W. A. Slywka, *J. Pharmacokinet. Biopharm.*, **2**, 287 (1974).

(2) A. V. Tembo, M. R. Hallmark, E. Sakmar, H. G. Bachmann, D. J. Weiller, and J. G. Wagner, *ibid.*, **5**, 257 (1977).

(3) K. S. Albert, S. W. Brown Jr., K. A. DeSante, A. R. DiSanto, R. D. Stewart, and T. T. Chen, *J. Pharm. Sci.*, **68**, 1312 (1979).

(4) E. Marlowe and R. F. Shangraw, *ibid.*, **56**, 498 (1967).

(5) T. A. Iranloye and E. L. Parrott, *ibid.*, **67**, 535 (1978).

(6) J. B. Schwartz, J. R. Flamholz, and R. H. Press, *ibid.*, **62**, 1165 (1973).

(7) J. M. Newton and F. N. Razzo, *J. Pharm. Pharmacol.*, **29**, 294 (1977).

(8) J. W. Smith, G. E. de Grey, and V. Patel, *Analyst*, **92**, 247 (1967).

(9) M. Llabrés, Tesis Doctoral, Santiago de Compostela (1975).

(10) M. Llabrés, R. Martínez-Pacheco, and J. L. Vila, *Il Farmaco Ed. Prat.*, **33**, 111 (1978).

(11) J. W. Tukey, *Biometrics*, **11**, 111 (1955).

(12) W. G. Cochran, *ibid.*, **3**, 22 (1947).

(13) M. B. Brown and A. B. Forsythe, *ibid.*, **30**, 719 (1974).

(14) W. G. Cochran and G. M. Cox. "Experimental Design," 2nd ed. Wiley, New York, N.Y., 1957 pp. 61–70.

(15) J. G. Wagner. "Fundamentals of Clinical Pharmacokinetics," Drug Intelligence Publications, Hamilton, Ill., 1975.

(16) W. J. Westlake, *J. Pharm. Sci.*, **62**, 1579 (1973).

(17) W. H. Barr, in "Dosage Form Design and Bioavailability," J. Swarbrick, Ed., Lea & Febiger, Philadelphia, Pa., 1973, pp. 31–75.

Quantification of the Effect of Excipients on Bioavailability by Means of Response Surfaces II: Amoxicillin in Fat–Silica Matrix

MATÍAS LLABRÉS, JOSÉ L. VILA ˣ, and RAMÓN MARTÍNEZ-PACHECO

Received April 11, 1980, from the *Departamento de Farmacia Galénica, Facultad de Farmacia, Universidad de Santiago de Compostela, Spain.* Accepted for publication November 17, 1981.

Abstract □ This report studies the bioavailability of amoxicillin in different fat–silica matrixes. A urinary excretion study was carried out on four formulations containing fat and silica excipients. The formulations were administered to 24 healthy volunteers according to a Latin-square design. The following percent proportions of fat–silica were used: 15:3.75, 15:7.50, 30:3.75, and 30:7.50. The urinary excretion curves were characterized using the quantity of unchanged drug excreted between 0–2 and 0–12 hr postadministration, respectively as parameters. The ANOVA results showed that both excipients had an additive effect on the quantity of drug excreted between 0 and 2 hr, whereas the effect on the quantity of drug excreted between 0 and 12 hr was also one of interaction between both excipients. Quantification of the ANOVA results in terms of excipient content was conducted by means of the adequate linear functions. At the same time, a dissolution study was carried out using the quantity of drug dissolved in 30 and 180 min as parameters. The behavior was similar to that encountered for the *in vivo* parameters.

Keyphrases □ Amoxicillin—effect of excipients on bioavailability by means of response surfaces, fat–silica matrix □ Bioavailability—effect of excipients by means of response surfaces, amoxicillin in fat–silica matrix □ Excipients—effect on bioavailability by means of response surfaces, amoxicillin in fat–silica matrix

The aim of the present study is to determine the effect which the combination of two excipients, a synthetic fat[1] and a silica colloid[2], has on the bioavailability of amoxicillin tablets.

EXPERIMENTAL

Assayed Formulations—Four formulations of amoxicillin trihydrate[3] tablets were manufacturerd and studied. Formulations, D, E, F, and G, contained 375 mg of anhydrous amoxicillin, and their percent composition is shown in Table I. Hardness, in each case, was 5 kg on the hardness tester scale[4].

Clinical Protocol—The urinary excretion of unchanged drug was studied in 24 healthy volunteers whose ages ranged from 20 to 30 years and who showed no evidence of renal insufficiency. The subjects were randomly divided into four equal groups. A Latin-square 4 × 4 design with 6 replicates was used, and the washing period was 5 days. Immediately before a standard breakfast, fasted subjects were given two tablets equivalent to 750 mg of anhydrous amoxicillin. Urine samples were collected at 1, 2, 3, 4, 5, 6, 8, 10, and 12 hr postadministration.

Pharmacokinetic Analysis—Characterization of the urinary excretion curves was achieved by means of the parameters mentioned in the previous report (1).

Dissolution Rate Studies—The apparatus and methodology used were both described in the previous report (1).

Statistical Analysis—Heterogeneous variances for the treatments

[1] Precirol, Gattefossè.

[2] Aerosil, Degussa.

[3] Antibióticos S.A. lot A30H-106, potency 859 μg/mg.

[4] Monsanto hardness tester.

0022-3549/82/0800-0927$01.00/0

Table I—Percent Composition of Formulations

Formulation	Amoxicillin Trihydrate, %	Fat, %	Silica, %	Talc, %
D	77.25	15	3.75	5
E	72.50	15	7.50	5
F	62.25	30	3.75	5
G	57.50	30	7.50	5

Table II—Mean Values and Variances [a] for the Excretion Parameters

Formulation	E_2	E_{12}
D	36.2 (763.3)	237.6 (11,322.6)
E	84.2 (4,407.8)	352.9 (16,708.0)
F	16.9 (113.7)	112.8 (3,366.3)
G	52.5 (1,982.4)	353.4 (7,306.9)

[a] Variances in parentheses.

were observed and exposed by means of Barlett's test (2). Once again, logarithmic transformation of data failed to stabilize the variances; therefore, Scheffé's test, modified by Brown and Forsythe (3), was again employed.

The study was carried out on four formulations combining two equally spaced levels of each of the excipients. Therefore, the subdivision of the sum of squares for the term treatments of the ANOVA, to obtain the response surfaces, was achieved by means of the following polynomials (Z):

Treatment	Z_1	Z_2	Z_3
T_1	−1	−1	1
T_2	1	−1	−1
T_3	−1	1	−1
T_4	1	1	1
Component	Fat mean response	Silica mean response	Interaction

These polynomials subdivide the sum of the squares in mean response for each excipient and interaction between the two excipients (4).

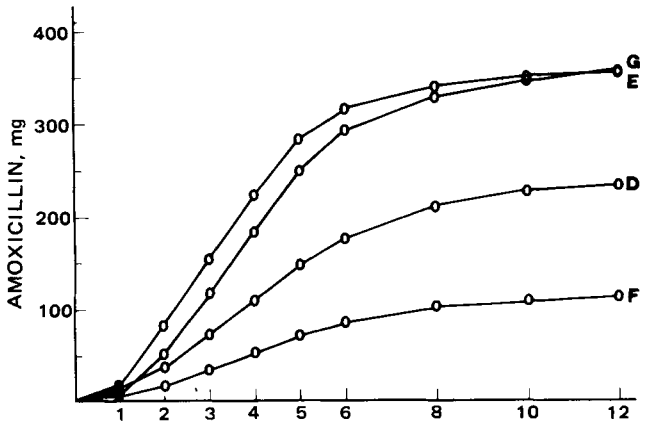

Figure 1—*Cumulative curves for urinary excretion of unchanged amoxicillin.*

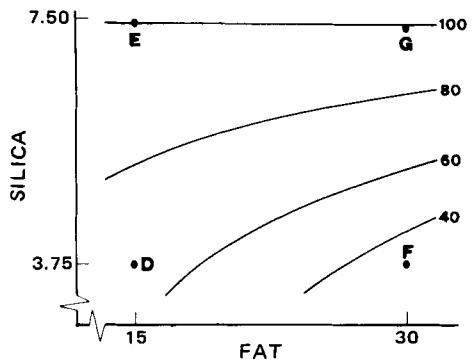

Figure 2—*Contour curves for* E_{12} *as function of fat and silica contents.*

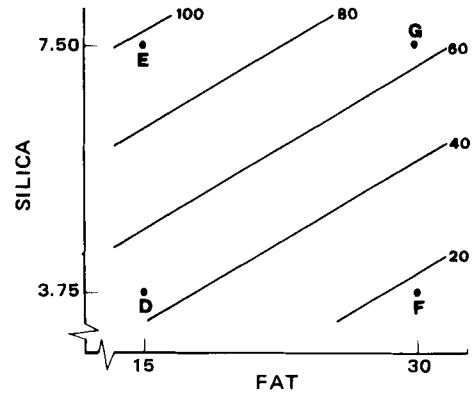

Figure 3—*Contour curves for* E_2 *as function of fat and silica contents.*

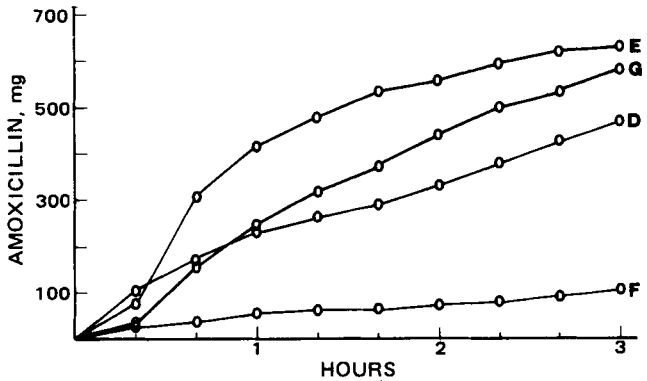

Figure 4—*Cumulative dissolution curves.*

Having inferred the factors that affect absorption, and the existence or nonexistence of interaction, the corresponding polynomial functions were then adjusted to the mean experimental values by means of the least-squares method. The results are shown graphically by means of the contour lines generated by these equations.

RESULTS AND DISCUSSION

The mean urine excretion curves are depicted in Fig. 1, whereas the mean values of the parameters used for their characterization, E_2 and E_{12}, and the respective variances, are shown in Table II. The ANOVA results appear in Tables III and IV. As mentioned previously (1), two parts must be distinguished, namely, the contrasts between pairs of formulations and the orthogonal contrasts used to monitor the effect of the excipients on bioavailability. The latter contrast shows that both excipients have a significant effect on the two parameters. With respect to the E_{12} parameter, significant interaction between both excipients is also observed. According to this, the following functions indicate the quantitative correlation between the bioavailability parameters and the fat (x_1) and (x_2) content, expressed as percent, for those formulations

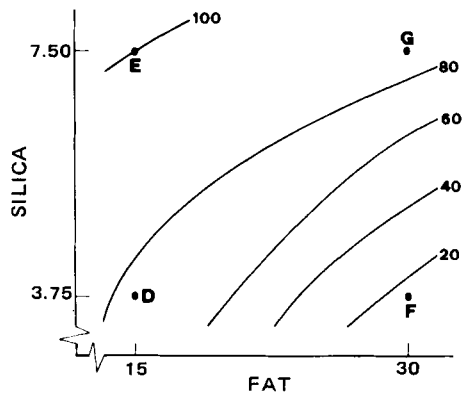

Figure 5—*Contour curves for* D_{180} *as function of fat and silica contents.*

Table III—Results of ANOVA for E_{12} [a]

i	H_i	$V(H)$	$g-1$	f	F	A	Results
1	−124.27	1612.66	3	73	2.72	114.71	Significant fat effect
2	355.85	1612.66	3	73	2.72	114.71	Significant silica effect
3	125.23	1612.66	3	73	2.72	114.71	Significant fat–silica interaction
4	−124.75	612.04	3	73	2.72	74.83	Significant contrast D *versus* F
5	115.31	1167.94	3	73	2.72	103.28	Significant contrast D *versus* E
6	115.79	776.23	3	73	2.72	84.28	Significant contrast D *versus* G
7	240.06	836.43	3	73	2.72	87.48	Significant contrast F *versus* E
8	240.98	444.71	3	73	2.72	63.79	Significant contrast F *versus* G
9	−0.48	1000.62	3	73	2.72	95.69	No significant contrast E *versus* G

[a] $\alpha = 0.05$. The minimum value for rejecting the null hypothesis is $A = \sqrt{(g-1)\,FV\,(H_i)}$ (Ref. 3).

Table IV—Results of ANOVA for E_2 [a]

i	H_i	$V(H)$	$g-1$	f	F	A	Results
1	−50.80	302.80	3	73	2.72	49.71	Significant fat effect
2	83.80	302.80	3	73	2.72	49.71	Significant silica effect
3	−12.46	302.80	3	73	2.72	49.71	No significant fat–silica interaction
4	−19.21	36.54	3	73	2.72	18.28	Significant contrast D *versus* F
5	48.03	215.46	3	73	2.72	44.40	Significant contrast D *versus* E
6	16.36	114.40	3	73	2.72	32.35	No significant contrast D *versus* G
7	67.24	188.40	3	73	2.72	41.52	Significant contrast F *versus* E
8	35.37	87.44	3	73	2.72	28.27	Significant contrast F *versus* G
9	−31.67	266.26	3	73	2.72	43.36	No significant contrast E *versus* G

[a] $\alpha = 0.05$ (see Table III).

Table V—Mean Values for the Chosen Dissolution Parameters

Formulation	D_{30}	D_{180}
D	141.3	470.0
E	204.8	634.0
F	49.3	106.3
G	135.4	580.0

Table VI—Results of ANOVA for D_{180}

Source of Variation	Sum of Squares	Degrees of Freedom	F	α
Treatments	462,925.01	3	35.23	<0.01
Fat	169,218.75	1	38.63	<0.01
Silica	242,013.44	1	55.25	<0.01
Fat and Silica	51,692.81	1	11.80	<0.01
Residual	35,044.37	8		
Total	497,969.37	11		

Table VII—Results of ANOVA for D_{30}

Source of Variation	Sum of Squares	Degrees of Freedom	F	α
Treatments	85,891.83	3	63.26	<0.01
Fat	70,878.76	1	156.61	<0.01
Silica	14,195.50	1	31.37	<0.01
Fat and Silica	817.58	1	1.81	—
Residual	3,620.63	8		
Total	89,512.46	11		

whose composition lie within the limits of the experiment:

$$E_{12} = 372.17 - 16.66\,x_1 - 2.63\,x_2 + 2.22\,x_1x_2 \qquad \text{(Eq. 1)}$$

$$E_2 = 22.90 - 1.70\,x_1 + 11.15\,x_2 \qquad \text{(Eq. 2)}$$

The response surfaces obtained are shown in Figs. 2 and 3. A value of 100% is assigned to Formulation E, to which the other formulations are referred. Observation of Fig. 2 leads to the conclusion that, in order to obtain acceptable physiological availabilities within the limits of the experiment, a silica content close to 7.5% should be used, no matter what the fat content may be; because at this level, the silica practically cancels out the effect of the fat on the E_{12} parameter. For this reason, Formulations E and G present equivalent absorption. Nevertheless, with low silica concentration (3.75%), the fat content produces a marked effect as can be seen by the differences observed between Formulations D and F. The response surface obtained for the E_2 parameter plane surface in this case, due to the nonexistence of interaction between excipients, is shown in Fig. 3. The observed response corresponds to the sum of the effects produced by both excipients: negative with regard to the fat content and positive in the case of silica. For this reason, Formulation E, with low content in fat and high content in silica, gives the highest value for the E_2 parameter and also shows significant differences with regard to the other formulations. It is also seen that those formulations characterized by incomplete absorption show higher variation coefficients, as pointed out previously (5).

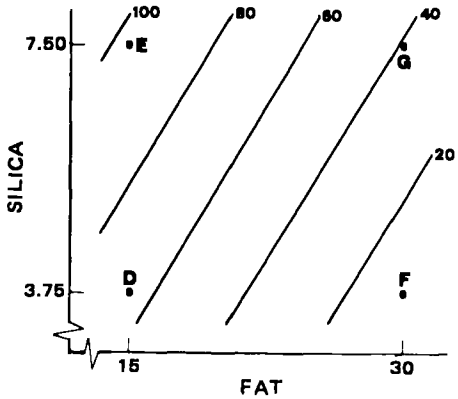

Figure 6—*Contour curves for* D_{30} *as function of fat and silica contents.*

With respect to the dissolution tests, the mean accumulative curves appear in Fig. 4, while the mean values of the chosen parameters are shown in Table V. The respective ANOVAs are shown in Tables VI and VII. It can inferred from Table VII that the two excipients have a significant effect on both parameters, whereas in the case of the D_{180} parameter, there is also significant interaction between both excipients. According to this, the following functions indicate the quantitative correlation between the dissolution parameters and the fat (x_1) and silica (x_2) content, expressed as a percent, for those formulations whose composition lie within the bounds of this study:

$$D_{180} = 964.39 - 42.06\,x_1 - 29.16\,x_2 + 4.66\,x_1x_2 \qquad \text{(Eq. 3)}$$

$$D_{30} = 267.20 - 10.25\,x_1 + 18.34\,x_2 \qquad \text{(Eq. 4)}$$

Commentaries similar to those made about the *in vivo* response may also be made about the response surfaces obtained *in vitro* which are depicted in Figs. 5 and 6. Nevertheless, with the conditions used in the dissolution studies, the order relationship *in vivo* (G, E, D, F, for E_{12} and E, G, D, F, for E_2) is not the same as *in vitro* (E, G, D, F for D_{180} and E, D, G, F for D_{30}).

REFERENCES

(1) M. Llabrés, J. L. Vila, and R. Martínez-Pacheco, *J. Pharm. Sci.*, **71**, 924 (1982).

(2) M. S. Barlett, *Biometrics*, **3**, 39 (1947).

(3) M. B. Brown and A. B. Forsythe, *Biometrics*, **30**, 719 (1974).

(4) W. G. Cochran and G. M. Cox, "Experimental Design," 2nd ed., Wiley, New York, N.Y., 1957, pp. 61–70.

(5) W. H. Barr, in "Dosage Forms Design and Bioavailability," J. Swarbrick, Ed., Lea & Febiger, Philadelphia, Pa., 1973, pp. 31–75.

Quantification of the Effect of Excipients on Bioavailability by Means of Response Surfaces III: *In Vivo–In Vitro* Correlations

MATÍAS LLABRÉS, JOSÉ L. VILA ˣ, and RAMÓN MARTÍNEZ-PACHECO

Received April 11, 1980, from the *Departamento de Farmacia Galénica, Facultad de Farmacia, Universidad de Santiago de Compostela, Spain.* Accepted for publication November 17, 1981.

Abstract □ This study compares one of the previously studied formulations with commercial amoxicillin capsules. The results indicate that the percentage of the dose absorbed is similar in both formulations; nevertheless, the amoxicillin capsules present a higher absorption rate. The *in vivo–in vitro* correlations in terms of response surfaces, and the general correlation among all the formulations studied in the three articles of this series is discussed. The quantity of drug excreted in 2 hr and the quantity of drug dissolved in 30 min presents a correlation coefficient $r = 0.9458$ ($p < 0.01$) and the quantity of amoxicillin excreted in 12 hr and the quantity dissolved in 180 min presents a correlation coefficient $r = 0.9761$ ($p < 0.01$).

Keyphrases □ Amoxicillin—effect of excipients on bioavailability by means of response surfaces, *in vivo–in vitro* correlations □ Bioavailability—effect of excipients by means of response surfaces, amoxicillin, *in vivo–in vitro* correlations □ Excipients—effect on bioavailability by means of response surfaces, amoxicillin, *in vivo–in vitro* correlations

The comparison between Formulation E (1), previously studied, and a commercial amoxicillin capsule (Formulation S) was carried out. This study has a double purpose: first, to determine whether the absorption of the drug in Formulation E (which showed good absorption in previous studies) is equivalent to the absorption shown by the conventional formulations; second, to determine the degree of the individual variation for both types of formulations.

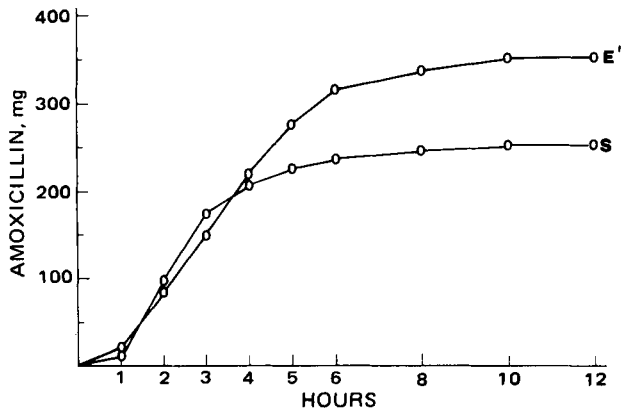

Figure 1—*Mean cumulative curves for urinary excretion of unchanged amoxicillin.*

EXPERIMENTAL

Assayed Formulations—A comparison is made between Formulation E, whose composition has been described (1) and commercial capsules[1] containing 500 mg of anhydrous amoxicillin. To differentiate the results of the present study from those obtained previously (1), Formulation E is termed E′ in the present report.

Clinical Protocol—Urinary excretion of unchanged drug was studied in 12 healthy volunteers of both sexes, whose ages ranged from 20 to 30 years and who showed no evidence of renal insufficiency. Subjects were divided at random into two equal groups of six. A Latin-square 2 × 2 design with 6 replicates was used, and the washing period was 5 days. The conditions of administration and sample times are the same as those described in the previous two reports (1, 2).

Pharmacokinetic Analysis—The parameters employed to characterize the excretion curves obtained are the same as those described previously (1, 2), E_2 and E_{12}.

Dissolution Rate Studies—The apparatus and methodology used were both described in Part I (2).

Statistical Analysis—Cochran's test (3) confirmed the existence of heterogeneous variances for the treatments. Therefore, Scheffé's test modified by Brown and Forsythe (4) was employed (even though the logarithmic transformation of data stabilized the variances) in order to maintain homogeneity in the statistical treatment of data.

RESULTS AND DISCUSSION

A commercial formulation of 500 mg was chosen because the urinary excretion curves obtained for Formulation E in the previous study indicated the possibility of obtaining peaks similar to those obtained with 500-mg doses in conventional formulations. This approach, together with the comparison of the parameters E_2 and E_{12}, permits the possibility of determining whether or not there is a prolongation in the release–absorption process with respect to Formulation E′. This would explain the large individual variations observed in previous studies.

Figures 1 and 2 show the excretion and dissolution mean cumulative curves for both formulations. With respect to the E_2 parameter, the mean values and variances (in parentheses) obtained for Formulations E′ and S were 85.3 (2824.2) and 98.1 (2188.9), respectively. The corresponding figures for the E_{12} parameter were 354.4 (9003.6) and 253.6 (1895.9). The dissolution parameter D_{30} yielded mean values of 204.8 and 404.0 for Formulations E′ and S, respectively, whereas the D_{180} parameter yielded mean values of 634.0 and 471.5 for the respective formulations. The ANOVA results, using the method of Brown and Forsythe (4), show that both formulations are equivalent with regards to the E_2 parameter ($F_{1,22} = 0.392$) but differ significantly (0.01) with regards to the E_{12} parameter ($F_{1,22} = 11.190$). The quantity of intact drug excreted in urine was ~50% of the administered dose in the case of each formulation, which has been

[1] Clamoxil, lot 2L26, F. Bonet.

0022-3549/82/0800-0930$01.00/0

REFERENCES

(1) M. Llabrés, J. L. Vila, and R. Martínez-Pacheco, *J. Pharm. Sci.*, **71**, 924 (1982).

(2) M. S. Barlett, *Biometrics*, **3**, 39 (1947).

(3) M. B. Brown and A. B. Forsythe, *Biometrics*, **30**, 719 (1974).

(4) W. G. Cochran and G. M. Cox, "Experimental Design," 2nd ed., Wiley, New York, N.Y., 1957, pp. 61–70.

(5) W. H. Barr, in "Dosage Forms Design and Bioavailability," J. Swarbrick, Ed., Lea & Febiger, Philadelphia, Pa., 1973, pp. 31–75.

Quantification of the Effect of Excipients on Bioavailability by Means of Response Surfaces III: *In Vivo–In Vitro* Correlations

MATÍAS LLABRÉS, JOSÉ L. VILA ˣ, and RAMÓN MARTÍNEZ-PACHECO

Received April 11, 1980, from the *Departamento de Farmacia Galénica, Facultad de Farmacia, Universidad de Santiago de Compostela, Spain.* Accepted for publication November 17, 1981.

Abstract □ This study compares one of the previously studied formulations with commercial amoxicillin capsules. The results indicate that the percentage of the dose absorbed is similar in both formulations; nevertheless, the amoxicillin capsules present a higher absorption rate. The *in vivo–in vitro* correlations in terms of response surfaces, and the general correlation among all the formulations studied in the three articles of this series is discussed. The quantity of drug excreted in 2 hr and the quantity of drug dissolved in 30 min presents a correlation coefficient $r = 0.9458$ ($p < 0.01$) and the quantity of amoxicillin excreted in 12 hr and the quantity dissolved in 180 min presents a correlation coefficient $r = 0.9761$ ($p < 0.01$).

Keyphrases □ Amoxicillin—effect of excipients on bioavailability by means of response surfaces, *in vivo–in vitro* correlations □ Bioavailability—effect of excipients by means of response surfaces, amoxicillin, *in vivo–in vitro* correlations □ Excipients—effect on bioavailability by means of response surfaces, amoxicillin, *in vivo–in vitro* correlations

The comparison between Formulation E (1), previously studied, and a commercial amoxicillin capsule (Formulation S) was carried out. This study has a double purpose: first, to determine whether the absorption of the drug in Formulation E (which showed good absorption in previous studies) is equivalent to the absorption shown by the conventional formulations; second, to determine the degree of the individual variation for both types of formulations.

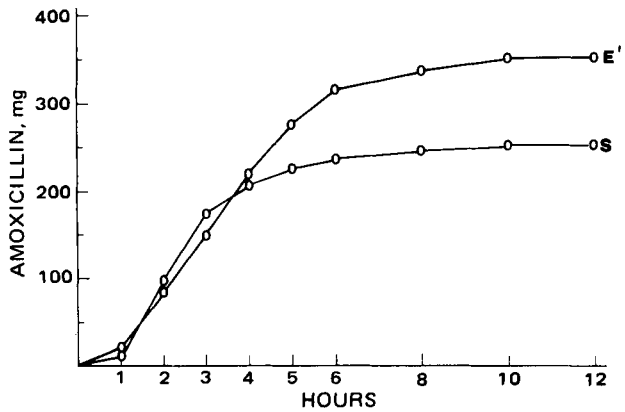

Figure 1—*Mean cumulative curves for urinary excretion of unchanged amoxicillin.*

EXPERIMENTAL

Assayed Formulations—A comparison is made between Formulation E, whose composition has been described (1) and commercial capsules[1] containing 500 mg of anhydrous amoxicillin. To differentiate the results of the present study from those obtained previously (1), Formulation E is termed E′ in the present report.

Clinical Protocol—Urinary excretion of unchanged drug was studied in 12 healthy volunteers of both sexes, whose ages ranged from 20 to 30 years and who showed no evidence of renal insufficiency. Subjects were divided at random into two equal groups of six. A Latin-square 2 × 2 design with 6 replicates was used, and the washing period was 5 days. The conditions of administration and sample times are the same as those described in the previous two reports (1, 2).

Pharmacokinetic Analysis—The parameters employed to characterize the excretion curves obtained are the same as those described previously (1, 2), E_2 and E_{12}.

Dissolution Rate Studies—The apparatus and methodology used were both described in Part I (2).

Statistical Analysis—Cochran's test (3) confirmed the existence of heterogeneous variances for the treatments. Therefore, Scheffé's test modified by Brown and Forsythe (4) was employed (even though the logarithmic transformation of data stabilized the variances) in order to maintain homogeneity in the statistical treatment of data.

RESULTS AND DISCUSSION

A commercial formulation of 500 mg was chosen because the urinary excretion curves obtained for Formulation E in the previous study indicated the possibility of obtaining peaks similar to those obtained with 500-mg doses in conventional formulations. This approach, together with the comparison of the parameters E_2 and E_{12}, permits the possibility of determining whether or not there is a prolongation in the release–absorption process with respect to Formulation E′. This would explain the large individual variations observed in previous studies.

Figures 1 and 2 show the excretion and dissolution mean cumulative curves for both formulations. With respect to the E_2 parameter, the mean values and variances (in parentheses) obtained for Formulations E′ and S were 85.3 (2824.2) and 98.1 (2188.9), respectively. The corresponding figures for the E_{12} parameter were 354.4 (9003.6) and 253.6 (1895.9). The dissolution parameter D_{30} yielded mean values of 204.8 and 404.0 for Formulations E′ and S, respectively, whereas the D_{180} parameter yielded mean values of 634.0 and 471.5 for the respective formulations. The ANOVA results, using the method of Brown and Forsythe (4), show that both formulations are equivalent with regards to the E_2 parameter ($F_{1,22} = 0.392$) but differ significantly (0.01) with regards to the E_{12} parameter ($F_{1,22} = 11.190$). The quantity of intact drug excreted in urine was ~50% of the administered dose in the case of each formulation, which has been

[1] Clamoxil, lot 2L26, F. Bonet.

0022-3549/82/0800-0930$01.00/0

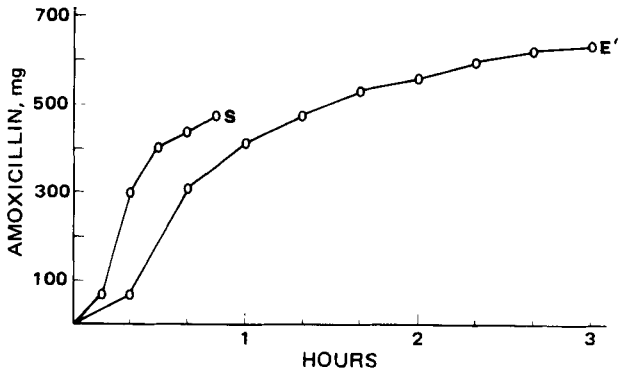

Figure 2—*Mean cumulative dissolution curves.*

discussed previously (5). The ratio between the observed values for the E_{12} parameter, in the case of each of the formulations, is the same as the ratio between doses, thus indicating equal absorption extent for both formulations. With respect to the E_2 parameter, statistically the ratio is equal to unity. This indicates a reduction in the absorption rate of Formulation E′ compared with Formulation S. Furthermore, there is a greater variation between subjects for Formulation E′, with respect to both parameters, which is why there are heterogeneous variances.

Response surfaces are not only useful for quantifying the effect of the different factors on bioavailability, but also serve as a basis for establishing the possible *in vivo–in vitro* correlations. Furthermore, this latter aspect is an important problem facing biopharmaceutics in the field of dosage form control. This importance is underlined by the numerous methods proposed for the study of such correlations (6, 7). Nevertheless, the fact that these methods are mainly empirical is not desirable. For this reason, some authors (6) point out that quantitative-type correlations, at least, "should probably be derived only when there is a theoretical reason for relating the variables."

Although the conditions found in the GI tract are difficult to simulate, it is possible to study a series of factors which presumably affect the processes of release–dissolution of the drug in a biological medium, assuming that these processes are the limiting steps in absorption. The rate with which a drug is liberated from the dosage form is conditioned by two types of factors: the effect of the different excipients and technological factors and their possible interaction with the drug and the interactions between the dosage form and the GI environment. Some kind of physicochemical model is necessary so that the interaction between the technological factors of the dosage form and the physiological environment can be simulated *in vitro*. However, no such model is readily available. However, statistical models can be used, as is the case here, to see if the effects of the technological factors studied *in vitro* by means of certain parameters are comparable to the effects produced *in vivo*. Furthermore, this approach affords the possibility of obtaining the optimum conditions for *in vitro* testing.

Obtaining a correlation between the *in vivo* and *in vitro* response surfaces implies that the polynomials obtained from both series of data are related by means of any one operator; nevertheless, from a practical

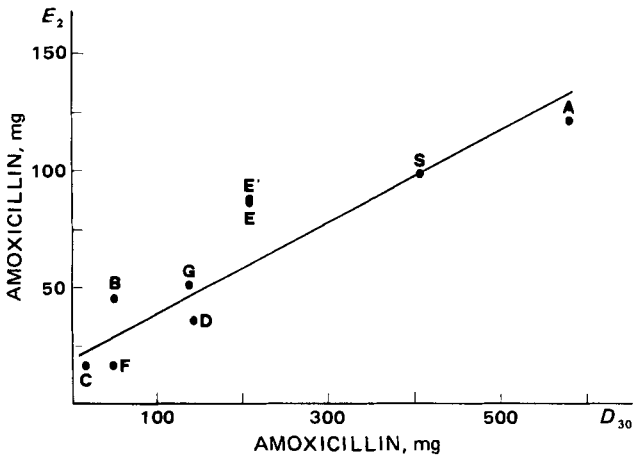

Figure 3—*Linear relationship between the amount of unchanged amoxicillin excreted in 2 hr and the amount dissolved in 30 min [y = 20.90 + 0.2169 x (r = 0.9458; F = 59.48; $\alpha < 0.01$)].*

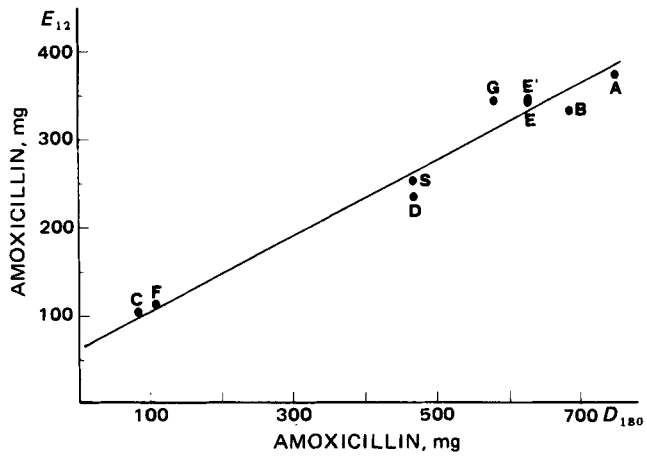

Figure 4—*Linear relationship between the amount of unchanged amoxicillin excreted in 12 hr and the amount dissolved in 180 min [y = 64.01 + 0.4278 x (r = 0.9761; F = 141.30; $\alpha < 0.01$)].*

point of view, it is desirable to have a linear relationship between both, that is, the polynomials obtained should have linear combination. Furthermore, the use of linear relations makes the predictions more plausible. Due to the nature of the experimental data, obtaining linear combinations, is not expected; nevertheless, the approximation to this situation can be tested by means of the linear regression of the polynomial coefficients obtained *in vivo versus* those obtained *in vitro*. If both polynomial functions are a linear combination, then a linear relationship with the ordinate at the origin, statistically equal to zero, will be obtained. This situation is analyzed by means of the ANOVA of the regression among coefficients, using as index the F value obtained for the regression term b_0. To establish precisely the coefficients of the polynomial function used *in vivo*, taking as a basis the *in vitro* counterparts, it is desirable to meet Wetz's criterion (8). According to Wetz, the minimum value of F necessary for equating prediction errors with experimental errors is four times the tabulated value. Another necessary condition is that the ordinate in the origin should be statistically equal to zero. It should also be noticed that the proportion constant for the polynomial coefficients is the same as one obtained by means of the regression between the *in vivo* and *in vitro* parameters.

The regression obtained among the polynomial coefficients corresponding to the E_2 and D_{30} parameters, for Formulations A, B, and C is:

$$y = 1.1419 + 0.1995\,x \quad (r = 0.9999;\ F = 25{,}200.8) \qquad \text{(Eq. 1)}$$

in which the ordinate in origin is statistically equal to zero; the F value is superior to the quadruple of the value tabulated (645.6). Thus, both polynomials must be considered a linear combination within the experimental limits. From this the relationship between the E_2 and D_{30} parameters is as follows:

$$E_2 = 16.04 + 0.200\,D_{30} \quad (r = 0.9977;\ F = 226.5) \qquad \text{(Eq. 2)}$$

in which the y intercept is statistically equal to zero and the slope is almost equal to that obtained in the regression among polynomial coefficients. This coincidence confirms the existence of a linear combination between the response surfaces *in vivo* and *in vitro*.

Nevertheless, the regression obtained between the polynomial coefficients corresponding to E_{12} and D_{180} is:

$$y = -12.473 + 0.768\,x \quad (r = 0.9912;\ F = 56.47) \qquad \text{(Eq. 3)}$$

where the F value is smaller than the critical value tabulated for $\alpha = 0.05$. For this reason, the existence of a linear combination between sets of coefficients cannot be considered. Nevertheless, the relation between the parameters E_{12} and D_{180}:

$$E_{12} = 64.227 + 0.400\,D_{180} \quad (r = 0.990;\ F = 549.19) \qquad \text{(Eq. 4)}$$

presents an excellent linear correlation, even though there is no relationship between the *in vivo* and *in vitro* response curves; the relation, in fact, is exclusively empirical.

The existence of a linear combination between the polynomials obtained for E_2 and D_{30}, but not for E_{12} and D_{180}, suggests an alteration of the intensity factor (7), since the times corresponding to the *in vivo* and *in vitro* parameters chosen are multiples in both cases.

In the second study carried out on Formulations D, E, F, and G, it was pointed out that the two systems do not arrange the different formulations in the same way, and therefore, the existence of response surfaces proportional for the chosen parameters must be ruled out.

With regards to the general correlations, Figs. 3 and 4 show the regression of E_2 against D_{30} and E_{12} against D_{180}, respectively, for all the formulations studied. In spite of the large differences existing between the various formulations, a significant linear regression is obtained, especially in the case of E_{12} against D_{180}. Even the F value obtained for the regression term, b_0, of the ANOVA of the regression was higher than the quadruple of the critical value tabulated. The high F values indicate the capability of the apparatus employed for the *in vitro* studies.

A study of response surfaces is not necessary for establishing a routine control. Nevertheless, in biopharmaceutics, a knowledge of the technological factors which can interact with drugs, as well as of the physicochemical properties responsible for this interaction, is essential. A mechanistic model which would include all variables, both technologically and physiologically dependent, is not feasible, therefore, the use of response surfaces to quantify the effect produced by the factor studied is necessary. This quantification should be independent of therapeutic implications and should insist on establishing the necessary guidelines for obtaining an exact formulation of the dosage forms.

REFERENCES

(1) M. Llabrés, J. L. Vila, and R. Martínez-Pacheco, *J. Pharm. Sci.*, **71**, 924 (1982).

(2) M. Llabrés, J. L. Vila, and R. Martínez-Pacheco, *ibid.*, **71**, 927 (1982).

(3) W. G. Cochran, *Biometrics*, **3**, 22 (1947).

(4) M. B. Brown and A. B. Forsythe, *Biometrics*, **30**, 719 (1974).

(5) M. Barza and L. Weinstein, *Clin. Pharmacokinet.*, **1**, 297 (1976).

(6) J. G. Wagner, "Biopharmaceutics and Relevant Pharmacokinetics," 1st ed., Drug Intelligence Publications, Hamilton, Ill., 1971, pp. 121–147.

(7) J. Swarbrick, "Biopharmaceutics," 1st ed. Lea & Febiger. Philadelphia, Pa., 1970, pp. 265–296.

(8) J. W. Wetz in "Applied Regression Analysis," 1st ed., N. Draper and H. Smith, Eds., Wiley, New York, N.Y., 1966, p. 64.

Determination of Isoetharine in Plasma by Reversed-Phase Chromatography with Amperometric Detection

GEORGE B. PARK *, RAYMOND F. KOSS *, JULIE UTTER *, BRIAN A. MAYES ‡, and JEROME EDELSON *x

Received August 26, 1981, from the **Department of Drug Metabolism and Disposition* and the ‡*Department of Toxicology, Sterling-Winthrop Research Institute, Rensselaer, NY 12144.* Accepted for publication November 12, 1981.

Abstract □ A reversed-phase liquid chromatographic method for the determination of isoetharine in blood plasma, utilizing amperometric detection, is described. Plasma samples were extracted utilizing an ion-pair reagent, di-(2-ethylhexyl)phosphoric acid, to concentrate the catecholamine. Only minor differences were observed in the relative bioavailability of isoetharine hydrochloride and isoetharine mesylate after oral administration to rats. Observed plasma levels, at 1 hr after oral medication, were highly variable in dose-ranging studies at doses of 800–2500 mg/kg/day for 2 weeks.

Keyphrases □ Bioavailability—determination of isoetharine in plasma by reversed-phase chromatography with amperometric detection □ Reversed-phase chromatography—determination of isoetharine in plasma with amperometric detection □ Isoetharine—determination in plasma by reversed-phase chromatography with amperometric detection

Isoetharine (4-[1-hydroxy-2-[(1-methylethyl)-amino]-butyl]-1,2-benzenediol) (I) is a β-agonist which is widely

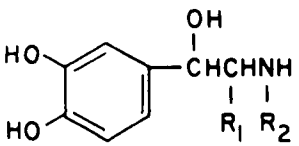

	R_1	R_2
I	CH_2CH_3	$-CH(CH_3)_2$
II	H	$-C(CH_3)_3$

used as a bronchodilator in inhalation therapy. Reversed-phase liquid chromatography with amperometric detection has been used extensively for the determination of endogenous and exogenous biogenic amines in various biological media (1). The most common methods for sample preparation include various modifications of the method of Anton and Sayre (2) in which the compound of interest is adsorbed to alumina through the catechol moiety. In addition, ion exchange resins (3) and boric acid gels (4) have been used to concentrate the analyte and separate it from interfering substances. In the present study, the catecholamine was extracted into an organic solvent through the formation of an ion-pair with di-(2-ethylhexyl)phosphoric acid (5).

The present report describes an analytical method developed for the determination of isoetharine in blood plasma, and the application of the method to the analysis of rat plasma in studies comparing the oral bioavailability of the hydrochloride and mesylate salts (the two marketed salt forms of isoetharine) and in dose-ranging toxicity studies.

EXPERIMENTAL

Reagents—Isoetharine[1] (hydrochloride and mesylate salts) (I), colterol[2] (mesylate salt, internal standard) (4-[2-[1,1-dimethylethyl)-amino]-1-hydroxyethyl]-1,2-benzenediol) (II), methanol[3], benzene[4], di-(2-ethylhexyl)phosphoric acid[5], were used as received. Water was deionized, distilled, and treated with high-intensity UV radiation[6]. All other chemicals were reagent grade or better and used without further purification.

A 1.5% (or 0.5%) solution of di-(2-ethylhexyl)phosphoric acid in ben-

[1] Breon Laboratories, New York, N.Y.
[2] Sterling-Winthrop Research Institute, Rensselaer, N.Y.
[3] OmniSolve, McB, Cincinnati, Oh.
[4] Nanograde, Mallinckrodt, St. Louis, Mo.
[5] Sigma Chemical Co., St. Louis, Mo.
[6] ORGANICpure, Sybron/Barnstead, Boston, Mass.

0022-3549/82/0800-0932$01.00/0

In the second study carried out on Formulations D, E, F, and G, it was pointed out that the two systems do not arrange the different formulations in the same way, and therefore, the existence of response surfaces proportional for the chosen parameters must be ruled out.

With regards to the general correlations, Figs. 3 and 4 show the regression of E_2 against D_{30} and E_{12} against D_{180}, respectively, for all the formulations studied. In spite of the large differences existing between the various formulations, a significant linear regression is obtained, especially in the case of E_{12} against D_{180}. Even the F value obtained for the regression term, b_0, of the ANOVA of the regression was higher than the quadruple of the critical value tabulated. The high F values indicate the capability of the apparatus employed for the *in vitro* studies.

A study of response surfaces is not necessary for establishing a routine control. Nevertheless, in biopharmaceutics, a knowledge of the technological factors which can interact with drugs, as well as of the physicochemical properties responsible for this interaction, is essential. A mechanistic model which would include all variables, both technologically and physiologically dependent, is not feasible, therefore, the use of response surfaces to quantify the effect produced by the factor studied is necessary. This quantification should be independent of therapeutic implications and should insist on establishing the necessary guidelines for obtaining an exact formulation of the dosage forms.

REFERENCES

(1) M. Llabrés, J. L. Vila, and R. Martínez-Pacheco, *J. Pharm. Sci.*, **71**, 924 (1982).

(2) M. Llabrés, J. L. Vila, and R. Martínez-Pacheco, *ibid.*, **71**, 927 (1982).

(3) W. G. Cochran, *Biometrics*, **3**, 22 (1947).

(4) M. B. Brown and A. B. Forsythe, *Biometrics*, **30**, 719 (1974).

(5) M. Barza and L. Weinstein, *Clin. Pharmacokinet.*, **1**, 297 (1976).

(6) J. G. Wagner, "Biopharmaceutics and Relevant Pharmacokinetics," 1st ed., Drug Intelligence Publications, Hamilton, Ill., 1971, pp. 121–147.

(7) J. Swarbrick, "Biopharmaceutics," 1st ed. Lea & Febiger. Philadelphia, Pa., 1970, pp. 265–296.

(8) J. W. Wetz in "Applied Regression Analysis," 1st ed., N. Draper and H. Smith, Eds., Wiley, New York, N.Y., 1966, p. 64.

Determination of Isoetharine in Plasma by Reversed-Phase Chromatography with Amperometric Detection

GEORGE B. PARK *, RAYMOND F. KOSS *, JULIE UTTER *, BRIAN A. MAYES ‡, and JEROME EDELSON *x

Received August 26, 1981, from the **Department of Drug Metabolism and Disposition* and the ‡*Department of Toxicology, Sterling-Winthrop Research Institute, Rensselaer, NY 12144.* Accepted for publication November 12, 1981.

Abstract □ A reversed-phase liquid chromatographic method for the determination of isoetharine in blood plasma, utilizing amperometric detection, is described. Plasma samples were extracted utilizing an ion-pair reagent, di-(2-ethylhexyl)phosphoric acid, to concentrate the catecholamine. Only minor differences were observed in the relative bioavailability of isoetharine hydrochloride and isoetharine mesylate after oral administration to rats. Observed plasma levels, at 1 hr after oral medication, were highly variable in dose-ranging studies at doses of 800–2500 mg/kg/day for 2 weeks.

Keyphrases □ Bioavailability—determination of isoetharine in plasma by reversed-phase chromatography with amperometric detection □ Reversed-phase chromatography—determination of isoetharine in plasma with amperometric detection □ Isoetharine—determination in plasma by reversed-phase chromatography with amperometric detection

Isoetharine (4-[1-hydroxy-2-[(1-methylethyl)-amino]-butyl]-1,2-benzenediol) (I) is a β-agonist which is widely

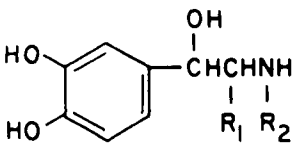

	R_1	R_2
I	CH_2CH_3	$-CH(CH_3)_2$
II	H	$-C(CH_3)_3$

used as a bronchodilator in inhalation therapy. Reversed-phase liquid chromatography with amperometric detection has been used extensively for the determination of endogenous and exogenous biogenic amines in various biological media (1). The most common methods for sample preparation include various modifications of the method of Anton and Sayre (2) in which the compound of interest is adsorbed to alumina through the catechol moiety. In addition, ion exchange resins (3) and boric acid gels (4) have been used to concentrate the analyte and separate it from interfering substances. In the present study, the catecholamine was extracted into an organic solvent through the formation of an ion-pair with di-(2-ethylhexyl)phosphoric acid (5).

The present report describes an analytical method developed for the determination of isoetharine in blood plasma, and the application of the method to the analysis of rat plasma in studies comparing the oral bioavailability of the hydrochloride and mesylate salts (the two marketed salt forms of isoetharine) and in dose-ranging toxicity studies.

EXPERIMENTAL

Reagents—Isoetharine[1] (hydrochloride and mesylate salts) (I), colterol[2] (mesylate salt, internal standard) (4-[2-[1,1-dimethylethyl)-amino]-1-hydroxyethyl]-1,2-benzenediol) (II), methanol[3], benzene[4], di-(2-ethylhexyl)phosphoric acid[5], were used as received. Water was deionized, distilled, and treated with high-intensity UV radiation[6]. All other chemicals were reagent grade or better and used without further purification.

A 1.5% (or 0.5%) solution of di-(2-ethylhexyl)phosphoric acid in ben-

[1] Breon Laboratories, New York, N.Y.
[2] Sterling-Winthrop Research Institute, Rensselaer, N.Y.
[3] OmniSolve, McB, Cincinnati, Oh.
[4] Nanograde, Mallinckrodt, St. Louis, Mo.
[5] Sigma Chemical Co., St. Louis, Mo.
[6] ORGANICpure, Sybron/Barnstead, Boston, Mass.

0022-3549/82/0800-0932$01.00/0

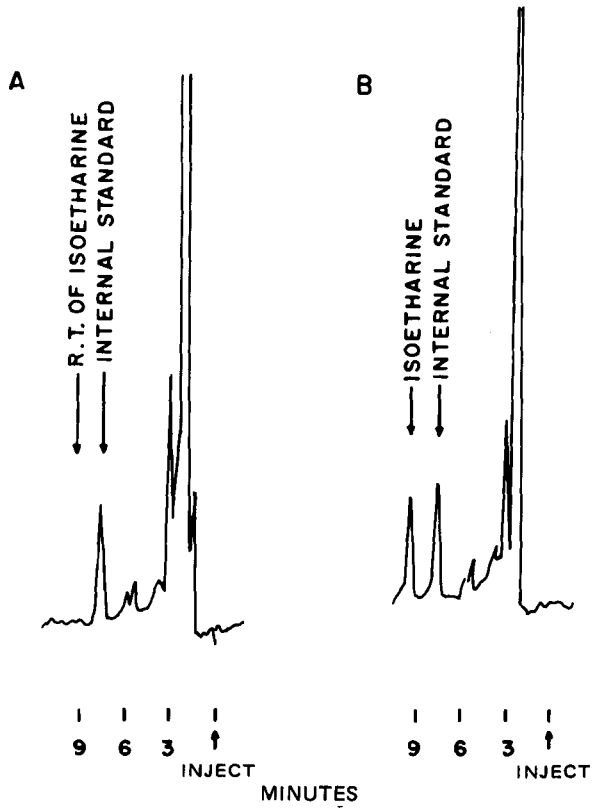

Figure 1—*Representative chromatograms of processed rat plasma: (A) control plasma containing only internal standard; (B) 4 ng/100μl standard. See text for chromatographic conditions. Attenuation 10 nA/V (full scale).*

zene was prepared by diluting 0.6 ml of reagent to 40.0 ml (or 0.5 ml of reagent to 100 ml) with benzene. Phosphate buffer, pH 6.9 (0.2 *M*), was prepared by dissolving 13.6 g of KH_2PO_4 in 300 ml of water, adding 50 ml of 1 *N* NaOH, diluting to 0.5 liter, and adjusting the pH to 6.9 with 1 *N* HCl. Fresh stock standard solutions of isoetharine and colterol were prepared in 0.05 *N* H_2SO_4 at concentrations of 100 μg/ml. All glassware was silanized before use.

Preparation of Standards—The chromatographic system was calibrated by analyzing duplicate plasma standards containing 0, 2.5, 5, 10, 20, 40, 60, 80, and 100 ng/ml of free base. The standards were prepared by adding 100-μl aliquots of isoetharine stock standards (made by serial dilution of the 100 μg/ml stock standard solution with 0.05 *N* H_2SO_4) to 1.0 ml of control human plasma (oxalate anticoagulant). Fresh standards were prepared for each analysis set and analyzed with the prepared samples. Values are reported as isoetharine.

Preparation of Spiked Plasma Samples—Two sets of samples, to be analyzed under single-blind conditions, were prepared in triplicate by adding appropriate volumes of isoetharine stock standard solutions to 1.0 ml of human control plasma. One set was analyzed upon preparation; the other set was frozen for 7 days at −70° before analysis.

Analytical Procedure for Spiked Samples—To each tube containing a sample or standard were added 50 ng of internal standard (100 μl of a 500-ng/ml solution in 0.05 *N* H_2SO_4), 2.0 ml of phosphate buffer (pH 6.9) and 10 ml of 1.5% di-(2-ethylhexyl)phosphoric acid in benzene solution. The tube was shaken and centrifuged. The organic phase was transferred, with methanol-washed disposable pipets, to a tube containing 130 μl of 0.2 *N* H_2SO_4. The tube was shaken and centrifuged, and the organic phase was discarded. The tube was placed in the laboratory freezer (−4°) until chromatographic analysis (usually the next day), at which time the aqueous phase was thawed, and a 100-μl aliquot was injected into the chromatograph.

Chromatography—The HPLC was a modular system constructed of commercially available components: a reciprocating pump[7], syringe-loaded injection valve[8], a 5-μm ODS (25 cm × 4.6-mm i.d.) column[9], and an amperometric (electrochemical) detector with a glassy carbon electrode[10]. The chromatographic conditions were as follows: mobile phase, 0.1 *M* Na_2SO_4 (adjusted to pH 2.8 with phosphoric acid and then adjusted to pH 3.0 with NaOH)–methanol (87.5:12.5, v/v); flow rate, 1.2 ml/min (~150 bar); applied potential, +0.60 V *versus* Ag/AgCl (3 *M* NaCl); at ambient temperature; an injection volume of 100 μl; and approximate retention times of 7.5 min for colterol (internal standard) and 9.3 min for isoetharine.

[7] Milton Roy Minipump, Riviera Beach, Fla.
[8] Model 7120, Rheodyne, Cotati, Calif.
[9] Ultrasphere-ODS, Altex, Woburn, Mass.

Table I—Concentrations of Isoetharine (Free Base) Found in Spiked Plasma Samples

Nominal Concentration, ng/ml	Mean Concentration Found[a], ng/ml	
Minimum Quantifiable Level[b]		
0		
5.5		5.7
	% *SEM*	2.1%
	Mean % Difference	+4.25%
	% *CV*[c]	5.1%
19		19.4
	% *SEM*	0.9%
	Mean % Difference	+1.9%
	% *CV*	2.1%
38		39.4
	% *SEM*	1.3%
	Mean % Difference	+3.6%
	% *CV*	3.2%
88		91.3
	% *SEM*	1.0%
	Mean % Difference	+3.8%
	% *CV*	2.4%

[a] $n = 6$. [b] Mean minimum quantifiable level = 0.92 ng/ml, $n = 2$. [c] Coefficient of variation.

Animal Dosing and Sample Collection—Two groups of six Sprague-Dawley rats[11] each were medicated orally with isoetharine hydrochloride or mesylate. Each animal received the equivalent of 120 mg of isoetharine base *via* a stomach tube as a solution in distilled water. A minimum of 0.2 ml of blood was collected from the orbital sinus in microcentrifuge tubes containing oxalate anticoagulant. Samples were collected prior to medication and at 1, 2, 4, 6, 8, and 10 hr after medication. At 12 hr after medication, blood was collected from the abdominal aorta. The blood was centrifuged and the plasma was separated. The plasma samples were stored in a low-temperature freezer (−70°) until analysis.

In a separate exploratory dose-ranging study, 10 rats/group were medicated orally with isoetharine hydrochloride for 2 weeks at doses of 0, 800, 1400, 2000, and 2500 mg/kg/day. At the end of two weeks, blood samples were obtained from the orbital sinus 1 hr after medication. Plasma was separated and frozen until analysis for isoetharine levels. One rat in the 2500-mg/kg group died during the study.

Sample Preparation—The plasma samples were analyzed by the procedure described for spiked samples with several modifications required because of the small sample volumes. Aliquots of the plasma samples (25–150 μl) were transferred to screw-cap tubes, and 100 μl (5.0 ng) of a solution of colterol (50 ng/ml in 0.05 *N* H_2SO_4) was added as internal standard. Two milliliters of 2% boric acid, 2 g of ammonium sulfate, and 10 ml of 0.5% di-(2-ethylhexyl)phosphoric acid in benzene solution were added. Each tube was shaken and centrifuged, and the organic phase was transferred into a conical tube containing 130 μl of 0.05 *N* H_2SO_4. The tube was shaken and centrifuged; the organic phase was aspirated and discarded. The aqueous phase was frozen until liquid chromatographic analysis on the following day. Duplicate standards containing 0, 0.5, 1, 2, 4, 6, 8, 10, and 15 ng of isoetharine (free base) in 100 μl of control plasma were used for calibration of the chromatograph. Fresh standards were prepared and extracted with each analysis set.

Statistical Analysis—A regression analysis of the peak height ratios (isoetharine/internal standard) obtained for the standards was performed to determine the linearity of the response with respect to concentration. The resulting linear regression was used to estimate the concentrations of isoetharine in the plasma samples. The minimum quantifiable level of the assay was estimated as the concentration whose 80% confidence limit just encompassed zero[12].

[10] Model LC-4 controller and model TL-5 cell, Bioanalytical Systems, West Lafayette, Ind.
[11] Charles River Co.
[12] R. W. Ross and H. Stander, paper presented at the Princeton Conference on Applied Statistics, Dec. 1975.

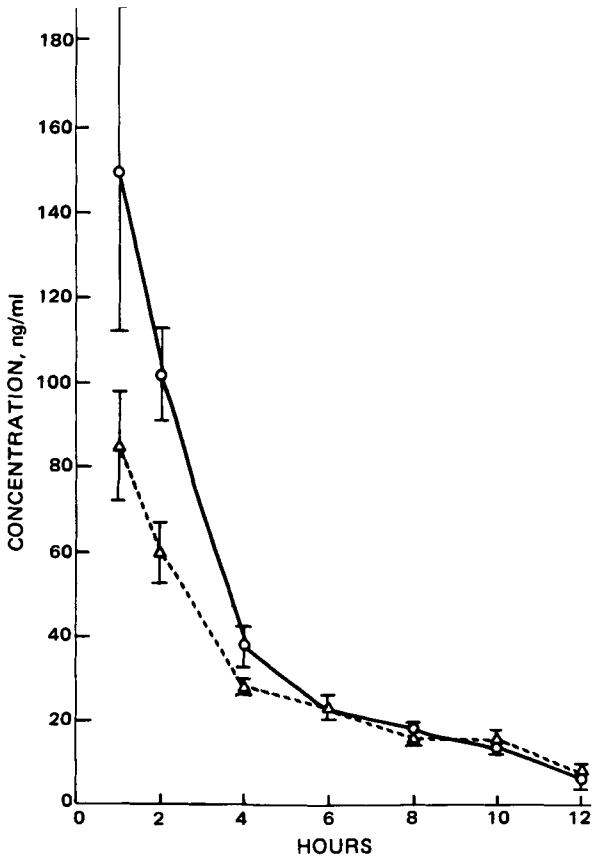

Figure 2—*Plot of mean isoetharine plasma concentration after oral administration of isoetharine hydrochloride or isoetharine mesylate. Key: (○) hydrochloride salt administered; (△) mesylate salt administered. Vertical bars represent the standard error of the mean.*

The assayed levels for the spiked samples were expressed as the percent differences from the nominal values, and a two-way ANOVA with replication was carried out to determine if there was a concentration effect, a time (fresh *versus* frozen) effect, or a concentration times time interaction.

An ANOVA was carried out to determine differences between the two salt forms in terms of maximum observed concentration (C_{max}), the time of the maximum observed concentration (t_{max}), apparent first-order elimination rate constant (K), and the area under the plasma concentration *versus* time curve (AUC). C_{max} and t_{max} were determined by direct observation; the elimination half-life for each rat was determined from a least-squares regression on the logarithm of the 4–12-hr plasma concentration data with time. This assumes first-order elimination kinetics. The AUC was determined from the plasma data by the trapezoidal rule. The data from the dose-ranging study were analyzed by a least-squares regression to determine if observed plasma levels were dose related.

RESULTS AND DISCUSSION

Representative chromatograms of extracted rat plasma standards are shown in Fig. 1. Linear least-squares analysis indicated that peak height ratio (isoetharine/internal standard) *versus* concentration was linear over a range of at least 0 and 0.5–100 ng/ml.

The results of the single-blind analysis of the spiked plasma samples are summarized in Table I. The accuracy of the assay, defined as the mean percent difference from the nominal level was >5%. The estimated assay precision, calculated from the overall mean square error term of the two-way ANOVA, was ±1.9%. The mean (±SE) minimum quantifiable level of the assay was 0.92 (±0.20) ng/ml, n = 2. The mean (±SE) percent recovery of the assay, determined by comparison with unextracted standards, at concentrations of 10, 50, and 100 ng of isoetharine/ml and 50 ng of internal standard/ml, was 78.4 (±2.31%) for isoetharine and 79.1 (±3.6%) for the internal standard.

The two-way ANOVA with replication on the percent differences for the samples indicate neither a concentration effect nor a concentration times time interaction. A highly significant time (fresh *versus* frozen) effect was indicated; however, the trend was to a higher concentration upon freezing. The observed differences were due to a slight difference in the slopes derived from the regression analysis on the standards for the two days, and the difference was statistically significant because of the good precision at each concentration. The observed time effect is considered of little practical significance. The stability of isoetharine and the internal standard in the final acid extract was shown by chromatographing the final acid extract for a set of standards twice, separated by 8 weeks of storage at −4°. The chromatograms obtained on the two days indicated no apparent decomposition of either isoetharine or the internal standard.

The results of the analysis of rat plasma samples, taken after the oral administration of isoetharine hydrochloride and isoetharine mesylate are plotted as means *versus* time of collection in Fig. 2. The mean (±SE) maximum observed plasma concentrations (C_{max}) for the hydrochloride and mesylate salts were 162 (±32) and 92.0 (±9.8) ng/ml, respectively. The mean (±SE) times to C_{max} (t_{max}) were 1.2 (±0.2) and 1.3 (±0.2) hr for the hydrochloride and mesylate salts, respectively.

The area under the plasma concentration *versus* time (AUC) plot was calculated for each rat by the trapezoidal rule using the experimental data. The mean (±SE) AUC was 498 (±56) ng hr/ml for the hydrochloride salt and 344 (±16) ng hr/ml for the mesylate salt.

The apparent first-order elimination rate constant, K, was determined for each animal using the 4- to 12-hr data. The mean (±SE) values of K were 0.21 (±0.04) hr^{-1} for the hydrochloride salt and 0.17 (±0.03) hr^{-1} for the mesylate salt. The corresponding half-lives are 3.3 and 4.1 hr, respectively. It should be emphasized that these are crude estimates of the rate constants since they were determined from data collected over a time period of approximately two half-lives.

ANOVA on the means of C_{max}, t_{max}, and K for the two salts indicated that the differences were not statistically significant ($p \geq 0.05$). The difference between the AUC means for the two salts was significant at the 5% level but not at the 1% level. The hydrochloride salt had the larger AUC (498 ng hr/ml *versus* 344 ng hr/ml).

The observed isoetharine concentrations in rats medicated orally for 2 weeks were highly variable. A least-squares analysis of the data was inconclusive in determining whether the observed plasma levels were proportional to dose in the range of 800–2500 mg/kg.

The formation of an ion-pair with di-(2-ethylhexyl)phosphoric acid provided a simple, rapid means of isolating two exogenous catecholamines from plasma for subsequent quantitation by reversed-phase liquid chromatography. The method is applicable to small (<100 μl) samples and samples up to 2 ml. In this study, the described extraction procedure proved more reliable and gave cleaner chromatograms than adsorption to either alumina or boric acid gels. The usefulness of the assay is demonstrated in that small samples could be analyzed, allowing serial samples to be taken from individual rats, and in the analysis of samples from rats medicated over a 20-fold range of doses.

REFERENCES

(1) W. R. Heineman and P. T. Kissinger, *Anal. Chem.*, **52**, 138R (1980).

(2) A. H. Anton and D. F. Sayre, *J. Pharmacol. Exp. Ther.*, **138**, 360 (1962).

(3) G. M. Tyce, N. S. Sharpless, and C. A. Owen, *Biochem. Pharmacol.*, **21**, 2409 (1972).

(4) S. Higa, T. Suzuki, A. Hayashi, I. Tsuge, and Y. Yamamura, *Anal. Biochem.*, **77**, 18 (1977).

(5) D. M. Temple and R. Gillespie, *Nature (London)*, **209**, 714 (1966).

N-Alkylated Derivatives of 5-Fluorouracil

NITYA G. KUNDU ˣ **and SCOTT A. SCHMITZ**

Received August 24, 1981, from the *School of Pharmacy and LAC-USC Cancer Center, Research Laboratory, University of Southern California, Los Angeles, CA 90033.* Accepted for publication November 16, 1981.

Abstract □ Some *N*-alkyl derivatives of 5-fluorouracil were designed to act as latent depot forms of 5-fluorouracil. A general and efficient method for the syntheses of the alkylated derivatives is described. As expected, the alkylated derivatives of 5-fluorouracil did not show any cytotoxicity in cell culture systems even up to 10^{-4} *M* concentration. The synthesis of 1,3-dimethyl-5-fluoro-5,6-dihydrouracil is also described.

Keyphrases □ 5-Fluorouracil—*N*-alkylated derivatives, synthesis, cytotoxicity □ Derivatives—*N*-alkylated, 5-fluorouracil, synthesis, cytotoxicity □ Cytotoxicity—5-fluorouracil, *N*-alkylated derivatives, synthesis

5-Fluorouracil (I) and its deoxyribonucleoside derivative, flouridine (II), have been found to be highly effective compounds for the treatment of various solid tumors (1–3). The tetrahydrofuryl derivative (III) of 5-fluorouracil has also been found to be clinically active (4). Efforts have been made to improve upon the efficacy of these drugs (5–11).

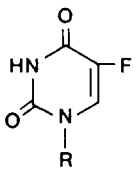

I, R = H

II, R = 2-DEOXYRIBOSE

III, R = 

Recently, 1-alkyl carbamoyl derivatives (IV) of 5-fluorouracil have been tested as masked forms of 5-fluorouracil and several of them have been found to be promising (12, 13). The synthesis and antitumor properties of various *N*-acyl and *N*-(alkoxycarbonyl)-5-fluorouracil derivatives (V) which probably act as depot forms of 5-fluorouracil have been reported (14). 5′-*O*-Glucuronide of 5-fluorouridine (VI) has been described recently (15). This is expected to be activated by the β-glucuronidase activity in tumor cells.

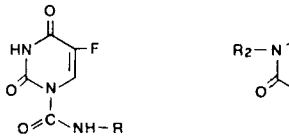

IV, R = CH_3, C_2H_5, C_3H_7, C_4H_9 etc.

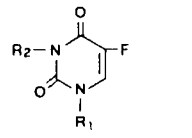

V, R_1, R_2, H, acyl, or, alkoxycarbonyl

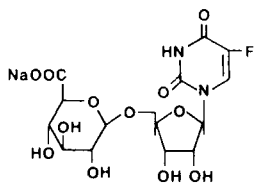

VI

In view of the success of the various acyl, alkoxycarbonyl, and carbamoyl derivatives of 5-fluorouracil, the authors became interested in suitable *N*-alkyl derivatives of 5-fluorouracil in which an activated methylene group is attached to the nitrogen atom of the fluorouracil ring. These compounds could act as latent depot forms of 5-fluorouracil (Scheme I). In this report, a general method for the syntheses of various N_1, N_3-dialkyl (VII–X) and N_1-monoalkyl (XI and XII) derivatives of 5-fluorouracil and the study of their toxicities in cell culture systems are reported. In addition, the synthesis of N_1, N_3-dimethyl-5-fluoro-5,6-dihydrouracil (XIII), a model for 5-fluoro-5,6-dihydrouracil, which is an intermediate in the catabolism of 5-fluorouracil, is also described.

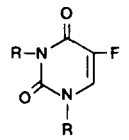

VII, R = CH_3

VIII, R = $CH_2C_6H_5$

IX, R = $CH_2-CH=CH_2$

X, R = $CH_2-C\equiv CH$

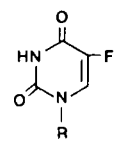

XI, R = $CH_2C_6H_5$

XII, R = $CH_2-CH=CH_2$

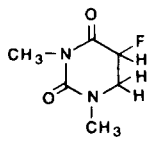

XIII

RESULTS

Chemistry—The direct *N*-alkylation of 5-fluorouracil has been studied previously (16). It was observed that by using dimethyl sulfoxide as solvent and potassium carbonate as base, alkylation of 5-fluorouracil with unreactive halides led to N_3-alkylation, whereas with reactive halides, alkylation was found to be N_1-alkylation. However, formation of N_1, N_3-dialkyl derivatives was not described. Since among the acyl derivatives of 5-fluorouracil, the diacylated derivative, N_1-acetyl-N_3-*O*-toluyl-5-fluorouracil was found to be the most promising (14), there has been a greater interest in studying the dialkylated species of 5-fluorouracil. Preformation of the potassium salts[1] of 5-fluorouracil and subsequent reaction of the potassium salts with different alkylating agents led to excellent yields of the alkylated species. The formation of the potassium salts of 5-fluorouracil was accomplished in dimethylformamide as a solvent in the presence of potassium carbonate as a base. The process was found to be relatively slow at room temperature and was completed by overnight stirring when a thick gel of the potassium salts of 5-fluorouracil was formed. Reaction of the gel with different alkylating agents yielded either a mixture of monoalkyl and dialkyl products or, exclusively, the dialkyl products dependent upon the amount of the alkylating agents used. However, in all cases the total yields of the alkylated species (as shown in Table I) were very high compared with the other reported methods (16–18) of alkylation. In Table II are shown the different proportions of mono- and dialkylated species which could be obtained by using different amounts of the alkylating agents.

[1] Probably a mixture of N_1-mono, N_3-mono, and N_1, N_3-dipotassium salts is formed.

0022-3549/82/0800-0935$01.00/0

Table I—*N*-Alkylated Derivatives of 5-Fluorouracil

Compound	Melting Point°	Yield, %		Molecular Formula		Analysis, % Calc.	Found
VII	130–131	90		$C_6H_7N_2O_2F$	C	45.57	45.48
					H	4.43	4.33
					N	17.72	17.52
VIII	oil	84	90	$C_{18}H_{15}N_2O_2F$	C	69.68	69.40
					H	4.84	4.64
					N	9.03	8.95
					F	6.13	6.25
XI	166–168	6		$C_{11}H_9N_2O_2F$	C	60.00	60.17
					H	4.09	4.25
					N	12.73	12.75
					F	8.64	8.83
IX	38	41.5	73.9	$C_{10}H_{11}N_2O_2F$	C	57.14	57.36
					H	5.24	5.31
					N	13.33	13.32
					F	9.05	9.36
XII	125	32.4		$C_7H_7N_2O_2F$	C	49.41	49.61
					H	4.12	4.32
					N	16.47	16.48
					F	11.18	11.47
X	98	92		$C_{10}H_7N_2O_2F$	C	58.25	58.26
					H	3.40	3.53
					N	13.59	13.50
					F	9.22	9.44
XIII	51	98.5		$C_6H_9N_2O_2F$	C	45.00	45.28
					H	5.63	5.80
					N	17.50	17.54
					F	11.18	11.84

The structures of the alkylated species were established by elemental analyses and by spectroscopic methods. The compounds gave satisfactory carbon, hydrogen, nitrogen, and fluorine analyses (Table I). In mass spectral measurements (see Experimental) all the compounds showed the molecular ions, and their fragmentation patterns confirmed their structures. The UV absorption spectra (Table III) of the dialkylated species showed them to be the N_1, N_3-dialkylated species. The monoalkylated species were found to be the N_1-alkylated derivatives by comparison of their melting points with those reported in the literature (16, 17) and also from the independence of their UV absorptions in neutral, acidic, and basic media (Table III). No N_3-alkylated compounds were isolated under the reaction conditions. A comparison of the PMR spectra of the mono- and dialkylated derivatives (Table IV) showed that N_1-CH_3 and N_1-CH_2- groups have higher field chemical shifts than the corresponding N_3-CH_3 and N_3-CH_2-groups. This provides an independent method for the identification of N_1- and N_3-substituted alkyl derivatives of 5-fluorouracil.

5-Fluoro-5,6-dihydrouracil is an intermediate in the catabolic degradation of 5-fluorouracil, and has been synthesized (2) in an extremely small yield by the catalytic hydrogenation of 5-fluorouracil. Lithium tri-*sec*-butyl borohydride has been used for the reduction of α,β-unsaturated ketones and esters to the corresponding saturated ketones and esters (19, 20). Recently, this reagent has been used successfully for the reduction of the 5,6-double bond of uracil and 5-fluorouracil derivatives (21). When 1,3-dimethyl-5-fluorouracil was reduced with lithium tri-*sec*-butyl borohydride, a quantitative yield of crystalline 1,3-dimethyl-5-fluoro-5,6-dihydrouracil (XIII) was obtained. Its structure was established by elemental analysis, lack of UV absorption, and its PMR spectrum. In the mass spectrum, a very strong peak due to the parent molecular ion was seen, confirming the structure of the compound.

Table II—Ratios of N_1, N_3-Diallyl and N_1-Allyl 5-Fluorouracils Formed

5-Fluorouracil	Potassium Carbonate	Allyl Bromide	Diallyl/Monoallyl
1 mole	1.04 mole	1.30 mole	1.28
1 mole	1.6 mole	1.63 mole	3.3

Table III—UV Spectroscopic Data for *N*-Alkylated Derivatives of 5-Fluorouracil

Compounds	λ_{max} (ϵ) 95% Ethyl Alcohol	0.1 *M* HCl	0.1 *M* NaOH
VII	274 (7413)	271 (7260)	271 (7820)
VIII	276 (7560)	[a]	[a]
XI	274 (8930)	275 (9220)	273 (6760)
IX	273 (6570)	275 (7410)	271 (7070)
XII	274 (8240)	273 (8640)	272 (6270)
X	267 (7330)	271 (7980)	264 (7600)
XIII	—	—	—

[a] The absorptions could not be determined due to a solubility problem.

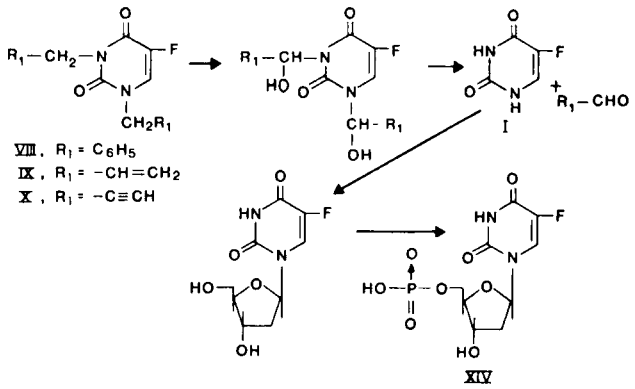

Scheme I

Growth Inhibition Studies—The growth inhibitory effects of the compounds (VII–XII) were studied against L-1210 (22) and CCRF-CEM leukemic cells in culture (23). As expected, none of the compounds showed any significant cell inhibitory effects even at concentrations up to 10^{-4} *M*.

DISCUSSION

N_1, N_3-Dialkylated (VII–X) and N_1-monoalkylated (XI and XII) derivatives of 5-fluorouracil were synthesized by a simple and highly efficient method. These compounds were chosen since they either have a small alkyl group (*e.g.*, methyl) or an active methylene group (attached to an unsaturated center) on nitrogen. These compounds, as expected, were found to have very little toxicity against leukemic cells in culture. However, like many anticancer agents (24, 25), these compounds could be activated by an oxidative mechanism (26, 27) in the whole animal as shown in Scheme I[2]. A slow formation of 5-fluorouracil (I) could provide the active compound (XIV) in a small steady state. Also, since the alkylated derivatives are much more soluble in nonpolar solvents in contrast to 5-fluorouracil, they are expected to have different pharmacological characteristics compared with 5-fluorouracil. Further biological studies of these compounds are in progress.

[2] Alternative metabolic transformation leading probably to inactive products are not ruled out by Scheme I.

Table IV—PMR Spectral Data for *N*-Alkylated Derivatives of 5-Fluorouracil

Compound	δ, ppm					
	H_6	N_1-CH_3	N_3-CH_3	N_1-CH_2-	N_3-CH_2	Other Hydrogens
VII	7.45 (d) ($J_{H_6,F}$ = 4.5 Hz)	3.4 (s)	3.5 (s)			
VIII	at 7.34	—	—	4.8 (s)	5.1 (s)	7.34 (aromatic)
XI	8.13 (d) ($J_{H_6,F}$ = 8 Hz)	—	—	4.84 (s)	—	7.38 (aromatic)
IX	7.32 (d) ($J_{H_6,F}$ = 6 Hz)	—	—	4.38 (d) (J = 6 Hz)	4.63 (d) (J = 6 Hz)	5.25 (m, CH_2 of vinyl) 5.87 (m, CH of vinyl)
XII	7.4 (d) ($J_{H_6,F}$ = 6 Hz)	—	—	4.33 (d) (J = 6 Hz)	—	5.32 (m, CH_2 of vinyl) 5.92 (m, CH of vinyl)
X	7.68 (d) ($J_{H_6,F}$ = 6 Hz)	—	—	4.65 (d) (J = 3 Hz)	4.75 (d) (J = 3 Hz)	2.2 (t, J = 3 Hz) and 2.57 (t, J = 3 Hz) (acetylenic Hs)
XIII	—	3.13 (s)	3.23 (s)	—	—	3.7 (m, 2H, C_6-H) 5.1 (2t, 1H, C_5-H, $J_{H_5,F}$ = 48 Hz)

5-Fluoro-5,6-dihydrouracil is an intermediate in the catabolism of 5-fluorouracil. There is no convenient method available for the synthesis of this compound. A highly efficient method for the synthesis of 1,3-dimethyl-5-fluoro-5,6-dihydrouracil has been developed. This compound in combination with 5-fluorouracil may show different toxicities to tumor systems. This aspect is also under extensive study.

EXPERIMENTAL[3]

***N_1, N_3*-Dimethyl 5-Fluorouracil (VII)**—5-Fluorouracil (2.0 g, 15.4 mmoles) was dissolved in dimethylformamide (50 ml) when a clear solution was formed. To this solution powdered anhydrous potassium carbonate (4.2 g, 30.4 mmoles) was added, and the mixture was stirred overnight at room temperature when a thick white gel of the potassium salts of 5-fluorouracil was formed. Methyl iodide (4.2 g, 29.6 mmoles) was added and the mixture was stirred for 3 days at room temperature. Dimethylformamide was removed under high vacuum and the residue was partitioned between chloroform (200 ml) and water (100 ml). The aqueous layer was again extracted with chloroform (2 × 100 ml). The combined chloroform extract was dried over anhydrous magnesium sulfate, filtered, and solvent was removed to yield a crystalline white solid (2.2 g, 13.9 mmoles, 90%), single spot on TLC, R_f = 0.12, 0.25, and 0.91 in Solvents A, B, and C, respectively. On crystallization from absolute ethanol this yields long white needles, mp 130–131° [lit. (18) mp 128–130°]; ν_{max} 3070, 1702, and 1650 cm^{-1}; MS m/z 158 (M^+, 100%).

***N_1,N_3*-Dibenzyl-5-fluorouracil (VIII) and *N_1*-Benzyl-5-fluorouracil (XI)**—Benzyl bromide (7.8 g, 45.6 mmoles) was added to the potassium salts of 5-fluorouracil made by stirring 5-fluorouracil (3 g, 23 mmoles) and anhydrous potassium carbonate (6.3 g, 45.6 mmoles) in dimethylformamide (80 ml). The mixture was stirred at room temperature for 6 days. Dimethylformamide was removed and the residue partitioned between chloroform and water. The chloroform extracts on removal of solvent yielded an oil which was chromatographed on silica gel. The column was washed with petroleum ether (bp 35–60°, 300 ml) and then the dibenzyl derivative (VIII) was eluted with chloroform–ethyl acetate (15:1 Fractions 2–4, total volume 250 ml) and was obtained on removal of solvent as a gum (6 g, 19.4 mmoles, 84%); TLC, R_f = 0.38, 0.90, and 0.95 in Solvents A, B, and C respectively; IR ν_{max} 3040, 3080, 1710, 1720, 1660, 1650 cm^{-1}; MS m/z 310 (M^+, 51.7%), 219 (M^+ − 91, 19.3%), 91 ($C_6H_7^+$, 100%).

***N_1*-Benzyl-5-fluorouracil (XI)**—N_1-Benzyl-5-fluorouracil was eluted with chloroform–methanol (10:1 fractions 6–7). On removal of solvent, a white solid (300 mg, 1.4 mmoles, 6%) was obtained. This was crystallized from absolute ethanol as white plates, mp 170° [lit. (16) mp 170–171°]; TLC R_f 0.06, 0.08, and 0.81 in solvents A, B, and C, respectively; IR ν_{max} 3070, 1720, 1665 cm^{-1}; MS m/z 220 (M^+), 91 ($C_7H_7^+$, 100%).

***N_1, N_3*-Diallyl-5-fluorouracil (IX) and *N_1*-Allyl-5-fluorouracil (XII)**—The potassium salts of 5-fluorouracil (10 g, 76.6 mmoles) were made by stirring with anhydrous potassium carbonate (11 g, 79.7 mmoles) in dimethyformamide (50 ml). Allyl bromide (12 g, 100 mmoles) was added and the mixture was stirred for 1 week at room temperature. Dimethylformamide was removed under vacuum and the residue was treated with water (100 ml) and 6 *N* HCl to pH 4. The mixture was extracted with methylene chloride. The methylene chloride layer was washed with water, dried over anhydrous magnesium sulfate, and solvent was removed yielding a gummy semisolid residue which was chromatographed on silica gel (40–140 mesh). The column was washed with petroleum ether (bp 40–60°) and then diallyl-5-fluorouracil (IX, 6.7 g, 31.9 mmoles, 41.5%) was eluted with methylene chloride. The monoallyl-5-fluorouracil (XII, 4.24 g, 24.9 mmoles, 32.4%) was eluted with methylene chloride–ethyl acetate (15:1) and chloroform–methanol (10:1). N_1, N_3-Diallyl-5-fluorouracil was crystallized from absolute ethanol in the cold as long white needles, mp 38°; TLC, R_f = 0.27, 0.69, and 0.98 in solvents A, B, and C, respectively; IR ν_{max} 1650, 1680 cm^{-1}; MS m/z 210 (M^+, 26.5%). N_1-Monoallyl-5-fluorouracil was crystallized from absolute ethanol in small white needles, mp 125–126°; TLC, R_f = 0.07, 0.08, and 0.71 in Solvents A, B, and C, respectively; IR ν_{max} 1650, 1680 cm^{-1}; MS m/z 170 (M^+).

***N_1,N_3*-Dipropargyl-5-fluorouracil (X)**—To the potassium salts made from 5-fluorouracil (5 g, 38.5 mmoles) and anhydrous potassium carbonate (8.0 g, 57.9 mmoles) in dimethylformamide (160 ml), propargyl bromide (9.5 ml of 80% solution in toluene) was added and stirred at room temperature for 4 days. Dimethylformamide was removed under high vacuum and the residue was partitioned between water (10 ml) and methylene chloride (300 ml). The methylene chloride layer was washed with water, dried over anhydrous magnesium sulfate, and solvent removed to obtain a residue (7.3 g, 35.42 mmoles, 92%) which crystallized readily at room temperature. The material was crystallized from methylene chloride into long colorless needles, mp 98°; TLC, R_f 0.23, 0.67, and 0.98 in solvents A, B, and C, respectively; IR ν_{max} 3280 (≡CH), 1655, 1670, 1718 cm^{-1}; MS m/z 206 (M^+), 167 (M^+—CH_2—C≡CH).

***N_1,N_3*-Dimethyl-5-fluoro-5,6-dihydrouracil (XIII)**—N_1, N_3-Dimethyl-5-fluorouracil (316 mg, 2 mmoles) was dissolved in dry tetrahydrofuran (10 ml) and cooled in a dry ice–acetone bath under argon atmosphere. Lithium tri-*sec*-butyl borohydride (2.2 ml of 1 *M* solution in tetrahydrofuran) was injected and the mixture was stirred in a dry ice–acetone bath for 10 min. The mixture was decomposed with saturated ammonium chloride solution which was injected and stirred in the cold bath for another 10 min. Tetrahydrofuran was removed under aspirator and the residue was extracted with methylene chloride. The methylene chloride layer was washed with water, dried over anhydrous magnesium sulfate, and solvent was removed to obtain a thick liquid which was chromatographed over silica gel. Compound XIII was eluted with methylene chloride–ethyl acetate (15:1). On removal of solvent, a thick colorless liquid (315 mg, 1.97 mmoles, 98.5%) was obtained which crystallized from ethanol, mp 51°; TLC, R_f = 0.15, 0.33, and 0.94 in Solvents A, B, and C, respectively; IR ν_{max} 1728, 1690 cm^{-1}; MS m/z 160 (M^+, 100%).

Growth Inhibition Assay—L-1210 cells and CCRF-CEM cells were grown in medium[4] supplemented with 10% dialyzed fetal calf serum with

[3] Melting points were determined on a Thomas-Hoover melting point apparatus and are uncorrected. The UV spectra were recorded on a Beckman model 25. Spectra were taken in 95% ethanol unless otherwise mentioned. The IR spectra were done on a Beckman 4210 in a fluorinated hydrocarbon. PMR spectra (δ) were recorded on a Varian EM-390 90-MHz NMR spectrometer in deuterated chloroform, using tetramethylsilane as internal reference. Elemental analyses were performed by Galbraith Laboratories, Inc., Knoxville, Tenn., or Spang Microanalytical Laboratory, Ann Arbor, Mich. Mass spectra were taken on a Hewlett-Packard, model 5985 spectrophotometer. TLC was performed on an Eastman Chromagram sheet (6060 silica gel with fluorescent indicator) in the indicated solvents: Solvent A, chloroform; Solvent B, methylene chloride–ethyl acetate (15:1); Solvent C, chloroform–methanol (10:1); R_f's for 5-fluorouracil are 00.0, 00.0, and 0.26 in Solvents A, B, and C, respectively.

[4] Roswell Park Memorial Institute (RPMI) 1640.

a doubling time of 10–12 and 18–24 hr, respectively. The solutions were diluted to a stock solution of 10^{-3} *M* with phosphate-buffered saline, sterilely filtered, and aseptically diluted by half-log increments. Each concentration (0.7 ml) was added to duplicate 13- × 75-mm test tubes. Cells from logarithmically growing stock culture were suspended in prewarmed medium[4] supplemented with 10% dialyzed fetal calf serum, 10 m*M* (morpholine-propanesulfonic acid, and 20 m*M* [*N*-(2-hydroxyethyl)piperazine-*N'*-2-ethanesulfonic acid]. Cell suspension (1.8 ml) was added to each tube. The tubes were incubated upright at 37° in a warm room or dry incubator. Under these conditions, L-1210 cells grew exponentially 15- to 25-fold from an initial density of 2–2.5 × 10^4/cm^3; CCRF-CEM cells grew exponentially 8- to 10-fold. After 48 hr (for L-1210 cells), or 72 hr (for CCRF-CEM cells), the incubation was terminated and the cell densities were determined[5]. The degree of proliferation of each 2-ml culture was expressed as the ratio of the final cell density to the initial cell density; this index was plotted against the drug concentration employed. The concentration of drug which depresses the ratio to 50% of control (the IC_{50}) was graphically determined. For the clinically effective drug, 5-fluorouracil, IC_{50} = 1.9 × 10^{-6} *M* for CCRF-CEM cells in culture.

REFERENCES

(1) C. Heidelberger, N. K. Chaudhuri, P. Danneberg, D. Mooren, L. Griesbach, R. Duschinsky, R. J. Schnitzer, E. Pleven, and J. Scheiner, *Nature (London)*, **179**, 663 (1957).

(2) R. Duschinsky, E. Pleven, and C. Heidelberger, *J. Am. Chem. Soc.*, **79**, 4559 (1957).

(3) C. Heidelberger, in "Cancer Medicine," J. F. Holland and E. Frei, Eds., Lea and Febiger, Philadelphia, Pa., 1973, p. 768.

(4) S. A. Hiller, R. A. Zhuk, and M. Yu. Lidak, *Dokl. Acad. Nauk SSSR*, **176**, 332 (1967); *Chem. Abstr. Jpn.*, **68**, 29664 (1968).

(5) C. Heidelberger, *Progr. Nucleic Acid Res. Mol. Biol.*, **4**, 1 (1965).

(6) G. J. Coomen, F. Alewijk, D. Blok, and U. K. Pandit, *Heterocycles*, **12**, 1535 (1979).

(7) S. A. Hiller, R. A. Zhuk, and G. Ya. Nashatyr, *Khim. Geterotstikl. Soedin. Sb.*, **3**, 577 (1968); Chem. Abstr. Jpn., **69**, 96641h (1968).

(8) M. Tada, *Bull. Chem. Soc. Jpn.*, **50**, 2406 (1977).

(9) S. Ozaki, Y. Ike, H. Mizuno, K. Ishikawa, and H. Mori, *ibid.*, **50**, 2406 (1977).

(10) T. T. Sakai, A. L. Pogolotti, and D. V. Santi, *J. Heterocycl. Chem.*, **5**, 849 (1968).

(11) M. Yasumoto, I. Yamawaki, T. Marunaka, and S. Hashimoto, *J. Med. Chem.*, **21**, 738 (1978).

(12) A. Hoshi, M. Iigo, M. Yoshida, and K. Kuretani, *Gann*, **66**, 673 (1975).

(13) M. Iigo, A. Hoshi, A. Nakamura, and K. Kuretani, *Cancer Chemother. Pharmacol.*, **1**, 203 (1978).

(14) T. Kametani *et al.*, *J. Med. Chem.*, **23**, 1324 (1980).

(15) K. A. Watanabe, A. Matsuda, M. J. Halat, D. H. Hollenberg, J. S. Nisselbaum, and J. J. Fox, *ibid.*, **24**, 893 (1981).

(16) B. R. Baker and G. D. F. Jackson, *J. Pharm. Sci.*, **54**, 1758 (1965).

(17) M. Gacek and K. Undheim, *Acta. Chem. Scand. Ser. B*, **33**, 515 (1979).

(18) M. Fikus, K. L. Wierzchowski, and D. Sugar, *Biochem. Biophys. Res. Commun.*, **16**, 478 (1964).

(19) B. Ganem, *J. Org. Chem.*, **41**, 146 (1975).

(20) J. M. Fotunato and B. Ganem, *ibid.*, **41**, 2194 (1976).

(21) S. J. Hannon, N. G. Kundu, R. P. Hertzberg, R. S. Bhatt, and C. Heidelbeger, *Tetrahedron Lett.*, **21**, 1105 (1980).

(22) G. E. Moore, A. A. Sandberg, and K. Ulrich, *J. Natl. Cancer Inst.*, **36**, 405 (1966).

(23) G. E. Foley, H. Lazarus, S. Farber, B. G. Uzman, B. A. Boone, and R. E. McCarthy, *Cancer*, **18**, 522 (1965).

(24) N. Brock, *Cancer Treat. Rep.*, **60**, 301 (1976); G. E. Foley, O. M. Friedman, and B. P. Drolet, *Cancer Res.*, **21**, 57 (1961).

(25) T. A. Connors, P. B. Farmer, A. B. Foster, A. M. Gilman, M. Jarman, and M. J. Tisdale, *Biochem. Pharmacol.*, **22**, 1971 (1973).

(26) B. Testa and P. Jenner, "Drug Metabolism: Chemical and Biological Aspects," M. Dekker, New York, N.Y., 1976, pp. 82–97.

(27) K. L. Khanna, G. S. Rao, and H. H. Cornish, *Toxicol. Appl. Pharmacol.*, **23**, 720 (1972).

ACKNOWLEDGMENTS

Supported by Grant RO1-CA 257125 from the Division of Cancer Treatment, National Cancer Institute, National Institutes of Health, Department of Health, Education, and Welfare.

The authors wish to thank Dr. Zoltan Tokes and Mr. Csaba Csipke for the cell culture studies, and Dr. K. Chan and Mr. E. Watson for the mass spectral data. Thanks are also due to Mrs. Suvra Kundu for her technical help and Ms. Margaret Soh for her patience and excellent typing.

[5] Determined by using a Coulter Counter.

High-Pressure Liquid Chromatographic Assay of Cloxacillin in Serum and Urine

F. W. TEARE *x, R. H. KWAN, M. SPINO, and S. M. MacLEOD

Received April 6, 1981, from the * *Faculty of Pharmacy, University of Toronto, Toronto, Canada, M5S 1A1* and the *Department of Clinical Pharmacology, The Hospital for Sick Children, Toronto, Canada.* Accepted for publication September 2, 1981.

Abstract □ Two rapid, specific, and sensitive high-pressure liquid chromatographic (HPLC) assays were developed for cloxacillin in serum and urine. A reversed-phase column (RP-8) was selected for use with two different sets of HPLC conditions and sample pretreatment procedures. Cloxacillin extraction efficiencies are reported from serum and urine. Equations are presented for linear relationships between peak height or peak area ratios of cloxacillin to nafcillin (internal standard) and the cloxacillin concentration over a range of 0–80 μg/ml. The sensitivity limit of these assays was ~0.3 μg/ml of a standard solution for one method and 0.05 μg/ml for the other HPLC assay.

Keyphrases □ Cloxacillin—high-pressure liquid chromatographic assay, serum, urine, nafcillin □ Nafcillin—cloxacillin, high-pressure liquid chromatographic assay, serum, urine □ High-pressure liquid chromatography—cloxacillin in serum and urine □ Penicillins—high-pressure liquid chromatography of cloxacillin

Cloxacillin sodium (I), [3-(*o*-chlorophenyl)-5-methyl-4-isoxazoyl] penicillin sodium, is a semisynthetic penicillin synthesized in 1962 (1). It can be administered both parenterally and orally. Like other penicillins, I is sensitive to nucleophilic and electrophilic attack catalysed by general bases and acids, respectively. Maximum stability of

0022-3549/82/0800-0938$01.00/0

a doubling time of 10–12 and 18–24 hr, respectively. The solutions were diluted to a stock solution of 10^{-3} *M* with phosphate-buffered saline, sterilely filtered, and aseptically diluted by half-log increments. Each concentration (0.7 ml) was added to duplicate 13- × 75-mm test tubes. Cells from logarithmically growing stock culture were suspended in prewarmed medium[4] supplemented with 10% dialyzed fetal calf serum, 10 m*M* (morpholine-propanesulfonic acid, and 20 m*M* [*N*-(2-hydroxyethyl)piperazine-*N'*-2-ethanesulfonic acid]. Cell suspension (1.8 ml) was added to each tube. The tubes were incubated upright at 37° in a warm room or dry incubator. Under these conditions, L-1210 cells grew exponentially 15- to 25-fold from an initial density of 2–2.5 × 10^4/cm^3; CCRF-CEM cells grew exponentially 8- to 10-fold. After 48 hr (for L-1210 cells), or 72 hr (for CCRF-CEM cells), the incubation was terminated and the cell densities were determined[5]. The degree of proliferation of each 2-ml culture was expressed as the ratio of the final cell density to the initial cell density; this index was plotted against the drug concentration employed. The concentration of drug which depresses the ratio to 50% of control (the IC_{50}) was graphically determined. For the clinically effective drug, 5-fluorouracil, IC_{50} = 1.9 × 10^{-6} *M* for CCRF-CEM cells in culture.

REFERENCES

(1) C. Heidelberger, N. K. Chaudhuri, P. Danneberg, D. Mooren, L. Griesbach, R. Duschinsky, R. J. Schnitzer, E. Pleven, and J. Scheiner, *Nature (London)*, **179**, 663 (1957).

(2) R. Duschinsky, E. Pleven, and C. Heidelberger, *J. Am. Chem. Soc.*, **79**, 4559 (1957).

(3) C. Heidelberger, in "Cancer Medicine," J. F. Holland and E. Frei, Eds., Lea and Febiger, Philadelphia, Pa., 1973, p. 768.

(4) S. A. Hiller, R. A. Zhuk, and M. Yu. Lidak, *Dokl. Acad. Nauk SSSR*, **176**, 332 (1967); *Chem. Abstr. Jpn.*, **68**, 29664 (1968).

(5) C. Heidelberger, *Progr. Nucleic Acid Res. Mol. Biol.*, **4**, 1 (1965).

(6) G. J. Coomen, F. Alewijk, D. Blok, and U. K. Pandit, *Heterocycles*, **12**, 1535 (1979).

(7) S. A. Hiller, R. A. Zhuk, and G. Ya. Nashatyr, *Khim. Geterotstikl. Soedin. Sb.*, **3**, 577 (1968); Chem. Abstr. Jpn., **69**, 96641h (1968).

(8) M. Tada, *Bull. Chem. Soc. Jpn.*, **50**, 2406 (1977).

(9) S. Ozaki, Y. Ike, H. Mizuno, K. Ishikawa, and H. Mori, *ibid.*, **50**, 2406 (1977).

(10) T. T. Sakai, A. L. Pogolotti, and D. V. Santi, *J. Heterocycl. Chem.*, **5**, 849 (1968).

(11) M. Yasumoto, I. Yamawaki, T. Marunaka, and S. Hashimoto, *J. Med. Chem.*, **21**, 738 (1978).

(12) A. Hoshi, M. Iigo, M. Yoshida, and K. Kuretani, *Gann*, **66**, 673 (1975).

(13) M. Iigo, A. Hoshi, A. Nakamura, and K. Kuretani, *Cancer Chemother. Pharmacol.*, **1**, 203 (1978).

(14) T. Kametani *et al.*, *J. Med. Chem.*, **23**, 1324 (1980).

(15) K. A. Watanabe, A. Matsuda, M. J. Halat, D. H. Hollenberg, J. S. Nisselbaum, and J. J. Fox, *ibid.*, **24**, 893 (1981).

(16) B. R. Baker and G. D. F. Jackson, *J. Pharm. Sci.*, **54**, 1758 (1965).

(17) M. Gacek and K. Undheim, *Acta. Chem. Scand. Ser. B*, **33**, 515 (1979).

(18) M. Fikus, K. L. Wierzchowski, and D. Sugar, *Biochem. Biophys. Res. Commun.*, **16**, 478 (1964).

(19) B. Ganem, *J. Org. Chem.*, **41**, 146 (1975).

(20) J. M. Fotunato and B. Ganem, *ibid.*, **41**, 2194 (1976).

(21) S. J. Hannon, N. G. Kundu, R. P. Hertzberg, R. S. Bhatt, and C. Heidelbeger, *Tetrahedron Lett.*, **21**, 1105 (1980).

(22) G. E. Moore, A. A. Sandberg, and K. Ulrich, *J. Natl. Cancer Inst.*, **36**, 405 (1966).

(23) G. E. Foley, H. Lazarus, S. Farber, B. G. Uzman, B. A. Boone, and R. E. McCarthy, *Cancer*, **18**, 522 (1965).

(24) N. Brock, *Cancer Treat. Rep.*, **60**, 301 (1976); G. E. Foley, O. M. Friedman, and B. P. Drolet, *Cancer Res.*, **21**, 57 (1961).

(25) T. A. Connors, P. B. Farmer, A. B. Foster, A. M. Gilman, M. Jarman, and M. J. Tisdale, *Biochem. Pharmacol.*, **22**, 1971 (1973).

(26) B. Testa and P. Jenner, "Drug Metabolism: Chemical and Biological Aspects," M. Dekker, New York, N.Y., 1976, pp. 82–97.

(27) K. L. Khanna, G. S. Rao, and H. H. Cornish, *Toxicol. Appl. Pharmacol.*, **23**, 720 (1972).

ACKNOWLEDGMENTS

Supported by Grant RO1-CA 257125 from the Division of Cancer Treatment, National Cancer Institute, National Institutes of Health, Department of Health, Education, and Welfare.

The authors wish to thank Dr. Zoltan Tokes and Mr. Csaba Csipke for the cell culture studies, and Dr. K. Chan and Mr. E. Watson for the mass spectral data. Thanks are also due to Mrs. Suvra Kundu for her technical help and Ms. Margaret Soh for her patience and excellent typing.

[5] Determined by using a Coulter Counter.

High-Pressure Liquid Chromatographic Assay of Cloxacillin in Serum and Urine

F. W. TEARE *x, R. H. KWAN, M. SPINO, and S. M. MacLEOD

Received April 6, 1981, from the * *Faculty of Pharmacy, University of Toronto, Toronto, Canada, M5S 1A1* and the *Department of Clinical Pharmacology, The Hospital for Sick Children, Toronto, Canada.* Accepted for publication September 2, 1981.

Abstract □ Two rapid, specific, and sensitive high-pressure liquid chromatographic (HPLC) assays were developed for cloxacillin in serum and urine. A reversed-phase column (RP-8) was selected for use with two different sets of HPLC conditions and sample pretreatment procedures. Cloxacillin extraction efficiencies are reported from serum and urine. Equations are presented for linear relationships between peak height or peak area ratios of cloxacillin to nafcillin (internal standard) and the cloxacillin concentration over a range of 0–80 μg/ml. The sensitivity limit of these assays was ~0.3 μg/ml of a standard solution for one method and 0.05 μg/ml for the other HPLC assay.

Keyphrases □ Cloxacillin—high-pressure liquid chromatographic assay, serum, urine, nafcillin □ Nafcillin—cloxacillin, high-pressure liquid chromatographic assay, serum, urine □ High-pressure liquid chromatography—cloxacillin in serum and urine □ Penicillins—high-pressure liquid chromatography of cloxacillin

Cloxacillin sodium (I), [3-(*o*-chlorophenyl)-5-methyl-4-isoxazoyl] penicillin sodium, is a semisynthetic penicillin synthesized in 1962 (1). It can be administered both parenterally and orally. Like other penicillins, I is sensitive to nucleophilic and electrophilic attack catalysed by general bases and acids, respectively. Maximum stability of

0022-3549/82/0800-0938$01.00/0

I occurs at pH 6.3 (2). The pKa of the carboxylic hydrogen is reported as 2.70–2.73 in water at 25° (3). Cloxacillin is 94–96% bound to serum proteins (4).

Previously reported assays for I include those based on spectrophotometry (5–10), titrimetric methods (6), microbiological methods (6, 7), an electrophoretic method (11), a polarimetric procedure (12), and an HPLC method for aqueous solutions (13).

Paper chromatograms of urine and serum samples following oral administration of I showed a similar ratio of unchanged I and a metabolite (14). Intramuscular injection of I is reported to give rise to metabolite formation as well. Cole *et al.* (15) reported that 21.6% of I appeared as the penicilloic acid metabolite in urine collected within 12 hr of a 500-mg oral dose but that none was found at half this dose.

Prompted by the apparent absence of any reported HPLC assay for cloxacillin in human serum or urine, two such methods were developed and are reported in this paper. These methods were developed for clinical studies and preliminary pharmacokinetic evaluation of I (16).

EXPERIMENTAL

The two distinct sets of HPLC assay conditions reported here will be referred to as HPLC Systems I and II. System I: RP-8 column; mobile phase, methanol–aqueous 0.04 *M* NaH_2PO_4 (4.1:5.9), pH 4.5; flow rate, 1.1 ml/min; detection wavelength, 225 nm; chart speed, 0.508 cm/min; retention time, cloxacillin, 8.75 min and nafcillin, 15.80 min. System II: RP-8 column; mobile phase, acetonitrile–aqueous 0.04 *M* NaH_2PO_4 (6.2:20), pH 4.5; flow rate, 1.6 ml/min; detection wavelength, 210 nm; chart speed, 0.508 cm/min; retention time, cloxacillin, 5.10 min and nafcillin, 6.60 min. Likewise, two different sample pretreatment procedures were used and are referred to as Procedures A and B.

Materials—A 10-cm × 4.6-mm i.d. stainless steel column[1] containing a chemical bonded reversed-phase (C_8) on 10-μM silica was selected. The modular HPLC system was comprised of a pump[2], an injection valve[3], a guard column[4], a variable wavelength UV-detector[5], and an integrator-plotter[6]. Other equipment used included a centrifuge[7] and mechanical mixer[8]. All inorganic buffer salts and acids were analytical grade and were dissolved in reagent grade water[9]. Organic solvents were acetonitrile[10] and methanol[10].

Mobile Phases I and II were deaerated and filtered through 1.0-μM pore membranes[11] under reduced pressure.

Standard Solutions—Cloxacillin sodium[12] (I) and nafcillin sodium[13] (II) were used as received for weekly preparation of stock standard and stock internal standard solutions, respectively. Human control serum[14] and control urine were used in the daily preparation of working standard solutions as well as simulated samples. Standard solutions of I were prepared in water, control serum, and control urine as follows: to each of seven appropriately labeled tubes[15] was added in succession 0.5 ml of water (or urine or serum), 0.01 ml of one of the working standards of I in the 0–54.3-μg range, and 0.05 ml (equivalent to 12.0 μg of II) of internal standard solution. The contents of each tube were thoroughly mixed by the mechanical mixer. These standards and similar simulated samples were subjected to one or the other of the pretreatment Procedures A or B, to compensate for recovery losses and other systematic errors.

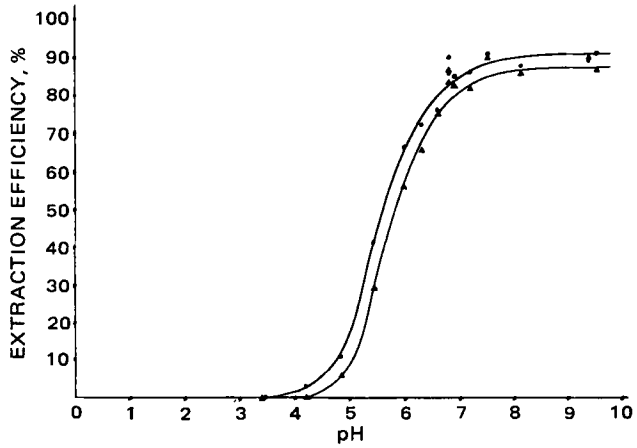

Figure 1—*Extraction efficiency of cloxacillin (●) and nafcillin (▲) from urine as a function of pH of the 0.04-*M *sodium dihydrogen phosphate buffer.*

Standard and Sample Pretreatment Procedures—*Procedure A*—Protein precipitation was performed by adding dropwise 0.5 ml of acetonitrile to a 0.5-ml sample of serum (or urine) in a small tube. This was followed by agitation for 20 sec by the mixer and centrifugation at 3000 rpm for 1 min. The clear supernate was filtered[16], and 10 μl of the filtrate was injected onto the column.

Procedure B—A drug extraction and back extraction procedure was performed as follows: to 0.5 ml of serum (or urine), in a small test tube, was added 0.05 ml of internal standard solution, equivalent to 12.0 μg of II. Then 0.05 ml of 1 *M* H_2SO_4 was added and the tube was mixed for 5 sec. Two milliliters of methylene chloride[17] was added and the tube was shaken for 2 min prior to centrifugation at 2000 rpm for 2 min. The organic layer was transferred to a second tube containing 1.0 ml of aqueous 0.04 *M* NaH_2PO_4, pH 6.80. This tube was stoppered and the shaking and centrifugation steps were repeated. An aliquot equivalent to ~75% of the aqueous layer containing the penicillins was transferred to a third tube, which was agitated vigorously on the mixer for 20 sec to dispel the volatile methylene chloride carried over in the aqueous layer. Injections (10 μl) of the final assay solution were used. Either integrated peak area ratios or peak height ratios of I–II were calculated and referred to a standard curve similarly constructed with standard solutions of I in accordance with the internal standard assay method. The sample concentrations were reported as micrograms of I per milliliter of serum or urine.

Precision and sensitivity limits were estimated for these assays.

RESULTS AND DISCUSSION

Preliminary trials were made using three reversed-phase columns[18] and mobile phases consisting of various ratios of aqueous buffers and either methanol or acetonitrile. Simple mixtures of water and methanol or acetonitrile proved inadequate for these assays. The effect of buffer pH was studied (16). The best results were obtained with an RP-8 column using aqueous 0.04 *M* NaH_2PO_4, pH 4.5, blended with methanol or acetonitrile in HPLC Systems I and II, respectively. These systems provided adequate resolution at desirable retention times. The wavelength of detection was selected to give maximum sensitivity consistent with minimum interference from trace endogenous biological materials. The method of sample pretreatment was developed to minimize interferences arising from the biological fluids.

Pretreatment Procedure A involving a simple protein precipitation step produced good results when HPLC System I was used. However, the addition of acetonitrile diluted the sample and, hence, decreased the level of sensitivity for I in the method. Procedure B involved the extraction of the undissociated acid forms of penicillins I and II with methylene chloride, followed by back-extraction of the ionized forms into aqueous phosphate buffer, pH 6.8. This procedure reduced the level of endogenous

[1] MPLC Concept RP-8 column and holder, Brownlee Labs, Santa Clara, CA 95050.
[2] Model 6000A, Waters Associates Inc., Milford, MA 01757.
[3] Model U6K, Waters Associates, Milford, MA 01757.
[4] Column survival kit packed with CO: Pell ODS (No. 6561-403), Whatman, Inc., Clifton, NJ 07014.
[5] Model 450, Waters Associates, Milford, MA 01757.
[6] Data module, model 730, Waters Associates, Milford, MA 01757.
[7] Sorvall Centrifuge, model GLC-2 with head adapter HL-4 and No. 575 tube holders, Du Pont Co., Wilmington, DE 19898.
[8] Vortex-Genie, Cat. No. 12-812-VI, Fisher Scientific Co.
[9] Millipore Corp., Bedford, MA 01730.
[10] Caledon Laboratories Ltd., Georgetown, Ontario, Canada.
[11] Gelman Instrument Co., Ann Arbor, MI 48106.
[12] Beecham Laboratories, Pointe Claire, Quebec, Canada.
[13] Wyeth Limited.
[14] Grand Island Biological Co., Grand Island, NY 14072.
[15] 12-mm × 75-mm polypropylene or glass tubes closed with polyethylene caps.
[16] Type FA, Teflon, 0.5-μm pore diameter, Millipore Corp.
[17] Methylene chloride, HPLC-grade, UV-Cutoff 230 nm, Caledon Laboratories, Ltd.
[18] Brownlee Labs, Santa Clara, CA 95050, MPLC Concept RP-2, RP-8, and RP-18, 10-cm × 4.6-mm i.d. columns.

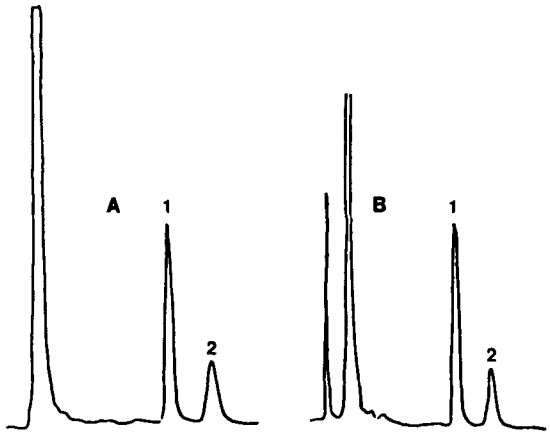

Figure 2—*(A) Representative chromatogram of a serum extract of (1) cloxacillin (9.04 min) and (2) nafcillin (11.42 min) on a 25-cm × 4.6-mm i.d. RP-8 column with a column guard. (B) Same as A except the column guard was removed: (1) cloxacillin (7.22 min), and (2) nafcillin (9.4 min).*

material interference and enhanced the sensitivity of the assay for I and II through the use of a detection wavelength of 210 nm.

Figure 1 shows the pronounced effect of buffer pH on the extraction efficiency of penicillins I and II in pretreatment Procedure B. A pH of 6.80 gave near optimal recovery and remains within the pH range of compatibility for these reversed-phase columns. A greater level of interference by endogenous biological materials occurs as the buffer pH becomes >pH 7.0 (16). The methylene chloride volume used in Procedure B also markedly affects the overall extraction efficiency of I and II. A 1:1 volume ratio of methylene chloride–serum produced a troublesome gelatinous globule due to proteins present. Although volume ratios of 4:1 or 5:1 gave similar and good drug recoveries, 6:1 or larger ratios caused lower recoveries of these drugs (16). The 4:1 volume ratio of methylene chloride–serum was selected for the sample (or standard) serum pretreatment Procedure B. The length of exposure of drugs I and II to sulfuric acid (Procedure B) is critical. This exposure to acid must be minimized and fixed at a value of <5 min. It has been found that ~1.5% of cloxacillin and 6.4% of nafcillin are degraded during 5 min when exposed to this strong mineral acid. Fortunately, this exposure to acid can easily be reduced if only a few serum samples are extracted at one time. The absence of degraded I and II peaks on HPLC chromatograms of samples pretreated by Procedure B indicates that insignificant, if any, degradation occurred during this short extraction period.

Figure 2 shows a representative chromatogram of cloxacillin and internal standard, nafcillin, extracted by Procedure B and chromatographed by System II, except that a longer column[19] of the same type packing was used. Figure 2 also shows the influence of the guard column. Figure 3 shows a typical chromatogram obtained with the shorter RP-8 column[18], using otherwise identical conditions. Note the small peak at 3.70 min due to residual methylene chloride, which was not adequately removed from this sample as it was in the normal procedure for Procedure B. This shorter RP-8 column had an advantage in that time and solvents were saved due to the shorter retention times for penicillins I and II.

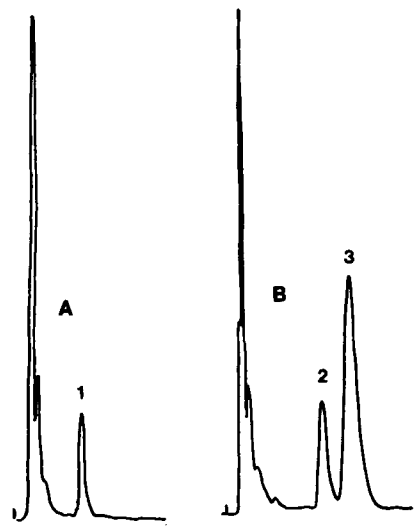

Figure 3—*Cloxacillin extracted from serum and chromatographed on a 10-cm × 4.6-mm i.d. RP-8 column. (A) Blank serum extract showing Peak 1 due to unremoved methylene chloride (3.70 min); (B) serum extracted cloxacillin (Peak 2, 5.3 min) and nafcillin (Peak 3, 6.85 min).*

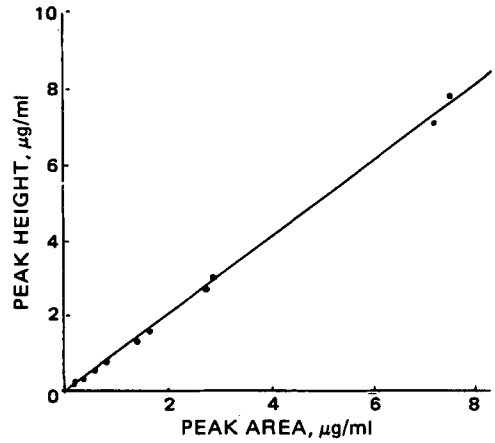

Figure 4—*Comparison of the serum cloxacillin concentrations from two human males as assayed by the internal standard method using peak height ratio and peak area ratio of cloxacillin to nafcillin. Linear regression analysis of this plot yields the equation* $y = 1.0117x - 0.0452$, *with a coefficient of correlation,* $r = 0.9990$. *A 250-mg iv dose of cloxacillin was given to each volunteer.*

The mean absolute extraction efficiencies for six replicate cloxacillin standards using Procedure B were 83.4 ± 1.4% *SD*, coefficient of variation (*CV*) = 1.6 and 91.4 ± 3.5%, *CV* = 3.8%, from serum and urine standards, respectively (16). Similarly determined mean extraction efficiencies for nafcillin (internal standard) were 78.9 ± 1.4%, *CV* = 1.8% and 84.5 ± 2.8%, *CV* = 3.3% for serum and urine standards, respectively. Neither serum nor urine standards containing both penicillins I and II gave rise to any extra peaks which could not be accounted for when the assay involved the pretreatment Procedure B with HPLC System II. This suggests the absence of any significant *in vitro* acid degradation of I and II. These reproducible high recoveries from both biological fluids ensure rather acceptable sensitivity for these assays of cloxacillin.

The precision of the HPLC System II was determined using a simulated serum sample containing 5 μg of I and 1.5 μg of II as well as 0.5 ml of control human serum. Sample pretreatment Procedure B was used and six replicate 10-μl injections of the final assay solution were assayed according to HPLC System II in which peak height ratios were calculated. The mean peak height ratio of I–II was 3.273 ± 0.032, *CV* = 1.0%.

The minimum quantitative limit, defined here as a signal–noise ratio of 3, for cloxacillin in an aqueous standard was ~0.3 μg/ml using HPLC System I and 0.05 μg/ml using HPLC System II. These do not represent overall assay sensitivity limits, since no pretreatment procedures were employed.

In the assay of cloxacillin using sample pretreatment Procedure B and HPLC System II, either peak height ratios or integrated peak area ratios of I–II can be used. Twelve serum samples were obtained from two male humans after different times following infusion of 250 mg iv of cloxacillin. Duplicate aliquots of each sample were extracted using Procedure B and assayed with HPLC System II. Figure 4 shows a comparison of the two methods of plotting, through regression analysis[20], in which the coefficient of correlation ($r = 0.9990$) indicates excellent agreement. Therefore, either I–II ratio can be used in the preparation of the internal standard method calibration curve for I. Figure 4 also confirms the excellent reproducibility of this assay over the concentration range used. The equation obtained by regressional analysis of the serum calibration curve, using peak height ratios of I–II *versus* concentration of I in six cloxacillin serum standards assayed by the same procedure, was $y = 0.591x + 0.0162$, ($r = 0.9976$).

Since both penicillins were somewhat more efficiently extracted

[19] Lichrosorb RP-8 packing in a HiBar II column, 25-cm × 4.6-mm i.d., EM Lab Inc., E. Merck, Darmstadt, W. Germany.

[20] Hewlett-Packard calculator model 9100A; Plotter, model 9125B; and program cards, model 9100.

(Procedure B) from urine than from serum, the calibration curves for I in these two biological fluids differed slightly. These calibration curves can be represented by equations obtained through linear regressional analysis: $y = 0.0437x + 0.0070$, ($r = 0.9991$) and $y = 0.0462x + 0.0270$, ($r = 0.9985$) for serum and urine cloxacillin standards, respectively. In these equations, y equals the integrated peak area ratio of I–II, and x equals the cloxacillin standard concentration in the serum or urine. HPLC System II was used to obtain these calibrations. The cloxacillin concentration covered the 0–80 μg/ml range of biological fluid.

The specificity of either HPLC System I or II is indicated by the fact that no endogenous material, metabolite of I, or degradation product of I or II gave peaks having the same retention times of I or II in chromatograms of *in vivo* serum or urine or of simulated *in vitro* serum or urine samples. The same was true for aqueous solutions of I or II deliberately degraded under acidic or alkaline conditions (16). No interfering peaks were detected in HPLC System II from extracts of human or rabbit serum or of human urine following intravenous administration of cloxacillin. Many other drugs which might be administered during cloxacillin therapy failed to interfere with this HPLC assay. The specific drugs tested for interference were penicillin G, amoxicillin, ticarcillin, carbenicillin, cephalexin, ampicillin, theophylline, acetaminophen, hydrocortisone acetate, vitamins A, C, D and E, and chloramphenicol (16). While this is not an exhaustive list, it represents many drugs that might be found in conjunction with I in urine or serum. Diazepam might partially interfere with this HPLC assay if its serum level is high (16).

The assay method involving pretreatment Procedure A and HPLC System I was initially developed to assay cloxacillin in human serum and urine but has also been used to determine I in rabbit plasma and serum. The same assay was used to establish that 51.35% of an intravenous dose of cloxacillin was excreted unchanged in the urine of one 75-kg human male volunteer within 24 hr. An extra peak was observed not previously seen in *in vitro* urine samples of cloxacillin. The peak may represent a metabolite, since it is not identical to any acidic or alkaline-degraded I peak. Cloxacillin had half-life values ($t_{1/2}$) of 26.9 and 26.5 min in two healthy human male volunteers who received intravenous doses of I (16). These values are in reasonable agreement with a reported value of 33 min in normal human adults (17). The overall elimination rate constants determined in the same two persons were 0.0258 min^{-1} and 0.0262 min^{-1} (16) and compare favorably with a reported value of 0.021 ± 0.003 min^{-1} (17).

In summary, two successful HPLC assays, together with serum and urine sample pretreatment procedures, have been developed. Pretreatment Procedure A used with HPLC System I, while slower, is superior for the resolution of peaks for I and II from each other and all biological endogenous materials or degradation compounds of I or II. The assay including pretreatment Procedure B and HPLC System II is preferred for the rapid assay of unchanged cloxacillin in urine and serum. This assay is specific, sensitive, rapid, precise, and has sufficient accuracy for the intended purposes.

REFERENCES

(1) J. H. C. Nayler, A. A. W. Long, D. M. Brown, P. Acred, G. N. Rolinson, F. R. Batchelor, S. Stevens, and R. Sunderland, *Nature (London)*, **195,** 1264 (1962).

(2) H. Bundgaard and K. Ilver, *Dan. Tidsskr. Farm.*, **44,** 365 (1970).

(3) D. C. Rapson and A. E. Bird, *J. Pharm. Pharmacol.*, **15,** 222T (1963).

(4) C. M. Kunin, *Clin. Pharmacol. Ther.*, **7,** 166, 180 (1966).

(5) M. W. Brandris, E. L. Denny, M. A. Huber, and H. G. Steinman, *Antimicrob. Ag. Chemother.*, **1962,** 627.

(6) "U.S. Pharmacopeia," XVIII Rev., U.S. Pharmacopeial Convention, Rockville, Md., (1970).

(7) "Code of Federal Regulations," U.S. Government Printing Office, Washington, D.C.

(8) F. Saccani and G. Pitrola, *Boll. Chim. Farm.*, **108,** 29 (1969).

(9) T. Yasuda and S. Shimada, *J. Antibiot.*, **24,** 290 (1971).

(10) A. G. Davidson and J. B. Stenlake, *J. Pharm. Pharmacol.*, **25,** 156P (1973).

(11) A. Carlström, K. Dornbusch, A. Hagelberg, and A. Malmborg, *Acta Pathol. Microbiol. Scand., Sec. B*, **82,** 67 (1974).

(12) C. E. Rasmussen and T. Higuchi, *J. Pharm. Sci.*, **60,** 1608 (1971).

(13) T. Yamana, A. T. Suji, E. Miyamoto, and O. Kubo, *ibid.*, **66,** 747 (1977).

(14) G. N. Rolinson and F. R. Batchelor, *Antimicrob. Ag. Chemother.*, **1962,** 654.

(15) M. Cole, M. D. Kenig, and V. A. Hewitt, *ibid.*, **3,** 463 (1973).

(16) R. H. B. Kwan, Thesis, University of Toronto, Toronto, Canada 1980.

(17) E. H. Nauta and H. Mattie, *Clin. Pharmacol. Ther.*, **20,** 98 (1976).

ACKNOWLEDGMENTS

Supported by a grant from Beecham Laboratories, Pointe Claire, Quebec, Canada.

Prolongation of Drug Half-Life due to Obesity: Studies of Desmethyldiazepam (Clorazepate)

DARRELL R. ABERNETHY [x], DAVID J. GREENBLATT, MARCIA DIVOLL, and RICHARD I. SHADER

Received August 17, 1981, from the *Division of Clinical Pharmacology, Departments of Psychiatry and Medicine, Tufts University School of Medicine and New England Medical Center Hospital, Boston, MA 02111.* Accepted for publication November 20, 1981.

Abstract □ Desmethyldiazepam pharmacokinetics were determined after oral administration of its precursor, clorazepate, to 12 obese subjects (mean weight: 105.4 kg; mean percent ideal body weight: 170%) who were matched for age, sex, and smoking habits with 12 normal controls (66.5 kg; percent ideal body weight: 103.3%). After an overnight fast, a single 15-mg clorazepate capsule, equivalent to 10.3 mg of desmethyldiazepam, was administered. Multiple plasma samples drawn 10–42 days postdose were analyzed for desmethyldiazepam by electron-capture GLC. Obese subjects compared to controls had a prolonged desmethyldiazepam elimination half-life ($t_{1/2}$) (154.1 hr *versus* 57.1 hr; $p < 0.005$). Assuming quantitative conversion of clorazepate to desmethyldiazepam and 100% systemic availability, volume of distribution (V_d) was greatly increased in the obese (158.8 liters *versus* 63.3 liters; $p < 0.001$). The value of V_d remained greater even after correction for body weight (1.52 liter/kg *versus* 0.94 liter/kg; $p < 0.005$). However, clearance of desmethyldiazepam was not different between groups (13.2 ml/min in obese *versus* 13.4 ml/min in controls). The percent ideal body weight was highly correlated with V_d ($r = 0.82$), as was total body weight ($r = 0.86$). The value of $t_{1/2}$ was correlated highly with V_d ($r = 0.89$) but only weakly with clearance ($r = -0.38$). Therefore, the large increase in the desmethyldiazepam $t_{1/2}$ value seen in obese subjects is predominantly due to the disproportionate distribution of this lipid-soluble drug into body fat as opposed to lean tissue. The contribution of clearance to desmethyldiazepam $t_{1/2}$ was of much less importance than was V_d in this obese study population.

Keyphrases □ Desmethyldiazepam—prolongation of drug half-life due to obesity □ Pharmacokinetics—prolongation of drug half-life due to obesity, desmethyldiazepam □ Obesity—prolongation of drug half-life, desmethyldiazepam

The elimination half-life ($t_{1/2}$) of drugs has often been equated with the rate of biotransformation and clearance (1). However, principles of pharmacokinetics indicate that half-life is a hybrid variable, depending upon both drug distribution and clearance (2):

$$t_{1/2} = \frac{0.693 \times \text{Volume of Distribution } (V_d)}{\text{Clearance}} \quad \text{(Eq. 1)}$$

To date only a few experimental circumstances have been described in which a high inverse correlation between clearance and elimination half-life did not exist, with a significant contribution to variability in elimination half-life being attributable instead to changes in the volume of distribution (3, 4). Clorazepate, a prodrug which is converted to desmethyldiazepam after oral administration (5), has been used in this laboratory and by others as a means of evaluating desmethyldiazepam pharmacokinetics (6, 7). The present study demonstrates that in obese individuals, comprising perhaps 20% of the population of the United States (8), a potentially serious misinterpretation of drug metabolizing capacity may occur with some lipid-soluble drugs when elimination half-life is used as a measure of drug metabolism.

EXPERIMENTAL

Subjects—Twelve obese (>133% ideal body weight) and 12 control (<125% ideal body weight) subjects participated in the study (Table I).

Table I—Subject Characteristics and Kinetic Variables for Diazepam

	Mean (with range) Values[a]	
	Obese ($n = 12$)	Control ($n = 12$)
Subject Characteristics		
Age, years	33(23–61)	33(24–74)
Sex, F/M	8/4	7/5
Total body weight, kg	105(77–197)	67(51–91)[b]
Ideal body weight, kg	62(41–77)	65(50–82)
Percent ideal body weight	170(134–257)	103(86–125)[c]
Smoking, no/yes	9/3	9/3
Kinetic Variables of Absorption		
Absorption lag time, hr	0.20(0.06–0.25)	0.40(0.18–0.73)[c]
Half-Time for absorption, hr	0.94(0.25–2.03)	0.48(0.02–1.85)
Time to peak plasma concentration, hr	1.3(0.5–2.5)	1.5(0.5–3.0)
Peak plasma concentration, ng/ml	149(90–239)	249(89–590)[d]
Kinetic Variables of Elimination		
Elimination half-life, hr	154(64–369)	57(30–77)[b]
V_d, liter	159(91–340)	63(38–119)[c]
V_d/kg total body weight, liter/kg	1.52(1.00–2.51)	0.94(0.63–1.30)[b]
V_d/kg ideal body weight, liter/kg	2.58(1.49–4.43)	0.98(0.60–1.45)[c]
Clearance, ml/min	13.2(7.4–18.2)	13.4(5.7–21.8)
Clearance/kg total body weight, ml/min/kg	0.14(0.05–0.23)	0.20(0.10–0.31)
Free fraction, percent	2.4(1.5–3.1)	2.5(1.8–3.7)

[a] Student t test for difference between control and obese groups; [b] $p < 0.005$. [c] $p < 0.001$. [d] $p < 0.02$.

The ideal body weight was defined from life insurance tables as follows (9):

Ideal body weight (males) = 50 kg ± 0.9 kg/cm above or below 150-cm height.

Ideal body weight (females) = 45 kg ± 0.9 kg/cm above or below 150-cm height.

The percent ideal body weight was calculated as the ratio of actual or total body weight to ideal body weight. Other measures of adiposity such as weight/height and weight/height^2 (10) have been evaluated in such populations, but it was found that none of these other indexes provides more information than dose comparison of total body weight and ideal body weight.

Obese and control subjects were matched for age, sex, and cigarette smoking habits. No subjects were on a special diet designed for weight loss and all remained at the same weight during the study.

Procedure—After an overnight fast, all subjects received a capsule containing 15 mg of clorazepate dipotassium[1] with 75 ml of water. Subjects remained fasting for 3 hr after drug ingestion. Venous blood samples were drawn into heparinized tubes before the dose, at 5, 15, 30, and 45 min, and 1, 1.5, 2.0, 2.5, 3, 4, 6, 8, 12, and 24 hr, and every 1 to 2 days for 10–42 days. An indwelling butterfly cannula, kept patent by a slow infusion (20 ml/hr) of physiologic saline, was used to obtain blood samples during the first 8 hr postdosing. All other samples were drawn by separate venipuncture. Samples on subsequent days were drawn in the nonfasting state. Blood specimens were centrifuged, and the plasma was separated and stored at −20° until assayed.

Analysis of Samples—Plasma desmethyldiazepam concentrations were determined by electron-capture GLC (6). The extent of diazepam binding to plasma protein for each subject was determined from pooled samples drawn in the nonfasting state at least 72 hr postdose. Binding

[1] Tranxene, Abbott Laboratories, North Chicago, Ill.

0022-3549/82/0800-0942$01.00/0

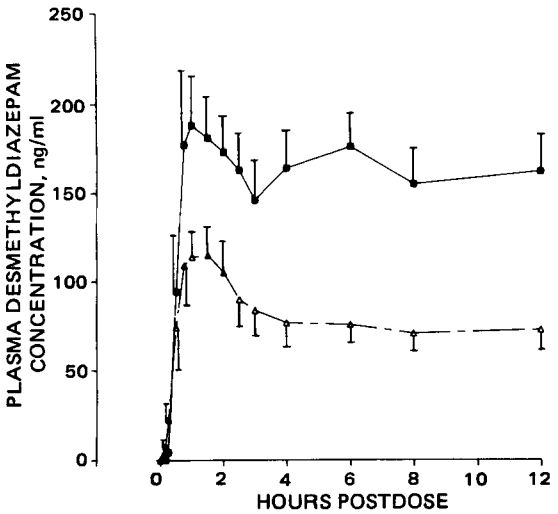

Figure 1—*Mean plasma desmethyldiazepam concentrations over the initial 12 hr after drug administration. Each value is the mean (±SE) for the 12 subjects in obese and control groups at the corresponding time. Pharmacokinetic variables of absorption are listed in Table I. Key: (■) control; (△) obese.*

was determined by equilibrium dialysis using duplicate 2-ml samples spiked to contain 500 ng of desmethyldiazepam/ml. Recovery of desmethyldiazepam from the dialysis system was 100% and the variation for replicate samples was <10%. Binding was independent of the total desmethyldiazepam plasma concentration up to levels of 5000 ng/ml (11, 12).

Data Analysis—Plasma desmethyldiazepam concentrations were analyzed by weighted iterative nonlinear least-squares regression techniques as described previously (13–15). Since desmethyldiazepam derived from orally ingested clorazepate is 100% bioavailable[2], coefficients and exponents from the function of best fit were used to calculate the following kinetic variables: lag time prior to the start of absorption, absorption half-life, total volume of distribution (V_d) using the area method, elimination half-life, and total clearance (16, 17). The data were further analyzed by determination of kinetic parameters for the fraction not bound to plasma protein (18, 19). Assuming that protein binding of desmethyldiazepam for a given subject was constant over time and independent of total concentration, values for V_d and clearance were divided by the subject's unbound fraction yielding values of unbound V_d and unbound (intrinsic) clearance.

Differences in kinetic variables between obese and control groups were

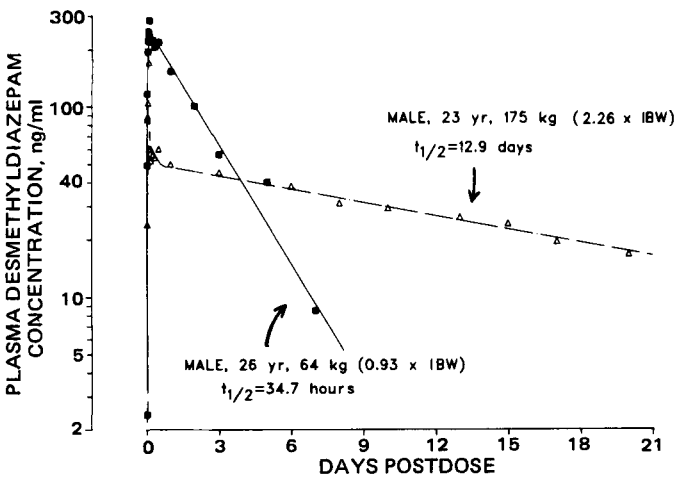

Figure 2—*Plasma desmethyldiazepam concentrations and pharmacokinetic functions following oral chlorazepate administration to a representative obese male [(△); 23 years; 175 kg (2.26 × IBW); $t_{1/2}$ = 12.9 days] and to a matched control male of normal weight [(■); 26 years; 64 kg (0.93 × IBW); $t_{1/2}$ = 34.7 hr].*

[2] Unpublished observation.

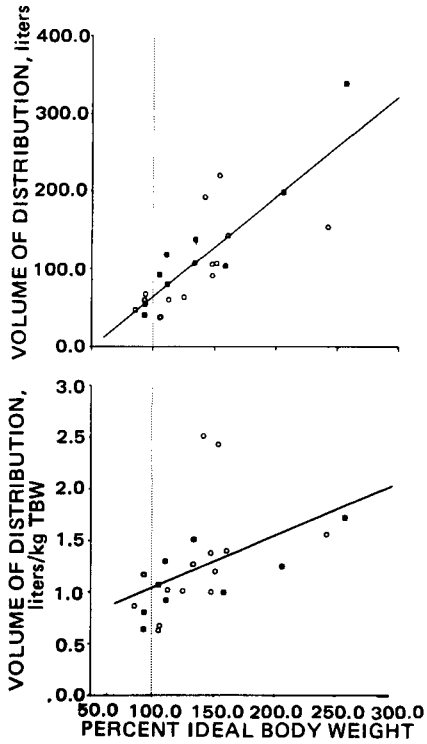

Figure 3—*Relation of percent ideal body weight (abscissa) to desmethyldiazepam absolute volume of distribution (top) and corrected for total body weight (r = 0.82) (bottom). Solid lines were determined by least-squares regression analysis. Key: (■) male; (○) female.*

assessed by Student t test. Relationships among kinetic variables and subject characteristics were evaluated by linear regression analysis.

RESULTS

Lag time elapsing prior to the appearance of desmethyldiazepam in plasma after clorazepate was significantly shorter in the obese than in the control subjects ($p < 0.001$). However, absorption half-life and the time to peak plasma concentration did not differ significantly between groups (Table I). Peak plasma concentrations were much lower in the obese subjects ($p < 0.02$), presumably reflecting the much more extensive distribution of desmethyldiazepam in obesity (Fig. 1, Table I).

Elimination of desmethyldiazepam from plasma after ingestion of clorazepate was adequately described in all subjects by a linear sum of exponential terms (Fig. 2). Pharmacokinetic variables (Table I) reveal a significantly prolonged elimination half-life ($p < 0.001$) in obese as compared to control subjects. This is not explained by a change in clearance, as total metabolic clearance was nearly identical in the two groups (Table I). Since the extent of protein binding was similar in obese and control groups (Table I), intrinsic (unbound) clearance was also similar in the two groups.

The V_d value, in liters, as well as V_d corrected for total body weight (V_d/kg of total body weight) and V_d corrected for ideal body weight (V_d/kg of ideal body weight), were significantly larger in obese subjects than controls (Table I). Represented as a continuous function among all subjects, there was a highly significant ($r = 0.82$; $p < 0.001$) positive correlation between percent ideal body weight and absolute V_d, as well as V_d/kg total body weight ($r = 0.49$, $p < 0.05$) (Fig. 3). This indicates disproportionate distribution of desmethyldiazepam into excess body weight over ideal body weight that is greater than distribution into ideal body weight. Using mean values for total body weight and V_d, distribution of desmethyldiazepam into excess body weight over ideal body weight is approximately twice as extensive as distribution into ideal body weight.

The difference in elimination half-life between groups is the result of the marked increase in V_d in the obese group. This is demonstrated by the highly significant correlation between elimination half-life and V_d ($r = 0.89$; $p < 0.001$) and the nonsignificant correlation between elimination half-life and clearance ($r = -0.38$; *NS*) (Fig. 4).

DISCUSSION

Many drugs are administered on the basis of dose per unit body weight. This assumes that drug clearance is proportional to weight, and that drug

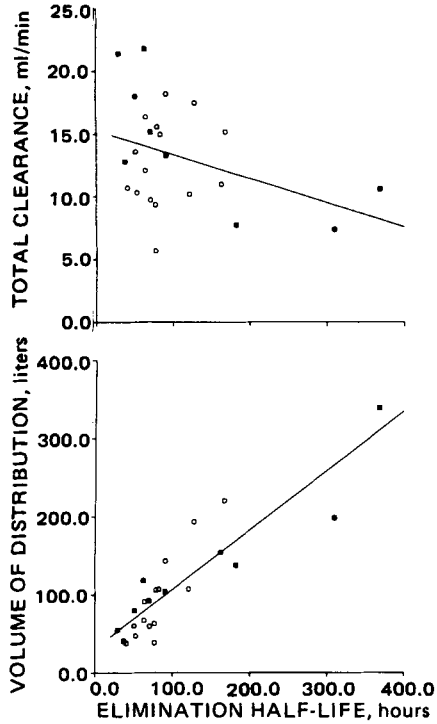

Figure 4—*Relation of desmethyldiazepam volume of distribution (top) and total clearance (bottom) to desmethyldiazepam elimination half-life (abscissa). Volume of distribution was highly correlated with half-life (r = 0.89), but clearance is not significantly related to half-life (r = −0.38). Key: (■) male; (○) female.*

distribution per unit weight is unchanged with large variations in body weight. However, such assumptions may not be warranted since obese individuals may have a significant incidence of hepatocellular disease (20), changes in renal blood flow (21), and marked deviation in body composition from normal (8). A recent report demonstrates a marked increase in tissue enflurane uptake and an increase in the rate and amount of metabolite appearing in peripheral blood in the obese state in the absence of other pathological processes (22). In addition, drug distribution may be quite different in the obese individual as compared to one of normal body weight. Evaluation of the kinetics of digoxin (23), gentamicin (24), tobramycin (24, 25), and amikacin (26) in obesity suggest that distribution of these drugs is mainly into lean body mass, such that an incorrect drug dosage may result from calculation based on total body weight. Similar results are reported for theophylline (27). In contrast, fat-soluble drugs such as diazepam may be much more extensively distributed into body weight in excess of ideal body weight than into ideal body weight (3). Again, this may result in incorrect drug dosage and/or prolongation of time to steady-state plasma concentration if loading and maintenance doses do not take the degree of obesity into consideration.

The present study assessed the effect of obesity on the absorption, distribution, and clearance of desmethyldiazepam, a lipid-soluble benzodiazepine antianxiety agent. Subjects in both obese and control groups varied in age, sex, and cigarette smoking habits, all of which can influence drug disposition. However, these factors are unlikely to have influenced the results, since control and obese subjects were matched for these characteristics. The findings indicate that distributional changes in obesity can remarkably alter the apparent half-life of elimination despite no change in metabolic clearance. Furthermore, the extent of distribution into excess body weight over ideal body weight is even more extensive than into ideal body weight. This is presumably due to the lipophilic character of desmethyldiazepam.

Thus, elimination half-life of lipid-soluble drugs changes greatly in obese patients in the absence of change in total metabolic clearance. Total clearance is the appropriate pharmacokinetic parameter to use for evaluation of the rate of biologic drug removal, as drug dose required to achieve a given steady-state plasma level is a function of this independent variable, not the dependent variable elimination half-life.

REFERENCES

(1) L. G. Sultatos, B. H. Dvorchik, E. S. Vesell, D. G. Shand, and R. A. Branch, *Clin. Pharmacokinet.*, **5**, 263 (1980).

(2) D. Perrier and M. Gibaldi, *J. Pharmacol. Exp. Ther.*, **191**, 17 (1974).

(3) D. R. Abernethy, D. J. Greenblatt, M. Divoll, J. S. Harmatz, and R. I. Shader, *ibid.*, **217**, 681 (1981).

(4) D. R. Abernethy, D. J. Greenblatt, and M. D. Allen, *Clin. Res.*, **28**, 233A (1980).

(5) P. J. Corrigan, G. C. Chao, W. M. Barker, D. J. Hoffman, and A. H. C. Chun, *J. Clin. Pharmacol.*, **17**, 18 (1977).

(6) D. J. Greenblatt, *J. Pharm. Sci.*, **67**, 427 (1978).

(7) E. Rey, P. D'Athis, P. Giraux, D. de Lautre, J. M. Turquois, J. Chavinie, and G. Olive, *Eur. J. Clin. Pharmacol.*, **15**, 175 (1979).

(8) G. A. Bray, *Disease-a-Month*, **26**, 7 (1979).

(9) ANON, *Stat. Bull. Metropol. Life Ins. Co.*, 40, Nov.–Dec. (1959).

(10) C. V. Florey, *J. Chronic Dis.*, **23**, 93 (1970).

(11) D. J. Greenblatt, M. D. Allen, J. S. Harmatz, and R. I. Shader, *Clin. Pharmacol. Ther.*, **27**, 301 (1980).

(12) E. Woo and D. J. Greenblatt, *J. Pharm. Sci.*, **68**, 466 (1979).

(13) D. J. Greenblatt and J. Koch-Weser, *N. Engl. J. Med.*, **293**, 702, 964 (1975).

(14) D. W. Marquardt, *J. Soc. Ind. Appl. Math.*, **11**, 431 (1963).

(15) R. A. Usanis, "NLIN-Nonlinear Least-Squares Estimation of Parameters (Library Services Series Document No. LSR-089-1)," Triangle Universities Computation Center, Research Triangle Park, N.C., 1972.

(16) J. G. Wagner, "Fundamentals of Clinical Pharmacokinetics," Drug Intelligence Publications, Hamilton, Ill., 1975.

(17) M. Gibaldi and D. Perrier, "Pharmacokinetics," Marcel Dekker, New York, N.Y., 1975.

(18) J. Koch-Weser and E. M. Sellers, *N. Engl. J. Med.*, **294**, 311, 526, (1976).

(19) J. G. Wagner, *Eur. J. Clin. Pharmacol.*, **10**, 425 (1976).

(20) M. Adler and F. Schaffner, *Am. J. Med.*, **67**, 811 (1979).

(21) J. K. Alexander, E. W. Dennis, and W. G. Smith, *Cardiovasc. Center Res. Bull.*, **1**, 39 (1962–1963).

(22) M. S. Miller, A. J. Gandolfi, R. W. Vaughan, and J. B. Bentley, *J. Pharmacol. Exp. Ther.*, **215**, 292 (1980).

(23) G. A. Ewy, B. M. Groves, M. F. Ball, L. Nimmo, B. Jackson, and F. Marcus, *Circulation*, **44**, 810 (1971).

(24) S. N. Schwartz, G. J. Pazin, J. A. Lyon, M. Ho, and A. W. Pasculle, *J. Infect. Dis.*, **138**, 499 (1978).

(25) R. A. Blouin, H. J. Mann, W. O. Griffen, L. A. Bauer, and K. E. Record, *Clin. Pharmacol. Ther.*, **26**, 508 (1979).

(26) L. A. Bauer, R. A. Blouin, W. O. Griffen, K. E. Record, and R. M. Bell, *Am. J. Hosp. Pharm.*, **37**, 519 (1980).

(27) P. Gal, W. J. Jusko, A. M. Yurchak, and B. A. Franklin, *Clin. Pharmacol. Ther.*, **23**, 438 (1978).

ACKNOWLEDGMENTS

Supported by Grants MH-34223, AG-00077, and GM-07611 from the United States Public Health Service.

The authors thank Ann Locniskar, Lawrence J. Moschitto, Ann M. Zumbo, Jerold S. Hamatz, Dr. Dean S. MacLaughlin, and the staff of the Clinical Study Unit, New England Medical Center Hospital (supported by USPHS Grant RR-24040) for their assistance.

Medicament Release from Suppository Bases I: Physicochemical Characteristics and Bioavailability of Indomethacin in Rabbits

NICHOLAS J. VIDRAS *, VINCENT E. REID *, N. R. BOHIDAR ‡, and FOTIOS M. PLAKOGIANNIS *x

Received August 2, 1979, from the *Division of Pharmaceutics, Arnold and Marie Schwartz College of Pharmacy and Health Sciences, Long Island University, Brooklyn, NY 11201 and ‡Merck, Sharp and Dohme Research Laboratories, West Point, PA 19486. Accepted for publication November 3, 1981.

Abstract □ This investigation was designed to determine the *in vitro* release of indomethacin from suppository bases and the *in vivo* bioavailability in rabbits. Suppositories containing 25 mg of indomethacin were made by the fusion method with theobroma oil, esterified fatty acids (C_{10}–C_{18}), and polyethylene glycol 1000. To produce an exact dosage form, a formula for the determination of the displacement value was derived, and it was found that theobroma oil > esterified fatty acids (C_{10}–C_{18}) > polyethylene glycol 1000. The suppository hardness was determined by using appropriate apparatus and it was found that the esterified fatty acids (C_{10}–C_{18}) allowed the formation of more brittle suppositories. The release rates were determined with the USP dissolution apparatus, with or without cellophane membrane, and it was found that polyethylene glycol 1000 > esterified fatty acids (C_{10}–C_{18}) > theobroma oil. The bioavailability of indomethacin after rectal administration was greater with polyethylene glycol base. Significant correlation was obtained during the first 45 min between the *in vitro* release (dialyzing tubing) and the *in vivo* bioavailability.

Keyphrases □ Indomethacin—physicochemical characteristics, bioavailability, rabbits, suppository bases □ Bioavailability—indomethacin physicochemical characteristics, rabbits, suppository bases □ Suppositories—bases, indomethacin, physicochemical characteristics, bioavailability, rabbits

Indomethacin, a nonsteroid drug, was first synthesized in 1961 (1). It has been proven to have anti-inflammatory and analgesic effects in rheumatoid arthritis (2–6), gout (7), osteoarthritis (8–10), ankylosing spondylitis (11), glomerulonephritis (12), and acute musculoskeletal disorders (13). Unfortunately, like other analgesic and anti-inflammatory agents, it carries the risk of GI irritation. The tablets and capsules, which are presently used, have led to peptic ulceration and anorexia (14, 15), nausea, vomiting, dyspepsia, and diarrhea (16). Other side-effects have involved the central nervous system, including headache, giddiness, mental changes, faintness, drowsiness, and blurring of vision. An attractive route of administration for patients with peptic ulcers and for those who are unable to tolerate the drug could be the rectal route.

Previous studies on the rectal administration of indomethacin (17–20) have given little information regarding the suppository bases used, the influence of the suppository base on the release of the drug, or the effects of the physicochemical properties such as hardness or melting range on *in vitro* and *in vivo* drug release. In this study, indomethacin suppositories in three different bases, polyethylene glycol 1000, esterified fatty acids (C_{10}–C_{18}), and theobroma oil were used to evaluate their physicochemical properties, to examine the *in vitro* release of indomethacin, its *in vivo* release in rabbits, and to correlate if possible the *in vitro* with *in vivo* data.

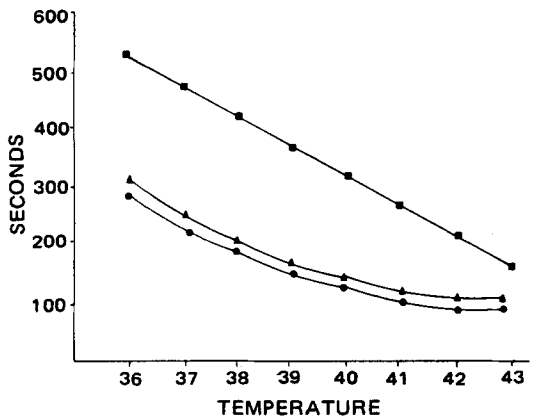

Figure 1—*Time interval for complete melting of indomethacin suppositories as a function of temperature using the USP disintegration apparatus. Key: (■) polyethylene glycol; (▲) esterified fatty acids (C_{10}–C_{18}); (●) theobroma oil.*

EXPERIMENTAL

Chemicals—Indomethacin[1], polyethelene glycol 1000[2], esterified fatty acids (C_{10}–C_{18})[3], theobroma oil[4], heptane[4], phosphate buffer[4] solutions, (pH 7–9), sodium hydroxide[4], and hydrochloric acid[4]. All reagents were analytical or reagent grade purity.

Preparation of Suppositories—All suppositories were prepared by the fusion method using a metal mold with 12 cavities (10). Drug displacement (3) in polyethylene glycol 1000, esterified fatty acids (C_{10}–C_{18}),

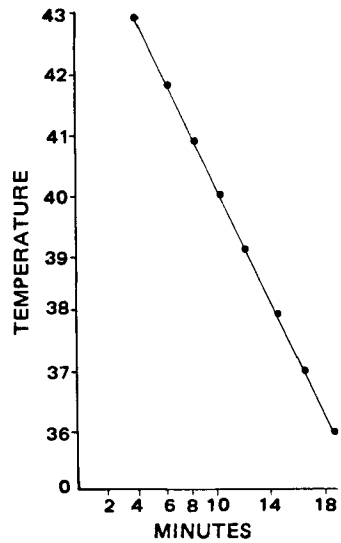

Figure 2—*Time interval for complete melting of indomethacin–polyethylene glycol base as a function of temperature using the commercial disintegration apparatus.*

[1] Merck, Sharp and Dohme, West Point, Pa.
[2] J. T. Baker Chemical Co., Philipsburg, N.J.
[3] Witepsol H-15, Kay-Fries Chemical Inc., Montvale, NJ 07645.
[4] Fisher Scientific Co., Springfield, N.J.

0022-3549/82/0800-0945$01.00/0

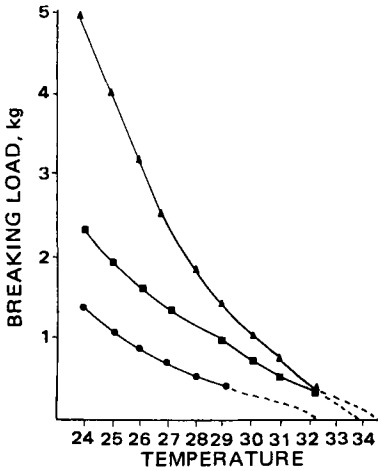

Figure 3—*Breaking load of the indomethacin suppositories as a function of temperature. Key: (■) polyethylene glycol; (▲) esterified fatty acids (C_{10}–C_{18}); (●) theobroma oil.*

and theobroma oil was first determined, and then the amount of indomethacin required was calculated.

Weight Variation—Twenty suppositories from each base were weighed, and the average weight and percent deviation for each suppository was calculated.

Content Uniformity Test—Although the USP does not specify a content uniformity for suppositories, the relative potency of the suppositories was determined. Thirty suppositories were randomly selected from each base, 10 of which were assayed individually. A preweighed suppository was melted and dissolved in 15 ml of phosphate buffer solution (pH 8). The buffer solution was added to a final yield of 1 liter. The adsorbance was measured on a spectrophotometer[5] at 318 nm. Blank suppositories were tested, and it was determined that the suppository vehicles had no effect on the UV absorbance at 318 nm. The concentration of indomethacin in the samples was determined from a standard curve.

Melting Range Test (Macro-Melting Range Test)—It has been shown (4, 5) that a narrow melting range is important in maintaining the shape of the suppository in ambient temperatures and in controlling the melting time of the suppository after insertion. The melting range test is a time measure for complete melting or dispersal of the suppository when immersed in a constant temperature water bath. Two apparatuses were used for the determination of the melting range. The USP tablet disintegration apparatus[6] was set as required in USP XIX, using water as the immersion fluid. A suppository, stored for at least 24 hr at room temperature, was placed in each tube of the basket, and each tube was covered with a disk. The time required for each suppository to completely melt at a specific temperature was determined. The temperature for this study ranged from 36 to 43°. The melting point testing apparatus for suppositories[7] was also used.

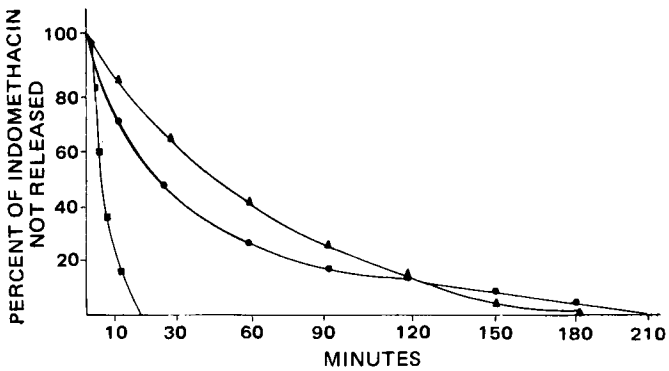

Figure 4—*Percentage of indomethacin not released from different suppository bases* versus *the time (min), using the USP dissolution apparatus. Key: (■) polyethylene glycol; (▲) esterified fatty acids (C_{10}–C_{18}); (●) theobroma oil.*

[5] Bausch-Lomb double beam spectronic 2000 UV by Shimadly.
[6] Erweaka, model ZT3, New York, N.Y.
[7] American Optical Co., New York, N.Y.

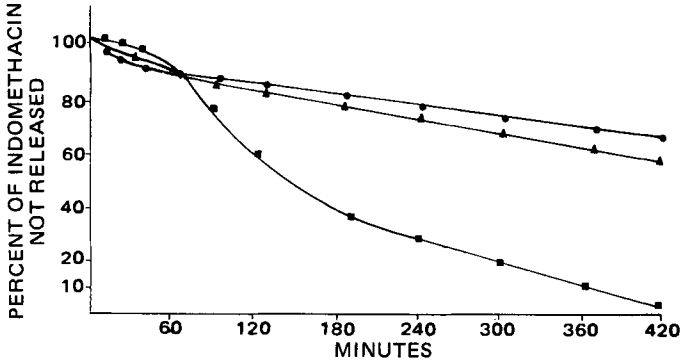

Figure 5—*Percentage of indomethacin not released from different suppository bases* versus *the time (min), using the USP dissolution apparatus and cellophane membrane. Key: (■) polyethylene glycol; (▲) esterified fatty acids (C_{10}–C_{18}); (●) theobroma oil.*

Breaking Test (Hardness)—The breaking test was designed to measure the brittleness and fragility of suppositories (1). This was measured by the weight in kilograms under which a suppository collapses at a specific temperature. The hardness of each suppository was determined by utilizing the fracture point testing apparatus for suppositories[7].

Release of Indomethacin from Suppository Bases—Three different methods were used for the determination of the release rates:

Method A—The USP rotating basket dissolution apparatus was used for the determination of release rates by this method. Each suppository was placed in the wire basket, which was lined from the inside with filter paper, and lowered into a flask containing 600 ml of phosphate buffer solution (pH 8). (The filter paper was used as a barrier for the diffusion of the suppository base.) The basket was rotated at 100 rpm at a constant temperature (37 ± 0.5°). Five-milliliter samples were withdrawn at appropriate time intervals and assayed to obtain a dissolution profile. Five milliliters of phosphate buffer was added to the dissolution medium to compensate for sampling. The absorbances of these solutions were measured at 318 nm on a spectrophotometer and the concentrations were determined from the standard curve.

Method B—The same apparatus and the conditions as previously described were employed. The modification was to place the suppository in a cellophane membrane[8] before exposure to the buffer solution.

Method C—This method employed dialysis. The dialyzing bags were prepared from dialysis tubing tied with plastic cord and soaked overnight in the phosphate buffer solution (pH 8). After rinsing the bags twice, 20 ml of phosphate buffer (pH 8) and one suppository were placed in each bag and suspended in a 500-ml wide-mouth bottle containing 400 ml of the phosphate buffer solution. The bottle was placed in a water bath at a constant temperature[9] of 39 ± 0.5° and agitated with a magnetic stirrer. At constant time intervals, a 5-ml sample was removed from the bottle and assayed to obtain a dissolution profile. Five milliliters of phosphate

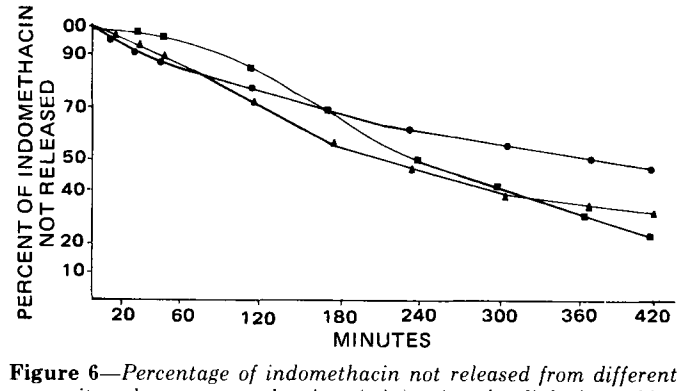

Figure 6—*Percentage of indomethacin not released from different suppository bases* versus *the time (min) using the dialyzing tubing method. Key: (■) polyethylene glycol; (▲) esterified fatty acids (C_{10}–C_{18}); (●) theobroma oil.*

[8] Dupont Co.
[9] The temperature, 39°, was chosen in order to initiate the *in vivo* conditions as closely as possible (the temperature of the rectum of the rabbits was 39°) and ensure complete melting of the suppositories.

Table I—Related Bioavailability Parameters from Serum Level Data

Parameter	Treatment A: Polyethylene Glycol 1000 Suppositories	Treatment B: Esterified Fatty Acids (C_{10}–C_{18}) Suppositories	Treatment C: Theobroma Oil Suppositories	Treatment D: Powder Suspension
Average of Peaks of Individual Serum Concentrations (Time Curve), μg/ml	1.35	1.12	1.17	1.64
Time of Peak Value of Individual Serum Concentration–Time Curves, min	60	90	90	90
Average of Area under Individual Serum Concentration–Time Curves, μg/ml min	178.53	182.42	177.92	215.10

buffer (pH 8) was added to the dissolution medium to compensate for sampling. The absorbances were measured at 318 nm in a spectrophotometer and the concentrations of indomethacin were obtained from the standard curve.

***In Vivo* Studies**—Twelve healthy white New Zealand male rabbits (3–4.5 kg) were randomly divided into four groups of three animals each. Four different dosage forms of indomethacin were administered, and each dosage form provided 25 mg of indomethacin.

At time zero, each rabbit received indomethacin as follows: Group A, one polyethylene glycol 1000 suppository; Group B, one esterified fatty acids (C_{10}–C_{18}) suppository; Group C, one theobroma oil suppository; and Group D, 25 mg of indomethacin suspended in ~100 ml of water administered orally. Retention of the suppositories by the rabbits was ensured by the use of an appropriately sized styrofoam disk taped to the rectum after insertion. Blood (2–5 ml) was taken by cardiac puncture from each rabbit at different time intervals up to 4 hr.

Assay of Serum—The serum samples were assayed by modifying a method described previously (17). One milliliter of serum was pipeted into a glass stoppered centrifuge tube containing 2 ml of a 1 *M* citrate buffer and 25 ml of heptane containing 5% isoamyl alcohol. The test tube was mechanically agitated for 30 min and then centrifuged. Twenty milliliters of the heptane phase was pipeted into a second centrifuge tube containing 5 ml of a 0.2 *M* citrate buffer. This was agitated for 25 min and then centrifuged. Ten milliliters of the organic phase was pipeted into a third centrifuge tube containing 3 ml of 0.1 *N* NaOH and shaken for 5 min. The organic phase was removed by aspiration and 2 ml of the aqueous phase transferred to a quartz cell for immediate spectrofluorophotometric determination (activation maximum, 305 nm; fluorescence maximum, 400 nm)[10,11].

RESULTS AND DISCUSSION

In the preparation of suppositories some difficulty is experienced in achieving the exact dosage. This is because the volume of suppositories from a particular mold is uniform, but its weight will vary because the density of the drug usually differs from the density of the base with which the mold is calibrated. Each mold should be calibrated before use by preparing suppositories using the base alone, weighing the blank suppositories, and taking the mean weight as the calibration factor. Therefore, to prepare accurate suppositories, it is essential to derive a general expression (Eq. 1) to account for the displacement value of a drug, which is defined as the number of parts by weight of the drug that displaces one part by weight of the base:

$$F = \frac{XB}{100\,(A - B) + XB} \qquad \text{(Eq. 1)}$$

where F is the displacement value of a drug; X is the percentage of drug used; B is the weight of n suppositories containing X% of a drug; and A is the calibration factor, *i.e.*, weight of unmedicated n suppositories.

According to the definition, the displacement value of a drug is:

$$F = \frac{\text{Amount of the drug in each suppository}}{\text{Amount of base displaced in each suppository}} \qquad \text{(Eq. 2)}$$

Since the amount of drug in each suppository is $X/100\,B$, and the amount of base displaced by the above amount of drug is $(A - (100 - X)/100\,B)$, Eq. 2 becomes:

$$F = \frac{\frac{X}{100}B}{A - \frac{100 - X}{100}B} = \frac{XB}{100\,(A - B) + XB} \qquad \text{(Eq. 3)}$$

Therefore, the quantity of base required is calculated using the following equation:

$$P = (N \times S) - \frac{D}{F} \qquad \text{(Eq. 4)}$$

where P is the amount of base required (in grams); N is the number of the prepared suppositories; S is the size of the mold used (in grams); and D is the amount of drug (in grams) that is required.

The displacement values of indomethacin were calculated in the polyethylene glycol 1000, esterified fatty acids (C_{10}–C_{18}), and theobroma oil suppository bases, and were found to be 1.72 ± 0.21, 2.06 ± 0.14, and 2.44 ± 0.39, respectively.

The weight variation of 20 randomly selected indomethacin suppositories containing 25 mg of the drug in the three bases was determined and found to be from 1.71 to 1.84 g for polyethylene glycol 1000, 1.38 to 1.48 g for esterified fatty acids (C_{10}–C_{18}), and 1.09 to 1.17 g for theobroma oil. All the suppositories prepared met the acceptable limits of the German, Russian, and Nordica pharmacopeias (21), which state that individual weight variations of rectal suppositories can vary by ±5, ±5, and ±10% of their average weight, respectively. The USP does not have any limits for acceptable weight variation of rectal suppositories. Although the USP does not specify content uniformity standards, the content uniformity of indomethacin suppositories in polyethylene glycol 1000, esterified fatty acids (C_{10}–C_{18}), and theobroma oil was determined and found to be within −5.2 to +12.2, −8.2 to +9.8, and −8.2 to +12.2 of the labeled amounts, respectively.

The definitions of rectal suppositories as reported in different pharmacopeias, specifically state the "suppositories should soften, melt, or dissolve at body temperature." However, these are of little value, as pointed out previously (22), unless the method of determining these characteristics is given. This is because different methods give different results and, consequently, suppositories may be accepted as satisfactory, although they do not melt, soften, or dissolve in the rectal environment. Furthermore, if a uniform method for determining the melting range could be developed, it would be quite useful in deciding if a suppository is sufficiently firm to be introduced into the rectum or handled and stored at ordinary room temperature or in warm environments. The melting range was determined by using the USP disintegration apparatus and a commercial disintegration apparatus[6]. Figure 1 shows the time for

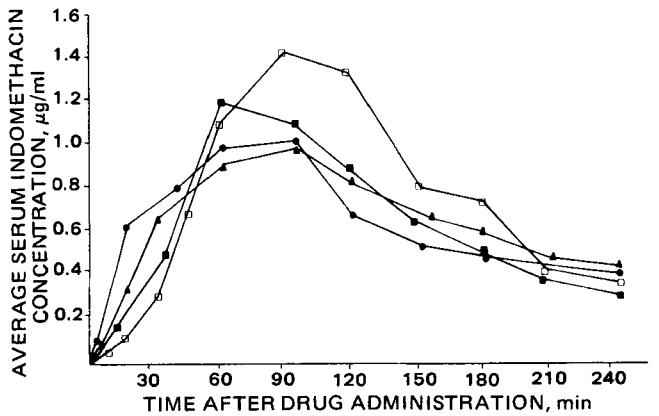

Figure 7—*Average serum indomethacin concentrations (μg/ml) obtained for three rabbits after receiving 25 mg of indomethacin given as: (■) polyethylene glycol; (▲) esterified fatty acids (C_{10}–C_{18}); (●) theobroma oil; (□) oral dose.*

[10] Aminco–Browman Spectrofluorophotometer, American Instrument Co.

[11] Prolonged exposure to daylight or delay in taking readings must be avoided because indomethacin is light sensitive.

Table II—Analysis of Variance of Plasma Concentration [a]

Source of Variation	Degrees of Freedom	Sum of Squares	Mean Square	F-ratio
Treatments (T), (A, B, C, D)	3	0.1618	0.0539	
Rabbits/Treatment (R) (Error-T)	8	3.9365	0.4921	
Time Period, (P)	10	21.7512	2.1751	
$T \times P$ interaction	30	2.9795	0.0993	2.31[b]
$(T \times R)/D$ Error P	80	3.4433	0.0430	
Total	131	32.2723		

[a] Based on a split-strip-plot configuration (31, 32). [b] Implies that the interaction is significant ($p < 0.05$).

complete melting of indomethacin suppositories as a function of temperature. It is apparent from Fig. 1 that the polyethylene glycol 1000 indomethacin suppositories require a longer time for complete dissolution than that of esterified fatty acids (C_{10}–C_{18}) and theobroma oil in the USP disintegration apparatus. Figure 2 shows the time that is required to dissolve the polyethylene glycol 1000 indomethacin suppository as a function of temperature in the commercial disintegration apparatus[6]. This apparatus can be used for bases having densities >1 g/cm^{-3}. Polyethylene glycol 1000 can be measured in the apparatus but esterified fatty acids (C_{10}–C_{18}) (0.97 g/cm^{-3}) and theobroma oil (0.86 g/cm^{-3}) cannot.

The breaking load of the indomethacin suppositories in the three bases as a function of temperature is shown in Fig. 3. As can be seen from these curves, it is possible to determine the degree of deformation. A steep curve (esterified fatty acids, C_{10}–C_{18}) indicates a brittle base, whereas a flat curve (theobroma oil) indicates greater elasticity of the suppository base and a longer softening interval. A large number of methods are available for determination of the release of medicament from suppository bases (23–30); however, to our knowledge none have been proven to be totally satisfactory in correlating *in vitro* release with *in vivo* bioavailability. The release of indomethacin from the three suppository bases was determined by using three methods: two existing methods and a new, modified method.

Using the USP dissolution apparatus, the percent of indomethacin released is shown in Fig. 4. The data indicate that the time required to release the total amount of indomethacin from the polyethylene glycol 1000 suppository base was ~10 times less than that of the other two bases due to the water solubility of polyethylene glycol 1000 base. Therefore, the USP dissolution apparatus cannot be used for the determination of the medicament release from water soluble suppository bases without the use of membranes or filters. The inability of the USP dissolution method to be used with water soluble bases led to the use of membranes to hinder the erosion process.

The plot of indomethacin released using Method B is shown in Fig. 5. The data indicate that in the first hour the order of release was theobroma oil > esterified fatty acids (C_{10}–C_{18}) > polyethylene glycol 1000, but after the first hour, the order changed to polyethylene glycol 1000 > esterified fatty acids (C_{10}–C_{18}) > theobroma oil. The use of cellophane membranes and the dialysis technique, Methods B and C (Fig. 6), may represent an additional slow step in the overall release of indomethacin from suppositories, which may prevent a comparison of the methods. Therefore, an investigation is under way to determine and calculate the possible lag time in the methods.

***In Vivo* Studies**—The plasma indomethacin concentration–time relationshihps obtained for three rabbits after administration of single

Table III—Analysis of Variance for Each Time Period

Time Period, min	Levene Test[a]	ANOVA[b] Test
0	no test	no test
5	NS[c]	NS
12–15	NS	—[d]
30–40	NS	NS
60	NS	NS
90–95	NS	NS
120	NS	NS
145–155	NS	NS
180	NS	NS
205–210	NS	NS
240	NS	NS

[a] Levene Test is used for the comparison of variabilities. [b] ANOVA: Analysis of variance. [c] NS: Not significant at $p = 0.05$. [d] Highly significant ($p < 0.01$).

Table IV—Analysis of Variance For the 12–15-Min Time Period

Source of Variation	Degrees of Freedom	Sum of Squares	Mean Square	F-Ratio
Treatments	3	0.6134	0.2045	8.127[a]
Within Treatments	8	0.2013	0.0252	
Total	11	0.8146		

[a] Highly significant ($p < 0.01$).

25-mg doses of indomethacin are shown in Table I and Fig. 7. As can be seen from the data, the peak levels obtained were 1.35 μg/ml for Treatment A, 1.12 μg/ml for Treatment B, 1.17 μg/ml for Treatment C, and 1.64 μg/ml for Treatment D. Furthermore, the average peak of indomethacin concentration obtained after rectal administration of 25 mg of indomethacin was 82.31, 68.29, and 71.34% for Treatments A, B, and C, respectively, of that when given orally.

The absorption of indomethacin from all suppository bases, as well as from those administered orally, was rapid, as reflected by the relatively short time to attain the peak plasma indomethacin level (Fig. 7 and Table I). The time of occurrence of the maximum peak level was considerably less after Treatment A (60 min) than that after Treatments B, C, and D (90 min).

The area under the plasma concentration–time curve (AUC) was calculated by the trapezoidal rule. The values of AUC measurements, as well as the average of peaks of individual serum concentration–time curves and the time of peak value of individual serum concentration–time curves, are given in Table I.

Statistical Analysis—The mean plasma concentration of indomethacin associated with polyethylene glycol 1000, esterified fatty acids (C_{10}–C_{18}), theobroma oil, and suspension was statistically compared, based on three rabbits per each treatment and 11 sampling time periods. The ANOVA for a split-strip-plot (31–32) design suitable for time-dependent responses was conducted and the results presented in Table II.

The ANOVA indicated that there is an interaction between treatment and time periods. The interpretation of the significant interaction indicates that there exists one or more time periods in which the mean plasma concentration of the treatments are significantly different. This information led to the second set of analyses in which an ANOVA was conducted for each time period to identify the time period in which the treatments were significantly different. These results are provided in Table III. Some of the collection times in Table III show a range of time periods and not a specific collection time, because the ANOVA is used to identify the time period in which the treatments are significantly different. Therefore, the exact collection time should be used. The 12–15 min time period indicates that some blood samples at the third collection time were collected at 12 min, while others at 15 min. Specifically, the collection time for the indomethacin–polyethylene glycol 1000 suppositories was 12 min, while for the other treatments it was 15 min.

It can be seen that there is a significant difference among the treatments in the 12–15-min time period. This is the most critical information of the experiment. The ANOVA for this period is given in Table IV. A Duncan's Multiple Range Test was conducted, and the results (Table V) revealed that Treatment C ($\bar{C} = 0.70$) was significantly higher) ($p > 0.05$) than that of Treatment A ($A = 0.18$) and Treatment D ($\bar{D} = 0.12$). There was no significant difference between Treatments B and C. As time increased, the variability of the plasma concentration increased, and thus, no significant differences among the treatments were detected (31, 32).

The present results indicate that the indomethacin is well absorbed from the rectum, although the peak serum concentration and AUC were less than after an equivalent oral dose, which is in accordance with previous experiments (17).

Table V—Analysis of Variance According To Duncan's Multiple Range Test

	Significance Triangle			
	D	A	B	C
0.6967 C	—[a]	—[a]	0[b]	
0.400 B	0			
0.1800 A	0			
0.1200 D				

[a] Implies significant difference between C and D and between C and A ($p < 0.05$). [b] 0 implies no significant difference at $p = 0.05$.

An attempt to correlate the *in vivo* with the *in vitro* release of the indomethacin proved to be unsatisfactory because of the wide variance in the results from three *in vivo* treatments and three dissolution methods. However, the dialyzing tubing method gave the best correlation with the *in vivo* data in three suppository bases, whereas the USP dissolution method gave the best correlation only with the use of fatty suppository bases (esterified fatty acids (C_{10}–C_{18}) and theobroma oil). Attempts to use a sequential order correlation between the three dissolution methods and the *in vivo* results show that the best correlation was found during the first 45 min of the experiment.

REFERENCES

(1) T. Y. Shen *et al.*, *J. Am. Chem. Soc.*, **85**, 488 (1963).
(2) B. M. Norcross, *Arthritis Rheum.*, **6**, 290 (1963).
(3) C. J. Smyth, *ibid.*, **8**, 921 (1965).
(4) F. D. Hart and P. L. Boardman, *Br. Med. J.*, **2**, 1281 (1965).
(5) W. M. O'Brien, *Clin. Pharm. Ther.*, **9**, 94 (1968).
(6) V. Wright and M. Roberts, *Clin. Med.*, **80**, 12 (1973).
(7) I. Haslock, *Br. Med. J.*, **2**, 121 (1974).
(8) N. Thompson and J. S. Percy, *ibid.*, **1**, 80 (1966).
(9) E. Zachariae, *Nord. Med. NM*, **75**, 384 (1966).
(10) R. Hodgkinson and D. Woolf, *Practitioner*, **210**, 392 (1973).
(11) A. C. Stevenson, *Ann. Rheum. Dis.*, **30**, 487 (1971).
(12) E. Renner and E. Held, *Arzneimi.-Forsch.*, **21**, 1849 (1970).
(13) J. H. Jacobs and M. F. Grayson, *Br. Med. J.*, **3**, 158 (1968).
(14) P. M. Catoggio, A. Centurion, H. Alberti, H. Roldan, and L. Canepa, *Arthritis Rheum.*, **7**, 300 (1964).
(15) M. Kelly, *Med. J. Aust.*, **2**, 541 (1964).
(16) F. D. Hart and P. L. Boardman, *Br. Med. J.*, **2**, 965 (1963).
(17) L. P. J. Holt and C. F. Hawkins, *ibid.*, **1**, 1354 (1965).
(18) D. L. Woolf, *ibid.*, **1**, 1497 (1965).
(19) E. C. Huskisson, R. T. Taylor, G. H. Whitehouse, D. F. Hart, D. H. Trapnell, *Ann. Rheum. Dis.*, **29**, 393 (1970).
(20) C. Alvan, M. Orme, L. Bertilsson, R. Ekstrand, and L. Palmer, *Clin. Pharmacol. Ther.*, **18**, 364 (1974).
(21) B. T. Emmerson, *Br. Med. J.*, **1**, 272 (1967).
(22) L. Lachman, H. A. Lieberman, and J. L. Kanig, "The Theory and Practice of Industrial Pharmacy," 2nd ed., Lea and Febiger, Philadelphia, Pa., 1976, pp. 245–269.
(23) A. Caldwell, *Q. J. Pharm. Pharmacol.*, **12**, 680 (1939).
(24) R. T. Yousef and A. A. Ghobashy, *Dan. Tidsskr. Farm.*, **43**, 31 (1969).
(25) H. M. Gross and C. H. Becker, *J. Am. Pharm. Assoc., Sci. Ed.*, **42**, 96 (1953).
(26) M. R. Baichwal and T. Y. Lohit, *J. Pharm. Pharmacol.*, **22**, 427 (1970).
(27) I. W. Kellaway and C. Marriott, *J. Pharm. Sci.*, **64**, 1161 (1975).
(28) W. H. Thomas and R. McCormack, *J. Pharm. Pharmacol.*, **23**, 490 (1971).
(29) Von F. Neuwald and F. Kunze, *Arzneim.-Forsch.*, **14**, 1162 (1964).
(30) A. L. Weiss and B. J. Sciarrone, *J. Pharm. Sci.*, **58**, 980 (1969).
(31) H. P. M. Kerhoffes and T. Huizinga, *Pharm. Weekblad.*, **102**, 1183 (1967).
(32) G. W. Snedecor and W. G. Cochran, "Statistical Methods," 6th ed., Iowa State University Press, Ames, Ia., 1967, Chap. 12, pp. 271, 369.
(33) H. Levene, "Robust Tests for Equality of Variances," Essays in Honor of Harold Hobelling, Stanford University Press, Stanford, Calif. 1961. pp. 278.

ACKNOWLEDGMENTS

Presented in part at the 25th Academy of Pharmaceutical Sciences National Meeting, Basic Pharmaceutics Section, Hollywood, Fla., November, 1978.

Abstracted from a thesis submitted by Nicholas J. Vidras to the Graduate Faculty, Arnold and Marie Schwartz College of Pharmacy and Health Sciences, Long Island University, in partial fulfillment of the MS degree requirements.

The authors thank Dr. Clement Stone, Merck, Sharp and Dohme, West Point, Pa., for providing indomethacin and Mr. Ronald Loucas, Kay-Fries Chemical, Montvale, N.J.

NOTES

High-Performance Liquid Chromatographic Determination of Proglumide in Plasma

TERUYOSHI MARUNAKA ˣ, YOSHINORI MINAMI, YUKIHIKO UMENO, and EIJI MATSUSHIMA

Received May 22, 1981, from the *Research Laboratory, Taiho Pharmaceutical Co., Ltd., Kawauchi-cho, Tokushima, 771-01, Japan.* Accepted for publication October 7, 1981.

Abstract □ A rapid and sensitive method for determining the anticholinergic agent, proglumide, in plasma by high-performance liquid chromatography is described. Samples were acidified with hydrochloric acid and extracted with chloroform. The dried extract was resolved in chloroform and chromatographed on an adsorption chromatographic column using a mobile phase of chloroform–methanol (24:1) on a high-performance liquid chromatograph equipped with a UV absorbance detector (240 nm). The detection limit for proglumide was 0.05 μg/ml.

Keyphrases □ Proglumide—high-performance liquid chromatographic determination in plasma □ High-performance liquid chromatography—analysis, proglumide in plasma □ Anticholinergic agent—proglumide, high-performance liquid chromatographic determination in plasma

Proglumide (xylamide, DL-4-benzamido-*N*,*N*-dipropylglutaramic acid) is a derivative of the amino acid that was developed as an anticholinergic agent (1–7). The GLC methods have been reported for the assay of proglumide in plasma (8–10). Proglumide has been assayed for its methyl derivative (8, 9), and its trimethylsilyl derivative determined (10).

The present report describes a rapid, precise, and sen-

0022-3549/82/0800-0949$01.00/0

An attempt to correlate the *in vivo* with the *in vitro* release of the indomethacin proved to be unsatisfactory because of the wide variance in the results from three *in vivo* treatments and three dissolution methods. However, the dialyzing tubing method gave the best correlation with the *in vivo* data in three suppository bases, whereas the USP dissolution method gave the best correlation only with the use of fatty suppository bases (esterified fatty acids (C_{10}–C_{18}) and theobroma oil). Attempts to use a sequential order correlation between the three dissolution methods and the *in vivo* results show that the best correlation was found during the first 45 min of the experiment.

REFERENCES

(1) T. Y. Shen *et al.*, *J. Am. Chem. Soc.*, **85**, 488 (1963).
(2) B. M. Norcross, *Arthritis Rheum.*, **6**, 290 (1963).
(3) C. J. Smyth, *ibid.*, **8**, 921 (1965).
(4) F. D. Hart and P. L. Boardman, *Br. Med. J.*, **2**, 1281 (1965).
(5) W. M. O'Brien, *Clin. Pharm. Ther.*, **9**, 94 (1968).
(6) V. Wright and M. Roberts, *Clin. Med.*, **80**, 12 (1973).
(7) I. Haslock, *Br. Med. J.*, **2**, 121 (1974).
(8) N. Thompson and J. S. Percy, *ibid.*, **1**, 80 (1966).
(9) E. Zachariae, *Nord. Med. NM*, **75**, 384 (1966).
(10) R. Hodgkinson and D. Woolf, *Practitioner*, **210**, 392 (1973).
(11) A. C. Stevenson, *Ann. Rheum. Dis.*, **30**, 487 (1971).
(12) E. Renner and E. Held, *Arzneimi.-Forsch.*, **21**, 1849 (1970).
(13) J. H. Jacobs and M. F. Grayson, *Br. Med. J.*, **3**, 158 (1968).
(14) P. M. Catoggio, A. Centurion, H. Alberti, H. Roldan, and L. Canepa, *Arthritis Rheum.*, **7**, 300 (1964).
(15) M. Kelly, *Med. J. Aust.*, **2**, 541 (1964).
(16) F. D. Hart and P. L. Boardman, *Br. Med. J.*, **2**, 965 (1963).
(17) L. P. J. Holt and C. F. Hawkins, *ibid.*, **1**, 1354 (1965).
(18) D. L. Woolf, *ibid.*, **1**, 1497 (1965).
(19) E. C. Huskisson, R. T. Taylor, G. H. Whitehouse, D. F. Hart, D. H. Trapnell, *Ann. Rheum. Dis.*, **29**, 393 (1970).
(20) C. Alvan, M. Orme, L. Bertilsson, R. Ekstrand, and L. Palmer, *Clin. Pharmacol. Ther.*, **18**, 364 (1974).
(21) B. T. Emmerson, *Br. Med. J.*, **1**, 272 (1967).
(22) L. Lachman, H. A. Lieberman, and J. L. Kanig, "The Theory and Practice of Industrial Pharmacy," 2nd ed., Lea and Febiger, Philadelphia, Pa., 1976, pp. 245–269.
(23) A. Caldwell, *Q. J. Pharm. Pharmacol.*, **12**, 680 (1939).
(24) R. T. Yousef and A. A. Ghobashy, *Dan. Tidsskr. Farm.*, **43**, 31 (1969).
(25) H. M. Gross and C. H. Becker, *J. Am. Pharm. Assoc., Sci. Ed.*, **42**, 96 (1953).
(26) M. R. Baichwal and T. Y. Lohit, *J. Pharm. Pharmacol.*, **22**, 427 (1970).
(27) I. W. Kellaway and C. Marriott, *J. Pharm. Sci.*, **64**, 1161 (1975).
(28) W. H. Thomas and R. McCormack, *J. Pharm. Pharmacol.*, **23**, 490 (1971).
(29) Von F. Neuwald and F. Kunze, *Arzneim.-Forsch.*, **14**, 1162 (1964).
(30) A. L. Weiss and B. J. Sciarrone, *J. Pharm. Sci.*, **58**, 980 (1969).
(31) H. P. M. Kerhoffes and T. Huizinga, *Pharm. Weekblad.*, **102**, 1183 (1967).
(32) G. W. Snedecor and W. G. Cochran, "Statistical Methods," 6th ed., Iowa State University Press, Ames, Ia., 1967, Chap. 12, pp. 271, 369.
(33) H. Levene, "Robust Tests for Equality of Variances," Essays in Honor of Harold Hobelling, Stanford University Press, Stanford, Calif. 1961. pp. 278.

ACKNOWLEDGMENTS

Presented in part at the 25th Academy of Pharmaceutical Sciences National Meeting, Basic Pharmaceutics Section, Hollywood, Fla., November, 1978.

Abstracted from a thesis submitted by Nicholas J. Vidras to the Graduate Faculty, Arnold and Marie Schwartz College of Pharmacy and Health Sciences, Long Island University, in partial fulfillment of the MS degree requirements.

The authors thank Dr. Clement Stone, Merck, Sharp and Dohme, West Point, Pa., for providing indomethacin and Mr. Ronald Loucas, Kay-Fries Chemical, Montvale, N.J.

NOTES

High-Performance Liquid Chromatographic Determination of Proglumide in Plasma

TERUYOSHI MARUNAKA ˣ, YOSHINORI MINAMI, YUKIHIKO UMENO, and EIJI MATSUSHIMA

Received May 22, 1981, from the *Research Laboratory, Taiho Pharmaceutical Co., Ltd., Kawauchi-cho, Tokushima, 771-01, Japan.* Accepted for publication October 7, 1981.

Abstract □ A rapid and sensitive method for determining the anticholinergic agent, proglumide, in plasma by high-performance liquid chromatography is described. Samples were acidified with hydrochloric acid and extracted with chloroform. The dried extract was resolved in chloroform and chromatographed on an adsorption chromatographic column using a mobile phase of chloroform–methanol (24:1) on a high-performance liquid chromatograph equipped with a UV absorbance detector (240 nm). The detection limit for proglumide was 0.05 μg/ml.

Keyphrases □ Proglumide—high-performance liquid chromatographic determination in plasma □ High-performance liquid chromatography—analysis, proglumide in plasma □ Anticholinergic agent—proglumide, high-performance liquid chromatographic determination in plasma

Proglumide (xylamide, DL-4-benzamido-*N*,*N*-dipropylglutaramic acid) is a derivative of the amino acid that was developed as an anticholinergic agent (1–7). The GLC methods have been reported for the assay of proglumide in plasma (8–10). Proglumide has been assayed for its methyl derivative (8, 9), and its trimethylsilyl derivative determined (10).

The present report describes a rapid, precise, and sen-

0022-3549/82/0800-0949$01.00/0

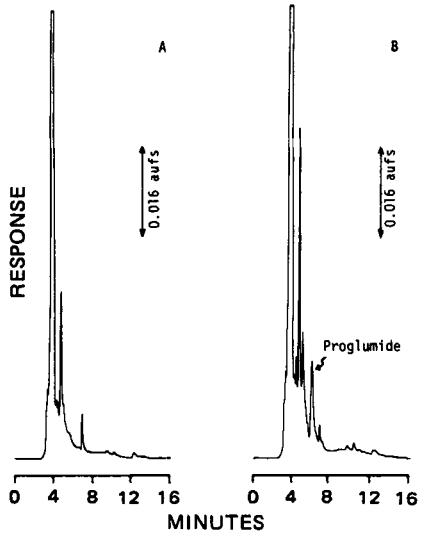

Figure 1—*High-performance liquid chromatograms of human control plasma (A) and human plasma extracts following addition of proglumide at 0.5 μg/ml (B). The conditions were: column (25-cm × 6.2-mm i.d.); mobile phase, chloroform–methanol (24:1); flow rate, 1.5 ml/min; and UV detector, 240 nm (room temperature).*

sitive high-performance liquid chromatographic (HPLC) method using an adsorption chromatographic column for determination of proglumide in plasma.

EXPERIMENTAL

Materials—Proglumide[1] was used as received. Chloroform and methanol were liquid chromatographic grade[2], and the other chemicals[2] were analytical reagent grade.

HPLC Conditions—The high-performance liquid chromatograph[3] was equipped with a high-pressure injection valve[4] and a variable-wavelength (240 nm) UV absorbance detector[5].

An adsorption chromatographic column[6] (25-cm × 6.2-mm i.d.) was used for the separation and maintained at room temperature. The mobile phase was chloroform–methanol (24:1) at a flow rate of 1.5 ml/min. A gradienter[7] was used for controlling the mobile phase concentration. A computer system[8] was employed for quantitative calculations.

Analytical Procedure—Blood samples were collected in heparinized containers and centrifuged to separate the plasma.

A sample of 1.0 ml of plasma was diluted to 2.0 ml with distilled water, adjusted to pH 3.0 with 1 *N* HCl, and then shaken vigorously with 20 ml of chloroform at room temperature for 10 min. This extraction was repeated once. The combined chloroform layer was evaporated to a suitable volume under reduced pressure at water temperature, then transferred to a test tube (5-ml capacity) by washing with chloroform, and dried under nitrogen. The residue was dissolved in 100 μl of chloroform, and 30-μl portions of this solution were injected into the liquid chromatograph with a 100-μl syringe[9].

Calibration curve for the determination of proglumide by HPLC was prepared by plotting the peak area against the concentration of this compound. This calibration curve was linear.

RESULTS AND DISCUSSION

The HPLC separation of proglumide extracted from plasma was first examined using a reversed-phase column[10]. When a linear gradient system with methanol–5 m*M* KH_2PO_4 (0–100% methanol, 6%/min) was used as the mobile phase, proglumide was well separated from plasma constituents.

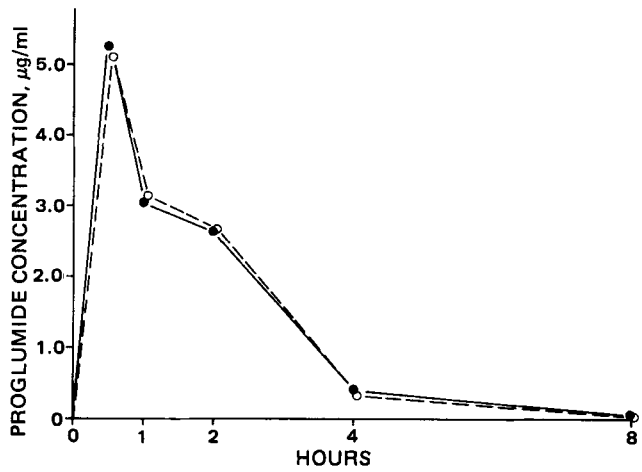

Figure 2—*Comparison of plasma levels of proglumide determined by HPLC (●) and GLC (○) methods after a single oral dose of 400 mg of proglumide to a healthy human.*

An adsorption chromatographic column[6] was used next for the separation of proglumide extracted from plasma. A mixture of a nonpolar solvent (*e.g.*, chloroform, methylene chloride, or ethylene chloride), containing 4–6% alcohol (*e.g.*, methanol or ethanol) as the mobile phase, gave a good separation of proglumide from plasma components. Of these columns and mobile phases tested, a column[6] and chloroform–methanol (24:1) as the mobile phase showed the most suitable chromatographic separation and analysis time and was chosen for the present experiments.

The HPLC separation pattern of proglumide extracted from human plasma following addition of 0.5 μg/ml of this compound and that of a control plasma extract are shown in Fig. 1. The retention time of proglumide was 6.0 min, and the time required for the assay was 15 min. The detection limit for proglumide under the present HPLC condition was 0.05 μg/ml of plasma. The present method had a precision of ±2.8% and good reproducibility.

Known amounts (0.1, 0.5, 1.0, 5.0, and 10.0 μg/ml) of proglumide were added to human plasma (1.0 ml) and the recovery of proglumide was examined five times at each concentration. The overall recovery of proglumide was 93.1 ± 3.2%.

A 400-mg dose of proglumide was administered orally to a healthy male, and the time course of change in concentration of proglumide in plasma was measured by the present HPLC method. The results were compared with those by the GLC method (8, 9). As shown in Fig. 2, the overall difference between the value obtained by the two methods was ± 3.7%.

The present HPLC method is simple and rapid since it does not require the preparation of derivatives and has high accuracy and sensitivity.

[1] Rotta Research Laboratorium S.p.A., Monza, Italy.
[2] Wako Pure Chemicals Co., Osaka, Japan.
[3] Model LC-3, Shimadzu, Kyoto, Japan.
[4] Model SIL-1A, Shimadzu.
[5] Model SPD-2, Shimadzu.
[6] Zorbax SIL (Du Pont), Shimadzu.
[7] Model GRE-2, Shimadzu.
[8] Chromatopac C-R1A, Shimadzu.
[9] Model 100A-RP-GP, Scientific Glass Engineering Ltd., North Melbourne, Australia.
[10] μ-Bondapak C_{18}, Waters Associates, Milford, Mass.

REFERENCES

(1) A. L. Rovati, P. L. Casula, and G. Da Re, *Minerva Med.*, **58**, 3656 (1967).
(2) I. E. Danhof, *ibid.*, **58**, 3670 (1967).
(3) S. Mainoli, C. Milvio, and D. Borellini, *ibid.*, **58**, 3708 (1967).
(4) P. R. De Carvalho, J. F. Penteado, and N. Zacharias, *J. Bras. Med.*, **17**, 51 (1967).
(5) D. Borellini and C. Milvio, *Minerva Med.*, **60**, 1053 (1969).
(6) M. Matsunaka, S. Kawakami, Y. Hitta, and Y. Yoshida, *Clin. Rep.*, **4**, 1969 (1970).
(7) H. Geoffroy, R. Viguie, M. Choisy, and P. Coudoux, *Therapie*, **48**, 471 (1972).
(8) A. L. Rovati and G. Picciola, *Boll. Chim. Farm.*, **110**, 595 (1971).
(9) A. A. Bignamini, P. L. Casula, and A. L. Rovati, *Arzneim.-Forsch./Drug Res.*, **29**, 639 (1979).
(10) J. F. Douglas and S. Shahinian, *Farmaco. Ed. Prat.*, **26**, 682 (1971).

Belladonna Alkaloids and Phenobarbital Combination Pharmaceuticals Analysis I: High-Performance Liquid Chromatographic Determinations of Hyoscyamine–Atropine and Scopolamine

LINDA J. PENNINGTON ˣ and WALTER F. SCHMIDT

Received March 3, 1981, from the *Food and Drug Administration, Atlanta, GA 30309.* Accepted for publication November 16, 1981.

Abstract □ High-performance liquid chromatographic separations are described for the analysis of hyoscyamine–atropine and scopolamine in combination pharmaceutical dosage forms containing phenobarbital. A mobile phase containing 0.034 *M* tetramethylammonium phosphate in water–methanol (21:10, pH 2.0) separated hyoscyamine or atropine from scopolamine on an octadecylsilane column in <9 min. Monitoring of the column effluent at 220 nm gave a detection limit of 0.02 μg for each alkaloid. Hyoscyamine sulfate and/or atropine sulfate were determined as total equivalent hyoscyamine sulfate, and scopolamine hydrobromide was determined as a separate entity. Data from the application of the method to commercial pharmaceutical products are also presented.

Keyphrases □ High-performance liquid chromatography—belladonna alkaloids and phenobarbital combination pharmaceuticals, determination of hyoscyamine–atropine and scopolamine □ Combination drugs—belladonna alkaloids, high-performance liquid chromatographic determination of hyoscyamine–atropine and scopolamine □ Alkaloids—belladonna, combination pharmaceuticals, high-performance liquid chromatographic determination of hyoscyamine–atropine and scopolamine

Microgram quantities of the belladonna alkaloids, hyoscyamine, atropine, and scopolamine, are widely used in combination with phenobarbital in pharmaceutical dosage forms for antispasmodic, anticholinergic, and sedative effects, especially in the treatment of functional GI disorders. Methodology was developed in this laboratory which would allow for the analysis of the belladonna alkaloids and for phenobarbital in such products. The present report presents the method, procedures, and data obtained on the determination of hyoscyamine–atropine and scopolamine.

The detection and quantitation of individual tablet levels of belladonna alkaloids in the common combination dosage forms is difficult for the following reasons: (*a*) low concentrations, (*b*) low UV absorptivity, (*c*) instability to the heat and pH ranges normally encountered in suitable sample analysis extraction procedures, and (*d*) interference from the large concentration and high UV absorptivity of phenobarbital. Currently available methodology for detection and quantitation of belladonna alkaloids includes colorimetry (1), fluorometry (2), GC (3–5), and HPLC (6, 7). The colorimetric procedure uses an ion-pair extraction with bromothymol blue at pH 5.6 for a total alkaloid determination and an ion-pair extraction with bromocresol purple at pH 6.6 for a hyoscyamine–atropine determination; scopolamine is estimated by the difference between the two assays (1). The fluorometric procedure consists of an extraction followed by ion-pair reaction with eosine yellow and determines only hyoscyamine and atropine (2). The simultaneous analysis of scopolamine and hyoscyamine–atropine can be achieved with GC but requires extensive column preparation and conditioning (3–5). Adsorption effects hamper especially the quantitation of scopolamine due to its low concentration in dosage forms as well as the peak broadening, which occurs due to its longer GC retention time. Loss of the alkaloids by adsorption on the sodium sulfate used to dry solvent extracts prior to GLC injection has also been noted (5). Due to the instability of the alkaloids' free bases, sample solutions must be injected on the day of extraction. The two HPLC (6, 7) procedures utilize reversed-phase ion-pairing chromatography with UV detection at 254 and 230 nm, respectively, to quantitate atropine and/or scopolamine. However, because of excessive background absorbance of the mobile phase, these methods lack sufficient sensitivity to quantitate the alkaloids at the microgram levels present in the common combination dosage forms.

Improved HPLC procedures are reported for the analysis of hyoscyamine, atropine, and scopolamine in combination pharmaceutical dosage forms containing phenobarbital. The method is applicable to a wide range of elixirs, tablets, and capsules for individual tablet assays (content uniformity test), as well as composite assays. In addition, the analysis of 22 commercial products using the described HPLC methods is presented.

EXPERIMENTAL

Apparatus—A liquid chromatograph[1] equipped with a 20-μl loop injector[2], a variable wavelength UV detector[3], and a recorder-integrator[4] were used. A 25 cm × 4-mm stainless steel column containing octadecylsilane chemically bonded to 5 μm silica[5] was employed.

Reagents—Methylene chloride[6] was passed through a 10 × 3-cm glass column containing 75 g of basic aluminum oxide[7] and stored over basic aluminum oxide (25 g/4 liters of solvent) in a light resistant glass container.

A carbonate buffer (pH 9.4) was prepared by mixing 5.3 g of anhydrous sodium carbonate and 4.2 g of sodium bicarbonate in 100 ml of distilled water.

A solution containing 1% concentrated HCl in methanol was prepared fresh daily.

A 0.05 *M* tetramethylammonium phosphate buffer was prepared by mixing 23 ml of 20% tetramethylammonium hydroxide in methanol[8] and 10 ml of concentrated phosphoric acid in 500 ml of distilled water, adjusting to pH 2.0 with concentrated phosphoric acid, and diluting to 1 liter with distilled water.

Preparation of Internal Standard Solutions—An internal standard solution was prepared for use in the drug standard solution by dissolving anhydrous theophylline[9] in methanol (300 μg/ml). The theophylline

[1] Constametric I Pump, Laboratory Data Control, Riviera Beach, Fla.
[2] Chromatography Accessory Module Injector, 20-μl loop, Laboratory Data Control, Riviera Beach, Fla.
[3] Spectromonitor II Variable Wavelength UV-Visible Detector, Laboratory Data Control, Riviera Beach, Fla.
[4] HP 3380A Integrator, Hewlett-Packard, Palo Alto, Calif.
[5] Spherisorb octadecylsilane, 5 μm. Prepacked column purchased from Laboratory Data Control, Riviera Beach, Fla.
[6] Burdick and Jackson Laboratories, Muskegon, Mich.
[7] Brockmann Activity Grade 1, J. T. Baker, Phillipsburg, N.J.
[8] Aldrich Chemical Co., Milwaukee, Wis.
[9] K&K Laboratories, Plainview, N.Y.

0022-3549/82/0800-0951$01.00/0

Table I—Recovery Data for Spiked Sample Determinations of Commercial Formulations [a]

Elixirs			Tablets and Capsules		
	Recovery, %			Recovery, %	
Formulation	Hyoscyamine Sulfate	Scopolamine Hydrobromide	Formulation	Hyoscyamine Sulfate	Scopolamine Hydrobromide
1	97.2	93.7	11	99.1	—[b]
2	101.1	94.3	12	94.8	99.6
3	101.0	98.0	13	102.7	94.3
4	100.6	106.1	14	101.0, 99.3[c]	95.7, 97.4[c]
5	102.7	93.0	15	94.4	93.6
6	105.1	[b]	16	98.3	106.1
7	94.7	[b]	17	99.0	104.4
8	95.6	96.5	18	102.2	105.2
9	97.3	93.3	19	99.8	100.4
10	103.1	[b]	20	99.3	95.6
—			21	98.2, 98.3[c]	102.8, 101.2[c]
—			22	103.0	—[b]
Mean Recovery	99.8	96.4		99.3	99.8
SD	3.46	4.65		2.75	4.74
RSD	±3.47	±4.82		±2.77	±4.75
Range	94.7–105.1	93.0–106.1		94.4–103.0	93.6–105.2

[a] Portions of sample spiked with standard solution containing hyoscyamine sulfate and scopolamine hydrobromide and analyzed according to procedure. [b] Product did not contain scopolamine hydrobromide. [c] Value obtained by second analyst. Value not included in statistics.

solution was then diluted with methylene chloride (2.25 μg/ml) for use in the assay procedure.

Preparation of Drug Standard Solutions—A standard solution of scopolamine hydrobromide[10] in distilled water (500 μg/ml) was prepared and stored in low-actinic glassware.

A mixed standard solution was prepared by weighing hyoscyamine sulfate[11] (16 mg) into a 50-ml low-actinic volumetric flask, adding 3.0 ml of the methanolic theophylline internal standard solution (300 μg/ml) and 2.0 ml of scopolamine hydrobromide standard solution, and diluting to ~40 ml with distilled water.

Preparation of Mobile Phase—The mobile phase was prepared by mixing 525 ml of 0.05 *M* tetramethylammonium phosphate buffer with 250 ml of methanol.

HPLC Conditions—A flow rate of 0.8 ml/min was used with UV detection set at 220 nm and the sensitivity set at 0.02 aufs.

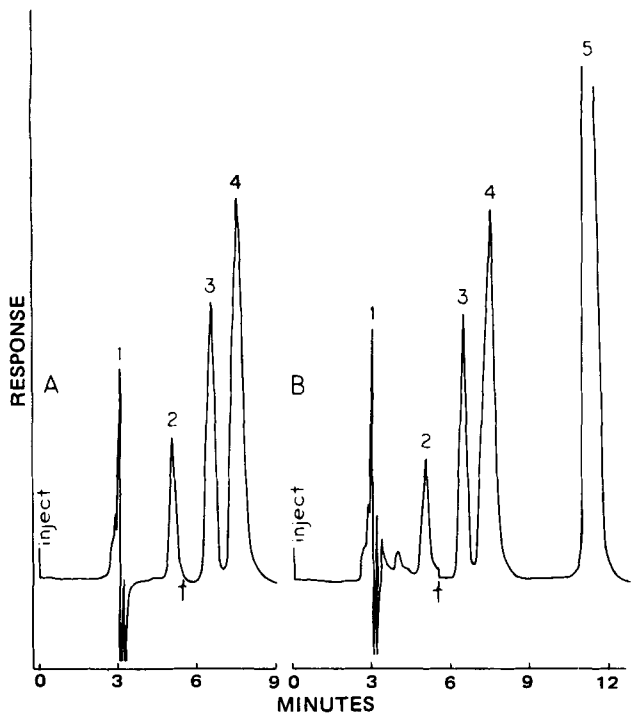

Figure 1—*Typical chromatograms of HPLC separations of A, the standard solution and B, the tablet sample. Key: 1, solvent; 2, scopolamine; 3, theophylline (internal standard); 4, hyoscyamine–atropine; 5, phenobarbital. Attenuation change of 4× after each scopolamine peak at the arrow.*

[10] USP Reference Standard.
[11] NF Reference Standard.

Assay for Tablets and Capsules—Twenty tablets were weighed and finely powdered, or the contents of 20 capsules were weighed and composited. A sample portion equivalent to ~0.6 mg of combined hyoscyamine sulfate–atropine sulfate was accurately weighed and quantitatively transferred to a 50-ml centrifuge tube; 25 ml of 0.05 *N* sulfuric acid then was added and the tube shaken for 15 min. The mixture was then centrifuged for 5 min at 3000 rpm. A 5.0-ml aliquot of the supernate was pipeted into a 125-ml separatory funnel where it was extracted with two 30-ml portions of methylene chloride. The organic phase was then discarded. Two milliliters of carbonate buffer (pH 9.4) was added to the aqueous phase remaining in the separatory funnel and the mixture was extracted with four 30-ml portions of methylene chloride. Each extract was filtered through a methylene chloride-rinsed glass wool plug into a flash evaporator[12] fitted with a concentrator tube[13]. Exactly 3 ml of theophylline internal standard solution (2.25 μg/ml) and 9–10/50 grit boiling chips[14] were added to the concentrator. A distilling column[15] was added to the concentrator and the methylene chloride evaporated on a steam bath to ~10 ml. The distilling column was then rinsed with 1–2 ml of methylene chloride and the solvent evaporated to 0.5–1 ml. The distilling column was removed and the column-concentrator junction rinsed with ~1 ml of methylene chloride into the concentrator tube. The concentrator tube was placed in a beaker of warm water (40 ± 5°) and the solvent evaporated to ~1 ml with the aid of a current of dry air. Next, 0.1 ml of acidic methanol was added, mixed, and the solution evaporated to dryness using the conditions described previously. The sides of the concentrator tube were rinsed with 0.5 ml of methanol and the solution again evaporated to dryness. The extract was then dissolved in 300 μl of distilled water and a 20-μl sample was injected onto a liquid chromatograph.

Content Uniformity Test—One tablet or the contents of one capsule were transferred to a 125-ml separatory funnel and 7 ml of 0.05 *N* sulfuric acid added. The funnel was shaken until the tablet disintegrated and then shaken for an additional 5 min. Thereafter, the "Assay for Tablets and Capsules" was followed beginning with, " . . . it was extracted with two 30-ml portions of methylene chloride . . .."

Assay for Elixirs—A sample equivalent to ~0.6 mg of combined hyoscyamine sulfate–atropine sulfate was pipeted into a 150-ml beaker. The solution was warmed in a 40 ± 5° water bath with a current of air for 30 min to remove alcohol. After cooling to room temperature, the sample was quantitatively transferred to a 25-ml volumetric flask and adjusted to volume with distilled water. Exactly 5 ml of this solution was pipeted into a 125-ml separatory funnel, 2 ml of 0.2 *N* sulfuric acid added, and the "Assay for Tablets and Capsules" was followed thereafter beginning with, " . . . it was extracted with two 30-ml portions of methylene chloride . . .."

Calculations—After obtaining the chromatograms, each peak response was determined by measurement of peak height or peak area. The quantity, in milligrams, of hyoscyamine sulfate–atropine sulfate and scopolamine hydrobromide in the portion of sample taken was calculated

[12] Kuderna-Danish Concentrator, Kontes Glass Co., Vineland, N.J.
[13] Mills Tube, Kontes Glass Co., Vineland, N.J.
[14] Carborundum.
[15] Snyder Distilling Column, Kontes Glass Co., Vineland, N.J.

Table II—HPLC Analysis Results for Commercial Formulations

Formulation	Form	Percent of Label Claim: Hyoscyamine Sulfate[a]–Atropine Sulfate	Percent of Label Claim: Scopolamine Hydrobromide[b]
1	Elixir	89.3	93.2
2	Elixir	106.6	88.6
3	Elixir	90.2	105.5
4	Elixir	101.1	100.7
5	Elixir	93.2	81.7
6	Elixir	105.1	[c]
7	Elixir	91.8	[c]
8	Elixir	95.3	81.4
9	Elixir	32.1	88.2
10	Elixir	106.4	[c]
11	Tablet	93.6, (95.2)[d]	[c]
12	Tablet	93.2, (94.7)	97.5, (95.2)[d]
13	Tablet	91.9, (92.5)	101.2, (100.6)
14	Tablet	99.4, 93.1[e], (98.1)	100.0, 94.5[e], (90.5)
15	Tablet	83.7, (85.2)	[c]
16	Tablet	95.8, (96.2)	83.2, (87.4)
17	Tablet	101.1, (97.7)	99.2, (99.4)
18	Tablet	95.5, (91.7)	103.4, (97.1)
19	Tablet	90.5, (89.3)	55.5, (50.5)
20	Tablet	91.6, (94.8)	88.9, (98.0)
21	Capsule	98.2, 96.2[e], (100.9)	90.0, 98.3[e], (104.6)
22	Capsule	11.7, (10.8)	[c]

[a] Label claim range from 0.1205–0.217 mg/unit dose. [b] Label claim range from 0.0060–0.0284 mg/unit dose; 0.006–0.0075 most common. [c] Product did not contain scopolamine hydrobromide. [d] Values in parentheses are the average of 10 individual tablet assays (content uniformity). [e] Value obtained by second analyst.

by the formula $0.3C \times (Ru/Rs)$. The values Ru and Rs are the ratios of the hyoscyamine sulfate (or scopolamine hydrobromide) response to the internal standard response for sample (u) and standard (s), respectively, and C is the concentration of hyoscyamine sulfate (or scopolamine hydrobromide) (milligrams per milliliter) in the standard solution.

RESULTS AND DISCUSSION

Mobile Phase Selection—The presence of tetramethylammonium ions at pH 2 in the methanol–water mobile phase was found to minimize column adsorption of the alkaloids resulting in decreased retention time. Their presence also provided a high resolution separation of scopolamine and hyoscyamine–atropine, as shown in Fig. 1. The mobile phase was sufficiently UV-transparent for the detector to be set at 220 nm where alkaloid absorptivity is considerably higher. Three octadecylsilane columns were used, and the separation of component peaks on each column was as good as or better than that shown.

Even though the pH of the mobile phase buffer was at the lower extreme of the range normally considered advisable for column stability, the columns maintained separation and reproducibility for 5 months with daily use. At the end of each day's use, the column was rinsed with water and then methanol and stored in methanol overnight to avoid column deterioration from prolonged contact with the low pH buffer in the mobile phase.

Interferences—Considerable interference in the area of the hyoscyamine–atropine peak was encountered when first testing the procedure. Upon checking the reagent blank, the interference was attributed to impurities in commercially available methylene chloride. Passing the methylene chloride through basic alumina eliminated the interference. Each commercial product analyzed was carried through the procedure without addition of internal standard to check for interference of excipients in the area of the internal standard peak. A synthetic preparation of excipients representative of those encountered in the commercial products analyzed was also prepared and carried through the procedure to test for interference in the areas of the scopolamine peak and hyoscyamine–atropine peak. No significant interferences were detected. Phenobarbital was not entirely removed by the extraction procedure but did not interfere with the HPLC determination because it was well separated from the peaks of interest, as shown in Fig. 1.

Stability of Standard Preparation and Sample Solutions—A standard solution was prepared and its peak areas checked each day against a freshly prepared standard solution for 1 week. No deterioration in standard peak responses was noted. A sample solution was treated in a similar manner and sample peak responses also did not deteriorate. When standards or samples were dissolved in 0.05 N sulfuric acid or mobile phase instead of water, peak responses deteriorated.

Validation Tests—Twenty microliters of each of a series of five standard solutions containing 0–0.5 mg of hyoscyamine sulfate/ml and 0–0.032 mg of scopolamine hydrobromide/ml were injected onto the HPLC. Linear responses were obtained for each drug in its respective range by both peak height and peak area. Six replicate injections of the procedural standard solution gave a coefficient of variation of 1.4% for scopolamine hydrobromide and 0.5% for hyoscyamine sulfate.

Precautions in Sample Extraction—To minimize decomposition of the alkaloids due to heat, acids, and bases, the sample was carried through the entire extraction procedure to final dilution without stopping. The evaporation of solvent was found to be the most critical step. Since the alkaloid free bases decompose above 45°, methylene chloride (bp 38°) was chosen as the extracting solvent. Use of the flash evaporator allowed for rapid evaporation without bumping and splattering of the solvent. During the evaporation, the sample was not allowed to go to dryness before addition of methanolic hydrochloric acid to prevent possible loss of the alkaloids' free bases. The final methanol rinse was added to drive off residual hydrochloric acid which would decompose scopolamine salt. Because the alkaloid concentrations are in the microgram range, and thus subject to minute interferences, all glassware was thoroughly rinsed with distilled water and methylene chloride to ensure cleanliness.

Recovery of Standards—An aliquot of each commercial formulation assay composite was spiked with a standard solution of scopolamine hydrobromide and hyoscyamine sulfate, extracted and assayed according to the procedure, and the percentage of standard recovered calculated. Recovery of alkaloid standards was also checked by a second analyst for Formulations 14 and 21. The recovery results for each product and the statistical evaluation of the recovery data are summarized in Table 1.

Analysis of Commercial Formulations—Twenty-two commercial formulations consisting of elixirs, tablets, and capsules were assayed. Tablets and capsules were also analyzed for content uniformity. Results of the analyses are summarized in Table II. The average content uniformity values generally agreed with the assay values, but individual tablet values often varied ±10% of the average value. This variation coupled with the low concentration of alkaloids caused difficulty in preparing a uniform assay composite for tablets and capsules. Assays on Formulations 14 and 21 were checked by a second analyst, and the results compared favorably with those of the first analyst.

REFERENCES

(1) S. El-Masry and S. A. H. Khalil, *J. Pharm. Sci.*, **62,** 1332 (1973).

(2) U. R. Cieri, *J. Assoc. Off. Anal. Chem.*, **61,**(4), 937 (1978).

(3) "U.S. Pharmacopeia," 19th Rev., U.S. Pharmacopeial Convention, Rockville, Md., pp. 40 and 447, (1975).

(4) *Pharmacopeial Forum*, **6,**(1), 20 (1980).

(5) D. K. Wyatt, W. G. Richardson, B. McEwan, J. M. Woodside, and L. T. Grady, *J. Pharm. Sci.*, **65,** 680, (1976).

(6) N. D. Brown and H. K. Sleeman, *J. Chromatogr.*, **150,** 225 (1978).

(7) M. J. Walters, *J. Assoc. Off. Anal. Chem.*, **61**(6), 1428 (1978).

ACKNOWLEDGMENTS

The authors acknowledge the technical assistance of Jay Martin, Lawrence Mitchell, and Annie Pitts and the editorial assistance of Dr. James T. Stewart.

Belladonna Alkaloids and Phenobarbital Combination Pharmaceuticals Analysis II: High-Performance Liquid Chromatographic Determination of Phenobarbital

WALTER F. SCHMIDT ˣ **and LINDA J. PENNINGTON**

Received March 9, 1981, from the *Food and Drug Administration, Atlanta, GA 30309.* Accepted for publication November 16, 1981.

Abstract □ A high-performance liquid chromatographic separation is described for the analysis of phenobarbital in combination pharmaceutical dosage forms containing belladonna alkaloids. A mobile phase of 0.003 *M* tetramethylammonium chloride in water–methanol (3:2, pH 7.4) was used to separate phenobarbital from belladonna alkaloids on an octadecylsilane column in <7 min. The column effluent was monitored at 240 nm, which resulted in a detection limit of 6 ng of phenobarbital. The method is applicable to elixirs, tablets, and capsules with no preliminary extraction procedure. Data from the application of the method to commercial products is also presented.

Keyphrases □ High-performance liquid chromatography—belladonna alkaloids and phenobarbital combination pharmaceuticals, determination of phenobarbital □ Phenobarbital—belladonna alkaloids, combination pharmaceuticals, high-performance liquid chromatographic determination □ Combination drugs—belladonna alkaloids, high-performance liquid chromatographic determination of phenobarbital

Phenobarbital is present in elixirs, tablets, and capsules with belladonna alkaloids for its sedative effects. It has been previously analyzed by such procedures as extraction with UV detection (1), partition chromatography with UV detection (2), derivative formation with gas chromatography (3–5), normal-phase high-performance liquid chromatography (HPLC) (6, 7), and reversed-phase HPLC (8–10). Since an assay was desired which would work as rapidly and as effectively with elixirs as with tablets and capsules with minimum sample preparation, reversed-phase HPLC was investigated.

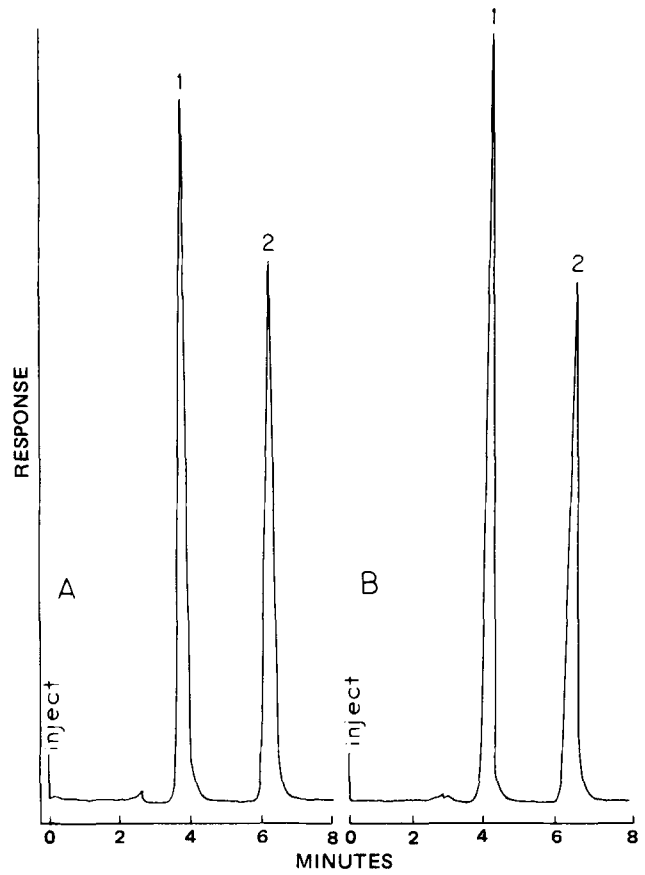

Figure 1—*Typical HPLC chromatograms showing separations of A, the standard solution and B, the sample solution. Key: 1, phenobarbital; 2, guaifenesin (internal standard).*

The HPLC retention properties of phenobarbital at different pH values of the mobile phase using ammonium phosphate and ammonium carbonate buffers was investigated previously (8). It was found that phenobarbital could not be resolved from the solvent front on 37–40-μm commercially packed reversed-phase columns, and that the phenobarbital peak resolution was not improved by variations in either pH or the methanol–water ratio. Others, also investigating the reversed-phase retention properties of phenobarbital at different pH values of the mobile phase (9) found, using sodium phosphate buffers, that retention volumes would change with the pH of the mobile phase on a 10-μm commercially packed reversed-phase column. However, no optimization of analytical conditions was attempted. Reversed-phase HPLC was used also for the analysis of phenobarbital in animal feeds with an unbuffered methanol–water mobile phase (10). However, the mobile phase was selected to minimize animal feed interferences.

A reversed-phase HPLC procedure was developed in this laboratory which is rapid, specific, and stability indicating for the analysis of phenobarbital in the presence of belladonna alkaloids in commercial elixirs, tablets, and capsules. Analytical data for selected commercial products using the proposed method are reported.

EXPERIMENTAL

Apparatus—A liquid chromatograph[1], equipped with a 20-μl loop injector[2], a variable wavelength UV detector[3], and a recorder-integrator[4], was used. A 25 cm × 4-mm i.d. stainless steel column containing octadecylsilane chemically bonded to 5-μm silica[5] was employed.

Reagents—A 0.01 *M* tetramethylammonium chloride solution was prepared by mixing 1.1 g of tetramethylammonium chloride[6] in 1 liter of distilled water. A 0.02 *M* phosphate buffer (pH 7.4) was prepared by dissolving 6.80 g of monobasic potassium phosphate in ~250 ml of distilled water, adjusting to pH 7.4 with ~39 ml of 1 *N* NaOH, and diluting to 1 liter.

Preparation of Internal Standard Solution—A guaifenesin[7] internal standard solution in methanol (3.2 mg/ml) was prepared (Fig. 1).

[1] Constametric I Pump, Laboratory Data Control, Riviera Beach, Fla.
[2] Chromatography Accessory Module Injector, 20-μl loop, Laboratory Data Control, Riviera Beach, Fla.
[3] Spectromonitor II Variable Wavelength UV-Visible Detector, Laboratory Data Control, Riviera Beach, Fla.
[4] HP 3380A Integrator, Hewlett-Packard, Palo Alto, Calif.
[5] Spherisorb octadecylsilane, 5 μm. Prepacked column purchased from Laboratory Data Control, Riviera Beach, Fla.
[6] Aldrich Chemical Co., Milwaukee, Wis.
[7] K&K Laboratories, Plainview, N.Y.

0022-3549/82/0800-0954$01.00/0

Table I—Recovery Data for Spiked Sample Determinations of Commercial Formulations for Phenobarbital [a]

Elixirs		Tablets and Capsules	
Formulation [b]	Percent Recovery	Formulation [b]	Percent Recovery
2	100.0	10	99.2
5	98.0	15	101.4
9	99.9	19	101.8
		20	100.8
Mean Recovery	99.3		100.8
SD	1.1		1.1
RSD	±1.1		±1.1
Range	98.0–100.0		99.2–101.8

[a] Portion of sample spiked with standard solution containing phenobarbital and analyzed according to procedure. [b] Numbering corresponds to formulations in Table II.

Preparation of Drug Standard Solution—A phenobarbital[8] standard solution was prepared in absolute methanol (260 μg/ml). Five milliliters of this solution was added to 4.0 ml of guaifenesin internal standard solution and 30 ml of 0.02 *M* phosphate buffer (pH 7.4), cooled to room temperature, and the volume adjusted to 50.0 ml with absolute methanol.

Preparation of Mobile Phase—A mobile phase was prepared by mixing 150 ml of 0.02 *M* phosphate buffer (pH 7.4), 150 ml of 0.01 *M* tetramethylammonium chloride solution, and 200 ml of absolute methanol.

HPLC Conditions—A flow rate of 1.0 ml/min was used with the UV detector set at 240 nm and the detector sensitivity set at 0.04 aufs.

Assay for Phenobarbital in Elixirs—A quantity of elixir equivalent to ~16 mg of phenobarbital was pipeted into a 50-ml volumetric flask. Thirty milliliters of methanol was added to the flask, the contents shaken for 4 min, and made to volume with methanol. About 5 ml of the solution was passed through a 0.5-μm filter. Aliquots of 2.0 ml of the filtrate and 2.0 ml of guaifenesin internal standard solution were combined with 15 ml of 0.02 *M* phosphate buffer (pH 7.4) into a 25-ml volumetric flask. The solution was mixed and made to volume with methanol. A 20-μl portion of the solution was injected into a liquid chromatograph. The peak response was compared with the peak response by peak height or peak area of 20 μl of phenobarbital standard solution. The quantity of phenobarbital in the portion of sample taken was calculated by the formula $(Ru/Rs) \times C$ in which Ru and Rs were the ratios of phenobarbital to guaifenesin peak response for sample (u) and standard (s), respectively, and C was the concentration of phenobarbital in the standard solution.

Assay for Phenobarbital in Tablets and Capsules—Twenty tablets or the contents of 20 capsules were weighed and finely powdered. A portion of sample composite equivalent to ~16 mg of phenobarbital was accurately weighed and transferred to a 50-ml volumetric flask. Five milliliters of distilled water was added and the contents of the flask shaken for 1 min. The procedure for "Assay for Phenobarbital in Elixirs" was then followed beginning with, "Thirty milliliters of methanol was added . . .."

Content Uniformity in Tablets and Capsules—A tablet or the contents of one capsule were quantitatively transferred to a volumetric flask which would yield a concentration of ~0.32 mg/ml of phenobarbital. Five milliliters of distilled water was added and the contents of the flask were mixed for 1 min. The "Assay for Phenobarbital in Elixirs" was then followed beginning with, "Thirty milliliters of methanol was added . . .."

RESULTS AND DISCUSSION

A slightly basic mobile phase (pH 7.4) was used to increase the UV absorptivity of phenobarbital, while avoiding the considerable column degradation normally observed with a mobile phase at a more basic pH. The addition of tetramethylammonium cations to the mobile phase resulted in selective increased retention of anionic compounds (*i.e.*, phenobarbital) through the formation of a tetramethylammonium ion-pair (11). Increased peak broadening with a resulting loss in peak resolution occurred when samples or standards were dissolved in methanol instead of in the mobile phase.

No intefering peaks were detected with 20 min of injection in any of the commercial products analyzed. The belladonna alkaloids did not interfere because of their separate retention times, lower absorptivities, and smaller sample concentrations. The column was found to be stable with daily usage for more than 1 month with no apparent loss in resolution of phenobarbital and guaifenesin internal standard.

[8] USP reference standard.

Table II—HPLC Analysis Results for Commercial Formulations

Formulation	Dosage Form	Percent of Label Claim [a]
1	Elixir	101.9
2	Elixir	102.2
3	Elixir	102.5
4	Elixir	98.8
5	Elixir	99.7
6	Elixir	98.1
7	Elixir	108.6
8	Elixir	101.2
9	Elixir	95.6
10	Tablet	99.0, (100.0) [b]
11	Tablet	104.7, (104.7)
12	Tablet	92.4, (96.9)
13	Tablet	104.6, (102.2)
14	Tablet	100.6, (100.6)
15	Tablet	104.4, (102.1)
16	Tablet	97.5, 100.6 [c], (101.2)
17	Tablet	104.9, 101.9 [c], (100.0)
18	Tablet	96.9, (100.6)
19	Tablet	100.4, 101.2 [c], (101.2)
20	Capsule	106.8, 106.8 [c], (109.2)
21	Capsule	105.0 (101.9)

[a] Label claim range 15–32 mg/unit dose. [b] Values in parentheses are the average of 10 individual tablet assays (content-uniformity). [c] Value obtained by second analyst.

Six replicate injections of a standard solution containing 0.026 mg/ml of phenobarbital gave a coefficient of variation of 0.5% for the ratio of the peak response of phenobarbital to that of internal standard. Linear response was obtained in the 0–0.055 mg/ml range for a series of five phenobarbital standards.

Seven commercial formulations were each spiked with a standard solution of phenobarbital, extracted and assayed, and the percentage of standard recovery calculated. The recovery results and the statistical evaluation of the recovery data are summarized in Table I.

Twenty-one commercial formulations consisting of elixirs, tablets, and capsules were assayed. Tablets and capsules were also analyzed for content uniformity. Results of the content uniformity analyses are summarized in Table II. The average content uniformity values agreed with the composite assay values. Composite assays on Formulations 16, 17, 19, and 20, listed in Table II, were performed by another analyst. These results compared favorably with the original findings.

REFERENCES

(1) "U.S. Pharmacopeia XX National Formulary XV," U.S. Pharmacopeial Convention, Inc., Rockville, Md., 1980, p. 609.

(2) "Methods of Analysis," 13th ed., Association of Official Analytical Chemists, Washington, D.C., 1980, p. 618.

(3) V. S. Venturella, V. M. Gualario, and R. E. Lang, *J. Pharm. Sci.*, **62,** 662 (1973).

(4) R. Osiewicz, V. Aggarwal, R. M. Young, and I. Sunshine, *J. Chromatogr.*, **88,** 157 (1974).

(5) K. Kurata, M. Takeuchi, and K. Yoshida, *J. Pharm. Sci.*, **68,** 1187 (1979).

(6) J. E. Evans, *Anal. Chem.*, **45,** 2428 (1973).

(7) S. H. Atwell, V. A. Green, and W. G. Haney, *J. Pharm. Sci.*, **64,** 806 (1975).

(8) I. L. Honigberg, J. T. Stewart, A. P. Smith, R. D. Plunkett, and E. L. Justice, *ibid.*, **64,** 1389 (1975).

(9) P. J. Twitchett and A. C. Moffat, *J. Chromatogr.*, **111,** 149 (1975).

(10) M. C. Bowman and L. G. Rushing, *J. Chromatogr. Sci.*, **16,** 23 (1978).

(11) R. Gloor and E. L. Johnson, *ibid.*, **15,** 413 (1977).

ACKNOWLEDGMENTS

The authors acknowledge the technical assistance of Sandford B. Clarke, Edward Lamar, Jay Martin, Lawrence Mitchell, and Carl Ponder and the editorial assistance of Dr. James T. Stewart.

Ion-Pair High-Performance Liquid Chromatography of Terbutaline and Catecholamines with Aminophylline in Intravenous Solutions

DAVID A. WILLIAMS *x, **ESTHER Y. Y. FUNG** ‡, and **DAVID W. NEWTON** §

Received June 15, 1981, from the *Department of Chemistry, Massachusetts College of Pharmacy and Allied Health Sciences, Boston, MA 02115, the ‡Tiers Drug Store, Uxbridge, Ontario, Canada LOC 1 KO, and the §Department of Pharmaceutics, College of Pharmacy, University of Nebraska Medical Center, Omaha, NE 68105. Accepted for publication November 12, 1981.

Abstract □ A stability-indicating ion-pair high-performance liquid chromatographic (HPLC) assay that is rapid and specific for epinephrine, isoproterenol, dopamine, norepinephrine, methyldopate, or terbutaline in intravenous solutions with aminophylline has been developed using a spectrofluorometric detector. A HPLC method for the analysis of terbutaline and methyldopate is introduced, and the superiority of fluorometric over UV detection of terbutaline and the catecholamines is illustrated.

Keyphrases □ High-performance liquid chromatography—ion-pair, terbutaline and catecholamines with aminophylline in intravenous solutions □ Fluorescence detector—high-performance liquid chromatographic analysis of catecholamines in presence of aminophylline □ Catecholamines—ion-pair high-performance liquid chromatography with aminophylline in intravenous solutions

Dopamine (I), epinephrine (II), isoproterenol (III), methyldopate (IV), norepinephrine (V), or terbutaline (VI) may be combined with aminophylline (VII) in intravenous admixtures prior to patient administration. Catecholamines and other phenolic sympathomimetic amines are reportedly more unstable in an alkaline media and can undergo rapid autoxidation to biologically inactive quinoid products (1). Thus, the therapeutic efficacy of these sympathomimetic amines is directly related to their stability in an alkaline aminophylline solution (pH 8.6–9.0) for injection. Little information has appeared regarding the stability of these sympathomimetic amines (I–VI) when combined with aminophylline solutions. This may be due in part to the lack of a rapid, specific, stability-indicating assay for I–VI in the presence of their degradation products and theophylline.

Over the years, catecholamines (I–V) have been assayed using UV or spectrofluorometric methods. However, the poor specificity of these commonly employed methods for I–V in the presence of quinone degradation products raises doubts about their validity.

One significant advantage of chromatographic assays is that they are stability-indicating (2, 3). This is of importance when determining the rate and extent of degradation of potent, potentially lifesaving pharmacologic agents such as sympathomimetic drugs which are diluted in parenteral solutions for clinical administration, sometimes in combination with other drugs.

Several HPLC procedures for the assay of catecholamines and related drugs or metabolites have employed UV detection (4–7), fluorescence detection with precolumn derivatization (8), or electrochemical detection (9–11). Finally, other less expedient chromatographic procedures have been applied to the analysis of some of these drugs (12, 13). Apparently, neither the HPLC assay for terbutaline and methyldopate, nor the use of fluorometric detection requiring no derivatization has been reported for the HPLC analysis of VI or the catecholamines (I–V) in solutions intended clinically for injection. The present report describes a rapid, sensitive, and stability-indicating method for I–VI in the presence of aminophylline and the superiority of fluorometric over UV detection.

Table I—Conditions for the High-Performance Liquid Chromatographic Assay of Terbutaline and Five Catecholamines in 5% Dextrose in Water Injection in the Absence and Presence of Aminophylline

Drug	Methanol in Eluant, % (v/v)	Fluorometer Sensitivity[a]	Volume Injected, μl
Dopamine Hydrochloride (I)	25	2 × 0.3	20
Epinephrine Hydrochloride (II)	25	4 × 3	20
Isoproterenol Hydrochloride (III)	35	4 × 10	20
Methyldopate Hydrochloride (IV)	35	4 × 1	15
Norepinephrine Bitartrate (V)	15	4 × 10	15
Terbutaline Sulfate (VI)	35	4 × 10	40
Aminophylline (VII)	—	—	—

[a] Fluorescence detector P.M. gain × sensitivity range. Maximum sensitivity = 4 × 10.

EXPERIMENTAL

Apparatus—A high-pressure liquid chromatograph[1] equipped with a septumless injector[2] and a variable wavelength spectrofluorometric[3] or a variable wavelength UV detector[4] was employed in conjunction with a microparticulate C_{18} column[5] for separation.

Reagents—All chemicals and reagents were analytical grade unless otherwise indicated. Dopamine hydrochloride[6], epinephrine hydrochloride[7], isoproterenol hydrochloride[8], methyldopate hydrochloride[9], norepinephrine bitartrate[7,8], terbutaline sulfate[10], aminophylline[7], and glass-distilled HPLC grade methanol[11] were used without further purification. Sodium heptanesulfonate[12] was recrystallized from an acetone–water mixture.

[1] M-6000A solvent delivery system, Waters Associates, Milford, Mass.
[2] U6K injector, Waters Associates, Milford, Mass.
[3] Model 204A Spectrofluorometer, Perkin-Elmer, Norwalk, Conn.
[4] Model LC-55 Spectrophotometer, Perkin-Elmer, Norwalk, Conn.
[5] Catalog No. 27324, Waters Associates, Milford, Mass.
[6] Arnar-Stone, McGaw Park, Ill.
[7] Sigma Chemical, St. Louis, Mo.
[8] Sterling-Winthrop, Rensselaer, N.Y.
[9] Merck, Sharp and Dohme, West Point, Pa.
[10] Ciba-Geigy, Summit, N.J.
[11] Fisher Scientific Co., Fairlawn, N.J.
[12] Eastman Chemicals, Rochester, N.Y.

0022-3549/82/0800-0956$01.00/0

Table II—Retention Time and Analysis of the Catecholamines and Terbutaline in Known Mixtures

Drug		t_R[a] min	t_R, min[a] aminophylline	Concentration, mg/liter Added	Concentration, mg/liter Found ± CL[b]	Error, %
I	(80–900)[c]	4.08	ND[d]	800.0	802.53 ± 7.09	0.32
II	(0.4–4.2)[c]	4.13	3.50	4.0	3.98 ± 0.02	0.50
III	(0.2–2.4)[c]	4.33	3.17	2.0	2.02 ± 0.06	1.0
IV	(120–1100)[c]	4.50	2.75	1000.0	996.92 ± 5.30	0.31
V	(0.8–8.5)[c]	4.75	5.33	8.0	8.05 ± 0.09	0.63
VI	(0.4–4.2)[c]	5.33	2.75	4.0	3.96 ± 0.05	1.0

[a] Flow rate = 1.6 ml/min. t_R for aminophylline is for theophylline. [b] 95% confidence limits. [c] Concentration range (μg/ml) used for preparing standard curves. [d] Not detected, sensitivity too low.

Analytical Procedure—Standard solutions (Table I) of each drug were freshly prepared by diluting a stock solution with 5% dextrose in water for injection, USP[13]. The mobile phase was 0.35 *M* acetic acid and 0.005 *M* sodium heptanesulfonate in different concentrations of methanol (Table II). The flow rate was 1.6–2.0 ml/min at ambient temperature. The injection volumes for the standard or sample solution are reported in Table II. The catecholamines (I–V) were detected using an excitation wavelength (λ_{ex}) of 285 nm and an emission wavelength (λ_{em}) of 315 nm. The values of λ_{ex} and λ_{em} for terbutaline were 280 and 310 nm, respectively. The UV detector was operated at 280 nm. The concentrations of I–VI were determined from their respective peak areas by comparison to a standard curve. Peak areas were calculated from the product of peak height times half-height peak widths. Good reproducibility was obtained without the use of an internal standard.

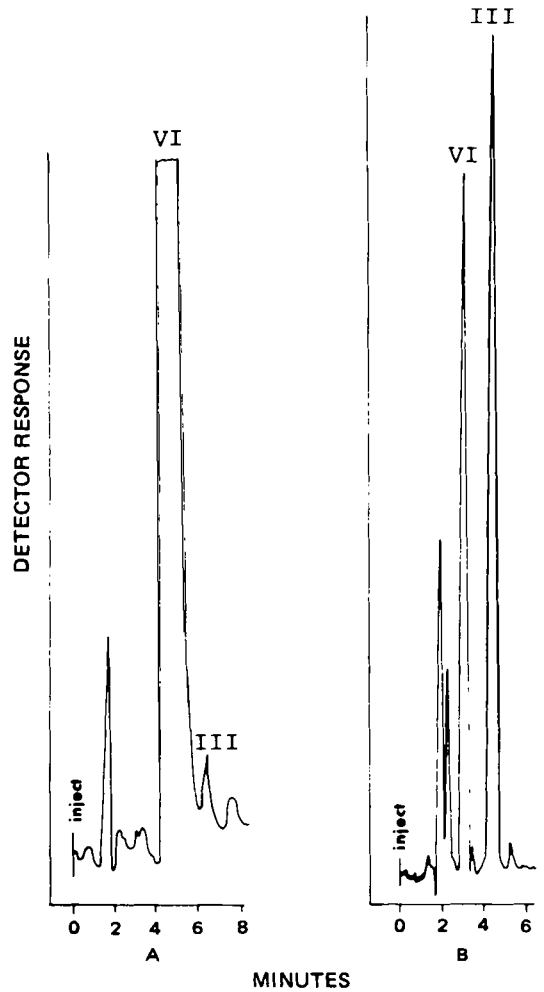

Figure 1—*(A) Chromatogram of isoproterenol hydrochloride (III), 2 μg/ml and aminophylline (VII), 500 μg/ml. UV detector = 280 nm, flow rate = 1.6 ml/min, 0.005* M *1-heptanesulfonate sodium and 0.35* M *acetic acid in 20% (v/v) methanol. The recorder was set at 1 mV; detector response = 0.004 aufs, and injection volume = 20 μl. (B) Chromatogram of isoproterenol hydrochloride (III), 2 μg/ml and aminophylline (VII), 500 μg/ml. Fluorometric detector (λ_{ex} = 285 nm, λ_{em} = 315 nm), flow rate = 1.6 ml/min, 0.005* M *1-heptanesulfonate sodium and 0.35* M *acetic acid in 35% (v/v) methanol. The recorder was set at 10 mV, and a chart speed of 0.5 cm/min; detector sensitivity and injection volume are given in Table I.*

[13] Abbott Laboratories, North Chicago, Ill.

RESULTS

The chromatogram peaks attributed to aminophylline actually represent theophylline, because at pH 2.4–3.0 of the mobile phase, aminophylline dissociates into theophylline and the ethylenediammonium ion. The high concentration and strong UV absorbance of theophylline makes the accurate HPLC analysis for dilute solutions of II, III, V, and VI difficult and poorly reproducible with a UV detector. Increasing the injection volume and/or retention time produced unsatisfactory results. The advantage of fluorescence detection in this study was to provide decreased response to theophylline concurrently with increased sensitivity and selectivity towards II, III, V, and VI without pre- or postcolumn derivatization. A typical chromatogram illustrating the advantage of using fluorescence detection is shown for III in Fig. 1. For I and IV, fluorescence detection offered no advantage over UV detection because of their much higher concentrations, relative to II, III, V, and VI (Table III). Theophylline may not be detectable when using the fluorescence detector at its lower sensitivity, which was the case for dopamine. The sensitivity of the fluorescent method permits quantitation of II, III, V, and VI to <0.1 μg/ml. The methanol concentration in the mobile phase needed to achieve the desired separation for I–VI from aminophylline is given in Table I, and their respective retention times, which are the mean of four replicate determinations, are reported in Table II. Standard curves of eight drug concentrations *versus* their peak height areas were constructed from triplicate injections for each drug in Table I. The linear plots showed that the peak height area of each drug was directly related to its concentration.

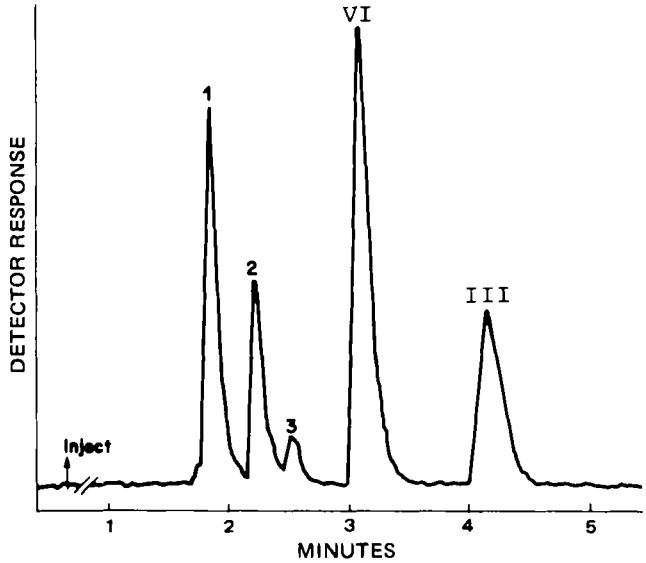

Figure 2—*Chromatogram of isoproterenol hydrochloride (III), 2 μg/ml and aminophylline (VII), 500 μg/ml, after 17 hr of exposure to fluorescent light. Fluorometric detector (λ_{ex} = 285 nm, λ_{em} = 315 nm), flow rate 1.6 ml/min 0.005* M *1-heptanesulfonate sodium and 0.35* M *acetic acid in 35% (v/v) methanol. The recorder was set at 10 mV and a chart speed of 4 cm/min; detector sensitivity and injection volume are given in Table I. Peaks 1 and 3 are degradation products, and Peak 2 is unidentified.*

The correlation coefficient for the standard curves over the concentration range used in this study was >0.997 (n = 22 or 25). The analysis of the concentrations of I–VI in the experimental samples compared favorably with the theoretical values of the drug formulations (Table II) with <1% error.

The described HPLC assay has been successfully applied as a stability-indicating method for determining the rate and percentage of autoxidation of commercially supplied injectable solutions of I–VI which had been diluted in 5% dextrose in water injection, with and without aminophylline (500 μg/ml) (14). The chromatographic separation of I–VI from their autoxidation products is illustrated in Fig. 2, with III, which has undergone 70% decomposition after being exposed to 17 hr of fluorescent light. Peak 1 represents the principal degradation product and Peak 3 a minor product. The unidentified Peak 2 is present in unexposed samples and does not appear to change after exposure to light. Similarly, the degradation products of I, II, and IV–VI elude within 2–3 min following injection. Figure 1B represents III before exposure to fluorescent light and decomposition has already commenced. This method has demonstrated the capability of separating degradation products from the analysis of pure I–VI.

The application of ion-pair HPLC for the analysis of formulations containing VI or IV has not been previously described. This reported method is applicable for the accurate determination of these drugs, using either UV or fluorescence detectors.

DISCUSSION

Various analytical methods have been used in stability studies for catecholamines but suffered from their inability to quantitate or separate degradation products from the parent substance. The combination of fluorescence detection with reversed-phase ion-pair HPLC yields a rapid and selective method for the quantitative separation and determination of I–VI in the presence of their autoxidation products and pharmaceutical adjuvants. The lowest concentration at which the sympathomimetic amines used in this study could be detected was 0.1 μg/ml.

The described method is applicable for the content uniformity and quality control of products containing VI and IV.

Despite the widespread use of UV detection in HPLC assays, the sensitive fluorescence measurement for low concentrations of sympathomimetic amines in pharmaceutical preparations has not been extensively reported except for their clinical analysis in biological fluids. The sensitive measurement of I–VI will allow studies of the purity of dosage forms and investigation of their degradation kinetics and pharmacokinetics. Without the use of a fluorescence detector, II, III, V, or VI could not be quantitatively measured in the presence of aminophylline. Also, the presence of pharmaceutical adjuvants should not interfere, because of their poor fluorescent properties.

REFERENCES

(1) A. Lund, *Acta Pharmacol. Toxicol.*, **5**, 75 (1949).

(2) J. B. Johnson and V. S. Venturella, *Bull. Parenter. Drug Assoc.*, **25**, 239 (1971).

(3) L. Chafetz, *J. Pharm. Sci.*, **60**, 335 (1971).

(4) A. G. Ghanekar and V. D. Gupta, *ibid.*, **67**, 1247 (1978).

(5) K. E. Rasmussen, F. Tonnesen, and S. N. Rasmussen, *Medd. Nor. Farm. Selsk.*, **39**, 128 (1977).

(6) G. A. Scratchley, A. N. Mosaud, S. J. Stohs, and D. W. Wingard, *J. Chromatogr.*, **169**, 313 (1979).

(7) B. A. Persson and B. L. Karger, *J. Chromatogr. Sci.*, **12**, 521 (1974).

(8) T. P. Davis, C. W. Gehrke, C. W. Gehrke, Jr., T. D. Cunningham, K. C. Kuo, K. O. Gerhardt, H. D. Johnson, and C. H. Williams, *Clin. Chem.*, **24**, 1317 (1978).

(9) G. M. Kochak and W. D. Mason, *J. Pharm. Sci.*, **69**, 897 (1980).

(10) T. P. Moyer and N. S. Jiang, *J. Chromatogr.*, **153**, 365 (1978).

(11) T. M. Kenyhercz and P. T. Kissinger, *J. Pharm. Sci.*, **67**, 112 (1978).

(12) J. R. Watson and R. C. Lawrence, *ibid.*, **66**, 560 (1977).

(13) F. N. Minard and D. S. Grant, *Biochem. Med.*, **6**, 46 (1972).

(14) D. W. Newton, E. Y. Y. Fung, and D. A. Williams, *Am. J. Hosp. Pharm.*, **38**, 1314 (1981).

ACKNOWLEDGMENTS

Abstracted in part from a thesis submitted by Esther Yin Yee Fung to the Graduate Council of the Massachusetts College of Pharmacy and Allied Health Sciences in partial fulfillment of the M.S. degree requirements.

The authors thank Arnar-Stone Laboratories, Ciba Pharmaceutical, Merck, Sharp and Dohme, and Sterling-Winthrop for their donation of analytical quality drug samples, and Mrs. Gail Williams for typing the manuscript.

Enhanced Entrapment of a Quaternary Ammonium Compound in Liposomes by Ion-Pairing

MICHAEL JAY ˣ and GEORGE A. DIGENIS

Received September 9, 1981, from the *Division of Medicinal Chemistry and Pharmacognosy, College of Pharmacy, University of Kentucky, Lexington, KY 40536.* Accepted for publication November 10, 1981.

Abstract □ The encapsulation of a quaternary ammonium compound by multilamellar liposomes was enhanced by formation of ion-pairs with a counterion. Thus, [^{14}C]methantheline bromide was synthesized and paired with a 25 M excess of trichloroacetate. Under these conditions, the amount of radioactivity entrapped by phosphatidylcholine liposomes was three times greater than when no trichloroacetate was present. The increased liposomal loading was probably due to the solubilization of the ion-pair in the lipid membrane of the liposome.

Keyphrases □ Liposomes—quaternary ammonium compound, entrapment, ion pairing □ Ion-pairing—quaternary ammonium compound, entrapment, liposomes □ Ammonium—quaternary compound, entrapment in liposomes, ion-pairing

Liposomes are microscopic lipid vesicles originally used to study the structure and function of biological membranes (1). In recent years, liposomes have demonstrated potential as carriers and transporters of biologically active compounds (2). A wide variety of compounds have been encapsulated in liposomes, ranging from RNA (3) and insulin (4) to small molecules like histamine (5). Liposomes have been administered intravenously and orally (6), and a recent report describes the delivery of drugs *via* liposomes by the topical route (7). Liposomes elicit no immunological or toxicological responses and are completely biodegradable. For these reasons, liposomes have been viewed as an attractive mechanism for drug delivery, especially for biologically unstable compounds, but not without certain drawbacks. Special techniques have been developed in an attempt to direct liposomes to specific targets or organ systems by immunological methods (8) and by producing pH-sensitive liposomes (9). Polymerized

0022-3549/82/0800-0958$01.00/0

The correlation coefficient for the standard curves over the concentration range used in this study was >0.997 (n = 22 or 25). The analysis of the concentrations of I–VI in the experimental samples compared favorably with the theoretical values of the drug formulations (Table II) with <1% error.

The described HPLC assay has been successfully applied as a stability-indicating method for determining the rate and percentage of autoxidation of commercially supplied injectable solutions of I–VI which had been diluted in 5% dextrose in water injection, with and without aminophylline (500 μg/ml) (14). The chromatographic separation of I–VI from their autoxidation products is illustrated in Fig. 2, with III, which has undergone 70% decomposition after being exposed to 17 hr of fluorescent light. Peak 1 represents the principal degradation product and Peak 3 a minor product. The unidentified Peak 2 is present in unexposed samples and does not appear to change after exposure to light. Similarly, the degradation products of I, II, and IV–VI elude within 2–3 min following injection. Figure 1B represents III before exposure to fluorescent light and decomposition has already commenced. This method has demonstrated the capability of separating degradation products from the analysis of pure I–VI.

The application of ion-pair HPLC for the analysis of formulations containing VI or IV has not been previously described. This reported method is applicable for the accurate determination of these drugs, using either UV or fluorescence detectors.

DISCUSSION

Various analytical methods have been used in stability studies for catecholamines but suffered from their inability to quantitate or separate degradation products from the parent substance. The combination of fluorescence detection with reversed-phase ion-pair HPLC yields a rapid and selective method for the quantitative separation and determination of I–VI in the presence of their autoxidation products and pharmaceutical adjuvants. The lowest concentration at which the sympathomimetic amines used in this study could be detected was 0.1 μg/ml.

The described method is applicable for the content uniformity and quality control of products containing VI and IV.

Despite the widespread use of UV detection in HPLC assays, the sensitive fluorescence measurement for low concentrations of sympathomimetic amines in pharmaceutical preparations has not been extensively reported except for their clinical analysis in biological fluids. The sensitive measurement of I–VI will allow studies of the purity of dosage forms and investigation of their degradation kinetics and pharmacokinetics. Without the use of a fluorescence detector, II, III, V, or VI could not be quantitatively measured in the presence of aminophylline. Also, the presence of pharmaceutical adjuvants should not interfere, because of their poor fluorescent properties.

REFERENCES

(1) A. Lund, *Acta Pharmacol. Toxicol.*, **5**, 75 (1949).

(2) J. B. Johnson and V. S. Venturella, *Bull. Parenter. Drug Assoc.*, **25**, 239 (1971).

(3) L. Chafetz, *J. Pharm. Sci.*, **60**, 335 (1971).

(4) A. G. Ghanekar and V. D. Gupta, *ibid.*, **67**, 1247 (1978).

(5) K. E. Rasmussen, F. Tonnesen, and S. N. Rasmussen, *Medd. Nor. Farm. Selsk.*, **39**, 128 (1977).

(6) G. A. Scratchley, A. N. Mosaud, S. J. Stohs, and D. W. Wingard, *J. Chromatogr.*, **169**, 313 (1979).

(7) B. A. Persson and B. L. Karger, *J. Chromatogr. Sci.*, **12**, 521 (1974).

(8) T. P. Davis, C. W. Gehrke, C. W. Gehrke, Jr., T. D. Cunningham, K. C. Kuo, K. O. Gerhardt, H. D. Johnson, and C. H. Williams, *Clin. Chem.*, **24**, 1317 (1978).

(9) G. M. Kochak and W. D. Mason, *J. Pharm. Sci.*, **69**, 897 (1980).

(10) T. P. Moyer and N. S. Jiang, *J. Chromatogr.*, **153**, 365 (1978).

(11) T. M. Kenyhercz and P. T. Kissinger, *J. Pharm. Sci.*, **67**, 112 (1978).

(12) J. R. Watson and R. C. Lawrence, *ibid.*, **66**, 560 (1977).

(13) F. N. Minard and D. S. Grant, *Biochem. Med.*, **6**, 46 (1972).

(14) D. W. Newton, E. Y. Y. Fung, and D. A. Williams, *Am. J. Hosp. Pharm.*, **38**, 1314 (1981).

ACKNOWLEDGMENTS

Abstracted in part from a thesis submitted by Esther Yin Yee Fung to the Graduate Council of the Massachusetts College of Pharmacy and Allied Health Sciences in partial fulfillment of the M.S. degree requirements.

The authors thank Arnar-Stone Laboratories, Ciba Pharmaceutical, Merck, Sharp and Dohme, and Sterling-Winthrop for their donation of analytical quality drug samples, and Mrs. Gail Williams for typing the manuscript.

Enhanced Entrapment of a Quaternary Ammonium Compound in Liposomes by Ion-Pairing

MICHAEL JAY ˣ and GEORGE A. DIGENIS

Received September 9, 1981, from the *Division of Medicinal Chemistry and Pharmacognosy, College of Pharmacy, University of Kentucky, Lexington, KY 40536.* Accepted for publication November 10, 1981.

Abstract □ The encapsulation of a quaternary ammonium compound by multilamellar liposomes was enhanced by formation of ion-pairs with a counterion. Thus, [^{14}C]methantheline bromide was synthesized and paired with a 25 M excess of trichloroacetate. Under these conditions, the amount of radioactivity entrapped by phosphatidylcholine liposomes was three times greater than when no trichloroacetate was present. The increased liposomal loading was probably due to the solubilization of the ion-pair in the lipid membrane of the liposome.

Keyphrases □ Liposomes—quaternary ammonium compound, entrapment, ion pairing □ Ion-pairing—quaternary ammonium compound, entrapment, liposomes □ Ammonium—quaternary compound, entrapment in liposomes, ion-pairing

Liposomes are microscopic lipid vesicles originally used to study the structure and function of biological membranes (1). In recent years, liposomes have demonstrated potential as carriers and transporters of biologically active compounds (2). A wide variety of compounds have been encapsulated in liposomes, ranging from RNA (3) and insulin (4) to small molecules like histamine (5). Liposomes have been administered intravenously and orally (6), and a recent report describes the delivery of drugs *via* liposomes by the topical route (7). Liposomes elicit no immunological or toxicological responses and are completely biodegradable. For these reasons, liposomes have been viewed as an attractive mechanism for drug delivery, especially for biologically unstable compounds, but not without certain drawbacks. Special techniques have been developed in an attempt to direct liposomes to specific targets or organ systems by immunological methods (8) and by producing pH-sensitive liposomes (9). Polymerized

0022-3549/82/0800-0958$01.00/0

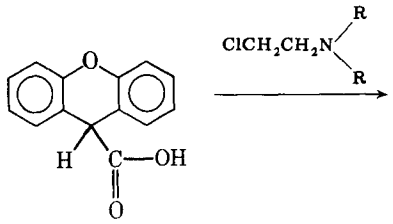

I

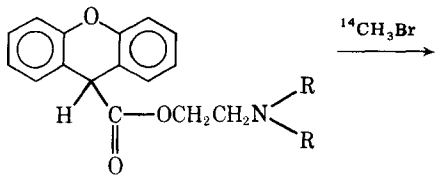

II

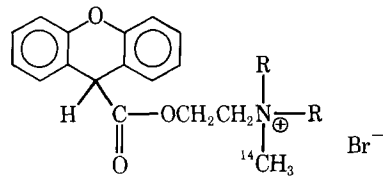

III

R = C_2H_5

vesicles have been produced to increase their stability (10), but one major problem still exists, *i.e.*, many drugs are very poorly encapsulated by lipsomes, especially water-soluble compounds (11).

Some progress in this case has been reported. The degree of encapsulation of the chemotherapeutic agents 6-mercaptopurine and 8-azaguanine in single compartment liposomes has been improved by the formation of charge-transfer complexes with chloranil (2,3,5,6-tetrachloro-*p*-benzoquinone) and cyanocobalamin (12, 13). In this report, the enhanced entrapment of a quaternary ammonium compound in multilamellar liposomes by the formation of ion-pairs is described. More specifically the entrapment of the antimuscarinic drug, methantheline bromide, in the presence and absence of trichloroacetate was compared. A relatively simple procedure for the synthesis of [^{14}C]methantheline bromide, based on the method of Cusic and Robinson (14) is reported. This differs from the product synthesized in a previous study in the position of the carbon 14 label (15).

EXPERIMENTAL[1]

***N,N*-Diethylaminoethyl Xanthene-9-carboxylate (II)**—2-Diethylaminoethyl chloride hydrochloride[2] (3.0 g, 0.017 mole) was added to 30 ml of 1.0 *N* NaOH and extracted three times with 30 ml of ether. The combined ether extracts were dried over sodium sulfate, filtered, and evaporated under reduced pressure yielding a viscous oil. To this oil was added 4.0 g (0.019 mole) of xanthene-9-carboxylic acid[3] (I) in 15 ml of isopropyl alcohol and the mixture was refluxed overnight. After filtering, the solvent was evaporated, yielding an oily residue which crystallized upon further drying. Recrystallization from ethyl acetate afforded 4.277 g (0.012 mole) of analytically pure material which melted at 145–147° [lit. (15) 143–145°], IR (KBr): 1735 (C=O) cm^{-1}, with a 68% yield.

[^{14}C]Methantheline Bromide (*N,N*-Diethylaminoethyl xanthene-9-carboxylate[^{14}C]methobromide) (III)—A 0.3-g aliquot of II was made alkaline and extracted into ether as described previously. After drying, the solvent was evaporated and the resultant oily residue was dissolved in 4 ml of absolute ethanol. The solution was transferred to a vial containing 0.25 mCi (4.75 mg) of [^{14}C]methyl bromide[4] (5 mCi/mmole) which was cooled to 0–4° in an ice bath. The vial was sealed and allowed to stand for 48 hr at room temperature. The addition of dry ether to the ethanolic solution resulted in the formation of a precipitate which, upon recrystallization from benzene, gave 12.1 mg (0.029 mmole, 0.144 mCi) of fine, white needles (58% yield). The product had an IR spectrum identical to the authentic material[5] and melted at 173–175° in close agreement with the literature value of 175° (6). A radiochromatogram of the product [(silica gel) ethanol–water–acetic acid (3:2:1), R_f = 0.56] verified its radiochemical purity.

For the experiments with liposome entrapment of III, unlabeled methantheline bromide was added to III resulting in a final specific activity of 1 μCi/μmole.

Preparation of Multilamellar Liposomes—Unsonicated multilamellar liposomes were prepared according to the method of Maghew *et al.* (16). Phosphatidylcholine[6] (10 μmoles) and cholesterol[6] (3 μmoles) were dissolved in 2 ml of chloroform and placed in a cylindrical test tube. The chloroform was evaporated leaving a thin film in the bottom of the tube. To this was added the aqueous phase which consisted of 1 μmole of III (1 μCi in 2 ml of phosphate buffer at pH 7.4). In the ion-pairing experiments, 25 μmoles of trichloroacetate[7] was added as well. The mixture was mechanically agitated for 10 min after which time the liposome-entrapped radioactivity (arising from III) was separated from the free radioactivity (*i.e.*, nonliposome-bound activity) by molecular sieves[8]. The extent of entrapment by liposomes of III in the presence and absence of trichloroacetate was calculated by comparing the total number of counts arising from liposome-bound radioactivity with the free radioactivity.

RESULTS AND DISCUSSION

The partitioning of charged species into a nonaqueous medium results from the masking of the hydrophilic site by a counterion. Some counterions are more effective than others in increasing the lipophilicity of the charged species. The use of ion-pairing techniques has been utilized to enhance the lipid solubility of certain ionic compounds (17) and, in this connection, has improved the GI absorption of large cationic drugs (18). The chloroform–water partition coefficient of methantheline bromide was shown to increase over 200-fold when ion-paired with a 25 *M* excess of trichloroacetate (19). Higher concentrations of trichloroacetate did not improve the partitioning of methantheline into the chloroform layer (20). The entrapment of this drug by multilamellar liposomes would presumably be enhanced by the formation of ion-pairs with trichloroacetate, which would allow methantheline to be solubilized in the lipid membrane of the liposome. Multilamellar liposomes have a high lipid content relative to the aqueous phase compared to sonicated unilamellar liposomes. As a result, the effects of ion pairing on increasing lipid solubility should be most pronounced in the multilamellar liposomes. Solubilization of methantheline in the liposomal membrane should significantly increase the total amount of drug carried by the liposome. In the absence of trichloroacetate, the drug would only be carried in the small aqueous core of the liposome and the thin aqueous layers between the lipid bilayers of the multilamellar liposome. In the presence of trichloroacetate, the drug would be carried in these aqueous compartments as well as in the membrane itself.

The addition of a 25 *M* excess of trichloroacetate (with respect to III) in the aqueous phase during liposome production resulted in a threefold increase in the amount of radioactivity, which was entrapped by the multilamellar liposomes (1005–3027 dpm). Varying the cholesterol content of the liposomal membrane from 0 to 5 μmoles per 10 μmoles of phosphatidylcholine, did not significantly alter the entrapment of III. The increase of entrapped radioactivity arising from [^{14}C]methantheline from 0.44–1.2% by ion-pairing could be increased further by utilizing phospholipid membranes with physical properties differing from phos-

[1] Infrared spectra (KBr) were recorded on a Perkin-Elmer 567 spectrophotometer. Melting points were determined using a Thomas-Hoover capillary apparatus and are uncorrected. Radiochemical purity was determined with a Packard 7201 radiochromatogram scanner. Radioactive samples were counted in a Packard 3375 Tri-Carb Liquid Scintillation Spectrometer. ACS (Amersham) was the cocktail used for radioactive samples.

[2] Aldrich Chemical Co., Milwaukee, Wis.

[3] K and K Laboratories, Plainview, N.Y.

[4] New England Nuclear, Boston, Mass.

[5] Searle and Co., San Juan, P.R.

[6] Sigma Chemical Co., St. Louis, Mo.

[7] Sodium trichloroacetate, Fisher Scientific Co., Pittsburg, Pa.

[8] Sephadex G-50, Pharmacia Fine Chemicals, Piscataway, N.J.

phatidylcholine. The use of a charged membrane as well as the addition of other membrane adjuvants may affect the entrapment of methantheline and other compounds by liposomes.

These ion-pairing techniques can be used to increase liposomal loading of a large number of ionic compounds. The liposome-entrapped compounds can be used to overcome some traditional problems in the oral administration of drugs such as acid lability, inadequate intestinal absorption, and poor palatability.

The administration of methantheline bromide *via* liposomes is particularly desirable considering the poor absorption observed for quaternary ammonium compounds. In addition, ion-pairing of quaternary ammonium compounds increases the loading of these poorly entrapped drugs in liposomal membranes.

REFERENCES

(1) A. D. Bangham, *Ann. N.Y. Acad. Sci.*, **308**, 2 (1978).

(2) J. H. Fendler and A. Romero, *Life Sci.*, **20**, 1109 (1977).

(3) D. Papahadjopoulos, T. Wilson, and R. Taber, *In Vitro*, **16**, 49 (1980).

(4) H. M. Patel and B. E. Ryman, *FEBS Lett.*, **62**, 60 (1976).

(5) G. Gregoriadis, *N. Engl. J. Med.*, **295**, 704 (1976).

(6) C. Weingarten, A. Moufti, J. F. Desjeux, T. T. Luong, G. Durand, J. F. Devissaguet, and F. Puisieux, *Life Sci.*, **28**, 2747 (1981).

(7) M. Mezei and V. Gulasekharam, *ibid.*, **26**, 1473 (1980).

(8) G. Gregoriadis, *N. Engl. J. Med.*, **295**, 765 (1976).

(9) M. B. Yatvin, W. Kreuz, B. A. Horwitz, and M. Shinitzky, *Science*, **210**, 1253 (1980).

(10) S. L. Regen, B. Czech, and A. Singh, *J. Am. Chem. Soc.*, **102**, 6640 (1980).

(11) D. Stamp and R. J. Juliano, *Can. J. Physiol. Pharmacol.*, **57**, 535 (1979).

(12) K. Tsujii, J. Sunamoto, and J. H. Fendler, *Life Sci.*, **19**, 1743 (1976).

(13) K. Kano and J. H. Fendler, *ibid.*, **20**, 1729 (1977).

(14) J. W. Cusic and R. A. Robinson, *J. Org. Chem.*, **16**, 1921 (1951).

(15) R. Nakai, M. Sugii, and H. Tomono, *J. Pharm. Soc. Jpn.*, **75**, 1014 (1955).

(16) E. Maghew, D. Papahadjopoulos, J. A. O'Malley, W. A. Carter, and W. Vail, *Mol. Pharmacol.*, **13**, 488 (1977).

(17) A. P. Michaelis and T. Higuchi, *J. Pharm. Sci.*, **58**, 201 (1969).

(18) G. M. Irwin, H. B. Kostenbauder, L. W. Dittert, R. Staples, A. Mischer, and J. V. Swintosky, *ibid.*, **58**, 323 (1969).

(19) M. N. Gillespie, L. Diamond, J. Newburger, and H. B. Kostenbauder, *Experientia*, **33**, 936 (1977).

(20) J. Newberger, Ph.D. Thesis, University of Kentucky, 1974.

ACKNOWLEDGMENTS

The authors thank Dr. Demetrios Papahadjopoulos for helpful suggestions in the preparation of liposomes.

pH-Sensitive Microcapsules for Drug Release

KIRAN BALA * and PADMA VASUDEVAN ‡x

Received July 24, 1981, from the **Centre for Biomedical Engineering, All India Institute of Medical Sciences*, and the *‡Centre for Rural Development and Appropriate Technology, Indian Institute of Technology, Hauz Khas, New Delhi-110 016 India.* Accepted for publication November 3, 1981.

Abstract □ Microcapsules were designed for a sustained drug release, where the external medium controls the rate of release of the drug. As a model, secretin was encapsulated in acryloyl chloride–lysine capsules, and the conditions of formation are described. The scanning electron micrographs show the formation of good spherical microcapsules in the size range of 5–10 μm. The release of secretin was studied in four media having different pH. Polymer dissolution was pH sensitive, and the capsules placed in different media eroded at a constant rate, depending on the pH of the medium. Dissolution of the microcapsules was limited to the polymer buffer media and the drug was released by zero-order kinetics. The possible use of such a system is in the treatment of duodenal ulcers and the diagnosis of pancreatic diseases.

Keyphrases □ Microcapsules—pH sensitive, drug release □ Drug release—pH sensitive microcapsules, polymerization □ Polymerization—pH sensitive microcapsules for drug release □ Dosage forms—pH-sensitive microcapsules for drug release

Microencapsulation is a process by which individual entities of a solid, liquid, or gas are discretely enclosed in a shell of inert polymeric materials. These inert shells may be designed to release their ingredients at a specific rate and/or under a specific set of conditions. Microencapsulation of a material may permit the alteration of its physical properties so that the desired availability is achieved and at the same time the encapsulated material is protected from its environment. Release of drug may be achieved *via* erosion, dissociation, or diffusion. Dosage forms have become more complex and now include such forms as sustained release, prolonged action, and repeat action. The technique of microencapsulation is one of the newer methods for sustained delivery which is receiving increasing attention (1, 2).

Precisely controlled sustained delivery does not always correspond to the optimum therapeutic regimen, however. In many applications a better delivery system is the one that delivers the active agent only when needed. In the present study secretin was microencapsulated in acryloyl chloride–lysine microcapsules, and the rate of release was studied in different media of varying pH.

BACKGROUND

Secretin (3), a small polypeptide (molecular weight ~3400), is present in the mucosa of the upper small intestine in the inactive form of prosecretin. When chyme enters the intestine, it causes the release and activation of secretin, which is subsequently absorbed into the blood. The constituent that causes greatest secretin release is hydrochloric acid, although almost any type of food will cause at least some release. Secretin is released any time the pH of the duodenal contents falls below ~4.0. This immediately causes large quantities of pancreatic juice containing abundant amounts of sodium bicarbonate to be secreted. Carbonic acid is formed by reaction of sodium bicarbonate with hydrogen chloride. The carbonic acid is immediately dissociated into carbon dioxide and water, and the carbon dioxide is absorbed into the body fluids, thus, leaving a neutral solution of sodium chloride in the duodenum. In this way, the acid contents emptied into the duodenum from the stomach become neutralized and the peptic activity of the gastric juices is immediately blocked. Since the mucosa of the small intestine cannot withstand the intense digestive properties of gastric juice, this is a highly important protective mechanism against the development of duodenal ulcers (4). A second function of hydrolytic secretin by the pancreas is to provide an appropriate pH for action of pancreatic enzymes. All such enzymes

0022-3549/82/0800-0960$01.00/0

phatidylcholine. The use of a charged membrane as well as the addition of other membrane adjuvants may affect the entrapment of methantheline and other compounds by liposomes.

These ion-pairing techniques can be used to increase liposomal loading of a large number of ionic compounds. The liposome-entrapped compounds can be used to overcome some traditional problems in the oral administration of drugs such as acid lability, inadequate intestinal absorption, and poor palatability.

The administration of methantheline bromide *via* liposomes is particularly desirable considering the poor absorption observed for quaternary ammonium compounds. In addition, ion-pairing of quaternary ammonium compounds increases the loading of these poorly entrapped drugs in liposomal membranes.

REFERENCES

(1) A. D. Bangham, *Ann. N.Y. Acad. Sci.*, **308**, 2 (1978).

(2) J. H. Fendler and A. Romero, *Life Sci.*, **20**, 1109 (1977).

(3) D. Papahadjopoulos, T. Wilson, and R. Taber, *In Vitro*, **16**, 49 (1980).

(4) H. M. Patel and B. E. Ryman, *FEBS Lett.*, **62**, 60 (1976).

(5) G. Gregoriadis, *N. Engl. J. Med.*, **295**, 704 (1976).

(6) C. Weingarten, A. Moufti, J. F. Desjeux, T. T. Luong, G. Durand, J. F. Devissaguet, and F. Puisieux, *Life Sci.*, **28**, 2747 (1981).

(7) M. Mezei and V. Gulasekharam, *ibid.*, **26**, 1473 (1980).

(8) G. Gregoriadis, *N. Engl. J. Med.*, **295**, 765 (1976).

(9) M. B. Yatvin, W. Kreuz, B. A. Horwitz, and M. Shinitzky, *Science*, **210**, 1253 (1980).

(10) S. L. Regen, B. Czech, and A. Singh, *J. Am. Chem. Soc.*, **102**, 6640 (1980).

(11) D. Stamp and R. J. Juliano, *Can. J. Physiol. Pharmacol.*, **57**, 535 (1979).

(12) K. Tsujii, J. Sunamoto, and J. H. Fendler, *Life Sci.*, **19**, 1743 (1976).

(13) K. Kano and J. H. Fendler, *ibid.*, **20**, 1729 (1977).

(14) J. W. Cusic and R. A. Robinson, *J. Org. Chem.*, **16**, 1921 (1951).

(15) R. Nakai, M. Sugii, and H. Tomono, *J. Pharm. Soc. Jpn.*, **75**, 1014 (1955).

(16) E. Maghew, D. Papahadjopoulos, J. A. O'Malley, W. A. Carter, and W. Vail, *Mol. Pharmacol.*, **13**, 488 (1977).

(17) A. P. Michaelis and T. Higuchi, *J. Pharm. Sci.*, **58**, 201 (1969).

(18) G. M. Irwin, H. B. Kostenbauder, L. W. Dittert, R. Staples, A. Mischer, and J. V. Swintosky, *ibid.*, **58**, 323 (1969).

(19) M. N. Gillespie, L. Diamond, J. Newburger, and H. B. Kostenbauder, *Experientia*, **33**, 936 (1977).

(20) J. Newberger, Ph.D. Thesis, University of Kentucky, 1974.

ACKNOWLEDGMENTS

The authors thank Dr. Demetrios Papahadjopoulos for helpful suggestions in the preparation of liposomes.

pH-Sensitive Microcapsules for Drug Release

KIRAN BALA * and PADMA VASUDEVAN ‡x

Received July 24, 1981, from the **Centre for Biomedical Engineering, All India Institute of Medical Sciences*, and the *‡Centre for Rural Development and Appropriate Technology, Indian Institute of Technology, Hauz Khas, New Delhi-110 016 India.* Accepted for publication November 3, 1981.

Abstract □ Microcapsules were designed for a sustained drug release, where the external medium controls the rate of release of the drug. As a model, secretin was encapsulated in acryloyl chloride–lysine capsules, and the conditions of formation are described. The scanning electron micrographs show the formation of good spherical microcapsules in the size range of 5–10 μm. The release of secretin was studied in four media having different pH. Polymer dissolution was pH sensitive, and the capsules placed in different media eroded at a constant rate, depending on the pH of the medium. Dissolution of the microcapsules was limited to the polymer buffer media and the drug was released by zero-order kinetics. The possible use of such a system is in the treatment of duodenal ulcers and the diagnosis of pancreatic diseases.

Keyphrases □ Microcapsules—pH sensitive, drug release □ Drug release—pH sensitive microcapsules, polymerization □ Polymerization—pH sensitive microcapsules for drug release □ Dosage forms—pH-sensitive microcapsules for drug release

Microencapsulation is a process by which individual entities of a solid, liquid, or gas are discretely enclosed in a shell of inert polymeric materials. These inert shells may be designed to release their ingredients at a specific rate and/or under a specific set of conditions. Microencapsulation of a material may permit the alteration of its physical properties so that the desired availability is achieved and at the same time the encapsulated material is protected from its environment. Release of drug may be achieved *via* erosion, dissociation, or diffusion. Dosage forms have become more complex and now include such forms as sustained release, prolonged action, and repeat action. The technique of microencapsulation is one of the newer methods for sustained delivery which is receiving increasing attention (1, 2).

Precisely controlled sustained delivery does not always correspond to the optimum therapeutic regimen, however. In many applications a better delivery system is the one that delivers the active agent only when needed. In the present study secretin was microencapsulated in acryloyl chloride–lysine microcapsules, and the rate of release was studied in different media of varying pH.

BACKGROUND

Secretin (3), a small polypeptide (molecular weight ~3400), is present in the mucosa of the upper small intestine in the inactive form of prosecretin. When chyme enters the intestine, it causes the release and activation of secretin, which is subsequently absorbed into the blood. The constituent that causes greatest secretin release is hydrochloric acid, although almost any type of food will cause at least some release. Secretin is released any time the pH of the duodenal contents falls below ~4.0. This immediately causes large quantities of pancreatic juice containing abundant amounts of sodium bicarbonate to be secreted. Carbonic acid is formed by reaction of sodium bicarbonate with hydrogen chloride. The carbonic acid is immediately dissociated into carbon dioxide and water, and the carbon dioxide is absorbed into the body fluids, thus, leaving a neutral solution of sodium chloride in the duodenum. In this way, the acid contents emptied into the duodenum from the stomach become neutralized and the peptic activity of the gastric juices is immediately blocked. Since the mucosa of the small intestine cannot withstand the intense digestive properties of gastric juice, this is a highly important protective mechanism against the development of duodenal ulcers (4). A second function of hydrolytic secretin by the pancreas is to provide an appropriate pH for action of pancreatic enzymes. All such enzymes

0022-3549/82/0800-0960$01.00/0

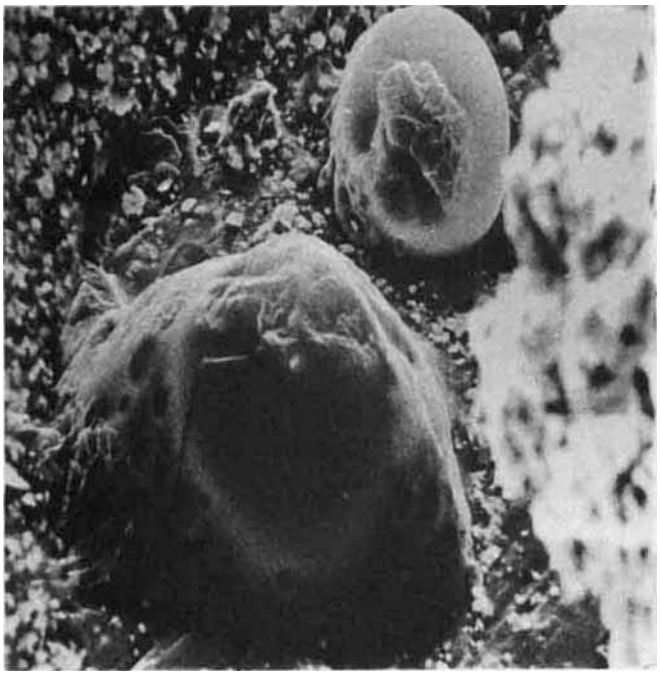

Figure 1—*Scanning electron micrograph of polyacryloyl chloride–lysine microcapsules containing secretin (5000×).*

function optimally in a slightly alkaline or neutral medium. The pH of the hydrolytic secretion averages 8.0.

Secretin release *in vivo* is pH-sensitive. To simulate this system, it was proposed to design a secretin microcapsule that would become more permeable at low pH. The acryloyl chloride–lysine encapsulation system was chosen as the wall material, since it was anticipated that the presence of unreacted amino groups in the capsule wall would likely cause the erodibility of the polymer to become pH dependent.

EXPERIMENTAL

Microcapsules were prepared by interfacial polymerization as described previously (5). Acrylic acid distilled under reduced pressure was polymerized under vacuum by gamma radiation from a cobalt 60 source. The polyacrylic acid was dissolved in distilled 1,6-dioxane and then converted into the acid chloride with thionyl chloride. The polyacryloyl chloride that precipitated out was dissolved in dimethylformamide.

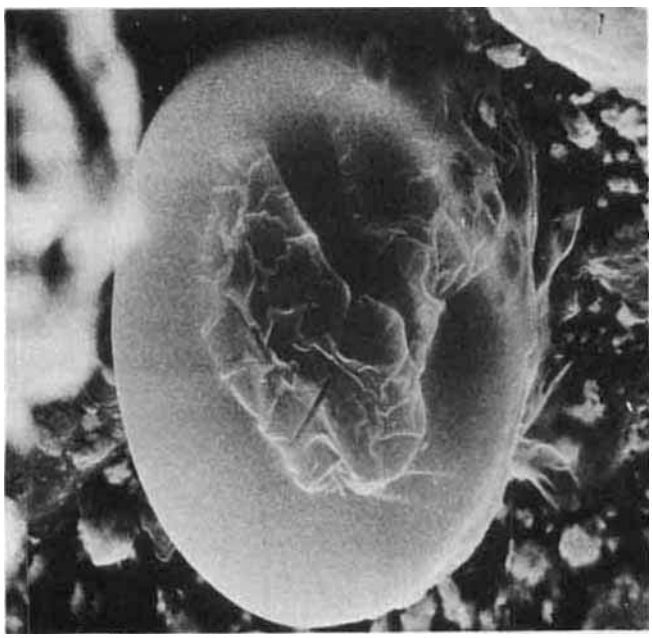

Figure 2—*Scanning electron micrograph of polyacryloyl chloride–lysine microcapsules containing secretin (5000× 2.5).*

Table I—Cumulative Release of Secretin at Different pH

Time, days	I pH 2 Amount, mg	I pH 2 Secretin, %	II pH 4 Amount, mg	II pH 4 Secretin, %	III pH 7 Amount, mg	III pH 7 Secretin, %
1	10.0	20	5.0	10	2.5	5
2	21.0	42	10.0	20	5.0	10
3	29.0	58	15.0	30	7.0	14
4	40.0	80	20.0	40	9.5	19
5	44.0	88	25.0	50	12.0	24
6	47.0	94	31.0	62	15.0	30
7	—	—	35.0	70	18.0	36
8	—	—	40.0	80	20.0	40
9	—	—	42.5	85	22.5	45
10	—	—	44.0	88	26.0	52
12	—	—	47.0	94	30.0	60
14	—	—	—	—	35.0	70
16	—	—	—	—	40.0	80
18	—	—	—	—	44.0	88
20	—	—	—	—	47.0	94
22	—	—	—	—	48.0	96

Secretin (50 mg) was mixed with an equal volume of 0.8 *M* lysine dissolved in a tromethamine buffer (pH 7.4), containing 2 ml of 0.45 *M* sodium bicarbonate solution. This mixture was freshly prepared and stirred in a 100-ml beaker at room temperature. The organic phase [a 15-ml mixture of chloroform–cyclohexane (1:4)] was added with stirring to the beaker. Stirring was continued for 45–60 sec at the maximum speed to disperse the aqueous droplets and to reduce their size, and polyacryloyl chloride solution in dimethylformamide was added. The amount of polyacryloyl chloride used was approximately equivalent to lysine. In this way polyacryloyl chloride–lysine microcapsules containing secretin were prepared.

The microcapsules were separated from the organic phase by centrifugation and transferred to the aqueous phase with the aid of polyoxyethylene sorbitol washed repeatedly with saline solution and dispersed in isotonic buffer. Scanning electron micrographs of the capsules were taken[1]. Release of encapsulated drug was studied by following its elution in buffer solutions of different pH. For a typical experiment the microcapsules were equilibrated with 15 ml of buffer for 24 hr. The supernate was separated by centrifugation and its optical density was determined at 245 nm. A fresh buffer (5 ml) was equilibrated until no more elution of the drug occurred.

RESULTS AND DISCUSSION

To check the reproducibility of the method of encapsulation and release, three sets of samples (labeled I, II, and III) were prepared under the same conditions just described. The electron micrograph of each sample was taken separately. In all cases, the capsules were 5–10 μm in diameter (Figs. 1 and 2).

The release rates of secretin at different pH values are given in Table I. Figure 3 shows the cumulative release of secretin as a function of time for all samples. In all cases, at least up to 80% of the drug was released by a zero-order mechanism; however, the rate of release was fastest at pH

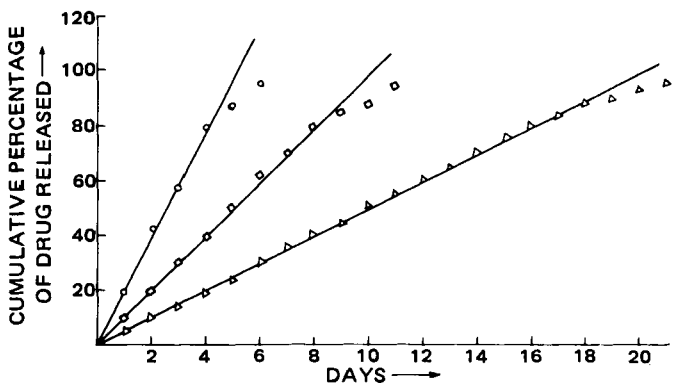

Figure 3—*Cumulative percentage of secretin released from acryloyl chloride–lysine microcapsules. Key: (○) pH 2, (□) pH 4, (△) pH 7.*

[1] Micrographs taken by a Cambridge Steroscan S_4-10 instrument.

2, and was prolonged for up to 6 days. At pH 4, the release sustained for up to 12 days, and on increasing the pH to 7, the duration of the release increased to 22 days. Thus, it was also observed that as the pH increased, the solubility of the wall material decreased and the quantity of drug released per day decreased. When the pH was raised to 10, no dissolution of the polymer wall occurred and no release of secretin was observed for several days.

The data indicated that the drug was perhaps released by polymer dissolution at the polymer–water interface by a mechanism similar to that discussed previously (6, 7). Detailed study of this polymer will be necessary before the complete mechanism for erosion can be understood; the mechanism of release is the subject of further study. However, in the present study the interest was more on controlled release of the drug at low pH, which has been achieved. The above type of capsules would be suitable for sustained drug release at low pH. Further, since the polymer was erodible up to pH 8, it can form a suitable biosoluble wall material for encapsulating other drugs. The biocompatibility of this material is being studied.

Notable features of the microcapsules described in this report are: their ability to undergo surface erosion and, hence, release of the core material by zero-order kinetics, and sensitivity of the erosion rate to the surrounding aqueous environment (pH). A pH environment has a major effect on the erosion rate and, thus, controls the drug release which is increased by decreasing the pH.

REFERENCES

(1) C. Tanquary and R. E. Lacey, Eds., "Controlled Release of Biologically Active Agent," Plenum, New York, N.Y., 1974.

(2) R. W. Baker and H. K. Lonsadle, *Chem. Technol.*, **5**, 668 (1975).

(3) A. C. Guyton, "Textbook of Medical Physiology," W. B. Saunders, Philadelphia, London, Toronto, 1976, p. 877.

(4) M. I. Grossman, *Gastroenterology*, **50**, 912 (1966).

(5) K. Tamotu, M. Arakwa, and B. Tamaushi, "Microencapsulation," J. R. Nixon, Ed., vol. 3, Marcel Dekker, New York, N.Y., 1976, p. 163.

(6) J. Heller, R. W. Baker, R. M. Gale, and J. O. Rodin, *J. Appl. Polym. Sci.*, **22**, 1991 (1978).

(7) J. Heller and P. V. Trescony, *J. Pharm. Sci.*, **68**, 919 (1979).

ACKNOWLEDGMENTS

The authors thank the Indian Council of Medical Research for financial support.

Reaction of Phenobarbital with Diphenhydramine

MELVIN F. W. DUNKER[x] and LAURENCE M. SIROIS

Received June 8, 1981, from the *College of Pharmacy and Allied Health Professions, Wayne State University, Detroit, MI 48202.* Accepted for Publication November 3, 1981.

Abstract □ A compound of low water solubility, consisting of phenobarbital–diphenhydramine in a 1:1 ratio and mp 109.5–110.5° was isolated from a prescription which had been dispensed as a clear solution and later returned with a white sediment. The information obtained suggested that it was either an easily dissociated complex or a salt.

Keyphrases □ Phenobarbital—reaction with diphenhydramine, complexation, salts □ Diphenhydramine—reaction with phenobarbital, complexation, salts □ Complexation—phenobarbital and diphenhydramine, salts

A number of salts, complexes, or addition compounds formed by barbiturates, particularly by phenobarbital, have been recorded previously (1–6). Similarly, there are recorded complexes and salts for diphenhydramine, the best known being dimenhydrinate, USP (7). The products formed by heating diphenhydramine and barbital or allobarbital in alcohol at 100–120° are reported to be 1:1 salts melting at 86 and 102–103°, respectively (8).

Literature pertaining to intravenous admixtures refers to diphenhydramine hydrochloride as being incompatible with phenobarbital sodium (9–11) as well as several other barbiturate salts; forming particulate matter (12, 13), forming a precipitate (14), or as not remaining clear for 24 hr after mixing (15). The only explanation provided is that solutions of sodium barbiturates and sodium diphenylhydantoin are alkaline and may lead to the formation of precipitates from solutions of acid salts. A previous study (16) pointed out that aqueous solutions of diphenhydramine hydrochloride and phenobarbital sodium will form a precipitate when mixed in low concentrations, even at pH values at which phenobarbital would be soluble. It was assumed that the precipitate was an undissociated, less soluble diphenhydramine–phenobarbital complex. No characteristics for this substance were reported.

The reported compound was first obtained from the crystalline settlement in a compounded prescription consisting of 250 ml of diphenhydramine hydrochloride elixir in which 750 mg of phenobarbital sodium had been dissolved in accordance with physician's instructions. When prepared, the mixture slowly became cloudy and then deposited crystals over several days. Upon filtration and recrystallization of the solid from ~75% alcohol, the hard, colorless crystals melted at 109.5–110.5° (uncorrected). The product was found to be composed of phenobarbital–diphenhydramine (1:1).

The formation of the crystals could be avoided by dissolving the equivalent amount of phenobarbital in 10 ml of alcohol and mixing it into the elixir. Such a sample was still free of crystals after 1 year. Since the crystals are very soluble in alcohol, somewhat soluble in water, and the pH of the elixir results in only a low concentration of diphenhydramine base, the product probably does not form in an amount sufficient to exceed its solubility in the hydroalcoholic medium.

EXPERIMENTAL

Diphenhydramine hydrochloride elixir[1], diphenhydramine[1], diphenhydramine hydrochloride[1], phenobarbital[2], and phenobarbital sodium[2] were obtained as indicated. The various solvents were USP or reagent grade.

[1] Elixir Benadryl, Parke-Davis & Co.; the diphenhydramine and its hydrochloride were provided by Parke-Davis & Co.

[2] Merck & Co., Rahway, N.J., commercial packages.

0022-3549/82/0800-0962$01.00/0

2, and was prolonged for up to 6 days. At pH 4, the release sustained for up to 12 days, and on increasing the pH to 7, the duration of the release increased to 22 days. Thus, it was also observed that as the pH increased, the solubility of the wall material decreased and the quantity of drug released per day decreased. When the pH was raised to 10, no dissolution of the polymer wall occurred and no release of secretin was observed for several days.

The data indicated that the drug was perhaps released by polymer dissolution at the polymer–water interface by a mechanism similar to that discussed previously (6, 7). Detailed study of this polymer will be necessary before the complete mechanism for erosion can be understood; the mechanism of release is the subject of further study. However, in the present study the interest was more on controlled release of the drug at low pH, which has been achieved. The above type of capsules would be suitable for sustained drug release at low pH. Further, since the polymer was erodible up to pH 8, it can form a suitable biosoluble wall material for encapsulating other drugs. The biocompatibility of this material is being studied.

Notable features of the microcapsules described in this report are: their ability to undergo surface erosion and, hence, release of the core material by zero-order kinetics, and sensitivity of the erosion rate to the surrounding aqueous environment (pH). A pH environment has a major effect on the erosion rate and, thus, controls the drug release which is increased by decreasing the pH.

REFERENCES

(1) C. Tanquary and R. E. Lacey, Eds., "Controlled Release of Biologically Active Agent," Plenum, New York, N.Y., 1974.

(2) R. W. Baker and H. K. Lonsadle, *Chem. Technol.*, **5**, 668 (1975).

(3) A. C. Guyton, "Textbook of Medical Physiology," W. B. Saunders, Philadelphia, London, Toronto, 1976, p. 877.

(4) M. I. Grossman, *Gastroenterology*, **50**, 912 (1966).

(5) K. Tamotu, M. Arakwa, and B. Tamaushi, "Microencapsulation," J. R. Nixon, Ed., vol. 3, Marcel Dekker, New York, N.Y., 1976, p. 163.

(6) J. Heller, R. W. Baker, R. M. Gale, and J. O. Rodin, *J. Appl. Polym. Sci.*, **22**, 1991 (1978).

(7) J. Heller and P. V. Trescony, *J. Pharm. Sci.*, **68**, 919 (1979).

ACKNOWLEDGMENTS

The authors thank the Indian Council of Medical Research for financial support.

Reaction of Phenobarbital with Diphenhydramine

MELVIN F. W. DUNKER[x] and LAURENCE M. SIROIS

Received June 8, 1981, from the *College of Pharmacy and Allied Health Professions, Wayne State University, Detroit, MI 48202.* Accepted for Publication November 3, 1981.

Abstract □ A compound of low water solubility, consisting of phenobarbital–diphenhydramine in a 1:1 ratio and mp 109.5–110.5° was isolated from a prescription which had been dispensed as a clear solution and later returned with a white sediment. The information obtained suggested that it was either an easily dissociated complex or a salt.

Keyphrases □ Phenobarbital—reaction with diphenhydramine, complexation, salts □ Diphenhydramine—reaction with phenobarbital, complexation, salts □ Complexation—phenobarbital and diphenhydramine, salts

A number of salts, complexes, or addition compounds formed by barbiturates, particularly by phenobarbital, have been recorded previously (1–6). Similarly, there are recorded complexes and salts for diphenhydramine, the best known being dimenhydrinate, USP (7). The products formed by heating diphenhydramine and barbital or allobarbital in alcohol at 100–120° are reported to be 1:1 salts melting at 86 and 102–103°, respectively (8).

Literature pertaining to intravenous admixtures refers to diphenhydramine hydrochloride as being incompatible with phenobarbital sodium (9–11) as well as several other barbiturate salts; forming particulate matter (12, 13), forming a precipitate (14), or as not remaining clear for 24 hr after mixing (15). The only explanation provided is that solutions of sodium barbiturates and sodium diphenylhydantoin are alkaline and may lead to the formation of precipitates from solutions of acid salts. A previous study (16) pointed out that aqueous solutions of diphenhydramine hydrochloride and phenobarbital sodium will form a precipitate when mixed in low concentrations, even at pH values at which phenobarbital would be soluble. It was assumed that the precipitate was an undissociated, less soluble diphenhydramine–phenobarbital complex. No characteristics for this substance were reported.

The reported compound was first obtained from the crystalline settlement in a compounded prescription consisting of 250 ml of diphenhydramine hydrochloride elixir in which 750 mg of phenobarbital sodium had been dissolved in accordance with physician's instructions. When prepared, the mixture slowly became cloudy and then deposited crystals over several days. Upon filtration and recrystallization of the solid from ~75% alcohol, the hard, colorless crystals melted at 109.5–110.5° (uncorrected). The product was found to be composed of phenobarbital–diphenhydramine (1:1).

The formation of the crystals could be avoided by dissolving the equivalent amount of phenobarbital in 10 ml of alcohol and mixing it into the elixir. Such a sample was still free of crystals after 1 year. Since the crystals are very soluble in alcohol, somewhat soluble in water, and the pH of the elixir results in only a low concentration of diphenhydramine base, the product probably does not form in an amount sufficient to exceed its solubility in the hydroalcoholic medium.

EXPERIMENTAL

Diphenhydramine hydrochloride elixir[1], diphenhydramine[1], diphenhydramine hydrochloride[1], phenobarbital[2], and phenobarbital sodium[2] were obtained as indicated. The various solvents were USP or reagent grade.

[1] Elixir Benadryl, Parke-Davis & Co.; the diphenhydramine and its hydrochloride were provided by Parke-Davis & Co.

[2] Merck & Co., Rahway, N.J., commercial packages.

0022-3549/82/0800-0962$01.00/0

The sample of diphenhydramine hydrochloride elixir had a pH of 6.8, which changed to 8.35 when 750 mg of phenobarbital sodium was dissolved in 250 ml of the sample. The mixture slowly became turbid, cleared as some oily droplets formed, and eventually crystallized over a period of several days. A crop of 833 mg of slightly pink crystals was collected. After treatment with charcoal and several crystallizations from ~30% alcohol, long, colorless needles, mp 109.5–110.5° (uncorrected)[3], were obtained. From 75–95% alcohol, clear, dense prisms of the same melting point were obtained. The crystals were dried *in vacuo* over phosphorus pentoxide at 80°.

Anal.—Calc. for $C_{29}H_{33}N_3O_4$: C, 71.45; H, 6.82; N, 8.62. Found[4]: C, 71.22; H, 6.77; N, 8.73.

After removal of the first crop of crystals, the filtrate was concentrated on a steam bath and then allowed to stand in open air. Large crystals formed (probably some sucrose since the elixir contains considerable syrup) and the mixture was extracted with three portions of ether. After removal of the ether the residue was taken up in 95% alcohol, treated with charcoal, and filtered. An additional 168 mg (mp 108–110° and giving no depression of melting point with previous crystals) of clear prisms was obtained, representing an overall yield of 95.9% based on the diphenhydramine hydrochloride present.

RESULTS AND DISCUSSION

The crystalline product from diphenhydramine hydrochloride elixir is easily soluble in 95% alcohol and is soluble in ether, acetone, chloroform, hot benzene, and somewhat soluble in water.

The same crystalline product could be obtained by dissolving phenobarbital in diphenhydramine with warming, followed by solution of the clear viscous material in alcohol. On cooling, prisms formed with mp 108–109°.

When a solution of 714 mg of phenobarbital in 10 ml of 95% alcohol was added to 240 ml of diphenhydramine hydrochloride elixir, the mixture remained clear and free of crystals for 1 year. There was no change in pH when the solution of phenobarbital was mixed with the elixir. It is probable that the small increase in alcohol concentration coupled with the low dissociation of the diphenhydramine hydrochloride in acid medium may not allow enough compound to form to exceed the solubility.

A solution of 300 mg of diphenhydramine hydrochloride in 30 ml of water had a pH of 5.5. When 261 mg of phenobarbital sodium was added with stirring, the mixture immediately became turbid. Droplets settled out, which quickly crystallized, and the pH changed to 7.5. After chilling, filtrating, washing, and drying, a crop of 425 mg (84.8%) of white crystals was obtained. The product melted sharply at 108–109° and gave no depression of melting point when mixed with material obtained from the prescription.

The UV spectra of phenobarbital, its sodium salt, diphenhydramine, its hydrochloride, and the product were compared, but no characteristics allowing distinction between a salt or a simple mixture could be observed. This agrees with observations reported for the phenobarbital–quinine complex (17).

A comparison of the IR spectra of potassium bromide pellets of phenobarbital, its sodium salt, diphenhydramine hydrochloride, and of the product indicated that the typical tertiary amine salt absorption at 2400–2700 cm^{-1} had disappeared in the product and the typical enolization band of phenobarbital (1620 cm^{-1}) is weak and shifted to ~1670 cm^{-1}. When the IR spectra of the product and of an equimolar mixture of phenobarbital and diphenydramine in chloroform were compared, no differences could be observed.

The NMR spectra of the product and an equimolar mixture of phenobarbital and diphenhydramine were run in deuterochloroform and compared. Most peaks were identical and could be assigned easily by comparison with spectra of the individual components. The only exception was a downfield signal (broad singlet accounting for two protons) which appeared at 10.9 ppm in the spectrum of the product and shifted upfield to 10.4 ppm in the spectrum of the mixture.

The sharp melting point of the product and the broad melting of mixtures [(102–147°) mixed with diphenhydramine hydrochloride and (106–155°) when mixed with phenobarbital] suggest that a new substance exists in the crystalline state. The evidence from the spectral measurements in solution indicates extensive dissociation.

[3] The melting points were obtained on a Hoover Melting Point Apparatus in open capillaries and are uncorrected. UV spectra were determined in 95% ethanol on a Beckman model DK-2A recording spectrophotometer. IR spectra were recorded either as potassium bromide pellets on a Beckman model 8 Infrared Spectrometer or in chloroform solution on Beckman model IR-33 Spectrometer. NMR spectra were recorded in deuterochloroform in a Varian model EM-360 Spectrometer using 1% tetramethylsilane as an internal reference standard.

[4] Spang Microanalytical Laboratory, Ann Arbor, Mich.

REFERENCES

(1) W. Mayo Higgins and Melvin F. W. Dunker, *J. Am. Pharm. Assoc. Sci. Ed.*, **33,** 310 (1944) references included.

(2) T. Higuchi and J. L. Lach, *ibid.*, **43,** 349 (1954).

(3) W. N. French and J. C. Morrison, *ibid.*, **54,** 1133 (1965).

(4) J. K. Guillory, S. C. Hwang, and J. L. Lach, *J. Pharm. Sci.*, **58,** 301 (1969).

(5) B. M. Craven and G. L. Gartland, *ibid.*, **59,** 1666 (1970).

(6) M. B. Mrtek, J. E. Gearien, and M. I. Blake, *ibid.*, **66,** 1019 (1977).

(7) United States Pharmacopeia, XX, U.S. Pharmacopeial Convention, Rockville, Md., 1980, p. 247.

(8) Japanese Patent 10, 499, Dec. 1, 1959 through *Chem. Abstracts*, **54,** 18564d (1960).

(9) T. J. Fowler, *Am. J. Hosp. Pharm.*, **24,** 450 (1967).

(10) N. A. Pelissier and S. L. Burge, *Hosp. Pharm.*, **3,** 15 (1968).

(11) J. G. Grayson, *Pharm. J.*, **206,** 64 (1971).

(12) R. Misgen, *Am. J. Hosp. Pharm.*, **22,** 92 (1965).

(13) W. Kramer, A. Inglott, and R. Cluxton, *Drug. Intell.*, **5,** 211 (1971).

(14) S. Garb, "Clinical Guide to Undesirable Drug Interactions and Interferences," Springer Publishing, New York, N.Y., 1971, p. 491.

(15) J. Patel and G. Phillips, *Am. J. Hosp. Pharm.*, **23,** 409 (1966).

(16) V. H. Bruin and W. H. Oliver, *Aust. J. Pharm.*, **38,** 226 (1957).

(17) W. N. French and J. C. Morrison, *J. Pharm. Sci.*, **54,** 1133 (1965).

ACKNOWLEDGMENTS

The authors thank Dr. Gerard Hokanson for the IR solution spectra, the NMR spectra and interpretation, and for helpful comments.

Effect of a Major Metabolite on the Plasma Protein Binding of Tolmetin

Keyphrases □ Tolmetin—effect of a major metabolite on plasma protein binding □ Metabolites—effect on the plasma protein binding of tolmetin □ Plasma protein binding—effect of a major metabolite, tolmetin

To the Editor:

The nonsteroidal anti-inflammatory agent, tolmetin, is highly bound (>99%) to plasma proteins (1). Recently, Selley *et al.* (2) reported that 3 μg/ml (10.4 μ*M*) of 1-methyl-5-(4-carboxybenzoyl)-1*H*-pyrrole-2-acetic acid (I), a major metabolite of tolmetin (3), caused a marked (245%) increase in tolmetin free fraction when dialyzed until equilibrium against 4% human serum albumin containing 26.4 μg/ml (84 μ*M*) of tolmetin. Such a result is unusual since these investigators also observed that I was bound only 72% to human serum albumin. This implies that the metabolite may have less affinity for albumin binding sites than tolmetin; yet, small concentrations of I were capable of displacing the extensively bound parent drug. We decided to investigate further the effect of I on tolmetin binding.

Plasma was obtained from three healthy volunteers and was seeded with 0 (control sample), 0.8 (0.23 μg/ml), 8 (2.3 μg/ml), 80 (23 μg/ml), and 800 μ*M* (230 μg/ml) concentrations of I[1] and dialyzed against 0.125 *M* Sørenson's sodium–potassium phosphate buffer (pH 7.4) containing 80 μ*M* (25.2 μg/ml) of [^{14}C]tolmetin (14.8 μCi/mg)[1]. Equilibrium was achieved after 4 hr of dialysis using an equilibrium dialysis system[2] equipped with a microcell accessory and cellulose dialysis membranes (MW cutoff, 6000–8000)[3]. This experiment was also performed using human serum albumin[4] instead of human plasma. Aliquots (100 or 150 μl) of dialysate and dialyzed plasma were assayed for radioactivity in 10 ml of scintillation cocktail[5] using a liquid scintillation spectrometer[6] and external standard quench correction.

In a second series of experiments, plasma aliquots (0.2 ml each) from 10 healthy volunteers were dialyzed against Sørenson's buffer (0.2 ml) containing 0.5, 5, and 50 μg/ml of [^{14}C]tolmetin, and the tolmetin free fraction was determined at each concentration. In addition, samples (1.0 ml) of pooled human plasma were seeded with 2, 20, and 200 μg/ml of I and dialyzed against 1.0-ml aliquots of 0.067 *M* Sørenson's buffer. Buffer and plasma samples (0.5 ml) were assayed for I using a sensitive HPLC procedure[7]. The percentage of free (unbound) I or tolmetin was calculated using:

$$\frac{C_d}{C_p} \times 100 = \% \text{ free} \qquad \text{(Eq. 1)}$$

where C_d is the concentration of ligand in the dialysate (unbound) and C_p is the concentration of ligand in dialyzed plasma (bound and unbound).

Table I lists the results obtained when 80 μ*M* [^{14}C]tolmetin was dialyzed in the presence of increasing concentrations of I in both plasma and 4% human serum albumin. The metabolite produced no effect on tolmetin protein binding when added at equimolar concentrations or less. In contrast, tolmetin free fraction increased when I was added in 10-fold molar excess over tolmetin. These results are consistent with the observation that tolmetin was much more highly bound to plasma proteins than I over the broad range of concentrations studied (Table II). The metabolite may have less affinity for binding sites shared with tolmetin on plasma proteins (probably albumin). Under these conditions I would not be expected to displace any protein-bound tolmetin except when added in great excess. These data differ from the study by Selley *et al.* (2), who reported that addition of 3 μg/ml of I yielded an in-

Table II—Binding of Tolmetin and its Major Metabolite I to Human Plasma

Seeded Concentration, μg/ml[a]	Percent Free
Tolmetin	
0.5	0.37 ± 0.14[b]
5	0.37 ± 0.10
50	0.63 ± 0.11
I	
2	19.6 ± 0.7[c]
20	23.8 ± 1.2
200	26.5 ± 1.0

[a] Expressed as micrograms of free acid per milliliter. [b] Mean ± *SD* of binding to plasma from 10 healthy volunteers. [c] Mean ± *SD* of 3–5 aliquots of pooled human plasma dialyzed separately.

Table I—The Effect of Metabolite I on Tolmetin Binding to Human Plasma and to 4% Human Serum Albumin

Concentration of [^{14}C]Tolmetin		Concentration of I		Percent Free Tolmetin[a]	
μ*M*	μg/ml[b]	μ*M*	μg/ml[b]	Plasma	4% Human Serum Albumin (fatty acid free)
80	25.2	0	0	0.42 ± 0.03	0.52 ± 0.07
80	25.2	0.8	0.23	0.39 ± 0.01	0.57 ± 0.08
80	25.2	8	2.3	0.53 ± 0.08	0.62 ± 0.06
80	25.2	80	23	0.42 ± 0.05	0.57 ± 0.07
80	25.2	800	230	0.68 ± 0.18	0.92 ± 0.21

[a] Mean ± *SD* of 4 aliquots dialyzed separately. [b] Expressed as micrograms of free acid per milliliter.

[1] McNeil Pharmaceutical, Spring House, Pa.
[2] Dianorm, Diachema Ag., Rüschlikon, Switzerland.
[3] Spectra/Por, Spectrum Medical Industries, Inc., Los Angeles, Calif.
[4] Fatty acid free; Sigma Chemical Co., St. Louis, Mo.
[5] BioFluor, New England Nuclear, Boston, Mass.
[6] Searle Analytical 81, Searle Analytic Inc., Des Plaines, Ill.

[7] T. Snyderman, N. L. Renzi, Jr., and K. T. Ng, data on file, McNeil Pharmaceutical, Spring House, Pa.

0022-3549/82/0800-0964$01.00/0

crease in free fraction of tolmetin (present at 26.7 μg/ml) from 0.29 ± 0.02% (Mean ± *SD*) to 1.0 ± 0.12%. It appears that factors other than the metabolite itself must have contributed to the increase in tolmetin free fraction observed by these investigators.

The fact that I does not readily displace tolmetin from plasma protein binding sites has important implications in the understanding of tolmetin disposition. Since the metabolite circulates at concentrations lower than those of tolmetin in healthy subjects (1, 4) and arthritic patients (5), no effect of I on tolmetin disposition would be anticipated based on the data presented in Table I. In anephric patients receiving tolmetin, I accumulates in plasma to concentrations often >10-fold those of tolmetin[8]. Some displacement of tolmetin by the metabolite in these patients might be expected. However, since uremic plasma has reduced binding affinity for tolmetin (6), it is difficult to assess the additional influence of high circulating metabolite concentrations on tolmetin disposition in the uremic patient.

(1) W. A. Cressman, G. F. Wortham, and J. Plostnieks, *Clin. Pharmacol. Ther.*, **19**, 224 (1976).

(2) M. L. Selley, B. W. Madsen, and J. Thomas, *Clin. Pharmacol. Ther.*, **24**, 694 (1978).

(3) D. D. Sumner, P. G. Dayton, S. A. Cucinell, and J. Plostnieks, *Drug Metab. Dispos.*, **3**, 283 (1975).

(4) J. W. Ayres, D. J. Weidler, J. Mackichan, E. Sakmar, M. R. Hallmark, E. F. Lemanowicz, and J. G. Wagner, *Eur. J. Clin. Pharmacol.*, **12**, 421 (1977).

(5) J. M. Grindel, B. H. Migdalof, and J. Plostnieks, *Clin. Pharmacol. Ther.*, **26**, 122 (1979).

(6) J. F. Pritchard, P. J. O'Neill, M. B. Affrime, and D. T. Lowenthal, *Abstracts APhA Acad. Pharm. Sci.*, 11(2), 137 (1981).

J. Frederick Pritchard[x]
Ravi K. Desiraju
Department of Drug Metabolism
McNeil Pharmaceutical
Spring House, PA 19477

Received January 18, 1982.
Accepted for publication April 9, 1982.

[8] R. K. Desiraju, N. L. Renzi, Jr., L. A. McKown, and R. K. Nayak, data on file, McNeil Pharmaceutical, Spring House, Pa.

Hydroxyisolongifolaldehyde: A New Metabolite of (+)-Longifolene in Rabbits

Keyphrases □ Longifolene—hydroxyisolongifolaldehyde, a new metabolite in rabbits □ Metabolites—hydroxyisolongifolaldehyde from longifolene in rabbits □ Hydroxyisolongifolaldehyde—a new metabolite of longifolene in rabbits

To the Editor:

In spite of daily usage of terpenoid-containing plant products such as fruits, drinks, tobacco, *etc.*, the metabolic fate of terpenoids is essentially unknown. The aim of this study is to clarify terpenoid biotransformation in mammalian biochemistry from the toxicological point of view. This will provide guidance for the effective usage of natural products and for preparation of starting materials for organic synthesis.

Wild rabbits damage the forests in Japan by feeding on the artificially planted young *Chamaecyparis obtusa*, an important tree used commercially in Japan. This Japanese cypress contains longifolene (I) as a major sesquiterpene hydrocarbon. The metabolism of α-pinene, camphene, and other related terpenoids in rabbits was studied previously (1–7).

Longifolene (36 g), $[\alpha]_D$ = +39.3°, in chloroform, was administered to rabbits and the metabolites were isolated according to the method described previously. The neutral crude alcohols (3.7 g), were acetylated and purified to afford the main acetate (II) (17% for total acetates), which gave the following spectral data: mass spectrum: *m/z* 278 ($C_{17}H_{26}O_3$); 2700 and 1710 cm^{-1}; and a small doublet (J = 1.5 Hz) at 9.88 ppm of an aldehyde group. It was hydrolyzed by potassium carbonate in methanol and on silica gel chromatography gave pure metabolic alcohol (III). The parent ion of III, *m/z* 236, means a molecular formula $C_{15}H_{24}O_2$ showing that two oxygen atoms were introduced into longifolene. These oxygen atoms are based on a hydroxyl group (3450 cm^{-1}) and an aldehyde group (2700 and 1720 cm^{-1}; 9.87 ppm). The signals at 3.46 and 3.31 ppm (AB quartet) of this alcohol shifted 0.5 ppm upfield compared with those of acetate, suggesting the presence of a primary hydroxyl group. The olefin group of longifolene was lost in this alcohol. Thus, the change of this *exo*-methylene group to an aldehyde or primary alcohol was expected. The positions of newly introduced groups were determined on the basis of IR, ^{1}H-NMR, and ^{13}C-NMR spectra.

First, the aldehyde proton signal of III split into a doublet (J = 2.0 Hz) indicating the presence of an adjacent 7-H proton. By this splitting, it was concluded that the position of the aldehyde group is not at C-12, C-14, and C-15 but at C-7. The 7-H configuration was determined on the basis of a coupling constant. Provided that 7-H is in an α-configuration, the coupling constants of this proton would be anticipated to be $J_{7,1}$ = 1.3–2.6 Hz and $J_{7,8}$ = ~0.5 Hz. However, if 7-H is in a β-configuration, these values would be expected to be: $J_{7,8}$ = 3.6–5.0 Hz, $J_{7,9}$ ~1.2 Hz, and $J_{7,11}$ = 0.5 Hz. In fact, $J_{7,8}$ in III was observed as 3.5 Hz meaning 7-H has the β-configuration. Thus, the configuration of this aldehyde group was determined to be in the C-7-*endo*-form, which is stable in isolongifolaldehyde (8).

Second, in the IR spectra of the metabolized alcohol and

Table I—^{13}C-NMR Chemical Shifts in Longifolene and Hydroxyisolongifolaldehyde

	Longifolene (I)	Hydroxyisolongifolaldehyde (III)
C-1	62.2	56.3
C-2	33.6	37.8
C-3	36.5	34.2
C-4	21.2	21.0
C-5	43.4	44.2
C-6	44.1	43.0
C-7	168.0	59.9
C-8	48.0	40.8
C-9	29.8	25.8
C-10	25.5	23.0
C-11	45.2	47.0
C-12	30.1[a]	26.0[a]
C-13	99.0	206.4
C-14	30.6[a]	22.6[a]
C-15	30.6[a]	72.6

[a] Assignments may be reversed in each compound.

0022-3549/82/0800-0965$01.00/0

crease in free fraction of tolmetin (present at 26.7 μg/ml) from 0.29 ± 0.02% (Mean ± *SD*) to 1.0 ± 0.12%. It appears that factors other than the metabolite itself must have contributed to the increase in tolmetin free fraction observed by these investigators.

The fact that I does not readily displace tolmetin from plasma protein binding sites has important implications in the understanding of tolmetin disposition. Since the metabolite circulates at concentrations lower than those of tolmetin in healthy subjects (1, 4) and arthritic patients (5), no effect of I on tolmetin disposition would be anticipated based on the data presented in Table I. In anephric patients receiving tolmetin, I accumulates in plasma to concentrations often >10-fold those of tolmetin[8]. Some displacement of tolmetin by the metabolite in these patients might be expected. However, since uremic plasma has reduced binding affinity for tolmetin (6), it is difficult to assess the additional influence of high circulating metabolite concentrations on tolmetin disposition in the uremic patient.

(1) W. A. Cressman, G. F. Wortham, and J. Plostnieks, *Clin. Pharmacol. Ther.*, **19**, 224 (1976).

(2) M. L. Selley, B. W. Madsen, and J. Thomas, *Clin. Pharmacol. Ther.*, **24**, 694 (1978).

(3) D. D. Sumner, P. G. Dayton, S. A. Cucinell, and J. Plostnieks, *Drug Metab. Dispos.*, **3**, 283 (1975).

(4) J. W. Ayres, D. J. Weidler, J. Mackichan, E. Sakmar, M. R. Hallmark, E. F. Lemanowicz, and J. G. Wagner, *Eur. J. Clin. Pharmacol.*, **12**, 421 (1977).

(5) J. M. Grindel, B. H. Migdalof, and J. Plostnieks, *Clin. Pharmacol. Ther.*, **26**, 122 (1979).

(6) J. F. Pritchard, P. J. O'Neill, M. B. Affrime, and D. T. Lowenthal, *Abstracts APhA Acad. Pharm. Sci.*, 11(2), 137 (1981).

J. Frederick Pritchard[x]
Ravi K. Desiraju
Department of Drug Metabolism
McNeil Pharmaceutical
Spring House, PA 19477

Received January 18, 1982.
Accepted for publication April 9, 1982.

[8] R. K. Desiraju, N. L. Renzi, Jr., L. A. McKown, and R. K. Nayak, data on file, McNeil Pharmaceutical, Spring House, Pa.

Hydroxyisolongifolaldehyde: A New Metabolite of (+)-Longifolene in Rabbits

Keyphrases □ Longifolene—hydroxyisolongifolaldehyde, a new metabolite in rabbits □ Metabolites—hydroxyisolongifolaldehyde from longifolene in rabbits □ Hydroxyisolongifolaldehyde—a new metabolite of longifolene in rabbits

To the Editor:

In spite of daily usage of terpenoid-containing plant products such as fruits, drinks, tobacco, *etc.*, the metabolic fate of terpenoids is essentially unknown. The aim of this study is to clarify terpenoid biotransformation in mammalian biochemistry from the toxicological point of view. This will provide guidance for the effective usage of natural products and for preparation of starting materials for organic synthesis.

Wild rabbits damage the forests in Japan by feeding on the artificially planted young *Chamaecyparis obtusa*, an important tree used commercially in Japan. This Japanese cypress contains longifolene (I) as a major sesquiterpene hydrocarbon. The metabolism of α-pinene, camphene, and other related terpenoids in rabbits was studied previously (1–7).

Longifolene (36 g), $[\alpha]_D$ = +39.3°, in chloroform, was administered to rabbits and the metabolites were isolated according to the method described previously. The neutral crude alcohols (3.7 g), were acetylated and purified to afford the main acetate (II) (17% for total acetates), which gave the following spectral data: mass spectrum: *m/z* 278 ($C_{17}H_{26}O_3$); 2700 and 1710 cm^{-1}; and a small doublet (J = 1.5 Hz) at 9.88 ppm of an aldehyde group. It was hydrolyzed by potassium carbonate in methanol and on silica gel chromatography gave pure metabolic alcohol (III). The parent ion of III, *m/z* 236, means a molecular formula $C_{15}H_{24}O_2$ showing that two oxygen atoms were introduced into longifolene. These oxygen atoms are based on a hydroxyl group (3450 cm^{-1}) and an aldehyde group (2700 and 1720 cm^{-1}; 9.87 ppm). The signals at 3.46 and 3.31 ppm (AB quartet) of this alcohol shifted 0.5 ppm upfield compared with those of acetate, suggesting the presence of a primary hydroxyl group. The olefin group of longifolene was lost in this alcohol. Thus, the change of this *exo*-methylene group to an aldehyde or primary alcohol was expected. The positions of newly introduced groups were determined on the basis of IR, ^{1}H-NMR, and ^{13}C-NMR spectra.

First, the aldehyde proton signal of III split into a doublet (J = 2.0 Hz) indicating the presence of an adjacent 7-H proton. By this splitting, it was concluded that the position of the aldehyde group is not at C-12, C-14, and C-15 but at C-7. The 7-H configuration was determined on the basis of a coupling constant. Provided that 7-H is in an α-configuration, the coupling constants of this proton would be anticipated to be $J_{7,1}$ = 1.3–2.6 Hz and $J_{7,8}$ = ~0.5 Hz. However, if 7-H is in a β-configuration, these values would be expected to be: $J_{7,8}$ = 3.6–5.0 Hz, $J_{7,9}$ ~1.2 Hz, and $J_{7,11}$ = 0.5 Hz. In fact, $J_{7,8}$ in III was observed as 3.5 Hz meaning 7-H has the β-configuration. Thus, the configuration of this aldehyde group was determined to be in the C-7-*endo*-form, which is stable in isolongifolaldehyde (8).

Second, in the IR spectra of the metabolized alcohol and

Table I—^{13}C-NMR Chemical Shifts in Longifolene and Hydroxyisolongifolaldehyde

	Longifolene (I)	Hydroxyisolongifolaldehyde (III)
C-1	62.2	56.3
C-2	33.6	37.8
C-3	36.5	34.2
C-4	21.2	21.0
C-5	43.4	44.2
C-6	44.1	43.0
C-7	168.0	59.9
C-8	48.0	40.8
C-9	29.8	25.8
C-10	25.5	23.0
C-11	45.2	47.0
C-12	30.1[a]	26.0[a]
C-13	99.0	206.4
C-14	30.6[a]	22.6[a]
C-15	30.6[a]	72.6

[a] Assignments may be reversed in each compound.

0022-3549/82/0800-0965$01.00/0

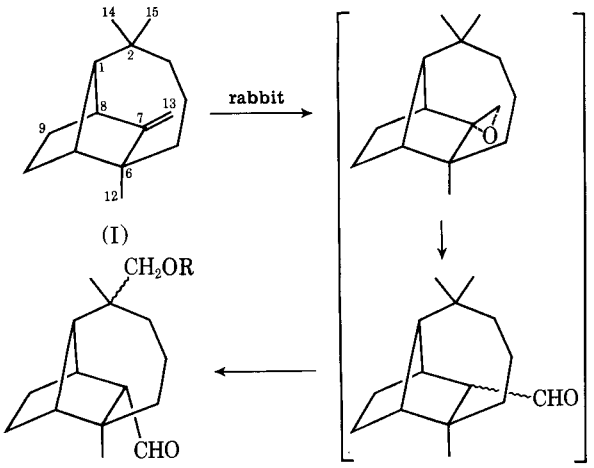

(II) R = CH_3CO
(III) R = H

Scheme I

its acetate, the absorption of the *gem*-dimethyl group, which appeared at 1355 and 1370 cm^{-1} in longifolene, was lost and instead a new single absorption (1360 cm^{-1}) appeared in this region. This suggests that one of the *gem*-dimethyl groups at C-2 was hydroxylated producing a primary alcohol. Furthermore, in the ^{13}C-NMR of III, the downfield shift of the C-2 carbon and the upfield shifts at C-1, C-3, and C-14 or C-15 were observed when compared with longifolene (Table I)[1].

The determination of which methyl (C-14 or C-15) was hydroxylated remains to be established. It is well known that the orientation of the C-7 substituent group in longifolene changes easily from the *exo*- to *endo*-form. However, such isomerization of the C-7 aldehyde during isolation processes was not found by TLC, GLC, or IR. Therefore, longifolene would be metabolized in rabbits as follows: (*a*) attack on the *exo*-methylene group from the *endo*-face to form its epoxide; and (*b*) isomerization of the epoxide to a stable *endo*-aldehyde. Thus, the metabolic route of longifolene would be written as in Scheme I.

In the metabolism of compounds having *exo*-methylene groups such as myrcene (2), camphene (3), and camphene epoxide (4), their glycols were obtained and their formation can be explained through epoxides. The reason for not finding longifolene-7,13-glycol can be attributed to the less stable longifolene-7,13-epoxide.

Terpenic aldehydes are biotransformed from camphor (dog) (9) and fenchone (rabbit) (10). Introduction of an aldehyde group in biotransformation is remarkable, and this isolongifolaldehyde may have some biological activity which is found in other sesquiterpene aldehydes such as polygodial. The hydroxylation of *gem*-dimethyl groups producing a primary alcohol has been reported on the compounds having three- (1, 2), four- (7), five- (10), and six- (11) membered rings in mammals. In this study, hydroxylation of the *gem*-dimethyl group on the seven-membered ring was newly added.

[1] The complete analysis of ^{13}C-NMR spectrum of longifolene was based on the comparison with that of longifolol, which was kindly furnished by Dr. K. Tori, Shionogi Research Laboratory, Shionogi & Co., Ltd., Japan.

(1) T. Ishida, Y. Asakawa, M. Okano, and T. Aratani, *Tetrahedron Lett.*, **1977**, 2437.

(2) T. Ishida, Y. Asakawa, T. Takemoto, and T. Aratani, *J. Pharm. Sci.*, **70**, 406 (1981).

(3) *Ibid.*, **68**, 928 (1979).

(4) T. Ishida, Y. Asakawa, T. Takemoto, and T. Aratani, "*The Abstracts of 23rd Symposium on the Chemistry of Terpenes, Essential Oils and Aromatics*," Chemical Society of Japan, Tokyo, Japan 1979, p. 39 (in Japanese).

(5) T. Ishida, Y. Asakawa, and T. Takemoto, and T. Aratani, *Res. Bull. Hiroshima Inst. Technol.*, **14**, 9 (1980).

(6) T. Ishida, Y. Asakawa, T. Takemoto, *ibid.*, **16**, 79 (1982).

(7) Y. Asakawa, Z. Taira, T. Takemoto, T. Ishida, M. Kido, and Y. Ichikawa, *J. Pharm. Sci.*, **70**, 710 (1981).

(8) S. Dev., *Prog. Chem. Org. Nat. Prod.*, **40**, 49 (1981).

(9) Y. Asahina and M. Ishidate, *Ber. Dtsch. Chem. Ges. B*, **68**, 947 (1935).

(10) M. Miyazawa, H. Kameoka, K. Morinaga, K. Negoro, and N. Mura, "*The Abstracts of 24th Symposium on the Chemistry of Terpenes, Essential Oils and Aromatics*," Chemical Society of Japan, Tokyo, Japan, 1980, p. 62 (in Japanese).

(11) R. Hanni, F. Bigler, W. Meister, and G. Fungert, *Helv. Chim. Acta*, **59**, 2221 (1976).

T. Ishida[x]
The Hiroshima Institute of Technology
Itsukaichi
Hiroshima 738, Japan

Y. Asakawa
T. Takemoto
Institute of Pharmacognosy
Tokushima Bunri University
Tokushima 770, Japan

Received March 4, 1982.
Accepted for publication May 6, 1982.

A publication of the
American Pharmaceutical Association—
the National Professional Society
of Pharmacists

JOURNAL OF PHARMACEUTICAL SCIENCES

INDEX TO AUTHORS
INDEX TO SUBJECTS

VOLUME 71
JANUARY TO DECEMBER, 1982

Published monthly under the supervision of the Board of Trustees

ACPE: Education's Measuring Stick

American drug products have long been regarded as meeting a level of quality and excellence generally unsurpassed throughout the world. In turn, the reasons often attributed to this phenomenon—in addition to the obvious capabilities and performance of the drug industry itself—are the elements of effective standards establishment and effective standards enforcement. In other words, the track record of drug quality is due, in large measure, to the impact or contribution made by the official compendia (*i.e.*, the USP/NF) and by the federal Food and Drug Administration.

Similarly, the graduates of American pharmacy schools have also been highly regarded worldwide as being uniformly well grounded in the art and science of the profession they have chosen. And, as in the case of American drug products, such consistency of quality and overall level of excellence is no accident.

Pharmacy education in the United States is blessed with a competent, effective, and efficient body that sets standards and accredits professional programs of the colleges and schools of pharmacy as well as the providers of continuing pharmaceutical education. The group responsible for these activities is the American Council on Pharmaceutical Education.

This national agency is not a government body. As in the case of the USP/NF, the ACPE represents the volunteer effort of the private sector to meet a perceived need and to establish a suitable level of performance that will give both the public and the health care community reasonable assurance of the quality of the products involved—in the former case high-quality pharmaceuticals and in the latter case high-quality pharmacy practitioners.

The Council is sponsored by three national groups in pharmacy: The American Association of Colleges of Pharmacy to represent academia and pharmacy educators; the American Pharmaceutical Association to represent the pharmacy profession and its practitioners; and the National Association of Boards of Pharmacy to represent governmental bodies responsible for the examination and licensure of pharmacy practitioners. Each of these three groups appoints three individual representatives to sit on the Council.

In addition, the public interest is represented on the ACPE through the participation of the American Council on Education, and that body appoints the tenth member to serve on the Council.

The ACPE is served by a very small but competent staff operating on a rather meager annual budget. This constitutes a dramatic illustration that big is not necessarily better, that empire building may not be beneficial for a particular agency, and that a key virtue of a lean operation often is maximum efficiency through minimum red tape.

Indeed, despite its very limited staff and resources, the ACPE has been very active in evaluating the professional degree programs of colleges and schools of pharmacy. Such evaluations and accreditations are made against standards of curriculum, of facilities, of staff, and of related considerations which the Council has developed and instituted over the years.

Similarly, evaluations are made of the providers of continuing pharmaceutical education, again judging such providers and their programs against criteria developed and adopted by the ACPE. Furthermore, the standards or criteria utilized are not static: they regularly undergo review and revision to ensure that they are meeting contemporary needs of the profession and of the public.

Our reason for choosing this particular time to comment on the ACPE and its work is due to the fact that the agency just celebrated its 50th Anniversary since its founding on August 26, 1932, by the above named sponsoring organizations.

Unquestionably, the ACPE has served well both pharmacy and the public. The uniformly high quality of the American network of higher education in pharmacy is a clear testimonial to that fact.

We take this opportunity to salute the Council, its members, its staff, its sponsors, and all those who now have, or who formerly had, a role in its successful operation. Its composition, structure, and operation make it unique among the accrediting agencies for the professions. Moreover, from our personal observation, it also appears to us to be the best and the most credible such accrediting agency.

—EDWARD G. FELDMANN
American Pharmaceutical Association
Washington, DC 20037

0022-3549/82/0900-0967$01.00/0

JOURNAL OF PHARMACEUTICAL SCIENCES

SEPTEMBER 1982
VOLUME 71 NUMBER 9

RESEARCH ARTICLES

Estimation of All Parameters from Nonisothermal Kinetic Data

IAN G. TUCKER and W. R. OWEN †

Received March 3, 1981, from the *Pharmacy Department, University of Queensland, St. Lucia, Australia 4067.* Accepted for publication August 3, 1981. † Deceased.

Abstract □ A method is described which estimates (using least-squares analysis) all parameters (kinetic parameters and also zero and infinite time assays) from nonisothermal kinetic data. This method overcomes the time delays required for infinite time assays and biased estimates caused by the use of those assay results. Flexible temperature and data collection programs can be used. The mathematical models account for thermal volume expansion and the appropriate model is selected by statistical tests (provided the reaction is studied over ~90% decomposition). The models use a reparameterized Arrhenius equation in which the frequency factor is replaced by k_a, the rate constant at a specified temperature. This improves the numerical procedure and allows room temperature stability to be estimated directly.

Keyphrases □ Kinetics—estimation of all parameters from nonisothermal data □ Models, mathematical—estimation of all parameters from nonisothermal kinetic data □ Drug stability—estimation from nonisothermal kinetic data

Nonisothermal kinetic methods enable drug stability to be estimated at any temperature from a single test rather than multiple experiments as required by the traditional isothermal approach.

A logarithmic nonisothermal method has been proposed (1) as well as reciprocal (2), linear (3), polynomial (4), and stepped (5) temperature programs. Most methods have used manual and/or approximate procedures to estimate the kinetic parameters. One method (6) employed numerical integration (trapezoidal method) within a nonlinear, least-squares regression; however, this is only applicable where dependent (concentration) and independent (time) variables can be separated in the model.

All methods thus far have treated time zero and time infinity concentrations as known. When these parameters are not known to a precision greatly exceeding that of the data, then they should be estimated from the data (7). This also avoids the lengthy time delays necessary to determine values at infinity. Treating them as constants may lead to biased kinetic parameter estimates as in isothermal experiments (8) and confidence limits might be falsely reduced (9).

In addition to these limitations of current methods, the effect of thermal volume expansion has not been considered.

The present report develops a nonrestrictive, numerical treatment which allows flexible temperature and data collection programs, estimates of all parameters, and accounts for thermal volume expansion in nonisothermal solution kinetics.

THEORY

The general form of the rate equation for a nonisochoric system (10) is:

$$-dM_1/dt = (1/V')^{\upsilon-1}\, k \prod_{i=1}^{i=j} M_i^{\upsilon_i} \qquad \text{(Eq. 1)}$$

where υ_i is the exponent of the ith reactant, υ is the reaction order ($= \upsilon_1 + \upsilon_2 + \ldots + \upsilon_j$), M_i is the number of moles of the ith reactant, V' is the solution volume which is a function of time, and k is the rate constant.

For a nonisothermal, nonisochoric system:

$$-dM_1/dt = (1/V')^{\upsilon-1}\, Ae^{-E/(RT)} \prod_{i=1}^{i=j} M_i^{\upsilon_i} \qquad \text{(Eq. 2)}$$

where A is the frequency factor, E is the apparent activation energy, R is the gas constant, and T is the absolute temperature.

From Eq. 2 the following apply:

$$-dM_1/dt = Ae^{-E/(RT)}\, V' \qquad \text{zero-order} \qquad \text{(Eq. 3)}$$

$$-dM_1/dt = Ae^{-E/(RT)}\, M_1 \qquad \text{first-order} \qquad \text{(Eq. 4)}$$

$$-dM_1/dt = Ae^{-E/(RT)}\, M_1\, M_2/V' \qquad \text{second-order} \qquad \text{(Eq. 5)}$$

It has been pointed out for isothermal kinetics (11) that if a reactant solution is prepared at room temperature and used at a different temperature, allowance should be made for thermal volume change. It is clear from Eq. 4 that first-order reactions are exempt from this requirement,

0022-3549/82/0900-0969$01.00/0

Table I—Convergence Rate of MARQDT when Minimizing on k_a and E, or A and E, for Typical First-Order Simulated Nonisothermal Data [a]

Initial Parameter Estimates[b]			Iterations Required	
k_a, min^{-1}	E, kcal mole^{-1}	$10^{-10}A$, min^{-1}	k_a/E	A/E
0.20	14.0	0.37	5	>20
0.20	16.0	10.70	6	>20
0.10	14.9	0.84	2	5
0.33	14.0	0.60	8	9
0.06	16.0	3.20	5	>15
0.06	14.0	0.11	5	>20
0.12	14.9	1.01	4	9

[a] Parametric values are E = 15.0 kcal/mole, $A = 1.0 \times 10^{10}$ min^{-1}, k_a = 0.10096 min^{-1}, where k_a is the rate constant at 25° and the linear temperature program range is 25–45°. [b] For each test, the two models have the same initial sum of squares.

since a volume term does not appear in the equation; however, pseudo first-order reactions for which Eq. 5, with M_2 constant, is applicable, are not exempt.

For nonisothermal experiments, the change in molar concentration, C', ($C' = M/V'$) of a reactant is due to reaction and thermal volume change. For the case where all samples are cooled to the same temperature (T_s) before analysis, the measured concentration (C) is independent of thermal volume change, and $C = M/V$ where V is the volume at T_s.

Since temperature and volume are functionally related to time [$T = f_1(t)$; $V' = V/f_2(t)$], Eqs. 3–5 can be rewritten as:

$$-dC_1/dt = Ae^{-E/[Rf_1(t)]}/f_2(t) \quad \text{zero-order} \quad \text{(Eq. 6)}$$

$$-dC_1/dt = Ae^{-E/[Rf_1(t)]}C_1 \quad \text{first-order} \quad \text{(Eq. 7)}$$

$$-dC_1/dt = Ae^{-E/[Rf_1(t)]}C_1C_2f_2(t) \quad \text{second-order} \quad \text{(Eq. 8)}$$

where C_2 is the concentration of Reactant 2 at volume V or the constant catalyst concentration at V in the pseudo first-order case.

Model for Absorbance Measurement—If change in absorbance (D) is used to follow the reaction and the following assumptions are made: (a) the reaction goes to completion; (b) the absorbance is the sum of component absorbances due to reactant, product, and constant background; (c) all component absorbances obey the Beer-Lambert law; and (d) the sum of the moles of reactant and moles of product is constant, then:

$$C_1 = (D - D_\infty)/[(a_r - a_p)b] \quad \text{(Eq. 9)}$$

$$C_{10} = (D_0 - D_\infty)/[(a_r - a_p)b] \quad \text{(Eq. 10)}$$

where D_0 and D_∞ are the absorbances at zero and infinite times, respectively, and are constant, a_r and a_p are the absorptivities of reactant and product, respectively, b the cell path length, and C_{10} is the concentration of reactant 1 at time zero and T_s.

Recalling that for pseudo first-order reactions, Eq. 8 with C_2 constant is applicable, then substituting Eq. 9 into Eqs. 6–8 yields:

$$-dD/dt = Ae^{-E/[Rf_1(t)]}(a_r - a_p)\,b/f_2(t) \quad \text{zero-order} \quad \text{(Eq. 11)}$$

$$-dD/dt = Ae^{-E/[Rf_1(t)]}(D - D_\infty) \quad \text{first-order} \quad \text{(Eq. 12)}$$

$$-dD/dt = Ae^{-E/[Rf_1(t)]}(D - D_\infty)\,C_2\,f_2(t) \quad \text{pseudo first-order} \quad \text{(Eq. 13)}$$

$$-dD/dt = Ae^{-E/[Rf_1(t)]}(D - D_\infty)^2\,f_2(t)/[(a_r - a_p)\,b] \quad \text{second-order} \quad \text{(Eq. 14)}$$

Similar equations can be derived for other situations where the sum of moles of reactant and moles of product is not constant.

Equations 11–14 cannot be integrated analytically. However, they can be solved numerically (*i.e.*, D values calculated at specified times) when initial values are supplied (*i.e.*, $D = D_0$ at $t = 0$).

For isothermal kinetics where $f_1(t)$ is constant, these equations can be integrated to give the familiar forms. For example, Eq. 12 yields:

$$D = D_\infty + (D_0 - D_\infty)e^{-kt} \quad \text{(Eq. 15)}$$

The parameters (D_0, D_∞, A, and E for nonisothermal; D_0, D_∞, and k for isothermal) are chosen so as to minimize Eq. 16:

$$SS = \sum_{i=1}^{i=N}(D_i - \hat{D}_i)^2 \quad \text{(Eq. 16)}$$

Table II—Parameter Estimates for Various Models Fitted to Nonisothermal First-Order Simulated Data [a]

Percent Reacted	Model			
	First-Order	Pseudo First-Order	Second-Order	Zero-Order
		k_a		
18	0.0537	0.0449	0.0063	0.1009
54	0.0992	0.0988	0.0469	0.1111
71	0.1002	0.0999	0.0605	0.1171
87	0.1004	0.1001	0.0735	0.1258
99	0.1002	0.1000	0.0866	0.1397
		E		
18	13.72	13.62	13.69	12.66
54	14.71	14.76	16.26	7.57
71	14.81	14.87	18.69	3.19
87	14.89	14.94	23.14	−2.91
99	14.97	15.02	41.32	−22.69
		D_0		
18	1.001	1.001	1.001	1.001
54	1.001	1.001	1.001	1.006
71	1.001	1.001	1.000	1.012
87	1.001	1.001	0.998	1.023
99	1.001	1.001	0.988	1.057
		D_∞		
18	−0.839	−1.198	−2.950	—[b]
54	0.031	0.030	−0.421	—
71	0.045	0.044	−0.240	—
87	0.049	0.049	−0.108	—
99	0.050	0.050	0.020	—

[a] Parameters and constants used to generate the first-order data were k_a = 0.1 hr^{-1}, E = 15 kcal/mole, D_o = 1.0, D_∞ = 0.05 with a linear temperature program over the range 25–45° in all cases. Also a_r = 1, a_p = 0, b = 1, with the random error variance of 0.56×10^{-6}. [b] The zero-order model has no D_∞ term.

where D_i and $\hat{D}_i$ are observed and calculated absorbances, respectively, at the ith datum, and N is the number of data.

Computational Procedures—*Temperature–Time Relationship* $f_1(t)$—For each data set, an orthogonal polynomial regression program, ORTHO (12), was used to establish the polynomial of lowest order which adequately described the temperature–time data. This enables flexible temperature programs to be employed. ORTHO uses the Gram–Schmidt orthonormalization procedure with an iterative straightening refinement (13).

Volume–Time Relationship $f_2(t)$—Data for the specific volume (V'_{sp}) of water at various temperatures are available (14). ORTHO was used to establish a polynomial relationship for this data over the experimental temperature range (30–92°),

$$V'_{sp} = 0.99992806 - 0.35791641 \times 10^{-4}\,T + 0.72094751 \times 10^{-5}\,T^2 - 0.42243321 \times 10^{-7}\,T^3 + 0.21949816 \times 10^{-9}\,T^4 - 0.47002556 \times 10^{-12}\,T^5 \quad \text{(Eq. 17)}$$

where T is degrees centrigrade for this equation only. All residuals about this regression were less than 7×10^{-7} ml/g and were randomly distributed.

Since the relationship $f_1(t)$ was established for each data set, and the general relationship $V'_{sp} = f(T)$ (Eq. 17) is available, the volume–time relationship $f_2(t)$ was established for each set.

Relationships $T = f_1(t)$ and $V'_{sp} = f(T)$ were used in the nonlinear regression program, MARQDT.

Optimization Routine—The function to be minimized (Eq. 16) contains nonlinear parameters so an iterative least-squares regression is required. A nonlinear regression program (MARQDT) was developed for this purpose. The program uses the Marquardt algorithm (15) with minor modifications (12). The advantages of this method have been described previously (16).

Initial estimates are required for the parameters. When these are not available from prior knowledge, satisfactory values can be obtained by one of the differential nonisothermal methods (17), provided thermal volume effects are neglected. These estimates are improved iteratively until the convergence test (the relative change in parametic estimates in consecutive iterations is less than 1 in 10^4) is satisfied.

Numerical Differentiation—The Marquardt algorithm requires partial derivatives with respect to each parameter at each datum. Since integrated functional equations are not available for nonisothermal kinetics, the partial derivatives were estimated numerically. These were computed using the two-point central difference method. Choice of the step length has been discussed previously (18).

Table III—Goodness of Fit Statistics for Various Models Fitted to Nonisothermal First-Order Simulated Data [a]

Percent Reacted	Model: First-Order	Pseudo First-Order	Second-Order	Zero-Order
		$10^6 V_r$ [b]		
18	0.56	0.56	0.56	0.55
54	0.56	0.56	0.59	5.5
71	0.56	0.56	0.72	21
87	0.56	0.56	1.6	73
99	0.56	0.56	13	279
		Probability[c]		
18	NS	NS	NS	NS
54	NS	NS	NS	S
71	NS	NS	NS	S
87	NS	NS	S	S
99	NS	NS	S	S

[a] See Table II. [b] V_r is the residual variance (*i.e.*, residual SS/df) and should be compared with the error variance of 0.56×10^{-6}. [c] Probabilities (NS = not significant at $p = 0.01$ level) for runs, mean square successive difference, and F tests were similar.

Numerical Integration—A fourth-order Runge–Kutta method with error estimation and step size control was used in MARQDT for the solution of Eqs. 11–14 (19). The method has been tested extensively on a number of derivative functions and found to perform excellently provided relative rather than absolute truncation errors are used to control step size.

In this work, a relative truncation error of 10^{-5} was used for sum of squares (SS) calculations, and 10^{-4} for partial derivative evaluations. This error in $\hat{D}_i$ for SS calculations was about one-fiftieth of the random error in the data and so did not contribute significantly to the calculated SS value. Further decrease in the truncation error did not lead to significant changes in the parameter estimates but only increased computational time.

Initial values are required for a particular solution of a differential equation. In the present work these were $D = D_0$ at $t = 0$ with D_0 being treated as a parameter.

Statistical Aspects—*Goodness of Fit*—The adequacy of the kinetic model was judged in two ways. First, the residuals were examined for nonrandomness or trends. If the model is adequate or the fit is good, the residuals should be randomly distributed in time. They were examined visually and by the runs (20) and mean square successive difference (21) statistical tests. Second, the residual variance about the regression was compared with the error variance of the experimental system (F-test) a knowledge of which was available from prior testing. However, in nonlinear regressions the residual variance is not an unbiased estimate of the pure error even when the model is correct, so this F-test is only approximate (16).

Confidence Limits—In nonlinear regressions, exact confidence limits for the parameters are not available; however, the linear estimates calculated from the variance–covariance matrix and residual variance are often adequate approximations (16). A Monte Carlo method has been described (22) to test the accuracy of these linear approximations. This test involves the following steps:

1. Estimate best-fit parameters and their approximate confidence limits;
2. Generate data using the best-fit estimates and add normally distributed random error with a variance equal to that of the original data set;
3. Estimate best-fit parameters for the data set;
4. Repeat steps 2 and 3 a number of times (15 has been used) and determine the confidence limits for the distribution of best-fit estimates.

This analysis need not be carried out every time a particular model is run, but should be used to check the linear approximations at least once for each model.

EXPERIMENTAL

Materials—p-Nitrophenyl acetate (I) was prepared by acetylation of p-nitrophenol (23) and recrystallized from fractionated benzene and petroleum ether (40–60° fraction) mixed solvent to a constant melting point (77.6°). p-Nitrophenol was recrystallized to constant melting point (115°) from fractionated benzene, and both materials were stored in vacuum desiccators in the dark until required for use. Thermal analysis indicated these samples to be greater than 99.9% pure.

Table IV—Parameter Estimates and Goodness of Fit Statistics for Various Models Fitted to Nonisothermal Second-Order Data [a]

Model	k_a	E	D_0	D_∞	Probability[b]
Second	0.1004	15.09	1.001	0.0512	NS
First	0.0739	−15.71	0.989	−0.1289	S
Pseudo first	0.0737	−15.64	0.989	−0.1287	S
Zero	0.0711	−30.57	0.968	—	S

[a] See Table II for parameter and constant values used to generate data over 90% reacted. [b] $p = 0.001$, S = significant, NS = not significant.

Concentrated hydrochloric acid[1] was diluted with glass distilled water to produce sufficient dilute acid for all experiments. This acid was standardized against freshly dried sodium carbonate (analytical reagent grade) using methyl orange indigo carmine indicator (24). Replicate analyses ($n = 4$) indicated the acid to be 0.2396 M (SE mean = ±0.0003 M).

Equipment—A 1-liter, closed, stirred, glass reaction vessel was immersed in a 60 liter polyethylene glycol 600 bath. In isothermal experiments the temperature was controlled by a circulating heater[2], while a variable speed programmer[3] was used for nonisothermal tests.

Temperatures inside the reaction vessel were monitored with a four-lead platinum resistance thermometer[4].

Samples were withdrawn automatically *via* polytef tubing, cooled to 32° in a jacketed coil, then passed into a 2-mm quartz flow-cell for spectrophotometric[5] analysis.

Analysis—The rate of hydrolysis was followed spectrophotometrically at 318 nm (2). Spectra recorded during the reaction showed a single iso-

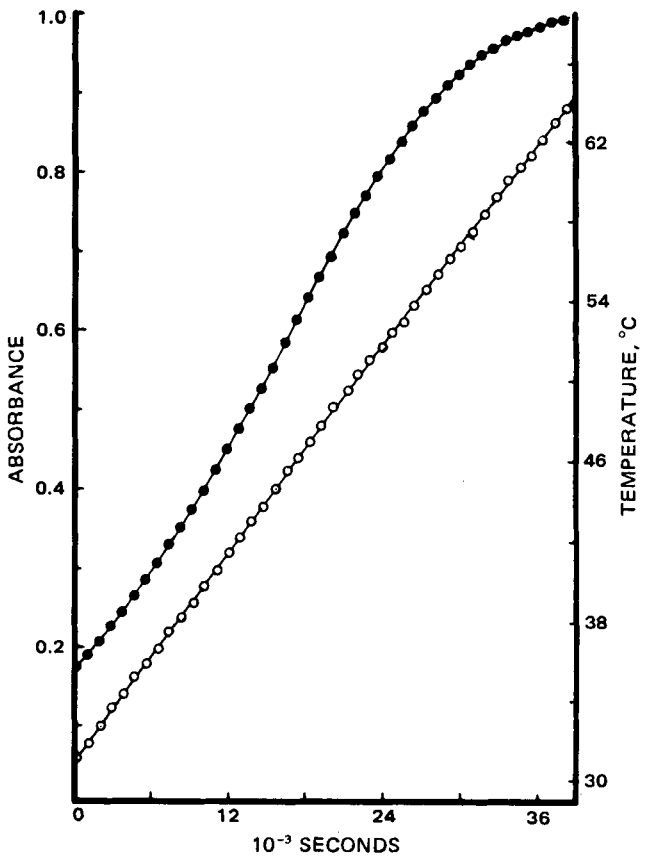

Figure 1—*Typical temperature program* (○) *and reaction data* (●) *with fitted curves for the nonisothermal acid catalysed (0.2396* M *HCl) hydrolysis of I. The temperature time relationship determined by ORTHO was* T(K) $303.911 + 0.904339 \times 10^{-3}\,t - 0.105973 \times 10^{-8}\,t^2$.

[1] Baker Analyzed Reagent, Baker Chemical Co.
[2] Model ED Unitherm, Gebruder Haake.
[3] Gebruder Haake Temperature Programmer, model PG12.
[4] Degussa element, type P4.
[5] Perkin-Elmer model 124 double-beam spectrophotometer.

Table V—Parameter Estimates and Goodness of Fit Statistics for Various Models Fitted to Nonisothermal Zero-Order Data [a]

Model	k_a	E	D_0	D_∞	Probability[b]
Zero	0.1004	14.95	1.000	—	NS
First	0.0019	15.19	1.000	−50.32	NS
Pseudo first	0.0018	15.25	1.000	−53.40	NS
Second	1×10^{-5}	15.16	1.000	−252.0	NS

[a] See Table II for parameter and constant values. [b] $p = 0.001$, NS = not significant.

bestic point (292 nm) indicating a one-to-one reaction and stability of the absorbing product, *p*-nitrophenol. The final spectrum was identical with that of *p*-nitrophenol.

A Beer–Lambert calibration, using replicate samples, confirmed linear concentration–absorbance relationships for I and *p*-nitrophenol, and that the component absorbances were additive. Since it was shown that spectra in acid and water were identical, this calibration was performed in distilled water, thereby minimizing decomposition problems.

Procedure—One liter of acid was allowed to equilibrate thermally in the closed reaction vessel. About 80 mg of I dissolved in 2 ml of fractionated ethanol was added to produce an ~0.0004 *M* solution which was bubbled with high purity nitrogen. The temperature programmer was started when I was added and the first sample withdrawn 2 min later. Samples were withdrawn automatically, cooled to 32°, and assayed directly, the concentrations used being such that the infinite time absorbance was ~1. At each sampling, reaction vessel temperature, sample absorbance, and time data were automatically recorded.

Design—About 30 data were collected during each experimental run. Triplicate isothermal tests were performed at 39.26, 49.03, 58.68, and 68.24°. Triplicate nonisothermal tests at each of four different approximately linear heating rates (~3, 6, 12, and 18°/hr) were used. These all started at about 30° and continued until decomposition exceeded 90% giving a maximum temperature of about 76° (for 18°/hr).

RESULTS AND DISCUSSION

Reparameterization of the Model—For first-order nonisothermal kinetics with a linear temperature program, exact simulated data were generated using parameter values of $A = 1 \times 10^{10}$ min^{-1}, $E = 15$ kcal/mole, $D_0 = 1$, $D_\infty = 0$, and $T = 298.15 + t$. D_0 and D_∞ were then held constant at their parametric values, while A and E were estimated. Convergence of the program was very slow, even for initial estimates close to the true values.

Sum of squares contours for the data in question were generated and found to be very elongated in the direction of the A parameter. It has been pointed out (16) that in such cases, slow convergence of any iterative estimation procedure is likely. Clearly, A is an ill-determined parameter; that is, large changes in A cause small changes in SS. In retrospect, it is apparent why A is ill-determined. It is the rate constant at infinite temperature. Since data are usually collected in the range 25–90°, estimation of A involves an extrapolation outside the data, and such estimates are poorly determined.

Conditioning can often be improved by reparameterizing the model. In the present study, this was done by replacing A with $k_a\, e^{E/(RT_a)}$ in Eqs. 11–14, where the new parameter k_a is the rate constant at T_a, a temperature within the experimental range. Sum of squares contours for various T_a values were found to be well-rounded ellipses, *i.e.*, the parameters were well-conditioned. Since little change occurs in the conditioning with changes in T_a, provided it is within or near the experimental range, it may be advantageous to choose $T_a = 25°$. This would allow the room temperature rate constant to be estimated directly, and approximate confidence limits would also be immediately available.

Table VI—Kinetic Parameter Estimates for the Acid Catalysed Hydrolysis of I [a]

Source	$E \pm SE$, kcal/mole	$10^5 k_a \pm SE$, sec^{-1}
Nonisothermal[b]	16.98 ± 0.03	1.904 ± 0.010
Isothermal[c]	17.00 ± 0.04	1.912 ± 0.009
Reference 2[d]	21 ± 2	1.9 ± 0.4
Reference 2[e]	18	
Reference 25[f]		2.054
Reference 26[g]	17.2	

[a] $T_a = 30°$. [b] Mean of 12 experiments. [c] Least-square estimates based on 12 experiments (three replicates at four temperatures). [d] Their nonisothermal estimates, k_a being calculated from their second-order rate constant at 25° using $[H^+] = 0.2396\ M$ and $E = 17.0$ kcal/mole. [e] Their isothermal estimate. [f] Determined from their second-order rate constant as above. [g] For phenyl acetate.

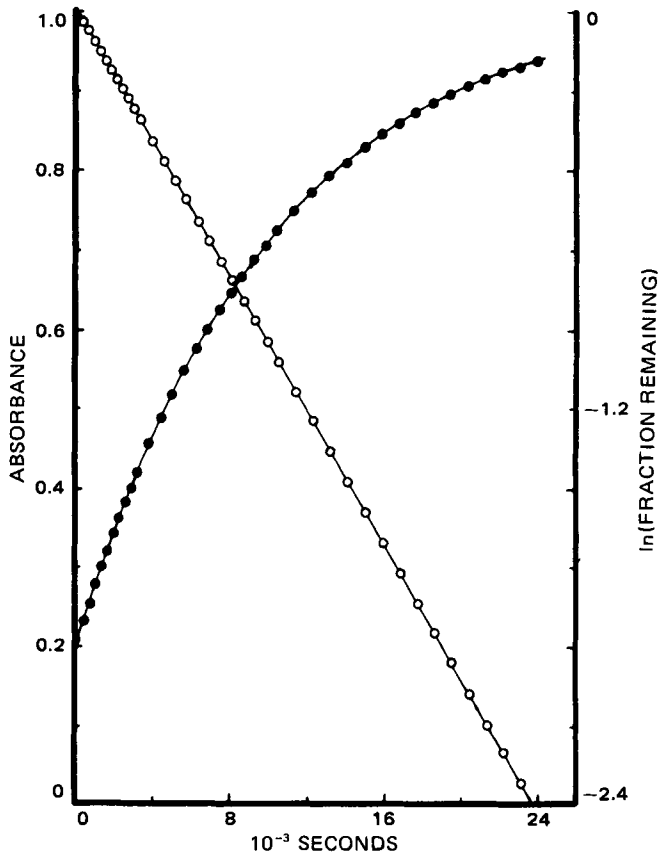

Figure 2—*Typical data for the isothermal acid catalysed (0.2396 M HCl) hydrolysis of I showing the first-order, nonlinear, least-squares curve (●) and the more usual linearized logarithmic plot (○). D_∞ from the nonlinear regression was used to calculate the fraction remaining.*

The new model was tried on the same first-order simulated data and convergence was rapid. A comparison of the new and old models for this typical data set, for differing initial estimates, is shown in Table I. In all cases the program converged to the parametric values and the new model was superior. Convergence was acceptable, since the initial estimates were far worse than normally would be expected.

It is clear that A may be of theoretical interest, but k_a is of greater interest in practical stability studies and its use facilitates the numerical procedure. In all subsequent computations, the reparameterized models were used.

Goodness of Fit—To test the ability to select the appropriate kinetic model, simulated data (40 pairs) were generated and normally distributed random error was added. The variance of the random error was that of the experimental system. The parameter estimates for zero-, first-, pseudo first-, and second-order fits to first-order data are given in Table II while the statistics for judging the goodness of fit are in Table III.

In all cases, ~95% confidence limits of the first-order estimates bracketed the parametric values. This, along with the excellent agreement between the residual variances (about the regression) and error variance (Table III), indicated the program was functioning correctly.

With the reaction 18% complete, the 95% confidence limits (−0.087–0.194) for the first-order estimate of k_a bracketed the parametric value, but the point estimate is about half the parametric value. This shows the danger of estimating rate constants from data covering a low percentage reacted, and of the need to compute confidence limits.

At high percentages reacted, the estimated E values for the zero-order model were negative. These values were expected, since the decrease in concentration causes a decrease in reaction rate for first-order kinetics; this is not accounted for in the zero-order model. Consequently, the reaction rate apparently decreased with temperature rise.

From Table III, it is clear that at the added random error level the various kinetic models could not be distinguished below 18% decomposition. At 54% reacted the zero-order model was inadequate, at 87% the second-order was inadequate, but the first- and pseudo first-order models

Table VII—Effect of Treating D_0 and/or D_∞ as Constants on the Remaining Parameter Estimates

Row	D_∞, Absorbance Units	D_0, Absorbance Units	$10^4\ k_a$, sec^{-1}	±95% Confidence Unit, %	E, kcal/mole	±95% Confidence Unit, %	10^6 Residual Variation, (absorbance units)^2
1	0.9825	0.1721	0.1897	0.54	17.06	0.48	0.16
2	I − CL[a]	0.1722	0.1896	0.47	17.08	0.22	0.16
3	I + CL	0.1720	0.1899	0.47	17.04	0.22	0.16
4	0.9845	II − CL[a]	0.1912	0.38	16.96	0.43	0.24
5	0.9805	II + CL	0.1882	0.39	17.16	0.43	0.24
6	I − CL	II + CL	0.1883	0.38	17.13	0.20	0.24
7	I + CL	II + CL	0.1883	0.40	17.10	0.22	0.27
8	I − 0.01	0.1729	0.1877	0.94	17.36	0.45	0.61
9	I + 0.01	0.1713	0.1916	0.87	16.78	0.43	0.55
10	I − 0.01	II	0.1891	0.65	17.30	0.35	0.70
11	I + 0.01	II	0.1902	0.60	16.83	0.33	0.63

[a] I and II are Row 1 estimates of D_∞ and D_0. I − CL means D_∞ was treated as a constant with value I minus the 95% confidence limit of a reading (0.0008 absorbance unit).

remained indistinguishable, even at 99% decomposition. When the error variance was reduced by a factor of 10, the second-order model was then inadequate at 71% reacted, but the first- and pseudo first-order models were adequate. Attempts to separate these two models by increasing the temperature range to 60° while maintaining 90% reacted were unsuccessful.

Second-order and zero-order data were generated using parameter and constant values given previously (Table II) and covering 90% reacted with a temperature range of 20°. The parameter estimates and probabilities for second-order data are given in Table IV and for zero-order data in Table V.

At 90% decomposition and at the random error level used, the second-order equation was the only adequate model (Table IV). The other models were shown to be inadequate by the statistical tests and the meaningless E estimates.

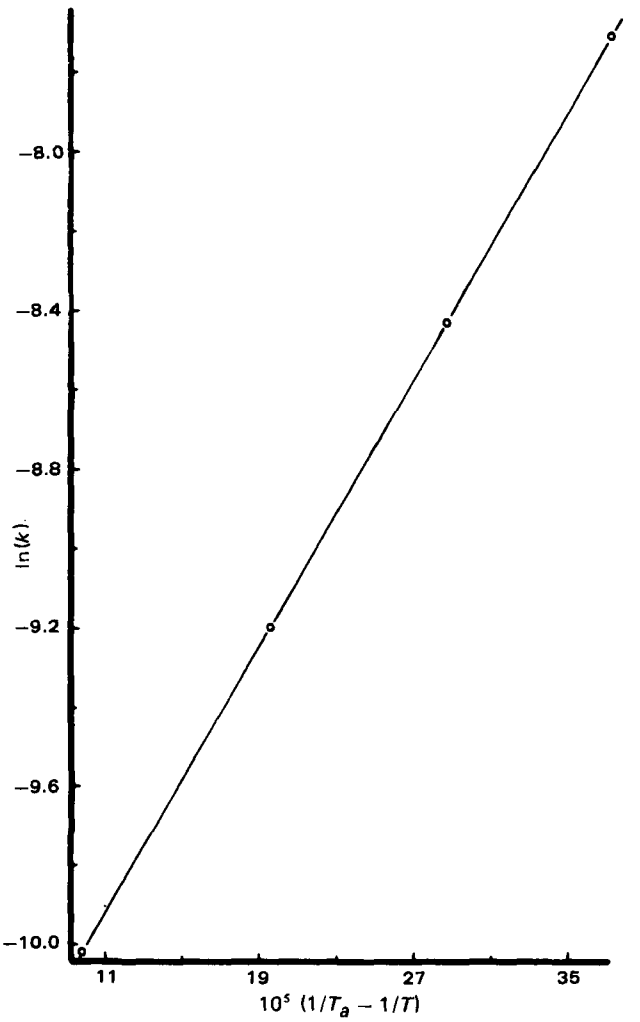

Figure 3—*Arrhenius plot for the acid catalysed (0.2396 M HCl) hydrolysis of I, T_a = 30°. Points cover the range of the experimental rate constants.*

The probabilities in Table V indicate that zero-order data can be described equally well by all models. Additionally, the kinetic parameter estimates (k_a,E) were reasonable for all models (although if prior stability information were available, the k_a estimates from the incorrect models would be suspect). However, the D_∞ estimates for the incorrect models were unacceptable, since absorbances of −50 and −252 are meaningless. Therefore, the first-, pseudo first-, and second-order models were rejected because of their D_∞ estimates and the zero-order model was accepted by default and because it was not rejected by the statistical tests.

For zero-order reactions, the rate increases continuously with time due to temperature rise and comes to an abrupt halt at zero concentration. For first-order, the rate increases initially but then decreases when the effect of lowered concentration exceeds that due to the increased k value. In second-order reactions, the decrease in rate occurs at a lower percentage reacted since rate is proportional to concentration squared. Therefore, all models appear similar before the inflection points and, consequently, zero-order reactions covering a high percentage decomposition appear like first- and second-order reactions covering a small percentage reacted. From Table V, the 90% reacted zero-order model was adequately fitted by first- and pseudo first-order models covering ~2% ($D_\infty \sim -50$) or a second-order model with ~0.5% decomposition ($D_\infty = -252$).

Data from the nonisothermal hydrolysis of I, over ~90% decomposition, were treated similarly. Graphs for a typical temperature program and reaction together with the ORTHO and MARQDT (pseudo first-order) fits are shown in Fig. 1. In all cases, zero- and second-order models were inadequate but the first- and pseudo first-order nonisothermal models were adequate. Pseudo first-order rate constants were estimated from isothermal data using nonlinear least-squares regression (Eq. 15). Plots of a typical data set and the fitted curve are shown in Fig. 2 along with the usual linearized graph. The rate constants were corrected for thermal volume expansion and then k_a and E were estimated by linear least-squares regression using the logarithmic form of the reparameterized Arrhenius equation (Fig. 3). Nonisothermal parameter estimates were in good agreement with isothermally determined values. These estimates are shown in Table VI with literature values.

Confidence Limits—In all cases tested, the approximate confidence limits did not greatly exceed the Monte Carlo limits (usually only by a factor of <1.5). This indicates that the approximate error estimates cause less confident parameter estimates than is justified. However, in a

Table VIII—Variations in Parameter Estimates when Thermal Volume Expansion is Neglected[a]

Temperature Range	Model: Zero-Order	Pseudo First-Order	Second-Order
		k_0	
20	0.09973	0.1002	0.1002
40	0.09949	0.1004	0.1003
60	0.09900	0.1007	0.1004
		E	
20	15.07	14.94	14.96
40	15.09	14.92	14.94
60	15.13	14.90	14.93

[a] Exact nonisothermal simulated data were generated using: $k_a = 0.1$, $E = 15.0$, $D_0 = 1.0$, $D_\infty = 0.05$, $a_r = 1$, $a_p = 0$, $b = 1$, $T = 298.15 + t$, and $T_a = 25°$ for various models incorporating the volume correction term.

practical sense, the differences were not large and errors caused by accepting the approximate values would be safe.

D_0 and D_∞ as Constants—The errors resulting from treating D_0 and D_∞ as constants were investigated using a typical set of I data. Initially, all parameters (k_a, E, D_0, and D_∞) were estimated (row 1, Table VII) and the residual variance from this fit was used to obtain the 95% confidence limits of a reading. Variables D_0 and/or D_∞ were then treated as constants and the remaining parameters were re-estimated from the data. Constant values for D_0 and D_∞ were best estimates from the four parameter fit ±95% confidence limits of a reading (0.0008 absorbance unit). It is acceptable that D_0 be determined to this precision, since for nonisothermal kinetics, the reaction initially proceeds slowly. However, determination of D_∞ may involve time delays with instrument drift, mechanism changes, *etc.*, so an uncertainty of 0.01 absorbance unit would not seem unreasonable. Table VII shows the results of these refits.

It is apparent that fixing D_0 and D_∞ reduces the 95% confidence limits of E as expected, while those of k_a are reduced except where the increase in residual variance outweighs the decrease caused by fixing D_0 and D_∞ (Table VII). In a practical sense it is unlikely that the decreases in 95% confidence limits would cause serious errors, but the inflated residual variances make the model suspect, making the choice of the appropriate reaction order difficult.

Errors in k_a and E estimates were quite small (0.16 and 0.23% range, respectively) when D_∞ was treated as a constant in error by the 95% confidence limit of a reading (Rows 2 and 3 in Table VII), but similar errors in D_0 caused considerable biases in the estimates (1.6 and 1.2% ranges for k_a and E, respectively). When the error in D_∞ was increased to 0.01 absorbance unit, k_a and E ranges were 2.1 and 3.4% in the worst case. These errors must be seen in light of the experimental precision and, hence, the approximate confidence limits. The 95% confidence limits for k_a and 99% limits for E for Rows 4 and 5 and 8 and 9 in Table VII do not bracket the best (Row 1) estimates. That is, biased estimates resulted from using constant (incorrect) values for D_0 and D_∞.

Thermal Volume Expansion—Comparison of the first- and pseudo first-order estimates in Table II indicates that errors caused by neglecting thermal volume expansion are small for this model. However, to ascertain the magnitude of expected biases for all models, exact simulated data (no added random error) were generated. Data (40 pairs) covering 90% decomposition and temperature ranges of 20, 40, and 60° were produced using reparameterized Eqs. 11, 13, and 14. Parameters were re-estimated using these equations and again without the volume correction term [$f_2(t)$]. In all cases where the complete equations were used, the estimates agreed (to 6 correct digits) with the parametric values. Errors caused by neglecting the volume correction are shown in Table VIII.

The biases observed are quite small (*e.g.*, pseudo first-order, 40° range, biases are +0.4% in k_a and −0.53% in E). These percentages varied little with parameter values (*e.g.*, with $k_a = 0.01$ and $E = 30$, the errors were +0.4% in k_a and −0.3% in E). Assuming an error variance of 0.56×10^{-6}, the 95% confidence limits for the 40° pseudo first-order range are ±0.61% for k_a and ±0.64% for E. These limits bracket the parametric values.

The bias in k_a depended on the T_a chosen. For $T_a = 90°$, the error was −1.9% but this increased error must be compared with the wider 95% confidence limits of ±2.5%. Thus, the bias errors are relatively small. As seen previously, fits with and without volume correction terms (first- and pseudo first-order, Table III) are equally good. Therefore, the need for a volume correction term was not evident from the experimental system, and justification for the term is theoretical (10).

From a practical viewpoint it appears that failure to correct for volume expansion has a negligible effect on kinetic parameter estimates from a single data set; however, in the long term, slightly biased estimates will result and the inclusion of the term is warranted.

REFERENCES

(1) A. R. Rogers, *J. Pharm. Pharmacol.*, **15**, 101T (1963).

(2) S. P. Eriksen and H. Stelmach, *J. Pharm. Sci.*, **54**, 1029 (1965).

(3) M. A. Zoglio, J. J. Windheuser, R. Vatti, H. V. Maulding, S. S. Kornblum, A. Jacobs, and H. Hamot, *ibid.*, **57**, 2080 (1968).

(4) H. V. Maulding and M. A. Zoglio, *ibid.*, **59**, 333 (1970).

(5) B. Edel and M. O. Baltzer, *ibid.*, **69**, 287 (1980).

(6) B. W. Madsen, R. A. Anderson, D. Herbison-Evans, and W. Sneddon, *ibid.*, **63**, 777 (1974).

(7) K. B. Wiberg, in "Techniques of Chemistry," vol. VI, part 1, Wiley, New York, N.Y., 1974, p. 748.

(8) E. A. Guggenheim, *Phil. Mag.*, **2**, 538 (1926).

(9) E. J. Williams, "Regression Analysis," Wiley, New York, N.Y., 1959, p. 15.

(10) R. Livingstone, in "Techniques of Organic Chemistry," vol. VIII, part 1, Interscience, New York, N.Y., 1961, p. 113.

(11) J. F. Bunnett, in "Techniques of Chemistry," vol. VI, part 1, Wiley, New York, N.Y., 1974, p. 174.

(12) P. J. Stewart, PhD thesis, University of Queensland, Australia, 1975.

(13) P. J. Davis, in "Survey of Numerical Analysis," J. Todd, Ed., McGraw-Hill, New York, N.Y., 1962, chap. 10.

(14) "CRC Handbook of Chemistry and Physics," R. C. Weast, Ed., 55th ed., CRC Press, Cleveland, Ohio, 1974, F5.

(15) D. W. Marquardt, *J. Soc. Indust. Appl. Math.*, **11**, 431 (1963).

(16) N. R. Draper and H. Smith, "Applied Regression Analysis," Wiley, New York, N.Y., 1966, chap. 10.

(17) R. A. Anderson and M. Campbell, *Aust. J. Pharm.*, **52**, S81 (1971).

(18) A. R. Curtis and J. K. Reid, *A.E.R.E.Report T.P.477*, (1972).

(19) L. Fox and D. F. Mayers, "Computing Methods for Scientists and Engineers," Clarendon, Oxford, England, 1968, p. 204.

(20) N. R. Draper and H. Smith, "Applied Regression Analysis," Wiley, New York, N.Y. 1966, p. 95.

(21) C. A. Bennett and N. L. Franklin, "Statistical Analysis in Chemistry and the Chemical Industry," Wiley, New York, N.Y., 1967, p. 677.

(22) J. P. Chandler, D. E. Hill, and H. O. Spivey, *Comput. Biomed. Res.*, **5**, 515 (1972).

(23) L. F. Fieser, "Experiments in Organic Chemistry," 2nd ed., Heath, New York, N.Y., 1941, p. 222.

(24) A. I. Vogel, "Quantitative Inorganic Analysis," 3rd ed., Longman, London, England, 1972, p. 235.

(25) K. A. Connors, *Interest*, **2**, 51 (1963).

(26) E. Tommila and C. N. Hinshelwood, *J. Chem. Soc.*, **1938**, 1801.

ACKNOWLEDGMENTS

The authors express their gratitude to Dr. P. J. Stewart for helpful comments in the preparation of this paper.

Development of a Method for Study of the Tendency of Drug Products to Adhere to the Esophagus

MARTTI MARVOLA *x, KARI VAHERVUO, ASLAK SOTHMANN, ESKO MARTTILA, and MARKKU RAJANIEMI

Received June 29, 1981, from the *Pharmaceutical Research Laboratories, Orion Pharmaceutical Co., Espoo, Finland*, and the **School of Pharmacy, University of Helsinki, Helsinki, Finland.* Accepted for publication November 9, 1981.

Abstract □ A method to determine the adherence of drugs to the esophagus was developed using isolated swine esophagi. A number of types of tablets and capsules (*e.g.*, of doxycycline) were tested. The results showed that the tendency of products to adhere to the esophagus can be regulated by pharmaceutical properties. It was concluded that the method described is simple, inexpensive, and accurate.

Keyphrases □ Esophagus—study of drug product adherence, doxycycline, swine esophagus □ Adherence—study of drug products in esophagus, doxycycline, swine esophagus

In recent years, many case reports concerning drug-induced esophageal ulceration or stricture in humans have been published. Serious damage has been caused by doxycycline (1–3), emepronium bromide (4–6), potassium chloride (7–9), alprenolol (3), and iron salts (3, 10). The mechanism of injury is not yet well understood, although it is obvious that the lesions were caused by drug substances. The primary reason has apparently been adherence of the drug product to the esophageal wall, allowing high local drug concentrations to be formed. The tendency to adhere is obviously greatest for hard gelatin capsules, but differences between various tablet formulations are also evident. The risk of esophageal lodging can generally be avoided by taking dosage forms with water and, if possible, in an upright position. Despite this, there is a great need for development of new drug products and product coatings with less tendency to adhere to the esophageal mucosa. However, no adequate and simple method for measuring adherence has been available.

The aim of the present investigation was to develop a method for study of the tendency of products to adhere to the esophageal wall, using the isolated swine esophagus. Our results on the effects of various pharmaceutical properties of products on adhesion will be published later.

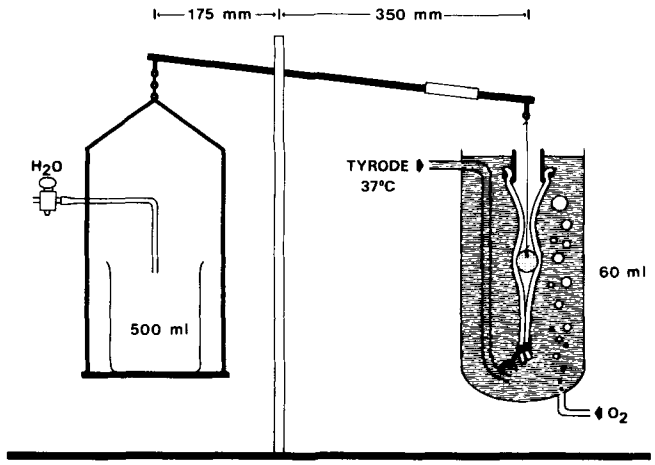

Figure 1—*Measurement system for force needed to detach product from the esophagus and organ bath I.*

EXPERIMENTAL

Isolated Esophagus Preparation—Pigs of both sexes of Landrace and Yorkshire breeds, weighing 90–100 kg were used. Immediately after slaughter, the esophagi were removed and transported to the laboratory in Tyrode solution, kept at ~4°. The composition of the Tyrode solution was (g liter^{-1}): sodium chloride 8.0, potassium chloride 0.2, calcium chloride · $2H_2O$ 0.134, sodium bicarbonate 1.0, sodium dihydrogen phosphate 0.05, and glucose · $1H_2O$ 1.0. During experiments the solution was aerated with pure oxygen and kept at 37°. Segments 6–7 cm long were cut from the esophagus. The segments were mounted in two kinds of organ baths. Organ bath I: The volume of the classic organ bath for isolated preparations was 60 ml (Fig. 1). The lower end of the esophageal segment was tied off and the upper end was attached around a glass tube (diameter 15 mm). The solution in the organ bath was changed at intervals of about 30 min. Organ bath II: The volume of the second organ bath was 2000 ml (Fig. 2). In this preparation, the lower end of the esophageal segment was also attached around a glass tube (diameter 8 mm). There was, therefore, free passage through the preparation, which allowed washing of the mucosa. The Tyrode solution in this organ bath was not changed during the 6-hr experiments.

Recording of Adherence—A hole (diameter of 1 mm) was drilled in the products to be tested. The product was attached to a copper wire (diameter of 0.25 mm) and placed, using a plastic tube as an applicator, in the esophageal preparation for a fixed time. The force needed to detach the product was measured using a modified prescription balance (maximum load 500 g; see Fig. 1). This force was used as a parameter for adherence. The force (F) in newtons was calculated by the equation:

$$F = \frac{0.00981W}{2}$$

where W = amount of water in the beaker in grams. The water flow rate was 280 g min^{-1} (corresponding to 1.37 N min^{-1}).

Characteristics Studied—To discover the usefulness of the preparation the following characteristics were studied: (*a*) the effect of the time for which the product remains in the esophagus upon the force needed to detach it; (*b*) the effect of the surface areas of different products on the force needed for detachment; (*c*) differences between the results obtained using the two different organ baths; (*d*) the effect of washing of the mucosa on adherence; and (*e*) differences in adherence to the esophagus of some commercially available doxycycline preparations.

Drug Products—Hard gelatin capsules[1], sizes 0, 1, 2, 3, 4, and 5, were filled with lactose. Placebo tablets were compressed from a mixture of basic granules (96%), talcum (3%), and magnesium stearate (1%). The

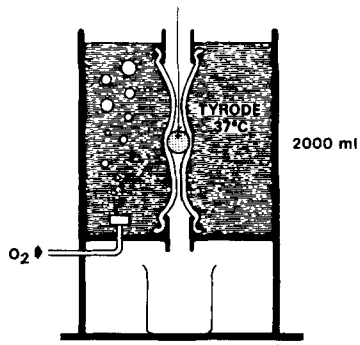

Figure 2—*Organ bath II for isolated esophageal preparations.*

[1] Capsugel AG, Switzerland.

0022-3549/82/0900-0975$01.00/0

Table I—Surface Areas of Products Studied

Capsule size	Area, mm^2	Placebo Tablet Diameter, mm	Area, mm^2	Potassium Chloride Tablet Diameter, mm	Area, mm^2
2	349	7	160	7	146
3	286	9	223	9	223
4	244	10	259	10	259
5	196	11	298	11	308
		12	358	12	358

Table II—Mean Force Newtons Per Unit Area (cm^2) Needed to Detach Products from the Isolated Swine Esophagus

Capsule Size	Force, N cm^{-2}	Placebo Tablet Diameter, mm	Force, N cm^{-2}	Potassium Chloride Tablet Diameter, mm	Force, N cm^{-2}
2	0.36	7	0.26	7	0.075
3	0.38	9	0.24	9	0.054
4	0.35	10	0.25	10	0.062
5	0.40	11	0.24	11	0.058
		12	0.24	12	0.056

basic granules contained lactose (78%), corn starch (19%), and gelatin (3%). Potassium chloride tablets were compressed from pure potassium chloride. The diameters of the placebo and potassium chloride tablets were 7, 9, 10, 11, or 12 mm. The shape of all tablets was biconvex. The surface areas of the capsules and tablets were calculated according to geometrical principles and are given in Table I.

As sugar-coated tablets, a commercial product[2] of 11-mm diameter was used. The diameter of the film-coated tablets[3] was also 11 mm. The film-forming material was hydroxypropylmethylcellulose.

In the final part of the present study, six commercially available doxycycline (100–150 mg) products (A–F) and two test formulations (G, H) were studied using the method developed. Products B–E were film-coated tablets. Product F was a capsule formulation (size 3). Products A, G, and H were uncoated tablets.

RESULTS AND DISCUSSION

Initially, the effect of the time interval between administration of the drug and commencement of detachment on the force needed for detachment was studied with four different products. As can be seen from

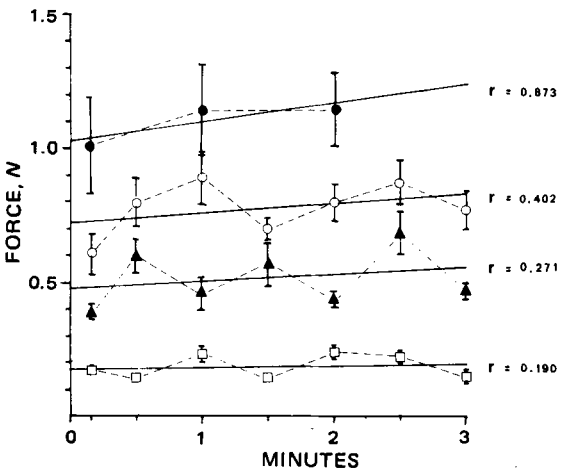

Figure 3—*Effect of the time interval between administration of the drug and commencement of detachment on force needed for detachment of drug. Key: (●) hard gelatin capsule size 2; (○) placebo tablet, diameter 11 mm; (▲) hydroxypropylmethylcellulose film-coated tablet, diameter 11 mm; (□) sugar-coated tablet, diameter 11 mm. Each point represents mean* ±SEM, n = *10.*

[2] Sembrina, Orion Pharmaceutical Co, Finland.
[3] Kaliduron, Orion Pharmaceutical Co, Finland.

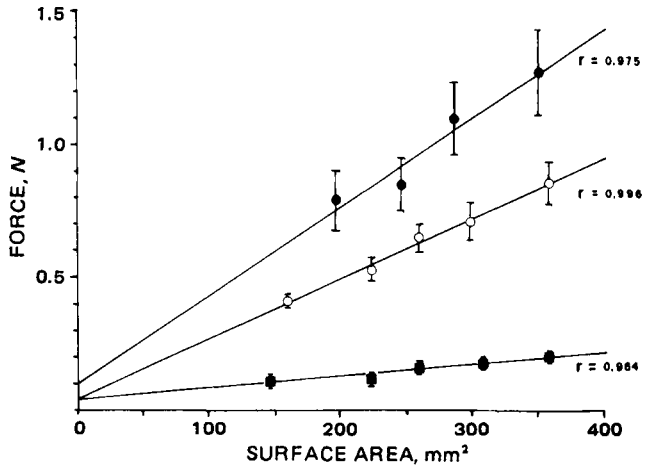

Figure 4—*Effect of surface area of product on the force needed for detachment. Key: (●) hard gelatin capsules, sizes 2, 3, 4, and 5: (○) placebo tablets, diameter 7, 9, 10, 11, and 12 mm; (■) potassium chloride tablets, diameter 7, 9, 10, 11, and 12 mm. Each point represents mean* ±SEM, n = *20.*

Fig. 3, no clear linear or exponential correlation between force and time was noted. In subsequent experiments, an interval of 2 min was usually used. Because of disintegration, hard gelatin capsules could not be left in the esophagus for longer than 2 min. For the same reason, the longest time in experiments using tablets was 3 min.

The results pertaining to the effect of surface area of product on the force exerted for detachment are shown in Fig. 4 and Table II. The forces for gelatin capsules larger than size 2 could not be measured, because the esophageal mucosa became detached from the preparation if forces greater than 1.5 N had to be used. As can be seen from Fig. 4, a significant (p = 0.05–0.001) linear correlation between force and area exists for every product. The force per unit of surface area appears independent of product size (Table II). The intercepts from extrapolation of the lines in Fig. 4 were 0.04–0.1 N. These can be regarded as the magnitudes of force needed to pull the products out of the esophagus, even though they are not adhering.

Three different sizes of placebo tablets (diameters 9, 11, and 12 mm), identical sizes of potassium chloride tablets, two different capsule sizes (2 and 4) and sugar-coated tablets were tested using identical procedures and organ baths I and II (n = 20). No statistically significant differences in results were observed. However, the classic organ bath for isolated preparations (I) was a little easier to handle. This is why most results in the present study were obtained with organ bath I.

Table III—Effect of Washing on Force Needed to Detach the Placebo Tablets from the Isolated Esophagus [a]

Diameter, mm	Force Without Washing, N, mean ± *SD* n = 20	Force after Washing with 5 ml Water, N, mean ± *SD* n = 10
10	0.65 ± 0.23	0.19 ± 0.07
11	0.71 ± 0.30	0.20 ± 0.04
12	0.86 ± 0.34	0.33 ± 0.09

[a] Student's t test; $p < 0.001$.

Table IV—Force Needed to Detach Doxycycline Products from the Isolated Swine Esophagus [a]

Product	Diameter, mm	Force, N, mean ± *SD*	n	t test[b]
Tablet A	9	0.29 ± 0.07	12	
Tablet B	9	0.27 ± 0.05	6	NS
Tablet C	9	0.30 ± 0.08	6	NS
Tablet D	10	0.58 ± 0.15	6	b
Tablet E	10	0.78 ± 0.22	6	b
Capsule F	(size 3)	1.21 ± 0.25	8	b
Tablet G	9	0.17 ± 0.04	8	b
Tablet H	10	0.16 ± 0.05	8	b

[a] Interval between administration and start of detachment was 2 min. [b] Student's t test comparison with Tablet A; $p < 0.001$. NS = not significant.

The effect of washing on adherence was tested using organ bath II. The preparation was washed with 5 ml of water immediately after administration of the drug. The results are shown in Table III. After washing, the force needed for detachment was only about 30% of that without washing.

Doxycycline has caused most of the reported drug-induced injuries to the esophagus (3, 11). The adherence properties of all doxycycline products at present being marketed in Finland were therfore studied. In addition, two experimental formulations of doxycycline were included in the study. As can be seen from Table IV, there were significant differences between the products. Hard gelatin capsules required the most force to dislodge. In addition, the forces for detachment of experimental formulations G and H were significantly lower than those for the best commercially available products.

In the present study about 60 esophageal preparations from 30 different pigs were used, but no marked interindividual variation was observed. The same preparation could be used for 20–30 consecutive measurements without excessive variation in results. If the mucosa was washed, 50–60 measurements with the same preparation were possible. In the experiments, esophagi stored at 4° in Tyrode solution for 24 hr as well as fresh esophagi were used, but no significant differences between the two were noted. The effect of possible spontaneous esophageal contractions on the detaching force was eliminated by using a large number of n-values (usually $n = 20$).

As can be seen from Figs. 3–4 and Table IV there were significant differences in the tendency for adherence, as between pharmaceutical formulations. The adherent tendency of uncoated potassium chloride tablets and sugar-coated tablets was only about 15–20% that of gelatin capsules. Thus, it is reasonable to try to develop drug products with less tendency to adhere. Large sizes should be avoided, especially in the case of drugs that are known to cause esophageal stricture or ulceration.

REFERENCES

(1) L. Bokey, and T. B. Hugh, *Med. J. Aust.*, **1**, 236 (1975).

(2) T. D. Crowson, L. H. Head, and W. A. Ferrante, *J. Am. Med. Assoc.*, **235**, 2747 (1976).

(3) B. Carlborg, A. Kumlien, and H. Olsson, *Läkartidningen*, **75**, 4609 (1978).

(4) H. Kavin, *Lancet*, **1**, 424 (1977).

(5) H. J. Puhakka, *J. Laryngol. Otol.*, **92**, 927 (1978).

(6) R. Hughes, *Br. Med. J.*, **2**, 132 (1979).

(7) J. Pemberton, *Br. Heart J.*, **32**, 267 (1970).

(8) T. Rosenthal, R. Adar, J. Militianu, and V. Deutsch, *Chest*, **65**, 463 (1974).

(9) J. R. Lambert and A. Newman, *Am. J. Gastroenterol.*, **73**, 508 (1980).

(10) B. Carlborg and O. Densert, *Eur. Surg. Res.*, **12**, 270 (1980).

(11) F. J. Collins, H. R. Matthews, S. E. Barker, and J. M. Strakova, *Br. Med. J.*, **1**, 1679 (1979).

ACKNOWLEDGMENTS

Presented in part at 41st International Congress of Pharmaceutical Sciences (FIP), Vienna, September 1981.

Supported by a grant from the National Research Council for Medical Sciences in Finland.

The authors wish to thank the staff of the Helsinki City Abattoir for their assistance.

Erythrocyte Changes in Aqueous Polyethylene Glycol Solutions Containing Sodium Chloride

TOMIKAZU NISHIO *x, SUMIKO HIROTA ‡, JUNKO YAMASHITA ‡, KIKUE KOBAYASHI ‡, YUKARI MOTOHASHI ‡, and YURIKO KATO ‡

Received November 17, 1980, from the **Research Laboratories, Ohta Pharmaceutical Co., Ltd., 21-25 Namiki 1-chome, Kawaguchishi, Saitama 332, Japan*, and the ‡*Faculty of Pharmaceutical Sciences, Science University of Tokyo, Ichigaya Funagawara-machi, Shinjukuku, Tokyo 162, Japan.* Accepted for publication November 19, 1981.

Abstract □ The behavior of rabbit erythrocytes in aqueous solutions of polyethylene glycol 300 (I) and polyethylene glycol 400 (II) containing sodium chloride was investigated during 2–120 min incubation at 37°. No hemolysis was found in I (0–10.1%) and II (0–12.9%) solutions in the presence of sodium chloride (0.45–1.35%), but prelytic potassium ion loss and changes in the appearance of the erythrocytes proceeded with the passage of time. The potassium ion loss increased with increasing concentration of polyethylene glycol and/or sodium chloride. The mean cellular volume of erythrocytes decreased temporarily (during the first 2 min) in both I (6.7%) and II (8.6%) solutions containing sodium chloride (0.68–1.35%), and then increased progressively to the same value as that determined by solution of sodium chloride at the same concentration but without polyethylene glycol (~30 and 120 min in I and II solutions, respectively). Both I (10.1%) and II (12.9%) induced a stomatocytic transformation of erythrocytes, but at the higher concentrations (0.9–1.35%) of sodium chloride, II accelerated the progress of spontaneous transformation to echinocytes. The results indicate that these solutions were not isotonic with rabbit erythrocytes.

Keyphrases □ Erythrocytes—changes in aqueous polyethylene glycol solutions, sodium chloride □ Sodium chloride—erythrocyte changes in aqueous polyethylene glycol solutions □ Polyethylene glycol—aqueous solutions containing sodium chloride, erythrocyte changes

The hemolysis of rabbit and human erythrocytes occurs in polyethylene glycol even at iso-osmotic concentrations, while the hemolysis is almost completely inhibited in the presence of a suitable amount of sodium chloride (1, 2). However, little is known about the retention of the normal characteristics of erythrocytes in polyethylene glycol solutions containing sodium chloride.

The experiments described deal with the quantitative variations of hemolysis, potassium ion loss, mean cellular volume, and shape of rabbit erythrocytes produced in aqueous polyethylene glycol 300 (I) and polyethylene glycol 400 (II) solutions with reduced sodium chloride content.

EXPERIMENTAL

Materials—Polyethylene glycol 300[1] and 400[1] in reagent grade were used without further purification. All other reagents and chemicals used were reagent grade or high purity.

Preparation of Solutions—The polyethylene glycol and sodium chloride solutions were weight-in-volume percentage preparations, and were adjusted to pH 7.4 by addition of 3 N HCl. Iso-osmotic concentration of polyethylene glycol was estimated by the freezing point depression data.

Preparation of Erythrocyte Suspension—Fresh rabbit (albino) erythrocytes, using heparin (100 U/ml of blood) as an anticoagulant re-

[1] Wako Pure Chemical Industries, Ltd., Osaka, Japan.

0022-3549/82/0900-0977$01.00/0

The effect of washing on adherence was tested using organ bath II. The preparation was washed with 5 ml of water immediately after administration of the drug. The results are shown in Table III. After washing, the force needed for detachment was only about 30% of that without washing.

Doxycycline has caused most of the reported drug-induced injuries to the esophagus (3, 11). The adherence properties of all doxycycline products at present being marketed in Finland were therfore studied. In addition, two experimental formulations of doxycycline were included in the study. As can be seen from Table IV, there were significant differences between the products. Hard gelatin capsules required the most force to dislodge. In addition, the forces for detachment of experimental formulations G and H were significantly lower than those for the best commercially available products.

In the present study about 60 esophageal preparations from 30 different pigs were used, but no marked interindividual variation was observed. The same preparation could be used for 20–30 consecutive measurements without excessive variation in results. If the mucosa was washed, 50–60 measurements with the same preparation were possible. In the experiments, esophagi stored at 4° in Tyrode solution for 24 hr as well as fresh esophagi were used, but no significant differences between the two were noted. The effect of possible spontaneous esophageal contractions on the detaching force was eliminated by using a large number of n-values (usually $n = 20$).

As can be seen from Figs. 3–4 and Table IV there were significant differences in the tendency for adherence, as between pharmaceutical formulations. The adherent tendency of uncoated potassium chloride tablets and sugar-coated tablets was only about 15–20% that of gelatin capsules. Thus, it is reasonable to try to develop drug products with less tendency to adhere. Large sizes should be avoided, especially in the case of drugs that are known to cause esophageal stricture or ulceration.

REFERENCES

(1) L. Bokey, and T. B. Hugh, *Med. J. Aust.*, **1**, 236 (1975).

(2) T. D. Crowson, L. H. Head, and W. A. Ferrante, *J. Am. Med. Assoc.*, **235**, 2747 (1976).

(3) B. Carlborg, A. Kumlien, and H. Olsson, *Läkartidningen*, **75**, 4609 (1978).

(4) H. Kavin, *Lancet*, **1**, 424 (1977).

(5) H. J. Puhakka, *J. Laryngol. Otol.*, **92**, 927 (1978).

(6) R. Hughes, *Br. Med. J.*, **2**, 132 (1979).

(7) J. Pemberton, *Br. Heart J.*, **32**, 267 (1970).

(8) T. Rosenthal, R. Adar, J. Militianu, and V. Deutsch, *Chest*, **65**, 463 (1974).

(9) J. R. Lambert and A. Newman, *Am. J. Gastroenterol.*, **73**, 508 (1980).

(10) B. Carlborg and O. Densert, *Eur. Surg. Res.*, **12**, 270 (1980).

(11) F. J. Collins, H. R. Matthews, S. E. Barker, and J. M. Strakova, *Br. Med. J.*, **1**, 1679 (1979).

ACKNOWLEDGMENTS

Presented in part at 41st International Congress of Pharmaceutical Sciences (FIP), Vienna, September 1981.

Supported by a grant from the National Research Council for Medical Sciences in Finland.

The authors wish to thank the staff of the Helsinki City Abattoir for their assistance.

Erythrocyte Changes in Aqueous Polyethylene Glycol Solutions Containing Sodium Chloride

TOMIKAZU NISHIO *x, SUMIKO HIROTA ‡, JUNKO YAMASHITA ‡, KIKUE KOBAYASHI ‡, YUKARI MOTOHASHI ‡, and YURIKO KATO ‡

Received November 17, 1980, from the **Research Laboratories, Ohta Pharmaceutical Co., Ltd., 21-25 Namiki 1-chome, Kawaguchishi, Saitama 332, Japan*, and the ‡*Faculty of Pharmaceutical Sciences, Science University of Tokyo, Ichigaya Funagawara-machi, Shinjukuku, Tokyo 162, Japan.* Accepted for publication November 19, 1981.

Abstract □ The behavior of rabbit erythrocytes in aqueous solutions of polyethylene glycol 300 (I) and polyethylene glycol 400 (II) containing sodium chloride was investigated during 2–120 min incubation at 37°. No hemolysis was found in I (0–10.1%) and II (0–12.9%) solutions in the presence of sodium chloride (0.45–1.35%), but prelytic potassium ion loss and changes in the appearance of the erythrocytes proceeded with the passage of time. The potassium ion loss increased with increasing concentration of polyethylene glycol and/or sodium chloride. The mean cellular volume of erythrocytes decreased temporarily (during the first 2 min) in both I (6.7%) and II (8.6%) solutions containing sodium chloride (0.68–1.35%), and then increased progressively to the same value as that determined by solution of sodium chloride at the same concentration but without polyethylene glycol (~30 and 120 min in I and II solutions, respectively). Both I (10.1%) and II (12.9%) induced a stomatocytic transformation of erythrocytes, but at the higher concentrations (0.9–1.35%) of sodium chloride, II accelerated the progress of spontaneous transformation to echinocytes. The results indicate that these solutions were not isotonic with rabbit erythrocytes.

Keyphrases □ Erythrocytes—changes in aqueous polyethylene glycol solutions, sodium chloride □ Sodium chloride—erythrocyte changes in aqueous polyethylene glycol solutions □ Polyethylene glycol—aqueous solutions containing sodium chloride, erythrocyte changes

The hemolysis of rabbit and human erythrocytes occurs in polyethylene glycol even at iso-osmotic concentrations, while the hemolysis is almost completely inhibited in the presence of a suitable amount of sodium chloride (1, 2). However, little is known about the retention of the normal characteristics of erythrocytes in polyethylene glycol solutions containing sodium chloride.

The experiments described deal with the quantitative variations of hemolysis, potassium ion loss, mean cellular volume, and shape of rabbit erythrocytes produced in aqueous polyethylene glycol 300 (I) and polyethylene glycol 400 (II) solutions with reduced sodium chloride content.

EXPERIMENTAL

Materials—Polyethylene glycol 300[1] and 400[1] in reagent grade were used without further purification. All other reagents and chemicals used were reagent grade or high purity.

Preparation of Solutions—The polyethylene glycol and sodium chloride solutions were weight-in-volume percentage preparations, and were adjusted to pH 7.4 by addition of 3 N HCl. Iso-osmotic concentration of polyethylene glycol was estimated by the freezing point depression data.

Preparation of Erythrocyte Suspension—Fresh rabbit (albino) erythrocytes, using heparin (100 U/ml of blood) as an anticoagulant re-

[1] Wako Pure Chemical Industries, Ltd., Osaka, Japan.

0022-3549/82/0900-0977$01.00/0

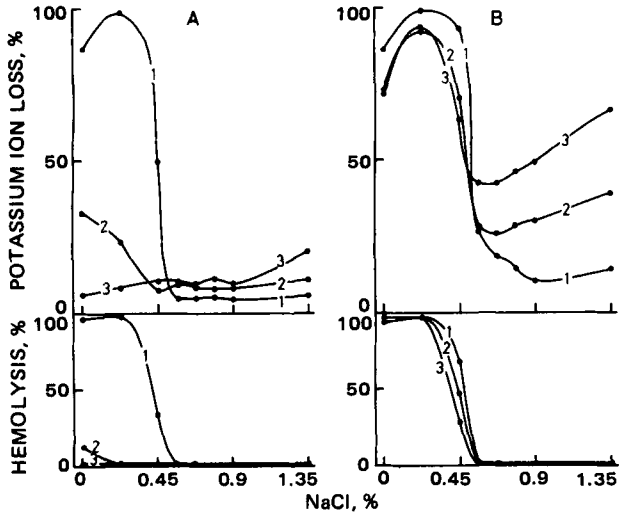

Figure 1—*The percent release of potassium ion (A, B upper) and hemoglobin (A, B lower) from rabbit erythrocytes in I–sodium chloride solutions in various proportions after incubation for 2 min (A) and 120 min (B) at 37°. Curves 1–3 represent the percent release in I (0, 6.7, and 10.1%, respectively) solutions. Each point is the mean value of three observations.*

agent, were washed three times with a chilled 0.9% NaCl solution to remove plasma and the buffy coat and resuspended at 80% hematocrit in the same solution.

Erythrocyte Incubation—To a mixture of 1 ml of polyethylene glycol solution (0–10.1% for I and 0–12.9% for II in the final medium) and 1 ml of NaCl solution (0–1.35% in the final medium), 0.5 ml of erythrocyte suspension (hematocrit value 80%) was added and mixed immediately. The mixture was incubated for a certain period (up to 120 min) at 37°, and an aliquot was withdrawn from the suspension and analyzed for the mean cellular volume and morphology of erythrocytes. The remaining suspension was centrifuged at 2000×*g* for 3 min, and both hemoglobin and potassium ion in the supernate were quantitatively determined. The degree of hemoglobin loss (hemolysis) and potassium ion loss were expressed as a percentage of their total losses induced by an aqueous saponin solution (100 mg/liter).

Estimation of Mean Cellular Volume—The mean volume of erythrocytes was calculated from the total cell volume, which was determined by the microhematocrit method and from the number of erythrocytes determined with a micro cell counter[2].

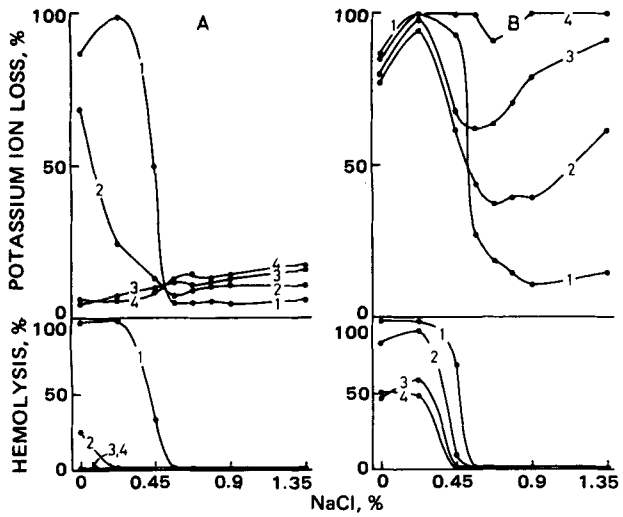

Figure 2—*The release percentage of potassium ion (A, B upper) and hemoglobin (A, B lower) from rabbit erythrocytes in II–sodium chloride solutions in various proportions after incubation for 2 min (A) and 120 min (B) at 37°. Curves 1–4 represent the percent release in II (0, 4.3, 8.6, and 12.9%, respectively) solutions. Each point is the mean value of three observations.*

[2] Model CC-107, Toa Medical Electronics Co., Ltd., Kobe, Japan.

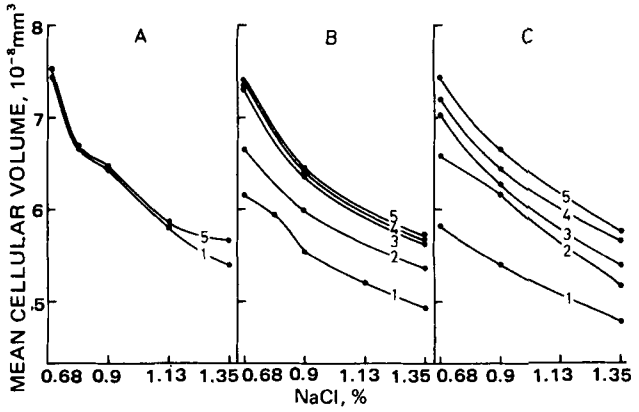

Figure 3—*The mean cellular volume of rabbit erythrocytes in the aqueous solutions of sodium chloride (A), 6.7% I–sodium chloride (B), and 8.6% II–sodium chloride (C) at 37°. Curves 1–5 represent the mean cellular volume after incubation for 2, 10, 30, 60, and 120 min, respectively. Each point is the mean value of three observations.*

Morphological Study of Erythrocytes with Scanning Electron Microscopy—Erythrocytes were fixed in 2.5% glutaraldehyde by standing overnight, followed by treatment in 2% osmium tetroxide for 2 hr in an isotonic phosphate-buffered saline solution (pH 7.4). The erythrocytes were dehydrated in a graded series of ethanol and air dried, followed by coating with gold–palladium alloy with an ion coater[3]. The erythrocytes were observed and photographed with a scanning electron microscope[4]. Morphology was defined according to Bessis' classification (3).

Determination of Hemoglobin (4)—The hemolyzates were added to ferricyanide–cyanide reagent, and the pigments were converted to cyanomethemoglobin. Their optical densities were analyzed with a spectrophotometer[5] at 540 nm.

Determination of Potassium Ion—Before measurements, proteins present in the hemolyzates were precipitated by boiling for 10 min and centrifuged. Potassium ion in the supernate was determined with an atomic absorption spectrophotometer[6] (air acetylene flame).

Measurement of Freezing Point Depression—The freezing point depression measurement was made on aqueous solutions of I and II by means of an osmometer[7].

RESULTS

Hemolysis and Potassium Ion Loss—Figures 1 and 2 show the release percentage of hemoglobin (hemolysis) and potassium ion from rabbit erythrocytes in various I and II solutions, respectively, with reduced content of sodium chloride at 37°.

After 2 min of incubation in I (Fig. 1A) and II (Fig. 2A) solutions with 0–0.45% NaCl, the percentage of hemolysis and potassium ion loss decreased with increased concentration of polyethylene glycol, and no loss occurred at iso- (I: 6.7%; II: 8.6%) or hyperosmotic concentration of polyethylene glycol. This finding was similar to that obtained for sodium chloride. Sodium chloride (>0.45%) prevented both the hemolysis and the potassium ion loss, regardless of the concentration of polyethylene glycol.

During a period from 2 to 120 min (I: Fig. 1B; II: Fig. 2B) at 0–0.45% NaCl, both hemolysis and potassium ion loss proceeded even at iso- or hyperosmotic concentration of polyethylene glycol (more rapidly in I than II solution) in contrast to the degree of hemolysis remaining unchanged for sodium chloride. At 0.45–1.35% NaCl, no hemolysis occurred, but potassium ion loss occurred depending upon the concentration of polyethylene glycol (remarkably in II solution). Furthermore the loss increased with increase of the concentration of sodium chloride. A minimal loss occurred at 0.6% NaCl.

Mean Cellular Volume of Erythrocytes—Figure 3 shows the mean cellular volumes of erythrocytes in solutions of I (6.7%) and II (8.6%) containing various concentrations of sodium chloride at 37°. Erythrocyte occupied a mean cellular volume of 6.4×10^{-8} mm^3 in 0.9% NaCl solution.

[3] Model IB-3, Eiko Engineering Co., Ltd., Ibaragi, Japan.
[4] Model Hitachi-Akashi MSM-4, Akashi Seisakusho Ltd., Tokyo, Japan.
[5] Model UV-VIS 193, Hitachi Ltd., Tokyo, Japan.
[6] Model 503, Perkin-Elmer Ltd., Norwalk, Conn.
[7] Model Osmette 2007, Precision Systems Inc., Sudbury, Mass.

Table I—The Distribution of Rabbit Erythrocyte Shapes[a] in Polyethylene Glycol–Sodium Chloride Solutions

Medium Composition, %	After 2-min Incubation, %			After 120-min Incubation, %		
	Stomatocyte	Discocyte	Echinocyte	Stomatocyte	Discocyte	Echinocyte
0.6 NaCl	3.3	82.6	14.1	2.0	64.8	33.2
0.9 NaCl	2.3	75.8	21.9	1.0	60.9	38.0
1.35 NaCl	8.5	79.2	12.4	0.5	37.6	62.0
10.1 I + 0.6 NaCl	4.4	91.2	4.4	6.4	86.6	7.0
10.1 I + 0.9 NaCl	7.6	90.7	1.7	8.6	70.4	21.0
10.1 I + 1.35 NaCl	24.8	65.2	9.9	11.0	38.2	50.9
12.9 II + 0.6 NaCl	39.5	60.1	0.4	5.4	89.8	4.8
12.9 II + 0.9 NaCl	29.1	69.6	1.4	11.7	44.5	43.8
12.9 II + 1.35 NaCl	31.2	62.8	6.0	3.5	21.5	75.0

[a] The percentage of each cell type (stomatocyte, discocyte, and echinocyte) was estimated in three fields of scanning electron micrograph each containing between 100 and 200 cells/field.

The value increased to 7.53×10^{-8} mm^3 in 0.68% NaCl solution or decreased to 5.39×10^{-8} mm^3 in 1.35% NaCl solution within 2 min. After that, each value remained unchanged. In polyethylene glycol–sodium chloride solutions, the mean cellular volume decreased temporarily and then increased progressively to the same value as that determined by solution of sodium chloride at the same concentration but without polyethylene glycol. It took ~30 and 120 min in I and II, respectively, to reach this stage.

Shape of Erythrocytes—Table I shows the distribution of erythrocyte shapes after a certain period of incubation at 37° in I (10.1%)–, or II (12.9%)–sodium chloride solutions. Both I and II slightly induced cup-formed erythrocytes (stomatocytic transformation) on 2-min incubation. On prolonged incubation the progressive echinocytic transformation was observed with all the solutions examined. After 120 min of incubation, the presence of I retarded the echinocytic transformation regardless of sodium chloride content. II also retarded the transformation at a low concentration (0.6%) of sodium chloride, whereas it accelerated it at a high concentration (0.9–1.35%) of sodium chloride.

DISCUSSION

A previous study (1) reported that sodium chloride prevented hemolysis in polyethylene glycol 200 (≤25%) or I (≤40%) solutions. The present investigation also indicates that ≥0.45% concentration of sodium chloride prevented almost completely the hemolysis of rabbit erythrocyte in I or II solutions, but did not prevent prelytic potassium ion loss, mean cellular volume change, and shape change. In addition, the present experimental data showed that the time course of these erythrocyte changes could be divided into the first phase which occurred during the first 2 min, and the second phase which occurred during further incubation. For example, as shown in Fig. 1 (Curves 2 and 3) and Fig. 2 (Curves 2–4), hemolysis and potassium ion loss in the first phase were prevented in the polyethylene glycol solutions with a small amount of sodium chloride (0–0.45%), while in the second phase it proceeded gradually. Similarly, it was reported (5, 6) that red cells were hemolyzed in hypotonic electrolyte solutions in two phases: an early fast phase due to rapid water entry followed by a slow phase. The time course of hemolysis in the polyethylene glycol solutions was approximately the same as that for the hypotonic electrolyte solutions except that the reaction (for the polyethylene glycol solutions) proceeded more rapidly in the second phase. The process of cellular volume change was also divided into two phases in the polyethylene glycol solutions containing sodium chloride (Fig. 3). In the first phase the mean cellular volume decreased temporarily, as if erythrocytes were placed in the solution in which polyethylene glycol exerted osmotic pressure as well as sodium chloride (Curve 1, Fig. 3). In the second phase the mean cellular volume increased progressively to the same value as that determined by solution of sodium chloride, at the same concentration but without polyethylene glycol (Curves 2–5, Fig. 3). This may be explained from the viewpoint of osmotic support. In the first phase polyethylene glycol acts as an osmotic particle, since most polyethylene glycol molecules remain outside the erythrocyte membrane, while in the second phase the osmotic pressure decreases gradually as they penetrate the membrane.

The potassium ion loss occurred at both hypo- and hypertonic concentration of polyethylene glycol and sodium chloride, and increased with increase in the concentration of polyethylene glycol and/or sodium chloride. This result suggests that polyethylene glycol disturbs the erythrocyte membranes and produces the prelytic potassium ion loss. Discoloration of rabbit erythrocytes has previously occurred at high concentration (>15%) of polyethylene glycol (1). The discoloration also indicates the damage of the cell membranes by polyethylene glycol. Both polyethylene glycol and sodium chloride exert osmotic pressure in the first phase, and such a high osmotic pressure may accelerate the potassium ion loss.

Polyethylene glycol exerted an influence upon the spontaneous transformation of erythrocyte shape to echinocyte, which was said to result from ATP depletion of erythrocytes by incubation (7). This mechanism, however, is yet unclear.

Observation of the behavior of erthrocytes that are suspended in a solution is the direct procedure for determining whether the solution is isotonic, hypotonic, or hypertonic. If the cells retain their normal characteristics, the solution is isotonic (8). The present investigation evaluates the tonicity of polyethylene glycol–sodium chloride solutions. The I and II solutions containing 0.6% NaCl are the most isotonic, because both the prelytic potassium ion loss and the transformation of erythrocyte shape (discocyte: 86.6% in I; 89.9% in II) were relatively inhibited by addition of 0.6% NaCl. Whereas, on the basis of mean cellular volume data (9), the I or II solution containing 0.9% NaCl is the most isotonic, because the mean cellular volume in this solution was the same as in 0.9% NaCl (after incubation for 120 min). An isotonic solution consisting of polyethylene glycol and sodium chloride was not obtained at any concentration of sodium chloride.

Because rabbit erythrocytes were employed in the present investigation, a quantitative transfer of the experimental data to a human erythrocyte system is not possible, however it may be expected that the data apply qualitatively.

A conclusion drawn from this experiment for rabbit erythrocytes was that hemolysis did not occur in I and II solutions with ≥0.45% NaCl, but prelytic potassium ion loss, mean cellular volume change, and shape transformation were observed. Therefore, these solutions were not isotonic.

REFERENCES

(1) B. L. Smith and D. E. Cadwallader, *J. Pharm. Sci.*, **56**, 351 (1967).

(2) E. R. Hammarlund and G. L. Van Pevenage, *ibid.*, **55**, 1448 (1966).

(3) M. Bessis, in "Red Cell Shape," M. Bessis, R. I. Weed, and P. F. Leblond, Eds., Springer-Verlag, New York, N.Y., 1973, pp. 1–25.

(4) E. Beutler, in "Red Cell Metabolism: A Manual of Biochemical Methods," 2nd ed., Grune and Stratton, New York, N.Y., 1975, pp. 8–18.

(5) A. J. Bowdler and T. K. Chan, *J. Physiol. (London)*, **201**, 437 (1969).

(6) T. K. Chan, P. L. La Celle, and R. I. Weed, *J. Cell Physiol.*, **85**, 47 (1975).

(7) M. Nakao, T. Nakao, S. Yamazoe, and H. Yoshikawa, *J. Biochem.*, **49**, 487 (1961).

(8) D. L. Deardorff, in "Remington's Pharmaceutical Sciences," 15th ed., J. E. Hoover, Ed., Mack Publishing Co., Easton, Pa., 1975, pp. 1405–1412.

(9) I. Setnikar and O. Temelcou, *J. Am. Pharm. Assoc. Sci. Ed.*, **48**, 628 (1959).

Anthralin: Chemical Instability and Glucose-6-phosphate Dehydrogenase Inhibition

DANIEL CAVEY ˣ, JEAN-CLAUDE CARON, and BRAHAM SHROOT

Received June 19, 1981, from the *Centre International de Recherches Dermatologiques, Sophia-Antipolis, F-06565 VALBONNE Cédex, France.* Accepted for publication November 20, 1981.

Abstract □ The chemical stability of the antipsoriatic drug, anthralin (1,8-dihydroxy-9-anthrone), in solution has been studied using high-performance liquid chromatographic analysis. The time course for decomposition in solution has been correlated with that of the inhibition of glucose-6-phosphate dehydrogenase, one of the most widely documented biochemical properties associated with anthralin. Solutions of anthralin in aqueous buffer (37°, pH 7.5, under light protection) decomposed completely within 4 hr giving the 10,10′-dimer (40%), no detectable 1,8-dihydroxy-9,10-anthraquinone, and a greatly increased potency of inhibition of glucose-6-phosphate dehydrogenase. This increased inhibitory potency could not be explained by formation of the dimer which, like anthralin and its quinone, were shown to be only weak inhibitors of the enzyme. In acetone solution exposed to light and air, anthralin decomposed completely within 4 days, in part *via* the dimer as intermediate. The final solution had the characteristic color of anthralin-brown, contained the quinone (20%), and like decomposed aqueous solutions of anthralin, completely inhibited glucose-6-phosphate dehydrogenase. The results show that neither anthralin, nor either of its two identified decomposition products, is the potent toxic species against glucose-6-phosphate dehydrogenase.

Keyphrases □ Anthralin—chemical instability and glucose-6-phosphate dehydrogenase inhibition □ High-performance liquid chromatography—chemical instability and glucose-6-phosphate dehydrogenase inhibition of anthralin □ Decomposition—anthralin, chemical instability and glucose-6-phosphate dehydrogenase inhibition

Anthralin (1,8-dihydroxy-9-anthrone, I) has been used successfully for over 60 years in the topical treatment of psoriasis (1–3). However, this treatment suffers from two main disadvantages: staining and irritation of the skin (4). It is well known that anthralin is unstable in solution and, depending on the conditions, can present a complex mixture of products and colors which have as their endpoint anthralin-brown (4, 5).

In view of this chemical instability, the *in vitro* biological properties which have been attributed to anthralin itself might, in fact, be related to some of its decomposition products. Furthermore, the therapeutic action and side effects following topical application of anthralin might result from the decomposition of this molecule into other chemical species having in turn antipsoriatic, irritating, and staining properties. Several attempts have been made to study the behavior of some known breakdown products in test systems which are claimed to give some indication of antipsoriatic or potentially toxic properties (6–8). Despite interest in the subject, little is known about which compounds play a major role in the action of this drug.

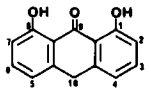

I

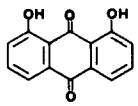

II

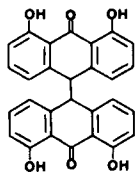

III

In a reinvestigation of anthralin, the first objective was to evaluate the stability of the molecule, particularly in a physiological buffer, using high-performance liquid chromatography (HPLC), and to relate the findings to one of the most widely documented biochemical properties attributed to anthralin itself: the inhibition of glucose-6-phosphate dehydrogenase (9, 10, and references therein)[1].

EXPERIMENTAL

Chemicals—The following chemicals were analytical grade reagents[2]: 2-[4-(2-hydroxyethyl)-1-piperazinyl]ethanesulfonic acid, iso-octane, diisopropyl ether, methanol, ethanol, 1-butanol, 1,3-butanediol, acetone, acetonitrile, 2-butanone, dimethylformamide, 1-propanol, 2-propanol, and acetic acid. 2-Butanol, tetrahydrofuran, and 1,4-dioxane were chromatographic grade[3]. 1,8-Dihydroxy-9-anthrone (anthralin/dithranol, I)[4] was purified by column chromatography (6). 1,8-Dihydroxy-9,10-anthraquinone (quinone, II) and bi(1,8-dihydroxy-9-anthron-10-yl) (dimer, III) were synthesized[5] following published procedures (7).

Enzymological studies were performed using pure yeast glucose-6-phosphate dehydrogenase[6], with glucose-6-phosphate and nicotinamide adenine dinucleotide phosphate as substrate and coenzyme, respectively[7]. All other chemicals were pure grade reagents[8].

High-Performance Liquid Chromatography—Analysis of anthralin and its derivatives was performed on an HPLC system[9] set at 254 nm (reference at 500 nm), and equipped with a reversed-phase 25-cm column[10], following the analytical conditions developed in this laboratory (11). In all experiments, samples (15 μl, either aqueous or organic solutions) were injected directly into the chromatographic system without previous solvent extraction.

Measurements of Glucose-6-phosphate Dehydrogenase Activity—All incubation experiments of glucose-6-phosphate dehydrogenase with anthralin and its derivatives were performed in a Ringer buffer composed of 140 m*M* NaCl, 5.2 m*M* KCl, 2.8 m*M* $CaCl_2$, 1.3 m*M* $MgSO_4$, and 20 m*M* 2-[4-(2-hydroxyethyl)-1-piperazinyl]ethanesulfonic acid at pH 7.5. In this buffer, the enzymatic activity remained almost constant over a 2-hr period at 37°. Before starting the experiments, the commercial enzyme suspension was diluted 300-fold in cold Ringer buffer and kept at 0°.

Time Course of the Influence of Anthralin, Dimer, and Quinone on

[1] This study was presented in part at the "Anthralin Symposium" Sophia-Antipolis, France, Oct. 1980.
[2] Merck.
[3] Carlo Erba.
[4] Bayer.
[5] Laboratoires de Recherches Fondamentales, L'Oréal, Aulnay-sous-Bois, France.
[6] Enzyme Commission Number 1.1.1. 49, yeast enzyme, grade II, Boehringer.
[7] Boehringer.
[8] Prolabo.
[9] Model 1084 B. Hewlett-Packard.
[10] Merck Lichrosorb RT 250-4/5 μm/RP 18.

0022-3549/82/0900-0980$01.00/0

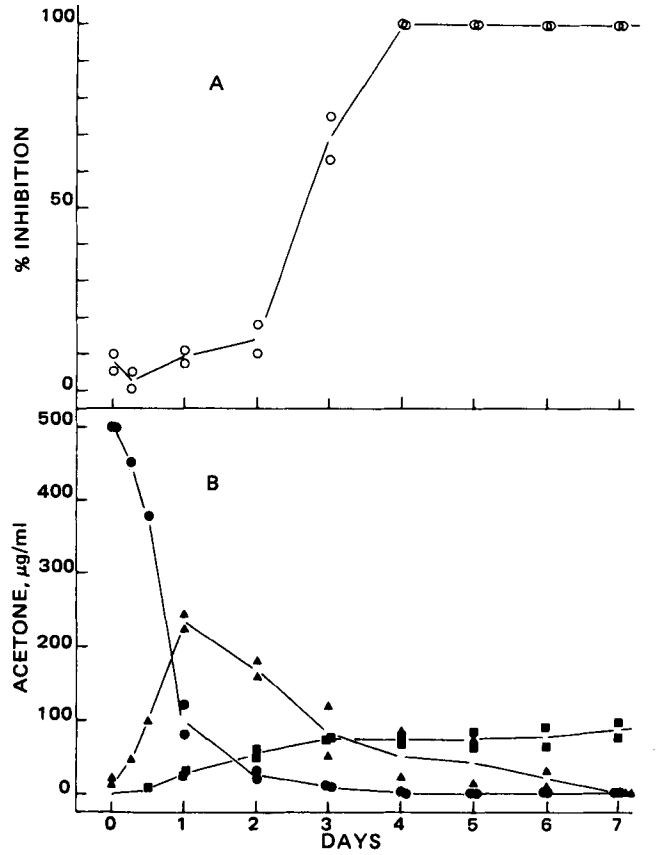

Figure 1—*Time course of the decomposition of anthralin in acetone (initial concentration = 0.5 mg/ml = 2.2 mM, 25°, continuous exposure to artificial light): inhibitory potency against glucose-6-phosphate dehydrogenase (A) and chemical composition of the medium as assayed by HPLC (B). Key: (○) percent of inhibition obtained by incubating the enzyme with 1% of the acetone solution for 5 min; (●) concentration of anthralin; (▲) concentration of dimer; (■) concentration of quinone.*

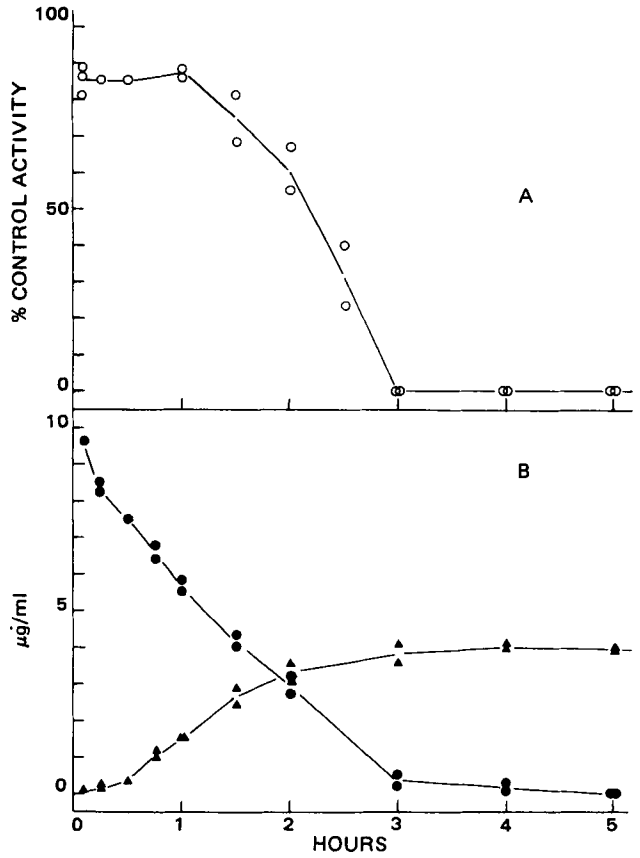

Figure 2—*Activity of glucose-6-phosphate dehydrogenase as a function of time of incubation with a solution of anthralin (A) (10 μg/ml in 1% acetone–Ringer buffer, pH 7.5, 37°, light protection), and the concurrent chemical composition of the medium, as determined by HPLC (B). Key: (○) percent of control enzymatic activity (the enzyme and anthralin were added at time zero); (●) concentration of anthralin; (▲) concentration of dimer.*

the Activity of Glucose-6-phosphate Dehydrogenase—The incubation medium (final volume = 3 ml) consisted of 2.92 ml of Ringer buffer, 50 μl of enzyme solution, and 30 μl of a 1 mg/ml solution of anthralin, dimer, or quinone in acetone to give a final concentration of 10 μg/ml in the incubation medium. Two test solutions and one control solution (to which acetone alone had been added) were kept for each specified time period at 37° in a water bath under light protection. The first test solution was then immediately analyzed by HPLC. To the second test solution and its control was added 50 μl of 10 m*M* nicotinamide adenine dinucleotide phosphate (final concentration 0.17 m*M* = 3 K_m under the present conditions)[11] and 50 μl of 18.6 m*M* glucose-6-phosphate (final concentration 0.31 m*M* = 3 K_m)[11], and the appearance of reduced nicotinamide adenine dinucleotide phosphate was immediately measured by its optical density at 340 nm at 37°[12].

At time zero of incubation, the control activity in the incubation medium (expressed as the variation of optical density per minute) was 0.21–0.23 ΔOD/min. Due to the presence of 1% acetone, this control activity decreased with increasing incubation time (to 50% of initial activity after 5 hr of incubation). To eliminate this unspecific solvent effect, each determination of the activity in the presence of anthralin or derivatives was corrected using the control activity in the presence of acetone alone at the same incubation time.

Time Course of Decomposition in Ringer Buffer and Inhibition of Glucose-6-phosphate Dehydrogenase—Duplicate solutions (30 μl of 1 mg anthralin/ml of acetone added to 2.92 ml of Ringer buffer) were kept for each selected time period at 37° in a water bath under light protection. To one solution, 50 μl of enzyme solution was then added and the solution (final volume = 3 ml, theoretical anthralin concentration 10 μg/ml = 44.2 μ*M*) maintained under light protection at 37° for an additional 5-min period. Enzymatic activity was measured as described earlier. To the second solution, 50 μl of enzyme solution was added and the mixture immediately analyzed by HPLC as described previously.

Time Course of Decomposition in Acetone and Inhibition of Glucose-6-phosphate Dehydrogenase—Anthralin was dissolved in acetone to a final concentration of 0.5 mg/ml. The solution was continuously exposed to air and artificial light[13] at 25° for a period of up to 1 week. At selected times the chemical composition of the medium was analyzed by HPLC, and its inhibitory potency against the enzyme was assessed by adding 30 μl of the acetone solution to a mixture of 2.92 ml of Ringer buffer and 50 μl of enzyme solution. The medium (final volume = 3 ml, theoretical anthralin concentration 5 μg/ml = 22.1 μ*M*) was maintained in a water bath at 37° for 5 min, and the enzymatic activity determined as described earlier.

RESULTS AND DISCUSSION

Selection of a Ringer Buffer–Solvent System—Despite the presence of the polar groups at C-1, C-8, and C-9, the anthralin molecule is quite lipophilic in nature. Consequently, an aqueous solution of anthralin (suitable for enzymological studies) must be prepared by adding a small volume of a concentrated solution of anthralin in an organic solvent to the aqueous medium. The criteria for a suitable organic solvent were solubility and relative stability of anthralin, water miscibility, and compatibility with the enzyme. Acetone was selected as the most suitable solvent (Table I). Stock solutions of anthralin (0.5 mg/ml or 1 mg/ml) in acetone could be used within 3 hr following the preparation.

The chemical decomposition of anthralin in acetone (0.5 mg/ml) was investigated over a 1-week period (Fig. 1B)[14]. At 25°, continuous exposure

[11] Under the present conditions (*i.e.*, Ringer buffer at pH 7.5 and 37°), the apparent Michaelis constants of glucose-6-phosphate and nicotinamide adenine dinucleotide phosphate were determined and found to be 0.1 m*M* and 0.05 m*M*, respectively.

[12] Model UV 25 spectrophotometer, Beckman.

[13] Mazda lamp, 75 watts.

[14] In all figures presented in this paper, each point is representative of one experiment.

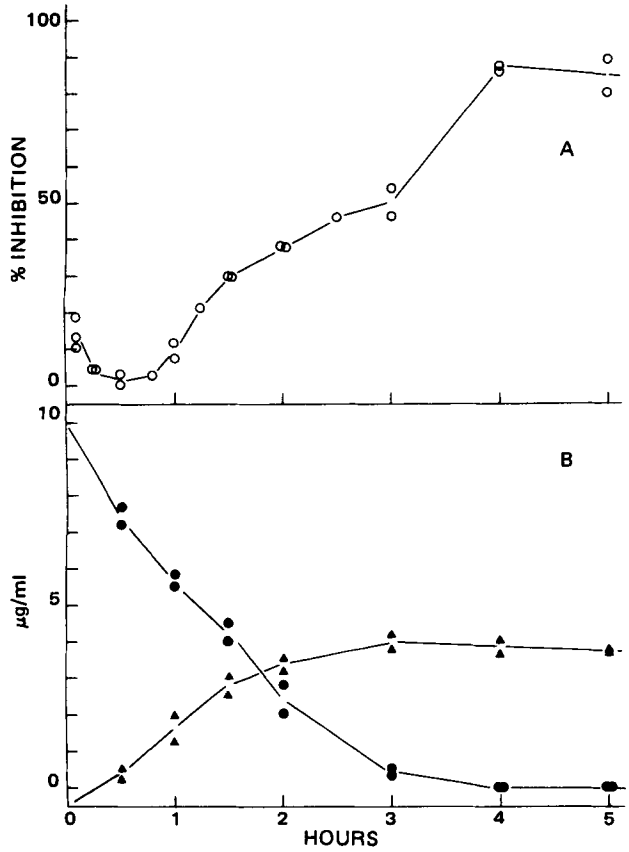

Figure 3—*Time course of the decomposition of anthralin in aqueous buffer (initial concentration = 10 µg/ml in 1% acetone–Ringer buffer, pH 7.5, 37°, light protection): inhibitory potency against glucose-6-phosphate dehydrogenase (A) and chemical composition of the medium as assayed by HPLC (B). Key: (○) percent of inhibition obtained by incubating the enzyme with the medium for 5 min; (●) concentration of anthralin; (▲) concentration of dimer.*

of the solution to light led to the decomposition of anthralin, in part *via* the dimer, and gave a final solution containing 20% quinone and having the characteristic color of anthralin-brown. For the studies in aqueous buffer, a 1% acetone–Ringer buffer system, in which the enzyme compatibility was even better than at 2% (Table I), was finally selected.

Time Dependence of Decomposition of Anthralin with Enzyme—The time dependence of the decomposition of anthralin in Ringer buffer and of the inhibition of glucose-6-phosphate dehydrogenase with enzyme present in the medium is as follows: Anthralin is unstable in aqueous solution at pH 7.5, irrespective of the organic solvent vehicle. When kept in 1% acetone–Ringer buffer at 37° under light protection, anthralin completely decomposed within 4 hr (Fig. 2B), undergoing, in part, oxidation to the dimer (40%), but not to detectable quantities of its quinone. The presence of glucose-6-phosphate dehydrogenase did not influence this process, since very similar results were obtained either in the presence (Fig. 2B) or in the absence (Fig. 3B) of enzyme in the Ringer buffer solution.

The corresponding time course of inhibition of glucose-6-phosphate dehydrogenase by anthralin (at its upper limit of solubility of 10 µg/ml) showed an initial slight inhibition (~15%) (Fig. 2A) which was rapidly established and lasted for ~1 hr, followed by an increasing inhibition, which was complete after 3 hr of incubation. Therefore, it was intriguing to speculate why enzyme inhibition should be initially maintained and then increased to reach its maximum over a 3-hr period, since HPLC analysis showed that anthralin was 25% degraded even after 30 min. The maintenance of the level of enzyme inhibition during the first phase could indicate that anthralin interacted slightly but irreversibly with the enzyme.

The second, slowly rising phase could be explained by the breakdown of anthralin into highly toxic species, which were responsible for the total destruction of enzymatic activity. Since the dimer was formed, it could have been suspected as being the highly toxic anthralin derivative. A solution of pure dimer (10 µg/ml = 22.1 µ*M*) was prepared in 1% acetone–Ringer buffer, at pH 7.5 and kept at 37° under light protection in the presence of the enzyme. At selected intervals, the composition of the medium was determined and the enzymatic activity was measured. The dimer was essentially stable over 2 hr (Fig. 4B) and caused only a modest, stable inhibition (10–20%) of glucose-6-phosphate dehydrogenase (Fig. 4A). Similar results were obtained with pure quinone (10 µg/ml, not shown).

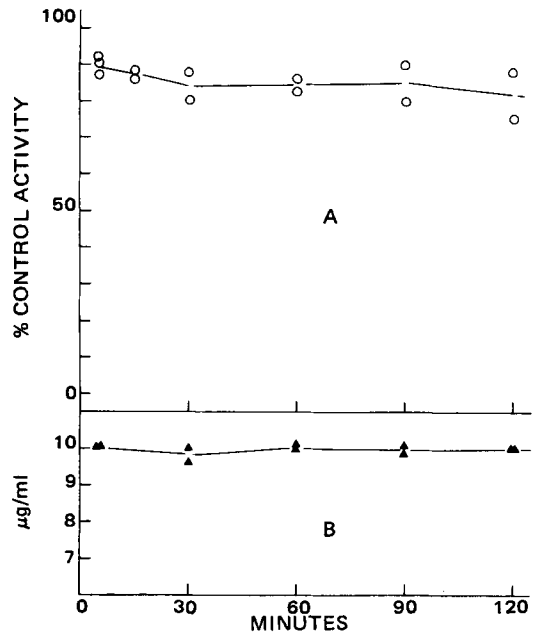

Figure 4—*Activity of glucose-6-phosphate dehydrogenase as a function of time of incubation with a solution of dimer (A) (10 µg/ml in 1% acetone–Ringer buffer, pH 7.5, 37°, light protection), and the concurrent chemical composition of the medium, as assayed by HPLC (B). Key: (○) percent of control enzymatic activity (the enzyme and dimer were added at time zero); (▲) concentration of dimer.*

These results demonstrate that the dramatic inhibition of glucose-6-phosphate dehydrogenase by anthralin solutions cannot be explained by the formation of dimer (40%), and suggest that one (or more) other unidentified breakdown products must be the toxic species. These breakdown products could not be detected under the present analytical conditions.

Time Dependence of Decomposition of Anthralin without Enzyme—The time dependence of the decomposition of anthralin in Ringer buffer, without enzyme and the inhibitory potency of the medium against glucose-6-phosphate dehydrogenase is as follows: Solutions of anthralin

Table I—Stability Properties of Anthralin in Pure Solvents and Compatibility of Solvent with Glucose-6-phosphate Dehydrogenase

Solvent	Stability[a]	Enzyme Compatibility[b] (percent solvent)
Methanol	– –	
1-Propanol	– –	ND[c]
1,3-Butanediol	– –	
Dimethylformamide	– –	
Ethanol	–	2
2-Propanol	–	1
1-Butanol	–	0
Tetrahydrofuran	–	0
2-Butanol	+	0
1,4-Dioxane	+	1
Acetonitrile	+	1
Acetone	++	2
2-Butanone	++	1
Acetic acid	++	0

[a] After 3 hr of exposure to day light at room temperature, the percentage of initial anthralin (0.5 mg/ml solvent) which has decomposed is >15% (– –), between 5 and 15% (–), between 1 and 5% (+), <1% (++). [b] Enzyme compatibility with solvent is expressed as the maximum percentage of solvent in the incubation medium, for which <10% of initial enzymatic activity is lost after 30 min of incubation at 37°. [c] Not done.

in 1% acetone–Ringer buffer (10 μg/ml) were left for appropriate periods at 37° under light protection in the absence of enzyme. The enzyme inhibitory potency of the aged solutions was assayed by adding glucose-6-phosphate dehydrogenase for an additional incubation period of 5 min.

The results shown in Fig. 3 indicate that the gradual disappearance of anthralin during the first 30 min was responsible for the concomitant decrease in the enzyme inhibitory potency of the solution. The reappearance of a stronger inhibitory activity, however, is in striking contrast with the complete degradation of anthralin which occurred during the following 2–3 hr and, as already noted, could not be attributed to the formation of the dimer.

Similarly, when anthralin was left in acetone (0.5 mg/ml) for several days under continuous exposure to light (Fig. 1), the final dark brown solution, which was totally devoid of anthralin or dimer, showed a strong toxicity against glucose-6-phosphate dehydrogenase (Fig. 1A). Incubation of 1% of the acetone solution with the enzyme in Ringer buffer (5 min) resulted in a total destruction of enzymatic activity, which could not be explained by the presence of quinone.

CONCLUSION

Using a highly sensitive and reproducible HPLC assay, additional evidence has been given for the chemical instability of anthralin in solution, particularly aqueous media. In acetone solution over long periods, anthralin decomposes, in part *via* the dimer, to give a final solution containing 20% quinone. In aqueous media at pH 7.5, 37°, and under light protection, the corresponding dimer (but not quinone) is formed. Near their upper limit of solubility in Ringer buffer, anthralin, dimer, and quinone interact with glucose-6-phosphate dehydrogenase, but this interaction leads to a fairly modest decrease of enzymatic activity. The dramatic changes regarding inhibition of the enzyme cannot be explained by the formation of dimer from anthralin and suggest that other breakdown products, unidentified as yet, must be the most active derivatives against glucose-6-phosphate dehydrogenase. Thus, if neutral aqueous buffers are used for the investigation of the mode of action of anthralin, the chemical instability of this molecule and the possible interference of highly active breakdown products should be kept in mind. Therefore, both *in vitro* and *in vivo* data should be interpreted cautiously.

REFERENCES

(1) B. Squire, *Br. Med. J.*, **1**, S, 546 (1877).

(2) B. Squire, *ibid.*, **1**, S, 199 (1877).

(3) B. Squire, *Arch. Dermatol. Syphilol.*, **10**, 332 (1878).

(4) K. K. Mustakallio, *Acta Dermato-Venereol.*, **59**, 125 (1979).

(5) H. Auterhoff and R. Sachdev, *Arch. Pharmacol.*, **295**, 850 (1962).

(6) L. B. Fisher and H. I. Maibach, *J. Invest. Dermatol.*, **64**, 338 (1975).

(7) A. Segal, C. Katz, and B. L. Van Duuren, *J. Med. Chem.*, **14**, 1152 (1971).

(8) B. L. Van Duuren, A. Segal, S. S. Tseng, G. M. Rusch, G. Loewengart, U. Maté, D. Roth, A. Smith, S. Melchionne, and I. Seidman, *J. Med. Chem.*, **21**, 26 (1978).

(9) W. Raab, *Hautarzt*, **26**, 452 (1975).

(10) W. Raab, *ibid.*, **26**, 456 (1975).

(11) J. C. Caron and B. Shroot, *J. Pharm. Sci.*, **70**, 1205 (1981).

ACKNOWLEDGMENTS

The authors thank Mr. Maignan, Laboratoires de Recherches Fondamentales, L'Ofeal, for the preparation and purification of the anthralin derivatives described in the text. They also thank Prof. H. Schaefer for his advice and encouragement concerning this work, and Dr. R. G. Dickinson for his helpful suggestions during the preparation of this manuscript, from Centre International de Recherches Dermatologiques, Sophia-Antipolis.

Steroidal Oxazoline Derivatives: Synthesis and *In Vitro* Effect on Bovine Pancreatic Ribonuclease Activity

A.-MOHSEN M. E. OMAR ˣ and OMAIMA M. ABOULWAFA

Received October 14, 1981, from the *Pharmaceutical Chemistry Department, Faculty of Pharmacy, University of Alexandria, Egypt.* Accepted for publication November 19, 1981.

Abstract □ A series of steroidal oxazoline derivatives, containing different chains attached to the heterocyclic ring, were synthesized and examined for *in vitro* effect on bovine pancreatic ribonuclease activity. The results indicated weak anabolic properties for all products except Compounds III and XII which showed mild catabolic activities.

Keyphrases □ Oxazoline—steroidal derivatives, synthesis and *in vitro* effect on bovine pancreatic ribonuclease activity □ Derivatives—steroidal oxazoline, synthesis and *in vitro* effect on bovine pancreatic ribonuclease activity □ Ribonuclease activity—bovine, pancreatic, steroidal oxazoline derivatives, synthesis and *in vitro* effects

In connection with a program studying modified steroids, a variety of *N,N*-disubstituted aminoethyl ethers of 6-phenyl, benzyl, or thiazolidinyl-17β-estradiol were synthesized and tested for antiestrogenic properties (1). In addition, various androgenic and estrogenic keto-steroids were converted into the corresponding 4-substituted-3-thiosemicarbazone (2) and acylhydrazone (3–5) derivatives, and the products evaluated for anticancer (2, 4) and endocrinological (2, 3, 5) activities.

Extending the studies to steroids containing fused heterocyclic systems, the synthesis of a series of 2′-thio-17-oxoestra-1(10),4-dieno[2,3-*d*]oxazolines (V, VII, IX, and XI) and the corresponding estra-1,5(10)-dieno[4,3-*d*]oxazolines (VI, VIII, X, and XII), possessing methyl or *N,N*-disubstituted aminoethyl moieties in the heterocyclic ring, was undertaken[1]. The *in vitro* effect of the product on the activity of the bovine pancreatic ribonuclease was evaluated as a preliminary measure for their anabolic and catabolic properties (6) (Scheme I).

RESULTS AND DISCUSSION

Chemistry—The 2- (I) and 4-aminoestrones (II), prepared by reduction of the 2- and 4-nitroestrones (7) with sodium dithionite in alkaline medium (8), were treated with carbon disulfide and potassium hydroxide in boiling ethanol to produce 2′-thio-17-oxoestra-1(10),4-dieno[2,3-*d*]oxazoline (III), and 2′-thio-17-oxoestra-1,5(10)-dieno[4,3-

[1] This paper constitutes Part VII of the series on Steroidal Derivatives: Part VI is Ref. 5.

0022-3549/82/0900-0983$01.00/0

in 1% acetone–Ringer buffer (10 μg/ml) were left for appropriate periods at 37° under light protection in the absence of enzyme. The enzyme inhibitory potency of the aged solutions was assayed by adding glucose-6-phosphate dehydrogenase for an additional incubation period of 5 min.

The results shown in Fig. 3 indicate that the gradual disappearance of anthralin during the first 30 min was responsible for the concomitant decrease in the enzyme inhibitory potency of the solution. The reappearance of a stronger inhibitory activity, however, is in striking contrast with the complete degradation of anthralin which occurred during the following 2–3 hr and, as already noted, could not be attributed to the formation of the dimer.

Similarly, when anthralin was left in acetone (0.5 mg/ml) for several days under continuous exposure to light (Fig. 1), the final dark brown solution, which was totally devoid of anthralin or dimer, showed a strong toxicity against glucose-6-phosphate dehydrogenase (Fig. 1A). Incubation of 1% of the acetone solution with the enzyme in Ringer buffer (5 min) resulted in a total destruction of enzymatic activity, which could not be explained by the presence of quinone.

CONCLUSION

Using a highly sensitive and reproducible HPLC assay, additional evidence has been given for the chemical instability of anthralin in solution, particularly aqueous media. In acetone solution over long periods, anthralin decomposes, in part *via* the dimer, to give a final solution containing 20% quinone. In aqueous media at pH 7.5, 37°, and under light protection, the corresponding dimer (but not quinone) is formed. Near their upper limit of solubility in Ringer buffer, anthralin, dimer, and quinone interact with glucose-6-phosphate dehydrogenase, but this interaction leads to a fairly modest decrease of enzymatic activity. The dramatic changes regarding inhibition of the enzyme cannot be explained by the formation of dimer from anthralin and suggest that other breakdown products, unidentified as yet, must be the most active derivatives against glucose-6-phosphate dehydrogenase. Thus, if neutral aqueous buffers are used for the investigation of the mode of action of anthralin, the chemical instability of this molecule and the possible interference of highly active breakdown products should be kept in mind. Therefore, both *in vitro* and *in vivo* data should be interpreted cautiously.

REFERENCES

(1) B. Squire, *Br. Med. J.*, **1**, S, 546 (1877).

(2) B. Squire, *ibid.*, **1**, S, 199 (1877).

(3) B. Squire, *Arch. Dermatol. Syphilol.*, **10**, 332 (1878).

(4) K. K. Mustakallio, *Acta Dermato-Venereol.*, **59**, 125 (1979).

(5) H. Auterhoff and R. Sachdev, *Arch. Pharmacol.*, **295**, 850 (1962).

(6) L. B. Fisher and H. I. Maibach, *J. Invest. Dermatol.*, **64**, 338 (1975).

(7) A. Segal, C. Katz, and B. L. Van Duuren, *J. Med. Chem.*, **14**, 1152 (1971).

(8) B. L. Van Duuren, A. Segal, S. S. Tseng, G. M. Rusch, G. Loewengart, U. Maté, D. Roth, A. Smith, S. Melchionne, and I. Seidman, *J. Med. Chem.*, **21**, 26 (1978).

(9) W. Raab, *Hautarzt*, **26**, 452 (1975).

(10) W. Raab, *ibid.*, **26**, 456 (1975).

(11) J. C. Caron and B. Shroot, *J. Pharm. Sci.*, **70**, 1205 (1981).

ACKNOWLEDGMENTS

The authors thank Mr. Maignan, Laboratoires de Recherches Fondamentales, L'Ofeal, for the preparation and purification of the anthralin derivatives described in the text. They also thank Prof. H. Schaefer for his advice and encouragement concerning this work, and Dr. R. G. Dickinson for his helpful suggestions during the preparation of this manuscript, from Centre International de Recherches Dermatologiques, Sophia-Antipolis.

Steroidal Oxazoline Derivatives: Synthesis and *In Vitro* Effect on Bovine Pancreatic Ribonuclease Activity

A.-MOHSEN M. E. OMAR ˣ and OMAIMA M. ABOULWAFA

Received October 14, 1981, from the *Pharmaceutical Chemistry Department, Faculty of Pharmacy, University of Alexandria, Egypt.* Accepted for publication November 19, 1981.

Abstract □ A series of steroidal oxazoline derivatives, containing different chains attached to the heterocyclic ring, were synthesized and examined for *in vitro* effect on bovine pancreatic ribonuclease activity. The results indicated weak anabolic properties for all products except Compounds III and XII which showed mild catabolic activities.

Keyphrases □ Oxazoline—steroidal derivatives, synthesis and *in vitro* effect on bovine pancreatic ribonuclease activity □ Derivatives—steroidal oxazoline, synthesis and *in vitro* effect on bovine pancreatic ribonuclease activity □ Ribonuclease activity—bovine, pancreatic, steroidal oxazoline derivatives, synthesis and *in vitro* effects

In connection with a program studying modified steroids, a variety of *N,N*-disubstituted aminoethyl ethers of 6-phenyl, benzyl, or thiazolidinyl-17β-estradiol were synthesized and tested for antiestrogenic properties (1). In addition, various androgenic and estrogenic keto-steroids were converted into the corresponding 4-substituted-3-thiosemicarbazone (2) and acylhydrazone (3–5) derivatives, and the products evaluated for anticancer (2, 4) and endocrinological (2, 3, 5) activities.

Extending the studies to steroids containing fused heterocyclic systems, the synthesis of a series of 2′-thio-17-oxoestra-1(10),4-dieno[2,3-*d*]oxazolines (V, VII, IX, and XI) and the corresponding estra-1,5(10)-dieno[4,3-*d*]oxazolines (VI, VIII, X, and XII), possessing methyl or *N,N*-disubstituted aminoethyl moieties in the heterocyclic ring, was undertaken[1]. The *in vitro* effect of the product on the activity of the bovine pancreatic ribonuclease was evaluated as a preliminary measure for their anabolic and catabolic properties (6) (Scheme I).

RESULTS AND DISCUSSION

Chemistry—The 2- (I) and 4-aminoestrones (II), prepared by reduction of the 2- and 4-nitroestrones (7) with sodium dithionite in alkaline medium (8), were treated with carbon disulfide and potassium hydroxide in boiling ethanol to produce 2′-thio-17-oxoestra-1(10),4-dieno[2,3-*d*]oxazoline (III), and 2′-thio-17-oxoestra-1,5(10)-dieno[4,3-

[1] This paper constitutes Part VII of the series on Steroidal Derivatives: Part VI is Ref. 5.

0022-3549/82/0900-0983$01.00/0

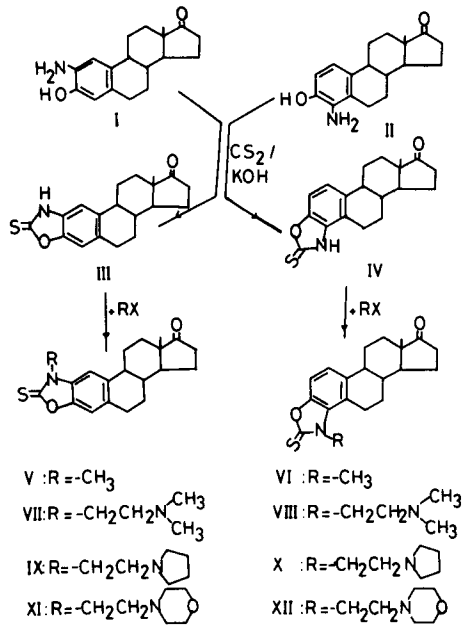

Scheme I

d]oxazoline (IV), respectively. The reaction of Compound III with methyl iodide in cold aqueous sodium hydroxide solution yielded the corresponding *N*-methylsteroidal oxazoline derivative (V). The application of the same procedure to synthesize the other required compounds (VI–XII) was fruitless. The preparation of the 3′-[2-(*N*-pyrrolidinyl)-ethyl] derivative (IX) necessitated the reaction of 2′-thioxazoline (III) with 2-(*N*-pyrrolidinyl)ethyl chloride hydrochloride salt in refluxing sodium ethoxide solution, while for compounds VI–VIII and X–XII, the use of potassium hydroxide in boiling acetone was the most effective in conducting the reaction to completion. The products (Table I) were identified by IR, UV, PMR, and, for one representative example, by mass spectra. The IR spectra of the products lacked the C=N absorption bands and exhibited a band at 930 cm^{-1} for the C=S absorption (9).

In the PMR spectra (Table II), the steroidal[2,3-*d*]oxazolines (V, VII, IX, and XI) showed two singlets at 7.08–7.20 and 7.27–7.59 ppm for the C_4 and C_1 protons of the steroidal skeleton. The analogous steroidal[4,3-*d*]oxazolines (VI, VIII, X, and XII) showed the C_1 and C_2 protons as a singlet at 7.20 ppm. The C_{18}—CH_3 of all products as well as the N—CH_3 of Compounds V and VI resonated as two singlets at 0.91–0.92 and 2.71–2.75 ppm, respectively. The protons of the 2-methylene chain of Compounds VII–XII were identified as two triplets resonating at

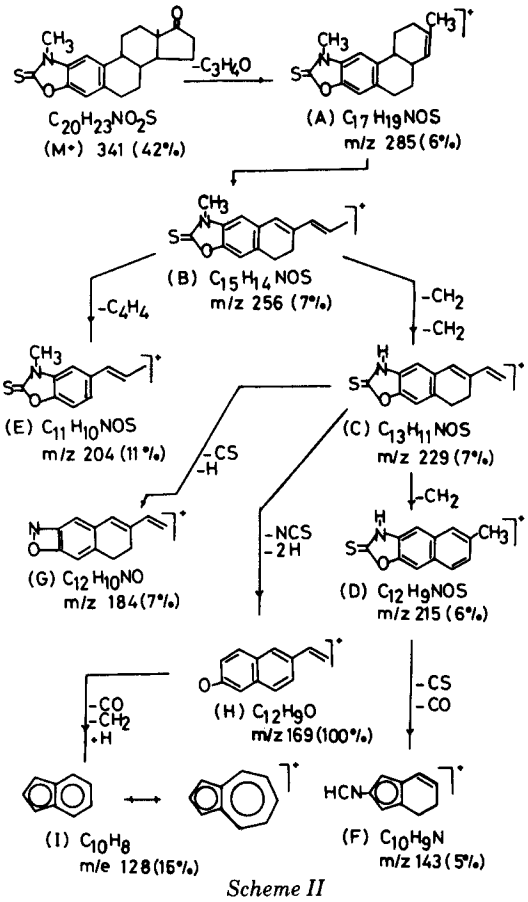

Scheme II

different chemical shifts. The first, appearing at 2.21–2.88 ppm, was assigned to the more shielded methylene protons adjacent to the *N*-dimethyl, pyrrolidino, or morpholino function. The other triplet, resonating at 3.42–3.49 ppm, was assigned to the relatively less shielded methylene protons attached to the oxazoline ring. The spectra also showed the signals for the pyrrolidine and morpholine protons at the expected chemical shift in the high field region.

The mass spectrum of Compound V showed a molecular ion peak at *m/z* 341. Its fragmentation as demonstrated in Scheme II involved the cleavage of Ring D to give Ion A at *m/z* 285 which after cleavage of Ring

Table I—Synthesized Steroidal Oxazoline Derivatives (V–XII)

Compound No.	Yield, %	Melting Point	Molecular Formula	Analysis, % Calc.	Found
V	63	204–205[a]	$C_{20}H_{23}NO_2S$	C 70.36	70.27
				H 6.79	6.82
				N 4.10	4.24
VI	87	186–187	$C_{20}H_{23}NO_2S$	C 70.36	70.37
				H 6.79	7.00
				N 4.10	4.26
VII	70	146–147	$C_{23}H_{30}N_2O_2S$	C 69.32	69.14
				H 7.59	7.85
				N 7.03	7.13
VIII	70	144–145	$C_{23}H_{30}N_2O_2S$	C 69.32	69.43
				H 7.59	7.74
				N 7.03	6.90
IX	93	157–158	$C_{25}H_{32}N_2O_2S$	C 70.72	70.54
				H 7.60	7.88
				N 6.60	6.47
X	85	157–158	$C_{25}H_{32}N_2O_2S$	C 70.72	70.37
				H 7.60	7.80
				N 6.60	6.60
XI	82	173–174	$C_{25}H_{32}N_2O_3S$	C 68.16	68.07
				H 7.32	7.29
				N 6.36	6.52
XII	67	179–180	$C_{25}H_{32}N_2O_3S$	C 68.16	67.98
				H 7.32	7.58
				N 6.36	6.54

[a] All products were crystallized from ethanol except compounds VII and X, which were crystallized from aqueous ethanol.

C produced Ion B at *m/z* 256. Successive elimination of methylene groups from Ion B gave Ions C, D, and E at *m/z* 229, 215, and 204, respectively. Ion D then lost a carbon monosulfide and a carbon monoxide function, and produced the isocyanide Ion F at *m/z* 143. Ion C either eliminated carbon monosulfide and a hydrogen to give Ion G at *m/z* 184 or underwent cleavage of an isothiocyanate ion and two hydrogens to yield Ion H as the base peak at *m/z* 169. This in turn eliminated carbon monoxide and a methylene ion and accepted a hydrogen giving Ion I at m/z 128. The spectrum has also shown the various ions reported for the normal fragmentation of estrone (10) and oxazole (11, 12).

Biological Screening—Compounds III–V, VII–IX, XI, and XII were *in vitro* tested for possible anabolic–catabolic activity by measuring their effects on the activity of the bovine pancreatic ribonuclease. The applied method, as reported (6), involved the utilization of four sets of incubation media: the medium containing the steroidal derivative and the enzyme, the blank lacking the enzyme, the control devoid of the steroidal derivative, and the control blank containing the enzyme and the phosphate buffer solution. After mixing the components of each set, the tubes were incubated at 37° for 15 min, and treated with an ethanol–glacial acetic acid mixture to terminate the reaction. They were stored for 1 hr in the refrigerator, centrifuged for 15 min, and the supernates were spectrophotometrically measured at 260 nm. The activity of the ribonuclease was calculated according to a previous report (13) and the data expressed as the mean values of five experiments ± standard deviation in units per milliliter.

In accordance with the results obtained (Table III), the majority of products caused a weak percentage inhibition of ribonuclease indicating mild anabolic properties. Compounds III and XII, induced a weak percentage activation of ribonuclease and hence proved to be of mild catabolic nature. In contrast to such findings, a variety of compounds having a heterocyclic ring fused to the 2,3- or 3,4-positions of various steroids have been reported to possess more potent endocrinological activity than the parent steroidal nuclei (14–19).

EXPERIMENTAL[2]

2′-Thiosteroidal-oxazolines III and IV—A mixture of the aminosterone (I or II) (8) (150 mg, 0.52 mmole), carbon disulfide (3.5 ml), and potassium hydroxide (30 mg) in ethanol (20 ml) was heated under reflux for 6 hr. The final solution was concentrated, cooled to room temperature, acidified with glacial acetic acid, treated with enough water until permanent turbidity, and left overnight in the refrigerator. The deposited white solid was filtered, washed with water, and crystallized from ethanol giving the required products. Compound III was obtained as white shiny scales darkening at 280°, mp 310°, yield: 87%. Compound IV was produced as white prisms, mp 188–192°, yield: 99%. IR (mineral oil): 1730 (C=O), 1510, 1495, 1140, and 930 cm^{-1} (H—N—C=S amide I, II, III, and IV bands, respectively) (9). UV of Compound IV, λ_{max} (ethanol) (log ϵ): 225 (4.477), 265 (4.202), 270 (4.180), 300 (sh) (4.503), and 310 nm (4.982). The products give microanalytical data within ±0.4% for C, H, and N.

2′-Thio-3′-methyl-17-oxoestra-1(10),4-dieno[2,3-*d*]oxazoline (V)—Methyl iodide (90 mg, 0.63 mmole) was added dropwise to an ice-cooled solution of 2′-thio-17-oxoestra-1(10),4-dieno[2,3-*d*]oxazoline (III) (200 mg, 0.61 mmole) in a mixture of ethanol (10 ml) and 10% aqueous potassium hydroxide solution (10 ml). The mixture was stirred for 1 hr, while being cooled in ice, and for an additional hour at room temperature. The final solution, containing some deposited products, was left overnight in the refrigerator, filtered, and the product crystallized from ethanol to give white shiny scales of the required Compound V. IR (mineral oil): 1720 (C=O) and 920 cm^{-1} (C=S). The yield and physical constants of the product are recorded in Table I. Mass spectrum of V showed *m/z* (relative abundance %) M^+ at 341 (42), 285 (6), 284 (6), 257 (4), 256 (7), 243 (8), 242 (4), 231 (9), 230 (13), 229 (7), 228 (11), 218 (5), 217 (18), 216 (13), 215 (6), 204 (11), 191 (11), 184 (7), 183 (11), 182 (9), 180 (3), 179 (5), 178 (26), 172 (5), 170 (9), 169 (100), 167 (5), 166 (4), 165 (6), 164 (6), 158 (7), 157 (15), 156 (5), 155 (7), 154 (6), 153 (8), 152 (5), 145 (4), 144 (4), 143 (5), 142 (6), 141 (11), 140 (5), 131 (8), 130 (6), 129 (15), 128 (15), 127 (6), 117 (5), 116 (15), 115 (22), 103 (15), 91 (6), 79 (4), 77 (6), 67 (6), 55 (6), and 41 (6).

2′-Thio-3′[2-(*N*-pyrrolidino)ethyl]-17-oxoestra-1(10),4-dieno-[2,3-*d*]oxazoline (IX)—2-(*N*-Pyrrolidinyl)ethyl chloride hydrochloride (110 mg, 0.6 mmole) was added to a solution of the thione derivative III (200 mg, 0.61 mmole) in sodium ethoxide (prepared from 30 mg of sodium metal and 10 ml of absolute ethanol) and the mixture was heated under reflux for 1 hr. The formed inorganic salt was filtered from the hot mixture and the filtrate concentrated to give, after cooling, the required product IX (Table I). IR (mineral oil): 1720 (C=O) and 920 cm^{-1} (C=S).

2′-Thio-3′-substituted-17-oxoestra-1(10),4-dieno[2,3-*d*]-and-1,5(10)-dieno[4,3-*d*]oxazolines (VI–VIII and X–XII)—A mixture of the steroidal 2′- (III) or 4′-thione (IV) derivative (200 mg, 0.61 mmole), potassium hydroxide (70 mg, 1.25 mmoles), and one molar equivalent of the selected alkyl, dialkylaminoalkyl, or *N*-heteroalkyl halide in acetone (15 ml) was heated under reflux for 2.5–12 hr (TLC). Filtration while hot, to remove the inorganic salt, and concentration of the acetone solution followed by treatment with water gave the required products identified as shown in Tables I and II. IR (mineral oil): 1730–1725 (C=O) and 965–920 cm^{-1} (C=S). UV of Compound VIII λ_{max} (ethanol) (log ϵ): 220 (4.449), 258 (4.303), 280 (4.181), and 290 nm (4.142).

Materials and Methods for the *In Vitro* Anabolic–Catabolic Activities—The following four sets of solutions were used in the evaluation procedures:

1. A 0.05 *M* phosphate buffer (pH 7.4);
2. A solution of 5 mg of a highly polymerized yeast RNA in 1 ml of the phosphate buffer;
3. A solution of 2.5 mg of bovine pancreatic ribonuclease[3] in 100 ml of distilled water;
4. Various molar concentrations (10^{-6} to 10^{-9}) of the steroidal derivatives in ethanol.

The media utilized were:

1. The medium containing the steroidal derivative and the enzyme was composed of a mixture of 0.4 ml of RNA solution, 0.4 ml of phosphate buffer, 0.1 ml of the steroidal solution, and 0.1 ml of ribonucleotase.
2. The blanks did not contain the enzyme but were composed of a mixture of 0.4 ml of RNA solution, 0.1 ml of the steroidal solution, and 0.5 ml of the buffer.
3. The control experiments were devoid of the steroidal components and contained a mixture of 0.1 ml of ribonucleotase, 0.4 ml of RNA, and 0.5 ml of the buffer solution.
4. The blank of the control contained only 0.4 ml of RNA completed to 1 ml volume by the buffer solution.

Table II—PMR Spectral Data of the Synthesized Steroidal Oxazoline Derivatives

Compound No.	Chemical Shift (δ ppm) in $CDCl_3$
III	0.92 (s, 3H, C_{18}—CH_3), 7.08 (s, 1H, C_4—H), 7.27 (s, 1H, C_1—H), 10.55 (broad and diffused singlet, disappearing on deuterization, 1H, N—H).
V	0.91 (s, 3H, C_{18}—CH_3), 2.71 (s, 3H, N—CH_3), 7.13 (s, 1H, C_4—H), 7.52 (s, 1H, C_1—H).
VI	0.93 (s, 3H, C_{18}—CH_3), 2.75 (s, 3H, N—CH_3), 7.2 (s, 2H, C_1 and C_2—H).
VII	0.91 (s, 3H, C_{18}—CH_3), 2.30 (s, 6H, $N(CH_3)_2$), 2.73 (t, 2H, J = 7 Hz, CH_2—$N(CH_3)_2$), 3.42 (t, 2H, J = 7 Hz, $CH_2CH_2N(CH_3)_2$), 7.13 (s, 1H, C_4—H), 7.51 (s, 1H, C_1—H).
VIII	0.92 (s, 3H, C_{18}—CH_3), 2.30 (s, 6H, —$N(CH_3)_2$), 2.21 (t, 2H, J = 7 Hz, —CH_2—$N(CH_3)_2$), 3.43 (t, 2H, J = 7 Hz, —$CH_2CH_2N(CH_3)_2$), 7.20 (s, 2H, C_1 and C_2—H).
IX	0.91 (s, 3H, C_{18}—CH_3), 2.9 (t, 2H, J = 7 Hz, CH_2—N), 3.49 (t, 2H, —CH_2CH_2N), 7.2 (s, 1H, C_4—H), 7.59 (s, 1H, C_1—H).
X	0.91 (s, 3H, C_{18}—CH_3), 2.88 (t, 2H, J = 7 Hz, CH_2—N), 3.46 (t, 2H, J = 7 Hz, —CH_2CH_2N), 7.2 (s, 2H, C_1 and C_2—H).
XI	0.91 (s, C_{18}—CH_3), 2.4–2.61 (m, 4H, morpholine protons), 2.77 (t, 2H, J = 7 Hz, —CH_2N), 3.45 (t, 2H, J = 7 Hz, —CH_2CH_2N), 3.62–3.80 (m, 4H, morpholine protons adjacent to oxygen), 7.15 (s, 1H, C_4—H), 7.50 (s, 1H, C_1—H).
XII	0.92 (s, 3H, C_{18}—CH_3), 2.45–2.65 (m, 4H, morpholine protons), 2.78 (t, 2H, J = 7 Hz, —CH_2—N), 3.46 (t, 2H, J = 7 Hz, —CH_2CH_2N), 3.63–3.81 (m, 4H, morpholine protons adjacent to oxygen), 7.20 (s, 2H, C_1 and C_2—H).

[2] All melting points are uncorrected. IR spectra were measured as Nujol mulls on a Beckman 4210 IR spectrophotometer. UV spectra for ethanol solution on a Perkin-Elmer 650 S spectrophotometer. PMR and MS were measured on a Perkin-Elmer R32 and an AEI-MS-50, respectively.

[3] Sigma Chemical Co., St. Louis, Mo.

Table III—*In Vitro* Effects of the Synthesized Steroidal Oxazoline Derivatives on the Activity of Bovine Pancreatic Ribonuclease

Compound No.		Molar Concentration of the Compound (M)			
		10^{-6}	10^{-7}	10^{-8}	10^{-9}
Estrone	Mean ± SE[a]	219.6 ± 10.03	225.4 ± 20.04	231.2 ± 14.4	230 ± 17.02
	% Activation	12.46	15.61	18.57	17.98
	p	>0.05	>0.05	>0.05	>0.05
	Control		(208.6 ± 18.6)		
III	Mean ± SE	235.8 ± 21.8	215.0 ± 12.9	205.8 ± 13.5	205.8 ± 23.5
	% Activation	12.89	3.37	1.45	1.45
	p	>0.05	>0.05	>0.05	>0.05
IV	Mean ± SE	187.28 ± 12.4	186.1 ± 12.7	215.0 ± 12.8	218.5 ± 11.7
	% Inhibition	10.1	10.62	3.36	4.81
	p	>0.05	>0.05	>0.05	>0.05
V	Mean ± SE	172.5 ± 13.2	179.3 ± 19.7	195.7 ± 18.5	198.2 ± 12.6
	% Inhibition	17.15	13.79	5.92	4.81
	p	>0.05	>0.05	>0.05	>0.05
VII	Mean ± SE	183.3 ± 13.3	183.3 ± 16.2	207.4 ± 17.4	205.5 ± 15.6
	% Inhibition	12.02	12.02	0.48	1.45
	p	>0.05	>0.05	>0.05	>0.05
VIII	Mean ± SE	194.4 ± 14.4	186.1 ± 16.6	197.22 ± 13.6	212.9 ± 18.9
	% Inhibition	6.62	10.58	5.29	1.92
	p	>0.05	>0.05	>0.05	>0.05
IX	Mean ± SE	200.9 ± 12.6	204.6 ± 12.9	234.3 ± 16.9	230.5 ± 15.6
	% Inhibition	3.51	1.73	12.5	10.58
	p	>0.05	>0.05	>0.05	>0.05
XI	Mean ± SE	200.8 ± 15.8	199.1 ± 16.3	213.7 ± 13.9	222.5 ± 17.6
	% Inhibition	3.55	4.37	2.74	6.87
	p	>0.05	>0.05	>0.05	>0.05
XII	Mean ± SE	221.3 ± 12.9	249.1 ± 17.4	211.8 ± 13.6	220.3 ± 17.7
	% Activation	6.25	19.71	1.45	5.77
	p	>0.05	>0.05	>0.05	>0.05

[a] The ribonuclease activity is expressed in units as the mean ± SE.

REFERENCES

(1) E. R. Clark, A.-Mohsen M. E. Omar, and G. Prestwich, *J. Med. Chem.*, **20,** 1096 (1977).

(2) A.-Mohsen M. E. Omar, S. M. El-Khawass, A. B. Makar, N. M. Bakry, and T. T. Dabees, *Pharmazie*, **33,** 577 (1978).

(3) S. M. El-Khawass, A.-Mohsen M. E. Omar, T. T. Dabees, and F. M. Sharaby, *ibid.*, **35,** 143 (1980).

(4) A.-Mohsen M. E. Omar, A. M. Farghaly, A. A. B. Hazzaa, and N. H. Eshba, *ibid.*, **35,** 809 (1980).

(5) E. A. Ibrahim, A.-Mohsen M. E. Omar, M. A. Khalil, A. B. Makar, and T. T. Dabees, *ibid.*, **35,** 810 (1980).

(6) S. M. El-Sewedy, E. A. El-Basyouni, and S. T. Assar, *Biochem. Pharmacol.*, **27,** 1831 (1978).

(7) H. Hamacher, *Arzneim.-Forsch.*, **29,** 463 (1979).

(8) S. Krayshy, *J. Am. Chem. Soc.*, **81,** 1702 (1959).

(9) A.-Mohsen M. E. Omar and S. A. Osman, *Pharmazie*, **28,** 30 (1973).

(10) C. Djerassi, J. M. Wilson, H. Budzikiewicz, and J. W. Chamberlain, *J. Am. Chem. Soc.*, **84,** 4544 (1962).

(11) H. Ogura, S. Sugimoto, and T. Itoh, *Org. Mass Spectrom.*, **3,** 1341 (1970).

(12) G. Barker and G. P. Ellis, *J. Chem. Soc. (C)*, **1971,** 1482.

(13) R. M. Sigulem, G. A. Brasel, E. G. Velasco, P. Rosso, and M. Winich, *Am. J. Clin. Nutr.*, **26,** 793 (1973).

(14) P. De Ruggieri, G. Gandolfi, U. Gozzi, D. Chiaramonti, and C. Ferrari, *Pharmaco. (Pavia) Ed. Sci.*, **20,** 280 (1965).

(15) R. O. Clinton, A. J. Manson, F. W. Stonner, R. G. Christiansen, A. L. Beyler, G. O. Potts, and A. Arnold, *J. Org. Chem.*, **26,** 279 (1961).

(16) R. G. Christiansen, U.S. pat. 4,055,562 (1977); through *Chem. Abstr.*, **88,** 121545g (1978).

(17) J. O. Zderic *et al.*, *Chem. Ind. (London)*, **1960,** 1625.

(18) M. Shimizu *et al.*, *Chem. Pharm. Bull. (Tokyo)*, **13,** 895 (1965).

(19) T. L. Popper, U.S. pat. 3,772,283 (1973); through *Chem. Abstr.*, **80,** 37391f (1974).

ACKNOWLEDGMENTS

Supported in part by Pharco Pharmaceuticals, Cairo, Egypt.

The authors thank Searle Pharmaceutical Co., U.S.A., Organon Pharmaceutical Co., Holland, and Hoffmann–La Roche Inc., Switzerland, for the donation of estrone. Thanks are also due to Dr. S. M. El-Sewedy, Laboratory of Applied Medical Chemistry, Medical Research Institute, University of Alexandria, for the biological data, and J. Bourdais, Laboratoire de Chimie des Hétérocycles D'Intérêt Biologique, Faculté de Médicine Nord, Université D'Aix-Marseille II, Marseille, France, for the analytical and spectral data.

Chromatographic Assay of Neomycin B and C in Neomycin Sulfate Powders

W. DECOSTER, P. CLAES, and H. VANDERHAEGHE ˣ

Received July 31, 1981, from the *Rega and Pharmaceutical Institutes, University of Leuven, B-3000 Leuven, Belgium.* Accepted for publication November 24, 1981.

Abstract □ A chromatographic assay of neomycin sulfate powders on strongly alkaline ion-exchange resin (hydroxide form) is described. D-(+)-α,α-Trehalose was used as an internal standard. The amount of neomycin B and C in commercial samples was determined with the proposed method, and the results are compared with those obtained by microbiological assay. In addition, minor neomycin components were estimated by TLC and GLC methods.

Keyphrases □ Neomycin—ion-exclusion chromatographic assay of neomycin B and C in neomycin sulfate powders □ Chromatography, ion-exclusion—assay of neomycin B and C in neomycin sulfate powders □ Neomycin sulfate powders—ion-exclusion chromatographic assay of neomycin B and C

The microbiological assay of neomycin prescribed by most pharmacopoeias presents more difficulties than usually encountered with other antibiotics. It shows large interlaboratory variation (1) and may be suspected of a lack of accuracy inherent to the mixture assay where the components have markedly different activities. The influence of the composition on the microbiological assay (2) requires a preliminary quantitation of neomycin C as a fraction of neomycin B to ascertain a similar composition of the unknown and standard preparation. Therefore, alternative methods of assaying neomycin have been developed. A GLC method of totally silylated neomycin was reported previously (3). Poor resolution and critical experimental conditions (4) make this method difficult to perform. A high-pressure liquid chromatographic (HLPC) method of *N*-dinitrophenylated neomycins on normal phase was also reported (5).

The present report deals with a chromatographic assay on a strongly basic ion-exchange resin (hydroxide form) using water as the mobile phase and refractometric detection. It was developed from a medium-pressure chromatographic method used in this laboratory for the determination of relative amounts of neomycin B and C (6) and has the advantage of avoiding pre- and postcolumn derivatization. The use of an internal standard allowed the quantitation of absolute amounts of neomycin B and C. With the proposed method, commercial neomycin samples of different origin were assayed and the amount of several minor components were estimated.

EXPERIMENTAL

Apparatus—A stainless steel column[1] (1.0 cm × 30 cm) was provided with the necessary ferules, fittings, and metal low-dead volume tubing. The usual metal fritted disks were replaced by porous polyethylene disks[1]. The outlet was connected to a differential refractometer[2] (attenuator setting, 8×). The strip chart recorder[3] (10-mV range, chart speed, 10 mm/min) was replaced in some experiments by an electronic integrator[4]. The column was held at constant temperature by submersion in a bath of circulating water[5], which also served for thermostatization of the refractometer. The column inlet was provided with an injector[6]. The mobile phase, carbon dioxide-free distilled water, was delivered at a constant rate by a reciprocating piston pump[7]. A Bourdon-type pressure gauge, which also served as a pulse dampener, was placed between the pump and injector, and a stainless steel guard column (1.0 cm × 10 cm) was filled with the same resin as in the analytical column.

The procedure for conversion of the resins into the hydroxide form was discussed in detail in a previous report (6).

Peak areas were determined with a polar planimeter or with an electronic integrator.

Materials—Samples of neomycin sulfates were obtained from different firms. The European Pharmacopoeia CRS of neomycin sulfate was used as received, the USP reference standard (Issue E) was previously dried at 60° for 3 hr *in vacuo* as prescribed. Four resins[8–10] were used without further purification or sizing.

Mobile Phase—Freshly distilled water was used in all experiments. The flasks were closed with a rubber stopper holding a soda-lime trap.

Standard and Sample Solution—Pure neomycin B and C free bases were obtained by preparative chromatography on a carboxylic ion-exchange resin (7). They were converted into sulfates by adding 0.5 *N* sulfuric acid to yield a product containing 30.0% sulfate, expressed on a dry weight basis. The solution was freeze-dried and its sulfuric acid content and weight loss on drying were determined. From these values the free base content of the neomycin B and C sulfates was calculated.

The $[\alpha]_D$ of D-(+)-α,α-trehalose dihydrate[11] (+181°) was in close agreement with the value given by the manufacturer (+179.9°). Weight loss on drying was 9.73% (theoretical water content 9.67%). The internal standard stock solution was prepared by dissolving 4.00 g of trehalose in 50.0 ml of distilled water.

Neomycin sulfate (100 mg) was weighed accurately in a test tube, and 1.000 ml of internal standard stock solution was added with a micrometer syringe[12]. A calibration curve was obtained by chromatographing mixtures of pure neomycin B and C sulfate in 1 ml of internal standard stock solution. Then, 100 μl of all solutions was injected onto the column.

Weight Loss on Drying—Weight loss was determined after heating a 100-mg sample in a drying pistol[13] at 60° in a vacuum of 0.1 mm Hg for 3 hr over phosphorus pentoxide. The mean absolute standard deviation of the method was 0.13, calculated for five sets of four assays[14].

Sulfuric Acid Content—A previously reported titrimetric method (8) was modified slightly. A 100-mg sample of neomycin sulfate was applied to a 1 × 5 cm column of strongly acidic ion-exchange resin[15]. The column was washed with water and the eluate collected in a 50-ml volumetric flask. A 20-ml aliquot was diluted with 20 ml of methanol and buffered with 2 drops of 0.5 *M* magnesium acetate. After addition of 3 drops of 0.25% thorin[16] solution and 3 drops of 0.0125% aqueous methylene blue solution, the titration was carried out under vigorous stirring with 0.01 *M* barium chloride until the color changed from green to pink. The mean absolute standard deviation of the method was 0.15, calculated for five sets of four assays[14].

Thin-Layer Chromatography of Minor Components—Some eluate fractions from the resin column were evaporated to dryness and dissolved

[1] Alltech Europe, Belgium.
[2] Waters Differential Refractometer R 403.
[3] Kipp BD 40.
[4] Hewlett-Packard 3390 A.
[5] Varian type 4100.
[6] Valco loop injector.
[7] Milton Roy MiniPump.
[8] Bio-Rex 9 resin (200–400 mesh), Bio-Rad Laboratories, Richmond, Calif.
[9] Bio-Rad AG 1-X2 and AG 1-X4 resins, Bio-Rad Laboratories, Richmond, Calif.
[10] Durrum DA-X2 resin, Pierce Chemical Co., Rockford, IL 61105.
[11] Fluka, Büchi, Switzerland.
[12] AGLA-Burroughs, Wellcome & Co., London, U.K.
[13] Desaga, Heidelberg, Germany.
[14] H. Vanderhaege, unpublished results.
[15] Dowex 50-X8 (100–200 mesh).
[16] Disodium salt of *O*-(2-hydroxy-3,6-disulfo-1-naftylazo)benzene arsonic acid.

0022-3549/82/0900-0987$01.00/0

Table I—Chromatographic Parameters on Different Strongly Alkaline Resins [a]

Parameter \ Resin	Resin[b]	Resin[c]	Resin[d]	Resin[e]	Two-Column System
t_R neomycin C, min	9.7	8.0	5.1	6.6	9.2
t_R neomycin B, min	20.4	17.0	9.7	14.2	18.4
t_R Internal Standard, min	30.0	43.0	17.0	25.1	29.3
N (calculated on neomycin B peak)	277 (923/m)	125 (417/m)	192 (1920/m)	200 (666/m)	220 (733/m)
Rs neomycin B – neomycin C	2.8	2.0	2.4	2.5	2.4
Rs neomycin B – paromomycin I	1.3	3.3	2.0	2.3	1.7
Rs paromomycin I–Internal Standard	Poor	Good	Poor	Good	Good
Symmetry factor neomycin B	0.77	0.91	0.95	0.92	0.90

[a] Hydroxide form resins in a 1 × 30-cm column at a flow rate of 270 ml/hr. [b] Bio-Rad AG I-X2 resin, minus 400 mesh. [c] Bio-Rad AG I-X4 resin, minus 400 mesh. [d] Durrum DA-X2, 1 × 10-cm column, flow rate 170 ml/hr. [e] Bio-Rex 9, 200–400 mesh.

in 0.5 ml of water. This solution (1, 2, 3, and 4 μl) was spotted on precoated silica gel plates[17], activated for 2 hr at 130°, and developed over 12 cm with a 15% (w/v) aqueous solution of potassium dihydrogen phosphate. It has been shown that these TLC plates[17] contain a polycarboxylic acid binder which is responsible for the separation of the aminoglycosides (9). After development, the dried plates were sprayed with a ninhydrin reagent (0.3 g in 100 ml of *n*-butanol containing 3% acetic acid) and heated for 5–7 min at 130°. Reference solutions of paromamine, mono-*N*-acetylneamine, mono-*N*-acetylneomycin B, and neamine contained 400 μg/ml. Comparison of the color intensities of the reference spots and the spots from the commercial samples allowed a semiquantitative determination of minor neomycin components.

GLC Determination of Acetyl Groups—In addition to the TLC method, the presence of acetylated products in commercial neomycin was also determined by a GLC method, preceded by acid hydrolysis and extraction of the liberated acetic acid with *tert*-butylmethyl ether. The stationary phase was 10% SP 1200[18] and 1% H_3PO_4 on 800/100 Chromosorb W AW (152.5 cm; o.d., 6 mm; i.d., 4 mm) at 95°. The flow rate of the carrier gas (nitrogen) was adjusted to 60 ml/min. The flame ion detector oven was set at 220°. Acid hydrolysis was performed on 100 mg of neomycin sulfate to which were added 0.4 ml of butyric acid internal standard solution (containing 1 mg/ml), 1 ml of concentrated sulfuric acid, and 0.8 ml of water. The test tube was sealed and heated at 100° for 4 hr in an oil bath. The reaction mixture was then extracted three times with 2.5 ml of *tert*-butyl methyl ether. The extracts were dried on anhydrous sodium sulfate, filtered, and reduced to ~0.5 ml with a stream of dry nitrogen; 5 μl of this concentrated extract then was injected on the column.

A calibration curve in the range of 50–500 μg/ml acetic acid was obtained by running known dilutions of acetic acid through the procedure described for the unknown samples. The peak height of acetic acid (retention time ~1 min) over the peak height of butyric acid (retention time ~2 min) was plotted against the amount of acetic acid present. The linear regression was $y = 0.471x - 0.008$ where the correlation coefficient is 0.9993.

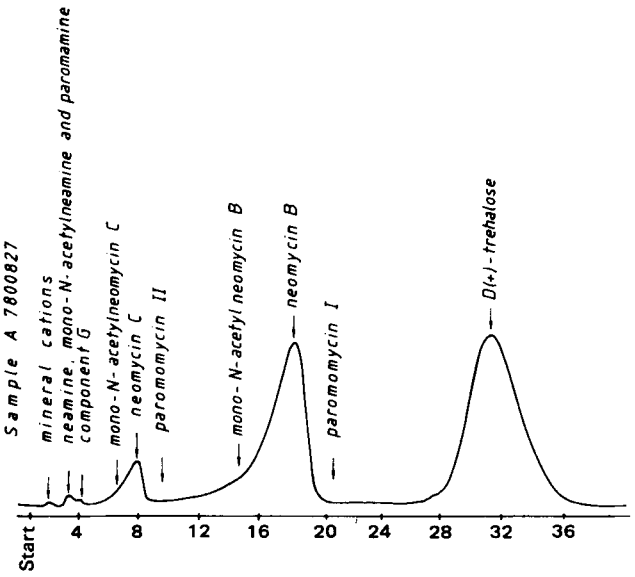

Figure 1—*Chromatogram of 10 mg of neomycin sulfate and 8 mg of internal standard, obtained on a 1 × 10 cm column of resin[21] connected to a 1 × 20 cm column of another resin[20]; flow rate, 270 ml/hr.*

[17] Merck Si60 precoated plates.

[18] Supelco, Bellefonte, Pa.

RESULTS AND DISCUSSION

Internal Standard—When examining a chromatogram of neomycin on strongly alkaline resin in the hydroxide form (Fig. 1), an internal standard should elute after neomycin B. The only aminoglycoside that is commercially available and has a larger retention time than neomycin B is paromomycin I (10). This product cannot be used, as it may be present in some neomycin samples. Since refractometric detection does not necessitate a compound with amino groups, as would be the case with ninhydrin–colorimetric or fluorimetric detection, nonreducing oligosaccharides were examined. Reducing sugars cannot be used because they react with the strongly basic resin (11). The retention times of saccharose and raffinose were too long, but D-(+)-α,α-trehalose was suitable (Fig. 1).

Selection of the Resin—Three resins with benzyltrimethylammonium groups and one resin with methylpyridinium groups were examined (Table I). This last type of resin[8] gave good separations of neomycin B and C and the internal standard, trehalose. However, it was observed that the resin in the hydroxide form deteriorated rapidly. When the column was run for 1 week, injecting only two samples a day, the area of the neomycin B peak, relative to that of the trehalose peak, decreased regularly (Fig. 2). The resin degradation also could be seen from the drastically changing column parameters. The t_R of neomycin C, B, and the internal standard decreased after 1 week to retention times of 5.3, 10.2, and 15.2 min. The resolution between neomycin B and C changed from 2.5 to 1.7, and the resolution between neomycin B and the internal standard changed from 2.3 to 1.1. It is probable that the resin decomposes at the

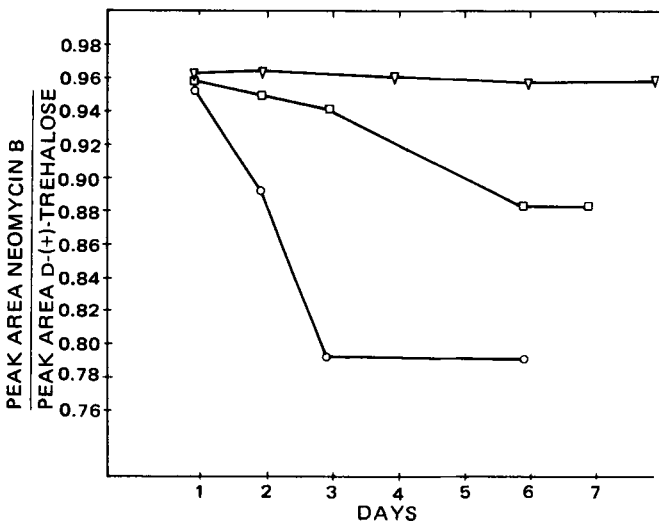

Figure 2—*Resin stability as a function of time. Key: (▽) resin[20] with guard column (>400 mesh); (□) resin[20] (>400 mesh); (○) resin[8] (200–400 mesh).*

Table II—Composition of Neomycin Samples of Different Origin

Sample	Number of Assays	Neomycin B Base[a], %	Neomycin C Base[a], %	Sulfuric Acid[b], %	Weight Loss on Drying[b], %	Paromomycin I, %	Mono-*N*-acetylneamine or Paromamine, %	Neamine, %	Component G	SUM[a], %	Mono-*N*-acetyl Neomycin B, % (TLC)	(GLC)	$[\alpha]_D^{20}$[c]
A	3	54.6 ± 1.0	7.0 ± 0.2	29.4	6.3	1–1.5	<0.5	–	–	98.6 ± 1.5	±0.75		+55.8°
B	9	54.4 ± 0.5	6.9 ± 0.2	30.1	5.9	1.2–1.7	–	–	–	98.7 ± 0.9			+56.8°
C	6	53.6 ± 0.7	8.9 ± 0.2	27.6	7.5	0.5–1	–	–	–	98.4 ± 1.2			+57.6°
D	8	59.4 ± 0.7	5.4 ± 0.3	26.5	9.4	–	<0.5	<0.5	+	100.6 ± 0.7	±3	4.2	+56.3°
E	8	56.3 ± 1.1	5.6 ± 0.2	26.0	11.9	–	<0.5	<0.5	+	99.8 ± 1.2	4 to 5	4.8	+55.9°
F	3	58.2 ± 1.8	4.9 ± 0.7	29.9	4.1	–	1.5–2	<0.5	+	97.7 ± 1.6	±0.75		+53.4°
G	8	56.1 ± 0.9	5.5 ± 0.4	30.8	6.5	–	2–3	<0.5	+	101.4 ± 1.7	±1		+54.4°
H	3	52.4 ± 0.7	6.0 ± 0.7	23.7	13.6	<0.5	±1	<0.5	+	96.5 ± 1.5	±1	0.9	+55.7°
I	8	55.2 ± 0.6	6.8 ± 0.7	25.6	13.0	<0.5	±1	<0.5	+	100.5 ± 0.8	±0.25		+55.6°
USP Reference Standard (Issue E)	4	70.8 ± 0.2	Trace	29.7	0	–	–	<0.5	–	100.5 ± 0.2	–	–	–
Standard European Pharmacopoeia	6	64.6 ± 0.2	6.3 ± 0.25	29.3	0	–	–	–	–	100.1 ± 0.5	–	–	+56.3°
First International Reference Standard Preparation	4	51.4 ± 1.6	16.4 ± 0.6	29.0[d]	0	–	–	3%[d]	–	99.8	–	–	–

[a] Confidence limits (95%) (*t* test). [b] Values represent the mean of two separate determinations. [c] Calculated on dry basis (*c* 1, H_2O). [d] Ref. (1).

site of the methylpyridinium groups yielding acidic functions. This would account for the regular decrease of the neomycin peaks.

One of the resins[19], which has a narrow particle size range (20 ± 5 μm for the resin in the chloride form) gave sharp peaks and a good separation of neomycin B and C. The separation of paromomycin I and the internal standard was not optimal (Table I). The main drawback was the low resistance to pressure of the resin in the hydroxide form. After 3 days at a pressure of 5 kg/cm², the resin bed was retracted to two-thirds of its original volume.

A second resin[20] gave good separation of neomycin B and C, but a poor resolution of paromomycin I and the internal standard, whereas for another resin[21] the opposite was true. With these resins a decrease with time of the neomycin peaks occurred also, although to a lesser extent than with a different resin[8] (Fig. 2). The pronounced change in column parameters was not observed.

Nonelution of a portion of the neomycin load is probably due to some carbon dioxide present in the water used as the mobile phase. Low concentrations could have an influence as large volumes of water are pumped through the columns during 1 week. When an aqueous solution of neomycin B base was saturated with carbon dioxide and applied to the column, no peak could be detected. When a freshly prepared column of resin[20] was loaded with 3 ml of carbon dioxide-saturated water or a 0.025% $NaHCO_3$ solution, the peak area of neomycin B relative to the peak area of trehalose decreased by 15 to 20%, although neomycin sulfate was applied. Formation of a carbonate link of the type $-\phi-CH_2-N^+(CH_3)_3$ CO_3^{-2} neomycin H^+ could explain the influence of carbon dioxide and carbonates on the elution of aminoglycosides. Similar problems have been encountered previously (12) when analyzing kanamycin free base on resin[22] in the hydroxide form. It was found that kanamycin base in aqueous solution converted partially into kanamycin carbonates by reaction with atmospheric carbon dioxide. The carbonates could only be eluted from the resin with water at pH 13 or 14 (12). The problem of carbonate accumulation on the analytical column was solved by connecting a guard column filled with one of the two resins[20,21] in the hydroxide form between the pump and the injector. This ensured a constant neomycin–internal standard ratio for at least 1 week (Fig. 2).

None of the two resins[20,21] gave an entirely satisfactory separation. Good separation of all components was obtained by replacing the 1 × 30 cm of resin[20] by a 1 × 10 cm column of resin[21] connected to a 1 × 20 cm column of resin[20] (Table I).

Calibration—Pure free bases of neomycin B and C were converted into their sulfates for reasons described. Since neomycin B and C had the same detector response in the experimental conditions (6), a mixture of known composition provided two points of the calibration curve per chromatogram. The peak area of the neomycin components over the internal standard peak area was plotted *versus* the calculated amount of free base present in the sample solution. In the 7–70 mg range of neomycin free base, the calibration curve was linear. The regression equation is $y = 0.0036 + 0.0130x$ and the correlation coefficient is 0.9995.

Interfering Compounds—Commercial neomycin contains mono-*N*-acetyl derivatives of the B and C compounds and of neamine (13) (the acetyl group is located at the amino function in the 3-position of the deoxystreptamine moiety) (14). Less active mono-*N*-acetylneomycins cause an overestimation of the B and C components, since they are eluted in the ascent of the main peaks (Fig. 1). Nevertheless, a TLC system allows the separation of neomycin B (or C) and mono-*N*-acetylneomycin B (or C) (Fig. 3). The eluate fractions corresponding to the first half of the neomycin B peak were collected and evaporated to dryness. The res-

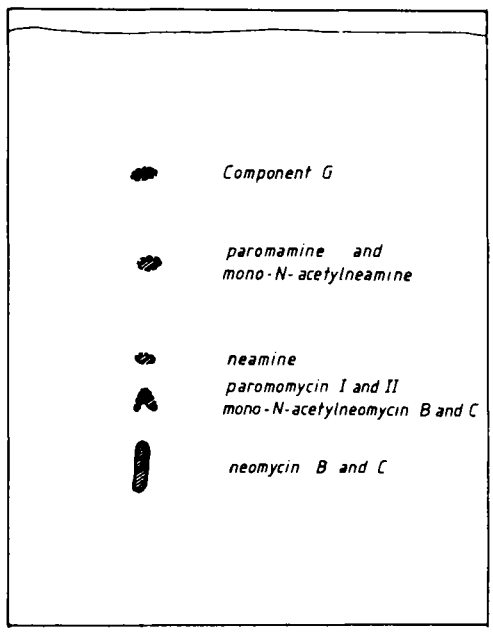

Figure 3—*TLC of a 10-μg sample of neomycin sulfate (silicagel plate[17], 15% potassium dihydrogen phosphate).*

[19] Durrum DA-X2 resin, Pierce Chemical Co., Rockford, IL 61105.
[20] Bio-Rad AG I-X2 resin, Bio-Rad Laboratories, Richmond, Calif.
[21] Bio-Rad AG I-X4 resin, Bio-Rad Laboratories, Richmond, Calif.
[22] Dowex 1-X2.

Table III—Potencies of Analyzed Samples Expressed on Dry Basis

Sample	Average Neomycin B Content, %	Average Neomycin C Content, %	Potency, U/mg	Microbiological Assay	
A	59.6[a]	7.5	725	724 IU/mg[c]	749 IU/mg[e]
B	59.3[a]	7.3	721	732 IU/mg[c]	721 IU/mg[e]
C	57.9[a]	9.6	718	696 IU/mg[c]	746 IU/mg[e]
D	62.3[b]	6.0	747	775 IU/mg[c]	
E	59.3[b]	6.4	715	744 IU/mg[c]	770 IU/mg[e]
F	60.7	5.1	724		
G	60.0	5.9	720		
H	60.6	6.9	733	700 μg/mg[c]	788 IU/mg[e]
I	63.4	7.9	770	710 μg/mg[c]	782 IU/mg[e]
USP Reference Standard (Issue E)	70.8		810	767 μg/mg[d]	
Standard European Pharmacopoeia	64.55	6.25	775	775 IU/mg[d]	
First International Reference Standard Preparation	51.4	16.4	682	680 IU/mg[d]	

[a] Including paromomycin I. [b] Corrected for mono-*N*-acetylneomycin B. [c] Declared by manufacturer. [d] Assigned potency. [e] Determined by Dr. Dubost, Rhône-Poulenc, Paris, France.

idue was then dissolved in 0.50 ml of water, and 1, 2, 3, and 4 μl were spotted on the activated TLC plates, together with 1, 2, 3, and 4 μl of the mono-*N*-acetylneomycin B reference solution. After development and resolution with ninhydrin, a semiquantitative determination of the amount of mono-*N*-acetylneomycin B was made by estimating which spot of the unknown series corresponds best to a spot of the reference dilution. The amount of acetylated products can also be estimated by GLC assay of acetic acid liberated by acid hydrolysis. The correlation between TLC and GLC figures is good, as can be seen from Table II. Mono-*N*-acetylneomycin C, if present, would only represent a fraction of neomycin C, so it was not necessary to estimate such a small amount. If no mono-*N*-acetylneomycin B is available as the reference, it can be replaced by paromomycin, taking into account the sulfuric acid and moisture content of this commercial product. No detectable difference of the ninhydrin response between mono-*N*-acetylneomycin B or C and paromomycin I or II was found.

Although not interfering directly in the assay of the main products, other minor components were analyzed also by TLC. The eluate fractions containing neamine, paromamine, *N*-acetylneamine, and component G were also evaporated to dryness and dissolved in 0.50 ml of water. TLC and semiquantitative determination of these components were performed in a similar way as for mono-*N*-acetylneomycin B. Component G, an *O*-(diaminodideoxyhexosyl)-*myo*-inositol (7) was available, but it was not sufficiently pure to allow such an estimation. Its presence in neomycin samples will be indicated only qualitatively. As can be seen from Fig. 3, it cannot be distinguished whether mono-*N*-acetylamine or paromamine is present. However, from results obtained in the laboratory with ion-pair chromatography on a reversed-phase column[23] it can be seen that mono-*N*-acetylneamine is generally present in a larger quantity than paromamine.

Assuming an equal detector response of paromomycin I and neomycin B (or C) to the differential refractometer, the paromomycin I content of neomycin samples was calculated as for the main products.

Composition of Commercial Samples—A survey of the composition of recent neomycin sulfate samples of French (A–C), Norwegian (D, E), Japanese (F, G), and American (H, I) origin is given in Table II. The neomycin B free base content ranges from 52–59%. These values include mono-*N*-acetylneomycin B which is eventually present. The amount of neomycin C free base is between 4 and 9%. In addition to neomycin B and C, sulfuric acid content, weight loss on drying, and an estimation of the minor components are tabulated. Disregarding components that represent <0.5%, a summation of all other components closely approaches 100%.

Although an assay or estimation of neamine is prescribed by many pharmacopoeias, the present results prove this substance to be virtually absent from all samples analyzed. However, mono-*N*-acetylated neomycins and paromomycin I may be present in appreciable amounts. The nature of the minor neomycin components is typical for a particular manufacturer, possibly as a result of different fermentation and isolation processes.

Correlation Between Chromatographic and Microbiological Assay—To make a correlation of the amounts of neomycin B and C found for different samples with the results of the microbiological assay, it is necessary to know the relative response of neomycin C to neomycin B. However, this response depends on the microorganisms and media used in a diffusion or a turbidimetric assay. Relative responses of 30–40% have been obtained (15). Past experience indicates that the variation is even larger, and it has been assumed that the potency of neomycin C is half that of neomycin B (5). Using the amount of neomycin B and C in the European Standard (which is from the same batch as the International Standard) and its titer (775 IU/mg), it can be calculated that 1 μg of free base of the European (or International) Standard corresponds to:

$$\frac{775}{645.5 + \frac{62.5}{2}} = 1.145 \text{ potency units.}$$

Although potency units correspond to international units, an alternative symbol is preferred since international units are, strictly speaking, only valid for microbiological assays.

This conversion was applied to the different neomycin samples (Table III). If they contained paromomycin I, the amount of this component was added to the amount of neomycin B, because their antimicrobial activity is almost identical. It is interesting to note that the potency units of the First International Standard are nearly identical to the assigned IU value. For samples A–E, H and I, the correlation is also acceptable. The results of the microbiological assays of two samples (C and E) differ somewhat from one laboratory to another, even if they were obtained by analysts having much experience with this type of assay.

An attempt can be made to correlate the International Standard with the USP Reference Standard, although the potency in micrograms per milligram is defined in a different way and despite the fact that the latter preparation contains almost exclusively neomycin B. From the calculated 810 potency U/mg and the 767 μg/mg figures, it can be deduced that 1 μg/mg = 1.056 IU/mg

These calculations are not essential for the proposed chromatographic assay, which gives information concerning relative and absolute amounts of neomycin B and C and related compounds. Nevertheless, the calculations indicate that the proposed method could replace a microbiological assay.

The proposed method allows a chromatographic quantitation of neomycin B and C in neomycin sulfate powders without cumbersome sample derivatizations. The absolute standard deviation (mean value) is 0.67% for the determination of neomycin B and 0.33% for neomycin C. It can be performed with relatively simple apparatus which can be automated easily. Taking the precaution of not analyzing free bases, reliable values can be obtained.

[23] Method described in a private communication of Dr. A. Sezerat, Roussel-UCLAF Co., Romainville, France.

REFERENCES

(1) J. W. Lightbown, A. H. Thomas, B. Grab, and H. Dixon, *J. Biol. Stand.*, **7**, 227 (1979).

(2) W. T. Sokolski, C. G. Chichester, and D. G. Kaiser, *J. Pharm Sci.*, **53**, 726 (1964).

(3) K. Tsuji and I. H. Robertson, *Anal. Chem.*, **41**, 1332 (1969).

(4) M. Margosis and K. Tsuji, *J. Pharm. Sci.*, **62**, 1836 (1973).

(5) K. Tsuji, W. F. Goetz, W. Van Meter, and K. A. Gusciora, *J. Chromatogr.*, **175**, 141 (1979).

(6) W. Decoster, P. Claes, and H. Vanderhaeghe, *ibid.*, **211**, 223 (1981).

(7) P. Claes, F. Compernolle, and H. Vanderhaeghe, *J. Antibiot.*, **27**, 931 (1974).
(8) E. Roets and H. Vanderhaeghe, *J. Pharm. Pharmacol.*, **24**, 795 (1972).
(9) M. Dubost, C. Pascal, B. Terlain, and J. P. Thomas, *J. Chromatogr.*, **86**, 274 (1974).
(10) S. Inouye and H. Ogawa, *J. Chromatogr.*, **13**, 536 (1964).
(11) A. Neuberger and A. P. Fletcher, *Carbohydr. Res.*, **17**, 89 (1971).
(12) K. S. Andrews and H. W. Coleman, *Annual General Meeting of Electrophoresis and Chromatography*. London, Nov. 12, 1975.
(13) W. S. Chilton, *Ph.D. Thesis*, University of Illinois, 1963.
(14) K. L. Rinehart, "The Neomycins and Related Antibiotics," Wiley, New York, N.Y., 1964.
(15) K. Tsuji, J. H. Robertson, R. Baas, and D. J. McInnis, *Appl. Microbiol.*, **18**, 396 (1969).

ACKNOWLEDGMENTS

The authors thank Dr. Dubost (Rhône-Poulenc, Paris, France) for the microbiological assay of neomycin samples, Dr. G. van Dedem (Diosynth, Oss, Holland) for information concerning the GLC determination of *N*-acetyl groups, Dr. J. Lightbown (National Institute for Biological Standards and Control, London, Great Britain) for providing a sample of the First International Reference Standard Preparation of neomycin, and to the firms Upjohn Belgium, (Puurs, Belgium), Apothekernes (Oslo, Norway), and Roussel-UCLAF (Romainville, France) for the supply of various neomycin sulfate samples.

Potential Alkylating Agents Derived from Benzimidazole and Benzothiazole

A.-MOHSEN M. E. OMAR ˣ, N. S. HABIB, and OMAIMA M. ABOULWAFA

Received October 14, 1981, from the *Pharmaceutical Chemistry Department, Faculty of Pharmacy, University of Alexandria, Egypt.* Accepted for publication November 19, 1981.

Abstract □ Several benzimidazole and benzothiazole alkylating agents, bearing structural modification of certain drugs, were synthesized and evaluated for anticancer activity. Among the products, the dihydrochloride salt of 2-[*p*-[2-(bis(2-chloroethyl)amino)ethoxy]phenyl]benzimidazole (VI) exhibited a high antileukemic activity in P-388 lymphocytic leukemia.

Keyphrases □ Alkylating agents—derived from benzimidazole and benzothiazole, potential □ Benzimidazole—potential alkylating agents, benzothiazole □ Benzothiazole—potential alkylating agents, benzimidazole

The studies of benzimidazole alkylating agents reported the production of a variety of compounds (1–5) of which 4 - [2 - [5(6) - bis - (2-chloroethyl)amino]benzimidazolyl]-butyric acid[1] (6) and 2-[bis(2-chloroethyl)aminoethyl]-benzimidazole[2] (7, 8) are the most effective and clinically useful anticancer agents. In a previous investigation of the effect of structural modification on the anticancer activity of these compounds, several benzimidazole-2-thioethylsulfonic esters and nitrogen mustard derivatives were synthesized and evaluated for antileukemic properties (9). In continuation of these studies, this study describes the preparation of several new benzimidazole and benzothiazole alkylating agents (III, IV, VI, and X) and reports on the results of their evaluation against P-388 lymphocytic leukemia (Scheme I).

RESULTS AND DISCUSSION

Chemistry—*p*-(2-Hydroxyethoxy)benzaldehyde (I), prepared by etherification of *p*-hydroxybenzaldehyde with ethylene chlorohydrin (10) in the presence of sodium methoxide, was reacted with *o*-phenylenediamine and copper acetate, in accordance with the modified Weidenhagen reaction (11), to give 2-[*p*-(2-hydroxyethoxy)-phenyl]-benzimidazole hydrochloride (II). This was reacted with methanesulfonyl chloride or *p*-toluenesulfonyl chloride in pyridine to produce the corresponding sulfonic esters (III and IV). The *p*-toluenesulfonic ester (IV) was fused with excess diethanolamine and the produced 2-[*p*-[2-(bis-(2-hydroxyethyl)amino)ethoxy]phenyl]benzimidazole (V) converted into the dihydrochloride salt of the nitrogen mustard 2-[*p*-[2-(bis-(2-chloroethyl)amino)ethoxy]phenyl]benzimidazole (VI) by boiling with thionyl chloride in dioxane.

The reaction of *p*-(2-hydroxyethoxy)benzaldehyde (I) with o-aminothiophenol in pyridine gave 2-[*p*-(2-hydroxyethoxy)phenyl]benzothiazole (VII). This, on treatment with *p-toluenesulfonyl* chloride or methanesulfonyl chloride, yielded 2-[*p*-(2-chloroethoxy)phenyl]benzothiazole (VIII) rather than the corresponding sulfonic esters. Compound VIII was also obtained when the hydroxybenzothiazole derivative

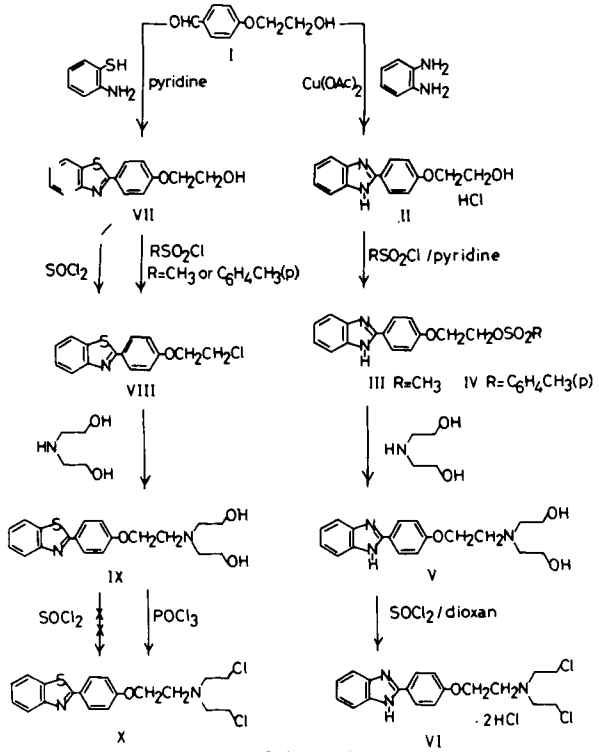

Scheme I

[1] Cytostasan, Imet 3393, A.
[2] Benzimidazole mustard NSC 23891, B.

0022-3549/82/0900-0991$01.00/0

(7) P. Claes, F. Compernolle, and H. Vanderhaeghe, *J. Antibiot.*, **27**, 931 (1974).
(8) E. Roets and H. Vanderhaeghe, *J. Pharm. Pharmacol.*, **24**, 795 (1972).
(9) M. Dubost, C. Pascal, B. Terlain, and J. P. Thomas, *J. Chromatogr.*, **86**, 274 (1974).
(10) S. Inouye and H. Ogawa, *J. Chromatogr.*, **13**, 536 (1964).
(11) A. Neuberger and A. P. Fletcher, *Carbohydr. Res.*, **17**, 89 (1971).
(12) K. S. Andrews and H. W. Coleman, *Annual General Meeting of Electrophoresis and Chromatography*. London, Nov. 12, 1975.
(13) W. S. Chilton, *Ph.D. Thesis*, University of Illinois, 1963.
(14) K. L. Rinehart, "The Neomycins and Related Antibiotics," Wiley, New York, N.Y., 1964.
(15) K. Tsuji, J. H. Robertson, R. Baas, and D. J. McInnis, *Appl. Microbiol.*, **18**, 396 (1969).

ACKNOWLEDGMENTS

The authors thank Dr. Dubost (Rhône-Poulenc, Paris, France) for the microbiological assay of neomycin samples, Dr. G. van Dedem (Diosynth, Oss, Holland) for information concerning the GLC determination of *N*-acetyl groups, Dr. J. Lightbown (National Institute for Biological Standards and Control, London, Great Britain) for providing a sample of the First International Reference Standard Preparation of neomycin, and to the firms Upjohn Belgium, (Puurs, Belgium), Apothekernes (Oslo, Norway), and Roussel-UCLAF (Romainville, France) for the supply of various neomycin sulfate samples.

Potential Alkylating Agents Derived from Benzimidazole and Benzothiazole

A.-MOHSEN M. E. OMAR ˣ, N. S. HABIB, and OMAIMA M. ABOULWAFA

Received October 14, 1981, from the *Pharmaceutical Chemistry Department, Faculty of Pharmacy, University of Alexandria, Egypt.* Accepted for publication November 19, 1981.

Abstract □ Several benzimidazole and benzothiazole alkylating agents, bearing structural modification of certain drugs, were synthesized and evaluated for anticancer activity. Among the products, the dihydrochloride salt of 2-[*p*-[2-(bis(2-chloroethyl)amino)ethoxy]phenyl]benzimidazole (VI) exhibited a high antileukemic activity in P-388 lymphocytic leukemia.

Keyphrases □ Alkylating agents—derived from benzimidazole and benzothiazole, potential □ Benzimidazole—potential alkylating agents, benzothiazole □ Benzothiazole—potential alkylating agents, benzimidazole

The studies of benzimidazole alkylating agents reported the production of a variety of compounds (1–5) of which 4 - [2 - [5(6) - bis - (2-chloroethyl)amino]benzimidazolyl]-butyric acid[1] (6) and 2-[bis(2-chloroethyl)aminoethyl]-benzimidazole[2] (7, 8) are the most effective and clinically useful anticancer agents. In a previous investigation of the effect of structural modification on the anticancer activity of these compounds, several benzimidazole-2-thioethylsulfonic esters and nitrogen mustard derivatives were synthesized and evaluated for antileukemic properties (9). In continuation of these studies, this study describes the preparation of several new benzimidazole and benzothiazole alkylating agents (III, IV, VI, and X) and reports on the results of their evaluation against P-388 lymphocytic leukemia (Scheme I).

RESULTS AND DISCUSSION

Chemistry—*p*-(2-Hydroxyethoxy)benzaldehyde (I), prepared by etherification of *p*-hydroxybenzaldehyde with ethylene chlorohydrin (10) in the presence of sodium methoxide, was reacted with *o*-phenylenediamine and copper acetate, in accordance with the modified Weidenhagen reaction (11), to give 2-[*p*-(2-hydroxyethoxy)-phenyl]-benzimidazole hydrochloride (II). This was reacted with methanesulfonyl chloride or *p*-toluenesulfonyl chloride in pyridine to produce the corresponding sulfonic esters (III and IV). The *p*-toluenesulfonic ester (IV) was fused with excess diethanolamine and the produced 2-[*p*-[2-(bis-(2-hydroxyethyl)amino)ethoxy]phenyl]benzimidazole (V) converted into the dihydrochloride salt of the nitrogen mustard 2-[*p*-[2-(bis-(2-chloroethyl)amino)ethoxy]phenyl]benzimidazole (VI) by boiling with thionyl chloride in dioxane.

The reaction of *p*-(2-hydroxyethoxy)benzaldehyde (I) with o-aminothiophenol in pyridine gave 2-[*p*-(2-hydroxyethoxy)phenyl]benzothiazole (VII). This, on treatment with *p-toluenesulfonyl* chloride or methanesulfonyl chloride, yielded 2-[*p*-(2-chloroethoxy)phenyl]benzothiazole (VIII) rather than the corresponding sulfonic esters. Compound VIII was also obtained when the hydroxybenzothiazole derivative

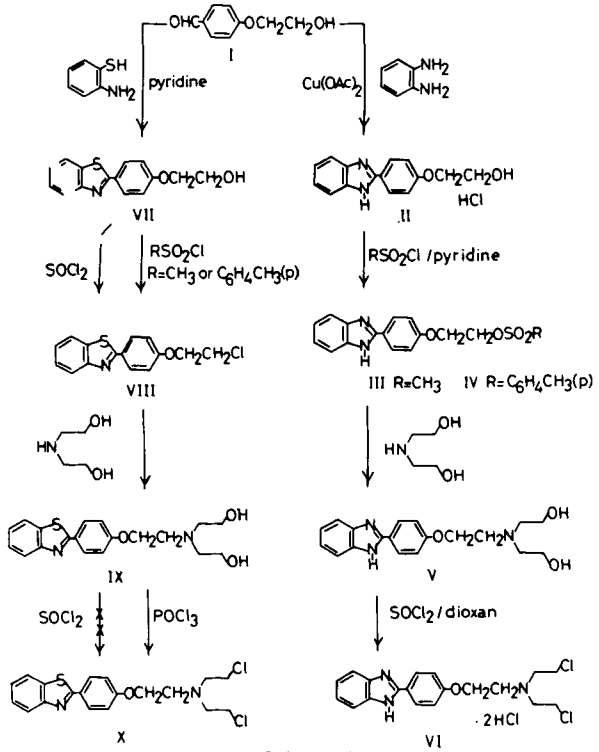

Scheme I

[1] Cytostasan, Imet 3393, A.
[2] Benzimidazole mustard NSC 23891, B.

0022-3549/82/0900-0991$01.00/0

(VII) was treated with thionyl chloride in chloroform. It was then fused with diethanolamine to form the dihydroxyethylaminobenzothiazole derivative (IX) which on reaction with excess phosphorous oxychloride yielded the required nitrogen mustard, 2-[*p*-[2-(bis(2-chloroethyl)amino)ethoxy]phenyl]benzothiazole (X). The products were identified by microanalysis, IR and UV spectra and for representative examples by PMR and mass spectra.

The mass spectrum of the benzimidazole nitrogen mustard (VI) indicated the absence of the molecular ion peak at *m/z* 449. However, it showed that the molecule underwent a successive elimination of two pairs of hydrogens to give Ion A at *m/z* 445 and at 447 and 449 (for M+2 and M+4, respectively) (Scheme II). It also showed that Compound VI lost 3 moles of hydrogen chloride and six hydrogens to form Ion B at *m/z* 335 and 337 (for M+2). In an alternative fragmentation pathway, Compound VI eliminated a chloroethyl and a chloromethyl group and accepted a hydrogen to give Ion C at *m/z* 266. This, on further elimination of a methylamino moiety and acceptance of a hydrogen, gave Ion D at *m/z* 238. The successive removal of two methylene groups from Ion D led to formation of 2-(*p*-hydroxyphenyl)benzimidazole, Ion E, at *m/z* 210. The latter lost carbon monoxide to yield 2-cyclopentadienylbenzimidazole, Ion F, at *m/z* 181. The base peak was identified at *m/z* 28 corresponding to a carbon monoxide, an ethylene, or —N—CH_2 ion. The mass spectrum of benzothiazole nitrogen mustard (X) showed the molecular ion peak at *m/z* 394, and at 396 and 398 (for M+2 and M+4, respectively). The cleavage of a chlorine ion from Compound X gave the ion at *m/z* 359 and 361 which successively cleaved a methylene and a chloromethylamino fragment giving the ion at *m/z* 254. This in turn lost two successive methylene groups to form the 2-(*p*-hydroxyphenyl)benzothiazole ion at *m/z* 227, which on elimination of carbon monoxide gave the 2-cyclopentadienylbenzothiazole ion at *m/z* 198. The base peak, as shown in the data in the Experimental section, was shown at *m/z* 154, and at 156 and 158 (for M+2 and M+4, respectively) corresponding to the bis(2-chloroethyl)aminomethyl ion. The spectra of both Compounds VI and X have also shown the ions corresponding to the reported fragmentation of the heterocyclic rings (12–15).

Anticancer Screening—The products were evaluated against P-388 lymphocytic leukemia in mice (9). The activities were measured as the ratio of the mean survival time of the test animals to that of the control animals, expressed as a percentage (T/C %). The nitrogen mustard (VI) was the only product which exhibited T/C % values of 189, 144, and 132 when administered in doses of 12.5, 6.25, and 3.13 mg/kg of body weight, respectively.

As revealed from the reported studies of the benzimidazole nitrogen mustards, the majority of active products (1, 3, 4, 7) either retained the methylene group of 2-[bis(2-chloroethyl)aminoethyl]benzimidazole[2] or in only a few cases replaced it by phenyl or styryl moieties having the alkylating function directly attached to their benzene rings. In the present investigation, the high antileukemic activity of Product VI has demonstrated the efficacy of the *p*-ethoxyphenyl function as an additional carrier chain for alkylating groups. To confirm this finding, the compounds in preparation now for other structural activity relationship studies of alkylating agents have been designed to contain this chain.

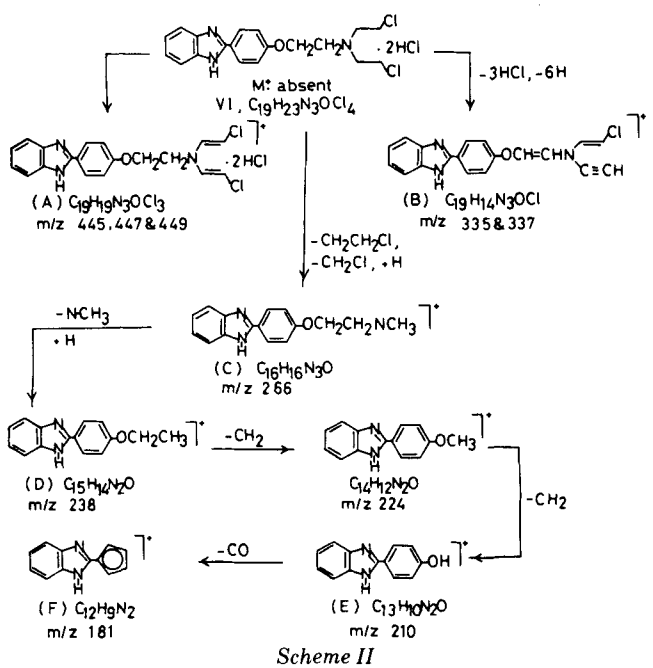

Scheme II

EXPERIMENTAL[3]

2-[*p*-(2-Hydroxyethoxy)phenyl]benzimidazole Hydrochloride (II)—A solution of copper acetate monohydrate (6 g, 30 mmoles) in water (25 ml) was added to the solution of *o*-phenylenediamine (1.6 g, 14.8 mmoles) and *p*-(2-hydroxyethoxy)benzaldehyde (I) (2.42 g, 14.5 mmoles) in ethanol (10 ml) and the mixture, developing an immediate green precipitate, was heated under reflux for 30 min. The product was filtered, washed with water until the washing became colorless, and dissolved by heating under reflux in 2 *N* HCl solution (50 ml) for 2 hr. After cooling, the deposited shiny dark brown crystals were filtered and crystallized from ethanol (charcoal) giving the required product (II) as small needles melting at 272–274°. Yield: 3.2 g (76%). IR (mineral oil): 3460–3320 (OH), 1620 and 1610 (C=N), 1575 and 1500 (C=C, Ar), 1555 (δ NH), 1300 (δ OH), 1260 and 1045 cm^{-1} (—C—O—C—, asym and sym). UV λ_{max} (ethanol) (log ε): 255 (4.124), 312 (4.467), and at 325 nm (sh) (4.222).

Anal.—Calc. for $C_{15}H_{15}N_2O_2Cl$: N, 9.62; Cl, 12.2. Found: N, 10.00; Cl, 12.00.

2-[*p*-[2-(*p*-Toluenesulfonyloxy)ethoxy]phenyl]benzimidazole (IV)—*p*-Toluenesulfonyl chloride (5.5 g, 28.8 mmoles) was added to a cooled (ice-salt) solution of the benzimidazole derivative (II) (2.8 g, 9.6 mmoles) in dry pyridine (25 ml), and the mixture was stirred during cooling for 6 hr to form a white precipitate. Ice cold water (10 ml) was added dropwise and stirring was continued until the precipitate dissolved, and an orange solution was obtained. Further addition of water (100 ml) separated a solid which was filtered, washed with water, and crystallized from ethanol giving the sulfonic ester (III) melting at 155–157°. Yield: 2.87 g (74%). IR (mineral oil): 1605 (C=N), 1580, 1490 (C=C, Ar), 1560 (δ OH), 1340, 1170 (SO_2, asym and sym), 1250 and 1030 cm^{-1} (—C—O—C—).

Anal.—Calc. for $C_{22}H_{20}N_2O_4S$: C, 64.70; H, 4.94; N, 6.86. Found: C, 64.70; H, 5.20; N, 6.70.

Mass spectrum: *m/z* (relative abundance %) 408 (M^+) (1), 407 (6), 390 (2), 328 (5), 327 (6), 326 (29), 264 (2), 263 (7), 262 (35), 235 (5), 199 (14), 157 (6), 156 (11), 155 (100), 139 (10), 107 (11), 105 (11), 92 (12), 91 (96), 90 (5), 89 (6), 78 (13), 65 (17), 44 (9).

2-[*p*-[2-(Methanesulfonyloxy)ethoxy]phenyl]benzimidazole (III)—By reacting methanesulfonyl chloride (1.18 g, 10.3 mmoles) with the benzimidazole derivative (II) (1 g, 3.4 moles) in dry pyridine (15 ml), in the same manner as described for the synthesis of compound IV, the required methanesulfonic ester (III) was obtained as small white shiny crystals melting at 206–208° (ethanol). Yield: 750 mg (96%).

IR (mineral oil): 1610 (C=N), 1580, 1490 (C=C, Ar), 1540 (δ NH), 1330, 1100 (SO_2 asym and sym), 1260 and 1040 cm^{-1} (—C—O—C—). UV λ_{max} (ethanol) (log ε): 252 (4.182), 312 (4.507), and at 325 nm (sh) (4.262).

Anal.—Calc. for $C_{16}H_{16}N_2O_4S$: C, 57.83; H, 4.85; N, 8.43; S, 9.63. Found: C, 57.80; H, 4.80; N, 8.30; S, 9.70.

2-[*p*-[2-(Bis(2-hydroxyethyl)amino)ethoxy]phenyl]benzimidazole (V)—Excess diethanolamine (1 g, 9.5 mmoles) was added to the *p*-toluenesulfonic ester (IV) (1.7 g, 4.1 mmoles) and the mixture was heated at 120–130° (external temperature) for 1 hr. After cooling, the pale yellow solution was diluted with water (100 ml) to separate a white precipitate which was filtered and washed with water (4 × 50 ml) and crystallized from aqueous ethanol to yield the dihydroxy-ethylamino derivative (V) as white amorphous powder melting at 185–187°. Yield: 900 mg (90%). IR (mineral oil): 3375 (OH), 1605 (C=N), 1595, 1490 (C=C, Ar), 1540 (δ NH), 1240 and 1060 cm^{-1} (—C—O—C—).

Anal.—Calc. for $C_{19}H_{23}N_3O_3$: C, 66.84; H, 6.79; N, 12.31. Found: C, 67.00; H, 6.70; N, 12.30.

2-[*p*-[2-(Bis(2-chloroethyl)amino)ethoxy]phenyl]benzimidazole Dihydrochloride (VI)—Thionyl chloride (2 ml) was added dropwise to a hot and stirred solution of Compound V (650 mg, 2.6 mmoles) in dioxane (25 ml) to form a white precipitate. This soon dissolved as the reflux started, and fine white crystals began to form and increased in volume during reflux for 2 hr. Filtration followed by successive washing of the product with hot dioxane and dry acetone gave the

[3] All melting points are uncorrected. IR spectra were measured on a Beckman 4210 IR spectrophotometer. UV spectra were measured on a Beckman 24 spectrophotometer. PMR spectra were measured on a Varian A60, and mass spectra on an AEI-MS-50.

dihydrochloride salt of the nitrogen mustard VI, which softened with darkening at 245° and completely melted with decomposition at 283–285°. Yield: 920 mg (97%). IR (mineral oil): 3110 (NH), 1640, 1610 (C=N), 1590, 1510 (C=C, Ar), 1550 (δ NH), 1260 and 1065 cm^{-1} (—C—O—C—).

Anal.—Calc. for $C_{19}H_{23}N_3O\,Cl_4$: C, 50.50; H, 5.09; N, 9.31; Cl, 31.48. Found: C, 50.60; H, 4.70; N, 8.90; Cl, 31.50.

Mass spectrum: *m/z* (relative abundance) (M^+ absent) 449 (4), 447 (12), 445 (32), 379 (1), 378 (3), 337 (4), 335 (13), 266 (17), 238 (11), 237 (25), 236 (38), 235 (36), 224 (17), 223 (47), 211 (54), 210 (92), 209 (38), 181 (32), 180 (22), 129 (12), 127 (18), 121 (8), 120 (20), 119 (26), 112 (30), 107 (13), 105 (37), 100 (16), 99 (38), 97 (11), 93 (12), 91 (36), 84 (15), 78 (28), 77 (35), 72 (10), 70 (29), 65 (33), 64 (34), 63 (38), 58 (29), 57 (42), 56 (57), 55 (52), 52 (39), 44 (20), 42 (81), 38 (41), 28 (100).

2-[*p*-(2-Hydroxyethoxy)phenyl]benzothiazole (VII)—A solution of *o*-aminothiophenol (730 mg, 5.8 mmoles) in pyridine (5 ml) was added to the solution of *p*-(2-hydroxyethoxy)benzaldehyde (I) (970 mg, 5.8 mmoles) in pyridine (5 ml) and the mixture was heated on a water bath for 1 hr. After cooling, the product was poured onto water (100 ml), and the yellowish white emulsion so obtained was left overnight to deposit a whitish precipitate. This was filtered, washed with water (3 × 50 ml) and crystallized from ethanol (charcoal) to deposit the required product (VII) as small whitish shiny crystals melting at 157–159°. Yield: 1.28 g (81%). IR (mineral oil): 3200 (OH), 1595, 1570 (C=N mixed with C=C, Ar), 1305 (δ OH), 1245 and 1040 cm^{-1} (—C—O—C—). UV λ_{max} (ethanol) (log ε): 322 nm (4.447).

Anal.—Calc. for $C_{15}H_{13}NO_2S$: C, 66.41; H, 4.83; S, 11.78. Found: C, 65.90; H, 4.70; S, 11.40.

2-[*p*-(2-Chloroethoxy)phenyl]benzothiazole (VIII)—p-*Toluenesulfonyl Chloride or Methanesulfonyl Chloride*—The sulfonyl chloride derivative (11 mmoles) was added to a solution of Compound VII (1 g, 3.6 mmoles) in dry pyridine (25 ml), and the orange clear solution was stirred at ~60–70° (external temperature) for 1 hr. The final dark mixture was left for 3 days at room temperature and then diluted with ice cold water (100 ml). The separated buffer product was filtered, washed with water (3 × 100 ml) and crystallized from ethanol (charcoal) to give colorless shiny scales melting at 144–145°. This was found to be 2-[*p*-(2-chloroethoxy)phenyl]benzothiazole. Yield: 70–80%.

Phosphorous Oxychloride—Phosphorous oxychloride (10 ml) was added to the hydroxy derivative (VII) (2.15 g, 7.9 mmoles) and the mixture heated under reflux for 1 hr. The dark brown solution was evaporated *in vacuo*, to remove excess phosphorous oxychloride, and the residue was dissolved in hot ethanol, treated with sodium hydrogen carbonate (2 g), and left overnight. The alcoholic solution was filtered, concentrated, and cooled to give a white precipitate of the chloro derivative (VIII) which melted at 143–145° (ethanol). Yield: 1.8 g (73%). Product VIII obtained from all experiments did not show melting point depression and showed superimposability in IR and UV spectra. IR (mineral oil): 1600, 1575 (C=N and C=C, Ar), 1250 and 1040 cm^{-1} (—C—O—C— asym and sym). UV λ_{max} (ethanol) (log ε): 320 nm (4.551).

Anal.—Calc. for $C_{15}H_{12}NOSCl$: C, 62.10; H, 4.10; N, 4.80; S, 11.00. Found: C, 62.40; H, 4.50; N, 4.80; S, 11.10.

PMR: δ ($CDCl_3$) 3.83 (t, 2H, CH_2Cl, J = 7 Hz), 4.28 (t, 2H, CH_2O, J = 7 Hz), 6.90–8.19 (m, 8H, Ar—H) ppm.

Mass spectrum: *m/z* (relative abundance %) 291 (M^+) (47), (M+2 at 293), 292 (7), 290 (23), 289 (100), 228 (5), 227 (22), 226 (19), 199 (4), 198 (11), 197 (4), 154 (5), 108 (9), 69 (7), 63 (9).

2-[*p*-[2-(Bis(2-hydroxyethyl)amino)ethoxy]phenyl]benzothiazole (IX)—Excess diethanolamine (1 g, 9.5 mmoles) was added to the chloro derivative (VIII) (0.5 g, 1.17 mmoles), and the mixture was heated at 110–120° (external temperature) for 30 min. After cooling, chloroform (50 ml) was added and the mixture was shaken with water (2 × 100 ml). The aqueous layer was again extracted with chloroform (2 × 50 ml), and the combined chloroform extracts were washed with water (3 × 100 ml) until free from diethanolamine, dried (anhydrous Na_2SO_4), and evaporated. The produced viscous oil was dissolved in benzene, treated with light petroleum (bp 60–80°) until a permanent turbidity developed, scratched, and stored in a refrigerator. The deposited brown solid was crystallized from a benzene–light petroleum mixture to give the required product (IX), as a creamy amorphous powder melting at 77–79°. Yield: 420 mg (99.7%). IR (mineral oil): 3400–3220 (OH), 1600, 1575 (C=N and C=C, Ar), 1300 (δ OH), 1245 and 1085 cm^{-1} (—C—O—C—). UV λ_{max} (ethanol) (log ε): 322 nm (4.397).

Anal.—Calc. for $C_{19}H_{22}N_2O_3S$: C, 63.67; H, 6.19; N, 7.82. Found: C, 63.30; H, 6.20; N, 7.40.

2-[*p*-[2-(Bis(2-chloroethyl)amino)ethoxy]phenyl]benzothiazole (X)—Phosphorous oxychloride (5 ml) was slowly added to the dihydroxyethylamino derivative (IX) (580 mg, 1.62 mmoles) while being cooled in ice, and the mixture was allowed to warm slowly to room temperature and then heated under reflux for 1 hr. Excess phosphorous oxychloride was evaporated *in vacuo* and the black viscous residue decomposed by addition of crushed ice. Water (50 ml) and a few drops of 10% aqueous HCl solution were then added, and the mixture was heated, filtered while hot, cooled, and rendered alkaline with sodium bicarbonate. The crude buffer product so obtained exhibited two spots on TLC and could not be purified by repeated crystallization from ethanol. Therefore, it was purified on a column of silica gel[4] (10 g) using chloroform as the eluent. Evaporation of chloroform gave 200 mg (31%) of the nitrogen mustard X, which on crystallization from methanol separated as shiny white crystals melting with decomposition at 90–91°. IR (mineral oil): 1600, 1570 (C=N and C=C, Ar), 1245 and 1070 cm^{-1} (—C—O—C— asym and sym). UV λ_{max} (ethanol) (log ε): 321 nm (4.416).

Anal.—Calc. for $C_{19}H_{20}N_2OSCl_2$: C, 57.70; H, 5.06; N, 7.08; S, 8.10; Cl, 17.90. Found: C, 57.60; H, 5.30; N, 6.60; S, 8.50; Cl, 17.50.

PMR δ ($CDCl_3$): 2.85–3.25 [*m*, 6H, $N(CH_2)_3$], 3.55 (t, 4H, 2 × —CH_2Cl, J = 7 Hz), 4.15 (t, 2H, O—CH_2—, J = 7 Hz), 6.90–8.20 (m, 8H, Ar—H)ppm.

Mass spectrum: *m/z* (relative abundance %) 398 (5), 397 (6), 396 (31), 395 (11), 394 (39), 359 (2), 347 (3), 345 (11), 254 (3), 240 (2), 227 (5), 226 (5), 210 (12), 198 (5), 172 (8), 170 (8), 168 (11), 158 (14), 156 (80), 154 (100), 65 (5), 63 (14), 56 (12), 42 (10), 32 (8), 28 (30).

REFERENCES

(1) O. F. Ginzburg, B. A. Porai-Koshits, M. I. Krylova, and S. M. Lotareichok, *Zh. Obshch. Khim.*, **27,** 411 (1957); through *Chem. Abstr. Jpn.*, **51,** 15500d (1957).

(2) R. C. Elderfield, I. S. Covey, J. B. Geiduschek, W. L. Meyer, A. B. Ross, and J. H. Ross, *J. Org. Chem.*, **23,** 1749 (1958).

(3) W. S. Gump and E. J. Nikawitz, *ibid.*, **24,** 712 (1959).

(4) W. A. Skinner, M. G. M. Schelstraete, and B. R. Baker, *ibid.*, **24,** 1827 (1959).

(5) K. C. Tsou, D. J. Rabiger, and D. Sobel, *J. Med. Chem.*, **12,** 818 (1969).

(6) P. N. Preston, *Chem. Rev.*, **74,** 310 (1974).

(7) E. Hirschberg, A. Gellhorn, and W. S. Gump, *Cancer Res.*, **17,** 904 (1957).

(8) M. Ochao, Jr. and E. Hirschberg, in "Experimental Chemotherapy," Vol. V, R. J. Schnitzer and F. Hawking, Eds., Academic, New York, N.Y., 1967, p. 19.

(9) E. A. Ibrahim, A.-Mohsen M. E. Omar, and M. A. Khalil, *J. Pharm. Sci.*, **69,** 1348 (1980).

(10) G. Hasegawa and S. Baba, Japan patent, 6,920,090, through *Chem. Abstr.*, **71,** 112628h (1969).

(11) L. L. Zaika and N. N. Joulie, *J. Heterocycl. Chem.*, **3,** 289 (1966).

(12) T. Nishiwaki, *J. Chem. Soc. C*, **1968,** 428.

(13) S. O. Lawesson, G. Schroll, J. H. Bowie, and R. G. Cooks, *Tetrahedron*, **24,** 1875 (1968).

(14) B. J. Millard and A. F. Temple, *Org. Mass Spectrom.*, **1,** 285 (1968).

(15) A. Maquestian, Y. Van Haverbeke, B. Flammang, and J. Pierard, *Bull. Soc. Chim. Belg.*, **84,** 213 (1975); through *Chem. Abstr.*, **83,** 77890m (1975).

ACKNOWLEDGMENTS

This work was partially supported by Pharco Pharmaceutical Co., Cairo, Egypt.

The authors thank the members of Drug Research and Development, Division of Cancer Research, National Cancer Institute, Bethesda, MD 20014, for screening the compounds. They also thank Prof. T. Kappe, Institute of Organic Chemistry, Graz, A-8010, Austria, for the mass spectra, and the members of the Microanalytical Unit, Faculty of Science, University of Cairo, for microanalytical data.

[4] Kieselgel 100 E. Merck; 70–230 mesh, ASTM.

Complexation of Procainamide with Dextrose

V. DAS GUPTA

Received June 8, 1981, from the *University of Houston, College of Pharmacy, Department of Pharmaceutics, Houston, TX 77030.* Accepted for publication November 20, 1981.

Abstract □ The percent of procainamide complexed with dextrose was determined to be directly related to the concentration per mole fraction of dextrose in the solution. The complexation process was reversible and did not proceed at lower pH (~1.5). The rate of formation of complex was dependent on the initial pH value of the solution and the pH decreased as the concentration of the complex increased. The increase in the concentration of procainamide did not change the equilibrium concentration of the complex. The addition of sodium chloride or edetate disodium did not alter the rate of formation of the complex or its equilibrium concentration. The addition of hydrochloric acid prevented the formation of the complex and on adding hydrochloric acid after the formation of the complex, procainamide was completely freed.

Keyphrases □ Dextrose—complexation of procainamide □ Procainamide—complexation, with dextrose □ Complexation—procainamide with dextrose

Procainamide (I) is often mixed with 0.9% NaCl or 5% dextrose solution in water. The mixture is usually administered by continuous intravenous infusion for the treatment of certain cardiovascular diseases.

Procainamide is stable when mixed with sodium chloride solution (1) but in 5% dextrose solution, the stability is doubtful (1, 2). For example, one such solution lost ~12% of potency after 24 hr of storage (1). It has been predicted that procainamide may be forming a reversible association complex with dextrose (2). Procainamide is considered unusually stable towards hydrolysis in the pH range of 2–7 (3) even at higher temperatures.

The separation of procainamide from *p*-aminobenzoic acid (the major product of degradation) using high-pressure liquid chromatography (HPLC) has been reported (2). The other product of degradation, diethylethylenediamine, did not absorb light to record a peak in the chromatogram. An additional peak from the interaction of dextrose and I was observed in the chromatogram.

The purpose of this investigation was to study the complexation of procainamide with dextrose. The study was conducted using an HPLC method similar to that previously reported (2) in the literature.

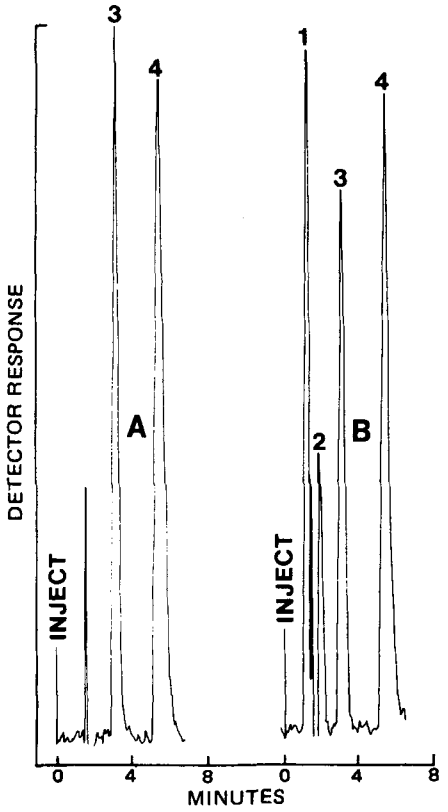

Figure 1—*Sample chromatograms: Peaks 1–4 are from* p-*aminobenzoic acid, complex of I with dextrose, free procainamide and methapyrilene (internal standard), respectively. Chromatogram A is from a standard solution and B from a 27-hr-old solution of procainamide (Solution 9 in Table I) to which 10.0 μg/ml of* p-*aminobenzoic acid was added before final dilution. For chromatographic conditions, see text.*

EXPERIMENTAL

Chemicals and Reagents—All chemicals and reagents were USP, NF, or American Chemical Society grade and were used as received. Procainamide hydrochloride[1] was used without further purification.

Apparatus—A high-pressure liquid chromatograph[2] equipped with a multiple wavelength detector[3], a recorder[4], and a digital integrator[5] was used.

Column—A semipolar column[6] (30 cm long × 4-mm i.d.) consisting of a monomolecular layer of cyanopropylsilane permanently bonded to silica gel was used.

Chromatographic Conditions—The mobile phase was 40% (v/v) acetonitrile in water containing 0.02 *M* ammonium acetate (pH ~7)[7], and

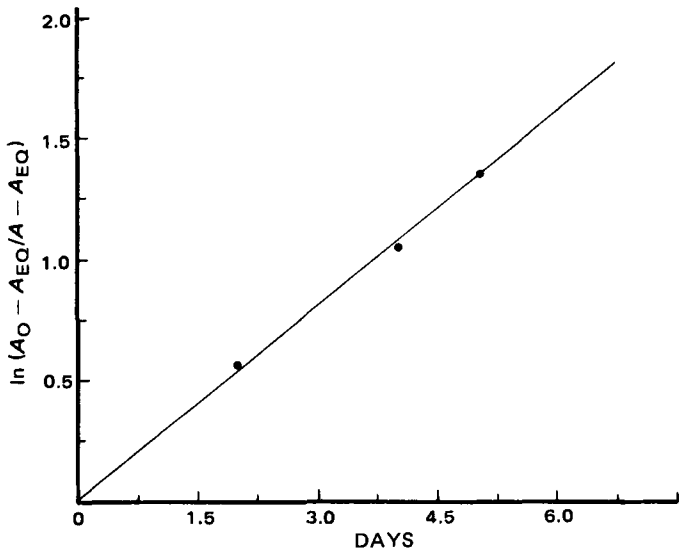

Figure 2—*A plot of complexation of dextrose with procainamide (Solution 6 in Table I) using the equation for a reversible reaction.*

[1] E. R. Squibb & Sons, Princeton, N.J.
[2] ALC 202 equipped with U6K universal injector, Waters Associates, Milford, Mass.
[3] Schoeffel SF770, Westwood, N.J.
[4] Omniscribe 1513-12, Houston Instruments, Austin, Tex.
[5] Autolab minigrator, Spectra Physics, Santa Clara, Calif.
[6] μBondapak/CN, Waters Associates, Milford, Mass.
[7] Zeromatic (SS-3) pH meter, Beckman, Fullerton, Calif.

0022-3549/82/0900-0994$01.00/0

Table I—Procainamide Hydrochloride Aqueous Solutions Prepared

Solution Number	Procainamide HCl, %	Dextrose, %	Other Ingredients (Final Conc)
1	0.1	0	—
2	0.1	0.2[a]	0.01 *N* HCl
3	0.1	0.2[a]	—
4	0.1	0.2[a]	0.45% NaCl[b]
5	0.1	1.0[a]	—
6	0.1	2.0[a]	—
7	0.1	3.0[a]	—
8	0.1	4.0[a]	—
9	0.1	5.0[a]	—
10	0.2	5.0[a]	—
11	0.4	5.0[a]	—
12	0.1	3.0[a]	0.18% NaCl[b]
13	0.1	3.0[a]	0.36% NaCl[b]
14	0.1	3.0[a]	0.54% NaCl[b]
15	0.1	3.0[a]	0.01 *N* HCl
16	0.1	0	0.5 *M* KH_2PO_4
17	0.1	1.0[a]	as above
18	0.1	2.0[a]	as above
19	0.2	2.0[a]	as above
20	0.1	3.0[a]	as above
21	0.1	5.0[a]	0.05% edetate disodium
22	0.1	5.0[c]	—
23	0.1	6.5[c]	—
24	0.1	8.0[c]	—
25	0.1	11.0[c]	—

[a] From dextrose 5% in water, Travenol Laboratories, Deerfield, Ill. [b] From sodium chloride, 0.9% in water, Travenol Laboratories, Deerfield, Ill. [c] From dextrose anhydrous, USP, J. T. Baker Chemical Co., Phillipsburg, N.J.

the flow rate was 2.0 ml/min. The detector was set at 280 nm (wavelength of maximum absorption), sensitivity was 0.04, the temperature was ambient, and the chart speed was 30.5 cm/hr.

Preparation of Solutions—The stock solutions of procainamide hydrochloride (1.0 mg/ml) and the internal standard, methapyrilene hydrochloride (5.0 mg/ml) in water, were prepared daily. A standard solution was prepared by transferring a 1.5-ml quantity of the stock solution of I and a 4.0-ml quantity of the stock solution of methapyrilene hydrochloride (II) to a 100-ml volumetric flask and then diluting with water to volume.

All solutions prepared for investigations of procainamide–dextrose

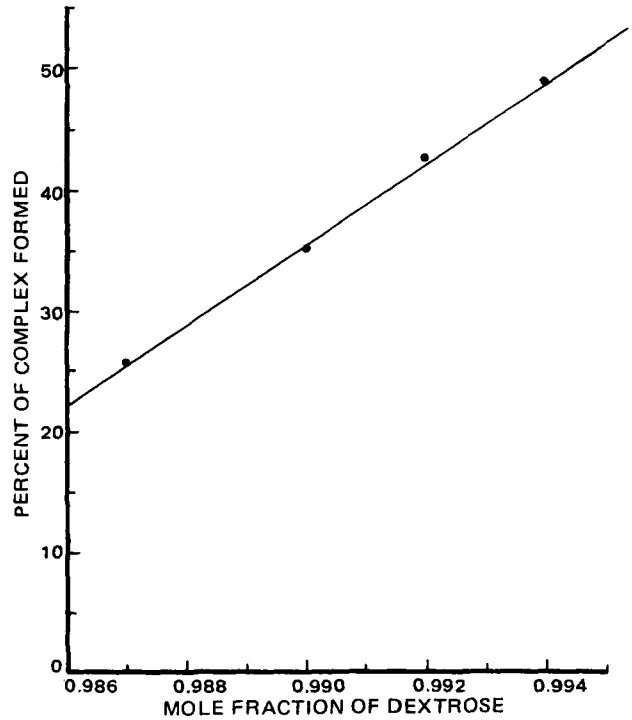

Figure 3—*A plot of mole fraction of dextrose* versus *percent of the complex formed after 4 days of storage (Solutions 22–25, Table I).*

Table II—Assay Results

Solution Number[a]	Percent of Label Claim Remaining, days							
	1	2	3	4	5	6	7	11
1	—	—	99.8	—	—	—	—	—
2	—	—	100.2	—	—	—	—	—
3	—	—	99.6	—	—	—	—	—
4	—	—	99.9	—	—	—	—	—
5	—	94.3	—	91.5	88.1	85.6	85.6	—
6	—	86.9	—	79.6	76.7	68.7	69.2	—
7	—	80.2	—	66.7	60.8	59.0	59.3	—
8	—	73.5	—	53.8	49.3	47.2	48.2	—
9	—	64.3	—	48.3	42.3	42.5	42.7	42.5
10	—	65.3	—	49.1	43.5	—	—	—
11	—	64.6	—	51.5	42.7	—	—	—
12	—	—	—	65.9	—	60.1	—	—
13	—	—	—	67.4	—	58.2	—	—
14	—	—	—	65.1	—	60.1	—	—
15	—	99.2	—	100.4	—	99.8	99.7	—
16	100.2	99.8	—	100.4	—	—	—	—
17	78.9	78.6	—	79.0	—	—	—	—
18	60.6	61.2	—	61.4	—	—	—	—
19	62.0	60.8	—	62.2	—	—	—	—
20	49.3	50.2	—	51.2	—	—	—	—
21	—	65.2	—	48.8	—	—	—	—
22	97.3	—	—	74.2	—	—	—	—
23	96.4	—	—	64.8	—	—	—	—
24	94.8	—	—	57.4	—	—	—	—
25	91.3	—	—	52.2	—	—	—	—

[a] For composition of the solution, see Table I.

complex are reported in Table I. All were prepared using a simple solution method. The solutions were assayed (see procedure following) and transferred to amber-colored bottles[8] and stored at room temperature (24 ±1°). They were reassayed after appropriate intervals and pH values were also determined.

Preparation of Assay Solution—All the solutions were diluted with water to contain 15.0 μg/ml of I (based on the label claim) and 200.0 μg/ml of II (internal standard).

Assay Procedure—A 20.0-μl aliquot of the assay solution was injected into the chromatograph using the described conditions. For comparison, an identical volume of the standard solution was injected after the assay solution eluted.

Calculations—The results were calculated using:

$$\frac{Ph_a}{Ph_s} \times 100 = \text{Percent of the label claim}$$

Where Ph_a is the ratio of the peak heights of procainamide and methapyrilene of the assay solution and Ph_s that of the standard solution of an identical concentration.

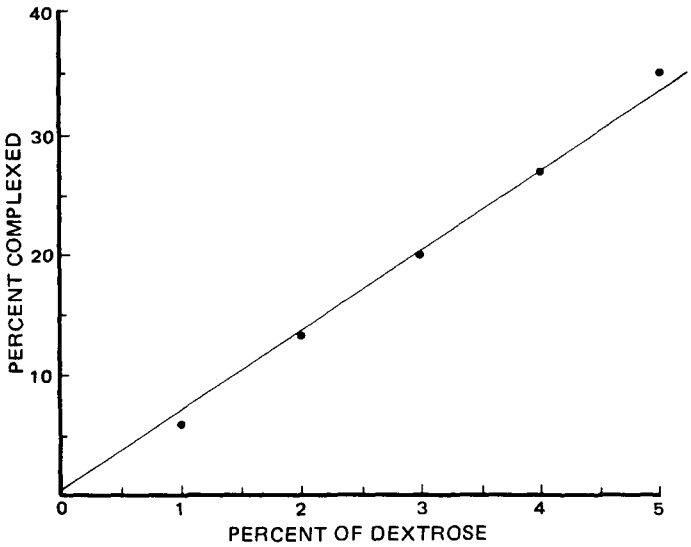

Figure 4—*A plot of dextrose concentration* versus *percent of procainamide–dextrose complex formed after 2 days of storage (Solutions 5–9 Table I).*

[8] Brockway Glass Co., Brockway, Pa.

Table III—pH Values of Solutions

Solution Number[a]	pH Value Remaining[b]						
	0	1	2	3	4	8	11
1	5.6	—	—	5.6	—	—	—
2	1.2	—	—	1.4	—	—	—
3	5.3	—	—	5.1	—	—	—
4	5.4	—	—	5.1	—	—	—
5	5.0	—	4.8	—	4.5	4.0	—
6	4.6	—	4.4	—	3.8	3.7	—
7	4.6	—	4.4	—	3.6	3.4	—
8	4.6	—	4.4	—	3.1	3.0	—
9	4.6	—	4.4	—	3.2	3.0	2.9
10	4.6	—	4.4	—	3.2	3.0	—
11	4.6	—	4.4	—	3.2	3.0	—
12	4.6	—	4.4	—	3.6	3.4	—
13	4.6	—	4.5	—	3.7	3.4	—
14	4.9	—	4.5	—	3.7	3.4	—
15	1.4	—	1.3	—	1.3	1.3	—
16	4.4	—	4.4	—	4.5	—	—
17	4.4	—	4.4	—	3.9	—	—
18	4.4	—	4.4	—	3.8	—	—
19	4.4	—	4.4	—	3.8	—	—
20	4.4	—	4.4	—	3.8	—	—
21	4.8	—	4.5	—	—	—	—
22	6.0	6.0	—	—	5.0	—	—
23	6.0	6.0	—	—	5.0	—	—
24	6.0	6.0	—	—	5.0	—	—
25	6.0	6.0	—	—	5.2	—	—

[a] For composition of the solution, see Table I. [b] Accuracy ± 0.1.

Other Experiments—A 1.5-ml quantity of a 4-day-old solution in 3% dextrose (Solution 7 in Table I) was mixed with 2 ml of ~5 *N* HCl. The mixture was allowed to stand for ~20 min, then 4.0 ml of the stock solution of the internal standard was added, the mixture was brought to volume (100.0 ml) with water, and assayed.

In another experiment, 50.0 mg of *p*-aminobenzoic acid was dissolved in enough 5% aqueous solution of dextrose to make 50.0 ml. This solution was assayed after 0-, 2-, and 4-day intervals to determine if there was a reaction between dextrose and *p*-aminobenzoic acid. The assay was conducted using the HPLC method described previously since *p*-aminobenzoic acid separated (Peak 1 in Fig. 1) from I, II, and the complex between I and dextrose. Before injecting, the solution was diluted to a ratio of 1.0:100 with water. The concentration of *p*-aminobenzoic acid was determined by comparing the peak heights of the assay solution with a standard solution of an identical concentration (10.0 μg/ml).

RESULTS AND DISCUSSION

The results indicated that procainamide and dextrose formed a reversible complex (Fig. 2). This complexation could be completely prevented by adding 0.01 *N* HCl (Solution 15 in Table II). Furthermore, procainamide could be completely released from the complex by treating with hydrochloric acid (see Other Experiments). On treatment with ~5 *N* HCl, all of the procainamide was freed from the complex formed over a 4-day period in 3% aqueous solution of dextrose (Solution 7 in Table II). Preliminary investigations indicated that aged solutions of dextrose with procainamide did not interfere with the assay procedure for procainamide and its complex.

The rate of complex formation was dependent on the initial pH value of the solution. For example, in Solutions 22–25 that had higher initial pH values (Table III), the formation of complex was slower than in Solutions 5–8 (initial pH value 4.6). A direct comparison was possible between Solutions 9 and 22, since both contained 5% dextrose. In Solution 9, a commercial sterile solution was used (Table I) and in Solution 22, anhydrous dextrose was used. The sterile solution of dextrose had a lower pH (~4) *versus* a fresh solution made from the powder (pH ~6). The pH values after adding 0.1% of procainamide hydrochloride were 4.6 and 6 for Solutions 9 and 22, respectively. It is well-known (4) that solutions of dextrose become acidic on autoclaving.

A new set of solutions (16–20 in Table I) were prepared containing 0.05 *M* phosphate buffer. The rate of complexation in these solutions was slightly higher than those without buffer (Table II) which might be an experimental error. There is also a possibility of interaction of phosphates with dextrose (5), which is under investigation.

The pH values of the solutions on storage were decreasing (Table III), which is probably due to release of hydrogen ions upon the formation of complex. The concentration of the complex formed was directly related to the mole ratio of dextrose (Fig. 3) in the solution. However, at lower concentrations of dextrose (~2–4%), especially after 2 days of storage, dextrose concentrations were directly related (Fig. 4) to the concentrations of the complex.

Keeping the dextrose concentration constant and increasing the concentration of procainamide did not affect the rate of formation of complex or the equilibrium concentration (Solutions 9–11, Table II). Also, the increase in the ionic strength with sodium chloride did not alter the equilibrium or rate of formation of the complex (Solutions 7, 12–14, Table II). The addition of 0.05% edetate disodium did not affect the process of complexation (Solutions 9 and 21, Table II).

The process of complexation (a reversible reaction, Fig. 2) is slow and the time required for the equilibrium to establish is dependent on the initial pH of the solution (see above and data in Table II). The equilibrium concentration itself depended on the initial concentration of dextrose and pH of the solution.

For Solution 6, the K, k_f, and k_r values for the complexation (reversible process) were estimated to be 0.456, 0.0858, and 0.188 day^{-1}, respectively.

None of the solutions showed any peak in the chromatogram due to *p*-aminobenzoic acid even with a complex concentration of 50%. This compound could be easily separated from I, II, and the complex (Fig. 1). Moreover, in a separate experiment (see Other Experiments), it was determined that *p*-aminobenzoic acid did not form a complex with dextrose. Letting *p*-aminobenzoic acid stand in the presence of dextrose (≤4 days) did not change its concentration or peak(s) in the chromatogram.

Since all of procainamide could be released from the complex (see above) by treating with hydrochloric acid (see Other Experiments), the drug probably did not decompose. The complex itself may be as active as procainamide[9]. If so, there may be no stability problem on mixing I with dextrose. Since blood also contains dextrose, the implications of this process in biosystems requires further investigation.

The possibility of formation of 5-hydroxymethylfurfural rather than the complex is ruled out since it is a reversible reaction (Fig. 2), the hydrolysis of glucose to 5-hydroxymethylfurfural cannot be reversed (6), and the hydrolysis of glucose to 5-hydroxymethylfurfural usually occurs at higher temperatures (no heat was used in these studies).

REFERENCES

(1) H. L. Kirschenbaum, L. J. Lesko, R. W. Mendes, and G. P. Sesin, *Am. J. Hosp. Pharm.*, **36**, 1464 (1979).

(2) D. M. Baaske and A. W. Malick, *ibid.*, **37**, 1050 (1980).

(3) A. D. Marcus and A. J. Taraszka, *J. Am. Pharm. Assoc., Sci. Ed.*, **46**, 28 (1957).

(4) A. Osol and G. E. Farrar, Jr., in "The Dispensatory of the United States of America," 25th. ed., Lippincott, Philadelphia, Pa., 1955, p. 428.

(5) L. Stryer, in "Biochemistry," Freeman, San Francisco, Calif., 1975, p. 283.

(6) A. N. Martin, J. Swarbrick, and A. Cammarata, in "Physical Pharmacy," 2nd ed. Lea & Febiger, Philadelphia, Pa., 1969, p. 369.

[9] This needs to be proven.

Stability Assay of Allantoin in Lotions and Creams by High-Pressure Liquid Chromatography

Z. R. ZAIDI ˣ, F. J. SENA, and C. P. BASILIO

Received September 1, 1981, from the *R&D Laboratories, Block Drug Co. Inc., Jersey City, NJ 07302.* Accepted for publication November 23, 1981.

Abstract □ A high-pressure liquid chromatographic method for indicating stability is described for the rapid quantitative analysis of allantoin in lotions and creams. Allantoin was extracted from the preparations using distilled water containing 70% (v/v) methanol and separated from interferences by reversed-phase chromatography. The separation was carried out using an amino column (250 × 4.5-mm i.d.) and a mobile phase of distilled water containing 70% (v/v) acetonitrile. Quantitation was accomplished using a UV detector at 220 nm. The assay has a relative standard deviation of ~1.7% (n = 10) and the average recovery from laboratory prepared samples was 100%.

Keyphrases □ Allantoin—stability assay in lotions and creams by high-pressure liquid chromatography, degradation □ Stability—assay of allantoin in lotions and creams, high-pressure liquid chromatography, degradation □ Degradation—allantoin in lotions and creams, stability assay, high-pressure liquid chromatography

Allantoin and its derivatives have been used in various cosmetic preparations including skin creams, lotions, shampoos, lipsticks, and shaving preparations. A suitable analytical method is required for routine quality control as well as stability studies in the pharmaceutical/cosmetic industry. Allantoin (I) can be unstable in alkaline conditions and is known to hydrolyze to urea (II) and glyoxylic acid (III), perhaps *via* allantoic acid (IV):

Several methods (1–3) have been reported that are based on this hydrolysis route and subsequent colorimetric determination of III with phenylhydrazine. A fluorometric determination of sodium glyoxylate using phenylephrine hydrochloride described previously has been applied to the determination of allantoin in pharmaceutical preparations (4). However, for stability tracking, these procedures are deficient, because they measure urea or glyoxylic acid which are the products of normal allantoin degradation, rather than the residual intact allantoin.

Other techniques reported include titration (5, 6), classical chromatography (7), and a TLC separation with UV assay of allantoin at 220 nm (8, 9). In addition, a chromatographic procedure had been followed in these laboratories based on the separation of allantoin *via* TLC and determination by densitometry after chromophore formation.

All of these procedures are either time consuming or nonspecific. To overcome these problems, an assay procedure for allantoin in topical cream and lotion products by high-pressure reversed-phase liquid chromatography was investigated. The method described provides rapid, specific determination of intact allantoin with minimal sample preparation.

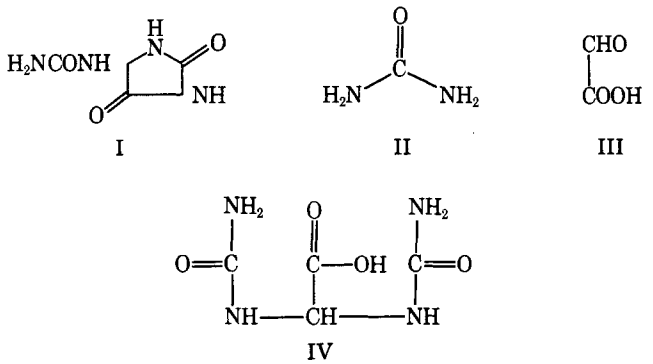

EXPERIMENTAL

Chemicals and Reagents—All reagents and chemicals were either HPLC or American Chemical Society grade and were used without further purification.

Apparatus—The liquid chromatograph[1] was fitted with a 50-μl septumless injector[2] and a variable wavelength UV detector[3] (set at 220 nm).

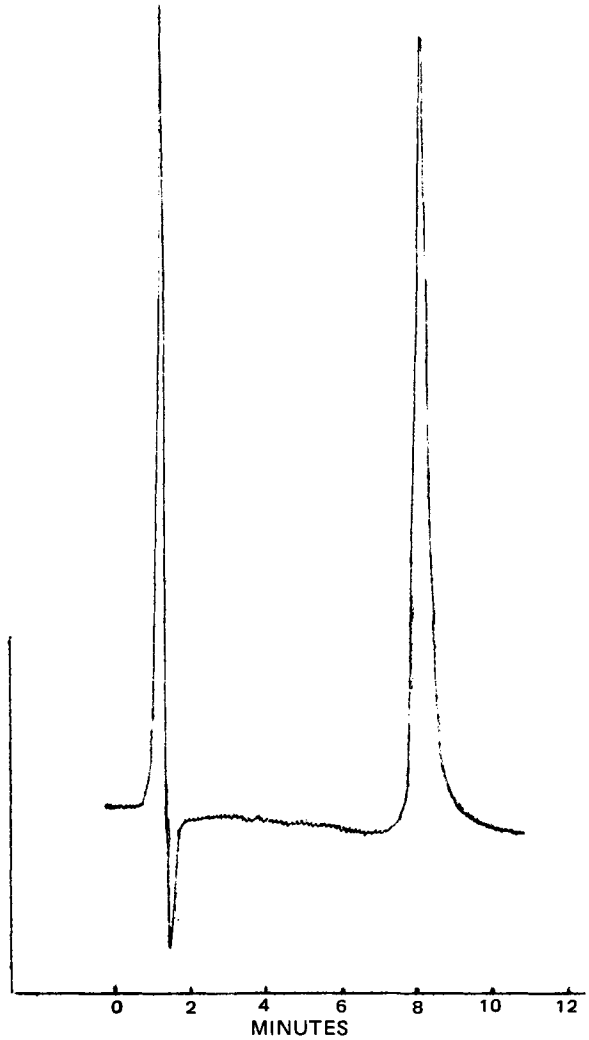

Figure 1—*HPLC of allantoin standard.*

[1] SP8000 Liquid Chromatograph equipped with a Printer/Plotter, Spectra-Physics, Santa Clara, Calif.
[2] Auto Injector model 725, Micromeritics Instruments Corp., Norcross, Ga.
[3] Spectroflow Monitor SF 770, Schoeffel Instruments Corp., Westwood, N.J.

0022-3549/82/0900-0997$01.00/0

Table I—Recovery Data for Spiked Samples

	Topical Lotion	Amount Added, mg	Amount Found, mg	Amount Recovered, %
	1	23.0	22.32	97.05
	2	26.0	26.35	101.35
	3	39.1	39.3	100.50
	4	45.0	44.82	99.6
	5	51.0	50.98	99.96
Average				99.69
RSD, %				1.62
	Topical Cream			
	1	26.2	26.25	100.2
	2	33.5	33.3	99.3
	3	37.5	38.2	101.8
	4	42.4	41.8	98.6
	5	46.4	46.4	100.0
Average				100.0
RSD, %				1.20

Column—A 250 mm × 4.5-mm i.d. column containing 5 μm amino (NH_2) packing[4] was used.

Chromatographic Conditions—The chromatographic solvent was 70% (v/v) acetonitrile in distilled water. The solvent was vacuum filtered through a 0.50-μm (47 mm) filter[5] and vacuum degassed for 2 min with stirring before use. The temperature was ambient, the solvent flow rate was 2.5 ml/min, and the inlet pressure was ~2000 psi. Detector sensitivity was 0.04 aufs and the chart speed was 5.08 mm/min.

Standard Solutions—Standard solutions containing 30, 40, and 50 mg of allantoin/100 ml were prepared in distilled water containing 70% (v/v) methanol. Sonication was used to complete dissolution and the solutions were filtered using a 0.5-μm syringe filter[5] (25 mm) prior to injection.

Table II—Assay Results for Topical Cream Containing 2.0% Allantoin

Topical Cream	Allantoin, %	Percent of Label
1	2.03	101.5
2	1.95	97.5
3	1.98	99.0
4	1.98	99.0
5	2.01	100.5
6	2.05	102.5
7	2.05	102.5
8	2.03	101.5
9	2.02	101.0
10	1.98	99.0
Average	2.01	100.4
RSD, %	1.7	

Assay for Commercial Products—Samples of creams and lotions were transferred from their commercial container to glass jars and mixed thoroughly. An accurately weighed 2.0-g sample was transferred to a 150-ml beaker, 30 ml of distilled water added, and the contents stirred for ~20 min. The contents of the beaker were then quantitatively

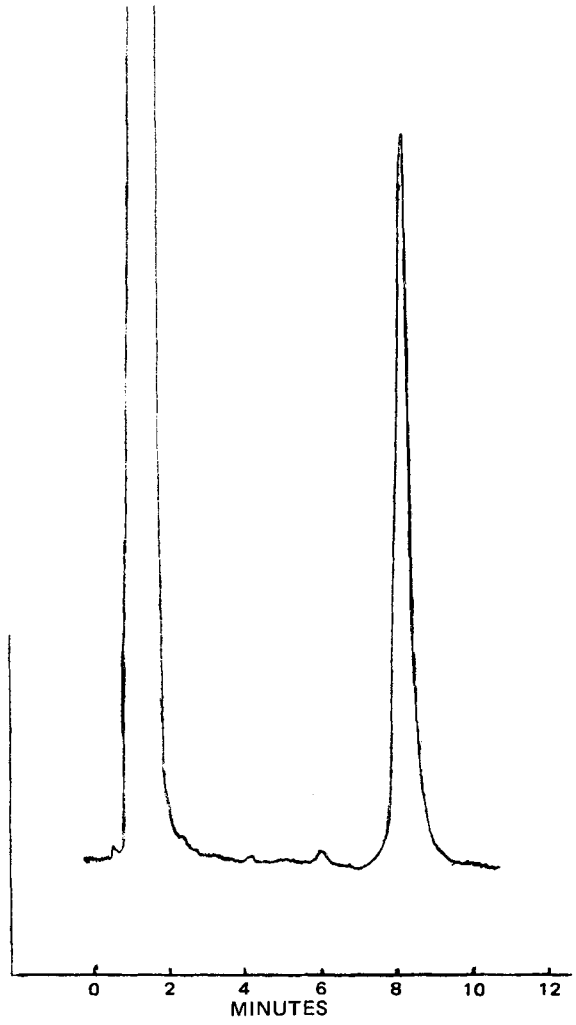

Figure 2—*HPLC of commercial cream sample.*

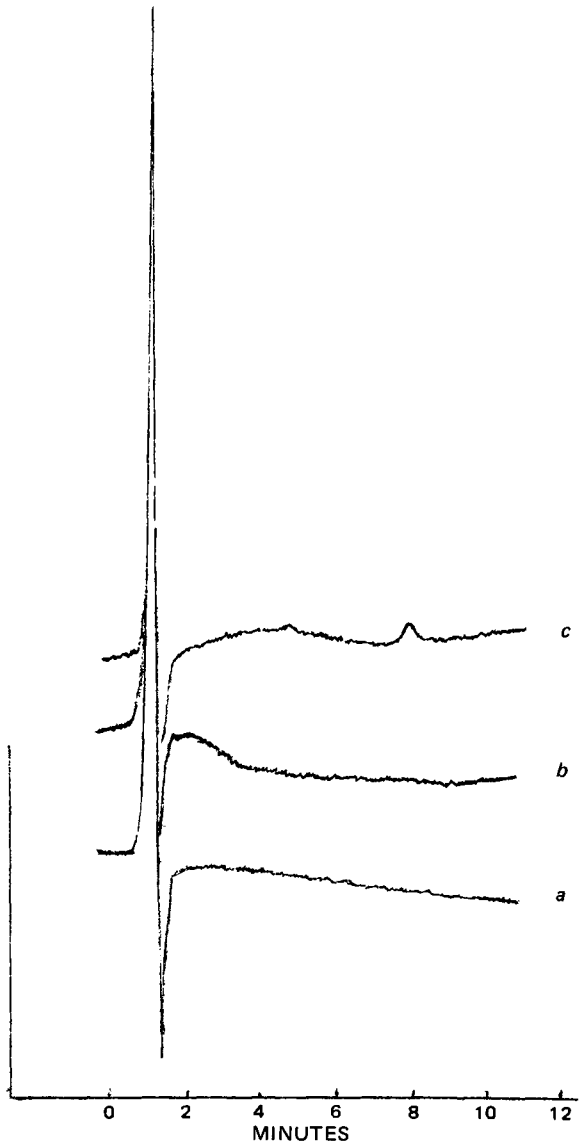

Figure 3—*HPLC of pure materials (a) blank, (b) urea, (c) allantoic acid.*

[4] Amino (NH_2) column, IBM Instruments Inc., Danberry, Conn.

[5] Type FH 0.5 μm, Fluoropore (PTFE), Millipore Corp., Bedford, Mass.

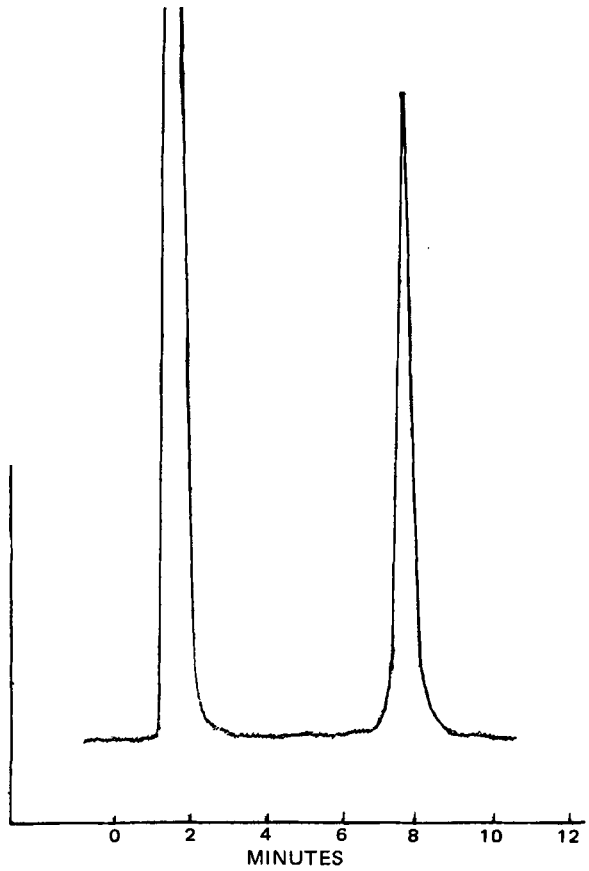

Figure 4—*HPLC of commercial lotion sample.*

transferred to a 100-ml volumetric flask, diluted to volume with methanol, mixed well, and filtered using a 0.5-μm syringe filter[5] (25 mm) prior to injection.

Spiked Samples—Accurately weighed quantities of allantoin were admixed with placebo portions of the topical creams and lotions. These samples were formulated to contain 1–2.5% (w/w) allantoin, and were assayed as described previously for commercial products.

Quantitation—Since peak heights of allantoin were directly proportional to concentration, all results were calculated by interpolation from a standard curve.

RESULTS AND DISCUSSION

Although satisfactory separations were achieved for samples of lotions and creams using distilled water containing 70% acetonitrile, for economic reasons, attempts were made to substitute methanol. However, no acceptable separations were obtained with various proportions of methanol water, therefore, acetonitrile was used for all further work.

The recovery data for allantoin from spiked samples of creams and lotions, presented in Table I, illustrate the validity of the method for these formulations. Average recoveries for cream and lotion were 100 and 99.7%, respectively. Linearity between peak height and concentration was excellent over the range of 0.3–0.5 mg of allantoin/ml with a correlation coefficient of 0.999. This method has been used routinely in a stability program and found to be accurate and precise with a *RSD* of 1.7% (n = 10). These data are summarized in Table II, and chromatograms obtained for allantoin standard and commercial cream sample are presented in Figs. 1 and 2, respectively. Since no sample clean up is required, assay time was ~15 min.

As noted earlier, allantoin is reported to degrade to urea and glyoxylic acid in alkaline conditions, perhaps through allantoic acid. To demonstrate the selectivity of the method for intact allantoin, standard and sample preparations containing allantoin were artificially degraded with alkali and analyzed according to the proposed conditions. No significant peaks were observed due to the degradation products at the retention time of allantoin peak, which was reduced in height.

To further demonstrate the stability-indicating nature of the method, several additional experiments were completed. Commercially available

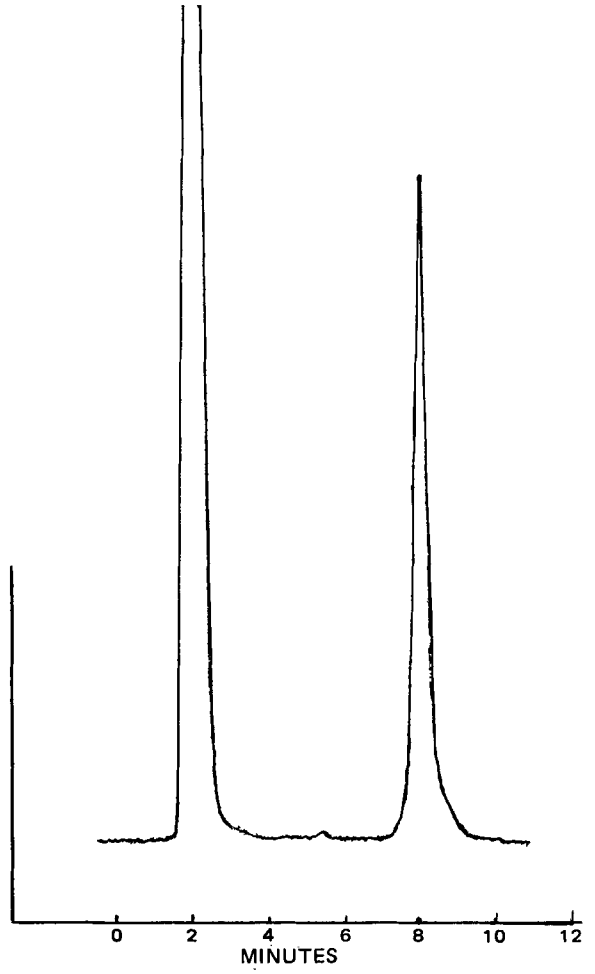

Figure 5—*HPLC of commercial lotion sample spiked with pure allantoic acid.*

urea and glyoxylic acid were chromatographed, and no peak was observed at the retention time of allantoin (Fig. 3). This was further confirmed by introducing 40–50 mg of these compounds to standard and sample preparations containing allantoin. In addition, commercially available allantoic acid was chromatographed as described (Fig. 3). It eluted at the same time as allantoin; however, when 0.4 mg/ml of allantoic acid (corresponding to 100% conversion from allantoin) was introduced to a standard allantoin solution (0.4 mg/ml) and chromatographed, an increase in allantoin peak height of <2% resulted.

A commercial lotion sample containing 40 mg of allantoin was analyzed in duplicate (Fig. 4). The samples were then spiked with 35–40 mg of allantoic acid and reanalyzed for allantoin (Fig. 5). Evaluation of these results indicated that within experimental error allantoic acid (if present) does not interfere in the analysis of allantoin.

It is concluded that the proposed method is selective for intact allantoin in the presence of probable degradation products.

REFERENCES

(1) E. Young and C. Conway, *J. Biol. Chem.*, **142,** 839 (1942).

(2) S. A. Katz, R. Turse, and S. B. Mecca, *J. Soc. Cosmet. Chem.*, **15,** 303 (1964).

(3) D. Zygmunt, *Farm. Pol.*, **25**(4), 255 (1969).

(4) T. Kaito, K. Sagara, Y. Ito, K. Nakamura, and T. Anmo, *Yakugaku Zasshi*, **97**(2) 165 (1977).

(5) D. J. Weber and J. W. Higgins, *J. Pharm. Sci.*, **59,** 1819 (1970).

(6) A. Billabert, J. Willemot, and G. Parry, *Ann. Pharm. Fr.*, **34,** 65 (1976).

(7) J. Deshusses and P. Desbaumes, *Parfums Cosmet. Savons*, **4,** 192, (1961).

(8) I. Bonadeo and G. Bottezzi, *Ital. Essenzy Profumi*, **50,** 78, (1968).

(9) J. Lutomski and B. Jernas, *Pharmazie*, **31,** 131 (1976).

Synthesis and Evaluation of Some Alkoxy-, Chloro-, and Acyloxy-Conjugated Styryl Ketones Against P-388 Lymphocytic Leukemia and an Examination of the Metabolism and Toxicological Effects of 1-(*m*-Ethoxymethyloxyphenyl)-1-nonen-3-one in Rats

J. R. DIMMOCK *x, D. L. KIRKPATRICK *, N. G. WEBB *, and B. M. CROSS ‡

Received August 24, 1981, from the **College of Pharmacy and* ‡*Department of Veterinary Pathology, Western College of Veterinary Medicine, University of Saskatchewan, Saskatoon, Saskatchewan, Canada S7N 0W0.* Accepted for publication December 15, 1981.

Abstract □ A number of analogs of a new antineoplastic agent, 1-(*m*-ethoxymethyloxyphenyl)-1-nonen-3-one (III*a*) were prepared and evaluated against murine P-388 lymphocytic leukemia. Metabolic studies of III*a* in rats showed that it was sequestered rapidly to the brain and hence probably to other adipose tissue, which may account for the absence of III*a* and metabolites in urine and feces. A detailed toxicological evaluation of III*a* in rats showed marked pathological changes principally in the liver and spleen as a result of erythrophagocytosis from bleeding into the abdomen.

Keyphrases □ Antineoplastics—alkoxy-, chloro-, and acyloxy-conjugated styryl ketones, synthesis and evaluation of activity □ Styryl ketones, conjugated—synthesis of alkoxy-, chloro-, and acyloxy-analogs, evaluation for antineoplastic activity □ 1-(*m*-Ethoxymethyloxyphenyl)-1-nonen-3-one—metabolic and toxicological studies

A number of Mannich bases (I) derived from conjugated styryl ketones synthesized in these laboratories displayed activity against P-388 lymphocytic leukemia, but murine toxicity was marked (1, 2). This observation was in contrast to the precursor α,β-unsaturated ketones (II) which, while not causing mortalities under the conditions of evaluation, were bereft of antineoplastic activity (1, 2). More recently, however, a number of conjugated styryl ketones, which were not Mannich bases, showed perceptible, beneficial responses in the P-388 lymphocytic leukemia screen. Thus, ethers III*a–c* increased the median survival time in mice by ~19% at the optimum dose levels, and assessment of III*a* against B-16 melanocarcinoma increased the lifespan by 30% with 1 mouse in 10 being cured (2). Furthermore, the unsubstituted and dichloro styryl ketones (IV*a–d*) also achieved increases in the lifespan of mice with P-388 lymphocytic leukemia of ~20% (3). With the exception of IV*b*, all of the compounds III and IV did not cause mortalities to mice during evaluation at the maximum doses administered (2, 3).

The purpose of the present investigation was twofold: First, molecular modification of the compounds in series III and IV to produce novel derivatives for evaluation in the P-388 screen was planned. Second, a study of the metabolism of III*a* was considered to be a viable undertaking, which may permit the identification of the breakdown products in the body followed by their antineoplastic evaluation and the subsequent design of new compounds on a rational basis.

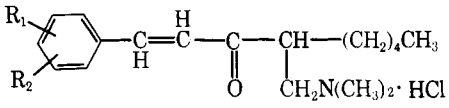

I

$R_1 = R_2 = H, Cl, OH$

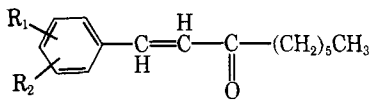

II

$R_1 = R_2 = H, Cl, OH$

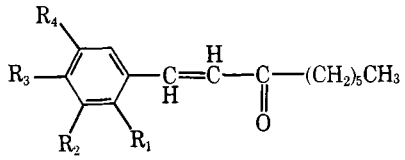

III

a: $R_1 = R_3 = R_4 = H$; $R_2 = OCH_2OC_2H_5$
b: $R_1 = R_4 = OCH_3$; $R_2 = R_3 = H$
c: $R_1 = R_4 = H$; $R_2 = R_3 = OCH_3$

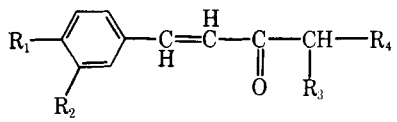

IV

a: $R_1 = R_2 = H$; $R_3 = CH_3$; $R_4 = (CH_2)_3CH_3$
b: $R_1 = R_2 = Cl$; $R_3 = CH_3$; $R_4 = (CH_2)_3CH_3$
c: $R_1 = R_2 = R_3 = R_4 = H$
d: $R_1 = R_2 = Cl$; $R_3 = R_4 = H$

RESULTS AND DISCUSSION

The synthetic program was directed toward the preparation of the ethers (V–VII), the ketones (VIII), the esters (IX), and finally some prodrugs of 4-phenyl-but-3-en-2-one, (X and XI). The reasons for proceeding in this direction were as follows. It has been claimed that the pH of a number of tumors is lower than normal tissue (4–6), and the average pH value for many tumors has been estimated to be ~6.5 (7). Therefore, it is conceivable that the levels of antineoplastic activity obtained with III*a*, namely, increases in mean survival times of 25 and 30% in mice bearing P-388 lymphocytic leukemia and B-16 melanocarcinoma, respectively (2), may be attributed to preferential hydrolysis to the corresponding phenol (II) (R_1 = 3-OH; R_2 = H) in the tumors. The inactivity of the precursor phenol (II) (R_1 = 3-OH; R_2 = H) may have been due to facile detoxification *via* the hydroxyl group prior to reaching the tumor. The synthesis of the corresponding *O*-benzyl ethers (V) was planned, since in simple nonbiological systems, many phenyl alkyl ethers regenerate the corresponding phenol under acidic conditions (8) but are stable under mildly alkaline conditions. In addition, alteration of the Hammett values of the nuclear substituents of the benzyl group in series V may permit variation in the rate of release of the precursor phenol (9) which may correlate with differences in antineoplastic activity. In the case of VI, the loss of the benzyl groups *in vivo* would permit the formation of an aromatic compound with vicinal hydroxy groups which may be con-

0022-3549/82/0900-1000$01.00/0

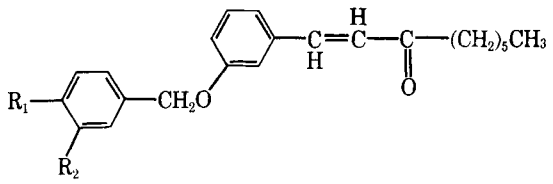

V

a: $R_1 = R_2 = H$
b: $R_1 = H$, $R_2 = Cl$
c: $R_1 = R_2 = Cl$
d: $R_1 = Cl$; $R_2 = H$
e: $R_1 = NO_2$; $R_2 = H$
f: $R_1 = CH_3$; $R_2 = H$

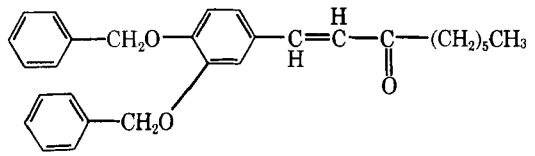

VI

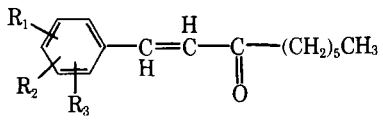

VII

a: $R_1 = 2\text{-}OCH_3$; $R_2 = R_3 = H$
b: $R_1 = 4\text{-}OCH_3$; $R_2 = R_3 = H$
c: $R_1 = 2\text{-}OCH_3$; $R_2 = 3\text{-}OCH_3$; $R_3 = H$
d: $R_1 = 2\text{-}OCH_3$; $R_2 = 4\text{-}OCH_3$; $R_3 = H$
e: $R_1 = 3\text{-}OCH_3$; $R_2 = 5\text{-}OCH_3$; $R_3 = H$
f: $R_1 = 2\text{-}OCH_3$; $R_2 = 3\text{-}OCH_3$; $R_3 = 4\text{-}OCH_3$
g: $R_1 = 2\text{-}OCH_3$; $R_2 = 4\text{-}OCH_3$; $R_3 = 5\text{-}OCH_3$
h: $R_1 = 2\text{-}OCH_3$; $R_2 = 4\text{-}OCH_3$; $R_3 = 6\text{-}OCH_3$
i: $R_1 = 3\text{-}OCH_3$; $R_2 = 4\text{-}OCH_3$; $R_3 = 5\text{-}OCH_3$

verted to an *ortho*-quinone. Since the two dimethoxy compounds (III*b* and *c*) were shown to possess some activity against P-388 lymphocytic leukemia, the question as to their mode of action was raised. *O*-Demethylation of phenols is a common metabolic pathway (10), and thus, the formation of the corresponding dihydroxy compounds could occur with subsequent oxidation to the corresponding *para*- and *ortho*-quinones (Scheme I), which may then interact with important cellular nucleophiles such as thiols (11, 12). Thus, the preparation of further nuclear methoxy styryl ketones (VII) was suggested, and in the absence of nuclear hydroxylation by metabolism, compounds VII*c*, *f*, *g*, and *i* are able to be converted *in vivo* into quinones, in contrast to VII*d*, *e*, and *h*.

In addition, while 1-phenyl-1-nonen-3-one (II, $R_1 = R_2 = H$) and the related dichloro derivative (II, $R_1 = 3\text{-}Cl$; $R_2 = 4\text{-}Cl$) are inactive against P-388 lymphocytic leukemia, branching of the alkyl chain α to the carbonyl group led to compounds IV*a* and *b* with perceptible beneficial responses in this screen (3). The increase in bioactivity could be due to a number of factors: Alignment at a receptor site with these branched-chain compounds may be favored, and also differences in the hydrophilic–lipophilic properties of IV*a* and *b* compared with the compounds containing the *n*-hexyl group are conceivable. Thus, increased branching of the alkyl chain in the case of three isomeric *n*-pentanols led to increased aqueous solubility (13), and a recent generalization that the biological activities of α,β-unsaturated carbonyl compounds depends largely on stereochemical considerations and modifications of the hydrophobic portion of the molecules (14) is of relevance. Furthermore, by altering the branching of the four-carbon alkyl group in compounds VIII*a–c* and *e–g*, the degree of enolization would be predicted to vary (15, 16), which in turn would affect the hydrophilic–lipophilic balance. In addition, since the bioactivities of α,β-unsaturated ketones are considered to be due to reaction in part with cellular nucleophiles (17, 18), chemical reaction would be expected to be reduced with increasing enolization. The cyclohexyl compounds (VIII*d* and *h*), like VIII*b* and *f*, have secondary carbon atoms adjacent to the carbonyl group, but differences in hydrophilic–lipophilic properties would be expected [*e.g.*, the aqueous solubilities of cyclohexanol and *s*-butanol at 20° are 3.6 and 12.5%, respectively (19)].

It has been shown recently that unsaturated alkyl ester groups, two carbon atoms distant from the carbonylene group, gave rise to compounds with antitumor properties, including activity against P-388 lymphocytic leukemia (20, 21), and hence, evaluation of the biological activity of series IX was deemed profitable.

Finally, the synthesis of prodrugs of 4-phenyl-but-3-en-2-one (IV*c*) was contemplated since the compound increased the median survival time in mice with P-388 lymphocytic leukemia by 26% (22). Since oximes may be prodrugs of ketones (23) and are known to be acid-labile (24), compound X may breakdown preferentially to IV*c* under the acidic conditions of certain neoplastic tissue. In addition, the dienol ether and related thio analog (XI*a* and *b*) would be expected to be stable under alkaline conditions but to be extremely sensitive to acid (25). The synthesis of these ethers (XI), if successful, could be applied to various Mannich bases (I) as well.

The second phase of the current investigation was to examine the metabolic route of III*a*. Primarily, this was to compare the antineoplastic activities of the metabolite(s) with the parent compound, and secondly, to observe the effect on anticancer properties of molecular modification of III*a* designed to retard metabolic processes.

The synthesis of compounds V–IX was achieved, and the effect on P-388 lymphocytic leukemia in mice for virtually all of the compounds is recorded in Table I. The *O*-benzyl ethers (V and VI), although not causing fatalities to mice under the test conditions, were inactive. An assessment of the stability of three of the ethers, (V*a*, *e*, and *f*) showed them to be stable in acetonitrile–phosphate buffer at physiological pH as well as at pH values of 6.9 and 6.4, which are likely to be found in various tumors. It is conceivable that a breakdown of the ethers V and VI to the corresponding phenols does not occur *in vivo*. None of the remaining ethers (VII) or ketones (VIII and IX) met the criterion for activity in the P-388 screen. Under the test conditions, no fatalities were noted at the maximum dose levels administered (200 mg/kg) for the compounds in Table I with the exception of VIII*g* and *h*. Oximation of the ketone IV*c* led to X which was nontoxic and inactive.

Attempts to synthesize the enol ether (XI*a*) were unsuccessful. Initially, a literature method used in the preparation of steroidal enol ethers (30) was employed but only unreacted ketone was isolated from the reaction mixture. When (*E*)-4-phenyl-3-buten-2-one and dimethoxypropane were heated in the presence of zinc chloride, two yellow oils, in ad-

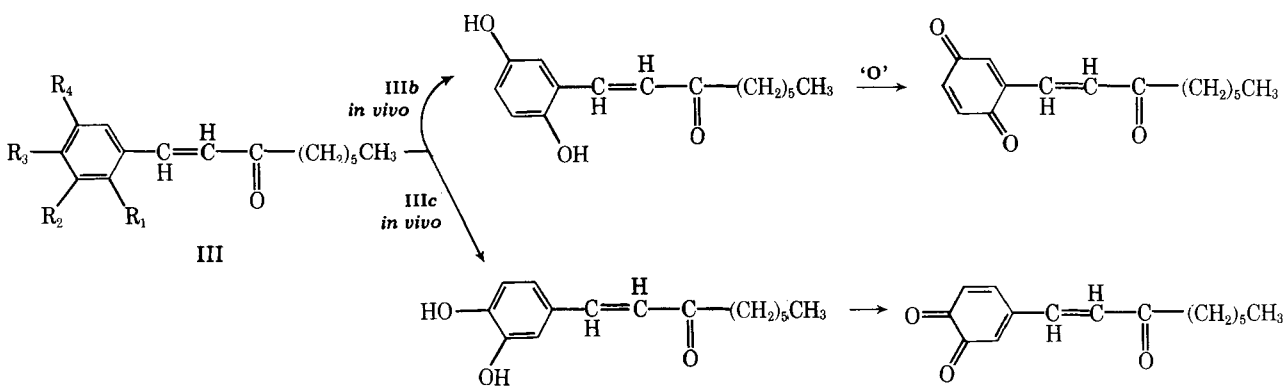

Scheme I

Table I—Physical Data on the Conjugated Styryl Ketones V–IX and Activity Against P-388 Lymphocytic Leukemia in Mice

Compound	Yield, %	Melting Point or Boiling Point, °C/mm	Formula	Analysis Calc. C	Calc. H	Found C	Found H	Max Increase in Median Survival Time[a] (Dose in mg/kg)
V*a*	35	55	$C_{22}H_{26}O_2$	81.99	8.07	82.07	8.19	NA
V*b*	49	27–28	$C_{22}H_{25}ClO_2$	74.16	7.02	74.12	7.01	96(200)
V*c*	30	57	$C_{22}H_{24}Cl_2O_2$	67.52	6.18	67.80	6.05	115(50)
V*d*	46	46	$C_{22}H_{25}ClO_2$	74.16	7.02	74.03	7.04	101(200)
V*e*	54	74–75	$C_{22}H_{25}NO_4$[b]	71.91	6.86	71.60	6.81	91(50)
V*f*	62	42	$C_{23}H_{28}O_2$	82.03	8.32	82.15	8.55	NA
VI	54	78–79	$C_{29}H_{32}O_3$	81.32	7.47	71.81	7.12	92(12.5)
VII*a*	53	145–146/0.45	$C_{16}H_{22}O_2$	78.00	9.01	77.93	9.04	117(200)
VII*b*	21	54	$C_{16}H_{22}O_2$	78.00	9.01	78.17	9.08	103(100)
VII*c*	39	146–148/0.24	$C_{17}H_{24}O_3$	73.88	8.75	74.12	8.74	107(100)
VII*d*	48	71	$C_{17}H_{24}O_3$	73.88	8.75	74.06	8.54	94(50)
VII*e*	56	66	$C_{17}H_{24}O_3$	73.88	8.75	73.64	8.39	103(100)
VII*f*	31	32	$C_{18}H_{26}O_4$	70.56	8.55	70.47	8.58	102(200)
VII*g*	72	90	$C_{18}H_{26}O_4$	70.56	8.55	70.66	8.59	100(50)
VII*h*	65	110	$C_{18}H_{26}O_4$	70.56	8.55	71.09	8.54	101(100)
VII*i*	44	80	$C_{18}H_{26}O_4$	70.56	8.55	70.68	8.48	101(50)
VIII*a*	66	37[c]	$C_{13}H_{16}O$	82.93	8.57	82.87	8.58	108(200)
VIII*b*	58	89–91/0.37	$C_{13}H_{16}O$	82.93	8.57	82.88	8.49	114(200)
VIII*c*	31	37[d]	$C_{13}H_{16}O$	82.93	8.57	83.08	8.77	105(200)
VIII*d*	51	57	$C_{15}H_{17}O$	84.46	8.04	84.49	8.32	107(100)
VIII*e*	49	49[e]	$C_{13}H_{14}Cl_2O$	60.72	5.49	60.72	5.52	98(50)
VIII*f*	54	34–35	$C_{13}H_{14}Cl_2O$	60.72	5.49	60.77	5.45	99(200)
VIII*g*	34	89[f]	$C_{13}H_{14}Cl_2O$	60.72	5.49	60.72	5.57	107(100)[g]
VIII*h*	45	65	$C_{15}H_{15}Cl_2O$	63.84	5.34	63.68	5.77	103(50)[g]
IX*a*	81	Oil	$C_{18}H_{22}O_3$	75.49	7.75	75.84	7.80	107(100)
IX*b*	83	Oil	$C_{19}H_{24}O_3$	75.97	8.05	75.87	7.80	100(200)
IX*c*	85	Oil	$C_{19}H_{24}O_3$	75.97	8.05	76.17	8.02	98(50)
IX*d*	95	Oil	$C_{24}H_{26}O_3$	79.53	7.23	79.80	7.19	96(50)

[a] The figures are the ratios of the survival time of treated animals to control animals expressed as a percentage. A compound should increase the median survival time by 20% to be considered active. NA result is not yet available. [b] *Anal.*—Calc. for $C_{22}H_{25}NO_4$: N, 3.81. Found: N, 3.78. [c] Lit. (26) mp 38–39°. [d] Lit. (27) mp 41°. [e] Lit. (28) mp 49°. [f] Lit. (29) mp 89–91°. [g] There were 5/6 and 6/6 survivors on Day 5 at dose levels of 200 and 100 mg/kg, respectively.

dition to unreacted ketone, were obtained. Separation of the three components showed that the molecular ions of both yellow oils was 274, and both purified compounds reverted to an equilibrium mixture of these two compounds. Initially, it was considered that a Diels-Alder reaction between the desired product (XI*a*) and unreacted ketone (IV*c*) had occurred to give a cyclohexene derivative such as XII (or alternatively, where the aromatic rings are vicinal to each other), which subsequently lost a molecule of methanol to give cyclohexadienes, which may be represented by structures XIII*a* and *b* (Scheme II). Interconversion between XIII*a* and *b* is possible since similar molecular rearrangements in conjugated systems are known (31). However, an alternative explanation was considered in that under the reaction conditions which contain a Lewis acid, two molecules of protonated ketone could undergo an aldol condensation, which on dehydration would lead to the triolefine (XIV) also possessing a molecular weight of 274 (Scheme II). This compound could undergo (*E*)–(*Z*) isomerization at the double bonds in the molecule. Recourse to ^{13}C-NMR spectroscopy supported the structures of the yellow compounds as XIV, based on a comparison of the observed values of carbon absorptions with the calculated values of chemical shifts calculated from tables (32). The presence of XII was eliminated since no

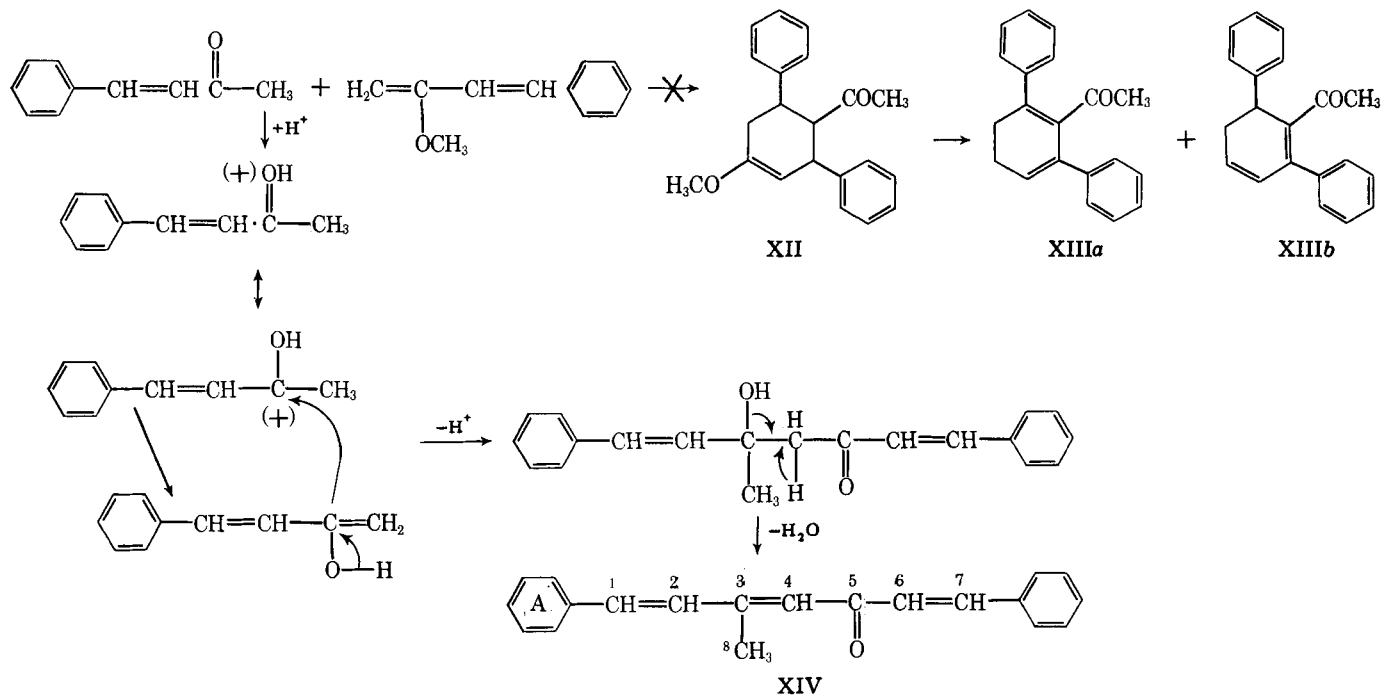

Scheme II

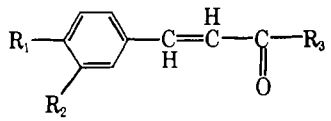

VIII

a: $R_1 = R_2 = H$; $R_3 = (CH_2)_3CH_3$
b: $R_1 = R_2 = H$; $R_3 = CH(CH_3)C_2H_5$
c: $R_1 = R_2 = H$; $R_3 = C(CH_3)_3$
d: $R_1 = R_2 = H$; $R_3 = C_6H_5$
e: $R_1 = R_2 = Cl$; $R_3 = (CH_2)_3CH_3$
f: $R_1 = R_2 = Cl$; $R_3 = CH(CH_3)C_2H_5$
g: $R_1 = R_2 = Cl$; $R_3 = C(CH_3)_3$
h: $R_1 = R_2 = Cl$; $R_3 = C_6H_5$

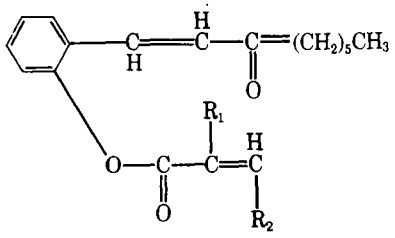

IX

a: $R_1 = R_2 = H$
b: $R_1 = H$; $R_2 = CH_3$
c: $R_1 = CH_3$; $R_2 = H$
d: $R_1 = H$; $R_2 = C_6H_5$

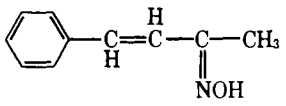

X

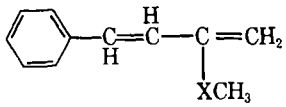

XI

c: X = O
b: X = S

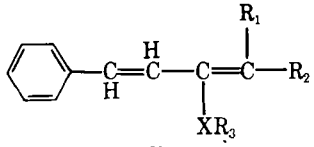

XV

a: $R_1 = H$, $R_2 = (CH_2)_4CH_3$; $R_3 = CH_3$; X = O
b: $R_1 = R_2 = H$; $R_3 = C_2H_5$; X = S
c: $R_1 = CH_3$; $R_2 = C_2H_5$; $R_3 = C_6H_5$, X = S
d: $R_1 = R_2 = H$; $R_3 = C_2H_5$; X = O

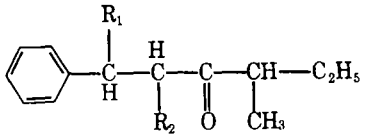

XVI

a: $R_1 = SC_6H_5$; $R_2 = H$
b: $R_1 = R_2 = Br$

absorbances at 30–40 ppm or 200–207 ppm were observed, indicating the absence of methylene and acetyl carbon atoms, respectively. No reaction was observed when II ($R_1 = R_2 = H$) was reacted with dimethoxypropane under the same experimental conditions in an attempt to produce XV*a*.

In an attempt to produce the thio ether (XV*b*) using a modification of the literature procedure (30), principally unreacted ketone (IV*c*) was found as well as two unidentified components. It has been observed that formation of thioenol ethers, in contrast to mercaptans, is enhanced by the carbon atom α to the carbonyl group being sterically hindered and having an electron-releasing group attached to it (33). These workers used thiophenol rather than ethanethiol, and hence, the reaction between VIII*b* and thiophenol was attempted. Examination of the product showed the presence of principally unreacted ketone (VIII*b*), the Michael adduct, 4-methyl-1-phenyl-1-phenylthiohexan-3-one (XVI*a*), and an unidentified product. To eliminate the formation of this Michael adduct, the dibromoketone (XVI*b*) was synthesized, but no reaction between this compound and thiophenol occurred under the experimental conditions employed.

Finally, a related enol ether (XV*d*) was synthesized essentially by literature procedures (34, 35) and shown to revert rapidly to 4-phenyl-3-buten-2-one (IV*c*). The marked instability of this compound precluded its assessment against P-388 lymphocytic leukemia. Hence, even if the desired compounds (XI) were prepared, it may be that they would be too unstable for pharmacological evaluation, even if the idea of XI reverting to 4-phenyl-3-buten-2-one is validated.

In an attempt to study the metabolism of III*a*, this compound was administered intraperitoneally into rats. No trace of III*a* nor metabolites was found in the urine and feces. Examination of rat plasma at different time intervals after intraperitoneal injection of III*a* did not reveal the presence of III*a* or metabolites, and it was considered that they may have been bound extensively to proteins [*e.g.*, an aromatic hydroxy compound used as a cholecystographic medium has been shown to be bound by covalent bonds to plasma protein albumin with a half-life of 2.5 years (36)]. However, analysis of plasma revealed the absence of xenobiotics. Since gross physiological effects were observed in the animals soon after intraperitoneal injection of III*a*, it was felt that this compound was being absorbed rapidly, so III*a* was administered by the intravenous route and blood obtained after short time intervals. Five minutes after injection of III*a*, the compound was detected, but after 10 min the concentration of this compound had been reduced 400 times compared to the quantity of III*a* measured at the end of 5 min. Since neither III*a* nor metabolites were found in the urine or feces, it was thought that rapid sequestration to adipose tissue in part could occur due to the lipophilicity of III*a*. Extraction of rat brain 15 min after intraperitoneal injection revealed the presence of ~5% of III*a*. This observation demonstrates that III*a* crosses the blood–brain barrier and is present in brain tissue not in the covalently bound state. This passage through the blood–brain barrier by III*a* may permit it to serve as a prototype of a series of compounds for evaluation against brain tumors. It is conceivable that this compound primarily is distributed to and retained by the fatty tissue of the rat.

After 6 weeks, some of the animals that had been dosed with III*a* died, and the remaining animals appeared sickly. The live animals were euthanized, and the gross pathological examination revealed peritonitis as well as enlarged livers and spleens. In addition, blood was found in various body cavities, and, although it did not clot on exposure to air, the prothrombin and partial thromboplastin times as well as platelet counts were normal. The capillaries in the reticular surface collagen surrounding livers and spleens seemed to be inadequately supported and may have permitted blood seepage into the organ capsules and abdomen. Changes in the mesenteric lymph nodes and the fact that no evident source of hemorrhage was found suggest that the bleeding into the abdomen noted in this group of treated rats occurred over several days. Histological examination revealed significant abnormalities in the liver and spleen. Figures 1 and 2 show the hepatic necrosis observed and the damage to the splenic capsules, respectively. In order to evaluate whether the pathological changes occurred soon after injection or gradually over a period of time, rats were injected with III*a* and euthanized at the end of 1, 2, 3, and 4 weeks. In general, the pathological changes noted were progressive. Finally, the dose of III*a* was reduced tenfold, and examination at the end of 4 weeks revealed cellular damage in the liver and spleen.

EXPERIMENTAL

Melting points and boiling points are uncorrected. Elemental analyses were undertaken locally[1], and the aluminum oxide[2] and silica gel[3] used in column chromatography were obtained commercially. TLC was carried out using aluminum oxide and silica gel with fluorescent indicator sheets[4],

[1] R. E. Teed, Department of Chemistry and Chemical Engineering, University of Saskatchewan, Saskatoon, Saskatchewan, Canada.
[2] Alcoa Chemicals aluminum oxide (F-20), Aluminum Co. of Canada.
[3] Silica gel 28-200 mesh, Sargent-Welch Scientific Co.
[4] Eastman Kodak Co.

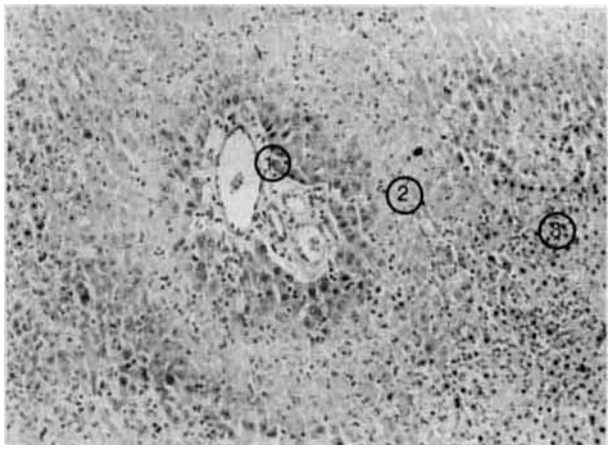

Figure 1—*Rat liver showing a viable portal triad ①, surrounded by an area of coagulation necrosis ②, and inflammation ③ (140×).*

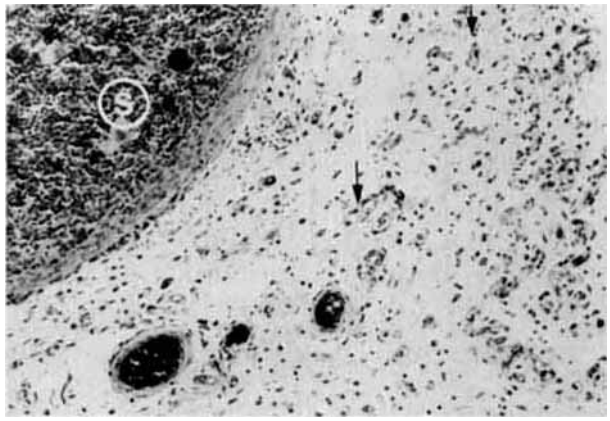

Figure 2—*Rat spleen (S) showing a thickened capsule composed of very fine reticular connective tissue and many poorly supported capillaries (arrows) (220×).*

while silica gel[5] (0.5-mm thick) on glass was used in preparative TLC. The plates were conditioned at 120° overnight and cooled prior to use. Unless otherwise stated, the boiling point of petroleum ether was 40–60°. Mass spectra[6-8] were run at 70 eV and the 60 MHz[9,10] and ^{13}C-NMR spectra[10] were determined using tetramethylsilane as the internal standard. GLC[11,12] analysis utilized a 122-cm × 3-mm column packed with phenylmethylsilicones on film calcined diatomite material of low density[13]. The injection port and detector temperatures were 250 and 300°, respectively, and the chromatograms were programmed from 150 to 250° at 4°/min. The physical data for Compounds V–IX are found in Table I.

1-(*m*-Benzyloxyphenyl)-1-nonen-3-ones (V*a–f*)—The compounds were prepared by alkylation of 1-(*m*-hydroxyphenyl)-1-nonen-3-one (2) with the appropriate benzyl chloride using a literature procedure (37) to give the crude product as a brown oil, purified as follows: The unsubstituted compound (V*a*) was chromatographed using a column of alumina and eluted with petroleum ether, followed by benzene and finally methanol. Recrystallization from petroleum ether afforded V*a* as a colorless powdery material. Compound V*b* was purified by trituration with cold petroleum ether to give colorless crystals which were recrystallized from petroleum ether. Compounds V*c* and *d* were purified by chromatography using alumina and a solvent system of chloroform–ethyl acetate–diethylamine (92:5:3). After the products were eluted, they were placed in a freezer (−5°) overnight and the solids obtained recrystallized from petroleum ether to give V*c* and *d* as a colorless powdery material. The nitro analog (V*e*) was purified by placing the crude oil in the freezer overnight and the crystals formed were recrystallized from anhydrous diethyl ether to give V*e* as a colorless product. The crude oil containing V*f* was placed in the freezer overnight and the crystals formed triturated with cold methanol. Recrystallization from methanol afforded V*f* as a colorless powdery material.

The stabilities of V*a*, *e*, and *f* in acetonitrile–phosphate buffers (1:1), which were prepared using the described methodology (38), were demonstrated as follows: The ketone (10^{-3} *M*) was dissolved in the buffer (250 ml) at pH values of 7.4, 6.9, and 6.4. The spectrum of the compound was obtained at dissolution ($t = 0$) and the solution retained at 37 ± 0.1° for 24 hr and monitored at regular time intervals. No change in the absorption at λ_{max} was noted.

1-(3,4-Dibenzyloxyphenyl)-1-nonen-3-one (VI)—A solution of 3,4-dibenzyloxybenzaldehyde (3.0 g, 0.010 mole), 2-octanone (1.4 g, 0.011 mole), piperidine (0.86 g, 0.01 mole), and glacial acetic acid (0.66 g, 0.011 mole) in benzene (50 ml) was heated under reflux for 36 hr. A Dean-Stark trap was attached to the reaction vessel. On cooling the solution was washed with water (3 × 20 ml) and the organic phase dried (anhydrous magnesium sulfate). After evaporation of benzene, the residue was cooled over ice to produce yellow crystals (2.6 g). Purification was accomplished by column chromatography using silica and benzene–acetone (4:1) to give VI as colorless needles (2.3 g). TLC using silica and developing with methylene chloride revealed one spot, $R_f = 0.80$. The mass spectrum of VI showed *m/z* 428 (M^+ 8%) and 91 (100%). NMR ($CDCl_3$): δ 7.30 (m, 13, aromatic H), 7.10 (d, 1, C_1H, J = 16 Hz), 6.55 (d, 1, C_2H, J = 16 Hz), 5.12 (s, 4, 2 × $CH_2C_6H_5$), 2.60 (t, 2, C_4H), and 1.40 [m, 11, $(CH_2)_4CH_3$]. Repeated elemental analyses invariably gave similar results to those quoted in Table I. Only unreacted aldehyde was isolated in an attempt to synthesize VI by the method employed for the preparation of V.

Methoxy-Substituted 1-Phenyl-1-nonen-3-ones (VII)—These ketones were prepared by a literature method (39). The yellow and colorless compounds obtained were recrystallized from methanol, except for VII*d* and *e*, which were recrystallized from petroleum ether.

Styryl Alkyl Ketones (VIII)—These compounds were prepared by the literature procedure (39). The crude products were recrystallized from petroleum ether to yield colorless crystals, except VIII*b*, which was distilled to give the desired compound as a pale yellow oil.

Esters of 1-(*o*-Hydroxyphenyl)-1-nonen-3-one (IX)—The esters (IX) were prepared from 1-(*o*-hydroxyphenyl)-1-nonen-3-one (40) and the appropriate acid chloride in the presence of triethylamine using a literature method (41), except that after the reactants were stirred at room temperature, diethyl ether was added to precipitate all of the triethylamine hydrochloride. Evaporation of the solvent produced yellow oils, which were passed through a column of alumina using methylene dichloride as the eluting solvent to give IX*a* and c as yellow oils, IX*b* as a pink oil, and IX*d* as a pale brown oil which solidified on standing. TLC using alumina and petroleum ether (bp 30–60°) as the eluting solvent showed only one spot.

(*E*)-4-Phenyl-3-buten-2-one oxime (X)—A mixture of (*E*)-4-phenyl-3-buten-2-one (5.0 g, 0.034 mole), hydroxylamine hydrochloride (1.2 g, 0.017 mole), sodium acetate (3.1 g, 0.038 mole), ethanol (25 ml), and water (25 ml) was heated under reflux for 5 hr. Water (200 ml) was added, and after cooling, the mixture was extracted with ether (3 × 50 ml) and the organic extracts washed with water, dried (anhydrous magnesium sulfate), and removal of the solvent afforded a yellow oil which solidified on standing. Recrystallization from petroleum ether (bp 40–60°) gave X as fawn crystals, mp 109° [lit. (42) mp 110°]; 52% yield.

Attempted Synthesis of (*E*)-3-Methoxy-1-phenyl-1,3-butadiene (XI*a*)—Conversion of (*E*)-4-phenyl-3-buten-2-one (IV*c*) into XI*a* was attempted initially using a literature procedure (30), but only unreacted ketone was isolated from the reaction mixture. The result was identical when the time of heating under reflux was extended from 3.5 to 24 hr. Employment of a published method (43) substituting dimethoxypropane for benzylmercaptan, gave a yellow-brown oil, which was shown by TLC using silica and a developing solvent of methylene chloride–benzene (4:1) to consist of unreacted ketone (IV*c*) $R_f = 0.44$ and two yellow components, $R_f = 0.52$ and 0.61. After replacement of the zinc chloride by stannic chloride, the reaction was monitored for 72 hr by TLC to observe the ratio of unreacted IV*c* to the two yellow compounds. After 3.5 hr, this ratio appeared to be constant. Attempts to separate the two yellow components by column chromatography using silica and a mixture of

[5] Silica gel GF Woelm TLC, ICN Pharmaceuticals, GMbH and Co., West Germany.
[6] AE1 MS-12 mass spectrometer, Picker X-Ray Engineering Ltd.
[7] VG Micromass MM16F mass spectrometer with 2025 data system.
[8] Finnigan model 4000 gas chromatograph mass spectrometer interfaced to a Finnigan Incos model 2300 data system. Samples were injected splitless on a 50 m × 0.3-mm fused silica capillary column coated with OV-1 at room temperature and the temperature raised ballistically to 150° and then programmed at 4°/min to 275°. The mass spectrometer was scanned from mass 40 to mass 650 every 2 sec. The temperature of the injector and separator oven were both at 250°.
[9] Varian T-60 spectrophotometer, Varian Associates of Canada Ltd.
[10] Brucker WP-60 spectrophotometer, Brucker Spectrospin (Canada) Ltd.
[11] Hewlett-Packard 5750 gas chromatograph.
[12] Perkin-Elmer Sigma 3B gas chromatograph.
[13] 3% OV-17 on Chromosorb W.

methylene chloride and benzene (4:1) were unsuccessful. Preparative TLC using silica (0.5 mm) and a developing solvent of methylene chloride and benzene (4:1) gave two distinct yellow bands which were eluted with methylene dichloride and the solvent removed *in vacuo* at room temperatures. Evaporation of the solvent gave the two compounds and were subject to mass spectral and ^{13}C-NMR evaluations. After refrigeration with protection from light for 24 hr, both compounds had reverted to an identical mixture of two yellow derivatives. The molecular ions of both compounds were 274 (100%). The ^{13}C-NMR chemical shifts were determined in deuterochloroform and are consistent with structure XIV (assignment, calculated value): 136.61 (C-1 aromatic ring A, 137.3); 128.18 (C-2 aromatic ring A, 127.9); 130.09 (C-3 aromatic ring A, 130.5); 126.39 (C-4 aromatic ring A, 126.2); 129.47 (C-1, 129.8); 135.13 (C-2, 135.3); 151.63 (C-3, 153.9); 125.35 (C-4, 123.9); 190.17 (C-5, –); 142.03 (C-6, 144.5); 150.34 (C-7, 151.1); and 14.30 (C-8, –) ppm. A further attempt to produce XI*a* by a literature procedure (44) produced an orange-brown oil shown by TLC [silica and a developing solvent of methylene chloride and benzene (4:1) to consist of unreacted ketone, R_f = 0.44, and two yellow components, R_f = 0.52 and 0.61].

Attempted Syntheses of the Butadienes (XV*a–c*)—An attempted conversion of (*E*)-1-phenyl-1-nonen-3-one (39) into the corresponding butadiene (XV*a*) by the reported procedure (43) led to the isolation of unreacted ketone from the reaction mixture (TLC evidence using silica and methylene chloride as the developing solvent). In the attempted synthesis of XV*b* from (*E*)-4-phenyl-3-buten-2-one (IV*c*) and ethanethiol by the published procedure (43), only unreacted ketone was isolated from the reaction mixture as revealed by TLC (silica and methylene chloride). Modification of a literature procedure (30) in a further attempt to produce XV*b* was as follows: A mixture of IV*c* (5.72 g, 0.035 mole), ethanethiol (2.67 g, 0.043 mole), and *p*-toluenesulfonic acid (0.50 g, 0.003 mole) in benzene (100 ml) were heated under reflux for 24 hr. On cooling, the mixture was neutralized with sodium bicarbonate (1.5 g), added to ice water (200 ml), and stirred at room temperature for 0.5 hr. After extraction with benzene, the organic layer was washed with water, dried (anhydrous sodium sulfate), and removal of benzene afforded a brown oil (3.6 g). TLC on silica using methylene chloride as the developing solvent revealed the presence of unreacted ketone, R_f = 0.55, and two yellow components, R_f = 0.69 and 0.80.

The attempted synthesis of the thioether (XV*c*) from 4-methyl-1-phenyl-1-hexen-3-one, VIII*b*, and thiophenol using the published procedure (33) yielded a yellow oil. TLC of the product using silica and a developing solvent of cyclohexanone–benzene (94:6) revealed the presence of unreacted ketone, R_f = 0.60, and two other compounds, R_f = 0.72 and 0.83. Separation of the components by preparative TLC using silica and cyclohexanone–benzene (94:6) was achieved and the compound with an R_f value of 0.72 was identified as 4-methyl-1-phenyl-1-phenylthiohexan-3-one (XVI*a*) as a yellow oil, NMR ($CDCl_3$): δ 7.05 (m, 10, aromatic H); 4.75 (t, 1, C_1H, J = 7 Hz); 3.00 (d, 2, C_2H, J = 7 Hz); 2.3 (broad q, 1, C_4H, J = 7 Hz); 1.40 (m, 2, C_5H); and 0.80 (m, 6, C_4HCH_3, C_6H).

Anal.—Calc. for $C_{19}H_{22}OS$: C, 76.46; H, 7.43. Found: C, 76.41; H, 7.49.

The remaining compound, R_f = 0.83, was not identified. However, mass spectrometry revealed the molecular weight to be 280 and the NMR spectrum showed the presence of aromatic protons and various aliphatic hydrogen atoms.

In an attempt to prepare the dibromo analog of XV*c*, the required intermediate ketone, 1,2-dibromo-4-methyl-1-phenyl-3-hexanone (XVI*b*), was prepared by a literature method (45) to give the desired product as colorless needles (mp 97.5°, 64% yield).

Anal.—Calc. for $C_{13}H_{16}Br_2O$: C, 44.82; H, 4.60. Found: C, 44.79; H, 4.60.

Reaction of 1,2-dibromo-4-methyl-1-phenyl-3-hexanone with thiophenol by the literature method (33) was unsuccessful and only unreacted ketone was isolated from the reaction mixture, mp 96–97°.

3-Ethoxy-1-phenyl-1,3-butadiene (XV*d*)—*n*-Butyl lithium (0.14 g, 0.002 mole) in hexane (0.64 ml) was added dropwise to a vigorously stirred suspension of 2-ethoxypropenyl-triphenylphosphine iodide (34) (0.948 g, 0.002 mole) in anhydrous tetrahydrofuran (10 ml) under nitrogen which was cooled to −50°. After the addition was complete, the orange mixture was allowed to warm to −25° and stirring was continued for 2 hr. On cooling to −78°, benzaldehyde (0.212 g, 0.002 mole) was added and the mixture stirred at this temperature for 15 min, 0° for 2 hr, and overnight at room temperature. After heating the reaction mixture under reflux for 6 hr, it was diluted with water (40 ml) and extracted with hexane. The hexane extracts were combined, washed with water, and dried (anhydrous magnesium sulfate), and evaporation of the organic solvent afforded XV*d* as a brown oil (0.15 g). NMR ($CDCl_3$) spectrum was identical to the published data for the (*E*) and (*Z*) isomers of XV*d* (35, 46). On standing overnight at room temperature in a sealed dark container, IV*d* was shown by mass spectral, NMR, and TLC evidence to have been converted into (*E*)-4-phenyl-3-buten-2-one (IV*c*). Attempts at purification of the butadiene (XV*d*) by preparative TLC using silica and a hexane–ether mixture (60:40) caused a breakdown of XV*d* into IV*c*. Column chromatography on alumina and eluting with a hexane–ether mixture (60:40) did not permit purification of the components, and vacuum distillation caused the reaction product to decompose.

Screening of Compounds—The anticancer screening was carried out[14] using protocols described previously (47). The compounds were administered by the intraperitoneal route into either male or female CD_2F_1 mice and male $B_6D_2F_1$ mice. The compounds were administered for 9 consecutive days except in the case of V*b*, VI, IX*a–d*, and X, which were injected for 5 consecutive days. The compounds were administered as suspensions in saline with polysorbate 80[15] except for VIII*d*, *e*, *g*, and *h*, X, and XVI, which were injected in hydroxypropylcellulose and also Compounds IX*d* and V*b*, which were administered in saline with alcohol and in saline with polysorbate 80[15] plus alcohol, respectively.

Examination of the Effect of III*a* in Rats—Unless stated otherwise, III*a* was suspended in normal saline containing 3% polysorbate 80[15] and injected by the intraperitoneal route into male albino Wistar rats. Control animals were injected with normal saline containing 3% polysorbate 80[15].

Metabolism Studies—Dose of III*a* used in metabolism studies is as follows: It has been shown[16] that two doses of III*a* of 400 mg/kg given by the intraperitoneal route on Days 1 and 7 caused no mortalities in the $B_6D_2F_1$ strain of mice by Day 5, and initially it was decided to examine the effect of III*a* in rats at single dose levels of 400, 300, and 200 mg/kg over a 72-hr period. Injection of III*a* at the 400-mg/kg dose level into two rats caused an onset of action between 3 and 5 min. The animals remained inactive for 24 hr, laying on their sides. Only slight movement was initiated by physical stimuli and slight hemorrhaging was observed around the nose. During the first 24 hr, the urine output was 16% that of two control rats. After 48 hr the urine output was normal. Four rats dosed with 300 mg/kg of III*a* had a urine output similar to two control animals, although after 3–5 min, the animals appeared to be sedated. Slight hemorrhaging around the nose was noted after 24 hr, but after 48 hr the animals appeared normal. Two rats dosed with 200 mg/kg of III*a* displayed similar gross physiological effects as the animals dosed with 300 mg/kg of III*a*. Hence, a dose of 300 mg/kg was chosen for the metabolism studies.

Efficiency of Extraction of III*a* from Urine, Feces, Plasma, and Brain of Rats—The percent efficiency of extraction of III*a* from urine, feces, plasma, and brain of rats was determined by GLC by a modification of a literature procedure (48). Compound III*a* (0.04 mg) was added to control urine (2.00 ml), and after basification with aqueous sodium hydroxide solution (0.45 *N*) to pH 10.50, it was extracted with ether (2 × 5 ml). After evaporation of the organic solvent, the extract was dissolved in a solution (0.10 ml) of promazine hydrochloride in methanol (1.00 mg/ml). The peak height ratio of III*a*, promazine hydrochloride, recorded when 1 μl of this solution was injected onto a GLC column, was compared to the ratio obtained after injecting 1 μl of a solution containing 0.40 mg of III*a* and 1.00 mg of promazine hydrochloride/ml. It was observed that 98% of III*a* was recovered by this method.

Compound III*a* (8.00 mg) was added to 25 g of control feces and extracted by the literature method (48). The ether-soluble basic fraction was evaporated to dryness, dissolved in 100 μl of a solution containing II (R_1 = 3-OH; R_2 = H) in methanol (1.00 mg/ml), and the peak height ratio of III*a*, II (R_1 = 3-OH; R_2 = H), was compared with the peak height ratio of a 1-μl sample of a solution containing III*a* (8.00 mg) and II(R_1 = 3-OH; R_2 = H; 0.1 mg) in methanol/100 μl. The percentage of III*a* extracted by this method was 61%.

Compound III*a* (0.04 mg) was added to plasma (1 ml), basified with aqueous sodium hydroxide solution (0.45 *N*) to pH 11.5, and extracted with ether (2 × 5 ml). After the ether was evaporated, the extract was dissolved in 100 μl of a solution containing II (R_1 = 3-OH; R_2 = H) in methanol (1 mg/ml). The peak height ratios of III*a* with II (R_1 = 3-OH; R_2 = H) were compared with a 1-μl sample of a solution containing 0.04 mg of III*a* and 0.10 mg of II (R_1 = 3-OH; R_2 = H) in 100 μl of methanol. It was found that the efficiency of extraction of III*a* from plasma was 71%.

[14] Anticancer screening was carried out by the Drug Research and Development Division of the National Cancer Institute, Bethesda, Md.

[15] Tween-80, Atlas Chemical Laboratories.

[16] The National Cancer Institute, Bethesda, Md.

The brain of a rat was removed, homogenized[17], and after the addition of IIIa, the compound was extracted by the literature method (49), except that no basification was undertaken and the extraction solvent was ether, not 1-chlorobutane. Comparison of the peak heights of IIIa with II (R_1 = 3-OH; R_2 = H) by the method already described, indicated a percentage efficiency of extraction of IIIa of 75%.

Examination of Rat Urine and Feces for IIIa and Metabolites—Compound IIIa was injected into rats weighing between 200 and 300 g. Normally a trial consisted of 10 dosed rats and 5 control animals. The urine and feces were collected every 24 hr for 3 days and then at 1-week intervals for 4 subsequent weeks. If the samples were not utilized on the day of collection, they were frozen immediately at −5°. Both 24-hr test and control urine were extracted with ether and fractionated into the strongly acidic, weakly acidic, neutral, amphoteric, and basic components essentially by the literature procedure (48). The extracts were dissolved in methanol (100 μl) and a 1-μl sample injected onto a GLC column. No peaks were found in the extracts from the urine of animals dosed with IIIa, which also were not found in the extracts from the urine of the control animals. A similar observation was made after extracting the urine collected between 24 and 48 hr and also between 48 and 72 hr after injection of IIIa. Extraction of the 24-hr test and control feces (25 g) with ether was undertaken by the published procedure (48), the extracts were dissolved in methanol (100 μl), and a 1-μl sample injected onto a GLC column. The chromatograms generated did not reveal the presence of unchanged IIIa nor metabolites in the test feces. At this time, the toxicity of IIIa became apparent and the dose of IIIa was reduced tenfold. Samples of the 24, 48, and 72 hr and 1–4 week urine from six rats dosed with 30 mg/kg of IIIa and two control animals were extracted as described above, and no unchanged IIIa nor metabolites were found. Both test and control urine (2 ml) were adjusted to pH 5.2 with an acetate buffer and sulfatase[18] (20 μl containing β-glucuronidase) was added and the mixture was incubated at 37° overnight. Extraction and analysis by GLC indicated the absence of IIIa and related metabolites.

Examination of Rat Plasma after Intraperitoneal Injection of IIIa—Compound IIIa (30 mg/kg) was injected by the intraperitoneal route into rats weighing between 200 and 500 g. Rats were decapitated 15 min and 2, 24, and 48 hr after injection; the blood was collected and extracted by the following methods. First, test plasma (1.0 ml) was basified to pH 11.5 with aqueous sodium hydroxide solution (0.45 *N*), extracted with ether, and the organic extracts evaporated to dryness. The original plasma was then acidified with aqueous sulfuric acid (1 *N*) to pH 2.4, extracted with ether (2 × 5 ml), and the ether extracts evaporated to dryness (Method A). Second, plasma (1.0 ml) and 4 *N* aqueous HCl (1.0 ml) were incubated at 85° for 10 min. The plasma (pH 2.4) was extracted with ether (2 × 5 ml) and the ether removed *in vacuo*. The original plasma was then basified with aqueous sodium hydroxide solution (0.45 *N*) to pH 11.5, extracted with ether (2 × 5 ml), and the ether removed by evaporation. Third, plasma from dosed animals (1.0 ml) and 4 *N* aqueous HCl (1.0 ml) were incubated at room temperature for 24 hr. The plasma (pH 2.4) was extracted with ether (2 × 5 ml) and the ether evaporated. Basification of the original plasma to pH 11.5 was accomplished with aqueous sodium hydroxide solution (0.45 *N*), extracted with ether (2 × 5 ml), and the ethereal extract evaporated to dryness. Fourth, plasma (1.0 ml) was extracted by a literature procedure (36). In all cases control plasma was extracted by identical methods. Extracts from the plasma of dosed and control animals were dissolved in 100 μl of methanol and a 1-μl sample examined by GLC. Chromatograms of the dosed and control plasma extracts appeared identical.

Examination of Rat Plasma after Intravenous Injection of IIIa—Rats weighing between 200 and 250 g were injected into the femoral vein with IIIa (300 mg/kg). In the first experiment, blood was collected after 5 and 10 min, and in the second, blood was collected by cardiac puncture after 5 and 8 min. Plasma was separated and extracted by Method A. The extracts were dissolved in 100 μl of a solution of II (R_1 = 3-OH; R_2 = H) in methanol (1 mg/ml), and a 1-μl sample was analyzed by GLC. The quantity of IIIa in the plasma samples was determined by comparing the peak height ratio of IIIa to II (R_1 = 3-OH; R_2 = H) with a standard curve prepared from standard solutions of these two compounds. The results were determined by calibration and revealed that the concentrations of IIIa were 1.974 (2.132, 1.816), 0.602, and 0.005 mg/ml after 5, 8, and 10 min, respectively.

Examination of Rat Brain after Intraperitoneal Injection of IIIa—A dose of 300 mg/kg of IIIa was injected intraperitoneally into a rat weighing 340 g and the animal decapitated 15 min after injection. The brain was removed, homogenized[17], and the compound extracted by the literature procedure (49), except that basification prior to extraction was omitted, and the extraction solvent was ether, not 1-chlorobutane. The quantity of IIIa in the brain was measured using II (R_1 = 3-OH; R_2 = H) as the reference compound by the same procedure described earlier and found to represent 4.78% of the injected dose of the compound.

Pathological Study of IIIa—A dose of 300 mg/kg of IIIa was injected intraperitoneally into 10 male Wistar rats and two control animals were utilized. Deaths occurred in three animals after 40, 41, and 42 days, and at the end of 43 days the remaining seven animals were weak and bloated. There was paralysis in the hind legs and hemorrhaging from the nose. Necropsy was undertaken on these seven animals. Tissues were fixed in 10% buffered formaldehyde solution, sectioned at 5 μm, and stained with hematoxylin and eosin.

Blood samples were obtained by cardiac puncture prior to necropsy of the seven rats. Hemoperitoneum was noted in six of the seven rats. The markedly distended abdomens and scrotal sacs contained blood. Hemopericardium was noted in the seventh rat. The blood found in body cavities did not clot on exposure to air; however, the prothrombin times, partial thromboplastin times, and platelet counts of representative test animals were comparable to those of the controls. Two rats had a chronic diffuse peritonitis, whereas in the other five, the peritonitis was confined to the cranial abdomen where the diaphragm, liver, spleen, stomach, proximal duodenum, colon, and cranial poles of the kidneys adhered to one another by fibrous strands. Both the liver and spleen were enlarged in all of the rats examined. The stomach and intestines contained food and the other organs appeared normal.

The significant histological changes were found in the spleen, liver, and mesenteric lymph nodes. Chronic perihepatitis was characterized by a markedly thickened fibrous capsule. Loose granulation tissue attached to the peritoneal surface of the capsule contained capillaries, fibroblasts, and an infiltrate of polymorphonuclear leukocytes. Liver parenchymal changes were observed throughout all lobes and ranged from periportal vacuolation, basophilic cytoplasmic clumping, single hepatocyte necrosis, and occasional mitosis to multifocal centrilobular and midzonal coagulation necrosis. The periportal areas seemed to have been spared, although single necrotic cells were visible in these areas. Polymorphonuclear leukocytes were noted in the areas of necrosis.

Changes in the splenic capsule were similar to those in the liver capsule. The splenic red pulp was congested. Extramedullary hematopoiesis varied in degree among the rats from the occasional focus to more diffuse areas of hemopoietic activity.

Numerous erythrocytes were present in the medullary and subcapsular sinuses of the mesenteric lymph nodes. Siderocytes were numerous and erythrophagocytosis was evident.

To evaluate whether these pathological changes occurred soon after injection of the compound or gradually, four rats were injected intraperitoneally with IIIa at a dose of 300 mg/kg and euthanized for necropsy after 1, 2, 3, and 4 weeks. No gross abnormalities were noted in the rat 1 week postinjection. Mild hepatomegaly was noted 2 weeks postinjection. Perihepatitis, hepatomegaly, perisplenitis, and hemoperitoneum were noted 3 weeks postinjection, although the amount of blood in the abdominal cavity was very small. Perisplenitis, hepatomegaly, and congestion were noted 4 weeks postinjection. Liver parenchymal changes appeared to be progressive. Hydropic degeneration of periportal hepatocytes was mild 1 week postinjection but marked 2, 3, and 4 weeks postinjection. Over the 4 weeks, the vacuolation progressed towards the central veins. Mitotic figures were frequent in hepatocytes during the first 2 weeks postinjection but decreased during weeks 3 and 4. Many of the mitoses observed were abnormal and unlikely to produce viable cells. Single hepatocyte necrosis was noted after 1 week and progressed to focal tissue necrosis, principally in centrilobular areas, after 3 weeks. Clumps of leukocytes phagocytosing debris were noted in the areas of necrosis. Kupffer cell hyperplasia was evident in all livers examined. Capsular thickening was focal 1 week postinjection with lymphocytic infiltration. Three and 4 weeks postinjection the changes were diffuse. Dense fibrous tissue was present adjacent to the liver parenchyma. However, the surface collagen was very fine and contained many normal capillaries. Areas of old hemorrhage were present in the surface collagen, as was an infiltrate of lymphocytes, mast cells, plasma cells, and eosinophils. Subcapsular veins were ectatic and congested. Perisplenitis was noted 3 and 4 weeks postinjection. The capsule was thickened with fibrous tissue and infiltrated with lymphocytes. The amount of extramedullary hematopoiesis paralleled that of the controls.

Finally, IIIa was administered intraperitoneally to one rat at a reduced dose of 30 mg/kg, while a control animal was given polysorbate 80[15] (3%) in normal saline. The animals were examined at the end of a 4-week pe-

[17] Virtis homogenizer, model 45.

[18] Sigma Type H-2, Sigma Chemical Co., St. Louis, MO 63178.

riod. Perisplenitis was noted on gross examination of the test rat. Histological examination revealed focal thickenings of the splenic capsule with very fine reticulate connective tissue. Large capillaries were prominent in these areas and small hemorrhages were noted. Mast cells, some of which were degranulated, were numerous in the thickened capsule. Histologically the degree of liver change was mild with centrilobular degeneration characterized by basophilic clumping of cytoplasm, single cell necrosis with phagocytosis by invading leucocytes, and prominence of Kupffer cells.

REFERENCES

(1) J. R. Dimmock and W. G. Taylor, *J. Pharm. Sci.*, **64,** 241 (1975).

(2) J. R. Dimmock, C. B. Nyathi, and P. J. Smith, *ibid.*, **68,** 1216 (1979).

(3) J. R. Dimmock, N. W. Hamon, E. W. K. Chow, D. L. Kirkpatrick, L. M. Smith, and M. G. Prior, *Can. J. Pharm. Sci.*, **15,** 84 (1980).

(4) M. Eden, B. Haines, and H. Kahler, *J. Natl. Cancer Inst.*, **16,** 541 (1955).

(5) H. Kahler and W. B. Robertson, *ibid.*, **3,** 495 (1943).

(6) K. A. Meyer, E. M. Kammerling, L. Amtman, M. Koller, and S. J. Hoffman, *Cancer Res.*, **8,** 513 (1948).

(7) G. Abel, T. A. Connors, P. Goddard, H. Hoellinger, Nguyen-Hoang-Nam, L. Pichat, W. C. J. Ross, and D. E. V. Wilman, *Eur. J. Cancer*, **11,** 787 (1975).

(8) E. Haslam, in "Protective Groups in Organic Chemistry," J. F. W. McOmie, Ed., Plenum, London, England, 1973, p. 157.

(9) B. Testa and P. Jenner, "Drug Metabolism: Chemical and Biochemical Aspects," Marcel Dekker, New York, N.Y. 1976, p. 99.

(10) J. B. Stenlake, "Foundations of Molecular Pharmacology," Vol. 2, Athlone Press, London, 1979, p. 239.

(11) M. M. Wick, *J. Invest. Dermatol.*, **71,** 163 (1978).

(12) M. M. Wick, *Science*, **199,** 775 (1978).

(13) P. Ginnings and R. Baum, *J. Am. Chem. Soc.*, **59,** 1111 (1937).

(14) A. Burger, *J. Med. Chem.*, **21,** 1 (1978).

(15) G. S. Hammond, in "Steric Effects in Organic Chemistry," M. S. Newman, Ed., John Wiley, New York, N.Y., 1956, p. 444.

(16) G. W. Wheland, "Advanced Organic Chemistry," 3rd ed., John Wiley, New York, N.Y., 1960, p. 675.

(17) J. R. Dimmock and M. L. C. Wong, *Can. J. Pharm. Sci.*, **11,** 35 (1976) and references cited therein.

(18) S. M. Kupchan, D. C. Fessler, M. A. Eakin, and T. J. Giacobbe, *Science*, **168,** 376 (1970).

(19) "Handbook of Chemistry," 10th ed., N. A. Lange and G. M. Forker, Eds., McGraw-Hill, New York, N.Y. 1961, pp. 441, 471.

(20) I. H. Hall, K.-H. Lee, C. O. Starnes, S. A. El Gebaly, T. Ibuka, Y.-S. Wa, T, Kimura, and M. Haruna, *J. Pharm. Sci.*, **67,** 1235 (1978).

(21) M. C. Wani, H. L. Taylor, J. B. Thompson, and M. E. Wall, *Lloydia*, **41,** 578 (1978).

(22) J. R. Dimmock and L. M. Smith, *J. Pharm. Sci.*, **69,** 575 (1980).

(23) R. T. Williams, "Detoxication Mechanisms," 2nd ed., Wiley, New York, N.Y., 1959, p. 166.

(24) H. J. E. Loewenthal, in "Protective Groups in Organic Chemistry," J. F. W. McOmie, Ed., Plenum, London, England, 1973, p. 341.

(25) *Ibid.*, p. 337.

(26) I. Iwai and K. Okajima, *J. Pharm. Soc. Jpn.*, **79,** 1284 (1959).

(27) J. M. Conia, *Bull. Soc. Chim. Fr.*, **1956,** 1392.

(28) J. R. Dimmock, P. L. Carter, and P. D. Ralph, *J. Chem. Soc. B.*, **1968,** 698.

(29) J. S. Gillespie, Jr., S. P. Acharya, D. A. Shamblee, and R. E. Davis, *Tetrahedron*, **31,** 3 (1975).

(30) A. L. Nussbaum, E. Yuan, D. Dincer, and E. P. Oliveto, *J. Am. Chem. Soc.*, **26,** 3925 (1961).

(31) M. Mousseron, *Pure Appl. Chem.*, **9,** 481 (1964).

(32) G. C. Levy and G. L. Nelson, "Carbon-13 Nuclear Magnetic Resonance for Organic Chemists," Wiley-Interscience, New York, N.Y., 1972.

(33) E. Campaigne and J. R. Leal, *J. Am. Chem. Soc.*, **76,** 1272 (1954).

(34) F. Ramirez and S. Dershowitz, *J. Org. Chem.*, **22,** 41 (1957).

(35) E. Vedejs, D. A. Engler, and M. J. Mullin, *ibid.*, **42,** 3109 (1977).

(36) E. B. Astwood, *Trans. Assoc. Am. Phys.*, **70,** 183 (1957).

(37) G. Buchi, D. M. Foulkes, M. Kurono, G. F. Mitchell, and R. S. Schneider, *J. Am. Chem. Soc.*, **89,** 6745 (1967).

(38) J. R. Dimmock, L. M. Smith, and P. J. Smith, *Can. J. Chem.*, **58,** 984 (1980).

(39) P. J. Smith, J. R. Dimmock, and W. G. Taylor, *ibid.*, **50,** 871 (1972).

(40) J. R. Dimmock, C. B. Nyathi, and P. J. Smith. *J. Pharm. Sci.*, **67,** 1543 (1978).

(41) BRIT. 815, 277, June 24, 1959; through *Chem. Abstr.*, **53,** 19651e (1959).

(42) M. Chambow, *Ann. Pharm. Fr.*, **2,** 98 (1944); through *Chem. Abstr.*, **40,** 4852 (1946).

(43) G. Rosenkranz, St. Kaufmann, and J. Romo, *J. Am. Chem. Soc.*, **71,** 3689 (1949).

(44) A. Serini and H. Köster, *ibid.*, **75,** 650 (1963).

(45) D. J. Marshall and R. Gaudry, *Can. J. Chem.*, **38,** 1495 (1960).

(46) M. L. Martin, R. Marrtione, and G. J. Martin, *C. R. Acad. Sci., Paris*, **260,** 4205 (1965).

(47) R. I. Geran, N. H. Greenberg, M. M. MacDonald, A. M. Schumacher, and B. J. Abbott, *Cancer Chemother. Rep., Part 3*, **3** (Sept. 1972).

(48) J. R. Dimmock, N. W. Hamon, K. W. Hindmarsh, A. P. Sellar, W. A. Turner, G. H. Rank, and A. J. Robertson, *J. Pharm. Sci.*, **65,** 538 (1976).

(49) B. H. Thomas, B. B. Coldwell, G. Solomonraj, W. Zeitz, and H. L. Trenholm, *Biochem. Pharmacol.*, **21,** 2605 (1972).

ACKNOWLEDGMENTS

Financial support to D. L. Kirkpatrick came principally from an award of a University of Saskatchewan Graduate Scholarship and the John and Mary Spinks Graduate Scholarship and is recorded with gratitude.

The authors thank the Medical Research Council of Canada for an operating grant (MA 5538) to J. R. Dimmock.

The authors thank Dr. K. K. Midha and Mr. J. K. Cooper, College of Pharmacy, University of Saskatchewan, Saskatoon, for their advice and assistance during the course of this project; Mr. L. Hogge, Prairie Regional Laboratory, Saskatoon for generating most of the GC–MS data; Mrs. L. M. Smith, College of Pharmacy, University of Saskatchewan who synthesized compounds IX and X; and Mr. Ian Shirley, Western College of Veterinary Medicine, Saskatoon who prepared Figs. 1 and 2. The cooperation of the Drug Research and Development Division of the National Cancer Institute, Bethesda, Md. for evaluating the antineoplastic potential of many of the compounds described in this study is greatly appreciated.

Placental Transfer of Ranitidine During Steady-State Infusions of Maternal and Fetal Sheep

G. W. MIHALY *x, D. J. MORGAN ‡, A. W. MARSHALL *, R. A. SMALLWOOD *, S. COCKBAIN *, D. MacLELLAN §, and K. J. HARDY §

Received May 11, 1981, from the *Gastroenterology Unit, Department of Medicine; the §Department of Surgery, Austin Hospital, Heidelberg, Victoria 3084, Australia; and the ‡Victorian College of Pharmacy, 381 Royal Parade, Parkville, 3052 Victoria, Australia. Accepted for publication November 24, 1981.

Abstract □ The placental transfer of ranitidine was studied at pharmacokinetic steady state in anesthetized, full-term, pregnant sheep. Ranitidine was administered to the ewe in three preparations and to the fetus in three other sheep. In all experiments, dose size was based on the combined maternal–fetal weight. Steady-state plasma levels were reached within 4 hr by using an initial intravenous bolus dose followed by continuous infusion. Following maternal dosage, the mean maternal (jugular vein) steady-state concentration ($C_{M_{ss}}$) at 4 hr was 842 ± 66 ng/ml (*SEM*), the mean fetal (carotid artery) steady-state concentration ($C_{F_{ss}}$) was 26.5 ± 4.2 ng/ml, and the mean fetal umbilical venous steady-state concentration was 28.9 ± 3.5 ng/ml. Both the fetal and umbilical plasma concentrations were significantly less than the maternal plasma concentration ($p < 0.01$). With fetal dosage, mean $C_{M_{ss}}$ was 414 ± 42 ng/ml at 4 hr and was significantly less than the mean $C_{F_{ss}}$ value at the same time, which was 6890 ± 360 ng/ml ($p < 0.005$). Ranitidine was not bound extensively to plasma proteins in the ewe or the fetus (range 12–55% bound). The reversal of the $C_{M_{ss}}/C_{F_{ss}}$ gradient with the change from maternal to fetal administration and the low binding of the drug shows that the gradient following maternal dosage cannot be explained by ion-trapping or differential plasma protein binding. As active placental transport is considered unlikely, the low fetal plasma concentrations are probably due to the presence of significant fetal elimination of ranitidine. Furthermore, the substantial gradient between maternal and umbilical venous plasma concentrations suggests that placental elimination of ranitidine should also be considered.

Keyphrases □ Ranitidine—placental transfer during steady-state infusions of maternal and fetal sheep □ Placental transfer—ranitidine, during steady-state infusions, maternal and fetal sheep

The use of H_2-receptor antagonists in pregnancy is becoming widespread (1, 2), although little is known of their placental transfer. Cimetidine has been shown to cross the placenta (1) but ranitidine, a new H_2-receptor antagonist, has not been studied.

Since opportunities to make observations in pregnant women are necessarily limited, we have used a pregnant sheep model to study the placental transfer of ranitidine. A similar model has been used recently to examine the placental transfer of meperidine (3), indomethacin (4), and aspirin (5). In contrast to earlier work, the bidirectional transfer of drug has been studied in this report. Results establish that ranitidine does cross the placenta. They also indicate that the comparatively low drug concentrations found in the fetus after maternal dosage are probably accounted for by fetal and/or placental elimination.

EXPERIMENTAL

Methods—Experiments were carried out in pregnant Merino or Dorset-Horn sheep, 2–5-years old, during the last 2 weeks of gestation (term = 147 days). The animals were treated with fenbendazole[1] to clear intestinal parasites. Anesthesia was induced with sodium thiopental[2] (15 mg/kg iv) and maintained with a mixture of halothane and oxygen using intermittent positive pressure respiration. The partial pressure of oxygen was kept in excess of 100 mm of Hg, while the partial pressure of carbon dioxide was 25–35 mm of Hg. Surgery was performed with strict sterile techniques.

The uterus was incised and the fetus was delivered onto a small draped platform. The fetus was kept on the platform through the experiments and its rectal temperature was maintained at 38–39° with a heating pad. The fetus and umbilical cord were kept moist with saline packs.

The maternal jugular vein was cannulated with a dimethicone cannula (1.2-mm i.d.) to allow collection of maternal blood samples. The fetal carotid artery was cannulated with a dimethicone catheter (0.76-mm i.d.) to allow fetal blood sampling. In fetal dosage experiments, the internal jugular vein was cannulated with a dimethicone catheter (0.76-mm i.d.) for drug administration.

Liver function tests were carried out in both ewe and fetus before and after every experiment. No abnormalities were encountered. Fetal and maternal hematocrits changed by <3% over the course of the experiment.

Calculation of Bolus Dose and Infusion Rate—Steady-state plasma levels of ranitidine were achieved by the combination of an initial bolus dose together with a continuous intravenous infusion that was maintained throughout the experiment. The bolus dose for both maternal and fetal administration was calculated as follows (6):

$$\text{Bolus Dose} = C_{ss} \times V_\beta \times W$$

where C_{ss} (μg/liter) is the desired steady-state plasma concentration, V_β (liter/kg) is the total apparent volume of distribution, and W is the animal's weight (kg) (*i.e.*, the combined weight of sheep and fetus). Maternal and fetal infusion rates were calculated as follows (6):

$$\text{Infusion rate} = C_{ss} \times Q \times W$$

where Q (liter/hr) is the systemic plasma clearance of ranitidine. The desired steady-state concentrations in maternal plasma following maternal dosage was between 500 and 1000 ng/ml (500 ng/ml was used in the calculations). The values used for V_β (1.6 liter/kg) and Q (0.5 liter/hr/kg) were previously determined from a pilot pharmacokinetic study in a single nonpregnant sheep.

Since $t_{1/2\beta}$ for the adult sheep was ~2 hr, a constant infusion would not have achieved steady-state concentrations until 8–10 hr. Using this procedure, steady-state plasma concentrations were approached within 2 hr and were then maintained for the duration of the experiment.

Maternal Dosage Experiments—Ranitidine[3] was administered intravenously to three pregnant ewes *via* a foreleg vein. A predose blood sample was collected from the maternal jugular vein (8 ml) and from the fetal carotid artery (5 ml) and further samples were then collected from both the ewe and the fetus at 2, 4, 10, 15, 120, 180, 210, and 240 min postbolus dose. A sample was taken from the umbilical vein of each fetus at 240 min.

Fetal Dosage Experiments—Ranitidine was administered to three fetuses *via* the internal jugular vein. The same dosage regimen as used for maternal administration was applied, using the weight of the pregnant ewe for calculations. Blood samples were collected as described above from both the ewe and the fetus. Additional samples were collected at 240 min from umbilical artery and vein.

Protein Binding—Plasma protein binding of ranitidine in maternal and fetal plasma samples collected at 240 min was estimated by ultrafiltration (7).

Drug Analysis—Plasma concentrations of ranitidine were determined

[1] Panacur, Hoescht, Melbourne, Australia.
[2] Pentothal, Abbott Pharmaceuticals, Australia.
[3] Glaxo Group Research Ltd.

0022-3549/82/0900-1008$01.00/0

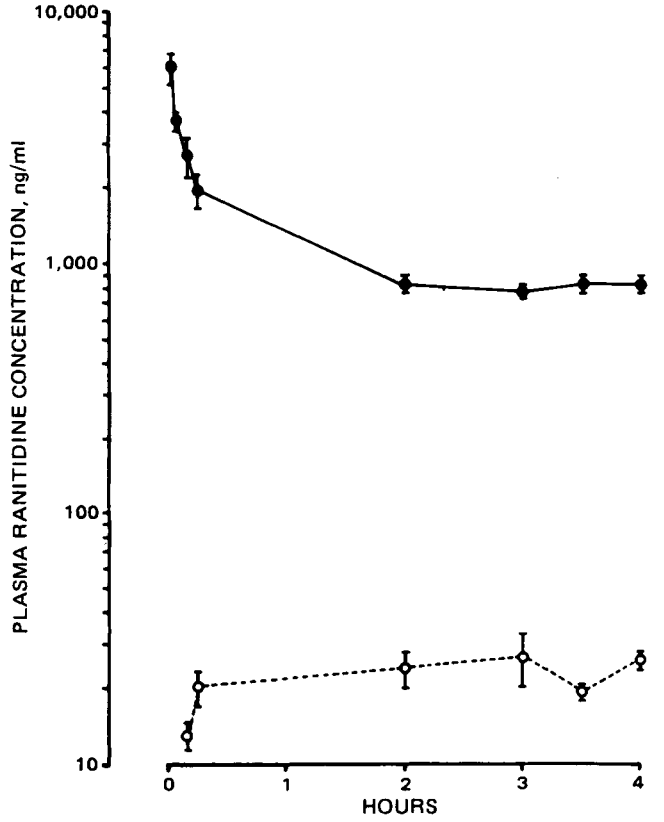

Figure 1—*Mean plasma ranitidine concentrations in ewes and fetuses during maternal administration (intravenous bolus plus constant rate infusion). Key: (●) maternal, (○) fetal.*

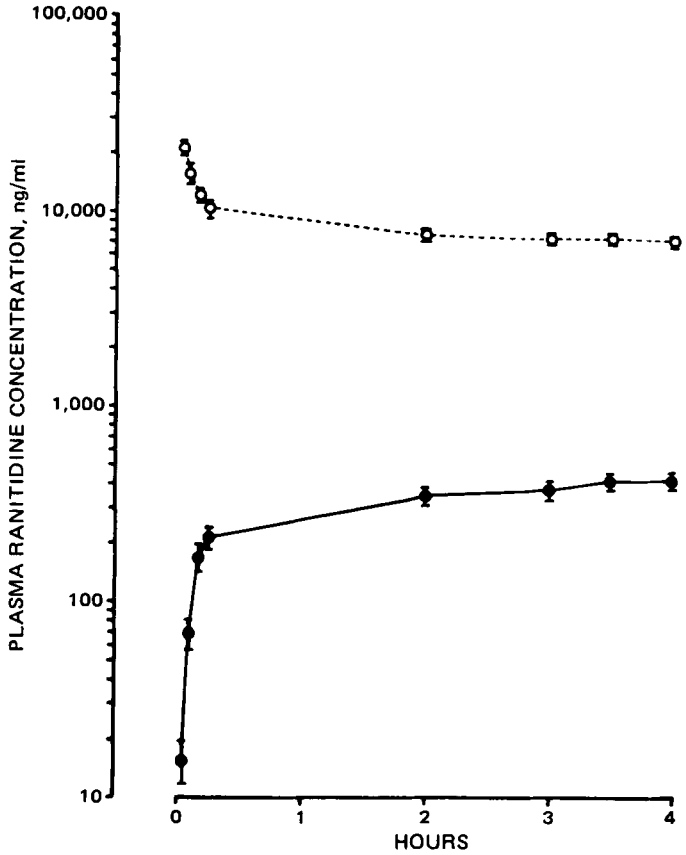

Figure 2—*Mean plasma ranitidine concentrations in ewes and fetuses during fetal administration (intravenous bolus plus constant rate infusion). Key: (●) maternal, (○) fetal.*

by a high-performance liquid chromatographic (HPLC) method (8). This method was specific for ranitidine and had a sensitivity of 5 ng/ml of compound in plasma.

Statistical Analysis—Data are presented as mean ±*SEM*. Statistical comparisons were made using the Student's t test or linear regression analysis and statistical significance accepted when $p < 0.05$.

RESULTS

Maternal Dosage Experiments—The mean plasma ranitidine concentration *versus* time curves in both the ewe and the fetus, following maternal dosage, are shown in Fig. 1. The initial bolus dose produced an early peak in maternal plasma levels and steady state was achieved by 4 hr, since the slope of the linear regression line through the plasma concentration–time data from 2 to 4 hr was not significantly different from zero ($p > 0.05$). The mean steady-state concentration of ranitidine at 4 hr was 842 ± 66 ng/ml. Ranitidine was detected in fetal plasma within 10 min and fetal plasma concentrations also achieved steady state by 4 hr ($p > 0.05$). The mean fetal steady-state concentration of ranitidine at 4 hr was 26.5 ± 4.2 ng/ml and this value was significantly less than the maternal concentration at 4 hr (paired t test, $p < 0.01$). The mean umbilical venous concentration of ranitidine at 4 hr was 28.9 ± 3.5 ng/ml and was also significantly less than the corresponding maternal concentration (paired t test, $p < 0.01$) but did not appear to differ from the fetal concentration.

Fetal Dosage Experiments—The mean plasma ranitidine concentration *versus* time curves in both the ewe and the fetus, after fetal dosage, are shown in Fig. 2. Placental transfer was detected within 2 min, and a steady state was again reached in both the ewe and the fetus by 4 hr ($p > 0.05$). Fetal mean carotid arterial, umbilical arterial, and umbilical venous plasma concentrations of ranitidine at 4 hr were 6890 ± 360 ng/ml, 8010 ± 544 ng/ml, and 6990 ± 433 ng/ml, respectively. The mean maternal steady-state plasma concentration of ranitidine at 4 hr was 414 ± 42 ng/ml, which was significantly less than each of the above three mean fetal concentrations (paired t test, $p < 0.005$).

Plasma Protein Binding of Ranitidine—Plasma protein binding experiments are summarized in Table I. Approximately 30% of plasma was bound in both maternal and fetal plasma.

DISCUSSION

Studies of placental drug transfer and fetal pharmacokinetics cannot be readily undertaken in humans, in whom observations have been largely confined to the comparison of drug concentrations in maternal and umbilical vein plasma at birth. Such observations contribute little to the understanding of placental transfer, or of fetal drug distribution and elimination. The pregnant sheep preparation is not limited in this way, and the increased flexibility of experimental design allows much greater insight into the fetal handling of drugs.

The present study was carried out in anesthetized sheep. General anesthesia may cause hemodynamic changes (9), and this should be borne in mind when considering these results. However, all maternal and fetal sheep remained in excellent condition, and previous work suggests that anesthesia does not significantly alter propranolol disposition in this pregnant sheep preparation (10). Blood gases, pH, biochemical, and hematological profiles remained within normal physiological values (11) in mothers and fetuses in all experiments. The comparatively large doses of ranitidine administered to fetuses produced no detectable adverse effects, despite steady-state fetal plasma levels which were tenfold greater than the maternal levels obtained after maternal dosage. Fetal dosage was based on the combined maternal–fetal rather than fetal weight, because it was presumed that most of the drug would be eliminated by the mother, and a small fetal dose might have resulted in undetectable maternal plasma concentrations.

Following maternal dosage, steady-state levels of ranitidine in the ewe were 30 times that in the fetus. This cannot be explained by a delay in placental transfer, since a steady state existed. Furthermore, ranitidine was detected within 10 min in fetal plasma, suggesting that any hold up at the placenta is short lived.

It has been argued (12) that, after maternal dosage, the fetal–maternal steady-state concentration ratio should equal one, unless one of the following applies: (*a*) there is active transport of drug across the placenta, (*b*) there is differential binding of drug to fetal and maternal plasma proteins, (*c*) there is differential ionization of drug in maternal and fetal plasma due to differences in plasma pH, (*d*) the fetus eliminates the drug, or (*e*) the placenta eliminates the drug. The fact that fetal dosage reversed the placental gradient obtained after maternal dosage (Figs. 1 and 2)

Table I—Percentage of Total Plasma Ranitidine Bound to Proteins in Both Maternal and Fetal Plasma after Both Maternal and Fetal Administration

Sheep Number	Maternal		Fetal	
	Total Plasma Concentration, ng/ml	Bound, %	Total Plasma Concentration, ng/ml	Bound, %
M1	838	45	[a]	[a]
M2	606	40	[a]	[a]
M3	714	21	1110[b]	36
Mean	719	35	—	—
SEM	67	7	—	—
F1	374	31	6300	12
F2	481	31	7680	40
F3	370	55	6630	20
Mean	408	39	6870	24
SEM	36	8	415	8

[a] Plasma not available for ultrafiltration. [b] Sample supplemented with pure ranitidine to ~1100 ng/ml.

effectively rules out *a*, *b*, and *c* above. These three mechanisms would tend to maintain a gradient in the same direction, whatever the route of administration. Furthermore, the plasma protein binding data (Table I) shows that ranitidine is not extensively bound in maternal or fetal plasma. This also rules out any possibility that differential binding of drug in maternal and fetal plasma could be responsible for the placental gradient, because the unbound fraction of drug in fetal plasma would need to exceed that in maternal plasma 30-fold. It could be argued that since active transport is likely to be unidirectional (*e.g.*, fetus → mother) the higher fetal concentrations produced by drug administration to the fetus might saturate an active transport system and alter the maternal–fetal ratio. Such an active transport mechanism is unlikely (13), although there is insufficient data to allow us to rule it out completely.

The placental transfer of the other drugs has been studied in pregnant sheep. Following maternal administration, meperidine (3), indomethacin (4), and aspirin (5) were found to have lower fetal than maternal steady-state plasma concentrations of drug. Szeto *et al.* (3) used a pharmacokinetic model to propose that the difference in fetal and maternal steady-state meperidine concentrations was due partly to fetal drug elimination. This proposal was subsequently supported when it was demonstrated that renal excretion of meperidine does take place in the ovine fetus (14, 15).

Following maternal dosage, the fact that umbilical venous plasma concentrations of ranitidine were substantially less than maternal concentrations suggests that the gradient in concentration occurs across the placenta. Hence, the possibility of placental drug elimination in addition to fetal drug elimination should be considered. Several drug biotransformation processes have been identified in animal and human placentas (16), but the role of the placenta in xenobiotic metabolism still remains unclear (17). A previous study (13), in discussing the theoretical relationships between metabolism and fetal plasma levels of drugs, concluded that enzymes in the fetus would usually be more effective than those in the placenta in protecting the fetus against lipid-soluble drugs. Therefore, the relative importance of placental compared with fetal elimination of ranitidine requires further investigation. It may be that fetal exposure to ranitidine encountered during pregnancy is reduced by placental metabolism, at a time when the fetus' own capacity to eliminate this foreign substance is greatly limited.

REFERENCES

(1) W. A. W. McGowan, *J. R. Soc. Med.*, **72**, 902 (1979).

(2) F. Glade, C. L. Saccar, and G. R. Pereira, *Am. J. Dis. Child.*, **134**, 87 (1980).

(3) H. H. Szeto, L. I. Mann, A. Bhakthavathsalan, M. Liu, and C. E. Inturrisi, *J. Pharmacol. Exp. Ther.*, **206**, 448 (1978).

(4) E. F. Anderson, T. M. Phernetton, and J. H. G. Rankin, *ibid.*, **213**, 100 (1980).

(5) D. F. Anderson, T. M. Phernetton, and J. H. G. Rankin, *Am. J. Obstet. Gynacol.*, **137**, 735 (1980).

(6) J. G. Wagner, in "Fundamentals of Clinical Pharmacokinetics," 1st ed., Drug Intelligence Public. Inc., Hamilton, Ill., 1975, pp. 57–128.

(7) J. Thomas, G. Long, G. Moore, and D. Morgan, *Clin. Pharm. Ther.*, **19**, 426 (1976).

(8) G. W. Mihaly, O. Drummer, A. Marshall, R. A. Smallwood, and W. J. Louis, *J. Pharm. Sci.*, **69**, 1155 (1980).

(9) M. A. Heymann, *Fed. Proc. Fed. Am. Soc. Exp. Biol.*, **31**, 44 (1972).

(10) A. W. Marshall, G. W. Mihaly, R. A. Smallwood, D. J. Morgan, and K. J. Hardy, *Res. Commun. Chem. Pathol. Pharmacol.*, **32**, 3 (1981).

(11) L. D. Longo and E. P.Hill, *Am. J. Physiol.*, **232**, H324 (1977).

(12) G. Levy and W. L. Hayton, in "Fetal Pharmacology," L. Boreus, Ed., Raven, New York, N.Y., 1973, pp. 29–39.

(13) J. R. Gillette, R. H. Menard, and B. Stripp, *Clin. Pharmacol. Ther.*, **14**, 680 (1973).

(14) H. H. Szeto, R. F. Kaiko, J. F. Clapp, R. W. Larrow, L. I. Mann, and C. E. Inturrisi, *J. Pharmacol. Exp. Ther.*, **209**, 244 (1979).

(15) H. H. Szeto, J. F. Clapp, R. W. Larrow, C. E. Inturrisi, and L. I. Mann, *ibid.*, **213**, 346 (1980).

(16) M. R. Juchau, in "Perinatal Pharmacology and Therapeutics," B. L. Mirkin, Ed., Academic, New York, N.Y., 1976, pp. 71–118.

(17) T. P. Green, R. F. O'Dea, and B. L. Mirkin, *Annu. Rev. Pharmacol. Toxicol.*, **19**, 285 (1979).

ACKNOWLEDGMENTS

Supported by the National Health and Medical Research Council of Australia.

The authors wish to acknowledge the invaluable technical assistance of Mrs. J. Anderson, Ms. P. Elias, Mr. P. Ballard, and Mr. Lech Mackiewicz, the clerical assistance of Mrs. S. Evans, and the cooperation of Toolka Partnership in obtaining pregnant sheep of known gestational age.

Species Differences in the Urinary Excretion of the Novel Primary Amine Conjugate: Tocainide Carbamoyl *O*-β-D-Glucuronide

KEVIN J. GIPPLE, KIN TUNG CHAN, ALFRED T. ELVIN, DAVID LALKA, and JAMES E. AXELSON *x

Received July 21, 1981, from the *Department of Pharmaceutics, School of Pharmacy, State University of New York at Buffalo, Amherst, NY 14260*, and the **Faculty of Pharmaceutical Sciences, University of British Columbia, Vancouver V6T 1W5 BC Canada.* Accepted for publication November 19, 1981.

Abstract □ The metabolism of the antiarrhythmic drug tocainide (I) has been shown previously to occur *via* a novel pathway involving the addition of carbon dioxide to the primary amine nitrogen of I followed by conjugation with glucuronic acid. The product of this reaction, tocainide carbamoyl *O*-β-D-glucuronide (II), the principal metabolite of I in humans, has been found to cyclize under strongly basic conditions to form 3-(2,6-xylyl)-5-methylhydantoin (III). Thus, evidence for the existence of II can be obtained by two different procedures: conversion of II to III in the presence of strong base and by hydrolysis of II with β-glucuronidase. The principal purpose of the present investigation was to identify suitable species for studies of the mechanism involved in the formation of II, as well as to find an animal model suitable for toxicological evaluation of tocainide and structurally related compounds. Eight animal species were examined to identify those capable of metabolizing I into II. The fraction of an intraperitoneal dose excreted in urine as II was estimated by measurement of tocainide released by β-glucuronidase mediated hydrolysis of urine and by the quantitation of III formed after alkalinization of urine samples. Urinary recovery of unchanged drug ranged from 9.5% of the dose in the gerbil to 48.7% in the cat. The percent of the dose excreted in urine as acid hydrolyzable conjugates ranged from <1% in the gerbil to a mean of 13% in the rabbit. Guinea pigs, dogs, cats, rabbits, and pigtail monkeys excreted amounts of II ranging from 0.2 to 2.4% of the dose. Thus, none of the species appeared to be a suitable model for the study of the mechanism of formation of II because of the quantitative insignificance of this pathway.

Keyphrases □ Excretion—urinary, novel primary amine conjugate, tocainide carbamoyl *O*-β-D-glucuronide, species differences □ Tocainide carbamoyl *O*-β-D-glucuronide—species differences in urinary excretion, novel primary amine conjugate □ Metabolism—tocainide carbamoyl *O*-β-D-glucuronide, species differences in urinary excretion

Tocainide (I) is an antiarrhythmic drug undergoing extensive clinical evaluation (1, 2). Substantial evidence suggests that the major pathway for the metabolism of I in humans is formation of a carbaminic acid from tocainide and carbon dioxide followed by conjugation with glucuronic acid (Scheme I). In normal healthy humans ~25–40% of a dose of I is excreted in urine as tocainide carbamoyl *O*-β-D-glucuronide (II) and another 25–40% is excreted as unchanged I (3). In the Wistar rat, urinary excretion of administered I was found to be dose-dependent with 15–50% of a dose excreted as I (4) and <10% as II (5, 6). Other mixed function oxidase products may account for the remainder of the dose in both species (5–7).

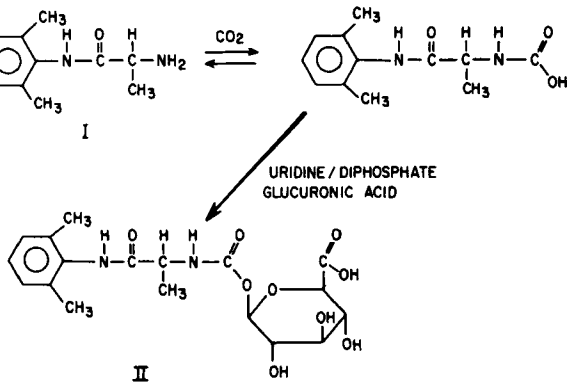

Scheme I

Formation of a carbaminic acid from an amine and carbon dioxide followed by conjugation with glucuronic acid is a metabolic pathway that has been reported only for tocainide (8). However, precedent exists for the formation of a glucuronide conjugate of a carbaminic acid in that formation of a carbamoyl glucuronide after administration of *p*-chlorophenyl cyanamide to rabbits has been reported (9). Furthermore, there is overwhelming evidence that covalent bonding of carbon dioxide to amine functions of hemoglobin (forming a carbaminic acid) is the principal mechanism of carbon dioxide transport in blood (10). Carbaminic acid formation followed by glucuronide conjugation may be an important metabolic pathway for primary amine drugs other than tocainide. However, substantial difficulties in isolation and detection may have prevented previous discovery of this pathway because acids of this type readily hydrolyze to parent drug and carbon dioxide (8). Compound II was discovered because the unique structural characteristics of I allowed facile cyclization of II to form 3-(2,6-xylyl)-5-methylhydantoin (III) under alkaline conditions (Scheme II). Since acid or β-glucuronidase mediated hydrolysis of II yields I (8), estimation of hydantoin (III) formed by alkalinization and the quantitation of free drug released by β-glucuronidase provide reliable independent methods to determine the concentration of this novel glucuronide in biological fluids[1].

Animal toxicological studies intended for extrapolation

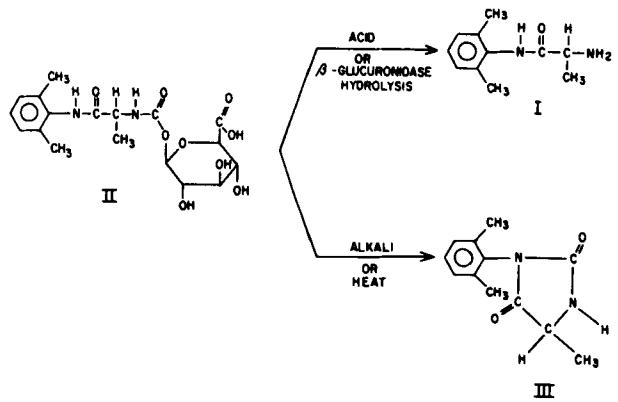

Scheme II

[1] R. A. Ronfeld and coworkers have established that II is quantitatively converted to III; unpublished observation.

0022-3549/82/0900-1011$01.00/0

Figure 1—*Urinary recovery of unchanged tocainide (□), total acid hydrolyzable conjugates (▨) and tocainide carbamoyl O-β-D-glucuronide (■). The figure presented for tocainide carbamoyl O-β-D-glucuronide is the estimate of III formed from II.*

to humans must be conducted in species that have qualitative (and preferably quantitative) metabolic profiles similar to that observed in humans. Furthermore, the identification of interspecies differences in the capacity to carry out specific types of drug biotransformation (*i.e.*, acetylation, formation of ester glucuronides, *etc.*) has been of fundamental concern to pharmacologists for decades, since such information can sometimes explain interspecies differences in the toxicology and pharmacology of drugs (11, 12). Thus, after the discovery of the novel metabolic pathway which results in the conversion of tocainide to II, it was appropriate to determine which common laboratory animal species could also form this type of glucuronide. In all, eight animal species received intraperitoneal doses of I to determine if any of them could be used effectively to study this metabolic process.

EXPERIMENTAL

Chemicals—Tocainide (2-amino-2′,6′-propionoxylidide), glycine xylidide, bupivacaine (prepared as the hydrochloride salts), and 3-(2,6-xylyl)-5-methylhydantoin were provided by the same source[2]. Heptafluorobutyrylimidazole[3], mollusk β-glucuronidase[4] (lyophilized; 0.7% arylsulfatase), and saccharo-1,4-lactone[4] were obtained from commercial sources. All solvents were spectral or high-pressure liquid chromatographic (HPLC) grade.

Instrumentation—GLC was performed on dual column gas chromatographs[5] equipped with flame ionization detectors (FID). The GLC conditions were: glass columns, 1.8 m × 2-mm i.d. packed with 3% OV-17, 10% OV-17, or 3% OV-101 on 80–100 mesh chromosorb W-HP[6]. Helium, hydrogen, and air flow rates were 30, 30, and 300 ml/min, respectively. Injector and detector temperatures were 250°. Column temperatures for the various assays will be described.

Extraction and Preextraction Treatment of Urine Samples—The extraction procedures used to quantitate unchanged tocainide and tocainide released from conjugates in urine have been described previously. The following is a summary of the information provided by each procedure (8).

The quantitative estimation of I extracted from alkalinized urine allows the determination of the concentration of unchanged I. Acid hydrolysis followed by this standard extraction procedure yields the concentration of unchanged I plus acid labile conjugates.

Incubation with β-glucuronidase followed by the standard extraction procedure yields the sum of unchanged I, glucuronide conjugates, and other conjugates released by commercial mollusk β-glucuronidase preparations.

Incubation of urine samples with the mollusk β-glucuronidase preparation described above in the presence of saccharo-1,4-lactone (a selective β-glucuronidase inhibitor) followed by the standard extraction procedure yields an estimate of the sum of unchanged I plus conjugates of I other than glucuronides (presumably sulfates).

Quantitative Estimation of I in Urine—After the urine samples were extracted using the procedures described above, tocainide concentrations were determined using the GLC method described previously (8).

Quantitative Estimation of III in Urine—The following extraction procedures were used to quantitate tocainide carbamoyl *O*-β-D-glucuronide by measuring III formed by base catalyzed cyclization.

One milliliter of 1 *N* NaOH, 0.25 ml of urine, 0.25 ml of bupivacaine solution (10 μg/ml in deionized water, used as an internal standard), and 3.0 ml of methylene chloride were added to 15-ml centrifuge tubes. The tubes were shaken, centrifuged, and the aqueous layer removed and discarded. The organic phase was evaporated at 50°, reconstituted with 20 μl of methylene chloride, and 1–2 μl was injected into a gas chromatograph (3% OV-17) at a column temperature of 250°. When a peak with retention time and shape identical to III was found, the same samples were reassayed on a 3% OV-101 column (210°) to confirm the observations made in the standard assay. This procedure quantitated III formed *in vitro* from II plus any III which may have formed *in vivo*. A second extraction procedure quantitated III formed *in vivo*, *i.e.*, III that existed prior to alkalinization. This procedure was identical to the above method, except that 1.0 ml of 0.2 *M* acetate buffer (pH 5) was substituted for 1.0 ml of 1.0 *N* NaOH.

Additional Experimental Control Procedures—Predose urine samples were assayed before and after acid or enzymatic hydrolysis to ensure the absence of interfering compounds in urine.

Table I—Physical Characteristics of Animal Species Studied

No. of Animals Studied	Species	Strain	Sex	Weight Range, kg
3	Rat	Sprague-Dawley	male	0.350–0.360
3	Rat	Gunn	male	0.190–0.210
3	Rat	Wistar, inbred	male	0.190–0.210
4	Mouse	Brown Bal	female	0.022–0.032
3	Guinea Pig	Mixed breed	male	0.740–0.850
2	Gerbil	Mixed breed	male	0.034–0.041
4	Dog	Mixed breed	males	8.6–12.7
1	Cat	Siamese	male	
2		Mixed breed	1 female; 1 male	3.4–5.4
3	Rabbit	New Zealand White	male	3.6–3.8
1	Monkey	African Green	female	2.7
2	Monkey	Pigtail	female	5.0–8.6

[2] Astra Pharmaceutical Products, Inc., Framingham, Mass.
[3] Pierce Chemical Co., Rockford, Ill.
[4] Calbiochem, La Jolla, Calif.
[5] Varian model 2400 Aerograph, Palo Alto, Calif.
[6] Alltech Associates, Arlington Heights, Ill.

Table II—Urinary Recovery of Tocainide and its Metabolites in Various Species[a]

Species (strain)	Unchanged Tocainide	Tocainide Carbamoyl O-β-D-Glucuronide: Measured as I[b], Released Enzymatically	Tocainide Carbamoyl O-β-D-Glucuronide: Measured as III, Formed upon Alkalinization	Tocainide Carbamoyl O-β-D-Glucuronide: Total Acid Hydrolyzable Conjugates
Rat				
Sprague-Dawley	20.3(17–22)	ND[c]	ND[d]	4.7(3–6)
Gunn	18.3(10–27)	ND[c]	ND[d]	4.8(2–9)
Wistar	30.3(24–34)	ND[c]	ND[d,e]	10.0(7–15)
Mouse	38.5(33–44)	—[f]	ND[d]	1.0(0–3)
Guinea Pig	36.3(30–42)	2.3(2–3)	1.0(0.9–1.1)	5.4(4–8)
Gerbil	9.5(7–12)	—[f]	ND[d]	0.55(0.3–1)
Dog	21.2(11–32)	1.5(1–2)	1.4(0.4–2.2)	4.9(2–8)
Cat	48.7(41–54)	0.3(0–1)	0.2(0.0–0.3)	11(5–20)
Rabbit	17.6(10–27)	1.4(0–3)	1.2(1.0–1.3)	13(9–29)
Monkey				
African Green	47.4	1.4	ND[d]	7.9 NA
Pigtail	44.6(39–50)	0.1(0–0.1)	2.4(0.8–4.0)	3.9(2–6)

[a] Expressed as percent of the dose excreted in urine; on a molar basis. Numbers in parentheses give the range of observed values. [b] Glucuronide conjugates were quantitated by measuring the difference between tocainide released by β-glucuronidase and β-glucuronidase plus saccharo-1,4-lactone. [c] Not detected. Based on the limited sensitivity of the GLC procedure utilized, the minimum percentage dose which could have been detected was between 1.0 and 1.5%. [d] Not detected. The minimum percentage of dose detectable was 0.02%. [e] The presence of III in urine of tocainide treated (intraperitoneally and orally in these species) Wistar-Vancouver rats has been noted (14, 15) using a highly sensitive qualitative electron-capture GC assay with confirmation by GLC–mass spectrometry. The quantitative study described here using GLC with FID failed to confirm the presence of III, due either to limitations in detection or because of differences in the animals studied. [f] Enzymatic hydrolysis was not performed because acid hydrolysis studies indicated that ≤1% of the dose was excreted as conjugated tocainide.

Three coded unknown urine samples, prepared to contain concentrations of tocainide from 0 to 135 μg/ml, were assayed every experimental day by an analyst blinded to the tocainide concentration. An error of ≥10% caused data to be rejected and mandated the reassay of all samples from that day. Since urine pH has previously been shown to influence the urinary excretion of tocainide in humans (13), the pH of all urine samples was measured.

A check for bacterial breakdown of II was performed by diluting urine known to contain approximately equal amounts of I and II (obtained from humans who had received tocainide) with blank animal urine in a 1:1 ratio. Both this sample and the undiluted sample were left at room temperature for 24 hr and were then assayed. If the 1:1 dilution contained <55% of the tocainide concentration seen in the undiluted sample, no significant bacterial breakdown of II to I was considered to have occurred. However, if >55% of the undiluted sample's concentration was in the 1:1 dilution, the extra tocainide was considered to have been liberated by the breakdown of II. In such cases the data obtained for the urinary recovery of II were considered to be an underestimate and were not to be used for further data analysis.

If acid hydrolysis failed to show significant generation (<10% increase in the concentration of I in the urine) of I from conjugates, urine was not subject to treatment with β-glucuronidase. However, these urines were assayed for the presence of III before and after treatment with NaOH to rule out the presence of II.

Animal Study Design—Animals were given an injection of 10 mg/kg ip of tocainide hydrochloride after fasting for 24 hr. Fasting was continued for at least 24 hr following injection. Water was allowed *ad libitum* throughout the experiment. Animals were housed in plexiglass or stainless steel metabolism cages. Predose urine specimens were obtained and urine was also collected until at least 24 hr following dosing. Urine specimens were frozen at −20° until assayed. The weight, sex, and strain of the animals used in these studies are detailed in Table I.

RESULTS

The principal observations made in the various species are summarized in Fig. 1 and Table II. The dogs, rabbits, guinea pigs, pigtail monkeys, and cats synthesized and excreted tocainide carbamoyl O-β-D-glucuronide (Table II). The amounts were small but were readily detectable as III formed upon alkalinization of the urine sample. No evidence was obtained to suggest the presence of II in the urine of mice, gerbils, the African green monkeys, or in any of the three strains of rats (*i.e.*, III was not observed upon alkalinization of the urine samples, and little or no I was released by β-glucuronidase mediated hydrolysis). All available evidence suggests that the III which was observed in the other species was formed from II; *i.e.*, no III was found in samples that had not been alkalinized.

The details of the urinary recovery studies are presented in Table II. The percent of the dose excreted as unchanged tocainide ranged from 9.5% in gerbils to 48.7% in cats. The percent of the dose recovered as II was ≤2.4% in all species studied (Table II). Total acid hydrolyzable conjugates accounted for ≤13% of the dose in all species. No evidence of bacterial breakdown of II to I by human or animal urine was observed. Furthermore, no trend in the urinary excretion of I or II was seen as a function of urine pH (data not presented).

DISCUSSION

A principal purpose of the present investigation was to identify a common laboratory animal that could biotransform tocainide into II. In an earlier investigation of tocainide metabolism (using GLC–mass spectrometry and electron capture GLC analysis), the presence of trace amounts of III in the urine of Wistar rats was reported prior to alkalinization (14, 15). Thus, it seemed reasonable to examine a number of rodents for their capacity to form II. However, the results from the present study suggested that among common rodents, only the guinea pig could form amounts of II measurable using FID detection methods. It was also observed that rabbits, cats, pigtail monkeys, and dogs excreted small amounts of II (~1% of the dose), but none approached the amount found in human urine (25–40% of dose). These results indicate that the enzyme(s) needed to produce II may be widespread in the animal kingdom, but the capacity to produce substantial amounts of II has only been documented in humans, following oral administration (3, 7, 8). Alternative explanations have not been ruled out. For example, the various animal species studied may have synthesized large amounts of II but eliminated it *via* an alternative pathway such as biliary excretion, or II may be formed by gut flora, and hence (in the absence of biliary excretion) could only be formed following oral administration. At present, no evidence exists suggesting the biliary excretion of II or metabolism of I to II by gut flora. Thus, it is reasonable to assume that none of the animals studied is an adequate model of humans. It is important to find a species that produces substantial amounts of II, both for toxicological studies and for investigations into the fundamental nature of this potentially widespread biochemical transformation. The toxicity, mechanism of formation, and factors that influence the rate of formation of II remain unknown. Such investigations will be greatly facilitated when an appropriate model (whole animal) study system has been identified.

From a toxicologic standpoint, the demonstrated lability of II, plus the large amount formed in humans raise questions as to whether II may play a role in the toxicity of tocainide. A recent publication noted that some patients exhibit allergic reactions (*i.e.*, rashes) when treated with tocainide (16). These reactions may be due to II. Though toxic glucuronide metabolites have only been recently recognized, two have been identified that irreversibly bind (covalently bond) to proteins (17) and nucleic acids (18). These reactive compounds share some structural analogy with tocainide carbamoyl O-β-D-glucuronide. However, it would be premature to attribute any of tocainide's toxicity to II or any of its other metabolites (5, 7).

Independent of the toxicological considerations, it is of fundamental interest to identify species producing carbamate glucuronides from amines, since such conjugates represent a category of drug metabolite which has been discovered only recently (8).

While precedents exist for enzymatic carbamylation of amine functional groups (10) and glucuronidation of carbamates (9), little is known of the mechanisms involved in the sequential carbamylation and glucuronidation of primary amine drugs. After an appropriate animal model has been identified, studies to ascertain these mechanisms will be possible. The elucidation of these mechanisms may substantially expand understanding of the glucuronidation process.

REFERENCES

(1) D. G. McDevitt, A. S. Nies, G. R. Wilkinson, R. F. Smith, R. L. Woosley, and J. A. Oates, *Clin. Pharmacol. Ther.*, **19**, 396 (1976).

(2) R. A. Winkle, P. J. Meffin, J. W. Fitzgerald, and D. C. Harrison, *Circulation*, **54**, 884 (1976).

(3) A. T. Elvin, D. Lalka, K. Stoeckel, P. duSouich, J. E. Axelson, L. H. Golden, and A. J. McLean, *Clin. Pharmacol. Ther.*, **28**, 652 (1980).

(4) R. Venkataramanan and J. E. Axelson, *J. Pharmacol. Exp. Ther.*, **215,** 231 (1980).

(5) R. Venkataramanan and J. E. Axelson, in "Abstracts," vol. 9 (1), A.Ph.A. Academy of Pharmaceutical Sciences, Anaheim, Calif., 1979, p 92.

(6) R. Venkataramanan, F. S. Abbott, and J. E. Axelson, *J. Pharm. Sci.*, 71, 491 (1982).

(7) R. A. Ronfeld, E. M. Wolshin, and A. J. Block, *Clin. Pharmacol. Ther.*, 31, 384 (1982).

(8) A. T. Elvin, J. B. Keenaghan, E. W. Byrnes, P. A. Tenthorey, P. D. McMaster, B. H. Takman, D. Lalka, C. V. Manion, D. T. Baer, E. M. Wolshin, M. B. Meyer, and R. A. Ronfeld, *J. Pharm. Sci.*, **69,** 47 (1980).

(9) R. L. Smith and R. T. Williams, *J. Med. Pharm. Chem.*, **4,** 147 (1961).

(10) J. V. Kilmartin and L. Rossi-Bernardi, *Physiol. Rev.*, **53,** 836 (1973).

(11) B. N. LaDu, H. G. Mandel, and E. L. Way, in "Fundamentals of Drug Metabolism and Drug Disposition," Williams and Wilkins, Baltimore, Md., 1971, pp. 187–205.

(12) P. L. Grover and P. Sims, *Biochem. J.*, **90,** 603 (1964).

(13) D. Lalka, M. B. Meyer, B. R. Duce, and A. T. Elvin, *Clin. Pharmacol. Ther.*, **19,** 757 (1976).

(14) R. Venkataramanan, Ph.D. Thesis, Faculty of Pharmaceutical Sciences, University of British Columbia, Vancouver, B.C., Canada, 1978.

(15) R. Venkataramanan and J. E. Axelson, *Xenobiotica*, **11,** 259 (1981).

(16) D. M. Roden, S. B. Reele, S. B. Higgins, R. K. Carr, R. F. Smith, J. A. Oates, and R. L. Woosley, *Am Heart J.*, **100,** 15 (1980).

(17) G. J. Mulder, J. A. Hinson, and J. R. Gillette, *Biochem. Pharmacol.*, **27,** 1641 (1978).

(18) R. A. Cardona and C. M. King, *ibid.*, **25,** 1051 (1976).

ACKNOWLEDGMENTS

Supported in part by Grant 65-0566 from the British Columbia Heart Association and by Grant GM-20852 from the Institute of General Medical Sciences, National Institutes of Health.

Dr. James E. Axelson (Visiting Scientist, January 1, 1981–December 31, 1981) expresses his appreciation to the Canadian Heart Foundation and Medical Research Council of Canada for their support.

In Vitro Skin Evaporation and Penetration Characteristics of Mosquito Repellents

WILLIAM G. REIFENRATH ˣ and PETER B. ROBINSON

Received June 8, 1981, from the *Division of Cutaneous Hazards, Letterman Army Institute of Research, Presidio of San Francisco, CA 94129.* Accepted for publication November 24, 1981.

Abstract □ An *in vitro* apparatus was used to study mosquito repellent evaporation and penetration characteristics with skin. The mosquito repellents 2-ethyl-1,3-hexanediol, *N,N*-diethyl-*m*-toluamide, *N,N*-diethyl-*p*-toluamide, 1-(butylsulfonyl)hexahydro-1*H*-azepine, and *N,N'*-dicyclohexamethyleneurea were studied. *In vitro* repellent duration, calculated from repellent evaporation rates, was compared to *in vivo* duration at the same dose (0.3 mg/cm^2) to assess the validity of the model. *In vitro* durations for 2-ethyl-1,3-hexanediol, *N,N*-diethyl-*m*-toluamide, *N,N*-diethyl-*p*-toluamide, and *N,N'*-dicyclohexamethyleneurea correlated with *in vivo* durations ($r^2 = 0.94$), although *in vitro* duration was longer than *in vivo* duration. 1-(Butylsulfonyl)hexahydro-1*H*-azepine, which had the longest *in vivo* duration, had an *in vitro* duration that exceeded the test period (12 hr). The 0–12-hr *in vitro* percutaneous penetration correlated with corresponding data available from *in vivo* studies.

Keyphrases □ Mosquito repellents—*in vitro* skin evaporation, penetration □ Evaporation—*in vitro* skin penetration, mosquito repellents □ Penetration—*in vitro* skin evaporation, mosquito repellents

Evaporation of mosquito repellents from the skin surface and percutaneous penetration represent important modes of loss of mosquito repellents from the skin surface. Various estimates of the percutaneous penetration of mosquito repellents have been made (1–4). However, only one repellent (*N,N*-diethyl-*m*-toluamide) whose loss from the skin surface by evaporation and skin penetration has been quantified (5). The percentages of *in vitro* skin evaporation and percutaneous penetration of the following five mosquito repellents are reported in this paper: 2-ethyl-1,3-hexanediol (I), *N,N*-diethyl-*m*-toluamide (II), *N,N*-diethyl-*p*-toluamide (III), 1-(butylsulfonyl)hexahydro-1*H*-azepine (IV), and *N,N'*-dicyclohexamethyleneurea (IV). Two dose levels were used: a dose corresponding to a repellent's minimum effective dose against *Aedes aegypti* mosquitoes (6) and a dose of 0.3 mg/cm^2, which has been used to determine the effective duration of the repellents on the skin of humans (6).

The duration of steady-state evaporation rate of repellents from aluminum planchets has been compared with the duration of effectiveness of several mosquito repellents on the skin of humans (7). The findings suggest a possible relationship between evaporation rate from skin and repellent duration. In this report, this possible relationship was examined by computing the *in vitro* durations for each repellent from *in vitro* evaporation rates and comparing them to previously reported values for *in vivo* duration (6).

EXPERIMENTAL

Labeled Compounds—The following radiolabeled mosquito repellents were used: [1,3-^{14}C]2-ethyl-1,3-hexanediol(Ia)[1], specific activity, 6.06×10^4 dpm/μg; [carbonyl-^{14}C]*N,N*-diethyl-*m*-toluamide(IIIa) (8), specific activity, 1.15×10^4 dpm/μg; [carbonyl-^{14}C]*N,N*-diethyl-*m*-toluamide(IIa) (8), specific activity, 2.47×10^4 dpm/μg; 1-(butylsulfonyl)-[2,2'-^{14}C] hexahydro-1*H*-azepine(IVa), specific activity, 332 dpm/μg; and *N,N'*-[2,2'-^{14}C]dicyclohexamethyleneurea(Va), specific activity, 174 dpm/μg. For skin applications of I at the minimum effective dose and the 0.3 mg/cm^2 dose, cold I[3] was used to dilute the radiolabeled samples to give total radioactive doses of 0.02 and 0.14 μCi, respectively. For one replicate (skin No. A8478) of skin application of III at 0.3 mg/cm^2, cold III[4] was used to dilute the radiolabeled sample to give a final ra-

[1] New England Nuclear Corp., Boston, Mass.
[2] SRI International, Menlo Park, Calif.
[3] Niagara Chemical Division, FMC, Middleport, N.Y.
[4] Hercules, Inc., Wilmington, Del.

0022-3549/82/0900-1014$01.00/0

(4) R. Venkataramanan and J. E. Axelson, *J. Pharmacol. Exp. Ther.*, **215,** 231 (1980).

(5) R. Venkataramanan and J. E. Axelson, in "Abstracts," vol. 9 (1), A.Ph.A. Academy of Pharmaceutical Sciences, Anaheim, Calif., 1979, p 92.

(6) R. Venkataramanan, F. S. Abbott, and J. E. Axelson, *J. Pharm. Sci.*, 71, 491 (1982).

(7) R. A. Ronfeld, E. M. Wolshin, and A. J. Block, *Clin. Pharmacol. Ther.*, 31, 384 (1982).

(8) A. T. Elvin, J. B. Keenaghan, E. W. Byrnes, P. A. Tenthorey, P. D. McMaster, B. H. Takman, D. Lalka, C. V. Manion, D. T. Baer, E. M. Wolshin, M. B. Meyer, and R. A. Ronfeld, *J. Pharm. Sci.*, **69,** 47 (1980).

(9) R. L. Smith and R. T. Williams, *J. Med. Pharm. Chem.*, **4,** 147 (1961).

(10) J. V. Kilmartin and L. Rossi-Bernardi, *Physiol. Rev.*, **53,** 836 (1973).

(11) B. N. LaDu, H. G. Mandel, and E. L. Way, in "Fundamentals of Drug Metabolism and Drug Disposition," Williams and Wilkins, Baltimore, Md., 1971, pp. 187–205.

(12) P. L. Grover and P. Sims, *Biochem. J.*, **90,** 603 (1964).

(13) D. Lalka, M. B. Meyer, B. R. Duce, and A. T. Elvin, *Clin. Pharmacol. Ther.*, **19,** 757 (1976).

(14) R. Venkataramanan, Ph.D. Thesis, Faculty of Pharmaceutical Sciences, University of British Columbia, Vancouver, B.C., Canada, 1978.

(15) R. Venkataramanan and J. E. Axelson, *Xenobiotica*, **11,** 259 (1981).

(16) D. M. Roden, S. B. Reele, S. B. Higgins, R. K. Carr, R. F. Smith, J. A. Oates, and R. L. Woosley, *Am Heart J.*, **100,** 15 (1980).

(17) G. J. Mulder, J. A. Hinson, and J. R. Gillette, *Biochem. Pharmacol.*, **27,** 1641 (1978).

(18) R. A. Cardona and C. M. King, *ibid.*, **25,** 1051 (1976).

ACKNOWLEDGMENTS

Supported in part by Grant 65-0566 from the British Columbia Heart Association and by Grant GM-20852 from the Institute of General Medical Sciences, National Institutes of Health.

Dr. James E. Axelson (Visiting Scientist, January 1, 1981–December 31, 1981) expresses his appreciation to the Canadian Heart Foundation and Medical Research Council of Canada for their support.

In Vitro Skin Evaporation and Penetration Characteristics of Mosquito Repellents

WILLIAM G. REIFENRATH ˣ and PETER B. ROBINSON

Received June 8, 1981, from the *Division of Cutaneous Hazards, Letterman Army Institute of Research, Presidio of San Francisco, CA 94129.* Accepted for publication November 24, 1981.

Abstract □ An *in vitro* apparatus was used to study mosquito repellent evaporation and penetration characteristics with skin. The mosquito repellents 2-ethyl-1,3-hexanediol, *N,N*-diethyl-*m*-toluamide, *N,N*-diethyl-*p*-toluamide, 1-(butylsulfonyl)hexahydro-1*H*-azepine, and *N,N'*-dicyclohexamethyleneurea were studied. *In vitro* repellent duration, calculated from repellent evaporation rates, was compared to *in vivo* duration at the same dose (0.3 mg/cm^2) to assess the validity of the model. *In vitro* durations for 2-ethyl-1,3-hexanediol, *N,N*-diethyl-*m*-toluamide, *N,N*-diethyl-*p*-toluamide, and *N,N'*-dicyclohexamethyleneurea correlated with *in vivo* durations ($r^2 = 0.94$), although *in vitro* duration was longer than *in vivo* duration. 1-(Butylsulfonyl)hexahydro-1*H*-azepine, which had the longest *in vivo* duration, had an *in vitro* duration that exceeded the test period (12 hr). The 0–12-hr *in vitro* percutaneous penetration correlated with corresponding data available from *in vivo* studies.

Keyphrases □ Mosquito repellents—*in vitro* skin evaporation, penetration □ Evaporation—*in vitro* skin penetration, mosquito repellents □ Penetration—*in vitro* skin evaporation, mosquito repellents

Evaporation of mosquito repellents from the skin surface and percutaneous penetration represent important modes of loss of mosquito repellents from the skin surface. Various estimates of the percutaneous penetration of mosquito repellents have been made (1–4). However, only one repellent (*N,N*-diethyl-*m*-toluamide) whose loss from the skin surface by evaporation and skin penetration has been quantified (5). The percentages of *in vitro* skin evaporation and percutaneous penetration of the following five mosquito repellents are reported in this paper: 2-ethyl-1,3-hexanediol (I), *N,N*-diethyl-*m*-toluamide (II), *N,N*-diethyl-*p*-toluamide (III), 1-(butylsulfonyl)hexahydro-1*H*-azepine (IV), and *N,N'*-dicyclohexamethyleneurea (IV). Two dose levels were used: a dose corresponding to a repellent's minimum effective dose against *Aedes aegypti* mosquitoes (6) and a dose of 0.3 mg/cm^2, which has been used to determine the effective duration of the repellents on the skin of humans (6).

The duration of steady-state evaporation rate of repellents from aluminum planchets has been compared with the duration of effectiveness of several mosquito repellents on the skin of humans (7). The findings suggest a possible relationship between evaporation rate from skin and repellent duration. In this report, this possible relationship was examined by computing the *in vitro* durations for each repellent from *in vitro* evaporation rates and comparing them to previously reported values for *in vivo* duration (6).

EXPERIMENTAL

Labeled Compounds—The following radiolabeled mosquito repellents were used: [1,3-^{14}C]2-ethyl-1,3-hexanediol(Ia)[1], specific activity, 6.06×10^4 dpm/μg; [carbonyl-^{14}C]*N,N*-diethyl-*m*-toluamide(IIIa) (8), specific activity, 1.15×10^4 dpm/μg; [carbonyl-^{14}C]*N,N*-diethyl-*m*-toluamide(IIa) (8), specific activity, 2.47×10^4 dpm/μg; 1-(butylsulfonyl)-[2,2'-^{14}C] hexahydro-1*H*-azepine(IVa), specific activity, 332 dpm/μg; and *N,N'*-[2,2'-^{14}C]dicyclohexamethyleneurea(Va), specific activity, 174 dpm/μg. For skin applications of I at the minimum effective dose and the 0.3 mg/cm^2 dose, cold I[3] was used to dilute the radiolabeled samples to give total radioactive doses of 0.02 and 0.14 μCi, respectively. For one replicate (skin No. A8478) of skin application of III at 0.3 mg/cm^2, cold III[4] was used to dilute the radiolabeled sample to give a final ra-

[1] New England Nuclear Corp., Boston, Mass.
[2] SRI International, Menlo Park, Calif.
[3] Niagara Chemical Division, FMC, Middleport, N.Y.
[4] Hercules, Inc., Wilmington, Del.

0022-3549/82/0900-1014$01.00/0

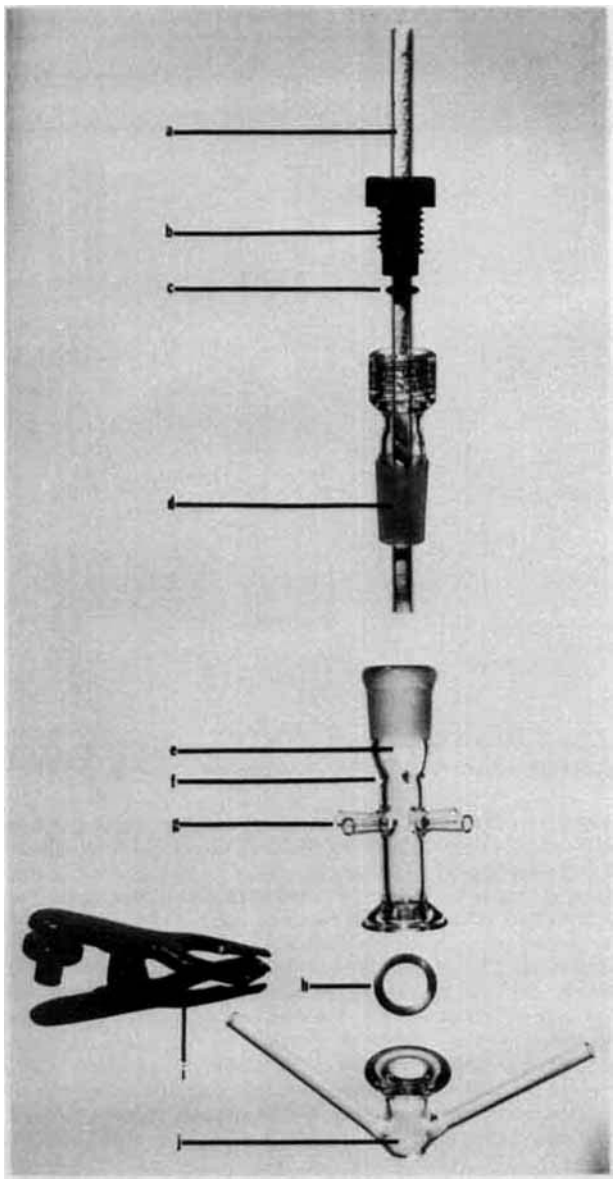

Figure 1—*Evaporation–penetration cell, Key: (a) vapor trap i.d. = 0.38 cm, o.d. = 0.63 cm, length = 15.2 cm; (b) threaded portion of adapter; (c) rubber o-ring; (d) 14/20 standard taper adapter; (e) evaporation manifold, joint size 18/9, i.d. = 0.9 cm, length = 7.25 cm; (f) indents for centering vapor trap located 1 cm above air inlets; (g) air inlets i.d. = 0.3 cm, o.d. = 0.5 cm, length = 1.5 cm, located 2.75 cm above lower joint; (h) polytetrafluoroethylene o-ring; (i) clamp No. 18A; (j) lower chamber, joint size 18/9, i.d. = 0.9 cm, length = 2.5 cm, inlet and outlet i.d. = 0.3 cm, o.d. = 0.5 cm, length = 4 cm.*

dioactive dose of 0.03 μCi. All compounds were homogeneous as determined by TLC (silica gel[5] and chloroform).

Procedure—Whole skin (abdominal), obtained at autopsy, was stored at −65° in sealed plastic bags before use. Storage time did not exceed 3 months. Subcutaneous fat was removed from the thawed sample (~7 cm^2) before use.

The apparatus shown in Fig. 1[6] was used. A magnetic stirrer was placed in the lower chamber filled with Ringer's lactate solution[7], a skin sample was placed over the lower chamber visceral side down, a polytef o-ring which served as a seal between the lower and upper chamber was placed on top of the skin, and the evaporation manifold was clamped into place. Air bubbles underneath the skin were removed by tipping the assembly, allowing the skin to come in contact with the Ringer's lactate. After 20

[5] Silica gel G Applied Science Division, Milton Roy Co. Laboratory Group, State College, Pa.
[6] Laboratory Glass Apparatus, Berkeley, Calif.
[7] Cutter Laboratories, Inc., Berkeley, Calif.

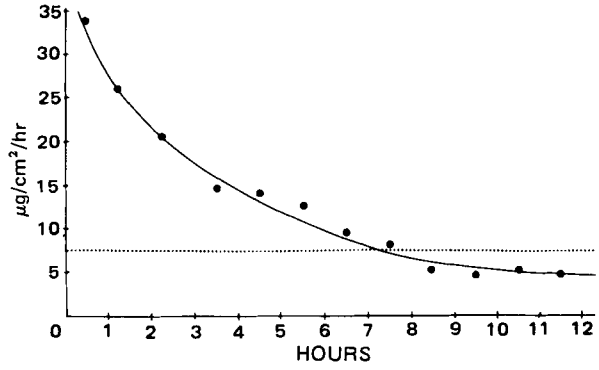

Figure 2—*Mean evaporation rate of I* versus *time at 0.3 mg/cm^2 (—); the minimum effective evaporation rate (·····).* In vitro *duration is 7 hr.*

min. the evaporation manifold was removed and the desired dose of labeled compound dissolved in ethanol (~10 μl) was applied to the skin area circumscribed by the o-ring (1.27 cm^2) by use of a syringe[8]. For controls, an equal volume was placed into counting vials. The evaporation manifold was then clamped to the lower chamber and the lower chamber was immersed in a water bath at 37°. One arm of the lower chamber was connected to a precision pump[9] which delivered 1.6 ml of Ringer's lactate/hr. The other arm of the lower chamber was connected to a short length of flexible tubing which led into a counting vial.

The vapor trap, a glass tube packed with 200 mg of absorbant[10] and plugged with cotton at its ends, was inserted into the threaded 14/20 standard taper adapter[11], and the assembly slipped into the ground-glass joint of the evaporation manifold so that the lower end of the vapor trap tube was 0.65 cm above the surface of the skin. The vapor trap was connected by flexible tubing to a bubbler trap which contained aqueous counting solution[12] and served as a safety trap. The bubbler trap was connected to a peristaltic pump[13], which pulled in air at 30 ml/min. The outlet from the peristaltic pump was connected to a flow gauge[14]. Air entering the evaporation manifold was entrained in the following manner: The four intake tubes of the evaporation manifold were connected by adapters to a common tube which was connected to a calcium sulfate drying tower. The inlet port of the drying tower was connected by tubing to an air flow gauge, whose reading corresponded to the other flow gauge reading if there were no leaks or plugged tubes in the system. Dry air at

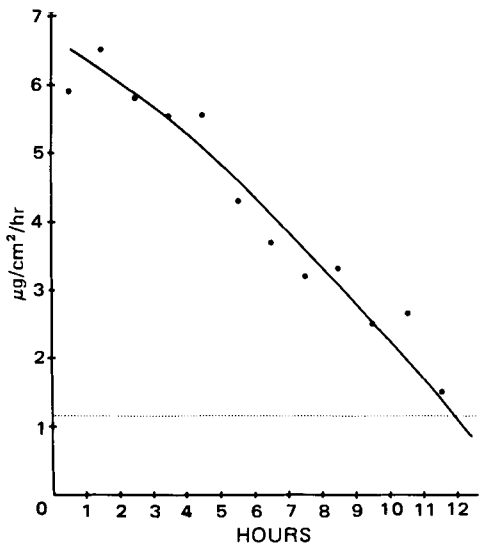

Figure 3—*Mean evaporation rate of II* versus *time at 0.3 mg/cm^2 (—); the minimum effective evaporation rate (·····).* In vitro *duration is 12 hr.*

[8] Hamilton Co., Reno, Nev.
[9] Bodine Electric Co., Chicago, Ill.
[10] Tenax GC, Alltech Associates, Arlington Heights, Ill.
[11] Ace Glass Inc., Vineland, N.J.
[12] Aqueous Counting Scintillant, Amersham Corp., Arlington Heights, Ill.
[13] Masterflex pump, Cole-Parmer Instrument Co., Chicago, Ill.
[14] Flowmeter No. 10, Gilmont Instruments, Inc., Great Neck, N.Y.

Table I—Disposition of Radioactivity 12 Hr after Application of Radiolabeled Repellents to Excised Skin at a Dose of 0.3 mg/cm²

Skin Code	Percent of Applied Radioactive Dose				
	Evaporation[a]	Percutaneous Penetration	Skin Surface	Skin Oxidation	Total Recovery[b]
			I		
A6178	45.9	12.9	13.2	10.9	83.0
A6178	42.7	15.0	10.3	19.0	87.7
A6178	50.6	10.7	16.9	9.4	90.5
A6178	44.0	13.6	7.3	20.1	86.6
—[c]	52.7	7.7	18.9	10.1	91.9
Mean ± *SD*	47.2 ± 4.3	12.0 ± 2.9	13.3 ± 4.7	13.9 ± 5.2	87.9 ± 3.5
			II		
A5578	12.6	8.6	17.9	35.7	80.5
A5578	17.5	4.2	32.6	19.1	75.3
A8378	19.9	6.9	16.2	34.4	77.7
Mean + *SD*	16.7 ± 3.7	6.6 ± 2.2	22.2 ± 9.0	29.7 ± 9.2	77.8 ± 2.6
			III		
A13479	15.6	—[d]	14.2	43.8	74.7
A13579	15.5	4.7	39.8	13.8	75.3
A13679	14.6	3.6	34.4	30.1	83.5
Mean ± *SD*	15.2 ± 0.6	4.2 ± 0.8	29.5 ± 13.5	29.2 ± 15.0	77.8 ± 4.9
			IV		
A1279	4.2	2.6	37.0	31.7	75.7
A2779	7.5	2.7	25.7	33.8	70.3
A2779	7.5	3.1	35.3	29.3	75.7
—[c]	5.4	1.8	61.6	15.0	86.8
Mean ± *SD*	6.2 ± 1.6	2.6 ± 0.5	39.9 ± 15.3	27.5 ± 8.5	77.1 ± 7.0
			V		
A5778	2.5	3.0	28.1	36.8	71.1
A8378	0.8	4.1	27.6	46.1	83.6
A8678	5.9	4.5	50.1	18.7	86.1
Mean ± *SD*	3.0 ± 2.6	3.9 ± 0.8	35.3 ± 12.9	33.9 ± 13.9	80.3 ± 8.0

[a] Radioactivity recovered from the vapor trap. [b] Total recovery includes small percentages of radioactivity recovered from the evaporation manifold. [c] Skin code not recorded. [d] Sample lost.

22° (ambient laboratory temperature) was thus drawn into the evaporation manifold, over the skin surface, and through the vapor trap, which absorbed any repellent evaporating from the skin surface. Air flowed above the skin and Ringer's lactate flowed below the skin for 1 hr after application of the minimum effective dose and for 12 hr after the 0.3 mg/cm² dose. During the 12-hr runs, the vapor trap and counting vial were changed at hourly intervals.

Radioactivity Measurements—After minimum effective dose applications, the Ringer's lactate in the lower chamber and the rinses of the lower chamber were combined with the Ringer's lactate in the counting vial used to collect lower chamber outflow. After the 0.3-mg/cm² dose, each of the 12 counting vials used to collect lower chamber outflow and the residual fluid in the lower chamber were counted separately[15]. The contents and counting solution rises of each vapor trap were placed in separate counting vials. The resultant disintegrations per minute were corrected for loss in counting efficiency introduced by the absorbant powder, determined by spiking vapor traps with a known amount of radiolabeled repellents. Efficiency varied from 89 to 92% of control for the five repellents. The stratum corneum surface of the skin sample was washed with aqueous counting solution and rinses were collected in a counting vial. The skin sample was then cut into pieces (each <250 mg in weight) and the separate pieces were oxidized[16]. The disintegration per minute was determined by the standard spike method. The evaporation manifold was rinsed with aqueous counting solution and the radioactivity recovered was added to the total percent recovery. The percentage of the applied radioactive dose, recovered from the polytef o-ring by counting solution rinse, was added to the percentage accounted for by the skin surface rinse.

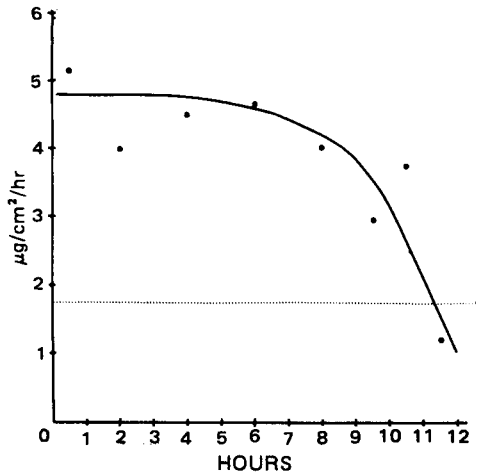

Figure 4—*Mean evaporation rate of III* versus *time at 0.3 mg/cm² (—); the minimum effective evaporation rate (·····).* In vitro *duration is 12 hr. Because of irregularly timed sample collection during the first 9 hr, hourly Sample 2 was combined with 3, 4 with 5, 6 with 7, and 8 with 9.*

RESULTS AND DISCUSSION

The mean evaporation rate *versus* time after the 0.3-mg/cm² dose for each repellent is plotted in Figs. 2–6 relative to the minimum effective evaporation rate of the repellent, the evaporation rate obtained from the

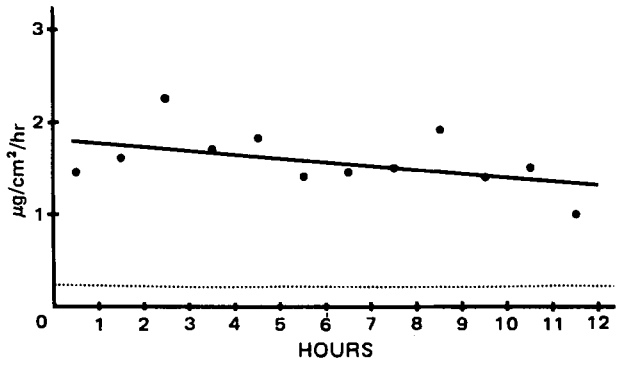

Figure 5—*Mean evaporation rate of IV* versus *time at 0.3 mg/cm² (—); the minimum effective evaporation rate (·····).* In vitro *duration is >12 hr.*

[15] Disintegration per minute determined by automatic external standard on a Packard model 3390-AAA scintillation spectrometer, Packard Instrument Co., Downers Grove, Ill.

[16] Samples were oxidized in a Packard model 306 Sample Oxidizer, liberated radioactive CO_2 trapped in Packard Carbo-sorb, and disintegration per minute determined on a Packard model 3375 scintillation spectrometer.

Table II—Disposition of Radioactivity 1 Hr after Application of Radiolabeled Repellents to Excised Skin at a Minimum Effective Dose Against *A. aegypti* Mosquitoes

Skin Code	Percent of Applied Radioactive Dose				
	Evaporation[a]	Percutaneous Penetration	Skin Surface	Skin Oxidation	Total Recovery[b]
			I, 0.046 mg/cm²		
A5778	16.5	0.3	40.1	30.8	89.5
A6178	12.3	2.0	23.5	41.6	80.1
A6378	19.8	0.8	30.7	33.5	87.6
Mean ± *SD*	16.2 ± 3.8	1.0 ± 0.9	31.4 ± 8.3	35.3 ± 5.6	85.7 ± 5.0
			II, 0.027 mg/cm²		
A5778	3.1	0.3	41.3	44.5	90.0
A8378	5.5	0.0	64.1	22.1	92.7
A5678	4.2	0.2	53.0	22.1	81.0
Mean ± *SD*	4.3 ± 1.2	0.2 ± 0.1	52.8 ± 11.4	29.6 ± 12.9	87.9 ± 6.1
			III, 0.032 mg/cm²		
A8678	8.4	0.4	47.6	25.0	83.1
A8378	4.6	0.2	37.0	38.4	80.7
A6378	3.6	0.1	44.1	26.0	78.8
Mean ± *SD*	5.5 ± 2.5	0.2 ± 0.1	42.9 ± 5.4	29.8 ± 7.5	80.9 ± 2.1
			IV, 0.020 mg/cm²		
A13479	1.4	0.2	81.2	15.5	98.6
A13579	0.6	0.0	65.7	10.8	84.6
A13679	0.9	0.1	82.5	17.4	101.3
Mean ± *SD*	1.0 ± 0.4	0.1 ± 0.1	76.5 ± 9.4	14.6 ± 3.4	94.8 ± 9.0
			V, 0.196 mg/cm²		
A6378	0.5	1.0	47.3	30.9	80.3
—[c]	0.6	0.3	52.6	24.4	78.5
A2779	0.5	0.6	67.8	18.8	88.4
Mean ± *SD*	0.5 ± 0.1	0.6 ± 0.3	55.9± 10.6	24.7 ± 6.1	82.4 ± 5.3

[a] Radioactivity recovered from the primary vapor trap. [b] Total recovery includes small percentage of radioactivity recovered from the evaporation manifold. [c] Skin code was not recorded.

minimum effective dose. (In Figs. 2–4, curves were fitted by eye. In Figs. 5 and 6, least-squares regression lines were drawn.)

The radioactivity recovered from each hour outflow from the lower chamber during the 0.3-mg/cm² dose–12-hr runs represents a time average of the amount of radioactivity in the lower chamber during a given hour. The amount of radioactivity recovered from the residual Ringer's lactate in the lower chamber at the end of the 12-hr runs was always higher than could be accounted for by the 12th-hr outflow. This was probably the result of adsorption of repellent to the glass walls of the lower chamber. Therefore, the amounts of radioactivity in each of the 12 counting vials from the lower chamber outflow, and residual radioactivity in the lower chamber were summed, expressed as the percent of applied dose, and termed as the percutaneous penetration (Table I).

The disposition of radioactivity, expressed as the percent of applied radioactive dose, following the minimum effective dose, is given in Table II, and following the 0.3-mg/cm² dose is given in Table I. The relative volatilities for the repellents are: V < IV < II < I[17]. The percent of radioactivity lost from the skin by evaporation was greater as volatility increased (Tables I and II). Except for I (the most volatile compound) in the 12-hr runs, the majority of the applied radioactive dose for each repellent was recovered from the skin surface and from the skin tissue.

In vitro duration for each repellent at the 0.3-mg/cm² dose was computed by determining the time it took for the evaporation rate from the 0.3-mg/cm² dose to reach the evaporation rate arising from the minimum effective dose or minimum effective evaporation rate for that repellent. The *in vitro* duration so obtained was plotted against the duration on humans (6) of each repellent at 0.3 mg/cm² (Fig. 7). Although *in vitro* duration was always longer than *in vivo* duration, a good correlation existed between them ($r^2 = 0.94$).

The minimum effective evaporation rate for each repellent represents the minimum amount of repellent vapor necessary to repel *A. aegypti* mosquitoes under given test conditions and, therefore, is a measure of the intrinsic repellency or potency of a compound. Minimum effective evaporation rate is calculated by dividing the amount (micrograms) of repellent evaporating from the skin surface by the skin surface area (1.27 cm²) and by the time (1 hr). The minimum effective evaporation rates (μg/cm²/hr ± *SD*) for the repellents studied are as follows: IV, 0.20 ± 0.09; V, 1.1 ± 0.1; II 1.2 ± 0.3; III, 1.8 ± 0.8; I, 7.5 ± 1.7. Compound IV is the most potent repellent, V, II, and III are equipotent, and I is the least potent repellent among the five. Repellent minimum effective evaporation rate will not necessarily be the same for different types of mosquitoes and would be expected to increase when test conditions are more severe (*e.g.*, increased avidity of mosquitoes). For V, the least volatile repellent, the evaporation rate following the 0.3-mg/cm² dose (Fig. 6) is essentially

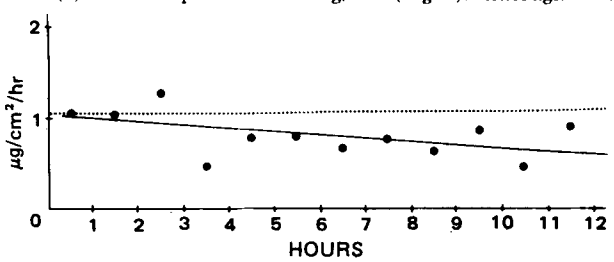

Figure 6—*Mean evaporation rate of V* versus *time at 0.3 mg/cm² (—); the minimum effective evaporation rate (·····).* In vitro *duration is 1 hr.*

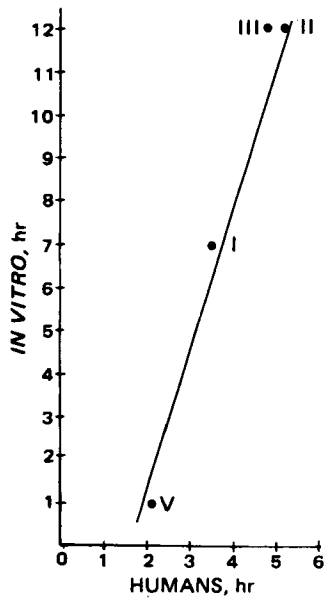

Figure 7—*Calculated* in vitro *duration* versus in vivo *duration of protection of five repellents at a dose of 0.3 mg/cm² against* A. aegypti *mosquitos.*

[17] June R. Jaeger, Research Chemist, Letterman Army Institute of Research, personal communication.

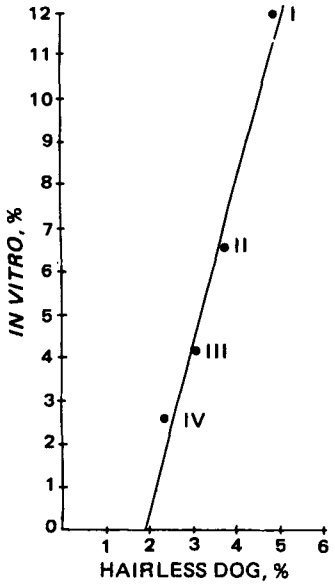

Figure 8—*Mean 12-hr percutaneous penetration (percent of applied radioactive dose)* in vitro versus *hairless dog.*

a horizontal line near its minimum effective evaporation rate. In this instance, the repellent failed almost immediately when challenged with mosquitoes (6). However, if the minimum effective evaporation rate were lower, the repellent could last a long time. The low volatility of V probably accounts for its sporadic performance[18].

In Fig. 8, 12-hr *in vitro* percutaneous penetration at the 0.3-mg/cm^2 dose is compared to 12-hr percutaneous penetration in the hairless dog at the same dose (2, 9) for four of the repellents studied (data for *in vivo–in vitro* comparison of IV were not available). Although *in vitro* percutaneous penetration was always greater than *in vivo* penetration, a good correlation exists between them ($r^2 = 0.96$).

The disposition of radioactivity 1 hr after topical application of radiolabeled II at its minimum effective dose (0.025 mg/cm^2) has been previously reported (5), both *in vitro* and *in vivo*. For the *in vitro* studies, 9.7 ± 5.9% of the applied radioactive dose evaporated, 19.7 ± 3.1% remained on the skin surface, and 50.8 ± 15.0% remained in the skin. For the *in vivo* studies, 9.6 ± 3.6% of the applied radioactive dose evaporated and 27.1 ± 11.6% remained on the skin surface. In this study, a lower percentage (4.3 ± 1.2%) of the radioactive dose of II evaporated 1 hr after *in vitro* application at the minimum effective dose. This difference may result from a closer proximity of the vapor entraining tube to the skin surface (1.5 mm *versus* 6.5 mm) in the previous report (5). A larger portion (52.8 ± 11.4%) of the applied radioactive dose was recovered from the skin surface and a correspondingly smaller portion (29.6 ± 12.9%) of the applied radioactive dose was recovered by skin oxidation, compared to the percentages cited in the previous study (5). This difference may result from the thoroughness of the skin surface rinse procedure, as the sum of the percentages of applied radioactive dose recovered by skin rinse and skin oxidation in the two studies are similar in magnitude.

The *in vitro* apparatus described here can be a useful tool for the screening of mosquito repellent formulations that incorporate a repellent whose evaporation and penetration characteristics and minimum effective evaporation rate are known. Formulations can be selected that reduce excessive evaporation, maintain evaporation rates above the minimum effective evaporation rate for longer periods of time, and reduce percutaneous penetration as compared with the unformulated repellent.

[18]W. Reifenrath and W. Akers, unpublished data.

REFERENCES

(1) R. J. Feldmann and H. I. Maibach, *J. Invest. Dermatol.*, **54**, 399 (1970).

(2) W. G. Reifenrath, J. A. Hill, P. B. Robinson, D. L. McVey, W. A. Akers, D. M. Anjo, and H. I. Maibach, *J. Environ. Pathol. Toxicol.*, **4**, 249 (1980).

(3) H. L. Snodgrass and M. H. Weeks, *Am. Ind. Hyg. Assoc. J.*, **39**, 540 (1978).

(4) L. Blomquist and W. Throsell, *Acta Pharmacol. Toxicol.*, **41**, 235 (1977).

(5) T. S. Spencer, J. A. Hill, R. J. Feldmann, and H. I. Maibach, *J. Invest. Dermatol.*, **72**, 317 (1979).

(6) J. A. Hill, P. B. Robinson, D. L. McVey, W. A. Akers, and W. G. Reifenrath, *Mosquito News*, **39**, 307 (1979).

(7) M. L. Gabel, T. S. Spencer, and W. A. Akers, *ibid.*, **36**, 141 (1976).

(8) A. P. Kurtz, "Annual Progress Report," Letterman Army Institute of Research, San Francisco, Calif., p. 5 (1971).

(9) W. G. Reifenrath, P. B. Robinson, V. Bolton, and R. E. Aliff, *Fd. Cosmet. Toxicol.*, **19**, 195 (1981).

High-Performance Liquid Chromatographic Analysis of Digitoxin Formulations

BELACHEW DESTA and K. M. McERLANE ˣ

Received June 25, 1981, from the *Faculty of Pharmaceutical Sciences, University of British Columbia, Vancouver, B.C. V6T 1W5, Canada.* Accepted for publication November 27, 1981.

Abstract □ A rapid, selective, and simple high-performance liquid chromatographic assay for digitoxin formulations is described. The method utilizes a conventional octadecyl-bonded phase column with detection at 220 nm. The isocratic solvent system resolves digitoxin from its potential degradation products and provides an accurate assay for tablet and injectable formulations with a relative standard deviation of 1.4 and 3.3%, respectively. The method is sufficiently sensitive to monitor content uniformity of tablets and the minimum quantifiable amount of digitoxin was determined to be 20 ng. The total chromatograph time was ~15 min.

Keyphrases □ Digitoxin—high-performance liquid chromatographic analysis of formulations, content uniformity □ Formulations—digitoxin, high-performance liquid chromatographic analysis, content uniformity □ High-performance liquid chromatography—content uniformity, analysis of digitoxin formulations

Digitoxin is a cardiac glycoside obtained from the leaves of *Digitalis purpurea* and is used in the treatment of congestive heart failure. Due to its long biological half-life the unit dose is generally low (0.1 mg). Assurance of potency and content uniformity of tablets is, therefore, a necessity for proper dosage. The determination of such a potent drug in the dosage form requires a method that is accurate, selective, and sensitive.

0022-3549/82/0900-1018$01.00/0

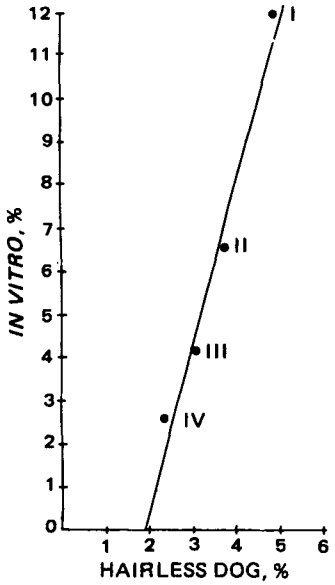

Figure 8—*Mean 12-hr percutaneous penetration (percent of applied radioactive dose)* in vitro versus *hairless dog.*

a horizontal line near its minimum effective evaporation rate. In this instance, the repellent failed almost immediately when challenged with mosquitoes (6). However, if the minimum effective evaporation rate were lower, the repellent could last a long time. The low volatility of V probably accounts for its sporadic performance[18].

In Fig. 8, 12-hr *in vitro* percutaneous penetration at the 0.3-mg/cm^2 dose is compared to 12-hr percutaneous penetration in the hairless dog at the same dose (2, 9) for four of the repellents studied (data for *in vivo–in vitro* comparison of IV were not available). Although *in vitro* percutaneous penetration was always greater than *in vivo* penetration, a good correlation exists between them ($r^2 = 0.96$).

The disposition of radioactivity 1 hr after topical application of radiolabeled II at its minimum effective dose (0.025 mg/cm^2) has been previously reported (5), both *in vitro* and *in vivo*. For the *in vitro* studies, 9.7 ± 5.9% of the applied radioactive dose evaporated, 19.7 ± 3.1% remained on the skin surface, and 50.8 ± 15.0% remained in the skin. For the *in vivo* studies, 9.6 ± 3.6% of the applied radioactive dose evaporated and 27.1 ± 11.6% remained on the skin surface. In this study, a lower percentage (4.3 ± 1.2%) of the radioactive dose of II evaporated 1 hr after *in vitro* application at the minimum effective dose. This difference may result from a closer proximity of the vapor entraining tube to the skin surface (1.5 mm *versus* 6.5 mm) in the previous report (5). A larger portion (52.8 ± 11.4%) of the applied radioactive dose was recovered from the skin surface and a correspondingly smaller portion (29.6 ± 12.9%) of the applied radioactive dose was recovered by skin oxidation, compared to the percentages cited in the previous study (5). This difference may result from the thoroughness of the skin surface rinse procedure, as the sum of the percentages of applied radioactive dose recovered by skin rinse and skin oxidation in the two studies are similar in magnitude.

The *in vitro* apparatus described here can be a useful tool for the screening of mosquito repellent formulations that incorporate a repellent whose evaporation and penetration characteristics and minimum effective evaporation rate are known. Formulations can be selected that reduce excessive evaporation, maintain evaporation rates above the minimum effective evaporation rate for longer periods of time, and reduce percutaneous penetration as compared with the unformulated repellent.

[18]W. Reifenrath and W. Akers, unpublished data.

REFERENCES

(1) R. J. Feldmann and H. I. Maibach, *J. Invest. Dermatol.*, **54**, 399 (1970).

(2) W. G. Reifenrath, J. A. Hill, P. B. Robinson, D. L. McVey, W. A. Akers, D. M. Anjo, and H. I. Maibach, *J. Environ. Pathol. Toxicol.*, **4**, 249 (1980).

(3) H. L. Snodgrass and M. H. Weeks, *Am. Ind. Hyg. Assoc. J.*, **39**, 540 (1978).

(4) L. Blomquist and W. Throsell, *Acta Pharmacol. Toxicol.*, **41**, 235 (1977).

(5) T. S. Spencer, J. A. Hill, R. J. Feldmann, and H. I. Maibach, *J. Invest. Dermatol.*, **72**, 317 (1979).

(6) J. A. Hill, P. B. Robinson, D. L. McVey, W. A. Akers, and W. G. Reifenrath, *Mosquito News*, **39**, 307 (1979).

(7) M. L. Gabel, T. S. Spencer, and W. A. Akers, *ibid.*, **36**, 141 (1976).

(8) A. P. Kurtz, "Annual Progress Report," Letterman Army Institute of Research, San Francisco, Calif., p. 5 (1971).

(9) W. G. Reifenrath, P. B. Robinson, V. Bolton, and R. E. Aliff, *Fd. Cosmet. Toxicol.*, **19**, 195 (1981).

High-Performance Liquid Chromatographic Analysis of Digitoxin Formulations

BELACHEW DESTA and K. M. McERLANE ˣ

Received June 25, 1981, from the *Faculty of Pharmaceutical Sciences, University of British Columbia, Vancouver, B.C. V6T 1W5, Canada.* Accepted for publication November 27, 1981.

Abstract □ A rapid, selective, and simple high-performance liquid chromatographic assay for digitoxin formulations is described. The method utilizes a conventional octadecyl-bonded phase column with detection at 220 nm. The isocratic solvent system resolves digitoxin from its potential degradation products and provides an accurate assay for tablet and injectable formulations with a relative standard deviation of 1.4 and 3.3%, respectively. The method is sufficiently sensitive to monitor content uniformity of tablets and the minimum quantifiable amount of digitoxin was determined to be 20 ng. The total chromatograph time was ~15 min.

Keyphrases □ Digitoxin—high-performance liquid chromatographic analysis of formulations, content uniformity □ Formulations—digitoxin, high-performance liquid chromatographic analysis, content uniformity □ High-performance liquid chromatography—content uniformity, analysis of digitoxin formulations

Digitoxin is a cardiac glycoside obtained from the leaves of *Digitalis purpurea* and is used in the treatment of congestive heart failure. Due to its long biological half-life the unit dose is generally low (0.1 mg). Assurance of potency and content uniformity of tablets is, therefore, a necessity for proper dosage. The determination of such a potent drug in the dosage form requires a method that is accurate, selective, and sensitive.

0022-3549/82/0900-1018$01.00/0

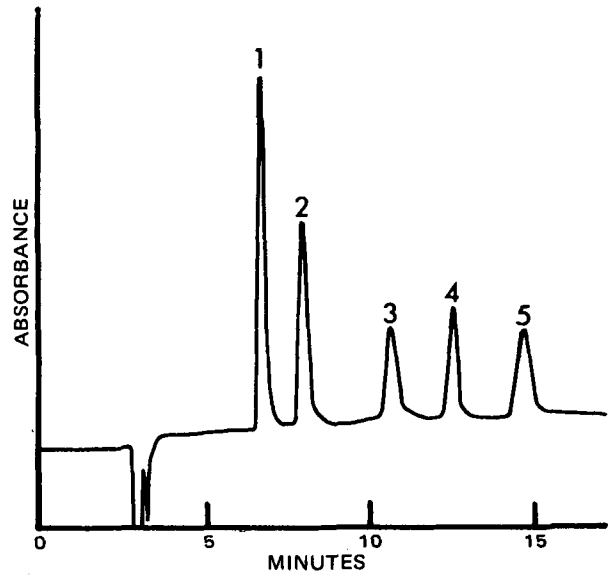

Figure 1—*Isocratic HPLC separation of digitoxin and its potential degradation products. Sequence of elution: digitoxigenin (1), digitoxigenin monodigitoxoside (2), digitoxigenin bisdigitoxoside (3), 17α-methyltestosterone (4), and digitoxin (5). Mobile phase: water–methanol–isopropanol–methylene chloride (45:38:11:6); flow rate: 1.1 ml/min.*

Quantitative colorimetric methods (1–8) lack selectivity, since the chromogenic agent reacts with either the lactone ring or the digitoxose sugar residue of the digitoxin molecule and would not determine the quantity of intact drug in the presence of any degradation products. In addition, these techniques are relatively insensitive. Fluorometric procedures (9–13) are based on the dehydration of the aglycone moiety, and although sensitive, are largely nonspecific. TLC techniques (14–17) although selective, are semiquantitative at best. A GC assay method (18) provided a highly sensitive method utilizing a heptafluorobutyrate derivative with electron-capture detection. However, the procedure requires conversion of the drug and potential impurities to the digitoxigenin portion of the glycoside and thus is nonselective. High-performance liquid chromatographic (HPLC) techniques have been reported (19–23) for the resolution of digitoxin and its potential metabolites, degradation products, and impurities; however, quantitative procedures for digitoxin in its dosage forms have not been reported.

This paper describes an HPLC method that is fast, selective, and sufficiently sensitive to allow accurate quantitation of digitoxin in single-tablet assays.

EXPERIMENTAL

Materials and Methods—A high-performance liquid chromatograph[1] equipped with dual pumps[2], a microprocessor system controller[3], a dynamically stirred mixing chamber[4], and a 20-μl loop injector[5] were used throughout. A variable wavelength detector[6] was operated at 220 nm. Data acquisition was accomplished with an electronic printer/plotter integrator[7]. The HPLC column[8] had a dimension of 4.6 mm × 250-mm i.d. and was packed with octadecyl (C-18) 5-μm bonded phase.

[1] Model 322, Beckman Instruments Inc., Toronto, Ontario, Canada.
[2] Model 100A and 110A, Beckman Instruments Inc.
[3] Model 420, Beckman Instruments Inc.
[4] Model 400, Beckman Instruments Inc.
[5] Model 210, Beckman Instruments Inc.
[6] Hitachi Ltd., Tokyo, Japan.
[7] Model C-R1A, Shimadzu Corp. Kyoto, Japan.
[8] Ultrasphere, Beckman Instruments Inc.

Table I—Recovery Data for the HPLC Analysis of Digitoxin Tablets[a]

Number	Theoretical Digitoxin Concentration, mg	Amount Added, mg	Recovery, %
1	1.0	0.5	98.6
2	1.0	0.5	102.6
3	1.0	0.5	95.8
4	1.0	0.5	101.9
Mean			99.7
RSD (%)[b]			3.1

[a] 0.1-mg tablet. [b] Relative standard deviation.

Water, methanol, isopropanol, and methylene chloride were of HPLC grade[9]. Digitoxin[10], digitoxigenin[10], digitoxigenin monodigitoxoside[10], digitoxigenin bisdigitoxoside[10], and 17α-methyltestosterone[11] were used without further purification.

The mobile phase used for the isocratic assay consisted of water–methanol–isopropanol–methylene chloride (45:38:11:6); flow rate was 1.1 ml/min and the UV detector was set at 220 nm.

An internal standard solution of 17α-methyltestosterone was prepared by dissolving 100 mg in 100 ml of methanol.

A standard solution of digitoxin was prepared by dissolving 10 mg in 60 ml of boiling methanol in a 100-ml volumetric flask. After cooling the resulting solution to room temperature, the flask was brought to volume with methanol and thoroughly mixed.

Calibration Curve—Aliquots of 1, 2, 5, 10, 20, and 30 ml of the digitoxin reference standard solution were added into 100-ml volumetric flasks along with 1 ml of internal standard solution. The solutions were diluted with methanol to produce a volume of 35 ml in each case. The resulting solutions were then brought to volume with water and thoroughly mixed. Three 20-μl aliquots of each of the calibration standards were used to determine the response ratio and linearity.

Tablet Formulation Assay—Forty tablets (0.1 mg/tablet) were weighed and triturated to a fine powder. An accurately weighed aliquot equivalent to ~1 mg of digitoxin was transferred to a 100-ml volumetric flask. Distilled water (10 ml) was added and the flask was swirled for 2–3 min, followed by the addition of 34 ml of methanol. The flask was shaken for 15 min, and the resulting suspension was filtered through filter paper[12] and the residue was washed with three, 5-ml portions of distilled water. The filtrate and washings were collected in a 100-ml volumetric flask containing 1 ml of the internal standard solution. The flask was brought to volume with water and a 20-μl aliquot was injected into the liquid chromatograph.

A single tablet assay was performed by placing one tablet in a 50-ml

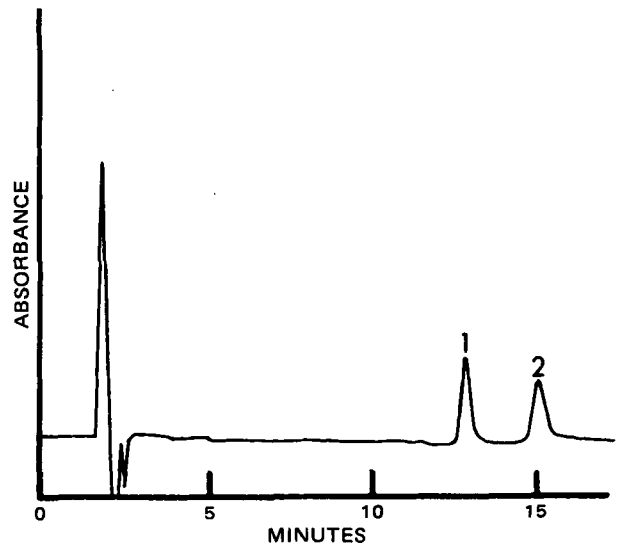

Figure 2—*High-performance liquid chromatogram of a digitoxin tablet formulation. Sequence of elution: 17α-methyltestosterone (1), digitoxin (2). Refer to Fig. 1 for HPLC conditions.*

[9] Fisher Scientific Co., Vancouver, British Columbia, Canada.
[10] Boehringer Mannheim Corp., Mannheim, G.F.R.
[11] Sigma Chemical Co., St. Louis, Mo.
[12] Whatman paper No. 1, W and R Balston Ltd., Eng.

Table II—Results of the HPLC Analysis of Digitoxin Tablet and Injectable Formulations

Number	Percent of Label Claim		
	Tablet Composite Assay[a]	Single Tablet Assay[a]	Injectable[b]
1	95.1	94.8	95.9
2	97.1	104.6	94.3
3	96.8	92.8	100.5
4	99.0	98.4	—
5	98.4	96.5	—
6	96.8	94.8	—
7	—	97.9	—
8	—	107.0	—
9	—	98.2	—
10	—	103.8	—
Mean	97.2	98.8	96.9
RSD (%)[c]	1.4	4.8	3.3

[a] 0.1-mg tablet. [b] 0.2 mg/ml. [c] Relative standard deviation.

volumetric flask and following the same procedure as for the tablet formulation assay.

Injectable Formulation Assay—Exactly 1 ml of digitoxin injection was quantitatively transferred to a 10-ml volumetric flask. A 0.1-ml aliquot of the internal standard solution along with 3.3 ml of methanol were added, and the flask was brought to volume with water.

To determine assay precision, 70 tablets were weighed and triturated to a fine powder. Six aliquots equivalent to ~1 mg of digitoxin were individually treated as described under tablet formulation assay. Three 20-μl injections were made from each of the six aliquots.

Recovery of Digitoxin from Tablets—Eighty tablets (0.1 mg/tablet) were weighed and ground to a fine powder. Three aliquots were treated and assayed in the same manner as for the tablet formulation to determine a mean assay value. Four aliquots of the ground digitoxin tablets, equivalent to an assay value of 1 mg, were prepared, and an accurately weighed quantity of digitoxin reference standard[9] equivalent to 0.5 mg was added to each sample. The samples were further treated as described under tablet assay. Three injections were made for each sample.

RESULTS AND DISCUSSION

A representative chromatogram for a standard mixture of digitoxin, its mono- and bisdigitoxosides, digitoxigenin, and the internal standard, 17α-methyltestosterone, is given in Fig. 1. From the chromatogram it can be determined that the potential impurities or degradation products are well resolved and are separated from the peak due to digitoxin. The overall chromatographic time of 15 min provides efficient assay capabilities.

The chromatogram obtained for a tablet composite assay is given in Fig. 2. The chromatogram is essentially devoid of any interfering peaks due to other glycosides or tablet excipients. As a further check, common tablet excipients such as lactose, starch, methylcellulose, and stearate lubricants were subjected to the extraction and assay procedures and were found not to interfere with the peaks due to the digitalis glycosides or the internal standard.

The composite sample used for the recovery study was initially assayed in triplicate and a mean value of 99.8% was obtained. The recovery of digitoxin from tablet formulations was thus determined by adding an amount equivalent to 50% of the tablet potency adjusted for the 99.8% potency observed. The data given in Table I indicate that the mean recovery was 99.7% of the expected total potency of the theoretical composite potency plus the amount of digitoxin added. The precision of the assay was determined by independent analysis of six tablet aliquots of a 0.1-mg tablet formulation and was found to yield a mean assay value of 97.2% with a 1.4% *RSD* (Table II).

USP assay (8) for digitoxin tablets is a relatively time-consuming procedure requiring column chromatographic isolation of the digitalis glycoside followed by a chromogenic reaction and colorimetric measurement. As such, the method requires several hours of analytical time. The HPLC method described in this paper, however, requires <1 hr to complete each assay determination. The USP limits for digitoxin tablets specify a content of 90–110% of label claim. From the data for a composite tablet assay given in Table II, the formulation examined falls within the pharmacopeial requirements. Because of the need to ensure content uniformity of digitoxin tablets, the USP specifies a sensitive but lengthy fluorometric procedure. The HPLC method described herein is sufficiently sensitive to determine content uniformity of 0.1-mg tablets. The resulting data obtained from a random sample of 10 tablets is given in Table II. The general pharmacopeial requirements for tablets specify that each dosage unit must contain 85–115% of the labeled potency. The data given in Table II indicate that the tablets examined have a mean potency of 98.8% with a 4.8% *RSD*. The range of 92.8 to 107.0% observed falls within the required limits.

Table III—Results of the Analysis of Digitoxin Tablets Using the USP XX Method[a]

Number	Label Claim, %
1	103.1
2	101.1
3	97.4
Mean	100.5
RSD (%)[b]	2.9

[a] 0.1-mg tablet. [b] Relative standard deviation.

As a final comparison with the USP assay for tablet potency, three aliquots of the 0.1-mg tablet composite used to determine the potencies given in Table II were assayed according to the pharmacopeial method. The results given in Table III for this analysis indicate that the formulation had a mean potency of 100.5% with a 2.9% *RSD*. It can be seen that the assay results obtained with the HPLC method compare favorably with those obtained with the USP method.

The HPLC analysis of a digitoxin injectable formulation is given in Table II. The assay mean (96.9%) indicates that the formulation is within the limits (90–110%) specified in the USP (8). The HPLC analytical procedure requires that the formulation only be diluted, whereas the USP method requires a prior column chromatographic procedure followed by timed chromogenic reaction and serial spectrophotometric readings. A significant time advantage is obtained with the HPLC procedure described.

The HPLC assay method described herein for tablet and injectable formulations is simple, rapid, and precise, and provides a sufficiently sensitive method for the determination of individual tablet content. The potency determinations compare favorably with those obtained with the USP assay method.

REFERENCES

(1) A. E. James, F. O. Laquer, and J. D. McIntyre, *J. Am. Pharm. Assoc., Sci. Ed.*, **36**, 1 (1947).

(2) F. K. Bell and J. C. Krantz, *ibid.*, **37**, 297 (1948).

(3) E. Soos, *Sci. Pharm.*, **16**, 29 (1948).

(4) E. E. Kennedy, *J. Am. Pharm. Assoc., Sci. Ed.*, **39**, 25 (1950).

(5) J. M. Rowson, *J. Pharm. Pharmacol.*, **4**, 814 (1952).

(6) D. H. Tattje, *Ann. Pharm. Fr.*, **12**, 267 (1954).

(7) D. H. Tattje, *J. Pharm. Pharmacol.*, **9**, 29 (1957).

(8) "United States Pharmacopeia," 20th Rev., U.S. Pharmacopeial Convention, Rockville, Md., 1980.

(9) L. J. Sciarini and W. T. Salter, *J. Pharmacol. Exp. Ther.*, **101**, 167 (1951).

(10) I. M. Jakovljevic, *Anal. Chem.*, **35**, 1513 (1963).

(11) D. Wells, B. Katzung, and F. H. Meyers, *J. Pharm. Pharmacol.*, **13**, 389 (1961).

(12) A. J. Khoury, "Automation in Analytical Chemistry, Technicon Symposia, 1966," Vol. I, Mediad, New York, N.Y., 1967.

(13) L. F. Cullen, D. L. Packman, and G. J. Papariello, *J. Pharm. Sci.*, **59**, 697 (1970).

(14) R. W. Jeliffe, *J. Chromatogr.*, **27**, 172 (1967).

(15) T. Bican-Fister and J. Merkas, *ibid.*, **41**, 91 (1969).

(16) J. M. G. J. Frijns, *Pharm. Weekblad*, **105**, 209 (1970).

(17) F. J. Evans, P. A. Flemons, C. F. Duignan, and P. S. Cowley, *J. Chromatogr.*, **88**, 341 (1974).

(18) E. Watson, P. Tramell, and S. M. Kalman, *ibid.*, **69**, 157 (1972).

(19) M. C. Castle, *ibid.*, **115**, 437 (1975).

(20) W. Lindner and R. W. Frei, *ibid.*, **117**, 81 (1976).

(21) F. Nachtmann, H. Spitzy, and R. W. Frei, *ibid.*, **122**, 293 (1976).

(22) F. Ernie and R. W. Frei, *ibid.*, **130**, 169 (1977).

(23) Y. Fujii, H. Fukuda, Y. Saito, and M. Yamazaki, *ibid.*, **202**, 139 (1980).

ACKNOWLEDGMENTS

This project was funded by a grant from the British Columbia Health Care Research Foundation. The World Health Organization provided a fellowship to Belachew Desta. The authors gratefully acknowledge all assistance.

Chromatographic Study of Interactions Between Polyvinylpyrrolidone and Drugs

D. HORN ˣ and W. DITTER

Received July 21, 1981, from the *Hauptlaboratorium der BASF Aktiengesellschaft, D-6700 Ludwigshafen/Rhein, West Germany.* Accepted for publication November 27, 1981.

Abstract □ A chromatographic technique for the study of possible interactions of drugs with soluble or insoluble polymer additives is proposed. Crospovidone was used as a stationary phase. The method allowed the rapid determination of interaction constants in the range of $>1\ M^{-1}$ as relevant for applications in practice. The interaction of 39 drugs and model compounds of diverse chemical structure with povidone and crospovidone was studied. The results closely agreed with data obtained from conventional equilibrium dialysis and sorption studies. The complexation reaction was found to be dominated by hydrogen binding. A close correspondence between the strength of interaction and the nature, number, and position of hydrogen-donating functional groups in the active ingredient was observed. The binding tendency was enhanced when the functional groups were connected with aromatic residues. The carboxyl group was more effective than the hydroxide or amino groups. The binding can be quantified by the binding constants, K_p and K_s, respectively, describing the interaction with polyvinylpyrrolidone *via* independent binding sites. At pH 1, with the exception of tannic acid, all investigated drugs exhibited K_p and/or K_s values well below an upper limit of $10\ M^{-1}$. Hence, with additive–drug ratios commonly used in pharmaceutical preparations, the bound amount of drug after oral administration can hardly exceed 3%. In view of this already low degree of potential binding and considering its reversible character and its decreasing tendency with increasing pH during GI passage, the presence of polyvinylpyrrolidone in pharmaceutical preparations is not expected to interfere with GI drug absorption.

Keyphrases □ Polyvinylpyrrolidone—chromatographic study of interactions with drugs, soluble and insoluble polymer additives □ Chromatography—study of interactions with polyvinylpyrrolidone and drugs, soluble and insoluble polymer additives □ Polymers—soluble and insoluble additives, chromatographic study of interactions between polyvinylpyrrolidone and drugs

N-Vinylpyrrolidone can be polymerized to yield povidone (I), a polymer readily soluble in water and numerous other solvents, producing solutions with remarkably low viscosities (1). It can also be transformed into an insoluble polymer, crospovidone (II), by proliferous polymerization (2, 3). In pharmaceutical technology, both forms of the polymer are used mainly in the production of tablets. The pronounced disintegrating effect of II is based on an exceptionally high swelling pressure in aqueous systems (4–6).

Additives used in formulations of drugs are expected to be nontoxic and therapeutically inactive. In both respects polyvinylpyrrolidone meets these requirements. The degree to which the additive might form complexes with the active component is another consideration; a low tendency for complex formation is preferred, unless a sustained-release effect is of interest.

BACKGROUND

Because of the dipolar character of I and II, specific interactions with certain drugs are possible and have been observed in several cases. A recent review covers the published data concerning the interaction properties of various macromolecular additives (7). Data characterizing the interaction properties of I have been reported in numerous studies (8–23).

Much more limited are relevant data concerning the interaction tendency of Compound II. The binding of phenolic substances and its relevance for their removal from beer has been studied (24–26). Similarly, II has been used to remove phenols from plant tissues in the process of isolating active enzymes from plants (27). Furthermore, tannic acid and related compounds are known to be bound strongly by II (3). Other compounds such as acetaminophen, benzocaine, metamizole, and salicylamide exhibited no stronger interaction with II than with corn starch, carboxymethyl starch, and microcrystalline cellulose (28). First results of a systematic study of the interaction properties of II with various pharmaceuticals have been reported (29).

The objectives of the present study are: to develop new experimental techniques that simplify the performance of binding studies, to study the binding of selected model compounds to improve the basic understanding of the mode of interaction with I and II, and to present the binding data obtained from various drugs of diverse chemical structure in a way ready to be applied to systems of practical interest. The application of a novel chromatographic technique is emphasized.

EXPERIMENTAL

Materials—The following were obtained from commercial sources: acetaminophen[1], aspirin[2], aniline[3], benzocaine[4], benzoic acid[2], benzyl alcohol[5], caffeine[2], chloramphenicol[6], 1,2-dicarboxybenzene[2], 1,3-dicarboxybenzene[3], 1,4-dicarboxybenzene[3], 1,2-dihydroxybenzene[2], resorcinol[2], 1,4-dihydroxybenzene[5], 2,4-dihydroxybenzoic acid[1], 3,4-dihydroxybenzoic acid[7], 3,5-dihydroxybenzoic acid[5], 2,4-dimethylphenol[1], salicylic acid[2], 3-hydroxybenzoic acid[1], 4-hydroxybenzoic acid[1], methotrimeprazine[5], methyldopa[6], methylparaben[8], 2-methylphenol[1], papaverine hydrochloride[2], phenol[2], promethazine hydrochloride[5], riboflavin[2], salicylamide[2], sorbic acid[9], sulfamethazine[10], sulfamoxole[11], sulfathiazole[12], tetracaine hydrochloride[13] gallic acid[2], trimethoprim[11], 2,4,6-trimethylphenol[7], and tannic acid[2]. All materials were of the highest available grade and were used without further purification.

Povidone[14] was used as received (weight average of molecular weight $\overline{M}_w = 49{,}000$; number average of molecular weight $\overline{M}_n = 10{,}000$).

The sorption studies were performed applying crospovidone[15], characterized by a specific surface area[16] of $S_{N_2} = 6.0\ m^2/g$ and a density of $1.2\ g/cm^3$. A coarse fraction of II was used for the stationary phase in the chromatographic column.

Chromatography—In preparing the chromatographic column (length, 10 cm; diameter, 0.25 cm) an aqueous slurry of a coarse fraction of II, as specified above, was poured into the column and allowed to pack by gravity flow. The column was coupled with a UV-visible spectrophotometer[17] equipped with a 1-cm micro flow-through cell. The column was charged with 10-μl samples of the drug solution. For the easily soluble substances, 1000 mg was dissolved in 1000 ml of 0.1 *N* HCl. Where the solubility was insufficient, saturated solutions at 25° were used. In general, 0.1 *N* HCl, plain or loaded with 10–30 g/liter of I, was used for elution[18] with a rate of 7.5 ml/hr at ambient temperature (25 ± 1°).

[1] Merck-Schuchardt, München, West Germany.
[2] Merck-AG, Darmstadt, West Germany.
[3] BASF-AG, Ludwigshafen/Rhein, West Germany.
[4] Dr. Rentschler & Co., Laupheim, West Germany.
[5] Bayer-AG, Leverkusen, West Germany.
[6] Boehringer GmbH, Mannheim, West Germany.
[7] EGA Chemie GmbH & Co. KG, Steinheim, West Germany.
[8] W. Damm, Hamburg, West Germany.
[9] Dr. Schuchardt & Co., München, West Germany.
[10] Cilag Orion GmbH, Alsbach, West Germany.
[11] Nordmark-Werke GmbH, Hamburg, West Germany.
[12] K.-W. Pfannenschmidt, Hamburg, West Germany.
[13] Hoechst-AG, Frankfurt, West Germany.
[14] Kollidon 30, BASF-AG, Ludwigshafen/Rhein, West Germany.
[15] Kollidon CL, BASF-AG, Ludwigshafen/Rhein, West Germany.
[16] Areameter, Ströhlein, Düsseldorf, West Germany.
[17] PM 2 DL, Zeiss, Oberkochen, West Germany.
[18] Prominent, Type A 2001, C.F.G., Heidelberg, West Germany.

0022-3549/82/0900-1021$01.00/0

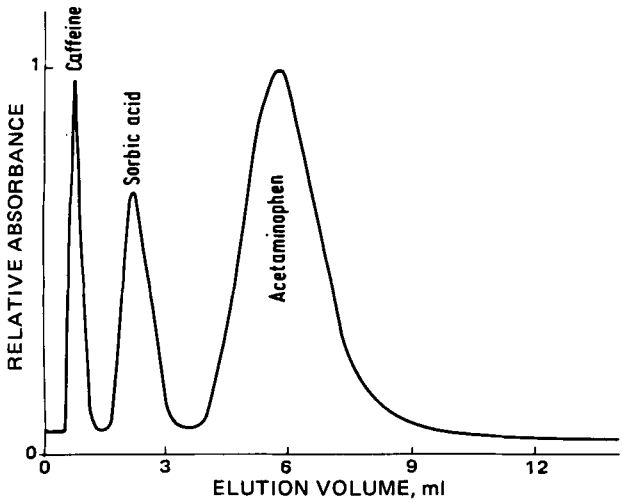

Figure 1—*Chromatographic fractionation of drugs using II as stationary phase and 0.1* N *HCl as eluent. The degree of interaction with II is indicated by specific retention volumes.*

Sorption Studies—For easily soluble substances, aqueous solutions containing 250 mg/liter of the active ingredient were prepared. The solution pH was adjusted in the range of 1.0–12.0 by adding the required amounts of hydrochloric acid or sodium hydroxide. For less soluble substances, saturated solutions were used as received at 25°.

The sorption experiments were performed in 250-ml flasks at 25 ± 0.5°. Compound II was added in amounts of 20–1000 mg/200 ml of solution. The suspension was maintained under steady vibration stirring for 10 min then centrifuged[19]. The amount of unbound drug was determined spectrophotometrically[20] in the supernate.

For the binding studies with Compound I, the sorption experiments were performed after I was added as a cosolute in amounts of 2–6 g/200 ml of solution.

Equilibrium Dialysis—Equilibrium dialysis[21] was carried out at controlled temperature (25 ± 0.5°) using cellulosehydrate membranes[22] with a molecular weight cutoff of 5000 daltons. The effective surface area was 11.3 cm^2 in each cell, separating two compartments of 2 ml of volume. Equilibration was attained under steady rotation after 2 hr. The distribution of the active ingredient was determined spectrophotometrically[21]. With the exception of tannic acid, with all drugs and model substances, no detrimental interaction with the membrane was observed.

THEORETICAL

Evaluation of Data—There have been only a few attempts to apply various modes of gel permeation chromatography for investigating the complex formation between macromolecules and drugs (7). Molecular sieves as a stationary phase are only useful in exceptional cases where the dissociation rate is small compared to the rate of elution (30–33). Certain precautions have to be taken in order to obtain significant experimental results (34–36).

In contrast, the chromatographic technique proposed in the present study requires a rapid adjustment of the equilibrium of complex formation. One component of the complex formation of interest, compound II, is used as a stationary phase. In a few cases a similar polymer has been used before to separate phenolic acids (37) and purine and pyrimidine bases (38, 39) by liquid chromatography.

As was shown in a previous study, interactions of drugs with II are volume-controlled, and any possible influence of the extent of the specific surface area of II is negligible (29). Hence, the active ingredient will be distributed between the insoluble polymer phase and the liquid phase according to the Nernst distribution law:

$$k = \frac{[A]_s}{[A]} \qquad \text{(Eq. 1)}$$

where $[A]_s$ and $[A]$ denote the drug concentrations in the insoluble polymer and the liquid compartment, respectively.

[19] Omnifuge, Heraeus, Hanau, West Germany.
[20] Cary 14 Spectrophotometer, Varian GmbH, Darmstadt, West Germany.
[21] DIANORM, Bachofer GmbH & Co. KG, Reutlingen, West Germany.
[22] DIACHEMA, Cut-off 5000 No. 10.14, Bachofer GmbH & Co. KG, Reutlingen, West Germany.

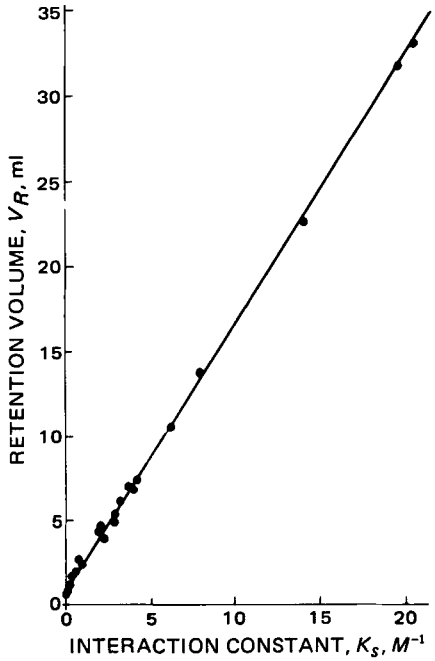

Figure 2—*Calibration of the chromatographic column. The retention volume,* V_R, *depends linearly on the interaction constant,* K_s, *as predicted by Eq. 11.* K_s *was determined by sorption experiments.*

Only part of $[A]_s$ is bound to active sites of the polymer (29). To first approximation, $[A]_s$ of Eq. 1 can be separated according to:

$$[A]_s = [A] + [FA]_s \qquad \text{(Eq. 2)}$$

where $[FA]_s$ denotes the portion of $[A]_s$ bound to active binding sites, while the concentration of the remaining fraction of $[A]_s$ that is unspecifically bound by the polymer compartment is assumed to be equilibrated to $[A]$ of the surrounding liquid phase (29).

With the liquid compartment containing, besides the active ingredient, A, an additional polymer cosolute, *e.g.*, Compound I, a similar relation holds true for $[A]_L$, the concentration of the drug in the liquid compartment:

$$[A]_L = [A] + [FA]_p \qquad \text{(Eq. 3)}$$

where $[FA]_p$ denotes the portion of $[A]_L$ bound in a drug–polymer complex.

For a system containing I and II simultaneously besides the active ingredient, A, the Nernst distribution law becomes:

$$k^* = \frac{[A] + [FA]_s}{[A] + [FA]_p} \qquad \text{(Eq. 4)}$$

Now, the equilibrium law of complex formation in the liquid phase and of the interaction in the insoluble polymer compartment becomes:

$$K_p = \frac{[FA]_p}{[A]([F_0]_p - [FA]_p)} \qquad \text{(Eq. 5)}$$

and:

$$K_s = \frac{[FA]_s}{[A]([F_0]_s - [FA]_s)} \qquad \text{(Eq. 6)}$$

respectively, where $[F]$, the concentration of free binding sites, is already replaced by the relation $[F] = [F_0] - [FA]$ in which $[F_0]$ represents the total concentration of available binding sites in the respective compartment of the system.

In distribution chromatography, the retention volume, V_R, is given by (40):

$$V_R = n(V'_L + kV'_s) \qquad \text{(Eq. 7)}$$

where n is the number of theoretical plates and V'_L and V'_s denote the volumes per theoretical plate of the mobile and the stationary phases, respectively. After introducing the phase ratio $\varphi = V_s/V_L$, and considering that for the chromatographic column: $V_s = nV'_s$ and $V_L = nV'_L$, Eq. 7 becomes:

$$V_R = V_L(1 + k\varphi) \qquad \text{(Eq. 8)}$$

Table I—Binding Data of the Interaction of Drugs with II in 0.1 *N* HCl at 25°

Compound	Interaction Constant, K_s, M^{-1} Sorption Method	Chromatographic Method
Acetaminophen	2.0	2.4
Aspirin	1.5	2.1
Benzocaine	~0	~0
Caffeine	~0	~0
Chloramphenicol	~0	~0
Methotrimeprazine	0.7	1.2
Methyldopa	0.2	~0
Methylparaben	4.2	4.2
Papaverine hydrochloride	0.1	0.2
Promethazine hydrochloride	0.4	0.6
Riboflavin	~0	~0
Salicylamide	3.7	4.0
Sorbic acid	0.5	0.7
Sulfamethazine	~0	~0
Sulfamoxole	~0	~0
Sulfathiazole	1.0	1.0
Tetracaine hydrochloride	~0	~0
Trimethoprim	~0	~0

where V_L and φ are constants for a given column. Hence, V_R is expected to be proportional to k.

As was shown earlier (29, 41), considering the mass balance of the drug:

$$[A_0]V_L = [A]V_L + [A]V_s + [FA]_sV_s \qquad \text{(Eq. 9)}$$

where $[A_0]$ represents the weighing-in concentration of the active ingredient, Eq. 6 can be combined with Eq. 1 to give:

$$k = 1 + \frac{[F_0]_sK_s}{1 + [A]K_s} \qquad \text{(Eq. 10)}$$

With the formal assumption that each monomeric subunit of the polymer may serve as a binding site, $[F_0]_s$ becomes ~9 M.

In most cases of interaction investigated in the present study, the approximation, $K_s[A] \ll 1$, holds true, since $K_s < 10$ and $[A] \approx 10^{-3}$ M. M.

Hence, substituting Eq. 10 into Eq. 8 gives:

$$K_s = \frac{1}{9}\left[\frac{V_R}{V_s} - \left(\frac{V_L}{V_s} + 1\right)\right] \qquad \text{(Eq. 11)}$$

Therefore, the retention volume, V_R, is linearly correlated with the interaction constant K_s.

Similarly, K_p can be determined by adding a definite amount of the soluble polymer (I) to the mobile phase. Considering Eqs. 4 and 8, the retention volume is altered to:

$$V_R^* = V_L(1 + k^*\varphi) \qquad \text{(Eq. 12)}$$

Dividing Eq. 12 by Eq. 8 yields for the ratio of the Nernst coefficients:

$$\frac{k^*}{k} = \frac{V_R^* - V_L}{V_R - V_L} \qquad \text{(Eq. 13)}$$

This ratio can be expressed in terms of the constant of complex formation in the liquid compartment, K_p, by combining Eqs. 1, 4, and 5:

$$\frac{k^*}{k} = \left(1 + \frac{K_p[F_0]_p}{1 + K_p[A]}\right)^{-1} \qquad \text{(Eq. 14)}$$

Again, the approximation $K_p[A] \ll 1$ is in general valid, and substituting Eq. 14 in Eq. 13 leads to:

$$K_p = \frac{(V_R - V_R^*)}{(V_R - V_L)}\frac{1}{[F_0]_p} \qquad \text{(Eq. 15)}$$

Therefore, K_p is readily determined by adding a certain amount of I, $[F_0]_p$, to the mobile phase and measuring the change of the retention volume, $V_R - V_R^*$, of the active ingredient.

In order to prove the validity of the chromatographic results, K_s and K_p were also determined by sorption studies, as reported previously (29). The variable K_s is readily evaluated from k (Eq. 1) according to the rearranged Eq. 10:

$$K_s = \frac{k - 1}{[F_0]_s - [A](k - 1)} \qquad \text{(Eq. 16)}$$

Table II—Binding Data of the Interaction of Model Compounds with II in 0.1 *N* HCl at 25°

Compound	Interaction Constant, K_s, M^{-1} Sorption Method	Chromatographic Method
Aniline	1.0	0
Benzyl alcohol	1.3	0.3
Phenol	1.9	2.3
2-Methylphenol	2.9	2.9
2,4-Dimethylphenol	2.3	2.0
2,4,6-Trimethylphenol	3.2	3.4
1,2-Dihydroxybenzene	3.9	3.9
Resorcinol	13.1	14.0
1,4-Dihydroxybenzene	8.0	8.3
1,2,3-Trihydroxybenzene	10.0	6.3
Benzoic acid	2.9	2.6
1,2-Dicarboxybenzene	5.0	4.7
1,3-Dicarboxybenzene	20.5	[a]
1,4-Dicarboxybenzene	50.0	[a]
Salicylic Acid	6.2	6.2
3-Hydroxybenzoic acid	20.8	20.5
4-Hydroxybenzoic acid	19.8	19.6
2,4-Dihydroxybenzoic acid	71.9	[a]
3,4-Dihydroxybenzoic acid	93.2	[a]
3,5-Dihydroxybenzoic acid	125.6	[a]
Gallic Acid	>1000	[a]

[a] Not measured: retention volume too large.

Then, after adding a definite amount of the soluble polymer, $[F_0]_p$, to the system, k^* is measured according to Eq. 4. For systems where $K_p[A] \ll 1$ is valid, the rearranged Eq. 14 gives:

$$K_p = \frac{k - k^*}{k^*[F_0]_p} \qquad \text{(Eq. 17)}$$

Equilibrium dialysis was used as a supplementary technique to perform binding studies of some systems.

In this case the evaluation of data is based on Eq. 5:

$$K_p = \frac{k^{**} - 1}{[F_0]_p - (k^{**} - 1)[A]} \qquad \text{(Eq. 18)}$$

where the experimentally accessible coefficient k^{**} is introduced describing the distribution of the drug between the polymer-free and polymer-containing dialysis compartments, according to:

$$k^{**} = \frac{[A] + [FA]_p}{[A]} \qquad \text{(Eq. 19)}$$

For the strongly interacting tannic acid, the approximation, $K_s[A] \ll 1$, is invalid, and the Nernst coefficient, k, becomes strongly dependent upon $[A]$. The experimental results of the interaction with II can be described with a model where two classes of independent binding sites are assumed to be operative. Each class is characterized by a specific interaction constant, $K_{s,1}$ and $K_{s,2}$, respectively. With reference to Eq. 10, the interaction can be described by:

$$k_{1,2} = 1 + \frac{K_{s,1}[F_0]_1}{1 + K_{s,1}[A]} + \frac{K_{s,2}[F_0]_2}{1 + K_{s,2}[A]} \qquad \text{(Eq. 20)}$$

where $[F_0]_1$ and $[F_0]_2$ refer to the concentration of available binding sites of Class 1 and Class 2.

There exists a simple relationship between K_p, as defined by Eq. 5, and the binding constant, K, defined by the basic theory of ligand–polymer interaction as advanced by Klotz *et al.* (42) and by Scatchard (43). The interaction with independent binding sites is described by:

$$r = \frac{nK[A]}{1 + K[A]} \qquad \text{(Eq. 21)}$$

where r is the number of moles of ligand bound per monomer unit of the polymer, $r = [FA]/[F_0]_p$, n represents the total number of sites available, and K is the binding constant. Introducing Eq. 5 into Eq. 21 and considering $[FA] \ll [F_0]_p$ gives:

$$K_p \approx \frac{nK}{1 + K[A]} \qquad \text{(Eq. 22)}$$

and for $K[A] \ll 1$:

$$K_p \approx nK \qquad \text{(Eq. 23)}$$

The product, nK, is equal to the first binding constant, k_1, which is a measure for the strength of the binding. Values of $nK = k_1$ are commonly

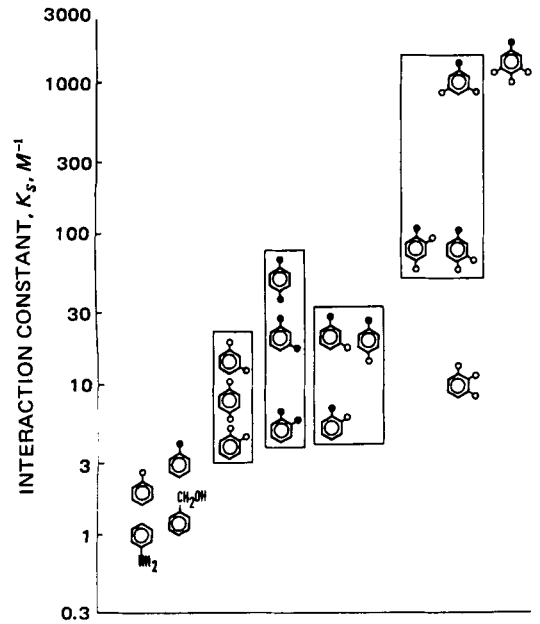

Figure 3—*Interaction constant, K_s, of various aromatic model compounds characterizing the influence of the nature, number, and position of hydrogen donating functional groups on the interaction with II. Key: (○) hydroxide group; (●) carboxyl group.*

deduced from the slopes of linear binding plots according to Klotz *et al.* (42) or Scatchard (43). Values of n, however, can be determined only with much uncertainty (44). Their physical relevance is doubtful.

RESULTS AND DISCUSSION

Figure 1 shows a typical chromatogram of a sample solution composed of three drugs. Each component is characterized by a specific retention volume indicating the degree of interaction with II. The theoretically proposed linear correlation between the interaction constant, K_s, and the retention volume, V_r, (Eq. 11) is experimentally corroborated in Fig. 2 where for a series of drugs and drug models the retention volume, V_R, is plotted against the interaction constant, K_s, as obtained from sorption studies. The linear correlation between the results of the sorption experiments and the chromatographic studies clearly indicates a reversible interaction of the active ingredients with II. Apparently, the adjustment of equilibrium takes place rapidly enough so that the provisions for true partition chromatography are satisfied. Hence, by the data of Fig. 2, a chromatographic technique is established that offers new and convenient means for the investigation of interactions between drugs and crospovidone. As was shown before, the method is readily extended to binding studies with soluble polymer additives by adding the respective polymer to the mobile phase.

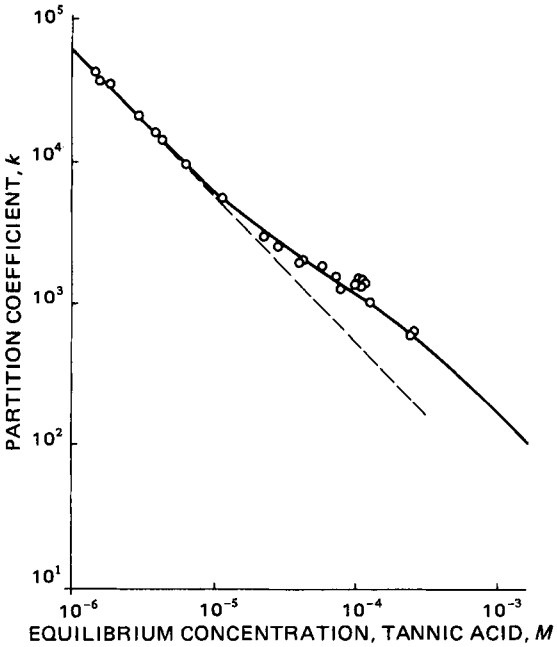

Figure 4—*Dependence of the Nernst coefficient, k, on the equilibrium concentration of tannic acid interacting with II in 0.1 N HCl suspensions. The curve was calculated according to Eq. 20 using $[F_0]_1 = 0.12$ M; $K_{s,1} = 10^4$ M^{-1}; $[F_0]_2 = 0.06$ M; $K_{s,2} = 10^7$ M^{-1}.*

Table III—Binding Data of the Interaction Model Compounds and Drugs with I in 0.1 *N* HCl at 25°

Compound	Binding Constant, K_p, M^{-1} Sorption Method	Chromatography Method	Dialysis Method
Acetaminophen	<1	<1	1.5
Aspirin	<1	<1	0.7
Benzoic acid	<1	<1	0.9
Chloramphenicol	[a]	[a]	0.4
1,2-Dihydroxybenzene	<1	<1	0.8
Resorcinol	1.3	2.2	2.4
1,4-Dihydroxybenzene	1.6	1.9	1.6
Salicylic Acid	1.7	1.1	1.5
3-Hydroxybenzoic acid	2.7	3.5	2.8
4-Hydroxybenzoic acid	5.2	5.3	3.6
Methotrimeprazine	4.6	5.2	3.2
2-Methylphenol	<1	<1	1.0
Methylparaben	2.6	<1	1.8
Phenol	<1	<1	0.8
Salicylamide	1.6	1.5	1.3
Sorbic acid	<1	<1	0.5
Sulfathiazole	<1	<1	0.4
Sulfamoxole	[a]	[a]	0.3
Trimethoprim	[a]	[a]	0.2

[a] Not measurable: K_s too small.

The chromatographically determined K_s-values of various drugs are listed in Table I. As expected from Fig. 2, they are found in close agreement with the corresponding values obtained from sorption experiments. All drugs are characterized by K_s-values <5 M^{-1}. The K_s-values of the model compounds are listed in Table II. They range from 1 M^{-1} to ~1000 M^{-1}.

The data of Tables I and II agree with findings of an earlier study (29) where the tendency for the complex formation with II was found closely correlated with the ability of the drugs to act as hydrogen donators. Accordingly, none of the compounds of Table I characterized by K_s-values <0.1 M^{-1} carries hydroxide or carboxyl groups bound to aromatic residues. The ability of aromatic amines to act as hydrogen donators is known to be small, and compounds of Table I belonging to this class exhibit K_s-values <1 M^{-1}. Besides hydrogen binding, mechanisms of hydrophobic interaction can be operative, as found with several phenothiazine derivatives, in close agreement with observations of Voigt *et al.* (18). However, interactions with I or II based on this hydrophobic mechanism are found to be moderate.

The significance of hydrogen binding for the occurrence of strong interactions with I or II can best be shown by the data obtained with the model compounds, as listed in Table II. In Fig. 3, the correspondence between the strength of interaction and the number and position of hydrogen-donating functional groups is documented. Aromatic carboxylic acids form stronger complexes than phenols. The complexation tendency increases with the number of hydrogen-donating functional groups. In all bifunctional compounds, the weakest complexes are formed by the *ortho* isomers. Steric effects are apparently responsible for the fact that with biphenols, the *meta* isomer, and with the corresponding carboxylic acids, the *para* isomer exhibit the strongest interaction tendency.

For trifunctional compounds the importance of the *meta* position of the active ligands is again emphasized: the K_s-value of 3,5-dihydroxybenzoic acid is by an order of magnitude larger than that of the corresponding 2,4- and 3,4-isomers, where in both cases an unfavorable *ortho* substitution reduces the interaction tendency. The accumulation of *ortho* substituents in 1,2,3-trihydroxybenzene causes a further reduction of K_s by an order of magnitude.

As reported earlier (29), tannic acid forms exceptionally strong complexes with II; the same is true for the interaction with I. An explanation for this exceptional interaction tendency immediately follows from its multifunctional chemical structure based on gallic acid and digallic acid. According to Fig. 3, gallic acid already exhibits a K_s-value of ~1000 M^{-1}. The accumulation of residues of this nature within the tannic acid mol-

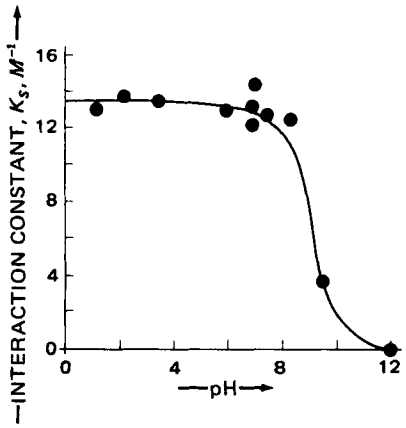

Figure 5—*Influence of pH on the interaction of resorcinol with II.*

ecule leads to a further increase of K_s. The approximation, $K_s\,[A] \ll 1$, is no longer valid and k becomes dependent on A.

Figure 4 shows the results of interaction studies with II extending beyond the concentration range of earlier investigations (29). The dependence of the partition coefficient, k, upon $[A]$ is satisfactorily described by model calculations based on Eq. 20, assuming two classes of binding sites, F_1 and F_2, on part of the polymer. The corresponding interaction constants, $K_{s,1}$ and $K_{s,2}$, are determined to be of the order of 10^4 and 10^7 M^{-1}, respectively. Hence, tannic acid exceeds other model compounds and drugs in its interaction tendency toward II by several orders of magnitude. Similar results were obtained for the interaction with I but are not shown here in detail. The concentration of available binding sites, $[F_o]_1$ and $[F_0]_2$, is determined to be 0.12 and 0.06 M, respectively. These figures are well below the theoretical limit of 9 M for polyvinylpyrrolidone, underlining the fact that one interacting molecule of tannic acid, owing to its extended molecular structure, covers many vinylpyrrolidone units in the polymer.

The results of the binding studies with I are listed in Table III. The chromatographically determined values of K_p satisfactorily agree with those data obtained by standard equilibrium dialysis. (In the present study all values of K_s or K_p are defined by relating to the molecular weight of a monomer segment of the polymer. This is preferable to using often ill-defined molecular weight data of the polymer.)

The application of the chromatographic technique for determining K_p requires a minimum interaction between the investigated active ingredient and II used as a stationary phase. In general, the interaction tendencies of drugs with both I and II are closely corresponding (29). Therefore, the chromatographic technique can best be applied in cases where moderate to strong interaction is occurring. In studies of weak interaction, equilibrium dialysis yields more reliable data.

All interaction data presented so far relate to pH conditions of gastric fluids. They define upper limits for the interaction constants for all systems where hydrogen binding dominates the complexation reaction. With increasing pH, the degree of dissociation of the hydrogen donating functional groups rises, and, correspondingly, the interaction tendency is expected to decrease. For example, Fig. 5 depicts the pH dependence of K_s as observed with resorcinol. Other examples of a similar pH dependence were recently reported (45). Even in cases of very strong interaction, as observed with several model compounds, the interaction constants start to drop at pH values >4. With tannic acid, a decrease of the K_s values was observed, starting from $\gg$10,000 M^{-1} at pH 1 and ending at ~50 M^{-1} at pH 12. These observations further support the notion of hydrogen-binding being the dominating mechanism in moderate to strong interactions with I or II, even in cases of high molecular weight compounds like tannic acid. In hydrophobically interacting systems, a significant influence of pH on the strength of interaction was observed only with some phenothiazines (18). The reason for the decrease with increasing pH is not fully understood.

The significance of the reported data for practical applications becomes apparent in calculations of the bound amount of an active ingredient in a pharmaceutical formulation or after administering the drug. Knowing the respective values of K_s or K_p, the assessment can be based on Eqs. 5 or 6, since reversibility of the interaction has been proved with a representative selection of systems by desorption studies (29). The feasibility of the chromatographic technique requiring a reversible interaction of the involved components further supports this notion.

In Fig. 6 the bound fraction of the active ingredient is plotted as a function of the interaction constant, K_s, for various concentrations of the polymer additive, II. The graph is applicable for weighing-in concentrations of the active ingredient between 1×10^{-4} and 2×10^{-3} M, covering the concentration range usually encountered in practice. If the oral administration of two tablets containing 10% by weight of the additive II is considered as an example of practical relevance, then the additive concentration in the gastric fluid can hardly exceed a value of 0.5 g/liter. In Fig. 6 the relevant area is marked by shading. Considering the fact that—with the exception of tannic acid and related compounds—K_s of active ingredients is limited to values <10 M^{-1}, the bound amount can not excel the 3% limit. Differences in the salt concentration, not accounted for in this estimate, cannot affect this figure to a significant degree. As was pointed out before, in respect to a possible dependence upon pH, this figure constitutes an upper limit.

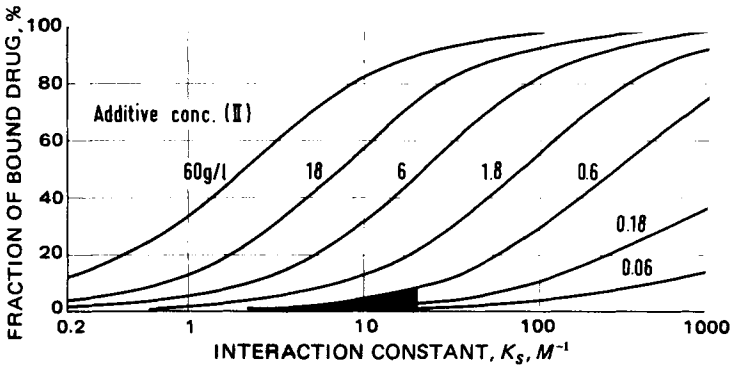

Figure 6—*Fraction of drug bound to II as a function of the interaction constant, K_s, for various concentrations of II. The graph is valid for concentrations of the active ingredient $[A_0]$, between 1×10^{-4} and 2×10^{-3} M, covering the range of practical interest. The significance of the shaded area is explained in the text.*

Another way of interpreting the data is offered in Fig. 7, where the bound fraction of the drug is plotted as a function of the additive I concentration for various values of K_p. Considering the data of Table III, it immediately follows that for all practical purposes the fraction of the drug bound by the additive after oral administration is estimated in the range of a few percent.

Graphs as shown in Figs. 6 and 7 offer the opportunity to transfer binding data that are sometimes, for experimental reasons, obtained at excessively high levels of additive concentration into a concentration range of more practical relevance. In studies of the interaction properties of I, polymer concentrations as high as 50 g/liter were frequently used (7, 10, 46, 47). From Fig. 7 it can be deduced that at this level of additive concentration, the bound fraction of compounds with even moderate binding tendency, as corresponding to $K_p \sim 1$ M^{-1}, amounts to ~30%. This is illustrated by a recent investigation of the inhibitory effect polyvinylpyrrolidone may exhibit on the absorption of acetaminophen (47). The binding constant, K, was determined (42) at pH 6.4 as 23 M^{-1} with $1/n = 18.5$. Considering Eq. 23, it follows that $k_1 = 1.24$ M^{-1}, which

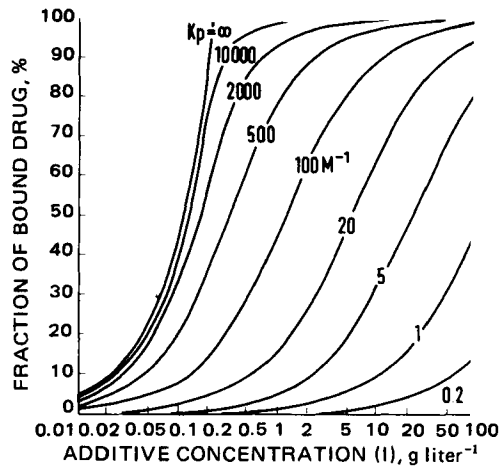

Figure 7—*Fraction of drug bound to I as a function of the additive concentration (I), for various values of the binding constant, K_p. The graph is valid for concentrations of the active ingredient, $[A_0]$, between 1×10^{-4} and 2×10^{-3} M.*

is in close agreement with $K_p = 1.5\ M^{-1}$ of the present study. By inspection of Fig. 7, a bound fraction of ~35% is estimated at an additive concentration of 50 g/liter as was applied in the respective study.

At an additive concentration of 0.5 g/liter, however, considered as typical for the oral administration of drugs, the bound fraction of the drug falls to a level close to zero, as shown in Fig. 7.

For tannic acid and related compounds in the acidic pH range, even at a polymer concentration as low as 0.5 g/liter, the bound fraction is >95%, a fact that is advantageously used in practice (24–26).

CONCLUSIONS

The chromatographic method proposed in the present study represents an easy to use experimental technique for a rapid assessment of interaction properties of drugs in systems containing soluble or insoluble polymer additives. The determination of interaction constants in the range of $>1\ M^{-1}$ is reduced to the readily performed determination of retention volumes. As was shown in detail, only interactions with K_s and/or K_p values above this limit are of practical interest. With the exception of tannic acid and related compounds, all drugs investigated in the present study exhibited K_p- or K_s-values well below an upper limit of $10\ M^{-1}$, indicating that with commonly used additive concentrations of I or II, the bound fraction of the drug after oral administration can hardly exceed a limit of the order of 3%. Considering further the fact that binding is reversible, and in view of the observed pH dependence of binding strength, the presence of these additives is not expected to interfere with the GI absorption of the pharmaceutical.

However, as can be seen from Fig. 7, at additive concentrations of 10–50 g/liter, often used in standard binding studies, the fraction of bound active ingredient can readily amount to 30%, even in cases of moderate binding. Additive concentrations of this order of magnitude are never applied in practice. The graphs of Figs. 6 and 7 may, therefore, assist in using the large body of available binding data for a sensible assessment of the degree of binding in systems of practical relevance.

REFERENCES

(1) "Kollidon®—Marken", BASF-Aktiengesellschaft, Ludwigshafen/Rhein, West Germany, Firmenschrift Nr. B 382 d, December 1980.

(2) H. F. Kauffmann and J. W. Breitenbach, *Angew. Makromol. Chem.*, **45,** 167 (1975).

(3) K. Seelert, *Acta Pharm. Technol.*, **21,** 211 (1975).

(4) P. H. List and U. A. Muazzam, *Pharm. Ind.*, **41,** 459 (1979).

(5) R. Hüttenrauch and I. Keiner, *Pharmazie*, **28,** 137 (1973).

(6) S. S. Kornblum and S. B. Stoopak, *J. Pharm. Sci.*, **62,** 43 (1973).

(7) S. Keipert, J. Becker, H.-H. Schultze, and R. Voigt, *Pharmazie*, **28,** 145 (1973).

(8) P. Molyneux and H. P. Frank, *J. Am. Chem. Soc.*, **83,** 3169 (1961).

(9) T. Higuchi and R. Kuramoto, *J. Am. Pharm. Assoc., Sci. Ed.*, **43,** 393 (1954).

(10) G. Jürgensen-Eide and P. Speiser, *Acta Pharm. Suec.*, **4,** 185 (1967).

(11) G. Jürgensen-Eide and P. Speiser, *Pharm. Acta Helv.*, **42,** 385 (1967).

(12) E. Ullmann, K. Thoma, and P. Mohrschulz, *Arch. Pharm. (Weinheim Ger.)*, **302,** 756 (1969).

(13) R. Ansel, H. Intorp, and E. Weisschedel, *Arzneim.-Forsch.*, **13,** 949 (1963).

(14) H. Jacobi, *ibid.*, **17,** 458 (1967).

(15) W. Scholtan, *ibid.*, **14,** 469 (1964).

(16) M. A. Kassem and A. G. Mattha, *Pharm. Acta Helv.*, **45,** 18 (1970).

(17) G. P. Polli and B. M. Frost, *J. Pharm. Sci.*, **58,** 1543 (1969).

(18) R. Voigt, H. H. Schultze, and S. Keipert, *Pharmazie*, **31,** 863 (1976).

(19) S. Keipert, I. Korner, and R. Voigt, *ibid.*, **32,** 357 (1977).

(20) K. Thoma and D. Steinbach, *Pharm. Ind.*, **38,** 841 (1976).

(21) R. Voigt, C. Gulde, and C. Fechner, *Pharmazie*, **33,** 732 (1978).

(22) S. Keipert, I. Korner, and R. Voigt, *ibid.*, **33,** 380 (1978).

(23) K. Thoma, E. Ullmann, and P. Mohrschulz, *Arch. Pharm. (Weinheim Ger.)*, **311,** 205 (1978).

(24) W. D. McFarlane, *J. Inst. Brew.*, **67,** 502 (1961).

(25) W. D. McFarlane and M. J. Vader, *ibid.*, **68,** 254 (1962).

(26) W. D. McFarlane and P. T. Sword, *ibid.*, **68,** 344 (1962).

(27) W. D. Loomis and J. Battaile, *Phytochemistry*, **5,** 423 (1966).

(28) S. Lang, in "Abstract," Jahreskongress der Arbeitsgemeinschaft für Pharmazeutische Verfahrenstechnik (APV), 1978, p. 61.

(29) K. H. Frömming, W. Ditter, and D. Horn, *J. Pharm. Sci.*, **70,** 738 (1981).

(30) R. V. Quincey and C. H. Gray, *J. Endocrinol.*, **26,** 509 (1963).

(31) W. Scholtan, *Arzneim.-Forsch.*, **14,** 146 (1964).

(32) J. Clausen, *J. Pharmacol. Exp. Ther.*, **153,** 167 (1966).

(33) W. Nichol and D. J. Winzer, *J. Phys. Chem.*, **68,** 2455 (1964).

(34) P. F. Cooper and G. C. Wood, *J. Pharm. Pharmacol.*, **20,** Suppl. 150 (1968).

(35) S. Keresztes-Nagy, R. F. Mais, Y. T. Oester, and J. F. Zaroslinski, *Anal. Biochem.*, **48,** 80 (1972).

(36) H. Kurz, H. Trunk, and B. Weitz, *Arzneim.-Forsch.*, **27,** 1373 (1977).

(37) G. Alibert, *J. Chromatogr.*, **80,** 173 (1973).

(38) Th. M. Dougherty and A. I. Schepartz, *ibid.*, **43,** 397 (1969).

(39) J. Lerner, Th. M. Dougherty, and A. I. Schepartz, *ibid.*, **37,** 453 (1968).

(40) E. Bayer, "Gaschromatographie," 2. Aufl., Springer-Verlag, Berlin, West Germany, 1962.

(41) W. A. P. Luck, *Kolloid Z. Z. Polym.*, **223,** 110 (1968).

(42) I. M. Klotz, F. M. Walker, and R. B. Pivan, *J. Am. Chem. Soc.*, **68,** 1486 (1946).

(43) G. Scatchard, *Ann. N.Y. Acad. Sci.*, **51,** 660 (1949).

(44) W. Scholtan, *Makromol. Chem.*, **11,** 131 (1953).

(45) J. A. Plaizier-Vercammen and R. E. DeNève, *J. Pharm. Sci.*, **69,** 1403 (1980).

(46) P. Speiser, *Dtsch. Apoth. Ztg.*, **115** (12), 389 (1975).

(47) H. Sekikawa, K. Ito, T. Artia, R. Hori, and M. Nakano, *Chem. Pharm. Bull.*, **27,** 1106 (1979).

ACKNOWLEDGMENTS

The authors thank Dr. S. Lang, Dr. V. Bühler, and Dr. K. Seelert for valuable discussions. The skillful technical assistance of Mr. H. P. Kaub is gratefully acknowledged. Dedicated to Professor Werner Reif on the occasion of his 60th birthday.

Isocratic High-Performance Liquid Chromatographic Method for the Determination of Tricyclic Antidepressants and Metabolites in Plasma

S. M. JOHNSON, C. CHAN, S. CHENG, J. L. SHIMEK, G. NYGARD, and S. K. WAHBA KHALIL ˣ

Received August 21, 1981, from the *Pharmacokinetic Drug Analysis Laboratory, College of Pharmacy, North Dakota State University and Veterans Administration Medical Center, Fargo, ND 58102.* Accepted for publication December 10, 1981.

Abstract □ An isocratic high-performance liquid chromatographic method for the determination of six tricyclic antidepressants and their major metabolites is presented. Hexane containing 0.5% diethylamine was used as an extraction solvent to minimize adsorption onto glass. A reversed-phase cyanopropylsilane column was used with a mobile phase consisting of 70% acetonitrile and 30% 0.03 *M* acetate buffer, pH 7.0. Good identification and quantitation were obtained by the use of both UV detection at 245 nm and spectrofluorometric detection with an excitation wavelength of 276 nm and an emission filter with a 370-nm cutoff. A minimum detectable limit of <5 ng/ml of plasma is possible with this system. The reproducibility and precision of the method are shown from the analysis of samples containing 20–400 ng/ml in plasma.

Keyphrases □ Antidepressants—tricyclic, isocratic high-performance liquid chromatographic method for the determination of metabolites in plasma □ Metabolites—isocratic high-performance liquid chromatographic method for the determination of tricyclic antidepressants in plasma □ High-performance liquid chromatography—isocratic determination of tricyclic antidepressants and metabolites in plasma

Tricyclic antidepressants have been used extensively in the treatment of psychiatric patients suffering from depression. The relationship between the plasma concentration of these drugs and their clinical effect on depressive symptoms is controversial (1), but monitoring therapeutic levels is important, since the side effects of these drugs are quite common and mainly dose related (2). The major metabolic pathways are demethylation and hydroxylation (3).

In a recent two-part review article (4, 5), both the methodology and the pharmacokinetics of tricyclics were reviewed. The methodology review lists several methods for the determination of tricyclics and their metabolites. Many of the methods, including UV spectrometry (6, 7), fluorimetry (8), and TLC (9), are nonspecific, since the compounds are difficult to separate and the major metabolites have spectral characteristics similar to the parent drugs. Radioimmunoassay has been used, although many antisera show substantial cross reactivity (10).

GLC methods require either derivatization of the compounds or a selective detector (11–14). Quantitation of tricyclic antidepressants and their metabolites have also been performed by high-performance liquid chromatography (HPLC) (15–19), but most of the reported methods did not include the hydroxy metabolites which have been shown to be pharmacologically active (20). Most methods also involve an elaborate multistep extraction procedure.

The present report describes the separation and determination of the most commonly prescribed tricyclic antidepressants. The method involves one extraction step followed by HPLC using a reversed-phase cyanopropylsilane column and dual UV and fluorescence detection. The method is applicable to the direct determination of plasma levels in the presence of one or more of several drugs which might be prescribed concurrently. The applicability of the method has been demonstrated by the analysis of plasma from patients receiving tricyclic antidepressants. The determination of amitriptyline includes the simultaneous analysis of its most important metabolites in plasma.

EXPERIMENTAL

Instrumentation—A high-performance liquid chromatograph[1] was equipped with a fluorometric detector[2] and a cyanopropylsilane[3] column (250 mm long, 4.6-mm i.d.). The degassed mobile phase was pumped through the column at 3.0 ml/min (20–22 mPa). The column compart-

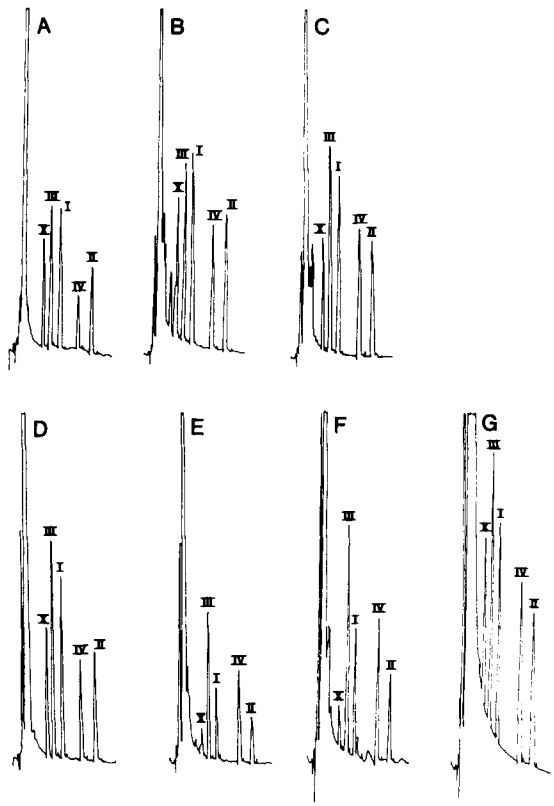

Figure 1—*Chromatograms of the extracts of 1.0 ml of plasma containing 200 ng/ml each of I, II, III, and IV. The extracts were reconstituted with 100 μl of methanol, injection volume 30 μl, absorbance at 245 nm. Key: (A) hexane; (B) hexane plus 2% isoamyl alcohol; (C) heptane plus 4% isobutyl alcohol; (D) hexane plus 0.5% diethylamine; (E) methylene chloride; (F) methylene chloride plus 0.5% diethylamine; (G) ethyl acetate.*

[1] Model 1084B chromatograph with variable wavelength UV detector and autoinjector, Hewlett-Packard Co., Avondale, Pa.
[2] FS-970, Schoeffel, Westwood, N.J.
[3] Ultrasphere Cyano, Beckman Instruments, Inc., Berkeley, Calif.

0022-3549/82/0900-1027$01.00/0

Table I—Precision of Tricyclic Antidepressant Assay

Amount Added, ng/ml	Amount Found, ng/ml[a,b] I	II	III	IV	V	VI	VII	VIII	IX
20	19.6 ± 1.1	14.6 ± 1.4	19.3 ± 2.5	17.6 ± 2.6	37.4 ± 3.1	30.5 ± 3.3	19.3 ± 2.7	17.7 ± 1.5	14.2 ± 1.5
50	42.1 ± 3.9	38.3 ± 2.4	48.2 ± 1.4	40.8 ± 6.0	62.6 ± 4.4	58.1 ± 4.9	50.1 ± 15.2	47.6 ± 6.7	47.7 ± 11.9
100	105.5 ± 2.3	96.9 ± 10.0	95.0 ± 5.0	87.5 ± 10.4	116.2 ± 6.8	101.8 ± 6.2	101.6 ± 11.9	95.8 ± 6.0	102.2 ± 2.2
150	150.4 ± 4.8	148.4 ± 5.9	134.2 ± 11.4	129.0 ± 8.3	182.1 ± 19.7	175.5 ± 25.5	159.4 ± 10.7	154.2 ± 14.6	149.3 ± 8.1
200	200.2 ± 8.9	183.4 ± 9.4	198.0 ± 10.6	184.7 ± 24.5	224.6 ± 11.7	211.3 ± 2.5	219.9 ± 12.9	203.2 ± 6.6	225.2 ± 13.0
300	289.2 ± 27.1	285.9 ± 29.1	310.1 ± 15.8	306.0 ± 31.4	318.9 ± 21.8	317.8 ± 37.0	304.7 ± 34.4	289.6 ± 27.2	300.1 ± 4.9
400	403.3 ± 21.0	402.5 ± 21.4	400.8 ± 26.5	404.1 ± 25.7	407.5 ± 26.7	394.2 ± 38.7	393.1 ± 16.4	402.0 ± 15.0	403.7 ± 19.3
Correlation coefficient	0.994	0.993	0.995	0.991	0.993	0.984	0.991	0.995	0.995
Total n	32	31	35	33	30	32	32	32	29
R^2	0.989	0.987	0.989	0.983	0.985	0.968	0.990	0.990	0.990

[a] Absorbance at 245 nm. [b] For each compound values are the mean ±*SD*.

ment was maintained at 45°. The UV was monitored at 245 nm and the fluorometer was set at an excitation wavelength of 276 nm. An emission cutoff filter (type 370 nm) was used.

Chemicals and Reagents—Sodium acetate, sodium phosphate, acetic acid, phosphoric acid, diethylamine, sodium hydroxide, isoamyl alcohol, and isobutyl alcohol were reagent grade. HPLC grade methanol, acetonitrile, hexane, heptane, ethyl acetate, and methylene chloride were used. Amitriptyline hydrochloride (I)[4], nortriptyline hydrochloride (II)[5], 10-hydroxyamitriptyline (III)[4], 10-hydroxynortriptyline hydrogen maleate (IV)[4], imipramine hydrochloride (V)[6], desipramine hydrochloride (VI)[7], doxepin hydrochloride (VII)[8], demethyldoxepin hydrochloride (VIII)[8], protriptyline hydrochloride (IX)[4], and trimipramine hydrochloride (X)[9] were obtained commercially.

Mobile Phase—Sodium acetate solution (0.03 *M*) was prepared in deionized distilled water, and the pH was adjusted to 7 by the gradual addition of acetic acid. The mobile phase consisted of 70% acetonitrile and 30% buffer.

Solution Preparation—*Drug Stock Solutions*—Separate solutions of each drug and metabolite were made containing 5 mg of free base/10 ml of methanol.

Working Drug Solutions—Dilutions to working concentrations (5 ng/μl) were made with methanol for drug–metabolite groups (I–IV; V–VI; VII–VIII) or for a single drug (IX).

Extraction Solution—The internal standard stock solution (X) was diluted with hexane containing 0.5% diethylamine to a concentration of 20 ng/ml.

Sample Preparation—An aliquot (4–80 μl) of the drug working solution containing 20–400 ng, 0.5 ml of 0.1 *M* NaOH, and 10 ml of extraction solution were added to 1.0 ml of heparinized plasma in a 15-ml screwcapped centrifuge tube. The tubes were vortexed for 10 sec and centrifuged for 5 min at 900×*g*. A 9-ml volume of the organic phase was transferred to special concentration tubes[10] and evaporated to dryness at 30° under a gentle stream of nitrogen.

HPLC Separation and Quantitation—The residue was dissolved in 100 μl of methanol and transferred to a polypropylene micro-vial[11] before injection of 30 μl into the HPLC. A standard curve was constructed utilizing a minimum of four replicate plasma extractions simulating concentrations of drugs and metabolites from 20 to 400 ng/ml. The chromatograms were recorded at a chart speed of 5 mm/min. The peak heights were measured, and the ratios (drug/internal standard and metabolite/internal standard) were calculated and plotted *versus* concentration expressed as nanograms per milliliter of plasma.

Interferences—Possible interferences from normal plasma constituents, as well as other drugs and metabolites, were studied.

Factors Affecting Extraction Efficiency—The amounts of drugs and their metabolites extracted at pH 12 were studied using hexane, methylene chloride, ethyl acetate, hexane containing 0.5% diethylamine, hexane containing 2% isoamyl alcohol, methylene chloride containing 0.5% diethylamine, and heptane containing 4% isobutyl alcohol. Extractions were carried out at three different pH values (7.4, 9.5, and 12) with the following solvents: hexane, hexane containing 0.5% diethylamine, and methylene chloride.

Adsorption onto Glass—The effect of several agents on the adsorption of tricyclics and their metabolites onto glass during extraction and evaporation was studied. Diethylamine, isoamyl alcohol, isobutyl alcohol, and silanization of glass were tried.

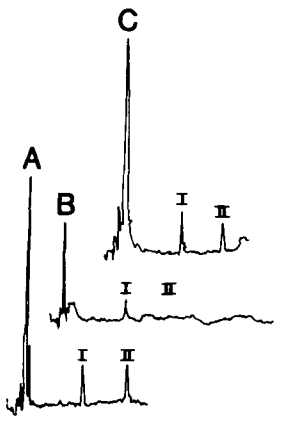

Figure 2—*Chromatograms showing the effect of solvents on adsorption of I and II onto glass. Injection volume 20 μl of 0.2 ng/μl, absorbance at 245 nm. Key: (A) methanol; (B) hexane; (c) hexane plus 0.5% diethylamine.*

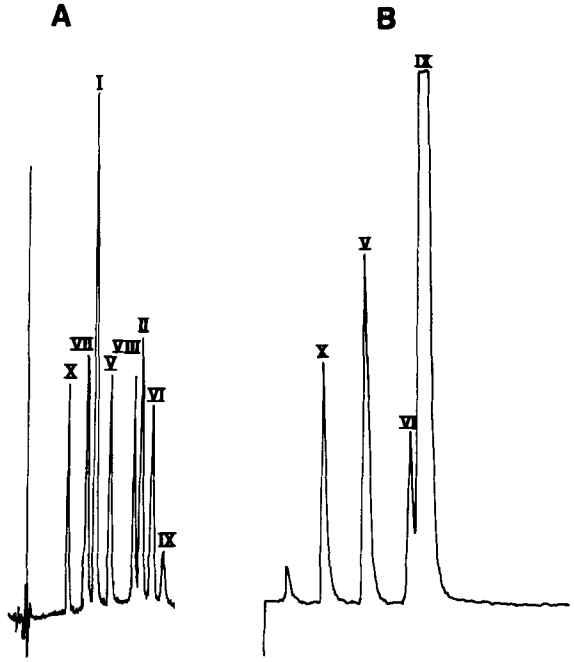

Figure 3—*Chromatograms of a mixture of 40 ng each of I, II, V–X. Key: (A) absorbance at 245 nm; (B) fluorescence at 276-nm excitation and 370-nm emission cutoff filter.*

[4] Merck, Sharp & Dohme Research Laboratory, Rahway, N.J.
[5] Eli Lilly and Co., Indianapolis, Ind.
[6] CIBA Pharmaceutical Co., Summit, N.J.
[7] Merrell-National Laboratories, Cincinnati, Ohio.
[8] Pfizer, Inc., New York, N.Y.
[9] Ives Laboratories, Inc., New York, N.Y.
[10] Concentratubes, Laboratory Research Co., Los Angeles, Calif.
[11] Micro-volume sample flask, P. Weidmann & Co., Romanshorn, Switzerland.

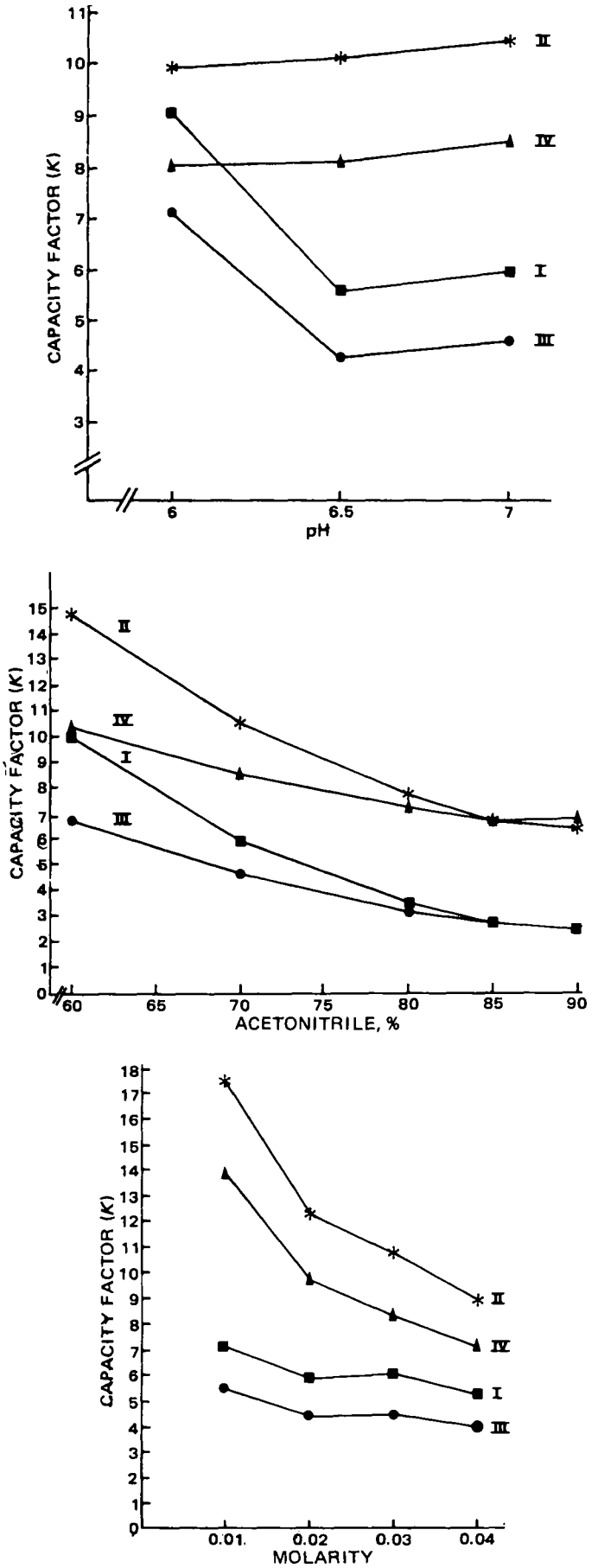

Figure 4—*Effect of pH, percent acetonitrile, and molarity of the mobile phase on capacity factor (K) of I–IV.*

Table II—Drugs Tested for Possible Interference

Drug	Retention Time, min	Absorbance[a]	Fluorescence[b]
Diazepam	SF[c]	+	–
Dextromethorphan	SF	+	+
Iminodibenzyl (Metabolite of Desipramine)	SF	+	+
Lidocaine	SF	+	–
Loxapine	1.90	+	–
Fluphenazine	2.05	+	+
Perphenazine	2.21	+	–
Haloperidol	2.29	+	–
Amoxapine	2.82	+	–
Trimipramine (X)	3.75	+	+
Thiothixene	3.90	+	+
Chlorprothixene	4.02	+	+
Quinidine	4.11	+	+
Trifluoperazine	4.55	+	+
10-Hydroxyamitriptyline (III)	4.66	+	–
Propranolol	4.82	–	+
Doxepin (VII)	5.08	+	–
Chlorpromazine	5.10	+	–
N-Acetylprocainamide	5.15	+	+
Amitriptyline (I)	5.22	+	–
Clomipramine	5.70	+	–
Procainamide	5.80	+	+
Imipramine (V)	6.20	+	+
10-Hydroxynortriptyline (IV)	6.41	+	–
Disopyramide	6.66	+	–
Thioridazine	6.88	+	+
Nortriptyline (II)	7.08	+	–
Demethyldoxepin (VIII)	7.12	+	–
Maprotiline	7.51	+	–
Desipramine (VI)	7.65	+	+
Protriptyline (IX)	7.90	+	+
Mesoridazine	8.75	+	+

[a] Absorbance at 245 nm. [b] Fluorescence at 276/370 nm. [c] SF is the solvent front.

Patient Samples—Heparinized plasma samples from patients receiving oral tricyclic antidepressant therapy were extracted in duplicate using the same procedure. The amounts of drug and metabolites in patient samples were calculated by comparison with a standard curve prepared daily.

RESULTS AND DISCUSSION

The choice of extraction conditions is based on a compromise between extraction yield and selectivity of extraction. Extraction with hexane afforded a cleaner extract than several other solvents (Fig. 1). The addition of 0.5% diethylamine to the hexane minimized the adsorption of the tricyclics onto the glass surface (Fig. 2). This observation confirms that reported previously (21). Evaporation under nitrogen at 30° minimized volatilization of drugs and metabolites and yet is sufficient for ready evaporation of diethylamine and hexane. In addition, the use of an organic phase–aqueous phase ratio in extraction of 10:1.5 made it possible to have a high yield in one extraction step. A slightly higher yield was obtained at pH 12 than pH 7.4 or 9.5. Reconstitution in methanol was chosen over the mobile phase because glass adsorption from acetonitrile considerably reduced the peak heights and prevented accurate quantitation. The effect was the greatest for the metabolites.

The use of a cyanopropylsilane column in a reversed-phase mode with a mobile phase of 70% acetonitrile and 30% acetate buffer (0.03 *M*, pH 7) produced good separation of several tricyclics (Fig. 3) and between each drug and its respective major metabolites. The separation of I–IV depends on the pH and molarity of the buffer as well as the percent acetonitrile in the mobile phase. This is illustrated by the change of *K* values (Fig. 4). The pH, molarity, and percent acetonitrile of the mobile phase may be varied slightly to obtain separation on cyanopropylsilane columns of different manufacturers or on a column after a period of use. The use of fluorescence detection is not necessary for the analysis, since all of the drugs and metabolites absorb at 245 nm and only V, VI, and IX fluoresce. Dual detection using both absorbance and fluorescence is helpful, however, to afford exact identification and good quantitation. The drugs may be monitored at 254 nm with only a slight loss of sensitivity. Monitoring at 288 nm or by fluorescence will enhance the sensitivity for IX. Trimipramine was chosen as the internal standard because it has almost equal absorbance and fluorescence under the experimental conditions and is well separated from all the drugs and metabolites.

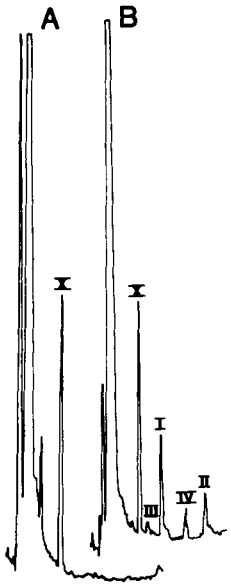

Figure 5—*Typical chromatograms of extracts of 1 ml of plasma, injection volume 30 μl, absorbance at 245 nm. Key: (A) drug free; (B) patient receiving I orally. Concentrations of compounds expressed as ng/ml of plasma are I = 87, II = 50, III = 7, and IV = 38.*

The ratios of the peak heights of the drugs and metabolites to the peak height of the internal standard were calculated. Statistical analysis of the data (Table I) by linear regression indicated linearity and reproducibility in the 20–400-ng/ml range of plasma. This range includes the therapeutic range of the drugs. Absolute recovery of the drugs and metabolites ranged from 55 to 80% of the theoretical amounts. This low recovery may be responsible for the variation in the amount found at low concentrations (Table I). The minimum detectable limit for the compounds is <5 ng/ml of plasma.

No interference from normal plasma constituents was observed (Fig. 5A). Also, several drugs which might be prescribed simultaneously with tricyclics were chromatographed. The retention times are listed in Table II.

The method has been applied to many patient samples and is being used routinely in the laboratory for monitoring therapeutic levels (Fig. 5B). Major advantages of the method are its simplicity, rapidity, and high sensitivity. All of the drugs and metabolites, including the 10-hydroxy metabolites of amitriptyline and nortriptyline, are determined using a single procedure. Adsorbance of the drugs onto glass has been minimized.

REFERENCES

(1) G. D. Burrows, B. A. Scoggins, L. R. Purecek, and B. Davis, *Clin. Pharmacol. Ther.*, **16,** 637 (1974).

(2) C. J. S. Walter, *Proc. R. Soc. Med.*, **64,** 282 (1971).

(3) B. R. Knapp, T. E. Gassney, R. E. McMahon, and G. Kiplinger, *J. Pharmacol. Exp. Ther.*, **180,** 784 (1972).

(4) B. A. Scoggins, K. P. Maguire, T. R. Norman, and G. D. Burrows, *Clin. Chem.*, **26,** 5 (1980).

(5) *Ibid.*, **26,** 805 (1980).

(6) J. E. Wallace and E. V. Dahl, *J. Forensic Sci.*, 12, 484 (1967).

(7) C. R. Henwood, *ibid.*, **15,** 47 (1975).

(8) J. P. Moody, S. F. White, and G. J. Naylor, *Clin. Chem. Acta*, **43,** 355 (1973).

(9) D. B. Faber, C. Mulder, and W. A. in't Veld, *J. Chromatogr.*, **100,** 55 (1974).

(10) K. P. Maguire, G. D. Burrows, T. R. Norman, and B. A. Scoggins, *Clin. Chem.*, **24,** 549 (1978).

(11) D. N. Bailey and P. I. Jatlow, *ibid.*, **22,** 777 (1976).

(12) S. Dawling and R. A. Braithwaite, *J. Chromatogr.*, **146,** 449 (1978).

(13) P. C. N. Eichholtz, *ibid.*, 111, 456 (1975).

(14) J. Vasillades and K. C. Bush, *Anal. Chem.*, **48,** 1708 (1976).

(15) P. A. Reece and R. Zacest, *J. Chromatogr.*, **163,** 310 (1979).

(16) B. Melström and R. Braithwaite, *ibid.*, **157,** 379 (1978).

(17) H. F. Proelss, H. J. Lohmann, and D. G. Miles, *Clin. Chem.*, **24,** 1948 (1978).

(18) R. F. Suckow and T. B. Cooper, *J. Pharm. Sci.*, **70,** 257 (1981).

(19) I. D. Watson and M. J. Stewart, *J. Chromatogr.*, **132,** 155 (1977).

(20) W. Z. Potter, H. M. Calil, A. A. Manian, A. P. Zavadil, and F. K. Goodwin, *Biol. Psychiatry*, **14,** 601 (1979).

(21) J. E. Burch, M. A. Raddats, and S. G. Thompson, *J. Chromatogr.*, **162,** 351 (1979).

ACKNOWLEDGMENTS

The authors acknowledge CIBA Pharmaceutical and Co., Eli Lilly and Co., Merck, Sharp & Dohme, Merrell-National Laboratories, and Pfizer, Inc., for providing free authentic samples of the drugs and their metabolites.

Chelation of Mercury by Polymercaptal Microspheres: New Potential Antidote for Mercury Poisoning

S. MARGEL ˣ **and J. HIRSH**

Received February 18, 1981, from the *Department of Plastics Research, The Weizmann Institute of Science, Rehovot, Israel.* Accepted for publication November 17, 1981.

Abstract □ Newly synthesized polymercaptal microspheres of 0.8 ± 0.02 μm were shown to have a specific and fast intake of mercury compounds over a whole range of pH while maintaining low toxicity. The microspheres bind easily with mercury compounds which are already bound to the biological mercury binders, albumin or cysteine. Mercury was recovered completely from the microspheres by using a solution of thiourea in hydrochloric acid. Due to their high surface area, low toxicity, and strong affinity toward mercury compounds, the microspheres have a potential use as a new oral drug for treatment in cases of mercury poisoning.

Keyphrases □ Microspheres—chelation of mercury, polymercaptal, new potential antidote for mercury poisoning □ Mercury—chelation by polymercaptal microspheres, new potential antidote for poisoning □ Chelation—mercury, polymercaptal microspheres, new potential antidote for mercury poisoning

Mercury compounds, both organic and inorganic, constitute an environmental and agricultural hazard (1, 2). Severe poisoning is known to cause brain damage, fetal disabilities, and death (2, 3). The therapy for mercury poisoning includes intravenous administration of the chelating drugs dimercaprol and/or penicillamine (4).

0022-3549/82/0900-1030$01.00/0

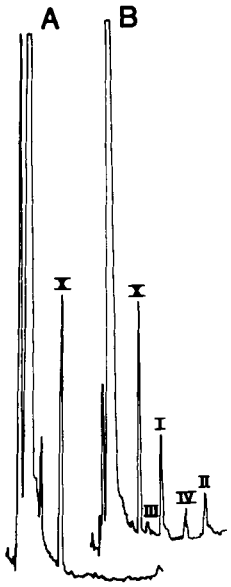

Figure 5—*Typical chromatograms of extracts of 1 ml of plasma, injection volume 30 μl, absorbance at 245 nm. Key: (A) drug free; (B) patient receiving I orally. Concentrations of compounds expressed as ng/ml of plasma are I = 87, II = 50, III = 7, and IV = 38.*

The ratios of the peak heights of the drugs and metabolites to the peak height of the internal standard were calculated. Statistical analysis of the data (Table I) by linear regression indicated linearity and reproducibility in the 20–400-ng/ml range of plasma. This range includes the therapeutic range of the drugs. Absolute recovery of the drugs and metabolites ranged from 55 to 80% of the theoretical amounts. This low recovery may be responsible for the variation in the amount found at low concentrations (Table I). The minimum detectable limit for the compounds is <5 ng/ml of plasma.

No interference from normal plasma constituents was observed (Fig. 5A). Also, several drugs which might be prescribed simultaneously with tricyclics were chromatographed. The retention times are listed in Table II.

The method has been applied to many patient samples and is being used routinely in the laboratory for monitoring therapeutic levels (Fig. 5B). Major advantages of the method are its simplicity, rapidity, and high sensitivity. All of the drugs and metabolites, including the 10-hydroxy metabolites of amitriptyline and nortriptyline, are determined using a single procedure. Adsorbance of the drugs onto glass has been minimized.

REFERENCES

(1) G. D. Burrows, B. A. Scoggins, L. R. Purecek, and B. Davis, *Clin. Pharmacol. Ther.*, **16,** 637 (1974).

(2) C. J. S. Walter, *Proc. R. Soc. Med.*, **64,** 282 (1971).

(3) B. R. Knapp, T. E. Gassney, R. E. McMahon, and G. Kiplinger, *J. Pharmacol. Exp. Ther.*, **180,** 784 (1972).

(4) B. A. Scoggins, K. P. Maguire, T. R. Norman, and G. D. Burrows, *Clin. Chem.*, **26,** 5 (1980).

(5) *Ibid.*, **26,** 805 (1980).

(6) J. E. Wallace and E. V. Dahl, *J. Forensic Sci.*, 12, 484 (1967).

(7) C. R. Henwood, *ibid.*, **15,** 47 (1975).

(8) J. P. Moody, S. F. White, and G. J. Naylor, *Clin. Chem. Acta*, **43,** 355 (1973).

(9) D. B. Faber, C. Mulder, and W. A. in't Veld, *J. Chromatogr.*, **100,** 55 (1974).

(10) K. P. Maguire, G. D. Burrows, T. R. Norman, and B. A. Scoggins, *Clin. Chem.*, **24,** 549 (1978).

(11) D. N. Bailey and P. I. Jatlow, *ibid.*, **22,** 777 (1976).

(12) S. Dawling and R. A. Braithwaite, *J. Chromatogr.*, **146,** 449 (1978).

(13) P. C. N. Eichholtz, *ibid.*, 111, 456 (1975).

(14) J. Vasillades and K. C. Bush, *Anal. Chem.*, **48,** 1708 (1976).

(15) P. A. Reece and R. Zacest, *J. Chromatogr.*, **163,** 310 (1979).

(16) B. Melström and R. Braithwaite, *ibid.*, **157,** 379 (1978).

(17) H. F. Proelss, H. J. Lohmann, and D. G. Miles, *Clin. Chem.*, **24,** 1948 (1978).

(18) R. F. Suckow and T. B. Cooper, *J. Pharm. Sci.*, **70,** 257 (1981).

(19) I. D. Watson and M. J. Stewart, *J. Chromatogr.*, **132,** 155 (1977).

(20) W. Z. Potter, H. M. Calil, A. A. Manian, A. P. Zavadil, and F. K. Goodwin, *Biol. Psychiatry*, **14,** 601 (1979).

(21) J. E. Burch, M. A. Raddats, and S. G. Thompson, *J. Chromatogr.*, **162,** 351 (1979).

ACKNOWLEDGMENTS

The authors acknowledge CIBA Pharmaceutical and Co., Eli Lilly and Co., Merck, Sharp & Dohme, Merrell-National Laboratories, and Pfizer, Inc., for providing free authentic samples of the drugs and their metabolites.

Chelation of Mercury by Polymercaptal Microspheres: New Potential Antidote for Mercury Poisoning

S. MARGEL ˣ **and J. HIRSH**

Received February 18, 1981, from the *Department of Plastics Research, The Weizmann Institute of Science, Rehovot, Israel.* Accepted for publication November 17, 1981.

Abstract □ Newly synthesized polymercaptal microspheres of 0.8 ± 0.02 μm were shown to have a specific and fast intake of mercury compounds over a whole range of pH while maintaining low toxicity. The microspheres bind easily with mercury compounds which are already bound to the biological mercury binders, albumin or cysteine. Mercury was recovered completely from the microspheres by using a solution of thiourea in hydrochloric acid. Due to their high surface area, low toxicity, and strong affinity toward mercury compounds, the microspheres have a potential use as a new oral drug for treatment in cases of mercury poisoning.

Keyphrases □ Microspheres—chelation of mercury, polymercaptal, new potential antidote for mercury poisoning □ Mercury—chelation by polymercaptal microspheres, new potential antidote for poisoning □ Chelation—mercury, polymercaptal microspheres, new potential antidote for mercury poisoning

Mercury compounds, both organic and inorganic, constitute an environmental and agricultural hazard (1, 2). Severe poisoning is known to cause brain damage, fetal disabilities, and death (2, 3). The therapy for mercury poisoning includes intravenous administration of the chelating drugs dimercaprol and/or penicillamine (4).

0022-3549/82/0900-1030$01.00/0

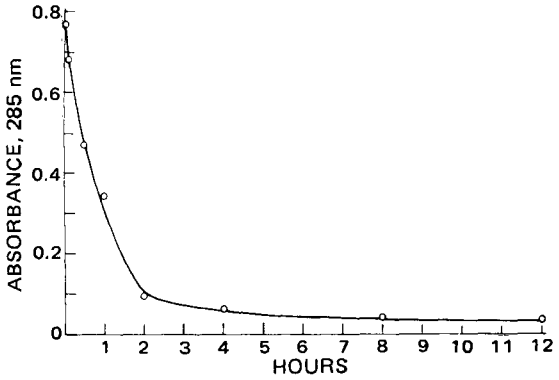

Figure 1—*Change of the absorbance at 285 nm during the reaction between glutaraldehyde and pentaerythritol tetrathioglycolate. The reaction was carried out by stirring 4.5 mmoles of glutaraldehyde with 4.5 mmole of pentaerythritol tetrathioglycolate in 30 ml of H_2O at pH 4.0, at room temperature.*

Recently, new types of water soluble drugs, 2,3-dimercapto-succinic acid (5) and dithiocarbamate compounds (6) were synthesized and suggested as intravenously administered antidotes for mercury poisoning. Another approach which has been tried successfully in cases of mercury poisoning, in particular methyl mercury, is based on the oral administration of insoluble polythiol resins which bind mercury compounds and thereby increase their fecal excretion (7–9).

In the present study the use of insoluble chelating microspheres specific for mercury compounds as a potential oral antidote for mercury poisoning is suggested. For this purpose polymercaptal microspheres of 0.8 ± 0.02 μm were synthesized. The large surface area of these microspheres, as well as their low toxicity and strong affinity toward mercury compounds renders them as good candidates to be used in cases of mercury poisoning.

EXPERIMENTAL

Reagents—All reagents were of analytical grade and used as received. A phosphate-buffered solution was prepared by adding sodium hydrogen phosphate solution (0.1 *M*) to an aqueous solution of sodium dihydrogen phosphate (0.1 *M*) until a pH of 7.2 was reached. The solution was then diluted 10 times with distilled water. Phosphate-buffered saline solution was prepared by adding sodium chloride to the phosphate-buffered solution to obtain a final concentration of 0.15 *M*. The following reagents gave a very small mercury blank value and could be used without further purification: sulfuric acid, hydrochloric acid, stannous chloride, hydroxylamine hydrochloride, potassium permanganate, and deionized water. The stock solution of mercuric chloride and of methyl mercury chloride was prepared in 10% HCl. Standards were prepared from the stock solution by diluting with 10% HCl. Glassware was soaked in concentrated nitric acid for several hours before use.

Mercury Analysis—Mercury was determined by cold vapor atomic absorption with a cold vapor analyser kit[1] (10). The limit of detection for this procedure is 0.15 ng in 1.0 ml of solution.

Binding of Mercury Compounds to Albumin—A phosphate-buffered saline solution containing 4.0% normal human albumin was shaken for 2 hr with methyl mercury chloride or with mercuric chloride (20 ppm Hg). The binding with mercuric chloride was determined by placing the solution into ultrafiltration membranes[2] and centrifuging it for 5 min at 1000 rpm. The binding with methyl mercury chloride was determined by ultrafiltration of the solution through a dialyzing membrane with a permeability corresponding to a molecular weight of 10,000. In both cases mercury was not detected in the ultrafiltrate, indicating that the mercury compounds were completely bound to albumin.

Chelating Microspheres—An aqueous solution containing 0.2% (v/v) polyoxyethylene sorbitan monolaurate[3] as surfactant and 5% (v/v) pentaerythritol tetrathioglycolate was vigorously stirred for several hours until a stable aqueous emulsion of pentaerythritol tetrathioglycolate was produced. Thereafter, 5.5 ml of 25% glutaraldehyde was added to the emulsion solution which was then shaken for 12 hr. The reaction product was composed of a solid sticky compound that resulted from the agglutination of chelating microspheres and 60% disperse solid chelating microspheres. The microspheres were separated by decantation from the sticky part and cleaned from impurities either by dialysis or by slow spinning. The appearance and size of the microspheres was determined by scanning electron and light microscopy.

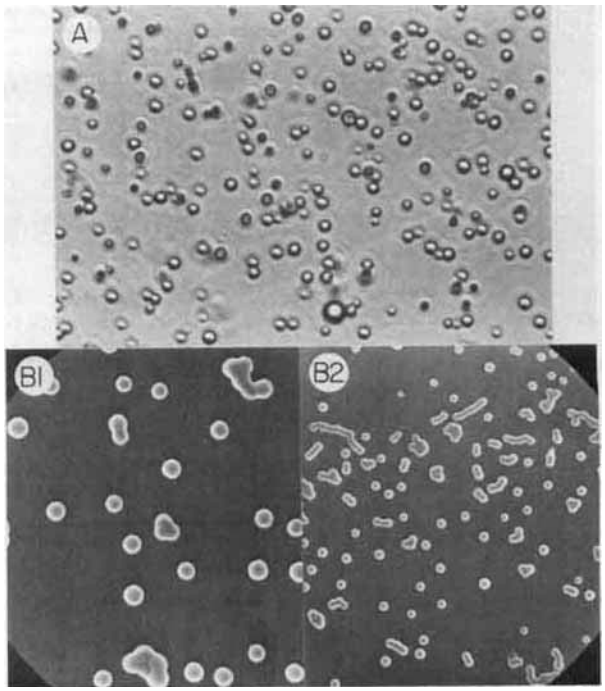

Figure 2—*(A) Light microscopy photomicrograph of chelating microspheres (×3000). (B) Scanning electron microscopic photomicrographs of chelating microspheres (1, 3100×; 2, 6300×).*

Toxicity—The acute median lethal dose (LD_{50} orally) to 40 mice[4] of the chelating microspheres was found to be 1.0 g/kg of body weight.

Intake of Mercury Compounds by Chelating Microspheres—The chelating microspheres were added to a stirred phosphate-buffered saline solution containing mercury compounds. Samples to be tested for mercury concentration were spun at 10,000 rpm for 10 min, thereby separating the solution from the precipitating microspheres. Control experiments were carried out in the same way but without chelating microspheres. (Spinning of the control samples did not show any precipitation of mercury compounds.)

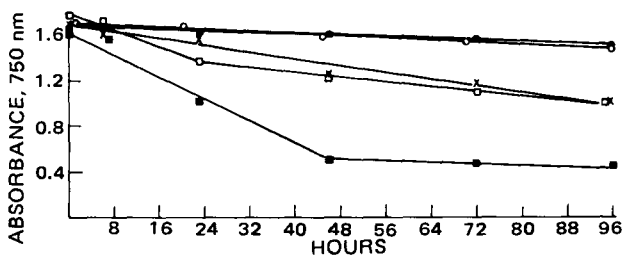

Figure 3—*Aggregation properties of the chelating microspheres. The absorbances at 750 nm were obtained by diluting 0.05 ml of the chelating microsphere suspension (containing 20 mg/ml) with 2.5 ml of H_2O. Key: (○) microspheres in H_2O; (×) microspheres in phosphate-buffered solution; (□) microspheres in phosphate-buffered saline solution; (■) microspheres in aqueous solution at pH 1.1; and (●) microspheres in phosphate-buffered saline solution under shaking.*

[1] Varian model 1200, Mulgrave, Victoria, Australia.
[2] Amicon 2100, CF-50, Lexington, Mass.
[3] Tween 20, Sigma Chemical Co., St. Louis, Mo.
[4] ICR mice.

Table I—Yield of Chelating Microspheres as a Function of pH [a]

pH [b]	Yield, %
7.0	70
4.0	60
2.0	6
0.5	1

[a] Glutaraldehyde (25%, 5.5 ml) was added to a shaken aqueous suspension (100 ml) of pentaerythritol tetrathioglycolate (5 ml), at various pHs. [b] pH 7.0 was obtained by adding sodium hydroxide to the aqueous suspension; pH 2.0 and pH 0.5 were obtained by adding hydrochloric acid to the aqueous suspension.

Recovery of Mercury Compounds from Chelating Microspheres—Fast and quantitative recovery of mercury compounds bound to microspheres was carried out by adding thiourea and hydrochloric acid to a stirred solution up to a final concentration of 1.0% CH_4N_2S and 0.5% HCl. In <10 min 100% of the mercuric chloride or of the methyl mercury chloride were recovered from the microspheres.

Photomicrographs—A photomicrograph of the microspheres was prepared by using a photographic flash light attached to a light microscope, thereby obtaining a focused picture of most of the moving microspheres.

A sample for scanning electron microscopy was prepared by drying a drop of a diluted solution of the microspheres on a cover slide which was then coated with gold.

RESULTS

The chelating microspheres were prepared by carrying out the reaction of glutaraldehyde and pentaerythritol tetrathioglycolate in the presence of the mentioned surfactant. The assumed reaction is shown in Scheme I:

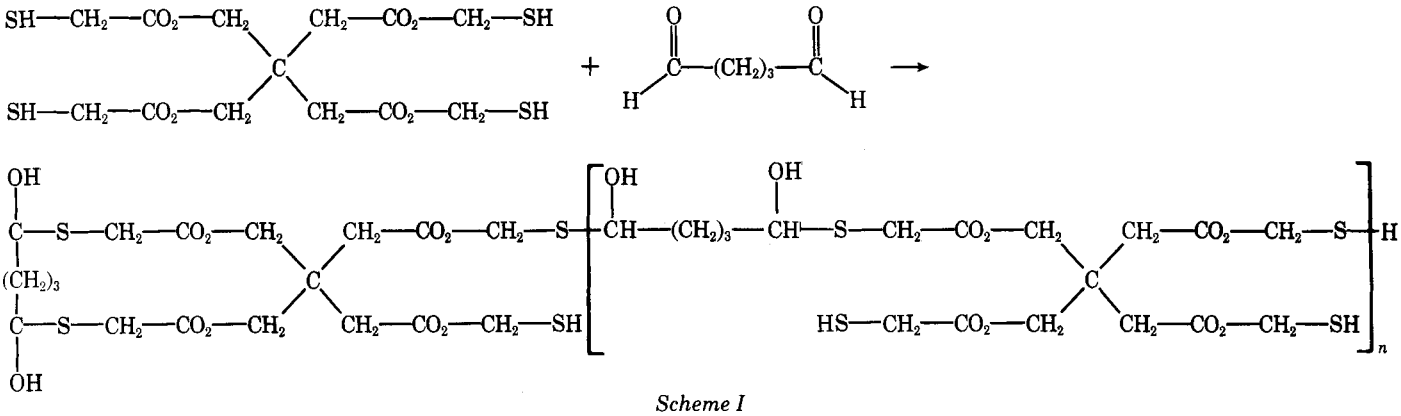

Scheme I

The rate of the reaction was measured by following the disappearance of the absorbance at 285 nm, related to the aldehyde groups of glutaraldehyde (Fig. 1). The surfactant stabilized micelles of pentaerythritol tetrathioglycolate which were interacted with glutaraldehyde to form the insoluble microspheres (Fig. 2).

The chelating microspheres were found to be monodispersed with a diameter of 0.8 ± 0.02 μm. They were spherical with a calculated surface area with an average microsphere size of 8.04×10^{-8} cm^2. The yield of the microspheres is dependent on the pH of the reaction. At a lower pH the microspheres tend to agglutinate more and therefore their yield is lower (Table I). The stability of the chelating microsphere suspension was checked by following the change in the turbidity of the suspension (Fig. 3). Aggregation of microspheres was indicated by the decrease in the turbidity. The chelating microsphere suspension is stable in water and there was no indication of aggregation even after a year. The microspheres tend to sink slowly to the bottom of the container and can be resuspended by shaking them again. The tendency of the microspheres to aggregate at acidic pH or at a high salt concentration was prevented by continuous shaking. Supporting evidence for the stability results was obtained by looking at the monodispersity of the microspheres under a light microscope (Fig. 2A). In water, the monodispersed microspheres moved in a Brownian motion, and there was no indication of agglutinated microspheres even after a year. Under strong acidic conditions (pH 1.0) large aggregates slowly formed. Attempts were made to obtain a scanning electron microscopic photomicrograph of the microspheres (Fig. 2B-1 and B-2). However, some small aggregates of microspheres were obtained

Table II—Intake of Mercury Compounds by Chelating Microspheres in Presence of Alkali and Alkaline Earth Metallic Compounds [a]

[Hg], ppm	Metallic Compounds, *M*	Microspheres, mg	Hg Intake, %	Ca, Na, and Mg Intake, %
20 (Mercuric Chloride)	0.001 $CaCl_2$	15	100	0
20 (Mercuric Chloride)	0.15 NaCl	15	100	0
1 (Mercuric Chloride)	0.1 NaCl + $CaCl_2$ + $MgCl_2$	10	~95	0
20 (Methyl Mercury Chloride)	0.15 NaCl	15	100	0
1 (Methyl Mercury Chloride)	0.1 NaCl + $CaCl_2$ + $MgCl_2$	10	~95	0

[a] The mercury compounds were stirred with chelating microspheres for 15 min in 20 ml of aqueous solution.

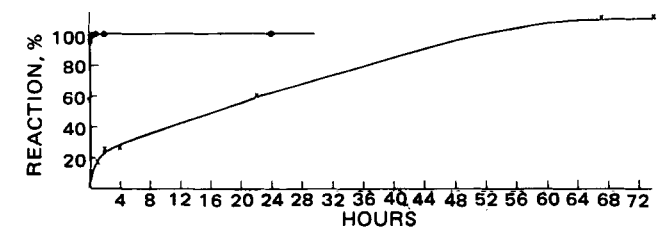

Figure 4—*Comparison of the rate of intake of mercuric chloride by chelating microspheres and agglutinated chelating microspheres. The reaction was carried out by stirring 10^{-4} M mercuric chloride (20 ppm Hg) and 20 mg of the chelating polymer in 50 ml of phosphate-buffered saline solution. Key: (●) chelating microspheres; (X) agglutinated chelating microspheres.*

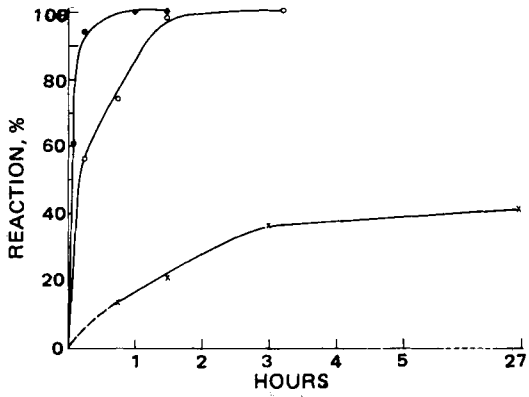

Figure 5—*Rate of intake of mercuric chloride by chelating microspheres. The reaction was carried out by stirring 10^{-4} M mercuric chloride in 80 ml of phosphate-buffered saline solution in presence of: (X) 3.5-mg microspheres; (○) 20-mg microspheres; (●) 60-mg microspheres.*

Table III—Percent Reaction of Mercuric Chloride with Chelating Microspheres at Various pH [a]

Time, min	pH [b]			
	2.0	4.0	7.1	8.5
10	98	98	97	98
120	100	100	100	97
240	100	100	100	95

[a] Mercuric chloride (10^{-4} *M*) was stirred with chelating microspheres (25 mg) in 50 ml of aqueous solution. [b] pH 2.0 and pH 4.0 were obtained by adding hydrochloric acid to 0.1 *M* sodium hydrogen phosphate aqueous solution. pH 8.5 was received by adding sodium hydroxide to 0.1 *M* H_2NaO_4P aqueous solution.

due to the drying of the sample. A photograph of higher concentration of microspheres could not be obtained since large aggregates of the microspheres were formed and single microspheres could not be found.

The chelating microspheres had a high surface area, and therefore, their rate of mercury intake was much higher than that of the same chelating compound in bulk (Fig. 4). Organic and inorganic mercury compounds are taken in by the microspheres very rapidly (Figs. 5 and 6), but do not interact with alkaline or alkaline earth metallic compounds (Table II). They bind the mercury compounds over a broad range of pH (Table III) and compete and bind mercury compounds which are already bound to albumin or to cysteine (Tables IV and V). Comparison with commercial resins reported to have a high affinity for mercury, *e.g.*, styrene–divinylbenzene derivatized either with iminodiacetates[5] or with Srafion NMRR[6] (11) showed that the iminodiacetate derivative did not bind methyl mercury chloride, although it bound quantitatively Hg^{2+}, while the Srafion NMRR bound mercury compounds under physiological conditions much slower than the chelating microspheres (Fig. 7). A quantitative elution of the bound mercury is obtained by adding thiourea and hydrochloric acid to the suspended microspheres.

DISCUSSION

The structure of the chelating compound produced by the reaction of the aldehyde groups of glutaraldehyde and the thiol groups of pentaerythritol tetrathioglycolate seems to be complicated, and does not agree with the ideal structure of a polymer as suggested previously (12). The mercury compounds are probably bound to the chelating compound through its free thiol groups, and the S—C(OH) groups (hemi thio acetal). The structure of the chelating compound and of its binding to mercury compounds is currently being investigated. The chelating microspheres bind the mercury compound very strongly and reverse the binding from the biological receptors to the microspheres:

$$\text{Metallic compounds (R—M)} \xrightarrow{\text{Biological receptor}} \text{R—M} \cdots \text{Biological receptor} \xrightarrow{\text{Microspheres}} \text{R—M} \cdots \text{Microspheres} + \text{Biological receptors}$$

Scheme II

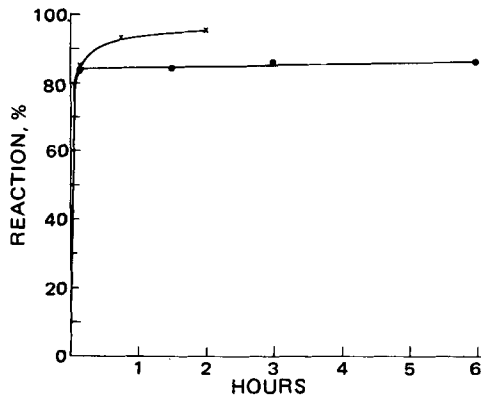

Figure 6—*Rate of intake of methyl mercury chloride by chelating microspheres. The reaction was carried out by stirring 10^{-4} M methyl mercury chloride in 80 ml of phosphate-buffered saline solution in the presence of: (●) 4.6-mg microspheres; (X) 60-mg microspheres.*

[5] Chelex 100 prepared by Bio-Rad Lab., Richmond, Calif.
[6] NMRR prepared by Ayalon Water Conditioning Co., Haifa, Israel.

Table IV—Rate of Intake of Mercury Compounds from Albumin [a]

Mercury Compound	Time, min	Reaction, %
Mercuric chloride	10	81
Mercuric chloride	60	81
Mercuric chloride	120	83
Mercuric chloride	1320	88
Methyl mercury chloride	10	78
Methyl mercury chloride	120	68
Methyl mercury chloride	1320	72

[a] Mercury compounds (5 ppm Hg) were stirred for 2 hr with 60 ml of 4% human albumin in phosphate-buffered saline solution, and then chelating microspheres were added (48 mg in the reaction with mercuric chloride and 60 mg in the reaction with methyl mercury chloride). In control experiments the loss of mercury compounds was negligible (<3%).

Many of the heavy metallic compounds are excreted by the liver *via* the bileduct and intestinal tract, but a great part of the metallic compound (~90% of methyl mercury chloride) is reabsorbed by the intestine. Therefore, it seems feasible that a nonabsorptive binding material, administered orally might bind the metallic compound secreted *via* the bile, prevent reabsorption of the metal, and greatly increase its fecal excretion. Several investigators (7–9) showed that oral administration of indigestible and nonabsorbable resin that binds methyl mercury enhances the fecal excretion of methyl mercury from animals. It was also observed (7) that nonabsorbable polythiol resin given orally can substantially reduce the level of methyl mercury in the blood, brain, kidney, and liver. In an epidemic of methyl mercury poisoning in Iraq (13) a group of scientists reported that oral administration of the same polythiol resin to humans significantly decreased their whole body levels of mercury. In most cases (diffusion control) the rate of mercury intake is directly proportional to the surface area of the mercury binder resin. For a resin with a spherical shape, the rate is directly proportional to the ratio $1/r$:

$$v \alpha n \pi r^2 = \frac{3V}{4\pi r^3} \pi r^2 = 0.75\, V \frac{1}{r} = k \frac{1}{r} \qquad \text{(Eq. 1)}$$

where v is the rate of mercury intake, V is the spherical volume, and n is the number of spheres having a radius r.

For example, spheres with a radius of 1 μm will intake mercury 100 times faster than those with a radius of 100 μm. The dramatic effect of the high surface area of the chelating microspheres (radius of 0.4 μm as compared with hundreds of micrometers of the polythiol resin) are clearly shown in Fig. 4. In 30 min 100% of mercuric chloride was taken in by the microspheres while during the same period of time the agglutinated microspheres bound only 5% of the mercuric chloride.

In conclusion, polymeric microspheres were shown to have a potential use for various applications such as cell labeling and cell separation (14, 15), drug delivery (16), and diagnostic purposes (17). A new application for microspheres is suggested. Chelating microspheres may be very useful

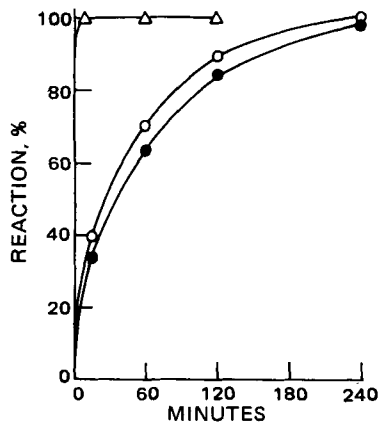

Figure 7—*Rate of intake of mercuric chloride and methyl mercury chloride by the Srafion NMRR–styrene divinylbenzene copolymer resin and the chelating microspheres. The reaction was carried out by stirring 50 ml of phosphate-buffered saline solution containing 10^{-4} M mercuric chloride or methyl mercury chloride with 100 mg of the chelating polymers. Key: (●) Srafion NMRR–styrene divinylbenzene copolymer resin with mercuric chloride; (○) Srafion NMRR–styrene divinylbenzene copolymer resin with methyl mercury chloride; (△) chelating microspheres with either mercuric chloride or methyl mercury chloride.*

Table V—Rate of Intake of Mercury Compounds from Cysteine [a]

Mercury Compounds	Time, min	Reaction, %
Mercuric chloride	10	95
Mercuric chloride	60	97
Mercuric chloride	240	99
Mercuric chloride	1320	100
Methyl mercury chloride	10	91
Methyl mercury chloride	60	91
Methyl mercury chloride	240	91

[a] Mercury compounds (20 ppm Hg) were stirred for 2 hr with 20 ml of 10^{-2} *M* cysteine in phosphate-buffered saline solution. Chelating microspheres were then added (20 mg in the reaction with methyl mercury chloride and 50 mg in the reaction with mercuric chloride). In control experiments the loss of mercury compounds was negligible.

as an oral antidote for treatment in cases of heavy metal poisoning, due to their high surface area. As a model, the potential of polymercaptal microspheres for mercury poisoning was demonstrated *in vitro* and future experiments will have to be carried out *in vivo* as well. Moreover, the affinity of chelating microspheres toward other heavy metallic compounds such as arsenic, cadmium, lead, and copper, *etc.*, will be investigated to evaluate their potential use for treatment of poisoning with these heavy metals.

REFERENCES

(1) T. Aaronson, *Environment*, **13**, 16 (1971).

(2) N. Nelson *et al.*, *Environ. Res.*, **4**, 1 (1971).

(3) N. Grant, *Environment*, **13**, 2 (1971).

(4) W. G. Levine, in "The Pharmacological Basis of Therapeutics," L. S. Goodman and A. Gilman, Eds., Macmillan, New York, N.Y., 1975, pp. 912, 923.

(5) E. Friedheim and C. Corvi, *J. Pharm. Pharmacol.*, **27**, 624 (1975).

(6) M. M. Jones, L. T. Burka, M. E. Hunter, M. Basinger, G. Campo, and A. D. Weaver, *J. Inorg. Nucl. Chem.*, **42**, 775 (1979).

(7) T. W. Clarkson, *Arch. Environ. Health*, **26**, 173 (1973).

(8) H. Takahashi and K. Hirayama, *Nature (London)*, **232**, 201 (1971).

(9) J. J. Benes, J. Stanberg, J. Peska, M. Tichy, and M. Cikrt, *Die Angewandte Makromolekular Chemie*, **44**, 67 (1975).

(10) A. Campe, N. Veighe, and A. Claeys, *At. Absorp. Newsl.*, **17**, 100 (1978).

(11) S. L. Law, *Science*, **174**, 285 (1971).

(12) G. A. Nyssen, M. M. Jones, J. D. Hernigan, D. R. Harbison, and J. S. MacDonald, *J. Inorg. Nucl. Chem.*, **39**, 1889 (1977).

(13) F. Bakir, *et al.*, *Science*, **181**, 230 (1973).

(14) S. Margel, S. Zisblat, and A. Rembaum, *J. Immunol. Methods*, **28**, 341 (1979).

(15) A. Rembaum and S. Margel, *Br. Polym. J.*, **10**, 275 (1978).

(16) K. J. Widder, A. E. Senyei, and D. G. Scarpelli, *Proc. Soc. Exp. Biol. Med.*, **158**, 141 (1978).

(17) J. M. Singer, *Am. J. Med.*, **31**, 766 (1961).

ACKNOWLEDGMENTS

The research was supported by the Committee on Prevention and Research in Occupational Health, The Government of Israel.

Relative Bioavailability of Commercially Available Ibuprofen Oral Dosage Forms in Humans

W. R. GILLESPIE, A. R. DiSANTO, R. E. MONOVICH, and K. S. ALBERT ˣ

Received August 20, 1981, from the *Clinical Biopharmaceutics Research Unit, The Upjohn Company, Kalamazoo, MI 49001.* Accepted for publication December 1, 1981.

Abstract □ Two human bioavailability studies were conducted to assess the *in vivo* performances of recently marketed 200-, 300-, and 400-mg ibuprofen capsules relative to the innovator's 300- and 400-mg tablets when administered as single oral 300- or 400-mg doses. An ibuprofen oral solution was also administered in each trial. Within each study, the products were equivalent to each other and to the oral solution with respect to the extent of ibuprofen absorption. Absorption rates, however, differed markedly among the products studied. Ibuprofen was more slowly absorbed from the 300- and 400-mg capsules than from the respective strength tablets. The 200-mg capsule exhibited an absorption rate comparable to the 400-mg tablet but more rapid than the 400-mg capsule. It was concluded that two of the duplicator's 200-mg capsules were bioequivalent to one of the innovator's 400-mg tablet. The duplicator's 300- and 400-mg capsules were bioinequivalent to the innovator's 300- and 400-mg tablets, respectively, due to their slower rates of absorption.

Keyphrases □ Bioavailability—commercially available ibuprofen oral dosage forms in humans □ Ibuprofen—bioavailability of commercially available oral dosage forms in humans □ Dosage forms, oral—bioavailability of commercially available ibuprofen in humans

Ibuprofen is a propionic acid derivative with anti-inflammatory, analgesic, and antipyretic activities and is widely utilized in the treatment of osteoarthritis, rheumatoid arthritis, and mild to moderate pain (1, 2). Recently, it has become a multiple-source drug product in Canada; thus, the question arises whether the new products are equivalent relative to the quality and performance of the innovator's products. Of particular importance is their *in vivo* performance in terms of the extent and rate of ibuprofen GI absorption from the solid oral dosage forms.

A previous study demonstrated the bioequivalence of a pilot plant lot of the 300-mg capsule product to the innovator's 300-mg tablet (3). The present studies were conducted to assess the bioavailability of full-scale production lots of the recently introduced 200-, 300-, and 400-mg capsules relative to the innovator's 300- and 400-mg tablets.

EXPERIMENTAL

Products Studied—Two comparative bioavailability studies were conducted to evaluate the five commercially available ibuprofen products (A, B, C, D, and E) listed in Table I.

An aqueous solution of sodium ibuprofen (F, Table I) was utilized as a reference standard to which the other formulations could be compared. With the exception of the solution, the products were obtained from usual commercial sources without any attempt to procure or select specific lots.

The ibuprofen dosage forms were administered as single, oral 300-mg doses in Study I and as single, oral 400-mg doses in Study II.

0022-3549/82/0900-1034$01.00/0

Table V—Rate of Intake of Mercury Compounds from Cysteine [a]

Mercury Compounds	Time, min	Reaction, %
Mercuric chloride	10	95
Mercuric chloride	60	97
Mercuric chloride	240	99
Mercuric chloride	1320	100
Methyl mercury chloride	10	91
Methyl mercury chloride	60	91
Methyl mercury chloride	240	91

[a] Mercury compounds (20 ppm Hg) were stirred for 2 hr with 20 ml of 10^{-2} *M* cysteine in phosphate-buffered saline solution. Chelating microspheres were then added (20 mg in the reaction with methyl mercury chloride and 50 mg in the reaction with mercuric chloride). In control experiments the loss of mercury compounds was negligible.

as an oral antidote for treatment in cases of heavy metal poisoning, due to their high surface area. As a model, the potential of polymercaptal microspheres for mercury poisoning was demonstrated *in vitro* and future experiments will have to be carried out *in vivo* as well. Moreover, the affinity of chelating microspheres toward other heavy metallic compounds such as arsenic, cadmium, lead, and copper, *etc.*, will be investigated to evaluate their potential use for treatment of poisoning with these heavy metals.

REFERENCES

(1) T. Aaronson, *Environment*, **13**, 16 (1971).

(2) N. Nelson *et al.*, *Environ. Res.*, **4**, 1 (1971).

(3) N. Grant, *Environment*, **13**, 2 (1971).

(4) W. G. Levine, in "The Pharmacological Basis of Therapeutics," L. S. Goodman and A. Gilman, Eds., Macmillan, New York, N.Y., 1975, pp. 912, 923.

(5) E. Friedheim and C. Corvi, *J. Pharm. Pharmacol.*, **27**, 624 (1975).

(6) M. M. Jones, L. T. Burka, M. E. Hunter, M. Basinger, G. Campo, and A. D. Weaver, *J. Inorg. Nucl. Chem.*, **42**, 775 (1979).

(7) T. W. Clarkson, *Arch. Environ. Health*, **26**, 173 (1973).

(8) H. Takahashi and K. Hirayama, *Nature (London)*, **232**, 201 (1971).

(9) J. J. Benes, J. Stanberg, J. Peska, M. Tichy, and M. Cikrt, *Die Angewandte Makromolekular Chemie*, **44**, 67 (1975).

(10) A. Campe, N. Veighe, and A. Claeys, *At. Absorp. Newsl.*, **17**, 100 (1978).

(11) S. L. Law, *Science*, **174**, 285 (1971).

(12) G. A. Nyssen, M. M. Jones, J. D. Hernigan, D. R. Harbison, and J. S. MacDonald, *J. Inorg. Nucl. Chem.*, **39**, 1889 (1977).

(13) F. Bakir, *et al.*, *Science*, **181**, 230 (1973).

(14) S. Margel, S. Zisblat, and A. Rembaum, *J. Immunol. Methods*, **28**, 341 (1979).

(15) A. Rembaum and S. Margel, *Br. Polym. J.*, **10**, 275 (1978).

(16) K. J. Widder, A. E. Senyei, and D. G. Scarpelli, *Proc. Soc. Exp. Biol. Med.*, **158**, 141 (1978).

(17) J. M. Singer, *Am. J. Med.*, **31**, 766 (1961).

ACKNOWLEDGMENTS

The research was supported by the Committee on Prevention and Research in Occupational Health, The Government of Israel.

Relative Bioavailability of Commercially Available Ibuprofen Oral Dosage Forms in Humans

W. R. GILLESPIE, A. R. DiSANTO, R. E. MONOVICH, and K. S. ALBERT ˣ

Received August 20, 1981, from the *Clinical Biopharmaceutics Research Unit, The Upjohn Company, Kalamazoo, MI 49001.* Accepted for publication December 1, 1981.

Abstract □ Two human bioavailability studies were conducted to assess the *in vivo* performances of recently marketed 200-, 300-, and 400-mg ibuprofen capsules relative to the innovator's 300- and 400-mg tablets when administered as single oral 300- or 400-mg doses. An ibuprofen oral solution was also administered in each trial. Within each study, the products were equivalent to each other and to the oral solution with respect to the extent of ibuprofen absorption. Absorption rates, however, differed markedly among the products studied. Ibuprofen was more slowly absorbed from the 300- and 400-mg capsules than from the respective strength tablets. The 200-mg capsule exhibited an absorption rate comparable to the 400-mg tablet but more rapid than the 400-mg capsule. It was concluded that two of the duplicator's 200-mg capsules were bioequivalent to one of the innovator's 400-mg tablet. The duplicator's 300- and 400-mg capsules were bioinequivalent to the innovator's 300- and 400-mg tablets, respectively, due to their slower rates of absorption.

Keyphrases □ Bioavailability—commercially available ibuprofen oral dosage forms in humans □ Ibuprofen—bioavailability of commercially available oral dosage forms in humans □ Dosage forms, oral—bioavailability of commercially available ibuprofen in humans

Ibuprofen is a propionic acid derivative with anti-inflammatory, analgesic, and antipyretic activities and is widely utilized in the treatment of osteoarthritis, rheumatoid arthritis, and mild to moderate pain (1, 2). Recently, it has become a multiple-source drug product in Canada; thus, the question arises whether the new products are equivalent relative to the quality and performance of the innovator's products. Of particular importance is their *in vivo* performance in terms of the extent and rate of ibuprofen GI absorption from the solid oral dosage forms.

A previous study demonstrated the bioequivalence of a pilot plant lot of the 300-mg capsule product to the innovator's 300-mg tablet (3). The present studies were conducted to assess the bioavailability of full-scale production lots of the recently introduced 200-, 300-, and 400-mg capsules relative to the innovator's 300- and 400-mg tablets.

EXPERIMENTAL

Products Studied—Two comparative bioavailability studies were conducted to evaluate the five commercially available ibuprofen products (A, B, C, D, and E) listed in Table I.

An aqueous solution of sodium ibuprofen (F, Table I) was utilized as a reference standard to which the other formulations could be compared. With the exception of the solution, the products were obtained from usual commercial sources without any attempt to procure or select specific lots.

The ibuprofen dosage forms were administered as single, oral 300-mg doses in Study I and as single, oral 400-mg doses in Study II.

0022-3549/82/0900-1034$01.00/0

Table I—Description of Ibuprofen Dosage Forms Tested

Formulation Type	Lot Number	Formulation Code
Capsule, 300 mg[a]	8E08N	A
Tablet, 300 mg[b]	E284	B
Capsule, 400 mg[a]	9D079	C
Capsule, 200 mg[a]	8E07N	D
Tablet, 400 mg[b]	E426	E
Solution, 20 mg/ml[c]	18,025-6	F

[a] Amersol capsules; manufactured and marketed by Frank W. Horner Ltd., Montreal, Quebec, Canada. [b] Motrin tablets; manufactured and marketed by The Upjohn Co. of Canada, Don Mills, Ontario, Canada. [c] Manufactured by The Upjohn Co., Kalamazoo, Mich.

Human Subjects—Eighteen normal volunteers between the ages of 18 and 35 years and 20 normal volunteers between the ages of 20 and 33 years were selected to participate in Study I and Study II, respectively. They were accepted into the studies following informed consent, a physical examination, and blood and urine analyses.

Study Design—In Study I, Formulations A, B, and F were administered according to a 3 × 3 Latin-square crossover design with six replications. In Study II, Formulations C, D, E, and F were administered according to a 4 × 4 Latin-square crossover design with five replications (Table II). The ibuprofen doses were separated by 4 days. Each dose was administered with 180 ml of water following an overnight fast. The fasting period continued for 2 hr following the dose. No food or beverage other than water was permitted during the fasting period.

Blood (7 ml) was collected from a forearm vein by individual venipunctures just prior to dosing and at 0.17 (10 min), 0.33 (20 min), 0.5, 1, 1.5, 2, 3, 4, 6, 8, 10, and 12 hr following drug administration. Serum was harvested from the blood samples ~40 min after collection, immediately frozen, and kept in a frozen state until assayed.

The serum specimens were quantitatively analyzed for unchanged ibuprofen utilizing GLC with flame ionization detection as described previously (4).

THEORETICAL

Symbols—The following symbols were used in the calculations and are defined as follows:

- AUC_t = area under the serum ibuprofen concentration–time curve from time zero through time t
- AUC_∞ = area under the serum ibuprofen concentration–time curve from time zero through infinite time
- $AUMC_t$ = area under the (first) moment curve from time zero through time t
- $AUMC_\infty$ = area under the (first) moment curve from time zero through infinite time
- C_t = ibuprofen serum concentration at time t (measured)
- $\hat{C}_t$ = ibuprofen serum concentration at time t (calculated)
- C_{max} = peak ibuprofen serum concentration
- CFA_{rel} = cumulative fraction absorbed relative to the oral solution
- MDT = mean *in vivo* dissolution time
- MRT = mean residence time
- t = elapsed time after ibuprofen administration
- T = time at which the last measurable ibuprofen serum concentration (≥1.0 μg/ml) was observed
- t_{max} = time at which C_{max} occurred
- λ_z = apparent ibuprofen elimination rate constant

Model Independent Parameters—AUC_t and $AUMC_t$ were calculated by trapezoidal rule. Extrapolations through infinite time utilized:

$$AUC_\infty = AUC_T + \frac{\hat{C}_T}{\lambda_z} \quad \text{(Eq. 1)}$$

$$AUMC_\infty = AUMC_T + \left[T + \frac{1}{\lambda_z}\right]\frac{\hat{C}_T}{\lambda_z} \quad \text{(Eq. 2)}$$

The apparent elimination rate constant (λ_z) was estimated by fitting the ibuprofen serum concentrations following administration of the oral solution (Formulation F) to a biexponential equation using nonlinear least-squares regression (NONLIN) (5). Estimates of $\hat{C}_T$ following administration of Formulation F were calculated from the same biexponential equation. Estimates of $\hat{C}_T$ following administration of the solid dosage forms were calculated from the equation of the line resulting from linear least-squares regression of $\ln C_t$ *versus* t using those data points in the terminal log-linear region. Attempts to estimate λ_z from the slope of that line resulted in significantly smaller values for Capsules A and C (Table III), suggesting prolonged GI absorption of ibuprofen. The elimination rate constant estimated from the oral solution data was considered a more reliable description of the elimination rate and was utilized in all subsequent calculations. This decision required the assumptions that λ_z remained constant for each volunteer throughout the study and that absorption was essentially complete by 12 hr following drug administration.

Table II—Latin-Square Crossover Designs for Ibuprofen Bioavailability Studies

Study I (Dose = 300 mg)

Group	Subjects	Formulation Phase I	Phase II	Phase III
1	5, 7, 8, 10, 13, 16	A	B	F
2	1, 2, 4, 6, 12, 18	B	F	A
3	3, 9, 11, 14, 15, 17	F	A	B

Study II (Dose = 400 mg)

Group	Subjects	Formulation Phase I	Phase II	Phase III	Phase IV
1	2, 10, 17[a], 18, 20	C	D	F	E
2	7, 13, 14, 15, 19	D	E	C	F
3	1, 4, 9, 11, 16	E	F	D	C
4	3, 5, 6, 8, 12	F	C	E	D

[a] Subject dropped from study following Phase I for reasons unrelated to the study.

The mean residence time of drug in the body (MRT) was calculated using (6):

$$MRT = \frac{AUMC_\infty}{AUC_\infty} \quad \text{(Eq. 3)}$$

The difference between the MRT for a solid oral dosage form and the

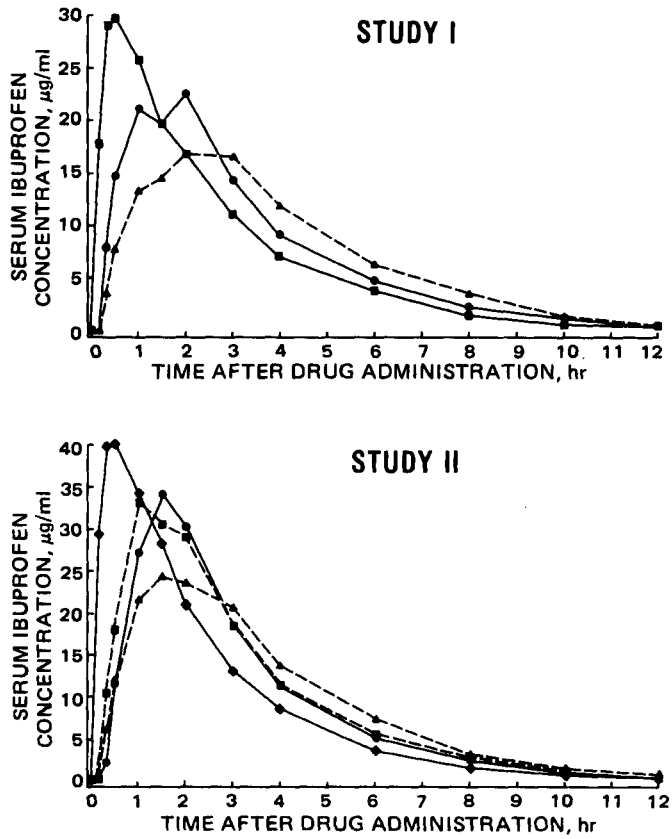

Figure 1—*Mean serum ibuprofen concentration–time curves. Key: Study I: (▲) 300-mg capsule (A); (●) 300-mg tablet (B); (■) oral solution (F); Study II: (▲) 400-mg capsule (C); (■) 200-mg capsule (D); (●) 400-mg tablet (E); (◆) oral solution (F).*

Table III—Mean Serum Ibuprofen Concentrations and Related Parameters

Study I ($N = 18$)

	Formulation			p^a	Pairwise[b] Comparisons
	A	B	F		
C_t, μg/ml at:					
0.0 hr	0.00	0.00	0.00	—	
0.167	0.06	0.16	17.8	< 0.0001	F B A
0.333	3.59	7.96	29.0	< 0.0001	F B A
0.5	7.79	14.7	29.7	< 0.0001	F B A
1	13.3	21.1	25.7	0.0066	F B A
1.5	14.5	19.6	19.7	0.075	F B A
2	16.9	22.5	17.0	0.0021	B F A
3	16.6	14.3	11.0	< 0.0001	A B F
4	11.9	9.09	7.10	< 0.0001	A B F
6	6.31	4.76	3.82	0.0006	A B F
8	3.54	2.25	1.44	< 0.0001	A B F
10	1.36	1.23	0.57	0.018	A B F
12	0.63	0.46	0.38	0.23	A B F
AUC_∞, μg hr/ml	91.5	89.9	88.5	0.75	A B F
C_{max}, μg/ml	21.1	32.4	31.9	< 0.0001	B F A
t_{max}, hr	2.17	1.32	0.46	< 0.0001	A B F
λ_z, hr^{-1}	0.347	0.414	0.455	0.0002	F B A

Study II ($N = 18$)

	Formulation				p^a	Pairwise[b] Comparisons
	C	D	E	F		
C_t, μg/ml at:						
0.0 hr	0.00	0.00	0.00	0.00	—	
0.167	0.12	0.22	0.06	29.4	< 0.0001	F D C E
0.333	6.09	10.4	2.12	39.7	< 0.0001	F D C E
0.5	12.0	18.0	11.4	40.0	< 0.0001	F D C E
1	21.6	33.1	27.1	34.2	0.0067	F D E C
1.5	24.3	30.5	34.1	28.2	0.0058	E D F C
2	23.5	29.0	30.2	21.0	0.0001	E D C F
3	20.7	18.4	18.7	13.0	0.0030	C E D F
4	13.7	11.4	11.1	8.51	0.0006	C D E F
6	7.33	5.58	5.06	3.58	< 0.0001	C D E F
8	3.11	2.61	2.42	1.55	0.0022	C D E F
10	1.52	1.10	0.92	0.72	0.025	C D E F
12	0.91	0.36	0.48	0.29	0.0074	C E D F
AUC_∞, μg hr/ml	116	119	112	110	0.48	D C E F
C_{max}, μg/ml	31.4	39.0	37.9	45.5	< 0.0001	F D E C
t_{max}, hr	2.00	1.25	1.39	0.53	< 0.0001	C E D F
λ_z, hr^{-1}	0.364	0.390	0.415	0.499	< 0.0001	F E D C

[a] Level of significance for test of equal treatment means. [b] The means for formulations connected by overhead bars were not significantly different ($p > 0.05$).

MRT for an oral solution (Eq. 4) has been termed the mean *in vivo* dissolution time (MDT) by Riegelman and Collier (7):

$$MDT = MRT_{solid} - MRT_{solution} \quad \text{(Eq. 4)}$$

Theoretically, MDT is an estimate of the mean time which a drug molecule remains as a solid in the GI tract. In reality, MDT is probably not an absolute estimator of dissolution rate due to the differing influences of stomach emptying rate on solid and solution dosage forms. It is, nonetheless, an excellent tool for comparing absorption rates among treatments administered to the same subjects in a bioavailability trial.

Model Dependent Parameters—The serum ibuprofen concentrations following the administration of the oral solution to each subject were well described by a biexponential equation. This indicated that the pharmacokinetics of ibuprofen could be explained in terms of a one-compartment open model. As a result, cumulative absorption profiles could be constructed according to the method of Wagner and Nelson (8). *Modification* of that method resulted in Eq. 5, which was utilized to estimate the cumulative amount of ibuprofen absorbed from the solid dosage form divided by the total amount absorbed from the oral solution, *e.g.*, cumulative fraction absorbed relative to the oral solution (CFA_{rel}):

$$CFA_{rel} = \frac{C_t + \lambda_z [AUC_t]}{\lambda_z [AUC_{\infty}^{solution}]} \quad \text{(Eq. 5)}$$

Estimates of cumulative fraction absorbed relative to the oral solution (CFA_{rel}) provided both visual and statistical comparisons of absorption rate and extent among the treatments.

Statistical Comparisons—Within each study, statistical comparisons of C_t, C_{max}, t_{max}, and AUC_∞ data were performed utilizing ANOVA with group, subject within group, phase, and treatment as factors. In cases where treatment effects were significant ($p < 0.05$), pairwise comparisons were evaluated with Tukey's multiple range test. A two-tailed paired t test was applied to MDT and CFA_{rel} data from Study I. The described ANOVA model was utilized to evaluate MDT and CFA_{rel} data from Study II except that the pairwise comparisons were performed using linear contrasts of the regression coefficients resulting from the ANOVA (9).

Table IV—Mean Estimates of Cumulative Fraction Absorbed Relative to the Oral Solution (CFA_{rel}) and Mean *In Vivo* Dissolution Time (*MDT*)

Study I (N = 18)

	Formulation A	Formulation B	p^a
CFA_{rel} at:			
0.0 hr	0.00	0.00	—
0.167	0.00	0.00	0.16
0.333	0.10	0.23	0.16
0.5	0.22	0.44	0.071
1	0.43	0.73	0.046
1.5	0.55	0.79	0.044
2	0.70	0.96	0.0023
3	0.89	0.96	0.15
4	0.93	0.96	0.54
6	1.00	1.00	0.89
MDT, hr	1.44	0.73	0.0052

Study II (N= 18)

	Formulation C	Formulation D	Formulation E	p^a	Pairwise[b] Comparisons
CFA_{rel} at:					
0.00 hr	0.00	0.00	0.00	—	
0.167	0.00	0.00	0.00	0.51	C D E
0.333	0.13	0.21	0.04	0.028	D C E
0.5	0.25	0.38	0.23	0.16	D C E
1	0.52	0.77	0.63	0.021	D E C
1.5	0.68	0.88	0.91	0.012	E D C
2	0.78	0.99	0.99	0.0056	D E C
3	0.93	1.02	1.00	0.0052	D E C
4	0.97	1.03	0.99	0.12	D E C
6	1.04	1.08	1.02	0.25	D C E
MDT, hr	1.27	0.80	0.79	0.0016	C D E

[a] Level of significance for test of equal treatment means. [b] The means for formulations connected by overhead bars were not significantly different ($p > 0.05$).

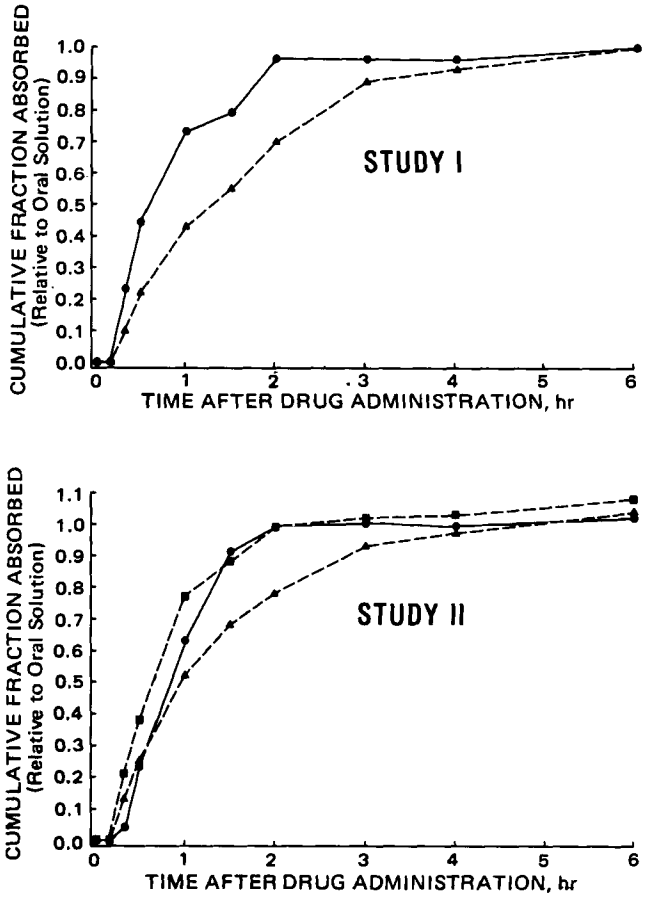

Figure 2—*Modified Wagner-Nelson absorption plots of mean cumulative fraction absorbed relative to the oral solution* (CFA_{rel}) versus *time. Key: Study I: (▲) 300-mg capsule (A); (●) 300-mg tablet (B); Study II: (▲) 400-mg capsule (C); (■) 200-mg capsule (D); (●) 400-mg tablet (E).*

RESULTS

All 18 subjects enrolled in Study I successfully completed the three treatment phases. Of the 20 subjects enrolled in Study II, one (Subject 17) discontinued participation following Phase I for reasons unrelated to the study. Another (Subject 18) exhibited such unusual ibuprofen concentration–time courses that the person was considered unrepresentative of a normal subject population. Neither of these subjects' results were utilized in any subsequent data analyses.

Concentration at Each Sampling Time (C_t)—Table III and Fig. 1 present the mean serum ibuprofen concentrations at each sampling time which resulted from the administration of Formulations A, B, and F as single, oral 300-mg doses in Study I and formulations C, D, E, and F as single, oral 400-mg doses in Study II.

In Study I, statistically significant ($p < 0.05$) differences were observed among the treatments at all but two sampling times. The pairwise comparisons indicated that those differences were predominantly the result of a concentration–time profile for the oral solution which differed markedly from those for the two solid dosage forms. Tablet B, however, did exhibit significantly lower concentrations than Capsule A at 2, 4, 6, and 8 hr following drug administration.

In Study II, statistically significant differences among the formulations were observed at each sampling time. Most of those differences were attributable to solid dosage form *versus* solution comparisons. Concentrations following Capsule C administration did differ significantly from those following Capsule D administration at 1, 6, and 12 hr, and from those following Tablet E administration at 1.5, 2, and 6 hr postdose. No significant differences were observed for Formulations D *versus* E comparisons at any sampling time.

Area Under the Concentration–Time Curve (AUC_∞)—The average areas under the serum ibuprofen concentration–time curves (AUC_∞) resulting from administration of each formulation are also shown in Table III. Within each study, no statistically significant differences were observed among the formulations. The following ratios of mean AUC_∞ for the solid dosage forms to the mean AUC_∞ for the oral solution were observed:

A/F	B/F	C/F	D/F	E/F
1.03	1.02	1.05	1.08	1.01

Those results indicated that the tablet and capsule products were equivalent to each other and to the oral solution with respect to the extent of ibuprofen absorption.

Peak Concentration (C_{max}) and Peak Time (t_{max})—Statistical analyses of the C_{max} and t_{max} values observed following the administration of the various ibuprofen formulations (Table III) yielded significant differences among the treatment means in both studies. The oral solution exhibited the most rapid rate of absorption with an average t_{max} in both studies of ~0.5 hr and average C_{max} estimates of 31.9 and 45.5 μg/ml in Studies I and II, respectively.

In Study I, the 300-mg capsule (A) resulted in an average C_{max} which was 35% less and a t_{max} which was 64% greater than those achieved by the 300-mg tablet (B). Those differences were statistically significant and indicated that ibuprofen was more rapidly absorbed from the tablet than from the capsule.

In Study II, the results of pairwise comparisons between the 400-mg tablet (E) and capsule (C) were similar to those seen in Study I for the 300-mg formulations. Capsule C produced an average C_{max} which was 17% less and a t_{max} which was 44% greater than those resulting from Tablet E. Only the t_{max} difference was statistically significant. The mean C_{max} and t_{max} results for the 200-mg capsule (D) were similar to those for the 400-mg tablet (E) and significantly different from those for the 400-mg capsule (C). These results indicated that Formulations D and E were absorbed at similar rates and that both were absorbed more rapidly than Formulation C.

Mean *In Vivo* Dissolution Time (*MDT*)—The average *MDT* estimates shown in Table IV distinguish the solid dosage forms on the basis of absorption rate. The 300-mg capsule (A) exhibited an average *MDT* nearly twice that for the 300-mg tablet (B) (1.44 *versus* 0.73 hr). In Study

II, the 200-mg capsule (D) and the 400-mg tablet (E) resulted in approximately equal *MDT* estimates (0.80 *versus* 0.79 hr). The 400-mg capsule (C), however, was more slowly absorbed with an average *MDT* of 1.27 hr. The differences for the pairwise comparisons of A *versus* B, C *versus* D, and C *versus* E were statistically significant.

Cumulative Fraction Absorbed Relative to the Oral Solution (CFA_{rel})—Modified Wagner-Nelson plots of mean CFA_{rel} *versus* time for the ibuprofen products are presented as Fig. 2. Inspection of the plots suggests that, on the average, Formulations A and C required 4–6 hr to achieve an extent of absorption within 95% of the oral solution. Formulations B, D, and E, however, reached the same endpoint by the 2-hr sampling time.

Statistical comparisons of the CFA_{rel} estimates at each sampling time up to 6 hr are shown in Table IV. The 300-mg tablet (B) resulted in significantly greater mean CFA_{rel} values at 1, 1.5, and 2 hr than the 300-mg capsule (A). The 400-mg tablet (E) and the 200-mg capsule (D) exhibited similar mean CFA_{rel} estimates with a significant difference occurring only at the 20-min sampling time. The 400-mg capsule (C) results were significantly less than those for Formulation D at 1, 1.5, 2, and 3 hr and those for Formulation E at 1.5, 2, and 3 hr. Since no differences were observed in the extent of absorption among the products studied, the relatively low estimates of CFA_{rel} resulting from Formulations A and C were indicative of their slower rates of absorption.

DISCUSSION

Though all of the commercially available ibuprofen products studied were equivalent with respect to the amount of drug absorbed from the dosage forms, they differed markedly in terms of absorption rate. Specifically, the 300-mg tablet (B) was more rapidly absorbed than the 300-mg capsule (A), and the 400-mg tablet (E) and the 200-mg capsule (D) were more rapidly absorbed than the 400-mg capsule (C).

The results of a previously reported study indicated that a pilot plant lot of the 300-mg capsule was bioequivalent to the innovator's 300-mg tablet (3). The present study suggested that some change associated with scale-up to commercial production resulted in a less rapidly absorbed dosage form.

Since bioequivalence has been defined as equivalence in both extent and rate of drug absorption (10), it has been concluded that Formulations A and C were bioinequivalent to the innovator's products (B and E) due to their slower absorption rates. Whether this conclusion could be translated to indicate clinical inequivalence could not be determined from these studies. It would be hypothesized, however, that differences in clinical efficacy might be observed when ibuprofen is administered as single doses for the relief of mild to moderate pain.

A more general conclusion resulting from these studies was that the potential exists for bioavailability problems among ibuprofen solid oral dosage forms.

REFERENCES

(1) S. S. Adams, K. F. McCullough, and J. S. Nicholson, *Arch. Int. Pharmacodyn. Ther.*, **178**, 115 (1969).

(2) T. G. Kantor, *Ann. Intern. Med.*, **91**, 877 (1979).

(3) D. L. Simmons, A. A. Legore, P. Picotte, and F. Cesari, *Can. J. Pharm. Sci.*, **15**, 26 (1980).

(4) D. G. Kaiser and G. J. VanGiessen, *J. Pharm. Sci.*, **63**, 219 (1974).

(5) C. M. Metzler, G. L. Elfring, and A. J. McEwen, *Biometrics*, **30**, 562 (1974).

(6) A. Rescigno and G. Segre, in "Drug and Tracer Kinetics," 1st American Edition, Blaisdell, Waltham, Mass., 1966, p. 161.

(7) S. Riegelman and P. Collier, *J. Pharmacokinet. Biopharm.*, **8**, 509 (1980).

(8) J. G. Wagner and E. Nelson, *J. Pharm. Sci.*, **52**, 610 (1963).

(9) J. Neter and W. Wasserman, in "Applied Linear Statistical Models," Irwin, Homewood, Ill., 1974, p. 795.

(10) U.S. Food and Drug Administration, *Fed. Reg.*, **42**, 1635 (1977).

ACKNOWLEDGMENTS

Presented in part before the American Pharmaceutical Association, Academy of Pharmaceutical Sciences, 29th National Meeting, San Antonio, Tex. (November 9–13, 1980).

The Role of Surfactants in the Release of Very Slightly Soluble Drugs from Tablets

HANS SCHOTT ˣ, LILIAN CHONG KWAN *, and STUART FELDMAN ‡

Received August 4, 1981, from the *School of Pharmacy, Temple University, Philadelphia, PA 19140.* Accepted for publication November 24, 1981.

*Present address: William H. Rorer, Inc., Fort Washington, PA 19034. ‡Present address: College of Pharmacy, University of Houston, Houston, TX 77030.

Abstract □ The ability of surfactants to accelerate the *in vitro* dissolution of very slightly soluble drugs has been ascribed to wetting and/or micellar solubilization. Deflocculation as a mechanism to accelerate dissolution has not been investigated. In the present study, the effect of a surfactant on the dissolution kinetics of prednisolone from tablets and the mode of action of the surfactant were investigated. The dissolution of prednisolone at 37° in 0.1 *N* HCl containing different concentrations of the nonionic surfactant, octoxynol 9, followed zero-order kinetics. The rate constant was increased by 15, 150, and 950% when octoxynol was added to the dissolution medium at 0.0039 and 0.032% (~0.5 and 4.0 times the critical micelle concentration) and incorporated into the tablets (for a final concentration of 0.0039%), respectively. The surface tensions of the dissolution media were 71, 35, and 31 dyne/cm for 0, 0.0039, and 0.032% octoxynol, respectively. The largest decrease in surface tension corresponded to the smallest increase in dissolution rate, indicating that wetting was unimportant. The micellar solubilization capacity of octoxynol was much too small to account for the increases in dissolution rate. Microscopic particle size measurements and sedimentation volume determinations showed the pronounced deflocculation of prednisolone by the surfactant. The observed increases in specific surface area at the two octoxynol concentrations were in good quantitative agreement with the increases in dissolution rate according to the Noyes–Whitney equation.

Keyphrases □ Deflocculation—surfactants, release of very slightly soluble drugs, tablets, dissolution kinetics □ Surfactants—release of very slightly soluble drugs, tablets, dissolution kinetics □ Kinetics—dissolution, surfactants, release of very slightly soluble drugs, tablets, deflocculation

The most likely mechanisms by which surfactants could speed up the release of very slightly soluble drugs from tablets are wetting, micellar solubilization, and deflocculation (1). The purpose of the present study was to assess their relative importance in accelerating the dissolution of prednisolone by octoxynol.

0022-3549/82/0900-1038$01.00/0

II, the 200-mg capsule (D) and the 400-mg tablet (E) resulted in approximately equal *MDT* estimates (0.80 *versus* 0.79 hr). The 400-mg capsule (C), however, was more slowly absorbed with an average *MDT* of 1.27 hr. The differences for the pairwise comparisons of A *versus* B, C *versus* D, and C *versus* E were statistically significant.

Cumulative Fraction Absorbed Relative to the Oral Solution (CFA_{rel})—Modified Wagner-Nelson plots of mean CFA_{rel} *versus* time for the ibuprofen products are presented as Fig. 2. Inspection of the plots suggests that, on the average, Formulations A and C required 4–6 hr to achieve an extent of absorption within 95% of the oral solution. Formulations B, D, and E, however, reached the same endpoint by the 2-hr sampling time.

Statistical comparisons of the CFA_{rel} estimates at each sampling time up to 6 hr are shown in Table IV. The 300-mg tablet (B) resulted in significantly greater mean CFA_{rel} values at 1, 1.5, and 2 hr than the 300-mg capsule (A). The 400-mg tablet (E) and the 200-mg capsule (D) exhibited similar mean CFA_{rel} estimates with a significant difference occurring only at the 20-min sampling time. The 400-mg capsule (C) results were significantly less than those for Formulation D at 1, 1.5, 2, and 3 hr and those for Formulation E at 1.5, 2, and 3 hr. Since no differences were observed in the extent of absorption among the products studied, the relatively low estimates of CFA_{rel} resulting from Formulations A and C were indicative of their slower rates of absorption.

DISCUSSION

Though all of the commercially available ibuprofen products studied were equivalent with respect to the amount of drug absorbed from the dosage forms, they differed markedly in terms of absorption rate. Specifically, the 300-mg tablet (B) was more rapidly absorbed than the 300-mg capsule (A), and the 400-mg tablet (E) and the 200-mg capsule (D) were more rapidly absorbed than the 400-mg capsule (C).

The results of a previously reported study indicated that a pilot plant lot of the 300-mg capsule was bioequivalent to the innovator's 300-mg tablet (3). The present study suggested that some change associated with scale-up to commercial production resulted in a less rapidly absorbed dosage form.

Since bioequivalence has been defined as equivalence in both extent and rate of drug absorption (10), it has been concluded that Formulations A and C were bioinequivalent to the innovator's products (B and E) due to their slower absorption rates. Whether this conclusion could be translated to indicate clinical inequivalence could not be determined from these studies. It would be hypothesized, however, that differences in clinical efficacy might be observed when ibuprofen is administered as single doses for the relief of mild to moderate pain.

A more general conclusion resulting from these studies was that the potential exists for bioavailability problems among ibuprofen solid oral dosage forms.

REFERENCES

(1) S. S. Adams, K. F. McCullough, and J. S. Nicholson, *Arch. Int. Pharmacodyn. Ther.*, **178**, 115 (1969).

(2) T. G. Kantor, *Ann. Intern. Med.*, **91**, 877 (1979).

(3) D. L. Simmons, A. A. Legore, P. Picotte, and F. Cesari, *Can. J. Pharm. Sci.*, **15**, 26 (1980).

(4) D. G. Kaiser and G. J. VanGiessen, *J. Pharm. Sci.*, **63**, 219 (1974).

(5) C. M. Metzler, G. L. Elfring, and A. J. McEwen, *Biometrics*, **30**, 562 (1974).

(6) A. Rescigno and G. Segre, in "Drug and Tracer Kinetics," 1st American Edition, Blaisdell, Waltham, Mass., 1966, p. 161.

(7) S. Riegelman and P. Collier, *J. Pharmacokinet. Biopharm.*, **8**, 509 (1980).

(8) J. G. Wagner and E. Nelson, *J. Pharm. Sci.*, **52**, 610 (1963).

(9) J. Neter and W. Wasserman, in "Applied Linear Statistical Models," Irwin, Homewood, Ill., 1974, p. 795.

(10) U.S. Food and Drug Administration, *Fed. Reg.*, **42**, 1635 (1977).

ACKNOWLEDGMENTS

Presented in part before the American Pharmaceutical Association, Academy of Pharmaceutical Sciences, 29th National Meeting, San Antonio, Tex. (November 9–13, 1980).

The Role of Surfactants in the Release of Very Slightly Soluble Drugs from Tablets

HANS SCHOTT ˣ, LILIAN CHONG KWAN *, and STUART FELDMAN ‡

Received August 4, 1981, from the *School of Pharmacy, Temple University, Philadelphia, PA 19140.* Accepted for publication November 24, 1981.

*Present address: William H. Rorer, Inc., Fort Washington, PA 19034. ‡Present address: College of Pharmacy, University of Houston, Houston, TX 77030.

Abstract □ The ability of surfactants to accelerate the *in vitro* dissolution of very slightly soluble drugs has been ascribed to wetting and/or micellar solubilization. Deflocculation as a mechanism to accelerate dissolution has not been investigated. In the present study, the effect of a surfactant on the dissolution kinetics of prednisolone from tablets and the mode of action of the surfactant were investigated. The dissolution of prednisolone at 37° in 0.1 *N* HCl containing different concentrations of the nonionic surfactant, octoxynol 9, followed zero-order kinetics. The rate constant was increased by 15, 150, and 950% when octoxynol was added to the dissolution medium at 0.0039 and 0.032% (~0.5 and 4.0 times the critical micelle concentration) and incorporated into the tablets (for a final concentration of 0.0039%), respectively. The surface tensions of the dissolution media were 71, 35, and 31 dyne/cm for 0, 0.0039, and 0.032% octoxynol, respectively. The largest decrease in surface tension corresponded to the smallest increase in dissolution rate, indicating that wetting was unimportant. The micellar solubilization capacity of octoxynol was much too small to account for the increases in dissolution rate. Microscopic particle size measurements and sedimentation volume determinations showed the pronounced deflocculation of prednisolone by the surfactant. The observed increases in specific surface area at the two octoxynol concentrations were in good quantitative agreement with the increases in dissolution rate according to the Noyes–Whitney equation.

Keyphrases □ Deflocculation—surfactants, release of very slightly soluble drugs, tablets, dissolution kinetics □ Surfactants—release of very slightly soluble drugs, tablets, dissolution kinetics □ Kinetics—dissolution, surfactants, release of very slightly soluble drugs, tablets, deflocculation

The most likely mechanisms by which surfactants could speed up the release of very slightly soluble drugs from tablets are wetting, micellar solubilization, and deflocculation (1). The purpose of the present study was to assess their relative importance in accelerating the dissolution of prednisolone by octoxynol.

0022-3549/82/0900-1038$01.00/0

Table I—Tablet Compositions

Ingredients[a]	Weight in Formulation, mg I	II	III
Microcrystalline cellulose	75	75	75
Octoxynol	—	35	35
Lactose	100	100	100
Prednisolone	25	25	—
Magnesium stearate	5	5	5
Lactose	295	260	285
Total	500	500	500

[a] Listed in order of addition.

BACKGROUND

Wetting—The wetting process consists in replacing a solid–air interface with a solid–liquid interface. Wetting agents speed up the penetration of gastric fluid into the tablets and, hence, tablet disintegration. This effect, which is due to the lowering of contact angles and of surface and interfacial tensions of the aqueous medium by the surfactants, has been well documented (2–22).

The improper use of surfactants could conceivably retard the dissolution of solid drugs by dewetting. When hydrophilic solid surfaces of relatively high charge density come into contact with aqueous solutions of ionic surfactants of the opposite charge, the surface-active ions are chemisorbed by an ion-exchange mechanism with their hydrocarbon chains oriented toward the aqueous phase. This process reduces the *zeta* potential of the solid surface to very low values or even zero (23). It also covers that surface with hydrocarbon chains, rendering it more hydrophobic and poorly wetted. The contact angles of water on such hydrophilic surfaces as barium sulfate (24) and glass (25) were thus increased from 0 to 60° or more.

The following observation also illustrates this point. The addition of the anionic surfactant, dioctyl sodium sulfosuccinate, to water increased the rate of penetration into a powder bed of negatively charged aspirin particles but lowered the rate of penetration into a bed of positively charged magnesium oxide particles (8).

Solubilization—Micellar solubilization occurs only when the dissolved surfactant is present at concentrations exceeding its critical micelle concentration. In most instances, the amount of surfactant that can be conveniently incorporated into a tablet supplies less than that needed to exceed the critical micelle concentration once the surfactant is dissolved and uniformly distributed throughout the gastric fluid. Owing to their size, shape, and chemical nature, most drug molecules capable of being solubilized by micelles cause little or no reduction in the critical micelle concentration.

Immediately after ingestion, aqueous fluid penetrates into tablets and begins to dissolve the surfactant contained therein. This process could temporarily produce, inside the tablets, a surfactant solution of concentration well in excess of the critical micelle concentration. This transitory micellar solution may temporarily dissolve a very slightly water-soluble drug by micellar solubilization. After the tablets disintegrate and/or the surfactant is leached out, the surfactant solution inside the tablets is diluted by the entire volume of gastric fluid and its concentration drops below the critical micelle concentration. As the micelles dissociate, the solubilized drug precipitates. However, this precipitation produces a colloidal dispersion of the drug characterized by a large specific surface area, and, therefore, by a high subsequent dissolution rate. The fine particle size of the drug during precipitation is maintained by the low drug solubility and a small concentration. This combination results in a low degree of supersaturation and provides little precipitating solid drug for growth of the nuclei. Adsorption of the surfactant and of pepsin and mucin dissolved in the gastric fluid onto the nuclei further limits their growth.

Numerous publications deal with the effect of micellar solubilization on the dissolution rate of very slightly soluble drugs from tablets (26–38).

Table II—Tablet Characteristics

Property	Formulation I	Formulation II
Weight ± *SE*[a], mg (*N*)[b]	499.7 ± 1.0 (30)	500.0 ± 1.0 (10)
Diameter ± *SE*, mm (*N*)	12.77 ± 0.01 (14)	12.84 ± 0.02 (5)
Thickness ± *SE*, mm (*N*)	2.76 ± 0.02 (30)	2.76 ± 0.02 (5)
Prednisolone Content ± *SE*, mg (*N*)	25.1 ± 0.1 (6)	Not assayed
Hardness ± *SE*, kg (*N*)	8.1 ± 0.1 (4)	1.4 ± 0.1 (4)

[a] Standard error. [b] Number of determinations.

Table III—Tablet Disintegration Times

Tablet Composition[a]	Liquid Medium[b]	Disintegration Times, min Mean[c] ± *SD*[d]	Range
I	A	107.0 ± 9.3	23.2
I	B	104.3 ± 14.5	44.6
I	C	67.4 ± 3.7	9.5
II	A	18.5 ± 0.8	2.0

[a] See Table I. [b] Medium A is 0.1 *N* HCl, B is 0.1 *N* HCl + 0.0039% octoxynol, and C is 0.1 *N* HCl + 0.032% octoxynol. See text for properties. [c] Mean of 6 tablets. [d] Standard deviation.

Miscellaneous—A few investigators found that surfactants incorporated into tablets or dissolution media had no effect on the disintegration and/or dissolution times (39, 40). Others observed reduced dissolution times in the presence of surfactants but did not identify the mode of action of the surfactants (41). Still other investigators rejected surface tension lowering and micellar solubilization as causes for the observed increase in dissolution rate, because these factors were not large enough to account for the magnitude of that increase, but offered no alternative explanation (42).

In the case of relatively hydrophilic tablets, surfactants reduced the disintegration times by weakening adhesion, as shown by reduced tablet hardness, rather than by enhancing the penetration of the dissolution medium (43–45). Nonionic surfactants increased the rate of dissolution according to their hydrophile–lipophile balance. Increases in the rate of disintegration depended on the chemical category of the nonionic surfactant (46).

Deflocculation—Deflocculation, deaggregation, or peptization is the breaking up or dispersing of aggregates or secondary particles into smaller aggregates or primary particles. This process increases the specific surface area of the solid drug particles and, thereby, their rate of dissolution. It enhances the bioavailability of very slightly soluble and practically insoluble drugs, whose absorption is limited by their dissolution rate.

The role of surfactants in deflocculating or deaggregating the solid phase in lyophobic aqueous and nonaqueous dispersions and suspensions is well recognized (47). However, the possibility that surfactants employed as tablet excipients increase the dissolution rate of very slightly soluble drugs by peptization or deflocculation has, to the best of our knowledge, neither been explicitly recognized nor documented (48).

However, it was postulated that the presence of sodium lauryl sulfate dissolved in the granulating liquid greatly increased the rate of dissolution by preventing the formation of agglomerates of hydrophobic drug particles in the tablet (49). The increase in the dissolution rate of aspirin from tablets in the presence of surfactants (17) was ascribed to "a wetting and/or deaggregation effect" (21).

The present data on the release of prednisolone from tablets in the presence of a nonionic surfactant show that the major mechanism through which the surfactant increased the dissolution rate of this very slightly soluble drug was a deflocculating or peptizing action.

EXPERIMENTAL

Materials—Prednisolone was anhydrous, USP grade, and micronized[1]. Octoxynol 9, an anhydrous, viscous liquid[2], and microcrystalline cellulose[3] were NF grade. Magnesium stearate[4], supplied as an impalpable powder, and spray-dried lactose[5] were USP grade. All other chemicals were American Chemical Society reagent grade. Water was twice distilled.

Tablet Preparation—Three formulations of 500-mg tablets were prepared by triturating 5.000 g of the ingredients, enough to make 10 tablets, in a mortar and pestle in the order of addition listed in Table I. Microcrystalline cellulose was included to absorb the liquid octoxynol and prevent it from rendering the tablet excessively soft. The 75-mg portion of microcrystalline cellulose was the minimum amount required to absorb 35 mg of octoxynol and maintain their mixture as a nonsoggy, free-flowing powder. The lactose was incorporated in two portions. The

[1] Schering Corp., Bloomfield, N.J.
[2] Triton X-100 of Rohm & Haas Co., Philadelphia, Pa. It is a branched octylphenol adduct with an average of 9–10 ethylene oxide units.
[3] Avicel PH 102, FMC Corp., Marcus Hook, Pa.
[4] Mallinckrodt Inc., St. Louis, Mo.
[5] Foremost Dairies, Inc., supplied by Smith Kline & French Labs., Philadelphia, Pa.

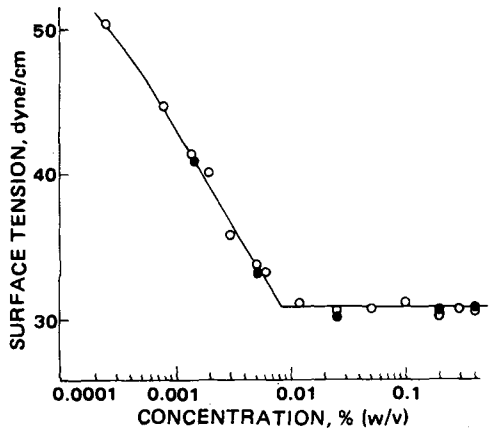

Figure 1—*Surface tension of octoxynol solutions in 0.1* N *HCl at 37° as a function of surfactant concentration. Key: (●) equilibration time 1 hr; (○) equilibration time 24 hr.*

first was added between the surfactant and the prednisolone to minimize direct contact between the latter two ingredients.

A cylindrical stainless steel die with a diameter of 1.27 cm (0.5 in) and a flat-faced punch were used on a hydraulic press[6] equipped with a pressure gauge. The 500-mg aliquots were compressed for 30 sec with a weight of 4536 kg (10,000 lbs), which corresponds to a pressure of 50,900 psi. This weight produced tablets of more uniform disintegration times than did 2268 kg (5000 lbs).

Tablet hardness was measured with a manual, spring-operated tester[7].

Liquid Media—The three media used for disintegration and dissolution studies consisted of 900 ml of 0.1 *N* HCl maintained at 37.0 ± 0.2°. Medium A contained no other additives. Its surface tension was 71.1 dyne/cm. Medium B contained 0.0039% (w/v) octoxynol, *i.e.*, 35 mg in 900 ml, and had a surface tension of 35.4 dyne/cm. Medium C contained 0.032% (w/v) octoxynol and had a surface tension of 30.9 dyne/cm. Since the critical micelle concentration of octoxynol in 0.1 *N* HCl at 37° is 0.0083%, the surfactant concentrations in Media B and C correspond approximately to 0.5 and 4.0 times the critical micelle concentration, respectively.

Tablet Disintegration—Disintegration times were measured with the USP apparatus[8]. The plastic disks (50) were omitted. The 1-liter beaker was jacketed, and water from a constant-temperature bath at 37° was circulated through the jacket. Individual disintegration times, measured for each tablet, were the times required for all fragments to fall through the 10-mesh bottom screen.

Prednisolone Dissolution—A USP single-position dissolution apparatus (50) was used with the basket rotating at 100 ±5 rpm[8]. Aliquots were withdrawn at predetermined intervals and filtered before analyzing for dissolved prednisolone to remove suspended, insoluble tablet ingredients as well as any colloidally dispersed prednisolone that may have been present. Pressure filtration through membrane filters[9] with a pore size of 0.22 μm was employed. The stainless steel barrel of the pressure filter holder was thermostated at 37°.

Prednisolone assay by direct UV absorption spectroscopy was not sensitive enough. Therefore, a colorimetric assay based on the Porter and Silber method (51) was developed. It will be described in a separate publication. Its accuracy and reproducibility in the presence of the tableting ingredients were evaluated as follows: A tablet containing 25.0 mg of prednisolone was triturated with 10 ml of methanol to dissolve the prednisolone and the entire mass was diluted to 1.000 liter with 0.1 *N* HCl. Prednisolone assays were performed in duplicate on filtered aliquots. This procedure was repeated with two additional tablets, for a total of six determinations.

Four to six dissolution experiments were conducted at each of the four experimental conditions. Octoxynol interacted with the acid phenylhydrazine solution to produce a faint yellow tint. To compensate for this effect, comparable concentrations of octoxynol were incorporated into the blank solutions.

Octoxynol Dissolution—The release rate of octoxynol from tablets made according to Formulation III was determined by measuring the

[6] Carver Laboratory Press, model C, Fred C. Carver Inc., Summit, N.J.
[7] Stokes Hardness Tester, Pennwalt Corp., Warminster, Pa.
[8] Scientific Glass Apparatus Co., Bloomfield, N.J.
[9] Millipore Corp., Bedford, Mass.

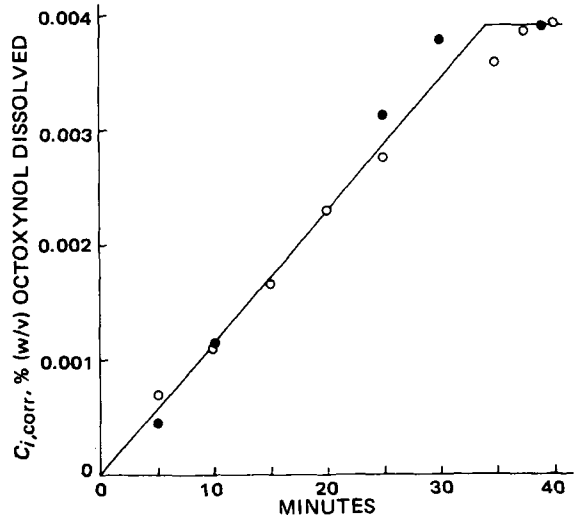

Figure 2—*Dissolution profile of octoxynol;* $C_{i,corr}$ *represents the concentration of dissolved octoxynol in percent (w/v) calculated according to Eq. 2. Key: (●) Tablet 1; (○) Tablet 2.*

surface tension of the dissolution medium as a function of time. A calibration plot of surface tension *versus* octoxynol concentration was prepared at 37° in 0.1 *N* HCl. When the octoxynol concentration in the dissolution medium exceeded the critical micelle concentration, octoxynol determinations were made by surface tension measurements at 37° on aliquots after appropriate dilution with 0.1 *N* HCl to concentrations below the critical micelle concentration.

Surface tensions were measured with a Wilhelmy balance[10] equipped with a sand-blasted platinum blade on 40-ml portions of octoxynol solutions or aliquots of the dissolution medium. These solutions were equilibrated at 37.0 ± 0.1° for 1 hr or 24 hr prior to the measurements.

Micellar Solubilization of Prednisolone—The solubility of prednisolone in 0.1 *N* HCl solutions containing octoxynol at concentrations ranging from 0 to 0.128% was determined by colorimetric and gravimetric assays. In both methods, 50-mg portions of prednisolone triturated to a fine powder were mixed with 50-ml portions of the dissolving media in amber glass bottles. The bottles were flushed with nitrogen, stoppered, and shaken on an oscillating water bath[11] at 37°.

For the colorimetric assay, 5-ml aliquots were withdrawn after 2, 6, and 16 days of shaking, filtered through 0.1-μm membrane filters, and assayed according to the modified Porter and Silber method (51). The blank solutions contained octoxynol at the same concentrations as the test solutions.

In the gravimetric method, the suspensions were shaken at 37° for 3, 6, or 22 days. The entire 50-ml suspension volumes containing 50 mg of prednisolone were then filtered through tared fritted glass filtering crucibles. The filters, containing the undissolved prednisolone, were washed and dried to constant weight at 100°.

Sedimentation Volumes of Prednisolone Suspensions—Suspensions containing 50 mg of prednisolone in 50 ml of 0.1 *N* HCl with different octoxynol concentrations were prepared as described under Micellar Solubilization. Each suspension was vigorously shaken on the shaker bath for 3 days at 140 oscillations/min and poured immediately into a glass funnel with a top diameter of 12 cm connected to a 12-ml graduated glass centrifuge tube with a conical bottom. The volume of the bottom milliliter could be read with an accuracy of ±0.01 ml.

Particle Size Distribution of Prednisolone Suspensions—The number and sizes of the coarse particles contained in 0.1 ml of suspensions prepared as in the preceding section were determined by withdrawing a 0.1-ml aliquot immediately after vigorous shaking, using a graduated pipet with a tip of 2-mm i.d. The size of every coarse particle in that volume was measured with a magnifying glass and a ruler. Since the coarse particles were irregular, their equivalent spherical diameters were recorded.

The number and sizes of the fine particles were measured with a hemacytometer. A drop of a suspension was put into the counting chamber. When the cover glass was placed over it, the liquid layer was reduced to a thickness of 0.1 mm. The dimensions of every particle in four adjacent

[10] Surface Tensiometer, VWR Scientific, Baltimore, Md.
[11] Shaker bath, model 50, Precision Scientific Co., Chicago, Ill.

Table IV—Dissolution Rate of Prednisolone from Tablets in Three Dissolution Media and Zero-Order Dissolution Rate Constants

Tablet Composition[a]	Dissolution Medium[b]	Dissolution Time, min	Prednisolone Dissolved, %[c] Mean ± SD[d]	(N')[e]	Rate Constant ± SD[f], %/min	(N)[g]
I	A	10	3.5 ± 0.8	(4)		
		30	6.7 ± 2.7	(6)		
		50	12.3 ± 1.4	(5)	0.218 ± 0.011	(32)
		75	18.8 ± 2.7	(5)		
		105	23.4 ± 3.2	(5)		
I	B	10	1.9 ± 0.5	(4)		
		30	7.7 ± 1.3	(4)		
		50	13.3 ± 3.0	(4)	0.251 ± 0.007	(20)
		80	20.5 ± 2.5	(4)		
		120	29.5 + 3.1	(4)		
I	C	10	6.4 ± 2.1	(4)		
		25	13.7 ± 2.3	(3)		
		40	22.0 ± 3.4	(3)	0.547 ± 0.010	(20)
		60	32.0 ± 1.8	(3)		
		90	48.3 ± 2.9	(3)		
II	A	5	15.8 ± 0.5	(2)		
		10	24.9 ± 4.6	(5)		
		15	30.8 ± 0.2	(2)		
		20	46.7 ± 5.8	(4)	2.284 ± 0.067	(16)
		25	56.3 ± 2.0	(3)		
		30	96.7 ± 3.8	(4)		
		35	104.2 ± 0.2	(2)		
		40	98.7 ± 2.0	(3)		
		60	100.2 ± 5.1	(3)		

[a] See Table I. [b] See Footnote *b* of Table III for composition and text for properties. [c] The amount in each tablet, namely, 25 mg, represents 100%. [d] Standard deviation. [e] Number of tablets. [f] Standard deviation calculated by Eqs. 5 and 6. [g] Total number of measurements; $N - 1$ is the degree of freedom.

0.2-mm squares, corresponding to a volume of $4 \times (0.2\text{ mm})^2 \times 0.1\text{ mm} = 0.016\text{ mm}^3$, was measured by means of a microscope equipped with an eyepiece micrometer. Since the fine particles were rod-shaped, their lengths and diameters were recorded.

RESULTS

The tablet characteristics are listed in Table II. The small standard errors of the averages indicate that the properties were reproducible.

Tablet Disintegration—Disintegration times are listed in Table III. All tablets, regardless of the presence or absence of octoxynol, retained their integrity during most of the duration of the disintegration test. Only toward the end did they break up into separate fragments.

In liquid Medium A (0.1 *N* HCl), the tablets disintegrated into coarse grains which settled quickly. When octoxynol was added to the disintegrating liquid (Media B and C) or incorporated into the tablets, they disintegrated into fine granules that remained suspended in the liquid, turning it turbid.

Comparing the mean disintegration time of 107.0 min in the absence of octoxynol with the mean value of 104.3 min in the presence of 0.0039% octoxynol by means of the *t* test shows that their 2.5% difference is not statistically significant even at the 20% probability level.

Increasing the octoxynol content of the liquid medium to 0.032% reduced the disintegration time by 37% compared to no octoxynol and by 35% compared to 0.0039% octoxynol. These differences are statistically significant because the two calculated *t* values are larger than the 0.1% critical value for *t*. Incorporation of octoxynol into the tablets reduced the disintegration time by 82%.

The observation that the shortest disintegration times were obtained when octoxynol was incorporated into the tablets may in part be due to their reduced hardness (Table II). However, the major cause is probably the temporary high concentration of dissolved octoxynol inside the tablets as the disintegration liquid penetrates them and leaches the surfactant out of the microcrystalline cellulose granules.

The spread of the individual disintegration times about their mean, as represented by the standard deviation and range, was largest when the medium contained 0.0039% octoxynol and smallest when the octoxynol was incorporated into the tablet, paralleling the rank order of the disintegration times themselves. The rank order of the breadth of the statistical dispersion of the individual values about their means remained the same regardless of whether the standard deviation and range were expressed as percent of the means or as absolute values.

Octoxynol Dissolution Rate—Micelles of nonionic surfactants are slow to dissociate and the nonassociated surfactant molecules are slow to reach equilibrium adsorption at the air–water interface. While most measurements to establish the concentration–surface tension relationship were made after equilibrating the octoxynol solutions at 37° for 1 hr, some surface tensions were measured after 24 hr of equilibration. As is seen in Fig. 1, longer equilibration times did not result in noticeably lower surface tensions.

The calibration plot of surface tension *versus* the log of concentration is linear between the critical micelle concentration of 0.0083% (w/v) (surface tension = 30.9 dyne/cm) and 0.0008% (surface tension = 44.7 dyne/cm). This concentration range corresponds to the region of saturation adsorption of the surfactant at the air–water interface. The least-squares correlation between surface tension, γ, in dyne/cm and octoxynol concentration, C %, (w/v), valid for this concentration range, is:

$$\gamma = 2.59 - 13.62 \log C \qquad \text{(Eq. 1)}$$

with a correlation coefficient of 0.993 ($N = 8$).

When determining the dissolution rate of octoxynol from tablets, 40-ml aliquots were withdrawn from the 900-ml medium for surface tension measurements. These withdrawals represented substantial reductions in the volume of the medium and in the amount of dissolved surfactant. Correction was made by the following equation, derived for that purpose:

$$C_{i,\text{corr}} = \left[\frac{900 - (i-1)40}{900}\right] C_{i,\text{obs}} + \frac{40}{900} \sum_{i-1=1}^{i-1} C_{i-1,\text{obs}} \qquad \text{(Eq. 2)}$$

where $C_{i,\text{corr}}$ is the surfactant concentration in the dissolution medium at the time when the ith aliquot was withdrawn, corrected for the withdrawal of all previous aliquots, *i.e.*, $C_{i,\text{corr}}$ is the concentration that would have been measured if no aliquots had been withdrawn previously. The surfactant concentration in the ith 40-ml aliquot is $C_{i,\text{obs}}$. Both $C_{i,\text{corr}}$ and $C_{i,\text{obs}}$ are expressed as percent (w/v). The summation term starts with the second aliquot, *i.e.*, with $i - 1 = 1$ or $i = 2$; in this term, $i \neq 1$. The summation term is always one aliquot behind the other two terms of Eq. 2.

The values for $C_{i,\text{obs}}$ were obtained from the surface tensions either by means of the calibration plot of Fig. 1 or at octoxynol concentrations between 0.008% and the critical micelle concentration, by Eq. 1.

The presence of debris of insoluble tablet ingredients suspended in the dissolution medium did not affect the surface tension measurements, nor was there substantial adsorption of octoxynol by the debris. The surface tensions of the following media were identical within the precision of the measurements, namely, ±0.1 dyne/cm, at comparable nominal octoxynol concentrations: (*a*) octoxynol solutions in 0.1 *N* HCl, before and after filtration through membrane filters with pore sizes of 0.22 and 0.1 μm; (*b*) octoxynol solutions in dissolution media containing disintegrated tablets, before and after filtration through 0.22- and 0.1-μm filters.

Tablets made from Formulation III and a dissolution medium of 0.1 *N* HCl were used to study the rate of release of octoxynol. A plot of the octoxynol concentration in the dissolution medium *versus* time, obtained with two tablets, was linear and went through the origin (Fig. 2). A plot of the logarithm of the concentration of dissolved octoxynol *versus* time

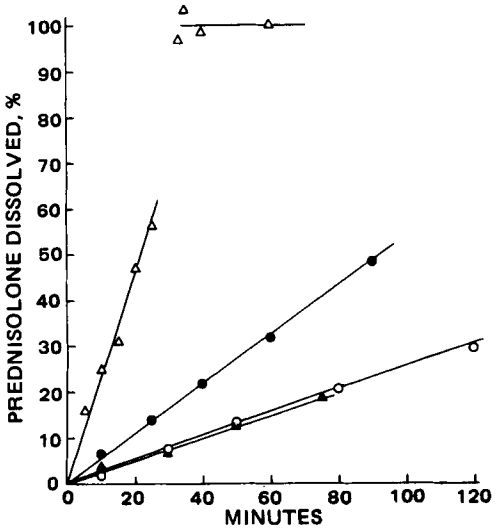

Figure 3—*Effect of octoxynol on the dissolution rate of prednisolone in 0.1 N HCl at 37°. Key: (▲) no octoxynol; (○) 0.0039%, (●) 0.032%; and (△) 0.0039% equivalent octoxynol in tablet but none added to medium.*

was concave toward the time axis. After a dissolution period of 35 min, at which time all of the octoxynol had been dissolved, the tablets disintegrated completely and all fragments fell through the screen of the dissolution basket.

The dissolution of octoxynol from tablets follows zero-order kinetics. The slope of Fig. 2, calculated by the method of least squares, is 0.000112% (w/v)/min, the correlation coefficient is 0.990. The total amount of octoxynol present in the tablet, 35 mg, dissolved in the 900-ml volume of dissolution liquid, would have produced a concentration of 0.00389% (w/v). Therefore, the dissolution rate constant of octoxynol is:

$$k = \frac{dC}{dt} = \left(\frac{0.000112\%\ (w/v)}{\text{min}}\right)\left(\frac{100\%}{0.00389\%\ (w/v)}\right) = 2.88\%/\text{min} \qquad \text{(Eq. 3)}$$

where percent refers to the amount of octoxynol released, expressed as percent of the total amount present or C_∞.

Prednisolone Dissolution Rate—Octoxynol is an effective deflocculating agent and may have dispersed some of the solid prednisolone into colloidal particles. If these particles passed the 0.22-μm membrane filter, they would be assayed together with the dissolved prednisolone, resulting in an excessively high dissolution rate.

When three 5-ml portions of a dissolution medium were filtered in succession through a membrane filter with a pore size of 0.22 μm and an additional three 5-ml portions of the same medium were filtered in succession through a membrane filter with a pore size of 0.1 μm, all six filtrates had identical prednisolone contents. Moreover, the filtrates were clear and did not exhibit Tyndall beams. These facts indicate that only molecularly dissolved prednisolone, and possibly prednisolone solubilized in micelles, were present in the filtrates, and that the membrane filters did not absorb measurable quantities of the steroid. No colloidally dispersed and undissolved prednisolone was present in the filtrates.

The accuracy and reproducibility of the prednisolone assay in the presence of the tableting ingredients was evaluated by assaying three tablets containing 25.0 mg each of prednisolone as described above. After trituration with methanol to dissolve the steroid, the entire mass was diluted to 1.000 liter with 0.1 *N* HCl. Duplicate assays on filtered aliquots for each tablet gave the following results: The mean of six values of prednisolone concentration was 25.05 mg/liter, the standard error 0.07 mg/liter, and the range 0.4 mg/liter. The standard error represents only 0.3% of the mean.

Table V—Sedimentation Volumes of Prednisolone Suspensions at Different Octoxynol Concentrations

Octoxynol Concentration, % (w/v)	Sedimentation Volume, ml		
	Coarse Particles	Fine Particles	Total
0	0.20	0.65	0.85
0.0039	0.19	0.23	0.42
0.012	0.16	0.39	0.55
0.016	0.14	1.02	1.16
0.032	0.13	1.32	1.45
0.128	0.05	2.00	2.05

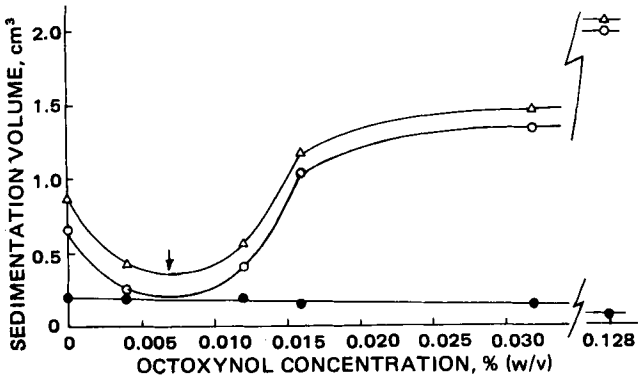

Figure 4—*Sedimentation volume of prednisolone suspensions in 0.1 N HCl at 25° as a function of octoxynol concentration. Key: (●) coarse aggregates; (○) fine; and (△) total volume. Arrow indicates critical micelle concentration.*

The dissolution data are summarized in Table IV. Plots of the logarithms of percent prednisolone dissolved *versus* dissolution time were concave toward the time axis. Plots of percent prednisolone dissolved *versus* dissolution time were straight lines going through the origin, indicating that the dissolution was zero order (Fig. 3).

Dissolution studies were conducted for up to 2 hr. In that period, tablets of Formulation I (no surfactant) in Media A and B released 25–30% of the prednisolone. Under these conditions, tablet disintegration times were somewhat under 2 hr. Nearly half of the prednisolone was dissolved within 1.5 hr in Medium C, where the disintegration time was somewhat >1 hr. When octoxynol was incorporated into the tablet, complete dissolution of the prednisolone occurred in ~30 min, compared with disintegration times of <20 min. Thus, tablet disintegration always preceded complete prednisolone dissolution.

The zero-order rate constants for the dissolution of prednisolone were calculated by (52):

$$k = \frac{\sum tp}{\sum t^2} \qquad \text{(Eq. 4)}$$

where p represents the percent prednisolone dissolved, based on the total amount of prednisolone present in the tablets, namely, 25 mg, and t represents dissolution time.

The standard deviation of k, S_k, was calculated by (52):

$$S_k = \sqrt{\frac{S^2_{t,p}}{\sum t^2}} \qquad \text{(Eq. 5)}$$

The variance of regression is:

$$S^2_{t,p} = \frac{1}{N-1}\left[\sum p^2 - \frac{(\sum tp)^2}{\sum t^2}\right] \qquad \text{(Eq. 6)}$$

where N is the number of measurements and $N-1$ the number of degrees of freedom.

Zero-order dissolution rate constants for the four systems and their standard deviations are listed in Table IV. The mean rate constant in Medium B, containing octoxynol at a concentration of 0.0039% (w/v) or 47% of the critical micelle concentration, is somewhat larger than the one in Medium A without octoxynol. However, the difference between the two values is not statistically significant because the observed t value of 1.816 is smaller than the critical t value at the 5% level for $N_1 + N_2 - 2 = 50$, namely, 2.008 (52).

A higher level of octoxynol in the dissolution medium, 3.9 times the critical micelle concentration, doubled the rate of dissolution. However, the rate of dissolution was increased tenfold when the surfactant was incorporated into the tablet rather than dissolved in the dissolution medium.

Micellar Solubilization of Prednisolone—To ascertain whether micellar solubilization of prednisolone by octoxynol could play a role in speeding up its dissolution from tablets, the solubility of prednisolone in 0.1 *N* HCl solutions containing different concentrations of octoxynol up to 0.128% (w/v) was measured at 37°.

To ensure that equilibration was attained, prednisolone suspensions in 0.1 *N* HCl containing different octoxynol concentrations were shaken at 37° for 2, 6, and 16 days prior to the colorimetric assay, and for 3, 6, and

Table VI—Particle Size Distribution of Prednisolone Suspensions at Different Octoxynol Concentrations

Octoxynol Concentration, % (w/v)	Size Range, μm	Mid-point, D^a, μm	N^b	Number Distribution, Frequency, %	Weight Distribution, Frequency, %
0		Rod-Shaped Particles			
	0–5	2.5	187,500	17.6	0.005
	5–10	7.5	375,000	35.3	0.28
	10–15	12.5	187,500	17.6	0.65
	15–20	17.5	125,000	11.8	1.18
	20–25	22.5	62,500	5.9	1.26
	25–30	27.5	62,500	5.9	2.29
	30–35	32.5	62,500	5.9	3.78
		Coarse Particles			
	0–200	100	380	0.036	0.67
	200–400	300	220	0.021	10.5
	400–600	500	110	0.010	24.2
	600–800	700	70	0.007	42.3
	800–1,000	900	10	0.001	12.9
	Total		1,063,290	100.075	100.015
0.0039		Rod-Shaped Particles			
	0–5	2.5	625,000	37.0	0.02
	5–10	7.5	375,000	22.2	0.36
	10–15	12.5	437,500	25.9	1.96
	15–20	17.5	250,000	14.8	3.07
		Coarse Particles			
	0–200	100	890	0.053	2.04
	200–400	300	360	0.021	22.3
	400–600	500	190	0.011	54.5
	600–800	700	20	0.001	15.7
	Total		1,688,960	99.986	99.95
0.032		Rod-Shaped Particles			
	0–5	2.5	5,562,500	55.3	0.26
	5–10	7.5	3,812,500	37.9	4.77
	10–15	12.5	687,500	6.8	3.98
		Coarse Particles			
	0–200	100	370	0.0037	1.10
	200–400	300	220	0.0022	17.6
	400–600	500	140	0.0014	51.9
	600–800	700	20	0.0002	20.4
	Total		10,063,250	100.0075	100.01

[a] Defined by Eq. 8. [b] Number of particles per milliliter.

22 days prior to analysis by the gravimetric method. In both methods, the longer shaking times did not significantly increase the amount of prednisolone solubilized, indicating that equilibrium had been reached within the shortest shaking times.

The linear relation between the solubility of prednisolone in 0.1 *N* HCl containing octoxynol at concentrations above the critical micelle concentration and the concentration of octoxynol was calculated by the least-squares method. If the solubility limit of prednisolone was expressed in milligrams per liter and the octoxynol concentration in percent (w/v), the colorimetric method yielded an intercept of 309 and a slope of 453. The gravimetric method yielded an intercept of 367 and a slope of 510. According to the *t* test (52), the difference between the two intercepts is not statistically significant at the 5% probability level. Moreover, the intercepts do not differ significantly from the solubility of prednisolone in 0.1 *N* HCl solutions with octoxynol levels between zero and the critical micelle concentration.

Because the difference between the slopes of the two regression lines was not statistically significant either, the two sets of data were pooled. The critical micelle concentration of 0.0083% was subtracted from the total octoxynol concentration C to give the concentration of octoxynol associated into micelles, expressed as percent (w/v). With the solubility of prednisolone S in milligrams per liter as the dependent variable, the equation of the regression line (N = 17) was:

$$S = 342 + 326\,(C - 0.0083) \qquad \text{(Eq. 7)}$$

with a correlation coefficient of 0.804.

The intercept, 342 mg/liter, represents the solubility of prednisolone in the aqueous environment. It is identical with the mean solubility value of prednisolone in 0.1 *N* HCl containing between 0 and 0.008% octoxynol, 343 ± 42 (N = 14).

The slope, 326 mg/liter of prednisolone/% (w/v) micellar octoxynol, represents the solubilizing capacity of octoxynol micelles for prednisolone. For Medium C, containing 0.0320 − 0.0083 = 0.0237% micellar octoxynol, the total solubility of prednisolone S is 350 mg/liter according to Eq. 7. Of this amount, only 8 mg/liter (350 − 342 = 0.0237 × 326 = 8) is solubilized in micelles.

Sedimentation Volumes of Prednisolone Suspensions—The sedimentation volumes of 50-ml suspensions containing 50 mg of prednisolone in 0.1 *N* HCl and different octoxynol concentrations are listed in Table V. Constant sedimentation volumes were reached within 24–48 hr. In the absence or at low concentrations of octoxynol, the suspensions consisted mostly of coarse particles, which were granular aggregates. At intermediate concentrations, in the vicinity of the critical micelle concentration, octoxynol broke these up progressively into fine particles which were rod-shaped. The latter tended to agglomerate into loose flocs at high octoxynol concentrations.

The sediments were stratified into two distinct layers consisting of the coarse and fine particles, respectively, separated by a sharp boundary. The sedimentation volumes of both types of particles were recorded separately and added together in Table V. Octoxynol decreased the sedimentation volumes of the coarse particles in two ways. With increasing concentration, the surfactant peptized progressive amounts of the coarse particles into fine, rod-shaped particles. It also caused the remaining coarse particles to pack more tightly into sediments that were more compact and, hence, occupied progressively smaller volumes.

The sedimentation volume of the fine, rod-shaped particles was not a monotonic function of the octoxynol concentration but went through a minimum in the vicinity of the critical micelle concentration (Fig. 4). The initial decrease was caused by deflocculation of the fine particles into primary rods. Flocs were rarely seen under the microscope below the critical micelle concentration.

As the surfactant concentration increased above the critical micelle concentration, the sedimentation volume of the fine particles increased in two ways. Their number increased because of the progressive breaking up of coarse particles. Moreover, the rod-shaped particles became more extensively aggregated into loose flocs of progressively larger size. Many flocs containing 40–60 rod-shaped particles were observed in 0.128% octoxynol.

Flocculation of the rod-shaped primary particles may be due to bridging by octoxynol micelles. As the surfactant concentration increased, the number and size of the micelles increased, thereby increasing their ability to bridge and bind together rod-shaped prednisolone particles. At concentrations exceeding the critical micelle concentration tenfold or more, cylindrical micelles probably begin to form which, at still higher

concentrations, produce the middle phase (53). Increasing micellar asymmetry increases the number of prednisolone particles on which a single micelle may be adsorbed, cementing them together into flocs.

Particle Size Distribution of Prednisolone Suspensions—Microscopic measurements were conducted on three suspensions in 0.1 *N* HCl containing 0, 0.0039, and 0.032% octoxynol, corresponding to dissolution Media A, B, and C, respectively. The fine particles were rods of length L and width or diameter W. To obtain a particle size distribution which included the fine rod-shaped particles and the coarse irregular particles, a single dimension was needed for the former. The dimension chosen was the surface diameter D (54, 55), *i.e.*, the diameter of a sphere having the same surface area as the rod, because the dissolution rate of very slightly soluble drugs depends largely on their surface area:

$$D = \sqrt{W(L + W/2)} \qquad \text{(Eq. 8)}$$

The particle size distribution data for the three media are listed in Table VI. Number- and weight-distribution frequencies were calculated by standard procedures (54–56). Cumulative plots yielding median diameters were not made because the size distributions are bimodal. However, mean volume–surface diameters D_{vs} (54–56) were calculated:

$$D_{vs} = \sum N_i D_i^3 / \sum N_i D_i^2 \qquad \text{(Eq. 9)}$$

where D_i is the diameter of the midpoint of the ith size range. For the rod-shaped particles, the D values were calculated by Eq. 8.

The D_{vs} values at different octoxynol concentrations and the corresponding specific surface areas, estimated as $6/D_{vs}$, are listed in Table VII. The surfactant increased the specific surface area A of the suspended prednisolone particles by only 10% below the critical micelle concentration but more than doubled it above that concentration.

Within the range of data of Table VII, there is a linear relation between the specific surface area A in cm^2/cm^3 and the octoxynol concentration C in % (w/v):

$$A = 347 + 12{,}900\,C \qquad \text{(Eq. 10)}$$

with a correlation coefficient of 0.99956. This proportionality cannot extend to higher octoxynol concentrations at which the coarse particles are completely broken down because, at these concentrations, the surfactant flocculates the primary, rod-shaped particles extensively.

DISCUSSION

The experimental data afford an assessment of the relative contributions of wetting, micellar solubilization, and deflocculation towards the enhancement of the dissolution rate of prednisolone by octoxynol.

Wetting—The first step in the disintegration of tablets and dissolution of the active ingredient is the displacement of air from the internal surface of the tablet by the dissolution medium, replacing the solid–air with a solid–liquid interface. This wetting process is expedited if the dissolution medium makes a small or zero contact angle on the solid surface. Small contact angles are generally produced by liquids of low surface tension.

The following facts demonstrate that wetting affected neither the disintegration time of the tablets nor the dissolution rate of the active ingredient. Medium A, consisting of 0.1 *N* HCl with a surface tension of 71.1 dyne/cm at 37°, produced only marginally greater disintegration times than Medium B, which consisted of 0.100 *N* HCl + 0.0039% octoxynol with only half the surface tension. Medium C, consisting of 0.1 *N* HCl + 0.032% octoxynol with a surface tension of 30.9 dyne/cm, which is only 4.5 dyne/cm below that of Medium B, reduced the disintegration time by one-third (Table III).

No additional air bubbles were released from the disintegrating tablets after the initial immersion time of 1 min. Therefore, wetting, *i.e.*, the penetration of the dissolution medium into the pores of the tablets and the displacement of the air therein, was completed within that period.

The dissolution rate of prednisolone in Medium B was only marginally higher than that in Medium A, despite the fact that the latter had twice the surface tension of the former. The dissolution rate in Medium C was twice that in Medium B (Table IV), despite the small difference in their surface tensions.

Since wetting depends markedly on surface tension, while the disintegration times and dissolution rates were not correlated with surface tension, wetting was not a rate-determining step for these processes.

Micellar Solubilization of Prednisolone—According to Eq. 7, 326 mg/liter prednisolone is solubilized by 1% (w/v) or 10,000 mg/liter micellar octoxynol at saturation. The solubilizing capacity of octoxynol is thus 0.0326 g of prednisolone/g of micellar octoxynol; *i.e.*, 0.057 mole of prednisolone/mole of micellar octoxynol, or 18 moles of micellar octoxynol/mole of solubilized prednisolone. This value is typical for micellar solubilization of steroids by nonionic surfactants (57, 58).

The following two facts demonstrate that micellar solubilization cannot play a significant role in the enhancement of the dissolution rate of prednisolone by octoxynol. Medium C, with 0.0320 − 0.0083 = 0.0237% micellar octoxynol, dissolves 350 mg/liter prednisolone at saturation, or a maximum of 315 mg for the actual 900-ml volume of the dissolution medium. Of the latter amount, only 7 mg is solubilized in micelles, while most of the prednisolone is dissolved in the aqueous environment.

Of the 25 mg of prednisolone contained in a tablet, only a small fraction will be solubilized by micelles, <3% if the partition coefficient of prednisolone dissolved in the aqueous phase and in the micelles of a 0.032% octoxynol solution equals the ratio of its solubility limits, namely, (350 − 8)/8 or 43:1.

The greatest enhancement of the dissolution rate of prednisolone was observed with Formulation III (Tables I and IV), where octoxynol was incorporated into the tablets. This 35 mg of octoxynol, if it existed entirely in the micellar form, could solubilize a maximum of 1.1 mg of prednisolone according to Eq. 7, *i.e.*, no more than 5% of the prednisolone present in the tablets. Thus, micellar solubilization cannot play a major role in speeding up the dissolution of prednisolone even in the hypothetical situation where the dissolution medium flowing into a tablet dissolves all of the octoxynol contained therein, and where the micellar solution thus produced becomes saturated with prednisolone inside the tablet before octoxynol begins to diffuse out.

Deflocculation—The tablet disintegration experiments provided a visual demonstration of deflocculation. Even at octoxynol concentrations below the critical micelle concentration, the tablets broke up into fine granules that remained in suspension, compared with coarse, quickly sedimenting grains in the absence of surfactant.

The data of Table VII and Eq. 10 indicate that octoxynol deflocculated the suspended prednisolone and that the extent of deflocculation was proportional to the surfactant concentration. It is interesting to compare quantitatively the increase in dissolution rate with the increase in specific surface area measured at comparable octoxynol concentrations to ascertain whether the deflocculation was extensive enough to produce the observed increases in dissolution rate.

The Noyes–Whitney (59) and Nernst–Brunner (60) equation relates the rate of change of drug concentration C in the dissolution medium with time t to the specific surface area A of the drug particles, the thickness h of the stagnant saturated solvent layer surrounding the drug particle, the solubility limit of the drug, C_s, which is its concentration in the stagnant layer, and the drug concentration C_t in the bulk solvent at time t:

$$\frac{dC}{dt} = \frac{DA}{h}(C_s - C_t) \qquad \text{(Eq. 11)}$$

where D represents the diffusion coefficient of the drug molecules in solution.

The maximum values of C_t in the present experiments, attained when the 25 mg of prednisolone present in the tablets is completely dissolved in the 0.9-liter volume of dissolution medium, is 25 mg/0.9 liter or 28 mg/liter. This value is <10% of the lower prednisolone solubility limit of 342 mg/liter obtained in the absence of octoxynol. Therefore, $C_s \gg C_t$ and $C_s - C_t \cong C_s$. The left term in Eq. 11 represents the zero-order dissolution rate constant k obtained from Fig. 3 and listed in Table IV. Thus, Eq. 11 simplifies to:

$$k = DAC_s/h \qquad \text{(Eq. 12)}$$

indicating that k should be directly proportional to A if h is independent of A.

The last column of Table VII lists the ratios k/A. They increased by a mere 16% while A and k more than doubled. The slight increase in the k/A ratio with increasing k and A values may not be statistically significant despite the consistent trend. If the increase is significant, it can be ascribed to a slight decrease in h caused by an increase in A. A slight decrease in the thickness of the stagnant layer caused by a large reduction in particle size is to be expected.

Of the three possible mechanisms by which octoxynol could have increased the rate of dissolution of prednisolone, only deflocculation was extensive enough to account for the magnitude of the observed rate enhancement. Neither wetting nor micellar solubilization made significant contributions to the observed effect.

Higher octoxynol concentrations, *e.g.*, 16 times its critical micelle concentration, produced extensive flocculation of the primary rod-shaped particles. However, these surfactant concentrations were much larger than those attainable in a practical situation.

Table VII—Mean Volume–Surface Diameters and Specific Surface Areas of Prednisolone Suspensions and Their Relation with Dissolution Rate Constants

Octoxynol Concentration, % (w/v)	D_{vs}, μm	A, cm^2/cm^3	k[a], %/min	k/A, 10^4(%/min)/(cm^2/cm^3)
0	170	353	0.218	6.2
0.0039	154	390	0.251	6.4
0.032	79	760	0.547	7.2

[a] Values of zero-order dissolution rate constant from Table IV.

The highest dissolution rates were obtained when the octoxynol was incorporated into the tablets. The transient, relatively concentrated octoxynol solutions produced inside tablets when the octoxynol was extracted from the microcrystalline cellulose by the inflowing dissolution medium produced the most extensive deflocculation of prednisolone. Even these solutions, however, broke up the coarse particles without flocculating the resulting rod-shaped particles. Moreover, flocs of the rod-shaped particles dispersed readily when the suspending medium of concentrated octoxynol was diluted with water or 0.1 *N* HCl.

Relation between Tablet Disintegration Time and Prednisolone Dissolution Rate—Octoxynol reduced the tablet disintegration time and increased the prednisolone dissolution rate considerably. Therefore, the mean tablet disintegration times t in minutes (Table III) and the zero-order rate constants for the dissolution of prednisolone k, in percent per minute (Table IV), were compared for tablets of Composition I in Media A, B, and C and for tablets of Composition II in Medium A.

The relation between log k and t was linear:

$$\log k = 0.546 - 0.0113\,t \qquad \text{(Eq. 13)}$$

with a correlation coefficient of 0.997. While it is to be expected that a given factor, such as the presence of a surfactant, which reduces disintegration times also increases dissolution rates (61, 62), no physical meaning is ascribed to the fact that the two parameters were related by a linear relationship on a semilogarithmic scale.

REFERENCES

(1) H. Schott and A. N. Martin, in "American Pharmacy," 7th ed., L. W. Dittert, Ed., Lippincott, Philadelphia, Pa., 1974, Chap. 6.

(2) W. Awe and H. Gelbrecht, *Pharm. Z.*, **101**, 1112 (1956).

(3) B. F. Cooper and E. A. Brecht, *J. Am. Pharm. Assoc., Sci. Ed.*, **46**, 520 (1957).

(4) D. E. Wurster and J. A. Seitz, *ibid.*, **49**, 335 (1960).

(5) L. Aradi, *Acta Pharm. Hung.*, **31**, 272 (1960).

(6) J. B. Ward and A. Trachtenberg, *Drug Cosmet. Ind.*, **91**(7), 35 (1962).

(7) G. Levy and R. H. Gumtow, *J. Pharm. Sci.*, **52**, 1139 (1963).

(8) H. Nogami, H. Fukuzawa, and Y. Nakai, *Chem. Pharm. Bull.*, **11**, 1389 (1963).

(9) J. K. C. Yen, *Can. Pharm. J., Sci. Sect.*, **97**, 493 (1964).

(10) E. E. Borzunov, S. M. Shevchenko, and S. A. Nosovitskaya, *Med. Prom. SSSR*, **19**(11), 31 (1965); through *Chem. Abstr.*, **64**, 4874h (1966).

(11) S. J. Desai, P. Singh, A. P. Simonelli, and W. I. Higuchi, *J. Pharm. Sci.*, **55**, 1230 (1966).

(12) J. T. Ingram and W. Lowenthal, *ibid.*, **57**, 187 (1968).

(13) P. Singh, S. J. Desai, A. P. Simonelli, and W. I. Higuchi, *ibid.*, **57**, 217 (1968).

(14) P. Finholt and S. Solvang, *ibid.*, **57**, 1322 (1968).

(15) B. Chodkowska-Granicka and L. Krowczynski, *Acta Pol. Pharm.*, **25**, 299 (1968); through *Chem. Abstr.*, **70**, 31665v (1969).

(16) *Ibid.*, **25**, 527 (1968); through *Chem. Abstr.*, **70**, 60786r (1969).

(17) H. Weintraub and M. Gibaldi, *J. Pharm. Sci.*, **58**, 1368 (1969).

(18) E. E. Borzunov, *Farm. Zh.*, **26**, 49 (1971); through *Chem. Abstr.*, **75**, 121361a (1971).

(19) W. Lowenthal, *Pharm. Acta Helv.*, **48**, 589 (1973).

(20) N. Watari and N. Kaneniwa, *Chem. Pharm. Bull.*, **24**, 2577 (1976).

(21) P. Finholt, in "Dissolution Technology," L. J. Leeson and J. T. Carstensen, Eds., The Industrial Pharmaceutical Technology Section of the Academy of Pharmaceutical Sciences, Washington, D.C., 1974, Chap. 4.

(22) B. R. Hajratwala and H. Taylor, *J. Pharm. Pharmacol.*, **28**, 934 (1976).

(23) H. Schott and I. J. Kazella, *J. Am. Oil Chem. Soc.*, **44**, 416 (1967).

(24) J. H. Schulman and J. Leja, *Trans. Faraday Soc.*, **50**, 598 (1954).

(25) L. Ter Minassian-Saraga, *J. Chim. Phys.*, **57**, 10 (1960).

(26) D. E. Wurster and P. W. Taylor, *J. Pharm. Sci.*, **54**, 169 (1965).

(27) P. W. Taylor and D. E. Wurster, *ibid.*, **54**, 1654 (1965).

(28) E. L. Parrott and V. K. Sharma, *ibid.*, **56**, 1341 (1967).

(29) T. R. Bates, S.-L. Lin, and M. Gibaldi, *ibid.*, **56**, 1492 (1967).

(30) M. Gibaldi, S. Feldman, R. Wynn, and N. D. Weiner, *ibid.*, **57**, 787 (1968).

(31) P. Singh, S. J. Desai, D. R. Flanagan, A. P. Simonelli, and W. I. Higuchi, *ibid.*, **57**, 959 (1968).

(32) A. P. Simonelli, D. R. Flanagan, and W. I. Higuchi, *ibid.*, **57**, 1629 (1968).

(33) P. H. Elworthy and F. J. Lipscomb, *J. Pharm. Pharmacol.*, **20**, 923 (1968).

(34) M. Gibaldi, S. Feldman, and N. D. Weiner, *J. Pharm. Sci.*, **58**, 132 (1969).

(35) M. Gibaldi, S. Feldman, and N. D. Weiner, *Chem. Pharm. Bull.*, **18**, 715 (1970).

(36) R. J. Braun and E. L. Parrott, *J. Pharm. Sci.*, **61**, 175 (1972).

(37) *Ibid.*, **61**, 592 (1972).

(38) J. A. Rees and J. H. Collett, *J. Pharm Pharmacol.*, **26**, 956 (1974).

(39) A. S. Alam and E. L. Parrott, *J. Pharm. Sci.*, **60**, 795 (1971).

(40) L. S. C. Wan, *Can. J. Pharm. Sci.*, **12**, 34 (1977).

(41) J. Sanchez-Morcillo and E. Selles, *Congr. Nac. Biofarm. Farmacocinet. (Actas)* **1**, 405 (1977).

(42) P. Fuchs, E. Schottky, and G. Schenck, *Pharm. Ind.*, **32**, 581 (1970).

(43) G. Kedvessy and E. Mucsi, *Pharm. Zentralhalle*, **104**, 309 (1965).

(44) R. Huettenrauch and U. Zahn, *Pharmazie*, **29**, 547 (1974).

(45) R. Huettenrauch, U. Zahn, and J. Jacob, *ibid.*, **30**, 57 (1975).

(46) D. Duchene, A. Djiane, and F. Puisieux, *Ann. Pharm. Franc.*, **28**, 289 (1970).

(47) M. J. Rosen, "Surfactants and Interfacial Phenomena," Wiley-Interscience, New York, N.Y., 1978, Chap. 9.

(48) M. Gibaldi, in "The Theory and Practice of Industrial Pharmacy," 2nd ed., L. Lachman, H. A. Lieberman, and J. L. Kanig, Eds., Lea & Febiger, Philadelphia, Pa., 1976, pp. 108–111.

(49) D. Ganderton, J. W. Hadgraft, W. T. Rispin, and A. G. Thompson, *Pharm. Acta Helv.*, **42**, 152 (1967).

(50) "The United States Pharmacopeia," 19th rev., U.S. Pharmacopeial Convention, Rockville, Md., 1975, pp. 650–651.

(51) C. C. Porter and R. H. Silber, *J. Biol. Chem.*, **185**, 201 (1950).

(52) W. J. Youden, "Statistical Methods for Chemists," Wiley, New York, N.Y., 1951, Chap. 5.

(53) J. M. Corkill and J. F. Goodman, *Adv. Colloid Interface Sci.*, **2**, 297 (1969).

(54) J. M. DallaValle, "Micromeritics," Pitman, New York, N.Y., 1943, Chap. 3.

(55) A. N. Martin, J. Swarbrick, and A. Cammarata, "Physical Pharmacy," 2nd ed., Lea & Febiger, Philadelphia, Pa., 1969, Chap. 17.

(56) R. R. Irani and C. F. Callis, in "Particle Size: Measurement, Interpretation and Application," Wiley, New York, N.Y., 1963, pp. 25–45.

(57) P. H. Elworthy, A. T. Florence, and C. B. MacFarlane, "Solubilization by Surface-Active Agents," Chapman & Hall, London, England, 1968, Chap. 3.

(58) L. Sjöblom, in "Solvent Properties of Surfactant Solutions," K. Shinoda, Ed., Dekker, New York, N.Y., 1967, Chap. 5.

(59) A. A. Noyes and W. R. Whitney, *J. Am. Chem. Soc.*, **19**, 930 (1897).

(60) W. Nernst and E. Brunner, *Z. Physik. Chem.*, **47**, 52 (1904).

(61) L. C. Schroeter, J. E. Tingstad, E. L. Knoechel, and J. G. Wagner, *J. Pharm. Sci.*, **51**, 865 (1962).

(62) J. T. Carstensen, "Solid Pharmaceutics: Mechanical Properties and Rate Phenomena," Academic, New York, N.Y., 1980, Chap. VI-5.

ACKNOWLEDGMENTS

Adapted from the dissertation submitted by Lilian Chong Kwan to Temple University in partial fulfillment of the Master of Science requirements.

Presented in part at the Fourth International Conference on Surface and Colloid Science, Jerusalem, Israel, July 1981.

The authors thank Dr. Irving I. A. Tabachnick, Vice-President, Drug Safety and Metabolism, Schering Corp., for the gift of prednisolone.

Synthesis of Some Benzofuran and Furocoumarin Derivatives for Possible Biological Activity

O. H. HISHMAT, A. H. ABD EL RAHMAN *x, Kh. M. A. KHALIL, M. I. MOAWAD, and M. M. ATALLA

Received December 18, 1980, *from the National Research Centre, Dokki, Cairo, Egypt.* Accepted for publication October 15, 1981. *Present address, Chemistry Department, Faculty of Science, Mansoura University, Mansoura, Egypt.

Abstract □ Condensation of 5-formyl-6-methoxy-2,3-diphenylbenzofuran (I) and 6-formyl-5-methoxy-2,3-diphenylbenzofuran (II) with aliphatic or aromatic primary amines led to the formation of the corresponding anils (III*a–k* and IV*a–c*). The anils (III*a,f,k* or IV*a–c*) reacted with ethyl cyanoacetate, ethyl acetoacetate, or diethyl malonate to form the respective esters (V*a–c* or VI*a–c*). When V*a–c* or VI*a–c* were treated with pyridine hydrochloride, demethylation occurred followed by cyclization to form the corresponding furocoumarins (VII*a–c* or VIII*a–c*). Reduction of the anils using sodium borohydride furnished the corresponding Mannich bases (X*a–d* and XI). The antimicrobial activity of compounds III*i*, IV*c*, V*a*, VI*a*, and VIII*a* was investigated.

Keyphrases □ Benzofuran—derivatives, synthesis for possible biological activity □ Furocoumarin—derivatives, synthesis for possible biological activity □ Antimicrobial activity—synthesis of some benzofuran and furocoumarin derivatives for possible biological activity

Furocoumarins (1–3) are used as photosensitizing agents, and some of their derivatives possess tuberculostatic (4) as well as molluskicidal (5) activity. Following up a previous investigation (6), synthesis of some new furocoumarins (VII and VIII) derived from 5-formyl-6-methoxy-2,3-diphenylbenzofuran (I) (7) and 6-formyl-5-methoxy-2,3-diphenylbenzofuran (II) (6, 7) was undertaken to investigate these compounds.

DISCUSSION

Condensation of I or II with equimolar quantities of the appropriate amines gave the corresponding anils (III or IV), respectively. The amines employed were propyl-, isopropyl-, hexyl-, cyclohexyl-, benzylamine; aniline; *m*-toluidine; *p*-toluidine; *p*-anisidine; and *m*-chloro- and *p*-chloroaniline.

The structure assigned to these anils was supported by IR spectra,

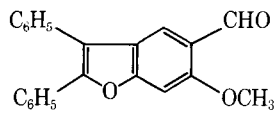

I

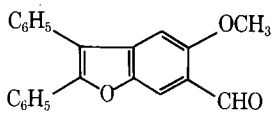

II

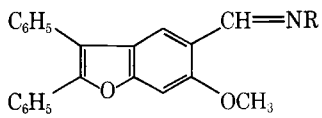

III

a, R=$(CH_2)_2CH_3$
b, R=$CH(CH_3)_2$
c, R=$(CH_2)_5CH_3$
d, R=cyclohexyl
e, R=$CH_2C_6H_5$
f, R=C_6H_5
g, R=$C_6H_4CH_3$ (*meta*)
h, R=$C_6H_4CH_3$ (*para*)
i, R=$C_6H_4OCH_3$ (*para*)
j, R=C_6H_4Cl (*meta*)
k, R=C_6H_4Cl (*para*)

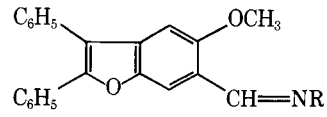

IV

a, R=C_6H_5
b, R=$C_6H_4CH_3$ (*para*)
c, R=$C_6H_4OCH_3$ (*para*)

which showed absorption at 1625–1635 cm^{-1} assignable to —CH=N (8). The PMR spectrum of III*e* showed singlets at δ 3.92 (OCH_3, 3H), 4.84 (CH_2—, 2H), 7.08 (C-4, 1H), and 8.18 (C-7, 1H). The aromatic protons appeared as multiplets at 7.40–7.66 (15H). The mass spectra of III*e* and *k* showed intense molecular ions (M^+) at *m/z* (relative intensity) 417 and 437/439, respectively. In both spectra the imino moieties were eliminated yielding a base peak at *m/z* 311.

Compounds III*e*, *f*, or *k* and IV*a–c* reacted with ethyl cyanoacetate in dry benzene to give the respective esters, V*a* and VI*a*. Compounds V*a* and VI*a* were also obtained by the reaction of I and II with ethyl cyanoacetate in the presence of piperidine. The IR spectrum of V*a* revealed a band at 2220 cm^{-1} characteristic for C≡N group and a band at 1705

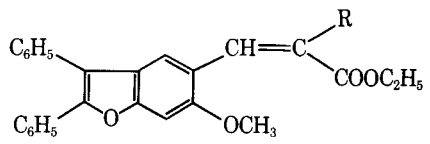

V

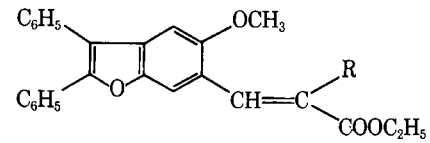

VI

a, R=CN
b, R=$COCH_3$
c, R=$COOC_2H_5$

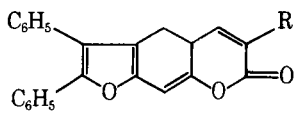

VII

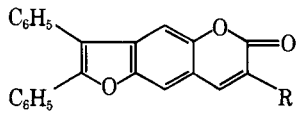

VIII

a, R=H
b, R=$COCH_3$
c, R=$COOC_2H_5$

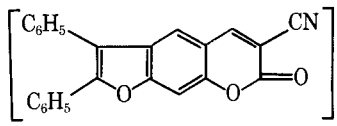

IX

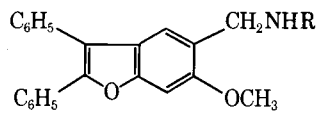

X

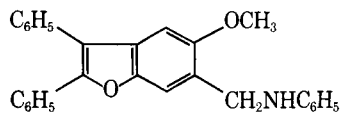

XI

a, R=$(CH_2)_2CH_3$
b, R=C_6H_5
c, R=$C_6H_4OCH_3$ (*para*)
d, R=C_6H_4Cl (*para*)

0022-3549/82/0900-1046$01.00/0

Table I—Physical Data for Anils IIIa–k and IVa–c

Compound	mp	Yield, %	Formula	Analysis Calc.	Analysis Found
IIIa	142–144	74	$C_{25}H_{23}NO_2$	C 81.31 H 6.23 N 3.79	C 81.10 H 5.96 N 3.52
IIIb	138–140	79	$C_{25}H_{23}NO_2$	C 81.31 H 6.23 N 3.79	C 40.96 H 5.91 N 3.47
IIIc	146–148	67	$C_{28}H_{29}NO_2$	C 81.75 H 7.06 N 3.40	C 81.72 H 6.89 N 3.49
IIId	154–156	78	$C_{28}H_{29}NO_2$	C 82.15 H 6.60 N 3.42	C 82.40 H 6.30 N 3.47
IIIe	163–165	85	$C_{29}H_{23}NO_2$	C 83.45 H 5.52 N 3.36	C 83.60 H 5.55 N 3.25
IIIf	192–194	91	$C_{28}N_{21}NO_2$	C 83.37 H 5.21 N 3.47	C 83.62 H 5.53 N 3.35
IIIg	155–157	74	$C_{29}H_{23}NO_2$	C 83.45 H 5.52 N 3.36	C 83.68 H 5.50 N 3.26
IIIh	180–182	63	$C_{29}H_{23}NO_2$	C 83.45 H 5.52 N 3.36	C 83.32 H 5.61 N 3.01
IIIi	148–150	77	$C_{29}H_{23}NO_3$	C 80.37 H 5.31 N 3.23	C 80.68 H 5.52 N 3.43
IIIj	148–150	86	$C_{28}H_{20}ClNO_2$	C 76.80 H 4.57 N 3.20 Cl 8.12	C 76.82 H 4.83 N 2.84 Cl 7.89
IIIk	162–164	78	$C_{28}H_{20}ClNO_2$	C 76.80 H 4.57 N 3.20 Cl 8.12	C 76.62 H 4.83 N 6.92 Cl 7.79
IVa	128–130	72	$C_{28}H_{21}NO_2$	C 83.37 H 5.21 N 3.47	C 83.44 H 5.46 N 3.24
IVb	150–152	76	$C_{29}H_{23}NO_2$	C 83.45 H 5.52 N 3.36	C 83.51 H 5.77 N 3.09
IVc	163–165	61	$C_{29}H_{23}NO_3$	C 80.37 H 5.31 N 3.23	C 79.99 H 5.32 N 2.94

Table II—Physical Data for Esters Va–c and VIa–c

Compound	mp	Yield, %	Formula	Analysis Calc.	Analysis Found
Va	192–194	74	$C_{27}H_{21}NO_4$	C 76.60 H 4.96 N 3.31	C 76.82 H 5.07 N 3.72
Vb	177–179	71	$C_{28}H_{24}O_5$	C 76.36 H 5.45	C 76.50 H 5.73
Vc	167–169	73	$C_{29}H_{26}O_6$	C 74.04 H 5.53	C 74.46 H 5.74
VIa	192–194	86	$C_{27}H_{21}NO_4$	C 76.60 H 4.96 N 3.31	C 76.45 H 5.23 N 2.99
VIb	168–170	76	$C_{28}H_{24}O_5$	C 76.36 H 5.45	C 76.68 H 5.50
VIc	103–105	75	$C_{29}H_{26}O_6$	C 74.04 H 5.53	C 74.39 H 5.29

cm^{-1}, indicating an ester carbonyl ($—COOC_2H_5$). The mass spectrum of Va showed an M^+ at m/z (relative intensity) 423.

When Va or VIa were treated with pyridine hydrochloride, the furocoumarins VIIa or VIIIa were formed, respectively. The reaction involved demethylation followed by cyclization to form the intermediate derivative IX, which underwent hydrolysis followed by decarboxylation.

The IR spectrum of VIIa showed a band at 1725 cm^{-1} characteristic for the >C=O vibration of coumarins (9). Moreover, absorption bands, corresponding to C≡N and ester >C=O, were not present as in the parent ester Va. The mass spectrum of VIIa showed an M^+ at m/z (relative intensity) 338.

In a similar manner, reaction of IIIf or IVa with ethyl acetoacetate and diethyl malonate yielded Vb and c or VIb and c, respectively.

The mass spectrum of Vb and c showed an M^+ at m/z 440 and 470, respectively.

Treatment of Vb and c and VIb and c with pyridine hydrochloride yielded the corresponding acetyl and carboethoxyfurocoumarin derivatives, VIIb and c and VIIIb and c, respectively.

The structures of VIIb and c and VIIIb and c were confirmed by their melting points and mixed melting points with authentic samples prepared by the reaction of I and II with ethyl acetoacetate and diethyl malonate in the presence of piperidine (7).

Sodium borohydride reduction of the benzofuran anils, IIIa, f, i, and k and IVa, were carried out in ethanol and gave the corresponding Mannich bases Xa–d and XI.

The IR spectrum of Xb showed absorption at 3380 cm^{-1} due to NH

Table III—Physical Data of Mannich Bases X*a–d* and XI

Compound	mp	Yield, %	Formula	Analysis Calc.	Found
X*a*	184–186	69	$C_{25}H_{25}NO_2$	C 80.86 H 6.74 N 3.77	C 81.23 H 7.01 N 3.98
X*b*	154–156	80	$C_{28}H_{23}NO_2$	C 82.96 H 5.68 N 3.46	C 83.17 H 5.82 N 3.58
X*c*	148–150	66	$C_{29}H_{25}NO_3$	C 80.00 H 5.75 N 3.22	C 79.69 H 5.60 N 2.97
X*d*	103–105	53	$C_{28}H_{22}ClNO_2$	C 76.45 H 5.01 Cl 8.08 N 3.19	C 76.71 H 5.35 Cl 8.24 N 3.22
X*I*	124–126	47	$C_{28}H_{23}NO_2$	C 82.96 H 5.68 N 3.45	C 82.76 H 5.80 N 3.07

and no absorption characteristic for C=N appeared. The PMR spectrum of X*b* revealed singlets at δ 3.85 (OCH_3, 3H), 4.40 (CH_2, 2H), 6.75 (C-4, 1H), and 7.72 (C-7, 1H). The NH proton appeared as a broad band at δ 4.00 which disappeared after adding deuterium oxide. Finally, the multiplets at δ 7.17–7.46 corresponded to 15 aromatic protons. The mass spectrum of X*b* showd an M^+ at *m/z* (relative intensity) 405 as a base peak.

EXPERIMENTAL[1]

Studies for Antimicrobial Activity—The activity of some compounds were tested on *Bacillus subtilis*, NRRL 543; *Escherichia coli*, NRRL 210; *Klebsiella pneumoniae*, NRRL 117; *Proteus mirabilis; Sarcina lutea; Salmonella typhosea*, NRRL 537 (bacteria); *Candida lypolitica; Candida pellicula; Sacharomyces cerviceae*, NRRL Y567 (yeasts); *Aspergillus nigar*, NRRL 599; *Fusarium moniliforme*, and *Penicillium funiculosum* (fungi[2]).

Preparation of Benzofuran Anils (III*a–k* and IV*a–c*)—The appropriate amine (0.03 mole) and piperidine (0.5 ml) were added to a solution of I or II (0.03 mole) in benzene or ethanol (50 ml). The reaction mixture was refluxed for 3 hr, then concentrated to ~10 ml and left to cool. The solid was filtered and crystallized from ethanol to give III*a–k* and IV*a–c* as white-yellow crystals (Table I).

Preparation of the Esters (V*a–c* and VI*a–c*)—*Method A*—A mixture of III or IV (1 g) in dry benzene (20 ml) and either ethyl cyanoacetate, ethyl acetoacetate, or diethyl malonate (1.5 ml) was stirred for 0.5 hr and left overnight. The solvent was evaporated under reduced pressure and 5 ml of water was added. The solution was heated and then left to cool. The solid that separated was filtered and crystallized from ethanol to give V*a–c* or VI*a–c* as yellow crystals.

Method B—A mixture of I or II (1 g), 1.5 ml of ethyl cyanoacetate, ethyl acetoacetate, and diethyl malonate esters and piperidine (0.5 ml) in ethanol (50 ml) was refluxed for 1 hr and left to cool. The solid that formed was crystallized from ethanol as yellow crystals.

Methods A and B gave the same products (melting point and mixed melting point gave no depression) (Table II).

Action of Pyridine Hydrochloride on V*a–c* and VI*a–c*—A mixture of V*a–c* or VI*a–c* (1 g) and freshly prepared pyridine hydrochloride (3 g) was kept at 200° for 20 min, left to cool, then acidified with dilute hydrochloric acid. The solid was filtered and crystallized from an appropriate solvent.

Compound VII*a* was obtained at a 56% yield as pale brownish crystals from ethanol, mp 223–225°.

Anal.—Calc. for $C_{23}H_{14}O_3$: C, 81.66; H, 4.14. Found: C, 81.93; H, 3.99.

Compound VII*b* was crystallized from ethanol as pale brownish crystals, mp 256–258°; yield 55% (melting point and mixed melting point with an authentic sample (7) gave no depression).

Compound VII*c* was obtained as pale brownish crystals from ethanol, mp 196–198°; yield 34% (melting point and mixed melting point with an authentic sample (7) gave no depression).

Compound VIII*a* gave a 53% yield as pale brownish crystals from methanol, mp 220–222°.

Anal.—Calc. for $C_{23}H_{14}O_3$: C, 81.66; H, 4.14. Found: C, 81.41; H, 4.36.

Compound VIII*b* produced a 49% yield as pale brownish crystals from ethanol, mp 256° (melting point and mixed melting point with an authentic sample (7) gave no depression).

Compound VIII*c* gave a 52% yield as pale brownish crystals from acetone, mp 195° (melting point and mixed melting point with an authentic sample (7) gave no depression).

Preparation of the Mannich Bases (X*a–d* and XI)—A mixture of III*c, f, i, k*, or IV*a* (1 g) and sodium borohydride (2 g) in ethanol (50 ml) was heated at 50° for 5 min to start the reaction. The reaction mixture was stirred for 2 hr, and 20 ml water was added and left overnight. The solution was filtered, and the solid washed with water and crystallized from ethanol to give the Mannich bases X*a–d* and XI as colorless needles (Table III).

Antimicrobial Activity—A freshly prepared suspension of the test organisms was used to inoculate three plates, each with nutrient agar (bacterial strain), media containing glucose (10 g), yeast extract (3 g), peptone (5 g), and agar (20 g). All ingredients were dissolved in 1 liter of distilled water and adjusted at pH 6.0. The fungi were cultivated on Dox's agar plates. Fungal inoculum was prepared from 14-day old cultures. The paper disk method was used to test III*i*, IV*c*, V*a*, VI*a*, and VII*a*; one representing each series selected at random to screen their antimicrobial activity. A filter paper disk (5-mm diameter) containing 100 μg from each compound was soaked, dried, and firmly applied to the surface of the inoculated agar plates and then the plates with the bacterial strain were incubated at 37° for 48 hr, while those containing yeast and fungi were

Table IV—Antimicrobial Activity of Compounds III*i*, IV*c*, V*a*, VI*a*, and VII*a* Against Bacteria, Yeasts, and Fungi

Micro-organism	Compound III*i*	IV*c*	V*a*	VI*a*	VII*a*
Bacillus subtilis	7[a]	11	7	7	—
Escherichia coli	7	11	7	7	7
Klebsiella pneumoniae	—	9	—	7	—
Proteus mirabilis	—	11	—	7	7
Salmonella typhosae	7	9	7	7	—
Sarcina lutea	8	11	7	10	—
Candida lypolitica	8	14	8	8	—
Candida pellicula	8	—	7	8	—
Sacharomyces cerviceae	—	9	—	8	—
Aspergillus nigar	—	—	—	—	—
Fusarium moniliforme	—	—	—	—	—
Penicillium funiculosum	7	17	8	—	—

[a] Diameters of inhibition zone in millimeters.

[1] All melting points are not corrected. The IR spectra were recorded on Carl-Zeiss Spectrophotometer model UR 10. The PMR spectra were run in $CDCl_3$ at 60 MHz, with tetramethylsilane as internal standard on a Varian instrument. Mass spectra were carried out at 70 eV on a Varian Mat 112 Spectrometer.

[2] The organisms with no identification numbers were isolated locally and were isolated by M. M. Fahim, Y. A. Abduo, and M. M. Atalla, Third Egypt. Phytopathol. Congress, Cairo, pp 734–744 (1979).

incubated at 30° for 48–72 hr. The inhibition zone was measured around each disk (Table IV).

CONCLUSIONS

The present results indicate that the microorganisms tested were sensitive to the action of the anils (IIIi and IVc) and the esters (Va and VIa) except for *A. nigar* and *F. moniliforme*. The results also illustrated that the anils potentiate the activity more than the esters. However, it was observed that the presence of the methoxy group in the *para* position to the benzofuran oxygen (IVc and VIa) increased the activity. The cyclization of Va blocked the activity against most of the microorganisms tested. Such preliminary results would encourage further studies to elucidate the relationship between structure and activity.

REFERENCES

(1) L. Musajo, G. Rodighiero, and G. Caporale, *Chim. Ind. (Milan)*, **35**, 13 (1953); *Chem. Abstr.*, **48**, 4111 (1954).

(2) L. Musajo, G. Rodighiero, and G. Caporale, *Bull. Soc. Chim. Biol.*, **36**, 1213 (1954); *Chem. Abstr.*, **49**, 4871 (1955).

(3) M. A. Pathak, J. H. Fellman, and K. D. Kaufman, *J. Invest. Dermatol.*, **35**, 165 (1960).

(4) G. Rodighiero, B. Perissinotto, and G. Caporale, *Atti Ist. Veneto Sci. Lett. Arti, Cl. Sci. Mat. Nat.*, **114**, 1(1955–56); *Chem. Abstr.*, **51**, 10736 (1957).

(5) A. Schonberg and N. Latif, *J. Am. Chem. Soc.*, **76**, 6208 (1954).

(6) O. H. Hishmat, A.-K. M. N. Gohar, and M. E. Wasef, *Acta Helv.*, **52**, 252 (1977).

(7) O. H. Hishmat and A. H. Abd el Rahman, *Aust. J. Chem.*, **27**, 2499 (1974).

(8) L. J. Bellamy "The Infra-Red Spectra of Complex Molecules," 2nd ed., Methuen, London, England, 1966, p. 269.

(9) R. N. Jones and F. Herling, *J. Org. Chem.*, **19**, 1252 (1954).

Aspirin—A National Survey V: Determination of Aspirin and Impurities in Enteric Coated Tablets and Suppository Formulations and *In Vitro* Dissolution of Enteric Coated Tablets

ROSS D. KIRCHHOEFER ˣ, EVERETT JEFFERSON, and PAUL E. FLINN

Received September 18, 1981, from the *National Center for Drug Analysis, Food and Drug Administration, St. Louis MO 63101.* Accepted for publication December 9, 1981.

Abstract □ The results of a national survey on the quality of enteric coated aspirin tablets and aspirin suppositories are presented. The tablets were analyzed for strength, salicylic acid content, *in vitro* dissolution rate, and related aspirin impurities. The suppositories were analyzed for strength and salicylic acid content. The methods of analysis and validation of data are also presented.

Keyphrases □ Aspirin—semiautomated procedure for enteric coated tablets □ Dissolution—automated *in vitro* profiles of enteric coated aspirin tablets □ Analgesics—determination of aspirin and impurities in enteric coated tablets

A national survey of aspirin tablet products was conducted at the National Center for Drug Analysis in 1978 and 1979 to ascertain the quality of these products.

Parts I–III (1–3) of this series deal with the analysis of aspirin, salicylic acid, and aspirin related impurities in plain and buffered tablets. Part IV (4) compares *in vitro* dissolution results for these dosage forms using both the USP XX paddle and basket procedures (5). The present report describes the quality of enteric coated tablets with respect to content uniformity, dissolution characteristics, and impurities. Suppository formulations were also checked for content uniformity and impurities.

The official compendia do not provide a method or criterion for the *in vitro* dissolution of enteric coated tablets. Embil and Torosian (6) described the dissolution behavior of two brands of enteric coated tablets using a basket procedure. Over 60% of the aspirin content in the two brands dissolved within 3 hr, but there were significant differences in the release rates. Johansen (7) investigated the correlation between dissolution and absorption rates for plain and enteric coated aspirin tablets. The dissolution rate determinations were made with both a Sartorius apparatus and a USP XIX basket apparatus. Johansen found that the USP XIX basket apparatus, when applied to enteric coated tablets, gave a poor *in vitro/in vivo* correlation. He attributed this to the fact that the USP apparatus dissolved aspirin rather quickly after changing from simulated gastric fluid to intestinal fluid. To obtain a better correlation he recommended decreasing the rotational speed of the basket.

The purpose of this study was to investigate a semiau-

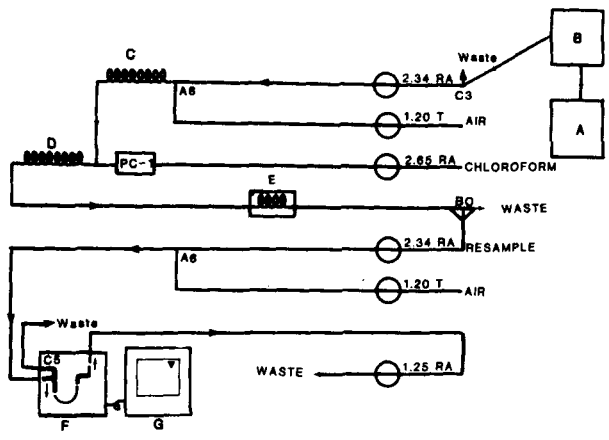

Figure 1—*Flow diagram of automated system for enteric coated aspirin dissolution. Key: (T) Tygon pump tube; (RA) red acidiflex pump tube; (C) 28-turn × 2.4-mm i.d. mixing coil; (D) 28-turn × 2.4-mm i.d. mixing coil with one double end; (E) 5.5-turn setting coil; (F) UV spectrophotometer; (G) recorder; (A) six-spindle dissolution apparatus; (B) automatic sampler. Pump tube sizes are in milliliters per minute. C-3, C-5, A6, and PC-1 are commercially available glass fittings.*

0022-3549/82/0900-1049$01.00/0

incubated at 30° for 48–72 hr. The inhibition zone was measured around each disk (Table IV).

CONCLUSIONS

The present results indicate that the microorganisms tested were sensitive to the action of the anils (IIIi and IVc) and the esters (Va and VIa) except for *A. nigar* and *F. moniliforme*. The results also illustrated that the anils potentiate the activity more than the esters. However, it was observed that the presence of the methoxy group in the *para* position to the benzofuran oxygen (IVc and VIa) increased the activity. The cyclization of Va blocked the activity against most of the microorganisms tested. Such preliminary results would encourage further studies to elucidate the relationship between structure and activity.

REFERENCES

(1) L. Musajo, G. Rodighiero, and G. Caporale, *Chim. Ind. (Milan)*, **35**, 13 (1953); *Chem. Abstr.*, **48**, 4111 (1954).

(2) L. Musajo, G. Rodighiero, and G. Caporale, *Bull. Soc. Chim. Biol.*, **36**, 1213 (1954); *Chem. Abstr.*, **49**, 4871 (1955).

(3) M. A. Pathak, J. H. Fellman, and K. D. Kaufman, *J. Invest. Dermatol.*, **35**, 165 (1960).

(4) G. Rodighiero, B. Perissinotto, and G. Caporale, *Atti Ist. Veneto Sci. Lett. Arti, Cl. Sci. Mat. Nat.*, **114**, 1(1955–56); *Chem. Abstr.*, **51**, 10736 (1957).

(5) A. Schonberg and N. Latif, *J. Am. Chem. Soc.*, **76**, 6208 (1954).

(6) O. H. Hishmat, A.-K. M. N. Gohar, and M. E. Wasef, *Acta Helv.*, **52**, 252 (1977).

(7) O. H. Hishmat and A. H. Abd el Rahman, *Aust. J. Chem.*, **27**, 2499 (1974).

(8) L. J. Bellamy "The Infra-Red Spectra of Complex Molecules," 2nd ed., Methuen, London, England, 1966, p. 269.

(9) R. N. Jones and F. Herling, *J. Org. Chem.*, **19**, 1252 (1954).

Aspirin—A National Survey V: Determination of Aspirin and Impurities in Enteric Coated Tablets and Suppository Formulations and *In Vitro* Dissolution of Enteric Coated Tablets

ROSS D. KIRCHHOEFER ˣ, EVERETT JEFFERSON, and PAUL E. FLINN

Received September 18, 1981, from the *National Center for Drug Analysis, Food and Drug Administration, St. Louis MO 63101.* Accepted for publication December 9, 1981.

Abstract □ The results of a national survey on the quality of enteric coated aspirin tablets and aspirin suppositories are presented. The tablets were analyzed for strength, salicylic acid content, *in vitro* dissolution rate, and related aspirin impurities. The suppositories were analyzed for strength and salicylic acid content. The methods of analysis and validation of data are also presented.

Keyphrases □ Aspirin—semiautomated procedure for enteric coated tablets □ Dissolution—automated *in vitro* profiles of enteric coated aspirin tablets □ Analgesics—determination of aspirin and impurities in enteric coated tablets

A national survey of aspirin tablet products was conducted at the National Center for Drug Analysis in 1978 and 1979 to ascertain the quality of these products.

Parts I–III (1–3) of this series deal with the analysis of aspirin, salicylic acid, and aspirin related impurities in plain and buffered tablets. Part IV (4) compares *in vitro* dissolution results for these dosage forms using both the USP XX paddle and basket procedures (5). The present report describes the quality of enteric coated tablets with respect to content uniformity, dissolution characteristics, and impurities. Suppository formulations were also checked for content uniformity and impurities.

The official compendia do not provide a method or criterion for the *in vitro* dissolution of enteric coated tablets. Embil and Torosian (6) described the dissolution behavior of two brands of enteric coated tablets using a basket procedure. Over 60% of the aspirin content in the two brands dissolved within 3 hr, but there were significant differences in the release rates. Johansen (7) investigated the correlation between dissolution and absorption rates for plain and enteric coated aspirin tablets. The dissolution rate determinations were made with both a Sartorius apparatus and a USP XIX basket apparatus. Johansen found that the USP XIX basket apparatus, when applied to enteric coated tablets, gave a poor *in vitro/in vivo* correlation. He attributed this to the fact that the USP apparatus dissolved aspirin rather quickly after changing from simulated gastric fluid to intestinal fluid. To obtain a better correlation he recommended decreasing the rotational speed of the basket.

The purpose of this study was to investigate a semiau-

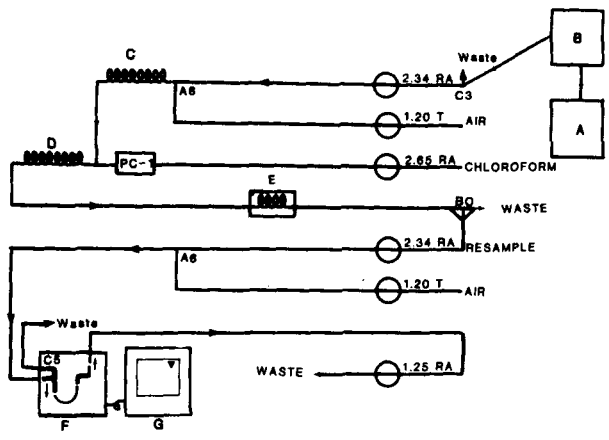

Figure 1—*Flow diagram of automated system for enteric coated aspirin dissolution. Key: (T) Tygon pump tube; (RA) red acidiflex pump tube; (C) 28-turn × 2.4-mm i.d. mixing coil; (D) 28-turn × 2.4-mm i.d. mixing coil with one double end; (E) 5.5-turn setting coil; (F) UV spectrophotometer; (G) recorder; (A) six-spindle dissolution apparatus; (B) automatic sampler. Pump tube sizes are in milliliters per minute. C-3, C-5, A6, and PC-1 are commercially available glass fittings.*

0022-3549/82/0900-1049$01.00/0

Table I—Aspirin in Enteric Coated Tablets by Semiautomated Procedure and Salicylic Acid as Percent of Aspirin Declaration

Manufacturer[a]	Tablet Dosage, mg	Aspirin[b], %	Salicylic Acid, %
A	324	101.1 (1.85)	0.3
A	648	96.8 (1.34)	0.2
A	648	95.8 (2.42)	0.1
A	324	99.8 (3.58)	0.1
B	324	100.5 (2.32)	[c]
B	324	100.3 (2.57)	[c]
B	324	99.8 (2.11)	[c]
B	324	100.8[d] (2.23)	[c]
B	324	100.8 (2.61)	[c]
C	320	97.9[d] (2.81)	0.1
C	320	100.0[d] (2.21)	0.2
D	648	100.2 (1.91)	0.2
D	648	99.9 (1.66)	0.1
D	648	100.5 (1.63)	[c]
D	325	99.8 (2.52)	1.2
D	325	96.1 (1.57)	0.6
D	486	99.5 (1.95)	0.4
D	324	100.8 (2.14)	0.1
D	324	100.4 (1.84)	0.5
D	650	97.3 (2.15)	0.6
D	325	99.3 (2.30)	1.6

[a] (A) Eli Lilly & Co., Indianapolis, Ind.; (B) Smith Kline Corp., Philadelphia, Pa.; (C) Vale Chemical Co., Allentown, Pa.; (D) Standard Pharmacal Co., Chicago, Ill. [b] Each value represents 60 determinations unless otherwise noted. Number in parentheses is standard deviation. [c] Met compendial requirements. [d] Represents 30 determinations.

tomated UV (1) method for the determination of aspirin in enteric coated tablets, an automated method for the determination of the *in vitro* dissolution rate of aspirin from enteric coated tablets, and a manual UV method for the determination of aspirin in suppositories. In addition, five batches of enteric coated tablets were tested for aspirin-related impurities by the procedures described previously (3).

EXPERIMENTAL

Content Uniformity of Enteric Coated Tablets—*Apparatus, Reagents, and Determination*—These have been described previously (1).

Standard Preparation—About 325 mg of USP reference standard aspirin was accurately weighed and dissolved in 50.0 ml of buffer–ethanol solution (1:1). The standard solution was prepared fresh daily.

Sample Preparation—Each 325-mg enteric coated tablet was cracked and partially crushed in a piece of weighing paper[1] with a hammer and then transferred to separate 50-ml volumetric flasks. Alcoholic pH 2.2 buffer solution was added, and the flasks were placed in an ultrasonic bath[2] for ~1.5 hr with frequent shaking. The flasks were kept cool with circulating tap water. The flasks then were removed and the contents diluted to volume with alcoholic pH 2.2 buffer solution. After settling for 30 min, the solution in the flasks was analyzed as described previously (1).

Dissolution—*Apparatus*—A dissolution apparatus[3], equipped with a paddle [apparatus 2, (5)], and an automated sampler described previously (8) were used. The USP paddle method was used because it has been preferred historically in the laboratory.

For the determinative step, an automatic analyzer with a pump[4], manifold, spectrophotometer[5], flowcell[6], and recorder[7] was connected to the automatic sampler (8).

Reagents—American Chemical Society (ACS) grade chloroform was washed with water and filtered through paper on the day of use. The 0.4 *N* HCl was prepared by diluting 34.0 ml of concentrated hydrochloric acid to 1.0 liter with water. The simulated gastric fluid and simulated intestinal fluid was prepared according to the procedure in the USP XX (5) but without enzyme.

Standard Preparation—About 324 mg of USP reference standard aspirin was accurately weighed and dissolved in 500.0 ml of simulated intestinal fluid. The standard was prepared fresh daily and used without delay. Similar standards were prepared for the 486- and 648-mg tablets.

Sample Preparation—One tablet was placed in each dissolution vessel, which contained 500 ml of simulated gastric fluid. The paddles were rotated at 50 rpm for 1 hr, then the fluid was replaced with 500 ml of simulated intestinal fluid.

Automated Sampling—The aliquots were removed automatically every 15 min. The six dissolution sample probes were first placed into the standard solution, and the standard was sampled through the first cycle. The probes were then removed from the standard solution and placed in the dissolution medium. The aliquots were diluted with simulated intestinal fluid and stored in the holding–mixing coil. As the aliquots were pumped sequentially out of the holding–mixing coil, the stream was acidified with 0.4 *N* HCl and mixed.

Automated Determination—The automated system was assembled as shown in Fig. 1. Air was first removed from the acidified stream, which was drawn continuously into the manifold. The acidified stream was extracted with chloroform and resampled. The absorbance of the chloroform solution was monitored at 280 nm. The standard reading obtained through each probe was used to calculate the result from the sample reading obtained through that probe.

Suppositories—A recording spectrophotometer[8] and ACS reagent grade chloroform and glacial acetic acid were used.

Standard Preparation—About 100 mg of USP reference standard aspirin was accurately weighed and dissolved in 100.0 ml of chloroform. A 5.0-ml aliquot was diluted to 100.0 ml with a 1% acetic acid in chloroform solution.

Sample Preparation—Each suppository was dissolved in chloroform and diluted to volume with chloroform in an appropriate volumetric flask. An aliquot was taken and diluted with 1% acetic acid in chloroform to give a concentration similar to the standard.

Quantitation—The absorbance of both the standard and sample was measured from 350 to 220 nm in a 1-cm cell with 1% acetic acid in chloroform as the reference solution. The corrected net absorbance at 280 nm was used for the calculation of aspirin in each suppository.

Aspirin Identification and Salicylic Acid Limit Test—An ascending chromatography tank[9] (use unlined), silica gel plates[10], and a fluorescence detector[11] were used. Petroleum ether (bp range 30–60°), ethyl acetate, chloroform, glacial acetic acid, methanol, and ferric chloride hexahydrate were ACS reagent grade and/or suitable for chromatography. The mobile phase consisted of petroleum ether–ethyl acetate–glacial acetic acid (85:18:3).

Standard Aspirin Preparation—A concentration of 20.0 mg/ml of aspirin in chloroform was prepared and used as quickly as possible.

Standard Salicylic Acid Preparation—Solutions containing 0.02, 0.05, 0.10, 0.20, 0.40, and 0.80 mg/ml of salicylic acid in chloroform were prepared by quantitative dilution of a stock solution.

Sample Preparation—For the tablets a portion of a powdered composite was mixed with a 1.5% acetic acid in methanol solution to give an aspirin concentration of 20 mg/ml. The solution was centrifuged to obtain a clear supernate.

The suppositories were dissolved in chloroform to give a concentration of 20 mg/ml, except the 60-mg dose, which was diluted to a final concentration of 10 mg/ml.

Determination—About 100 ml of mobile phase was poured into the developing tank. The TLC plate was prewashed. The plate was removed and protected from evaporation by covering with two clear glass plates. The protective glass plates were separated to expose the origin or spotting line. One-microliter aliquots of each sample and standard were spotted 2 cm apart on the origin line. The mobile phase used for prewash was replaced with fresh mobile phase. The plate was developed until the solvent front had migrated at least 10 cm from the origin line. The plate was removed and dried on a hot plate until only a faint odor of acetic acid remained.

[1] Glassine paper (8.5 × 8.5 cm), Scientific Products, McGaw Park, IL 60085.
[2] Sonicor Model SC 400T, ultrasonic cleaner with timer, Randall Manufacturing Co., Hillside, NJ 08406.
[3] Model 72RL, Easi-Lift multiple spindle dissolution drive, Hanson Research Corp., Northridge, CA 91324.
[4] AutoAnalyzer proportioning pump III, 133-A014-04, Technicon Instruments Corp., Tarrytown, NY 10591.
[5] Model PM2DL, Carl Zeiss, Oberkochen, West Germany.
[6] Ten millimeters, 18 μl (886881), or 80 μl (886878), Beckman Instruments, Fullerton, CA 92634.
[7] Servo/Riter II, PS01WGA, Texas Instruments, Houston, TX 77001.
[8] Cary 118C, Varian Corp., Sunnyvale, CA 94086.
[9] Brinkmann Instruments, Inc., Westbury, CT 11590.
[10] Silica gel 60 F-254, 250 μm on a 20 × 20-cm plate, Curtis Matheson Scientific, Inc., Maryland Heights, MO 63043.
[11] Schoeffel Model SD 3000 spectrodensitometer. Excitation 310 nm, emission 440 nm. Schoeffel Instrument Corp., Westward, NJ 07675.

Table II—Dissolution Results [a] of Enteric Aspirin (Percent of Label Declaration) with Paddle at 50 rpm

Time, min	Manufacturer/Batch [b] A_1 Dosage, mg 324	A_2 648	B_1 324	C_1 324	D_1 324	D_2 486	D_3 486
15	49.5 (3.30)	40.0 (3.37)	44.8 (9.40)	0	0	0.1 (0.01)	0
30	63.3 (6.02)	52.8 (2.82)	55.9 (7.03)	0	0.1 (0.19)	0.1 (0.01)	0
45	70.3 (5.09)	61.9 (4.41)	61.1 (6.05)	0	1.0 (0.58)	0.6 (0.01)	0
60	74.3 (3.73)	67.1 (4.50)	65.7 (4.91)	0	1.7 (0.99)	1.1 (0.01)	0.9 (0.43)
75	77.6 (3.07)	71.3 (4.92)	68.4 (4.87)	0	2.6 (0.99)	1.5 (0.31)	1.5 (0.46)
90	79.0 (2.42)	74.4 (5.83)	69.8 (3.23)	0.2 (0.39)	3.2 (1.11)	2.1 (0.39)	2.0 (1.02)
105	81.3 (3.26)	75.1 (7.64)	69.8 (1.53)	0.6 (0.70)	3.7 (1.34)	2.1 (0.48)	2.9 (0.82)
120	82.4 (3.88)	76.9 (8.74)	68.6 (3.59)	1.2 (1.12)	4.3 (1.59)	2.1 (0.52)	3.5 (0.90)
135	82.8 (4.57)	76.9 (8.74)	67.9 (4.58)	1.7 (1.49)	5.0 (1.70)	2.4 (0.67)	4.1 (1.18)
150	84.4 (4.57)	76.6 (11.01)	66.2 (6.54)	2.5 (1.86)	5.5 (1.86)	2.7 (0.81)	4.7 (1.21)
165	83.4 (6.91)	75.8 (11.17)	62.3 (11.56)	3.1 (2.50)	6.1 (2.03)	2.9 (0.88)	5.2 (1.34)
180	84.8 (9.47)		57.8 (15.65)	3.7 (3.22)	6.7 (2.17)	3.1 (0.93)	5.6 (1.54)
195	83.0 (12.13)	—	56.0 (14.22)	4.3 (3.48)	7.2 (2.23)	3.3 (1.00)	6.0 (1.68)
210	82.6 (8.57)	—	52.3 (11.33)	5.3 (4.60)	7.8 (4.24)	3.5 (0.97)	6.6 (1.47)
225	83.4 (10.54)	—	—	6.3 (5.46)	8.3 (2.53)	3.6 (1.02)	6.8 (1.83)
240	81.7 (12.01)	—	—	7.2 (6.09)	9.0 (2.74)	—	7.3 (2.02)
255	—	—	—	8.4 (7.04)	9.5 (2.88)	—	7.7 (2.13)
270	—	—	—	9.3 (7.79)	10.2 (2.96)	—	8.4 (2.25)
285	—	—	—	10.4 (8.89)	—	—	—
300	—	—	—	11.7 (10.09)	—	—	—

[a] Average of six tablets; number in parenthesis is standard deviation. [b] See Table I, footnote *a*.

Salicylic acid was determined by scanning the plate with the densitometer. The spot intensities of the standard and sample were compared. An amount of salicylic acid in the spotted sample corresponding to the 0.20-mg/ml standard would be equivalent to the 1% limit. After the limit test, the remaining spots were visualized by spraying with ferric chloride TS (5) and heating at 110° for 10 min. Aspirin was identified by comparison of the R_f of the sample and standard spots.

Table III—National Survey Results (Percent of Label Declaration) for Aspirin in Suppositories and Salicylic Acid Results

Manufacturer [a]	Dosage, mg	Aspirin [b], %	Salicylic Acid, %
A	648	100.2 [c] (2.12)	0.3
A	648	100.8 [c] (1.15)	0.6
A	648	99.9 [c] (2.99)	0.3
A	648	102.0 [c] (2.07)	[d]
A	324	102.4 [c] (2.50)	0.7
A	324	102.7 [c] (2.84)	0.8
A	324	104.7 [c] (2.99)	0.6
E	600	102.8 (1.60)	0.2
E	300	103.1 (2.69)	0.4
E	300	105.0 (3.00)	0.2
E	200	104.8 (1.31)	0.5
E	200	104.2 (1.70)	0.4
E	150	102.5 (0.98)	0.8
E	120	106.1 (2.12)	0.7
E	120	105.1 [c] (3.88)	0.8
E	60	107.4 (1.79)	0.9
E	120	101.0 (1.88)	0.3
E	600	103.2 (4.32)	0.2
E	600	102.8 (1.61)	0.2
E	120	104.7 (0.99)	0.7
E	120	103.5 (1.56)	0.6
E	120	103.8 (1.63)	0.4
E	60	105.8 (2.53)	1.7 [e]
E	60	107.0 (1.09)	1.9 [f]
E	60	106.3 (2.88)	2.0 [g]
F	600	103.8 (2.23)	[d]
G	600	102.8 (4.03)	0.3
G	600	100.9 (3.63)	0.3
G	600	101.9 (3.56)	0.3
G	300	97.3 (1.14)	0.5
G	300	94.4 (2.27)	0.7
G	300	95.3 (2.64)	0.4
G	125	102.1 (1.71)	0.4
G	125	96.5 (1.29)	0.4
H	650	102.9 [c] (4.44)	0.1
H	325	106.4 [c] (12.29)	0.1

[a] (A) Eli Lilly & Co., Indianapolis, Ind.; (E) Suppositoria Labs, Inc., Farmingdale, N.Y.; (F) Wyeth Labs, Inc., Malvern, Pa.; (G) G&W Labs, Inc., So. Plainfield, N.J.; (H) Dr. Rose, Inc., Madison, Conn. [b] Each value represents 10 determinations unless otherwise noted; number in parentheses is standard deviation. [c] Thirty determinations. [d] Met compendial requirements. [e] The result for salicylic acid using the USP procedure was 2.3%. [f] The result for salicylic acid using the USP procedure was 1.5%. [g] The result for salicylic acid using the USP procedure was 2.1%.

Table IV—Comparison of Salicylic Acid (Percent of Aspirin) Data from the TLC and USP XX Procedures

Material	TLC	USP
648-mg Enteric coated tablet composite	1.3	1.3
Aspirin powder	0.1	0.1
324-mg Enteric coated tablet composite	0.6	0.5
648-mg Suppository composite	0.7	0.6
120-mg Suppository composite	0.2	0.3

RESULTS AND DISCUSSION

Tablet Content Uniformity Validation Test—The original validation for the content uniformity determination was described previously (1). Portions of a ground tablet composite equivalent to single tablets were analyzed by the proposed method and the USP XX (5). The ground tablet composite was prepared from a commercial 648-mg enteric coated tablet. The average of 22 results was 102.0% with a coefficient of variation of 1.91%. The USP XX result was 103.2%. The results obtained for the content uniformity determination of aspirin and the salicylic acid concentrations in enteric coated tablets are given in Table I. No batches were found outside USP XX specifications for strength or salicylic acid.

Dissolution Validation Tests—A series of validation tests were performed on the automated dissolution system. A linear response was obtained when four solutions of standard containing from 0.324 to 1.296 mg of aspirin/ml (corresponding to 50–200% of a 324-mg label declaration) were tested. Carry-over for 100–200–100–50% series of aspirin solutions was also determined with satisfactory results. A portion of the ground composite equivalent to one tablet was accurately weighed and subjected to the dissolution test for 5 hr. The analysis obtained for aspirin was 101.3% of that declared. The hydrolysis rate of aspirin determined on this sample over 5 hr was calculated to be 2.1%/hr.

Table V—Impurities [a] as Percent of Label Declaration of Aspirin Found in Enteric Coated Aspirin Tablets

Manufacturer [b] Batch	Tablet Dosage, mg	I,%	II,%	III,%
A_1	324	— [c]	0.243	— [d]
A_2	648	— [c]	0.224	— [d]
B_1	324	— [c]	0.094	Trace [e]
C_1	324	— [c]	0.050	— [d]
D_2	486	0.006	0.087	— [d]

[a] Impurities: I, acetylsalicylic anhydride; II, acetylsalicylsalicylic acid; III, *O*-salicylsalicylic acid. [b] See Table I, footnote *a*. [c] Assay could not be performed on this formulation. Colloidal suspension in benzene layer. [d] Not detected. [e] Trace = 0.01%.

Table II shows the dissolution rates for the batches representing various manufacturers. The batch results are not corrected for aspirin hydrolysis. Only three of the seven batches showed significant amounts of dissolution in the 3–4 hr period. A physical inspection of the residues from batches C_1, D_1, D_2, and D_3 revealed that the tablets were still firm and 90% intact. Batch D_3, which gave one of the lowest percentage rates, was analyzed again at a paddle speed of 100 rpm. There was no increase in dissolution. The percentages were almost identical to the results obtained at 50 rpm. No sample showed signs of dissolution in the 1-hr pretreatment with gastric fluid.

Both batch A_1 and D_1 gave similar salicylate blood level concentrations[12]. Therefore, this dissolution test, in its present form, is not satisfactory for predicting bioavailability.

Suppository Validation Test—Portions of a composite prepared from a commercial 324-mg suppository were analyzed by the USP XX and the dilute-and-read procedures. The result for the USP procedure was 102.5% of declared and 104.9% for the proposed procedure. The UV curves obtained from the standard and sample solutions were nearly identical and showed very little background interference from the suppository excipients. The results obtained for the content uniformity determination of aspirin and the salicylic acid concentrations in suppositories are given in Table III. Three batches from Manufacturer E exceeded the USP XX limit for salicylic acid.

Salicylic Acid Limit Test Validation by TLC—A linear calibration curve was obtained for salicylic acid when concentrations from 0 to 800 ng/μl were spotted. The fluorescent readings were made by scanning the chromatogram with the spectrodensitometer in the reflectance mode at a fluorescence excitation wavelength of 310 nm and an emission wavelength of 410 nm. Table IV shows the data obtained by the TLC and USP XX (5) procedures on commercial samples. Salicylic acid has a relative R_f value of 1.7 compared to aspirin. In addition, five batches of enteric coated tablets (A_1, A_2, B_1, C_1, and D_2) were analyzed for aspirin-related impurities by the HPLC method described previously (3). Table V shows the amounts of impurities found in these batches. Suppository samples were not tested for impurities.

[12] R. D. Kirchhoefer, unpublished data.

REFERENCES

(1) W. E. Juhl and R. D. Kirchhoefer, *J. Pharm. Sci.*, **69**, 544 (1980).

(2) R. D. Kirchhoefer and W. E. Juhl, *ibid.*, **69**, 548 (1980).

(3) R. D. Kirchhoefer, J. C. Reepmeyer, and W. E. Juhl, *ibid.*, **69**, 550 (1980).

(4) W. E. Juhl and R. D. Kirchhoefer, *ibid.*, **69**, 967 (1980).

(5) "The United States Pharmacopeia," 20th rev., U.S. Pharmacopeial Convention, Rockville, Md., 1980, pp. 57, 1104.

(6) K. Embil and G. Torosian, *J. Pharm. Sci.*, **68**, 1290 (1979).

(7) H. Johansen, *Arch. Pharm. Chem. Sci. Ed.*, **7**, 33 (1978).

(8) J. W. Myrick and C. E. Wells, *J. Assoc. Off. Anal. Chem.*, **62**, 56 (1979).

NOTES

Potential Anticonvulsants IV: Condensation of Isatin with Benzoylacetone and Isopropyl Methyl Ketone

FRANK D. POPP ˣ and HOSSEIN PAJOUHESH

Received June 8, 1981, from the *Department of Chemistry, University of Missouri-Kansas City, Kansas City, MO 64110.* Accepted for publication November 16, 1981.

Abstract □ A series of new 3-hydroxy-3-substituted oxindoles were prepared and screened for anticonvulsant activity. A number of these 3-hydroxyoxindoles had activity in the maximal electroshock seizure test.

Keyphrases □ Anticonvulsants—condensation of isatin, benzoylacetone, isopropyl methyl ketone □ Isatin—anticonvulsants, condensation, benzoylacetone, isopropyl methyl ketone □ Benzoylacetone—anticonvulsants, condensation of isatin, isopropyl methyl ketone □ Isopropyl methyl ketone—anticonvulsants, condensation of isatin, benzoylacetone

The anticonvulsant activity[1] of 3-hydroxy-3-phenacyloxindole (I) (1) and 3-hydroxy-3-acetonyloxindole (II) has been reported previously. In a study of analogs of I and II (2) it was found in initial screening that III, derived from isatin and benzoylacetone and having features of both I and II, was inactive at 600 mg/kg in the maximal electroshock seizure test (MES)[1] but was active at 100 mg/kg in the pentylenetetrazol seizure threshold test (Met)[1]. Compound IV related to II and derived from isatin and isopropyl methyl ketone, was active at 100 mg/kg in the MES test and inactive in the Met test. This report de-

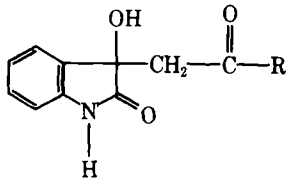

I R = C_6H_5
II R = CH_3
IV R = $CH(CH_3)_2$

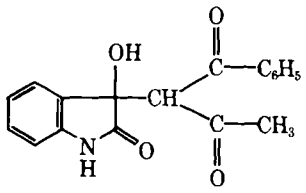

III

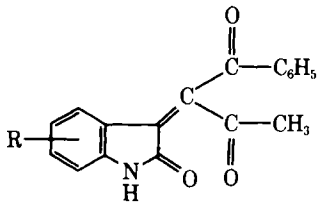

V

[1] Anticonvulsant screening was carried out through the Antiepileptic Drug Development Program, National Institutes of Health. The standard screening protocol of that group was followed.

0022-3549/82/0900-1052$01.00/0

Table II shows the dissolution rates for the batches representing various manufacturers. The batch results are not corrected for aspirin hydrolysis. Only three of the seven batches showed significant amounts of dissolution in the 3–4 hr period. A physical inspection of the residues from batches C_1, D_1, D_2, and D_3 revealed that the tablets were still firm and 90% intact. Batch D_3, which gave one of the lowest percentage rates, was analyzed again at a paddle speed of 100 rpm. There was no increase in dissolution. The percentages were almost identical to the results obtained at 50 rpm. No sample showed signs of dissolution in the 1-hr pretreatment with gastric fluid.

Both batch A_1 and D_1 gave similar salicylate blood level concentrations[12]. Therefore, this dissolution test, in its present form, is not satisfactory for predicting bioavailability.

Suppository Validation Test—Portions of a composite prepared from a commercial 324-mg suppository were analyzed by the USP XX and the dilute-and-read procedures. The result for the USP procedure was 102.5% of declared and 104.9% for the proposed procedure. The UV curves obtained from the standard and sample solutions were nearly identical and showed very little background interference from the suppository excipients. The results obtained for the content uniformity determination of aspirin and the salicylic acid concentrations in suppositories are given in Table III. Three batches from Manufacturer E exceeded the USP XX limit for salicylic acid.

Salicylic Acid Limit Test Validation by TLC—A linear calibration curve was obtained for salicylic acid when concentrations from 0 to 800 ng/μl were spotted. The fluorescent readings were made by scanning the chromatogram with the spectrodensitometer in the reflectance mode at a fluorescence excitation wavelength of 310 nm and an emission wavelength of 410 nm. Table IV shows the data obtained by the TLC and USP XX (5) procedures on commercial samples. Salicylic acid has a relative R_f value of 1.7 compared to aspirin. In addition, five batches of enteric coated tablets (A_1, A_2, B_1, C_1, and D_2) were analyzed for aspirin-related impurities by the HPLC method described previously (3). Table V shows the amounts of impurities found in these batches. Suppository samples were not tested for impurities.

[12] R. D. Kirchhoefer, unpublished data.

REFERENCES

(1) W. E. Juhl and R. D. Kirchhoefer, *J. Pharm. Sci.*, **69**, 544 (1980).

(2) R. D. Kirchhoefer and W. E. Juhl, *ibid.*, **69**, 548 (1980).

(3) R. D. Kirchhoefer, J. C. Reepmeyer, and W. E. Juhl, *ibid.*, **69**, 550 (1980).

(4) W. E. Juhl and R. D. Kirchhoefer, *ibid.*, **69**, 967 (1980).

(5) "The United States Pharmacopeia," 20th rev., U.S. Pharmacopeial Convention, Rockville, Md., 1980, pp. 57, 1104.

(6) K. Embil and G. Torosian, *J. Pharm. Sci.*, **68**, 1290 (1979).

(7) H. Johansen, *Arch. Pharm. Chem. Sci. Ed.*, **7**, 33 (1978).

(8) J. W. Myrick and C. E. Wells, *J. Assoc. Off. Anal. Chem.*, **62**, 56 (1979).

NOTES

Potential Anticonvulsants IV: Condensation of Isatin with Benzoylacetone and Isopropyl Methyl Ketone

FRANK D. POPP ˣ and HOSSEIN PAJOUHESH

Received June 8, 1981, from the *Department of Chemistry, University of Missouri-Kansas City, Kansas City, MO 64110.* Accepted for publication November 16, 1981.

Abstract □ A series of new 3-hydroxy-3-substituted oxindoles were prepared and screened for anticonvulsant activity. A number of these 3-hydroxyoxindoles had activity in the maximal electroshock seizure test.

Keyphrases □ Anticonvulsants—condensation of isatin, benzoylacetone, isopropyl methyl ketone □ Isatin—anticonvulsants, condensation, benzoylacetone, isopropyl methyl ketone □ Benzoylacetone—anticonvulsants, condensation of isatin, isopropyl methyl ketone □ Isopropyl methyl ketone—anticonvulsants, condensation of isatin, benzoylacetone

The anticonvulsant activity[1] of 3-hydroxy-3-phenacyloxindole (I) (1) and 3-hydroxy-3-acetonyloxindole (II) has been reported previously. In a study of analogs of I and II (2) it was found in initial screening that III, derived from isatin and benzoylacetone and having features of both I and II, was inactive at 600 mg/kg in the maximal electroshock seizure test (MES)[1] but was active at 100 mg/kg in the pentylenetetrazol seizure threshold test (Met)[1]. Compound IV related to II and derived from isatin and isopropyl methyl ketone, was active at 100 mg/kg in the MES test and inactive in the Met test. This report de-

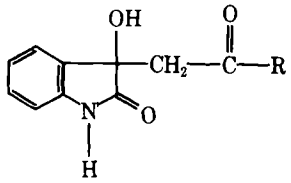

I R = C_6H_5
II R = CH_3
IV R = $CH(CH_3)_2$

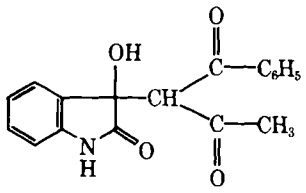

III

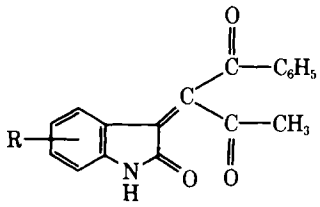

V

[1] Anticonvulsant screening was carried out through the Antiepileptic Drug Development Program, National Institutes of Health. The standard screening protocol of that group was followed.

0022-3549/82/0900-1052$01.00/0

Table I—Reaction of Isatins with Isopropyl Methyl Ketone

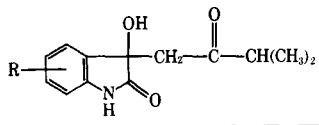

R	Melting Point[a]	Formula	Analysis Calc.	Analysis Found	Anticonvulsant Activity, mg/kg MES	Anticonvulsant Activity, mg/kg Met
H[b]	128–130°	$C_{13}H_{15}NO_3$	—	—	100[c]	NA[c]
4-Cl-7-CH_3	149–150[d]	$C_{14}H_{16}ClNO_3$	C 59.68	59.29	300	600
			H 5.72	5.62		
			N 4.97	4.87		
4-Cl-7-OCH_3	139–140	$C_{14}H_{16}ClNO_4$	C 56.48	56.74	NA[e]	600
			H 5.42	5.38		
			N 4.71	4.62		
1-$C_6H_5CH_2$	155–156[f]	$C_{20}H_{21}NO_3$	C 74.28	74.38	NA[e]	300
			H 6.55	6.51		
			N 4.33	4.27		
5-NO_2	261–263	$C_{13}H_{14}N_2O_5$	C 56.11	56.00	NA[e]	NA[e]
			H 5.07	4.97		
5-Br	240–241	$C_{13}H_{14}BrNO_3$	C 50.14	49.95	NA[e]	600
			H 4.53	4.29		

[a] Recrystallized from ethanol unless otherwise noted, melting point uncorrected, spectral data consistent with structure. [b] Described in Reference 2. [c] Additional screening indicated an ED_{50} of 151.8 in the MES test, an ED_{50} of 242.9 in the Met test, and a TD_{50} of 843.6. [d] Recrystallized from chloroform. [e] Not active at 600 mg/kg. [f] Recrystallized from ethyl acetate.

Table II—Reactions of Isatins with Benzoylacetone

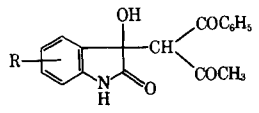

R	Melting Point[a]	Formula	Analysis Calc.	Analysis Found	Anticonvulsant Activity, mg/kg MES	Anticonvulsant Activity, mg/kg Met
H[b]	184–185	$C_{18}H_{15}NO_4$	—	—	NA[c]	100
1-CH_3	158–159	$C_{19}H_{17}NO_4$	C 70.57	70.52	NA[c]	NA[c]
			H 5.30	5.19		
			N 4.33	4.40		
1-C_6H_5-CH_2	136–137	$C_{25}H_{21}NO_4$	C 75.20	75.43	NA[c]	NA[c]
			H 5.26	5.33		
			N 3.51	3.58		
5-Br	187–189	$C_{18}H_{14}BrNO_4$	C 55.68	55.38	NA[c]	100
			H 3.64	3.37		
			N 3.61	3.81		
5-Cl	190–192	$C_{18}H_{14}ClNO_4$	C 62.89	62.81	NA[c]	600
			H 4.10	4.16		
			N 4.08	4.07		
5-CH_3	173–174	$C_{19}H_{17}NO_4$	C 70.57	70.16	NA[c]	NAc
			H 5.30	5.71		
			N 4.33	4.06		
5-NO_2	215–217	$C_{18}H_{14}N_2O_6$	C 61.01	60.92	NA[c]	NA[c]
			H 3.98	3.97		
			N 7.91	7.95		
6-Cl	200–201	$C_{18}H_{14}ClNO_4$	C 62.89	62.52	NA[c]	300
			H 4.10	4.11		
			N 4.08	3.80		
4-Cl-7-CH_3	200–201	$C_{19}H_{16}ClNO_4$	C 63.78	63.74	NA[c]	300
			H 4.51	4.63		
			N 3.91	3.86		
4-Cl-7-OCH_3	190–191	$C_{19}H_{16}ClNO_5$	C 61.05	61.24	NA[c]	NA[c]
			H 4.32	4.39		
			N 3.75	3.73		

[a] Recrystallized from ethanol, mp uncorrected, spectral data consistent with structure. [b] Reference 2. [c] Not active at 600 mg/kg.

scribes the synthesis and anticonvulsant activity of analogs of III and IV and related compounds.

RESULTS AND DISCUSSION

A number of substituted isatins were condensed with isopropyl methyl ketone to give the analogs of IV shown in Table I. None of these compounds were as active as II. Benzoylacetone was also condensed with a number of substituted isatins to give the analogs of III shown in Table II. None of these compounds were active in the MES test and only the 5-bromo analog of III was as active as III in the Met test. Subsequent screening of IV has shown an ED_{50} of 151.8 in the MES test, 242.9 in the Met test, and 211.8 in the subcutaneous picrotoxin test with a TD_{50} of 843.6. This compound gave a maximum protection of 62.5% at 200 mg/kg in the subcutaneous bicuculline test.

Dehydration of analogs of III derived from 5-bromoisatin and from 4-chloro-7-methoxyisatin gave compounds (V) inactive at 600 mg/kg in both the MES and Met screens.

Anticonvulsant screening results of a number of related compounds are included in Table III and further screening results on analogs of II (2) are included in Table IV.

In the 3-hydroxyoxindoles studied to date, II has the best activity and protective index in the MES test. None of the compounds in this report

Table III—3-Substituted-3-Hydroxyoxindoles

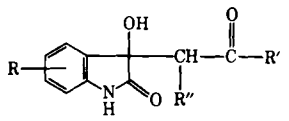

R	R′	R″	Melting Point[a]	Formula	Analysis Calc.	Analysis Found	Anticonvulsant Activity, mg/kg MES	Anticonvulsant Activity, mg/kg Met
1-$C_6H_5CH_2$	C_6H_5	H	197–198[b]	$C_{23}H_{19}NO_3$	C 77.29	77.38	NA[c]	NA[c]
					H 5.36	5.43		
					N 3.92	4.00		
1-$C_6H_5CH_2$	CH_3	H	162–163	$C_{18}H_{17}NO_3$	C 73.20	73.07	NA[c]	600
					H 5.80	5.70		
					N 4.74	4.81		
1-(4-BrC_6H_4)$NHCH_2$	CH_3	H	163–165	$C_{18}H_{17}BrN_2O_3$	C 55.54	55.40	NA[c]	NA[c]
					H 4.40	4.21		
					N 7.20	7.31		
1-(*N*-morpholino)CH_2	CH_3	H	168–169	$C_{16}H_{20}N_2O_4$	C 63.14	63.20	300	NA[c]
					H 6.62	6.64		
					N 9.21	9.11		
H	C_6H_5	C_6H_5	156–158[d]	$C_{22}H_{17}NO_3$	—	—	NA[c]	600
H	$CH_2C_6H_5$	C_6H_5	163–164	$C_{23}H_{19}NO_3$	C 77.29	77.06	NA[c]	NA[c]
					H 5.36	5.31		
					N 3.92	3.87		
6-Cl-7-CH_3	C_6H_{11} (cyclo)	H	148–150[e]	$C_{17}H_{20}ClNO_3$	C 63.45	63.31	600	600
					H 6.26	6.28		
					N 4.35	4.33		
H	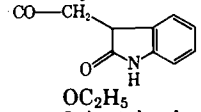	H	221–223	$C_{20}H_{16}N_2O_6$	C 63.15	62.96	NA[c]	NA[c]
					H 4.24	4.25		
					N 7.37	7.32		
H	OC_2H_5	$CO_2C_2H_5$	155–157[f]	$C_{15}H_{17}NO_6$	—	—	NA[c]	NA[c]
H	2-Acetylcyclohexanone[g]		215–216	$C_{24}H_{22}N_2O_6$	C 66.35	66.38	600	NA[c]
					H 5.10	5.05		
					N 6.45	6.51		

[a] Recrystallized from ethanol unless otherwise noted. [b] Recrystallized from *n*-butanol. [c] Not active at 600 mg/kg. [d] Reported (5) mp 156–158°. [e] Recrystallized from benzene. [f] Reported (6) mp 156–158°. [g] Condensation with 2 moles of isatin.

have outstanding activity in the Met test. The effect of structure to activity in the 3-hydroxyoxindoles is still not clear, although it appears that substituents on the oxindole portion of the molecule do not enhance and generally decrease the activity. The study of the effect of substituents in the 3-position is being continued.

EXPERIMENTAL[2]

Condensation of Isatins with Ketones—The compounds in Tables I, II, and III were prepared, as previously described (1–3), by heating a solution of isatin and the appropriate ketone in absolute ethanol containing a few drops of diethylamine on a steam bath.

Dehydration of 3-Hydroxyoxindoles.—Following the procedure of Braude and Lindwall (4) the product from 5-bromoisatin and benzoylacetone was heated on a steam bath in acetic acid containing a small amount of hydrochloric acid to give V (R = 5-Br), mp 232–234° (ethanol).

Anal.—Calc. for $C_{18}H_{12}BrNO_3$: C, 58.40; H, 3.27; N, 3.78. Found: C, 58.22; H, 3.55; N, 3.64.

In a similar manner V (R = 4-Cl-7-OCH_3), mp 225–226° (ethanol), was obtained.

Anal.—Calc. for $C_{19}H_{14}ClNO_4$: C, 64.14; H, 3.97; N, 3.94. Found: C, 64.18; H, 4.03; N, 3.86.

[2] All compounds exhibited IR spectra consistent with the structures shown and with those previously reported (1–3). Melting points are uncorrected, and analyses were carried out by the Spang Microanalytical Laboratory.

Table IV—Analogs of II[a]

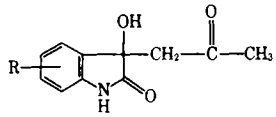

R	MES ED_{50}	Met ED_{50}	TD_{50}
H	40	—	490
6-Cl	337.5	279.2	585.2
7-Cl	64.4	131.8	297.9
4-Cl-7-OCH_3	802.4	404.8	>1500
4-Cl-7-CH_3	90.2	211.5	615.4
4,7-Cl_2	127.8	242.8	~00

[a] Reference 2.

REFERENCES

(1) F. D. Popp and B. E. Donigan, *J. Pharm. Sci.*, **68**, 519 (1979).

(2) F. D. Popp, R. Parson, and B. E. Donigan, *ibid.*, **69**, 1235 (1980).

(3) F. D. Popp, R. Parson, and B. E. Donigan, *J. Heterocycl. Chem.*, **17**, 1329 (1980).

(4) F. Braude and H. G. Lindwall, *J. Am. Chem. Soc.*, **55**, 325 (1933).

(5) S. Pietra and G. Tacconi, *Farmaco, Ed. Sci.*, **16**, 483 (1961).

(6) G. L. Papayan, *Arm. Khim. Zh.*, **22**, 457 (1967).

GC Analysis of Imidazopyrazole in Plasma Using Nitrogen-Specific Detection

GARRY W. BOSWELL * **and JORDAN L. COHEN** ˣ

Received September 18, 1981, from the *School of Pharmacy, University of Southern California, Los Angeles, CA 90033.* Accepted for publication December 15, 1981. *Present address: Letterman Army Institute of Research, San Francisco, CA 94129.

Abstract □ A sensitive, specific GC assay for imidazopyrazole in plasma was developed using nitrogen-specific detection. The samples are extracted with methylene chloride containing 7-bromo-imidazopyrazole as the internal standard and the extract derivatized with pentaflourobenzoyl chloride prior to isothermal chromatography on an OV-17 column. Peak-height ratio measurements produced linear standard curves over the concentration range of 0.045–40 μg/ml. The practical limit of sensitivity was 50 ng/ml and typical between-run variability for replicate analysis of a control specimen produced a coefficient of variation of 5.1%. This method is applicable to the study of the pharmacokinetics of imidazopyrazole following therapeutic doses and was used to support such studies in parallel with Phase I clinical studies in children.

Keyphrases □ Imidazopyrazole—GC analysis, plasma, nitrogen-specific detection □ Plasma—GC analysis of imidazopyrazole, nitrogen-specific detection □ Nitrogen-specific detection—GC analysis of imidazopyrazole, plasma □ GC analysis—imidazopyrazole in plasma

Imidazopyrazole[1] (2,3-dihydro-1-H-imidazo[1,2,-6]-pyrazole[2], I) is an investigational antineoplastic agent which selectively inhibits DNA synthesis (1). Preclinical studies have shown I to have significant antitumor activity especially against L-1210 leukemia cells, including those variants resistant to similar chemotherapeutic agents (2). The suggested mechanism of action is inhibition of ribonucleotide reductase, and in mice the drug showed the capacity to synchronize tumor, bone marrow, and duodenal crypt cells in the S-phase of the cell cycle (3). Phase I clinical trials of this novel agent have been initiated in children and adults with initial doses of 150 mg/m^3 body surface area (4), and an obvious need to collect early pharmacologic disposition data exists.

A limited number of methods for determining I in biological media have been preliminarily reported including liquid scintillation of radiolabeled drug (5), radioimmunoassay (6), and electron-capture GC (7). The former two methods require reagents not readily available and lack evidence of specificity, while the latter suffers from the lack of ruggedness generally associated with electron-capture detection when applied to analysis of biological specimens. The present method was developed to allow nitrogen-specific detection and still maintain adequate sensitivity to support Phase I clinical and pharmacokinetic studies in children being treated for cancer.

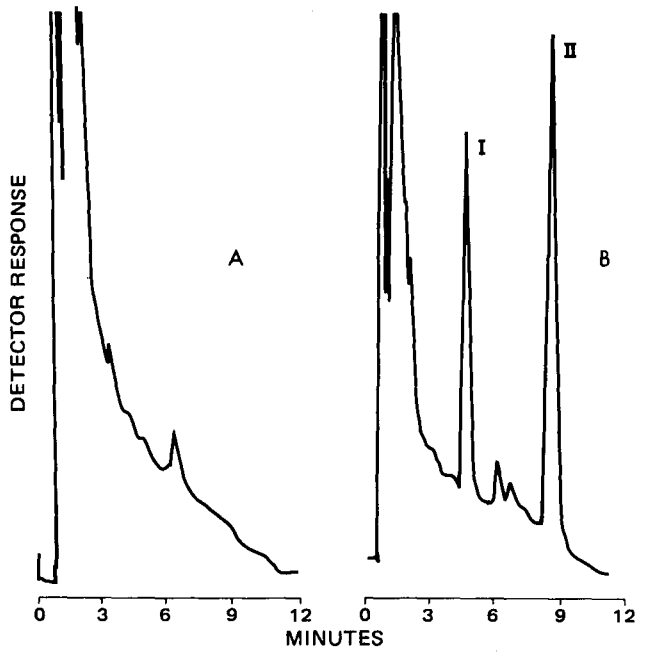

Figure 1—*Gas-liquid chromatographic tracing of (A) a blank serum sample and (B) a serum sample to which was added 2.37 μg/ml of I and internal standard at an attenuation of 16 × 10^{-11}.*

EXPERIMENTAL

Chemicals and Reagents—Compound I and 7-bromoimidazopyrazole[3] (7-bromo,2,3-dihydro-1-H-imidazo[1,2-6]pyrazole, II) were used directly. Pentafluorobenzoyl chloride[4] was used as received and stored under dry nitrogen at −20° in 1-ml ampules to protect from moisture. A 1.0 *M*, pH 10.5 carbonate buffer was prepared using reagent grade sodium carbonate[5] and sodium bicarbonate[5]. Methanol and methylene chloride were both HPLC grade[6]; all other chemicals and solvents were reagent grade. All glassware was acid washed then treated with 5% dichloromethylsilane in toluene[5] and rinsed successively with toluene and

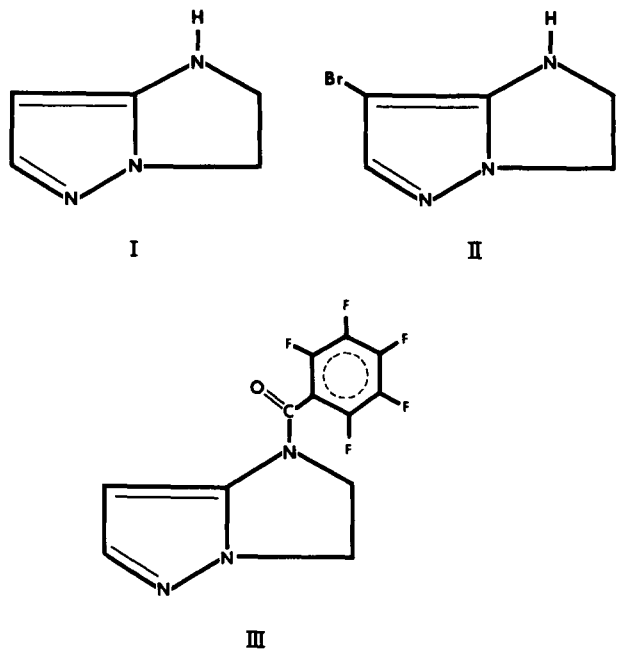

[1] National Cancer Institute, Bethesda, Md.
[2] NSC 51143.
[3] Dr. Louis Malspeis, Ohio State University, Columbus, Ohio.
[4] Aldrich Chemical Co., Milwaukee, Wis.
[5] Matheson, Coleman and Bell, Norwood, Ohio.
[6] Fisher Scientific, Fairlawn, N.J.

0022-3549/82/0900-1055$01.00/0

Table I—Recovery of I Added to Human Serum

I Added, μg/ml	n	I Found, μg/ml (mean ± SE)
0.048	10	0.054 ± 0.003
0.48	9	0.47 ± 0.011
1.91	10	2.03 ± 0.069
4.93	4	4.71 ± 0.32
9.85	4	10.27 ± 0.30
19.70	4	18.59 ± 0.56
39.40	4	40.37 ± 0.92

methanol and then oven dried. Deionized water was prepared using a filter reverse osmosis system[7].

Instrumentation—A gas chromatograph[8] equipped with a nitrogen phosphorous thermionic detector and 1-mV recorder was used. Chromatography was performed on a U-shaped glass column (1.8 m × 2 mm i.d.) packed with 3% OV-17 on 100/120 mesh[9], which was conditioned overnight at 250° and pretreated with several injections (10–25 μl)[10]. Nitrogen at a flow rate of 30 ml/min was used as the carrier gas, and air and hydrogen flows were optimized for maximum detector response. Operating temperatures were: oven, 195°; injector, 235°; and detector, 250°. Mass spectral data were obtained using a GC–MS–computer system[11]. Chromatography was performed using a coiled glass column (1.2 m × 2-mm i.d.) packed with 3% OV-101 on 100/120 mesh[9] operated isothermally at 170° with an injector temperature of 250°. The instrument was equipped with a jet separator and used 70 V as the ionization energy.

Standard Curves—Stock standards were prepared by dissolving 1 mg of I in 10 ml of water and 1 mg of II in 10 ml of methylene chloride. These were diluted to produce working standards of 10 μg/ml and stored at 4° where they were stable for at least 2 weeks. Appropriate aliquots were added to human serum[12] to produce either a low-concentration series of 0.05, 0.1, 0.5, 1.0, and 2.0 μg/ml of I (1 μg of II), or a high-concentration series of 1, 5, 10, 20, 30, and 40 μg/ml of I (28 μg of II). Calibration curves were constructed from peak-height ratio measurement of I/II.

Analytical Procedure—Seven milliliters of methylene chloride, 50 μl (5 μg) of internal standard (II) solution, 2 g of sodium chloride, and 1 ml of carbonate buffer (1.0 *M*, pH 10.5) were added to 1.0 ml of a patient

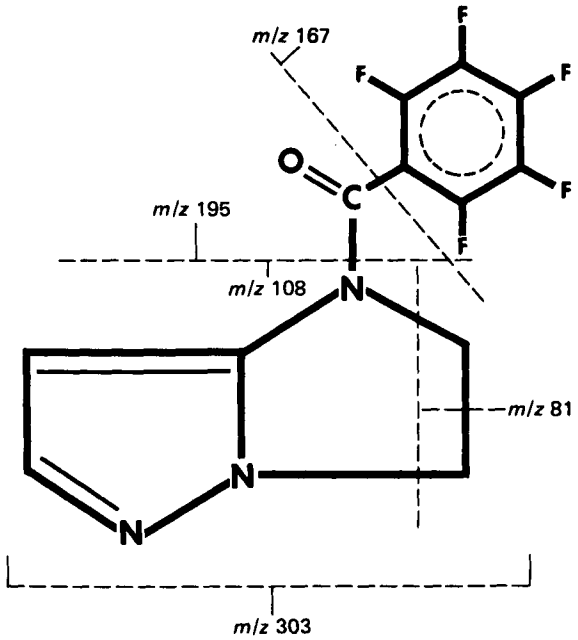

Figure 2—*Proposed mass fragmentation of III. See text for conditions.*

[7] Millipore Corp., Bedford, Mass.
[8] Varian Aerograph Model 2100, Varian Assoc., Palo Alto, Calif.
[9] Applied Science Laboratories, State College, Pa.
[10] Aquasil Pierce Chemical Co., Rockford, Ill.
[11] Hewlett-Packard Model 5992B/9825A, Hewlett-Packard, Santa Clara, Calif.
[12] Irvine Scientific, Santa Ana, Calif.

Table II—*In Vitro* Stability of I [a]

Hours	Concentration of I, μg/ml: pH 7.4 Phosphate Buffer, 0.1 *M*	Human Serum	5% Serum Albumin
0	1.04	0.95	1.01
1	1.03	0.77	0.88
2	1.10	0.79	0.92
4	1.06	0.69	0.79
8	1.03	0.67	0.81
24	1.01	0.62	0.73
48	—	0.62	—

[a] Solutions originally spiked with 1.0 μg/ml of I and stored under refrigeration.

plasma or spiked serum sample in a 15-ml centrifuge tube. The tube was then mechanically shaken for 30 min, centrifuged at 2000 rpm for 10 min, and the lower (organic) layer filtered into a clean tube containing 1 g of sodium sulfate. This was vortexed for 1 min and allowed to stand for 10 min. The organic phase was transferred to a clean tube to which was added 5 μl of pentafluorobenzoyl chloride. This was incubated for 30 min in a 50° water bath, and 0.5 ml of methanol was added. The tube was reincubated for 15 min and then evaporated to dryness under a stream of dry air at room temperature. The residue was redissolved in 2 ml of methylene chloride, shaken with 5 ml of carbonate buffer for 20 min, centrifuged for 10 min, and the lower (organic) layer transferred to a 5 ml conical centrifuge tube. This was evaporated to dryness under air and redissolved in 50 μl of methanol prior to injection of 1–2 μl into the gas chromatograph.

Clinical Study—Human plasma samples were obtained from pediatric oncology patients receiving I under an approved Phase I study protocol of the Childrens Cancer Study Group. Doses were administered by rapid intravenous infusion over 30–60 min, and blood samples of 1–3 ml were collected prior to dosing and at 0.25, 0.5, 1.0, 2.0, 6.0, 12.0, and 24.0 hr postdose. Blood samples were immediately centrifuged and the plasma separated and stored at −80° until analyzed.

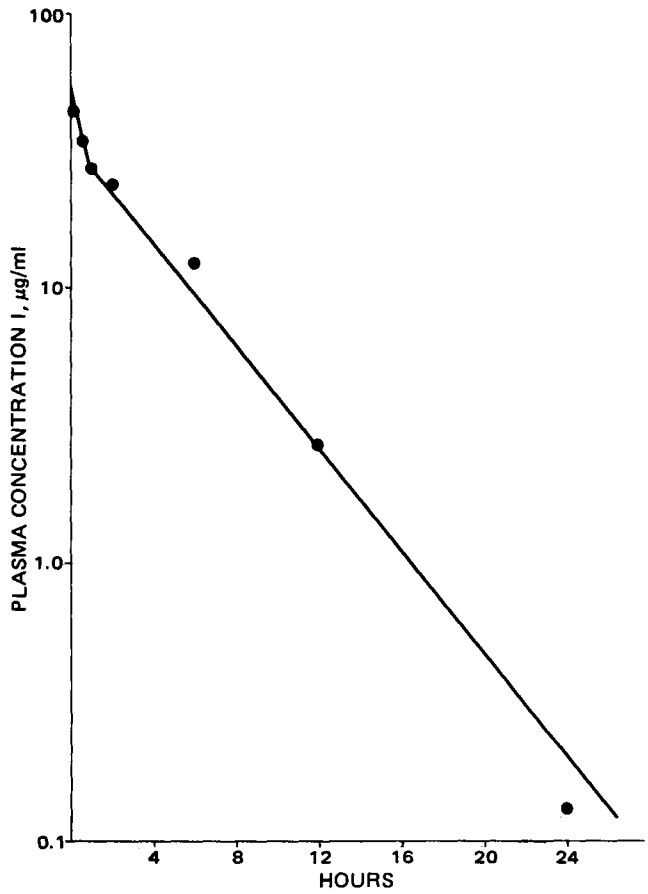

Figure 3—*Patient plasma–time profile of I following an intravenous bolus infusion of 450 mg.*

RESULTS AND DISCUSSION

Typical chromatograms from the analysis of a human serum blank and a spiked serum standard are shown in Fig. 1. Under the analytical conditions described, the retention times of derivatized I and II were 4.0 and 8.7 min, respectively. Standard curves prepared from a series of duplicate serum standards were linear over two concentration ranges typically encountered in pharmacokinetic monitoring. Linear regression for a series of low concentration standard (0.05–2.0 μg/ml) curves produced a slope of 1.642 ± 0.068, an intercept of −0.043 ± 0.063 with a mean correlation coefficient of 0.992. Corresponding results for the high-concentration range (1–40 μg/ml) produced a slope of 0.106 ± 0.002, an intercept of −0.0119 ± 0.031, and a mean (r) of 0.998. This reflects excellent between-run reproducibility, which is further supported by the recovery data over a wide concentration range shown in Table I. Replicate analysis of two spiked serum control specimens resulted in between-run coefficients of variation of 6.3% ($\bar{x}$ = 0.107 μg/ml) and 3.8% ($\bar{x}$ = 4.54 μg/ml). The practical lower limit of sensitivity for this procedure, for which a signal–baseline noise ratio of 3:1 can be seen, was 50 ng/ml. This is the same as that reported using a GC–electron-capture detection procedure (7). The entire procedure requires ~4 hr and allows analysis of ~20 specimens/analyst/working day.

The identity of the derivatized I GC peak was confirmed by comparing its mass spectrum to that of authentic, synthesized pentafluorobenzoyl imidazopyrazole (III). These were identical and demonstrated a parent peak at m/z 303 and a base peak at m/z 195, which corresponded to the pentafluorobenzoyl fragment. Other characteristic peaks occurred at m/z 167, 108, and 81 as seen in the proposed fragmentation pattern in Fig. 2.

The pharmacokinetic behavior of I was followed in four pediatric patients receiving intravenous bolus doses in a Phase I clinical trial. The plasma time course for one patient who received 450 mg is shown in Fig. 3. The mean terminal phase half-life and volume of distribution for all patients was 4.4 hr and 1.5 liters/kg, respectively. These values were in reasonable agreement with those reported for adult patients (6) ($t_{1/2}$ = 3–10 hr, Vd = 5–15 liters), although other widely divergent values using less specific radioactivity detection methods have also been reported (8). No other data in pediatric patients have been reported to date.

In the course of studying the reproducibility of the assay, it was observed that significant decreases in measured concentrations of I occurred if the spiked serum sample was allowed to sit unfrozen over a few hours. This had not been reported in the previous literature and appears to have serious implications for I measurements in biological media. A limited stability study was performed of I in pH 7.4 buffer, human serum, and 5% purified serum albumin. The results are summarized in Table II and indicate a relatively rapid decline in I in the presence of protein, which appears to stabilize at a level of 65–70% of the initial level over time.

A preliminary experiment examining the possibility of rapid irreversible protein binding suggested that this did not explain the relatively rapid decline observed. Although this problem can be circumvented by either immediate analysis of samples or quick freezing in methanol–dry ice, the mechanism of this apparent instability merits further study. Lack of recognition of this problem could lead to altered serum concentrations and errors in pharmacokinetic analysis *in vivo*.

The method reported appears sufficiently sensitive, reproducible, and rapid to support extended pharmacokinetic studies of I in humans or animals provided caution is used in rapidly handling samples to avoid an apparent instability in biological specimens.

REFERENCES

(1) H. L. Ennis, L. H. Moller, J. J. Wang, and O. S. Selawry, *Biochem. Pharmacol.*, **20**, 2639 (1971).

(2) R. W. Brockman, S. C. Shaddix, J. W. Carpenter, N. F. DuBois, and R. F. Struck, *Proc. Am. Assoc. Cancer Res.*, Abstract 81, 19 (1978).

(3) A. Krishran and R. Ganapathi, *Cancer Res.*, **40**, 1103 (1980).

(4) B. Yap, W. Murphy, M. A. Burgess, M. Valdivieso, and G. P. Bodey, *Cancer Treat. Rep.*, **63**, 1849 (1979).

(5) L. M. Allen, *Proc. Am. Assoc. Cancer Res.*, Abstract 433, 107 (1979).

(6) K. L. L. Fong, D. H. W. Ho, G. P. Bodey, B. S. Yap, R. S. Benjamin, N. S. Brown, and E. J. Freireich, *ibid.*, Abstract 826, 204, (1979).

(7) L. Malspeis, J. J. V. DeSousa, A. E. Staubus, and H. B. Bhat, *ibid.*, Abstract 617, 153 (1979).

(8) L. M. Allen, M. Feely, and J. Denefrio, *J. Clin. Pharmacol.*, **20**, 34, (1980).

ACKNOWLEDGMENTS

The participation of Dr. Denise Jamin and the late Gussie Higgins in Phase I clinical study collaboration at Childrens Hospital of Los Angeles is gratefully acknowledged.

Stability of Concentrated Aqueous Solutions of Pralidoxime Chloride

ROBERT I. ELLIN

Received August 18, 1981, from the *U.S. Army Medical Research Institute of Chemical Defense, Aberdeen Proving Ground, MD 21010.* Accepted for publication November 20, 1981.

Abstract □ Concentrated aqueous solutions of pralidoxime chloride degrade more rapidly than dilute solutions. The rate and degree of degradation is dependent on the initial and final pH as well as the container in which the solution is stored. The effects of glass, metal, plastic, and rubber stoppers on the stability of concentrated and dilute solutions are discussed. The stability and shelf lives of 50% aqueous concentrates at different temperatures were determined.

Keyphrases □ Pralidoxime chloride—stability of concentrated aqueous solutions, kinetics □ Stability—concentrated aqueous solutions of pralidoxime chloride, kinetics □ Kinetics—comparison of stability in concentrated aqueous solutions of pralidoxime chloride

Pyridinium oximes in combination with atropine provide effective therapy in poisoning by many organophosphorus cholinesterase inhibitors (1). More clinical data are available for pralidoxime salts than other pyridinium oximes, as this oxime is in wider use. Pralidoxime also reportedly produces few undesirable side effects (2, 3). It is generally accepted that, for therapeutic efficacy, pralidoxime plasma concentrations should be at least 4 μg/ml (4). A 600-mg im dose is required to produce this level. A dilute solution would require an injection of an impractical volume. Since pralidoxime chloride is very water soluble, 30–50% concentrates can be used to provide a 4-μg/ml plasma level (5, 6). The purpose of this study was to determine stabilities and the effect of containers on the shelf life of aqueous concentrates of pralidoxime chloride[1].

[1] The opinions or assertions contained herein are the private views of the author and not to be construed as reflecting the views of the Department of the Army or the Department of Defense.

0022-3549/82/0900-1057$01.00/0

RESULTS AND DISCUSSION

Typical chromatograms from the analysis of a human serum blank and a spiked serum standard are shown in Fig. 1. Under the analytical conditions described, the retention times of derivatized I and II were 4.0 and 8.7 min, respectively. Standard curves prepared from a series of duplicate serum standards were linear over two concentration ranges typically encountered in pharmacokinetic monitoring. Linear regression for a series of low concentration standard (0.05–2.0 μg/ml) curves produced a slope of 1.642 ± 0.068, an intercept of −0.043 ± 0.063 with a mean correlation coefficient of 0.992. Corresponding results for the high-concentration range (1–40 μg/ml) produced a slope of 0.106 ± 0.002, an intercept of −0.0119 ± 0.031, and a mean (r) of 0.998. This reflects excellent between-run reproducibility, which is further supported by the recovery data over a wide concentration range shown in Table I. Replicate analysis of two spiked serum control specimens resulted in between-run coefficients of variation of 6.3% ($\bar{x}$ = 0.107 μg/ml) and 3.8% ($\bar{x}$ = 4.54 μg/ml). The practical lower limit of sensitivity for this procedure, for which a signal–baseline noise ratio of 3:1 can be seen, was 50 ng/ml. This is the same as that reported using a GC–electron-capture detection procedure (7). The entire procedure requires ~4 hr and allows analysis of ~20 specimens/analyst/working day.

The identity of the derivatized I GC peak was confirmed by comparing its mass spectrum to that of authentic, synthesized pentafluorobenzoyl imidazopyrazole (III). These were identical and demonstrated a parent peak at m/z 303 and a base peak at m/z 195, which corresponded to the pentafluorobenzoyl fragment. Other characteristic peaks occurred at m/z 167, 108, and 81 as seen in the proposed fragmentation pattern in Fig. 2.

The pharmacokinetic behavior of I was followed in four pediatric patients receiving intravenous bolus doses in a Phase I clinical trial. The plasma time course for one patient who received 450 mg is shown in Fig. 3. The mean terminal phase half-life and volume of distribution for all patients was 4.4 hr and 1.5 liters/kg, respectively. These values were in reasonable agreement with those reported for adult patients (6) ($t_{1/2}$ = 3–10 hr, Vd = 5–15 liters), although other widely divergent values using less specific radioactivity detection methods have also been reported (8). No other data in pediatric patients have been reported to date.

In the course of studying the reproducibility of the assay, it was observed that significant decreases in measured concentrations of I occurred if the spiked serum sample was allowed to sit unfrozen over a few hours. This had not been reported in the previous literature and appears to have serious implications for I measurements in biological media. A limited stability study was performed of I in pH 7.4 buffer, human serum, and 5% purified serum albumin. The results are summarized in Table II and indicate a relatively rapid decline in I in the presence of protein, which appears to stabilize at a level of 65–70% of the initial level over time.

A preliminary experiment examining the possibility of rapid irreversible protein binding suggested that this did not explain the relatively rapid decline observed. Although this problem can be circumvented by either immediate analysis of samples or quick freezing in methanol–dry ice, the mechanism of this apparent instability merits further study. Lack of recognition of this problem could lead to altered serum concentrations and errors in pharmacokinetic analysis *in vivo*.

The method reported appears sufficiently sensitive, reproducible, and rapid to support extended pharmacokinetic studies of I in humans or animals provided caution is used in rapidly handling samples to avoid an apparent instability in biological specimens.

REFERENCES

(1) H. L. Ennis, L. H. Moller, J. J. Wang, and O. S. Selawry, *Biochem. Pharmacol.*, **20**, 2639 (1971).

(2) R. W. Brockman, S. C. Shaddix, J. W. Carpenter, N. F. DuBois, and R. F. Struck, *Proc. Am. Assoc. Cancer Res.*, Abstract 81, 19 (1978).

(3) A. Krishran and R. Ganapathi, *Cancer Res.*, **40**, 1103 (1980).

(4) B. Yap, W. Murphy, M. A. Burgess, M. Valdivieso, and G. P. Bodey, *Cancer Treat. Rep.*, **63**, 1849 (1979).

(5) L. M. Allen, *Proc. Am. Assoc. Cancer Res.*, Abstract 433, 107 (1979).

(6) K. L. L. Fong, D. H. W. Ho, G. P. Bodey, B. S. Yap, R. S. Benjamin, N. S. Brown, and E. J. Freireich, *ibid.*, Abstract 826, 204, (1979).

(7) L. Malspeis, J. J. V. DeSousa, A. E. Staubus, and H. B. Bhat, *ibid.*, Abstract 617, 153 (1979).

(8) L. M. Allen, M. Feely, and J. Denefrio, *J. Clin. Pharmacol.*, **20**, 34, (1980).

ACKNOWLEDGMENTS

The participation of Dr. Denise Jamin and the late Gussie Higgins in Phase I clinical study collaboration at Childrens Hospital of Los Angeles is gratefully acknowledged.

Stability of Concentrated Aqueous Solutions of Pralidoxime Chloride

ROBERT I. ELLIN

Received August 18, 1981, from the *U.S. Army Medical Research Institute of Chemical Defense, Aberdeen Proving Ground, MD 21010.* Accepted for publication November 20, 1981.

Abstract □ Concentrated aqueous solutions of pralidoxime chloride degrade more rapidly than dilute solutions. The rate and degree of degradation is dependent on the initial and final pH as well as the container in which the solution is stored. The effects of glass, metal, plastic, and rubber stoppers on the stability of concentrated and dilute solutions are discussed. The stability and shelf lives of 50% aqueous concentrates at different temperatures were determined.

Keyphrases □ Pralidoxime chloride—stability of concentrated aqueous solutions, kinetics □ Stability—concentrated aqueous solutions of pralidoxime chloride, kinetics □ Kinetics—comparison of stability in concentrated aqueous solutions of pralidoxime chloride

Pyridinium oximes in combination with atropine provide effective therapy in poisoning by many organophosphorus cholinesterase inhibitors (1). More clinical data are available for pralidoxime salts than other pyridinium oximes, as this oxime is in wider use. Pralidoxime also reportedly produces few undesirable side effects (2, 3). It is generally accepted that, for therapeutic efficacy, pralidoxime plasma concentrations should be at least 4 μg/ml (4). A 600-mg im dose is required to produce this level. A dilute solution would require an injection of an impractical volume. Since pralidoxime chloride is very water soluble, 30–50% concentrates can be used to provide a 4-μg/ml plasma level (5, 6). The purpose of this study was to determine stabilities and the effect of containers on the shelf life of aqueous concentrates of pralidoxime chloride[1].

[1] The opinions or assertions contained herein are the private views of the author and not to be construed as reflecting the views of the Department of the Army or the Department of Defense.

0022-3549/82/0900-1057$01.00/0

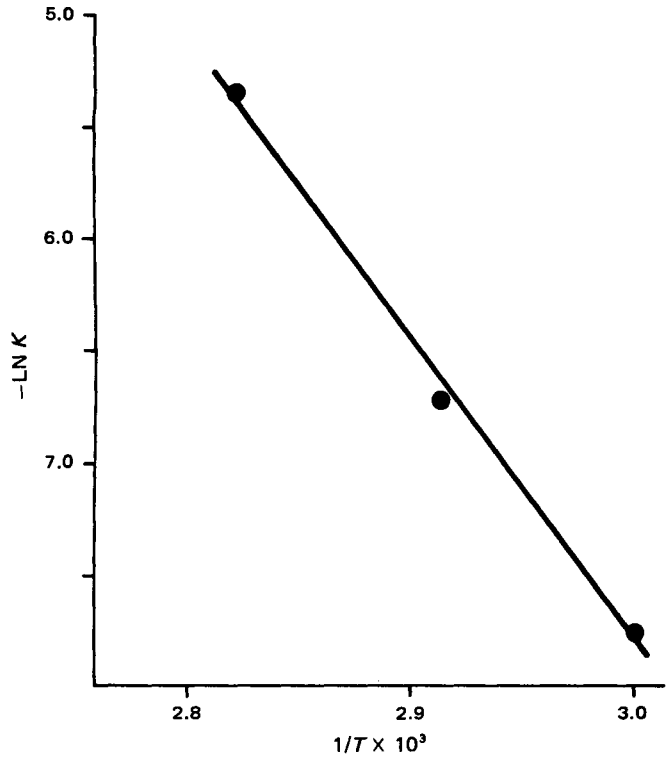

Figure 1—*Temperature Dependency of the Degradation of 50% Aqueous Solution of Pralidoxime in Glass Ampuls.*

EXPERIMENTAL

Twenty-five grams of pralidoxime chloride were transferred into a 50-ml volumetric flask and brought to volume with triple distilled water. Approximately 1.0-ml volumes were added to 2-ml glass ampuls which had been acid washed (0.01 *N* HCl), water-rinsed, and dried in an oven at 110°. The ampuls were sealed with an oxygen torch, then placed in hot air ovens at 60, 70, and 81°. Ampuls were removed at selected time periods. An aliquot was diluted with distilled water (0.2–500), then rediluted with 0.05 *N* NaOH (3.0–100) to obtain a final concentration of ~6 μg/ml. Samples were assayed by UV analysis at 336 nm (7).

Approximately 1.0-ml volumes were also added to glass, metal, stainless steel, and plastic (polypropylene) cylinders which were sealed at one end with a neoprene rubber stopper. After filling, the cylinder was closed with another neoprene rubber stopper, then weighed on a balance. Cylinders were placed in a holding device which consisted of a plastic base, 1.91-cm thick, containing holes slightly wider than the diameter of the glass cylinders. A plastic cap was placed over the top of each filled cylinder and a metal plate placed over the filled cylinders. The cylinders were secured by two screws. The holder containing the cylinders was placed in the oven, and the cylinders were removed as needed. Prior to analysis, cylinders were reweighed to determine possible losses due to evaporation or leakage. Pralidoxime chloride concentrations were determined as described above.

RESULTS

Stability of 50% Aqueous Solutions of Pralidoxime in Glass Ampuls—The rate of degradation of concentrates of pralidoxime at 60, 70, and 81° conforms to a first-order equation. As a 50% solution of pralidoxime at initial pH 3.65 is hypertonic, buffer was not added to maintain a constant pH. The rate constants at 60, 70, and 81° were 4.27×10^{-4}, 1.22×10^{-3}, and 4.68×10^{-3} hr^{-1}, respectively. The logarithm of velocity constants was plotted against the reciprocal of the absolute temperatures (Fig. 1). A linear relationship indicated the mechanism responsible for oxime decay is not altered by changes in temperature. The relationship is shown by the Arrhenius equation:

$$k = Ae^{-Ea/RT} \qquad \text{(Eq. 1)}$$

where Ea, the energy of activation, was 26,755 cal/mole; A was 4.08×10^{10} min^{-1}; R was the molar gas constant; and T the absolute temperature.

[2] Unpublished data.

Table I—Calculated Shelf Lives for 50% Aqueous Solutions of Pralidoxime Chloride in Glass Ampuls

Temperature°	Shelf Life[a] 10%	25%
10	37.0 *y*	101.0 *y*
15	16.0 *y*	44.0 *y*
20	7.3 *y*	20.0 *y*
25	3.4 *y*	9.3 *y*
30	1.6 *y*	4.4 *y*
35	286.0 *d*	2.1 *y*
40	142.0 *d*	1.1 *y*
45	72.0 *d*	198.0 *d*
50	38.0 *d*	103.0 *d*

[a] *y* = years; *d* = days.

Degradation of Concentrated Aqueous Solution of Pralidoxime—Glass ampuls and glass, metal, and plastic cylinders sealed with neoprene and butyl rubber stoppers were used. The degradation rates of 50% aqueous solutions of pralidoxime chloride were similar in plastic and glass cylinders sealed with neoprene stoppers and more rapid in metal cylinders when determined at 40°. The pH dropped with time, 3.6–3.2 after 40 days in glass and plastic, but increased in metal 3.6–4.2. When performed at 45 and 60° in glass with 30% solutions of pralidoxime chloride in cylinders stoppered with either neoprene or butyl rubber, the pH fell more rapidly in the butyl rubber than in the neoprene-stoppered containers[2].

DISCUSSION

The stability of 50% concentrates of pralidoxime chloride in unbuffered aqueous solutions in glass ampuls was studied under accelerated temperatures. Calculated 10 and 25% shelf lives are shown in Table I. At 25°, 10 and 25% shelf lives were found to be 3.4 and 9.3 years, respectively. The report also indicates the importance of considering the effects of material(s) in the container in which a formulation is packaged.

When results of the report are compared with the results of related investigations (5, 8), discrepancies in reported stabilities of pralidoxime might be assumed by the reader. However, on examination of data, one finds this is not so. Stability studies on 16% (w/v) solutions of pralidoxime methanesulfonate in sealed glass ampuls buffered at pH values 2.0–3.5 have been reported (5). Stability efforts on unbuffered solutions of 10–33% (w/v) pralidoxime chloride in glass ampuls and also glass vials sealed with butyl rubber stoppers have also been performed (8). Acid was added to obtain initial pH values of 1.3–2.0. In this study the stabilities of unbuffered, pH-unadjusted 50% solutions of pralidoxime chloride (w/v) in glass ampuls were investigated. In preliminary studies[3] with concentrates of pralidoxime chloride in cylinders made of glass, plastic, and metal sealed with rubber enclosures, significant variations in stability were found. Consequently, when comparing stability data, the reader must take into consideration different oxime salts, oxime concentrations, initial pH values, formulations, and storage containers. Fortunately, there are data where direct comparisons can be made. Stabilities for pralidoxime concentrates in sealed glass ampuls at 25 and 45° have been reported (5, 8).

Previous studies (9) on solutions (0.1%) of pralidoxime chloride showed that pralidoxime solutions possess maximum stability at pH 4.3 with a shelf life to 10 years at 25°. Here equilibria at pH 1–3 were noted but not considered in the shelf life estimations. If equilibria data had been included, the predicted shelf lives at these pHs would have been significantly greater. In later efforts 30% concentrated solutions were found to be less stable than 0.1% solutions, in that concentrated solutions of pralidoxime chloride degraded 2.5 times more rapidly than the dilute solution[2].

On examination of all data, one finds that: (*a*) oxime loss in a 50% solution of pralidoxime chloride and a 16% buffered solution of pralidoxime methanesulfonate, both stored in glass ampuls at 45°, are similar (a 16% solution of pralidoxime methanesulfonate is equivalent in oxime content to a 12% solution of pralidoxime chloride), (*b*) lowering of the initial pH in unbuffered concentrates results in greater stability (8), (*c*) use of buffer at pH 2.5 in 16% solutions of pralidoxime methanesulfonate decreased stability drastically when compared with 30% unbuffered solutions, (*d*) rubber closures affect the pH and stability of pralidoxime chloride concentrates stored in glass, plastic, and metal cylinders[2,3]. The drop in pH

[3] J. R. May, U.S. Chemical Research and Development Laboratories, Aberdeen Proving Ground, MD 21010, 1965.

was greater in the glass and plastic containers than in metal. When butyl rubber was used, a lower pH resulted than when neoprene rubber was tested. A lower pH is desirable because of the unique occurrence of equilibria.

The reason(s) that high concentrations of pralidoxime chloride degrade more rapidly than dilute concentrations is not known. To resolve this problem, studies should be carried out to determine and quantitate degradation products and their rate of formation. By establishing the proper mechanism(s) one should be able to design stable formulations of concentrated solutions of drugs.

REFERENCES

(1) A. G. Gilman, L. S. Goodman, and A. Gilman, Eds., in "The Pharmacological Basis of Therapeutics," 6th ed., Macmillan, New York, N.Y., 1980, p. 110.

(2) G. Calesnick, J. A. Christensen, and M. Richter, *Arch. Environ. Health*, **15**, 599 (1967).

(3) G. E. Quinby, *J. Am. Med. Assoc.*, **187**, 202 (1964).

(4) A. Sundwall, *Biochem. Pharmacol.*, **11**, 377 (1962).

(5) R. Barkman, B. Edgren, and A. Sundwall, *J. Pharm. Pharmacol.*, **15**, 671 (1963).

(6) F. R. Sidell, J. E. Markis, W. Groff, and A. Kaminskis, *J. Pharmacokinet. Biopharm.*, **2**, 197 (1974).

(7) R. I. Ellin and A. A. Kondritzer, *Anal. Chem.*, **31**, 200 (1959).

(8) A. A. Hussain, U.S. Pat. 3,629,425, Dec. 21 (1972).

(9) R. I. Ellin, J. S. Carlese, and A. A. Kondritzer, *J. Pharm. Sci.*, **51**, 141 (1962).

Growth and Characterization of Calcium Oxalate Dihydrate Crystals (Weddellite)

L. LEPAGE and R. TAWASHI[x]

Received July 14, 1980, from the *Faculté de Pharmacie, Université de Montréal, Montreal, Quebec, Canada.* Accepted for publication November 25, 1981.

Abstract □ Conditions are given for the growth of calcium oxalate dihydrate crystals (weddellite) in aqueous solution. The crystals obtained were characterized by scanning electron microscopic, spectroscopic, and thermal methods. The dissolution kinetics and electrophoretic mobility were determined; the thermodynamically unstable calcium oxalate dihydrate had a higher dissolution rate and a lower zeta potential than the monohydrate and underwent a phase transformation into the more stable calcium oxalate monohydrate. The results obtained on the chemical stability and the surface charge of calcium oxalate dihydrate offered additional information for assessing the current theories on the formation of calcium oxalate renal stones.

Keyphrases □ Crystals—calcium oxalate dihydrate, growth and characterization □ Dissolution, kinetics—determination, calcium oxalate dihydrate crystals, growth and characterization □ Electrophoretic mobility—determination, calcium oxalate dihydrate crystals, growth and characterization

In recent years there has been much discussion on the role of different hydrated calcium oxalate crystals in the formation of calcium oxalate stones (1–4). Chemically, two varieties of calcium oxalate crystals occur in renal calculi: calcium oxalate monohydrate (whewellite) and calcium oxalate dihydrate (weddellite). The variable amount of water of crystallization is a direct consequence of the urine composition. The formation of these phases and the possible transformation between them is important from the urinary calcification standpoint.

The growth of calcium oxalate dihydrate in natural urine, synthetic urine, and in a mixture of both has been a subject of a number of investigations (5–7). In a recent study from this laboratory, it has been noticed that the calcium oxalate dihydrate was formed in the rat kidney after the injection of 4-hydroxy-L-proline. These crystals transformed gradually into the more stable calcium oxalate monohydrate (8). Previously it was reported that it is possible to grow calcium oxalate dihydrate crystals from a medium consisting of natural and synthetic urine (9). The chemical reaction between the sodium oxalate (0.005 *M*) and calcium chloride (1 *M*) at 37° in the previously described medium produced the octahedral dipyramidal calcium oxalate dihydrate. The crystals obtained were mixed with ~5% monohydrate. This work is intended to describe an improved technique for the growth of calcium oxalate dihydrate in aqueous solution and to study the dissolution kinetics and electrophoretic mobility of this form. Some aspects of the structure-dependent properties of both whewellite and weddellite crystals will be discussed.

EXPERIMENTAL

Materials—The following materials were used: synthetic urine [an aqueous medium containing various electrolytes present in normal urine which has been described previously (5, 9)], calcium chloride dihydrate[1], sodium oxalate[1], and calcium oxalate monohydrate[1] (high purity reagent grade), and freshly bidistilled water.

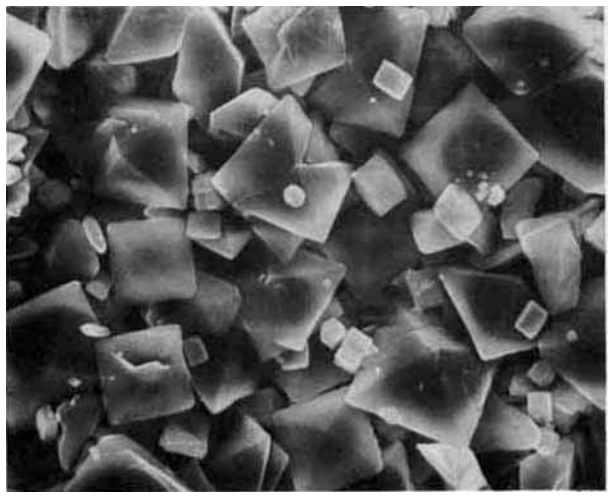

Figure 1—*Scanning electron micrograph of calcium oxalate dihydrate (2000×).*

[1] Fisher Scientific Co., Fair Lawn, N.J.

0022-3549/82/0900-1059$01.00/0

was greater in the glass and plastic containers than in metal. When butyl rubber was used, a lower pH resulted than when neoprene rubber was tested. A lower pH is desirable because of the unique occurrence of equilibria.

The reason(s) that high concentrations of pralidoxime chloride degrade more rapidly than dilute concentrations is not known. To resolve this problem, studies should be carried out to determine and quantitate degradation products and their rate of formation. By establishing the proper mechanism(s) one should be able to design stable formulations of concentrated solutions of drugs.

REFERENCES

(1) A. G. Gilman, L. S. Goodman, and A. Gilman, Eds., in "The Pharmacological Basis of Therapeutics," 6th ed., Macmillan, New York, N.Y., 1980, p. 110.

(2) G. Calesnick, J. A. Christensen, and M. Richter, *Arch. Environ. Health*, **15**, 599 (1967).

(3) G. E. Quinby, *J. Am. Med. Assoc.*, **187**, 202 (1964).

(4) A. Sundwall, *Biochem. Pharmacol.*, **11**, 377 (1962).

(5) R. Barkman, B. Edgren, and A. Sundwall, *J. Pharm. Pharmacol.*, **15**, 671 (1963).

(6) F. R. Sidell, J. E. Markis, W. Groff, and A. Kaminskis, *J. Pharmacokinet. Biopharm.*, **2**, 197 (1974).

(7) R. I. Ellin and A. A. Kondritzer, *Anal. Chem.*, **31**, 200 (1959).

(8) A. A. Hussain, U.S. Pat. 3,629,425, Dec. 21 (1972).

(9) R. I. Ellin, J. S. Carlese, and A. A. Kondritzer, *J. Pharm. Sci.*, **51**, 141 (1962).

Growth and Characterization of Calcium Oxalate Dihydrate Crystals (Weddellite)

L. LEPAGE and R. TAWASHI[x]

Received July 14, 1980, from the *Faculté de Pharmacie, Université de Montréal, Montreal, Quebec, Canada.* Accepted for publication November 25, 1981.

Abstract □ Conditions are given for the growth of calcium oxalate dihydrate crystals (weddellite) in aqueous solution. The crystals obtained were characterized by scanning electron microscopic, spectroscopic, and thermal methods. The dissolution kinetics and electrophoretic mobility were determined; the thermodynamically unstable calcium oxalate dihydrate had a higher dissolution rate and a lower zeta potential than the monohydrate and underwent a phase transformation into the more stable calcium oxalate monohydrate. The results obtained on the chemical stability and the surface charge of calcium oxalate dihydrate offered additional information for assessing the current theories on the formation of calcium oxalate renal stones.

Keyphrases □ Crystals—calcium oxalate dihydrate, growth and characterization □ Dissolution, kinetics—determination, calcium oxalate dihydrate crystals, growth and characterization □ Electrophoretic mobility—determination, calcium oxalate dihydrate crystals, growth and characterization

In recent years there has been much discussion on the role of different hydrated calcium oxalate crystals in the formation of calcium oxalate stones (1–4). Chemically, two varieties of calcium oxalate crystals occur in renal calculi: calcium oxalate monohydrate (whewellite) and calcium oxalate dihydrate (weddellite). The variable amount of water of crystallization is a direct consequence of the urine composition. The formation of these phases and the possible transformation between them is important from the urinary calcification standpoint.

The growth of calcium oxalate dihydrate in natural urine, synthetic urine, and in a mixture of both has been a subject of a number of investigations (5–7). In a recent study from this laboratory, it has been noticed that the calcium oxalate dihydrate was formed in the rat kidney after the injection of 4-hydroxy-L-proline. These crystals transformed gradually into the more stable calcium oxalate monohydrate (8). Previously it was reported that it is possible to grow calcium oxalate dihydrate crystals from a medium consisting of natural and synthetic urine (9). The chemical reaction between the sodium oxalate (0.005 *M*) and calcium chloride (1 *M*) at 37° in the previously described medium produced the octahedral dipyramidal calcium oxalate dihydrate. The crystals obtained were mixed with ~5% monohydrate. This work is intended to describe an improved technique for the growth of calcium oxalate dihydrate in aqueous solution and to study the dissolution kinetics and electrophoretic mobility of this form. Some aspects of the structure-dependent properties of both whewellite and weddellite crystals will be discussed.

EXPERIMENTAL

Materials—The following materials were used: synthetic urine [an aqueous medium containing various electrolytes present in normal urine which has been described previously (5, 9)], calcium chloride dihydrate[1], sodium oxalate[1], and calcium oxalate monohydrate[1] (high purity reagent grade), and freshly bidistilled water.

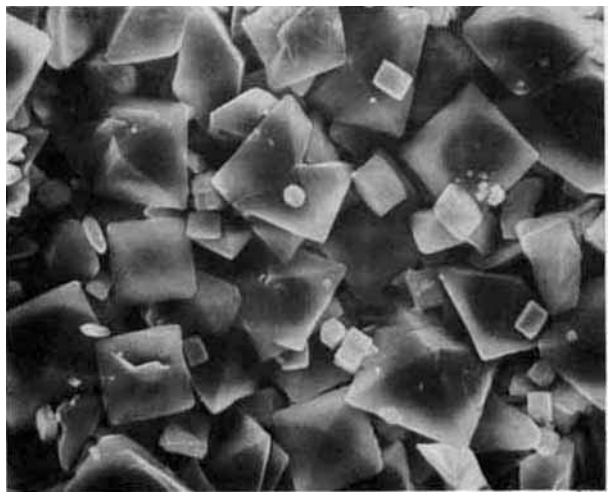

Figure 1—*Scanning electron micrograph of calcium oxalate dihydrate (2000×).*

[1] Fisher Scientific Co., Fair Lawn, N.J.

0022-3549/82/0900-1059$01.00/0

Table I—Powder Diffraction Patterns of Calcium Oxalate Monohydrate and Calcium Oxalate Dihydrate[a]

Whewellite		Calcium Oxalate Monohydrate		Weddellite		Calcium Oxalate Dihydrate	
d-Spacing, Å	Intensity, I/I_0	d-Spacing, Å	Intensity, I/I_0	d-Spacing, Å	Intensity, I/I_0	d-Spacing, Å	Intensity, I/I_0
5.93	100	5.94	100	8.73	4	8.70	3.3
5.79	30	5.79	32	6.32	6		
4.77	2	4.77	2.1	6.18	100	6.18	48.4
4.52	4	4.52	7.2			5.94	2.8
3.78	6	3.78	12.3	4.42	30	4.41	29.1
3.65	70	3.64	100	4.37	2		
3.41	2	3.39	3.1	3.91	8	3.91	9.8
3.12	2	3.30	3.1	3.68	12	3.66	19.7
3.11	10	3.09	4.6	3.59	2		
		3.01	17	3.39	4	3.39	4.1
2.97	45	2.96	67.7	3.16	4	3.16	5.7
2.92	10			3.12	2		
2.90	8	2.90	23.6	3.09	10	3.09	13.6
		2.83	18			2.96	4.9
2.52	4			2.82	14	2.81	21.4
2.49	18	2.49	39	2.78	65	2.77	100
2.45	4	2.44	7.2	2.76	4		
2.42	6	2.41	8.2	2.68	2	2.68	2.1
2.38	4					2.49	2.5
2.36	30			2.42	8		
2.35	12	2.35	67.2	2.41	16	2.40	27.5
2.30	2			2.37	2		
2.26	8			2.34	4	2.34	12.3
2.25	6	2.25	26.7	2.28	2	2.27	3.3
2.21	6	2.20	10.3	2.24	25	2.24	45.5
2.13	2	2.12	5.1	2.21	6	2.20	10.7
2.09	2			2.19	2		
2.08	14	2.07	25.1	2.12	8	2.12	13.5
2.00	2	1.99	5.1	2.02	6	2.02	9.0
1.98	10	1.97	19.5	2.00	4	1.99	5.5
1.96	2			1.96	10	1.95	18.9
1.95	10	1.95	19.5				
1.93	8	1.92	21.5	1.90	16	1.89	20.5
				1.84	10	1.83	19.7

[a] Diffraction patterns compared with those of the mineral whewellite (calcium oxalate monohydrate) and weddellite (calcium oxalate dihydrate) from powder diffraction File 20-231 and File 17-540, Joint Committee Powder Diffraction Standards.

Table II—Summary of the Structure-Dependent Properties of Calcium Oxalate Monohydrate and Calcium Oxalate Dihydrate

	Crystal Morphology	Density (12), g/cm³	Solubility at 37° in Normal Saline, mg of $Ca_2C_2O_4$/liter	Dissolution rate Constant, $g^{1/3}$/sec	Zeta Potential, ± SE, mV	Stability at 37° in Normal Saline
Calcium Oxalate Monohydrate	Prisms Tabular	2.23	24.37	5.67×10^{-5}	−32.67 ± 0.49	Stable
Calcium Oxalate Dihydrate	Bipyramidal Octahedral	1.99	38.74	11.3×10^{-5}	−29.46 ± 0.13	Transformed to Monohydrate after 24 hr

Crystal Growth—The precise conditions necessary for the growth of uncontaminated calcium oxalate dihydrate are as follows: 24 ml of sodium oxalate in bidistilled water (0.005 *M*) at room temperature was added to 40 ml of calcium chloride solution in bidistilled water (1 *M*) at 4° in glass tubes (2-cm diameter, 20-cm height). The sodium oxalate solution was added to the center of the air–liquid interface of the calcium chloride solution using a pipet. The mixture was left without agitation for 24 hr at 4°. The calcium oxalate dihydrate crystals deposited were separated by filtration[2]. The crystals obtained were characterized by scanning electron microscopy[3], IR spectra[4], X-ray powder diffraction[5], and differential thermal analysis[6]. The results of the diffractometer scan, the d-spacing, and the intensities matched those listed for the mineral weddellite in powder diffraction file[7]. Those of the standard calcium oxalate monohydrate used in this study matched the data for the mineral whewellite[8] (Table I). The differential thermal analysis and the IR spectra of calcium oxalate dihydrate grown in this study and calcium oxalate monohydrate used as the standard agree with previously reported data (9, 10).

Dissolution Rates Studies—The dissolution rate of calcium oxalate dihydrate was determined in normal saline at 37° (under sink conditions). Calcium oxalate dihydrate (5 mg) was added to 500 ml of normal saline and agitated by a mechanical stirrer at 150 rpm. Samples were taken from the dissolution media at different time periods, filtered[9], and analyzed for calcium by a complexometric method using a calcium autoanalyzer[10] (11). The solubility of both calcium oxalate dihydrate and monohydrate were also determined in normal saline at 37° (Table II).

Electrophoretic Mobility Studies—The electrophoretic mobility of calcium oxalate dihydrate was measured by a zeta-meter[11] in a synthetic urine at pH 7.5. The zeta potential was determined by tracking 150 particles of the calcium oxalate crystals. The technique of measuring the zeta potential is described elsewhere (13, 14).

Phase Transformation—The conversion of calcium oxalate dihydrate to calcium oxalate monohydrate was studied at 37° in normal saline. Calcium oxalate dihydrate (50 mg) was suspended in 100 ml of normal saline and the concentration of calcium was determined as a function of time using a calcium autoanalyzer. A drop in the concentration of calcium oxalate from 38.43 mg/liter (solubility of calcium oxalate dihydrate) to

[2] Millipore, 0.22 μm.
[3] Cambridge S-4. Cambridge, England.
[4] Perkin-Elmer 257.
[5] Phillips model PN 1130 diffractometer.
[6] Mettler T-WG-68.
[7] Powder diffraction, file 17-541, for calcium oxalate (whewellite); Joint Committee on Powder Diffraction Standards.
[8] Powder diffraction, file 20-231, for calcium oxalate dihydrate (weddellite); Joint Committee on Powder Diffraction Standards.
[9] Millipore, 0.22 μm.
[10] Corning calcium autoanalyser 940.
[11] Zeta-Meter Inc., New York, N.Y.

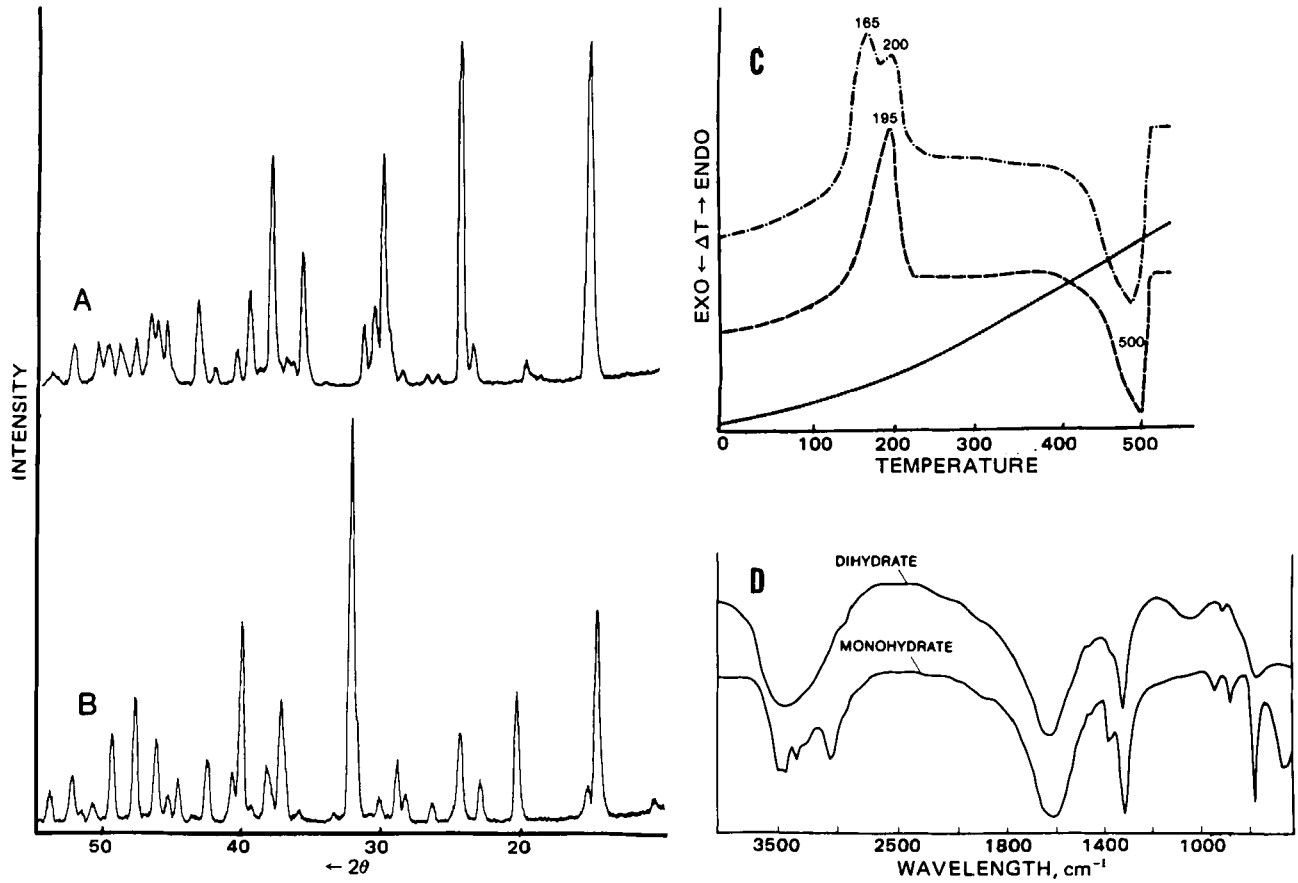

Figure 2—*X-Ray diffraction spectra of calcium oxalate monohydrate (A) and dihydrate (B); differential thermal analysis of calcium oxalate monohydrate (- - -) and calcium oxalate dihydrate (----); temperature: 10°/min (C); and IR spectra (D) of calcium oxalate monohydrate and dihydrate crystals, which were grown by the method described in the text. Calcium oxalate monohydrate crystals are the standard crystals described in the text.*

24.37 mg/liter (solubility of calcium oxalate monohydrate) was observed after 24 hr suggesting phase transformation. This transformation was confirmed by optical and spectroscopic examination of the oxalate crystals.

RESULTS AND DISCUSSION

Figure 1 shows the characteristic octahedral bipyramidal calcium oxalate dihydrate crystals grown by the described method. These crystals have different IR and X-ray powder diffraction spectra and differential thermal analysis from the standard calcium oxalate monohydrate crystals (Fig. 2). Table I shows powder diffraction patterns of the two calcium oxalate crystals compared with the phase of the minerals whewellite and weddellite.

The dissolution data of calcium oxalate dihydrate is given in Fig. 3. The results were presented according to the cube root law (15): $Kt = W_0^{1/3} - W^{1/3}$, where W_0 is the weight of crystals at the start or when time $t = 0$, W is the weight of the crystals at time t, and K is the dissolution rate constant (Fig. 4). Figure 4 shows that the calcium oxalate dihydrate dissolves faster than the calcium oxalate monohydrate. The higher dissolution rate of the dihydrate cannot be attributed to surface area effect, because the size distribution analysis indicated that calcium oxalate monohydrate crystals are smaller in size than calcium oxalate dihydrate

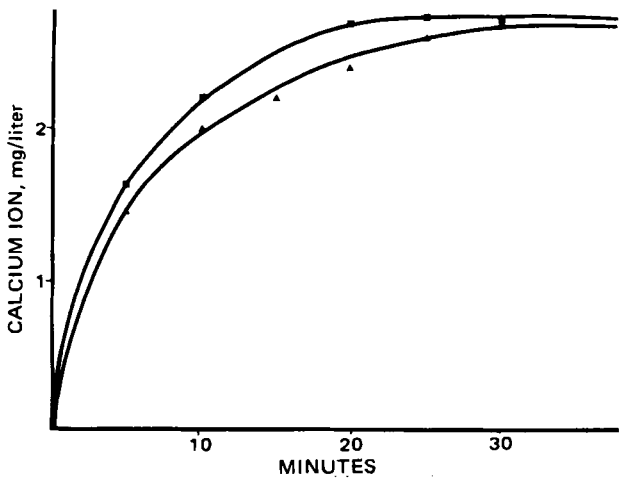

Figure 3—*Dissolution curves of calcium oxalate dihydrate prepared by the method described in the text (■) and calcium oxalate monohydrate standard (▲) under sink conditions at 37°.*

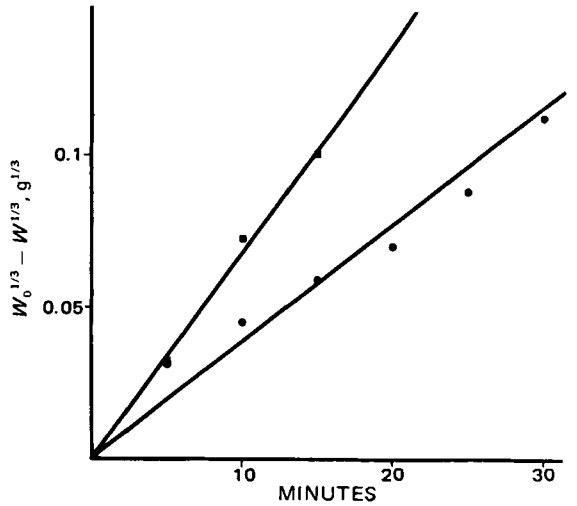

Figure 4—*Cube root plot of the dissolution data of calcium oxalate monohydrate (●) and calcium oxalate dihydrate (■).*

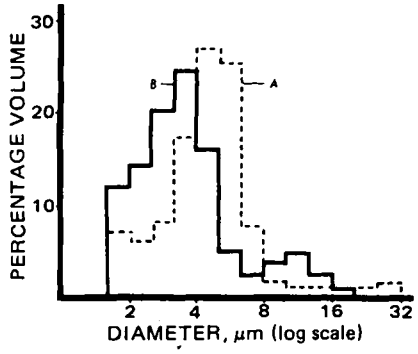

Figure 5—*Crystal size distribution of calcium oxalate dihydrate (A) and calcium oxalate monohydrate (B) used for the dissolution rate studies.*

[determined by automated particle counter[12] (Fig. 5)]. Table II summarizes the structure-dependent properties of calcium oxalate monohydrate and dihydrate. The dihydrate has a higher solubility and dissolution rate and a lower zeta potential than the monohydrate. The dihydrate crystals are stable in air at 4° for 2 weeks; however, when these crystals are kept in normal saline at 37°, they are stable for only 24 hr. After 24 hr, gradual conversion to monohydrate occurs.

The observation that calcium oxalate dihydrate has a higher solubility, higher dissolution rate, and undergoes gradual dissolution–recrystallization to calcium oxalate monohydrate is consistent with recent results reported on the crystallization of calcium oxalate in the rat kidney (8). It offers the most probable explanation for the gradual transformation of calcium oxalate dihydrate to calcium oxalate monohydrate in rat kidney following the administration of 4-hydroxy-L-proline. Detailed study of the difference in the zeta potential between the monohydrate and the dihydrate could lead to a better understanding of the role of crystal aggregation in stone formation.

[12] Coulter Counter model TA II.

REFERENCES

(1) M. Berenyi, D. Franc, and J. Legrady, *Int. Urol. Nephrol.*, **4**, 341 (1972).

(2) B. Tomazic and G. H. Nancollas, *J. Cryst. Growth*, **46**, 355 (1979).

(3) B. B. Tomazic and G. H. Nancollas, *Invest. Urol.*, **16**, 329 (1979).

(4) W. Berg, P. Lange, C. Bothor, and D. Rossler, *Eur. Urol.*, **5**, 136 (1979).

(5) G. L. Gardner and R. H. Doremus, *Invest. Urol.*, **15**, 478 (1978).

(6) A. Hesse, W. Berg, H-J. Schneider, and E. Hienzsch, *Urol. Res.*, **4**, 125 (1976).

(7) A. Hesse, W. Berg, H-J. Schneider, and E. Hienzsch, *ibid.*, **4**, 157 (1976).

(8) R. Tawashi, M. Cousineau, and M. Sharkawi, *ibid.*, **8**, 121 (1980).

(9) R. Tawashi and M. Cousineau, *Invest. Urol.*, **18**, 86 (1980).

(10) J. Bellanato, L. Cifuentes Delatte, A. Hidalgo, and M. Santos, in "Urinary Calculi," International Symposium on Renal Stone Research, Madrid, 1972, p. 237.

(11) H. C. Holtkamp, P. A. Nantel, H. J. Brouwer, T. L. Lien, and J. C. Van Zwam. *Clin. Chem. Acta*, **76**, 125 (1977).

(12) A. S. Meyer, B. Finlayson, and L. Dubois, *Br. J. Urol.*, **43**, 154 (1971).

(13) P. Curreri, G. Y. Onoda, and B. Finlayson, *J. Colloid Interface Sci.*, **69**, 170 (1979).

(14) T. M. Riddick, in "Control of Colloidal Stability through Zeta Potential," Zeta-Meter New York, N.Y., 1968, p. 320.

(15) A. W. Hixson and J. H. Crowell, *Ind. Eng. Chem.*, **23**, 923 (1931).

ACKNOWLEDGMENTS

Presented to the APhA Academy of Pharmaceutical Sciences, Washington, D.C., April 1980.

Supported by the Medical Research Council of Canada.

The authors thank Mr. M. Cousineau for his technical assistance.

Potential Thyroliberin Affinity Labels II: Chloroacetyl Substituted Phenylalanyl Prolineamides

RICHARD J. GOEBEL *, BRUCE L. CURRIE *x, and CYRIL Y. BOWERS ‡

Received August 3, 1981, from the **Department of Medicinal Chemistry, College of Pharmacy, University of Illinois at the Medical Center, Chicago, IL 60680*, and the ‡*Department of Medicine, School of Medicine, Tulane University, New Orleans, LA 70112.* Accepted for publication December 9, 1981.

Abstract □ Three analogs of thyroliberin (I) were prepared. These compounds, *N-m*-chloroacetylbenzoyl-phenylalanyl-prolineamide (VI*a*), *N-p*-chloroacetylbenzoyl-phenylalanyl-prolineamide (VI*b*) and *N*-chloroacetyl-alanyl-phenylalanyl-prolineamide (IX), were designed as potential I antagonist affinity labels. However, no significant antagonist activity was observed. Compounds VI*a* and IX were found to have weak agonist activity. Cyclo (Phe-Pro) an analog of the I metabolite, cyclo (His-Pro), was found, however, to have significant I antagonist activity, but no agonist activity.

Keyphrases □ Thyroliberin—potential affinity labels, chloroacetyl substituted phenylalanyl prolineamides □ Hormones—peptide, thyroliberin affinity labels, chloroacetyl substituted phenylalanyl prolineamides □ Receptor-hormone interactions—affinity label analogs, characterization, thyroliberin

Thyroliberin (I) is a peptide hormone from the hypothalamus that can release thyrotropin (1) and prolactin (2) from the anterior pituitary both *in vivo* and *in vitro*. Affinity label analogs of I that irreversibly bind to the I receptor could aid in the characterization of the I receptor and the study of receptor–hormone interactions. The use of a naltrexamine affinity label to isolate a complex with an opiate receptor, which was recently reported (3) while these studies were in progress, is a similar approach.

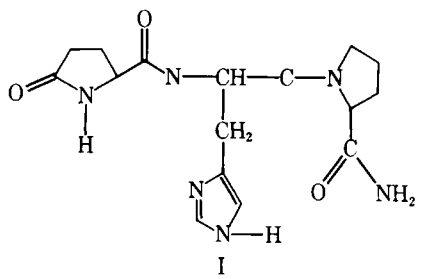

I

Initial attempts to develop analogs of I as potential af-

0022-3549/82/0900-1062$01.00/0

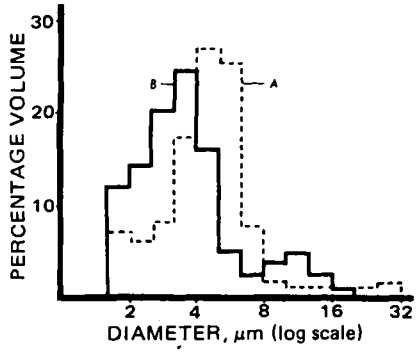

Figure 5—*Crystal size distribution of calcium oxalate dihydrate (A) and calcium oxalate monohydrate (B) used for the dissolution rate studies.*

[determined by automated particle counter[12] (Fig. 5)]. Table II summarizes the structure-dependent properties of calcium oxalate monohydrate and dihydrate. The dihydrate has a higher solubility and dissolution rate and a lower zeta potential than the monohydrate. The dihydrate crystals are stable in air at 4° for 2 weeks; however, when these crystals are kept in normal saline at 37°, they are stable for only 24 hr. After 24 hr, gradual conversion to monohydrate occurs.

The observation that calcium oxalate dihydrate has a higher solubility, higher dissolution rate, and undergoes gradual dissolution–recrystallization to calcium oxalate monohydrate is consistent with recent results reported on the crystallization of calcium oxalate in the rat kidney (8). It offers the most probable explanation for the gradual transformation of calcium oxalate dihydrate to calcium oxalate monohydrate in rat kidney following the administration of 4-hydroxy-L-proline. Detailed study of the difference in the zeta potential between the monohydrate and the dihydrate could lead to a better understanding of the role of crystal aggregation in stone formation.

[12] Coulter Counter model TA II.

REFERENCES

(1) M. Berenyi, D. Franc, and J. Legrady, *Int. Urol. Nephrol.*, **4**, 341 (1972).

(2) B. Tomazic and G. H. Nancollas, *J. Cryst. Growth*, **46**, 355 (1979).

(3) B. B. Tomazic and G. H. Nancollas, *Invest. Urol.*, **16**, 329 (1979).

(4) W. Berg, P. Lange, C. Bothor, and D. Rossler, *Eur. Urol.*, **5**, 136 (1979).

(5) G. L. Gardner and R. H. Doremus, *Invest. Urol.*, **15**, 478 (1978).

(6) A. Hesse, W. Berg, H-J. Schneider, and E. Hienzsch, *Urol. Res.*, **4**, 125 (1976).

(7) A. Hesse, W. Berg, H-J. Schneider, and E. Hienzsch, *ibid.*, **4**, 157 (1976).

(8) R. Tawashi, M. Cousineau, and M. Sharkawi, *ibid.*, **8**, 121 (1980).

(9) R. Tawashi and M. Cousineau, *Invest. Urol.*, **18**, 86 (1980).

(10) J. Bellanato, L. Cifuentes Delatte, A. Hidalgo, and M. Santos, in "Urinary Calculi," International Symposium on Renal Stone Research, Madrid, 1972, p. 237.

(11) H. C. Holtkamp, P. A. Nantel, H. J. Brouwer, T. L. Lien, and J. C. Van Zwam. *Clin. Chem. Acta*, **76**, 125 (1977).

(12) A. S. Meyer, B. Finlayson, and L. Dubois, *Br. J. Urol.*, **43**, 154 (1971).

(13) P. Curreri, G. Y. Onoda, and B. Finlayson, *J. Colloid Interface Sci.*, **69**, 170 (1979).

(14) T. M. Riddick, in "Control of Colloidal Stability through Zeta Potential," Zeta-Meter New York, N.Y., 1968, p. 320.

(15) A. W. Hixson and J. H. Crowell, *Ind. Eng. Chem.*, **23**, 923 (1931).

ACKNOWLEDGMENTS

Presented to the APhA Academy of Pharmaceutical Sciences, Washington, D.C., April 1980.

Supported by the Medical Research Council of Canada.

The authors thank Mr. M. Cousineau for his technical assistance.

Potential Thyroliberin Affinity Labels II: Chloroacetyl Substituted Phenylalanyl Prolineamides

RICHARD J. GOEBEL *, BRUCE L. CURRIE *x, and CYRIL Y. BOWERS ‡

Received August 3, 1981, from the **Department of Medicinal Chemistry, College of Pharmacy, University of Illinois at the Medical Center, Chicago, IL 60680*, and the ‡*Department of Medicine, School of Medicine, Tulane University, New Orleans, LA 70112.* Accepted for publication December 9, 1981.

Abstract □ Three analogs of thyroliberin (I) were prepared. These compounds, *N-m*-chloroacetylbenzoyl-phenylalanyl-prolineamide (VI*a*), *N-p*-chloroacetylbenzoyl-phenylalanyl-prolineamide (VI*b*) and *N*-chloroacetyl-alanyl-phenylalanyl-prolineamide (IX), were designed as potential I antagonist affinity labels. However, no significant antagonist activity was observed. Compounds VI*a* and IX were found to have weak agonist activity. Cyclo (Phe-Pro) an analog of the I metabolite, cyclo (His-Pro), was found, however, to have significant I antagonist activity, but no agonist activity.

Keyphrases □ Thyroliberin—potential affinity labels, chloroacetyl substituted phenylalanyl prolineamides □ Hormones—peptide, thyroliberin affinity labels, chloroacetyl substituted phenylalanyl prolineamides □ Receptor-hormone interactions—affinity label analogs, characterization, thyroliberin

Thyroliberin (I) is a peptide hormone from the hypothalamus that can release thyrotropin (1) and prolactin (2) from the anterior pituitary both *in vivo* and *in vitro*. Affinity label analogs of I that irreversibly bind to the I receptor could aid in the characterization of the I receptor and the study of receptor–hormone interactions. The use of a naltrexamine affinity label to isolate a complex with an opiate receptor, which was recently reported (3) while these studies were in progress, is a similar approach.

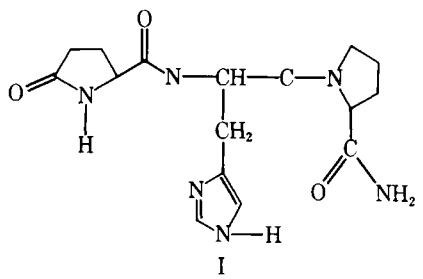

I

Initial attempts to develop analogs of I as potential af-

0022-3549/82/0900-1062$01.00/0

finity labels were based on previously reported structure–activity relationships and were expected to result in compounds that were antagonists of I. These compounds, with general structure *N*-chloroacetyl [ ]Phe-Pyrr, were found, however, to be only weak agonists (4).

In an effort to improve receptor binding affinity, the prolineamide moiety was included in the present compounds. The resulting analogs were expected to have improved agonist potency based on previously reported structure–activity relationships (5). Therefore, compounds of general structure, *N*-chloroacetyl[ ]Phe-Pro-NH_2, were synthesized. Cyclo (Phe-Pro) was also synthesized as an analog of cyclo (His-Pro), a metabolite of I (6, 7).

EXPERIMENTAL

Melting points[1] reported are uncorrected. All amino acid derivatives used were of the L configuration. Thin-layer chromatography was performed on 250 μm silica gel G plates with fluorescent indicator[2]. The following solvent systems were used: (A) chloroform–methanol (39:1); (B) chloroform–methanol (19:1); (C) chloroform–methanol–concentrated ammonium hydroxide (18:1:1), lower phase; (D) chloroform–methanol–concentrated ammonium hydroxide (17:2:1), lower phase. Methods of detection are indicated with the data. Proton magnetic resonance[3] spectra were recorded at 60 MHz in the solvent indicated for each compound and the data are reported in parts per million (δ) downfield from internal tetramethylsilane. Optical rotations were determined with a digital readout polarimeter[4], and the solvent used is indicated with the data. Elemental analyses are reported for new compounds[5].

L-Phe-L-Pro-NH_2 Hydrochloride (III)—*N*-Carbobenzoxy-L-Phe (1.5 g, 5.02 mmoles) was dissolved in dry ethyl acetate (60 ml) with stirring and cooled to −40°. *N*-methylmorpholine (0.61 ml, 5.55 mmoles) was added followed immediately with isobutyl chloroformate (8) (0.62 ml, 4.78 mmoles). After 8 min, L-Pro-NH_2 hydrochloride (0.72 g, 4.78 mmoles) was added followed by additional *N*-methylmorpholine (0.53 ml). The reaction mixture was allowed to warm to room temperature and stirred overnight. The mixture was washed with 5% $NaHCO_3$ (2 × 25 ml), 1 *N* HCl (2 × 25 ml), water (2 × 25 ml), dried over anhydrous magnesium sulfate, and evaporated to dryness (3.95 g).

Chromatographic purification on a silica gel column (90 g, 2.5 × 51.5 cm) and elution with chloroform (450 ml) and 5% methanol in chloroform (600 ml) yielded 3.05 g of *N*-carbobenzoxy-L-Phe-L-Pro-NH_2 (II) as a sticky foam from fractions (4 ml) 205 through 230; one spot on TLC, Solvent B, UV and chlorine–tolidine positive, ninhydrin negative; with a confirming PMR spectrum.

A solution of II (3.05 g) in methanol (55 ml) containing gaseous hydrogen chloride (0.16 g) was hydrogenolyzed for 1 hr at 10 psi and room temperature over 5% palladium on charcoal. Removal of the catalyst and concentration *in vacuo* provided III as a hygroscopic solid which could be used directly in subsequent reactions. Further purification was not possible due to conversion into cyclo (L-Phe-L-Pro) (IV) during crystallization attempts. The PMR spectrum confirmed the assigned structure; one spot on TLC, Solvent D, UV, ninhydrin and chlorine–tolidine positive.

Cyclo (L-Phe-L-Pro) (IV)—Hydrogenolysis of II (2.75 g) in methanol (20 ml) and glacial acetic acid (0.5 ml) at 10 psi over 5% palladium on charcoal for 2 hr, removal of the catalyst, and evaporation to dryness gave a residue. This residue was refluxed for 1 hr in benzene (20 ml), filtered hot, and crystals of IV obtained upon addition of petroleum ether, 0.28 g, mp 126–128° [lit. (9) mp 125–127°], one spot on TLC, Solvent A, UV and iodine positive, ninhydrin negative.

3-Chloroacetylbenzoyl-L-Phe-L-Pro-NH_2 (VI*a*)—To a solution of III (0.40 g, 1.34 mmoles), in dry dimethylformamide (4 ml), methylene chloride (6 ml), and *N*-methylmorpholine (0.14 ml), was added 0.21 g of 3-chloroacetylbenzoyl chloride (V*a*) (4) in methylene chloride (4 ml) followed by additional *N*-methylmorpholine (0.11 ml). The reaction mixture was stirred for 3 hr at room temperature.

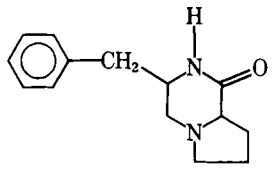

IV

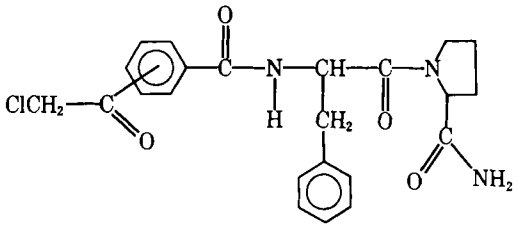

VI*a*: = *m*-$ClCH_2CO$—
VI*b*: = *p*-$ClCH_2CO$—

Methylene chloride (25 ml) was added, and the mixture was washed with 5% $NaHCO_3$ (35 ml), 1 *N* HCl (25 ml), and water (25 ml). The organic layer was dried over magnesium sulfate, evaporated to dryness, and crystalline VI*a* obtained from ethyl acetate–petroleum ether; yield 0.11 g (25%); mp 152–154°; one spot on TLC, Solvent B, UV and chlorine–tolidine positive, ninhydrin negative; $[\alpha]_D^{28} = -52.4°$ (*C* = 0.867, chloroform). The NMR spectrum supported the assigned structure.

Anal.—Calc. for $C_{23}H_{24}ClN_3O_4$: C, 62.51; H, 5.47; Cl, 8.02; N, 9.51. Found: C, 62.49; H, 5.54; Cl, 8.22; N, 9.44.

4-Chloroacetylbenzoyl-L-Phe-L-Pro-NH_2 (VI*b*)—A solution of III (0.40 g, 1.34 mmoles), in dimethylformamide (4 ml), methylene chloride (6 ml), and *N*-methylmorpholine (0.14 ml), was treated with 0.25 g of 4-chloroacetylbenzoyl chloride (V*b*) (4) in methylene chloride (4 ml) followed by additional *N*-methylmorpholine (0.11 ml). The reaction was stirred for 3 hr at room temperature. Workup was similar to that for VI*a*.

Crude VI*b* (0.44 g) required column purification on a chloroform packed silica gel column (35 g, 2.5 × 28 cm) eluted with chloroform (200 ml), 30% ethyl acetate in chloroform (200 ml), 60% ethyl acetate in chloroform (200 ml), and ethyl acetate (600 ml). Fractions (4 ml) 235 through 285 contained VI*b* which was crystallized from ethyl acetate–petroleum ether. Purified VI*b* crystallized with 0.5 mole of ethyl acetate, which was confirmed in the PMR spectrum; yield 0.17 g (35%); mp 103–107°; one spot on TLC, Solvent B, UV and chlorine–tolidine positive, ninhydrin negative; $[\alpha]_D^{28} = -32.4°$ (*C* = 1.125, chloroform).

Anal.—Calc. for $C_{23}H_{24}ClN_3O_4 \cdot 0.5\ C_4H_8O_2$: C, 61.79; H, 5.81; Cl, 7.29; N, 8.65. Found: C, 61.77; H, 5.72; Cl, 7.11; N, 8.74.

***N*-Chloroacetyl-L-Ala-L-Phe-L-Pro-NH_2 (IX)**—A solution of *N*-carbobenzoxy-L-Ala (0.95 g, 4.26 mmoles) in dry tetrahydrofuran (80 ml) was cooled to −40°, *N*-methylmorpholine (0.52 ml, 4.73 mmoles) was added, followed by isobutyl chloroformate (0.53 ml, 4.09 mmoles). After 15 sec, III (1.25 g, 4.20 mmoles) was added followed by additional *N*-methylmorpholine (0.46 ml, 4.18 mmoles). The reaction was warmed to room temperature, stirred overnight, and then evaporated to dryness.

The residue was dissolved in methylene chloride (100 ml) and washed with bicarbonate, acid, and water similar to the procedure used for II. The organic layer was dried over magnesium sulfate and taken to dryness. The residue was applied to a chloroform packed silica gel column (35 g, 28 × 2.5 cm) which was eluted with chloroform (250 ml), 1% methanol in chloroform (300 ml), and 1.5% methanol in chloroform (400 ml). The desired product was collected in fractions (4 ml) 167 to 202 that were concentrated to a residue (0.80 g), one spot on TLC, Solvent B, UV and

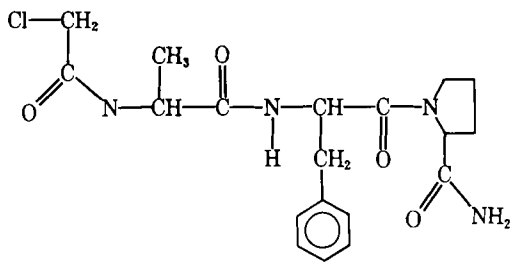

IX

[1] Determined on a Mel-Temp block; values are uncorrected.
[2] Obtained from E. Merck.
[3] Determined with a Varian Associates T-60A instrument equipped with a Nicolet Instrument Corp. TT-7 Fourier Transform Accessory.
[4] Determined with a Perkin-Elmer model 241.
[5] Performed by Micro-Tech Laboratories, Skokie, Ill.

Table I—Relative Agonist Activity

Peptide	Relative Activity, %
I	100[a]
IV	None[b]
VI*a*	0.0006
VI*b*	None[b]
IX	0.0002

[a] Compound I dose of 0.6 ng. [b] At a dose up to 30 μg.

chlorine–tolidine positive, ninhydrin negative. The PMR spectrum indicated the expected product, *N*-carbobenzoxy-Ala-Phe-Pro-NH_2 (VII) which could be used directly in the next step.

A solution of VII (1.04 g) in methanol (40 ml) containing gaseous hydrogen chloride (0.10 g) and 5% palladium on charcoal (0.35 g) was hydrogenolyzed for 1 hr at 10 psi and room temperature. Removal of the catalyst by filtration, concentration *in vacuo*, and coevaporation with benzene gave Ala-Phe-Pro-NH_2 hydrochloride (VIII) (0.82 g) as a glass which gave the appropriate PMR spectrum, and was one spot on TLC, Solvent C, UV, chlorine–tolidine, and ninhydrin positive.

Chloroacetic anhydride (0.20 g, 1.17 nmoles) was added to a solution of VIII (0.47 g, 1.27 mmoles) in dimethylformamide (3 ml) and methylene chloride (7 ml) followed by *N*-methylmorpholine (0.14 ml, 1.27 mmoles). The reaction was stirred for 6 hr, methylene chloride (10 ml) was added, and the mixture was washed with 5% $NaHCO_3$ (2 × 10 ml), 1 *N* HCl (2 × 10 ml), and water (2 × 10 ml). The organic layer was dried over magnesium sulfate and concentrated to dryness to yield 0.27 g of IX.

The crude product was applied to a silica gel column (35 g, 28 × 2.5 cm) packed in chloroform and eluted with chloroform (200 ml), 10% acetone in chloroform (200 ml), 20% acetone in chloroform (200 ml), and acetone (200 ml). The desired product was collected in fractions (4 ml) 265 to 280. Pure IX was obtained by crystallization from ethyl acetate–petroleum ether; yield 0.02 g (4%); one spot on TLC, Solvent B, UV and chlorine–tolidine positive, ninhydrin negative; mp 198–202°; $[\alpha]_D^{28} = -68.0°$ (C = 0.883, chloroform); PMR spectrum in deuterochloroform: δ 1.31 [d, $J \simeq$ 7 Hz, 3H(β—CH_3 of Ala)], 1.75 [m, 2H(δ—CH_2 of Pro—NH_2)], 2.06 [m, 4H(β and γ—CH_2 of Pro—NH_2)], 3.00 [m, 2H(β—CH_2 of Phe)], 4.01 [s, 2H (—$COCH_2Cl$)], 4.53–5.25 [m, 3H(overlapping α—CH)], 7.23 [s, 5H (aromatic H of Phe)].

Anal.—Calc. for $C_{19}H_{25}ClN_4O_4$: C, 55.81; H, 6.16; Cl, 8.67; N, 13.71. Found: C, 55.52; H, 6.17; Cl, 8.62; N, 13.43.

Biological Assay—The initial evaluation of the thyroliberin agonist and antagonist activity of these compounds was by the *in vitro* method of Bowers *et al.* (10). Freshly excised whole pituitaries from 20-day-old female rats were incubated in Krebs–Ringer bicarbonate for six 1-hr periods. The incubation medium was replaced after each hour. Test samples were added during the third through the sixth hours (I_3–I_6), and the resultant thyrotropin concentration in the incubation media was measured by radioimmunoassay and compared with the second hour (P_2). Agonist activity was measured by the effects of the analogs alone on the pituitaries. Antagonist activity was measured by the net effect of the analog in combination with synthetic thyroliberin. The bioassay results are summarized in Table I.

RESULTS AND DISCUSSION

As shown in Table I, the agonist potency is weak and is on the same order as that reported previously (4) for the pyrrolidine analogs. The incorporation of prolineamide into thyroliberin analogs has usually resulted in a significant increase in the agonist potency of the resulting peptides relative to the corresponding pyrrolidine derivatives. However, this was not the case for the reported analogs.

The case of IX is striking. Chloroacetylalanyl can be considered to be an open ring analog of pyroglutamyl. Thus, there is only a minor change in structure from the relatively potent analog, *p*-Glu-Phe-Pro-NH_2 (11). Compound IX, however, had only 0.0002% of the agonist potency of thyroliberin. No significant antagonist activity was found for VI*a*, VI*b*, or IX.

The synthesis of IV has been previously reported (9) in conjunction with some spectroscopic studies. The evaluation of the endocrine activity of IV was of interest because of the importance of cyclo (His-Pro) as a metabolite (6, 7) of thyroliberin and the observation that cyclo (His-Pro) could inhibit the thyroliberin-stimulated release of prolactin both *in vitro* (12, 13) and *in vivo* (12). An uncharacterized pineal substance that can inhibit thyroliberin-stimulated thyrotropin release has also been recently reported (14).

Cyclo (Phe-Pro) had no significant agonist activity up to a 30-μg dose; however, antagonist activity was apparent. Thyroliberin (0.6 ng) alone caused the release of 17.3 μg of thyrotropin. In the presence of IV (3 μg and 30 μg), the thyrotropin release was 11.0 μg ($p < 0.01$) and 13.1 μg ($p < 0.05$), respectively. This is of interest because cyclo (His-Pro) has not been reported to have thyroliberin antagonist activity.

REFERENCES

(1) C. Y. Bowers, H. G. Friesen, R. Hwang, H. J. Guyda, and K. Folkers, *Biochem. Biophys. Res. Commun.*, **45**, 1033 (1972).

(2) P. S. Dannies and A. H. Tashjian, Jr., *Nature (London)*, **261**, 707 (1976) and references therein.

(3) T. P. Caruso, D. L. Larson, P. S. Portoghese, and A. E. Takemori, *Life Sci.*, **27**, 2063 (1980).

(4) R. J. Goebel, B. L. Currie, and C. Y. Bowers, *J. Med. Chem.*, **24**, 366 (1981).

(5) W. Vale, G. Grant, and R. Guillemin, in, "Frontiers in Neuroendocrinology," W. F. Ganong and L. Martini, Eds., Oxford University Press, London, 1973, p. 375.

(6) C. Prasad and A. Peterkofsky, *J. Biol. Chem.*, **251**, 3229 (1976).

(7) C. Prasad, T. Matsui, and A. Peterkofsky, *Nature (London)*, **268**, 142 (1977).

(8) M. A. Tilak, *Tetrahedron Lett.*, 849 (1970).

(9) P. E. Young, V. Madison, and E. R. Blout, *J. Am. Chem. Soc.*, **98**, 5365 (1976).

(10) C. Y. Bowers, H. Sievertsson, J. Chang, J. Stewart, S. Castensson, J. Bjorkman, D. Chang, and K. Folkers, in *Proceedings of the 7th International Thyroid Conference*, Boston, June, 1975, Excerpta Medica, Amsterdam, 1976, p. 1.

(11) H. Sievertsson, J.-K. Chang, K. Folkers, and C. Y. Bowers, *J. Med. Chem.*, **15**, 219 (1972).

(12) K. Bauer, K. J. Graf, A. Faivre-Bauman, A. Tixier-Vidal, and H. Kleinauf, *Nature (London)*, **274**, 174 (1978).

(13) C. Prasad, J. F. Wilber, V. Akerstrom, and A. Banerji, *Life Sci.*, **27**, 1979 (1980).

(14) J. Vriend, P. M. Hinkle, and K. M. Knigge, *Endocrinology*, **107**, 1791 (1980).

ACKNOWLEDGMENTS

Presented in part at the 180th National Meeting of the American Chemical Society, Las Vegas, Nev., August 24–29, 1980, abstract MEDI 47.

This work forms part of a thesis submitted by R. J. Goebel to the University of Illinois at the Medical Center in partial fulfillment of the requirements for the degree of Doctor of Philosophy.

The authors thank Ms. George Ann Reynolds for her expert technical assistance in the performance of the bioassays and Ms. Marion Roberts for her assistance in the preparation of this manuscript.

Fast Atom Bombardment Mass Spectra of Azthreonam and Its Salts

Keyphrases □ Fast atom bombardment—mass spectra of azthreonam and its salts □ Azthreonam—biologically active azetidinesulfonic acids, monobactams, fast atom bombardment mass spectra □ Mass spectrometry—fast atom bombardment of azthreonam and its salts □ Monobactams—biologically active azetidinesulfonic acids, azthreonam, fast atom bombardment mass spectra

To the Editor:

Recently, Cimarusti *et al.* (1) reported the synthesis of a new class of biologically active azetidinesulfonic acids, termed monobactams. One of these monobactams, azthreonam[1], is highly selective against aerobic Gram-negative bacteria (2), including *Pseudomonas aeruginosa* (3).

This communication reports the results of the mass spectra of the named compound and its monosodium and dipotassium salts by the fast atom bombardment technique pioneered by Barber *et al.* (4) and applied by various investigators in the analysis of vexatious polar compounds (5–12).

Mass spectra were obtained on a double-focusing magnetic sector instrument[2] equipped with a fast atom bombardment source using 4–8 kV xenon neutral atoms. Azthreonam (I) gave a very prominent $[M—H]^-$ ion (base peak) in the negative-ion detection mode[3] (Table I) and a significant MH^+ ion in the positive-ion detection mode (Table II). Weak, but perceptible, dimeric ions were also observed. Based upon the expected losses, the fragmentation patterns in each ion detection mode yielded diagnostic information.

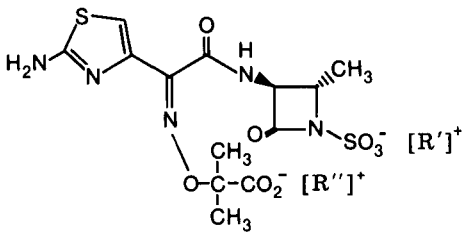

	R′	R″	MW	MH^+	$[M·H]^-$
I Azthreonam	H	H	435	436	434
II	Na	H	457	458	456
III	K	K	511	512	510

In the negative ion spectrum, the ions resulting from the direct N—O bond cleavage yields the $[m/z\ 332]^-$ ion and its $[m/z\ 103]^-$ ion complement (Table I). The principal high mass fragment ion in the positive-ion mass spectrum results from the loss of sulfur trioxide from the MH^+ ion (Table II). Cleavage of the monobactam ring of I gives rise to the $[m/z\ 313]^+$ ion in the positive-ion detection mode and its $[m/z\ 122]^-$ complement in the negative-ion detection mode.

Because polar acids are often isolated as alkali salts, the fast atom bombardment spectra of the monosodium (II) and dipotassium (III) salts (13) were compared to the spectra of azthreonam (I). The negative-ion spectra produced readily assignable $[M—H]^-$ and $[M—R']^-$ ions (Table I). The positive-ion spectra yielded complimentary information, although ions generated from mono- and dicationization were more intense than the MH^+ ions. Consequently, care should be taken to introduce as minimum extraneous inorganic salts, or, if unavoidable, only a single species of cation. Fast atom bombardment mass spectrometry has been used in the characterization of related naturally occurring monobactams, synthetic intermediates for azthreonam, and impurities.

Table I—Negative-Ion Fast Atom Bombardment Mass Spectra [a,b]

Negative-Ion Compound Assignment	I R′ = R″ = H	II R′ = Na, R″ = H	III R′ = R″ = K
	[mass/charge (Relative Intensity)]		
2M+R′—2H	—	935(5)	—
2M—H	869(1)	913(5)	—
2M—R′	—	891(8)	983(2)
M+R′—2H	—	478(4)	548(3)
M—H	434(100)	456(76)	510(20)
M—R′	434(100)	434(76)	472(39)
M—R″$O_2CC_3H_6O$	332(16)	354(11)	370(24)
M—R′$O_2CC_3H_6O$	332(16)	332(13)	370(24)
$HO_3SNC_4H_4NCO$	205(16)	205(65)	205(100)
O_3SNCO and/or $O_3SNC_2H_4$	122(58)	122(100)	122(80)
$HO_2CC_3H_6O$	103(10)	103(18)	103(59)
SO_3NH_2	96(26)	96(39)	96(20)
SO_3	80(48)	80(87)	80(85)

[a] Xenon neutral gas. [b] Glycerin matrix.

Table II—Positive-Ion Fast Atom Bombardment Mass Spectra [a,b]

Positive-Ion Compound Assignment	I R′ = R″ = H	II R′ = Na, R″ = H	III R′ = R″ = K
	[mass/charge (Relative Intensity)]		
2M+2R′—H	—	959(9)	1099(1)
2M+R′	871(1)	937(24)	1061(4)
2M+H	871(1)	915(3)	1023(2)
M+2R′—H	—	502(44)	588(14)
M+R′	436(30)	480(100)	550(47)
MH	436(30)	458(21)	512(16)
M+R′—SO_3	356(44)	400(14)	432(11)
MH—SO_3	356(44)	378(?)	—
M—H—SO_3	354(3)	377(83)	—
MH—HO_3SNCO and/or MH—$HO_3SNC_2H_4$	313(65)	335(22)	389(11)
MH—$O_2CC_3H_6O$	334(4)	356(5)	410(13)
$C_4H_6N_3S$	126(100)	126(93)	—

[a] Xenon neutral gas. [b] Glycerin matrix.

[1] {2*S*-[2α,3β(*Z*)]}-3[[2-amino-4-thiazolyl-[(1-carboxy-1-methyl-ethoxy)imino]-acetyl]-amino]-2-methyl-4-oxo-1-azetidinesulfonic acid; CAS 78110-38-0, SQ 26,776.

[2] Model ZAB 1F, VG Analytical Ltd., Altrincham, U.K.

[3] A similar negative-ion mass spectrum of I was obtained on the Kratos MS 50 mass spectrometer, with xenon gas, at the Middle Atlantic Mass Spectrometry (MAMS) Laboratory, Baltimore, Md.

(1) C. M. Cimarusti, H. Breuer, T. Denzel, D. K. Kronenthal, U. D. Treuner, D. P. Bonner, and R. B. Sykes, Abstract 487, 21st Interscience Conference on Antimicrobial Agents and Chemotherapy, Chicago, Ill., November 4–6, 1981.

0022-3549/82/0900-1065$01.00/0

(2) R. B. Sykes, K. Bush, and J. S. Freudenberger, Abstract 479, *ibid.*

(3) P. B. Fernandes, D. P. Bonner, R. R. Whitney, B. H. Miller, C. O. Baughn, and R. B. Sykes, Abstract 490, *ibid.*

(4) M. Barber, R. S. Bardoli, R. D. Sedwick, and A. N. Tyler, *J. Chem. Soc. Chem. Commun.*, **1981**, 325.

(5) C. Fenselau and R. J. Cotter, *Pure Appl. Chem.*, in press.

(6) D. H. Williams, C. Bradley, G. Bojesen, S. Santikarn, and L. C. E. Taylor, *J. Am. Chem. Soc.*, **103**, 5700 (1981).

(7) M. Barber, R. S. Bardoli, R. D. Sedwick, and A. N. Tyler, *Biomed. Mass. Spectrom.*, **8**, 492–495 (1981).

(8) A. Dell, H. R. Morris, M. D. Levin, and S. M. Hecht, *Biochem. Biophys. Res. Commun.*, **102**, 730 (1981).

(9) M. Barber, R. S. Bardoli, R. D. Sedwick, and L. W. Tetler, *Org. Mass Spectrom.*, **16**, 256 (1981).

(10) C. Fenselau, R. Cotter, G. Hansen, T. Chen, and D. Heller, *J. Chromatogr.*, **218**, 21 (1981).

(11) C. Fenselau, *Anal. Chem.*, **54**, 105A (1982).

(12) C. J. McNeal, *ibid.*, **54**, 43A (1982).

(13) H. Breuer, C. M. Cimarusti, Th. Denzel, W. H. Koster, W. A. Slusarchyk, and U. D. Treuner, *J. Antimicrob. Agents Chemother.*, **8**, Suppl. E, 21 (1981).

Allen I. Cohen[x]
Phillip T. Funke
Department of Analytical Research
Squibb Institute for Medical Research
New Brunswick, NJ 08903

Brian N. Green
VG Analytical Ltd.
Altrincham, U.K.

Received March 17, 1982.
Accepted for publication May 12, 1982.

The authors recognize the Middle Atlantic Mass Spectrometry (MAMS) Laboratory, a National Science Foundation shared instrument facility, directed by Drs. C. Fenselau and R. J. Cotter, as an important resource for the early evaluation of fast atom bombardment mass spectrometry. Some of the preliminary spectra were expertly run by Dr. G. Hansen on the MAMS instrument. Characterized samples were graciously furnished by Dr. C. M. Cimarusti.

Effect of Initial Conditions and Drug–Protein Binding on the Time to Equilibrium in Dialysis Systems

Keyphrases □ Drug–protein binding—effect of initial conditions on the time to equilibrium in dialysis systems □ Equilibrium dialysis—effect of initial conditions and drug–protein binding

To The Editor:

A major disadvantage of using equilibrium dialysis methods for determining *in vitro* plasma protein binding of drugs is the time needed to reach equilibrium. Recently, Øie and Guentert (1) mathematically showed that equilibration is more rapid when the drug is initially added to the plasma side as opposed to the buffer side. The approach to equilibrium was described by integrated equations for the concentration of drug on the buffer side as a function of time. The relative time to equilibrium for the two initial configurations was found to be:

$$R = \frac{t_B}{t_P} = \frac{\ln \delta + \ln \alpha}{\ln \delta} = 1 + \frac{\ln \alpha}{\ln \delta} \qquad \text{(Eq. 1)}$$

where t_B and t_P are the times to reach some fraction (δ) from the equilibrium concentration when the drug is initially added to the buffer or plasma side, respectively, and α is the unbound fraction in plasma which is assumed to be constant during the dialysis. For example, a δ value of 0.05 indicates a deviation of 5% from the true equilibrium value.

The authors indicated that the closer to the true equilibrium value one wants to be, the closer the ratio is to unity. Furthermore, a smaller α (stronger binding) or a larger δ increases the advantage of spiking the plasma side. While we are in complete agreement with these conclusions, some interesting and practical information may be lost if the examination of this system is limited only to the ratio of the times to equilibrium. In this communication the concept of approach to equilibrium in dialysis systems will be further developed and factors affecting comparative equilibration times will be discussed.

When drug is initially added to the plasma side, the concentration on the buffer side (C_B) at any time (t) is:

$$C_B = \frac{C_0\alpha}{1+\alpha}(1 - e^{-K_T(1+\alpha)t}) \qquad \text{(Eq. 2)}$$

where C_0 is the initial concentration, and K_T is the rate constant governing the transfer of drug across the membrane (1).

When drug is initially placed in the buffer side, a similar equation is obtained:

$$C_B = \frac{C_0}{1+\alpha}(\alpha + e^{-K_T(1+\alpha)t}) \qquad \text{(Eq. 3)}$$

Although the actual concentration on the buffer side is the variable of interest, a more useful relationship for examining the influence of α on equilibrium times would be an expression of C_B in relative terms. A fraction away from the equilibrium concentration in the buffer side (δ) is defined as:

$$\delta = \frac{\text{Absolute Value } (C_B^\infty - C_B)}{C_B^\infty} \qquad \text{(Eq. 4)}$$

where C_B^∞ is the concentration of C_B as $t \to \infty$ and $C_B^\infty = C_0\alpha/(1+\alpha)$ for both cases (buffer or plasma spiked).

In a form analogous to Eq. 2, the time course of this fraction when drug is initially on the plasma side is then described by:

$$\delta_P = e^{-K_T(1+\alpha)t} \qquad \text{(Eq. 5)}$$

When drug is initially placed on the buffer side, the time course of δ is described by:

$$\delta_B = \frac{e^{-K_T(1+\alpha)t}}{\alpha} \qquad \text{(Eq. 6)}$$

A hypothetical semilog plot for the time course of these fractions from equilibrium concentration is shown in Fig. 1. As dictated by Eqs. 5 and 6, the δ values decline exponentially with time. For a given value of α, $\ln \delta_P$ and $\ln \delta_B$ decrease at the same rate with slope $= -K_T(1+\alpha)$. As $\alpha \to 0$, the slopes become $-K_T$ and as $\alpha \to 1$, the slopes become $-2K_T$. At $t = 0$, $\delta_P = 1$, whereas the $\delta_B = 1/\alpha$. Thus, δ_P values are always ≤ 1 whereas δ_B has no limit. Although the actual rate constants for approach to equilibrium are the same for both buffer and plasma spiked systems, the buffer spiked system requires more time to reach comparable δ values, because a greater amount of drug must be

0022-3549/82/0900-1066$01.00/0

(2) R. B. Sykes, K. Bush, and J. S. Freudenberger, Abstract 479, *ibid.*

(3) P. B. Fernandes, D. P. Bonner, R. R. Whitney, B. H. Miller, C. O. Baughn, and R. B. Sykes, Abstract 490, *ibid.*

(4) M. Barber, R. S. Bardoli, R. D. Sedwick, and A. N. Tyler, *J. Chem. Soc. Chem. Commun.*, **1981**, 325.

(5) C. Fenselau and R. J. Cotter, *Pure Appl. Chem.*, in press.

(6) D. H. Williams, C. Bradley, G. Bojesen, S. Santikarn, and L. C. E. Taylor, *J. Am. Chem. Soc.*, **103**, 5700 (1981).

(7) M. Barber, R. S. Bardoli, R. D. Sedwick, and A. N. Tyler, *Biomed. Mass. Spectrom.*, **8**, 492–495 (1981).

(8) A. Dell, H. R. Morris, M. D. Levin, and S. M. Hecht, *Biochem. Biophys. Res. Commun.*, **102**, 730 (1981).

(9) M. Barber, R. S. Bardoli, R. D. Sedwick, and L. W. Tetler, *Org. Mass Spectrom.*, **16**, 256 (1981).

(10) C. Fenselau, R. Cotter, G. Hansen, T. Chen, and D. Heller, *J. Chromatogr.*, **218**, 21 (1981).

(11) C. Fenselau, *Anal. Chem.*, **54**, 105A (1982).

(12) C. J. McNeal, *ibid.*, **54**, 43A (1982).

(13) H. Breuer, C. M. Cimarusti, Th. Denzel, W. H. Koster, W. A. Slusarchyk, and U. D. Treuner, *J. Antimicrob. Agents Chemother.*, **8**, Suppl. E, 21 (1981).

Allen I. Cohen[x]
Phillip T. Funke
Department of Analytical Research
Squibb Institute for Medical Research
New Brunswick, NJ 08903

Brian N. Green
VG Analytical Ltd.
Altrincham, U.K.

Received March 17, 1982.
Accepted for publication May 12, 1982.

The authors recognize the Middle Atlantic Mass Spectrometry (MAMS) Laboratory, a National Science Foundation shared instrument facility, directed by Drs. C. Fenselau and R. J. Cotter, as an important resource for the early evaluation of fast atom bombardment mass spectrometry. Some of the preliminary spectra were expertly run by Dr. G. Hansen on the MAMS instrument. Characterized samples were graciously furnished by Dr. C. M. Cimarusti.

Effect of Initial Conditions and Drug–Protein Binding on the Time to Equilibrium in Dialysis Systems

Keyphrases □ Drug–protein binding—effect of initial conditions on the time to equilibrium in dialysis systems □ Equilibrium dialysis—effect of initial conditions and drug–protein binding

To The Editor:

A major disadvantage of using equilibrium dialysis methods for determining *in vitro* plasma protein binding of drugs is the time needed to reach equilibrium. Recently, Øie and Guentert (1) mathematically showed that equilibration is more rapid when the drug is initially added to the plasma side as opposed to the buffer side. The approach to equilibrium was described by integrated equations for the concentration of drug on the buffer side as a function of time. The relative time to equilibrium for the two initial configurations was found to be:

$$R = \frac{t_B}{t_P} = \frac{\ln \delta + \ln \alpha}{\ln \delta} = 1 + \frac{\ln \alpha}{\ln \delta} \qquad \text{(Eq. 1)}$$

where t_B and t_P are the times to reach some fraction (δ) from the equilibrium concentration when the drug is initially added to the buffer or plasma side, respectively, and α is the unbound fraction in plasma which is assumed to be constant during the dialysis. For example, a δ value of 0.05 indicates a deviation of 5% from the true equilibrium value.

The authors indicated that the closer to the true equilibrium value one wants to be, the closer the ratio is to unity. Furthermore, a smaller α (stronger binding) or a larger δ increases the advantage of spiking the plasma side. While we are in complete agreement with these conclusions, some interesting and practical information may be lost if the examination of this system is limited only to the ratio of the times to equilibrium. In this communication the concept of approach to equilibrium in dialysis systems will be further developed and factors affecting comparative equilibration times will be discussed.

When drug is initially added to the plasma side, the concentration on the buffer side (C_B) at any time (t) is:

$$C_B = \frac{C_0\alpha}{1+\alpha}(1 - e^{-K_T(1+\alpha)t}) \qquad \text{(Eq. 2)}$$

where C_0 is the initial concentration, and K_T is the rate constant governing the transfer of drug across the membrane (1).

When drug is initially placed in the buffer side, a similar equation is obtained:

$$C_B = \frac{C_0}{1+\alpha}(\alpha + e^{-K_T(1+\alpha)t}) \qquad \text{(Eq. 3)}$$

Although the actual concentration on the buffer side is the variable of interest, a more useful relationship for examining the influence of α on equilibrium times would be an expression of C_B in relative terms. A fraction away from the equilibrium concentration in the buffer side (δ) is defined as:

$$\delta = \frac{\text{Absolute Value } (C_B^\infty - C_B)}{C_B^\infty} \qquad \text{(Eq. 4)}$$

where C_B^∞ is the concentration of C_B as $t \to \infty$ and $C_B^\infty = C_0\alpha/(1+\alpha)$ for both cases (buffer or plasma spiked).

In a form analogous to Eq. 2, the time course of this fraction when drug is initially on the plasma side is then described by:

$$\delta_P = e^{-K_T(1+\alpha)t} \qquad \text{(Eq. 5)}$$

When drug is initially placed on the buffer side, the time course of δ is described by:

$$\delta_B = \frac{e^{-K_T(1+\alpha)t}}{\alpha} \qquad \text{(Eq. 6)}$$

A hypothetical semilog plot for the time course of these fractions from equilibrium concentration is shown in Fig. 1. As dictated by Eqs. 5 and 6, the δ values decline exponentially with time. For a given value of α, $\ln \delta_P$ and $\ln \delta_B$ decrease at the same rate with slope $= -K_T(1+\alpha)$. As $\alpha \to 0$, the slopes become $-K_T$ and as $\alpha \to 1$, the slopes become $-2K_T$. At $t = 0$, $\delta_P = 1$, whereas the $\delta_B = 1/\alpha$. Thus, δ_P values are always ≤ 1 whereas δ_B has no limit. Although the actual rate constants for approach to equilibrium are the same for both buffer and plasma spiked systems, the buffer spiked system requires more time to reach comparable δ values, because a greater amount of drug must be

0022-3549/82/0900-1066$01.00/0

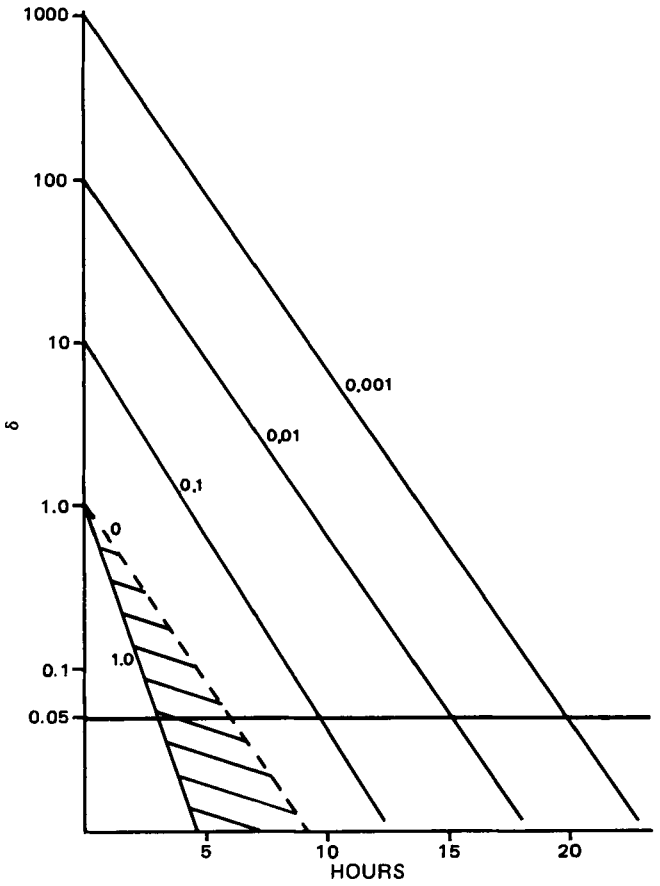

Figure 1—*The time course of the fraction away from equilibrium buffer concentration (δ) when* $K_T = 0.5\ hr^{-1}$. *The α values are given on the continuous lines representing* δ_B. *The dashed line is* δ_P *as* $\alpha \to 0$. *All plasma spiked systems fall within the shaded area bounded by the α = 1.0 (*$\delta_B = \delta_P$*) and dashed lines. The horizontal line at δ = 0.05 indicates a 5% deviation from the true equilibrium value for all conditions.*

transported across the membrane. For example, 99% of the initial mass present in a buffer spiked system ($\alpha = 0.01$) must cross the membrane to reach equilibrium. In a comparable plasma spiked system, only 1% of the initial mass must diffuse to the buffer side at equilibrium.

These comparisons can be shown more clearly by considering the times required to reach a given δ level. Rearrangement of Eq. 5 for the plasma spiked system gives:

$$t_p = \frac{-\ln \delta_P}{K_T(1 + \alpha)} \qquad \text{(Eq. 7)}$$

Thus, as α becomes smaller, t_p reaches a limiting value [$\lim_{\alpha \to 0} t_P = -(\ln \delta_P / K_T)$].

Conversely, when the buffer is spiked, the value of t_B is written as:

$$t_B = \frac{-(\ln \delta + \ln \alpha)}{K_T(1 + \alpha)} \qquad \text{(Eq. 8)}$$

Instead of reaching a limiting value as α decreases, t_B continues to increase in proportion to the negative logarithm of α ($\lim_{\alpha \to 0} t_B = \infty$).

Table I compares the time to reach concentrations 5 and 1% from the true equilibrium concentration. These levels were chosen since they are similar to differences which would be experimentally acceptable. The practical advantage of initially placing drug in the plasma side is obvious throughout the range of α, but becomes most striking below $\alpha \simeq 0.05$. Although t_P becomes essentially constant, t_B continues to increase with decreasing α. If only the ratio of t_B/t_P were used, the important observation of an essentially constant equilibration time (t_P) below $\alpha \simeq 0.05$ would be overlooked. Table I also illustrates a second point brought out by Øie and Guentert (1): the closer to the true equilibrium value one wishes to be, the closer the ratio is to unity. Thus, at $\delta = 0.05$ spiking of plasma would be 78% faster, whereas at $\delta = 0.01$, the advantage is 51%, assuming a constant α value of 0.1.

Table 1—Influence of Initial Conditions and Fraction Unbound in Plasma (α) on the Time to Reach a Fraction (δ) away from Equilibrium Concentration [a]

	α	t_B	t_P	t_B/t_P
$\delta = 0.05$				
	1.0	3.0	3.0	1.00
	0.5	4.9	4.0	1.22
	0.1	9.6	5.4	1.78
	0.05	11.4	5.7	2.00
	0.01	15.0	5.9	2.54
	0.005	16.5	6.0	2.75
	0.001	19.8	6.0	3.30
$\delta = 0.01$				
	1.0	4.6	4.6	1.00
	0.5	7.1	6.1	1.15
	0.1	12.6	8.4	1.51
	0.05	14.5	8.8	1.65
	0.01	18.2	9.1	2.00
	0.005	19.7	9.2	2.15
	0.001	23.0	9.2	2.50

[a] $K_T = 0.5\ hr^{-1}$.

Most clinically important drug–protein interactions occur with compounds having unbound fractions (α) of ≤0.2. Experimentally, the time to equilibrium is usually established (and fixed) in preliminary studies using plasma obtained from healthy subjects, and it is rarely re-examined, even if the extent of binding varies in subsequent samples. To avoid potentially serious errors in binding data, the following points should be considered when conducting equilibrium dialysis experiments:

1. Preliminary studies should include establishment of the equilibration time in a buffer *versus* buffer system. If the logarithm of δ is plotted *versus* time (Eq. 5 or 6 with $\alpha = 1$), the slope = $2K_T$. Changes in the membrane, drug, cell volume, or agitation method may require that K_T be redetermined. With a value for K_T and an estimate for α in plasma for a particular drug, the time to equilibrium and time difference between plasma- and buffer-spiked configurations can be estimated.

2. The time to equilibrium when spiking buffer increases with decreasing α values, whereas when spiking plasma it is essentially independent of α. The maximum equilibration time in a plasma spiked system should not be more than twice that of a buffer *versus* buffer system. No such maximum exists when drug is initially added to the buffer side (Table I).

3. Unbound (buffer) drug concentrations or fraction unbound should be used to monitor the approach to equilibrium, since total (plasma) concentrations and the fraction bound are relatively insensitive parameters at low α values.

4. If there are no significant advantages in sample preparation, the drug should be added on the plasma side. This minimizes equilibration time and reduces potential

problems such as drug degradation, microbiological growth (2), protein dilution (3), and lipolysis (4).

5. When spiking the buffer side is desirable, establish the time to equilibrium for the system with the smallest expected α value. The smallest α values do not always occur with healthy adult plasma. For example, the interaction of cationic drugs with α_1-acid glycoprotein increased in certain disease states and under various stress conditions (5, 6). When spiking plasma under these conditions, the apparent α value would be smaller than the true equilibrium value, whereas the opposite would occur when spiking the buffer side.

(1) S. Øie and T. W. Guentert, *J. Pharm. Sci.*, **71**, 127 (1982).
(2) T. W. Guentert and S. Øie, *ibid.*, **71**, 325 (1982).
(3) T. Tozer, Abstracts of the Sidney Riegelman Memorial Symposium, San Francisco, Calif., April 1982.
(4) K. M. Giacomini, S. E. Swezey, J. C. Giacomini, and T. F. Blaschke, *Life Sci.*, **27**, 771 (1980).
(5) K. M. Piafsky, O. Borgå, I. Odar-Cederlöf, C. Johansson, and F. Sjögvist, *N. Engl. J. Med.*, **299**, 1435 (1978).
(6) D. J. Edwards, D. Lalka, F. Cerra, and R. L. Slaughter, *Clin. Pharmacol. Ther.*, **31**, 62 (1982).

Patrick J. McNamara[x]
Joseph B. Bogardus
College of Pharmacy
University of Kentucky
Lexington, KY 40536-0053

Received March 17, 1982.
Accepted for publication May 24, 1982.

BOOKS

REVIEWS

The Peptides. Analysis, Synthesis, Biology. Vol. 4. Edited by ERHARD GROSS and JOHANNES MEIENHOFFER. Academic, 111 Fifth Ave., New York, NY 10017. 1981. 309 pp. 15 × 23 cm.

The first three volumes of *The Peptides* were devoted to the methodology concerning the synthesis of peptides. The fourth volume is the first of several volumes planned, according to the editors, dealing with the analytical aspects of peptides. The fourth volume eminently succeeds in reaching the high standards set for it by its predecessors.

The six chapters are divided evenly among the physical and chemical methods for peptide–protein-structure determination. Of those concerned with the physical methods, the first two focus on the crystal structure analysis by X-ray studies. In the first chapter, I. L. Karle discusses the crystal structures of linear and cyclic peptides containing 2 to 15 peptide units. Several useful generalizations are mentioned; for example, "4 → 1 H-bonds begin to appear in cyclic hexapeptides" and "the possibility for several different conformations assumed by the same compound arises starting with the cyclic heptapeptides." The author has made liberal use of tables and figures, which also list pertinent references.

J. Gunning and T. Blundell present in Chapter 2 a crystal structure analysis of the larger peptide hormones. The crystal structures of insulin (A-chain, 21 residues; B-chain, 30 residues), glucagon (29 residues), and the pancreatic polypeptide (36 residues) have been determined. On the basis of the known homology with the amino acid sequence of insulin, the structures of proinsulin and relaxin have been proposed and are discussed.

The chiroptical method for the determination of the absolute configuration of α-amino acids and small peptides is the topic of Chapter 3 by V. Toome and M. Weigle. The chiroptical properties of both the free α-amino acids and of the free oligopeptides, as well as of their metal complexes and chromophoric derivatives, are discussed.

In the fourth chapter, S. Stein describes the technique of peptide and protein-analysis at the picomole level employing HPLC and fluorescence spectrophotometry. The combination of HPLC and fluorescence detection raises the possibility of determination of peptides and proteins in tissues and organs of individual animals. This combination of techniques has also been employed for the determination of the amino acid sequence.

Chapter 5, by J. R. Benson, P. C. Louie, and R. A. Bradshaw, deals with the single-column amino acid analysis of peptides. For the purpose of discussion, the authors have divided the amino acids into four categories according to whether they are (*a*) normally found in proteins, (*b*) formed *in vivo* from the first group by post- or cotranslation, (*c*) formed by chemical modification from Group 1, or (*d*) nonprotein amino acids. Several protocols are given for the separation of these amino acids.

R. A. Laursen in Chapter 6 probes in exquisite detail the solid-phase sequencing technique, which would help overcome problems (such as overlap, increased-background, amino-terminal blocking) experienced with the Edman method.

Both the editors and the authors are to be congratulated for the excellence of this volume, which is a must for those concerned with any and all aspects of proteins and peptides, and for those contemplating a start in this area of research.

Received by Amrit Kapoor
College of Pharmacy
St. John's University
Jamaica, NY 11439

Medicinal Chemistry VI (Proceedings of the 6th International Symposium on Medicinal Chemistry). Edited by M. A. SIMKINS. Wiley, 605 Third Ave., New York, NY 10016. 1979. 477 pp. 16 × 24 cm. Price $94.00.

Medicinal Chemistry VI is a collection of papers presented at the 6th Internation Symposium on Medicinal Chemistry held in Brighton, England in 1978. They were chosen for this volume by the members of the Society for Drug Research and cover a wide range of interests, many being a blend of chemistry, biology, biochemistry, and medicine. The majority of the papers are based on disease states while others discuss theoretical concepts relating to substrate–receptor interactions or predicting activity of molecules based solely on structure.

This volume is divided into plenary lectures and symposium papers. The plenary lectures are given by Dr. Linus Pauling, who speaks of "orthomolecular medicine," a new concept in treating diseases, which he defines as the achievement and preservation of the best of health and the prevention and treatment of disease by using substances (right molecules in the right amounts) that are normally present in the body; professor Sir John Cornforth provides the reader with a greater awareness of

problems such as drug degradation, microbiological growth (2), protein dilution (3), and lipolysis (4).

5. When spiking the buffer side is desirable, establish the time to equilibrium for the system with the smallest expected α value. The smallest α values do not always occur with healthy adult plasma. For example, the interaction of cationic drugs with α_1-acid glycoprotein increased in certain disease states and under various stress conditions (5, 6). When spiking plasma under these conditions, the apparent α value would be smaller than the true equilibrium value, whereas the opposite would occur when spiking the buffer side.

(1) S. Øie and T. W. Guentert, *J. Pharm. Sci.*, **71**, 127 (1982).
(2) T. W. Guentert and S. Øie, *ibid.*, **71**, 325 (1982).
(3) T. Tozer, Abstracts of the Sidney Riegelman Memorial Symposium, San Francisco, Calif., April 1982.
(4) K. M. Giacomini, S. E. Swezey, J. C. Giacomini, and T. F. Blaschke, *Life Sci.*, **27**, 771 (1980).
(5) K. M. Piafsky, O. Borgå, I. Odar-Cederlöf, C. Johansson, and F. Sjögvist, *N. Engl. J. Med.*, **299**, 1435 (1978).
(6) D. J. Edwards, D. Lalka, F. Cerra, and R. L. Slaughter, *Clin. Pharmacol. Ther.*, **31**, 62 (1982).

Patrick J. McNamara[x]
Joseph B. Bogardus
College of Pharmacy
University of Kentucky
Lexington, KY 40536-0053

Received March 17, 1982.
Accepted for publication May 24, 1982.

BOOKS

REVIEWS

The Peptides. Analysis, Synthesis, Biology. Vol. 4. Edited by ERHARD GROSS and JOHANNES MEIENHOFFER. Academic, 111 Fifth Ave., New York, NY 10017. 1981. 309 pp. 15 × 23 cm.

The first three volumes of *The Peptides* were devoted to the methodology concerning the synthesis of peptides. The fourth volume is the first of several volumes planned, according to the editors, dealing with the analytical aspects of peptides. The fourth volume eminently succeeds in reaching the high standards set for it by its predecessors.

The six chapters are divided evenly among the physical and chemical methods for peptide–protein-structure determination. Of those concerned with the physical methods, the first two focus on the crystal structure analysis by X-ray studies. In the first chapter, I. L. Karle discusses the crystal structures of linear and cyclic peptides containing 2 to 15 peptide units. Several useful generalizations are mentioned; for example, "4 → 1 H-bonds begin to appear in cyclic hexapeptides" and "the possibility for several different conformations assumed by the same compound arises starting with the cyclic heptapeptides." The author has made liberal use of tables and figures, which also list pertinent references.

J. Gunning and T. Blundell present in Chapter 2 a crystal structure analysis of the larger peptide hormones. The crystal structures of insulin (A-chain, 21 residues; B-chain, 30 residues), glucagon (29 residues), and the pancreatic polypeptide (36 residues) have been determined. On the basis of the known homology with the amino acid sequence of insulin, the structures of proinsulin and relaxin have been proposed and are discussed.

The chiroptical method for the determination of the absolute configuration of α-amino acids and small peptides is the topic of Chapter 3 by V. Toome and M. Weigle. The chiroptical properties of both the free α-amino acids and of the free oligopeptides, as well as of their metal complexes and chromophoric derivatives, are discussed.

In the fourth chapter, S. Stein describes the technique of peptide and protein-analysis at the picomole level employing HPLC and fluorescence spectrophotometry. The combination of HPLC and fluorescence detection raises the possibility of determination of peptides and proteins in tissues and organs of individual animals. This combination of techniques has also been employed for the determination of the amino acid sequence.

Chapter 5, by J. R. Benson, P. C. Louie, and R. A. Bradshaw, deals with the single-column amino acid analysis of peptides. For the purpose of discussion, the authors have divided the amino acids into four categories according to whether they are (*a*) normally found in proteins, (*b*) formed *in vivo* from the first group by post- or cotranslation, (*c*) formed by chemical modification from Group 1, or (*d*) nonprotein amino acids. Several protocols are given for the separation of these amino acids.

R. A. Laursen in Chapter 6 probes in exquisite detail the solid-phase sequencing technique, which would help overcome problems (such as overlap, increased-background, amino-terminal blocking) experienced with the Edman method.

Both the editors and the authors are to be congratulated for the excellence of this volume, which is a must for those concerned with any and all aspects of proteins and peptides, and for those contemplating a start in this area of research.

Received by Amrit Kapoor
College of Pharmacy
St. John's University
Jamaica, NY 11439

Medicinal Chemistry VI (Proceedings of the 6th International Symposium on Medicinal Chemistry). Edited by M. A. SIMKINS. Wiley, 605 Third Ave., New York, NY 10016. 1979. 477 pp. 16 × 24 cm. Price $94.00.

Medicinal Chemistry VI is a collection of papers presented at the 6th Internation Symposium on Medicinal Chemistry held in Brighton, England in 1978. They were chosen for this volume by the members of the Society for Drug Research and cover a wide range of interests, many being a blend of chemistry, biology, biochemistry, and medicine. The majority of the papers are based on disease states while others discuss theoretical concepts relating to substrate–receptor interactions or predicting activity of molecules based solely on structure.

This volume is divided into plenary lectures and symposium papers. The plenary lectures are given by Dr. Linus Pauling, who speaks of "orthomolecular medicine," a new concept in treating diseases, which he defines as the achievement and preservation of the best of health and the prevention and treatment of disease by using substances (right molecules in the right amounts) that are normally present in the body; professor Sir John Cornforth provides the reader with a greater awareness of

problems such as drug degradation, microbiological growth (2), protein dilution (3), and lipolysis (4).

5. When spiking the buffer side is desirable, establish the time to equilibrium for the system with the smallest expected α value. The smallest α values do not always occur with healthy adult plasma. For example, the interaction of cationic drugs with α_1-acid glycoprotein increased in certain disease states and under various stress conditions (5, 6). When spiking plasma under these conditions, the apparent α value would be smaller than the true equilibrium value, whereas the opposite would occur when spiking the buffer side.

(1) S. Øie and T. W. Guentert, *J. Pharm. Sci.*, **71**, 127 (1982).
(2) T. W. Guentert and S. Øie, *ibid.*, **71**, 325 (1982).
(3) T. Tozer, Abstracts of the Sidney Riegelman Memorial Symposium, San Francisco, Calif., April 1982.
(4) K. M. Giacomini, S. E. Swezey, J. C. Giacomini, and T. F. Blaschke, *Life Sci.*, **27**, 771 (1980).
(5) K. M. Piafsky, O. Borgå, I. Odar-Cederlöf, C. Johansson, and F. Sjögvist, *N. Engl. J. Med.*, **299**, 1435 (1978).
(6) D. J. Edwards, D. Lalka, F. Cerra, and R. L. Slaughter, *Clin. Pharmacol. Ther.*, **31**, 62 (1982).

Patrick J. McNamara[x]
Joseph B. Bogardus
College of Pharmacy
University of Kentucky
Lexington, KY 40536-0053

Received March 17, 1982.
Accepted for publication May 24, 1982.

BOOKS

REVIEWS

The Peptides. Analysis, Synthesis, Biology. Vol. 4. Edited by ERHARD GROSS and JOHANNES MEIENHOFFER. Academic, 111 Fifth Ave., New York, NY 10017. 1981. 309 pp. 15 × 23 cm.

The first three volumes of *The Peptides* were devoted to the methodology concerning the synthesis of peptides. The fourth volume is the first of several volumes planned, according to the editors, dealing with the analytical aspects of peptides. The fourth volume eminently succeeds in reaching the high standards set for it by its predecessors.

The six chapters are divided evenly among the physical and chemical methods for peptide–protein-structure determination. Of those concerned with the physical methods, the first two focus on the crystal structure analysis by X-ray studies. In the first chapter, I. L. Karle discusses the crystal structures of linear and cyclic peptides containing 2 to 15 peptide units. Several useful generalizations are mentioned; for example, "4 → 1 H-bonds begin to appear in cyclic hexapeptides" and "the possibility for several different conformations assumed by the same compound arises starting with the cyclic heptapeptides." The author has made liberal use of tables and figures, which also list pertinent references.

J. Gunning and T. Blundell present in Chapter 2 a crystal structure analysis of the larger peptide hormones. The crystal structures of insulin (A-chain, 21 residues; B-chain, 30 residues), glucagon (29 residues), and the pancreatic polypeptide (36 residues) have been determined. On the basis of the known homology with the amino acid sequence of insulin, the structures of proinsulin and relaxin have been proposed and are discussed.

The chiroptical method for the determination of the absolute configuration of α-amino acids and small peptides is the topic of Chapter 3 by V. Toome and M. Weigle. The chiroptical properties of both the free α-amino acids and of the free oligopeptides, as well as of their metal complexes and chromophoric derivatives, are discussed.

In the fourth chapter, S. Stein describes the technique of peptide and protein-analysis at the picomole level employing HPLC and fluorescence spectrophotometry. The combination of HPLC and fluorescence detection raises the possibility of determination of peptides and proteins in tissues and organs of individual animals. This combination of techniques has also been employed for the determination of the amino acid sequence.

Chapter 5, by J. R. Benson, P. C. Louie, and R. A. Bradshaw, deals with the single-column amino acid analysis of peptides. For the purpose of discussion, the authors have divided the amino acids into four categories according to whether they are (*a*) normally found in proteins, (*b*) formed *in vivo* from the first group by post- or cotranslation, (*c*) formed by chemical modification from Group 1, or (*d*) nonprotein amino acids. Several protocols are given for the separation of these amino acids.

R. A. Laursen in Chapter 6 probes in exquisite detail the solid-phase sequencing technique, which would help overcome problems (such as overlap, increased-background, amino-terminal blocking) experienced with the Edman method.

Both the editors and the authors are to be congratulated for the excellence of this volume, which is a must for those concerned with any and all aspects of proteins and peptides, and for those contemplating a start in this area of research.

Received by Amrit Kapoor
College of Pharmacy
St. John's University
Jamaica, NY 11439

Medicinal Chemistry VI (Proceedings of the 6th International Symposium on Medicinal Chemistry). Edited by M. A. SIMKINS. Wiley, 605 Third Ave., New York, NY 10016. 1979. 477 pp. 16 × 24 cm. Price $94.00.

Medicinal Chemistry VI is a collection of papers presented at the 6th Internation Symposium on Medicinal Chemistry held in Brighton, England in 1978. They were chosen for this volume by the members of the Society for Drug Research and cover a wide range of interests, many being a blend of chemistry, biology, biochemistry, and medicine. The majority of the papers are based on disease states while others discuss theoretical concepts relating to substrate–receptor interactions or predicting activity of molecules based solely on structure.

This volume is divided into plenary lectures and symposium papers. The plenary lectures are given by Dr. Linus Pauling, who speaks of "orthomolecular medicine," a new concept in treating diseases, which he defines as the achievement and preservation of the best of health and the prevention and treatment of disease by using substances (right molecules in the right amounts) that are normally present in the body; professor Sir John Cornforth provides the reader with a greater awareness of

structural characteristics of enzymes; and Sir Arnold Burgen along with N. J. M. Birdsall and E. C. Hume introduce the reader to modern techniques which provide a better understanding of receptors.

In the foreword J. F. Cavalla and M. A. Simkin offer an interesting proposal about what it takes for a medicinal chemist to become successful. They propose that the medicinal chemist must associate himself/herself with a biologist, and for further success, must acquire a working knowledge of basic pharmacology in the area in which he/she is working, coupled with a detailed awareness of structure–activity relationships; then, they say, the medicinal chemist should succeed in discovering new and better medicines. This reviewer finds himself in agreement with their offer, except that I would propose the use of the adjective "molecular" before biologist (and pharmacologist) to describe the needs of medicinal chemists today. Much more knowledge at the molecular level is needed, and it is a pleasure to find the theoretical papers of this volume fulfilling this need.

Overall, the volume is quite good and makes a worthwhile contribution to medicinal chemistry and allied fields. The authors are experts in their field and their papers are well-written, containing sufficient references. The organization of this book is not unlike most proceedings of meetings and symposia in which there is the absence of major sections and chapter numbers.

The greatest use of this volume will be by graduate students and researchers in the areas for which this volume was intended: medicinal chemistry, pharmacology (pharmacokinetics), and medicine. It also can be recommended as an important source for new ideas and for use in many graduate courses.

Reviewed by Robert A. Magarian
Department of Medicinal Chemistry
College of Pharmacy
Health Sciences Center
University of Oklahoma
Oklahoma City, OK 73190

Textbook of Adverse Drug Reactions. 2nd ed. Edited by D. M. DAVIES. Oxford University Press. 200 Madison Ave., New York, NY 10016. 1981. 693 pp. 18 × 25 cm. Price $67.50.

This second edition is an expansion of the first that originally filled the void that had existed for an authoritative reference source for all major and minor adverse drug reactions. It is the work of 36 contributors authoring 30 chapters and 4 appendixes. The newest chapter discusses disorders of temperature regulation brought upon by disease, hypersensitivity, and drugs. The remaining chapters have been slightly rewritten with the addition of material and updated references.

This reference text makes it clear that perhaps 10% of patients suffer from physicians' efforts to treat them and that iatrogenic diseases and side-effects are certain consequences to drug therapy. Therefore, the public should be made aware that risk in any treatment is always there, and particularly so when new drugs and regimens come along that have not been used extensively in large numbers of patients. In addition, the problem of risk *versus* benefit is compounded when there is excessive or even irresponsible prescribing.

Most chapters use a classification of adverse drug reactions that divides them into two types. The first, Type A, are augmented effects but predictable on their known pharmacologic action and affect many people but cause few deaths. The second, Type B, are bizarre effects, not predictable from their known pharmacologic action when administered in regular doses to patients with average metabolic processes. These types of adverse drug reactions have a low incidence but, when they occur, often are lethal. It is also pointed out that some adverse drug reactions must be tolerated, because for a drug to work, it always shows toxicity at some dosage level. So, some reactions to medications are a necessary cross to bear in order to remedy the myriad of maladies that affect mankind.

This edition maintains the clarity of the earlier edition. Its first appendix lists the drugs alphabetically with the most outstanding possible untoward effects and includes the pages on which they are discussed. This makes it a quick reference source without having to resort to the index, which often leads to delay.

This book is recommended for individuals requiring the most up-to-date information on adverse drug reactions. Specifically, hospital pharmacists; clinical pharmacologists; internists; medical clinics; and all pharmacy, medical, and dental libraries.

Reviewed by Ronald F. Gautieri
Department of Pharmacology
Temple University
School of Pharmacy
Philadelphia, PA 19140

Tableting Specifications Manual. American Pharmaceutical Association, Washington, DC 20037. 1981. 39 pp. 20 × 28 cm (three-holed punch, loose-leaf format). Price $42.00 ($28.00 for APhA members).

This extensively updated and revised version of the original (1971) book, *IPT Standard Specifications for Tableting Tools*, contains the latest information available on tablet tooling and available equipment. *The Tableting Specifications Manual* is a new book prepared by the Industrial Pharmaceutical Technology Section of the American Pharmaceutical Association's Academy of Pharmaceutical Sciences with the cooperation of tableting tool suppliers.

The manual supplies the standards needed by both drug manufacturers and tool suppliers: Drug manufacturers will find the publication useful in preventing premature tool wear and costly work stoppages, while improving tablet quality and production rate. Pharmaceutical tool suppliers will benefit from the reduced lead times and manufacturing costs possible and the smaller inventory that standardization allows.

The manual also includes: a set of dimensional specifications and tolerances for rotary tableting machines in both graphic and tabular forms; a tool interchangeability chart with the five most commonly used tablet machines in the United States; a list of tool manufacturers and suppliers; and additional information on the bisection bar.

With numerous tables and IPT drawings and a loose-leaf, shrink-wrapped format for greater convenience and ease of updating, this manual will be a useful resource for those needing the most up-to-date information on tableting.

Staff Review

NOTICES

Adolescent Marijuana Abusers and Their Families. (NIDA Research 40—9/81). By HERBERT HENDIN, ANN POLLINGER, RICHARD ULMAN, and ARTHUR C. CARR. National Institute on Drug Abuse, Division of Research, 5600 Fishers Lane, Rockville, MD 20857.

Amino Acids, Peptides and Proteins. Vol. 12. Senior Reporter, R. C. SHEPPARD. Royal Society of Chemistry, Burlington House, London, WIV OBN, England. 1982. 634 pp. 13 × 22 cm. Price $153.00.

The Aminoglycosides: Microbiology, Clinical Use and Toxicology. (Kindley Disease Series, Vol. 2). Edited by ANDREW WHELTON and HAROLD C. NEU. Dekker, 270 Madison Ave., New York, NY 10016. 1982. 640 pp. 17 × 26 cm. Price $75.00.

Assessment of Public Health and Social Problems Associated with the Use of Psychotropic Drugs. (Report of the WHO Expert Committee on Implementation of the Convention on Psychotropic Substances 1971). World Health Organization, 1211 Geneva 27, Switzerland. 1981. 54 pp. 14 × 20 cm. Price Sw. fr. 4.

Bailey's Industrial Oil and Fat Products. Vol. 2. 4th Ed. Edited by DANIEL SWERN. By ROBERT R. ALLEN, MARVIN W. FORMO, R. G. KRISHNAMURTHY, G. N. McDERMOTT, FRANK A. NORRIS, and NORMAL O. V. SONNTAG. Wiley, 605 Third Ave., New York, NY 10016. 1982. 603 pp. 15 × 23 cm.

Behavioral Pharmacology of Human Drug Dependence. (NIDA Research Monograph 37, 7/81). Edited by TRAVIS THOMPSON and

structural characteristics of enzymes; and Sir Arnold Burgen along with N. J. M. Birdsall and E. C. Hume introduce the reader to modern techniques which provide a better understanding of receptors.

In the foreword J. F. Cavalla and M. A. Simkin offer an interesting proposal about what it takes for a medicinal chemist to become successful. They propose that the medicinal chemist must associate himself/herself with a biologist, and for further success, must acquire a working knowledge of basic pharmacology in the area in which he/she is working, coupled with a detailed awareness of structure–activity relationships; then, they say, the medicinal chemist should succeed in discovering new and better medicines. This reviewer finds himself in agreement with their offer, except that I would propose the use of the adjective "molecular" before biologist (and pharmacologist) to describe the needs of medicinal chemists today. Much more knowledge at the molecular level is needed, and it is a pleasure to find the theoretical papers of this volume fulfilling this need.

Overall, the volume is quite good and makes a worthwhile contribution to medicinal chemistry and allied fields. The authors are experts in their field and their papers are well-written, containing sufficient references. The organization of this book is not unlike most proceedings of meetings and symposia in which there is the absence of major sections and chapter numbers.

The greatest use of this volume will be by graduate students and researchers in the areas for which this volume was intended: medicinal chemistry, pharmacology (pharmacokinetics), and medicine. It also can be recommended as an important source for new ideas and for use in many graduate courses.

Reviewed by Robert A. Magarian
Department of Medicinal Chemistry
College of Pharmacy
Health Sciences Center
University of Oklahoma
Oklahoma City, OK 73190

Textbook of Adverse Drug Reactions. 2nd ed. Edited by D. M. DAVIES. Oxford University Press. 200 Madison Ave., New York, NY 10016. 1981. 693 pp. 18 × 25 cm. Price $67.50.

This second edition is an expansion of the first that originally filled the void that had existed for an authoritative reference source for all major and minor adverse drug reactions. It is the work of 36 contributors authoring 30 chapters and 4 appendixes. The newest chapter discusses disorders of temperature regulation brought upon by disease, hypersensitivity, and drugs. The remaining chapters have been slightly rewritten with the addition of material and updated references.

This reference text makes it clear that perhaps 10% of patients suffer from physicians' efforts to treat them and that iatrogenic diseases and side-effects are certain consequences to drug therapy. Therefore, the public should be made aware that risk in any treatment is always there, and particularly so when new drugs and regimens come along that have not been used extensively in large numbers of patients. In addition, the problem of risk *versus* benefit is compounded when there is excessive or even irresponsible prescribing.

Most chapters use a classification of adverse drug reactions that divides them into two types. The first, Type A, are augmented effects but predictable on their known pharmacologic action and affect many people but cause few deaths. The second, Type B, are bizarre effects, not predictable from their known pharmacologic action when administered in regular doses to patients with average metabolic processes. These types of adverse drug reactions have a low incidence but, when they occur, often are lethal. It is also pointed out that some adverse drug reactions must be tolerated, because for a drug to work, it always shows toxicity at some dosage level. So, some reactions to medications are a necessary cross to bear in order to remedy the myriad of maladies that affect mankind.

This edition maintains the clarity of the earlier edition. Its first appendix lists the drugs alphabetically with the most outstanding possible untoward effects and includes the pages on which they are discussed. This makes it a quick reference source without having to resort to the index, which often leads to delay.

This book is recommended for individuals requiring the most up-to-date information on adverse drug reactions. Specifically, hospital pharmacists; clinical pharmacologists; internists; medical clinics; and all pharmacy, medical, and dental libraries.

Reviewed by Ronald F. Gautieri
Department of Pharmacology
Temple University
School of Pharmacy
Philadelphia, PA 19140

Tableting Specifications Manual. American Pharmaceutical Association, Washington, DC 20037. 1981. 39 pp. 20 × 28 cm (three-holed punch, loose-leaf format). Price $42.00 ($28.00 for APhA members).

This extensively updated and revised version of the original (1971) book, *IPT Standard Specifications for Tableting Tools*, contains the latest information available on tablet tooling and available equipment. *The Tableting Specifications Manual* is a new book prepared by the Industrial Pharmaceutical Technology Section of the American Pharmaceutical Association's Academy of Pharmaceutical Sciences with the cooperation of tableting tool suppliers.

The manual supplies the standards needed by both drug manufacturers and tool suppliers: Drug manufacturers will find the publication useful in preventing premature tool wear and costly work stoppages, while improving tablet quality and production rate. Pharmaceutical tool suppliers will benefit from the reduced lead times and manufacturing costs possible and the smaller inventory that standardization allows.

The manual also includes: a set of dimensional specifications and tolerances for rotary tableting machines in both graphic and tabular forms; a tool interchangeability chart with the five most commonly used tablet machines in the United States; a list of tool manufacturers and suppliers; and additional information on the bisection bar.

With numerous tables and IPT drawings and a loose-leaf, shrink-wrapped format for greater convenience and ease of updating, this manual will be a useful resource for those needing the most up-to-date information on tableting.

Staff Review

NOTICES

Adolescent Marijuana Abusers and Their Families. (NIDA Research 40—9/81). By HERBERT HENDIN, ANN POLLINGER, RICHARD ULMAN, and ARTHUR C. CARR. National Institute on Drug Abuse, Division of Research, 5600 Fishers Lane, Rockville, MD 20857.

Amino Acids, Peptides and Proteins. Vol. 12. Senior Reporter, R. C. SHEPPARD. Royal Society of Chemistry, Burlington House, London, WIV OBN, England. 1982. 634 pp. 13 × 22 cm. Price $153.00.

The Aminoglycosides: Microbiology, Clinical Use and Toxicology. (Kindley Disease Series, Vol. 2). Edited by ANDREW WHELTON and HAROLD C. NEU. Dekker, 270 Madison Ave., New York, NY 10016. 1982. 640 pp. 17 × 26 cm. Price $75.00.

Assessment of Public Health and Social Problems Associated with the Use of Psychotropic Drugs. (Report of the WHO Expert Committee on Implementation of the Convention on Psychotropic Substances 1971). World Health Organization, 1211 Geneva 27, Switzerland. 1981. 54 pp. 14 × 20 cm. Price Sw. fr. 4.

Bailey's Industrial Oil and Fat Products. Vol. 2. 4th Ed. Edited by DANIEL SWERN. By ROBERT R. ALLEN, MARVIN W. FORMO, R. G. KRISHNAMURTHY, G. N. McDERMOTT, FRANK A. NORRIS, and NORMAL O. V. SONNTAG. Wiley, 605 Third Ave., New York, NY 10016. 1982. 603 pp. 15 × 23 cm.

Behavioral Pharmacology of Human Drug Dependence. (NIDA Research Monograph 37, 7/81). Edited by TRAVIS THOMPSON and

structural characteristics of enzymes; and Sir Arnold Burgen along with N. J. M. Birdsall and E. C. Hume introduce the reader to modern techniques which provide a better understanding of receptors.

In the foreword J. F. Cavalla and M. A. Simkin offer an interesting proposal about what it takes for a medicinal chemist to become successful. They propose that the medicinal chemist must associate himself/herself with a biologist, and for further success, must acquire a working knowledge of basic pharmacology in the area in which he/she is working, coupled with a detailed awareness of structure–activity relationships; then, they say, the medicinal chemist should succeed in discovering new and better medicines. This reviewer finds himself in agreement with their offer, except that I would propose the use of the adjective "molecular" before biologist (and pharmacologist) to describe the needs of medicinal chemists today. Much more knowledge at the molecular level is needed, and it is a pleasure to find the theoretical papers of this volume fulfilling this need.

Overall, the volume is quite good and makes a worthwhile contribution to medicinal chemistry and allied fields. The authors are experts in their field and their papers are well-written, containing sufficient references. The organization of this book is not unlike most proceedings of meetings and symposia in which there is the absence of major sections and chapter numbers.

The greatest use of this volume will be by graduate students and researchers in the areas for which this volume was intended: medicinal chemistry, pharmacology (pharmacokinetics), and medicine. It also can be recommended as an important source for new ideas and for use in many graduate courses.

Reviewed by Robert A. Magarian
Department of Medicinal Chemistry
College of Pharmacy
Health Sciences Center
University of Oklahoma
Oklahoma City, OK 73190

Textbook of Adverse Drug Reactions. 2nd ed. Edited by D. M. DAVIES. Oxford University Press. 200 Madison Ave., New York, NY 10016. 1981. 693 pp. 18 × 25 cm. Price $67.50.

This second edition is an expansion of the first that originally filled the void that had existed for an authoritative reference source for all major and minor adverse drug reactions. It is the work of 36 contributors authoring 30 chapters and 4 appendixes. The newest chapter discusses disorders of temperature regulation brought upon by disease, hypersensitivity, and drugs. The remaining chapters have been slightly rewritten with the addition of material and updated references.

This reference text makes it clear that perhaps 10% of patients suffer from physicians' efforts to treat them and that iatrogenic diseases and side-effects are certain consequences to drug therapy. Therefore, the public should be made aware that risk in any treatment is always there, and particularly so when new drugs and regimens come along that have not been used extensively in large numbers of patients. In addition, the problem of risk *versus* benefit is compounded when there is excessive or even irresponsible prescribing.

Most chapters use a classification of adverse drug reactions that divides them into two types. The first, Type A, are augmented effects but predictable on their known pharmacologic action and affect many people but cause few deaths. The second, Type B, are bizarre effects, not predictable from their known pharmacologic action when administered in regular doses to patients with average metabolic processes. These types of adverse drug reactions have a low incidence but, when they occur, often are lethal. It is also pointed out that some adverse drug reactions must be tolerated, because for a drug to work, it always shows toxicity at some dosage level. So, some reactions to medications are a necessary cross to bear in order to remedy the myriad of maladies that affect mankind.

This edition maintains the clarity of the earlier edition. Its first appendix lists the drugs alphabetically with the most outstanding possible untoward effects and includes the pages on which they are discussed. This makes it a quick reference source without having to resort to the index, which often leads to delay.

This book is recommended for individuals requiring the most up-to-date information on adverse drug reactions. Specifically, hospital pharmacists; clinical pharmacologists; internists; medical clinics; and all pharmacy, medical, and dental libraries.

Reviewed by Ronald F. Gautieri
Department of Pharmacology
Temple University
School of Pharmacy
Philadelphia, PA 19140

Tableting Specifications Manual. American Pharmaceutical Association, Washington, DC 20037. 1981. 39 pp. 20 × 28 cm (three-holed punch, loose-leaf format). Price $42.00 ($28.00 for APhA members).

This extensively updated and revised version of the original (1971) book, *IPT Standard Specifications for Tableting Tools*, contains the latest information available on tablet tooling and available equipment. *The Tableting Specifications Manual* is a new book prepared by the Industrial Pharmaceutical Technology Section of the American Pharmaceutical Association's Academy of Pharmaceutical Sciences with the cooperation of tableting tool suppliers.

The manual supplies the standards needed by both drug manufacturers and tool suppliers: Drug manufacturers will find the publication useful in preventing premature tool wear and costly work stoppages, while improving tablet quality and production rate. Pharmaceutical tool suppliers will benefit from the reduced lead times and manufacturing costs possible and the smaller inventory that standardization allows.

The manual also includes: a set of dimensional specifications and tolerances for rotary tableting machines in both graphic and tabular forms; a tool interchangeability chart with the five most commonly used tablet machines in the United States; a list of tool manufacturers and suppliers; and additional information on the bisection bar.

With numerous tables and IPT drawings and a loose-leaf, shrink-wrapped format for greater convenience and ease of updating, this manual will be a useful resource for those needing the most up-to-date information on tableting.

Staff Review

NOTICES

Adolescent Marijuana Abusers and Their Families. (NIDA Research 40—9/81). By HERBERT HENDIN, ANN POLLINGER, RICHARD ULMAN, and ARTHUR C. CARR. National Institute on Drug Abuse, Division of Research, 5600 Fishers Lane, Rockville, MD 20857.

Amino Acids, Peptides and Proteins. Vol. 12. Senior Reporter, R. C. SHEPPARD. Royal Society of Chemistry, Burlington House, London, WIV OBN, England. 1982. 634 pp. 13 × 22 cm. Price $153.00.

The Aminoglycosides: Microbiology, Clinical Use and Toxicology. (Kindley Disease Series, Vol. 2). Edited by ANDREW WHELTON and HAROLD C. NEU. Dekker, 270 Madison Ave., New York, NY 10016. 1982. 640 pp. 17 × 26 cm. Price $75.00.

Assessment of Public Health and Social Problems Associated with the Use of Psychotropic Drugs. (Report of the WHO Expert Committee on Implementation of the Convention on Psychotropic Substances 1971). World Health Organization, 1211 Geneva 27, Switzerland. 1981. 54 pp. 14 × 20 cm. Price Sw. fr. 4.

Bailey's Industrial Oil and Fat Products. Vol. 2. 4th Ed. Edited by DANIEL SWERN. By ROBERT R. ALLEN, MARVIN W. FORMO, R. G. KRISHNAMURTHY, G. N. McDERMOTT, FRANK A. NORRIS, and NORMAL O. V. SONNTAG. Wiley, 605 Third Ave., New York, NY 10016. 1982. 603 pp. 15 × 23 cm.

Behavioral Pharmacology of Human Drug Dependence. (NIDA Research Monograph 37, 7/81). Edited by TRAVIS THOMPSON and

structural characteristics of enzymes; and Sir Arnold Burgen along with N. J. M. Birdsall and E. C. Hume introduce the reader to modern techniques which provide a better understanding of receptors.

In the foreword J. F. Cavalla and M. A. Simkin offer an interesting proposal about what it takes for a medicinal chemist to become successful. They propose that the medicinal chemist must associate himself/herself with a biologist, and for further success, must acquire a working knowledge of basic pharmacology in the area in which he/she is working, coupled with a detailed awareness of structure–activity relationships; then, they say, the medicinal chemist should succeed in discovering new and better medicines. This reviewer finds himself in agreement with their offer, except that I would propose the use of the adjective "molecular" before biologist (and pharmacologist) to describe the needs of medicinal chemists today. Much more knowledge at the molecular level is needed, and it is a pleasure to find the theoretical papers of this volume fulfilling this need.

Overall, the volume is quite good and makes a worthwhile contribution to medicinal chemistry and allied fields. The authors are experts in their field and their papers are well-written, containing sufficient references. The organization of this book is not unlike most proceedings of meetings and symposia in which there is the absence of major sections and chapter numbers.

The greatest use of this volume will be by graduate students and researchers in the areas for which this volume was intended: medicinal chemistry, pharmacology (pharmacokinetics), and medicine. It also can be recommended as an important source for new ideas and for use in many graduate courses.

Reviewed by Robert A. Magarian
Department of Medicinal Chemistry
College of Pharmacy
Health Sciences Center
University of Oklahoma
Oklahoma City, OK 73190

Textbook of Adverse Drug Reactions. 2nd ed. Edited by D. M. DAVIES. Oxford University Press. 200 Madison Ave., New York, NY 10016. 1981. 693 pp. 18 × 25 cm. Price $67.50.

This second edition is an expansion of the first that originally filled the void that had existed for an authoritative reference source for all major and minor adverse drug reactions. It is the work of 36 contributors authoring 30 chapters and 4 appendixes. The newest chapter discusses disorders of temperature regulation brought upon by disease, hypersensitivity, and drugs. The remaining chapters have been slightly rewritten with the addition of material and updated references.

This reference text makes it clear that perhaps 10% of patients suffer from physicians' efforts to treat them and that iatrogenic diseases and side-effects are certain consequences to drug therapy. Therefore, the public should be made aware that risk in any treatment is always there, and particularly so when new drugs and regimens come along that have not been used extensively in large numbers of patients. In addition, the problem of risk *versus* benefit is compounded when there is excessive or even irresponsible prescribing.

Most chapters use a classification of adverse drug reactions that divides them into two types. The first, Type A, are augmented effects but predictable on their known pharmacologic action and affect many people but cause few deaths. The second, Type B, are bizarre effects, not predictable from their known pharmacologic action when administered in regular doses to patients with average metabolic processes. These types of adverse drug reactions have a low incidence but, when they occur, often are lethal. It is also pointed out that some adverse drug reactions must be tolerated, because for a drug to work, it always shows toxicity at some dosage level. So, some reactions to medications are a necessary cross to bear in order to remedy the myriad of maladies that affect mankind.

This edition maintains the clarity of the earlier edition. Its first appendix lists the drugs alphabetically with the most outstanding possible untoward effects and includes the pages on which they are discussed. This makes it a quick reference source without having to resort to the index, which often leads to delay.

This book is recommended for individuals requiring the most up-to-date information on adverse drug reactions. Specifically, hospital pharmacists; clinical pharmacologists; internists; medical clinics; and all pharmacy, medical, and dental libraries.

Reviewed by Ronald F. Gautieri
Department of Pharmacology
Temple University
School of Pharmacy
Philadelphia, PA 19140

Tableting Specifications Manual. American Pharmaceutical Association, Washington, DC 20037. 1981. 39 pp. 20 × 28 cm (three-holed punch, loose-leaf format). Price $42.00 ($28.00 for APhA members).

This extensively updated and revised version of the original (1971) book, *IPT Standard Specifications for Tableting Tools*, contains the latest information available on tablet tooling and available equipment. *The Tableting Specifications Manual* is a new book prepared by the Industrial Pharmaceutical Technology Section of the American Pharmaceutical Association's Academy of Pharmaceutical Sciences with the cooperation of tableting tool suppliers.

The manual supplies the standards needed by both drug manufacturers and tool suppliers: Drug manufacturers will find the publication useful in preventing premature tool wear and costly work stoppages, while improving tablet quality and production rate. Pharmaceutical tool suppliers will benefit from the reduced lead times and manufacturing costs possible and the smaller inventory that standardization allows.

The manual also includes: a set of dimensional specifications and tolerances for rotary tableting machines in both graphic and tabular forms; a tool interchangeability chart with the five most commonly used tablet machines in the United States; a list of tool manufacturers and suppliers; and additional information on the bisection bar.

With numerous tables and IPT drawings and a loose-leaf, shrink-wrapped format for greater convenience and ease of updating, this manual will be a useful resource for those needing the most up-to-date information on tableting.

Staff Review

NOTICES

Adolescent Marijuana Abusers and Their Families. (NIDA Research 40—9/81). By HERBERT HENDIN, ANN POLLINGER, RICHARD ULMAN, and ARTHUR C. CARR. National Institute on Drug Abuse, Division of Research, 5600 Fishers Lane, Rockville, MD 20857.

Amino Acids, Peptides and Proteins. Vol. 12. Senior Reporter, R. C. SHEPPARD. Royal Society of Chemistry, Burlington House, London, WIV OBN, England. 1982. 634 pp. 13 × 22 cm. Price $153.00.

The Aminoglycosides: Microbiology, Clinical Use and Toxicology. (Kindley Disease Series, Vol. 2). Edited by ANDREW WHELTON and HAROLD C. NEU. Dekker, 270 Madison Ave., New York, NY 10016. 1982. 640 pp. 17 × 26 cm. Price $75.00.

Assessment of Public Health and Social Problems Associated with the Use of Psychotropic Drugs. (Report of the WHO Expert Committee on Implementation of the Convention on Psychotropic Substances 1971). World Health Organization, 1211 Geneva 27, Switzerland. 1981. 54 pp. 14 × 20 cm. Price Sw. fr. 4.

Bailey's Industrial Oil and Fat Products. Vol. 2. 4th Ed. Edited by DANIEL SWERN. By ROBERT R. ALLEN, MARVIN W. FORMO, R. G. KRISHNAMURTHY, G. N. McDERMOTT, FRANK A. NORRIS, and NORMAL O. V. SONNTAG. Wiley, 605 Third Ave., New York, NY 10016. 1982. 603 pp. 15 × 23 cm.

Behavioral Pharmacology of Human Drug Dependence. (NIDA Research Monograph 37, 7/81). Edited by TRAVIS THOMPSON and

CHRIS E. JOHANSON. National Institute on Drug Abuse, Division of Research, 5600 Fishers Lane, Rockville, MD 20857. 294 pp. 15 × 23 cm.

Benzodiazepines: A Review of Research Results, 1980. (NIDA Research Monograph 33). A RAUS Review Report. By STEPHEN I. SZARA and JACQUELINE P. LUDFORD. National Institute on Drug Abuse, Division of Research, 5600 Fishers Lane, Rockville, MD 20867. 101 pp. 15 × 13 cm.

Calculator Programming for Chemistry and the Life Sciences. By FRANK H. CLARKE. Academic, 111 5th Ave., New York, NY 10003. 1981. 225 pp. 15 × 23 cm.

Calculator Programs for Chemical Engineers. Edited by VINCENT CAVASENO, and THE STAFF OF CHEMICAL ENGINEERING. McGraw-Hill, 1221 Avenue of the Americas, New York, NY 10020. 1982. 328 pp. 20 × 28 cm. Price $27.50.

Calculus with Analytic Geometry. 2nd Ed. By NATHAN O. NILES and GEORGE E. HARORAK. Prentice-Hall, Englewood Cliffs, NJ 07632. 1981. 635 pp. 15 × 23 cm. Price $24.95.

Chronicles of Drug Discovery. Vol. 1. Edited by JASJIT S. BINDRA and DANIEL LEDNICER. Wiley, 605 Third Ave., New York, NY 10016. 1982. 283 pp. 15 × 23 cm.

Clinical Hypertension and Hypotension. Edited by HANS R. BRUNNER and HARALAMBOS GAVRAS. Dekker, 270 Madison Ave., New York, NY 10016. 1982. 503 pp. 15 × 23 cm. Price $67.50.

Directory of On-Going Research In Cancer Epidemiology. By C. S. MUIR and G. WAGNER. International Agency for Research on Cancer, 150, cours Albert Thomas, F69372 Lyon Cedex 2, France. 1981. 696 pp. 17 × 24 cm. Price $20.00.

Drug Abuse and the American Adolescent. NIDA Research Monograph 38, A RAUS Review Report. Edited by DAN J. LETTIERI and JACQUELINE P. LUDFORD. National Institute of Drug Abuse, Division of Research, 5600 Fishers Lane, Rockville, MD 20857. 132 pp. 14 × 23 cm.

Drug Development Regulatory Assessment, and Postmarketing Surveillance. Edited by WILLIAM M. WARDELL and GIAMPAOLO VELO. Plenum, 223 Spring St., New York, NY 10013. 1981. 355 pp. 15 × 25 cm. Price $45.00.

IARC Monographs on the Evaluation of the Carcinogenic Risk of Chemicals to Humans. Some Antineoplastic and Immunosuppressive Agents, Vol. 26. International Agency for Research on Cancer. World Health Organization, 1211 Geneva 27, Switzerland. 411 pp. 17 × 24 cm. Price $30.00.

IARC Monographs on the Evaluation of the Carcinogenic Risk of Chemicals to Humans. Wood, Leather and Some Associated Industries. Vol. 25. Health & Biomedical Information Programme, World Health Organization, 1211 Geneva 27, Switzerland. 1981. 412 pp. 17 × 24 cm. Price $30.00.

Iatrogenic Diseases. 2nd Ed. Update 1981. By P. F. D'ARCY and J. P. GRIFFIN. Oxford, 200 Madison Ave., New York, NY 10016. 1981. 262 pp. 18 × 24 cm. Price $67.50.

Identifizierung von Arzneistoffen. By HARRY AUTERHOFF and KARL-ARTUR KOVAR. Wissenchaftiche Verlagagesellschaft mbH, 7000 Stuttgart 1, Germany. 1981, 286 pp. 17 × 24 cm. Price $36.00.

Introductory Medicinal Chemistry. By J. B. TAYLOR and P. D. KENNEWELL. Wiley, One Wiley Drive, Somerset, NJ 08873. 1981. 202 pp. 15 × 23 cm. Price $59.95.

Kinetic Data Analysis. Design and Analysis of Enzyme and Pharmacokinetic Experiments. Edited by LASZLO ENDRENYI. Plenum, 233 Spring St., New York, NY 10013. 1981. 427 pp. 16 × 24 cm. Price $47.50.

Modern Pharmacology. Edited by CHARLES R. CRAIG and ROBERT E. STITZEL. Little Brown, 34 Beacon St., Boston, MA 02106. 1981. 1038 pp. 18 × 23 cm. Price $34.50.

New Perspectives on Calcium Antagonists. Edited by GEORGE B. WEISS. Williams & Wilkins, 300 Idlewild Ave., Easton, MD 21601. 1981. 241 pp. 16 × 25 cm. Price $38.50.

Opiate Receptors, Neurotransmitters, & Drug Dependence: Basic Science–Clinical Correlates, By BARRY STIMMEL. Haworth Press, 149 5th Ave., New York, NY 10010. 1981. 129 pp. 13 × 21 cm. Price $25.00.

PAR Pseudo-Allergic Reactions. Involvement of Drugs and Chemicals. Vol. 3. Cell Mediated Reactions Miscellaneous Topics. By P. DUKOR, P. KALLOS, H. D. SCHLUMBERGER, and C. B. WEST. S. Karger Ag, Basel, P.O. Box Postfach, CH-4009 Basel, Switzerland. 159 pp. 17 × 24 cm. Price: $47.50, US; DM 95. SFr. 79.

Pharmaceutical Applications of Polymers. (A Selected Bibliography.) Edited by RICHARD JUNIPER. Rubber and Plastics Research Association of Great Britain, Shawbury Shrewsbury Salop, SY44NR, England, 1981. 245 pp. 15 × 21 cm.

Principles and Applications of Medicolegal Alcohol Determination. By E. M. P. WIDMARK. Urben & Schwarzenberg, N 24, Friedrichstraffe 105B, Germany. 163 pp. 15 × 20 cm.

Progress in the Quality Control of Medicines. By P. B. DEASY and R. F. TIMONEY. Elsevier Biomedical Press, P.O. Box 211, Amsterdam, The Netherlands. 1981. 297 pp. 16 × 24 cm. Price $86.00.

Psychiatry, Psychopharmacology, and Alternative Therapies. Trends for the 80's. Edited by JOHN J. SCHWAB. Dekker, 270 Madison Ave., New York, NY 10016. 1981. 227 pp. 15 × 23 cm. Price $37.50.

Radionuclide Imaging in Drug Research. Edited by CLIVE GEORGE WILSON and JOHN G. HARDY with M. FRIER and S. S. DAVIS. Groom Helm Ltd. 2-10 St. John's Rd., London, SW11, England. 1981, 329 pp. 13 × 22 cm. Price $44.00.

Recombinant DNA. Proceedings of the Third Cleveland Symposium on Macromolecules, Cleveland, Ohio. 22–26 June 1981. Edited by A. G. WALTON. Elsevier Scientific, P.O. Box 330, Amsterdam, The Netherlands. 1981. 310 pp. 16 × 24 cm. Price $78.75.

Short-Term Bioassays in the Analysis of Complex Environmental Mixtures II. Edited by MICHAEL D. WATERS, SHAHBEG S. SANDHU, JOELLEN LEWTAS HUISINGH, LARRY CLAXTON, and STEPHEN NESNOW. Plenum, 223 Spring St., New York, NY 10013. 1981. 524 pp. 16 × 25 cm. Price $59.50.

Supplement 3. Cumulative with First Two Supplements. NF XV. USP XX. By authority of the U.S. Pharmacopeial Convention, Inc. Prepared by the Board of Trustees. 1982. 440 pp. 20 × 30 cm.

Testing for Toxicity. Edited by J. W. GORROD. Taylor & Francis, Ltd, 4 John St., London WCIN 3ET, England. 1981. 381 pp. 15 × 23 cm.

Young Men and Drugs in Manhattan: A Causal Analysis. (NIDA Research Monograph 39—9/81). By RICHARD R. CLAYTON and HARWIN L. VOSS. National Institute on Drug Abuse, Division of Research, 5600 Fishers Lane, Rockville, MD 20857.

A publication of the
American Pharmaceutical Association—
the National Professional Society
of Pharmacists

JOURNAL OF PHARMACEUTICAL SCIENCES

INDEX TO AUTHORS
INDEX TO SUBJECTS

VOLUME 71
JANUARY TO DECEMBER, 1982

Published monthly under the supervision of the Board of Trustees

On "Being There"—Professionally

On about half the Sunday afternoons each autumn, a sell-out crowd of approximately 55,000 Washington, DC, area residents will pack RFK Stadium to watch the Washington Redskins professional football team do battle with one or another of its league rivals. This phenomenon occurs despite the fact that (a) each of those games can be watched on television for free from the comfort of one's home, (b) both the admission tickets and various incidental costs—such as parking and refreshments—are all very expensive, and (c) the stadium, its seats, and often the weather conditions leave much to be desired in the way of creature comforts. In fact, thousands of other people clamor for the opportunity to buy Redskins tickets even at prices above their already costly face value.

Similar fan enthusiasm is apparent in many other cities and with regard to various other sports both professional and amateur.

If one were to ask those sports fans why it is worth the expense, inconvenience, and discomfort to see the game in person when they can see it more clearly on color television, with professional audio commentary, and with the added dimension of instant replays, they will offer a variety of explanations. However, no matter how the replies are stated, virtually all of the explanations boil down to: "There is no adequate substitute for personally being there—namely, where the real action is!"

The same can be said with respect to professional and scientific meetings or conferences.

Reading newsletter summaries of the highlights of a conference, or reviewing journal articles covering research presented at a technical session, amounts to a very inadequate substitute for first-hand attendance at the meeting itself.

Moreover, in contrast to the sporting event, personal attendance at a meeting or symposium gives one many additional advantages and benefits. For example, one can personally meet and talk to the researcher, and ask questions and obtain clarifications and insights. There is also the opportunity to meet other experts or notables in the field; the opportunity to share experiences through informal conversation; and the opportunity to exchange other important career-related information such as job openings, employment benefits, and comparative remuneration. Finally, there is the built-in vehicle to become more active professionally and organization-wise through opening the door to voluntary participation, committee appointments, and elective office.

Many meetings or conferences can provide such opportunities. But for American pharmaceutical scientists, there are really two meetings that annually offer the greatest means of satisfying such needs and expectations. These are the combined APhA–APS Annual Meeting in the spring of each year, and the APS mid-year meeting in the fall.

The special benefit to be derived from these meetings is that the pharmaceutical scientist has the ready opportunity to broaden horizons via direct contact, dialog, and interchange with colleagues in other scientific fields as well as in other environments of practice. Hence, pharmaceutical scientists who are primarily chemists mingle and exchange views with others who are primarily pharmacologists, or biologists, or analysts, or whatever. And the person employed in industry not only associates with other industry colleagues but also others in academia, government, and elsewhere.

Furthermore, at the combined APhA–APS meetings, the scientist rubs elbows with and can have dialog with people not in science or research but who share a common interest and concern regarding pharmaceuticals and pharmaceutical products; namely, community and hospital practitioners, pharmacy officials, and students.

All of this cannot help but have some effect and beneficial influence on the person so exposed.

In an effort to maximize the opportunity for professional growth and to make the experience of attending an APhA Annual Meeting even more valuable, the programming for the 1983 Annual Meeting in New Orleans is being organized into a series of four "tracks." One or more of these "tracks" will be of major interest and value to each registrant.

In the past, many registrants might have overlooked a session that would have been of interest simply because the session was sponsored by a group in another discipline. For example, the FDA pharmaceutical analyst might have ignored sessions dealing with institutional pharmacy on the assumption that he or she had no interest in "hospital pharmacy." As a result, that person completely overlooked the session on "Complying with FDA's Good Manufacturing Practice (GMP) Regulations in the Hospital Pharmacy Manufacturing Laboratory."

Hopefully, the "track" system will eliminate future such oversights. Program content of special interest to practitioners, to scientists, and to students will be grouped in separate lists for ready and convenient reference by these respective people. So, too, will be grouped the broader, more general program content involving Association policy and general information. As a result, the "scientist track" will list not only APS sessions but also SAPhA programs on increasing graduate student enrollment, APP programs on comparative bioavailability of competing drug products, and APhA General Session speakers such as the Director of the National Institutes of Health or the Commissioner of the Food and Drug Administration.

Consequently, we urge our readers to make plans now to attend the up-coming APS National Meeting, November 14–18, 1982, in San Diego, California, and APhA–APS Annual Meeting, April 9–14, 1983, in New Orleans, Louisiana. "Being there" will be more important and rewarding than ever before.

—EDWARD G. FELDMANN
American Pharmaceutical Association
Washington, DC 20037

0022-3549/82/01000-1071$01.00/0

JOURNAL OF PHARMACEUTICAL SCIENCES

OCTOBER 1982
VOLUME 71 NUMBER 10

LITERATURE SURVEY

Vitamins in Pharmaceutical Formulations

ELMER DeRITTER

Received from the *Product Development and Application, Roche Chemical Division, Hoffmann-LaRoche, Nutley, NJ 07110.*

Keyphrases □ Vitamins—pharmaceutical formulations, literature survey □ Pharmaceutical formulations—vitamins, literature survey

CONTENTS

The formulation of pharmaceutical vitamin products having adequate physical and chemical stability as well as suitable taste, odor, color, and freedom from bacterial contamination can entail numerous problems arising from the differing physical form, stability, and solubility characteristics of the individual vitamins. For liquid products, choice of the optimal pH is a crucial factor. Interactions between some of the vitamins and between vitamins and other product constituents must also be considered. Successful development of vitamin products requires knowledge of the fundamental aspects of the physical and chemical properties of the various forms of the vitamins available, the use of adequate techniques of manufacture, and the addition of suitable manufacturing overages based on critical stability studies.

SOLUBILITY OF THE VITAMINS

Vitamins are categorized into two general groups: fat-soluble and water-soluble. The fat-soluble vitamins include vitamins A, E, and K and cholecalciferol (vitamin D). Vitamin A is available as the free alcohol, retinol, and its acetate, palmitate, and propionate esters. Vitamin E is listed by USP as both *d*- and *dl*-forms of tocopherol and its acetate and acid succinate esters. Cholecalciferol is normally utilized in pharmaceuticals as ergocalciferol (vitamin D_2) or cholecalciferol (vitamin D_3), both of which are equally active in humans. Oil-soluble forms of vitamin K include phytonadione (vitamin K_1), menadione, menadiol diacetate, and menadiol dibutyrate. Incorporation of fat-soluble vitamins into an aqueous preparation requires the use of an efficient emulsifying agent (*e.g.*, polysorbate 80) to produce homogeneous and physically stable formulations. In the case of vitamin K, there are a number of water-soluble forms such as menadiol sodium diphosphate, the dipotassium salt of menadiol disulfate, and menadione sodium bisulfite.

Solubilities of the water-soluble vitamins at 25° in water are listed in Table I. For several of the relatively insoluble vitamins such as riboflavin and biotin, the solubility is dependent on the nature of the crystal structure. For acids such as biotin and folic acid, addition of alkali significantly increases solubility. In the case of biotin it is possible to prepare a 20% aqueous solution of the sodium salt by this method. Figure 1 illustrates the increasing solubility of

0022-3549/82/01000-1073$01.00/0

Table I—Solubility of Vitamins in Water at 25°

	mg/ml
Panthenol	Freely soluble
Thiamine hydrochloride	1000
Thiamine mononitrate	27
Niacinamide	1000
Sodium ascorbate	620
Ascorbic acid	333
Calcium pantothenate	356
Pyridoxine hydrochloride	220
Riboflavin-5′-phosphate sodium	43–112
Riboflavin	0.066–0.33
Cyanocobalamin	12.5
Biotin	0.3–0.4
Folic acid	0.0016

folic acid with increasing pH and shows the solubilizing effect on folic acid of gentisic acid ethanolamide as related to pH (1). An amorphous form of *d*-calcium pantothenate was reported (2) to dissolve ~10% faster than the crystalline form in aqueous media (pH 7.0 buffer).

STABILITY CHARACTERISTICS OF THE VITAMINS

Factors influencing the stability of the individual vitamins and their relative effects on different forms of a particular vitamin are listed in Table II. Although temperature is not mentioned in the tabulation, it is normal that an increase in temperature will accelerate any of the decomposition reactions. Macek (5) has reviewed the stability problems encountered with some vitamins.

A number of the vitamins may be classified as stable since they usually present no major problems regarding stability in pharmaceutical dosage forms. These include cholecalciferol, vitamin E acetate or acid succinate, biotin, niacin or niacinamide, pyridoxine, and riboflavin. The labile vitamins which are likely to present problems of instability in dosage forms are vitamin A (retinol and retinyl esters), vitamin K, ascorbic acid, cyanocobalamin, folic acid, pantothenic acid, panthenol, and thiamine.

The presence of one or more double bonds in the structures of vitamin A, cholecalciferol, and phytonadione makes them subject to isomerization under conditions frequently encountered in pharmaceutical products. For example, vitamin A undergoes isomerization in aqueous preparations at an acid pH. Vitamin A added to such products as essentially the all-*trans* form will isomerize on storage to an equilibrium mixture of approximately two-thirds all-*trans* and one-third *cis* isomers, the predominant *cis* isomer being 2-*cis* or neovitamin A, which has biological activity of 75% of that of the all-*trans* isomer. Lesser amounts of the 6-*cis* and 2,6-di-*cis* isomers may also form. The latter have only ~23% of the biological potency of all-*trans* vitamin A. Lehman *et al.* (6) have reported on the extent of isomerization that occurs in stored multivitamin drops. Equations have been proposed (7, 8) for calculating the biological potency of the isomerized vitamin A from the maleic values determined by Carr-Price colorimetry before and after reaction of vitamin A with maleic anhydride, in which isomers having a *cis* configuration at the terminal double bond (the 2-position) do not react to form an adduct.

Vitamin A suppliers have made available mixtures of vitamin A palmitate isomers at the equilibrium ratio of

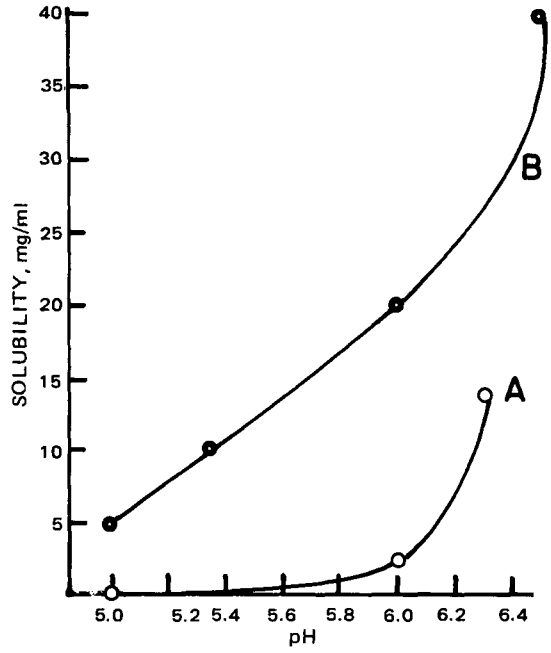

Figure 1—*Solubility of folic acid* versus *pH. Key: (A) with no solubilizer, (B) with 3% gentisic acid ethanolamide.*

Table II—Stability Characteristics of Vitamins

Vitamin A	sensitive to atmospheric oxygen (retinol less stable than its esters); trace metals catalyze decomposition; inactivated by UV light; isomerizes at acid pH; stable in alkali; in aqueous dispersions palmitate ester more stable to heat than retinol <pH 5.5; palmitate most stable ester under moisture stress; stabilized by antioxidants and protective coatings.
Cholecalciferol (vitamin D)	sensitive to atmospheric oxygen; trace metals and carriers with acid surface activity catalyze isomerization or decomposition; generally more stable than vitamin A; stabilized by antioxidants and protective coatings.
Vitamin E	tocopherol sensitive to atmospheric oxygen, especially in alkali and sensitive to UV light; esters very stable.
Vitamin K	fairly stable to heat; decomposed by sunlight and alkali.
Ascorbic acid (vitamin C)	stable when dry; readily oxidized in solution; decomposition catalyzed by metal ions (copper and iron); greatest instability at ~pH 4.
Biotin	stable to air and acid and at neutral pH; slightly unstable in alkali.
Cyanocobalamin (vitamin B_{12})	decomposed by oxidizing and reducing agents; slightly unstable in acid or alkaline solution; ascorbic acid and thiamine–niacinamide accelerate the decomposition; sensitive to light in very dilute solutions for assay.
Folic acid	unstable <pH 5; decomposed by sunlight and riboflavin; decomposed by reducing agents.
Niacin and niacinamide	normally very stable.
Calcium pantothenate	unstable in acid (< pH 5) and alkali; maximum stability at pH 6–7.
Panthenol	more stable than calcium pantothenate at ≤pH 5.
Pyridoxine (vitamin B_6)	normally very stable; metal ions can catalyze decomposition; dilute solutions for assay are sensitive to light.
Riboflavin (vitamin B_2)	stable in acid solution; unstable in alkaline solution; sensitive to light, especially in alkaline solution or in very dilute acid solutions for assay; decomposed by reducing agents.
Thiamine (vitamin B_1)	increasingly unstable in solution as pH rises; decomposed by oxidizing or reducing agents; cleaved by sulfite very rapidly at high pH (Ref. 3); hydrochloride more hygroscopic than mononitrate (Ref. 4).

two-thirds all-*trans* and one-third *cis* for use in aqueous products where isomerization is known to occur (9). With such use, the drop in potency by USP assay due to isomerization does not occur in the multivitamin product and, consequently, the stability of vitamin A in the product is somewhat better with the preisomerized mixtures than with all-*trans* vitamin A. Figure 2 illustrates this advantage of the preisomerized equilibrium mixture over all-*trans* vitamin A palmitate in a number of multivitamin drop preparations at pH 5.0 stored at room temperature for 12 months. On the average, after 6–12 months, vitamin A retention is 7% greater with the preisomerized vitamin A. A similar difference was found in storage tests at 45°.

The reversible isomerization reaction in solutions of cholecalciferol has been discussed by Keverling Buisman *et al.* (10). In this reaction an equilibrium is formed over time between ergocalciferol and precalciferol, the equilibrium ratio of the isomers being dependent on temperature. The isomerization rates of ergocalciferol and cholecalciferol are virtually equal (11) and are not influenced by the solvent, acidity, UV light, catalysts, and free-radical reaction inhibitors (12, 13).

Inactive byproducts that may be present from the irradiation process used for manufacture of cholecalciferol, such as tachysterol, isotachysterol, and *trans*-cholecalciferol, give the same pink color with Nield's reagent used for assay of ergocalciferol plus precalciferol. The interference by tachysterol and *trans*-cholecalciferol can be eliminated by forming an adduct of those compounds with maleic anhydride, which can be done in 30 min at 20°. Isotachysterol can be estimated after formation of adducts of ergocalciferol and precalciferol with maleic anhydride by heating for 3 hr at 100°. Isotachysterol does not react significantly with maleic anhydride (14) under these conditions.

In a series of papers, Takahashi and Yamamoto (15) studied the isomerization of ergocalciferol that occurs in powders prepared with various excipients such as $CaSO_4$, $CaHPO_4$, talc, aluminum silicate, and magnesium trisilicate. This isomerization is catalyzed by the surface acid of the excipients. Compounds such as monoethanolamine and polyoxyethylene glycol 4000, which are able to reduce the surface acidity of the excipients, act as stabilizers of ergocalciferol. Storage of ergocalciferol powders at high humidity increases their stability because the surface acidity is reduced through absorption of moisture. However, coating agents such as shellac, ethylcellulose, or cellulose acetate phthalate were unable to prevent the isomerization of the vitamin. The isomers identified were 5,6-*trans*-ergocalciferol, precalciferol, isocalciferol, a *cis* isomer of isocalciferol, isotachysterol, and tachysterol.

Phytonadione, having a double bond in the side chain, exists in the form of both *trans* and *cis* isomers. The *trans* isomer is the naturally occurring form, which is biologically active. The *cis* form has no significant biological activity.

DEGRADATION STUDIES

Vitamin A—The degradation of retinol in solution in an oil with polysorbate 80 was shown by Carstensen (16) to be a pseudo first-order reaction. Carstensen (16) and Tardif (17) reported first-order decomposition of vitamin A in tablets with adherence to an Arrhenius equation, and Shah *et al.* (18) found that vitamin A in two multivitamin preparations decomposed in accordance with a first-order reaction.

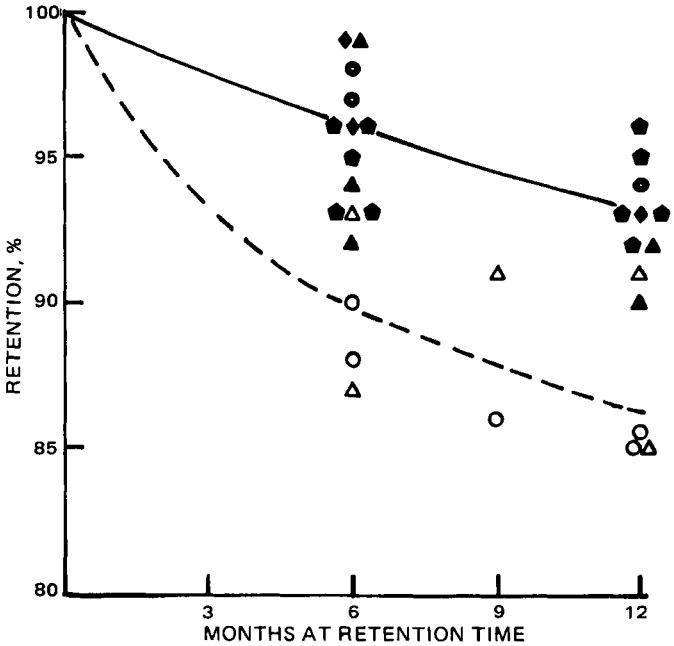

Figure 2—*Stability of vitamin A palmitate in aqueous multivitamin drops at pH 5; symbols represent different formulations with all-*trans *(●, △) or preisomerized (○, ▲, ■, ◆) vitamin A.*

Cholecalciferol (Vitamin D)—The decomposition of ergocalciferol and cholecalciferol at 25 and 40° under dry, humid conditions was studied by Grady and Thakker (19). Ergocalciferol decomposed rapidly at both temperatures in dry air, leading to formation of products of higher polarity. It was more stable at higher humidity than in dry air. Cholecalciferol was not as labile in dry air but decomposed rapidly at 40° and high humidity levels.

Vitamin E (α-Tocopheryl Acetate)—Vitamin E is relatively stable, but the unesterified α-tocopherol is less stable due to the free phenolic hydroxy group. Oxidation of α-tocopherol with agents such as nitric acid, ferric chloride, or ceric sulfate leads successively to the formation of α-tocopherolquinone, α-tocored, the *para*-quinone, and α-tocopurple (20, 21). In the absence of air, α-tocopherol is stable to heat but will be degraded if exposed to air. Thus, during saponification for analysis, protection by an antioxidant such as ascorbic acid or pyrogallol is practiced. Exposure to light will cause gradual darkening.

Vitamin K—Vire *et al.* (22) studied the degradation of menadione and menadione bisulfite in neutral and alkaline solution using polarographic methods. In alkaline solution the predominant degradation of the bisulfite addition product is to menadione, but in neutral solution isomerization to a naphthoquinone sulfinate becomes significant. In the absence of oxygen, menadione is degraded primarily *via* rearrangement to epoxynaphthohydroquinone.

Thiamine (Vitamin B_1)—The chemistry of the degradation of thiamine under the influence of heat and pH has been reported by Dwivedi *et al.* (23–25). The kinetics of the degradation of thiamine have been studied by various workers (17, 18, 25–29) who have reported first-order reactions with a rate increasing with increasing pH. Mulley *et al.* (28) also studied the degradation of cocarboxylase,

which was less stable than thiamine hydrochloride between pH 4.5 and 6.5 in phosphate buffer. Kobayashi (30) found that decomposition of thiamine in the neutral range is accelerated by the presence of Cu^{+2} at high temperature. The decomposition was affected by initial concentrations of thiamine and Cu^{+2}, time and temperature of heating, pH, and kind of buffer. In the presence of sodium nitrite, Kaya (31) found that heating of thiamine solutions for 60 min at 75° caused formation of elemental sulfur and thiochrome as well as 4-methyl-5-(β-hydroxyethyl)thiazole. The cleavage of thiamine by sulfite or bisulfite as noted in Table II is very rapid at high pH. Almost complete destruction of thiamine within 24 hr has been observed when thiamine was added to parenteral infusion fluids containing bisulfite as a preservative and having a pH ≥6.

Stepuro and Ostrovskii (32) studied the effect of pH on the photochemical reaction rate of thiamine, thiamine derivatives, and decomposition products using UV irradiation at 253.7 nm. The reactions take place at pH 3.0–9.0 with a rapid speeding up at pH 4–5 for thiamines. At pH < 3, the photolyzed thiazoles produce thiamide precipitates. Moorthy *et al.* (33) reported the reversible 1-electron redox potential of thiamine to be ~−0.5 V.

Riboflavin—Irradiation of riboflavin in neutral or acid solution yields lumichrome and in alkaline solution lumiflavine (34). The rate of decomposition is dependent on temperature, pH, and light intensity and wavelength. The decay of riboflavin-5′-phosphate exposed to light is dependent on the same factors (35).

Pantothenic Acid—Degradation has been shown to be a first-order reaction in solution at pH 3.8 by Frost and McIntire (36), in tablets by Campbell *et al.* (37–39), and in multivitamin liquids by Shah *et al.* (18).

Cyanocobalamin (Vitamin B_{12})—The decomposition of cyanocobalamin in tablets follows a first-order reaction (37–39). Marcus and Stanley (40) stored solutions of hydroxocobalamin in either acetate or citrate–phosphate buffer at 70, 80, and 90° and found the vitamin to degrade by a first-order reaction. Macek and Feller (41) show the decomposition of cyanocobalamin at higher temperatures to be catalyzed by thiamine decomposition and, hence, to be complicated. Shah *et al.* (18) found that cyanocobalamin in two multivitamin liquids stored at higher temperatures did not decompose in accordance with first-order kinetics. The oxidation–reduction thermodynamics of cyanocobalamin, cobalamins, and cobinamides have been reported by Ely (42).

The rates of destruction of cyanocobalamin in neutral aqueous solutions when exposed to various light sources have been reported by DeMerre and Wilson (43). Below 300 foot candles no destruction is noticeable. Sunlight at a brightness of 8000 foot candles caused 10% loss for each 30 min of exposure.

Losses of cyanocobalamin in solutions sterilized by gamma irradiation were lower at −78 and −196° than at −22 or −50° and were greatest at 0 and 18° (44).

Folic Acid—Dick *et al.* (45) studied the thermal stability of folic acid in buffered solutions at 100 and 120 ± 1°. Considerable destruction was found <pH 4, but >pH 5 there was no destruction in 1 hr at 100° or 15 min at 121°. Stokstad *et al.* (46) found rapid destruction of folic acid when a solution was exposed to direct sunlight. Degradation was most rapid at pH 7.0 and most slow in alkaline solution. Exposure to fluorescent light for 6 hr produced only slight inactivation. By extrapolation of results obtained at 55, 70, and 85° and 30, 50, and 70% relative humidity, Tripet and Kesselring (47) calculated 1%/year decomposition rate for folic acid either in solid form or in solutions with 5, 10, and 50% avicel. In two multivitamin liquids at higher temperatures, Shah *et al.* (18) found that folic acid did not follow first-order kinetics.

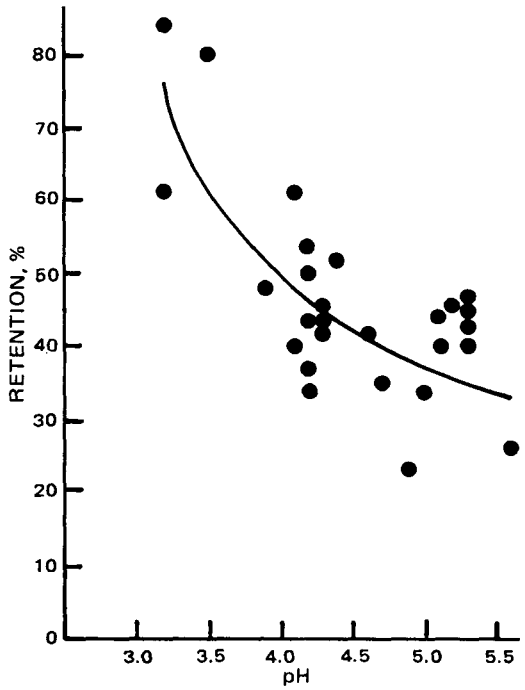

Figure 3—*Stability of thiamine* versus *pH in multivitamin drops; 6 weeks/45°.*

Ascorbic Acid (Vitamin C)—Reversible oxidation of ascorbic acid yields dehydroascorbic acid which has full ascorbic acid activity. Levandoski *et al.* (48) demonstrated that this reaction proceeds through an intermediate compound, identified as monodehydroascorbic acid, which may be complexed with ascorbic acid. Ascorbic acid stability in certain aqueous and fruit juice vehicles was reported by Uprety *et al.* (49). Ogata *et al.* (50) studied the kinetics of cupric salt-catalyzed autoxidation of ascorbic acid in aqueous solutions. Kassem *et al.* (51) reported that metal-catalyzed degradation of ascorbic acid in 10% injectable solutions took place by first-order kinetics. The order of effectiveness of metal ions as catalysts was $Cu^{+2} > Fe^{+2} > Zn^{+2}$; Fe^{+3}, Mn^{+2}, and Mg^{+2} had negligible effect. Dissolved oxygen had a deleterious effect increasing with concentration. Hayakawa and Hayashi (52) identified a Cu^{+2}–ascorbate complex as intermediate in the oxidation of ascorbic acid in the presence of Cu^{+2} ions.

The rate of anaerobic degradation of ascorbic acid in aqueous solution and the corresponding rate of formation of carbon dioxide as a breakdown product were reported by Finholt *et al.* (53, 54). Rogers and Yacomeni (55) and Blaug and Hajratwala (56) studied the effect of pH on the aerobic degradation of ascorbic acid in aqueous solution, which proceeded by a first-order reaction. Maximum rate of degradation occurred at pH 4 near the pK_{a_1} of ascorbic acid, and the minimum rate was at pH 5.6. Tingstad *et al.* (57) reported first-order degradation of ascorbic acid in a

multivitamin emulsion containing sodium fluoride stored at 70° and pH 3.15, 3.40, and 3.80.

Sattar *et al.* (58) found fluorescent light to have practically no effect on the destruction of ascorbic acid in pure solution, but the addition of riboflavin accelerated the decomposition. Losses of ascorbic acid were markedly increased by Cu^{+2} and Fe^{+3} under light exposed and unexposed conditions. The pro-oxidant effect of Cu^{+2} increased with increasing temperature and was relatively low under limited oxygen supply as compared to that in air, whereas oxygen supply had no influence on the effect of Fe^{+3}. Addition of Zn^{+2}, Ni^{+2}, and Mn^{+2} exhibited almost no effect under limited or excess oxygen availability. Uno *et al.* (59) and Switek and Modrzejewski (60) described the decomposition of ascorbic acid due to high frequency or gamma radiation used to sterilize aqueous solutions.

Vitamins, General—Huettenrauch (61) recommended the following as useful experimental parameters for kinetic studies of interactions and degradation of water-soluble vitamin preparations: temperature, pressure, solvent, degree of ionization, pH, concentration, and catalytic activity.

MUTUAL INTERACTIONS OF THE VITAMINS

Thiamine–Riboflavin—An incompatibility in aqueous vitamin B complex solutions has been described by Gambier and Rahn (62). The oxidative action of riboflavin on thiamine leads to the formation and precipitation of thiochrome. Subsequently, chloroflavin, the reduction product of riboflavin, may also precipitate. In vitamin B complex solutions containing ascorbic acid, thiochrome formation is not observed.

Thiamine–Folic Acid—Biamonte and Schneller (63) found thiamine to cause considerable decomposition of folic acid at pH 5.9 and 6.9 in aqueous, buffered solutions. Darnule and Colah (64) found the breakdown of folic acid to be accelerated by the presence of decomposition products of thiamine. The key element was the hydrogen sulfide produced during the breakdown of thiamine.

Thiamine–Cyanocobalamin—Blitz *et al.* (65) reported that the combination of thiamine and niacinamide in a vitamin B complex solution caused considerable decomposition of cyanocobalamin. It was shown by Macek and Feller (41, 66) that the breakdown of cyanocobalamin could be attributed largely to the 4-methyl-5-(β-hydroxyethyl)thiazole formed by cleavage of thiamine. At low levels of thiamine (1–10 mg/ml) losses of cyanocobalamin after a year at room temperature were small, but the losses were much higher at higher levels of thiamine or at elevated temperatures.

Riboflavin–Niacinamide—The presence of niacinamide in aqueous solution increases the solubility of riboflavin, due apparently to a complex formation between the two vitamins. This effect of niacinamide was useful in the preparation of vitamin solutions before the more soluble riboflavin-5′-phosphate became available. El-Khawas and El-Gindy (67) studied this interaction and reported that below 1% niacinamide, the effect on the solubility of riboflavin is small, but as the concentration of niacinamide is increased above 1%, the solubilizing effect on riboflavin becomes more pronounced and greater than that of urea.

Riboflavin–Folic Acid—Biamonte and Schneller (63) reported the deleterious effect of riboflavin on folic acid in aqueous, buffered solutions, particularly at pH ≥ 5.0. The combined action of light and riboflavin causes rapid oxidative cleavage of folic acid. Scheindlin *et al.* (68) studied this reaction and found it to occur more rapidly at pH 6.5 than at pH 4.0. The reaction is retarded, but not halted, by the exclusion of air and will proceed even when the solution is kept in amber glass.

Riboflavin–Ascorbic Acid—Hand *et al.* (69) and Sattar *et al.* (58) have reported that riboflavin catalyzes the photochemical decomposition of ascorbic acid during exposure of solutions to light and air.

Niacinamide–Ascorbic Acid—Wenner (70) described the preparation of a niacinamide–ascorbic acid complex in solid form. This yellow compound (71), containing one molecule each of niacinamide and ascorbic acid, forms readily in solution by what appears to be a charge–transfer reaction. It has been claimed (72) that preforming of this complex prevents difficulties with thickening and hardening of the mixtures employed in soft gelatin capsules. Guttman and Brooke (73) studied the formation of this yellow complex in the acid pH range at room temperature by measuring the absorbance at 365 nm. Maximum color was formed at pH 3.8 under the conditions employed. Osberger (74) described the commercial preparation of this complex and its applications in direct-compression tablets.

Niacinamide–Folic Acid—Taub and Lieberman (75) found that niacinamide acts as a solubilizer of folic acid. A 10% solution of niacinamide maintained a concentration of 5 mg/ml of folic acid at pH as low as 5.6, whereas the normal solubility of folic acid at pH 6.0 is 2 mg/ml.

Ascorbic Acid–Folic Acid—The cleavage of folic acid due to the reducing action of ascorbic acid was studied by Scheindlin and Griffith (76). In an acid medium the reaction products are *p*-aminobenzoylglutamic acid and 2-amino-4-hydroxy-6-methylpteridine. The free amino group of *p*-aminobenzoylglutamic acid is then destroyed by ascorbic acid or its oxidation products. The decomposition of folic acid was rapid at pH 3.0–3.3 and slow at pH 6.5–6.7.

Ascorbic Acid–Cyanocobalamin—Gakenheimer and Feller (77) observed an incompatibility between ascorbic acid and cyanocobalamin with losses of cyanocobalamin being least at pH 0–1 and increasing to a maximum at pH 7. Trenner *et al.* (78) found that hydroxycobalamin was much less stable in the presence of ascorbic acid then cyanocobalamin. Studies by Frost *et al.* (79) indicated that cyanocobalamin analogs in which the cobalt atom is strongly coordinated are the most stable toward ascorbate. Bartilucci and Foss (80) reported that decomposition products of ascorbic acid may play an important role in the effect on cyanocobalamin stability. Since copper ions catalyze the decomposition of ascorbic acid, it is not surprising that Stapert *et al.* (81) found that copper ions greatly enhance the destructive action of ascorbic acid on cyanocobalamin. Studies by Rosenberg (82) showed that Cu^{+2} itself has no effect on cyanocobalamin, and that ascorbic acid in the complete absence of Cu^{+2} causes relatively little decomposition of cyanocobalamin, but the combinations of ascorbic acid–Cu^{+2} or dehydroascorbic acid–Cu^{+2} were destructive of cyanocobalamin.

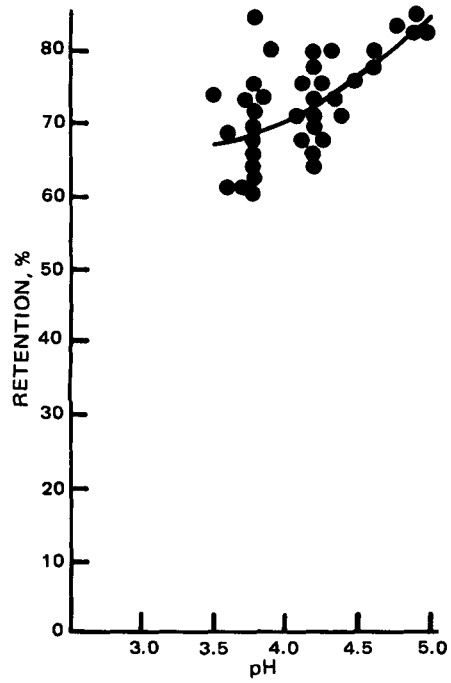

Figure 4—*Stability of ascorbic acid* versus *pH in vitamin B complex–ascorbic acid injectables; 6 weeks/45°.*

Utsumi *et al.* (83) studied the effect of various cobalamin analogs in catalyzing the oxidation of ascorbic acid in solution in acetate buffer at pH 5. The catalytic activity decreased in the order of hydroxycobalamin > hydroxocobinamide > cyanocobalamin coenzyme > cyanocobalamin > cyanocobinamide.

Other Interactions—Papp *et al.* (84) reported that several binary mixtures of thiamine, riboflavin, pyridoxine, niacin, and ascorbic acid showed nonlinear interferometric and conductometric curves, suggesting interactions. Hsu (85) found that niacinamide added to a solution of riboflavin-5′-phosphate sodium and ascorbic acid significantly increased the loss of riboflavin-5′-phosphate during photolysis, whereas added tryptophan stabilized both vitamins. Valls *et al.* (86) determined the stability of pyridoxal-5-phosphate and found it to be poor at pH 6 in aqueous solution. Increase in the degradation rate was caused by either thiamine, thiamine diphosphate, riboflavin-5′-phosphate, cobamamide, pyridoxal, or pyridoxine but not by riboflavin or cyanocobalamin. Takahashi and Yamamoto (87) found that ergocalciferol in powder preparations was readily isomerized by ascorbic acid, folic acid, thiamine hydrochloride, or pyridoxine hydrochloride but not by niacinamide or calcium pantothenate.

pH-STABILITY RELATIONSHIPS

In Aqueous Model Systems—*Thiamine versus Pantothenic Acid*—As noted in Table II, the stability of thiamine is best at low pH and decreases rapidly as the pH increases toward neutrality. In contrast, the stability of calcium pantothenate is optimal at pH 6.5–7 and decreases as the pH decreases. Frost and McIntire (36) studied the retention of thiamine hydrochloride and calcium pantothenate in 0.1% solutions at various pH levels after autoclaving for 15 min at 6.81 kg. Equal retentions of thiamine and calcium pantothenate were found at ~pH 4.5, the point at which the two curves of stability *versus* pH

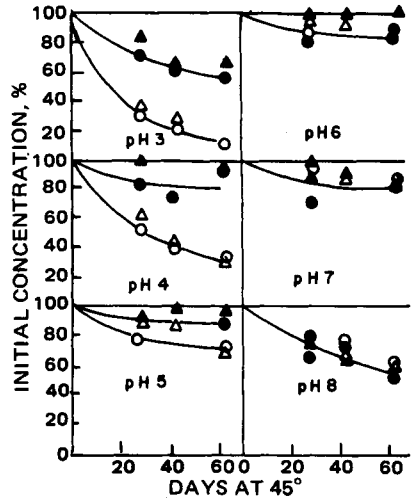

Figure 5—*Comparative stability of pantothenic acid (○, △) and panthenol (●, ▲) at pH 3–8.*

intersected. It may be noted that Figs. 3 and 4, which show 6 week/45° stability curves for thiamine and calcium pantothenate, respectively, in multivitamin drops, indicate 40% retention of both vitamins at pH 4.7.

Panthenol versus Calcium Pantothenate—Rubin (88) studied the comparative stability of these two forms of the vitamin in pure solutions with added buffers and a preservative. Both microbiological and rat bioassays were employed to assess stability. Figure 5 shows the comparative stability data obtained in tests at 45° for as much as 63 days. In the pH range of 3–5, commonly encountered in multivitamin liquids, panthenol shows markedly better stability than pantothenic acid.

Ascorbic Acid—The degradation of ascorbic acid in

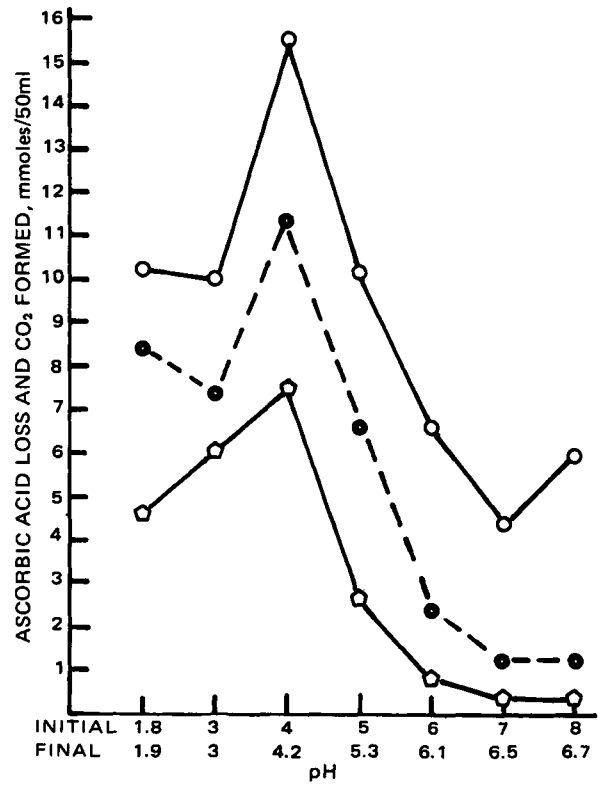

Figure 6—*Effect of pH on decomposition of ascorbic acid in 25% aqueous solution sealed in ampuls and stored 93 hr at 55°. Key: (○) ascorbic acid; (●) total ascorbic acid; (□) carbon dioxide formed.*

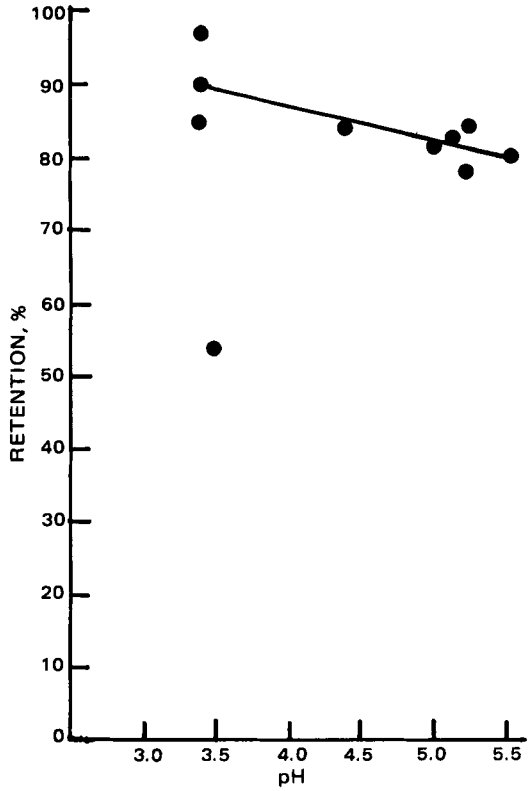

Figure 7—*Stability of thiamine* versus *pH in multivitamin products for teaspoon dosage; 6 weeks/45°.*

solution is pH-dependent. Finholt *et al.* (53) studied the pH–rate profile of the anaerobic degradation of ascorbic acid in solution at 96°. A maximum rate was observed at pH 4.1 which corresponds to the pK_1 of ascorbic acid. A study conducted in the author's laboratory also showed maximum degradation at ~pH 4.1 in solutions of 25% ascorbic acid in 50-ml sealed ampuls stored for 93 hr at 55°. Assays were made for ascorbic acid and dehydroascorbic acid contents and carbon dioxide formed. The results are shown in Fig. 6. The three graphs showing losses of ascorbic acid and total ascorbic acid (reduced and dehydro) and carbon dioxide formed all show a peak at ~pH 4.1. Pressure build-up in containers of products containing ascorbic acid can be especially troublesome at that pH as compared to either lower or higher pH.

In Aqueous Multivitamin Products—The influence of pH on the stability of some of the labile vitamins has been studied in a number of commercial as well as experimental multivitamin formulations. The pH–stability relationships are illustrated in Figs. 3, 4, 7–12 which show the results of storage for 6 weeks at 45°.

Thiamine—Figures 3, 7, and 8 show the retention of thiamine over the usual pH range for multivitamin drops, teaspoon dosage forms, and vitamin B complex and ascorbic acid injectables, respectively. All three types of products show progressively decreasing stability with increasing pH. Thiamine stability is particularly poor in the drop preparations, intermediate in the injectables, and best in the syrups and elixirs for teaspoon dosage. In the latter case, the better stability may be due to the influence of a high sugar content.

Ascorbic Acid—Figures 4, 9, and 10 show the pH–stability relations for ascorbic acid in multivitamin drops, teaspoon dosage forms, and vitamin B complex–ascorbic

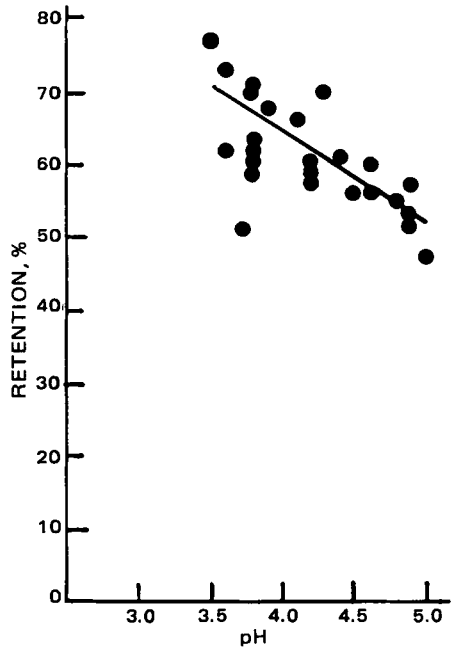

Figure 8—*Stability of thiamine* versus *pH in vitamin B complex–ascorbic acid injectables; 6 weeks/45°.*

acid injectables, respectively. In the drop preparations (Fig. 9), the curve shows maximum loss to occur at ~pH 4.2, which is similar to the pattern found in model systems (Fig. 6). In the other two types of preparation (Figs. 4 and 10), the losses at a given pH are similar and both show progressively decreasing loss as the pH increases from 3.5 to 5 or 5.5.

Panthenol and Calcium Pantothenate—The relative stability of panthenol and calcium pantothenate *versus* pH is shown in Fig. 11 for multivitamin drops and teaspoon dosage forms, which show similar stability patterns for panthenol. Figure 12 gives a similar comparison for vitamin B complex–ascorbic acid injectables. Panthenol shows the expected trend toward increasing losses with decreasing pH similar to the losses observed in the model systems shown in Fig. 5. Below pH 5 the losses of calcium pantothenate are much higher than those of panthenol.

Vitamin A—The relation of vitamin A palmitate stability to pH in multivitamin preparations for teaspoon dosage is shown in Fig. 13. Increasing the pH improves vitamin A stability. In the case of multivitamin drops, no clear-cut pattern of pH stability could be established due to wide variations found at any given pH level due to non-pH-related factors in the formulations tested.

FACTORS THAT ENHANCE VITAMIN STABILITY

Reduction of Water Content—Anmo *et al.* (89) determined the stability of retinol in 60–100% aqueous ethanol and found increasing losses as the water content increased. In a study of an oral liquid vitamin preparation made with various proportions of water, glycerin, and/or propylene glycol, Delgado *et al.* (90) reached the general conclusion that formulations containing lesser amounts of water possessed relatively higher stability values than those containing larger amounts of water. Parikh and Lofgren (91) demonstrated increased stability of ascorbic acid and thiamine when glycerin or propylene glycol was substituted for part of the water in an oral multivitamin

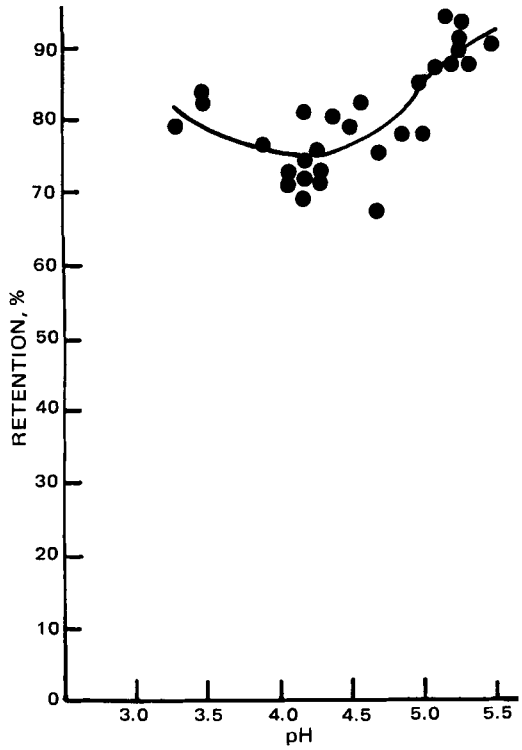

Figure 9—*Stability of ascorbic acid* versus *pH in multivitamin drops; 6 weeks/45°.*

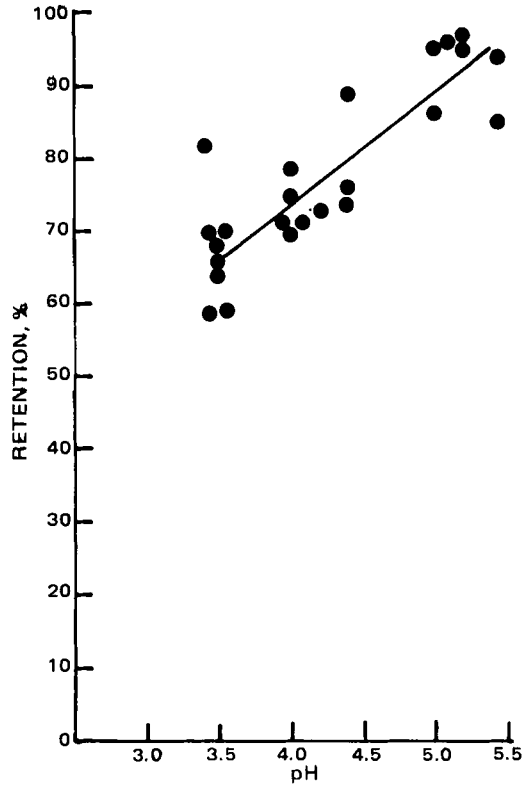

Figure 10—*Stability of ascorbic acid* versus *pH in multivitamin products for teaspoon dosage; 6 weeks/45°.*

liquid. Bandelin and Tuschhoff (92) reported similar findings on ascorbic acid and, in addition, found that ethanol or sugars such as sucrose, corn syrup, and dextrose also provide a stabilizing effect on ascorbic acid. Poust and Colaizzi (93) found that the first-order rate constants for oxidative decomposition of ascorbic acid at 30° decrease as a function of polysorbate 80 concentration up to 30%. In a study of the stability of ascorbic acid *per se* for 3 weeks at 45°, DeRitter *et al.* (94) found increasing stability as the moisture content decreased. Gerber *et al.* (95) reported increased stability of cyanocobalamin with high levels of sorbitol or sorbitol and glycerin. These authors found reasonable stability of both cyanocobalamin and ascorbic acid in a mixture with ferrous gluconate in 70% sorbitol. Gulesich (96) described an aqueous preparation containing ascorbic acid and iron, preferably ferrous sulfate, with 60–75% sorbitol.

Antioxidants—The stability of vitamins sensitive to oxidative decomposition can be increased in many cases by addition of antioxidants. Vitamin A and cholecalciferol are decomposed by exposure to air and are generally stabilized, in concentrates as well as pharmaceutical products, by addition of small amounts of antioxidants such as tocopherol, butylated hydroxyanisole, butylated hydroxytoluene, propyl gallate, ascorbyl palmitate, or a combination of several antioxidants (97–100). Koslov *et al.* (101) described model systems for studying the effectiveness of antioxidants in stabilizing vitamin A acetate and palmitate in thin films. At 10–40° butylated hydroxytoluene was superior to butylated hydroxyanisole, but ≥50° both were equally effective.

Ascorbic acid may also be more stable in the presence of antioxidants. Gladkikh (102) has reviewed methods for increasing the stability of ascorbic acid in medicinal forms. According to Tansey and Schneller (103), phenolic antioxidants such as butylated hydroxyanisole, nordihydroguaiaretic acid, and ethyl hydrocaffeate at levels of 0.02–0.05% retard the decomposition of folic acid by light in the presence of riboflavin and also protect folic acid somewhat in the dark.

Chelating Agents—The presence of trace metal ions, especially Cu^{+2} and to a lesser extent Fe^{+2}, accelerate the breakdown of ascorbic acid. The addition of a chelating agent such as edetic acid and its salts has been shown to enhance the stability of ascorbic acid *via* formation of metal chelates (90, 104). Kirkova *et al.* (105) tested nine stabilizers for ascorbic acid solutions and found a mixture of 0.1% disodium edetic acid and 0.25% $Na_2S_2O_4$ most effective. Reyes (106) found chelates of ascorbic acid with stearates of magnesium, calcium, or aluminum to provide improved stability of ascorbic acid in aqueous solutions.

Pyridoxine in solution is also sensitive to trace metal ions (107). Huang (108) found that Fe^{+2} in multivitamin products led to low recoveries of pyridoxine in microbiological assays. Recoveries of pyridoxine were 75 or 77% for 20:1 or 12:1 ratios of Fe^{+2}–pyridoxine, respectively. Addition of edetic acid before acid hydrolysis of such samples brought recovery of pyridoxine to 100%.

Cort *et al.* (109) found that the degradation of *dl*-α-tocopherol and *dl*-γ-tocopherol by Cu^{+2} could be completely inhibited by the combination of ascorbic acid and edetic acid, whereas ascorbic acid alone could prevent the oxidation of tocopherol in the presence of Fe^{+3}. Pure tocopherols when undiluted were stable to air and light over a period of years.

Other Compounds—Knobloch *et al.* (110) reported that the decomposition of vitamin A and cholecalciferol catalyzed by fine grain silicic acid can be inhibited by trolamine. An adduct of cholecalciferol with cholesterol

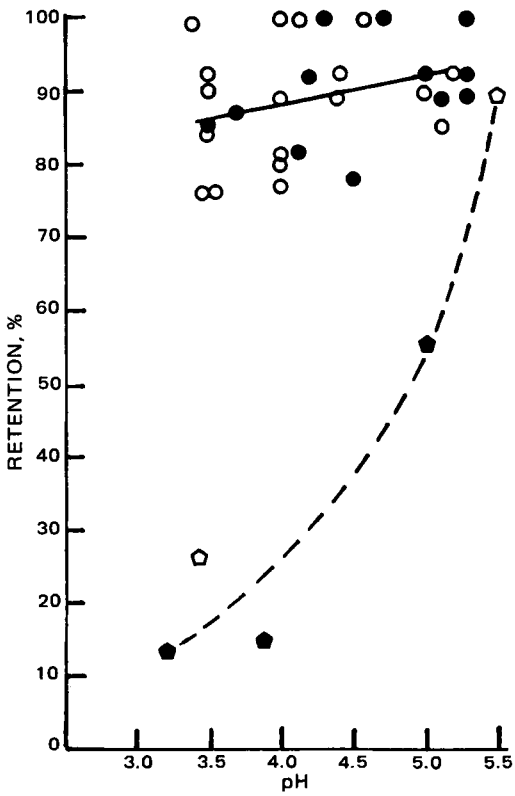

Figure 11—*Stability of panthenol (—●, ○) and pantothenate (- - -■, □) versus pH in multivitamin solutions-drops (●, ■) and teaspoon dosage forms (○, □); 6 weeks/45°.*

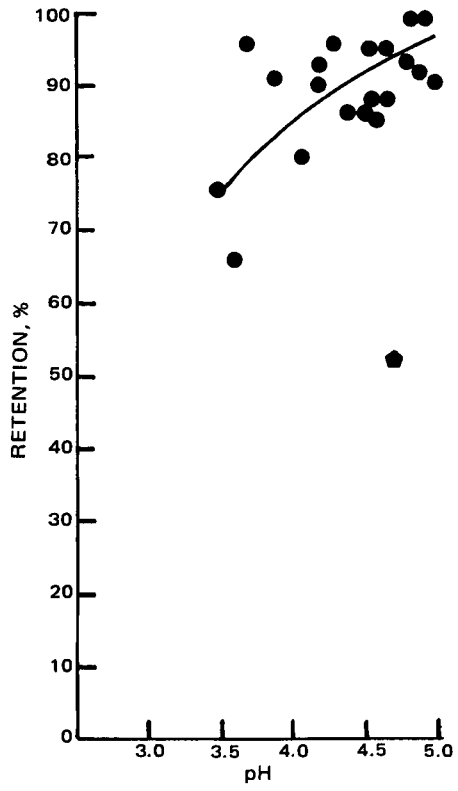

Figure 12—*Stability of panthenol (●) and pantothenate (■) versus pH in vitamin B complex injectables; 6 weeks/45°.*

was also found to be more stable than ergocalciferol or cholecalciferol.

Stabilization of riboflavin was achieved by Nobukuni *et al.* (111) by the addition of 1–20 moles of 2′-, 3′- and/or 5′-guanylic acid/mole of riboflavin. Protection of riboflavin, flavin mononucleotide, and flavin-adenine dinucleotide from photodecomposition was studied by Hata *et al.* (112–114). *para*-Substituted phenol derivatives, salicylic acid, tryptophan, and caffeine increased the stability of flavin mononucleotide through interactions in aqueous solution. Antipyrine and sulpyrine added to solutions of the flavins caused changes in their absorption spectra in the visible region suggesting interactions.

O'Broin *et al.* (115) compared the stability of folic acid to that of 5-formyl-, 10-formyl-, 5-methyl-, and unsubstituted tetrahydropteroylglutamate. Ascorbate was a superior stabilizing agent to 2-mercaptoethanol at comparable concentrations.

The effect of various compounds as stabilizers of B complex vitamins during gamma irradiation for the purpose of sterilizing aqueous solutions has been determined by Kishore *et al.* (116, 117). The combinations of nitrous oxide and glucose or oxygen and glucose as well as thiourea, tryptophan, and tyrosine provided good protection to thiamine, riboflavin, pyridoxine, niacinamide, and folic acid. Irradiation of aqueous solutions of these vitamins in the frozen state and with addition of glucose reduces radiolytic degradation. Irradiation in the dry, solid state causes no detectable damage, indicating that the best method for radiation sterilization of vitamin preparations may be to irradiate the components in the dry, solid state and then compound them together.

Rosenblum and Woodbury (118) reported the stabilizing effect of ferrous and ferric ions on cyanocobalamin in a multiple vitamin capsule. Newmark (119) described the effective stabilization of cyanocobalamin in solution in the presence of thiamine, niacinamide, and ascorbic acid by addition of various iron compounds and salts, including iron peptonate, ferric ammonium citrate, ferric chloride, ferrous gluconate, ferric glycerophosphate, ferric or ferrous sulfate, ferric or ferrous oxide, and ferric or ferrous complexes with such substances as edetic acid and its salts. Zuck and Conine (120) compared the relative effectiveness of complex cyanides and iron salts and found the cyanides to provide more effective stabilization of cyanocobalamin under conditions designed to exclude air as well as in partially filled containers having a large volume of air over the product. The complex cyanides were also effective in reducing the destruction of cyanocobalamin induced by UV irradiation.

Stabilization of thiamine solutions by addition of 0.05–5% monothioglycerol, thiosorbitol, or thioglucose has been the subject of a patent by Bray (121). Sodium formaldehyde sulfoxylate is used also for stabilizing injectable solutions of thiamine.

A considerable number of compounds have been reported to be stabilizers of ascorbic acid in solutions. In extracting solutions used in analyses of ascorbic acid, the stabilizers that have been used include metaphosphoric acid (122), oxalic acid (123), acetic acid (124, 125), and trichloroacetic acid. A combination of metaphosphoric acid and edetic acid has been recommended for use in the presence of Cu^{+2} and Fe^{+2} (104). Flavonoids inhibit the Cu^{+2} catalyzed oxidation of ascorbic acid (126). The order of activity reported by Takamura and Ito (127) is 3-hydroxyflavone < rutin < quercetin, and no inhibition was observed for flavone. Other compounds reported to have

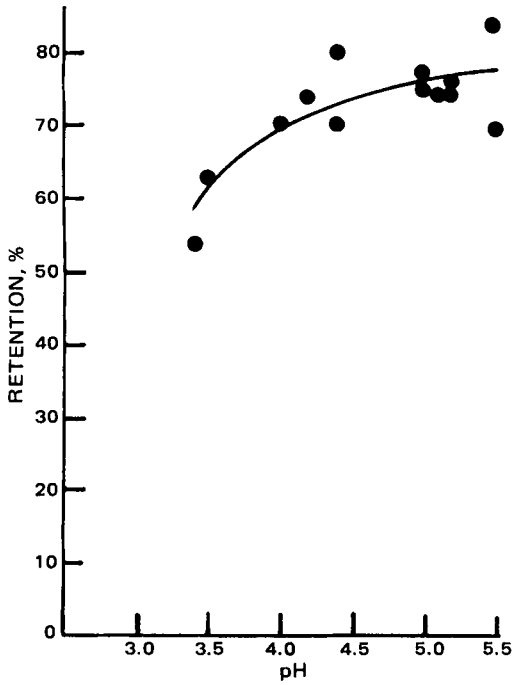

Figure 13—*Stability of vitamin A palmitate* versus *pH in multivitamin products for teaspoon dosage; 6 weeks/45°.*

similar activity are *O*-diphenols (128), aryl thioureas (129), rubeanic acid (130), acidic polysaccharides (131), sodium alginate (132), high concentrations of sucrose, glucose, or fructose (133), lysine and glutamic acid (117), a combination of *dl*-*N*-acetylhomocystine-thiolactone and sodium sulfite (134), gelatin (135), urocanic acid and/or its alkyl esters (136), and RNA, DNA, or salts (137). A review on the stabilization of ascorbic acid in liquid and solid preparations has been published by Gladkikh (102).

Coating and Encapsulation—A list of the various coating materials and processes used on single vitamins or combinations of several vitamins is given in Table III. Improving stability of labile vitamins under stress conditions is an important function of coating agents, but they are also useful for converting liquid vitamins into free-flowing, dry powders, masking taste in chewable tablets, improving handling and tableting characteristics, or stabilizing the color of ascorbic acid tablets, which otherwise may develop a tan color on aging.

Preparation of Adsorbates—Adsorption of fat-soluble vitamins on suitable adsorbents has been utilized as a means of conversion of the vitamins to dry, free-flowing powders as well as to enhance their stability. Espoy (182) described the preparation of an adsorbate of vitamin A on calcium silicate[1]. Neutral or weakly alkaline carriers such as magnesium oxide tend to stabilize vitamin A and cholecalciferol, whereas carriers with acid surface activity catalyze their decomposition (110, 183). This acid catalysis on fine grain silicic acid[2] can be inhibited by trolamine. Takahashi and Yamamoto (15) reported that ethanolamines and polyoxyethylene compounds were effective in preventing the isomerization of ergocalciferol caused by surface acidity of excipients.

Cannalonga and Czarecki (184) described a process for preparing agglomerated, free-flowing powders containing

[1] Microcel-E.
[2] Aerosil.

Table III—Coating or Encapsulation Processes for Vitamins

Vitamin	Stabilization Process	Reference
	Fat-Soluble Vitamins[a]	
A	Emulsify oil solution in gelatin, agar, or pectin or combinations thereof, plus sugar solution, cast into sheets, dry, freeze, and grind.	138, 139
A	Emulsify in gelatin–sugar solution and spray into starch ester containing hydrophobic groups[b].	140
A	Emulsify solution in hot well oil in wax and spray chill.	141
A	Granulate with partially hydrolyzed casein–formaldehyde and dry.	142
A	Emulsify in water-soluble gelable colloid, freeze, grind, and dry.	143
A	Emulsify in alkaline gelatin solution–pectin and water-soluble calcium salt and spray dry.	144
A	Emulsify in solution of low molecular weight amylose–glucose, dry on glass plate, and powder.	145
A	Emulsify vitamin A palmitate in hydrolyzed gelatin solution, spray dry, and agglomerate.	146
A and/or cholecalciferol	Emulsify in solution of gelatin–dextrin and maltose and spray dry.	147
A and/or cholecalciferol	Prepare clathrate in desoxycholic acid and subdivide.	148
A and/or cholecalciferol	Emulsify in wax or hydrogenated oil–vegetable flour and lecithin or polyoxyethylene sorbitan monopalmitate and spray.	149
A and/or cholecalciferol	Emulsify in film former (selected from dextrin, gelatin, casein or sodium carboxymethyl cellulose, maltose, sucrose, gum arabic)–emulsifier and spray into a current of atomized dehydrating agent (ethylene glycol, propylene glycol, glycerin, sorbitol, benzyl alcohol, ethanol, propanol, or butanol).	150
E	Emulsify in gum acacia–sugar solution and drum dry.	151
E	Emulsify in gum acacia solution–surface-active agent and convert into dry product.	152
E (acetate)	Emulsify in hydrolyzed gelatin solution with preservatives and spray dry.	153, 154
E (acetate)	Emulsify in hydrolyzed gelatin solution with preservatives and spray dry with agglomeration.	155
A, E, K, and/or cholecalciferol	Emulsify in solution of gum acacia or polyoxyethylene derivative of a partial ester of sorbitol and a fatty acid–glucose, sucrose, or corn syrup, cool and drop from a candy drop machine.	156
A, E, K, and/or cholecalciferol	Emulsify in gelatin and/or gum–a sugar alcohol–emulsifier such as lecithin and spray dry.	98
A, E, K, and/or cholecalciferol	Emulsify in solution of gum arabic or gum ghatti–lactose and spray dry; add 2% calcium silicate[c] as flour agent.	157
A, E, K, and/or cholecalciferol	Emulsify in wax, lecithin–synthetic polysaccharide[d], spray, and dust with one part soya flour to two parts of vitamin beadlets.	158
A, E, K, and/or cholecalciferol	Emulsify in solvent solution of a prolamine[e]–polymerized corn syrup and spray onto warm surface to remove solvent.	159
A, E, K, and/or cholecalciferol	Mix with gum acacia solution and dry gum acacia to form a plastic dough, dry, and comminute.	160
A, E, K, and/or cholecalciferol	Emulsify into gelatin solution previously heated with ascorbic acid–citric acid–plasticizer and spray into alcohol.	161

Continued on next page

Table III—*Continued*

Vitamin	Stabilization Process	Reference
A, E, K, and/or cholecalciferol	Emulsify into gelatin solution–powdered milk–a solid fat (mp 35–70°).	162
A, E, K, and/or cholecalciferol	Emulsify in a starch ester containing hydrophobic groups[b]–gelatin and sucrose or glucose and spray dry or spray into mineral oil or water.	163
A, E, K, and/or cholecalciferol	Solution in sunflower oil microencapsulated in gelatin.	164
A, E, or cholecalciferol	Emulsify into gelatin solution–chelating agent, protective polymer, antifoaming agent, and powdered whey.	165
	Water-Soluble Vitamins	
Thiamine	Microencapsulation in cellulose acetate phthalate with an acetone–benzene mixture as solvent.	166
Cyanocobalamin	Spray dry in starch succinate base–buffers and preservatives and add silicic acid.	167
Cyanocobalamin	Spray or vacuum dry in a galactomannan base from guar seed.	168
Ascorbic acid	Spray dry in methylcellulose, gum acacia, or gelatin–sucrose or lactose and magnesium stearate.	169
Ascorbic acid–salts and esters	Coating with small percentage of methyl polysiloxane.	170
Ascorbic acid	Spray with silicone lacquer and ethanol in fluidized bed dryer.	171
Ascorbic acid	Application of silicone oil coating.	172
Ascorbic acid	Microencapsulation in ethyl polymers using methyl ethyl ketone or with acetylcellulose in acetone.	166
Ascorbic acid	Disperse solid ascorbic acid in polyethylene glycol 6000 or 4000.	173
Ascorbic acid (calcium salt)	Microencapsulate in hydrogenated castor oil in ethanol.	174
Ascorbic acid	Coating with fats (mp 50–80°), lecithin, and glycerin esters.	175
Thiamine, riboflavin, or pyridoxine	Suspend in molten mixture of mono- and diglycerides of fatty acids and spray chill.	176
Niacinamide	Suspend in molten stearic acid, spray chill, heat for 14 days at 45°, and dust with silicic acid.	177
Niacinamide	Suspend in molten mixture of mono- and diglycerides of fatty acids, heat 14 days at 45°, and dust with silicic acid.	178
Thiamine, riboflavin, or niacinamide	Suspend in molten stearic, palmitic, or myristic acid or combinations thereof, and spray chill.	179
Thiamine, riboflavin, or niacinamide	Encapsulate in ethylcellulose–polyethylene in cyclohexane.	180
Vitamins	Coat with resins and polyvinyl compounds.	181

[a] Antioxidants and preservatives added are not listed. [b] Dry-Flo. [c] Micro-Cel. [d] Polyose D. [e] Zein.

vitamin A palmitate, *dl*-α-tocopheryl acetate, riboflavin, or perfumes which could be easily tableted. The adsorbents used included SiO_2, kaolin, $CaHPO_4$, and $MgCO_3$.

Protection from Light—Vitamins such as riboflavin and phytonadione, which are sensitive to light, particularly in solution, should be protected from light by suitable packaging of the vitamin solution. Surowiecki and Krowcznyski (185) reported that decay of riboflavin-5′-phosphate depended on temperature and intensity and wavelength of light. To prevent such decomposition, storage in amber glass capable of absorbing light up to a wavelength of 650 nm was recommended.

Lyophilization—For single or multivitamin solutions where instability of one or more vitamins in the formulation is a serious problem, lyophilization is an effective means of achieving improved vitamin stability. The lyophilization process has been applied in the preparation of multidose vials of vitamin B complex vitamins for parenteral use.

FORMULATION OF VITAMIN PRODUCTS

Aqueous Emulsions of Fat-Soluble Vitamins—Various surface-active agents (Table IV) have been used in the preparation of aqueous dispersions of fat-soluble vitamins. Optically clear dispersions can be made with efficient surfactants. Dispersions of single vitamins and multivitamin products containing vitamins A and E and cholecalciferol are prepared in aqueous media for both oral and intramuscular uses. A water-dispersible vitamin E compound was prepared by Cawley and Stern (193), namely, the polyethylene glycol ester of α-tocopheryl acid succinate.

Injectables—*Vitamins A and E and Cholecalciferol (vitamin D)*—Sobel (194) prepared veterinary injectables containing 0.0001–0.1% of vitamin A ester plus 0.005–0.06 g/ml of sorethytan monooleate in an aqueous, isotonic vehicle. Robeson (195) described a clear parenteral preparation in which vitamin A and cholecalciferol plus α-tocopherol or α-tocopheryl acetate were dispersed in an aqueous solution of α-tocopheryl polyoxyethylene glycol 1000 succinate. Aiello and Bauernfeind (196) prepared veterinary injectables of vitamins A, A–cholecalciferol, and A–E–cholecalciferol using a glyceryl triester of low molecular weight fatty acids (6–12 carbons and not more than 10% C-14 or greater) plus a polyoxyethylene-sorbitan ester of palmitic, stearic, oleic, or ricinoleic acid. A semisolid preparation for intramuscular injection of vitamins A and E and cholecalciferol was described by Feigh (197) as a substantially water-free mixture of the vitamins with polyethylene glycol 4000 and 200 plus antioxidant and preservative. Gherghinof *et al.* (198) prepared an aqueous injectable solution containing 22,000 IU/ml of vitamin A palmitate with 10 parts of polysorbate 80[3] to 1.1 parts of vitamin A. Butylated hydroxytoluene was added as antioxidant, the pH adjusted to 3–4 with ascorbic acid, and the solution sealed in vials under nitrogen and sterilized three times at 80° for 60 min with intervals of 24 hr. A solution was described which contained 300,000 IU of cholecalciferol/ml made with 15% (w/v) polysorbate 80[3] and 2.25% (w/v) isoamyl alcohol with ascorbic acid added to bring pH to 3–4. The vials were sealed under nitrogen without heat sterilization.

Vitamin K—Water-soluble derivatives of menadione such as menadiol tetrasodium diphosphate salt are used in injectable formulations. The fat-soluble phytonadione has been prepared in colloidal emulsion form with an efficient surfactant such as polyoxyethylene vegetable oil[4]. Fujita *et al.* (199, 200) prepared an injectable in which vitamin K was dissolved in a mixture of a hardened castor oil polyoxyethylene derivative and propylene glycol, after which sorbitol, trolamine, and water were added prior to sealing in ampuls and autoclaving for 30 min at 4.54 kg. Koshiro *et al.* (201) studied the compatibility of three

[3] Tween 80.
[4] Emulphor-620.

Table IV—Surfactants Used in Preparation of Aqueous Dispersions of Fat-Soluble Vitamins

Surfactants or Dispersing Agents	Reference
Polyalkalene oxide derivatives of partially esterified polyhydric alcohols or their anhydrides.	186
Bone gelatin from the lime process, ascorbyl palmitate, and a monoester of glycerin or of propylene glycol.	187
Polyoxyethylene glycol monoricinoleate containing 30–50 oxyethylene units.	188
Monoester (laurate, oleate, *etc.*) of polyethylene glycol 400 and a predominantly nonionic surfactant.	189
Polyoxyethylene vegetable oil[a] or other emulsifier[b].	190
Polysorbate[c] 40, 60, or 80–polyethylene glycol 200–600.	191
Polysorbate[d] 20 and algin[e].	192

[a] Emulphor EL-620. [b] Prosol E-4329. [c] Tween 40, 60, or 80. [d] Tween 20. [e] Tagat R, S, or O.

parenteral solutions of vitamin K with 98 commercial injectables.

Thiamine—For a single vitamin injectable with thiamine, the hydrochloride salt is generally preferred, but purity of the vitamin is an important factor. A special ampul grade of thiamine hydrochloride has been made for this purpose. Monciu and Boteanu (202) prepared 2.5 and 5% solutions of thiamine hydrochloride and found retention of at least 90% of initial concentration in the 2.5% solution after 4 years at room temperature and in the 5% solution after 5 years at room temperature. Various additives have been tested for their effect on the stability of thiamine hydrochloride solutions for injection. Ammar (203) compared the effects of edetic acid, *N*-hydroxyethyledetic acid, and pentetic acid and found the latter two to be superior to edetic acid in stabilizing thiamine. The optimum concentration of edetic acid was 3 mmoles/liter and 0.5 mmole/liter of *N*-hydroxyethyledetic acid. Ammar (204) also studied the effect of DL-α-lipoic acid, which at low concentrations (0.5–1.0 mmole/liter) increased the stability of solutions of thiamine hydrochloride for injection, but at higher concentrations (3–10 mmoles/liter) decreased the stability of thiamine hydrochloride. In the presence of 20 ppm of copper, the concentration of lipoic acid for maximum stability of thiamine was shifted from 0.5–1.0 mmole/liter, indicating that the concentration of additive for maximum stability of thiamine is dependent on the level of trace metals in the solution. Kirkova and Nedelova (205) studied the effect of different buffers, propyl gallate, benzyl alcohol, sodium edetate, sorbitol, glucose, and heat sterilization on the stability of thiamine solutions for injection. The most important factor was found to be the quality of the thiamine hydrochloride.

Taub *et al.* (206) reported that thiamine in parenteral solutions in admixture with riboflavin and niacinamide exhibited maximum stability with respect to potency and clarity of solution at pH 4 under a nitrogen atmosphere. In admixture with iron compounds, thiamine was more stable in the presence of ferrous gluconate than of iron peptonate or ferric ammonium citrate, and again, the optimum pH was 4. In these studies it was found that thiamine mononitrate is somewhat more stable than the hydrochloride.

Ascorbic Acid—Stable, buffered solutions containing 50–200 mg of ascorbic acid/ml were prepared by Cimenera and Wilcox (207) by buffering to pH 6.0–6.5 with trisodium phosphate, adding 0.5% phenol, heating 2-ml sealed ampuls at 100° for 10 min and cooling rapidly. Stability was achieved by adhering to rigid anaerobic conditions by the use of nitrogen throughout manufacture and avoiding contact with metals. Popovic *et al.* (208) obtained best stability in a parenteral solution containing 10 g of ascorbic acid, 4.75 g of $NaHCO_3$, 1 g of $Na_2S_2O_5$ and 0.1 g of edetic acid/liter and through which carbon dioxide was passed. Kassem *et al.* (209) studied the stabilizing effect of various metal complexing agents on ascorbic acid solutions. *N*-Hydroxyethylethylenediaminetriacetic acid was most effective, but the optimum concentration depended on the amount of heavy metal ions in the solution and had to be determined experimentally for each formulation.

Pyridoxine (Vitamin B_6)—Stabilized 2.5 and 5.0% solutions of pyridoxine were prepared by Nikolov and Nedelova (210) at pH 2.8–3.0 with 0.1% Na_2SO_3 added. The filling was done under a stream of nitrogen and aseptic conditions were used. Inoue *et al.* (211) determined the stability of an injectable solution of pyridoxamine phosphate in the presence of 70 other injectables.

Multivitamins—Ban (212) reviewed the preparation, storage, and usage of injectable solutions of the water-soluble vitamins. Boyazhieva *et al.* (213) described a veterinary preparation for intramuscular use containing ferro-dextran, gamma globulin, trace elements, and vitamins, which was claimed to be stable for 1 year. Blitz *et al.* (214) studied the stability of cyanocobalamin in vitamin B complex injectables and found cyanocobalamin to be unstable in the presence of thiamine and niacinamide at concentrations from 25–100 mg/cm^3 of each at pH 4.25 but relatively stable at lower concentrations of each component. Rigoli (215) reported good stability of cyanocobalamin and ascorbic acid after lyophilization of a solution containing both vitamins. Haeger and Nash (216) described a two-compartment syringe for injectable water-soluble vitamins with sodium ascorbate, folic acid, and niacinamide in the upper compartment and thiamine hydrochloride, riboflavin-5′-phosphate sodium, niacinamide, panthenol, pyridoxine, cyanocobalamin, and ferrous citrate in the lower compartment. A complete multivitamin injectable preparation was also described (217) which is similar to that described previously but with vitamin A palmitate, *d*-α-tocopheryl acetate, and ergocalciferol emulsified in the solution in the upper compartment by means of polysorbate 80 and propylene glycol.

The stability of vitamins after addition of injectable preparations to intravenous fluids is also a matter of concern. Although storage of such mixtures is normally for short periods, losses of labile vitamins such as vitamin A, thiamine, cyanocobalamin, and ascorbic acid can be significant and are higher during light exposure than in the dark. In addition, sorption of vitamins on the surface of plastic infusion fluid bags can contribute to unavailability of a portion of the vitamin content to the patient. Moorhatch and Chiou (218) studied the sorption of 10 vitamins on such bags. Howard *et al.* (219) studied the effect on vitamin A activity of storage of a parenteral nutrient solution in polyvinyl bags in the dark at 4°. After 8 and 72 hr and 2 weeks, the vitamin A content was 86, 73, and 23% of the initial concentration. Approximately 30% of the vitamin A losses were due to sorption on the plastic bags. The

use of bisulfite as a preservative in parenteral infusion fluids can cause high losses of added thiamine, particularly at ≥pH 5.5. In the laboratory only 3–8% retention of thiamine was found after 24 hr at room temperature in an amino acid infusion fluid at pH 6.5 and containing, according to label, 1 mg of sodium bisulfite/ml. Kobayashi and King (220) reported that the addition of vitamins to a protein hydrolysate–dextrose parenteral solution caused no physical incompatibilities.

Tablets—The fat-soluble vitamins A and E and cholecalciferol are normally incorporated into tablets in the form of dry, stabilized coated products or adsorbates as described above. The B complex vitamins, thiamine, riboflavin, niacinamide, and pyridoxine, which can contribute off-flavor to chewable tablets, are available in coated forms, usually containing 25–33% of the vitamin. Fatty acids or mono- and diglycerides of fatty acids are utilized as coating agents for effective masking of taste and also contribute to the stability of thiamine. Ascorbic acid is stabilized with a small percentage of ethylcellulose and is also available as granulations containing 90–95% ascorbic acid, which are particularly suited for preparation of high-potency ascorbic acid tablets by direct compression. Biotin and cyanocobalamin are used in tablets in the form of triturates, adsorbates, or spray-dried powders containing 0.1–1.0% of the vitamin to facilitate the distribution of the microgram quantities normally used. Nessel *et al.* (221) have studied the uniformity of distribution of cyanocobalamin in tablet formulations using 0.1 and 1% gelatin products and a 1% resinate in both wet-granulated and dry-blended formulations.

Single or multiple vitamin tablets have been made by both wet and dry granulation processes and by direct compression and either left uncoated or coated by compression, film, or sugar-coating processes. A number of reports dealing with vitamin tablet technology are listed in Table V. Seugling (239) has reviewed the use of various tableting aids in the development of pharmaceutical products, including conventional and chewable vitamin tablets. Lieberman and Lachman (240) have presented a comprehensive review of tablet technology which also deals with vitamin products. Wai *et al.* (241) studied stability of vitamin A, thiamine, and ascorbic acid compressed in eight commonly used solid vehicle matrixes. Mannitol and lactose were found to yield superior stability. All three vitamins were quite stable when the moisture content of the tablets was ≤1%. In multivitamin chewable tablets, these authors found that the use of coated ascorbic acid, thiamine, riboflavin, and niacinamide enhanced vitamin stability. The best stability results were obtained when vitamin A, ergocalciferol, and thiamine were granulated with one-fourth of the mannitol-magnesium stearate, ascorbic acid with one-half of the matrix, and the remaining B vitamins with one-fourth of the matrix. The use of water or dilute alcohol for granulation caused more rapid discoloration on storage than did alcohol granulation or dry slugging procedures.

Campbell and McLeod (39) studied the stability of vitamins in several commercial tablet formulations and found a rather wide range of stability for some of the labile vitamins. Maekawa *et al.* (242) studied the stability of vitamins in sugar-coated decavitamin tablets and the mutual interactions of the various vitamins. The best stability was obtained when vitamin A, ergocalciferol, calcium pantothenate, cyanocobalamin, and folic acid were in the coatings and the other vitamins in the tablet core. Bojarski *et al.* (243) compared vitamin stability in decavitamin tablets and dragees and found better stability in the tablets. Only thiamine and calcium pantothenate were unstable, and water had a major influence, especially on the stability of thiamine. Thiamine nitrate was more stable in these tests than thiamine hydrochloride. Ragazzi and Veronese (244) reported much better stability of vitamin A, ergocalciferol, and cyanocobalamin when these vitamins were protected by gelatin-sugar coating prior to incorporation into multivitamin tablets. Coated ascorbic acid, however, was not different from uncoated. Maekawa *et al.* (245) found much better stability of ascorbic acid in sugar-coated tablets than in uncoated tablets upon storage for 3 weeks at 37° and 74% relative humidity. Bolatre *et al.* (246) determined that ascorbic acid in tablets can discolor badly without much change in ascorbic acid content. Carstensen *et al.* (247) studied the degradation of thiamine tableted with magnesium stearate and microcrystalline cellulose. As the moisture level was increased to 5.5%, thiamine loss increased, but at higher moisture levels stability was enhanced with increased moisture content. The model proposed to explain this phenomenon was that thiamine dissolved in the water present adsorbs on the microcrystalline cellulose, and the thiamine present in the monolayer degrades totally, whereas the thiamine in layers beyond the monolayer does not degrade.

The preparation of sustained-release vitamin tablets has been a matter of interest, particularly in the case of high-potency ascorbic acid, but very little has been published on the technology of formulation of such tablets. Nuernberg *et al.* (248) described the preparation and *in vitro* release testing of 250-mg ascorbic acid tablets in which the release of the vitamin was sustained by the addition of more than 20% galactomannans. Cazals (249) prepared tablets of cyanocobalamin containing a mixture of mannitol and aminoacetic acid, which were claimed to yield prolonged and enhanced effectiveness. Kassem *et al.* (250) described a tablet of riboflavin-5′-phosphate with a maintenance dose in the core and an initial dose in the coating. The vitamin was embedded in a matrix of tragacanth, acacia, ethylcellulose, and stearic acid and granulated through a sieve to an optimal size of 1.6 μm. Subsequent coating with a thin layer of ethylcellulose suppressed the initial release. Hardening the granules at 30° for 2 hr improved the release. Lubrication with magnesium stearate and talc was recommended.

The major problem in formulating a sustained-release multivitamin product is to achieve full bioavailability of the vitamins in addition to sustained-release for a significant number of hours. Riboflavin is particularly troublesome in this regard due to its very low solubility in water. Morrison *et al.* (251) studied *in vitro* release rates and the corresponding physiological availability of riboflavin in sustained-release vitamin preparations and pointed out the frequent association of incomplete bioavailability with prolonged *in vitro* release. Other work by this group (252–255) pointed out similar difficulties with availability of riboflavin in normal, enteric coated, and chewable vitamin tablets. It was concluded that *in vitro* disintegration times longer than 1 hr or coating processes

Table V—Vitamin Tablet Technology

Vitamins	Formulation Technology	Reference
A, E, and cholecalciferol	Absorbed from oil solution on magnesium oxide with ascorbic acid and *dl*-α-tocopherol added; granulate with calcium pantothenate, starch, and calcium stearate before tableting.	184
Thiamine	Granulation with 1.5% ethylcellulose or 15% polyethylene glycol in alcohol plus dry binder.	222
Ascorbic acid	Addition of ~1% of sorbose, lactose, or a mixture of the two in the granulation tends to stabilize tablet color.	223
Ascorbic acid	Granulate 50–80 parts of ascorbic acid with 5–16 parts starch and 2.5–5 parts hydroxypropyl methylcellulose (viscosity 20–4000); add 0.25–0.35 liter of alcohol/kg and 5.5–16 parts starch; dry and pass through 10–16 mesh screen. Add lubricants (0.25–2 parts colloidal silicon, 0.5–2 parts hydrogenated vegetable oil, 0.1–0.5 parts zinc stearate, and 2.8–8 parts starch) and compress.	224
Ascorbic acid	Add physically modified starch, magnesium silicate as hardener, and hydrogenated vegetable oil as lubricant and compress directly.	225
Ascorbic acid	Vinyl acetate–crotonic acid copolymer yields harder and less friable tablets by direct compression than polyethylene glycol 6000.	226
Ascorbic acid	Microcrystalline cellulose is superior to microfine cellulose (less compression required and less capping).	227
Thiamine, ascorbic acid, or folic acid	Tablets formulated[a] and subjected to accelerated aging; ascorbic acid was unstable but thiamine and folic acid were stable.	228
Thiamine and ascorbic acid	Tablets coated with 2% aqueous solution of hydroxypropyl cellulose (viscosity 6.1 cps at 20°) were more stable than tablets coated with a sugar solution.	229
Thiamine and ascorbic acid	Tablets coated with syrup containing sugar, gelatin, and gum arabic over a subcoating of carboxymethyl–starch–talc disintegrated in 14 min while controls without the carboxymethyl–starch in subcoating took 42 min.	230
Thiamine and ascorbic acid	pH of tablets also containing aspirin adjusted to 2.5–4 with tartaric acid; tablets coated with 10% povidone and 4% shellac.	231
Cyanocobalamin and ascorbic acid	Granulating cyanocobalamin and ascorbic acid with trace element caseinates improved vitamin stability; without ascorbic acid caseinates did not improve cyanocobalamin stability.	232
Cyanocobalamin, thiamine, and pyridoxine	Best stability of cyanocobalamin achieved with cyanocobalamin in a separate layer in a sugar-coated tablet.	233
Multivitamin	Granulation with alcohol and addition of 5% povidone.	234
Multivitamin	Vitamin E adsorbed on silica gel and 0.5–5% finely divided silica gel added to smoothing syrup.	235
Multivitamin	Granulation of vitamin E and ascorbic acid.	236
Multivitamin	Effervescent tablets stabilized with 0.1 g of cyclamic acid and 0.2 g of α-aminoacetic acid/tablet.	237
Multivitamin	Lyophilization of vitamin substance in a solvent containing a binder, granulating and compressing; binders used were gum arabic, alginates, pectins, dextrins, glucose, povidone, polyvinyl alcohol, carboxymethyl cellulose, polyethylene glycol, *etc.*	238

[a] Formulated with Encompress Std.

can reduce the bioavailability of vitamins to humans and that any product with such characteristics should be tested in humans to determine that the vitamins are available.

Oral Single Vitamin Liquids—Vitamin A, in the form of an aqueous dispersion with an effective surface-active agent, yields much more rapid absorption *in vivo* than oil solutions. Adamski and Sawick (256) found the stability of vitamin A palmitate in aqueous dispersions to depend on the concentration of the vitamin A, the nature of the surfactant, and the buffer applied. A derivative of castor oil and ethylene oxide[5] yielded the best stability.

Stabilized aqueous solutions of thiamine were prepared by Bray (121) using thioglycerol, thiosorbitol, and thioglucose as stabilizing agents. Italfarmaco S.p.A. (257) described a 1% solution of thiamine hydrochloride with 5% povidone, 0.05% propyl gallate, and 0.005% sodium edetic acid, which was chemically and organoleptically stable for more than 2 years. Riboflavin and pyridoxine were also incorporated into similar compositions. Genova and Papazova (258) found cyanocobalamin stable for 5 months at 40° in a solution containing 100 μg/ml of cyanocobalamin in 1% solutions of orotic acid and monoethanolamine. Exposure to UV light caused destruction of cyanocobalamin, which was more rapid at pH 4.9–5.2 than at pH 3.9–4.2. Bajeva and Jonega (259) studied the stability of ascorbic acid–citrate formulations and found maximum stability with addition of 30% (v/v) propylene glycol and 0.1% cysteine hydrochloride.

Oral Multivitamin Liquids—General directions for preparation of stabilized multivitamin liquids have been given by Djourno and Thoumyre (260) and Belova and Litvinenko (261). Delgado *et al.* (90) prepared 10 different multivitamin drop formulations with various combinations of water, glycerin, and/or propylene glycol as vehicle. The most stable preparation contained 80% propylene glycol + 20% water with ethyl hydrocaffeate and Na_2Ca edetic acid. Parikh and Lofgren (91) studied the stability of seven different oral multivitamin drop preparations with sorbitol alone or in combinations with propylene glycel and glycerin in the aqueous vehicle. The studies showed: (*a*) butylated hydroxyanisole retards oxidative decomposition of vitamin A; (*b*) glycerin is a better substitute for a portion of the water than propylene glycol as far as stability of thiamine is concerned; (*c*) reducing the percentage of water by substituting propylene glycol or glycerin yields better stability of ascorbic acid; (*d*) stability of cyanocobalamin increased as pH was increased from 3.5 to 4.5; (*e*) folic acid, when in solution in preparations containing propylene glycol, was very unstable at pH 3.4. Biamonte and Schneller (63) also found folic acid in solution very un-

[5] Cremophor EL.

stable at acid pH, but when in suspension at low pH due to insolubility, folic acid is quite stable.

Stone (262) determined the stability of drop formulations containing thiamine, riboflavin, and niacinamide with and without ascorbic acid, using propylene glycol as a vehicle either alone or with 25 and 50% glycerin, simple syrup, or water. Greater retention of thiamine was found in solutions containing the greater percentage of water, whereas higher stability values were obtained for ascorbic acid in formulations containing lesser amounts of water. Similar relationships are seen in Figs. 3, 7, 9, and 10 where drop preparations show higher losses of thiamine than the more dilute elixirs or syrups, whereas ascorbic acid is more stable at pH 4 in the drop formulations than in the teaspoon dosage forms. Discoloration by yellowing and darkening was found by Stone (262) to be proportional to the percentage of water present.

Zoni and Lazzeretti (263) obtained satisfactory stability in a drop preparation containing B vitamins and L-lysine by adding povidone to the aqueous base. Synergistic enhancement of the stabilizing effect of povidone was found with the addition of polymerized povidone[6], 0.05% propyl gallate, and 0.005% (w/v) edetate disodium at pH 4. Maekawa and Egawa (264) achieved stability of an aqueous multivitamin preparation by the use of a partitioned container with vitamin A palmitate, niacinamide, and ascorbic acid in one chamber and thiamine in the other. The liquids contained stabilizing and flavoring agents and were admixed just prior to use. Youssef *et al.* (265) reported that the decomposition of vitamins and sodium metabisulfite is accelerated by storage of aqueous solutions in polyethylene containers.

Ointments, Creams, and Lotions—The utility of topically applied vitamins has been discussed by Siemers and Sleezer (266), DeRitter *et al.* (267), and Clement and Jones (268). Rubin (269) reviewed the percutaneous absorption of vitamins. Formulations of topical preparations containing panthenol were described by Rubin *et al.* (270), and the incorporation of various topically active vitamins into application forms was reviewed by DeRitter *et al.* (267). Anmo and Fueller (271) described a stable vitamin A ointment, and Haronikova and Mandak (272) found that the stability of vitamin A and cholecalciferol in an ointment was increased by adding a mixture of two antioxidants, nordihydroguaiaretic acid, butylated hydroxyanisole, and/or quercitin, or one antioxidant plus edetic acid or potassium pectinate. The composition of the ointment base influences the stability of vitamin A in the ointment (273, 274); the presence of polyethylene glycol and sodium lauryl sulfate in the base enhances the degradation of vitamin A. The decomposition of vitamin A palmitate in emulsion ointments is accelerated by lime water and lavindin (275), and the stability of vitamin A in cosmetic creams has been reported to be highly variable (276).

Syrups—Yashiki *et al.* (277) described a stable vitamin A palmitate syrup that prevented the sorption of vitamin A to plastic containers on storage. Bandelin and Tuschhoff (278) studied the stability of ascorbic acid in syrups at pH 3.0 and at concentrations of 25 and 100 mg/teaspoonful with two sucrose and one glycerin–sorbitol bases. Smaller losses of ascorbic acid were found with the glycerin–sorbitol combination, and the losses were relatively less at the higher concentration of ascorbic acid. The rate of loss of ascorbic acid in solution was determined (92) with ethanol, glycerin, propylene glycol, sorbitol, sucrose, corn sugar, or dextrose added and all yielded a stabilizing effect on ascorbic acid. Sucrose, sorbitol, glycerin, and propylene glycol were superior to the others in this respect. Vegetable gums added to such solutions to increase viscosity accelerated destruction of the vitamin. Vitamin B complex factors added to ascorbic acid syrups in USP syrup and in sorbitol appeared to increase the stability of ascorbic acid. The stability of ascorbic acid in glycerin and sorbitol bases containing salts and stabilizers was investigated by Agarwal and Agarwal (279). In solutions at pH 4 stored for 90 days at 47°, glycerin afforded better protection to ascorbic acid than sorbitol; the effect of stabilizers was less pronounced in the case of the glycerin base. Yao and Hsu (280) prepared multivitamin solutions in syrup, glucose, sorbitol, or sucrose solutions at pH 3.2, 4.5, and 7.0. In stability tests at 41.5 and 60° thiamine was more stable at pH 3.2 and ascorbic acid at pH 7.0. The use of antioxidants, including ascorbyl palmitate and butylated hydroxyanisole, and lecithin and an oxidized starch derivative, W14/S, was found by Fabrizzi *et al.* (281) to stabilize vitamin A, thiamine, and ascorbic acid in a syrup having low vitamin content. Ismaiel and Ismaiel (282) reported that thiamine, riboflavin, and ascorbic acid in syrups could be stabilized by replacing sucrose, vanillin, and various aldehyde-rich essential oils with sorbitol, sodium saccharin, sodium edetate, and essence of banana or apple.

Bartilucci *et al.* (283) studied the stability of cyanocobalamin in aqueous solutions of sorbitol, glycerin, dextrose, and sucrose stored at 25 and 45° for up to 140 days. Cyanocobalamin was compatible with sorbitol and glycerin, but dextrose and sucrose caused losses of cyanocobalamin with dextrose being worse. Gerber *et al.* (284) found that the instability of cyanocobalamin and ascorbic acid in solution with ferrous sulfate could be largely overcome by using 70% sorbitol as the vehicle.

Capsules—Campbell and McLeod (39) determined the vitamin contents of three multivitamin capsule products purchased on the retail market in Canada. Pantothenic acid appeared to be markedly affected by shelf life and storage conditions. In a shelf storage test of one product, pantothenic acid showed high losses and vitamin A, thiamine, and ascorbic acid small losses, while riboflavin, pyridoxine, and niacinamide were stable.

Stability tests of soft gelatin capsules in the laboratory revealed riboflavin, pyridoxine, vitamin E, ascorbic acid, biotin, and niacinamide to have excellent stability. Vitamin A and cholecalciferol showed reasonably good stability, while cyanocobalamin and folic acid tended to vary from product to product. Calcium pantothenate generally had poor stability at pH levels < 3.5, and panthenol was more stable than calcium pantothenate at < pH 4.5; > pH 4 both forms have good stability. Thiamine hydrochloride suffered high losses at pH > 4, whereas thiamine mononitrate showed fair to good stability up to pH 6.4. Macek *et al.* (4) also found thiamine mononitrate to be more stable than the hydrochloride salt in soft gelatin capsules as well as in multivitamin and vitamin B complex, dry-filled capsules. Acidification of the contents of the vitamin B complex capsules was necessary to stabilize the hydrochloride, but

[6] 15% Kollidon 17.

the mononitrate was stable without acidification, which was very destructive of calcium pantothenate. With thiamine mononitrate and a higher pH, it was possible to achieve good stability of both thiamine and calcium pantothenate.

PREDICTION OF VITAMIN STABILITY FROM ACCELERATED AGING TESTS

Garrett and Carper (285) proposed a procedure for predicting degradation of vitamins in liquid multivitamin preparations at normal shelf-life temperatures by measurement of degradation at several elevated temperatures and application of the Arrhenius equation. Garrett (286–288) applied this method in studies of complex multivitamin liquids and demonstrated the validity of the stability predictions for vitamin A, thiamine, ascorbic acid, dexpanthenol, folic acid, and cyanocobalamin. Since a slight change in vehicle composition does not significantly change the heat of activation or the rate of change of degradation with temperature, it was suggested by Garrett (287) that it may be practical in such cases to predict stability on the basis of one elevated temperature once the behavior of the system has been established at several elevated temperatures. The Arrhenius approach to stability prediction is limited according to Garrett (287) to degradation mechanisms that have heats of activation of sufficiently high magnitude (*i.e.*, in excess of 10 kcal/mole), but too high a heat of activation of components (sugars, *etc.*) that trigger a degradation of other components may give unreliable estimates of stability.

McLeod *et al.* (289) confirmed the validity of Garrett's method of predicting degradation rates of liquid multivitamin preparations at room temperature and described a simple graphical method of extrapolation to avoid the time-consuming mathematical calculations. Tardif (17) verified the applicability of the graphical method to the prediction of stability of a multivitamin tablet. Pelletier (290) found that storage tests at 50, 60, and 70° were suitable to predict the stability of thiamine and ascorbic acid in several multivitamin tablets and capsules and verified the predictions by analysis of samples stored at room temperature for 3 years. A short preliminary test at 70° was suggested for guidance in the selection of the most appropriate elevated temperatures, the equations used for the calculations were summarized, and a computer program for handling the calculations listed.

BIOAVAILABILITY TESTING OF VITAMIN PRODUCTS

Bioavailability of a vitamin may be defined as the relative amount of that vitamin contained in a dosage form, which enters the systemic circulation in an active form after administration as compared to the amount after administration of a comparable standard dose of the vitamin in fully available form such as a solution.

Various biochemical laboratory techniques have been employed in assessing bioavailability (291). The majority of these techniques fall into the following categories: (*a*) measurement of the nutrient level in the blood; (*b*) measurement of the urinary excretion rate of the nutrient; (*c*) measurement of urinary metabolites of the nutrient; (*d*) measurement of changes in blood components or enzyme activities that can be related to intakes of the nutrient; and (*e*) load, saturation, and isotopic tests. In the human population one is limited to urine and blood samples. Generally, one is restricted to measuring the concentration of a particular nutrient which is either excreted in the urine or circulating in the vascular system. Blood samples do permit the investigator a slightly greater latitude than urine, since the former can be partitioned into whole blood, serum, plasma, and/or red blood cells if a refinement of technique is justified. It is important that appropriate guidelines are available for the interpretation of the meaning of these measurements. A serum vitamin A level or a urinary value for riboflavin has little meaning until it can be compared with standard levels which have been measured experimentally under comparable conditions.

Measurement of absorption of vitamins *in vivo* requires specific and sensitive methods for determining the concentration of the vitamins or their metabolic products in human body fluids. For the fat-soluble vitamins A and E and cholecalciferol, measurement of blood levels provides a means of assessing absorption directly. For the water-soluble vitamins, except cyanocobalamin, urinary excretion of the vitamins or vitamin metabolites (indirect measurements) are most commonly used. Since normal human subjects consuming average diets without additional supplementation with vitamin products vary widely in the degree of saturation of their tissues with vitamins, relatively uniform excretion patterns can only be achieved by saturating the subjects with the vitamin under test before administering the test doses of the vitamin and measuring urinary excretions. For example, little or no urinary excretion of ascorbic acid is frequently observed following a 500-mg dose of ascorbic acid to subjects not previously saturated, whereas ~50% of such a dose is excreted in the urine of subjects after a state of saturation is reached.

Absorption and Excretion Patterns of the Vitamins—The patterns of absorption, metabolism, and excretion of the individual vitamins that serve as a basis for the test procedures are as follows:

Vitamin A—For evaluation studies in humans, blood level measurements are the only practical means of assessing the absorption of this nutrient. There are, however, many factors that influence the absorption of vitamin A, including type and amount of fat in the diet; interfering substances in diet such as nitrites, ethanol, absorbants, and drugs; size of dose; emulsion (rapid absorption) *versus* oil solution (slower absorption); vitamin E adequacy of subject; zinc adequacy of subject; state of protein nutrition of subject; respiratory, intestinal, renal, or parasitic disease in subject.

By the use of normal subjects in a cross-over design, control of diet, size of dose and the vitamin E level accompanying the dose, and measurement at specific time intervals after dosing to establish a tolerance curve, it is possible to utilize blood levels in humans for assessment of bioavailability of vitamin A products. Although adequate analytical methods are available for measuring blood levels of vitamin A, the difficulties in withdrawing repeated samples of blood under proper supervision make this type of testing unattractive, even when the facilities for conducting such tests are available. In addition, large numbers of subjects are needed if results within a small error range are desired.

Cholecalciferol—The metabolism of cholecalciferol in humans involves conversion to hydroxylated derivatives. Measurement of cholecalciferol or its metabolites in the blood is possible but has not been applied for bioavailability testing. Since cholecalciferol is normally present in a multivitamin product in the same physical form as vitamin A (*i.e.*, as an oil solution, an emulsion, or a dry stabilized beadlet or powder), evidence for bioavailability of vitamin A is likely to be valid for cholecalciferol as well in the majority of products.

Vitamin E—Bioavailability of vitamin E can also be evaluated by determining blood level curves after loading doses. Methodology for determining blood levels of tocopherol has been reviewed by Bunnell (292). The factors listed earlier which influence the absorption of vitamin A may also affect absorption of vitamin E. In addition, the differing biopotencies of the *d*- and *dl*-forms of tocopherol, the differences in absorption between tocopherol, tocopheryl acetate, tocopheryl succinate, and tocopheryl polyethylene glycol 1000 succinate (293) and the possible need to measure specific tocopherols in blood are factors which must be considered in interpreting blood level data. The practical difficulties in conducting blood level studies, as noted under *Vitamin A*, apply also to such tests of vitamin E in blood.

Vitamin K—Increases in blood levels of vitamin K after loading doses have not been used as a measure of bioavailability of dosage forms since most supplemental vitamin K is given parenterally. Oral doses in the form of an oil solution or emulsion would not be expected to present significant problems with bioavailability. Water-dispersible beadlets containing phytonadione have been demonstrated to be biologically available *via* animal tests and are used as a reference standard for animal bioassays (294). Hence, if these are used in solid dosage forms, a rapid *in vitro* disintegration would be indicative of adequate bioavailability.

Thiamine—Of the various biochemical procedures which have been developed for assessing thiamine absorption, the most common one is the measurement of urinary levels. At levels in the range of the daily requirement, thiamine is absorbed fairly well. Thomson (295) reported that 54% of the 1-mg dose of ^{35}S-labeled thiamine hydrochloride given orally after an overnight fast was found in the urine within 24 hr by radioactivity measurements. Continuing the urine collection in one subject for 9 days gave only an additional 7.5% of the dose in the standard test. It appears that the absorption of thiamine in humans is mainly in the upper small intestine. Melnick *et al.* (296) and Jowett (297) also concluded that the absorption of thiamine seems to be confined largely to the upper intestinal tract.

As the oral dose of thiamine is increased (298, 299), the percentage absorption decreases progressively although the total amount absorbed increases. With a single oral dose of 5 mg given on successive days, Schultz *et al.* (300) reported recoveries in urine of 24–42% of the dose and levels of thiamine in the stools were increased. On giving 10-mg doses, only 19–21% was recovered in the urine. The percentage of a thiamine test dose excreted is increased slightly when the dose is given with food (298).

Riboflavin—Riboflavin is absorbed efficiently by humans in any practical dosage range. Friedemann *et al.* (298) state that at least several hundred milligrams of riboflavin is absorbed readily. Human urinary excretion studies by Morrison and Campbell (299) showed that the total extra excretion of riboflavin averaged close to 60% of the oral dose over the dosage range of 1–20 mg. The studies have shown also that 50% or more of an oral dose of riboflavin up to 30 mg is excreted in the urine within 24 hr when the dose was given after breakfast. Levy and Hewitt (301) obtained only 19.3% excretion of a dose of 41 mg of riboflavin phosphate given on an empty stomach as compared to 52.6% when the same dose was given after breakfast.

Niacin or Niacinamide—Hundreds of milligrams of niacin or niacinamide are absorbed readily after oral dosage. Approximately three-fourths of such large doses can be accounted for in the urine of human subjects within 72 hr as a combination of niacin, niacinamide, trigonelline, N^1-methylnicotinamide, and N^1-methyl-2-pyridone-5-carboxamide. The latter is the main metabolite appearing in the urine. If the rate of release of niacin is retarded, the metabolism proceeds to a somewhat greater extent to the end product, the pyridone.

Pyridoxine—Pyridoxine is absorbed readily from the intestinal tract by human subjects. Efficient absorption of several hundred milligrams is normal. Only a small fraction of ingested pyridoxine is excreted unchanged in the urine (only 4–8% of doses in the range of 8–100 mg). In humans, 4-pyridoxic acid accounts for 70–90% of the urinary excretion products of pyridoxine (302).

Calcium Pantothenate or Panthenol—Both pantothenic acid (or its calcium salt) and panthenol are absorbed readily from the intestinal tract. At RDA dose levels, only a small percentage of the dose is excreted in the urine as pantothenic acid but the excretion of the vitamin *per se* increases to ~16% after a 100-mg oral dose and to 36% of a 250-mg dose (303).

Biotin—One milligram of biotin was administered orally to a human male subject on each of two successive days. Urinary excretion of biotin, measured microbiologically with *Lactobacillus arabinosus* as the test organism, amounted to 20 and 48% of the dose in the 24-hr periods after the two doses (304). Although bioavailability of biotin in vitamin products has not been reported, urinary excretion measurements of biotin after oral dosage to saturated subjects may represent a possible approach to this problem.

Folic Acid—By saturating human subjects with high doses of folic acid (10 mg on the first day, 5 mg on the second day, 2 mg on the third and fourth days, and every second day thereafter while excretion tests are in progress), it is possible to obtain urinary excretion of a reasonable percentage of a normal test dose (305). In the author's trials, this technique yielded 5–13% excretion of an oral dose of 0.65 mg of folic acid in a group of five subjects.

Cyanocobalamin—Cyanocobalamin is absorbed maximally in the middle segment of the small intestine and is poorly absorbed in the distal segments (306–308). The size of the dose significantly influences the percent absorption (309). Conley *et al.* (310) reported that oral doses up to 10 mg of cyanocobalamin resulted in no detectable increase of the vitamin in urine within 48 hr. Normal subjects and patients with pernicious anemia behaved similarly. Thus, no bioavailability test for cyanocobalamin can be based on

urinary excretion measurements. Adams *et al.* (311) state that cyanocobalamin absorption can only be studied by using radioactive cyanocobalamin. These authors used a whole-body counting technique in their absorption studies on human subjects. Such techniques are beyond the capability of many laboratories. It is evident that there is no simple method of assessing the bioavailability of cyanocobalamin in pharmaceutical products which would permit testing of bioavailability.

Ascorbic Acid—Ascorbic acid is absorbed efficiently from the upper part of the small intestine. Nicholson and Chornock (312), using an intubation technique, found that 50% of an oral dose of 600 mg of ascorbic acid given in 600 ml of water or saline was absorbed in 1 hr. Saturation of the subjects by giving 500 mg of ascorbic acid daily in addition to the regular diet had no significant effect on their absorption of ascorbic acid. The authors state that the upper part of the small intestine has a capacity for absorption of ascorbic acid far in excess of the optimal daily requirement. Kübler and Gehler (313) studied blood serum levels and rates of urinary excretion of ascorbic acid in previously saturated subjects and concluded that the rate of absorption in the distal part of the absorbing intestine was about half the rate in the proximal portion. These authors found that with increasing doses of ascorbic acid the percent absorption decreases. They reported 71.5% absorption of a dose of 180 mg, 49.5% for 1.5 g, and 16.1% for 12 g. In the dose range of 1.5–12 g, the mean urinary excretion was 62 ± 3.7% of the absorbed ascorbic acid. Proportionality between ingestion and intestinal absorption was claimed up to a single dose of ~180 mg.

Stewart and Booth (314) gave one subject single doses of ascorbic acid at 4-day intervals of 0.2, 0.4, 0.5, 0.7, 1.0, 1.5, 2, and 3 g. Total urinary excretion in up to 30 hr rose steeply up to the 0.5-g dose where ~50% was excreted, and then much less steeply with increasing doses, with an excretion of ~16.7% of the 3-g dose. At the lowest dosage in the range (200 mg) there is practically no excretion of the ascorbic acid dose in the feces. Chieffi and Kirk (315) reported fecal excretion averaging 1.2 mg of ascorbic acid daily by 13 elderly men on an ordinary diet. With a 200-mg supplement of ascorbic acid in the form of a tablet, the fecal excretion averaged 1.5 mg/day, indicating no significant excretion of the supplement in the feces.

Absorption Tests—*Fat-Soluble Vitamins (Blood Level Tolerance Test): Vitamin A*—The application of the blood level tolerance test to determination of the biological availability of vitamin A in three different multivitamin capsules was reported by Sobel and Rosenberg (316). Either 1000 or 2000 IU of vitamin/kg of body weight was administered to eight normal adults in the postabsorptive state. Blood specimens were taken prior to the test and 3, 6, 9, and 24 hr posttreatment. The capsules were swallowed without chewing. As a reference of absorption, oleovitamins A and D was used. Intervals betweeen doses were 2–7 days. If the response as serum vitamin A for the oil dose is taken as 100%, the three capsules showed comparative responses of 198, 185, and 70% based on the mean maximal rise and ~150, 170, and 50% based on the area within the tolerance curves for the 24-hr period.

The authors mention three factors that influence the physiological availability of fat-soluble vitamins: (*a*) the site at which the capsule releases its contents, (*b*) the stability of vitamin A in the GI contents, (*c*) the state of dispersion of the vitamin A released to the GI content (finely dispersed particles are absorbed more readily). The study of Sobel and Rosenberg illustrates some of the difficulties in assessing bioavailability in humans by measuring blood levels of a fat-soluble vitamin such as vitamin A. Such tests have not been utilized to any great extent for determining bioavailability of pharmaceutical products.

Vitamin E—Increases in blood plasma levels of tocopherol in response to oral doses have been reported. For example, Filer *et al.* (317) gave premature and full-term infants oral doses of α-tocopherol and α-tocopheryl esters of 20 mg/kg of body weight and measured blood level increases after 3, 6, 9, 12, and 24 hr. No significant differences in plasma tolerance curves were found between tocopherol and its esters in healthy infants. In disease states diagnosed as fibrocystic disease of the pancreas, diarrhea, and cirrhosis, low vitamin E tolerance curves were observed. Metabolic disorders associated with hypercholesterolemia gave abnormally high values for the areas under the tolerance curve.

Week *et al.* (318) gave oral doses of 1000 mg of *dl*-α-tocopherol or an equivalent amount of *dl*-α-tocopheryl acetate in corn oil in capsules to 10 male and 10 female adult subjects. Blood levels of tocopherol were measured at 0, 2, 4, 5, 6, 8, 12, and 24 hr. The average area under the tolerance curve was 35% higher for free tocopherol than for the acetate ester.

Overman *et al.* (319) found higher blood levels after oral doses of *dl*-α-tocopheryl acetate to humans in the form of aqueous emulsion than after a capsule dosage. They concluded that the amount of vitamin E given and the vehicle are important in determining the effectiveness of vitamin E preparations in increasing the plasma levels of free tocopherol.

Water-Soluble Vitamins (Urinary Excretion Tests)—The human bioassay technique for determining bioavailability of water-soluble vitamins was introduced by Melnick *et al.* in 1945 (320, 321). The principle of this method was summarized as follows: "In normal human subjects the urinary excretion of the water-soluble vitamins, as such or as their derivatives, is directly proportionial to the quantity consumed, provided that at the time of the tests the subjects are subsisting on an adequate diet. The linear dose–response relationship established by feeding the vitamins in pure solution, *i.e.*, in their most completely available form, constitutes the basis of the bioassay."

Outline of the Testing Program—A group of at least five nutritionally normal subjects is chosen. If possible, the subjects should keep their diet the same on two consecutive urine collection days and avoid vitamin supplements and foods unusually high in vitamins such as liver. Urine is collected over a 24-hr period for each of these 2 days. Tuesday and Wednesday are the days of choice for conducting the experiment. Thus, urine collections are made from Tuesday morning after the first voiding and continued until after the first voiding the following morning and repeated the second day similarly. The two 24-hr samples are collected in amber bottles containing a total of 20 ml of 3.5 *N* H_2SO_4 or 2 g of thymol and kept in the refrigerator whenever feasible. On the first day the subjects ingest nothing but their usual diet; the urinary

excretion for this period represents the basal urinary excretion. At the beginning of the second day the subjects take either a standard control dose or a test dose which is reversed to each subject the following week. The control dose contains known amounts of the pure vitamins on test in aqueous solution or suspension. By subtracting the basal excretion from the excretion after the control or test dose, the extra urinary excretion due to dose is determined. The results for each subject are expressed in terms of percent of dose. These tests can be run weekly. The control dose and the test dose should contain similar concentrations of the vitamins.

Saturation Dosage—To ensure maximum and uniform urinary excretion of the extra vitamins fed, it is necessary to saturate the subjects with the vitamins under test. Since the excretion of an individual vitamin is relatively independent of the other vitamins, a high potency multiple vitamin preparation can be used, provided it contains at least the following quantities of the vitamins under test: thiamine (5 mg); riboflavin (5 mg); ascorbic acid (500 mg); calcium pantothenate (50 mg); niacinamide (50 mg); pyridoxine (5 mg). The saturating dose is taken for 4 days and 1 day without this dosage is allowed before the day on which the basal urine is collected. (The saturating dosage schedule for folic acid was mentioned previously.)

Control and Test Doses—The standard control dose of pure vitamins is given in water. The amount of the control dose of each vitamin should be as nearly equal as possible to the amount of each vitamin in the pharmaceutical product to be tested. Following are suggested dosing ranges of the vitamins for use in bioavailability tests:

Thiamine	5–15 mg
Riboflavin	5–30 mg
Niacinamide	50–100 mg
Ascorbic acid	500–1000 mg
Calcium pantothenate or panthenol	25–100 mg
Pyridoxine	5–15 mg
Folic acid	0.5–1 mg

Urine Assay Methods—The following methods may be used for measuring excretions of the vitamins or metabolites:

Thiamine	—fluorometric assay by the thiochrome method of Mawson and Thompson (322)
Riboflavin	—direct dilution with pH 6 acetate buffer in final solution for fluorometric measurement
Niacinamide	—assay of the metabolite, N^1-methylnicotinamide, by the method of Pelletier and Campbell (323)
Calcium pantothenate	—microbiologically with *L. plantarum* as test organism and the medium of Skeggs and Wright (324)
Pyridoxine	—assay of the metabolite, 4-pyridoxic acid, by the method of Pearson (325)
Folic acid	—microbiologically with *Streptococcus faecalis* as test organism and the medium of Rabinowitz and Snell (326) modified by the omission of folic acid and the addition of 2 μg of pyridoxamine/tube
Ascorbic acid	—colorimetrically, using the dichlorophenolindophenol–xylene technique of Rubin *et al.* (327)

Basal and Extra Excretions—In Table VI the average basal excretions and average extra urinary excretions for saturated subjects receiving the above doses are presented.

Availability of a Test Dose—The physiological availability of a test preparation is ascertained by the following calculation:

$$\frac{\text{Percent recovery of test dose}}{\text{Percent recovery of control dose}} \times 100 = \text{Percent availability}$$

Due to the variability of physiological responses in different subjects and in the same subject from time to time, the analytical errors, and the fact that availability is measured as the ratio of two recoveries, which in themselves are the difference between two excretion values, an error of ±20% is not thought excessive. Therefore, a value ≥80% is considered indicative of satisfactory availability. Oser *et al.* (321) present data obtained by this technique on various multivitamin tablets and discuss some factors that might lead to low availabilities.

Rate of Excretion of Dose—According to Johnson *et al.* (328) urinary excretion of oral vitamin doses dissolved in water is practically complete in 8–10 hr. Results obtained in the author's laboratory using the sodium salt of riboflavin phosphate as the test material indicate that this is essentially correct. In these studies a dose of the phosphate, equivalent to 30 mg of riboflavin, was dissolved in water and taken by the test subjects. The hourly excretion (as percent of dose) is summarized below.

Hours after Dose	Average Excretion of Dose, %
0–1	6.5
1–2	12.9
2–3	9.4
3–4	6.0
4–5	3.8
5–6	2.8
6–7	2.2
7–8	1.3
Total percentage of dose excreted in 8 hr	44.9

From the data, one would not expect much excretion beyond a 10-hr collection period. Excretion data after oral dosage of thiamine, ascorbic acid, and niacinamide show that the bulk of the urinary output occurs in the first 12 hr postdose.

However, when the dose is taken in capsule or tablet form, significant excretion may occur in the 12–24-hr period postdose. Therefore, as a standard procedure, it is advisable to run both test and control collections for 24 hr.

Correlation of Excretion Tests with In Vitro *Disintegration and Dissolution Tests*—There is considerable evidence that the pharmaceutical form has a marked influence on the availability of vitamins to the body. Chap-

Table VI—Average Basal Urinary Excretions and Average Extra Excretions of Vitamins or Metabolites After Control Doses

Vitamin	Vitamin or Metabolite Measured	Basal Excretion (on normal diets), mg	Approximate Extra Excretion Due to Control Dose[a]
			Percent of dose
Riboflavin	Riboflavin	0.5–2.5	45–70
Thiamine	Thiamine	0.3–0.5	5–20[b]
Ascorbic acid	Ascorbic acid	30–60	40–60
Calcium pantothenate	Pantothenic acid	4–9[c]	10–20
Panthenol	Pantothenic acid	4–9[c]	10–20
Niacinamide	N^1-Methylnicotinamide[d]	6–12	10–20
Pyridoxine	4-Pyridoxic acid[e]	0.6–1.2	10–15
Folic acid	Folic acid	0.003–0.006	10–15

[a] If the test product is completely available, the percent excretion of the test dose will be equivalent within experimental limits to the percent excretion of the control dose given in aqueous solution. [b] In the case of thiamine, the percent of dose excreted diminishes markedly as the dose is increased; in the case of a 30-mg dose, the excretion may be only ~2–5% of the dose. [c] Expressed in terms of pantothenic acid. [d] When N^1-methylnicotinamide hydrochloride is used as the standard, multiplication of the urinary results by 0.707 converts them to the equivalent niacinamide levels. [e] To convert milligrams of 4-pyridoxic acid to pyridoxine hydrochloride, multiply by 1.123. At higher doses the percent of dose excreted as 4-pyridoxic acid will be higher.

man *et al.* (252) found by a specified *in vitro* test that vitamin tablets that did not disintegrate in 1 hr were not fully available to the body, as judged by the amount of riboflavin excreted in the urine. This was confirmed by Morrison *et al.* (253) and has been the basis for a regulation promulgated under the Canadian Food and Drugs Act setting a 1-hr time limit for the disintegration of ordinary tablets. Middleton *et al.* (329) examined the relationships between *in vitro* dissolution rate, disintegration time, and physiological availability of riboflavin in sugar-coated tablets. They found a close relationship between disintegration time and dissolution rate, and both *in vitro* procedures correlated reasonably well with physiological availablity as measured by urinary excretion of riboflavin. It was concluded that either of these two *in vitro* procedures can provide a useful estimate of the availability to the body of riboflavin in sugar-coated tablets.

Libby *et al.* (330) studied riboflavin excretion by human subjects ingesting sustained-release capsules or tablets which did not pass the official USP disintegration test. Urinary recoveries of riboflavin from these preparations were extremely low in comparison to those obtained with an equal dose of riboflavin standard. These authors also showed reduced urinary excretion of riboflavin when six tablets containing calcium, ascorbic acid and cholecalciferol were fed together with fully available riboflavin tablets. Ida *et al.* (331) reported a lower rate of excretion in the first 6 hr after dose of compressed film-coated tablets, even though these disintegrated in 4 min in water and in 5–10 min in simulated gastric juice by the USP XVI method. These workers, however, did not measure excretions in later hours, which may have indicated complete absorption of the riboflavin over a longer period.

Evaluation of the absorption of most of the vitamins in a multivitamin preparation is a very time-consuming and expensive operation, involving skilled staff and analytical methodology for vitamin metabolites which is not normally used in vitamin assay laboratories. Emphasis in various studies of vitamin absorption has been placed on the excretion of riboflavin, primarily because of its relative insolubility compared with most other water-soluble vitamins. With the exception of biotin, the solubility of which is close to that of riboflavin in water, and folic acid, the solubility of which is strongly dependent on pH, all other vitamins are many times more soluble than riboflavin. Thus, if a tablet granulation is made with a uniform mixture of the water-soluble vitamins and water-dispersible beadlets or powders containing the fat-soluble vitamins (a usual procedure), the finding in a urinary excretion test that the riboflavin from the finished tablet is fully available to the body makes it evident that the tablet has disintegrated suitably. Since the riboflavin has then obviously dissolved in order to have been absorbed in the upper part of the intestinal tract, it is most likely that the more soluble vitamins and the readily dispersible powders have also been readily available for absorption. If, on the other hand, any of the other individual vitamins are coated or added to the tablet mix in a different manner for a special solid dosage form than the riboflavin component, then it becomes desirable to establish the correlation of disintegration and/or dissolution tests with an *in vivo* absorption test for such vitamins. Once a relationship of *in vivo* tests to *in vitro* tests has been established, the *in vitro* tests should be an adequate means of control for ensuring suitable absorption characteristics of solid pharmaceutical dosage forms in routine pharmaceutical manufacturing operations.

REFERENCES

(1) H. L. Newmark, U.S. Patent 2,759,870, Aug. 21, 1956.

(2) M. Kuhnert-Brandstaetter and A. Burger, *Pharm. Ind.*, **31**, 496 (1972).

(3) R. R. Williams, R. E. Waterman, J. C. Keresztesy, and E. R. Buchman, *J. Am. Chem. Soc.*, **57**, 536 (1935).

(4) T. J. Macek, B. A. Feller, and E. J. Hanus, *J. Am. Pharm. Assoc., Sci. Ed.*, **39**, 365 (1950).

(5) T. J. Macek, *Am. J. Pharm.*, **132**, 433 (1960).

(6) R. W. Lehman, J. M. Dieterle, W. T. Fisher, and S. R. Ames, *J. Am. Pharm. Assoc., Sci. Ed.*, **49**, 363 (1960).

(7) S. R. Ames,W. J. Swanson, and R. W. Lehman, *ibid.*, **49**, 366 (1960).

(8) E. DeRitter, *J. Pharm. Sci.*, **50**, 510 (1961).

(9) W. E. Stieg and J. A. Kardys, U.S. Patent 2,907,696, Oct. 6, 1959.

(10) J. A. Keverling Buisman, K. H. Hanewald, F. J. Mulder, J. R. Roborgh, and K. J. Keuning, *J. Pharm. Sci.*, **57**, 1326 (1968).

(11) K. H. Hanewald, F. J. Mulder, and K. J. Keuning, *ibid.*, **57**, 1308 (1968).

(12) A. Verloop, A. L. Koevoet, and E. Havinga, *Rec. Trav. Chim.*, **76**, 689 (1957).

(13) J. L. M. A. Schlatmann, J. Pot, and E. Havinga, *ibid.*, **83**, 1173 (1964).

(14) E. J. DeVries, F. J. Mulder, and B. Borsje, *J. Assoc. Off. Anal. Chem.*, **60**, 989 (1977).

(15) T. Takahashi and R. Yamamoto, *J. Pharm. Soc. Jpn.*, **89**, 909, 914, 919, 925, 943 (1969).

(16) J. T. Carstensen, *J. Pharm. Sci.*, **53**, 839 (1964).

(17) R. Tardif, *ibid.*, **54**, 281 (1965).

(18) R. C. Shah, P. V. Raman, B. M. Shah, and H. H. Vora, *Drug Dev. Commun.*, **2**, 393 (1976).

(19) L. T. Grady and K. D. Thakker, *J. Pharm. Sci.*, **69**, 1099 (1980).

(20) W. John and W. Emte, *Hoppe-Seyler's Z. Physiol. Chem.*, **268**, 85 (1940).

(21) V. L. Frampton, W. A. Skinner, P. Cambour, and P. S. Bailey, *J. Am. Chem. Soc.*, **82**, 4632 (1960).

(22) J. C. Vire, G. J. Patriarche, and G. D. Christian, *Anal. Chem.*,

51, 752 (1979).
(23) B. K. Dwivedi, R. G. Arnold, and L. M. Libbey, *J. Food Sci.*, **37,** 689 (1972).
(24) B. K. Dwivedi and R. G. Arnold, *J. Agric. Food Chem.*, **21,** 54 (1973).
(25) B. K. Dwivedi, *Diss. Abstr. Int. B.*, **83,** 4851 (1973). Available from University Microfilms, Ann Arbor, Mich., Order No. 72-31, 863.
(26) E. R. Garrett, *Am. Perfum. Aromat.* **8,** 23, (1959).
(27) N. N. Mosolov, *Ref. Nauchn. Soobshch.-Vses. Biokhim, S'ezd., 3rd*, **2,** 61 (1974).
(28) E.A. Mulley, C. R. Stumbo, and W. M. Hunting, *J. Food Sci.*, **40,** 989 (1975).
(29) E. Ralchovska, *Khranit. Prom.*, **26,** 19 (1977).
(30) K. Kobayashi, *Vitamins*, **45,** 239 (1972).
(31) K. Kaya, *Agric. Biol. Chem.*, **41,** 2055 (1977).
(32) I. Stepuro and Y. M. Ostrovskii, *Vestsi Akad. Navuk BSSR Ser. Biyal Navuk*, **3,** 51 (1974).
(33) P. N. Moorthy, K. N. Rao, and K. Kishore, *Radiat. Eff. Lett.*, **43,** 1 (1979).
(34) P. Karrer, H. Salomon, K. Schöpp, E. Schlitter, and H. Fritsche, *Helv. Chim. Acta*, **17,** 1010 (1934).
(35) J. Surowiecki and L. Krowcznyski, *Acta Pol. Pharm.*, **29,** 399 (1972).
(36) D. V. Frost and F. C. McIntire, *J. Am. Chem. Soc.*, **66,** 425 (1944).
(37) J. A. Campbell, *Can. Med. Assoc. J.*, **68,** 103 (1953).
(38) J. A. Campbell, *J. Am. Pharm. Assoc., Sci. Ed.*, **44,** 598 (1955).
(39) J. A. Campbell and H. A. McLeod, *ibid.*, **44,** 263 (1955).
(40) A. D. Marcus and J. L. Stanley, *J. Pharm. Sci.*, **53,** 91 (1964).
(41) T. Macek and B. Feller, *J. Am. Pharm. Assoc., Sci. Ed.*, **44,** 662 (1955).
(42) D. L. Ely, Jr., *Diss. Abstr. Ind. B* **39,** 1753 (1978). Available University Microfilms, Ann Arbor, Mich., Order No. 78-18755.
(43) L. J. DeMerre and C. Wilson, *J. Am. Pharm. Assoc., Sci. Ed.*, **45,** 129 (1956).
(44) E. Berelko, G. S. Babakina, I. V. Berezovskaya, V. S. Degilova, V. V. Sukhanov, and V. L. Tal'roze, *Khim.-Farm. Zh.*, **11,** 94 (1977).
(45) M. I. B. Dick, I. T. Harrison, and K. T. H. Farrer, *Austr. J. Exp. Biol. Med.*, **26,** 239 (1948).
(46) E. L. R. Stokstad, D. Fordham, and A. DeGrunigen, *J. Biol. Chem.*, **167,** 877 (1947).
(47) F. Y. Tripet and U. W. Kesselring, *Pharm. Acta Helv.*, **50,** 318 (1975).
(48) N. G. Levandoski, E. M. Baker, and J. E. Canham, "Abstracts," 6th Intern. Congr. of Biochem., New York, N.Y., 1964, V-G-176.
(49) M. C. Uprety, B. Revis, and S. M. Jafar, *J. Pharm. Sci.*, **52,** 1001 (1963).
(50) Y. Ogata, Y. Kosugi, and T. Morimoto, *Tetrahedron*, **24,** 4057 (1968).
(51) M. A. Kassem, A. A. Kassem, and H. O. Ammar, *Pharm. Acta Helv.*, **44,** 667 (1969).
(52) K. Hayakawa and Y. Hayashi, *J. Nutr. Sci. Vitaminol.*, **23,** 395 (1977).
(53) P. Finholt, R. B. Paulssen, and T. Higuchi, *J. Pharm. Sci.*, **52,** 948 (1963).
(54) P. Finholt, R. B. Paulssen, I. Alsos, and T. Higuchi, *ibid.*, **54,** 124 (1965).
(55) A. R. Rogers and J. A. Yacomeni, *J. Pharm. Pharmacol.*, **23** (Supp.), 218 S (1971).
(56) S. M. Blaug and B. Hajratwala, *J. Pharm. Sci.*, **61,** 556 (1972).
(57) J. E. Tingstad, L. H. MacDonald, and P. D. Meister, *ibid.*, **52,** 343 (1963).
(58) A. Sattar, J. M. DeMan, and J. C. Alexander, *Can. Inst. Food Sci. Technol. J.*, **10,** 65 (1977).
(59) T. Uno, S. Kitazawa, M. Kubota, A. Maeda, S. Terramura, and Y. Okada, *Yakuzaigaku*, **33,** 101 (1973).
(60) W. Switek and F. Modrzejewski, *Pharmazie*, **31,** 181 (1976).
(61) R. Huettenrauch, *ibid.*, **23,** 150 (1968).
(62) A. S. Gambier and E. P. G. Rahn, *J. Am. Pharm. Assoc., Sci. Ed.*, **46,** 134 (1957).
(63) A. R. Biamonte and G. H. Schneller, *ibid.*, **40,** 313 (1951).
(64) A. T. Darnule and R. B. M. Colah, *J. Inst. Chem. (India)*, **44,** 188 (1972).
(65) M. Blitz, E. Eigen, and E. Gunsberg, *J. Am. Pharm. Assoc., Sci. Ed.*, **46,** 134 (1957).
(66) B. A. Feller and T. J. Macek, *ibid.*, **44,** 662 (1955).
(67) F. El-Khawas and N. A. El-Gindy, *Pharm. Ind.*, **39,** 1019 (1977).
(68) S. Scheindlin, A. Lee, and I. Griffith, *J. Am. Pharm. Assoc., Sci. Ed.*, **41,** 420 (1952).
(69) D. B. Hand, E. S. Guthrie, and P. F. Sharp, *Science*, **87,** 439 (1938).
(70) W. Wenner, *J. Org. Chem.*, **14,** 22 (1949).
(71) T. H. Milhorat, *Proc. Soc. Exp. Biol. Med.*, **55,** 52 (1944).
(72) C. W. Bailey, J. R. Bright, and J. J. Jasper, *J. Am. Chem. Soc.*, **67,** 1184 (1945).
(73) D. E. Guttman and D. Brooke, *J. Am. Pharm. Assoc., Sci. Ed.*, **52,** 941 (1963).
(74) T. F. Osberger, *Pharm. Technol.*, **4,** 53 (1980).
(75) A. Taub and H. Lieberman, *J. Am. Pharm. Assoc., Sci. Ed.*, **42,** 183 (1953).
(76) S. Scheindlin and I. Griffith, *Am. J. Pharm.*, **123,** 78 (1951).
(77) W. C. Gakenheimer and B. A. Feller, *J. Am. Pharm. Assoc., Sci. Ed.*, **38,** 660 (1949).
(78) N. R. Trenner, R. F. Buhs, F. A. Bacher, and W. C. Gakenheimer, *ibid.*, **39,** 361 (1950).
(79) D. V. Frost, M. Lapidus, K. A. Plaut, E. Scherfling, and H. H. Fricke, *Science*, **116,** 119 (1952).
(80) A. Bartilucci and N. E. Foss, *J. Am. Pharm. Assoc., Sci. Ed.*, **43,** 159 (1954).
(81) E. M. Stapert, E. B. Ferrer, and I. Stubberfield, *ibid.*, **43,** 87 (1954).
(82) A. J. Rosenberg, *J. Biol. Chem.*, **219,** 951 (1956).
(83) I. Utsumi, K. Harada, and H. Miura, *Vitamins (Japan)*, **49,** 1 (1975).
(84) I. Papp, A. Popovici, M. Rogoscu, and A. Aron, *Rev. Med. (Tirgu-Mures, Rom.)*, **22,** 168 (1976).
(85) H.-C. Hsu, *Tai-wan Yao Hsueh Tsa Chih*, **30,** 20 (1978).
(86) O. Valls, J. M. Lopez, M. Castillo, and V. Vilas, *Circ. Farm.*, **30,** 67 (1972).
(87) T. Takahashi and R. Yamamoto, *J. Pharm. Soc. Jpn.*, **89,** 938 (1969).
(88) S. H. Rubin, *J. Am. Pharm. Assoc., Sci. Ed.*, **37,** 502 (1948).
(89) T. Anmo, M. Washitake, Y. Takashima, M. Isohata, M. Furuya, and K. Koike, *Vitamins (Japan)*, **46,** 193 (1972).
(90) J. N. Delgado, F. V. Lofgren, and H. M. Burlage, *Drug Stand.*, **26,** 51 (1958).
(91) B. D. Parikh and F. V. Lofgren, *ibid.*, **26,** 56 (1958).
(92) F. J. Bandelin and J. V. Tuschhoff, *J. Am. Pharm. Assoc., Sci. Ed.*, **44,** 241 (1955).
(93) R. I. Paust and J. L. Colaizzi, *J. Pharm. Sci.*, **57,** 2119 (1968).
(94) E. DeRitter, L. Magid, M. Osadca, and S. H. Rubin, *ibid.*, **59,** 229 (1970).
(95) C. F. Gerber, C. P. Hetzel, O. Klioze, and A. F. Leyden, *J.Am. Pharm. Assoc., Sci. Ed.*, **46,** 635 (1957).
(96) J. J. Gulesich, U.S. Patent 2,822,317, Feb. 4, 1958.
(97) J. A. Elder, Jr., Canadian Patent 511,033, Mar. 15, 1955.
(98) M. A. Cannalonga and L. Magid, U.S. Patent 2,756,177, July 24, 1956.
(99) R. W. Lehman, U.S. Patent 2,895,878, July 21, 1959.
(100) N. D. Embree and H. M. Kascher, U.S. Patent 2,686,751, Aug. 17, 1954.
(101) E. I. Koslov, R. A. Ivanova, E. I. Finkle'shtein, E. Lopatnikova, and E. V. Alekseev, *Khim.-Farm. Zh.*, **11,** 100 (1977).
(102) S. P. Gladkikh, *ibid.*, **4,** 37 (1970).
(103) R. P. Tansey and G. H. Schneller, *J. Am. Pharm. Assoc., Sci. Ed.*, **44,** 34 (1955).
(104) H. Jager, *Pharmazie*, **3,** 536 (1948).
(105) M. Kirkova, L. Nedelova, and N. Gospodinov, *Tr. Nauchnoizled. Khim.-Farm. Inst.*, **9,** 435 (1974).
(106) Z. Reyes, U.S. Patent 3,178,451, Apr. 13, 1965.
(107) J. C. Bauernfeind and O. N. Miller, Proceedings of a Workshop, San Francisco, Calif., June 11–12, 1976, p. 78. Available from National Acad. Sci., Washington, DC 20418.
(108) J.-H. Huang, *J. Pharm. Sci.*, **60,** 1481 (1971).
(109) W. M. Cort, W. Mergens, and A. Greene, *J. Food Sci.*, **43,** 797 (1978).
(110) E. Knobloch, V. Janata, M. Auskova, K. Mnoucek, O. Matousova, and M. Likarova, *Cesk. Farm.*, **20,** 244 (1971).
(111) T. Nobukuni, N. Yano, M. Fukushima, A. Mizuno, and F. Nagayoshi, Japan Patent 69 27,399, Nov. 13, 1969.
(112) S. Hata, K. Mizuno, and S. Tomioka, *Yakuzaigaku*, **27,** 130

(1967).
(113) S. Hata, T. Anraku, and H. Sano, *ibid.*, **27,** 132 (1967).
(114) S. Hata and S. Tomioka, *ibid.*, **27,** 199 (1967).
(115) J. D. O'Broin, I. J. Temperley, J. P. Brown, and J. M. Scott, *Am. J. Clin. Nutr.*, **28,** 438 (1975).
(116) K. Kishore, P. N. Moorthy, and K. N. Rao, *Radiat. Eff.*, **38,** 97 (1978).
(117) K. N. Rao, P. N. Moorthy, and K. Kishore, *INIS Atomindex*, **9,** (20), Abstr. No. 404840 (1978).
(118) C. Rosenblum and D. T. Woodbury, *J. Am. Pharm. Assoc., Sci. Ed.*, **41,** 368 (1952).
(119) H. L. Newmark, U.S. Patent 2,823,167, Feb. 11, 1958.
(120) D. A. Zuck and J. W. Conine, *J. Pharm. Sci.*, **52,** 59 (1963).
(121) M. D. Bray, U.S. Patent 2,498,200, Feb. 21, 1950.
(122) A. Fujita and D. Iwatake, *Biochem. Z.*, **277,** 293 (1935).
(123) J. D. Ponting, *Ind. Eng. Chem. Anal. Ed.*, **15,** 389 (1943).
(124) O. Gawron and R. Berg, *ibid.*, **16,** 757 (1944).
(125) A. J. Lorenz and L. J. Arnold, *ibid.*, **10,** 687 (1938).
(126) W. Heimann and B. Heinrich, *Fette, Seifen, Anstrichm.*, **61,** 1024 (1959).
(127) K. Takamura and M. Ito, *Chem. Pharm. Bull.*, **25,** 3218 (1977).
(128) E. Géro, *Compt. Rend.*, **240,** 1818 (1955).
(129) C. Inagaki, H. Fukuba, M. Mukai, and S. Toyosato, *Nippon Nogei Kagaku Kaishi*, **29,** 416 (1955).
(130) A. Smoczkiewiczowa and J. Grochmalicka, *Nature (London)*, **192,** 161 (1961).
(131) J. Herrmann and H. G. Grossman, *Pharm. Zentralhalle*, **101,** 743 (1962).
(132) T. Fukuda, K. Miyakawa, and K. Ro, *Shokuhin Eiseigaku Zasshi*, **7,** 508 (1966).
(133) S. Baczyk, A. Lempka, and K. Baranowska, *Pr. Zakresu Towarozn Chem., Wyzza Szk. Ekon. u Poznaniu Zesg. Nauk., Ser. I*, **26,** 39 (1966).
(134) T. Katari, J. Sato, T. Iida, and S. Makino, Japan. Kokai, 74 92,219, Sept. 3, 1974.
(135) R. D. Davis, Japan. Kokai, 77 66,672, June 2, 1977.
(136) K. Hasunuma, Japan. Kokai 74 86,524, Aug. 19, 1974.
(137) K. Hasunuma, Japan. Kokai 74 32,935, Sept. 4, 1974.
(138) A. Bavley, C. J. Knuth, W. A. Laxler, and A. E. Timreck, U.S. Patent 2,689,202, Sept. 14, 1954.
(139) A. Bavley and A. E. Timreck, U.S. Patent 2,702,262, Feb. 15, 1955.
(140) J. C. Bauernfeind and L. Magid, U.S. Patent 2,708,628, May 17, 1955.
(141) A. Rosenberg, U.S. Patent 2,855,306, Oct. 7, 1958.
(142) J. E. Allegretti, U.S. Patent 2,897,118, July 28, 1959.
(143) H. W. Flandreau, Jr., U.S. Patent 3,529,065, Sept. 15, 1970.
(144) W. Cort and H. L. Newmark, U.S. Patent 3,749,799, July 31, 1973.
(145) T. Furuhashi and T. Hayashibara, Japan. Kokai 75 13,521, Feb. 13, 1975.
(146) M. A. Cannalonga and L. V. Czarecki, U.S. Patent 3,947,596, Mar. 30, 1976.
(147) J. C. Wallenmeyer, F. G. McDonald, and R. L. Henry, U.S. Patent 2,650,895, Sept. 1, 1953.
(148) R. D. Wakely, U.S. Patents 2,758,923 and 2,758,924, Aug. 14, 1956.
(149) M. Hochberg, U.S. Patents 2,777,797 and 2,777,798, Jan. 15, 1957.
(150) S. Ohtaki, U.S. Patent 3,050,728, Oct. 2, 1962.
(151) C. H. Benton, Jr. and L. A. Anderson, U.S. Patent 2,940,900, Jan. 14, 1960.
(152) G. Brooks, U.S. Patent 3,173,838, Mar. 16, 1965.
(153) R. H. Bunnell and M. A. Cannalonga, U.S. Patent 3,608,083, Sept. 21, 1971.
(154) R. H. Bunnell and M. A. Cannalonga, Ger. Offen. 2,135,247, Jan. 25, 1973.
(155) M. A. Cannalonga and L. V. Czarecki, U.S. Patent 3,914,430, Oct. 21, 1975.
(156) J. Myhre, U.S. Patent, 2,676,136, Apr. 20, 1954.
(157) H. J. Dunn, U.S. Patent 2,897,119, July 28, 1959.
(158) M. Hochberg and C. Ely, U.S. Patent 3,067,104, Dec. 4, 1962.
(159) H. D. Ratish and M. Hochberg, U.S. Patent, 3,067,105, Dec. 4, 1962.
(160) L. A. Anderson, U.S. Patent 3,099,602, July 30, 1963.
(161) R. E. Aiello and P. P. Eisenstein, U.S. Patent 3,138,532, June 23, 1964.
(162) A. Rosenberg, U.S. Patent 3,124,510, Mar. 10, 1964.
(163) L. A. Anderson, U.S. Patent 3,184,385, May 18, 1965.
(164) A. Berseneva, *Khim.-Farm. Zh.*, **11,** 131 (1977).
(165) J. Spaleny, J. Kucharsky, J. Lomjansky, and P. Tomlein, Czech. Patent 172,543, May 15, 1978.
(166) I. V. Kozlova, G. I. Dontsova, V. A. Chenov, V. Y. Lebedenko, and G. P. Gryadunova, *Farmatsiya (Moscow)*, **26,** 37, (1977).
(167) M. A. Cannalonga and J. E. Raymond, Ger. Offen. 2,402,413, July 25, 1974.
(168) E. Nuernberg, German Patent 1,290,611, Mar. 13, 1969.
(169) L. E. Stoyle, Jr., U.S. Patent 3,293,132, Dec. 20, 1966.
(170) W. Haas and H. G. Zeller, S. Afr. Patent 68 03,687, Jan. 15, 1969.
(171) W. Haas and H. G. Zeller, U.S. Patent 3,873,713, Mar. 25, 1975.
(172) A. Kassem, S. Said, and S. El-Bassouni, *Manuf. Chem. Aerosol News*, **46,** 53 (1975).
(173) I. Chaudry, J. A. Concha, and N. F. deCastro, *Asian J. Pharm.*, **3,** 10 (1977).
(174) S. Kondo and H. Nakano, Ger. Offen. 2,706,705, Feb. 23, 1978.
(175) H. Tamura, M. Kawasaki, and T. Yamaguchi, Japan. Kokai Tokyo Koho 78 127,819, Nov. 8, 1978.
(176) A. Koff, U.S. Patent 3,080,292, Mar. 5, 1963.
(177) A. Koff, U.S. Patent, 3,080,293, Mar. 5, 1963.
(178) E. DeRitter and J. E. Raymond, U.S. Patent 3,676,556, July 11, 1972.
(179) L. E. Stoyle, Jr., P. A. Owellette, and E. J. Hanus, U.S. Patent 3,037,911, June 5, 1962.
(180) L. D. Morse and P. A. Hammes, Ger. Offen. 2,255,236, May 16, 1974 and Brit. Patent 1,371,840, Oct. 30, 1974.
(181) C. N. Andersen, U.S. Patent 2,410,417, Nov. 5, 1946.
(182) H. M. Espoy, U.S. Patent 2,858,215, Oct. 28, 1958.
(183) E. Knobloch, V. Janata, and E. Likarova, Czech. Patent 159,454, Aug. 15, 1975.
(184) M. Cannalonga and L. V. Czarecki, Fr. Demande 2,179,899, Dec. 28, 1973.
(185) J. Surowiecki and L. Krowcznyski, *Acta Pol. Pharm.*, **29,** 399 (1972).
(186) L. Freedman and E. Green, U.S. Patent 2,417,299, Mar. 11, 1947.
(187) M. R. Zentner, U.S. Patent 2,628,930, Feb. 17, 1953.
(188) A. Wander, Brit. Patent 710,817, June 16, 1954.
(189) R. A. Lehman, U.S. Patent 3,036,957, May 29, 1962.
(190) J. D. Mullins and T. J. Macek, U.S. Patent 3,070,499, Dec. 25, 1962.
(191) A. E. Timreck, U.S. Patent 3,359,167, Dec. 19, 1967.
(192) L. Tomasini, E. Trandafilova, V. Boyanova, and P. Grigorov, *Farmatsiya (Sofia)*, **25,** 33 (1975).
(193) J. D. Cawley and M. H. Stern, U.S. Patent 2,680,749, June 8, 1954.
(194) A. E. Sobel, U.S. Patent 2,816,855, Dec. 17, 1957.
(195) C. D. Robeson, U.S. Patent 3,102,078, Aug. 27, 1963.
(196) R. E. Aiello and J. C. Bauernfeind, U.S. Patent 3,149,037, Sept. 15, 1964.
(197) W. H. Feigh, U.S. Patent 3,244,595, Apr. 5, 1966.
(198) R. Gherghinof, V. Pilea, M. Ionescu, and R. Paiusan, *Farmacia (Bucharest)*, **14,** 681 (1966).
(199) M. Fujita, T. Shimamoto, and J. Takahashi, Japan. Kokai 74 42,818, Apr. 22, 1974.
(200) M. Fujita, T. Shimamoto, J. Takahashi, and K. Ishizuka, Japan. Kokai 78 07,489, Mar. 18, 1978.
(201) A. Koshiro, K. Fujimoto, K. Ishimoto, K. Matsuoka, E. Uchida, K. Fujimura, S. Harada, K. Takahama, and T. Ogata, *Kyushu Yakugakkai Kaiho*, **32,** 31 (1978).
(202) D. Monciu and M. Boteanu, *Farmacia (Bucharest)*, **25,** 159 (1977).
(203) H. O. Ammar, *Pharmazie*, **31,** 235 (1976).
(204) *Ibid.*, **31,** 373 (1976).
(205) M. Kirkova and L. Nedelova, *Farmatsiya (Sofia)*, **22,** 34 (1972).
(206) A. Taub, I. Katz, and M. Katz, *J. Am. Pharm. Assoc., Sci. Ed.*, **38,** 119 (1949).
(207) J. L. Cimenera and P. W. Wilcox, *ibid.*, **35,** 363 (1946).
(208) R. Popovic, J. Grujic-Vasic, and I. Pilipovic, *Arch. Farm.*, **21,** 199 (1971).

(209) M. A. Kassem, A. A. Kassem, and H. O. Ammar, *Pharm. Acta Helv.*, **47,** 89 (1972).
(210) S. Nikolov and L. Nedelova, *Farmatsiya (Sofia)*, **16,** 35 (1966).
(211) Y. Inoue, C. Honke, and N. Hashiguchi, *Hiroshima-ken Byoin Yakuzaishikai Gakujutsu Nempo*, **13,** 42 (1978).
(212) P. Ban, *Farmacia (Bucharest)*, **18,** 1 (1970).
(213) A. Boyazhieva, M. Iotov, and P. Dilov, *Vet.-Med. Naukr*, **12,** 45 (1975).
(214) M. Blitz, E. Eigen, and E. Gunsberg, *J. Am. Pharm. Assoc., Sci. Ed.*, **45,** 803 (1956).
(215) A. Rigoli, *Boll. Chim. Farm.*, **107,** 229 (1968).
(216) B. E. Haeger and R. A. Nash, Ger. Offen. 2,433,440, Feb. 13, 1975.
(217) B. E. Haeger and R. A. Nash, U.S. Patent 3,914,419, Oct. 21, 1975.
(218) P. Moorhatch and W. L. Chiou, *Am. J. Hosp. Pharm.*, **31,** 72 (1974).
(219) L. Howard, R. Chu, S. Feman, H. Mintz, L. Ovesen, and B. Wolf, *Ann. Int. Med.*, **93,** 576 (1980).
(220) N. H. Kobayashi and J. C. King, *Am. J. Hosp. Pharm.*, **34,** 589 (1977).
(221) R. J. Nessel, H. M. Apelian, and J. Blodinger, *J. Pharm. Sci.*, **59,** 254 (1970).
(222) A. K. Shukla and J. G. Asthana, *Indian Drugs*, **15,** 177 (1978).
(223) L. Magid, U.S. Patent 3,446,894, May 27, 1969.
(224) H. M. Apelian and J. Blodinger, U.S. Patent 3,459,863, Aug. 5, 1969.
(225) R. Couchoud and J. Willemot, Fr. Demande 2,128,046, Nov. 24, 1972.
(226) F. M. El-Khawas, M. M. Abdel-Khalek, and R. M. El-Rashedy, *Pharm. Ind.*, **38,** 648 (1976).
(227) R. L. Lamberson and G. E. Raynor, Jr., *Manuf. Chem. Aerosol News*, **47,** 55 (1976).
(228) D. H. Shah and A. S. Arambulo, *Drug Dev. Commun.*, **1,** 495 (1974–1975, Pub. 1976).
(229) S. Ohno, N. Hoshi, and F. Sekigawa, Ger. Offen. 2,528,190, Jan. 15, 1976.
(230) H. Maekawa and K. Noda, Japan. Kokai 74 31,816, Mar. 22, 1974.
(231) St. Nikolov, L. Nedelova, and E. Velikova, *Farmatsiya (Sofia)*, **17,** 60 (1967).
(232) E. I. Rzheuskii, *Farm. Zh. (Kiev)*, **5,** 92 (1977).
(233) A. A. Kassem and W. Darwish, *Bull. Fac. Pharm. (Cairo Univ.)*, **11,** 129 (1972).
(234) D. Casicioli, P. Celletti, B. Petrangeli, and A. Pullo, *Boll. Chim. Farm.*, **110,** 408 (1971).
(235) L. Magid, U.S. Patent 3,646,192, Feb. 29, 1972.
(236) A. Koff and L. Magid, U.S. Patent 3,655,852, Apr. 11, 1972.
(237) I. Cruceanu, I. Selmiciu, S. Motet, and M. Mosang, Rom. 54,704, Mar. 20, 1973.
(238) P. Sorbini, Ger. Offen. 2,217,652, Oct. 18, 1973.
(239) E. W. Seugling, *Pharm. Technol.*, **5,** 50 (1981).
(240) H. A. Lieberman and L. Lachman, "Pharmaceutical Dosage Forms: Tablets," vol. I, Marcel Dekker, New York, N.Y., 1980.
(241) K.-N. Wai, H. G. DeKay, and G. S. Banker, *J. Pharm. Sci.*, **51,** 1076 (1962).
(242) H. Maekawa, Y. Hayase, K. Noda, T. Sadamoto, and Y. Takagishi, *Yakuzaigaku*, **26,** 120 (1966).
(243) A. Bojarski, D. Blitek, and B. Borkowski, *Diss. Pharm. Pharmacol.*, **19,** 297 (1967).
(244) E. Ragazzi and G. Veronese, *Farmaco, Ed. Prat.*, **22,** 96 (1967).
(245) H. Maekawa, T. Takeda, K. Noda, and K. Tsutsumi, *Yakuzaigaku*, **37,** 8 (1977).
(246) P. Bolatre, R. Bouche, V. Henschel, J. Jonas, R. Kinget, A. Marcq, M. Pocket, H. Robert, and M. Roland, *J. Pharm. Belg.*, **27,** 417 (1972).
(247) J. T. Carstensen, M. Osadca, and S. H. Rubin, *J. Pharm. Sci.*, **58,** 549 (1969).
(248) E. Nuernberg, E. Rettig, and H. Mueller, Ger. Offen. 2,130,545, Dec. 21, 1972.
(249) B. Cazals, Fr. Demande 2,096,949, Apr. 7, 1972.
(250) A. A. Kassem, A. M. Fouli, A. A. Badawi, and Y. A. Moustafa, *Bull. Fac. Pharm. (Cairo Univ.)*, **15,** 133 (1976).
(251) A. B. Morrison, C. B. Perusse, and J. A. Campbell, *N. Engl. J. Med.*, **263,** 115 (1960).
(252) D. G. Chapman, R. Crisafio, and J. A. Campbell, *J. Am. Pharm. Assoc., Sci. Ed.*, **43,** 297 (1954).
(253) A. B. Morrison, D. G. Chapman, and J. A. Campbell, *ibid.*, **48,** 634 (1959).
(254) A. B. Morrison and J. A. Campbell, *ibid.*, **49,** 473 (1960).
(255) A. B. Morrison and J. A. Campbell, *Am. J. Clin. Nutr.*, **10,** 212 (1962).
(256) R. Adamski and J. Sawick, *Herba Pol.*, **20,** 50 (1974).
(257) Italfarmaco S.p.A., Fr. Demande 2,042,326, Mar. 19, 1971.
(258) A. Genova and P. Papazova, *Farmatsiya (Sofia)*, **22,** 25 (1972).
(259) S. K. Bajeva and M. P. Jonega, *Indian J. Technol.*, **6,** 96 (1968).
(260) M. Djourno and D. Thoumyre, *Prod. Probl. Pharm.*, **22,** 153 (1967).
(261) O. I. Belova and T. N. Litvinenko, *Farmatsiya (Moscow)*, **22,** 84 (1973).
(262) G. B. Stone, *J. Am. Pharm. Assoc., Sci. Ed.*, **39,** 159 (1950).
(263) G. Zoni and V. Lazzeretti, *Boll. Chim. Farm.*, **106,** 872 (1967).
(264) H. Maekawa and S. Egawa, U.S. Patent 3,626,065, Dec. 7, 1971.
(265) M. K. Youssef, A. Sina, A. A. Kassem, S. A. Ibrahim, and M. A. Attia, *Ind. J. Pharm.*, **35,** 155 (1973).
(266) G. F. Siemers and P. E. Sleezer, *Drug Cosmet. Ind.*, **74,** 38 (1954).
(267) E. DeRitter, L. Magid, and P. E. Sleezer, *Am. Perf. Aromat.*, **73,** 54 (1959).
(268) G. H. Clement and M. Jones, *Chem. Prod. Aerosol News*, July (1962).
(269) S. H. Rubin, *J. Soc. Cosmet. Chem.*, **11,** 160 (1960).
(270) S. H. Rubin, L. Magid, and J. Scheiner, *Proc. Sci. Sect. Toilet Goods Assoc.*, **32,** Dec. (1959).
(271) T. Anmo and W. Fueller, Japan. Kokai 73 48,617, July 10, 1973.
(272) K. Haronikova and M. Mandak, *Farm. Obz.*, **46,** 311 (1977).
(273) A. Popovici, *Farmacia (Bucharest)*, **21,** 109 (1973).
(274) A. Popovici and M. Rogosa, *Rev. Med. (Tirgu-Mures, Rom.)*, **21,** 24 (1975).
(275) R. Adamski and R. Dobrucki, *Farm. Pol.*, **30,** 25 (1974).
(276) E. Selles-Flores and R. Gimeno, *Cienc. Ind. Farm.*, **9,** 254 (1977).
(277) T. Yashiki, Y. Nishida, K. Aoki, N. Nakajima, M. Godo, and N. Tan, Japan. Kokai 75 06,710, Jan. 23, 1975.
(278) F. J. Bandelin and J. V. Tuschhoff, *J. Am. Pharm. Assoc., Pract. Pharm. Ed.*, **15,** 761 (1954).
(279) K. C. Agarwal and D. K. Agarwal, *Indian J. Technol.*, **1,** 410 (1969).
(280) S. Yao and H. Hsu, *Tai-Wan Yao Hsueh Tsa Chih*, **24,** 37 (1972).
(281) G. Fabrizzi, M. Galloni, B. Lotti, and O. Vezzosi, *Boll. Chim. Farm.*, **110,** 726 (1971).
(282) S. A. Ismaiel and E. A. Ismaiel, *Pharmazie*, **30,** 59 (1975).
(283) A. J. Bartilucci and R. DiGirolamo, Abstracts of the 104th Meeting of APS of the American Pharmaceutical Association, 1957, p. 26.
(284) C. F. Gerber, C. P. Hetzel, O. Klioze, and A. F. Leyden, *ibid.*, 1957, p. 25.
(285) E. R. Garrett and R. F. Carper, *J. Pharm. Sci.*, **44,** 515 (1955).
(286) E. R. Garrett, *ibid.*, **45,** 171 (1956).
(287) *Ibid.*, **45,** 470 (1956).
(288) *Ibid.*, **51,** 811 (1962).
(289) H. A. McLeod, O. Pelletier, and J. A. Campbell, *Can. Pharm. J.*, **91,** 173 (1958).
(290) O. Pelletier, *Can. J. Pharm. Sci.*, **8,** 103 (1973).
(291) H. E. Sauberlich, R. P. Dowdy, and J. H. Skala, "Laboratory Tests for the Assessment of Nutritional Status," CRC Press, Cleveland, Ohio, 1974.
(292) R. H. Bunnell, in "The Vitamins," vol. VI, P. György and W. N. Pearson, Eds., Academic Press, New York, N.Y., 1967, p. 298.
(293) S. Gross and D. K. Melhorn, *J. Pediatr.*, **85,** 753 (1974).
(294) H. S. Perdue, *Feedstuffs*, **37,** No. 10, 30 (1965).
(295) A. D. Thomson, *Clin. Sci.*, **31,** 167 (1966).
(296) D. Melnick, H. Field, Jr., and W. D. Robinson, *J. Nutr.*, **18,** 593 (1939).
(297) M. Jowett, *Biochem. J.*, **34,** 1348 (1940).
(298) T. E. Friedemann, T. C. Kmieciak, P. K. Keegan, and B. B. Sheft, *Gastroenterology*, **11,** 100 (1948).

(299) A. B. Morrison and J. A. Campbell, *J. Nutr.*, **72,** 435 (1960).
(300) A. S. Schultz, R. F. Light, and C. N. Frey, *Proc. Soc. Exp. Biol. Med.*, **38,** 404 (1938).
(301) G. Levy and R. R. Hewitt, *Am. J. Clin. Nutr.*, **24,** 401 (1971).
(302) H. Linkswiler and M. S. Reynolds, *J. Nutr.*, **41,** 523 (1950).
(303) S. H. Rubin, J. M. Cooperman, M. E. Moore, and J. Scheiner, *ibid.*, **35,** 499 (1948).
(304) L. Drekter, J. Scheiner, E. DeRitter, and S. H. Rubin, *Proc. Soc. Exp. Biol. Med.*, **78,** 381 (1951).
(305) T. Tamura and E. L. R. Stokstad, *Br. J. Haematol.*, **25,** 513 (1973).
(306) C. C. Booth, I. Chanarin, B. B. Anderson, and D. L. Mollin, *ibid.*, **13,** 253 (1957).
(307) C. C. Booth and D. L. Mollin, *Lancet*, **1,** 13 (1959).
(308) P. R. Dallman and L. K. Diamond, *J. Pediatr.*, **57,** 689 (1960).
(309) J. A. Campbell and A. B. Morrison, *Am. J. Clin. Nutr.*, **12,** 162 (1963).
(310) C. L. Conley, J. R. Krevans, B. F. Chow, C. Barrows, and C. A. Lang, *J. Lab. Clin. Med.*, **38,** 84 (1951).
(311) J. F. Adams, D. J. Clow, S. K. Ross, K. Boddy, P. King, and M. A. Mahaffy, *Clin. Sci.*, **43,** 233 (1972).
(312) J. T. L. Nicholson and F. W. Chornock, *J. Clin. Invest.*, **21,** 505 (1942).
(313) W. Kübler and J. Gehler, *Int. Z. Vitaminforsch.*, **40,** 442 (1970).
(314) J. S. Stewart and C. C. Booth, *Clin. Sci.*, **27,** 15 (1964).
(315) M. Chieffi and J. E. Kirk, *J. Nutr.*, **59,** 273 (1956).
(316) A. E. Sobel and A. A. Rosenberg, *Am. J. Dis. Child.*, **84,** 609 (1952).
(317) L. J. Filer, Jr., S. W. Wright, M. P. Manning, and K. E. Mason, *Pediatrics*, **8,** 328 (1951).
(318) E. F. Week, F. J. Sevigne, and M. E. Ellis, *J. Nutr.*, **46,** 353 (1952).
(319) R. S. Overman, M. M. McNeely, N. E. Todd, and J. S. Wright, *Am. J. Clin. Nutr.*, **2,** 168 (1954).
(320) D. Melnick, M. Hochberg, and B. L. Oser, *J. Nutr.*, **30,** 67 (1945).
(321) B. L. Oser, D. Melnick, and M. Hochberg, *Ind. Eng. Chem. Anal. Ed.*, **17,** 405 (1945).
(322) E. H. Mawson and S. Y. Thompson, *Biochem. J.*, **43,** 2 (1948).
(323) O. Pelletier and J. A. Campbell, *Anal. Biochem.*, **3,** 60 (1962).
(324) H. R. Skeggs and L. D. Wright, *J. Biol. Chem.*, **156,** 21 (1944).
(325) W. N. Pearson, in "The Vitamins," vol. VII, P. György and W. N. Pearson, Eds., Academic Press, New York, N.Y., 1967, p. 191.
(326) J. C. Rabinowitz and E. E. Snell, *J. Biol. Chem.*, **169,** 131 (1947).
(327) S. H. Rubin, F. W. Jahns, and J. C. Bauernfeind, *Fruit Prod. J. Am. Food Manuf.*, **24,** 327 (1945).
(328) R. E. Johnson, L. A. Contreras, F. C. Consolazio, and P. F. Robinson, *Am. J. Physiol.*, **144,** 58 (1945).
(329) E. J. Middleton, J. Davies, and A. B. Morrison, *J. Pharm. Sci.*, **54,** 1 (1965).
(330) D. A. Libby, M. E. Schertel, and H. W. Loy, *J. Assoc. Off. Agr. Chem.*, **48,** 981 (1965).
(331) T. Ida, S. Takahashi, K. Noda, S. Kishi, S. Nakagami, and I. Utsumi, *J. Pharm. Sci.*, **52,** 472 (1963).

RESEARCH ARTICLES

Solid-State Stability of Aspirin in the Presence of Excipients: Kinetic Interpretation, Modeling, and Prediction

P. V. MROSO, A. LI WAN PO ˣ, and W. J. IRWIN

Received August 7, 1981, from the *Department of Pharmacy, University of Aston, Gosta Green, Birmingham B4 7ET England.* Accepted for publication December 14, 1981.

Abstract □ Salicylsalicylic acid and acetylsalicylsalicylic acid were identified as decomposition products of aspirin when mixtures of the drug, with magnesium stearate, were stored in the solid state at 60° and 75% relative humidity. The effect of increasing the concentration of magnesium stearate and the addition of other alkali stearates on the rate of decomposition of aspirin were studied. The validity of the theory that pH changes induced by the alkali stearates account for the catalytic effect of the lubricants on the decomposition was tested. The changes observed were modeled and the mechanism involved elucidated. The potential use of the melting points of aspirin mixtures in predicting the stability of the drug in such drug–excipient mixtures is demonstrated.

Keyphrases □ Aspirin—solid-state stability in presence of excipients, kinetic interpretation, modeling and prediction, decomposition □ Decomposition—solid-state stability, aspirin, excipients, kinetic interpretation, modeling and prediction □ Stability—solid state, aspirin, in presence of excipients, kinetic interpretation, modeling and prediction

The mechanisms of decomposition of drugs in the solid state are complex and difficult to unravel (1–3). The problems are compounded by the fact that most drugs are formulated with excipients, and decomposition in such systems is even more complicated. This, together with the usually slow rates of decomposition in the solid state relative to solutions, may explain the comparatively small number of reports on the quantitation of decomposition of drugs in formulated solid-dosage forms. Many of the reports that have appeared have tended to be semiquantitative, although a few detailed studies have been reported (4–9). To overcome the time constraints, some workers have resorted to the prediction of the solid-state stability of hydrolabile drugs by studying their decomposition in suspension systems. Kornblum and Zoglio (10) for example attempted to predict the stability of aspirin in the presence of tablet lubricants in the solid state by this approach. Although the method described is attractive, the mechanisms of decomposition in solid dosage systems may be different from those observed in systems containing a higher proportion of water.

More recent studies have shown that in addition to

0022-3549/82/01000-1096$01.00/0

(299) A. B. Morrison and J. A. Campbell, *J. Nutr.*, **72,** 435 (1960).
(300) A. S. Schultz, R. F. Light, and C. N. Frey, *Proc. Soc. Exp. Biol. Med.*, **38,** 404 (1938).
(301) G. Levy and R. R. Hewitt, *Am. J. Clin. Nutr.*, **24,** 401 (1971).
(302) H. Linkswiler and M. S. Reynolds, *J. Nutr.*, **41,** 523 (1950).
(303) S. H. Rubin, J. M. Cooperman, M. E. Moore, and J. Scheiner, *ibid.*, **35,** 499 (1948).
(304) L. Drekter, J. Scheiner, E. DeRitter, and S. H. Rubin, *Proc. Soc. Exp. Biol. Med.*, **78,** 381 (1951).
(305) T. Tamura and E. L. R. Stokstad, *Br. J. Haematol.*, **25,** 513 (1973).
(306) C. C. Booth, I. Chanarin, B. B. Anderson, and D. L. Mollin, *ibid.*, **13,** 253 (1957).
(307) C. C. Booth and D. L. Mollin, *Lancet*, **1,** 13 (1959).
(308) P. R. Dallman and L. K. Diamond, *J. Pediatr.*, **57,** 689 (1960).
(309) J. A. Campbell and A. B. Morrison, *Am. J. Clin. Nutr.*, **12,** 162 (1963).
(310) C. L. Conley, J. R. Krevans, B. F. Chow, C. Barrows, and C. A. Lang, *J. Lab. Clin. Med.*, **38,** 84 (1951).
(311) J. F. Adams, D. J. Clow, S. K. Ross, K. Boddy, P. King, and M. A. Mahaffy, *Clin. Sci.*, **43,** 233 (1972).
(312) J. T. L. Nicholson and F. W. Chornock, *J. Clin. Invest.*, **21,** 505 (1942).
(313) W. Kübler and J. Gehler, *Int. Z. Vitaminforsch.*, **40,** 442 (1970).
(314) J. S. Stewart and C. C. Booth, *Clin. Sci.*, **27,** 15 (1964).
(315) M. Chieffi and J. E. Kirk, *J. Nutr.*, **59,** 273 (1956).
(316) A. E. Sobel and A. A. Rosenberg, *Am. J. Dis. Child.*, **84,** 609 (1952).
(317) L. J. Filer, Jr., S. W. Wright, M. P. Manning, and K. E. Mason, *Pediatrics*, **8,** 328 (1951).
(318) E. F. Week, F. J. Sevigne, and M. E. Ellis, *J. Nutr.*, **46,** 353 (1952).
(319) R. S. Overman, M. M. McNeely, N. E. Todd, and J. S. Wright, *Am. J. Clin. Nutr.*, **2,** 168 (1954).
(320) D. Melnick, M. Hochberg, and B. L. Oser, *J. Nutr.*, **30,** 67 (1945).
(321) B. L. Oser, D. Melnick, and M. Hochberg, *Ind. Eng. Chem. Anal. Ed.*, **17,** 405 (1945).
(322) E. H. Mawson and S. Y. Thompson, *Biochem. J.*, **43,** 2 (1948).
(323) O. Pelletier and J. A. Campbell, *Anal. Biochem.*, **3,** 60 (1962).
(324) H. R. Skeggs and L. D. Wright, *J. Biol. Chem.*, **156,** 21 (1944).
(325) W. N. Pearson, in "The Vitamins," vol. VII, P. György and W. N. Pearson, Eds., Academic Press, New York, N.Y., 1967, p. 191.
(326) J. C. Rabinowitz and E. E. Snell, *J. Biol. Chem.*, **169,** 131 (1947).
(327) S. H. Rubin, F. W. Jahns, and J. C. Bauernfeind, *Fruit Prod. J. Am. Food Manuf.*, **24,** 327 (1945).
(328) R. E. Johnson, L. A. Contreras, F. C. Consolazio, and P. F. Robinson, *Am. J. Physiol.*, **144,** 58 (1945).
(329) E. J. Middleton, J. Davies, and A. B. Morrison, *J. Pharm. Sci.*, **54,** 1 (1965).
(330) D. A. Libby, M. E. Schertel, and H. W. Loy, *J. Assoc. Off. Agr. Chem.*, **48,** 981 (1965).
(331) T. Ida, S. Takahashi, K. Noda, S. Kishi, S. Nakagami, and I. Utsumi, *J. Pharm. Sci.*, **52,** 472 (1963).

RESEARCH ARTICLES

Solid-State Stability of Aspirin in the Presence of Excipients: Kinetic Interpretation, Modeling, and Prediction

P. V. MROSO, A. LI WAN PO ˣ, and W. J. IRWIN

Received August 7, 1981, from the *Department of Pharmacy, University of Aston, Gosta Green, Birmingham B4 7ET England.* Accepted for publication December 14, 1981.

Abstract □ Salicylsalicylic acid and acetylsalicylsalicylic acid were identified as decomposition products of aspirin when mixtures of the drug, with magnesium stearate, were stored in the solid state at 60° and 75% relative humidity. The effect of increasing the concentration of magnesium stearate and the addition of other alkali stearates on the rate of decomposition of aspirin were studied. The validity of the theory that pH changes induced by the alkali stearates account for the catalytic effect of the lubricants on the decomposition was tested. The changes observed were modeled and the mechanism involved elucidated. The potential use of the melting points of aspirin mixtures in predicting the stability of the drug in such drug–excipient mixtures is demonstrated.

Keyphrases □ Aspirin—solid-state stability in presence of excipients, kinetic interpretation, modeling and prediction, decomposition □ Decomposition—solid-state stability, aspirin, excipients, kinetic interpretation, modeling and prediction □ Stability—solid state, aspirin, in presence of excipients, kinetic interpretation, modeling and prediction

The mechanisms of decomposition of drugs in the solid state are complex and difficult to unravel (1–3). The problems are compounded by the fact that most drugs are formulated with excipients, and decomposition in such systems is even more complicated. This, together with the usually slow rates of decomposition in the solid state relative to solutions, may explain the comparatively small number of reports on the quantitation of decomposition of drugs in formulated solid-dosage forms. Many of the reports that have appeared have tended to be semiquantitative, although a few detailed studies have been reported (4–9). To overcome the time constraints, some workers have resorted to the prediction of the solid-state stability of hydrolabile drugs by studying their decomposition in suspension systems. Kornblum and Zoglio (10) for example attempted to predict the stability of aspirin in the presence of tablet lubricants in the solid state by this approach. Although the method described is attractive, the mechanisms of decomposition in solid dosage systems may be different from those observed in systems containing a higher proportion of water.

More recent studies have shown that in addition to

0022-3549/82/01000-1096$01.00/0

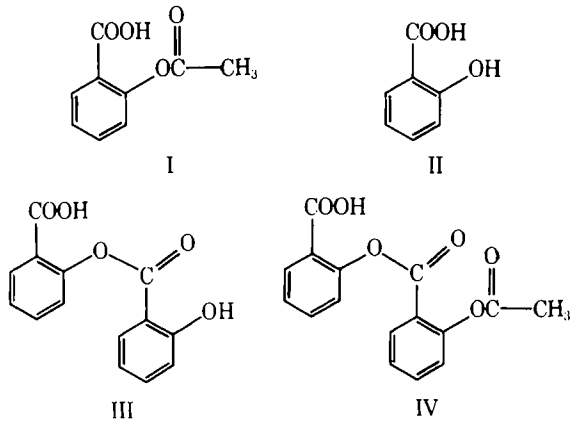

salicylic acid (II), salicylsalicylic acid (III) and acetylsalicylsalicylic acid (IV) could be detected in aspirin tablets (11–13). Since these compounds (III and IV) have been shown (14, 15) to be potentially immunogenic, limiting their presence in formulated products is important. It has been previously reported that although III was detected in aspirin tablets, it was not detected in various aspirin samples, thus suggesting that its formation could be excipient-induced (12).

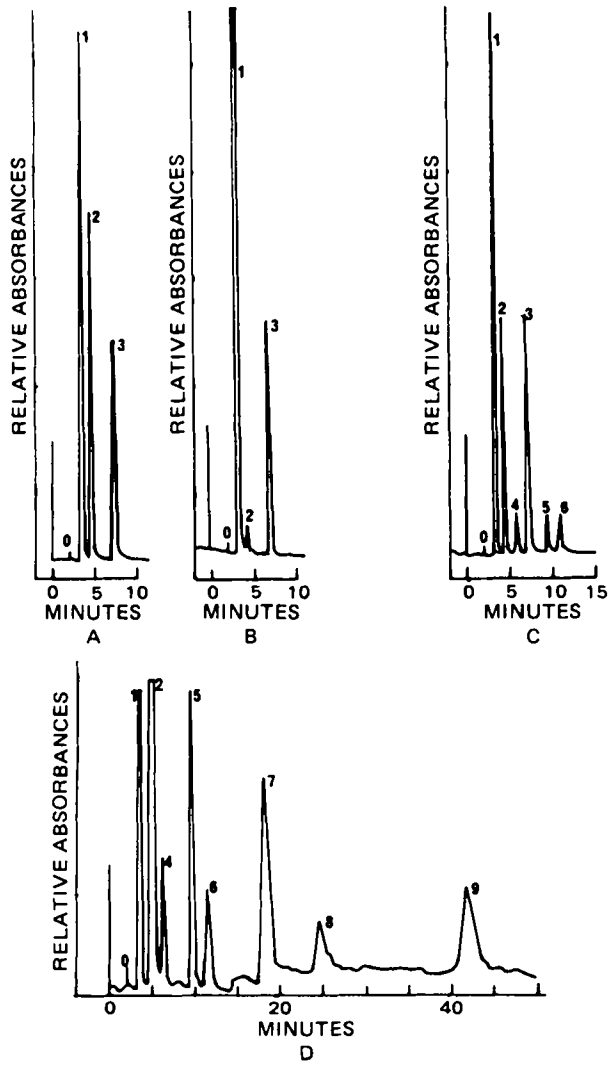

Figure 1—*High-performance liquid chromatograms of aspirin and its decomposition products: (A) aspirin in the presence of salicylic acid and propyl paraben (n-propyl-p-hydroxybenzoate); (B) aspirin–1% magnesium stearate mixture at time 0; (C) mixture after storage for 18 days at 60° and 75% humidity; (D) mixture after 21 days without internal standard. Key: (0) solvent front; (1) aspirin; (2) salicylic acid; (3) internal standard; (4) acetylsalicylsalicylic acid; (5) salicylsalicylic acid; (6–9) unidentified products.*

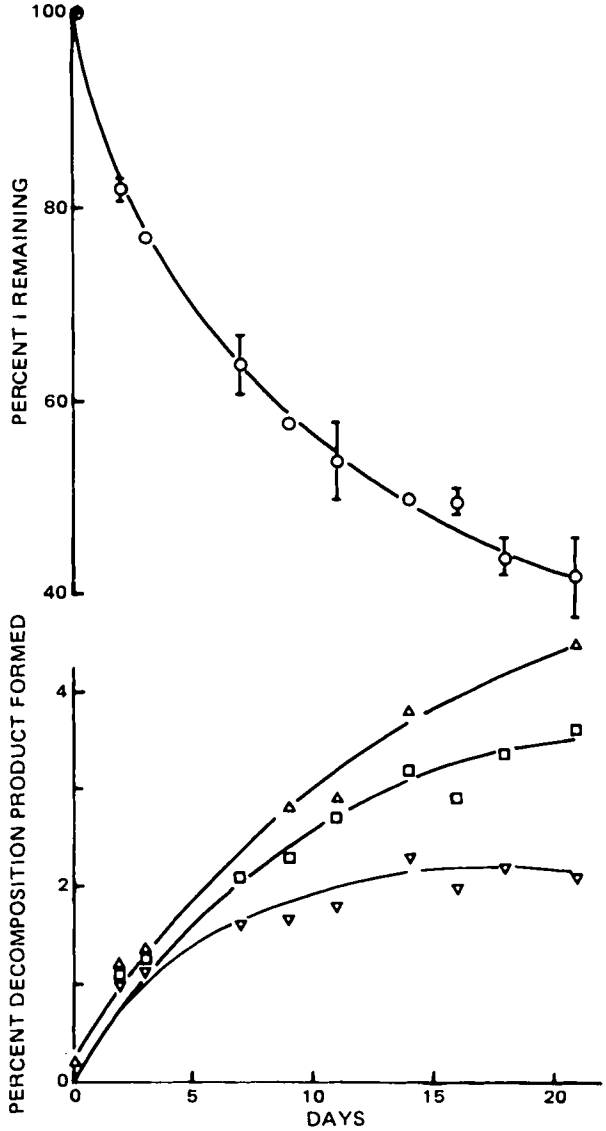

Figure 2—*Kinetics of decomposition of aspirin (I) in the presence of 1% magnesium stearate (60° and 75% relative humidity) and amounts of II, III, and IV. Key: (○) aspirin remaining; (△) II detected, (□) III; (▽) IV.*

The present study was initiated to determine whether III and IV were formed during the decomposition of aspirin in the presence of excipients in the solid state, to quantify the kinetics of decomposition of aspirin in the presence of excipients, and to elucidate the mechanisms of interaction of aspirin with tablet lubricants and in particular with magnesium stearate.

EXPERIMENTAL

Materials—Salicylic acid[1], phosphoric acid[1], *n*-propyl-*p*-hydroxy benzoate[2], and calcium, aluminum, sodium, and zinc stearates[3] were obtained from a single manufacturer[4]. Magnesium stearate samples were

[1] Analar grade.
[2] Laboratory grade.
[3] Technical grade.
[4] British Drug Houses, Poole, England, UK.

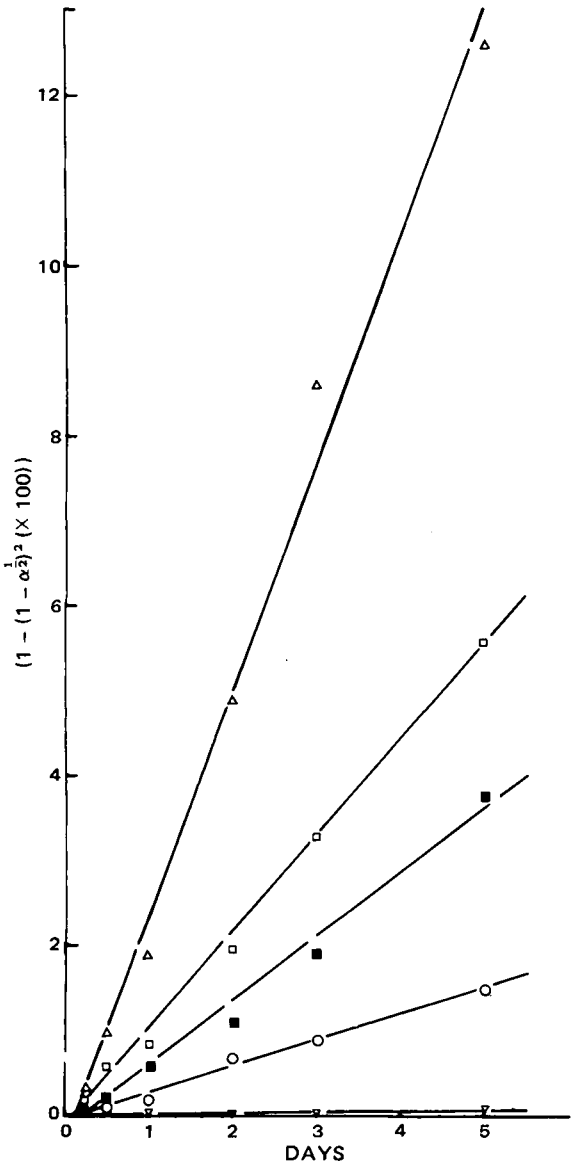

Figure 3—*Effect of magnesium stearate concentration on the rate of decomposition of aspirin plot according to Eq. 6. Key: (▽) aspirin without additive; (○) 1%; (■) 2%; (□) 3%; (△) 5% magnesium stearate.*

obtained from two different sources[4,5]. Sodium chloride (BP)[6], methanol[7], and salicylsalicylic acid[8] were used as obtained. Acetylsalicylsalicylic acid was synthesized as described (16) and tested for chromatographic purity by high-performance liquid chromatography (HPLC).

Methods—*Analysis of the Metal Stearates*—For the assay of free fatty acid 100 mg of each metal stearate was weighed out and extracted with 5 ml of chloroform. The chloroformic extract was filtered through a glass fiber filter paper and 1 ml of the filtrate was analyzed by GLC. For the assay of total fatty acid 60 mg of each stearate was weighed into a separating funnel and 30 ml of concentrated hydrochloric acid was added. The free acids liberated were extracted with 50 ml of chloroform and 1 ml of the extract assayed by GLC. Preliminary studies showed that concentrated acid was necessary to obtain clear chloroformic extracts.

GLC Analysis for Stearic, Palmitic and Myristic Acids—The GC system used for assaying the free and the total fatty acids in the alkali stearates consisted of a gas chromatograph[9] fitted with a silicone[10] coated open tubular glass capillary column (10 m × 0.8-mm o.d.) and an all-glass solids injector. Temperature settings were at 200° for the column and 250° for the detector and injector. Nitrogen, hydrogen, and air pressures were 0.9, 1.0, and 0.75 kg/cm^2, respectively. The nitrogen flow rate was 1 ml/min. Peak areas were obtained by integration.

One milliliter of extract was mixed with 0.8 ml of a chloroformic linoleic acid (1 mg/ml) solution and evaporated to dryness at 60° under nitrogen. The residues were methylated using a boron trifluoride–methanol mixture[11] maintained at 60° for 15 min. The product was extracted with 1 ml of *n*-hexane and 1 μl was injected into the chromatograph. Standard solutions prepared from the pure free acids[12] were derivatized and assayed simultaneously.

Analysis of the Salicylates—Analyses were performed using an HPLC constructed from a constant-flow solvent-metering pump[13], a valve[14] fitted with a 20-μl loop, and a variable wavelength monitor[15] equipped with an 8-μl flow cell and operated at 285 nm with a sensitivity of 0.32 aufs. Reversed-phase chromatography was performed using a 5-μm ODS (25-cm × 4.6-mm i.d.) column[16] and a mobile phase consisting of 0.02% phosphoric acid in 60% methanol in water and delivered at 1.4 ml/min.

Sample Preparation and Storage—Aspirin crystals were mixed with fixed proportions of magnesium, zinc, aluminum, sodium, or calcium stearate, and 100-mg quantities of each of the mixtures or of pure aspirin were weighed into individual glass vials[17] and loosely covered with cotton wool to prevent entry of condensed water droplets. The samples were then stored in a humidity cabinet[18] maintained at 60°. A 75% relative humidity environment was maintained at this temperature using a saturated sodium chloride solution. Samples were taken at predetermined intervals and assayed for aspirin and its decomposition products by the HPLC method.

Sample Preparation for HPLC—The contents of the vial sampled were dissolved in methanol, quantitatively transferred to a 25-ml volumetric flask, and brought up to volume with methanol. The resultant solution was analyzed by HPLC.

Particle-Size Analysis—The aspirin crystals were sized by sieve analysis (17) and a geometric mean of 280 ± 1.85 μm was obtained.

Washed Magnesium Stearate—Samples of magnesium stearate were washed by adding 5 g to 200 ml of 0.1 *M* HCl to remove any alkaline impurities and filtering the residues through a No. 3 sintered glass filter. The stearate was then washed by shaking with 50 ml of alcohol to remove stearic acid precipitated out during the acid wash. The powder was rinsed with several changes of double-distilled water until the resultant pH was in the 6.9–7.0 range. After a second filtration, the residues were dried overnight on filter paper at room temperature and finally at 50° for one-half hour before storage in tightly closed glass containers.

Melting-Point Determinations—The melting points of aspirin and its mixtures were determined by the standard capillary-tube method using an electrothermal melting point apparatus[19]. A second set of melting points were also obtained using a differential scanning calorimeter[20] operated at a heating rate of 8°/min and a nitrogen atmosphere of 2 bar. Samples (20–30 mg) were used with aluminum as the reference material.

Mathematical Model—The model used for explaining the results obtained in this study is based on liquid reaction-product layer formation during the decomposition of the aspirin. Jander (18) first showed that if one considers the formation of a liquid reaction-product layer, during the decomposition of spherical particles and if the reaction is diffusion limited, then it is possible to derive an expression relating the fraction decomposed with time. Such a model has been used previously (19).

Microscopic examination of the particles shows that the shape of the aspirin crystals used in this study were better approximated by cylinders than by spheres. Using Jander's assumptions of a diffusion-limited reaction and of a rate of thickening of the liquid layer dy/dt being inversely proportional to its thickness, y, Eq. 1 is obtained:

$$dy/dt = k/y \qquad \text{(Eq. 1)}$$

On integration:

$$y^2 = 2kt \qquad \text{(Eq. 2)}$$

[5] Griffin and George Ltd.
[6] McCarthys, UK.
[7] Analar Grade, Fisons, UK.
[8] Riker 3M, UK.
[9] Model Pye GC-V.
[10] CP-Sil 5.
[11] Pierce Chemical Co.
[12] Stearic and palmitic acids, specially pure grade, British Drug Houses myristic acid; Sigma Grade, Sigma Chemical Co., UK.
[13] Altex 100A.
[14] Rheodyne 7120.
[15] Pye LC3.
[16] Spherisorb.
[17] Fisons Ltd., Loughborough, UK.
[18] Townson and Mercer Ltd., Croydon, UK.
[19] Electrothermal Ltd., London, UK.
[20] Perkin-Elmer model DSC-1B.

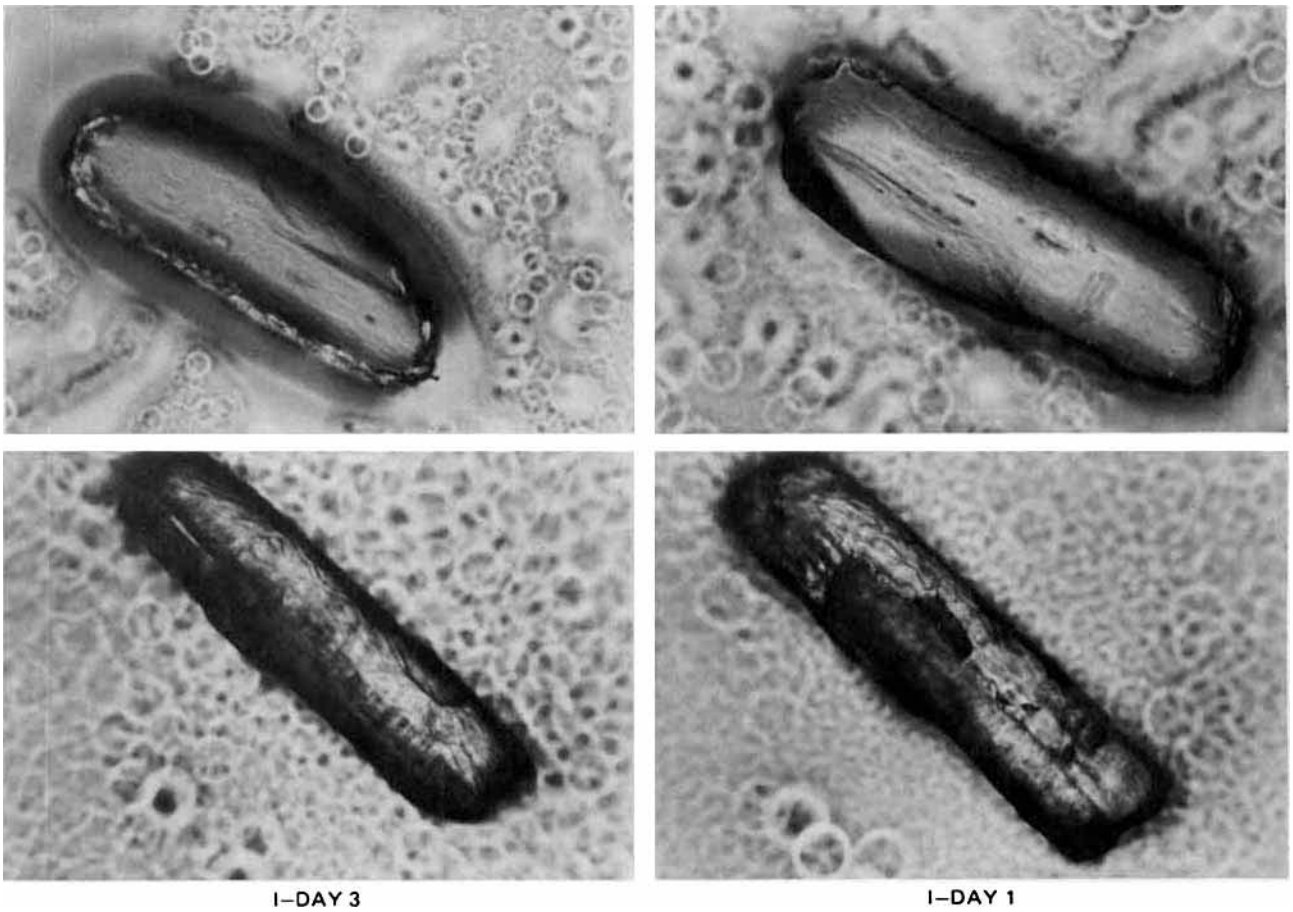

Figure 4—*Photomicrographs of decomposing aspirin (I) crystals with and without magnesium stearate at 50° and 75% relative humidity.*

The fraction decomposed (x) after time (t) can be expressed in terms of the total weight of the cylindrical particles studied:

$$\frac{\eta\rho\pi r_0^2 h - \eta\rho\pi(r_0 - y)^2}{\eta\rho\pi r_0^2 h} h = x \qquad \text{(Eq. 3)}$$

where r_0 = initial radius, h = height of cylinder, η = number of cylinders, ρ = density.

$$r_0^2 - (r_0 - y)^2 = x r_0^2 \qquad \text{(Eq. 4)}$$

Rearranging Eq. 4:

$$r_0[1 - (1 - x)^{1/2}] = y \qquad \text{(Eq. 5)}$$

Substituting for y in Eq. 5 from Eq. 2 and squaring:

$$[1 - (1 - x)^{1/2}]^2 = \frac{2k}{r_0^2} t \qquad \text{(Eq. 6)}$$

A plot of $[(1 - (1 - x)^{1/2}]^2$ against t should therefore give a straight line with zero intercept if the liquid-layer diffusion-controlled model describes the system studied. The model assumes that the length–diameter ratio of the aspirin crystals is such that end effects are negligible.

RESULTS AND DISCUSSION

Analysis of the stored samples by HPLC showed that II, III, and IV (Fig. 1) were formed during storage of aspirin at 60° and 75% relative humidity in the presence of magnesium stearate. Samples of aspirin on its own stored under identical conditions did not lead to the formation of III and IV when followed over the same time period. Figure 1 shows chromatograms of nonstored (Fig. 1B) as well as of stored samples (Fig. 1C) of aspirin.

Peak identification was achieved by comparison of retention times with authentic specimens as well as the ratio of the wavelength (20). HPLC of samples stored for longer periods of time showed that the decomposition is even more complex and several products which have not yet been identified were observed (Fig. 1D). These results are in agreement with those reported by Taguchi *et al.* (21) who showed that storage of aspirin tablets at 50° led to the formation of II, III, and IV, and that when further stressed at 95°, additional components could be detected in significant amounts. HPLC analysis of an aspirin sample stored for 4 weeks at 60° and 75% relative humidity showed traces of all the decomposition products detected in the presence of magnesium stearate. This shows that the stearates accelerate rather than induce their formation.

The decomposition of aspirin in the presence of 1% magnesium stearate is shown in Fig. 2 together with the amounts of II, III, and IV detected in the samples. It is important to note that these amounts of decomposition products can only be used as guide values since an open system was used. This particularly applies to salicylic acid which has been shown to sublime readily (22). Studies in which aspirin decomposition has been followed in the solid state, by following the kinetics of formation of salicylic acid, will therefore lead to erroneous results unless closed systems are used. In the present study an open system that allowed exposure of the samples to a constant relative humidity was preferred. Aspirin was assayed in addition to salicylic acid.

To investigate whether the concentration of lubricant present affected the rate of decomposition of aspirin, the degradation was followed in the presence of a series of concentrations of magnesium stearate. The results of these studies are shown in Fig. 3. An increase in magnesium stearate concentration quite clearly accelerated the decomposition of aspirin.

Various authors have reported on the catalytic effect of excipients on aspirin decomposition (23–25). The explanation put forward for explaining the effect of magnesium stearate has generally been based on hydrolysis taking place in an adsorbed moisture layer and on an alteration in the pH of this layer by the added excipient (26). It is known that the magnesium stearate used for tablet lubrication contains a significant amount of magnesium oxide. The USP and the BP specifications for magnesium stearate allow for up to 8.5% of magnesium oxide (27, 28). The 1980 BP however now defines the pH range of a 5% suspension and states that it should be between 6.2 and 7.4 (29).

A relationship between the observed zero rate constant of salicylic acid formation and the pH of the suspension after addition of the lubricants has been shown previously (10) in aspirin–tablet lubricant suspension

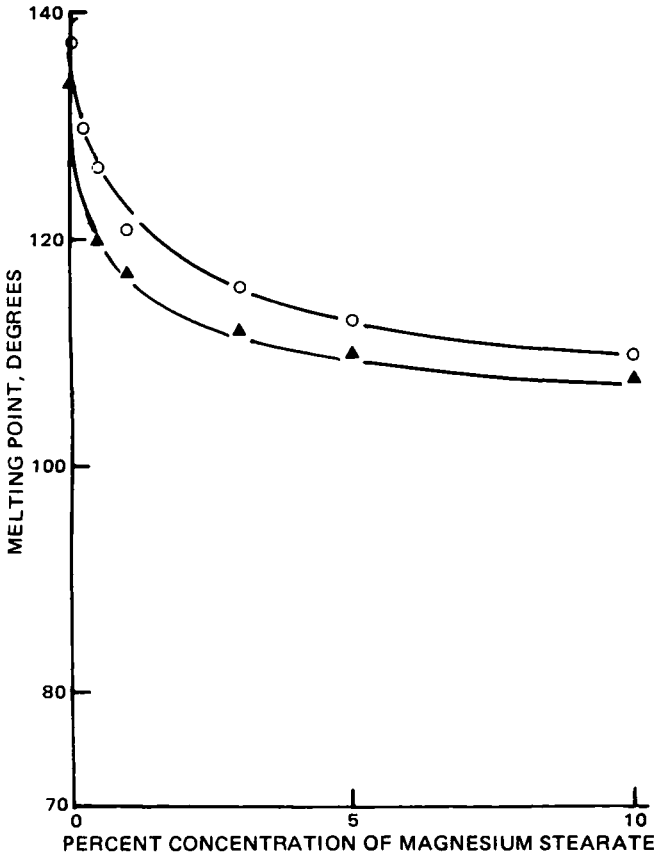

Figure 5—*Effect of addition of different concentrations of magnesium stearate on the melting point of aspirin; (○) using traditional melting point apparatus and (▲) using differential scanning calorimetry.*

systems. Magnesium stearate produced the largest pH shift and the highest rate constant. It has not been conclusively shown, however, that the pH change plays a significant part in the decomposition of aspirin in the solid state. To test this, the rate of decomposition of aspirin was measured in the presence of washed and unwashed magnesium stearate. The washed sample gave a suspension (1%) with a pH near neutrality (6.9), whereas an unwashed sample prepared similarly gave a pH of 9.9. The observed rate constants as mirrored by the slope of Eq. 6 were almost identical; the slopes were 0.0033 and 0.0030/day, respectively. Clearly the results do not exclude pH-induced changes in the rates of decomposition. The results indicate that any such change was too small to be detected during the study and was swamped by other effects when the stability of pure aspirin is compared with aspirin in the presence of magnesium stearate. GLC analysis of the magnesium stearate used both before and after washing showed that the total acids recovered (89.5 and 88.3%) were not significantly different. The amount of free acid recovered increased from 0.6 to 5.8% upon washing. It has been suggested (30) that because sublimation of II is observed on the surface of aspirin under stress conditions (22), factors other than those involved in solutions must be operable. However, sublimation out of a solution is also conceivable. Once the moisture microfilm is saturated with II, additional formation will lead to precipitation, decomposition onto adjacent surfaces, and eventually sublimation.

Microscopic (Fig. 4) and visual examination of the stored samples showed the presence of liquid films around the decomposing particles. Any theory put forward for explaining the observed increase in decomposition of aspirin in the presence of magnesium stearate must therefore take this into account.

A linear relationship between the logarithm of the observed rate constant of decomposition, and the reciprocal of the melting temperature (°K), has been found in a previous study on the solid-state stability of Vitamin A compounds (5). This was derived from the relationship between the fraction of material in the liquid state (x_1) and the melting point of the pure crystalline solid (T_m):

$$\ln x_1 = \frac{-L_f}{R}\left(\frac{1}{T} - \frac{1}{T_m}\right) \qquad \text{(Eq. 7)}$$

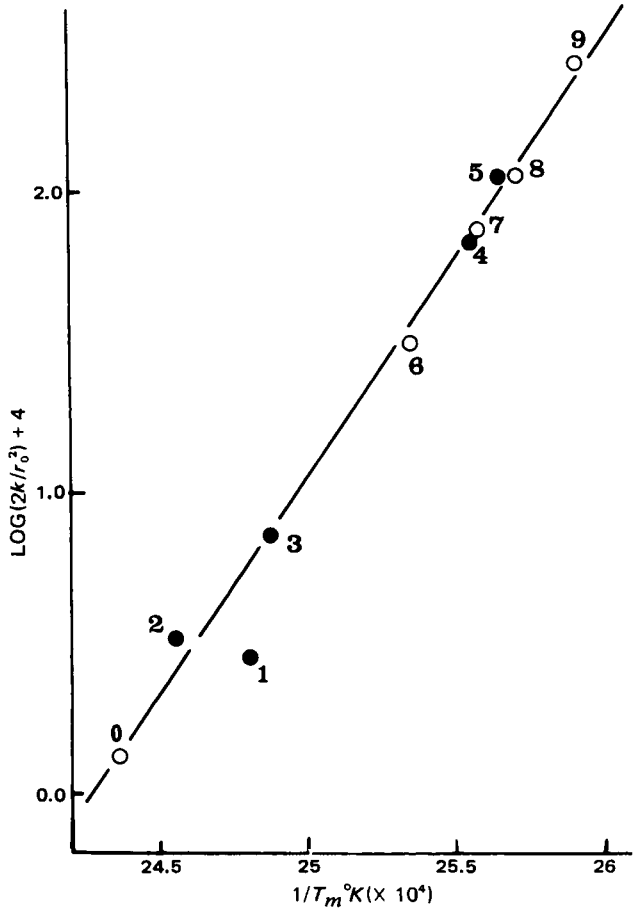

Figure 6—*Relationship between the rate constant of decomposition of aspirin in the presence of alkali stearates as mirrored by the slopes of Eq. 6 and the reciprocal of the melting points of the mixtures. Key: (0) aspirin on its own; (●) with 3% Zn (1), Al (2), Na (3), Ca (4), and Mg (5) stearates; (○) aspirin with 1% (6), 2% (7), 3% (8) and, 5% (9) magnesium stearates.*

where L_f is the molar heat of fusion and represents the difference in internal energy between the two states, the liquid being much more reactive than the solid; T is the temperature of storage; and R is the gas constant.

To test whether this relationship might explain the effect of magnesium stearate on the decomposition of aspirin the melting points of the mixtures were determined. Figure 5 shows the relationship between the melting point observed and the magnesium stearate content. The same trend was observed using both the traditional capillary tube melting point determinations and differential scanning calorimetry although differences in the absolute values were observed.

The slopes of Eq. 6 for the reactions shown in Fig. 4 were then plotted against the reciprocal of the corresponding melting points. Figure 6 shows that this relationship holds for the systems studied. One would also expect that other stearates would also alter the decomposition rates of aspirin, the magnitude of the change being determined by the size of the depression in melting point. Experiments were carried out to test this and the results are superimposed on the magnesium stearate results (Fig. 6). It is evident that the general relation holds here too.

Analysis of the stearates used in this study showed that the acid composition of the samples was significantly different (Table I). In addition to the samples used in the stability studies, other batches of magnesium and sodium stearates were also assayed for the three acids. As can be seen, interbatch and intermanufacturer variability in relative compositions were obvious. These can, in turn, be expected to produce different effects on aspirin decomposition and should be screened for during formulation studies.

CONCLUSIONS

The present study shows that III and IV are decomposition products of aspirin when the latter is stored in the solid state in the presence of alkaline lubricants such as magnesium stearate. Compounds III and IV

Table I—GLC Analysis of Alkali Stearates Used in the Stability Study

Metal Stearate	Relative Composition, % Myristate	Palmitate	Stearate	Recovery, %[a]	Free Acid, %[a]
Zinc stearate	1.9	39.2	58.9	90.5	0.3
Calcium stearate	3.7	33.4	62.9	97.1	2.8
Aluminum stearate	2.8	33.9	63.3	85.7	3.5
Sodium stearate (Manufacturer A, Batch 1)	2.4	53.0	44.6	89.1	2.8
Sodium stearate[b] (Manufacturer A, Batch 2)	4.0	40.6	55.4	95.5	1.8
Magnesium stearate (Manufacturer A, Batch 1)	5.7	37.2	57.1	87.1	0.6
Magnesium stearate (Manufacturer A, Batch 2)[b]	5.2	38.5	56.3	83.7	0.6
Magnesium stearate (Manufacturer B, Batch 1)[b]	3.2	54.0	42.8	76.7	1.2

[a] Refers to percent of initial weight accounted for by the three stearates. [b] These batches were not used in the stability studies.

were not detected in samples of aspirin stored under identical conditions for the same length of time. More prolonged storage, however, led to the formation of traces of the products. These data would suggest that the stearates accelerate the formation of these products and provide an explanation for the earlier report showing that III was detected in most of the commercial aspirin tablets analyzed but not in bulk aspirin samples. A direct relationship was shown between the rate constant of decomposition, as expressed by the slopes of plots of Eq. 6, and the concentration of magnesium stearate present. It has further been demonstrated that there was a linear relationship between the logarithm of slopes of Eq. 6 and the reciprocal of the melting points of the aspirin–stearate mixtures. Using a series of stearates it was shown that the relationship is of wide applicability. Changes in melting point rather than shifts in pH of the moisture microfilms surrounding the particles would appear to be the more plausible explanation for the observed effects of magnesium and other alkali stearates on aspirin stability. Melting point determinations would appear to provide a rapid method for predicting the stability of aspirin in aspirin–lubricant mixtures. The inverse relationship between aspirin decomposition in aspirin–lubricant mixtures and the reciprocal of the melting point (31) is quantitatively confirmed. Alkali stearates show batch-to-batch and intermanufacturer variability in acid composition and should be screened for during formulation studies.

REFERENCES

(1) J. T. Carstensen, *J. Pharm. Sci.*, **63,** 1 (1974).

(2) S. R. Byrn, *ibid.*, **65,** 1 (1976).

(3) E. R. Garrett, *Adv. Pharm. Sci.*, **2,** 1 (1967).

(4) E. R. Garrett, *J. Am. Pharm. Assoc., Sci. Ed.*, **43,** 539 (1954).

(5) J. K. Guillory and T. Higuchi, *J. Pharm. Sci.*, **51,** 100 (1962).

(6) L. J. Leeson and A. M. Mattocks, *J. Am. Pharm. Assoc., Sci. Ed.*, **47,** 329 (1958).

(7) J. T. Carstensen and M. N. Musa, *J. Pharm. Sci.*, **61,** 1112 (1972).

(8) J. T. Carstensen and P. Pothisiri, *ibid.*, **64,** 37 (1975).

(9) J. T. Cartensen and R. Kothari, *ibid.*, **69,** 123 (1980).

(10) S. S. Kornblum and M. A. Zoglio, *ibid.*, **56,** 1569 (1967).

(11) S. Patel, J. H. Perrin, and J. J. Windheuser, *ibid.*, **61,** 1794 (1972).

(12) H. Bundgaard and A. L. DeWeck, *Int. Arch. Allergy Appl. Immunol.*, **49,** 119 (1975).

(13) J. C. Reepmeyer and R. D. Kirchhoefer, *J. Pharm. Sci.*, **68,** 1167 (1979).

(14) H. Bundgaard, *J. Pharm. Pharmacol.*, **26,** 18 (1974).

(15) A. L. DeWeck, *Int. Arch. Allergy Appl. Immunol.*, **41,** 393 (1971).

(16) F. D. Chattaway, *J. Chem. Soc.*, **1931** 2495.

(17) I. C. Edmundson, in "Advances in Pharmaceutical Sciences," vol. 2. H. B. Bean, A. H. Beckett, and J. E. Carless, Eds., Academic, London, 1967, p. 95.

(18) W. Jander, *Z. Anorg. Allg. Chem.*, **163,** 1 (1927).

(19) E. Nelson, D. Eppich, and J. T. Carstensen, *J. Pharm. Sci.*, **63,** 755 (1974).

(20) A. Li Wan Po and W. J. Irwin, *J. Clin. Hosp. Pharm.*, **5,** 107 (1980).

(21) V. Y. Taguchi, M. L. Cotton, C. H. Yates, and J. F. Miller, *J. Pharm. Sci.*, **70,** 64 (1981).

(22) A. Y. Gore, K. B. Naik, D. O. Kildsig, G. E. Peck, V. F. Smolen, and G. S. Banker, *ibid.*, **57,** 1850 (1968).

(23) M. R. Nazareth and C. Lee Huyck, *ibid.*, **50,** 620 (1961).

(24) *Ibid.*, **50,** 608 (1961).

(25) H. Delonca, A. Puech, G. Seguva, and Y. Youakim, *J. Pharm. Belg.*, **24,** 5 (1969).

(26) Fr. Jaminet and G. Louis, *Pharm. Acta Helv.*, **43,** 153 (1968).

(27) "United States Pharmacopeia," 20th ed. United States Pharmacopoeial Convention, Rockville, Md., 1980.

(28) "British Pharmacopeia," Pharmaceutical Press (London) 1973.

(29) *Ibid.*, 1980.

(30) A. Y. Gore and G. S. Banker, *J. Pharm. Sci.*, **68,** 197 (1979).

(31) H. V. Maulding, M. A. Zoglio, and E. J. Johnston, *ibid.*, **57,** 1873 (1968).

ACKNOWLEDGMENTS

The authors thank the World Health Organization for the fellowship awarded to P. V. Mroso, and the West Midlands Regional Health Authority for the HPLC equipment used in this study.

In Vivo Pharmacokinetics of Triazinate in L-1210 and W-256 Cells

J. GREGORY TOWNSEND *§, **RAKESH K. JAIN** *x, and **ARLENE R. CASHMORE** ‡

Received April 6, 1981, from the *Department of Chemical Engineering, Carnegie-Mellon University, Pittsburgh, PA 15213 and the ‡Department of Pharmacology, Yale University, New Haven, CT 06510. Accepted for publication November 20, 1981. §Present Address: Sun Tech Inc., Process Development, Marcus Hook, PA 19061.

Abstract □ A pharmacokinetic model for triazinate uptake in L-1210 cells in mice and W-256 cells in rats was developed to describe the observed concentration profiles with time in these cells following a 36 mg/m^2 ip injection. The L-1210 cell permeability to triazinate was found to be ~15 times smaller compared with W-256 cells. Similarly, the partition coefficient for L-1210 cells was calculated to be ~175 times smaller than for W-256 cells. Cell membrane permeability appears to be the key parameter determining drug transport at a short time after injection.

Keyphrases □ Pharmacokinetics—of triazinate *in vivo* in L-1210 and W-256 cells □ Binding—*in vivo* pharmacokinetics of triazinate in L-1210 and W-256 cells □ Permeability, cell membrane—*in vivo* pharmacokinetics of triazinate in L-1210 and W-256 cells

Triazinate[1] (I) (NSC-139105) is a triazine folate antagonist which inhibits the enzyme dihydrofolate reductase in nucleic acid synthesis. Triazinate penetrates cells passively (1) unlike another prominent dihydrofolate reductase inhibitor, methotrexate, which enters cells by active transport. Although effective in the cure of Walker 256 ascites tumors, triazinate is not active against the L-1210 leukemia (2). This contrast in antineoplastic activity appears related to the significant accumulation of triazinate in the W-256 cells compared with the L-1210 cells (3). Since differences in drug transport probably account for the marked differences in triazinate activity observed in these cell lines (3), a quantitative analysis of triazinate transport and uptake through a mathematical model may be useful in understanding this behavior.

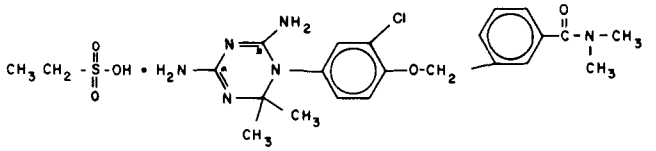

I

A preliminary pharmacokinetic model for triazinate transport in L-1210 leukemia and W-256 ascites cells is reported based on the uptake data in tumor-bearing mice and rats of Cashmore *et al.* (2). The model parameters include: cell permeabilities, drug–dihydrofolate reductase binding constants, and drug partition coefficients.

EXPERIMENTAL

Details of the experimental procedures are given elsewhere (2). Normal male rats weighing 55 to 60 g were given intraperitoneal inoculations of 5 × 10^6 W-256 ascites cells; normal male mice weighing 25 to 30 g were given intraperitoneal inoculations of 5 × 10^6 L-1210 ascites cells. Four days later, the animals were given intraperitoneal injections of 0.2 μCi[^{14}C]triazinate (0.3 μCi/μmole); this corresponded to dosage levels of 36 mg/m^2 (12 mg/kg in mice and 6 mg/kg in rats).

At intervals from 15 min to 6 hr, three animals of each species were sacrificed. Twelve milliliters of Eagle's minimal essential medium were then injected into the peritoneal cavity, and the ascites cells and fluid were removed. After separation by centrifugation, the cells and supernatant fluids were stored frozen.

The ascites cells were lysed by freeze-thawing twice in four volumes of 0.9% NaCl solution. After centrifugation, 0.5 ml of each supernatant was added to 10.0 ml of scintillation fluid[2] and counted. The counting efficiency, as determined by external standardization and standard curves for the carbon 14 radioactivity in the scintillation fluid, was 80–85%.

Thin-layer chromatography was used to determine whether triazinate was metabolized when administered *in vivo*. Silica gel glass plates[3], 5 × 20 cm, with 0.25-mm coating, were prewashed with ethyl acetate. The solvent system of either 2-methoxyethanol–ethanesulfonic acid (1000:3) or 2-methoxyethanol–glacial acetic acid (1000:3) was used. One milliliter

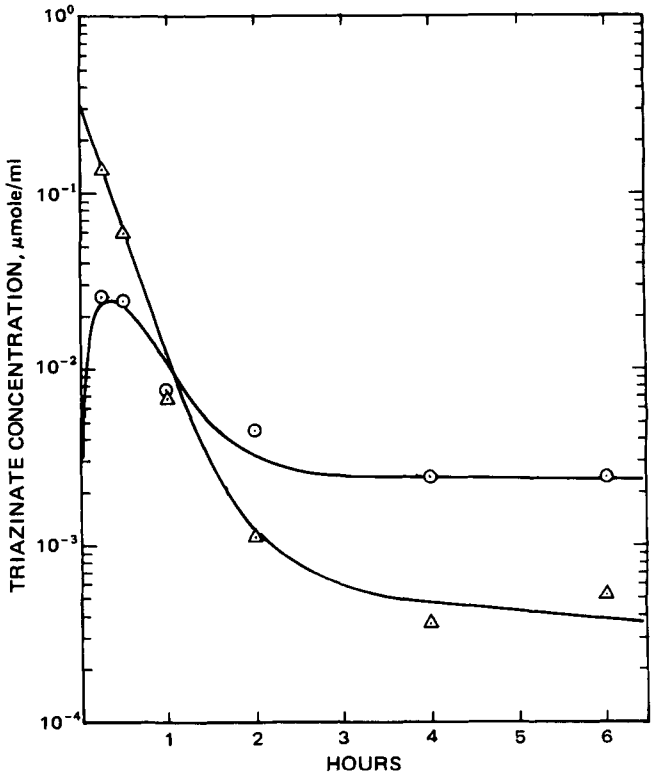

Figure 1—*Concentrations of triazinate in the peritoneal fluid and L-1210 cells as a function of time following injections of 12 mg/kg ip (36 mg/m^2) in mice. Points represent experimental determinations (2). The solid lines represent the peritoneal fluid-forcing function (C_{pe}) and the model predictions of L-1210 cell triazinate concentrations (C_c). The peritoneal fluid triazinate concentration was fitted by the expression:*

$$C_{pe} = 0.286\, e^{-0.0691t} + 0.0741\, e^{-0.0414t} + 0.000707\, e^{-0.00165t}$$

Other parameters are given in Table I. Key: (⊙) L-1210 cells; (△) peritoneal fluid.

[1] Triazinate: ethanesulfonic acid compounded with α-(2-chloro-4-(4,6-diamino-2,2-dimethyl-*s*-triazine-1(2*H*)-yl)phenoxy)-*N*,*N*-dimethyl-*m*-toluamide (1:1).

[2] Aquafluor.

[3] Brinkmann Silica Gel F-254.

0022-3549/82/01000-1102$01.00/0

Table I—Model Parameters for L-1210 Ascites Cells in Male Mice and W-256 Ascites Cells in Male Rats

Parameter	Mice (L-1210 cells)	Rats (W-256 cells)
V_c, cell volume, ml	0.21[a]	
V_{pe}, peritoneal cavity volume, ml	1.5[b]	3.1[b]
a, dihydrofolate reductase binding constant, μmole/ml	2.3×10^{-3} [c]	2.2×10^{-4} [d]
ϵ, dissociation constant, μmole/ml	2.2×10^{-8} [e]	
Average protein content[f]		
Cells, mg	69	140
Peritoneal fluid, mg	32.4	56.1
Estimated physicochemical parameters		
PA/V_c, cell permeability or passive transfer coefficient, min^{-1}	0.01	0.15
R, fluid–cell partition coefficient, dimensionless	0.2	35

[a] Calculated from average of experimental measurements of L-1210 cell numbers with time (2) and properties of tumor cells given by Sirotnak and Donsbach(4). [b] Estimated from values of Weissbrod *et al.* (5). [c] Adapted from Goldman *et al.* (6). [d] From Werkheiser (7). [e] Methotrexate dissociation constant from Bischoff *et al.* (8). [f] Experimentally measured.

of methanol was added to 0.5 ml of crude cell extract, mixed, and centrifuged, and the resulting solution was evaporated to 0.2 ml. Five microliters of this solution was applied onto the silica gel plates. Reference and control samples consisting of [^{14}C]triazinate, unlabeled triazinate, and control tissue extracts plus [^{14}C]triazinate were run with each set. The plates were run for 3 hr at room temperature and then air dried. Examination under UV light revealed a fluorescent green background with dark quenching spots. The spots were scraped and placed in a counting vial containing the scintillation fluid, and the radioactivity was determined.

No evidence for drug metabolism was obtained using the methanol extracts of tumor cells, as well as liver, kidney, and spleen cells, obtained up to 8 hr after drug administration. Analysis of methanol extracts of urine and feces also indicated no evidence for metabolism of ^{14}C-labeled triazinate in mice or rats.

The values of drug concentrations (in micromoles per milligram of protein) reported previously (2) were converted into micromoles per gram of cells or micromoles per milliliter of ascites fluid in this study using the values given in Table I.

MODEL DEVELOPMENT

A schematic of the model for triazinate pharmacokinetics in tumor cells is shown in Scheme I. The drug is injected into the peritoneal cavity, from which it enters the tumor cells and other body tissues and blood. Previous investigators of methotrexate transport *in vivo* simulated plasma or peritoneal fluid drug concentrations with multiple exponential expressions, which then served as inputs to the tumor model simulations (5, 9, 10). This approach focuses on drug kinetics in the tumor cells and obviates the need to consider details of triazinate distribution in the rest of the body.

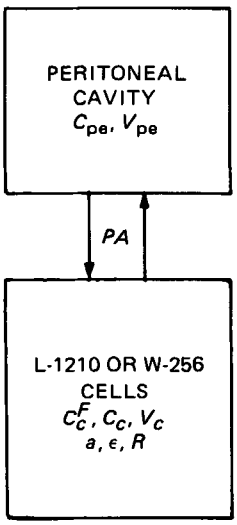

Scheme I—*The pharmacokinetic model for triazinate in L-1210 and W-256 cells. Symbols are defined in the text.*

In this study, instantaneous mixing of drug in the peritoneal cavity following intraperitoneal injection is assumed. A three-term exponential decay function of the form:

$$C_{pe} = a_1 e^{-b_1 t} + a_2 e^{-b_2 t} + a_3 e^{-b_3 t} \quad \text{(Eq. 1)}$$

is fit to the available peritoneal fluid concentration (C_{pe}) data as a function of time (t). (Here, $a_1 - a_3$ and $b_1 - b_3$ are empirical constants.) This expression serves as a forcing function in the mass balance for drug accumulation in the tumor cells:

$$\frac{dC_c}{dt} = \left(\frac{PA}{V_c}\right)\left(C_{pe} - \frac{C_c^F}{R}\right) \quad \text{(Eq. 2)}$$

where V_c is the volume of the tumor cells in milliliters; C_c is the total concentration of free and bound triazinate in the cells in micromoles per milliliter; PA is the cell permeability to drug in milliliters per minute; C_{pe} is the triazinate concentration in the peritoneal fluid in micromoles per milliliter; C_c^F is the concentration of free triazinate in the cells in micromoles per milliliter; and R is the partition coefficient relating peritoneal fluid concentration to free tumor cell concentration of triazinate at equilibrium (dimensionless). Drug transport in the model is considered to occur by passive diffusion, with drug binding to dihydrofolate reductase occurring in the cells.

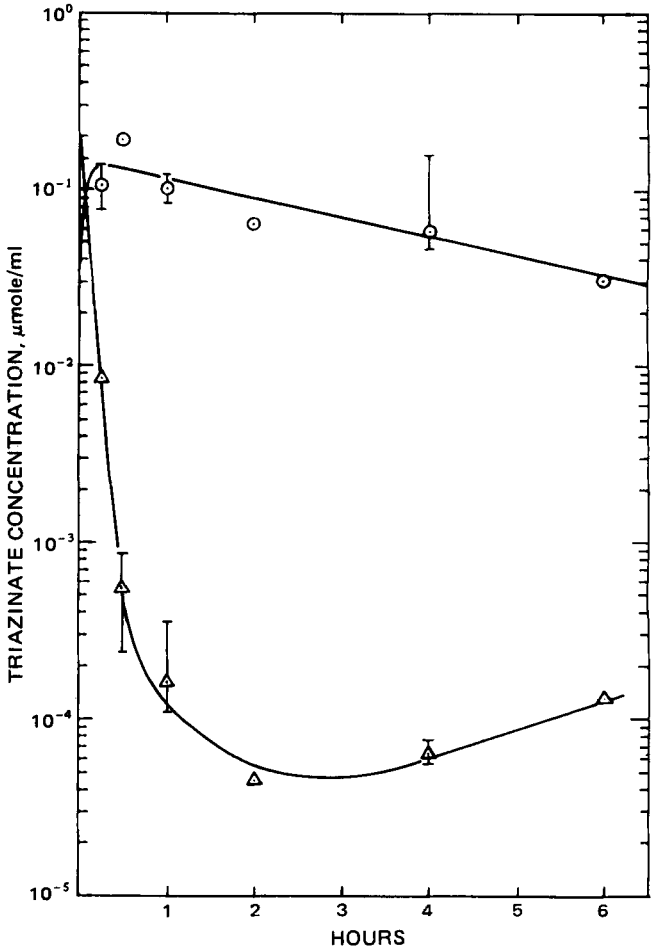

Figure 2—*Concentrations of triazinate in the peritoneal fluid and W-256 cells as a function of time following injections of 6 mg/kg ip (36 mg/m^2) in rats. Points represent experimental determinations (2). The solid lines represent the peritoneal fluid-forcing function (C_{pe}) and the model predictions of W-256 cell triazinate concentration (C_c). The peritoneal fluid triazinate concentration was fitted by the expression:*

$$C_{pe} = 0.203\, e^{-0.213t} + 4.31 \times 10^{-4}\, e^{-0.0224t} + 1.33 \times 10^{-5}\, e^{+0.00639t}$$

Other parameters are given in Table I. The bars represent ranges of the determinations. Key: (⊙) W-256 cells; (△) peritoneal fluid.

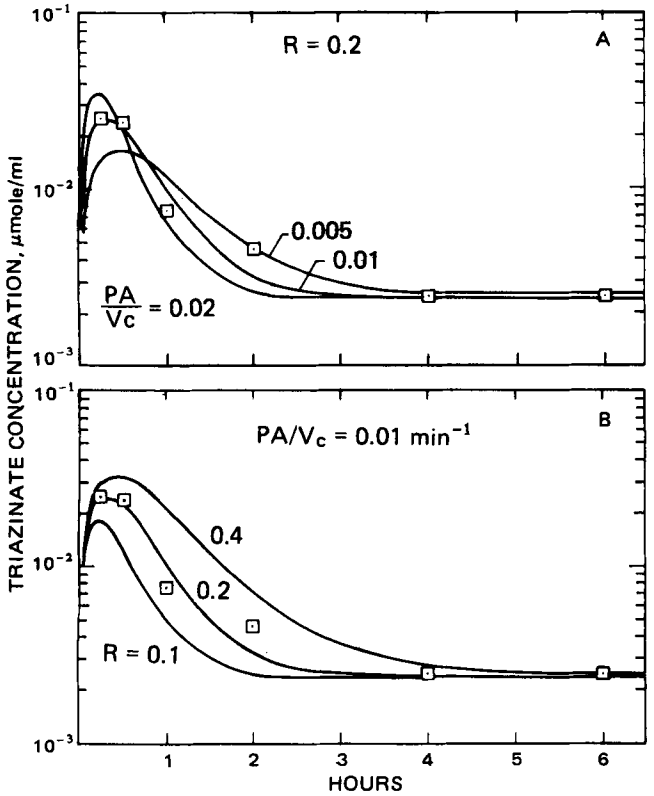

Figure 3—*Sensitivity of the model to changes in the parameters of (A) cell permeability (PA/V$_c$); and (B) partition coefficient (R) for the L-1210 cells in mice following injections of 12 mg/kg ip (36 mg/m^2). The points represent experimental determinations (2). The solid lines represent the model predictions of triazinate concentration in the L-1210 cells as a function of time.*

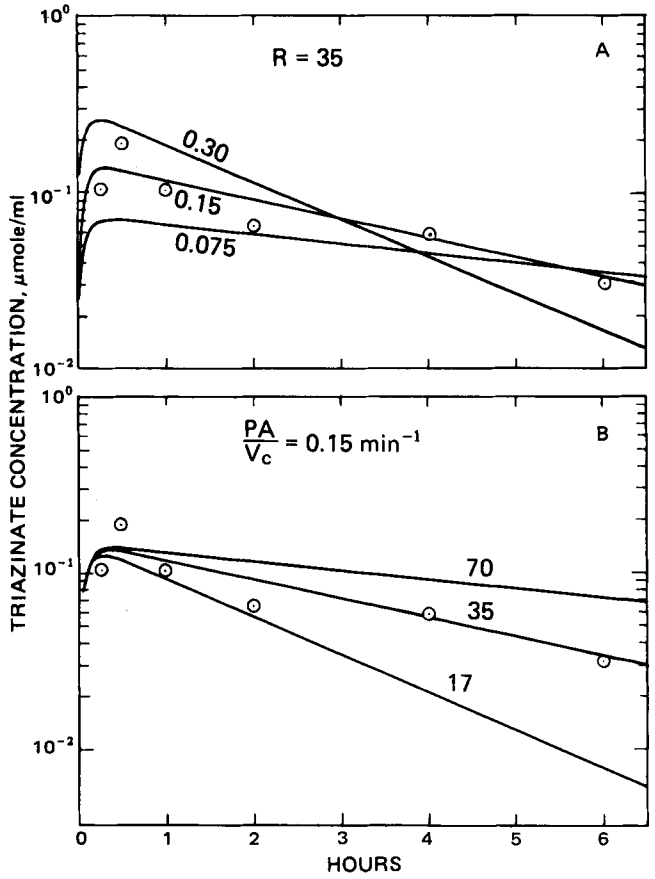

Figure 4—*Sensitivity of the model to changes in the parameters of (A) cell permeability (PA/V$_c$); and (B) partition coefficient (R) for the W-256 cells in rats following injections of 6 mg/kg ip (36 mg/m^2). The points represent experimental determinations (2). The solid lines represent the model predictions of triazinate concentration in the W-256 cells as a function of time.*

The total intracellular triazinate concentration in the tumor cells is the sum of free drug and drug bound to dihydrofolate reductase. The total tumor concentration in the model is related to the free drug concentration by the following relationship used previously for methotrexate (8):

$$C_c = C_c^F + \frac{aC_c^F}{\epsilon + C_c^F} \qquad \text{(Eq. 3)}$$

where a is the drug binding capacity of dihydrofolate reductase and ϵ is the dissociation constant of the drug–enzyme complex, both in micromoles per milliliter.

Values of the tumor cell permeabilities to triazinate, expressed as the quantity PA/V_c (min^{-1}), and the fluid–cell partition coefficients (R) are estimated by fitting Eq. 2 to the available data. These physicochemical parameters are summarized in Table I with the other model parameters. The system equations are solved by a Runge-Kutta routine (11) by computer to yield predictions of tumor cell triazinate concentration as a function of time.

RESULTS

Figures 1 and 2 show the peritoneal fluid and tumor cell concentrations of triazinate after injections of 36 mg/m^2 ip in mice and rats (12 and 6 mg/kg, respectively). The points represent the average of three individual determinations. The solid lines indicate the multiple exponential fits to the peritoneal fluid data and the model predictions of drug uptake by the L-1210 cells in mice (Fig. 1) and the W-256 cells in rats (Fig. 2). The average errors between model predictions and data are 16% for the L-1210 cells and 20% for the W-256 cells.

DISCUSSION

A pharmacokinetic model for triazinate uptake by L-1210 and W-256 ascites cells *in vivo* following a 36 mg/m^2 ip injection adequately simulates the observed concentration–time behavior in these cells. The model includes passive drug transport into the cells and binding of triazinate to intracellular dihydrofolate reductase. Values of binding constants and peritoneal fluid volumes are estimated from the literature (Table I), while the tumor cell volumes and other transport parameters (PA/V_c, R) are determined from the data (2).

A precise value for the dissociation constant (ϵ) for the triazinate–dihydrofolate reductase complex is not available. The value used here is that for methotrexate (8). Because triazinate is more tightly bound to dihydrofolate reductase than methotrexate, the ϵ for triazinate–dihydrofolate reductase should be smaller than ϵ for methotrexate–dihydrofolate reductase. However, since concentrations of free drug in the cells considered here are much greater than the magnitude of ϵ (of order 10^{-8} μmole/ml or less for triazinate), the expression for the amount of intracellular bound drug reduces to:

$$\frac{aC_c^F}{\epsilon + C_c^F} \rightarrow a \text{ (for } C_c^F \gg \epsilon) \qquad \text{(Eq. 4)}$$

Thus, a precise value of ϵ is not required.

The dramatic differences in triazinate uptake by the L-1210 and W-256 ascites cells are reflected in the model parameters determined from this study. The L-1210 cell permeability to drug (0.01 min^{-1}) is significantly smaller than that of the W-256 cells (0.15 min^{-1}), consistent with the observed difficulty of triazinate penetration in the leukemic cells compared with the W-256 cells (2, 3). While a partition coefficient of less than unity was determined for L-1210 cells, the W-256 partition coefficient is 35. These values also reflect the marked differences in drug accumulation in the two cell lines.

To assess the relative importance of permeability and partitioning in drug uptake and retention, a series of computer simulations was carried out. The effects of changing the transport parameters (PA/V_c) and distribution coefficients (R) are shown in Figs. 3 and 4 for the L-1210 cells and the W-256 cells, respectively. Each parameter is increased or decreased twofold while holding the remaining parameter constant. These simulations suggest that the cell permeability (PA/V_c) is the primary determinant of early accumulation of drug in tumor cells.

The preliminary model for triazinate pharmacokinetics presented here provides a logical basis for further investigation of the mechanism of triazinate transport and activity in different tumor lines.

REFERENCES

(1) B. R. Baker, *Ann. N.Y. Acad. Sci.*, **186**, 214 (1971).

(2) A. R. Cashmore, R. T. Skeel, D. R. Makulu, E. J. Gralla, and J. R. Bertino, *Cancer Res.*, **35**, 17 (1975).

(3) R. T. Skeel, W. L. Sawicki, A. R. Cashmore, and J. R. Bertino, *ibid.*, **33**, 2972 (1973).

(4) F. M. Sirotnak and R. C. Donsbach, *Cancer Res.*, **36**, 1151 (1976).

(5) J. M. Weissbrod, R. K. Jain, and F. M. Sirotnak, *J. Pharmacol. Biopharm.*, **6**, 487 (1978).

(6) I. D. Goldman, N. S. Lichtenstein, and V. T. Oliverio, *J. Biol. Chem.*, **243**, 5007 (1968).

(7) W. C. Werkheiser, *J. Biol. Chem.*, **236**, 888 (1961).

(8) K. B. Bischoff, R. L. Dedrick, D. S. Zaharko, and J. A. Longstreth, *J. Pharm. Sci.*, **60**, 1128 (1971).

(9) R. J. Lutz, R. L. Dedrick, J. A. Straw, M. M. Hart, P. Klubes, and D. S. Zaharko, *J. Pharmacol. Biopharm.*, **3**, 77 (1975).

(10) R. K. Jain, J. M. Weissbrod, and J. Wei, *Adv. Cancer Res.*, **33**, 251 (1980).

(11) R. K. Jain, Ph.D. Thesis, Department of Chemical Engineering, University of Delaware, Newark, Del. (1976).

ACKNOWLEDGMENTS

This work was supported by the Chemical Hygiene Fellowship of Mellon Institute of Research to J. G. Townsend and a Research Career Development Award to R. K. Jain.

Disposition and Absolute Bioavailability of Furosemide in Healthy Males

ELAINE S. WALLER *[x], STEPHEN F. HAMILTON *, JOSEPH W. MASSARELLA *, MOTRIA A. SHARANEVYCH [‡], ROBERT V. SMITH *, GERALD J. YAKATAN [§], and JAMES T. DOLUISIO *

Received October 23, 1981, from the **Drug Dynamics Institute, College of Pharmacy, The University of Texas at Austin, Austin, TX 78712*, the [‡]*Hoechst-Roussel Pharmaceuticals Inc., Somerville, NJ 08876*, and the [§]*Warner-Lambert Company, Ann Arbor, MI 48105.* Accepted for publication December 10, 1981.

Abstract □ Furosemide (40 mg) was administered to 18 healthy adult males as an intravenous dose, an oral solution, and in tablet form. The pharmacokinetics of intravenous furosemide were studied, determining a total body clearance rate of 117.6 ± 41.3 ml/min and a harmonic mean half-life of 78 min. The mean absolute bioavailability determined by ratio of areas under the plasma–time curves was 64 and 71% for the solution and tablet, respectively. The mean absolute bioavailability determined by the ratio of urinary cumulative excretion data was 61 and 66% for the solution and tablet, respectively. The absolute bioavailabilities of furosemide determined with plasma and urine data were not significantly different. Thus, urine data alone may be used to establish bioavailability of furosemide. Inspection of plasma–time curves revealed secondary maxima in several subjects, suggesting enterohepatic cycling.

Keyphrases □ Furosemide—disposition and absolute bioavailability in healthy males □ Pharmacokinetics—disposition and absolute bioavailability of furosemide in healthy males □ Bioavailability—disposition, furosemide in healthy males

Furosemide is one of a series of anthranilic acid derivatives which is commonly used as a potent diuretic. Depending on the severity of clinical indication for its use, it is usually administered either orally or intravenously. Therefore, it is of interest to determine the bioavailability of oral preparations with respect to intravenous dosing.

Absolute bioavailability of furosemide has been studied previously by several investigators. Intravenous and oral doses of furosemide were administered previously to four subjects and the absolute bioavailability of tablets was determined to be 65%; the oral aqueous solution was 69% bioavailable (1). [^{35}S]Furosemide was administered orally as an aqueous solution to seven volunteers and intravenously to two different volunteers in another study (2). Comparison of the areas under the plasma curves across subjects determined the solution was 67% bioavailable. In a study with six volunteers (3), absolute bioavailability of oral furosemide (dosage form not identified) was found to be 49%. Eleven normal volunteers were studied (4); tablet and solution preparations were determined to be 69% bioavailable.

The present study was conducted to determine the absolute bioavailability of furosemide (40 mg) given in tablet form and as an oral solution to a large population of healthy males. In addition, the feasibility of using urinary excretion data alone to establish bioavailability was investigated. This would allow future bioavailability studies to be conducted without exposing subjects to numerous blood collections.

Absolute bioavailability of furosemide tablets and solution was established by both ratio of the areas under the plasma–time curves and ratio of cumulative excretion data. The disposition of furosemide given intravenously was also determined. Analysis of the resulting data strongly suggests enterohepatic cycling of furosemide.

EXPERIMENTAL

Subject Selection—Twenty-one healthy males, 20–31 years of age (mean 24) weighing between 61 and 83 kg (mean 71), who were in good physical condition as determined by physical examination, volunteered to participate in the study. Informed consent was obtained from each subject[1].

Study Design—An open Latin-square design was used to study 21 subjects divided into three groups of seven. Subjects were randomly as-

[1] The protocol has approval of the University of Texas at Austin Human Investigation Review Committee.

0022-3549/82/01000-1105$01.00/0

The preliminary model for triazinate pharmacokinetics presented here provides a logical basis for further investigation of the mechanism of triazinate transport and activity in different tumor lines.

REFERENCES

(1) B. R. Baker, *Ann. N.Y. Acad. Sci.*, **186**, 214 (1971).

(2) A. R. Cashmore, R. T. Skeel, D. R. Makulu, E. J. Gralla, and J. R. Bertino, *Cancer Res.*, **35**, 17 (1975).

(3) R. T. Skeel, W. L. Sawicki, A. R. Cashmore, and J. R. Bertino, *ibid.*, **33**, 2972 (1973).

(4) F. M. Sirotnak and R. C. Donsbach, *Cancer Res.*, **36**, 1151 (1976).

(5) J. M. Weissbrod, R. K. Jain, and F. M. Sirotnak, *J. Pharmacol. Biopharm.*, **6**, 487 (1978).

(6) I. D. Goldman, N. S. Lichtenstein, and V. T. Oliverio, *J. Biol. Chem.*, **243**, 5007 (1968).

(7) W. C. Werkheiser, *J. Biol. Chem.*, **236**, 888 (1961).

(8) K. B. Bischoff, R. L. Dedrick, D. S. Zaharko, and J. A. Longstreth, *J. Pharm. Sci.*, **60**, 1128 (1971).

(9) R. J. Lutz, R. L. Dedrick, J. A. Straw, M. M. Hart, P. Klubes, and D. S. Zaharko, *J. Pharmacol. Biopharm.*, **3**, 77 (1975).

(10) R. K. Jain, J. M. Weissbrod, and J. Wei, *Adv. Cancer Res.*, **33**, 251 (1980).

(11) R. K. Jain, Ph.D. Thesis, Department of Chemical Engineering, University of Delaware, Newark, Del. (1976).

ACKNOWLEDGMENTS

This work was supported by the Chemical Hygiene Fellowship of Mellon Institute of Research to J. G. Townsend and a Research Career Development Award to R. K. Jain.

Disposition and Absolute Bioavailability of Furosemide in Healthy Males

ELAINE S. WALLER *[x], STEPHEN F. HAMILTON *, JOSEPH W. MASSARELLA *, MOTRIA A. SHARANEVYCH [‡], ROBERT V. SMITH *, GERALD J. YAKATAN [§], and JAMES T. DOLUISIO *

Received October 23, 1981, from the **Drug Dynamics Institute, College of Pharmacy, The University of Texas at Austin, Austin, TX 78712*, the [‡]*Hoechst-Roussel Pharmaceuticals Inc., Somerville, NJ 08876*, and the [§]*Warner-Lambert Company, Ann Arbor, MI 48105.* Accepted for publication December 10, 1981.

Abstract □ Furosemide (40 mg) was administered to 18 healthy adult males as an intravenous dose, an oral solution, and in tablet form. The pharmacokinetics of intravenous furosemide were studied, determining a total body clearance rate of 117.6 ± 41.3 ml/min and a harmonic mean half-life of 78 min. The mean absolute bioavailability determined by ratio of areas under the plasma–time curves was 64 and 71% for the solution and tablet, respectively. The mean absolute bioavailability determined by the ratio of urinary cumulative excretion data was 61 and 66% for the solution and tablet, respectively. The absolute bioavailabilities of furosemide determined with plasma and urine data were not significantly different. Thus, urine data alone may be used to establish bioavailability of furosemide. Inspection of plasma–time curves revealed secondary maxima in several subjects, suggesting enterohepatic cycling.

Keyphrases □ Furosemide—disposition and absolute bioavailability in healthy males □ Pharmacokinetics—disposition and absolute bioavailability of furosemide in healthy males □ Bioavailability—disposition, furosemide in healthy males

Furosemide is one of a series of anthranilic acid derivatives which is commonly used as a potent diuretic. Depending on the severity of clinical indication for its use, it is usually administered either orally or intravenously. Therefore, it is of interest to determine the bioavailability of oral preparations with respect to intravenous dosing.

Absolute bioavailability of furosemide has been studied previously by several investigators. Intravenous and oral doses of furosemide were administered previously to four subjects and the absolute bioavailability of tablets was determined to be 65%; the oral aqueous solution was 69% bioavailable (1). [^{35}S]Furosemide was administered orally as an aqueous solution to seven volunteers and intravenously to two different volunteers in another study (2). Comparison of the areas under the plasma curves across subjects determined the solution was 67% bioavailable. In a study with six volunteers (3), absolute bioavailability of oral furosemide (dosage form not identified) was found to be 49%. Eleven normal volunteers were studied (4); tablet and solution preparations were determined to be 69% bioavailable.

The present study was conducted to determine the absolute bioavailability of furosemide (40 mg) given in tablet form and as an oral solution to a large population of healthy males. In addition, the feasibility of using urinary excretion data alone to establish bioavailability was investigated. This would allow future bioavailability studies to be conducted without exposing subjects to numerous blood collections.

Absolute bioavailability of furosemide tablets and solution was established by both ratio of the areas under the plasma–time curves and ratio of cumulative excretion data. The disposition of furosemide given intravenously was also determined. Analysis of the resulting data strongly suggests enterohepatic cycling of furosemide.

EXPERIMENTAL

Subject Selection—Twenty-one healthy males, 20–31 years of age (mean 24) weighing between 61 and 83 kg (mean 71), who were in good physical condition as determined by physical examination, volunteered to participate in the study. Informed consent was obtained from each subject[1].

Study Design—An open Latin-square design was used to study 21 subjects divided into three groups of seven. Subjects were randomly as-

[1] The protocol has approval of the University of Texas at Austin Human Investigation Review Committee.

0022-3549/82/01000-1105$01.00/0

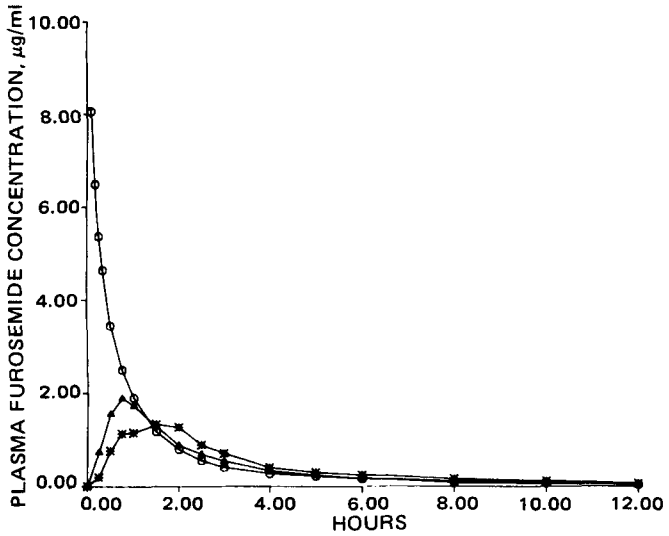

Figure 1—*Mean furosemide plasma concentrations following 40 mg administered as an intravenous solution (○), oral solution (△), and tablet (*) to 18 healthy adult males.*

signed to each group. A single dose of furosemide[2] (40 mg) was administered on 3 different days as an intravenous injection, oral aqueous solution, and tablet. Seven-day washout periods separated the study days.

All subjects abstained from medications, smoking, and alcohol for 1 week prior to and throughout the study. Subjects fasted for 12 hr before each drug administration and 3 hr thereafter. Furosemide tablets were taken with 200 ml of water. Four milliliters of furosemide oral solution was administered with 200 ml of water. The intravenous furosemide dose was injected over a 2-min period.

Following drug administration, blood samples (10 ml) were collected from a forearm vein using a plastic syringe with immediate transfer to heparinized tubes. Blood was collected immediately before and at 0.25, 0.5, 0.75, 1, 1.5, 2, 2.5, 3, 4, 5, 6, 8, 10, and 12 hr after oral drug administration. Blood was collected immediately before and at 5, 10, 15, 20, 30, and 45 min and 1, 1.5, 2, 2.5, 3, 4, 5, 6, 8, 10, and 12 hr after the intravenous injection was completed. Plasma was separated and frozen at −20° until assayed. During each study day, urine was collected immediately before drug administration and for the following periods: 0–1, 1–2, 2–3, 3–4, 4–5, 5–6, 6–8, 8–12, and 12–24 hr. Urine volumes were recorded and an aliquot was frozen at −20° until assayed.

Assay—The plasma and urine specimens were assayed by reversed-phase high-performance liquid chromatography (HPLC) using a method described previously (5). The only substantive change in procedure was the use of hydroflumethiazide as internal standard instead of furosemide methyl ester. The methods described in the literature and used in the author's laboratories are specific for the intact furosemide and showed no interference from its hydrolysis product, 4-chloro-5-sulfamoyl anthranilic acid. Furthermore, no interference was observed at the retention time for the internal standard, hydroflumethiazide.

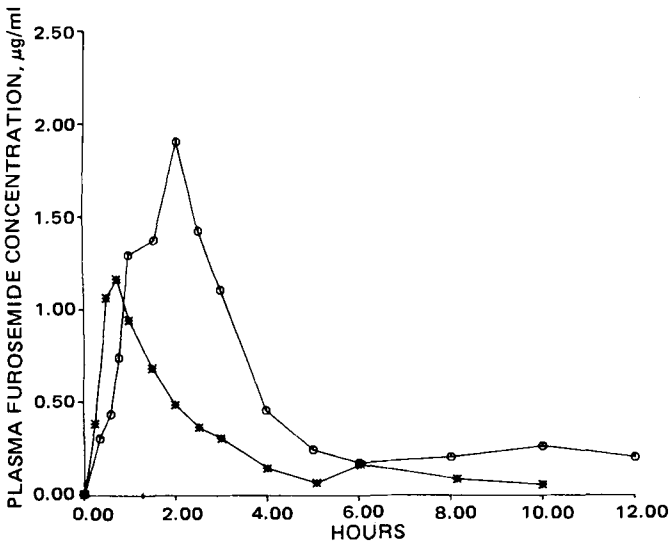

Figure 2—*Furosemide plasma concentrations following 40 mg administered as an intravenous solution to two healthy adult males (Subjects 2 and 13).*

[2] Lasix, supplied by Hoechst-Roussel Pharmaceuticals Inc., tablet: Lot #601160; oral solution: Lot #680010; intravenous solution: Lot #619513.

Table I—Pharmacokinetic Parameters (Mean ± *SD*) in 16 Normal Males Following Intravenous Administration of Furosemide (40 mg)

Parameter	Value
A, μg/ml	8.7 ± 2.7
B, μg/ml	2.1 ± 1.3
α, min^{-1}	0.063 ± 0.051
β, min^{-1}	0.0089 ± 0.0052
Ke, min^{-1}	0.028 ± 0.014
K_{21}, min^{-1}	0.021 ± 0.017
K_{12}, min^{-1}	0.024 ± 0.027
$AUC_{0\to\infty}$ μg $min\ ml^{-1}$	374.28 ± 110.49
Vc, liter/kg	0.056 ± 0.017
Vd_{ss}, liter/kg	0.13 ± 0.06
Cl_T, ml/min	117.6 ± 41.3
Cl_R, ml/min	88.9 ± 44.8 (n = 13)
Cl_{NR}, ml/min	32.4 ± 11.9 (n = 13)

The analytical method employed involved extraction of acidified urine or plasma (spiked with internal standard) with a fivefold excess of diethyl ether. In the case of plasma, the ether was reduced to dryness under a stream of nitrogen, the residue reconstituted in glycine buffer (pH 11.0), and subjected to chromatographic development. Urine ether extracts were back-extracted with glycine buffer (pH 11.0) and the latter alkaline extracts subjected to HPLC. Peak areas (furosemide and internal standard) were determined with a computing integrator dedicated to the HPLC apparatus used in the determinations. Peak area ratios from samples were compared with similar data developed from eight standard samples for plasma determinations (in the range of 0.05–20.05 μg/ml) and five standard samples for urine determinations (in the range of 0.1–50.0 μg/ml), which were used in preparing standard curves ($r \geq 0.999$). The average relative standard deviation of the standard samples for plasma determinations was 7.3%; 2.6% was found for urine determinations. All samples were protected from light prior to analysis.

Data Analysis—Area under the plasma concentration–time curve (AUC) was calculated for 0–12 hr using the trapezoidal rule. The $AUC_{0\to\infty}$ for intravenously administered furosemide included a terminal slope correction factor, Cp^n/β, where Cp^n is the last measured concentration–time point, and β is the slope of the terminal log-linear phase of the semilog plot of concentration *versus* time. The maximum plasma concentration achieved (Cp_{max}) and time to maximum plasma concentration (t_{max}) were observed from the measured plasma concentrations following oral drug administration.

Plasma concentration data following termination of the rapid intravenous infusion were fitted to the biexponential equation:

$$Cp = Ae^{-\alpha t} + Be^{-\beta t} \qquad \text{(Eq. 1)}$$

where Cp is the plasma concentration in micrograms per milliliter at time t, A and B are pre-exponential terms in units of concentration, and α and β are hybrid first-order rate constants with units of reciprocal time. The data were fitted using nonlinear least-squares regression analysis with the program NONLIN (6) (weight = $1/Cp$). Microconstants were calculated for each individual subject using:

$$K_{21} = \frac{A\beta + B\alpha}{A + B} \qquad Ke = \frac{\alpha\beta}{K_{21}} \qquad K_{12} = \alpha + \beta - K_{21} - Ke$$

(Eq. 2)

The volume of distribution of the central compartment (Vc) was calculated from:

$$Vc = \frac{\text{Dose}}{A + B} \qquad \text{(Eq. 3)}$$

The steady-state volume of distribution (Vd_{ss}) was calculated from the definition:

$$Vd_{ss} = \left(1 + \frac{K_{12}}{K_{21}}\right) Vc \qquad \text{(Eq. 4)}$$

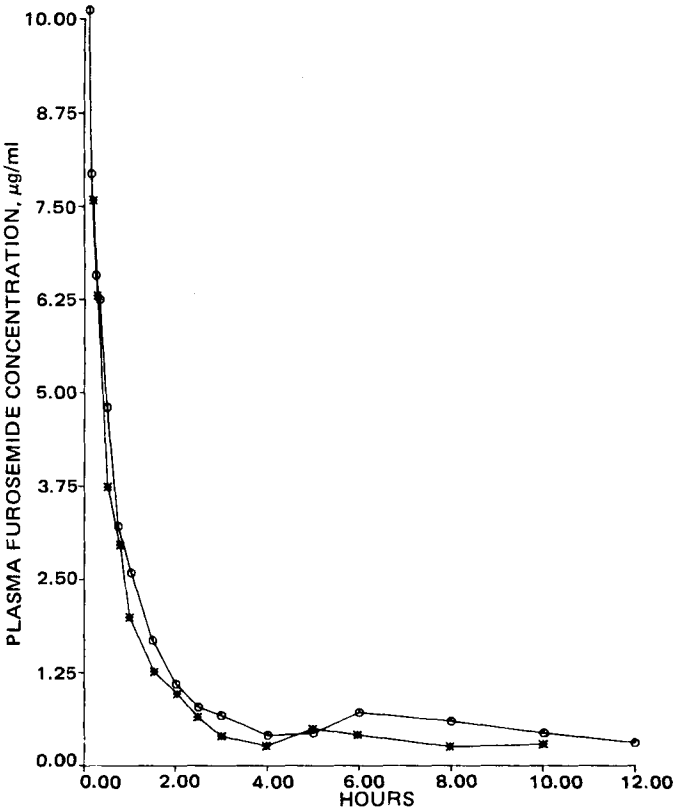

Figure 3—*Furosemide plasma concentrations following 40 mg administered as tablet (*) and oral solution (O) to two healthy adult males (Subjects 8 and 16).*

Total body clearance (Cl_T) was determined from:

$$Cl_T = \frac{\text{Dose}}{AUC_{0\to\infty}} \qquad \text{(Eq. 5)}$$

Renal clearance (Cl_R) was calculated from the relation:

$$Cl_R = \frac{X_{u0\text{-}24}}{AUC_{0\to\infty}} \qquad \text{(Eq. 6)}$$

where $X_{u0\text{-}24}$ is the total amount of unchanged drug eliminated in the urine in 24 hr. The difference between total body clearance and renal clearance was labeled the nonrenal clearance (Cl_{NR}).

The absolute bioavailability (F) was determined from plasma and urine data from:

$$F_{\text{plasma}} = \frac{AUC_{0\text{-}12}^{\text{oral}}}{AUC_{0\text{-}12}^{\text{iv}}} \qquad \text{(Eq. 7)}$$

$$F_{\text{urine}} = \frac{X_{u0\text{-}24}^{\text{oral}}}{X_{u0\text{-}24}^{\text{iv}}} \qquad \text{(Eq. 8)}$$

Analysis of variance with the least significant difference test utilized for *a posteriori* comparison and Student's t test for paired data were used to make statistical evaluations of the data. An α-level of <0.05 was accepted as evidence of statistical significance.

RESULTS AND DISCUSSION

Eighteen subjects completed the study. Three subjects dropped from the study for reasons unrelated to the administered drug. Data collected from these three subjects were not included in the data analysis.

Mean plasma furosemide concentrations given intravenously and orally are depicted in Fig. 1. Two subjects administered the intravenous dose had a second peak in their plasma furosemide concentrations at 5–6 hr. The data from these two subjects were not included in the determination of the disposition of intravenous furosemide. The pharmacokinetic parameters for the remaining 16 subjects are given in Table I. The mean terminal log-linear phase disposition rate constant corresponds to a half-life of 78 min. This is reasonably consistent with other half-life values of 26–72 min following intravenous furosemide dosing (7). Other pharmacokinetic parameters are in agreement with those previously reported in the literature, though the total body clearance of 118 ml/min is among the lower clearance values reported (112–268 ml/min) (7).

Table II—Bioavailability Parameters (Mean ± *SD*) in 18 Normal Males Following Administration of Furosemide (40 mg) [a]

Parameter	Value
$AUC_{0\text{-}12}$ iv, μg min ml^{-1}	383.9 ± 121.9
$AUC_{0\text{-}12}$ solution (μg min ml^{-1})	240.9 ± 98.8
$AUC_{0\text{-}12}$ tablet (μg min ml^{-1})	250.0 ± 116.2
$X_u^{0\text{-}24}$/dose iv	0.71 ± 0.10 (n = 14)
$X_u^{0\text{-}24}$/dose solution	0.41 ± 0.02 (n = 16)
$X_u^{0\text{-}24}$/dose tablet	0.44 ± 0.15
$AUC^{\text{solution}}/AUC^{\text{iv}}$	0.64 ± 0.22
$AUC^{\text{tablet}}/AUC^{\text{iv}}$	0.71 ± 0.35
$X_u^{\text{solution}}/X_u^{\text{iv}}$	0.61 ± 0.17 (n = 12)
$X_u^{\text{tablet}}/X_u^{\text{iv}}$	0.66 ± 0.23 (n = 14)
$Cp_{\max}$ solution, μg/ml	1.8 ± 0.6
$Cp_{\max}$ tablet, μg/ml	1.7 ± 0.9
$t_{\max}$ solution, min	50.1 ± 23.8
$t_{\max}$ tablet, min	86.2 ± 50.3

[a] Given as tablet, oral solution, and intravenous solution.

Individual plasma concentrations in the two subjects with a second peak in plasma furosemide concentrations are displayed in Fig. 2. The appearance of this second peak suggests the possibility of biliary secretion of furosemide and/or metabolite(s) with subsequent reabsorption of the parent drug. An attempt to study biliary secretion of furosemide in humans was made previously (2). This group found increased radioactivity counts in duodenal aspirates of two subjects given intravenous [^{35}S]furosemide with cholecystokinin stimulation. It was not determined if the increased counts represented intact furosemide or metabolites. [^{35}S]-Furosemide was administered intravenously to two dogs, and an average of 51.4% was found in the feces (8). It was deduced that biliary secretion may play a major role in the elimination of furosemide and/or metabolites. In additional work, cannulation of the bile duct with complete bile collection in one dog given intravenous furosemide showed furosemide to be present in the bile[3]. Secondary maxima have been reported in normal subjects given oral furosemide, and biliary recycling was suggested as an explanation (9).

While no conclusive studies have been conducted in humans to determine if furosemide undergoes enterohepatic cycling, the presence of intact furosemide in the bile of one animal species and the observed secondary maxima in the plasma concentration–time curves in two subjects in the present study suggest enterohepatic cycling may occur. This hypothesis is further supported by plasma concentration–time curves obtained from data following oral doses of furosemide. Secondary maxima were seen in several subjects receiving the drug orally; representative curves are shown in Fig. 3.

Mean bioavailability parameters are displayed in Table II. The AUC was truncated at 12 hr because secondary maxima in plasma concentrations obscured the terminal log-linear phase in many subjects, making corrections to $AUC_{0\to\infty}$ unreliable. Because most subjects had plasma concentrations below assay sensitivity or near the sensitivity limit at the time of the last blood sample, a significant portion of the AUC was not lost by not calculating the AUC to infinity. The $AUC_{0\text{-}12}$ for the intravenous dose was significantly greater than the $AUC_{0\text{-}12}$ for either the oral solution or tablet. The mean absolute bioavailability determined from the plasma data was 64 and 71% for the solution and tablet, respectively. The bioavailabilities for the solution and tablet preparations were not statistically significantly different for either the plasma or urine determinations.

The absolute bioavailabilities of furosemide determined with plasma and urine data were not significantly different ($p > 0.05$); however, there was a trend toward a greater bioavailability ratio determined from plasma data, compared with the ratio determined from the urine data. This is similar to previously reported data (2), in which 67% bioavailability of furosemide solution determined from plasma data and 65% bioavailability determined from urinary data was reported. In contrast, 49% bioavailability determined from plasma data was reported and 52% bioavailability determined from urinary data (3). The slightly greater bioavailability determined with plasma data in the present study may possibly be explained by biliary recycling of furosemide. The observed secondary maxima increased the AUC. There was also considerable intrasubject variability in the appearance of these peaks. The bioavailability determined by AUC may be inflated from secondary plasma peaks while the

[3] G. Yakatan and J. Johnston, unpublished data.

bioavailability determined from urine data may give a more accurate reflection of the true bioavailability. Thus, the feasibility of using urinary excretion data alone to determine bioavailability of furosemide is good, given the statistical agreement of absolute bioavailability determined by plasma and urine data. Also, the possibility of overestimation of bioavailability by plasma data because of enterohepatic recycling makes bioavailability determined from urine data appear more reliable.

The t_{max} and Cp_{max} determinations were not statistically significantly different for the tablet and solution. There was a trend toward later peak plasma concentrations following tablet administration, probably due to time required for tablet disintegration and dissolution. The seeming disagreement of Cp_{max} determinations presented in Table II and Fig. 1 is a function of mean data being graphically presented, while the means of individual subjects are presented in the table.

The bioavailabilities of the tablet and solution are essentially the same, though <70% of the dose was absorbed. This suggests the absorption may not be solely dependent on solubility, but may also be limited by absorption occurring only from a specific site in the GI tract. Site-limited absorption may explain intrasubject variability in absolute bioavailability.

In summary, the disposition of intravenous furosemide as determined by this study is in agreement with previous reports. The mean absolute bioavailability determined from cumulative urinary excretion data was 61 and 66% for the solution and tablet, respectively. The bioavailability determined with urine data may be more reliable than bioavailability determined with plasma data because of a possible enterohepatic recycling process. Site-limited absorption of furosemide is suggested.

REFERENCES

(1) M. Kelly, R. Cutler, A. Forrey, and B. Kimpel, *Clin. Pharmacol. Ther.*, **15**, 178 (1973).

(2) B. Beermann, E. Dalén, B. Lindström, and A. Rosén, *Eur. J. Clin. Pharmacol.*, **9**, 57 (1975).

(3) R. Branch, C. Roberts, M. Homeida, and D. Levine, *Br. J. Clin. Pharmacol.*, **4**, 121 (1977).

(4) W. Tilstone and A. Fine, *Clin. Pharmacol. Ther.*, **23**, 644 (1978).

(5) K. Carr, A. Rane, and J. Frolich, *J. Chromatogr.*, **145**, 421 (1978).

(6) C. M. Metzler, "*A User's Manual for NONLIN*," Technical Report 7292/69/7292/005, The Upjohn Co., Kalamazoo, Mich., 1969.

(7) L. Z. Benet, *J. Pharmacokin. Biopharm.*, **7**, 1 (1979).

(8) G. Yakatan, D. Maness, J. Scholler, W. Novick, Jr., and J. Doluisio, *J. Pharm. Sci.*, **65**, 1456 (1976).

(9) D. Smith, E. Lin, and L. Benet, *Drug Metab. Dispos.* **8**, 337 (1980).

ACKNOWLEDGMENTS

This work was supported by a grant provided by Hoechst-Roussel Pharmaceuticals Inc.

Determination of Amine Ingredients in Cough–Cold Liquids by Reversed-Phase Ion-Pair High-Performance Liquid Chromatography

G. W. HALSTEAD

Received October 9, 1981, from *Control Analytical Research and Development, The Upjohn Company, Kalamazoo, MI 49001.* Accepted for publication December 14, 1981.

Abstract □ The chromatographic behavior of phenylephrine, codeine, pseudoephedrine, phenylpropanolamine, methoxyphenamine, pheniramine, pyrilamine, dextromethorphan, and chlorpheniramine was examined by reversed-phase, ion-pair high-performance liquid chromatography. An isocratic chromatographic system was devised for the analysis of cough–cold liquids containing these amine drugs by optimization of the mobile phase ionic strength, buffer pH, pairing ion concentration, and secondary ion concentration. Quantitative recovery and excellent precision were demonstrated for the simultaneous determination of phenylpropanolamine, dextromethorphan, and chlorpheniramine in a typical formulation. The method was successfully applied to various commercial cough–cold liquids for the analysis of a wide range of amine drugs.

Keyphrases □ Cough–cold liquids—determination of amine ingredients by reversed-phase, ion-pair high-performance liquid chromatography □ High-performance liquid chromatography—determination of amine ingredients in cough–cold liquids □ Amine drugs—determination in cough–cold liquids by reversed-phase ion-pair high-performance liquid chromatography

Cough–cold liquids are usually complex formulations containing several active ingredients and a broad spectrum of excipients such as dyes, flavors, sweeteners, and preservatives. Many of these products are designed to be multisymptom preparations typically containing a variety of basic amino compounds acting as antihistamines, decongestants, or cough suppressants. Some of the common amino agents utilized include phenylephrine, phenylpropanolamine, pseudoephedrine, pyrilamine, pheniramine, chlorpheniramine, codeine, and dextromethorphan. The analgesics, phenacetin and acetaminophen, are also commonly found in cough–cold liquids adding further complexity to the list of possible ingredients. Preservatives such as methyl- and propylparaben or sodium benzoate are normally present in a formulation. It was the purpose of this study to develop a simple high-performance liquid

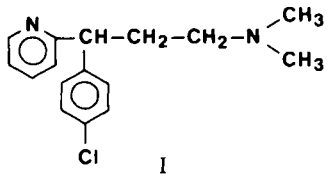

I

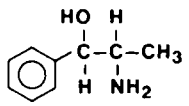

II

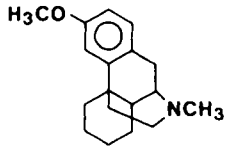

III

0022-3549/82/01000-1108$01.00/0

bioavailability determined from urine data may give a more accurate reflection of the true bioavailability. Thus, the feasibility of using urinary excretion data alone to determine bioavailability of furosemide is good, given the statistical agreement of absolute bioavailability determined by plasma and urine data. Also, the possibility of overestimation of bioavailability by plasma data because of enterohepatic recycling makes bioavailability determined from urine data appear more reliable.

The t_{max} and Cp_{max} determinations were not statistically significantly different for the tablet and solution. There was a trend toward later peak plasma concentrations following tablet administration, probably due to time required for tablet disintegration and dissolution. The seeming disagreement of Cp_{max} determinations presented in Table II and Fig. 1 is a function of mean data being graphically presented, while the means of individual subjects are presented in the table.

The bioavailabilities of the tablet and solution are essentially the same, though <70% of the dose was absorbed. This suggests the absorption may not be solely dependent on solubility, but may also be limited by absorption occurring only from a specific site in the GI tract. Site-limited absorption may explain intrasubject variability in absolute bioavailability.

In summary, the disposition of intravenous furosemide as determined by this study is in agreement with previous reports. The mean absolute bioavailability determined from cumulative urinary excretion data was 61 and 66% for the solution and tablet, respectively. The bioavailability determined with urine data may be more reliable than bioavailability determined with plasma data because of a possible enterohepatic recycling process. Site-limited absorption of furosemide is suggested.

REFERENCES

(1) M. Kelly, R. Cutler, A. Forrey, and B. Kimpel, *Clin. Pharmacol. Ther.*, **15**, 178 (1973).

(2) B. Beermann, E. Dalén, B. Lindström, and A. Rosén, *Eur. J. Clin. Pharmacol.*, **9**, 57 (1975).

(3) R. Branch, C. Roberts, M. Homeida, and D. Levine, *Br. J. Clin. Pharmacol.*, **4**, 121 (1977).

(4) W. Tilstone and A. Fine, *Clin. Pharmacol. Ther.*, **23**, 644 (1978).

(5) K. Carr, A. Rane, and J. Frolich, *J. Chromatogr.*, **145**, 421 (1978).

(6) C. M. Metzler, "*A User's Manual for NONLIN*," Technical Report 7292/69/7292/005, The Upjohn Co., Kalamazoo, Mich., 1969.

(7) L. Z. Benet, *J. Pharmacokin. Biopharm.*, **7**, 1 (1979).

(8) G. Yakatan, D. Maness, J. Scholler, W. Novick, Jr., and J. Doluisio, *J. Pharm. Sci.*, **65**, 1456 (1976).

(9) D. Smith, E. Lin, and L. Benet, *Drug Metab. Dispos.* **8**, 337 (1980).

ACKNOWLEDGMENTS

This work was supported by a grant provided by Hoechst-Roussel Pharmaceuticals Inc.

Determination of Amine Ingredients in Cough–Cold Liquids by Reversed-Phase Ion-Pair High-Performance Liquid Chromatography

G. W. HALSTEAD

Received October 9, 1981, from *Control Analytical Research and Development, The Upjohn Company, Kalamazoo, MI 49001.* Accepted for publication December 14, 1981.

Abstract □ The chromatographic behavior of phenylephrine, codeine, pseudoephedrine, phenylpropanolamine, methoxyphenamine, pheniramine, pyrilamine, dextromethorphan, and chlorpheniramine was examined by reversed-phase, ion-pair high-performance liquid chromatography. An isocratic chromatographic system was devised for the analysis of cough–cold liquids containing these amine drugs by optimization of the mobile phase ionic strength, buffer pH, pairing ion concentration, and secondary ion concentration. Quantitative recovery and excellent precision were demonstrated for the simultaneous determination of phenylpropanolamine, dextromethorphan, and chlorpheniramine in a typical formulation. The method was successfully applied to various commercial cough–cold liquids for the analysis of a wide range of amine drugs.

Keyphrases □ Cough–cold liquids—determination of amine ingredients by reversed-phase, ion-pair high-performance liquid chromatography □ High-performance liquid chromatography—determination of amine ingredients in cough–cold liquids □ Amine drugs—determination in cough–cold liquids by reversed-phase ion-pair high-performance liquid chromatography

Cough–cold liquids are usually complex formulations containing several active ingredients and a broad spectrum of excipients such as dyes, flavors, sweeteners, and preservatives. Many of these products are designed to be multisymptom preparations typically containing a variety of basic amino compounds acting as antihistamines, decongestants, or cough suppressants. Some of the common amino agents utilized include phenylephrine, phenylpropanolamine, pseudoephedrine, pyrilamine, pheniramine, chlorpheniramine, codeine, and dextromethorphan. The analgesics, phenacetin and acetaminophen, are also commonly found in cough–cold liquids adding further complexity to the list of possible ingredients. Preservatives such as methyl- and propylparaben or sodium benzoate are normally present in a formulation. It was the purpose of this study to develop a simple high-performance liquid

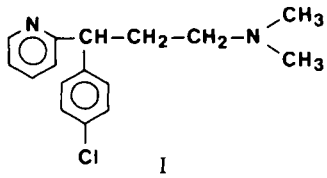

I

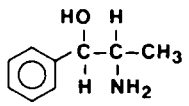

II

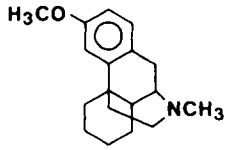

III

0022-3549/82/01000-1108$01.00/0

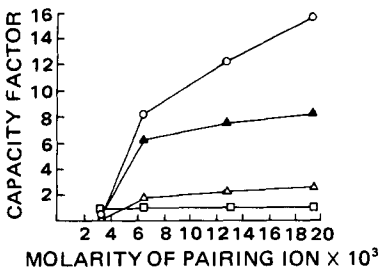

Figure 1—*Relationship between retention and pairing ion concentration of the mobile phase. Key: (△) phenylpropanolamine; (▲) dextromethorphan; (○) chlorpheniramine; (□) propylparaben. Mobile phase: 0.02* M *ammonium nitrate, 70% methanol, 1.5% glacial acetic acid. The pairing ion is sodium dioctyl sulfosuccinate.*

chromatographic (HPLC) procedure capable of determining the full range of amines commonly found in cough–cold liquids. Efforts were concentrated on the simultaneous determination of the antihistamine, chlorpheniramine (I); the decongestant, phenylpropanolamine (II); and the cough suppressant, dextromethorphan (III) in a typical cough–cold liquid. Applicability of the chromatographic separation to these and other amine drugs in a variety of different formulations was demonstrated by the analysis of cough–cold liquids from a variety of different sources.

BACKGROUND

Chromatographic determination of cough–cold amines has previously been performed using GLC (1–3) and ion-pair, reversed-phase HPLC (4–10). The GLC methods are generally less efficient due to the necessity of derivatization of some or all of the amines, and because the sample preparation usually involves an extraction step or evaporation of the sample and redissolution in a suitable solvent. Several of the available HPLC procedures were designed for the determination of one component and are not able to handle all of the amine ingredients found in combination products (4–6, 8). Another chromatographic system for the determination of pseudoephedrine, brompheniramine, and dextromethorphan elutes pseudoephedrine near the solvent front before major excipient peaks (7). This situation is undesirable, since excipient interferences are likely to arise when different formulations from a variety of sources are analyzed. The determination of codeine, phenylpropanolamine, pheniramine, and pyrilamine has also been described (10). This procedure fails to separate the two antihistamines, pheniramine and pyrilamine, and they must be quantitated separately by a spectrophotometric method.

Reversed-phase, ion-paired HPLC was chosen as the most suitable chromatographic system due to the desire for a sample preparation that would require only dilution of the cough–cold liquid prior to injection onto the column. The ideal chromatographic system would use a pairing ion that would not cause precipitation in the samples and yet provide enough retention to resolve the drugs of interest from the formulation excipients. All of the drugs would be adequately resolved and the analysis time should be sufficiently short (*i.e.*, ≤20 min). These goals were accomplished by the manipulation of the mobile phase ionic strength, mobile phase solvent strength, buffer pH, pairing ion concentration, and secondary ion concentration. The results of these studies and an HPLC method for a variety of cough–cold amines that requires a minimum of sample treatment are presented.

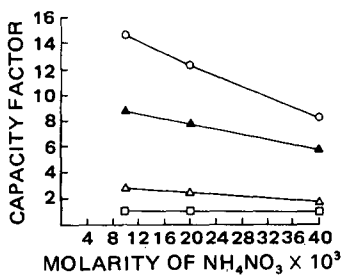

Figure 2—*Relationship between the capacity factor and the concentration of the secondary ion, ammonium nitrate. Key: (△) phenylpropanolamine; (▲) dextromethorphan; (○) chlorpheniramine; (□) propylparaben. Mobile phase: 70% methanol, 0.013* M *sodium dioctylsulfosuccinate, 1.5% glacial acetic acid.*

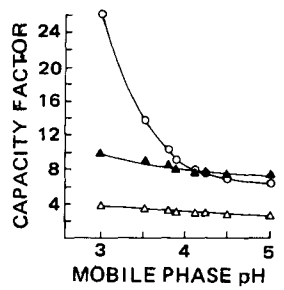

Figure 3—*Relationship between retention and pH of the mobile phase. Key: (△) phenylpropanolamine; (▲) dextromethorphan; (○) chlorpheniramine. Mobile phase: methanol–water–tetrahydrofuran–85% phosphoric acid (68:29:4:1); the sodium dioctyl sulfosuccinate concentration was 0.013* M. *Ammonium hydroxide was used for pH adjustment.*

EXPERIMENTAL

Materials—The various cough–cold ingredients, acetaminophen, guaifenesin, phenacetin, phenylephrine hydrochloride, codeine sulfate, ephedrine sulfate, phenylpropanolamine hydrochloride, methoxyphenamine hydrochloride, pheniramine maleate, benzphetamine hydrochloride, pyrilamine maleate, dextromethorphan hydrobromide, chlorpheniramine maleate, and α-aminopropiophenone were USP-NF quality. Sodium dioctyl sulfosuccinate[1], 3-hydroxy-*N*-methylmorphinan[2], *N*,*N*-dimethylaniline[1], acetophenone[1], methylparaben[2], and propylparaben[2] were used as received. Methanol and tetrahydrofuran were distilled in glass[3], and distilled water was used in all mobile phases. All other chemicals were reagent grade. The cough–cold liquids from various manufacturers were nonprescription products purchased at local drugstores.

Apparatus—A modular high-performance liquid chromatograph, consisting of a reciprocating piston pump equipped with a pulse dampener[4], an automated autosampler[5], a UV detector[6] (254 nm), and a recorder[7], was used for all measurements. For quantitative measurements, data were collected and processed by a digital computer[8].

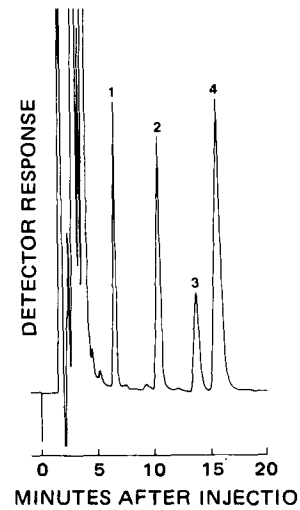

Figure 4—*Chromatogram of a typical cough–cold syrup containing phenylpropanolamine (Peak 1), benzphetamine (Peak 2, the internal standard), dextromethorphan (Peak 3), and chlorpheniramine (Peak 4) at 0.03 aufs.*

[1] Aldrich Chemical Co., Milwaukee, WI 53233.
[2] The Upjohn Co.
[3] Burdick & Jackson Laboratories, Muskegon, MI 49442.
[4] Model 110, Altex Corp., Berkeley, CA 94710.
[5] Model 8050, Varian Associates, Palo Alto, CA 94303.
[6] UVIII, Laboratory Data Control, Riviera Beach, Fla.
[7] Model XKR, Sargent Welch Co., Skokie, IL 60067.
[8] PDP 11, Digital Equipment Co., Maynard, MA 01754.

Table I—Replicate Analyses of Chlorpheniramine (I), Phenylpropanolamine (II), and Dextromethorphan (III) in a Single Cough–Cold Syrup Lot [a]

	I	II	III
Day 1	3.98	24.6	19.9
	4.00	25.1	20.1
	3.97	24.8	19.7
	3.90	24.9	19.6
	4.05	25.4	20.2
	3.96	24.6	19.7
	3.93	24.8	19.6
	3.97 ± 0.5	24.9 ± 0.2	19.8 ± 0.2
RSD	1.2%	1.1%	1.2%
Label	99.2	99.6	99.1
Day 2	3.98	25.0	19.9
	4.01	24.9	19.9
	4.03	25.1	20.1
	4.00	25.0	19.8
	3.96	25.1	19.9
	4.00	25.2	19.9
	4.01	25.1	20.0
	4.00 ± .02	25.1 ± 0.1	19.9 ± 0.1
RSD	0.5%	0.4%	0.4%
Label	100.0	100.2	99.6

[a] Internal standard method.

Mobile Phase—The mobile phase was prepared as follows. Methanol (680 ml) was added to 5.8 g of sodium dioctyl sulfosuccinate. Stirring was continued and 290 ml of distilled water, 40 ml of tetrahydrofuran, and 1 ml of 85% phosphoric acid were added. The pH was adjusted to 3.80 ± 0.05 with concentrated ammonium hydroxide solution. The solution was filtered through a 5-μm filter before use.

Separation between dextromethorphan and chlorpheniramine could be increased without affecting the other components by decreasing the pH of the mobile phase. If greater separation was necessary between phenylpropanolamine and the excipients, the methanol content of the mobile phase was decreased.

Columns—A microparticulate octadecylsilane column[9] (10-μm particles, 30 cm × 4 mm) was used throughout this study. The column was washed with a mobile phase consisting of methanol–water–tetrahydrofuran (68:29:4) when not in use to ensure long column life. The column temperature was ambient, column pressure ~2000 psi, injection volume ~50 μl, and the flow rate was 1.3 ml/min. These conditions gave satisfactory chromatography.

Internal Standard Solution—A solution with a concentration of ~7.0 mg/ml of benzphetamine hydrochloride was prepared.

Standard Preparation—About 8.3 mg of phenylpropanolamine hydrochloride, 6.7 mg of dextromethorphan hydrobromide, and 1.3 mg of chlorpheniramine maleate were accurately weighed, and 1.0 ml of the internal standard solution and ~35 ml of the mobile phase were added.

Sample Preparation—An appropriate amount of sample (accurately measured) was diluted with 1.0 ml of internal standard solution and ~30 ml of mobile phase. The resulting solution was mixed for 5 min. The amounts of commercial cough–cold liquid and mobile phase used were varied depending on the drug concentrations in the various products.

Procedure—The sample or standard (50 μl) was chromatographed using the conditions described. The detector setting was ~0.03 aufs. Concentrations were determined by comparison of peak height ratios from sample preparations to those from the standard preparation (USP reference standards were used).

RESULTS AND DISCUSSION

The primary requirements of the chromatographic system would be its ability to separate the amine drugs from the latest eluting excipient peak and yet maintain a chromatographic run time of <20 min. If adequate separation could be obtained, then sample preparation for the cough–cold liquids would merely require dilution of the sample with the mobile phase. Preliminary experiments indicated that the preservative, propylparaben, was the latest eluting excipient in the formulation chosen for initial development. Its retention behavior was compared with those of phenylpropanolamine, dextromethorphan, and chlorpheniramine in later studies to optimize the mobile phase.

The effects of the carbon chain length of the pairing ion on the capacity factors of phenylpropanolamine, dextromethorphan, and chlorpheniramine were initially investigated. The capacity factor of propylparaben was observed to remain nearly constant as the pairing ion was varied due to its presence in the unionized state at the pH of the initial mobile phase (pH 3.3). The chain length of alkylsulfonate or alkylsulfate pairing ions was varied from 6 to 20. It was observed that a pairing ion with a chain length of >12 carbons would be necessary to ensure adequate resolution of phenylpropanolamine from propylparaben. An upper limit on the size of the pairing ion was established by the fact that the C_{20} (eicosyl) pairing ion caused precipitates to form in the diluted syrup samples. Sodium dioctyl sulfosuccinate was ultimately chosen as the pairing ion based on its ability to produce adequate retention of phenylpropanolamine, dextromethorphan, and chlorpheniramine and its solubility, availability, and low cost.

By lowering the methanol content of the mobile phase, the resolution between propylparaben and phenylpropanolamine can be increased to obtain the desired degree of separation but only at the expense of extremely long retention times for chlorpheniramine. At this point it was clear that what was needed was greater selectivity between the amine drugs and propylparaben. Increasing the size of the pairing ion would increase the resolution between phenylpropanolamine and propylparaben, but this approach was unsuccessful due to the formation of precipitates when the samples were diluted with the mobile phase containing these larger pairing ions. Examination of a possible mechanism for retention in ion-paired, reversed-phase chromatography (Eqs. 1 and 2) suggested that a smaller, more soluble pairing ion could be used by increasing its concentration in the mobile phase to increase the k' of the amines while leaving the k' of propylparaben unaffected:

$$k' = \frac{V_s}{V_m}\frac{[R^+ I^-]_{org}}{[R^+]_{aq}} \quad \text{(Eq. 1)}$$

$$k' = \frac{V_s}{V_m} E\,[I^-]_{aq} \quad \text{(Eq. 2)}$$

where

$$E = \frac{[R^+ I^-]_{org}}{[R^+]_{aq}[I^-]_{aq}}$$

k' is the capacity factor, V_s is the volume of the stationary phase, V_m is

Table II—Analyses of Chlorpheniramine (I), Phenylpropanolamine (II), and Dextromethorphan (III) in Nonprescription Cough–Cold Liquids

Sample	Content, mg/ml I	II	III
A[a]	NP[b]	2.58 (103)[c]	C[d]
B	0.404 (101)	2.53 (101)	NP
C	0.681 (102)	C	0.676 (101)
D	0.133 (100)	NP	0.667 (100)
E	NP	1.22 (98)	0.998 (100)
F	0.396 (99)	NP	NP
G	0.401 (100)	NP	2.03 (102)
H	0.265 (99)	1.66 (100)	1.32 (99)

[a] Sample A was done by an external standard method. [b] NP refers to an amine not present in the formulation. [c] The numbers in parentheses refer to percent of label. [d] C refers to a chromatographic interference that prevented quantitation.

Table III—Approximate Retention of Various Cough–Cold Component Compounds [a]

Compound	Retention Time, min	k'
Acetaminophen	2.4	0.5
Guaifenesin	2.6	0.6
Phenacetin	2.9	0.7
Phenylephrine	5.1	2.1
Codeine	5.6	2.5
Ephedrine	7.0	3.2
Phenylpropanolamine	7.1	3.3
Methoxyphenamine	8.3	4.1
Pheniramine	11.0	5.9
Benzphetamine	11.2	6.0
Pyrilamine	14.4	8.0
Dextromethorphan	14.9	8.2
Chlorpheniramine	17.5	9.6

[a] Mobile phase: methanol–water–tetrahydrofuran–80% phosphoric acid (67:29:4:0.1) with 5.8 g of dioctyl sulfosuccinate adjusted to pH 3.8.

[9] μBondapak C_{18}, Waters Associates, Milford, MA 01757.

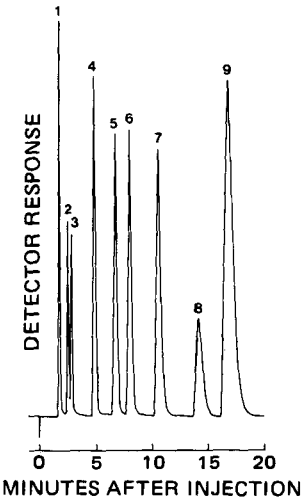

Figure 5—*Chromatogram demonstrating the retention behavior of a variety of cough–cold ingredients: maleic acid (1), guaifenesin (2), phenacetin (3), phenylephrine (4), phenylpropanolamine (5), methoxyphenamine (6), benzphetamine (7, internal standard), dextromethorphan (8), and chlorpheniramine (9). See Table III for mobile phase composition.*

the volume of the mobile phase, $[I^-]$ is the concentration of the pairing ion, $[R^+]$ is the concentration of the protonated amine, $[R^+ I^-]$ is the concentration of the ion pair, and E is the extraction constant (11).

The relationship between the capacity factors (k') and the pairing ion concentration for phenylpropanolamine, dextromethorphan, chlorpheniramine, and propylparaben is shown in Fig. 1. Equation 2 predicts k' to be proportional to the pairing ion concentration, and this type of behavior is observed in the early portions of the curves. The optimum pairing ion concentration was chosen as 0.013 M. As expected, the protonated form of propylparaben exhibited no change in capacity factor with increasing pairing ion concentration in the acetate buffer.

In the past, ammonium nitrate had been used in the mobile phase as a secondary ion to improve peak shape and reduce tailing (4, 5). It was initially included here based mainly on past history. Secondary ions compete with the pairing ion to form ion pairs and would be expected to decrease the retention of the amines by effectively decreasing the concentration of dioctyl sulfosuccinate ion pairs in the stationary phase. The effect of the nitrate ion concentration on the retention of phenylpropanolamine, dextromethorphan, chlorpheniramine, and propylparaben is shown in Fig. 2. The retention of the amines is observed to decrease with increasing nitrate ion concentration. As expected, the retention of propylparaben is unaffected by the concentration of the secondary ion. When ammonium nitrate was completely removed from the mobile phase, retention increased while tailing was changed very little. Tetrahydrofuran was added to the mobile phase and was found to be more effective in reducing tailing than nitrate ion.

Adequate resolution between propylparaben and phenylpropanolamine was obtained by increasing the retention with increased pairing ion concentration and removal of the secondary ion from the mobile phase, but the retention time of chlorpheniramine became excessive. The retention of chlorpheniramine was reduced relative to dextromethorphan, phenylpropanolamine, and propylparaben by changing from an acetate buffer to a carefully controlled phosphate buffer system of lower ionic strength. Figure 3 demonstrates the relationship between retention of the amines and mobile phase pH. In the pH region of 3–5, the capacity factors of phenylpropanolamine and dextromethorphan remain relatively constant, while chlorpheniramine's retention changes dramatically. The amine groups of phenylpropanolamine and dextromethorphan (pKa ~10) are fully protonated in this pH range and are behaving as monocations with respect to the ion-pairing system. Chlorpheniramine is capable of being protonated twice with reported pKa values of 4.0 (pyridinium group) and 9.2 (tertiary amine group) (12). In the pH 5.0 region, chlorpheniramine is exhibiting retention behavior more compatible with that of a monocation, while at pH 3.0 the increased retention is due to large concentrations of the dication form. For bivalent sample ions, the capacity factor is predicted to be proportional to the square of the pairing ion concentration (11), and the rapid increase in retention of chlorpheniramine at lower pH is consistent with this proposition. A mobile phase pH of 3.8 was chosen to shorten the chromatographic run time and still retain

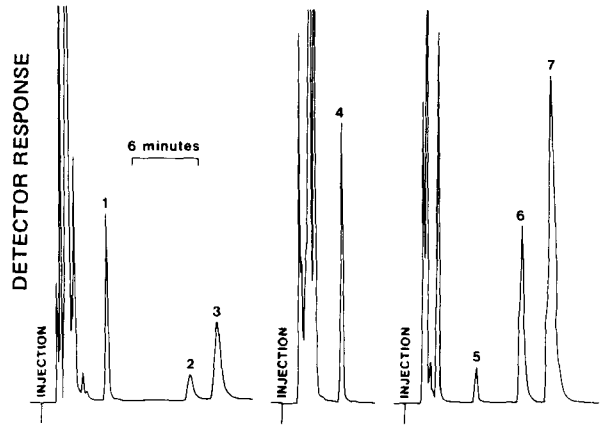

Figure 6—*Chromatograms of three different commercial cough–cold syrups demonstrating the separation of pseudoephedrine (1), dextromethorphan (2), chlorpheniramine (3), codeine (4), phenylpropanolamine (5), pheniramine (6), and pyrilamine (7) from the excipients found in these syrups.*

baseline separation of chlorpheniramine and dextromethorphan. Selectivity between dextromethorphan and chlorpheniramine is affected to such a great extent that the order of elution can be reversed by adjusting the pH of the mobile phase (Fig. 3).

Figure 4 shows a typical chromatogram of a 5.0-ml syrup sample (8.3 mg of phenylpropanolamine hydrochloride, 6.7 mg of dextromethorphan hydrobromide, and 1.3 mg of chlorpheniramine maleate/5 ml) spiked with 1.0 ml of internal standard solution and diluted to ~35 ml with mobile phase. Excellent separation of the three drugs and the internal standard were obtained with all syrup excipients eluting in the early portions of the chromatogram. The percent recovery of phenylpropanolamine, dextromethorphan, and chlorpheniramine from spiked syrup placebo averaged 100.0 ± 0.7 (n = 9), 99.9 ± 1.4 (n = 8), and 99.9 ± 1.1 (n = 8), respectively, over the ranges of 4.1–12.5, 3.2–9.9, and 0.8–1.9 mg/5 ml. Replicate analyses of one lot of cough–cold syrup gave average values of 24.9 ± 0.2 (phenylpropanolamine, theoretical: 25 mg/15 ml), 19.8 ± 0.2 (dextromethorphan, theoretical: 20 mg/15 ml), and 3.97 ± 0.05 (chlorpheniramine, theoretical: 4 mg/15 ml). Data for the first and second day analyses of this lot are given in Table I.

Eight samples of commercial cough–cold liquids containing phenylpropanolamine, dextromethorphan, or chloropheniramine, alone or in combination, were analyzed with no changes in the mobile phase or chromatographic parameters. Good agreement with the labeled content for phenylpropanolamine, dextromethorphan, and chlorpheniramine was obtained (Table II). In each case simple dilution of the sample with mobile phase was used, and no excipient inteference problems were noted with the exception of Sample C where an unknown excipient peak obscured phenylpropanolamine. However, dextromethorphan and chlorpheniramine were successfully quantitated in Sample C. In Sample A dextromethorphan was not adequately resolved from pyrilamine (also present in Sample A) to allow quantitation. Adjustment of the mobile phase pH would undoubtedly increase the separation of dextromethorphan and pyrilamine, since analogous behavior to that observed for chlorpheniramine and dextromethorphan in Fig. 3 would be expected in this case.

The retention behavior of other cough–cold ingredients was also investigated using this assay methodology to test the applicability of the chromatographic system to a wider range of product formulations. Table III lists the capacity factors (k') found for some common cough–cold drugs. Figure 5 contains a chromatogram of the separation of a synthetic mixture of many of these compounds. Commercial cough–cold liquids containing amine drugs other than or in addition to phenylpropanolamine, dextromethorphan, and chlorpheniramine were also investigated (Fig. 6). No excipient interferences were noted in commercial samples containing codeine, pseudoephedrine, methoxyphenamine, pheniramine, and pyrilamine. Analgesics such as acetaminophen eluted near the solvent front and were easily separated from the amine drugs of interest. While quantitation of these amine drugs was not attempted, the applicability of the present methodology to a wide range of amine drugs was confirmed.

The reversed-phase, ion-pairing HPLC procedure described is shown to be precise and accurate for the simultaneous determination of phenylpropanolamine, dextromethorphan, and chlorpheniramine in

cough–cold liquids. In addition, the results indicate that the methodology is applicable to a wide range of amine drugs commonly found in cough–cold liquids. The chromatographic system is capable of separating the amines of interest from the dyes, preservatives, and flavorings normally associated with a liquid cough–cold formulation. In all cases the sample preparation consisted of dissolution of the sample in the mobile phase and the total chromatographic run time was <20 min.

REFERENCES

(1) F. DeFabrizio, *J. Pharm. Sci.*, **69**, 854 (1980).
(2) R. E. Madsen and D. F. Magin, *ibid.*, **65**, 924 (1976).
(3) C. Hishta and R. G. Lauback, *ibid.*, **58**, 745 (1969).
(4) E. J. Kubiak and J. W. Munson, *ibid.*, **69**, 152 (1980).
(5) E. J. Kubiak and J. W. Munson, *ibid.*, **69**, 1380 (1980).
(6) W. O. McSharry and I. V. E. Savage, *ibid.*, **69**, 212 (1980).
(7) M. K. Chao, I. J. Holcomb, and S. A. Fusari, *ibid.*, **68**, 1463 (1979).
(8) N. Muhammad and J. A. Bodnar, *J. Liquid Chromatogr.*, **3**, 113 (1980).
(9) D. L. Massart and M. R. Detaevernier, *J. Chromatogr. Sci.*, **18**, 139 (1980).
(10) V. Das Gupta and A. G. Ghanekar, *J. Pharm. Sci.*, **66**, 895 (1977).
(11) L. R. Snyder and J. J. Kirkland, in "Introduction to Modern Liquid Chromatography," 2nd ed., Wiley, New York, N.Y., 1979, p. 457.
(12) C. G. Eckhart and T. McCorkle in "Analytical Profiles of Drug Substances," Vol 7, K. Florey, Ed., Academic, New York, N.Y., 1978, p. 43.

Precise High-Performance Liquid Chromatographic Procedure for the Determination of Cefsulodin, a New Antipseudomonal Cephalosporin Antibiotic, in Plasma

G. RICHARD GRANNEMAN and LAWRENCE T. SENNELLO ˣ

Received August 25, 1981, from the *Drug Metabolism Department, Division of Drug Safety Evaluation, Abbott Laboratories, North Chicago, IL 60064.* Accepted for publication December 9, 1981.

Abstract □ A simple and precise high-performance liquid chromatographic (HPLC) procedure was developed for the determination of cefsulodin, a new antipseudomonal cephalosporin antibiotic, in plasma. The analytical procedure involved ultrafiltration of samples that were buffered to prevent cefsulodin degradation, followed by injection into an HPLC system, utilizing a C_{18} reversed-phase analytical column, a mobile phase of acetonitrile–modified aqueous acetate buffer, and a UV spectrophotometric detector. Because of the simplicity of the procedure, the intraassay (~2%) and interassay (~3–4%) coefficients of variation were extremely low. Recoveries of drug were essentially quantitative in freshly buffered specimens and in those stored buffered and frozen for nearly 3 months. Calibration curves were rectilinear from the limit of quantification (~0.2 μg/ml) to 200 μg/ml, as demonstrated by regression correlation coefficients averaging >0.999 during routine analyses.

Keyphrases □ High-performance liquid chromatography—procedure for the determination of cefsulodin in plasma, new antipseudomonal cephalosporin antibiotic □ Cefsulodin—new cephalosporin antibiotic, high-performance liquid chromatographic determination □ Ultrafiltration—high-performance liquid chromatographic determination of cefsulodin in plasma, new antipseudomonal cephalosporin antibiotic

Cefsulodin sodium [3-(4-carbamoyl-1-pyridiniomethyl) - 7β - (D - α -sulfophenylacetamido) - ceph - 3 - em-4-carboxylate monosodium salt] (I), a semisynthetic cephalosporin antibiotic (Fig. 1)[1], has been shown to have excellent antipseudomonal activity (1, 2).

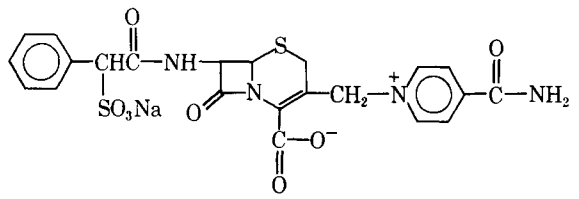

I

Microbiological assays have traditionally been used for analysis of biological specimens containing antibiotics; however, such procedures are occasionally disadvantageous due to long analysis times, nonlinear calibration curves, inadequate specificity, and relatively poor precision. In addition, preliminary experiments suggested that problems might arise during microbiological assays for cefsulodin due to drug hydrolysis during incubation of inoculated analysis plates.

With these factors in mind, work was started to develop an alternate procedure which had adequate sensitivity, high precision, short analysis time, and which did not allow hydrolysis of the cefsulodin. High-performance liquid chromatography (HPLC) is ideally suited for the analysis of the relatively polar, nonvolatile cephalosporins. Since the therapeutic concentrations of these compounds are usually in the microgram per milliliter range, concentrating techniques are usually not required. However, the majority of the high molecular weight proteins and fibrin must be removed from plasma samples to prevent column filter and bed damage. Several HPLC procedures for cephalosporins, employing classical deproteination reagents such as tri-

Table I—Precision and Linearity of the HPLC Procedure for Cefsulodin

Concentration of Cefsulodin, μg/ml		Coefficient of Variation, %
Actual	Calculated[a]	
0.78	0.76 (0.74)[b]	4.5 (3.3)[b]
1.56	1.57 (1.57)	1.9 (1.7)
3.13	3.10 (3.13)	1.7 (0.4)
6.25	6.31 (6.44)	3.2 (2.1)
12.50	12.71 (12.70)	0.9 (0.6)
25.00	25.05 (25.17)	1.3 (0.4)
50.00	49.40 (50.41)	1.1 (0.4)
100.00	97.34 (98.87)	1.7 (0.3)

[a] Based on results of linear regression of means from quadruplicate determinations for each concentration using reciprocal variance weights (r = 0.9999). [b] Data in parentheses were obtained neglecting responses of the internal standard.

[1] Developed by Takeda Chemical Industries; also known as SCE-129. Currently under clinical investigation by Abbott Laboratories.

0022-3549/82/01000-1112$01.00/0

cough–cold liquids. In addition, the results indicate that the methodology is applicable to a wide range of amine drugs commonly found in cough–cold liquids. The chromatographic system is capable of separating the amines of interest from the dyes, preservatives, and flavorings normally associated with a liquid cough–cold formulation. In all cases the sample preparation consisted of dissolution of the sample in the mobile phase and the total chromatographic run time was <20 min.

REFERENCES

(1) F. DeFabrizio, *J. Pharm. Sci.*, **69**, 854 (1980).
(2) R. E. Madsen and D. F. Magin, *ibid.*, **65**, 924 (1976).
(3) C. Hishta and R. G. Lauback, *ibid.*, **58**, 745 (1969).
(4) E. J. Kubiak and J. W. Munson, *ibid.*, **69**, 152 (1980).
(5) E. J. Kubiak and J. W. Munson, *ibid.*, **69**, 1380 (1980).
(6) W. O. McSharry and I. V. E. Savage, *ibid.*, **69**, 212 (1980).
(7) M. K. Chao, I. J. Holcomb, and S. A. Fusari, *ibid.*, **68**, 1463 (1979).
(8) N. Muhammad and J. A. Bodnar, *J. Liquid Chromatogr.*, **3**, 113 (1980).
(9) D. L. Massart and M. R. Detaevernier, *J. Chromatogr. Sci.*, **18**, 139 (1980).
(10) V. Das Gupta and A. G. Ghanekar, *J. Pharm. Sci.*, **66**, 895 (1977).
(11) L. R. Snyder and J. J. Kirkland, in "Introduction to Modern Liquid Chromatography," 2nd ed., Wiley, New York, N.Y., 1979, p. 457.
(12) C. G. Eckhart and T. McCorkle in "Analytical Profiles of Drug Substances," Vol 7, K. Florey, Ed., Academic, New York, N.Y., 1978, p. 43.

Precise High-Performance Liquid Chromatographic Procedure for the Determination of Cefsulodin, a New Antipseudomonal Cephalosporin Antibiotic, in Plasma

G. RICHARD GRANNEMAN and LAWRENCE T. SENNELLO ˣ

Received August 25, 1981, from the *Drug Metabolism Department, Division of Drug Safety Evaluation, Abbott Laboratories, North Chicago, IL 60064.* Accepted for publication December 9, 1981.

Abstract □ A simple and precise high-performance liquid chromatographic (HPLC) procedure was developed for the determination of cefsulodin, a new antipseudomonal cephalosporin antibiotic, in plasma. The analytical procedure involved ultrafiltration of samples that were buffered to prevent cefsulodin degradation, followed by injection into an HPLC system, utilizing a C_{18} reversed-phase analytical column, a mobile phase of acetonitrile–modified aqueous acetate buffer, and a UV spectrophotometric detector. Because of the simplicity of the procedure, the intraassay (~2%) and interassay (~3–4%) coefficients of variation were extremely low. Recoveries of drug were essentially quantitative in freshly buffered specimens and in those stored buffered and frozen for nearly 3 months. Calibration curves were rectilinear from the limit of quantification (~0.2 μg/ml) to 200 μg/ml, as demonstrated by regression correlation coefficients averaging >0.999 during routine analyses.

Keyphrases □ High-performance liquid chromatography—procedure for the determination of cefsulodin in plasma, new antipseudomonal cephalosporin antibiotic □ Cefsulodin—new cephalosporin antibiotic, high-performance liquid chromatographic determination □ Ultrafiltration—high-performance liquid chromatographic determination of cefsulodin in plasma, new antipseudomonal cephalosporin antibiotic

Cefsulodin sodium [3-(4-carbamoyl-1-pyridiniomethyl) - 7β - (D - α -sulfophenylacetamido) - ceph - 3 - em-4-carboxylate monosodium salt] (I), a semisynthetic cephalosporin antibiotic (Fig. 1)[1], has been shown to have excellent antipseudomonal activity (1, 2).

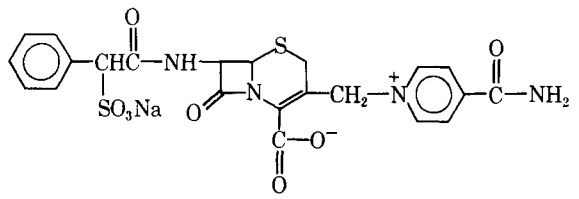

I

Microbiological assays have traditionally been used for analysis of biological specimens containing antibiotics; however, such procedures are occasionally disadvantageous due to long analysis times, nonlinear calibration curves, inadequate specificity, and relatively poor precision. In addition, preliminary experiments suggested that problems might arise during microbiological assays for cefsulodin due to drug hydrolysis during incubation of inoculated analysis plates.

With these factors in mind, work was started to develop an alternate procedure which had adequate sensitivity, high precision, short analysis time, and which did not allow hydrolysis of the cefsulodin. High-performance liquid chromatography (HPLC) is ideally suited for the analysis of the relatively polar, nonvolatile cephalosporins. Since the therapeutic concentrations of these compounds are usually in the microgram per milliliter range, concentrating techniques are usually not required. However, the majority of the high molecular weight proteins and fibrin must be removed from plasma samples to prevent column filter and bed damage. Several HPLC procedures for cephalosporins, employing classical deproteination reagents such as tri-

Table I—Precision and Linearity of the HPLC Procedure for Cefsulodin

Concentration of Cefsulodin, μg/ml		Coefficient of Variation, %
Actual	Calculated[a]	
0.78	0.76 (0.74)[b]	4.5 (3.3)[b]
1.56	1.57 (1.57)	1.9 (1.7)
3.13	3.10 (3.13)	1.7 (0.4)
6.25	6.31 (6.44)	3.2 (2.1)
12.50	12.71 (12.70)	0.9 (0.6)
25.00	25.05 (25.17)	1.3 (0.4)
50.00	49.40 (50.41)	1.1 (0.4)
100.00	97.34 (98.87)	1.7 (0.3)

[a] Based on results of linear regression of means from quadruplicate determinations for each concentration using reciprocal variance weights (r = 0.9999). [b] Data in parentheses were obtained neglecting responses of the internal standard.

[1] Developed by Takeda Chemical Industries; also known as SCE-129. Currently under clinical investigation by Abbott Laboratories.

0022-3549/82/01000-1112$01.00/0

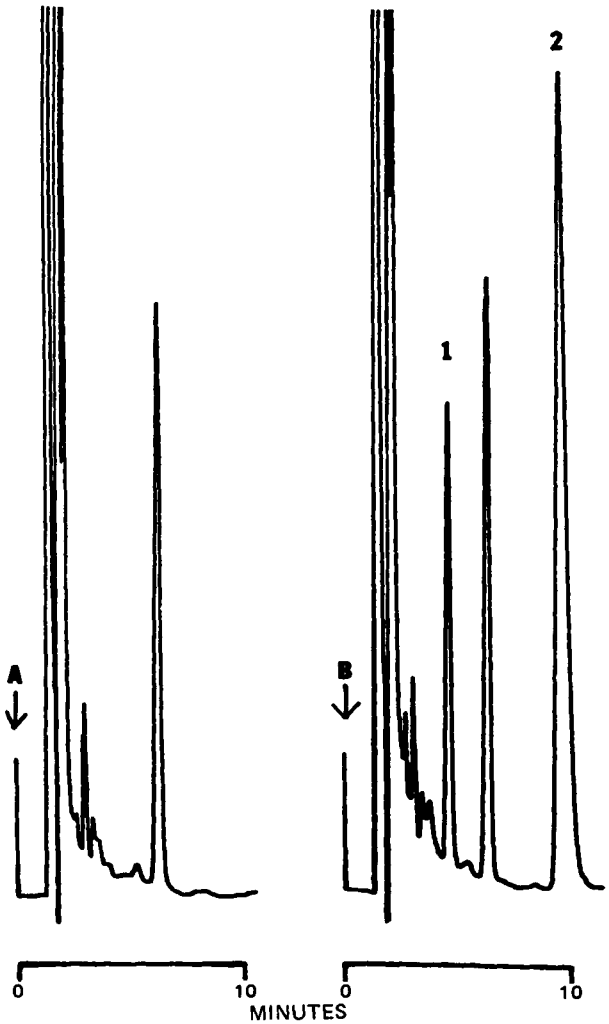

Figure 1—*Typical HPLC traces for ultrafiltrates of (A) predose and (B) postdose plasma from a subject who received a 500-mg dose of cefsulodin. The calculated concentration of cefsulodin was 4.3 μg/ml. Compound II was added to a final concentration in plasma of 400 μg/ml. Key: (1) cefsulodin; (2) II.*

chloroacetic acid (3, 4) or organic solvents (5–8) have been reported recently. The described HPLC procedure, involving removal of plasma proteins by ultrafiltration, offers the advantages of simplicity and high reproducibility, obviating the problems associated with the precipitation procedures, such as sample dilution, incomplete protein precipitation, drug coprecipitation, and acid catalyzed degradation of labile drugs. Furthermore, the ultrafiltration procedure would allow the determination of the free and total drug concentrations in plasma, if desired.

EXPERIMENTAL

Chromatography—HPLC analyses were conducted using a reciprocating pump[2] in conjunction with a UV detector[3] operated at an analytical wavelength of 254 nm. The mobile phase, consisting of 4.5% acetonitrile[4] in 0.02 *M* ammonium acetate, which was adjusted to pH 4.2 with glacial acetic acid, was maintained at a flow rate of 2.0 ml/min through a C_{18}[5] analytical column.

Ultrafiltration Apparatus—Ultrafiltrates of plasma samples were obtained using conical centrifuge tubes[6], conical supports[7], and membrane cones[8], with respective molecular weight cutoff values of 25,000 and 50,000. Use of the former cone model was slightly favored due to its higher apparent flux and protein retentivity. For reasons to be discussed, the two types of cones should not be mixed within an analytical run.

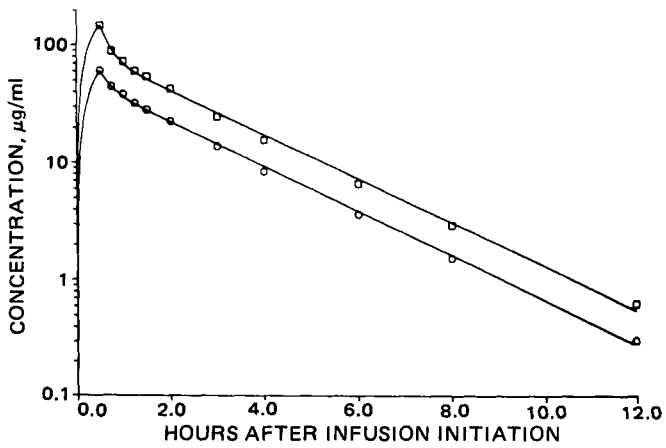

Figure 2—*Plasma cefsulodin levels determined for two subjects receiving 1000-mg (○) and 2000-mg (□), 30-min intravenous infusions of cefsulodin. Plotted curves represent nonlinear best-fit regressions.*

Sample Preparation—The stability of cefsulodin in plasma was demonstrated to be greatly improved by addition of phosphate buffer to bring the final pH to 6.5 or less. Thus, plasma samples should be mixed with an equal volume of 1.0 *M* phosphate buffer (pH 6) prior to freezing.

The 1.0 *M* phosphate buffer (pH 6) was prepared by addition of three parts (by weight) of 1.0 *M* $NaH_2PO_4 \cdot H_2O$ to one part 1.0 *M* $Na_2HPO_4 \cdot 7H_2O$, which was equivalent to 103.5 g of $NaH_2PO_4 \cdot H_2O$ and 67.05 g of $Na_2HPO_4 \cdot 7H_2O$/liter of solution. Mixture of this solution with an equal volume of plasma resulted in a solution with pH 6.1–6.3.

Standard Preparation—Since the plasma samples were diluted by the 1:1 mixture with phosphate buffer, standards had to be diluted similarly. Typically, a 200 μg/ml solution of the reference material, freshly prepared in 1.0 *M* phosphate buffer (pH 6) was mixed with an equal volume of fresh plasma. This standard thereafter was serially diluted with an equivolume mixture of phosphate buffer and plasma to provide the remaining standards.

Sample Workup—Sample processing involved ultrafiltration of a mixture of accurately pipeted aliquants of the sample and internal standard. The use of *p*-fluoro-α-methylbenzylamine hydrochloride (II) as an internal standard was found to be satisfactory. Typically, 0.05 ml of an 8.0 mg/ml solution of II hydrochloride was thoroughly mixed with 2.0 ml of the standards and unknowns. Control blanks and predose samples were processed without internal standard. After transfer to a clean filtration apparatus, the samples were centrifuged at the same relative centrifugal force for the same length of time. Centrifugation at 450×*g* for ~20 min produced ~1.0 ml of ultrafiltrate. Whenever possible, samples in the various stages of workup were refrigerated until all samples were processed. Thereafter, the ultrafiltrates could be stored frozen for several days prior to analysis.

Injection of 70 μl of these ultrafiltrates into the described HPLC system resulted in a nearly full-scale recorder reading for the internal standard (retention volume ~22 ml) at a detector attenuation of 0.02 aufs. Under the same conditions, the response for a sample containing 0.2 g of cefsulodin/ml would be two to three times greater than instrumental noise. To minimize the degradation of cefsulodin in the ultrafiltrates, they should not be allowed to stand at room temperature for more than 2 hr prior to analysis. Typical chromatograms are shown in Fig. 1.

RESULTS AND DISCUSSION

Method Development—*Cleanup Procedures*—Several of the classical procedures for the removal of protein from samples were investigated. Procedures involving deproteination with organic solvents, such as methanol, acetonitrile, and acetone, were all unsatisfactory due to coprecipitation of cefsulodin, chromatographic aberrations due to the

[2] Model 6000A, Waters Associates, Milford, Mass.
[3] Model 440, Waters Associates, Milford, Mass.
[4] HPLC Grade, Burdick and Johnson.
[5] μBondapak C_{18}, Waters Associates, Milford, Mass.
[6] Centriflo system, Amicon Corp., Lexington, Mass.
[7] Model CS1A, Amicon Corp., Lexington, Mass.
[8] Either model CF25 or CF50A, Amicon Corp., Lexington, Mass.

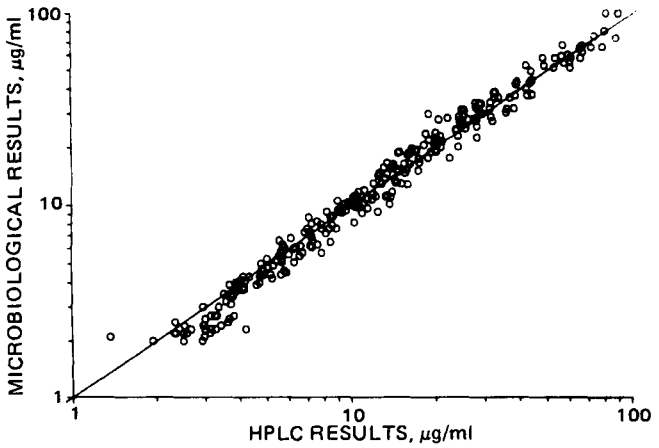

Figure 3—*Correlation of HPLC and microbiological assay results; 270 assays.*

high organic content of directly injected supernates, and degradation of cefsulodin during the evaporation of the supernates. Similarly, other deproteination reagents such as concentrated salt solutions (*e.g.*, sodium sulfate) and acids (*e.g.*, trichloroacetic, sulfosalicylic) were unacceptable due to coprecipitation of cefsulodin, incomplete protein precipitation, cefsulodin degradation, and chromatographic difficulties. Isolation of cefsulodin by column chromatographic techniques, such as anion and cation exchange, silica absorption, alumina absorption, and gel exclusion, was also not feasible due to inadequate protein removal, sample dilution, and the limited number of samples that could be analyzed per day.

Ultrafiltration proved to be ideally suited for the removal of protein from cefsulodin-containing plasma samples. Due to the low apparent protein binding of cefsulodin in the buffered plasma samples, recoveries were nearly quantitative. However, pressurized ultrafiltration techniques using cells or membrane tubing were slow, cumbersome, and involved variable sample dilution due to the necessity of prewetting the membrane. Alternatively, ultrafiltration by centrifugation with the apparatus described was found to be simple, fast, and highly reproducible.

Recovery—The recoveries of cefsulodin and II in the first 50–100 μl of ultrafiltrate were slightly lower than in subsequent fractions. Additionally, in some experiments, the peak height ratio from the initial ultrafiltrate was higher than the true ratio. Lower recoveries for the initial ultrafiltrate may be attributed to one or more of the following phenomena: (*a*) leaching of glycerin or other liquid materials from the membrane; (*b*) low-level binding to the membrane; and/or (*c*) molecular sieving. Regardless, when ultrafiltrate volumes approaching or exceeding 0.50 ml were collected, recoveries were nearly quantitative for both cefsulodin (>95%) and II (>93%), and their peak height ratio became constant.

Intersubject variability in ultrafiltration recovery was assessed by supplementing plasma samples from six subjects with cefsulodin and II. The intersubject coefficient of variation for cefsulodin recovery was 1.3% without II and 1.2% with II as the internal standard. Recovery also did not appear to be dependent on the concentration of cefsulodin in the sample. Mean recoveries for quadruplicate standards ranging from 0.8 to 100 μg/ml averaged 99.1%.

The 25,000 and 50,000 molecular weight cutoff membranes were compared for samples spiked with 2, 20, and 200 μg of cefsulodin/ml. Although the recoveries of cefsulodin were essentially the same for both types of membranes, recoveries of II were slightly lower for the lower cutoff cones. Thus, it is recommended that the two types of filters not be mixed within the same assay run.

Precision and Linearity—The precision and linearity of the procedure was assessed by quadruplicate analyses of buffered plasma samples supplemented with cefsulodin in the concentration range of 0.78–100 μg/ml. The results are summarized in Table I. With no correction made for the internal standard response, the mean assay coefficient of variation (*CV*) was 1.2 ± 1.1%. Correction of the data with the internal standard responses resulted in a mean *CV* of 2.0 ± 1.2%. The errors involved with either approach are uncharacteristically low for the analysis of drugs in biological matrixes. This is due to the simplicity of the workup procedure and the high recoveries.

Linear regression analyses were performed with the mean data from the above experiment, using reciprocal analytical variances as the weights (9). The same data were then refitted using 1, 1/concentration (1/*C*), and 1/concentration-squared ($1/C^2$) as the weighting schemes.

The high correlation coefficients from the regressions (~0.9999) demonstrate that the responses are rectilinearly related to the concentration of cefsulodin in the samples. The near-zero intercepts demonstrate that the blank plasma had negligible interferences for cefsulodin, and that recovery of drug in the ultrafiltrates was not concentration dependent. From careful consideration of the dispersion of the residual errors, the $1/C^2$ weighting scheme was found to best represent the reciprocal analytical variances when the internal standard was not used; hence, weighting by reciprocal squared concentrations should be used in regression analyses of peak height ratio data obtained during sample analyses. Alternatively, if an internal standard is not used, the best choice of the weighting scheme is $1/C$.

The interassay precision of the procedure was assessed from quality control data obtained during routine analyses. For the first application of the procedure to a clinical study, plasma was supplemented on-site at concentrations of 4 and 20 μg/ml of cefsulodin/ml. For the first group of subjects, the quality control standards averaged 3.9 ± 0.2 (n = 9) and 20.0 ± 0.7 (n = 9) μg/ml, respectively. In a second series of analyses, the references averaged 4.0 ± 0.2 (n = 5) and 19.9 ± 0.6 (n = 8) μg/ml. In the most recent use of the procedure, the mean value for a 10.0 μg/ml quality control pool, determined in 20 analytical runs performed over a 1-month period by two technicians, was 10.2 ± 0.3 μg/ml. The mean regression correlation coefficient for the 6–8 point calibration curves was 0.9996. Thus, under routine conditions, the interassay coefficient of variation is ~3–4%, and accuracy errors are negligible.

Stability—Preliminary experiments in this laboratory suggested that 15–40% of the cefsulodin activity in plasma or serum could be lost after storage at ~−17° for 7 weeks, and that the rate of degradation was dependent on the freshness of the plasma. The stability of the compound in buffer was considerably greater, especially in the pH range of 3–7. Degradation of cefsulodin in aqueous media is most pronounced under alkaline conditions, which facilitate isomerization, hydrolysis, and nucleophilic displacement at the various functional centers of the compound. As a result, acidification with phosphate buffer was evaluated as a means of enhancing the stability of cefsulodin in plasma. After incubation at 8° for 3 days, or 24° for 1 day, essentially quantitative recoveries of drug were realized from plasmas which were acidified within the pH range of 3–6.5 with 1.0 *M* phosphate buffer. In contrast, cefsulodin was ~50 and 80% inactivated when stored in unbuffered plasma under the same conditions.

Since sensitivity reduction of the microbiological assay, and protein denaturation were encountered in plasma samples buffered in the pH range of 3–5.5, a final pH of ~6 was found to be the most desirable. An equivolume mixture of plasma and buffer was deemed the most convenient and accurate acidification procedure for diverse clinical settings. Since the implementation of this stabilization procedure, degradation of cefsulodin during frozen storage or workup has not been encountered based on quality control data. In another experiment, the recovery of cefsulodin in frozen plasma was 101.4 ± 1.7% after 36 days and 98.5 ± 1.7% after 81 days; thus, prolonged frozen storage of cefsulodin-containing samples appears to present no significant problems.

Since the half-life of cefsulodin in unbuffered plasma at room temperature is roughly 8 hr, care must be taken to prevent appreciable degradation. Whole blood samples should be cooled prior to the harvest of serum or plasma and the subsequent acidification. After the specimens have been buffered, drug degradation is no longer a serious problem.

Sample Analysis—There are indications that cefsulodin may degrade in the ultrafiltrates at a slightly greater rate than in buffered plasma. Hourly analyses of an ultrafiltrate of a buffered plasma sample containing cefsulodin and internal standard showed that after 15 hr, ~11.7% of the cefsulodin had been lost, and that the concentration was declining at ~0.8%/hr.

Accordingly, on the day of analysis, ultrafiltrates are refrigerated before and after manual injection into the HPLC system, and are usually left at room temperature for <2–3 hr. For automated analyses of large numbers of samples, the ultrafiltrates can be loaded into the sampler in batches of 10–20. Alternatively, for long unattended analyses, standards allowing for compensation for degradation may be interspersed among the samples.

After analysis of over 2000 plasma samples with this procedure, the necessity of altering the described chromatographic conditions has been rare; however, column efficiency loss or chromatographic interference from atypical plasma samples, such as those from patients with severe renal impairment, has occasionally required alternate mobile phases. Generally, small changes in the pH of the eluent greatly affects the relative retention volume of cefsulodin and plasma components, providing flexibility for difficult separations. For extremely difficult separations, the use of an ion-pair reversed-phase system, employing tetrabutylam-

monium (III) as the counter ion, has been used successfully. To compensate for addition of 0.005 *M* III to the regular mobile phase, the acetonitrile content must be increased to ~12%. Since cefsulodin, by virtue of its sulfonic acid moiety, is more acidic than most compounds encountered in plasma, the III-containing mobile phases provide additional versatility. Although II cannot be used as the internal standard in such a system, analytical precision is not compromised, due to the extreme simplicity and quantitative recoveries of the ultrafiltration procedure.

Figure 2 shows the results of the analysis of plasma samples from two subjects who received single 1000- and 2000-mg, 30-min intravenous infusions of cefsulodin. The solid lines represent the nonlinear best-fit regressions calculated for these data.

Comparison to Microbiological Assay Procedures—In the first application of this HPLC procedure to a clinical study, 270 plasma samples were assayed both microbiologically, using *Pseudomonas aeruginosa* (NCTC 10490) as the test organism, and with HPLC as described. Figure 3 shows that results from the two procedures were highly correlated. Linear regression of the data yielded a correlation coefficient of 0.993.

The centrifugal ultrafiltration technique is a good alternative to classical deproteinization procedures because it is rapid and simple and requires no sample adulteration. For more highly protein-bound compounds, the ultrafiltration procedure allows direct quantification of unbound drug levels.

REFERENCES

(1) K. Tsuchiya, M. Kondo, and K. Nagatoma, *Antimicrob. Agents Chemother.*, **13,** 137 (1978).

(2) M. Kondo and K. Tsuchiya, *ibid.*, **14,** 151 (1978).

(3) E. Crombez, G. Van der Weken, W. Van den Bossche, and P. de Moerloose, *J. Chromatogr.*, **177,** 323 (1979).

(4) J. S. Wold and S. A. Turnipseed, *Clin. Chim. Acta*, **78,** 203 (1977).

(5) M. G. Torchina and R. G. Danzinger, *J. Chromatogr.*, **181,** 120 (1980).

(6) A. Suzuki, K. Nods, and H. Noguchi, *ibid.*, **182,** 448 (1980).

(7) J. G. Aziz, J. Gambertoglio, E. T. Lin, H. Grausz, and L. Z. Benet, *J. Pharmacokinet. Biopharm.*, **6,** 153 (1978).

(8) I. Nilsson-Ehle, T. T. Yoshikawa, M. C. Schotz, and L. B. Guze, *Antimicrob. Agents Chemother.*, **13,** 221 (1978).

(9) H. G. Boxenbaum, S. Riegelman, and R. M. Elashoff, *J. Pharmacokinet. Biopharm.*, **2,** 123 (1974).

ACKNOWLEDGMENTS

The authors thank Dr. Walton Grundy and Mrs. Barbara Zorc for their help in performing the microbiological analyses.

Simultaneous Assay of Hydrocodone Bitartrate and Acetaminophen in a Tablet Formulation

WARREN E. WALLO ˣ and ANTHONY D'ADAMO

Received September 1, 1981, from the *Analytical Research Department, Knoll Pharmaceutical Co., Whippany, NJ 07981.* Accepted for publication December 11, 1981.

Abstract □ A reversed-phase pressurized liquid chromatographic procedure is presented for the simultaneous quantitation of hydrocodone bitartrate and acetaminophen in a tablet formulation. The separation method was based on an octadecylsilane column with a buffered (pH 4.5) methanol–water mobile phase. Measurement was with a UV spectrophotometer set at 283 nm, compared to external standards. Assays for the active ingredients in tablet samples averaged 99.7% of the label claim for hydrocodone bitartrate and 100.3% for acetaminophen. The respective relative standard deviations of the retention time and precision were 2.2 and 1.75% for hydrocodone and 3.3 and 0.95% for acetaminophen. The range of interest studied was 0.035 to 0.065 mg/ml for hydrocodone bitartrate and 3.50 to 6.50 mg/ml for acetaminophen. The assay method was also compared to colorimetric and USP procedures for the active ingredients. The method was suitable for control, content uniformity, and stability-indicating use.

Keyphrases □ Hydrocodone bitartrate—simultaneous assay in a tablet formulation, acetaminophen □ Acetaminophen—simultaneous assay in a tablet formulation, hydrocodone bitartrate □ Tablet formulation—simultaneous assay of hydrocodone bitartrate and acetaminophen

The determinations of acetaminophen (I), hydrocodone (II), and related compounds have been reported by gas (1–3) and high-pressure liquid chromatographic (HPLC) methods (4–14). However, none of the methods has been applied to the simultaneous determination of these compounds.

Due to interferences, the pharmacopeial procedures for the individual drugs are also unsuitable for simultaneous analysis (15, 16). In addition, the authors are not aware of any published stability-indicating method for hydrocodone.

The present report presents an HPLC method for the quantitative analysis of both substances in a two-component tablet formulation. The content uniformity test of the minor component (II) in the tablet formulation is also feasible by this method. An analysis can be conducted in <13 min and separates possible impurities and degradation products.

EXPERIMENTAL

Reagents and Materials—Water and methanol were HPLC grade solvents. Hydrocodone bitartrate, acetaminophen, codeine phosphate, and hydromorphone hydrochloride were USP reference standards. Other materials were ACS grade or the highest quality commercial grade available.

The high-pressure liquid chromatograph[1] was connected to an automatic sampler[2], a variable wavelength UV detector[3], and an integrator/recorder[4]. A bonded reversed-phase C_{18} column[5] was used.

Chromatographic Conditions—The mobile phase consisted of 25% methanol and 75% of an aqueous solution containing 0.01 *N* monobasic potassium phosphate and 0.05 *N* potassium nitrate, adjusted to a pH of ~4.5 by dropwise addition of 3 *N* phosphoric acid solution. The mobile phase was degassed prior to use by vacuum. A flow rate of ~1.1 ml/min was established. The detector sensitivity was 2.0 aufs for acetaminophen and 0.010 aufs for hydrocodone, both measured at 283 nm. The chart speed was 0.7 cm/min.

External Standard Solutions—A two-component standard solution containing 5 mg/ml of I and 0.05 mg/ml of II bitartrate was prepared in water.

[1] Waters ALC 204, Waters Associates, Milford, MA 01757.
[2] WISP, 710B Waters Assoc., Milford, MA 01757.
[3] SF 770 Spectroflow Monitor, Schoeffel Instruments, Westwood, NJ 07675.
[4] DATA Module, Waters Assoc., Milford, MA 01757.
[5] μBondapak C_{18} column, Waters Assoc., Milford, MA 01757.

0022-3549/82/01000-1115$01.00/0

monium (III) as the counter ion, has been used successfully. To compensate for addition of 0.005 *M* III to the regular mobile phase, the acetonitrile content must be increased to ~12%. Since cefsulodin, by virtue of its sulfonic acid moiety, is more acidic than most compounds encountered in plasma, the III-containing mobile phases provide additional versatility. Although II cannot be used as the internal standard in such a system, analytical precision is not compromised, due to the extreme simplicity and quantitative recoveries of the ultrafiltration procedure.

Figure 2 shows the results of the analysis of plasma samples from two subjects who received single 1000- and 2000-mg, 30-min intravenous infusions of cefsulodin. The solid lines represent the nonlinear best-fit regressions calculated for these data.

Comparison to Microbiological Assay Procedures—In the first application of this HPLC procedure to a clinical study, 270 plasma samples were assayed both microbiologically, using *Pseudomonas aeruginosa* (NCTC 10490) as the test organism, and with HPLC as described. Figure 3 shows that results from the two procedures were highly correlated. Linear regression of the data yielded a correlation coefficient of 0.993.

The centrifugal ultrafiltration technique is a good alternative to classical deproteinization procedures because it is rapid and simple and requires no sample adulteration. For more highly protein-bound compounds, the ultrafiltration procedure allows direct quantification of unbound drug levels.

REFERENCES

(1) K. Tsuchiya, M. Kondo, and K. Nagatoma, *Antimicrob. Agents Chemother.*, **13,** 137 (1978).

(2) M. Kondo and K. Tsuchiya, *ibid.*, **14,** 151 (1978).

(3) E. Crombez, G. Van der Weken, W. Van den Bossche, and P. de Moerloose, *J. Chromatogr.*, **177,** 323 (1979).

(4) J. S. Wold and S. A. Turnipseed, *Clin. Chim. Acta*, **78,** 203 (1977).

(5) M. G. Torchina and R. G. Danzinger, *J. Chromatogr.*, **181,** 120 (1980).

(6) A. Suzuki, K. Nods, and H. Noguchi, *ibid.*, **182,** 448 (1980).

(7) J. G. Aziz, J. Gambertoglio, E. T. Lin, H. Grausz, and L. Z. Benet, *J. Pharmacokinet. Biopharm.*, **6,** 153 (1978).

(8) I. Nilsson-Ehle, T. T. Yoshikawa, M. C. Schotz, and L. B. Guze, *Antimicrob. Agents Chemother.*, **13,** 221 (1978).

(9) H. G. Boxenbaum, S. Riegelman, and R. M. Elashoff, *J. Pharmacokinet. Biopharm.*, **2,** 123 (1974).

ACKNOWLEDGMENTS

The authors thank Dr. Walton Grundy and Mrs. Barbara Zorc for their help in performing the microbiological analyses.

Simultaneous Assay of Hydrocodone Bitartrate and Acetaminophen in a Tablet Formulation

WARREN E. WALLO ˣ and ANTHONY D'ADAMO

Received September 1, 1981, from the *Analytical Research Department, Knoll Pharmaceutical Co., Whippany, NJ 07981.* Accepted for publication December 11, 1981.

Abstract □ A reversed-phase pressurized liquid chromatographic procedure is presented for the simultaneous quantitation of hydrocodone bitartrate and acetaminophen in a tablet formulation. The separation method was based on an octadecylsilane column with a buffered (pH 4.5) methanol–water mobile phase. Measurement was with a UV spectrophotometer set at 283 nm, compared to external standards. Assays for the active ingredients in tablet samples averaged 99.7% of the label claim for hydrocodone bitartrate and 100.3% for acetaminophen. The respective relative standard deviations of the retention time and precision were 2.2 and 1.75% for hydrocodone and 3.3 and 0.95% for acetaminophen. The range of interest studied was 0.035 to 0.065 mg/ml for hydrocodone bitartrate and 3.50 to 6.50 mg/ml for acetaminophen. The assay method was also compared to colorimetric and USP procedures for the active ingredients. The method was suitable for control, content uniformity, and stability-indicating use.

Keyphrases □ Hydrocodone bitartrate—simultaneous assay in a tablet formulation, acetaminophen □ Acetaminophen—simultaneous assay in a tablet formulation, hydrocodone bitartrate □ Tablet formulation—simultaneous assay of hydrocodone bitartrate and acetaminophen

The determinations of acetaminophen (I), hydrocodone (II), and related compounds have been reported by gas (1–3) and high-pressure liquid chromatographic (HPLC) methods (4–14). However, none of the methods has been applied to the simultaneous determination of these compounds.

Due to interferences, the pharmacopeial procedures for the individual drugs are also unsuitable for simultaneous analysis (15, 16). In addition, the authors are not aware of any published stability-indicating method for hydrocodone.

The present report presents an HPLC method for the quantitative analysis of both substances in a two-component tablet formulation. The content uniformity test of the minor component (II) in the tablet formulation is also feasible by this method. An analysis can be conducted in <13 min and separates possible impurities and degradation products.

EXPERIMENTAL

Reagents and Materials—Water and methanol were HPLC grade solvents. Hydrocodone bitartrate, acetaminophen, codeine phosphate, and hydromorphone hydrochloride were USP reference standards. Other materials were ACS grade or the highest quality commercial grade available.

The high-pressure liquid chromatograph[1] was connected to an automatic sampler[2], a variable wavelength UV detector[3], and an integrator/recorder[4]. A bonded reversed-phase C_{18} column[5] was used.

Chromatographic Conditions—The mobile phase consisted of 25% methanol and 75% of an aqueous solution containing 0.01 *N* monobasic potassium phosphate and 0.05 *N* potassium nitrate, adjusted to a pH of ~4.5 by dropwise addition of 3 *N* phosphoric acid solution. The mobile phase was degassed prior to use by vacuum. A flow rate of ~1.1 ml/min was established. The detector sensitivity was 2.0 aufs for acetaminophen and 0.010 aufs for hydrocodone, both measured at 283 nm. The chart speed was 0.7 cm/min.

External Standard Solutions—A two-component standard solution containing 5 mg/ml of I and 0.05 mg/ml of II bitartrate was prepared in water.

[1] Waters ALC 204, Waters Associates, Milford, MA 01757.
[2] WISP, 710B Waters Assoc., Milford, MA 01757.
[3] SF 770 Spectroflow Monitor, Schoeffel Instruments, Westwood, NJ 07675.
[4] DATA Module, Waters Assoc., Milford, MA 01757.
[5] μBondapak C_{18} column, Waters Assoc., Milford, MA 01757.

0022-3549/82/01000-1115$01.00/0

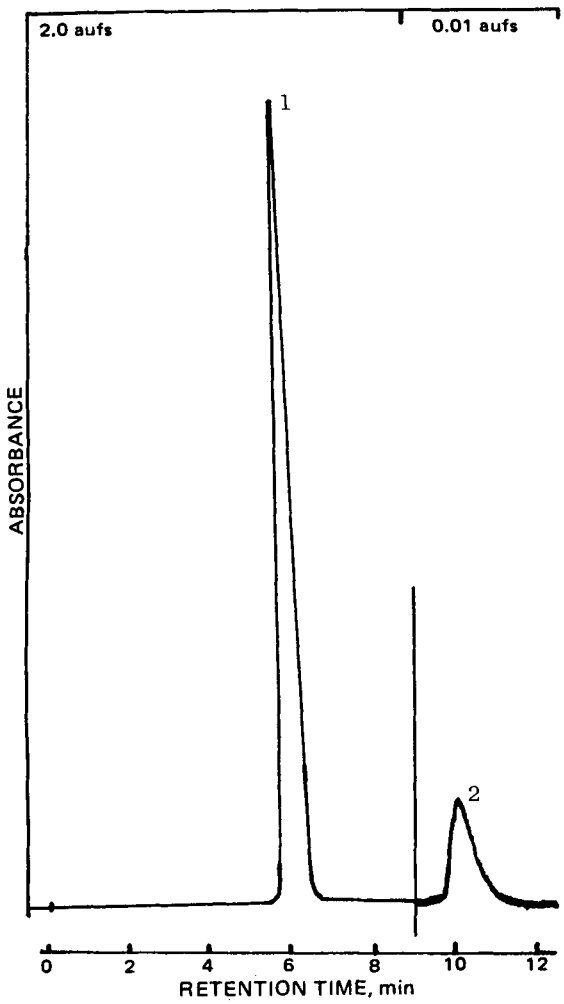

Figure 1—*HPLC chromatogram for standard preparation of (1) acetaminophen and (2) hydrocodone.*

Sample Preparation—For the content uniformity test and tablet composite assay, a tablet[6] or an amount equivalent to 1 average tablet was transferred to a 100-ml volumetric flask. About 95 ml of water was added and the flask was placed on a steam bath. After 15 min, the flask was removed, mixed for 15 min, sonicated, and allowed to stand. A portion of this solution was filtered[7] and placed in a sealed vial[8].

Assay Method—Equal volumes (~13 μl) of standard preparations and assay preparations were introduced into the HPLC operated at room temperature by means of the automatic injector.

Calculation—Quantitation was done by measuring peak heights electronically compared to external standards. To determine the number of milligrams per tablet of acetaminophen, the following equation was used:

$$\frac{Pha}{Phs} \times \frac{Ws}{5} \times \frac{ATW}{Wa} \qquad \text{(Eq. 1)}$$

Similarly, for the mg/tablet hydrocodone bitartrate:

$$\frac{Pha}{Phs} \times Ws \times 4 \times \frac{ATW}{Wa} \qquad \text{(Eq. 2)}$$

where *Pha* is the average peak height of the assay preparation; *Phs* is the average peak height of the standard preparation; *Ws* is the weight of the standard in milligrams; *Wa* is the weight of the assay sample in milligrams; and *ATW* is the average tablet weight in milligrams.

Accelerated Decomposition Studies—Accelerated, extreme degradation of hydrocodone bitartrate was accomplished by several methods and its peak height was measured by data module integration:

[6] Vicodin, Knoll Pharmaceutical Co., Whippany, NJ 07981.
[7] Waters Associates Aqueous Sample Clarification Kit part No. 26865, Milford, MA 01757.
[8] Waters Associates Standard 4-ml vial assembly part No. 73018, Milford, MA 01757.

Table I—Retention Time of Hydrocodone, Acetaminophen, and Related Compounds

Compound	Retention Time, min
p-Aminophenol	3.4
Hydromorphone	5.2
Acetaminophen	5.9
Codeine	7.3
Hydrocodone	10.0
p-Chloracetanilide	43.3

Table II—Reproducibility of Retention Times for Hydrocodone and Acetaminophen

Run	Retention Time, min: Acetaminophen (I)	Retention Time, min: Hydrocodone (II)	RRT (II)/(I)
1	5.2	10.4	2.00
2	5.1	10.1	1.98
3	5.5	10.1	1.84
4	5.2	9.9	1.90
5	5.5	10.4	1.89
6	5.1	9.9	1.94
7	5.3	10.3	1.94
8	5.1	9.9	1.94
$\bar{X}$	5.2	10.1	1.93
RSD, %	3.2	2.2	2.6

(a) Hydrocodone bitartrate powder was heated at 105° for 1-week.
(b) Hydrocodone bitartrate (1 mg/ml) was refluxed in 0.1 *N* NaOH for 24 hr.
(c) Hydrocodone bitartrate (1 mg/ml) was refluxed in 1.0 *N* HCl for 48 hr.
(d) Hydrocodone bitartrate (1 mg/ml) was dissolved in water, placed in a quartz cell, and irradiated with a 275-watt sunlamp for 2 hr.
(e) Hydrocodone bitartrate (1 mg/ml) was dissolved in 3% H_2O_2 and allowed to stand for 1 month.

These decomposition studies were compared with the following control samples:
(a) Hydrocodone bitartrate dissolved in water (1 mg/ml).
(b) Hydrocodone bitartrate refluxed in aqueous solution (1 mg/ml) for 24 hr.

Precision Analysis—Ten tablets were weighed then powdered by mortar and pestle. An amount of powder equivalent to about one average tablet was accurately weighed and transferred to each of eight separate 100-ml volumetric flasks. These samples were treated as described in *Sample Preparation*. Duplicate injections of each sample solution were made.

Accuracy Analysis—Known amounts at the 100% of tablet claim of hydrocodone bitartrate and acetaminophen were added to a placebo powder mixture dissolved in water. This sample was treated as described and six replicate injections were made into the high-pressure liquid chromatograph.

RESULTS

In a typical standard run, good separation of I and II can be seen (Fig. 1). The following related compounds were shown to be separable by this

Table III—Precision of HPLC Assay of Hydrocodone Bitartrate and Acetaminophen in Commercial Tablets [a]

Tablet Sample	Acetaminophen Found, %	Hydrocodone Bitartrate Found, %
1	98.4	96.4
2	97.0	96.4
3	98.2	100.4
4	97.8	98.2
5	100.2	101.0
6	99.0	98.6
7	98.0	98.2
8	98.4	100.0
Mean ($\bar{x}$)	98.4	98.6
SD ($n-1$)	0.93	1.73
RSD, %	0.95	1.75

[a] Vicodin tablets contain 5 mg of hydrocodone bitartrate and 500 mg of acetaminophen.

Table IV—Comparison of HPLC with USP Column Assays for Acetaminophen and Ion-Pairing Assays for Hydrocodone Bitartrate in Tablets [a]

Batch Number	Acetaminophen Found, %			Hydrocodone Bitartrate Found, %		
	HPLC	USP Column	Variation	HPLC	Ion-Pairing	Variation
1	100.4	99.1	1.3	100.3	102.8	2.5
2	99.9	99.3	0.6	97.1	98.2	1.1
3	101.3	99.9	1.4	98.2	98.4	0.2
4	97.6	101.8	4.2	97.8	95.6	2.2
5	97.7	97.2	0.5	97.2	96.8	0.4
6	97.6	94.5	3.1	98.8	101.8	3.0
7	99.8	94.6	5.2	99.8	99.0	0.8

[a] Vicodin tablets. [b] Based on method by Das Gupta (Ref. 17).

method: *p*-aminophenol, *p*-chloroacetanilide, codeine, and hydromorphone. The two compounds, *p*-aminophenol and *p*-chloroacetanilide, are possible hydrolysis and precursor compounds, respectively, of acetaminophen (17). Codeine and hydromorphone are narcotic drugs chemically related to hydrocodone. This separation demonstrates the specificity of the assay. The respective retention times of the related compounds are listed in Table I.

Linearity—Calibration standard solutions were prepared at 10% intervals between 70 and 130% levels in the expected range of analysis. A plot of peak heights *versus* the amount of the two components injected was linear as evidenced by a correlation coefficient of 0.998 for I between 3.5 and 6.5 mg/ml and 0.996 for II between 0.035 and 0.065 mg/ml.

Accuracy—In a study of a spiked placebo, results showed a mean accuracy of 100.3% for I and 99.7% for II. No interference due to the placebo ingredients could be detected in the chromatograms produced. Reproducibility of retention time was sufficiently precise to ensure separation and identity of I and II (Table II).

Precision—The relative standard deviations for eight samples of a commercial tablet were 0.95% for I and 1.75% for II (Table III). Comparison of this HPLC method and the bromothymol blue complex method for II and the USP method for I are shown in Table IV. HPLC assay results on these commercial tablet samples varied on an average of 2.3% from those of the USP assay for I and 1.45% from those of the dye complex assay for II.

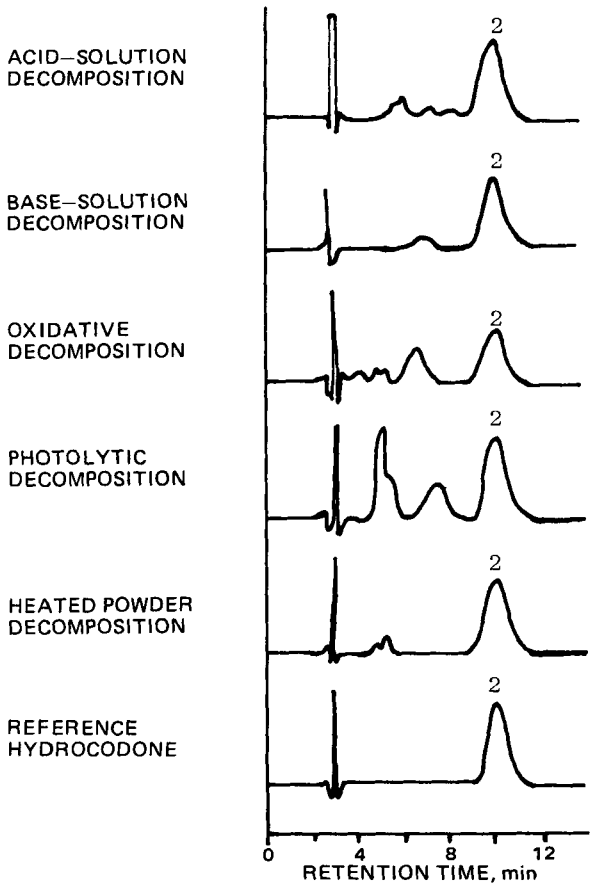

Figure 2—*Retention times of decomposition products resulting from extreme, accelerated decomposition studies of (Ref. 2) hydrocodone.*

Decomposition—No extraneous peak was detected in the analysis of the sample hydrocodone refluxed in water for 24 hr. Comparison of the chromatogram with USP reference standard hydrocodone bitartrate control solution showed a 100% quantitative recovery. Similar measurements of the main chromatographic peak from the decomposed solutions showed various amounts of residual drug depending on its treatment (Fig. 2).

The quantities remaining were found to be 81% after thermal, 79% after base hydrolysis, 87% after acid hydrolysis, 94% after UV photolysis, and 62% after oxidative treatment.

DISCUSSION

The proposed method requires less time than the USP method for acetaminophen tablets (15) which requires column preparation, elution, and absorbance measurements. A titration of an extract is reported for hydrocodone bitartrate tablets (16). For control assay purposes, a colorimetric ion-pairing assay has been adapted in this laboratory for determining II as described for codeine (17).

The chromatographic difficulty associated with the simultaneous quantitation of acetaminophen and codeine has been reported (12). The problem is even more severe in this dosage form. The quantitation of the 100:1 ratio of I to II is made possible by the electronic data module and optimum wavelength absorbance for II. For the tablet product, extracting the dosage form with water completely dissolved both components. Attention to detail in the chromatographic process was necessary so that the peak height of acetaminophen would be as large as possible without overloading the detector, thereby allowing the hydrocodone peak to be more easily and reproducibly quantitated. The elution times are also important, since band broadening increases with increasing elution time and subsequently decreases the peak height. In an additional analysis using the above method, a 10:1 weight ratio of acetaminophen to codeine was assayed simultaneously by measurements at the maximum wavelength of codeine.

The HPLC separation of degradation impurities that result when II is subjected to accelerated extreme decomposition is demonstrated in Fig. 2. The quantitative and qualitative content of unchanged II is easily determined, showing the stability-indicating nature of the analysis. To eliminate the possibility of an interference, no internal standard is employed. In this two-component solid dosage with many possible impurities and degradation products, this approach appears preferable.

It may be possible for a stress-produced degradation product of II to be within the peak for I. However, the response for I (>100:1) is so large

Table V—Comparison of Content Uniformity Assay for Hydrocodone Bitartrate by HPLC and by Ion-Pairing Method

Sample	Hydrocodone Bitartrate, %		
	HPLC	Ion-Pairing	Deviation
1	94.5	90.5	−4.0
2	95.9	96.1	+0.2
3	102.3	98.2	−4.1
4	95.4	91.8	−3.6
5	101.0	100.5	−0.5
6	96.1	94.3	−1.8
7	103.7	100.0	−3.7
8	98.4	98.6	+0.2
9	102.5	100.9	−1.6
10	103.4	102.3	−1.1
Average	99.3	97.3	−2.0

compared with II that the effect on I would be insignificant. In addition, the analysis for intact II is sufficiently specific and quantitative for stability purposes. The known degradation product, *p*-aminophenol, and the impurity of I have different retention times compared with II (Table I). Good assay data have been obtained for several 5-year-old tablet samples. Since there was only an interest in the strength of the hydrocodone, no attempt was made to identify the decomposition products formed under stress.

For the content uniformity run, aliquots of the same 10 tablet samples were assayed by the HPLC and ion-pairing methods for II as paired comparison. Assay data for the ion-pairing analysis are generally lower compared with HPLC (Table V).

Through the utilization of the selected wavelength of maximum absorbance for II, this procedure is being routinely used as an automated simultaneous determination. The HPLC method reported in this study allows for rapid, specific, stability-indicating, and simultaneous quantitation of both substances in a two-component tablet formulation.

REFERENCES

(1) E. Brochmann-Hanssen and A. Baerheim Svendsen, *J. Pharm. Sci.*, **51**, 1096 (1962).

(2) J. W. Barnhart and W. J. Caldwell, *J. Chromatogr.*, **130**, 243 (1977).

(3) F. M. Plakogiannis and A. M. Saad, *J. Pharm. Sci.*, **66**, 604 (1977).

(4) M. K. Chao, I. J. Holcomb, and S. A. Fusari, *ibid.*, **68**, 1463 (1979).

(5) E. J. Kubiak and J. W. Munson, *ibid.*, **69**, 152 (1980).

(6) A. Menyharth, F. P. Mahn, and J. E. Heveran, *ibid.*, **63**, 430 (1974).

(7) F. J. Sena, J. T. Piechocki, and K. L. Li, *ibid.*, **68**, 1465 (1979).

(8) S. K. Soni and S. M. Dugar, *J. Forensic Sci.*, **24** 437 (1979).

(9) V. Das Gupta, *J. Pharm. Sci.*, **69**, 110 (1980).

(10) D. Burke and H. Sokoloff, *ibid.*, **69**, 138 (1980).

(11) W. O. McSharry and I. V. E. Savage, *ibid.*, **69**, 212 (1980).

(12) C. Y. Ko, F. C. Marziani, and C. A. Janicki, *ibid.*, **69**, 1081 (1980).

(13) E. Townley and P. Roden, *ibid.*, **69**, 523 (1980).

(14) J. W. Munson and E. J. Kubiak, *Anal. Lett*, **13**(B8) 705 (1980).

(15) "The United States Pharmacopeia," 20th Rev., U.S. Pharmacopeial Convention, Rockville, Md., 1980, p. 12.

(16) *Ibid.*, p. 379.

(17) J. E. Fairbrother in "Analytical Profiles of Drug Substances," vol. 3, K. Florey, Ed., Academic, New York, N.Y., 1974 p. 34.

(18) V. Das Gupta, *Am. J. Hosp. Pharm.*, **28**, 55 (1971).

High-Pressure Liquid Chromatographic Assays for Ticarcillin in Serum and Urine

R. H. KWAN, S. M. MacLEOD, M. SPINO, and F. W. TEARE *x

Received April 6, 1981, from the **Faculty of Pharmacy, University of Toronto, Toronto, Ontario M5S 1A1, Canada*, and the *Department of Clinical Pharmacology, The Hospital for Sick Children, Toronto, Ontario M5S 1A1, Canada.* Accepted for publication December 9, 1981.

Abstract □ Rapid and sensitive high-pressure liquid chromatographic (HPLC) assays for ticarcillin in serum and urine have been developed. Sample pretreatment and optimized chromatographic conditions are presented for a C-18-bonded reversed-phase column used in an internal standard assay method. Ticarcillin has a retention time of ~5.3 min at a flow rate of 1.5 ml/min for a mobile phase of acetonitrile–aqueous 0.06 *M* sodium biphosphate, pH 2.05, (50.5:100). In a two-step extraction procedure, the ticarcillin extraction efficiencies from serum and urine were 76.1 ± 4.7 and 80.9 ± 3.2%, respectively. The assay sensitivity limit for ticarcillin in these fluids is ~1.0 μg/ml. A comparison is made of the HPLC and microbiological assay results for ticarcillin in 20 different but equally divided serum samples obtained from two volunteers.

Keyphrases □ Ticarcillin—high-pressure liquid chromatographic assays, serum and urine □ Urine—ticarcillin, high-pressure liquid chromatographic assays, serum □ Serum—ticarcillin, high-pressure liquid chromatographic assays, urine □ High-pressure liquid chromatography—ticarcillin in serum and urine

During the past decade, measurements of ticarcillin concentrations in clinical studies have been performed mainly by microbiological assays (1–9). A microtitration method (10, 11) has been applied to broth. Although numerous chemical and physical assay methods have been reported for the detection and assay of penicillins, they suffer from a variety of disadvantages. For instance, iodometric titration (12–15) cannot be applied to penicillins having unsaturated side chains. Spectrophotometric methods (16–18) are not very sensitive and a colorimetric assay (19–21) involving the reaction of hydroxylamine with penicillins in the presence of ferric ions to form a colored salt lacks both specificity and sensitivity, having a limit of ~20 μg/ml. A spectrofluorometric assay (22) has application only for fluorophoric penicillins. More recently, precise, convenient, and specific HPLC assays for various penicillins have been reported (23–29).

At the time the present study commenced there was, to the best of our knowledge, no HPLC assay reported for ticarcillin in biological fluids. This report presents a rapid, specific, and accurate HPLC assay for ticarcillin in human serum and urine.

EXPERIMENTAL

Materials—Powdered ticarcillin[1] (disodium salt) and carbenicillin[2], the internal standard, were used as received without further purification as standards. All solvents and reagents were analytical reagent grade, except for acetonitrile[3] which was HPLC grade, 190 nm cutoff.

Apparatus—The HPLC pump[4] was fitted with an injector[5] and variable wavelength detector[6] set at 210 nm and attenuated at 0.04 aufs. The signal was recorded either on a 10-mV recorder[7] at a speed of 0.5 cm/min or an integrator-plotter[8].

Columns—A prepacked 10- × 0.8-cm i.d. cartridge[9] containing a reversed-phase, C-18, chemically bonded to 10 μm of silica, and contained in a radial compression device[10] was employed at ambient temperature. A guard column[11] was placed between the injector and the column. Ti-

[1] Beecham Laboratories, Pointe Claire, Ontario, Quebec.
[2] Ayerst Laboratories Saint-Laurent, Quebec.
[3] Caledon Laboratories Ltd., Georgetown, Ontario, Canada.
[4] Waters Associates Inc., Milford, Mass., model 6000A.
[5] Waters Associates, model U6K.
[6] Waters Association, model 450.
[7] Beckman 10 inch Recorder, model 1005.
[8] Waters Associates, Data Module, model 730.
[9] Waters Associates, Radial-Pak-A.
[10] Waters Associates, RCM-100 Radial Compression System.
[11] Whatman Inc., Column Survival Kit with Co-Pell ODS.

0022-3549/82/01000-1118$01.00/0

compared with II that the effect on I would be insignificant. In addition, the analysis for intact II is sufficiently specific and quantitative for stability purposes. The known degradation product, *p*-aminophenol, and the impurity of I have different retention times compared with II (Table I). Good assay data have been obtained for several 5-year-old tablet samples. Since there was only an interest in the strength of the hydrocodone, no attempt was made to identify the decomposition products formed under stress.

For the content uniformity run, aliquots of the same 10 tablet samples were assayed by the HPLC and ion-pairing methods for II as paired comparison. Assay data for the ion-pairing analysis are generally lower compared with HPLC (Table V).

Through the utilization of the selected wavelength of maximum absorbance for II, this procedure is being routinely used as an automated simultaneous determination. The HPLC method reported in this study allows for rapid, specific, stability-indicating, and simultaneous quantitation of both substances in a two-component tablet formulation.

REFERENCES

(1) E. Brochmann-Hanssen and A. Baerheim Svendsen, *J. Pharm. Sci.*, **51**, 1096 (1962).

(2) J. W. Barnhart and W. J. Caldwell, *J. Chromatogr.*, **130**, 243 (1977).

(3) F. M. Plakogiannis and A. M. Saad, *J. Pharm. Sci.*, **66**, 604 (1977).

(4) M. K. Chao, I. J. Holcomb, and S. A. Fusari, *ibid.*, **68**, 1463 (1979).

(5) E. J. Kubiak and J. W. Munson, *ibid.*, **69**, 152 (1980).

(6) A. Menyharth, F. P. Mahn, and J. E. Heveran, *ibid.*, **63**, 430 (1974).

(7) F. J. Sena, J. T. Piechocki, and K. L. Li, *ibid.*, **68**, 1465 (1979).

(8) S. K. Soni and S. M. Dugar, *J. Forensic Sci.*, **24** 437 (1979).

(9) V. Das Gupta, *J. Pharm. Sci.*, **69**, 110 (1980).

(10) D. Burke and H. Sokoloff, *ibid.*, **69**, 138 (1980).

(11) W. O. McSharry and I. V. E. Savage, *ibid.*, **69**, 212 (1980).

(12) C. Y. Ko, F. C. Marziani, and C. A. Janicki, *ibid.*, **69**, 1081 (1980).

(13) E. Townley and P. Roden, *ibid.*, **69**, 523 (1980).

(14) J. W. Munson and E. J. Kubiak, *Anal. Lett*, **13**(B8) 705 (1980).

(15) "The United States Pharmacopeia," 20th Rev., U.S. Pharmacopeial Convention, Rockville, Md., 1980, p. 12.

(16) *Ibid.*, p. 379.

(17) J. E. Fairbrother in "Analytical Profiles of Drug Substances," vol. 3, K. Florey, Ed., Academic, New York, N.Y., 1974 p. 34.

(18) V. Das Gupta, *Am. J. Hosp. Pharm.*, **28**, 55 (1971).

High-Pressure Liquid Chromatographic Assays for Ticarcillin in Serum and Urine

R. H. KWAN, S. M. MacLEOD, M. SPINO, and F. W. TEARE *x

Received April 6, 1981, from the **Faculty of Pharmacy, University of Toronto, Toronto, Ontario M5S 1A1, Canada*, and the *Department of Clinical Pharmacology, The Hospital for Sick Children, Toronto, Ontario M5S 1A1, Canada.* Accepted for publication December 9, 1981.

Abstract □ Rapid and sensitive high-pressure liquid chromatographic (HPLC) assays for ticarcillin in serum and urine have been developed. Sample pretreatment and optimized chromatographic conditions are presented for a C-18-bonded reversed-phase column used in an internal standard assay method. Ticarcillin has a retention time of ~5.3 min at a flow rate of 1.5 ml/min for a mobile phase of acetonitrile–aqueous 0.06 *M* sodium biphosphate, pH 2.05, (50.5:100). In a two-step extraction procedure, the ticarcillin extraction efficiencies from serum and urine were 76.1 ± 4.7 and 80.9 ± 3.2%, respectively. The assay sensitivity limit for ticarcillin in these fluids is ~1.0 μg/ml. A comparison is made of the HPLC and microbiological assay results for ticarcillin in 20 different but equally divided serum samples obtained from two volunteers.

Keyphrases □ Ticarcillin—high-pressure liquid chromatographic assays, serum and urine □ Urine—ticarcillin, high-pressure liquid chromatographic assays, serum □ Serum—ticarcillin, high-pressure liquid chromatographic assays, urine □ High-pressure liquid chromatography—ticarcillin in serum and urine

During the past decade, measurements of ticarcillin concentrations in clinical studies have been performed mainly by microbiological assays (1–9). A microtitration method (10, 11) has been applied to broth. Although numerous chemical and physical assay methods have been reported for the detection and assay of penicillins, they suffer from a variety of disadvantages. For instance, iodometric titration (12–15) cannot be applied to penicillins having unsaturated side chains. Spectrophotometric methods (16–18) are not very sensitive and a colorimetric assay (19–21) involving the reaction of hydroxylamine with penicillins in the presence of ferric ions to form a colored salt lacks both specificity and sensitivity, having a limit of ~20 μg/ml. A spectrofluorometric assay (22) has application only for fluorophoric penicillins. More recently, precise, convenient, and specific HPLC assays for various penicillins have been reported (23–29).

At the time the present study commenced there was, to the best of our knowledge, no HPLC assay reported for ticarcillin in biological fluids. This report presents a rapid, specific, and accurate HPLC assay for ticarcillin in human serum and urine.

EXPERIMENTAL

Materials—Powdered ticarcillin[1] (disodium salt) and carbenicillin[2], the internal standard, were used as received without further purification as standards. All solvents and reagents were analytical reagent grade, except for acetonitrile[3] which was HPLC grade, 190 nm cutoff.

Apparatus—The HPLC pump[4] was fitted with an injector[5] and variable wavelength detector[6] set at 210 nm and attenuated at 0.04 aufs. The signal was recorded either on a 10-mV recorder[7] at a speed of 0.5 cm/min or an integrator-plotter[8].

Columns—A prepacked 10- × 0.8-cm i.d. cartridge[9] containing a reversed-phase, C-18, chemically bonded to 10 μm of silica, and contained in a radial compression device[10] was employed at ambient temperature. A guard column[11] was placed between the injector and the column. Ti-

[1] Beecham Laboratories, Pointe Claire, Ontario, Quebec.
[2] Ayerst Laboratories Saint-Laurent, Quebec.
[3] Caledon Laboratories Ltd., Georgetown, Ontario, Canada.
[4] Waters Associates Inc., Milford, Mass., model 6000A.
[5] Waters Associates, model U6K.
[6] Waters Association, model 450.
[7] Beckman 10 inch Recorder, model 1005.
[8] Waters Associates, Data Module, model 730.
[9] Waters Associates, Radial-Pak-A.
[10] Waters Associates, RCM-100 Radial Compression System.
[11] Whatman Inc., Column Survival Kit with Co-Pell ODS.

0022-3549/82/01000-1118$01.00/0

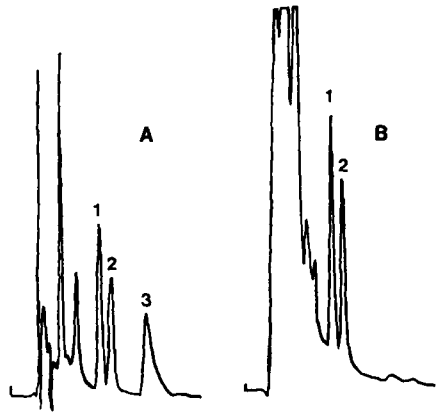

Figure 1—*Typical chromatograms of ticarcillin and carbenicillin (internal standard) in(A) serum and (B) urine sample. Peaks: (1) ticarcillin, (2) carbenicillin, and (3) endogenous material.*

carcillin sample and standard solutions containing the internal standard were injected in 10-, 25-, and 50-μl volumes with microliter syringes[12] into the injector valve.

Mobile Phase—A solution was prepared consisting of acetonitrile–aqueous 0.06 *M* sodium biphosphate (50.5:100), and the pH was adjusted to 2.05 with ~35 ml of 85% phosphoric acid. This solution was filtered and degassed by passage through a membrane filter[13] under reduced pressure. The mobile phase was pumped isocratically through the column at ambient temperature with a flow rate of 1.5 ml/min under a back pressure of ~350 psi/g.

Internal Standard—Aqueous carbenicillin sodium stock solution containing 59 mg/liter was prepared fresh weekly and stored at 4°. Accurate volume aliquots equivalent to 2.95 μg/50 μl of serum and 14.75 μg/250 μl of urine were used as internal standards in the assay for ticarcillin.

Standard Solutions—An aqueous stock solution of ticarcillin disodium (0.5113 g/100 ml) was prepared weekly and stored at 4°. Serial dilutions were performed daily to prepare six working standards in the range of 0–1400 μg/ml. Serum standards contained 200 μl of human control serum, 10 μl of a working ticarcillin standard solution, and 50 μl of the internal standard solution. Urine standards contained 500 μl of control human urine, 50 μl of a ticarcillin working standard, and 250 μl of the internal standard solution. In each instance calibration curves were initially constructed by plotting the integrated peak area ratios of the standard ticarcillin to internal standard against the corresponding ticarcillin standard concentration. Sample serums and urines were similarly prepared and the measured peak area ratios referred to the calibration curve to read the concentration of ticarcillin present.

Assay Method for Serum—A serum sample (200 μl) was transferred to a 12- × 75-mm polypropylene test tube, followed in succession by 50 μl of internal standard, and 50 μl of 1 *M* sulfuric acid. The tube contents were vigorously agitated with a mechanical mixer[14] for 5 sec, then 1.0 ml of ethyl acetate was added and the tube capped and shaken for 2 min prior to centrifugation[15] for another 2 min. The supernate was transferred to another similar tube and evaporated to dryness under reduced pressure at 35°. To this extract residue was added 200 μl each of methylene chloride and aqueous 0.04 *M* sodium biphosphate, pH 6.8. The tube contents were gently agitated for 1 min then centrifuged for 2 min. The top aqueous layer (~75%) was accurately transferred to another similar test tube and briefly shaken mechanically in a water bath at 35° to remove traces of methylene chloride. An accurate aliquot of 10–50 μl of this final sample solution was injected onto the RP-18 column.

Method for Urine—A 500-μl urine sample was treated in a manner similar to that described for serum, except for the volumes of solvents employed. A 250-μl volume of the internal standard solution was added to the 500-μl urine sample (or known dilution if required) and the mixture extracted once with 2 ml of ethyl acetate. The extract was evaporated to dryness as described for serum and the residue reconstituted in a mixture of 1.0 ml of methylene chloride and 1.0 ml of aqueous 0.04 *M* sodium biphosphate, pH 6.80. Beyond this point the sample was handled in the same manner as that for the serum.

[12] Hamilton Co., Reno, Nev., 25- and 100-μl syringes.
[13] Millipore Corp., No. FALP 04700, 1.0-μm pore.
[14] Vortex-Genie—Fisher Scientific Co.
[15] Sorvall, Newton, Conn. Model GLC-2, at 2000 rpm.

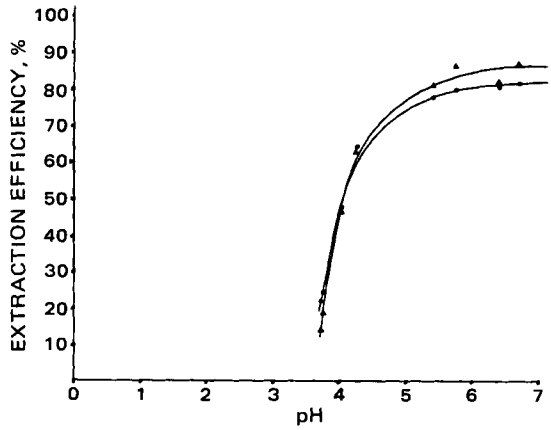

Figure 2—*Extraction efficiency of ticarcillin (●) and carbenicillin (▲) from urine as a function of the pH of the back-extraction phosphate buffer.*

Serum and Urine Collection and Assay—In an HPLC assay *versus* microbiological assay, nine 5-ml blood samples were obtained at specified intervals from each of two healthy volunteers following a 10-min intravenous infusion of a solution containing 2.0 g of ticarcillin disodium. Sera were separated by centrifugation and each was divided into two identical portions. One portion was subjected to a microbiological assay procedure analogous to that of Bannatyne and Cheung (30) and the other to the HPLC assay described. Triplicate determinations were made on each serum sample with both methods.

Concomitantly, urine samples were obtained from one of the volunteers receiving the 2.0-g dose of ticarcillin. Both time and urine volumes were recorded at each collection. Triplicate determinations were performed by the HPLC method only on each urine sample.

RESULTS AND DISCUSSION

The goals were to select a suitable reversed-phase column and mobile phase to separate the two penicillins, then develop a rapid and sensitive HPLC assay for ticarcillin in both serum and urine. The choices of columns and mobile phases studied were made on the basis of good peak symmetry, resolution, and short retention times suitable for measuring many biological samples in a relatively short period with good accuracy.

When the RP-8[16] column was used with several mobile phases, the ticarcillin was either poorly retained or eluted as asymmetric or fused peaks. Whether this result is due to varying degrees of ionization of the two carboxylic acid groups present, to the presence of sterisomeric structures, or to some other cause remains to be shown.

When these same solvent systems were used to elute ticarcillin from

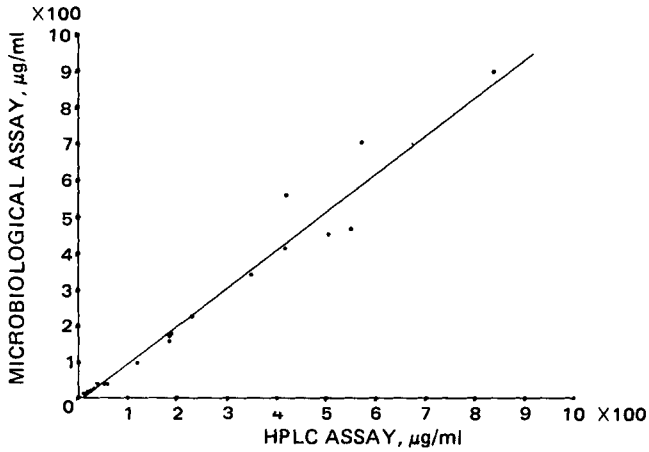

Figure 3—*Comparison of assays for ticarcillin in human urine. Identical samples were assayed by HPLC and microbiological methods. Linear regression analysis of this data yields the equation* $y = 1.0716x - 13.2182$, $r = 0.9809$.

[16] MPLC, Brownlee Labs, Santa Clara, CA 95050.

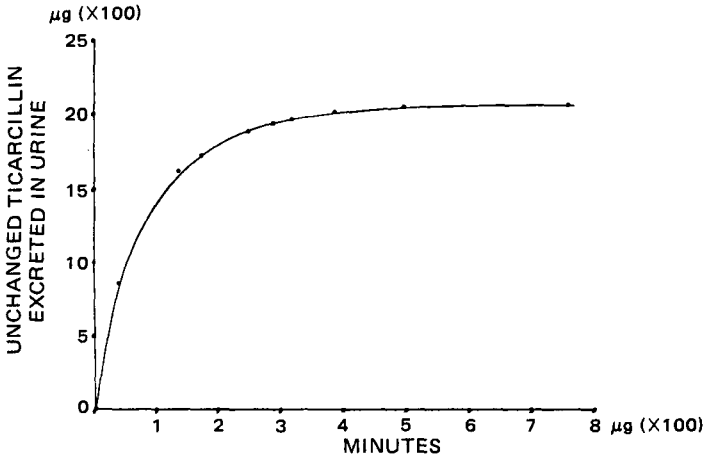

Figure 4—*Cumulative ticarcillin excreted in urine following slow intravenous infusion of a 2-g dose to a 70-kg normal male.*

a RP-2[16] column, retention times were improved, but the problem of fused or asymmetric peaks remains. Among the solvent systems tried was one comprised of 1 liter of aqueous 0.06 *M* sodium biphosphate and 125 ml of acetonitrile plus ~5 ml of 95% phosphoric acid to give a final pH value of 2.75. This mobile phase gave rise to a symmetrical peak for ticarcillin with a reasonable retention time of 5.50 min at a flow rate of 2.0 ml/min. Using the same conditions, except for the adjustment of pH values ranging from 5.0 to 2.0, the retention time was observed to increase from 1.5 to 11.0 min as the acidity increased. At pH values between 2.8 and 3.3, the ticarcillin peak was sharp but too close to the solvent peak resulting from each injection. At a pH of 2.75, both ticarcillin and carbenicillin gave symmetrical and well-resolved peaks having favorable retention times of 5.30 and 6.80 min, respectively.

Another reversed-phase column, RP-18[9], was found to work very well. Since ticarcillin is potentially a relatively polar compound having two carboxylic acid groups, its retention on the nonpolar RP-18 column could be increased through either ion-suppression or the ion-pairing techniques. The former was attempted due to its simplicity. Ticarcillin has a reported pKa value of between 2.70 and 2.73 (31); therefore, a new mobile phase consisting of 505 ml of acetonitrile and 1 liter of 0.06 *M* sodium biphosphate monobasic was adjusted by means of 85% phosphoric acid to a pH of 2.05. Use of this solvent system produced well-resolved, sharp symmetrical peaks at ~5.30 min and 6.00 min for ticarcillin and carbenicillin, respectively, at a flow rate of 1.50 ml/min (Fig. 1). If the pH was 2.20, ticarcillin eluted as two fused peaks at 4.42 and 4.85 min. These observations underscore the necessity of having the mobile phase accurately buffered to a pH of 2.05.

Serum and Urine Assays—Assays were developed using simulated samples. Penicillins lack a strong chromophoric group in their structure. The wavelength of maximum absorption for ticarcillin occurs slightly below 200 nm, and this region would give the highest sensitivity for measurement. However, several endogenous substances in these biological fluids also give rise to absorption leading to interference in this region. Therefore, in order to obtain specificity and maximum sensitivity for ticarcillin, these interferences had to be eliminated. Several approaches (32) were taken to solve this problem. First, several deproteinizing agents such as acetonitrile, cold methanol, and 5% trichloroacetic acid in methanol were investigated. Second, drug extractions using various organic solvents alone were attempted. Finally, organic solvent extraction followed with back-extraction into aqueous buffers was attempted. The protein precipitation method met with little success. The one-step organic solvent extraction of ticarcillin and carbenicillin from serum and urine at pH 2.0 using four volumes of ethyl acetate showed some promise but also extracted interfering endogenous materials. These were slow to elute from the column, interfered with the separation of subsequent sample, and necessitated frequent column cleaning.

A back-extraction of the ethyl acetate extract with 0.04 *M* sodium biphosphate, pH 6.8, to separate the ticarcillin and the internal standard from these biological interferences proved very successful. However, when the UV detector was set at 210 nm, an intense peak appeared (t_r = 5.52 min) which severely interfered with the quantitation of the ticarcillin peak. It was subsequently identified as a peak due to ethyl acetate in the aqueous buffer extract. This problem was circumvented by evaporating the ethyl acetate extract to dryness under reduced pressure at 35°, then adding to the residue equal 0.2-ml volumes of methylene chloride and aqueous 0.04 *M* sodium biphosphate (pH 6.8), and vigorously agitating for 1 min prior to centrifugation for 2 min to separate the immiscible phases. The interfering ethyl acetate remained in the methylene chloride phase, while the two penicillins passed into the aqueous buffer layer. A small trace of interference by methylene chloride was readily removed from the aqueous layer by a brief vigorous agitation at 35° prior to the injection of an aliquot of this phase.

Extraction Efficiency—This was expressed as a percent recovery, defined here as the quotient of the peak height of a ticarcillin standard extracted from the biological fluid divided by the peak height of the corresponding amount of drug prepared as a standard solution in the mobile phase and injected directly, all multiplied by 100. The pH value of the aqueous 0.04 *M* sodium biphosphate used in the back-extraction step had a very important effect on the extraction efficiency of both ticarcillin and carbenicillin as shown in Fig. 2. The recovery of both drugs was optimized at >pH 6.0, and the ratio of the ticarcillin peak height divided by that for carbenicillin became constant. A pH >7 was avoided due to possible base-catalyzed degradation of these penicillins. The mean recovery of six replicate serum standards of ticarcillin and carbenicillin was 76.1 ± 4.7% (*CV* = 6.2%) and 76.3 ± 4.5% (*CV* = 5.8%), respectively. The mean recovery of nine urine standards was 80.9 ± 3.2% (*CV* = 4.0%) and 84.5 ± 5.3% (*CV* = 6.3%), for ticarcillin and carbenicillin, respectively.

Accuracy of the HPLC Assays—The quantitation was based on the internal standard method, *i.e.*, the linearity of the plot of the peak area ratios of ticarcillin standards divided by carbenicillin, *versus* the known concentrations of ticarcillin used in the preparation of the standards in mixed human control serum and urine. The linearity of this plot was determined by linear regression analysis using six serum and six urine ticarcillin standards with each standard concentration measured in duplicate. The results were found to be: $y = 0.0061 + 0.0371x$ ($r = 0.9998$), and $y = 0.0150 + 0.343x$ ($r = 0.9995$), for serum and urine standard curves, respectively. The concentration of ticarcillin in the biological sample was obtained by calculating the peak area ratio, substituting the value for y in the appropriate equation, and solving for x.

HPLC and Microbiological Assay Comparison—In the comparison of the HPLC and microbiological assays for ticarcillin in identical *in vivo* serum samples, it is evident from Fig. 3 that these methods are in good agreement having an excellent correlation coefficient ($r = 0.9809$). The overall mean of the percent difference between the microbiological and HPLC values was 13.1%, when all serum samples were considered. One reason for this seemingly large difference is due to the fact that a broad range of ticarcillin concentrations (0–1000 μg/ml) in serum was compared. It must be remembered that the microbiological assay was less accurate at the lower end of the concentration range, *i.e.*, at <50 μg/ml, while the HPLC method was more accurate at <200 μg/ml.

Precision—One simulated ticarcillin serum sample and one urine sample were treated and extracted in the manner outlined earlier. Six replicate injections of each sample were made onto the RP-18 column, and the integrated peak area ratios were calculated. The mean peak area ratios of ticarcillin–carbenicillin were 0.711 ± 0.010 (*CV* = 1.3%) and 1.148 ± 0.013 (*CV* = 1.2%) for serum and urine samples, respectively.

The minimum quantitation limit was ~1 μg/ml for ticarcillin in these biological fluids based on a signal to noise level ratio of three.

Ticarcillin urine levels from one human volunteer were measured with the HPLC assay described. The cumulative amount of unchanged ticarcillin excreted is shown in Fig. 4. Over a period of 12 hr, 103.5% of the administered intravenous dose was measured in the urine. This value agrees well with the 6-hr urine excretion of 99% of a dose administered intramuscularly (33). No degradation product of ticarcillin was detected in any urine sample assayed.

Preliminary pharmacokinetic results (32) obtained using the developed HPLC assay are in very good agreement with those reported in the literature using other assays (34, 35). Further pharmacokinetic studies employing this assay are in progress.

The results indicate that a rapid, convenient, sensitive, specific, and accurate HPLC assay for ticarcillin in serum and urine has been developed and shown to have potential application for pharmacokinetic and clinical studies with this penicillin.

REFERENCES

(1) H. C. Neu and H. Swartz, *J. Gen. Microbiol.*, **58**, 301 (1970).

(2) P. Acred, D. M. Brown, B. F. Clark, and L. Mizen, *Br. J. Pharmacol.*, **39**, 439 (1970).

(3) V. Rodriguez, J. Inagaki, and G. Bodey, *Antimicrob. Agents Chemother.*, **4**, 31 (1973).

(4) T. R. Weibrauch, H. J. Prior, D. Höffler, and J. Kreiglstein, *Klin. Wochenshr.*, **52**, 842 (1974).
(5) D. Phaneuf and H. C. Neu, *Antimicrob. Agents Chemother.*, **16**, 625 (1979).
(6) R. D. Libke, J. T. Clarke, E. D. Ralph, R. P. Luthy, and W. M. M. Kirby, *Clin. Pharmacol. Ther.*, **17**, 441 (1975).
(7) E. Kalkani and N. Marketos, *Antimicrol. Agents Chemother.*, **9**, 89 (1976).
(8) J. S. Tan and S. J. Salstrom, *ibid.*, **11**, 698 (1977).
(9) P. Chanbusarokum and P. R. Murray, *ibid.*, **14**, 505 (1978).
(10) H. J. Harwick, P. Weiss, and F. R. Fekety, *J. Lab. Clin. Med.*, **72**, 511 (1968).
(11) E. R. Ervin and W. E. Bullock, *Antimicrob. Agents Chemother.*, **9**, 94 (1976).
(12) R. G. Tucker, *Nature (London)*, **173**, 85 (1954).
(13) C. J. Perret, *ibid.*, **174**, 1012 (1954).
(14) D. C. Grove and P. R. Randall, in "Assay Methods of Antibiotics," Medical Encyclopedia, New York, N.Y., 1955, p. 16.
(15) P. J. Weiss, *Antibiot. Chemother.*, **9**, 660 (1959).
(16) R. M. Herriot, *J. Biol. Chem.*, **194**, 725 (1946).
(17) M. W. Brandriss, M. L. Denny, M. A. Huber, and H. G. Steinman, *Antimicrob. Agents Chemother.*, **1962**, (627).
(18) T. Yasuda and S. Shimada, *J. Antibiot.*, **24**, 290 (1971).
(19) F. W. Staab, E. A. Ragan, and S. B. Binkley, *Abstracts of the 109th Meeting American Chemical Society 3B*, (1946).
(20) G. E. Boxer and P. M. Everett, *Anal. Chem.*, **21**, 670 (1949).
(21) F. R. Batchler, E. B. Chain, R. Hardy, K. R. L. Mansford, and G. N. Rolinson, *Proc. R. Soc. London, Ser. B*, **154**, 498 (1961).
(22) D. M. Lichtenwalner, B. Suh, B. Lorber, and A. Sugar, *Antimicrob. Agents Chemother.*, **16**, 210 (1979).
(23) J. M. Blaha, A. M. Knevel, and S. L. Hun, *J. Pharm. Sci.*, **64**, 1384 (1975).
(24) K. Tsuji and J. H. Robertson, *ibid.*, **64**, 1542 (1975).
(25) A. Tsuji, E. Miyamoto, O. Kubo, and T. Yamana, *ibid.*, **68**, 812 (1979).
(26) E. R. White, M. A. Carrol, J. E. Zarembo, and A. D. Bender, *J. Antibiot.*, **28**, 205 (1975).
(27) E. R. White, M. A. Carrol, and J. E. Zarembo, *ibid.*, **30**, 811 (1977).
(28) T. L. Lee, L. D'arconte, and M. A. Brooks, *J. Pharm. Sci.*, **68**, 454 (1979).
(29) W. A. Vadino, E. T. Sugita, R. L. Schnaare, H. Y. Ando, and P. J. Niebergall, *ibid.*, **68**, 1316 (1979).
(30) R. M. Bannatyne and R. Cheung, *Antimicrob. Agents Chemother.* **16**, 43 (1979).
(31) D. C. Rapson and A. E. Bird, *J. Pharm. Pharmacol.*, **15**, 222T (1963).
(32) R. H. Kwan, Thesis, University of Toronto, Toronto, Canada (1980).
(33) R. Sutherland, J. Burnett, and G. N. Rolinson, *Antimicrob. Agents Chemother.*, **1970**, 390.
(34) R. D. Libke, *Clin. Pharmacol. Ther.*, **17**, 441 (1975).
(35) M. J. Perry and H. C. Neu, *Chemother. Proc. Int. Congr. Chemother., 9th*, (1975), 5.

ACKNOWLEDGMENTS

Supported by a generous grant from Beecham Laboratories, Pointe Claire, Quebec.

The authors also wish to acknowledge the kind cooperation of Dr. R. M. Bannatyne and Ms. R. Cheung of the Department of Bacteriology, The Hospital for Sick Children, Toronto in performing the microbiological assays of ticarcillin and for their helpful comments.

Concomitant Adsorption and Stability of Some Anthracycline Antibiotics

E. TOMLINSON *x and L. MALSPEIS

Received October 20, 1981, from the *Division of Pharmaceutics and Pharmaceutical Chemistry, College of Pharmacy, Ohio State University, Columbus, OH 43210.* Accepted for publication December 14, 1981. *Present address: Department of Pharmacy, University of Amsterdam, Plantage Muidergracht 24, 1018 TV Amsterdam, The Netherlands.

Abstract □ Using liquid scintillation counting and liquid chromatographic techniques, it has been demonstrated that the anthracycline antibiotics, doxorubicin hydrochloride, *N*-trifluoroacetyladriamycin-14-valerate, and *N*-trifluoroacetyladriamycin-14-octanoate, can be strongly adsorbed to the walls of containers, depending on the nature of both the container material and the solute. It also has been shown that the esters are unstable in the chemical growth media commonly used in cell culture studies. Both the adsorption and stability effects are suggested as being factors which should be carefully considered in interpretation of the *in vitro* and perhaps *in vivo* activities of the anthracycline esters.

Keyphrases □ Anthracyclines—concomitant adsorption and stability, esters, cell culture studies □ Antibiotics—anthracyclines, concomitant adsorption and stability, cell culture studies □ Adsorption—concomitant adsorption and stability of some anthracyclines, cell culture studies

The anthracycline antibiotic, doxorubicin hydrochloride (I), has a wide range of antitumor activity (1). Although I given singly or in combination is now used extensively in the treatment of a variety of tumors (2, 3), its clinical value is limited due to its acute myelotoxicity and to the frequent development of irreversible cardiomyopathy [normally observed when the accumulated dose is >550 mg m^{-2} (4)]. The use of structural analogs of I has been proposed (5, 6) as a means of obviating these two effects; in this respect particular interest has been given to the proposed use of the esters of I and its *O*- and *N*-acetylated derivatives (7–14).

During a study examining the uptake of I and its analogs into tumor cells *in vitro* using both cell monolayers and suspensions, effects were observed on the mass balances of some radiolabeled anthracyclines which could only be reconciled in terms of solute adsorption to container walls. Accordingly, the role of adsorption and stability on the solution properties of I and two of its *N*-trifluoroacetyl esters (*i.e.*, the 14-valerate and the 14-octanoate) have been investigated more completely. The present report presents the results found in this investigation.

EXPERIMENTAL

Chemicals—Anthracycline antibiotics were obtained commercially[1]. ^{14}C-Labeled antibiotics were synthesized as described previously (15). Samples of solid I, *N*-trifluoroacetyladriamycin-14-valerate (II), and *N*-trifluoroacetyladriamycin-14-octanoate (III) had specific activities of 17.1, 22.5, and 28.3 μCi $\mu mole^{-1}$, respectively.

[1] Adria, Ohio.

0022-3549/82/01000-1121$01.00/0

(4) T. R. Weibrauch, H. J. Prior, D. Höffler, and J. Kreiglstein, *Klin. Wochenshr.*, **52**, 842 (1974).
(5) D. Phaneuf and H. C. Neu, *Antimicrob. Agents Chemother.*, **16**, 625 (1979).
(6) R. D. Libke, J. T. Clarke, E. D. Ralph, R. P. Luthy, and W. M. M. Kirby, *Clin. Pharmacol. Ther.*, **17**, 441 (1975).
(7) E. Kalkani and N. Marketos, *Antimicrol. Agents Chemother.*, **9**, 89 (1976).
(8) J. S. Tan and S. J. Salstrom, *ibid.*, **11**, 698 (1977).
(9) P. Chanbusarokum and P. R. Murray, *ibid.*, **14**, 505 (1978).
(10) H. J. Harwick, P. Weiss, and F. R. Fekety, *J. Lab. Clin. Med.*, **72**, 511 (1968).
(11) E. R. Ervin and W. E. Bullock, *Antimicrob. Agents Chemother.*, **9**, 94 (1976).
(12) R. G. Tucker, *Nature (London)*, **173**, 85 (1954).
(13) C. J. Perret, *ibid.*, **174**, 1012 (1954).
(14) D. C. Grove and P. R. Randall, in "Assay Methods of Antibiotics," Medical Encyclopedia, New York, N.Y., 1955, p. 16.
(15) P. J. Weiss, *Antibiot. Chemother.*, **9**, 660 (1959).
(16) R. M. Herriot, *J. Biol. Chem.*, **194**, 725 (1946).
(17) M. W. Brandriss, M. L. Denny, M. A. Huber, and H. G. Steinman, *Antimicrob. Agents Chemother.*, **1962**, (627).
(18) T. Yasuda and S. Shimada, *J. Antibiot.*, **24**, 290 (1971).
(19) F. W. Staab, E. A. Ragan, and S. B. Binkley, *Abstracts of the 109th Meeting American Chemical Society 3B*, (1946).
(20) G. E. Boxer and P. M. Everett, *Anal. Chem.*, **21**, 670 (1949).
(21) F. R. Batchler, E. B. Chain, R. Hardy, K. R. L. Mansford, and G. N. Rolinson, *Proc. R. Soc. London, Ser. B*, **154**, 498 (1961).
(22) D. M. Lichtenwalner, B. Suh, B. Lorber, and A. Sugar, *Antimicrob. Agents Chemother.*, **16**, 210 (1979).
(23) J. M. Blaha, A. M. Knevel, and S. L. Hun, *J. Pharm. Sci.*, **64**, 1384 (1975).
(24) K. Tsuji and J. H. Robertson, *ibid.*, **64**, 1542 (1975).
(25) A. Tsuji, E. Miyamoto, O. Kubo, and T. Yamana, *ibid.*, **68**, 812 (1979).
(26) E. R. White, M. A. Carrol, J. E. Zarembo, and A. D. Bender, *J. Antibiot.*, **28**, 205 (1975).
(27) E. R. White, M. A. Carrol, and J. E. Zarembo, *ibid.*, **30**, 811 (1977).
(28) T. L. Lee, L. D'arconte, and M. A. Brooks, *J. Pharm. Sci.*, **68**, 454 (1979).
(29) W. A. Vadino, E. T. Sugita, R. L. Schnaare, H. Y. Ando, and P. J. Niebergall, *ibid.*, **68**, 1316 (1979).
(30) R. M. Bannatyne and R. Cheung, *Antimicrob. Agents Chemother.* **16**, 43 (1979).
(31) D. C. Rapson and A. E. Bird, *J. Pharm. Pharmacol.*, **15**, 222T (1963).
(32) R. H. Kwan, Thesis, University of Toronto, Toronto, Canada (1980).
(33) R. Sutherland, J. Burnett, and G. N. Rolinson, *Antimicrob. Agents Chemother.*, **1970**, 390.
(34) R. D. Libke, *Clin. Pharmacol. Ther.*, **17**, 441 (1975).
(35) M. J. Perry and H. C. Neu, *Chemother. Proc. Int. Congr. Chemother., 9th*, (1975), 5.

ACKNOWLEDGMENTS

Supported by a generous grant from Beecham Laboratories, Pointe Claire, Quebec.

The authors also wish to acknowledge the kind cooperation of Dr. R. M. Bannatyne and Ms. R. Cheung of the Department of Bacteriology, The Hospital for Sick Children, Toronto in performing the microbiological assays of ticarcillin and for their helpful comments.

Concomitant Adsorption and Stability of Some Anthracycline Antibiotics

E. TOMLINSON *x and L. MALSPEIS

Received October 20, 1981, from the *Division of Pharmaceutics and Pharmaceutical Chemistry, College of Pharmacy, Ohio State University, Columbus, OH 43210.* Accepted for publication December 14, 1981. *Present address: Department of Pharmacy, University of Amsterdam, Plantage Muidergracht 24, 1018 TV Amsterdam, The Netherlands.

Abstract □ Using liquid scintillation counting and liquid chromatographic techniques, it has been demonstrated that the anthracycline antibiotics, doxorubicin hydrochloride, *N*-trifluoroacetyladriamycin-14-valerate, and *N*-trifluoroacetyladriamycin-14-octanoate, can be strongly adsorbed to the walls of containers, depending on the nature of both the container material and the solute. It also has been shown that the esters are unstable in the chemical growth media commonly used in cell culture studies. Both the adsorption and stability effects are suggested as being factors which should be carefully considered in interpretation of the *in vitro* and perhaps *in vivo* activities of the anthracycline esters.

Keyphrases □ Anthracyclines—concomitant adsorption and stability, esters, cell culture studies □ Antibiotics—anthracyclines, concomitant adsorption and stability, cell culture studies □ Adsorption—concomitant adsorption and stability of some anthracyclines, cell culture studies

The anthracycline antibiotic, doxorubicin hydrochloride (I), has a wide range of antitumor activity (1). Although I given singly or in combination is now used extensively in the treatment of a variety of tumors (2, 3), its clinical value is limited due to its acute myelotoxicity and to the frequent development of irreversible cardiomyopathy [normally observed when the accumulated dose is >550 mg m^{-2} (4)]. The use of structural analogs of I has been proposed (5, 6) as a means of obviating these two effects; in this respect particular interest has been given to the proposed use of the esters of I and its *O*- and *N*-acetylated derivatives (7–14).

During a study examining the uptake of I and its analogs into tumor cells *in vitro* using both cell monolayers and suspensions, effects were observed on the mass balances of some radiolabeled anthracyclines which could only be reconciled in terms of solute adsorption to container walls. Accordingly, the role of adsorption and stability on the solution properties of I and two of its *N*-trifluoroacetyl esters (*i.e.*, the 14-valerate and the 14-octanoate) have been investigated more completely. The present report presents the results found in this investigation.

EXPERIMENTAL

Chemicals—Anthracycline antibiotics were obtained commercially[1]. ^{14}C-Labeled antibiotics were synthesized as described previously (15). Samples of solid I, *N*-trifluoroacetyladriamycin-14-valerate (II), and *N*-trifluoroacetyladriamycin-14-octanoate (III) had specific activities of 17.1, 22.5, and 28.3 μCi $\mu mole^{-1}$, respectively.

[1] Adria, Ohio.

0022-3549/82/01000-1121$01.00/0

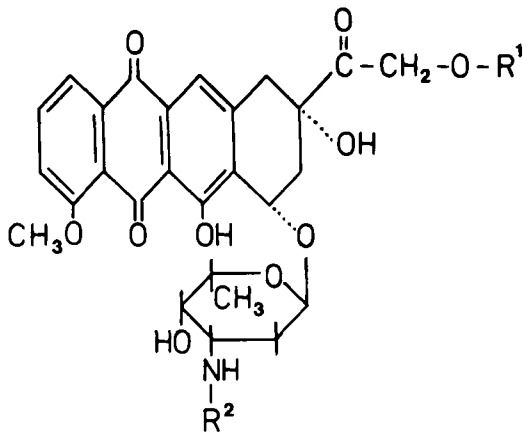

	R^1	R	k′
I	H	H	
II	$CO(CH_2)_3.CH_3$	$COCF_3$	1.6
III	$CO(CH_2)_6.CH_3$	$COCF_3$	3.1
IV	H	$COCF_3$	0.6

The Hanks culture media used was an isotonic buffered (pH 7.2–7.6) solution[2] containing essential salts and glucose, together with 10% fetal calf serum, streptomycin, penicillin, gentamicin, and glutamine. For studies examining only adsorption effects, the Hanks solution contained only the essential salts and glucose.

Analysis—^{14}C-labeled anthracycline was assayed using a liquid scintillation counter[3]. Unlabeled anthracycline was assayed by high-performance liquid chromatography (HPLC) using a stationary phase packing of RP-18[4]: mobile phase, methanol–water (9:1); fluorescence detection[5] with 239 nm excitation and a 550 nm cutoff filter; potassium dichromate as nonretained compound; and quantitation using total integrated peak areas[6]. During assay care was taken to ensure that inner-filter effects (16) were avoided by measuring only in the linear portion region of the anthracycline concentration *versus* peak area relationship. The good reproducibility of the method (coefficient of variation <1.0%) permitted the use of an internal standard to be avoided. The chromatographic capacity ratios measured using this system were 1.6, 3.1, and 0.6 for II, III, and IV, respectively.

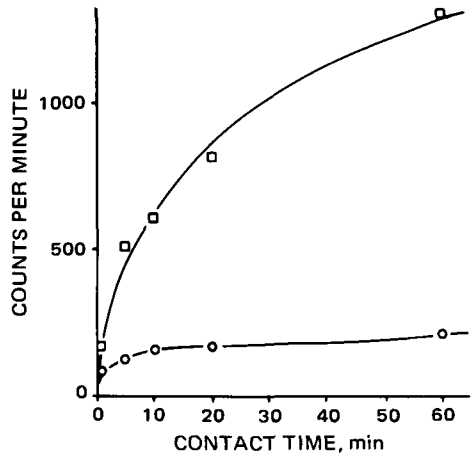

Figure 1—*Total radioactivity (cpm) of 0.5 ml of sodium lauryl sulfate lysis wash after incubation of benzpyrene-induced adenocarcinoma tumor cells (in monolayer aspect) for varying drug solution contact times using polyethylene petri dish containers. Key: (○) I; (□) II.*

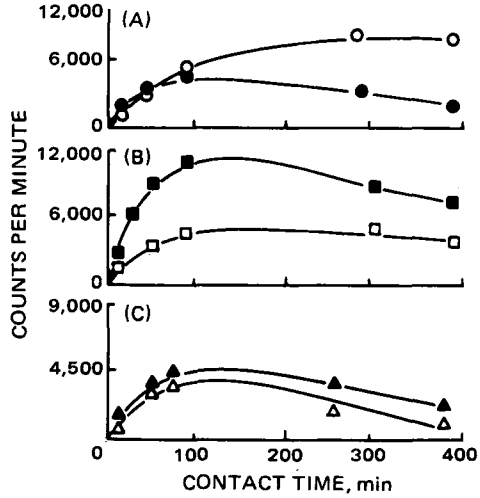

Figure 2—*Total radioactivity (cpm) of 0.5 ml of sodium lauryl sulfate lysis wash after various incubation times with antibiotic solution at 37° in the absence (closed data points) and presence (open data points) of tumor cells (in the monolayer aspect) using polyethylene petri dish containers. Key: (○●) I; (□■) II; (△▲) III.*

Adsorption-Stability Studies—*With Tumor Cells*—Hamster benzpyrene-induced adenocarcinoma cells were prepared as monolayers by seeding 10^5 cells into either 35-mm diameter sterile polyethylene petri dishes[7], or glass (silica) monolayer growth tubes (area of growth was ~2 cm^2) followed by incubation at 37° for 24 hr. The incubation media was removed by suction, and 1 ml of Hanks media was added to wash the cells. This solution was then removed and 1 ml of radiolabeled anthracycline was added (2 μM in Hanks media). Tubes or dishes were then placed in an incubator at 37°. After appropriate incubation times, the drug solution was removed from the culture vessels by suction, and these vessels were washed three times with 1 ml of Hanks solution; 1 ml of 0.5% sodium

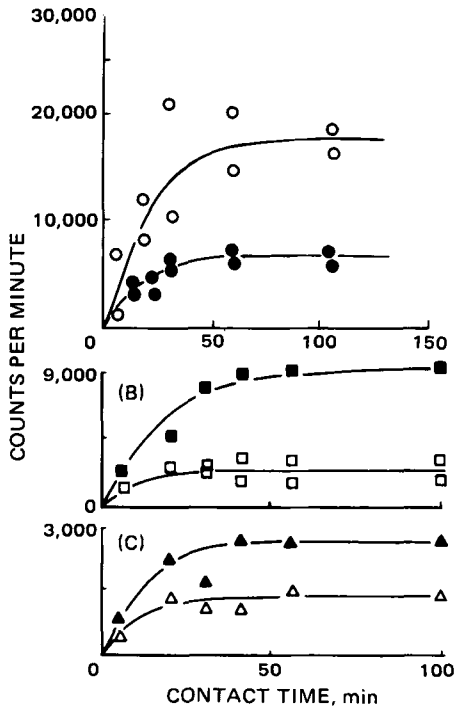

Figure 3—*Total radioactivity (cpm) of 0.5 ml of sodium lauryl sulfate lysis wash after various incubation times with antibiotic solution at 37° in the absence and presence of benzpyrene-induced adenocarcinoma tumor cells (monolayers) using silica glass culture tubes. Key: (○●) I: (□■) II; (△▲) III, and as Fig. 2.*

[2] Grand Island Minimum Essential Media.
[3] Packard Tricarb, model 3375.
[4] Spherisorb ODS 5 μm, (PhaseSep).
[5] Schoeffel flow through detector, model GM 970.
[6] Infotronics, model 308.
[7] Corning #25000, Corning Works, Corning, N.Y.

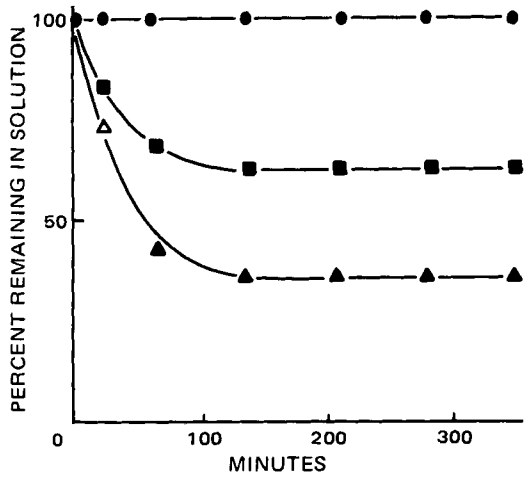

Figure 4—*Percent total radioactivity in Hanks solution with time (pH 7.4, 37°) using a polypropylene container and 1 and 2 μM initial concentrations of antibiotic. Key: (●) I; (■) II; (▲) III, and as Fig. 2.*

lauryl sulfate (as cell digestion agent) was added. After an additional 10 min, 0.5 ml of this digestion fluid was transferred to 19.5 ml of scintillation cocktail and the radioactivity measured. All data given are the mean of three separate determinations carried out in duplicate. For the blank experiments, the described procedure was followed; however, no cells were present in the culture vessels.

Absence of Tumor Cells—Solutions (1 or 2 μM) of the anthracyclines were prepared in Hanks media by dilution of a 100- or 200-μM stock methanolic solution of compound, which was stored in the dark at 0° for not longer than 7 days. (Storage of the stock solution for this length of time was shown by HPLC analysis to be possible without any significant deterioration in the solution.) The dilution was performed by adding 0.1–0.4 ml of stock solution to 19.6–19.9 ml of Hanks media at 37°. The solutions were stirred at 100 rpm using an overhead stirrer and a stirring paddle constructed of the same material as the container. Containers examined were 150-ml silica glass beakers siliconized by immersion in 5% silicone solution with oven drying, 100-ml polytetrafluoroethylene beakers, 50-ml polypropylene conical tapered tubes, and 100-ml stainless steel beakers. All containers were new when used and were discarded after use. For assay using HPLC, 5-, 10-, or 20-μl samples were taken using an HPLC syringe[8] aged using a 2-μM solution of antibiotic. For assay by scintillation counting, 0.1-ml samples were taken using an automatic syringe having polypropylene tips, transferring in the minimum amount of time to 19.9 ml of scintillation cocktail fluid. Anthracycline solutions were kept in the dark whenever possible. All data given are the means of three separate determinations.

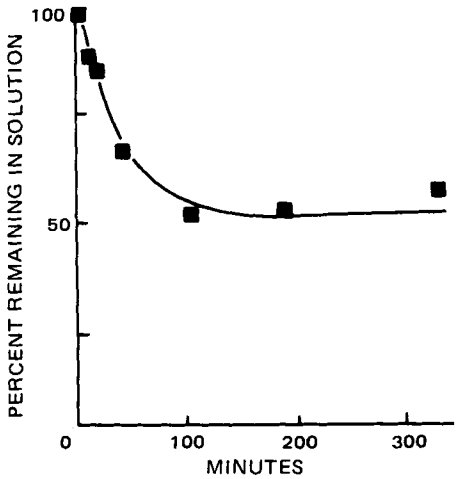

Figure 5—*Percent total radioactivity in Hanks solution with time (pH 7.4, 37°) using a siliconized glass container and 1 and 2 μM initial concentrations of II.*

[8] Hamilton HPLC syringe.

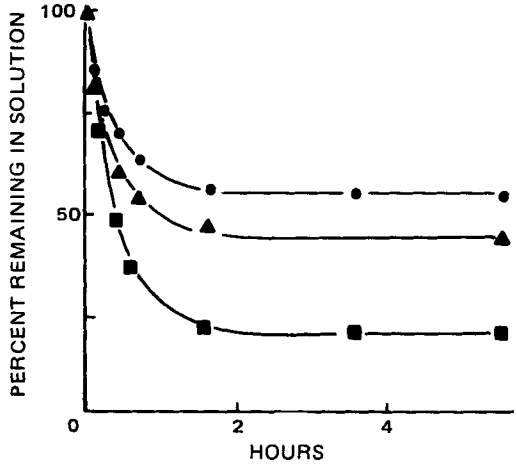

Figure 6—*Percent total radioactivity remaining in Hanks solution with time (pH 7.4, 37°) using a polytetrafluoroethylene container and 1 and 2 μM initial concentrations of antibiotic. Key: (●) I; (■) II; (▲) III.*

RESULTS AND DISCUSSION

Adsorption effects by large hydrophobic drugs have been reported (17–23) with respect to their apparent loss from solution onto and into the walls of their containers. The adsorption of I onto container walls, although a recognized phenomenon, has been noted only briefly in the literature as the probable cause of the observed nonideal behavior of I in its analysis (24) and during its sampling from solution (25). In addition, the use of various cosolvent extraction schemes have been proposed (24, 26, 27) to overcome these effects. Although it has been shown that I undergoes self-association in water (28), others have suggested (29) that no evidence for air–water interfacial adsorption of I can be found.

Although the *in vivo* metabolism of I and its esters have been reported (11), little attention has been given to their solution stability. Kaniewska (30) showed that the aqueous stability of I over a temperature range of 50–60° and a pH range of 2.6–5.5 is greater at lower temperatures and the higher pHs, with a half-life of 136 hr in water at 25° and pH 5.5 (0.2% phosphate buffer) being suggested by extrapolation. Other workers have studied recently the photostability of doxorubicin (31) and the stability of some anthracyclines in infusion fluids (32).

Using the described procedures, Fig. 1 shows the amount of radioactive anthracycline antibiotic determined in the cell digestion fluid after various contact times. Similar cell uptake kinetics are reported often in the literature for these molecules and show that the more hydrophobic the molecule, the greater its rate and extent of uptake by cells (7, 8, 14, 33, 34). However, using the same digestion technique, but in the absence of cells, it can be demonstrated (Figs. 2 and 3) that for I, II, and III, more or less anthracycline antibiotic can be extracted from the system, de-

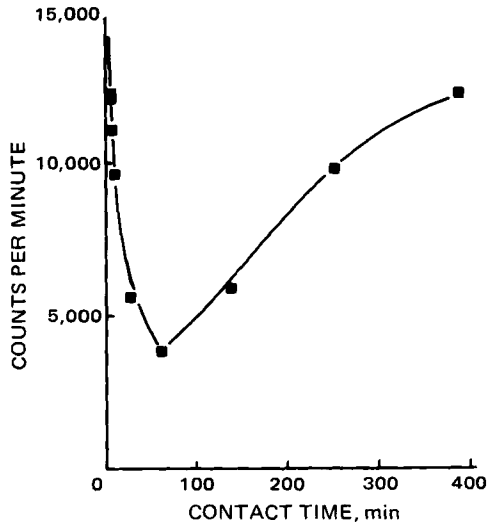

Figure 7—*Percent total radioactivity in Hanks solution (pH 7.4, 37°), for II (2 μM) using a stainless steel container.*

Table I—Percent Maximum Loss of Anthracycline from Solution to Container Wall

Material	Percent Maximum Loss[a] Compound I	II	III	IV[b]
Polypropylene	0	32 (110 min)	67 (190 min)	6 (20 min)
Polytetrafluoroethylene	45 (60 min)	83 (100 min)	57 (100 min)	—
Siliconized glass	0	50 (100 min)	74 (90 min)	—
Stainless steel	—	68 (60 min)	—	—
Glass tubes[c]	7.3 (5 min)	30 (60 min)	8.5 (25 min)	—
Polyethylene petri dishes[c]	4.6 (50 min)	8.7 (70 min)	11 (50 min)	—

[a] Initially 1- or 2-μM solution of radioactive-labeled molecule in Hanks media at 37° in the absence of cells and assayed using scintillation counting; number in parentheses, time for maximum adsorption. [b] By HPLC. [c] Solution 2 μM left in contact, no stirring, all external solution removed by suction, surface washed four times, 1 ml of sodium lauryl sulfate to surface for 30 min, aliquot of this control.

Table II—Rate Constants According to Scheme I

Rate constant	k, hr^{-1} II	III
k_{12}	1.900	2.150
k_{21}	0.005	0.001
k_{13}	1.150	1.150
k_{34}	0.012	0.012
k_{43}	0.001	0.001
k_{35}	0.085	0.085

pending on the analog and the type of container material used. This suggests an adsorption of anthracycline onto the container walls.

Loss of Radioactive Label from Solution—Figures 4–7 show how the loss of anthracycline is affected by the type of container material in use. Although polypropylene has no adsorbent properties, glass, polyethylene, polytetrafluoroethylene, and stainless steel do have adsorbent properties for I. Both esters are taken up well by all the materials studied, with the more hydrophobic molecule being taken up at a faster rate and to a greater extent. Table I is a summary of these effects. The unusual phenomenon found with stainless steel will be discussed.

All three anthracycline antibiotics studied can be lost from aqueous solution solely by adsorption or sorption. The extent of this adsorption depends on the nature of the container material used. Similar effects have been observed (19) for hydrophobic amines on wall adsorption material dependency. The present results indicate strongly that it is necessary to take care in practice to avoid these effects by: (*a*) reducing the number of wall surface contacts made; (*b*) choosing a container material with care;

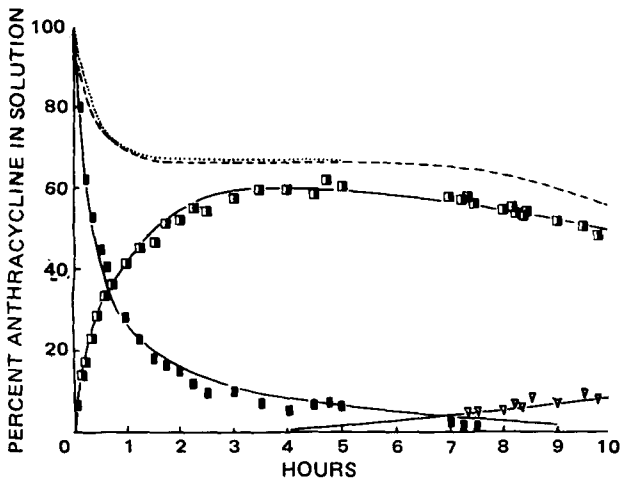

Figure 8—*Concomitant adsorption and stability of II at pH 7.4 and 37° using polypropylene containers. Solid lines are generated using the model given by Scheme I and the rate constants of Table II. Key: (■) II; (◨) IV; (▽) breakdown product of IV; (·····) total radioactivity found in solution; (- - -) the total normalized HPLC peak area.*

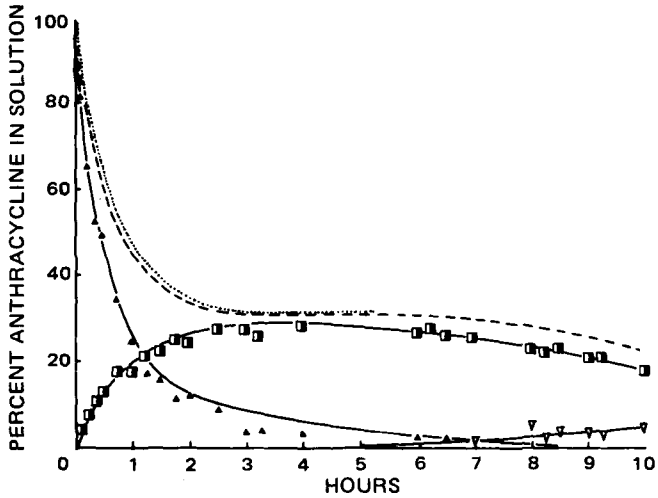

Figure 9—*Concomitant adsorption and stability of III at pH 7.4 and 37° using polypropylene containers. Solid lines are generated as for Fig. 8. Key: (▲) III; (◨) IV; (▽) breakdown product of IV; (·····) total radioactivity found in solution; (- - -) the total normalized HPLC peak area.*

(*c*) making use of possible preaging of containers with compound before use; and (*d*) using cosolvents (19, 24, 26, 27).

Concomitant Stability and Adsorption of II and III—Israel *et al.* (11, 12) demonstrated that *in vivo* II is not metabolized extensively to I, but that *N*-trifluoroacetyladriamycin (IV) and *N*-trifluoroacetyladriamycinol are important metabolites of this drug. In addition, the lack of DNA binding of II suggests that its *in vivo* antitumor activity is due to either its conversion to a DNA-binding metabolite or to a mechanism of action different from that accepted (10) for I. Thus, since II and other esters of I are proposed as antitumor agents with a high therapeutic index, and with the knowledge that both the esters examined in this study are adsorbed onto container walls, it was appropriate to examine ester stability in conjunction with these adsorption effects. Figures 8 and 9 give the combined HPLC and radioactivity information for II and III. The initial breakdown product of both II and III is considered to be IV, since the chromatographic capacity ratio of this product corresponded exactly to the value for authentic samples of IV. The second breakdown product had a chromatographic capacity factor which indicated that it was more hydrophobic than the parent molecule.

Although the initial HPLC data up to 4 hr indicate that the total anthracycline mass detected is equal to that found using radioactivity measurements, the subsequent falls in the total fluorescent peak values (Figs. 8 and 9) suggest that the first breakdown product is itself weakly adsorbed onto the polypropylene container wall. These data suggest that the solution equilibria for II and III in aqueous solution at pH 7.4 can be described by Scheme I when adsorption effects are in evidence. These schemes have been modeled using an analog computer[9], and the lines drawn in Figs. 8 and 9 are computer generated using the rate constants determined (Table II).

Good agreement is obtained between the experimental results and the theoretical results using Scheme I as a model of the equilibria occurring in these systems. Thus, the rapid loss of either ester from solution can be attributed to both adsorption and chemical transformation to IV.

Notable features of the rate constants are that the desorption steps are small, and, although for III adsorption is faster, for neither ester can hydrolysis or adsorption be described as the rate-determining step in the loss process. Combination of the peak areas for either ester and IV (normalized for differences in extinction) gives mass balances equivalent to those found using radioactivity measurements. Compound IV is unstable to a small extent and also adsorbs, which is confirmed by inspection of Fig. 10 where the results of an HPLC examination of the behavior of this compound in Hanks media are given.

If it is assumed that the ester is stable in the adsorbed state, then the container acts as a reservoir. For the polypropylene material, since the degradation products of the esters are less adsorbed due to their lower hydrophobicity, it follows that the relationship between total anthracycline concentration in solution and time should exhibit a minimum. Due to the slow rates of desorption (Table II), these minima are not seen

[9] Type RA 742, Telefunken.

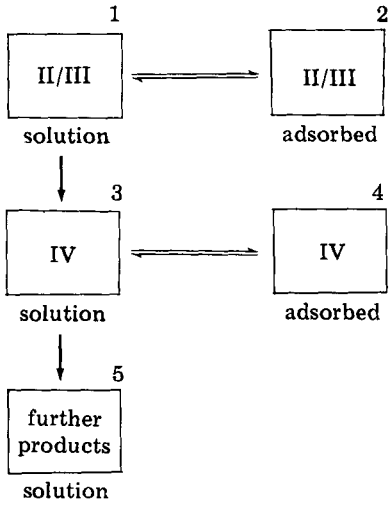

Scheme I

within the experimental time, although there is some indication of this effect in the case of II and siliconized glass (Fig. 5). A similar phenomenon would be observed if the ester were unstable at the container surface resulting in the production of a species with a high desorption rate. This effect is observed for II adsorbed at the stainless steel surface (Fig. 7). If this were the case, the altered stability of II at the stainless steel surface could be indicative of metal ion catalysis, which is possible since the structures of these anthracycline antibiotics suggest that they can act as chelating agents.

The results indicate that anthracycline antibiotics can adsorb strongly onto the walls of containers, and that the rate and extent of adsorption depends on both the nature of the anthracycline and the wall material

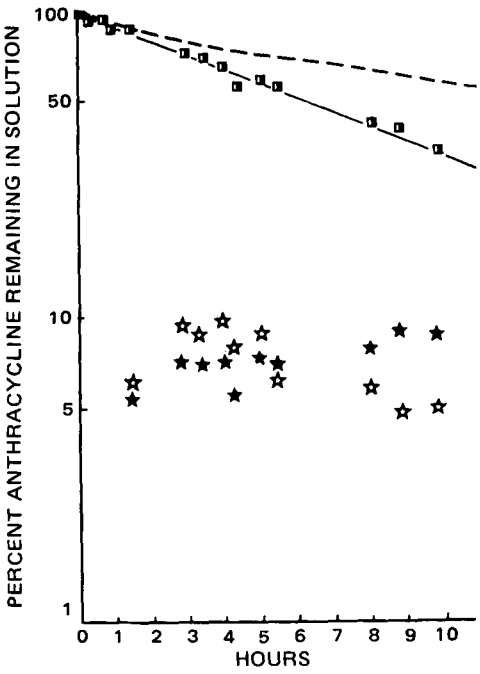

Figure 10—*Stability of IV in Hanks media (pH 7.4, 37°) using polypropylene containers. Key: (- - -) total peak area obtained by summation of the IV HPLC peak area (■) and the peak areas of its two fluorescent breakdown products (☆ ★).*

used. It is believed that these effects have an importance in the analysis of these compounds, as well as in those studies attempting to measure the effect of these antibiotics in living cell cultures. Finally, it can be argued that the combined effects of adsorption and ester instability have implications for the bioavailability and delivery of these drugs.

REFERENCES

(1) R. H. Blum and S. K. Carter, *Ann. Intern. Med.*, **80,** 249 (1974).

(2) A. Dimarco and L. Lenaz, in "Cancer Medicine," J. F. Holland and E. Frei, Eds., Lea and Febiger, Philadelphia, Pa., 1973, p. 826.

(3) T. Skovsgaard and N. I. Nissen, *Dan. Med. Bull.*, **22,** 64 (1975).

(4) E. A. Lefrak, J. Pitha, S. Rosenheim, and J. A. Gottlieb, *Cancer*, **32,** 302 (1973).

(5) P. Chandra, *Cancer Chemother. Rep. Part 3*, **6,** 115 (1975).

(6) M. Israel, E. J. Modest, and E. Frei, *Cancer Res.*, **35,** 1365 (1975).

(7) F. Arcamone *et al.*, *J. Med. Chem.*, **17,** 335 (1974).

(8) N. R. Bachur, M. Steele, W. D. Meriwether, and R. C. Hildebrand, *ibid.*, **19,** 651 (1976).

(9) S. Neidle, *Cancer Treat. Rep.*, **60,** 217 (1976).

(10) S. K. Sengupta, S. Seshadri, E. J. Modest, and M. Israel, *AACR Abstracts*, 109 (1976).

(11) M. Israel, N. J. Pegg, and P. M. Wilkinson, *J. Pharmacol. Exp. Ther.*, **204,** 696 (1978).

(12) M. Israel, P. M. Wilkinson, W. J. Pegg, and E. Frei, *Cancer Res.*, **38,** 365 (1978).

(13) G. Cassinelli, D. Ruggieri, and F. Arcamone, *J. Med. Chem.*, **22,** 121 (1979).

(14) P. M. Kanter and H. S. Schwartz, *Cancer Res.*, **39,** 448 (1979).

(15) B. R. Vishnuvajjala, T. Kataoka, F. D. Cazer, D. T. Witiak, and L. Malspeis, *J. Labeled Comp. Radiopharm.*, **14,** 77 (1978).

(16) R. B. Mikkelsen, P. S. Lin, and D. F. H. Wallach, *J. Mol. Med.*, **2,** 33 (1977).

(17) L. H. Bird, *N. Z. Sci. Technol.* **30,** 344 (1949).

(18) K. T. H. Farrer and E. C. J. Hollenberg, *Analyst*, **78,** 730 (1953).

(19) K. D. Thakker, T. Higuchi, and L. A. Sternson, *J. Pharm. Sci.*, **68,** 93 (1979).

(20) T. Mitzutani and A. Mitzutani, *ibid.*, **67,** 1102 (1978).

(21) T. Mitzutani and A. Mitzutani, *ibid.*, **69,** 279 (1980).

(22) T. Mitzutani, *ibid.*, **70,** 493 (1981).

(23) W. G. Crouthamel and K. van Dyke, *Anal. Biochem.*, **66,** 234 (1975).

(24) S. Eksborg, H. Ehrsson, B. Andersson, and M. Beran, *J. Chromatogr.*, **153,** 211 (1978).

(25) K. Danø, *Biochem. Biophys. Acta*, **323,** 466 (1973).

(26) R. Baurain, A. Zenebergh, and A. Trouet, *J. Chromatogr.*, **157,** 331 (1978).

(27) J. F. Strauss, R. L. Kitchens, V. W. Patrizi, and E. P. Frenkel, *ibid.*, **221,** 139 (1980).

(28) S. Eksborg, *J. Pharm. Sci.*, **67,** 783 (1978).

(29) F. A. Vilallonga and E. W. Phillips, *ibid.*, **67,** 773 (1978).

(30) T. Kaniewska, *Farm. Pol.*, **33,** 539 (1977).

(31) N. Tavoloni, A. M. Guarino, and P. D. Berk, *J. Pharm. Pharmacol.*, **32,** 860 (1980).

(32) G. K. Poochikian, J. C. Cradock, and K. P. Flora, *Am. J. Hosp. Pharm.*, **38,** 483 (1981).

(33) T. Skovsgaard, *Biochem. Pharmacol.*, **26,** 215 (1977).

(34) *Ibid.*, **27,** 1221 (1978).

ACKNOWLEDGMENTS

The authors thank Dr. B. S. Zwilling, Department of Microbiology, The Ohio State University, for assistance in the cell culture studies.

Synthesis and Biological Evaluation of *gem*-Dichlorocyclopropyl and Cyclopropyl Analogs of Stilbene Congeners as Potential Antiestrogens

JOHN F. STOBAUGH *, ROBERT A. MAGARIAN ‡x, and J. THOMAS PENTO §

Received October 6, 1981, from the ‡*Department of Medicinal Chemistry and the* §*Department of Pharmacodynamics and Toxicology, College of Pharmacy, University of Oklahoma Health Sciences Center, Oklahoma City, OK 73190.* Accepted for publication December 15, 1981. * Present address: Department of Pharmaceutical Chemistry, College of Pharmacy, University of Kansas, Lawrence, KS 66045.

Abstract □ A series of *gem*-dichlorocyclopropyl and cyclopropyl analogs of stilbene congeners was synthesized and examined for estrogenic and antiestrogenic activity using the uterotropic assay in the immature mouse. The relative receptor affinity *in vitro* was determined by measuring [^{3}H]estradiol displacement from the rat uterine cytosol receptor. The 11 test compounds synthesized in this study did not produce estrogenic or antiestrogenic activity at the dosage levels used (1–25 μg), but did produce a significant displacement of [^{3}H]estradiol in the rat uterine receptor binding assay with analog XVIII possessing the greatest binding affinity and compound XI the lowest affinity. Structure–affinity relationships of this series were established from the receptor binding assay and comparisons between these analogs and a previously reported series are summarized.

Keyphrases □ *gem*-Dichlorocyclopropyl analogs—synthesis, biological evaluation, cyclopropyl analogs, stilbene congeners, potential antiestrogens □ Stilbene—congeners, potential antiestrogens, synthesis, biological evaluation of *gem*-dichlorocyclopropyl and cyclopropyl analogs □ Antiestrogens—synthesis, biological evaluation of *gem*-dichlorocyclopropyl and cyclopropyl analogs of stilbene congeners □ Biological evaluation—synthesis, *gem*-dichlorocyclopropyl and cyclopropyl analogs of stilbene congeners, potential antiestrogens □ Cyclopropyl analogs—synthesis and biological evaluation, stilbene congeners, potential antiestrogens

In a previous paper (1)[1], a series of cyclopropyl analogs (I–X) of stilbene and stilbenediol was reported as a novel class of nonsteroidal estrogens and antiestrogens. The interesting pharmacological properties of these analogs prompted the investigation of a new series of related compounds. The preparation of some related cyclopropyl analogs (XI–XXI), their estrogenic, antiestrogenic, and receptor binding activities are reported here. The receptor binding effects of this new series were compared to the first series (1) to examine more fully the total structure–affinity relationships with the hope of providing additional insight into the steric requirements of the ligand that binds to the estrogenic receptor. This relationship between the ligand–receptor binding and biological response is of great interest, because elucidation of this relationship would help to clarify the mechanism of action of both estrogenic and antiestrogenic compounds at the cellular level.

EXPERIMENTAL[2]

Preparation of Starting Olefins—These compounds were not available and were prepared by previously reported procedures (2–12).

General Method for the Preparation of *gem*-Dichlorocyclopropyl Analogs XI–XVI (Table I) (13–15)—A molar ratio (1:10) of triethylbenzylammonium chloride to the starting olefin was dissolved in excess chloroform (10 times the molar concentration of olefin) contained in a three-neck flask fitted with an air condenser and dropping funnel. The

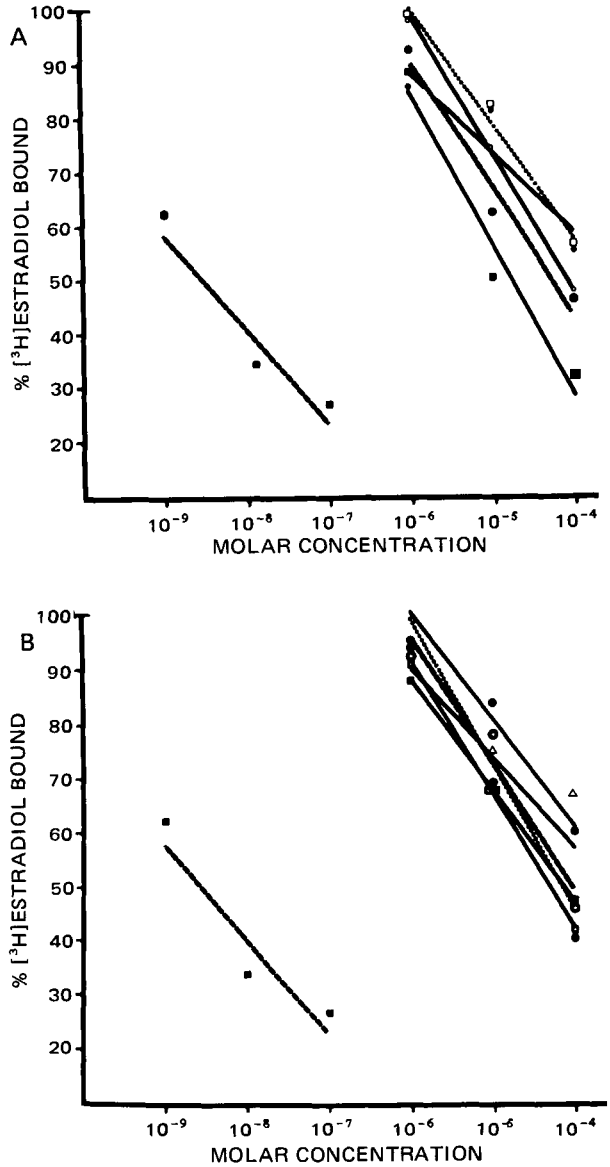

Figure 1—*Uterine receptor binding activity of the cyclopropyl analogs XI–XXI. The receptor binding data is presented in two parts (A and B) due to the overlap in binding between these compounds. Each point represents the mean of two determinations. Key: (A) (●) XI; (○) XIII; (⊙) XV; (⊡) XVIII; (□) XIX. (B) (▣) XII; (◉) XIV; (◘) XVII; (◉) XVI; (⊙) XX; (△) XXI. (A, B) (■) 17β-estradiol.*

[1] This is the third paper in a series. See Refs. 1 and 14 for previous papers.

[2] Melting points were determined on a Thomas-Hoover capillary melting point apparatus. Neither melting points nor boiling points are corrected. The elemental analyses were determined by Midwest Microlab, Inc., Indianapolis, Ind. IR spectra were determined with a Beckman IR20A spectrophotometer using polystyrene film as a standard to ascertain reproducibility. The PMR spectroscopic analyses were recorded in a Varian T-60 spectrometer using deuterochloroform as a solvent, and chemical shifts are reported relative to the internal standards tetramethylsilane. Analytical samples had compatible IR and PMR spectra.

0022-3549/82/01000-1126$01.00/0

Table I—*gem*-Dichlorocyclopropyl Analogs of Stilbene Congeners

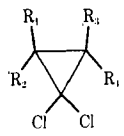

Compound No.	R_1	R_2	R_3	R_4	Formula	mp°	Yield, %	Analysis, % Calc.	Found
XI	H	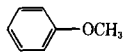	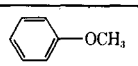	CH_3	$C_{18}H_{18}O_2Cl_2$	99–100[a]	77	C 64.10 H 5.37 Cl 21.02	63.93 5.28 21.31
XII	CH_3	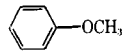	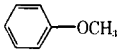	CH_3	$C_{19}H_{20}O_2Cl_2$	112[b]	48	C 64.96 H 5.74 Cl 20.19	64.97 5.69 20.10
XIII	H			CH_3	$C_{16}H_{14}Cl_2$	71–71.5[b]	57	C 69.33 H 5.09 Cl 25.58	69.32 5.21 25.73
XIV	CH_3			CH_3	$C_{17}H_{16}Cl_2$	142–143[c]	60	C 70.11 H 5.54 Cl 24.35	70.38 5.79 24.19
XV		H		CH_3	$C_{16}H_{14}Cl_2$	74.5–75.5[b]	62	C 69.33 H 5.09 Cl 25.58	69.58 5.15 25.51
XVI		CH_3		CH_3	$C_{17}H_{16}Cl_2$	109.5–110.5[b]	37	C 70.11 H 5.54 Cl 24.35	69.95 5.63 24.56

[a] Recrystallized from methanol. [b] Purified by sublimation. [c] Recrystallized from *n*-propyl alcohol.

Table II—Cyclopropyl Analogs of Stilbene Congeners

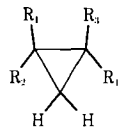

Compound No.	R_1	R_2	R_3	R_4	Formula	mp or bp°	Yield, %	Analysis, % Calc.	Found
XVII	H	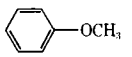	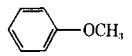	CH_3	$C_{18}H_{20}O_2$	156–159/0.01 mm[a]	61	C 80.56 H 7.51	80.85 7.72
XVIII	CH_3	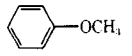	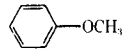	CH_3	$C_{19}H_{22}O_2$	105–106°[b]	68	C 80.81 H 7.86	81.10 7.62
IX	H			CH_3	$C_{16}H_{16}$	96–99/0.05 mm[a]	55	C 92.26 H 7.74	91.88 7.74
XX	CH_3			CH_3	$C_{17}H_{18}$	116.5–117.5[c]	80	C 91.84 H 8.16	91.58 7.92
XXI		H		CH_3	$C_{16}H_{16}$	97–99/0.05 mm[a]	69	C 92.26 H 7.74	91.29 8.13

[a] Distillation. [b] Purified by sublimation. [c] Recrystallized from methanol.

flask was cooled in an ice water bath and a 33–50% aqueous sodium hydroxide solution (sodium hydroxide–chloroform, 2:1) was added dropwise while the mixture was magnetically stirred. After the addition was completed, the ice bath was removed and stirring continued for 6–120 hr. The dark mixture was diluted with excess water and the aqueous layer was separated and extracted three times with chloroform. The chloroform extracts were combined, washed three times with water, dried over anhydrous magnesium sulfate, and filtered to remove the drying agent. The chloroform was removed under reduced pressure, yielding a dark liquid or solid which was purified as described in Table I. PMR ($CDCl_3$): XI, 7.13 (q, 8H), 3.80 (s, 6H), 3.05 (s, 1H), 1.40 (s, 3H); XII, 7.13 (q, 8H), 3.82 (s, 6H), 1.40 (s, 6H); XIII, 7.37 (s, 10H), 3.17 (s, 1H), 1.43 (s, 3H); XIV, 7.32 (s, 10H), 1.40 (s, 6H); XV, 7.13 (m, 10H), 2.85 (s, 1H), 1.80 (s, 3H); XVI, 7.33 (m, 10H), 1.77 (s, 6H).

General Method for the Preparation of Cyclopropyl Analogs XVII–XXI (Table II)—The method of Gassman and Pape (16) was modified. *gem*-Dichloro intermediates XI–XVI and tetrahydrofuran were added to a 100-ml flask fitted with a reflux condenser. This solution was stirred by means of a magnetic stirrer and sodium metal was cut in small pieces and added to the solution followed by *tert*-butyl alcohol. The mixture was stirred and heated at reflux for 12 hr. The unreacted sodium was consumed with methanol and then water was added. The aqueous layer was separated and extracted twice with ether. The ether extracts were combined, dried over anhydrous magnesium sulfate, filtered, and the solvent removed under reduced pressure yielding a solid or liquid which was purified as described in Table II. PMR ($CDCl_3$): XVII, δ 7.04 (m, 8H), 3.70 (s, 6H), 2.23 (m, 3H), 1.18 (m, 3H); XVIII, δ 7.10 (q, 8H), 3.80 (s, 6H), 1.10 (s, 2H), 1.00 (s, 6H); XIX, δ 7.41 (m, 10H), 2.33 (m, 1H), 1.29 (m, 2H), 1.03 (s, 3H); XX, δ 7.35 (s, 10H), 1.18 (s, 2H), 1.03 (s, 6H); XXI, δ 7.16 (m, 10H), 2.60 (m, 2H), 1.93 (m, 1H), 1.36 (m, 3H).

Uterotropic Assay for Estrogenic and Antiestrogenic Activity—The assay for estrogenic activity was a modification (1) of the original uterotropic method of Rubin *et al.* (17) using Swiss-Webster mice. Each cyclopropyl analog was examined over a dosage range of 1–25 μg (total dose).

The uterotropic assay also was used to evaluate the antiestrogenic activity of the test compounds which did not produce an estrogenic response in the previous assay. The antiestrogenic assay was conducted as described for estrogenic activity, except that each animal in the cyclopropyl analog treatment groups received a standard stimulating dose of estradiol (0.04 μg). The test compounds and estradiol were administered separately at different injection sites to minimize possible physical interaction or reduced absorption of either compound. Antiestrogenic activity was measured as a decrease in estradiol-stimulated uterotropic response in groups which received both the test compound and estradiol as compared to a group that received estradiol alone.

Table III—Receptor Binding Assay

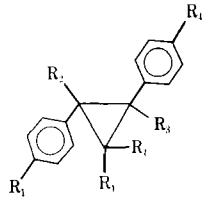

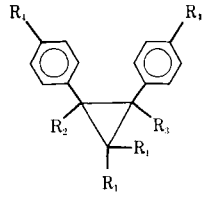

Compound No.	Configuration	R_1	R_2	R_3	R_4	Relative Binding Activity[a] (Estradiol Response, %)
Estradiol						100
XI	*trans*	Cl	CH_3	H	O—CH_3	8.3×10^{-5}
XII	*trans*	Cl	CH_3	CH_3	O—CH_3	5.9×10^{-4}
XIII	*trans*	Cl	CH_3	H	H	5.3×10^{-4}
XIV	*trans*	Cl	CH_3	CH_3	H	5.1×10^{-4}
XV	*cis*	Cl	CH_3	H	H	6.3×10^{-4}
XVI	*cis*	Cl	CH_3	CH_3	H	5.5×10^{-4}
XVII	*trans*	H	CH_3	H	O—CH_3	7.3×10^{-4}
XVIII	*trans*	H	CH_3	CH_3	O—CH_3	2.2×10^{-3}
XIX	*trans*	H	CH_3	H	H	1.5×10^{-4}
XX	*trans*	H	CH_3	CH_3	H	1.1×10^{-4}
XXI	*cis*	H	CH_3	H	H	8.0×10^{-4}

[a] $\frac{\text{Concentration of estradiol that displaced 50\% [}^3\text{H]estradiol}}{\text{Concentration of analog that displaced 50\% [}^3\text{H]estradiol}} \times 100$.

Receptor Binding Assay—A modification (1) of the competitive receptor binding assay method of Korenman (18) was used in this study. Uteri from mature (250 g) female Sprague-Dawley rats were used to prepare the cytosol receptor agent for this assay. Each test compound was assayed at three concentrations over a range of 10^{-4} to 10^{-6} *M* for the cyclopropyl analogs and 10^{-7} to 10^{-9} *M* for the estradiol standard. The test compounds were dissolved in ethanol, and in all cases the final concentration of ethanol was <2% of the total incubation volume.

The [^{3}H]estradiol displacement curve for each test compound was determined by linear regression analysis and plotted graphically. The relative receptor binding activity of each analog was determined using the ratio (concentration of unlabeled estradiol producing 50% displacement of [^{3}H]estradiol/concentration of cyclopropyl analog producing 50% displacement of [^{3}H]estradiol) × 100. Parallelism between the curve produced by each of the analogs and the unlabeled estradiol standard (an index of assay displacement specificity) was determined according to the method of Bliss (19).

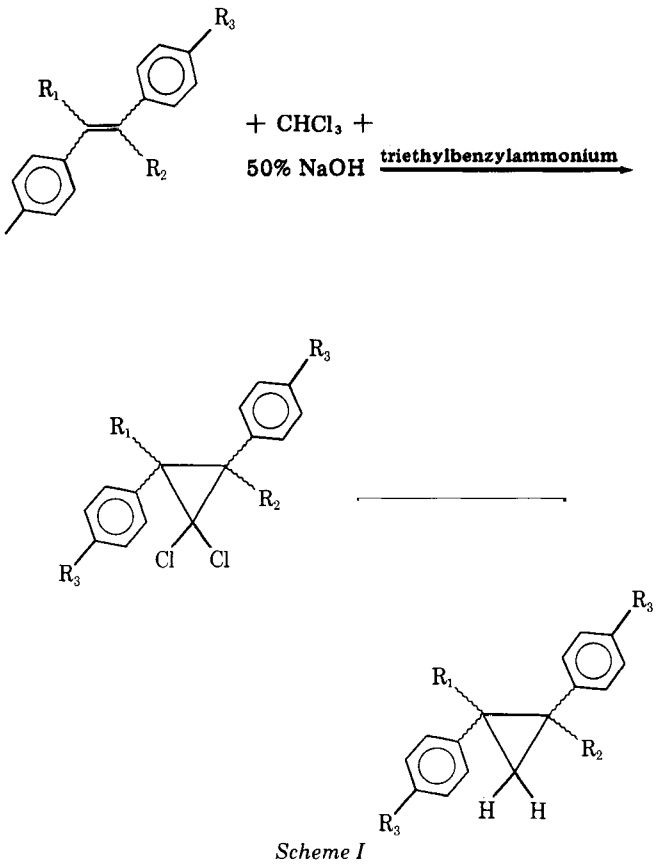

Scheme I

RESULTS AND DISCUSSION

Chemistry—Scheme I illustrates the method of Dehmlow and Schonefeld (13) used for the synthesis of the *gem*-dichloropropanes (Table I) in this study. This is a phase transfer reaction catalyzed by triethylbenzylammonium chloride using chloroform and concentrated aqueous sodium hydroxide solution (33%) to generate a dichlorocarbene. The carbene adds stereospecifically across the double bond in the starting olefins, thus, generating the desired *gem*-dichlorocyclopropyl intermediate (Table I). This reaction was easily carried out and provided yields between 50 and 70%; however, analog XVI was obtained in only 37% yield, and XI and XII yielded dark mixtures before purification. The method of Gassman and Pape (16) was modified to remove the *gem*-dichloro groups from the cyclopropyl ring, and is illustrated in Scheme I. This modified reaction involved the use of the dichloro intermediate, sodium metal, and *tert*-butyl alcohol in refluxing tetrahydrofuran. The dehalogenated cyclopropyl analogs (Table II) were isolated in 60–80% yields.

Pharmacology—All cyclopropyl analogs prepared were tested for estrogenic and antiestrogenic activity in a concentration range of 1–25 μg (total dose) using the immature mouse uterotropic assay (17). None of the test compounds produced an estrogenic response (increase in uterine weight) or an antiestrogenic response (antagonism of estradiol-induced increase in uterine weight) within the dosage range used in this assay system.

Each test compound produced a significant displacement of [^{3}H]estradiol in the rat uterine receptor binding assay (Table III, Figs. 1A and 1B) with analog XVIII displaying the greatest binding affinity and compound XI the lowest. However, the binding affinity of most of the test compounds was similar and in the order of 10^{-3} to 10^{-5}% of 17β-estradiol on a molar basis. Accordingly, receptor binding curves were illustrated in two separate figures due to the significant overlap in analog-induced [^{3}H]estradiol displacement activity.

Since substituents play an important role in the receptor recognition of substrates, it was of interest to look at the nature of the substituent and its contribution to the binding processes. Consequently, the structure–affinity relationships exhibited by this substituted *cis*- and *trans*-diphenylcyclopropane series (Table III) are discussed briefly.

Structural modifications restricted to monomethyl (R_2) and dimethyl (R_2 and R_3) substitutions in *gem*-dichloro-*cis*- and *trans*-2,3-diphenylcyclopropanes (XIII–XVI) did not alter binding activity. The additional methyl group (R_3) in dimethyl substitution does appear, however, to increase activity when in combination with *p*-methoxyphenyl substituents (XII *versus* XI and XVIII *versus* XVII). *gem*-Dichloro substitution (R_1 = Cl) in monomethyl *trans*-diphenylcyclopropanes (XIX *versus*

XIII) and dimethyl analogs (XX *versus* XIV) generally produced a small increase in binding affinity. *p*-Methoxy groups increased activity in the dehalogenated cyclopropyl analogs (XIX *versus* XVII and XX *versus* XVIII) with the greatest receptor binding affinity found in compound XVIII. The *cis*-isomer XXI displayed greater receptor affinity than the *trans*-isomer XIX, but there were no apparent differences in the *gem*-dichloro analogs (XV *versus* XIII and XVI *versus* XIV).

When the receptor binding activities of these analogs were compared to the present compounds (1), it was found that the monomethyl and dimethyl substituents at R_2 and R_3 (Table III) in the hydrophobic cyclopropyl skeleton led to a reduction in receptor binding affinity of the derivatives, while diethyl substitution increased receptor binding ability.

REFERENCES

(1) J. T. Pento, R. A. Magarian, R. J. Wright, M. M. King, and E. J. Benjamin, *J. Pharm. Sci.*, **70**, 399 (1981).

(2) I. A. Allen and L. S. Buck, *J. Am. Chem. Soc.*, **52**, 312 (1930).

(3) A. F. Casy, A. Parulkar, and P. Pocha, *Tetrahedron*, **24**, 3031 (1968).

(4) H. O. House, "Modern Synthetic Reactions," 2nd ed., W. A. Benjamin, Menlo Park, Calif., 1972, pp. 546–570.

(5) D. J. Cram and F. A. A. Elhafez, *J. Am. Chem. Soc.*, **74**, 5828 (1952).

(6) W. R. Kirner and W. Windus, *Org. Syn. Coll.*, **2**, 136 (1943).

(7) A. Zwierzak and H. Pines, *J. Org. Chem.*, **27**, 4084 (1962).

(8) D. J. Cram, F. O. Greene, and C.H. DePuy, *J. Am. Chem. Soc.*, **78**, 790 (1956).

(9) W. R. Brasen, J. W. Kantor, P. S. Skell, and C. R. Hauser, *ibid.*, **79**, 397 (1957).

(10) D. J. Cram and F. A. A. Elhafez, *ibid.*, **74**, 5851 (1952).

(11) W. Marshall, *J. Chem. Soc.*, **107**, 523 (1915).

(12) M. Norris, Z. Watt, and J. Thomas, *J. Am. Chem. Soc.*, **38**, 1078 (1916).

(13) E. V. Dehmlow and J. Schonefeld, *Liebigs Ann. Chem.*, **744**, 42 (1971).

(14) R. A. Magarian and E. J. Benjamin, *J. Pharm. Sci.*, **64**, 1626 (1975).

(15) M. Makosza and W. Wawrzyniewiez, *Tetrahedron Lett. (London)*, **1969**, 4659.

(16) P. G. Gassman and P. G. Pape, *J. Org. Chem.*, **29**, 160 (1964).

(17) B. L. Rubin, A. S. Dorfman, L. Black, and R. D. Dorfman, *Endocrinology*, **49**, 429 (1951).

(18) S. G. Korenman, *Steroids*, **13**, 163 (1969).

(19) C. I. Bliss, "The Statistics of Bioassay," Academic, New York, N.Y., 1952.

ACKNOWLEDGMENTS

Abstracted in part from a thesis submitted by John F. Stobaugh to the University of Oklahoma in partial fulfillment of the Master of Science degree requirement.

Moment Analysis for the Separation of Mean *In Vivo* Disintegration, Dissolution, Absorption, and Disposition Time of Ampicillin Products

YUSUKE TANIGAWARA ˣ, KIYOSHI YAMAOKA, TERUMICHI NAKAGAWA, and TOYOZO UNO

Received September 28, 1981, from the *Faculty of Pharmaceutical Sciences, Kyoto University, Sakyo-ku, Kyoto 606, Japan.* Accepted for publication December 18, 1981.

Abstract □ The *in vivo* disintegration, dissolution, absorption, and disposition processes of ampicillin products are separated by means of moment analysis. This method is model-independent, that is, any specific model is not assumed. The mean residence time (MRT), mean absorption time (MAT), mean dissolution time (MDT), and mean disintegration time (MDIT) are calculated for several dosage forms of ampicillin. The fraction of dose absorbed (F) is also separated into several fractions corresponding to these *in vivo* processes. Bioavailability and bioequivalence are discussed in terms of the zero and first moments. The flip-flop behavior of ampicillin is proved by the fact that the MRT following intravenous injection is less than the MAT of any oral dosage form. Absorption of released ampicillin is proved to be a rate-determining step, since the MRT of released ampicillin in the GI tract is the greatest of all MRT corresponding to the *in vivo* processes. Moment analysis is compared with classical compartment theory, and a new component concept is introduced.

Keyphrases □ Ampicillin—moment analysis, *in vivo* disintegration, dissolution, absorption, disposition time □ Disintegration—ampicillin, moment analysis, *in vivo* dissolution, absorption, disposition time □ Dissolution—ampicillin, moment analysis, *in vivo* disintegration, absorption, disposition time □ Absorption—ampicillin, moment analysis, *in vivo* disintegration, dissolution, disposition time

In recent years moment analysis has been developed in the pharmacokinetic field as a method to comprehend drug behavior in the body, that is, absorption, distribution, metabolism, and excretion (1–10)[1]. Since statistical moments are characteristic of the shape of the statistical distribution curves such as plasma concentration–time curve or urinary excretion rate–time curve, they are only dependent on the observed time course data and are independent of the pharmacokinetic compartment model. Zero moment represents the area under the plasma concentration–time curve (AUC) or the total amount of drug excreted in urine, which is widely used as a model-independent parameter. The first moment, which is defined as the mean residence time (MRT), gives significant information with respect to kinetic features of the process which a drug undergoes in the GI tract and the body (1).

The absorption of a drug from its oral preparation involves a process too complex to be described by a simple mathematical equation. Therefore, a model-independent approach has been undertaken to evaluate the absorption rate (1–3, 11–13). These methods are based on deconvolution. The mean absorption time (MAT) is the useful index of the rate of bioavailability (1–3). The *in vivo* drug absorption involves disintegration and dissolution steps

[1] Y. Tanigawara, K. Yamaoka, T. Nakagawa, and T. Uno, *Chem. Pharm. Bull.*, **30**, 2174 (1982).

0022-3549/82/01000-1129$01.00/0

XIII) and dimethyl analogs (XX *versus* XIV) generally produced a small increase in binding affinity. *p*-Methoxy groups increased activity in the dehalogenated cyclopropyl analogs (XIX *versus* XVII and XX *versus* XVIII) with the greatest receptor binding affinity found in compound XVIII. The *cis*-isomer XXI displayed greater receptor affinity than the *trans*-isomer XIX, but there were no apparent differences in the *gem*-dichloro analogs (XV *versus* XIII and XVI *versus* XIV).

When the receptor binding activities of these analogs were compared to the present compounds (1), it was found that the monomethyl and dimethyl substituents at R_2 and R_3 (Table III) in the hydrophobic cyclopropyl skeleton led to a reduction in receptor binding affinity of the derivatives, while diethyl substitution increased receptor binding ability.

REFERENCES

(1) J. T. Pento, R. A. Magarian, R. J. Wright, M. M. King, and E. J. Benjamin, *J. Pharm. Sci.*, **70**, 399 (1981).

(2) I. A. Allen and L. S. Buck, *J. Am. Chem. Soc.*, **52**, 312 (1930).

(3) A. F. Casy, A. Parulkar, and P. Pocha, *Tetrahedron*, **24**, 3031 (1968).

(4) H. O. House, "Modern Synthetic Reactions," 2nd ed., W. A. Benjamin, Menlo Park, Calif., 1972, pp. 546–570.

(5) D. J. Cram and F. A. A. Elhafez, *J. Am. Chem. Soc.*, **74**, 5828 (1952).

(6) W. R. Kirner and W. Windus, *Org. Syn. Coll.*, **2**, 136 (1943).

(7) A. Zwierzak and H. Pines, *J. Org. Chem.*, **27**, 4084 (1962).

(8) D. J. Cram, F. O. Greene, and C.H. DePuy, *J. Am. Chem. Soc.*, **78**, 790 (1956).

(9) W. R. Brasen, J. W. Kantor, P. S. Skell, and C. R. Hauser, *ibid.*, **79**, 397 (1957).

(10) D. J. Cram and F. A. A. Elhafez, *ibid.*, **74**, 5851 (1952).

(11) W. Marshall, *J. Chem. Soc.*, **107**, 523 (1915).

(12) M. Norris, Z. Watt, and J. Thomas, *J. Am. Chem. Soc.*, **38**, 1078 (1916).

(13) E. V. Dehmlow and J. Schonefeld, *Liebigs Ann. Chem.*, **744**, 42 (1971).

(14) R. A. Magarian and E. J. Benjamin, *J. Pharm. Sci.*, **64**, 1626 (1975).

(15) M. Makosza and W. Wawrzyniewiez, *Tetrahedron Lett. (London)*, **1969**, 4659.

(16) P. G. Gassman and P. G. Pape, *J. Org. Chem.*, **29**, 160 (1964).

(17) B. L. Rubin, A. S. Dorfman, L. Black, and R. D. Dorfman, *Endocrinology*, **49**, 429 (1951).

(18) S. G. Korenman, *Steroids*, **13**, 163 (1969).

(19) C. I. Bliss, "The Statistics of Bioassay," Academic, New York, N.Y., 1952.

ACKNOWLEDGMENTS

Abstracted in part from a thesis submitted by John F. Stobaugh to the University of Oklahoma in partial fulfillment of the Master of Science degree requirement.

Moment Analysis for the Separation of Mean *In Vivo* Disintegration, Dissolution, Absorption, and Disposition Time of Ampicillin Products

YUSUKE TANIGAWARA ˣ, KIYOSHI YAMAOKA, TERUMICHI NAKAGAWA, and TOYOZO UNO

Received September 28, 1981, from the *Faculty of Pharmaceutical Sciences, Kyoto University, Sakyo-ku, Kyoto 606, Japan.* Accepted for publication December 18, 1981.

Abstract □ The *in vivo* disintegration, dissolution, absorption, and disposition processes of ampicillin products are separated by means of moment analysis. This method is model-independent, that is, any specific model is not assumed. The mean residence time (MRT), mean absorption time (MAT), mean dissolution time (MDT), and mean disintegration time (MDIT) are calculated for several dosage forms of ampicillin. The fraction of dose absorbed (F) is also separated into several fractions corresponding to these *in vivo* processes. Bioavailability and bioequivalence are discussed in terms of the zero and first moments. The flip-flop behavior of ampicillin is proved by the fact that the MRT following intravenous injection is less than the MAT of any oral dosage form. Absorption of released ampicillin is proved to be a rate-determining step, since the MRT of released ampicillin in the GI tract is the greatest of all MRT corresponding to the *in vivo* processes. Moment analysis is compared with classical compartment theory, and a new component concept is introduced.

Keyphrases □ Ampicillin—moment analysis, *in vivo* disintegration, dissolution, absorption, disposition time □ Disintegration—ampicillin, moment analysis, *in vivo* dissolution, absorption, disposition time □ Dissolution—ampicillin, moment analysis, *in vivo* disintegration, absorption, disposition time □ Absorption—ampicillin, moment analysis, *in vivo* disintegration, dissolution, disposition time

In recent years moment analysis has been developed in the pharmacokinetic field as a method to comprehend drug behavior in the body, that is, absorption, distribution, metabolism, and excretion (1–10)[1]. Since statistical moments are characteristic of the shape of the statistical distribution curves such as plasma concentration–time curve or urinary excretion rate–time curve, they are only dependent on the observed time course data and are independent of the pharmacokinetic compartment model. Zero moment represents the area under the plasma concentration–time curve (AUC) or the total amount of drug excreted in urine, which is widely used as a model-independent parameter. The first moment, which is defined as the mean residence time (MRT), gives significant information with respect to kinetic features of the process which a drug undergoes in the GI tract and the body (1).

The absorption of a drug from its oral preparation involves a process too complex to be described by a simple mathematical equation. Therefore, a model-independent approach has been undertaken to evaluate the absorption rate (1–3, 11–13). These methods are based on deconvolution. The mean absorption time (MAT) is the useful index of the rate of bioavailability (1–3). The *in vivo* drug absorption involves disintegration and dissolution steps

[1] Y. Tanigawara, K. Yamaoka, T. Nakagawa, and T. Uno, *Chem. Pharm. Bull.*, **30**, 2174 (1982).

0022-3549/82/01000-1129$01.00/0

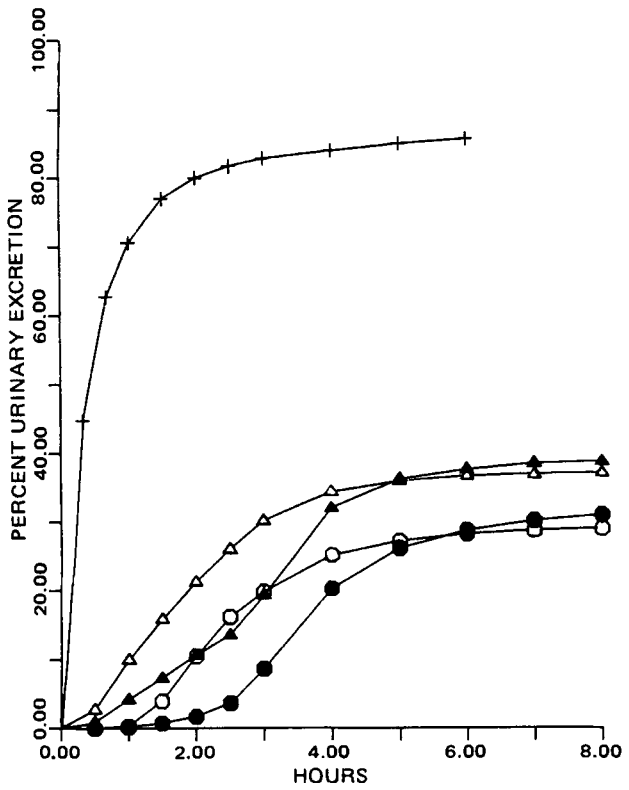

Figure 1—*Cumulative urinary excretion of ampicillin after intravenous and oral administrations to Subject 2. Key: (+) intravenous injection; (△) solution; (▲) Powder A; (●) Capsule A; (○) Capsule B.*

prior to absorption of released drug. The evaluation of *in vivo* disintegration and dissolution of a drug product is necessary for the development of a drug delivery system. It is also necessary to know the rate-determining step in these *in vivo* processes.

Recently the mean dissolution time (MDT) was defined as the magnitude of *in vivo* dissolution rate (3). In this article, moment analysis using urinary excretion data is carried out to separate four *in vivo* steps from administration of an ampicillin product through urinary excretion, that is, disintegration, dissolution, absorption, and disposition steps. The rate-determining step is specified by comparing the mean residence time intrinsic to each step. The extent and rate of bioavailability of the anhydrate and trihydrate forms of ampicillin are estimated in terms of the zero and first moments. Bioequivalence is discussed from the results for the urinary recovery and the mean residence time.

EXPERIMENTAL

Procedure—Four healthy male volunteers, 25–32 years of age, weighing 62–76 kg participated in this study. The subjects were fasted overnight before each dosage and were permitted to eat no food until 3 hr after dosing except for intravenous administration. No other drugs were taken for at least 1 week prior to and during the study. All subjects received single doses of ampicillin in five different dosage forms (*a–e*). Each dosage was separated by at least 1 week:

(a) *Intravenous injection*—A 2.5-ml injectable ampicillin[2] solution containing 125 mg (as potency) was intravenously administered in 1 min.

(b) *Solution*—A solution of 500-mg (as potency) of ampicillin sodium[2] dissolved in 100 ml of water was orally administered.

(c) *Powder* A—The contents of a 500-mg (as potency) ampicillin trihydrate capsule[3] were removed and orally administered with 100 ml of water.

(d) *Capsule* A—One 500-mg (as potency) capsule[3] was orally administered with 100 ml of water. The ampicillin was in trihydrate form.

(e) *Capsule* B—One 500-mg (as potency) ampicillin anhydrate capsule[4] was orally administered with 100 ml of water.

The maximum plasma concentration after intravenous injection is much higher than that after oral administration of the same dose. Therefore, a quarter of the oral dose was used for the intravenous dose in order to avoid saturation in drug disposition.

Urine samples were collected immediately before and at 0.5, 1, 1.5, 2, 2.5, 3, 4, 5, 6, 7, and 8 hr after oral dosing, or at 20 and 40 min and 1, 1.5, 2, 2.5, 3, 4, 5, and 6 hr after intravenous dosing. After the urine volume was measured, a portion was frozen until assayed.

Assay of Ampicillin—The antibiotic concentration was determined by reversed-phase high-pressure liquid chromatography (HPLC). The chromatograph[5] was equipped with a UV detector[6] adjusted at 220 nm. The stationary phase was octadecylsilane chemically bonded on totally porous silica gel (particle size 5 μm), packed in a 150-mm stainless steel column[7] (4-mm i.d.). The mobile phase was a mixture of methanol–0.0167 *M* phosphate buffer (pH 7.0, 1:2 v/v). The flow rate was 0.6 ml/min and column oven temperature was set at 28°. Peak area was used for quantitation[8].

Evaluation of Moments and Statistical Analysis—The urinary recovery, *f*(percent), and the mean residence time, MRT(hour), were evaluated from the time course data for the urinary excretion by means of the linear trapezoidal integration and extrapolation (1). The statistical evaluation of the differences in MRT and *f* values between dosage forms and subjects was achieved by two-way ANOVA. The subsequent pairing test was carried out when significant differences were found ($p < 0.05$).

Table I—Mean Residence Time, MRT(hr), of Ampicillin Products

Dosage Form	Subject 1	2	3	4	Mean ± *SD*
Intravenous injection	0.766	0.752	0.816	0.752	0.772 ± 0.026
Solution	2.53	2.00	2.78	2.10	2.35 ± 0.32
Powder A	3.18	2.95	2.88	2.56	2.89 ± 0.22
Capsule A	3.40	3.98	3.33	2.23	3.24 ± 0.63
Capsule B	3.08	2.73	2.51	2.24	2.64 ± 0.31

Table II—Percent Urinary Recoveries, *f*(%), of Ampicillin at Infinite Time

Dosage Form	Subject 1	2	3	4	Mean ± *SD*
Intravenous injection	83.4	86.9	64.1	77.5	78.0 ± 8.7
Solution	39.0	37.2	37.8	52.5	41.6 ± 6.3
Powder A	45.2	38.9	39.0	45.8	42.2 ± 3.3
Capsule A	40.9	31.9	30.7	42.2	36.4 ± 5.2
Capsule B	38.7	29.2	26.1	31.2	31.3 ± 4.6

RESULTS

Mean Residence Time and Urinary Recovery—Figure 1 shows the time courses for the cumulative urinary excretion of ampicillin administered to Subject 2 in various dosage forms. The MRT and *f* values are listed in Tables I and II. In calculating the moments, the contributions of the extrapolated area to MRT and *f* values were evaluated. The increases of MRT and *f* by extrapolation to infinite time were <1%, which demonstrates that the urinary time courses were measured in an adequate period of time. The differences in MRT and *f* values among the dosage forms were statistically significant at the 0.01 level by ANOVA. The MRT and *f* values after intravenous injection are very different from those after any other oral dosage forms. For example, ampicillin is retained in the

[2] Pentrex for injection, Banyu Pharmaceutical Co. Ltd., Tokyo, Japan.

[3] Pentrex capsules, Banyu Pharmaceutical Co. Ltd., Tokyo, Japan.
[4] Solcillin capsules, Takeda Chemical Industries, Ltd., Osaka, Japan.
[5] Model TRIROTAR-III, Japan Spectroscopic Co., Tokyo, Japan.
[6] Model UVIDEC-100-III, Japan Spectroscopic Co., Tokyo, Japan.
[7] Develosil ODS-5, Nomura Chemicals, Seto, Japan.
[8] CHROMATOPAC C-R1A, Shimadzu, Kyoto, Japan.

GI tract and the body for ~3 hr when the trihydrate capsule (Capsule A) is orally administered, whereas only 46 min of residence time follows intravenous injection. The differences in MRT values are insignificant at the 0.05 level between Powder A and Capsule A, between Solution B and Capsule B, and between Powder A and Capsule B. The differences in f values are insignificant at the 0.05 level between Powder A and Capsule A, between Solution A and Powder A, between Solution A and Capsule A, and between Capsule A and Capsule B. Therefore, from the viewpoint of extent and rate of bioavailability, it follows that Powder A and Capsule A are bioequivalent, but that any other pairs are not bioequivalent at the 0.05 level.

Mean Absorption Time and Extent of Absorption—The following discussions are based on the assumptions (1) that the pharmacokinetic system is linear, and the oral response is given by the convolution of weight functions which correspond to each step, such as disintegration, dissolution, absorption, and disposition.

The mean absorption time, MAT, and the fraction of dose absorbed, F, for a drug administered orally have been defined as (1, 2):

$$MAT = MRT_{po} - MRT_{iv} \quad \text{(Eq. 1)}$$

$$F = f_{po}/f_{iv} \quad \text{(Eq. 2)}$$

where po and iv reveal oral and intravenous bolus administrations, respectively. MAT expresses the mean overall time since a drug is administered until it enters into the systemic circulation. Table III lists the MAT (hour) and F (percent) for four ampicillin dosage forms. The MAT values are estimated by the subtraction of the average of MRT_{iv} from that of MRT_{po}. Absorption rate from the solution is the fastest of all oral dosage forms. Absorption from Capsule B, which contains ampicillin anhydrate is as fast as that from the solution, but absorption from Capsule A, which contains the trihydrate form, is clearly slower than that from the solution. Difference in MAT values between these two capsules is 0.60 hr (36 min). The fact that the MRT_{iv} is less than the MAT of any oral dosage form shows that the pharmacokinetic profile of ampicillin is flip-flop (14).

Mean Disintegration Time and Mean Dissolution Time—Though the discussion below can be applied to tablets and sustained-release preparations, the case of capsules is considered here as a representative example. Prior to the absorption of released drug through the GI wall, a drug administered as a capsule undergoes *in vivo* disintegration of the capsule shell and subsequent dispersion of drug powder, and dissolution of the dispersed drug into GI fluid. Therefore, the MAT for capsules was separated into three steps as follows (Scheme I):

Table III—MAT, MDT, F, and F_{rel} of Orally Administered Ampicillin Preparations

	Solution	Powder A	Capsule A	Capsule B
MAT (hr)	1.58	2.12	2.47	1.87
MDT (hr)	—	0.54	0.89	0.29
F (%)	53.3	54.1	46.7	40.1
F_{rel} (%)	—	101.4	87.5	75.2

$$MAT_{capsule} = T_1 + T_2 + T_3 \quad \text{(Eq. 3)}$$

where T_1 is the mean time for the disintegration of a capsule, T_2 is the mean time for the dissolution of dispersed drug powder, and T_3 is the mean time for the absorption of the released drug. Accordingly, it is possible to estimate the *in vivo* mean time of each step by comparing the MAT values for several different dosage forms. When a drug is administered as a solution:

$$MAT_{solution} = T_3 \quad \text{(Eq. 4)}$$

When a drug is administered as a powder (or suspension):

$$MAT_{powder} = T_2 + T_3 \quad \text{(Eq. 5)}$$

The mean *in vivo* dissolution time, MDT, was defined (3):

$$MDT_{capsule} = MAT_{capsule} - MAT_{solution} \quad \text{(Eq. 6)}$$

In the same manner, we define the mean *in vivo* disintegration time, MDIT, as follows:

$$MDIT_{capsule} = MAT_{capsule} - MAT_{powder} \quad \text{(Eq. 7)}$$

Substitution of Eq. 1 into Eqs. 6 and 7 yields:

$$MDT_{capsule} = MRT_{capsule} - MRT_{solution} \quad \text{(Eq. 8)}$$

$$MDIT_{capsule} = MRT_{capsule} - MRT_{powder} \quad \text{(Eq. 9)}$$

Table III lists the MDT values for three solid dosage forms. The MDIT of Capsule A is 0.35 hr which is statistically negligible, and it means that the disintegration of capsule shell in the GI tract is a very rapid process. The MDT of Capsule A is greater than that of Capsule B, which coincides with the previously reported fact that the *in vitro* dissolution rate of anhydrous ampicillin is faster than that of the trihydrate form (15–18).

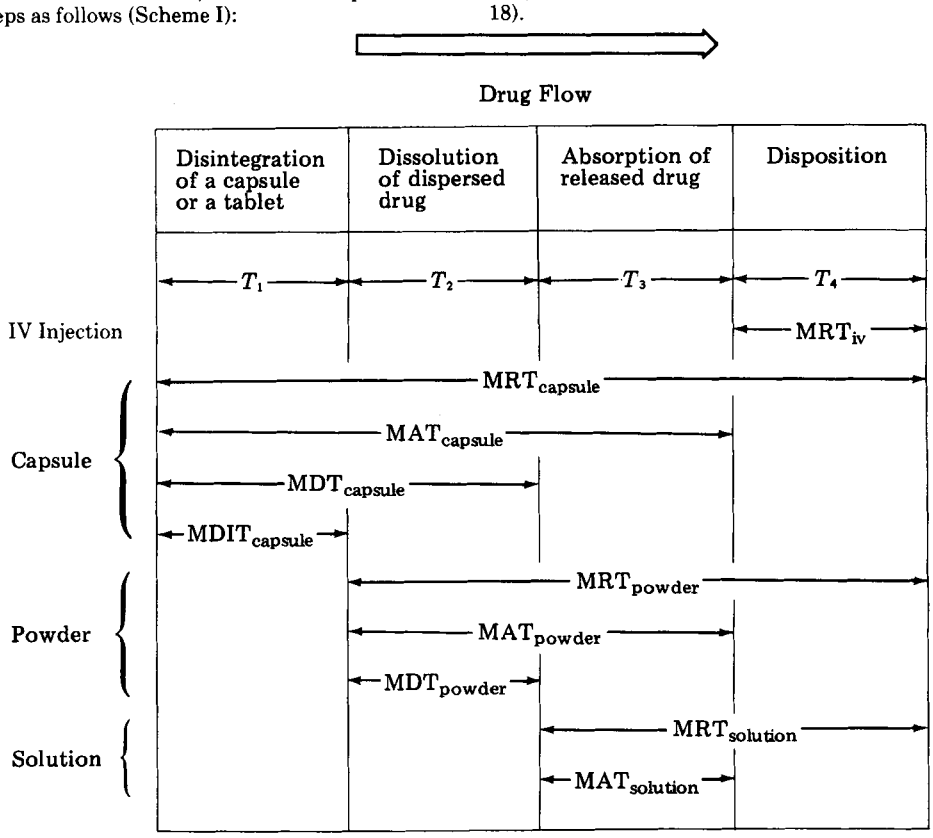

Scheme I—Illustration of the meanings of the MRT, MAT, MDT, and MDIT.

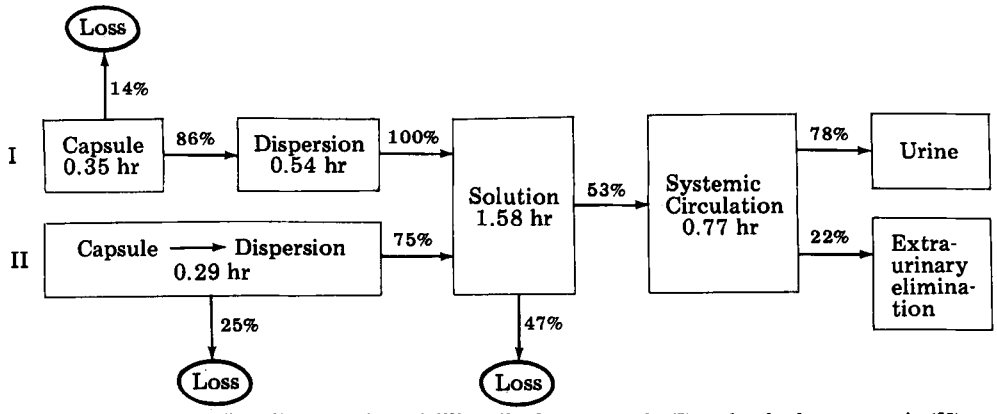

Scheme II—Drug flow diagram of ampicillin trihydrate capsule (I) and anhydrate capsule (II).

The zero moment of each step for a capsule can be separated as:

$$F_{capsule} = F_1 \cdot F_2 \cdot F_3 \qquad \text{(Eq. 10)}$$

where F_1, F_2, and F_3 reveal the ratio of ampicillin amount which transfers as an intact form from step to step. The zero moments for solution and powder thus become:

$$F_{solution} = F_3 \qquad \text{(Eq. 11)}$$

$$F_{powder} = F_2 \cdot F_3 \qquad \text{(Eq. 12)}$$

Corresponding to MDT, the relative extent of absorption, F_{rel}, is defined as:

$$F_{rel} = F_{capsule\ (or\ powder)}/F_{solution} \qquad \text{(Eq. 13)}$$

The F and F_{rel} values are listed in Table III.

Drug Flow Diagram of Ampicillin Products—Scheme II depicts the drug flow diagram summarizing the drug flow after oral administration of two kinds of ampicillin capsules. The intrinsic MRT, which is a time component related to each step in the total MRT, is given in the box and the transfer ratio from step to step is written on the arrow. It should be noted that this box exhibits a quite different concept from the classical compartment. We call the box a component. This is very similar to the strong component concept (19). The detailed discussion is given later.

The absorption kinetics of some ampicillin products were compared by means of a previous method (20), but that report did not give a clear explanation for the incomplete absorption of orally administered ampicillin. Scheme II clearly shows that some portions of ampicillin are lost before entering the systemic circulation. This may be due to incomplete disintegration of a capsule or incomplete dissolution or degradation to an unavailable form. In the case of the trihydrate form, the loss in the disintegration process is 14%, but the dissolution of the dispersed drug is perfect, whereas the loss of the anhydrate form in the dissolution process is 25%.

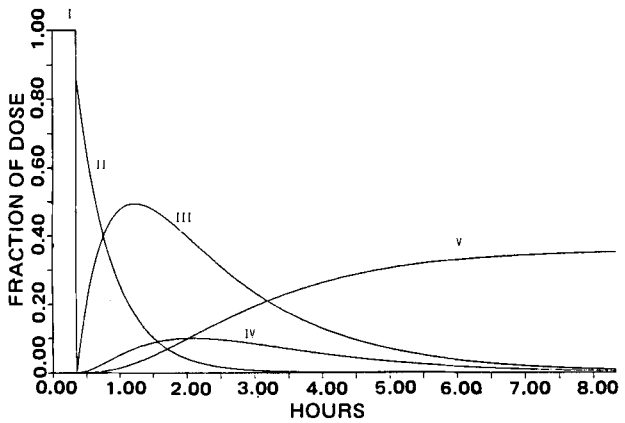

Figure 2—*Computer simulations of ampicillin amount* versus *time curves in five components for the trihydrate form. The drug levels are simulated by a convolution method. Key: (I) capsule form; (II) dispersed drug; (III) released drug in the GI tract; (IV) drug amount in body; (V) amount of urinary excreted drug.*

The interesting observation is that the intrinsic MRT of released drug in the GI tract is the greatest of all time components, and it means that the absorption of released ampicillin is the rate-determining step. Therefore, the dissolution rate does not appreciably affect the plasma peak levels. Besides, the transfer ratio from solution to systemic circulation is the lowest (53%) of all transfer ratios. It is suggested that the pharmaceutical improvement of absorption in the released state (esterification, *etc.*) is more effective than that of dissolution in order to obtain high plasma peak levels.

Simulations of Ampicillin Levels in Each Component—To simulate the ampicillin levels in each component shown in Scheme II, the following approximation was adopted. It was assumed that all the steps except for disintegration were expressed by the monoexponential equations, and that the disintegration step was represented by the lag time, because the collapse of a capsule is expected to occur abruptly. Actually the lag time was observed in the experimental time course data for a capsule form. The weight function of each step except for disintegration is represented by:

$$G_i = \frac{F_i}{T_i} \times \exp\left(-\frac{t}{T_i}\right) \qquad i = 2, 3, \text{ and } 4 \qquad \text{(Eq. 14)}$$

where 2, 3, and 4 reveal the dissolution, absorption, and disposition processes, respectively. It is noted that the zero and first moments of G_i *versus* time curve just become F_i and T_i, respectively.

Figure 2 shows ampicillin fraction *versus* time curves in five components after oral administration of trihydrate capsules. Drug levels in the body are much less than those in the GI tract, and the area under the curve (*AUC*) of body levels (Curve IV) is only 25% of released drug (Curve III).

DISCUSSION

Bioavailability is defined as the rate and extent of absorption of a drug from its dosage form (21). The absolute bioavailability is determined by a comparison of the measured characteristics after oral and intravenous administration, so long as instantaneous and complete bioavailability is assumed for intravenous injection. The zero moment (*AUC* or urinary recovery) expresses the amount profile, and the first moment (MRT) expresses the time profile. Therefore, the rate of absolute bioavailability is represented by the MAT, and the extent of absolute bioavailability is the fraction of dose absorbed (F). The relative bioavailability is determined by comparing the absorption behavior of a test preparation of a drug with that of its standard preparation. Thus, the MDT or MDIT is the indication of the rate of relative bioavailability, when solution or powder is specified as the reference standard. The extent of relative bioavailability is expressed by F_{rel}.

The absorption time of pharmaceutical alternatives can be compared by using MAT. Though MAT is a useful index of the overall absorption time of several drug products, the intravenous administration is not always possible because of toxicity or hydrophobicity of a drug. The MDT and MDIT can be useful in that case. Pharmaceutical equivalents, which lead to the identical resolved state in the GI tract, are compared in terms of MDT. In the case of poorly soluble drugs, the use of semiaqueous solutions, *e.g.*, polyethylene glycol–water solution, has been proposed as the reference standards in estimating MDT (3). However, since polyethylene glycol can have an effect not only on the dissolution process but also on the GI wall as an adjuvant, the latter effect could interfere in estimation of MDT. Hence, the MDIT is a useful indicator for relative bioavailability of very poorly soluble drugs.

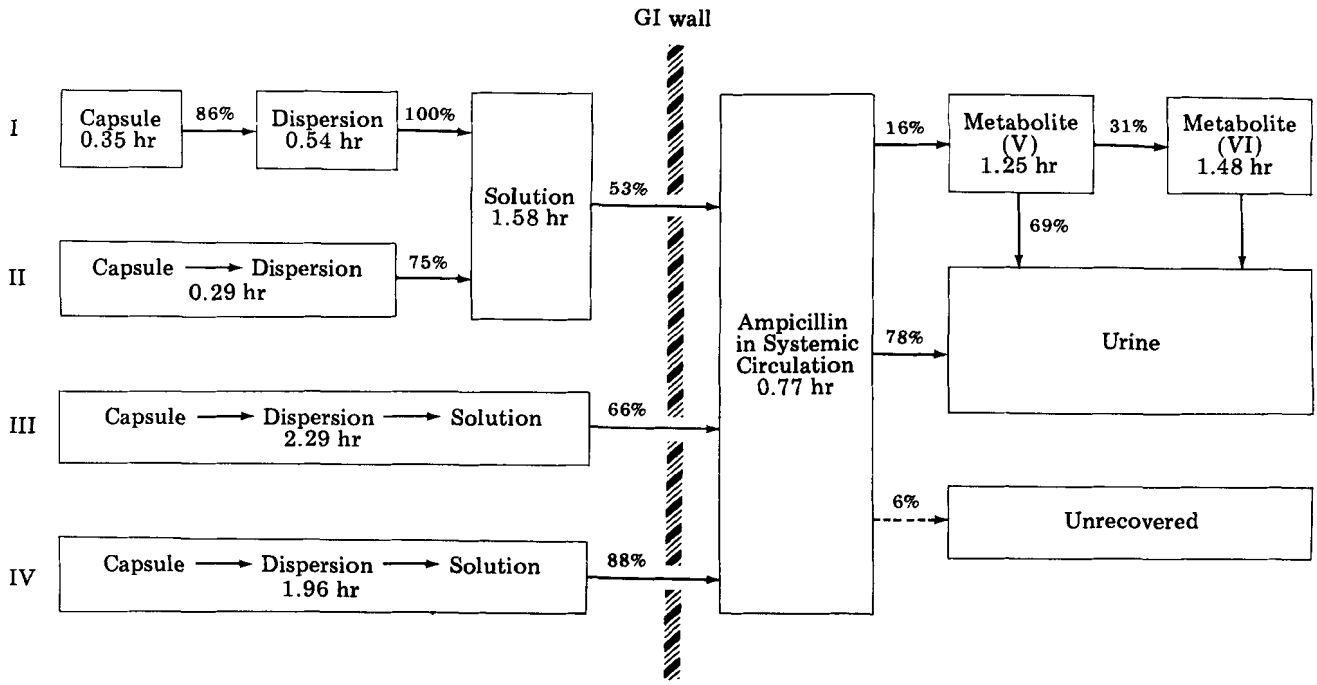

Scheme III—Drug flow diagram of ampicillin and its prodrugs. Key: (I) ampicillin trihydrate; (II) ampicillin anhydrate; (III) hetacillin potassium; (IV) talampicillin hydrochloride; (V) α-aminobenzyl penicilloic acid; (VI) α-aminobenzyl penamaldic acid.

It is of interest to correlate *in vitro* tests with *in vivo* bioavailability. Because MDT and MDIT are just the extracted characteristics of *in vivo* dissolution and disintegration from a complicated biopharmaceutical process, the *in vitro* dissolution and disintegration tests can be directly correlated to these quantities.

The component is a concept that should be distinguished from the classical compartment. The compartment is related to the pharmacokinetic model which is expressed by simultaneous ordinary differential equations. The complete mixing or the steady state is assumed in a certain compartment. The number of compartments in a system is determined according to the number of exponential terms in a pharmacokinetic equation that fits well to the experimental time course data. In contrast, the component is derived from the moment analysis, which is a model-independent method. A component specifies a biological or physicochemical state of a drug, that is, in a capsule, in intestinal fluid, in plasma, as a prodrug, or as a metabolite. The drug flow diagram constructed by components gives the intuitive information about rate and extent profiles of a drug in the GI tract and systemic circulation. The diagram can be more detailed as the experimental information increases. For example, Scheme III shows the more detailed flow diagram of four ampicillin preparations. This diagram was prepared by combining the data in this article with those reported previously (8). Six percent of absorbed ampicillin was unrecovered as shown by the dotted arrow. This process is not yet confirmed and another disposition route is possible.

REFERENCES

(1) K. Yamaoka, T. Nakagawa, and T. Uno, *J. Pharmacokinet. Biopharm.*, **6**, 547 (1978).

(2) D. J. Cutler, *J. Pharm. Pharmacol.* **30**, 476 (1978).

(3) S. Riegelman and P. Collier, *J. Pharmacokinet. Biopharm.*, **8**, 509 (1980).

(4) D. J. Cutler, *ibid.*, **7**, 101 (1979).

(5) L. Z. Benet and R. L. Galeazzi, *J. Pharm. Sci.*, **68**, 1071 (1979).

(6) J. Haginaka, K, Yamaoka, T. Nakagawa, Y. Nishimura, and T. Uno, *Chem. Pharm. Bull.*, **27**, 3156 (1979).

(7) J. Haginaka, T. Nakagawa, and T. Uno, *J. Antibiot.*, **33**, 236 (1980).

(8) T. Uno, M. Masada, K. Yamaoka, and T. Nakagawa, *Chem. Pharm. Bull.*, **29**, 1957 (1981).

(9) Y. Murai, T. Nakagawa, K. Yamaoka, and T. Uno, *ibid.*, **29**, 3290 (1982).

(10) K. Yamaoka, Y. Tanigawara, T. Nakagawa, and T. Uno, *Int. J. Pharm.*, **10**, 291 (1982).

(11) J. G. Wagner and E. Nelson, *J. Pharm. Sci.*, **53**, 1392 (1964).

(12) J. C. K. Loo and S. Riegelman, *ibid.*, **57**, 918 (1968).

(13) A. Rescigno and G. Segre, in "Drugs and Tracer Kinetics," Blaisdell, Waltham, Mass., 1966, p. 102.

(14) P. R. Byron and R. E. Notari, *J. Pharm. Sci.*, **65**, 1140 (1976).

(15) J. W. Poole and C. K. Bahal, *ibid.*, **57**, 1945 (1968).

(16) D. A. Wadke and G. E. Reier, *ibid.*, **61**, 868 (1972).

(17) S. A. Hill, K. H. Jones, H. Seager, and C. B. Taskis, *J. Pharm. Pharmacol.*, **27**, 594 (1975).

(18) A. Tsuji, E. Nakashima, S. Hamano, and T. Yamana, *J. Pharm. Sci.*, **67**, 1059 (1978).

(19) C. D. Thron, *Fed. Proc. Fed. Am. Soc. Exp. Biol.*, **39**, 2443 (1980).

(20) J. C. K. Loo, E. L. Foltz, H. Wallick, and K. C. Kwan, *Clin. Pharmacol. Ther.*, **16**, 35 (1974).

(21) *Fed. Regis.*, **42**(5), 1624 (January 7, 1977).

ACKNOWLEDGMENTS

The authors thank Banyu Pharmaceutical Co. and Takeda Chemical Industries for the gifts of penicillins.

Sequential Electrochemical Reduction, Solvent Partition, and Automated Thiol Colorimetry for Urinary Captopril and its Disulfides

HAROLD KADIN ˣ **and RAYMOND B. POET**

Received June 8, 1981, from the *Squibb Institute for Medical Research, New Brunswick, NJ 08903.* Accepted for publication December 10, 1981.

Abstract □ Analysis of urinary captopril was necessary for dosage form bioavailability and dose titration studies. The necessity for long-term storage of samples prior to analysis and the presence of an oxidation-prone thiol of captopril required development of an acid-chelate stabilization method for urinary captopril. An electrochemical reduction released disulfide-conjugated captopril for thiol colorimetry. Of several rugged reduction cells evaluated, one with a porous glass disk separating the anode and the mercury pool cathode was preferred. Methylene chloride partitions from acidified salt-saturated urines, before and after reduction, allowed the measurement of free and disulfide-conjugated captopril. The drug partitioned into the solvent, whereas the aqueous phase retained acid protonated, amino group-bearing thiols like cysteine. Subsequent solvent evaporation volatilized other potential colorimetric interferences. An automated thiol colorimetry of 25 samples/hr was developed for analysis of the aqueous reconstitutes. Results were confirmed by a subsequently developed HPLC method with electrochemical detection.

Keyphrases □ Captopril—urinary, disulfides, automated thiol colorimetry, solvent partition, sequential electrochemical reduction □ Colorimetry—automated thiol, urinary captopril and disulfides, solvent partition, sequential electrochemical reduction □ Electrochemical, reduction—sequential, solvent partition, automated thiol colorimetry, urinary captopril, disulfides

Captopril, 1-(3-mercapto-2-D-methyl-1-oxopropyl)-L-proline (*S,S*)

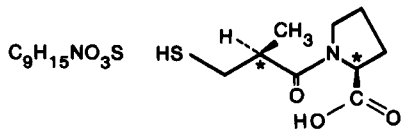

MW 217.29

is the first clinically potent oral hypotensive agent designed for highly selective inhibition of the angiotensin-converting enzyme (1). Captopril has been found effective for treatment of hypertension and congestive heart failure (2–4).

BACKGROUND

Captopril[1] is readily oxidized in human urine. Acidification minimizes excessive oxidation for only 1–2 days. However, an anticipated large sample load required storage for several weeks before analysis. This provided the impetus for a urinary captopril stability study to determine sample stability under various storage conditions prior to analysis. Satisfactory stabilization was attained by acidification, trace metal removal, and quick refrigeration. A very simple, direct automated colorimetry of pre- and postdosage urines, developed first, appeared adequate. Attempts were made to minimize the predosage urine blank by automating additional thiol colorimetries. These included the alkaline nitroprusside (5) and *S*-nitroso-Bratton–Marshall (6) colorimetries. An automated version of the reaction of Ellman and Lysko (7) gave the lowest blanks.

This simple, direct analysis was quickly found to lack sensitivity by comparison with thin-layer radiochromatographic analysis (8, 9) performed on divided samples from subjects dosed with radioactive captopril. Consequently, the direct colorimetry was preceded by a solvent partition clean-up. To assay for total captopril, which includes captopril, its disulfide, and captopril mixed disulfides (*e.g.*, captopril–cysteine), the urine sample was electrochemically reduced prior to solvent extraction.

The present method, intended as an interim method until development of an HPLC–electrochemical detection (ECD) procedure (10), offers an alternative to laboratories not equipped for HPLC-ECD.

EXPERIMENTAL

Reagents and Apparatus—The reagents included captopril, captopril disulfide, captopril–cysteine disulfide, 8% diethylenetriamine pentaacetic acid (I) in 0.8 *N* NaOH (refrigerate), 10.5% citric acid monohydrate in 6.3% oxalic acid dihydrate, acid-chelating mixture of 0.4% I and 1.05% citric acid monohydrate in 0.63% oxalic acid dihydrate (constituted from the preceding concentrates), freshly water washed methylene chloride, sodium sulfate (anhydrous, fine, granular, or ball milled for rapid dissolution), 1.86% disodium ethylenediaminetetraacetic acid dihydrate (II) plus 0.02% polyoxyethylene sorbitan monooleate[2] in 20% triethanolamine (III)[3], 0.08% 5,5′ dithio-bis(2-nitrobenzoic acid) (Ellman's reagent) in 50% methanol–50% 0.01 *M* sodium acetate–acetic acid buffer[3] (pH 4.7), 0.1 *N* HCl[3], 10% mercuric chloride in 1 *N* HCl, aqueous saturated sodium chloride, and 0.5 *M* Na_2CO_3. In constituting Ellman's reagent, refrigerated buffer was used to minimize heat generated on dilution of the methanol, since heat hydrolyzes the reagent to produce the same yellow color characteristic of its colorimetric reaction with thiols. Since it is also sensitive to light, the reagent was dispensed from an amber container. To further minimize yellow background the triethanolamine used was water-white rather than the yellow of amines stored for long periods of time. Water referred to in this report is distilled water.

The apparatus included centrifuge tubes (50-ml round-bottom, screw capped, with flat polytetrafluoroethylene[4] or polyethylene cone liners), nitrogen evaporation assembly with a 40° bath, ultrasonic bath, plastic caps[5], and an autoanalysis system[6] as illustrated in Fig. 1. The system included an automatic sampler[7] equipped with a 50-2/1 cam. The cam facilitates 50 sample transfers per hour, with samplings twice as long as intermediate washes. The asterisks in Fig. 1 identify solvent resistant tubing[8], whereas the other tubing[9] was not required to be solvent resistant. The peristaltic pump transferred Ellman's reagent, the II–III mixture, and other solutions as indicated in Fig. 1 and in the *Reagents* section.

Colorimetric Standards—Exactly 25.0 mg of captopril was accurately weighed into a 100-ml volumetric flask, dissolved, and diluted to volume with the acid-chelating mixture. Ten-milliliter portions of this primary standard were transferred to 25-, 50-, and 100-ml volumetric flasks. Each flask was diluted to volume with the acid-chelating mixture. These secondary working standard solutions contained 100, 50, and 25 μg of captopril/ml. The primary standard solution was refrigerated up to 1 week. Fresh secondary working standards were prepared daily.

Sample Collection—Five milliliters of I concentrate was added to each subject's plastic, urine collection container. Subjects voided into these containers and the contents were mixed by swirling. The total volume was immediately measured and recorded. Without delay, each

[1] Capoten, Lopirin, SQ 14,225, E. R. Squibb, Princeton, N.J.

[2] Tween 80, I.C.I. Americas, Inc., Wilmington, Del.

[3] Autoanalysis reagents were gravity filtered through a funnel with coarse sintered disk prior to use.

[4] Teflon, E. I. duPont de Nemours & Co., Wilmington, Del.

[5] From polyethylene containers, Nalgene No. 6250, Nalge Co., Rochester, N.Y.

[6] Technicon Autoanalyzer, Technicon Industrial Systems, Tarrytown, N.Y.

[7] Technicon Sampler II, Technicon Industrial Systems.

[8] Solvaflex, Norton Plastics and Synthetics Divison, Akron, Ohio.

[9] Tygon, Norton Plastics and Synthetics Division.

0022-3549/82/01000-1134$01.00/0

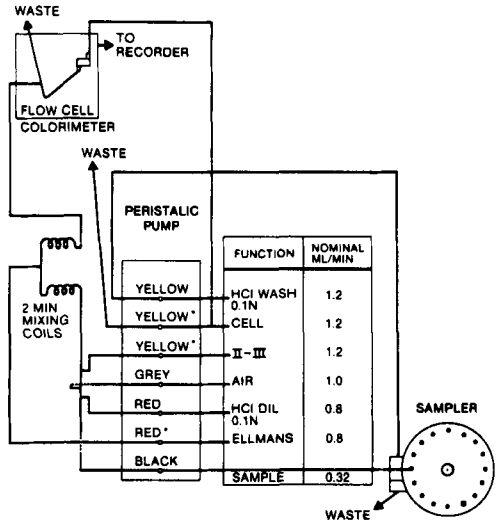

Figure 1—*Autoanalysis of Ellman colorimetry. See Reagents and Apparatus section.*

sample was then poured into central, plastic storage vessels (one for each subject), containing 100 ml of cold citric–oxalic concentrate. The solutions were mixed by swirling and the sample rapidly chilled to about refrigerator temperature (3–5°). Each subject's urine voided during a desired collection period was treated as described and collected in that individual's central storage vessel. The volume of urine plus stabilizers in the central storage vessel was measured and recorded. About 50 ml of the settled, measured urine was transferred to a suitably labeled tube. All such tubes were refrigerated during storage or transportation pending assay. The collections for each subject included a predosage control urine.

Electrochemical Reduction Cell—The cell in Fig. 2 was a scale-up from that of previous study (11), and was used for most of the studies. The 5.05 × 1.85-cm i.d. tube contained a magnetically stirred mercury pool in electrical contact with a platinum wire extending to the exterior of the tube. An inverted U side arm (3.5-mm i.d.) was attached ~2 cm from the bottom of the tube. The latter contained a saturated sodium chloride 2% agar bridge constituted and maintained as described previously (12). The agar salt bridge isolates the negative reductive mercury pool cathode from the positive oxidative platinum anode. The anode is positioned at the tip of the bridge in a small container of saturated sodium chloride. The cells were connected in series with miniature alligator clip jumper leads through a 0–5 milliammeter and a power supply[10] capable of supplying 2.5 mA/hr. The integrity of the agar bridge was maintained optimally by storage with saturated sodium chloride solution at both

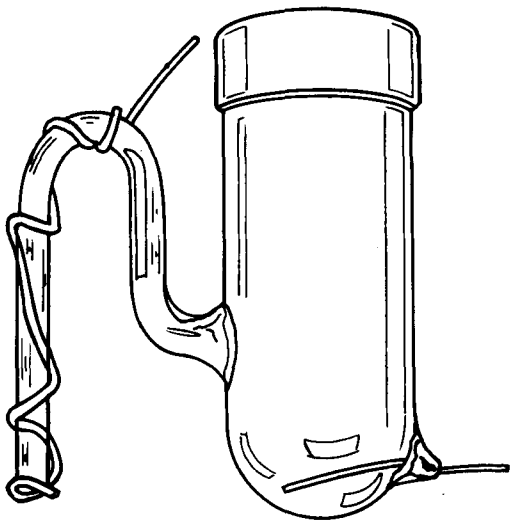

Figure 2—*Saetre-Rabenstein (see Ref. 11) agar bridged electrochemical reduction cell.*

[10] Power Supply No. 6212A, Hewlett-Packard Co., Palto Alto, Calif.

ends. During electrolysis the mercury pool–urine interface was magnetically stirred[11] minimizing vortexing or dispersed mercury droplets. Two cells were stirred over each stirrer. As many as 12 cells were operated in series. To minimize chlorine generation at the anode the saturated sodium chloride electrolyte was made alkaline, as recommended previously (13). Five to six drops of 0.5 *M* Na_2CO_3 were mixed in 9 ml of the anode electrolyte, and the reduction assembly was operated in a hood to sweep chlorine away. The alligator clips were placed well away from the anodic electrolyte to minimize corrosion by chlorine. To minimize chlorine retention in the gel, the bridge tip was removed from the electrolyte soon after a run. Near quantitative disulfide reduction was obtained without widely recommended (13–18) nitrogen blanketing of the cathode compartment. Almost complete sulfhydryl recovery was ensured by l-citric–oxalic thiol stabilization, slight electrolytic hydrogen generation, and a minimum headspace beneath a pinhole vented plastic cap.

Electrochemical Reduction of Sample—Prior to analysis, the saturated sodium chloride and three subsequent water washes were aspirated from the mercury in each cell. The wet mercury and stirring bar were then poured into a 100-ml beaker containing a generous piece of filter paper on the bottom. The mercury was cleaned and dried by swirling it several times over the paper. The mercury and stirring bar were returned to the cell. The cell was then clamp mounted over a magnetic stirrer with its salt bridge exit tip immersed in a small container of alkaline saturated sodium chloride. Washed, dried, and mounted cells were filled with urine samples, leaving minimal headspace beneath the pinhole vented plastic caps[5]. Moderate magnetic stirring was initiated. The cells were securely connected in series to the milliammeter and power supply with the miniature alligator clip jumper leads as follows. The black negative terminal of the power supply was attached with a clip lead to the platinum–mercury cathode of the first cell, then its positive salt bridge platinum anode was clip attached to the platinum–mercury cathode of the next cell in the series. This series clip lead connection between adjoining cells was continued until the last platinum salt bridge anode was connected to the red positive terminal of the power source through the milliammeter. The power supply current was adjusted to 2.5 mA. The voltage across each cell was measured to locate those with abnormally high voltage drops due to a high resistance, deteriorated agar bridge. When a cell had a voltage drop greater than 5 V it was replaced. The electrolysis proceeded for 1 hr with adjustment of the 2.5-mA current, if required. The reduced urine samples were solvent partitioned as subsequently described.

Cells were prepared for the next electrolysis by first shutting off the power supply and stirrers. The urine and three successive, briefly stirred water washes were aspirated. Saturated sodium chloride was added to each cell. The electrolysis as just described for urine samples was performed for 30 min. After 30 min, the electrolysis leads at the power supply terminals were reversed for 10 sec. The power source was then turned off. Leads were disconnected. Cells were demounted for storage in large covered beakers with salt bridges moistened with saturated sodium chloride at both ends.

Solvent Partition—This was performed on reduced urine (section above) to determine free plus disulfide conjugated captopril and on nonreduced urines to determine free captopril. To prepare for the solvent partition 1.0 ± 0.1-g portions of the fine, granular, anhydrous sodium sulfate were weighed into screw-capped 50-ml round bottom tubes. In addition, methylene chloride was freshly water washed (250 ml of methylene chloride washed with 3 × 150 ml of water).

Reduced urine samples were handled as follows: the electrolysis was allowed to proceed while exactly 5.0 ml of the urine was removed by pipet then gradually and vigorously swirled into the sodium sulfate in the 50-ml screw-capped tube to effect salt dissolution[12]. Nonreduced urine samples were likewise transferred to other sodium sulfate containing tubes. Ten milliliters of the washed methylene chloride was gradually added to each tube over the surface of the aqueous phase. Each tube was firmly capped. A pair of tubes was gently rocked to effect emulsion-free extraction[13]. The tubes were centrifuged for ~2 min at ~2500 rpm. With tissue-wiped

[11] Micro V magnetic stirrers, Cole-Parmer Instrument Co., Chicago, Ill.

[12] This was done with a vigorous, circular motion to prevent refractory caking. This vigorous swirling was successively repeated down a line of tubes to effect a gradual salt dissolution. To aid the dissolution the lower portion of the tubes was agitated in the active portion of an ultrasonic bath immediately after the initial swirling.

[13] The extraction was effected by enclosing a pair of tubes within both hands. The tubes were gently rocked 3× within 60° from the horizontal then placed vertically in a rack for at least 30 sec to allow maximum phase separation. The rocking extraction-standing sequence was then repeated two more times. This gentle rocking technique was developed when ordinary shaking oxidized captopril and yielded very stable emulsions.

Table I—Percent Recovery of Captopril [a] in Pooled, Refrigerated, and Frozen Human Urine

Storage Time, days	Stabilized by: Citric–Oxalic-I pH 2 Refrig	Citric–Oxalic-I pH 2 Frozen	Perchloric Acid pH 1 Refrig	Perchloric Acid pH 1 Frozen
Initial	101.0	—	94.9	—
6	97.1	96.8	—	—
7	—	—	84.6	85.3
9	92.6	91.9	—	—
21	92.5	92.8	—	—
27	91.8	86.1	73.2	57.6
29	91.6	—	—	—
42	87.5	82.4	70.5	52.0
63	84.3	—	—	—

[a] 25 and 50 μg/ml.

10-ml pipets and using a pipet filler all of the possible lower phase was carefully transferred to another 50-ml screw-capped tube. Two additional extractions were performed. The combined extracts were evaporated under nitrogen at 40°. Residues were reconstituted in 5.0 ml of the acid chelating mixture, sonicated, and vortexed briefly to dissolve any particles. The tubes were then centrifuged for 5 min at ~2500 rpm. Automated colorimetry with associated blanking was then performed as described.

Automated Colorimetry—Figure 1 shows the apparatus for automated colorimetry. The centrifuge clarified samples were transferred to sample cups[6] by careful decantation[14]. The filled cups were then placed in sampler turntable slots with each sample cup bracketed by full washout water cups. In the same manner single cups containing the acid chelating mixture (reagent blank) and duplicate cups containing 25-, 50-, and 100-μg/ml standards were placed in the turntable prior to and after the sample sequence. The automated analysis was allowed to proceed while preparing the mercuric treated samples as follows. Two milliliters of the above clarified urine sample and reagent blanks was transferred into suitable test tubes containing 0.2 ml of mercuric chloride solution. These were capped, mixed, then centrifuged to optical clarity. Each supernate was carefully transferred[14] (to avoid disturbing sediment) into a sample cup. These were placed on the sampler, bracketed by water cups, following the second set of standards. Five sample cups containing the primary standard dilution followed the mercuric blanked samples. The latter solutions were used to remove trace, potential sulfhydryl blocking mercuric ion from the autoanalysis system (absorbance data were discarded).

Calculations—Percent dose voided = $[100\,(X - B)\,SV]/(1000\,D) = [(X - B)\,SV]/(10\,D)$, where X is absorbance of sample minus the reagent blank, B is 1.1 (absorbance of mercuric treated sample minus the mercuric treated reagent blank), where 1.1 is the mercuric solution sample dilution factor, S is average of three standards calculated as (micrograms per milliliter)/(absorbance of standard), V is urine + stabilizers volume, ml, D is captopril dose, in milligrams.

RESULTS AND DISCUSSION

Urinary Captopril and Its Disulfides—This method was used to analyze captopril in 8-hr postdosage urine of normal subjects before and after electrochemical reduction. Results with 10 subjects expressed as percent of dose (100 mg) were:

$$\text{Free Captopril} - 30.3 \pm 7.74\ SD$$

$$\text{Captopril + Disulfides} - 54.9 \pm 14.6\ SD$$

Thin-layer radiochromatography (8) indicated that human urinary captopril was primarily free (unchanged) and, in almost equal proportion, disulfide conjugated with cysteine. Relatively small amounts of captopril disulfide were observed. Consequently, the present results suggest that ~25% of the dose in the 8-hr urine is principally captopril–cysteine.

Urinary Captopril Stabilization—Long-term urinary captopril stabilization studies were performed by the simple, direct automated analysis on pooled human urine in screw-capped tubes containing 25 and 50 μg of captopril/ml at room, refrigerator, and freezer temperatures. Direct automated analysis of the unfortified pooled urine served as a blank. Data obtained are presented in Table I.

Note that long-term freezing seemed to enhance degradation relative to refrigeration storage particularly with perchloric acid acidified urine. Acid–chelate stabilized urine freezing did not seem to increase stabilization, and in the long-term slightly enhanced degradation.

The stabilization attained by the acid–chelate mixture was attributed to efficient (19) trace metal binding by I at the pH of human urine (pH 5–6), acidification, and refrigeration.

Selectivity, Recovery, Precision, Sensitivity—Selectivity was shown by analysis of predosage 8-hr urines collected from 34 individuals. All yielded essentially zero colorimetric response. Interference from occasionally extracted urinary pigments is obviated by subtracting the colorimetric response of the mercuric blank from that of the sample (see Calculations). Mercuric ion added to a portion of the sample (reconstituted from the methylene chloride extract–nitrogen evaporation residue) prevents captopril colorization of Ellman's reagent by formation of thiol mercaptides. This allows measurement and correction for nonsulfhydryl color.

Pooled predosage and postdosage urines from six individuals were fortified with captopril at 25 and 50 μg/ml, respectively. In two experiments the recoveries with predosage urine were 96.4 and 98.8%. The analysis of the unfortified postdosage pool was subtracted from that fortified to 50 μg/ml to yield a recovery for added captopril of 96.6%. The precision and sensitivity were evaluated by pooling blank urine from 12 subjects. Six replicate assays of this pool determined the apparent micrograms of captopril per milliliter. The pooled urine was fortified with captopril at ~46 μg/ml. Two chemists each performed eight replicate assays of thiol content as described.

Chemist 1 achieved a mean of 45.1 ± *SD* 0.26 with an *RSD* of 1.2. Chemist 2 obtained 45.4 ± *SD* 0.72 with an *RSD* of 2.0. The apparent micrograms per milliliter of captopril in the blank pooled urine was 0.24. The average blank value (subtracted for the recovery data) was calculated from absorbances of 0.002–0.003. Zero and negative absorbance values in this range were frequently obtained and were considered essentially zero blanks. The sensitivity of this method is conservatively estimated at 0.5 μg/ml, which is approximately twice the average blank found in this precision study.

Solvent Partition—To reduce the large predosage blank obtained in direct colorimetry of the urine, the multiple methylene chloride extraction and evaporation was performed, as described in *Experimental* section. Solvent partition of highly polar captopril required salting out from the acidic urines. Appreciable captopril oxidation was observed when using sodium chloride as a salting out agent instead of sodium sulfate. This oxidation was attributed to chlorine from metal catalyzed, solvent mediated air oxidation of chloride (20). Attempts were made to substitute a column solvent partition in which the acidified urine–sodium sulfate was held by a column of polar stationary phase (*e.g.*, diatomaceous earth, silica gel, or cellulose) and a readily evaporated mobile phase (*e.g.*, ethyl acetate, methylene chloride, or 10% isopropanol in methylene chloride) percolates through the column to efficiently perform continuous, multiple extractions. If successful, this column partition would have considerably decreased operator time. However, incomplete recoveries (60–80%), possibly attributable to irreversible adsorption and/or oxidation, were obtained. Attempts at a reversed-phase partitioning into particulate polystyrene divinylbenzene[15] or octadecylsilane bonded to silica particles[16] followed by solvent elution also resulted in recoveries of 85–90%, short of the goal of 95% or better.

Automated Colorimetry—In the design of the colorimetry from a preexisting manual colorimetry (7), the sequence of adding Ellman's reagent before the alkali was reversed to maintain solubility of the reagent within the autoanalysis system. In addition, methanol and acidic aqueous buffer were added to Ellman's reagent to enhance both solubility and stability.

Electrochemical Reduction—The electrical characteristics of the cell included the resistance across the agar bridge of 1600–1700 ohms, a voltage drop across the cell of 3–4 V, and a cathode voltage, *versus* silver–silver chloride, of −0.9 to −1.0 V. These characteristics allowed efficient disulfide reduction by minimizing parasitic reductions of hydrogen ion, oxalic acid (14), and I–metal complexes.

Part of a pool of five normal human urine, stabilized with I–citric–oxalic acids, was fortified with captopril disulfide at 50 μg/ml. Table II presents results of a time and current study of the electrochemical re-

[14] When commercially available pasteur pipets were used to transfer the reconstituted acid captopril solutions to autoanalyzer cups, the first transfer yielded appreciably lower results than the second transfer with the same pipet. This was not encountered when previously washed and dried volumetric pipets or decantation transfers were made.

[15] XAD-2 Resin, Rohm and Haas Co., Philadelphia, Pa.

[16] SEP-PAK Columns, Waters Associates, Inc., Milford, Mass.

Table II—Effect of Time and Current on Reduction of Captopril Disulfide [a] in Normal Human Urine Pool

Min	Percent Recovery at Current, mA		
	2	2.5	5
20	53.4	—	68.7
40	84.4	—	92.0
60	97.3	99.3, 98.1, 100.1	93.0

[a] 50 μg/ml.

duction of this fortified urine followed by the extraction analysis. The unfortified human urine pool (control) reduced electrochemically at 2.5 mA for 1 hr yielded a colorimetric response, through the extraction analysis, of 0.003 absorbance units. This is equivalent to a blank (see preceding discussion on sensitivity of the solvent partition).

Table II indicates a possible fall off of reduction at 5 mA. Subsequently, a current of 2.5 mA for 1 hr was used with the encouraging results indicated. Whereas a 1-hr reduction was necessary here, Saetre and Rabenstein (11, 13) reported a complete 10-min reduction with cystine and the penicillamine and the glutathione disulfides. Possibly the amino groups of the latter three disulfides facilitate disulfide reduction by shifting electrons from the disulfide linkage in a manner described previously (21). The 1-hr electrochemical reduction was also valid for captopril–cysteine disulfide. However, a time–current study comparable to that in Table II was not done with the mixed disulfide.

In view of the agar bridge fragility in routine use, several substitutes were considered including a sturdy polyacrylamide gel (22), sintered glass disks (17), tightly rolled paper wads in each end of a glass U tube containing the saturated sodium chloride[17], and 4-mm porous glass[18] disks[19]. The porous (pore diameter 4 μm) glass[18] acts as a semipermeable membrane providing ultra-low liquid leakage rates and minimum IR drop through the tip (23). A rather simple porous glass[18] disk bridge[19] (Fig. 3) had the same resistance as the agar bridge and gave captopril analyses very comparable to that with the agar bridge. It is considered a preferable substitute for the agar bridge. Incorporating the porous glass[18] disk at its end, a tapered glass tube enters a hole in the previously needle-punctured plastic cap (from a 5-ml plastic container)[5] at the top of the cell illustrated. The 4 × 2.9 mm (diameter × width) porous glass disk in heat shrink polytetrafluoroethylene tubing[19] was previously slipped over the glass taper. The heat shrink tubing, well away from the porous glass[18] disk, was then heat shrunk with a heat gun. The assembly was completed with a platinum electrode clipped to the wide top of the glass tube, which contained saturated aqueous sodium chloride. The electrochemical reduction was chosen over other disulfide reduction procedures since it is performed at an acid pH which stabilizes the sulfhydryl. It adds no reducing agents (dithiothreitol, mercaptoethanol, or sulfite) which colorize Ellman's reagent. It is not toxic as is the highly effective disulfide reductant tributylphosphine (24). Finally, several reports (13–16) indicated that borohydride and zinc-acid reductions yielded incomplete reduction or reoxidations in biological samples, whereas electrochemical reductions were quantitative.

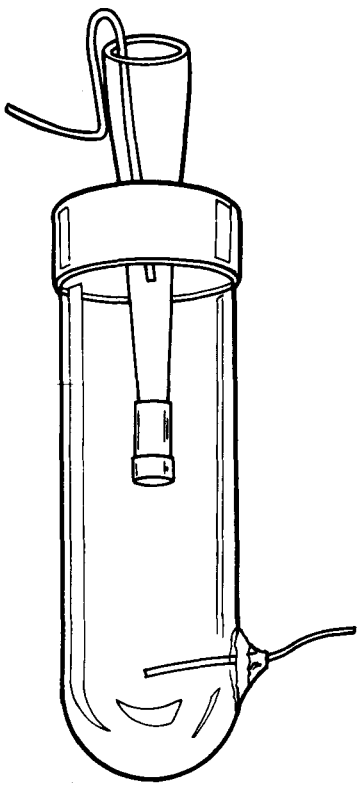

Figure 3—*Porous glass*[18] *bridged electrochemical reduction cell.*

[17] Dr. M. Szyper, Squibb Institute for Medical Research, New Brunswick, N.J., personal communication.

[18] Vycor, Corning Glass Company, Corning, N.Y.

[19] The disk and heat shrink tubing were obtained as Catalog No. G0100 from Princeton Applied Research, Princeton, N.J.

Table III—Analysis of Captopril and Its Disulfides in 0–4 Hr Predosage Urine by HPLC–ECD and the Present Method [a]

Subject No.	μg/ml			
	Captopril		Captopril Plus Disulfides	
	HPLC-ECD	PM	HPLC-ECD	PM
2D	13.7	14.7	22.0	23.4
3B	30.6	32.5	47.0	49.3
4A	32.0	33.1	50.5	51.3
5C	25.1	33.5	39.4	32.9
6C	29.7	28.7	52.6	50.7
7B	45.6	43.3	74.2	73.5
8B	34.4	33.2	58.1	59.6

[a] Present method = PM.

The reported electrochemical reduction utilizes a meter, a relatively sophisticated power supply, and an integrated reduction cell. It should be pointed out that simpler versions using a battery, a variable resistor, beakers, and detached agar U-bridges have been implemented (18).

Confirmatory Analysis *via* HPLC–Electrochemical Detection (ECD)—Analysis performed by the presently reported method and the subsequently developed HPLC method (10) are compared in Table III. Agreement is very satisfactory. The assay conformity appears more remarkable when it is learned that the HPLC–ECD assays were performed on samples stored for 90–120 days after their colorimetric analyses.

REFERENCES

(1) M. A. Ondetti, B. Rubin, and D. W. Cushman, *Science*, **196**, 441 (1977).

(2) A. B. Atkinson and J. I. S. Robertson, *Lancet*, **ii**, 836 (1979).

(3) R. C. Heel, R. N. Brogden, T. M. Speight, and G. S. Avery, *Drugs*, **20**, 409 (1980).

(4) H. Gavras, I. Gavras, P. Hadzinikolaou, and H. R. Brunner, *J. Cardiovasc. Med.*, **5**(4), 327 (1980).

(5) J. H. Karchmer, in "Treatise on Analytical Chemistry," Part II, vol. 13, I. M. Kolthoff and P. J. Elving, Eds., Wiley-Interscience New York, N.Y., 1966, p. 465.

(6) H. Liddell and B. Saville, *Analyst*, **84**, 188 (1959).

(7) G. L. Ellman and H. Lysko, *J. Lab. Clin. Med.*, **70**, 518 (1967).

(8) K. J. Kripalani, F. S. Meeker, Jr., A. V. Dean, D. N. McKinstry, and B. H. Migdaloff, *Fed. Proc. Fed. Am. Soc. Exp. Biol.*, **39**, 307 (1980).

(9) B. H. Migdaloff, S. M. Singhvi, and K. J. Kripalani, *J. Liquid Chromatogr.*, **3**, 857 (1980).

(10) P. Yeh, Abstracts, No. 60, page 54, Eastern Analytical Symposium, New York, N.Y., Nov. 1980.

(11) R. Saetre and D. L. Rabenstein, *Anal. Chem.*, **50**, 276 (1978).

(12) L. Meites, "Polarographic Techniques," 2nd ed., Wiley-Interscience, New York, N.Y., 1965, pp. 63, 388.

(13) R. Saetre, "Determination of Biologically Active Sulfur-Containing Compounds by HPLC with a Mercury-Based Electrochemical Detector," Ph.D. Thesis, March 1, 1978, University of Alberta, Edmonton, Alberta, Canada.

(14) J. S. Dohan and G. E. Woodward, *J. Biol. Chem.*, **129**, 393 (1939).

(15) T. Hata, *Bull. Res. Inst. Food Sci.*, **3**, 63 (1950).

(16) S. K. Bhattacharya, J. S. Robson, and C. P. Stewart, *Biochem. J.*, **60**, 696 (1955).

(17) E. G. Sement, M. L. Girard, F. Rousselet, and M. Chemla, *Ann. Pharm. Franc.*, **37**, 513 (1979).

(18) P. D. J. Weitzman, J. K. Hanson, and M. G. Parker, *FEBS Lett.*, **43**, 101 (1974).
(19) "Versene, Products and Properties—Comparison Chart," Dow Chemical Co., Midland, Mich., 1977.
(20) "Kirk-Othmer Encyclopedia of Chemical Technology," vol. 1, 3rd ed., Wiley-Interscience, New York, N.Y., 1978, p. 826.
(21) W. W. C. Chan, *Biochemistry*, **7**, 4247 (1968).
(22) J. A. Rothfus, *Anal. Biochem.*, **16**, 167 (1966).
(23) Princeton Applied Research, Princeton, N.J., "Handling Instructions for Glassware Incorporating Vycor Tips," No. 11328-A-MD.
(24) U. T. Rüegg and J. Rudinger, in "Methods in Enzymology, Enzyme Structure," Part E, Vol. 47, H. Timasheff, Ed., Academic Press, New York, N.Y., 1977, p. 111.

ACKNOWLEDGMENTS

The authors thank Drs. Glen Brewer, Klaus Florey, Doris McKinstry, Bruce Migdaloff, and Sampat Singhvi for support and suggestions; Drs. Peter Yeh and Joel Kirschbaum for the HPLC-ECD data; Peter Hazlett for constructing the electrochemical reduction cells; Jose Alcantara for designing Figs. 1–3; and Eva Johnson, Lois George, and Rita Kalasin for technical assistance.

Intestinal Absorption of Amino Acid Derivatives: Importance of the Free α-Amino Group

G. L. AMIDON *[x], M. CHANG, D. FLEISHER, and R. ALLEN

Received August 14, 1981, from the *School of Pharmacy, University of Wisconsin, Madison, WI 53706.* Accepted for publication December 18, 1981. *Present Address: INTER$_x$ Research Corporation, Lawrence KS 66044.

Abstract ■ The intestinal absorption of L-lysine-*p*-nitroanilide, L-alanine-*p*-nitroanilide, and glycine-*p*-nitroanilide was studied in the presence of competitive inhibitors in a perfused rat intestine. It was observed that L-lysine-*p*-nitroanilide absorption was inhibited by L-lysine methyl ester and L-arginine-β-naphthylamide but not by N_α-acetyl-L-lysine methyl esters. L-Alanine-*p*-nitroanilide absorption was inhibited by L-alanine methyl ester but not by β-alanine methyl ester. It was further observed that N_α-benzoyl-L-arginine-*p*-nitroanilide and N_α-succinyl-L-phenylalanine-*p*-nitroanilide were poorly absorbed. It was concluded that the peptidase in the brush border region that serves as the hydrolysis site requires a free α-amino group (an aminopeptidase), and that passive absorption of these compounds occurs only to a small extent.

Keyphrases □ Absorption, intestinal—amino acid derivatives, importance of the free α-amino group □ Amino acid derivatives—intestinal absorption importance of the free α-amino group □ α-Amino groups—importance of the free α-amino group in the intestinal absorption of amino acid derivatives

Recent investigations have demonstrated that brush border hydrolysis of soluble derivatives of insoluble drugs may significantly increase the absorption rate of the drug (1). Since the approach is based on enzymatic hydrolysis, the specificity of the hydrolytic enzymes in the brush border region must be investigated. While many enzymes have been reported to be present in this region (1), the aminopeptidases represent a likely site for reconversion of compounds previously studied (2–4). Furthermore, a free amino group on the substrate is required for aminopeptidase activity. The objective of this study was to determine the importance, for absorption, of a free α-amino group in amino acid derivatives of drugs.

EXPERIMENTAL

Materials—α-*N*-Benzoyl-DL-arginine-*p*-nitroanilide, *n*-succinyl-L-phenylalanine-*p*-nitroanilide, L-lysine-*p*-nitroanilide, L-lysine methyl ester, N_α-acetyl-L-lysine methyl ester, L-arginine-β-naphthylamide, L-alanine-*p*-nitroanilide, L-alanine methyl ester, β-alanine-*p*-nitroanilide, L-lysine methyl ester, β-alanine methyl ester, glycine-*p*-nitroanilide[1], and glycine methyl ester were used as received.

[1] U.S. Biochemical Corp., Cleveland, Ohio.

Perfusion Experiments—Drug absorption was measured in a perfused rat intestine segment as previously reported (1, 5). The inlet (C_o) and exit (C_m) concentrations were measured spectrophotometrically for the *p*-nitroanilide derivatives. The free *p*-nitroanilide was released by overnight (12 hr) hydrolysis of the syringe and perfusate samples after addition of sodium hydroxide (pH 11–12). A three-point analysis of the spectrum (350, 375, and 400 nm) was used in order to subtract the usually small protein background at these wavelengths.

THEORETICAL

The method of data analysis is the same as previously reported (1, 6). The method is appropriate as long as the boundary condition is linear:

$$J_w = -D\left.\frac{dc}{dr}\right|_{r=R} = P_w C_w \qquad \text{(Eq. 1)}$$

where J_w is the flux at the wall, P_w the wall permeability, and C_w the wall concentration. The dimensionless wall permeability (P_w*) is:

$$P_w^* = \frac{P_w R}{D} \qquad \text{(Eq. 2)}$$

where R is the radius of the intestine and D the solute diffusivity. The wall permeability ($^\circ P_w$*) is calculated using the measured ratio of exit to inlet concentrations (C_m/C_o) and the Graetz number (Gz) where $Gz = \pi DL/2Q$ and where L is the length of the intestinal segment and Q the fluid flow rate. The calculations follow the method previously reported (6). Diffusion coefficients are given in Table I. Analysis is based on the uncorrected $^\circ P_w$* values since the correction is small (6).

For the test compounds used in the present report (*e.g.*, L-lysine-*p*-nitroanilide) it is assumed that hydrolysis at the wall provides the driving force for transport to the wall, with the released *p*-nitroanilide being taken up by the wall (1). The wall permeability is, consequently, a heterogeneous reaction rate constant. The general case has been discussed (1) and gives:

$$P_w = \alpha D \operatorname{Tanh}(\alpha\delta_E) \qquad \text{(Eq. 3)}$$

or

$$P_w^* = \alpha R \operatorname{Tanh}(\alpha\delta_e) \qquad \text{(Eq. 4)}$$

where

$$\alpha^2 = k/D \qquad \text{(Eq. 5)}$$

where k is the first-order reaction rate constant, and δ_E is the (unknown) thickness of the enzyme layer. Two special cases of Eq. 4 are:

High reactivity ($\alpha\delta_e > 1$):

$$P_w^* = \alpha R \qquad \text{(Eq. 6)}$$

(18) P. D. J. Weitzman, J. K. Hanson, and M. G. Parker, *FEBS Lett.*, **43**, 101 (1974).
(19) "Versene, Products and Properties—Comparison Chart," Dow Chemical Co., Midland, Mich., 1977.
(20) "Kirk-Othmer Encyclopedia of Chemical Technology," vol. 1, 3rd ed., Wiley-Interscience, New York, N.Y., 1978, p. 826.
(21) W. W. C. Chan, *Biochemistry*, **7**, 4247 (1968).
(22) J. A. Rothfus, *Anal. Biochem.*, **16**, 167 (1966).
(23) Princeton Applied Research, Princeton, N.J., "Handling Instructions for Glassware Incorporating Vycor Tips," No. 11328-A-MD.
(24) U. T. Rüegg and J. Rudinger, in "Methods in Enzymology, Enzyme Structure," Part E, Vol. 47, H. Timasheff, Ed., Academic Press, New York, N.Y., 1977, p. 111.

ACKNOWLEDGMENTS

The authors thank Drs. Glen Brewer, Klaus Florey, Doris McKinstry, Bruce Migdaloff, and Sampat Singhvi for support and suggestions; Drs. Peter Yeh and Joel Kirschbaum for the HPLC-ECD data; Peter Hazlett for constructing the electrochemical reduction cells; Jose Alcantara for designing Figs. 1–3; and Eva Johnson, Lois George, and Rita Kalasin for technical assistance.

Intestinal Absorption of Amino Acid Derivatives: Importance of the Free α-Amino Group

G. L. AMIDON *[x], M. CHANG, D. FLEISHER, and R. ALLEN

Received August 14, 1981, from the *School of Pharmacy, University of Wisconsin, Madison, WI 53706.* Accepted for publication December 18, 1981. *Present Address: INTER$_x$ Research Corporation, Lawrence KS 66044.

Abstract ■ The intestinal absorption of L-lysine-*p*-nitroanilide, L-alanine-*p*-nitroanilide, and glycine-*p*-nitroanilide was studied in the presence of competitive inhibitors in a perfused rat intestine. It was observed that L-lysine-*p*-nitroanilide absorption was inhibited by L-lysine methyl ester and L-arginine-β-naphthylamide but not by N_α-acetyl-L-lysine methyl esters. L-Alanine-*p*-nitroanilide absorption was inhibited by L-alanine methyl ester but not by β-alanine methyl ester. It was further observed that N_α-benzoyl-L-arginine-*p*-nitroanilide and N_α-succinyl-L-phenylalanine-*p*-nitroanilide were poorly absorbed. It was concluded that the peptidase in the brush border region that serves as the hydrolysis site requires a free α-amino group (an aminopeptidase), and that passive absorption of these compounds occurs only to a small extent.

Keyphrases □ Absorption, intestinal—amino acid derivatives, importance of the free α-amino group □ Amino acid derivatives—intestinal absorption importance of the free α-amino group □ α-Amino groups—importance of the free α-amino group in the intestinal absorption of amino acid derivatives

Recent investigations have demonstrated that brush border hydrolysis of soluble derivatives of insoluble drugs may significantly increase the absorption rate of the drug (1). Since the approach is based on enzymatic hydrolysis, the specificity of the hydrolytic enzymes in the brush border region must be investigated. While many enzymes have been reported to be present in this region (1), the aminopeptidases represent a likely site for reconversion of compounds previously studied (2–4). Furthermore, a free amino group on the substrate is required for aminopeptidase activity. The objective of this study was to determine the importance, for absorption, of a free α-amino group in amino acid derivatives of drugs.

EXPERIMENTAL

Materials—α-*N*-Benzoyl-DL-arginine-*p*-nitroanilide, *n*-succinyl-L-phenylalanine-*p*-nitroanilide, L-lysine-*p*-nitroanilide, L-lysine methyl ester, N_α-acetyl-L-lysine methyl ester, L-arginine-β-naphthylamide, L-alanine-*p*-nitroanilide, L-alanine methyl ester, β-alanine-*p*-nitroanilide, L-lysine methyl ester, β-alanine methyl ester, glycine-*p*-nitroanilide[1], and glycine methyl ester were used as received.

[1] U.S. Biochemical Corp., Cleveland, Ohio.

Perfusion Experiments—Drug absorption was measured in a perfused rat intestine segment as previously reported (1, 5). The inlet (C_o) and exit (C_m) concentrations were measured spectrophotometrically for the *p*-nitroanilide derivatives. The free *p*-nitroanilide was released by overnight (12 hr) hydrolysis of the syringe and perfusate samples after addition of sodium hydroxide (pH 11–12). A three-point analysis of the spectrum (350, 375, and 400 nm) was used in order to subtract the usually small protein background at these wavelengths.

THEORETICAL

The method of data analysis is the same as previously reported (1, 6). The method is appropriate as long as the boundary condition is linear:

$$J_w = -D\left.\frac{dc}{dr}\right|_{r=R} = P_w C_w \qquad \text{(Eq. 1)}$$

where J_w is the flux at the wall, P_w the wall permeability, and C_w the wall concentration. The dimensionless wall permeability (P_w*) is:

$$P_w^* = \frac{P_w R}{D} \qquad \text{(Eq. 2)}$$

where R is the radius of the intestine and D the solute diffusivity. The wall permeability ($^\circ P_w$*) is calculated using the measured ratio of exit to inlet concentrations (C_m/C_o) and the Graetz number (Gz) where $Gz = \pi DL/2Q$ and where L is the length of the intestinal segment and Q the fluid flow rate. The calculations follow the method previously reported (6). Diffusion coefficients are given in Table I. Analysis is based on the uncorrected $^\circ P_w$* values since the correction is small (6).

For the test compounds used in the present report (*e.g.*, L-lysine-*p*-nitroanilide) it is assumed that hydrolysis at the wall provides the driving force for transport to the wall, with the released *p*-nitroanilide being taken up by the wall (1). The wall permeability is, consequently, a heterogeneous reaction rate constant. The general case has been discussed (1) and gives:

$$P_w = \alpha D \operatorname{Tanh}(\alpha\delta_E) \qquad \text{(Eq. 3)}$$

or

$$P_w^* = \alpha R \operatorname{Tanh}(\alpha\delta_e) \qquad \text{(Eq. 4)}$$

where

$$\alpha^2 = k/D \qquad \text{(Eq. 5)}$$

where k is the first-order reaction rate constant, and δ_E is the (unknown) thickness of the enzyme layer. Two special cases of Eq. 4 are:

High reactivity ($\alpha\delta_e > 1$):

$$P_w^* = \alpha R \qquad \text{(Eq. 6)}$$

Table I—Diffusion Coefficients

Compound	D, × 10^6, cm^2/sec
Lysine-*p*-nitroanilide	6.7
Alanine-*p*-nitroanilide	7.0
Glycine-*p*-nitroanilide	7.4

Low reactivity ($\alpha\delta_E < 1$):

$$P_w^* = \alpha^2\delta_E \qquad \text{(Eq. 7)}$$

Assuming Michaelis-Menten kinetics at the wall and limiting substrate concentration to the first-order region, the first-order reaction rate constant (k) (Eq. 5) becomes:

$$k = V_{max}/K_m \qquad \text{(Eq. 8)}$$

where V_{max} (moles/liter/second) is the maximal velocity and K_m (moles/liter) is the Michaelis constant. In the presence of a competitive inhibitor[2] (*e.g.*, lysine-*p*-nitroanilide in the presence of lysine methyl ester) Eq. 8 becomes:

$$k = V_{max}/\left(1 + \frac{I}{K_I}\right)K_m \qquad \text{(Eq. 9)}$$

where I is the inhibitor concentration (in the enzyme layer) and K_I the inhibition constant. Combining Eqs. 5, 6, 7, and 9 gives:

High reactivity case:

$$P_w^{*2} = (V_m R^2/DK_m)[1/(1 + I/K_I)] \qquad \text{(Eq. 10)}$$

Low reactivity case:

$$P_w^* = (V_m \delta_E/DK_m)[1/(1 + I/K_I)] \qquad \text{(Eq. 11)}$$

Both Eqs. 10 and 11 can be linearized, but this aspect is not explored in this report. The main point of Eqs. 10 and 11 is that P_w^* is reduced in the presence of a competitive inhibitor. This investigation uses as substrates the *p*-nitroanilide derivatives and the remaining compounds as competitive inhibitors.

Rough estimates of the inhibition constants (K_I) can be made on the basis of this model. From Eqs. 6–11 the following relationships can be obtained:

High reactivity:

$$K_I = I/\{[P_w^*(S)/P_w^*(I)]^2 - 1\} \qquad \text{(Eq. 12)}$$

Low reactivity:

$$K_I = I/\{[P_w^*(S)/P_w^*(I)] - 1\} \qquad \text{(Eq. 13)}$$

where $P_w^*(S)$ is the (dimensionless) substrate permeability and $P_w^*(I)$ is the substrate permeability in the presence of the inhibitor. The inhibitor concentration, $[I]$, would be the concentration in the enzyme layer which is unknown. However, using as $[I]$ its value in the profusing solution allows the calculation of an apparent K_I.

RESULTS AND DISCUSSION

The experimental C_m/C_o ratios and Graetz numbers (Gz), along with the calculated dimensionless wall permeabilities ($^\circ P_w^*$), are presented in Tables II–XIV. Figure 1 presents a summary of the results.

Figure 2 is a graph of the data in Table II where the lysine-*p*-nitroanilide permeability was studied as a function of concentration. The results do not provide any evidence of saturation. While saturation would be expected at some point, it apparently would require concentrations above the 0.8 mM used in these studies. All subsequent studies were done using a lysine-*p*-nitroanilide concentration of 4×10^{-5} M. At this concentration the enzymatic reaction at the wall is in the apparent first-order region, and the analysis in the theoretical section would apply.

The results for the L-lysine-*p*-nitroanilide permeability in the presence of the competitive inhibitors L-lysine, L-lysine methyl ester, N_α-acetyl-L-lysine methyl ester, and arginine-β-naphthylamide are given in Tables IV–VII and Fig. 1. L-Lysine and N_α-acetyl-L-lysine methyl ester did not reduce the L-lysine-*p*-nitroanilide permeability at concentrations of 4×10^{-4} M. L-Lysine methyl ester and arginine-β-naphthylamide did significantly (t test) reduce the L-lysine permeability. These results are consistent with the hydrolysis site being an enzyme of the aminopeptidase type, *i.e.*, requiring a free α-amino group. The fact that L-lysine itself is not a good competitive inhibitor is probably related to the fact that it is the product of the enzymatic reaction. The surface enzyme responsible for hydrolysis apparently does not show significant product inhibition[3].

[2] Compounds used are actually competitive substrates, but since the assay is specific for only one of the substrates, the other acts as a competitive inhibitor (7).

Table II—L-Lysine-*p*-nitroanilide Dimensionless Wall Permeability *versus* Concentration

Concentration, × 10^5 M	$[C_m/C_o]$	Gz, × 10^2		$^\circ P_w^*$[a]	log C_o
4	0.84	1.97		5.4	
4	0.91	1.64		2.2	
4	0.75	1.64		∞	
4	0.78	2.63		8.4	−4.4
4	0.93	1.31		1.9	
4	0.90	1.23		3.9	
			$\overline{^\circ P_w^*}$	4.4 (1.2)	
8	0.87	1.074		12.2	
8	0.88	1.40		4.6	−4.1
			$\overline{^\circ P_w^*}$	6.5 (3.7)	
40	0.81	2.0		8.2	
40	0.82	2.0		7.4	−3.4
40	0.85	2.0		4.5	
			$\overline{^\circ P_w^*}$	6.7 (1.1)	
80	0.85	2.0		4.3	−3.1

[a] Values in parentheses are the standard error of the mean.

Table III—L-Lysine-*p*-nitroanilide [a] Dimensionless Wall Permeabilities

C_m/C_o	Gz, × 10^2		$^\circ P_w^*$
0.84	1.97		5.5
0.91	1.64		2.2
0.78	2.63		8.4
0.91	1.23		3.9
0.87	1.07		12.2
0.89	1.40		4.7
0.86	2.0		4.3
0.82	2.0		8.3
0.82	2.0		7.5
0.85	2.0		4.6
		$\overline{^\circ P_w^*}$	6.2
		SEM	0.9

[a] 4×10^{-5} M.

Table IV—L-Lysine-*p*-nitroanilide Dimensionless Wall Permeability *versus* L-Lysine Concentration

[L-Lysine-*p*-nitroanilide] × 10^5 M	[Lysine] × 10^3 M	$[C_m/C_o]$	Gz, × 10^2		$^\circ P_w^*$
8	5	0.83	1.074		131.0
40	5	0.61	2.0		∞
40	5	0.84	2.0		5.1
80	5	0.83	2.0		5.8
80	5	0.83	2.06		6.0
80	5	0.78	2.60		7.3
				$\overline{^\circ P_w^*}$	6.0
				SEM	0.5

Table V—L-Lysine-*p*-nitroanilide [a] Dimensionless Wall Permeability in the Presence of L-Arginine-β-naphthylamide [a]

C_m/C_o	Gz, × 10^2		$^\circ P_w^*$
0.93	1.81		1.34
0.92	1.32		2.45
0.90	1.23		4.41
0.95	1.32		1.4
		$\overline{^\circ P_w^*}$	2.4
		SEM	0.72

[a] 4×10^{-5} M.

[3] The proteolytic enzyme, trypsin, for example, does not show significant product inhibition. Apparently the carboxyl group generated by either amide or ester hydrolysis of the substrate and its subsequent ionization significantly reduces the binding constant for the product to the enzyme.

Table VI—L-Lysine-*p*-nitroanilide [a] Dimensionless Wall Permeabilities in the Presence of *N*-Acetyl-L-lysine-Methyl Ester [b]

C_m/C_o	$Gz, \times 10^2$		^oP_w*
0.86	1.55		6.1
0.92	1.23		8.3
0.86	1.32		9.9
0.88	1.32		6.7
0.82	1.73		11.9
0.82	1.89		10.5
		$\overline{^oP_w}$*	8.8
		SEM	0.9

[a] 4×10^{-5} *M*. [b] 4×10^{-4} *M*.

Table VII—L-Lysine-*p*-nitroanilide [a] Dimensionless Wall Permeability in the Presence of L-Lysine Methyl Ester [b]

C_m/C_o	$Gz, \times 10^2$		^oP_w*
0.91	1.32		3.1
0.91	1.32		2.9
0.96	1.40		1.0
0.87	1.73		4.2
0.94	1.32		1.8
0.94	1.20		1.9
0.88	1.81		3.5
0.87	1.89		4.0
		$\overline{^oP_w}$*	2.8
		SEM	0.4

[a] 4×10^{-5} *M*. [b] 4×10^{-4} *M*.

Table VIII—L-Alanine-*p*-nitroanilide Dimensionless Wall Permeabilities

C_m/C_o	$Gz, \times 10^{-2}$		^oP_w*
0.82	1.56		13.6
0.78	1.82		32.9
0.85	1.82		5.1
0.84	1.56		8.9
0.86	1.29		7.9
0.88	1.29		5.4
0.72	1.82		∞
0.88	0.963		11.5
0.87	0.963		14.3
0.87	1.34		7.2
		$\overline{^oP_w}$*	11.9
		SEM	2.8

[a] 4×10^{-5} *M*.

Table IX—L-Alanine-*p*-nitroanilide [a] Dimensionless Wall Permeabilities in the Presence of L-Alanine Methyl Ester [b]

C_m/C_o	$Gz, \times 10^{-2}$		^oP_w*
0.82	1.91		7.5
0.87	1.91		3.2
0.86	1.91		3.8
0.81	1.91		9.5
0.91	1.27		3.2
0.95	1.27		1.3
0.96	1.27		0.97
0.94	1.37		1.2
		$\overline{^oP_w}$*	3.9
		SEM	1.1

[a] 4×10^{-5} *M*. [b] 4×10^{-3} *M*.

The results for the L-alanine-*p*-nitroanilide permeability in the presence of L-alanine methyl ester and β-alanine methyl ester (Tables VIII–X) are also consistent with the hydrolysis site being an enzyme of the aminopeptidase class. The β-alanine methyl ester, with the primary amino group on the β-carbon rather than the α-carbon, is not a good competitive inhibitor. This is consistent with structural specificity of an aminopeptidase enzyme.

The results for N_α-benzoyl-arginine-*p*-nitroanilide and N_α-succinyl-phenylalanine-*p*-nitroanilide, (Tables XI and XII) provide direct evidence for the importance of a free α-amino group. Both compounds are poorly absorbed as evidenced by their very low permeabilities. The

Table X—L-Alanine-*p*-nitroanilide [a] Dimensionless Wall Permeabilities in the Presence of β-Alanine Methyl Ester [b]

C_m/C_o	$Gz, \times 10^{-2}$		^oP_w*
0.843	1.24		19.6
0.843	1.55		9.4
0.848	1.82		5.8
0.810	1.56		27.1
0.853	1.56		7.5
0.789	1.38		∞
0.881	1.34		5.6
0.827	1.38		23.1
0.843	1.55		9.4
		$\overline{^oP_w}$*	13.5
		SEM	3.0

[a] 4×10^{-5} *M*. [b] 4×10^{-3} *M*.

Table XI—*N*-α-Benzoyl-arginine-*p*-nitroanilide [a] Dimensionless Wall Permeabilities

C_m/C_o	$Gz, \times 10^{-2}$		^oP_w*
0.963	1.48		0.8
1.06	1.32		0.0
1.03	2.64		0.0
0.913	1.92		1.8
0.982	3.85		0.1
0.955	1.58		0.9
1.035	1.23		0.0
1.082	1.23		0.0
0.978	1.15		0.6
0.969	1.15		0.8
		$\overline{^oP_w}$*	0.5
		SEM	0.2

[a] 4×10^{-5} *M*.

Table XII—Succinyl-L-phenylalanine-*p*-nitroanilide [a] Dimensionless Wall Permeabilities

C_m/C_o	$Gz, \times 10^{-2}$		^oP_w*
1.000	1.24		0.0
1.11	1.27		0.0
1.04	2.55		0.0
0.969	1.41		0.7
0.954	2.82		0.5
0.892	7.07		0.5
1.003	1.65		0.0
0.993	1.65		0.1
1.103	1.68		0.0
1.131	1.29		0.0
1.021	1.20		0.0
1.004	1.20		0.0
		$\overline{^oP_w}$*	0.1
		SEM	0.04

[a] 4×10^{-5} *M*.

Table XIII—Glycine-*p*-nitroanilide [a] Dimensionless Wall Permeability

C_m/C_o	$Gz, \times 10^2$		^oP_w*
0.78	2.19		13.7
0.87	1.82		3.7
0.76	2.92		8.6
0.90	2.10		1.9
0.85	1.91		4.8
0.87	1.64		4.3
0.89	1.55		3.61
0.77	1.55		∞
0.83	1.55		12.0
0.95	1.27		1.32
0.88	1.27		5.4
0.88	1.64		3.54
0.86	1.8		4.01
		$\overline{^oP_w}$*	5.6
		SEM	1.1

[a] 4×10^{-5} *M*.

Table XIV—Glycine-*p*-nitroanilide [a] Dimensionless Wall Permeability in the Presence of Glycine Methyl Ester [b]

C_m/C_o	$Gz, \times 10^2$		$°P_w*$
0.84	1.92		6.4
0.88	1.55		4.6
0.91	1.55		2.5
0.88	1.55		4.5
0.88	1.28		6.6
0.91	1.28		3.1
0.87	1.74		4.1
0.87	1.74		4.5
0.86	1.83		5.1
0.90	1.65		2.9
		$\overline{°P_w*}$	4.4
		SEM	0.4

[a] 4×10^{-5} *M*. [b] 4×10^{-3} *M*.

fact that L-arginine-β-naphthylamide is a good competitive inhibitor for L-lysine-*p*-nitroanilide, while the N_α-benzoyl-arginine-*p*-nitroanilide is not absorbed well at all, further illustrates the importance of a free α-amino group. In addition, the low permeabilities for N_α-benzoyl-arginine-*p*-nitroanilide and N_α-succinyl-phenylalanine-*p*-nitroanilide suggest that passive absorption for both compounds is very small. This is expected since both compounds are ionized at pH 7.4. It further suggests that passive permeation of the other compounds studied is not significant, providing further evidence (in addition to the observed competition) that the absorption mechanism is through membrane hydrolysis (1).

The results for glycine-*p*-nitroanilide and glycine methyl ester (Tables XIII and XIV) do not fit with the above results. That is, it would be expected that glycine methyl ester would be a competitive inhibitor for glycine-*p*-nitroanilide. This suggests that glycine derivatives may be absorbed by a different mechanism (*e.g.*, passive diffusion) or that the enzyme binding constants for the glycine derivative are small. Peptide absorption studies on glycine peptides (*e.g.*, Gly-Gly) indicate that the peptide is taken up intact and is not a good substrate for the brush border peptidases (3, 8). Studies with peptide transport inhibitors need to be

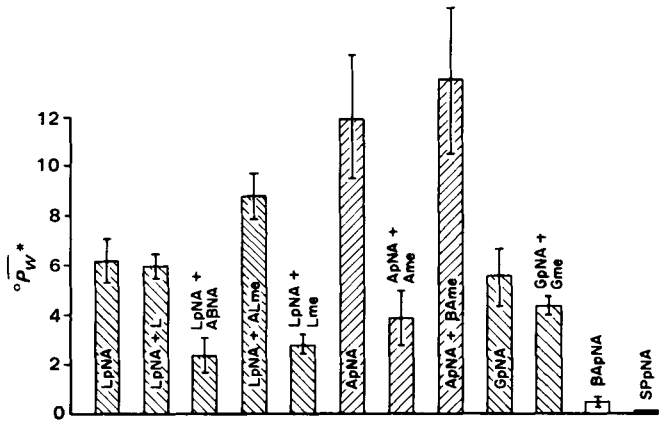

Figure 1—*Summary of intestinal wall permeability ($°P_w*$) results. Key: (LpNA) L-lysine-p-nitroanilide; (L) L-lysine; (Lme) L-lysine methyl ester; (AβNA) L-arginine-β-naphthylamide; (ALme) N-acetyl-L-lysine methyl ester; (ApNA) L-alanine-p-nitroanilide; (Ame) L-alanine methyl ester; (βAme) β-alanine methyl ester; (GpNA) glycine-p-nitroanilide; (Gme) glycine methyl ester; (βApNA) N_α-benzoyl-arginine-p-nitroanilide; (SPpNA) N_α-succinyl-phenylalanine-p-nitroanilide.*

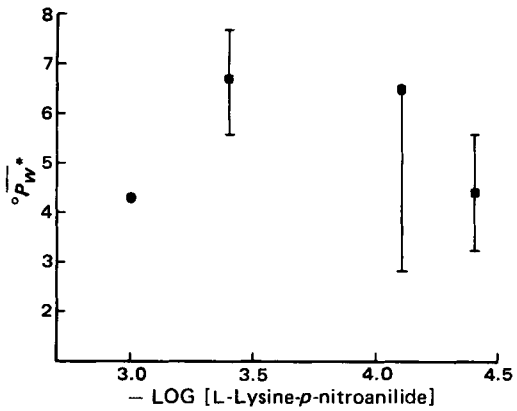

Figure 2—*Wall permeability of L-lysine-p-nitroanilide as a function of concentration in the perfusing solution.*

done to further establish the absorption mechanism for glycine-*p*-nitroanilide.

Using Eqs. XII and XIII, rough estimates of a k_I value can be made where significant inhibition is observed. For L-arginine-β-naphthylamide and L-lysine methyl ester respective values of 0.7×10^{-4} and 1.0×10^{-4} *M* are obtained for the high reactivity case, while respective values of 2.5×10^{-4} and 3.3×10^{-4} *M* are obtained for the low reactivity case. The values for L-alanine methyl ester are 0.6×10^{-4} and 2.2×10^{-4} *M* for the high and low reactivity cases, respectively. Since the inhibitor concentration in the enzyme layer is certainly lower than that in the perfusing solutions, these values would represent upper limits on the estimate.

Studies on the intestinal absorption of *p*-nitroanilide derivatives of the amino acids, L-lysine and L-alanine, in the presence of various competitive inhibitors have shown that only those compounds with a free α-amino group are good competitive inhibitors, *i.e.*, reduce the wall permeability, $°P_w*$. This suggests a free α-amino group is essential for good brush border peptidase activity. The fact that N_α-benzoyl-arginine-*p*-nitroanilide and N_α-succinyl-phenylalanine-*p*-nitroanilide are poorly absorbed is also consistent with this inference.

REFERENCES

(1) G. L. Amidon, G. D. Leesman, and R. L. Elliott, *J. Pharm. Sci.*, **69,** 1363 (1980).

(2) F. Wojnarowska and G. M. Gray, *Biochim. Biophys. Acta*, **403,** 147 (1975).

(3) E. M. Rosen-Levin, K. W. Smithson, and G. M. Gray, *ibid.*, **629,** 126 (1980).

(4) G. M. Gray and N. A. Santiago, *J. Biol. Chem.*, **252,** 4922 (1977).

(5) G. L. Amidon, J. Kou, R. L. Elliott, and E. N. Lightfoot, *J. Pharm. Sci.*, **69,** 1369 (1980).

(6) R. L. Elliott, G. L. Amidon, and E. N. Lightfoot, *J. Theor. Biol.*, **87,** 757 (1980).

(7) I. H. Segel, "Enzyme Kinetics," Wiley-Interscience, New York, N.Y., 1975, p. 113.

(8) D. M. Matthews and J. W. Payne, *Curr. Top. Memb. Transp.*, **14,** 331 (1980).

ACKNOWLEDGMENTS

This work was supported by Grant GM 27680 from the Public Health Service.

The authors thank Mr. H. Lee for his assistance.

Determination of Sulfadiazine and N^4-Acetylsulfadiazine in Biological Fluids by Liquid Chromatography on Silica Gel with an Aqueous Buffer as Mobile Phase

DOUGLAS WESTERLUND ˣ **and AGNETA WIJKSTRÖM**

Received June 8, 1981, from the *Astra Läkemedel AB, Research and Development Laboratories Analytical Chemistry, S-151 85 Södertälje, Sweden.* Accepted for publication December 15, 1981.

Abstract □ Sulfadiazine and N^4-acetylsulfadiazine were determined in biological fluids by the direct injection (plasma after protein precipitation and urine after dilution 100 times) of 20 μl on a silica gel column. The mobile phase was an aqueous citrate buffer (pH 4.0) and UV detection was at 264 nm. Chromatographic selectivity was optimized by the silica gel surface and pH of the mobile phase. Detection limits were ~0.4 μg/ml for sulfadiazine in plasma and ~5 and 7 μg/ml for sulfadiazine and N^4-acetylsulfadiazine in urine, respectively. In quantitations by peak heights relative to an internal standard (sulfamerazine), within-run precisions ($s_{rel\%}$) for sulfadiazine were 1.7 and 4.0% at 40 and 2 μg/ml, respectively, in plasma and 0.76 and 1.7% at 750 and 25 μg/ml, respectively, in urine.

Keyphrases □ Sulfadiazine—N^4-acetylsulfadiazine, determination in biological fluids by liquid chromatography □ Biological fluids—determination of sulfadiazine and N^4-acetylsulfadiazine by liquid chromatography □ Liquid chromatography—determination of sulfadiazine and N^4-acetylsulfadiazine in biological fluids

It has been demonstrated recently that the antibacterial (1) and pharmacokinetic (2–4) properties of sulfadiazine indicate that it is a suitable sulfonamide for combination with trimethoprim in order to utilize optimally the synergistic antibacterial effect that is exerted by such a composition.

Sulfonamides have been determined by tradition in biological material by the colorimetric Bratton–Marshall technique (5) or modifications that partly overcome its lack of specificity. The most important of these was developed by Rieder (6). Recently, the Bratton–Marshall reaction has been automated for determination of sulfisoxazole and sulfamethoxazole in biological fluids (7). Sulfasalazine could be determined in biological samples by direct spectrophotometric measurement at 455 nm (8). Sulfamethoxazole has been determined in serum by spectrofluorometry after extraction with *n*-butyl chloride (9). There have also been published methods in which gas chromatography with both flame ionization (10) and electron capture detection (11), thin-layer chromatography with spectrophotometric scanning (12, 13), and spectrofluorimetric scanning after derivatization with fluorescamine (14), have been used.

Most new methods have utilized HPLC as the separation tool, either after a preliminary extraction (15–17), or by the direct injection of the biological fluid after a preliminary precipitation of proteins and/or dilution (18–24). Nonpolar bonded phases have been used mainly as the support, but underivatized silica gel (15), amino-bonded (18) and cyano-bonded (20) reversed-phase materials have also been utilized. Thus far, no method has been published for determination of sulfadiazine and its main metabolite, N^4-acetylsulfadiazine, in biological material by HPLC. To study in detail the pharmacokinetics of sulfadiazine, the desired limit of determination should be ~1 μg/ml for plasma and ~10 μg/ml in urine.

The present method relies on the direct injection of biological fluid: either plasma after precipitation of proteins or urine after dilution onto the chromatographic column. The support was silica gel with a large specific surface area, and the chromatogram was developed with an aqueous buffer as the mobile phase. The UV absorbance was recorded at 264 nm.

EXPERIMENTAL

Apparatus—The chemicals were weighed on analytical[1] or microanalytical[2] balances. Samples were vortexed[3], and precipitated proteins and tissue were removed by centrifugation[4] at 1000×*g*. The pH was measured[5] when necessary. For column packing a constant pressure gas amplifier pump[6] was used connected to a 30-ml reservoir[7].

The liquid chromatograph consisted of a reciprocating piston pump[8], an injection valve[9] equipped with a 20-μl loop, and a variable wavelength UV detector[10,11] monitored at 264 nm by a recorder[12].

Chemicals—Sulfadiazine[13], N^4-acetylsulfadiazine[13] and sulfamerazine[13] were from approved batches. The buffer substances, citric acid[14], phosphoric acid[14], sodium dihydrogen phosphate[14], and sodium hydroxide[15], were of analytical quality. From stock solutions of the sulfonamides (0.5 mg/ml in 0.01 *M* NaOH), suitable dilutions were made with deionized and doubly distilled water, which also was used for preparation of the chromatographic mobile phases.

Chromatographic Technique—A spherical silica gel[16] with a mean particle diameter of 5 μm and a specific surface area of 500 m^2/g was packed into a precision bore stainless steel column[17] (150 × 4.0 mm) by an upwards slurry packing technique (25). The slurry (1.5-g support in 25 ml of methyl isobutyl ketone[18]) was sonicated[19] for 5 min and forced into the column by methylene chloride at 400 bars. After packing, the column was washed with methanol and water (100 ml each), and the mobile phase was deaerated by vacuum. Equilibrium was obtained after the passage of ~25 ml of mobile phase at a flow rate of 0.85 ml/min. The column void volume (~1.3 ml) was determined by the injection of potassium nitrate.

Sample Preparation—*Plasma*—A 0.5-ml sample of plasma containing sulfadiazine and 125 μl of sulfamerazine (internal standard) solution (1.0 μg/μl) were acidified by the addition of 25 μl of hydrochloric acid. The proteins were precipitated by the addition of 1 ml of 45% ammonium sulfate solution, mixing, and keeping at room temperature for 0.5 hr. After centrifugation at 1000×*g* for 10 min, the clear supernatant was transferred by a Pasteur pipet, equipped with a piece of cotton at the

[1] Analytical balance HL 52, Mettler Instrumente AG, Greifensee, Switzerland.
[2] Microbalance M5 SA, Mettler Instrumente AG, Greifensee, Switzerland.
[3] Fisons Whirlimixer, Fisons Scientific Apparatus, Loughborough, U.K.
[4] FP 10 Centrifuge, Labsystems Oy, Helsinki, Finland.
[5] pH-Meter 26, Radiometer, Copenhagen, Denmark.
[6] Haskel AO 15, Haskel Engineering & Supply Co., Burbank, Calif.
[7] Specac packing bomb, Anal. Accessories Ltd., Orpington, Kent, U.K.
[8] Model 711-47, Laboratory Data Control, Riviera Beach, Fla.
[9] Rheodyne Model 7120, Rheodyne Inc., Berkeley, Calif.
[10] Cecil CE 212, Cecil Instruments Ltd., Cambridge, U.K.
[11] Spectromonitor III, Laboratory Data Control, Riviera Beach, Fla.
[12] Tekman TE 200, Tekman Electronics Ltd., Bicester, U.K.
[13] Department of Organic Chemistry, Astra Läkemedel AB, Södertälje, Sweden.
[14] Merck, Darmstadt, West Germany.
[15] EKA, Bohus, Sweden.
[16] Nucleosil 50-5, Macherey-Nagel & Co, Düren, West Germany.
[17] Handy & Harman, USA.
[18] Fisher Scientific Co., N.J.
[19] Bransonic 220, Branson, Heusenstamm, West Germany.

0022-3549/82/01000-1142$01.00/0

tip, to another tube, and 20 μl of the filtrate was injected onto the column. A standard curve (2–40 μg/ml) was obtained by treating 0.5 ml of pooled plasma, 100 μl of sulfadiazine standard solution (0.01–0.20 μg/μl), and 25 μl of sulfamerazine solution (0.5 μg/μl) in the same way as the samples.

Urine—Urine (containing sulfadiazine) (0.5 ml) and 200 μl of sulfamerazine solution (0.5 μg/μl) were diluted to 50.0 ml with water, and 20 μl was injected onto the column after careful mixing. A standard curve (25–750 μg/ml) was obtained by adding 25–750 μl of sulfadiazine and N^4-acetylsulfadiazine solutions (0.5 μg/μl) to 0.5 ml of pooled urine portions, which were treated equivalently to the samples.

Chromatography—Plasma and urine samples were run with the same mobile phase, citric acid buffer (pH 4.0; ionic strength = 0.1; 70 ml of 1 *M* citric acid–83 ml of 1 *M* NaOH were diluted to 1000 ml with water). The flow rate was 0.8–0.9 ml/min and the UV absorbance was recorded at 264 nm. After continuous running the chromatographic performance slowly changed (decreasing capacity ratios and efficiencies), probably because of the adsorption of endogenous compounds onto the support. For column maintenance after each working day, the column was washed first with water (50 ml), then overnight with methanol at a low flow rate (0.1 ml/min), and again just before use with 50 ml of water. By treating in this way, a column could be used for routine analysis (300 plasma or urine samples per week) giving reproducible results for several months.

RESULTS AND DISCUSSION

Chromatography—Sulfadiazine is an amphoteric polar compound which is difficult to extract quantitatively into an organic phase. It is possible to achieve such an extraction, but this necessitates the use of a strongly polar organic medium and/or the addition of ion-pairing counter ions. As a consequence, the obtained extract will contain many coextracted endogenous compounds that may disturb the chromatogram when nonselective UV detection is used. Under such circumstances the introduction of an extraction step only means an unnecessary and roundabout way and time loss in the analytical method. The method was developed to avoid extractions and design the necessary selectivity within the chromatographic system to allow for the direct injection of biological fluids. Preliminary experience with a conventional reversed-phase system (LiChrosorb RP-8 with an acidic methanolic mobile phase) showed significant chromatographic interferences that were hard to control, especially within the retention times for N^4-acetylsulfadiazine.

Underivatized silica gel has been used successfully with aqueous mobile phases for forensic purposes (26, 27) for the determination of the new antidepressant, zimelidine (28), and in studies on ion-pair retention mechanisms (29). A system of this kind was tried for the sulfonamides. It was found at an early stage during the method development that the addition of even small amounts (2%) of organic modifier (*e.g.*, methanol) to the aqueous mobile phase causes the compounds to elute with the front, so neat aqueous buffer solutions had to be used for optimization of the chromatographic system. The actual sulfonamides are only slightly retained by the support in systems of this kind, and it is important to use supports with the largest possible effective surface area. The capacity ratios of sulfadiazine, N^4-acetylsulfadiazine, and sulfamerazine were nearly linearly related to the nominal specific surface area of three different commercial supports (Fig. 1); a citrate buffer (pH 4) was used as the mobile phase in all cases. The pore diameter of the supports decrease with increasing surface area, and this may account for the retentions obtained for the support with the largest area, since all the area may not be available to the comparatively large eluates in this case.

The chromatographic performance of the 800-m^2/g support was, however, not acceptable, giving low efficiency and tailing peaks. Furthermore, it gave coincident retention times for sulfadiazine and sulfamethoxazole, as well as for their N^4-acetylated metabolites. Therefore, the 500-m^2/g support was utilized for further studies.

There is not a marked dependence of the retention on pH (Fig. 2). The capacity ratios are generally somewhat larger at higher pH, but a retention reversal between sulfamerazine and N^4-acetylsulfadiazine occurs with an acidic mobile phase. Crommen (29) has shown that in this kind of chromatography the support seems to work as the more unpolar phase relative to the aqueous mobile phase, and demonstrated that the addition of counterions gave an ion-pair effect similar to that obtained in conventional reversed-phase liquid chromatography. It was found that a large hydrophobic counterion (tetrahexylammonium) was required to give an ion-pair effect in this system. At pH 6.5 the capacity ratios increased about three times in the presence of this counterion, but the time needed for column stabilization was long (~15 hr). Later experience also showed

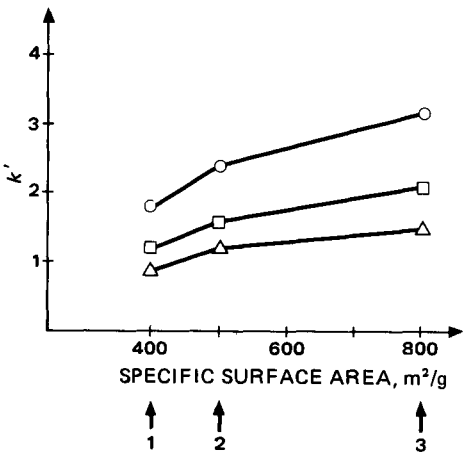

Figure 1—*The dependence of capacity ratios on the support surface area. Mobile phase: citrate buffer (pH 4, μm = 0.1) Column packings: (1) Partisil 5; (2) Nucleosil 50-5;(3) Spherosil XOA-800. Key: (○) sulfamerazine; (□) N^4-acetylsulfadiazine; (△) sulfadiazine.*

that in blank chromatograms from body fluids, endogenous compounds, whose retention times also were influenced by the hydrophobic counterion, interfered with the sulfonamides.

The chromatographic efficiency is typically in the range of 35–45 μm (HETP), while the asymmetry factor (back/front at 10% of peak height) normally is in the range of 1.3–1.8.

The selectivity against trimethoprim is high for all three sulfonamides (α = 2.2) at pH 4 which is used in the bioanalysis, but with this mobile phase it is not as satisfactory relative to other sulfonamides. N^4-Acetylsulfadiazine almost coelutes with sulfamethoxazole (α = 1.07) and N^4-acetylsulfamethoxazole interferes with sulfamerazine (α = 1.05). Changing the pH of the mobile phase, however, will also change the selectivity, since the retentions in this system are dependent on the pKa values of the compounds.

Analysis in Biological Material—The only useful parameter remaining for optimization of the mobile phase for bioanalytical work is pH. The result of such a procedure for urine is demonstrated in Fig. 2. Sulfadiazine is severely interfered with by endogenous compounds at most pH values, but at pH 4 all three actual eluates are resolved from the main interfering compounds. An equivalent optimization for plasma determinations resulted in the same mobile phase pH as for urine. Unfortunately, however, endogenous compounds severely disturbed the N^4-acetylsulfadiazine peak and prevented quantitative determination in plasma by the present method at the very low concentrations of this

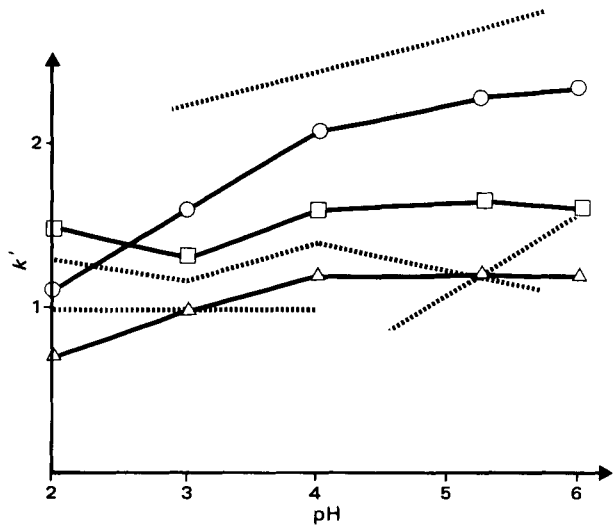

Figure 2—*Optimization of mobile phase pH for urine determinations. Mobile phase: pH ≥4 citrate buffer (μm = 0.1); pH <4 phosphate buffer (μm = 0.1). Key: (△) sulfadiazine; (□) N^4-acetylsulfadiazine; (○) sulfamerazine (internal standard); (·····) endogenous peaks.*

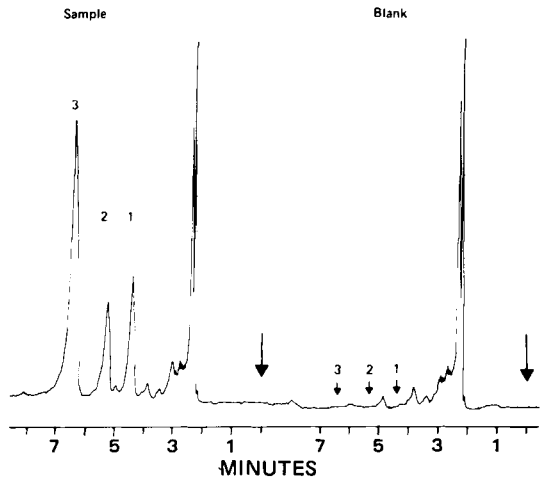

Figure 3—*Chromatograms for determinations in urine (column: 200 × 3.8 mm). Spiked with: (1) sulfadiazine (100 μg/ml); (2) N^4-acetylsulfadiazine (100 mg/ml); (3) sulfamerazine (400 μg/ml). See text for experimental details.*

compound that normally are encountered in most volunteers and patients. Representative chromatograms from spiked urine and plasma samples are shown in Figs. 3 and 4, respectively.

For plasma determinations, the proteins are precipitated by the addition of ammonium sulfate followed by acidification; this procedure was found to give reasonably clean blank chromatograms and acceptable recoveries. The addition of acetonitrile or methanol for this purpose is not possible, since the chromatographic performance (decreased retention times, the appearance of double peaks, *etc.*) is affected by the presence of an organic solvent in the injected sample. A comparison of peak heights of sulfadiazine (1–15 μg/ml) obtained from plasma samples after protein precipitation by the adopted method and from pure buffer samples, respectively, indicated that the absolute recovery from pooled plasma samples is ~76%. A similar comparison of peak height ratios of sulfadiazine and sulfamerazine, the internal standard, gave congruent standard curves (1–15 μg/ml) from pure mobile phase and plasma, respectively, showing that the recovery of sulfamerazine from plasma is of the same magnitude as for sulfadiazine.

The concentrations of sulfadiazine and N^4-acetylsulfadiazine in human urine are high after the recommended dose (0.82 g × 1 or × 2), even after

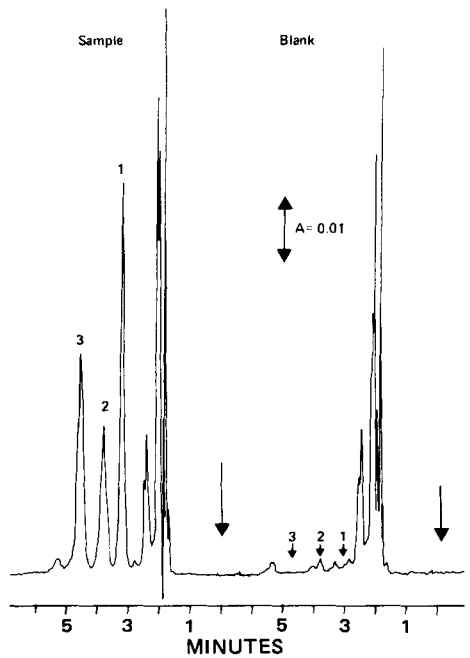

Figure 4—*Chromatograms for determinations in plasma. Spiked with: (1) sulfadiazine (25 μg/ml) in plasma; (2) N^4-acetylsulfadiazine (15 μg/ml) in plasma; (3) sulfamerazine (20 μg/ml) in plasma. See text for experimental details.*

Table I—Studies on Quantitative Determinations and Within-Run Precisions

	Added μg/ml of Plasma	$s_{rel\%}$	Mode[a]
Plasma[b]			
Sulfadiazine	40	1.68	IS
	40	2.85	NIS
Sulfadiazine	2	3.97[c]	IS
	2	3.74	NIS
Urine[d]			
Sulfadiazine	750	0.76	IS
	750	2.12	NIS
N^4-Acetylsulfadiazine	750	0.69	IS
	750	1.73	NIS
Sulfadiazine	25	1.67	IS
	25	3.42	NIS
N^4-Acetylsulfadiazine	25	2.46	IS
	25	4.16	NIS

[a] IS, with internal standard; NIS, without internal standard. [b] Internal standard: 25 μg of sulfamerazine/ml of plasma (n = 10). [c] Change of detector sensitivity during the run. [d] Internal standard: sulfamerazine 500 μg/ml and 200 μg/ml, respectively (n = 8).

a single dose, so that a simple dilution of the urine 100 times and the injection of 20 μl of the resultant solution is an adequate procedure for quantitative determinations. The limits of detection for sulfadiazine and N^4-acetylsulfadiazine are ~5 and 7 μg/ml, respectively, under these conditions, corresponding to the injection of 1–1.4 ng of the compounds. It was observed, however, that the selectivity of the chromatographic system may differ between different batches of the support. In some cases the N^4-acetylsulfadiazine peak was interfered with by endogenous compounds also in the urine determinations. In plasma determinations the detection limit for sulfadiazine is ~0.4 μg/ml, *i.e.*, an injected amount of 2.4 ng.

For characterization of the methods, some repeatability studies were performed where the results were calculated in two ways on the same sample: by peak height measurements of sulfadiazine (*i.e.*, no internal standard involved in the calculations) and by peak height ratio calculations (Table I). In accordance with some earlier studies (30, 31), the incorporation of an internal standard, structurally related to the compounds of interest, significantly improves the within-run precisions of the method, presumably by the compensation for the slight changes in chromatographic performance of the column that occur during a working day, and by the elimination of deviations due to small differences in volume between the samples.

REFERENCES

(1) B. Ekström, U. Forsgren, B. Örtengren, and T. Bergan, *Infection 7, Suppl.*, **4**, 359 (1979).

(2) T. Bergan, H. Vik-Mo, and U. Ånstad, *Clin. Pharmacol. Ther.*, **22**, 211 (1977).

(3) B. Örtengren, H. Fellner, and T. Bergan, *Infection*, *7, Suppl.*, **4**, 367 (1979).

(4) B. Örtengren, L. Magni, and T. Bergan, *ibid.*, **4**, 371 (1979).

(5) A. D. Bratton and E. V. Marshall, *J. Biol. Chem.*, **128**, 537 (1939).

(6) J. Rieder, *Chemotherapy*, **17**, 1 (1972).

(7) R. E. Weinfeld and T. L. Lee, *J. Pharm. Sci.*, **68**, 1387 (1979).

(8) M. Sandberg and K.-A. Hansson, *Acta Pharm. Suec.*, **10**, 107 (1973).

(9) D. M. Lichtenwalner, B. Suh, B. Lorber, and A. M. Sugar, *Antimicrob. Agents Chemother.*, **16**, 579 (1979).

(10) E. Röder and W. Stuthe, *Z. Anal. Chem.*, **271**, 281 (1974).

(11) O. Gyllenhaal, B. Näslund, and P. Hartvig, *J. Chromatogr.*, **156**, 330 (1978).

(12) B. Örtengren and L. R. Treiber, *Res. Commun. Chem. Pathol. Pharmacol.*, **9**, 339 (1974).

(13) C. W. Sigel, M. E. Grace, C. A. Nichol, and G. H. Hitchings, *J. Pharm. Sci.*, **63**, 1202 (1974).

(14) C. W. Sigel, J. L. Woolley, Jr., and C. A. Nichol, *ibid.*, **64**, 973 (1975).

(15) A. Bye and M. E. Brown, *J. Chromatogr. Sci.*, **15**, 365 (1977).

(16) K. Lanbeck and B. Lindström, *J. Chromatogr.*, **154**, 321 (1978).

(17) C. Fischer and U. Klotz, *ibid.*, **146**, 157 (1978).

(18) J. P. Sharma, E. G. Perkins, and R. F. Bevill, *J. Pharm. Sci.*, **65**, 1606 (1976).

(19) G. W. Peng, M. A. F. Gadalla, and W. L. Chiou, *Res. Commun. Chem. Pathol. Pharmacol.*, **18**, 233 (1977).
(20) J. Overbach, N. F. Johnson, T. R. Bates, H. J. Pieniaszek, Jr., and W. J. Jusko, *J. Pharm. Sci.*, **67**, 1250 (1978).
(21) K. Harzer, *J. Chromatogr.*, **155**, 399 (1978).
(22) T. B. Vree, Y. A. Hekster, A. M. Baars, J. E. Damsma and E. van der Kleijn, *J. Chromatogr.*, **146**, 103 (1978).
(23) R. W. Bury and M. L. Mashford, *ibid.*, **163**, 114 (1979).
(24) D. Jung and S. Øie, *Clin. Chem.*, **26**, 51 (1980).
(25) P. A. Bristow, P. N. Brittain, C. M. Riley, and B. F. Williamson, *J. Chromatogr.*, **131**, 57 (1977).
(26) I. Jane, *ibid.*, **111**, 227 (1975).
(27) B. B. Wheals, *ibid.*, **122**, 85 (1976).
(28) B. Emanuelsson and R. G. Moore, *ibid.*, **146**, 113 (1978).
(29) J. Crommen, in "Advances in Chromatography," A. Zlatkis, ed., 1979, p. 783.
(30) D. Westerlund, A. Theodorsen and Y. Jaksch, *J. Liq. Chromatogr.*, **2**, 969 (1979).
(31) D. Westerlund and E. Erixson, *J. Chromatogr.*, **185**, 593 (1979).

Binding of Selected Phenol Derivatives to Human Serum Proteins

JOSEPH JUDIS

Received March 10, 1981, from the *College of Pharmacy, The University of Toledo, Toledo, OH 43606.* Accepted for Publication December 17, 1981.

Abstract □ The binding of phenol and four of its derivatives to whole human serum and several human serum proteins was investigated. ^{14}C-labeled derivatives were utilized and binding was studied by either equilibrium or dynamic dialysis. Phenol itself was bound least to most of the serum proteins as compared to the derivatives and albumin, and whole human serum exhibited the highest percent binding of the proteins used. Percent binding to albumin and serum paralleled molecular weights of the derivatives, but no definite pattern was observed in ranking the percent binding of the other derivatives to the other serum proteins. Binding constants (K_1, K_2, n_1 and n_2) were determined from Scatchard plots for all the derivatives except *p*-chloro-*m*-xylenol. Phenol was found to have the highest association constant (K_1) and *p-tert*-amylphenol, the lowest. For the entire group of five derivatives and albumin as the protein, a direct, statistically significant correlation was found between percent binding and Hansch π values. No correlation could be found with Hammett σ values. It is concluded that binding of the phenol derivatives to albumin involves primarily hydrophobic bonds.

Keyphrases □ Binding—selected phenol derivatives, human serum proteins ■ Phenol—selected derivatives, binding, selected human serum proteins □ Serum—human, binding of selected phenol derivatives to proteins ■ Derivatives—phenol, selected, binding to human serum proteins

Since the discovery of phenol in 1834 and its introduction to antiseptic surgery by Lister in 1867 (1), both phenol and many of its derivatives have become firmly established as germicidal agents (2, 3). Phenol derivatives, unlike many other germicides, have been shown to be less active in the presence of organic matter (2–4). Blood is a common organic contaminant in materials to be sterilized. Preliminary investigations of the binding of phenol derivatives to human serum proteins were carried out as part of the work in this study on the mechanism of action of phenol derivatives (5, 6). These preliminary studies were expanded to include individual major human serum proteins, percent binding to each, and binding parameters for human serum albumin for a selected group of phenol derivatives.

EXPERIMENTAL

Materials—The phenol derivatives used were obtained with carbon-14 labels[1]. The compounds used and specific activities were as follows: [^{14}C]phenol, 1.57 mCi/mmole; [2,4-^{14}C]dichlorophenol, 0.68 mCi/mmole; [2,4,6-^{14}C]trichlorophenol, 0.68 mCi/mmole; [^{14}C]*p-tert*-amylphenol, 0.27 mCi/mmole; [^{14}C]*p*-chloro-*m*-xylenol, 0.0027 mCi/mmole. Phenol stock solutions were made in distilled water and those of the other derivatives were made with 0.1% NaOH as the solvent. Crystalline human serum albumin and the other human serum proteins were obtained commercially[2] and the whole human serum was of tissue culture quality[3]. All other chemicals used were of reagent grade.

Methods—Dialysis methods (equilibrium and dynamic) were carried out as previously described (7). Radioactivity was determined in a liquid scintillation system using techniques previously described (7, 8). Estimates of binding parameters were calculated using the method of Sandberg (8) and standard Scatchard techniques. All averages were based on a minimum of three replicates.

Table I—Binding of [^{14}C]Phenol and [^{14}C]-*p-tert*-Amylphenol to Human Serum Proteins [a]

Serum Proteins		Ligands Percent Bound[b]	
Fraction	Concentration[c], mg/ml	Phenol	*p-tert*-Amylphenol
Albumin	40.0	48.7 (0.68)	89.1 (0.74)
α Globulin IV-1	1.0	7.9 (0.47)	28.5 (1.92)
α Globulin IV-4	5.0	23.0 (0.63)	46.5 (1.60)
β Globulin III	7.0	3.13 (0.14)	35.2 (0.60)
γ-Globulin II	11.0	8.21 (0.63)	13.0 (0.69)
Human serum	—	52.7 (1.16)	95.3 (0.18)

[a] Each system contained a total of 1.00×10^{-7} mole of [^{14}C]phenol or 1.86×10^{-7} mole of [^{14}C]*p-tert*-amylphenol. [b] The values in parentheses are standard deviations. Data obtained using equilibrium dialysis method. [c] Concentrations used approximate those normally found in human serum.

RESULTS AND DISCUSSION

The values obtained for percent binding to whole human serum and the several serum proteins for the five derivatives studied are listed in Tables I and II. Weakest binding was found with phenol and the latter was bound primarily to albumin. Although phenol was bound to the other serum proteins, the extent was <10% except for α-globulin IV-4. The addition of alkyl groups or halogens to the phenol molecule has been found to increase the latter's germicidal activity (9). It would appear from the results in Tables I and II that alkylation and/or halogenation of phenol also increases the latter's binding affinity for serum proteins. The addition of a tertiary amyl group to phenol increased percent binding of phenol almost twofold (Table I) for albumin and whole human serum and

[1] New England Nuclear Corp.

[2] Nutritional Biochemicals Division of ICN Life Sciences Group.
[3] Difco Laboratories (desiccated TC human serum).

0022-3549/82/01000-1145$01.00/0

(19) G. W. Peng, M. A. F. Gadalla, and W. L. Chiou, *Res. Commun. Chem. Pathol. Pharmacol.*, **18**, 233 (1977).
(20) J. Overbach, N. F. Johnson, T. R. Bates, H. J. Pieniaszek, Jr., and W. J. Jusko, *J. Pharm. Sci.*, **67**, 1250 (1978).
(21) K. Harzer, *J. Chromatogr.*, **155**, 399 (1978).
(22) T. B. Vree, Y. A. Hekster, A. M. Baars, J. E. Damsma and E. van der Kleijn, *J. Chromatogr.*, **146**, 103 (1978).
(23) R. W. Bury and M. L. Mashford, *ibid.*, **163**, 114 (1979).
(24) D. Jung and S. Øie, *Clin. Chem.*, **26**, 51 (1980).
(25) P. A. Bristow, P. N. Brittain, C. M. Riley, and B. F. Williamson, *J. Chromatogr.*, **131**, 57 (1977).
(26) I. Jane, *ibid.*, **111**, 227 (1975).
(27) B. B. Wheals, *ibid.*, **122**, 85 (1976).
(28) B. Emanuelsson and R. G. Moore, *ibid.*, **146**, 113 (1978).
(29) J. Crommen, in "Advances in Chromatography," A. Zlatkis, ed., 1979, p. 783.
(30) D. Westerlund, A. Theodorsen and Y. Jaksch, *J. Liq. Chromatogr.*, **2**, 969 (1979).
(31) D. Westerlund and E. Erixson, *J. Chromatogr.*, **185**, 593 (1979).

Binding of Selected Phenol Derivatives to Human Serum Proteins

JOSEPH JUDIS

Received March 10, 1981, from the *College of Pharmacy, The University of Toledo, Toledo, OH 43606.* Accepted for Publication December 17, 1981.

Abstract □ The binding of phenol and four of its derivatives to whole human serum and several human serum proteins was investigated. ^{14}C-labeled derivatives were utilized and binding was studied by either equilibrium or dynamic dialysis. Phenol itself was bound least to most of the serum proteins as compared to the derivatives and albumin, and whole human serum exhibited the highest percent binding of the proteins used. Percent binding to albumin and serum paralleled molecular weights of the derivatives, but no definite pattern was observed in ranking the percent binding of the other derivatives to the other serum proteins. Binding constants (K_1, K_2, n_1 and n_2) were determined from Scatchard plots for all the derivatives except *p*-chloro-*m*-xylenol. Phenol was found to have the highest association constant (K_1) and *p-tert*-amylphenol, the lowest. For the entire group of five derivatives and albumin as the protein, a direct, statistically significant correlation was found between percent binding and Hansch π values. No correlation could be found with Hammett σ values. It is concluded that binding of the phenol derivatives to albumin involves primarily hydrophobic bonds.

Keyphrases □ Binding—selected phenol derivatives, human serum proteins ■ Phenol—selected derivatives, binding, selected human serum proteins □ Serum—human, binding of selected phenol derivatives to proteins ■ Derivatives—phenol, selected, binding to human serum proteins

Since the discovery of phenol in 1834 and its introduction to antiseptic surgery by Lister in 1867 (1), both phenol and many of its derivatives have become firmly established as germicidal agents (2, 3). Phenol derivatives, unlike many other germicides, have been shown to be less active in the presence of organic matter (2–4). Blood is a common organic contaminant in materials to be sterilized. Preliminary investigations of the binding of phenol derivatives to human serum proteins were carried out as part of the work in this study on the mechanism of action of phenol derivatives (5, 6). These preliminary studies were expanded to include individual major human serum proteins, percent binding to each, and binding parameters for human serum albumin for a selected group of phenol derivatives.

EXPERIMENTAL

Materials—The phenol derivatives used were obtained with carbon-14 labels[1]. The compounds used and specific activities were as follows: [^{14}C]phenol, 1.57 mCi/mmole; [2,4-^{14}C]dichlorophenol, 0.68 mCi/mmole; [2,4,6-^{14}C]trichlorophenol, 0.68 mCi/mmole; [^{14}C]*p-tert*-amylphenol, 0.27 mCi/mmole; [^{14}C]*p*-chloro-*m*-xylenol, 0.0027 mCi/mmole. Phenol stock solutions were made in distilled water and those of the other derivatives were made with 0.1% NaOH as the solvent. Crystalline human serum albumin and the other human serum proteins were obtained commercially[2] and the whole human serum was of tissue culture quality[3]. All other chemicals used were of reagent grade.

Methods—Dialysis methods (equilibrium and dynamic) were carried out as previously described (7). Radioactivity was determined in a liquid scintillation system using techniques previously described (7, 8). Estimates of binding parameters were calculated using the method of Sandberg (8) and standard Scatchard techniques. All averages were based on a minimum of three replicates.

Table I—Binding of [^{14}C]Phenol and [^{14}C]-*p-tert*-Amylphenol to Human Serum Proteins [a]

Serum Proteins		Ligands Percent Bound[b]	
Fraction	Concentration[c], mg/ml	Phenol	*p-tert*-Amylphenol
Albumin	40.0	48.7 (0.68)	89.1 (0.74)
α Globulin IV-1	1.0	7.9 (0.47)	28.5 (1.92)
α Globulin IV-4	5.0	23.0 (0.63)	46.5 (1.60)
β Globulin III	7.0	3.13 (0.14)	35.2 (0.60)
γ-Globulin II	11.0	8.21 (0.63)	13.0 (0.69)
Human serum	—	52.7 (1.16)	95.3 (0.18)

[a] Each system contained a total of 1.00×10^{-7} mole of [^{14}C]phenol or 1.86×10^{-7} mole of [^{14}C]*p-tert*-amylphenol. [b] The values in parentheses are standard deviations. Data obtained using equilibrium dialysis method. [c] Concentrations used approximate those normally found in human serum.

RESULTS AND DISCUSSION

The values obtained for percent binding to whole human serum and the several serum proteins for the five derivatives studied are listed in Tables I and II. Weakest binding was found with phenol and the latter was bound primarily to albumin. Although phenol was bound to the other serum proteins, the extent was <10% except for α-globulin IV-4. The addition of alkyl groups or halogens to the phenol molecule has been found to increase the latter's germicidal activity (9). It would appear from the results in Tables I and II that alkylation and/or halogenation of phenol also increases the latter's binding affinity for serum proteins. The addition of a tertiary amyl group to phenol increased percent binding of phenol almost twofold (Table I) for albumin and whole human serum and

[1] New England Nuclear Corp.

[2] Nutritional Biochemicals Division of ICN Life Sciences Group.
[3] Difco Laboratories (desiccated TC human serum).

0022-3549/82/01000-1145$01.00/0

Table II—Binding of [2,4-^{14}C]Dichlorophenol, [2,4,6-^{14}C]Trichlorophenol, and [^{14}C]-*p*-Chloro-*m*-Xylenol to Human Serum Proteins [a]

Serum Proteins		Ligands Percent Bound [b]		
Fraction	Concentration, mg/ml	2,4-Dichlorophenol	2,4,6-Trichlorophenol	*p*-Chloro-*m*-xylenol
Albumin	40.0	87.7 (0.45)	94.1 (0.36)	85.2 (2.32)
α-Globulin IV-1	1.0	17.3 (0.30)	8.09 (0.139)	23.8 (0.20)
α-Globulin IV-4	5.0	57.5 (0.28)	55.2 (0.93)	10.9 (0.88)
β-Globulin III	7.0	20.5 (0.53)	13.0 (1.66)	23.8 (2.57)
γ-Globulin II	11.0	8.0 (0.51)	6.4 (0.55)	14.9 (1.12)
Human serum	—	94.6 (0.40)	95.8 (0.15)	89.8 (2.99)

[a] Each system contained a total of 1.56×10^{-7} mole of [2,4-^{14}C]dichlorophenol, or 2.21×10^{-7} mole of [2,4,6-^{14}C]trichlorophenol or 2.04×10^{-7} mole of [^{14}C]*p*-chloro-*m*-xylenol. [b] The values in parentheses are standard deviations. Data obtained using equilibium dialysis method.

Table III—Binding Parameters [a] (Albumin) of Phenol, 2,4-Dichlorophenol, 2,4,6-Trichlorophenol, and *p-tert*-Amylphenol

Ligand [b]	Percent Binding	K_1 [c]	n_1	K_2	n_2
Phenol	48.7	67,200,000	0.0487	16,020	0.186
2,4-Dichlorophenol	87.7	1,010,000	0.1930	71,900	0.345
p-tert-Amylphenol	89.1	64,600	0.3670	21,500	0.714
2,4,6-Trichlorophenol	94.1	30,200,000	0.2940	1,470,000	0.323

[a] Data obtained by dynamic dialysis method. [b] Initial number of moles added to each system: phenol, 1.03×10^{-6}; *p-tert*-amylphenol, 9×10^{-7}; 2,4-dichlorophenol, 9.2×10^{-7}; 2,4,6-trichlorophenol, 9.95×10^{-7}. Dynamic dialysis method was used to obtain data. [c] Liters per mole.

Table IV—Ranking of Phenol Derivatives [a] in Order of Percent Binding to Various Serum Proteins

Serum Protein	Ranking by Percent Binding
Whole human serum	III > IV > II > V > I
Human serum albumin	III > IV > II > V > I
α-Globulin IV-1	IV > V > II > III > I
α-Globulin IV-4	II > III > IV > I > V
β-Globulin III	IV > V > II > III > I
γ-Globulin II	V > IV > I > II > III
Ranking on basis of molecular weight	III > IV > II > V > I

[a] Phenol derivatives above are: phenol, I; 2,4-dichlorophenol, II; 2,4,6-trichlorophenol, III; *p-tert*-amylphenol, IV; and *p*-chloro-*m*-xylenol, V.

also substantially for the other serum proteins. Again, the serum protein showing the highest percent binding was albumin, and α-globulin IV-4 also exhibited substantial binding (46.5%).

Halogenation of phenol also caused a great increase in binding with whole serum and the serum proteins. 2,4,6-Trichlorophenol was found to be bound to a higher percent to whole serum and albumin than 2,4-dichlorophenol ($p < 0.05$), but binding to the other serum proteins did not show a similar pattern. The derivative that was both a halogenated and alkylated derivative of phenol, *p*-chloro-*m*-xylenol, exhibited a higher percent binding to whole serum and most of the serum proteins than phenol itself, but not higher than the two halogenated derivatives for albumin and human serum.

The Scatchard plot for *p-tert*-amylphenol and albumin is shown in Fig. 1. Data for Scatchard plots were limited, in this study, to albumin as the protein, because all of the derivatives showed the highest percent binding to albumin. The plots for phenol, 2,4-dichlorophenol, and 2,4,6-trichlorophenol were similar, differing only in values for the axes. It can be seen that the curve is not a straight line as would be expected for a single binding system. It appears that the curve has two distinct segments indicative of two binding systems. The binding parameters calculated are given in Table III[4]. The two derivatives exhibiting the highest percent binding to whole serum and albumin, did not yield the largest K_1 association constants. Phenol itself had the highest calculated association constant (K_1) and *p-tert*-amylphenol's constant (K_1) was the lowest of all. All of the *n* values, the number of binding sites, were fractional. Values for $n < 1$ have been reported in other studies (10–12) and present difficulties in interpretation in terms of a physical model.

The ranking by percent binding of the several phenol derivatives to the protein fractions studied is illustrated in Table IV. The only obvious pattern is that ranking of the phenols with respect to binding to albumin or whole human serum is exactly the same as ranking by molecular weight. No clearcut pattern is apparent for the other proteins. Hansch (13–15), in his studies of the relationships between structure and biological activity, found correlation of the latter with partition coefficients expressed as the constant, π. An additional constant, σ, was developed by Hammett (16) to express the electronic activity of the substituents on an organic molecule. Thus, π is an expression of the degree of lipophilicity of a compound and σ is the electronic (polar) nature of a compound. The Hansch equation attempts to take into account the contribution of both lipophilic and electronic properties of a compound with respect to its biological activity. The latter is usually represented as the log of the reciprocal of the measure of biological activity.

The π and σ values for the phenol derivatives were determined, either from literature values reported (15) or calculated on the basis of the sum of the values of substituent groups (14–17). The log of the reciprocal of percent binding to each protein was analyzed by regression analysis with the π and σ values to search for possible correlations. The results obtained are listed in Table V. For those values (π or σ values and log of 1/percent bound) yielding a correlation coefficient of at least 0.900 ($p \leq 0.05$), correlation coefficients are listed. A direct relationship with π values would indicate that the percent binding increased with an increase in lipophilic properties. Significant correlation with σ values would suggest increased binding with more polar properties if the relationship was direct

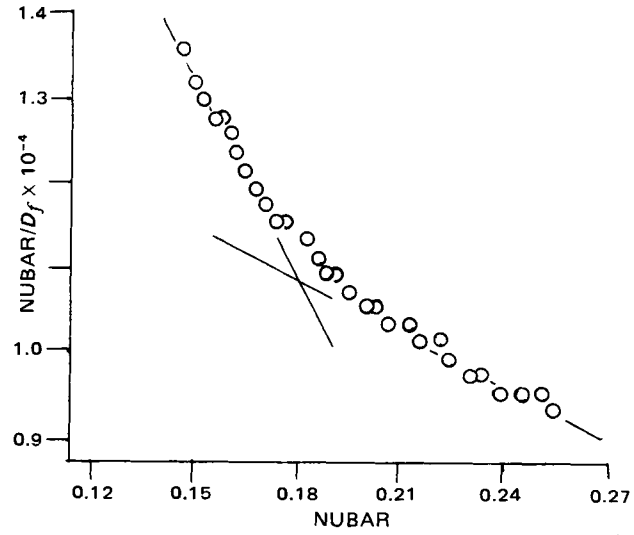

Figure 1—*Scatchard plot of data for binding of* p-tert-*amylphenol to human serum albumin, determined by dynamic dialysis. A total of 9.3* $\times 10^{-7}$ *moles of* p-tert-*amylphenol were added at the beginning of the run and albumin concentration in the bag (5 ml volume) was* 5.797×10^{-4} *M (40 mg/ml). Nubar is equal to total bound moles of ligand divided by moles of albumin in the system and* D_f *is the molar concentration of unbound ligand.*

[4] It was not possible to obtain binding parameters for *p*-chloro-*m*-xylenol because a sufficient quantity of the labeled compound was not available.

Table V—Relationships Between Percent Binding of Phenol Derivatives to Various Serum Proteins and π or σ Values or Molecular Weights of Phenol Derivatives

Phenol Derivative[a] Groups	Serum Protein	Relationship[b] π[c] Values	σ Values	Molecular Weight
I–V	Albumin	Direct (0.963)	—	Direct (0.964)
II–V	α-Globulin IV-1	—	Inverse (−0.964)	—
	β-Globulin III	—	Inverse (−0.954)	—
I–III	Albumin	Direct (0.98)	Direct (0.979)	Direct (0.98)
	α-Globulin IV-4	Direct (0.924)	Direct (0.920)	Direct (0.924)
I, IV, V	Albumin	Direct (0.979)	—	Direct (1.0)
	α-Globulin IV-1	Direct (.997)	—	Direct (1.0)
	β-Globulin III	Direct (0.998)	—	Direct (0.966)
	γ-Globulin II			Direct (0.931)

[a] Phenol derivatives above are: I, phenol; II, 2,4-dichlorophenol; III, 2,4,6-trichlorophenol; IV, *p*-chloro-*m*-xylenol; V, *p*-*tert*-amylphenol. [b] Figures in parentheses are coefficients of correlation. [c] π Values for I–V, respectively, were 1.46, 3.0, 3.69, 3.27, and 3.59. σ Values, respectively, were −0.36, 0.10, 0.33, −0.47, and 0.85.

and the reverse, if inverse. For the entire group of five phenol derivatives, correlation was direct with increasing molecular weight (as pointed out previously) and with increasing π values. The relationship with σ values was not statistically significant.

It would appear that for the entire group of five derivatives, the more lipophilic the molecule, the higher the binding to albumin. Other statistically significant relationships were found when the phenol derivatives were divided into other groups. Namely, either the halogenated phenols plus phenol or the alkylated phenols (including *p*-chloro-*m*-xylenol) and phenol. The data in Table V also suggest something about the hydrophilic–hydrophobic properties of several of the proteins. Albumin appears to have both hydrophobic and polar binding sites in that there was a direct relationship between binding and π values and also with σ values for the more polar derivatives (Group 3). On the other hand, α-globulin IV-1 had a direct relationship with π values and an inverse relationship with σ values for the more polar derivatives (Group 2.) suggesting capability for a polar binding primarily. Like albumin, α-globulin IV-4 appears to have both nonpolar and polar binding sites as indicated by the direct relationship with both π and σ values for the more polar derivatives.

In one form of the Hansch equation (17):

$$\log 1/C = a\pi + b\sigma + c \qquad \text{(Eq. 1)}$$

where C represents the measure of biological activity. The values a, b, and c are constants characteristic of the system, while π is the Hansch constant and σ is the Hammett constant. It was possible to fit this equation with statistical significance ($p = 0.05$) only in the cases of binding of the five phenols to either albumin or human serum. The constants obtained were:

For albumin:

$$\log 1/\text{percent binding} = -0.13\pi + 0.016\sigma - 1.51 \qquad \text{(Eq. 2)}$$

For human serum:

$$\log 1/\text{percent binding} = -0.12\pi + 0.0091\sigma - 1.56 \qquad \text{(Eq. 3)}$$

In studies of the toxicity of phenol derivatives to two microorganisms (18) the Hansch equations calculated suggested that the σ value was of little consequence. This would also appear to be true in the equations describing the binding of the phenol derivatives to either albumin or human serum in that the coefficient for the σ term is relatively small.

In conclusion, it would appear from the data obtained that for the derivatives of phenol studied, serum protein binding is significant, especially to whole human serum and albumin and that binding is related to molecular weight and Hansch π values. Binding to albumin apparently involves primarily hydrophobic bonds rather than polar bonding. This conclusion would be consistent with the findings of Teresi (19) that treatment of bovine serum albumin to remove epsilon-amino positive charges had little effect on binding of 2,4-dichlorophenolate (pH 7.6). In addition, Scholtan (20) concluded that nonspecific hydrophobic binding to human serum albumin is the major mechanism for a wide variety of organic molecules.

REFERENCES

(1) J. Lister, *Lancet*, **2**, 353 (1867).

(2) F. Putnam, *Adv. Protein Chem.*, **IV**, 79 (1948).

(3) G. Sykes, "Disinfection and Sterilization," D. Van Nostrand Co., Princeton, N.J., 1958, p. 244.

(4) E. Bennett, "Advances in Applied Microbiology," vol. 1, Academic, New York, N.Y., 1958, p. 123.

(5) J. Judis, *J. Pharm. Sci.*, **55**, 803 (1966).

(6) *Ibid.*, **57**, 768 (1968).

(7) *Ibid.*, **66**, 802 (1977).

(8) A. Sandberg, H. Rosenthal, S. Schneider, and M. Slaunwhite, in "Steroid Dynamics," T. Nkro, G. Pincus, and J. Tait, Eds., Academic, New York, N.Y. 1966, p. 33.

(9) S. Block, "Disinfection, Sterilization and Preservation," Lea & Febiger, Philadelphia, Pa., 1977, p. 227.

(10) J. Vallner, *J. Pharm. Sci.*, **66**, 447 (1977).

(11) C. Bowmer and W. Lindup, *Biochim. Biophys. Acta*, **624** 260 (1980).

(12) G. Powis, *J. Pharm. Pharmacol.*, **26**, 113 (1974).

(13) C. Hansch, P. Maloney, T. Fujita, and R. Muir, *Nature (London)*, **194**, 178 (1962).

(14) T. Fujita, J. Iwasa, and C. Hansch, *J. Am. Chem. Soc.*, **86**, 5175 (1964).

(15) A. Leo, C. Hansch, and D. Elkins, *Chem. Rev.*, **71**, 525 (1971).

(16) H. Jaffe, *ibid.*, **53**, 191 (1953).

(17) C. Hansch, R. Muir, T. Fujita, P. Maloney, F. Geiger, and M. Streich, *J. Am. Chem. Soc.*, **85**, 2817 (1963).

(18) C. Hansch and T. Fijita, *ibid.*, **86**, 1616 (1964).

(19) J. Teresi, *ibid.*, **72**, 3972 (1950).

(20) V. Scholtan, *Arzneim.-Forsch.*, **18**, 505 (1968).

ACKNOWLEDGMENTS

The author thanks Mrs. Virginia Matusek for technical assistance.

Determination of Bacmecillinam, an Amdinocillin Prodrug, in Human and Canine Whole Blood by Reversed-Phase Liquid Chromatography

DOUGLAS WESTERLUND ˣ, BODIL PETTERSSON, and JAN CARLQVIST

Received June 8, 1981, from the *Astra Läkemedel AB, Research and Development Laboratories, Analytical Chemistry, S-151 85 Södertälje, Sweden.* Accepted for publication December 15, 1981.

Abstract □ Bacmecillinam is an amdinocillin prodrug designed to be easily hydrolyzed in biological materials, so special procedures were developed for the collection of blood specimens. Whole blood was collected in tubes containing bacampicillin as an adsorption inhibitor and kept at −70°; the extracting solvent, hexane–methylene chloride (9:1, v/v), was added to the cold tubes, and the extraction was performed during the thawing of the samples. The organic phase was partially evaporated before a reextraction to a small volume of acidic aqueous phase was made. The separation was performed on a microparticulate C_{18}-alkyl bonded silica packed in glass-lined stainless steel columns. Mobile phase was a buffer (pH 6)–acetonitrile mixture containing *N*-hexyl-*N*-methylamine as an adsorption inhibitor. The detection limit was 600 pg/ml of whole blood, and the within-run precision ($s_{rel\%}$) was ~8% at the 5-ng/ml level.

Keyphrases □ Bacmecillinam—determination in biological fluids by reversed-phase liquid chromatography □ Biological fluids—determination of bacmecillinam by reversed-phase liquid chromatography □ Reversed-phase liquid chromatography—determination of bacmecillinam in biological fluids

Amdinocillin, a 6β-amidinopenicillanic acid, is a relatively new antibiotic agent for which a synergistic effect *in vitro* and *in vivo* has been demonstrated, in combination with β-lactam antibiotics, against many strains of Gram-negative bacteria. Since amdinocillin is poorly absorbed after oral administration, prodrugs such as amdinocillin pivoxil and bacmecillinam have been developed in order to enhance the oral drug absorption efficiency. Bacmecillinam, the 1′-ethoxycarbonyloxyethyl ester, is rapidly hydrolyzed by endogenous esterases in blood and tissues releasing ethanol, acetaldehyde, and carbon dioxide. Recently (1), the superior pharmacokinetic properties of bacmecillinam compared with amdinocillin pivoxil were demonstrated in studies on healthy volunteers, resulting in statistically significant differences regarding areas under the curve, urinary excretion, and peak plasma concentrations.

During the evaluation of the toxicological and clinical properties of the drug, a need for the determination of the intact prodrug, bacmecillinam, arose. This report presents such a method for the quantitative determination of the compound in whole blood and bile. Since the compound is very unstable in the presence of biological fluids, special precautions in sample handling had to be developed. At the very low concentration levels encountered, severe adsorption tendencies of the compound had to be overcome by careful handling of the sample. An extraction procedure comprising a base extraction and a reextraction to an acidic aqueous phase precedes the chromatographic step which relies on reversed-phase liquid chromatography and UV detection. Amdinocillin pivoxil was utilized as the internal standard.

EXPERIMENTAL

Apparatus—Chemicals were weighed on analytical[1] or microanalytical[2] balances; a shaker[3] was used for extraction, speed control 6.5; and the extraction tubes were centrifuged at 300×*g*[4] (Step 1 in the extraction) or at 650×*g*[5] (Step 2). The equipment for liquid chromatography was comprised of a dual reciprocating piston pump[6], an injection valve[7] equipped with a 20- or 200-μl loop, an injection syringe[8] with a total volume of 1 ml, a variable UV detector[9] monitored at 230 nm, and a recorder[10] with an input of 10 mV and a paperspeed of 40 cm/hr.

Chemicals—Bacampicillin[11], bacmecillinam[11], and amdinocillin pivoxil[12] were from released batches. *N*-Hexyl-*N*-methylamine[13] of pure quality, phosphoric acid (85%)[14] of analytical quality, and acetonitrile[13] of HPLC quality were used for preparation of the mobile phases. Methylene chloride[13] of HPLC quality and *n*-hexane[14] of spectroscopic quality were used in the extractions. The water was deionized.

Standard Solutions—Solution S consisted of 5 mg of bacmecillinam/250 ml of water in a polypropylene flask[15]; Solution I: amdinocillin pivoxil, internal standard, 1.25 mg/250 ml of water in a polypropylene flask; Solution A: bacampicillin, adsorption inhibitor, 100 mg/100 ml of water in a polypropylene flask. Solutions S, I, and A were divided into 1-ml portions and stored at −70° in tubes[16]. Each day of analysis, appropriate amounts were thawed, and out of Solution S, a series of seven twofold dilutions (S_1–S_7), containing 10–0.156 μg/ml, were made in tubes[16].

Solution IA was made by mixing 1.0 ml of I and 0.5 ml of A in a tube[16] and Solution ID was made by mixing 1.0 ml of I and 0.5 ml of water in a tube[16]. Solvent for extraction (Solvent E): methylene chloride (50.0 ml) was added by pipet into a 500-ml flask and *n*-hexane was added to the mark. Solution S_4 (200 μl), 300 μl of Solution IA, and 3500 μl of 0.01 *M* H_3PO_4 were mixed to make the chromatographic test solution.

Control of Standards—Two independent weighings for the preparation of standard solutions were made. The solutions were diluted with an equal volume of deionized water and the absorbances at 220 nm were measured on a spectrophotometer. If the absorbances agreed within 2%, one of the standard solutions was prepared and stored according to the described procedure. If the absorbances deviated, new sets of dilutions were prepared and the control performed once more. If disagreement still persisted, new weighings had to be made.

Instrument Control—The performance of the HPLC instrumentation was controlled each day of operation by the injection of two standard solutions (S_2 and S_5). The slope of this standard curve was calculated, and the baseline noise level was observed. If data were in accordance with previously reported data (results within ±10% of established data) the instrument performance was approved.

Sample Collection—*Whole Blood*—Whole blood (0.25–2 ml) was collected by means of a cannula[17] in 5-ml tubes[18], containing 10–100 μl

[1] Mettler 2002 MP 1, Mettler Instrumente AG, Greifensee, Switzerland.
[2] Mettler M5 SA, Mettler Instrumente AG, Greifensee, Switzerland.
[3] Universal Shaking Machine, SM BI, Edmund Bühler, Tübingen, West Germany.
[4] Wifug X-1, AB Winkelcentrifug, Stockholm, Sweden.
[5] Labsystem OY CF 510 A, Helsinki, Finland.
[6] Constametric I, Laboratory Data Control, Riviera Beach, Fla.
[7] Rheodyne 7120, Rheodyne, Berkeley, Calif.
[8] Gilette Scimitar, Gilette Surgical, Isleworth, Middlesex, U.K.
[9] SpectroMonitor III, Laboratory Data Control, Riviera Beach, Fla.
[10] Linear 255, Linear Instruments Corp., Irvine, Calif.
[11] Astra Läkemedel AB, Södertälje, Sweden.
[12] Løvens Kemiske Fabrik, Ballerup, Denmark.
[13] Fluka AG, Buchs, Switzerland.
[14] Merck, Darmstadt, West Germany.
[15] Kartell, Binasco, Italy.
[16] Ellerman tubes Cerbo, Trollhättan, Sweden.
[17] Vacutainer Needle, Becton & Dickinson, Rutherford, N.J.
[18] Venoject, Terumo Corp., Tokyo, Japan.

0022-3549/82/01000-1148$01.00/0

of Solution A, diluted 10 times, with each dilution containing 10 μg of bacampicillin. Care was taken to avoid blood coming into contact with the stopper. The content was then rapidly poured into preweighed centrifuge glass tubes, which were placed in a carbon dioxide–ethanol bath in order to rapidly freeze the content. The whole procedure had to be performed within 10 sec.

Bile—Bile from dogs was collected directly in preweighed centrifuge tubes, containing ~10 μg of bacampicillin as an adsorption inhibitor, and kept in a carbon dioxide–ethanol bath, which was isolated[19] to prevent the freezing of the bile in the tube coming from the dog.

Sample Preparation—For preparation of standards, 2.00 ml of human whole blood or 1.00 ml of canine whole blood or bile was added by pipet into 14 centrifuge tubes and the tubes were chilled in an ice bath. A 20 μl volume of Solutions S_1–S_7 was added to the standard tubes, each solution to two tubes leaving two tubes as blanks; the tubes were mixed for 5 sec and put in a carbon dioxide–ethanol bath (~−70°) in a fast and reproducible manner. All sample handling from then on was performed by keeping the samples cold in the carbon dioxide–ethanol bath. The sample tubes were weighed on an analytical balance and put in the freezing mixture. Solution IA (30 μl) was added to all standard tubes, and 30 μl of Solution ID was added to all sample tubes.

Extraction—While keeping the tubes at −70°, 5.00 ml of Solvent E/ml of sample was added to each tube. The stoppers were sealed by rubber bands and the tubes were put in the shaker horizontally for 20 min. After loosening the stoppers, the tubes were centrifuged[4] for 10 min. The organic phase was carefully transferred to new glass centrifuge tubes (10-ml volume) and evaporated to 4 ml under a gentle stream of air or nitrogen at room temperature, 400 μl of 0.01 *M* H_3PO_4 was added, the stoppers were sealed by rubber bands, and the tubes were put in the shaker horizontally for 15 min. After centrifugation[5] for 5 min the organic phase was removed carefully by a Pasteur pipet and remaining traces were evaporated by compressed air. The aqueous phase (200 μl) was injected into the chromatographic column.

Chromatography—The support[20] was packed in glass-lined stainless steel columns[21] (100 × 4-mm, i.d.) by an upwards slurry packing technique (2) with methylene chloride as solvent. Mobile phase was pH 6 phosphate buffer (ionic strength = 0.05)–acetonitrile (6:4, v/v) containing *N*-hexyl-*N*-methylamine (10^{-4} *M*); the mixture was degassed for 2 hr by magnetic stirring before use. The chromatographic procedure was as follows. The column was equilibrated with the mobile phase for ~1 hr before starting the analysis. Samples (200 μl) were injected in the following order: (*a*) 0.01 *M* H_3PO_4 for control of chromatographic purity; (*b*) chromatographic test solution; (*c*) extract from a whole blood blank sample; (*d*) Standard S_1, (*e*) sample; (*f*) Standard S_2 and so on from there. (This sequence of injections is not critical to the outcome of the analysis but is recommended in order to get as reliable results as possible from the quantitations.) The standard injecting frequency depended on the number of samples and was distributed as evenly as possible among the samples. Finally, the injections were concluded by another sample of the chromatographic test solution, and its chromatographic appearance was compared with the first sample injected in order to confirm the column retention throughout the study.

For quantitation a standard curve was constructed by plotting the peak height ratio of sample–internal standard against the concentration of bacmecillinam in the standards.

RESULTS AND DISCUSSION

Sample Handling—Bacmecillinam as a prodrug is designed to be unstable in biological material, and the compound is rapidly hydrolyzed in whole blood as demonstrated in Fig. 1 (~30% of the compound is lost within 1 min at 37°). The enzyme systems responsible for the degradation are not identified, but similar studies on other prodrugs, amdinocillin pivoxil, talampicillin, and bacampicillin (3), have revealed that blood, plasma, and serum, as well as homogenates from liver, gastric, and duodenal mucosa from humans, dogs, and rats, are capable of efficiently hydrolyzing these types of prodrugs. A fast procedure for collection of samples, involving an immediate freezing of the sample to −70° and subsequent storage at this temperature, therefore, is an essential step in the method.

In bile the compound was more stable: after 10 min at 23° and 37°, ~4.0 and 6.5%, respectively, was lost.

Table I—Stability of Bacmecillinam in Canine Biological Fluids[a]

Day of Analysis	Mean, ng/ml	*s*, ng/ml	Confidence Interval[b]	*n*
Whole Blood				
1	7480	—	—	2
42	7310	134	7090–7520	4
1	89	—	—	2
42	83	6.2	73–92	4
Bile				
1	105	4.8	93–117	3
42	100	1.7	97–103	4

[a] At −70°. [b] $p = 0.05$.

Bacmecillinam is stable both in canine whole blood and bile (Table I) at −70° for at least 40 days; although, the mean values of the analyses indicate a small decrease in concentration after this time, it is not statistically significant.

Extraction—The extraction was optimized by mixing a nonpolar organic solvent, *n*-hexane, with a more polar one, methylene chloride. Preliminary experiments gave log $k_d \times K'_s = 6.3$ and 2, respectively, for the two solvents (k_d is the partition coefficient, K'_s is the acid dissociation constant = $10^{-6.83}$ at 21° and ionic strength = 0.1[22]). The extraction yield was optimized at pH 7.4, ionic strength = 0.5 (equal to the plasma pH) to eliminate the need of buffer addition to the whole blood. Under these conditions the percent extraction from buffer increased from 92 to 97% (Fig. 2) by adding 10% methylene chloride. It can be calculated that with a phase ratio (V_{org}/V_{aq}) equal to three, a quantitative extraction (99%) is achieved with such an organic phase, compared to $V_{org}/V_{aq} = 9$ required with pure *n*-hexane. In extractions from biological fluids, a phase ratio of five was used in order to compensate for the influence of biological material on the extraction.

For a quantitative reextraction of bacmecillinam to an aqueous phase, 0.01 *M* H_3PO_4 was used. It was found empirically that even with $V_{org}/V_{aq} = 20$, the compound is completely reextracted onto the aqueous phase. In the analytical procedure, the initial organic extract is partially evaporated to about half the volume prior to extraction resulting in $V_{org}/V_{aq} = \sim 12$.

In extractions from bile using a mechanical shaker, a heavy emulsion was obtained. It could be decreased by mixing the phases more gently in a rotating device[23], but to break up the emulsion completely, it was necessary to freeze the samples to −25° after a preliminary centrifugation

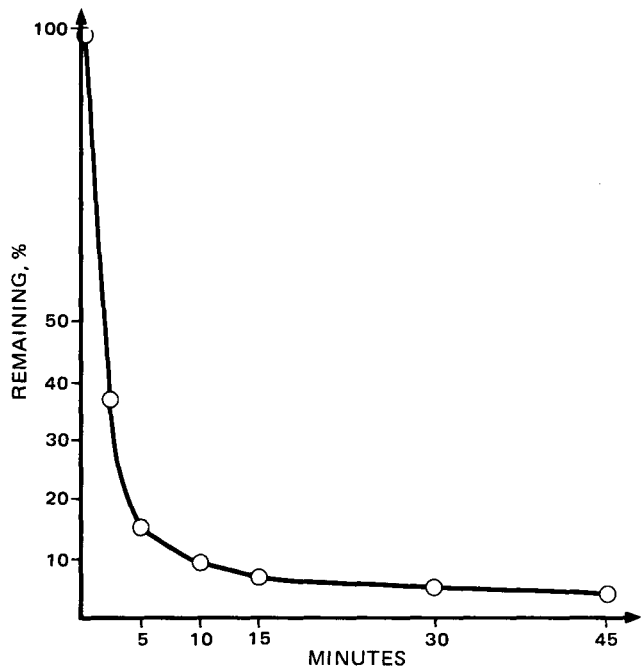

Figure 1—*Stability of bacmecillinam in whole blood at 37°.*

[19] Frigolit, Plastolit, Täby, Sweden.
[20] Nucleosil C_{18} (5 μm), Macherey-Nagel & Co., Düren, West Germany.
[21] Scientific Glass Engineering, Australia.
[22] J. Lindqvist, personnal communication.
[23] Test Tube Rotator Rotamix RK 20 VS, Heto Lab Equipment A.S., Birkerød, Denmark.

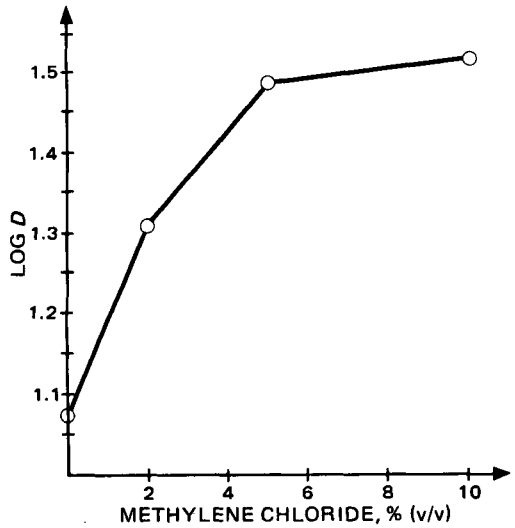

Figure 2—*Extraction of bacmecillinam: Aqueous phase: phosphate buffer pH 7.4 (ionic strength = 0.1); organic phase:* n*-hexane–methylene chloride;* D = *distribution ratio = total concentration in organic phase–total concentration in aqueous phase.*

(900×*g* for 5 min), followed by another identical centrifugation. Bacmecillinam also has a tendency to adsorb at certain interfaces. This was first observed in studies on extraction properties of the compound during method development when nonreproducible results initially were obtained. Silanization of glassware or use of plastic (polypropylene) tubes did not improve the results; only by the addition of a comparatively large excess (100–5000 times) of a related prodrug, bacampicillin, the results became reproducible. The adsorption of bacmecillinam to glass surfaces was further illustrated in an experiment (Table II) where whole blood containing bacmecillinam was transferred by Pasteur pipets. The recovery in the transferred samples was ~57% (median value), and with a large variation, the difference was statistically significant compared with controls.

Considering the facts on hydrolysis and absorption, the blood is collected in sampling tubes which contain an aqueous solution of the adsorption inhibitor, bacampicillin. The content is then rapidly poured into preweighed centrifuge tubes of glass placed in a freezing bath. The whole procedure must be performed within 10 sec to avoid significant hydrolysis of the compound.

Chromatography—Nucleosil C_{18} (5 μm) has been found suitable for the chromatography of hydrophobic amines (4) and was chosen as the support in this study. Initial experiments indicated that bacmecillinam

Table II—Adsorption of Bacmecillinam onto Pasteur Pipets [a]

Treatment	Range Found, ng/g	Median, ng/g	Median Recovery, %
Not transferred	20.7–32.0	27.6	99.3
Transferred	0.5–16.8	15.8	56.8

[a] Procedure: From five centrifuge tubes with 4 ml of whole blood, each containing bacmecillinam (27.8 ng/g), ~2 ml was transferred to new centrifuge tubes by Pasteur pipets during 30 sec maximally. The tubes were then immediately frozen to −70° and later analyzed by HPLC.

Table III—Adsorption of Bacmecillinam onto Glass-Lined Stainless Steel Columns [a]

Mobile Phase	Amount Injected, ng	Peak Height Range, mm	Peak Height Median, mm	*n*
Without *N*-hexyl-*N*-methylamine	23	30–68	61	7
With *N*-hexyl-*N*-methylamine	20	78–80	79	6

[a] Procedure: Bacmecillinam was dissolved in water and analyzed by HPLC with and without the addition of *N*-hexyl-*N*-methylamine (10^{-4} *M*) to the mobile phase.

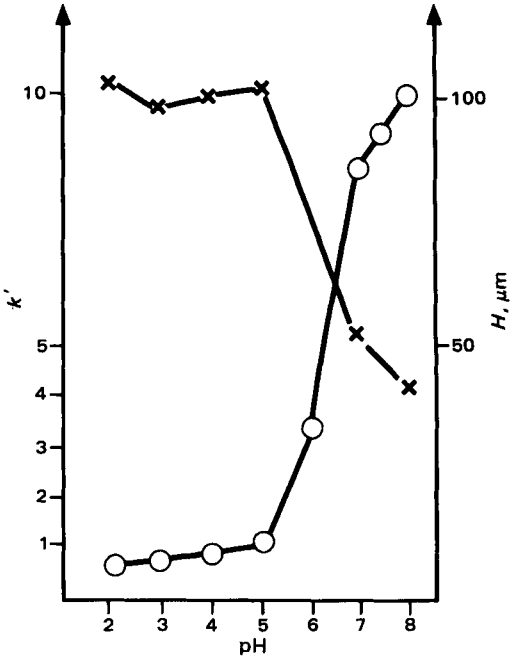

Figure 3—*Relation of pH in mobile phase with capacity ratio and efficiency. Mobile phase: phosphate or citrate buffer (ionic strength = 0.1)–acetonitrile (4:6, v/v). Key: X = H and O = k'.*

gave unacceptable asymmetric peaks ($As_{10\%}$ = 2.4–3.0) when the support was packed in conventional stainless steel columns and run with phosphate buffer (pH 7; ionic strength = 0.05)–acetonitrile (3.5–4.0—6.5–6.0, v/v) as mobile phase. With glass-lined stainless steel columns, however, the peaks were symmetrical ($As_{10\%}$ = 1.0–1.2) and had equally good efficiencies (h ~ 5: h = reduced plate height; HETP/dp; dp = support particle diameter). With this system, however, nonreproducible peak heights were obtained, although other chromatographic parameters were unaffected. The phenomenon was interpreted as being due to adsorption of the compound to the glass walls, similar to the problems encountered during the development of the described extraction procedure, and the effect could be avoided by the addition of a secondary amine (*N*-hexyl-

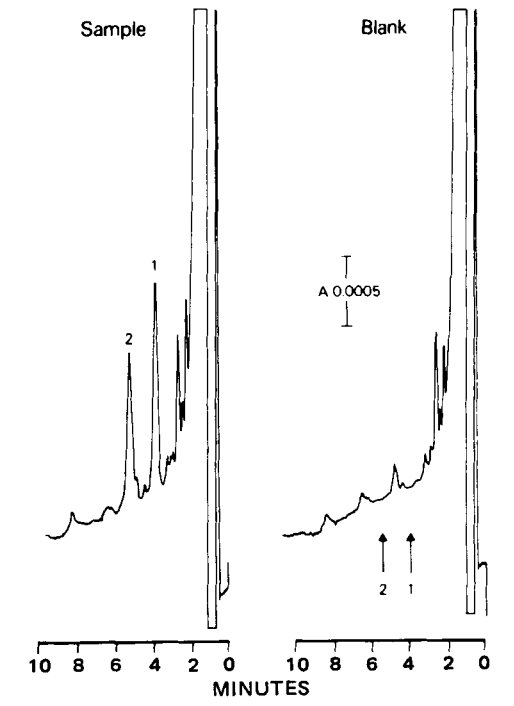

Figure 4—*Blank and sample chromatograms of (1) bacmecillinam (21 ng) and (2) amdinocillin pivoxil (20 ng). Analysis was performed as described in the text.*

Table IV—Repeatability in Quantitative Determinations of Bacmecillinam [a]

Added, ng/ml	Found, %	*CV*, %
4.7	100.4	8.3
18.6	95.7	4.1

[a] Four samples were analyzed as described in *Experimental* relative to five standards in the range of 3.3–53 ng/ml.

N-methylamine) as an adsorption inhibitor (Table III). The chromatographic parameters (efficiency, peak symmetry, and capacity ratio) were virtually unaffected by the amine addition. Later experiments with stainless steel columns indicate that peak asymmetries observed initially, and described above, were also eliminated by the presence of *N*-hexyl-*N*-methylamine in the mobile phase.

The capacity factor of bacmecillinam was optimized by varying the pH of the mobile phase while keeping the volume ratio between buffer and acetonitrile constant (4:6, v/v) (Fig. 3). At pH 6 the retention time is suitable and the chromatographic efficiency is acceptable, while at pH 5 the capacity ratios are too low and the efficiencies are about half of those at higher pH. The compound used as the adsorption inhibitor for the extraction, bacampicillin, is almost nonretained at the chosen conditions and elutes near the front of the chromatogram. Amdinocillin, the antibiotically active compound, also elutes near the front in this chromatographic system, and the compound, furthermore, is not extracted to a significant amount in the extraction step. The quantitative determination of amdinocillin in biological fluids still requires the methodology described earlier (5).

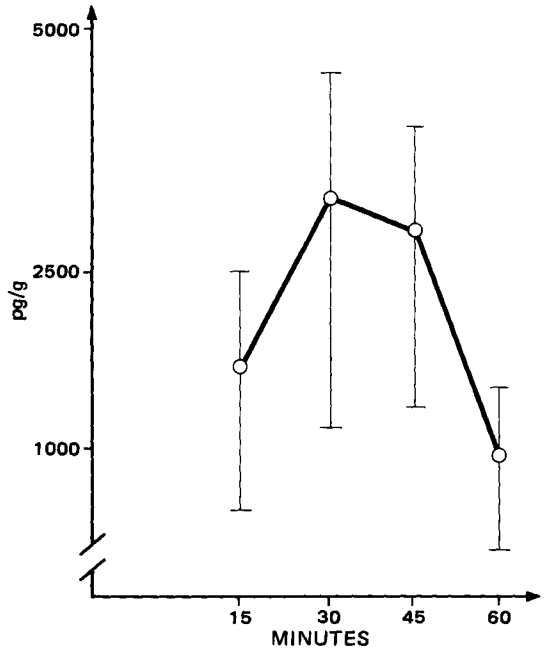

Figure 5—*Mean levels of bacmecillinam from three volunteers. Dose: 244 mg of bacmecillinam hydrochloride orally.*

Representative blank and sample chromatograms from whole blood (Fig. 4) illustrate that the chosen conditions are suitable for the analysis of bacmecillinam, and that the internal standard, amdinocillin pivoxil, elutes largely unaffected by blank disturbances.

The injected sample differs in composition from the mobile phase, and some of the small peaks that appear in the chromatogram originate from the resulting composition disturbance and not from the biological sample. Late in the chromatogram, after ~2 hr, an additional broad composition disturbance peak elutes and has to be taken into account in routine determinations in order to avoid interferences. This kind of disturbance can be reduced by the injection of smaller sample volumes. Some preliminary experiments have indicated the possibility of reextracting and injecting a volume 10 times smaller (*i.e.*, 20 μl instead of 200 μl).

Quantitative Determinations—The limit of detection, defined as a signal equal to twice the background noise level of the baseline, is ~600 pg/ml of whole blood. The repeatability of the method (Table IV) is ~8% (*CV*) at the level of 5 ng/ml, and it is estimated that at 1–2 ng/ml, the precision still is acceptable (*i.e.*, 15–20%, *CV*) for quantitative determinations.

Mean levels from three volunteers receiving 244 mg of bacmecillinam as a single dose are in the range of 1–3 ng/g of whole blood (Fig. 5).

The method has also been applied to determination of the compound in canine portal and peripheral whole blood as well as bile.

REFERENCES

(1) J.-O. Lernestedt, B. Pring, and D. Westerlund, in "Current Chemotherapy and Infectious Disease, Proceedings of the 11th ICC and the 19th ICAAC," American Society of Microbiology, Washington D.C., 1980, p. 314.

(2) P. A. Bristow, P. N. Brittain, G. M. Riley, and B. F. Williamson, *J. Chromatogr.*, **131**, 57 (1977).

(3) D. Westerlund, in "Formulation and Preparation of Dosage Forms," J. Polderman, Ed., Elsevier/North Holland Biomedical Press, 1977, p. 113.

(4) D. Westerlund, and E. Erixson, *J. Chromatogr.*, **185**, 593 (1979).

(5) D. Westerlund, J. Carlqvist, and A. Theodorsen, *Acta Pharm. Suec.*, **16**, 187 (1979).

Biotransformation and Excretion of Nitromethaqualone in Rats and Humans

M. VAN BOVEN and P. DAENENS ˣ

Received April 27, 1981, from the *Laboratory of Toxicology, University of Louvain, Louvain, Belgium.* Accepted for publication December 23, 1981.

Abstract □ The metabolic disposition of ^{14}C-labeled nitromethaqualone was investigated in rats. Unlabeled nitromethaqualone was used for studies on humans. Nitromethaqualone was eliminated from the body after most of it had undergone biotransformation. Both humans and rats reduced the nitro group of nitromethaqualone to the corresponding amino derivative, which was partially transformed to the corresponding acetylated form. Cleavage of the quinazolinone nucleus resulting in 2-methoxy-4-nitroaniline was also observed in humans. In rats additional major metabolites arose from the oxidation of the 2-methyl group into hydroxymethyl resulting in 2-hydroxymethyl-3-(2′-methoxy-4′-nitrophenyl)-4(3*H*)-quinazolinone and concomitant *in vivo* reduction of the latter resulting in 2-hydroxymethyl-3-(2′-methoxy-4′-aminophenyl)-4(3*H*)-quinazolinone. Both metabolites were also excreted as glucuronides. In rats fecal excretion accounted for 55–60% of the administered dose, while 24–27% was excreted in the urine. Protracted excretion in both humans and rats indicated an extensive enterohepatic circulation.

Keyphrases □ Biotransformation—excretion, nitromethaqualone in rats and humans, metabolism □ Nitromethaqualone—biotransformation and excretion in rats and humans, metabolism □ Metabolism—biotransformation and excretion of nitromethaqualone in rats and humans

Nitromethaqualone[1] (I) or 2-methyl-3-(2′-methoxy-4′-nitrophenyl)-4(3*H*)-quinazolinone has been available in Europe since 1967 as a nonbarbituric hypnotic of the quinazolinone series, which includes methaqualone [2-methyl-3-*o*-tolyl-4(3*H*)-quinazolinone (II)] and mecloqualone [2-methyl-3-(2′-chlorophenyl)-4(3*H*)-quinazolinone (III)].

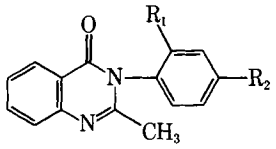

$R_1 = OCH_3$, $R_2 = NO_2$ (Nitromethaqualone, I)
$R_1 = CH_3$, $R_2 = H$ (methaqualone, II)
$R_1 = Cl$, $R_2 = H$ (mecloqualone, III)

The abuse of methaqualone (1–3) and mecloqualone (4) has been reported previously. Both drugs are metabolized extremely well in humans and animals (5–12), with detection of the unchanged drug in the urine being difficult when therapeutic amounts have been ingested. Detection in urine samples is usually done by means of the metabolites (13, 14).

Neither the metabolism of nitromethaqualone nor its analysis in urine samples has been established previously.

The present report deals with the metabolism of nitromethaqualone in humans and rats, along with the detection of the drug in urine samples for clinical and medicolegal practice. The excretion in rats was studied with [2-^{14}C]2-methyl -3- (2′-methoxy-4′-nitrophenyl)-4(3*H*)-quinazolinone.

[1] Parnox, Sopar, Brussels, Belgium.

EXPERIMENTAL

Synthesis of [2-^{14}C]2-Methyl-3-(2′-methoxy-4′-nitrophenyl)-4(3*H*) - quinazolinone—[2-^{14}C]2-Methyl-3-(2′-methoxy-4′-nitrophenyl)-4(3*H*)-quinazolinone was synthesized as shown in Scheme I by condensation of labeled *N*-acetylanthranilic acid with 2-methoxy-4-nitroaniline in toluene in the presence of phosphorus trichloride according to a procedure described previously (15). Labeled *N*-acetylanthranilic acid was prepared by refluxing 1 mmole of anthranilic acid in toluene with 1 mmole of [1-^{14}C]acetyl chloride (specific activity, 5.0 mCi/mmole) until no more hydrochloric acid was liberated. The reaction mixture was cooled to 70°. 2-Methoxy-4-nitroaniline (1 mmole) was added followed by the addition of phosphorus trichloride in toluene over a 10-min period (Scheme I). The mixture then was mixed thoroughly and refluxed for 2 hr in an oil bath. Toluene was evaporated under vacuum and the yellow residue was shaken with 10% aqueous sodium carbonate and extracted twice with 50 ml of chloroform. After evaporation of the solvent, the residue was taken up in benzene and purified on a 10-g column[2]. The column was eluted with 1 liter of benzene. Benzene was removed under vacuum and the residue recrystallized from methanol–water.

The specific activity determined by liquid scintillation counting was 5.0 mCi/mmole. The purity of the prepared compound was tested by TLC using two different solvents: chloroform–acetone–ammonia (50:50:1) and cyclohexane–chloroform–diethylamine (70:20:10). In both solvent systems only one spot could be detected accounting for the complete radioactivity with an R_f value identical to a standard of unlabeled nitromethaqualone. The radioactive spots were localized with a thin-layer scanner[3].

Animal Experiments—A single 2-mg dose of [^{14}C]nitromethaqualone with an activity of 5 μCi/mg suspended in medicinal oil was introduced directly into the stomach of two male Wistar rats, 260 and 312 g, respectively. The rats were housed in metabolic cages; urine and feces were collected separately at 12-hr intervals over 6 days. Urine samples were counted without any treatment; feces samples were counted as described under quantification of radioactivity. Two other rats were each given 30 mg of unlabeled nitromethaqualone. Urine was collected during 6 days and examined for metabolites.

Clinical Study—Two male volunteers were administered single 25-mg nitromethaqualone tablets[1]. Urine was collected at 2–4-hr intervals on the first day and 12-hr specimens were sampled over the next 6 days.

Quantification of Radioactivity—The isotope disintegration rates of all specimens were determined by liquid scintillation spectrometry[4]. Counting mixtures were prepared as follows: 2-ml urine samples were taken up in 15 ml of scintillation liquid[5]; 20- to 40-mg feces samples were rehydrated for 2 hr with 200 μl of water in plastic counting vials and 1 ml of tissue solubilizer[6] was added. The mixtures were incubated for 5 hr

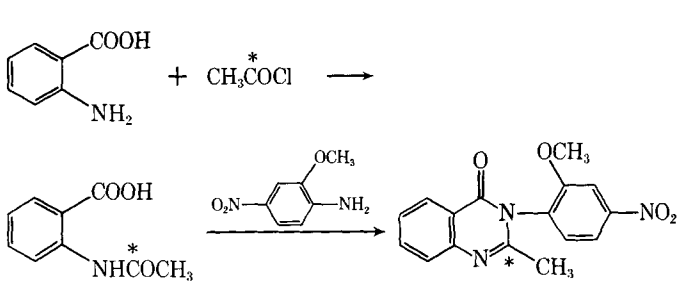

Scheme I—Synthesis of [^{14}C]nitromethaqualone.

[2] Florisil column.
[3] Dünnschicht Scanner LB 2723, Berthold Instruments.
[4] Liquid scintillation counter, model BF 5000/300, Berthold Instruments.
[5] Insta-Gel, Packard.
[6] Soluene-350, Packard.

0022-3549/82/01000-1152$01.00/0

Table I—TLC and GLC of Nitromethaqualone and Metabolites (R_f and R_t Values)

	TLC Solvent System[a] A	B	C	GLC (R_t, min)[b]
2-Methyl-3-(2′-methoxy-4′-nitrophenyl)-4(3*H*)-quinazolinone (nitromethaqualone)	0.79	0.90	0.60	10.6
2-Methyl-3-(4′-nitrophenyl)-4(3*H*)-quinazolinone (internal standard for GLC)	—	—	—	9.0
2-Hydroxymethyl-3-(2′-methoxy-4′-nitrophenyl)-4(3*H*)-quinazolinone (Metabolite I)	0.77	0.84	0.30	Decomposition
2-Methyl-3-(2′-methoxy-4′-aminophenyl)-4(3*H*)-quinazolinone (Metabolite II)	0.52	0.70	0.00	12.8
2-Hydroxymethyl-3-(2′-methoxy-4′-aminophenyl)-4(3*H*)-quinazolinone (Metabolite III)	0.45	0.61	0.00	Decomposition
2-Methyl-3-(2′-methoxy-4′-acetylaminophenyl)-4(3*H*)-quinazolinone (Metabolite IV)	0.52	0.61	0.00	38.4
4-Nitro-2-methoxyaniline (Metabolite V)	0.75	0.92	0.08	1.0
2-Methyl-3-(2′-hydroxy-4′-aminophenyl)-4(3*H*)-quinazolinone (Metabolite VI)	0.25	0.16	0.00	Not eluted
2-Methyl-3-(2′-hydroxy-4′-nitrophenyl)-4(3*H*)-quinazolinone	0.18	0.05	0.00	Not eluted
Trimethylsilyl derivative of Metabolite I	—	—	—	13.4
Trimethylsilyl derivative of Metabolite III	—	—	—	16.6

[a] Solvent A: benzene–*n*-propanol–ammonia (80:20:1); Solvent B: chloroform–acetone–ammonia (50:50:1); Solvent C: cyclohexane–chloroform–diethylamine (70:20:10). [b] OV-17/QF, (1.5%); 260°.

at 60°. After cooling to room temperature, 0.5 ml of isopropanol was added followed by 0.2 ml of hydrogen peroxide (30%) for bleaching. The mixtures were kept at room temperature for 4 hr until transparent.

Finally, 15 ml of a mixture of 9 parts scintillation liquid[5] and 1 part 0.5 *N* HCl was added and the sample counted. Counting efficiency was determined by the internal standard method with ^{14}C-labeled toluene. Efficiency of the different urine samples examined varied between 85 and 99% and of the feces between 65 and 90%. Silica gel zones scraped from thin-layer chromatograms were suspended in 15 ml of scintillation fluid. Solvent extracts were measured following evaporation of the solvent and dissolution of the residue in 15 ml of scintillation liquid[7].

Extraction and Fractionation of Drug Components from Urine Samples—Urine samples were extracted on prepacked kieselguhr columns[8]. Twenty-milliliter samples were poured onto the columns, the aqueous solution was distributed as stationary phase on the chemically inert support, and then eluted with 100 ml of extraction solvent consisting of a mixture of dichloromethane–*n*-propanol (85:15). In this way the lipophilic substances were extracted from the aqueous phase into the organic phase, the aqueous phase remaining on the support (16, 17). The solvent was evaporated under vacuum and the residue taken up in 100 μl of methanol for TLC, GC, and GC–MS examination.

For the study of glucuronides, urine samples were extracted with chloroform at pH 3.0 followed by an extraction with ethyl acetate at pH 9.0. The remaining aqueous phases were submitted to an enzymatic hydrolysis. Therefore, 5 ml of the previously extracted samples were adjusted to pH 5.2 and incubated for 24 hr at 37° with 0.1 ml of β-glucuronidase[9]. The treated samples were handled on columns as described for the direct extraction. TLC examination of radioactive extracts was performed on precoated silica gel plates[10].

The presence of intact [^{14}C]nitromethaqualone was determined by one-dimensional TLC of extracts[8] using System C (Table I). For metabolites, Systems A and B (Table I) were used. Measurements of the isotope disintegration rates of the silica gel areas were carried out as described. For nonradioactive extracts, different metabolites were located by spraying the plates with different reagents specific for definite chemical functions. Aromatic amino functions were detected by the Bratton–Marshall reaction. The plates were sprayed first with a 1:1 mixture of 1% sodium nitrite in water and 1 *N* HCl followed by a solution of 200 mg of *N*-(1-naphthyl)ethylenediamine dihydrochloride in methanol.

Aromatic acetyl amino functions were detected in the same way as described for the aromatic amino functions following acid hydrolysis on the TLC plate to the free amino function. Plates were first sprayed with 2 *N* H_2SO_4 and put in an oven at 130° for 15 min. After cooling, the plates were sprayed as described earlier. Aromatic nitro functions were first reduced to an aromatic amino function by spraying the plates with a 1% titanium trichloride solution. After drying with warm air, the aromatic amino function was detected as described. Phenols were detected by the Folin–Ciocalteu reagent.

The metabolites present in the extracts from human urine samples were isolated by preparative TLC. Silica gel plates (20 × 20 cm, 250-μm thick[11]) were used. The extracts were applied as a band across the plate. Following development with Solvent System B, the separated zones were scraped off and eluted in minicolumns with 10 ml of methanol. The solvent was evaporated under a stream of nitrogen. The residues were then analyzed by GC and GC–MS.

Metabolite Characterization—Metabolites were identified by comparing their mass spectra and chromatographic data (TLC and GLC) with those of synthesized metabolites. The structure of the synthesized nitromethaqualone was confirmed by comparing the obtained physicochemical data with those of the literature (18). The structure of the synthesized metabolites was proved by NMR and mass spectrometry.

The mass spectra were recorded on a single-focusing apparatus[12] operated at 8-kV accelerating voltage, 100-μA trap current, and 70-eV ionization energy. The spectra were recorded either by the direct inlet method for isolated metabolites or synthesized products or by coupling the gas chromatograph to the mass spectrometer.

Optimal GC conditions were as follows: mixed phase, 1.5% OV-17-1.5% QF_1 on 80–100 mesh Gaschrom Q (180 cm × 2-mm i.d.) at 260° or with temperature programming (4°/min from 100 to 260°). The carrier gas was either helium at 60 ml/min (GC–MS) or nitrogen at 30 ml/min (GC).

Products were detected with a nitrogen-phosphorus detector for conventional GC. Identity of the proposed structures from the metabolites were confirmed by synthesis, and NMR spectra[13] were recorded in deuterochloroform as a solvent and tetramethylsilane as an internal standard.

Synthesis of Metabolites—*2-Methyl-3-(2′-hydroxy-4′-nitrophenyl)-4(3H)-quinazolinone*—Acetylanthranilic acid was condensed with 2-hydroxy-4-nitroaniline (15). White crystals with mp 225° were obtained.

2-Methyl-3-(2′-methoxy-4′-nitrophenyl)-4(3H)-quinazolinone (Nitromethaqualone)—The previous product was dissolved in methanol and a solution of diazomethane in ether added in excess. After 30 min the solvents were evaporated and the residue was crystallized. Light yellow crystals with mp 193° were obtained. The structure was identical with the product isolated from commercial nitromethaqualone tablets and confirmed by mass spectrometry and NMR (18). Nitromethaqualone was also prepared by direct condensation of acetylanthranilic acid with 2-methoxy-4-nitroaniline, yield 70%.

2-Methyl-3-(2′-methoxy-4′-aminophenyl)-4(3H)-quinazolinone—Nitromethaqualone (0.5 g) was dissolved in 200 ml of warm 0.2 *N* NaOH; 1 g of sodium dithionite was added and the mixture kept at 80° for 10 min, then it was cooled and extracted twice with a mixture of chloroform–1-propanol (85:15). The solvent was evaporated under vacuum and the yellow residue recrystallized from ethanol. White crystals (mp 205–206°) were obtained, yield 80%. The NMR spectrum of the synthesized compound showed a broad singlet integrating for two protons at $\delta = 4.9$ proving the presence of an amino group. The latter gave a positive reaction with the Bratton–Marshall reagent proving its aromatic nature. The mass spectrum (Table II) confirmed the proposed structure.

Anal.—Calc. for $C_{16}H_{15}N_3O_2$: C, 68.31; H, 5.37; N, 14.94. Found: C, 68.26; H, 5.41; N, 14.82.

2-Methyl-3-(2′-methoxy-4′-acetylaminophenyl)-4(3H)-quinazolinone—2-Methyl-3-(2′-methoxy-4′-aminophenyl)-4(3*H*)-quinazolinone (250 mg) was heated in 200 ml of dry toluene, an equivalent quantity

[7] LipoLuma, Lumac Systems AG, Basel, Switzerland.
[8] Extrelut, Diagnostica Merck, Darmstadt, West Germany.
[9] β-glucuronidase *Escherichia coli*, 100 U/ml, Boehringer, Mannheim, West Germany.
[10] Sil G-25UV$_{254+366}$, Machery-Nagel, Düren, Germany.
[11] DC Fertig Platten Kieselgel 60, F 254, Merck, Darmstadt, West Germany.
[12] A Kratos AEI MS-12 apparatus was used.
[13] NMR spectra were obtained with a Hitachi Perkin-Elmer R 24, 60-MHz apparatus.

Table II—Mass Spectra of Nitromethaqualone and Synthesized Metabolites

		Molecular Ion	Major Peaks m/z (Relative Intensity)				
2-Methyl-3-(2′-methoxy-4′-nitrophenyl)-4(3*H*)-quinazolinone		311 (85)	296 (32)	280 (100)	250 (38)	143 (27)	
2-Hydroxymethyl-3-(2′-methoxy-4′-nitrophenyl)-4(3*H*)-quinazolinone	A	327 (52)	296 (100)		250 (19)		
Corresponding trimethylsilyl derivative	B	384(M-15) (30)	368 (100)	324 (32)	264 (40)		
2-Methyl-3-(2′-methoxy-4′-aminophenyl)-4(3*H*)-quinazolinone	C	281 (100)		264 (27)	250 (80)	143 (35)	
Corresponding trimethylsilyl derivative	D	369 (53)	354 (100)	266 (42)	248 (53)		
2-Hydroxymethyl-3-(2′-methoxy-4′-aminophenyl)-4(3*H*)-quinazolinone	E	297 (41)	266 (21)	123 (100)			
2-Methyl-3-(2′-methoxy-4′-acetylaminophenyl)-4(3*H*)-quinazolinone	F	323 (75)	308 (25)	292 (100)	281 (45)	250 (50)	143 (90)
2-Nitro-2-methoxyaniline	G	168 (100)	153 (18)	137 (20)	58 (26)		
2-Methyl-3-(2′-hydroxy-4′-aminophenyl)-4(3*H*)-quinazolinone	H	267 (100)	252 (33)	251 (26)	225 (60)	143 (20)	

of acetic anhydride was added, and the mixture refluxed for 30 min. The reaction mixture was allowed to cool then neutralized and extracted with ether. The extract was dried on anhydrous sodium sulfate and evaporated. The residue was recrystallized from methanol. White crystals (mp 256°) were obtained, yield 82%. The NMR spectrum showed a singlet at δ = 2.15 integrating for three protons proving the presence of an acetyl group in the molecule. The mass spectrum from this compound (Table II) confirmed the proposed structure.

Anal.—Calc. for $C_{18}H_{17}N_3O_3$: C, 66.86; H, 5.30; N, 13.00. Found: C, 66.91; H, 5.21; N, 13.09.

2-Hydroxymethyl-3-(2′-methoxy-4′-nitrophenyl)-4(3H)-quinazolinone—The synthesis of an analogous methaqualone metabolite (Scheme II) was carried out using a procedure described previously (19). Glycolic acid was taken up in an excess of thionyl chloride and the mixture kept at room temperature for 25 hr. The excess thionyl chloride was then evaporated and the residue taken up in dry toluene, along with an equivalent amount of anthranilic acid, and refluxed for 1 hr. The solvent was evaporated under vacuum, and the residue was taken up in acetic acid and treated with sodium acetate and acetic anhydride in slight excess [1.5 mole of both for 1 mole of *N*-(hydroxyacetyl)anthranilic acid]. The mixture was heated to 100° for 2 hr and then concentrated *in vacuo*. The residue was taken up in chloroform and washed with 5% sodium carbonate. The chloroform was evaporated under vacuum and the resulting *N*-(acetoxyacetyl)anthranilic acid condensed with 2-methoxy-4-nitroaniline in the usual way (15).

The obtained ester was dissolved in a 100:25 mixture of dioxane–5 *M* HCl. The mixture was boiled for 10 min then cooled and the hydrochloride filtered off. The base was isolated by dissolving the hydrochloride in chloroform and adding 0.2 *N* NaOH. The chloroform was evaporated and the residue crystallized from methanol–water. White crystals with mp 169–170° were obtained, yield 10%. The NMR spectrum of this compound showed a singlet at δ = 4,2 integrating for two protons replacing the singlet at δ = 2,2 integrating for three protons in nitromethaqualone. An additional broad singlet integrating for one proton was observed at δ = 3,4 corresponding to an hydroxyl proton.

Anal.—Calc. for $C_{16}H_{13}N_3O_5$: C, 58.72; H, 4.00; N, 12.84. Found: C, 58.62; H, 3.94; N, 12.77.

2-Hydroxymethyl-3-(2′-methoxy-4′-aminophenyl)-4(3H)-quinazolinone—This compound was prepared by alkaline reduction of 2-methyl-3-(2′-methoxy-4′-nitrophenyl)-4(3*H*)-quinazolinone in alkaline medium with sodium dithionite. The reaction product was extracted with a mixture of chloroform–2-propanol (85:15). White crystals (mp 290°, dec.) were obtained, yield 92%. The NMR spectrum of the compound showed an additional broad singlet at δ = 4,9 in comparison to the starting compound proving the presence of an amino group. The last gives a positive Bratton–Marshall reaction proving its aromatic nature. The mass spectrum (Table II) confirms the proposed structure.

Anal.—Calc. for $C_{16}H_{15}N_3O_3$: C, 64.64; H, 5.09; N, 14.13. Found: C, 64.69; H, 5.13; N, 14.22.

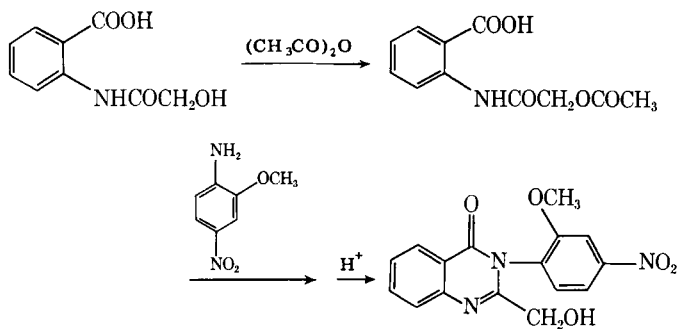

Scheme II—Synthesis of 2-hydroxymethyl-3-(2′-methoxy-4′-nitrophenyl)-4(3H)-quinazolinone.

RESULTS

Rat Experiments—*Identification of Urinary Metabolites*—After counting the individual urine samples, the residual collected samples were pooled and extracted on columns[8], and 21–25% of the total urinary radioactivity was extracted. TLC of the extract using Solvent System C separated a compound with R_f = 0.30 (Metabolite I). The remaining radioactivity was located at the start of the chromatogram. Intact [^{14}C]nitromethaqualone (R_f = 0.6) could not be detected. The same plate was now run with Solvent System B allowing the detection of two additional radioactive zones with R_f = 0.7 (Zone II) and 0.61 (Zone III). This made it possible to locate on a plate the corresponding zones of metabolites in urine extracts of rats treated with unlabeled nitromethaqualone. The latter were applied in 10-cm bands across the plates. One centimeter of this band was overspotted with the extract from [^{14}C]nitromethaqualone-treated rats and the plates run in Solvent System B. After localizing the radioactive zones, the corresponding nonradioactive zones were scraped off and extracted with methanol. The solvent was evaporated and the residue examined by GC and GC–MS.

Metabolite I—The metabolite isolated from Zone I appeared to consist of one single spot on TLC with all solvent systems, A, B, and C. GC of the product, however, showed a broad peak of two maxima with R_t = 13.4 and 13.6 min, respectively. Following silylation with trimethylsilylimidazole[14], only one homogeneous peak was observed. The mass spectrum of the product recorded *via* solid probe (Table II,A) was different from the product recorded by GC–MS indicating that the metabolite decomposed under the described gas chromatographic conditions. The mass spectrum of Metabolite I recorded by the direct inlet method indicated a molecular ion at *m/z* 327 representing an addition of one oxygen to nitromethaqualone. The mass spectrum of the trimethylsilyl derivative (Table II,B) showed one silylated function, indicating the presence of an hydroxyl group in the molecule. This, however, is not located on one of the phenyl nuclei as could be shown from the fragmentation pattern of both silylated and underivatized metabolites. This metabolite proved to be identical with the synthesized 2-hydroxymethyl-3-(2′-methoxy-4′-nitrophenyl)-4(3*H*)-quinazolinone.

Metabolites II, III, and IV—The product isolated from Zone II was examined by GC and showed one homogeneous peak with an R_t value of 12.8 min (Metabolite II). The mass spectrum obtained with GC–MS (Table II,C) revealed a molecular ion at *m/z* 281 and a fragment ion at *m/z* 250 indicating the loss of a methoxy fragment. The metabolite showed a positive Bratton–Marshall reaction. All those characteristics

[14] Pierce Eurochemie NV, Rotterdam, Holland.

Table III—Excretion of Total Radioactivity in Urine and Feces of [^{14}C]Nitromethaqualone-Treated Rats [a]

Excretion, End of Period, hr	Dose Excreted, % Urine Rat I	Urine Rat II	Feces Rat I	Feces Rat II
24	10.0	10.2	9.8	13.1
48	23.5	18.2	45.5	26.3
72	26.0	22.0	56.8	48.1
96	27.0	24.0	58.7	54.2
120	27.2	24.4	59.7	54.9
144	27.3	24.6	59.9	55.0

[a] Expressed as cumulative percent.

Table IV—Percent of [^{14}C]Nitromethaqualone and Metabolites Present in the Direct Extracts from Rat Urine

Drug and Metabolites	Recovered Radioactivity (Extract, %)[a]
Nitromethaqualone	0
Metabolite[b] I	8
Metabolite II	40
Metabolite III	19
Metabolite IV	14
Not identified	19

[a] The values are averages of results on two rats. [b] Symbols correspond to metabolites given in the text.

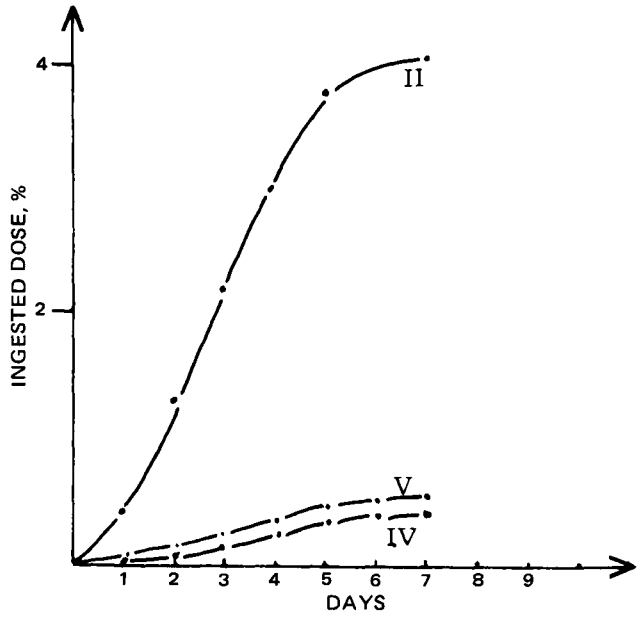

Figure 1—*Cumulative excretion graph of nitromethaqualone Metabolites II, IV, and V in humans.*

were identical with those of synthesized 2-methyl-3-(2′-methoxy-4′-aminophenyl)-4(3*H*)-quinazolinone.

Zone III, isolated with Solvent System B, was reexamined with Solvent System A and consisted of two distinct products with R_f values of 0.45 and 0.52. In this way both compounds of Zone III were separated on a preparative scale and examined separately with GC and GC–MS. The zone with R_f = 0.52 on GC showed different peaks when analyzed without derivatization. Following silylation with trimethylsilylimidazole, one homogeneous peak eluted with R_t = 16.6 min. The mass spectrum of this product obtained with the direct inlet method indicated a molecular ion at *m/z* 297 (Table II,E). The silylated derivative showed one silylated hydroxyl function (Table II,D). Fragmentation patterns of both the underivatized metabolite and silylated derivative showed that this is not located on one of the phenyl nuclei of the molecule. The metabolite showed also a positive Bratton–Marshall reaction. These characteristics suggest 2-hydroxymethyl-3-(2′-methoxy-4′-aminophenyl)-4(3*H*)-quinazolinone as a possible structure for this metabolite. This structure was confirmed by synthesis of the expected metabolite (Metabolite III). The zone with an R_f value of 0.45 in Solvent System A showed one homogeneous peak with an R_t value of 43 min on GC (Metabolite IV).

The mass spectrum recorded by GC–MS indicated a molecular ion at *m/z* 323 (Table II,F). The transition *m/z* 292 to *m/z* 250 proved by the presence of a metastable peak corresponds to the loss of ketene and indicates the presence of an acetyl group in the molecule. The metabolite showed only a positive Bratton–Marshall reaction on the plate following acid hydrolysis, indicating the presence of an aromatic acetylamino group. Those characteristics suggest that Metabolite IV is the acetylated form of Metabolite II. The structure could be confirmed by synthesis of the metabolite. Table I represents the TLC and GC data of nitromethaqualone and its metabolites.

Quantitation of the Metabolites—The cumulative urinary and fecal excretion of nitromethaqualone after a single oral dose of 10-μCi [^{14}C]-nitromethaqualone is given in Table III. Within 6 days, 55–60% of the dose is excreted in the feces while 25–27% is excreted in the urine.

Aliquots of the collected urine samples were extracted on kieselguhr columns. In this way 21 and 25%, respectively, of the radioactivity present in the urine of the two rats could be extracted.

The concentrated extracts were chromatographed on silica gel plates using the described solvent. The radioactive zones were scraped off and counted as described. The quantitative amounts of the different metabolites present in definite areas are given in Table IV. Metabolite II is the major metabolite (40%). Unchanged nitromethaqualone could not be detected. The measured radioactivity (19%) remained at the start of the chromatogram and was not further examined. From the kieselguhr columns used for extraction, remaining polar metabolites, probably consisting of glucuronides, could not be eluted. Following enzymatic hydrolysis with β-glucuronidase of urine samples previously extracted with chloroform and ethyl acetate at pH 3.0 and 9.0, only Metabolites I and III could be identified in the same way as described above, proving their excretion as conjugates with glucuronic acid. No quantitative data, however, could be obtained due to the instability of the amino compound during the reaction procedure.

Human Studies—The metabolism in humans was studied only with unlabeled nitromethaqualone. Aliquots of the different urine samples were pooled and extracted as described. The extracts were examined by analytical and preparative TLC as for the study on urine from rats. Solvent System C was used for detecting unchanged nitromethaqualone and the hydroxymethyl derivative (Metabolite I). Neither nitromethaqualone nor Metabolite I could be detected in human urine. TLC with Solvent System B resulted in three spots showing a positive Bratton–Marshall reaction corresponding to R_f values of 0.90, 0.70, and 0.16 and one additional spot at R_f = 0.61 reacting positively only following acid hydrolysis on the plate. Preparative TLC allowed isolation of all four metabolites. The zone with R_f = 0.90 showed on GC one single homogeneous peak at 170°. The mass spectrum (Table II,G) revealed a molecular ion at *m/z* 168. Loss of 31 indicates the presence of an intact methoxy group.

Furthermore, a positive Bratton–Marshall reaction indicates the presence of an aromatic amino group. The spectrum is compatible with 2-methoxy-4-nitroaniline as a possible structure of this metabolite (Metabolite V). This product could be obtained from a commercial source[15] and proved to be identical with the isolated metabolite. The zone

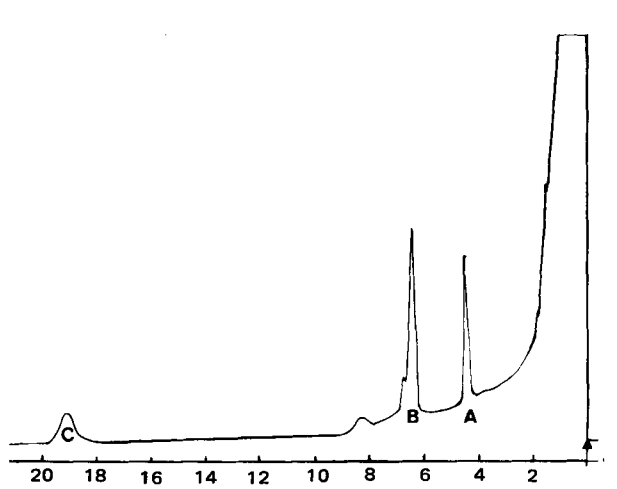

Figure 2—*Typical gas chromatogram from a urine extract. Key: (A) internal standard; (B) Metabolite III; (C) Metabolite IV.*

[15] Riedel-de-Haën AG, Seelze, Hannover, West Germany.

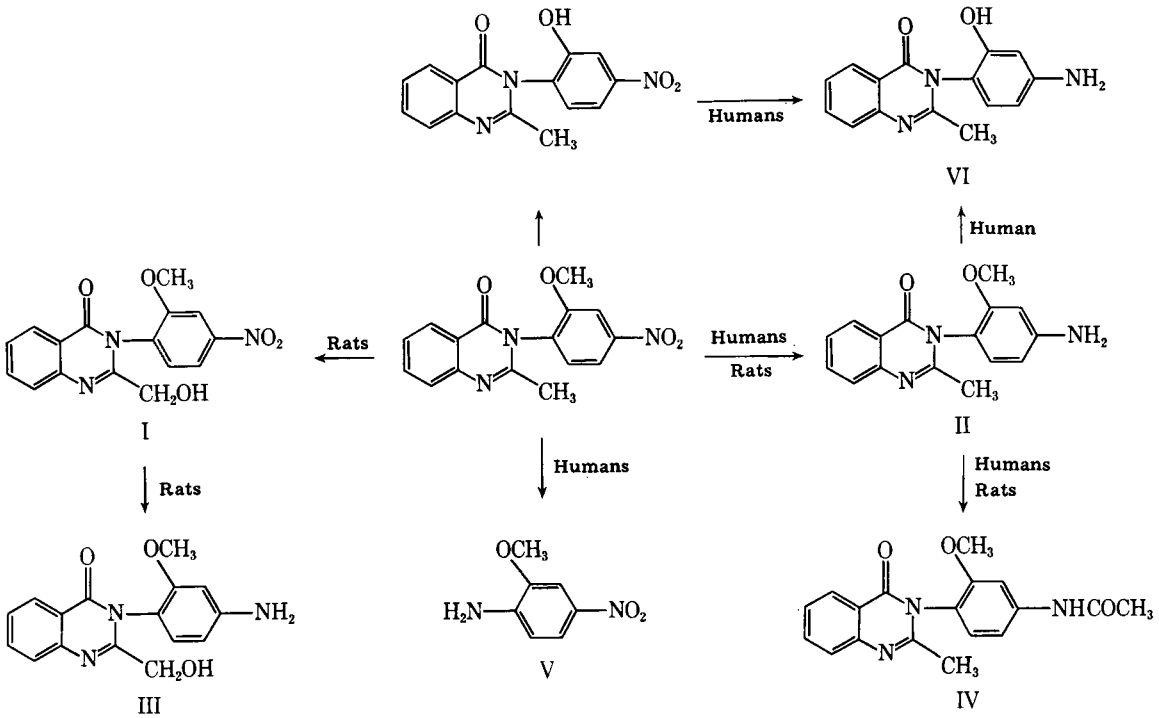

Scheme III—Metabolic pathways of nitromethaqualone in humans and rats.

with an R_f value of 0.70 showed one peak on GC at 260°. The mass spectrum proved to be identical with the spectrum of Metabolite II already identified in the urine of treated rats. Likewise, the zone with R_f = 0.61 appeared to be identical with Metabolite IV. The zone with R_f = 0.16 reacts not only positively with the Bratton–Marshall reagent but also with the Folin–Ciocalteu reagent. The product could only be analyzed by GC following methylation with diazomethane. The resulting peak showed the R_f value of Metabolite II along with an identical mass spectrum. The most important fragment ions of the mass spectrum of the metabolite prior to methylation are represented in Table II,H. The molecular ion shows at m/z 267. All these characteristics suggest 2-methyl-3-(2′-hydroxy-4′-aminophenyl)-4(3*H*)-quinazolinone as a possible structure (Metabolite VI). This structure was proved to be correct by synthesis. After enzymatic hydrolysis with β-glucuronidase, Metabolite VI could be detected in the extract. No quantitative data could be obtained, since the metabolite was not stable in the course of the reaction.

Cumulative excretion curves (Fig. 1) in humans were established for Metabolites II, IV, and V. Therefore, following administration of nitromethaqualone, urine samples were collected at regular intervals and the metabolite concentration per milliliter determined. Upon multiplication by the volume of urine excreted during the collecting period, the amount of metabolites was obtained. The additive amounts excreted for each collecting period were then plotted *versus* time of collecting intervals.

Metabolites II and IV were determined by GC. Therefore, 20-ml urine samples, to which 2-methyl-3-(4′-nitrophenyl)-4(3*H*)-quinazolinone had been added as an internal standard, were extracted as described above. The concentrated extracts were injected on a mixed phase 1.5% OV-17, 1.5% QF_1 column at 260° and detected with a nitrogen-phosphorus detector. Figure 2 shows a typical gas chromatogram of a urine extract. Metabolite V was determined by TLC. The violet color of the spots following a Bratton–Marshall reaction was measured on the plate in comparison with known amounts of the reference compound.

DISCUSSION

Nitromethaqualone is eliminated from rats and humans by biotransformation. No unchanged drug can be detected in urine samples. In both rats and humans, 2-methyl-3-(2′-methoxy-4′-aminophenyl)-4(3*H*)-quinazolinone is quantitatively the most important unconjugated metabolite. Both species excrete this metabolite partially in the acetylated form. In rats but not in humans, oxidation of the 2-methyl group to 2-hydroxymethyl-3-(2′-methoxy -4′ -nitrophenyl)-4(3*H*)-quinazolinone along with reduction of the nitro function of the latter to 2-hydroxymethyl-3-(2′-methoxy-4′-aminophenyl)-4(3*H*)-quinazolinone represents two other important metabolites, both being excreted also as conjugates with glucuronic acid. The slow urinary excretion along with the protracted fecal excretion of carbon 14 in the rats suggests an extensive enterohepatic circulation. In addition, human subjects excrete 2-methoxy-4-nitroaniline indicating cleavage of the quinazolinone nucleus. *O*-Demethylation followed by reduction of the nitro group is a minor metabolic pathway in humans (Scheme III). The slow urinary excretion in the urine of the formed metabolites in humans may be related to a continuous reabsorption of the biliary fraction. The method, as described for the extraction and analysis of urine extracts, using Solvent System B and the reagents for the Bratton–Marshall reaction, makes it possible to demonstrate nitromethaqualone intake even in a therapeutic dose. For legal practice, a GC–MS examination for the presence of the major metabolite in humans [2-methyl-3-(2′-methoxy-4′-aminophenyl)-4(3*H*)-quinazolinone] should confirm the TLC results.

REFERENCES

(1) D. S. Inaba, G. R. Gray, J. A. Newmeyer, and C. Whitehead, *J. Am. Med. Assoc.*, **224**, 1505 (1973).

(2) E. F. Pascarelli, *ibid.*, **224**, 1512 (1973).

(3) M. Schwartzburg, J. Lieb, and A. H. Schwartz, *Arch. Gen. Psychiatry*, **29**, 46 (1973).

(4) Anonymous, *Microgram*, **7**, 64 (1974).

(5) F. R. Preusz, H. M. Hassler, and R. Kopf, *Arzneim-Forsch.* (*Drug Research*), **16**, 395 (1966).

(6) F. R. Preusz, H. M. Hassler, and R. Kopf, *ibid.*, **16**, 401 (1966).

(7) F. R. Preusz and H. M. Hassler, *ibid.*, **20**, 1920 (1970).

(8) F. R. Preusz, H. Hoffman-Pinther, H. Achenbach, and H. Friebolon, *Pharmazie*, **25**, 752 (1970).

(9) H. Nowak, G. Schorre, and R. Struller, *Arzneim-Forsch.* (*Drug Research*), **16**, 407 (1966).

(10) M. Akagi, Y. Oketani, and S. Yamane, *Chem. Pharm. Bull.*, **11**, 1216 (1963).

(11) P. Daenens and M. Van Boven, *Arzneim-Forsch.* (*Drug Research*), **24**, 195 (1974).

(12) B. Dubnick and C. A. Towne, *Toxicol. Appl. Pharmacol.*, **15**, 632 (1969).

(13) R. C. Permisohn, L. H. Hilpert, and L. Kazyak, *J. Forensic Sci.*, **21**, 98 (1976).

(14) M. Van Boven, G. Janssen, and P. Daenens, *Mikrochim. Acta*, **1974**, 603.

(15) H. W. Grimmel, A. Guenther, and J. F. Morgan, *J. Am. Chem.*

Soc., 68, 542 (1946).
(16) J. Breiter, *J. Clin. Chem. Biochem.*, 14, 46 (1976).
(17) J. Breiter and R. Helger, *Z. Clin. Chem. Biochem.*, 13, 254 (1975).
(18) P. Daenens and M. Van Boven, *J. Forensic Sci.*, 21, 552 (1976).
(19) C. Bogentoft, O. Ericsson, and B. Danielsson, *Acta Pharm. Suecica*, 11, 59 (1974).

ACKNOWLEDGMENTS

The authors thank the NFWO for financial assistance.

Guinea Pig Ear as a New Model for *In Vivo* Percutaneous Absorption

H. Y. ANDO ˣ, E. T. SUGITA, R. L. SCHNAARE, and L. BOGDANOWICH

Received October 29, 1981, from the *Department of Pharmacy, Philadelphia College of Pharmacy and Science, Philadelphia, PA 19104.* Accepted for publication December 29, 1981.

Abstract □ A new animal model for *in vivo* percutaneous absorption utilizing the hairless, relatively thick skin of the guinea pig ear is proposed. Topical absorption studies were carried out with [^{14}C]hydrocortisone and [^{14}C]testosterone. Systemic studies were also conducted to correct for incomplete urinary excretion. In addition, a single stratum corneum correction factor was developed from published data to enable the guinea pig ear skin to be directly compared with human forearm skin. A comparison of human percutaneous absorption with the corrected guinea pig ear absorption shows a high correlation for both hydrocortisone and testosterone. The effects of ambient changes in relative humidity are also discussed with respect to *in vivo* percutaneous absorption.

Keyphrases □ Guinea pig ear—model for *in vivo* percutaneous absorption, hydrocortisone, testosterone □ Absorption—percutaneous, guinea pig ear, *in vivo* model, hydrocortisone, testosterone □ Hydrocortisone—guinea pig ear, model for *in vivo* percutaneous absorption, testosterone □ Testosterone—guinea pig ear, model for *in vivo* percutaneous absorption, hydrocortisone

Various animal species have been used to study percutaneous absorption *in vivo*. Percutaneous absorption rates of common laboratory rodents such as rats and rabbits have been studied (1). These studies have shown that the back skin of these animals absorb a selected number of substances much more rapidly than the ventral surface of the human forearm (2, 3). Higher species of mammals including hairless dogs (4), rhesus monkeys (5), and miniature swine (1) have also been studied. Of these species, it has been concluded (6) that the rhesus monkey and the miniature swine percutaneous absorption characteristics correlated best with human penetration. The obvious disadvantage of using swine and monkeys include cost and the need for special animal facilities.

One important determinant of percutaneous absorption is the thickness of the stratum corneum. If two areas of skin are sufficiently similar, then one would expect percutaneous absorption to be inversely proportional to the number of stratum corneum layers in the skin. The percutaneous absorption of hydrocortisone from a number of different anatomical sites in humans has been determined previously (7). The number of stratum corneum layers at these sites has also been determined (8). If a proportional relationship between thickness and absorption can be established in humans, this provides a rationale to correct animal model data for thickness. However, the problem with most animal models is that skin with fur generally has a thin stratum corneum (9). Consequently, changes of one or two layers could cause corrections as much as 50% if the stratum corneum is very thin. An ideal animal surface would have to be relatively large and essentially hairless. The guinea pig ear appeared to meet the desired criteria.

EXPERIMENTAL

Male albino guinea pigs, 250–300 g, were individually acclimated for 1 day in metabolism cages[1]. Water and guinea pig chow were given *ad libitum*. For topical application of [^{14}C]hydrocortisone (I) or [^{14}C]testosterone (II), the animals were lightly anesthetized in a bell jar with methoxyflurane[2]. One ear of an animal was sandwiched with medium pressure between two halves of Karush-type dialysis chambers without caps[3]. A 4 μg/cm^3 volume of one of the ^{14}C-labeled compounds reconstituted in acetone was applied in a 40-μl volume to a 1.77-cm^2 area with a flat tip 50-μl syringe[4] to the dorsal surface of the ear. After the acetone had evaporated, the dialysis chambers were removed, and the animals were returned to their metabolism cages. For systemic administration, the ^{14}C-compounds were solubilized first in 50 μl of ethanol and then in 1 ml of sterile saline. The animals were then dosed intraperitoneally with a 0.5-ml volume.

Urine samples were collected daily. The urine was acidified with glacial acetic acid to a pH of 5 to solubilize the magnesium and calcium phosphate precipitates. A 1-ml aliquot was counted on a liquid scintillation counter[5] using 10 ml of liquid scintillation cocktail[6]. The internal standard method using [^{14}C]toluene[7] was used to correct for quench. Relative humidity readings were taken daily using a wet–dry thermometer.

RESULTS

Thickness of the Stratum Corneum and Absorption—Table I presents the determination of:

$$N \times A = K \qquad \text{(Eq. 1)}$$

where N is the number of cell layers in the stratum corneum (8), A is the percent of drug absorbed in 5 days (7), and K is the inverse proportionality constant. These results from human data show that K (forearm) differs from K (back) by only 9.8%. It would be desirable to have more data to confirm this result for different compounds besides hydrocortisone in humans. Nevertheless, one form of verification would be to use a single correction factor to relate guinea pig ear data to the human forearm for a number of different compounds. If Eq. 1 holds, then this

[1] Nalge Co., Rochester, N.Y.
[2] Abbott Lab., North Chicago, Ill.
[3] Belco Glass Co., Vineland, N.J.
[4] Hamilton.
[5] Model 3385 Tri-Carb.
[6] Fisher Scientific Co., Fair Lawn, N.J.
[7] New England Nuclear, Boston, Mass.

0022-3549/82/01000-1157$01.00/0

Soc., 68, 542 (1946).
(16) J. Breiter, *J. Clin. Chem. Biochem.*, 14, 46 (1976).
(17) J. Breiter and R. Helger, *Z. Clin. Chem. Biochem.*, 13, 254 (1975).
(18) P. Daenens and M. Van Boven, *J. Forensic Sci.*, 21, 552 (1976).
(19) C. Bogentoft, O. Ericsson, and B. Danielsson, *Acta Pharm. Suecica*, 11, 59 (1974).

ACKNOWLEDGMENTS

The authors thank the NFWO for financial assistance.

Guinea Pig Ear as a New Model for *In Vivo* Percutaneous Absorption

H. Y. ANDO ˣ, E. T. SUGITA, R. L. SCHNAARE, and L. BOGDANOWICH

Received October 29, 1981, from the *Department of Pharmacy, Philadelphia College of Pharmacy and Science, Philadelphia, PA 19104.* Accepted for publication December 29, 1981.

Abstract □ A new animal model for *in vivo* percutaneous absorption utilizing the hairless, relatively thick skin of the guinea pig ear is proposed. Topical absorption studies were carried out with [^{14}C]hydrocortisone and [^{14}C]testosterone. Systemic studies were also conducted to correct for incomplete urinary excretion. In addition, a single stratum corneum correction factor was developed from published data to enable the guinea pig ear skin to be directly compared with human forearm skin. A comparison of human percutaneous absorption with the corrected guinea pig ear absorption shows a high correlation for both hydrocortisone and testosterone. The effects of ambient changes in relative humidity are also discussed with respect to *in vivo* percutaneous absorption.

Keyphrases □ Guinea pig ear—model for *in vivo* percutaneous absorption, hydrocortisone, testosterone □ Absorption—percutaneous, guinea pig ear, *in vivo* model, hydrocortisone, testosterone □ Hydrocortisone—guinea pig ear, model for *in vivo* percutaneous absorption, testosterone □ Testosterone—guinea pig ear, model for *in vivo* percutaneous absorption, hydrocortisone

Various animal species have been used to study percutaneous absorption *in vivo*. Percutaneous absorption rates of common laboratory rodents such as rats and rabbits have been studied (1). These studies have shown that the back skin of these animals absorb a selected number of substances much more rapidly than the ventral surface of the human forearm (2, 3). Higher species of mammals including hairless dogs (4), rhesus monkeys (5), and miniature swine (1) have also been studied. Of these species, it has been concluded (6) that the rhesus monkey and the miniature swine percutaneous absorption characteristics correlated best with human penetration. The obvious disadvantage of using swine and monkeys include cost and the need for special animal facilities.

One important determinant of percutaneous absorption is the thickness of the stratum corneum. If two areas of skin are sufficiently similar, then one would expect percutaneous absorption to be inversely proportional to the number of stratum corneum layers in the skin. The percutaneous absorption of hydrocortisone from a number of different anatomical sites in humans has been determined previously (7). The number of stratum corneum layers at these sites has also been determined (8). If a proportional relationship between thickness and absorption can be established in humans, this provides a rationale to correct animal model data for thickness. However, the problem with most animal models is that skin with fur generally has a thin stratum corneum (9). Consequently, changes of one or two layers could cause corrections as much as 50% if the stratum corneum is very thin. An ideal animal surface would have to be relatively large and essentially hairless. The guinea pig ear appeared to meet the desired criteria.

EXPERIMENTAL

Male albino guinea pigs, 250–300 g, were individually acclimated for 1 day in metabolism cages[1]. Water and guinea pig chow were given *ad libitum*. For topical application of [^{14}C]hydrocortisone (I) or [^{14}C]testosterone (II), the animals were lightly anesthetized in a bell jar with methoxyflurane[2]. One ear of an animal was sandwiched with medium pressure between two halves of Karush-type dialysis chambers without caps[3]. A 4 μg/cm^3 volume of one of the ^{14}C-labeled compounds reconstituted in acetone was applied in a 40-μl volume to a 1.77-cm^2 area with a flat tip 50-μl syringe[4] to the dorsal surface of the ear. After the acetone had evaporated, the dialysis chambers were removed, and the animals were returned to their metabolism cages. For systemic administration, the ^{14}C-compounds were solubilized first in 50 μl of ethanol and then in 1 ml of sterile saline. The animals were then dosed intraperitoneally with a 0.5-ml volume.

Urine samples were collected daily. The urine was acidified with glacial acetic acid to a pH of 5 to solubilize the magnesium and calcium phosphate precipitates. A 1-ml aliquot was counted on a liquid scintillation counter[5] using 10 ml of liquid scintillation cocktail[6]. The internal standard method using [^{14}C]toluene[7] was used to correct for quench. Relative humidity readings were taken daily using a wet–dry thermometer.

RESULTS

Thickness of the Stratum Corneum and Absorption—Table I presents the determination of:

$$N \times A = K \qquad \text{(Eq. 1)}$$

where N is the number of cell layers in the stratum corneum (8), A is the percent of drug absorbed in 5 days (7), and K is the inverse proportionality constant. These results from human data show that K (forearm) differs from K (back) by only 9.8%. It would be desirable to have more data to confirm this result for different compounds besides hydrocortisone in humans. Nevertheless, one form of verification would be to use a single correction factor to relate guinea pig ear data to the human forearm for a number of different compounds. If Eq. 1 holds, then this

[1] Nalge Co., Rochester, N.Y.
[2] Abbott Lab., North Chicago, Ill.
[3] Belco Glass Co., Vineland, N.J.
[4] Hamilton.
[5] Model 3385 Tri-Carb.
[6] Fisher Scientific Co., Fair Lawn, N.J.
[7] New England Nuclear, Boston, Mass.

0022-3549/82/01000-1157$01.00/0

Table I—Inverse Relationship for Hydrocortisone Between Absorption and Stratum Corneum Thickness (Cell Layers)

	Number of Cell Layers[a] (N)	Absorbed/ 5 Days[b], % (A)	Inverse Constant[c] (K)
Forearm (ventral)	21.9	1.04	22.78
Back	16.3	1.26	20.54

[a] See ref. 8. [b] See ref. 7. [c] $K = NA$.

Table II—Recovery of Radioactivity in Urine Following Intraperitoneal (ip) and Topical (t) Administration

Penetrant	n	Admin. Dose/Day (d), % d 1	d 2	d 3	d 4	d 5	Total Absorption Dose, %	Range
I,ip	2	82.1	4.9	1.3	0.9	1.3	93.1	(89.1, 96.8)
I,t[a]	4	0.3	0.8	1.0	0.9	0.9	3.9	(2.8, 5.5)
II,ip	2	62.9	7.2	2.1	1.3	1.0	74.5	(74.4, 74.6)
II,t[a]	3	7.5	7.3	6.4	1.8	2.5	25.9	(22.8, 29.3)

[a] Corrected for recovery following intraperitoneal administration and for stratum corneum thickness of the guinea pig ear.

correction factor would be determined from the relation:

$$A_h = (N_g/N_h)\, A_g \qquad \text{(Eq. 2)}$$

where the subscripts h and g refer to the human forearm and the guinea pig ear, respectively. The values, N_g is 11 and N_h is 21.9, have been determined previously (8, 10). The correction factor, N_g/N_h, is therefore 0.502.

Guinea Pig Ear Absorption—Table II shows the recovery of ^{14}C-labeled compound following intraperitoneal and topical administration of hydrocortisone and testosterone for a 5-day period. The intraperitoneal data were used to correct the topical studies for incomplete excretion. Equation 2 was also used to correct the topical studies for stratum corneum thickness. Figure 1 shows a comparison of the corrected percent of topical hydrocortisone not absorbed for humans (2) and for the guinea pig ear. Similarly, Fig. 2 shows a comparison for testosterone between humans (2), rats (1), rabbits (1), and the guinea pig ear. In Fig. 3, the corrected percent of the dose absorbed is shown for hydrocortisone and testosterone on days 1 and 5. On day 1, the ratio of guinea pig ear to human forearm absorption is nearly 1, whereas by day 5, this ratio is nearly 2.

Effect of Ambient Relative Humidity—In Fig. 4, the corrected percent of drug absorbed by the guinea pig ear is shown for hydrocortisone and testosterone over a 10-day period. Each point is plotted

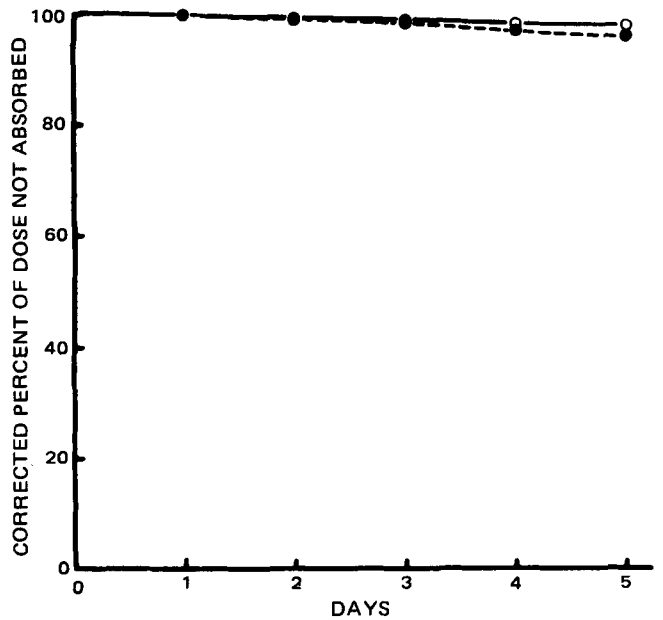

Figure 1—*Percutaneous absorption of hydrocortisone in humans and guinea pig ear. Key: (○) human (2); (●) guinea pig. All data are corrected for recovery following systemic administration. Guinea pig ear data are also corrected for thickness using Eq. 2.*

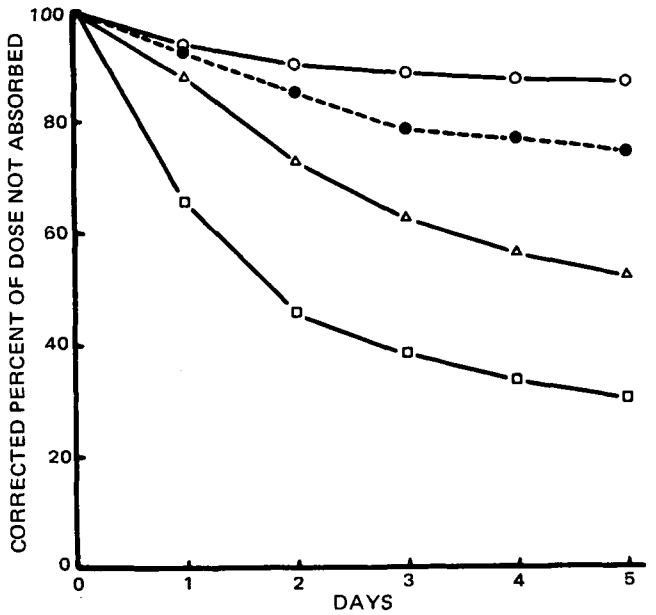

Figure 2—*Percutaneous absorption of testosterone in humans, rats, rabbits, and guinea pig ear. Key: (○) human (2); (●) guinea pig; (△) rat (1); (□) rabbit (1). All data are corrected for recovery following systemic administration. Guinea pig ear data are also corrected for thickness using Eq. 2.*

at the end of its respective 24-hr collection period. Figure 5 shows the relative humidity at the time of urine collection for the hydrocortisone and testosterone experiments. Note in Fig. 4 the drop in the testosterone curve on day 4 and the rise in the hydrocortisone curve on day 5. Corresponding changes in relative humidity can be seen in Fig. 5. It appears that these countertrend changes in percutaneous absorption reflect changes in the ambient relative humidity. Moreover, these changes in relative humidity are also reflected in the volume of urine excreted (Fig.

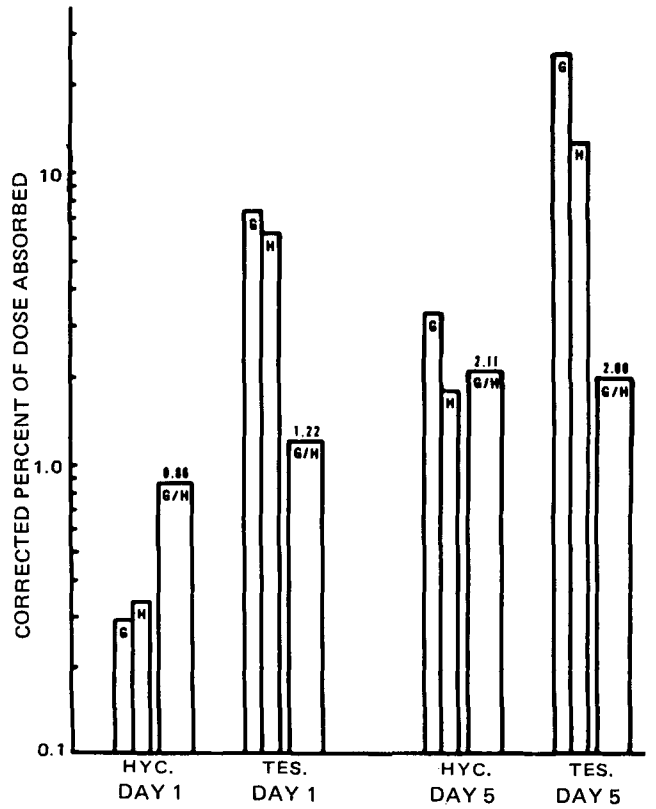

Figure 3—*Comparison of percutaneous absorption in guinea pig ear and humans (2) 1 day and 5 days following topical application. Key: (G) guinea pig; (H) humans.*

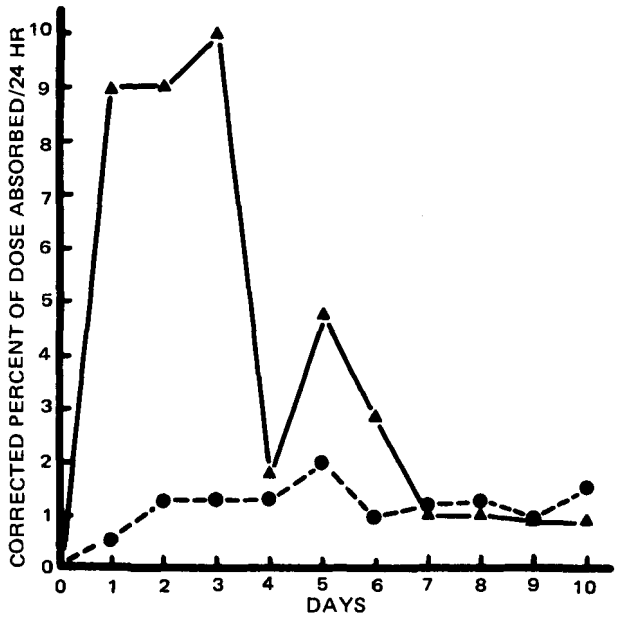

Figure 4—*Percutaneous absorption of hydrocortisone and testosterone over a 10-day period. Key: (▲) testosterone; (●) hydrocortisone. Each point is the average of two animals.*

6) and in the urine color quench (Fig. 7). This can be seen by comparing Fig. 5 with Figs. 6 and 7.

DISCUSSION

To be useful, an animal model should correlate with the desired parameter, and it should be accessible to a large number of researchers. Use of the guinea pig ear as a model for human percutaneous absorption may meet these criteria.

The animal is relatively inexpensive to acquire and house, its ears each have an area of ~3 cm^2, and are essentially hairless. Hairless guinea pig ear skin, as in humans, would be expected to have a thicker stratum corneum than back skin with hair because it must adapt to greater mechanical and temperature stress (1).

Human stratum corneum is on the average of 15 cells thick with a viable layer of 6–10 cells (9, 10). The guinea pig ear skin compares favorably with human skin, having a viable thickness of 7–8 cell layers and a stratum corneum thickness of 10–12 cells (12, 13). In addition, the correlation between epidermal thickness and turnover time (maturation) for human and guinea pig ear epidermises are nearly identical (14). This is important, since the structural organization of normal stratum corneum is dependent upon a slow rate of cell maturation (14).

Percutaneous absorption studies presented here using the guinea pig ear show that for hydrocortisone and testosterone the initial 24-hr period of absorption is comparable to human absorption if a correction is made for differences in stratum corneum thickness. Five-day cumulative absorption in this model is twice as great as in humans. This might be attributed to three possible factors. First, in the human studies (2, 3), the subjects were allowed to wash the application site after the first 24 hr. Thus, some material could have been removed. Second, in our studies no attempt was made to prevent exfoliation of the stratum corneum. It is possible that radioactive squama contamination could have elevated the urine counts. We did not attempt to prevent this because almost any attempt to prevent exfoliation would most likely increase the local moisture content of the stratum corneum. As the relative humidity studies have shown, this can increase absorption. Finally, there may be physical differences between human stratum corneum and guinea pig squama as there may be human differences (15).

In a recent study (16), the guinea pig back skin was used as a model for percutaneous absorption; the much thicker and hairless skin of the guinea pig ear was used as a model in this study. A comparison of the 1-day guinea pig back skin to human forearm absorption ratio (G/H) for hydrocortisone and testosterone (0.30 and 2.23, respectively) showed a much larger variation than the ratios of 0.86 and 1.22, respectively, obtained with the ear model in this report. Similarly, the G/H for the 5-day absorption studies for hydrocortisone and testosterone (1.33 and 3.83, respectively) also showed a much greater variation than the ratios of 2.11 and 2.00, respectively, obtained in this study with the guinea pig ear. The ear skin model would be expected to be a superior model compared to the back skin because the stratum corneum is thicker in accordance with the inverse relationship between stratum corneum thickness and hairiness (9) and the ear is hairless so that no depilation is necessary as it is for the furred back skin.

Hydrocortisone and testosterone were chosen for this study because these compounds are among the slowest and the fastest steroids absorbed by humans. If further studies show that the ratio between the guinea pig ear model and human percutaneous absorption remain constant as they do for these steroids, the guinea pig ear model may prove to be an inexpensive, accessible model for human percutaneous absorption.

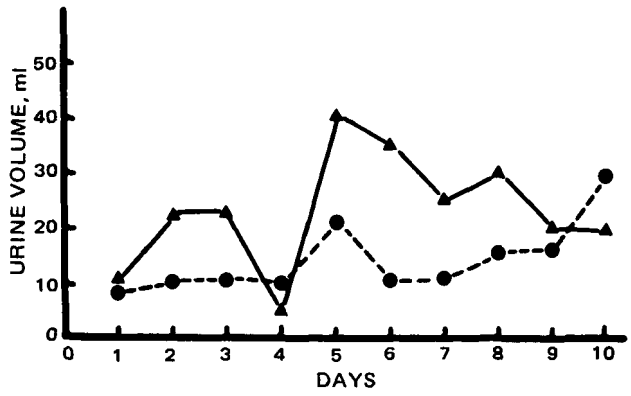

Figure 6—*Volume of urine excreted during 10-day hydrocortisone and testosterone experiments. Key: (▲) testosterone; (●) hydrocortisone.*

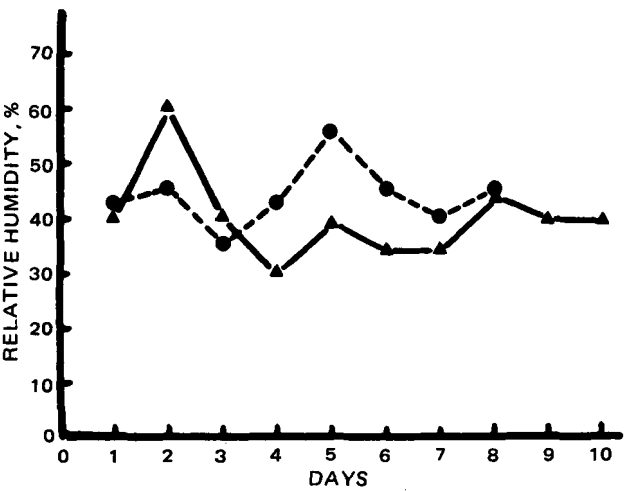

Figure 5—*Relative humidity during 10-day hydrocortisone and testosterone experiments. Key: (▲) testosterone; (●) hydrocortisone.*

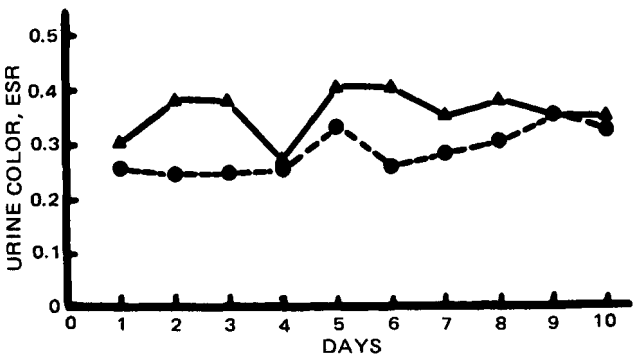

Figure 7—*Urine color during 10-day hydrocortisone and testosterone experiments. Key: (▲) testosterone; (●) hydrocortisone. Urine color was quantified as quench changes in the external standard ratio (ESR) standardization during liquid scintillation counting.*

REFERENCES

(1) M. J. Bartek, J. A. LaBudde, and H. L. Maibach, *J. Invest. Dermatol.*, **58**, 114 (1972).

(2) R. J. Feldmann and H. I. Maibach, *ibid.*, **52**, 89 (1969).

(3) *Ibid.*, **54**, 399 (1970).

(4) N. Hunziger, R. J. Feldmann, and H. I. Maibach, *Dermatologica*, **156**, 79 (1978).

(5) R. C. Wester and H. I. Maibach, *Toxicol. Appl. Pharmacol.*, **32**, 394 (1975).

(6) D. M. Anjo, R. J. Feldmann, and H. I. Maibach, in "Percutaneous Absorption of Steroids," P. Mauvais-Jarvis, C. F. H. Vickers, and J. Wepierre, Eds., Academic, New York, N.Y., 1980, p. 31.

(7) R. J. Feldmann and H. I. Maibach, *J. Invest. Dermatol.*, **48**, 181 (1967).

(8) K. A. Holbrook and G. F. Odland, *ibid.*, **62**, 415 (1974).

(9) A. M. Kligman, in "The Epidermis," W. Montagna and W. C. Lobitz, Jr., Eds., Academic, New York, N.Y., 1964, p. 387.

(10) E. Christophers and A. M. Kligman, *J. Invest. Dermatol.*, **42**, 407 (1964).

(11) M. M. Mershon and J. F. Callahan, in "Animal Models in Dermatology," H. I. Maibach, Ed., Churchill Livingstone, New York, N.Y., 1975, p. 36.

(12) E. Christophers, *J. Invest. Dermatol.*, **56**, 165 (1971).

(13) E. Christophers, *Virchows Arch. B: Zellpath.*, **10**, 286 (1972).

(14) E. Christophers and E. B. Laurence, *Curr. Probl. Dermatol.*, **6**, 87 (1976).

(15) D. A. Weigand, C. Haygood, J. R. Gaylor, and J. H. Anglin, in "Current Concepts in Cutaneous Toxicity," V. A. Drill and P. Lazar, Eds., Academic, New York, N.Y., 1980, p. 221.

(16) K. E. Andersen, H. I. Maibach, and M. D. Anjo, *Br. J. Dermatol.*, **102**, 447 (1980).

Improved High-Pressure Liquid Chromatographic Method for the Analysis of Erythromycin in Solid Dosage Forms

KIYOSHI TSUJI ˣ **and MICHAEL P. KANE**

Received September 18, 1981, from the *Control Analytical Research and Development, The Upjohn Company, Kalamazoo, MI 49001.* Accepted for publication December 23, 1981.

Abstract □ A stability-indicating high-pressure liquid chromatographic (HPLC) method for the assay of erythromycin in enteric film-coated tablets was developed. The method used a reversed-phase column at 70° with a mobile phase of acetonitrile–methanol–0.2 *M* ammonium acetate–water (45:10:10:35) at pH 7.0. The column effluent was monitored at 215 nm. Several reversed-phase columns were evaluated for the analysis of erythromycin. The HPLC method was also applicable for the analysis of salts and esters of erythromycin. The linearity and precision of the HPLC assay method for erythromycin in the solid dosage form were examined by spiking erythromycin into a tablet placebo at 60–120% of the label. The recovery of erythromycin was 99.9% with a relative standard deviation of <1%. The correction factors to express the results of HPLC in terms of antimicrobial bioequivalency against *Staphylococcus aureus* ATCC 6538P for erythromycins A, B, and C were determined to be 1.0, 0.92, and 0.48, respectively. Eight lots of tablets were assayed by the HPLC method, and the results, expressed in terms of erythromycin bioequivalency, showed no statistically significant difference from those of the microbiological assay method.

Keyphrases □ High-pressure liquid chromatography—improved method for the analysis of erythromycin in solid dosage forms □ Dosage forms—improved high-pressure liquid chromatographic method for the analysis of erythromycin □ Erythromycin—solid dosage forms, improved high-pressure liquid chromatographic method for analysis

Erythromycin, a macrolide antibiotic, is normally administered orally and is marketed in several forms. These include the free base, salts such as the stearate, and esters such as ethyl succinate and 2′-*O*-propionyl. Erythromycin free base is formulated as an enteric coated tablet to protect erythromycin from acid degradation and to allow absorption in the intestinal tract.

High-pressure liquid chromatographic (HPLC) methods for the determination of erythromycin free base and an ester of erythromycin, erythromycin ethyl succinate, have been reported (1–4). The HPLC assay method for erythromycin ethyl succinate uses an elevated column temperature at 70° to minimize peak tailing and to improve peak resolution (4). This HPLC method was adopted for monitoring the clinical blood level of erythromycin and erythromycin ethyl succinate by use of a postcolumn extraction and derivatization technique for fluorimetric detection (5).

Since the HPLC method reported for the assay of erythromycin uses ambient column temperature (1), considerable peak tailing and lack of peak resolution have been experienced. The method reported in this paper uses elevated column temperature for optimum peak resolution and minimum peak tailing for the assay of erythromycin in a solid dosage form.

EXPERIMENTAL

Apparatus—A modular liquid chromatograph equipped with a variable wavelength detector at 215 nm[1], a high-pressure pump[2], and a 100-μl fixed loop injector[3] were used. A reversed-phase HPLC column[4] was water jacketed and maintained at 70° with a circulating water bath[5]. The peak area was electronically determined by use of an electronic integrator[6].

Reagent—All the solvents used were distilled in glass and were UV grade[7]. Ammonium acetate used was analytical reagent grade. The mobile phase composed of acetonitrile–methanol–0.2 *M* ammonium acetate–water (45:10:10:35) was filtered through a membrane filter[8]. The flow rate of the mobile phase was ~1.0 ml/min.

The 0.2 *M* ammonium acetate was prepared by weighing 15.5 g of ammonium acetate[9] into a 1-liter graduated cylinder and adding water to volume.

[1] Model 1201 Spectromonitor I, Laboratory Data Control, Riviera Beach, Fla.

[2] Model 196-0066-02 High-Pressure Mini Pump, Laboratory Data Control.

[3] Model 70-10 Loop Injector, Rheodyne, Berkeley, Calif.

[4] 18-5A, LiChrosorb RP-18, Brownlee Labs, Santa Clara, Calif.

[5] Lauda K-2/R controlled-temperature circulating water bath, Brinkmann, Lauda, GFR West Germany.

[6] Chromatopac-E1A, Shimadzu Seisakusho, Ltd., Kyoto, Japan.

[7] Burdick and Jackson Labs, Muskegon, Mich.

[8] Catalog No. FHLP04700 Fluoropore Filter, Millipore Corp., Bedford, Mass.

[9] Mallinckrodt, Inc., Paris, Ky.

0022-3549/82/01000-1160$01.00/0

REFERENCES

(1) M. J. Bartek, J. A. LaBudde, and H. L. Maibach, *J. Invest. Dermatol.*, **58**, 114 (1972).

(2) R. J. Feldmann and H. I. Maibach, *ibid.*, **52**, 89 (1969).

(3) *Ibid.*, **54**, 399 (1970).

(4) N. Hunziger, R. J. Feldmann, and H. I. Maibach, *Dermatologica*, **156**, 79 (1978).

(5) R. C. Wester and H. I. Maibach, *Toxicol. Appl. Pharmacol.*, **32**, 394 (1975).

(6) D. M. Anjo, R. J. Feldmann, and H. I. Maibach, in "Percutaneous Absorption of Steroids," P. Mauvais-Jarvis, C. F. H. Vickers, and J. Wepierre, Eds., Academic, New York, N.Y., 1980, p. 31.

(7) R. J. Feldmann and H. I. Maibach, *J. Invest. Dermatol.*, **48**, 181 (1967).

(8) K. A. Holbrook and G. F. Odland, *ibid.*, **62**, 415 (1974).

(9) A. M. Kligman, in "The Epidermis," W. Montagna and W. C. Lobitz, Jr., Eds., Academic, New York, N.Y., 1964, p. 387.

(10) E. Christophers and A. M. Kligman, *J. Invest. Dermatol.*, **42**, 407 (1964).

(11) M. M. Mershon and J. F. Callahan, in "Animal Models in Dermatology," H. I. Maibach, Ed., Churchill Livingstone, New York, N.Y., 1975, p. 36.

(12) E. Christophers, *J. Invest. Dermatol.*, **56**, 165 (1971).

(13) E. Christophers, *Virchows Arch. B: Zellpath.*, **10**, 286 (1972).

(14) E. Christophers and E. B. Laurence, *Curr. Probl. Dermatol.*, **6**, 87 (1976).

(15) D. A. Weigand, C. Haygood, J. R. Gaylor, and J. H. Anglin, in "Current Concepts in Cutaneous Toxicity," V. A. Drill and P. Lazar, Eds., Academic, New York, N.Y., 1980, p. 221.

(16) K. E. Andersen, H. I. Maibach, and M. D. Anjo, *Br. J. Dermatol.*, **102**, 447 (1980).

Improved High-Pressure Liquid Chromatographic Method for the Analysis of Erythromycin in Solid Dosage Forms

KIYOSHI TSUJI ˣ **and MICHAEL P. KANE**

Received September 18, 1981, from the *Control Analytical Research and Development, The Upjohn Company, Kalamazoo, MI 49001.* Accepted for publication December 23, 1981.

Abstract □ A stability-indicating high-pressure liquid chromatographic (HPLC) method for the assay of erythromycin in enteric film-coated tablets was developed. The method used a reversed-phase column at 70° with a mobile phase of acetonitrile–methanol–0.2 *M* ammonium acetate–water (45:10:10:35) at pH 7.0. The column effluent was monitored at 215 nm. Several reversed-phase columns were evaluated for the analysis of erythromycin. The HPLC method was also applicable for the analysis of salts and esters of erythromycin. The linearity and precision of the HPLC assay method for erythromycin in the solid dosage form were examined by spiking erythromycin into a tablet placebo at 60–120% of the label. The recovery of erythromycin was 99.9% with a relative standard deviation of <1%. The correction factors to express the results of HPLC in terms of antimicrobial bioequivalency against *Staphylococcus aureus* ATCC 6538P for erythromycins A, B, and C were determined to be 1.0, 0.92, and 0.48, respectively. Eight lots of tablets were assayed by the HPLC method, and the results, expressed in terms of erythromycin bioequivalency, showed no statistically significant difference from those of the microbiological assay method.

Keyphrases □ High-pressure liquid chromatography—improved method for the analysis of erythromycin in solid dosage forms □ Dosage forms—improved high-pressure liquid chromatographic method for the analysis of erythromycin □ Erythromycin—solid dosage forms, improved high-pressure liquid chromatographic method for analysis

Erythromycin, a macrolide antibiotic, is normally administered orally and is marketed in several forms. These include the free base, salts such as the stearate, and esters such as ethyl succinate and 2′-*O*-propionyl. Erythromycin free base is formulated as an enteric coated tablet to protect erythromycin from acid degradation and to allow absorption in the intestinal tract.

High-pressure liquid chromatographic (HPLC) methods for the determination of erythromycin free base and an ester of erythromycin, erythromycin ethyl succinate, have been reported (1–4). The HPLC assay method for erythromycin ethyl succinate uses an elevated column temperature at 70° to minimize peak tailing and to improve peak resolution (4). This HPLC method was adopted for monitoring the clinical blood level of erythromycin and erythromycin ethyl succinate by use of a postcolumn extraction and derivatization technique for fluorimetric detection (5).

Since the HPLC method reported for the assay of erythromycin uses ambient column temperature (1), considerable peak tailing and lack of peak resolution have been experienced. The method reported in this paper uses elevated column temperature for optimum peak resolution and minimum peak tailing for the assay of erythromycin in a solid dosage form.

EXPERIMENTAL

Apparatus—A modular liquid chromatograph equipped with a variable wavelength detector at 215 nm[1], a high-pressure pump[2], and a 100-μl fixed loop injector[3] were used. A reversed-phase HPLC column[4] was water jacketed and maintained at 70° with a circulating water bath[5]. The peak area was electronically determined by use of an electronic integrator[6].

Reagent—All the solvents used were distilled in glass and were UV grade[7]. Ammonium acetate used was analytical reagent grade. The mobile phase composed of acetonitrile–methanol–0.2 *M* ammonium acetate–water (45:10:10:35) was filtered through a membrane filter[8]. The flow rate of the mobile phase was ~1.0 ml/min.

The 0.2 *M* ammonium acetate was prepared by weighing 15.5 g of ammonium acetate[9] into a 1-liter graduated cylinder and adding water to volume.

[1] Model 1201 Spectromonitor I, Laboratory Data Control, Riviera Beach, Fla.

[2] Model 196-0066-02 High-Pressure Mini Pump, Laboratory Data Control.

[3] Model 70-10 Loop Injector, Rheodyne, Berkeley, Calif.

[4] 18-5A, LiChrosorb RP-18, Brownlee Labs, Santa Clara, Calif.

[5] Lauda K-2/R controlled-temperature circulating water bath, Brinkmann, Lauda, GFR West Germany.

[6] Chromatopac-E1A, Shimadzu Seisakusho, Ltd., Kyoto, Japan.

[7] Burdick and Jackson Labs, Muskegon, Mich.

[8] Catalog No. FHLP04700 Fluoropore Filter, Millipore Corp., Bedford, Mass.

[9] Mallinckrodt, Inc., Paris, Ky.

0022-3549/82/01000-1160$01.00/0

Reference Standard Solution—USP erythromycin reference standard was dried at 60° for 3 hr under <5-mm Hg pressure. The dried bottle was capped and placed in a desiccator to cool. Approximately 10 mg of the reference standard was weighed accurately using an electronic balance[10] and placed in a 10-ml volumetric flask. The standard was dissolved and diluted to volume with the internal standard solution.

Internal Standard Solution—A sufficient quantity of megestrol acetate was dissolved in the mobile phase to give a final concentration of ~0.025 mg/ml.

Sample Preparation—Approximately 10 mg of erythromycin powder was accurately weighed into a 10-ml volumetric flask. The powder was dissolved and diluted to volume with the internal standard solution.

To assay solid dosage forms, 10 tablets were accurately weighed to compute an average tablet weight. Tablets were ground to a fine powder using a laboratory mill[11] with a 40-mesh screen. Approximately 18 mg of the ground tablet, or an equivalent quantity of the powder to contain ~10 mg of erythromycin, was accurately weighed using an electronic balance[10] into a 10-ml volumetric flask. The internal standard solution was added to the flask, sonicated for ~1 min, and shaken briefly to facilitate dissolution. The suspension was then centrifuged at 2000 rpm for ~2 min to remove tablet excipients.

Calculation—The erythromycin content in a tablet was calculated using:

$$\text{Erythromycin (mg/tablet)} = \frac{Pa + 0.9Pb + 0.5Pc}{Ta + 0.9Tb + 0.5Tc} \times \frac{W_t}{W_p} \times \frac{I_t}{I_p} \times F_1 \times \frac{F_2}{1000} \quad \text{(Eq. 1)}$$

where Pa is the peak area of erythromycin A of the sample; Pb is the peak area of erythromycin B of the sample; Pc is the peak area of erythromycin C of the sample; Ta is the peak area of erythromycin A of the reference standard; Tb is the peak area of erythromycin B of the reference standard; Tc is the peak area of erythromycin C of the reference standard; W_t is the weight of the reference standard in milligrams per milliliter; I_t is the peak area of the internal standard in the reference standard; I_p is the peak area of the internal standard of the sample; W_p is the weight of the sample in milligrams per milliliter; F_1 is an average tablet weight in milligrams per tablet; F_2 is the assigned potency of the reference standard in micrograms per milligram; and 1000 is a factor to convert the potency of the reference standard to a fraction.

Microbiological Assay Method—The turbidimetric assay method using *Staphylococcus aureus* ATCC 6538P as the test microorganism as described in the Code of Federal Regulations (6) was used to assay erythromycin.

RESULTS AND DISCUSSION

Chromatographic Conditions—The effect of mobile phase composition and pH on the chromatographic behavior of erythromycins A, B, and C have been reported (1). Increasing the concentration of acetonitrile or methanol or decreasing the pH of the mobile phase was found to reduce the retention times of erythromycins A, B, and C. The selection of pH for the mobile phase was determined by the type of sample under investigation, with pH 6.2 for the bulk drug and pH 7.8 for biological extracts.

Increase in the column temperature was found to significantly improve column performance for the assay of erythromycin. The effects of column temperature on the height equivalent to theoretical plate (HETP) for LiChrosorb RP-18[4] and μ-Bondapak C_{18}[12] columns are presented in Fig. 1. The HETP for the μ-Bondapak C_{18} column was significantly smaller than that of the LiChrosorb RP-18 at a column temperature <50°. However, lines of two-column performance intersected at ~70°. The HETP for the LiChrosorb RP-18 was slightly smaller than that of μ-Bondapak C_{18} at the column temperature of 80°. Although column performances increased up to 80°, 70° was selected for the assay of erythromycin. The 70° temperature represents a compromise between column performance and column stability. Most column manufacturers recommend that the column not exceed 70°. The HPLC column was stable for more than 1 month when operated at 70° if the mobile phase was saturated with silica.

Increase in temperature has been shown to increase the rate of mass transfer or diffusion of the solute to the stationary phase (7). This most likely has resulted in improved column efficiency.

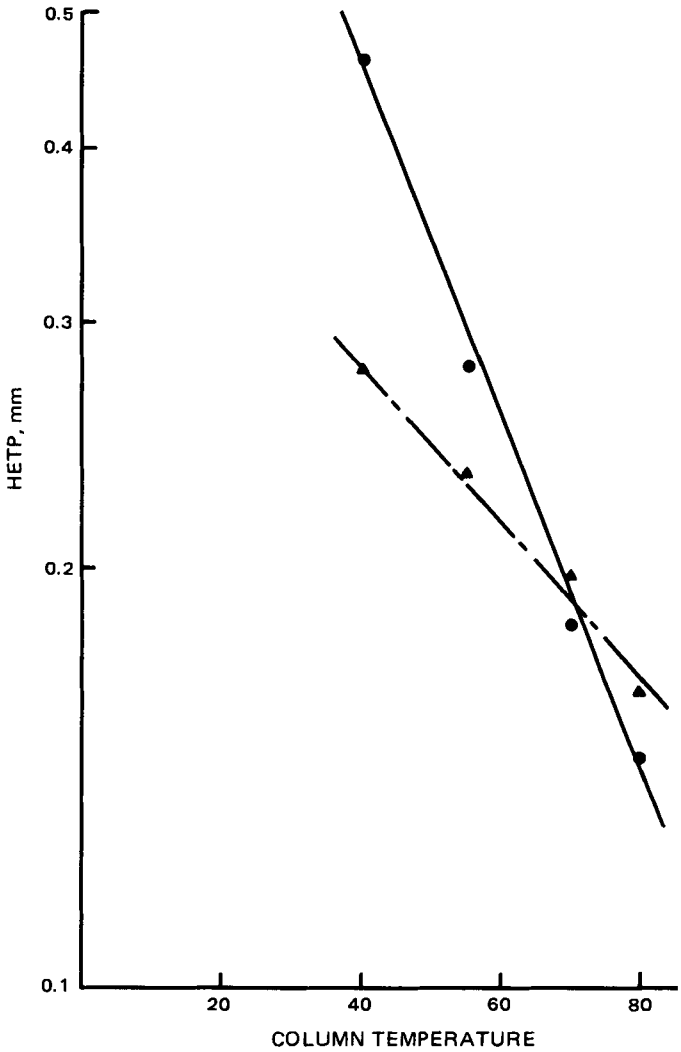

Figure 1—*Effect of column temperature on HETP. Key: (●) LiChrosorb RP-18; (▲) μ-Bondapak C_{18}.*

Selection of Column—Several HPLC columns were evaluated for analysis of erythromycin using the mobile phase composed of acetonitrile–methanol–0.2 *M* ammonium acetate–water (45:10:10:35) at pH 7.0. This pH was selected as a compromise between shorter retention times and better resolution. The following HPLC columns were evaluated: LiChrosorb RP-18[4], μ-Bondapak C_{18}[12], Spherisorb RP-18[13], Partisil ODS[14], Partisil ODS-3[14], and Zorbax ODS[15]. Erythromycin A eluted in 8–10 min from LiChrosorb RP-18, Partisil ODS, and Partisil ODS-3 columns. However, it was found necessary to increase the acetonitrile concentration to 60% to obtain comparative retention time for the erythromycin A peak from Spherisorb RP-18 and Zorbax ODS columns. These latter columns are packed with spherical particles.

The columns were evaluated on the basis of HETP, tailing factor for the erythromycin A peak, and the peak resolution between erythromycins A and C. The data are presented in Table I. The LiChrosorb RP-18 and μ-Bondapak C_{18} columns were judged to give good overall performance for the analysis of erythromycin. A typical chromatogram of erythromycin powder using the LiChrosorb RP-18 column is shown in Fig. 2.

The relative retentions of erythromycins A, B, and C, as well as various impurities and degradation products on the LiChrosorb RP-18 column, are listed in Table II. Although the relative retentions of these compounds were slightly different from those reported previously using a μ-Bondapak C_{18} column at room temperature (1), the order of elution was not affected.

A peak which frequently appears on GLC chromatograms using an

[10] Cahn 21 Automatic Electrobalance, Ventron Corp., Cerritos, Calif.
[11] Wiley Mill model 3383, A. H. Thomas, Philadelphia, Pa.
[12] Waters Associates, Milford, Mass.
[13] Brownlee Labs.
[14] Whatman Ltd., Clifton, N.J.
[15] DuPont Instrument Co., Wilmington, Del.

Table I—Evaluation of Various Reversed-Phase HPLC Columns for the Analysis of Erythromycin

Column at 70°	Column Parameters		
	HETP, mm	Tailing Factor[a]	Resolution[b]
LiChrosorb RP-18	0.182	2.0	2.5
μ-Bondapak C_{18}	0.198	2.0	2.5
Spherisorb RP-18	0.227	2.1	1.9
Partisil ODS	0.244	2.1	1.6
Partisil ODS-3	0.303	2.0	1.9
Zorbax ODS	0.530	2.8	1.7

[a] For erythromycin A peak. [b] Between peaks of erythromycins A and C.

Table II—Relative Retention of Various Erythromycins [a]

Compound	Relative Retention
Erythronolide B	0.73
Erythromycin C	0.78
Erythromycin A	1.00
8-Epi-10,11-anhydroerythromycin A	1.22
Erythralosamine	1.32
Anhydroerythromycin A	1.38
Erythromycin B	1.46
Dihydroerythromycin A	1.74
8,9-Anhydro-6,9-hemiketal erythromycin	2.20

[a] LiChrosorb RP-18 at 70°; mobile phase: acetonitrile–methanol–0.2 *M* ammonium acetate–water (45:10:10:35), pH 7.0.

OV-225 column and tentatively reported as an acid hydrolyzed erythromycin (8) was identified as 8,9-anhydro-6,9-hemiketal erythromycin (9). Although this compound is often inherently present in erythromycin powder, additional amounts can easily be formed from erythromycin under the silylation conditions employed for the GLC assay method. This was not a problem for this HPLC method.

Megestrol acetate, selected as the internal standard for the LiChrosorb RP-18 column, eluted between erythromycin B and 8,9-anhydro-6,9-hemiketal erythromycin peaks (Fig. 3). Calusterone, which elutes immediately after the erythromycin peak, would be suitable as an internal standard when a μ-Bondapak C_{18} column is used (Fig. 4).

Antimicrobial Activity—Since erythromycins A, B, and C differ in both peak response and antimicrobial activity, correction factors must be applied to each of these biologically active compounds so that the total antimicrobial potency of a sample as determined by HPLC correlates with that of the microbiological assay method. The correction factors for

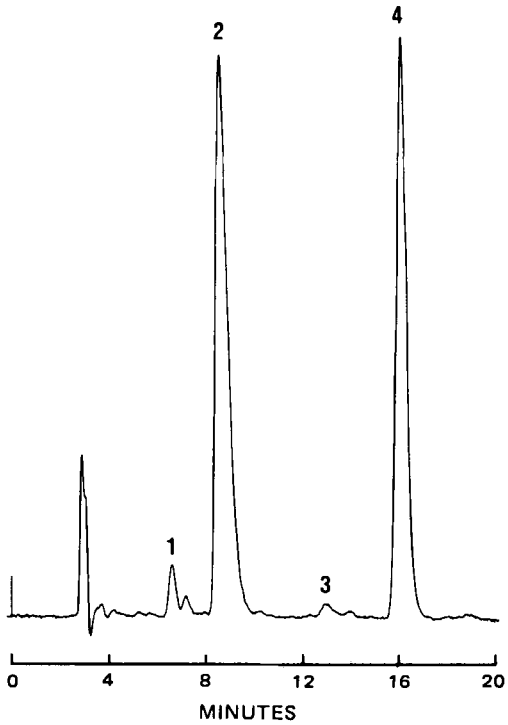

Figure 3—*Reversed-phase HPLC chromatogram of erythromycin USP with internal standard on LiChrosorb RP-18 at 70°. Mobile phase: acetonitrile–methanol–0.2 M ammonium acetate–water (45:10:10:35) at pH 7.0. Peak identification: 1, erythromycin C; 2, erythromycin A; 3, erythromycin B; 4, megestrol acetate.*

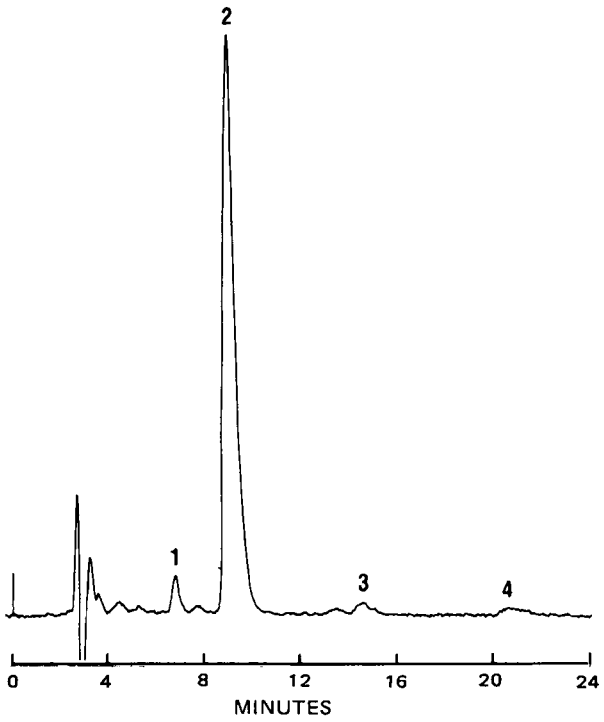

Figure 2—*Reversed-phase HPLC chromatogram of erythromycin USP on μ-Bondapak C_{18} at 70°. Mobile phase: acetonitrile–methanol–0.2 M ammonium acetate–water (45:10:10:35) pH 7.0. Peak identification: 1, erythromycin C; 2, erythromycin A; 3, erythromycin B; 4, 8,9-anhydro-6,9-hemiketal erythromycin.*

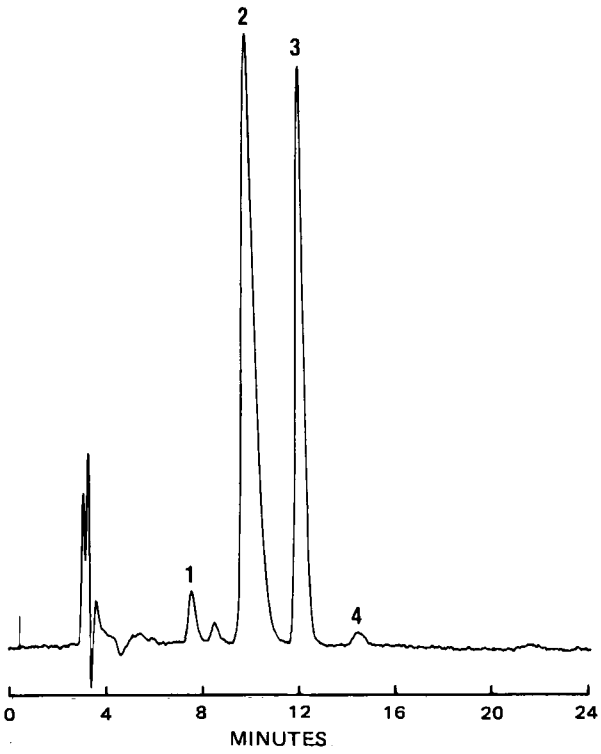

Figure 4—*Reversed-phase HPLC chromatogram of erythromycin USP with calusterone internal standard on μ-Bondapak C_{18} at 70°. Mobile phase: acetonitrile–methanol–0.2 M ammonium acetate–water (45:10:10:35) at pH 7.0. Peak identification: 1, erythromycin C; 2, erythromycin A; 3, calusterone; 4, erythromycin B.*

Table III—Correction Factors in the Determination of Erythromycin Bioequivalency

	Relative Response[a], area/weight	Potency[a], μg/mg	Correction Factor
Erythromycin A[b]	1.00	1000	1.00
Erythromycin B	0.86	787	0.92
Eryythromycin C	1.02	487	0.48

[a] Values obtained against *S. aureus* ATCC 6538P were corrected for purity determined by HPLC. Unidentified impurities were assumed to have an equal peak response. [b] USP Reference Standard Issue H-1.

Table IV—Relative Retention of Erythromycin Ethyl Succinate and Impurities[a]

Compound	Relative Retention
Erythromycin A	0.45
Anhydroerythromycin A	0.56
Erythromycin C ethyl succinate	0.69
8,9-Anhydro-6,9-hemiketal erythromycin A	0.78
Erythromycin A ethyl succinate	1.0
Erythromycin B ethyl succinate	1.4
Anhydroerythromycin ethyl succinate	1.7
8,9-Anhydro-6,9-hemiketal erythromycin ethyl succinate	2.2

[a] LiChrosorb RP-18 at 70°; mobile phase: acetonitrile–0.2 *M* ammonium acetate–water (60:10:30), pH 7.4.

erythromycins A, B, and C are 1.0, 0.92, and 0.48, respectively, when tested turbidimetrically using *S. aureus* ATCC 6538P (6) (Table III). These values were obtained by comparison of the relative chromatographic area responses and antimicrobial activities of erythromycins B and C with the erythromycin A reference standard. The relative response factors for erythromycins A, B, and C of 1.0, 0.5, and 0.4, respectively, reported previously were obtained by use of less pure samples of erythromycins B and C and a different test microorganism, *S. aureus* ATCC 9144 (8). Differences in the strain of *S. aureus* could account for the difference in the relative responses of erythromycin B and erythromycin A.

Assay of Erythromycins—Versatility of the HPLC method for the analysis of esters and salts of erythromycin has been demonstrated. HPLC chromatograms of erythromycin estolate, erythromycin ethyl-

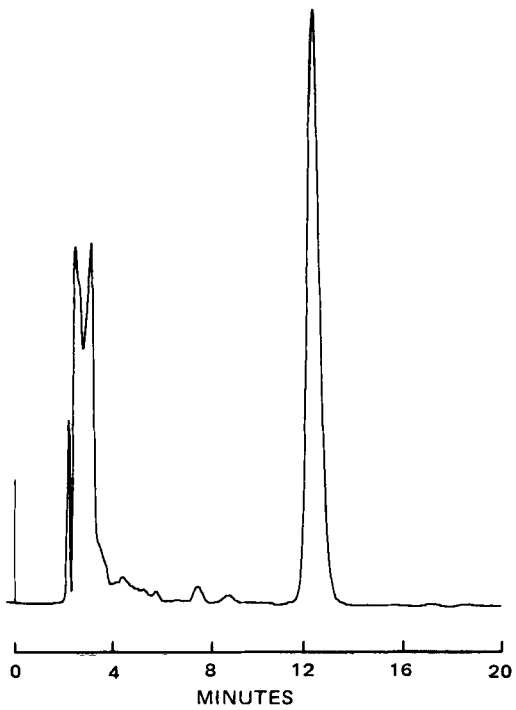

Figure 5—*HPLC chromatogram of erythromycin estolate on μ-Bondapak C_{18} at 70°. Mobile phase: acetonitrile–0.2* M *ammonium acetate–water (60:10:30) at pH 7.0.*

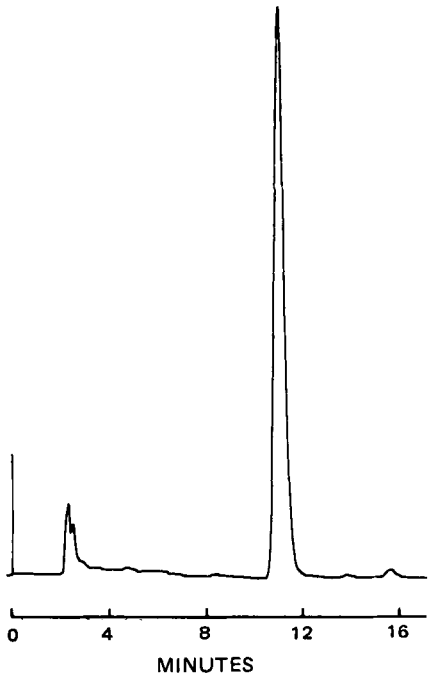

Figure 6—*HPLC chromatogram of erythromycin ethyl carbonate on μ-Bondapak C_{18} at 70°. Mobile phase: acetonitrile–0.2* M *ammonium acetate–water (60:10:30) at pH 7.0.*

carbonate, and erythromycin propionate are shown in Figs. 5–7. Chromatograms were obtained with a μ-Bondapak C_{18} column at 70° with mobile phase of acetonitrile–0.2 *M* ammonium acetate–water (60:10:30) at pH 7.0. The data shown in Table IV indicate the capability of HPLC

Table V—Precision of HPLC Assay for Erythromycin

Erythromycin, mg/ml	Peak Area Ratio, Erythromycin/Internal Standard	Peak Area Ratio/ Erythromycin Concentration
0.9256	1.039	1.123
0.8907	1.013	1.137
0.9126	1.030	1.129
0.8981	1.011	1.126
0.9042	1.015	1.123
0.9150	1.016	1.110
		RSD: 0.8%

Table VI—Linearity of Recovery of Erythromycin from Tablet Placebo

Erythromycin Added, mg	Erythromycin Recovered, mg	Recovery, %
6.242	6.273	100.5
7.928	7.841	98.9
9.969	10.069	101.0
11.949	11.830	99.0
13.993	14.035	100.3
		Mean: 99.9%
		RSD: 0.9%
		Correlation Coefficient: 0.9996
		$y = 0.9999x - 0.0058$

Table VII—Precision of Recovery of Erythromycin from Tablet Placebo

Erythromycin Added, mg	Erythromycin Recovered, mg	Recovered, %
9.969	10.069	101.0
9.974	9.884	99.1
10.123	9.981	98.6
10.359	10.266	99.1
9.984	10.014	100.3
10.276	10.297	100.2
		Mean: 99.7
		RSD: 0.9%

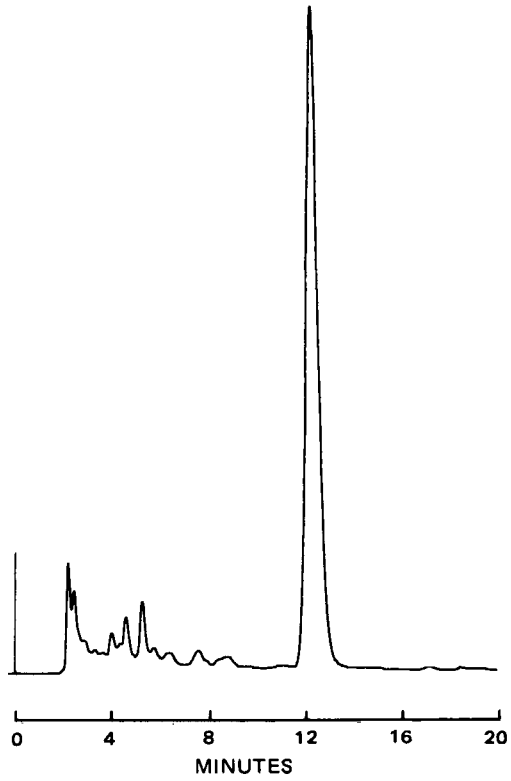

Figure 7—*HPLC chromatogram of erythromycin propionate on μ-Bondapak C_{18} at 70°. Mobile phase: acetonitrile–0.2 M ammonium acetate–water (60:10:30) at pH 7.0.*

to differentiate an ester of erythromycin, erythromycin ethyl succinate, from its impurities. The peaks, EES-C1 and EES-C2, reported previously (2) have been identified as erythromycin C ethyl succinate and 8,9-anhydro-6,9-hemiketal erythromycin A. For quantification of erythromycin, the HPLC response was linear over a concentration range of 0.5–1.3 mg of erythromycin/ml with a correlation coefficient of 0.9999. Six individually weighed and prepared samples were analyzed at an erythromycin concentration of 0.9 mg/ml. The relative standard deviation (*RSD*) of the assay was 0.8% (Table V).

Enteric film coated tablets were then examined for erythromycin content by HPLC. No interference from placebo was experienced. Linearity of recovery was studied by spiking erythromycin into placebo at ~60–120% of label. The average recovery was 99.9% (*RSD* 0.9%). The correlation coefficient for linearity was 0.9996 with the slope of 0.9999 (Table VI). The precision of the HPLC assay for tablets was determined by analyzing six replicate samples prepared at 100% of the label requirements. The average recovery was 99.7% (*RSD* 0.9%) (Table VII).

Table VIII—Comparison of HPLC and Microbiological Assay Methods for the Determination of Erythromycin in Enteric Film Coated Tablets

Lot Number	Erythromycin Content, mg/tablet	
	HPLC (bioequivalency)	Microbiology (potency)
A	263	257
B	261	250
C	267	250
D	262	260
E	251	251
F	263	246
G	335	347
H	328	347

Eight lots of tablets were assayed. The results of HPLC were expressed in terms of bioequivalency using the correction factors described earlier. The results of the HPLC and the microbiological assay methods are shown in Table VIII. No statistically significant difference was noted between the HPLC and the microbiological assay methods.

REFERENCES

(1) K. Tsuji and J. F. Goetz, *J. Chromatogr.*, **147**, 359 (1978).

(2) *Ibid.*, **157**, 185 (1978).

(3) K. Tsuji and J. F. Goetz, *J. Antibiot.*, **31**, 302 (1978).

(4) K. Tsuji, in "GLC and HPLC Determination of Therapeutic Agents," part 2, K. Tsuji, Ed., Dekker, New York, N.Y., 1978, pp. 759–764.

(5) K. Tsuji, *J. Chromatogr.*, **158**, 337 (1978).

(6) Code of Federal Regulations, Title 21, Food and Drug Administration, U.S. Government Printing Office, Washington, D.C., 1980.

(7) J. A. Schmidt, R. A. Henry, R. C. Williams, and J. F. Diekman, *J. Chromatogr. Sci.*, **9**, 645 (1971).

(8) K. Tsuji and J. H. Robertson, *Anal. Chem.*, **43**, 818 (1971).

(9) P. Kurath, P. H. Jones, R. S. Tegan, and T. J. Perum, *Experientia*, **27**, 362 (1971).

ACKNOWLEDGMENTS

The authors thank Abbott Laboratories for providing erythromycins B and C impurity standards.

Bioavailability of Griseofulvin from Tablets in Humans and the Correlation with its Dissolution Rate

NOBUO AOYAGI ˣ, HIROYASU OGATA, NAHOKO KANIWA, MASANOBU KOIBUCHI †, TOSHIO SHIBAZAKI, and AKIRA EJIMA

Received July 31, 1981, from the *Division of Drugs, National Institute of Hygienic Sciences, 18-1, Kamiyoga 1-chome, Setagaya-ku, Tokyo 158, Japan.* †Deceased. Accepted for publication December 30, 1981.

Abstract □ Dissolution rates of 10 commercial microsize griseofulvin tablets and one ultramicrosize griseofulvin tablet were preliminarily determined in 18 liters of pH 7.2 phosphate buffer and in 900 ml of 40% dimethylformamide as test media. Addition of dimethylformamide affected the dissolution behavior of the formulations. The products, three microsize and one ultramicrosize, were selected for further studies on the bioavailability in humans and dissolution. Significant differences among the formulations were found in serum levels, C_{max}, and $AUC_{47.5\ hr}$, but not in AUC_{∞} and t_{max}. The maximum difference of C_{max} was ~40%. The ultramicrosize product showed lower C_{max} and serum levels at earlier sampling times than two microsize products. The dissolution rates determined under sink and nonsink conditions without pretreatment significantly correlated with the serum level at 1 hr but not with the other *in vivo* parameters. Only the dissolution rate determined by the sink method with pretreatment with a small quantity of water (1.0 ml) and plastic beads significantly correlated with serum levels at 3 and 5 hr, C_{max}, and $AUC_{47.5\ hr}$.

Keyphrases □ Bioavailability—griseofulvin from tablets in humans, correlation with dissolution rate □ Dissolution, rates—correlation with bioavailability of griseofulvin from tablets in humans □ Griseofulvin—bioavailability from tablets in humans, correlation with dissolution rate

The absorption of a poorly water soluble drug is considered to be dissolution rate limited. Griseofulvin used as an antifungal agent is a practically insoluble compound. The *in vivo* availability is enhanced by increasing the dissolution rate by means of reduction of particle size of the crystals (1–6). A good correlation between the bioavailability and dissolution rate was found for griseofulvin tablets (7, 8). However, fine particles may not necessarily produce the expected dissolution rate and bioavailability due to their aggregation and agglomeration (4, 9). A microsize griseofulvin powder has been widely used in commercial tablets, and now a new formulation, an ultramicrosize griseofulvin tablet, can be obtained, which has been formulated with the drug dispersed in polyethylene glycol 6000 (10–12) and has been shown to have better bioavailability than microsize products (11, 12). However, recently lower absorption of the drug from an ultramicrosize than from a microsize formulation was shown (13).

The present investigation was undertaken to study the dissolution rate and bioavailability in humans for commercial microsize griseofulvin tablets and an ultramicrosize griseofulvin tablet, and to clarify the relation between the *in vitro* and *in vivo* findings.

EXPERIMENTAL

Formulation—Ten commercial microsize griseofulvin tablets available in Japan and one ultramicrosize griseofulvin tablet[1] were used for the preliminary dissolution test. Each tablet contained 125 mg of griseofulvin. Based on preliminary dissolution data, four formulations, including an ultramicrosize formulation, were selected to provide a broad range of dissolution rates with the expectation that those formulations would show a wide variation in their bioavailabilities.

Table I—t_{50} for Griseofulvin Tablets [a]

Tablet	Method	
	Beaker[b]	Paddle[c]
1 (A)	13.8	8.3
2	25.4	24.7
3	102.6	9.1
4	80.3	10.6
5 (B)	8.1	11.0
6	73.9	37.0
7	85.0	6.0
8 (D)	211.0	38.8
9 (C)	107.8	9.0
10	86.8	—
11	66.0	29.5

[a] Time (t_{50}) in minutes. [b] 18 liters of pH 7.2 phosphate buffer. [c] 40% Dimethylformamide (900 ml).

Solubility—The solubility of griseofulvin in water [pH 7.2 sodium phosphate buffer (0.01 *M*) and 40% dimethylformamide] was determined at 37° spectrophotometrically after filtration of the equilibrated solution of griseofulvin through a 1.0-μm membrane filter.

Disintegration Time—Disintegration times of the griseofulvin formulations were determined with six tablets in pH 7.2 sodium phosphate buffer (0.01 *M*) according to Japanese Pharmacopeia IX specifications (30 strokes/min, 37°). The time when there were no particles of tablets or only a trace amount of soft residue on the screen was selected as the disintegration time.

Dissolution Rate—The dissolution rate of the drug from each dosage form was determined at 37° in pH 7.2 sodium phosphate buffer (0.01 *M*) unless otherwise specified. Hydrochloric acid solution (pH 1.2) and 40% dimethylformamide were also used as solvents. The amount of the drug dissolved was monitored spectrophotometrically by passing the solution through a glass filter stick (porosity G-3) to a flow cell and was expressed as a percentage of the labeled amount. An average dissolution rate was obtained after three dissolution runs. The dissolution rate was represented as t_5, t_{30}, and t_{50}, which indicate, respectively, the time required for 5, 30, and 50% of the drug to be dissolved. Polysorbate 80[2] and diastase (Japanese Pharmacopeia IX grade) were used to investigate their effects on the dissolution.

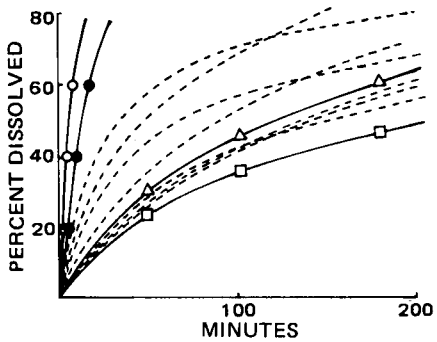

Figure 1—*Dissolution curves of griseofulvin tablets with the beaker method at pH 7.2. Key (●) Tablet A; (○) Tablet B; (△) Tablet C; (□) Tablet D; (- - -) dissolution curves of the other tablets.*

[1] Dorsey Laboratories, Division of Sandoz Inc.

[2] Tween 80, Wako Pure Chemical Industries Ltd., Osaka, Japan.

0022-3549/82/01000-1165$01.00/0

Table II—Dissolution Rates of Griseofulvin from Four Different Tablets with Sink Methods

In Vitro Test		t_{30}, min				t_{50}, min			
Method	Condition	A	B	C	D	A	B	C	D
Beaker	—	8.7	4.8	32.8	63.3	14.1	6.5	80.6	157.5
	0.1% Polysorbate 80	9.1	4.8	27.4	44.3	13.6	6.6	70.2	105.3
	0.014% Diastase	8.0	4.8	34.0	31.5	14.5	6.3	76.0	71.7
	848 rpm	6.5	4.1	28.7	48.0	9.5	5.6	65.3	119.0
	pH 1.2	10.0	3.0	31.5	85.0	—	—	—	—
	pH 1.2, 0.1% Polysorbate 80	7.5	3.5	16.0	30.0	—	—	—	—
Basket	—	6.5	5.0	26.0	21.5	9.0	7.0	75.0	57.0
Method I	—	3.1	1.7	8.3	2.7	6.1	2.5	26.7	4.6
Method II	—	1.8	1.9	6.6	3.3	2.7	3.2	17.3	6.4

Sink Method—*Nonpretreatment Method*—The beaker method consisted of agitating the solution with a three-bladed screw-type impeller (5.0-cm i.d., stirring rate: 512 rpm) in the middle of the solvent (18 liters) in a 20-liter flat-bottom beaker (29.0-cm i.d.).

The basket method consisted of placing a tablet in a cylindrical basket (1.7-cm i.d. × 2.3 cm) of 80-mesh stainless steel cloth. This basket was placed in a basket (Apparatus 1) as used in USP XX. The basket was held ~10 cm below the surface of the solvent and rotated at 400 rpm, ~7 cm from the wall of the beaker. The dissolution medium was agitated with a three-bladed impeller as described for the 18-liter beaker method.

With the paddle method (USP XX), 900 ml of 40% dimethylformamide was used as a solvent and was stirred at 120 rpm.

Pretreatment Method—Method I: A tablet was put into a 100-ml round bottle containing 1.0 ml of water and was gently shaken for 1 min. After standing for 5 min, 20 g of plastic beads (8-mm i.d.)[3] was added to the bottle. The bottle was fixed at an angle of 5° and was rotated at 3.8 rpm in a water bath (37°) for 15 min. The contents then were poured into 18 liters of the solvent with 100 ml of water for washing through a sieve to remove the plastic beads. Then the dissolution rate was determined according to the 18-liter beaker method procedure.

Method II: A tablet was gently shaken in 20 ml of water contained in a 50-ml round bottle for 5 min, and then 27 g of the plastic beads used in Method I was added. The subsequent procedure was the same as method I.

Nonsink Method—A 900 ml volume of the solvent was used in each experiment. The following procedures were used:

1. Rotating basket method (USP XX): The basket was rotated at 120 rpm.
2. Paddle method (USP XX): The stirring rate was 120 rpm.
3. Beaker method: A three-bladed screw-type impeller (5.0-cm i.d.) used as a stirring device was rotated at 2.5 cm from the bottom of the beaker which was used for the paddle method at 120 rpm.

Bioavailability—Twelve healthy male volunteers who participated in a Latin square crossover study were randomly assigned to one of four groups of equal size. The subjects ranged in age from 22 to 51 years (22, 22, 22, 22, 23, 24, 30, 32, 37, 37, 50, and 51; mean 31), in height from 160 to 180 cm (mean 170), and in weight from 53 to 69 kg (mean 60). Before the studies the participants were given a clinical examination to ensure they were healthy. All of the subjects were prohibited from taking medicines and alcoholic beverges from 3 days before the drug administration to the end of the test. Each subject took a test tablet orally with 200 ml of water at 9:00 am after fasting overnight. No foods or liquids were allowed until 4 hr after ingestion of the tablet. Blood samples (5 ml) were obtained at 1, 3, 5, 8, 23.5, 33, and 47.5 hr after administration of a tablet and the serum samples were kept frozen at −15° until assayed. The experiments were repeated every 2 weeks according to the dosage schedule. The following parameters were statistically subjected to ANOVA, and the differences among the treatments were examined by Tukey's test:

1. Serum levels at each sampling time.
2. Peak serum level (C_{max}).
3. Time to reach peak serum level (t_{max}).
4. Area under serum concentration–time curves from zero to the time t (AUC_t) calculated by the trapezoidal rule

The AUC_∞ was calculated by the method of Wagner (14).

Dose–Bioavailability Relation—A single tablet and one-half tablet of Formulation B, corresponding to 125 and 62.5 mg of griseofulvin, respectively, were given orally to three subjects according to a crossover design. The sampling times were the same as described in the bioavailability study.

Assay—The serum griseofulvin concentration was determined by the GLC method described previously (15). To a 0.5-ml aliquot of serum were added 0.5 ml of saturated sodium chloride solution and 5 ml of ether. After shaking for 10 min, a 4-ml aliquot of the ether phase was taken and evaporated to dryness *in vacuo*. The residue was dissolved with 0.4 ml of benzene containing 1.1 μg of clothiapine as internal standard, and 5 μl of the solution was taken for the GLC assay. GLC conditions: column, glass column (3-mm i.d. × 70 cm) packed with 5% OV-17 on 60–80 mesh Chromosorb W; injection temperature, 260°; detector temperature, 260°.

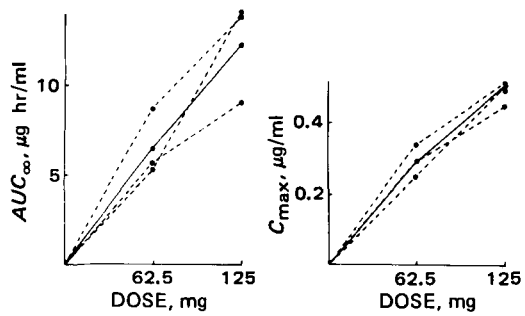

Figure 2—*Relations of griseofulvin dose with* AUC_∞ *and peak concentration after oral administration of the drug. Key: (- - -) responses of the individual subjects; (—) the average response.*

[3] Sartorius-Membranfilter GmbH.

RESULTS

Dissolution Rate—The solubilities of griseofulvin at 37° in water, pH 7.2 buffer, and 40% dimethylformamide were 31.8, 32.2, and 482.1 μg/ml, respectively; therefore, the preliminary dissolution tests were carried out with 18 liters of the aqueous medium (18-liter beaker method) and 900 ml of 40% dimethylformamide (paddle method) in order to get a sink condition. Figure 1 shows the dissolution profiles with the 18-liter beaker method. Relatively large differences were observed among the microsize griseofulvin formulations. The ultramicrosize formulation (A) showed rapid dissolution. Table I lists t_{50} in 18 liters of aqueous solvent and in 40% dimethylformamide. Addition of the organic solvent to aqueous medium altered the dissolution behavior of griseofulvin; however, the use of a partially alcoholic medium was described for the dissolution test of water insoluble drugs (16). On the basis of the *in vitro* data, four formulations (A, B, C, D), including an ultramicrosize formulation, were selected for further investigations concerning their dissolution rates and bioavailabilities.

Table II lists the dissolution rates (t_{30} and t_{50}) of these formulations determined under the sink condition. With the 18-liter beaker method

Table III—Dissolution Rate of Griseofulvin from Tablets with Nonsink Methods [a]

Method	Polysorbate 80	t_5, min A	B	C	D
Rotating basket	0	6.4	5.0	21.0	24.0
	0.1%	2.7	3.0	15.0	18.5
Paddle	0	4.5	4.7	9.9	18.6
	0.1%	4.2	4.0	9.0	11.0
Beaker	0	3.4	3.6	6.5	14.8
	0.1%	3.0	2.8	4.6	8.2

[a] At pH 7.2.

Table IV—Serum Levels, C_{max}, t_{max}, and AUC After Oral Administration of 125-mg Griseofulvin Tablets

In Vivo Parameter	Time, hr	Formulation[a] A	B	C	D	ANOVA[b]	Tukey's[c] Test
Serum levels, μg/ml	1.0	0.250 ± 0.058	0.331 ± 0.048	0.154 ± 0.025	0.126 ± 0.023	$p < 0.01$	B>A>C>D
	3.0	0.446 ± 0.065	0.593 ± 0.052	0.340 ± 0.041	0.462 ± 0.074	$p < 0.01$	B>D>A>C
	5.0	0.408 ± 0.036	0.576 ± 0.045	0.365 ± 0.038	0.486 ± 0.063	$p < 0.01$	B>D>A>C
	8.0	0.326 ± 0.035	0.462 ± 0.039	0.320 ± 0.035	0.439 ± 0.041	$p < 0.01$	B>D>A>C
	23.5	0.234 ± 0.021	0.199 ± 0.022	0.192 ± 0.019	0.243 ± 0.025	$p < 0.01$	D>A>B>C
	33.0	0.152 ± 0.018	0.109 ± 0.015	0.146 ± 0.020	0.133 ± 0.024	$p < 0.05$	A>C>D>B
	47.5	0.071 ± 0.011	0.046 ± 0.006	0.072 ± 0.010	0.062 ± 0.011	$p < 0.05$	C>A>D>B
C_{max}, μg/ml		0.502 ± 0.049	0.660 ± 0.046	0.395 ± 0.036	0.546 ± 0.070	$p < 0.01$	B>D>A>C
t_{max}, hr		5.3 ± 1.7	3.6 ± 0.3	6.0 ± 1.7	7.9 ± 2.1	NS	
$AUC_{47.5}$, μg hr/ml		10.57 ± 0.86	11.53 ± 0.76	9.46 ± 0.73	11.47 ± 0.67	$p < 0.01$	B>D>A>C
AUC_∞ μg hr/ml		11.83 ± 0.95	12.30 ± 0.86	11.27 ± 0.91	12.76 ± 0.81	NS	

[a] The figures indicate means ± standard errors. [b] NS: not significant. [c] Formulations underlined by a common line did not differ significantly; $p < 0.05$.

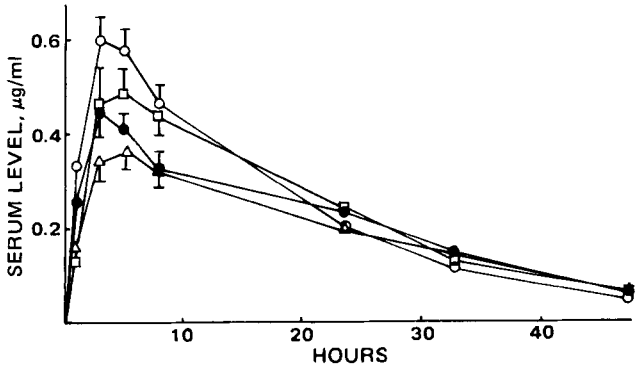

Figure 3—*Mean serum griseofulvin concentration after oral administration of 125-mg griseofulvin tablets to humans. Key: (●) Tablet A; (○) Tablet B; (△) Tablet C; (□) Tablet D. The vertical lines indicate standard errors.*

at either pH 7.2 or 1.2 without additives, the drug rapidly dissolved from Formulations A and B due to their rapid disintegration into fine particles. It slowly dissolved, however, from Formulations C and D due to the large particles resulting from disintegration. Polysorbate 80 and diastase, which was used to investigate the digestive action on the starch widely employed in tablets as the disintegrant or excipient, enhanced the dissolution from Formulation D, and in the presence of diastase its dissolution rate was faster than that from Formulation C. This can be attributed to a wetting action of the surfactant and a digestive one of the diastase. The dissolution rates were not enhanced by an increase of agitation intensity, but the dissolution from Formulation D was specifically facilitated with the basket method in which its deaggregation into fine particles seemed to be promoted due to being rubbed against the sieve wall of the basket as it was rotated. This suggests that deaggregation, especially for Formulation D, must be more accelerated by mechanical forces than by the flow of the dissolution medium. This was further ascertained by the pretreatment methods in which the dissolution of the drug, especially from Formulation D, was greatly enhanced. This is probably due to the strong deaggregation effects of the plastic beads.

The volume of water used in the pretreatment affected the dissolution, especially from the ultramicrosize formulation (A). It formed a pastelike agglomerate and showed slower dissolution when a small quantity of water (1.0 ml) was used (Method I) than when 20 ml of water was employed. In the latter case the formulation rapidly disintegrated into fine particles.

Table V—Power Analysis with $\alpha = 0.05$ and $\beta = 0.2$

Parameter	Time, hr	Subjects for 20% difference	Minimum Detectable Difference, %
Serum level	1	76	53
	3	28	30
	5	24	28
	8	20	26
	23.5	20	25
	33	44	39
	47.5	60	47
C_{max}		20	24
t_{max}		216	90
$AUC_{47.5}$		12	17
AUC_∞		16	21

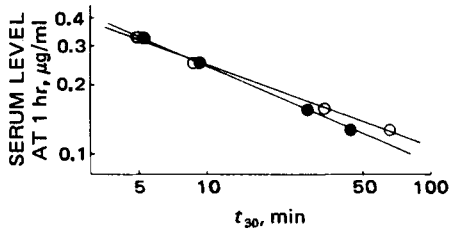

Figure 4—*Log–log plots of serum level of griseofulvin at 1 hr against t_{30} determined by the beaker method at pH 7.2 without an additive (○) and in the presence of polysorbate 80 (●).*

The initial dissolution rates (t_5) determined under the nonsink condition are shown in Table III. The results were similar to those determined with nonpretreatment methods under the sink condition, which suggests that by using the initial dissolution rates, the dissolution under the sink condition can be predicted.

Disintegration Time—The mean disintegration times of Formulations A, B, C, and D were 9.3, 12.5, 0.4, and 2.4 min, respectively. Contrary to the disintegration findings, the slow dissolution of the drug from Formulations C and D led to the conclusion that the resultant particulate state after disintegration is more important for the dissolution of griseofulvin than the disintegration time.

Bioavailability—The relations of griseofulvin dose with AUC_∞ and C_{max} are shown in Fig. 2. The nearly linear relationships of dose–AUC_∞ ($r = 0.829$) and dose–C_{max} ($r = 0.944$) indicate that linear pharmacokinetics can be applied to the serum level of griseofulvin within the dose ranges studied.

Figure 3 shows the mean serum concentration–time curves of griseofulvin in humans after oral administration of four formulations. Table IV lists the mean values of each parameter for these formulations. The rank order of serum level at 1 hr was B>A>C>D, but the serum levels during 3–8 hr, C_{max} and $AUC_{47.5}$, were B>D>A>C. The lowest peak

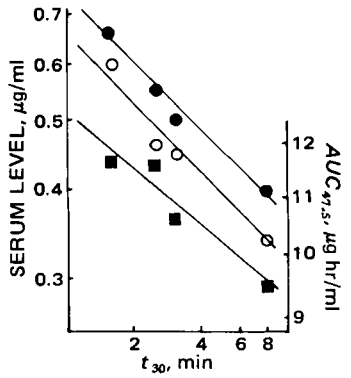

Figure 5—*Log–log plots of serum level at 3 hr (○), C_{max} (●), and $AUC_{47.5}$ (■) against t_{30} determined by Method I.*

Table VI—Correlation Coefficients Between *In Vivo* Parameters (X) and t_{30} (Y) Determined by Sink Methods

In Vitro Test		$X - Y^{-1}$					log (X) − log (Y)				
		Serum Level					Serum Level				
Method	Condition	1 hr	3 hr	5 hr	C_{max}	$AUC_{47.5}$	1 hr	3 hr	5 hr	C_{max}	$AUC_{47.5}$
Beaker	—	0.995[a]	0.809	0.655	0.727	0.430	−0.998[a]	−0.608	−0.399	−0.508	−0.229
	Polysorbate 80	0.990[a]	0.820	0.679	0.471	0.441	−0.999[a]	−0.650	−0.453	−0.554	−0.276
	Diastase	0.990[a]	0.840	0.680	0.763	0.489	−0.975[b]	−0.771	−0.564	−0.689	−0.460
	848 rpm	0.998[a]	0.792	0.617	0.708	0.420	−0.995[a]	−0.624	−0.403	−0.526	−0.259
	pH 1.2	0.942	0.848	0.765	0.782	0.482	−0.991[a]	−0.611	−0.442	−0.514	−0.217
	pH 1.2 Polysorbate 80	0.976[b]	0.813	0.696	0.736	0.423	−0.992[a]	−0.613	−0.442	−0.516	−0.220
Basket	—	0.978	0.796	0.598	0.716	0.466	−0.951	−0.769	−0.545	−0.690	−0.483
Method I	—	0.719	0.998[a]	0.965[b]	0.997[a]	0.896	−0.559	−0.982[b]	−0.917	−0.987[b]	−0.953[b]
Method II	—	0.814	0.742	0.513	0.686	0.570	−0.742	−0.824	−0.601	−0.780	−0.697

[a] $p < 0.01$. [b] $p < 0.05$.

Table VII—Correlation Coefficients Between *In Vivo* Parameters (X) and t_5 (Y) Determined by Nonsink Methods

In Vitro Test		$X - Y^{-1}$					log (X) − log (Y)				
		Serum Level					Serum Level				
Method	Additive	1 hr	3 hr	5 hr	C_{max}	$AUC_{47.5}$	1 hr	3 hr	5 hr	C_{max}	$AUC_{47.5}$
Rotating basket	none	0.986[a]	0.758	0.554	0.670	0.402	−0.954[a]	−0.627	−0.387	−0.527	−0.260
	Polysorbate 80	0.895	0.591	0.329	0.498	0.380	−0.947	−0.591	−0.325	−0.494	−0.269
Paddle	none	0.912	0.503	0.245	0.394	0.120	−0.939	−0.387	−0.135	−0.274	0.002
	Polysorbate 80	0.954[a]	0.641	0.402	0.544	0.282	−0.974[a]	−0.584	−0.335	−0.484	−0.235
Beaker	none	0.892	0.428	0.170	0.313	0.220	−0.907	−0.287	−0.044	−0.169	0.118
	Polysorbate 80	0.937	0.492	0.262	0.378	0.553	−0.934	−0.345	−0.119	−0.229	0.068

[a] $p < 0.05$.

concentration (Formulation C) was only 60% of the highest one (Formulation B). Significant differences were found among the formulations; however, there were no significant differences in AUC_∞, which suggests that the four formulations were equivalent in the extent of bioavailability.

The mean peak times did not show significant differences, though the maximum difference (3.6–7.9 hr) was relatively large. This can be attributed to the large variations in the parameter which will be due in some degree to a few peak times of 23.5 hr, which occurred with all formulations except B. It may have been artificially caused by the long interval of the sampling time from 8 to 23.5 hr. The power analysis was employed to estimate the minimum detectable difference between the formulations which would be statistically significant ($\alpha = 0.05$, $\beta = 0.2$) or the number of subjects required for a 20% difference to be significant (Table V). The results of this analysis indicate considerably low detectability of t_{max} compared with the other parameters; only 90% of the minimum difference could be detected in this study, and >200 subjects would have been required for a 20% difference to be significant. The parameters of $AUC_{47.5}$ and AUC_∞ provided better detectabilities, which must be due to the small variabilities in the parameters.

The ultramicrosize formulation (A) did not show good bioavailability, which is coincident with previous results (13), though absorption of the drug from the formulation was reported to be approximately twice that from microsize formulations (11, 12).

Correlation Between Dissolution Rate and Bioavailability—The correlation coefficients between the *in vivo* and *in vitro* parameters (t_{30} and t_5 determined by sink and nonsink methods, respectively) are shown in Tables VI and VII. The t_{30} determined by sink methods without pretreatment correlated significantly with the serum level at 1 hr in normal–reciprocal and log–log regressions but not with the other *in vivo* parameters. Similar relations were found between t_5 determined by nonsink methods and the *in vivo* parameters. The t_{30} determined by Method I with pretreatment with 1.0 ml of water was significantly correlated with serum levels at 3–5 hr and C_{max} in normal–reciprocal regression and even with $AUC_{47.5}$ in log–log regression. Those determined by Method II using 20 ml of water, however, did not correlate significantly with any of the *in vivo* parameters. Figures 4 and 5 illustrate the log–log regression lines that were significantly correlated between *in vivo* and *in vitro* findings.

DISCUSSION

The *in vivo* and *in vitro* findings for griseofulvin formulations suggest the complex dissolution behavior of the drug from its dosage forms in the GI tract in humans. The serum levels 1 hr after administration of the formulation correlated well with the dissolution rates determined under sink and nonsink conditions without pretreatment, which leads to the conclusion that initial absorption is mainly controlled by relatively simple dissolution behavior as shown artificially in the dissolution tests without pretreatment. However, the serum levels during 3–5 hr and C_{max} did not correlate well with these dissolution rates, which is probably due to the unexpectedly low values for Formulation A and high values for D for the *in vivo* parameters. It may be considered that for a drug having as low solubility in water or biological fluids as griseofulvin, the *in vivo* disintegration and dissolution must be affected more by physiological factors in the GI tract than those of a drug having high solubility, because the former drug must stay in the GI tract longer. The *in vitro* pretreatment, which decreases the sizes of aggregates or particles available from dissolution with plastic beads, markedly increased the dissolution, especially from Formulation D. The resulting dissolution rates highly correlated with the serum levels at 3 and 5 hr, C_{max}, and $AUC_{47.5}$. These findings suggest a strong deaggregation action on the aggregates and/or particles while the drug having low solubility stays in the GI tract.

A previous report on sugar-coated tablets of chloramphenicol also suggested the violent destructive force on the formulations *in vivo* (17). Therefore, the absorption of a drug having low solubility from its dosage forms seems to be correlated more with the dissolution rates determined under the conditions of vigorous agitation and destructive intensities than under mild conditions, though the absorption of a drug having high solubility such as aspirin may be correlated more with the dissolution rates determined under the latter conditions (18, 19).

Formulation A showed rapid dissolution under sink and nonsink conditions without pretreatment, which is probably due to the original ultramicrosize particulate state of the drug. But the rapid dissolution did not contribute to the *in vivo* absorption. Formulation A formed a pastelike agglomerate when treated with a small quantity of water (1.0 ml). Such an agglomerate may be also produced in the GI tract after rapid gastric emptying and rapid absorption of water coadministered with the formulation and may be responsible for slower dissolution and the resulting lower absorption of the drug.

REFERENCES

(1) R. M. Atkinson, C. Bedford, K. J. Child, and E. G. Tomich, *Nature (London)*, **193,** 588 (1962).

(2) P. Kabasakalian, M. Katz, B. Rosenkrantz, and E. Townley, *J. Pharm. Sci.*, **59,** 595 (1970).

(3) M. Kraml, J. Dubac, and D. Beall, *Can. J. Biochem. Physiol.*, **40,** 1449 (1962).

(4) R. M. Atkinson, C. Bedford, K. J. Child, and E. G. Tomich, *Antibiot. Chemother.*, **12,** 232 (1962).

(5) M. Kraml, J. Dubuc, and D. Dvornik, *Arch. Dermatol.*, **87**, 179 (1963).
(6) J. R. Marvel, D. A. Schlichting, D. Denton, E. J. Levy, and M. M. Cahn, *J. Invest. Dermatol.*, **42**, 197 (1964).
(7) B. Katchen and S. Symchowicz, *J. Pharm. Sci.*, **56**, 1108 (1967).
(8) S. Symchowicz and B. Katchen, *ibid.*, **57**, 1383 (1968).
(9) S. Lin, J. Menig, and L. Lachman, *ibid.*, **57**, 2143 (1968).
(10) W. L. Chiou and S. Riegelman, *ibid.*, **60**, 1376 (1971).
(11) W. E. Barrett, *Curr. Ther. Res.*, **18**, 501 (1975).
(12) *Ibid.*, **18**, 491 (1975).
(13) A. B. Straughn, M. C. Meyer, G. Raghow, and K. Rotenberg, *J. Pharmacokinet. Biopharm.*, **8**, 347 (1980).
(14) J. G. Wagner, "Fundamentals of Clinical Pharmacokinetics," Drug Intelligence Publications, Hamilton, Ill., 1975, p. 344.
(15) H. J. Schwarz, B. A. Waldman, and V. Madrid, *J. Pharm. Sci.*, **65**, 370 (1976).
(16) "USP Pharmacopeial Forum," **3**, 22–25 (1977).
(17) H. Ogata, T. Shibazaki, T. Inoue, and A. Ejima, *J. Pharm. Sci.*, **68**, 712 (1979).
(18) G. Levy, *ibid.*, **50**, 388 (1961).
(19) *Ibid.*, **52**, 1039 (1963).

Bioavailability of Griseofulvin from Tablets in Beagle Dogs and Correlation with Dissolution Rate and Bioavailability in Humans

NOBUO AOYAGI *x, HIROYASU OGATA *, NAHOKO KANIWA *, MASANOBU KOIBUCHI *†, TOSHIO SHIBAZAKI *, AKIRA EJIMA *, NORIYASU TAMAKI ‡, HIDETAKA KAMIMURA §, YOSHIO KATOUGI ‡, and YUKIO OMI §

Received July 31, 1981, from the **Division of Drugs, National Institute of Hygienic Sciences, 18-1, Kamiyoga 1-chome, Setagaya-ku, Tokyo 158, Japan;* the ‡*Yaizu Plant, Yamanouchi Pharmaceutical Co. Ltd., Ozumi-180, Yaizu-shi, Shizuoka-ken 425, Japan;* and the §*Institute of Research and Development, Yamanouchi Pharmaceutical Co. Ltd., 1-8, Azusawa 1-chome, Itabashi-ku, Tokyo 174, Japan.*
†Deceased. Accepted for publication December 30, 1981.

Abstract □ The bioavailability of four griseofulvin tablets in beagle dogs, including an ultramicrosize tablet used previously in a human bioavailability study, was investigated on the basis of the plasma 6-demethylgriseofulvin concentration. The relations with the *in vivo* findings in humans and the *in vitro* dissolution rates also were examined. Contrary to the lower bioavailability of the ultramicrosize formulation in humans, it provided the best bioavailability in beagles. The microsize griseofulvin formulations showed similar *in vivo* results to those in humans. Poor correlation of *in vivo* parameters between humans and beagles was attributed to the discrepancy of the availability of the ultramicrosize formulation between the two species. The dissolution rates determined by the pretreatment method using plastic beads were correlated more with the *in vivo* findings than those determined by the other methods. Beagles were a useful animal model for bioavailability studies of certain griseofulvin formulations but not ultramicrosize ones.

Keyphrases □ Bioavailability—griseofulvin from tablets in beagle dogs, correlation with dissolution rate and bioavailability in humans □ Dissolution rates—bioavailability of griseofulvin from tablets in beagle dogs, bioavailability in humans □ Griseofulvin—bioavailability from tablets in beagle dogs, dissolution rate and bioavailability in humans

The bioavailabilities for four lots of griseofulvin tablets in humans have been reported previously, and the relations with *in vitro* dissolution rates have been discussed (1).

Beagle dogs are often used as an animal model for bioavailability studies, but their suitability has not been clarified sufficiently. A good relation of penicillin bioavailability between humans and dogs was reported (2). Previous studies on bioavailability of diazepam formulations in humans and beagles revealed no good relations between the results from both species. The discrepancy was considered to be due to the differences of physiological states of the GI tract, especially of gastric emptying rate and GI transition time (3).

In the present study the bioavailability of griseofulvin from tablets in beagles was studied, and the relations with *in vivo* results in humans and *in vitro* dissolution rates were investigated.

EXPERIMENTAL

Formulations—Four lots of tablets containing 125 mg of griseofulvin employed in the human bioavailability study (1) were used. One formu-

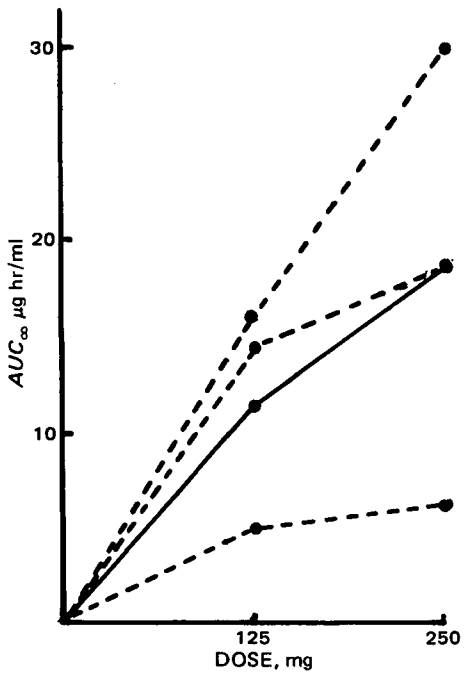

Figure 1—*Relation between griseofulvin dose and* AUC_∞ *of 6-demethylgriseofulvin. Key: (---) responses of the individual dogs; (—) average response.*

0022-3549/82/01000-1169$01.00/0

(5) M. Kraml, J. Dubuc, and D. Dvornik, *Arch. Dermatol.*, **87**, 179 (1963).
(6) J. R. Marvel, D. A. Schlichting, D. Denton, E. J. Levy, and M. M. Cahn, *J. Invest. Dermatol.*, **42**, 197 (1964).
(7) B. Katchen and S. Symchowicz, *J. Pharm. Sci.*, **56**, 1108 (1967).
(8) S. Symchowicz and B. Katchen, *ibid.*, **57**, 1383 (1968).
(9) S. Lin, J. Menig, and L. Lachman, *ibid.*, **57**, 2143 (1968).
(10) W. L. Chiou and S. Riegelman, *ibid.*, **60**, 1376 (1971).
(11) W. E. Barrett, *Curr. Ther. Res.*, **18**, 501 (1975).
(12) *Ibid.*, **18**, 491 (1975).
(13) A. B. Straughn, M. C. Meyer, G. Raghow, and K. Rotenberg, *J. Pharmacokinet. Biopharm.*, **8**, 347 (1980).
(14) J. G. Wagner, "Fundamentals of Clinical Pharmacokinetics," Drug Intelligence Publications, Hamilton, Ill., 1975, p. 344.
(15) H. J. Schwarz, B. A. Waldman, and V. Madrid, *J. Pharm. Sci.*, **65**, 370 (1976).
(16) "USP Pharmacopeial Forum," **3**, 22–25 (1977).
(17) H. Ogata, T. Shibazaki, T. Inoue, and A. Ejima, *J. Pharm. Sci.*, **68**, 712 (1979).
(18) G. Levy, *ibid.*, **50**, 388 (1961).
(19) *Ibid.*, **52**, 1039 (1963).

Bioavailability of Griseofulvin from Tablets in Beagle Dogs and Correlation with Dissolution Rate and Bioavailability in Humans

NOBUO AOYAGI *x, HIROYASU OGATA *, NAHOKO KANIWA *, MASANOBU KOIBUCHI *†, TOSHIO SHIBAZAKI *, AKIRA EJIMA *, NORIYASU TAMAKI ‡, HIDETAKA KAMIMURA §, YOSHIO KATOUGI ‡, and YUKIO OMI §

Received July 31, 1981, from the **Division of Drugs, National Institute of Hygienic Sciences, 18-1, Kamiyoga 1-chome, Setagaya-ku, Tokyo 158, Japan;* the ‡*Yaizu Plant, Yamanouchi Pharmaceutical Co. Ltd., Ozumi-180, Yaizu-shi, Shizuoka-ken 425, Japan;* and the §*Institute of Research and Development, Yamanouchi Pharmaceutical Co. Ltd., 1-8, Azusawa 1-chome, Itabashi-ku, Tokyo 174, Japan.*
†Deceased. Accepted for publication December 30, 1981.

Abstract □ The bioavailability of four griseofulvin tablets in beagle dogs, including an ultramicrosize tablet used previously in a human bioavailability study, was investigated on the basis of the plasma 6-demethylgriseofulvin concentration. The relations with the *in vivo* findings in humans and the *in vitro* dissolution rates also were examined. Contrary to the lower bioavailability of the ultramicrosize formulation in humans, it provided the best bioavailability in beagles. The microsize griseofulvin formulations showed similar *in vivo* results to those in humans. Poor correlation of *in vivo* parameters between humans and beagles was attributed to the discrepancy of the availability of the ultramicrosize formulation between the two species. The dissolution rates determined by the pretreatment method using plastic beads were correlated more with the *in vivo* findings than those determined by the other methods. Beagles were a useful animal model for bioavailability studies of certain griseofulvin formulations but not ultramicrosize ones.

Keyphrases □ Bioavailability—griseofulvin from tablets in beagle dogs, correlation with dissolution rate and bioavailability in humans □ Dissolution rates—bioavailability of griseofulvin from tablets in beagle dogs, bioavailability in humans □ Griseofulvin—bioavailability from tablets in beagle dogs, dissolution rate and bioavailability in humans

The bioavailabilities for four lots of griseofulvin tablets in humans have been reported previously, and the relations with *in vitro* dissolution rates have been discussed (1).

Beagle dogs are often used as an animal model for bioavailability studies, but their suitability has not been clarified sufficiently. A good relation of penicillin bioavailability between humans and dogs was reported (2). Previous studies on bioavailability of diazepam formulations in humans and beagles revealed no good relations between the results from both species. The discrepancy was considered to be due to the differences of physiological states of the GI tract, especially of gastric emptying rate and GI transition time (3).

In the present study the bioavailability of griseofulvin from tablets in beagles was studied, and the relations with *in vivo* results in humans and *in vitro* dissolution rates were investigated.

EXPERIMENTAL

Formulations—Four lots of tablets containing 125 mg of griseofulvin employed in the human bioavailability study (1) were used. One formu-

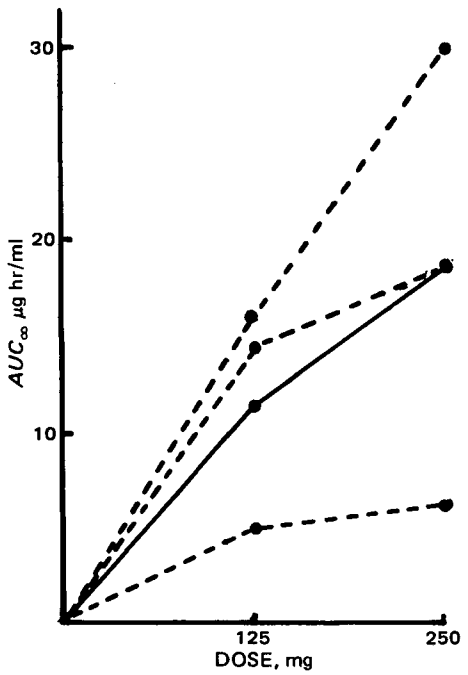

Figure 1—*Relation between griseofulvin dose and* AUC_∞ *of 6-demethylgriseofulvin. Key: (---) responses of the individual dogs; (—) average response.*

0022-3549/82/01000-1169$01.00/0

Table I—Plasma Concentrations of Griseofulvin and 6-Demethylgriseofulvin Following Oral Administration of Formulation A to 12 Beagles

In Vivo Parameter		Griseofulvin Means ± *SD*	Griseofulvin Coefficient of Variation, %	6-Demethylgriseofulvin Means ± *SD*	6-Demethylgriseofulvin Coefficient of Variation, %
Plasma Concentration μg/ml	0.5 hr	0.209 ± 0.202	97	1.559 ± 1.128	72
	1	0.494 ± 0.481	97	2.562 ± 1.264	49
	2	0.429 ± 0.298	70	2.059 ± 1.138	55
	3	0.327 ± 0.196	60	1.519 ± 0.763	50
	4	0.203 ± 0.116	57	1.092 ± 0.468	43
	6	0.103 ± 0.036	35	0.843 ± 0.259	31
	8	0.065 ± 0.033	51	0.753 ± 0.298	40
	10	0.050 ± 0.036	73	0.544 ± 0.289	53
	24	0.003 ± 0.010	333	0.127 ± 0.199	157
C_{max}, μg/ml		0.626 ± 0.458	73	3.083 ± 1.114	36

Table II—Plasma Levels, C_{max}, t_{max}, and AUC_{24} of 6-Demethylgriseofulvin Following Oral Administration of Four Lots of 125-mg Griseofulvin Tablets to Beagles

In Vivo Parameter		Formulation[a] A	B	C	D	Result[b] of ANOVA	Tukey's[c] Test
Plasma level, μg/ml	0.5 hr	1.559 ± 0.325	1.265 ± 0.290	0.640 ± 0.123	0.699 ± 0.229	$p < 0.05$	A > B > D > C
	1	2.562 ± 0.365	1.857 ± 0.342	0.925 ± 0.112	1.222 ± 0.272	$p < 0.01$	A > B > D > C
	2	2.059 ± 0.329	1.482 ± 0.314	0.977 ± 0.135	1.234 ± 0.105	$p < 0.01$	A > B > D > C
	3	1.519 ± 0.220	1.170 ± 0.256	0.850 ± 0.138	0.951 ± 0.093	$p < 0.05$	A > B > D > C
	4	1.092 ± 0.135	0.924 ± 0.199	0.845 ± 0.202	0.813 ± 0.136	NS	
	6	0.843 ± 0.075	0.714 ± 0.135	0.540 ± 0.101	0.540 ± 0.098	NS	
	8	0.753 ± 0.086	0.584 ± 0.110	0.434 ± 0.086	0.483 ± 0.081	NS	
	10	0.544 ± 0.083	0.463 ± 0.102	0.282 ± 0.040	0.442 ± 0.102	NS	
	24	0.127 ± 0.057	0.071 ± 0.017	0.077 ± 0.029	0.053 ± 0.015	NS	
C_{max}, μg/ml		3.083 ± 0.321	2.340 ± 0.322	1.369 ± 0.156	1.749 ± 0.190	$p < 0.01$	A > B > D > C
t_{max}, hr		1.5 ± 0.2	1.3 ± 0.2	1.9 ± 0.5	1.7 ± 0.3	NS	
AUC_{24}, μg hr/ml		16.34 ± 1.38	12.86 ± 2.77	8.86 ± 1.05	10.62 ± 1.48	< 0.01	A > B > D > C

[a] The figures indicate means ± standard error. [b] NS: not significant. [c] Formulations underlined by a common line did not differ significantly ($p < 0.05$).

lation was an ultramicrosize griseofulvin tablet (A); the others were commercial microsize griseofulvin tablets (B, C, D).

Dissolution Rate—The methods to determine the dissolution rates were carried out as reported previously (1). Sink methods included nonpretreatment (18-liter beaker method and basket method) and pretreatment (Methods I and II). The dissolution rate was expressed as t_{30} the time taken for 30% of the drug to dissolve.

Bioavailability—Twelve beagles (12.0–14.0 kg; mean 12.9) were randomly divided into four groups according to a Latin square crossover design. The beagles, having fasted for 20 hr, were given a test tablet and then forced to take 30 ml of water. The beagles were not given any food until 10 hr after drug administration. Blood samples were taken at 0.5, 1, 2, 3, 4, 6, 8, 10, and 24 hr after administration, and the plasma samples were frozen and stored until assay. The experiments were repeated every week according to the dosage schedule. The bioavailability for each formulation was evaluated from the plasma concentrations of 6-demethylgriseofulvin, a metabolite of griseofulvin, at each sampling time, peak plasma concentration (C_{max}), time to C_{max} (t_{max}), and area under plasma concentration–time curves from 0 to the sampling time t (AUC_t). The value for AUC_∞ was calculated by the method of Wagner (4).

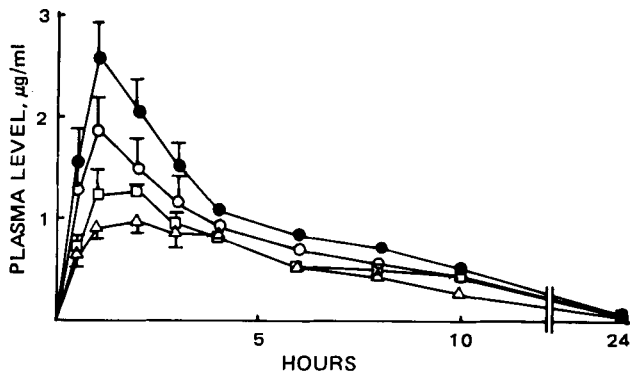

Figure 2—*Mean plasma 6-demethylgriseofulvin concentration after oral administration of 125-mg griseofulvin formulations to beagles. Key: (●) Tablet A; (○) Tablet B; (△) Tablet C; (□) Tablet D. The vertical lines show standard errors.*

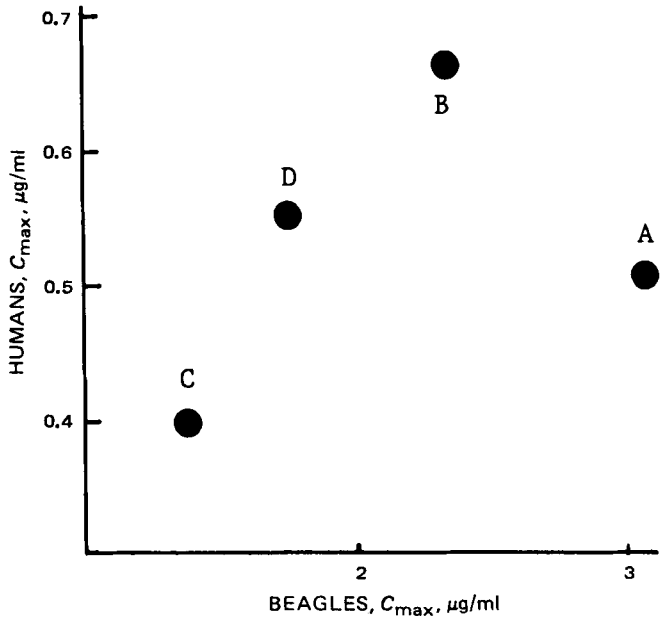

Figure 3—*Correlation of C_{max} values after oral administration of four griseofulvin formulations between humans and beagles.*

Table III—C_{max}, t_{max}, and AUC_{24} of 6-Demethylgriseofulvin Following Oral Administration of Three Griseofulvin Formulations [a]

Parameter	Formulation	Volume of Water 30 ml	Volume of Water 200 ml	Paired [b] t test
C_{max}, μg/ml	A	3.038 ± 0.287 [c]	2.608 ± 0.167	NS
	B	2.290 ± 0.490	2.067 ± 0.160	NS
	D	1.787 ± 0.270	1.388 ± 0.381	NS
t_{max}, hr	A	1.6 ± 0.2	1.8 ± 0.2	NS
	B	1.2 ± 0.2	1.7 ± 0.4	NS
	D	1.9 ± 0.4	3.6 ± 1.0	NS
AUC_{24}, μg hr/ml	A	18.89 ± 1.15	17.59 ± 0.88	NS
	B	11.13 ± 2.56	14.46 ± 1.79	NS
	D	11.68 ± 2.10	11.50 ± 1.96	NS

[a] With 30 and 200 ml of water. [b] NS: not significant. [c] Mean ± standard error.

Dose–AUC_∞ Relation—Three beagles were fasted overnight and given one and two tablets of Formulation C, corresponding to 125 and 250 mg of griseofulvin, respectively. The other procedures were the same as described for the bioavailability test.

Effects of Volume of Water Coadministered—Three formulations, including the ultramicrosize formulation, were used. Eight beagles were given a tablet with 30 and 200 ml of water in a crossover design. The other procedures were the same as described for the bioavailability test.

Assay—Griseofulvin and 6-demethylgriseofulvin in plasma were determined by GC (5).

RESULTS

Plasma Levels of Griseofulvin and 6-Demethylgriseofulvin—Table I shows the mean plasma griseofulvin and 6-demethylgriseofulvin concentrations after oral administration of Formulation A. The plasma griseofulvin concentrations were below one-fifth of those of 6-demethylgriseofulvin, and only a trace of griseofulvin was detected at 24 hr after administration of the drug. This can be attributed to the greater clearance of griseofulvin in dogs than in humans (6, 7), and hence, a considerable fraction of the dose administered orally will be converted to 6-demethylgriseofulvin by first-pass metabolism before reaching the blood circulation (8). The great clearance of griseofulvin probably leads to the greater coefficients of variation found in the plasma levels of griseofulvin than those of 6-demethylgriseofulvin. Considering the findings, the bioavailability of griseofulvin in beagles was estimated on the basis of the plasma level of 6-demethylgriseofulvin.

Bioavailability—The relation of the griseofulvin dose and the AUC_∞ of 6-demethylgriseofulvin is shown in Fig. 1. Large differences in the AUC_∞ values among the beagles were found. With the high dose, the unabsorbed fraction of the drug may increase by being not fully dissolved in the GI tract.

Figure 2 shows the mean plasma level–time curves of 6-demethylgriseofulvin following oral administration of four formulations. Table II lists their mean values for *in vivo* parameters. The plasma levels of 6-demethylgriseofulvin at 24 hr were very low, so the AUC_{24} can be considered as AUC_∞. Although the ultramicrosize formulation (A) showed relatively low bioavailability in humans (1), this formulation showed the highest values in the plasma concentrations, C_{max} and AUC_{24}, in beagles. The ratios of C_{max} and AUC_{24} of the ultramicrosize formulation to those of Formulation B, which showed the highest availability of all microsize formulations, were 132 and 127%, respectively. Significant differences were found between Formulation A and two microsize formulations (C and D) in the plasma levels at earlier sampling times, C_{max} and AUC_{24}.

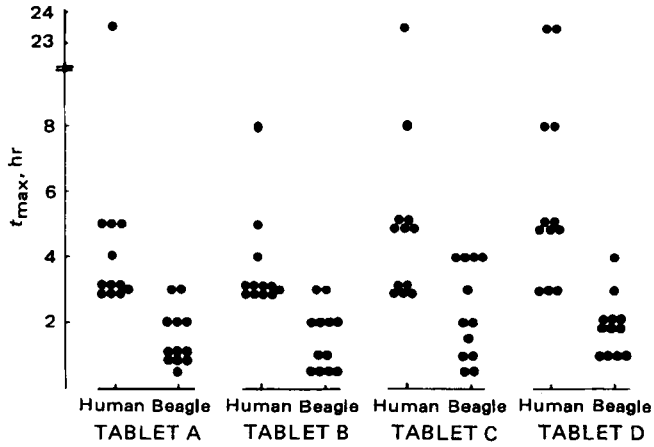

Figure 4—*Individual t_{max} values in beagles and humans after oral administration of four griseofulvin formulations.*

For microsize formulations, the *in vivo* results were similar to those in humans: Formulation B had the best bioavailability as expected from the *in vitro* dissolution rate and Formulation D showed better bioavailability than Formulation C. A significant difference was found in C_{max} between Formulations B and C but not in plasma levels and AUC_{24}. The t_{max} values in beagles, which seemed shorter than those in humans (3.6–7.9 hr), did not show significant differences among the formulations.

Effects of Volume of Water Coadministered—Thirty milliliters of water was given to beagles; however, 200 ml was used in the human bioavailability study (1). The large volume of water enhanced the *in vivo* absorption of erythromycin stearate and amoxicillin which are poorly soluble in water (9). The different volumes of water used in the human and beagle tests might lead to a discrepancy in the *in vivo* results, especially for the ultramicrosize formulation. To clarify this, the bioavailabilities were tested with 30 and 200 ml of water. As shown in Table III, the fluid volume did not significantly affect the bioavailabilities, which leads to the conclusion that the discrepancy of bioavailabilities between humans and beagles is not due to the difference of the volume of water administered. As another explanation, the physiological differences in the GI tract between the two species may be considered.

Correlation Between the Bioavailability and Dissolution Rates—The correlation coefficients between the *in vivo* parameters and *in vitro* dissolution rates (t_{30}) determined by sink methods are shown in Table IV. The *in vivo* parameters are correlated more in the log–log and normal–reciprocal regressions with t_{30} determined by Method II (Table IV), in which the tablets were treated in 20 ml of water with plastic beads before the determination of dissolution rates.

Correlation Between Humans and Beagles—As shown in Table V, low correlation coefficients were found between humans and beagles. The poor relations are attributed mainly to the discrepancy of the ultramicrosize formulation (A) between them. Figure 3 shows that the microsize formulations (B, C, D) showed a good relation (r = 0.976) in C_{max} values between humans and beagles, which suggests that the bioavailabilities of microsize formulations can be evaluated in beagles instead of humans.

DISCUSSION

The *in vivo* findings in beagles did not correlate well with those in humans. The ultramicrosize formulation provided the best availability

Table IV—Correlation Coefficients Between *In Vivo* Parameters (X) and t_{30} (Y) Determined by Sink Methods

In Vitro Test Method	Condition	X − Y^{-1} Serum Level 1 hr	3 hr	5 hr	C_{max}	AUC_{24}	log X − log Y Serum Level 1 hr	3 hr	5 hr	C_{max}	AUC_{24}
Beaker	—	0.747	0.631	0.514	0.613	0.579	−0.872	−0.760	−0.655	−0.731	−0.701
	Polysorbate 80	0.714	0.595	0.474	0.577	0.541	−0.859	−0.748	−0.638	−0.719	−0.686
	Diastase	0.776	0.672	0.562	0.658	0.625	−0.916	−0.846	−0.751	−0.824	−0.793
	848 rpm	0.803	0.697	0.587	0.680	0.648	−0.903	−0.802	−0.704	−0.775	−0.747
	pH 1.2	0.556	0.423	0.292	0.405	0.366	−0.788	−0.656	−0.535	−0.623	−0.587
	pH 1.2 Polysorbate 80	0.641	0.510	0.382	0.491	0.453	−0.793	−0.663	−0.542	−0.630	−0.594
Basket	—	0.872	0.790	0.695	0.777	0.749	−0.948	−0.896	−0.815	−0.878	−0.851
Method I	—	0.472	0.422	0.341	0.429	0.404	−0.589	−0.636	−0.575	−0.635	−0.602
Method II	—	0.943	0.932	0.889	0.933	0.903	−0.910	−0.945	−0.910	−0.943	−0.927

Table V—Correlation Coefficients of Bioavailability Parameters Between Humans and Beagles

Beagle	Human	r
$C_{0.5}$[a]	C_1	0.789
	C_3	0.505
C_1	C_1	0.678
	C_3	0.448
C_{max}	C_{max}	0.388
t_{max}	t_{max}	0.711
AUC_{24}	$AUC_{47.5}$	0.306

[a] C_t shows the plasma or serum concentration at time t.

in beagles contrary to its lower absorption in humans. Considering the insignificant effects of the volume of water on the bioavailability, the ultramicrosize formulation discrepancy may be attributed to the physiological differences in the GI tract. None of the *in vitro* dissolution methods indicated such a superiority of the ultramicrosize formulation in beagles. These findings suggest that this formulation may disintegrate into the original ultramicrosize particulate state of the drug and allow rapid dissolution in the GI tract in beagles beyond the expectation from the *in vitro* dissolution findings.

The t_{max} values in beagles for different formulations were smaller than those in humans (Fig. 4). This suggests rapid transition of the drug to the absorption site, namely, fast gastric emptying of the drug in beagles. The good bioavailability of the ultramicrosize formulation may be related to the rapid gastric emptying of the drug which leads to dissolution of the drug in the small intestinal tract.

Formulation D provided higher C_{max} and plasma levels at earlier sampling times than Formulation C as observed in the human test. The *in vitro* dissolution rate of the drug from Formulation D was enhanced over that from Formulation C by pretreatment with plastic beads. These findings suggest that in beagles and humans there is a strong intensive deaggregation action on the particles or aggregates of the drug during their transition into the GI tract.

Although there was no significant difference in AUC_∞ values among the formulations in humans, the AUC_{24} (considered as AUC_∞) of Formulations C and D were significantly lower than that of Formulation A in beagles. This suggests their incomplete dissolution during passage through the GI tract and also suggests the short absorption site and/or fast transition of the drug in the GI tract in beagles as previously shown for the bioavailability of diazepam in beagles (3).

Although the *in vivo* findings of the ultramicrosize formulation in beagles did not agree with those in humans, the bioavailabilities of the microsize formulations showed good agreement. Considering this, beagles may serve as a useful animal model for bioavailability studies of certain griseofulvin tablet formulations, but not ultramicrosize ones.

REFERENCES

(1) N. Aoyagi, H. Ogata, N. Kaniwa, M. Koibuchi, T. Shibazaki, and A. Ejima, *J. Pharm. Sci.*, **71**, 1165 (1982).

(2) J. W. Poole, *Rev. Can. Biol.* Suppl., **32**, 43 (1973).

(3) H. Ogata, N. Aoyagi, N. Kaniwa, M. Koibuchi, T. Shibazaki, A. Ejima, T. Shimamoto, T. Yashiki, Y. Ogawa, Y. Uda, and Y. Nishida, *Int. J. Clin. Pharmacol. Toxicol.*, in press.

(4) J. G. Wagner, "Fundamentals of Clinical Pharmacokinetics," Drug Intelligence Publications, Hamilton, Ill., 1975, p. 344.

(5) H. Kamimura, Y. Omi, Y. Shiobara, N. Tamaki, and Y. Katogi, *J. Chromatogr.*, 163, 271 (1979).

(6) M. Rowland, S. Riegelman, and W. L. Epstein, *J. Pharm. Sci.*, **57**, 984 (1968).

(7) P. A. Harris and S. Riegelman, *ibid.*, **58**, 93 (1969).

(8) W. L. Chiou and S. Riegelman, *ibid.*, **59**, 937 (1970).

(9) P. G. Welling, *Pharm. Int.*, **1**, 14 (1980).

NOTES

Antibradykinin Active Material in *Aloe saponaria*

AKIRA YAGI *x, NOBUO HARADA ‡, HIDENORI YAMADA *, SHUICHI IWADARE ‡, and ITSUO NISHIOKA *

Received October 27, 1981, from the **Faculty of Pharmaceutical Sciences, Kyushu University, Maidashi, Higashi-ku, Fukuoka, Japan*, and the ‡*Banyu Pharmaceutical Co., Ltd., Nihonbashi honcho, Chuo-ku, Tokyo, Japan.* Accepted for publication December 31, 1981.

Abstract □ A material having antibradykinin activity on isolated guinea pig ileum was partially purified from the nondialysate of the pulp of *Aloe saponaria* by repetition of gel chromatography using a hydrophilic polyvinyl gel and dextran gels. From the results of amino acid and carbohydrate analyses, the antibradykinin-active material was estimated to be a glycoprotein. It was found that this material catalyzes the hydrolysis of bradykinin at pH 7.4. The results of peptide analysis using reversed-phase high-performance liquid chromatography coupled with amino acid analysis indicate that this glycoprotein cleaves the Gly^4-Phe^5 and Pro^7-Phe^8 bonds of the bradykinin molecule.

Keyphrases □ Antibradykinin—active material in *Aloe saponaria*, guinea pig ileum, glycoprotein, high-performance liquid chromatography □ Glycoprotein—antibradykinin active material in *Aloe saponaria*, high-performance liquid chromatography, guinea pig ileum □ *Aloe saponaria*—antibradykinin active material, glycoprotein, high-performance liquid chromatography, guinea pig ileum

Cardiac stimulant action of the constituents in the dialysate of the pulp from *Aloe saponaria*[1] on isolated cardiac muscles has been reported (1). Antibradykinin activity of the nondialysate of the pulp has been examined here to obtain pharmacological evidence for its anti-inflammatory action (2). In this report, the results of partial purification of material having antibradykinin activity from *A. saponaria* on isolated guinea pig ileum and its proteolytic property against bradykinin are presented.

EXPERIMENTAL

Materials—The following materials were purchased from suppliers: dextran gel[2,3], hydrophilic polyvinyl gel[4], dialysis membrane[5], synthetic bradykinin[6], and bromelain[7]. The gel filtrations were performed at room temperature at a flow rate of 21 ml/hr using a microtube pump[8].

Methods of Analysis—Protein and carbohydrate contents in samples

[1] *Aloe saponaria* is also known as white spotted *aloe* or soap *aloe*.

[2] Sephadex G-100, Pharmacia Fine Chemicals, Uppsala, Sweden.
[3] Sephadex G-25, Pharmacia Fine Chemicals, Uppsala, Sweden.
[4] Toyopearl HW 40, Toyo Soda Mfg., Co. Ltd., Tokyo, Japan.
[5] Visking tube, Visking Co., Union Carbide Corp.
[6] The Protein Research Foundation, Osaka, Japan.
[7] Nakarai Chemical Co., Ltd., Kyoto, Japan.
[8] Tokyo Riakkikai Co., Ltd., Tokyo, Japan.

0022-3549/82/01000-1172$01.00/0

Table V—Correlation Coefficients of Bioavailability Parameters Between Humans and Beagles

Beagle	Human	r
$C_{0.5}$[a]	C_1	0.789
	C_3	0.505
C_1	C_1	0.678
	C_3	0.448
C_{max}	C_{max}	0.388
t_{max}	t_{max}	0.711
AUC_{24}	$AUC_{47.5}$	0.306

[a] C_t shows the plasma or serum concentration at time t.

in beagles contrary to its lower absorption in humans. Considering the insignificant effects of the volume of water on the bioavailability, the ultramicrosize formulation discrepancy may be attributed to the physiological differences in the GI tract. None of the *in vitro* dissolution methods indicated such a superiority of the ultramicrosize formulation in beagles. These findings suggest that this formulation may disintegrate into the original ultramicrosize particulate state of the drug and allow rapid dissolution in the GI tract in beagles beyond the expectation from the *in vitro* dissolution findings.

The t_{max} values in beagles for different formulations were smaller than those in humans (Fig. 4). This suggests rapid transition of the drug to the absorption site, namely, fast gastric emptying of the drug in beagles. The good bioavailability of the ultramicrosize formulation may be related to the rapid gastric emptying of the drug which leads to dissolution of the drug in the small intestinal tract.

Formulation D provided higher C_{max} and plasma levels at earlier sampling times than Formulation C as observed in the human test. The *in vitro* dissolution rate of the drug from Formulation D was enhanced over that from Formulation C by pretreatment with plastic beads. These findings suggest that in beagles and humans there is a strong intensive deaggregation action on the particles or aggregates of the drug during their transition into the GI tract.

Although there was no significant difference in AUC_∞ values among the formulations in humans, the AUC_{24} (considered as AUC_∞) of Formulations C and D were significantly lower than that of Formulation A in beagles. This suggests their incomplete dissolution during passage through the GI tract and also suggests the short absorption site and/or fast transition of the drug in the GI tract in beagles as previously shown for the bioavailability of diazepam in beagles (3).

Although the *in vivo* findings of the ultramicrosize formulation in beagles did not agree with those in humans, the bioavailabilities of the microsize formulations showed good agreement. Considering this, beagles may serve as a useful animal model for bioavailability studies of certain griseofulvin tablet formulations, but not ultramicrosize ones.

REFERENCES

(1) N. Aoyagi, H. Ogata, N. Kaniwa, M. Koibuchi, T. Shibazaki, and A. Ejima, *J. Pharm. Sci.*, **71**, 1165 (1982).

(2) J. W. Poole, *Rev. Can. Biol.* Suppl., **32**, 43 (1973).

(3) H. Ogata, N. Aoyagi, N. Kaniwa, M. Koibuchi, T. Shibazaki, A. Ejima, T. Shimamoto, T. Yashiki, Y. Ogawa, Y. Uda, and Y. Nishida, *Int. J. Clin. Pharmacol. Toxicol.*, in press.

(4) J. G. Wagner, "Fundamentals of Clinical Pharmacokinetics," Drug Intelligence Publications, Hamilton, Ill., 1975, p. 344.

(5) H. Kamimura, Y. Omi, Y. Shiobara, N. Tamaki, and Y. Katogi, *J. Chromatogr.*, 163, 271 (1979).

(6) M. Rowland, S. Riegelman, and W. L. Epstein, *J. Pharm. Sci.*, **57**, 984 (1968).

(7) P. A. Harris and S. Riegelman, *ibid.*, **58**, 93 (1969).

(8) W. L. Chiou and S. Riegelman, *ibid.*, **59**, 937 (1970).

(9) P. G. Welling, *Pharm. Int.*, **1**, 14 (1980).

NOTES

Antibradykinin Active Material in *Aloe saponaria*

AKIRA YAGI *x, NOBUO HARADA ‡, HIDENORI YAMADA *, SHUICHI IWADARE ‡, and ITSUO NISHIOKA *

Received October 27, 1981, from the **Faculty of Pharmaceutical Sciences, Kyushu University, Maidashi, Higashi-ku, Fukuoka, Japan*, and the ‡*Banyu Pharmaceutical Co., Ltd., Nihonbashi honcho, Chuo-ku, Tokyo, Japan.* Accepted for publication December 31, 1981.

Abstract □ A material having antibradykinin activity on isolated guinea pig ileum was partially purified from the nondialysate of the pulp of *Aloe saponaria* by repetition of gel chromatography using a hydrophilic polyvinyl gel and dextran gels. From the results of amino acid and carbohydrate analyses, the antibradykinin-active material was estimated to be a glycoprotein. It was found that this material catalyzes the hydrolysis of bradykinin at pH 7.4. The results of peptide analysis using reversed-phase high-performance liquid chromatography coupled with amino acid analysis indicate that this glycoprotein cleaves the Gly^4-Phe^5 and Pro^7-Phe^8 bonds of the bradykinin molecule.

Keyphrases □ Antibradykinin—active material in *Aloe saponaria*, guinea pig ileum, glycoprotein, high-performance liquid chromatography □ Glycoprotein—antibradykinin active material in *Aloe saponaria*, high-performance liquid chromatography, guinea pig ileum □ *Aloe saponaria*—antibradykinin active material, glycoprotein, high-performance liquid chromatography, guinea pig ileum

Cardiac stimulant action of the constituents in the dialysate of the pulp from *Aloe saponaria*[1] on isolated cardiac muscles has been reported (1). Antibradykinin activity of the nondialysate of the pulp has been examined here to obtain pharmacological evidence for its anti-inflammatory action (2). In this report, the results of partial purification of material having antibradykinin activity from *A. saponaria* on isolated guinea pig ileum and its proteolytic property against bradykinin are presented.

EXPERIMENTAL

Materials—The following materials were purchased from suppliers: dextran gel[2,3], hydrophilic polyvinyl gel[4], dialysis membrane[5], synthetic bradykinin[6], and bromelain[7]. The gel filtrations were performed at room temperature at a flow rate of 21 ml/hr using a microtube pump[8].

Methods of Analysis—Protein and carbohydrate contents in samples

[1] *Aloe saponaria* is also known as white spotted *aloe* or soap *aloe*.

[2] Sephadex G-100, Pharmacia Fine Chemicals, Uppsala, Sweden.
[3] Sephadex G-25, Pharmacia Fine Chemicals, Uppsala, Sweden.
[4] Toyopearl HW 40, Toyo Soda Mfg., Co. Ltd., Tokyo, Japan.
[5] Visking tube, Visking Co., Union Carbide Corp.
[6] The Protein Research Foundation, Osaka, Japan.
[7] Nakarai Chemical Co., Ltd., Kyoto, Japan.
[8] Tokyo Riakkikai Co., Ltd., Tokyo, Japan.

0022-3549/82/01000-1172$01.00/0

were determined colorimetrically by a previously reported method (3) and the phenol–sulfuric acid method (4), respectively. Elution of materials through gel filtration was monitored by absorbance of effluents at 260 nm[9]. Paper electrophoresis[10] was carried out with a buffer solution of pyridine–acetic acid–water (1:10:489, pH 3.5) at 600 V for 2 hr. Paper chromatography was performed by developing the paper[10] with the solvent of butanol–pyridine–water (6:4:3). Peptide separation was accomplished by reversed-phase[11] high-performance liquid chromatography (HPLC)[12]. Peptides were applied to a column (4 × 250 mm), and the column was eluted with a linear gradient of ethanol concentration from 1% (40 ml) to 50% (40 ml), both containing 0.1% concentrated HCl at a flow rate of 0.4 ml/min (5). Peptide elution was monitored by absorbances of effluents at 210 and 260 nm[13]. The elution volume of bradykinin was 48 ml. For amino acid analysis the sample was hydrolyzed in 6 *N* HCl at 110° for 20 hr in evacuated sealed tubes. At the end, the hydrolysates were evaporated to dryness, dissolved in 0.02 *N* HCl, and analyzed with an amino acid analyzer[14]. Ultracentrifugation was performed on an analytical ultracentrifuge with an optical system[15] in a single sector at 20° and 56,000 rpm.

Assay Method for Antibradykinin—Antibradykinin activity was estimated by the biological assay on the guinea pig ileum by a previously described method (6). Briefly, a strip from 2 to 3 cm of guinea pig ileum was suspended in 10 ml of magnesium ion-free Tyrode solution which was oxygenated with oxygen–carbon dioxide (95:5) in an organ bath at 30°. The contractile responses of various concentrations of bradykinin were measured with a mechanoelectric transducer[16] equipped with a recorder[17] for 45 sec after injection. At the beginning of the assay, responses to a series of four doses of bradykinin (usually 25, 50, 75, and 100 ng dissolved in 1 ml of 10 m*M* phosphate buffer at pH 7.4) were checked, and each of them was repeated two or three times to obtain a standard dose–response curve. For measurement of anti-bradykinin activity, 0.2 ml of bradykinin solution (1 μg/ml) was incubated with 0.2 ml of a sample for 5 min at 30°, and the contractile response by 0.2 ml of this mixture (100 ng bradykinin equivalent) was measured. When the activity of a sample was so potent that >70% of bradykinin was inactivated, the sample was diluted with the same buffer to give at least 30 ng of bradykinin remaining after 5 min of incubation.

Extraction and Purification of Antibradykinin Active Material from *A. saponaria*—*Water Extraction*—The fresh leaves of *A. saponaria*[18] were harvested from the green house of the herbal garden of Kyushu University in September or December, 1979. The leaves (7 kg) were cut in half and colorless gelatinous pulp was separated carefully by scraping the green cortical layer containing yellow phenolics. The homogenized pulp (3 kg) was centrifuged at 10,000 rpm for 30 min. The supernatant was dialyzed with cellulose tubing[5] against distilled water for 48 hr. The nondialyzable fraction was lyophilized to yield colorless, soft crude Extract A (obtained from the leaves harvested in September, 5.8 g) or B (obtained from the leaves harvested in December, 7.0 g). No considerable difference between crude Extracts A and B in antibradykinin activity was observed (Table I).

Ammonium Sulfate Precipitation—Ammonium sulfate was added to a solution of crude Extract A (5.8 g) in distilled water (200 ml) to make 35% saturation, and after standing overnight it was centrifuged at 10,000 rpm for 30 min. The precipitate was dissolved in distilled water, dialyzed against distilled water for 48 hr, and then lyophilized to yield ammonium sulfate fraction (1.2 g).

Gel Filtration on Hydrophilic Polyvinyl Gel and Dextran Gels—Ammonium sulfate fraction (0.1 g) dissolved in 0.3 *M* NaCl (6 ml) was applied to a column of hydrophilic polyvinyl gel[4] (20 × 690 mm), and the column was eluted with the same solution. The eluate (108 ml) was dialyzed against distilled water followed by lyophilization to give polyvinyl gel fraction (50 mg). The fraction (50 mg) was subjected to filtration through a column of dextran gel[2] (20 × 790 mm) using 0.3 *M* NaCl as a solvent, and the eluate from the column was fractionated to three portions. Each portion was dialyzed against distilled water followed by lyophilization to yield gel filtration Fractions A (20 mg), B (10 mg), and C (negligible amount). Fraction B (120 mg) was further chromatographed through a column of dextran gel[3] (16 × 880 mm) using distilled water as a solvent followed by lyophilization to give Fraction D (26.3 mg).

[9] Hitachi 200-10 spectrophotometer.
[10] Toyo filter paper No 50, Toyo Roshi, Co. Ltd., Tokyo, Japan.
[11] Lichrosorb RP-8, 5 μm, Merck, Darmstadt, West Germany.
[12] Hitachi 635A liquid chromatograph.
[13] Hitachi 635M liquid chromatograph detector.
[14] Hitachi 835 amino acid analyzer.
[15] Schlieren, Spinco Model E, Beckman Instrument Inc.
[16] FD-Pick up SB-L-TH, Nihon Koden, Tokyo, Japan.
[17] VP-651B, National Co., Ltd., Tokyo, Japan.
[18] A voucher specimen is available for inspection at Higashiyama Botanical Garden, Nagoya, Japan.

Table I—Antibradykinin Activity of Fractions on Isolated Guinea Pig Ileum

Sample	Protein, %	Carbohydrate, %	Unit/g[a]	Ratio
Crude Extract A	1.7	66[b]	6.34	1.00
Crude Extract B	1.9	63	8.94	1.41
Ammonium sulfate precipitate	2.4	68	27.9	4.40
Gel filtration Fraction A	—	72	6.0	0.94
Gel filtration Fraction B	7.2	63	85.4	13.47
Bromelain			1114.0	175.70

[a] One kininase unit was defined as the amount of enzyme preparation that could degrade 1 μg of bradykinin for 1 min, at 30°, pH 7.4. For statistical purposes 3–5 guinea pigs were used for each assay. [b] The measured content of carbohydrate and protein does not account for 100% of the material. This may reflect the presence of water, since a polymer is extremely hygroscopic.

RESULTS AND DISCUSSION

Extraction and Concentration of Antibradykinin Active Material from *A. saponaria*—The pulp of *A. saponaria* leaves was extracted with water and the extract was dialyzed against distilled water. The nondialyzable fraction (crude extract) showed antibradykinin activity when assayed on the inhibition of the contractile response on isolated guinea pig ileum. As can be seen in Table I, no considerable difference in antibradykinin activity was observed between crude Extracts A and B, which were obtained from the leaves harvested in September and December, respectively. Crude Extract A was precipitated with ammonium sulfate at 35% saturation. The precipitate gained 4.4 times the increased specific activity compared with crude Extract A (Table I). Several attempts to increase the specific activity by means of dextran gel chromatographies were unsuccessful, because the material was too viscous to obtain a practical flow rate. Thus, the chromatography over hydrophilic polyvinyl gel[4] was performed first to remove viscous material from the antibradykinin active material, which was then chromatographed on dextran gel[2] to give three fractions (A–C). As shown in Table I, Fraction A having low specific activity is composed of only carbohydrate, while Fraction B with 13.5 times higher specific activity than crude Extract A is composed of carbohydrate and a low content of protein. Fraction C was not analyzed because of its low yield. To remove contaminated salts completely, Fraction B was chromatographed over dextran gel[3] using distilled water as an eluting solvent to yield Fraction D. Further purification was not continued because of shortage of the sample (total yield, 0.003%). As a positive control, bromelain containing ~2% carbohydrate was employed for the assay and extremely potent antibradykinin activity was observed (7).

Characterization of Antibradykinin Active Material—To clarify the nature of the antibradykinin active material, the pH-dependency of antibradykinin activity and the thermal stability were studied using crude Extract A. Each solution of crude Extract A (10 mg) in 0.067 *M* phosphate buffer (1.0 ml) at various pH values (4.5, 5.0, 6.0, 7.0, 8.0, and 8.5) was kept standing at 30° for 1 hr.

After the dialysis, followed by lyophilization, antibradykinin activity of crude Extract A at each pH was estimated and expressed as percent of the activity at pH 7.4. The results showed that crude Extract A is comparably active at pH 5.0–7.0, but <20% of antibradykinin activity was observed at pH 4.5, 8.0, or 8.5. Antibradykinin activity was completely lost when crude Extract A was treated at 90° for 10 min. These results suggest that the antibradykinin active material may be a protein or a glycoprotein having enzymatic activity rather than a small molecule such as norepinephrine (8).

To ascertain this speculation, the purest material obtained here, Fraction D, was subjected to an ultracentrifugation experiment, uv spectral absorption measurement, amino acid analysis, and carbohydrate analysis. Fraction D in 0.3 *M* NaCl was analyzed by ultracentrifugation with an optical system[15] for determination of the sedimentation coefficient. Since Fraction D (10 mg/ml of 0.3 *M* NaCl) indicated a single peak having $S_{20,w}$ = 0.79 *S*, it appeared to be homogeneous in size. The UV absorption spectrum of Fraction D in 0.3 *M* NaCl indicated the presence of an absorption band with a maximum at 260 nm. On acid hydrolysis of Fraction D, only D-mannose was observed as sugar moiety on paper chromatography, and Asp, Thr, Ser, Glu, Gly, Ala, Val, Ile, Leu, Phe, Lys,

Arg, and Pro as amino acid moieties were observed on amino acid analysis. All of these results support the theory that the antibradykinin active material is a protein or a glycoprotein.

Action of the Antibradykinin Active Material Against Bradykinin Molecule—Bradykinin (0.5 mg) in 10 m*M* phosphate buffer (0.7 ml, pH 7.4) was incubated with 1.0 mg of Fraction D at 30° for 2 hr. The lyophilized mixture was subjected to paper electrophoresis with acetate–pyridine buffer (pH 3.5) to afford two ninhydrin positive spots of fast and slow moving ones compared with that of bradykinin which migrates towards the cathode. These two spots were not observed in the blank experiments without bradykinin or Fraction D.

The fast moving spot was eluted from unstained paper strips and the extract was subjected to amino acid analysis. The fast moving spot was confirmed to be a peptide composed of Arg, Pro, and Gly in the ratio of 1:2:1, which was consistent with the residues 1–4 (Arg^1-Pro^2-Pro^3-Gly^4) of bradykinin, indicating that Fraction D cleaved the bond between Gly^4 and Phe^5 in bradykinin and, therefore, had a kininase activity. The slow moving spot, however, was not clearly separated from the spot due to bradykinin on paper electrophoresis.

The incubation mixture after lyophilization was subjected to HPLC on a reversed-phase column. Three major peaks were observed at an elution volume of 6, 38, or 48 ml in HPLC, and each peak was collected and subjected to amino acid analysis to afford the following amino acid composition, respectively: Arg, Pro, Gly (1:2:1); Arg, Pro, Gly, Phe, Ser (1:3:1:1:1); and Arg, Pro, Gly, Phe, Ser (2:3:1:2:1).

Each composition was consistent with the structures Arg^1-Pro^2-Pro^3-Gly^4, Arg^1-Pro^2-Pro^3-Gly^4-Phe^5-Ser^6-Pro^7, and Arg^1-Pro^2-Pro^3-Gly^4-Phe^5-Ser^6-Pro^7-Phe^8-Arg^9 (bradykinin), respectively. All of these results indicate that the antibradykinin active material in *A. saponaria* has a kininase activity and cleaves the peptide bonds at *N*-terminuses of two phenylalanine residues in bradykinin.

As a kininase from plant origin, bromelain, papain, and ficin are known to cleave Gly^4-Phe^5 and Phe^5-Ser^6 bonds of the bradykinin molecule, while both shimejikininase (9) from mushroom, *Tricholoma congluobatum*, and kinonase AI (10) from microbes, *Streptomyces* species, cleave Gly^4-Phe^5 and Pro^7-Phe^8 bonds of the bradykinin molecule. Thus, the action of the glycoprotein obtained here is similar to that of shimejikininase and kinonase AI.

As one of the pharmacological evidences for anti-inflammatory activity of *A. saponaria*, the presence of an antibradykinin active glycoprotein was confirmed here. Further study on the anti-inflammation effect is in progress.

REFERENCES

(1) A. Yagi, S. Shibata, I. Nishioka, S. Iwadare, and Y. Ishida, *J. Pharm. Sci.*, **71**, 739 (1982).

(2) R. H. Cheney, *Quart. J. Crude Res.*, **10**, 1523 (1970) and references cited therein.

(3) O. H. Lowry, N. J. Rosebrough, A. L. Farr, and R. J. Randall, *J. Biol. Chem.*, **193**, 265 (1951).

(4) M. Dubois, K. A. Gilles, J. K. Hamilton, P. A. Rebers, and F. Smith, *Anal. Chem.*, **28**, 350 (1956).

(5) T. Imoto and K. Okazaki, *J. Biochem.*, **89**, 437 (1981).

(6) K. Fujita, R. Teradaira, and T. Nagatsu, *Biochem. Pharmacol.*, **25**, 205 (1976).

(7) T. Murachi, H. Yasui, and Y. Yasuda, *Biochemistry*, **3**, 48 (1964).

(8) M. Ikekita, H. Moriya, C. Moriwaki, and T. Rurikawa, *Yakugaku Zasshi*, **99**, 607 (1979).

(9) K. Kizuki, C. Moriwaki, Y. Hojima, and H. Moriya, *Chem. Pharm. Bull.*, **24**, 1742 (1976).

(10) S. Nakamura, Y. Marumoto, H. Yamaki, T. Nishimura, N. Tanaka, M. Hamada, M. Ishizuka, T. Takeuchi, and H. Umezawa, *ibid.*, **17**, 714 (1969).

ACKNOWLEDGMENTS

The authors wish to thank Professor T. Imoto of this faculty for giving us the opportunity for using many instruments. They also express deep thanks to Miss Nagai for her technical assistance and to Dr. T. Fukamizo, Faculty of Agricultural Sciences, Kyushu University, for measurement of sedimentation coefficient.

Cardiotonic Principles of Ginger (*Zingiber officinale* Roscoe)

N. SHOJI *, A. IWASA *, T. TAKEMOTO *, Y. ISHIDA ‡ and Y. OHIZUMI ‡x

Received May 12, 1981, from the **Faculty of Pharmacy, Tokushima-Bunri University, Tokushima-shi, Tokushima 770, Japan* and ‡*Mitsubishi-Kasei Institute of Life Sciences, Machida-shi, Tokyo 194, Japan.* Accepted for publication December 9, 1981.

Abstract □ Crude methanol extracts of the rhizome of ginger (*Zingiber officinale* Roscoe) showed potent, positive inotropic effects on the guinea pig isolated left atria. The extract of this rhizome has been fractionated, monitored by the cardiotonic activity, to yield gingerols as active principles.

Keyphrases □ Ginger (*Zingiber officinale* Roscoe)—cardiotonic principles, gingerols, □ Cardiotonic principles—ginger (*Zingiber officinale* Roscoe), gingerols □ Gingerols—cardiotonic principles of ginger (*Zingiber officinale* Roscoe)

The rhizome of ginger (*Zingiber officinale* Roscoe) has been used not only as a seasoning spice but also as an important medicine in Japan and China. It is considered to possess stomachic, carminative, stimulant, diuretic, bechic, and antiemetic properties (1). Chemical studies on the pungent principles of ginger have been carried out by a number of investigators (2–8). Recently, gingerols have been isolated from ginger as pungent substances (3).

It was found that the crude methanol extract of ginger had a powerful positive inotropic effect on the guinea pig isolated atria. The present report describes the isolation of cardiotonic principles from ginger and determination of their chemical structures.

EXPERIMENTAL[1]

Isolation—The dried rhizome (580 g) of ginger (*Z. officinale* Roscoe), zingiberis rhizoma, was crushed mechanically and soaked in methanol at room temperature. The mixture was filtered and the filtrate was evaporated *in vacuo*. The residue (106 g) was partitioned between water and ethyl acetate. The ethyl acetate layer was evaporated *in vacuo* and the residue (30 g) was dissolved in methanol and extracted with *n*-hexane. The pharmacologically active methanol fraction was again evaporated *in vacuo*. The residue (25.4 g) was dissolved in a small amount of benzene,

[1] Melting points were obtained on a Yanagimoto micro melting point apparatus and are uncorrected. Optical rotation was recorded on a Jasco ORD/UV-5 spectrometer with a circular dichroism attachment. UV spectra were obtained with a Hitachi 200-20 spectrophotometer. IR spectra were obtained on a Shimadzu LKB-9000B. PMR spectra were recorded on a Varian XL-100A spectrometer. CMR spectra were recorded on a Hitachi R-22 spectrometer.

0022-3549/82/01000-1174$01.00/0

Arg, and Pro as amino acid moieties were observed on amino acid analysis. All of these results support the theory that the antibradykinin active material is a protein or a glycoprotein.

Action of the Antibradykinin Active Material Against Bradykinin Molecule—Bradykinin (0.5 mg) in 10 m*M* phosphate buffer (0.7 ml, pH 7.4) was incubated with 1.0 mg of Fraction D at 30° for 2 hr. The lyophilized mixture was subjected to paper electrophoresis with acetate–pyridine buffer (pH 3.5) to afford two ninhydrin positive spots of fast and slow moving ones compared with that of bradykinin which migrates towards the cathode. These two spots were not observed in the blank experiments without bradykinin or Fraction D.

The fast moving spot was eluted from unstained paper strips and the extract was subjected to amino acid analysis. The fast moving spot was confirmed to be a peptide composed of Arg, Pro, and Gly in the ratio of 1:2:1, which was consistent with the residues 1–4 (Arg^1-Pro^2-Pro^3-Gly^4) of bradykinin, indicating that Fraction D cleaved the bond between Gly^4 and Phe^5 in bradykinin and, therefore, had a kininase activity. The slow moving spot, however, was not clearly separated from the spot due to bradykinin on paper electrophoresis.

The incubation mixture after lyophilization was subjected to HPLC on a reversed-phase column. Three major peaks were observed at an elution volume of 6, 38, or 48 ml in HPLC, and each peak was collected and subjected to amino acid analysis to afford the following amino acid composition, respectively: Arg, Pro, Gly (1:2:1); Arg, Pro, Gly, Phe, Ser (1:3:1:1:1); and Arg, Pro, Gly, Phe, Ser (2:3:1:2:1).

Each composition was consistent with the structures Arg^1-Pro^2-Pro^3-Gly^4, Arg^1-Pro^2-Pro^3-Gly^4-Phe^5-Ser^6-Pro^7, and Arg^1-Pro^2-Pro^3-Gly^4-Phe^5-Ser^6-Pro^7-Phe^8-Arg^9 (bradykinin), respectively. All of these results indicate that the antibradykinin active material in *A. saponaria* has a kininase activity and cleaves the peptide bonds at *N*-terminuses of two phenylalanine residues in bradykinin.

As a kininase from plant origin, bromelain, papain, and ficin are known to cleave Gly^4-Phe^5 and Phe^5-Ser^6 bonds of the bradykinin molecule, while both shimejikininase (9) from mushroom, *Tricholoma congluobatum*, and kinonase AI (10) from microbes, *Streptomyces* species, cleave Gly^4-Phe^5 and Pro^7-Phe^8 bonds of the bradykinin molecule. Thus, the action of the glycoprotein obtained here is similar to that of shimejikininase and kinonase AI.

As one of the pharmacological evidences for anti-inflammatory activity of *A. saponaria*, the presence of an antibradykinin active glycoprotein was confirmed here. Further study on the anti-inflammation effect is in progress.

REFERENCES

(1) A. Yagi, S. Shibata, I. Nishioka, S. Iwadare, and Y. Ishida, *J. Pharm. Sci.*, **71**, 739 (1982).

(2) R. H. Cheney, *Quart. J. Crude Res.*, **10**, 1523 (1970) and references cited therein.

(3) O. H. Lowry, N. J. Rosebrough, A. L. Farr, and R. J. Randall, *J. Biol. Chem.*, **193**, 265 (1951).

(4) M. Dubois, K. A. Gilles, J. K. Hamilton, P. A. Rebers, and F. Smith, *Anal. Chem.*, **28**, 350 (1956).

(5) T. Imoto and K. Okazaki, *J. Biochem.*, **89**, 437 (1981).

(6) K. Fujita, R. Teradaira, and T. Nagatsu, *Biochem. Pharmacol.*, **25**, 205 (1976).

(7) T. Murachi, H. Yasui, and Y. Yasuda, *Biochemistry*, **3**, 48 (1964).

(8) M. Ikekita, H. Moriya, C. Moriwaki, and T. Rurikawa, *Yakugaku Zasshi*, **99**, 607 (1979).

(9) K. Kizuki, C. Moriwaki, Y. Hojima, and H. Moriya, *Chem. Pharm. Bull.*, **24**, 1742 (1976).

(10) S. Nakamura, Y. Marumoto, H. Yamaki, T. Nishimura, N. Tanaka, M. Hamada, M. Ishizuka, T. Takeuchi, and H. Umezawa, *ibid.*, **17**, 714 (1969).

ACKNOWLEDGMENTS

The authors wish to thank Professor T. Imoto of this faculty for giving us the opportunity for using many instruments. They also express deep thanks to Miss Nagai for her technical assistance and to Dr. T. Fukamizo, Faculty of Agricultural Sciences, Kyushu University, for measurement of sedimentation coefficient.

Cardiotonic Principles of Ginger (*Zingiber officinale* Roscoe)

N. SHOJI *, A. IWASA *, T. TAKEMOTO *, Y. ISHIDA ‡ and Y. OHIZUMI ‡x

Received May 12, 1981, from the **Faculty of Pharmacy, Tokushima-Bunri University, Tokushima-shi, Tokushima 770, Japan* and ‡*Mitsubishi-Kasei Institute of Life Sciences, Machida-shi, Tokyo 194, Japan.* Accepted for publication December 9, 1981.

Abstract □ Crude methanol extracts of the rhizome of ginger (*Zingiber officinale* Roscoe) showed potent, positive inotropic effects on the guinea pig isolated left atria. The extract of this rhizome has been fractionated, monitored by the cardiotonic activity, to yield gingerols as active principles.

Keyphrases □ Ginger (*Zingiber officinale* Roscoe)—cardiotonic principles, gingerols, □ Cardiotonic principles—ginger (*Zingiber officinale* Roscoe), gingerols □ Gingerols—cardiotonic principles of ginger (*Zingiber officinale* Roscoe)

The rhizome of ginger (*Zingiber officinale* Roscoe) has been used not only as a seasoning spice but also as an important medicine in Japan and China. It is considered to possess stomachic, carminative, stimulant, diuretic, bechic, and antiemetic properties (1). Chemical studies on the pungent principles of ginger have been carried out by a number of investigators (2–8). Recently, gingerols have been isolated from ginger as pungent substances (3).

It was found that the crude methanol extract of ginger had a powerful positive inotropic effect on the guinea pig isolated atria. The present report describes the isolation of cardiotonic principles from ginger and determination of their chemical structures.

EXPERIMENTAL[1]

Isolation—The dried rhizome (580 g) of ginger (*Z. officinale* Roscoe), zingiberis rhizoma, was crushed mechanically and soaked in methanol at room temperature. The mixture was filtered and the filtrate was evaporated *in vacuo*. The residue (106 g) was partitioned between water and ethyl acetate. The ethyl acetate layer was evaporated *in vacuo* and the residue (30 g) was dissolved in methanol and extracted with *n*-hexane. The pharmacologically active methanol fraction was again evaporated *in vacuo*. The residue (25.4 g) was dissolved in a small amount of benzene,

[1] Melting points were obtained on a Yanagimoto micro melting point apparatus and are uncorrected. Optical rotation was recorded on a Jasco ORD/UV-5 spectrometer with a circular dichroism attachment. UV spectra were obtained with a Hitachi 200-20 spectrophotometer. IR spectra were obtained on a Shimadzu LKB-9000B. PMR spectra were recorded on a Varian XL-100A spectrometer. CMR spectra were recorded on a Hitachi R-22 spectrometer.

0022-3549/82/01000-1174$01.00/0

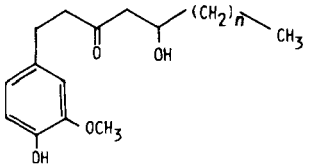

I : n=4 [6]-gingerol

II : n=6 [8]-gingerol

III: n=8 [10]-gingerol

put on a silica gel[2] column packed with benzene, and eluted with a mixture of benzene–ethyl acetate (9:1). Each fraction was monitored using TLC[3] with a mixture of benzene–acetonitrile (9:1) as a developing solution. Fractions showing the bioactivity were combined and rechromatographed five times on silica gel to afford three active substances, I–III:

Compound I—$C_{17}H_{26}O_4$, mp 30–32°, $[\alpha]_D$ = +27.8° (*C*, 1.0 chloroform); UV (ethanol): 284 nm (ϵ 2700); IR (neat): 1700 cm^{-1} (C=O); mass spectrum: *m/z* 294 (M^+, 61.8%), 137 (100), PMR (deuterochloroform): δ 0.88 (3H, broad t, J = 7 Hz, —$(CH_2)_4$—CH_3), 1.06–1.62 [8H, m, —$(CH_2)_4$—CH_3], 2.42–2.61 (2H, m, —CO—CH_2—CHOH—), 2.61–2.95 (4H, m, —CH_2—CH_2—CO—), 3.07 (1H, broad s, —*OH*), 3.84 (3H, s, —OCH_3), 3.86–4.16 (1H, m, —CH_2—*CH*OH—), 5.82 (1H, broad s, —*OH*), 6.54–6.86 (3H, m, aromatic H); CMR (deuterochloroform): δ 14.02 (q), 22.61 (t), 25.19 (t), 29.31 (t), 31.78 (t), 36.59 (t), 45.45 (t), 49.50 (t), 55.89 (q), 67.83 (d), 111.29 (d), 114.72 (d), 120.85 (d), 132.75 (s), 144.23 (s), 146.77 (s), 211.50 (s).

Compound II—$C_{19}H_{30}O_4$, mp 28–30°, $[\alpha]_D$ = +26.2° (*C*, 1.0 chloroform); UV (ethanol): 284 nm (ϵ 2700); IR (KBr): 1700 cm^{-1} (C=O); mass spectrum: *m/z* 322 (M^+, 13.9%), 137 (100); PMR (deuterochloroform): δ 0.88 [3H, broad t, J = 7 Hz, —$(CH_2)_6$—CH_3], 1.06–1.55 [12H, m, —$(CH_2)_6$—CH_3], 2.43–2.62 (2H, m, —CO—CH_2—CHOH—), 2.62–2.92 (4H, m, —CH_2—CH_2—CO—), 2.89 (1H, broad s, —*OH*), 3.86 (3H, s, —OCH_3), 3.88–4.16 (1H, m, —CH_2—*CH*OH—), 5.71 (1H, s, —*OH*), 6.56–6.88 (3H, m, aromatic H); CMR (deuterochloroform): δ 14.06 (q), 22.65 (t), 25.50 (t), 29.27 (t) × 2, 29.54 (t), 31.82 (t), 36.63 (t), 45.41 (t), 49.46 (t), 55.85 (q), 67.83 (d), 111.33 (d), 114.76 (d), 120.81 (d), 132.71 (s), 144.23 (s), 146.81 (s), 211.46 (s).

Compound III—$C_{21}H_{34}O_4$, mp 42–43°, $[\alpha]_D$ = +19.8 (*C*, 1.0 chloroform); UV (ethanol): 284 nm (ϵ 3100); IR (KBr): 1700 cm^{-1} (C=O); mass spectrum: *m/z* 350 (M^+, 13.4%), 137 (100); PMR (deuterochloroform): δ 0.80 (3H, broad t, J = 7 Hz, —$(CH_2)_8$—CH_3), 1.20 (16H, broad s, —$(CH_2)_8$—CH_3), 2.39–2.54 (2H, m, —CO—CH_2—CHOH—), 2.54–2.84 (4H, m, —CH_2—CH_2—), 2.91 (1H, broad s, —*OH*), 3.78 (3H, s, —OCH_3), 3.82–4.08 (1H, m, —CH_2—*CH*OH—), 5.63 (1H, broad s, —*OH*), 6.48–6.82 (3H, m, aromatic H); CMR (deuterochloroform): δ 14.09 (q), 22.69 (t), 25.50 (t), 29.35 (t) × 4, 29.62 (t), 31.93 (t), 36.63 (t), 45.45 (t), 49.46 (t), 55.89 (q), 67.83 (d), 111.25 (d), 114.68 (d), 120.85 (d), 132.75 (s), 144.19 (s), 146.73 (s), 211.50 (s).

Guinea Pig Isolated Left Atria—Bioassay of the fraction being tested was performed on the isolated left atria of guinea pigs. Guinea pigs (300–400 g) were sacrificed by cervical dislocation. The atrium was separated from the rest of the heart and mounted vertically in 50 ml of tissue bath containing Krebs-Ringer bicarbonate solution of the following

Rhizhome of ginger (580 g)
↓ extracted with methanol
Methanol extract (106 g)(+)
↓ partitioned with ethyl acetate and water

Ethyl acetate soluble portion (30 g)(+) — Water soluble portion (76 g)(−)
↓ partitioned with n-hexane and methanol

Methanol soluble portion (25.4 g)(+) — n-Hexane soluble portion (4.4 g)(−)
↓ chromatographed over silica gel
eluted with benzene-ethyl acetate (9:1)

(7.19 g)(−) | (7.29 g)(+) | (8.30 g)(−)
↓ chromatographed five times over silica gel
eluted with benzene-ethyl acetate (9:1)

Substance I (4.14 g)(+) | Substance II (0.62 g)(+) | Substance III (1.08 g)(+)

Scheme I—Procedure of the isolation of the cardiotonic principles from ginger (Z. officinale Roscoe); (+) active, (−) inactive.

[2] Silica gel 60, Merck.
[3] TLC plates silica gel 60 F_{254}, Merck.

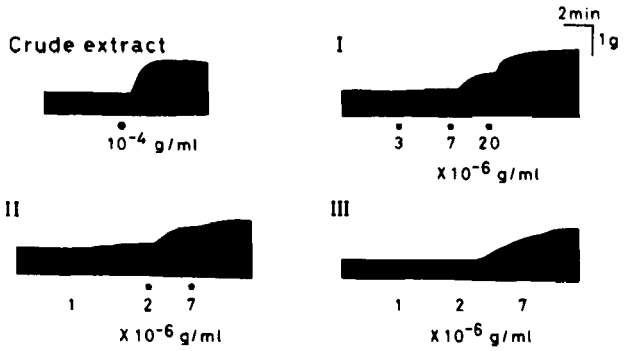

Figure 1—*The inotropic effect of the crude methanol extract of ginger (Z. officinale Roscoe) and gingerols on the guinea pig isolated left atria. Crude extract and gingerols were cumulatively added at (●). (I) [6]-gingerol; (II) [8]-gingerol; (III) [10]-gingerol.*

composition (in millimoles): sodium chloride, 120; potassium chloride, 4.8; calcium chloride, 1.2: magnesium sulfate, 1.3; potassium dihydrogenphosphate, 1.2; sodium hydrogen carbonate, 25.2; and glucose, 5.8; pH 7.4. The solution was bubbled with a gas mixture of oxygen–carbon dioxide (95:5) and maintained at 30°. A resting tension of 800 mg was applied to each strip. Tissues were driven by an electrical stimulator[4] at a frequency of 2 Hz with square-wave pulses of 5 msec at 4–5 V. Isometric contractions were measured by the force-displacement transducer and recorded on a polygraph. Four preparations from different animals were used for one sample being tested.

RESULTS AND DISCUSSION

The methanol extract (6×10^{-5}–3×10^{-4} g/ml) of rhizome of ginger caused a dose-dependent positive inotropic effect on the guinea pig isolated atria. A representative pattern of a positive inotropic effect of the methanol extract (10^{-4} g/ml) is shown in Fig. 1. In order to isolate the cardiotonic principles from ginger, fractionation of the methanol extract of ginger was performed, being monitored by the positive inotropic action as shown in Scheme I. Active fractions, 37–117, eluted with benzene–ethyl acetate (9:1) from the silica gel column, contained three components. The mixture was chromatographed five times over silica gel to give three active substances, I–III. Their yields were 0.71, 0.11, and 0.19%, respectively. Each substance tasted pungent, suggesting that they might be known pungent principles of ginger. Their physicochemical properties confirm that substances I–III are [6]-, [8]-, and [10]-gingerol, respectively, which had been isolated previously as pungent constituents (9).

As shown in Fig. 1, treatment with [6]-, [8]-, and [10]- gingerol of the atria induced a dose-dependent positive inotropic action. The minimum effective doses were 10^{-5}, 10^{-6}, and 3×10^{-5} g/ml for [6]-, [8]-, and [10]-gingerol, respectively. The activity appears to be in the decreasing order: [8]-gingerol > [10]-gingerol > [6]-gingerol.

On the basis of the present results, it is concluded that ginger has a powerful positive inotropic effect on the guinea pig isolated atria and that cardiotonic principles of ginger were identified as [6]-, [8]-, and [10]-gingerol.

REFERENCES

(1) L. M. Perry, "Medicinal Plants of East and Southeast Asia," The MIT Press, Boston, Mass., 1980, p. 443.
(2) H. Nomura, *J. Chem. Soc.*, **1917,** 769.
(3) H. Nomura, *Sci. Rep. Tohoku Imp. Univ.*, **6**(i), 41 (1917).
(4) H. Nomura, *ibid.*, **7**(i), 67 (1918).
(5) D. W. Connell and M. D. Sutherland, *Aust. J. Chem.*, **22,** 1033 (1969).
(6) D. W. Connell, *ibid.*, **23,** 369 (1970).
(7) Y. Masada, T. Inoue, K. Hashimoto, M. Fujioka, and K. Shiraki, *Yakugaku Zasshi*, **93,** 318 (1973).
(8) Y. Masada, T. Inoue, K. Hashimoto, M. Fujioka, and C. Uchino, *ibid.*, **94,** 735 (1974).
(9) T. Murata, M. Shinohara, and M. Miyamoto, *Chem. Pharm. Bull.*, **20,** 2291 (1972).

ACKNOWLEDGMENTS

The authors are grateful to Nippon Hunmatsu Yakuhin Co., Ltd. for a generous supply for rhizoma of *Z. officinale*.

[4] Grass stimulator (model S9B).

Lipid-Soluble Inhibitors of Dihydrofolate Reductase III: Quantitative Thin-Layer and High-Performance Liquid Chromatographic Methods for Measuring Plasma Concentrations of the Antifolate, 2,4-Diamino-6-(2,5-dimethoxybenzyl)-5-methylpyrido-[2,3-*d*]pyrimidine

ROBERT G. FOSS and CARL W. SIGEL ˣ

Received November 20, 1981, from the *Department of Medicinal Biochemistry, Wellcome Research Laboratories, Research Triangle Park, NC 27709.* Accepted for publication January 4, 1982.

Abstract □ Specific methods using high-performance liquid chromatography (HPLC) and thin-layer chromatography (TLC) for the analysis of the potent antifolate, 2,4-diamino-6-(2,5-dimethoxybenzyl)-5-methylpyrido-[2,3-*d*]pyrimidine (I) in plasma were developed. The HPLC system employed paired-ion chromatography using a mobile phase of water–acetonitrile (65:35, v/v) in conjunction with a reversed-phase C-1 column and detection by UV absorbance measurement. The TLC system utilized a scanning densitometer operating in the reflectance mode with detection of I by fluorescence measurement. The lower limits of detection for the HPLC and TLC methods were ~0.005 μg/ml. The coefficients of variation for the measurement of drug concentrations over the range of 0.04–1.0 μg/ml of plasma were 5 and 6%, respectively.

Keyphrases □ Dihydrofolate reductase—quantitative thin-layer chromatographic and high-performance liquid chromatographic methods for measuring plasma concentrations of antifolate □ Antifolate—thin-layer chromatographic and high-performance liquid chromatographic methods for measuring concentrations of plasma, lipid-soluble inhibitors of dihydrofolate reductase □ High-performance liquid chromatography—method for measuring concentrations of an antifolate, lipid-soluble inhibitors of dihydrofolate reductase

2,4-Diamino-6-(2,5-dimethoxybenzyl)-5-methylpyrido-[2,3-*d*]pyrimidine (I)[1] is a new lipid-soluble folate antagonist for the treatment of neoplastic diseases (1, 2). Methods using high-performance liquid chromatography (HPLC) and quantitative TLC for assaying this drug in plasma were developed and compared. For the measurement of I by HPLC, a reversed-phase C-1 column coupled with UV detection at 254 nm was employed; the TLC method fluorescence was measured after chromatography on conventional §silica gel plates. Chromatographic analyses were facilitated by the use of a microcomputer-based system for the acquisition and reduction of data (3).

BACKGROUND

In contrast to some other antifolate drugs, I exhibits activity comparable to methotrexate against mammalian dihydrofolate reductase, while minimally inhibiting the catabolism of histamine *via* histamine-*N*-methyltransferase (2, 4). The moderate lipophilicity [log *P* (octanol–water) = 1.73] of I facilitates cellular entry of the drug by diffusion, thus avoiding the dependence on the reduced folate facilitated transport system (2, 5). The short half-life of the drug (0.38 hr in the rat) and its response to calcium leucovorin rescue alleviate the problems of cumulative toxicity to normal cells (2, 6). Studies *in vivo* of the effect of I on solid W256 carcinoma in the rat resulted in reductions in mean tumor volumes of 70–90%, relative to tumorous control animals (1, 2).

The encouraging properties of I prompted development of specific analytical methods that could be used for measuring I in biological samples for chemotherapy, disposition, and toxicological studies. HPLC and TLC methods were evaluated and found to be comparable with respect to the analytical precision and net recovery of I.

[1] Wellcome Research Laboratories, Research Triangle Park, N.C.

EXPERIMENTAL

Reagents—Acetonitrile[2], chloroform[2], methylene chloride[2], methanol[2], 2-propanol[2], ammonium hydroxide[3], sodium bicarbonate[3], and sodium hydroxide[3] were reagent grade. The ion-pairing reagent[4] was used as received. Distilled water was filtered through a 0.45-μm membrane filter[5] prior to use.

Apparatus—A liquid chromatograph[6] equipped with a valve-loop injector[7], strip-chart recorder[8], and a microcomputer-based data system was used with a commercially packed 25 cm × 4.6-mm i.d. column[9] containing 6-μm C-1 reversed-phase packing. A precolumn[10] filled with C-18 pellicular packing[11] was also used.

A motor-driven multispotter[12] was used to spot 20 × 20-cm nonfluorescing 0.25-mm layer thickness silica gel 60 TLC plates[13]. The plates were quantified using a scanning densitometer[14] interfaced with a microcomputer.

Standard Solutions—A stock solution of I was prepared in methanol that was diluted with either methanol or chloroform–methanol (90:10, v/v) to produce standard solutions for liquid and thin-layer chromatography, respectively.

Reference solutions of I for HPLC analyses were prepared at concentrations of 0.25, 1.0, and 4.0 ng/μl; those for TLC analyses were prepared at concentrations of 1.0 and 5.0 ng/μl. No apparent degradation of stock

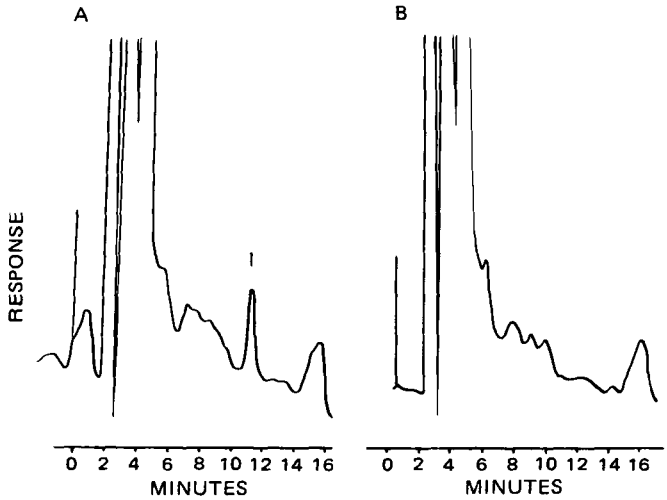

Figure 1—*Typical HPLC chromatograms of extracts from plasma (1 ml) (A) containing 0.040 μg of I and from blank plasma (1 ml) (B).*

[2] "Distilled in Glass," Burdick & Jackson, Muskegon, Mich.
[3] Analytical Reagent, Mallinckrodt, Inc. Paris, Ky.
[4] PIC B-8, Waters Associates, Milford, Mass.
[5] Millipore, Bedford, Mass.
[6] Series ALC 200, Waters Associates, Milford, Mass.
[7] Model U6K, Waters Associates, Milford, Mass.
[8] Omniscribe, Houston Instruments, Austin, Tex.
[9] ZORBAX TMS, E. I. Dupont de Nemours & Co., Wilmington, Del.
[10] Guard Column, Waters Associates, Milford, Mass.
[11] Permaphase ODS, E. I. Dupont de Nemours & Co., Wilmington, Del.
[12] AIS, Libertyville, Ill.
[13] No. 5763, E. Merck Laboratories, Elmsford, N.Y.
[14] Model SD3000, Schoeffel Instrument Corp., Westbrook, N.J.

0022-3549/82/01000-1176$01.00/0

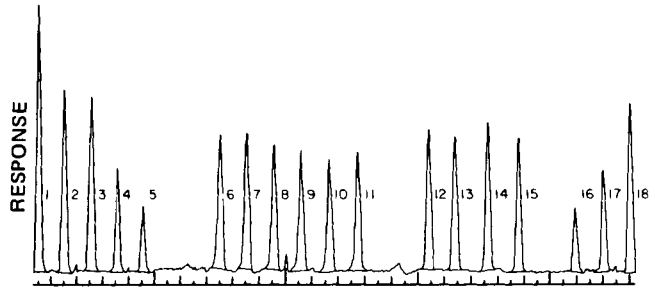

Figure 2—*Typical TLC chromatogram of extracts from plasma (1 ml) and I. Peaks corresponding to known amounts of I are as follows: 1, 0.080 μg; 2, 0.050 μg; 3, 0.050 μg; 4, 0.030 μg; 5, 0.020 μg; 16, 0.020 μg; 17, 0.030 μg; 18, 0.050 μg. Peaks 6–11 are the extracts from replicate plasma (1 ml) samples, each containing 0.040 μg of I. Peaks 12–15 are 20% of the extracts from replicate plasma (1 ml) samples, each containing 0.20 μg of I.*

or standard solutions was observed over a period of 6 months, when stored at −15°.

Sample Preparation—To a 12-ml culture tube[15], fitted with a polytef[16]-lined screw cap, was added 1.0 ml of plasma. The pH of the plasma was adjusted with 1.0 ml of pH 10 bicarbonate buffer and vortex mixed[17] for 5 sec. The basified plasma was extracted by addition of 4.0 ml of methylene chloride and rotary mixing[18] for 10 min. The organic phase was transferred and retained. A second 4.0-ml portion of methylene chloride was used to extract the aqueous phase, as above, and the organic extracts were combined and concentrated at ~40° to 1.0 ml using a gentle stream of dry nitrogen. Extraneous material was separated from I by passing the concentrated extract through a disposable silica gel cartridge[19] that was preeluted sequentially with 25 ml of methanol and 15 ml of methylene chloride. Ten milliliters of methylene chloride was passed through the silica cartridge and discarded. A 6.5-ml eluate of methanol was collected and evaporated at ~55° with nitrogen. The residue was reconstituted, using methanol for HPLC analysis or chloroform–methanol (90:10, v/v) for TLC analysis, to a final volume dependent on the expected concentration of I in the plasma. For both analyses, if low levels (5–200 ng) of I were anticipated, sample tubes were washed with two 40-μl portions of the appropriate solvent, which were drawn into a 100-μl syringe; for higher levels, residues were dissolved in 250–1000 μl of solvent and a suitable volume (10–100 μl) was drawn into a syringe.

Analytical Procedure for HPLC—The mobile phase, filtered distilled water containing 0.005 *M* 1-octane sulfonic acid–acetonitrile (65:35, v/v), was degassed by agitation under reduced pressure. The C-1 column was operated isocratically with an eluent flow rate of 1.5 ml/min and a column inlet pressure of 2500 psi. The retention time for I was ~11 min. Volumes of reference solution (20–100 μl) were injected to bracket expected amounts of I in the samples. The column effluent was monitored by UV absorbance measurement at 254 nm. Chromatograms were obtained in an analog form using a recorder with a chart speed of 0.5 cm/min and in a digital form using a microcomputer[20] with a data sampling rate of 1 point/sec. The use of a microcomputer in this laboratory as an adjunct to the acquisition and reduction of chromatographic data has been described previously (3).

Analytical Procedure for TLC—A motor-driven multispotter was used to spot gradually the extracts and reference solutions onto a nonfluorescing silica gel plate. Volumes of reference solution (10–100 μl), containing a sufficient quantity of I to bracket expected amounts in the sample residues, were drawn into 100-μl syringes for deposit on the TLC plate. Warm air from a 460-watt hair dryer[21] was blown across the plate to hasten evaporation of the solvent and to minimize spot diffusion. Plates were developed to 10 cm with chloroform–2-propanol–concentrated ammonium hydroxide (25:20:01, v/v). The plate was air dried in a hood for 30 min, then the fluorescence of I was measured using a scanning densitometer operated in the single-beam reflectance mode at 340 nm excitation wavelength with a 400-nm cutoff interference filter. Plates that were spotted with quantities of I at the low end of the concentration range were stored overnight and scanned the next day after the intensity of the fluorescence of I had increased.

[15] KIMAX, Owens-Illinois, Inc., Toledo, Ohio.
[16] TEFLON, E. I. Dupont de Nemours & Co., Wilmington, Del.
[17] Vortex-Genie, Scientific Industries, Inc., Bohemia, N.Y.
[18] Multi-Purpose Rotator, Scientific Industries, Inc., Bohemia, N.Y.
[19] SEP-Pak, Waters Associates, Milford, Mass.
[20] Lilliputer, Digital Specialities, Carrboro, N.C.
[21] Model 202, Oster Corp., Milwaukee, Wis.

Table I—Recovery of I from Spiked Plasma

Compound I, μg/ml	HPLC			TLC		
	N	Recovery, %	*CV*	*N*	Recovery, %	*CV*
0.040	4	84	6	10	95	7
0.200	4	80	0	10	89	5
1.00	4	86	5	10	93	5
Composite	12	84	5	30	92	6

Identification and Quantification of I in Plasma—Programmable microcomputers were interfaced with the HPLC and TLC equipment to provide for ready assessment of chromatograms (3). The microcomputers monitored either the output of the HPLC absorbance detector or the output of the TLC scanning densitometer.

The chromatographic peak corresponding to I in samples was identified by comparison of retention time or R_f value with those for reference solutions containing I. Quantification was achieved by calculating the ratio of the peak area of I in the sample to the peak areas of varying amounts of external reference I as determined by least-squares regression fit. Although peak heights were also available, calculations based on peak areas were found to provide more reliable results (3).

RESULTS

High-Performance Liquid Chromatography—Typical chromatograms of the entire extracts from 1.0 ml of control (blank) plasma and 1.0 ml of plasma to which was added 0.040 μg of I are presented in Fig. 1. At a capacity factor (k') of 6, the linear calibration range for I was 0.010–0.320 μg. A correlation coefficient of 0.999 was obtained for a typical regression analysis, $y = 0.2134x - 0.0008$, where y is the peak area and x is the peak amount in micrograms. At a signal-to-noise ratio of 2.5, the HPLC limit of detection for I in plasma was 0.005 μg/ml. The mean recovery of I in plasma over the range of 0.04–1.0 μg/ml was 84% with a coefficient of variation (CV) of 5% ($n = 12$) (Table I).

Thin-Layer Chromatography—Using the chromatographic conditions indicated, I had an R_f of 0.35. A microcomputer-generated plot of peaks obtained for I by scanning an entire TLC plate is presented in Fig. 2. No peaks corresponding to the drug were found in control samples. A typical TLC calibration curve was linear over the range of 0.004–0.300 μg with a correlation coefficient of 0.997 for the line $y = 1.167x + 0.0128$, where y is the peak area and x is the peak amount in micrograms. The limit of detection for plasma extracts, at a signal-to-noise ratio of 2.5, was 0.004 μg/ml. The mean recovery of I over the range of 0.040–1.0 μg/ml of plasma was 92% with a CV of 6% ($n = 30$) (Table I).

DISCUSSION

Concentration-dependent variations in the extraction efficiency of BW 301U were observed over the measured range when a one-step methylene chloride extraction procedure was utilized; consequently, a two-step extraction procedure was investigated. Although this refinement did decrease the variability to an acceptable level, an excessive amount of endogenous material was extracted also. The coextractives resulted in considerable streaking from the origin to the solvent front of TLC silica gel plates, deforming the spots of compound I. Silica gel cartridges were used to remove these relatively nonpolar materials. Prior to use, the cartridges were eluted with methanol to reduce plate streaking and to remove a contaminant, R_f of ~0.85, that fluoresced when exposed to long wavelength (366 nm) UV radiation. Once the sample extract was loaded, the cartridge was eluted with methylene chloride to remove the sample components responsible for the streaking. Compound I, strongly retained on silica gel, was not eluted until methanol was passed through the cartridge.

Immediately after removal of the TLC plate from the developing chamber the fluorescence of I was most intense, but it diminished markedly to a minimum within 20 min. Plates could be analyzed at that time; however, for increased sensitivity, plates were retained for 24 hr before scanning to permit the fluorescence of I to increase to an intensity that was comparable to that observed initially. The change in fluorescence intensity did not require the presence of light. Following this initial interval, the enhanced fluorescence was stable for at least 1 month.

The substances responsible for the streaking of TLC silica gel plates initially did not appear to adversely affect HPLC chromatograms; however, the silica gel cartridges and a C-18 guard column were used to maximize column longevity, providing a useful column life in excess of several months.

The tendency of I to exhibit fluorescence in solution is potentially useful for analysis by HPLC. However, this fluorescence is readily quenched in aqueous solutions, thereby hindering its use in many reversed-phase liquid chromatographic systems. Normal-phase liquid chromatography does not appear promising due to the strong affinity of I for silica gel columns, resulting in asymmetric peak shapes and excessive capacity factors. Thus, paired-ion reversed-phase chromatography in conjunction with detection by UV absorbance is used for the analysis of I by HPLC. The parameters chosen provided good peak shape, a moderate retention time, and analytical sensitivity comparable to that obtained by fluorescence detection.

The selection of one procedure in preference to the other for the analysis of plasma samples from clinical studies is a matter of available equipment and efficiency. TLC is used preferentially to HPLC in this laboratory for the rapid analysis of limited numbers of samples (typically 1–20). Larger numbers of samples may be analyzed more efficiently by HPLC using an auto-injector to provide for unattended operation. The chromatographic equipment is interfaced with microcomputers to facilitate quantification, thereby achieving high levels of precision and accuracy.

REFERENCES

(1) E. M. Grivsky, S. Lee, C. W. Sigel, D. S. Duch, and C. A. Nichol, *J. Med. Chem.*, **23**, 327 (1980).

(2) D. S. Duch, C. W. Sigel, S. W. Bowers, M. P. Edelstein, J. C. Cavallito, R. G. Foss, and C. A. Nichol, in "Current Chemotherapy and Infectious Disease," Proceedings of the 11th International Congress of Chemotherapy and the 19th Interscience Conference on Antimicrobial Agents and Chemotherapy, American Society for Microbiology, Washington, D.C., 1980, p. 1597.

(3) R. G. Foss, C. W. Sigel, R. J. Harvey, and R. L. DeAngelis, *J. Liq. Chromatogr.*, **3**, 1843 (1980).

(4) D. S. Duch, S. W. Bowers, and C. A. Nichol, *Mol. Pharmacol.*, **18**, 100 (1980).

(5) W. D. Sedwick, R. Birdwell, and J. Laszlo, in "Current Chemotherapy and Infectious Disease," Proceedings of the 11th International Congress of Chemotherapy and the 19th Interscience Conference on Antimicrobial Agents and Chemotherapy, American Society for Microbiology, Washington, D.C., 1980, p. 1593.

(6) D. S. Duch, M. P. Edelstein, S. W. Bowers, and C. A. Nichol, *Proc. Am. Assoc. Cancer Res.*, **22**, 264 (1981).

NMR Determination of Isosorbide Dinitrate and β-Adrenergic Blocking Agents in Tablets

SILVIA N. CHIARELLI, MABEL T. ROSSI, MARÍA T. PIZZORNO, and SEM M. ALBONICO ˣ

Received August 26, 1981, from the *Universidad de Buenos Aires, Faculdad de Farmacia y Bioquímica, 1113 Buenos Aires, Argentina.* Accepted for publication January 11, 1982.

Abstract □ An NMR spectroscopic method for the determination of isosorbide dinitrate, alone or together with alprenolol or propranolol, is described. Spectra are determined in dimethyl sulfoxide-d_6 containing maleic acid or 1,4-dinitrobenzene as internal standards. Both synthetic mixtures and commercial formulations were assayed, and the results were compared using compendial procedures.

Keyphrases □ Isosorbide dinitrate—NMR determination, β-adrenergic blocking agents in tablets □ β-Adrenergic blocking agents—NMR determination of isosorbide dinitrate, tablets □ NMR spectroscopy—determination of isosorbide dinitrate and β-adrenergic blocking agents in tablets

Isosorbide dinitrate (I) is a member of the group of vasodilator drugs, having a nitrite or nitrate function, that are used particularly in the treatment of angina pectoris and ischemia of skeletal muscle (1). It is used alone or together with β-adrenergic blocking agents such as propranolol (II) (2) or alprenolol (III) (3).

Several methods for the analysis of I, II, and III have been described. The official compendia describe a polarographic titration (4) or a colorimetric reaction with *p*-phenolsulfonic acid (5) for isosorbide dinitrate and a spectrophotometric assay for alprenolol (6) and propranolol (7). However, their application for the quantitative determination of I in tablets is laborious and time consuming. The present report describes a new quantitative method for the determination of I alone or together with II or III by ^{1}H-NMR spectroscopy. Furthermore, it allows the simultaneous analysis of II or III.

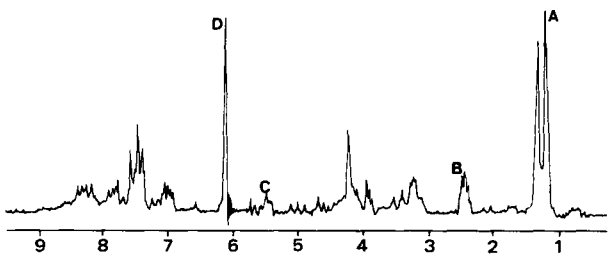

Figure 1—*NMR spectrum of a typical I and II mixture analysis in dimethyl sulfoxide-*d_6. *Key: (A) methyl protons of II; (B) solvent impurity; (C) protons on* C_2 *and* C_5 *of I; (D) single signal of IV.*

EXPERIMENTAL[1]

Materials—Standard isosorbide dinitrate (I), propranolol hydrochloride (II), and alprenolol hydrochloride (III) were purified by recrystallization from ethanol–water, *n*-propanol, and ethyl acetate, respectively.

Maleic acid (IV) was used as internal standard after recrystallization from water, mp 130–131°; 1,4-dinitrobenzene (V) (8), also used as internal standard, was purified by sublimation, mp 173–174°. Dimethyl sulfoxide-d_6 (VI) was used as the solvent and tetramethylsilane was the internal standard.

Samples—Tablets from two batches of each brand locally obtained were used.

Isosorbide Dinitrate Tablets—Twenty tablets were weighed and a sample equivalent to 50 mg of I was dissolved in 10 ml of 2% sodium bicarbonate solution and extracted from methylene chloride (3 × 7 ml). The solution was evaporated in a Craig tube, and 75 mg of IV was added. The mixture was dissolved in 1.0 ml of VI, and ~0.4 ml of the solution was transferred to an NMR tube where the spectrum was obtained (Table I).

Isosorbide Dinitrate and Propranolol Hydrochloride Tablets—The same procedure as just described was used with a sample equivalent

[1] A Perkin-Elmer R12 NMR spectrometer, 60 MHz was used. All spectra were scanned at a probe temperature of 35°.

0022-3549/82/01000-1178$01.00/0

The tendency of I to exhibit fluorescence in solution is potentially useful for analysis by HPLC. However, this fluorescence is readily quenched in aqueous solutions, thereby hindering its use in many reversed-phase liquid chromatographic systems. Normal-phase liquid chromatography does not appear promising due to the strong affinity of I for silica gel columns, resulting in asymmetric peak shapes and excessive capacity factors. Thus, paired-ion reversed-phase chromatography in conjunction with detection by UV absorbance is used for the analysis of I by HPLC. The parameters chosen provided good peak shape, a moderate retention time, and analytical sensitivity comparable to that obtained by fluorescence detection.

The selection of one procedure in preference to the other for the analysis of plasma samples from clinical studies is a matter of available equipment and efficiency. TLC is used preferentially to HPLC in this laboratory for the rapid analysis of limited numbers of samples (typically 1–20). Larger numbers of samples may be analyzed more efficiently by HPLC using an auto-injector to provide for unattended operation. The chromatographic equipment is interfaced with microcomputers to facilitate quantification, thereby achieving high levels of precision and accuracy.

REFERENCES

(1) E. M. Grivsky, S. Lee, C. W. Sigel, D. S. Duch, and C. A. Nichol, *J. Med. Chem.*, **23**, 327 (1980).

(2) D. S. Duch, C. W. Sigel, S. W. Bowers, M. P. Edelstein, J. C. Cavallito, R. G. Foss, and C. A. Nichol, in "Current Chemotherapy and Infectious Disease," Proceedings of the 11th International Congress of Chemotherapy and the 19th Interscience Conference on Antimicrobial Agents and Chemotherapy, American Society for Microbiology, Washington, D.C., 1980, p. 1597.

(3) R. G. Foss, C. W. Sigel, R. J. Harvey, and R. L. DeAngelis, *J. Liq. Chromatogr.*, **3**, 1843 (1980).

(4) D. S. Duch, S. W. Bowers, and C. A. Nichol, *Mol. Pharmacol.*, **18**, 100 (1980).

(5) W. D. Sedwick, R. Birdwell, and J. Laszlo, in "Current Chemotherapy and Infectious Disease," Proceedings of the 11th International Congress of Chemotherapy and the 19th Interscience Conference on Antimicrobial Agents and Chemotherapy, American Society for Microbiology, Washington, D.C., 1980, p. 1593.

(6) D. S. Duch, M. P. Edelstein, S. W. Bowers, and C. A. Nichol, *Proc. Am. Assoc. Cancer Res.*, **22**, 264 (1981).

NMR Determination of Isosorbide Dinitrate and β-Adrenergic Blocking Agents in Tablets

SILVIA N. CHIARELLI, MABEL T. ROSSI, MARÍA T. PIZZORNO, and SEM M. ALBONICO ˣ

Received August 26, 1981, from the *Universidad de Buenos Aires, Faculdad de Farmacia y Bioquímica, 1113 Buenos Aires, Argentina.* Accepted for publication January 11, 1982.

Abstract □ An NMR spectroscopic method for the determination of isosorbide dinitrate, alone or together with alprenolol or propranolol, is described. Spectra are determined in dimethyl sulfoxide-d_6 containing maleic acid or 1,4-dinitrobenzene as internal standards. Both synthetic mixtures and commercial formulations were assayed, and the results were compared using compendial procedures.

Keyphrases □ Isosorbide dinitrate—NMR determination, β-adrenergic blocking agents in tablets □ β-Adrenergic blocking agents—NMR determination of isosorbide dinitrate, tablets □ NMR spectroscopy—determination of isosorbide dinitrate and β-adrenergic blocking agents in tablets

Isosorbide dinitrate (I) is a member of the group of vasodilator drugs, having a nitrite or nitrate function, that are used particularly in the treatment of angina pectoris and ischemia of skeletal muscle (1). It is used alone or together with β-adrenergic blocking agents such as propranolol (II) (2) or alprenolol (III) (3).

Several methods for the analysis of I, II, and III have been described. The official compendia describe a polarographic titration (4) or a colorimetric reaction with *p*-phenolsulfonic acid (5) for isosorbide dinitrate and a spectrophotometric assay for alprenolol (6) and propranolol (7). However, their application for the quantitative determination of I in tablets is laborious and time consuming. The present report describes a new quantitative method for the determination of I alone or together with II or III by ^{1}H-NMR spectroscopy. Furthermore, it allows the simultaneous analysis of II or III.

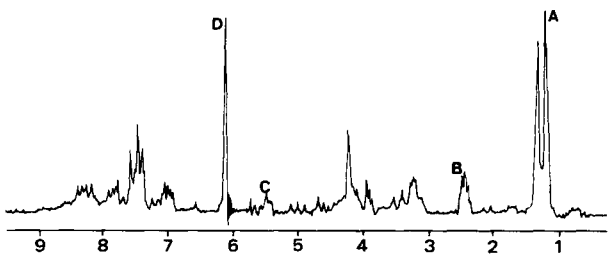

Figure 1—*NMR spectrum of a typical I and II mixture analysis in dimethyl sulfoxide-*d_6. *Key: (A) methyl protons of II; (B) solvent impurity; (C) protons on* C_2 *and* C_5 *of I; (D) single signal of IV.*

EXPERIMENTAL[1]

Materials—Standard isosorbide dinitrate (I), propranolol hydrochloride (II), and alprenolol hydrochloride (III) were purified by recrystallization from ethanol–water, *n*-propanol, and ethyl acetate, respectively.

Maleic acid (IV) was used as internal standard after recrystallization from water, mp 130–131°; 1,4-dinitrobenzene (V) (8), also used as internal standard, was purified by sublimation, mp 173–174°. Dimethyl sulfoxide-d_6 (VI) was used as the solvent and tetramethylsilane was the internal standard.

Samples—Tablets from two batches of each brand locally obtained were used.

Isosorbide Dinitrate Tablets—Twenty tablets were weighed and a sample equivalent to 50 mg of I was dissolved in 10 ml of 2% sodium bicarbonate solution and extracted from methylene chloride (3 × 7 ml). The solution was evaporated in a Craig tube, and 75 mg of IV was added. The mixture was dissolved in 1.0 ml of VI, and ~0.4 ml of the solution was transferred to an NMR tube where the spectrum was obtained (Table I).

Isosorbide Dinitrate and Propranolol Hydrochloride Tablets—The same procedure as just described was used with a sample equivalent

[1] A Perkin-Elmer R12 NMR spectrometer, 60 MHz was used. All spectra were scanned at a probe temperature of 35°.

0022-3549/82/01000-1178$01.00/0

Table I—Analysis of Isosorbide Dinitrate (I) Tablets

Sample	Declared dosage, mg	NMR		USP XX[a]		FA VI[b]	
		mg	Percent	mg	Percent	mg	Percent
A	20.0	19.6	98.0	20.1	100.5	20.3	101.4
B	20.0	19.3	96.4	19.6	98.0	19.9	99.5
C	20.0	20.0	100.0	20.4	102.0	20.6	103.2
D	20.0	19.7	98.6	20.3	101.5	20.4	102.1

[a] See Ref. 4. [b] Formacopea Naconial Argentina (see Ref. 5).

Table II—Analysis of Tablets of Isosorbide Dinitrate (I) and Propranolol Hydrochloride (II)

Tablets	Propranolol Hydrochloride					Isosorbide Dinitrate				
	Declared dosage, mg	NMR		BP[a]		Declared dosage, mg	NMR		USP XX[b]	
		mg	Percent	mg	Percent		mg	Percent	mg	Percent
A	40.0	39.9	99.7	40.7	101.8	10.0	10.5	105.3	9.8	97.8
B	40.0	39.7	99.2	39.9	97.5	10.0	10.2	102.2	10.1	100.9
C	40.0	41.2	102.9	41.2	103.0	10.0	10.2	101.9	9.8	98.5
D	40.0	40.0	100.0	39.4	98.4	10.0	9.9	98.7	9.9	99.4

[a] British Pharmacopoeia (see Ref. 7). [b] See Ref. 4.

Table III—Analysis of Tablets of Isosorbide Dinitrate (I) and Alprenolol Hydrochloride (III)

Tablets	Alprenolol Hydrochloride					Isosorbide Dinitrate				
	Declared dosage, mg	NMR		BP[a]		Declared dosage, mg	NMR		USP XX[b]	
		mg	Percent	mg	Percent		mg	Percent	mg	Percent
A	50.0	51.6	103.2	51.1	102.2	10.0	10.5	104.9	10.2	102.5
B	50.0	50.7	101.4	49.9	99.8	10.0	10.3	102.7	10.1	101.1
C	50.0	51.3	102.6	51.4	102.9	10.0	10.3	102.6	9.8	99.7
D	50.0	46.4	92.8	47.6	95.2	10.0	10.3	102.8	10.2	102.0

[a] British Pharmacopoeia (see Ref. 6). [b] See Ref. 7.

Table IV—Analysis of Standard Mixtures of Isosorbide Dinitrate (I) and Propranolol Hydrochloride

Standard Mixture	Internal Standard, mg	Propranolol Hydrochloride			Isosorbide Dinitrate		
		Added, mg	Found, mg	Recovery, %	Added, mg	Found, mg	Recovery, %
1	75.5	188.7	187.0	99.1	40.3	39.2	97.2
2	63.2	204.3	206.8	101.2	46.9	47.8	101.8
3	70.7	233.2	227.3	97.5	50.0	47.2	94.3
4	73.2	204.8	205.0	99.9	47.0	47.2	100.5
5	77.0	209.4	210.0	100.3	55.5	53.1	95.6
6	75.0	238.5	231.1	96.9	41.7	39.7	95.2
7	78.0	201.7	198.2	98.3	49.8	50.2	100.7
8	74.5	202.2	206.0	101.9	51.5	50.5	98.0
				Mean = 99.4			Mean = 97.9
				% *SD* = ±1.80			%*SD* = ±2.90

to 50 mg of I and 200 mg of II using 75 mg of IV as the internal standard (Table II).

Isosorbide Dinitrate and Alprenolol Hydrochloride Tablets—The same procedure as described for isosorbide dinitrate was used, with a sample equivalent to 20 mg of I and 100 mg of III using 60 mg of V as the internal standard (Table III).

Calculations—The amount of I was calculated as follows:

$$\frac{\text{I, mg}}{\text{tablet}} = \frac{EW_I}{EW_{ST}} \times \frac{A_I}{A_{ST}} \times \frac{ST, \text{mg}}{W_S} \times ATW$$

Where EW_I is the molecular weight of I divided by the number of protons in the signal chosen, EW_{ST} is the molecular weight of the internal standard divided by the number of protons in its signal, A_I is the integral value of the signal representing I, A_{ST} is the integral value of the signal representing the internal standard, W_S is the weight of the sample in milligrams, and ATW is the average tablet weight.

The amount of II and III was calculated by a similar procedure.

RESULTS AND DISCUSSION

All the drugs and internal standards were soluble in dimethyl sulfoxide. Its impurity appeared at 2.5 ppm and it did not interfere with the signals chosen. The stability of the drugs in this solvent during testing was ensured by running the spectra twice.

Maleic acid was selected as the internal standard because it provides a signal at 6.2 ppm, which is near the signal chosen for the analysis; therefore, the error due to drift is small. Furthermore, it has an equivalent of 58, larger than the equivalent of most internal standards. For the analysis of III, V was used due to the overlapping of the signals of III and IV.

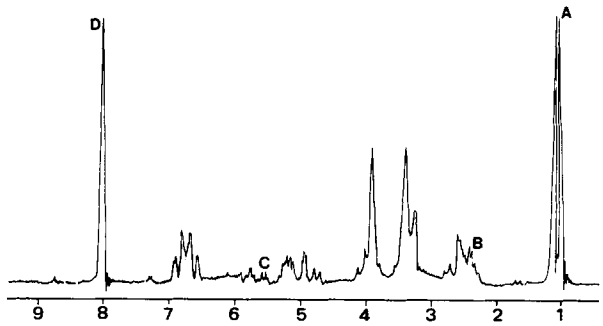

Figure 2—*NMR spectrum of a typical I and III mixture analysis in dimethyl sulfoxide-*d_6. *Key: (A) methyl protons of III; (B) solvent impurity; (C) protons on* C_2 *and* C_5 *of I; (D) single signal of V.*

Table V—Analysis of Standard Mixtures of Isosorbide Dinitrate and Alprenolol Hydrochloride

Standard Mixture	Internal Standard, mg	Alprenolol Hydrochloride			Isosorbide Dinitrate		
		Added, mg	Found, mg	Recovery, %	Added, mg	Found, mg	Recovery, %
1	101.7	253.0	252.5	99.7	53.2	53.5	100.6
2	102.7	250.7	261.0	104.1	53.5	53.5	100.0
3	114.0	258.2	252.2	101.5	52.5	54.2	103.3
4	97.7	260.5	256.5	98.5	57.5	56.5	98.3
5	94.5	251.0	256.5	102.2	57.0	56.0	98.2
6	94.8	252.0	258.0	102.4	57.0	58.5	102.6
7	91.2	249.5	254.0	101.8	52.5	49.0	93.3
8	91.5	258.5	266.0	102.9	62.0	63.0	101.6
				Mean = 101.6			Mean = 99.7
				%SD = ±1.78			%SD = ±3.18

The signal chosen for the analysis of I was the multiplet at 5.5 ppm due to the protons on C_2 and C_5. The presence of this signal at low fields is due to the electronegativity of the nitrate ester group as in 1,4:3,6-dianhydro-D-glucital. In this compound both diacetoxy and dimesyloxy derivatives have their C_2 and C_5 protons shifted to lower fields (9).

The doublet at 1.25 ppm due to both methyl groups was chosen for II. The signal given by the same group in III, a doublet at 1.30 ppm, was selected for III. The singlets at 6.2 ppm for IV and 8 ppm for V were used for the internal standards.

The results of the analysis of a group of known standard mixtures of I and II and I and III are summarized in Tables IV and V (Figs. 1 and 2). The method is accurate and precise, with an $SD \pm 3.06$ for I. The standard deviation is ±1.80 and ±1.78 for II and III, respectively, for the standard mixtures.

This procedure was also applied to commercial lots of tablets from three companies containing I and its mixtures with II and III.

The results obtained are in agreement with those obtained using the official USP procedure for I (4) and the BP procedures for II (6) and III (7).

REFERENCES

(1) P. Needleman and E. M. Johnson, Jr., in "The Pharmacological Basis of Therapeutics," L. S. Goodman and A. Gilman, Eds., McMillan, New York, N.Y., 1980, p. 819.

(2) M. Marmo, *Clin. Ter.*, **56**, 121 (1971).

(3) A. M. Barrett and V. A. Cullum, *Br. J. Pharmacol.*, **34**, 43 (1968).

(4) "The United States Pharmacopeia," 20th, U.S. Pharmacopeial Convention, Rockville, Md., 1980, p. 439.

(5) "Farmacopea Nacional Argentina," 6ª ed., Editorial Codex, Buenos Aires, Argentina, 1978, p. 413.

(6) "British Pharmacopoeia 1980," Her Majesty's Stationery Office, London, England, 1980, p. 729.

(7) Ibid., p. 815.

(8) Maria R. Rodríguez, María T. Pizzorno, and S. M. Albonico, *J. Pharm. Sci.*, **66**, 121 (1977).

(9) F. J. Hopton and G. H. S. Thomas, *Can. J. Chem.*, **47**, 2395 (1969).

Ion-Specific Electrode Study of Copper Binding to Serum Albumins

P. MOHANAKRISHNAN and C. F. CHIGNELL[x]

Received October 26, 1981, from the *Laboratory of Environmental Biophysics, National Institute of Environmental Health Sciences, Research Triangle Park, NC 27709.* Accepted for publication December 23, 1981.

Abstract □ The binding of copper to bovine, human, rabbit, rat, and porcine albumin has been studied using a cupric ion-specific electrode. The results were analyzed in terms of Scatchard expression assuming two classes of independent binding sites. The high-affinity constants for copper binding to the albumin show the same trend as the first association constants for nickel binding, namely, rabbit > human > rat > pig. Despite the similarity in the primary amino acid sequence for human and bovine serum albumin, the former has only one high-affinity site for copper, while the latter has more than three sites.

Keyphrases □ Binding—copper to serum albumin, ion-specific electrode study, bovine, human, rabbit, rat, porcine □ Serum albumin—bovine, human, rabbit, rat, porcine, ion-specific electrode study, copper binding □ Ion-specific electrode—copper binding to serum albumin, bovine, rabbit, human, rat, porcine

Serum copper levels play a dual role in several pathological conditions, both in humans and experimental animals (1, 2). Anti-inflammatory properties are associated with several salts and chelates of copper (3–9). On the other hand, increased copper levels have been observed in several diseases such as tuberculosis and pneumonia (10), rheumatoid arthritis (11, 12), and ankylosing spondilitis (13). In serum the weakly bound form of copper is associated with the transport protein, albumin. Sequence analysis studies have shown that the first three amino acids at the *N*-terminal constitute a high-affinity copper binding site in bovine (14–16), human, and rat albumin (17). Nickel, which has been implicated as a carcinogen in humans and experimental animals (18), also binds to this *N*-terminal site.

There have been several previous attempts to measure the binding of copper to serum albumins from different animal species. In an early study (19) the thermodynamics of copper binding to bovine serum albumin using absorption spectroscopy were examined. However, the insensitivity of the spectroscopic method necessitated the use of high protein concentrations, which precluded the determination of the high-affinity binding constants. A later study (20) estimated the number of copper binding sites on bovine and human albumin but the relative affinity constants were not determined. A more recent study (21)

0022-3549/82/01000-1180$01.00/0

Table V—Analysis of Standard Mixtures of Isosorbide Dinitrate and Alprenolol Hydrochloride

Standard Mixture	Internal Standard, mg	Alprenolol Hydrochloride			Isosorbide Dinitrate		
		Added, mg	Found, mg	Recovery, %	Added, mg	Found, mg	Recovery, %
1	101.7	253.0	252.5	99.7	53.2	53.5	100.6
2	102.7	250.7	261.0	104.1	53.5	53.5	100.0
3	114.0	258.2	252.2	101.5	52.5	54.2	103.3
4	97.7	260.5	256.5	98.5	57.5	56.5	98.3
5	94.5	251.0	256.5	102.2	57.0	56.0	98.2
6	94.8	252.0	258.0	102.4	57.0	58.5	102.6
7	91.2	249.5	254.0	101.8	52.5	49.0	93.3
8	91.5	258.5	266.0	102.9	62.0	63.0	101.6
				Mean = 101.6			Mean = 99.7
				%SD = ±1.78			%SD = ±3.18

The signal chosen for the analysis of I was the multiplet at 5.5 ppm due to the protons on C_2 and C_5. The presence of this signal at low fields is due to the electronegativity of the nitrate ester group as in 1,4:3,6-dianhydro-D-glucital. In this compound both diacetoxy and dimesyloxy derivatives have their C_2 and C_5 protons shifted to lower fields (9).

The doublet at 1.25 ppm due to both methyl groups was chosen for II. The signal given by the same group in III, a doublet at 1.30 ppm, was selected for III. The singlets at 6.2 ppm for IV and 8 ppm for V were used for the internal standards.

The results of the analysis of a group of known standard mixtures of I and II and I and III are summarized in Tables IV and V (Figs. 1 and 2). The method is accurate and precise, with an $SD \pm 3.06$ for I. The standard deviation is ±1.80 and ±1.78 for II and III, respectively, for the standard mixtures.

This procedure was also applied to commercial lots of tablets from three companies containing I and its mixtures with II and III.

The results obtained are in agreement with those obtained using the official USP procedure for I (4) and the BP procedures for II (6) and III (7).

REFERENCES

(1) P. Needleman and E. M. Johnson, Jr., in "The Pharmacological Basis of Therapeutics," L. S. Goodman and A. Gilman, Eds., McMillan, New York, N.Y., 1980, p. 819.

(2) M. Marmo, *Clin. Ter.*, **56**, 121 (1971).

(3) A. M. Barrett and V. A. Cullum, *Br. J. Pharmacol.*, **34**, 43 (1968).

(4) "The United States Pharmacopeia," 20th, U.S. Pharmacopeial Convention, Rockville, Md., 1980, p. 439.

(5) "Farmacopea Nacional Argentina," 6ª ed., Editorial Codex, Buenos Aires, Argentina, 1978, p. 413.

(6) "British Pharmacopoeia 1980," Her Majesty's Stationery Office, London, England, 1980, p. 729.

(7) Ibid., p. 815.

(8) Maria R. Rodríguez, María T. Pizzorno, and S. M. Albonico, *J. Pharm. Sci.*, **66**, 121 (1977).

(9) F. J. Hopton and G. H. S. Thomas, *Can. J. Chem.*, **47**, 2395 (1969).

Ion-Specific Electrode Study of Copper Binding to Serum Albumins

P. MOHANAKRISHNAN and C. F. CHIGNELL[x]

Received October 26, 1981, from the *Laboratory of Environmental Biophysics, National Institute of Environmental Health Sciences, Research Triangle Park, NC 27709.* Accepted for publication December 23, 1981.

Abstract □ The binding of copper to bovine, human, rabbit, rat, and porcine albumin has been studied using a cupric ion-specific electrode. The results were analyzed in terms of Scatchard expression assuming two classes of independent binding sites. The high-affinity constants for copper binding to the albumin show the same trend as the first association constants for nickel binding, namely, rabbit > human > rat > pig. Despite the similarity in the primary amino acid sequence for human and bovine serum albumin, the former has only one high-affinity site for copper, while the latter has more than three sites.

Keyphrases □ Binding—copper to serum albumin, ion-specific electrode study, bovine, human, rabbit, rat, porcine □ Serum albumin—bovine, human, rabbit, rat, porcine, ion-specific electrode study, copper binding □ Ion-specific electrode—copper binding to serum albumin, bovine, rabbit, human, rat, porcine

Serum copper levels play a dual role in several pathological conditions, both in humans and experimental animals (1, 2). Anti-inflammatory properties are associated with several salts and chelates of copper (3–9). On the other hand, increased copper levels have been observed in several diseases such as tuberculosis and pneumonia (10), rheumatoid arthritis (11, 12), and ankylosing spondilitis (13). In serum the weakly bound form of copper is associated with the transport protein, albumin. Sequence analysis studies have shown that the first three amino acids at the *N*-terminal constitute a high-affinity copper binding site in bovine (14–16), human, and rat albumin (17). Nickel, which has been implicated as a carcinogen in humans and experimental animals (18), also binds to this *N*-terminal site.

There have been several previous attempts to measure the binding of copper to serum albumins from different animal species. In an early study (19) the thermodynamics of copper binding to bovine serum albumin using absorption spectroscopy were examined. However, the insensitivity of the spectroscopic method necessitated the use of high protein concentrations, which precluded the determination of the high-affinity binding constants. A later study (20) estimated the number of copper binding sites on bovine and human albumin but the relative affinity constants were not determined. A more recent study (21)

0022-3549/82/01000-1180$01.00/0

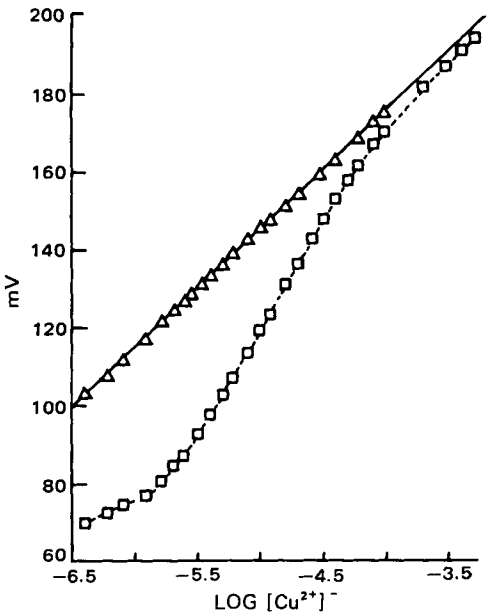

Figure 1—*Response of the electrode to the addition of Cu^{2+} Cu^{2+} was added in microliter quantities to a stirred solution of 0.1 M KNO_3 (50 ml) in the absence (△) and in the presence (□) of human serum albumin, and the change in potential was measured after each addition.*

employed a cupric ion-specific electrode to determine the copper binding parameters of bovine serum albumin. In this report the copper binding parameters for bovine, human, rat, porcine, and rabbit albumins have been estimated using a cupric ion-specific electrode. The sensitivity of this technique is such that it permits the determination of the association constant of copper for the high-affinity primary albumin binding site(s).

EXPERIMENTAL

Materials—Crystallized bovine, human, and rabbit serum albumins[1] were used without further purification. Rat serum albumin[1] (Fraction V) was extensively dialyzed against large volumes of 5 m*M* edetic acid and deionized water, freeze-dried, and stored at 4° until use. Porcine Fraction V[2] was decolorized with charcoal at pH 3 and eluted with 0.2 *M* NaCl over a cross-linked dextran gel column (100 × 3.5 cm). The albumin fractions from the column were concentrated by ultrafiltration[3], dialyzed against large volumes of 5 m*M* edetic acid, lyophilized after dialysis against large volumes of deionized water, and stored cold (4°). The monomer and higher oligomers were pooled together before use. Human and bovine albumin concentrations in the solutions were estimated from their respective absorbances at 279 nm (22, 23). Other albumin solutions were prepared by dissolving a known amount of protein in a desired volume of 0.1 *M* KNO_3 solution. Typically, the titration solutions contained 10–40 μ*M* albumin. Stock solutions of 2 and 100 m*M* $CuSO_4$ were prepared and their concentrations were estimated by atomic absorption spectroscopy.

Titration Experiments—The titrations were carried out with a cupric ion-specific electrode[4] and a single-junction electrode[5] both connected to a digital pH/mV meter and dipped in a 0.1 *M* KNO_3 solution (with or without albumin). Aliquots of the copper sulfate solution (first 2 and later 100 m*M*) were added to the albumin solutions (20–50 ml) using a microsyringe such that the logarithm of the cupric ion concentration in the medium increased linearly with each addition. The corresponding potential as shown by the pH/mV meter was noted after each addition. The parameters of the electrode (the slope and the intercept) were determined from control (no protein) titrations in each case. All titrations were performed at room temperature (23–25°). The pH of the solution at the beginning and end of each titration was 5.2–5.4.

[1] Miles Laboratories, Elkhart, Ind.
[2] Sephadex G-150 Sigma Chemical Co., St. Louis, Mo.
[3] UM-10 membrane, Amicon, Danvers, Mass.
[4] Model 94-29, Orion Res. Inc., Cambridge, Mass.
[5] Model 90-01, Orion Res. Inc., Cambridge, Mass.

Table I—Parameters of Cu^{2+} Binding to Serum Albumins [a]

Source	n_1	$K_1 \times 10^{-6}, M^{-1}$	n_2	$K_2 \times 10^{-3}, M^{-1}$
Bovine	3.68	3.14	12.73	20.15
	3.0[b]	3.0[b]	16.0[b]	20.0[a]
Human	1.13	2.33	4.5	67.54
Rabbit	3.9	2.83	15.14	7.52
Rat	2.62	1.85	26.4	4.34
Porcine	1.86	0.41	18.01	5.76

[a] The values represent the computer analysis of the results of three or more titration experiments. The values are the best fit for both *R versus C* and *(R/C) versus R* Scatchard analysis. The standard deviation was <8% for the computer fittings. [b] Taken from Reference 21.

It is known that above pH 4 at the concentrations employed in this study, the Cu^{2+} ion begins to hydrolyze and precipitates as the oxide or hydroxide soon thereafter (24). Although a more physiological pH of 7.4 would have been the ideal choice, the sensitivity of the electrode may decrease above pH 6 because of the formation of both soluble and insoluble hydroxo–oxo complexes under experimental conditions. Hence, no pH adjustments were made before each titration.

Data Analysis—The titration data were analyzed in terms of the Nernst equation to find the concentration of free and bound copper in solution. Since the resultant Scatchard plots exhibited considerable curvature, the assumption was made that there were two sets of independent binding sites and the data were fitted to the expression (25):

$$r = \frac{n_1 K_1 C}{1 + K_1 C} + \frac{n_2 K_2 C}{1 + K_2 C}$$

where r is the number of Cu^{2+} bound per mole of protein, n_1 and n_2 are the number of binding sites, K_1 and K_2 are the corresponding constants[6], and C the molar concentration of free Cu^{2+}. The curve fitting was performed using a modeling program[7] (26) running on a computer[8,9].

RESULTS AND DISCUSSION

A typical titration curve is shown in Fig. 1. Figure 2 is a computer-fitted Scatchard plot for human serum albumin. The binding parameters determined in this study for albumins from different species are listed in Table I. Also listed in Table I are the binding parameters for bovine serum albumin reported previously (21) for comparison. It can be seen that the results of the present study are in reasonable agreement with previous results (21).

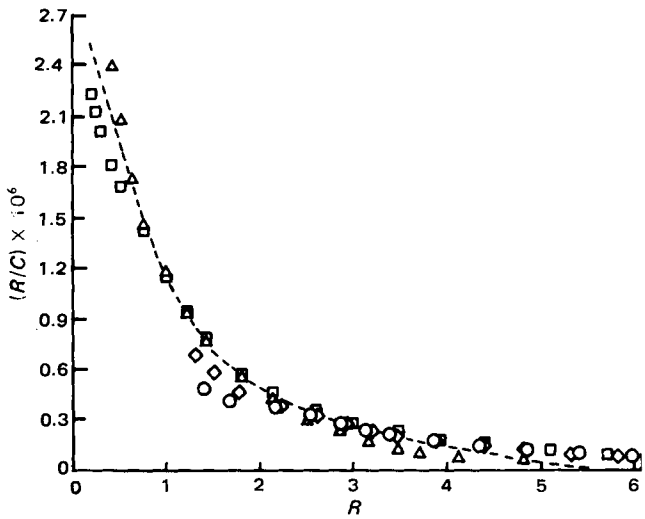

Figure 2—*Scatchard analysis of Cu^{2+} binding to human serum albumin. R and C are the number of Cu^{2+} ions bound per mole of albumin and the molar concentration of free Cu^{2+}, respectively. The figure is the result of a computer fit of the results from four different (○,△,□,◇) titration experiments.*

[6] K_1 and K_2 above are defined for the equilibrium: albumin + n Cu^{2+} ⇌ (albumin-n Cu^{2+}).
[7] Modeling Laboratory, MLAB.
[8] DEC-10, Digital Equipment Company, Marlborough, Mass.
[9] Computer at the Division of Computer Research & Technology, the National Institutes of Health, Bethesda, Md.

The trend in the high-affinity association constants, namely, rabbit > human > rat > pig, parallels that observed for nickel binding to the same albumins as determined previously (27). While it was not possible to obtain consistent values for copper binding to dog serum albumin, the results seemed to indicate that the primary binding sites for canine albumin had a lower affinity than those found in porcine albumin. Again, this is the case for nickel binding (27). If both Cu^{2+} and Ni^{2+} occupy the same albumin binding sites and form complexes of the same geometry type, then one would expect the same trend for both copper and nickel binding. This suggests that the *N*-terminal Cu^{2+}-binding site may also constitute the primary binding site for nickel. The relatively lower binding constants for dog and pig albumins are probably due to the absence of a histidine at the third amino acid position from the *N*-terminal end of these proteins (26).

The number of high-affinity sites for human albumin is less than that for bovine (Table I). From a comparison of the proposed primary structures of these proteins (28, 29), and based on the assumption that the geometry at the additional sites should be comparable to that at the *N*-terminal site, two extra high-affinity sites in bovine albumin may be provided by the amino acid sequences of Glu^{16}–Glu–His^{18} near the *N*-terminal and Asp^{373}–Lys–Leu–Lys–His–Leu–Val–Asp^{380} between the second and the third domains. However, it should be pointed out that this assignment is only tentative and needs to be further substantiated experimentally. It is our experience that the extrinsic circular dichroism spectra of bound copper are not the same for human and bovine albumins[10]. Obviously, there must be some significant differences in both the number and the nature of the copper binding sites for these two types of albumin.

REFERENCES

(1) M. W. Whitehouse, *Agents Actions*, **6**, 201 (1976).

(2) R. Milanino, E. Passarella, and G. P. Velo, in "Advances in Inflammation Research," G. D. Weissman, B. Samuelsson, and R. Raoletti, Eds., Academic, New York, N.Y., 1979, p. 281.

(3) T. Richardson, *J. Pharm. Pharmacol.*, **28**, 66 (1976).

(4) T. R. J. Sorenson, *ibid.*, **29**, 450 (1977).

(5) T. R. J. Sorenson, *J. Med. Chem.*, **19**, 135 (1976).

(6) A. J. Lewis, *Agents Actions*, **8**, 244 (1978).

(7) K. D. Rainsford and M. W. Whitehouse, *J. Pharm. Pharmacol.*, **28**, 83 (1976).

(8) M. W. Whitehouse and W. R. Walker, *Agents Actions*, **8**, 85 (1978).

(9) D. A. Williams, D. T. Waltz, and W. O. Foye, *J. Pharm. Sci.*, **65**, 126 (1976).

(10) M. E. Lahey, C. J. Gubler, M. S. Chase, G. E. Cartwright, and M. M. Wintrobe, *J. Clin. Invest.*, **32**, 329 (1953).

(11) I. L. Pshetakovsky, *Vop Reum.*, **13**, 17 (1973).

(12) D. P. Bajpayee, *Ann. Rheum. Dis.*, **34**, 162 (1975).

(13) P. R. Scudder, D. Al-Timini, W. McMurray, A. G. White, B. C. Zoob, and T. L. Dormandy, *ibid.*, **37**, 67 (1978).

(14) W. T. Shearer, R. A. Bradshaw, F. R. N. Gurd, and T. Peters, Jr., *J. Biol. Chem.*, **242**, 5451 (1967).

(15) T. Peters, Jr. and F. A. Blumenstock, *ibid.*, **242**, 1574 (1967).

(16) R. A. Bradshaw, W. T. Shearer, and F. R. N. Gurd, *ibid.*, **243**, 3817 (1967).

(17) R. A. Bradshaw and T. Peters, Jr., *ibid.*, **244**, 5582 (1969).

(18) F. W. Sunderman, Jr., *Fd. Cosmet. Toxicol.*, **9**, 105 (1971).

(19) I. M. Klotz and H. G. Curme, *J. Am. Chem Soc.*, **70**, 939 (1948).

(20) C. K. Luk, *Biopolymers*, **10**, 1229 (1971).

(21) D. V. Naik, C. F. Jewell, and S. G. Schulman, *J. Pharm. Sci.*, **64**, 1243 (1975).

(22) F. B. Edwards, R. B. Rombauer, and B. J. Campbell, *Biochim. Biophys. Acta*, **194**, 234 (1969).

(23) J. Janatova, J. K. Fuller, and M. J. Hunter, *J. Biol. Chem.*, **243**, 3612 (1968).

(24) C. F. Baes, Jr. and R. E. Mesmer, "The Hydrolysis of Cations," Wiley, New York, N.Y., 1976, p. 267.

(25) G. Scatchard, *Ann. N.Y. Acad. Sci.*, **51**, 660 (1949).

(26) G. D. Knott and D. K. Reece, Proceedings of the ON LINE 1972 Conference, vol. 1, Brunel University, England, 1972, p. 497.

(27) W. M. Callan and F. W. Sunderman, Jr., *Rec. Commun. Chem. Path. Pharmacol.*, **5**, 459 (1973).

(28) J. R. Brown, in "Albumin Function and Uses," V. M. Rosenoer, M. Oratz, and M. A. Rothschild, Eds., Pergamon, Oxford, 1977, p. 27.

(29) B. Meloun, L. Moravek, and V. Kostka, *FEBS Lett.*, **58**, 134 (1975).

[10] P. Mohanakrishnan and C. F. Chignell, unpublished results.

Effect of Dose Size on the Pharmacokinetics of Oral Hydrocortisone Suspension

ROGER D. TOOTHAKER *‡, **WILLIAM A. CRAIG** §, and **PETER G. WELLING** *x

Received September 1, 1981, from the *School of Pharmacy, University of Wisconsin, Madison, WI 53706 and the §Veterans Administration Hospital, Madison, WI 53705. Accepted for publication December 31, 1981. ‡Present address: School of Pharmacy, University of Washington, Seattle, WA 98195.

Abstract □ The pharmacokinetics of hydrocortisone were examined following single doses of 5-, 10-, 20-, and 40-mg hydrocortisone suspensions to healthy male volunteers. Endogenous hydrocortisone was suppressed by giving 2 mg of dexamethasone the night before hydrocortisone administration. Plasma samples obtained serially for 12 hr after hydrocortisone administration were assayed by reversed-phase high-pressure liquid chromatography using a fixed-wavelength (254 nm) UV absorbance detector. Drug absorption was rapid, with mean maximum plasma hydrocortisone concentrations occurring within 60 min of dosing. Subsequent drug elimination was monophasic with mean elimination half-lives increasing from 1.2 hr for the 5-mg dose to 1.7 hr for the 40-mg dose. Increases in *AUC* and C_{max} with increasing dose were linear but not directly proportional to dose size. This was attributed to dose-dependent absorption or to loss of drug during the first-pass through the liver.

Keyphrases □ Hydrocortisone—effect of dose size on pharmacokinetics of oral suspension, absorption, elimination □ Pharmacokinetics—oral hydrocortisone suspension, absorption, elimination, effect of dose size □ Absorption—oral hydrocortisone suspension, elimination, effect of dose size on pharmacokinetics □ Suspension—oral hydrocortisone, absorption, elimination, effect of dose size on pharmacokinetics

Hydrocortisone was designated by the U.S. Food and Drug Administration as a drug whose different brands and dosage forms should be examined for bioequivalence (1). A series of studies was initiated to examine the pharmacokinetics of hydrocortisone and to assess the feasibility of conducting bioequivalence studies on commercial products.

In a previous study (2), dexamethasone was shown to

0022-3549/82/01000-1182$01.00/0

The trend in the high-affinity association constants, namely, rabbit > human > rat > pig, parallels that observed for nickel binding to the same albumins as determined previously (27). While it was not possible to obtain consistent values for copper binding to dog serum albumin, the results seemed to indicate that the primary binding sites for canine albumin had a lower affinity than those found in porcine albumin. Again, this is the case for nickel binding (27). If both Cu^{2+} and Ni^{2+} occupy the same albumin binding sites and form complexes of the same geometry type, then one would expect the same trend for both copper and nickel binding. This suggests that the *N*-terminal Cu^{2+}-binding site may also constitute the primary binding site for nickel. The relatively lower binding constants for dog and pig albumins are probably due to the absence of a histidine at the third amino acid position from the *N*-terminal end of these proteins (26).

The number of high-affinity sites for human albumin is less than that for bovine (Table I). From a comparison of the proposed primary structures of these proteins (28, 29), and based on the assumption that the geometry at the additional sites should be comparable to that at the *N*-terminal site, two extra high-affinity sites in bovine albumin may be provided by the amino acid sequences of Glu^{16}–Glu–His^{18} near the *N*-terminal and Asp^{373}–Lys–Leu–Lys–His–Leu–Val–Asp^{380} between the second and the third domains. However, it should be pointed out that this assignment is only tentative and needs to be further substantiated experimentally. It is our experience that the extrinsic circular dichroism spectra of bound copper are not the same for human and bovine albumins[10]. Obviously, there must be some significant differences in both the number and the nature of the copper binding sites for these two types of albumin.

REFERENCES

(1) M. W. Whitehouse, *Agents Actions*, **6**, 201 (1976).

(2) R. Milanino, E. Passarella, and G. P. Velo, in "Advances in Inflammation Research," G. D. Weissman, B. Samuelsson, and R. Raoletti, Eds., Academic, New York, N.Y., 1979, p. 281.

(3) T. Richardson, *J. Pharm. Pharmacol.*, **28**, 66 (1976).

(4) T. R. J. Sorenson, *ibid.*, **29**, 450 (1977).

(5) T. R. J. Sorenson, *J. Med. Chem.*, **19**, 135 (1976).

(6) A. J. Lewis, *Agents Actions*, **8**, 244 (1978).

(7) K. D. Rainsford and M. W. Whitehouse, *J. Pharm. Pharmacol.*, **28**, 83 (1976).

(8) M. W. Whitehouse and W. R. Walker, *Agents Actions*, **8**, 85 (1978).

(9) D. A. Williams, D. T. Waltz, and W. O. Foye, *J. Pharm. Sci.*, **65**, 126 (1976).

(10) M. E. Lahey, C. J. Gubler, M. S. Chase, G. E. Cartwright, and M. M. Wintrobe, *J. Clin. Invest.*, **32**, 329 (1953).

(11) I. L. Pshetakovsky, *Vop Reum.*, **13**, 17 (1973).

(12) D. P. Bajpayee, *Ann. Rheum. Dis.*, **34**, 162 (1975).

(13) P. R. Scudder, D. Al-Timini, W. McMurray, A. G. White, B. C. Zoob, and T. L. Dormandy, *ibid.*, **37**, 67 (1978).

(14) W. T. Shearer, R. A. Bradshaw, F. R. N. Gurd, and T. Peters, Jr., *J. Biol. Chem.*, **242**, 5451 (1967).

(15) T. Peters, Jr. and F. A. Blumenstock, *ibid.*, **242**, 1574 (1967).

(16) R. A. Bradshaw, W. T. Shearer, and F. R. N. Gurd, *ibid.*, **243**, 3817 (1967).

(17) R. A. Bradshaw and T. Peters, Jr., *ibid.*, **244**, 5582 (1969).

(18) F. W. Sunderman, Jr., *Fd. Cosmet. Toxicol.*, **9**, 105 (1971).

(19) I. M. Klotz and H. G. Curme, *J. Am. Chem Soc.*, **70**, 939 (1948).

(20) C. K. Luk, *Biopolymers*, **10**, 1229 (1971).

(21) D. V. Naik, C. F. Jewell, and S. G. Schulman, *J. Pharm. Sci.*, **64**, 1243 (1975).

(22) F. B. Edwards, R. B. Rombauer, and B. J. Campbell, *Biochim. Biophys. Acta*, **194**, 234 (1969).

(23) J. Janatova, J. K. Fuller, and M. J. Hunter, *J. Biol. Chem.*, **243**, 3612 (1968).

(24) C. F. Baes, Jr. and R. E. Mesmer, "The Hydrolysis of Cations," Wiley, New York, N.Y., 1976, p. 267.

(25) G. Scatchard, *Ann. N.Y. Acad. Sci.*, **51**, 660 (1949).

(26) G. D. Knott and D. K. Reece, Proceedings of the ON LINE 1972 Conference, vol. 1, Brunel University, England, 1972, p. 497.

(27) W. M. Callan and F. W. Sunderman, Jr., *Rec. Commun. Chem. Path. Pharmacol.*, **5**, 459 (1973).

(28) J. R. Brown, in "Albumin Function and Uses," V. M. Rosenoer, M. Oratz, and M. A. Rothschild, Eds., Pergamon, Oxford, 1977, p. 27.

(29) B. Meloun, L. Moravek, and V. Kostka, *FEBS Lett.*, **58**, 134 (1975).

[10] P. Mohanakrishnan and C. F. Chignell, unpublished results.

Effect of Dose Size on the Pharmacokinetics of Oral Hydrocortisone Suspension

ROGER D. TOOTHAKER *‡, **WILLIAM A. CRAIG** §, and **PETER G. WELLING** *x

Received September 1, 1981, from the *School of Pharmacy, University of Wisconsin, Madison, WI 53706 and the §Veterans Administration Hospital, Madison, WI 53705. Accepted for publication December 31, 1981. ‡Present address: School of Pharmacy, University of Washington, Seattle, WA 98195.

Abstract □ The pharmacokinetics of hydrocortisone were examined following single doses of 5-, 10-, 20-, and 40-mg hydrocortisone suspensions to healthy male volunteers. Endogenous hydrocortisone was suppressed by giving 2 mg of dexamethasone the night before hydrocortisone administration. Plasma samples obtained serially for 12 hr after hydrocortisone administration were assayed by reversed-phase high-pressure liquid chromatography using a fixed-wavelength (254 nm) UV absorbance detector. Drug absorption was rapid, with mean maximum plasma hydrocortisone concentrations occurring within 60 min of dosing. Subsequent drug elimination was monophasic with mean elimination half-lives increasing from 1.2 hr for the 5-mg dose to 1.7 hr for the 40-mg dose. Increases in *AUC* and C_{max} with increasing dose were linear but not directly proportional to dose size. This was attributed to dose-dependent absorption or to loss of drug during the first-pass through the liver.

Keyphrases □ Hydrocortisone—effect of dose size on pharmacokinetics of oral suspension, absorption, elimination □ Pharmacokinetics—oral hydrocortisone suspension, absorption, elimination, effect of dose size □ Absorption—oral hydrocortisone suspension, elimination, effect of dose size on pharmacokinetics □ Suspension—oral hydrocortisone, absorption, elimination, effect of dose size on pharmacokinetics

Hydrocortisone was designated by the U.S. Food and Drug Administration as a drug whose different brands and dosage forms should be examined for bioequivalence (1). A series of studies was initiated to examine the pharmacokinetics of hydrocortisone and to assess the feasibility of conducting bioequivalence studies on commercial products.

In a previous study (2), dexamethasone was shown to

0022-3549/82/01000-1182$01.00/0

Table I—Mean Pharmacokinetic Parameter Values[a] Obtained following 5-, 10-, 20-, and 40-mg Oral Doses of Hydrocortisone

Parameter	Value				Statistic[b]
	5-mg Dose	10-mg Dose	20-mg Dose	40-mg Dose	
k_{el}, hr^{-1}	0.60 ± 0.07	0.57 ± 0.01	0.46 ± 0.04	0.42 ± 0.07	$\overline{ABCD}$[c]
$t_{1/2\ el}$, hr	1.2 ± 0.1	1.3 ± 0.2	1.5 ± 0.14	1.7 ± 0.3	$\overline{DCBA}$
C_{max}[d], ng/ml	119 ± 23	175 ± 119	263 ± 55	389 ± 103	$\overline{DCBA}$
t_{max}[d], hr	0.7 ± 0.4	0.8 ± 0.5	0.9 ± 0.5	1.0 ± 0.5	$\overline{DCBA}$
AUC, ng·hr/ml	293 ± 57	447 ± 75	835 ± 148	1340 ± 360	$\overline{DCBA}$
$AUC\ k_{el}$, ng/ml	171 ± 26	248 ± 21	377 ± 44	553 ± 90	DCBA
$AUC\ k_{el}\ D\ 10^{-6}$/ml	34 ± 5	25 ± 2	19 ± 2	14 ± 2	ABCD
C_{max}/D, 10^{-6}/ml	24 ± 5	18 ± 2	13 ± 3	10 ± 3	ABCD

[a] ±1 *SD*. [b] Differences were considered significant at the 95% level. [c] A = 5 mg, B = 10 mg, C = 20 mg, D = 40 mg. [d] Observed values.

suppress endogenous hydrocortisone plasma levels from normal values of 40–200 ng/ml to 6–14 ng/ml for at least 21 hr, thus permitting accurate measurement of circulating exogenous hydrocortisone with negligible interference by endogenous compounds. A reversed-phase high-pressure liquid chromatographic (HPLC) assay for hydrocortisone in plasma, capable of measuring concentrations as low as 5 ng/ml, was used to determine the pharmacokinetics from 10-, 30-, and 50-mg doses of hydrocortisone given as oral tablets to healthy male volunteers (3). Results obtained in this study suggested that hydrocortisone pharmacokinetics may be dose-dependent, and that increases in circulating levels may not be dose-proportional. Similar results to these were observed following oral doses of cortisone acetate (4). A subsequent study, in which 5-, 10-, 20-, and 40-mg doses of hydrocortisone sodium succinate were given intravenously, demonstrated dose-proportional hydrocortisone levels and dose-independence of most pharmacokinetic values (5). Dose-nonproportionality following oral doses was thus attributed either to tablet effects or to nonlinear absorption or first-pass metabolism.

In the present study, hydrocortisone pharmacokinetics were examined in healthy male volunteers following oral doses of 5, 10, 20, and 40 mg of hydrocortisone suspension.

EXPERIMENTAL

Materials—Chemical standard hydrocortisone[1] and internal standard Δ^4-pregnen-17α,20β,21-triol-3,11-dione[1] were analytical grade. Reagent grade methylene chloride[2] was distilled prior to use. All other solvents and chemicals were reagent grade and were used as supplied. Plasma for construction of standard curves was obtained from healthy volunteers between 7 and 9 am subsequent to administration of 2 mg of dexamethasone at 11 pm the previous day.

Subjects—After giving informed consent, eight male volunteers (age 22–39 years, height 170–183 cm, weight 64–77 kg) underwent physical examinations including blood and urine analyses. Vital signs and laboratory values for all subjects were normal.

Protocol—Each subject received 5-, 10-, 20-, and 40-mg doses of hydrocortisone as an oral suspension[3] at least 1 week apart in a randomized block design. Subjects were fasted from 10 pm on the day prior to dosing until 12 noon the next day. All subjects received 2 mg of dexamethasone[4] together with 180 ml of water at 11 pm hr on the day before dosing. Hydrocortisone suspension (0.1–0.8 ml) was mixed with 60 ml of orange juice immediately before dosing. The orange juice–hydrocortisone mixture was swallowed, rapidly followed by three 40-ml rinses of orange juice. Dosing containers were assayed for residual hydrocortisone and contained 0.41 ± 0.25% (*SD*) of the dose; this was considered negligible. Subjects were permitted to ingest no other liquid until 4 hr after dosing.

Blood samples (10 ml) were taken from a forearm vein into heparinized vacuum tubes immediately before and then serially from 15 min to 12 hr after hydrocortisone administration. Blood samples were centrifuged immediately and the plasma was stored at −20° until assayed. Subjects were ambulatory during blood sampling.

Assay—The HPLC assay used in this study was described previously (3). Hydrocortisone and added internal standard were extracted from 1 ml of plasma into methylene chloride. The residue from the evaporated organic layer was reconstituted in the liquid chromatographic mobile phase (60% aqueous methanol), and 30 μl was injected onto the column. Components were detected at 254 nm, and concentrations of hydrocortisone were calculated by peak height ratio. Separate standard curves were run with each batch of samples. Suppressed hydrocortisone concentrations obtained just before hydrocortisone administration were subtracted from all concentrations obtained after dosing for each subject.

Data Analysis—Model-independent estimates of areas under plasma hydrocortisone concentration curves from zero to infinite time (AUC) were calculated by trapezoidal rule, with end correction where necessary (6). Elimination rate constants were calculated by regression analysis of the postabsorption phase of hydrocortisone plasma profiles.

Pharmacokinetic parameters were examined by ANOVA for crossover design. Differences between individual doses were analyzed using Tukey's test (7).

RESULTS

Mean plasma hydrocortisone concentrations, corrected for endogenous hydrocortisone, are shown for all four dose levels in Fig. 1. Drug absorption was rapid, with maximum drug concentrations occurring within 1 hr of dosing. Drug levels then declined monoexponentially in all cases. Mean hydrocortisone levels resulting from the 10-, 20-, and 40-mg doses were slightly elevated at the last sampling times, suggesting the possibility of a more prolonged terminal elimination phase. However, the drug levels at these times approached the lower sensitivity limit of the assay, so that their significance is uncertain. This effect was not noted following the 5-mg dose. Exclusion of the terminal data points did not significantly affect the calculated drug half-lives. Hydrocortisone concentrations were above predose suppressed values for up to 8 hr following the 5- and 10-mg doses, and up to 12 hr following the 20- and 40-mg doses.

Pharmacokinetic parameters and statistical analysis are presented in Table I. Mean peak levels of hydrocortisone increased from 119 ng/ml following the 5-mg dose, to 389 ng/ml following the 40-mg dose. The time of peak levels was independent of dose. The elimination half-life was affected by dose size, increasing from a mean value of 1.2 hr following the 5-mg dose to 1.7 hr following the 40-mg dose. The area under the hydrocortisone plasma curve, and also the area corrected for variance in the elimination rate constant, $AUC\ k_{el}$, both increased with increasing dose. However, the increases in both the area and C_{max} values were not dose-proportional. Doubling the dose at 5, 10, and 20 mg resulted in mean area increases of 1.5-, 1.9-, and 1.6-fold, respectively, while the value of C_{max} increased 1.5-fold with each two-fold increase in dose.

The nonproportional relationship between AUC, C_{max}, and dose size is shown graphically in Fig. 2. Linear regression analysis resulted in positive y-intercepts which were significantly >0 ($p < 0.05$). When $AUC\ k_{el}$ and C_{max} values were corrected for dose size (Table I) the resulting values significantly decreased between each incremental dose of hydrocortisone.

DISCUSSION

In this study, the pharmacokinetics of hydrocortisone have been described following 5-, 10-, 20-, and 40-mg oral suspension doses to healthy

[1] Sigma Chemical Co., St. Louis, MO 63178.
[2] Burdick and Jackson Laboratories, Muskegon, MI 49442.
[3] Cortef intramuscular suspension, 50 mg/ml, Upjohn, Kalamazoo, MI 49001.
[4] Decadron elixir, 0.1 mg/ml, Merck, Sharp and Dohme, West Point, PA 19486.

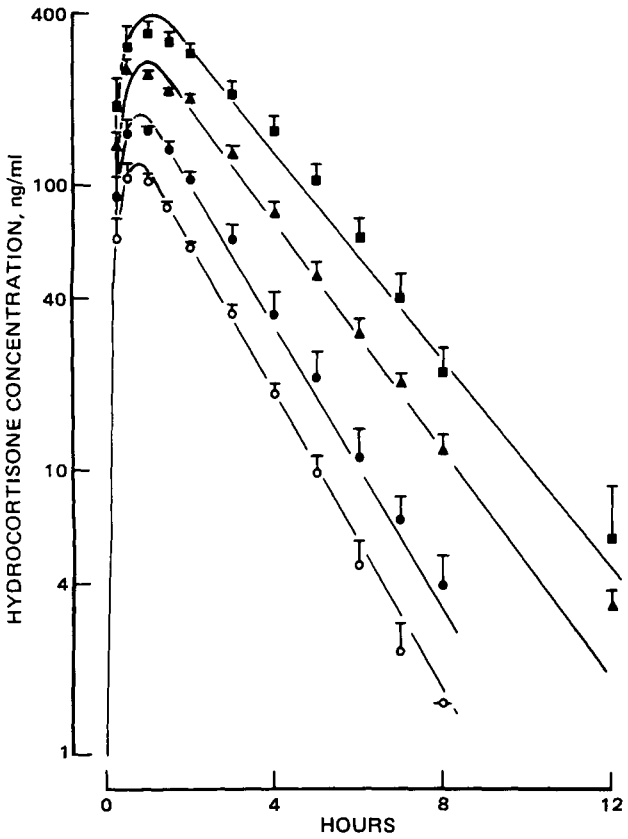

Figure 1—*Mean plasma hydrocortisone concentrations (±1 SEM, n = 8) versus time for subjects receiving oral hydrocortisone suspensions. Key: (○) 5 mg; (●) 10 mg; (▲) 20 mg; (■) 40 mg.*

volunteers. The plasma profiles, and also the values of pharmacokinetic parameters, obtained under these conditions are generally consistent with values reported elsewhere (8–12). The drug is absorbed rapidly into the circulation, achieving peak plasma concentrations within 1 hr. Plasma levels then decline with a half-life of 1.2–1.7 hr. The plasma levels of hydrocortisone obtained in this study are comparable to those obtained previously when a tablet dosage form was used (3). The only dose size that was common to both studies, 10 mg, yielded almost identical C_{max} and *AUC* values.

Increases in circulating levels of hydrocortisone have thus been shown not to be proportional to increasing doses following both tablet (3) and suspension dosage forms. An overall five-fold increase in the tablet dose (10–50 mg) resulted in a 2.1-fold increase in mean C_{max}, and a 3.3-fold increase in *AUC* values. In the present study an overall eight-fold increase in the suspension dose (5–40 mg) resulted in a 3.3-fold increase in C_{max} and a 4.6-fold increase in *AUC*. The somewhat greater increase in *AUC* compared to C_{max} with increasing dose in both studies is due to the somewhat slower absorption and elimination of hydrocortisone at higher doses resulting in flatter and somewhat more prolonged drug profiles.

A number of explanations was originally proposed to account for the nonproportional relationship between circulating hydrocortisone levels and the size of the oral dose (3). These included changes in the binding characteristics of hydrocortisone to plasma proteins, limited tablet dissolution, saturable absorption, and an increased first-pass effect following higher doses. Of these, changes in binding characteristics appear unlikely as plasma levels of hydrocortisone have been shown to be dose-proportional following those intravenous doses that yielded similar circulating drug levels to those obtained following the oral doses (5). Limited tablet dissolution at higher doses is also an unlikely explanation as similar effects occurred with both tablet and suspension dosages.

It is difficult to distinguish the other possibilities, limited absorption and greater first-pass metabolism, from the present data. Previous studies have indicated that hydrocortisone is well-absorbed from the small intestine (13), and absorption appears not to be saturable at dosages used in the present study (14). Dividing the mean *AUC* values obtained following the suspension dose by those obtained after equivalent intravenous doses (5) shows that the systemic availability of hydrocortisone is 71, 57, and 56% from the 5-, 10-, and 20-mg doses, respectively. Similar

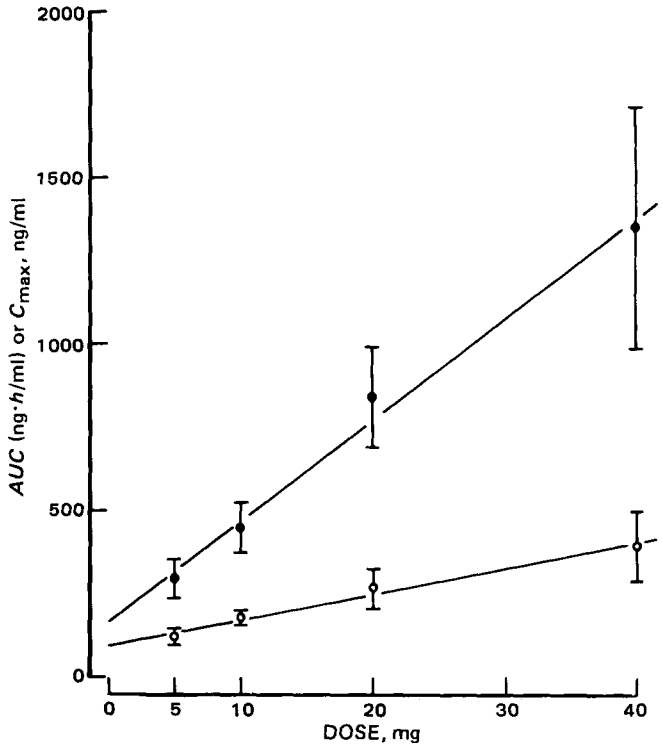

Figure 2—*Relationship between mean (±1 SD) AUC and C_{max} values, and oral hydrocortisone dose (n = 8). Key: (●) AUC; (○) C_{max}.*

comparison of the tablet dose data indicates that systemic availability of hydrocortisone was 60% from a 10-mg dose, and 40% from 30- and 50-mg doses.

In the absence of additional information, the most likely cause of the apparent dose dependency of hydrocortisone absorption is that of increased first-pass metabolism at higher doses. The rapid absorption of hydrocortisone from the GI tract will give rise to transient, high drug levels in the splanchnic circulation. These levels are likely to exceed the binding capacity of the high-affinity, low-capacity binding protein transcortin (15), resulting in a large proportion of drug passing through the liver during the first-pass either loosely bound to the low-affinity, high-capacity protein albumin or in free form. The percentage of drug that is in the loosely bound or unbound form during the first-pass will increase, while the percentage of drug tightly bound to transcortin will decrease, as the size of the dose increases. An increased free fraction during the first-pass is likely to permit greater hepatic clearance, and to decrease the overall systemic availability of unchanged drug. While this hypothesis is attractive, further studies are needed to identify the intrinsic relationships between the protein binding and hepatic clearance of hydrocortisone.

The results obtained in the present study have confirmed that plasma levels of oral hydrocortisone are not proportional to the administered dose. However, as peak plasma levels and *AUC* are approximately linearly related to dose size within the dosage range studied (Fig. 2), we conclude that meaningful bioavailability comparisons can be made for hydrocortisone at therapeutic dose levels.

REFERENCES

(1) *Fed. Reg.*, **42**, 1624 (1976).

(2) T. J. Goehl, G. M. Sundaresan, J. P. Hunt, V. K. Prasad, R. D. Toothaker, and P. G. Welling, *J. Pharm. Sci.*, **69**, 1409 (1980).

(3) R. D. Toothaker, G. M. Sundaresan, J. P. Hunt, T. J. Goehl, K. S. Rotenberg, V. K. Prasad, W. A. Craig, and P. G. Welling, *ibid.*, **71**, 573 (1982).

(4) W. A. Colburn, A. R. DiSanto, S. S. Stubbs, R. E. Monovich, and K. A. DeSante, *J. Clin. Pharmacol.*, **20**, 428 (1980).

(5) R. D. Toothaker and P. G. Welling, *J. Pharmacokinet. Biopharm.*, in press.

(6) M. Gibaldi and G. Perrier, "Pharmacokinetics," M. Dekker, New York, N.Y., 1975, p. 293.

(7) J. Netter and W. Wasserman, "Applied Linear Statistical Models," Irwin, Inc., Homewood, Ill., 1974, p. 474.

(8) W. R. Beisel, V. C. Diraimondo, P. Y. Chao, J. M. Rosner, and P. H. Forsham, *Metabolism*, **13**, 942 (1964).
(9) P. J. Fell, *Clin. Endocrinol.*, **1**, 65 (1972).
(10) P. L. Morselli, V. Marc, S. Garattini, and M. Zaccala, *Biochem. Pharmacol.*, **19**, 1643 (1970).
(11) R. E. Peterson, J. B. Wyngaarden, S. L. Guerra, B. B. Brodie, and J. J. Bunim, *J. Clin. Invest.*, **34**, 1779 (1955).
(12) J. Scheuer and P. K. Bondy, *ibid.*, **36**, 67 (1957).
(13) H. P. Schedl, J. A. Clifton, and G. Nokes, *J. Clin. Endocrinol.*, **24**, 224 (1964).
(14) H. P. Schedl, *ibid.*, **25**, 1309 (1965).
(15) W. H. Daughaday and I. K. Mariz, *Metabolism*, **10**, 937 (1961).

ACKNOWLEDGMENTS

Funds were provided by FDA Contract 223-78-3006 and by NIH Grant 20327.

COMMUNICATIONS

The Effect of Thermal History on the Transition Temperature of Citric Acid Glass

Keyphrases □ Transition temperature—effect of thermal history, citric acid glass □ Citric acid glass—effect of thermal history on the transition temperature

To the Editor:

Glass is a noncrystalline solid which does not exhibit long-range order of its molecules and has a characteristic temperature where its physical state changes from a rigid, brittle material to a flexible, rubbery material. In addition, glass is not thermodynamically stable and will readily revert to the crystalline state under the proper environmental conditions (1, 2). As a result of these characteristics, materials capable of glass formation have been suggested as vehicles for solid dispersion systems, because it has been theorized that they should exhibit more rapid dissolution than their crystalline counterparts (3–5).

One compound often mentioned as a potential vehicle is citric acid (6–12). In the crystalline state, this material is highly hydrogen bonded (13), a property that apparently is responsible for its glass formation, because it has been reported that hydrogen bonding tendency helps prevent crystallization from occurring when a liquid melt is cooled below its liquidus temperature (14–16).

Recently, there has been a reported discrepancy in the transition temperature (T_g) of citric acid glass. This discrepancy was explained (17) to be due to residual moisture contamination in the samples. These studies (7–10) utilized citric acid monohydrate, while another study (12) employed anhydrous citric acid.

We do not dispute this explanation of the discrepancy. However, we thought it would be helpful to future investigators if the effect of thermal history of the melt and the presence of impurities on the T_g of citric acid glass was reported.

Anhydrous citric acid[1] was used in this study in order to eliminate possible effects of residual moisture contamination. The procedures used for sample preparation and determination of the T_g of a glass by differential scanning calorimetry (DSC) have already been discussed in detail (12). In examination of the effect of the thermal history of the molten citric acid on the T_g of citric acid glass, the DSC procedure was modified such that after heating the citric acid to melting, the molten citric acid was raised to the desired temperature and held isothermally for a specified time before rapidly being cooled.

Table I—The Transition Temperatures Obtained for Citric Acid Glass after Holding Molten Citric Acid Isothermally above Its Melting Temperature for Specified Times

Temperature°	Time, min	T_g Values°
172	5	10.0[a]
	15	7.0
	30	2.0
177	5	10.0
	20	4.0
180	5	8.0
	15	3.0
	30	0.0
190	5	6.5
	15	1.0
	30	—[b]

[a] Average of at least duplicate determinations. [b] Material discolored, not able to detect a T_g from −60 to 200°.

Table I shows the effect of thermal history on the T_g of citric acid glass. Results indicate that the higher the temperature and the longer the exposure time at a given temperature, the lower the T_g value of citric acid glass. Accompanying this decrease in the T_g value was a progressive discoloration of the molten citric acid from a clear transparent liquid to a yellowish brown liquid.

Aconitic acid[2], a dehydration decomposition product of citric acid, degrades upon melting. By adding the material to citric acid in varying proportions and then preparing glass dispersions of the mixture, it is possible to simulate the effect of degradation product impurities on the T_g of citric acid glass. Figure 1 shows that as the level of impurities increases, the T_g of citric acid glass decreases.

The thermal stability of citric acid has been of concern to previous solid dispersion investigators (6–10, 12). Available thermal analysis literature on citric acid is limited. One study (18) suggests that citric acid may begin to decompose at ~185°, while another study (19) states that thermal degradation of citric acid does not begin to occur until 200–225°. The data presented in this communication indicate that citric acid does exhibit some degree of thermal instability. However, thermal degradation does not appear to begin immediately upon initial melting but only

[1] J. T. Baker Chemical Co., Phillipsburg, N.J.

[2] Aldrich Chemical Co., Milwaukee, Wis.

0022-3549/82/01000-1185$01.00/0

(8) W. R. Beisel, V. C. Diraimondo, P. Y. Chao, J. M. Rosner, and P. H. Forsham, *Metabolism*, **13**, 942 (1964).
(9) P. J. Fell, *Clin. Endocrinol.*, **1**, 65 (1972).
(10) P. L. Morselli, V. Marc, S. Garattini, and M. Zaccala, *Biochem. Pharmacol.*, **19**, 1643 (1970).
(11) R. E. Peterson, J. B. Wyngaarden, S. L. Guerra, B. B. Brodie, and J. J. Bunim, *J. Clin. Invest.*, **34**, 1779 (1955).
(12) J. Scheuer and P. K. Bondy, *ibid.*, **36**, 67 (1957).
(13) H. P. Schedl, J. A. Clifton, and G. Nokes, *J. Clin. Endocrinol.*, **24**, 224 (1964).
(14) H. P. Schedl, *ibid.*, **25**, 1309 (1965).
(15) W. H. Daughaday and I. K. Mariz, *Metabolism*, **10**, 937 (1961).

ACKNOWLEDGMENTS

Funds were provided by FDA Contract 223-78-3006 and by NIH Grant 20327.

COMMUNICATIONS

The Effect of Thermal History on the Transition Temperature of Citric Acid Glass

Keyphrases □ Transition temperature—effect of thermal history, citric acid glass □ Citric acid glass—effect of thermal history on the transition temperature

To the Editor:

Glass is a noncrystalline solid which does not exhibit long-range order of its molecules and has a characteristic temperature where its physical state changes from a rigid, brittle material to a flexible, rubbery material. In addition, glass is not thermodynamically stable and will readily revert to the crystalline state under the proper environmental conditions (1, 2). As a result of these characteristics, materials capable of glass formation have been suggested as vehicles for solid dispersion systems, because it has been theorized that they should exhibit more rapid dissolution than their crystalline counterparts (3–5).

One compound often mentioned as a potential vehicle is citric acid (6–12). In the crystalline state, this material is highly hydrogen bonded (13), a property that apparently is responsible for its glass formation, because it has been reported that hydrogen bonding tendency helps prevent crystallization from occurring when a liquid melt is cooled below its liquidus temperature (14–16).

Recently, there has been a reported discrepancy in the transition temperature (T_g) of citric acid glass. This discrepancy was explained (17) to be due to residual moisture contamination in the samples. These studies (7–10) utilized citric acid monohydrate, while another study (12) employed anhydrous citric acid.

We do not dispute this explanation of the discrepancy. However, we thought it would be helpful to future investigators if the effect of thermal history of the melt and the presence of impurities on the T_g of citric acid glass was reported.

Anhydrous citric acid[1] was used in this study in order to eliminate possible effects of residual moisture contamination. The procedures used for sample preparation and determination of the T_g of a glass by differential scanning calorimetry (DSC) have already been discussed in detail (12). In examination of the effect of the thermal history of the molten citric acid on the T_g of citric acid glass, the DSC procedure was modified such that after heating the citric acid to melting, the molten citric acid was raised to the desired temperature and held isothermally for a specified time before rapidly being cooled.

Table I—The Transition Temperatures Obtained for Citric Acid Glass after Holding Molten Citric Acid Isothermally above Its Melting Temperature for Specified Times

Temperature°	Time, min	T_g Values°
172	5	10.0[a]
	15	7.0
	30	2.0
177	5	10.0
	20	4.0
180	5	8.0
	15	3.0
	30	0.0
190	5	6.5
	15	1.0
	30	—[b]

[a] Average of at least duplicate determinations. [b] Material discolored, not able to detect a T_g from −60 to 200°.

Table I shows the effect of thermal history on the T_g of citric acid glass. Results indicate that the higher the temperature and the longer the exposure time at a given temperature, the lower the T_g value of citric acid glass. Accompanying this decrease in the T_g value was a progressive discoloration of the molten citric acid from a clear transparent liquid to a yellowish brown liquid.

Aconitic acid[2], a dehydration decomposition product of citric acid, degrades upon melting. By adding the material to citric acid in varying proportions and then preparing glass dispersions of the mixture, it is possible to simulate the effect of degradation product impurities on the T_g of citric acid glass. Figure 1 shows that as the level of impurities increases, the T_g of citric acid glass decreases.

The thermal stability of citric acid has been of concern to previous solid dispersion investigators (6–10, 12). Available thermal analysis literature on citric acid is limited. One study (18) suggests that citric acid may begin to decompose at ~185°, while another study (19) states that thermal degradation of citric acid does not begin to occur until 200–225°. The data presented in this communication indicate that citric acid does exhibit some degree of thermal instability. However, thermal degradation does not appear to begin immediately upon initial melting but only

[1] J. T. Baker Chemical Co., Phillipsburg, N.J.

[2] Aldrich Chemical Co., Milwaukee, Wis.

0022-3549/82/01000-1185$01.00/0

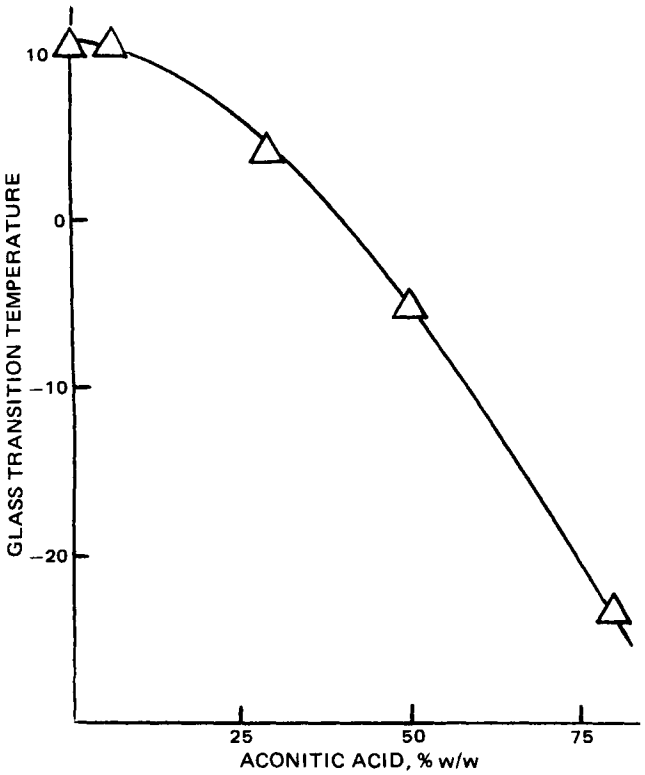

Figure 1—*The effect of aconitic acid on the transition temperature of citric acid glass.*

on prolonged exposure of molten citric acid to temperatures above its melting temperature. It has been shown previously that the sample preparation techniques used in this study did not adversely affect citric acid (12). In addition, the data also imply that low levels of impurities (<5% w/w) cannot be readily detected by DSC.

In preparation of citric acid glass, care should be taken to use the minimum amount of heat necessary to melt the citric acid, to avoid prolonged heating at temperatures of its melting point, and to employ a procedure in which there is some means of temperature control. Although these suggestions for the preparation of citric acid glass may make this material unsuitable for use in the commercial preparation of solid dispersion systems, it should not eliminate the use of this glassy vehicle as a tool for the examination of the compatability, miscibility, and stabilization of the glassy states of materials.

(1) P. Chaudhari and D. Turnbull, *Science*, **199**, 11 (1978).
(2) P. Chaudhari, B. C. Giessen, and D. Turnbull, *Sci. Am.*, **242**, 98 (1980).
(3) W. L. Chiou and S. Riegelman, *J. Pharm. Sci.*, **60**, 1281 (1971).
(4) B. R. Hajratwala, *Aust. J. Pharm. Sci.*, **NS3**, 101 (1974).
(5) J. W. McGinity, *Pharm. Tech.*, **2**, 48 (1978).
(6) W. L. Chiou and S. Riegelman, *J. Pharm. Sci.*, **58**, 1505 (1969).
(7) M. P. Summers and R. P. Enever, *J. Pharm. Pharmacol.*, **26**, 83P (1974).
(8) M. P. Summers and R. P. Enever, *J. Pharm. Sci.*, **65**, 1613 (1976).
(9) *Ibid.*, **66**, 825 (1977).
(10) M. P. Summers, *ibid.*, **67**, 1606 (1978).
(11) J. W. McGinity, D. D. Maness, and G. J. Yakatan, *Drug Dev. Commun.*, **1**, 369 (1974–1975).
(12) R. J. Timko and N. G. Lordi, *J. Pharm. Sci.*, **68**, 601 (1979).
(13) C. E. Nordman, A. S. Weldon, and A. L. Patterson, *Acta Crystallogr.*, **13**, 418 (1960).
(14) G. S. Parks and H. M. Huffman, *J. Phys. Chem.*, **31**, 1842 (1927).
(15) D. Fox, M. M. Labes, and A. Weissberger, Eds., "Physics and Chemistry of the Organic Solid State," vol. 1, Wiley Interscience, New York, N.Y., 1963.
(16) A. R. Ubbelohde, "Melting and Crystal Structure," Oxford University Press, London, England, 1965.
(17) M. P. Summers and R. P. Enever, *J. Pharm. Sci.*, **69**, 612 (1980).
(18) W. W. Wendlandt and J. A. Hoiberg, *Anal. Chim. Acta*, **28**, 506 (1963).
(19) M. T. Saibova, V. K. Bukins, and E. L. Abromova, *Usb. Khim. Zh.*, **9**, 54 (1965); through *Chem. Abstr.*, **63**, 16197c (1965).

Robert J. Timko *
Nicholas G. Lordi [x]
College of Pharmacy
Rutgers—The State University
Piscataway, NJ 08854

Present address: *Ortho Pharmaceutical Corporation, Raritan, NJ 08869.

Received November 27, 1978.
Accepted for publication June 23, 1982.

Dose-Dependent Decrease in Heparin Elimination

Keyphrases □ Heparin—dose-dependent pharmacokinetics □ Pharmacokinetics—dose-dependent decrease in heparin elimination

To the Editor:

Studies on the pharmacokinetics of heparin have revealed dose-dependent (1–4), time-dependent (5), and assay-dependent (4) characteristics. The mechanisms underlying these characteristics are unknown but are likely to reside in the heterogeneity of heparin. Heparin is a natural mammalian glycosaminoglycan consisting of polymeric constituents arranged linearly, with different chain length and chemical composition and with a molecular weight ranging from 3000 to 45,000 (6–8). Recent studies have demonstrated that the antithrombin-III binding site of heparin, which is necessary for its pharmacological action, appears to reside in an oligosaccharide segment of the molecule that has a specific sequence of four to eight monosaccharides, *i.e.*, iduronic and glucuronic acids and glucosamines, with *N*-sulfate, *O*-sulfate, and *N*-acetyl groups being required at specific sites (9–11). The metabolism of heparin is not well understood. Although the metabolic processes involved are thought to include depolymerization and desulfation, the relationship between different metabolic processes and the decline in anticoagulant activity is unclear.

The biologic half-life of heparin increases with increasing dose in humans and animals (1–4). This dose-dependence is without any indication of Michaelis-Menten type kinetic characteristics (3, 4) and recently has been demonstrated in humans to be due to a dose-dependent decrease in the total clearance of the anticoagulant (4). The total clearance of heparin in humans usually is reported to be between 0.5 and 2 ml/min/kg, while the apparent volume of distribution is usually reported to be between 40 and 100 ml/kg (2, 4, 12–14). However, reported values for both of these pharmacokinetic parameters vary widely

0022-3549/82/01000-1186$01.00/0

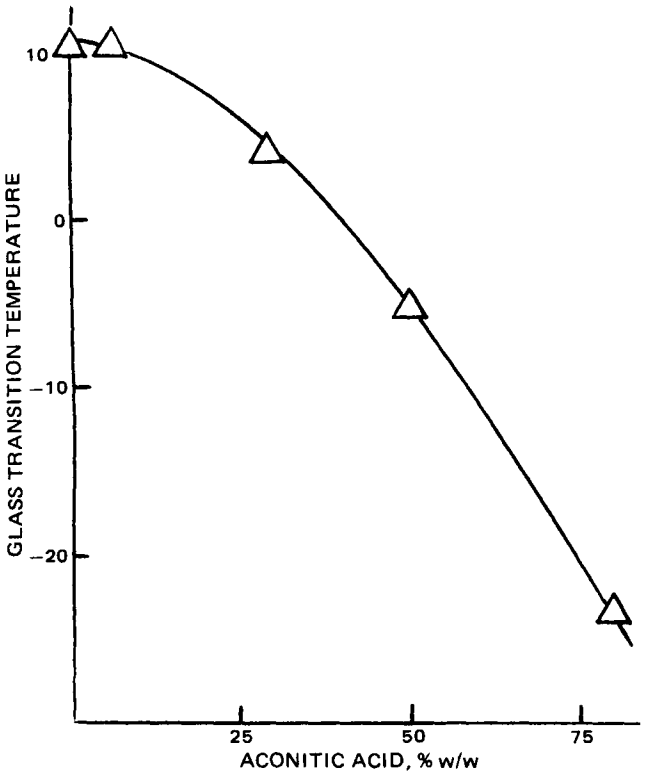

Figure 1—*The effect of aconitic acid on the transition temperature of citric acid glass.*

on prolonged exposure of molten citric acid to temperatures above its melting temperature. It has been shown previously that the sample preparation techniques used in this study did not adversely affect citric acid (12). In addition, the data also imply that low levels of impurities (<5% w/w) cannot be readily detected by DSC.

In preparation of citric acid glass, care should be taken to use the minimum amount of heat necessary to melt the citric acid, to avoid prolonged heating at temperatures of its melting point, and to employ a procedure in which there is some means of temperature control. Although these suggestions for the preparation of citric acid glass may make this material unsuitable for use in the commercial preparation of solid dispersion systems, it should not eliminate the use of this glassy vehicle as a tool for the examination of the compatability, miscibility, and stabilization of the glassy states of materials.

(1) P. Chaudhari and D. Turnbull, *Science*, **199**, 11 (1978).
(2) P. Chaudhari, B. C. Giessen, and D. Turnbull, *Sci. Am.*, **242**, 98 (1980).
(3) W. L. Chiou and S. Riegelman, *J. Pharm. Sci.*, **60**, 1281 (1971).
(4) B. R. Hajratwala, *Aust. J. Pharm. Sci.*, **NS3**, 101 (1974).
(5) J. W. McGinity, *Pharm. Tech.*, **2**, 48 (1978).
(6) W. L. Chiou and S. Riegelman, *J. Pharm. Sci.*, **58**, 1505 (1969).
(7) M. P. Summers and R. P. Enever, *J. Pharm. Pharmacol.*, **26**, 83P (1974).
(8) M. P. Summers and R. P. Enever, *J. Pharm. Sci.*, **65**, 1613 (1976).
(9) *Ibid.*, **66**, 825 (1977).
(10) M. P. Summers, *ibid.*, **67**, 1606 (1978).
(11) J. W. McGinity, D. D. Maness, and G. J. Yakatan, *Drug Dev. Commun.*, **1**, 369 (1974–1975).
(12) R. J. Timko and N. G. Lordi, *J. Pharm. Sci.*, **68**, 601 (1979).
(13) C. E. Nordman, A. S. Weldon, and A. L. Patterson, *Acta Crystallogr.*, **13**, 418 (1960).
(14) G. S. Parks and H. M. Huffman, *J. Phys. Chem.*, **31**, 1842 (1927).
(15) D. Fox, M. M. Labes, and A. Weissberger, Eds., "Physics and Chemistry of the Organic Solid State," vol. 1, Wiley Interscience, New York, N.Y., 1963.
(16) A. R. Ubbelohde, "Melting and Crystal Structure," Oxford University Press, London, England, 1965.
(17) M. P. Summers and R. P. Enever, *J. Pharm. Sci.*, **69**, 612 (1980).
(18) W. W. Wendlandt and J. A. Hoiberg, *Anal. Chim. Acta*, **28**, 506 (1963).
(19) M. T. Saibova, V. K. Bukins, and E. L. Abromova, *Usb. Khim. Zh.*, **9**, 54 (1965); through *Chem. Abstr.*, **63**, 16197c (1965).

Robert J. Timko *
Nicholas G. Lordi [x]
College of Pharmacy
Rutgers—The State University
Piscataway, NJ 08854

Present address: *Ortho Pharmaceutical Corporation, Raritan, NJ 08869.

Received November 27, 1978.
Accepted for publication June 23, 1982.

Dose-Dependent Decrease in Heparin Elimination

Keyphrases □ Heparin—dose-dependent pharmacokinetics □ Pharmacokinetics—dose-dependent decrease in heparin elimination

To the Editor:

Studies on the pharmacokinetics of heparin have revealed dose-dependent (1–4), time-dependent (5), and assay-dependent (4) characteristics. The mechanisms underlying these characteristics are unknown but are likely to reside in the heterogeneity of heparin. Heparin is a natural mammalian glycosaminoglycan consisting of polymeric constituents arranged linearly, with different chain length and chemical composition and with a molecular weight ranging from 3000 to 45,000 (6–8). Recent studies have demonstrated that the antithrombin-III binding site of heparin, which is necessary for its pharmacological action, appears to reside in an oligosaccharide segment of the molecule that has a specific sequence of four to eight monosaccharides, *i.e.*, iduronic and glucuronic acids and glucosamines, with *N*-sulfate, *O*-sulfate, and *N*-acetyl groups being required at specific sites (9–11). The metabolism of heparin is not well understood. Although the metabolic processes involved are thought to include depolymerization and desulfation, the relationship between different metabolic processes and the decline in anticoagulant activity is unclear.

The biologic half-life of heparin increases with increasing dose in humans and animals (1–4). This dose-dependence is without any indication of Michaelis-Menten type kinetic characteristics (3, 4) and recently has been demonstrated in humans to be due to a dose-dependent decrease in the total clearance of the anticoagulant (4). The total clearance of heparin in humans usually is reported to be between 0.5 and 2 ml/min/kg, while the apparent volume of distribution is usually reported to be between 40 and 100 ml/kg (2, 4, 12–14). However, reported values for both of these pharmacokinetic parameters vary widely

0022-3549/82/01000-1186$01.00/0

among studies. Although this variability in part may be due to the nonlinearity in the elimination kinetics of heparin, it is in part due to differences in heparin assay methods used, since recent studies in humans have shown that there are significant differences among values of individual pharmacokinetic parameters obtained, depending on heparin assay methodology (4). This applies primarily to total clearance and apparent volume of distribution, both of which were on the average ~1.5- to twofold larger when based on hexadimethrine bromide[1] neutralization assay of heparin than when based on bioassays using the coagulation tests activated partial thromboplastin time and thrombin clotting time. However, no significant differences were noted in values of biologic half-life. The immediate practical consequences of the assay-dependent pharmacokinetics of heparin are that when summarizing published pharmacokinetic parameters for heparin, the assay methods have to be specified, and only data obtained by the same heparin assay can be treated together. This becomes particularly important when exploring relationships between dose and individual pharmacokinetic parameters of heparin. Two studies have been published on heparin pharmacokinetics in normal subjects using heparin assays based on thrombin-induced clotting times, with doses ranging from 50 to 400 U/kg (1, 4). Therefore, it was of interest to use data from these two studies to explore relationships between dose and pharmacokinetic parameters of heparin, particularly since one of the studies had not provided values for the latter.

The subjects studied in these two studies were four healthy males, ages 27–35 years, who received intravenous injections of heparin of 50 and 75 U/kg body weight each (4), and six healthy males and seven healthy females, ages 19–45 years, who received intravenous injections of heparin of either 100 (five subjects), 200 (four subjects), or 400 (four subjects) U/kg body weight (1). Multiple blood samples were collected after each dose, and plasma heparin activity was determined by bioassays based on thrombin clotting time. These assays are described in detail elsewhere (4, 15). They involve first establishing the relationship between the thrombin-induced clotting times and heparin added to plasma *in vitro*, and then deriving the plasma heparin activity in the samples obtained after the dose from the observed clotting times. One of these assays uses addition of bovine plasma to the plasma sample (15). While this will attenuate intersubject differences in the relationship between clotting time and added heparin, it will not affect the determination of heparin activity in plasma. It should be noted that the relationship between thrombin-induced clotting times and heparin activity in plasma is log linear (4, 15, 16).

The pharmacokinetic parameters, biologic half-life ($t_{1/2}$), total clearance (Cl), and apparent volume of distribution (V_d), were calculated as described previously (4). As is shown in Fig. 1, the biologic half-life of heparin increases with increasing dose. The average ($\pm SD$) $t_{1/2}$ values for the 50, 75, 100, 200, and 400 U/kg doses were 42 ± 5, 49 ± 15, 57 ± 8, 96 ± 10, and 153 ± 10 min, respectively. The positive relationship between the biologic half-life and dose of heparin is statistically highly significant ($p < 0.001$).

[1] Polybrene.

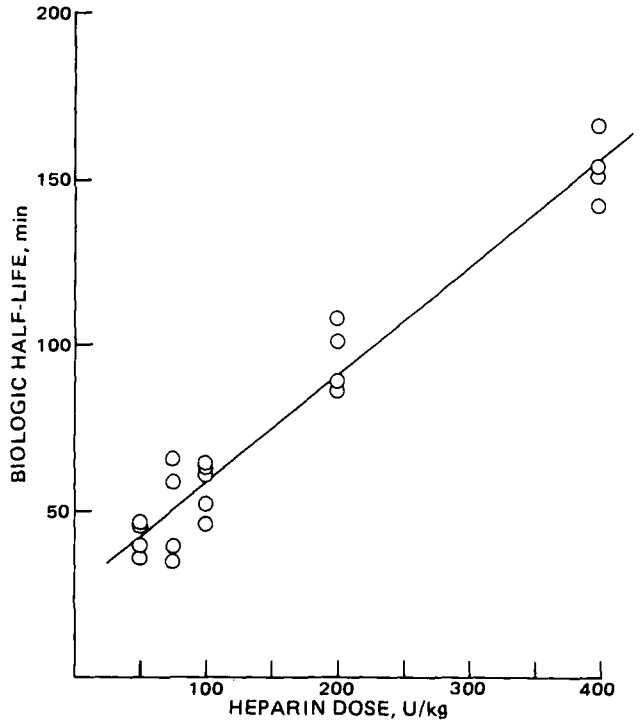

Figure 1—*Relationship between biologic half-life and dose of heparin in humans when heparin activity in plasma is determined by a bioassay based on thrombin-induced clotting times. (Data are from Refs. 1 and 4). The line represents the best-fitted line for the relationship between these parameters (intercept, 26.2 min; slope, 0.323 min kg U^{-1}; r^2 = 0.952).*

Figure 2 shows that there is also a statistically highly significant positive linear relationship between the biologic half-life and total clearance of heparin ($p < 0.001$). The

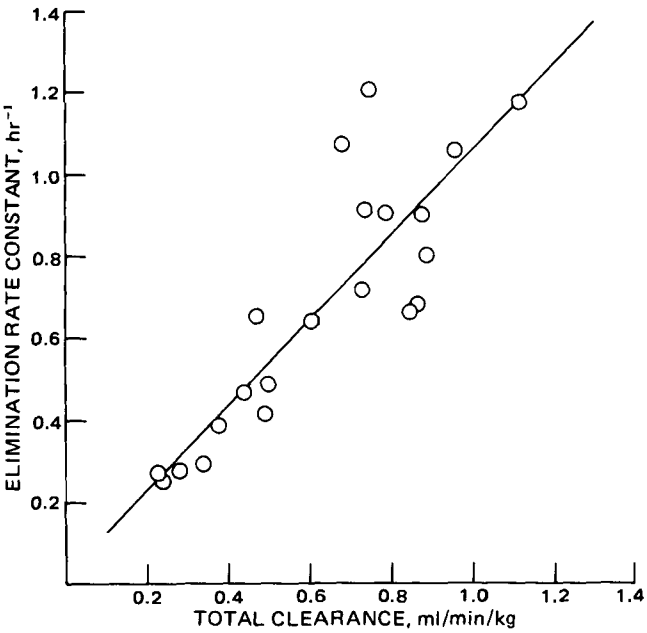

Figure 2—*Relationship between the elimination rate constant and total clearance of heparin in humans when heparin activity in plasma is determined by a bioassay based on thrombin-induced clotting times. (Data are from Refs. 1 and 4.) The line represents the best-fitted line for the relationship between these parameters (intercept, 0.030 hr^{-1}; slope, 1.025 t ml^{-1} kg^{-1}, where t is a time unit correction factor; r^2 = 0.739).*

total clearance of heparin ranged from 0.23 to 1.12 ml/min/kg for the 400 and 50 U/kg doses, respectively, representing about a fivefold variation in total clearance for eightfold difference in dose. The reason for this linear positive relationship is that the apparent volume of distribution of heparin changes only very modestly with dose. The average ($\pm SD$) V_d was 58 ± 11 ml/kg body weight over the entire dose range, with small but statistically insignificant changes in V_d when it was evaluated with respect to dose (intercept, 55 ml/kg; slope, 0.018 ml/kg/U; r^2 = 0.046).

The results presented in this report are in support of and extend recent findings that the dose-dependent increase in the biologic half-life of heparin in humans is due to a dose-dependent decrease in the total clearance of the anticoagulant (4). In humans, there is no significant increase in the apparent volume of distribution of heparin with dose. This is in contrast to findings in rats and dogs, which have shown a dose-dependent increase in V_d with dose (2, 3). While the mechanism underlying the nonlinear pharmacokinetics of heparin in humans is presently not understood, however, the linear relationship between dose and dose-dependent pharmacokinetic parameters is noteworthy.

(1) P. Olsson, H. Lagergren, and S. Ek, *Acta Med. Scand.*, **173**, 619 (1963).

(2) J. W. Estes, E. W. Pelikan, and E. Kruger-Thiemer, *Clin. Pharmacol. Ther.*, **10**, 329 (1969).

(3) T. D. Bjornsson and G. Levy, *J. Pharmacol. Exp. Ther.*, **210**, 237 (1979).

(4) T. D. Bjornsson, K. M. Wolfram, and B. B. Kitchell, *Clin. Pharmacol. Ther.*, **31**, 104 (1982).

(5) T. D. Bjornsson and G. Levy, *J. Pharmacol. Exp. Ther.*, **210**, 243 (1979).

(6) H. B. Nader, H. M. McDuffie, and C. P. Dietrich, *Biochem. Biophys. Res. Commun.*, **57**, 488 (1974).

(7) U. Lindahl and M. Hook, *Annu. Rev. Biochem.*, **47**, 385 (1978).

(8) L. Jaques, *Pharmacol. Rev.*, **31**, 99 (1979).

(9) R. D. Rosenberg, G. M. Oosta, R. E. Jordan, and W. T. Gardner, in "Chemistry and Biology of Heparin," R. L. Lundblad, W. V. Brown, K. G. Mann, and H. R. Roberts, Eds., Elsevier/North Holland, New York, N.Y., 1981, p. 249.

(10) M. Hook, L. Thunberg, J. Riesenfeld, G. Backstrom, I. Pattersson, and U. Lindahl, in "Chemistry and Biology of Heparin," R. L. Lundblad, W. V. Brown, K. G. Mann, and H. R. Roberts, Eds., Elsevier/North Holland, New York, N.Y., 1981, p. 271.

(11) J. Choay, J. C. Lormeau, M. Petitou, P. Sinay, and J. Fareed, *Ann. N.Y. Acad. Sci.*, **370**, 644 (1981).

(12) R. J. Cipolle, R. D. Seifert, B. A. Neilan, D. E. Zaske, and E. Haus, *Clin. Pharmacol. Ther.*, **29**, 387 (1981).

(13) J. Hirsh, W. G. Van Aken, A. S. Gallus, C. T. Dollery, J. F. Cade, and W. L. Yung, *Circulation*, **53**, 691 (1976).

(14) T. L. Simon, T. M. Hyers, J. P. Gaston, and L. A. Harker, *Br. J. Haematol.*, **39**, 111 (1978).

(15) M. Blomback, B. Blomback, P. Olsson, G. William-Olsson, and A. Senning, *Acta Chir. Scand., Suppl.*, **245**, 259 (1959).

(16) T. D. Bjornsson and K. M. Wolfram, *Eur. J. Clin. Pharmacol.*, **21**, 491 (1982).

Thorir D. Bjornsson

Division of Clinical Pharmacology
Departments of Pharmacology and Medicine
Duke University Medical Center
Durham, NC 27710

Received June 1, 1982.

Accepted for publication July 14, 1982.

Supported by Grant No. HL24343 from the National Institutes of Health.

Thorir D. Bjornsson is a Nanaline Duke Scholar and a recipient of a Pharmaceutical Manufacturers Association Foundation Faculty Development Award in Clinical Pharmacology.

Renal Excretion of *R*- and *S*-Epimers of Moxalactam in Dogs

Keyphrases □ Stereoisomers—arylmalonylamino 1-oxacephem, renal clearance, dog, plasma protein binding □ Renal clearance—arylmalonylamino 1-oxacephem, comparison between stereoisomers, relation to plasma protein binding □ Protein binding—dog plasma, arylmalonylamino 1-oxacephem, comparison between stereoisomers, relation to renal clearance

To the Editor:

Moxalactam[1] (latamoxef[2], I) is a mixture of *R* (II) and *S* (III) epimers, and both forms are usually eliminated unchanged by the kidney (1, 2). Studies with humans (3) show that the biological half-life of the *R*-epimer is shorter than that of the *S*-epimer. To obtain a better understanding of the elimination kinetics, we studied the renal clearance and binding of moxalactam epimers to plasma protein in beagle dogs.

Two male beagle dogs were anesthetized with sodium pentobarbital (30 mg/kg iv). After a tracheotomy was performed, an incision was made in the left flank. The retroperitoneal space was explored and the left ureter was cannulated. Urine was collected through the cannula (4). After completion of the operation, 20 mg of sodium *p*-aminohippurate/kg and 100 mg of creatinine/kg were injected as the priming dose into the axillary vein. As the sustaining dose, a solution containing 15% mannitol, 0.9% NaCl, 0.25% creatinine, and 0.1% sodium *p*-aminohippurate was injected at the rate of 5 ml/min/10 kg. Moxalactam[3] was injected at a priming dose of 10 mg/kg followed by a sustaining dose of 5.0 mg/kg/hr. Approximately 1 hr after beginning the infusion, the urinary output was stabilized at 3–5 ml/min and urine samples were collected three or four times from the left ureter at 3-min intervals. Blood samples were taken at the middle point of each clearance period. The same procedure was repeated in the presence of probenecid (30 mg/kg iv). Collected urine and plasma samples were analyzed for creatinine (5), *p*-ami-

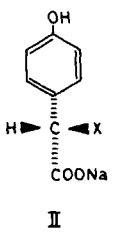

II

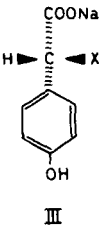

III

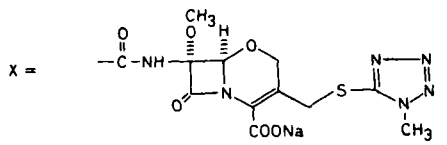

[1] United States Adopted Name (USAN).
[2] International Nonproprietary Name (INN), 6059-S.
[3] Shionogi & Co., Ltd., Osaka, Japan.

0022-3549/82/01000-1188$01.00/0

total clearance of heparin ranged from 0.23 to 1.12 ml/min/kg for the 400 and 50 U/kg doses, respectively, representing about a fivefold variation in total clearance for eightfold difference in dose. The reason for this linear positive relationship is that the apparent volume of distribution of heparin changes only very modestly with dose. The average ($\pm SD$) V_d was 58 ± 11 ml/kg body weight over the entire dose range, with small but statistically insignificant changes in V_d when it was evaluated with respect to dose (intercept, 55 ml/kg; slope, 0.018 ml/kg/U; r^2 = 0.046).

The results presented in this report are in support of and extend recent findings that the dose-dependent increase in the biologic half-life of heparin in humans is due to a dose-dependent decrease in the total clearance of the anticoagulant (4). In humans, there is no significant increase in the apparent volume of distribution of heparin with dose. This is in contrast to findings in rats and dogs, which have shown a dose-dependent increase in V_d with dose (2, 3). While the mechanism underlying the nonlinear pharmacokinetics of heparin in humans is presently not understood, however, the linear relationship between dose and dose-dependent pharmacokinetic parameters is noteworthy.

(1) P. Olsson, H. Lagergren, and S. Ek, *Acta Med. Scand.*, **173**, 619 (1963).

(2) J. W. Estes, E. W. Pelikan, and E. Kruger-Thiemer, *Clin. Pharmacol. Ther.*, **10**, 329 (1969).

(3) T. D. Bjornsson and G. Levy, *J. Pharmacol. Exp. Ther.*, **210**, 237 (1979).

(4) T. D. Bjornsson, K. M. Wolfram, and B. B. Kitchell, *Clin. Pharmacol. Ther.*, **31**, 104 (1982).

(5) T. D. Bjornsson and G. Levy, *J. Pharmacol. Exp. Ther.*, **210**, 243 (1979).

(6) H. B. Nader, H. M. McDuffie, and C. P. Dietrich, *Biochem. Biophys. Res. Commun.*, **57**, 488 (1974).

(7) U. Lindahl and M. Hook, *Annu. Rev. Biochem.*, **47**, 385 (1978).

(8) L. Jaques, *Pharmacol. Rev.*, **31**, 99 (1979).

(9) R. D. Rosenberg, G. M. Oosta, R. E. Jordan, and W. T. Gardner, in "Chemistry and Biology of Heparin," R. L. Lundblad, W. V. Brown, K. G. Mann, and H. R. Roberts, Eds., Elsevier/North Holland, New York, N.Y., 1981, p. 249.

(10) M. Hook, L. Thunberg, J. Riesenfeld, G. Backstrom, I. Pattersson, and U. Lindahl, in "Chemistry and Biology of Heparin," R. L. Lundblad, W. V. Brown, K. G. Mann, and H. R. Roberts, Eds., Elsevier/North Holland, New York, N.Y., 1981, p. 271.

(11) J. Choay, J. C. Lormeau, M. Petitou, P. Sinay, and J. Fareed, *Ann. N.Y. Acad. Sci.*, **370**, 644 (1981).

(12) R. J. Cipolle, R. D. Seifert, B. A. Neilan, D. E. Zaske, and E. Haus, *Clin. Pharmacol. Ther.*, **29**, 387 (1981).

(13) J. Hirsh, W. G. Van Aken, A. S. Gallus, C. T. Dollery, J. F. Cade, and W. L. Yung, *Circulation*, **53**, 691 (1976).

(14) T. L. Simon, T. M. Hyers, J. P. Gaston, and L. A. Harker, *Br. J. Haematol.*, **39**, 111 (1978).

(15) M. Blomback, B. Blomback, P. Olsson, G. William-Olsson, and A. Senning, *Acta Chir. Scand., Suppl.*, **245**, 259 (1959).

(16) T. D. Bjornsson and K. M. Wolfram, *Eur. J. Clin. Pharmacol.*, **21**, 491 (1982).

Thorir D. Bjornsson

Division of Clinical Pharmacology
Departments of Pharmacology and Medicine
Duke University Medical Center
Durham, NC 27710

Received June 1, 1982.

Accepted for publication July 14, 1982.

Supported by Grant No. HL24343 from the National Institutes of Health.

Thorir D. Bjornsson is a Nanaline Duke Scholar and a recipient of a Pharmaceutical Manufacturers Association Foundation Faculty Development Award in Clinical Pharmacology.

Renal Excretion of *R*- and *S*-Epimers of Moxalactam in Dogs

Keyphrases □ Stereoisomers—arylmalonylamino 1-oxacephem, renal clearance, dog, plasma protein binding □ Renal clearance—arylmalonylamino 1-oxacephem, comparison between stereoisomers, relation to plasma protein binding □ Protein binding—dog plasma, arylmalonylamino 1-oxacephem, comparison between stereoisomers, relation to renal clearance

To the Editor:

Moxalactam[1] (latamoxef[2], I) is a mixture of *R* (II) and *S* (III) epimers, and both forms are usually eliminated unchanged by the kidney (1, 2). Studies with humans (3) show that the biological half-life of the *R*-epimer is shorter than that of the *S*-epimer. To obtain a better understanding of the elimination kinetics, we studied the renal clearance and binding of moxalactam epimers to plasma protein in beagle dogs.

Two male beagle dogs were anesthetized with sodium pentobarbital (30 mg/kg iv). After a tracheotomy was performed, an incision was made in the left flank. The retroperitoneal space was explored and the left ureter was cannulated. Urine was collected through the cannula (4). After completion of the operation, 20 mg of sodium *p*-aminohippurate/kg and 100 mg of creatinine/kg were injected as the priming dose into the axillary vein. As the sustaining dose, a solution containing 15% mannitol, 0.9% NaCl, 0.25% creatinine, and 0.1% sodium *p*-aminohippurate was injected at the rate of 5 ml/min/10 kg. Moxalactam[3] was injected at a priming dose of 10 mg/kg followed by a sustaining dose of 5.0 mg/kg/hr. Approximately 1 hr after beginning the infusion, the urinary output was stabilized at 3–5 ml/min and urine samples were collected three or four times from the left ureter at 3-min intervals. Blood samples were taken at the middle point of each clearance period. The same procedure was repeated in the presence of probenecid (30 mg/kg iv). Collected urine and plasma samples were analyzed for creatinine (5), *p*-ami-

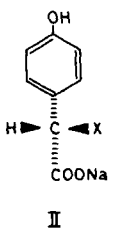

II

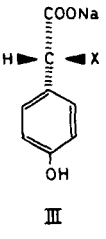

III

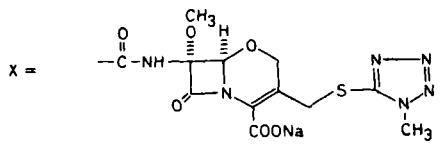

[1] United States Adopted Name (USAN).
[2] International Nonproprietary Name (INN), 6059-S.
[3] Shionogi & Co., Ltd., Osaka, Japan.

0022-3549/82/01000-1188$01.00/0

Table I—Renal Clearance (ml/min/kidney) of *R*- and *S*-Epimers of Moxalactam in Anesthetized Male Beagle Dogs

	Dog 1		Dog 2	
	Control phase[a]	Probenecid phase[b]	Control phase[a]	Probenecid phase[a]
Apparent clearances				
R-epimer, total	16.29 ± 0.68[a]	10.81 ± 0.17[b]	17.32 ± 1.18	15.90 ± 0.58
S-epimer, total	9.21 ± 0.52	6.97 ± 0.85[b]	10.48 ± 0.43	10.76 ± 0.25
Clearance ratio *R*/*S*, I	1.81 ± 0.11	1.59 ± 0.19[b]	1.66 ± 0.10	1.48 ± 0.07
Corrected clearances				
R-epimer, 23.7% binding	21.73 ± 0.74	14.19 ± 0.20[b]	22.57 ± 1.55	20.01 ± 0.26
S-epimer, 44.9% binding	16.68 ± 0.95	12.67 ± 1.56[b]	19.03 ± 0.82	19.52 ± 0.44
Clearance ratio *R*/*S*, II	1.32 ± 0.09	1.16 ± 0.14[b]	1.19 ± 0.07	1.07 ± 0.05
Statistical differences[c] of *R*/*S* values between I (total) and II (unbound)	$p < 0.05$	NS	$p < 0.01$	$p < 0.01$
Glomerular filtration rate (Creatinine clearance)	18.16 ± 0.19	14.33 ± 0.88[b]	18.67 ± 0.37	17.04 ± 0.44

[a] Value represents mean ± *SE* (number of samples: $n = 4$). [b] Number of samples: $n = 3$. [c] Student's t test.

nohippuric acid (6), and moxalactam (7). The ratios of *R*- to *S*-epimer in plasma and urine were determined using high-performance liquid chromatography (8). The fractions of the *R*- and *S*-epimers of moxalactam bound to dog plasma were determined at 37° by an ultrafiltration method[4].

The renal clearances of the moxalactam epimers in Table I were calculated by dividing the urinary excretion (micrograms per milliliter) by the total (bound and unbound) concentrations of the epimers. Clearance of the *R*-epimer was 1.4–1.8 times that of the *S*-epimer. The clearance ratios of *R*- and *S*-epimers to creatinine were less than unity. Since only unbound moxalactam would have been available for glomerular filtration, the clearance value based on the total concentration of the epimer in plasma may be underestimated. To determine the actual glomerular filtration, the protein binding of moxalactam epimers was determined at concentrations of 25, 50, and 100 μg/ml of dog plasma. The mean percentage of the bound fraction calculated from these values was 23.7 ± 1.6% *SEM* ($n = 3$) for the *R*-form and 44.9 ± 0.4% ($n = 3$) for the *S*-form.

As indicated in Table I, the data were corrected for the binding of the *R*- and *S*-epimers, *e.g.*, the clearances were calculated by dividing the urinary excretion (micrograms per minute) by the concentrations of the unbound epimers. The calculated renal clearances of the epimers were nearly equal to the glomerular filtration rate (creatinine clearance) and the *R*-epimer/*S*-epimer clearance ratio was closer to unity. When probenecid was given to Dog 1, the *p*-aminohippurate clearance decreased from 55.3 ± 0.6 to 17.0 ± 1.0 ml/min/kidney (mean ± standard error, $n = 3$), but the *R*- or *S*-epimer/creatinine clearance ratio was not affected.

Stereospecific differences in protein binding have been reported for other drugs (9–12) and vary from one animal species to another (3, 13). Our findings indicate that in the dog, both epimers of moxalactam are excreted by glomerular filtration, and the striking difference in renal clearance of the *R*- and *S*-epimers is due mainly to differences in binding to plasma protein.

(1) J. N. Parson, J. M. Romano, and M. E. Levison, *Antimicrob. Agents Chemother.*, **17**, 226 (1980).

(2) J. Shimada, Y. Ueda, T. Yamaji, Y. Abe, and M. Nakamura, in "Current Chemotherapy and Infectious Disease," Proceedings of the 11th ICC and the 19th ICAAC, American Society of Microbiology, 1980, p. 109.

(3) H. Yamada, T. Ichihashi, K. Hirano, and H. Kinoshita, *J. Pharm. Sci.*, **70**, 112 (1981).

(4) T. Higashio, Y. Abe, and K. Yamamoto, *J. Pharmacol. Exp. Ther.*, **207**, 212 (1978).

(5) A. L. Chasson, H. T. Grady, and M. A. Stanly, *Am. J. Clin. Pathol.*, **35**, 83 (1961).

(6) H. W. Smith, N. Finkelstein, L. Aliminosa, B. Crawford, and M. Graber, *J. Clin. Invest.*, **24**, 338 (1945).

(7) T. Yoshida, S. Matsuura, M. Mayama, Y. Kameda, and S. Kuwahara, *Antimicrob. Agents Chemother.*, **17**, 302 (1980).

(8) R. Konaka, K. Kuruma, R. Nishimura, Y. Kimura, and T. Yoshida, *J. Chromatogr.*, **225**, 169 (1981).

(9) W. E. Müller and U. Wollert, *Mol. Pharmacol.*, **11**, 52 (1975).

(10) W. Schmit and E. Jähnchen, *Experientia*, **34**, 1323 (1978).

(11) D. T. Witiak and M. W. Whitehouse, *Biochem. Pharmacol.*, **18**, 971 (1969).

(12) A. Yacobi and G. Levy, *J. Pharmacokinet. Biopharm.*, **5**, 123 (1977).

(13) H. Yamada, Y. Ichihashi, K. Hirano, and H. Kinoshita, *J. Pharm. Sci.*, **70**, 113 (1981).

M. Nakamura[x]
K. Sugeno
R. Konaka
H. Yamada
T. Yoshida
Shionogi Research Laboratories
Shionogi & Co., Ltd.
Fukushima-ku, Osaka 553, Japan

Received May 18, 1981.
Accepted for publication May 12, 1982.
The authors thank Dr. Jingoro Shimada, Jikei University School of Medicine, for his helpful comments and Mr. Tomoji Kawabata for his technical assistance.

[4] Centriflo CF25, Amicon Corp., Lexington, Mass.

Effect of Ascorbic Acid on Renal Excretion of Lead in the Rat

Keyphrases □ Ascorbic acid—effect on renal excretion of lead, rats □ Lead—effect of ascorbic acid on renal excretion, rats □ Renal excretion—effect of ascorbic acid, lead, rats

To the Editor:

Lead poisoning is currently treated by chelation therapy using edetate disodium and dimercaprol, both of which have serious side effects. Few studies have been carried out

0022-3549/82/01000-1189$01.00/0

Table I—Renal Clearance (ml/min/kidney) of *R*- and *S*-Epimers of Moxalactam in Anesthetized Male Beagle Dogs

	Dog 1		Dog 2	
	Control phase[a]	Probenecid phase[b]	Control phase[a]	Probenecid phase[a]
Apparent clearances				
R-epimer, total	16.29 ± 0.68[a]	10.81 ± 0.17[b]	17.32 ± 1.18	15.90 ± 0.58
S-epimer, total	9.21 ± 0.52	6.97 ± 0.85[b]	10.48 ± 0.43	10.76 ± 0.25
Clearance ratio *R*/*S*, I	1.81 ± 0.11	1.59 ± 0.19[b]	1.66 ± 0.10	1.48 ± 0.07
Corrected clearances				
R-epimer, 23.7% binding	21.73 ± 0.74	14.19 ± 0.20[b]	22.57 ± 1.55	20.01 ± 0.26
S-epimer, 44.9% binding	16.68 ± 0.95	12.67 ± 1.56[b]	19.03 ± 0.82	19.52 ± 0.44
Clearance ratio *R*/*S*, II	1.32 ± 0.09	1.16 ± 0.14[b]	1.19 ± 0.07	1.07 ± 0.05
Statistical differences[c] of *R*/*S* values between I (total) and II (unbound)	$p < 0.05$	NS	$p < 0.01$	$p < 0.01$
Glomerular filtration rate (Creatinine clearance)	18.16 ± 0.19	14.33 ± 0.88[b]	18.67 ± 0.37	17.04 ± 0.44

[a] Value represents mean ± *SE* (number of samples: $n = 4$). [b] Number of samples: $n = 3$. [c] Student's t test.

nohippuric acid (6), and moxalactam (7). The ratios of *R*- to *S*-epimer in plasma and urine were determined using high-performance liquid chromatography (8). The fractions of the *R*- and *S*-epimers of moxalactam bound to dog plasma were determined at 37° by an ultrafiltration method[4].

The renal clearances of the moxalactam epimers in Table I were calculated by dividing the urinary excretion (micrograms per milliliter) by the total (bound and unbound) concentrations of the epimers. Clearance of the *R*-epimer was 1.4–1.8 times that of the *S*-epimer. The clearance ratios of *R*- and *S*-epimers to creatinine were less than unity. Since only unbound moxalactam would have been available for glomerular filtration, the clearance value based on the total concentration of the epimer in plasma may be underestimated. To determine the actual glomerular filtration, the protein binding of moxalactam epimers was determined at concentrations of 25, 50, and 100 μg/ml of dog plasma. The mean percentage of the bound fraction calculated from these values was 23.7 ± 1.6% *SEM* ($n = 3$) for the *R*-form and 44.9 ± 0.4% ($n = 3$) for the *S*-form.

As indicated in Table I, the data were corrected for the binding of the *R*- and *S*-epimers, *e.g.*, the clearances were calculated by dividing the urinary excretion (micrograms per minute) by the concentrations of the unbound epimers. The calculated renal clearances of the epimers were nearly equal to the glomerular filtration rate (creatinine clearance) and the *R*-epimer/*S*-epimer clearance ratio was closer to unity. When probenecid was given to Dog 1, the *p*-aminohippurate clearance decreased from 55.3 ± 0.6 to 17.0 ± 1.0 ml/min/kidney (mean ± standard error, $n = 3$), but the *R*- or *S*-epimer/creatinine clearance ratio was not affected.

Stereospecific differences in protein binding have been reported for other drugs (9–12) and vary from one animal species to another (3, 13). Our findings indicate that in the dog, both epimers of moxalactam are excreted by glomerular filtration, and the striking difference in renal clearance of the *R*- and *S*-epimers is due mainly to differences in binding to plasma protein.

(1) J. N. Parson, J. M. Romano, and M. E. Levison, *Antimicrob. Agents Chemother.*, **17**, 226 (1980).

(2) J. Shimada, Y. Ueda, T. Yamaji, Y. Abe, and M. Nakamura, in "Current Chemotherapy and Infectious Disease," Proceedings of the 11th ICC and the 19th ICAAC, American Society of Microbiology, 1980, p. 109.

(3) H. Yamada, T. Ichihashi, K. Hirano, and H. Kinoshita, *J. Pharm. Sci.*, **70**, 112 (1981).

(4) T. Higashio, Y. Abe, and K. Yamamoto, *J. Pharmacol. Exp. Ther.*, **207**, 212 (1978).

(5) A. L. Chasson, H. T. Grady, and M. A. Stanly, *Am. J. Clin. Pathol.*, **35**, 83 (1961).

(6) H. W. Smith, N. Finkelstein, L. Aliminosa, B. Crawford, and M. Graber, *J. Clin. Invest.*, **24**, 338 (1945).

(7) T. Yoshida, S. Matsuura, M. Mayama, Y. Kameda, and S. Kuwahara, *Antimicrob. Agents Chemother.*, **17**, 302 (1980).

(8) R. Konaka, K. Kuruma, R. Nishimura, Y. Kimura, and T. Yoshida, *J. Chromatogr.*, **225**, 169 (1981).

(9) W. E. Müller and U. Wollert, *Mol. Pharmacol.*, **11**, 52 (1975).

(10) W. Schmit and E. Jähnchen, *Experientia*, **34**, 1323 (1978).

(11) D. T. Witiak and M. W. Whitehouse, *Biochem. Pharmacol.*, **18**, 971 (1969).

(12) A. Yacobi and G. Levy, *J. Pharmacokinet. Biopharm.*, **5**, 123 (1977).

(13) H. Yamada, Y. Ichihashi, K. Hirano, and H. Kinoshita, *J. Pharm. Sci.*, **70**, 113 (1981).

M. Nakamura[x]
K. Sugeno
R. Konaka
H. Yamada
T. Yoshida
Shionogi Research Laboratories
Shionogi & Co., Ltd.
Fukushima-ku, Osaka 553, Japan

Received May 18, 1981.
Accepted for publication May 12, 1982.
The authors thank Dr. Jingoro Shimada, Jikei University School of Medicine, for his helpful comments and Mr. Tomoji Kawabata for his technical assistance.

[4] Centriflo CF25, Amicon Corp., Lexington, Mass.

Effect of Ascorbic Acid on Renal Excretion of Lead in the Rat

Keyphrases □ Ascorbic acid—effect on renal excretion of lead, rats □ Lead—effect of ascorbic acid on renal excretion, rats □ Renal excretion—effect of ascorbic acid, lead, rats

To the Editor:

Lead poisoning is currently treated by chelation therapy using edetate disodium and dimercaprol, both of which have serious side effects. Few studies have been carried out

0022-3549/82/01000-1189$01.00/0

on the use of natural compounds such as ascorbic acid to remove heavy metals from the body, and these few studies and anecdotal observations have not provided any direct evidence for ascorbic acid on the excretion of lead from the body (1–4).

In the present communication we report a direct effect of ascorbic acid on the excretion profile of lead in the rat. The control group of rats (weight 300–450 g) were given demineralized water for 4 weeks; the treatment group received 4% ascorbic acid (pH 7.4) as drinking water. Food was given *ad libitum* to both groups ($n = 16$). Lead was administered as lead acetate solution in 5% dextrose intravenously at a dose of 0.637 μg of lead/g of body weight. The treatment group also received a bolus dose of ascorbic acid (1 mg/g of body weight) following administration of lead acetate solution. This was followed by 0.25 mg of ascorbic acid/g of body weight given subcutaneously every 6 hr. The blood samples were collected from the tail vein periodically for up to 163 hr, and urine samples were collected in 24-hr pools for up to 1 week. All samples were analyzed for total lead using a flameless atomic absorption spectrophotometer with graphite furnace[1].

The initial blood levels in the treatment group were higher than the control in accordance with previous findings (3). The urinary clearance of lead was calculated from the plots of blood concentration (C_b) against the urinary excretion (X_u) rate:

$$\text{Control: } \frac{dX_u}{dt} = 0.0049 + 0.1932\ C_b \quad (r > 0.92) \qquad \text{(Eq. 1)}$$

$$\text{Treatment: } \frac{dX_u}{dt} = -0.02089 + 0.4261\ C_b \quad (r > 0.99) \qquad \text{(Eq. 2)}$$

[1] Atomic Absorption Spectrophotometer model 503, Perkin-Elmer, Norwalk, Conn.

The good linear correlation coefficient signifies the relationship between blood concentration and the urinary excretion according to clearance principles; the slopes of Eqs. 1 and 2 were statistically different ($p < 0.05$). An increase of almost 120% in the urinary clearance of lead was recorded as a result of treatment with ascorbic acid. This finding was also reflected in a similar increase in the total amount of lead excreted in the urine (6.5 *versus* 12.8%) within 1 week (difference significant at $p < 0.05$).

Despite the complications involved in the disposition kinetics of lead in the body, such direct observation of the effect of ascorbic acid attests to the many anecdotal uses of ascorbic acid in the treatment and prevention of lead poisoning.

(1) H. N. Holmes, K. Campbell, and E. J. Amberg, *J. Lab Clin. Med.*, **24**, 1119 (1939).

(2) L. Pillemer, J. Seifter, A. I. Kuehn, and E. E. Eskes, *Am. J. Med. Sci.*, **200**, 322 (1940).

(3) R. Papionnou and A. Solher, *Fed. Proc. Fed. Am. Soc. Exp. Biol.*, **37**, 405 (1978).

(4) R. A. Goyer and M. G. Chirian, *Life Sci.*, **24**, 433 (1979).

S. Niazi [x]
J. Lim
Department of Pharmacodynamics
College of Pharmacy
University of Illinois Medical Center
Chicago, IL 60680

J. P. Bederka
Department of Toxicology
University of Illinois Medical Center
Chicago, IL 60680

Received March 3, 1982.
Accepted for publication June 9, 1982.

BOOKS

REVIEWS

The International Pharmacopoeia, Third Edition, Vol. 2: Quality specifications, Health and Biomedical Information Programme, World Health Organization, 1211 Geneva 27, Switzerland. 1981. 342 pp. 16 × 24 cm. Price 36 Sw fr.

By virtue of a resolution of the Third World Health Assembly, the *International Pharmacopoeia* is published to improve the quality control of all drugs and pharmaceutical substances. The quality specification establishment and revision process was carried out with the help of members of the World Health Organization's Expert Advisory Panel on the International Pharmacopoeia and Pharmaceutical Preparations and other specialists.

The present (third) edition of the *International Pharmacopoeia* will appear in five volumes. This volume, the second, contains quality specifications for 126 individual drugs widely used in health care. The first volume was published in 1979 and describes 42 general methods of analysis and should be used along with the general notices given in the present volume. The remaining three volumes will contain further specifications.

Specifications included in the second edition of the *International Pharmacopoeia* have been subjected to thorough revision. For other substances, no international quality specifications have been previously issued. While these specifications have no legal status in any country, unless expressly introduced into the national legislation, they are intended to serve as references for national authorities; it is expected that they will be applied by many developing countries for pharmaceuticals used by their health systems.

As for the monographs themselves, for substances used in more than one form (*e.g.*, anhydrous and hydrated, or noninjectable and sterile) the requirements for the relevant forms have been put together in a single monograph, but separate tests have been provided, as required, for each specific form. Also, IR spectra are mentioned in a number of monographs; however, a separate publication containing reproductions of such spectra will be issued at a later date.

Staff Review

on the use of natural compounds such as ascorbic acid to remove heavy metals from the body, and these few studies and anecdotal observations have not provided any direct evidence for ascorbic acid on the excretion of lead from the body (1–4).

In the present communication we report a direct effect of ascorbic acid on the excretion profile of lead in the rat. The control group of rats (weight 300–450 g) were given demineralized water for 4 weeks; the treatment group received 4% ascorbic acid (pH 7.4) as drinking water. Food was given *ad libitum* to both groups ($n = 16$). Lead was administered as lead acetate solution in 5% dextrose intravenously at a dose of 0.637 μg of lead/g of body weight. The treatment group also received a bolus dose of ascorbic acid (1 mg/g of body weight) following administration of lead acetate solution. This was followed by 0.25 mg of ascorbic acid/g of body weight given subcutaneously every 6 hr. The blood samples were collected from the tail vein periodically for up to 163 hr, and urine samples were collected in 24-hr pools for up to 1 week. All samples were analyzed for total lead using a flameless atomic absorption spectrophotometer with graphite furnace[1].

The initial blood levels in the treatment group were higher than the control in accordance with previous findings (3). The urinary clearance of lead was calculated from the plots of blood concentration (C_b) against the urinary excretion (X_u) rate:

$$\text{Control: } \frac{dX_u}{dt} = 0.0049 + 0.1932\ C_b \quad (r > 0.92) \qquad \text{(Eq. 1)}$$

$$\text{Treatment: } \frac{dX_u}{dt} = -0.02089 + 0.4261\ C_b \quad (r > 0.99) \qquad \text{(Eq. 2)}$$

[1] Atomic Absorption Spectrophotometer model 503, Perkin-Elmer, Norwalk, Conn.

The good linear correlation coefficient signifies the relationship between blood concentration and the urinary excretion according to clearance principles; the slopes of Eqs. 1 and 2 were statistically different ($p < 0.05$). An increase of almost 120% in the urinary clearance of lead was recorded as a result of treatment with ascorbic acid. This finding was also reflected in a similar increase in the total amount of lead excreted in the urine (6.5 *versus* 12.8%) within 1 week (difference significant at $p < 0.05$).

Despite the complications involved in the disposition kinetics of lead in the body, such direct observation of the effect of ascorbic acid attests to the many anecdotal uses of ascorbic acid in the treatment and prevention of lead poisoning.

(1) H. N. Holmes, K. Campbell, and E. J. Amberg, *J. Lab Clin. Med.*, **24**, 1119 (1939).

(2) L. Pillemer, J. Seifter, A. I. Kuehn, and E. E. Eskes, *Am. J. Med. Sci.*, **200**, 322 (1940).

(3) R. Papionnou and A. Solher, *Fed. Proc. Fed. Am. Soc. Exp. Biol.*, **37**, 405 (1978).

(4) R. A. Goyer and M. G. Chirian, *Life Sci.*, **24**, 433 (1979).

S. Niazi [x]
J. Lim
Department of Pharmacodynamics
College of Pharmacy
University of Illinois Medical Center
Chicago, IL 60680

J. P. Bederka
Department of Toxicology
University of Illinois Medical Center
Chicago, IL 60680

Received March 3, 1982.
Accepted for publication June 9, 1982.

BOOKS

REVIEWS

The International Pharmacopoeia, Third Edition, Vol. 2: Quality specifications, Health and Biomedical Information Programme, World Health Organization, 1211 Geneva 27, Switzerland. 1981. 342 pp. 16 × 24 cm. Price 36 Sw fr.

By virtue of a resolution of the Third World Health Assembly, the *International Pharmacopoeia* is published to improve the quality control of all drugs and pharmaceutical substances. The quality specification establishment and revision process was carried out with the help of members of the World Health Organization's Expert Advisory Panel on the International Pharmacopoeia and Pharmaceutical Preparations and other specialists.

The present (third) edition of the *International Pharmacopoeia* will appear in five volumes. This volume, the second, contains quality specifications for 126 individual drugs widely used in health care. The first volume was published in 1979 and describes 42 general methods of analysis and should be used along with the general notices given in the present volume. The remaining three volumes will contain further specifications.

Specifications included in the second edition of the *International Pharmacopoeia* have been subjected to thorough revision. For other substances, no international quality specifications have been previously issued. While these specifications have no legal status in any country, unless expressly introduced into the national legislation, they are intended to serve as references for national authorities; it is expected that they will be applied by many developing countries for pharmaceuticals used by their health systems.

As for the monographs themselves, for substances used in more than one form (*e.g.*, anhydrous and hydrated, or noninjectable and sterile) the requirements for the relevant forms have been put together in a single monograph, but separate tests have been provided, as required, for each specific form. Also, IR spectra are mentioned in a number of monographs; however, a separate publication containing reproductions of such spectra will be issued at a later date.

Staff Review

A publication of the
American Pharmaceutical Association—
the National Professional Society
of Pharmacists

JOURNAL OF PHARMACEUTICAL SCIENCES

INDEX TO AUTHORS
INDEX TO SUBJECTS

VOLUME 71
JANUARY TO DECEMBER, 1982

Published monthly under the supervision of the Board of Trustees

Solving the Orphan Drug Problem

"Motherhood, the Flag, and apple pie" need to move over to make room for another revered entity. "Orphan drugs" constitute the newest member of this select group.

Every government official, every drug firm, every consumer representative, and every health care organization seemingly has a policy position or other means of indicating their support for research, development, and marketing of drugs of little commercial value, otherwise popularly known as "orphan drugs."

Moreover, various bills on the subject have been introduced in the U.S. Congress; the Food and Drug Administration has established a separate unit within the Commissioner's Office on Orphan Product Development; the Pharmaceutical Manufacturers Association has set up a blue-ribbon Commission on Drugs for Rare Diseases; and there has been a host of other activities ranging from congressional hearings to lay audience-prime time television shows.

Indeed, things seemed to be moving along in fine fashion insofar as solving the "orphan drugs" problem. The PMA's Commission wasted no time in getting itself off and running. In mid-June it announced that it had made its first selection: *"At its recent meeting on June 10, 1982, the PMA Commission on Drugs for Rare Diseases unanimously recommended further development of L-5-hydroxytryptophan (L-5HTP) in the treatment of post-hypoxic myoclonus."* Accompanying the announcement was an array of impressive information disclosing the scientific and medical considerations that went into the selection process, the expertise of consultants who participated, and the importance of the drug chosen and its value in treatment of the disease involved.

Moreover, the regulatory wheels over at FDA also seemed to be moving with rather unaccustomed speed. A statement from the FDA's office of Orphan Products Development outlining the NDA approval requirements was released simultaneously with the PMA Commission's announcement. Finally, a summary report was included that described the disease, myoclonus, and the reasons why the group felt that this disease and this drug clearly were their first choice in launching what we might refer to as "the war on orphan drugs."

So far, so good. We all had reason to believe that a great start had been made and concrete progress would be right around the corner.

But not so.

An "Orphan Drug Update" newsletter, published by the National Coalition for Rare Disorders, carried in its September 1982 issue an article entitled **"L-5HTP NOT ADOPTED!!"** The article described the situation as follows:

"However, despite the (PMA) Commission's massive effort to publicize the need for a sponsor of L-5HTP (more than 2,000 announcements were distributed by PMA), not one PMA member has stepped forward *to give hope to people with Myoclonus . . . A small generic manufacturer is interested (not a PMA member), but a final commitment has not been made by the manufacturer.*

"Consumers must question why none of the multi-million dollar pharmaceutical corporations stepped forward to adopt L-5HTP. Why would a small manufacturer, who has much more to lose, offer to adopt this drug? At press time, we are still in doubt as to the future of L-5HTP, and people with Myoclonus are suffering needlessly. Since the government and industry claim they will both solve the orphan drug dilemma 'voluntarily,' why are people with Myoclonus without their therapy? In this instance, HHS, FDA, NIH and the PMA have all failed to live up to their promises! In the absence of a legislative mandate, the Coalition feels that the saga of L-5HTP will be repeated again and again by other drugs for a great variety of orphan diseases."

More recent information appears to confirm that Bolar Laboratories—which has been described in the pharmaceutical press as a small, generic, non-PMA member drug company—is *"assuming the responsibility for financing clinical trials on the product (L-5HTP) and the administrative role of shepherding an NDA through FDA."*

Hence, it appears that a fairy godmother, or godfather, has been found for this particular agent. But although this immediate crisis has passed, what about the second orphan drug selected? and the third? and the next after those? What firm, if any, will step forward to undertake the financially unrewarding, but humanely necessary, task of sponsoring those agents through the drug approval process?

When the cry went up for patient information on prescribed drugs, FDA responded by proposing mandatory Patient Package Inserts (PPIs). But that proposed regulation was withdrawn because the health professions—and pharmacy and medicine particularly—moved decisively to embrace voluntary systems of patient education and information regarding prescribed and dispensed drugs.

Similarly, it appears to us that the drug industry now is faced with comparable options. Everyone else, including the industry's own trade association (PMA), has done all they can do to solve the orphan drugs problem. Whether the voluntary approach will work depends on individual drug companies making the necessary financial commitment.

If individual companies fail to respond in a positive fashion, legislation—and with it regulations, government intrusion, red tape, and all the other things that run contrary to the free enterprise system—is bound to ensue. But is the industry, on a company-by-company basis, willing to pay the relatively small price of voluntary service in order to retain its freedom of operation in this area?

—EDWARD G. FELDMANN
American Pharmaceutical Association
Washington, DC 20037

0022-3549/82/1100-1191$01.00/0

JOURNAL OF PHARMACEUTICAL SCIENCES

NOVEMBER 1982
VOLUME 71 NUMBER 11

RESEARCH ARTICLES

In Vitro Adsorption–Desorption of Fluphenazine Dihydrochloride and Promethazine Hydrochloride by Microcrystalline Cellulose

ROBERT M. FRANZ * and GARNET E. PECK ˣ

Received December 26, 1980, from the *Industrial and Physical Pharmacy Department, School of Pharmacy and Pharmacal Sciences, Purdue University, West Lafayette, IN 47907.* Accepted for publication January 29, 1982. *Present Address: The Upjohn Co., Kalamazoo, MI 49001.

Abstract □ Fluphenazine dihydrochloride and promethazine hydrochloride were adsorbed *in vitro* from suspensions of the tableting excipient, microcrystalline cellulose. Studies were undertaken to determine how this adsorption phenomenon was affected by the type of phenothiazine derivative, the type of microcrystalline cellulose, and pH and ionic strength adjustment. The smaller the microcrystalline cellulose particle size, the more drug was adsorbed. Changes in the pH, the ionic strength, and the valency of the cation used to adjust the ionic strength all had a major effect on the extent of adsorption. The adsorption process was rapidly and completely reversed *in vitro* at gastric pH and ionic strength values.

Keyphrases □ Fluphenazine dihydrochloride—*in vitro* adsorption-desorption by microcrystalline cellulose, promethazine hydrochloride □ Promethazine hydrochloride—*in vitro* adsorption-desorption by microcrystalline cellulose, fluphenazine dihydrochloride □ Adsorption—*in vitro* desorption of fluphenazine dihydrochloride and promethazine hydrochloride by microcrystalline cellulose

Microcrystalline cellulose has been extensively used as a tablet diluent, disintegrant, and dry binder in tablet formulations prepared by direct compression. More recently it has been used as a tablet excipient in formulations prepared by wet granulation (1). This process often involves dissolving the active ingredient or ingredients in the granulating liquid. When the active ingredient is dissolved, the possibility of its being adsorbed by microcrystalline cellulose or other tablet excipients is increased due to the greater number of drug molecules available for interaction with the sorbent surface.

Cellulose derivatives and their adsorption properties have been studied extensively in the textile and paper industries. These studies have often involved dye and surfactant adsorption (2–7). Cellulose, including microcrystalline cellulose, has also been used to coat TLC plates for use in the separation of various chemical and biological agents (8, 9). The adsorptive properties of cellulose cannot be disputed. Even so, very few studies have been undertaken to determine if drug substances (*i.e.*, phenothiazines) adsorb to the insoluble cellulose derivatives that are used as excipients in the manufacture of tablets (10).

This study was undertaken to characterize the interaction, if any, between the phenothiazine derivatives, fluphenazine dihydrochloride (I) and promethazine hydrochloride (II), and two different grades of microcrystalline cellulose. It was hoped that by understanding the basic principles of drug–microcrystalline cellulose interactions a greater insight into the formulation of phenothiazine tablets could be gained.

EXPERIMENTAL

Materials—Fluphenazine dihydrochloride[1], promethazine hydrochloride[2], and all other chemicals used in this study were either USP, NF, or reagent grade. All water was doubled distilled, deionized, and degassed. Microcrystalline cellulose, in both a medium grade (III)[3] and a fine grade (IV)[4] was obtained directly from the supplier and was used without further modification. Actinic glassware was used to avoid photodecomposition of the phenothiazines.

Methods—The analytical procedure used for determining drug concentrations in solutions or suspension supernatants was a 3-point UV spectrophotometric technique (11) subsequently adopted for phenothiazine analysis (12, 13). This method was used in order to remove linear background absorbance due to UV absorbing trace substances released into the suspension media by the microcrystalline cellulose. Wavelengths used for the adsorption measurements are shown in Table I.

[1] Fluphenazine dihydrochloride, Schering Corp., Kenilworth, N.J.
[2] Promethazine hydrochloride, Wyeth Laboratories, Philadelphia, Pa.
[3] Avicel pH 101, FMC Corp., Philadelphia, Pa.
[4] Avicel pH 105, FMC Corp., Philadelphia, Pa.

0022-3549/82/1100-1193$01.00/0

Table I—Wavelengths Used for UV Absorption Measurements

Compound	Wavelengths, nm		
	WL^{a}_{short}	WL^{b}_{max}	WL^{c}_{long}
I	234	256	268
II	225	250	260

[a] Wavelength shorter than WL_{max}. [b] Wavelength of maximum absorption. [c] Wavelength longer than WL_{max}.

The accuracy of the assay was determined at different drug concentrations, as well as at the different ionic strengths and pH values used in this study. The range of measured drug concentrations was 97.60–105.17% of the theoretical drug concentrations. The appropriate pH and ionic strength adjusted solution was used in the reference cell.

Adsorption *versus* pH—The preparation of a series of drug–cellulose suspensions involved the addition of 100 ml of distilled water to a 250-ml actinic glass flask containing 3 g of the appropriate grade of microcrystalline cellulose. The suspensions were then shaken or placed in a bath-type sonifier[5] for 30 sec to ensure dispersion. To each suspension was added 1.3 ml of a 1 mg/ml stock solution of the appropriate drug. The pH of these suspensions was adjusted to 2.1, 3.0, 4.0, 5.0, or 6.1, using 0.1 *N* HCl or 0.009 *N* KOH, while the added[6] ionic strengths were adjusted to 0.0107 or 0.107 using 2 *N* KCl. The pH and ionic strengths of the suspensions were adjusted by the addition of ~95% of the total 2 *N* KCl necessary for ionic strength adjustment (determined by a trial run), followed by pH adjustment using 0.1 *N* HCl or 0.009 *N* KOH, and finally the addition of enough 2 *N* KCl to bring the added ionic strengths to the desired level. This was necessary since the initial addition of 2 *N* KCl caused a significant drop in the pH of the suspensions. The final small addition of 2 *N* KCl to bring the added ionic strength to the desired level caused no significant pH change. A final small dilution with distilled water brought the total volume of the suspensions to 120 ml. The pH was monitored using a combination hydrogen ion electrode[7] and pH meter[8].

Preliminary experiments indicated no significant drug degradation took place at the pH values used in this study, nor in the presence of

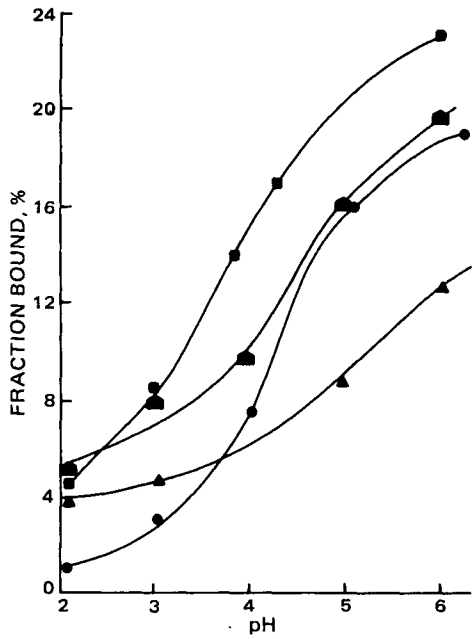

Figure 1—*Effect of pH on the percent fraction of fluphenazine dihydrochloride bound to 3 g of microcrystalline cellulose (1.3 mg of drug/120 ml of external phase). Key: (●) III, added ionic strength (μ′) = 0.0107; (■) IV, μ′ = 0.0107; (▲) III, μ′ = 0.107; (▲) IV, μ′ = 0.107.*

[5] Coulter Ultrasonic Bath, Branson Instruments, Stamford, Conn.

[6] The added ionic strength refers to the total contribution from the hydrochloric acid or the potassium hydroxide and the potassium chloride used in pH and ionic strength adjustment, respectively. It does not include contributions from ions released from the microcrystalline cellulose itself, nor does it include contributions from the drug molecules themselves.

[7] Combination pH Electrode, Sargent-Welch Scientific Co., Skokie, Ill.

[7] Expandomatic SS-2 pH meter, Beckman Instruments, Inc., Scientific Instruments Div., Fullerton, Calif.

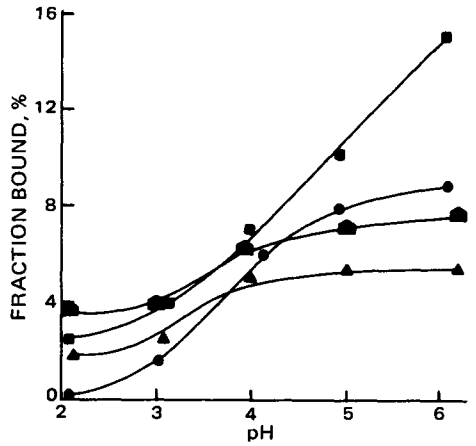

Figure 2—*Effect of pH on the percent fraction of promethazine hydrochloride bound to 3 g of microcrystalline cellulose (1.3 mg of drug/120 ml of external phase). Key: (●) III, μ′ = 0.0107; (■) IV, μ′ = 0.0107; (▲) III, μ′ = 0.107; (▲) IV, μ′ = 0.107.*

microcrystalline cellulose. Blanks were prepared at the same drug concentrations, pH, and added ionic strengths as the samples, but they contained no microcrystalline cellulose. The suspensions and blanks were equilibrated for 1 hr at 23 ± 0.5° on a mechanical shaker water bath[9]. Preliminary experiments performed over a 24-hr period indicated that equilibrium between the adsorbates and adsorbents was reached in <30 min. The suspensions were then centrifuged for 20 min at 23 ± 0.5° on a refrigerated centrifuge[10] at 15,100 rpm. The supernatants were decanted and recentrifuged for an additional 20 min at the same temperature and rpm. The supernatants and blanks were then assayed by the previously described UV spectrophotometric technique. Two separate readings were performed on each sample, and the average was used in the final calculations. The pH values of the final supernatants were monitored and they did not differ by > ±2% of the original adjusted value. The percent fraction of drug bound was calculated as:

$$\% \text{ Fraction Bound} = \frac{[\text{Drug}]_B - [\text{Drug}]_S}{[\text{Drug}]_B} \times 100\% \qquad \text{(Eq. 1)}$$

where $[\text{Drug}]_B$ was the concentration of drug found in the blank and $[\text{Drug}]_S$ was the concentration of drug found in the suspension supernatant. Throughout this study it was assumed that only a minimal amount of water was adsorbed by the microcrystalline cellulose. Even so, the uptake of water by the adsorbent will alter slightly the actual drug concentrations in the suspension supernatants. For this reason, the adsorption discussed throughout this work is actually the apparent adsorption and includes the effect of water uptake by microcrystalline cellulose.

Adsorption Isotherms—Adsorption isotherms were determined for suspensions where the external medium was distilled water (*i.e.*, no pH or ionic strength adjustment), as well as for pH and ionic strength adjusted suspensions. The suspensions were prepared as previously described, with only the drug concentrations being different. For the un-

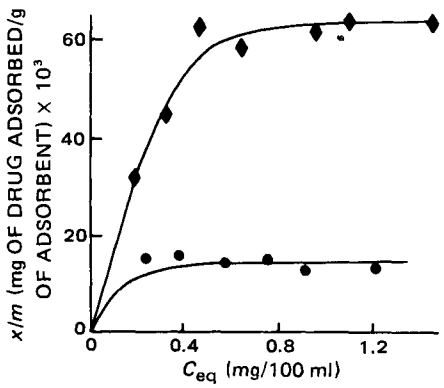

Figure 3—*Adsorption isotherms of fluphenazine dihydrochloride on III at an added ionic strength of 0.107. Key: (●) pH 2.1; (♦) pH 6.1.*

[9] Thermo Shake Incubator Shaker, Forma Scientific, Inc., Marietta, Ohio.

[10] Sorvall Superspeed RC 2-B, Ivan Sorvall, Inc., Newtown, Conn.

Table II—Summary of Constants Obtained from Linear Plots of Langmuir and Freundlich Equations for Fluphenazine Dihydrochloride

Suspension pH	2.1				6.1				Unadjusted (Distilled Water)	
Added ionic strength	0.0107		0.1070		0.0107		0.1070		Unadjusted	
Type of microcrystalline cellulose	III	IV	III	IV	III	IV	III	IV	III	IV
Langmuir constants:										
Adsorptive capacity $k_2 \times 10^3$ (mg of drug adsorbed/g of III or IV) $\times 10^3$	9.6	16.1	11.3	17.6	77.6	106.2	74.9	96.4		
Affinity constant k_1k_2	0.137	0.284	−0.121	9.804	1.218	1.068	0.353	0.767		
Freundlich constants:										
Relative adsorptive capacity $K \times 10^3$									15.2	36.1
Affinity constant N									0.572	0.414
R^2 for linear plots	0.96	0.99	0.98	0.98	0.98	0.99	0.98	0.96	0.98	0.99

adjusted suspensions, the initial drug concentration ranged from 2.5×10^{-3} to 3.33×10^{-2} mg/ml, while for the pH and ionic strength adjusted suspensions the initial concentration of drug was between 2.5×10^{-3} and 1.67×10^{-2} mg/ml. The pH values of the adjusted suspensions were held at 2.1 and 6.1, while the added ionic strengths were held at 0.0107 and 0.1070. The pH values were considered to approximate gastric and intestinal conditions. Blanks were prepared at the same drug concentration, pH, and added ionic strength as the appropriate suspension, only containing no microcrystalline cellulose. The suspensions and blanks were adjusted to the above-mentioned pH and added ionic strength values, equilibrated, and assayed as described previously. The amount of drug adsorbed to the microcrystalline cellulose was determined by the difference in drug concentrations between the suspension supernatant and the appropriate blank. The amount of drug adsorbed in milligrams per gram of microcrystalline cellulose was calculated.

Adsorption *versus* Electrolyte Addition—Suspensions and blanks were prepared at constant pH values of 2.1 and 6.1 exactly as described in the Adsorption *versus* pH section except the added ionic strengths were adjusted. Only III was used. Suspensions prepared at pH 6.1 were adjusted to added ionic strengths of 0, 0.000107, 0.00107, 0.0107, 0.107, and 1.070. Appropriate dilutions were made in a 2 *N* KCl solution so that measurable volumes could be added to the suspensions for ionic strength adjustment. At pH 2.1 the suspensions were adjusted to added ionic strength values of 0.0107, 0.107, and 1.07, using 2 *N* KCl. The suspensions and blanks were equilibrated and assayed as previously described. The percent fraction of drug adsorbed was calculated usng Eq. 1.

Adsorption *versus* Ionic Species—Individual suspensions were prepared by adding 100 ml of distilled water to 250-ml actinic glass flasks containing 3 g of III. Compound III was dispersed, and 1 ml of the appropriate 1-mg/ml drug solution was added. Blanks were prepared containing no adsorbent. Enough sodium chloride, potassium chloride, magnesium chloride, or calcium chloride was added to make the suspensions and blanks 9.804×10^{-4} *M* in added electrolyte. All salt solutions used were 0.1 *N*. These electrolytes were selected due to their frequency of occurrence in the GI tract. Another group of suspensions and blanks were adjusted to a constant added ionic strength of 9.804×10^{-4} using the same salts. Total volume was kept constant at 102 ml, and no pH adjustments were made. The suspensions and blanks were equilibrated, centrifuged, and assayed as previously described. The percent fraction of drug adsorbed was calculated using Eq. 1, and the supernatant pH was monitored.

Desorption *versus* Elution—Individual adsorption complexes were prepared by the addition of 39 ml of distilled water to 50-ml plastic centrifuge tubes containing 1 g of III or IV. The adsorbent was dispersed by shaking. To these suspensions was added 1 ml of a 1-mg/ml solution of the appropriate drug. Blanks were prepared without III or IV. The suspensions and blanks were then equilibrated, centrifuged, and assayed as previously described. Preliminary experiments performed over a 24-hr period indicated that desorption equilibrium was attained in <30 min.

The amount of drug adsorbed to III or IV in the suspension sediment was calculated as the difference between the total drug concentration in the blank and the total drug concentration in the supernatant. This adsorbed amount was considered to be 100% of the possible drug that could be desorbed during an elution. After carefully decanting the supernatant, the remaining drug–microcrystalline cellulose sediment was eluted with either distilled water, or medium adjusted to pH values of 2.1 or 6.2 and added ionic strengths of 0.0107 or 0.1070. The pH and added ionic strength adjustments were performed as previously described after the addition of 35 ml of distilled water to resuspend the sediment. The total volume of elution medium was kept constant at 40 ml. Sediment and elution media were equilibrated, centrifuged, and assayed as described previously, and the elution procedure was repeated a maximum of five times on each drug–microcrystalline cellulose sediment. The pH values of the supernatants were determined and they did not differ significantly from the original adjusted pH values. The cumulative percent desorbed was calculated after each elution using the following equation:

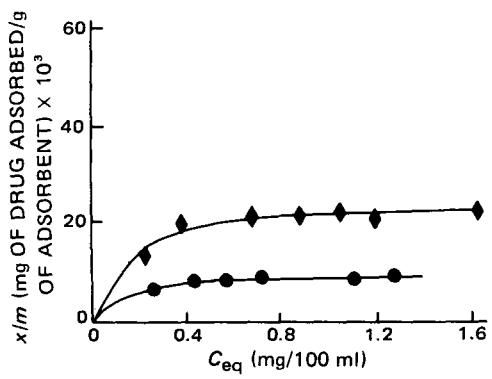

Figure 4—*Adsorption isotherms of promethazine hydrochloride on III at an added ionic strength of 0.107. Key: (●) pH 2.1; (♦) pH 6.1.*

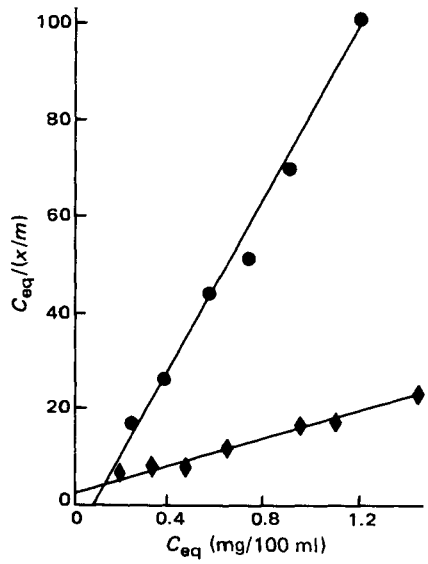

Figure 5—*Langmuir plots for the adsorption of fluphenazine dihydrochloride on III at an added ionic strength of 0.107. Key: (●) pH 2.1; (♦) pH 6.1.*

Table III—Summary of Constants Obtained from Linear Plots of the Langmuir and Freundlich Equations for Promethazine Hydrochloride

Suspenion pH	2.1				6.1				Unadjusted (Distilled Water)	
Added ionic strength	0.0107		0.1070		0.0107		0.1070		Unadjusted	
Type of microcrystalline cellulose	III	IV	III	IV	III	IV	III	IV	III	IV
Langmuir constants:										
Adsorptive capacity $k_2 \times 10^3$ (mg of drug adsorbed/g of III or IV) $\times 10^3$	0	10.1	9.9	19.1	70.3	93.6	25.0	40.5		
Affinity constant k_1k_2	0	0.465	0.073	0.093	0.080	0.185	0.168	0.164		
Freundlich constants:										
Relative adsorptive capacity $K \times 10^3$									4.6	5.8
Affinity constant N									0.703	0.628
R^2 for linear plots	—	0.99	0.99	0.96	0.96	0.94	0.97	0.98	0.99	0.99

$$\text{Cumulative \% Desorbed} = \frac{[\text{Drug}]_C - \sum_{i=1}^{m} [\text{Drug}]_i}{[\text{Drug}]_C} \times 100\% \qquad \text{(Eq. 2)}$$

where $i = 1, 2, 3, \ldots m$ elutions, $[\text{Drug}]_C$ is the total amount of drug initially adsorbed in the drug–microcrystalline cellulose adsorption complex, and $[\text{Drug}]_i$ is the total amount of drug found in the supernatant after the ith elution. Each elution was performed on two separate samples and the values were averaged.

RESULTS AND DISCUSSION

Effect of pH on Adsorption—Figures 1 and 2 illustrate the effect of pH on the adsorption of fluphenazine dihydrochloride and promethazine hydrochloride from suspensions of microcrystalline cellulose adjusted to two different added ionic strengths. Both figures show that at a given added ionic strength and pH, IV always adsorbs a greater amount of drug than does III. This is probably due to the greater total surface area of IV when compared with an equal weight of III. The average particle size of III is 50 μm, while the average particle size of IV is 20 μm (1).

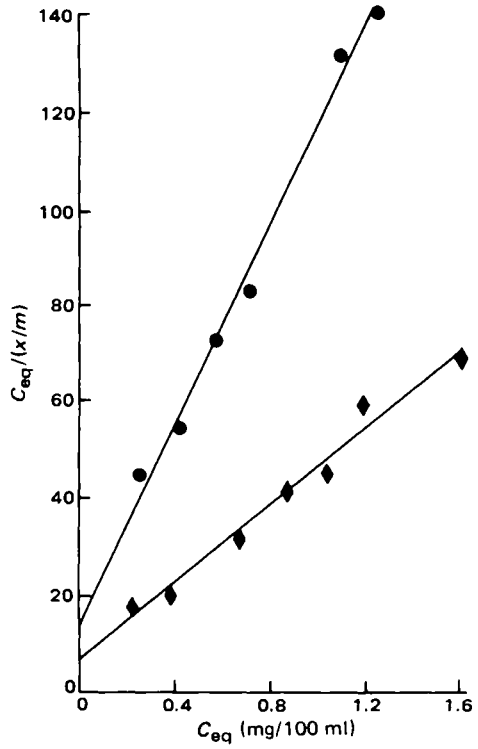

Figure 6—*Langmuir plots for the adsorption of promethazine hydrochloride on III at an added ionic strength of 0.107. Key: (●) pH 2.1; (♦) pH 6.1.*

Table IV—Percent Fraction of Drug Adsorbed by III (3 g) from Suspensions Containing 1.3 mg of Drug/120 ml of Adjusted Medium [a]

Total Added Ionic Strength	Fraction of Drug Adsorbed, %	
	I	II
0.0	82.48	68.98
0.000107	65.17	54.33
0.00107	42.04	27.05
0.0107	16.83	8.77
0.107	13.50	5.28
1.07	11.99	5.84

[a] At a fixed pH of 6.1.

As the pH increases from 2.1 to 6.1, the amount of drug adsorbed by the microcrystalline cellulose also increases (Figs. 1 and 2). This is most likely due to the ionization of carboxyl groups on the cellulose surface. These carboxyl groups are formed by oxidation of the hydroxy groups on individual anhydro-glucose units (14–16). The pKa of these carboxyl groups is ~4.0 (14). As the pH values of the suspensions are increased from 2.1 to 6.1, the number of negatively charged carboxylate groups on the surface of the microcrystalline cellulose particles increases. The increased number of anionic surface sites leads to increased adsorption of the predominantly positively charged drugs at the surface of the particles. The pKa values of these weakly basic drugs are 3.90 and 8.05 for fluphenazine dihydrochloride and 9.08 for promethazine hydrochloride (13).

The possibility also exists that these hydrophobic drugs are adsorbed from solution as the nonprotonated free bases. As the pH values of the suspensions approach the highest pKa values of the phenothiazines, more free base will be found in solution. The free base could then be removed from solution by adsorption to the microcrystalline cellulose surface. As free base is removed from solution, new free base will replace it from the

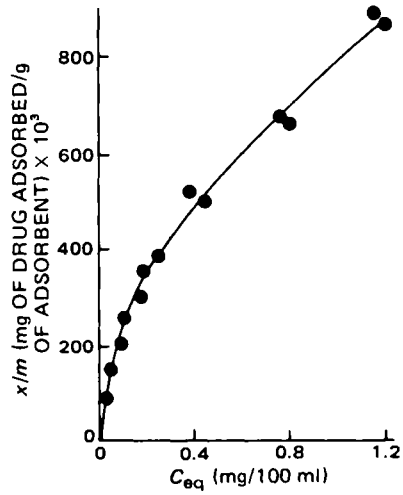

Figure 7—*Adsorption isotherm of fluphenazine dihydrochloride on III in distilled water.*

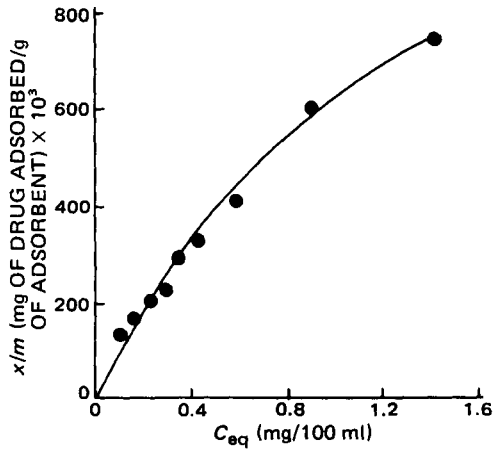

Figure 8—*Adsorption isotherm of promethazine hydrochloride on III in distilled water.*

protonated excess. This will continue until an equilibrium is established between the free base in solution and the base adsorbed to the cellulose surface. This explanation does not seem as likely as the one previously described since pH levels are kept two or more units below the highest pKa of the drugs, and there is an abundance of literature describing the negative surface of microcrystalline cellulose (14, 17–19) as well as other cellulosic materials (2, 15, 20).

Increasing the added ionic strength has different effects on the extent of adsorption depending on the pH of the suspension (Figs. 1 and 2). At high pH values (*i.e.*, pH 6.1), an increase in added ionic strength caused a decrease in the amount of drug adsorbed. This is most likely caused by increased competition between positively charged drug molecules and potassium and hydrogen ions for the negatively charged microcrystalline cellulose surface.

At low pH values (*i.e.*, pH 2.1), where the cellulose carboxy groups are predominantly in their nonionized form, an increase in the added ionic strength causes a slight increase in the amount of drug adsorbed by a particular type of microcrystalline cellulose (Figs. 1 and 2). This could be due to the increased surface activity of these phenothiazines at higher ionic strengths (21). The increased surface activity of these drugs at higher ionic strengths could be caused by the suppression of adsorbed drug–drug electrical repulsions due to the screening effect of the added ions. This would allow more drug to be adsorbed to the cellulosic surface. At higher pH values, where the surface of the microcrystalline cellulose is predominantly negative, this suppression effect may be absent or hidden by the attraction between oppositely charged particles. There is also a possibility that these drugs adsorb by different mechanisms depending on the pH of the suspension and the interrelated surface charge of the microcrystalline cellulose.

The experimental results of this adsorption study give only indirect evidence for the mechanism of adsorption. Further experiments using IR spectroscopy and X-ray diffraction would be needed to determine the exact adsorption mechanism (22, 23).

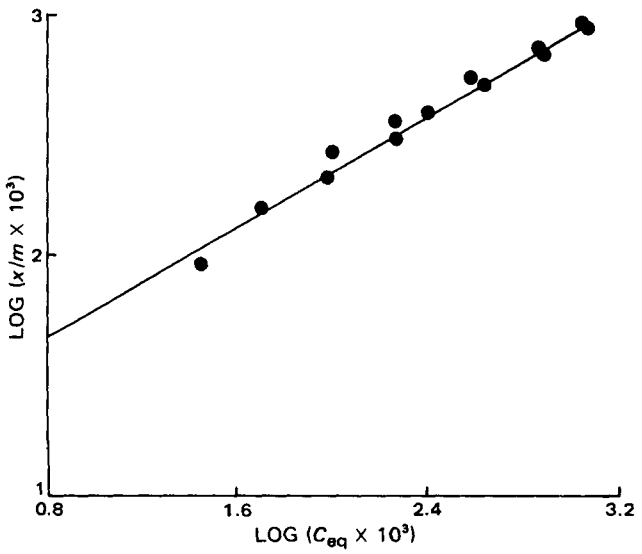

Figure 9—*Freundlich plot for the adsorption of fluphenazine dihydrochloride on III in distilled water.*

Table V—Percent Fraction of Drug Adsorbed by III (3 g) from Suspensions Containing 1.3 mg of Drug/120 ml of Adjusted Medium [a]

Total Added Ionic Strength	Fraction of Drug Adsorbed, % I	II
0.0107	1.01	0.00
0.107	4.66	1.85
1.07	6.27	4.23

[a] At a fixed pH of 2.1.

Table VI—Effect of Electrolytic Species on the Fraction of Promethazine Hydrochloride (0.98 mg/100 ml) Bound to III (3 g)

Electrolyte	Constant Molarity of Added Electrolyte (9.804×10^{-4} *M*) Fraction Bound, %	pH of Supernatant	Constant Ionic Strength of Added Electrolyte (9.804×10^{-4} *M*) Fraction Bound, %	pH of Supernatant
Potassium chloride	28.6	5.55	28.6	5.55
Sodium chloride	31.8	5.52	31.8	5.52
Magnesium chloride	9.9	5.45	14.2	5.60
Calcium chloride	9.5	4.90	15.4	5.30

Adsorption Isotherms—Adsorption isotherms prepared from suspension data where the pH and ionic strength were adjusted to fixed values adhered to the theoretical Langmuir equation, while those prepared from distilled water conformed to the empirical Freundlich equation (24–26). Fit to one or the other type of isotherm was based solely on the comparison of R^2 values obtained from the linear plots (using least squares) of the respective isotherms.

Drug aggregates often exist below the apparent critical micelle concentration for surface active agents such as the phenothiazines (27). The apparent critical micelle concentration will change with varying pH and ionic strength levels (28). Adsorption of aggregates of drug molecules (*i.e.*, ion-pair adsorption) has been reported in the literature (2). This type of phenomenon is often accompanied by a drastic increase in adsorption as the drug concentration approaches its apparent critical micelle concentration (2). No such changes in the adsorption isotherms were observed during this study. It was felt that this fact, coupled with the low concentrations of drugs used, indicated that adsorption was predominantly occurring at a monomolecular level.

The linear form of the Langmuir adsorption isotherm is given by:

$$\frac{C_{eq}}{x/m} = \frac{1}{k_1 k_2} + \frac{C_{eq}}{k_2} \qquad \text{(Eq. 3)}$$

where C_{eq} is the concentration of drug remaining in the suspension supernatant in mg/100 ml after equilibrium adsorption is obtained, x/m is the amount of drug adsorbed in milligrams per gram of microcrystalline cellulose, and k_1 and k_2 are constants. The constant k_2 is the limiting adsorptive capacity. It is the maximum amount of adsorbate, in milligrams, that can be adsorbed by 1 g of adsorbent. Due to the lack of data points at extremely low drug concentrations (*i.e.*, infinite dilution), k_1k_2, instead of k_1, is often used as a measure of the relative affinity of the adsorbate for the adsorbent (13, 29, 30). Typically, calculated k_1k_2 values have been shown to be subject to some error (31). Figures 3 and 4 are typical examples of the isotherms obtained from pH and ionic strength adjusted suspensions. Figures 5 and 6 are the linear plots of these same Langmuir adsorption isotherms.

Adsorption isotherms determined for the phenothiazine–microcrystalline cellulose suspensions where the external phase was distilled water conformed to the Freundlich equation given in the linear form as:

$$\log \frac{x}{m} = \log K + N \log C_{eq} \qquad \text{(Eq. 4)}$$

where x/m and C_{eq} are defined as before and K and N are constants. According to Adamson, the constant K gives a rough measure of the relative adsorbent capacity for a given drug, while N gives a general idea of the affinity of the adsorbate for the adsorbent (32). Typically, the

Table VII—Summary of Desorption *versus* Elution Data for Fluphenazine Dihydrochloride

Elution pH	2.1				6.2				Unadjusted (Distilled Water)	
Added ionic strength	0.0107		0.1070		0.0107		0.1070		Unadjusted	
Type of microcrystalline cellulose	III	IV	III	IV	III	IV	III	IV	III	IV
Cumulative percent desorbed										
Elution 1	97.2	94.4	93.7	92.0	88.5	81.9	86.5	84.9	6.6	5.7
Elution 2	100	100	100	100	98.6	94.2	96.1	97.3	9.9	9.5
Elution 3					100	97.8	97.1	100	12.9	13.1
Elution 4									16.3	16.3
Elution 5									20.5	18.1

Table VIII—Summary of Desorption *versus* Elution Data for Promethazine Hydrochloride

Elution pH	2.1				6.2				Unadjusted (Distilled Water)	
Added ionic strength	0.0107		0.1070		0.0107		0.1070		Unadjusted	
Type of microcrystalline cellulose	III	IV	III	IV	III	IV	III	IV	III	IV
Cumulative percent desorbed										
Elution 1	96.0	96.3	95.1	96.8	86.6	90.5	89.6	92.7	11.8	14.0
Elution 2	100	100	100	100	96.6	100	97.8	100	21.6	24.3
Elution 3									30.6	32.7
Elution 4									37.7	39.0
Elution 5									44.3	45.4

constants k_1 and k_2 (Langmuir constants) are not compared to the constants K or N (Freundlich constants) since they are determined from different types of isotherms (*i.e.*, theoretical *versus* empirical). Figures 7 and 8 are typical examples of the isotherms obtained from suspensions where the external medium was distilled water. Figures 9 and 10 are the linear plots of these same Freundlich adsorption isotherms.

Tables II and III show the constants obtained from the different isotherms, as well as the squared correlation coefficients of the linear plots for fluphenazine dihydrochloride and promethazine hydrochloride, respectively. Comparison of isotherms determined from suspensions in which the external medium was distilled water (Figs. 7 and 8) to isotherms where the external medium was pH and ionic strength adjusted (Figs. 3 and 4) indicates that the electrolyte concentration of the suspension has a major effect on the extent of adsorption.

Effect of Added Electrolyte—Tables IV and V show how changes in the added ionic strength of the suspensions affects the percent fraction of drug adsorbed at constant pH values of 6.1 and 2.1, respectively.

Effect of Ionic Species—The results shown in Table VI indicate that divalent cations have a major effect on the extent of promethazine hydrochloride adsorption by III at both constant electrolyte molarity and added ionic strength. There seems to be little difference in the fraction of drug bound when comparing cations with equal valences. Divalent cations seem to cause a major decrease in the amount of drug adsorbed to III, as compared with monovalent cations. This could be due to divalent cations neutralizing twice as much negative charge on the surface of the microcrystalline cellulose as monovalent cations, which would decrease the number of anionic surface sites available for the protonated drug molecules to interact with, and therefore less drug would be adsorbed. The divalent cations may also have a greater affinity for the surface of III than the monovalent cations and, therefore, less drug would be adsorbed due to increased competition for the negative surface of the microcrystalline cellulose.

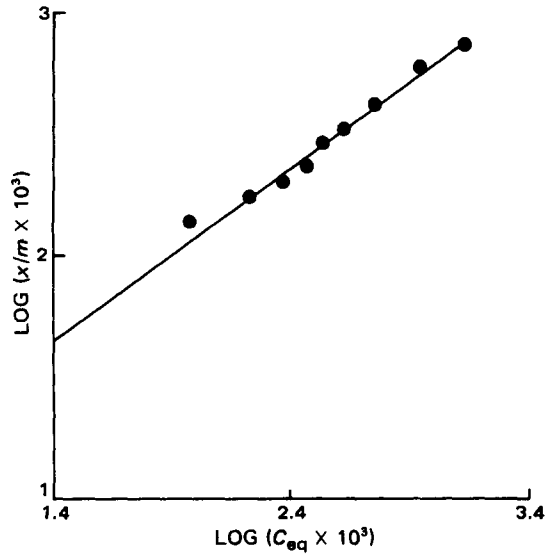

Figure 10—*Freundlich plot for the adsorption of promethazine hydrochloride on III in distilled water.*

Even though the above are hypothesized mechanisms, they seem likely due to the fact that oxidized celluloses, such as microcrystalline cellulose (14, 18), have been shown to adsorb inorganic cations (16, 20, 33). The pH values of the final supernatants were approximately the same after the addition of potassium chloride, sodium chloride, magnesium chloride, and only slightly lower for calcium chloride, indicating that pH was not the reason for the differences seen in the fraction of drug adsorbed.

Desorption—Preliminary experiments indicated that desorption equilibrium was attained in <30 min. Tables VII and VIII show the results of the desorption experiments for fluphenazine dihydrochloride and promethazine hydrochloride, respectively. These results demonstrate the importance that electrolytes play in the desorption phenomenon. It would appear that the inorganic cations in the elution medium have an affinity for the negative surface of the microcrystalline cellulose and, therefore, displace the adsorbed drugs into the external media. This is evidenced by small amounts of the drugs being desorbed from microcrystalline cellulose after five elutions with distilled water, as compared with almost 100% being desorbed with pH and ionic strength adjusted media after three or less washes (Tables VII and VIII). The pH values of the elution supernatants of samples washed with distilled water were close to the adjusted elution pH of 6.2. This indicates that the added electrolytes in the adjusted elution samples must cause the increased desorption, not differences in pH.

The results of these *in vitro* desorption studies indicate that the adsorption of these drugs by microcrystalline cellulose should be rapidly and completely reversed at gastric and intestinal pH values and ionic strengths.

REFERENCES

(1) J. W. Wallace, "FMC Technical Bulletin PH-59," FMC Corp., Philadelphia, Pa., 1978.

(2) F. H. Sexsmith and H. J. White, *J. Colloid Sci.*, **14**, 598 (1959).

(3) Y. Gotshal, L. Rebenfeld, and H. J. White, *ibid.*, **14**, 619 (1959).

(4) A. S. Weatherburn and C. H. Bayley, *Text. Res. J.*, Dec. 797 (1952).

(5) I. D. Rattee and M. M. Breuer, in "The Physical Chemistry of Dye Adsorption," Academic, New York, N.Y., 1974, pp. 179–220.

(6) F. H. Sexsmith and H. J. White, *J. Colloid Sci.*, **14**, 630 (1959).

(7) A. L. Meader and B. A. Fries, *Ind. Eng. Chem.*, **44**, 1636 (1952).

(8) L. Lepri, P. G. Desideri, and M. Lepori, *J. Chromatogr.*, **116**, 131 (1976).
(9) M. L. Wolfrom, D. L. Patin, and R. M. Lederkremer, *ibid.*, **17**, 488 (1965).
(10) H. Nyqvist, P. Lundgren, and C. Nystrom, *Acta. Pharm. Suc.*, **15**, 150 (1978).
(11) R. A. Morton and A. L. Stubbs, *Analyst*, **71**, 348 (1946).
(12) T. L. Flanagan, T. H. Lin, W. J. Novick, I. M. Rondish, C. A. Bocher, and E. J. Van Loon, *J. Med. Pharm. Chem.*, **1**, 263 (1959).
(13) D. L. Sorby, E. M. Plein, and J. D. Benmaman, *J. Pharm. Sci.*, **55**, 785 (1966).
(14) M. R. Edelson and J. Hermans, *J. Polym. Sci., Part C, No. 2*, 145 (1963).
(15) L. F. McBurney, "High Polymers, Vol 5, Part 2: Cellulose and Cellulose-Derivatives," Wiley Interscience, New York, N.Y., 1954.
(16) H. F. Mark, N. G. Gaylord, and N. M. Bikales, in "The Encyclopedia of Polymer Science and Technology," vol. 3, Wiley, New York, N.Y., 1965, pp. 170–178.
(17) L. S. Sandell and P. Luner, *J. Appl. Polym. Sci.*, **18**, 2075 (1974).
(18) S. Kratohvil, G. E. Janauer, and E. Matijevic, *J. Colloid Interface Sci.*, **29**, 187 (1969).
(19) O. A. Battista, in "Microcrystal Polymer Science," McGraw-Hill, New York, N.Y., 1975, pp. 17–57.
(20) T. C. Allen and J. A. Cuculo, *Macromol. Rev.*, **7**, 189 (1973).
(21) G. Zografi and M. V. Munshi, *J. Pharm. Sci.*, **59**, 819 (1970).
(22) L. S. Porubcan, C. J. Serna, J. L. White, and S. L. Hem, *ibid.*, **67**, 1081 (1978).
(23) L. S. Porubcan, G. S. Born, J. W. White, and S. L. Hem, *ibid.*, **68**, 358 (1979).
(24) G. W. Bailey and J. L. White, *Residue Rev.*, **32**, 29 (1970).
(25) C. H. Giles, T. H. MacEwan, S. N. Makhwa, and D. Smith, *J. Chem. Soc.*, **1960**, 2973.
(26) B. A. G. Knight and T. E. Tomlinson, *J. Soil Sci.*, **18**, 233 (1967).
(27) P. Mukerjee, *J. Pharm. Sci.*, **63**, 972 (1974).
(28) D. Attwood, A. T. Florence, and J. M. N. Gillan, *ibid.*, **63**, 988 (1974).
(29) C. A. Bainbridge, E. L. Kelly, and W. D. Walkling, *ibid.*, **66**, 480 (1977).
(30) E. M. Sellers, V. Khouw, and L. Dolman, *ibid.*, **66**, 1640 (1977).
(31) J. B. Milne and G. L. Chatten, *J. Pharm. Pharmacol.*, **9**, 686 (1959).
(32) A. W. Adamson, in "Physical Chemistry of Surfaces," Wiley Interscience, New York, N.Y., 1967, pp. 397–429.
(33) D. A. McLean and L. A. Wooten, *Ind. Eng. Chem.*, **31**, 1138 (1939).

ACKNOWLEDGMENTS

Presented at the Industrial Pharmaceutical Technology Section, APhA Academy of Pharmaceutical Sciences, San Antonio meeting, November 1980.

Supported by a fellowship awarded by the FMC Corp., Philadelphia, PA 19103.

The authors wish to thank the reviewer for the time spent to prepare the recommendations for revision of the manuscript.

Isolation, Identification, and Synthesis of the Major Sulpiride Metabolite in Primates

J. J. BRENNAN *[x], A. R. IMONDI [‡], D. G. WESTMORELAND [§], and M. J. WILLIAMSON [‡]

Received March 27, 1981, from the *Corporate Health & Safety Department, Rohm and Haas Co., Bristol, PA 19007;* the [‡]*Adria Laboratories, Inc., Columbus, OH 43216;* and the [§]*Rohm and Haas Company, Research Laboratories, Spring House, PA 19477.* Accepted for publication January 6, 1982.

Abstract □ The major metabolite of sulpiride, *N*-[(1-ethyl-2-pyrrolidinyl)methyl]-5-sulfamoyl-2-anisamide (I), in the monkey is *N*-[(1-ethyl-5-oxo-2-pyrrolidinyl)methyl]-5-sulfamoyl-2-anisamide (II). It is also a metabolite in other laboratory animal species and possibly at very low levels in humans. Treatment of the urine from a monkey dosed orally with ^{14}C-I by dry column chromatography and high-pressure liquid chromatography (HPLC) produced the major metabolite in pure form. Characterization of the purified ^{14}C-radiolabeled metabolite by proton NMR, TLC, HPLC, and chemical ionization mass spectroscopy, along with subsequent comparison of a synthetically prepared sample, gave unequivocal structural confirmation.

Keyphrases □ Sulpiride—isolation, identification, and synthesis of major metabolites, monkeys □ High-pressure liquid chromatography—analysis, major sulpiride metabolites, monkeys □ Metabolites—sulpiride, isolation, identification, and synthesis, monkeys

Sulpiride (I) is a structurally unique antipsychotic drug. Studies utilizing ^{14}C-labeled I indicated that, while this drug is metabolized to a very small extent in humans, the monkey produces a major metabolite which accounts for 10–30% of a single dose (1). Column chromatography on a strong cation exchange resin, with dilute acid, rapidly eluted this major metabolite, whereas I was retained. This behavior suggested that the metabolite was rendered less basic than the parent drug by a metabolic change on the pyrrolidine ring.

There are several model chemical compounds that possess a pyrrolidinyl moiety either as a fused five-membered ring or as the saturated heterocyclic structure analogous to I. Among these are mazindol (III), prolintane (IV), and tremorine (V).

One of the major biotransformations of these chemical models (Structures II, III–V) in analogous animal species is the oxidation of the alpha position of the five-membered ring to the lactam structures (VI, VII, and VIII). These metabolic changes suggest that I would be similarly biotransformed. It has been reported (2) that the metabolite oxytremorine (VI) is physiologically active and provided

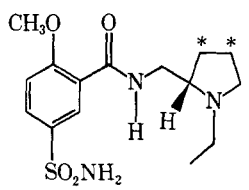

I

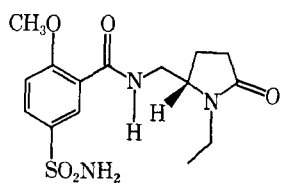

II

0022-3549/82/1100-1199$01.00/0

(8) L. Lepri, P. G. Desideri, and M. Lepori, *J. Chromatogr.*, **116**, 131 (1976).
(9) M. L. Wolfrom, D. L. Patin, and R. M. Lederkremer, *ibid.*, **17**, 488 (1965).
(10) H. Nyqvist, P. Lundgren, and C. Nystrom, *Acta. Pharm. Suc.*, **15**, 150 (1978).
(11) R. A. Morton and A. L. Stubbs, *Analyst*, **71**, 348 (1946).
(12) T. L. Flanagan, T. H. Lin, W. J. Novick, I. M. Rondish, C. A. Bocher, and E. J. Van Loon, *J. Med. Pharm. Chem.*, **1**, 263 (1959).
(13) D. L. Sorby, E. M. Plein, and J. D. Benmaman, *J. Pharm. Sci.*, **55**, 785 (1966).
(14) M. R. Edelson and J. Hermans, *J. Polym. Sci., Part C, No. 2*, 145 (1963).
(15) L. F. McBurney, "High Polymers, Vol 5, Part 2: Cellulose and Cellulose-Derivatives," Wiley Interscience, New York, N.Y., 1954.
(16) H. F. Mark, N. G. Gaylord, and N. M. Bikales, in "The Encyclopedia of Polymer Science and Technology," vol. 3, Wiley, New York, N.Y., 1965, pp. 170–178.
(17) L. S. Sandell and P. Luner, *J. Appl. Polym. Sci.*, **18**, 2075 (1974).
(18) S. Kratohvil, G. E. Janauer, and E. Matijevic, *J. Colloid Interface Sci.*, **29**, 187 (1969).
(19) O. A. Battista, in "Microcrystal Polymer Science," McGraw-Hill, New York, N.Y., 1975, pp. 17–57.
(20) T. C. Allen and J. A. Cuculo, *Macromol. Rev.*, **7**, 189 (1973).
(21) G. Zografi and M. V. Munshi, *J. Pharm. Sci.*, **59**, 819 (1970).
(22) L. S. Porubcan, C. J. Serna, J. L. White, and S. L. Hem, *ibid.*, **67**, 1081 (1978).
(23) L. S. Porubcan, G. S. Born, J. W. White, and S. L. Hem, *ibid.*, **68**, 358 (1979).
(24) G. W. Bailey and J. L. White, *Residue Rev.*, **32**, 29 (1970).
(25) C. H. Giles, T. H. MacEwan, S. N. Makhwa, and D. Smith, *J. Chem. Soc.*, **1960**, 2973.
(26) B. A. G. Knight and T. E. Tomlinson, *J. Soil Sci.*, **18**, 233 (1967).
(27) P. Mukerjee, *J. Pharm. Sci.*, **63**, 972 (1974).
(28) D. Attwood, A. T. Florence, and J. M. N. Gillan, *ibid.*, **63**, 988 (1974).
(29) C. A. Bainbridge, E. L. Kelly, and W. D. Walkling, *ibid.*, **66**, 480 (1977).
(30) E. M. Sellers, V. Khouw, and L. Dolman, *ibid.*, **66**, 1640 (1977).
(31) J. B. Milne and G. L. Chatten, *J. Pharm. Pharmacol.*, **9**, 686 (1959).
(32) A. W. Adamson, in "Physical Chemistry of Surfaces," Wiley Interscience, New York, N.Y., 1967, pp. 397–429.
(33) D. A. McLean and L. A. Wooten, *Ind. Eng. Chem.*, **31**, 1138 (1939).

ACKNOWLEDGMENTS

Presented at the Industrial Pharmaceutical Technology Section, APhA Academy of Pharmaceutical Sciences, San Antonio meeting, November 1980.

Supported by a fellowship awarded by the FMC Corp., Philadelphia, PA 19103.

The authors wish to thank the reviewer for the time spent to prepare the recommendations for revision of the manuscript.

Isolation, Identification, and Synthesis of the Major Sulpiride Metabolite in Primates

J. J. BRENNAN *[x], A. R. IMONDI [‡], D. G. WESTMORELAND [§], and M. J. WILLIAMSON [‡]

Received March 27, 1981, from the *Corporate Health & Safety Department, Rohm and Haas Co., Bristol, PA 19007;* the [‡]*Adria Laboratories, Inc., Columbus, OH 43216;* and the [§]*Rohm and Haas Company, Research Laboratories, Spring House, PA 19477.* Accepted for publication January 6, 1982.

Abstract □ The major metabolite of sulpiride, *N*-[(1-ethyl-2-pyrrolidinyl)methyl]-5-sulfamoyl-2-anisamide (I), in the monkey is *N*-[(1-ethyl-5-oxo-2-pyrrolidinyl)methyl]-5-sulfamoyl-2-anisamide (II). It is also a metabolite in other laboratory animal species and possibly at very low levels in humans. Treatment of the urine from a monkey dosed orally with ^{14}C-I by dry column chromatography and high-pressure liquid chromatography (HPLC) produced the major metabolite in pure form. Characterization of the purified ^{14}C-radiolabeled metabolite by proton NMR, TLC, HPLC, and chemical ionization mass spectroscopy, along with subsequent comparison of a synthetically prepared sample, gave unequivocal structural confirmation.

Keyphrases □ Sulpiride—isolation, identification, and synthesis of major metabolites, monkeys □ High-pressure liquid chromatography—analysis, major sulpiride metabolites, monkeys □ Metabolites—sulpiride, isolation, identification, and synthesis, monkeys

Sulpiride (I) is a structurally unique antipsychotic drug. Studies utilizing ^{14}C-labeled I indicated that, while this drug is metabolized to a very small extent in humans, the monkey produces a major metabolite which accounts for 10–30% of a single dose (1). Column chromatography on a strong cation exchange resin, with dilute acid, rapidly eluted this major metabolite, whereas I was retained. This behavior suggested that the metabolite was rendered less basic than the parent drug by a metabolic change on the pyrrolidine ring.

There are several model chemical compounds that possess a pyrrolidinyl moiety either as a fused five-membered ring or as the saturated heterocyclic structure analogous to I. Among these are mazindol (III), prolintane (IV), and tremorine (V).

One of the major biotransformations of these chemical models (Structures II, III–V) in analogous animal species is the oxidation of the alpha position of the five-membered ring to the lactam structures (VI, VII, and VIII). These metabolic changes suggest that I would be similarly biotransformed. It has been reported (2) that the metabolite oxytremorine (VI) is physiologically active and provided

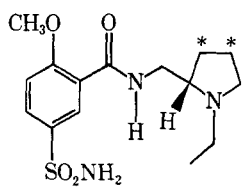

I

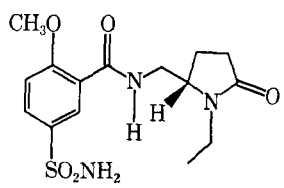

II

0022-3549/82/1100-1199$01.00/0

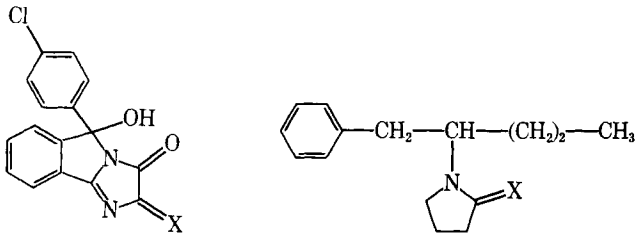

III: X = 2H; VI: X = O

IV: X = 2H; VII: X = O

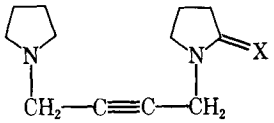

V: X = 2H; VIII: X = O

further impetus for identification, synthesis, and biological evaluation of this suspected metabolite.

EXPERIMENTAL

Isolation of the Metabolite by Dry Column Chromatography—Urine from a male monkey (*Macaca mulatta*) which had been dosed orally with [^{14}C]3,4-pyrrolidine sulpiride (I) was dissolved in Solvent System I [1-butanol-acetic acid–water (2:2:1)] and placed on a nylon column (25-mm flat width × 280-mm flat length) packed with dry silica gel[1] to a height of 250 mm. When the elution was complete, the column was divided into 11 segments (25 mm each), excluding the upper and lower portions of the column which were discarded. The segments were slurried with absolute methanol (25 ml) and 10-μl aliquot portions were collected, diluted with 10 ml of scintillation cocktail[2], and counted in liquid scintillation counter. The results are plotted in Fig. 1. Fractions from segments II–V were slurried with methanol, filtered (0.5-μm filter), and concentrated under dry nitrogen. The residue was dissolved in Solvent System V [5 ml of propanol–NH_4OH (9:1)] and eluted with the same size column used for Solvent System I. When the elution was complete, the column was treated as above; the data are plotted in Fig. 2. Fractions 6–8 were diluted further, filtered, and concentrated under dry nitrogen. The residue was extracted with methylene chloride (25 ml), and two aliquot portions (50 μl) were removed and counted. The results showed that 239 μg of crude metabolite had been isolated.

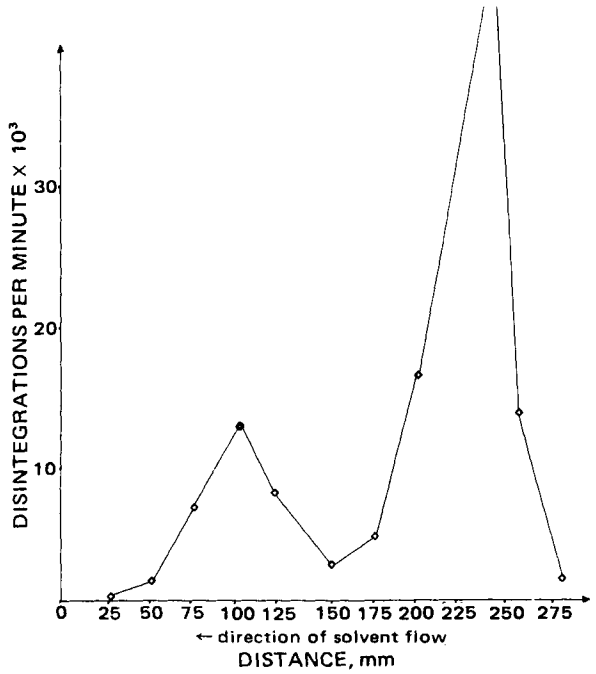

Figure 1—*Radiolabeled sulpiride and the metabolite.*

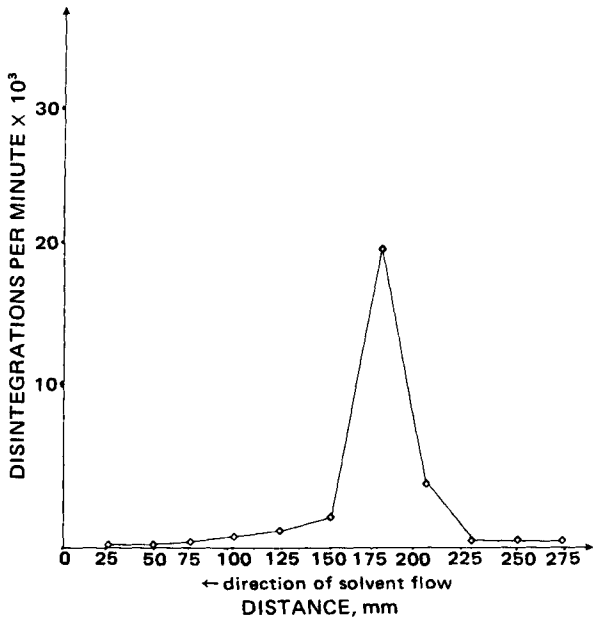

Figure 2—*Radiolabeled metabolite.*

Purification of the Metabolite by HPLC—The methylene chloride solution containing ~239 μg of radioactive material was concentrated to ~1.2 ml under nitrogen and filtered through a 0.5-μm filter. The filtered solution was loaded into a high-pressure liquid chromatographic (HPLC) injection assembly and the solvent overflow was collected and counted; it contained no detectable radioactivity. At zero time, the sample was injected on a preparative HPLC column[3] and the program initiated. A 50-min concave program from 100% water to 100% acetonitrile at 2.8 ml/min and with UV detection at 290 nm was used. The fractions were collected at 5-min intervals or when necessary by elution of a peak. Aliquots of up to 0.5 ml were taken from each vial for liquid scintillation counting. After four runs, it was determined by UV absorption and liquid scintillation counting that three vials (Fig. 3) contained ~77, 17, and 7 μg, respectively, of radioactive material. The vial with the highest radioactivity was concentrated under nitrogen and examined by ^{1}H-NMR.

Identification—*NMR Analysis of the Metabolite*—The sulpiride metabolite sample which had been purified by dry column chromatography and HPLC was dried in a conical vial. The vial was placed under a nitrogen blanket (water free), and 6 μl of dimethyl sulfoxide[4] was added

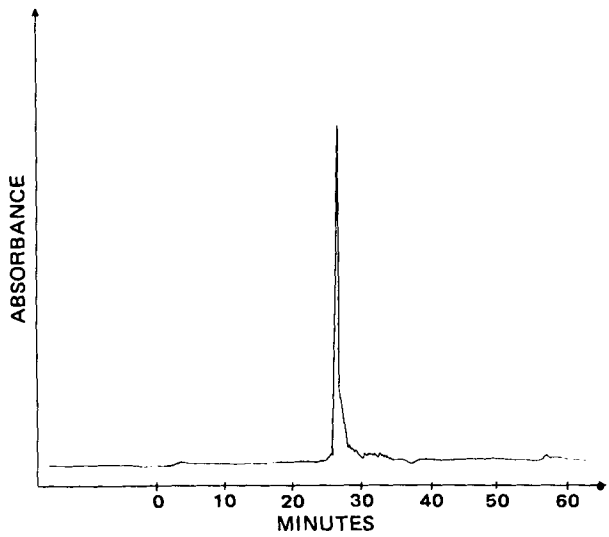

Figure 3—*Isolation of the radiolabeled metabolite by HPLC.*

[1] Grace, 60–200 mesh.
[2] Hydromix.
[3] Varian Micropak C-H.
[4] 100% deuterated, Merck.

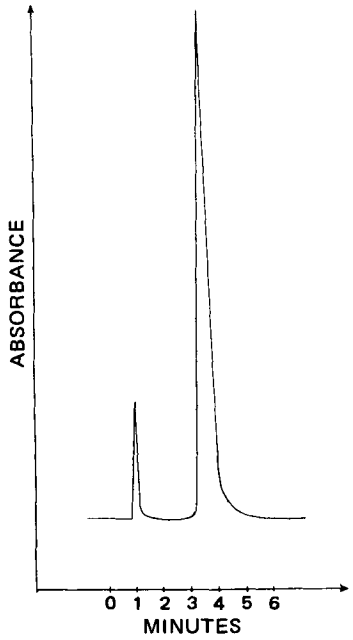

Figure 4—*Comparison of the elution times of radiolabeled metabolite and internal standard.*

to the vial. When the material had dissolved, the solution was transferred *via* capillary action to a 1-mm glass tube and the ends sealed with corks. The tube was removed from the nitrogen blanket and sealed immediately with a torch. The 100 MHz ^{1}H-NMR spectrum was obtained using Fourier transform spectroscopy. The time average of 4872 free induction decays (collected with a 1-sec acquisition time) yielded the following spectrum: δ 0.98 (triplet, J = 7 Hz, CH_3), 1.75–2.26 (multiplet, $2CH_2$), 2.87–3.59 (multiplet, CH, $2CH_2$), 3.88 (singlet, CH_3), 7.21 (singlet, NH_2), and 7.29–8.31 (multiplet, 3 aromatic). Analysis of this spectrum compared to that of sulpiride suggested that the metabolite had the structure of II. The ^{1}H-NMR spectrum of synthetic II was obtained at a later date in a similar manner and was essentially identical to that of the metabolite.

Chemical Ionization Mass Spectral Analysis of the Metabolite and the Synthetically Prepared Material—The data for the purified metabolite sample were of good quality, probably because of the higher purity. The methane chemical ionization mass spectrum shows the protonated molecular ion of the α-pyrrolidinone derivative at mass spectrum 356 and also association ion peaks for $(M+, C_2H_5)^+$ at 384 and $(M+, C_3H_5)^+$ at 396. However, a second component was also observed with peaks at 370 and 398, implying a molecular weight of 369. The amount of this component cannot be estimated from the chemical ionization mass spectroscopic data, but is probably <10% of II, since it was not readily observed in the ^{1}H-NMR data. This second component was probably a derivative of sulpiride which was oxidized at two positions on XVI.
A mass spectral scan of synthetic II showed a multitude of ions and could not be readily interpreted. Evidently the impurities in the preparation were masking the major component, perhaps due to higher volatility or stability.

HPLC Analysis of the Metabolite—A high-pressure liquid chromatograph equipped with a valve-loop injector (10 μl), an amino column[5], and a variable wavelength detector set at 240 nm was used. The mobile phase was prepared by adding 15 ml of concentrated ammonium hydroxide to a 400-ml mixture of 97.5 acetonitrile–2.5% water. This mixture was pumped through the column at 1 ml/min. Using this system I eluted at 3.3 min, with an internal standard of *p*-toluenesulfonamide eluting at 1.0 min (Fig. 4).

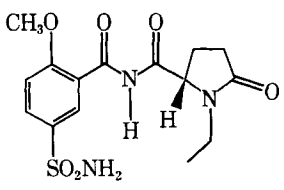

XVI

[5] Varian Micropak-NH_2.

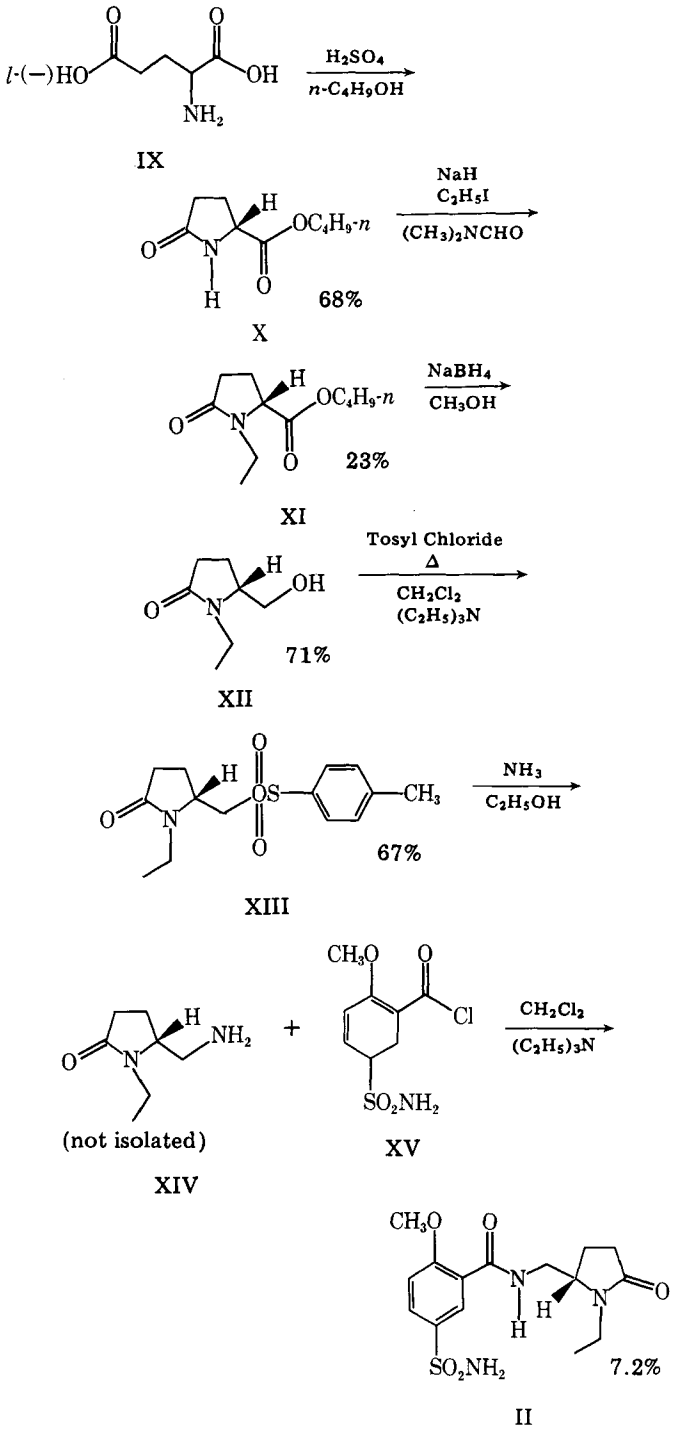

Scheme I—Synthetic route to II.

A solution of 1.8 mg of II in 5 ml of acetonitrile was prepared. A 10-μl aliquot was injected and a retention time of 1.9 min measured (Fig. 5A). A sample of the radioactive metabolite was dissolved in 1 ml of acetonitrile, and a 5-μl aliquot was injected. The retention time by UV absorption and collected radioactivity was found to be 1.9 min (Fig. 5B), identical to that of the synthetic material. The two chromatograms are shown in Fig. 5.

Synthesis of Metabolite II—*Butyl-5-oxopyroglutamate (X)*—Scheme I shows the synthesis of II: A 2-liter flask containing *l*(−)-glutamic acid (IX) (147 g, 1.0 mole) and 1-butanol (625.0 g, 8.45 moles) was stirred at room temperature. The suspension was treated with concentrated sulfuric acid (125.0 g, 1.27 moles) in portions and gave a clear solution. The reaction was heated at reflux with the removal of water for 25 hr and the pH adjusted to 4.5 with 1 *N* Na_2CO_3 and concentrated *in vacuo*. The viscous oil obtained was stirred with benzene (500 ml) while adjusting the pH to 9.5 with 2 *N* NaOH. The organic layer was separated,

Table I—Elemental Analysis of Compounds II, X-XIV

Compound Number	Empirical Formula	mp/bp°	Elemental analyses: (Calc) Found			
			C	H	N	S
X	$C_9H_{15}NO_3$	162–3, 1.7 mm	58.74	8.56	8.53	—
			(58.36)	(8.16)	(7.55)	—
XI	$C_{11}H_{19}NO_3$	135–6, 0.75 mm	63.25	9.63	7.05	—
			(61.95)	(8.98)	(6.56)	—
XII	$C_7H_{13}NO_2$	159, 3.5 mm	58.26	9.38	9.72	—
			(58.72)	(9.15)	(9.77)	—
XIII	$C_{14}H_{19}NO_4S$	84–85	56.65	6.51	4.99	10.76
			(56.54)	(6.44)	(4.70)	(10.78)
XIV	$C_7H_{14}N_2O$	Oil	59.53	9.79	—	—
			(59.13)	(9.92)	—	—
II	$C_{15}H_{21}N_3O_5S$	227–228	48.70	5.83	10.98	11.30
			(50.69)	(5.95)	(11.82)	(9.02)

and the aqueous layer was further extracted with benzene (2 × 250 ml). The organic layers were combined, washed with saturated sodium chloride solution, and concentrated to give a lightly colored oil. The oil was distilled (160–165°, 1.7 mm) to give 126.0 g (68%) of a colorless product.

Butyl-N-ethyl-5-oxopyroglutamate (XI)—A 500-ml flask equipped with a mechanical stirrer, reflux condenser, thermometer, and funnel was used. Compound X (37.0 g, 0.2 mole) was dissolved in dimethylformamide (200 ml, previously dried over 4-Å molecular sieves for 24 hr). Sodium hydride (9.5 g of 50% dispersion, 0.2 mole) was added in portions, the reaction exothermed to 50°, and the solution became amber. The reaction was maintained at 50° for 1 hr and then cooled. Ethyl iodide (31.2 g, 0.2 mole) was then added dropwise at a rate sufficient to maintain a temperature of 50°. After the addition was complete, the reaction was heated at 50° for 2 hr and stirred to room temperature overnight. The reaction mixture was poured into water (1000 ml), extracted with carbon tetrachloride (3 × 600 ml), dried over magnesium sulfate, filtered, and concentrated to give 35.5 g of crude product. The crude material was distilled (136°, 0.75 mm) to give 18.7 g (44%) of pure product.

N-Ethyl-5-hydroxymethyl-2-pyrrolidinone (XII)—A 250-ml flask equipped with a magnetic stirrer, reflux condenser, thermometer, and funnel was used. Compound XI (25.0 g, 0.12 mole) was added dropwise to a solution of absolute methanol (120 ml) containing sodium borohydride (11.4 g, 0.30 mole) at room temperature. The addition of the ester caused an exotherm and the reaction temperature was maintained below 50° with ice. When the addition was complete, the reaction was heated at reflux overnight. The reaction mixture was concentrated, the viscous oil slurried with a minimum amount of anhydrous ethanol, then chromatographed on a glass column (58 mm × 600 mm) which had been packed with slurried silica gel[1]. The product was eluted with ethanol, concentrated, and the oil obtained was extracted into benzene, dried over magnesium sulfate, filtered, and concentrated to give 12.2 g (71.2%) of pure product.

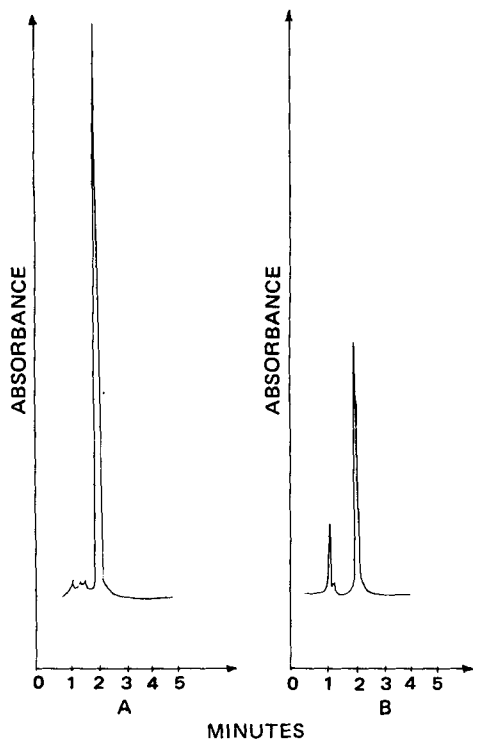

Figure 5—*Comparison of the elution times of the synthetic (A) and radiolabeled metabolite (B).*

N-Ethyl-5-tosylmethyl-2-pyrrolidinone (XIII)—A 100-ml flask equipped with a reflux condenser and drying tube was used. Compound XII (7.24 g, 50.77 mmoles), 4-toluenesulfonyl chloride (19.1 g, 100.0 mmoles), and triethylamine (10.1 g, 100.0 mmoles) were dissolved in methylene chloride (50 ml) and heated overnight. The rection mixture was poured into dilute sodium bicarbonate solution (10 ml of a saturated solution was diluted to 100 ml), the layers were separated, and the organic layer was extracted with 0.1 *N* HCl (2 × 100 ml), dried over magnesium sulfate, filtered, concentrated, and refrigerated, overnight. The tan solid obtained was stirred with heptane (5 × 100 ml), filtered, and air dried to give 10.15 g of product (mp 80–82°). The product was crystallized from ethyl acetate–heptane (1:1) (mp 84–85°, 67% yield).

N-Ethyl-α-aminomethyl-2-pyrrolidinone (XIV)—A 300-ml stainless steel autoclave equipped with a pressure gauge (1 × 10^3 psi) was employed. Ethanol (200 proof, 100 ml) was cooled and saturated with ammonia for 1.5 hr. *N*-Ethyl-5-tosylmethyl-2-pyrrolidinone (XIII) (5.0 g, 16.9 mmoles) was added and the solution was stirred and heated at 80° overnight. The resulting amber solution was diluted with water (30 ml) and then the ethanol was removed *in vacuo*. The remaining aqueous solution was cooled and the pH adjusted to 14 with solid potassium hydroxide. The resulting alkaline solution was extracted with ethyl acetate (3 × 100 ml) and the aqueous solution was readjusted to pH 14 and further extracted with ethyl acetate (2 × 100 ml). The organic layers were combined and concentrated to a minimum volume and further extracted with 1 *N* HCl (30 ml). The acid solution was made alkaline to litmus, extracted with ethyl acetate (3 × 300 ml), dried over magnesium sulfate, filtered, and concentrated to give 220 mg of an amber oil (9.3% yield).

N-[(1-Ethyl-2-pyrrolidinyl)methyl-5-oxo]-5-sulfamoyl-2-anisamide (II)—A 100-ml single-neck flask equipped with a magnetic stirrer, reflux condenser, and drying tube was used. Thionyl chloride (50 ml, 0.68 mole) and 2-methoxy-5-sulfamoyl-benzoic acid (7.0 g, 26.6 mmole) were mixed, pyridine (4 drops) was added, and the reaction was heated at reflux overnight. The thionyl chloride was removed *in vacuo*, and benzene (2 × 50 ml) was added and removed *in vacuo* to remove the final traces of thionyl chloride.

α-Aminomethyl-*N*-ethyl-2-pyrrolidinone (XIV) (220 mg, 1.55 mmoles) and triethylamine (160 mg, 1.58 mmoles) were dissolved in 10 ml of chloroform in a 50-ml flask equipped with a magnetic stirrer and a reflux condenser, and cooled in ice. A chloroform solution (3.5 ml) containing 2-methoxy-5-sulfamoyl-benzoyl chloride (402 mg, 1.61 mmoles) was added dropwise (a slight exotherm was observed). The reaction was stirred to room temperature and then heated at reflux for 3.5 hr. The mixture was cooled, concentrated, and the resulting gummy black tar was triturated with water and allowed to stand. A gray solid formed, which was filtered and air dried, to yield 40 mg of the desired product. Further trituration of the solid with absolute methanol followed by filtering and air drying gave a gray solid (mp 228° with decomposition, 7.2%).

The melting points were obtained on a melting point apparatus[6] and are uncorrected. The elemental analyses for these compounds are given in Table I.

[6] Thomas–Hoover.

DISCUSSION

The major metabolite of sulpiride in monkeys was obtained by isolation from urine followed by chromatographic purification. The chromatogram in Fig. 3 represents the sample that was submitted for identification by ^{1}H-NMR, chemical ionization mass spectroscopy, and HPLC. Comparison for the ^{1}H-NMR spectra of the metabolite and sulpiride showed that some biotransformation had occurred to the pyrrolidine ring, where it appeared that alpha oxidation had taken place similar to the model compounds, VI–VIII.

This conclusion was further supported by the fact that sulpiride is retained on a cation exchange column, while metabolite II can be eluted with an acidic solvent system. The different chemical behavior of these two species was attributed to the differences in the basicity of the sulpiride pyrrolidine ring nitrogen, which was a tertiary amine prior to biotransformation and subsequently was converted into a cyclic amide of lesser basicity. The synthesis of compound II by an unambiguous route (Scheme I) and analysis by ^{1}H-NMR of the synthetic material gave unequivocal evidence that alpha oxidation had occurred. In addition, a sample of the radiolabeled metabolite and the synthetically prepared sample were compared by HPLC and found to have identical retention times (Fig. 5).

Previous attempts to obtain a mass spectrum on II by electron impact had failed, probably due to the presence of impurities. Subsequently, chemical ionization mass spectral data were obtained on the same sample that had been subjected to ^{1}H-NMR. The spectrum was of good quality and demonstrated that II has a molecular weight of 355. A compound of molecular weight 369 ($\simeq$10%) was also observed. Although its structure has not been identified, it has undergone oxidation at two methylene groups and may be the compound shown by XVI.

Isolation of the metabolite by column chromatography and purification by HPLC with subsequent identification by Fourier transform-NMR, chemical ionization mass spectroscopy, HPLC, and unambiguous chemical synthesis has shown that the structure of the major metabolite of sulpiride is II.

REFERENCES

(1) A. R. Imondi, A. S. Alam, J. J. Brennan, and L. M. Hagerman, *Arch. Int. Pharmacodyn. Ther.*, **232**, 79 (1978).

(2) A. K. Cho, W. L. Haslett, and D. J. Jenden, *Biochem. Biophys. Res. Commun.*, **5**, 276 (1961).

ACKNOWLEDGMENTS

The authors thank Mrs. F. Burnley for her assistance in interpreting the ^{1}H-NMR data and Mr. John P. Helfrich for the comparative HPLC work of the metabolite and synthetic oxysulpiride.

Potential Radiosensitizing Agents III: 2-Nitro-4-Acetylimidazole Analogs

RAJ K. SEHGAL and KRISHNA C. AGRAWAL ˣ

Received November 2, 1981, from the *Department of Pharmacology, Tulane University School of Medicine, New Orleans, LA 70112.* Accepted for publication, December 31, 1981.

Abstract □ New analogs of 2-nitroimidazole have been synthesized in an effort to minimize the toxicity and increase selective sensitization of hypoxic mammalian cells toward lethal effects of ionizing radiation. 2-Nitro-4(5)-acetyl-5(4)-methylimidazole was synthesized from the corresponding 2-amino analog and then reacted with oxiranes to produce the corresponding 1-substituted 2-propanol and 3-methoxy-2-propanol derivatives. The biological results of radiosensitizing activity of these agents against Chinese hamster cells (V-79) indicated that the 3-methoxy-2-propanol derivative was a more effective radiosensitizer than misonidazole *in vitro*. Evaluation of the acute toxicity of these agents as determined by LD_{50} demonstrated no significant difference between these agents and misonidazole suggesting that the 3-methoxy-2-propanol analog may possess a therapeutic advantage over misonidazole.

Keyphrases □ Radiosensitizing agents, potential—2-nitro-4-acetylimidazole analogs □ 2-Nitro-4-acetylimidazole—analogs, potential radiosensitizing agents □ Analogs—2-nitro-4-acetylimidazole, potential radiosensitizing agents

In a continuing effort to develop new effective radiosensitizers to sensitize selectively the relatively resistant hypoxic tumor cells toward radiotherapy, an additional electron affinic acetyl function has been incorporated into the 2-nitroimidazole nucleus. A direct correlation between the sensitizing efficiency and electron affinity of the radiosensitizers has been demonstrated (1). Initially, a series of 2,4-dinitroimidazoles were synthesized in an effort to increase the electron affinity of the 2-nitroimidazole nucleus (2, 3). The 1-(2-hydroxy-3-methoxypropyl)-2,4-dinitroimidazole was found to be the most effective radiosensitizer of this series (4). However, the 2,4-dinitroimidazole derivatives were found to be generally more toxic than misonidazole (5), an agent currently under clinical trials for evaluation as a radiosensitizer. It was deemed desirable to study the effect of another electron affinic group other than the nitro function at the 4-position of the 2-nitroimidazole nucleus. Accordingly, 4-acetyl substituted 2-nitroimidazole analogs have been synthesized. This modification was thought to be of interest in view of the report that 1-methyl-2-nitroimidazole-5-carboxaldehyde sensitized the hypoxic Chinese hamster cells *in vitro* to ionizing radiation at much lower concentrations (25 μM) than misonidazole (1).

BACKGROUND

It is obvious that an aldehyde function is a metabolically unstable group, and perhaps in addition to high electron affinity, lack of an hydroxyl group in the side chain at the 1-position may have contributed toward enhanced cytotoxicity of this agent. Therefore, the synthesis of 4-acetyl analogs of 2-nitroimidazole with a 2-hydroxypropyl side chain at the 1-position was undertaken. The molecular design of agents described in this report was also related to the structure of metronidazole, a known but less potent radiosensitizer than misonidazole, in that the functional groups at 2- and 5-positions were reversed to provide a 2-nitro-5-methyl analog, since 2-nitroimidazoles have been reported to be more effective radiosensitizers (6).

The synthesis of the required intermediate 2-amino-4(5)-acetyl-5(4)-methylimidazole (III) was accomplished by the known mononuclear 1,2,4-oxadiazole imidazole rearrangement with minor modification of utilizing sodium methoxide in dimethylformamide rather than sodium ethoxide as a base (7). The starting material 3-amino-5-phenyl-1,2,4-oxadiazole, readily obtained from hydrolysis of the *N,O*-dibenzoyl hydroxyguanidine (8), was condensed with an equimolar amount of acetylacetone in anhydrous toluene in the presence of *p*-toluenesulfonic acid

0022-3549/82/1100-1203$01.00/0

DISCUSSION

The major metabolite of sulpiride in monkeys was obtained by isolation from urine followed by chromatographic purification. The chromatogram in Fig. 3 represents the sample that was submitted for identification by ^{1}H-NMR, chemical ionization mass spectroscopy, and HPLC. Comparison for the ^{1}H-NMR spectra of the metabolite and sulpiride showed that some biotransformation had occurred to the pyrrolidine ring, where it appeared that alpha oxidation had taken place similar to the model compounds, VI–VIII.

This conclusion was further supported by the fact that sulpiride is retained on a cation exchange column, while metabolite II can be eluted with an acidic solvent system. The different chemical behavior of these two species was attributed to the differences in the basicity of the sulpiride pyrrolidine ring nitrogen, which was a tertiary amine prior to biotransformation and subsequently was converted into a cyclic amide of lesser basicity. The synthesis of compound II by an unambiguous route (Scheme I) and analysis by ^{1}H-NMR of the synthetic material gave unequivocal evidence that alpha oxidation had occurred. In addition, a sample of the radiolabeled metabolite and the synthetically prepared sample were compared by HPLC and found to have identical retention times (Fig. 5).

Previous attempts to obtain a mass spectrum on II by electron impact had failed, probably due to the presence of impurities. Subsequently, chemical ionization mass spectral data were obtained on the same sample that had been subjected to ^{1}H-NMR. The spectrum was of good quality and demonstrated that II has a molecular weight of 355. A compound of molecular weight 369 ($\simeq$10%) was also observed. Although its structure has not been identified, it has undergone oxidation at two methylene groups and may be the compound shown by XVI.

Isolation of the metabolite by column chromatography and purification by HPLC with subsequent identification by Fourier transform-NMR, chemical ionization mass spectroscopy, HPLC, and unambiguous chemical synthesis has shown that the structure of the major metabolite of sulpiride is II.

REFERENCES

(1) A. R. Imondi, A. S. Alam, J. J. Brennan, and L. M. Hagerman, *Arch. Int. Pharmacodyn. Ther.*, **232**, 79 (1978).

(2) A. K. Cho, W. L. Haslett, and D. J. Jenden, *Biochem. Biophys. Res. Commun.*, **5**, 276 (1961).

ACKNOWLEDGMENTS

The authors thank Mrs. F. Burnley for her assistance in interpreting the ^{1}H-NMR data and Mr. John P. Helfrich for the comparative HPLC work of the metabolite and synthetic oxysulpiride.

Potential Radiosensitizing Agents III: 2-Nitro-4-Acetylimidazole Analogs

RAJ K. SEHGAL and KRISHNA C. AGRAWAL ˣ

Received November 2, 1981, from the *Department of Pharmacology, Tulane University School of Medicine, New Orleans, LA 70112.* Accepted for publication, December 31, 1981.

Abstract □ New analogs of 2-nitroimidazole have been synthesized in an effort to minimize the toxicity and increase selective sensitization of hypoxic mammalian cells toward lethal effects of ionizing radiation. 2-Nitro-4(5)-acetyl-5(4)-methylimidazole was synthesized from the corresponding 2-amino analog and then reacted with oxiranes to produce the corresponding 1-substituted 2-propanol and 3-methoxy-2-propanol derivatives. The biological results of radiosensitizing activity of these agents against Chinese hamster cells (V-79) indicated that the 3-methoxy-2-propanol derivative was a more effective radiosensitizer than misonidazole *in vitro*. Evaluation of the acute toxicity of these agents as determined by LD_{50} demonstrated no significant difference between these agents and misonidazole suggesting that the 3-methoxy-2-propanol analog may possess a therapeutic advantage over misonidazole.

Keyphrases □ Radiosensitizing agents, potential—2-nitro-4-acetylimidazole analogs □ 2-Nitro-4-acetylimidazole—analogs, potential radiosensitizing agents □ Analogs—2-nitro-4-acetylimidazole, potential radiosensitizing agents

In a continuing effort to develop new effective radiosensitizers to sensitize selectively the relatively resistant hypoxic tumor cells toward radiotherapy, an additional electron affinic acetyl function has been incorporated into the 2-nitroimidazole nucleus. A direct correlation between the sensitizing efficiency and electron affinity of the radiosensitizers has been demonstrated (1). Initially, a series of 2,4-dinitroimidazoles were synthesized in an effort to increase the electron affinity of the 2-nitroimidazole nucleus (2, 3). The 1-(2-hydroxy-3-methoxypropyl)-2,4-dinitroimidazole was found to be the most effective radiosensitizer of this series (4). However, the 2,4-dinitroimidazole derivatives were found to be generally more toxic than misonidazole (5), an agent currently under clinical trials for evaluation as a radiosensitizer. It was deemed desirable to study the effect of another electron affinic group other than the nitro function at the 4-position of the 2-nitroimidazole nucleus. Accordingly, 4-acetyl substituted 2-nitroimidazole analogs have been synthesized. This modification was thought to be of interest in view of the report that 1-methyl-2-nitroimidazole-5-carboxaldehyde sensitized the hypoxic Chinese hamster cells *in vitro* to ionizing radiation at much lower concentrations (25 μM) than misonidazole (1).

BACKGROUND

It is obvious that an aldehyde function is a metabolically unstable group, and perhaps in addition to high electron affinity, lack of an hydroxyl group in the side chain at the 1-position may have contributed toward enhanced cytotoxicity of this agent. Therefore, the synthesis of 4-acetyl analogs of 2-nitroimidazole with a 2-hydroxypropyl side chain at the 1-position was undertaken. The molecular design of agents described in this report was also related to the structure of metronidazole, a known but less potent radiosensitizer than misonidazole, in that the functional groups at 2- and 5-positions were reversed to provide a 2-nitro-5-methyl analog, since 2-nitroimidazoles have been reported to be more effective radiosensitizers (6).

The synthesis of the required intermediate 2-amino-4(5)-acetyl-5(4)-methylimidazole (III) was accomplished by the known mononuclear 1,2,4-oxadiazole imidazole rearrangement with minor modification of utilizing sodium methoxide in dimethylformamide rather than sodium ethoxide as a base (7). The starting material 3-amino-5-phenyl-1,2,4-oxadiazole, readily obtained from hydrolysis of the *N,O*-dibenzoyl hydroxyguanidine (8), was condensed with an equimolar amount of acetylacetone in anhydrous toluene in the presence of *p*-toluenesulfonic acid

0022-3549/82/1100-1203$01.00/0

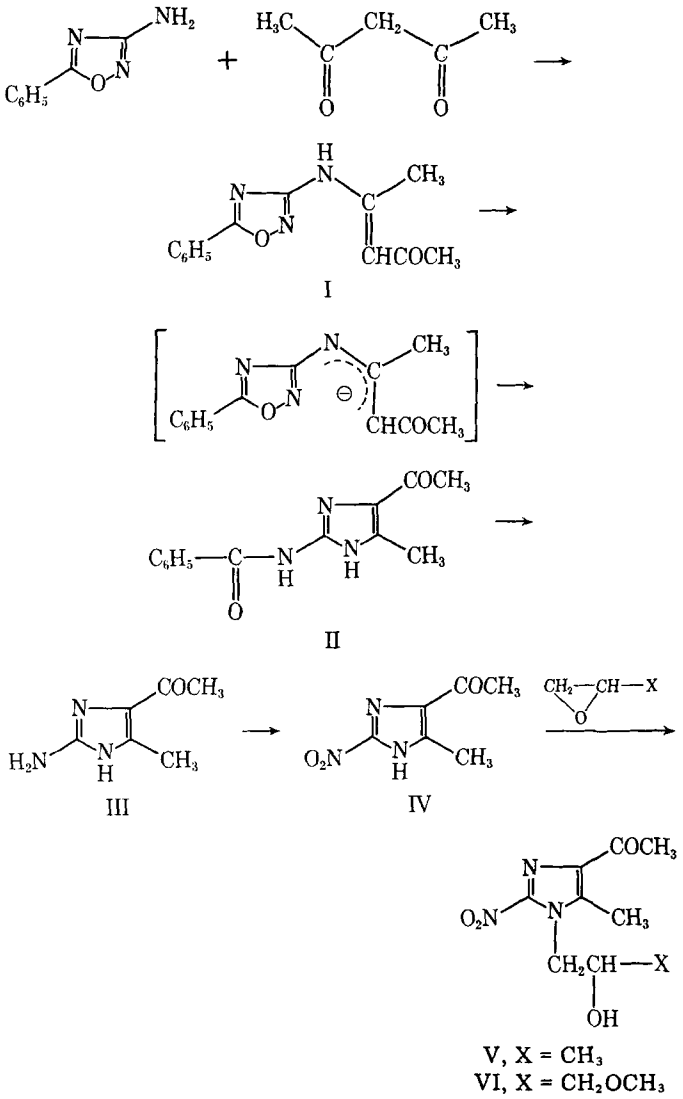

Scheme I

as a catalyst, removing azeotropically the reaction water to give the enaminoketone I (Scheme I). Treatment of I with a molar equivalent amount of sodium methoxide in anhydrous dimethylformamide caused isomerization to the anticipated 2-benzoylaminoimidazole (II). Acid hydrolysis of II afforded the 2-aminoimidazole analog (III). 2-Nitro-4(5)-acetyl-5(4)-methylimidazole (IV) was prepared from the corresponding 2-aminoimidazole derivative (III) by diazotization in fluoroboric acid followed by the reaction of the diazonium salt with nitrous acid in the presence of copper sulfate. Treatment of IV with propylene oxide in absolute ethanol, in the presence of a catalytic amount of sodium hydroxide, afforded Alcohol V. Reaction of IV with 1,2-epoxy-3-methoxypropane during 16 hr at 80° under reflux afforded alcohol VI. In each case the reaction with oxiranes produced the corresponding 4-acetyl analog and not the 5-acetyl isomer, suggesting that the reaction mechanism may be similar to the reaction of 2,4(5)-dinitroimidazoles with oxiranes as reported earlier (4).

EXPERIMENTAL

IR spectra were recorded on a spectrophotometer[1] as potassium bromide pellets. PMR spectra were recorded on a 90-MHz spectrometer[2] using tetramethylsilane as the internal reference. Electron-impact mass spectra were run on a spectrometer[3] at 70 eV ionization potential using direct inlet injection. The elemental analyses[4] were within ±0.4% of the theoretical values. Melting points were determined on glass cover slips[5] and are uncorrected. Analytical TLC was performed on plastic plates coated with a 0.25-mm layer of silica gel[6] GF_{254} and the compounds were detected by visual examination under UV light (254 nm).

[1] Beckman IR-10.
[2] JOEL.
[3] Hitachi Perkin-Elmer RMU-6E.
[4] Performed by the Integral Microanalytical Laboratories, Raleigh, N.C.
[5] Fisher-Johns melting point apparatus.

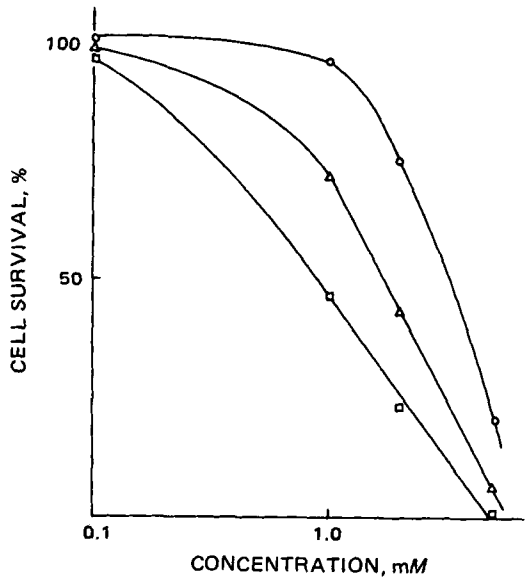

Figure 1—*The effect of Compound V at various time intervals on the survival of hypoxic Chinese hamster cells as a function of drug concentration.*

4(5)-Acetyl-5(4)-methyl-2-nitroimidazole (IV)—4(5)-Acetyl-5(4)-methyl-2-aminoimidazole (III) (0.556 g, 4 mmoles) (7) was dissolved in a mixture containing 10 ml of water, 0.5 ml of sulfuric acid, and 3.5 ml of 50% fluoroboric acid. The solution was then cooled to −20° in an ice–salt bath and a solution of sodium nitrite (2.76 g, 40 mmoles) in 5 ml of water was added dropwise to the cooled 2-aminoimidazolium sulfate solution. The mixture was stirred at −10° for 1 hr and then added to a solution of copper sulfate (19.97 g, 80 mmoles) in 150 ml of water. An additional 2.76 g of sodium nitrite was added to this mixture and stirred at room temperature overnight. The pH of the mixture was then adjusted to ~2.0 with dilute nitric acid. The mixture was repeatedly extracted with ethyl acetate (8 × 30 ml), dried over sodium sulfate, and the solvent removed under reduced pressure to leave a yellow residue, which was recrystallized (ethyl ether–hexane) to afford 210 mg (31%): mp 155–156°; IR (KBr) 1652 (CO) 1540 and 1342 (NO_2) cm^{-1}; NMR ($CDCl_3$) δ 2.68 [s, CH_3CO (CH_3)], 2.72 [s, $CH_3(CH_3CO)$]; MS, *m/z* 169 (M^+), 154 (M—CH_3), 122 [M—(NO_2+H)], 108 [M—(NO_2+CH_3)].

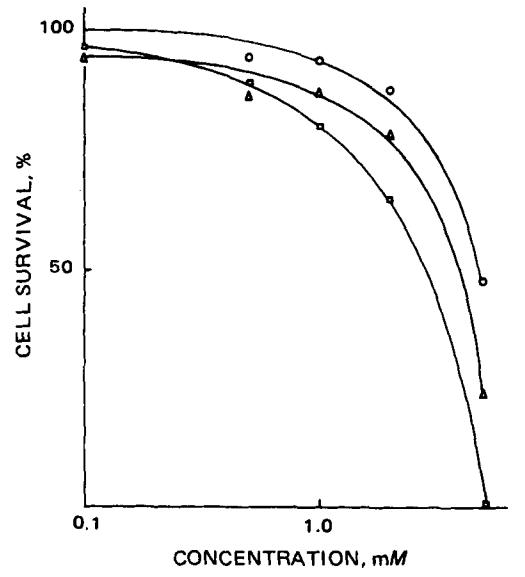

Figure 2—*The effect of Compound VI at various time intervals on the survival of hypoxic Chinese hamster cells as a function of drug concentration.*

[6] E-Merck AG, Darmstadt, Germany.

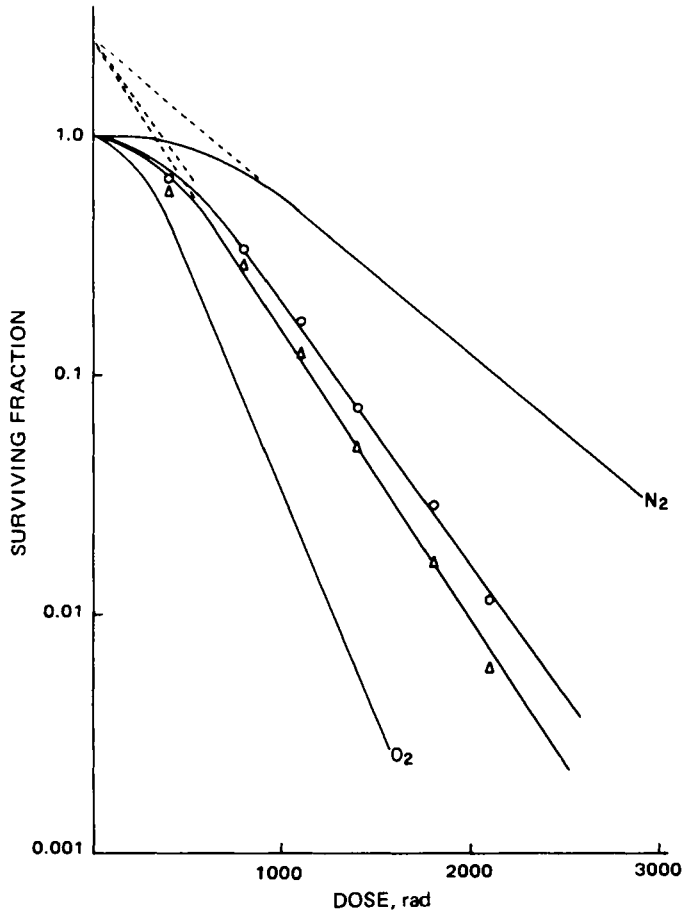

Figure 3—*The radiation survival curves of 2-nitro-4-acetylimidazole analogs by employing Chinese hamster cells (V-79). Key: N_2, cells irradiated in nitrogen; O_2, cells irradiated in air; (○) Compound VI, 1 mM; (△) Compound V, 1 mM. Each point represents the mean of three different experiments.*

Anal.—Calc. for $C_6H_7N_3O_3 \cdot H_2O$: C, 38.50; H, 4.81; N, 22.46. Found: C, 38.23; H, 4.75; N, 22.39.

Reaction of 4(5)-Acetyl-5(4)-methyl-2-nitroimidazole (IV) with Propylene Oxide—Propylene oxide (10 ml) and sodium hydroxide (15 mg) were added to a solution of IV (0.169 g, 1 mmole) in 25 ml of absolute ethanol. The reaction mixture was stirred at room temperature for 8 hr. However, the reaction was found to be negligible as followed by TLC in ethyl acetate. This reaction was completed upon heating the mixture to 40–45° under reflux for 60 hr. The solvent and excess oxirane were removed under reduced pressure to leave a residual oil which was recrystallized (ethyl ether–hexane) to afford 125 mg (55%) of alcohol (V): mp 134–135°; IR (KBr) 3360 (OH), 1650 (CO), 1540 and 1340 (NO_2) cm^{-1}; NMR ($CDCl_3$) δ 2.60 [s, $CH_3CO(CH_3)$], 2.72 [s, $CH_3(CH_3CO)$], 4.36 (m, NCH_2), 4.60 (m, CHO), 1.36 (d, CH_3): MS, *m/z* 227 (M^+), 212 (M—CH_3) 210 (M—OH), 180 [M—(NO_2+H)].

Anal.—Calc. for $C_9H_{13}N_3O_4$: C, 47.58; H, 5.73; N, 18.50. Found: C, 47.61; H, 5.68; N, 18.46.

Reaction of 4(5)-Acetyl-5(4)-methyl-2-nitroimidazole (IV) with 1,2-Epoxy-3-methoxypropane—A solution of IV (0.169 g, 1 mmole) in 2.5 ml of 1,2-epoxy-3-methoxypropane was initially stirred at room temperature for 8 hr. The reaction was found to be negligible as followed by TLC in ethyl acetate; however, it was completed upon further heating the solution to 80° under reflux for 16 hr. The excess oxirane was removed under diminished pressure to leave a residual oil, which was recrystallized (ethyl ether) to afford 148 mg (58%) of VI: mp 126–127°; IR (KBr) 3367 (OH), 1667 (CO), 1540 and 1350 (NO_2) cm^{-1}; NMR ($CDCl_3$) δ 2.64 [s, $CH_3CO(CH_3)$], 2.76 [s, $CH_3(CH_3CO)$], 4.28 (m, NCH_2), 4.64 (m, CHO), 3.60 (d), and 3.51 (s, CH_2OCH_3): MS, *m/z* 257 (M+), 242 (M—CH_3), 240 (M—OH), 211 (M—NO_2).

Anal.—Calc. for $C_{10}H_{15}N_3O_5$: C, 46.69; H, 5.84; N, 16.34. Found: C, 46.75; H, 5.62; N, 16.41.

Biological Studies—The cytotoxicity studies were carried out by employing asynchronous monolayer cultures of Chinese hamster cells (V-79). The techniques used for culturing and handling this cell line were followed as previously reported (2). To determine differential cytotoxicity between the oxic and hypoxic cells, ~200 cells were plated in petri dishes[7] (60 × 15 mm) containing 3 ml of minimum essential medium with 15% fetal calf serum and allowed to attach for 2 hr. The medium was then removed by aspiration and replaced by the medium containing an appropriate concentration of the compound under study. The cells were exposed to a range of concentrations of each compound for intervals of 2, 4, and 8 hr at 37° in air or in hypoxia. The hypoxia was achieved by placing the open petri dishes in sealed containers and then purging with nitrogen–carbon dioxide (95:5). The gas mixture was bubbled through a flask containing sterile water before entering the sealed containers to maintain humidity inside the chambers. At the end of the specific time interval, the medium containing the drug was removed and replaced with 3 ml of fresh medium. Cultures were incubated for 6 days at 37° in an atmosphere of air–carbon dioxide (95:5); the resulting colonies were fixed in absolute ethanol, stained with methylene blue, and counted.

The radiosensitization studies were carried out by irradiating the cells inside the sealed containers under hypoxia by employing a cobalt 60 source at a dose rate of ~240 rad/min. Complete survival curves were obtained for each compound at radiation doses of 400–3000 rad under oxic and hypoxic conditions. The D_0 values were calculated for the hypoxic control cells and for the hypoxic cells treated with the drug. The ratio of these two D_0 values provided the sensitizer enhancement ratio of the corresponding agent.

Partition Coefficients—The compounds were dissolved in phosphate buffer (0.1 *M*, pH 7.4) and were then stirred with an equal volume of octanol at room temperature for 1 hr. The concentration of the nitroimidazoles in the aqueous phase was determined spectrophotometrically at 320 nm.

Table I—Sensitizer Enhancement Ratios, LD_{50} Values, and Partition Coefficients of 2-Nitro-4-acetylimidazole Analogs

Compound	SER[a]	LD_{50}[b], mg/kg	PC[c]
V	2.1	1,200	2.46
VI	1.9	1,400	1.07
Misonidazole	1.9	1,300	0.43

[a] Sensitizer enhancement ratio determined by dividing the D_0 value for the control hypoxic cells with the D_0 value obtained for the cells irradiated in the presence of the sensitizer. [b] LD_{50} values were determined in C57BL mice by the standard procedures. [c] Partition coefficients.

RESULTS AND DISCUSSION

Both Compounds V and VI were essentially nontoxic to the Chinese hamster cells up to a concentration of 5 m*M* when exposed to a maximum period of 8 hr under oxic conditions. However, when the cells were exposed to various drug concentrations under nitrogen, Compounds V and VI were differentially more toxic to the hypoxic cells, and the toxicity increased as a function of time with increased concentration (Figs. 1 and 2, respectively). Similar differential cytotoxicity has been reported for other nitroimidazoles (9) and has been related to the metabolic reduction of the drug under hypoxia, causing the production of the reduced intermediates that are toxic to the cells (10). Compound V was comparatively more toxic to the hypoxic Chinese hamster cells than VI. The hypoxic toxicity increased with time and drug concentration. Compound V, although nontoxic, at 1.0 m*M* concentration upon 2 hr of exposure, caused >50% inhibition by 8 hr (Fig. 1). Compound VI did not show significant differential cytotoxicity up to a concentration of 1 m*M* and required higher concentrations and increasing incubation time for hypoxic cytotoxicity (Fig. 2).

The radiosensitizing efficiency of these agents was assessed from the radiation survival curves of hypoxic Chinese hamster cells (Fig. 3). These experiments were conducted at a nontoxic concentration of 1 m*M*, and the sensitizer enhancement ratios were calculated by dividing the D_0 value for the control hypoxic cells with the D_0 value obtained for the cells irradiated in the presence of the radiosensitizer under nitrogen. The enhancement ratios for Compounds V and VI were found to be 2.1 and 1.9, respectively (Table I). Misonidazole, under similar conditions, produced an enhancement ratio of 1.9 at 1 m*M* concentration, suggesting that V is, comparatively, a more effective radiosensitizer.

Although 2,4-dinitroimidazole derivatives have been shown to be more efficient radiosensitizers than 2-nitroimidazoles *in vitro* (4), the powerful electron withdrawing group at the 4-position also causes an increase in

[7] Permanox, Lux Scientific Corp.

cytotoxicity (5). In attempts to develop radiosensitizers relatively less toxic than misonidazole, the results obtained upon introducing an acetyl function at the 4-position of 2-nitroimidazole have been described in this report. The acetyl function, although relatively less powerful than the nitro group with respect to the electron withdrawing capacity, has been reported to possess radiosensitizing properties (11). It was contemplated that the insertion of an acetyl function in the 2-nitroimidazole molecule may provide analogs which are comparatively less toxic than the 2,4-dinitroimidazoles. The *in vivo* acute toxicity of these agents was assessed by determining the LD_{50} in C57BL mice. Compounds V and VI were found to have an LD_{50} of 1.2 and 1.4 g/kg, respectively (Table I). These values are similar to misonidazole, which had an LD_{50} of 1.3 g/kg but are greater than the LD_{50} of 2,4-dinitroimidazoles (5). These agents are relatively less toxic than the corresponding dinitroimidazoles as expressed by the doses required for acute toxicity. The partition coefficients of these agents were determined in an octanol–phosphate buffer (pH 7.4) mixture. Compounds V and VI are more lipophilic than misonidazole (Table I), a property that would be expected to be favorable for *in vivo* diffusion into the hypoxic region of the tumors. This work has demonstrated that an additional electron affinic group could be inserted in the misonidazole molecule without significantly increasing the acute toxicity and yet enhancing the sensitizing efficiency. Thus, V may possess a therapeutic advantage over misonidazole as a radiosensitizer.

REFERENCES

(1) G. E. Adams, I. R. Flockhart, C. E. Smithen, I. J. Stratford, P. Wardman, and M. E. Watts, *Radiat. Res.*, **67**, 9 (1976).

(2) K. C. Agrawal, B. C. Millar, and P. Neta, *ibid.*, **78**, 532 (1978).

(3) K. C. Agrawal, K. B. Bears, R. K. Sehgal, J. N. Brown, P. E. Rist, and W. D. Rupp, *J. Med. Chem.*, **22**, 583 (1978).

(4) R. K. Sehgal, M. W. Webb, and K. C. Agrawal, *ibid.*, **24**, 601 (1981).

(5) K. C. Agrawal, M. W. Webb, and R. K. Sehgal, *Proc. Am. Assoc. Cancer Res.*, **21**, 304 (1980).

(6) J. C. Asquith, M. E. Watts, K. Patel, C. E. Smithen, and G. E. Adams, *Radiat. Res.*, **60**, 108 (1974).

(7) M. Riccoa, N. Vivona, and G. Cusmano, *Tetrahedron*, **30**, 3859 (1974).

(8) P. Adams, D. W. Kaiser, and G. A. Peters, *J. Org. Chem.*, **18**, 934 (1953).

(9) E. J. Hall and J. Biaglow, *Int. J. Radiat. Oncol. Biol. Phys.*, **2**, 521 (1977).

(10) S. H. Basaga, J. R. Dunlop, A. J. F. Searle, and R. L. Wilson, *Br. J. Cancer, Suppl. III.*, **37**, 132 (1978).

(11) G. E. Adams and M. S. Cooke, *Int. J. Radiat. Biol.*, **15**, 457 (1969).

The Hydrolysis of Spirohydantoin Mustard

K. P. FLORA, J. C. CRADOCK, and J. A. KELLEY ˣ

Received July 23, 1981, from the *Pharmaceutical Resources Branch, and the Laboratory of Medicinal Chemistry and Biology, Division of Cancer Treatment, National Cancer Institute, National Institutes of Health, Bethesda, MD 20205.* Accepted for publication January 13, 1982.

Abstract □ Spirohydantoin mustard (I) is a rationally designed antitumor agent with substantial *in vivo* activity against intracranially implanted tumors in mice. However, hydrolysis of I was much faster than that of mechlorethamine hydrochloride or melphalan, two parenterally administered mustards. The hydrolysis products of I were identified by GC–MS of their silylated derivatives. The decomposition of I (at 25° in 10% dimethylacetamide at pH 4–6), as monitored by GLC was pseudo first-order. The half-life of I ranged from 20 min at pH 4.0 to 14 min at pH 6.0. Nonionic surfactants enhanced the stability of I, but this effect was diminished at lower pH, presumably due to decreased solubility of I in the micelle as more drug was protonated. Several dilute parenterally suitable solvents exhibited no marked effect on the hydrolysis of I. The drug was most stable in a 10% fat emulsion system where the time for 10% decomposition of I was 49 ± 5 min. Plots of the concentration of I *versus* time were linear indicating the disappearance was zero order in the 10% fat emulsion system.

Keyphrases □ Spirohydantoin mustard—hydrolysis, antitumor agent, mechlorethamine hydrochloride, melphalan, mice □ Hydrolysis—spirohydantoin mustard, antitumor agent, mechlorethamine hydrochloride, melphalan, mice □ Antitumor agents—hydrolysis of spirohydantoin mustard, mice

Spirohydantoin mustard (I) (NSC-172112), 3-[2-[bis(2′- chloroethyl)amino] - ethyl] - 5,5 - pentamethylenehydantoin, is a potential antitumor agent that has been designed specifically for use against central nervous system tumors. Compound I has demonstrated significant antitumor activity against L-1210 leukemia, P-388 leukemia, B-16 melanoma, and ependymoblastoma when administered in an aqueous suspension by the intraperitoneal route (1). Compound I was designed to incorporate a mustard alkylating function coupled to a substituted hydantoin carrier to provide an overall optimum partition coefficient for crossing the blood–brain barrier (1). A preliminary pharmacological study in dogs indicates that I does enter the central nervous system, although actual concentrations in cerebrospinal fluid are low (2).

As is often the case with nitrogen mustard derivatives, solution decomposition problems are evident. The aqueous stability of I and related compounds is such that octanol–water partition coefficients could not be determined (1). Preliminary chloride titration data also indicate that the decomposition of I in aqueous solution is rapid. In fact, the decomposition of I is more rapid than the hydrolysis of either of two clinically useful mustards, melphalan or mechlorethamine hydrochloride. In addition, the aqueous solubility of I is limited (<10 μg/ml) (3). Dissolution in concentrated acid with subsequent dilution is possible (1.25 mg/ml); however, the upward adjustment of pH usually results in precipitation of the drug. Likewise, I has

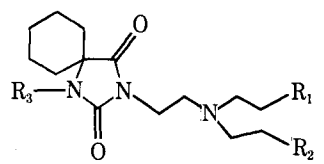

I $R_1 = R_2 = -Cl$; $R_3 = -H$
Ia $R_1 = R_2 = -Cl$; $R_3 = -$Trimethylsilyl or $-Si(CH_3)_3$
II $R_1 = -Cl$; $R_2 = -OH$; $R_3 = -H$
IIa $R_1 = -Cl$; $R_2 = -OSi(CH_3)_3$; $R_3 = -Si(CH_3)_3$
III $R_1 = R_2 = -OH$; $R_3 = -H$
IIIa $R_1 = R_2 = -OSi(CH_3)_3$; $R_3 = -Si(CH_3)_3$
IV $R_1 = -OH$; $R_2 = -OCOCH_3$; $R_3 = -H$
IVa $R_1 = -OSi(CH_3)_3$; $R_2 = -OCOCH_3$; $R_3 = -Si(CH_3)_3$

0022-3549/82/1100-1206$01.00/0

cytotoxicity (5). In attempts to develop radiosensitizers relatively less toxic than misonidazole, the results obtained upon introducing an acetyl function at the 4-position of 2-nitroimidazole have been described in this report. The acetyl function, although relatively less powerful than the nitro group with respect to the electron withdrawing capacity, has been reported to possess radiosensitizing properties (11). It was contemplated that the insertion of an acetyl function in the 2-nitroimidazole molecule may provide analogs which are comparatively less toxic than the 2,4-dinitroimidazoles. The *in vivo* acute toxicity of these agents was assessed by determining the LD_{50} in C57BL mice. Compounds V and VI were found to have an LD_{50} of 1.2 and 1.4 g/kg, respectively (Table I). These values are similar to misonidazole, which had an LD_{50} of 1.3 g/kg but are greater than the LD_{50} of 2,4-dinitroimidazoles (5). These agents are relatively less toxic than the corresponding dinitroimidazoles as expressed by the doses required for acute toxicity. The partition coefficients of these agents were determined in an octanol–phosphate buffer (pH 7.4) mixture. Compounds V and VI are more lipophilic than misonidazole (Table I), a property that would be expected to be favorable for *in vivo* diffusion into the hypoxic region of the tumors. This work has demonstrated that an additional electron affinic group could be inserted in the misonidazole molecule without significantly increasing the acute toxicity and yet enhancing the sensitizing efficiency. Thus, V may possess a therapeutic advantage over misonidazole as a radiosensitizer.

REFERENCES

(1) G. E. Adams, I. R. Flockhart, C. E. Smithen, I. J. Stratford, P. Wardman, and M. E. Watts, *Radiat. Res.*, **67**, 9 (1976).

(2) K. C. Agrawal, B. C. Millar, and P. Neta, *ibid.*, **78**, 532 (1978).

(3) K. C. Agrawal, K. B. Bears, R. K. Sehgal, J. N. Brown, P. E. Rist, and W. D. Rupp, *J. Med. Chem.*, **22**, 583 (1978).

(4) R. K. Sehgal, M. W. Webb, and K. C. Agrawal, *ibid.*, **24**, 601 (1981).

(5) K. C. Agrawal, M. W. Webb, and R. K. Sehgal, *Proc. Am. Assoc. Cancer Res.*, **21**, 304 (1980).

(6) J. C. Asquith, M. E. Watts, K. Patel, C. E. Smithen, and G. E. Adams, *Radiat. Res.*, **60**, 108 (1974).

(7) M. Riccoa, N. Vivona, and G. Cusmano, *Tetrahedron*, **30**, 3859 (1974).

(8) P. Adams, D. W. Kaiser, and G. A. Peters, *J. Org. Chem.*, **18**, 934 (1953).

(9) E. J. Hall and J. Biaglow, *Int. J. Radiat. Oncol. Biol. Phys.*, **2**, 521 (1977).

(10) S. H. Basaga, J. R. Dunlop, A. J. F. Searle, and R. L. Wilson, *Br. J. Cancer, Suppl. III.*, **37**, 132 (1978).

(11) G. E. Adams and M. S. Cooke, *Int. J. Radiat. Biol.*, **15**, 457 (1969).

The Hydrolysis of Spirohydantoin Mustard

K. P. FLORA, J. C. CRADOCK, and J. A. KELLEY ˣ

Received July 23, 1981, from the *Pharmaceutical Resources Branch, and the Laboratory of Medicinal Chemistry and Biology, Division of Cancer Treatment, National Cancer Institute, National Institutes of Health, Bethesda, MD 20205.* Accepted for publication January 13, 1982.

Abstract □ Spirohydantoin mustard (I) is a rationally designed antitumor agent with substantial *in vivo* activity against intracranially implanted tumors in mice. However, hydrolysis of I was much faster than that of mechlorethamine hydrochloride or melphalan, two parenterally administered mustards. The hydrolysis products of I were identified by GC–MS of their silylated derivatives. The decomposition of I (at 25° in 10% dimethylacetamide at pH 4–6), as monitored by GLC was pseudo first-order. The half-life of I ranged from 20 min at pH 4.0 to 14 min at pH 6.0. Nonionic surfactants enhanced the stability of I, but this effect was diminished at lower pH, presumably due to decreased solubility of I in the micelle as more drug was protonated. Several dilute parenterally suitable solvents exhibited no marked effect on the hydrolysis of I. The drug was most stable in a 10% fat emulsion system where the time for 10% decomposition of I was 49 ± 5 min. Plots of the concentration of I *versus* time were linear indicating the disappearance was zero order in the 10% fat emulsion system.

Keyphrases □ Spirohydantoin mustard—hydrolysis, antitumor agent, mechlorethamine hydrochloride, melphalan, mice □ Hydrolysis—spirohydantoin mustard, antitumor agent, mechlorethamine hydrochloride, melphalan, mice □ Antitumor agents—hydrolysis of spirohydantoin mustard, mice

Spirohydantoin mustard (I) (NSC-172112), 3-[2-[bis(2′- chloroethyl)amino] - ethyl] - 5,5 - pentamethylenehydantoin, is a potential antitumor agent that has been designed specifically for use against central nervous system tumors. Compound I has demonstrated significant antitumor activity against L-1210 leukemia, P-388 leukemia, B-16 melanoma, and ependymoblastoma when administered in an aqueous suspension by the intraperitoneal route (1). Compound I was designed to incorporate a mustard alkylating function coupled to a substituted hydantoin carrier to provide an overall optimum partition coefficient for crossing the blood–brain barrier (1). A preliminary pharmacological study in dogs indicates that I does enter the central nervous system, although actual concentrations in cerebrospinal fluid are low (2).

As is often the case with nitrogen mustard derivatives, solution decomposition problems are evident. The aqueous stability of I and related compounds is such that octanol–water partition coefficients could not be determined (1). Preliminary chloride titration data also indicate that the decomposition of I in aqueous solution is rapid. In fact, the decomposition of I is more rapid than the hydrolysis of either of two clinically useful mustards, melphalan or mechlorethamine hydrochloride. In addition, the aqueous solubility of I is limited (<10 μg/ml) (3). Dissolution in concentrated acid with subsequent dilution is possible (1.25 mg/ml); however, the upward adjustment of pH usually results in precipitation of the drug. Likewise, I has

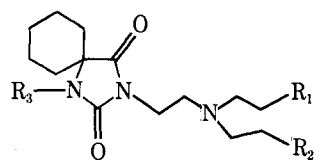

I $R_1 = R_2 = -Cl$; $R_3 = -H$
Ia $R_1 = R_2 = -Cl$; $R_3 = -$Trimethylsilyl or $-Si(CH_3)_3$
II $R_1 = -Cl$; $R_2 = -OH$; $R_3 = -H$
IIa $R_1 = -Cl$; $R_2 = -OSi(CH_3)_3$; $R_3 = -Si(CH_3)_3$
III $R_1 = R_2 = -OH$; $R_3 = -H$
IIIa $R_1 = R_2 = -OSi(CH_3)_3$; $R_3 = -Si(CH_3)_3$
IV $R_1 = -OH$; $R_2 = -OCOCH_3$; $R_3 = -H$
IVa $R_1 = -OSi(CH_3)_3$; $R_2 = -OCOCH_3$; $R_3 = -Si(CH_3)_3$

0022-3549/82/1100-1206$01.00/0

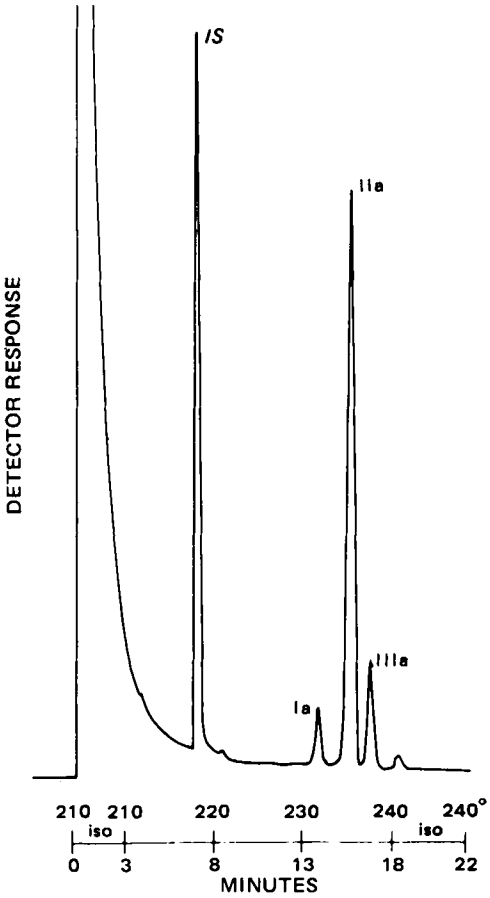

Figure 1—*Chromatogram of the trimethylsilyl derivatives of I, II, III (Ia, IIa, IIIa) and internal standard (IS) in a typical hydrolysis mixture (t = 60 min, apparent pH = 4.0).*

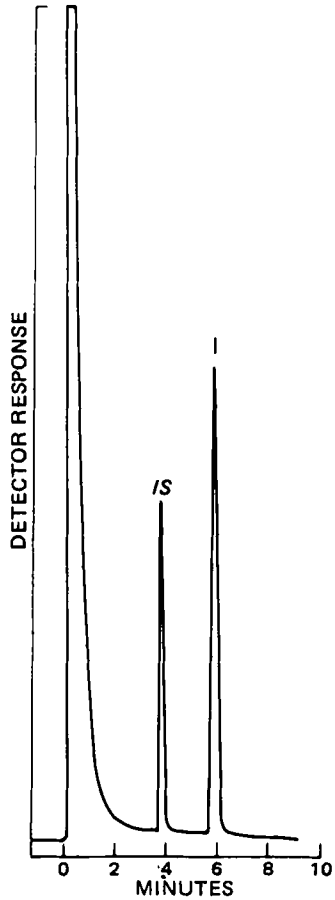

Figure 2—*Chromatogram of I and internal standard (IS) after extraction from 10% fat emulsion (1.0 mg/ml of I).*

considerable solubility in some organic solvents (*e.g.*, >300 mg/ml in dimethylacetamide); however, dilution with aqueous solutions usually causes the drug to precipitate.

The purpose of this study was to investigate the effect of pH and the presence of various excipients on the hydrolysis of I with emphasis on impeding degradation. Successful approaches would be applied to the development of a parenteral dosage form suitable for clinical trial.

EXPERIMENTAL

Materials—Dimethylacetamide[1], polysorbate 20[2], polysorbate 80[2], two polyoxyethylated castor oils[3,4], stearylcetyl alcohol ethoxylate[5], propylene glycol[6], bovine albumin[7], thymol[8], thymol blue[8], gelatin[9], spirohydantoin mustard (I)[10] (NSC-172112), mechlorethamine hydrochloride[10] (NSC-762), and melphalan (NSC-8806) were used as received. Compound III[10] was twice recrystallized from isopropanol–benzene (1:50) before use. All other chemicals were reagent grade. Citrate buffers (pH 3–6) were prepared by dilution of a 0.42 *M* stock solution of citric acid with subsequent addition of sodium hydroxide to the desired pH.

Hydrolysis Studies—Due to the limited solubility of I, studies of the hydrolysis at various pHs were conducted in 10% dimethylacetamide in citrate or ammonium acetate buffer (4.2×10^{-2} *M*), or under pH stat control. All reported pH values are in fact apparent pH values unless otherwise indicated. The mustard I was weighed, dissolved in dimethylacetamide, and then diluted with thermally equilibrated (25 ± 0.1°) water, buffer, or buffer plus excipient. Final drug concentration was 0.35 mg/ml unless otherwise indicated. All hydrolysis studies were run at 25 ± 0.1°.

Chloride Titration—The concentration of chloride ion was determined by the coulometric–amperometric titration[11] of aliquots of the hydrolysis mixture. A 0.5- or 1.0-ml aliquot was removed and diluted with 3.0 ml of 0.1 *N* nitric acid–10% acetic acid reagent. When a 0.5-ml aliquot was used, 0.5 ml of distilled water was added to keep the titration volume consistent at 4.0 ml. Four drops of a gelatin reagent containing 6.0 mg/ml of gelatin, 0.1 mg/ml of thymol blue, and 0.1 mg/ml of thymol were added prior to each titration. The titration was performed only if a red color, indicating that the mixture was sufficiently acidic (pH ~ 1.2), was present. The titrator was calibrated at the low titration rate using standard sodium chloride solutions. Blanks and standards were prepared to be of identical composition to the hydrolysis solution in terms of the buffers and excipients present.

Disappearance of I by GLC—Preliminary studies at pH 4.0 indicated that the efficient and simultaneous extraction of I, II, and III from sodium citrate or sodium acetate buffers was impractical, presumably because of the low pH. Extraction of I, II, and III could be avoided by using an ammonium acetate buffer which could be removed by freeze-drying the hydrolysis mixture. However, in this case, small peaks corresponding to acetate esters of III were detected within 90 min. Therefore, a bufferless system, which also required no extractive cleanup, was employed by using a titrator[12] operating in the pH stat mode. Sodium hydroxide (0.05 *M*) was used as the titrant. This system was capable of maintaining the pH of the solution at ±0.1 pH units during the course of the experiment.

In these hydrolysis studies a 2-ml aliquot of the hydrolysis mixture initially containing I at a concentration of 0.15 mg/ml and internal standard (phenytoin) was removed at appropriate times and immediately

[1] Burdick and Jackson Co., Muskegon, Mich.
[2] Tween 20, Tween 80, Sigma Chemical Co., St. Louis, Mo.
[3] Emulphor EL-719, GAF Corp., New York, N.Y.
[4] Cremophor EL, Sandoz, Basel, Switzerland.
[5] Siponic E-7, Alcolac Inc., Baltimore, Md.
[6] Matheson, Coleman and Bell, East Rutherford, N.J.
[7] Sigma Chemical Co., St. Louis, Mo.
[8] Fisher Scientific Co., Fair Lawn, N.J.
[9] Knox Gelatin, Inc. Johnstown, N.Y.
[10] Provided by the Division of Cancer Treatment, National Cancer Institute, Bethesda, Md.

[11] Buchler-Cotlove Chloridometer, Buchler Instruments Inc., Fort Lee, N.J.
[12] Radiometer Type TTTld Titrator, Radiometer, Copenhagen, Denmark.

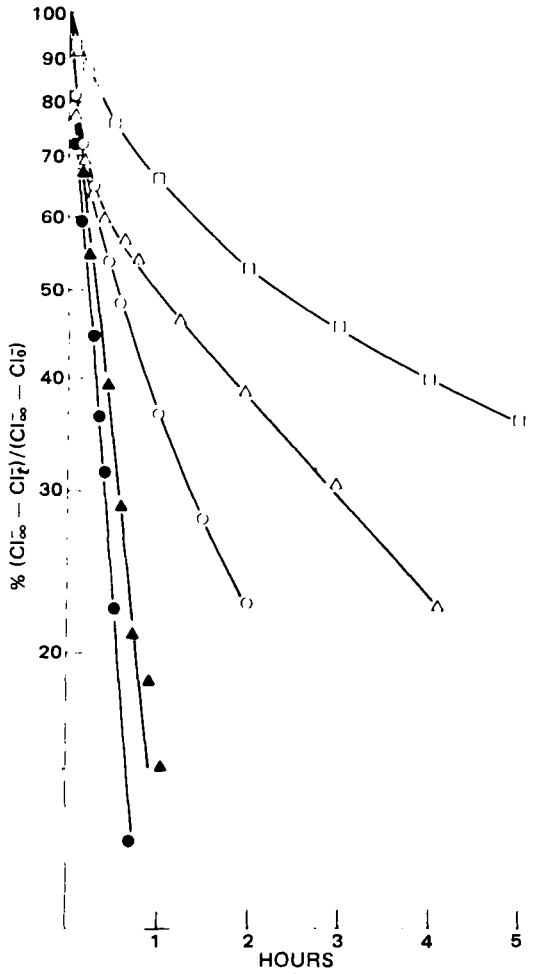

Figure 3—*The effect of pH on the hydrolysis of I (0.35 mg/ml) as determined by chloride titration. All pHs (apparent) are with sodium citrate buffer (4.2×10^{-2} M). Key: (□) pH 3.0; (△) pH 3.5; (○) pH 4.0; (▲) pH 5.0; (●) pH 6.0.*

frozen in glass vials (37.4 ml) prechilled on dry ice. Appropriate standards of I and III plus internal standard were similarly frozen. All samples were then placed on a prechilled shelf and freeze-dried[13]. The freeze-dried samples and standards were derivatized by reaction with 0.30 ml of a mixture of *N,O*-bis(trimethylsilyl)trifluoroacetamide[14]–acetonitrile (1:2) at room temperature for a minimum of 30 min. Shaking and sonication were employed to effect solution and reaction of the freeze-dried samples. Aliquots (4.0 μl) of the trimethylsilylation reaction mixture were analyzed by GLC[15] on a 1.83-m × 2-mm i.d. glass column packed with 3% SE-30 100/120 mesh Gas-Chrom Q[14] and installed for on-column injection. The gas chromatograph was temperature programmed from 210 to 240° at 2°/min after an initial delay of 3 min. Other operating parameters were: helium carrier gas flow, 30 ml/min; hydrogen, 30 ml/min; air, 300 ml/min; injector port, 255°; and flame ionization detector (FID), 260°. Samples were analyzed interspersed with standards so that standard curves of the peak area ratios of both I and III to internal standard were prepared for each hydrolysis experiment. The direct quantitation of I and III allowed II to be calculated by difference as well as a calculation of chloride ion so that a direct comparison with the coulometric–amperometric titrations could be made. A typical chromatogram is presented in Fig. 1.

GC–MS Analysis—Representative hydrolysis mixtures were also analyzed by GC–MS[16] under data system[17] control to identify the hydrolysis products. GC analysis parameters were identical to those used above, while the mass spectrometer operating conditions were: transfer line and jet separator, 255°; ion source, 260°; electron energy, 75 eV; ionizing current, 250 μamps; accelerating voltage, 1.6 kV; and scan speed, 2 sec/decade.

[13] Virtis Model 10-146 MR-BA Freeze-Mobile, The Virtis Company, Gardiner, N.Y.
[14] Applied Science Laboratories, Inc., State College, Pa.
[15] Model 2740, Varian Aerograph, Walnut Creek, Calif.
[16] DuPont 21-492B, Dupont Instruments, Monrovia, Calif.
[17] VG 2040 Data System, VG Data Systems Limited, Altrincham, England.

Table I—Comparison of Percent Total Chloride Liberated from I after Hydrolysis at pH 4.0 (apparent) in 0.042 *M* Ammonium Acetate Calculated from GLC and by Titration

Minutes	Percent Total Chloride Liberated: Calculated from GLC Data	Percent Total Chloride Liberated: Determined by Direct Titration
5	12.3	10.3
10	16.2	16.6
20	31.7	29.8
30	39.3	38.2
60	52.1	53.0

Stability in 10% Fat Emulsion by GLC—The disappearance of I in 10% fat emulsion[18] was monitored by GLC[19]. A measured volume of 10% fat emulsion (49.4 ml) was placed in a 50-ml flint serum vial which was closed with a butyl rubber stopper and an aluminum seal. The vial was secured to a mechanical mixer with tape. The mixer was started, and a solution of I in dimethylacetamide (50 mg in 0.6 ml) was injected directly into the emulsion using a 1-ml glass syringe equipped with an 8.89-cm, 22-gauge needle. The solution of I was injected at ~1 ml/min while the vigorous mixing continued. Duplicate 2-ml aliquots were drawn at designated times, placed in glass screw-capped vials (149.6 ml each) and were immediately frozen in a dry ice–acetone bath. A series of standards corresponding to 0.2, 0.5, 0.7, 1.0, and 1.5 mg/ml of I were prepared by adding appropriate amounts of I in ethyl acetate to the emulsion. Samples were immediately frozen. All samples and standards were freeze-dried in a shelf-type unit[13]. The freeze-dried residue was extracted with 5.0 ml of ethyl acetate containing 40 mg/ml tetraphenylethylene as an internal standard. Aliquots (2 μl) of the samples and standards were analyzed by GLC on a 1.83-m × 2-mm i.d. glass column packed with 3% OV-17 on 80/100 mesh Chromosorb WHP[20] and installed for on-column injection. The gas chromatograph was operated isothermally at 230°. Other operating parameters were: helium carrier gas flow, 22 ml/min; hydrogen, 28 ml/min; air, 350 ml/min; injector port, 240°, and FID, 250°. Samples were analyzed interspersed with standards. Quantitation was accomplished by an internal standard method using the ratio of peak heights of I to tetraphenylethylene. A typical chromatogram is seen in Fig. 2.

Antitumor Activity—The antitumor activity of I in an experimental formulation (5% dimethylacetamide in 10% fat emulsion[18]) was evaluated against a suspension of bulk I in the P-388 tumor. Studies were conducted according to standard National Cancer Institute protocols (4). The tumor inoculum was injected intraperitoneally. Drug treatment began the following day and continued for a total of 9 daily intraperitoneal injections.

RESULTS AND DISCUSSION

Chloride titrations of the bulk drug I used as received indicated no free chloride was present. Hydrolysis mixtures that were allowed to proceed

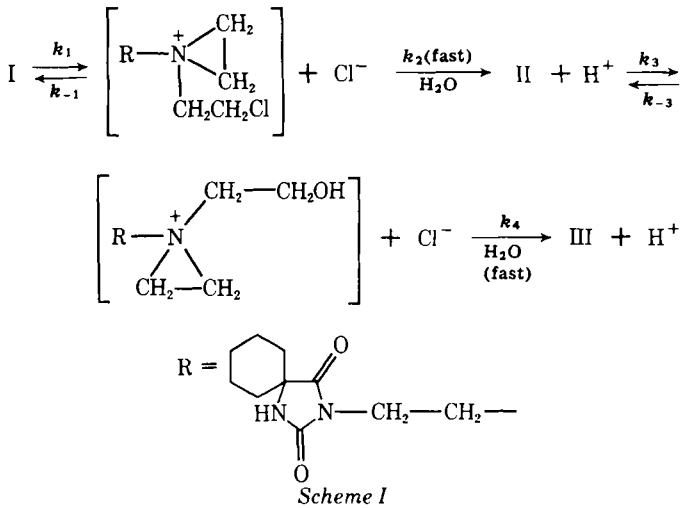

Scheme I

[18] Intralipid 10%, Cutter Laboratories, Inc., Berkeley, Calif.
[19] Model 5754, Hewlett-Packard, Avondale, Pa.
[20] Supelco, Inc., Bellefonte, Pa.

Table II—GC-MS Characteristics of Silylated Derivatives of I

Compound	Ia	IIa	IIIa	IVa
Retention Index (SE-30, 220°)	2490	2543	2578	2629
Mass Spectrum probable structure	*m/z* (relative intensity)			
M^+	407(0.3)	461(0.4)	515(0.6)	485(0.3)
$M-CH_3$	392(2.3)	446(7.0)	500(10)	470(8.4)
M−HCl	371(3.7)	425(4.8)	—	—
$M-CH_2Cl$	358(3.8)	412(3.4)	—	—
M−HCl	335(17)	—	—	—
$M-CH_2O(CH_3CO)$	—	—	—	412(9.4)
$M-Si(CH_3)_3OH$	—	371(1.8)	425(1.5)	395(2.8)
$M-CH_2OSi(CH_3)_3$	—	358(80)	412(100)	382(65)
$M-Si(CH_3)_3OH$—HCl	—	335(6.4)	—	—
$M-CH_2OSi(CH_3)_3$—CH_2Cl	—	309(3.7)	—	—
B	267(7.5)	267(34)	267(8.8)	267(14)
A	154(100)	208(100)	262(62)	232(100)
A−HCl	118(15)	—	—	—
$C_4H_7O_2^+$	—	—	—	87(70)
$Si(CH_3)_3^+$	73(16)	73(77)	73(19)	73(66)

to completion yielded, by titration, the theoretical amount of chloride ion. The hydrolysis products, II and III, were identified as their trimethylsilyl derivatives (IIa and IIIa) by GC–MS analysis of a typical hydrolysis mixture.

Stability *Versus* pH by Chloride Titration—The hydrolysis of I in 10% dimethylacetamide and sodium citrate buffer (4.2×10^{-2} *M*) as a function of pH between pH 3.0 and pH 6.0 is shown in Fig. 3. The percent of chlorine remaining covalently bound in I and II is calculated based on the percent of the theoretical amount of chloride that has been liberated at a given time.

The liberation of chloride from I is a function of pH of the media as seen in Fig. 3. The rate of hydrolysis increases as the pH increases. The slower rate at lower pH may be due to the protonation of the nitrogen of the alkylating function which inhibits the formation of the postulated aziridinium ion intermediate (Scheme I). Over the pH range studied (3.0–6.0) the rate of hydrolysis is too rapid for practical application.

Stability *Versus* pH by GLC—Table I compares the percentage of total chloride liberated from I in 0.042 *M* ammonium acetate buffer at pH 4.0 as determined by immediate direct titration and as calculated on the basis of the amounts of I, II, and III present determined by GLC analysis. These data indicate that the required manipulations prior to GLC analysis (freezing, freeze-drying, and derivatization) did not produce additional hydrolysis of I. Similar data demonstrate the comparability of the two methods in the pH stat controlled experiments. However, in this instance, it was necessary to apply corrections to the titration data to compensate for chloride bleed from the pH electrode.

The concentrations of I, II, and III *versus* time at pH 4.0 (pH stat control) as determined by GLC are seen in Fig. 4. Trimethylsilylation was essential for forming volatile derivatives with good GC properties from the degradation products of I. Combined GC–MS analysis showed that the hydantoin nitrogen as well as any free hydroxyl groups were derivatized by *N,O-bis*(trimethylsilyl)trifluoroacetamide. Table II lists the isothermal retention indexes of these derivatives and summarizes their mass spectral fragmentation patterns. The predominant mode of fragmentation was cleavage at bonds α to the mustard nitrogen with charge retention on this nitrogen. When the ethylene moiety between the hydantoin ring and mustard nitrogen was cleaved, Fragment A resulted as a major ion. Cleavage of the other C—C bonds α to the mustard nitrogen resulted in loss of substituted methyl radicals to form abundant ions such as *m/z* 358 in IIa, *m/z* 412 in IIIa, and *m/z* 382 in IVa. Cleavage of the bond adjacent to the mustard nitrogen and charge retention on the hydantoin moiety produced Fragment B at *m/z* 267, which was found in the MS of every derivative. The presence or absence and number of chlorine atoms was also evident from the distinctive isotopic pattern of this element. This information, plus an indication of the molecular weight from the molecular ion and fragmentation due to neutral losses (*e.g.*, $M-CH_3$, M−HCl), was more than sufficient to determine the identity of these derivatives.

The disappearance of I was pseudo first-order as indicated by the linearity ($r > 0.998$) of plots of the log of concentration of I *versus* time at pH 4.0, 5.0, and 6.0 (pH stat control). Pseudo first-order rate constants (k_1) at pH 4.0, 5.0, and 6.0 were 0.0336, 0.0472, and 0.0492/min, respectively. This pH–hydrolysis rate relationship demonstrates the same trend seen with the chloride titration data (Fig. 3). If the hydrolysis of I is

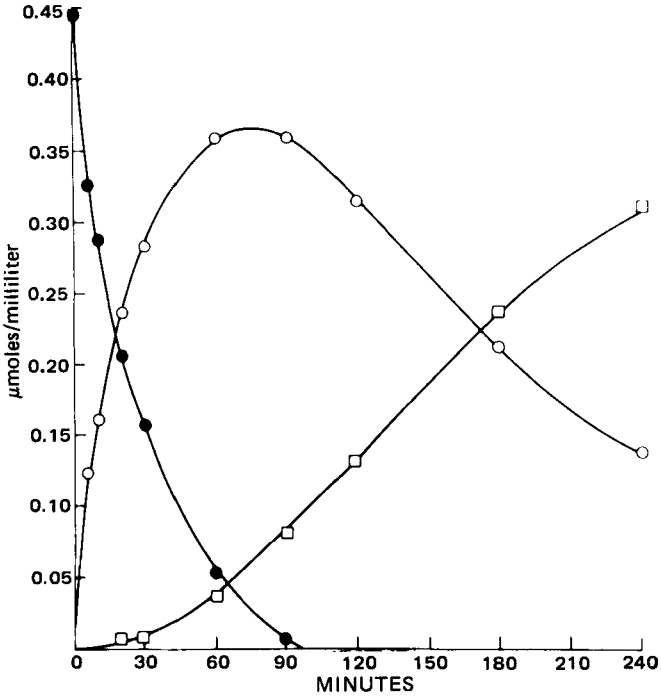

Figure 4—*Concentration* versus *time curves at pH 4.0 (apparent) and 25 ± 0.1°. Key: (●) I; (○) II; (□) III.*

represented by a mechanism comprised of consecutive pseudo first-order reactions (*i.e.*, $k_1 \gg k_{-1}$, $k_1 \ll k_2$, and $k_3 \gg k_{-3}$, $k_3 \ll k_4$),

$$I \xrightarrow{K_1} II \xrightarrow{k_3} III$$

where k_1 and k_3 are pseudo first-order rate constants, and it is possible to obtain estimates of k_3 by a method using dimensionless parameters and variables (5, 6). Application of this method gave $k_3 = k_1/14.0$ at pH 4.0 and $k_3 = k_1/1.9$ at pH 6.0.

Interpretation of Chloride Titration Data at Various pHs—The decomposition of I as a function of solution pH (Fig. 3) as determined by the titration of chloride ion shows a significant deviation from linearity in plots of percent chloride remaining $[\%(Cl_\infty^- - Cl_t^-)/(Cl_\infty^- - Cl_0^-)]$ *versus* time at ≤pH 4.0. To investigate any relationship these deviations might have with the protonation of I, II, or III, it was necessary to have information regarding their pKa values. The instability and limited solubility of I rendered pKa measurements impractical. However, it was possible to estimate by potentiometric titration with 0.05 *N* HCl a pKa of 6.4 for III. A spectrophotometric estimation of the pKa value for the dialcohol hydrolysis product of aniline mustard (NSC-18429) by a standard method (7) is 4.3. A published pKa for aniline mustard is 2.2 (8) indicating a 2.1-U difference between the pKa values of aniline mustard and its final hydrolysis product. If the aniline mustard–dialcohol model is roughly analogous the pKa of I may be ~4.3. The rate of hydrolysis of I or II decreases as pH decreases, presumably due to the protonation of the alkylating function nitrogen which inhibits aziridinium ion formation (an intermediate in the hydrolytic cleavage). A decrease in the rate of hydrolysis of I as pH decreases is reflected in the GLC data at pH 6.0, 5.0, and 4.0. If the pKa of II is taken to be intermediate between I and III the value would be 5.3. At pH 4.0 Compound II would be >95% protonated, which should significantly affect the hydrolysis rate (k_3) when compared to the rate at pH 6.0. This is supported by the data which indicate a sevenfold decrease in k_3 between pH 6.0 and 4.0. The decrease in the hydrolysis of I (k_1) between pH 6.0 and 4.0 is less dramatic, because with a pKa of 4.3 significant amounts of I remain unprotonated even at pH 4.0. The shape of the decomposition curves based on the release of chloride ion (Fig. 3) at ≤pH 4.0 are consistent with the lower rate (k_3) at which II releases chloride at low pH. The effect of various values of k_3/k_1 on the linearity of theoretical chloride ion plots have been described (9). It has also been shown (10) that an inverse relationship exists between hydrolysis rate and degree of protonation of a nitrogen mustard.

Chloride titration, although lacking specificity, is a useful tool in the investigation of the hydrolysis of nitrogen mustards. This is particularly true when used in a screening context (*e.g.*, to evaluate the effect of various solvent mixtures and other excipients on the hydrolysis rate).

Table III—Comparison of Stability of I to Melphalan and Mechlorethamine at 25°

Drug[a]	pH (apparent)	Time, Liberation of 50% Theoretical Cl^-, hr[b]
I	5.0	0.3
Melphalan	5.0	9.0
Mechlorethamine hydrochloride	5.0	8.4

[a] All drugs were 1×10^{-3} *M* in 10% dimethylacetamide–citrate buffer (4.2×10^{-2} *M*). [b] Determined graphically from a plot of log $(Cl_\infty^- - Cl_t^-)/(Cl_\infty^- - Cl_0^-)$ *versus* time.

However, particular care must be taken in the interpretation of chloride ion titration data derived from the hydrolysis of nitrogen mustards at pH near or between the pKa values for the intact mustard and its hydrolysis products. Since the titration of chloride is not a specific method (*i.e.*, the disappearance of I is not measured independently), the rate of chloride ion release measures the combined effect of both chloride generating reactions. Therefore, it is important to be aware of the effect of the relative magnitudes of k_1 and k_3 when interpreting such data.

Comparisons to Other Mustards—A comparison of the rates of hydrolysis as indicated by the liberation of chloride at pH 5.0 of I and two clinically useful mustards, mechlorethamine hydrochloride (NSC-762) and melphalan (NSC-8806), is presented in Table III. Compound I is much less stable than either of these mustards. The aromatic nitrogen mustards (melphalan and the aromatic hydantoin mustards described previously) (11) are inherently more stable due to the decreased basicity of the alkylating function nitrogen when attached to an aromatic ring. The apparent superior stability of mechlorethamine hydrochloride relative to I (Table III) is probably because of the fact that its more stable hydrochloride salt is formed (the formation of the aziridinium ion intermediate is blocked) and can be administered at a pharmaceutically acceptable pH (3.0–5.0 for the reconstituted USP product) (12). In contrast, the hydrochloride salt of I could be isolated only at pH <1 and upon storage was unstable[21]. Salt formation was effective for increasing solubility only at very low, pharmaceutically unacceptable pH values. Subsequent upward adjustment of pH caused precipitation of I.

Attempts to Stabilize I—The stability of I in the presence of a chemically diverse group of additives is seen in Table IV. Significant increases in the stability of some aromatic nitrogen mustards in the presence of surface active agents has been shown (13). Several surfactants slowed the hydrolysis of I (Table IV) with the best, stearylcetyl alcohol ethoxylate[5], increasing the half-life of I six- to sevenfold at pH 5.0. The increases in the stability of I appear to parallel the lipophilicity of the surface active agents. At lower pH (3.0 and 4.0) in the presence of 5% polyoxyethylated castor oil[3] the relative increases in stability of I are less. This diminished effect is probably due to a decreased solubility of I in the micelle as more drug is protonated. Solutions of up to 30% ethanol or 50% propylene glycol have no significant effect on the hydrolysis of I. Some mustards were found to be more stable in the presence of albumin (13, 14). However, the hydrolysis of I was very rapid in the presence of 5% albumin.

The disappearance of I as monitored by GLC at pH 4.0 in the presence of 0.15 *M* NaCl demonstrates the inhibitory effect of chloride ion on the hydrolysis of I. The pseudo first-order rate constant for the disappearance of I under these conditions is 0.00925/min. This reduced hydrolysis rate is not unexpected, since it has been shown previously with other nitrogen mustards using specific assay procedures (15, 16). None of these approaches has dramatically increased the stability of I.

10% Fat Emulsion System—The 10% fat emulsion system combines two approaches which have increased the stability of I (*i.e.*, isolation of I from the aqueous component of the vehicle as with the surfactants and inhibition by the presence of chloride ion).

The stability of I in a 10% fat emulsion was determined by GLC. Attempts to extract I directly from the 10% fat emulsion with ethyl acetate for GLC analysis were erratic with the recovery varying from 80 to 37% in the 1.0–0.2 mg/ml concentration range. Other extraction solvents gave similar results. However, the extraction of I with ethyl acetate from the residue remaining after freeze drying the 10% fat emulsion was more consistent. An extraction efficiency of 89.4 ± 3.3% was observed over the 1–0.15 mg/ml concentration range. Compounds II and III were not extracted under these conditions. The relative standard deviation for the overall extraction GLC procedure was 5.0% on the basis of 10 extracted samples (0.7 mg/ml of I). Determination of the concentration of I by GLC in the emulsion system with subsequent filtration through a 0.45-μm filter and reassay indicated that the drug does not precipitate at 1 mg/ml. However, at 2 mg/ml considerable precipitation had occurred.

[21] J. S. Driscoll, Laboratory of Medicinal Chemistry and Biology, National Cancer Institute, personal communication, 1979.

Table IV—Stability of I in Various Media at 25 ± 0.1°

pH (apparent)	Media[a]	Time, Liberation of 50% Theoretical Cl^-, hr[b]
	Buffers	
5.0	4.2×10^{-2} *M* citrate	0.3
4.0	4.2×10^{-2} *M* citrate	0.9
3.5	4.2×10^{-2} *M* citrate	0.9
3.0	4.2×10^{-2} *M* citrate	2.5
	Surfactants	
5.0	5% polysorbate 20[c]	0.7
5.0	5% polysorbate 80[d]	0.9
5.0	5% polyoxyethylated castor oil[e]	1.1
5.0	5% stearylcetyl alcohol ethoxylate[f]	1.6
5.0	5% polyoxyethylated vegetable oil[g]	0.9
4.0	5% polyoxyethylated vegetable oil[g]	1.2
3.0	5% polyoxyethylated vegetable oil[g]	1.5
	Solvents	
5.0	30% ethanol	0.6
5.0	50% propylene glycol	1.0
4.0	30% propylene glycol	0.6
3.5	50% propylene glycol	1.1
3.5	50% polyethylene glycol 400	1.2
	Miscellaneous	
7.0	5% albumin	0.3

[a] In addition to the component listed, each solution contained 10% dimethylacetamide and sodium citrate buffer 4.2×10^{-2} *M*. [b] Graphically estimated from a plot of log $(Cl_\infty^- - Cl_t^-)/(Cl_\infty^- - Cl_0^-)$ *versus* time. [c] Tween 20. [d] Tween 80. [e] Cremophor El. [f] Siponic E-7. [g] Emulphor EL-719.

The disappearance of I in 10% fat emulsion was monitored by GLC. Plots of the concentration of I *versus* time were linear ($r > 0.99$). The release of I from the fat component of the emulsion may be the rate-limiting step.

A fat emulsion identical to the one used in this report has been used as a vehicle for another unstable antitumor agent (17). Also, large volumes of the fat emulsion alone have been used clinically as a nutritional source (17, 18). A projected human dose for I derived by the application of equivalent surface area dosage conversion factors described previously (19) to the mouse antitumor data would indicate a dose of 6–48 mg for a 60-kg human. This would require the administration of 6–48 ml of the 10% fat emulsion formulation (1 mg/ml of I). A formulation of another antitumor agent in 10% fat emulsion has been given at 1 ml/min with no adverse effects (17). At the time of use, a vial containing I produced by low temperature vacuum drying (20) would be dissolved in dimethylacetamide with the resulting solution being added to the fat emulsion as described in the Experimental section. Administration of appropriate doses of the formulation of I could be accomplished by an infusion at 1 ml/min or slightly faster. This would allow the entire dose to be administered before unacceptable decomposition (≥10%) occurred.

Biological Activity—The antitumor activity of I in the emulsion formulation was compared with a suspension of I *versus* intraperitoneally implanted P-388 leukemia cells in three experiments. The antitumor response of I in both emulsion and suspension preparations was comparable.

Summary—The hydrolysis of I is quite rapid. Several attempts (Table IV) to increase the stability of I have provided less than dramatic results. Although the 10% fat emulsion system has significantly stabilized I, the decomposition rate remains rather rapid resulting in a formulation that is only marginally acceptable. It is unfortunate that I exhibits poor solubility in addition to the instability. Other nitrogen mustards are inherently more stable, such as the aromatic mustards (*e.g.*, melphalan) or they are more soluble allowing for more rapid administration in a small volume (*e.g.*, mechlorethamine).

REFERENCES

(1) G. W. Peng, V. E. Marquez, and J. S. Driscoll, *J. Med. Chem.*, 18, 846 (1975).

(2) J. Plowman, D. B. Lakings, E. S. Owens, and R. H. Adamson, *Pharmacology*, **15**, 359 (1977).
(3) C. A. Hewitt, Chemical Information Sheet on Spirohydantoin Mustard NSC-172112, Division of Cancer Treatment, National Cancer Institute, Bethesda, Md., May 1976.
(4) R. I. Geran, N. H. Greenberg, M. M. MacDonald, A. M. Schumacher, and B. J. Abbott, *Cancer Chemother. Rep., Part 3*, **3**, 1 (1972).
(5) A. A. Frost and R. G. Pearson, "Kinetics and Mechanism," 2nd ed., Wiley, New York, N.Y., 1961, p. 166.
(6) E. H. Jensen and D. J. Lamb, *J. Pharm. Sci.*, **53**, 402 (1964).
(7) A. Albert and E. P. Serjeant, "The Determination of Ionization Constants," 2nd ed., Chapman and Hall, London, 1971.
(8) W. C. J. Ross, *J. Chem. Soc.*, **1949**, 183.
(9) D. Chatterji, *J. Pharm. Sci.*, **69**, 859 (1980).
(10) W. R. Owen and P. J. Stewart, *ibid.*, **68**, 992 (1979).
(11) A. B. Mauger and W. C. J. Ross, *Biochem. Pharmacol.*, **11**, 847 (1962).
(12) "The United States Pharmacopeia," 19th rev., U.S. Pharmacopeial Convention, Rockville, Md., 1975, p. 297.
(13) J. A. Stock and W. J. Hopwood, *Chem.-Biol. Interact.*, **4**, 31 (1971/1972).
(14) M. Szekerke, R. Wade, and R. E. Whisson, *Neoplasma*, **19**, 211 (1972).
(15) K. P. Flora, S. L. Smith, and J. C. Cradock, *J. Chromatogr.*, **177**, 91 (1979).
(16) S. Y. Chang, T. L. Evans, and D. S. Alberts, *J. Pharm. Pharmacol.*, **31**, 853 (1979).
(17) C. L. Fortner, W. R. Grove, D. Bowie, and M. D. Walker, *Am. J. Hosp. Pharm.*, **32**, 582 (1975).
(18) D. Hallberg, I. Holm, and A. L. Abel, *Postgrad. Med. J.*, **43**, 307 (1967).
(19) E. J. Freireich, E. A. Gehan, D. P. Rall, L. H. Schmidt, and H. E. Skipper, *Cancer Chemother. Rep.*, **50**, 219 (1966).
(20) D. W. Flamberg, D. L. Francis, S. L. Morgan, and G. F. Wickes, *Bull. Parenter. Drug Assoc.*, **24**, 209 (1970).

ACKNOWLEDGMENTS

The authors thank Mr. Douglas J. Wiederrich for technical assistance and Dr. Randall K. Johnson, Arthur D. Little, Inc., Cambridge, Mass. for performing the tumor studies.

The Use of *N,N*-Diethyl-*m*-Toluamide to Enhance Dermal and Transdermal Delivery of Drugs

JOHN J. WINDHEUSER *, JOHN L. HASLAM ˣ, LARRY CALDWELL, and RICHARD D. SHAFFER

Received October 16, 1981, from the *INTERx Research Corporation, Lawrence, KS 66044.* Accepted for publication January, 11, 1982. *Present address: Luitpold-Werk, Munich, West Germany.

Abstract □ A dermal penetration enhancer has been found which improves the dermal delivery of a wide variety of drugs and at the same time has a history of low toxicity for human dermal application. *N,N*-Diethyl-*m*-toluamide (I) has been shown to improve the delivery of many drugs through hairless mouse skin in an *in vitro* diffusion cell model. A topically applied steroid, hydrocortisone, has been used to demonstrate the *in vivo* effectiveness of I on human skin. The degree of pallor produced on human skin by the corticosteroids was used as a measure of the relative delivery of hydrocortisone from formulations with and without I.

Keyphrases □ *N,N*-Diethyl-*m*-toluamide—enhancement of dermal and transdermal drug delivery, hydrocortisone □ Hydrocortisone—enhancement of *N,N*-diethyl-*m*-toluamide on drug delivery, dermal and transdermal delivery □ Delivery, drug—dermal and transdermal, *N,N*-diethyl-*m*-toluamide enhancement, hydrocortisone

Improved dermal delivery of drugs has been the focus of pharmaceutical research worldwide for many years. The goal in most cases has been to find a substance of low toxicity which is nonirritating and will deliver a wide variety of compounds effectively.

Efforts to improve dermal delivery of drugs have included traditional formulation approaches and studies on the effects of surfactants, fatty acids, and glycols (1, 2). Although these approaches attained some degree of success, in no case was the enhancement of drug delivery spectacular. In contrast, dimethyl sulfoxide has been shown to greatly enhance dermal and transdermal delivery of a wide variety of drugs (3–11). Unfortunately, the use of this substance has been limited in humans to the treatment of interstitial cystitis by intravesical instillation. Dimethylacetamide has been found to enhance the delivery of a number of drugs for the treatment of skin diseases (12–14). However, the lack of long-term safety information has limited the use of this compound.

In the present study, the effects of *N,N*-diethyl-*m*-toluamide (I) on skin permeability was examined for a wide variety of drugs. Formulations of I have been used extensively as insect repellents. The compound was first reported to be an effective insect repellent in 1954 (15) and has been applied *ad libitum* to the skin in concentrations ranging from 10 to 100%. Despite prolonged and widespread use in humans, major side effects due to the penetration enhancer itself have not been encountered.

EXPERIMENTAL

Reagents and Drugs—Hydrocortisone[1], hydrocortisone acetate[1], hydrocortisone 17-butyrate[2], and hydrocortisone 17-valerate[3] were among the compounds used. Also used were dibucaine[1], benzocaine[4], indomethacin[1], ibuprofen[5], erythromycin[6], tetracycline hydrochloride[7], griseofulvin[8], mycophenolic acid[9], and methyl salicylate[10]. Triethanolamine salicylate was prepared by adding equal molar amounts of

[1] Sigma Chemical Co.
[2] Analysis calculated: C, 70.24; H, 8.16. Analysis found: C, 70.20; H, 8.12. Assay by HPLC to contain <2% hydrocortisone-21-butyrate.
[3] Analysis calculated: C, 69.96; H, 8.52. Analysis found: C, 69.69; H, 8.50.
[4] ICN Pharmaceuticals, Inc.
[5] Industrie Chemicle Farmaceutiche Italiane SpA.
[6] Assay 959 μg/mg, Sigma Chemical Co.
[7] Solid supplied with Topicycline.
[8] Ayerst Laboratories.
[9] Eli Lilly and Co.
[10] Matheson Coleman and Bell.

0022-3549/82/1100-1211$01.00/0

(2) J. Plowman, D. B. Lakings, E. S. Owens, and R. H. Adamson, *Pharmacology*, **15**, 359 (1977).
(3) C. A. Hewitt, Chemical Information Sheet on Spirohydantoin Mustard NSC-172112, Division of Cancer Treatment, National Cancer Institute, Bethesda, Md., May 1976.
(4) R. I. Geran, N. H. Greenberg, M. M. MacDonald, A. M. Schumacher, and B. J. Abbott, *Cancer Chemother. Rep., Part 3*, **3**, 1 (1972).
(5) A. A. Frost and R. G. Pearson, "Kinetics and Mechanism," 2nd ed., Wiley, New York, N.Y., 1961, p. 166.
(6) E. H. Jensen and D. J. Lamb, *J. Pharm. Sci.*, **53**, 402 (1964).
(7) A. Albert and E. P. Serjeant, "The Determination of Ionization Constants," 2nd ed., Chapman and Hall, London, 1971.
(8) W. C. J. Ross, *J. Chem. Soc.*, **1949**, 183.
(9) D. Chatterji, *J. Pharm. Sci.*, **69**, 859 (1980).
(10) W. R. Owen and P. J. Stewart, *ibid.*, **68**, 992 (1979).
(11) A. B. Mauger and W. C. J. Ross, *Biochem. Pharmacol.*, **11**, 847 (1962).
(12) "The United States Pharmacopeia," 19th rev., U.S. Pharmacopeial Convention, Rockville, Md., 1975, p. 297.
(13) J. A. Stock and W. J. Hopwood, *Chem.-Biol. Interact.*, **4**, 31 (1971/1972).
(14) M. Szekerke, R. Wade, and R. E. Whisson, *Neoplasma*, **19**, 211 (1972).
(15) K. P. Flora, S. L. Smith, and J. C. Cradock, *J. Chromatogr.*, **177**, 91 (1979).
(16) S. Y. Chang, T. L. Evans, and D. S. Alberts, *J. Pharm. Pharmacol.*, **31**, 853 (1979).
(17) C. L. Fortner, W. R. Grove, D. Bowie, and M. D. Walker, *Am. J. Hosp. Pharm.*, **32**, 582 (1975).
(18) D. Hallberg, I. Holm, and A. L. Abel, *Postgrad. Med. J.*, **43**, 307 (1967).
(19) E. J. Freireich, E. A. Gehan, D. P. Rall, L. H. Schmidt, and H. E. Skipper, *Cancer Chemother. Rep.*, **50**, 219 (1966).
(20) D. W. Flamberg, D. L. Francis, S. L. Morgan, and G. F. Wickes, *Bull. Parenter. Drug Assoc.*, **24**, 209 (1970).

ACKNOWLEDGMENTS

The authors thank Mr. Douglas J. Wiederrich for technical assistance and Dr. Randall K. Johnson, Arthur D. Little, Inc., Cambridge, Mass. for performing the tumor studies.

The Use of *N,N*-Diethyl-*m*-Toluamide to Enhance Dermal and Transdermal Delivery of Drugs

JOHN J. WINDHEUSER *, JOHN L. HASLAM ˣ, LARRY CALDWELL, and RICHARD D. SHAFFER

Received October 16, 1981, from the *INTERx Research Corporation, Lawrence, KS 66044.* Accepted for publication January, 11, 1982. *Present address: Luitpold-Werk, Munich, West Germany.

Abstract □ A dermal penetration enhancer has been found which improves the dermal delivery of a wide variety of drugs and at the same time has a history of low toxicity for human dermal application. *N,N*-Diethyl-*m*-toluamide (I) has been shown to improve the delivery of many drugs through hairless mouse skin in an *in vitro* diffusion cell model. A topically applied steroid, hydrocortisone, has been used to demonstrate the *in vivo* effectiveness of I on human skin. The degree of pallor produced on human skin by the corticosteroids was used as a measure of the relative delivery of hydrocortisone from formulations with and without I.

Keyphrases □ *N,N*-Diethyl-*m*-toluamide—enhancement of dermal and transdermal drug delivery, hydrocortisone □ Hydrocortisone—enhancement of *N,N*-diethyl-*m*-toluamide on drug delivery, dermal and transdermal delivery □ Delivery, drug—dermal and transdermal, *N,N*-diethyl-*m*-toluamide enhancement, hydrocortisone

Improved dermal delivery of drugs has been the focus of pharmaceutical research worldwide for many years. The goal in most cases has been to find a substance of low toxicity which is nonirritating and will deliver a wide variety of compounds effectively.

Efforts to improve dermal delivery of drugs have included traditional formulation approaches and studies on the effects of surfactants, fatty acids, and glycols (1, 2). Although these approaches attained some degree of success, in no case was the enhancement of drug delivery spectacular. In contrast, dimethyl sulfoxide has been shown to greatly enhance dermal and transdermal delivery of a wide variety of drugs (3–11). Unfortunately, the use of this substance has been limited in humans to the treatment of interstitial cystitis by intravesical instillation. Dimethylacetamide has been found to enhance the delivery of a number of drugs for the treatment of skin diseases (12–14). However, the lack of long-term safety information has limited the use of this compound.

In the present study, the effects of *N,N*-diethyl-*m*-toluamide (I) on skin permeability was examined for a wide variety of drugs. Formulations of I have been used extensively as insect repellents. The compound was first reported to be an effective insect repellent in 1954 (15) and has been applied *ad libitum* to the skin in concentrations ranging from 10 to 100%. Despite prolonged and widespread use in humans, major side effects due to the penetration enhancer itself have not been encountered.

EXPERIMENTAL

Reagents and Drugs—Hydrocortisone[1], hydrocortisone acetate[1], hydrocortisone 17-butyrate[2], and hydrocortisone 17-valerate[3] were among the compounds used. Also used were dibucaine[1], benzocaine[4], indomethacin[1], ibuprofen[5], erythromycin[6], tetracycline hydrochloride[7], griseofulvin[8], mycophenolic acid[9], and methyl salicylate[10]. Triethanolamine salicylate was prepared by adding equal molar amounts of

[1] Sigma Chemical Co.
[2] Analysis calculated: C, 70.24; H, 8.16. Analysis found: C, 70.20; H, 8.12. Assay by HPLC to contain <2% hydrocortisone-21-butyrate.
[3] Analysis calculated: C, 69.96; H, 8.52. Analysis found: C, 69.69; H, 8.50.
[4] ICN Pharmaceuticals, Inc.
[5] Industrie Chemicle Farmaceutiche Italiane SpA.
[6] Assay 959 μg/mg, Sigma Chemical Co.
[7] Solid supplied with Topicycline.
[8] Ayerst Laboratories.
[9] Eli Lilly and Co.
[10] Matheson Coleman and Bell.

0022-3549/82/1100-1211$01.00/0

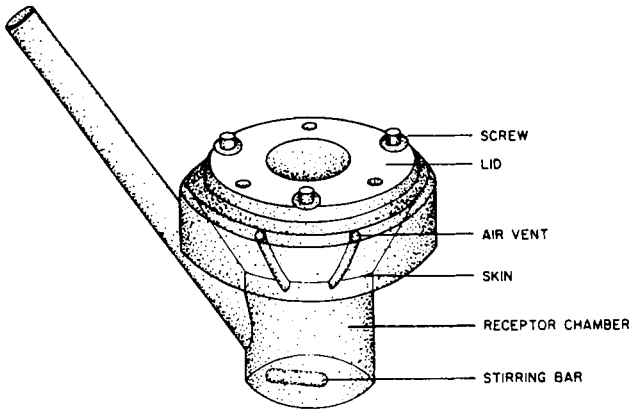

Figure 1—*Plexiglass diffusion cell with polytef lid.*

triethanolamine[11] and salicylic acid[12]. Idoxuridine[13], petrolatum USP, mineral oil[14], isopropyl myristate[1], *N,N*-diethyl-*m*-toluamide (I)[1], polyoxyethylene (2) stearyl ether[15], and polyoxyethylene 40 stearate[15] were additional compounds used. Other chemicals were reagent grade.

Procedure for Hairless Mouse Skin Diffusion Model—Transdermal drug delivery rates were determined using an *in vitro* diffusion cell procedure. Diffusion cells consisted of a plexiglass receptor chamber with a side arm to allow receptor phase sampling and a polytef lid[16] (Fig. 1). A polytef-coated stirring bar was used for receptor mixing. Female hairless mice[17] were sacrificed by cervical dislocation and the dorsal skin was removed in one piece. The skin was placed over the lower opening of the polytef lid and secured with a neoprene rubber gasket. The lid was then secured on the chamber. The exposed epidermal surface measured 8.0 cm^2. The receptor fluid was 45 ml of buffer solution consisting of 1.5×10^{-1} *M* NaCl, 5.0×10^{-4} *M* NaH_2PO_4, 2.0×10^{-4} *M* Na_2HPO_4, and 200 ppm gentamicin sulfate adjusted to pH 7.2 with sodium hydroxide or hydrochloric acid. In most cases, test formulations were applied in the amount of 0.1 ml (~100 mg/cell). The cell was placed in a thermostated chamber maintained at 32 ± 1°. The reservoir was stirred by a magnetic stirrer at 2.5 Hz. After 24 hr, a sample of the receptor fluid was withdrawn by a pipet through the side arm and emptied into a test tube. The test tube was then capped and frozen. The concentration of applied drug in the receptor fluid was measured using high-pressure liquid chromatography (HPLC). The results reported for each experiment were the average values from three replicate diffusion cells.

Procedures for Human Blanching Studies—Test formulations were applied to test areas (2 × 2 cm) on the lower backs of healthy human volunteers. Each formulation was applied to four or more test areas per subject and the results were averaged. All test areas were exposed to air (nonoccluded) for 3.5 hr after application. Any remaining formulation was then wiped off with ethanol. Blanching was evaluated at 5, 6, 7, and 8 hr postapplication. The blanching at each test area was visually appraised on a scale of 0–4, where 0 is no blanching, 1 is barely discernible blanching, and 4 is maximum blanching. Individual values for each formulation were averaged (n = 8–10). This value became the basis for comparisons.

Chromatographic Analysis—Samples of the *in vitro* receptor fluid were analyzed for the drug substance in each experiment by HPLC. The chromatographic components included pump[18], injector[19], detector[20], and recorder[21] coupled with a microparticulate column. The column type, mobile phase, and detection wavelength used for each drug substance are detailed in Table I.

Table I—HPLC Conditions for Analysis

Compound	Mobile Phase	Detection Wavelength, nm
Hydrocortisone[a]	35% acetonitrile–65% water	254
Hydrocortisone 21-acetate[b]	20% acetonitrile–20% tetrahydrofuran–60% water	254
Hydrocortisone 17-butyrate[b]	40% Tetrahydrofuran–60% water	254
Hydrocortisone 17-valerate[b]	30% acetonitrile–20% tetrahydrofuran–50% water	254
Dibucaine[c]	2 m*M* $NH_4H_2PO_4$ in 40% acetonitrile–60% water	254
Benzocaine[b]	15% acetonitrile–20% tetrahydrofuran–65% water	254
Indomethacin[c]	2 m*M* $NH_4H_2PO_4$ in 40% acetonitrile–60% water	254
Ibuprofen[c]	2 m*M* $NH_4H_2PO_4$ in 35% acetonitrile–65% water	205
Erythromycin[a]	2 m*M* $NH_4H_2PO_4$ in 30% acetonitrile–70% water	215
Tetracycline hydrochloride[a]	1 m*M* Na_2EDTA; 2 m*M* H_3PO_4 in 28% acetonitrile–72% water	254
Griseofulvin[c]	2 m*M* $NH_4H_2PO_4$ in 25% acetonitrile–75% water	295
Mycophenolic acid[c]	2 m*M* $NH_4H_2PO_4$ in 25% acetonitrile–75% water	295
Methyl salicylate[b]	4 m*M* H_3PO_4 in 40% tetrahydrofuran–60% water	254
Triethanolamine salicylate[b]	10 m*M* H_3PO_4 in 60% methanol–40% water	254

[a] Waters Associates, μBondapak, C18. [b] Brownlee Labs, RP-8. [c] Waters Associates, μBondapak, CN-RP.

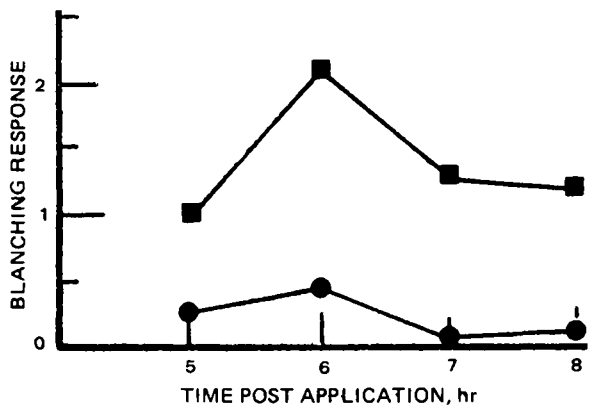

Figure 2—*Blanching results for hydrocortisone ointments in two subjects. Key: (■) 1% hydrocortisone in 5% I-petrolatum; (●) 1% hydrocortisone in petrolatum.*

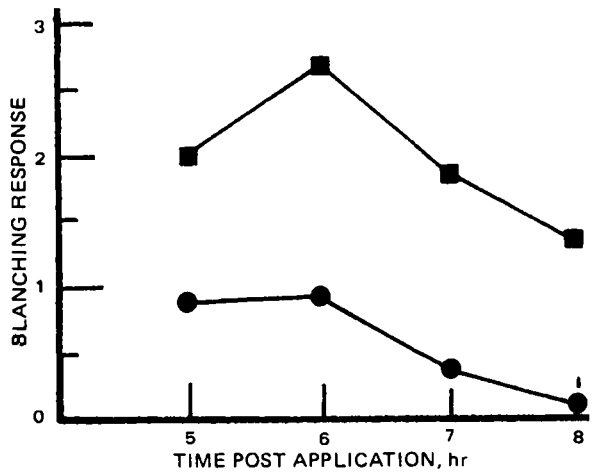

Figure 3—*Blanching results for hydrocortisone creams in two subjects. Key: (■) 1% hydrocortisone in 5% I-cream; (●) 1% hydrocortisone in cream.*

[11] Baker and Adamson Products.
[12] Fisher Scientific Co.
[13] Byron Chemical Co., Inc.
[14] Nujol, Plough, Inc.
[15] Brij 72 and Myrj 52, respectively, ICI United States, Inc.
[16] Kersco Engineering Consultants, Palo Alto, CA 94305.
[17] HRSJ, Jackson Labs, Bar Harbor, ME 04609.
[18] Model 6000A, Waters Associates.
[19] Model U6K, Waters Associates.
[20] Model 440 (at 254 nm) or Model 450 (variable), Waters Associates.
[21] Omniscribe model B5000.

Table II—*In Vitro* Diffusion of Various Drugs through Hairless Mouse Skin at 32° for 24 hr

Drug	Formulations	Applied Drug Delivered, %
Hydrocortisone	Hydrocortisone cream[a] 1% *versus* 1% drug in I	1.6 *versus* 35.0
Hydrocortisone acetate	Hydrocortisone acetate cream[b] 1% *versus* 1% drug in I	0.67 *versus* 27.6
Hydrocortisone 17-butyrate	Hydrocortisone 17-butyrate cream[c] 0.1% *versus* 0.1% drug in I	4.7 *versus* 63.1
	Hydrocortisone 17-butyrate ointment[b] 0.1% *versus* 0.1% drug in I	2.0 *versus* 63.1
Hydrocortisone 17-valerate	Hydrocortisone 17-valerate cream[d] 0.2% *versus* 0.2% drug in I	6.1 *versus* 40.8
Dibucaine	Dibucaine cream[e] 0.5% *versus* 0.5% drug in I	15.0 *versus* 82.0
Benzocaine	Benzocaine cream[f] 1% *versus* 1% drug in I	12.3 *versus* 35.7
Indomethacin	1% drug in petrolatum *versus* 1% drug in I	0.9 *versus* 37.6
Ibuprofen	1% drug in petrolatum *versus* 1% drug in I	63.5 *versus* ≃100
Erythromycin	1% drug in petrolatum *versus* 1% drug in I	not detectable *versus* 83.4
Tetracycline hydrochloride	Tetracycline lotion[g] *versus* 0.22% drug in I	not detectable *versus* ≃100
Griseofulvin	0.5% drug in petrolatum *versus* 0.5% drug in I	0.4 *versus* 29
Mycophenolic acid	1% drug in petrolatum *versus* 1% drug in I	not detectable *versus* 42
Methyl salicylate	5% drug in petrolatum *versus* 5% drug in I	not detectable *versus* 9
Triethanolamine salicylate	Triethanolamine salicylate lotion[h] 10% *versus* 1% drug in I	16 *versus* 89

[a] Hytone Cream, Dermik Laboratories, Inc., Fort Washington, PA 19034. [b] Carmol Cream and Locoid Ointment, respectively, Ingram Pharmaceutical Co., San Francisco, CA 94111. [c] Locoid Cream, Torii Pharmaceutical Co., Tokyo, Japan. [d] Westcort Cream, Westwood Pharmaceuticals, Inc., Buffalo, NY 14213. [e] Nupercainal Cream, Ciba Pharmaceuticals, Summit, NJ 07901. [f] Solarcaine Cream, Plough, Inc., Memphis, TN 38151. [g] Topicycline Lotion, Proctor and Gamble, Cincinnati, OH 45202. [h] Asper Lotion, Thompson Medical Co., Inc., New York, NY 10022.

Table III—*In Vitro* Diffusion of Hydrocortisone through Hairless Mouse Skin at 32°

Hydrocortisone in	Percent of Applied Drug[a] Delivered in 24 hr
Petrolatum	0.3
5% I-petrolatum	0.8
Cream	0.5
5% I cream	1.5

[a] One hundred milligrams (~0.1 ml, containing 1 mg of hydrocortisone) of the formulation was applied.

RESULTS AND DISCUSSION

In the *in vitro* diffusion experiments, hairless mouse skin was used as the barrier membrane. The data were generally reproducible allowing for comparisons between the relative rates of penetration of a wide variety of drugs. These diffusion cell results are not necessarily applicable to skin *in vivo*, but they do provide an indication of the relative penetration enhancement. Literature references suggest that a correlation between human and hairless mouse skin can be expected for some drugs (16, 17). Table II contains diffusion results for various drugs dissolved in pure Compound I and allowed to diffuse through the hairless mouse skin at 32° for 24 hr. All the drugs in I were solutions; however, griseofulvin required warming to obtain a solution rapidly. The I formulation was compared to a commercial product whenever possible. Where no comparable product was available, the drug was dispersed in petrolatum USP. It should be noted, however, that both ibuprofen and methyl salicylate dissolve in petrolatum, while the others are suspensions. From the results presented in Table II, it is apparent that enhancement of drug delivery is dramatic when I is present in the formulation.

The amount of pure I which diffused through the barrier membrane was also measured. Over 90% of the sample of I diffused across the hairless mouse skin in 24 hr. In an investigation (18) studying the evaporation of I from human skin *in vivo*, it was found that ~50% of the applied amount of I (25 $\mu g/cm^2$) could be recovered by evaporation, skin wiping, and skin stripping after 30 min. The remaining 50% of I, therefore, appeared to have been absorbed or associated with nonstripped skin.

Although solution preparations dissolved in I were used in the *in vitro* studies, they are less commonly used for topical application *in vivo*. Creams and ointments are the more conventional mode. To investigate enhanced drug delivery with I *in vivo*, hydrocortisone cream and ointment formulations were prepared. Hydrocortisone was chosen as the model drug due to the blanching effect it causes on human skin. The amount of skin blanching due to local vasoconstriction occurring after corticosteroid application was used as a relative measure of drug penetration.

As a preliminary experiment to examine hydrocortisone delivery, the following formulations were prepared: 1, 1% hydrocortisone in petrolatum; 2, 1% hydrocortisone in petrolatum plus 5% I; 3, 1% hydrocortisone cream; and 4, 1% hydrocortisone cream plus 5% I. These formulations differed only in that 2 and 4 contained 5% I. These preparations were examined in the hairless mouse skin diffusion test, the results of which are shown in Table III.

The hydrocortisone preparations were then applied to humans as described in the *Experimental* section. Figures 2 and 3 show the results obtained from two subjects. A large increase in the blanching response was observed for Formulations 2 and 4 relative to 1 and 3. Control experiments demonstrated that I alone does not cause skin blanching. Therefore, the increase in the blanching response clearly indicates enhanced dermal delivery of hydrocortisone effected by the presence of I in the hydrocortisone formulations. It is interesting to note that hydrocortisone delivery is improved with as little as 5% I, whereas studies with other dermal penetration enhancers such as dimethyl sulfoxide appear to require higher concentrations.

REFERENCES

(1) P. Grasso and A. B. G. Lansdown, *J. Soc. Cosmet. Chem.*, **23**, 481 (1972).

(2) M. Katz and B. J. Poulson, in "Handbook of Pharmacology Concepts in Biochemical Pharmacology Part I," B. B. Brodie and J. R. Gillette, Eds., Springer-Verlag, New York, N.Y., 1971, p. 103.

(3) C. F. H. Vickers, *Br. J. Dermatol.*, **81**, 902 (1969).

(4) R. B. Stoughton and W. Fritsch, *Arch. Dermatol.*, **90**, 512 (1964).

(5) A. C. Allenby, J. Fletcher, C. Schock, and T. F. S. Tees, *Br. J. Dermatol.*, **81**, 31 (1969).

(6) V. L. Brechner, D. D. Chen, and J. Pretsky, *Ann. N.Y. Acad. Sci.*, **141**, 524 (1967).

(7) W. D. Collom and V. L. Winek, *Clin. Toxicol.*, **1**, 309 (1968).

(8) L. D. Davis, *Clin. Med.*, **73**, 70 (1966).

(9) R. L. Dobson, S. W. Jacob, and R. J. Herschler, U.S. Pat. 3,499,961 (1970).

(10) A. M. Kligman, *J. Am. Med. Assoc.*, **193**, 140, 151 (1965).

(11) G. F. Schumacher, *Drug Intell.*, **1**, 188 (1967).

(12) D. D. Munro and R. B. Stoughton, *Arch. Dermatol.*, **92**, 585 (1965).

(13) R. B. Stoughton, U.S. Pat. 3,472,931 (1969).

(14) D. D. Munro, *Br. J. Dermatol.*, **81**, 92 (1969).

(15) E. T. McCabe, W. F. Barthel, S. T. Gertler, and S. A. Hall, *J. Org. Chem.*, **19**, 493 (1954).

(16) R. B. Stoughton, in "Animal Models in Dermatology," H. I. Maibach, Ed., Churchill Livingstone, New York, N.Y., 1975, p. 121.

(17) H. Durrheim, G. L. Flynn, W. I. Higuchi, and C. R. Behl, *J. Pharm. Sci.*, **69**, 781 (1980).

(18) T. S. Spencer, J. A. Hill, R. J. Feldmann and H. I. Maibach, *J. Invest. Dermatol.*, **72**, 317 (1979).

ACKNOWLEDGMENTS

The authors wish to acknowledge the technical assistance of Ms. Robyn Cargill and Ms. Maure Dillsaver.

Esters of Nipecotic and Isonipecotic Acids as Potential Anticonvulsants

A. MICHAEL CRIDER *x, TERENCE T. TITA *, J. D. WOOD ‡, and CHRISTINE N. HINKO *

Received September 24, 1981, from the **College of Pharmacy, University of Toledo, Toledo, OH 43606* and the ‡*Department of Biochemistry, University of Saskatchewan, Saskatoon, Saskatchewan.* Accepted for publication January 11, 1982.

Abstract □ A variety of esters of nipecotic and isonipecotic acids were synthesized and evaluated for anticonvulsant activity. The ester group was varied in terms of lipophilicity and reactivity toward hydrolysis. The esters were screened against seizures induced by electroshock, pentylenetetrazol, and the putative γ-aminobutyric acid antagonist, bicuculline. The most significant activity was demonstrated by the *p*-nitrophenyl esters of nipecotic and isonipecotic acids against bicuculline-induced seizures. Esters of nipecotic acid were tested for *in vitro* inhibition of γ-aminobutyric acid and L-proline uptakes into mouse whole brain minislices. The *p*-nitrophenyl, *n*-octyl, and succinimidyl esters were the most potent inhibitors of γ-aminobutyric acid uptake. The uptake of γ-aminobutyric acid by the ester derivatives appeared to involve specific and nonspecific mechanisms.

Keyphrases □ Anticonvulsants—potential, esters of nipecotic and isonipecotic acids, mice □ Nipecotic acid—esters, isonipecotic acid, potential anticonvulsants, mice □ Isonipecotic acid—esters, nipecotic acid, potential anticonvulsants, mice

Over the past several years evidence has been accumulated to implicate γ-aminobutyric acid as a major central nervous system (CNS) inhibitory neurotransmitter (1, 2). Impairment of γ-aminobutyric acid neurotransmission may cause a variety of neurological disorders such as epilepsy and certain psychiatric conditions (2, 3). As a result, considerable research has been directed toward the search for compounds that act as agonists, uptake inhibitors, or inhibitors of the metabolizing enzymes of γ-aminobutyric acid (4). The hope has been that agents that potentiate γ-aminobutyric acid neurotransmission could be potentially useful anticonvulsants.

BACKGROUND

(±)-Nipecotic acid (I*a*) was shown to be a potent inhibitor of neuronal γ-aminobutyric acid uptake into rat cerebral cortex (5) and mouse whole brain minislices (6). Additional studies found that the *R*-(−) enantiomer was more active as a γ-aminobutyric acid uptake inhibitor than the *S*-(+) enantiomer (7).

Due to its polarity, nipecotic acid does not readily penetrate the blood–brain barrier (8). However, it was previously shown (9) that (+)-ethyl nipecotate, when administered intraperitoneally, protected mice against audiogenic seizures. Furthermore, it was found (10) that (−)-ethyl nipecotate raised the threshold for convulsions induced by electroshock in mice. These same investigators also demonstrated that (−)- and (+)-ethyl nipecotate significantly elevated the threshold for clonic convulsions induced by pentylenetetrazol. (−)-Nipecotic acid had no effect in these anticonvulsant tests when administered intraperitoneally.

Recently, it was found that (*R*)-ethyl nipecotate given intramuscularly in mice resulted in a dose-dependent increase in γ-aminobutyric acid levels in the synaptosomes (11). The speculation was that such an increase in γ-aminobutryic acid levels in the nerve endings possibly could bring about an anticonvulsant effect.

During the final stages of this work, the anticonvulsant activity of a series of esters of the γ-aminobutyric acid agonist, isoguvacine, was reported (12). Most of the esters exhibited weak anticonvulsant activity against seizures induced by bicuculline or isoniazid. However, a good correlation existed between the onset of electroshock activity and the rates of *in vitro* enzymatic hydrolysis.

Isonipecotic acid (I*b*) was shown to be a potent and specific γ-aminobutyric acid agonist in the [^{3}H]γ-aminobutyric acid-binding assay procedure (13, 14). As in the case of nipecotic acid, isonipecotic acid was also too polar to penetrate the blood–brain barrier.

The purpose of this investigation was to prepare and evaluate the anticonvulsant activity of ester derivatives of nipecotic and isonipecotic acids. The ester group was varied in terms of lipophilicity and reactivity toward hydrolysis. Since the amino acids (I*a* and I*b*) are too polar to penetrate the CNS, it was anticipated that the ester derivatives would enter the brain and be hydrolyzed to yield the respective amino acids.

The synthesis and anticonvulsant activity of the ester derivatives of nipecotic and isonipecotic acids are described in the present report. Additionally, γ-aminobutyric acid and L-proline uptake studies into mice whole brain minislices by the ester derivatives of nipecotic acid are reported.

RESULTS AND DISCUSSION

Chemistry—Esterification of carboxylic acids can be accomplished by the use of dehydrating agents such as dicyclohexylcarbodiimide, provided an acid catalyst is present (15). Although *N*-hydroxysuccinimide and *p*-nitrophenol are acidic enough to furnish a proton, the aliphatic alcohols are not. As a result, the reaction between 1-(*tert*-butoxycarbonyl)piperidine-4-carboxylic acid (II*b*) and *n*-hexanol initially gave a thermally unstable *O*-acylisourea (16), which rearranged to the more stable *N*-acylurea (III). The alkyl esters (IV*a–f*) were successfully synthesized by Fischer esterification of the piperidine carboxylic acids (I*a* and I*b*) with an appropriate alcohol in the presence of dry hydrogen chloride. The remaining esters were conveniently prepared by standard procedures (Scheme I). The physical properties of these derivatives are given in Tables I and II.

Biological Testing—In initial investigations[1], three of the piperidinyl esters showed some activity against the subcutaneous pentylenetetrazol seizure test. The octyl ester (IV*f*) exhibited an ED_{50} of 165 mg/kg in the subcutaneous pentylenetetrazol seizure test at the time of peak effect (4 hr). However, IV*f* showed considerable toxicity (TD_{50} = 178 mg/kg) when evaluated in the rotorod test at 4 hr after administration of the compound. Compounds II*a* and VI*a* protected one out of four animals when administered 0.5 hr before pentylenetetrazol in doses of 600 and 300 mg/kg, respectively. Although no neurotoxicity was reported for II*a*, compound VI*a* produced deficiency in rotorod performance in two out of four animals when administered in a dose of 300 mg/kg.

The subcutaneous pentylenetetrazol test was repeated in the laboratory with three of the esters, which were administered 1 hr prior to the con-

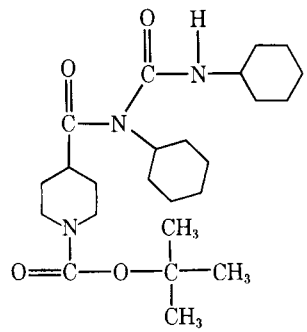

III

[1] All compounds were tested for anticonvulsant activity by the Antiepileptic Drug Development Program, Epilepsy Branch, Neurological Disorders Program, National Institutes of Health, Bethesda, MD 20225.

0022-3549/82/1100-1214$01.00/0

vulsant by subcutaneous injection in an attempt to reduce peripheral hydrolysis that might occur with the intraperitoneal route. The results are shown in Table III. Sodium phenobarbital (25 mg/kg sc), the reference compound, completely protected the mice tested from clonic and tonic seizure. Esters VIII*a*, VIII*b*, and VI*a*, in 150-mg/kg doses, all significantly lengthened the onset time for myoclonic activity as compared to the saline-treated control animals. The succinimidyl ester (VI*a*) was most active, protecting three out of the eight animals from clonic convulsions. All three esters protected the animals tested from tonic seizure and death. These results, however, are difficult to interpret since only 2 of the 16 control animals died after exhibiting tonic convulsions, and pentylenetetrazol is most commonly used for its ability to produce threshold or minimal (clonic) seizures (17). Neurotoxicity was not observed with any of the three esters at the 150-mg/kg dose.

These three compounds were also evaluated for their ability to protect against bicuculline-induced convulsions. The results are shown in Table IV. Each of the three esters at a 150-mg/kg dose significantly prolonged the onset time of clonic seizures when administered by subcutaneous injection. The *p*-nitrophenyl ester (VIII*a*) was most active against bicuculline, protecting four out of eight animals from any clonic activity and completely protecting all eight mice from tonic seizure and death. These results are especially significant when compared to the controls where bicuculline produced clonic and tonic seizures and resulted in fatality in 100% of the saline-treated mice. The *p*-nitrophenyl ester (VIII*b*), although not as effective as VIII*a*, protected three out of eight mice from clonic seizure and seven out of eight from tonic convulsions and death. The succinimidyl ester (VI*a*), which showed activity against pentylenetetrazol produced no protection from myoclonus and only minimal protection (two out of eight mice) from tonic seizures. Four out of eight animals, however, were protected from fatality. Additional experiments were performed in an attempt to maximize the anticonvulsant activity of VI*a*. However, increasing the dose to 225 mg/kg and varying the pretreatment time did not alter its effects. The reference compound, diazepam (10 mg/kg ip), prevented bicuculline-induced seizure activity in all animals tested.

The results of the uptake studies of the esters of nipecotic acid, with respect to γ-aminobutyric acid and L-proline into mouse whole brain minislices, are given in Table V. Although all esters showed appreciable inhibition of γ-aminobutyric acid uptake, IV*c*, VI*a*, and VIII*a* were the most potent. In order for the esters to exhibit inhibition of γ-aminobutyric acid uptake, hydrolysis to the parent amino acid (I*a*) is necessary. Thus, it is not surprising that VI*a* inhibited γ-aminobutyric acid uptake in a manner identical to nipecotic acid. NMR analysis of VI*a* indicates that the ester is hydrolyzed very rapidly to the parent amino acid. (±)-ethyl nipecotate demonstrated moderate inhibition (47%) as contrasted with an earlier report (7) indicating that the (−)-isomer was inactive.

In all probability, the octyl ester (IV*c*) is acting as a nonspecific inhibitor of γ-aminobutyric acid uptake. In comparison with I*a*, IV*c* is a much more potent inhibitor of L-proline (99 *versus* 21% inhibition). The octyl ester (IV*c*) may well be exerting its inhibitory activity by a nonspecific detergent-like effect. Compound IV*c* probably interrupts all types of membrane functions, causing γ-aminobutyric acid and L-proline inhibition.

Compound VIII*a* presents a different case than IV*c*. Although VIII*a* seems to exhibit nonspecificity, as evidenced by its 70% inhibition of L-proline uptake at 1×10^{-3} *M*, it does not inhibit L-proline as potently as IV*c*. Dilution of VIII*a* does not decrease the γ-aminobutyric acid uptake inhibition as drastically as that for IV*c*.

One possible explanation for these results is that the observed effects of IV*c* and VIII*a* are the summation of two different types of inhibition, specific and nonspecific. The nonspecific effect is due to the intact ester, while the specific effect is caused by hydrolysis of IV*c* and VIII*a* to nipecotic acid. Support for this hypothesis can be obtained by noting that at 1×10^{-3} *M*, both IV*c* and VIII*a* are more potent than I*a* in the γ-aminobutyric acid uptake assay. Furthermore, pipecolic acid is a much weaker inhibitor of γ-aminobutyric acid uptake than I*a* (Table V). However, the octyl esters (IV*c* and IV*g*) of the amino acids were equal in potency as γ-aminobutyric acid uptake inhibitors. These results suggest that IV*c* and IV*g* are not hydrolyzed under the assay conditions, and that their inhibition is due to a nonspecific cationic detergent effect.

If this hypothesis is correct, the nonspecific mechanism appears to assume a greater role in the case of IV*c* than VIII*a*. Support for this can be gathered by noting that VIII*a* did not inhibit L-proline to the extent of IV*c*. Furthermore, the inhibition of L-proline by VIII*a* was always much less than that of IV*c*.

Further studies are in progress to define more accurately the anti-

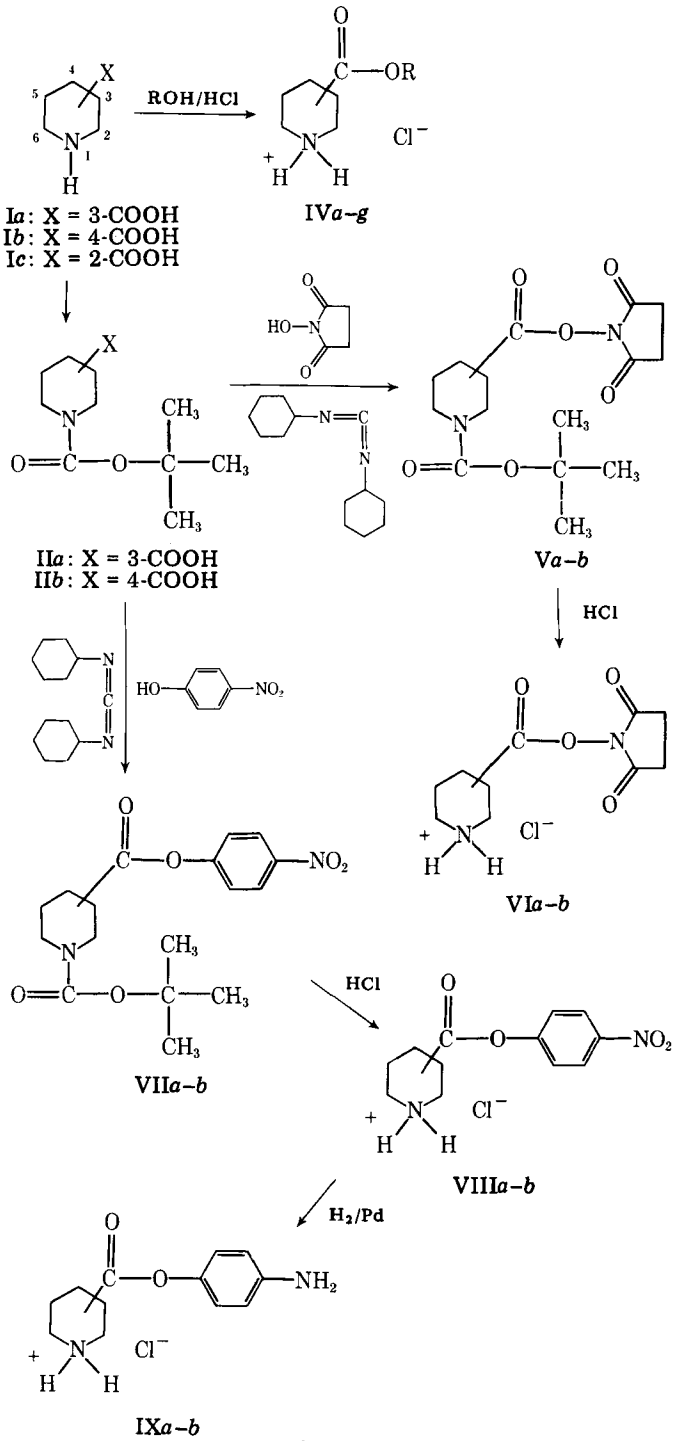

Scheme I

convulsant activity of VIII*a* as well as to determine the effect of VIII*a* on the γ-aminobutyric acid content of nerve endings using a synaptosomal model.

EXPERIMENTAL[2]

Nipecotic Acid (I*a*)—Compound I*a* was prepared by the method of Freifelder (18) in 62% yield, mp 258–260° [lit. (19) mp 260–261°].

1-(tert-Butyloxycarbonyl)piperidine-3-carboxylic Acid (*II*a)—A solution of I*a* (10.0 g, 0.077 mole) in 50 ml of water was treated with tri-

[2] Melting points were determined on a Fisher-Johns melting point apparatus and are uncorrected. IR spectra were recorded as potassium bromide pellets with a Perkin-Elmer 137 spectrophotomer. NMR spectra were recorded on a Varian EM 360A spectrometer. Chemical shifts are reported in parts per million (δ) relative to tetramethylsilane (1%) or in the case of D_2O (1%) sodium 2,2-dimethyl-2-silapentane-5-sulfonate.

Table I—Physical Properties of *n*-Alkyl Piperidinecarboxylate Hydrochlorides

Compound	R	Substituent Ring Position	Melting Point	Yield, %[a]	Formula	Analysis, % Calc.	Found
IV*a*	$-(CH_2)_3CH_3$	3	51–53°	39	$C_{10}H_{20}ClNO_2$	C 54.13	54.36
						H 9.11	9.04
						N 6.32	6.12
IV*b*	$-(CH_2)_5CH_3$	3	32–34°	34	$C_{12}H_{24}ClNO_2$	C 57.69	57.64
						H 9.70	9.76
						N 5.61	5.86
IV*c*	$-(CH_2)_7CH_3$	3	43–45°	57	$C_{14}H_{28}ClNO_2$	C 60.51	60.31
						H 10.18	10.12
						N 5.61	5.86
IV*d*	$-(CH_2)_3CH_3$	4	113–115°	66	$C_{10}H_{20}ClNO_2$	C 54.16	54.31
						H 9.11	9.27
						N 6.32	6.18
IV*e*	$-(CH_2)_5CH_3$	4	73–75°	50	$C_{12}H_{24}ClNO_2$	C 57.69	57.61
						H 9.70	9.54
						N 5.61	5.38
IV*f*	$-(CH_2)_7CH_3$	4	75–77°	60	$C_{14}H_{28}ClNO_2$	C 60.51	60.75
						H 10.18	10.32
						N 5.04	4.91
IV*g*	$-(CH_2)_7CH_3$	2	128–129°	82	$C_{14}H_{28}ClNO_2$	C 60.51	59.83
						H 10.18	10.33
						N 5.04	5.06

[a] The yield of analytically pure hydrochloride after one recrystallization from ethyl acetate, except IV*f* which was recrystallized from chloroform–ethyl acetate.

ethylamine (11.9 g, 0.116 mole) followed by the addition of 2-(*tert*-butoxycarbonyloxyimino)-2-phenylacetonitrile (21.0 g, 0.085 mole) in 50 ml of acetone. After stirring overnight, the reaction mixture was treated with 250 ml of an equal ethyl acetate–water mixture. The water layer was separated and the ethyl acetate phase was washed with an additional 100 ml of water. The combined aqueous phases were washed with 100 ml of ethyl acetate and acidified with cold 1 *N* HCl to pH 2. Upon cooling, a white solid precipitated from solution. Recrystallization from absolute ethanol–water gave 14.4 g (81%) of II*a*, mp 149–151°; IR (KBr): 1750 (C=O, acid) and 1680 (C=O, carbamate) cm^{-1}; NMR ($CDCl_3$): δ 1.45 [s, 9H, $C(CH_3)_3$], 1.65 (m, 4H, CH_2CH_2CH), 2.30–3.20 (broad m, CHNCH and CH overlap), 4.0 (m, 2H, CHNCH), and 10.1 (broad s, 1H, COOH) ppm.

Anal.—Calc. for $C_{11}H_{19}NO_4$: C, 57.61; H, 8.37; N, 6.11. Found: C, 57.80; H, 8.32; N, 5.99.

*1-(tert-Butyloxycarbonyl)piperidine-4-carboxylic Acid (II*b*)*—Compound II*b* was prepared, as described for II*a*, from I*b* (10.0 g, 0.077 mole), triethylamine (11.9 g, 0.116 mole) and 2-(*tert*-butoxycarbonyloxyimino)-2-phenylacetonitrile (21.0 g, 0.085 mole). Recrystallization of the product from absolute ethanol–water yielded 13.3 g (75%) of ana-

Table II—Physical Properties of Piperidine Derivatives

Compound	Substituent Ring Position	Melting Point	Yield, %	Recrystallization Solvent[a]	Formula	Analysis, % Calc.	Found
II*a*	3	149–151°	81	A	$C_{11}H_{19}NO_4$	C 57.61	57.80
						H 8.37	8.32
						N 6.11	5.99
II*b*	4	135–137°	75	A	$C_{11}H_{19}NO_4$	C 57.61	57.62
						H 8.37	8.32
						N 6.11	6.21
V*a*	3	125–127°	61	B	$C_{15}H_{22}N_2O_6$	C 55.19	55.19
						H 6.81	6.85
						N 8.58	8.76
V*b*	4	139–141°	67	B	$C_{15}H_{22}NO_6$	C 55.19	54.95
						H 6.81	6.71
						N 8.58	8.82
VI*a*	3	168–170°	69	B	$C_{10}H_{15}ClN_2O_4$	C 45.71	45.95
						H 5.77	5.94
						N 10.66	10.83
VI*b*	4	205–207°	62	B	$C_{10}H_{15}ClN_2O_4$	C 45.71	45.83
						H 5.77	5.61
						N 10.66	10.95
VII*a*	3	73–75°	59	C	$C_{17}H_{22}N_2O_6$	C 58.27	58.33
						H 6.34	6.50
						N 8.00	8.16
VII*b*	4	91–93°	60	B	$C_{17}H_{22}N_2O_6$	C 58.27	58.29
						H 6.34	6.24
						N 8.00	8.19
VIII*a*	3	160–162°	60	B	$C_{12}H_{15}ClN_2O_4$	C 50.26	50.39
						H 5.28	5.30
						N 9.77	9.92
VIII*b*	4	215–217°	77	A	$C_{12}H_{15}ClN_2O_4$	C 50.26	50.03
						H 5.28	5.09
						N 9.77	10.01
IX*a*	3	217–219°	73	D	$C_{12}H_{17}ClN_2O_2$	C 56.13	55.96
						H 6.69	6.62
						N 10.91	10.77
IX*b*	4	237–239°	66	D	$C_{12}H_{17}ClN_2O_2$	C 56.13	55.90
						H 6.69	6.51
						N 10.91	10.78

[a] (A) ethanol–water; (B) absolute ethanol; (C) ethanol–hexane; and (D) 95% ethanol.

Table III—Antagonism of Pentylenetetrazol-Induced Convulsions by Esters of Nipecotic Acid

Effect	Saline	Pretreatment[a] Sodium Phenobarbital (25 mg/kg sc)	VIII*a* (150 mg/kg sc)	VIII*b* (150 mg/kg sc)	VI*a* (150 mg/kg sc)
Onset of myoclonus[b], min (Mean ± *SEM*)	8.50 ± 0.5	—	19.7 ± 0.7[c]	21.5 ± 3.8[c]	18.2 ± 1.9[c]
Protected, %	0 (0/16)	100 (4/4)[c]	12.5 (1/8)	14.3 (1/7)	37.5 (3/8)[d]
Onset of tonic seizure, min	20; 25	—	—	—	—
Protected, %	87.5 (14/16)	100 (4/4)	100 (8/8)	100 (7/7)	100 (8/8)
Time of death, min	20; 60	—	—	—	—
Protected, %	87.5 (14/16)	100 (4/4)	100 (8/8)	100 (8/8)	100 (8/8)

[a] Pretreatments were administered 1 hr before injection of pentylenetetrazol (85 mg/kg sc). [b] Onset of myoclonus was defined as one episode of clonic activity persisting for at least 5 sec. [c] Significantly different from saline controls, ($p < 0.01$). [d] $p < 0.05$.

Table IV—Antagonism of Bicuculline-Induced Convulsions by Esters of Nipecotic Acid

Effect	Saline	Pretreatment[a] Diazepam[b] (10 mg/kg ip)	VIII*a* (150 mg/kg sc)	VIII*b* (150 mg/kg sc)	VI*a* (150 mg/kg sc)
Onset of myoclonus[c], min (Mean ± *SEM*)	5.5 ± 0.3	—	20.3 ± 2.8[d]	17.6 ± 3.0[d]	11.0 ± 2.5[d]
Protected, %	0 (0/23)	100 (4/4)	50 (4/8)[d]	37.5 (3/8)[e]	0 (0/8)
Onset of tonic seizure, min (Mean ± *SEM*)	7.7 ± 0.4	—	—	22.0	11.6 ± 1.5[d]
Protected, %	0 (0/23)	100 (4/4)	100 (8/8)[e]	87.5 (7/8)[e]	25 (2/8)
Time of death, min	9.2 ± 1.3	—	—	22.0	15.7 ± 2.5[f]
Protected, %	0 (0/23)	100 (4/4)	100 (8/8)[d]	87.5 (7/8)[d]	50 (4/8)[d]

[a] Pretreatments were administered 1 hr before injection of bicuculline (3 mg/kg sc). [b] Diazepam completely protected the mice from seizures as compared to the solvent for diazepam (40% propylene glycol–10% ethanol). [c] Onset of myoclonus was defined as one episode of clonic activity persisting for at least 5 sec. [d] Significantly different from saline controls ($p < 0.01$). [e] $p < 0.05$. [f] This mean is based on $n = 3$, with the fourth animal dying ~2 hr postinjection of bicuculline.

lytically pure product, mp 135–137°; IR (KBr): 1750 (C=O, acid) and 1680 (C=O, carbamate) cm^{-1}; NMR ($CDCl_3$): δ 1.40 [s, 9H, $C(CH_3)_3$], 1.80 (m, 4H, CH_2CHCH_2), 2.60 (m, 3H, CHNCH and CH overlap), 4.0 (m, 2H, CHNCH), and 10.2 (broad s, 1H, COOH) ppm.

Anal.—Calc. for $C_{11}H_{19}NO_4$: C, 56.61; H, 8.37; N, 6.11. Found: C, 56.62; H, 8.32; N, 6.21.

N,N′-*Dicyclohexyl*-N-(1-tert-*butyloxycarbonyl-4-piperidinocarbonyl)urea* (III)—A solution of II*b* (2.50 g, 0.011 mole) and *n*-hexanol (1.10 g, 0.011 mole) in 155 ml of acetonitrile was treated in one portion with 2.30 g (0.011 mole) of dicyclohexylcarbodiimide. The reaction mixture was stirred overnight, filtered, and the filtrate was concentrated under reduced pressure. The resulting oil was triturated with diethyl ether to afford after recrystallization from hexane 1.30 g (28%) of white solid, mp 166–168°; IR (KBr): 3350 (NH), 1700 (C=O, amide) and 1670 (C=O, carbamate and urea) cm^{-1}; NMR ($CDCl_3$): δ 1.30 [s, 9H, $C(CH_3)_3$], 1.40–1.80 (broad m, 26H, CH_2NCH_2 and cyclohexyl overlap), 2.20–2.60 (broad m, 3H, CHNCH and CHCO overlap), 4.0 (m, 2H, CHNCH), and 6.15 (d, 1H, NH) ppm.

Anal.—Calc. for $C_{24}H_{41}N_3O_4$: C, 66.16; H, 9.50; N, 9.65. Found: C, 65.91; H, 9.49; N, 9.44.

n-*Alkyl Piperidinecarboxylate Hydrochlorides* (*IV*a–g)—The synthesis of *n*-butyl 4-piperidinecarboxylate hydrochloride (IV*d*) was representative of the general method. A suspension of isonipecotic acid in 20 ml of *n*-butanol was saturated with dry hydrogen chloride and refluxed for 2 hr. The resulting solution was cooled, diluted with ether, and washed with four 50-ml portions of water. The aqueous phase was washed with 50 ml of ether, basified with sodium bicarbonate to pH 8, and extracted with four 50-ml portions of chloroform. The combined chloroform layer was dried (sodium sulfate) and evaporated to give a colorless oil. The oil was dissolved in anhydrous chloroform and was saturated with hydrogen chloride at 0°. Recrystallization of the hydrochloride from ethyl acetate gave 2.3 g (67%) of white crystalline solid, mp 113–115°; IR (KBr): 2500 (NH_2^+), 1760 (C=O), and 1225 (C—O) cm^{-1}; NMR ($CDCl_3$): δ 0.90 (t, 3H, CH_3), 1.50 (m, 4H, CH_2CH_2), 2.15 (t, 4H, CH_2CHCH_2), 2.50 (m, 1H, CH), 3.20 (m, 4H, $CH_2NH_2^+CH_2$), 4.1 (t, 2H, OCH_2), and 8.50–9.30 (broad s, 1H, NH_2^+).

Anal.—Calc. for $C_{10}H_{20}ClNO_2$: C, 54.16; H, 9.11; N, 6.32. Found: C, 54.31; H, 9.27; N, 6.18.

Preparation of *tert*-Butyloxycarbonyl Esters V*a–b* and VII*a–b*)—The synthesis of *p*-nitrophenyl-1-(*tert*-butyloxycarbonyl)-4-piperdinecarboxylate (VII*b*) is representative of the general procedure. A mixture of II*b* (2.5 g, 0.011 mole) and *p*-nitrophenol (1.50 g, 0.011 mole) in 115 ml of acetonitrile was treated with dicyclohexylcarbodiimide (2.30 g, 0.011 mole). Immediately, a white precipitate of dicyclohexylurea formed. Stirring was continued overnight and the precipitated dicyclohexylurea was filtered, and the filtrate was concentrated. Recrystallization of the solid from absolute ethanol gave 2.30 g (60%) of white crystalline solid, mp 91–93°; IR (KBr): 1790 (C=O, ester) and 1700 (C=O, carbamate) cm^{-1}; NMR ($CDCl_3$): δ 1.40 [s, 9H, $C(CH_3)_3$], 1.80 (m, 4H, CH_2CHCH_2), 2.80 (m, 3H, CHNCH and CH), 4.0 (m, 2H, CHNCH), 7.20–8.20 (m, 4H, ArH).

Anal.—Calc. for $C_{17}H_{22}NO_6$: C, 58.27; H, 6.34; N, 8.00. Found: C, 58.29; H, 6.24; N, 8.19.

Removal of the *tert*-Butyloxycarbonyl Group from V*a–b* and VII*a–b*—p-*Nitrophenyl 4-Piperidinecarboxylate Hydrochloride* (*VIIIb*)—Synthesis of VIII*b* is typical of the general method. A solution of VII*b* (2.70 g, 0.008 mole) in 100 ml of chloroform was saturated with hydrogen chloride at 0–5° for 1 hr. The solvent was evaporated and the resulting solid was recrystallized from ethanol–water to afford 1.70 g (78%) of a white crystalline solid, mp 215–217°; IR (KBr): 2500 (NH_2^+), 1750 (C=O, ester), and 1180 (C—O) cm^{-1}; NMR (D_2O): δ 2.45 (m, 4H, CH_2CHCH_2), 3.10–3.65 (broad m, 5H, CH_2NCH_2 and CH overlap), and 7.45–8.35 (m, 4H, ArH).

Anal.—Calc. for $C_{12}H_{15}ClN_2O_4$: C, 50.26; H, 5.28; N, 9.77. Found: C, 50.03, H, 5.09; N, 10.01.

p-*Aminophenyl 3-Piperidinecarboxylate Hydrochloride* (*IX*a)—A suspension of VIII*a* (1.40 g, 0.0049 mole) and 0.2 g of 10% palladium on carbon in 250 ml of ethanol was hydrogenated on a hydrogenator[3] at an initial pressure of 3 atm. After 1 hr, the theoretical amount of hydrogen had been absorbed. The mixture was warmed gently to dissolve the product, filtered, and evaporated under reduced pressure. The solid product was recrystallized twice from ethanol to yield 0.92 g (73%) of a brown crystalline solid, mp 217–219°; IR (KBr): 3550 and 3450 (NH_2), 2500 (NH_2^+), 1780 (C=O, ester), and 1220 (C—O) cm^{-1}; NMR (D_2O): δ 1.90 (m, 4H, CH_2CH_2CH), 2.70–3.70 (broad m, 5H, $CH_2NH_2^+CH_2CH$) and 6.85 (s, 4H, ArH).

Anal.—Calc. for $C_{12}H_{17}ClN_2O_2$: C, 56.13; H, 6.69; N, 10.91. Found: C, 55.96; H, 6.62; N, 10.77.

p-*Aminophenyl 4-Piperidinecarboxylate Hydrochloride* (*IX*b)—Compound IX*b* was prepared from VIII*b* (1.50 g, 0.005 mole), 0.2 g of 10% palladium on carbon in 250 ml of ethanol in the same manner as described for the synthesis of IX*a*. Recrystallization of the product from ethanol gave 0.89 g (66%) of analytically pure product, mp 237–239°; IR (KBr): 3550 and 3400 (NH_2), 2500 (NH_2^+), 1750 (C=O, ester), and 1190 (C—O) cm^{-1}; NMR (D_2O): δ 2.20 (m, 4H, CH_2CHCH_2), 2.80–3.50 (broad m, 5H, $CH_2NH_2^+CH_2$ and CH overlap) and 6.90 (s, 4H, ArH).

Anal.—Calc. for $C_{12}H_{17}ClN_2O_2$: C, 56.13; H, 6.69; N, 10.91. Found: C, 55.90; H, 6.51; N, 10.78.

Biological Testing—Initial evaluation for anticonvulsant activity was done by an antiepileptic drug development program[1] using the test systems as previously described (19). The testing included the maximal electroshock seizure test, the subcutaneous pentylenetetrazol seizure threshold test, and the rotorod test to evaluate neurotoxicity. In these

[3] Parr hydrogenator.

Table V—Effect of Piperidine Derivatives on the Uptakes of γ-Aminobutyric Acid [a] and L-Proline [b]

Inhibitor	Concentration of Inhibitor, m*M*	Uptake System	Uptake, pmole/g/min [c] Control	Inhibitor	Inhibition, %
I*a*	1.0	GABA	112.9 ± 6.7	4.1 ± 0.3	96.3 ± 0.2
	0.2		126.2 ± 5.8	13.7 ± 0.6	89.0 ± 0.7
	0.05		134.0 ± 2.7	33.4 ± 1.6	75.1 ± 0.9
	0.02		112.3 ± 8.7	40.2 ± 2.1	63.8 ± 1.4
	1.0	Proline	47.2 ± 1.4	37.4 ± 1.9	21.0 ± 2.9
	0.2		45.6 ± 1.2	40.2 ± 2.2	11.7 ± 5.1
I*c*	1.0	GABA	117.8 ± 2.2	80.7 ± 1.7	32.6 ± 0.8
	0.2		111.6 ± 7.0	95.0 ± 3.9	14.2 ± 2.8
(±)-Ethyl nipecotate	1.0	GABA	112.6 ± 5.2	62.3 ± 3.2	47.4 ± 1.6
IV*a*	1.0	GABA	112.7 ± 4.9	46.5 ± 1.9	59.7 ± 1.3
IV*b*	1.0	GABA	112.6 ± 4.3	53.2 ± 0.7	52.7 ± 1.6
IV*c*	1.0	GABA	112.7 ± 4.2	0.1 ± 0.1	99.7 ± 0.1
	0.2		128.8 ± 8.7	66.4 ± 2.7	47.8 ± 2.6
	0.05		136.6 ± 6.4	114.6 ± 4.8	16.0 ± 2.5
	1.0	Proline	36.5 ± 2.4	0.5 ± 0.2	98.8 ± 0.5
	0.2		45.9 ± 1.5	13.3 ± 1.0	70.9 ± 2.4
IV*g*	1.0	GABA	116.5 ± 2.6	0.2 ± 0.1	99.8 ± 0.1
	0.2		107.6 ± 4.6	50.6 ± 3.3	53.1 ± 1.6
	0.05		94.3 ± 4.9	73.0 ± 3.3	22.4 ± 1.4
VI*a*	1.0	GABA	119.0 ± 2.4	4.3 ± 0.3	96.4 ± 0.3
	0.2		115.8 ± 5.8	11.8 ± 0.8	89.7 ± 0.6
	0.05		123.5 ± 5.2	30.9 ± 1.2	74.9 ± 0.9
VIII*a*	1.0	GABA	138.9 ± 5.5	1.3 ± 0.1	99.0 ± 0.1
	0.5		154.1 ± 6.0	6.2 ± 0.4	95.8 ± 0.3 [d]
	0.2		162.1 ± 4.1	20.0 ± 1.2	87.6 ± 0.8
	0.05		154.0 ± 6.6	62.4 ± 6.0	59.7 ± 2.7
	1.0	Proline	45.1 ± 0.6	13.5 ± 0.8	70.0 ± 1.8
	0.5		45.3 ± 1.5	16.3 ± 1.1	63.7 ± 2.8 [d]
	0.2		45.9 ± 1.7	23.7 ± 1.6	47.4 ± 3.9
	0.05		44.1 ± 1.6	37.0 ± 1.7	15.9 ± 3.0
IX*a*	1.0	GABA	138.9 ± 5.5	40.2 ± 1.1	70.6 ± 2.0

[a] GABA = γ-aminobutyric acid. [b] Uptake measured in mouse whole brain minislices. [c] All values are mean ± *SEM* for six samples except where indicated and for the control group where 18 samples were used. [d] Mean ± *SEM* for five samples.

tests the compounds being evaluated were administered by intraperitoneal injection.

Based on the data obtained from the initial screening, additional tests were performed on the piperidinyl esters using male Sprague-Dawley mice[4]. To assess the activity of these compounds against convulsions induced by the putative γ-aminobutyric acid antagonist, bicuculline, the experimental animals received a subcutaneous injection of 3 mg/kg of bicuculline in a volume of 0.01 ml/g. The bicuculline solution was freshly prepared on the day of the experiment by dissolving the solid in 0.1 *N* HCl and adjusting to pH 5 with 0.1 *N* NaOH solution (20). The compounds evaluated against bicuculline-induced seizures were administered by intraperitoneal or subcutaneous injection prior to challenge with the convulsant. Diazepam, dissolved in a 40% propylene glycol–10% ethanol solution, was used as a reference compound in these studies.

The mice were divided into groups of four to eight animals, with Group 1 receiving injection of 0.9% NaCl solution (0.01 ml/g sc); Group 2, an injection of the diazepam solvent (0.01 ml/g ip); Group 3, 10 mg/kg ip of diazepam by injection; and Group 4, 150 mg/kg sc of the ester by injection. The incidence of clonic and tonic convulsions induced by bicuculline was determined at 0.5, 1.0, and 4.0 hr after administration of the test compound. A clonic convulsion was defined as a single episode of clonic spasms of at least a 5-sec duration. A tonic seizure was defined as a brief period of hindlimb flection followed by a prolonged period of hindlimb extension.

In addition, the piperidinyl esters were reevaluated for their ability to protect against pentylenetetrazol-induced seizures. In the initial evaluation, the test compounds were administered by intraperitoneal injection. It was theorized that subcutaneous administration might increase anticonvulsant activity by preventing the peripheral hepatic hydrolysis of the esters that might occur with intraperitoneal dosing. Therefore, experimental animals received a subcutaneous injection of 85 mg/kg of pentylenetetrazol in a 0.01-ml/g volume. Sodium phenobarbital dissolved in saline was used as a reference compound. Groups of four to eight mice were used to determine the anticonvulsant activity, with Group 1 receiving a subcutaneous injection of 0.9% NaCl solution (0.01 ml/g); Group 2, 25 mg/kg sc of sodium phenobarbital by injection; and Group 3, 150 mg/kg sc of the ester by injection. The incidence of clonic and tonic convulsions induced by pentylenetetrazol was determined as described for bicuculline.

[4] Obtained from Harlan Sprague-Dawley, Madison, Wis.

Uptake of Amino Acids—The uptakes of [^{3}H]γ-aminobutyric acid and tritiated L-proline were carried out according to described procedures (6, 21).

REFERENCES

(1) J. K. Saelens and F. J. Vinick, in "Annual Report in Medicinal Chemistry," vol. 13, F. H. Clarke, Ed., Academic, New York, N.Y., 1978, p. 31.

(2) D. R. Curtis, in "GABA-Neurotransmitters, Pharmacochemical, Biochemical and Pharmacological Aspects," P. Krogsgaard-Larsen, J. Scheel-Krüger, and H. Kofod, Eds., Academic, New York, N.Y., 1979, p. 18.

(3) B. S. Meldrum, *Int. Rev. Neurobiol.*, **17**, 1 (1975).

(4) W. Löscher, *Naunyn-Schmiedeberg's Arch. Pharmacol.*, **315**, 119 (1980).

(5) P. Krogsgaard-Larsen and G. A. R. Johnston, *J. Neurochem.*, **25**, 797 (1975).

(6) J. D. Wood, D. Tsui, and J. W. Phillis, *Can. J. Physiol. Pharmacol.*, **57**, 581 (1979).

(7) G. A. R. Johnston, P, Krogsgaard-Larsen, A. L. Stephanson, and B. Twitchin, *J. Neurochem.*, **26**, 1029 (1976).

(8) D. Lodge, G. A. R. Johnston, D. R. Curtis, and S. J. Brand, *Brain Res.*, **136**, 513 (1977).

(9) R. W. Horton, J. F. Collins, G. M. Anlezark, and B. S. Meldrum, *Eur. J. Pharmacol.*, **59**, 75 (1979).

(10) H. H. Frey, C. Popp, and W. Löscher, *Neuropharmacology*, **18**, 581 (1979).

(11) J. D. Wood, A. Schousboe, and P. Krogsgaard-Larsen, *ibid.*, **19**, 1149 (1980).

(12) E. Falch, P. Krogsgaard-Larsen, and A. V. Christensen, *J. Med. Chem.*, **24**, 285 (1981).

(13) P. Krogsgaard-Larsen and G. A. R. Johnston, *J. Neurochem.*, **30**, 1377 (1978).

(14) P. Krogsgaard-Larsen, G. A. R. Johnston, P. Lodge, and D. R. Curtis, *Nature (London)*, **268**, 53 (1977).

(15) J. March, in "Advanced Organic Chemistry: Reactions, Mechanisms, and Structure," McGraw-Hill, New York, N.Y., 1968, p. 320.

(16) L. J. Mathias, *Synthesis*, **1979**, 561.

(17) J. A. Vida, in "Principles of Medicinal Chemistry," 2nd ed., W. O. Foye, Ed., Lea and Febiger, Philadelphia, 1981, p. 183.

(18) M. Freifelder, *J. Org. Chem.*, **28**, 1135 (1963).
(19) A. M. Crider, T. M. Kolczynski, and D. L. Miskell, *J. Pharm. Sci.*, **70**, 192 (1981).
(20) J. B. Patel, L. R. Nelson, and J. B. Malick, *Brain Res. Bull. Supp 2*, **5**, 639 (1980).
(21) L. L. Iversen and M. J. Neal, *J. Neurochem.*, **15**, 1141 (1968).

ACKNOWLEDGMENTS

This investigation was supported by a research grant from the Epilepsy Foundation of America (A.M.C.). J. D. Wood gratefully acknowledges the grant support of the Medical Research Council of Canada. The authors thank Dr. W. E. Scott at Hoffmann-LaRoche for a generous supply of diazepam.

The arrangement of anticonvulsant testing through the Antiepileptic Drug Development Program administered by the National Institutes of Health by Mr. Gill D. Gladding is greatly appreciated.

The authors thank Catherine Forster, David Miskell, and Eugene Kurylo for their technical assistance, and the helpful suggestions by Dr. K. A. Bachmann are appreciated.

Simultaneous Determination of Hydrocortisone and Benzyl Alcohol in Pharmaceutical Formulations by Reversed-Phase High-Pressure Liquid Chromatography

ALBERT REGO ˣ **and BRETT NELSON**

Received May 13, 1981, from the *Analytical Development Group, Allergan Pharmaceuticals, Inc., Irvine, CA 92713.* Accepted for publication January 12, 1982.

Abstract □ An accurate, reproducible, and specific reversed-phase high-pressure liquid chromatographic (HPLC) procedure that simultaneously determines hydrocortisone and benzyl alcohol in a variety of pharmaceutical formulations is presented. Cream, gel, ointment, and solution formulations containing varying hydrocortisone and benzyl alcohol concentrations can be analyzed with only minor modifications in sample preparation. To provide optimum accuracy and reproducibility, phenethyl alcohol is used as an internal standard. The specificity of the procedure allows for the quantitative determination of hydrocortisone and benzyl alcohol in the presence of their degradation products and without interference from the phenethyl alcohol. The determinations can be performed with an analysis time of 10–13 min/sample.

Keyphrases □ Hydrocortisone—simultaneous determination with benzyl alcohol, pharmaceutical formulations, reversed-phase high-pressure liquid chromatography □ Benzyl alcohol—simultaneous determination with hydrocortisone, pharmaceutical formulations, reversed-phase high-pressure liquid chromatography □ High-pressure liquid chromatography, reversed-phase—hydrocortisone, simultaneous determination with benzyl alcohol, pharmaceutical formulations

Hydrocortisone (I) has gained wide acceptance as a topical agent for the relief of inflammatory manifestations of corticosteroid-responsive dermatoses (1). Benzyl alcohol (II) is commonly used as an antimicrobial agent in a variety of topical formulations (2).

Various methods have been used for the determination of hydrocortisone, including TLC, polarography, colorimetry, GC, and high-pressure liquid chromatography (HPLC). TLC, though somewhat specific, lacks precision and short analysis time (1, 3–6). Polarographic determinations can be erroneous due to interferences, and they can

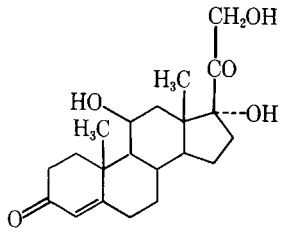

I

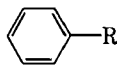

II: R = CH_2OH
III: R = CH_2CH_2OH

be nonspecific in that a variety of similar steroids can elicit the same reduction potential for the same functional groups (7–10). Colorimetric methods include reaction with aldehyde–sulfuric acid (11), ammonium molybdate (12), and 4,5-dimethyl-*o*-phenylenediamine (13). These methods lack specificity, because degradation products may provide a colorimetric response not indicative of actual steroid concentration. Numerous GC methods are available (14–18); however, most steroids cannot be directly analyzed but must be initially derivatized. The complexity of steroids precludes the direct formation of a single derivative (19). The USP methods for hydrocortisone formulations were recently changed from a colorimetric reaction with tetrazolium blue (1, 20–23) to HPLC procedures (1). Recently, literature on hydrocortisone analysis *via* HPLC has been published (19, 24–29). While these methods may be specific, the sample preparation and analysis time can be prohibitive to a rapid assay. Benzyl alcohol can be determined by spectrophotometry and GC. Spectrophotometric methods have the inherent problems of nonspecificity and formulation base interferences. GC methods, including the USP compendial method, are specific and efficient (2). However, these methods may have interferences due to longer retained compounds from the formulation base[1].

The described procedure allows for the simultaneous determination of hydrocortisone and benzyl alcohol in cream, gel, ointment, and solution formulations with a general sample preparation. The procedure incorporates phenethyl alcohol (III) as an internal standard to achieve optimum accuracy and reproducibility with an analysis

[1] Unpublished data.

0022-3549/82/1100-1219$01.00/0

(18) M. Freifelder, *J. Org. Chem.*, **28**, 1135 (1963).
(19) A. M. Crider, T. M. Kolczynski, and D. L. Miskell, *J. Pharm. Sci.*, **70**, 192 (1981).
(20) J. B. Patel, L. R. Nelson, and J. B. Malick, *Brain Res. Bull. Supp 2*, **5**, 639 (1980).
(21) L. L. Iversen and M. J. Neal, *J. Neurochem.*, **15**, 1141 (1968).

ACKNOWLEDGMENTS

This investigation was supported by a research grant from the Epilepsy Foundation of America (A.M.C.). J. D. Wood gratefully acknowledges the grant support of the Medical Research Council of Canada. The authors thank Dr. W. E. Scott at Hoffmann-LaRoche for a generous supply of diazepam.

The arrangement of anticonvulsant testing through the Antiepileptic Drug Development Program administered by the National Institutes of Health by Mr. Gill D. Gladding is greatly appreciated.

The authors thank Catherine Forster, David Miskell, and Eugene Kurylo for their technical assistance, and the helpful suggestions by Dr. K. A. Bachmann are appreciated.

Simultaneous Determination of Hydrocortisone and Benzyl Alcohol in Pharmaceutical Formulations by Reversed-Phase High-Pressure Liquid Chromatography

ALBERT REGO ˣ **and BRETT NELSON**

Received May 13, 1981, from the *Analytical Development Group, Allergan Pharmaceuticals, Inc., Irvine, CA 92713.* Accepted for publication January 12, 1982.

Abstract □ An accurate, reproducible, and specific reversed-phase high-pressure liquid chromatographic (HPLC) procedure that simultaneously determines hydrocortisone and benzyl alcohol in a variety of pharmaceutical formulations is presented. Cream, gel, ointment, and solution formulations containing varying hydrocortisone and benzyl alcohol concentrations can be analyzed with only minor modifications in sample preparation. To provide optimum accuracy and reproducibility, phenethyl alcohol is used as an internal standard. The specificity of the procedure allows for the quantitative determination of hydrocortisone and benzyl alcohol in the presence of their degradation products and without interference from the phenethyl alcohol. The determinations can be performed with an analysis time of 10–13 min/sample.

Keyphrases □ Hydrocortisone—simultaneous determination with benzyl alcohol, pharmaceutical formulations, reversed-phase high-pressure liquid chromatography □ Benzyl alcohol—simultaneous determination with hydrocortisone, pharmaceutical formulations, reversed-phase high-pressure liquid chromatography □ High-pressure liquid chromatography, reversed-phase—hydrocortisone, simultaneous determination with benzyl alcohol, pharmaceutical formulations

Hydrocortisone (I) has gained wide acceptance as a topical agent for the relief of inflammatory manifestations of corticosteroid-responsive dermatoses (1). Benzyl alcohol (II) is commonly used as an antimicrobial agent in a variety of topical formulations (2).

Various methods have been used for the determination of hydrocortisone, including TLC, polarography, colorimetry, GC, and high-pressure liquid chromatography (HPLC). TLC, though somewhat specific, lacks precision and short analysis time (1, 3–6). Polarographic determinations can be erroneous due to interferences, and they can

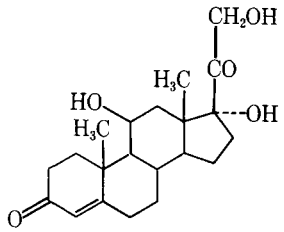

I

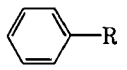

II: R = CH_2OH
III: R = CH_2CH_2OH

be nonspecific in that a variety of similar steroids can elicit the same reduction potential for the same functional groups (7–10). Colorimetric methods include reaction with aldehyde–sulfuric acid (11), ammonium molybdate (12), and 4,5-dimethyl-*o*-phenylenediamine (13). These methods lack specificity, because degradation products may provide a colorimetric response not indicative of actual steroid concentration. Numerous GC methods are available (14–18); however, most steroids cannot be directly analyzed but must be initially derivatized. The complexity of steroids precludes the direct formation of a single derivative (19). The USP methods for hydrocortisone formulations were recently changed from a colorimetric reaction with tetrazolium blue (1, 20–23) to HPLC procedures (1). Recently, literature on hydrocortisone analysis *via* HPLC has been published (19, 24–29). While these methods may be specific, the sample preparation and analysis time can be prohibitive to a rapid assay. Benzyl alcohol can be determined by spectrophotometry and GC. Spectrophotometric methods have the inherent problems of nonspecificity and formulation base interferences. GC methods, including the USP compendial method, are specific and efficient (2). However, these methods may have interferences due to longer retained compounds from the formulation base[1].

The described procedure allows for the simultaneous determination of hydrocortisone and benzyl alcohol in cream, gel, ointment, and solution formulations with a general sample preparation. The procedure incorporates phenethyl alcohol (III) as an internal standard to achieve optimum accuracy and reproducibility with an analysis

[1] Unpublished data.

0022-3549/82/1100-1219$01.00/0

Table I—Recovery Studies[a]

Formulation	Hydrocortisone			Benzyl Alcohol		
	Spike, %	N	Recovery, %	Spike, %	N	Recovery, %
A	0.460	6	99.60 ± 0.46	0.730	3	99.85 ± 0.34
B	1.02	3	100.17 ± 0.05	1.06	4	100.27 ± 1.15
C	2.52	3	99.14 ± 0.05	0.99	4	99.81 ± 1.07
D	0.553	3	100.10 ± 0.20	1.16	3	100.54 ± 0.03
E	1.00	3	100.08 ± 0.23	2.00	4	99.87 ± 0.68
F	1.05	5	100.08 ± 0.17	—[b]	—	—
G	0.500	3	100.67 ± 1.53	—	—	—
H	2.36	3	100.20 ± 0.82	—	—	—

[a] Mean ± %*RSD* for *N* samples. [b] The dash denotes formulations not containing benzyl alcohol.

time of 10–13 min/sample. Phenethyl alcohol cannot be used as an internal standard for those formulations containing methylparaben, as these compounds elute at the same time. Benzyl alcohol could be used as an internal standard for those formulations containing methylparaben and propylparaben. The procedure is shown to be specific for hydrocortisone and benzyl alcohol in the presence of their degradation products in these formulations.

EXPERIMENTAL

Materials—Hydrocortisone[2], benzyl alcohol[3], methylparaben[4], propylparaben[4], and phenethyl alcohol[5] were used as standards. HPLC grade acetonitrile[6] and distilled, deionized water were used as reagents.

The HPLC system consisted of a pump[7], an automatic injector[8], a 254-nm detector[9], a radial compression module[10], and a reversed-phase octadecylsilane cartridge[11] fitted with a 2-μm precolumn filter and a recorder[12]. All peaks were electronically integrated with the laboratory data system[13].

The system was operated at ambient temperature, and the detector sensitivity was 0.1 or 0.2 aufs, depending on the hydrocortisone concentration. The chromatographic parameters include a 10-μl loop, an analysis time of 10 min, and a chart speed of 0.25 cm/min. After the baseline had stabilized, replicate standards were run to ensure reproducibility.

Mobile Phase—The mobile phase was 22.5% (v/v) acetonitrile in distilled, deionized water. Prior to use, the mobile phase was filtered through a 3.0-μm filter[14] and degassed with a water aspirator. A flow rate of 6.0 ml/min was used with a cartridge pressure of 1500–2000 psi.

Internal Standard Preparation—The stock phenethyl alcohol internal standard solution was prepared as 1.0% (w/v) in acetonitrile.

Standard Preparations—The hydrocortisone reference standard and benzyl alcohol reference standard were diluted to give the required working standard concentration levels. To provide accuracy and reproducibility, 25.0 ml of the phenethyl alcohol internal standard solution

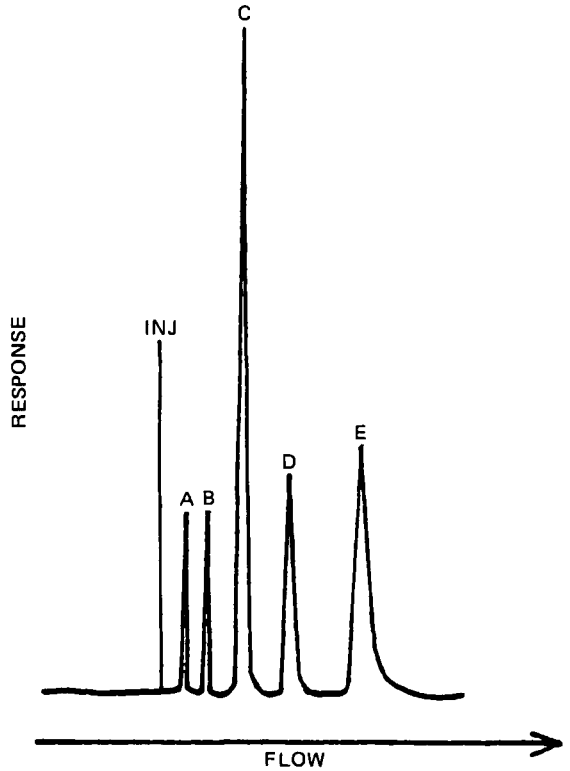

Figure 1—*A chromatogram showing the separation of components from benzyl alcohol degradation products. Key: (A) benzoic acid; (B) benzyl alcohol; (C) phenethyl alcohol (internal standard); (D) benzaldehyde; (E) hydrocortisone.*

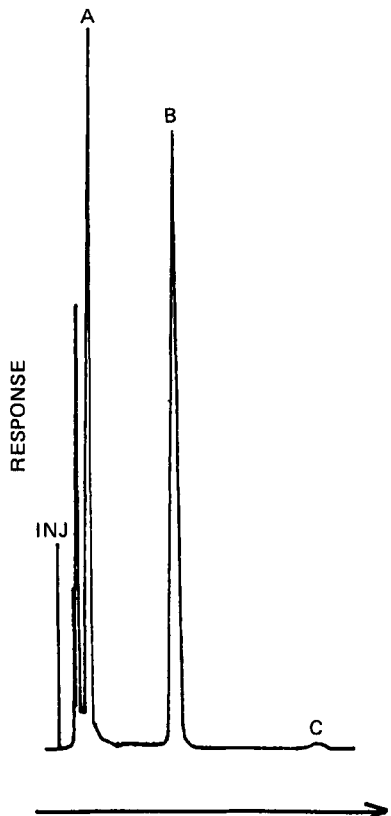

Figure 2—*A chromatogram showing the separation of components from hydrocortisone degradation products. Key: (A) polar degradation products of hydrocortisone; (B) hydrocortisone; (C) nonpolar degradation product of hydrocortisone.*

[2] The Upjohn Co., Kalamazoo, Mich.
[3] Stauffer Chemicals, Westport, Conn.
[4] Quad Chemicals, Long Beach, Calif.
[5] Matheson, Coleman, and Bell, Los Angeles, Calif.
[6] J. T. Baker, Phillipsburg, N.J.
[7] Model 6000A, Waters Associates, Milford, Mass.
[8] Model 725, Micromeritics Instrument Corp., Norcross, Ga.
[9] Model 440, Waters Associates, Milford, Mass.
[10] RCM-100 Radial Compression Module, Waters Associates, Milford, Mass.
[11] Radial Pak A, 10-cm × 8-mm cartridge (10-μm particles), Waters Associates, Milford, Mass.
[12] Omniscribe, Houston Instruments, Austin, Tex.
[13] Model 3352B, Hewlett-Packard, Fullerton, Calif.
[14] Millipore Type FS, Millipore, Corp., Bedford, Mass.

Table II—Reproducibility Studies[a]

Formulation	Hydrocortisone				Benzyl Alcohol			
	Day-to-Day	*N*	Operator-to-Operator	*N*	Day-to-Day	*N*	Operator-to-Operator	*N*
A	0.545 ± 1.91	19	0.550 ± 1.15	19	1.06 ± 0.83	19	1.06 ± 0.90	19
B	1.04 ± 1.30	20	1.05 ± 0.64	20	1.05 ± 0.58	19	1.05 ± 0.58	19
C	2.70 ± 0.72	19	2.71 ± 0.50	20	1.05 ± 0.85	19	1.05 ± 1.36	20
D	0.559 ± 0.89	20	0.557 ± 0.73	20	1.09 ± 0.81	20	1.08 ± 1.11	20
E	1.13 ± 0.94	19	1.13 ± 1.02	19	2.23 ± 0.56	19	2.22 ± 0.57	19
F	1.05 ± 0.85	18	1.04 ± 1.05	19	—[b]	—	—[b]	—
G	0.484 ± 0.97	18	0.484 ± 1.05	19	—	—	—	—
H	2.54 ± 0.74	18	2.54 ± 9.90	18	—	—	—	—

[a] Mean ± %*RSD* for *N* samples. [b] The dash denotes formulations not containing benzyl alcohol.

was added before the diluted standards were brought to 100 ml final volume with acetonitrile. The diluted working standard concentrations included 0.125 mg/ml, 0.250 mg/ml, and 0.625 mg/ml of hydrocortisone (equivalent to 0.5, 1.0, and 2.5% hydrocortisone on a product basis) and 0.250 and 0.500 mg/ml of benzyl alcohol (equivalent to 1.0 and 2.0% benzyl alcohol on a product basis).

Sample Preparation for Hydrocortisone and Benzyl Alcohol Determinations—*Cream and Gel Formulations*—Five-hundred milligrams of the sample was weighed into a 30-ml screw-capped culture tube. Acetonitrile (15.0 ml) and 5.0 ml of phenethyl alcohol internal standard solution, were accurately added and tightly capped. The tube was vigorously shaken by hand to disperse the sample and shaken for an additional 30 min on a mechanical shaker. The sample was centrifuged for 20 min, and the injector vial was filled with the clear supernatant. An aliquot (10 μl) was injected onto the liquid chromatograph.

Ointment Formulations—Five-hundred milligrams of the sample was accurately weighed into a 30-ml screw-capped culture tube. HPLC mobile phase (15.0 ml) and 5.0 ml of the phenethyl alcohol internal standard solution were accurately added, then tightly capped. The sample was then placed into a constant temperature (60–65°) water bath for 30 min and shaken by hand at 5-min intervals. The solution was then cooled to room temperature and centrifuged for 20 min. An aliquot was injected onto the liquid chromatograph following the procedure used for cream and gel formulations.

Solution Formulations—Five-hundred milligrams of the sample was accurately weighed into a 30-ml screw-capped culture tube. Acetonitrile (15.0 ml) and 5.0 ml of the phenethyl alcohol internal standard solution were accurately added and tightly capped. The sample was then shaken for 20 min on a mechanical shaker. The solution was injected as described in the previous two preparations.

RESULTS AND DISCUSSION

Linearity—To determine the linearity of the detector response, separate calibration curves for hydrocortisone (0.5, 1.0, and 2.5% product level) and benzyl alcohol (1.0 and 2.0% product level) were obtained. Each curve contained points equivalent to 50 and 150% of label claim and three intermediate points. In all cases, the component concentration was plotted *versus* the ratio of component peak area over internal standard peak area. The internal standard was held constant throughout the study. A composite hydrocortisone calibration curve passed through zero and was linear from 0.050 to 1.008 mg/ml with a correlation coefficient of 0.999. A composite benzyl alcohol calibration curve passed through zero and was linear from 0.129 to 0.854 mg/ml with a correlation coefficient of 0.999.

Recovery Studies—Each formulation was received with the appropriate placebo base. Each base was prepared and analyzed by HPLC to ensure that no UV absorbing peaks were present in the regions of benzyl alcohol, phenethyl alcohol, and hydrocortisone. To determine method accuracy, each placebo was spiked a minimum of three times with benzyl alcohol to the appropriate levels (1.0 and 2.0% on a product basis). A second placebo series was spiked a minimum of three times with hydrocortisone to the appropriate levels (0.5, 1.0, and 2.5% on a product basis). The samples were prepared and subjected to HPLC analysis. In all cases, satisfactory recoveries were obtained (Table I).

Reproducibility Studies—The reproducibility of the HPLC procedure was determined by the criteria of day-to-day reproducibility and operator-to-operator reproducibility. The following scheme was applied to each formulation: Day 1, Operator 1; Day 2, Operator 1; and Day 2, Operator 2 (Table II).

Limit of Detection—The limit of detection, defined here as an acceptable signal to noise level of >2:1 was performed by diluting the working standard 1–100 with acetonitrile and performing the analysis at 0.01 aufs. In all cases, benzyl alcohol, phenethyl alcohol, and hydrocortisone were easily detected and within acceptable limits.

Specificity Studies—It is known that benzyl alcohol degrades *via* oxidation to yield benzoic acid and benzaldehyde[15]. As confirmation of method specificity, a sample was spiked with benzoic acid and benzaldehyde and analyzed. The two peaks were noted and did not create any interference problems (Fig. 1).

The degradation of a steroid, such as hydrocortisone, is complex and involves hydrolysis, oxidation, and possible transesterification (19). Each formulation and formulation base placebo was artificially degraded by adjusting the sample to ~pH 12 with 50% NaOH and also by heating a second series of samples at 100° for 1 hr.

The four base formulation placebos, with or without benzyl alcohol depending on the formulation, were analyzed by the HPLC procedure. In all cases, no interfering peaks were noted in the area of benzyl alcohol, phenethyl alcohol, or hydrocortisone.

Further work demonstrated that degradation products of hydrocor-

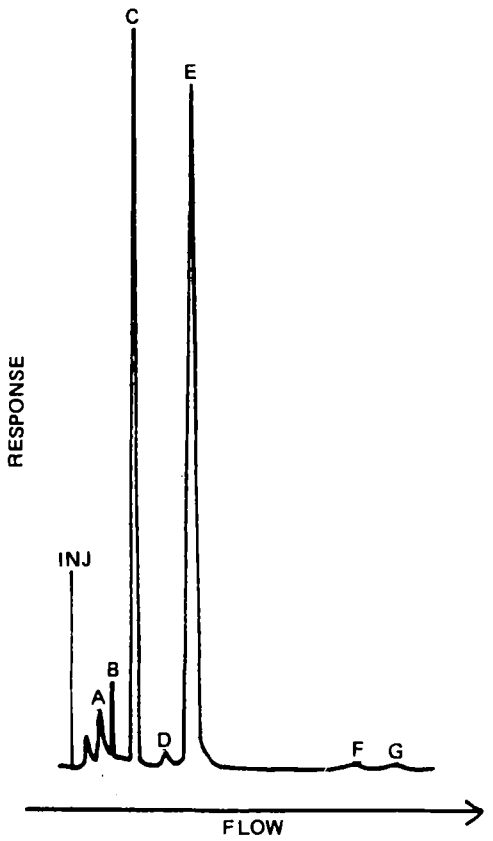

Figure 3—*A chromatogram showing the separation of components from degradation products of an aged sample. Key: (A) benzoic acid and polar degradation products of hydrocortisone; (B) benzyl alcohol; (C) phenethyl alcohol; (D) benzaldehyde; (E) intact hydrocortisone; (F, G) nonpolar degradation products of hydrocortisone.*

[15] The degradation products benzaldehyde and benzoic acid were verified by GC using 1.83-m × 0.318-cm stainless steel Porapak P column (Waters Associates, Milford, Mass.). Chromatographic parameters include gas flow of 45 ml/min, nitrogen, 220° oven temperature, and a flame ionization detector.

Table III—Stability Study[a]

Age, Days	Percent Hydrocortisone Found[b] Lot A	Lot B	Lot C	Percent Benzyl Alcohol Found[b] Lot A	Lot B	Lot C
0	0.517	0.527	0.528	1.06	1.06	1.05
36	0.517	0.519	0.518	1.02	1.04	1.04
49	0.472	0.476	0.480	1.05	1.07	1.06
86	0.467	0.470	0.464	1.06	1.07	1.04
119	0.391	0.390	0.393	1.00	0.99	1.00

[a] Claim was 0.525% hydrocortisone and 1.0% benzyl alcohol. [b] Each result represents the mean of four values.

tisone do not interfere with benzyl alcohol or the internal standard phenethyl alcohol. An artificially degraded gel formulation, not containing benzyl alcohol or phenethyl alcohol, gave a similar pattern of degradation peaks as noted in Fig. 2 with no benzyl alcohol or phenethyl alcohol interferences.

As a final test, a tube of a sample stored at 45° for >300 days was analyzed. The hydrocortisone level was 72% of label claim, substantially below the allowed lower specification limit. The chromatogram revealed a variety of peaks, none of which interfere with the benzyl alcohol, phenethyl alcohol, or hydrocortisone (Fig. 3). To ensure that there were no extraneous peaks under the hydrocortisone peaks, the sample was injected onto the HPLC coupled with a UV-visible spectrophotometer[16].

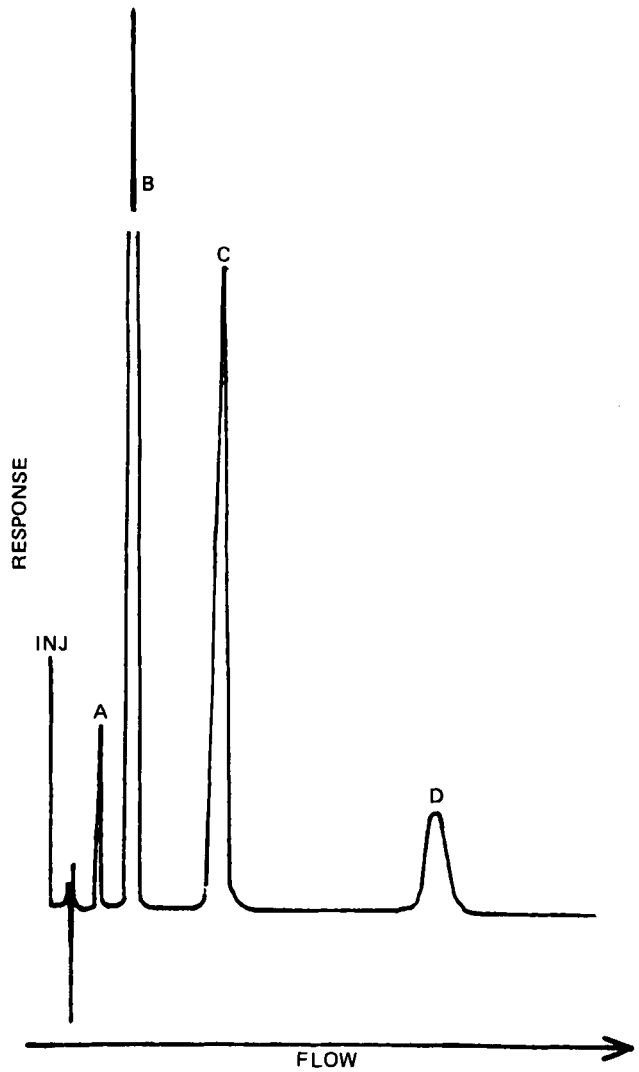

Figure 4—*A chromatogram showing the separation of preservatives and hydrocortisone. Key: (A) benzyl alcohol; (B) methylparaben; (C) intact hydrocortisone; (D) propylparaben.*

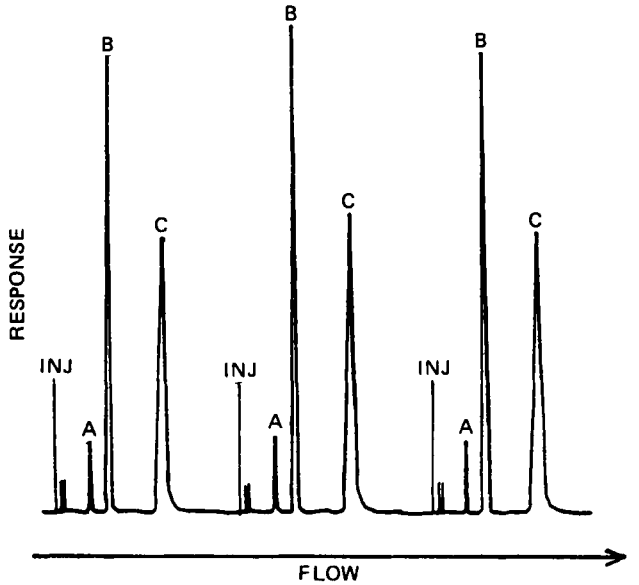

Figure 5—*A typical chromatogram of an experimental formulation. Key: (A) benzyl alcohol; (B) phenethyl alcohol; (C) hydrocortisone.*

As the hydrocortisone peak eluted, a UV scan was taken every 3 sec. These 14 scans were compared to a standard hydrocortisone UV scan. No differences were noted during the elution of the peak. As a further check, the first derivatives of the peak segments were subtracted from the first derivative of the hydrocortisone standard. In all cases, the predicted waveform was noted, indicating there are no UV absorbing interferences at the location of hydrocortisone. No attempt was made to identify the peaks associated with the degradation of hydrocortisone.

Phenethyl alcohol was used as a chromatographically pure reagent for all studies and was not subjected to a simulated degradation.

Stability Study—Actual data were generated with this procedure (Table III). The samples were a 0.5% hydrocortisone experimental formulation stored at 45° for accelerated stability studies for 120 days. The data for hydrocortisone revealed the expected downward trend and demonstrated the method could easily detect changes in hydrocortisone concentration. The data for benzyl alcohol revealed no significant loss throughout the study. Note that specificity was previously established to confirm the validity of the data.

Paraben Study—The methylparaben reference standard and propylparaben reference standard were diluted to 0.005 and 0.016 mg/ml, respectively. The hydrocortisone reference standard was added equivalent to 0.125 mg/ml to the diluted paraben standard. The three components are completely resolved. The methylparaben would interfere with the phenethyl alcohol. A second injection showed benzyl alcohol does not interfere with the parabens (Fig. 4). In formulations containing parabens the benzyl alcohol could be utilized as the internal standard in place of phenethyl alcohol.

The principal goal of any analytical separation procedure is to achieve maximum resolution in minimum time. Initial studies were conducted with a reversed-phase stainless steel column[17] and a 25% (v/v) acetonitrile solution in distilled, deionized water mobile phase pumped at 2.0 ml/min. Under these conditions, 15–25 min were required to achieve baseline to baseline resolution of the benzyl alcohol, phenethyl alcohol, and hydrocortisone, as well as the total elution of the degradation products. In comparison, the radial compression system with the modified mobile phase pumped at 6.0 ml/min achieved the same analysis in 10–13 min. The time factor was of obvious importance in the choice of this approach, allowing for the analysis of a large number of samples in a short period of time (Fig. 5).

An efficient feature of this procedure is the general sample preparation scheme and analysis parameters. The sample weights, sample dilution volumes, and internal standard concentration are constant. There are only two minor variations in sample preparation. The first is the centrifugation step for the cream, gel, and ointment formulations (relative to the solution) prior to injection. The second is the heating of the ointment formulation in the HPLC solvent prior to centrifugation. With this

[16] Model 8450A UV/VIS Spectrophotometer, Hewlett-Packard, Palo Alto, Calif.

[17] μ Bondapak C-18, 30 cm × 3.9-mm i.d. (10-μm particles), Waters Associates, Milford, Mass.

general scheme, the analysis parameters do not require solvent modification, variable injection volumes, or a change in analysis time. The only chromatographic variation is an attenuation change from 0.1 to 0.2 aufs for the 2.5% hydrocortisone formulations.

A variety of hydrocortisone formulations may contain methylparaben and propylparaben as preservatives. Though methylparaben interferes with phenethyl alcohol, benzyl alcohol could be substituted as the internal standard and yield satisfactory chromatographic separation.

REFERENCES

(1) "The United States Pharmacopeia," 20th rev., United States Pharmacopeial Convention, Rockville, Md., 1980, p. 172.

(2) *Ibid*, p. 1212.

(3) H. C. Van Dame, *J. Assoc. Off. Anal. Chem.*, **63**, 1184 (1980).

(4) M. Lanouette and B. A. Lodge, *J. Chromatogr.*, **129**, 475 (1976).

(5) T. Okumura and A. Azuma, *Bunseki Kagaku*, **28**, 235 (1979).

(6) S. Hara and K. Mibe, *Chem. Pharm. Bull.*, **15**, 1036 (1967).

(7) H. S. De Boer, P. H. Lansaat, K. R. Kooistna, and W. J. Van Oort, *Anal. Chim. Acta.*, **111**, 275 (1979).

(8) H. S. De Boer, J. Den Hartigh, and H. H. J. L. Ploegmakers, *ibid.*, **102**, 141 (1978).

(9) A. Y. Taira, *EDRO SARAP Res. Tech. Rep.*, **3**, 243 (1978).

(10) H. S. Boer, P. H. Lansaat, and W. J. Van Oort, *Anal. Chim. Acta*, **116**, 69 (1980).

(11) E. A. Ibraham, A. M. Wahbi, and M. A. Abdel-Salam, *Pharmazie*, **28**, 232 (1973).

(12) *Ibid.*, **28**, 195 (1973).

(13) G. Szepesi and S. Gorog, *Boll. Chim. Farm.*, **114**, 98 (1975).

(14) G. Garzo, M. Blazso, and S. Gorog, *Proc. Conf. Appl. Phys. Chem.*, **2**, 301 (1971).

(15) E. M. Chambaz and E. C. Horning, *Anal. Lett.*, **1**, 201 (1968).

(16) W. L. Gardiner and E. C. Horning, *Biochem. Biophys. Acta*, **115**, 425 (1968).

(17) B. Mahme, W. E. Wilson, and E. C. Horning, *Anal. Lett.*, **1**, 746 (1968).

(18) M. G. Horning, A. M. Moss, and E. C. Horning, *Anal. Biochem.*, **22**, 284 (1968).

(19) J. A. Mollica and R. F. Stursz, *J. Pharm. Sci.*, **61**, 445 (1972).

(20) S. Gorog and P. Horvath, *Analyist (London)*, **103**, 346 (1978).

(21) R. E. Graham, E. R. Biehl, C. T. Kenner, G. H. Luttrell, and D. L. Middleton, *J. Pharm. Sci.*, **64**, 226 (1975).

(22) R. E. Graham and C. T. Kenner, *ibid.*, **62**, 103 (1973).

(23) W. J. Mader and R. R. Buck, *Anal. Chem.*, **24**, 666 (1952).

(24) A. R. Lea, J. M. Kennedy, and G. K. C. Loa, *J. Chromatogr.*, **198**, 41 (1980).

(25) N. W. Tymes, *J. Chromatogr. Sci.*, **15**, 151 (1977).

(26) G. Cavina, G. Moretti, B. Gallinella, R. Alimenti, and R. Barchiesi, *Boll. Chim. Farm.*, **117**, 534 (1978).

(27) J. Q. Rose and W. J. Jusko, *J. Chromatogr.*, **162**, 273 (1979).

(28) S. Shoji and K. Mibe, *Chem. Pharm. Bull.*, **23**, 2850 (1975).

(29) P. A. Williams and E. R. Biehl, *J. Pharm. Sci.*, **70**, 530 (1981).

ACKNOWLEDGMENTS

Presented in part at the APhA Academy of Pharmaceutical Sciences, Newport Beach, Calif. meeting, October 1980.

The authors thank Dancoise Beard, Patricia Loh, Linda O'Shea, and Heidemarie Wierzba for technical assistance.

Synthesis and Evaluation of an ^{111}In-labeled Porphyrin for Lymph Node Imaging

RICHARD VAUM *, NED D. HEINDEL *‡ˣ, H. DONALD BURNS *, JACQUELINE EMRICH*, and NATALIE FOSTER‡

Received October 20, 1981, from the **Department of Radiation Therapy and Nuclear Medicine, Hahnemann Medical College and Hospital, Philadelphia, PA 19102* and the ‡*Center for Health Sciences, Lehigh University, Bethlehem, PA 18015.* Accepted for publication January 18, 1982.

Abstract □ ^{111}In-labeled tetra(4-*N*-methylpyridyl)porphyrin was investigated as a possible lymph node imaging agent. A clinically feasible method for the preparation of this radioactive pharmaceutical was developed from experiments with the synthesis and characterization of the unlabeled complex. The *in vivo* distribution of the compound in Wistar rats was determined as a function of time. Favorable lymph node–blood, lymph node–muscle, and specific lymph node–surrounding tissue ratios were obtained.

Keyphrases □ Porphyrin—^{111}In-labeled, synthesis and evaluation, biodistribution, lymph node imaging, rats □ Imaging, lymph node—^{111}In-labeled porphyrin, synthesis and evaluation, biodistribution, rats □ Biodistribution—^{111}In-labeled porphyrin, synthesis, lymph node imaging, evaluation, rats

The diagnostic imaging methods now being used for evaluating disease in the lymphatic system, oil lymphography and technetium Tc 99m antimony trisulfide colloid lymphoscintigraphy, possess significant inherent limitations. These methods image only those nodal groups that drain the subcutaneous injection site, and thus, require patent lymphatic vessels between the injection site and the nodes to be imaged (1–3). An intravenously administered radiopharmaceutical agent that allows the visualization of all nodal groups with a single injection would be an improvement in the diagnosis of lymph node involvement in malignancy.

BACKGROUND

It has been known since the 1940s that many porphyrins and metalloporphyrins display an affinity for lymphatic and neoplastic tissues when injected intravenously (4, 5). These early studies, however, depended solely upon differential fluorescence to detect the presence of the porphyrin in the target tissue and, consequently, were of limited diagnostic utility. A method is available for introducing indium, an electronic isostere of iron, into porphyrins (6). Two nuclides of that element, indium 111 and indium 113m, would be clinically acceptable from the viewpoint of decay energies, gamma-emission, and half-life for use in *in vivo* diagnostic radiopharmaceuticals. Furthermore, it has been shown that several porphyrins can transport β-emitting nuclides (cobalt 58, zinc 65, and palladium 109) to nodal tissue where their ionizing radiation results in selective nodal ablation and diminished rejection rate for skin homographs in dogs dosed with these radio porphyrins (7–9). It has also been demonstrated that an intravenously administered cobalt 57 derivative of a water-soluble porphyrin developed a tumor–blood ratio of 44:1 at 5 days postdosing in the TCT-4904 rat bladder tumor (10). Sufficient precedent exists to indicate that a soluble indium-labeled porphyrin might be nodal specific. This study reports a facile synthesis for radioactive [^{111}In]tetra(4-*N*-methylpyridyl)porphyrin (I) whose biodistribution in rats illustrates its potential as a radiodiagnostic agent for major nodal systems.

0022-3549/82/1100-1223$01.00/0

general scheme, the analysis parameters do not require solvent modification, variable injection volumes, or a change in analysis time. The only chromatographic variation is an attenuation change from 0.1 to 0.2 aufs for the 2.5% hydrocortisone formulations.

A variety of hydrocortisone formulations may contain methylparaben and propylparaben as preservatives. Though methylparaben interferes with phenethyl alcohol, benzyl alcohol could be substituted as the internal standard and yield satisfactory chromatographic separation.

REFERENCES

(1) "The United States Pharmacopeia," 20th rev., United States Pharmacopeial Convention, Rockville, Md., 1980, p. 172.

(2) *Ibid*, p. 1212.

(3) H. C. Van Dame, *J. Assoc. Off. Anal. Chem.*, **63**, 1184 (1980).

(4) M. Lanouette and B. A. Lodge, *J. Chromatogr.*, **129**, 475 (1976).

(5) T. Okumura and A. Azuma, *Bunseki Kagaku*, **28**, 235 (1979).

(6) S. Hara and K. Mibe, *Chem. Pharm. Bull.*, **15**, 1036 (1967).

(7) H. S. De Boer, P. H. Lansaat, K. R. Kooistna, and W. J. Van Oort, *Anal. Chim. Acta.*, **111**, 275 (1979).

(8) H. S. De Boer, J. Den Hartigh, and H. H. J. L. Ploegmakers, *ibid.*, **102**, 141 (1978).

(9) A. Y. Taira, *EDRO SARAP Res. Tech. Rep.*, **3**, 243 (1978).

(10) H. S. Boer, P. H. Lansaat, and W. J. Van Oort, *Anal. Chim. Acta*, **116**, 69 (1980).

(11) E. A. Ibraham, A. M. Wahbi, and M. A. Abdel-Salam, *Pharmazie*, **28**, 232 (1973).

(12) *Ibid.*, **28**, 195 (1973).

(13) G. Szepesi and S. Gorog, *Boll. Chim. Farm.*, **114**, 98 (1975).

(14) G. Garzo, M. Blazso, and S. Gorog, *Proc. Conf. Appl. Phys. Chem.*, **2**, 301 (1971).

(15) E. M. Chambaz and E. C. Horning, *Anal. Lett.*, **1**, 201 (1968).

(16) W. L. Gardiner and E. C. Horning, *Biochem. Biophys. Acta*, **115**, 425 (1968).

(17) B. Mahme, W. E. Wilson, and E. C. Horning, *Anal. Lett.*, **1**, 746 (1968).

(18) M. G. Horning, A. M. Moss, and E. C. Horning, *Anal. Biochem.*, **22**, 284 (1968).

(19) J. A. Mollica and R. F. Stursz, *J. Pharm. Sci.*, **61**, 445 (1972).

(20) S. Gorog and P. Horvath, *Analyist (London)*, **103**, 346 (1978).

(21) R. E. Graham, E. R. Biehl, C. T. Kenner, G. H. Luttrell, and D. L. Middleton, *J. Pharm. Sci.*, **64**, 226 (1975).

(22) R. E. Graham and C. T. Kenner, *ibid.*, **62**, 103 (1973).

(23) W. J. Mader and R. R. Buck, *Anal. Chem.*, **24**, 666 (1952).

(24) A. R. Lea, J. M. Kennedy, and G. K. C. Loa, *J. Chromatogr.*, **198**, 41 (1980).

(25) N. W. Tymes, *J. Chromatogr. Sci.*, **15**, 151 (1977).

(26) G. Cavina, G. Moretti, B. Gallinella, R. Alimenti, and R. Barchiesi, *Boll. Chim. Farm.*, **117**, 534 (1978).

(27) J. Q. Rose and W. J. Jusko, *J. Chromatogr.*, **162**, 273 (1979).

(28) S. Shoji and K. Mibe, *Chem. Pharm. Bull.*, **23**, 2850 (1975).

(29) P. A. Williams and E. R. Biehl, *J. Pharm. Sci.*, **70**, 530 (1981).

ACKNOWLEDGMENTS

Presented in part at the APhA Academy of Pharmaceutical Sciences, Newport Beach, Calif. meeting, October 1980.

The authors thank Dancoise Beard, Patricia Loh, Linda O'Shea, and Heidemarie Wierzba for technical assistance.

Synthesis and Evaluation of an ^{111}In-labeled Porphyrin for Lymph Node Imaging

RICHARD VAUM *, NED D. HEINDEL *‡ˣ, H. DONALD BURNS *, JACQUELINE EMRICH*, and NATALIE FOSTER‡

Received October 20, 1981, from the **Department of Radiation Therapy and Nuclear Medicine, Hahnemann Medical College and Hospital, Philadelphia, PA 19102* and the ‡*Center for Health Sciences, Lehigh University, Bethlehem, PA 18015.* Accepted for publication January 18, 1982.

Abstract □ ^{111}In-labeled tetra(4-*N*-methylpyridyl)porphyrin was investigated as a possible lymph node imaging agent. A clinically feasible method for the preparation of this radioactive pharmaceutical was developed from experiments with the synthesis and characterization of the unlabeled complex. The *in vivo* distribution of the compound in Wistar rats was determined as a function of time. Favorable lymph node–blood, lymph node–muscle, and specific lymph node–surrounding tissue ratios were obtained.

Keyphrases □ Porphyrin—^{111}In-labeled, synthesis and evaluation, biodistribution, lymph node imaging, rats □ Imaging, lymph node—^{111}In-labeled porphyrin, synthesis and evaluation, biodistribution, rats □ Biodistribution—^{111}In-labeled porphyrin, synthesis, lymph node imaging, evaluation, rats

The diagnostic imaging methods now being used for evaluating disease in the lymphatic system, oil lymphography and technetium Tc 99m antimony trisulfide colloid lymphoscintigraphy, possess significant inherent limitations. These methods image only those nodal groups that drain the subcutaneous injection site, and thus, require patent lymphatic vessels between the injection site and the nodes to be imaged (1–3). An intravenously administered radiopharmaceutical agent that allows the visualization of all nodal groups with a single injection would be an improvement in the diagnosis of lymph node involvement in malignancy.

BACKGROUND

It has been known since the 1940s that many porphyrins and metalloporphyrins display an affinity for lymphatic and neoplastic tissues when injected intravenously (4, 5). These early studies, however, depended solely upon differential fluorescence to detect the presence of the porphyrin in the target tissue and, consequently, were of limited diagnostic utility. A method is available for introducing indium, an electronic isostere of iron, into porphyrins (6). Two nuclides of that element, indium 111 and indium 113m, would be clinically acceptable from the viewpoint of decay energies, gamma-emission, and half-life for use in *in vivo* diagnostic radiopharmaceuticals. Furthermore, it has been shown that several porphyrins can transport β-emitting nuclides (cobalt 58, zinc 65, and palladium 109) to nodal tissue where their ionizing radiation results in selective nodal ablation and diminished rejection rate for skin homographs in dogs dosed with these radio porphyrins (7–9). It has also been demonstrated that an intravenously administered cobalt 57 derivative of a water-soluble porphyrin developed a tumor–blood ratio of 44:1 at 5 days postdosing in the TCT-4904 rat bladder tumor (10). Sufficient precedent exists to indicate that a soluble indium-labeled porphyrin might be nodal specific. This study reports a facile synthesis for radioactive [^{111}In]tetra(4-*N*-methylpyridyl)porphyrin (I) whose biodistribution in rats illustrates its potential as a radiodiagnostic agent for major nodal systems.

0022-3549/82/1100-1223$01.00/0

Table I—Percent Dose per Gram Uptake of I in Rat Tissues [a]

Organ	1 hr	4 hr	24 hr	48 hr
Blood	0.179 ± 0.04	0.097 ± 0.03	0.009 ± 0.00	0.006 ± 0.004
Heart	0.125 ± 0.03	0.077 ± 0.03	0.035 ± 0.00	0.023± 0.01
Lungs	0.360 ± 0.10	0.229 ± 0.06	0.119 ± 0.06	0.076 ± 0.02
Pancreas	0.074 ± 0.02	0.049 ± 0.01	0.043 ± 0.01	0.027 ± 0.004
Spleen	0.260 ± 0.09	0.370 ± 0.12	0.530 ± 0.06	0.517 ± 0.42
Liver	0.177 ± 0.06	0.291 ± 0.13	0.526 ± 0.07	0.334 ± 0.08
Fat pad	0.042 ± 0.01	0.025 ± 0.005	0.058 ± 0.07	0.017 ± 0.005
Muscle	0.045 ± 0.01	0.025 ± 0.01	0.012 ± 0.01	0.009 ± 0.004
Femur	0.183 ± 0.08	0.153 ± 0.07	0.080 ± 0.04	0.040 ± 0.02
Testes	0.053 ± 0.02	0.058 ± 0.02	0.031 ± 0.01	0.036 ± 0.03
Kidneys	2.284 ± 0.68	3.652 ± 1.38	4.963 ± 1.00	3.076 ± 0.64
Adrenals	0.256 ± 0.06	0.214 ± 0.11	0.294 ± 0.29	0.120 ± 0.07
Stomach	0.194 ± 0.04	0.127 ± 0.04	0.067 ± 0.02	0.050 ± 0.01
Intestines	0.096 ± 0.03	0.108 ± 0.04	0.063 ± 0.01	0.040 ± 0.01
Thyroid	0.469 ± 0.78	0.214 ± 0.19	0.356 ± 0.34	0.115 ± 0.14
Brain	0.009 ± 0.005	0.004 ± 0.002	0.019 ± 0.03	0.003 ± 0.002
Node	**1 hr**	**4 hr**	**24 hr**	**48 hr**
Inguinal	0.455 ± 0.47	1.317 ± 1.53	0.707 ± 0.55	0.607 ± 0.30
Aortic bifurcation	0.548 ± 0.48	0.836 ± 1.18	0.647 ± 0.39	1.126 ± 1.21
Superior mesenteric	0.387 ± 0.09	0.476 ± 0.10	0.727 ± 0.28	0.562 ± 0.20
Renal and abdominal	0.442 ± 0.42	0.415 ± 0.69	0.851 ± 1.07	1.116 ± 1.13
Thoracic	0.218 ± 0.17	0.242 ± 0.23	0.333 ± 0.42	0.382 ± 0.41
Axillary	0.234 ± 0.07	0.216 ± 0.09	0.458 ± 0.32	0.371 ± 0.03
Cervical	0.291 ± 0.10	0.240 ± 0.08	0.353 ± 0.34	0.384 ± 0.27
Total nodes	0.368 ± 0.12	0.535 ± 0.41	0.582 ± 0.20	0.650 ± 0.34

[a] Each figure is the average of five animals normalized for a 500-g rat.

EXPERIMENTAL

The reactants, indium chloride[1], [^{111}In]indium chloride[2], and tetra(4-*N*-methylpyridyl)porphyrin tosylate salt[3], were obtained commercially. The tosylate salt of the porphyrin was converted to the chloride by passage through an anion-exchange column in the chloride form and the tetra(4-*N*-methylpyridyl) porphyrin chloride (II) used in all subsequent syntheses. UV spectra were obtained on a UV-visible spectrophotometer[4] in aqueous solution. Combustion analyses were performed by a microanalytical laboratory[5].

Synthesis of Indium Tetra(4-*N*-methylpyridyl)porphyrin—Indium chloride (66.0 mg, 0.30 mmole) was dissolved in 2.0 ml of 0.05 *N* HCl. In a 3.0-ml capped vial, 0.02 ml of this solution was evaporated to dryness under nitrogen in a 115° oil bath. Tetra(4-*N*-methylpyridyl)-porphyrin chloride (II) (25.0 mg, 0.03 mmole) was dissolved in 1.0 ml of distilled water and added to the indium chloride residue. This reaction mixture was stirred in a capped vial in a 115° oil bath for 1 hr. The visible spectra of both this reaction mixture and the starting ligand (II) were obtained. The majority of the reaction mixture was retained for elemental analysis. The aliquot portion of the mixture was applied to a 1.0 × 19.0-cm cation exchange column, which had been pretreated by eluting it with 10 ml of 5×10^{-5} *N* HCl. This column was then eluted sequentially with 10 ml of 5×10^{-5} *N* HCl, 30 ml of 5×10^{-4} *N* HCl, 10 ml of 5×10^{-3} *N* HCl, and 100 ml of 5×10^{-2} *N* HCl. The eluate was collected in 180 0.8-ml fractions.

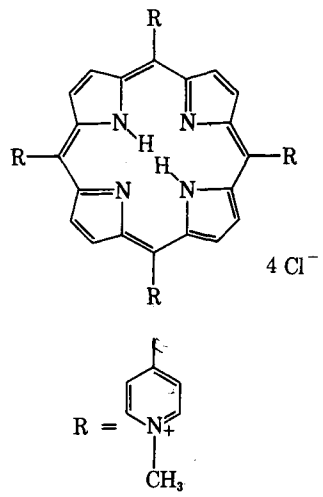

A sample of the porphyrin ligand (II) was passed through an identically prepared column in the same manner. Visible spectra were obtained of representative samples of the colored eluate fractions from both indium tetra(4-*N*-methylpyridyl)porphyrin and the ligand (II) columns. Tubes (130–160 fractions) inclusive from the complex's eluate were then combined, the pH of the resulting solution adjusted to neutrality, and a visible spectrum obtained.

The portion of the original reaction mixture, retained for analysis, was solubilized in 2.5 ml of distilled water and treated with 5 ml of 4 *M* lithium perchlorate. The perchlorate salt precipitated. It was vacuum filtered with a fine frit, washed with cold water, dried under 0.5 torr, transferred carefully with a porcelain spatula (similar perchlorate salts have been reported to explode when rubbed or heated), and a portion subjected to combustion analyses. Chemical yields of the precipitated perchlorates were always in excess of 90% of theoretical. No defined melting point could be observed.

Anal.—Calc. for $C_{44}H_{36}N_8In(ClO_4)_5$: C, 41.12; H, 2.80; N, 8.72. Found: C, 41.28; H, 3.01; N, 8.87.

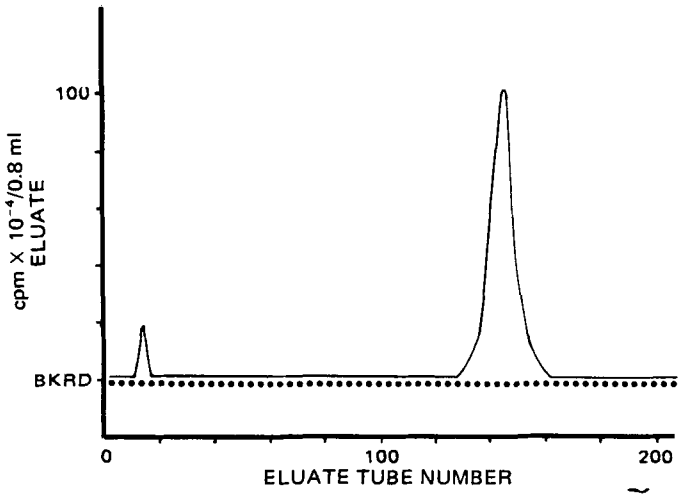

Figure 1—*Elution profile of [^{111}In]indium chloride and of porphyrin complex (I) from cation exchange column. Key: (—) compound I; (. . . .) [^{111}In]indium chloride.*

[1] Alfa Products Thiokol/Ventron Division, lot 041179.
[2] New England Nuclear Corp., carrier free grade as 0.3 ml of a 16-mCi/ml solution in 0.05 *N* HCl.
[3] Man-win Chemical Co.
[4] Beckman, model DK-2A.
[5] G.I. Robertson Microanalytical Laboratory, Florham Park, N.J.

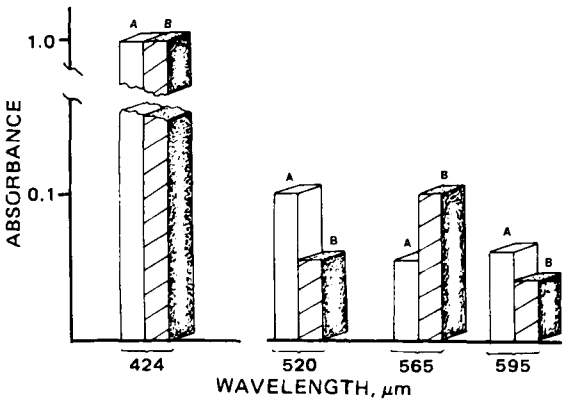

Figure 2—*UV and visible absorption spectra of free porphyrin ligand (II) and of the indium complex of II. Key: (A) indium complex; (B) porphyrin ligand.*

Synthesis of [^{111}In]tetra(4-*N*-methylpyridyl)porphyrin (I)—[^{111}In]indium chloride (3.8×10^{-6} mg, 1.7×10^{-8} mmoles, 1.57 mCi) in 0.05 *N* HCl was evaporated to dryness as described previously for nonradioactive indium chloride. Carrier indium chloride (3.8×10^{-4} mg, 1.7×10^{-6} mmoles) was added to the residue in 100 μl 0.05 *N* HCl, which was once again evaporated to dryness. The ligand (II) (0.14 mg, 1.7×10^{-4} mmoles) in 1.0 ml distilled water was added, and the reaction vial was stirred in a 115° oil bath for 1 hr. The cooled reaction mixture was applied to a cation exchange column prepared identically to those previously described and eluted in the same manner, and the activity of each 0.8-ml fraction was determined. Fractions 130–160 inclusive were combined, and the pH of the resulting solution was adjusted to neutrality by the addition of dilute sodium hydroxide. The neutralized solution was evaporated to a volume appropriate for the animal studies. The effective specific activity of I prepared in this manner was ~9 Ci/mmole as determined by dividing the total indium 111 activity used (1.57 mCi) by the total ligand (II) used (1.7×10^{-4} mmoles).

One microcurie of [^{111}In]indium chloride (2.39×10^{-9} mg, 1.08×10^{-11} mmoles) in 1.0 ml of distilled water was applied to a cation exchange column as previously described for I and was eluted in an identical manner. The activity of every one-tenth fraction plus a tube containing the contents of the eluted column was determined (Fig. 1).

Biodistribution Studies—Biodistribution studies using Wistar rats, average age 6.5 months and average weight 500 g, were carried out over a 4-day period. The animals were sacrificed in groups of 5 at four time periods: 1, 4, 24, and 48 hr. Each rat was injected with 0.2 ml of a 10-μCi/ml concentration of the neutralized solution of I in a caudal vein while under ether anesthesia. Just prior to the end of each time period each rat was again anesthetized with ether and a cardiac puncture was performed. Each rat was then sacrificed by cardiac removal and autopsied. The organs and tissues listed in Table I were removed, weighed, and counted in the gamma scintillation counter. The data for each organ or tissue have been normalized for a rat weighing 500 g, and the percentage of the total injection dose per gram weight has been calculated. The technique for tissue sampling and animal weight normalization has been described previously (11).

RESULTS AND DISCUSSION

Elemental analysis of the indium tetra(4-*N*-methylpyridyl)porphyrin correlated well with the calculated values. Since the amount of I synthesized for this study was too small to be characterized by the same method, another technique for its identification in solution was sought. When II was dissolved in distilled water the resulting solution was dark brown; after being heated with the indium chloride for 1 hr the reaction mixture turned violet in color. This color change was further manifested by a major difference in the visible spectral properties of the complex *versus* the porphyrin ligand. The spectra are compared at equimolar concentrations in Fig. 2. The change in the peak height ratios was used as a convenient tool to detect the complex in the presence of unreacted porphyrin. Cation exchange chromatography was used to isolate I from the crude reaction mixture. This method was capable of demonstrating small quantities of the radioactive complex in the presence of both unlabeled complex and free radioindium. Both the labeled and the unlabeled complexes were shown to elute from the column in the same elution volume (fractions 130–160): the former being demonstrated by a sharp rise in total counts per sample when each tube was examined in a gamma counter (Fig. 1), and the latter being demonstrated by the characteristic color which appeared only in those 30 fractions, and which possessed a visible spectrum identical to that of the complex prior to passing through the column.

Table II—Significant Lymph Node–Background Ratios

	1 hr	4 hr	24 hr	48 hr
Average node–bone	2.0:1	3.5:1	7.3:1	16.3:1
Average node–muscle	8.2:1	21.4:1	48.5:1	72.2:1
Thoracic nodes–heart	1.7:1	3.1:1	9.5:1	16.6:1
Thoracic nodes–blood	1.2:1	2.5:1	37.0:1	63.7:1
Superior mesenteric nodes–intestine	4.0:1	4.4:1	11.5:1	14.0:1

The identification of the labeled complex was considered conclusive when [^{111}In]indium chloride was placed on an identically prepared column, and no counts significantly over the background tissue were detected in the eluate, while the substance of the column was shown to retain all the counts that were applied as the radioactive indium chloride. The final manipulation of I was to neutralize the eluate that contained it with dilute sodium hydroxide before injection. This procedure was examined with the unlabeled complex and was shown to have no effect on the visible spectrum of that compound.

The distribution of I in rats as a function of time is presented in Table I. The percentage of the total injected dose per gram in the lymph nodes is surpassed only by that of the kidneys. More importantly, some node–surrounding tissue ratios, which would be pertinent for imaging both abdominal and thoracic nodal groups, have been expressed in Table II and show considerable prominence of the nodes over background tissue. The nodal groups in these areas are among the most difficult, if not impossible, to image by the best existing techniques, which depend on drainage of the injection site by the lymphatics of the nodes in question.

Earlier studies that reported the node ablation with β-emitting metalloporphyrins did not indicate, however, any property unique to porphyrins which causes their affinity for lymphatic tissue (7–10). It has been theorized in one report that porphyrins and metalloporphyrins are concentrated by tissues with a high mitotic index (4). Bone marrow and duodenal mucosa are two tissues with extremely high turnover rates, and yet in one quantitative study, it was noted that lymph node activity was 16.7 times that of duodenal mucosa and 7.5 times that of bone marrow (7). These data tend to indicate that some quality other than a high mitotic index may be required to explain the localization of these complexes in lymph nodes. It is possible that the complexes localize in the lymph nodes by the mechanism recently proposed for particulate antigens (12). This study showed that colloidal carbon was concentrated in lymph nodes in the region of the high endothelial venules. These unique vessels have been extensively examined (13), and this work suggests that the highly permeable nature of these venules, coupled with the intricate system of hemodynamic controls inherent in the nodal microvasculature, could provide functional lymph node–venous communications. Further study, however, will be required before the porphyrin localization mechanism can be clearly identified.

The potential of I as a diagnostic imaging agent is apparent. The intravenous route of administration would provide an easy and reproducible clinical procedure superior to oil lymphography and to technetium Tc 99m–antimony sulfide lymphoscintigraphy, while the possibility of examining abdominal and thoracic nodal groups by a relatively noninvasive technique would be an invaluable aid in monitoring both neoplastic metastasis and alterations in the immune system in response to a host of other pathologies. Further study of this compound is currently in progress.

REFERENCES

(1) K. D. Kaplan, W. F. Whitmore, and R. F. Gittes, *Invest. Radiol.*, **15**, 34 (1980).

(2) G. N. Ege, *Radiology*, **118**, 101 (1976).

(3) I. Kazem, A. Nedwich, R. Mortel, and T. Honda, *Clin. Radiol.*, **22**, 382 (1971).

(4) F. H. J. Figge, G. S. Weiland, and L. O. J. Manganiello, *Proc. Soc. Exp. Biol. Med.*, **68**, 640 (1948).

(5) D. S. Rassmussen-Taxdal, G. E. Ward, and F. H. J. Figge, *Cancer*, **8**, 78 (1955).

(6) A. D. Nunn, *J. Radioanal. Chem.*, **53**, 291 (1979).

(7) R. A. Fawwaz, H. S. Winchell, F. Frye, W. Hemphill, and J. H. Lawrence, *J. Nucl. Med.*, **10**, 581 (1969).

(8) R. A. Fawwaz, W. Hemphill, and H. S. Winchell, *ibid.*, **12**, 231 (1971).
(9) R. A. Fawwaz, F. Frye, W. D. Loughman, and W. Hemphill, *ibid.*, **15**, 997 (1974).
(10) R. A. Fawwaz, T. S. T. Wang, and P. O. Alderson, *ibid.*, **22**, 50 (1981).
(11) V. R. Risch, A. M. Markow, and T. Honda, in "The Chemistry of Radiopharamceuticals," N. D. Heindel, H. D. Burns, T. Honda, and L. W. Brady, Eds., Masson, New York, N.Y., 1978, p. 145.
(12) J. N. Blau, *Br. J. Exp. Pathol.*, **59**, 558 (1978).
(13) A. O. Anderson and N. D. Anderson, *Am. J. Pathol.*, **80**, 387 (1975).

ACKNOWLEDGMENTS

This investigation was supported in part by PHS Grant CA-22578 awarded by the National Cancer Institute, and by generous support from the Ruth Estrin Goldberg Memorial for Cancer Research and the Elsa U. Pardee Foundation. J. Emrich was supported by the American Cancer Society Biomedical Support Grant IN-146.

Simultaneous Self-Association and Diffusion of Phenol in Isooctane

J. B. DRESSMAN *§, **K. J. HIMMELSTEIN** *‡§x, **and T. HIGUCHI** *

Received June 11, 1981, from the *Department of Pharmaceutical Chemistry, ‡Department of Chemical and Petroleum Engineering, University of Kansas, Lawrence, KS 66045. Accepted for publication January 8, 1982. §Present Address: INTER$_x$ Research Corp., Lawrence, KS 66044

Abstract □ The impact of self-association on mass transport was studied. The model system chosen was the diffusion of phenol through an immobilized layer of isooctane. In the theoretical development, self-associated phenol contributed to diffusion, with the fluxes being interdependent because of the self-association equilibrium. Predictions from theory were then compared with experimental results. It was shown that self-association can significantly affect flux of diffusing species.

Keyphrases □ Phenol—self-association and diffusion in isooctane □ Isooctane—simultaneous self-association and diffusion of phenol □ Diffusion—phenol in isooctane, simultaneous self-association

Associative interactions are of interest to those concerned with pharmaceutics for two reasons. First, associative interactions affect many processes such as dissolution, partitioning, and diffusion, all of which are vitally important to drug delivery. Second, most drugs contain at least one interactive functional group and, thus, are able to participate in associative interactions with many substances found in dosage forms and in the body.

The effects of association and related processes on various aspects of drug delivery have been examined in several studies. Dissolution rate is known to be altered significantly when dissociation reactions (1, 2) or complexation (3) occur within the dissolution layer. It has also been observed that when a diffusing species self-associates (4) or forms micelles (5) there is a pronounced effect on the rate of transport of that substance. Another study (6) has indicated that in a self-associating system, where diffusion of the self-associated species is blocked by its inability to penetrate the membrane used, the observed mass transport behavior can be accounted for by assuming that the compound is transported only in its monomeric form.

Where simultaneous self-association and diffusion occur, the direct application of Fick's laws fails to predict the diffusion rates observed. In the current study, a more comprehensive approach to the theoretical analysis of diffusion under such circumstances is presented. It is postulated that (*a*) by taking into account the interdependence of the fluxes of the associated and unassociated species arising from associative equilibrium within the diffusional layer, (*b*) by applying Fick's laws to each kind of species present, and (*c*) by numerically solving the differential equations derived on this basis, it is possible to predict the mass transport behavior of self-associating systems.

The model system used to test this postulate was one in which phenol was allowed to diffuse from a donor phase of isooctane, through an immobilized layer of isooctane which served as the diffusion layer, into an aqueous receptor phase. Phenol is known to self-associate significantly (>50%) at high concentrations in isooctane (7). This interaction was expected to cause the rate of mass transport into the aqueous phase to deviate markedly from that predicted by simply applying Fick's laws to the overall concentration of phenol present. Using the scheme outlined above, the diffusional behavior of phenol in the model system was predicted mathematically. The predicted results were then compared with the experimental data obtained.

THEORETICAL

Previous studies have shown that when phenol self-associates in isooctane, the dominant species formed is probably the pentamer[1] (7). The equilibrium expression for this interaction has been reported as:

$$5\,P_m \rightleftharpoons P_5$$

where P_m represents monomeric phenol and P_5 represents the pentameric species. The equilibrium constant for this interaction is $K_{1\text{-}5} = 6300\ M^{-4}$ at 25° in isooctane. This model appears to provide an adequate description of self-association of phenol over a wide range of concentrations.

In the present investigation a silanized sintered glass filter with a presilanization pore size range of 4.5–5.5 μm was used to form a diffusional barrier between the donor isooctane and the receptor aqueous phases. Because of the large pore size and equilibration of the filter with the donor phase prior to each experiment, the barrier actually consisted of a layer of isooctane immobilized within the sintered glass filter. As

[1] J. B. Dressman and T. Higuchi, unpublished results.

0022-3549/82/1100-1226$01.00/0

(8) R. A. Fawwaz, W. Hemphill, and H. S. Winchell, *ibid.*, **12**, 231 (1971).
(9) R. A. Fawwaz, F. Frye, W. D. Loughman, and W. Hemphill, *ibid.*, **15**, 997 (1974).
(10) R. A. Fawwaz, T. S. T. Wang, and P. O. Alderson, *ibid.*, **22**, 50 (1981).
(11) V. R. Risch, A. M. Markow, and T. Honda, in "The Chemistry of Radiopharamceuticals," N. D. Heindel, H. D. Burns, T. Honda, and L. W. Brady, Eds., Masson, New York, N.Y., 1978, p. 145.
(12) J. N. Blau, *Br. J. Exp. Pathol.*, **59**, 558 (1978).
(13) A. O. Anderson and N. D. Anderson, *Am. J. Pathol.*, **80**, 387 (1975).

ACKNOWLEDGMENTS

This investigation was supported in part by PHS Grant CA-22578 awarded by the National Cancer Institute, and by generous support from the Ruth Estrin Goldberg Memorial for Cancer Research and the Elsa U. Pardee Foundation. J. Emrich was supported by the American Cancer Society Biomedical Support Grant IN-146.

Simultaneous Self-Association and Diffusion of Phenol in Isooctane

J. B. DRESSMAN *§, **K. J. HIMMELSTEIN** *‡§x, **and T. HIGUCHI** *

Received June 11, 1981, from the *Department of Pharmaceutical Chemistry, ‡Department of Chemical and Petroleum Engineering, University of Kansas, Lawrence, KS 66045. Accepted for publication January 8, 1982. §Present Address: INTER$_x$ Research Corp., Lawrence, KS 66044

Abstract □ The impact of self-association on mass transport was studied. The model system chosen was the diffusion of phenol through an immobilized layer of isooctane. In the theoretical development, self-associated phenol contributed to diffusion, with the fluxes being interdependent because of the self-association equilibrium. Predictions from theory were then compared with experimental results. It was shown that self-association can significantly affect flux of diffusing species.

Keyphrases □ Phenol—self-association and diffusion in isooctane □ Isooctane—simultaneous self-association and diffusion of phenol □ Diffusion—phenol in isooctane, simultaneous self-association

Associative interactions are of interest to those concerned with pharmaceutics for two reasons. First, associative interactions affect many processes such as dissolution, partitioning, and diffusion, all of which are vitally important to drug delivery. Second, most drugs contain at least one interactive functional group and, thus, are able to participate in associative interactions with many substances found in dosage forms and in the body.

The effects of association and related processes on various aspects of drug delivery have been examined in several studies. Dissolution rate is known to be altered significantly when dissociation reactions (1, 2) or complexation (3) occur within the dissolution layer. It has also been observed that when a diffusing species self-associates (4) or forms micelles (5) there is a pronounced effect on the rate of transport of that substance. Another study (6) has indicated that in a self-associating system, where diffusion of the self-associated species is blocked by its inability to penetrate the membrane used, the observed mass transport behavior can be accounted for by assuming that the compound is transported only in its monomeric form.

Where simultaneous self-association and diffusion occur, the direct application of Fick's laws fails to predict the diffusion rates observed. In the current study, a more comprehensive approach to the theoretical analysis of diffusion under such circumstances is presented. It is postulated that (*a*) by taking into account the interdependence of the fluxes of the associated and unassociated species arising from associative equilibrium within the diffusional layer, (*b*) by applying Fick's laws to each kind of species present, and (*c*) by numerically solving the differential equations derived on this basis, it is possible to predict the mass transport behavior of self-associating systems.

The model system used to test this postulate was one in which phenol was allowed to diffuse from a donor phase of isooctane, through an immobilized layer of isooctane which served as the diffusion layer, into an aqueous receptor phase. Phenol is known to self-associate significantly (>50%) at high concentrations in isooctane (7). This interaction was expected to cause the rate of mass transport into the aqueous phase to deviate markedly from that predicted by simply applying Fick's laws to the overall concentration of phenol present. Using the scheme outlined above, the diffusional behavior of phenol in the model system was predicted mathematically. The predicted results were then compared with the experimental data obtained.

THEORETICAL

Previous studies have shown that when phenol self-associates in isooctane, the dominant species formed is probably the pentamer[1] (7). The equilibrium expression for this interaction has been reported as:

$$5\,P_m \rightleftharpoons P_5$$

where P_m represents monomeric phenol and P_5 represents the pentameric species. The equilibrium constant for this interaction is $K_{1\text{-}5} = 6300\ M^{-4}$ at 25° in isooctane. This model appears to provide an adequate description of self-association of phenol over a wide range of concentrations.

In the present investigation a silanized sintered glass filter with a presilanization pore size range of 4.5–5.5 μm was used to form a diffusional barrier between the donor isooctane and the receptor aqueous phases. Because of the large pore size and equilibration of the filter with the donor phase prior to each experiment, the barrier actually consisted of a layer of isooctane immobilized within the sintered glass filter. As

[1] J. B. Dressman and T. Higuchi, unpublished results.

0022-3549/82/1100-1226$01.00/0

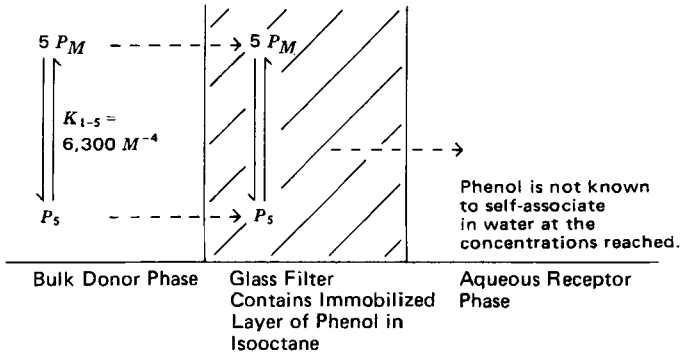

Figure 1—*Interactions of phenol in the silanized sintered glass filter system.*

shown in Fig. 1, self-association would be expected to occur within the diffusional layer as well as in the donor phase. Over the time span of the experiment, phenol concentrations remained sufficiently low in the aqueous phase to allow the assumption that self-association in that phase was negligible.

Consider an infinitesimal element within the diffusion layer. Expressions for the net flux of the monomer and pentamer species into the element can be obtained assuming that the self-association equilibrium between the two species is established very quickly compared to the rate of diffusion, and Fick's laws can be applied to the diffusion of each species within the element. Influx of the monomer can be represented as:

$$\left(\frac{\partial P_m}{\partial t}\right)_{IN} = -D_m\left(\frac{\partial P_m}{\partial h}\right) \qquad \text{(Eq. 1)}$$

where D_m is the diffusivity of the phenol monomer, h is distance, and t is time. The efflux of the monomer from the element can be written as:

$$\left(\frac{\partial P_m}{\partial t}\right)_{OUT} = -D_m\left[\left(\frac{\partial P_m}{\partial h}\right) + \frac{\partial}{\partial h}\left(\frac{\partial P_m}{\partial h}\right)\right] \qquad \text{(Eq. 2)}$$

The net flux of the monomer into the element is given by the difference between the influx and efflux of the monomer from the element:

$$\left(\frac{\partial P_m}{\partial t}\right) = \left(\frac{\partial P_m}{\partial t}\right)_{IN} - \left(\frac{\partial P_m}{\partial t}\right)_{OUT} = D_m\frac{\partial}{\partial h}\left(\frac{\partial P_m}{\partial h}\right) \qquad \text{(Eq. 3)}$$

as given by Fick's second law. Similarly, the following expression is obtained for the net flux of the pentamer:

$$\left(\frac{\partial P_5}{\partial t}\right) = D_5\left(\frac{\partial^2 P_5}{\partial h^2}\right) \qquad \text{(Eq. 4)}$$

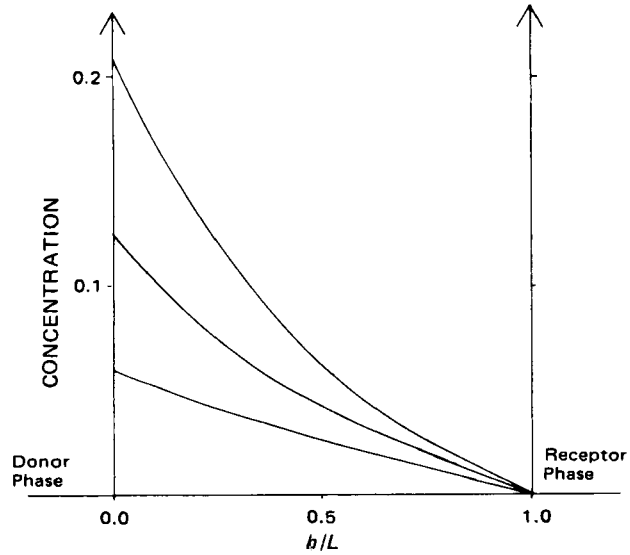

Figure 2—*Profile of total concentration of phenol in the immobilized layer of isooctane constituting the diffusion layer, calculated from Eqs. 9 and 15 for three donor phase concentrations of phenol: 0.2063, 0.1226, and 0.0432* M, *under steady-state and sink conditions.*

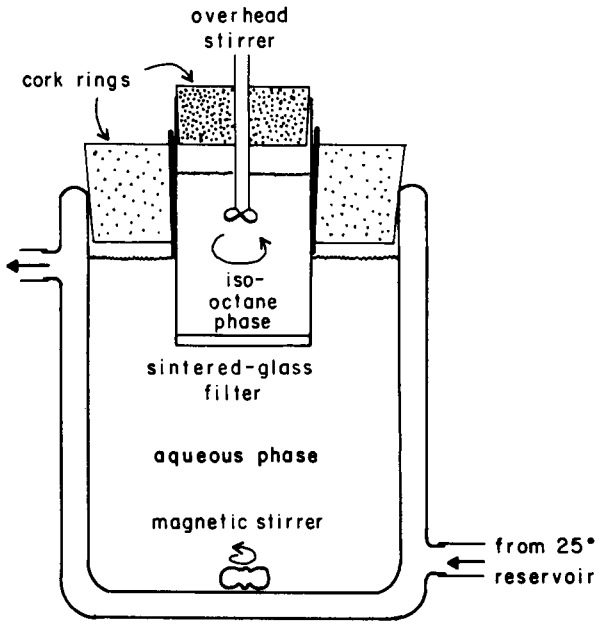

Figure 3—*Apparatus for diffusion studies.*

where D_5 is the diffusivity of the pentamer species. Given that P_T is the total concentration of phenol present, one can write:

$$P_T = P_m + 5P_5 \qquad \text{(Eq. 5)}$$

The expressions for the flux of the monomer and pentamer can therefore be combined into one expression as follows:

$$\left(\frac{\partial P_T}{\partial t}\right) = D_m\left(\frac{\partial^2 P_m}{\partial h^2}\right) + 5D_5\left(\frac{\partial^2 P_5}{\partial h^2}\right) \qquad \text{(Eq. 6)}$$

Using the equilibrium expression:

$$P_5 = K_{1-5}P_m^5 \qquad \text{(Eq. 7)}$$

it can be shown then by repeated application of the chain rule that:

$$\left(\frac{\partial^2 P_5}{\partial h^2}\right) = 20K_{1-5}P_m^3\left(\frac{\partial P_m}{\partial h}\right)^2 + 5K_{1-5}P_m^4\left(\frac{\partial^2 P_m}{\partial h^2}\right) \qquad \text{(Eq. 8)}$$

By substituting Eq. 7 into Eq. 5 one obtains the expression:

$$P_T = P_m + 5K_{1-5}P_m^5 \qquad \text{(Eq. 9)}$$

Taking the derivative of both sides of Eq. 9 with respect to time it can be shown that:

$$\left(\frac{\partial P_T}{\partial t}\right) = \left(\frac{\partial P_m}{\partial t}\right)(1 + 25K_{1-5}P_m^4) \qquad \text{(Eq. 10)}$$

Then, by substituting Eqs. 8 and 10 into Eq. 6 one can produce a partial differential equation in terms of the monomer concentration only:

$$\left(\frac{\partial P_m}{\partial t}\right)(1 + 25K_{1-5}P_m^4) = \left(\frac{\partial^2 P_m}{\partial h^2}\right)(D_m + 25D_5K_{1-5}P_m^4) + \left(\frac{\partial P_m}{\partial h}\right)^2 100D_5K_{1-5}P_m^3 \qquad \text{(Eq. 11)}$$

Steady-State Solution Under Sink Conditions—At steady state there is no net accumulation of either form of phenol at any point within the diffusion layer, so there is no net flux into any element, *i.e.*, $\partial P_T/\partial t = 0$. Applying this condition to Eq. 11 one finds that:

$$\left(\frac{\partial P_T}{\partial t}\right) = \left(\frac{\partial^2 P_m}{\partial h^2}\right)(D_m + 25D_5K_{1-5}P_m^4) + \left(\frac{\partial P_m}{\partial h}\right)^2 100K_{1-5}K_5P_m^3 = 0 \qquad \text{(Eq. 12)}$$

Letting $y = (dP_m/dh)$ in the above expression and then separating the variables and integrating, one obtains:

$$\left(\frac{dy}{y}\right) = -\left(\frac{100K_{1-5}D_5P_m^3}{D_m + 25K_{1-5}D_5P_m^4}\right)dP_m$$

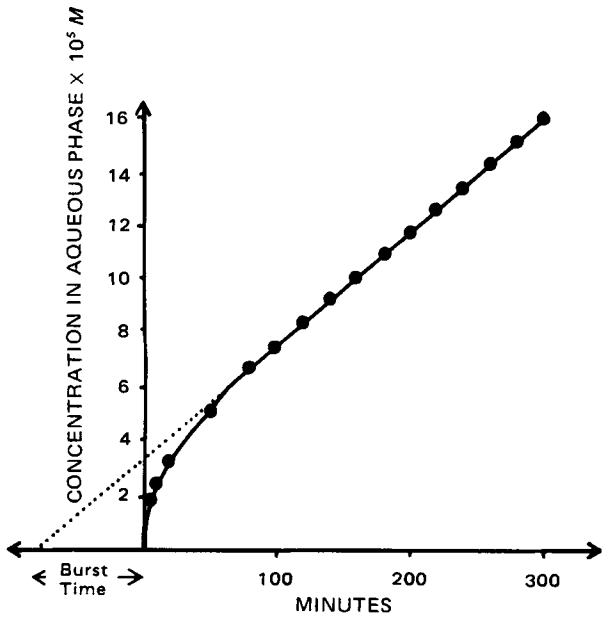

Figure 4—*Cumulative concentration of phenol in the aqueous phase* versus *time for diffusion through a sintered glass filter from a 0.1403* M *solution of phenol in isooctane. Key: (●) experimental data; (—) results obtained by numerical solution of Eq. 11.*

which leads to:

$$y = \left(\frac{dP_m}{d\,h}\right) = \frac{C_1}{D_m + 25\,K_{1\text{-}5}\,D_5 P_m^4} \qquad \text{(Eq. 13)}$$

where C_1 is the first constant of integration. Separating variables and integrating again gives the equation:

$$D_m P_m + 5\,K_{1\text{-}5}\,D_5 P_m^5 = C_1\,h + C_2 \qquad \text{(Eq. 14)}$$

where C_2 is the second constant of integration.

Appropriate boundary conditions can then be applied to solve for the constants of integration. Since the concentration in the bulk of the donor phase remains effectively constant during the course of the experiment, one can write:

$$P_m = P_0 \text{ at } h = 0$$

The second constant of integration C_2 can be found by substituting this condition into Eq. 14 to give:

$$C_2 = D_m\,P_0 + 5\,K_{1\text{-}5}\,D_5\,P_0^5$$

If sink conditions are assumed to hold at the aqueous interface, *i.e.*, $P_m = 0$ at $h = L$ where L is the distance across the diffusion barrier, this condition can be used in conjunction with the expression for C_2 in Eq. 14 to obtain the first constant of integration, which is thus given by:

$$C_1 = \frac{-D_m\,P_0 - 5\,K_{1\text{-}5}\,D_5\,P_0^5}{L}$$

Substituting for C_1 and C_2 in Eq. 14 gives the expression:

$$\frac{h}{L} = \frac{D_m(P_0 - P_m) + 5\,K_{1\text{-}5}\,D_5\,(P_0^5 - P_m^5)}{D_m\,P_0 + 5\,K_{1\text{-}5}\,D_5 P_0^5} \qquad \text{(Eq. 15)}$$

Equation 15 can be used to find the concentration of monomer and total phenol at any point in the diffusion layer at steady state, under sink conditions. Using Eq. 9 and the monomer concentration obtained using Eq. 15, the total concentration profile can be calculated. Figure 2 shows the total concentration profiles at three representative donor phase concentrations of phenol. These plots show that at higher concentrations of phenol where the self-associated species accounts for a large percentage of phenol present, the concentration profile is predicted to deviate from linearity in a pronounced manner. The values of D_m and D_5 were 5.5×10^{-6} and 2.0×10^{-6} cm²/sec, respectively. They were obtained initially from the Stokes–Einstein equation and then adjusted to give a reasonable representation of the experimental data. Filter tortuosity characterization with a substance with a known diffusion coefficient would have allowed a more accurate determination of D_m, at least at low concentrations.

Nonsteady-State Solution—To determine whether the self-association model can be used to successfully predict the data obtained for the cumulative amount of phenol in the aqueous phase over the course of the experiment and subsequently to predict burst time and steady-state flux data, it was necessary to obtain solutions to Eq. 11 for both presteady-state and steady-state behavior under nonsink conditions.

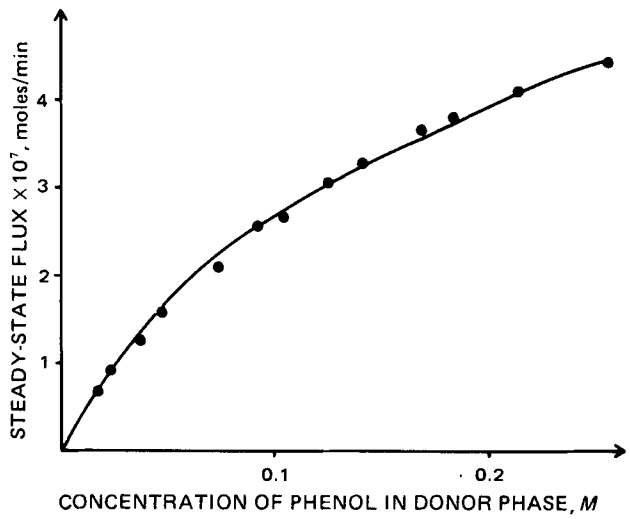

Figure 5—*Steady-state flux (moles per minute) over the entire diffusion layer surface area* versus *total concentration of phenol in the donor phase. Key: (●) mean of the experimental data at a given concentration of phenol; (—) results obtained by numerical solution of Eq. 11.*

Equation 11 is a nonlinear second-order partial differential equation and cannot be conveniently solved analytically under the required conditions. Therefore, it was necessary to transform the equation into an approximate algebraic expression that could be solved numerically. The derivatives were expressed as finite differences using the central and backward difference formulas outlined in a previous report (8) for use in implicit solution methods. The square term in the first derivative of P_m with respect to distance was handled by splitting it into two parts: a constant coefficient calculated on the previous time step and a backward difference expression for the derivative calculated on the current time step. This enabled a set of linear equations to be established for each time step, the coefficients of which were arranged in a tridiagonal matrix. This matrix system was then solved using a Gaussian elimination method as described previously (8). The nonlinear elements of the equation could then be updated from the solution obtained. The entire procedure was repeated until the solution obtained did not differ from the assumed elements by more than a predetermined tolerance. However, it was found that the first approximation used for the nonlinear elements was within the desired tolerance and the iterative solution was not employed subsequently.

Burst Time—Burst time methodology was employed because of the apparatus design. That is, the glass filter initially contained phenol at the same concentration as the bulk isooctane phase. As with the more commonly used lag time, the burst time should be independent of the donor phase concentration in a system where only one species is responsible for the total observed rate of diffusion. This can be shown by following the derivation presented in a previous report (9) and applying boundary and initial conditions appropriate for burst effect conditions to obtain:

$$t_{\text{burst}} = \frac{-L^2}{3.1\,D} \qquad \text{(Eq. 16)}$$

where L is the distance across the diffusion layer and D is the diffusivity (10). Deviation from this relationship was predicted in the current study as it was postulated that more than one species contributed to the overall rate of diffusion.

EXPERIMENTAL

Materials—Phenol[2] (Analytical reagent grade) was fractionally distilled under vacuum to remove the preservative and other contaminants, then stored under nitrogen in a desiccator. Certified ACS isooctane (2,2,4-trimethylpentane)[3] was used without further purification.

[2] Mallinckrodt.
[3] Fisher Scientific Co.

Table I—Experimental and Calculated Steady-State Flux and Burst Time Values for Diffusion of Phenol Through an Immobilized Layer of Isooctane in a Sintered Glass Filter

Concentration in Donor Phase, M	N^a	Steady-State Flux × 10^7, moles/min		Burst Time, min	
		Computer	Experimental ±SEM	Computer	Experimental ±SEM
0.0132	1	0.500	0.467	34.6	40
0.0166	1	0.630	0.689	34.8	39
0.0233	1	0.881	0.922	35	51
0.0365	4	1.332	1.270 ± 0.02	36	45 ± 3
0.0461	4	1.625	1.584 ± 0.05	39	51 ± 3
0.0913	4	2.556	2.576 ± 0.03	54	66 ± 3
0.1030	4	2.741	2.687 ± 0.06	57.5	69 ± 5
0.1240	4	3.010	3.069 ± 0.01	64	68 ± 3
0.1403	4	3.244	3.269 ± 0.07	69	86 ± 9
0.1680	4	3.592	3.676 ± 0.04	76	81 ± 5
0.1826	4	3.740	3.824 ± 0.10	80.5	92 ± 5
0.2130	4	4.018	4.109 ± 0.05	87	88 ± 3
0.2550	1	4.460	4.440	97	111

[a] Number of experiments.

The single sintered glass filter (pore size 4.5–5.5 μm; 2-mm thick; 30-mm radius) was obtained commercially[4] and silanized by soaking overnight in a solution of dichloromethylsilane in toluene. Excess silanizing agent was later removed with a solution of acetic acid in hexane.

Analytical Method—Two-milliliter samples were removed from the aqueous phase at suitable time intervals up to 300 min. At the conclusion of the experiment the UV absorbance at 269 nm, the wavelength of maximum absorbance for phenol in the UV region, was determined for each sample[5]. Deoxygenated, distilled water was used as the reference solution. In the aqueous solution with ~pH 6 ionization was >99.9% suppressed.

Diffusion Apparatus and Study—The experimental apparatus is depicted in Fig. 3. Five hundred milliliters of freshly deoxygenated distilled water was placed in a water-jacketed beaker connected to a controlled-temperature reservoir which was used to maintain the temperature of the system at 25°. A magnetic stirrer was used to keep the aqueous phase well mixed. Fifty milliliters of a solution of phenol in isooctane was poured into the tube containing the silanized sintered glass filter and allowed to sit for 3 min. The lower side of the filter was then wiped dry and the tube placed in the aqueous phase in such a position that bulging of the isooctane phase down into the aqueous phase was avoided. Silanization of the filter prevented the hydrostatic pressure of the aqueous phase forcing any water up into the filter. Cork rings fitted above both phases prevented evaporation. The isooctane phase was stirred from above. Optimal stirring rates for the isooctane and aqueous phases were used to ensure even mixing without vortexing problems. This allowed the assumption to be made that the boundary layers in the bulk isooctane and aqueous phases were a negligible barrier to diffusion compared to the immobilized isooctane layer in the sintered glass filter. Thus, the principal barrier to diffusion was the layer of isooctane immobilized in the sintered glass filter.

At suitable time intervals, 2-ml samples were removed from the aqueous phase and the volume replaced with deoxygenated distilled water. The samples were analyzed by UV spectroscopy at the conclusion of each experiment on the same day, so that chemical stability was not a problem.

RESULTS AND DISCUSSION

Phenol was diffused from a donor phase solution in isooctane (at concentrations ranging from 0.0123 to 0.255 M) through a layer of isooctane immobilized within a sintered glass filter into an aqueous phase. The concentration of phenol was determined in the aqueous phase at times up to 300 min. Figure 4 shows a typical plot of the data obtained. For all donor phase concentrations studied, the plot became linear for times >100 min as the system reached a pseudo steady state. Data for these points were analyzed by linear regression to determine the steady-state flux and burst time values. Results from runs in which the correlation coefficient was <0.999 were discarded to minimize uncertainty in calculations of steady-state flux. Extrapolation of the best-fitting linear relationship to zero phenol concentration in the aqueous phase provided the burst time measurement. The slope of the line was used to calculate the steady-state flux in moles per minute over the entire surface area of the diffusion layer (7.069 cm^2) after adjusting the units from molarity per minute by using the aqueous phase volume. Table I summarizes steady-state flux and burst time values obtained.

Steady-State Flux—The experimentally observed relationship between steady-state flux and total concentration in the donor phase obtained in these studies is shown in Fig. 5. This relationship may be compared with classical behavior predicted from Fick's laws. Fick's first law is given by:

$$J = -D\frac{\partial C}{\partial h} \qquad \text{(Eq. 17)}$$

$$J \approx -D\left(\frac{C_0 - C_L}{h}\right) \qquad \text{(Eq. 18)}$$

where J is the flux across the diffusion layer, D is the diffusivity, C_0 is the concentration at $h = 0$ (the donor phase interface), C_L is the concentration at $h = L$ (the receptor phase interface), and h is distance. Provided the receptor phase concentration remains low, *i.e.*, $C_L \approx 0$, the flux can be written as:

$$J \propto C_0 \qquad \text{(Eq. 19)}$$

Under these conditions, one would expect the steady-state flux to increase linearly with increasing concentration in the donor phase. Figure 5 shows, however, that steady-state flux is not directly proportional to donor phase concentration, since the plot deviates significantly from linearity. Anomalous behavior of this type has also been noted for diffusion of phenol through high-density polyethylene membranes by

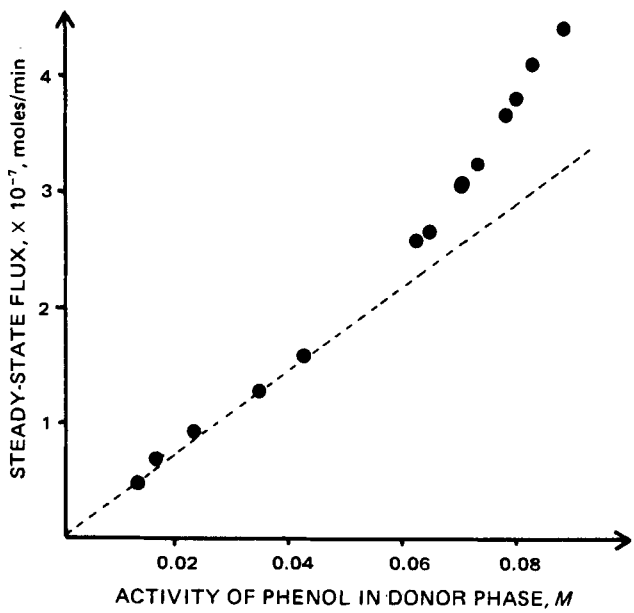

Figure 6—*Steady-state flux (moles per minute) over the entire diffusion layer surface area* versus *activity of phenol (concentration of monomeric phenol) in the donor phase. Key: (●) experimental data; (- - -) linear plot which would be expected if only the monomer species was contributing to the observed flux.*

[4] Lab glass.
[5] Cary 118 model UV/VIS spectrophotometer.

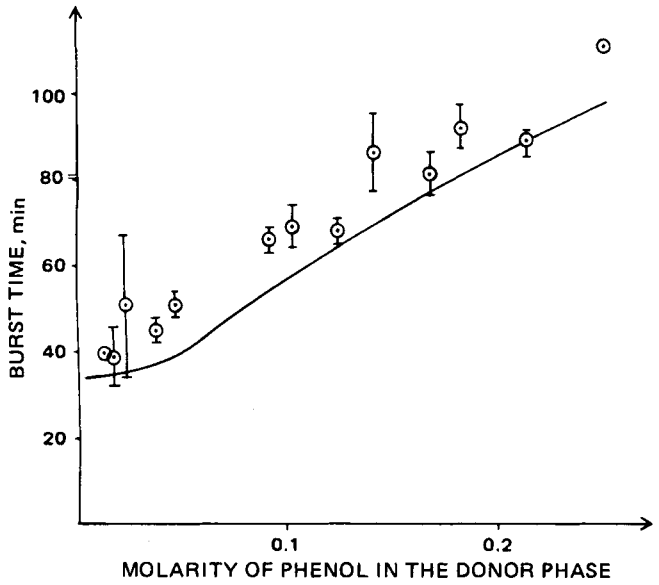

Figure 7—*Burst time (minutes)* versus *total concentration of phenol in the donor phase. Key: (O) experimental data points; (—) obtained from the numerical solution of Eq. 11.*

Mikkelson *et al.* (6) who were subsequently able to obtain a linear relationship by plotting the steady-state flux *versus* activity of phenol present. For that system it was suggested that only the monomeric phenol could partition into the membrane and, hence, contribute to the observed rate of flux. The steady-state flux data for the sintered glass filter system used in the current study was replotted *versus* activity of phenol (defined as the concentration of monomeric phenol) as shown in Fig. 6. The plot exhibits pronounced positive deviation from linearity which indicates that the monomeric portion of the phenol was not solely responsible for the transport of phenol into the aqueous phase in this system. The fraction of phenol present as monomer is ~0.35 at a total phenol concentration of 0.255 *M* as compared to >0.99 at 0.0132 *M*.

On the basis of the pentamer model for self-association of phenol in isooctane, it was proposed that both the monomer and the pentamer species of phenol contribute to the overall observed flux according to Eq. 11. This equation was solved numerically as outlined in the *Theoretical* section and the results compared with the experimental data. For both the individual plots of cumulative concentration in the aqueous phase *versus* time (Fig. 4) and the overall plot of steady-state flux *versus* total concentration of phenol on the donor phase (Fig. 5), the numerical solution is in good agreement with the observed results, indicating that the pentamer species was able to form in the diffusion layer and, hence, contribute proportionately to the flux into the aqueous phase.

Transient Behavior—A second way to study the effect of self-association on diffusion is to analyze the transient (burst time) data. The burst time for a single diffusing species should be independent of the concentration in the donor phase when the diffusion of one species accounts for the observed flux. Burst time data for the system under study are presented in Table I. Figure 7 shows a plot of measured burst time *versus* concentration in the donor phase. The burst time increased with increasing concentration rather than being entirely concentration independent. Since burst time is inversely proportional to diffusivity, the apparent diffusivity appears to have become smaller as the concentration in the donor phase increased. This type of behavior has also been noted for solutions of phenol in carbon tetrachloride (11).

An explanation can be offered for this behavior by considering the monomer–pentamer equilibrium. As the total concentration of phenol increased in the donor phase, the percentage present in the self-associated form increased. Since diffusivity is inversely related to the size of the diffusing species, one would expect that when the pentamer accounts for a large percentage of the phenol present, the apparent diffusivity would be lower, and thus, the burst time would be longer than at low concentrations where the much smaller monomer species accounts for virtually all of the phenol in solution.

The solid line in Fig. 7 represents burst time values calculated from the computer-generated data by applying linear regression analysis to predicted steady-state cumulative concentrations of phenol in the aqueous phase and extrapolating back to zero phenol concentration. Although there is considerable scatter in the experimental data, they appear to follow the same trend as the results derived from Eq. 11. In most instances the observed burst time tends to be greater than the theoretical value. This is probably due to a small amount of phenol solution on the lower face of the glass filter when it was positioned into the aqueous phase. This would have caused the immediate release of phenol into the aqueous phase by nondiffusive means, which in turn would result in falsely high observed values for the cumulative amount in the aqueous phase and, therefore, for the burst time.

The burst time and the steady-state flux data both support the conclusion that the apparent deviation of the diffusion characteristics of phenol in isooctane from Fick's laws can be entirely accounted for by considering the self-association equilibrium of phenol in isooctane. From Eq. 11 one can note that the diffusion of each species, monomer and pentamer, fundamentally obeys Fick's laws and that the diffusivity of each species is constant. The apparent diffusivity, as reflected in the burst time, only changes because of the variation with concentration of the relative proportions of the monomer and pentamer present.

CONCLUSIONS

In these studies it has been shown that the apparent deviation from classical behavior of the diffusion of phenol through an immobilized solution of isooctane can be explained by the specific interaction effects rather than needing to resort to an empirical description in terms of the apparent diffusivity of the overall system. This approach to describe concomitant self-association and mass transport can be used to help predict delivery rates of drugs for which diffusion is the rate-controlling step in release from the dosage form or in the absorption process, and self-association occurs under physiological conditions. Caffeine (4) and some analgesics and antihistamines (12–17) have been shown to self-associate at high concentrations in aqueous solution.

The rate of transport of these drugs across the dissolution layer when they are released from solid dosage forms, therefore, may be affected by the self-association interaction. Other substances such as alcohols and carboxylic acids are known to self-associate in organic solvents (18). Absorption through lipoidal membrane barriers or release from dosage forms which are coated with polymeric films are examples of steps in the drug delivery process at which self-association of drugs containing such groups may significantly affect the rate of transport.

REFERENCES

(1) K. G. Mooney, M. Mintun, K. J. Himmelstein, and V. J. Stella, *J. Pharm. Sci.*, **70,** 13 (1981).

(2) K. G. Mooney, M. G. Rodriguez, M. Mintun, K. J. Himmelstein, and V. J. Stella, *ibid.*, **70,** 1358 (1981).

(3) M. Donbrow and E. Touitou, *ibid.*, **67,** 95 (1978).

(4) R. H. Reuning and G. Levy, *ibid.*, **57,** 1335 (1968).

(5) G. E. Amidon, Ph.D. Thesis, University of Michigan, 1979, p. 44.

(6) T. J. Mikkelson, S. Watanabe, J. H. Rytting, and T. Higuchi, *J. Pharm. Sci.*, **69,** 133 (1980).

(7) B. D. Anderson, J. H. Rytting, and T. Higuchi, *J. Am. Chem. Soc.*, **101,** 5194 (1979).

(8) B. Carnahan, H. A. Luther, and J. O. Wilkes, "Applied Numerical Methods," Wiley, New York, N.Y., 1969, pp. 440–442, 464.

(9) J. Crank, "The Mathematics of Diffusion," 2nd ed., Clarendon, Oxford, 1975, pp. 49–51.

(10) A. C. Tanquary and R. E. Lacey, "Advances in Experimental Medicine and Biology," vol. 47, Plenum, New York, N.Y., 1974, p. 33.

(11) L. G. Longsworth, *J. Coll. Int. Sci.*, **22,** 3 (1966).

(12) D. Attwood and J. A. Tolley, *J. Pharm. Pharmacol.*, **32,** 533 (1980).

(13) D. Attwood, *ibid.*, **24,** 751 (1972).

(14) D. Attwood and O. K. Udeala, *ibid.*, **26,** 854 (1974).

(15) D. Attwood and O. K. Udeala, *ibid.*, **27,** 395 (1975).

(16) D. Attwood and J. A. Tolley, *ibid.*, **27,** 754 (1975).

(17) D. Attwood, *ibid.*, **28,** 407 (1976).

(18) M. D. Joesten and L. J. Schaad, "Hydrogen Bonding," Dekker, New York, N.Y., 1974, pp. 283–288.

ACKNOWLEDGMENTS

This work was supported by Grant GM-22357 from the National Institutes of Health.

Factors Affecting Survival of *Pseudomonas cepacia* in Decongestant Nasal Sprays Containing Thimerosal as Preservative

B. T. DECICCO *x, E. C. LEE *, and J. V. SORRENTINO ‡

Received July 6, 1981, from the **Department of Biology, The Catholic University of America, Washington, DC 20064*, and ‡*Vick Health Care Division, Richardson-Vicks, Inc., Wilton, CT 06897.* Accepted for publication January 18, 1982.

Abstract □ Strains of *Pseudomonas cepacia*, isolated from packages of nasal spray preserved with thimerosal, showed a high degree of resistance to the organomercurial, as compared to low and moderate resistance of standard laboratory strains or isolates from water. The product isolates were shown to degrade the thimerosal to metallic mercury which volatilized from the product or assay medium. The addition of organic nutrient was essential for survival of unadapted cells in the product. However, when cells were first grown in diluted product containing added nutrient and then inoculated into the full-strength product, survival and growth occurred even in the absence of added nutrient. The time required for growth to occur was inversely related to the amount of added nutrient. At low nutrient concentrations, ~99.9% of the inoculated cells were killed rapidly, but after a lag time of 7–12 days, the few survivors began to increase in numbers and eventually attained high cell concentrations. These findings should be useful in planning production and testing programs with thimerosal-preserved products.

Keyphrases □ Thimerosal—preservative, factors affecting survival of *Pseudomonas cepacia* in decongestant nasal sprays □ *Pseudomonas cepacia*—factors affecting survival in decongestant nasal sprays containing thimerosal as preservative □ Decongestants—nasal sprays containing thimerosal as preservative, factors affecting survival

Although generally considered nonpathogenic, *Pseudomonas cepacia* can cause severe and sometimes fatal infections, especially when accidently introduced directly from contaminated materials into wounds, blood vessels, or the urinary tract (1–9). Recently, it has been implicated as the cause of contamination of decongestant nasal sprays produced by two different companies. In one case the affected products contained the cationic surfactant benzalkonium chloride as the preservative, while in the other instance, the products contained the organomercurial, thimerosal. The present report describes studies with organisms isolated as contaminants in the latter products.

BACKGROUND

The bacterium, *P. cepacia*, was first reported as the causative agent of yellow rot in onions (10) and was given the species name on the basis of that ability. A taxonomic study of the genus *Pseudomonas* described an organism which was versatile nutritionally (11); based on that characteristic it was named *P. multivorans*. It was suggested that this species, which can utilize over 150 different organic compounds as sources of carbon and energy, had not been described earlier because of its geographic restriction, but it is now known to occur widely in soil and water. The two species, *P. cepacia* and *P. multivorans*, plus a third, *P. kingii*, have since been shown to be identical, and the designation *P. cepacia* has been adopted (12, 13).

In addition to its nutritional versatility, *P. cepacia* possesses the ability to grow in distilled water without added nutrients (14), and most isolates are highly resistant to antibiotics and other antibacterial agents (15, 16). This combination has led to numerous nosocomial problems due to its presence in water reservoirs, hospital aqueous solutions, and disinfectants (17–22). Like some of the other pseudomonads, *P. cepacia* has been isolated from numerous commercial products and rivals *P. aeruginosa* as to its presence and persistance in various pharmaceuticals.

In 1978, pseudomonads were isolated from several lots of both the regular and long-acting formulations of nasal sprays. The regular formulation contains phenylephrine hydrochloride while the long-acting variety contains xylometazoline as the adrenergic component. Both formulations contain 10 ppm of thimerosal as a preservative. Cetylpyridinium chloride also is present in the regular formulation but not in the long-acting brand. A number of separate bacterial isolates from both formulations were identified as *P. cepacia* of several different biotypes[1].

The occurrence of resistance to high levels of thimerosal and other organomercurials has been demonstrated in numerous bacterial species including the pseudomonads, *P. cepacia* and *P. aeruginosa*, and, although the mechanism of resistance varies with the microbial strain and the type of mercurial compound, with organomercurials it normally involves plasmid-determined inducible enzymes which hydrolyze the carbon–mercury linkage and then reduce the released Hg^{+2} to volatile metallic mercury (Hg°) (23, 24).

In this report some physiological characteristics of strains of *P. cepacia* isolated from products containing thimerosal are described. They are compared with strains from other sources, and the conditions under which successful contamination may or may not occur are examined.

EXPERIMENTAL

The bacterial strains employed in these studies were obtained from various sources, as shown in Table I.

Thimerosal sensitivity assays were performed in test tubes containing 7.5 g/liter (one-fourth strength) trypticase soy broth[2] plus various concentrations of thimerosal[3] ranging from 0 to 10,000 ppm in a final volume of 6.0 ml. Tubes were inoculated to cell densities of $\sim 5 \times 10^6$ organisms/ml using 0.05 ml of inocula grown in 7.5 g/liter trypticase soy broth, and were incubated with slow shaking at 30°. The highest concentration yielding growth, as indicated by visible turbidity, was noted. In the thimerosal sensitivity assay, turbidity was always present by Day 5 if growth was to occur. Negative tubes were verified to be free of viable cells by streaking onto trypticase soy agar[2] plates.

Chemical analyses for thimerosal were performed by determining mercury contents using atomic absorption spectrophotometry (25).

Microbiological assays for thimerosal were performed on trypticase soy agar and Mueller–Hinton agar plates using a sensitive strain of *Staphylococcus aureus* as the indicator organism. Filter paper disks were 12.5 mm in diameter. The plates were incubated at 35° and read at 24 hr. Challenge testing of the product was performed by growing test organisms in trypticase soy broth at 30 or 35° and inoculating the product to concentrations ranging from 1.5×10^5 to 2.4×10^7 organisms/ml. In some instances a second challenge was performed with the same organism. Both types of nasal spray were employed and were either freshly prepared or were from commercial lots of different ages.

Tests to determine the ability of the isolates to utilize product components as sole sources of carbon and energy were performed using a mineral salts basal medium. The mineral medium consisted of the following components per liter of distilled water: 80 mg K_2HPO_4, 200 mg NaH_2PO_4, 100 mg $(NH_4)_2SO_4$, 14 mg $MgSO_4 \cdot 7H_2O$, and 2 mg $Fe(NH_4)_2 \cdot 6H_2O$. Organic components of the nasal sprays were tested separately by adding them to the mineral medium to final concentrations of 0.1 and 1.0 g/liter. Thimerosal could not be tested as a carbon and energy source, since in mineral salts medium it was lethal to all strains at concentrations >5 ppm. Inocula for these studies were grown overnight on mineral salts agar containing 1 g/liter monosodium glutamate. Cells were transferred to sterile distilled water and shaken overnight, then

[1] Identified by G. Gilardi, Hospital for Joint Diseases, N.Y.
[2] Baltimore Biological Laboratories, Baltimore, Md.
[3] Sigma Chemical Co., St. Louis, Mo.

0022-3549/82/1100-1231$01.00/0

Table I—Thimerosal Sensitivity of Bacterial Strains from Various Sources

Organism		Source	Highest Concentration of Thimerosal-Yielding Growth, ppm	Inoculum Size, cells/ml
S. aureus	19636	ATCC[a]	0.03	5×10^{6}[b]
E. coli	11303	ATCC[a]	1	5×10^{6}
P. fluorescens	12633	ATCC[a]	3	5×10^{6}
P. aeruginosa	10145	ATCC[a]	10	5×10^{6}
P. aeruginosa	9027	ATCC[a]	3	5×10^{6}
P. cepacia	25416	R. Hugh	3	5×10^{6}
P. fluorescens	(2 isolates)	City water entering plant	10	5×10^{6}
P. cepacia	(4 isolates)	City water entering plant	30	5×10^{6}
Pseudomonas sp.	(7 isolates)	City water entering plant	10–100	5×10^{6}
P. cepacia	B7L	Product Isolate	500	5×10^{6}
P. cepacia	CAT	Product Isolate	300	5×10^{6}
P. cepacia	CWJ	Product Isolate	1000	5×10^{6}
P. cepacia	CWO	Product Isolate	1000	5×10^{6}
P. cepacia	CXN	Product Isolate	500	5×10^{6}
P. cepacia	CXN	Product Isolate	300	5×10^{4}
P. cepacia	CXN	Product Isolate	100	5×10^{2}

[a] American Type Culture Collection. [b] Standard.

diluted in distilled water to yield the desired inoculum size, which was calculated to be $\sim 1 \times 10^{2}$ cells/ml. The actual number of cells present at the time of inoculation and at daily intervals for 5 days was determined by spreading samples onto trypticase soy agar plates.

When adapted cultures were employed, they were prepared by growing inocula in a fourfold dilution of product (diluted with deionized water) containing 300 ppm of phytone[2] (soy peptone). In this medium organisms reached visible turbidity in 1–2 days.

In those experiments where nutrient supplementation of the product was employed, individual substances or complex media were prepared at concentrations of 120 g/liter (or lower if solubilities did not permit the higher levels), sterilized by membrane filtration, and added to tubes containing product to yield the desired range of concentrations. As with assays for thimerosal resistance, growth was noted by observing tubes for turbidity. Tubes showing no turbidity were checked periodically for viable cells by streaking or spreading aliquots onto trypticase soy agar plates.

RESULTS AND DISCUSSION

The thimerosal sensitivities of a number of well-characterized bacterial strains, as well as some water and product isolates, are shown in Table I. A difference in resistance is evident between the ATCC strains (growth up to 10 ppm) and the product isolates, which grew in the presence of 300–1000 ppm of thimerosal. No organism was isolated from the product which was not resistant to high levels of thimerosal. Thus, resistance to thimerosal appeared to be essential for survival in the product. Strains of *Pseudomonas* isolated from city water entering the production site had resistance levels intermediate between the laboratory strains and the product isolates. The effect of inoculum size also can be seen in Table I. When strain CXN was inoculated at concentrations 100- and 10,000-fold below the standard level of 5×10^{6} organisms/ml, the highest thimerosal concentration yielding survival and growth fell slightly, but even with the lowest inoculum of 500 cells/ml, the organisms still grew in 100 ppm of thimerosal. A similar effect was noted when strain CWJ was inoculated directly from a contaminated bottle into assay tubes to produce an inoculum level ~100-fold below the standard level (growth was to 500 ppm).

Table II—Microbiological and Chemical Assays[a] for Thimerosal in Uninoculated Samples and in Media Inoculated with Resistant Strains of *P. cepacia*

Sample	Initial Thimerosal Concentration, ppm	Microbial Assay Zone Diameter, mm	Chemical Assay, ppm
Thimerosal in deionized water	1	19	NA[b]
	10	26	NA
	100	36	NA
Thimerosal in uninoculated medium[c]	0	No zone	0
	1	18	0.8
	10	26	10
	100	36	107
Thimerosal in medium + strain CXN	0	No zone	0
	1	No zone	Trace
	10	No zone	0.5
	100	No zone	3.3
Thimerosal in medium + strain B7L	0	NA	0
	1	NA	Trace
	3	NA	Trace
	10	NA	Trace
	30	NA	4.5
	100	NA	2.4

[a] Both uninoculated and inoculated samples were assayed after 4-days incubation at 30°. [b] Not assayed. [c] Trypticase soy broth.

Table II shows the results of chemical and microbial assays for thimerosal using various solutions containing thimerosal, both uninoculated and after growth of two resistant strains. Comparison of thimerosal in deionized water with 4-day-old uninoculated trypticase soy–thimerosal tubes, using the microbiological assay, showed that the one-fourth strength trypticase soy medium had no neutralizing effect on thimerosal. Tubes inoculated with *P. cepacia* strain CXN showed the absence of detectable thimerosal by microbial assay, even when the initial concentration was 100 ppm and even though this assay easily detected 1-ppm concentration in the uninoculated deionized water and in trypticase soy broth controls. Chemical analyses for thimerosal mercury confirmed the inactivation of thimerosal by strains CXN and B7L. Since the chemical assay determines mercury levels, it can be assumed that strains B7L and CXN are resistant to thimerosal by virtue of enzymes which liberate metallic mercury from the media. This also was observed by chemical determination of mercury levels in numerous contaminated and uncontaminated packages of nasal spray. The analyses showed that 1-year-old uncontaminated packages all contained the expected levels of 6.8–7.4 ppm of thimerosal, whereas contaminated packages from the same lots and cases contained 0.1–1.5 ppm. Thus, when the contaminating organisms survived and grew in the product, the thimerosal was degraded.

When strains CWO and CXN were used to challenge both the regular and the long-acting product at levels of 1.5×10^{5}–2.4×10^{7} organisms/ml, no viable organisms could be recovered after 1 hr. In all, over 70 challenge tests were performed with uniformly negative results. This was true whether the products were freshly prepared in the laboratory or were uncontaminated packages taken from cases that contained one or more contaminated packages. Thus, no differences were noted between old and fresh product or between regular and long-acting product with regard to survival of *P. cepacia* strains isolated from the product. Since the long-acting product does not contain cetylpyridinium chloride, while the regular product does, the absence of cetylpyridinium chloride did not allow for survival of the challenge organisms.

It was assumed that the contaminating strains of *P. cepacia* were capable of utilizing some component(s) of the nasal sprays as a source of carbon and energy. To explore this assumption, each component was individually tested for its ability to support growth of *P. cepacia* strains CWO, B7L, and 25416. Within 72 hr, inoculum levels increased from between 40 and 200 organisms/ml to $\sim 2 \times 10^{6}$ organisms/ml in the presence of each tested component. However, the same increase in cell

Table III—Effect of Organic Nutrients on Survival and Growth of *P. cepacia* in Nasal Spray Containing Thimerosal

Nutrient, ppm	Nutrient Source: Trypticase soy broth	Trypticase	Yeast extract	Phytone	Dextrose	Glutamine	Proteose peptone	Acetate	Aspartate	Pyruvate	Benzoate	Monosodium glutamate	Starch	Maltose	Asparagine
20,000	+[a]				+					−[b]	−	+	−		
17,000					+					−	−	−	−		
15,000						−		−	−						−
13,000					+					−	−	−	−		
10,000	+				−				−						
9,000	+				−					−	−	−	−		
7,500						−		−	−						−
6,000					−							−			
5,000	+	+	+	+			+							−	
4,600					−					−	−	−	−		
4,100	+	+	+	+			+							−	
3,800						−		−	−						−
3,200	+	+	+	+	−		+					−		−	
2,200	−	+	+	+	−		−			−	−	−	−	−	
1,800			−			−		−	−						−
1,200	−	−	−	+	−		−		−	−	−	−	−	−	
900						−		−						−	
600	−	−	−	−			−							−	

[a] Growth to $>10^7$ cells/ml. [b] No viable cells present.

population occurred in the mineral salts medium without added substances. When acid-washed glassware and ultrapure reagents were employed, cell yields between 9×10^5 and 1.2×10^6 organisms/ml still were obtained both in mineral salts alone and with product components. When cells were passed repeatedly in sterile distilled water obtained from a quartz element glass still-fed from a deionizer unit, cell densities between 4 and 5×10^5 were maintained. Thus, the addition to water of usable organic nutrient is not necessary for the survival and growth of the product isolates. Growth of *P. cepacia* previously has been reported in mist therapy unit water and commercial distilled water (14).

An explanation was needed for the apparent contradiction between the observed high degree of thimerosal resistance of the product isolates as measured by tube or plate assay in trypticase soy media and the failure of the isolates to survive when introduced back into products similar to those from which they were originally isolated. Since none of the product ingredients stimulated growth of the isolates in minimal media, and since the absence of cetylpyridinium chloride did not enhance survival, two other factors were studied for their effect on survival of the isolates in the product: the addition of nutrient and adaptation of the isolates to the product.

Since the product isolates all showed high levels of thimerosal resistance in the trypticase soy tube assays, this complex medium was employed as a source of nutrient. As shown in Table III, when trypticase soy broth was added to the regular nasal spray formulation at concentrations ≥3200 ppm, survival and growth to visible turbidity was observed. When the organic components of trypticase soy broth (trypticase, phytone, dextrose) were tested individually, phytone (soy peptone) was most effective and supported growth in the regular product at concentrations ≥1200 ppm. Since the concentrations of nutrient required to support growth were higher than the nutrient levels present in the treated water or other components used in formulating the product, organic substances other than those present in trypticase soy broth were also tested in an attempt to find a more efficacious stimulator of successful contamination. The test substrates included the amino acids glutamine, glutamate, asparagine, and aspartate; the organic acids acetate, pyruvate, and benzoate; proteose peptone and yeast extract as complex nutrients; and starch and maltose as nonutilizable organics (for *P. cepacia*). As shown in Table III, none of these compounds was as effective as phytone in allowing survival of *P. cepacia* strain CWO. Of the single substrates, only dextrose and glutamate supported contamination of the product and neither of these was effective in concentrations that were comparable to those yielding growth when the complex nutrients were used. Since the tested organic substrates spanned a variety of utilizable and nonutilizable compounds, it seemed unlikely that a more effective supporter of survival would be found.

Since an alternative explanation was necessary to account for the survival of the contaminant organisms in the product in the absence of high quantities of nutrient, the effect of cultivating strain CWO in diluted product and then inoculating this adapted culture into undiluted commercial product containing a range of phytone concentrations was determined.

The effect of adaptation on the ability of thimerosal-resistant organisms to survive in the product is shown in Table IV. The inocula for these studies were grown in a fourfold dilution of product (regular formulation) containing 300 ppm of phytone, as contrasted with the unadapted inocula employed for the data shown in Table III, which were grown in trypticase soy broth. Table IV shows three significant effects. First, the adapted cells were able to survive and proliferate in the product in the absence of any added nutrient. Second, the time required for growth and turbidity to be evident was inversely related to the added nutrient concentration. Third, at low nutrient levels (0–120 ppm) the number of viable cells declined dramatically from the initial concentration of 1×10^6 cells/ml to between 1 and 15×10^2 cells/ml and remained at the lower levels for up to 2 weeks before an increase in viable cells was noted. The third effect was observed by periodically plating calibrated loops (0.01 ml) of culture from those tubes which showed no turbidity on day 5. These were the tubes containing the four lowest concentrations of phytone. Samples were plated on days 5, 7, and 12. The numbers of viable cells were low and remained stable for at least 7 days in the tubes containing the three lowest concentrations of nutrients (0, 60, and 120 ppm of phytone) (Table IV). The tube containing 240 ppm of phytone, which was not yet turbid on day 5, contained $\sim 10^5$ cells/ml at the time and became turbid on day 7. In the two tubes that became turbid on days 14 and 17 (0 and 120 ppm), increases in cell numbers were evident on day 12. The tube that became turbid on day 19 (60 ppm of phytone) still showed no increase in viable cells on day 12. Thus, inoculation into the product containing low concentrations of extraneous organic matter led to the death of most resistant cells, but the survivors persisted and eventually grew. A similar effect was noted by Pinney when a strain of *P. aeruginosa* resistant to thimerosal was inoculated into a minimal medium containing glucose as the energy source (26).

As expected, the turbidy attained in each tube was related to the level of nutrient present; when survival and growth occurred in the absence of added organic nutrient, the cultures were barely turbid. Similar levels were observed when strain CWO was inoculated into laboratory deionized water containing no added components. Thus, none of the organic components of the nasal spray need serve as a nutrient source in order to allow survival and growth of certain bacteria.

The data shown in Table IV were obtained using the product taken

Table IV—Persistence and Growth of *P. cepacia*[a] in Nasal Spray with Various Concentrations of Nutrient

Days Post Inoculation	Concentration of Soy Peptone, ppm: 0	60	120	240	360	480
5	1[b]	6	15	~1000	TNTC[c]	TNTC
7	0	6	10	TNTC	TNTC	TNTC
12	200	3	260	TNTC	TNTC	TNTC
Day on which culture became turbid	17	19	14	7	3	2

[a] Inoculum was adapted in diluted product (see text) and was adjusted to yield initial concentrations of 1×10^6 cells/ml. [b] Number of colonies present on trypticase soy agar after plating 0.01 ml of product. [c] Too numerous to count.

from commercial polyethylene containers. That product contained thimerosal levels of 8.0–8.5 ppm, which is the usual concentration present several months after manufacture due to the absorption of some thimerosal by the container. When similar challenges were performed with product formulated in glass containers containing thimerosal at 10 ppm, the same inverse relationship between nutrient concentrations and lag time was observed, except that with 10 ppm of thimerosal, cultures in the product containing low nutrient levels took up to 37 days to become turbid. Under these circumstances, low numbers of cells persisted for as long as 1 month before growth occurred. It is likely that during these long lag periods, small numbers of surviving cells were producing thimerosal-inactivating enzymes, which then reduced the thimerosal concentration to a level which allowed growth. The greater enhancement of survival and growth of resistant cells by peptone mixtures as compared with single carbohydrates or amino acids probably was due to the utilization of the peptone amino acids for efficient and rapid synthesis of the thimerosal-inactivating enzymes.

When the product containing thimerosal levels >10 ppm was tested, strain CWO survived and grew only when nutrient was added. The required nutrient levels increased with increasing thimerosal, *e.g.*, at 60 ppm of thimerosal; survival and subsequent growth of adapted cells required the presence of 1000 ppm of phytone. It is suspected that in the presence of thimerosal, the levels of inactivating enzymes are related to the amount of phytone present. Thus, high phytone levels are necessary for survival at higher thimerosal concentrations. At lower thimerosal concentrations, higher phytone levels and, consequently, greater levels of inactivating enzymes more quickly reduce thimerosal below the inhibitory level with the resultant shorter lag time.

One concern emanating from this study results from the long lag period which may precede growth. Thus, samples of the product which are tested microbiologically shortly after manufacture may contain only small numbers of viable organisms, yet if those organisms are resistant strains, eventual growth to high levels may occur. Some measures that would reduce the risk of such an occurrence are as follows:

1. Composite samples must not be made except in neutralizing solutions, since reduction or elimination of resistant cells can occur upon mixing with additional product.
2. Vegetative cells isolated from the product, even in very small numbers, should be checked for resistance to the preservative if the isolates are of a suspect species, especially one of the Gram-negative nonfermentative bacilli.
3. If low counts of an organism are obtained and the organism is shown to be resistant to the preservative by tube or plate testing, the product should be retested at intervals to determine whether counts are increasing. It is preferable to encode and hold individual packages for this purpose. With thimerosal preserved products, if viable vegetative cells are recovered after several days, eventual increases in counts are likely.
4. Challenge testing of product with suspected contaminants may give false assurance if the inocula for the challenges are grown in the absence of preservative. A 10- or 20-fold dilution of the product in water is a useful medium for growth of challenge organisms. In many cases it is not necessary to add additional nutrient to allow growth of Gram-negative organisms. Survival of adapted organisms in the full-strength product then can be compared with unadapted inocula grown in the usual culture media.

REFERENCES

(1) R. H. Daily and E. J. Benner, *N. Engl. J. Med.*, **279,** 361 (1968).

(2) D. C. J. Bassett, K. J. Stokes, and W. R. G. Thomas, *Lancet*, **i,** 1188 (1970).

(3) E. Yabuuchi, N. Miyajima, H. Hotta, and A. Ohyama, *Med. J. Osaka Univ.*, **21,** 1 (1970).

(4) I. Phillips, S. Eykyn, M. A. Curtis, and J. J. S. Snell, *Lancet*, **i,** 375 (1971).

(5) D. Taplin, D. C. Bassett, and P. M. Mertz, *ibid.*, **ii,** 568 (1971).

(6) R. H. Poe, H. R. Marcus, and G. L. Emerson, *Am. Rev. Respir. Dis.*, **115,** 861 (1977).

(7) A. C. Steer, J. H. Tenney, D. C. Mackel, M. J. Snyder, S. Polakavetz, M. E. Dunne, and R. E. Dixon, *J. Infect. Dis.*, **135,** 729 (1977).

(8) F. S. Rhame and J. McCullough, *Morbidity and Mortality Weekly Report*, **28,** 409 (1979).

(9) C. Randal, *Can. J. Public Health*, **71,** 119 (1980).

(10) W. H. Burkholder, *Phytopathology*, **40,** 115 (1950).

(11) R. Y. Stanier, N. J. Palleroni, and M. Doudoroff, *J. Gen. Microbial.*, **43,** 159 (1966).

(12) J. J. S. Snell, L. R. Hill, S. P. Lapage, and M. A. Curtis, *Int. J. Syst. Bacteriol.*, **22,** 127 (1972).

(13) H. A. Sinsabaugh and G. W. Howard, *ibid.*, **25,** 187 (1975).

(14) L. A. Carson, M. S. Favero, W. W. Bond, and N. J. Peterson, *Appl. Microbiol.*, **25,** 476 (1973).

(15) G. L. Gilardi, *ibid.*, **22,** 821 (1971).

(16) R. M. E. Richards and J. M. Richards, *J. Pharm. Sci.*, **68,** 1436 (1979).

(17) H. L. Moffet and T. Williams, *Am. J. Dis. Child.*, **114,** 7 (1967).

(18) D. W. Burdon and J. L. Whitby, *Br. Med. J.*, **2,** 153 (1967).

(19) P. C. Hardy, G. M. Ederer, and J. M. Matsen, *N. Engl. J. Med.*, **282,** 33 (1970).

(20) D. C. E. Speller, M. E. Stephens, and A. C. Viant, *Lancet*, **i,** 798 (1971).

(21) S. M. Gelbart, G. F. Reinhardt, and H. B. Greenlee, *J. Clin. Microbiol.*, **3,** 62 (1976).

(22) S. Lewin, *et al.*, *Morbidity and Mortality Weekly Report*, **29,** 553 (1980).

(23) T. Tezuka and K. Tonomura, *J. Biochem. (Tokyo)*, **80,** 79 (1976).

(24) D. L. Clark, A. A. Weiss, and S. Silver, *J. Bacteriol.*, **132,** 186 (1977).

(25) "United States Pharmacopeia," 20th rev., U.S. Pharmacopeial Convention, Rockville, Md., 1980, p. 791.

(26) R. J. Pinney, *J. Pharm. Pharmacol.*, **30,** 228 (1978).

ACKNOWLEDGMENTS

The authors thank Lura S. Oravec and Theresa A. Hoffman for technical assistance.

Water Vapor Sorption and Desorption by Human Callus I: Anomalous Diffusion

DALE E. WURSTER [x] **and KIN-HAI YANG** *

Received September 1, 1981, from the *College of Pharmacy, University of Iowa, Iowa City, IA 52242.* Accepted for publication January 18, 1982. * Present address: School of Pharmacy and Allied Health Sciences, University of Montana, Missoula, MT 59812.

Abstract □ The rates of sorption and desorption of water in membranes of varying thickness of excised human callus were determined for several relative vapor pressures and temperatures. Under the conditions studied, the diffusion of water in these membranes was interpreted as non-Fickian in nature. It was concluded that at low water concentration this type of membrane exists in the glassy state. The effect of the relative vapor pressure on the water sorption rates was examined in the context of the free volume theory.

Keyphrases □ Diffusion—anomalous, water vapor sorption and desorption by human callus □ Sorption—water vapor, by human callus, anomalous diffusion □ Desorption—water vapor, by human callus, anomalous diffusion

The hydration of the skin has been found to increase the percutaneous absorption rates of several substances in humans (1). *In vivo* studies have demonstrated this effect for salicylate esters (2) and methyl ethyl ketone (3); whereas, an *in vitro* study has shown the same effect for sarin (4). The transport of water itself in skin is affected similarly (5–7). In an early study (8), water was shown to plasticize human callus when the concentration was ~10%. Since the glass transition temperature of stratum corneum is reported as 53° (9), it might be anticipated that non-Fickian diffusion of water in stratum corneum would occur below this temperature. The purpose of this study was to study the rates of water vapor sorption and desorption, to elucidate the nature of the diffusional process, and to provide a theoretical basis for the above observations.

THEORETICAL

The experimental system can be defined as consisting of water in the vapor state in equilibrium with sorbed water in a membrane of human callus. The rate of sorption to attain the equilibrium amount (Q_e), however, is considered to be controlled by the rate at which water molecules diffuse in the membrane. For isothermal diffusion in a two-component system, the rate of diffusion is governed by Fick's second law:

$$\partial C/\partial t = \partial/\partial x\,[D(C)(\partial C/\partial x)] \qquad \text{(Eq. 1)}$$

where C is the concentration of the diffusing molecules in the system at time t and distance x, and $D(C)$ is the mutual diffusion coefficient of the system, assuming that diffusion is one-dimensional and the diffusion coefficient depends on concentration only. The initial and boundary conditions assumed for sorption are:

$$C(x, 0) = 0, 0 < x < L \qquad \text{(Eq. 2)}$$

$$C(0, t) = C(L, t) = C_e, t > 0 \qquad \text{(Eq. 3)}$$

and for desorption:

$$C(x, 0) = C_e, 0 < x < L \qquad \text{(Eq. 4)}$$

$$C(0, t) = C(L, t) = 0, t > 0 \qquad \text{(Eq. 5)}$$

where L is the thickness of the membrane, and C_e is the equilibrium concentration at given temperature (T) and pressure (p). Solution of Eq. 1, subject to Eqs. 2–5, indicates (10) that the fractional uptake, $Q(t)/Q_e$, should theoretically increase linearly with $t^{1/2}$ during the initial period for both sorption and desorption, and the initial slope, $K(C_e)$, of the plot of $Q(t)/Q_e$ *versus* $t^{1/2}$ is given by (11):

$$K(C_e) = 4\bar{D}^{1/2}(C_e)/\pi^{1/2}L \qquad \text{(Eq. 6)}$$

In this instance, $Q(t)$ is the amount sorbed or desorbed at time t and $\bar{D}(C_e)$ is the mean value of the mutual diffusion coefficient over the concentration range taken. Thus, the slope will vary with C_e for any given membrane. It was also shown that for $D(C)$ increasing with C, $K(C_e)$ for sorption is always greater than $K(C_e)$ for desorption, the difference being an indication of how strongly $D(C)$ depends on C for the given concentration range. For D independent of C, it can be seen from Eq. 6 that for a given membrane, the slope K will be independent of C_e and identical for both sorption and desorption. It can also be seen that when $Q(t)/Q_e$ is plotted against $t^{1/2}/L$, the slope should be independent of L.

Deviations from these theoretical predictions for the conditions considered, however, have been observed in many polymer–diluent systems (12–14). These deviations generally implicate the role of slow relaxation processes for glassy polymers (14, 15).

To meet the conditions imposed on the mathematical representation of the system, thin membranes of callus devoid of lipid were used. Since kinetic data for the initial period were emphasized and studies were limited to the relative vapor pressures below unity, any swelling effect on the membrane thickness was considered negligible. Thus, from measurements of $Q(t)$ as a function of time for varied relative vapor pressures and thicknesses at constant temperatures, the nature of the diffusion process for the membrane–water system can be examined.

EXPERIMENTAL

Sorption–Desorption System—The system, constructed of glass[1], consists of a sorption tube connected to a manifold leading to both the vapor source and the vacuum system. A sensitive quartz spring[2] was placed inside the sorption tube. The entire sorption system was enclosed in a thermostated chamber and the temperature was controlled to within ±0.05°. A two-stage mercury-vapor diffusion pump[3] backed by a two-stage mechanical forepump[4] provided a base vacuum of $<10^{-4}$ torr. For measuring the extension of the spring, a precision cathetometer[5], which

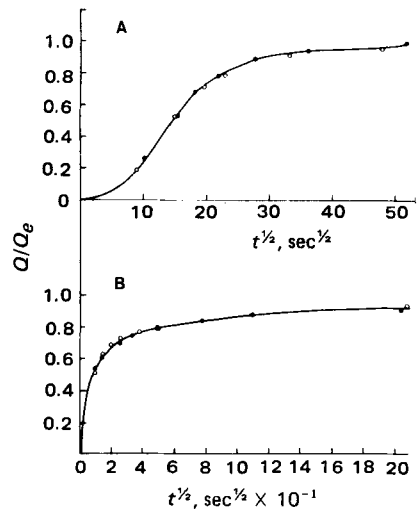

Figure 1—*Sorption and desorption of water vapor in human callus (Membrane 3) at 28°, p/p° = 0.84. Two repeated experiments. Key: (A) sorption, (○) Spring A; (●) Spring B; (B) desorption, (○) Spring A; (●) Spring B.*

[1] Pyrex.
[2] Worden.
[3] Pope, model 20045.
[4] Welch, model 1400.
[5] Gaertner, model M912.

0022-3549/82/1100-1235$01.00/0

Table I—Relative Vapor Pressure ($p/p°$) of the Saturated Salt Solutions

Salt	$p/p°$ 20°	30°	40°
Sodium tartrate[a]	0.91	0.91	0.91
Potassium chloride[b]	0.86	0.84	0.83
Sodium chloride[b]	0.75	0.75	0.75
Cupric chloride[b]	0.68	0.67	0.67
Magnesium nitrate[b]	0.52	0.52	0.51
Magnesium chloride[b]	0.33	0.32	0.31

[a] Data from Ref. 17. [b] Data from Ref. 18.

Table II—Physical Constants of the Test Membranes

Membrane	Weight, mg	Diameter, mm	Thickness, μm	Density, g/ml, 25°
1	1.364 ± 0.005	4.85 ± 0.05	57.3 ± 1.6	1.288 ± 0.005
2	0.786 ± 0.005	4.585 ± 0.007	37.0 ± 0.5	
3	0.826 ± 0.005	5.032 ± 0.007	32.3 ± 0.4	
4	1.152 ± 0.005	4.941 ± 0.007	46.7 ± 0.5	

reads to 0.01 mm, was used. Thus, with a spring sensitivity of 20 mm/mg, a change in weight of 0.5 μg could be detected. This system was similar in principle to the one employed by Prager and Long (16).

The quartz springs were calibrated with small standard weights which were weighed to 0.1 μg on an electrobalance[6]. Four quartz springs (A, B, C, and D) having calibrated sensitivities of 9.36, 9.59, 18.73, and 17.60 mm/mg, respectively, were used.

Conventional salt solutions were employed to obtain the relative water vapor pressures in the system. The relative vapor pressures of these salt solutions (17, 18) are shown in Table I.

Membrane Preparation and Physical Measurements—Human callus was used as a convenient and readily available model for stratum corneum in an attempt to study water sorption, desorption, and the influences on the water transport mechanism in skin. Excised human callus tissue was microtomed to thin membranes of different thicknesses and delipidized in anhydrous ether as reported (4). To prepare a test membrane, the membrane was first partially hydrated and then cut with a 4.76-mm punch. The diameter of each test membrane was measured with a filar eyepiece micrometer[7] attached to an optical micrometer[8], which was calibrated with a micrometer disk[9]. The weights of the test membranes were obtained using an electrobalance[6]. All test membranes were dried over Drierite to constant weight. The thickness of the membrane was calculated from its diameter, weight, and density (19).

The weights, diameters, and calculated thicknesses of the membranes used in this study are given in Table II.

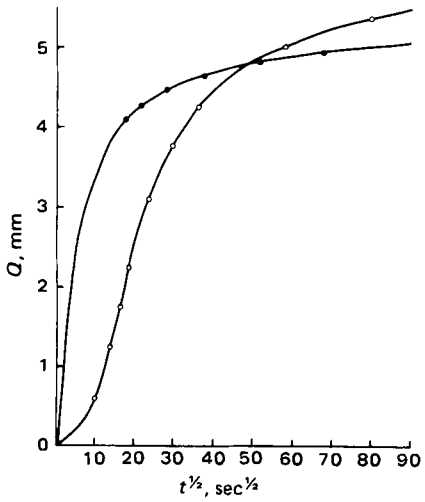

Figure 2—*Sorption and desorption of water vapor in human callus (Membrane 4) at 28°, p/p° = 0.91. Key: (○) sorption, (●) desorption, Spring B; Q_e (sorption) 5.58 mm.*

[6] Cahn, model 4200.
[7] Gaertner, model M202.
[8] Cenco.
[9] Bausch and Lomb.

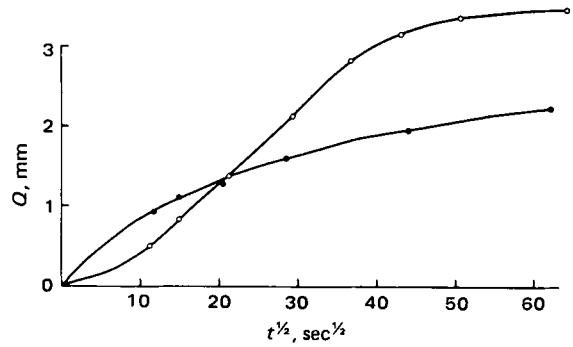

Figure 3—*Sorption and desorption of water vapor in human callus (Membrane 4) at 28°, p/p° = 0.67. Key: (○) sorption, (●) desorption, Spring C; Q_e (sorption) 3.53 mm.*

Sorption–Desorption Studies—For the sorption studies, the test membrane was attached to the quartz spring and kept at base vacuum at the given temperature until constant weight was reached. The membrane was then exposed to a given vapor pressure. The amount of water absorbed was followed by measuring the change in extension, $Q(t)$, of the spring with the cathetometer as a function of time until Q remained constant for a period of 24 hr. This value was taken as $Q_e(T,p)$. Upon the completion of the sorption run, the sorption tube was switched to the vacuum to initiate the desorption experiment. At that time $Q(t)$ represented the amount of water desorbed at the time t when Q was measured. Sorption and desorption rates were measured at relative vapor pressures of 0.32, 0.52, 0.67, 0.75, 0.84, and 0.91 and temperatures of 21, 28, 32, and 39°. The membrane thicknesses were 32.3, 37.0, 46.7, and 57.3 μm.

RESULTS AND DISCUSSION

Repeated experiments with the described system showed good reproducibility of the experimental procedure. A typical example showing the reproducibility of the experimental data is given in Fig. 1.

Effect of Relative Vapor Pressure—The rates of sorption and desorption were determined for various relative vapor pressures ($p/p°$) at 28° using Membrane 4. Paired sorption and desorption curves obtained for $p/p°$ = 0.91, 0.67, and 0.32 are shown in Figs. 2–4, respectively. The sorption curves obtained for four different relative vapor pressures are compared in Fig. 5. Similar results were obtained with test Membrane 1. Thus, the possibility of a constant, D, for the concentration range studied here does not seem plausible. Also, from the sigmoidal shape of the sorption curves and the relative positions of the sorption and desorption curves, it can be seen that the sorption and desorption of water vapor by the membranes are non-Fickian in nature. This would suggest that under the conditions studied, these membranes behave like glassy polymers, and some slow relaxation processes are taking place concurrently with the diffusion process when sorption occurs. The glass transition temperature of the callus was estimated to be ~55° (20). Thus, at 28° all experiments were started with a test membrane which was in a glassy state. At low water concentrations, for which the relaxation effect may be expected to be small, the rates of sorption or desorption could be essentially diffusion-controlled. This has been shown to be the case for a cellulose–water system (21), a wool–water system (22), and also appears to be true for the human callus–water system (Fig. 4). The sorption curve in Fig. 4, however, still exhibits the sigmoidal shape, which indicates that

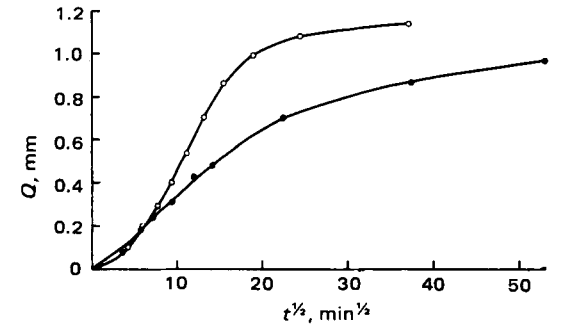

Figure 4—*Sorption and desorption of water vapor in human callus (Membrane 4) at 28°, p/p° = 0.32. Key: (○) sorption, (●) desorption, Spring C; Q_e (sorption) 1.14 mm.*

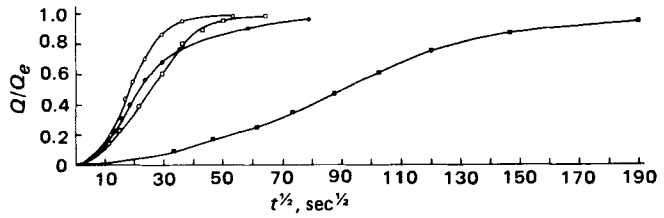

Figure 5—*Sorption of water vapor in human callus (Membrane 4) at 28°, p/p° = 0.32. (■); 0.67 (□); 0.84 (○); 0.91 (●).*

some relaxation effects are still present and cannot be totally ignored. For a cellulose–water system (21), this was previously attributed to a time-dependent surface concentration which approaches its equilibrium value shortly after the start of the experiment. A similar explanation could be suggested for the present system at $p/p° = 0.32$, which corresponds to an equilibrium water concentration of ~5% (w/w). It has been shown (12, 23, 24) that sigmoidal sorption curves can be obtained from the solution of Eq. 1 subject to the boundary condition of a variable surface concentration, $C_s(t)$. Both the theoretical consideration (25) and experimental evidence (23) for $C_s(t)$ have been utilized by others.

At high water concentrations, relaxation effects became more obvious (Figs. 2 and 3) and are not likely to be limited only to the surface region. A further complication may also arise. Since the glass transition temperature of the system is a function of the diluent concentration (26), these membranes may undergo transition from the glassy state to a rubbery state as sorption proceeds at the higher relative vapor pressures. Following Frisch (27), the glass transition temperature of the callus containing x (g/g) water can be estimated from the equation (28) based on the free volume theory:

$$T_g = T_g^\circ - (\beta/\alpha)x \qquad \text{(Eq. 7)}$$

where T_g is the glass transition temperature of the system, T_g° is the glass transition temperature of the callus, x is the water concentration (g/g), α is the difference between the thermal expansion coefficient above and below the glass transition temperature, and β is a parameter representing the contribution of water to the increase in free volume of the system. The value of β was found to be 0.16 for both collagen–water and wool–water systems (29). It also was shown (28) that for a limited range, β is independent of C and T. Using this same value for the present system and the suggested value of $\alpha = 4.8 \times 10^{-4}$ (deg^{-1}) for polymeric systems (30), T_g was calculated to be ~38° for $x = 0.05$ ($p/p° = 0.32$), and 15° for $x = 0.12$ ($p/p° = 0.60$). At $p/p° = 0.67$, which corresponds to an equilibrium water concentration of 0.16 g/g, the lowering of T_g will be even greater. Thus, at 28° and $p/p° = 0.67$, the callus membrane, initially in a glassy state, becomes rubbery whenever the concentration reaches its equilibrium value or lower, as long as it is sufficient to lower the T_g to <28°. This is in contrast to the absorption at 28° and the low $p/p° = 0.32$, where the membrane will remain in essentially the glassy state throughout the entire experiment.

While the exact shapes of the sorption curves in Fig. 5 reflect the total effect of both the relaxation and diffusion processes, in general they are in agreement with the presented analysis. In Fig. 5 the curves for $p/p°$ = 0.32, 0.67, and 0.84 all have an extended portion centered around $Q/Q_e = 0.5$, which is linear within the experimental error. The slopes of these linear portions are in order in accordance with an apparent diffusion coefficient increasing monotonically with the concentration. The slope of the curve for $p/p° = 0.91$, however, is smaller than that of the curve for $p/p° = 0.84$, indicating that the apparent diffusion coefficient decreases as the concentration increases above that corresponding to $p/p°$ = 0.84. A similar trend was confirmed with Membrane 1. The existence

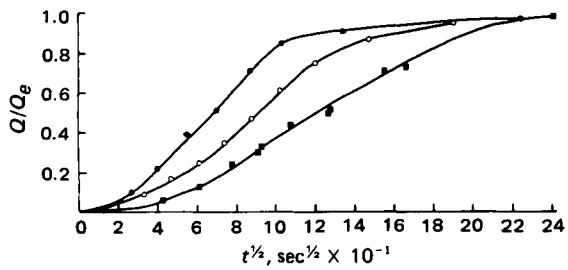

Figure 6—*Sorption of water vapor in human callus (Membrane 4) at p/p° = 0.32 and T = 21°. (■); 28° (○); 39° (●).*

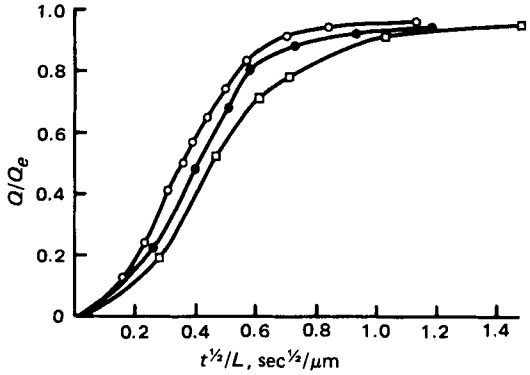

Figure 7—*Sorption of water vapor in human callus. Key: Membranes 1 (○) 57.3 μm; 2 (●) 37.0 μm; 3 (□) 32.4 μm at 28°; p/p° = 0.84.*

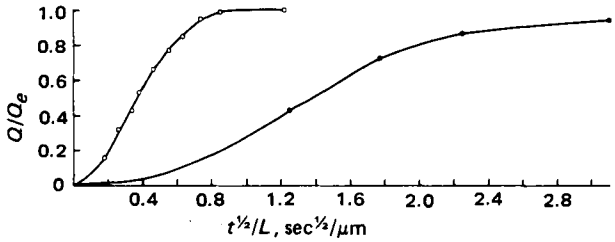

Figure 8—*Sorption of water vapor in human callus; Membrane 1. (○) 57.3 μm; and a human stratum corneum membrane (●) 9.7 μm at 28° and p/p° = 0.75.*

of a limiting value of the diffusion coefficient was also noted in a wool–water system (31). Thus, as absorption proceeds at 28° and $p/p° = 0.91$, not only is there a transition from glassy state to rubbery state for the callus–water system, but also a change in the functional dependence of D on C. This can be seen by the shapes of the curves for $p/p° = 0.84$ and 0.91 in Fig. 5.

The observation made by Blank (8) that the callus tissue became soft and pliable at 23° when it contained 10% water now can be understood. At this concentration, T_g of the system is effectively lowered to ~22°. Also, the same amount of water will not be sufficient to soften or plasticize the tissue at lower temperatures. The general effect of hydration on percutaneous absorption rates can be understood in the same context. The diffusion coefficients of organic vapors in glassy polymers are $\leq 10^{-10}$ cm^2/sec, while in the rubbery polymers they are in the order of 10^{-6} cm^2/sec (27).

Effect of Temperature—Absorption data obtained at 21, 28, and 39° for $p/p° = 0.32$ are compared in Fig. 6. The slopes of the linear portions of the curves increase as the temperature increases, which indicates that the apparent diffusion coefficient increases with the temperature, as would be expected. Since the relaxation time will also decrease as the temperature increases, the general effect of increasing the temperature to 39° was to reduce the role of the relaxation processes. The shape of the upper curve in the figure reflects this effect. A similar trend was seen for $p/p° = 0.67$ at these temperatures.

Effect of Thickness—In an attempt to confirm the non-Fickian mechanism, membranes of different thicknesses were used for the measurements of the rates of absorption under otherwise identical conditions. Results obtained at 28° and $p/p° = 0.84$ with Membranes 1–3 are compared in Fig. 7 in plots of Q/Q_e *versus* $t^{1/2}/L$. For a Fickian mechanism, the curves as plotted should be superimposable, but they are not. Repeated experiments for $p/p° = 0.75$ gave similar results. Such behavior was noted in a wool–water system (31) and a methylene chloride–polystyrene system (32). In both cases they were attributed to the time-dependence of D and/or C_s. The trend shown in Fig. 7 indicates that the apparent diffusion coefficient of the system studied depends on the membrane thickness which is smaller with the thinner membrane. Similar results are shown in Fig. 8 where a membrane, 1, of human callus having a 57.3-μm thickness is compared with a stratum corneum membrane of 9.7 μm at 28° and $p/p° = 0.75$. In the present report it appears that little difference other than thickness exists between these two different membrane types; however, this requires experimental verification.

REFERENCES

(1) B. Idson, *J. Soc. Cosmet. Chem.*, **24**, 197 (1973).

(2) D. E. Wurster and S. F. Kramer, *J. Pharm. Sci.*, **50**, 288 (1961).
(3) D. E. Wurster and R. Munies, *ibid.*, **54**, 1281 (1965).
(4) D. E. Wurster, J. A. Ostrenga, and L. E. Matheson, Jr., *ibid.*, **68**, 1406 (1979).
(5) R. J. Scheuplein and L. Ross, *J. Soc. Cosmet. Chem.*, **21**, 853 (1970).
(6) R. J. Scheuplein and I. H. Blank, *Physiol. Rev.*, **51**, 702 (1971).
(7) T. Higuchi, *J. Soc. Cosmet. Chem.*, **11**, 85 (1960).
(8) I. H. Blank, *J. Invest. Dermatol.*, **18**, 433 (1952).
(9) W. T. Humphries and R. H. Wildnauer, *ibid.*, **58**, 9 (1972).
(10) J. Crank, "The Mathematics of Diffusion," 1st ed., Oxford University Press, London, 1967, p. 276.
(11) Idem., p. 248.
(12) H. Fujita, *Fortschr. Hochpolym.-Forsch.*, **3**, 1 (1961).
(13) C. E. Rogers, in "Physics and Chemistry of the Organic Solid State," Vol. 2, D. Fox, Ed., Interscience, New York, N.Y., 1965.
(14) G. S. Park, in "Diffusion in Polymers," J. Crank and G. S. Park, Eds., Academic, New York, N.Y., 1968.
(15) J. Crank, "The Mathematics of Diffusion," 2nd ed., Oxford University Press, London, 1975, p. 254.
(16) S. Prager and F. A. Long, *J. Am. Chem. Soc.*, **73**, 4272 (1952).
(17) American Society for Testing Materials, ASTM Designation: E104-51 (1951).
(18) L. B. Rockland, *Anal. Chem.*, **32**, 1375 (1960).
(19) J. Reilly and W. N. Rae, "Physico-Chemical Methods," Vol. 1, van Nostrand, New York, N.Y., 1953.
(20) K. H. Yang, Ph.D. Thesis, University of Iowa, Iowa City, Iowa, 1975, p. 184.
(21) A. C. Newns, *J. Chem. Soc. Faraday Trans. 1*, **69**, 444 (1973).
(22) I. C. Watt, *Text. Res. J.*, **30**, 443 (1960).
(23) F. A. Long and D. Richman, *J. Am. Chem. Soc.*, **82**, 513 (1960).
(24) A. Kishimoto and T. Kitahara, *J. Polym. Sci., Part A-1*, **5**, 2147 (1967).
(25) H. L. Frisch, *J. Chem. Phys.*, **41**, 3679 (1964).
(26) J. D. Ferry, "Viscoelastic Properties of Polymers," 3rd ed., Wiley, New York, N.Y., 1980, p. 487.
(27) H. L. Frisch, *J. Polym. Sci., Part A-2*, **7**, 879 (1969).
(28) H. Fujita and A. Kishimoto, *ibid.*, **28**, 547 (1958).
(29) A. Tanioka, E. Jojima, K. Miyasaka, and K. Ishikawa, *J. Polym. Sci. Polym. Phys. Ed.*, **11**, 1489 (1973).
(30) M. L. Williams, R. F. Landel, and J. D. Ferry, *J. Am. Chem. Soc.*, **77**, 3701 (1955).
(31) P. Nordon, B. H. Mackay, J. G. Downes, and G. B. McMahon, *Text. Res. J.*, **30**, 761 (1960).
(32) G. S. Park, *J. Polym. Sci.*, **11**, 97 (1953).

ACKNOWLEDGMENTS

Abstracted in part from a dissertation submitted by K. H. Yang to the Graduate College of the University of Iowa in partial fulfillment of the Doctor of Philosophy degree requirements.

Supported by Vick Divisions Research, Richardson-Merrell Inc., Mount Vernon, N.Y.

Pharmacokinetics of Probenecid Following Oral Doses to Human Volunteers

ARZU SELEN, G. L. AMIDON, and P. G. WELLING ˣ

Received November 23, 1981, from the *School of Pharmacy, University of Wisconsin, Madison, WI 53706.* Accepted for publication January 19, 1982.

Abstract □ The pharmacokinetics of probenecid were examined following single 0.5-, 1.0-, and 2.0-g oral doses to healthy male volunteers. Doses were administered following overnight fast, according to a randomized design. Plasma levels of probenecid were determined by high-pressure liquid chromatography (HPLC), using sulfamethazine as the internal standard. Mean peak probenecid levels of 35.3, 69.6, and 148.6 μg/ml were obtained at 3–4 hr following the 0.5-, 1.0-, and 2.0-g doses, respectively. Probenecid levels from the 0.5- and 1.0-g doses declined in apparent monoexponential fashion, with mean elimination half-lives of 4.2 and 4.9 hr. Interpretation of the 2.0-g data by a kinetic model incorporating first-order elimination resulted in a plasma drug half-life of 8.5 hr. When first-order elimination was replaced by a Michaelis–Menten-type function, the mean value of the resulting V_m/K_m ratios was 0.20, equivalent to a plasma drug half-life [$0.693/(V_m/K_m)$] of 3.8 hr. Plasma probenecid curves from all three dosages were successfully fitted to the saturable elimination model using nonlinear regression and numerical integration routines. The results suggest that probenecid elimination may be saturable at therapeutic dose levels.

Keyphrases □ Probenecid—pharmacokinetics following oral doses to humans, high-pressure liquid chromatography, elimination □ Pharmacokinetics—probenecid following oral doses to humans, high-pressure liquid chromatography, elimination □ High-pressure liquid chromatography—probenecid following oral doses to humans, pharmacokinetics

Probenecid is used for the treatment of gout and gouty arthritis and also as an adjuvant in therapy to prolong the plasma levels of other compounds, particularly the β-lactam antibiotics (1).

Although it has been used clinically for several years, the pharmacokinetics of probenecid are not well documented. It is efficiently absorbed after oral doses (2–4) with peak plasma concentrations occurring at 1–5 hr. Probenecid is 83–95% bound to plasma proteins at concentrations of 20–176 μg/ml (3). It is cleared from the body predominantly by metabolism, which occurs mainly by side-chain oxidation and glucuronide conjugation (3, 5). Only 5–11% of orally dosed probenecid is excreted in unchanged form in urine (6, 7).

The rate at which probenecid is cleared from plasma was shown to be dose-dependent in dogs (8) and humans (3). In the latter study, the plasma half-life of probenecid increased from 3–8 hr following a 0.5-g iv dose, to 6–12 hr following a 2.0-g iv dose in three subjects.

Since probenecid is extensively metabolized, dose-dependent elimination may be due to saturation of one or more metabolic pathways. However, a subsequent study demonstrated an unchanged pattern of urinary metabolites from oral doses of 0.5, 1.0, and 2.0 g of probenecid (6).

In view of the uncertainty regarding the nature and possible dose-dependency of probenecid pharmacokinetics, this study was undertaken to examine plasma levels of probenecid following 0.5-, 1.0-, and 2.0-g oral doses to healthy male volunteers.

0022-3549/82/1100-1238$01.00/0

(2) D. E. Wurster and S. F. Kramer, *J. Pharm. Sci.*, **50**, 288 (1961).
(3) D. E. Wurster and R. Munies, *ibid.*, **54**, 1281 (1965).
(4) D. E. Wurster, J. A. Ostrenga, and L. E. Matheson, Jr., *ibid.*, **68**, 1406 (1979).
(5) R. J. Scheuplein and L. Ross, *J. Soc. Cosmet. Chem.*, **21**, 853 (1970).
(6) R. J. Scheuplein and I. H. Blank, *Physiol. Rev.*, **51**, 702 (1971).
(7) T. Higuchi, *J. Soc. Cosmet. Chem.*, **11**, 85 (1960).
(8) I. H. Blank, *J. Invest. Dermatol.*, **18**, 433 (1952).
(9) W. T. Humphries and R. H. Wildnauer, *ibid.*, **58**, 9 (1972).
(10) J. Crank, "The Mathematics of Diffusion," 1st ed., Oxford University Press, London, 1967, p. 276.
(11) Idem., p. 248.
(12) H. Fujita, *Fortschr. Hochpolym.-Forsch.*, **3**, 1 (1961).
(13) C. E. Rogers, in "Physics and Chemistry of the Organic Solid State," Vol. 2, D. Fox, Ed., Interscience, New York, N.Y., 1965.
(14) G. S. Park, in "Diffusion in Polymers," J. Crank and G. S. Park, Eds., Academic, New York, N.Y., 1968.
(15) J. Crank, "The Mathematics of Diffusion," 2nd ed., Oxford University Press, London, 1975, p. 254.
(16) S. Prager and F. A. Long, *J. Am. Chem. Soc.*, **73**, 4272 (1952).
(17) American Society for Testing Materials, ASTM Designation: E104-51 (1951).
(18) L. B. Rockland, *Anal. Chem.*, **32**, 1375 (1960).
(19) J. Reilly and W. N. Rae, "Physico-Chemical Methods," Vol. 1, van Nostrand, New York, N.Y., 1953.
(20) K. H. Yang, Ph.D. Thesis, University of Iowa, Iowa City, Iowa, 1975, p. 184.
(21) A. C. Newns, *J. Chem. Soc. Faraday Trans. 1*, **69**, 444 (1973).
(22) I. C. Watt, *Text. Res. J.*, **30**, 443 (1960).
(23) F. A. Long and D. Richman, *J. Am. Chem. Soc.*, **82**, 513 (1960).
(24) A. Kishimoto and T. Kitahara, *J. Polym. Sci., Part A-1*, **5**, 2147 (1967).
(25) H. L. Frisch, *J. Chem. Phys.*, **41**, 3679 (1964).
(26) J. D. Ferry, "Viscoelastic Properties of Polymers," 3rd ed., Wiley, New York, N.Y., 1980, p. 487.
(27) H. L. Frisch, *J. Polym. Sci., Part A-2*, **7**, 879 (1969).
(28) H. Fujita and A. Kishimoto, *ibid.*, **28**, 547 (1958).
(29) A. Tanioka, E. Jojima, K. Miyasaka, and K. Ishikawa, *J. Polym. Sci. Polym. Phys. Ed.*, **11**, 1489 (1973).
(30) M. L. Williams, R. F. Landel, and J. D. Ferry, *J. Am. Chem. Soc.*, **77**, 3701 (1955).
(31) P. Nordon, B. H. Mackay, J. G. Downes, and G. B. McMahon, *Text. Res. J.*, **30**, 761 (1960).
(32) G. S. Park, *J. Polym. Sci.*, **11**, 97 (1953).

ACKNOWLEDGMENTS

Abstracted in part from a dissertation submitted by K. H. Yang to the Graduate College of the University of Iowa in partial fulfillment of the Doctor of Philosophy degree requirements.

Supported by Vick Divisions Research, Richardson-Merrell Inc., Mount Vernon, N.Y.

Pharmacokinetics of Probenecid Following Oral Doses to Human Volunteers

ARZU SELEN, G. L. AMIDON, and P. G. WELLING ˣ

Received November 23, 1981, from the *School of Pharmacy, University of Wisconsin, Madison, WI 53706.* Accepted for publication January 19, 1982.

Abstract □ The pharmacokinetics of probenecid were examined following single 0.5-, 1.0-, and 2.0-g oral doses to healthy male volunteers. Doses were administered following overnight fast, according to a randomized design. Plasma levels of probenecid were determined by high-pressure liquid chromatography (HPLC), using sulfamethazine as the internal standard. Mean peak probenecid levels of 35.3, 69.6, and 148.6 μg/ml were obtained at 3–4 hr following the 0.5-, 1.0-, and 2.0-g doses, respectively. Probenecid levels from the 0.5- and 1.0-g doses declined in apparent monoexponential fashion, with mean elimination half-lives of 4.2 and 4.9 hr. Interpretation of the 2.0-g data by a kinetic model incorporating first-order elimination resulted in a plasma drug half-life of 8.5 hr. When first-order elimination was replaced by a Michaelis–Menten-type function, the mean value of the resulting V_m/K_m ratios was 0.20, equivalent to a plasma drug half-life [$0.693/(V_m/K_m)$] of 3.8 hr. Plasma probenecid curves from all three dosages were successfully fitted to the saturable elimination model using nonlinear regression and numerical integration routines. The results suggest that probenecid elimination may be saturable at therapeutic dose levels.

Keyphrases □ Probenecid—pharmacokinetics following oral doses to humans, high-pressure liquid chromatography, elimination □ Pharmacokinetics—probenecid following oral doses to humans, high-pressure liquid chromatography, elimination □ High-pressure liquid chromatography—probenecid following oral doses to humans, pharmacokinetics

Probenecid is used for the treatment of gout and gouty arthritis and also as an adjuvant in therapy to prolong the plasma levels of other compounds, particularly the β-lactam antibiotics (1).

Although it has been used clinically for several years, the pharmacokinetics of probenecid are not well documented. It is efficiently absorbed after oral doses (2–4) with peak plasma concentrations occurring at 1–5 hr. Probenecid is 83–95% bound to plasma proteins at concentrations of 20–176 μg/ml (3). It is cleared from the body predominantly by metabolism, which occurs mainly by side-chain oxidation and glucuronide conjugation (3, 5). Only 5–11% of orally dosed probenecid is excreted in unchanged form in urine (6, 7).

The rate at which probenecid is cleared from plasma was shown to be dose-dependent in dogs (8) and humans (3). In the latter study, the plasma half-life of probenecid increased from 3–8 hr following a 0.5-g iv dose, to 6–12 hr following a 2.0-g iv dose in three subjects.

Since probenecid is extensively metabolized, dose-dependent elimination may be due to saturation of one or more metabolic pathways. However, a subsequent study demonstrated an unchanged pattern of urinary metabolites from oral doses of 0.5, 1.0, and 2.0 g of probenecid (6).

In view of the uncertainty regarding the nature and possible dose-dependency of probenecid pharmacokinetics, this study was undertaken to examine plasma levels of probenecid following 0.5-, 1.0-, and 2.0-g oral doses to healthy male volunteers.

0022-3549/82/1100-1238$01.00/0

Table I—Mean Plasma Probenecid Concentrations Following Single Oral Doses of 0.5, 1.0, or 2.0 g of Probenecid

Dose	Concentration of Probenecid, μg/ml												
	0.5 hr	1 hr	1.5 hr	2 hr	2.5 hr	3 hr	4 hr	6 hr	12 hr	24 hr	30 hr	36 hr	48 hr
0.5 g													
Mean	3.4	13.8	22.2	25.6	27.7	32.9	31.7	23.1	9.1	1.7	—[a]	—	—
SD[b]	2.1	8.2	14.9	19.3	17.2	8.5	4.5	4.0	1.7	0.6	—	—	—
1.0 g													
Mean	1.8	15.5	31.2	40.6	48.6	51.6	65.7	56.3	32.2	5.7	2.6	—	—
SD	1.8	19.7	30.3	41.9	40.3	34.6	28.0	12.3	7.5	3.0	2.0	—	—
2.0 g													
Mean	11.3	39.4	61.7	85.2	124.2	103.5	120.1	122.4	79.7	32.6	18.9	7.5	1.1
SD	11.6	28.2	33.2	45.1	77.8	60.1	31.7	21.6	12.6	9.9	6.7	3.6	1.1

[a] Below the limit of detection. [b] $n = 5$.

EXPERIMENTAL

Protocol—Five healthy male volunteers (20–39 years, 53–86 kg), whose weight–height relationships were within ±10% of normal (9), participated in the study after giving informed consent. Subjects were instructed to take no other medication for 1 week before the study and during the study. Subjects received single doses of 0.5, 1.0, and 2.0 g of probenecid[1] on three separate occasions, at least 1 week apart, according to a randomized design. Doses were administered with 250 ml of water at 8 am following an overnight fast. The tablets were swallowed whole. Food and water were withheld until 4 hr postdose, then normal eating and drinking were resumed.

Blood samples (~10 ml) were taken from a forearm vein into heparinized evacuated tubes[2] immediately before and then serially to 48 hr postdose. Plasma was separated by centrifugation and stored at −20° until assayed. No deterioration of samples was observed during storage.

Assay—Probenecid concentrations in plasma were determined by a modification of a previously described high-pressure liquid chromatographic (HPLC) procedure (10). Plasma (1 ml), pH 4 phosphate buffer (1 ml), sodium chloride (1 g), 0.1–0.3 ml of methanol containing 25–75 μg/ml sulfamethazine as internal standard, and ether (8 ml) were combined in a 15-ml centrifuge tube, vortex mixed for 15 sec, and shaken for 30 min on a horizontal shaker. After centrifuging at 3000×*g* for 10 min, 5 ml of the ether layer was transferred to a clean tube, and evaporated to dryness in a water bath at 40° under nitrogen. The residue was reconstituted in 1.0 ml of chromatographic mobile phase by vortex mixing for 30 sec, and 20 μl of this was injected onto the column.

The chromatographic system consisted of a solvent pump[3], a fixed-volume (20 μl) sample injection valve[4], a 10-μm particle size reversed-phase octadecyl column (4.6 mm × 250 mm)[5], and a fixed-wavelength (254 nm) UV detector[6]. All chromatograms were recorded at a chart speed of 10 cm/hr.

The mobile phase was 27.5% acetonitrile in 0.01 *M* phosphate buffer, at pH 6, and the flow rate was 1 ml/min. Under these conditions, the retention times of probenecid and sulfamethazine were 9 and 6 min, respectively. There was no interference from endogenous substances. Concentrations of probenecid were determined by peak height ratios. Standard curves using each individual's predose plasma were run together with each batch of postdose plasma samples.

The extraction efficiency of probenecid in this system was 94.3 ± 5.8% *SD* ($n = 20$). The chromatographic assay was linearly responsive to probenecid concentrations between 1 and 200 μg/ml, and assay reproducibility was within 10% of the mean in this concentration range. Probenecid metabolites, all of which are more polar than the parent compound, do not interfere with the assay for probenecid under these assay conditions (10).

Reagents—Human plasma for assay development was purchased[7]. Probenecid[8] and sulfamethazine[9] were of reference standard quality. All other chemicals and solvents were analytical reagent grade and were used as received.

Data Analysis—Individual probenecid profiles in plasma resulting from the three doses were examined using two different pharmacokinetic models. The first of these was a one-compartment kinetic model with first-order appearance of drug into and loss of drug from plasma and an absorption lag time. With this model, plasma concentrations of probenecid were fitted to Eq. 1 in which F is the fraction of the oral dose (D) which is absorbed into the systemic circulation, V_d is the apparent homogenous distribution volume for probenecid, k_a and k_{el} are first-order rate constants for appearance and loss of drug, respectively, and t_0 is the absorption lag time (11):

$$C = \frac{FD}{V_d}\left(\frac{k_a}{k_a - k_{el}}\right)\left(e^{-k_{el}(t-t_0)} - e^{-k_a(t-t_0)}\right) \qquad \text{(Eq. 1)}$$

Initial estimates of parameter values were obtained by standard graphical procedures. Final estimates were obtained by nonlinear regression analysis using the program NREG (12) on a digital computer[10].

The second model, which was investigated primarily as a result of the plasma data resulting from the 2.0-g dose of probenecid, is different from the first in that the elimination phase is described in terms of a saturable Michaelis–Menten-type term. The rate equation for time-dependent change in probenecid plasma levels with this model is:

$$\frac{dc}{dt} = \frac{FDk_a}{V} e^{-k_a(t-t_0)} - \frac{V_m C}{K_m + C} \qquad \text{(Eq. 2)}$$

where V_m and K_m are Michaelis–Menten-type functions describing the maximum rate of probenecid elimination and the drug concentration when the rate of elimination is one-half the maximum value, respectively, and all other parameters are as described for Eq. 1. This rate equation cannot be solved analytically, and nonlinear regression analysis was done by coupling the program NREG with the numerical integration program DGEAR (13). Initial estimates of the values of V_m and K_m were obtained graphically by a previous method (14). Final computer estimates of values for k_a and FD/V_d from Eq. 1 were used as initial estimates for these parameters when fitting data to Eq. 2.

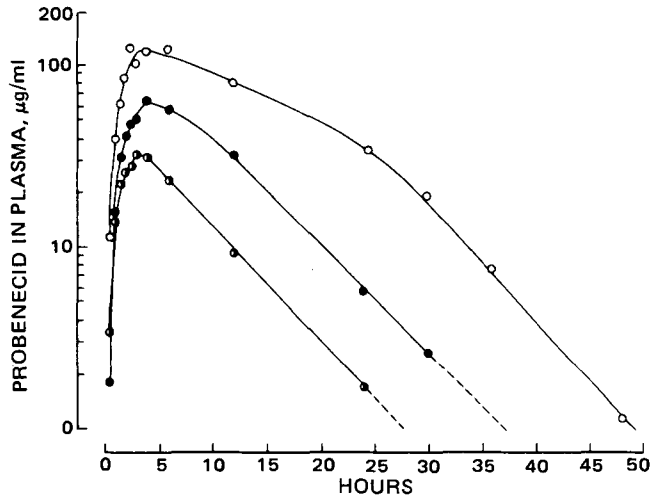

Figure 1—*Mean plasma levels of probenecid in five subjects following single oral doses. Key: 0.5-g (◑); 1.0-g (●); and 2.0-g (○) doses of probenecid.*

[1] Probenecid 500-mg tablets USP, lot No. E002Erl, Mylan Pharmaceuticals Inc., Morgantown, W.Va.
[2] Vacutainer.
[3] Model 110, Altex Scientific Inc., Berkeley, Calif.
[4] Model 210, Altex Scientific Inc., Berkeley, Calif.
[5] Lichrosorb C-18, Altex Scientific, Berkeley, Calif.
[6] Model 153, Altex Scientific, Berkeley, Calif.
[7] American Red Cross, Madison, Wis.
[8] Merck, Sharp and Dohme, West Point, Pa.
[9] Sigma Chemical Co., Saint Louis, Mo.
[10] Univac model 1100.

Table II—Pharmacokinetic Parameter Values (±1 *SD*) for Probenecid [a]

Parameter	Value 0.5-g Dose	1.0-g Dose	2.0-g Dose	Statistic[b]
C_{max}[c] (μg/ml)	35.3 ±8.5	69.6 ±26.9	148.6 ±47.4	C > B > A[d]
t_{max}[e] (hr)	3.1 ±0.9	3.9 ±1.3	3.5 ±1.5	NSD[f]
$AUC^{0\rightarrow 48hr}$[g] (μg hr/ml)	292 ±66	772 ±237	2109 ±429	C > B > A
$AUC^{0\rightarrow 48hr}/D$[h] (hr/ml × 10^{-6})	584 ±131	772 ±237	1054 ±214	C > A, B
k_a (hr^{-1})	0.98 ±0.49	0.56 ±0.41	0.66 ±0.29	NSD
t_0 (hr)	0.80 ±0.71	1.1 ±0.6	0.56 ±0.32	NSD
k_{el} (hr^{-1})	0.18 ±0.05	0.15 ±0.03	0.08 ±0.004	A, B > C
$t_{1/2(el)}$[i] (hr)	4.2 ±1.1	4.9 ±0.8	8.5 ±0.4	C > A, B
FD/V[j] (μg/ml)	50 ±10	109 ±22	176 ±30	C > B > A
F/V^k (10^{-6}/ml)	100 ±21	109 ±22	80 ±10	B > C
r^{2l}	0.98 ±0.02	0.98 ±0.02	0.95 ±0.07	NSD

[a] The model-dependent parameter values were obtained by fitting plasma data to Eq. 1. [b] Differences between doses are significant if $p < 0.05$. [c] Observed maximum concentration of probenecid in plasma. [d] A = 0.5-g dose, B = 1.0-g dose, and C = 2.0-g dose. [e] Time of C_{max}. [f] No significant differences. [g] Area under plasma–probenecid curve (0–48 hr), calculated by trapezoidal rule. [h] Area normalized for administered dose. [i] Calculated from $t_{1/2(el)} = \ln 2/k_{el}$. [j] Fraction of the dose absorbed, expressed as a concentration in its volume of distribution. [k] FD/V_d normalized for administered dose. [l] Coefficient of determination, $r^2 = (\Sigma obs^2 - \Sigma dev^2)/\Sigma obs^2$.

Statistical analysis of plasma levels, and also pharmacokinetic parameter values, resulting from the three doses were examined by ANOVA for crossover design. Significant effects between specific doses were examined by Tukey's test (15). Differences between pharmacokinetic parameter values, and also coefficients of determination, obtained by nonlinear regression analysis of plasma data using the first-order and saturable kinetic models were examined by paired *t*-test.

RESULTS

The mean plasma levels of probenecid obtained from the three doses are given in Table I, and the data are summarized graphically in Fig. 1. Some model-independent pharmacokinetic parameter values and also pharmacokinetic constants obtained after fitting individual data sets to Eq. 1 are given in Table II.

Following the 0.5-g dose, plasma probenecid levels reached a mean peak value of 35.3 μg/ml at 3 hr and then declined in apparent monoexponential fashion. Probenecid could be detected in all subjects up to 24 hr postdose. Following the 1.0-g dose, the mean peak probenecid level increased twofold to 69.6 μg/ml and occurred at 4 hr postdose. Drug levels again declined in apparent monoexponential fashion and could be detected in all subjects up to 30 hr postdose.

Individual plasma probenecid profiles following the 2.0-g dose were different from those resulting from the lower doses. The mean peak level was again doubled, compared with that from the 1.0-g dose, to 148.6 μg/ml and occurred at 3.5 hr. After peak levels had been reached from this dose, plasma levels of probenecid declined initially at a slower rate compared with the lower doses, and the rate of decline in the logarithm of plasma levels *versus* time during this period was curvilinear. It was not until 24–30 hr after dosing, when probenecid plasma levels had fallen to similar values to those obtained from the 0.5- and 1.0-g doses, that the rate of loss of probenecid from plasma became log-linear, with a similar rate to that obtained from the lower doses. Following the 2.0-g dose, probenecid could be detected in the plasma of all subjects at 36 hr, and in three of the five subjects at 48 hr, postdose.

Table III—Pharmacokinetic Parameter Values (±1 *SD*) Obtained by Analyzing Plasma Probenecid Levels from the 2.0-g Dose According to First-order or Saturable Kinetic Models

Parameter	Value First-Order Model[a]	Saturable Model[b]	Statistic[c]
k_a (hr^{-1})	0.66 ± 0.29	0.63 ± 0.26	NS[d]
t_0 (hr)	0.56 ± 0.32	0.40 ± 0.52	NS
k_{el} (hr^{-1})	0.082 ± 0.504	—[e]	
$t_{1/2(el)}$ (hr)	8.5 ± 0.4[f]	3.8 ± 1.1[g]	S[h]
V_m (μg/ml·hr)	—	8.6 ± 2.1	
K_m (μg/ml)	—	46.6 ± 26.5	
V_m/K_m (hr^{-1})	—	0.20 ± 0.06	
FD/V_d	176 ± 30	160 ± 19	NS
r^2	0.95 ± 0.07	0.96 ± 0.04	NS

[a] Data was fitted to Eq. 1. [b] Data was fitted to Eq. 2 with numerical integration. [c] Data compared using a paired *t* test. [d] Not significant ($p > 0.05$). [e] Does not apply. [f] Calculated from $t_{1/2(el)} = \ln 2/k_{el}$. [g] Calculated from $t_{1/2(el)} = \ln 2/(V_m/K_m)$. [h] Significant ($p < 0.05$).

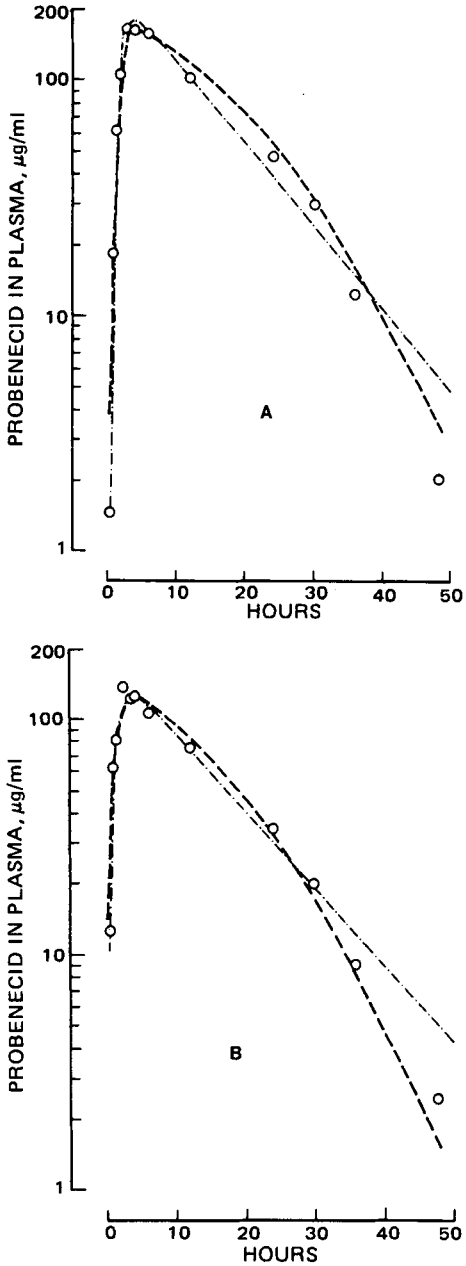

Figure 2—*Plasma levels (○) of probenecid in two subjects and nonlinear regression curves obtained from Eq. 1 (·--) and Eq. 2 (---). Key: (A) subject 1; (B) subject 2.*

Although the value of C_{max} was dose-proportional between the three dosages of probenecid, the 0–48-hr area under the plasma curve, $AUC^{0\rightarrow 48\ hr}$, increased 2.6-fold between the 0.5- and 1.0-g doses, and 2.9-fold between the 1.0- and 2.0-g doses. When the areas were normalized for the administered dose, there appeared to be a progressive increase in the values with increasing dose, and the value for the 2.0-g dose was significantly larger than those from the other two doses.

While the increases in area values were greater than expected with increasing dose size, the opposite effect was observed in the values of FD/V_d, which is a rate-independent measure of drug availability to the systemic circulation. The value of this parameter increased 2.2-fold between the 0.5- and 1.0-g doses, but only 1.5-fold between the 1.0- and 2.0-g doses. Normalizing this value for the administered dose resulted in a somewhat lower F/V_d value for the 2.0-g dose compared with the other two doses, but only the difference between the 2.0- and 1.0-g doses reached the 95% significance level.

No significant differences were observed in the lag times or in the absorption rate constants between doses. The elimination rate constant was

similar for the 0.5- and 1.0-g doses, yielding mean plasma half-lives of 4.2 and 4.9 hr, respectively. Following the 2.0-g dose, however, the elimination half-life of probenecid was significantly increased to a mean value of 8.5 hr. The coefficient of determination for nonlinear regression analysis of data using Eq. 1 was slightly lower following the 2.0-g dose compared to the other two doses, but differences in this value between treatments were not significant.

The discrepancies observed in the $AUC^{0\rightarrow 48}/D$ values between the 2.0-g dose and the 0.5- and 1.0-g doses, and the similar dose-dependency of the value of k_{el} and $t_{1/2(el)}$, prompted the analysis of the 2.0-g data in terms of Eq. 2. The results obtained using this equation are compared with those using Eq. 1 in Table III. No significant differences were observed in the values of k_a, t_0, or FD/V_d calculated by the two methods. The coefficient of determination r^2 was also similar, indicating that neither equation described the overall data significantly better than the other. However the ratio V_m/K_m, which is analogous to k_{el} at low drug concentrations, of 0.20 yielded a drug half-life in plasma of 3.8 hr. This value is less than one-half the value calculated using Eq.1, and is not statistically different from the values obtained from the two lower doses.

Although the saturable elimination model did not provide a better fit to the 2.0-g data compared to the first-order elimination model, it did provide a superior fit to the elimination phase of each drug profile. This is clearly demonstrated for two subjects in Fig. 2. The mean coefficient of determination between observed and predicted probenecid levels for all subjects during the 12–48-hr sampling period was 0.973 when Eq. 2 was used for nonlinear regression analysis. This value was significantly higher than the value of 0.953 obtained when the data were fitted by means of Eq. 1.

To determine whether Eq. 2 also described the probenecid data resulting from the 0.5- and 1.0-g doses, nonlinear regressions were carried out on these data using k_a, t_0, and FD/V_d values obtained from the analysis using Eq. 1, and V_m and K_m values obtained from the 2.0-g dose data for each individual. The mean coefficients obtained by this method were 0.96 and 0.97 for the 0.5- and 1.0-g doses, respectively. These values were not significantly different from those obtained when these data were fitted to Eq. 1.

DISCUSSION

The data generated in this study provide evidence that the elimination of probenecid from plasma is saturable at therapeutic dose levels. Following the 0.5- and 1.0-g oral doses of probenecid, plasma curves could be described adequately by a kinetic model incorporating first-order absorption and elimination. Although a satisfactory description of probenecid plasma levels following the 2.0-g dose was obtained also with this model, the probenecid elimination half-life obtained was twice that following the lower doses. When saturable elimination of probenecid from the 2.0-g dose was assumed, however, the terminal elimination half-life of probenecid was similar for all three dosages. Also a more satisfactory description of the elimination phase of probenecid plasma levels following the 2.0-g dose was obtained by incorporating a saturable component in the kinetic model.

These observations are consistent with previous suggestions that the elimination of probenecid is dose-dependent (3, 8), the drug half-life increasing with increasing dose size. In this respect probenecid behaves similarly to salicylate (16, 17), phenytoin (18), theophylline (19, 20), and alcohol (21); all of which exhibit saturable elimination kinetics at drug levels below those considered to be toxic.

An alternative explanation for the prolonged probenecid profiles in plasma following the 2.0-g dose, and to a smaller extent following the 1.0-g dose (Fig. 1), involves drug absorption rather than elimination. This argument, which was used previously in this context (6), is based on the low aqueous solubility of probenecid, and proposes that slow dissolution of the drug in the GI tract from larger doses may give rise to prolonged absorption. While the data obtained in the present study do not preclude this possibility, the similar absorption rate constants, absorption lag times, and times that maximum drug concentrations occur in plasma from the three dosages make it unlikely. Also, dose-dependent elimination of probenecid was previously demonstrated in humans following intravenous doses (3). Although the value of F/V_d from the 2.0-g dose was statistically smaller than that from the 1.0-g dose (Table II), it cannot be determined from the present data whether this is due to a change in drug absorption or in drug distribution at the higher dose.

The plasma levels at which Michaelis–Menten-type elimination became evident in this study, 40–50 μg/ml, are in excellent agreement with the observation (3) that probenecid levels measured in the 50–220-μg/ml range declined at slower rates than levels in the 10–55-μg/ml range. The higher levels in that study were obtained following a 2.0-g iv dose, while the lower levels were obtained following a 0.5-g dose. Unfortunately, the plasma sampling in that study was not extended for a sufficient time following the 2.0-g dose to monitor plasma levels in the lower concentration range.

The mechanism causing slower elimination of probenecid at high circulating levels is uncertain. Altered renal clearance is unlikely. Probenecid is actively secreted into the kidney tubules, but it is efficiently reabsorbed into the peritubular capillaries, and only a small fraction of the drug is cleared by this route. Probenecid is extensively metabolized, the principal metabolites involving side-chain oxidation (~70%) and glucuronide conjugation (~20%) (1). The dose-dependency of the amounts of these metabolites formed in two individuals has been investigated (6), and relative urinary recoveries of unchanged drug, probenecid acyl glucuronide, and the mono-*N*-propyl, carboxylic acid, and secondary alcohol metabolites from 0.5-, 1.0-, and 2.0-g doses were obtained. The investigators concluded that no individual metabolic pathway was saturated at high probenecid levels as this would have altered the relative amounts of the different metabolites that were formed. However, some of the side-chain oxidation metabolites of probenecid may be formed through a single intermediate, *i.e.*, an epoxide. Saturation of this common step may lead to a reduced rate of metabolism without affecting the ratio of formation of some of the major metabolites (22). One also cannot exclude product inhibition by one or more of the metabolites formed or saturation of a transport step governing access of probenecid to the site(s) of metabolism, causing clearance of drug from plasma to be delayed. More studies are needed to identify the rate-limiting process(es), and also the possible influence of other drugs on the saturable elimination of probenecid.

While attempting to describe plasma probenecid data in terms of Eq. 2, the authors are aware of the problems inherent in applying this type of equation to drug–concentration profiles, and also to the uncertainty regarding the numerical values assigned to the parameters V_m and K_m (23). However, notwithstanding these limitations, use of the saturable model is felt to be justified in terms of the similarity of the pharmacokinetic parameters which were common to the saturable and first-order models from the different doses, the realistic values of V_m and K_m obtained, and also the close agreement between the drug elimination half-lives obtained from the V_m/K_m ratios and from k_{el}.

The clinical significance of saturable probenecid elimination is uncertain. In view of the profound effect that saturable elimination may have on the degree of drug accumulation with repeated doses (24), it is likely that probenecid levels may increase with repeated dosing to an extent greater than might be predicted if first-order elimination is assumed. The clinical implication of saturable probenecid elimination may be further complicated, as the uricosuric potency of the oxidized metabolites has been shown to be approximately the same as the parent drug in experimental animals (25, 26).

REFERENCES

(1) R. F. Cunningham, Z. H. Israili, and P. G. Dayton, *Clin. Pharmacokinet.*, **6,** 135 (1981).

(2) W. P. Boger, W. P. Forrest, and M. E. Gallagher, *J. Lab. Clin. Med.*, **36,** 276 (1951).

(3) P. G. Dayton, T. F. Yü, W. Chen, L. Berger, L. A. West, and A. B. Gutman, *J. Pharmacol. Exp. Ther.*, **140,** 278 (1963).

(4) T. B. Tjandramaga, S. A. Cucinell, Z. H. Israili, J. M. Perel, P. G. Dayton, T. F. Yü, and A. B. Gutman, *Pharmacology*, **8,** 259 (1972).

(5) A. M. Guarino and L. S. Schanker, *J. Pharmacol. Exp. Ther.*, **164,** 387 (1968).

(6) S. Melethil and W. D. Conway, *J. Pharm. Sci.*, **65,** 861 (1976).

(7) J. M. Perel, R. F. Cunningham, H. M. Fales, and P. G. Dayton, *Life Sci.*, **9,** 1337 (1970).

(8) P. G. Dayton, S. A. Cucinell, M. Weiss, and J. M. Perel, *J. Pharmacol. Exp. Ther.*, **158,** 305 (1967).

(9) "Scientific Tables" Documenta, 7th ed., K. Kiem and C. Lentner, Eds., Geigy Pharmaceuticals, 1973, p. 712.

(10) R. K. Harle and T. Cowen, *Analyst*, **103,** 492 (1978).

(11) J. G. Wagner, "Fundamentals of Clinical Pharmacokinetics," Drug Intelligence Publications, Hamilton, Ill., 1975, p. 74.

(12) "Nonlinear Regression Subroutines," Madison Academic Computer Center, University of Wisconsin.

(13) "Reference Manual IMSL LIB-0008," International Mathematical and Statistical Libraries, Inc., Madison Academic Computer Center, Univ. of Wisconsin, June 1980.

(14) J. G. Wagner, "Fundamentals of Clinical Pharmacokinetics,"

Drug Intelligence Publications, Hamilton, Ill., 1975, p. 260.
(15) J. Neter and W. Wasserman, "Applied Linear Statistical Models," Richard D. Irwin, Inc., Homewood, Ill., 1974, p. 474.
(16) G. Levy, *J. Pharm. Sci.*, **54**, 959 (1965).
(17) G. Levy, T. Tsuchiya, and L. P. Amsel, *Clin. Pharmacol. Ther.*, **13**, 258 (1972).
(18) K. Arnold and N. Gerber, *ibid.*, **11**, 121 (1970).
(19) L. J. Lesko, *Clin. Pharmacokinet.*, **4**, 449 (1979).
(20) M. Weinberger and E. Gincansky, *J. Pediatr.*, **91**, 820 (1977).
(21) F. Lundquist and H. Wolthers, *Acta Pharmacol. Toxicol.*, **14**, 265 (1958).
(22) P. G. Dayton and J. M. Perel, *Ann. NY Acad. Sci.*, **179**, 339 (1971).
(23) D. D. M. Tong and C. M. Metzler, *Math. Biosci.*, **48**, 293 (1980).
(24) G. Levy and T. Tsuchiya, *N. Engl. J. Med.*, **287**, 430 (1972).
(25) P. G. Dayton, J. M. Perel, R. F. Cunningham, Z. H. Israili, and I. M. Weiner, *Drug. Metab. Dispos.* **1**, 742 (1973).
(26) Z. H. Israili *et al.*, *J. Med. Chem.* **15**, 709 (1972).

ACKNOWLEDGMENTS

Funds for this study were provided in part from grant GM20327, from the National Institutes of Health.

Purity Profiles of Pteroylglutamate Reference Substances by High-Performance Liquid Chromatography

L. V. FEYNS ˣ, K. D. THAKKER, V. D. REIF, and L. T. GRADY

Received October 5, 1981, from the *Drug Research and Testing Laboratory, United States Pharmacopeia, Rockville, MD 20852.* Accepted for publication January 21, 1982.

Abstract □ High-performance liquid chromatography (HPLC) in the reversed-phase mode was used for the purity analysis of three pteroylglutamic acid-type reference substances (folic acid, leucovorin calcium, and methotrexate). The influence of the pH of the mobile phase on the separation of an artificial mixture of six pteroylglutamic acid derivatives and three potential impurities was studied. Results of purity analysis of current lots of USP reference standards are reported. A better separation of methotrexate from its major impurities was achieved by using a standard buffer, rather than an ion-pairing mobile phase. A separation of methotrexate and its biologically inactive 7-isomer is reported.

Keyphrases □ Pteroylglutamate—purity profiles, reference substances, high-performance liquid chromatography, methotrexate □ High-performance liquid chromatography—pteroylglutamate, purity profiles, reference substances, methotrexate □ Methotrexate—pteroylglutamate, purity profiles, reference substances, high-performance liquid chromatography

Three USP drug substances, available as USP reference standards, belong to the class of pteroylglutamic acid derivatives: folic acid (I), methotrexate (II), and leucovorin calcium (III) (authentic substance as calcium formyltetrahydrofolate). This class of compounds exhibits high hydrolytic and oxidative reactivity. High-performance liquid chromatography (HPLC) has proved to be the method of choice for purity analysis in this laboratory because of similarities of structure within this series. Additional purity profile data were gained from 5 to 8 collateral determinations, but are not reported here as these results are independent of chromatographic purity.

Almost all the HPLC techniques have been used for the separation and analysis of this class of compounds. Anion-exchange columns were used first in 1973 for the separation of folic acid from a mixture of water-soluble vitamins (1) and then for the separation of folic acid and its reduced and N^5- and N^{10}-substituted derivatives (2). Anion-exchange chromatography alone, or coupled with an amine column operated in the reversed-phase mode, has also been used for the analysis and quantitative determination of methotrexate (3).

An extensive study (4) resulted in the development of a reversed-phase HPLC assay and purity analysis method for folic acid. The assay was made the object of a collaborative study (5), and it has been adopted into the folic acid monograph in the USP (6).

For the reversed-phase chromatographic analysis of methotrexate, mixtures of methanol or acetonitrile with the following buffers have been suggested as mobile phases: pH 3.5, 0.005 *M* ammonium formate (7); pH 5, 0.005 *M* ammonium acetate (7); pH 6.7, 0.1 *M* KH_2PO_4 (8); pH 6.8, 2-amino-2-hydroxymethyl-1,3-propanediol (tris) (9); pH 7.2, 0.05 *M* KH_2PO_4[1]; pH 6, 0.1 *M* citric acid–0.2 *M* Na_2HPO_4[2]. The latter is used in the assay of methotrexate in USP XX–NF XV (10). Mobile phases consisting of pH 5 phosphate buffer–acetonitrile (9) and pH 4 citrate buffer–dioxane (11) were recommended for the analysis and assay of leucovorin calcium. The effect of pH on the retention behavior of pteroyloligo-glutamates in reversed-phase HPLC has also been reported (12).

A third technique, ion-pair chromatography, separated 21 UV-absorbing impurities in a clinical sample of methotrexate (13) and has also been utilized in the separation of folic acid and its dihydro- and tetrahydro derivatives (14).

The object of this investigation was to study the influence of the pH of the mobile phase on the chromatographic separation of some pteryolglutamic acid derivatives and to determine optimum conditions for the purity analysis of the USP reference standards by HPLC.

EXPERIMENTAL

Apparatus—An isocratic high-performance liquid chromatograph[3] with a 254-nm detector and a gradient chromatograph[4] equipped with a variable wavelength UV detector[5] were used. The instruments were

[1] United States Pharmacopeia, Drug Research and Testing Laboratory, unpublished research.
[2] Lederle Laboratories, private communication.
[3] Altex Model 110, Altex Scientific Inc., Berkeley, Calif.
[4] Model 3500B, SpectraPhysics, Santa Clara, Calif.
[5] Model 770 Spectrophotometric detector, SpectraPhysics, Santa Clara, Calif.

0022-3549/82/1100-1242$01.00/0

Drug Intelligence Publications, Hamilton, Ill., 1975, p. 260.
(15) J. Neter and W. Wasserman, "Applied Linear Statistical Models," Richard D. Irwin, Inc., Homewood, Ill., 1974, p. 474.
(16) G. Levy, *J. Pharm. Sci.*, **54**, 959 (1965).
(17) G. Levy, T. Tsuchiya, and L. P. Amsel, *Clin. Pharmacol. Ther.*, **13**, 258 (1972).
(18) K. Arnold and N. Gerber, *ibid.*, **11**, 121 (1970).
(19) L. J. Lesko, *Clin. Pharmacokinet.*, **4**, 449 (1979).
(20) M. Weinberger and E. Gincansky, *J. Pediatr.*, **91**, 820 (1977).
(21) F. Lundquist and H. Wolthers, *Acta Pharmacol. Toxicol.*, **14**, 265 (1958).
(22) P. G. Dayton and J. M. Perel, *Ann. NY Acad. Sci.*, **179**, 339 (1971).
(23) D. D. M. Tong and C. M. Metzler, *Math. Biosci.*, **48**, 293 (1980).
(24) G. Levy and T. Tsuchiya, *N. Engl. J. Med.*, **287**, 430 (1972).
(25) P. G. Dayton, J. M. Perel, R. F. Cunningham, Z. H. Israili, and I. M. Weiner, *Drug. Metab. Dispos.* **1**, 742 (1973).
(26) Z. H. Israili *et al.*, *J. Med. Chem.* **15**, 709 (1972).

ACKNOWLEDGMENTS

Funds for this study were provided in part from grant GM20327, from the National Institutes of Health.

Purity Profiles of Pteroylglutamate Reference Substances by High-Performance Liquid Chromatography

L. V. FEYNS ˣ, K. D. THAKKER, V. D. REIF, and L. T. GRADY

Received October 5, 1981, from the *Drug Research and Testing Laboratory, United States Pharmacopeia, Rockville, MD 20852.* Accepted for publication January 21, 1982.

Abstract □ High-performance liquid chromatography (HPLC) in the reversed-phase mode was used for the purity analysis of three pteroylglutamic acid-type reference substances (folic acid, leucovorin calcium, and methotrexate). The influence of the pH of the mobile phase on the separation of an artificial mixture of six pteroylglutamic acid derivatives and three potential impurities was studied. Results of purity analysis of current lots of USP reference standards are reported. A better separation of methotrexate from its major impurities was achieved by using a standard buffer, rather than an ion-pairing mobile phase. A separation of methotrexate and its biologically inactive 7-isomer is reported.

Keyphrases □ Pteroylglutamate—purity profiles, reference substances, high-performance liquid chromatography, methotrexate □ High-performance liquid chromatography—pteroylglutamate, purity profiles, reference substances, methotrexate □ Methotrexate—pteroylglutamate, purity profiles, reference substances, high-performance liquid chromatography

Three USP drug substances, available as USP reference standards, belong to the class of pteroylglutamic acid derivatives: folic acid (I), methotrexate (II), and leucovorin calcium (III) (authentic substance as calcium formyltetrahydrofolate). This class of compounds exhibits high hydrolytic and oxidative reactivity. High-performance liquid chromatography (HPLC) has proved to be the method of choice for purity analysis in this laboratory because of similarities of structure within this series. Additional purity profile data were gained from 5 to 8 collateral determinations, but are not reported here as these results are independent of chromatographic purity.

Almost all the HPLC techniques have been used for the separation and analysis of this class of compounds. Anion-exchange columns were used first in 1973 for the separation of folic acid from a mixture of water-soluble vitamins (1) and then for the separation of folic acid and its reduced and N^5- and N^{10}-substituted derivatives (2). Anion-exchange chromatography alone, or coupled with an amine column operated in the reversed-phase mode, has also been used for the analysis and quantitative determination of methotrexate (3).

An extensive study (4) resulted in the development of a reversed-phase HPLC assay and purity analysis method for folic acid. The assay was made the object of a collaborative study (5), and it has been adopted into the folic acid monograph in the USP (6).

For the reversed-phase chromatographic analysis of methotrexate, mixtures of methanol or acetonitrile with the following buffers have been suggested as mobile phases: pH 3.5, 0.005 *M* ammonium formate (7); pH 5, 0.005 *M* ammonium acetate (7); pH 6.7, 0.1 *M* KH_2PO_4 (8); pH 6.8, 2-amino-2-hydroxymethyl-1,3-propanediol (tris) (9); pH 7.2, 0.05 *M* KH_2PO_4[1]; pH 6, 0.1 *M* citric acid–0.2 *M* Na_2HPO_4[2]. The latter is used in the assay of methotrexate in USP XX–NF XV (10). Mobile phases consisting of pH 5 phosphate buffer–acetonitrile (9) and pH 4 citrate buffer–dioxane (11) were recommended for the analysis and assay of leucovorin calcium. The effect of pH on the retention behavior of pteroyloligo-glutamates in reversed-phase HPLC has also been reported (12).

A third technique, ion-pair chromatography, separated 21 UV-absorbing impurities in a clinical sample of methotrexate (13) and has also been utilized in the separation of folic acid and its dihydro- and tetrahydro derivatives (14).

The object of this investigation was to study the influence of the pH of the mobile phase on the chromatographic separation of some pteryolglutamic acid derivatives and to determine optimum conditions for the purity analysis of the USP reference standards by HPLC.

EXPERIMENTAL

Apparatus—An isocratic high-performance liquid chromatograph[3] with a 254-nm detector and a gradient chromatograph[4] equipped with a variable wavelength UV detector[5] were used. The instruments were

[1] United States Pharmacopeia, Drug Research and Testing Laboratory, unpublished research.
[2] Lederle Laboratories, private communication.
[3] Altex Model 110, Altex Scientific Inc., Berkeley, Calif.
[4] Model 3500B, SpectraPhysics, Santa Clara, Calif.
[5] Model 770 Spectrophotometric detector, SpectraPhysics, Santa Clara, Calif.

0022-3549/82/1100-1242$01.00/0

Table I—Chromatographic Separation of Some Pteroylglutamic Acid Derivatives and Potential Contaminants

Mobile Phase[a]	3.0–Methanol (100:18)		4.0–Methanol (100:14)		5.0–Methanol (100:14)		6.0–Methanol (100:13)		7.0–Methanol (100:15)		7.5–Methanol (100:13)	
Flow Rate, ml/min	2.0		2.2		2.0		1.8		2.0		1.8	
Compound	$t_{R,i}$, min	α_{II}[b]	$t_{R,i}$, min	α_{II}	$t_{R,i}$, min	α_{II}	$t_{R,i}$, min	α_{II}	$t_{r,i}$, min	α_{II}	$t_{R,i}$, min	α_{II}
IX	1.5	0.16	1.25	0.13	1.2	0.12	1.06	0.12	1.1	0.12	1.15	0.12
VIII	—	—	0.9	0.09	1.0	0.10	—	—	—	—	—	—
Leucovorin (III)	4.4	0.46	3.0	0.31	2.0	0.21	1.57	0.17	1.45	0.16	1.55	0.17
Folic acid (I)	7.9	0.82	6.0	0.63	3.45	0.36	2.1	0.23	1.8	0.20	1.8	0.19
Aminopterin (V)	5.9	0.61	5.1	0.53	4.0	0.41	3.45	0.38	3.1	0.34	3.45	0.37
Methopterin (VI)	12.2	1.27	9.55	1	5.85	0.61	3.65	0.40	3.25	0.36	3.05	0.33
7-Methotrexate (IV)	10.3	1.03	9.9	1.03	8.8	0.91	8.1	0.88	8.15	0.90	8.25	0.88
Methotrexate (II)	9.6	1	9.55	1	9.65	1	9.17	1	9.05	1	9.35	1
VII	15.7	1.64	25.2	2.64	26.8	2.78	19.0	2.07	14.35	1.59	13.35	1.43

[a] 0.05 *M* KH_2PO_4 brought to either pH 3.0 or 4.0 with 85% H_3PO_4 and to pH 5.0, 6.0, 7.0, 7.2, and 7.5 with 1 *N* NaOH (Buffers pH 3–7.5, respectively). [b] $t_{R,i}$ = individual retention time; $\alpha_{II} = t_{R,i}/t_{R,II}$.

fitted with a recorder[6] and an electronic integrator[7]. Stainless steel columns containing reversed-phase packing material[8] were operated at room temperature. The samples were introduced by means of a loop injector[9] with a fixed volume of 10 or 20 μl. A digital pH meter[10] was used to measure the pH value of the buffers.

Samples, Reagents, and Solvents—Three methotrexate samples (a candidate lot for USP reference standard referred to as Lot A and two old lots kept at room temperature, referred to as Lots B and C), USP folic acid reference standard Lot J, and USP leucovorin calcium reference standard Lot F were analyzed for chromatographic purity. The following

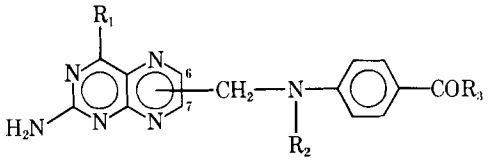

	Position side chain	R_1	R_2	R_3
I:	6	OH	H	L-Glu
II:	6	NH_2	CH_3	L-Glu
IV:	7	NH_2	CH_3	L-Glu
V:	6	NH_2	H	L-Glu
VI:	6	OH	CH_3	L-Glu
VII:	6	NH_2	CH_3	OH

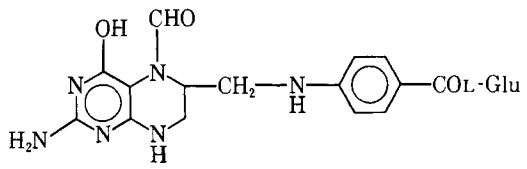

III

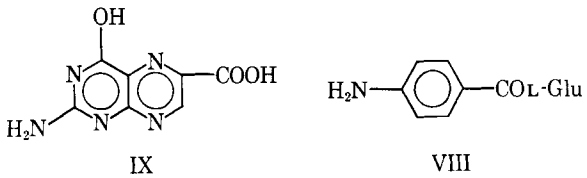

IX VIII

L-Glu = —NH—CH(COOH)—CH_2—CH_2—COOH (L-form)

[6] Linear model 261, Linear Instruments Corp., Irvine, Calif.
[7] System I Computing Integrator, SpectraPhysics, Santa Clara, Calif.
[8] 250 × 4.0-mm RP-18, Chromanetics, Baltimore, Md.; (b) 300 × 3.9-mm μ-Bondapak C-18, Waters Associates, Milford, Mass.; (c) 250 × 4.6-mm Zorbax ODS, DuPont, Wilmington, Del.; (d) 250 × 4.6-mm Partisil-10 ODS Whatman, Inc., Clifton, N.J.
[9] Altex 210, Altex Scientific Inc., Berkeley, Calif. or Valco sample injector CV-6-UHPa-N60.
[10] Model 701A, Orion Research Inc., Cambridge, Mass.

materials were used as received: 7-methotrexate (IV)[11], aminopterin (V)[12], methopterin (VI)[13], 4-amino-4-deoxy-N^{10}-methylpteroic acid (VII)[12], *N*-(*p*-aminobenzoyl)-L-glutamic acid (VIII)[13], 2-amino-4-hydroxypteridine-6-carboxylic acid (IX)[13]. Solvents were chromatographic grade. Tetrabutylammonium bromide and the materials used in the preparation of the buffers were reagent grade.

Mobile Phases—Premixed, degassed solvents were used. The following buffers were used as the aqueous component of the mobile phase:

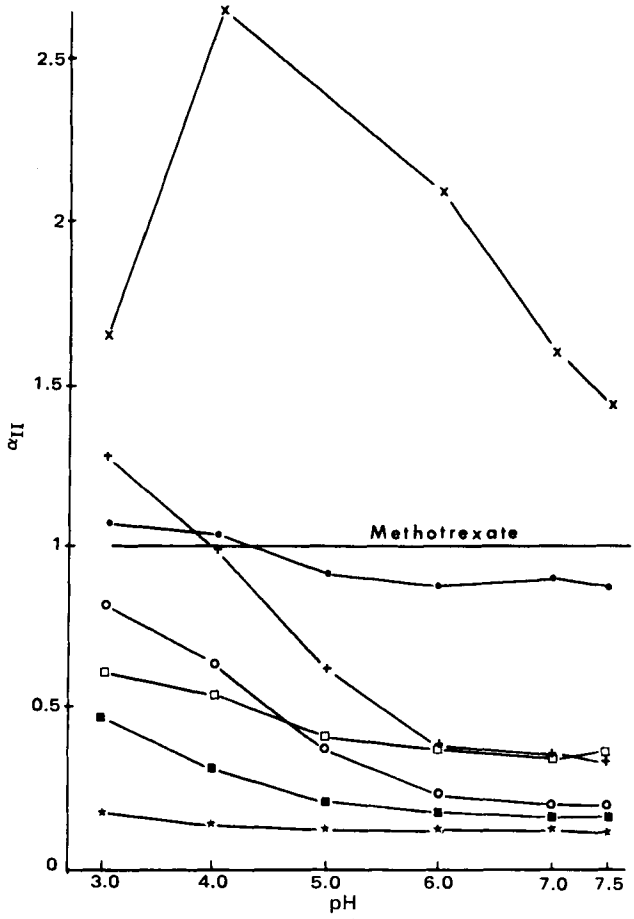

Figure 1—*Order of elution and separation as a function of the mobile phase pH. Key: (×) VII; (+) methopterin; (●) 7-methotrexate; (○) folic acid; (□) aminopterin; (■) leucovorin; (★) VIII.*

[11] Received on a complimentary basis from the Oncological Institute, Bucharest, Romania.
[12] Lederle Laboratories Division, American Cyanamid Company, Pearl River, N.Y.
[13] Sigma Chemical Company, St. Louis, Mo.

Table II—Purity Analysis of Methotrexate [a]

Lot A, 4 mg/ml						Lot B, 4 mg/ml					
Ion-Pairing Mobile Phase[b]			Standard Buffer[c]			Ion-Pairing Mobile Phase[b]			Standard Buffer[d]		
Peak No.	t_R, min	%[e]	Peak No.	t_R, min	%[e]	Peak No.	t_R, min	%[e]	Peak No.	t_R, min	%[e]
1	4.8	0.01	1	2.6	0.1	1	3.9	0.03	1	2.3	0.09
2	5.1	0.03	2[f]	4.7	0.45	2	4.5	0.09	2	2.5	0.10
3	5.8	0.08	3[g]	5.1	0.20	3	4.8	0.09	3	3.1	0.37
4	6.6	0.15	4	6.7	0.02	4	5.5	0.22	4[f]	4.1	6.18
5[f]	7.1	0.72	5	7.1	0.01	5[f]	6.7	7.67	5[g]	5.9	0.16
II	9.0	98.53	6	8.2	0.03	II	8.6	90.16[i]	6	6.8	0.11
6	11.2	0.10	II	9.7	98.84	6	9.8	0.38	II	8.0	90.64
7	13.7	0.04	7	12.9	0.03	7	12.9	0.02	7	9.5	0.03
8	14.7	0.02	8	13.5	0.05	8	13.3	0.01	8	11.1	0.06
9	15.7	0.02	9	20.1	0.04	9	14.4	0.22	9	15.6	0.53
10	18.4	0.30	10	21.0	0.05	10	17.9	0.07	10[h]	18.9	1.44
			11[h]	23.5	0.26	11	21.3	0.04	11	35.8	0.3 (est)
						12	25.6	0.07			
						13	29.2	0.93			

[a] Instrument—SpectraPhysics 3500B, column-μ-Bondapak C-18 300 × 3.9 mm, detector 302 nm-0.1 aufs. [b] 0.005 *M* Tetrabutylammonium bromide in pH 7.5 0.05 *M* KH_2PO_4-acetonitrile (82:18), flow rate 0.8 ml/min. [c] Buffer A-acetonitrile (10:1), flow rate 1 ml/min. [d] Buffer A-acetonitrile (10:1), flow rate 1.2 ml/min. [e] By area normalization. [f] Eluted at the same retention time as an authentic sample of methopterin. [g] Eluted at the same retention time as an authentic sample of aminopterin. [h] Eluted at the same retention time as an authentic sample of 4-amino-4-deoxy-N^{10}-methylpteroic acid. [i] Poorly resolved from Peak 5.

pH 6.0, 0.1 *M* citric acid–0.2 *M* Na_2HPO_4 (37:63, Buffer A); 0.05 *M* KH_2PO_4 brought to either pH 3.0 or 4.0 with 85% H_3PO_4 and to pH 5.0, 6.0, 7.0, 7.2, and 7.5 with 1 *N* NaOH (Buffers P-3–P-7.5, respectively); and pH 7.2, 0.05 *M* KH_2PO_4–0.25 *M* $NaClO_4$ (Buffer B).

As an ion-pairing mobile phase a 0.005 *M* solution of tetrabutylammonium bromide in pH 7.5, 0.05 *M* KH_2PO_4 buffer was used.

Sample Solutions—Mixtures of 0.25–4 mg of compound/ml of mobile phase were sonicated for 15–20 min and filtered through a 5-μm membrane filter prior to injection[14]. Fresh solutions were prepared daily.

RESULTS AND DISCUSSION

Analysis—In Table I and Fig. 1 the results are presented both as absolute values of the retention times (obtained from chromatograms of individual compounds) and as their ratios to the retention time of methotrexate (α_{II}). The quantitative data were calculated by area normalization. Unless otherwise mentioned, all the analyses were run in duplicate.

Influence of Buffer pH—Only a few of the impurities typical of commercial production of compounds in this class have been identified. To gain information on the influence of buffer pH on the chromatographic behavior, a synthetic mixture of Compounds I–IX was prepared and the separation has been studied over a pH range limited by the stability of the packing material (3.0–7.5). Buffers of 0.05 *M* KH_2PO_4 were prepared in this range in increments of whole pH units, and the amount of methanol in the mobile phase was adjusted to keep the retention time of the methotrexate peak between 9 and 10 min at a flow rate of 2 ± 0.2 ml/min.

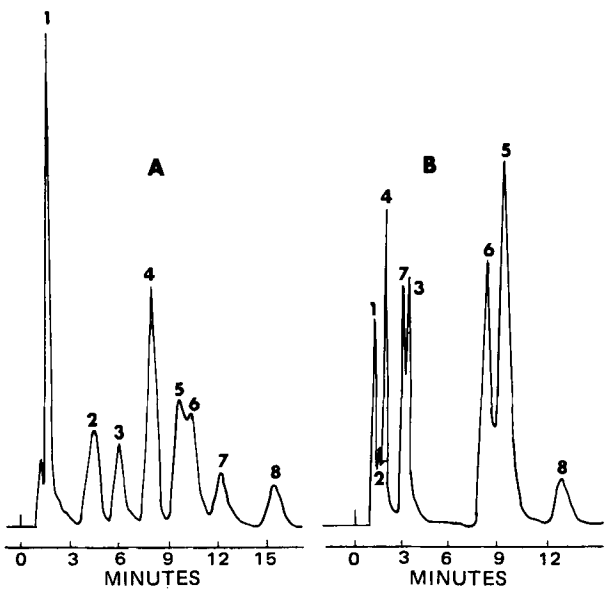

Figure 2—*High-pressure liquid chromatograms of a synthetic mixture. Key: (A) mobile phase pH 3.0; (B) mobile phase pH 7.5; peak identity: (1) VIII; (2) leucovorin; (3) aminopterin; (4) folic acid; (5) 7-methotrexate; (6) methotrexate; (7) methopterin; (8) VII.*

[14] Fluoropore membrane filter, Millipore Corp., Bedford, Mass.

No attempts were made to obtain baseline separation of all nine compounds, since their simultaneous presence in any one specimen is unlikely. The results are presented in Table I and Fig. 1.

A few aspects of the strong influence of the pH value of the buffer on the separation and order of elution of the peaks can be outlined as follows:

1. The α_{II} values for methopterin, aminopterin, folic acid, and leucovorin calcium increase with the decrease of pH value of the buffer. The most pH-sensitive is the methopterin peak. At pH 7.5 it elutes before the aminopterin peak; at pH 7.0 this order is reversed; at pH 4.0 it overlaps the methotrexate peak; and at pH 3.0 it is eluted after both methotrexate isomers.
2. At pH 3.0, methotrexate elutes before the 7-isomer; at pH 4.0 the two peaks overlap and the order of elution is reversed at all pH values above 4.0.
3. A reversal in the elution order of the folic acid and aminopterin peaks takes place at a pH value between 4.0 and 5.0.
4. The retention time of Compound VII reaches a maximum at pH 5.0. For practical reasons (long analysis time) it is probably better to avoid the use of this pH value in the analysis of mixtures containing VII.

The change in the order of elution is illustrated by the chromatograms at pH 3.0 and 7.5 (Fig. 2).

It is apparent that in this class of compounds the pH value of the buffer is the most powerful parameter in adjusting the separation of any given combination of components in a mixture, with optimization of a particular separation making use of other capabilities of HPLC such as selection of a percentage of the organic solvent or gradient elution.

Purity Analysis—*Folic Acid*—Using Buffer B and UV detection at 254 nm, the chromatographic purity of the current lot of USP folic acid RS (J) was found to be 99.8%. Four minor impurities were separated (three before the main peak, one after), none of them at the locus of formyltetrahydrofolate, which as calcium salt is used as an internal standard in the USP assay of folic acid.

Leucovorin Calcium—A 2-year-old sample was recently reanalyzed using two mobile phases. With Buffer B–methanol mixtures a 95.6% chromatographic purity was obtained, eight impurities being separated before the main peak and one after it.

Using a mobile phase recommended in the literature, pH 5.0, 0.05 *M* KH_2PO_4–acetonitrile (95:5) (9), a chromatographic purity of 95.8% was obtained (average of seven injections, 10 impurities separated).

Methotrexate—From the data in Table I, it appears that the best separation of methotrexate from closely related compounds takes place in the pH range of 6.0–7.5. A comparison between the pH 6.0 citrate buffer and the pH 7.5 phosphate buffer in the purity analysis of a 2-year-old sample (C) shows that the same number of impurities (13) was separated. Quantitation by area normalization indicated a chromatographic purity of 92.7% with either pH 6.0 or 7.5 mobile phases.

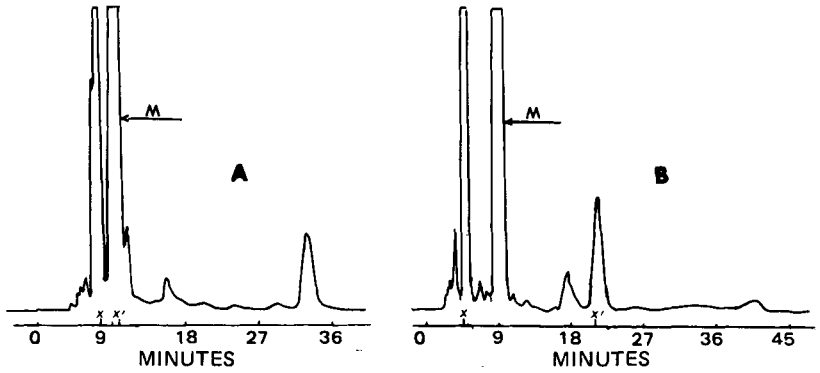

Figure 3—*High-pressure liquid chromatogram of methotrexate Sample B. Key: (A) ion-pairing mobile phase; (B) mobile phase–citrate buffer A: acetonitrile 10:1; (M) methotrexate peak; (X) retention time of an authentic sample of methopterin; (X′) retention time of an authentic sample of VII.*

To compare the pH 6.0 citrate buffer and the ion-pairing mobile phases, two methotrexate samples (A and B) were analyzed for chromatographic purity by the two procedures. The results are shown in Table II. The two methods separate the same number of major impurities, but there are significant advantages for the citrate buffer method:

1. The resolution between the peaks corresponding to methotrexate and methopterin (the major degradation product) is considerably larger using the citrate buffer. The average ratio of the retention times of the two peaks is 2.1 for the citrate buffer method and 1.3 for the ion-pair method. As a result, the resolution of the two peaks by the ion-pair method is acceptable at rather low concentrations of methopterin (V) (Sample A, <1%), but the peaks overlap at a 6% concentration (Sample B) (Fig. 3A). In Reference 13, although the methotrexate peak has a retention time of >40 min, V still elutes as a shoulder on the main peak. The better separation of the two peaks by the citrate buffer method is illustrated in the chromatogram of Sample B (Fig. 3).

2. Another potential impurity in methotrexate is 4-amino-4-deoxy-N^{10}-methylpteroic acid (VII). Again, the citrate buffer provided better separation. In the reported ion-pair chromatography[13], VII is well separated from methotrexate ($t_{R,VII}$ = 18 min, $t_{R,II}$ > 40 min). However, in conditions that, for practical purposes, bring the retention time of the methotrexate peak <10 min, the two peaks overlap ($t_{R,VII}$ = 8.4 min; $t_{R,II}$ = 8.5–8.6 min), and VII could not be identified by spiking a methotrexate sample. Using the citrate buffer mobile phase, with the methotrexate peak eluting between 8 and 10 min, the retention time of VII was ~20 min.

3. The ion-pairing procedure did not separate methotrexate and its 7-isomer. Without giving baseline resolution, the citrate buffer method allowed the detection of 0.2% of the 7-isomer in a spiked sample of methotrexate.

The ion-pairing method proved to be an excellent tool for biochemical studies on methotrexate and its metabolites, but from the previously mentioned considerations it may be concluded that standard buffers should be used as mobile phases for the purity analysis of methotrexate.

The chromatogram of the candidate lot for USP methotrexate reference standard is presented in Fig. 4. Additional chromatograms with mobile phases containing 5–20% acetonitrile ascertained the absence of late-eluting peaks or of potential impurities overlapping the main peak in Fig. 4. The chromatographic purity by area normalization with UV detection at 302 nm was 98.8%.

Separation of the 6- and 7-Isomers of Methotrexate—The formation of 6- and 7-pteridyl isomers in the reaction between 4,5-diaminopyrimidines and polyfunctional 3-carbon compounds is well known (15, 16). Isomerically pure 6- and 7-methotrexate have been synthesized and it was found that the position of the side chain is mainly a function of the pH of the reaction mixture in the pteridine ring closing step and that 7-methotrexate is biologically inactive (17). The two isomers have similar physical chemical characteristics, differing significantly only in the NMR spectra. By TLC or paper chromatography they could be separated only after a preliminary hydrolysis and oxidation to the 2-hydroxy-pteridine-6-carboxylic acid and 2-hydroxy-pteridine-7-carboxylic acid (17).

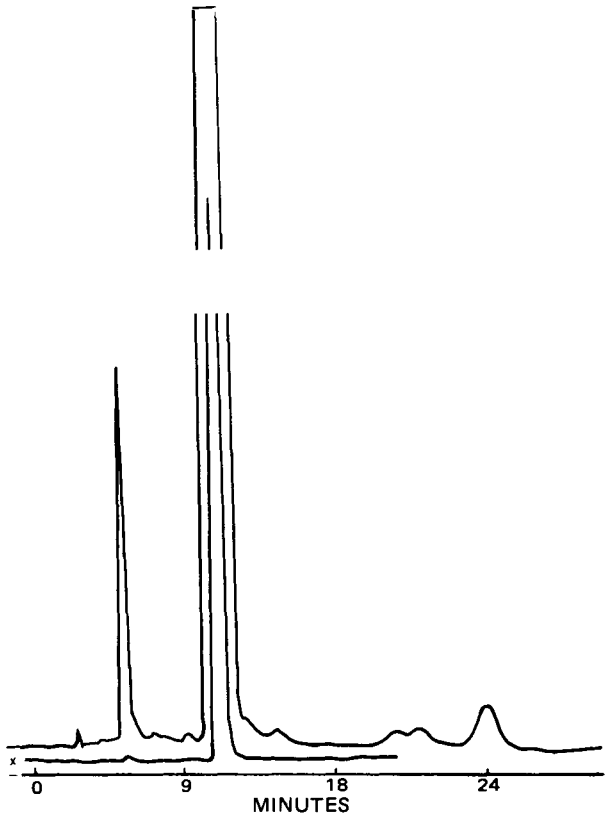

Figure 4—*High-pressure liquid chromatogram of a candidate lot for USP methotrexate reference standard. Mobile phase–Buffer A: acetonitrile 10:1, flow rate 1 ml/min. Key: (X) attenuation 32.*

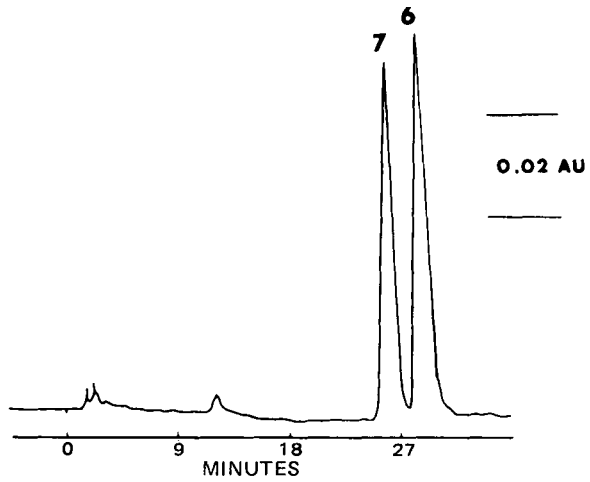

Figure 5—*HPLC separation of the 6- and 7-isomers of methotrexate. Mobile phase–Buffer P-7–CH_3OH; initial 100:5; final 100:12.5; sweep time 15 min, flow rate 2 ml/min. Sample 0.25 mg each/ml.*

Reversed-phase HPLC has been used for the separation of 6- and 7-methyl- (and-methanol-)2,4-diaminopteridines (9).

A nearly baseline separation of 6- and 7-methotrexate (R = 1.4) was obtained using a gradient elution system illustrated in Fig. 5.

REFERENCES

(1) R. C. Williams, D. R. Baker, and J. A. Schmit, *J. Chromatogr. Sci.*, **11**, 618 (1973).

(2) L. S. Reed and M. C. Archer, *J. Chromatogr.*, **121**, 100 (1976).

(3) D. C. Chatterjee and J. F. Gallelli, *J. Pharm. Sci.*, **66**, 1219 (1977).

(4) V. D. Reif, J. T. Reamer, and L. T. Grady, *ibid.*, **66**, 1112, (1977).

(5) W. O. McSharry and F. P. Mahn, *ibid.*, **68**, 241 (1979).

(6) "The United States Pharmacopeia," 20th rev., United States Pharmacopeial Convention, Inc., Rockville, Md., 1980, p. 341.

(7) W. P. Tong, J. Rosenberg, and D. B. Ludlum, *Lancet*, **ii**, 719 (1975).

(8) J. R. Piper and J. A. Montgomery, *J. Org. Chem.*, **42**, 208 (1977).

(9) J. A. Montgomery, T. P. Johnston, H. J. Thomas, J. R. Piper, and C. Temple, Jr., *Adv. Chromatogr.*, **15**, 169 (1977).

(10) "The United States Pharmacopeia," 20th rev., United States Pharmacopeial Convention, Rockville, Md., 1980, p. 508.

(11) C. Temple, Jr., A. T. Shortnacy, and J. A. Montgomery, *J. Chromatogr.*, **140**, 114 (1977).

(12) B. T. Bush, J. H. Frenz, W. R. Melander, C. Horvath, A. R. Cashmore, R. N. Dryer, J. O. Knipe, J. K. Coward, and J. R. Bertino, *ibid.*, **168**, 343 (1979).

(13) J. L. Wisnicki, W. P. Tong, and D. B. Ludlum, *Cancer Treat. Rep.*, **62**, 520 (1978).

(14) A. R. Branfman and M. McComish, *J. Chromatogr.*, **151**, 87 (1978).

(15) F. E. King and P. C. Spensley, *Nature (London)*, **164**, 574 (1949).

(16) R. B. Angier, C. W. Waler, J. H. Bote, H. H. Mowat, J. Semb, E. L. R. Stokstad, and Y. Subbarow, *J. Am. Chem. Soc.*, **70**, 3029 (1948).

(17) D. C. Suster, L. V. Feyns, G. Ciustea, G. Botez, V. Dobre, R. Bick, and I. Niculescu-Duvaz, *J. Med. Chem.*, **17**, 758 (1974).

Microbial Transformations of Natural Antitumor Agents XVIII: Conversions of Vindoline with Copper Oxidases

FRANCES ECKENRODE, WANDA PECZYNSKA-CZOCH, and JOHN P. ROSAZZA ˣ

Received November 20, 1981, from the *Division of Medicinal Chemistry and Natural Products, College of Pharmacy, The University of Iowa, Iowa City, IA 52242.* Accepted for publication January 22, 1982.

Abstract □ Vindoline occurs structurally intact in the clinically important *Vinca* alkaloids vinblastine and vincristine. It is oxidized by human ceruloplasmin and fungal and plant laccases into a reactive intermediate which undergoes intramolecular cyclization to an enamine which ultimately dimerizes. Transformations of vindoline by these copper oxidases are enhanced when enzyme incubations are performed with cofactors such as chlorpromazine. The role of copper oxidases in alkaloid metabolic interconversions and the possible implications of these reactions in *Vinca* alkaloid toxicity are discussed.

Keyphrases □ Vindoline—microbial transformations, natural antitumor agents, conversions with copper oxidase, *Vinca* alkaloids □ Alkaloids, *Vinca*—vindoline, microbial transformations, natural antitumor agents, conversions with copper oxidase □ Antitumor agents—vindoline, microbial transformations, natural antitumor agents, conversions with copper oxidase, *Vinca* alkaloids

Vincristine (II) and vinblastine (I) are widely used dimeric antitumor alkaloids obtained from species of *Catharanthus rosea*. These compounds differ structurally only in the oxidation state of one carbon atom which is attached to the dihydroindole nitrogen atom of the *Aspidosperma* portion of the molecule. Studies concerned with the metabolism of I and II are intended to reveal pathways of metabolic transformations which might ultimately be implicated in mechanism(s) of action and/or the toxicities associated with their use. Several attempts have been made to date (1–5) to study the metabolism of *Vinca* alkaloids, but no metabolites of these compounds have been isolated and fully identified. Low amounts of metabolites produced, very low doses of compounds employed, high molecular weights, and structural complexities probably rendered the identification of presumed metabolites difficult in previous studies.

Copper oxidases are widely occurring enzymes found in mammals, plants, and microorganisms. Enzymes from these different sources possess different physical characteristics including molecular weight, the number and oxidation states of copper, and the nature of copper ligands at presumed active sites (6, 7). Recognized similarities also exist among these enzymes, and direct comparisons between the catalytic capabilities of ceruloplasmin and laccases have been made previously (8, 9). The enzymes achieve the oxidation of substrates by the direct removal of substrate electrons and protons with the subsequent transfer of electrons to molecular oxygen *via* copper (6, 7, 10, 11). True substrates interact directly with copper oxidase enzymes to yield products, while pseudosubstrates require substances capable of interfacing between them and the enzyme during oxidations (6). The requirement for such cofactors has been noted primarily in work with ceruloplasmin in the oxidation of xenobiotics such as arylamines, phenols, and some centrally acting drugs and their analogs (6).

It was discovered that vindoline, a dihydroindole monomer found in the structure of I undergoes oxidation in the presence of copper oxidase enzymes including human ceruloplasmin, fungal, and plant laccases. This report describes the types of chemical transformations of vindoline catalyzed by the copper oxidases which result

0022-3549/82/1100-1246$01.00/0

Reversed-phase HPLC has been used for the separation of 6- and 7-methyl- (and-methanol-)2,4-diaminopteridines (9).

A nearly baseline separation of 6- and 7-methotrexate (R = 1.4) was obtained using a gradient elution system illustrated in Fig. 5.

REFERENCES

(1) R. C. Williams, D. R. Baker, and J. A. Schmit, *J. Chromatogr. Sci.*, **11**, 618 (1973).

(2) L. S. Reed and M. C. Archer, *J. Chromatogr.*, **121**, 100 (1976).

(3) D. C. Chatterjee and J. F. Gallelli, *J. Pharm. Sci.*, **66**, 1219 (1977).

(4) V. D. Reif, J. T. Reamer, and L. T. Grady, *ibid.*, **66**, 1112, (1977).

(5) W. O. McSharry and F. P. Mahn, *ibid.*, **68**, 241 (1979).

(6) "The United States Pharmacopeia," 20th rev., United States Pharmacopeial Convention, Inc., Rockville, Md., 1980, p. 341.

(7) W. P. Tong, J. Rosenberg, and D. B. Ludlum, *Lancet*, **ii**, 719 (1975).

(8) J. R. Piper and J. A. Montgomery, *J. Org. Chem.*, **42**, 208 (1977).

(9) J. A. Montgomery, T. P. Johnston, H. J. Thomas, J. R. Piper, and C. Temple, Jr., *Adv. Chromatogr.*, **15**, 169 (1977).

(10) "The United States Pharmacopeia," 20th rev., United States Pharmacopeial Convention, Rockville, Md., 1980, p. 508.

(11) C. Temple, Jr., A. T. Shortnacy, and J. A. Montgomery, *J. Chromatogr.*, **140**, 114 (1977).

(12) B. T. Bush, J. H. Frenz, W. R. Melander, C. Horvath, A. R. Cashmore, R. N. Dryer, J. O. Knipe, J. K. Coward, and J. R. Bertino, *ibid.*, **168**, 343 (1979).

(13) J. L. Wisnicki, W. P. Tong, and D. B. Ludlum, *Cancer Treat. Rep.*, **62**, 520 (1978).

(14) A. R. Branfman and M. McComish, *J. Chromatogr.*, **151**, 87 (1978).

(15) F. E. King and P. C. Spensley, *Nature (London)*, **164**, 574 (1949).

(16) R. B. Angier, C. W. Waler, J. H. Bote, H. H. Mowat, J. Semb, E. L. R. Stokstad, and Y. Subbarow, *J. Am. Chem. Soc.*, **70**, 3029 (1948).

(17) D. C. Suster, L. V. Feyns, G. Ciustea, G. Botez, V. Dobre, R. Bick, and I. Niculescu-Duvaz, *J. Med. Chem.*, **17**, 758 (1974).

Microbial Transformations of Natural Antitumor Agents XVIII: Conversions of Vindoline with Copper Oxidases

FRANCES ECKENRODE, WANDA PECZYNSKA-CZOCH, and JOHN P. ROSAZZA ˣ

Received November 20, 1981, from the *Division of Medicinal Chemistry and Natural Products, College of Pharmacy, The University of Iowa, Iowa City, IA 52242.* Accepted for publication January 22, 1982.

Abstract □ Vindoline occurs structurally intact in the clinically important *Vinca* alkaloids vinblastine and vincristine. It is oxidized by human ceruloplasmin and fungal and plant laccases into a reactive intermediate which undergoes intramolecular cyclization to an enamine which ultimately dimerizes. Transformations of vindoline by these copper oxidases are enhanced when enzyme incubations are performed with cofactors such as chlorpromazine. The role of copper oxidases in alkaloid metabolic interconversions and the possible implications of these reactions in *Vinca* alkaloid toxicity are discussed.

Keyphrases □ Vindoline—microbial transformations, natural antitumor agents, conversions with copper oxidase, *Vinca* alkaloids □ Alkaloids, *Vinca*—vindoline, microbial transformations, natural antitumor agents, conversions with copper oxidase □ Antitumor agents—vindoline, microbial transformations, natural antitumor agents, conversions with copper oxidase, *Vinca* alkaloids

Vincristine (II) and vinblastine (I) are widely used dimeric antitumor alkaloids obtained from species of *Catharanthus rosea*. These compounds differ structurally only in the oxidation state of one carbon atom which is attached to the dihydroindole nitrogen atom of the *Aspidosperma* portion of the molecule. Studies concerned with the metabolism of I and II are intended to reveal pathways of metabolic transformations which might ultimately be implicated in mechanism(s) of action and/or the toxicities associated with their use. Several attempts have been made to date (1–5) to study the metabolism of *Vinca* alkaloids, but no metabolites of these compounds have been isolated and fully identified. Low amounts of metabolites produced, very low doses of compounds employed, high molecular weights, and structural complexities probably rendered the identification of presumed metabolites difficult in previous studies.

Copper oxidases are widely occurring enzymes found in mammals, plants, and microorganisms. Enzymes from these different sources possess different physical characteristics including molecular weight, the number and oxidation states of copper, and the nature of copper ligands at presumed active sites (6, 7). Recognized similarities also exist among these enzymes, and direct comparisons between the catalytic capabilities of ceruloplasmin and laccases have been made previously (8, 9). The enzymes achieve the oxidation of substrates by the direct removal of substrate electrons and protons with the subsequent transfer of electrons to molecular oxygen *via* copper (6, 7, 10, 11). True substrates interact directly with copper oxidase enzymes to yield products, while pseudosubstrates require substances capable of interfacing between them and the enzyme during oxidations (6). The requirement for such cofactors has been noted primarily in work with ceruloplasmin in the oxidation of xenobiotics such as arylamines, phenols, and some centrally acting drugs and their analogs (6).

It was discovered that vindoline, a dihydroindole monomer found in the structure of I undergoes oxidation in the presence of copper oxidase enzymes including human ceruloplasmin, fungal, and plant laccases. This report describes the types of chemical transformations of vindoline catalyzed by the copper oxidases which result

0022-3549/82/1100-1246$01.00/0

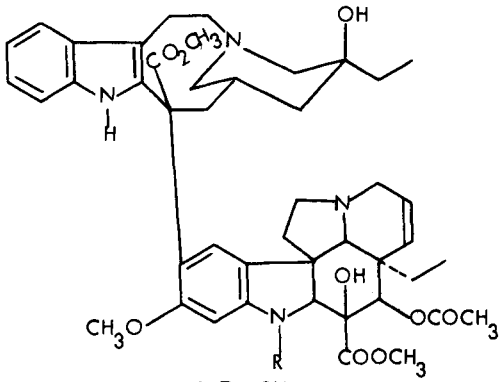

I: R = CH_3
II: R = CHO

in the formation of a reactive enamine intermediate which dimerizes.

EXPERIMENTAL

Compounds—Vindoline (III)[1] was fully characterized (melting point, NMR, UV,and IR spectra) before being used in these experiments (12). Dihydrovindoline ether (IV) and the enamine dimer (V) were authentic standards from previous work (12, 13). These compounds were previously characterized by high resolution mass spectral, carbon-13 and proton NMR analyses.

General—IR spectra[2] were determined using potassium bromide disks, UV spectra[3] were measured in alcohol solution, proton NMR spectra[4] were obtained using deuterochloroform as the solvent and tetramethylsilane as an internal standard, and low resolution mass spectra[5] were obtained using a direct inlet probe.

Chromatography—TLC was performed on 0.25-, 0.50-, or 1.0-mm thick layers of silica gel GF_{254}[6] on glass plates. Prior to use, TLC plates were activated at 120° for 30 min. Solvent systems employed were: A, ethyl acetate–methanol (3:1); B, ethyl acetate–benzene (3:1); C, ethyl acetate–benzene (1:1); and D, ethyl acetate 100%. Compounds were detected on developed chromatograms by fluorescence quenching <254- or 365-nm UV light and were later visualized by spraying with cerium (VI) ammonium sulfate (1% in 50% H_3PO_4, v/v). Column chromatography was performed with silica gel[7] activated for 30 min at 120° prior to use. Columns were packed wet by slurrying silica gel in developing solvent. High-performance liquid chromatography (HPLC) was performed using a reversed-phase column[8] (0.4 × 30 cm), a septumless injector[9], a solvent delivery system consisting of a dual-piston pump[10], and a dual fixed wavelength 254-nm UV absorbance detector[11]. Separations were best achieved using acetonitrile and 0.1% $(NH_4)_2CO_3$–water (50:50) at an average flow rate of 1 ml/min, and an operating pressure of 2000 psi. Authentic standards were injected singly to establish individual retention volumes, and mixtures of metabolites were well-resolved. The identities of individual metabolite peaks were confirmed by spiking with analytical standards. Retention volumes of various compounds were: III, 6.59 ml; IV, 7.78 ml; and V, 23.95 ml.

Enzymes—Methods used in the production, isolation, and analysis of *Polyporus anceps* laccase enzyme were described previously (14). Laccase enzyme activities were determined using a simple colorimetric assay procedure based on the oxidation of syringaldazine (14–16). For these assays, a standard laccase unit was defined as the amount of enzyme catalyzing the oxidation of 1 μmole of syringaldazine to its quinone form (ϵ = 65,000 at 526 nm)/min at 25° in pH 5.0, 0.2 *M* phosphate (K_2HPO_4–KH_2PO_4) (14).

Rhus vernicifera laccase[12] enzyme activities were determined in pH 7.5, 0.1 *M* phosphate buffer using the syringaldazine method.

The purity of ceruloplasmin (human, type III)[13] was ascertained by determining the ratio of absorbances at 610/280 nm, which was measured at 0.046. Pure crystalline enzyme was reportedly measured at A_{610}/A_{280} of 0.047 (17). Enzyme concentrations were calculated from the 610-nm absorption (ϵ = 10,900/*M*) (18) based on a molecular weight of 132,000 (19). Ceruloplasmin activity was standardized in terms of international units according to a previous procedure (20). A single variation of this procedure was the use of the sulfate rather than the oxalate salt of *N*,*N*-dimethyl-*p*-phenylenediamine for this determination. Based on these measurements, human ceruloplasmin contained a specific activity of 123 U/mg of protein. Ceruloplasmin activity was significantly lower at 25°, providing a measured specific activity of only 29 U/mg of protein.

Enzyme Incubation Procedures—Most incubations were conducted in 50-ml flasks which were shaken at 250 rpm[14].

Laccase incubations of *P. anceps* were conducted at 27°. Incubation mixtures were prepared by adding 2 mg (4.39×10^{-6} moles) of vindoline in 0.1 ml of methanol to 7 ml of phosphate buffer (pH 5.0, 0.2 *M*) containing 1.05 U of laccase.

Incubations with *R. vernicifera* laccase were also conducted at 27°, and incubation mixtures were prepared by adding 2 mg of vindoline in 0.1 ml of methanol to 5.2 ml of phosphate buffer (pH 7.0, 0.1 *M*) containing 0.019 U of *Rhus* laccase.

Incubations with human ceruloplasmin were conducted at 37°. These were prepared by adding 2 mg of vindoline in 0.1 ml of methanol to 7.05 ml of acetate buffer (0.2 *M*, pH 5.5) containing 54 U of ceruloplasmin activity.

Several cofactors were also employed in enzyme incubation mixtures. Where used, they were employed in molar ratios of 1:1 and 3:1 *versus* the substrate vindoline. Cofactors examined in this work were 3-hydroxy-4-methoxyphenethylamine; harmine; harmol hydrochloride; histamine; levodopa; syringaldazine; hydroquinone; *N*,*N*-dimethyl-*p*-phenylendiamine; and chlorpromazine. Cofactors were added to incubation mixtures in 0.1 ml of methanol.

Controls consisted of incubations containing enzyme alone, mixtures containing only substrates plus cofactors, and complete incubations containing boiled enzymes. No reactions were observable when boiled enzymes were used or when no enzymes were present in incubation mixtures.

Rates of enzyme reactions were determined by measuring oxygen uptake with an electrode[15] connected to a stirred, water-jacketed reaction chamber 3.73 ml in volume (21). Incubations were conducted as described before using 54 U of ceruloplasmin, and 0.25 U of *P. anceps* laccase. Vindoline (1.02 mg, 2.24×10^{-6} moles) was added to incubations in 0.05 ml of methanol, and chlorpromazine (9.4 mg, 2.65×10^{-6} moles) was added as a cofactor for most incubations.

Analyses of enzyme incubation reactions were also performed by withdrawing samples of 1.0 ml at various time intervals. Reaction samples were adjusted to pH 10 with 58% NH_4OH and extracted with 1 ml of ethyl acetate. Extracts were examined by TLC using solvent systems A and B or by HPLC.

Preparative Scale Production of the Dimer (V) Using *P. anceps* Laccase—Vindoline (300 mg) dissolved in 25 ml of dimethylformamide was added to 300 ml of pH 5.0, 0.2 *M* phosphate buffer containing 66 units of *P. anceps* laccase enzyme and 3.2 mg of syringaldazine added in 2 ml of methanol. This mixture was incubated for 24 hr at room temperature to ensure a complete bioconversion reaction before being adjusted to pH 10 with 58% NH_4OH and extracted four times with equal portions of ethyl acetate. The extracts were dried over anhydrous sodium sulfate and concentrated to a red oil (0.635 g). The oil was dissolved in 1 ml of ethyl acetate, applied to a silica gel column (3 × 33 cm, 100 g) and eluted with solvent system C at a flow rate of 2 ml/min while 10-ml fractions were collected. Fractions 269–300 contained the major reaction product, and these were combined, dried over anhydrous sodium sulfate, and concentrated to a brown solid (143 mg). This material was further purified by dissolving in 1 ml of acetone and applying to a 0.5-mm silica gel preparative layer TLC plate which was developed in solvent system B. The band at R_f 0.39 was scraped from the plate, mixed with 10-ml portions of acetone (4X), stirred, and filtered. Evaporation of the combined filtrates yielded 81 mg of pure V as an amorphous glass.

Trapping a Reactive Enamine Intermediate (VI) by Reduction to IV with Sodium Borohydride—Two milligrams of III dissolved in 0.1 ml of methanol was added to 7 ml of 0.2 *M* phosphate buffer, pH 6.5,

[1] Eli Lilly and Co., Indianapolis, Ind.
[2] Model 267, Perkin-Elmer, Norwalk, Conn.
[3] Model SP1800, Pye Unicam Ltd., Cambridge, England.
[4] Model EM360, Varian Associates, Palo Alto, Calif.
[5] Model 3200, Finnigan Corp., Sunnyvale, Calif.
[6] Merck and Co., Rahway, N.J.
[7] Baker 3405, J.T. Baker Chemical Co., Phillipsburg, N.J.
[8] μBondapak phenyl, Waters Associates, Milford, Mass.
[9] Model U6K, Waters Associates, Milford, Mass.
[10] Model 6000, Waters Associates, Milford, Mass.
[11] Model ALC/GPC 202, Waters Associates, Milford, Mass.
[12] H. B. Gray, California Institute of Technology, Pasadena, Calif.
[13] Sigma Chemical Co., St. Louis, Mo.
[14] Delong, Model G24, New Brunswick Scientific Co., Edison, N.J.
[15] Clark, YSI Co., Yellow Spring, Ohio.

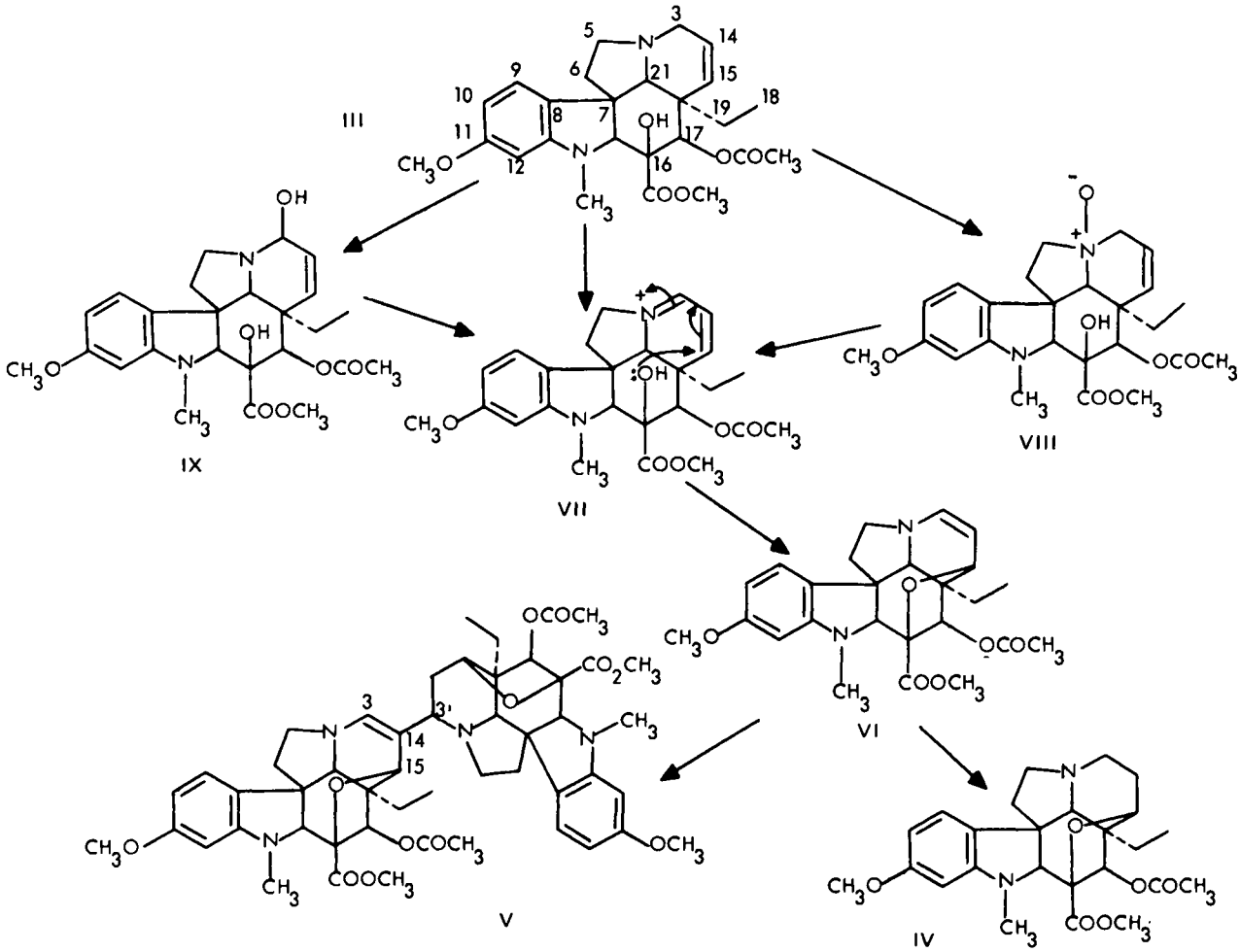

***Scheme I**—Pathways for the oxidation of vindoline (III).*

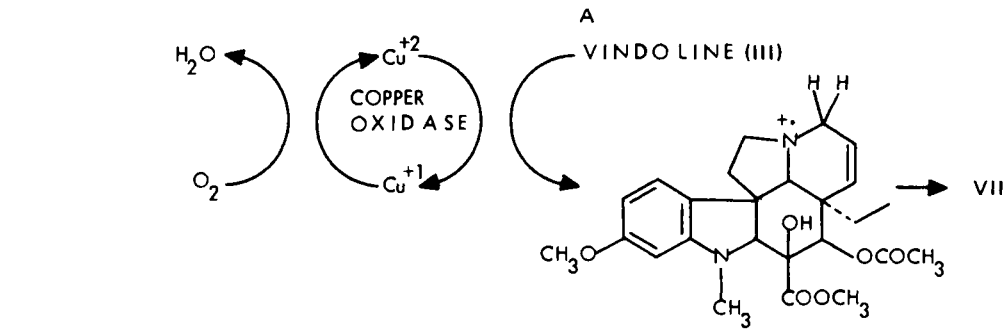

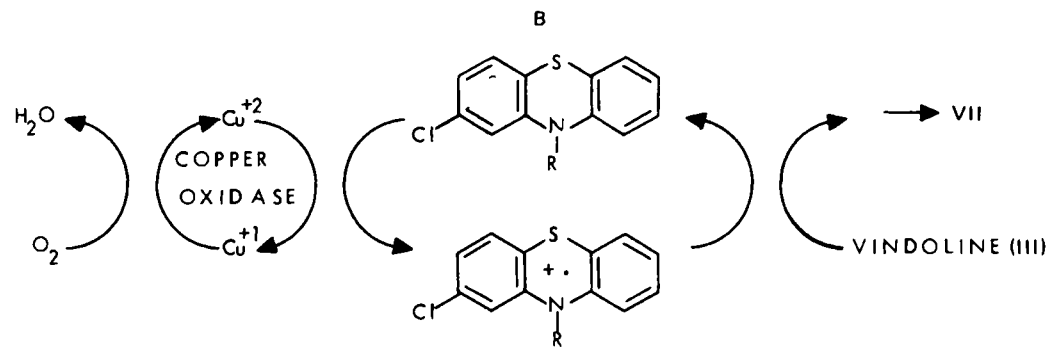

***Scheme II**—Pathways for the flow of electrons in the oxidation of vindoline by the copper oxidases.*

containing 1.2 units of *P. anceps* laccase. The mixture was incubated for 2.5 hr before being adjusted to pH 9.6 with 58% NH_4OH and extracted with 7 ml of ethyl acetate. TLC of the crude extract on silica gel plates (solvent system A) *versus* authentic standards revealed the presence of III R_f 0.7, V R_f 0.82, and the presumed enamine VI, R_f 0.9. The extract was evaporated to dryness, redissolved in 1 ml of methanol and treated with 10 mg of sodium borohydride. After 30 min, this reaction mixture was evaporated to 1 ml, quenched with 5 ml of water and extracted with ethyl acetate. This extract was evaporated to dryness and TLC examination on silica gel GF_{254} (solvent system A) revealed the presence of a substance with chromatographic mobility of R_f 0.25, identical to known dihydrovindoline ether (IV). The extract was dissolved in ethyl acetate, applied to a preparative 0.5-mm silica gel plate, and developed with solvent system A. The band at R_f 0.25 was removed and extracted from silica gel with acetone. TLC and HPLC (retention volume of 7.78 ml) determined that the eluted compound was identical to authentic IV.

RESULTS AND DISCUSSION

The monomeric *Vinca* alkaloid III has been the subject of a previous metabolic study. This compound is the most abundant and available of the alkaloids of *C. rosea*, and it is found essentially intact in the dimeric structures of I and II. Enzymatic transformations observed with III also might be expected to occur in the appropriate functionalities of the dimeric alkaloids like I and II.

Early work with microorganisms as metabolic tools (22) resulted in the elaboration of a unique vindoline metabolic pathway (Scheme I) (12, 13). *Streptomyces griseus* whole cells oxidized vindoline to V and IV, both of which accumulated in incubation media in high yield. A reactive enamine VI was identified as a key intermediate in transformations of III (13). Although the enzyme systems of *S. griseus* responsible for the biotransformation reactions remain unknown, it is possible to postulate four different pathways by which III might undergo initial oxidation to VI (Scheme I). The first pathway involves initial *N*-oxidation of III to VIII, conjugation through the *N*-oxide and elimination of ROH to form VII; and subsequent intramolecular cyclization to VI. This pathway would represent a biochemical equivalent to the modified Polonovsky reaction observed in the chemical treatment of these alkaloids (12). A second path involves direct oxidation of vindoline to VII by the removal of two electrons and a proton. The third possibility would invoke a direct hydroxylation of vindoline at position 3 to form a carbinolamine (IX) which provides VII by elimination of a hydroxide ion. Finally, and perhaps least likely, initial epoxidation of the 14,15-double bond followed by intramolecular etherification and subsequent dehydration could also provide VI. The need to elaborate the precise steps involved in oxidations of III has stimulated a search for more highly defined enzyme systems such as the copper oxidases.

Since crude fungal laccase could be reproducibly obtained in relatively large amounts, it was employed in preparative scale incubations designed to afford sufficient amounts of metabolites for isolation and structure elucidation. Incubations of III with *P. anceps* laccase (14) produced two metabolites with similar TLC mobilities to III derivatives VI and V (12, 13). The major and stable metabolite produced by *P. anceps* laccase was obtained by column and preparative layer chromatography in 27% yield from 300 mg of III. This metabolite was identified as V by spectral and chromatographic comparison with an authentic sample of the dimer (12). Pertinent spectral properties included the UV spectrum in ethanol with λ_{max} values at 252 nm (log ϵ, 4.13) and 309 (log ϵ, 3.84). Highly characteristic NMR signals were also obtained for the metabolite and included the following: ppm, 0.8 (6H, m, 2 overlapping 18H), 1.9 (3H, s, $COCH_3$), 2.0 (3H, s, $COCH_3$), 2.65 (3H, s, NCH_3), 2.75 (3H, s, NCH_3), 3.75 (12H, s, two overlapping CO_2CH_3 and OCH_3 groups), 4.05 (1H, m, 15′H), 4.2 (1H, s, 15H), 5.35 (2H, d, J = 2 Hz, overlapping 17H), 5.99 (2H, d, J = 2 Hz, overlapping 12H), 6.05 (1H, s, 3H), 6.25 (2H, q, overlapping 10H), 6.9 (2H, dd, overlapping 9H). Confirmation of the structure of the major and stable laccase metabolite as V is a significant finding, because the mechanism of copper oxidase reactions is reasonably well understood.

It was mechanistically important to confirm the involvement of the enamine (VI), in copper oxidase transformations of vindoline. The second and unstable laccase metabolite possessed similar TLC mobility to VI previously obtained from *S. griseus* incubations. Since the presumed enamine intermediate was considerably more stable at pH values near neutrality, enzyme incubations were conducted at pH 6.5 to favor its accumulation. Extracts of laccase incubation mixtures were concentrated, and reduced with sodium borohydride to convert the enamine to the known dihydrovindoline ether IV. This technique was employed earlier as a means of stabilizing and identifying the enamine VI (12, 13). Chromatographic (HPLC, retention volume 7.78 ml; TLC, R_f 0.25) analysis of the reduced laccase extract clearly demonstrated the presence of IV. Thus, it has been shown that the copper oxidase oxidations of III result in the formation of VI as well as V.

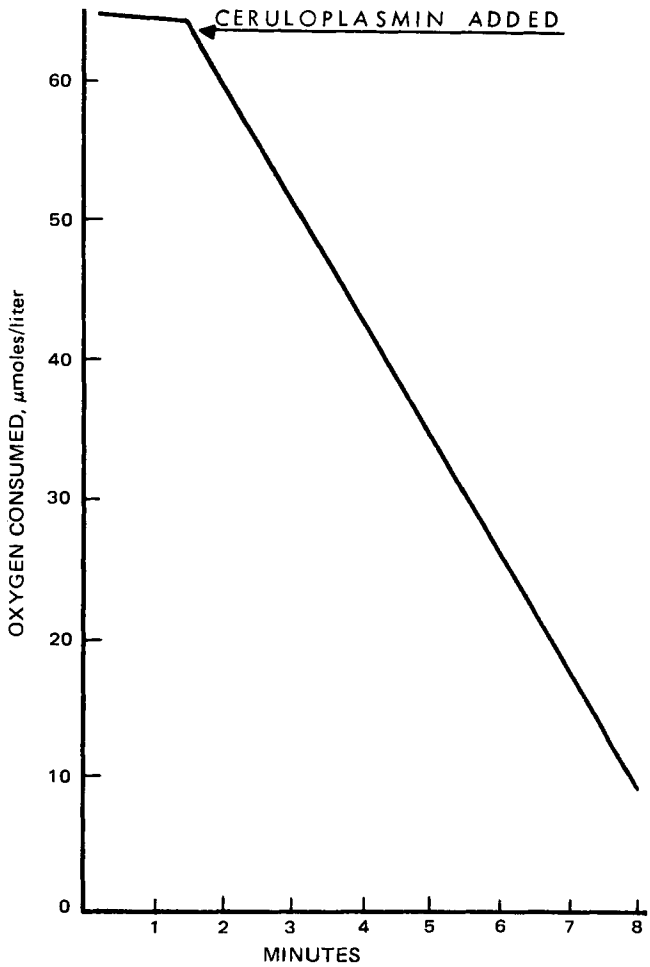

***Figure 1**—Rate of oxidation of vindoline by ceruloplasmin as shown by the uptake of molecular oxygen using a Clark oxygen electrode.*

The involvement of chlorpromazine and other cofactors in copper oxidase oxidations of III is illustrated in Scheme II. When III is a true substrate for ceruloplasmin, it is directly oxidized by the transfer of electrons through the copper oxidase enzyme to molecular oxygen (A). With chlorpromazine and syringaldazine, III is a pseudosubstrate which is oxidized directly by a chlorpromazine radical species which serves as a cycling intermediate between it and ceruloplasmin (Scheme IIB) (23). The oxidation of chlorpromazine to a radical species by ceruloplasmin has been associated with the formation of a red pigment with an absorption maximum at 529 nm by simultaneous optical-absorption, electron paramagnetic resonance measurements (23). With both laccase and ceruloplasmin, chlorpromazine forms a visible red pigment with an absorption maximum at 529 nm. Similar radical intermediates have been implicated in other oxidation reactions catalyzed by ceruloplasmin (23–26).

Human ceruloplasmin and *R. vernificera* laccase also oxidized III to the dimer (V). As with *P. anceps* laccase, III was an apparent true substrate for serum ceruloplasmin, forming products in the absence of added cofactors. However, reaction rates were increased sixfold when an ~1-mole equivalent of chlorpromazine was added to the reaction mixtures. A similar effect was observed when III was incubated with laccase alone or in the presence of laccase plus chlorpromazine. Results obtained using the oxygen electrode illustrate the rate enhancements obtained when chlorpromazine was added to enzyme incubation mixtures, and these are shown in Fig. 1. No reactions were observed at all with *Rhus* laccase unless cofactors were present.

Chlorpromazine clearly enhanced oxidation rates with all of the copper oxidases examined. Of the other cofactors examined, only syringaldazine, a known substrate for laccase (14), increased *Rhus* and *P. anceps* laccase oxidations. However, this compound had no measurable effect with ce-

ruloplasmin. Other substrates listed in the *Experimental* section had no effect on copper oxidase reactions. This was surprising since these compounds had previously been shown to facilitate oxidations of biogenic amine substrates with ceruloplasmin (23, 24, 27, 28).

This is the first report of any type of metabolic conversion of a *Vinca* alkaloid by mammalian enzymes, and the first demonstrating the oxidation of a nitrogen heterocycle of the *Aspidosperma* class of alkaloid by copper oxidases. It is an excellent example of the principle of microbial models for mammalian drug metabolism (22), and it clearly demonstrates the similarities with which microbial and mammalian enzymes achieve xenobiotic transformations. By their nature, copper oxidases most likely cause the elimination of two electrons and a proton from III as the first step in the biotransformation pathway. It appears that protons at position 3 of III are activated toward copper oxidase oxidations by virtue of their allylic nature and their proximity to the heterocyclic nitrogen atom. It can be expected that similar functionalities in other substrates will also be oxidized by the copper oxidases. While *N*-oxides, carbinolamines, and epoxides may be ruled out as possible intermediates in copper oxidase-mediated transformation of the *Vinca* alkaloids, it is possible that derivatives such as VIII and IX may be formed as a result of oxidation catalyzed by other types of enzymes such as the mixed function oxygenases found in mammalian liver (29–31).

This work provides a biochemical basis for understanding possible interactions of drugs like chlorpromazine and perhaps others with compounds like vindoline (III) and other copper oxidase substrates. The presence of cofactors that enhance conversions of their alkaloids and their congeners to chemically reactive species may have profound toxicological implications. The potential for chemically reactive imminium and enamine species to partake in reactions of pharmacological significance is enhanced by virtue of the stabilities of these substances in aqueous media (12, 13), which would allow for their facile distribution throughout the body. In this connection, ceruloplasmin levels are elevated in individuals afflicted with various types of cancer (32, 33). Further studies designed to elaborate enzymatic transformations of *Iboga* alkaloids representing the other half of dimers such as I and *Vinca* dimers themselves are in progress.

REFERENCES

(1) R. J. Owellen and D. W. Donigian, *J. Med. Chem.*, **15,** 894 (1972).

(2) C. T. Beer and J. F. Richards, *Lloydia*, **27,** 352 (1964).

(3) W. A. Creasey, A. I. Scott, C. Wei, J. Kutcher, A. Schwartz, and J. C. Marsh, *Cancer Res.*, **35,** 1116 (1975).

(4) R. J. Owellen and C. A. Hartke, *ibid.*, **35,** 975 (1975).

(5) H. D. Weiss, M. D. Walker, and P. H. Wiernik, *N. Engl. J. Med.*, **291,** 127 (1974).

(6) E. Frieden and H. S. Hsieh, in "Advances in Enzymology 44," A. Meister, Ed., Wiley Interscience, New York, N.Y., 1976, p. 187.

(7) A. M. Mayer and E. Harel, *Phytochemistry*, **18,** 193 (1979).

(8) J. Peisach and W. G. Levine, *J. Biol. Chem.*, **240,** 2284 (1965).

(9) C. Briving, E. Gandvik, and P. O. Nyman, *Biochem. Biophys. Res. Commun.*, **93,** 454 (1980).

(10) J. M. Bollag, R. D. Sjoblad, and S. Y. Liu, *Can. J. Microbiol.*, **25,** 229 (1979).

(11) B. R. Brown, in "Oxidative Coupling of Phenols," W. I. Taylor and A. R. Battersby, Eds., Dekker, New York, N.Y., 1967, p. 167.

(12) T. Nabih, L. Youel, and J. P. Rosazza, *J. Chem. Soc., Perkin Trans. 1*, **1978,** 757.

(13) M. E. Gustafson and J. P. Rosazza, *J. Chem. Res., Synop.*, 166 (1979).

(14) R. Petroski, W. Pecyznska Czoch, and J. P. Rosazza, *Appl. Environ. Microbiol.*, **40,** 1003 (1980).

(15) J. M. Harkin and J. R. Obst, *Science*, **180,** 296 (1973).

(16) J. M. Harkin and J. R. Obst, *Experientia*, **29,** 381 (1973).

(17) R. A. Lovstad, *Biochem. Pharmacol.*, **25,** 1877 (1976).

(18) H. F. Deutsch, *Arch. Biochem. Biophys.*, **89,** 225 (1960).

(19) J. A. Fee, *Struct. Bonding (Berlin)*, **23,** (1975).

(20) G. Curzon and L. Vallet, *Biochem. J.*, **74,** 279 (1960).

(21) R. W. Estabrook, in "Methods of Enzymology," vol. 10, R. W. Estabrook and M. E. Pullman, Eds., Academic, New York, N.Y., 1967, pp. 41–47.

(22) J. P. Rosazza and R. V. Smith, *Adv. Appl. Microbiol.*, **25,** 169 (1979).

(23) R. A. Lovstad, *ibid.*, **23,** 1045 (1974).

(24) B. C. Barass and D. B. Coult, *Biochem. Pharmacol.*, **21,** 677 (1972).

(25) E. Walaas and O. Walass, *Arch. Biochem. Biophys.*, **95,** 151 (1961).

(26) G. Curzon, *Biochem. J.*, **103,** 289 (1967).

(27) R. A. Lovstad, *Biochem. Pharmacol.*, **24,** 475 (1975).

(28) B. C. Barass, D. B. Coult, P. Rich, and K. J. Tutt, *ibid.*, **23,** 47 (1974).

(29) T. L. Nguyen, L. D. Gruenke, and N. Castagnoli, Jr., *J. Med. Chem.*, **19,** 1168 (1976).

(30) T. L. Nguyen, L. D. Gruenke, and N. Castagnoli, Jr., *ibid.*, **22,** 259 (1979).

(31) B. Ho and N. Castagnoli, Jr., *ibid.*, **23,** 133 (1980).

(32) G. L. Fisher and M. Shifrine, *Oncology*, **35,** 22 (1978).

(33) H. Ungar-Waron, A. Gluckran, E. Spira, M. Waron, and Z. Trainin, *Cancer Res.*, **38,** 1296 (1978).

ACKNOWLEDGMENTS

The authors wish to thank the NIH for grant support through CA 13786-06, Dr. H. B. Gray for a sample of *Rhus vernicifera* laccase, and Dr. G. Thompson of Eli Lilly and Company for providing vindoline used in this work.

Determination of Captopril in Human Blood and Urine by GLC–Selected Ion Monitoring Mass Spectrometry after Oral Coadministration with Its Isotopomer

ALLEN I. COHEN ˣ, RICHARD G. DEVLIN, EUGENE IVASHKIV, PHILLIP T. FUNKE, and TERRENCE McCORMICK

Received September 17, 1981, from the *Departments of Analytical Research and Clinical Pharmacology, The Squibb Institute for Medical Research, New Brunswick, NJ 08903.* Accepted for publication January 26, 1982.

Abstract □ A modified electron-impact GLC-selected ion monitoring mass spectrometric method for captopril is described. Positive chemical ionization GLC-selected ion monitoring and direct chemical ionization confirms the specificity of this procedure for captopril and establishes the chemical ionization techniques as potential analytical methods. This procedure has been adapted to the simultaneous measurement of captopril and its isotopomer. The results of a pilot oral bioavailability study of four subjects receiving either 100 mg of captopril as a direct compression tablet or a solution concomitantly with a 100-mg solution of isotopomer is discussed.

Keyphrases □ Captopril—determination in human blood and urine, GLC-selected ion monitoring mass spectrometry, oral coadministration with isotopomer □ GLC-selected ion monitoring mass spectrometry—determination of captopril in human blood and urine, oral coadministration with isotopomer □ Urine, human—determination of captopril in urine blood, GLC-selected ion monitoring mass spectrometry, oral coadministration with isotopomer

Captopril (I) is an orally active inhibitor of the angiotensin-converting enzyme (1, 2). A specific determination of I was performed by GLC–selected ion monitoring mass spectrometry (3). The succinimide (I*a*) was formed in whole blood by the addition of *N*-ethylmaleimide (IV), which was then adsorbed onto XAD-2 resin, eluted, methylated, and measured as the ester (I*b*). The collaborative studies obtained by the GLC selected ion monitoring and radiometric-TLC methods (4) established a high degree of specificity for the determination of the administered compound, in the presence of other captopril biotransformation products (5). Other recent assays for captopril in blood and urine employ GC (6) and high-performance liquid chromatography (HPLC) (7, 8).

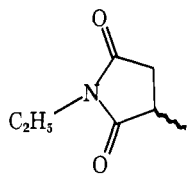

$C_6H_8NO_2$

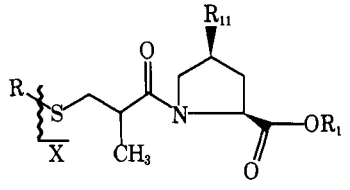

I, I*a*, I*b*, III, III*a*, III*b*

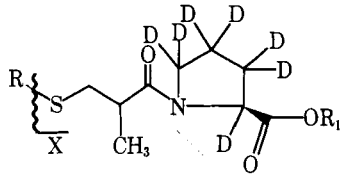

II, II*a*, II*b*

		R	R_I	R_{II}	MW	X EI	MH^+ PCI
Captopril	I	H	H	H	217		
	I *a*	$C_6H_8NO_2$	H	H	342		
	I *b*	$C_6H_8NO_2$	CH_3	H	356	230	357
Isotopomer	II	H	H	—	224		
	II *a*	$C_6H_8NO_2$	H	—	349		
	II *b*	$C_6H_8NO_2$	CH_3	—	363	237	364
Fluoroanalog	III	H	H	F	235		
	III *a*	$C_6H_8NO_2$	H	F	360		
	III *b*	$C_6H_8NO_2$	CH_3	F	374	248	

BACKGROUND

Based on the experience gained from the analysis of blood samples from more than 200 normotensive subjects, a number of modifications of the method (3) evolved to achieve more ease and reliability in processing samples as well as increased precision in making measurements. Currently, 1000 samples, typically collected in one multiple crossover bioavailability study, are processed monthly.

This highly specific and precise analytical method has shown the variability that exists in the disposition of the drug by individual subjects. Using the statistical criteria, a significant subject population is required to demonstrate bioequivalence of formulations. A number of investigators have successfully employed the coadministration of a drug with an isotopomeric formulation in absolute (9) and relative bioavailability (10–15) studies with fewer subjects and at a substantial savings in expense and time. Use of coadministered formulations places more emphasis on a comparison of intra- and intersubject variabilities and at the same time provides data better suited to the evaluation of pharmacokinetic parameters (16).

EXPERIMENTAL

Reagents—Captopril (I, 1-[*S*(2)-mercapto-2-methylpropionyl]-L-proline, CAS registry 62571-86-2), its heptadeutero-isotopomer(II) and 1-[(*S*,4*S*)-4-fluoro-1-(D-3-mercapto-2-methyl -1- oxopropyl)]-L-proline (III) were pharmaceutical grade materials[1] used with additional purification. Methanol, *N*-ethylmaleimide (IV), hydrochloric acid, sodium bicarbonate, diethylenetriaminetetraacetic acid[2] (V), citric acid, oxalic acid dihydrate, sodium phosphate dibasic ($Na_2HPO_4 \cdot 7H_2O$), ammonium phosphate dibasic, instant methanolic hydrochloric acid kit[3], 80–200 mesh Brockman Activity 1 neutral alumina, and sodium chloride were used without purification. Purified XAD-2 resin[3] was conditioned as previously described (3). Ethyl acetate was purified immediately before use by passing 600 ml through a neutral alumina 2.5 × 40-cm column to remove oxidizing impurities (3). Preparation of the phosphate buffer (pH 7.0) and methanolic hydrochloric acid have been previously described (3).

The solutions used for processing urine samples were prepared by a previous method (17). The 0.8% V solution was prepared by dissolving 4 g of V in 500 ml of 0.08 *M* NaOH, sonicated for ~30 min in an ultrasonic bath. The 0.08 *M* NaOH solution was prepared by dissolving 3.2 g in 1 liter of distilled water. The citric acid–oxalic acid solution was prepared by dissolving 105 g of citric acid monohydrate and 63 g of oxalic acid in 1 liter of distilled water.

Blood and Urine Collection—From 12 to 15 ml of blood was drawn[4] and processed as previously described (3) by the addition of 75 mg of IV to each sample. Frozen citrated whole blood was used for calibration and control samples. Urine samples were collected according to a previous

[1] E. R. Squibb & Sons, Princeton, N.J.
[2] G. F. Smith Chemical Co., Columbus, Oh.
[3] Applied Science Lab. Inc., State College, Pa.
[4] Becton-Dickinson, Vacutainer.

0022-3549/82/1100-1251$01.00/0

Table I—Summary of Calibration Data GLC–Selected Ion Monitoring Mass Spectrometry

Sample Type	Analyte		Ion m/z	Internal Reference Standard		Ion m/z	n	Intercept I_n	Slope k_n
Blood	Captopril	I	230.1	Isotopomer	II	237.1	1	0.0192	1.2991
	Captopril	I	230.1	Fluoroanalog	III	248.1	2	0.0275	2.0463
	Isotopomer	II	237.1	Fluoroanalog	III	248.1	3	0.0047	1.7396
Urine									
High	Captopril	I	230.1	Fluoroanalog	III	248.1	2	0.0911	1.9316
	Isotopomer	II	237.1	Fluoroanalog	III	248.1	3	0.0595	1.7111
Low	Captopril	I	230.1	Fluoroanalog	III	248.1	2	0.0157	2.3417
	Isotopomer	II	237.1	Fluoroanalog	III	248.1	3	0.009	2.0428

Table II—Comparison of Captopril Blood Levels Determined by Electron-Impact and Chemical Ionization GLC–MS

Time, hr	Captopril Blood Levels, ng/ml Subject A EI	CI	Diff, Δ EI–CI	Captopril Blood Levels, ng/ml Subject B EI	CI	Diff, Δ EI–CI
0.0	2.3	7.4	−5.1	4.1	1.7	2.4
0.25	21.1	26.1	−5.0	59.8	61.5	−1.7
0.50	272.0	265.0	7.0	318.0	317.0	1.0
0.75	432.0	437.0	−5.0	450.0	433.0	17.0
1.0	375.0	378.0	−3.0	337.0	344.0	−7.0
1.5	186.0	176.0	10.0	165.0	148.0	17.0
2.0	104.0	98.3	5.7	69.9	81.7	−11.8
3.0	31.4	28.4	3.0	20.4	20.9	−0.5
4.0	21.1	14.8	6.3	10.3	10.3	0.0
6.0	7.8	16.6	−8.8	6.4	5.6	0.8
8.0	1.8	1.6	0.2	2.2	2.9	−0.7
12.0	0.8	2.2	−1.4	2.0	1.8	0.2

procedure (17) for the colorimetric determination of captopril. The urine for each subject was collected over the prescribed time period, and 5 ml of refrigerated solution was added to the temporary container. Each subject's sample was swirled and added to the permanent container which contained 100 ml of citric acid–oxalic acid solution. The permanent container was returned to a 5° refrigerator, and at the end of the collection period the pH was tested with pH 2–4 paper. An additional 100 ml of citric acid–oxalic acid solution was added if the pH exceeded 2. Each volume of urine and citric acid–oxalic acid solution added to the container was measured and recorded, and 50–100 ml of this solution was transferred to a smaller container for storage in a refrigerator.

Before an elapsed time of 48 hr, 0.2 ml of a solution of IV (5 g/ml in acetone) was added to 5 ml of refrigerated urine sample, followed by 5 ml of ammonium phosphate dibasic solution (250 g/liter in water). After standing for 15 min, the solution was sampled for analysis or frozen if the analysis was to be performed at a later date.

Extraction of Blood Samples—The extraction procedure remained essentially the same (3), except that the samples were processed in batches of 11 plus one control. For samples containing the isotopomer, 2.5 μg of III was added as an internal reference to each 5-ml aliquot of blood sample, while 2.5 μg of II was added as the internal reference for the measurement if only captopril was administered. For coadministration studies, the control was composed of 5 μg each of I and II and 2.5 μg of the internal reference III. For the single administration samples, the control sample was 5 μg of I and 2.5 μg of the internal reference II. The samples were methylated after extraction, and just prior to measurement they were reconstituted with 20 μl of acetone.

Table III—Comparison of Captopril Blood Levels Determined by Electron-Impact GLC–MS and Direct Chemical Ionization

Electron Impact GLC–MS, ng/ml	Direct Chemical Ionization, ng/ml	Diff, GLC–MS–Direct Chemical Ionization
0.0	5.8	−5.8
2.3	2.5	−0.2
5.4	5.8	−0.4
9.6	1.3	8.3
13.3	13.8	−0.5
15.0	0.6	14.4
30.5	26.7	3.8
84.6	81.9	2.7
77.1	78.1	−1.0
196.0	180.0	16.0
213.0	204.0	9.0
312.0	303.0	9.0
408.0	417.0	−9.0
430.0	430.0	0.0
447.0	443.0	4.0
500.0	479.0	21.0
642.0	621.0	21.0

Extraction of Urine Samples—Urine samples collected just prior to and 4 hr after administration were processed in the same manner as the blood samples (3). To each 3-ml aliquot, 0.1 ml of the fluoro internal reference III containing 2.5 μg was added.

Samples collected during the first 4 hr after administration, were processed by adding 0.1 ml of internal reference containing 25 μg of internal reference III to a 2-ml aliquot of urine sample. The control urine sample contained 50 μg each of I and II and 25 μg of III. To each 150-mm screw-capped culture containing the urine sample, 2 g of sodium chloride and 2 ml of 6 N H_3PO_4 were added, the tubes covered with caps, and agitated on a shaker for 5 min. Five milliliters of purified ethyl acetate was added, the tubes were shaken for 5 min, and then centrifuged at 2000 rpm for 5 min. Five-tenths milliliter of the ethyl acetate layer (top) was then transferred to a 1-ml reaction vial[5] and the solvent was evaporated under nitrogen[6]. The contents of the reaction vials were then further dried under vacuum at room temperature for 15 min in an oven or dessicator. The samples were then methylated as described (3) and stored in a freezer. Just prior to measurement, the samples were dissolved in 20 μl of acetone.

Calibration and Preparation of Control Blood and Urine Samples—Varying amounts of I (and an equal amount of II for simultaneous measurements) were added to 5 ml of citrated blood (containing 25 mg of IV, in a 150-mm screw-capped culture tube), to yield blood concentrations of 0–1500 ng/ml. For the simultaneous measurements of captopril and its isotopomer, 0.1 ml of solution containing 2.5 μg of internal reference III was added, while an equivalent amount of internal reference II was added if only I was to be measured. The control sample represents the calibration point of 1000 ng of analyte(s) and 500 ng of internal reference per milliliter of blood.

The standard curve for the low-concentration urine samples was prepared from 3-ml urine samples containing 0–7.5 μg of I and II and 2.5 μg of internal reference III, which were processed as described for urine samples collected during the first 4 hr after administration. Control urines, containing either 5 or 50 μg of analytes I and II and 50% of internal reference III were processed for either low or high concentrations of captopril.

[5] Hewlett-Packard, Palo Alto, Calif.
[6] Mini-Vap.

Table IV—Statistical Evaluation of Captopril Blood Calibration Data

Ratio ng Captopril I / ng Isotopomer II[a]	$Int_{m/z\ 230}/Int_{m/z\ 237}$ Mean[b]	Standard Deviation (s)	s/Mean
0.0	0.01915	0.002783	0.145
0.0625	0.09775	0.01099	0.112
0.125	0.19146	0.02515	0.131
0.25	0.34287	0.01893	0.055
0.50	0.68678	0.02410	0.035
1.0	1.3050	0.04248	0.033
2.0	2.5694	0.1344	0.052
3.0	3.8928	0.1659	0.043

[a] 2500 ng internal reference standard added. [b] Based on nine measurements.

The ratio of the maximum peaks heights, R_n, was plotted *versus* the respective nanogram ratio R'_n:

n	R_n	R'_n
1	$I_{m/z\ 230}/I_{m/z\ 237}$	1/2
2	$I_{m/z\ 230}/I_{m/z\ 248}$	1/3
3	$I_{m/z\ 237}/I_{m/z\ 248}$	2/3

The intercept, I_n, is the ratio R_n for the blank extract ($R'_n = 0$). Linear regression:

$$R_n = I_n + k_n R'_n \qquad \text{(Eq. 1)}$$

establishes the slopes, k_n, and the intercepts I_n for Eq. 1 (Table I).

Selected Ion Monitoring—From 1 to 2 μl of solution, added to the tip of a GLC solids injector[7], was allowed to evaporate. The appropriate ion profiles (m/z 230.1, m/z 237.1, m/z 248.1) were obtained by selected ion monitoring. The maximum peak heights were measured using a program written especially for the batch processing of the data[8]. The program selects the baseline-corrected maximum peak heights of the requested ions. The mean ratio, R''_n, and standard deviation for three to five injections of the control sample bracketing the samples were determined for subsequent use to correct the data for differences in response from the calibration slope, k_n. The adjustment factor, A, is related to the calibration slope and the measured ratio of the control, R''_n, by Eq. 2:

$$A = \frac{R''_n}{I_n + 2k_n} \qquad \text{(Eq. 2)}$$

The measured ratio of the sample, R^*_n, is related to R_n by Eq. 3:

$$R_n = R^*_n/A \qquad \text{(Eq. 3)}$$

which is then used to calculate the ng (or μg) ratio of analyte to internal reference, R'_n:

$$R_n = R^*_n/A = I_n + k_n R'_n \qquad \text{(Eq. 4)}$$

The concentration of analyte, C_x, is calculated from Eq. 5:

$$C_x = R'_n(F/M) \qquad \text{(Eq. 5)}$$

where C_x is the concentration of analyte in nanograms per milliliter (blood) or micrograms per milliliter (urine), F is the quantity of internal reference (ng for blood; μg for urine) added to M milliliters of sample, and R'_n is the ratio of analyte to internal reference calculated from Eq. 1.

Instrumental Procedure—The combined GLC–MS with data system[9] was operated under selected ion monitoring mode. The instrument was tuned[10] for electron-impact (EI) MS from 69 to 502 Daltons using perfluorotributylamine at an ionization voltage of 70 eV and at an emission of 300 μA. The ion source was controlled at a constant temperature of 200°.

A septum guide[11] was attached to the GLC injector. The analyses were carried out on an 80- cm × 2-mm i.d. silanized glass column packed with 3% OV-101[12] which was connected through a single-stage jet separator.

[7] Scientific Glass Equipment Co., SI-1RDS, Penzias Assoc., Roslyn Heights, N.Y.
[8] The BASIC program for the HP 5985B GCL–MS is available upon request.
[9] Hewlett-Packard, Model 5985B, Palo Alto, Calif.
[10] AUTOTUNE.
[11] Supelco, Cat. No. 2-0839, Bellefonte, Pa.
[12] On 80/100 Supelcoport, Supelco, Bellefonte, Pa.

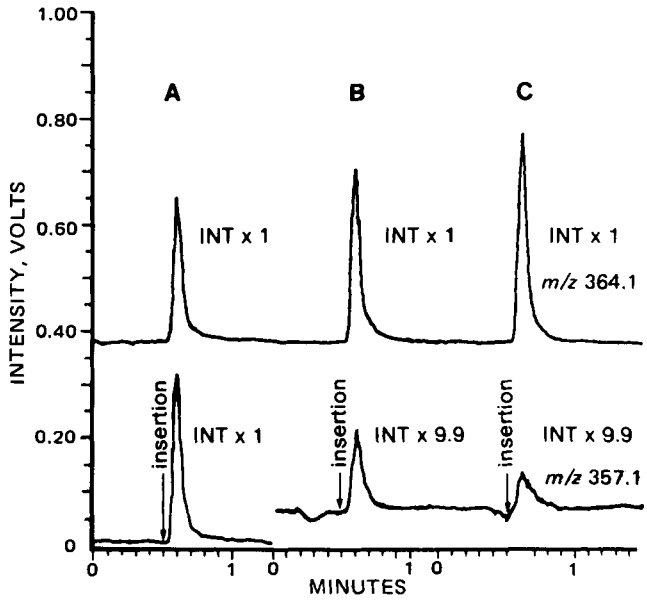

Figure 1—*Direct chemical ionization of captopril blood samples containing 500 ng/ml of internal reference as IIb and (A) 442, (B) 13.8, and (C) 2.5 ng/ml of captopril as Ib*

The separator and transfer line were maintained at 275° while the column was kept at an isothermal temperature of 260° and the injector was heated to 290°. A typical retention time of 0.6 min was obtained at a helium flow rate of 30 cm³/min. Slight adjustments in the column temperature were made to keep the retention time within the desired time window, when necessary. Helium, otherwise diverted, was allowed to flow into the ion source from 0.1 to 1.3 min after sample injection. The multiplier and electron voltages were only applied during the data collection period from 0.3 min until the termination of the GLC run. When required, portions of the column packing or the entire column was replaced to maintain optimum chromatographic conditions. The septum was replaced each day.

Positive chemical ionization GLC–MS was obtained with methane as the GLC carrier gas, at a flow rate of 20 cm³/min, directly into the source to create a 1-torr source pressure. Otherwise, the chromatographic conditions were identical to that of the electron impact-GLC–MS.

Direct chemical ionization mass spectra and measurements were taken on a modified quadrupole mass spectrometer[13] equipped with a data acquisition system[14]. The respective emission and electron energy were 1000 μA and 300 V. Resolution, sensitivity, and mass calibration were made according to the recommended procedures. Water was employed as the reagent gas, admitted from behind the sample and from a separate line into the chemical ionization source. The selected ion monitoring data were recorded on the MH^+ at a nominal source pressure of 1 torr and a source temperature of 250°. For the direct chemical ionization experiments ~1 μl of solution was deposited on a quartz probe.

RESULTS AND DISCUSSION

While the extraction procedure remains essentially unchanged (3), organizational efficiencies permitted each of four technicians to extract daily 11 samples plus the control. The sample data collection procedure was modified to increase the daily capacity to approximately twice the number of samples extracted. An isothermal column, a solids sample injector, and a retention time of the analyte of 0.6 min allowed sample injections at the rate of 12–15/hr. There was also a noticeable decrease in the background from the elimination of the solvent. Otherwise diverted by a dump valve, the helium carrier gas flowed into the source only during data acquisition to reduce column bleed. Instrument maintenance was also reduced by operating the ion source and multiplier only while collecting data.

Because the manual peak height measurement routine provided with the instrument was time consuming, a program was written to scan each data file, determine the baselines, the net peak heights for each acquired ion, and calculate the peak height ratios and concentrations. As elabo-

[13] SIMULSCAN, Extranuclear Corp., Pittsburgh, Pa.
[14] Model 69KD, Technivent Corp., St. Louis, Mo.

Table V—Comparative and Relative Bioavailability Parameters of 100-mg Direct Compression Tablet and Solution Formulations of Captopril Coadministered with Isotopomer Solution

Parameter	Mean Bioavailability Parameter: Direct Compression Tablet[a] Captopril	Solution[b] Isotopomer		Relative[c] Parameter
C_{max}, μg/ml, Mean[e]	0.931	0.678	C_{m1}	1.59
⟶ (± *SEM*)	(0.156)	(0.180)	C_{m2}	(0.38)
T_{max}, hr Mean	0.63	0.63		1.0
(±*SEM*)	(0.07)	(0.07)		(0)
$AUC_{0\rightarrow12}$ hr Mean	1.209	0.903	AUC_1	1.59
(± *SEM*)	(0.099)	(0.187)	AUC_2	(0.44)
	Solution[d] Captopril	Solution[b] Isotopomer		
C_{max}, μg/ml Mean	0.790	0.753	C_{m1}	1.06
(± *SEM*)	(0.054)	(0.052)	C_{m2}	(0.07)
T_{max}, hr Mean	0.75	0.81		0.94
(± *SEM*)	(0)	(0)		(0.06)
$AUC_{0\rightarrow12}$, hr Mean	1.065	1.061	AUC_1	1.01
(± *SEM*)	(0.065)	(0.039)	AUC_2	(0.07)

[a] Direct compression tablet (100 mg) coadministered. [b] Solution of isotopomer (100 mg) coadministered. [c] Parameter direct compression tablet (or solution)/parameter isotopomer. [d] Solution (100 mg) coadministered. [e] For four subjects.

rated in the experimental section, multiple measurements of the control sample allows for the single-point calibration to increase the accuracy of the measurements. It is also essential to keep the ion source at a controlled temperature to achieve the most precise measurements. Changes in the control ratio value may result from contaminant deposits on the source and quadrupole rods. In the case of the low-concentration urine extracts, the repeller was frequently shorted out because of the extraneous materials present in the extract. When this occurred, a sudden loss in sensitivity and a drastic change in the value of the control ratio was noted. While not capable of the same limit of detection, the extraction procedure for the higher concentration urine is preferred.

The specificity of the measurements of captopril was independently validated using positive chemical ionization GLC–selected ion monitoring by measuring the MH^+ of the reference (II*b*) and analyte (I*b*) derivatives. A comparison with the electron-impact data of two subjects demonstrates good correlation between the two data sets (Table II) reconfirming the specificity of the electron-impact method and also qualifying the positive chemical ionization GLC–selected ion monitoring procedure as an alternate method.

A limited set of data compares the electron-impact GLC–selected ion monitoring data with results obtained by direct chemical ionization. Nanogram quantities of a sample deposited on the direct insertion probe produce readily measureable intensities (Fig. 1) that can be used in the quantitative measurement of captopril related compounds (Table III).

The limit of detection and sensitivity of the method using the isotopomer as the internal reference was established (18) (Table IV). Three sets of calibration extracts were each measured three times to provide a total of nine measurements per calibration point. The weighted regression was chosen because the ratio of the standard deviations (s) to respective mean varies over the concentration range. From 0 to 60 ng/ml, the coefficient of variation (CV) is 13%. The 3s value of the lowest calibration point puts the limit of detection at 13 ng/ml (99% confidence limit). The actual distribution of 108 zero-hour samples has two-thirds of the values at ≤6 ng/ml and 95% of the values at ≤14.5 ng/ml (Fig. 2), in good agreement with the value derived from the detection limit of the lowest nonzero calibration 3s value. The limit of detection and the sensitivity could have been enhanced if a low level calibration curve were employed using one-tenth the amount of internal reference. No significant benefit would have been derived for these bioavailability studies, however.

Table VI—Comparative Bioavailability Parameters of 100-mg Direct Compression Tablets and Solution Formulations of Captopril

Parameter	Direct Compression Tablet[a] Captopril	Solution[b] Captopril
C_{max}, μg/ml Mean[c]	0.90	0.82
(SEM)	(0.05)	(0.05)
T_{max}, hr Mean	0.74	0.84
(SEM)	(0.04)	(0.07)
$AUC_{0\rightarrow12}$, hr Mean	1.23	1.16
μg × hr/ml (*SEM*)	(0.05)	(0.04)

[a] Captopril (100 mg) as a direct compression tablet. [b] Captopril (100 mg) as a solution. [c] For 18 subjects.

The relative standard deviation (RSD)[15] of 53 pairs of duplicate extracts of 0.75-hr blood samples is 3.9%, which is in good agreement with the CV ≤5.5% calculated from the 125 to 1500 ng/ml calibration data.

Because of intra- and intersubject variation in the disposition of drugs, a significant number of subjects, usually ≥16, are required to demonstrate bioequivalence in a multiple crossover study. Using simultaneous administration with isotopomeric formulations (9–15), superior bioavailability data may be obtained with fewer subjects. A pilot two-way crossover study was performed to compare the bioavailability of a 100-mg direct compression tablet with a 100-mg solution of I, given orally, along with a coadministered solution of 100 mg of the isotopomer, II.

The mean bioavailability parameters determined for the tablet and oral solution given to four subjects in this study compare favorably (Table V) with data obtained from 18 subjects administered in the usual way (Table VI). No significant difference was found for the mean bioavailability data derived from the coadministration of captopril and isotopomer as solutions (Tables V and VII). Consequently, the relative bioavailability parameters, C_{m1}/C_{m2} and AUC_1/AUC_2[16] are approximately in unity. However, the relative bioavailability parameters, C_{m1}/C_{m2} and AUC_1/AUC_2, for the direct compression tablet and isotopomer solution are significantly different. Examination of the data (Table VIII) reveals the captopril blood levels of subject 1 were approximately three times

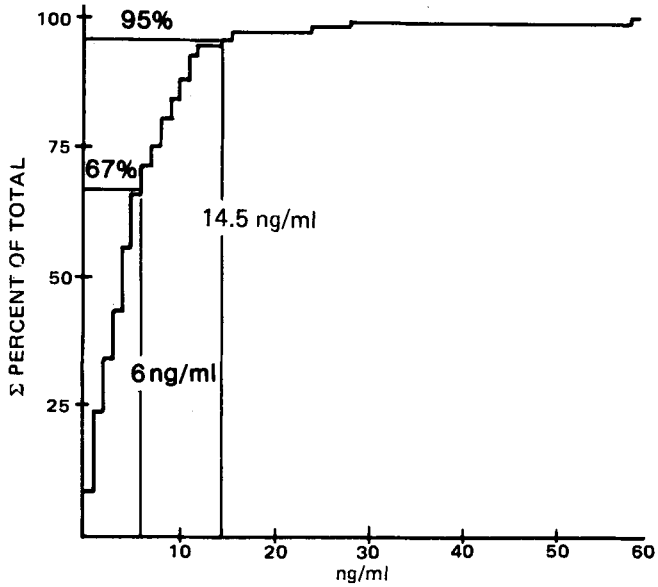

Figure 2—*Distribution of measured values of 108 zero-hour blood samples as a percent of total number of samples: maximum concentrations containing 67 and 95% of values are shown.*

[15] $RSD = (\Delta/M) \times 100$; $\Delta = (Ext_1 - Ext_2)$, $M = (Ext_1 + Ext_2)/2$.

[16] C_{m1}/C_{m2}—relative maximum concentrations of captopril (I) and isotopomer (II) AUC_1/AUC_2–relative area under the curve of I and II.

Table VII—Concentrations of Captopril and Isotopomer Each Sampling Time—Solution *versus* Solution

Time, hr	Captopril Solution[a], ng/ml Subject No. 1	2	3	4	Mean	Isotopomer Solution[b], ng/ml Subject No. 1	2	3	4	Mean
0.25	50	175	239	197	165	50	121	208	125	126
0.5	281	637	761	550	557	311	573	674	466	506
0.75	714	788	944	716	790	834	727	828	612	750
1.0	554	755	698	648	664	708	738	630	591	667
1.5	314	327	377	336	339	408	324	346	322	350
2.0	169	239	159	176	186	214	240	146	165	191
3.0	48	58	53	69	57	66	61	48	67	61
4.0	24	27	18	29	25	32	27	21	27	27
6.0	10	11	6	11	10	14	12	8	13	12
8.0	9	5	0	4	5	10	7	2	6	6
12.0	0	5	0	1	2	4	5	0	2	3

[a] Captopril (100 mg) coadministered as a solution. [b] Isotopomer (100 mg) coadministered as a solution.

Table VIII—Blood Concentrations of Captopril and Isotopomer at Each Sampling Time—Tablet *versus* Solution

Time, hr	Direct Compression Tablet[a], ng/ml Subject No. 1	2	3	4	Mean	Isotopomer Solution[b], ng/ml Subject No. 1	2	3	4	Mean
0.25	83	157	361	299	225	43	131	321	230	181
0.5	424	455	991	1322	806	199	360	892	1068	630
0.75	840	572	969	962	836	310	440	856	824	608
1.0	827	497	604	785	678	277	415	541	656	472
1.5	411	308	291	395	351	126	260	270	327	246
2.0	139	278	133	183	183	59	242	126	175	151
3.0	67	81	76	65	72	23	76	71	61	58
4.0	31	29	38	33	33	9	28	42	33	28
6.0	13	8	11	11	11	4	9	12	10	9
8.0	6	1	6	18	8	1	6	8	6	5
12.0	1	0	0	1	1	0	0	3	3	2

[a] Captopril (100 mg) coadministered as a direct compression tablet. [b] Isotopomer (100 mg) coadministered as a solution.

Table IX—Urinary Excretion of Captopril and Isotopomer as a Percent of Dose

Time, hr	Captopril Direct Compression Tablet[a], % of Dose Subject No. 1	2	3	4	Isotopomer Solution[b], % of Dose Subject No. 1	2	3	4
0–4	22.0	18.3	78.4[c]	22.8	8.0	14.6	72.4[c]	21.7
4–8	2.4	3.0	1.7	4.2	0.87	2.6	1.5	3.7
8–12	0.67	0.63	0.31	0.28	0.22	0.51	0.30	0.28
Total 0–12	25.1	20.3	—	27.3	9.1[d]	17.7	—	25.7
	Captopril Solution[e], % of Dose Subject No. 1	2	3	4	Isotopomer Solution[b], % of Dose Subject No. 1	2	3	4
0–4	19.2	24.3	8.2	8.2	22.9	23.1	7.2	7.4
4–8	3.3	1.5	1.7	2.7	4.3	1.5	1.5	2.4
8–12	0.38	0.45	0.29	0.48	0.58	0.51	0.28	0.54
Total 0–12	22.9	26.3	10.2	11.4	27.8	25.1	8.7	10.3

[a] Captopril (100 mg) coadministered as a direct compression tablet. [b] Isotopomer (100 mg) coadministered as a solution. [c] Urine appears to be in error. [d] Total isotopomer excreted from 0–12 hr is ~ one-third of excreted captopril for this subject. [e] Captopril (100 mg) coadministered as a solution.

greater than the isotopomer levels, as were the levels of compounds excreted in urine (Table IX). Significantly, this difference would have gone undetected in a conventional study. If the data for this subject are eliminated, the relative bioavailability parameters, while not in unity, are significantly lower. Previous bioavailability studies have also shown that a small difference in bioavailability parameters exists between direct compression tablet and solution formulations (Table VI).

The statistical evaluation of the coadministration bioavailability data was made to determine the power of the method to meet criteria for establishing differences in bioavailability. Excluding the suspect data of subject 1, data from only two of the three remaining subjects would be sufficient to establish differences in bioavailability that might require 14–40 subjects in a conventional study. However, from a practical point of view, it would seem more appropriate to expand such a study as this to ~6 subjects to provide a wider range of disposition, which would still result in a substantial savings in clinical and laboratory expense.

REFERENCES

(1) M. A. Ondetti, B. Rubin, and D. W. Cushman, *Science*, **196**, 441 (1977).

(2) *Drugs of the Future*, **5**, 576 (1980).

(3) P. T. Funke, E. Ivashkiv, M. F. Malley, and A. I. Cohen, *Anal. Chem.*, **52**, 1086 (1980).

(4) B. H. Migdalof, S. M. Singhvi, and K. J. Kripalani, *J. Liquid Chromatogr.*, **3**, 857 (1980).

(5) K. J. Kripalani, D. N. McKinistry, S. M. Singhvi, D. A. Willard, R. A. Vukovich, and B. H. Migdalof, *Clin. Pharmacol. Ther.*, **27**, 636 (1980).

(6) Y. Matsuki, K. Fukuhara, T. Ito, H. Ono, N. Ohara, T. Yui, and T. Nambara, *J. Chromatogr.*, **188**, 177 (1980).

(7) Y. Kawahara, M. Hisaoka, Y. Yamazaki, A. Inage, and T. Morioka, *Chem. Pharm. Bull.*, **29**, 150 (1981).

(8) B. Jarrott, A. Anderson, R. Hooper, and W. J. Louis, *J. Pharm. Sci.*, **70**, 665 (1981).

(9) J. M. Strong, J. S. Dutcher, W.-K. Lee, and A. J. Atkinson, Jr., *Clin. Pharmacol. Ther.*, **18**, 613 (1975).

(10) R. L. Wolen, R. H. Carmichael, A. S. Ridolfo, L. Thompkins, and E. A. Ziege, *Biomed. Mass Spectrom.*, **6**, 173 (1979).

(11) H. d'A. Heck, S. E. Buttrill, Jr., N. W. Flynn, R. L. Dyer, M. Anbar, T. Cairns, S. Dighe, and B. E. Cabana, *J. Pharmacokinet. Bio-*

pharm., 7, 233 (1979).
(12) J. R. Carlin, R. W. Walker, R. O. Davies, R. T. Ferguson, and W. J. A. VandenHeuvel, *J. Pharm. Sci.*, **69**, 1111 (1980).
(13) D. Alkalay, W. E. Wagner, Jr., S. Carlsen, L. Khemani. J. Volk, M. F. Barlett and A. LeSher, *Clin. Pharmacol. Ther.*, **27**, 697 (1980).
(14) P. J. Murphy and H. R. Sullivan, *Annu. Rev. Pharmacol. Toxicol.*, **20**, 609 (1980).
(15) R. L. Wolen and C. M. Gruber, Jr., in "Drug Absorption and Disposition: Statistical Considerations," K. S. Albert, Ed., Academy of Pharmaceutical Sciences, American Pharmaceutical Association, Washington, D.C., 1981, pp. 69–76.
(16) J. G. Wagner, *Pharmacol. Ther.*, **12**, 537 (1981).
(17) H. Kadin and R. B. Pacl, *J. Pharm. Sci.*, **71**, 1134 (1982).
(18) *Clin. Chim. Acta*, **98**, 145F (1979).

ACKNOWLEDGMENTS

The statistical evaluation of the data, provided by A. G. Itkin and M. Stern, and the technical advice concerning the processing of urine samples, given by H. Kadin, is gratefully acknowledged. One of the authors, A. I. Cohen, acknowledges the timely consultation by Dr. Myra Gordon, Merck of Canada, that stimulated this study.

Pharmacokinetics of Procainamide in Rats with Extrahepatic Biliary Obstruction

PETER J. BASSECHES *x and G. JOHN DiGREGORIO

Received August 3, 1981, from the *Department of Pharmacology, Hahnemann Medical College, Philadelphia, PA 19102.* Accepted for publication January 19, 1982. *Present address: Division of Developmental Oncology Research, Department of Oncology, Mayo Clinic, Rochester, MN 55905.

Abstract □ The pharmacokinetics of the widely used antiarrhythmic agent, procainamide, was studied in rats with extrahepatic biliary obstruction produced by ligation of the common bile duct. Various biological fluids, including plasma, saliva, and urine, were analyzed for procainamide and/or its major metabolite, *N*-acetylprocainamide. Ligation of the common bile duct immediately prior to intravenous administration of 50 mg/kg procainamide did not alter plasma, saliva, or urine concentrations of procainamide, indicating that biliary excretion was of minor importance in the elimination of procainamide. However, bile duct ligation allowed to persist for 4 days significantly elevated plasma, saliva, and urine levels of procainamide. While the increase in urinary procainamide paralleled the increase observed in plasma, salivary concentrations did not. Bile duct ligation did not appear to impair nonmicrosomal acetylation of procainamide, although a significantly greater amount of unchanged drug was found in the urine after 24 hr. Pharmacokinetic analysis *via* the two-compartment open model showed that bile duct ligation caused a decrease in overall clearance from ~61.94 to 28.71 ml/kg/min. This reduction probably resulted from the decreased microsomal metabolism of procainamide. The significant reduction in the apparent volume of distribution from 3.76 to 2.72 liter/kg could be the result of reduced binding sites. There was also a significant increase in the elimination half-life of procainamide from 47.39 to 78.64 min in bile duct ligated rats.

Keyphrases □ Pharmacokinetics—procainamide, rats with extrahepatic biliary obstruction □ Procainamide—pharmacokinetics in rats with extrahepatic biliary obstruction □ Biliary obstruction—extrahepatic, pharmacokinetics of procainamide in rats

Biliary stasis in humans can be caused by tumors, drugs, or various pathophysiological alterations. Many patients with biliary stasis are also critically ill with other serious conditions and therefore are under treatment with a number of pharmacological agents. Inhibition of bile flow and/or biliary excretion may have profound consequences on the pharmacokinetics of drugs, not only because bile can be a route of irreversible elimination, but also because cholestasis may affect microsomal drug metabolism. Tavolini and Guarino (1) demonstrated altered disposition of doxorubicin[1], an antineoplastic agent eliminated extensively in the bile. Other investigators (2–5) demonstrated that microsomal metabolism of a number of drugs that are not extensively excreted in bile is significantly decreased, thus prolonging the elimination half-life ($t_{1/2\beta}$). However, the effects of biliary stasis on the pharmacokinetics of drugs with minimal biliary excretion and minimal microsomal metabolism are unclear. The antiarrhythmic agent procainamide (I) is such a drug. It was the purpose of this investigation to study the effects of cholestasis, induced by mechanical obstruction of the common bile duct, on the pharmacokinetics of I. Salivary levels were measured as an index of drug distribution to the peripheral tissue compartment, and urine levels were assayed to obtain an estimate of the renal clearance of procainamide and the relative urinary metabolic profile.

[1] Adriamycin.

EXPERIMENTAL

Urine, saliva, and plasma were obtained from a group of normal Wistar rats (weight 190–260 g) for the quantitation of I. Rats were anesthetized with 50 mg/kg ip pentobarbital[2]. Initially, a tracheotomy was performed to facilitate breathing, and then the animals were prepared for collection of parotid saliva according to a previously described method (6). Stimulation of salivation was accomplished by infusing pilocarpine[3] (0.25 mg/ml) into the right brachial artery at a rate of 0.11 ml/min for 90 min. For the administration of I[4] (50 mg/kg), the femoral vein was cannulated. Urine was collected *via* cannulation of the ureters. Urine and saliva were collected over three 30-min collection periods, and 1.5 ml of whole blood was collected at 30, 60, and 90 min postinjection from a cannula placed in the femoral artery. From a separate group of normal rats, plasma was obtained at 30, 60, and 90 min following administration of 50 or 100 mg/kg of I for the quantitation of the acetylated metabolite, *N*-acetylprocainamide (II).

In anticipation of the fact that saliva was to be collected simultaneously with the other biological fluids, preliminary studies were performed to determine the effects of pilocarpine infusion of plasma procainamide concentration and urinary procainamide excretion. Ten control (no pilocarpine) and 10 test rats were used for plasma collection, and another group of five controls and five test animals were used for urine collection.

Extrahepatic biliary obstruction was produced in another group of

[2] Nembutal, Abbott Laboratories, North Chicago, Ill.
[3] Sigma Chemical Co., St. Louis, Mo.
[4] Squibb Institute for Medical Research, Princeton, N.J.

0022-3549/82/1100-1256$01.00/0

pharm., 7, 233 (1979).
(12) J. R. Carlin, R. W. Walker, R. O. Davies, R. T. Ferguson, and W. J. A. VandenHeuvel, *J. Pharm. Sci.*, **69**, 1111 (1980).
(13) D. Alkalay, W. E. Wagner, Jr., S. Carlsen, L. Khemani. J. Volk, M. F. Barlett and A. LeSher, *Clin. Pharmacol. Ther.*, **27**, 697 (1980).
(14) P. J. Murphy and H. R. Sullivan, *Annu. Rev. Pharmacol. Toxicol.*, **20**, 609 (1980).
(15) R. L. Wolen and C. M. Gruber, Jr., in "Drug Absorption and Disposition: Statistical Considerations," K. S. Albert, Ed., Academy of Pharmaceutical Sciences, American Pharmaceutical Association, Washington, D.C., 1981, pp. 69–76.
(16) J. G. Wagner, *Pharmacol. Ther.*, **12**, 537 (1981).
(17) H. Kadin and R. B. Pacl, *J. Pharm. Sci.*, **71**, 1134 (1982).
(18) *Clin. Chim. Acta*, **98**, 145F (1979).

ACKNOWLEDGMENTS

The statistical evaluation of the data, provided by A. G. Itkin and M. Stern, and the technical advice concerning the processing of urine samples, given by H. Kadin, is gratefully acknowledged. One of the authors, A. I. Cohen, acknowledges the timely consultation by Dr. Myra Gordon, Merck of Canada, that stimulated this study.

Pharmacokinetics of Procainamide in Rats with Extrahepatic Biliary Obstruction

PETER J. BASSECHES *x and G. JOHN DiGREGORIO

Received August 3, 1981, from the *Department of Pharmacology, Hahnemann Medical College, Philadelphia, PA 19102.* Accepted for publication January 19, 1982. *Present address: Division of Developmental Oncology Research, Department of Oncology, Mayo Clinic, Rochester, MN 55905.

Abstract □ The pharmacokinetics of the widely used antiarrhythmic agent, procainamide, was studied in rats with extrahepatic biliary obstruction produced by ligation of the common bile duct. Various biological fluids, including plasma, saliva, and urine, were analyzed for procainamide and/or its major metabolite, *N*-acetylprocainamide. Ligation of the common bile duct immediately prior to intravenous administration of 50 mg/kg procainamide did not alter plasma, saliva, or urine concentrations of procainamide, indicating that biliary excretion was of minor importance in the elimination of procainamide. However, bile duct ligation allowed to persist for 4 days significantly elevated plasma, saliva, and urine levels of procainamide. While the increase in urinary procainamide paralleled the increase observed in plasma, salivary concentrations did not. Bile duct ligation did not appear to impair nonmicrosomal acetylation of procainamide, although a significantly greater amount of unchanged drug was found in the urine after 24 hr. Pharmacokinetic analysis *via* the two-compartment open model showed that bile duct ligation caused a decrease in overall clearance from ~61.94 to 28.71 ml/kg/min. This reduction probably resulted from the decreased microsomal metabolism of procainamide. The significant reduction in the apparent volume of distribution from 3.76 to 2.72 liter/kg could be the result of reduced binding sites. There was also a significant increase in the elimination half-life of procainamide from 47.39 to 78.64 min in bile duct ligated rats.

Keyphrases □ Pharmacokinetics—procainamide, rats with extrahepatic biliary obstruction □ Procainamide—pharmacokinetics in rats with extrahepatic biliary obstruction □ Biliary obstruction—extrahepatic, pharmacokinetics of procainamide in rats

Biliary stasis in humans can be caused by tumors, drugs, or various pathophysiological alterations. Many patients with biliary stasis are also critically ill with other serious conditions and therefore are under treatment with a number of pharmacological agents. Inhibition of bile flow and/or biliary excretion may have profound consequences on the pharmacokinetics of drugs, not only because bile can be a route of irreversible elimination, but also because cholestasis may affect microsomal drug metabolism. Tavolini and Guarino (1) demonstrated altered disposition of doxorubicin[1], an antineoplastic agent eliminated extensively in the bile. Other investigators (2–5) demonstrated that microsomal metabolism of a number of drugs that are not extensively excreted in bile is significantly decreased, thus prolonging the elimination half-life ($t_{1/2\beta}$). However, the effects of biliary stasis on the pharmacokinetics of drugs with minimal biliary excretion and minimal microsomal metabolism are unclear. The antiarrhythmic agent procainamide (I) is such a drug. It was the purpose of this investigation to study the effects of cholestasis, induced by mechanical obstruction of the common bile duct, on the pharmacokinetics of I. Salivary levels were measured as an index of drug distribution to the peripheral tissue compartment, and urine levels were assayed to obtain an estimate of the renal clearance of procainamide and the relative urinary metabolic profile.

[1] Adriamycin.

EXPERIMENTAL

Urine, saliva, and plasma were obtained from a group of normal Wistar rats (weight 190–260 g) for the quantitation of I. Rats were anesthetized with 50 mg/kg ip pentobarbital[2]. Initially, a tracheotomy was performed to facilitate breathing, and then the animals were prepared for collection of parotid saliva according to a previously described method (6). Stimulation of salivation was accomplished by infusing pilocarpine[3] (0.25 mg/ml) into the right brachial artery at a rate of 0.11 ml/min for 90 min. For the administration of I[4] (50 mg/kg), the femoral vein was cannulated. Urine was collected *via* cannulation of the ureters. Urine and saliva were collected over three 30-min collection periods, and 1.5 ml of whole blood was collected at 30, 60, and 90 min postinjection from a cannula placed in the femoral artery. From a separate group of normal rats, plasma was obtained at 30, 60, and 90 min following administration of 50 or 100 mg/kg of I for the quantitation of the acetylated metabolite, *N*-acetylprocainamide (II).

In anticipation of the fact that saliva was to be collected simultaneously with the other biological fluids, preliminary studies were performed to determine the effects of pilocarpine infusion of plasma procainamide concentration and urinary procainamide excretion. Ten control (no pilocarpine) and 10 test rats were used for plasma collection, and another group of five controls and five test animals were used for urine collection.

Extrahepatic biliary obstruction was produced in another group of

[2] Nembutal, Abbott Laboratories, North Chicago, Ill.
[3] Sigma Chemical Co., St. Louis, Mo.
[4] Squibb Institute for Medical Research, Princeton, N.J.

0022-3549/82/1100-1256$01.00/0

Table I—Mean 24-hr Urinary Excretion of Procainamide and *N*-Acetylprocainamide before and after 4-Day Bile Duct Ligation Following Procainamide Administration

Administered dose, mg	Procainamide excreted, %[a]	*N*-Acetylprocainamide excreted, %
	Before Bile Duct Ligation	
11.59 ± 0.90	36.6 ± 3.38	26.2 ± 1.66
	After Bile Duct Ligation	
11.92 ± 0.63	45.5 ± 3.22[b]	30.58 ± 1.12[c]

[a] Percent excretion corrected for 90% recovery. [b] $p < 0.001$. [c] Not significant.

animals by double ligation of the common bile duct following anesthesia with 100 mg/kg of 98% ketamine[5]–2% acepromazine[6] ip. The animals were then sutured and allowed to recover for 4 days. On the fourth day, bile duct ligated animals were prepared for the simultaneous collection of saliva, urine, and plasma after administration of 50 mg/kg iv of I as described above, and the samples were quantitated for I. Plasma samples were also quantitated for II. Animals that did not exhibit jaundice, as evidenced by yellowish skin and bright yellow urine, were not used. Sham operated animals (with laparotomies) were also prepared in a manner identical to actual bile duct ligated animals. A group of six animals were utilized for I determinations immediately after bile duct ligation (Day 0).

To determine the effects of bile duct ligation on the metabolic disposition of I, control rats were injected with 50 mg/kg ip and placed in metabolic cages[7] for 24-hr urine collection. During this period the animals were allowed no food but were given water *ad libitum*. After the 24-hr period of urine collection, a period of 3 days was allowed to elapse to permit the animals to regain a normal metabolic profile. The animals were then anesthetized and the bile ducts were ligated. After 4 days these animals were again administered 50 mg/kg ip of I and placed in metabolic cages for 24-hr urine collection.

Six control and six bile duct ligated animals were prepared for pharmacokinetic studies by performing tracheotomies and cannulating the femoral vein and artery. After administration of 50 mg/kg iv of I, 0.4–0.5 ml of blood was sampled at 5, 15, 30, 45, 60, 90, and 120 min for analysis of the plasma I kinetics. To prevent major perturbation of drug levels, a separate group of six control and six bile duct ligated animals were used to obtain 1- and 5-min levels. The 1-min levels were then included with the values for the other animals for mathematical analysis on the basis of how closely matched the 5-min values were. The two-compartment open pharmacokinetic model was used to describe the kinetics of I, utilizing the biexponential function:

$$C_t = Ae^{-\alpha t} + Be^{-\beta t} \qquad \text{(Eq. 1)}$$

where C_t is the plasma concentration at time t, A and B are the zero-time intercepts of the fast and slow linear components, respectively, and α and β are the distribution and elimination rate constants, respectively. The pharmacokinetic parameters, A, B, α, and β, were calculated by linear regression of the two linear components of the plasma disappearance curve. Distribution half-life ($t_{1/2\alpha}$), elimination half-life ($t_{1/2\beta}$), volume of distribution (V_d), and clearance (Cl) were calculated by conventional techniques (7).

Analysis of I in all fluid samples and II in urine involved organic extraction of samples into 10 ml of methylene chloride and quantitation *via* a gas chromatograph[8] using dipropylprocainamide[4] as an internal standard as previously described (8). For reasons of sensitivity, plasma of II was quantitated *via* an enzyme–immunoassay method[9]. All statistical determinations of significance were done using the Student's t test. In all cases, except the 24-hr urinary disposition studies (Table I), the unpaired t test was used; in the case of the latter, the paired t test was employed.

RESULTS

Preliminary studies on the effect of pilocarpine infusion indicated that infusion of 0.25 mg/ml pilocarpine at a rate of 0.11 ml/min for 90 min had no effect on the plasma I concentration at any time period studied; however, urinary excretion did show significant decreases during the second and third 30-min collection periods (Table II).

[5] Bristol Inc., Syracuse, N.Y.
[6] Ayerst Laboratories, New York, N.Y.
[7] Wahman Co.
[8] Model 3920, Perkin-Elmer Corp., Norwalk, Conn.
[9] EMIT, Syva Co., Palo Alto, Calif.

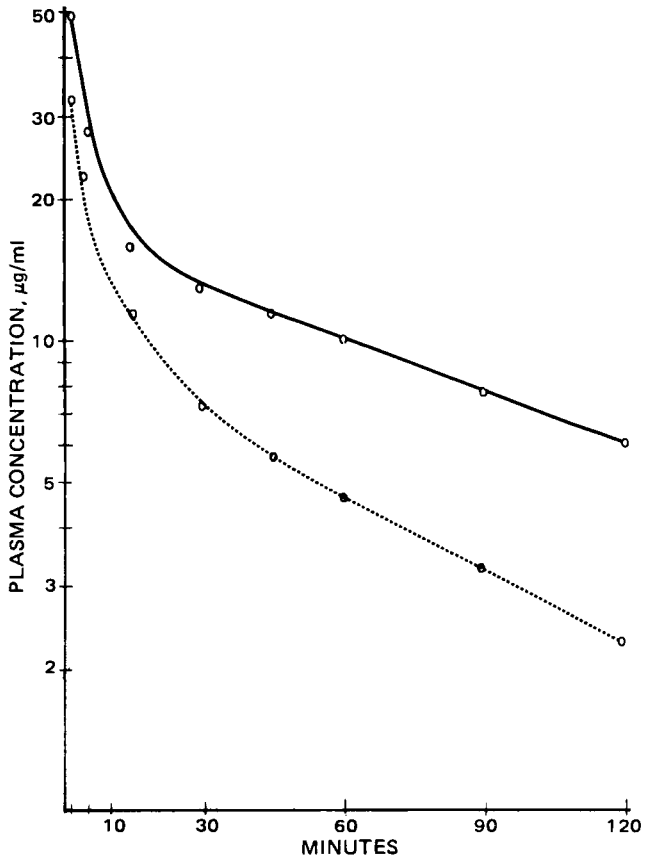

Figure 1—*Plasma disappearance of procainamide.*

The results of GC analysis of plasma, saliva, and urine samples from normal animals receiving a dose of 50 mg/kg iv of I are shown in Table III. The mean I levels in the three biological fluids of sham-operated rats were not significantly different from those of the normal rats at any time period studied. Similarly, in rats whose bile ducts were ligated immediately prior to administration of I (day 0), there were no significant differences in I levels of any of the biological fluids at any time period compared to normal rats. However, when bile duct ligation was allowed to persist for 4 days, significantly higher plasma, saliva, and urine levels were observed at all time periods. Plasma I concentrations increased 100, 125, and 105% at 30, 60, and 90 min, respectively. The increase in urinary excretion paralleled the increase in plasma levels with increases of 94, 125, and 133% over the three respective 30-min collections, indicating that renal excretion is not impaired by bile duct ligation. Salivary I concentrations also increased, but the increases did not parallel those observed in plasma except during the last collection periods. The salivary levels increased ~47, 77, and 125% over the three respective time periods (Table III).

Figure 1 illustrates the disappearance of I from plasma with time for normal animals and animals with 4-day bile duct ligation. The mean pharmacokinetic parameters for both groups are shown in Table IV. Distribution half-life ($t_{1/2\alpha}$) in 4-day bile duct ligated rats is not significantly different compared to normal rats. Elimination half-life ($t_{1/2\beta}$), however, is significantly prolonged ($p < 0.025$). Volume of distribution (V_d) is significantly decreased in 4-day bile duct ligated rats compared to normals ($p < 0.05$). Clearance (Cl) is also decreased by 115% ($p < 0.025$).

To determine whether the observed pharmacokinetic alterations were the result of bile duct ligation-induced metabolic changes, the urinary disposition of I was examined. Table I shows that in the 4-day bile duct ligated rats, the percentage of the drug excreted as II did not change significantly compared to controls. However, the amount of drug excreted unchanged increased significantly ($p < 0.025$). The absence of a change in the production of II during 4-day bile duct ligation was confirmed by measurement of plasma II concentrations in normal and 4-day bile duct ligated rats. In normal rats mean plasma II concentrations at 30, 60, and 90 min were 4.48 ± 0.48, 5.43 ± 0.59, and 7.72 ± 4.77 μg/ml, respectively. In 4-day bile duct ligated rats, mean plasma II concentrations at the same time periods were 4.54 ± 0.36, 7.06 ± 0.72, and 8.96 ± 0.06 μg/ml, respectively.

Table II—Effects of Pilocarpine Infusion on Plasma Procainamide Concentration and Urinary Excretion

	n	30 min		60 min		90 min	
		C[a]	P[b]	C	P	C	P
Plasma procainamide[c]	10	7.49 ± 0.60	8.65 ± 0.73	4.44 ± 0.43	4.53 ± 0.68	3.24 ± 0.28	2.95 ± 0.46
Urinary procainamide[d]	5	0.76 ± 0.17	0.65 ± 0.26	0.50 ± 0.07	0.30 ± 0.10	0.33 ± 0.06	0.20 ± 0.04

[a] C = control (no pilocarpine). [b] P = pilocarpine (0.25 mg/ml) infused at a rate of 0.11 ml/min; the dose was 50 mg/kg iv procainamide. [c] Data expressed as micrograms per milliliter (± *SE*). [d] Data expressed as milligrams (± *SE*).

Table III—Mean Procainamide Concentrations in Various Biological Fluids[a]

Condition	n	Plasma[b]			Saliva[b]			Urine[c]		
		30 min	60 min	90 min	30 min	60 min	90 min	30 min	60 min	90 min
Normal rats	8–10	8.65 ± 0.73	4.53 ± 0.68	2.95 ± 0.46	16.73 ± 1.69	7.75 ± 1.32	2.82 ± 0.35	0.65 ± 0.26	0.30 ± 0.10	0.20 ± 0.04
Sham-operated rats	5	8.58 ± 0.59	5.42 ± 0.69	3.20 ± 0.33	16.62 ± 1.17	8.00 ± 1.15	3.5 ± 0.41	0.61 ± 0.11	0.33 ± 0.08	0.22 ± 0.06
Day 0 bile duct ligation	6	9.40 ± 0.69	5.43 ± 0.96	4.23 ± 0.85	17.48 ± 1.84	7.56 ± 1.46	3.55 ± 0.60	0.51 ± 0.08	0.31 ± 0.03	0.21 ± 0.05
4-Day bile duct ligation	5–8	17.32 ± 2.15	10.20 ± 2.13	6.06 ± 1.06	24.55 ± 2.23	13.71 ± 1.98	5.68 ± 0.92	1.26 ± 0.19	0.70 ± 0.11	0.46 ± 0.10

[a] Dose of procainamide = 50 mg/kg iv; 0.25 mg/ml pilocarpine infused at a rate of 0.11 ml/min. [b] Data expressed as micrograms per milliliter (± *SE*). [c] Data expressed as milligrams (± *SE*).

It was thought that the higher plasma I levels observed in bile duct ligated animals should result in higher plasma II levels, since more I was apparently available to the liver for acetylation. Since no increase was noted, it was theorized that either bile duct ligation was inhibiting acetylation due to liver damage or that the enzyme responsible for conversion of I to II, *N*-acetyltransferase, was being saturated. To test these alternative hypotheses, a 100-mg/kg dose of I was administered to control animals to achieve blood levels comparable to those in bile duct ligated animals receiving 50 mg/kg. Plasma I concentrations in normal rats receiving 100 mg/kg iv at 30, 60, and 90 min were 18.22 ± 2.45, 10.93 ± 1.69, and 6.48 ± 1.25 μg/ml, respectively, while plasma II concentrations in those animals were 5.28 ± 0.47, 6.90 ± 0.66, and 7.53 ± 0.75 μg/ml at the three respective time periods. These data show that while plasma I levels in these animals did approximate those seen in bile duct ligated animals receiving half the dose, plasma II levels did not differ from either control or bile duct ligated animals receiving half the dose, suggesting that a saturation of the acetylation process was occurring even at the 50-mg/kg dose.

DISCUSSION

It has been demonstrated (9) that the transport of I into bile is an active process, since the biliary excretion exhibited a concentrative mechanism that was saturable and could be competitively inhibited by other tertiary and quaternary amines. However, since ligation of the bile duct immediately prior to intravenous administration of I did not significantly elevate plasma, saliva, or urine levels of the drug at any time period studied, it is apparent that biliary excretion of I is a minor component in its overall elimination (Table III). This is in agreement with previous findings (10), which state that renal excretion is the major route of elimination for this drug. Furthermore, simply shutting off the biliary route of excretion cannot be invoked as the primary explanation for pharmacokinetic alterations observed in 4-day bile duct ligation in the case of I. However, the small amount of I that normally appears in bile, which according to a previous report (11) amounts to 3–5% of the administrated dose, would be reabsorbed and contribute to elevated plasma levels.

The most logical hypothesis concerning the underlying mechanism for the altered kinetics would be that the metabolism of I was being inhibited due to liver damage resulting from the reflux of bile acids in a manner similar to that proposed for a number of drugs by various investigators (2–5) (*i.e.*, destruction or decreased synthesis of cytochrome P_{450}).

Table IV—Mean Pharmacokinetic Parameters of Procainamide in Normal and 4-Day Bile Duct Ligated Rats[a]

Parameters	Control	Bile Duct Ligated
$t_{1/2\alpha}$, min ± *SE*	4.87 ± 1.06	2.95 ± 0.90
$t_{1/2\beta}$, min ± *SE*[b]	47.39 ± 3.81	78.64 ± 13.13
V_d, liter/kg ± *SE*[c]	3.72 ± 0.47	2.76 ± 0.21
Cl, ml/kg/min ± *SE*[b]	61.94 ± 13.68	28.71 ± 3.80

[a] Dose of procainamide was 50 mg/kg iv; $n = 6$ rats. [b] $p < 0.025$. [c] $p < 0.05$.

However, the 24-hr urinary II levels as well as plasma II levels indicate that there is no difference in the amount of II produced by 4-day bile duct ligated rats compared to normal rats. Since II, the major metabolite of I, is a product of a nonmicrosomal metabolism (*i.e.*, not dependent on the mixed-function oxidase system), it appears that nonmicrosomal acetylation of I is relatively resistant to inhibition by ligation of the common bile duct. Furthermore, the studies with 100 mg/kg I in normal rats indicate that the acetylation enzyme, *N*-acetyltransferase, is saturable at the 50-mg/kg dose level of I, and thus, the activity of the enzyme in normal and 4-day bile duct ligated animals is apparently the same. These results also indicate that decreased production of II is not the primary mechanism responsible for the elevation of I concentrations in the various biological fluids.

However, inhibition of microsomal metabolism may play a contributing role in the altered kinetics of I, since a small percentage of the drug undergoes some microsomal metabolism. Recently, two other metabolites of I were found (12): desethylprocainamide and *N*-acetyldesethylprocainamide; the former being the primary intermediate in the formation of the latter. Since bile duct ligation has been shown to inhibit microsomal metabolism and the data in this study show significantly greater amounts of unchanged drug excreted (Table I), it is probable that these metabolites are not produced to the normal extent, thereby contributing to higher plasma levels of the parent compound. This may explain the prolonged $t_{1/2\beta}$ calculated in this study.

Since elimination by the biliary route of excretion or decreased acetylation apparently are not the major mechanisms underlying the bile duct ligation-induced alteration in the pharmacokinetics of I, other mechanisms must be operative. Calculation of various pharmacokinetic parameters (Table IV) revealed that there is a significant reduction in V_d of I in 4-day bile duct ligated rats. The reduction in V_d suggests that the drug is not leaving the central compartment as readily as in normal rats, thus contributing to higher than normal plasma concentrations. The fact that there was no significant difference in the calculated $t_{1/2\alpha}$ indicates that the rate of distribution is not affected by 4-day bile duct ligation, only the extent of the distribution is. The idea that bile duct ligation can induce a change in drug distribution has also been advanced in a previous report (2) where it was postulated that increased thiopental sleeping times may be due to this phenomenon. The decreased distribution to the peripheral compartment observed in this study is borne out by the salivary excretion data which showed that while there was an increase in saliva I concentration, it was not of the same magnitude as the increase in plasma except at the 90-min mark. One possible explanation for the decreased V_d may involve elevated bilirubin levels, which result from bile duct ligation (13). High levels of bilirubin have been associated with displacement of drugs from plasma proteins. Since plasma protein binding of I is negligible (10–15%) but tissue protein binding is extensive, it is possible that hyperbilirubinemia caused a significant reduction in tissue binding. Such an idea has been suggested previously (14). A significant decrease in tissue binding of a drug, which is normally bound to tissues extensively, would cause a decrease in the V_d of the drug.

Thus, although biliary excretion of I is of minor importance as a route of elimination, this study demonstrates that extrahepatic biliary obstruction induced by bile duct ligation can still lead to a significant al-

teration in the pharmacokinetics of I through a combination of effects including decreased microsomal metabolism and decreased volume of distribution. Furthermore, this study shows that nonmicrosomal hepatic metabolism, such as acetylation, is relatively resistant to pathological insults such as bile duct ligation.

REFERENCES

(1) N. Tavolini and A. M. Guarino, *Arch. Int. Pharmacodyn.*, **245,** 180 (1980).

(2) R. Drew and B. G. Priestly, *Biochem. Pharmacol.*, **25,** 1659 (1976).

(3) F. Hutterer, P. G. Bacchin, J. H. Raisfield, J. B. Schenkman, F. Schaffner, and H. Popper, *Life Sci.*, **9,** 1159 (1970 b).

(4) A. M. MacKinnon, E. S. Sutherland, and F. Simon, *Gastroenterology*, **65,** 558 (1973).

(5) E. F. McLuen and J. R. Fouts, *J. Pharmacol. Exp. Ther.*, **131,** 7 (1961).

(6) G. J. DiGregorio, A. J. Piraino, B. T. Nagle, and E. K. Kniaz, *J. Dent. Res*, **56,** 502 (1977).

(7) M. Gibaldi and D. Perrier, *Pharmacokinetics*, Marcel Dekker, New York, N.Y., 1975.

(8) D. W. Schneck, K. Grove, F. O. DeWitt, R. A. Schiroff, and A. H. Hayes, Jr., *J. Pharmacol. Exp. Ther.*, **204,** 219 (1978).

(9) P. K. Nayak and L. S. Schanker, *Am. J. Physiol.*, **217,** 1639 (1969).

(10) J. Koch-Weser and S. W. Klein, *J. Am. Med. Assoc.*, **215,** 1454 (1971).

(11) B. L. Kamath, C. M. Lai, S. D. Gupta, M. J. Durrani, and A. Yacobi, *J. Pharm. Sci.*, **70,** 299 (1981).

(12) T. I. Ruo, Y. Morita, A. J. Atkinson, Jr., T. Henthorn, and J. P. Thenot, *J. Pharmacol. Exp. Ther.*, **216,** 357 (1981).

(13) M. Birns, B. Mosek, and O. Auerbach, *Am. J. Pathol.*, **40,** 95 (1962).

(14) M. Rowland, T. F. Blaschke, P. J. Meffin, and R. L. Williams, in "Effect of Disease States on Drug Pharmacokinetics," L. Z. Benet, Ed., American Pharmaceutical Association, Washington, D.C., 1976, p. 64.

Bioavailability of Tolazamide from Tablets: Comparison of *In Vitro* and *In Vivo* Results

P. G. WELLING *x, R. B. PATEL *, U. R. PATEL *, W. R. GILLESPIE ¶, W. A. CRAIG ‡§, and K. S. ALBERT ¶

Received September 24, 1981, from the *Schools of *Pharmacy and ‡Medicine, University of Wisconsin, Madison, WI 53706,* the *§Veterans Administration Hospital, Madison, WI 53705,* and *¶The Upjohn Co., Kalamazoo, MI 49001.* Accepted for publication January 26, 1982.

Abstract □ The relative bioavailability of tolazamide was determined, in healthy male volunteers, from four different tablet formulations manufactured by direct compaction or granulation processes and the results were compared with *in vitro* disintegration and dissolution values. Serum tolazamide levels were determined by a high-pressure liquid chromatographic method developed in this laboratory. Serum tolazamide levels from the formulation that gave rise to rapid absorption were described by one-compartment model kinetics with a mean absorption half-time of 1.0 hr and an elimination half-life of 4.6 hr. Peak serum levels occurred at 3.3 hr after drug administration. Marked differences were observed in drug bioavailability from the four tablets, and the mean cumulative relative fraction of dose absorbed was 1.0, 0.42, 0.75, and 0.91 from Formulations A, B, C, and D, respectively. The hypoglycemic effect was closely related to serum tolazamide levels. Disintegration times did not predict *in vivo* tolazamide bioavailability. Dissolution rates provided an approximate rank order correlation with *in vivo* absorption but failed to be predictive among formulations. Currently available *in vitro* tests do not accurately predict tolazamide *in vivo* bioavailability characteristics among different formulations and manufacturing processes but may be useful to ensure lot-to-lot uniformity in bioavailability for a given formulation and specific method of manufacture.

Keyphrases □ Bioavailability—tolazamide from tablets, comparison of *in vitro* and *in vivo* results, humans □ Tolazamide—bioavailability from tablets, comparison of *in vitro* and *in vivo* results, humans □ High-pressure liquid chromatography—determination of tolazamide bioavailability from tablets, comparison of *in vitro* and *in vivo* results, humans

The hypoglycemic effect of oral sulfonylureas is related to the size of the dose and to the bioavailability of administered drug to the systemic circulation (1, 2). Large differences in circulating levels of chlorpropamide (3, 4) and tolbutamide (5) have been reported from different generic brands, and the *in vivo* bioavailability of tolbutamide did not correlate well with *in vitro* dissolution rates (6).

Although the sulfonylurea tolazamide has been used clinically since 1965, there appears to be little or no information on its pharmacokinetic or bioavailability characteristics. Therefore, this study was designed to investigate the pharmacokinetics of tolazamide after administration of oral tablets to healthy volunteers and to compare relative *in vivo* bioavailability of different tablets with their *in vitro* disintegration and dissolution rates.

EXPERIMENTAL

Tolazamide Formulations—The four tolazamide tablet formulations selected for study were:

A: Tolazamide 250-mg tablets, marketed Formulation[1]

B: Tolazamide 250-mg tablets, experimental Formulation 1[2]

C: Tolazamide 250-mg tablets, experimental Formulation 2[3]

D: Tolazamide 250-mg tablets, experimental Formulation 3[4]

Formulation A was the commercial brand of tolazamide. Formulations B, C, and D were experimental tablets containing similar excipients as Formulation A but in different quantities to produce different *in vitro* dissolution characteristics. Tablets A and D were wet granulation formulations; B and C were direct compression formulations.

***In Vitro* Studies**—Disintegration times were determined by the official USP XX method for uncoated tablets (7).

Tablet dissolution rates were determined by a rotating paddle procedure. The apparatus[5] consisted of a 1000-ml flask containing 900 ml of 0.05 *M tris*(hydroxymethyl)aminomethane aqueous buffer (pH 7.6) and a paddle stirring rate of 75 rpm. Drug dissolution was monitored by continuously pumping the dissolution medium through a 0.5-mm pathlength flow cell[6] and measuring UV absorbance at 224 nm.

***In Vivo* Studies**—*Subjects*—Subjects[7] were 20 healthy male volun-

[1] Tolinase tablets, Lot No. 901HK, The Upjohn Co., Kalamazoo, Mich.
[2] No. 19356, The Upjohn Co., Kalamazoo, Mich.
[3] No. 19357, The Upjohn Co., Kalamazoo, Mich.
[4] No. 19358, The Upjohn Co., Kalamazoo, Mich.
[5] SPADRA, The Upjohn Co., Kalamazoo, Mich.
[6] Kintrac VII, Beckman Instruments, Fullerton, Calif.
[7] Technical and administrative staff and graduate students.

0022-3549/82/1100-1259$01.00/0

teration in the pharmacokinetics of I through a combination of effects including decreased microsomal metabolism and decreased volume of distribution. Furthermore, this study shows that nonmicrosomal hepatic metabolism, such as acetylation, is relatively resistant to pathological insults such as bile duct ligation.

REFERENCES

(1) N. Tavolini and A. M. Guarino, *Arch. Int. Pharmacodyn.*, **245,** 180 (1980).

(2) R. Drew and B. G. Priestly, *Biochem. Pharmacol.*, **25,** 1659 (1976).

(3) F. Hutterer, P. G. Bacchin, J. H. Raisfield, J. B. Schenkman, F. Schaffner, and H. Popper, *Life Sci.*, **9,** 1159 (1970 b).

(4) A. M. MacKinnon, E. S. Sutherland, and F. Simon, *Gastroenterology*, **65,** 558 (1973).

(5) E. F. McLuen and J. R. Fouts, *J. Pharmacol. Exp. Ther.*, **131,** 7 (1961).

(6) G. J. DiGregorio, A. J. Piraino, B. T. Nagle, and E. K. Kniaz, *J. Dent. Res*, **56,** 502 (1977).

(7) M. Gibaldi and D. Perrier, *Pharmacokinetics*, Marcel Dekker, New York, N.Y., 1975.

(8) D. W. Schneck, K. Grove, F. O. DeWitt, R. A. Schiroff, and A. H. Hayes, Jr., *J. Pharmacol. Exp. Ther.*, **204,** 219 (1978).

(9) P. K. Nayak and L. S. Schanker, *Am. J. Physiol.*, **217,** 1639 (1969).

(10) J. Koch-Weser and S. W. Klein, *J. Am. Med. Assoc.*, **215,** 1454 (1971).

(11) B. L. Kamath, C. M. Lai, S. D. Gupta, M. J. Durrani, and A. Yacobi, *J. Pharm. Sci.*, **70,** 299 (1981).

(12) T. I. Ruo, Y. Morita, A. J. Atkinson, Jr., T. Henthorn, and J. P. Thenot, *J. Pharmacol. Exp. Ther.*, **216,** 357 (1981).

(13) M. Birns, B. Mosek, and O. Auerbach, *Am. J. Pathol.*, **40,** 95 (1962).

(14) M. Rowland, T. F. Blaschke, P. J. Meffin, and R. L. Williams, in "Effect of Disease States on Drug Pharmacokinetics," L. Z. Benet, Ed., American Pharmaceutical Association, Washington, D.C., 1976, p. 64.

Bioavailability of Tolazamide from Tablets: Comparison of *In Vitro* and *In Vivo* Results

P. G. WELLING *x, R. B. PATEL *, U. R. PATEL *, W. R. GILLESPIE ¶, W. A. CRAIG ‡§, and K. S. ALBERT ¶

Received September 24, 1981, from the *Schools of *Pharmacy and ‡Medicine, University of Wisconsin, Madison, WI 53706,* the *§Veterans Administration Hospital, Madison, WI 53705,* and *¶The Upjohn Co., Kalamazoo, MI 49001.* Accepted for publication January 26, 1982.

Abstract □ The relative bioavailability of tolazamide was determined, in healthy male volunteers, from four different tablet formulations manufactured by direct compaction or granulation processes and the results were compared with *in vitro* disintegration and dissolution values. Serum tolazamide levels were determined by a high-pressure liquid chromatographic method developed in this laboratory. Serum tolazamide levels from the formulation that gave rise to rapid absorption were described by one-compartment model kinetics with a mean absorption half-time of 1.0 hr and an elimination half-life of 4.6 hr. Peak serum levels occurred at 3.3 hr after drug administration. Marked differences were observed in drug bioavailability from the four tablets, and the mean cumulative relative fraction of dose absorbed was 1.0, 0.42, 0.75, and 0.91 from Formulations A, B, C, and D, respectively. The hypoglycemic effect was closely related to serum tolazamide levels. Disintegration times did not predict *in vivo* tolazamide bioavailability. Dissolution rates provided an approximate rank order correlation with *in vivo* absorption but failed to be predictive among formulations. Currently available *in vitro* tests do not accurately predict tolazamide *in vivo* bioavailability characteristics among different formulations and manufacturing processes but may be useful to ensure lot-to-lot uniformity in bioavailability for a given formulation and specific method of manufacture.

Keyphrases □ Bioavailability—tolazamide from tablets, comparison of *in vitro* and *in vivo* results, humans □ Tolazamide—bioavailability from tablets, comparison of *in vitro* and *in vivo* results, humans □ High-pressure liquid chromatography—determination of tolazamide bioavailability from tablets, comparison of *in vitro* and *in vivo* results, humans

The hypoglycemic effect of oral sulfonylureas is related to the size of the dose and to the bioavailability of administered drug to the systemic circulation (1, 2). Large differences in circulating levels of chlorpropamide (3, 4) and tolbutamide (5) have been reported from different generic brands, and the *in vivo* bioavailability of tolbutamide did not correlate well with *in vitro* dissolution rates (6).

Although the sulfonylurea tolazamide has been used clinically since 1965, there appears to be little or no information on its pharmacokinetic or bioavailability characteristics. Therefore, this study was designed to investigate the pharmacokinetics of tolazamide after administration of oral tablets to healthy volunteers and to compare relative *in vivo* bioavailability of different tablets with their *in vitro* disintegration and dissolution rates.

EXPERIMENTAL

Tolazamide Formulations—The four tolazamide tablet formulations selected for study were:

A: Tolazamide 250-mg tablets, marketed Formulation[1]

B: Tolazamide 250-mg tablets, experimental Formulation 1[2]

C: Tolazamide 250-mg tablets, experimental Formulation 2[3]

D: Tolazamide 250-mg tablets, experimental Formulation 3[4]

Formulation A was the commercial brand of tolazamide. Formulations B, C, and D were experimental tablets containing similar excipients as Formulation A but in different quantities to produce different *in vitro* dissolution characteristics. Tablets A and D were wet granulation formulations; B and C were direct compression formulations.

***In Vitro* Studies**—Disintegration times were determined by the official USP XX method for uncoated tablets (7).

Tablet dissolution rates were determined by a rotating paddle procedure. The apparatus[5] consisted of a 1000-ml flask containing 900 ml of 0.05 *M tris*(hydroxymethyl)aminomethane aqueous buffer (pH 7.6) and a paddle stirring rate of 75 rpm. Drug dissolution was monitored by continuously pumping the dissolution medium through a 0.5-mm pathlength flow cell[6] and measuring UV absorbance at 224 nm.

***In Vivo* Studies**—*Subjects*—Subjects[7] were 20 healthy male volun-

[1] Tolinase tablets, Lot No. 901HK, The Upjohn Co., Kalamazoo, Mich.
[2] No. 19356, The Upjohn Co., Kalamazoo, Mich.
[3] No. 19357, The Upjohn Co., Kalamazoo, Mich.
[4] No. 19358, The Upjohn Co., Kalamazoo, Mich.
[5] SPADRA, The Upjohn Co., Kalamazoo, Mich.
[6] Kintrac VII, Beckman Instruments, Fullerton, Calif.
[7] Technical and administrative staff and graduate students.

0022-3549/82/1100-1259$01.00/0

Table I—Disintegration Times and Dissolution Rates of Tolazamide Tablets[a]

Tablet	Mean Disintegration Time[b], min (range)	Percent Dissolved in 30 min[c] (range)
A	3.8 (3.0–4.0)	103.9 (100.5–106.3)
B	2.2 (1.8–2.5)	10.9 (9.3–13.5)
C	2.3 (2.0–2.5)	31.6 (26.4–37.2)
D	26.5 (22.5–30.5)	29.7 (20.8–38.4)

[a] n = 6. [b] By the method of USP XX (Ref. 7). [c] Dissolution rates in pH 7.6 buffer.

teers between 18 and 38 years of age (mean 26) and weighing between 61.4 and 95.5 kg (mean 74.5). Two subjects were classified as heavy frame, 14 as medium, and four as small (8). Sixteen subjects were nonsmokers, and four were moderate smokers.

Before participation in the study, subjects were shown to be healthy by physical examination, including complete blood and urine biochemistry. All values were within the normal range.

Any individual with peptic ulcer, psychosis, who had ever had a myocardial infarction, or who had a history of drug allergy or diabetes was automatically excluded. Subjects were instructed to take no enzyme-inducing agents for 1 month prior to and no drugs other than the required doses of tolazamide during the study.

Subjects were advised to ingest an adequate diet of ~2500 cal/day, high in carbohydrate (minimum 300 g) for 3 days before each dose of tolazamide.

Protocol—The 20 subjects were randomly assigned to four groups of five each, and the four treatments were administered according to a 4 × 4 Latin square design. Each subject received the four treatments at 1-week intervals.

At 10 pm on the day before a tolazamide dose, subjects received a snack of two cupcakes and 240 ml (8 oz) of whole milk. Following an overnight fast, subjects reported to the clinic at 6:45 am. At 7 am 500 mg of tolazamide was administered with 180 ml of water. No food or further water were permitted until 5 hr postdose when a standard meal, consisting of one cheese sandwich, one packet of potato chips, and a small carton of milk, was provided. Food and liquid intake was unrestricted after that time.

Blood samples (10 ml) were taken from a forearm vein into evacuated glass tubes[8] (containing no anticoagulant) immediately before and then at 1, 2, 3, 4, 5, 6, 8, 12, 16, and 24 hr following tolazamide administration. Blood was allowed to clot and serum was separated by centrifugation. Serum was divided into two portions. One portion was assayed for glucose by utilizing the potassium ferricyanide–ferrocyanide oxidation reduction reaction[9] (9). The other portion was assayed for tolazamide by the high-pressure liquid chromatographic (HPLC) method described below. All samples were stored at −20° until assayed. Assays were done within 4 weeks of sampling. Assay of selected serum samples immediately after sampling and during storage showed that both tolazamide and glucose were stable at −20° for 4 weeks.

Side Effects—Subjects were monitored for drug-related side effects following each dose of tolazamide. Subjects were requested to classify each side effect as mild, moderate, or severe. Classification was subjective and no attempt was made to assess any effect quantitatively.

Assay for Tolazamide in Serum—Concentrations of tolazamide in serum were determined by an HPLC procedure developed in this laboratory. To 0.5 ml of serum was added 0.5 ml of internal standard, 5-(*p*-methylphenyl)-5-phenylhydantoin[10] in chloroform[11], 0.5 ml of aqueous sodium acetate buffer (pH 4.5), and 5 ml of methylene chloride[11]. After shaking for 5 min on a horizontal shaker and centrifuging at 3000×*g* for 3 min, the aqueous layer was discarded and the organic layer was transferred to a clean tube and evaporated to dryness under nitrogen at room temperature. The residue was reconstituted in 80 μl of methanol by vortexing, and 20 μl was injected onto the chromatograph.

The HPLC system consisted of a solvent pump[12], a fixed-volume (20 μl) sample injection valve[13], a 10-μm particle size reversed-phase octadecyl column[14] (25 cm × 4.6 mm), and a 254-nm fixed wavelength detector[15]. All chromatograms were recorded at a chart speed of 20 cm/hr.

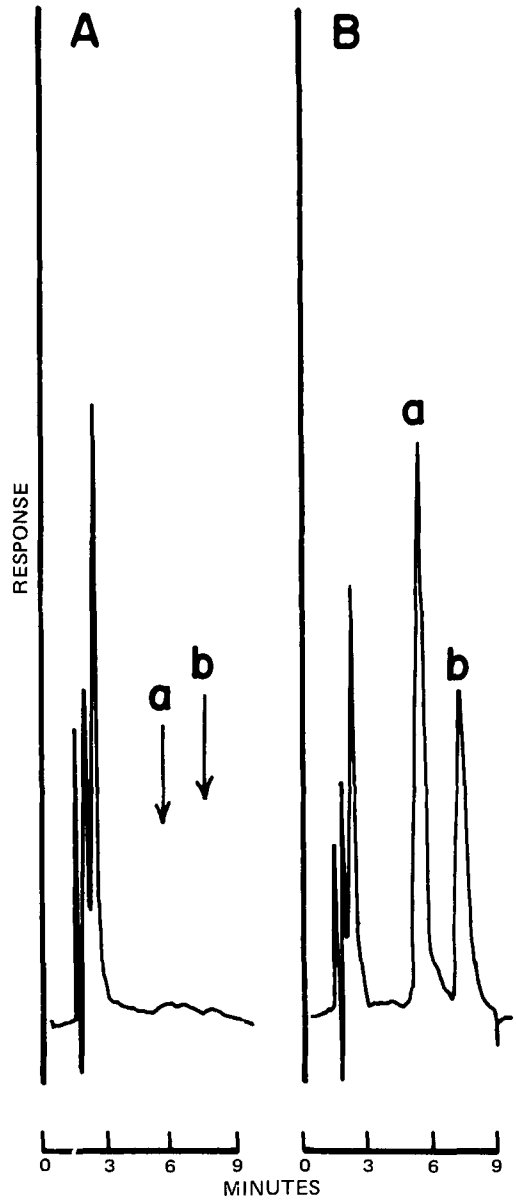

Figure 1—*Chromatograms obtained from HPLC analysis of serum containing (A) no added compounds and (B) 25 μg/ml tolazamide (a) and internal standard (b).*

The mobile phase was 52.3% methanol in pH 5.6 acetate buffer. The flow rate was 2 ml/min at a pump pressure of ~1000 psi. Concentrations of tolazamide were determined by the method of peak height ratios. Tolazamide[16] for assay standardization was reference standard quality.

Analysis of the Data—Individual serum tolazamide profiles from Formulation A were analyzed according to a single-compartment kinetic model with first-order drug appearance and elimination and an absorption lag time (10). Nonlinear regression analysis of the data was done using the program NONLIN (11) on a digital computer[17].

Estimates of the cumulative relative fraction of drug absorbed (*CRFA*) during 16 hr following each tolazamide dose were calculated by means of Eq. 1, which was derived from a previously described method for generating percent absorbed *versus* time plots (12):

$$CRFA = \frac{C_t + k_{el}^A (AUC)_{0-t}}{k_{el}^A (AUC)_{0-\infty}^A} \qquad \text{(Eq. 1)}$$

[8] Vacutainer, Becton-Dickinson, Rutherford, N.J.
[9] Technicon Auto Analyzer method No. N-2[b], Glucose, Technicon Instruments, Tarrytown, N.Y.
[10] Analytical grade, Aldrich Chemical Co., Milwaukee, Wis.
[11] Analytical grade, Burdick and Jackson, Muskegon, Mich.
[12] Model 110, Altex Scientific, Berkeley, Calif.
[13] Model 210, Altex Scientific, Berkeley, Calif.
[14] Lichrosorb C-18, Altex Scientific, Berkeley, Calif.
[15] Model 153, Altex Scientific, Berkeley, Calif.
[16] The Upjohn Co., Kalamazoo, Mich.
[17] IBM System/3033, IBM, White Plains, N.Y.

Table II—Mean Tolazamide Concentrations[a] in Serum

Time, hr	Treatment, μg/ml A	B	C	D	Statistic[b]
0	10.8 ± 7.4	1.3 ± 1.4	1.8 ± 1.9	3.5 ± 2.6	A D C B
1	20.5 ± 7.3	2.8 ± 2.8	5.4 ± 4.8	13.5 ± 6.6	A D C B
3	23.9 ± 5.3	4.4 ± 4.3	9.8 ± 5.6	20.0 ± 6.4	A D C B
4	25.4 ± 5.2	5.7 ± 4.1	13.6 ± 5.3	22.0 ± 5.4	A D C B
5	24.1 ± 6.3	6.6 ± 4.0	15.1 ± 4.7	22.6 ± 5.0	A D C B
6	19.9 ± 5.9	6.8 ± 3.4	14.3 ± 3.9	19.7 ± 4.7	A D C B
8	15.2 ± 5.5	6.6 ± 3.2	12.8 ± 4.1	14.6 ± 4.2	A D C B
12	8.8 ± 4.8	5.5 ± 3.2	9.1 ± 4.0	8.5 ± 4.1	C A D B
16	5.6 ± 3.8	4.6 ± 3.3	6.4 ± 3.9	5.4 ± 3.1	C A D B
24	2.7 ± 2.4	3.1 ± 2.6	3.1 ± 3.3	2.4 ± 1.8	C B A D
C_{max}[c], μg/ml	27.8 ± 5.3	7.7 ± 4.1	16.4 ± 4.4	24.0 ± 4.5	A D C B
T_{max}[d], hr	3.3 ± 0.9	7.0 ± 2.2	5.4 ± 2.0	4.0 ± 0.9	B C D A
AUC_{0-24}[e], μg hr/ml	260 ± 81	112 ± 63	193 ± 70	231 ± 67	A D C B

[a] Concentrations ±1 *SD*, $n = 20$. [b] For explanation see text. [c] Maximum concentration of tolazamide in serum. [d] Time of maximum concentration. [e] Area under the 0–24-hr serum tolazamide concentration curve calculated by trapezoidal rule.

where

$$(AUC)^A_{0-\infty} = (AUC)^A_{0-T} + \frac{C_T}{k^A_{el}},$$

C_t is the concentration of tolazamide in serum at time t, $(AUC)_{0-t}$ is the area under the tolazamide concentration *versus* time curve to time t calculated by trapezoidal rule, and C_T is the tolazamide concentration in serum at the last sampling time T. The values $k_{el}{}^A$, $(AUC)_{0-T}{}^A$, and $(AUC)_{0-\infty}{}^A$ are the first-order rate constants for loss of tolazamide from serum, the area under the tolazamide concentration curve to time T, and the area to infinite time, respectively, following Formulation A. This method permits the cumulative absorption of drug from each treatment to be calculated in individual subjects, relative to that from Formulation A.

Serum tolazamide and glucose levels from the four treatments were examined by analysis of variance for crossover design. When significant treatment effects were obtained, differences between individual products were examined by Tukey's significant difference test (13). In the statistics columns of Tables II and IV, the various values obtained from the different treatments are given in descending order of magnitude. All values under a common bar are statistically indistinguishable ($p > 0.05$); whereas, all values not under a common bar are statistically different ($p \leq 0.05$).

RESULTS

***In Vitro* Studies**—The disintegration times and dissolution rates of the four tablets are shown in Table I. While Formulations A, B, and C disintegrated within 4 min, Formulation D disintegrated more slowly with a mean time of 26.5 min. In the dissolution system used, Formulation A dissolved completely within 30 min. Formulations C and D exhibited similar dissolution characteristics to each other, with both tablets dissolving ~30%. Formulation B dissolved slowly, releasing only 10.9% of the drug during the 30-min period.

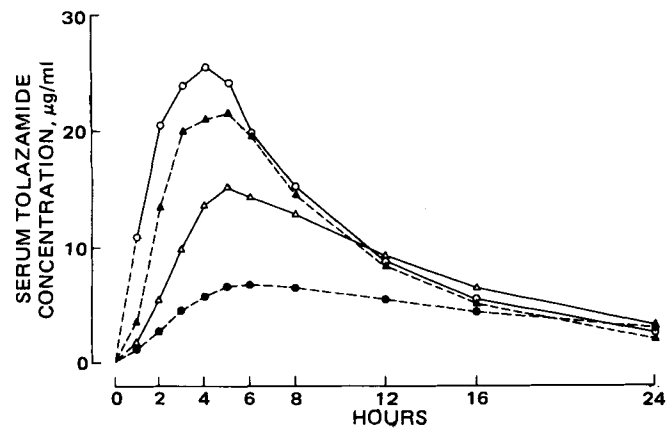

Figure 2—*Mean serum tolazamide levels as a function of time. Key: (○) Treatment A; (●) Treatment B; (△) Treatment C; (▲) Treatment D.*

Table III—Tolazamide Pharmacokinetic Parameter Values[a]

Parameter	Value
k_a[b], hr^{-1}	1.2 ± 1.3
$t_{1/2abs}$[c], hr	1.0 ± 0.7
k_{el}[d], hr^{-1}	0.18 ± 0.08
$t_{1/2elim}$[e], hr	4.6 ± 1.9
t_0[f], hr	0.75 ± 0.49
FD/V[g], μg/ml	43 ± 14
r^{2h}	0.99 ± 0.02

[a] Values ±1 *SD*, $n = 20$. [b] First-order rate constant for absorption of tolazamide in serum. [c] Absorption half-life (ln $2/k_a$). [d] First-order rate constant for loss of tolazamide from serum. [e] Elimination half-life (ln $2/k_{el}$). [f] Lag time between dosing and appearance of drug in serum. [g] Fraction of dose absorbed expressed as a concentration in the body distribution volume. [h] Coefficient of determination from nonlinear regression analysis [$r^2 = (\Sigma obs^2 - \Sigma dev^2)/\Sigma obs^2$].

Assay for Tolazamide in Serum—Typical chromatograms from serum containing both tolazamide and internal standard and from serum containing neither compound are shown in Fig. 1. Retention times for tolazamide and internal standard were 5.5 and 7.5 min, respectively. The procedure was highly specific and reproducible. Chromatographic response was linear for serum tolazamide concentrations between 1 and 100 μg/ml, and assay reproducibility from multiple replicates ($n \simeq 20$) done throughout the analytical procedures was within ±3% *SD* at the highest concentration and within ±12% at the lowest.

Drug-Related Side Effects—Side effects were noted following 41 of the 80 tolazamide doses. In each case the effect was judged by the subject as mild. On no occasion was supplementary medication or glucose considered to be necessary by the attending physician.

Side-effects were noted primarily 1–4 hr postdose and were generally typical manifestations of transient, mild hypoglycemia. In all there were 21 reports of lightheadedness or dizziness, 14 of excess perspiration, 12 of headache, 12 of tremor, 7 of weakness, 2 of dry mouth, 2 of drowsiness, 1 of constipation, and 1 of blurred vision.

The number of subjects reporting side effects was independent of the

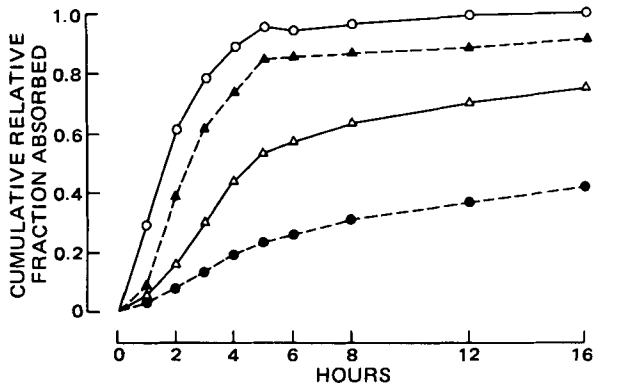

Figure 3—*Mean cumulative relative fractions of tolazamide absorbed as a function of time. Key: (○) Treatment A; (●) Treatment B; (△) Treatment C; (▲) Treatment D.*

Table IV—Parameter Values[a] for Glucose Response Following Four Tolazamide Treatments

Value	Treatment A	Treatment B	Treatment C	Treatment D	Statistic
G_{min}[b], mg/dl	54.6 ± 8.5	70.1 ± 6.2	66.0 ± 5.0	59.2 ± 6.5	B C D A
T_{min}[c], hr	1.7 ± 0.9	2.8 ± 1.0	2.6 ± 1.3	2.3 ± 1.1	B C D A
G_{dec}[d], mg/dl	41.2 ± 12.5	22.1 ± 10.2	29.2 ± 8.1	34.8 ± 6.8	A D C B
AUC_{0-5}, mg hr/dl	136 ± 41	71 ± 42	99 ± 32	116 ± 24	A D C B

[a] Values ±1 *SD*, $n = 20$. [b] Minimum serum glucose level. [c] Time of minimum serum glucose level. [d] Maximum decrease in serum glucose level. [e] Area under serum glucose reduction curve during 5 hr following tolazamide administration calculated by trapezoidal rule.

study phase but was dependent on treatment. Seventeen individuals reported side effects following Treatment A compared to 13 following Treatment D, 7 following Treatment C, and 4 following Treatment B.

Serum Tolazamide Levels—The mean concentrations of tolazamide in serum at each sampling time, maximum values, times of maximum values, and areas under serum tolazamide concentration curves from 0 to 24 hr, are shown in Table II. The mean data are summarized in Fig. 2.

Formulations A and D yielded serum drug profiles that were statistically indistinguishable ($p > 0.05$) at all times except 1 and 2 hr. Both treatments yielded mean peak drug levels >20 μg/ml at 3–4 hr. At 24 hr, drug levels had decreased to ~2.5 μg/ml. Serum tolazamide levels from Formulation C were lower than from A and D, the difference being significant ($p < 0.05$) at most sampling times. Formulation B yielded lower serum drug profiles than all other treatments, and the mean peak drug level of 7.7 μg/ml was not achieved from this tablet until 7 hr after drug administration.

The value of C_{max} increased in the treatment order B < C < D < A, and differences between all treatments were significant. The values of T_{max} and AUC_{0-24} were similar for Formulations A and D but were significantly different among all other pairs of treatments.

Pharmacokinetic Analysis—Analysis of individual data from Treatment A in terms of the pharmacokinetic one-compartment model yielded the values in Table III. From this product serum tolazamide levels are characterized by a mean lag time of 45 min, an absorption half-time of 1 hr, and an elimination half-life of 4.6 hr. The high coefficient of determination attests to the accuracy of the kinetic model employed. Pharmacokinetic analysis of data resulting from the other treatments is not presented, since delayed or prolonged tolazamide absorption prevented accurate determination of drug elimination parameters in some individuals receiving these products.

Estimates of *CRFA* values for each sampling time to 16 hr postdose from all four treatments are summarized in Fig. 3. The values confirm that tolazamide was absorbed at a similar rate and with similar overall efficiency from Formulations A and D. Absorption from the other two tablets was slower and less efficient, with Formulations B and C yielding *CRFA* values 42 and 75%, respectively, of Formulation A.

Serum Glucose Levels—The mean serum glucose levels during the initial 5-hr period following the four treatments are shown in Fig. 4.

The effects by the treatment on glucose levels are related to circulating drug levels. Formulations A and D caused rapid and marked reductions in serum glucose. Minimum values were observed at 1–2 hr. The reduction following Formulation C was less than from A and D and occurred at a slower rate. Formulation B had the least effect on serum glucose, and minimum levels were not achieved until 3 hr postdose.

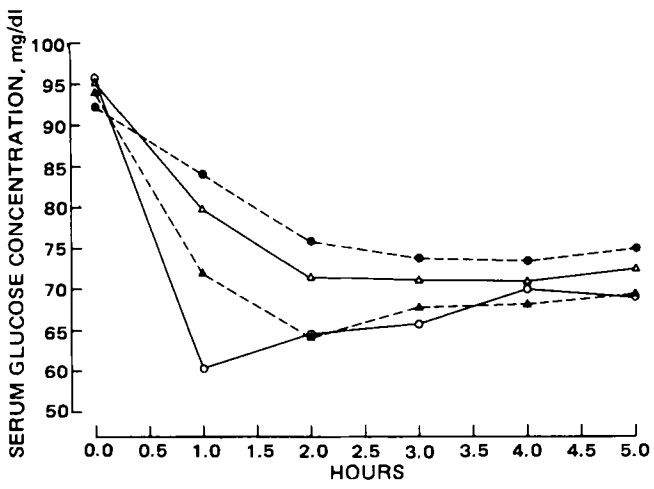

Figure 4—*Mean serum glucose concentrations as a function of time. Key: (○) Treatment A; (●) Treatment B; (△) Treatment C; (▲) Treatment D.*

Comparison of glucose levels at each sampling time indicates differences in glucose response between Treatments A and B and between B and D. Significant differences between Treatments A and C were observed at two sampling times and between Treatments C and D at one sampling time.

Some parameters defining the overall decrease in serum glucose are summarized in Table IV. The differences in minimum glucose levels and the maximum reduction in glucose levels were significant between all treatments. The area under the glucose response curve during the initial 5 hr following tolazamide administration was similar from Treatments A and D and from Treatments D and C but was different among all other treatment pairs. While a similar trend was observed in the 0–24-hr area, differences between treatments did not reach the 95% confidence level.

DISCUSSION

Increasing interest in the use of *in vitro* disintegration and dissolution testing procedures is reflected in the proliferation of such tests in national compendia (7). The use of such tests to determine drug product bioavailability or bioequivalence has been emphasized by the U.S. Food and Drug Administration (14).

The data obtained in this study have shown that different formulations of tolazamide may give rise to marked variations in drug bioavailability and in hypoglycemic response. The ability of *in vitro* tests to predict product-related *in vivo* bioavailability changes is less clear. The official disintegration test (7) yielded similar disintegration times for Formulations A, B, and C but a more prolonged time for D. These results are at variance with the relative *in vivo* bioavailability of the four products. The dissolution test yielded rapid dissolution for Formulation A, slow dissolution for B, and intermediate values for C and D, which were indistinguishable from each other. Although this test provided a reasonable rank-order correlation with *in vivo* bioavailability, there were some important discrepancies.

Formulations C and D yielded almost identical dissolution rates to each other, which were significantly slower than A, yet Formulation D yielded serum tolazamide levels similar to those from A, and significantly higher than those from C. Thus, while the dissolution test suggests that Formulations C and D are bioequivalent to each other and that both are bioinequivalent to A, the *in vivo* results show that Formulations A and D are bioequivalent, while C is not. The two formulations giving rise to superior *in vivo* bioavailability, A and D, were prepared by wet granulation; whereas Tablets B and C were prepared by direct compression. The absolute bioavailability of tolazamide could not be determined from any treatment in this study.

Although serum glucose reduction and resulting drug-related side effects (transient, mild hypoglycemia) were less well defined between treatments than drug levels, a similar product-related trend was observed. This was particularly evident at early sampling times before food was ingested.

These results indicate that bioavailability of tolazamide from oral tablets is dissolution-rate controlled, but *in vitro* methods currently available do not predict *in vivo* drug absorption and hypoglycemic response among formulations and manufacturing processes with acceptable accuracy. For a specific formulation and manufacturing process, *in vitro* tests may be useful to assure lot-to-lot uniformity in bioavailability. However, human trials may be necessary to demonstrate that bioavailability remains reasonably constant within a given range of dissolution rates and/or disintegration times.

REFERENCES

(1) F. H. McMahon, H. L. Upjohn, O. S. Carpenter, J. B. Wright, H. L. Oster, and W. E. Dulin, *Curr. Ther. Res.*, **4**, 330 (1962).

(2) G. Sartor, A. Melander, B. Scherstén, and E. Wahlin-Boll, *Eur. J. Clin. Pharmacol.*, **17**, 285 (1980).

(3) A. M. Monro and P. G. Welling, *ibid.*, **7**, 47 (1974).

(4) J. A. Taylor, D. F. Assinder, L. F. Chasseaud, P. M. Bradford, and J. S. Burton, *ibid.*, **11**, 207 (1977).

(5) F. C. Lu, W. B. Rice, and C. W. Mainville, *Can. Med. Assoc. J.*, **92**, 1166 (1965).

(6) C. B. Tuttle, M. Mayersohn, and G. C. Walker, *Can. J. Pharm. Sci.*, **8**, 31 (1973).

(7) "The United States Pharmacopeia," 20th rev., United States Pharmacopeial Convention, Rockville, Md., 1980, p. 958.

(8) "Documenta Geigy Scientific Tables," 7th ed., K. Diem and C. Lentner, Eds., Ciba-Geigy, Basle, Switzerland 1970, p. 712.

(9) W. S. Hoffman, *J. Biol. Chem.*, **120**, 51 (1937).

(10) J. G. Wagner, "Fundamentals of Clinical Pharmacokinetics," Drug Intelligence Publications, Hamilton, Ill., 1975, p. 81.

(11) C. M. Metzler, G. L. Elfring, and A. J. McEwen, *Biometrics*, **30**, 562 (1974).

(12) J. G. Wagner and E. Nelson, *J. Pharm. Sci.*, **52**, 610 (1963).

(13) J. Neter and W. Wasserman, "Applied Linear Statistical Models," Richard D. Irwin, Homewood, Ill., 1974, p. 475.

(14) *Fed. Reg.*, **42**, 1624 (1977).

ACKNOWLEDGMENTS

Funds for this study were provided from NIH Grant GM 20327 and from The Upjohn Co.

Antitumor Agents LV: Effects of Genkwadaphnin and Yuanhuacine on Nucleic Acid Synthesis of P-388 Lymphocytic Leukemia Cells

I. H. HALL ˣ, R. KASAI, R. Y. WU, K. TAGAHARA, and K. H. LEE

Received August 26, 1981, from the *Division of Medicinal Chemistry, School of Pharmacy, University of North Carolina at Chapel Hill, Chapel Hill, NC 27514.* Accepted for publication January 26, 1982.

Abstract □ The diterpene esters, genkwadaphnin and yuanhuacine, have been shown to possess significant antileukemic activity in the P-388 screen. The major metabolic effects of the diterpene esters were on DNA and protein synthesis. The effects on DNA synthesis *in vitro* were evoked at a lower concentration than that required for protein synthesis inhibition. The sites in DNA synthesis which were inhibited were DNA polymerase and purine synthesis. In the latter pathway the enzyme activities inhibited were phosphoribosyl aminotransferase, inosinic acid dehydrogenase, and dihydrofolate reductase. *In vivo* administration of the diterpene esters at 0.8 mg/kg afforded identical types of effects on purine and DNA synthesis and in addition suppressed histone phosphorylation and reduced the number of surviving tumor cells. The *in vivo* effects on purine and DNA synthesis were evident as early as 6 and 24 hr after administration of a single dose of the diterpene esters.

Keyphrases □ Antitumor agents—nucleic acid synthesis by genkwadaphnin and yuanhuacine of P-388 lymphocytic leukemia cells, diterpene esters □ Genkwadaphnin—antitumor agents, nucleic acid synthesis by yuanhuacine of P-388 lymphocytic leukemia cells, diterpene esters □ Yuanhuacine—antitumor agents, nucleic acid synthesis by genkwadaphnin of P-388 lymphocytic leukemia cells, diterpene esters

Genkwadaphnin (I) and yuanhuacine (II) are two *ortho* esters bearing daphnane type diterpenes which possess an isopropylene side chain at C_{13}. Compounds belonging to the daphnane diterpene esters have previously been shown to have antileukemic activity as opposed to tigliane diterpene esters, *e.g.*, phorbol esters, which are known to be carcinogenic promoting agents (1). Compound II (odoracin or gnidilatidin) has previously been isolated from *Daphne genkwa*, *Daphne odorata*, *Gnidia latifolia*, and *Gnidia glaucus* Fres, and like other diterpene esters, such as 12-hydroxydaphnetoxin, gnidimacrin, gnidimacrin-20-palmitate, gnidilatidin-20-palmitate, gnididin, gniditrin, and gnidicin, has been demonstrated to have antileukemic activity in the 20- to 100-μg/kg dose range in rodents (2–6). The isolation and chemical characterization of a new diterpene ester (I) has recently been reported (7) which also has demonstrated antileukemic activity. The effects of daphnane diterpene esters on nucleic acid and protein synthesis in P-388 lymphocytic leukemia is now reported to establish a mode of action in P-388 lymphocytic leukemia cells to explain their *in vivo* antileukemic activity.

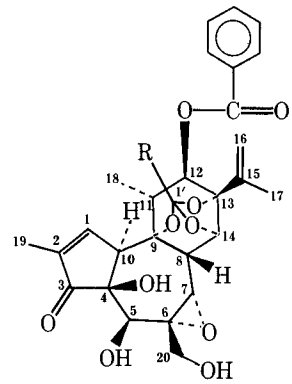

I: R = —C₆H₅

II: R = —CH=CH—CH=CH—$(CH_2)_4$—CH_3

EXPERIMENTAL

The air-dried flowers of *Daphne genkwa*[1] (9 kg) (known as Yuán-Huā in Chinese folklore; Thymelaeaceae) were extracted with methanol. Guided by the *in vivo* P-388 lymphocytic leukemia rodent screen as conducted by the NCI protocol (6), the resulting active residue was dis-

[1] The plant material utilized in this investigation was identified as *Daphne genkwa* Sieb and Zucc (Thymelaeaceae) by H. C. Huang (7). A voucher sample (No. HCH-DG-771022) representing material collected for this investigation is available for inspection at the Herbarium of the School of Pharmacy, Kaohsiung Medical College, Kaohsiung, Taiwan, Republic of China.

0022-3549/82/1100-1263$01.00/0

REFERENCES

(1) F. H. McMahon, H. L. Upjohn, O. S. Carpenter, J. B. Wright, H. L. Oster, and W. E. Dulin, *Curr. Ther. Res.*, **4**, 330 (1962).

(2) G. Sartor, A. Melander, B. Scherstén, and E. Wahlin-Boll, *Eur. J. Clin. Pharmacol.*, **17**, 285 (1980).

(3) A. M. Monro and P. G. Welling, *ibid.*, **7**, 47 (1974).

(4) J. A. Taylor, D. F. Assinder, L. F. Chasseaud, P. M. Bradford, and J. S. Burton, *ibid.*, **11**, 207 (1977).

(5) F. C. Lu, W. B. Rice, and C. W. Mainville, *Can. Med. Assoc. J.*, **92**, 1166 (1965).

(6) C. B. Tuttle, M. Mayersohn, and G. C. Walker, *Can. J. Pharm. Sci.*, **8**, 31 (1973).

(7) "The United States Pharmacopeia," 20th rev., United States Pharmacopeial Convention, Rockville, Md., 1980, p. 958.

(8) "Documenta Geigy Scientific Tables," 7th ed., K. Diem and C. Lentner, Eds., Ciba-Geigy, Basle, Switzerland 1970, p. 712.

(9) W. S. Hoffman, *J. Biol. Chem.*, **120**, 51 (1937).

(10) J. G. Wagner, "Fundamentals of Clinical Pharmacokinetics," Drug Intelligence Publications, Hamilton, Ill., 1975, p. 81.

(11) C. M. Metzler, G. L. Elfring, and A. J. McEwen, *Biometrics*, **30**, 562 (1974).

(12) J. G. Wagner and E. Nelson, *J. Pharm. Sci.*, **52**, 610 (1963).

(13) J. Neter and W. Wasserman, "Applied Linear Statistical Models," Richard D. Irwin, Homewood, Ill., 1974, p. 475.

(14) *Fed. Reg.*, **42**, 1624 (1977).

ACKNOWLEDGMENTS

Funds for this study were provided from NIH Grant GM 20327 and from The Upjohn Co.

Antitumor Agents LV: Effects of Genkwadaphnin and Yuanhuacine on Nucleic Acid Synthesis of P-388 Lymphocytic Leukemia Cells

I. H. HALL ˣ, R. KASAI, R. Y. WU, K. TAGAHARA, and K. H. LEE

Received August 26, 1981, from the *Division of Medicinal Chemistry, School of Pharmacy, University of North Carolina at Chapel Hill, Chapel Hill, NC 27514.* Accepted for publication January 26, 1982.

Abstract □ The diterpene esters, genkwadaphnin and yuanhuacine, have been shown to possess significant antileukemic activity in the P-388 screen. The major metabolic effects of the diterpene esters were on DNA and protein synthesis. The effects on DNA synthesis *in vitro* were evoked at a lower concentration than that required for protein synthesis inhibition. The sites in DNA synthesis which were inhibited were DNA polymerase and purine synthesis. In the latter pathway the enzyme activities inhibited were phosphoribosyl aminotransferase, inosinic acid dehydrogenase, and dihydrofolate reductase. *In vivo* administration of the diterpene esters at 0.8 mg/kg afforded identical types of effects on purine and DNA synthesis and in addition suppressed histone phosphorylation and reduced the number of surviving tumor cells. The *in vivo* effects on purine and DNA synthesis were evident as early as 6 and 24 hr after administration of a single dose of the diterpene esters.

Keyphrases □ Antitumor agents—nucleic acid synthesis by genkwadaphnin and yuanhuacine of P-388 lymphocytic leukemia cells, diterpene esters □ Genkwadaphnin—antitumor agents, nucleic acid synthesis by yuanhuacine of P-388 lymphocytic leukemia cells, diterpene esters □ Yuanhuacine—antitumor agents, nucleic acid synthesis by genkwadaphnin of P-388 lymphocytic leukemia cells, diterpene esters

Genkwadaphnin (I) and yuanhuacine (II) are two *ortho* esters bearing daphnane type diterpenes which possess an isopropylene side chain at C_{13}. Compounds belonging to the daphnane diterpene esters have previously been shown to have antileukemic activity as opposed to tigliane diterpene esters, *e.g.*, phorbol esters, which are known to be carcinogenic promoting agents (1). Compound II (odoracin or gnidilatidin) has previously been isolated from *Daphne genkwa*, *Daphne odorata*, *Gnidia latifolia*, and *Gnidia glaucus* Fres, and like other diterpene esters, such as 12-hydroxydaphnetoxin, gnidimacrin, gnidimacrin-20-palmitate, gnidilatidin-20-palmitate, gnididin, gniditrin, and gnidicin, has been demonstrated to have antileukemic activity in the 20- to 100-μg/kg dose range in rodents (2–6). The isolation and chemical characterization of a new diterpene ester (I) has recently been reported (7) which also has demonstrated antileukemic activity. The effects of daphnane diterpene esters on nucleic acid and protein synthesis in P-388 lymphocytic leukemia is now reported to establish a mode of action in P-388 lymphocytic leukemia cells to explain their *in vivo* antileukemic activity.

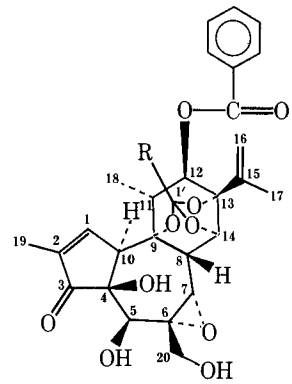

I: R = —C₆H₅

II: R = —CH=CH—CH=CH—$(CH_2)_4$—CH_3

EXPERIMENTAL

The air-dried flowers of *Daphne genkwa*[1] (9 kg) (known as Yuán-Huā in Chinese folklore; Thymelaeaceae) were extracted with methanol. Guided by the *in vivo* P-388 lymphocytic leukemia rodent screen as conducted by the NCI protocol (6), the resulting active residue was dis-

[1] The plant material utilized in this investigation was identified as *Daphne genkwa* Sieb and Zucc (Thymelaeaceae) by H. C. Huang (7). A voucher sample (No. HCH-DG-771022) representing material collected for this investigation is available for inspection at the Herbarium of the School of Pharmacy, Kaohsiung Medical College, Kaohsiung, Taiwan, Republic of China.

0022-3549/82/1100-1263$01.00/0

Table I—The Antineoplastic Activity of Genkwadaphnin and Yuanhuacine in the P-388 Lymphocytic Leukemia Screen in BDF_1 Male Mice

Compound (n = 6)	Dose, mg/kg/day	Average Survival Days, (T/C)	T/C %[a]
0.05% Polysorbate 80		11.0/11.0	100
Genkwadaphnin	0.4	15.5/11.0	141
	0.8	19.0/11.0	173
Yuanhuacine	0.4	16.0/11.0	145
	0.8	16.6/11.0	151
5-Fluorouracil	12.5	19.6/11.0	178

[a] (Number of days survived by the treated group/number of days survived by the control group) × 100.

solved in a methanol–water mixture (1:1) and then partitioned into n-hexane and ether successively. Column chromatography of the active ethereal extract (55 g) on silica gel[2] (500 g) in chloroform afforded two fractions (fraction A, 540 mg and fraction B, 820 mg), which possessed P-388 antileukemic activity. Subsequent purification of fraction B by preparative TLC led to the isolation of the new antileukemic principle I, as reported previously (7).

Column chromatography of fraction A (540 mg) on modified dextran beads[3] (3 g) in chloroform afforded a fraction (420 mg), which was further purified by preparative TLC[4] eluted with n-hexane–2-propanol (10:1) and then ether–n-hexane (5:1) to yield compound II (132.5 mg). Final purification of II was achieved by high-performance liquid chromatography (HPLC)[5] to give 82.3 mg of pure II: $[\alpha]_D^{25}$ + 62.4 (c = 0.242, $CHCl_3$) [previously reported: $[\alpha]_D^{24}$ + 34.3° (c = 0.184, $CHCl_3$) for odoracin (8), $[\alpha]_D^{23}$ + 28° (c = 0.16, $CHCl_3$) for gnidilatidin (2), and $[\alpha]_D^{32}$ + 61.7° (c = 1.07, $CHCl_3$) for yuanhuacine (9)]; UV_{max} (ethanol) 227 nm (ϵ, 44,300) [previously reported λ_{max} (ethanol) 232 nm (ϵ 36,000) and λ_{max} 232 nm (ϵ 52,706); MS m/z 648.2939 (M^+, Calc. for $C_{37}H_{44}O_{10}$: 648.2935 (9)].

The IR, ^1H-NMR, and ^{13}C-NMR spectra of II were identical to those of odoracin (8). Since the structure of odoracin is also identical to that of gnidilatidin (2) or yuanhuacine (9), yuanhuacine is thereby used as the name of II, since the work dealing with the isolation and structural determination of II was submitted for publication earlier than odoracin or gnidilatidin.

The P-388 lymphocytic leukemia tumor line was maintained in DBA/2 male mice (~20 g) and the antineoplastic activity was established by using the NCI protocol (6). For the *in vitro* studies, P-388 cells were harvested from the peritoneal cavity 10 days after administering 10^6 P-388 ip lymphocytic leukemia cells into BDF_1 male mice (~20 g) on day 0 (10).

In the *in vivo* studies, BDF_1 male mice were inoculated on day 0 with 10^6 P-388 cells ip, and on days 7, 8, and 9 the mice were administered 0.8 mg/kg, the optimum dose for antineoplastic activity, of I or II intraperitoneally. The biochemical studies were performed on cells harvested from the peritoneal cavity on day 10. Alternately, mice were injected with a single dose of drug at 0.8 mg/kg, the optimum dose for antineoplastic activity, on day 7 and sacrificed either 6 or 24 hr later.

The *in vitro* incorporation studies were conducted using 1 μCi of thymidine (6-^3H, 21.8 Ci/mmole), uridine (6-^3H, 22.4 Ci/mmole), or L-leucine (4.5-^3H(N), 56.5 Ci/mmole) with 10^6 P-388 whole cells or homogenized cells in minimum essential growth medium[6], pH 7.2, in a total volume of 1 ml, incubated for 60 min at 37°. Thymidine incorporation into DNA was terminated with perchloric acid containing pyrophosphate, which was filtered on glass fiber paper (GF/F) by vacuum suction. RNA and protein assays were terminated with trichloroacetic acid and collected on nitrocellulose membranes by vacuum suction. The acid-insoluble nucleic acid or protein precipitated on the filter papers was placed in scintillation vials and counted[7]. The control value for *in vitro* DNA synthesis for 10-day P-388 cells was 31,777 dpm/mg of DNA, for RNA 38,615 dpm/mg, and for protein 76,518 dpm/mg (11). *In vivo* thymidine incorporation into DNA was determined by injecting into the animal 1 hr before sacrifice 10 μCi ip of [^3H](methyl)thymidine (21.5 Ci/mmole).

[2] SilicAR, CC-7.
[3] Sephadex LH-20.
[4] Silica Gel GF, 1000 μm, 6 plates.
[5] Waters Associates model ALC/GPC 244 Liquid Chromatograph using a Whatman Partisil M9 (500 × 12.8 mm) column and a mixture of n-hexane–isopropanol (5:1) in a recycle mode with a flow rate of 4 ml/min.
[6] Eagle MEM × 1 supplemented with 10% fetal calf serum, penicillin, and streptomycin.
[7] Fisher Scintiverse.

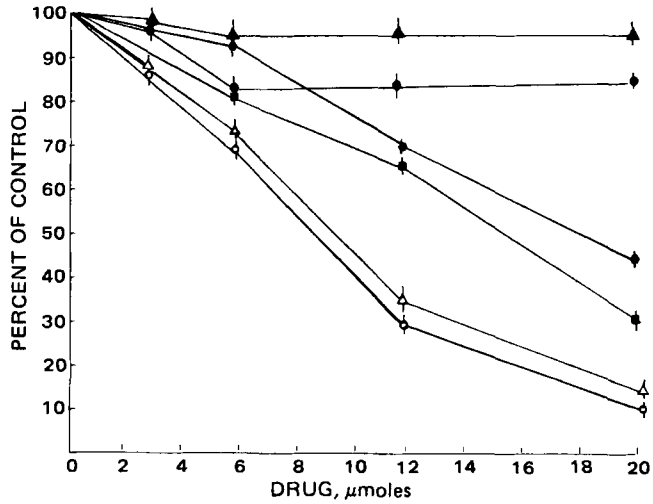

Figure 1—*The* in vitro *effects of genkwadaphnin (I) and yuanhuacine (II) on nucleic acid and protein synthesis of P-388 lymphocytic leukemia cells (60-min incubation)* (n = 5). *Key: [^3H]uridine into RNA, (▲) yuanhuacine, (●) genkwadaphnin; [^3H]leucine into protein, (■) yuanhuacine, (□) genkwadaphnin; [^3H]thymidine into DNA, (△) yuanhuacine, (○) genkwadaphnin; (|) standard deviation.*

The DNA was isolated (12), and the tritium content determined in scintillation fluid[7] and corrected for quenching. The DNA concentration was determined by the diphenylamine reaction using calf thymus DNA as the standard. The results were expressed as disintegrations per minute per milliliter of DNA isolated. Uridine incorporation into RNA was determined in an analogous manner with 10 μCi of 6-[^3H]uridine (22.4 Ci/mmole) and the RNA extracted (13). Leucine incorporation into protein was determined by a previous method (14) with 10 μCi [^3H]4,5(N)-L-leucine (52.0 Ci/mmole). The control values for DNA incorporation were 202,098 dpm/mg DNA, for RNA incorporation 356,926 dpm/mg RNA, and for leucine incorporation 319,300 dpm/mg of protein isolated.

After *in vivo* administration of the drug, on day 10, the number of tumor cells per milliliter and the 0.4% trypan blue uptake were determined with a hemocytometer (15). The *in vitro* UV binding studies were conducted with diterpene esters (5 μg/ml) incubated with DNA (38 μg/ml) in 0.1 M phosphate buffer, pH 7.2 from 0–24 hr and measured over the range of 200–340 nm (15).

The *in vitro* enzymatic studies were conducted with diterpene esters present in a final concentration of 12 μM[8]. The *in vitro* and *in vivo* enzymatic assays have been described previously (10). Briefly, nuclear DNA polymerase activity was determined on isolated P-388 cell nuclei (16) using a previous incubation medium (17), except that [^3H]methyldeoxyribothymidine triphosphate (82.4 Ci/mmole) was used. The insoluble nucleic acids were collected on glass fiber papers (GF/F). The control value was 24,568 dpm/mg of nuclear protein. Messenger, ribosomal, and transfer RNA polymerase enzymes were isolated using different concentrations of ammonium sulfate (18), namely, 0.3 M, 0.04 M, and 0.00 M, respectively, and the individual polymerase activities were measured using 5-[^3H]uridine-5-triphosphate (23.2 Ci/mmole).

Insoluble RNAs were collected on nitrocellulose filters (18, 19). Control values for messenger, ribosomal, and transfer RNA polymerase activities were, respectively, 21,434; 25,408; and 2,082 dpm/mg of nucleic protein. Ribonucleotide reductase activity was measured by a previous method (20) using 5-[^3H]cytidine-5′-diphosphate (21.5 Ci/mmole). The deoxyribonucleotides were separated from ribonucleotides by poly(ethyleneimine)cellulose TLC. The control value for the reductase was 577,720 dpm/mg of protein. Deoxythymidine kinase, deoxythymidylate monophosphate kinase, and deoxythymidylate diphosphate kinase activities were measured by spectrophotometric assay (21) based on the disappearance of nicotinamide dinucleotide at 340 nm. Control values using a postnuclear supernatant fraction (600×g, 10 min) were a change in absorbance of 0.385, 0.386, and 0.378 optical density units/20 min/mg of protein, respectively. Thymidine incorporation into the nucleotides was evaluated by using a previous medium (21). The reaction was extracted with ether and the aqueous layer plated on poly(ethylene)imine cellulose F plates eluted with 0.5 N formic acid–lithium chloride (1:1).

[8] Concentration of drug was selected because the micromolar range would be between ID_{50} values required to inhibit DNA and protein synthesis.

Table II—The *In Vitro* Effects of Genkwadaphnin and Yuanhuacine (12 μM) on P-388 Lymphocytic Leukemia Cell Metabolism

Biochemical Parameter (n = 6)	Control	Percent Control	
		Genkwadaphnin	Yuanhuacine
[^{3}H]Thymidine incorporation into DNA	100 ±8	23 ±4[a]	33 ±5[a]
[^{3}H]Uridine incorporation into RNA	100 ±10	84 ±8	92 ±5
[^{3}H]Leucine incorporation into protein	100 ±9	66 ±7[a]	70 ± 8
[^{14}C]Formate into purines	100 ±6	51 ±8[a]	76 ±9[a]
DNA polymerase	100 ±6	71 ±9[a]	84 ±4[a]
tRNA polymerase	100 ±5	92 ±6	95 ±3
rRNA polymerase	100 ±6	81 ±3[a]	106 ±4
mRNA polymerase	100 ±6	109 ±8	126 ± 5
Carbamyl phosphate synthetase	100 ±9	114 ±8	110 ±11
Aspartate transcarbamylase	100 ±7	113 ±4	89 ± 9
Orotidine monophosphate decarboxylase	100 ±8	89 ±5	96 ±6
Thymidylate synthetase	100 ±3	95 ±4	99 ±2
Thymidine kinase	100 ±7	98 ±5	102 ±6
Thymidylate monophosphate kinase	100 ±6	99 ±7	110 ±8
Thymidylate diphosphate kinase	100 ±4	97 ±4	93 ±6
Phosphoribosyl aminotransferase	100 ±7	68 ±7[a]	74 ± 9[a]
Inosinic acid dehydrogenase	100 ±5	66 ±8[a]	67 ±6[a]
Dihydrofolate reductase	100 ±12	55 ±8[a]	61 ±9[a]
Ribonucleotide reductase	100 ±7	96 ±5	114 ±7
Nonhistone phosphorylation	100 ±6	100 ±4	88 ±6

[a] $p \leq 0.001$.

Table III—The *In Vivo* Effects of Genkwadaphnin and Yuanhuacine on P-388 Lymphocytic Leukemia Cell Metabolism After 3 Days of Dosing at 0.8 mg/kg/day

Biochemical Parameter (n = 6)	Control	Percent Control, Day 10	
		Genkwadaphnin	Yuanhuacine
[^{3}H]Thymidine incorporation into DNA	100 ±6	14 ±3[a]	19 ±4[a]
[^{3}H]Uridine incorporation into RNA	100 ±11	23 ±5[a]	68 ±8[a]
[^{3}H]Leucine incorporation into protein	100 ±8	40 ±5[a]	51 ±5[a]
[^{14}C]Formate into purines	100 ±9	60 ±6[a]	66 ±4[a]
DNA polymerase	100 ±6	43 ±6[a]	40 ±5[a]
tRNA polymerase	100 ±8	118 ±6	111 ±9
rRNA polymerase	100 ±4	86 ±8[a]	81 ±5[a]
mRNA polymerase	100 ±8	115 ±10	81 ±9[a]
Carbamyl phosphate synthetase	100 ±7	91 ±8	94 ±8
Aspartate transcarbamylase	100 ±12	84 ±6	78 ±13
Orotidine monophosphate decarboxylase	100 ±6	99 ±5	117 ±17
Thymidylate synthetase	100 ±7	91 ±10	98 ±5
Thymidine kinase	100 ±8	118 ±9[a]	105 ±6
Thymidylate monophosphate kinase	100 ±8	125 ±9[a]	98 ±8
Thymidylate diphosphate kinase	100 ±7	109 ±10	93 ±8
Phosphoribosyl aminotransferase	100 ±8	70 ±7[a]	69 ±11[a]
Inosinic acid dehydrogenase	100 ±8	58 ±5[a]	51 ±5[a]
Dihydrofolate reductase	100 ±7	35 ±4[a]	51 ±6[a]
Ribonucleotide reductase	100 ±8	108 ±16	94 ±10
Histone phosphorylation	100 ±11	65 ±4[a]	51 ±5[a]
Number of cells per milliliter	100 ±3	16 ±2[a]	27 ±5[a]

[a] $p \leq 0.001$.

Areas that correlated with R_f values of thymidine monophosphate, diphosphate, and triphosphate standards were scraped and counted[9]. Enzymes of the pyrimidine synthetic pathway were also measured. Carbamyl phosphate synthetase activity was determined by a previous method (22). The colorimetric determination of citrulline was performed according to another method (23), resulting in 3.26 mg of citrulline formed/hr/μg of protein.

Aspartate carbamyl transferase activity was carried out in the presence of aspartate transcarbamylase (22), and the colorimetric determination of the carbamyl aspartate formed was according to a previous method (24), resulting in 0.301 μmole formed/hr/mg of protein. Orotidine monophosphate decarboxylase activity was measured using a (16,300×g, 20 min) supernatant fraction by a previous technique (25) using [^{14}C]-(*carboxyl*)*orotidine monophosphate* (34.9 mCi/mmole). The control value was 41,760 dpm/mg of protein. Thymidylate synthetase activity was determined by a previous method (26), utilizing a postmitochondrial (9000×g, 10 min) supernatant fraction with 5 μCi of 5-[^{3}H]deoxyuridine monophosphate (14 Ci/mmole), affording a control value of 14,500 dpm/hr/mg of protein.

Dihydrofolate reductase activity was determined using a (600×g, 10 min) supernatant fraction by a spectrophotometric method (27) based on the disappearance of reduced nicotinamide adenine dinucleotide resulting in a value of 0.761 optical density U/hr/mg of protein for 10-day P-388 cells. [^{14}C]Formate incorporation into purines was measured by a method used previously (28), using 0.5 μCi of [^{14}C]formic acid (52.0 mCi/mmole). Purine separation was achieved by silica gel TLC eluting with n-butanol–acetic acid–water (4:1:5). Using the standards, guanine and adenine, the appropriate spots were scraped and the radioactivity determined. The control value for purine synthesis was 23,682 dpm/mg of protein. Phosphoribosyl pyrophosphate aminotransferase activity was determined by a previous spectrophotometric method (29) at 340 nm using a (600×g, 10 min) supernatant fraction resulting in a control value of 0.806 optical density U/hr/mg of protein. Inosinic acid dehydrogenase activity was determined by a previous method (30) using 8-[^{14}C]inosine-5′-monophosphate (61 mCi/mmole). The control value was 5745 dpm/mg of protein.

Histone phosphorylation was determined by injecting 10 μCi ip of γ-[^{32}P]adenosine triphosphate (27 Ci/mmole). The nuclei were isolated 1 hr later, and the histone chromatin protein was extracted by a method used previously (31). Nonhistone chromatin phosphorylation by nucleic acid kinase was determined on isolated nuclei (16) utilizing 2 nmoles of γ-[^{32}P]adenosine triphosphate. Chromatin protein was collected on nitrocellulose membrane filters (32). The control value for histone phosphorylation was 2612 dpm/mg of chromatin protein isolated. Nonhistone phosphorylation was 18,616 dpm/mg of protein. Protein was determined by a previous method (33).

Data are expressed in the tables as percent of control with standard

[9] Packard Scintillation Counter in Fisher scintillation fluid and corrected for quenching.

Table IV—The *In Vivo* Effects of Genkwadaphnin and Yuanhuacine on P-388 Lymphocytic Leukemia Cell Metabolism 24 hr After a Single Dose at 0.8 mg/kg

Biochemical Parameter (n = 6)	Control	Percent Control, Day 8	
		Genkwadaphnin	Yuanhuacine
[^{3}H]Thymidine incorporation into DNA	100 ±7	17 ±4[a]	16 ±5[a]
[^{3}H]Uridine incorporation into RNA	100 ±12	82 ±9	84 ±8
[^{3}H]Leucine incorporation into protein	100 ±9	80 ±8[a]	103 ±8
[^{14}C]Formate incorporation into purines	100 ±7	69 ±5[a]	75 ±6[a]
DNA polymerase	100 ±5	75 ±5[a]	70 ±6[a]
tRNA polymerase	100 ±6	95 ±5	84 ±7[a]
rRNA polymerase	100 ±7	95 ±6	63 ±9[a]
mRNA polymerase	100 ±8	111 ±10	96 ±8
Orotidine monophosphate decarboxylase	100 ±7	99 ±8	117 ±9
Phosphoribosyl aminotransferase	100 ±8	48 ±9[a]	46 ±11[a]
Inosinic acid dehydrogenase	100 ±7	58 ±8[a]	53 ±8[a]
Dihydrofolate reductase	100 ±7	54 ±5[a]	53 ±5[a]
Ribonucleotide reductase	100 ±9	126 ±10[a]	91 ±8

[a] $p \leq 0.001$.

Table V—The *In Vivo* Effects of Genkwadaphnin and Yuanhuacine on P-388 Lymphocytic Leukemia Cell Metabolism 6 hr After a Single Dose at 0.8 mg/kg

Biochemical Parameter (n = 6)	Control	Percent Control, Day 7	
		Genkwadaphnin	Yuanhuacine
[^{3}H]Thymidine incorporation into DNA	100 ±8	13 ±5[a]	35 ±8[a]
[^{14}C]Formate incorporation into purines	100 ±7	67 ±6[a]	73 ±7[a]
DNA polymerase	100 ±7	71 ±6[a]	69 ±7[a]
Phosphoribosyl aminotransferase	100 ±9	47 ±5[a]	80 ±7[a]
Inosinic acid dehydrogenase	100 ±8	50 ±6[a]	49 ±7[a]
Dihydrofolate reductase	100 ±6	77 ±5[a]	68 ±4[a]

[a] $p \leq 0.001$.

deviation. The number of animals per group is represented by n. The probable (p) significant differences were determined by Student's t test.

RESULTS

Genkwadaphnin (I) and yuanhuacine (II) both demonstrated significant antineoplastic activity against the growth of P-388 lymphocytic leukemia. Compound I at 0.8 mg/kg/day afforded a T/C % value of 173, whereas II afforded a T/C % value of 151 (Table I). The antileukemic activity of the diterpene esters was comparable to the standard, 5-fluorouracil (T/C = 178% at 12.5 mg/kg) in their ability to inhibit P-388 tumor growth.

The *in vitro* studies involving whole cells and homogenized cells showed pellucidly that the major effect of the diterpene esters was on DNA synthesis, with I producing a 77% suppression and II producing a 67% suppression at 12 μM concentrations (Fig. 1). The effects of diterpene esters on DNA synthesis were identical in the studies on whole cells and homogenized cells, indicating that the effects of diterpene esters were not on the membrane transport of the radiolabeled precursor, but rather on cellular synthesis. The ID_{50} for the inhibition of DNA was 5.62 μM for I and 7.11 μM for II. The studies demonstrated that the diterpene esters inhibited *in vitro* protein synthesis at a higher concentration, compared with the concentration required to inhibit DNA synthesis, affording an ID_{50} of ~14.8 μM for I and an ID_{50} of 18.5 μM for II.

Further *in vitro* studies (Table II) showed that the principal pathway in nucleic acid synthesis which was suppressed by the diterpene esters was the purine pathway. Formate incorporation into purines was reduced 49% by I and 24% by II. A number of enzyme sites in purine synthesis appeared to be blocked by the diterpene esters. Phosphoribosyl aminotransferase activity was reduced 32% by I and 26% by II. Inosinic acid dehydrogenase activity was reduced 34% by I and 33% by II. Dihydrofolate reductase activity was suppressed 45% by I and 39% by II *in vitro*. Marginal inhibition of DNA polymerase activity was observed with 29% reduction by I and 16% by II. *In vitro* the diterpene esters had little effect on the enzymatic activities of the pyrimidine pathway, on the thymidylate kinases, or on the RNA polymerases.

In the *in vivo* studies, after dosing for 3 days at 0.8 mg/kg/day ip, I reduced the number of cells per milliliter from 206 to 33 × 10^6, and II reduced this number from 206 to 56 × 10^6 (Table III). The diterpene esters, *in vivo*, suppressed DNA synthesis significantly, with I causing an 86% reduction and II producing an 81% reduction after 3 days of dosing. Inhibition of RNA synthesis was observed *in vivo* with I causing a 77% reduction and II causing a 32% reduction. Likewise, protein synthesis was also reduced *in vivo* with I administration resulting in a 60% reduction and II a 49% reduction. *In vivo* purine synthesis was suppressed 40% by I and 34% by II. As observed in the *in vitro* studies, key enzymes of the purine pathway were blocked by the diterpene esters. Phosphoribosyl aminotransferase activity was reduced 30% by I and 31% by II after 3 days of administration. Inosinic acid dehydrogenase activity was suppressed *in vivo* 42% by I and 49% by II. Dihydrofolate reductase activity was inhibited 65% by I and 49% by II therapy. DNA polymerase activity *in vivo* was suppressed 57% by I and 60% by II administration. Phosphorylation of the chromatin basic histones was reduced by the administration of the diterpene esters, such that I caused 35% suppression and II caused 49% reduction. *In vivo* administration of the diterpene esters had little effect on the pyrimidine synthetic pathway or on the RNA polymerase activities.

Examination of the studies (Table IV) 24 hr after a single dose of the agents showed that DNA synthesis was inhibited significantly, with I resulting in 83% inhibition and II resulting in 84% inhibition. However, RNA synthesis and protein synthesis produced <20% inhibition 24 hr after a single dose of the diterpene esters. Formate incorporation into purines was reduced 31% by I and 25% by II administration. Phosphoribosyl aminotransferase activity was inhibited 52% by I and 54% by II therapy. Similarly, inosinic acid dehydrogenase activity was reduced 42% by I and 47% by II and dihydrofolate reductase activity was inhibited 46% by I and 47% by II after a single dose. DNA polymerase activity was inhibited 25% by I and 30% by II administration.

In vivo administration of a single dose of daphnane diterpene esters (Table V) with sacrifice of the mice 6 hr later demonstrated that DNA synthesis was suppressed 87% by I and 65% by II. Formate incorporation into purines after 6 hr demonstrated that I caused 33% reduction and II caused 27% reduction. Phosphoribosyl aminotransferase activity was reduced 53% by I and 20% by II administration. Inosinic acid dehydrogenase activity was reduced ~50% by a single dose of the diterpene esters. Dihydrofolate reductase activity was reduced 23% by I and reduced 32% by II therapy. DNA polymerase activity was reduced ~30% by the diterpene esters using a single dose.

The *in vitro* UV studies with DNA indicated that there were no hyperchromic effects or shift of absorbance to a higher wavelength. These studies indicate the diterpene esters did not bind to DNA or interfere with template activity for nucleic acid synthesis.

DISCUSSION

The diterpene esters, I and II, had significant effects on cellular metabolism which would explain their antineoplastic activity in the P-388 screen. The major effect is the suppression of DNA synthesis of P-388

lymphocytic leukemia cells. The observed inhibition of key regulatory steps of the purine pathway are of a sufficient magnitude to account for the reductions observed in DNA synthesis. In addition, other sites of inhibition by the diterpenes were DNA polymerase and dihydrofolate reductase activity. The inhibition DNA synthesis occurs within 6 hr, suggesting that it is not directly related to the abilities of the agents to suppress protein synthesis.

The effects on P-388 cellular metabolism induced by the daphnane diterpene esters are in direct contrast to the reported cellular effects of the tigliane diterpenes, croton oil, and 12-*O*-tetradecanoyl-phorbol-13-acetate. These esters are hyperplasia-inducing agents (34) and induce cell proliferation (35, 36) augmenting carcinogenesis. It has been suggested that they act on cellular or intercellular membranes causing irritation and inflammation (37). Both crude extracts and esters have been observed to stimulate DNA and RNA synthesis, which was positively related to their ability to induce tumors (38). Stimulation of protein synthesis also occurs after the increase in RNA synthesis but before stimulation of DNA synthesis (38, 39). Stimulation of phosphorylation of histones by the croton esters (40) has been observed. Increased histone phosphorylation is related to the ability of the croton oil esters to promote tumors and stimulate nucleic acid synthesis. Further studies have indicated that the croton oil esters inhibit the DNA repair enzyme system (41).

Plants of the Euphorbiaceae family are known for their toxic effects on cells (42). However, these plants historically were used in herbal medicine to treat human cancer and warts (42). An antileukemic phorbol ester has been isolated from *Croton tiglium* and an antileukemic ingenol ester has been isolated from *Euphorbia eoula* (43). Two of the more potent diterpene esters are the macrocyclic diterpenoid gnidimacrin and its C-20 palmitate (44). It has been suggested that the C-20 and C-12 ester groups are necessary for antileukemic activity and that these groups enable the agent to pass through the cellular membrane (2, 44), thus facilitating its antineoplastic effect on cell metabolism. Compounds I and II have an ester in the C-12 position but not the C-20 which contains a hydroxy group.

Studies on structural requirements for the antileukemic activity such as the effect of the cyclopentenone ring, 6,7-epoxide group, the ortho esters and the configuration of A/B rings of the daphnane nucleus are currently in progress.

REFERENCES

(1) F. J. Evans and C. J. Soper, *Lloydia*, **41**(3), 93 (1978).

(2) S. M. Kupchan, Y. Shizuri, W. C. Summer, R. Haynes, A. P. Leighton, and B. R. Sickles, *J. Org. Chem.* **41,** 3850 (1976).

(3) S. M. Kupchan, Y. Shizuri, T. Murae, J. G. Sweeny, H. R. Haynes, M. S. Shen, J. C. Barrick, and R. F. Bryan, *J. Am. Chem. Soc.*, **98,** 5719 (1976).

(4) S. M. Kupchan, J. G. Sweeny, R. L. Baxter, T. Murae, V. A. Zimmerly, and B. R. Sickles, *ibid.*, **97,** 672 (1975).

(5) J. Nyborg and T. LaCour, *Nature (London)*, **257,** 284 (1975).

(6) R. I. Geran, N. H. Greenberg, M. M. Macdonald, A. M. Schumacher, and B. J. Abbott, *Cancer Chem. Rep.*, **3,** 9 (1972).

(7) R. Kasai, K. H. Lee and H. C. Huang, *Phytochemistry*, **20,** 2592 (1981).

(8) S. Kogiso, K. Wada, and K. Munakata, *Agr. Biol. Chem.*, **40,** 2119 (1976).

(9) B. P. Ying, C. S. Wang, P. N. Chou, P. C. Pan, and J. S. Liu, *Hua Hseuh Pao*, **35,** 103 (1976).

(10) I. H. Hall, K. H. Lee, S. A. ElGebaly, Y. Imakura, Y. Sumida, and R. Y. Wu, *J. Pharm. Sci.*, **68,** 883 (1979).

(11) I. H. Hall, K. H. Lee, M. Okano, D. Sims, T. Ibuka, Y. F. Liou, and Y. Imakura, *ibid.*, **70,** 1147 (1981).

(12) C. B. Chae, J. L. Irvine, and C. Piantadosi, *Proc. Am. Assoc. Cancer Res.*, **9,** 44 (1978).

(13) R. G. Wilson, R. H. Bodner, and G. E. MacHorter, *Biochim. Biophys. Acta*, **378,** 260 (1975).

(14) A. C. Sartorelli, *Biochem. Biophys. Res. Commun.*, **27,** 26 (1967).

(15) I. H. Hall, K. H. Lee, E. C. Mar, C. O. Starnes, and T. G. Waddell, *J. Med. Chem.*, **20,** 333 (1977).

(16) W. C. Hymer and E. L. Kuff, *J. Histochem. Cytochem.*, **12,** 359 (1964).

(17) H. Sawada, K. Tatsumi, M. Sasada, S. Shirakawa, T. Nakumura, and G. Wakisaka, *Cancer Res.*, **34,** 3341 (1974).

(18) I. H. Hall, G. L. Carlson, G. S. Abernethy, and C. Piantadosi, *J. Med. Chem.*, **17,** 1253 (1974).

(19) K. M. Anderson, I. S. Mendelson, and G. Guzik, *Biochim. Biophys. Acta*, **383,** 56 (1975).

(20) E. C. Moore and R. B. Hurlbert, *J. Biol. Chem.*, **241,** 4802 (1966).

(21) F. Maley and S. Ochoa, *ibid.*, **233,** 1538 (1958).

(22) S. M. Kalman, P. H. Duffield, and T. Brzozwski, *J. Biol. Chem.*, **241,** 1871 (1966).

(23) R. M. Archibald, *J. Biol. Chem.*, **156,** 121 (1944).

(24) S. B. Koritz and P. P. Cohen, *ibid.*, **209,** 145 (1954).

(25) S. H. Appel, *ibid.*, **243,** 3924 (1968).

(26) A. Kampf, R. L. Barfknecht, P. J. Schaffer, S. Osaki, and M. P. Mertes, *J. Med. Chem.*, **19,** 903 (1976).

(27) M. K. Ho, T. Hakalo, and S. F. Zakrzwski, *Cancer Res.*, **32,** 1023 (1972).

(28) M. K. Spassova, G. C. Russev, and E. V. Golovinsky, *Biochem. Pharmacol.*, **25,** 923 (1976).

(29) J. B. Wyngaarden and D. M. Ashton, *J. Biol. Chem.*, **234,** 1492 (1959).

(30) H. J. Becker and G. W. Löhr, *Klin. Wochenschr.*, **57,** 1109 (1979).

(31) A. Raineri, R. C. Simsiman, and R. K. Boutwell, *Cancer Res.*, **33,** 134 (1973).

(32) Y. M. Kish and L. J. Kleinsmith, *Methods Enzymol.*, **40,** 201 (1975).

(33) O. H. Lowry, N. J. Rosebrough, A. L. Farr, and R. J. Randall, *J. Biol. Chem.*, **193,** 265 (1951).

(34) J. V. Frei and P. Stevens, *Br. J. Cancer*, **22,** 63 (1968).

(35) I. Berenblum, *Cancer Res.*, **4,** 44 (1941).

(36) W. M. Baird and R. K. Boutwell, *Cancer Res.*, **31,** 1074 (1971).

(37) R. J. Schmidt and F. J. Evans, *Lloydia*, **40,** 225 (1977).

(38) W. M. Baird, J. A. Sedgwick, and R. K. Boutwell, *Cancer Res.*, **31,** 1434 (1971).

(39) A. N. Raick, *ibid.*, **33,** 269 (1973).

(40) R. Raineri, R. C. Simsiman, and R. K. Boutwell, *ibid.*, **33,** 34 (1973).

(41) H. W. Lieberman, S. Sell, and E. Farber, *Proc. Am. Assoc. Can. Res.*, **12,** 5 (1971).

(42) J. L. Hartwell, *Lloydia*, **32,** 153 (1969).

(43) S. M. Kupchan, I. Uchida, A. R. Brantman, R. G. Dailey, and B. Yufei, *Science*, **191,** 571 (1976).

(44) S. M. Kupchan, Y. Shizuri, T. Murae, J. G. Sweeny, H. R. Haynes, M. S. Shen, J. C. Barrick, F. R. Bryan, D. Van der Helm, and K. K. Wu, *J. Am. Chem. Soc.*, **98,** 5719 (1976).

ACKNOWLEDGMENT

Supported by American Cancer Society Grant CH-19 (K. H. Lee and I. H. Hall), American Cancer Society Institutional Grant (UNC) (I. H. Hall), and National Cancer Institute Grant CA 17625 (K. H. Lee).

Isolated Perfused Rabbit Lung As a Model for Intravascular and Intrabronchial Administration of Bronchodilator Drugs I: Isoproterenol

R. K. BRAZZELL ‡, R. B. SMITH §, and H. B. KOSTENBAUDER *x

Received November 12, 1981, from the **College of Pharmacy, University of Kentucky, Lexington, KY 40506.* Accepted for publication January 29, 1982. ‡Present address: Hoffmann-La Roche Inc., Department of Pharmacokinetics and Biopharmaceutics, Nutley, NJ 07110, §The Upjohn Co., Kalamazoo, MI 49001.

Abstract □ The absorption, uptake, and metabolism of isoproterenol was studied following intravascular, intrabronchial, and aerosol administration of the drug to the isolated perfused rabbit lung. Capacity-limited metabolism of isoproterenol was observed following the addition of five doses, ranging from 10^{-7} to 10^{-5} moles, directly into the circulation of the lung system. A physiologically based perfusion model was developed to describe the disposition of the drug and metabolite in the isolated lung preparation. This model was also used to analyze data collected following intrabronchial and aerosol administration of isoproterenol.

Keyphrases □ Isoproterenol—intravascular and intrabronchial administration, isolated perfused rabbit lung □ Bronchodilators—isoproterenol, intravascular and intrabronchial administration, isolated perfused rabbit lung □ Pharmacokinetics—isolated perfused rabbit lung as a model for intravascular and intrabronchial administration of isoproterenol

Isoproterenol is often administered directly into the lungs by aerosol inhalation in the treatment of bronchial asthma. Little of the inhaled dose actually reaches the airways (1), but that which does is responsible for the bronchodilating effect. Little is known of the fate of the small fraction which reaches the airways and of the role of the lung in the disposition of the drug. The objective of this study was to evaluate the absorption, uptake, and metabolism of isoproterenol in the isolated perfused rabbit lung following intravascular, intrabronchial, and aerosol administration.

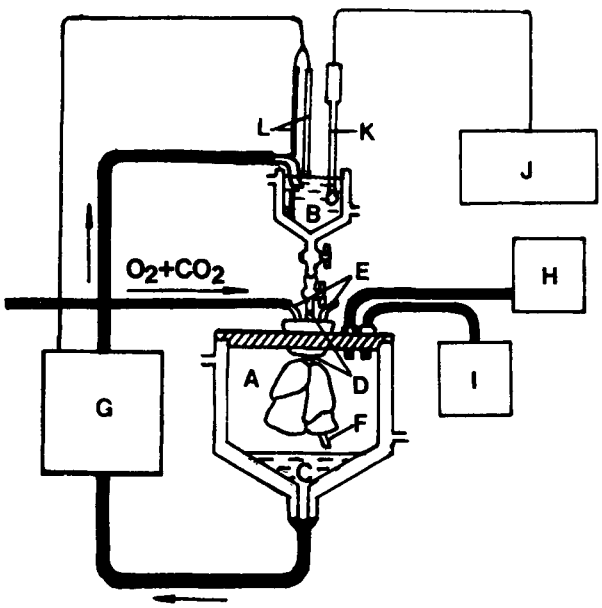

Figure 1—*Diagram of the isolated perfused rabbit lung apparatus. Key: (A) lung chamber; (B) upper reservoir; (C) lower reservoir; (D) pulmonary artery cannula; (E) tracheal cannula; (F) pulmonary venous cannula; (G) perfusion pump; (H) animal respirator; (I) pressure gauges; (J) pH meter; (K) pH electrode; (L) level-sensing probes.*

The isolated perfused rabbit lung preparation offers an ideal experimental system for studying the disposition of drugs by the lung, as it allows the lung to be studied independent of the rest of the body. The design of the system facilitates rapid and convenient sample withdrawal and complete recovery of the lung tissue and perfusate. Viability of the isolated perfused rabbit lung preparation has been documented by physiological, hematological, histological, and biochemical methods for periods up to 4 hr (2–5). Similar preparations have been used in the past to study the uptake and metabolism of various pharmacological agents. Little has been done, however, to apply pharmacokinetic concepts to the analysis of the data generated from these studies.

Previous experiments dealing with the disposition of isoproterenol in isolated lung preparations indicate that the drug is not taken up extensively by the lung (6) and that 3-*O*-methylisoproterenol is the only metabolite formed by the lung (7). The drug appears to be well-ab-

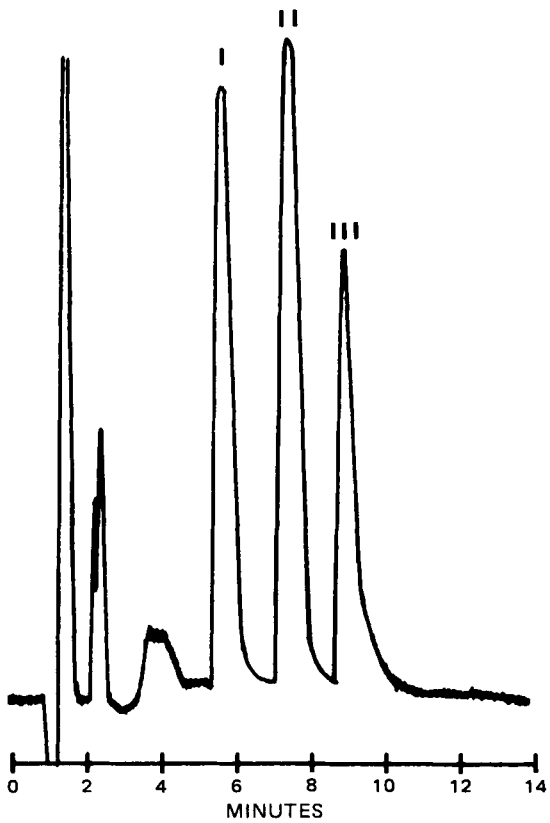

Figure 2—*Sample chromatogram of a diethylhexylphosphoric acid perfusate extract containing (I) isoproterenol, (II) isoproterenone, and (III) 3-O-methylisoproterenol separated on a strong cation exchange column with a phosphate buffer–methanol mobile phase.*

0022-3549/82/1100-1268$01.00/0

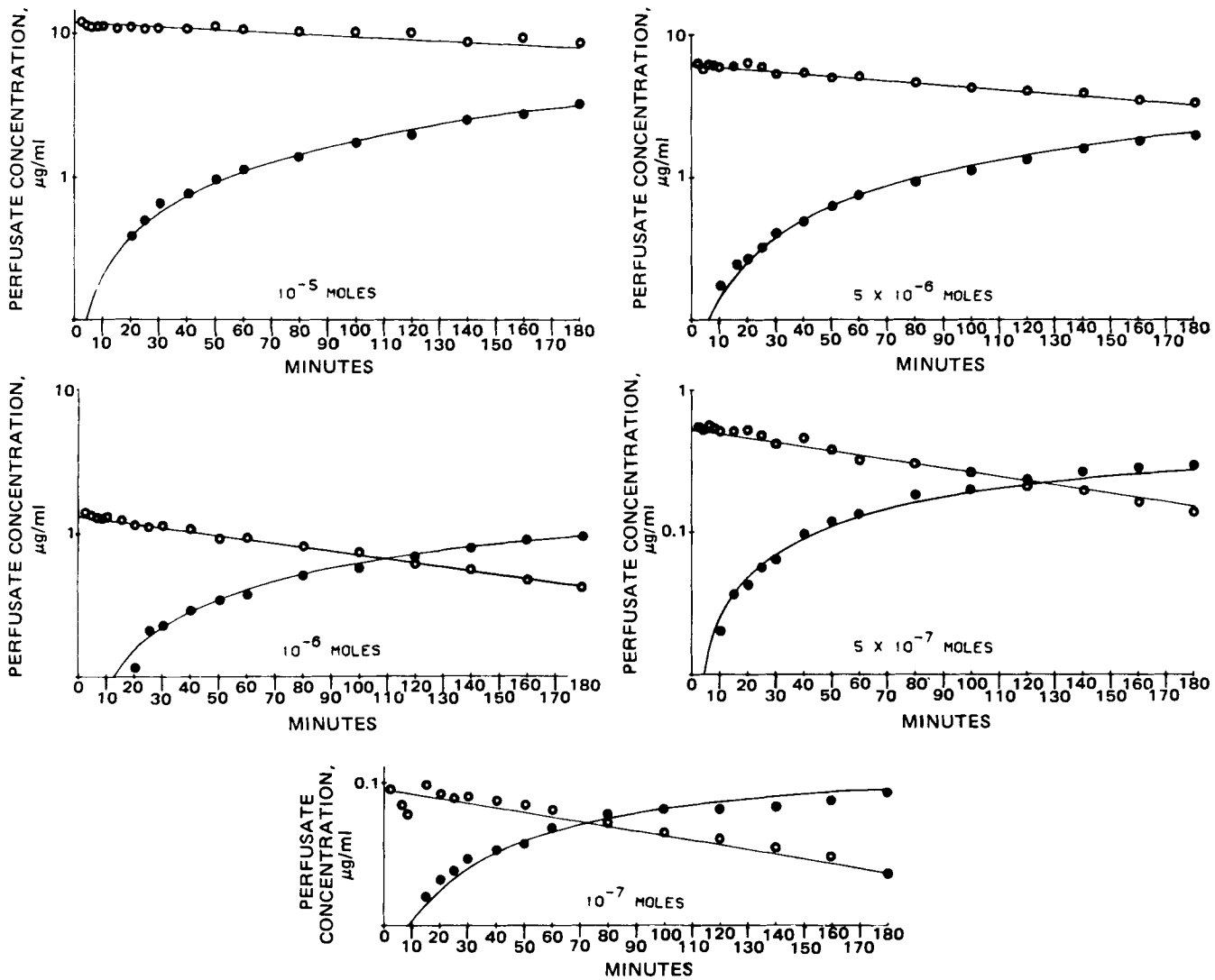

Figure 3—*Semilogarithmic plots of concentration* versus *time for (○) isoproterenol and (●) 3-O-methylisoproterenol, comparing observed values with those predicted by compartmental model fits for five intravascular doses of isoproterenol hydrochloride administered to the isolated perfused rabbit lung.*

sorbed when administered directly into the airways, and a 30% first-pass *O*-methylation during absorption has been reported (7).

EXPERIMENTAL

Isolated Perfused Rabbit Lung—The isolated perfused rabbit lung system has been described previously (2, 3). A schematic drawing of the apparatus is shown in Fig. 1. Male New Zealand rabbits (3–5 kg) were anesthetized with sodium pentobarbital and treated with heparin. The animals were exsanguinated *via* cardiac puncture; the heart, lungs, and trachea were removed; and the trachea, pulmonary artery, and left atrium were cannulated. The lung preparation was suspended in a cylindrical thorax[1] and connected to an upper reservoir such that perfusion medium could flow from the reservoir through the pulmonary vasculature and exit *via* a cannula inserted in the left atrium. The pooling perfusate was pumped back to the reservoir by a perfusion pump[2], providing constant circulation through the lung system. The lungs were ventilated with warm humidified air containing carbon dioxide by operating a small animal respirator[2] to create an alternating negative pressure within the lung chamber. This resulted in expansion and contraction of the lung and inspiration and expiration much like that in the intact animal. The thorax and the reservoir were water-jacketed to regulate the temperature at 37°. Once the system was in operation, it was allowed to equilibrate 15–20 min prior to drug administration. Sampling (1-ml specimens) was from the upper reservoir. For each perfusion, Krebs-Ringer bicarbonate solution (150 ml) containing 4.5% bovine serum albumin and the following in grams per liter was used: NaCl, 6.57; KCl, 0.355; $CaCl_2$, 0.28; KH_2PO_4, 0.16; $MgSO_4$, 0.145; $NaHCO_3$, 2.1; and glucose, 0.18. The pH was adjusted to 7.4 with sodium hydroxide.

Drug Administration—Isoproterenol hydrochloride was administered to the isolated lung system by intravascular, intrabronchial, and aerosol administration. One milliliter aliquots of aqueous isoproterenol hydrochloride solutions containing 10^{-5}, 5×10^{-6}, 10^{-6}, 5×10^{-7}, and 10^{-7} moles/ml were added to the upper reservoir for intravenous administration. For intrabronchial dosing, 250-μl aliquots containing 10^{-5} and 10^{-6} moles of drug were delivered to the airways as a bolus *via* a small bore plastic tubing inserted through the tracheal cannula. For aerosol administration, a 50-mg/ml aqueous solution of isoproterenol hydrochloride was nebulized[3] and delivered to the airways through a plastic tubing attached to the tracheal cannula for a 1-min dosing period. During drug administration, the respirator controls were changed from the normal settings of 30-ml stroke volume and 50% inspiration to 50-ml stroke volume and 70% inspiration. This maximized the flow of aerosolized drug into the lung by causing deep inspirations.

Chromatography—The perfusate concentrations of isoproterenol and 3-*O*-methylisoproterenol[4] were determined by high-pressure liquid chromatography (HPLC). The compounds were separated on a strong cation exchange column[5] and detected with a variable wavelength UV

[1] Fabricated by Thomas Burcar, Cincinnati, Ohio.
[2] Harvard Apparatus, So. Natuck, Mass.
[3] Model 35B Ultrasonic Nebulizer, DeVilbiss Co., Somerset, Pa.
[4] Provided by C. H. Boehringer Sohn, Postfach 200, Germany.
[5] PXS 10/25 SCX, Whatman, Inc., Clifton, N.J.

Table I—Parameter Estimates Generated by a Composite Fit of the Intravascular Isoproterenol Data to the Compartmental Model

Dose, moles	Vm μg/ml min	Km, μg/ml	V_1, ml	V_2, ml	SS[a] Isoproterenol	r^2 Isoproterenol	SS 3-O-Methylisoproterenol	r^2 3-O-Methylisoproterenol
10^{-5}	0.021	1.95	206	199	146.0	0.997	0.084	0.997
5×10^{-6}	0.021	1.95	200	262	39.6	0.992	0.025	0.996
10^{-6}	0.021	1.95	177	198	1.98	0.995	0.012	0.992
5×10^{-7}	0.021	1.95	209	345	0.362	0.984	0.0011	0.985
10^{-7}	0.021	1.95	250	247	0.013	0.387	0.0002	0.943

[a] Sum of squared deviations.

detector[6]. Due to the column-to-column variability and the tendency of the columns to lose efficiency during use, various mobile phases were utilized during the study. Potassium phosphate buffers (0.003–0.03 M) containing 5–30% methanol (pH 3.0) were used at a flow rate of 2 ml/min. The compounds were detected at either 278 or 220 nm. The higher wavelength was used when large concentrations of isoproterenol were present and isoproterenone hydrochloride[7] was used as an internal standard. A sample chromatogram is shown in Fig. 2. Detection at 220 nm afforded greater sensitivity, but the chromatographic conditions needed to separate isoproterenol and 3-O-methylisoproterenol from interfering extraneous peaks precluded the use of isoproterenone as the internal standard; morphine hydrochloride was used as the standard in this case.

Extraction of Perfusate Samples—All procedures were performed under yellow light to protect isoproterenol against photodecomposition. To each sample was added 1 ml of 0.1 N acetate buffer (pH 4.0) containing internal standard (isoproterenone hydrochloride or morphine hydrochloride) and 3 ml of 5% (v/v) diethylhexylphosphoric acid in freshly distilled diethyl ether. This was vortexed 1 min and centrifuged, and the ethereal layer was decanted into a conical centrifuge tube. To this was added 25–100 μl of 1 N HCl with 1% ascorbic acid, and the mixture was vortexed 1 min and centrifuged. An aliquot of the aqueous phase was injected into the chromatographic system.

Standard curves were prepared for each experiment by spiking 1-ml blank perfusate samples with 100 μl of 1% ascorbic acid and varying concentrations of isoproterenol and 3-O-methylisoproterenol. These standards were extracted and analyzed in the same manner as experimental samples.

Preparation of Lung Homogenate Samples—The lungs were thawed and blotted dry. Extraneous tissue was removed and the lung was weighed. The tissue was cut into small slices, diluted with 40 or 60 ml of normal saline containing 1% ascorbic acid, and homogenized[8]. A 1-ml aliquot of the homogenate was then extracted in the same manner as the perfusate samples previously described. Standard curves were prepared by adding varying amounts of isoproterenol and 3-O-methylisoproterenol to blank homogenate samples and analyzing these along with the unknown samples.

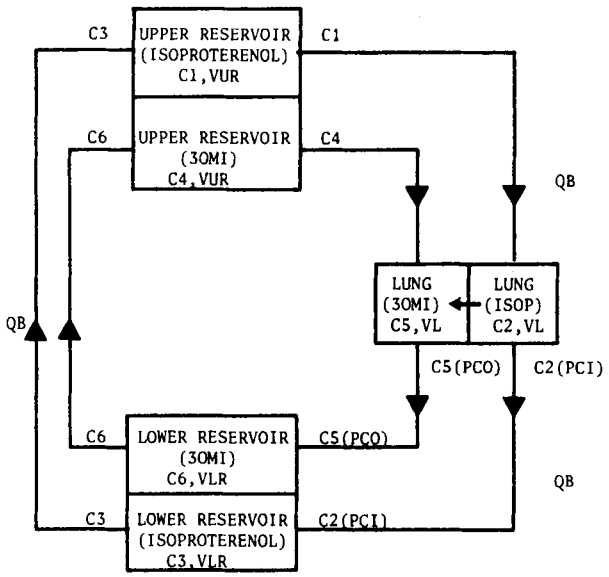

Figure 4—*Perfusion model used to describe the disposition of isoproterenol and 3-O-methylisoproterenol by the isolated perfused rabbit lung.*

[6] Vari-Chrom, Varian Associates, Palo Alto, Calif.
[7] Synthesized in this laboratory.
[8] Model SDT-182 Tissumizer, Tekmar Co., Cincinnati, Oh.

RESULTS

Intravascular Administration—Five doses of isoproterenol hydrochloride ranging from 10^{-7} to 10^{-5} moles were administered directly into the circulating perfusion medium, and samples were withdrawn for 180 min and analyzed for isoproterenol and 3-O-methylisoproterenol. In each experiment, isoproterenol concentrations appeared to decline monoexponentially with a corresponding increase in metabolite levels. The apparent half-life for drug elimination from the perfusate decreased with decreasing dose as the fraction of the dose appearing as 3-O-methylisoproterenol increased. This suggested a capacity-limited process for metabolism of isoproterenol. To investigate this possibility, data were analyzed pharmacokinetically using both a compartmental and perfusion model.

Compartmental Analysis—Each set of isoproterenol and 3-O-methylisoproterenol perfusate concentration–time data were fitted to a simple one-compartment model with the metabolism of isoproterenol to 3-O-methylisoproterenol being described by the Michaelis–Menten equation. The rates of change of drug and metabolic concentrations were described by the differential equations:

$$\frac{dC_1}{dt} = -\frac{Vm \times C_1}{Km + C_1} \quad \text{(Eq. 1)}$$

$$\frac{dC_2}{dt} = \frac{(Vm \times C_1)V_1}{(Km + C_1)V_2} \quad \text{(Eq. 2)}$$

where

C_1 = perfusate concentration of isoproterenol (μg/ml);
C_2 = perfusate concentration of 3-O-methylisoproterenol (μg/ml);
Vm = theoretical maximum metabolic rate (μg $ml^{-1}min^{-1}$);
Km = Michaelis constant (μg/ml);
V_1 = apparent volume of distribution of isoproterenol (ml);
V_2 = apparent volume of distribution of 3-O-methylisoproterenol (ml).

The isoproterenol and 3-O-methylisoproterenol perfusate concentration–time data from the intravascular studies were fitted to the differential equations using the NONLIN (8) digital computer program for nonlinear least-squares regression. The entire set of data (*i.e.*, isoproterenol and 3-O-methylisoproterenol from all five experiments) were fitted to this model resulting in unique estimates of Vm and Km describing the metabolism over the entire range of doses, whereas, V_1 and V_2 were allowed to vary for each dose independent of the others. Table I shows the parameter estimates obtained from these fits. Semilogarithmic plots comparing the observed data to that predicted from the composite fit are shown in Fig. 3.

Perfusion Model—A perfusion model was developed to describe the isolated perfused rabbit lung system and to assist in the analysis and interpretation of the observed data.

Figure 4 depicts the isolated perfused lung model as used to describe the concentration–time course for isoproterenol and 3-O-methylisoproterenol following intravascular administration of isoproterenol. This model is based on the following assumptions: (*a*) the concentration of isoproterenol and 3-O-methylisoproterenol entering the lung vasculature is the same as that in the upper reservoir; (*b*) the concentration of the two compounds in the lung tissue is in equilibrium with that in the perfusion medium leaving the lung and entering the lower reservoir; (*c*) the concentration entering the upper reservoir is the same as that leaving the lower reservoir; (*d*) the metabolism of isoproterenol to 3-O-methylisoproterenol occurs in the lung tissue by a capacity-limited process described by the Michaelis–Menten equation.

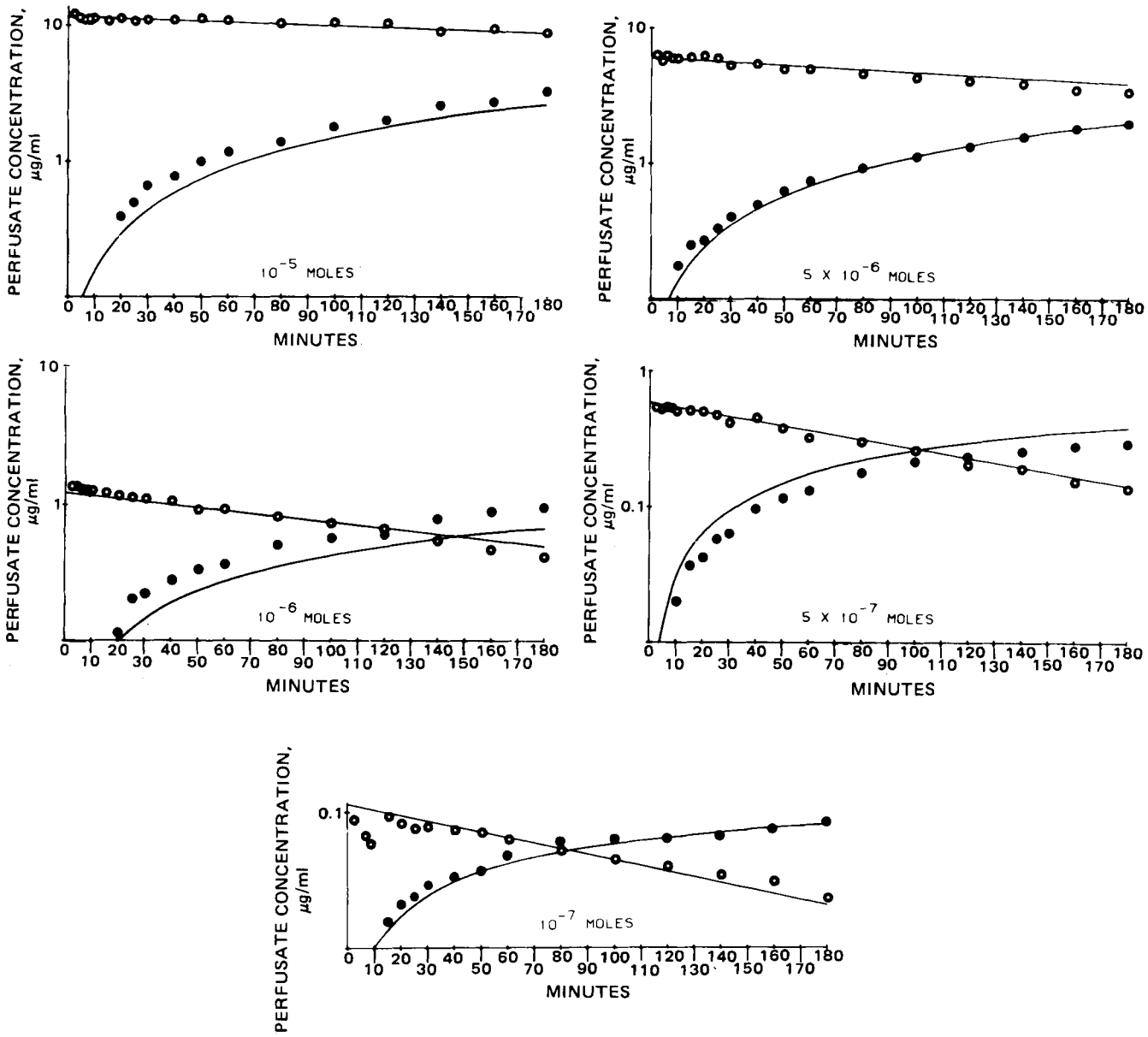

Figure 5—*Semilogarithmic plots of concentration* versus *time for (○) isoproterenol and (●) 3-O-methylisoproterenol comparing observed values with those predicted from perfusion model simulations for five intravascular doses of isoproterenol administered to the isolated perfused rabbit lung.*

The following differential equations describe the rate of change of isoproterenol and 3-*O*-methylisoproterenol concentrations in the lung tissue and in the reservoir compartments following introduction of a bolus of isoproterenol into the upper reservoir:

$$\frac{dC_1}{dt} = \frac{Q_b}{V_{UR}}(C_3 - C_1) \qquad \text{(Eq. 3)}$$

$$\frac{dC_2}{dt} = \frac{Q_b \times C_1}{V_L} - \frac{Q_b \times C_2}{PC_I \times V_L} - \frac{Vm \times C_2}{Km + C_2} \qquad \text{(Eq. 4)}$$

$$\frac{dC_3}{dt} = \frac{Q_b \times C_2}{PC_I \times V_{LR}} - \frac{Q_b \times C_3}{V_{LR}} \qquad \text{(Eq. 5)}$$

$$\frac{dC_4}{dt} = \frac{Q_b(C_6 - C_4)}{V_{UR}} \qquad \text{(Eq. 6)}$$

$$\frac{dC_5}{dt} = \frac{Q_b \times C_4}{V_L} - \frac{Q_b \times C_5}{PC_0 \times V_1} + \frac{Vm \times C_2}{Km + C_2} \qquad \text{(Eq. 7)}$$

$$\frac{dC_6}{dt} = \frac{Q_b \times C_5}{PC_0 \times V_{LR}} - \frac{Q_b \times C_6}{V_{LR}} \qquad \text{(Eq. 8)}$$

where

C_1 = concentration of isoproterenol in the upper reservoir (μmoles/ml);
C_2 = concentration of isoproterenol in the lung tissue (μmoles/ml);
C_3 = concentration of isoproterenol in the lower reservoir (μmoles/ml);
C_4 = concentration of 3-*O*-methylisoproterenol in the upper reservoir (μmoles/ml);
C_5 = concentration of 3-*O*-methylisoproterenol in the lung (μmoles/ml);
C_6 = concentration of 3-*O*-methylisoproterenol in the lower reservoir (μmoles/ml);
V_{UR} = volume of the upper reservoir (ml);
V_L = volume of the lung (ml);
V_{LR} = volume of the lower reservoir (ml);
PC_I = apparent partition coefficient for isoproterenol between the lung tissue and the emergent perfusion medium;
PC_0 = apparent partition coefficient for 3-*O*-methylisoproterenol between the lung tissue and the emergent perfusate;
Vm = maximum rate of metabolism of isoproterenol to 3-*O*-methylisoproterenol in the lung tissue (μmoles $ml^{-1}min^{-1}$);
Km = Michaelis constant (μmoles/ml);
Q_b = rate of flow of perfusion medium (ml/min).

The parameters used to describe this model were derived from actual

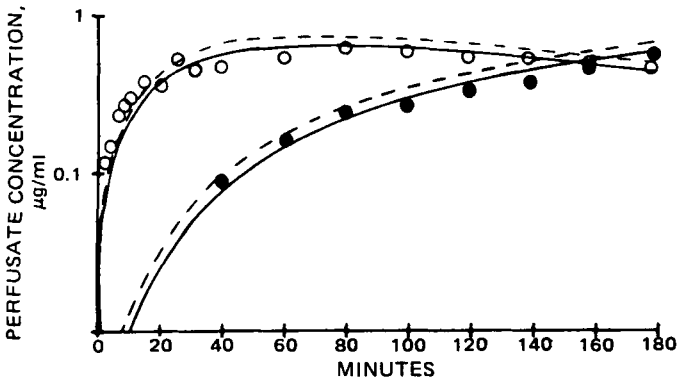

Figure 6—*Semilogarithimic plot of concentration* versus *time for (○) isoproterenol and (●) 3-O-methylisoproterenol following intrabronchial administration of 10^{-6} moles of isoproterenol assuming (- - -) 100% and (—) 90% absorption.*

experimental conditions associated with the isolated lung system. The values for V_{UR}, V_{LR}, PC_I, PC_0, Vm, Km, and Q_b were the same for all simulations. Only the dose and V_L were varied. The volumes of the upper and lower reservoirs were measured as 62 and 88 ml, respectively. The flow rate was constant at 150 ml/min. The partition coefficients for isoproterenol and 3-*O*-methylisoproterenol were determined experimentally from several experiments and an average value for each was used (1.5 for isoproterenol and 3.8 for 3-*O*-methylisoproterenol). Michaelis–Menten constants were estimated from those obtained with the compartmental model fits and were adjusted to represent metabolism occurring from the lung tissue. The following conversions were used to determine these constants from those reported in Table I:

$$Vm^* = \frac{Vm \times V_1}{MW \times V_L} \qquad \text{(Eq. 9)}$$

$$Km^* = \frac{Km \times PC_I}{MW} \qquad \text{(Eq. 10)}$$

where

Vm and Km = Michaelis–Menten constant generated from the composite compartmental fit assuming metabolism from the central compartment (perfusate);
Vm^* and Km^* = Michaelis–Menten constants representing metabolism from the lung tissue;
V_1 = volume of the central compartment of the compartmental model;
V_L = volume of the lung;
MW = molecular weight of isoproterenol;
PC_I = apparent partition coefficient for isoproterenol.

The Vm obtained from this conversion was 0.001 µmoles $ml^{-1}min^{-1}$ while the Km was 0.014 µmoles/ml. The weight of each lung was used as the lung volume.

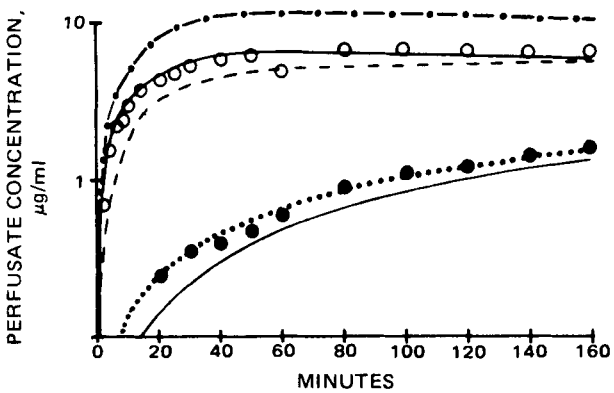

Figure 7—*Semilogarithmic plot of concentration* versus *time for (○) isoproterenol and (●) 3-O-methylisoproterenol following intrabronchial administration of 10^{-5} moles of isoproterenol hydrochloride. Perfusion model predictions for isoproterenol assuming (- · · · · ·) 100% and (—) 60% absorption are shown along with predicted 3-O-methylisoproterenol profiles assuming (- - - -) 40%, (· · · · ·) 2.5%, and (—) no first-pass metabolism.*

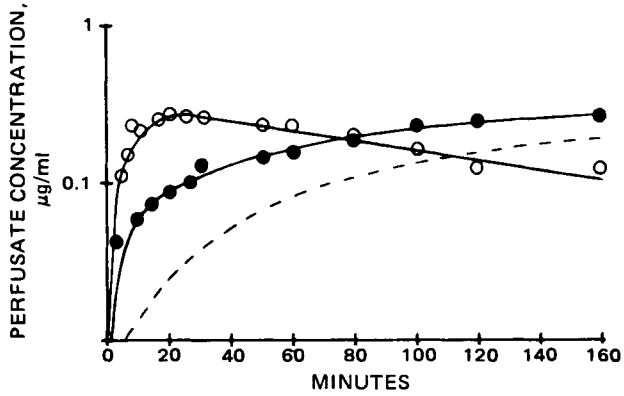

Figure 8—*Semilogarithmic plot of concentration* versus *time for (○) isoproterenol and (●) 3-O-methylisoproterenol following aerosol administration of isoproterenol hydrochloride. Perfusion model predictions for the absorption of 2.75×10^{-7} moles of (—) isoproterenol are shown along with predicted 3-O-methylisoproterenol concentrations with (—) and without (- - - -) 20% first-pass metabolism.*

These equations and parameter estimates were used to produce simulations of the isoproterenol and 3-*O*-methylisoproterenol concentration–time profile in the upper reservoir of the isolated lung system following administration of isoproterenol into the upper reservoir. These simulations were compared to the observed data to determine how the model actually described that which was occurring. These comparisons are shown in Fig. 5. There was good agreement for the isoproterenol data, whereas, slight deviations from the observed metabolite data are observed in some cases.

Intrabronchial Studies—The absorption and subsequent metabolism of isoproterenol was studied following endotracheal instillation of aqueous solutions containing 10^{-5} and 10^{-6} moles of isoproterenol hydrochloride. In both cases the absorption was relatively slow with peak drug levels occurring at 60–80 min. Comparison of isoproterenol and 3-*O*-methylisoproterenol concentrations to those observed following equivalent intravascular doses suggest that less drug and metabolite appeared in the circulation following intrabronchial administration. Determining the fraction of the dose absorbed by the usual method of comparing areas under the curves was not possible, because an accurate estimate of the area under the curve could not be obtained due to nonlinear pharmacokinetics.

The perfusion model was used to assist in the interpretation of the data. The only modification from the previous model was the addition of a first-order pathway for the absorption of isoproterenol from the airways into the lung tissue. In this case the dose was entered into the absorption site rather than the upper reservoir. All other parameters and estimates were identical to those used in the previous flow model.

The simulations produced by this model adequately matched the 10^{-6} mole dose (Fig. 6) but predicted higher isoproterenol concentrations than actually observed for the 10^{-5} mole dose (Fig. 7). The intravascular data suggested that if first-pass metabolism were occurring, it would most likely be due to conversion of isoproterenol to 3-*O*-methylisoproterenol as the drug was being absorbed. This preabsorptive first-pass metabolism was incorporated into the model as the absorption of a fraction of the dose as the metabolite (with the same rate of absorption as isoproterenol). Simulations involving various fractions of the dose being absorbed as intact isoproterenol and as 3-*O*-methylisoproterenol were compared to the observed data to determine if the first-pass model could describe the data.

The results of some of these simulations for the 10^{-5} mole dose are shown in Fig. 6. An absorption rate constant of 0.056 min^{-1} was used in these simulations. Comparing the simulations to the observed data shows that the model with 60% of the dose being absorbed intact and 2.5% as the metabolite best agrees with the data. This suggests that the intrabronchial dose was not totally absorbed but does not indicate an extensive first-pass effect. Similar simulations were produced for the 10^{-6} mole dose. The best agreement with the observed data was achieved with a model assuming that 90% of the dose was absorbed as isoproterenol with no first-pass effect occurring (Fig. 6). An absorption rate constant of 0.025 min^{-1} was used in these simulations.

Aerosol Studies—Isoproterenol hydrochloride was administered to the lung as a nebulized aqueous solution and the resulting concentrations of drug and metabolite were determined. Absorption following aerosol administration was faster than that with intrabronchial administration

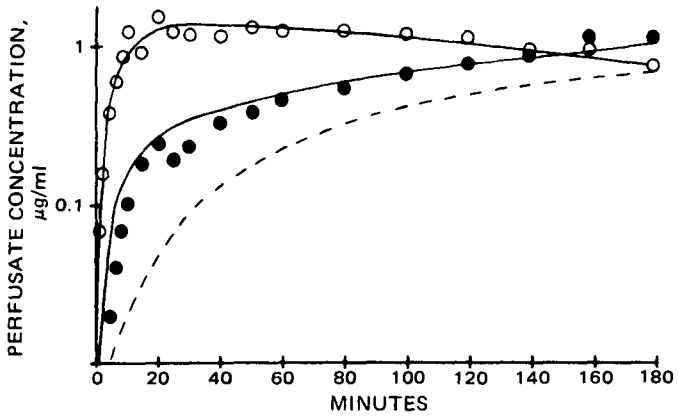

Figure 9—*Semilogarithmic plot of concentration* versus *time for (○) isoproterenol and (●) 3-O-methylisoproterenol following aerosol administration of isoproterenol hydrochloride. Perfusion model predictions for the absorption of 1.3 × 10^{-6} moles of (—) isoproterenol are shown along with predicted 3-O-methylisoproterenol concentrations with (—) and without (- - -) 16% first-pass metabolism.*

(Figs. 8 and 9). The *O*-methyl metabolite also appeared at a faster rate than that following intrabronchial administration. Data were analyzed in the same manner as were the intrabronchial data. The dose delivered to the lung by the nebulizer was not known and was estimated by the simulations. Simulations representing absorption of various fractions of the dose as the metabolite were generated and compared to the observed data. Figure 8 shows observed isoproterenol and 3-*O*-methylisoproterenol concentrations compared to that predicted for the absorption of 2.75 × 10^{-7} moles of aerosolized isoproterenol with and without a simulated 20% first-pass effect represented as absorption of the metabolite. An absorption rate constant of 0.12 min^{-1} was employed for both drug and metabolite. In Fig. 9, the simulated amount of drug absorbed was 1.3 × 10^{-6} moles while that of 3-*O*-methylisoproterenol was 2.5 × 10^{-7} moles (16% of the dose). The absorption rate constant for both was 0.08 min^{-1}. In both cases the incorporation of the first-pass phenomenon into the model provided simulations which matched the observed data much better than that seen when the phenomenon was not included in the model. Although this in itself is not sufficient documentation for concluding that first-pass metabolism was occurring, it does support similar findings by other investigators (7).

Lung Uptake—Lungs were homogenized and analyzed for isoproterenol and 3-*O*-methylisoproterenol. Partition coefficients were calculated for isoproterenol and the metabolite by dividing the lung concentration by the concentration in the final perfusate sample. The mean partition coefficient for isoproterenol was 1.49 ± 0.56 (n = 5), while that for the *O*-methyl metabolite was 3.79 ± 0.66 (n = 7). A plot of the amount of drug in the lung as a function of perfusate concentration for the two (Figs. 10 and 11) shows that uptake was linear over a 100-fold range of concentrations for both drug and metabolite.

DISCUSSION

The results of these studies suggest that pulmonary disposition is of little significance in the overall systemic clearance of isoproterenol when the drug is administered orally or parenterally. When administered *via* the airways, however, isoproterenol may be subject to first-pass metabolism, and the lung may play a significant role in the overall disposition of the drug.

Isoproterenol was metabolized in the lung tissue to 3-*O*-methylisoproterenol. The rate and extent of metabolism was dependent on the amount of drug administered to the lung system, and the kinetics of this process could be described by the Michaelis–Menten equation. The pulmonary clearance of the drug following intravascular administration of the lowest dose (10^{-7} moles) was ~2 ml/min. Lower doses would not be expected to be cleared much faster. Accumulation of the drug by the lung was limited, with concentrations in the lung tissue ~1.5 times those in the perfusion medium. The perfusate concentration profiles following intravascular administration displayed no discernible distribution phase, suggesting rapid equilibration of drug between the perfusate and lung tissue.

Interpretation of the data following intrabronchial and aerosol administration was complicated by the capacity-limited metabolism of isoproterenol. Reports in the literature have suggested a 30% first-pass

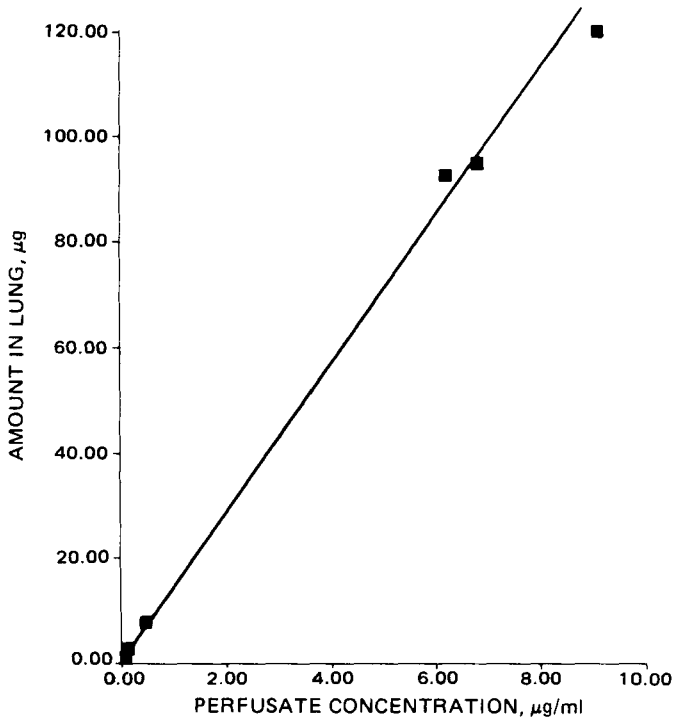

Figure 10—*Uptake of isoproterenol by the lung.*

metabolism of isoproterenol to its *O*-methyl metabolite following administration of the drug *via* the airways (7). Usual methods for evaluating first-pass metabolism (*i.e.*, *AUC* comparisons) were not applicable, as accurate estimates of infinity *AUC* values could not be obtained. As an alternative for interpreting the data, a mathematical model similar to the perfusion model described previously (9) was developed, based upon mass balance and the flow of perfusion medium through the various compartments of the isolated perfused lung system. The model described the drug and metabolite data following intravascular administration of isoproterenol.

Before the perfusion model could be modified to simulate first-pass metabolism, the nature of the first-pass effect had to be established. Two possible mechanisms for first-pass metabolism were discussed previously in a review of presystemic drug elimination (10). Postabsorptive first-pass metabolism occurs when a drug is absorbed into an eliminating organ; the fraction eliminated presystemically is equivalent to the organ extraction ratio (Cl/Q_h) following systemic administration (where Cl is the

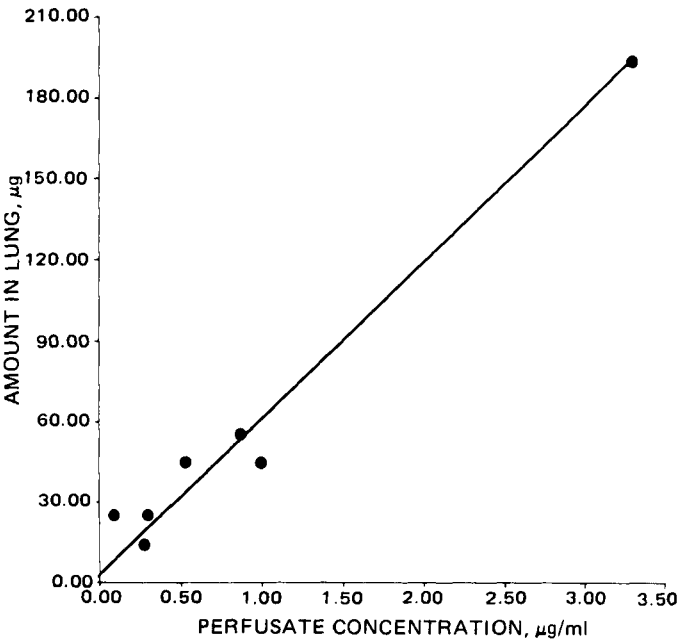

Figure 11—*Uptake of 3-O-methylisoproterenol by the lung.*

organ clearance of the drug following systemic administration, and Q_b is the flow rate through the organ). In this case the fraction of the absorbed dose reaching the circulation intact (F) is given as:

$$F = 1 - Cl/Q_b \qquad \text{(Eq. 11)}$$

Preabsorptive first-pass metabolism involves metabolism of a drug as it is absorbed into the circulation from the site of administration. In this case the fraction eliminated presystemically is not equal to the systemic extraction ratio.

The maximum pulmonary clearance of isoproterenol following systemic administration to the rabbit lung was ~2 ml/min, representing an extraction ratio of ~0.01. If only postabsorptive first-pass metabolism were occurring, this would predict that 99% of an intrabronchial or aerosol dose of isoproterenol should reach the circulation intact. If >1% first-pass metabolism occurs, as has been reported (7), preabsorptive first-pass metabolism must be involved. The preabsorptive metabolism would be observed experimentally as absorption of the metabolite into the circulation along with the parent drug. This was incorporated into the perfusion model as first-order absorption of both drug and metabolite, and various simulations with this model were compared to the experimental results following intrabronchial and aerosol administration of isoproterenol. These comparisons indicate little or no first-pass metabolism of isoproterenol following intrabronchial instillation of an aqueous solution of isoproterenol but suggest the possibility of a substantial first-pass effect when the drug was inhaled as an aerosol. The drug was also more rapidly absorbed following aerosol administration; it may be that this route of administration delivers the drug over a larger surface area in the airways than is achieved with intrabronchial administration. This may result in greater exposure of the drug to the epithelial cells of the bronchi and small airways, leading to more rapid absorption and avoiding local saturation of metabolizing capacity during absorption. This would hinder extrapolation of data following intrabronchial administration to situations involving aerosol inhalation of a drug and suggests that intrabronchial or endotracheal administration may be an inappropriate technique for studying drugs which are intended for aerosol administration.

REFERENCES

(1) J. W. Paterson, M. E. Conolly, D. S. Davies, and C. T. Dollery, *Lancet*, **2**, 426 (1968).

(2) R. W. Neimeir and E. Bingham, *Life Sci.*, Part II, **11**, 807 (1972).

(3) J. P. McGovren, W. C. Lubawy, and H. B. Kostenbauder, *J. Pharmacol. Exp. Ther.*, **199**, 198 (1976).

(4) T. C. Orton, M. W. Anderson, R. D. Pickett, T. E. Eling, and J. R. Fouts, *ibid.*, **186**, 482 (1973).

(5) F. C. P. Law, T. E. Eling, J. R. Bend, and J. R. Fouts, *Drug Metab. Dispos.*, **2**, 433 (1974).

(6) E. H. Butler, K. M. Moser, and P. A. Kot, *J. Lab. Clin. Med.*, **74**, 129 (1974).

(7) R. H. Briant, E. W. Blackwell, F. M. Williams, D. S. Davies, and C. T. Dollery, *Xenobiotica*, **3**, 787 (1973).

(8) C. M. Metzler, G. L. Elfring, and A. J. McEwen, *Biometrics*, **30**, 512 (1974).

(9) M. Rowland, L. Z. Benet, and G. G. Graham, *J. Pharmacokinet. Biopharm.*, **1**, 123 (1973).

(10) P. A. Routledge and D. G. Shand, *Annu. Rev. Pharmacol. Toxicol.*, **19**, 447 (1979).

Isolated Perfused Rabbit Lung as a Model for Intravascular and Intrabronchial Administration of Bronchodilator Drugs II: Isoproterenol Prodrugs

R. K. BRAZZELL * and H. B. KOSTENBAUDER ˣ

Received November 12, 1981, from the *College of Pharmacy, University of Kentucky, Lexington, KY 40506.* Accepted for publication January 29, 1982.

*Present address: Hoffmann-LaRoche Inc., Department of Pharmacokinetics and Biopharmaceutics, Nutley, NJ 07110.

Abstract □ The pulmonary disposition of two diester prodrugs of isoproterenol (di-*p*-toluoylisoproterenol and dipivaloylisoproterenol) was studied in the isolated perfused rabbit lung preparation. High-pressure liquid chromatographic methods were developed to measure diester, monoester, isoproterenol, and 3-*O*-methylisoproterenol from a single 1-ml perfusate sample. The prodrugs were administered directly into the circulating perfusion medium and by endotracheal instillation. Perfusate concentrations of diester, monoester, isoproterenol, and 3-*O*-methylisoproterenol were measured for 180 min. The diesters were rapidly eliminated from the perfusate with a subsequent increase in monoester concentrations. Isoproterenol levels were observed within minutes of prodrug administration, peaked at 60–80 min, and declined slowly thereafter. The prodrugs were rapidly absorbed following endotracheal administration with 30–50% of the diester being metabolized during the first pass through the lung.

Keyphrases □ Isoproterenol prodrugs—isolated rabbit lung as model for intravascular and intrabronchial administration of bronchodilator drugs, high-pressure liquid chromatography □ Prodrugs—isoproterenol, isolated rabbit lung as model for intravascular and intrabronchial administration of bronchodilator drugs, perfusion, high-pressure liquid chromatography □ Perfusion—isolated rabbit lung as model for intravascular and intrabronchial administration of bronchodilator drugs, high-pressure liquid chromatography □ High-pressure liquid chromatography—isolated rabbit lung as model for intravascular and intrabronchial administration of bronchodilator drugs, prodrugs, perfusion, isoproterenol

Isoproterenol is a β-adrenergic agonist which is often employed in the treatment of bronchial asthma. The drug has limited oral activity because of the extensive first-pass metabolism which occurs during absorption of the drug from the GI tract (1, 2). Aerosol inhalation is the most commonly used route of administration and offers the advantages of a rapid onset of activity and delivery of the drug directly to the airways (3). The duration of action following inhalation is short, however, and frequent dosing is often required to maintain the desired effect. This can result in side effects such as cardiac stimulation, which can hinder effective therapy with the drug. Increasing the duration of action of isoproterenol would offer a significant improvement in the clinical use of the drug for the treatment of asthma.

Prodrugs have been used in the past to improve the delivery of pharmacological agents, and this approach seems feasible with isoproterenol. An inactive derivative of isoproterenol, which itself possesses more favorable physicochemical and pharmacokinetic properties than the

0022-3549/82/1100-1274$01.00/0

organ clearance of the drug following systemic administration, and Q_b is the flow rate through the organ). In this case the fraction of the absorbed dose reaching the circulation intact (F) is given as:

$$F = 1 - Cl/Q_b \qquad \text{(Eq. 11)}$$

Preabsorptive first-pass metabolism involves metabolism of a drug as it is absorbed into the circulation from the site of administration. In this case the fraction eliminated presystemically is not equal to the systemic extraction ratio.

The maximum pulmonary clearance of isoproterenol following systemic administration to the rabbit lung was ~2 ml/min, representing an extraction ratio of ~0.01. If only postabsorptive first-pass metabolism were occurring, this would predict that 99% of an intrabronchial or aerosol dose of isoproterenol should reach the circulation intact. If >1% first-pass metabolism occurs, as has been reported (7), preabsorptive first-pass metabolism must be involved. The preabsorptive metabolism would be observed experimentally as absorption of the metabolite into the circulation along with the parent drug. This was incorporated into the perfusion model as first-order absorption of both drug and metabolite, and various simulations with this model were compared to the experimental results following intrabronchial and aerosol administration of isoproterenol. These comparisons indicate little or no first-pass metabolism of isoproterenol following intrabronchial instillation of an aqueous solution of isoproterenol but suggest the possibility of a substantial first-pass effect when the drug was inhaled as an aerosol. The drug was also more rapidly absorbed following aerosol administration; it may be that this route of administration delivers the drug over a larger surface area in the airways than is achieved with intrabronchial administration. This may result in greater exposure of the drug to the epithelial cells of the bronchi and small airways, leading to more rapid absorption and avoiding local saturation of metabolizing capacity during absorption. This would hinder extrapolation of data following intrabronchial administration to situations involving aerosol inhalation of a drug and suggests that intrabronchial or endotracheal administration may be an inappropriate technique for studying drugs which are intended for aerosol administration.

REFERENCES

(1) J. W. Paterson, M. E. Conolly, D. S. Davies, and C. T. Dollery, *Lancet*, **2**, 426 (1968).

(2) R. W. Neimeir and E. Bingham, *Life Sci.*, Part II, **11**, 807 (1972).

(3) J. P. McGovren, W. C. Lubawy, and H. B. Kostenbauder, *J. Pharmacol. Exp. Ther.*, **199**, 198 (1976).

(4) T. C. Orton, M. W. Anderson, R. D. Pickett, T. E. Eling, and J. R. Fouts, *ibid.*, **186**, 482 (1973).

(5) F. C. P. Law, T. E. Eling, J. R. Bend, and J. R. Fouts, *Drug Metab. Dispos.*, **2**, 433 (1974).

(6) E. H. Butler, K. M. Moser, and P. A. Kot, *J. Lab. Clin. Med.*, **74**, 129 (1974).

(7) R. H. Briant, E. W. Blackwell, F. M. Williams, D. S. Davies, and C. T. Dollery, *Xenobiotica*, **3**, 787 (1973).

(8) C. M. Metzler, G. L. Elfring, and A. J. McEwen, *Biometrics*, **30**, 512 (1974).

(9) M. Rowland, L. Z. Benet, and G. G. Graham, *J. Pharmacokinet. Biopharm.*, **1**, 123 (1973).

(10) P. A. Routledge and D. G. Shand, *Annu. Rev. Pharmacol. Toxicol.*, **19**, 447 (1979).

Isolated Perfused Rabbit Lung as a Model for Intravascular and Intrabronchial Administration of Bronchodilator Drugs II: Isoproterenol Prodrugs

R. K. BRAZZELL * and H. B. KOSTENBAUDER ˣ

Received November 12, 1981, from the *College of Pharmacy, University of Kentucky, Lexington, KY 40506.* Accepted for publication January 29, 1982.

*Present address: Hoffmann-LaRoche Inc., Department of Pharmacokinetics and Biopharmaceutics, Nutley, NJ 07110.

Abstract □ The pulmonary disposition of two diester prodrugs of isoproterenol (di-*p*-toluoylisoproterenol and dipivaloylisoproterenol) was studied in the isolated perfused rabbit lung preparation. High-pressure liquid chromatographic methods were developed to measure diester, monoester, isoproterenol, and 3-*O*-methylisoproterenol from a single 1-ml perfusate sample. The prodrugs were administered directly into the circulating perfusion medium and by endotracheal instillation. Perfusate concentrations of diester, monoester, isoproterenol, and 3-*O*-methylisoproterenol were measured for 180 min. The diesters were rapidly eliminated from the perfusate with a subsequent increase in monoester concentrations. Isoproterenol levels were observed within minutes of prodrug administration, peaked at 60–80 min, and declined slowly thereafter. The prodrugs were rapidly absorbed following endotracheal administration with 30–50% of the diester being metabolized during the first pass through the lung.

Keyphrases □ Isoproterenol prodrugs—isolated rabbit lung as model for intravascular and intrabronchial administration of bronchodilator drugs, high-pressure liquid chromatography □ Prodrugs—isoproterenol, isolated rabbit lung as model for intravascular and intrabronchial administration of bronchodilator drugs, perfusion, high-pressure liquid chromatography □ Perfusion—isolated rabbit lung as model for intravascular and intrabronchial administration of bronchodilator drugs, high-pressure liquid chromatography □ High-pressure liquid chromatography—isolated rabbit lung as model for intravascular and intrabronchial administration of bronchodilator drugs, prodrugs, perfusion, isoproterenol

Isoproterenol is a β-adrenergic agonist which is often employed in the treatment of bronchial asthma. The drug has limited oral activity because of the extensive first-pass metabolism which occurs during absorption of the drug from the GI tract (1, 2). Aerosol inhalation is the most commonly used route of administration and offers the advantages of a rapid onset of activity and delivery of the drug directly to the airways (3). The duration of action following inhalation is short, however, and frequent dosing is often required to maintain the desired effect. This can result in side effects such as cardiac stimulation, which can hinder effective therapy with the drug. Increasing the duration of action of isoproterenol would offer a significant improvement in the clinical use of the drug for the treatment of asthma.

Prodrugs have been used in the past to improve the delivery of pharmacological agents, and this approach seems feasible with isoproterenol. An inactive derivative of isoproterenol, which itself possesses more favorable physicochemical and pharmacokinetic properties than the

0022-3549/82/1100-1274$01.00/0

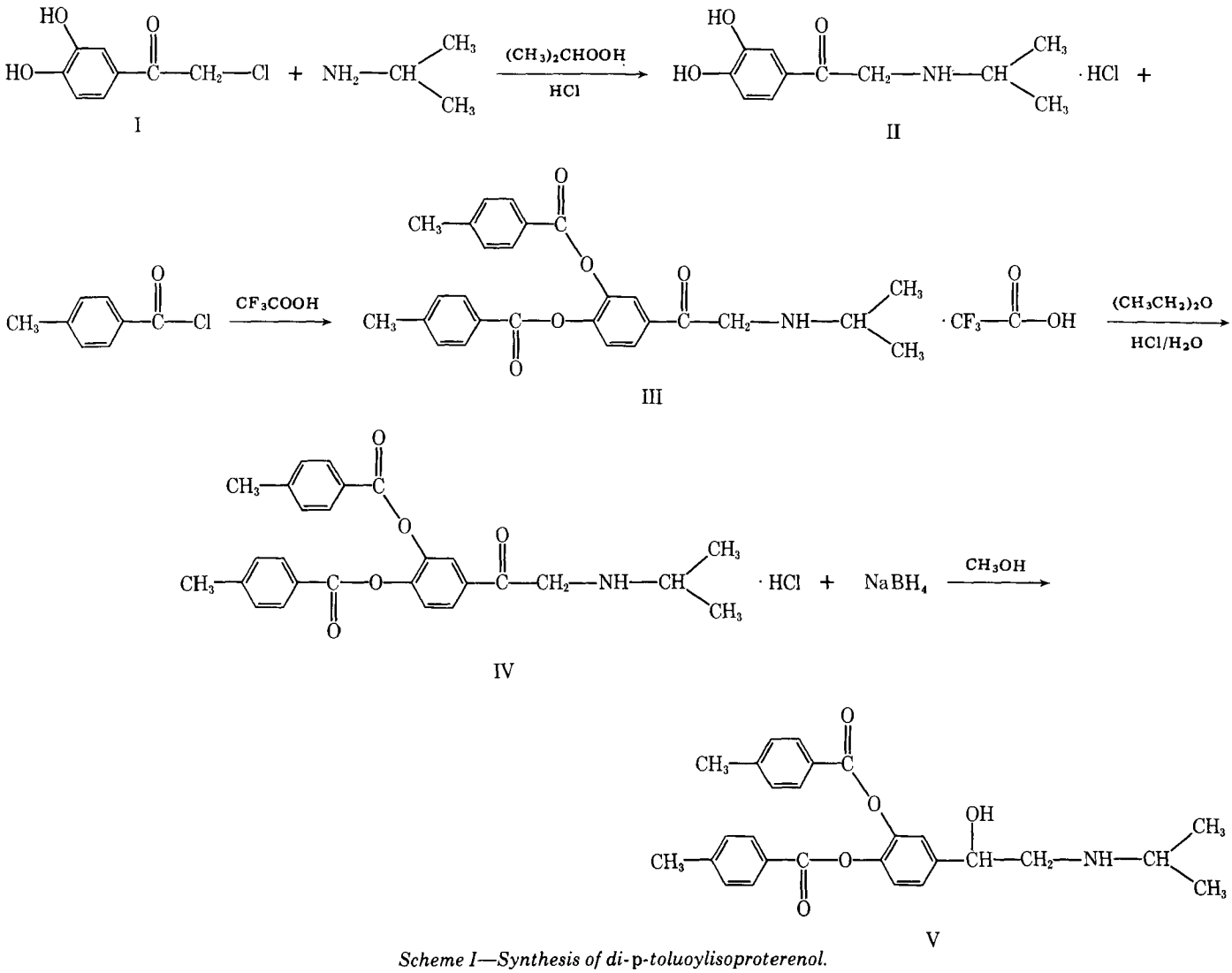

Scheme I—Synthesis of di-p-toluoylisoproterenol.

parent drug, and which would be converted to the active compound in the body, could provide a mechanism for improving the efficacy of the drug while eliminating some of its problems. Esterifying the phenolic hydroxyl groups of isoproterenol is a practical approach as these functionalities are involved in the metabolism and chemical degradation of the drug. Esterases capable of hydrolyzing these esters are distributed throughout the body and have been demonstrated in the lung tissue itself (4–6). The rate of hydrolysis of the ester could be controlled somewhat by the choice of the ester moiety (7–9); a slowly hydrolyzed hydrophobic ester might be taken up extensively by the lung tissue with subsequent slow release of the parent compound, resulting in a prolonged bronchodilating effect.

The present report details the preliminary evaluation of two prodrugs of isoproterenol, di-*p*-toluoylisoproterenol and dipivaloylisoproterenol. The absorption, uptake, and metabolism of these two drugs by the isolated perfused rabbit lung system were evaluated following their administration into the circulation of the system and into the airways of the lung. Disposition of isoproterenol in the isolated perfused rabbit lung has been discussed previously (10). The drug was converted to its *O*-methyl metabolite in the lung by a dose-dependent process. Uptake of the drug by the lung tissue, however, was linear over a 100-fold concentration range. A physiological pharmacokinetic perfusion model was developed to describe the disposition of isoproterenol and 3-*O*-methylisoproterenol by the isolated lung system, and a similar model is used in the evaluation of the data from this investigation.

EXPERIMENTAL

Di-*p*-toluoylisoproterenol—Synthetic procedures were modeled after published methods for preparation of esters of isoproterenol (7) and *N-tert*-butylarterenol (9). The overall reaction scheme is shown in Scheme I.

3,4-Dihydroxy-α-(isopropylamino)acetophenone Hydrochloride—A mixture of 37.5 g (0.2 mole) α-chloro-3′,4′-dihydroxyacetophenone[1] (I), 125 ml of isopropyl alcohol, and 60 ml of isopropylamine was slowly heated to 75° and maintained at that temperature for 5 min. While cooling, the mixture was acidified with hydrochloric acid. The hydrochloride salt was precipitated by the addition of 400 ml of acetone and overnight refrigeration. The filtered product (II) was slurried with 100 ml of acetone, filtered, and dried to yield 21.2 g (43%) of II, mp 239–242°.

3,4-Di-*p*-toluoyl-α-(isopropylamino)acetophenone Hydrochloride—Twenty grams of II was suspended in 60 ml of trifluoroacetic acid, and 35 ml of *p*-toluoyl chloride was added slowly, with stirring, over a period of 20 min. The mixture was heated slowly to 80° and held at that

[1] Aldrich Chemical Co., Milwaukee, Wis.

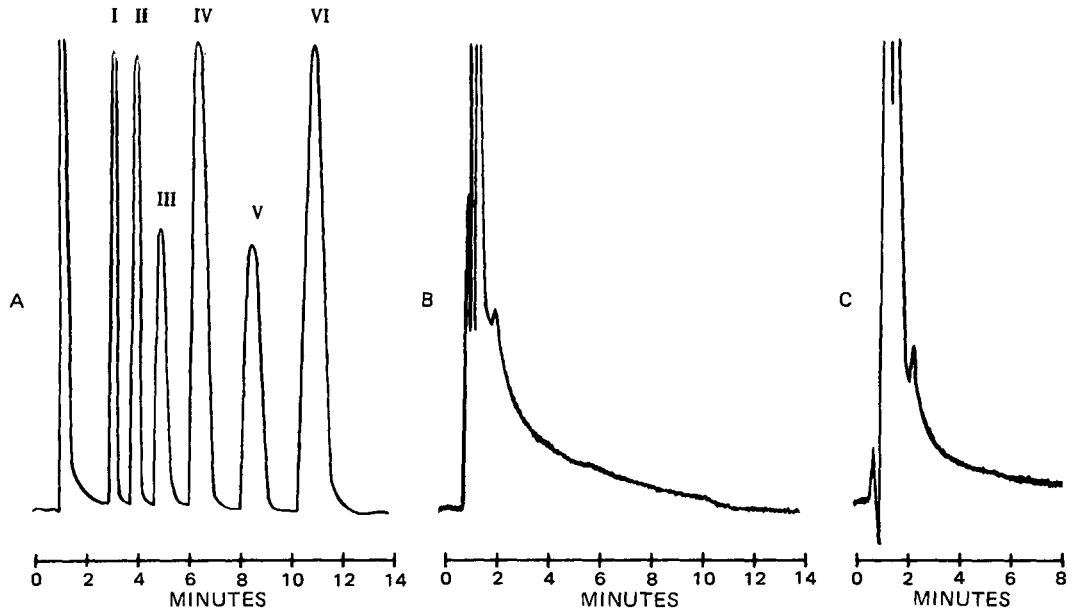

Figure 1—*(A) Separation of (I) isoproterenol, (II) 3-O-methylisoproterenol, (III) mono-p-toluoylisoproterenol, (IV) morphine, (V) di-p-toluoylisoproterenol, and (VI) codeine on a strong cation exchange column with 0.03 M KH_2PO_4–25% acetonitrile (pH 3.0) flowing at 2.5 ml/min. (B) Blank methylene chloride perfusate extract. (C) Blank diethylhexyl phosphoric acid perfusate extract.*

temperature for 75 min. Most of the solvent was evaporated *in vacuo* and the residue stirred with 400 ml of ether and refrigerated. Filtration yielded 40 g of III. Compound III was partitioned between ether and water and made basic with sodium hydroxide. The ether layer was removed and 40 ml of 20% HCl was added slowly with constant stirring. The crystalline product that precipitated was filtered, dried, and recrystallized from isopropyl acetate–methanol (9:1) to yield 20 g of IV, mp 198–202°.

Di-*p*-toluoylisoproterenol (V)—A cold solution of 0.5 g of sodium borohydride in methanol was added to 5 g of IV in 25 ml of methanol over a 1-hr period in an ice bath. Most of the solvent was evaporated *in vacuo* and the residue was suspended in 20 ml of isopropyl acetate. This mixture was rapidly stirred and 25 ml of 10% sodium bicarbonate (pH 10.5) was slowly added. The organic layer was separated and dried over magnesium sulfate. The solution was partially concentrated *in vacuo* and refrigerated. The precipitated product was filtered and dried to yield 2 g (40%) of di-*p*-toluoyl isoproterenol (V), mp 110–111°.

cipitated product was filtered and dried to yield 2 g (40%) of di-*p*-toluoyl isoproterenol (V), mp 110–111°.

Anal.—Calc. for $C_{27}H_{29}NO_5$: C, 72.48; H, 6.48; N, 3.13; O, 17.89. Found: C, 72.49; H, 6.4; N, 3.12; O, 17.6. NMR (CD_3COCD_3): δ 6.9–8.3 (m, 11, aromatic); δ 4.5–4.9 (s, 1, —CHO*H*); δ 2.5–3.2 (m, 5, —CH_2—N*H*—CH_2—); δ 2.2–2.5 (s, 6, p-methyl); δ 0.9–1.2 [d, 6, —CH—(CH_3)$_2$]. The UV spectrum displayed a maximum of 245 nm with a molar absorptivity of 3.4×10^{-4} liters/mole/cm.

Isolated Perfused Rabbit Lung—Details of the perfusion technique have been described in detail in previous reports (10–12). Krebs-Ringer bicarbonate solution with 4.5% bovine serum albumin was used as the perfusion medium. Di-*p*-toluoylisoproterenol and dipivaloylisoproterenol were administered to the system by intravascular and intrabronchial administration. Doses of 10^{-5} and 5×10^{-5} moles of the two drugs were administered intravascularly as aqueous solutions added to the perfusion medium in the upper reservoir of the lung system. Intrabronchial administration of 5×10^{-6} and 10^{-5} moles of di-*p*-toluoylisoproterenol and 10^{-5} moles of dipivaloylisoproterenol was accomplished by delivering

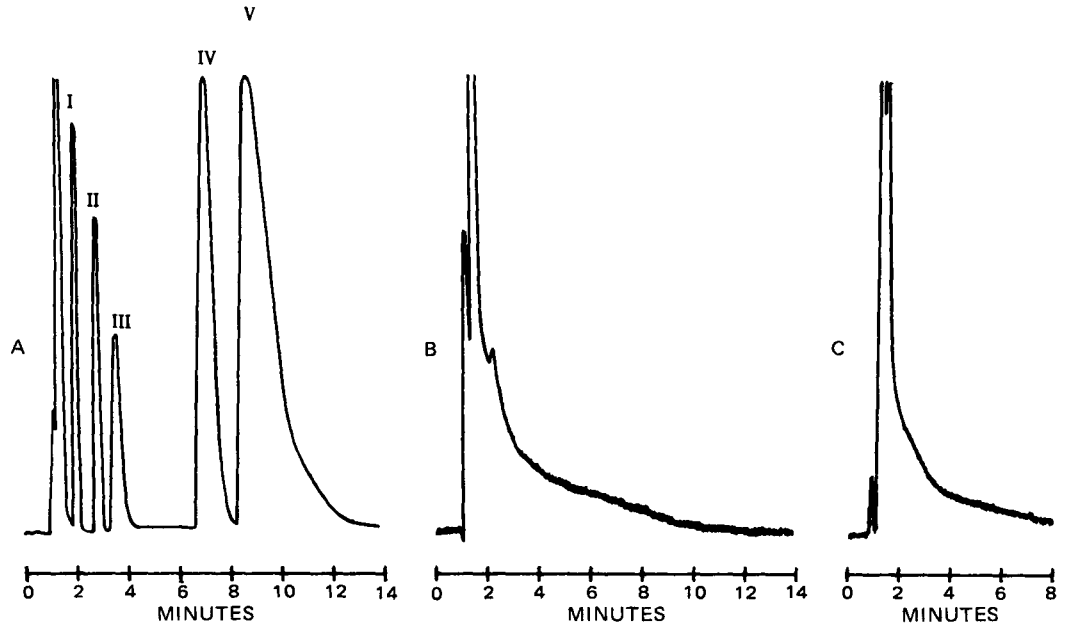

Figure 2—*(A) Separation of (I) isoproterenol, (II) 3-O-methylisoproterenol, (III) monopivaloylisoproterenol, (IV) dipivaloylisoproterenol, and (V) codeine on a strong cation exchange column with 0.01 KH_2PO_4–10% methanol (pH 3.0) flowing at 2.5 ml/min. (B) Blank methylene chloride perfusate extract. (C) Blank diethylhexyl phosphoric acid perfusate extract.*

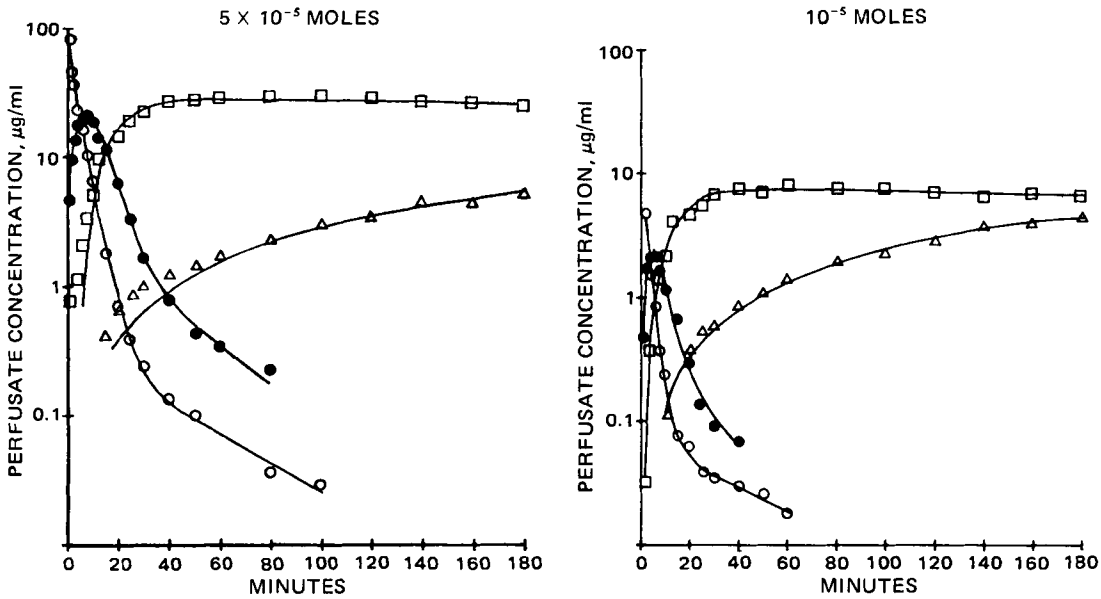

Figure 3—*Perfusate concentrations following the administration of 5 X 10^{-5} moles and 10^{-5} moles of di-p-toluoylisoproterenol into the circulation of the isolated perfused rabbit lung. Key: (○) di-p-toluoylisoproterenol; (●) mono-p-toluoylisoproterenol; (□) isoproterenol; (△) 3-O-methylisoproterenol.*

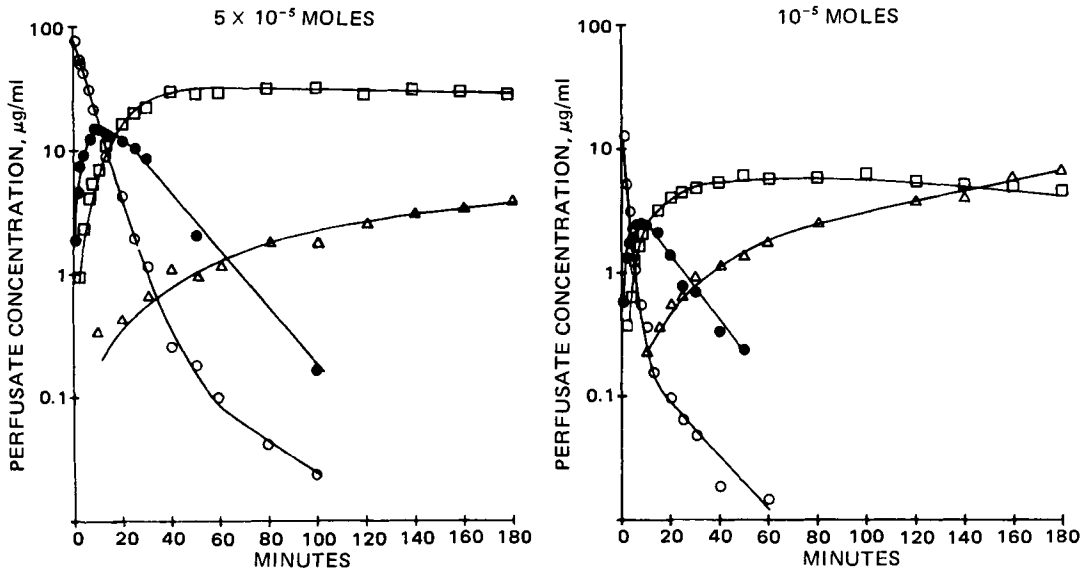

Figure 4—*Perfusate concentrations following 5 X 10^{-5} and 10^{-5} moles of dipivaloylisoproterenol administered to the circulation of the isolated perfused rabbit lung. Key: (○) dipivaloylisoproterenol; (■) monopivaloylisoproterenol; (□) isoproterenol; (△) 3-O-methylisoproterenol.*

250-μl aliquots of drug solution into the airways *via* a small polytef tube attached to a 1-ml syringe. Dipivaloylisoproterenol was dissolved in isotonic saline while di-*p*-toluoylisoproterenol was dissolved in saline which had been adjusted to pH 4.0 with hydrochloric acid.

Analysis—The perfusate concentrations of diester (di-*p*-toluoylisoproterenol or dipivaloylisoproterenol[2]), the corresponding monoester, isoproterenol, and 3-*O*-methylisoproterenol[3] were measured by high-pressure liquid chromatography (HPLC). The compounds were separated on a strong cation exchange column[4] and detected with a variable-wavelength UV detector[5]. Differences in physicochemical properties prevented the extraction of the four compounds with one procedure, and a double extraction technique was developed.

The same extraction procedure was used for both prodrugs. Samples were thawed to room temperature and 10 ml of methylene chloride containing codeine phosphate (internal standard) was added; this was vortexed for 1 min and centrifuged. The aqueous layer (750 μl) was transferred to a 15-ml culture tube and 100 μl of 1% ascorbic acid was added. This was stored at −20° and later analyzed for isoproterenol. The organic phase was evaporated under nitrogen, the residue reconstituted with 100 μl of methanol, and an aliquot was injected onto the HPLC system to measure the concentrations of the diester along with the monoester and 3-*O*-methylisoproterenol.

The 750-μl aqueous aliquot was thawed and 1 ml of 0.1 *N* acetate buffer (pH 4.0) containing morphine hydrochloride (internal standard) was added followed by 3 ml of 5% diethylhexyl phosphoric acid in ether. This was vortexed and centrifuged and the ether layer was transferred to a centrifuge tube; 100 μl of 1 *N* HCl containing 1% ascorbic acid was added, the mixture was vortexed and centrifuged, and a 10–50-μl aliquot was injected onto the HPLC system to measure isoproterenol.

Separation of di-*p*-toluoylisoproterenol, the monotoluoyl ester, isoproterenol, 3-*O*-methylisoproterenol, and codeine and morphine (internal standards) was accomplished with a strong cation exchange column and a mobile phase of 0.03 *M* KH_2PO_4 with 25% methanol and a final pH of 3.0. Flow rate was 2.5 ml/min and detection was at 220 nm. Aliquots

[2] Provided by the INTERx Corp., Lawrence, KS.
[3] Provided by C. H. Boehringer Sohn, Postfach 200, Germany.
[4] PXS 10/25 5CX, Whatman, Inc., Clifton, N.J.
[5] Vari-Chrom, Varian Associates, Palo Alto, Calif.

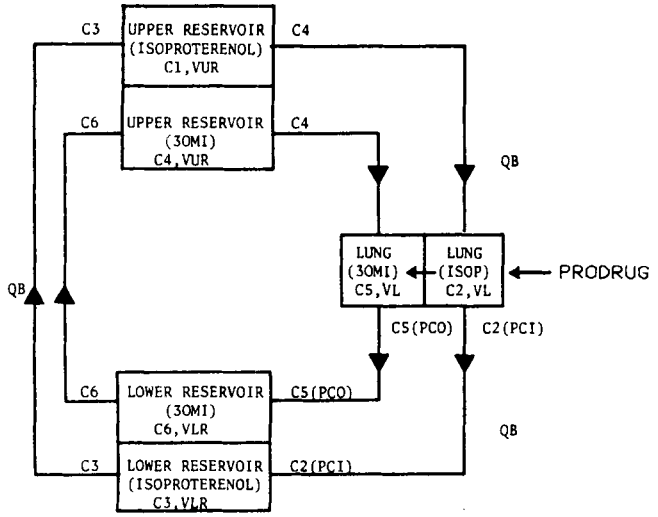

Figure 5—*Flow model used to describe the disposition of isoproterenol and 3-O-methylisoproterenol by the isolated perfused rabbit lung following administration of the diester prodrugs.*

(10–50 μl) from the methylene chloride extractions were injected onto this system to quantitate the diester, monoester, and 3-*O*-methylisoproterenol while aliquots (10–50 μl) from the diethylhexyl phosphoric acid extractions were injected to measure isoproterenol. This procedure provided adequate sensitivity for the monoester, isoproterenol, and 3-*O*-methylisoproterenol but was not capable of measuring diester concentrations <0.1 μg/ml. When diester concentrations below this limit were encountered, the methylene chloride extraction aliquots were also analyzed with an alternate chromatographic system utilizing a mobile phase of 0.04 *M* KH_2PO_4 with 20% acetonitrile and a final pH of 3.0 pumped through the cation exchange column at 3.0 ml/min with 250-nm detection. This provided sensitivity for the diester down to 0.01 μg/ml. Sample chromatograms are shown in Fig. 1.

A similar procedure was used for measuring dipivaloylisoproterenol. A cation exchange column was used; the mobile phase consisted of 0.01 *M* KH_2PO_4 with 10% methanol (pH 3.0) pumped at 2.5 ml/min with 220-nm detection. This system was used for measuring the monoester, isoproterenol, 3-*O*-methylisoproterenol, and concentrations of dipivaloylisoproterenol exceeding 0.5 μg/ml. The alternate system used to measure dipivalylisoproterenol concentrations <0.5 μg/ml also employed the cation exchange column with 0.045 *M* KH_2PO_4 with 20% methanol (pH 3.0) at a flow rate of 2.5 ml/min and 220-nm detection. Sample chromatograms are presented in Fig. 2.

For standard curves, the monoesters of di-*p*-toluoylisoproterenol and dipivaloylisoproterenol were produced by hydrolysis of the diesters in deoxygenated 1 *N* HCl containing 5% ascorbic acid as an antioxidant. Hydrolysis was relatively slow under these conditions and appreciable amounts of monoester could be produced while maintaining measurable amounts of the diester and isoproterenol by heating the solutions for 12–24 hr protected from light and air. These solutions were injected onto one of the previously described HPLC systems, and the concentrations of the diester and isoproterenol were determined by comparing their response to calibration curves prepared for the two compounds. Using the amounts of these two compounds and the diester initially added, the amount of monoester present in the solutions was determined using mass balance calculations.

Aliquots of these solutions were added to fresh blank perfusate samples along with equivalent volumes of 1 *N* NaOH such that the final perfusate sample volume was 1 ml. To each sample, 100 μl of 1 *M* phosphate buffer (pH 7.4) with 1% ascorbic acid was added. These samples were assayed in the manner described for the unknown samples. Standard curves for the diester, isoproterenol, and 3-*O*-methylisoproterenol were also generated. Peak heights were measured manually and the concentration *versus* peak height ratio of each compound to internal standard were fitted to a linear regression line. Correlation coefficients ≥0.98 were obtained using these methods. Standard curves for all compounds were produced on each day that samples were analyzed.

Care was taken in the storage, processing, and analysis of samples to minimize hydrolysis of the esters during this time. Small amounts of monoester and isoproterenol were observed in some diester standard perfusate samples processed in the same manner as the unknown samples, but these amounts never exceeded 5%.

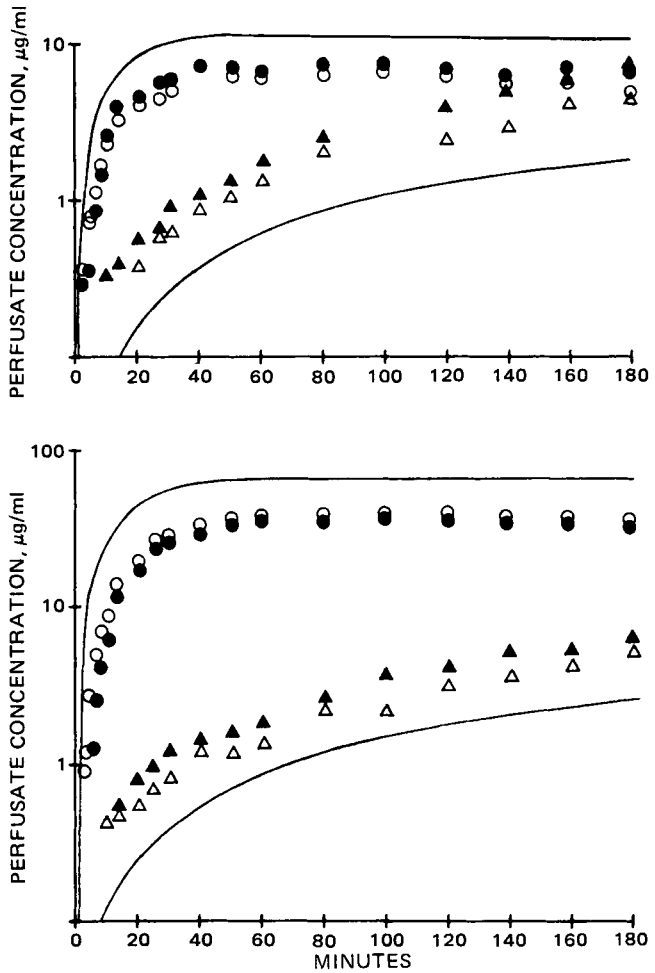

Figure 6—*Comparisons of observed concentrations to those predicted by the flow model for the intravascular administration of 10^{-5} moles of di-p-toluoylisoproterenol and dipivaloylisoproterenol (upper) and 5×10^{-5} moles of di-p-toluoylisoproterenol and dipivaloylisoproterenol (lower). Open symbols represent data from di-p-toluoylisoproterenol experiments, while closed symbols represent data from dipivalylisoproterenol experiments. Key: (○,●) isoproterenol; (△,▲) 3-O-methylisoproterenol.*

RESULTS AND DISCUSSION

Initial Studies—Preliminary studies involved administration of 10^{-5}-mole doses of dipivaloylisoproterenol and di-*p*-toluoylisoproterenol into the circulation of the isolated lung system. In each experiment, samples were withdrawn periodically from the upper reservoir and assayed for the prodrug, isoproterenol, and 3-*O*-methylisoproterenol. Both prodrugs were rapidly cleared from the perfusion medium, and in both cases isoproterenol appeared within 4–6 min. Following administration of each diester, an unidentified chromatographic peak was observed on the early sample chromatograms which eluted between 3-*O*-methylisoproterenol and the diester.

The peak height ratio *versus* time profile of this unknown component was suggestive of a monoester intermediate formed during the hydrolysis of the diester. The chromatographic behavior of this component under various conditions was identical to a similar component observed in partially hydrolyzed aqueous solutions of the corresponding diester. Earlier spectral kinetic studies with dipivaloylisoproterenol in diluted serum solutions had suggested the possibility of an intermediate in the hydrolysis of the diester[6].

These analytical comparisons help substantiate the presence of the monoester in the lung perfusate after administration of the prodrug, and chromatographic procedures were developed to separate and quantitate this compound in the perfusate samples.

Intravascular Administration—Dipivaloylisoproterenol and di-

[6] Unpublished data.

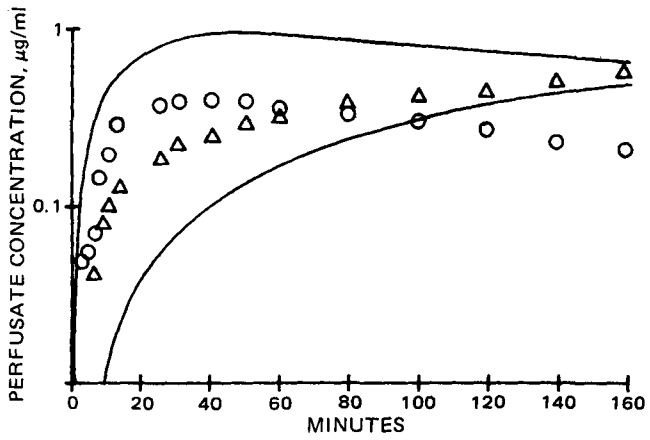

Figure 7—*Comparison of observed concentrations to those predicted by the flow model of the intravascular administration of 10^{-6} moles of di-p-toluoylisoproterenol to the isolated perfused rabbit lung. Key: (○) isoproterenol; (△) 3-O-methylisoproterenol.*

p-toluoylisoproterenol were administered to the circulation of the isolated lung system at 10^{-5}- and 5×10^{-5}-mole doses. Perfusate concentrations of diester, monoester, isoproterenol, and 3-*O*-methylisoproterenol were measured periodically for 180 min. A 10^{-6}-mole dose was also administered, but only isoproterenol and 3-*O*-methylisoproterenol were measured. The perfusate concentration–time profiles generated from these experiments are presented in Figs. 3 and 4.

Both diesters were rapidly cleared from the perfusion medium following their administration directly into the circulation. At the two 10^{-5}-mole doses, the clearance of di-*p*-toluoylisoproterenol was 92 and 106 ml/min, while that for dipivaloylisoproterenol was 59 and 89 ml/min. The diester perfusate concentration–time data were fitted best with a triexponential equation. The two initial rapid phases were barely distinguished from one another, but a slow terminal phase was observed for both diesters at very low concentrations. Detectable concentrations of the monoester intermediates were observed within 2–4 min of drug administration, indicating rapid uptake and hydrolysis of the diesters. Peak monoester concentrations occurred at 6–8 min. Isoproterenol appeared in the circulation within 6 min of prodrug administration but its elimination was very slow, as was the appearance of 3-*O*-methylisoproterenol. The perfusate concentration–time profiles of the four compounds of interest from the intravascular studies were initially fitted with complex compartmental pharmacokinetic models; the concentration–time profiles predicted from the curve fitting are represented by the solid lines in Figs. 3 and 4.

These models were successful in describing the data but provided little useful information about the disposition of these prodrugs. The limited number of experiments performed minimized the amount of pharmacokinetic information obtained, but the use of a physiologically based flow model provides some basic information concerning the disposition of isoproterenol following prodrug administration.

Perfusion Model Analysis—The perfusion model had been developed previously to describe the disposition of isoproterenol and 3-*O*-methylisoproterenol in the isolated perfused rabbit lung and was discussed previously (10). A similar model was used to evaluate the isoproterenol and 3-*O*-methylisoproterenol data resulting from the prodrug administrations (Fig. 5). Appearance of isoproterenol in the circulation of the lung system was modeled as a first-order release of the drug (from the prodrug) into the lung tissue with instantaneous partitioning into the perfusion medium. The parameters utilized to describe the model were, for the most part, identical to those described previously (10). An average lung volume of 11.7 ml and a rate constant for the appearance of isoproterenol of 0.05 min^{-1} were employed. The isoproterenol and 3-*O*-methylisoproterenol perfusate concentration–time profiles predicted by the perfusion model simulations are shown in Fig. 6 (5×10^{-5}- and 10^{-5}-mole doses) and Fig. 7 (10^{-6}-mole dose) along with the observed data.

These comparisons illustrate consistent disagreement between the observed and predicted data; the observed isoproterenol concentrations were lower than the predicted values, whereas the observed 3-*O*-methylisoproterenol concentrations were higher than those predicted by the model. This suggests that the disposition of isoproterenol is altered when the drug is delivered into the tissue *via* a prodrug. This might result from penetration of the more lipophilic prodrug into tissues to which isoproterenol does not penetrate.

Intrabronchial Administration—Solutions of the prodrugs in saline were instilled into the airways of the isolated lung; the upper reservoir was sampled periodically and perfusate concentrations of the diester, monoester, isoproterenol, and 3-*O*-methylisoproterenol were measured. Di-*p*-toluoylisoproterenol was administered at doses of 10^{-5} and 5×10^{-6} moles while dipivaloylisoproterenol was given at 10^{-5}-mole doses. In some studies, samples were initially collected at 15-sec intervals to characterize the absorption of the diester. The perfusate concentration–time profiles from these experiments are presented in Figs. 8 and 9.

Absorption of both prodrugs from the airways was quite rapid, with maximum concentrations of the intact diesters observed at ~2 min. Feathering the diester perfusate concentration–time curves yielded absorption rate constants of 1.4 min^{-1} and 0.9 min^{-1} for dipivaloylisoproterenol and di-*p*-toluoylisoproterenol, respectively, suggesting that absorption is virtually complete within 5 min. The subsequent metabolic profiles were quite similar to those following intravascular administration, except that the diester concentrations following intrabronchial administration were somewhat lower. Isoproterenol and 3-O-methylisoproterenol concentrations, however, were comparable to those following intravascular administration, and mass balance calculations suggest that most of the administered dose was absorbed.

A comparison of the apparent clearances of the diesters following in-

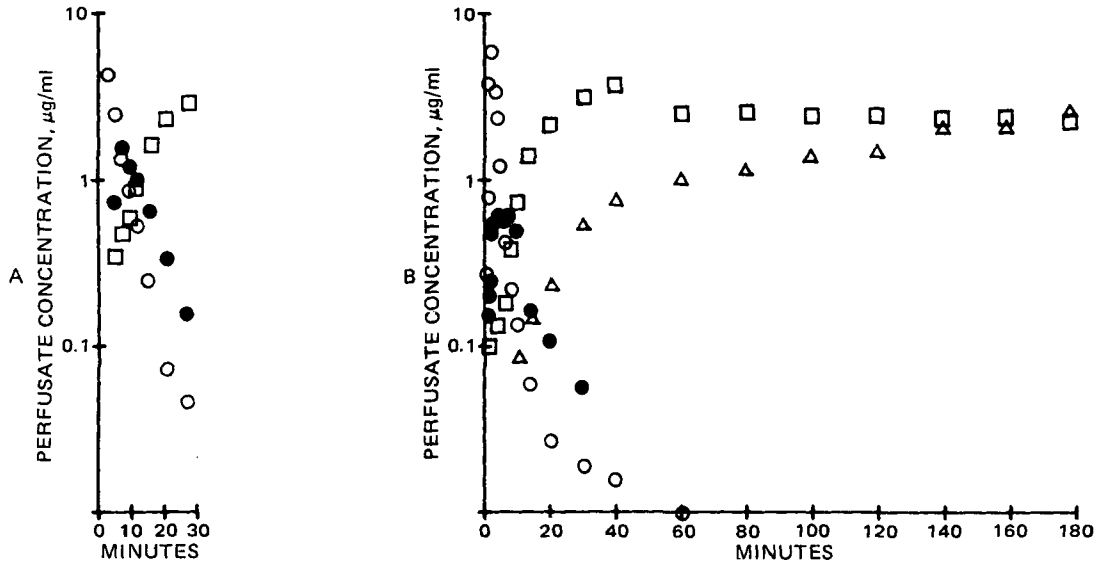

Figure 8—*Perfusate concentrations following the endotracheal instillation of 10^{-5} moles of di-p-toluoylisoproterenol (A) and 5×10^{-6} moles of di-p-toluoylisoproterenol (B). Key: (○) di-p-toluoylisoproterenol; (●) mono-p-toluoylisoproterenol; (□) isoproterenol; (△) 3-O-methylisoprotrenol.*

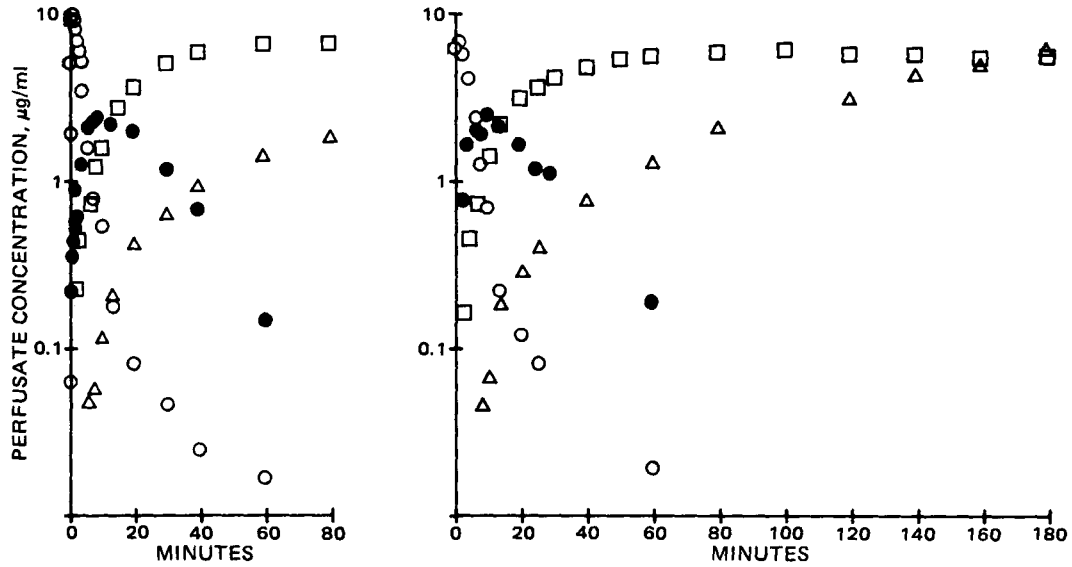

Figure 9—*Perfusate concentrations following the endotracheal instillation of two 10^{-5}-mole doses of dipivaloylisoproterenol. Key: (○) dipivaloylisoproterenol; (●) monopivalylisoproterenol; (□) isoproterenol; (△) 3-O-methylisoproterenol.*

trabronchial administration (172–203 ml/min for di-*p*-toluoylisoproterenol and 96–102 ml/min for dipivaloylisoproterenol) with those following intravascular administration (92–106 ml/min for di-*p*-toluoylisoproterenol and 59–89 ml/min for dipivaloylisoproterenol) suggests that a substantial portion of the intrabronchial dose does not reach the circulation as intact diester. From the data it appears that only ~50% of the di-*p*-toluoylisoproterenol and 75% of the dipivaloylisoproterenol reached the circulation intact after intrabronchial administration. This suggests that first-pass metabolism of the diesters following intrabronchial administration likely involves hydrolysis of the diester to the corresponding monoester (or isoproterenol) during the passage of the diester from the site of absorption to the systemic circulation. This possibility is consistent with the diester perfusate concentration data following intravascular administration to the lung from which an extraction ratio of 0.67 for di-*p*-toluoylisoproterenol and 0.5 for dipivaloylisoproterenol was calculated.

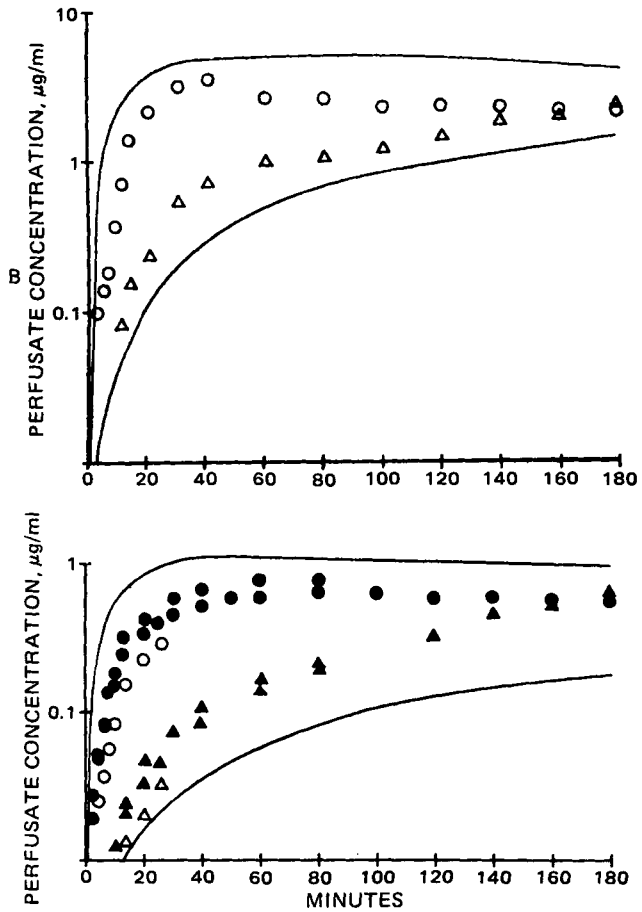

Figure 10—*Comparisons of observed concentrations to those predicted by the flow model for the intrabronchial administration of 10^{-5} moles of di-p-toluoylisoproterenol and dipivaloylisoproterenol (upper) and 5×10^{-6} moles of di-p-toluoylisoproterenol (lower). Key: (○,●) isoproterenol; (△,▲) 3-O-methylisoproterenol.*

The isoproterenol and 3-*O*-methylisoproterenol perfusate concentration data from the intrabronchial experiments were compared with perfusion model predictions in the same manner as the intravascular data. These comparisons are presented in Fig. 10 and exhibit a pattern very similar to that seen with intravascular data. Isoproterenol concentrations were lower than predicted, whereas 3-*O*-methylisoproterenol concentrations were higher, again suggesting that the disposition of isoproterenol by the lung was altered when the drug was administered as a prodrug.

Diester prodrugs of sympathomimetic amines have been suggested to increase the potency and duration of action of these drugs. Bitolterol, the di-*p*-toluate ester of *N*-*tert*-butylarterenol, has been studied rather extensively (13–15). This compound is very similar in structure to di-*p*-toluoylisoproterenol, and the disposition of the two might be expected to be similar. When administered to humans by aerosol inhalation, bitolterol displayed a 5-hr duration of activity compared with 1 hr for the parent compound (15). This has been attributed to uptake of the intact diester by the lung followed by slow release and subsequent hydrolysis to *N*-*tert*-butylarterenol, an active β_2 adrenoceptor agonist (14). Studies with dipivaloylisoproterenol and di-*p*-toluoylisoproterenol were designed to determine if these prodrugs exhibited a similar pattern.

These results suggest that the isoproterenol prodrugs do not accumulate to a great extent in the lung tissue and do not support the assumption that the prolonged activity of similar prodrugs is related to accumulation in the lung. Both dipivalylisoproterenol and di-*p*-toluoylisoproterenol were rapidly taken up by the lung but were quickly hydrolyzed, first to monoesters and then to active drug. The monoesters appeared in the circulation in appreciable concentrations and under normal conditions, *i.e.*, in the whole body, most of this intermediate would be swept away into the general circulation. These results do not explain the prolonged activity displayed by bitolterol and suggest the need for further studies in this area.

REFERENCES

(1) M. E. Conolly, D. S. Davies, C. T. Dollery, C. D. Morgan, J. W. Paterson, and M. Sandler, *Br. J. Pharmacol.*, **46**, 458 (1972).

(2) C. F. George, E. W. Blackwell, and D. S. Davies, *J. Pharm. Pharmacol.*, **26**, 265 (1974).

(3) D. C. Webb-Johnson and J. L. Andrews, *N. Engl. J. Med.*, **297**, 476 (1977).

(4) B. W. Blase and T. A. Loomis, *Toxic. Appl. Pharmacol.*, **37**, 481 (1976).
(5) J. Hartiala, P. Uotila, and W. Nienstedt, *Br. J. Pharmacol.*, **57**, 422 (1976).
(6) E. A. B. Brown, in "Drug Metabolism Reviews, Vol. 3," F. J. DiCarlo, Ed., Marcel Dekker, New York, N.Y., 1974, p. 33.
(7) A. A. Hussain and J. E. Truelove, U.S. Pat. No. 3,868,461 (1975).
(8) J. Kristoffersson, L. A. Svennson, and K. Tegner, *Acta Pharm. Suec.*, **11**, 427 (1974).
(9) B. F. Tullar, H. Minatoya, and R. R. Lorenz, *J. Med. Chem.*, **19**, 834 (1976).
(10) R. K. Brazzell, R. A. Smith, and H. B. Kostenbauder, *J. Pharm. Sci.*, **71**, 1268 (1982).
(11) R. W. Neimeier and E. Bingham, *Life Sci.*, Part II, **11**, 807 (1972).
(12) J. P. McGovren, W. C. Lubawy, and H. B. Kostenbauder, *J. Pharmacol. Exp. Ther.*, **199**, 198 (1976).
(13) H. Minatoya, *ibid.*, **206**, 515 (1978).
(14) L. Shargel, S. A. Dorrbecker, and M. Levitt, *Drug Metab. Dispos.*, **4**, 65 (1976).
(15) L. Shargel and S. A. Dorrbecker, *ibid.*, **4**, 72 (1976).

NOTES

An Improved High-Pressure Liquid Chromatographic Assay for Secobarbital in Serum

H. L. LEVINE *‡, M. E. COHEN §, P. K. DUFFNER§, K. A. KUSTAS *, and D. D. SHEN *x

Received July 22, 1981, from the **Department of Pharmaceutics, School of Pharmacy*, and the §*Department of Neurology, School of Medicine, State University of New York at Buffalo, Buffalo, NY 14260.* Accepted for Publication January 12, 1982. ‡Present address: Department of Clinical Pharmacy, School of Pharmacy, Duquesne University, Pittsburgh, PA 15219.

Abstract □ A high-pressure liquid chromatographic method for the analysis of secobarbital in serum was developed. Secobarbital was extracted from buffered serum (pH 5.5) with a solvent mix of hexane–ether–*n*-propanol. 5-(4-Methylphenyl)-5-phenylhydantoin was added as an internal standard. Separation of secobarbital and internal standard from serum constituents and other drugs was achieved on a 5-μm C-18 reversed-phase column using an acetonitrile–phosphate buffer (pH 4.4) mobile phase. The eluent was monitored at 195 nm. The sensitivity limit of the assay was ~0.02 μg/ml with 0.5 ml of serum sample. The application of this method to pharmacokinetic studies in pediatric patients was demonstrated.

Keyphrases □ Secobarbital—high-pressure liquid chromatographic assay in human serum, anticonvulsants, pharmacokinetics □ High-pressure liquid chromatography—secobarbital, anticonvulsant, pharmacokinetics, human serum □ Anticonvulsants—secobarbital, high-pressure liquid chromatographic assay in human serum, pharmacokinetics □ Pharmacokinetics—secobarbital, high-pressure liquid chromatographic assay in human serum, anticonvulsant

Secobarbital is used primarily as a hypnotic agent. Like many other barbiturates, when administered in anesthetic doses it is an effective anticonvulsant (1). Rectal secobarbital is prescribed for the emergency home treatment of prolonged seizures in poorly controlled epileptic children (2). In an attempt to study the bioavailability of rectally administered secobarbital in pediatric patients, a sensitive method for quantitating the drug in serum was required.

A number of analytical procedures for determining secobarbital in serum have been described in the literature. These include spectrophotometry (3), gas-liquid chromatography (GLC) (4–8), and high-pressure liquid chromatography (HPLC) (9, 10). However, many of these existing procedures are aimed at detecting high concentrations (>5 μg/ml) of secobarbital for screening purposes related to drug abuse. The more sensitive methods such as GLC with electron capture detection require tedious sample clean up and derivatization procedure prior to analysis. Also, with many of these methods, the problem of interference from other drugs and their metabolites in serum has not been evaluated. This report describes an improved HPLC method that permits the determination of submicrogram quantities of secobarbital in small volumes of serum in the presence of various antiepileptic drugs.

EXPERIMENTAL

Reagents and Chemicals—Secobarbital[1] and 5-(4-methylphenyl)-5-phenylhydantoin[2] (internal standard) were used as supplied. The solvents used for extraction and chromatography were all of HPLC grade[3,4]. All chemicals were of analytical reagent grade.

A stock solution of sodium secobarbital (120 μg/ml) and the internal standard (7 μg/ml) were prepared in water. The phosphate buffer component of the mobile phase was prepared by adding 300 μl of 1.0 *M* KH_2PO_4 and 50 μl of 0.9 *M* H_3PO_4 to 1800 ml of water (pH 4.4). For the extraction procedure, a pH 5.5 acetate buffer consisting of 0.01 *M* sodium acetate–0.01 *M* acetic acid (88.5:11.5, v/v) was prepared.

Apparatus and Operating Conditions—The liquid chromatograph consisted of a constant flow pump[5], a variable volume sampling valve[6], and a variable wavelength detector[7]. A 4.6-mm × 25-cm column packed with 5 μm of microporous silica chemically bonded with octadecylsilane was obtained from a commercial source[8]. The mobile phase consisting of 28% acetonitrile and 72% pH 4.4 phosphate buffer (v/v) was filtered[9]

[1] Eli Lilly and Co., Indianapolis, Ind.
[2] Aldrich Chemical Co., Milwaukee, Wis.
[3] Fisher Scientific Co., Rochester, NY.
[4] J. T. Baker Chemical Co., Rochester, NY.
[5] Model M6000A, Waters Associates, Milford, Mass.
[6] Model U6K, Waters Associates, Milford, Mass.
[7] Model SF770, Kratos Inc., Schoeffel Instrument Div., Westwood, N.J.
[8] Partisil 5 ODS-3, Whatman Inc., Clifton, NJ 07014.
[9] 0.5 μm FH type filter, Millipore, Bedford, Mass.

0022-3549/82/1100-1281$01.00/0

(4) B. W. Blase and T. A. Loomis, *Toxic. Appl. Pharmacol.*, **37**, 481 (1976).
(5) J. Hartiala, P. Uotila, and W. Nienstedt, *Br. J. Pharmacol.*, **57**, 422 (1976).
(6) E. A. B. Brown, in "Drug Metabolism Reviews, Vol. 3," F. J. DiCarlo, Ed., Marcel Dekker, New York, N.Y., 1974, p. 33.
(7) A. A. Hussain and J. E. Truelove, U.S. Pat. No. 3,868,461 (1975).
(8) J. Kristoffersson, L. A. Svennson, and K. Tegner, *Acta Pharm. Suec.*, **11**, 427 (1974).
(9) B. F. Tullar, H. Minatoya, and R. R. Lorenz, *J. Med. Chem.*, **19**, 834 (1976).
(10) R. K. Brazzell, R. A. Smith, and H. B. Kostenbauder, *J. Pharm. Sci.*, **71**, 1268 (1982).
(11) R. W. Neimeier and E. Bingham, *Life Sci.*, Part II, **11**, 807 (1972).
(12) J. P. McGovren, W. C. Lubawy, and H. B. Kostenbauder, *J. Pharmacol. Exp. Ther.*, **199**, 198 (1976).
(13) H. Minatoya, *ibid.*, **206**, 515 (1978).
(14) L. Shargel, S. A. Dorrbecker, and M. Levitt, *Drug Metab. Dispos.*, **4**, 65 (1976).
(15) L. Shargel and S. A. Dorrbecker, *ibid.*, **4**, 72 (1976).

NOTES

An Improved High-Pressure Liquid Chromatographic Assay for Secobarbital in Serum

H. L. LEVINE *‡, M. E. COHEN §, P. K. DUFFNER§, K. A. KUSTAS *, and D. D. SHEN *x

Received July 22, 1981, from the **Department of Pharmaceutics, School of Pharmacy*, and the §*Department of Neurology, School of Medicine, State University of New York at Buffalo, Buffalo, NY 14260.* Accepted for Publication January 12, 1982. ‡Present address: Department of Clinical Pharmacy, School of Pharmacy, Duquesne University, Pittsburgh, PA 15219.

Abstract □ A high-pressure liquid chromatographic method for the analysis of secobarbital in serum was developed. Secobarbital was extracted from buffered serum (pH 5.5) with a solvent mix of hexane–ether–*n*-propanol. 5-(4-Methylphenyl)-5-phenylhydantoin was added as an internal standard. Separation of secobarbital and internal standard from serum constituents and other drugs was achieved on a 5-μm C-18 reversed-phase column using an acetonitrile–phosphate buffer (pH 4.4) mobile phase. The eluent was monitored at 195 nm. The sensitivity limit of the assay was ~0.02 μg/ml with 0.5 ml of serum sample. The application of this method to pharmacokinetic studies in pediatric patients was demonstrated.

Keyphrases □ Secobarbital—high-pressure liquid chromatographic assay in human serum, anticonvulsants, pharmacokinetics □ High-pressure liquid chromatography—secobarbital, anticonvulsant, pharmacokinetics, human serum □ Anticonvulsants—secobarbital, high-pressure liquid chromatographic assay in human serum, pharmacokinetics □ Pharmacokinetics—secobarbital, high-pressure liquid chromatographic assay in human serum, anticonvulsant

Secobarbital is used primarily as a hypnotic agent. Like many other barbiturates, when administered in anesthetic doses it is an effective anticonvulsant (1). Rectal secobarbital is prescribed for the emergency home treatment of prolonged seizures in poorly controlled epileptic children (2). In an attempt to study the bioavailability of rectally administered secobarbital in pediatric patients, a sensitive method for quantitating the drug in serum was required.

A number of analytical procedures for determining secobarbital in serum have been described in the literature. These include spectrophotometry (3), gas-liquid chromatography (GLC) (4–8), and high-pressure liquid chromatography (HPLC) (9, 10). However, many of these existing procedures are aimed at detecting high concentrations (>5 μg/ml) of secobarbital for screening purposes related to drug abuse. The more sensitive methods such as GLC with electron capture detection require tedious sample clean up and derivatization procedure prior to analysis. Also, with many of these methods, the problem of interference from other drugs and their metabolites in serum has not been evaluated. This report describes an improved HPLC method that permits the determination of submicrogram quantities of secobarbital in small volumes of serum in the presence of various antiepileptic drugs.

EXPERIMENTAL

Reagents and Chemicals—Secobarbital[1] and 5-(4-methylphenyl)-5-phenylhydantoin[2] (internal standard) were used as supplied. The solvents used for extraction and chromatography were all of HPLC grade[3,4]. All chemicals were of analytical reagent grade.

A stock solution of sodium secobarbital (120 μg/ml) and the internal standard (7 μg/ml) were prepared in water. The phosphate buffer component of the mobile phase was prepared by adding 300 μl of 1.0 *M* KH_2PO_4 and 50 μl of 0.9 *M* H_3PO_4 to 1800 ml of water (pH 4.4). For the extraction procedure, a pH 5.5 acetate buffer consisting of 0.01 *M* sodium acetate–0.01 *M* acetic acid (88.5:11.5, v/v) was prepared.

Apparatus and Operating Conditions—The liquid chromatograph consisted of a constant flow pump[5], a variable volume sampling valve[6], and a variable wavelength detector[7]. A 4.6-mm × 25-cm column packed with 5 μm of microporous silica chemically bonded with octadecylsilane was obtained from a commercial source[8]. The mobile phase consisting of 28% acetonitrile and 72% pH 4.4 phosphate buffer (v/v) was filtered[9]

[1] Eli Lilly and Co., Indianapolis, Ind.
[2] Aldrich Chemical Co., Milwaukee, Wis.
[3] Fisher Scientific Co., Rochester, NY.
[4] J. T. Baker Chemical Co., Rochester, NY.
[5] Model M6000A, Waters Associates, Milford, Mass.
[6] Model U6K, Waters Associates, Milford, Mass.
[7] Model SF770, Kratos Inc., Schoeffel Instrument Div., Westwood, N.J.
[8] Partisil 5 ODS-3, Whatman Inc., Clifton, NJ 07014.
[9] 0.5 μm FH type filter, Millipore, Bedford, Mass.

0022-3549/82/1100-1281$01.00/0

Table I—Calibration Curve Linearity and Precision for the Concentration Range of 0.022–4.4 μg/ml (n = 8)

Day	Mean Normalized PHR[a], μg/ml	SD, μg/ml	CV, %
1	1.067	0.022	2.1
2	1.110	0.078	7.0
3	1.058	0.061	5.8
4	1.134	0.062	5.2
5	1.191	0.062	5.2
6	1.196	0.043	3.6
Mean	1.124	0.053	4.7

[a] Normalized peak height ratio defined as the peak height ratio of each secobarbital standard divided by the corresponding concentration.

Table II—Day-to-Day Precision Data Pooled From Six Separate Days of Analysis

Concentration, μg/ml	Mean Normalized PHR[a], μg/ml	SD, μg/ml	CV, %
4.4	1.150	0.004	0.3
2.2	1.093	0.044	4.0
1.1	1.132	0.071	6.3
0.55	1.138	0.100	8.8
0.275	1.127	0.107	9.5
0.11	1.091	0.047	4.3
0.055	1.128	0.109	9.7
0.022	1.138	0.057	5.0
Mean	1.125	0.067	6.0

[a] Normalized peak height ratio defined as the peak height ratio of each secobarbital standard divided by the corresponding concentration.

and degassed before use. The column was heated to 50° and the eluting solvent was pumped through the column at a flow rate of 2.8 ml/min with precolumn pressure of ~2800 psi. The column effluent was monitored at 195 nm.

Extraction—Extraction of serum samples was carried out in 15 glass centrifuge tubes sealed with polytef-lined screw caps. One milliliter of the acetate buffer and 50 μl of internal standard solution were added to 0.5 ml of serum. The mixture was agitated in a vortex mixer for 10 sec, followed by gentle shaking with 5 ml of hexane–ether–n-propanol (49:49:2, v/v/v) for 20 min. The organic and aqueous phases were separated by centrifugation at 1000×g for 5 min. The upper organic layer was transferred to a 1.5-ml polypropylene microcentrifuge tube[10]. The aqueous layer was reextracted with another 5-ml aliquot of the hexane–ether–n-propanol mixture. The second organic phase aliquot was pooled with the first and evaporated to dryness under nitrogen in a water bath at 50°. The residue was reconstituted in 300 μl of mobile phase and 50–100 μl was injected onto the column.

Standard Curves—Standardization samples were prepared by spiking blank serum (0.5 ml) with 50-μl aliquots of various dilutions of secobarbital stock solution to yield a concentration range between 0.022 and 4.4 μg/ml. Standard curves were constructed by plotting peak height ratios (secobarbital–internal standard) against the corresponding secobarbital concentration.

RESULTS AND DISCUSSION

Figure 1 shows typical chromatograms of serum samples from a pediatric patient before and after a single 5-mg/kg rectal dose of secobarbital. The drug and its internal standard were eluted at 8.5 ± 0.5 and 11.5 ± 0.7 min, respectively, under the described chromatographic conditions. Extraction recovery was evaluated by analyzing spiked serum samples. In these experiments, internal standard was added after transfer of organic phases to reduce error due to injection and chromatography. The extraction yield from serum was nearly complete and reasonably consistent (85–95%) over the chosen concentration range (0–4.4 μg/ml).

The detection limit with a 0.5-ml sample was ~0.02 μg/ml. This limit corresponded to a serum concentration that yields a peak height with a signal to noise ratio of at least 4.

Linear calibration curves were observed over the 0–4.4 μg/ml range. Calibration data obtained on six separate days are summarized in Table I. Precision was assessed by estimating the variations on normalized peak height ratios (*i.e.*, peak height ratios of each standard divided by the corresponding secobarbital concentration) (11). The coefficient of variation varied from 2.1 to 7.0%. Within-day reproducibility was also evaluated by replicate analysis of a 1.1-μg/ml serum standard. The coefficient of variation was 4.2% (n = 9). The day-to-day precision data are shown in Table II. The range of coefficient of variation for the eight concentrations was 0.3–9.7%.

Interference from endogenous materials and other drugs posed a major problem during the development of this assay. To attain good sensitivity, the loss of drug during sample preparation must be minimized. Precipitation of serum proteins with acetonitrile followed by direct injection of

[10] Walter Sarstedt Co., Princeton, N.J.

Table III—Retention Times of Anticonvulsants Detectable in the Present Chromatographic System[a]

Drugs	Retention Time, min
Ethosuximide	1.8
Primidone	2.0
Phenobarbital	2.6
Carbamazepine-10,11-epoxide	3.4
Paramethadione	3.8
Mephobarbital	7.4
Carbamazepine	7.8
Phenytoin	7.8
Secobarbital	8.5
5-(4-methylphenyl)-5-phenylhydantoin[b]	11.4

[a] Anticonvulsants that are either not detectable or not extracted include valproic acid, clonazepam, diazepam, chlorazepate, and thioridazine. [b] Internal standard.

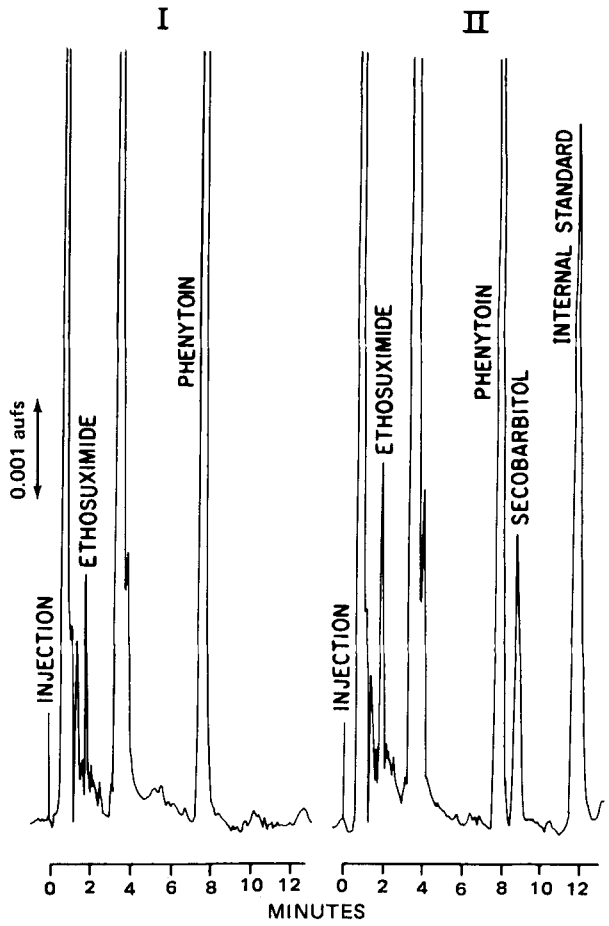

Figure 1—*Chromatogram of 0.5-ml serum extracts from a patient immediately before (I) and 90 min after (II) rectal administration of a 120-mg dose of secobarbital. The extract was reconstituted in 300 μl of eluting solvent; 50 μl was injected. The patient was a 7-year-old boy weighing 23 kg. The serum concentration of secobarbital was 0.447 μg/ml. The patient was also receiving phenytoin, ethosuximide, and clonazepam at the time of study. The observed peaks for ethosuximide and phenytoin represent serum drug concentrations of 20 and 21 μg/ml, respectively. Note the baseline separation between the secobarbital and phenytoin peaks.*

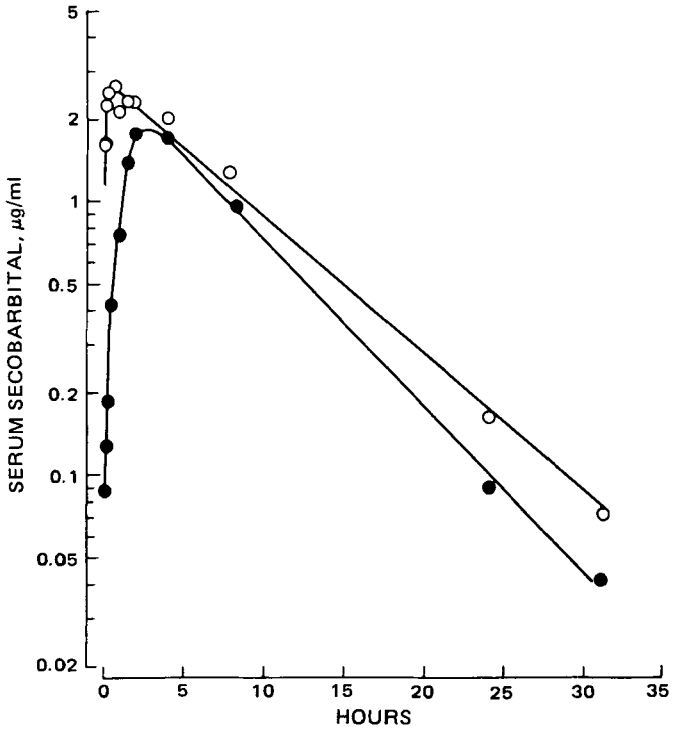

Figure 2—*Serum concentration–time course of secobarbital following separate rectal administration of a solution (○) and a suppository (●) to two 5-year-old female epileptic children with respective body weights of 17 and 19 kg.*

supernatant on the column as suggested previously (9) did produce a high recovery yield, but interference from serum constituents was observed on the chromatograms of blank samples from some patients. The problem was readily overcome by solvent extraction with hexane–ether–*n*-propranol, which provided good recovery with no interference seen in serum blanks. The extraction procedure is relatively simple, and up to 40 samples can be processed in ~1 hr.

Reversed-phase chromatography was chosen because of its versatility in separating compounds over a wide spectrum of polarity. A 10-μm reversed-phase octadecylsilane column[11] was used. Both phenytoin and carbamazepine, which coextracted with secobarbital, were eluted sufficiently close to secobarbital to hamper detection at low concentration limits. Although carbamazepine as a base can be eliminated by acid wash or back extraction, these procedures would not remove phenytoin. Also, multiple extractions reduced the recovery of secobarbital. Separation of secobarbital was achieved from both phenytoin and carbamazepine by an addition of a small quantity of tetrahydrofuran (1–2%) to the mobile phase (12). Unfortunately, this also resulted in an unstable baseline at the highest sensitivity setting (*i.e.*, 0.01 aufs) on a detector. This is probably due to the high absorptivity of tetrahydrofuran at 195 nm.

[11] μBondapak C-18, Waters Associates, Milford, Mass.

Complete resolution of secobarbital from the interfering drugs was achieved when a high-efficiency 5-μm C-18 reversed-phase column was employed. The chromatograms, as shown in Fig. 1, are taken from a patient receiving high doses of phenytoin (serum phenytoin concentration of 21 μg/ml). The phenytoin and secobarbital peaks were clearly separated.

Table III compares the retention times of secobarbital to those anticonvulsants that are detectable in our chromatographic system.

As an illustration of the applicability of our assay procedure to a single-dose pharmacokinetic study, the serum concentration–time course after rectal administration of a 5-mg/kg dose of sodium secobarbital in solution[12] and by suppository[13] in two age and weight matched epileptic children is shown in Fig. 2. The rate of absorption of secobarbital from the fatty base suppository was much slower as compared with that from the solution. Peak serum concentration was not reached until 3–4 hr after administration of the suppository, whereas peak serum concentration was achieved within 30 min with the solution preparation. The serum half-life of secobarbital in these two patients, being 6.0 and 4.9 hr, are shorter than estimates reported for adults (13).

In summary, a rapid procedure for analyzing nanogram quantities of secobarbital in serum is described. Sample preparation is minimal, and there is no interference from many other anticonvulsants.

REFERENCES

(1) L. S. Goodman and A. S. Gilman, "The Pharmacological Basis of Therapeutics," 5th ed., MacMillan, New York, N.Y., 1974, p. 108.

(2) H. L. Levine, M. E. Cohen, P. Duffner, D. Lacey, R. Karpynec, and D. D. Shen, *Pediat. Pharmacol.*, **2**, 33 (1982).

(3) E. C. White, J. R. Briggs, and I. Sunshine, *Am. J. Clin. Pathol.*, **29**, 506 (1958).

(4) H. V. Street and C. McMartin, *Nature (London)*, **199**, 456 (1963).

(5) G. Kananen, R. Osiewicz, and I. Sunshine, *J. Chromatogr. Sci.*, **10**, 283 (1972).

(6) T. P. Faulkner, J. W. Hayden, and E. G. Comstock, *Clin. Toxicol. Bull.*, **3**, 205 (1973).

(7) S. Sun and A. H. C. Chun, *J. Pharm. Sci.*, **66**, 477 (1977).

(8) S. Sun and D. J. Hoffman, *ibid.*, **68**, 386 (1979).

(9) P. M. Kabra, H. Y. Koo, and L. J. Marton, *Clin. Chem.*, **24**, 657 (1978).

(10) U. R. Tjaden, J. C. Kraak, and J. F. K. Huber, *J. Chromatogr.*, **143**, 183 (1977).

(11) A. P. DeLeenheer and H. J. C. F. Neils, *J. Pharm. Sci.*, **68**, 1527 (1979).

(12) F. Klink, *Am. Lab.*, **12**, 81 (1980).

(13) T. P. Faulkner, J. W. McGinity, J. H. Hayden, D. A. Olson, and E. G. Comstock, *J. Clin. Pharmacol.*, **19**, 605 (1979).

ACKNOWLEDGMENTS

Supported in part by the General Research Support Grant 2-S07-RR-05454-17 from the National Institutes of Health.

[12] Intravenous preparation of sodium secobarbital (seconal sodium) was diluted to a concentration of 15 mg/ml with water and administered through a rectal syringe.

[13] Seconal sodium suppositories, Eli Lilly and Co., Indianapolis, Ind.

Differential Pulse Polarography of Some Degradation Products of Tetracycline

T. JOCHSBERGER ˣ, A. J. CUTIE, HOU-YEH WANG, and N. Y. MARY

Received October 6, 1981, from the *Arnold and Marie Schwartz College of Pharmacy and Health Sciences, Long Island University, Brooklyn, NY 11201.* Accepted for publication January 19, 1982.

Abstract □ In an attempt to develop a more rapid, convenient, and precise method for the direct detection and analysis of the degradation products of tetracycline, a study of those products utilizing differential pulse polarography was initiated. The investigation was concentrated on the subject of the kinetics of the epimerization of anhydrotetracycline to 4-epianhydrotetracycline in acetate buffer. The reaction was followed at 25 and 50°. Duplicate experiments were run at each temperature. The apparent rate constants obtained were $4.17 \pm 0.13 \times 10^{-1}$/hr (25°) and $6.97 \pm 1.00 \times 10^{-2}$/hr (50°).

Keyphrases □ Tetracycline—differential pulse polarography, degradation products, kinetics, epimerization □ Kinetics—differential pulse polarography, degradation products of tetracycline, epimerization □ Epimerization—differential pulse polarography of degradation products of tetracycline, kinetics □ Degradation—differential pulse polarography, products of tetracycline, epimerization, kinetics

A unique method is reported for the determination of degradation products of tetracycline. It is well known that tetracycline undergoes spontaneous degradation to an epimer, 4-epitetracycline and dehydration to anhydrotetracycline. In addition, both of the latter compounds undergo further transformation to produce 4-epianhydrotetracycline (1–3). There has been much concern over the kinetics and mechanisms (4–6) of these reactions and methods for determining the various products (7–15). The application of differential pulse polarography to the detection of tetracycline and a number of its derivatives has been described previously (16). This report describes the use of differential pulse polarography for detecting anhydrotetracycline in the presence of epianhydrotetracycline and for following the conversion of the former compound to the latter.

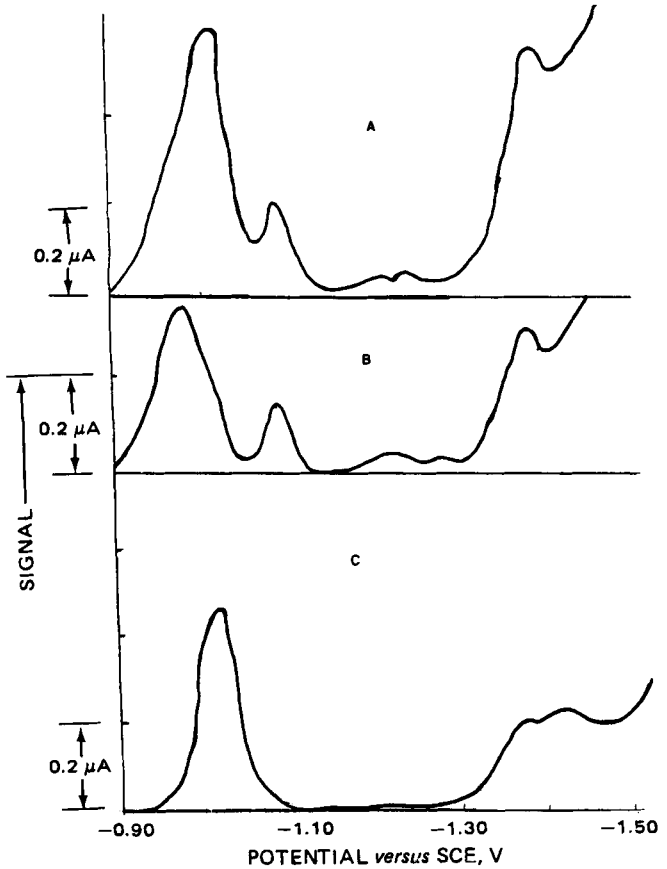

Figure 1—*(A) Differential pulse polarogram of a mixture of anhydrotetracycline and epianhydrotetracycline; (B) differential pulse polarogram of anhydrotetracycline; (C) differential pulse polarogram of epianhydrotetracycline.*

EXPERIMENTAL

Apparatus—The apparatus and technique used in this work have been described previously (17).

Materials—Anhydrotetracycline and 4-epianhydrotetracycline reference grade[1], were used as received. Acetate buffer (pH 4.31) was freshly prepared from reagent grade acetic acid and sodium acetate[2].

Procedure—Known amounts of anhydrotetracycline hydrochloride and/or 4-epianhydrotetracycline hydrochloride were added to a 250-ml volumetric flask. The materials were dissolved and brought to volume with acetate buffer solution. A fixed volume (25 ml) of each solution was withdrawn, deaerated, and assayed polarographically. Polarograms were recorded between −0.9 and −1.5 V.

In the rate studies, four different concentrations of anhydrotetracycline hydrochloride ($5.0–8.0 \times 10^{-5}$ *M*) in acetate buffer solution (pH 4.31) were followed as a function of time at the desired temperature. Polarograms of each sample were run immediately upon preparing the solution. Each solution was transferred into two separate 56.8-ml prescription bottles. The bottles were sealed with plastic covers and immediately placed in a thermostated shaker bath.

At appropriate time intervals, each sample bottle was withdrawn and immersed in ice to reduce the possibility of further reaction. The samples were analyzed by differential pulse polarography as described. Duplicate kinetic experiments were run at 25 and 50°.

RESULTS AND DISCUSSION

Figure 1A is a typical polarogram of a mixture of anhydrotetracycline and epianhydrotetracycline showing separate peaks attributable to the two compounds. The polarograms demonstrate clearly diverse curves at a peak potential of −1.09 V (Figs. 1B and 1C). A linear relationship between current and concentration exists at the peak potential at which these currents were measured. This is the major reduction potential in the polarographic spectrum for the compound.

At appropriate time intervals, solutions of anhydrotetracycline kept at various temperatures and concentrations were analyzed polarographically by the measurement of peak currents of the polarograms at the peak potential of −1.09 V.

The epimerization was observed to follow first-order kinetics as reported previously (18). The rate constants obtained from semilogarithmic plots are 0.0417 ± 0.0013 at 25° and 0.0697 ± 0.0100 at 50°. The values obtained in this study are somewhat lower than those reported (18) for the same reaction in phosphate buffer at pH 1.5. It is suspected that acid catalysis plays a role in the conversion.

Estimation of the activation energy for this reaction based on the two

[1] Lot Ph Eur 1, European Pharmacopoeia.
[2] Scientific Products, Inc. Edison, N.J.

0022-3549/82/1100-1284$01.00/0

temperatures studied leads to a low apparent value. It may be speculated that the reaction involves a low-energy bond rotation. However, it is not the intent of this report to provide a detailed mechanistic evaluation of the process. Such studies are to be conducted.

The technique of differential pulse polarography has been applied to the detection of anhydrotetracycline in the presence of epianhydrotetracycline and used to study the rate of conversion of anhydrotetracycline to its epimer. The authors feel this is a unique application of this technique. It is also felt that this work proves that this method, which is somewhat simpler to utilize than most commonly employed analytical procedures, might be useful in studying the reactions of other tetracycline derivatives.

REFERENCES

(1) A. P. Doerschuk, B. A. Bitler, and J. R. D. McCormick, *J. Am. Chem. Soc.*, **77**, 4687 (1955).

(2) J. R. D. McCormick, S. M. Fox, L. L. Smith, B. A. Bitler, J. Reichenthal, V. E. Origoni, W. H. Muller, R. Winterbottom, and A. P. Doerschuk, *ibid.*, **79**, 2849 (1957).

(3) K. D. Schlecht and C. W. Frank, *J. Pharm. Sci.*, **64**, 352 (1975).

(4) E. G. Remmers, G. M. Sieger, and A. P. Doerschuk, *ibid.*, **52**, 752 (1963).

(5) D. A. Hussar, P. J. Niebergall, E. T. Sugita, and J. T. Doluisio, *J. Pharm. Pharmacol.*, **20**, 539 (1968).

(6) T. D. Sokolski, L. A. Mitscher, P. H. Yuen, J. V. Juvarkar, and B. Hoener, *J. Pharm. Sci.*, **66**, 1159 (1977).

(7) E. Addison and R. G. Clark, *J. Pharm. Pharmacol.*, **15**, 268 (1963).

(8) B. W. Griffiths, *J. Pharm. Sci.*, **55**, 353 (1966).

(9) D. L. Simmons, H. S. L. Woo, C. M. Koorengevel, and P. Seers, *ibid.*, **55**, 1313 (1966).

(10) A. A. Fernandez, V. T. Noceda, and E. S. Carrera, *ibid.*, **58**, 443 (1969).

(11) M. Pernarowski, R. O. Searl, and J. Naylor, *ibid.*, **58**, 470 (1969).

(12) V. C. Walton, M. R. Howlett, and G. B. Selzer, *ibid.*, **59**, 1160 (1970).

(13) P. P. Ascione and G. P. Chrekian, *ibid.*, **59**, 1480 (1970).

(14) A. G. Butterfield, D. W. Hughes, N. J. Pound, and W. L. Wilson, *Antimicrob. Agents. Chemother.*, **4**, 11 (1973).

(15) K. Tsuji and J. H. Robertson, *J. Pharm. Sci.*, **65**, 400 (1976).

(16) A. J. Cutie, J. Mills, and T. Jochsberger, *Drug Dev. Ind. Pharm.*, **6**, 77 (1980).

(17) T. Jochsberger, A. Cutie, and J. Mills, *J. Pharm. Sci.*, **68**, 1061 (1979).

(18) P. H. Yuen and T. D. Sokolski, *ibid.*, **66**, 1648 (1977).

Extended Hansen Approach: Calculating Partial Solubility Parameters of Solid Solutes

P. L. WU *, A. BEERBOWER ‡, and A. MARTIN *x

Received October 13, 1981, from the **Drug Dynamics Institute, College of Pharmacy, University of Texas, Austin, TX 78712*, and the ‡*Energy Center, University of California at San Diego, La Jolla, CA 92093.* Accepted for publication January 21, 1982.

Abstract □ A multiple linear regression method, known as the extended Hansen solubility approach, was used to estimate the partial solubility parameters, δ_d, δ_p, and δ_h for crystalline solutes. The method is useful, since organic compounds may decompose near their melting points, and it is not possible to determine solubility parameters for these solid compounds by the methods used for liquid solvents. The method gives good partial and total solubility parameters for naphthalene; with related compounds, less satisfactory results were obtained. At least three conditions, pertaining to the regression equation and the solvent systems, must be met in order to obtain reasonable solute solubility parameters. In addition to providing partial solubility parameters, the regression equations afford a calculation of solute solubility in both polar and nonpolar solvents.

Keyphrases □ Solubility, partial—extended Hansen approach, parameters of solid solutes, naphthalene, decomposition □ Naphthalene—extended Hansen approach, partial solubility parameters of solid solutes, decomposition □ Decomposition—extended Hansen approach, partial solubility parameters of solid solutes, naphthalene

A multiple regression method using Hansen partial solubility parameters, δ_d, δ_p, and δ_h, was reported (1) for calculating the solubility of naphthalene in pure polar and nonpolar solvents.

THEORETICAL

The method, called the extended Hansen solubility approach, uses a regression equation of three terms involving solvent and solute solubility parameters:

$$-\log X_2 = -\log X_2{}^i + A[C_1(\delta_{1d} - \delta_{2d})^2 + C_2(\delta_{1p} - \delta_{2p})^2 + C_3(\delta_{1h} - \delta_{2h})^2] + C_0 \quad \text{(Eq. 1)}$$

where X_2 and $X_2{}^i$ are the mole fraction solubility and mole fraction ideal solubility, and A is a term from regular solution theory:

$$A = \frac{V_2\phi_1{}^2}{2.303RT} \quad \text{(Eq. 2)}$$

where V_2 is the molar volume of the solute in the supercooled liquid state, ϕ_1 is the volume fraction of solvent, R is the gas constant, and T is the absolute temperature.

The partial solubility parameters for dispersion, δ_d, dipolar interaction forces, δ_p, and hydrogen bonding and other Lewis acid–base interactions, δ_h, are found in Eq. 1 for solvent (subscript 1) and solute (subscript 2). The coefficients C_0, C_1, C_2, and C_3 are provided in the computer output resulting from the least-squares analysis.

The equation obtained for naphthalene in 24 solvents by the extended Hansen solubility approach was (1):

$$\log \alpha_2 = \log \frac{X_2{}^i}{X_2} = 1.0488A(\delta_{1d} - \delta_{2d})^2 - 0.3148A(\delta_{1p} - \delta_{2p})^2 + 0.2252A(\delta_{1h} - \delta_{2h})^2 + 0.0451 \quad \text{(Eq. 3)}$$

This equation provided solubilities of naphthalene in polar and nonpolar solvents at 40° with <30% error (except for *tert*-butanol, 53% error); for ~50% of the cases results were obtained within <5% error. The method allowed the calculation of the solubility of naphthalene in solvents not included in the series under investigation. The extended Hansen solubility approach was tested against the UNIFAC method (2) and the extended Hildebrand solubility approach (3), two alternate methods undergoing recent development.

RESULTS AND DISCUSSION

The partial solubility parameters of Hansen and Beerbower (4) are available for a large number of liquids, but the values for only a few solids (represented as supercooled liquids) are found in the literature. A table was prepared of group contributions for calculating partial solubility

temperatures studied leads to a low apparent value. It may be speculated that the reaction involves a low-energy bond rotation. However, it is not the intent of this report to provide a detailed mechanistic evaluation of the process. Such studies are to be conducted.

The technique of differential pulse polarography has been applied to the detection of anhydrotetracycline in the presence of epianhydrotetracycline and used to study the rate of conversion of anhydrotetracycline to its epimer. The authors feel this is a unique application of this technique. It is also felt that this work proves that this method, which is somewhat simpler to utilize than most commonly employed analytical procedures, might be useful in studying the reactions of other tetracycline derivatives.

REFERENCES

(1) A. P. Doerschuk, B. A. Bitler, and J. R. D. McCormick, *J. Am. Chem. Soc.*, **77**, 4687 (1955).

(2) J. R. D. McCormick, S. M. Fox, L. L. Smith, B. A. Bitler, J. Reichenthal, V. E. Origoni, W. H. Muller, R. Winterbottom, and A. P. Doerschuk, *ibid.*, **79**, 2849 (1957).

(3) K. D. Schlecht and C. W. Frank, *J. Pharm. Sci.*, **64**, 352 (1975).

(4) E. G. Remmers, G. M. Sieger, and A. P. Doerschuk, *ibid.*, **52**, 752 (1963).

(5) D. A. Hussar, P. J. Niebergall, E. T. Sugita, and J. T. Doluisio, *J. Pharm. Pharmacol.*, **20**, 539 (1968).

(6) T. D. Sokolski, L. A. Mitscher, P. H. Yuen, J. V. Juvarkar, and B. Hoener, *J. Pharm. Sci.*, **66**, 1159 (1977).

(7) E. Addison and R. G. Clark, *J. Pharm. Pharmacol.*, **15**, 268 (1963).

(8) B. W. Griffiths, *J. Pharm. Sci.*, **55**, 353 (1966).

(9) D. L. Simmons, H. S. L. Woo, C. M. Koorengevel, and P. Seers, *ibid.*, **55**, 1313 (1966).

(10) A. A. Fernandez, V. T. Noceda, and E. S. Carrera, *ibid.*, **58**, 443 (1969).

(11) M. Pernarowski, R. O. Searl, and J. Naylor, *ibid.*, **58**, 470 (1969).

(12) V. C. Walton, M. R. Howlett, and G. B. Selzer, *ibid.*, **59**, 1160 (1970).

(13) P. P. Ascione and G. P. Chrekian, *ibid.*, **59**, 1480 (1970).

(14) A. G. Butterfield, D. W. Hughes, N. J. Pound, and W. L. Wilson, *Antimicrob. Agents. Chemother.*, **4**, 11 (1973).

(15) K. Tsuji and J. H. Robertson, *J. Pharm. Sci.*, **65**, 400 (1976).

(16) A. J. Cutie, J. Mills, and T. Jochsberger, *Drug Dev. Ind. Pharm.*, **6**, 77 (1980).

(17) T. Jochsberger, A. Cutie, and J. Mills, *J. Pharm. Sci.*, **68**, 1061 (1979).

(18) P. H. Yuen and T. D. Sokolski, *ibid.*, **66**, 1648 (1977).

Extended Hansen Approach: Calculating Partial Solubility Parameters of Solid Solutes

P. L. WU *, A. BEERBOWER ‡, and A. MARTIN *x

Received October 13, 1981, from the **Drug Dynamics Institute, College of Pharmacy, University of Texas, Austin, TX 78712*, and the ‡*Energy Center, University of California at San Diego, La Jolla, CA 92093.* Accepted for publication January 21, 1982.

Abstract □ A multiple linear regression method, known as the extended Hansen solubility approach, was used to estimate the partial solubility parameters, δ_d, δ_p, and δ_h for crystalline solutes. The method is useful, since organic compounds may decompose near their melting points, and it is not possible to determine solubility parameters for these solid compounds by the methods used for liquid solvents. The method gives good partial and total solubility parameters for naphthalene; with related compounds, less satisfactory results were obtained. At least three conditions, pertaining to the regression equation and the solvent systems, must be met in order to obtain reasonable solute solubility parameters. In addition to providing partial solubility parameters, the regression equations afford a calculation of solute solubility in both polar and nonpolar solvents.

Keyphrases □ Solubility, partial—extended Hansen approach, parameters of solid solutes, naphthalene, decomposition □ Naphthalene—extended Hansen approach, partial solubility parameters of solid solutes, decomposition □ Decomposition—extended Hansen approach, partial solubility parameters of solid solutes, naphthalene

A multiple regression method using Hansen partial solubility parameters, δ_d, δ_p, and δ_h, was reported (1) for calculating the solubility of naphthalene in pure polar and nonpolar solvents.

THEORETICAL

The method, called the extended Hansen solubility approach, uses a regression equation of three terms involving solvent and solute solubility parameters:

$$-\log X_2 = -\log X_2{}^i + A[C_1(\delta_{1d} - \delta_{2d})^2 + C_2(\delta_{1p} - \delta_{2p})^2 + C_3(\delta_{1h} - \delta_{2h})^2] + C_0 \quad \text{(Eq. 1)}$$

where X_2 and $X_2{}^i$ are the mole fraction solubility and mole fraction ideal solubility, and A is a term from regular solution theory:

$$A = \frac{V_2\phi_1{}^2}{2.303RT} \quad \text{(Eq. 2)}$$

where V_2 is the molar volume of the solute in the supercooled liquid state, ϕ_1 is the volume fraction of solvent, R is the gas constant, and T is the absolute temperature.

The partial solubility parameters for dispersion, δ_d, dipolar interaction forces, δ_p, and hydrogen bonding and other Lewis acid–base interactions, δ_h, are found in Eq. 1 for solvent (subscript 1) and solute (subscript 2). The coefficients C_0, C_1, C_2, and C_3 are provided in the computer output resulting from the least-squares analysis.

The equation obtained for naphthalene in 24 solvents by the extended Hansen solubility approach was (1):

$$\log \alpha_2 = \log \frac{X_2{}^i}{X_2} = 1.0488A(\delta_{1d} - \delta_{2d})^2 - 0.3148A(\delta_{1p} - \delta_{2p})^2 + 0.2252A(\delta_{1h} - \delta_{2h})^2 + 0.0451 \quad \text{(Eq. 3)}$$

This equation provided solubilities of naphthalene in polar and nonpolar solvents at 40° with <30% error (except for *tert*-butanol, 53% error); for ~50% of the cases results were obtained within <5% error. The method allowed the calculation of the solubility of naphthalene in solvents not included in the series under investigation. The extended Hansen solubility approach was tested against the UNIFAC method (2) and the extended Hildebrand solubility approach (3), two alternate methods undergoing recent development.

RESULTS AND DISCUSSION

The partial solubility parameters of Hansen and Beerbower (4) are available for a large number of liquids, but the values for only a few solids (represented as supercooled liquids) are found in the literature. A table was prepared of group contributions for calculating partial solubility

Table I—Solubility of Naphthalene in Individual Solvents at 40° [a]

Solvent	Molar Volume, V_1	Dispersion Solubility Parameter, δ_{1d}	Polar Solubility Parameter, δ_{1p}	Hydrogen Bonding Solubility Parameter, δ_{1h}	Mole Fraction Solubility, X_2	Eq. 7 $X_{2(calc)}$	Eq. 7 Error, %	Eq. 10 $X_{2(calc)}$	Eq. 10 Error, %	Eq. 12 $X_{2(calc)}$	Eq. 12 Error, %
Hexane	131.6	7.3	0.0	0.0	0.222	0.264	−18.9	0.305	−37.3	0.283	−27.5
Carbon tetrachloride	97.1	8.7	0.0	0.3	0.395	0.438	−10.9	0.420	−6.4	0.448	−3.4
Toluene	106.8	8.8	0.7	1.0	0.422	0.435	−3.1	0.419	0.7	0.442	−4.7
Ethylidene chloride	84.8	8.1	4.0	0.2	0.437	0.413	5.5	0.414	5.3	0.424	3.0
Benzene	89.4	9.0	0.5[b]	1.0	0.428	0.449	−4.9	0.431	−0.7	0.453	−5.8
Chloroform	80.7	8.7	1.5	2.8	0.467	0.425	9.0	0.421	9.8	0.431	7.7
Chlorobenzene	102.1	9.3	2.1	1.0	0.444	0.448	−0.9	0.416	6.3	0.445	−0.2
Acetone	74.0	7.6	5.1	3.4	0.378	0.388	−2.6	0.413	−9.3	0.394	−4.2
Carbon disulfide	60.0	10.0	0.0	0.3	0.494	0.467	5.5	0.437	11.5	0.458	7.3
1,1-Dibromoethane	92.9	8.4	3.7	4.1	0.456	0.387	15.1	0.390	14.5	0.394	13.6
Ethylene dichloride	79.4	9.3	3.6	2.0	0.452	0.456	−0.9	0.437	3.3	0.453	−0.2
sec-Butanol	92.5	7.7	2.8	7.1	0.1122	0.135	−20.3	0.139	−23.9	0.142	−26.6
Nitrobenzene	102.7	9.8	4.2	2.0	0.432	0.469	−8.6	0.427	1.2	0.453	−4.9
tert-Butanol	94.3	7.3[b]	2.5[b]	6.8[b]	0.1009	0.103	−2.1	0.1224	−21.3	0.1049	−4.0
Cyclohexanol	106.0	8.5	2.0	6.6	0.232	0.237	−2.2	0.209	9.9	0.246	−6.0
Aniline	91.5	9.5	2.5	5.0	0.306	0.400	−30.7	0.355	−16.0	0.387	−26.5
Isobutanol	92.8	7.4	2.8	7.8	0.0925	0.0745	19.5	0.0761	17.7	0.0760	17.8
Butanol	91.5	7.8	2.8	7.7	0.116	0.113	2.6	0.104	10.3	0.118	−1.7
Isopropanol	76.8	7.7	3.0	8.0	0.0764	0.104	−36.1	0.0943	−23.4	0.1094	−43.2
Ethylene dibromide	87.0	10.3[b]	1.7[b]	4.2[b]	0.439	0.428	2.5	0.360	17.9	0.392	0.7
Propanol	75.2	7.8	3.3	8.5	0.0944	0.0903	4.3	0.0729	22.8	0.0946	−0.2
Acetic acid	57.6	7.1[c]	3.9[c]	6.6[c]	0.117	0.200	−70.9	0.254	−117.	0.196	−67.5
Ethanol	58.5	7.7	4.3	9.5	0.0726	0.0637	12.3	0.0431	40.6	0.0659	9.2
Methanol	40.7	7.4	6.0	10.9	0.0412	0.0356	13.6	0.0190	53.9	0.0353	14.3
Butyric acid[d]	91.9	7.3	2.0	5.2	0.251	0.148	26.7	0.238	5.5	0.189	24.7
Water	18.0	7.6	7.8	20.7	1.76×10^{-5}	1.76×10^{-5}	0.0	7.57×10^{-7}	95.7	1.7×10^{-5}	1.7

[a] V_2 = 123 cm³/mole, X_2^i (40°) = 0.46594. [b] Values recalculated from Reference 1. [c] Changed from values used in Reference 1 to those found in Reference 4. [d] From Reference 7.

parameters for both liquids and solids (4). This method provides only rough estimates of δ_d, δ_p, and δ_h for crystalline solids, and it would be advantageous to have another method to obtain these values.

The approach suggested here involves regressing $(\log \alpha_2)/A$ against δ_{1d}, δ_{1p}, δ_{1h}, δ_{1d}^2, δ_{1p}^2, and δ_{1h}^2 using a number of solvents. The result of this procedure using an SPSS regression program (5) is the expression:

$$(\log \alpha_2)/A = -13.5114\delta_{1d} + 0.6702\delta_{1d}^2 + 0.5570\delta_{1p} - 0.1418\delta_{1p}^2 - 0.2448\delta_{1h} + 0.1326\delta_{1h}^2 + 68.0377 \quad \text{(Eq. 4)}$$

$n = 26$, $s = 1.45$, $R^2 = 0.986$, $F = 276$, $F(6, 20, 0.01) = 3.87$.

The terms for δ_{1d}, δ_{1d}^2, δ_{1p}, δ_{1p}^2, δ_{1h}, and δ_{1h}^2 are paired together with the coefficient of the squared term taken outside the parenthesis in each instance:

$$(\log \alpha_2)/A = 0.6702(\delta_{1d}^2 - 20.1603\delta_{1d}) - 0.1418(\delta_{1p}^2 - 3.9281\delta_{1p}) + 0.1326(\delta_{1h}^2 - 1.8462\delta_{1h}) + 68.0377 \quad \text{(Eq. 5)}$$

The terms in parentheses can be cast into the form of perfect squares if 20.1603 is taken as $2\delta_{2d}$, 3.9281 as $2\delta_{2p}$, and 1.8462 as $2\delta_{2h}$ in Eq. 5. This leads to the result:

$$(\log \alpha_2)/A = 0.6702(\delta_{1d}^2 - 20.1603\delta_{1d} + 101.6094) - 0.1418(\delta_{1p}^2 - 3.9281\delta_{1p} + 3.8575) + 0.1326(\delta_{1h}^2 - 1.8462\delta_{1h} + 0.8521) - (0.6702)(101.6094) + (0.1418)(3.8575) - (0.1326)(0.8521) + 68.0377 \quad \text{(Eq. 6)}$$

Therefore, 101.6094 is δ_{2d}^2 and $(101.6094)^{1/2} = 10.08 = \delta_{2d}$; and likewise for δ_{2p} and δ_{2h}:

$$(\log \alpha_2)/A = 0.6702(\delta_{1d} - 10.08)^2 - 0.1418(\delta_{1p} - 1.964)^2 + 0.1326(\delta_{1h} - 0.923)^2 + 0.3731 \quad \text{(Eq. 7)}$$

It is observed that the partial solubility parameters, $\delta_{2d} = 10.08$, $\delta_{2p} = 1.964$, and $\delta_{2h} = 0.923$, have been obtained by a regression method involving only solvent partial solubility parameters, together with experimental solubility data from which $(\log \alpha_2)/A$ is calculated. The total solubility parameter δ_T for naphthalene by this method is:

$$\delta_T^2 = \delta_{2d}^2 + \delta_{2p}^2 + \delta_{2h}^2 = (10.08)^2 + (1.964)^2 + (0.923)^2 = 106.32$$
$$\delta_T = (106.32)^{1/2} = 10.31 \quad \text{(Eq. 8)}$$

The partial solubility parameters from the literature (4) are $\delta_d = 9.4$, $\delta_p = 1.0$, and $\delta_h = 1.9$[1], leading to a $\delta_T = 9.64$. The total solubility parameter of naphthalene from its maximum solubility in 24 solvents has been estimated to be $\delta_T = 9.6$ (1); the value $\delta_T = 10.31$ was obtained in the present study (Eq. 8). When a different number of solvents or different kinds of solvents are employed in the regression, the δ values may vary, since the coefficients of the equation change with various solvents. The δ_T value obtained by multiple regression was 10.43 when 23 solvents were used.

Nonlinear regression (6) led to the following results:

$$(\log \alpha_2)/A = 0.7429\delta_{1d}^2 - 13.5559\delta_{1d} - 0.1440\delta_{1p}^2 + 0.5781\delta_{1p} + 0.1883\delta_{1h}^2 - 0.5987\delta_{1h} + 63.6363 \quad \text{(Eq. 9)}$$

$$(\log \alpha_2)/A = 0.7429(\delta_{1d} - 9.124)^2 - 0.1440(\delta_{1p} - 2.007)^2 + 0.1883(\delta_{1h} - 1.590)^2 + 1.902 \quad \text{(Eq. 10)}$$

$n = 26$, s(based on X_2) = 0.052, R^2(based on X_2) = 0.927

The total solubility parameter is obtained:

$$\delta_T^2 = \delta_{2d}^2 + \delta_{2p}^2 + \delta_{2h}^2 = (9.12)^2 + (2.01)^2 + (1.59)^2$$
$$\delta_T = (89.74)^{1/2} = 9.47 \quad \text{(Eq. 11)}$$

It is too early to claim validity for the use of multiple regression as a means of establishing total and partial solubility parameters for solid solutes. However, if multiple regression can be shown to yield consistent results in the future, the method may be useful for drugs, biochemicals, and similar organic solutes, the solubility parameters of which cannot be obtained by the methods used for solvents. The regression procedure would also provide a check on the group contribution method of Hansen and Beerbower (4) for obtaining partial solubility parameters.

In preliminary work with similar systems, it appears that certain conditions must apply for the method to be successful: (*a*) The constant term C_0 of Eq. 1 should be <1.0 or 2.0, as observed in Eqs. 7 and 10. (*b*) The regression equation must be one that successfully predicts solubilities of the solute in the solvent systems employed. (*c*) The regression equation must be obtained by using a sufficient number of solvents (20 is good, 40 is much better) with solubility parameters both below and above that of the solute. The larger the number of known solubilities used in the regression analysis, the better the chance of obtaining reasonable solute solubility parameters.

[1] The δ_h for naphthalene is given in Reference 4 as 2.9 but this is in error; the value was intended to be 1.9.

The first right hand term of Eqs. 7 and 10 express London interaction (dispersion forces) between solute and solvent. These omnidirectional forces do not operate only on 67% of the nearest neighbor molecules, as suggested by the coefficient of Eq. 7, nor on 74%, as shown in Eq. 10. Instead, the coefficient of the $(\delta_{1d} - \delta_{2d})^2$ term should be unity. This can be ensured in the regression method by moving this term to the left hand side of the expression for the calculation of coefficients, then returning it to the right side to display the final equation. The δ_{2d} was taken as 9.40 and the equation obtained was:

$$(\log\alpha_2)/A = (\delta_{1d} - 9.40)^2 - 0.1463(\delta_{1p} - 2.059)^2 + 0.1319(\delta_{1h} - 0.778)^2 + 0.8640 \quad \text{(Eq. 12)}$$

This method reduces the variables of regression by one, but it does not seriously reduce the correlation coefficient: R^2 of Eq. 7 is 0.986 and of Eq. 12 is 0.980. Also from Eq. 13, $\delta_T{}^2 = 9.42 + 2.059^2 + 0.7782$; $\delta_T = (93.205)^{1/2} = 9.65$.

Although this report is devoted to the calculation of solubility parameters for crystalline solids, Eqs. 7, 10, and 12 provide the calculation of the solubility of naphthalene in both polar and nonpolar solvents, as was demonstrated in an earlier report (1). The results, $X_{2(calc)}$, are found in Table I together with the percentage error for naphthalene solubility in each of the 26 solvents studied. Most of the solubilities were very satisfactory, ~50% exhibiting errors of <10%. Most values have an error of < ~30%. Isopropanol and acetic acid exhibited errors of >30% when Eqs. 7 and 12 were used. The predicted solubilities for naphthalene in hexane, acetic acid, ethanol, methanol, and water were >30% error using Eq. 10. The reason that solubilities in these five solvents are >30% cannot be stated definitively at this time. Ethanol, methanol, isopropanol, acetic acid, and water are highly hydrogen bonded and exhibit self-association. However, other polar solvents such as propanol, butanol, and cyclohexanol have reasonable values in this work. The error of 37% for hexane is surprising, as this solvent tends to form regular solutions with nonpolar solutes such as naphthalene.

REFERENCES

(1) A. Martin, P. L. Wu, A. Adjei, A. Beerbower, and J. M. Prausnitz, *J. Pharm. Sci.*, **70**, 1260 (1981).

(2) A. Fredenslund, J. Gmehling, and P. Rasmussen, "Vapor–Liquid Equilibria Using UNIFAC," Elsevier, New York, N.Y., 1977.

(3) A. Martin, J. Newburger, and A. Adjei, *J. Pharm. Sci.*, **69**, 487 (1980).

(4) C. M. Hansen and A. Beerbower, in "Encyclopedia of Chemical Technology," Suppl. vol., 2nd ed., J. Wiley, New York, N.Y., 1971, p. 889.

(5) N. H. Nie, C. H. Hull, J. G. Jenkins, K. Steinbrenner, and D. H. Bent, "SPSS, Statistical Package for the Social Sciences," 2nd. ed., McGraw-Hill, New York, N.Y., 1975, chap. 20.

(6) A. Martin, P. L. Wu, A. Adjei, M. Mehdizadeh, K. C. James and C. Metzler, *J. Pharm. Sci.*, in press.

(7) C. M. Metzler, G. L. Elving, and A. J. McEwen, *Biometrics*, **30**, 562 (1974).

(8) "Solubilities of Inorganic and Organic Compounds," vol. 1, H. Stephen and T. Stephen, Eds., Pergamon, New York, N.Y. 1964, No. 6282.

ACKNOWLEDGMENTS

This study was funded in part by the endowed professorship provided to A. Martin by Coulter R. Sublett.

GLC Determination of Phenacemide in Tablets

PAUL CONNOLLY, SUSAN SIRMANS, ALBERT A. BELMONTE *x, and CHARLES M. DARLING

Received March 3, 1981, from the *School of Pharmacy, Auburn University, Auburn, Alabama 36849.* Accepted for publication January 13, 1982. *Present address: St. John's University, College of Pharmacy and Allied Health Professions, Jamaica, NY 11439

Abstract □ A GLC procedure was developed for phenacemide and was shown to be less time consuming than the official assay without sacrificing accuracy. The procedure involves extraction from powdered tablets and addition of pentylenetetrazol as the internal standard. The amount of phenacemide is determined by comparison of the ratio of the area under the curves to that of a standard.

Keyphrases □ Phenacemide—analysis in tablets, GLC determination, pentylenetetrazol □ Pentylenetetrazol—analysis of phenacemide in tablets, GLC determination □ GLC—phenacemide, analysis in tablets, pentylenetetrazol.

Phenacemide, an open chain analog of 5-phenylhydantoin, is used in temporal lobe epilepsy (psychomotor) which is refractory to other agents (1, 2). It is a white, odorless, and tasteless crystalline solid (3). While performing routine analyses in another experiment, a rapid method of analysis for phenacemide was needed. The official assay involves acid hydrolysis, extraction of the acidic products into chloroform, and back titration (4). The procedure is time consuming and requires much handling and transfer. Other methods for phenacemide determination have been developed but offer no distinct advantages (5–7).

This report outlines a rapid GLC method that has proven to be less time consuming. In addition to requiring less handling and transfer, it does not appear to sacrifice accuracy.

EXPERIMENTAL

Materials—Phenacemide powder[1] and phenacemide tablets[1] were utilized in the assay as received. Pentylenetetrazol[2] was used as the internal standard. Methanol[3] and isopropyl alcohol[3], ACS reagent grade, were used as solvents.

Apparatus—A basic gas chromatograph[4] with a flame ionization detector (FID) was used. A 3.17-mm, 1.83-m silicone column[5] was used. The temperature of the column and detector was maintained at 200 ± 20°. The flow rate of the carrier gas (helium) was ~20 ml/min. The detector was connected to an integrating recorder[6] for easy and accurate determination of area under the curve.

Standard Curve—Seven samples of varying ratios of phenacemide to pentylenetetrazol in methanol (Table I) were used to obtain a standard curve. Exact amounts of phenacemide and pentylenetetrazol were weighed directly into 10-ml volumetric flasks. A small volume of methanol was added to dissolve the sample and then made to volume with methanol.

Three microliters of each of the seven solutions was chromatographed and the results recorded. A standard curve was obtained by plotting the

[1] Abbott Laboratories, North Chicago, IL 60064.
[2] Knoll Pharmaceutical, Whippany, NJ 07981.
[3] Fisher Scientific, Norcross, GA 30091.
[4] Model 9500, Carle Instruments, Fullerton, CA 92631.
[5] 8% G.E. SF96 Carle Instruments, Fullerton, CA 92631.
[6] Model 1005, Beckman Instruments, Fullerton, CA 92631.

0022-3549/82/1100-1287$01.00/0

The first right hand term of Eqs. 7 and 10 express London interaction (dispersion forces) between solute and solvent. These omnidirectional forces do not operate only on 67% of the nearest neighbor molecules, as suggested by the coefficient of Eq. 7, nor on 74%, as shown in Eq. 10. Instead, the coefficient of the $(\delta_{1d} - \delta_{2d})^2$ term should be unity. This can be ensured in the regression method by moving this term to the left hand side of the expression for the calculation of coefficients, then returning it to the right side to display the final equation. The δ_{2d} was taken as 9.40 and the equation obtained was:

$$(\log\alpha_2)/A = (\delta_{1d} - 9.40)^2 - 0.1463(\delta_{1p} - 2.059)^2 + 0.1319(\delta_{1h} - 0.778)^2 + 0.8640 \quad \text{(Eq. 12)}$$

This method reduces the variables of regression by one, but it does not seriously reduce the correlation coefficient: R^2 of Eq. 7 is 0.986 and of Eq. 12 is 0.980. Also from Eq. 13, $\delta_T{}^2 = 9.42 + 2.059^2 + 0.7782$; $\delta_T = (93.205)^{1/2} = 9.65$.

Although this report is devoted to the calculation of solubility parameters for crystalline solids, Eqs. 7, 10, and 12 provide the calculation of the solubility of naphthalene in both polar and nonpolar solvents, as was demonstrated in an earlier report (1). The results, $X_{2(calc)}$, are found in Table I together with the percentage error for naphthalene solubility in each of the 26 solvents studied. Most of the solubilities were very satisfactory, ~50% exhibiting errors of <10%. Most values have an error of < ~30%. Isopropanol and acetic acid exhibited errors of >30% when Eqs. 7 and 12 were used. The predicted solubilities for naphthalene in hexane, acetic acid, ethanol, methanol, and water were >30% error using Eq. 10. The reason that solubilities in these five solvents are >30% cannot be stated definitively at this time. Ethanol, methanol, isopropanol, acetic acid, and water are highly hydrogen bonded and exhibit self-association. However, other polar solvents such as propanol, butanol, and cyclohexanol have reasonable values in this work. The error of 37% for hexane is surprising, as this solvent tends to form regular solutions with nonpolar solutes such as naphthalene.

REFERENCES

(1) A. Martin, P. L. Wu, A. Adjei, A. Beerbower, and J. M. Prausnitz, *J. Pharm. Sci.*, **70**, 1260 (1981).

(2) A. Fredenslund, J. Gmehling, and P. Rasmussen, "Vapor–Liquid Equilibria Using UNIFAC," Elsevier, New York, N.Y., 1977.

(3) A. Martin, J. Newburger, and A. Adjei, *J. Pharm. Sci.*, **69**, 487 (1980).

(4) C. M. Hansen and A. Beerbower, in "Encyclopedia of Chemical Technology," Suppl. vol., 2nd ed., J. Wiley, New York, N.Y., 1971, p. 889.

(5) N. H. Nie, C. H. Hull, J. G. Jenkins, K. Steinbrenner, and D. H. Bent, "SPSS, Statistical Package for the Social Sciences," 2nd. ed., McGraw-Hill, New York, N.Y., 1975, chap. 20.

(6) A. Martin, P. L. Wu, A. Adjei, M. Mehdizadeh, K. C. James and C. Metzler, *J. Pharm. Sci.*, in press.

(7) C. M. Metzler, G. L. Elving, and A. J. McEwen, *Biometrics*, **30**, 562 (1974).

(8) "Solubilities of Inorganic and Organic Compounds," vol. 1, H. Stephen and T. Stephen, Eds., Pergamon, New York, N.Y. 1964, No. 6282.

ACKNOWLEDGMENTS

This study was funded in part by the endowed professorship provided to A. Martin by Coulter R. Sublett.

GLC Determination of Phenacemide in Tablets

PAUL CONNOLLY, SUSAN SIRMANS, ALBERT A. BELMONTE *x, and CHARLES M. DARLING

Received March 3, 1981, from the *School of Pharmacy, Auburn University, Auburn, Alabama 36849.* Accepted for publication January 13, 1982. *Present address: St. John's University, College of Pharmacy and Allied Health Professions, Jamaica, NY 11439

Abstract □ A GLC procedure was developed for phenacemide and was shown to be less time consuming than the official assay without sacrificing accuracy. The procedure involves extraction from powdered tablets and addition of pentylenetetrazol as the internal standard. The amount of phenacemide is determined by comparison of the ratio of the area under the curves to that of a standard.

Keyphrases □ Phenacemide—analysis in tablets, GLC determination, pentylenetetrazol □ Pentylenetetrazol—analysis of phenacemide in tablets, GLC determination □ GLC—phenacemide, analysis in tablets, pentylenetetrazol.

Phenacemide, an open chain analog of 5-phenylhydantoin, is used in temporal lobe epilepsy (psychomotor) which is refractory to other agents (1, 2). It is a white, odorless, and tasteless crystalline solid (3). While performing routine analyses in another experiment, a rapid method of analysis for phenacemide was needed. The official assay involves acid hydrolysis, extraction of the acidic products into chloroform, and back titration (4). The procedure is time consuming and requires much handling and transfer. Other methods for phenacemide determination have been developed but offer no distinct advantages (5–7).

This report outlines a rapid GLC method that has proven to be less time consuming. In addition to requiring less handling and transfer, it does not appear to sacrifice accuracy.

EXPERIMENTAL

Materials—Phenacemide powder[1] and phenacemide tablets[1] were utilized in the assay as received. Pentylenetetrazol[2] was used as the internal standard. Methanol[3] and isopropyl alcohol[3], ACS reagent grade, were used as solvents.

Apparatus—A basic gas chromatograph[4] with a flame ionization detector (FID) was used. A 3.17-mm, 1.83-m silicone column[5] was used. The temperature of the column and detector was maintained at 200 ± 20°. The flow rate of the carrier gas (helium) was ~20 ml/min. The detector was connected to an integrating recorder[6] for easy and accurate determination of area under the curve.

Standard Curve—Seven samples of varying ratios of phenacemide to pentylenetetrazol in methanol (Table I) were used to obtain a standard curve. Exact amounts of phenacemide and pentylenetetrazol were weighed directly into 10-ml volumetric flasks. A small volume of methanol was added to dissolve the sample and then made to volume with methanol.

Three microliters of each of the seven solutions was chromatographed and the results recorded. A standard curve was obtained by plotting the

[1] Abbott Laboratories, North Chicago, IL 60064.
[2] Knoll Pharmaceutical, Whippany, NJ 07981.
[3] Fisher Scientific, Norcross, GA 30091.
[4] Model 9500, Carle Instruments, Fullerton, CA 92631.
[5] 8% G.E. SF96 Carle Instruments, Fullerton, CA 92631.
[6] Model 1005, Beckman Instruments, Fullerton, CA 92631.

0022-3549/82/1100-1287$01.00/0

Table I—Samples Used to Construct the Standard Curve

Sample Number	Phenacemide, g/10 ml	Pentylenetetrazol, g/10 ml
1	0.0405	0.0215
2	0.0133	0.0501
3	0.0308	0.0535
4	0.0320	0.0399
5	0.0507	0.0506
6	0.0200	0.0520
7	0.0377	0.0305

ratio of the area under the curve of phenacemide to pentylenetetrazol *versus* the ratio of the concentration of phenacemide to pentylenetetrazol in moles per liter.

Analysis of Phenacemide—In keeping with the USP method, 20 tablets were crushed in a porcelain mortar and pestle. The powder was dried over anhydrous calcium sulfate[7] in a dessicator. Samples containing ~400 mg of drug were accurately weighed and placed in a 500-ml round bottom flask. Approximately 450 ml of isopropyl alcohol was added and the solution was refluxed for 1 hr, cooled to room temperature, and filtered. Approximately 500 mg of an accurately weighed sample of pentylenetetrazol was added and the solution was brought to volume (1 liter) with isopropyl alcohol. A 3-μl sample was injected onto the chromatograph and the area under the curve recorded. The average of at least three determinations was used in the subsequent calculations.

RESULTS AND DISCUSSION

The equation of the standard curve using regression analysis[8] was found to be:

$$y = 1.30x - 0.0612 \qquad \text{(Eq. 1)}$$

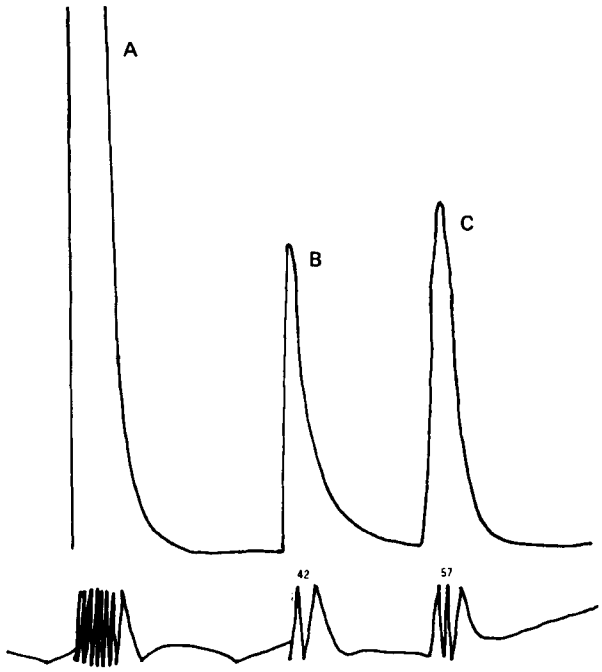

Figure 1—*A sample chromatogram from phenacemide tablets. Key: (A) solvent isopropyl alcohol; (B) phenacemide; (C) pentylenetetrazol.*

[7] Hammond Drierite Co., Xenia, OH 45385.
[8] Statistical Analysis System, SAS Institute, Raleigh, NC 27605.

Table II—Recovery and Assay Results from USP and GLC Methods

Phenacemide[a], g	Expected Phenacemide Control, g	Phenacemide Found, g	Recovery, %
	GLC Method		
0.5726	0.3843	0.3985	103.8
0.5966	0.4004	0.4120	102.9
0.5946	0.3991	0.4152	104.0
0.5950	0.3993	0.3993	100.1
	USP Method		
0.5944	0.4002	0.3976	99.4
0.5969	0.4006	0.4148	100.6
0.5962	0.4002	0.3992	99.8

[a] Powdered tablet weighed.

where:

$$y = \frac{\text{area under the curve of phenacemide}}{\text{area under the curve of pentylenetetrazol}} = \frac{AUCP}{AUCM} \qquad \text{(Eq. 2)}$$

$$= \frac{\text{concentration of phenacemide}}{\text{concentration of pentylenetetrazol}} = \frac{CONCP}{CONCM} \qquad \text{(Eq. 3)}$$

The standard curve was linear and the amount of phenacemide was determined using Eq. 1. The values are recorded in Table II.

The gas chromatogram resulting from each sample injection exhibited three peaks: the solvent (isopropyl alcohol), phenacemide, and pentylenetetrazol. Tailing was minimal and each peak approached the base line before the appearance of the next peak. A typical chromatogram is shown in Fig. 1.

The standard curve was linear in the range used for this study. The correlation coefficient of concentration *versus* area under the curve was 0.9996. Statistical comparison, using Student's t test for independent samples, showed no statistical difference between recovery of phenacemide using the USP assay and the GLC method. The calculated t-value was 0.7649, while the critical value was $t_{0.95} = 2.571$, with 5 df.

The GLC determination of phenacemide in tablets offers an improvement over the USP method without sacrificing accuracy in the samples assayed. The GLC determination of phenacemide in tablets is a simpler and quicker method which produces results essentially the same as that of the time-consuming official assay.

REFERENCES

(1) A. G. Gilman, L. S. Goodman, and A. Gilman, "The Pharmacological Basis of Therapeutics," 6th ed., MacMillan, New York, N.Y., 1980, p. 467.

(2) D. M. Woodbury, J. K. Penry, and R. P. Schmidt, "Antiepileptic Drugs," Raven Press, New York, N.Y., 1972, p. 275.

(3) A. Osol, "Remington's Pharmaceutical Sciences," 16th ed., Mack, Easton, Pa., 1980, p. 1025.

(4) "The United States Pharmacopeia," 20th rev., USP Convention, Rockville, Md., 1980, p. 605.

(5) J. Kracmar and J. Kracmova, *Cesk. Farm.*, **15,** 16 (1966); through *Chem. Abstr.*, **64,** 19323b (1966).

(6) E. Kassau, *Dtsch. Apoth.-Zg.*, **104,** 613 (1964); through *Chem. Abstr.*, **61,** 5460b (1964).

(7) J. W. Heusman, *Clin. Chim. Acta*, **13,** 323 (1966).

The Desolvation and Oxidation of Crystals of Dialuric Acid Monohydrate

RONALD J. CLAY, ADELBERT M. KNEVEL, and STEPHEN R. BYRN ˣ

Received June 29, 1981, from the *Department of Medicinal Chemistry and Pharmacognosy, School of Pharmacy and Pharmacal Sciences, Purdue University, West Lafayette, IN 47907.* Accepted for publication January 13, 1982.

Abstract □ Examination of the influence of the solvent of crystallization on the solid-state oxidation of dialuric acid (I) monohydrate to alloxantin (II) is reported. This reaction was investigated at low and high humidities using photomicrography, X-ray crystallography, and IR and mass spectrometry. Crystals of dialuric acid desolvated somewhat anisotropically; this behavior was consistent with crystal packing. The desolvated crystals of dialuric acid monohydrate had approximately the same crystal structure as the monohydrate and were stable in air at room temperature at low humidities. At high humidity, these crystals rehydrated and rapidly oxidized to alloxantin. These studies showed for the first time that desolvation was not a necessary prerequisite to solid-state oxidation and that solid-state oxidation reactions could be accelerated by high humidity.

Keyphrases □ Dialuric acid monohydrate—desolvation and solid-state oxidation of crystals □ Crystallization—desolvation and solid-state oxidation of dialuric acid monohydrate □ Solid-state oxidation—crystals of dialuric acid monohydrate, desolvation □ Desolvation—crystals of dialuric acid monohydrate, solid-state oxidation

Recent studies (1, 2) have correlated desolvation patterns of crystalline hydrates of drugs and related compounds with crystal packing (1, 2). Several crystal solvates, including those of dihydrophenylalanine (2, 3), ergosterol (4), hydrocortisone *tert*-butylacetate (5), dialuric aicd (6), bis(salicylidene)ethylenediimine Co(II) (7), and the picket fence porphyrins, are oxygen sensitive (8). In many of these solvates, desolvation precedes or coincides with reaction with oxygen.

The present report represents an extension of previous research (1, 2) and is aimed at understanding the relationship between desolvation and oxygen reactivity; the oxidation of dialuric acid monohydrate (I) is discussed as well.

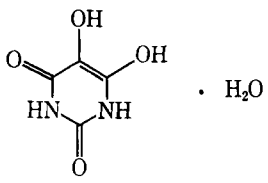

I

The results of this study, which show that moisture and factors other than oxygen permeability of the crystal influence solid-state oxidation reactions, may have important implications for the proper design and storage of drugs and dosage forms.

EXPERIMENTAL

Photomicrography of crystals was performed with a microscope[1] equipped with a hot stage[2]. The X-ray powder diffraction patterns were measured on film using CuKα radiation on a powder camera[3], and elemental analyses were obtained[4]. The extent of reaction was determined using polarographic[5] analysis (quantitative) and IR spectroscopy[6] (qualitative). The constant humidity experiments were performed in chambers with the humidity controlled by various saturated salt solutions: LiCl, 15%; NaCl + KNO_3 + $NaNO_3$, 30%; KSCN, 47%; NH_4Cl + KNO_3, 72%; KBr, 84%; and $NH_4H_2PO_4$, 93%. MS were measured on a mass spectrometer[7] in the chemical ionization mode.

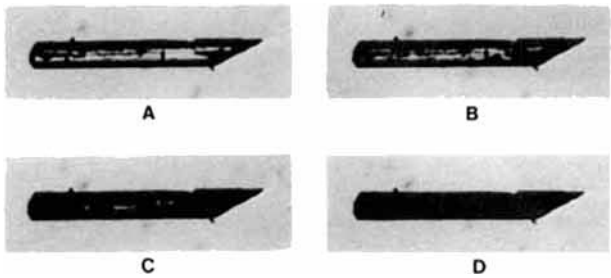

Figure 1—*Behavior of a crystal of dialuric acid monohydrate at 100°: (A) start (B) after 18 min; (C) after 28 min; (D) after 36 min.*

Dialuric acid was prepared according to a previous method (9). Two grams of recrystallized alloxan[5] was dissolved in 100 ml of freshly boiled deoxygenated water. Hydrogen sulfide[6] (5% H_2S, 95% N_2) was then passed through this solution until it became opalescent and free sulfur was liberated. Carbon disulfide (10 ml) then was added and the hydrogen sulfide passed through the solution for an additional 10 min. The carbon disulfide layer was removed and this process repeated for another 10 min. The aqueous solution then was filtered and evaporated to dryness. The product, dialuric acid monohydrate, was obtained by recrystallization from boiled, deoxygenated water. Dialuric acid gave an IR spectrum, elemental analysis, and X-ray diffraction patterns consistent with those in the literature (9).

Anal.—Calc. for $C_4H_6N_2O_5$: C, 29.64; H, 3.73; N, 17.28. Found: C, 29.56; H, 3.90; N, 17.00.

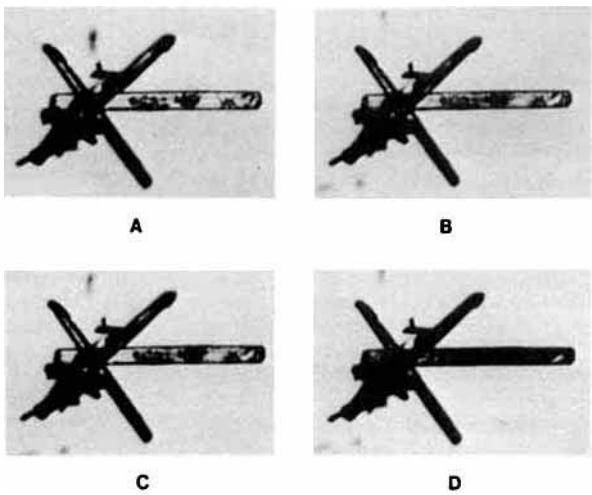

Figure 2—*Oxidation of a clump of crystals of dialuric acid monohydrate at room temperature and 100% relative humidity: (A) start; (B) after 30 min; (C) after 60 min; (D) after 120 min.*

[1] Carl Zeiss.
[2] Mettler FP5/52.
[3] Debye-Scherrer.
[4] Microanalysis laboratory, Purdue University.
[5] Eastman Organic Chemicals.
[6] Matheson.
[7] Dupont.

0022-3549/82/1100-1289$01.00/0

Table I—Calculated *d*-Spacings for Oxidized Dialuric Acid and Anhydrous Alloxantin

Sample 1		Sample 2		Anhydrous Alloxantin	
d-Spacing Å	Intensity[a]	*d*-Spacing Å	Intensity	*d*-Spacing Å	Intensity
6.036	w	5.996	w	6.026	m
5.556	s	5.522	vs	5.635	m
5.301	vw	5.262	vw	5.262	vw
5.082	vw	5.053	vw	5.046	vw
4.338	m	4.311	m	4.338	vw
3.754	w	3.723	w	3.708	vw
3.594	vvw	3.590	vvw	—	—
3.447	s	3.433	ms	3.417	vs
3.320	m	3.305	m	3.308	ms
3.164	m	3.145	mw	3.209	ms
3.056	vvw	3.048	vvw	3.069	vw
2.974	s	2.971	s	2.952	s
2.901	s	2.885	s	2.905	m
2.784	vw	2.767	vw	2.759	m
2.708	vw	2.692	vw	2.696	m
2.543	m	2.534	m	2.525	ms

[a] Key: (s) strong; (m) moderate; (w) weak; (v) very.

RESULTS

Dialuric acid monohydrate was prepared following literature procedures. It gave a satisfactory elemental analysis and its IR spectrum and X-ray powder pattern were identical to the published data (9). Heating at 76 or 100° led to the formation of the anhydrous form. The X-ray powder pattern of this anhydrous form, as measured on film, was approximately identical to that of the monohydrate. Crystals of dialuric acid monohydrate heated to 100° generally behaved anisotropically, with the reaction proceeding from the ends of the needle-like crystals toward the middle as shown in Fig. 1. The dehydrated solid was polycrystalline since it gave only a powder pattern, had approximately the same crystal structure as dialuric acid monohydrate, and was stable to oxidation. The dehydrated crystals had to be heated at 76° at room humidity for 56–70 days to be completely oxidized.

The structure of the oxidation product was shown to be alloxantin (II) rather than alloxan (III) as had been previously suggested (6). The X-ray powder diffraction pattern of two oxidized samples essentially was identical to that of alloxantin as shown in Table I. In addition, elemental

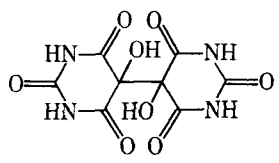

II

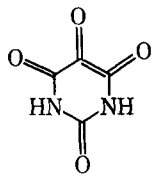

III

analysis of oxidized dialuric acid gave C, 29.77; H, 3.38; and N, 17.40%. The data calculated for alloxantin ($C_8H_6N_4O_8$) are C, 29.82; H, 3.13; and N, 17.39%; while the calculated values for alloxan are C, 30.01; H, 2.52; and N, 17.50%. Infrared and mass spectral measurements on alloxan and alloxantin and oxidized dialuric acid confirmed that dialuric acid is oxidized to alloxantin not alloxan (10).

The dehydrated crystals could be rehydrated at room temperature at humidities ranging from 30 to 84% in a constant humidity chamber. The results of these rehydration studies are shown in Table II. At 93 and 100% relative humidity, a rapid and unexpected oxidation to alloxantin occurs at room temperature. This oxidation complicates the weight gain measurements, which indicate that the equivalent of one molecule of water has been absorbed. In addition, the higher the humidity the faster the reaction, since complete oxidation occurs in <3 hr at 100% relative humidity.

Figure 2 shows the behavior of a clump of crystals of dialuric acid monohydrate at 100% relative humidity. The oxidation reaction begins at several nucleation sites and is nearly complete after 2 hr.

DISCUSSION

Dehydration of Dialuric Acid—The anisotropic behavior of dialuric acid monohydrate crystals during dehydration is probably due to the preferential exit of the water molecules along the tunnel direction (1, 2).

Table II—Structure Changes of Anhydrous Dialuric Acid at Room Temperature and Various Relative Humidities

Relative Humidity, %	Initial Weight Gain Equivalent	Structure Change[a]
2	None	None
15	None	None
30	0.018 g (1·H_2O)	Anhydrous to hydrate
47	0.018 g (1·H_2O)	
72	0.018 g (1·H_2O)	
84	0.018 g (1·H_2O)	
93	0.018 g	Anhydrous to hydrate to alloxantin hydrate (<24 hr)
100	0.018 g	Anhydrous to hydrate to alloxantin hydrate (<3 hr)

[a] As determined by IR and X-ray powder diffraction after 5-days exposure, except where noted.

An examination of the crystal packing of dialuric acid monohydrate (Fig. 3) shows that tunnels of water molecules lie approximately parallel to the needle axis of the crystal. Thus, an individual water molecule exits out these tunnels rather than penetrating the closely packed dialuric acid layers. Similar but more dramatic behavior has been observed for other crystals during desolvation (1, 2).

In addition, the crystal structure of the dehydrated crystals is approximately the same as the hydrate, since the X-ray powder patterns of dialuric acid monohydrate and anhydrous dialuric acid are nearly identical. Thus, dialuric acid is an example of crystal pseudomorphism, a term used to describe similar behavior of the solvates and anhydrous forms of the cephalosporin antibiotics (11).

Oxidation of Desolvated Dialuric Acid Monohydrate—The stability of the desolvated crystals toward oxidation in air was unexpected. Dialuric acid is unstable in solutions exposed to air and has a half-life of ~30 sec at room temperature in aqueous solution. In contrast, the desolvated crystals required 56–70 days at 76° for complete oxidation. Unlike dialuric acid, desolvated crystals of dihydrophenylalanine and bis(salicylidene)ethylenediamine Co(II) (1, 2) react with oxygen at room temperature in a few days. Also, anhydrous dialuric acid has approximately the same crystal structure as dialuric acid monohydrate and, thus, should contain voids previously occupied by water molecules. These voids do not result in facile oxidation. This shows that factors other than the ability of oxygen to penetrate the crystal can influence solid-state oxidation reactions.

Rehydration of Anhydrous Dialuric Acid—Exposure of desolvated crystals of dialuric acid to water vapor results in rehydration at humidities >30%. This is a well-known process for pharmaceuticals with the cephalosporin antibiotics exhibiting unusual ability to desolvate and resolvate (11). As with the cephalosporins, the crystal structures of dialuric acid monohydrate and anhydrous dialuric acid are nearly the same.

Rehydration and Oxidation of Anhydrous Dialuric Acid at High Humidities—If crystals of anhydrous dialuric acid are exposed to room temperature and relative humidities >93%, they rehydrate and oxidize. An increase in the rate of reaction at increased relative humidity is also apparent from the data. The rate of the decarboxylation of solid *p*-aminosalicylic acid and the hydrolysis of solid aspirin also increased with increasing relative humidities (12). The decreased stabilities of these compounds at increased relative humidities were interpreted in terms of the formation of a moisture layer a few molecules thick on the crystals and solution reaction in this moisture layer (12). A similar process may also explain the behavior of dialuric acid. However, because of the rehydration and the rapid oxidation, it is impossible to interpret the weight gain of the crystals at high humidities. For batches of crystals of

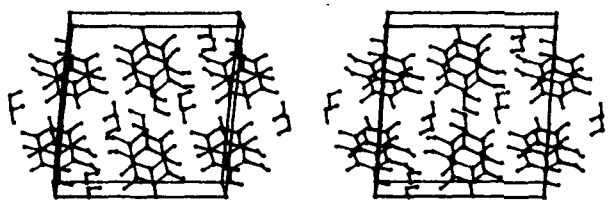

Figure 3—*Crystal packing of dialuric acid. The direction of the crystal axes are: with origin at top left a across b out of the plane of the paper, and c down. (Data from Ref. 6 were used to make this figure.)*

dialuric acid with an (assumed) area of 0.01 m^2/g, a monolayer of water molecules on a 0.100-g sample would weigh 2.14×10^{-7} g. Thus, a water layer 1000 molecules thick would barely be detectable in the absence of the complicating oxidation reaction.

These results indicate that factors other than the apparent permeability of oxygen into the crystal can govern solid-state oxidation reactions. Desolvated crystals of dialuric acid, which are expected to contain voids, are unreactive. Thus, desolvation does not always increase the reactivity of a crystal toward oxygen. Instead, solvated crystals exposed to high humidities react very rapidly, showing that high humidities can accelerate solid oxygen reactions. Also, reactions of the type: solid + gas → solid can be accelerated in high humidities presumably *via* reaction in an invisible moisture layer.

In contrast to other solids, these results indicate that stabilization of pharmaceuticals with solid-state behavior related to dialuric acid would best be accomplished, not by avoiding desolvation as indicated by some published results (1–3, 7, 8), but rather by preventing exposure to high humidities.

REFERENCES

(1) S. R. Byrn and C. T. Lin, *J. Am. Chem. Soc.*, **98**, 4004 (1976).

(2) C. T. Lin and S. R. Byrn, *Mol. Cryst. Liq. Cryst.*, **50**, 99 (1979).

(3) C. Ressler, *J. Org. Chem.*, **37**, 2933 (1972).

(4) R. K. Callow, *Biochem. J.*, **25**, 79 (1931).

(5) G. Brener, F. E. Roberts, A. Hoinowski, J. Budavari, B. Powell, D. Hinkley, and E. Schoenwaldt, *Angew. Chem. Intl. Ed.*, **8**, 975 (1969).

(6) W. Bolton, *Acta Crystallogr.*, **19**, 1051 (1965).

(7) R. M. Hochstrasser, *Can. J. Chem.*, **36**, 1123 (1959).

(8) J. D. Coleman, J. I. Brauman, K. M. Doxsee, T. R. Halbert, S. E. Hayes, and K. S. Suslick, *J. Am. Chem. Soc.*, **100**, 2761 (1978).

(9) R. S. Tipson and L. H. Cretchen, *J. Org. Chem.*, **16**, 1091 (1951).

(10) R. J. Clay, Ph.D. Thesis, Purdue University, W. Lafayette, Ind. (1979).

(11) R. Pfeiffer, K. S. Yang, and M. A. Tucker, *J. Pharm. Sci.*, **59**, 1809 (1970).

(12) J. T. Carstensen, *ibid.*, **63**, 1 (1974).

ACKNOWLEDGMENTS

This research was supported by Grant GM21174 and an American Foundation for Pharmaceutical Education Fellowship to R. J. Clay.

A Rapid Quantitative Determination of Acetaminophen in Plasma

SANDRA E. O'CONNELL[x] and FRANK J. ZURZOLA

Received August 26, 1981, from the *Research and Development Center, Bristol-Myers Products Division, Hillside, NJ 07207.* Accepted for publication January 27, 1982.

Abstract □ A simple method is described for the rapid, quantitative analysis of acetaminophen in plasma. The nonconjugated acetaminophen present in the plasma following drug administration is determined after plasma protein precipitation by high-pressure liquid chromatography (HPLC) at a wavelength of 240 nm. Acetaminophen (I) is detectable at levels as low as 0.1 μg/ml. Mean recoveries of 94% with a coefficient of variation of 3% were obtained for plasma standards whose concentrations ranged from 0 to 32 μg/ml. Interassay variability of the slope of the standard curve had a coefficient of variation of 2.7%. Application and verification of this method by comparison with another procedure run simultaneously during several human bioavailability studies are described.

Keyphrases □ Acetaminophen—high-performance liquid chromatographic analysis in human plasma □ High-performance liquid chromatography—analysis, acetaminophen in human plasma and blood □ Analgesics—acetaminophen, high-performance liquid chromatographic analysis in human plasma

The widespread use of acetaminophen (I) as an analgesic and antipyretic has stimulated an interest in the development of a simple and rapid free acetaminophen plasma determination suitable for analyzing multiple samples. The pharmacology of acetaminophen is such that ~80% of a dose is conjugated predominately with glucuronic acid and to a lesser extent with sulfuric acid. These conjugated metabolites lack efficacious biological activity (1). Most of the published methods determine total (*i.e.*, free plus conjugated) acetaminophen in plasma (2–4), while those that determine free acetaminophen by a variety of techniques (5–14), including HPLC (7–14), involve time-consuming and labor intensive organic extractions, solvent evaporations (7–10), deal with toxic levels rather than the lower therapeutic levels (11, 12), or are unsuitable for routine multiple therapeutic level samples because of lack of sensitivity, insufficient sample cleanup (11–14), or long analysis time (14).

The present method involves a single plasma protein precipitation step followed by liquid chromatographic determination of acetaminophen in the clear supernatant. The plasma proteins are denatured and precipitated using 0.3 *N* $Ba(OH)_2$ and 5% $ZnSO_4$ solutions described previously (15). The method is capable of detecting <0.1 μg/ml, and the reproducibility eliminates the need for an internal standard. Furthermore, the ease and rapidity of sample workup make this method ideal for multiple sample analysis.

This method has been used routinely for over a year with good results and has been verified by a comparison with an extraction–HPLC acetaminophen method[1] and a colorimetric procedure (16).

EXPERIMENTAL

Reagents—Standard solutions were prepared in distilled water. The 0.3 *N* $Ba(OH)_2$ and 5% $ZnSO_4$ solutions were obtained commercially[2]. The combination of these two salt solutions has been known for years as an effective plasma protein precipitant.

Instrumentation and Operating Conditions—The analysis was performed using a high-performance liquid chromatograph[3] with a variable wavelength UV detector[4] set at 240 nm, an automated injection system[5] fitted with a 75-μl loop, and a 30 cm × 4-mm i.d. reversed-phase,

[1] N. Kalish and S. O'Connell, Bristol-Myers Products, Analytical Chemistry Department, unpublished data, 1977.
[2] Fisher Scientific Co.
[3] Model 6000, Waters Associates, Milford, Mass.
[4] Model 450, Waters Associates, Milford, Mass.
[5] Model 834, Dupont Instrument Co., Wilmington, Del.

0022-3549/82/1100-1291$01.00/0

dialuric acid with an (assumed) area of 0.01 m^2/g, a monolayer of water molecules on a 0.100-g sample would weigh 2.14×10^{-7} g. Thus, a water layer 1000 molecules thick would barely be detectable in the absence of the complicating oxidation reaction.

These results indicate that factors other than the apparent permeability of oxygen into the crystal can govern solid-state oxidation reactions. Desolvated crystals of dialuric acid, which are expected to contain voids, are unreactive. Thus, desolvation does not always increase the reactivity of a crystal toward oxygen. Instead, solvated crystals exposed to high humidities react very rapidly, showing that high humidities can accelerate solid oxygen reactions. Also, reactions of the type: solid + gas → solid can be accelerated in high humidities presumably *via* reaction in an invisible moisture layer.

In contrast to other solids, these results indicate that stabilization of pharmaceuticals with solid-state behavior related to dialuric acid would best be accomplished, not by avoiding desolvation as indicated by some published results (1–3, 7, 8), but rather by preventing exposure to high humidities.

REFERENCES

(1) S. R. Byrn and C. T. Lin, *J. Am. Chem. Soc.*, **98**, 4004 (1976).

(2) C. T. Lin and S. R. Byrn, *Mol. Cryst. Liq. Cryst.*, **50**, 99 (1979).

(3) C. Ressler, *J. Org. Chem.*, **37**, 2933 (1972).

(4) R. K. Callow, *Biochem. J.*, **25**, 79 (1931).

(5) G. Brener, F. E. Roberts, A. Hoinowski, J. Budavari, B. Powell, D. Hinkley, and E. Schoenwaldt, *Angew. Chem. Intl. Ed.*, **8**, 975 (1969).

(6) W. Bolton, *Acta Crystallogr.*, **19**, 1051 (1965).

(7) R. M. Hochstrasser, *Can. J. Chem.*, **36**, 1123 (1959).

(8) J. D. Coleman, J. I. Brauman, K. M. Doxsee, T. R. Halbert, S. E. Hayes, and K. S. Suslick, *J. Am. Chem. Soc.*, **100**, 2761 (1978).

(9) R. S. Tipson and L. H. Cretchen, *J. Org. Chem.*, **16**, 1091 (1951).

(10) R. J. Clay, Ph.D. Thesis, Purdue University, W. Lafayette, Ind. (1979).

(11) R. Pfeiffer, K. S. Yang, and M. A. Tucker, *J. Pharm. Sci.*, **59**, 1809 (1970).

(12) J. T. Carstensen, *ibid.*, **63**, 1 (1974).

ACKNOWLEDGMENTS

This research was supported by Grant GM21174 and an American Foundation for Pharmaceutical Education Fellowship to R. J. Clay.

A Rapid Quantitative Determination of Acetaminophen in Plasma

SANDRA E. O'CONNELL[x] and FRANK J. ZURZOLA

Received August 26, 1981, from the *Research and Development Center, Bristol-Myers Products Division, Hillside, NJ 07207.* Accepted for publication January 27, 1982.

Abstract □ A simple method is described for the rapid, quantitative analysis of acetaminophen in plasma. The nonconjugated acetaminophen present in the plasma following drug administration is determined after plasma protein precipitation by high-pressure liquid chromatography (HPLC) at a wavelength of 240 nm. Acetaminophen (I) is detectable at levels as low as 0.1 μg/ml. Mean recoveries of 94% with a coefficient of variation of 3% were obtained for plasma standards whose concentrations ranged from 0 to 32 μg/ml. Interassay variability of the slope of the standard curve had a coefficient of variation of 2.7%. Application and verification of this method by comparison with another procedure run simultaneously during several human bioavailability studies are described.

Keyphrases □ Acetaminophen—high-performance liquid chromatographic analysis in human plasma □ High-performance liquid chromatography—analysis, acetaminophen in human plasma and blood □ Analgesics—acetaminophen, high-performance liquid chromatographic analysis in human plasma

The widespread use of acetaminophen (I) as an analgesic and antipyretic has stimulated an interest in the development of a simple and rapid free acetaminophen plasma determination suitable for analyzing multiple samples. The pharmacology of acetaminophen is such that ~80% of a dose is conjugated predominately with glucuronic acid and to a lesser extent with sulfuric acid. These conjugated metabolites lack efficacious biological activity (1). Most of the published methods determine total (*i.e.*, free plus conjugated) acetaminophen in plasma (2–4), while those that determine free acetaminophen by a variety of techniques (5–14), including HPLC (7–14), involve time-consuming and labor intensive organic extractions, solvent evaporations (7–10), deal with toxic levels rather than the lower therapeutic levels (11, 12), or are unsuitable for routine multiple therapeutic level samples because of lack of sensitivity, insufficient sample cleanup (11–14), or long analysis time (14).

The present method involves a single plasma protein precipitation step followed by liquid chromatographic determination of acetaminophen in the clear supernatant. The plasma proteins are denatured and precipitated using 0.3 *N* $Ba(OH)_2$ and 5% $ZnSO_4$ solutions described previously (15). The method is capable of detecting <0.1 μg/ml, and the reproducibility eliminates the need for an internal standard. Furthermore, the ease and rapidity of sample workup make this method ideal for multiple sample analysis.

This method has been used routinely for over a year with good results and has been verified by a comparison with an extraction–HPLC acetaminophen method[1] and a colorimetric procedure (16).

EXPERIMENTAL

Reagents—Standard solutions were prepared in distilled water. The 0.3 *N* $Ba(OH)_2$ and 5% $ZnSO_4$ solutions were obtained commercially[2]. The combination of these two salt solutions has been known for years as an effective plasma protein precipitant.

Instrumentation and Operating Conditions—The analysis was performed using a high-performance liquid chromatograph[3] with a variable wavelength UV detector[4] set at 240 nm, an automated injection system[5] fitted with a 75-μl loop, and a 30 cm × 4-mm i.d. reversed-phase,

[1] N. Kalish and S. O'Connell, Bristol-Myers Products, Analytical Chemistry Department, unpublished data, 1977.
[2] Fisher Scientific Co.
[3] Model 6000, Waters Associates, Milford, Mass.
[4] Model 450, Waters Associates, Milford, Mass.
[5] Model 834, Dupont Instrument Co., Wilmington, Del.

0022-3549/82/1100-1291$01.00/0

Table I—Accuracy of HPLC Assay For Acetaminophen in Plasma

Amount Added, μg	Experiment 1 Amount Found, μg	Experiment 1 Percent Error	Experiment 2 Amount Found, μg	Experiment 2 Percent Error	Experiment 3 Amount Found, μg	Experiment 3 Percent Error	Experiment 4 Amount Found, μg	Experiment 4 Percent Error	Experiment 5 Amount Found, μg	Experiment 5 Percent Error
1.0	1.05	5.0	1.03	3.0	1.04	4.0	1.07	7.0	1.07	7.0
1.0	1.05	5.0	1.07	7.0	1.00	0.0	0.98	2.0	0.99	1.0
2.0	2.10	5.0	2.05	2.5	2.09	4.5	2.14	7.0	2.12	6.0
2.0	2.05	2.5	2.09	4.5	2.09	4.5	2.04	2.0	2.12	6.0
4.0	4.10	2.5	4.00	0.0	4.00	0.0	4.07	1.8	4.15	3.8
4.0	4.02	0.5	4.08	2.0	4.04	1.0	3.95	1.3	3.97	0.8
8.0	7.99	0.1	7.80	2.5	7.99	0.1	7.84	2.0	8.16	2.0
8.0	8.03	0.4	7.93	0.9	7.91	1.1	7.93	0.9	7.67	4.1
16.0	16.19	1.2	15.81	1.2	16.11	0.7	15.97	0.2	16.28	1.8
16.0	16.23	1.4	16.51	3.2	16.03	0.2	15.85	0.9	15.47	3.3
24.0	24.04	0.2	23.68	1.3	24.06	0.3	24.28	1.2	24.45	1.9
24.0	22.74	5.2	24.17	0.7	23.67	1.3	23.90	0.4	23.73	1.1
32.0	32.29	0.9	—	—	32.14	0.4	—	—	—	—
32.0	32.38	1.2	—	—	32.00	0.0	—	—	—	—

high efficiency C_{18} column[6]. The mobile phase was methanol–water (15:85), which was filtered through a 0.45-μm pore filter[7] and degassed before use. The flow rate was 1.0 ml/min. The column was fitted with a precolumn packed with C_{18} Corasil 37–50 μm[8]. This precolumn was repacked once a week during panel use since particulate matter accumulated on the precolumn frit and would cause an increase in column pressure after the weekly load of 300 to 400 injections. The detector was set at a sensitivity of 0.2 aufs.

Plasma Acetaminophen Study in Humans—Patients were fasted overnight and were drug free for 72 hr prior to dosing. Each subject received a 650-mg oral dose of acetaminophen consisting of two 325-mg tablets taken with 100 ml of water. Venous blood specimens were withdrawn by syringe and discharged into centrifuge tubes containing heparin as an anticoagulant. Specimens were taken prior to and at specified times after drug administration through 1 hr. Collected specimens were centrifuged immediately for 15 min at 3500 rpm using a bench-top centrifuge. Plasma was separated and analyzed for free acetaminophen by the proposed method.

Analysis—One milliliter of freshly drawn plasma was added to a 16 × 100-mm screw top culture tube. To each tube was added 1 ml of the saturated 0.3 *N* $Ba(OH)_2$ solution. The tubes were vortexed at sufficient speed to ensure thorough mixing for 2 min on a multiple tube vortex mixer[9]. One milliliter of the 5% $ZnSO_4$ solution was then added to each sample which should have a milky opaque appearance. Each tube was capped and vortexed at high speed for 1 min. The tubes were then centrifuged in a bench-top centrifuge at high speed for 10 min. The resulting clear water-like supernatant was separated from the precipitate and filtered directly into an auto injector vial using a Pasteur pipet plugged

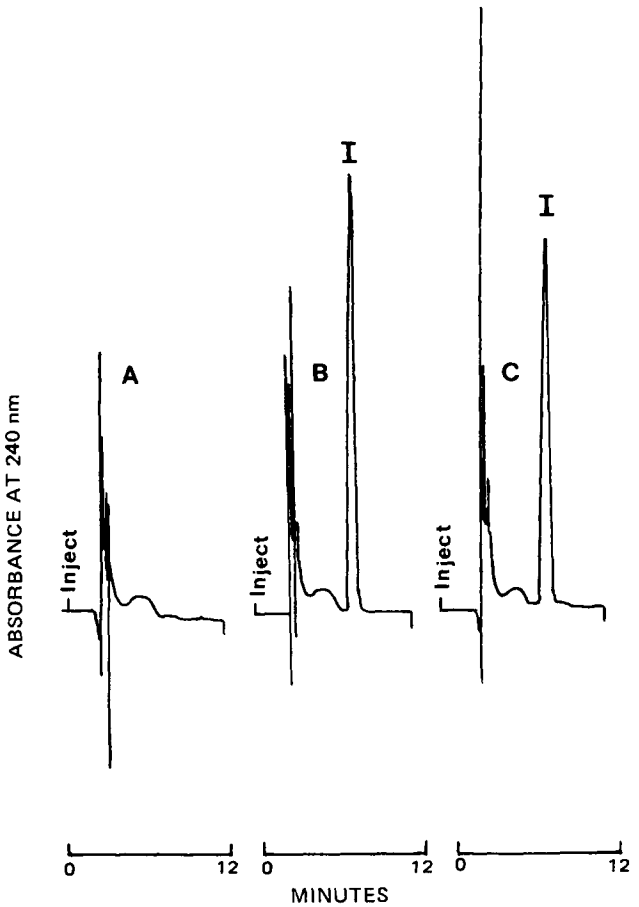

Figure 1—*Chromatograms for a typical subject. Key: (A) taken prior to acetaminophen (I) administration; (B) taken 20 min after oral administration of two 325-mg tablets; (C) taken 40-min postdosing.*

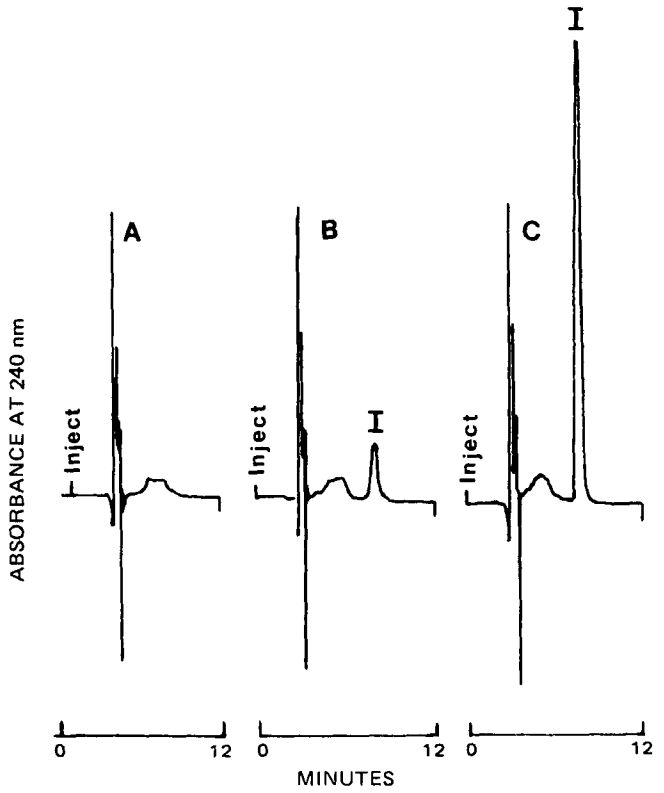

Figure 2—*Chromatograms of 1-ml human plasma sample processed by the described precipitation method. Key: (A) blank; (B) spiked with 1 μg of acetaminophen (I); (C) spiked with 8 μg of I. The mobile phase was 15% (v/v) methanol at a flow rate of 1.0 ml/min, and the chart speed was 15 cm/hr.*

[6] μ-Bondapak C_{18}, Waters Associates, Milford, Mass.
[7] Millipore Corp., Bedford, Mass.
[8] Waters Associates, Milford, Mass.
[9] Kraft Apparatus, Inc., Mineola, N.Y.

Table II—Comparison of Acetaminophen Levels in Plasma Analyzed Simultaneously by Plasma Protein Precipitation HPLC Assay and a Second Extraction Method

	Acetaminophen by Extraction				Acetaminophen by Precipitation–HPLC			
				Tablet A				
Time, min Subject	10	20	40	60	10	20	40	60
1	3.2	12.9	8.2	6.7	3.4	13.8	8.8	6.9
2	0.7	4.3	5.0	4.7	0.8	4.2	5.0	4.7
3	0	1.1	3.4	3.1	0	1.1	3.3	3.2
4	0.8	2.8	5.5	5.9	0.8	2.9	5.7	6.0
5	1.3	8.5	7.0	6.6	1.2	8.7	7.0	6.0
6	0	1.2	7.4	6.1	0	1.2	7.2	6.5
7	0	2.2	6.8	7.4	0	2.8	6.9	7.4
8	0	6.8	7.6	6.4	0	7.0	7.7	6.1
9	0.9	3.2	5.3	5.2	1.2	3.5	5.9	5.7
10	0	0.7	9.3	7.6	0	1.1	9.8	8.0
11	0.7	4.5	9.1	7.6	1.0	5.1	8.8	7.2
12	11.3	15.1	14.0	12.3	11.2	14.7	13.3	12.1
13	0	5.7	11.3	9.6	0	5.4	11.2	10.5
14	0	0.9	3.0	3.9	0	1.0	3.1	4.1
15	0	1.0	2.5	4.1	0	0.6	2.9	4.3
16	0	1.2	5.4	7.3	0	1.0	4.8	7.1
				Tablet B				
Time, min Subject	10	20	40	60	10	20	40	60
1	1.5	5.5	6.5	8.0	1.6	5.8	6.7	7.9
2	0	0.7	2.6	4.9	0	0.5	2.6	4.8
3	0	8.1	7.5	5.7	0	7.7	7.4	5.6
4	0	0	0.8	1.0	0	0	0.8	1.0
5	2.8	6.5	6.4	5.3	2.7	7.0	6.9	5.1
6	2.1	9.7	7.1	5.9	2.1	9.8	7.3	6.0
7	0	2.6	11.5	8.4	0	2.6	10.9	8.4
8	0	6.5	6.9	5.9	0	6.4	6.7	5.8
9	0	0.6	2.8	3.4	0	0.9	3.1	3.7
10	5.4	4.2	3.8	3.4	5.1	4.7	4.3	3.8
11	4.2	12.8	7.9	6.5	4.5	13.2	8.2	7.0
12	11.7	14.3	13.3	12.1	11.9	14.3	13.3	12.0
13	0.7	1.6	5.0	8.9	0.8	1.8	5.3	8.9
14	0	1.4	4.0	5.8	0	1.5	4.0	6.1
15	0	0	1.3	3.6	0	0	1.7	4.0
16	0	1.8	6.2	7.4	0	2.0	6.2	7.4
				Tablet C				
Time, min Subject	10	20	40	60	10	20	40	60
1	0.7	3.3	8.4	7.0	0.8	3.6	8.6	7.4
2	0	2.5	12.2	8.7	0	2.5	12.3	8.9
3	0	1.6	4.7	7.0	0	1.5	4.7	6.3
4	5.3	5.6	7.2	6.0	5.2	5.5	7.0	6.1
5	1.1	2.2	4.1	4.6	1.1	2.2	4.2	4.8
6	0	6.0	7.3	5.9	0	6.4	7.4	6.1
7	4.9	12.9	9.2	7.3	5.4	13.1	9.5	7.5
8	0	2.0	7.7	6.9	0	2.0	7.3	7.2
9	0	0	1.6	3.5	0	0	1.8	3.6
10	0	1.0	3.0	4.1	0	1.2	3.3	4.3
11	1.4	5.6	8.0	7.5	1.6	5.8	8.1	7.6
12	2.6	12.6	14.1	13.3	2.3	12.3	14.1	13.1
13	0.5	17.0	11.7	9.3	0.6	17.3	11.9	9.5
14	0	0.9	2.5	4.2	0	1.0	2.7	4.1
15	0	0	2.2	3.3	0	0	2.3	3.4
16	1.6	5.7	9.4	7.6	1.8	5.6	9.3	7.7

with glass wool. This ensured a minimal volume loss and a particulate-free sample.

Standard Curves—Calculations were carried out using standard curves constructed by analyzing 1-ml samples of the pooled predose plasma spiked with 1–32 μg of acetaminophen and plotting the area counts *versus* the corresponding concentration. The standard curve data were subjected to least-squares linear regression analysis, and the resulting equation was utilized for the calculation of the drug concentration in the unknown samples.

RESULTS AND DISCUSSION

Typical chromatograms of a predose plasma sample (Fig. 1A) and the 20- and 40-min postdose plasma samples (Fig. 1B and C) obtained for a typical subject, demonstrate the specificity of this method by the absence of interfering peaks. With 15% methanol in water as the eluent at a flow rate of 1.0 ml/min, the retention time for acetaminophen was 7 min. Additional peaks are observed eluting close to the solvent front. They are ascribed to the more polar metabolites of acetaminophen. Earlier elution of the acetaminophen is possible by increasing the methanol content of the mobile phase, but an occasional interfering peak was observed eluting close to the peak of interest.

Figure 2 represents the chromatograms of a 1-ml blank plasma sample, a 1-ml plasma sample spiked with 1 μg of acetaminophen, and a 1-ml plasma sample spiked with 8 μg of acetaminophen. The standards and samples are chromatographically clean to the extent that acetaminophen concentrations <1 μg/ml can be detected with this procedure. Since therapeutic acetaminophen levels normally encountered in blood plasma monitoring require detection of ≥1 μg/ml, the sensitivity of this method is more than adequate for use in blood level studies.

Recovery—The recovery of free acetaminophen from plasma relative to its recovery from water as measured by the ratio of the slopes of the

standard curves in plasma and water, respectively, was 0.94 ± 0.03 with a coefficient of variation of 3%. Interassay variability of the slope and y-intercept of the five standard curves generated during the bioavailability study had coefficients of variation of 2.7 and 8%, respectively. A typical calibration regression line is $y = 0.229x + 0.0296$ and is linear over a 1–32-μg/ml concentration range. The good linearity between the peak area and acetaminophen concentration in plasma is indicated by the correlation coefficient of $r > 0.999$.

Accuracy—Table I shows the actual amounts with which 1-ml blank plasma samples were spiked and the amounts found when the plasma was analyzed according to the described method. The experiment was performed in duplicate on each of 5 days. The percent error for each unknown sample was calculated according to (17):

$$\text{percent error} = \frac{\text{amount added} - \text{amount found}}{\text{amount added}} \times 100 \quad \text{(Eq.1)}$$

The average percent error was 2.2%. In no case did it exceed 7.0%.

Reliability—A comparison was made of acetaminophen levels determined by the described method with levels determined simultaneously by a previously validated extraction procedure. Table II shows the acetaminophen levels found with both methods for 16 subjects who had been studied on a three-way crossover with samples taken at 10, 20, 40, and 60 min postdosing. The comparison gave a correlation coefficient of 0.993. In addition, the application of a paired Student's t test and the Wilcoxon-Mann-Whitney rank-sum test to the two sets of data indicated at the 95% confidence level that there was no significant difference between results obtained by the two methods.

Summary—The proposed method is simple and sensitive for the rapid determination of nonconjugated acetaminophen in plasma or blood at levels likely to be encountererd after a usual 650- or 1000-mg total dose. Plasma proteins are denatured by the addition of a saturated $Ba(OH)_2$ solution and then precipitated with 5% $ZnSO_4$ solution. The resulting clear supernatant is analyzed by HPLC. The reproducibility, sensitivity, and selectivity of the method make the use of an internal standard unnecessary.

Since the major biotransformation of acetaminophen in humans is direct conjugation with sulfate and glucuronic acid to form the sulfate and glucuronic metabolites, these polar metabolites do not interfere in the assay as they are eluted along with the solvent. The accuracy and reliability of this method have been proven by comparison of results obtained with an established extraction procedure in over 400 comparative determinations.

REFERENCES

(1) J. Koch-Weser, *N. Engl. J. Med.*, **295,** 1297 (1976).

(2) G. Levy and H. Yamada, *J. Pharm. Sci.*, **60,** 215 (1971).

(3) F. Plakogiannis and A. Saad, *ibid.*, **67,** 581 (1978).

(4) G. Wilkinson, *Ann. Clin. Biochem.*, **13,** 435 (1976).

(5) J. I. Routh, N. A. Shane, E. G. Arrendondo, and W. D. Paul, *Clin. Chem.*, **14,** 882 (1968).

(6) J. W. Munson and H. Abdine, *J. Pharm. Sci.*, **67,** 1775 (1978).

(7) J. W. Munson, R. Weierstall, and H. B. Kostenbauder, *J. Chromatogr.*, **145,** 328 (1978).

(8) D. J. Miner and P. T. Kissinger, *J. Pharm. Sci.*, **68,** 96 (1979).

(9) R. A. Horvitz and P. I. Jatlow, *Clin. Chem.*, **23,** 1596 (1977).

(10) L. T. Wong, G. Solomonraj, and B. Thomas, *J. Pharm. Sci.*, **65,** 1064 (1976).

(11) M. Fowler and D. Altmiller, *Clin. Chem.*, **24,** 1007 (1978).

(12) J. C. West, *J. Anal. Toxicol.*, **5,** 118 (1981).

(13) B. R. Manno, J. E. Manno, C. Dempsey, and M. Wood, *ibid.*, **5,** 24 (1981).

(14) D. Blair and B. H. Rumack, *Clin. Chem.*, **23,** 743 (1977).

(15) M. J. Somogyi, *J. Biol. Chem.*, **160,** 69 (1945).

(16) H. M. Ederma, J. Skerpac, V. F. Cotty, and F. Sterbenz, "Use of Automated Systems in Drug Investigations, Automation in Analytical Chemistry," Technicon Symposia, 228 (1966).

(17) M. A. Schwartz and J. A. De Silva, in "Principles and Perspectives in Drug Bioavailability," J. Blanchard, R. W. Sawchuck, and B. B. Brodie, Eds., S. Karger, Basel, Switzerland, 1979, p. 92.

Pharmacokinetics of Bretylium in Dogs and the Effect of Hemoperfusion on Elimination

B. L. KAMATH *§, T. P. GIBSON ‡, Z. M. LOOK *, C. M. McENTEGART *, E. B. COMRIE *, and A. YACOBI *x

Received September 25, 1981, from the **Research and Development Department, American Critical Care, McGaw Park, IL 60085,* and the ‡*Section of Nephrology/Hypertension and Department of Medicine, Northwestern University Medical School, Northwestern Memorial Hospital and Veterans Administration Lakeside Medical Center, Chicago, IL 60611.* Accepted for publication January 29, 1982.

§ Present address: Xavier University, New Orleans, LA 70125.

Abstract □ The pharmacokinetics of bretylium in dogs and the efficacy of hemoperfusion with a resin column in its removal from the body following intravenous administration of bretylium tosylate were investigated. Five mongrel dogs weighing 18–26 kg were given a bolus dose of 15 mg/kg. Serial blood samples were taken for 24 hr. Hemoperfusion, through a resin column, was then initiated and continued for 4 hr under pentobarbital anesthesia. During hemoperfusion, arterial and venous blood samples were collected several times; venous blood samples were then withdrawn for an additional 8 hr. Urine was collected from each dog in three portions for up to 48–54 hr. Pharmacokinetics of bretylium in dogs could be characterized by a two-compartment open model with a distribution half-life of 7 min and biological half-life of 15.9 ± 1.9 hr. Plasma levels declined rapidly from ~20 μg/ml at 6 min to <2 μg/ml within 1 hr. The ratio of intercompartmental rate constants, k_{12}/k_{21}, was 16.7, and the volume of the central compartment and apparent volume of distribution were 0.245 and 5.22 liter/kg, respectively, indicating a wide distribution of bretylium into the tissues. Plasma dialysis clearance averaged 29.7 ml/min, which is 30% of the total body clearance (98.8 ml/min). These data suggest that resin hemoperfusion may not be useful in the treatment of bretylium intoxication.

Keyphrases □ Pharmacokinetics—bretylium and the effect of hemoperfusion on elimination, distribution, dogs □ Bretylium—pharmacokinetics and the effect of hemoperfusion on elimination, distribution, dogs □ Distribution—pharmacokinetics of bretylium and the effect of hemoperfusion on elimination, dogs

Bretylium tosylate is a quaternary ammonium compound used in the treatment of ventricular tachycardia or ventricular fibrillation. It has been demonstrated that bretylium increases the action potential duration along the entire left ventricular conducting system (1).

In humans and rats, bretylium is primarily eliminated unchanged *via* the kidneys. No metabolites have been identified following administration of bretylium in humans (2–5). A half-life of 9.75 ± 4.19 (*SD*) hr in eight patients aged 48.4 ± 10.8 years has been reported (6). The longest

0022-3549/82/1100-1294$01.00/0

standard curves in plasma and water, respectively, was 0.94 ± 0.03 with a coefficient of variation of 3%. Interassay variability of the slope and y-intercept of the five standard curves generated during the bioavailability study had coefficients of variation of 2.7 and 8%, respectively. A typical calibration regression line is $y = 0.229x + 0.0296$ and is linear over a 1–32-μg/ml concentration range. The good linearity between the peak area and acetaminophen concentration in plasma is indicated by the correlation coefficient of $r > 0.999$.

Accuracy—Table I shows the actual amounts with which 1-ml blank plasma samples were spiked and the amounts found when the plasma was analyzed according to the described method. The experiment was performed in duplicate on each of 5 days. The percent error for each unknown sample was calculated according to (17):

$$\text{percent error} = \frac{\text{amount added} - \text{amount found}}{\text{amount added}} \times 100 \quad \text{(Eq.1)}$$

The average percent error was 2.2%. In no case did it exceed 7.0%.

Reliability—A comparison was made of acetaminophen levels determined by the described method with levels determined simultaneously by a previously validated extraction procedure. Table II shows the acetaminophen levels found with both methods for 16 subjects who had been studied on a three-way crossover with samples taken at 10, 20, 40, and 60 min postdosing. The comparison gave a correlation coefficient of 0.993. In addition, the application of a paired Student's t test and the Wilcoxon-Mann-Whitney rank-sum test to the two sets of data indicated at the 95% confidence level that there was no significant difference between results obtained by the two methods.

Summary—The proposed method is simple and sensitive for the rapid determination of nonconjugated acetaminophen in plasma or blood at levels likely to be encountererd after a usual 650- or 1000-mg total dose. Plasma proteins are denatured by the addition of a saturated $Ba(OH)_2$ solution and then precipitated with 5% $ZnSO_4$ solution. The resulting clear supernatant is analyzed by HPLC. The reproducibility, sensitivity, and selectivity of the method make the use of an internal standard unnecessary.

Since the major biotransformation of acetaminophen in humans is direct conjugation with sulfate and glucuronic acid to form the sulfate and glucuronic metabolites, these polar metabolites do not interfere in the assay as they are eluted along with the solvent. The accuracy and reliability of this method have been proven by comparison of results obtained with an established extraction procedure in over 400 comparative determinations.

REFERENCES

(1) J. Koch-Weser, *N. Engl. J. Med.*, **295,** 1297 (1976).

(2) G. Levy and H. Yamada, *J. Pharm. Sci.*, **60,** 215 (1971).

(3) F. Plakogiannis and A. Saad, *ibid.*, **67,** 581 (1978).

(4) G. Wilkinson, *Ann. Clin. Biochem.*, **13,** 435 (1976).

(5) J. I. Routh, N. A. Shane, E. G. Arrendondo, and W. D. Paul, *Clin. Chem.*, **14,** 882 (1968).

(6) J. W. Munson and H. Abdine, *J. Pharm. Sci.*, **67,** 1775 (1978).

(7) J. W. Munson, R. Weierstall, and H. B. Kostenbauder, *J. Chromatogr.*, **145,** 328 (1978).

(8) D. J. Miner and P. T. Kissinger, *J. Pharm. Sci.*, **68,** 96 (1979).

(9) R. A. Horvitz and P. I. Jatlow, *Clin. Chem.*, **23,** 1596 (1977).

(10) L. T. Wong, G. Solomonraj, and B. Thomas, *J. Pharm. Sci.*, **65,** 1064 (1976).

(11) M. Fowler and D. Altmiller, *Clin. Chem.*, **24,** 1007 (1978).

(12) J. C. West, *J. Anal. Toxicol.*, **5,** 118 (1981).

(13) B. R. Manno, J. E. Manno, C. Dempsey, and M. Wood, *ibid.*, **5,** 24 (1981).

(14) D. Blair and B. H. Rumack, *Clin. Chem.*, **23,** 743 (1977).

(15) M. J. Somogyi, *J. Biol. Chem.*, **160,** 69 (1945).

(16) H. M. Ederma, J. Skerpac, V. F. Cotty, and F. Sterbenz, "Use of Automated Systems in Drug Investigations, Automation in Analytical Chemistry," Technicon Symposia, 228 (1966).

(17) M. A. Schwartz and J. A. De Silva, in "Principles and Perspectives in Drug Bioavailability," J. Blanchard, R. W. Sawchuck, and B. B. Brodie, Eds., S. Karger, Basel, Switzerland, 1979, p. 92.

Pharmacokinetics of Bretylium in Dogs and the Effect of Hemoperfusion on Elimination

B. L. KAMATH *§, T. P. GIBSON ‡, Z. M. LOOK *, C. M. McENTEGART *, E. B. COMRIE *, and A. YACOBI *x

Received September 25, 1981, from the **Research and Development Department, American Critical Care, McGaw Park, IL 60085,* and the ‡*Section of Nephrology/Hypertension and Department of Medicine, Northwestern University Medical School, Northwestern Memorial Hospital and Veterans Administration Lakeside Medical Center, Chicago, IL 60611.* Accepted for publication January 29, 1982.

§ Present address: Xavier University, New Orleans, LA 70125.

Abstract □ The pharmacokinetics of bretylium in dogs and the efficacy of hemoperfusion with a resin column in its removal from the body following intravenous administration of bretylium tosylate were investigated. Five mongrel dogs weighing 18–26 kg were given a bolus dose of 15 mg/kg. Serial blood samples were taken for 24 hr. Hemoperfusion, through a resin column, was then initiated and continued for 4 hr under pentobarbital anesthesia. During hemoperfusion, arterial and venous blood samples were collected several times; venous blood samples were then withdrawn for an additional 8 hr. Urine was collected from each dog in three portions for up to 48–54 hr. Pharmacokinetics of bretylium in dogs could be characterized by a two-compartment open model with a distribution half-life of 7 min and biological half-life of 15.9 ± 1.9 hr. Plasma levels declined rapidly from ~20 μg/ml at 6 min to <2 μg/ml within 1 hr. The ratio of intercompartmental rate constants, k_{12}/k_{21}, was 16.7, and the volume of the central compartment and apparent volume of distribution were 0.245 and 5.22 liter/kg, respectively, indicating a wide distribution of bretylium into the tissues. Plasma dialysis clearance averaged 29.7 ml/min, which is 30% of the total body clearance (98.8 ml/min). These data suggest that resin hemoperfusion may not be useful in the treatment of bretylium intoxication.

Keyphrases □ Pharmacokinetics—bretylium and the effect of hemoperfusion on elimination, distribution, dogs □ Bretylium—pharmacokinetics and the effect of hemoperfusion on elimination, distribution, dogs □ Distribution—pharmacokinetics of bretylium and the effect of hemoperfusion on elimination, dogs

Bretylium tosylate is a quaternary ammonium compound used in the treatment of ventricular tachycardia or ventricular fibrillation. It has been demonstrated that bretylium increases the action potential duration along the entire left ventricular conducting system (1).

In humans and rats, bretylium is primarily eliminated unchanged *via* the kidneys. No metabolites have been identified following administration of bretylium in humans (2–5). A half-life of 9.75 ± 4.19 (*SD*) hr in eight patients aged 48.4 ± 10.8 years has been reported (6). The longest

0022-3549/82/1100-1294$01.00/0

Table I—Pharmacokinetic Parameters of Bretylium in Dogs

Parameter	Preperfusion Data			Pre- and Postperfusion Data		Mean	*SD*
	217	224	256	289	299		
α (hr^{-1})	7.61	5.11	5.30	6.93	6.76	6.34	1.09
$t_{1/2}$, α (min)	5.46	8.14	7.85	6.00	6.15	6.72	1.20
β (hr^{-1})	0.043	0.051	0.044	0.045	0.037	0.044	0.005
$t_{1/2}$, β (hr)	16.20	13.50	15.90	15.40	18.70	15.90	1.87
k_{12} (hr^{-1})	6.02	3.95	4.37	5.34	5.76	5.09	0.894
k_{21} (hr^{-1})	0.233	0.279	0.405	0.221	0.382	0.304	0.085
k_{10} (hr^{-1})	1.40	0.942	0.569	1.42	0.655	0.997	0.401
V_c (liter/kg)	0.189	0.273	0.294	0.204	0.265	0.245	0.046
$V_{d,\beta}$ (liter/kg)	6.18	5.01	3.84	6.40	4.68	5.22	1.07
TBC (liter/hr/kg)	0.265	0.258	0.167	0.289	0.174	0.231	0.056
Percent Dose in Urine							
Collection period, hours	54.0	48.0	48.0	56.0	54.0		
Recovery, %	102.2	72.6	73.6	72.0	74.1	78.9	13.1

half-lives were found in the oldest patients, which would be consistent with the reduction in the renal function known to occur with aging. More recently, an average half-life of 8.1 hr for normal subjects and 16.1 and 31.5 hr for two patients with creatinine clearance of 21.0 and 1.0 ml/min, respectively, has been reported (3, 4). As renal function declines, dosage alteration may be required to avoid toxicity. A half-life of 13.6 hr has been reported (5) for 10 normal volunteers given 5 mg/kg iv of bretylium.

The purpose of this investigation was to study the efficacy of hemoperfusion with a clinically used resin[1] column in the removal of bretylium from the body following intravenous administration of bretylium tosylate to dogs. This resin[1] is a macroreticular copolymer of styrene and divinyl benzene with a surface area of 750 m^2/g, a porosity of 51%, and an affinity for lipid-soluble materials. This column is used clinically to treat intoxication (7).

EXPERIMENTAL

Five mongrel dogs weighing 23.3 ± 3.1 (*SD*) kg were randomly selected. Each dog received a rapid intravenous bolus dose of 15 mg/kg bretylium tosylate[2]. Blood samples (3 ml each) were taken frequently during the first 2 hr for characterization of distribution phase and then every 2–4 hr for the next 14–18 hr and at 24 hr to characterize the elimination phase.

Twenty-four hours after administration of bretylium, the dogs were hemoperfused for 4 hr using clinically available columns[3] containing 312 ± 15 g (dry weight) of loosely packed resins[1]. Immediately prior to hemoperfusion, the animals were anesthetized with pentobarbital (30 mg/kg iv) and intubated with an endotracheal tube. A femoral artery and vein were cannulated, and 10,000 U of heparin was given. The extracorporeal circuit (~300 ml) was washed with 3 liters of normal saline containing 1000 U/liter of heparin and primed with the same solution. The primer was infused at the beginning of hemoperfusion. Blood was pumped through the circuit at a constant antigravity flow of ~112 ml/min as determined by timed collections of saline before and after each experiment.

During hemoperfusion samples of blood were withdrawn from the arterial (inlet) and venous (outlet) lines at 0.5, 1.0, 2.0, 3.0, and 4.0 hr following the start of hemoperfusion. At the conclusion of hemoperfusion, blood was returned to the dog by gravity. The artery and vein were then closed and blood sampled for an additional 8 hr. Immediately after the collection of blood samples, they were centrifuged and plasma was separated and frozen until assayed. The hematocrit of all blood samples taken during hemoperfusion was measured.

After the hemoperfusion, the column was eluted with methanol to remove all the adsorbed bretylium. The final volume was measured and an aliquot was stored for bretylium assay.

Quantitative urine samples were collected from each dog and divided into three time intervals: prehemoperfusion, during, and posthemoperfusion urine. Aliquots were frozen until assayed for bretylium.

Bretylium Assay—Plasma, urine, and methanol eluate of the hemoperfusion column were assayed for bretylium as described previously (8). The sensitivity of this procedure was not sufficient enough to determine the bretylium levels in the methanol eluate. Therefore, the same eluate was concentrated 10–50 times and assayed again.

Pharmacokinetic Analysis—The prehemoperfusion plasma concentration *versus* time profiles were fitted to a two-compartment open model using the NLIN procedure (9). Pharmacokinetic parameters were obtained for three of the five dogs (numbers 217, 224, and 256). For dogs 289 and 299, the best fit was obtained when the postperfusion plasma concentrations were used. Bretylium plasma dialysis clearance during hemoperfusion (Cl_d) was calculated as previously described (10):

$$Cl_d = Q_p(A - V)/A$$

where Q_p is plasma flow, and A and V are arterial and venous plasma concentrations of bretylium, respectively.

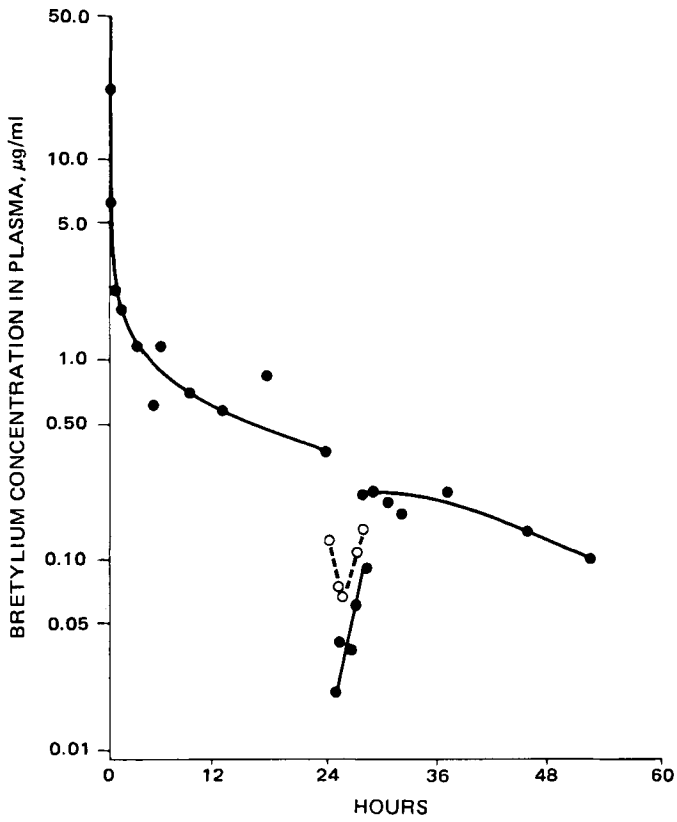

Figure 1—*Semilogarithmic plot of plasma concentrations of bretylium versus time following intravenous administration of bretylium tosylate, 15 mg/kg, in one dog (No. 217). Hemoperfusion was done 24 hr after administration of the drug. Key: (●) venous concentrations; (○) arterial concentrations; the solid line, through the first 24 hr, represents the least-squares computer fit.*

[1] Amberlite XAD-4, Extracorporeal Medical Specialties, Inc., King of Prussia, Pa.
[2] Bretylol, American Critical Care, McGaw Park, Ill.
[3] Extracorporeal Medical Specialties, Inc., King of Prussia, Pa.

Table II—Hemoperfusion Parameters in Dogs

Parameter	217	224	256	289	299	Mean	*SD*
Weight (kg)	24.9	26.1	18.1	24.0	23.6	23.3	3.1
Hematocrit	40.7	40.3	37.5	28.3	32.9	35.9	5.3
Blood flow (ml/min)	115.0	110.6	106.0	116.3	114.0	112.4	4.1
Plasma flow (ml/min)	68.2	66.0	66.3	83.4	76.5	72.1	7.63
Cl_d[a] (ml/min)	35.4	23.1	49.7	19.3	20.9	29.7	12.8
TBC[b] (ml/min)	110.2	112.4	87.4	115.8	68.4	98.8	20.4

[a] Plasma dialysis clearance during hemoperfusion. [b] Preperfusion total body clearance.

RESULTS AND DISCUSSION

The plasma concentration *versus* time plot, for a typical dog, is shown in Fig. 1. Immediately after the intravenous dose of 15 mg/kg, bretylium is distributed rapidly in the body. The plasma levels decreased from ~20 μg/ml at 6 min to <2 μg/ml within 1 hr. During the elimination phase, the levels declined more slowly with an average half-life of ~16 hr. In three dogs (217, 224, and 256), the preperfusion elimination phases were well defined with a half-life ranging from 13.5–16.2 hr. In dogs 289 and 299, the plasma concentrations could be best fitted to the model by using also the postperfusion data that were in line with the preperfusion levels.

Pharmacokinetic parameters, derived constants, and the means, are listed in Table I. The parameters were in good agreement in all dogs. As seen from Table I, bretylium is widely distributed in the body, with a volume of distribution of 5.22 liter/kg (±1.07) and a very small volume of central compartment of 0.245 ± 0.046 liter/kg. The average distribution half-life was 6.72 min. The intercompartmental rate constants, k_{12} and k_{21}, were 5.09 and 0.304 hr^{-1}, respectively. The extremely large volume of distribution and the very high ratio of k_{12}/k_{21} (16.7) signify strong affinity of bretylium to the tissues in the peripheral compartment. Earlier studies in dogs and rats (11, 12, and unpublished data) have shown an extremely high affinity of bretylium to the myocardium, with heart to plasma concentration ratio >20. The heart was found to be a part of the peripheral compartment in rats (12). The elimination rate constant, k_{10}, averaged 1.0 hr^{-1}, with a total body clearance (TBC) of 0.231 liter/hr/kg or 3.85 ml/min/kg.

The percentage of dose recovered in urine collected during the study period is also shown in Table I. An average of 79% of the dose was recovered unchanged in urine 48–54 hr following intravenous administration, and only an insignificant amount was cleared during hemoperfusion through the column. Available data on glomerular filtration rate in dogs (13) show that it ranges from 3.33–4.75 ml/min/kg. Total body clearance of bretylium in the dogs was 3.85 ml/min/kg and the renal clearance was ~3.0 ml/min/kg. These values indicate that bretylium might not be eliminated by an active mechanism in dogs. In humans and rats, bretylium is excreted extensively by active tubular secretion (4, 12).

A hemoperfusion 24 hr after the bretylium tosylate dose caused an immediate decrease (twofold–tenfold) in the arterial as well as venous plasma levels within 1 hr; this was followed by a gradual increase and reached a normal expected level by the completion of hemoperfusion in all animals (Fig. 1). Pertinent hemoperfusion parameters for each dog are given in Table II. Plasma dialysis clearance (Cl_d) averaged 29.7 ± 12.8 ml/min or 30% of the endogenous (preperfusion) TBC. The actual amount of bretylium removed from each dog *via* hemoperfusion and, consequently, recovery clearance (14) could not be calculated.

The rapid fall in the plasma concentration (central compartment), due to perfusion clearance, causes a shift in the equilibrium between the two compartments resulting in redistribution of bretylium from the peripheral compartment to the central compartment. When the rate of this redistribution exceeds the clearance from the central compartment, ~1 hr following the initiation of hemoperfusion, the plasma concentration rises (Fig. 1).

The efforts to determine the concentration of bretylium in the methanol eluate of the perfusion column did not succeed because the concentration was below the detection limit of 10 ng/ml. Concentrating the eluate, 10- to 50-fold, did not indicate a significant removal of bretylium by the column. Because of low bretylium concentrations and high background, the gas chromatogram did not provide any meaningful data. Even assuming a 10-ng/ml concentration of the eluate, the total amount removed would not be >10 μg total. Theoretically, the rate of removal of drug from plasma depends on the concentration in plasma. Because of the wide distribution in the tissues, *i.e.*, very large k_{12}/k_{21}, the plasma concentrations are very low and the rate of removal is very slow. These data are quite similar to those after digoxin in dogs and confirm that the rate-limiting step may be the clearance from tissues and not from plasma (15).

After the hemoperfusion was stopped, the plasma levels increased further till a new equilibrium was reached. Thereafter, levels declined exponentially as shown in Fig. 1. The plasma levels in the postperfusion equilibrium phase were very close to the levels that could be predicted by extrapolation of the curve fitted to the preperfusion data. This fact indicates that (resin) hemoperfusion may not be capable of substantially increasing the total body clearance of bretylium in subjects with normal renal function. Similar increase in the plasma levels after hemoperfusion has also been demonstrated for digoxin (15) and has been attributed to reequilibration of digoxin between two compartments.

In patients with severely impaired renal function, in whom the plasma concentrations are relatively high and the total body clearance of bretylium is markedly reduced, it is not clear whether resin hemoperfusions will be of any benefit in removing the drug. However, marked differences may exist in the ability of different commercially available hemoperfusion devices to remove a specific drug (16). Therefore, the results of this study should not be taken to indicate that hemoperfusion with other devices will produce identical results.

This study describes the pharmacokinetics of bretylium in dogs and demonstrates that hemoperfusion with a resin column does not remove bretylium equilibrated in the body. These data suggest that resin hemoperfusion may not be useful in the treatment of human bretylium intoxication.

REFERENCES

(1) R. Cardinal and B. I. Sasyniuk, *J. Pharmacol. Exp. Ther.*, **204,** 159 (1978).

(2) R. Kuntzman, I. Tsai, R. Chang, and A. H. Conney, *Clin. Pharmacol. Ther.*, **11,** 829 (1970).

(3) J. Adir, P. K. Narang, J. Josselson, and J. Sadler, *N. Engl. J. Med.*, **300,** 1390 (1979).

(4) P. K. Narang, J. Adir, J. Josselson, A. Yacobi, and J. Sadler, *J. Pharmacokinet. Biopharm.*, **8,** 363 (1980).

(5) J. L. Anderson, E. Patterson, J. G. Wagner, J. R. Stewart, H. R. Behm, and B. R. Lucchesi, *Clin. Pharmacol. Ther.*, **28,** 468 (1980).

(6) D. W. Romhilt, S. S. Bloomfield, R. J. Lipicky, R. M. Welch, and N. O. Fowler, *Circulation*, **45,** 880 (1972).

(7) J. F. Winchester, M. C. Gelfand, J. H. Knepshield, and G. E. Schreiner, *ASAIO J.*, **23,** 762 (1977).

(8) C. M. Lai, B. L. Kamath, J. E. Carter, P. Erhardt, Z. M. Look, and A. Yacobi, *J. Pharm. Sci.*, **69,** 681 (1980).

(9) "SAS User's Guide," 1979 ed., SAS Institute, Inc., Raleigh, N.C.

(10) G. Shah, H. A. Nelson, A. J. Atkinson, Jr., G. T. Okita, P. Ivanovich, and T. P. Gibson, *J. Lab. Clin. Med.*, **93,** 370 (1979).

(11) J. L. Anderson, E. Patterson, M. Conlon, S. Pasyk, B. Pitt, and B. R. Lucchesi, *Am. J. Cardiol.*, **46,** 583 (1980).

(12) B. L. Kamath, H. F. Stampfli, C. M. Lai, and A. Yacobi, *J. Pharm. Sci.*, **70,** 667 (1981).

(13) E. M. Renkin and J. P. Gilmore, in "Handbook of Physiology, Section 8: Renal Physiology," J. Orloff, R. W. Berliner, and S. R. Geiger, Eds., American Physiological Society, Washington, D.C., 1973, p. 229.

(14) T. P. Gibson, E. Matusek, L. D. Nelson, and W. A. Briggs, *Clin. Pharmacol. Ther.*, **20,** 720 (1976).

(15) T. P. Gibson, S. V. Lucas, H. A. Nelson, A. J. Atkinson, Jr., Okita, G. T., and P. Ivanovich, *J. Lab. Clin. Med.*, **91,** 673 (1978).

(16) T. P. Gibson, *Kidney Int.*, **18,** S101 (1980).

ACKNOWLEDGMENTS

This work was supported in part by the Research and Development Service of the Veterans Administration; the Clinical Research Center of Northwestern University, RR-48, Division of Research Resources, National Institutes of Health; and the Kidney Research Fund of Northwestern Memorial Hospital.

Determination of Sodium Fusidate and Fusidic Acid In Dosage Forms by High-Performance Liquid Chromatography and a Microbiological Method

AHMED H. HIKAL ˣ, ATEF SHIBL, and SAMMY EL-HOOFY

Received November 2, 1981, from the *Department of Pharmaceutics, College of Pharmacy, King Saud University of Riyadh, Riyadh, Saudi Arabia.* Accepted for publication January 21, 1982.

Abstract □ A new High-performance liquid chromatographic (HPLC) method for the assay of sodium fusidate (I) or fusidic acid in dosage forms was developed and compared to a microbiological assay. A linear relationship was obtained between absolute peak area and amount of I (r = 0.99+) in the 50–1000-μg/ml range. In the microbiological assay, *Staphylococcus aureus* (NCTC 6571) was the test organism, using an agar diffusion technique. With five test levels of the standard, potencies were interpolated from standard curve using a log transformation straight-line method with least-squares fitting (r = 0.99+). Both methods were applied to assay I (or fusidic acid) in tablets, a suspension, and an ointment. Excellent agreement was observed between results of the two methods.

Keyphrases □ Fusidate sodium—determination in dosage forms, high-performance liquid chromatography, microbiological method, tablets, suspension, ointment □ Fusidic acid—determination in dosage forms, sodium fusidate, high-performance liquid chromatography, microbiological method, tablets, suspension, ointment □ High-performance liquid chromatography—determination of fusidate sodium and fusidic acid in dosage forms, microbiological method, tablets, suspension, ointment

Fusidic acid is an antibiotic produced by the growth of certain strains of *Fusidium coccineum* (K. Tubaki). Its structure is related to helvolic acid and to cephalosporins. The structure also includes the cyclopentanoperhydrophenanthrene ring system, thus, it belongs to the steroid group of substances. Fusidic acid, or its sodium salt, shows a very high antistaphylococcal activity (1, 2). Available methods for the quantitative determination of fusidic acid are based mainly on microbiological procedures (3, 4). A colorimetric assay has been reported (5) which involved modification of an earlier sulfuric acid color test for steroids and measurement in the visible range of the spectrum (365–595 nm). Microbiological procedures are, by nature, time consuming and call for specialized technique, while the colorimetric assay involves the added steps of producing the color.

The present report describes a simple, sensitive, and specific procedure for the quantitative determination of fusidic acid and its sodium salt using high-performance liquid chromatography (HPLC). This new procedure was compared to a microbiological assay and was applied to the determination of fusidic acid or its sodium salt in tablets, a suspension, and an ointment.

EXPERIMENTAL

Reagents—Sodium fusidate, BP[1], was purified by crystallization from absolute ethanol before use. All other chemicals were USP or analytical reagent grade, and were used as obtained. All solvents were spectroscopic or chromatographic grade; water used in the mobile phase was double-distilled in an all-glass still. Drug products containing sodium fusidate or fusidic acid were purchased from commercial sources.

[1] Leo Pharmaceutical Products, Ballerup, Switzerland, lot no. 22176.

Apparatus—The liquid chromatograph[2] used was equipped with an automatic sample injector[3], a variable wavelength detector[4] set at 254 nm, a dual-pen recorder[5], and a data system[6]. The column was stainless steel 30 cm × 4-mm i.d. packed with microparticulate silica (5 μm) bonded with octadecylsilane[7]. Experiments were conducted at ambient temperature (25°).

Mobile Phase—The mobile phase consisted of a 3:1 mixture of

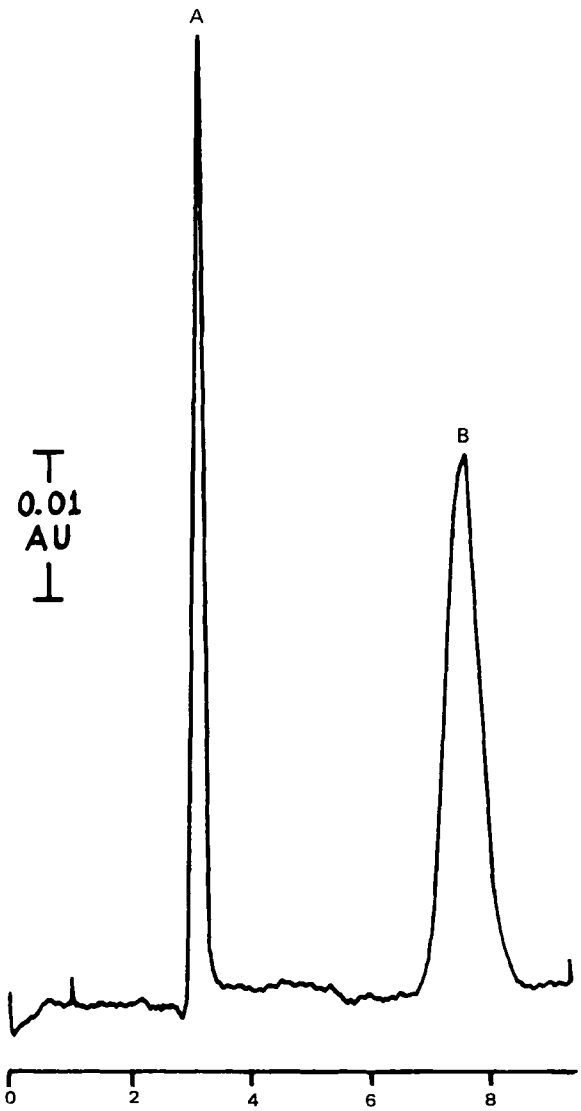

Figure 1—*Chromatogram of extract of sodium fusidate tablets. Key: (A) unassigned peak; (b) sodium fusidate.*

[2] Model 5021, Varian Instrument Group, Palo Alto, Calif.
[3] Model 8055, Varian Instrument Group.
[4] Model UV-50 Varian Instrument Group.
[5] Model 9176, Varian Instrument Group.
[6] Model CDS 111L, Varian Instrument Group.
[7] Micropak MCH, Varian Instrument Group.

0022-3549/82/1100-1297$01.00/0

Table I—Percent of Label Sodium Fusidate or Fusidic Acid Found in Dosage Forms

Dosage Form	Run Number	HPLC Method	Microbiological Method
Tablets	1	96.70	98.80
	2	93.22	95.60
	3	89.90	92.10
	4	95.07	94.50
	5	95.70	91.86
	6	87.90	86.81
	Mean ± *SD*	93.08 ± 3.49	93.28 ± 4.06
Suspension	1	100.47	98.71
	2	108.13	108.66
	3	102.13	104.57
	4	103.81	97.21
	5	105.84	100.00
	6	100.52	99.86
	Mean ± *SD*	103.48 ± 3.06	101.50 ± 4.29
Ointment	1	94.40	94.45
	2	101.60	100.00
	3	99.52	99.36
	4	101.93	100.00
	5	103.80	100.00
	6	99.97	94.50
	Mean ± *SD*	100.20 ± 3.23	98.05 ± 2.78
Overall	Mean ± *SD*	97.42 ± 8.77	97.61 ± 4.96

methanol[8] and 0.01 *M* KH_2PO_4 (pH ~6.6, not adjusted), at a flow rate of 2 ml/min.

Calibration Curve—Using the mobile phase as the solvent, nine different solutions of fusidate sodium were prepared to cover the 50–1000-μg/ml range. Duplicate injections of 10 μl were made, and the peak area was plotted against concentration. The line of best fit was calculated by linear regression, and was used to determine concentrations of the test solutions. The standard solutions were interspersed with solutions obtained from the extraction of dosage forms (see below), and all were run on the same working day.

Extraction Procedure—*Tablets*[9]—Six tablets were individually crushed in glass stoppered flasks, and shaken with 100 ml of methanol for 30 min. The extract was filtered through a membrane filter[10]. A 10-ml aliquot was diluted with 65 ml of methanol and 25 ml of 0.01 *M* KH_2PO_4 for HPLC assay. A 1-ml aliquot was used for microbiological assay as described below.

Suspension[11]—After shaking the bottle thoroughly, six 5-ml aliquots were pipeted using a wide-mouthed pipet, individually placed in 100-ml volumetric flasks, and treated with 0.5 ml of 1 N NaOH solution. Methanol was then added to volume, and the solution was filtered through a membrane filter[10].

Ointment[12]—Six 1-g aliquots were accurately weighed in small beakers and individually extracted as follows: Five milliliters of benzene was added, the mixture was transferred to a separatory funnel, and extracted with three 10-ml portions of 0.01 N NaOH. The combined aqueous extracts were filtered through a membrane filter[13]. A 10-ml aliquot was diluted with the mobile phase to a concentration of ~200 μg/ml for HPLC assay. A 1-ml aliquot was used for microbiological assay as described below.

Microbiological Assay—Aliquots obtained from extraction of tablets or suspension were evaporated at 50° and redissolved in 10 ml of saline. Solutions were transferred to 100-ml volumetric flasks, and saline was added to volume. Aliquots obtained from extraction of ointment were placed in 50-ml volumetric flasks, and saline was added to volume. An agar plate diffusion technique was employed using *Staphylococcus aureus* (NCTC 6571) as the test organism. A 1:10 dilution of an 18-hr culture in antibiotic assay broth[14] was added to melted and cooled (50°) antibiotic assay agar medium[14], mixed thoroughly, and poured into replica plate petri dishes. After the agar had solidified, wells (4-mm i.d.) were punched out, and a drop of a standard or test dilution was applied. Standard dilutions contained 10, 5, 2.5, 1.25, or 0.625 μg/ml of fusidate sodium in saline. Test solutions were diluted similarly. The zone of inhibition diameter was measured after an 18-hr incubation at 37°. Potencies were interpolated from a standard curve using a log transformation straight-line method with least-squares fitting.

RESULTS AND DISCUSSION

Inasmuch as fusidic acid is structurally related to steroid hormones, HPLC conditions that previously (6, 7) have been employed for steroid hormones were tried before the conditions described herein were selected. Under the experimental conditions described, sodium fusidate showed a single peak with a retention time of 7.4 min. A plot of peak area *versus* concentration produced a linear relationship (r for the least-squares line = 0.999, y-intercept = −294851, and slope = 22456); thus, no internal standard was needed. Figure 1 shows a representative chromatogram of the solution obtained from the extraction of tablets. It can be seen that the chromatogram shows an additional peak prior to the fusidate sodium peak. A similar peak appeared in the chromatogram of the solution obtained from the suspension. These additional peaks may be caused by formula additives or decomposition products; however, no definite assignment can be made at present. The absence of any interference with the sodium fusidate peak is an indication of the specificity of this procedure.

Table I gives the results of assaying commercial dosage forms by HPLC and by microbiological procedure. Good agreement is seen between results of the two methods. When six tablets were assayed by both methods, the mean (±*SD*) percent of labeled amount was 93.08 ± 3.49 by HPLC, and 93.28 ± 4.06 by microbiological procedure. The mean (±*SD*) percent of labeled amount obtained in the assay of the suspension was 103 ± 3.06 by HPLC and 101 ± 4.29 by microbiological method. HPLC assay of the ointment gave a mean (±*SD*) percent of labeled amount of 100.20 ± 3.23 compared to 98.05 ± 2.78 obtained by the microbiological method.

Microbiological procedures require considerable expenditure of time and effort and call for specialized skills. The HPLC procedure described is simple, sensitive, specific, and can be applied in routine quality control.

REFERENCES

(1) E. F. Scowen and L. P. Garrod, *Lancet*, **i**, 933 (1962).

(2) B. Dodson, *Br. Med. J.*, **1**, 190 (1963).

(3) Y. Kanazawa and T. Kuramata, *J. Antibiot., Ser. B.*, **17**, 7 (1964).

(4) J. Williamson, F. Russell, W. M. Doig, and R. W. W. Paterson, *Br. J. Ophthalmol.*, **54**, 126 (1970).

(5) J. E. Presser, F. T. Wilkomirsky, and A. J. Brieva, *Rev. Real Acad. Cienc. Exactas., Fis. Natur. Madrid*, **59**, 237 (1965); through Chem. Abstr., **64**, 6409a (1966).

(6) V. D. Gupta, *J. Pharm. Sci.*, **67**, 299 (1978).

(7) M. D. Smith, *ibid.*, **69**, 960 (1980).

[8] BDH Chemicals, Ltd., Poole, England.

[9] Fucidin Leo, fusidate sodium, 250 mg/tablet, Leo Pharmaceutical Products, Ballerup, Denmark, Lot No. A85K.

[10] Type FH, 0.5 μm, Millipore Corp., Bedford, Mass.

[11] Fucidin Leo, fusidic acid, 50 mg/ml, Leo Pharmaceutical Products, Lot. No. B08AA.

[12] Fucidin Leo, fusidate sodium, 20 mg/g, Leo Pharmaceutical Products, Lot No. L06B.

[13] Type AH, 0.45 μm, Millipore Corp.

[14] Oxoid Ltd., London, England.

2-Bromo-1-hydroxyquinolizinium Bromide Substituted Anilinium Salts: A New Class of Anti-inflammatory Agents

ROBERT J. ALAIMO *x **and MARVIN M. GOLDENBERG** ‡

Received October 6, 1981, from the *Chemical and ‡Biological Research Divisions, Norwich Eaton Pharmaceuticals, Inc., Norwich, NY 13815. Accepted for publication January 28, 1982.

Abstract □ A series of 2-bromo-1-hydroxyquinolizinium bromide substituted anilinium salts have been prepared by reaction of 1-acetoxy-2-bromoquinolizinium bromide with an appropriately substituted aniline. The resulting anilinium derivatives exhibited a moderate to high degree of anti-inflammatory activity in the carrageenin-induced rat paw edema assay. The most active anilinium salt of the series was evaluated for antiarthritic activity in the adjuvant induced arthritis rat model.

Keyphrases □ Anti-inflammatory agents—2-bromo-1-hydroxyquinolizinium bromide substituted anilinium derivatives, antiarthritic activity, rat □ 2-Bromo-1-hydroxyquinolizinium bromide—anti-inflammatory agents, substituted anilinium derivatives, antiarthritic activity, rat □ Derivatives, anilinium—2-bromo-1-hydroxyquinolizinium bromide, anti-inflammatory agents, antiarthritic activity, rat

As part of an investigation of the chemistry of quinolizinium salts, a number of 2-bromo-1-hydroxyquinolizinium bromide substituted anilinium salts were prepared and screened for biological activity. These anilinium compounds exhibited a moderate to high degree of anti-inflammatory activity in the carrageenin-induced rat paw edema assay. No structure–activity relationships, however, were found.

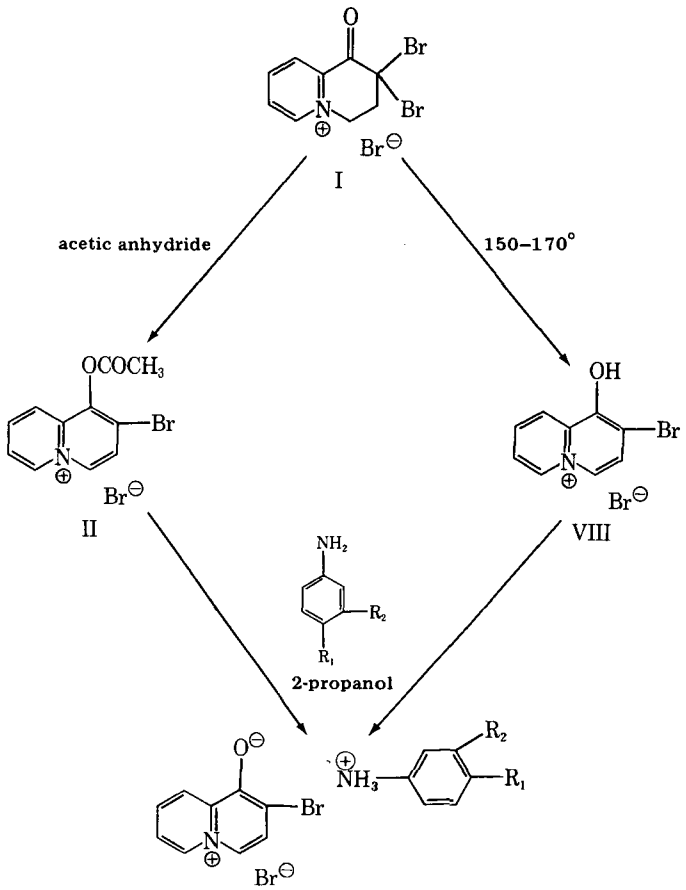

Scheme I

EXPERIMENTAL[1]

Chemistry—2-Bromo-1-hydroxyquinolizinium bromide-*p*-phenetidinium salt (III) was prepared by adding *p*-phenetidine (24 g, 0.18 mole) to a solution of 1-acetoxy-2-bromoquinolizinium bromide (30 g, 0.09 mole) (II) (1–3) in 2-propanol (600 ml). The stirred mixture was boiled under reflux for 4 hr, then chilled and filtered. The yellow crystalline product was washed thoroughly with ether and weighed 37 g (97%).

The remaining compounds in Table I were prepared in a similar manner from II and the appropriately substituted aniline. The reaction of 2-bromo-1-hydroxyquinolizinium bromide (VIII) (3) with the appropriate aniline under similar conditions provided the corresponding substituted anilinium compound III–VII in comparable yields (4). The microanalytical data for compounds III–VII are given in Table II.

Pharmacologic Testing—The compounds were tested for anti-inflammatory activity according to the carrageenin method as described previously (5). Each compound was suspended in distilled water by sonification and administered orally, 300 mg/kg in three male Wistar rats, 1 hr before subplantar injection of 0.05 ml of a 1% solution of carrageenin[2] into the left hind foot. The percentage reduction in edema formation (as compared to a nondrug-tested control) of the rat foot was recorded 4 hr after carrageenin administration.

Examination of VI for antiarthritic activity was determined by use of the adjuvant-induced arthritis model described previously (6). Ten male Wistar rats per treatment group were used in the antiarthritic evaluation. Three principal areas were considered in determining the efficacy of a drug: edema formation, body weight changes, and arthritic scores.

The arthritic lesion scores are based on a modification of previous procedures (6), in which a maximum lesion score of 27 is possible. The results are given in Table III.

RESULTS AND DISCUSSION

The 1-hydroxy-2-(substituted anilino)quinolizinium bromides (III–VII) (Table I) were readily prepared by the reaction of the known 1-acetoxy-2-bromoquinolizinium bromide (II) (1–3) or 2-bromo-1-hydroxyquinolizinium bromide (VIII) (3) with an appropriately substituted aniline in 2-propanol as shown in Scheme I (4). The preparation of the intermediate (II or VIII) proceeded through 2,2-dibromo-1,2,3,4-tetrahydro-1-oxo-quinolizinium bromide (I) either by reaction with acetic anhydride or by heating at 150–170° as shown in Scheme I. The synthesis of I has been described earlier (3).

Since II was more readily available synthetically than VIII, the procedure for the preparation of III–VII involving the use of II was favored. The yields of the final products III–VII were comparable, proceeding through either intermediate. The spectra of compounds III–VII (IR, NMR, UV), as well as the microanalytical data were consistent with the assigned structures. Further confirmation of the structure assignment was obtained when the starting material VIII was regenerated and the corresponding aniline hydrobromide salt isolated during treatment of III–VII with 48% hydrogen bromide.

These quinolizinium anilinium salts (III–VII) were evaluated for anti-inflammatory activity in the carrageenin-induced rat paw edema assay (5). The results are shown in Table I. The reference drug phenylbutazone (IX) is included for purposes of comparison. No apparent un-

[1] Melting points were determined in open capillary tubes using a Mel-Temp melting point apparatus and are uncorrected.

[2] Viscarin, Algin Corporation of America.

0022-3549/82/1100-1299$01.00/0

Table I—Anti-Inflammatory Evaluation and Physical Data for New Compounds

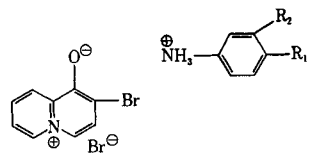

No.	R_1	R_2	Melting Point	Yield, %	Recrystallization Solvent	Formula[a]	Inhibition of Edema Formation, %[b,c]
I	OC_2H_5	H	161–162°	97	Ethanol–Ether	$C_{17}H_{18}Br_2N_2O_2$	31.4
IV	OCH_3	H	129–133°	74	2-Propanol–Ethyl Acetate	$C_{16}H_{16}Br_2N_2O_2$	44.1
V	OC_6H_5	H	123–125°	65	2-Propanol–Ether	$C_{21}H_{18}Br_2N_2O_2$	37.0
VI	$OCH_2CH{=}CH_2$	H	125–127°	77	2-Propanol	$C_{18}H_{18}Br_2N_2O_2$	63.0
VII	OCH_3	OCH_3	160–162°	76	Ethanol	$C_{17}H_{18}Br_2N_2O_3$	46.4
IX	Phenylbutazone						58.5[d]

[a] Analytical results for C, H, N, and Br are within ±0.24% of the theoretical values and shown in Table II. [b] Dosed at 300 mg/kg orally 60 min before carrageenin injection. [c] Compared to control (nondrug treated) hind paw 4 hr after carrageenin injection. [d] Dosed at 100 mg/kg orally.

Table II—Microanalytical Data

No.	Formula	Calc. C	Calc. H	Calc. N	Calc. Br	Found C	Found H	Found N	Found Br
I	$C_{17}H_{18}Br_2N_2O_2$	46.18	4.10	6.34	36.15	46.20	4.30	6.42	35.92
IV	$C_{16}H_{16}Br_2N_2O_2$	44.88	3.77	6.54	37.33	44.70	3.70	6.57	37.16
V	$C_{21}H_{18}Br_2N_2O_2$	51.45	3.70	5.72	32.61	51.42	3.74	5.72	32.77
VI	$C_{18}H_{18}Br_2N_2O_2$	47.60	3.99	6.17	35.19	47.69	4.09	6.12	35.26
VII	$C_{17}H_{18}Br_2N_2O_3$	44.56	3.96	6.12	34.89	44.80	4.01	5.96	34.88

Table III—Antiarthritic Evaluation of Compound VI

Compound	Dose, *per os* mg/kg (21-day)	Inhibition of Primary Lesion Injected Paw, % (22-day)	Inhibition of Secondary Lesion Noninjected Paw, % (22-day)	Increase in Body Weight, % (22-day)	Mean Arthritic Score
VI	50	0	10	22	13
	200	20	30	33	12
Aspirin	300	36	39	27	14
Phenylbutazone IX	100	78	82	40	8
Adjuvant control 0.5% methylcellulose	—	0	0	22	17

toward gross signs of drug action were observed for compounds III–VII.

The most active member of the series (VI) was examined for antiarthritic activity by use of the adjuvant-induced arthritis model (6). The results of the study were grouped into three principal areas: edema formation, body weight changes, and arthritic scores. All three areas are equally important in determining the anti-inflammatory efficacy of a drug. The results indicate that VI is at least as active as aspirin but less active than phenylbutazone. The results are presented in Table III.

The anti-inflammatory activity of compounds III–VII as revealed by the percent inhibition of edema formation was less than that elicited by several of the 2-(substituted amino)quinolizinium bromides reported previously (7).

REFERENCES

(1) R. J. Alaimo, C. J. Hatton, and M. K. Eckman, *J. Med. Chem.*, **13,** 554 (1970).

(2) T. Miyadera and I. Iwal, *Chem. Pharm. Bull. (Tokyo)*, **12,** 1338 (1964).

(3) A. Fozard and G. Jones, *J. Chem. Soc.*, **1963,** 2203.

(4) R. J. Alaimo and M. M. Goldenberg, U.S. Pat. 4,020,075 (1977).

(5) C. A. Winter, E. A. Risley, and G. V. Nuss, *Proc. Soc. Exp. Biol. Med.*, **111,** 544 (1962).

(6) M. E. Rosenthale, *Arch. Int. Pharmacodyn. Ther.*, **188,** 14 (1970).

(7) R. J. Alaimo and M. M. Goldenberg, *J. Pharm. Sci.*, **63,** 1939 (1974).

ACKNOWLEDGMENTS

The authors acknowledge the technical assistance of Miss Yvonne Miller in the preparation of chemical intermediates and the evaluation of these compounds for anti-inflammatory activity by Mr. Arthur C. Ilse, Jr. Microanalytical data were provided by Mr. Marvin Tefft and Mr. Grant Gustin.

Theophylline Bioavailability in the Dog

FRANCIS L. S. TSE *x **and DANIEL W. SZETO** ‡

Received July 16, 1981, from the *College of Pharmacy, Rutgers—The State University, Piscataway, NJ 08854.* Accepted for publication February 4, 1982. Present address: *Drug Metabolism Section, Sandoz Pharmaceuticals, East Hanover, NJ 07936; ‡Department of Basic Research, Berlex Laboratories, Cedar Knolls, NJ 07927.

Abstract □ The bioavailability of theophylline following single oral doses of a theophylline capsule, a theophylline tablet, and an aminophylline tablet in beagle dogs was compared against an intravenous standard. Plasma theophylline levels after oral and intravenous drug administration were described by the one-compartment open model. The onset of theophylline absorption from the oral products was rapid. While the theophylline tablet showed a slower absorption rate than the capsule or the aminophylline tablet, all three products appeared to be completely bioavailable.

Keyphrases □ Theophylline—absorption, bioavailability in the dog, capsule, tablet, aminophylline tablet □ Bioavailability—theophylline absorption in the dog, capsule, tablet, aminophylline tablet □ Absorption—theophylline bioavailability in the dog, capsule, tablet, aminophylline tablet

The absorption of the bronchodilator theophylline from conventional and sustained-release dosage forms has been extensively studied in humans (1–11). In one study using an aqueous solution as a standard (5), the absolute bioavailability of 13 different types of theophylline tablets marketed in the United States was determined. All yielded an absorption of >90%.

Similar comparative bioavailability data in animal models are limited. The absolute bioavailability of theophylline from five commercial dosage forms in rabbits has been examined (12). In that study significant interproduct differences in the percent of dose absorbed were reported. The data showed no evidence of dose-dependent kinetics after single oral doses (65–200 mg) of capsules or tablets.

The present report concerns theophylline bioavailability in the dog following single oral doses of a theophylline capsule, a theophylline tablet, and an aminophylline tablet, using an intravenous aminophylline dose as a reference standard.

EXPERIMENTAL

A 1-year-old male beagle dog (dog 1, 11.4 kg) and a 2-year-old female beagle dog (dog 2, 11.7 kg) each received four single doses of aminophylline or theophylline in separate experiments. The dogs were fasted overnight predose and 4 hr postdose, but had access to water at all times. During the experiment, the dogs were initially placed in a restraining sling to facilitate accurate dosing and blood sample collection.

Intravenous Administration—Each dog received a single 50-mg aminophylline[1] (85% theophylline) dose by rapid injection into a cephalic vein. Blood samples (5 ml) were collected from a cephalic or femoral vein immediately before and at 7, 10, 15, 30, and 45 min and 1, 1.5, 2, 3, 4, 6, 8, 12, and 24 hr after dosing.

Oral Administration—The capsule (A)[2] or tablet (B[3] or C[4]) was administered by placing it on the posterior portion of the dog's tongue so that it was not fractured or chewed before swallowing. The dose was followed by 20 ml of water. Venous blood samples were collected in the same manner as described for the intravenous dosing experiments, but the 7- and 10-min samples were omitted.

Blood samples were placed in heparinized tubes[5]. Plasma was separated by centrifugation and stored at −20° until analyzed.

Experiments were performed 3 weeks apart to avoid changes in pharmacokinetic parameters due to prior drug exposure and to allow complete drug washout from previous doses.

Plasma Assay—Plasma concentrations of theophylline were measured by reversed-phase high-performance liquid chromatography (HPLC) as previously described (13).

Data Interpretation—Plasma theophylline data after intravenous and oral dosing were analyzed in terms of the pharmacokinetic one-compartment open model. The equations and symbols pertaining to this model have been described (14). Intravenous pharmacokinetic parameters were calculated by linear regression of the natural log of the theophylline concentration against time. Oral data were analyzed on a digital computer[6] following standard graphical treatment; individual data sets were fitted to the appropriate equation by iterative least-squares methods using the NONLIN program (15).

RESULTS

Individual plasma levels of theophylline obtained from the four treatments are given in Table I. The results of the pharmacokinetic analysis are described in Table II.

Following intravenous dosing, plasma theophylline levels were highest (~5 μg/ml) at the first sampling time (7–10 min). Drug levels then declined monoexponentially, with plasma half-lives of 6.4 and 3.8 hr in dogs 1 and 2, respectively. The distribution volume, calculated from the y-intercept of the regression line, was 9.6 liter (84% of body weight) for dog 1 and 8.1 liter (70% of body weight) for dog 2. The plasma clearance was 1.5 ml/min/kg for dog 1 and 2.1 ml/min/kg for dog 2.

Following oral administration of each of the three products tested, theophylline was detected in plasma within 30 min. The observed onset was in good agreement with the computer estimated lag time of absorption (Table II). Product B appeared to be absorbed at a slower rate than products A and C, as indicated by its longer absorption half-time and time of peak concentration, although statistical comparison of data was not possible due to the small number of animals used. Normalized peak theophylline levels were similar for products A and B, but the level was lower for product C. The half-life of drug elimination was consistent between products, although variation between dogs was apparent. Plasma clearance values were calculated using the distribution volumes obtained from intravenous dosing.

Comparison of the areas under the plasma theophylline curves from the oral and intravenous doses, corrected for the different dose sizes, suggested complete absorption of theophylline from the three products. Correction for plasma clearance yielded F values of approximately unity in all cases.

DISCUSSION

Aminophylline, the ethylenediamine salt of theophylline, is generally used for the intravenous administration of this drug, primarily because of the low aqueous solubility of the weak acid (theophylline). A study using three volunteers (16) showed that, when given intravenously as aminophylline, theophylline was metabolized more rapidly and extensively than when given as the free acid. A previous study (17) compared the pharmacokinetics of theophylline and aminophylline after oral and intravenous administration in eight healthy male subjects, and reported virtually identical serum concentration–time curves for the two drug entities. While data in the present study also showed no apparent differences between aminophylline and theophylline disposition kinetics, plasma clearance was corrected for in the bioavailability calculations.

[1] Aminophyllin injection USP, 25 mg/ml, Gibco/Invenex, Chagrin Falls, Ohio.
[2] Elixophyllin (theophylline, 100-mg capsules), Berlex, Cedar Knolls, N.J.
[3] Theolair (theophylline, 125-mg tablets), Riker, Northridge, Calif.
[4] Aminophyllin (aminophylline, 200-mg tablets), Searle, Chicago, Ill.
[5] Vacutainer, Becton-Dickinson, Rutherford, N.J.
[6] IBM 370/168 digital computer, Rutgers Computer Center for Informational Services.

0022-3549/82/1100-1301$01.00/0

Table I—Individual Plasma Levels of Theophylline

Hours	Plasma Theophylline, μg/ml							
	Intravenous		Oral					
			A		B		C	
	Dog 1	Dog 2	Dog 1	Dog 2	Dog 1	Dog 2	Dog 1	Dog 2
0.12	—[a]	5.0	—	—	—	—	—	—
0.17	4.6	—	—	—	—	—	—	—
0.25	4.6	4.8	0	0.4	2.7	0	2.3	1.0
0.5	4.3	4.5	0.3	4.5	5.3	0.2	16.0	9.3
0.75	4.1	—	4.7	9.2	7.5	0.5	15.6	13.0
1	4.1	4.4	10.9	11.4	8.9	1.7	16.3	15.1
1.5	4.0	4.2	11.3	11.0	13.4	6.6	12.9	14.9
2	3.7	3.9	9.3	9.7	13.8	13.9	13.0	17.2
3	2.8	3.1	8.9	8.0	12.6	12.6	13.0	14.5
4	3.0	2.5	8.7	7.6	12.3	10.4	10.4	11.9
5	—	—	8.1	—	—	—	—	—
6	2.3	1.8	7.5	5.8	9.8	8.6	10.5	9.5
8	1.7	1.2	5.4	4.0	7.6	6.7	7.1	7.5
12	1.0	0.6	4.0	1.8	4.6	4.1	3.5	3.7
24	0.4	—	1.6	0.6	2.0	0.6	1.1	0.6

[a] Not determined.

Table II—Pharmacokinetic Parameters Obtained from Plasma Theophylline Data

Parameter[a]	Intravenous		Oral					
			A		B		C	
	Dog 1	Dog 2	Dog 1[b]	Dog 2	Dog 1	Dog 2[b]	Dog 1[b]	Dog 2
D, mg	42.5	42.5	100	100	125	125	170	170
k_a, hr^{-1}	—[c]	—	2.8 (1.6–4.1)[d]	4.5 (2.8–6.3)	1.0 (0.61–1.4)	0.70 (0.16–1.2)	17.3 (−58.6–93.3)	2.2 (1.7–2.8)
$t_{1/2,abs}$, hr	—	—	0.24	0.15	0.69	0.99	0.04	0.31
k_{el}, hr^{-1}	0.11	0.18	0.092 (0.066–0.12)	0.16 (0.13–0.18)	0.12 (0.084–0.16)	0.16 (0.066–0.26)	0.12 (0.096–0.14)	0.14 (0.11–0.17)
$t_{1/2}$, hr	6.4	3.8	7.5	4.3	5.6	4.3	5.8	5.0
FD/V, μg/ml	4.4	5.2	11.5 (9.9–13.1)	12.4 (11.5–13.3)	18.0 (15.0–21.0)	17.8 (9.6–25.9)	16.6 (15.2–18.0)	19.7 (17.9–21.4)
t_0, hr	—	—	0.49 (0.48–0.51)	0.40 (0.35–0.45)	0.12 (0.0037–0.24)	0.73 (0.66–0.81)	0.24 (0.21–0.28)	0.22 (0.18–0.26)
r	0.99	1.00	0.98	1.00	0.99	0.96	0.99	1.00
Vd, liter/kg	0.84	0.70	—	—	—	—	—	—
F	1	1	1.1	1.0	1.4	1.2	0.93	0.94
Normalized AUC, (μg hr)/ml	40.4	29.0	53.1	33.0	49.6	37.7	34.5	35.1
PCl, ml/min/kg	1.5	2.1	1.3	1.9	1.7	1.9	1.7	1.6
C_{max}, μg/ml	—	—	10.3	11.0	13.4	11.5	16.0	16.3
t_{max}, hr	—	—	1.7	1.2	2.5	3.5	0.5	1.6

[a] D, dose of theophylline or equivalent; k_a, first-order rate constant for drug absorption; $t_{1/2,abs}$, half-time of absorption = $0.693/k_a$; k_{el}, first-order rate constant for drug elimination; $t_{1/2}$, half-life of elimination = $0.693/k_{el}$; F, fraction of dose absorbed; Vd, apparent distribution volume of theophylline in the body; t_0, lag time between dosing and the appearance of drug in plasma; r, correlation coefficient; Normalized AUC, area under theophylline plasma concentration *versus* time curve = FD/Vk_{el}, normalized to a dose of 42.5 mg theophylline; PCl, plasma clearance = Vk_{el}; C_{max}, maximum concentration of theophylline in plasma after oral dosing = $(FD/V)(k_a/k_{el})^{k_{el}/(k_{el}-k_a)}$; t_{max}, time at which C_{max} occurs = $\ln(k_a/k_{el})/(k_a - k_{el}) + t_0$. [b] Plasma concentration data were weighted by their reciprocals during computer analysis. [c] Not relevant. [d] The 95% confidence interval.

In experiments with rabbits (12), no dose-dependent theophylline pharmacokinetics after single oral doses in the 65–200-mg range were found. In the dogs used in the present study, elimination half-lives and distribution volumes following a 50-mg iv dose were similar to those obtained previously (18) after a 100-mg iv aminophylline dose. Therefore, the 50-mg iv aminophylline dose was adequate as a reference dose for oral bioavailability assessment. It should be noted, however, that dose-dependent characteristics in theophylline distribution and elimination were observed at higher doses (13.8–52.0 mg/kg of aminophylline) in guinea pigs (19) and in children (20, 21).

Although the decline in plasma theophylline levels after intravenous dosing is biphasic (22), the distribution of theophylline into peripheral tissues is so rapid that a one-compartment model has been shown appropriate for the analysis of data obtained in rabbits (12), dogs (18), and humans (23, 24). This was also the case in this study.

Based on the results shown in Table II, the GI absorption of theophylline is efficient in dogs given an oral dose of either theophylline or aminophylline, despite the lower aqueous solubility of the former. This observation supports previous findings in humans (2, 17). All three products studied here were immediate-release formulations. They were similar to each other with respect to the onset of drug absorption, but the absorption rate from the theophylline tablet (B) was slower than that from the theophylline capsule (A) or aminophylline tablet (C). However, all three products showed virtually complete bioavailability.

The efficient absorption of theophylline from these different dosage forms is consistent with available data in humans (5). However, experiments with rabbits showed erratic drug absorption from commercial tablets and capsules of theophylline or aminophylline; the same brand products as used in the present study yielded F values of 0.50 to 1.20 (12). Thus, the beagle dog appears to be a more appropriate animal model for conducting theophylline pharmacokinetic studies.

REFERENCES

(1) P. A. Mitenko and R. I. Ogilvie, *Clin. Pharmacol. Ther.*, **16**, 720 (1974).

(2) L. Hendeles, M. Weinberger, and L. Bighley, *Am. J. Hosp. Pharm.*, **34**, 525 (1977).

(3) R. A. Upton, J.-F. Thiercelin, T. W. Guentert, L. Sansom, J. R. Powell, P. E. Coates, and S. Riegelman, *J. Pharmacokinet. Biopharm.*, **8**, 131 (1980).

(4) R. A. Upton, J. R. Powell, T. W. Guentert, J.-F. Thiercelin, L. Sansom, P. E. Coates, and S. Riegelman, *ibid.*, **8**, 151 (1980).

(5) R. A. Upton, L. Sansom, T. W. Guentert, J. R. Powell, J.-F. Thiercelin, V. P. Shah, P. E. Coates, and S. Riegelman, *ibid.*, **8**, 229 (1980).

(6) B. G. Charles, P. J. Ravenscroft, and F. Bochner, *Med. J. Aust.*, **2**, 264 (1980).

(7) D. T. Jones and M. R. Sears, *N. Z. Med. J.*, **92**, 196 (1980).

(8) J. G. Prior, D. Berry, and G. M. Cochrane, *Postgrad. Med. J.*, **56**, 638 (1980).
(9) W. E. Barrett, *Curr. Ther. Res.*, **28**, 669 (1980).
(10) D. L. Spangler, G. E. Vanderpool, M. S. Carroll, and D. G. Tinkelman, *Ann. Allergy*, **45**, 355 (1980).
(11) P. O. Fagerström, T. Mellstrand, and N. Svedmyr, *Int. J. Clin. Pharmacol. Ther. Toxicol.*, **19**, 131 (1981).
(12) A. El-Yazigi and R. J. Sawchuk, *J. Pharm. Sci.*, **70**, 452 (1981).
(13) F. L. S. Tse and D. W. Szeto, *J. Chromatogr.*, **226**, 231 (1981).
(14) M. Gibaldi and D. Perrier, "Pharmacokinetics," Dekker, New York, N.Y., 1975, p. 36.
(15) C. M. Metzler, G. L. Elfring, and A. J. McEwen, *Biometrics*, **30**, 562 (1974).
(16) T. J. Monks, R. L. Smith, and J. Caldwell, *J. Pharm. Pharmacol.*, **33**, 93 (1981).
(17) A. Aslaksen, O. M. Bakke, and T. Vigander, *Br. J. Clin. Pharmacol.*, **11**, 269 (1981).
(18) F. L. S. Tse, K. H. Valia, D. W. Szeto, T. J. Raimondo, and B. Koplowitz, *J. Pharm. Sci.*, **70**, 395 (1981).
(19) S. M. Madsen and U. Ribel, *Acta Pharmacol. Toxicol.*, **48**, 1 (1981).
(20) M. Weinberger and E. Ginchansky, *J. Pediatr.*, **91**, 820 (1977).
(21) E. Sarrazin, L. Hendeles, M. Weinberger, K. Muir, and S. Riegelman, *ibid.*, **97**, 825 (1980).
(22) P. A. Mitenko and R. I. Ogilvie, *Clin. Pharmacol. Ther.*, **13**, 329 (1972).
(23) R. I. Ogilvie, *Clin. Pharmacokinet.*, **3**, 267 (1978).
(24) J. P. Rosen, M. Danish, M. C. Ragni, C. L. Saccar, S. J. Yaffe, and H. I. Lecks, *Pediatrics*, **64**, 248 (1979).

ACKNOWLEDGMENTS

The authors thank Messrs. K. Valia and B. Koplowitz for their technical assistance.

COMMUNICATIONS

A New Technique for Determining *In Vitro* Release Rates of Drugs From Creams

Keyphrases □ Dosage forms, topical—new technique for determining *in vitro* release rates of drugs from creams □ Release rate, *in vitro*—new technique for determination, drugs from creams

To the Editor:

Within about the last 10 years, dissolution testing has become recognized as one of the most useful methods for evaluating tablets and capsules. In fact, such testing has all but supplanted the traditional disintegration test. Equipment and procedures for measuring the rate and extent of drug dissolution are now becoming standardized as a result of intensive research and, necessarily, some compromises.

No such standardization appears to be occurring, however, with the equipment or procedures used for testing the release of drugs from topical dosage forms (*i.e.*, creams, ointments, gels, suppositories, *etc.*). Many investigators have done extensive research on the release of drugs from such carriers, but it seems that, almost without exception, each used a unique method for presenting the drug to some receptor phase. The reason for this may be that each was faced with unique problems with regard to the formulations.

We present here a convenient and versatile technique for the *in vitro* testing of the release of drugs from creams or ointments. This technique could be used for a wide variety of vehicles, although it was developed specifically for cream formulations which are oil in water emulsions containing 0.01% estradiol.

The ideal procedure would be one in which the sample is in direct contact with the receptor phase, because barriers used to isolate the sample from that phase have a potential leveling effect on the rate of appearance of drug (in the receptor phase). Thus, the absence of barriers should maximize the probability of measuring differences between creams which differ only slightly in their drug-release characteristics. Therefore, we first tried filling shallow cups with the cream and immersing these in water at 37° in a fashion similar to that reported previously (1). This was attempted with a variety of cups of different dimensions supported upright or inverted in the receptor phase (water). These attempts failed because the cream swelled and eventually sloughed into the water. We noted also that the creams were no longer homogeneous, *i.e.*, the first few millimeters of sample nearest the water were physically different from the bulk of the sample before the end of the test time. In addition, samples were necessarily so large (a few grams) that only a small fraction of the total estradiol was near the surface where it could be expected to be released in a reasonable length of time.

Attempts were made to isolate the cream samples from the receptor phase using semipermeable membranes. Two membranes were tested, dialysis tubing and filter paper, in procedures similar to those reported previously (2). When these barriers were used, drug appeared in the receptor phase more slowly than when they were not. Although the problems associated with sample swelling and subsequent sloughing could be alleviated by using these barriers, this approach was abandoned because of the effects on the rate of appearance of drug in the receptor phase.

With these results in mind, we developed a simple technique which allows direct contact between the cream sample and the receptor phase (water) and which eliminates or minimizes sample sloughing. Cream samples are spread into the interstices of an 80-mesh stainless steel screen. The samples prepared in this way can be submerged in gently stirred water for long periods of time. The equipment and procedure are as follows.

A number of appropriately sized pieces of stainless steel screen were first prepared by cutting 7.5 × 7.5-cm squares and removing ~1 cm from each corner (Fig. 1).

Each screen was covered on both sides along the top edge with a piece of 2.54 cm wide masking tape such that 30 cm^2

0022-3549/82/1100-1303$01.00/0

(8) J. G. Prior, D. Berry, and G. M. Cochrane, *Postgrad. Med. J.*, **56**, 638 (1980).
(9) W. E. Barrett, *Curr. Ther. Res.*, **28**, 669 (1980).
(10) D. L. Spangler, G. E. Vanderpool, M. S. Carroll, and D. G. Tinkelman, *Ann. Allergy*, **45**, 355 (1980).
(11) P. O. Fagerström, T. Mellstrand, and N. Svedmyr, *Int. J. Clin. Pharmacol. Ther. Toxicol.*, **19**, 131 (1981).
(12) A. El-Yazigi and R. J. Sawchuk, *J. Pharm. Sci.*, **70**, 452 (1981).
(13) F. L. S. Tse and D. W. Szeto, *J. Chromatogr.*, **226**, 231 (1981).
(14) M. Gibaldi and D. Perrier, "Pharmacokinetics," Dekker, New York, N.Y., 1975, p. 36.
(15) C. M. Metzler, G. L. Elfring, and A. J. McEwen, *Biometrics*, **30**, 562 (1974).
(16) T. J. Monks, R. L. Smith, and J. Caldwell, *J. Pharm. Pharmacol.*, **33**, 93 (1981).
(17) A. Aslaksen, O. M. Bakke, and T. Vigander, *Br. J. Clin. Pharmacol.*, **11**, 269 (1981).
(18) F. L. S. Tse, K. H. Valia, D. W. Szeto, T. J. Raimondo, and B. Koplowitz, *J. Pharm. Sci.*, **70**, 395 (1981).
(19) S. M. Madsen and U. Ribel, *Acta Pharmacol. Toxicol.*, **48**, 1 (1981).
(20) M. Weinberger and E. Ginchansky, *J. Pediatr.*, **91**, 820 (1977).
(21) E. Sarrazin, L. Hendeles, M. Weinberger, K. Muir, and S. Riegelman, *ibid.*, **97**, 825 (1980).
(22) P. A. Mitenko and R. I. Ogilvie, *Clin. Pharmacol. Ther.*, **13**, 329 (1972).
(23) R. I. Ogilvie, *Clin. Pharmacokinet.*, **3**, 267 (1978).
(24) J. P. Rosen, M. Danish, M. C. Ragni, C. L. Saccar, S. J. Yaffe, and H. I. Lecks, *Pediatrics*, **64**, 248 (1979).

ACKNOWLEDGMENTS

The authors thank Messrs. K. Valia and B. Koplowitz for their technical assistance.

COMMUNICATIONS

A New Technique for Determining *In Vitro* Release Rates of Drugs From Creams

Keyphrases □ Dosage forms, topical—new technique for determining *in vitro* release rates of drugs from creams □ Release rate, *in vitro*—new technique for determination, drugs from creams

To the Editor:

Within about the last 10 years, dissolution testing has become recognized as one of the most useful methods for evaluating tablets and capsules. In fact, such testing has all but supplanted the traditional disintegration test. Equipment and procedures for measuring the rate and extent of drug dissolution are now becoming standardized as a result of intensive research and, necessarily, some compromises.

No such standardization appears to be occurring, however, with the equipment or procedures used for testing the release of drugs from topical dosage forms (*i.e.*, creams, ointments, gels, suppositories, *etc.*). Many investigators have done extensive research on the release of drugs from such carriers, but it seems that, almost without exception, each used a unique method for presenting the drug to some receptor phase. The reason for this may be that each was faced with unique problems with regard to the formulations.

We present here a convenient and versatile technique for the *in vitro* testing of the release of drugs from creams or ointments. This technique could be used for a wide variety of vehicles, although it was developed specifically for cream formulations which are oil in water emulsions containing 0.01% estradiol.

The ideal procedure would be one in which the sample is in direct contact with the receptor phase, because barriers used to isolate the sample from that phase have a potential leveling effect on the rate of appearance of drug (in the receptor phase). Thus, the absence of barriers should maximize the probability of measuring differences between creams which differ only slightly in their drug-release characteristics. Therefore, we first tried filling shallow cups with the cream and immersing these in water at 37° in a fashion similar to that reported previously (1). This was attempted with a variety of cups of different dimensions supported upright or inverted in the receptor phase (water). These attempts failed because the cream swelled and eventually sloughed into the water. We noted also that the creams were no longer homogeneous, *i.e.*, the first few millimeters of sample nearest the water were physically different from the bulk of the sample before the end of the test time. In addition, samples were necessarily so large (a few grams) that only a small fraction of the total estradiol was near the surface where it could be expected to be released in a reasonable length of time.

Attempts were made to isolate the cream samples from the receptor phase using semipermeable membranes. Two membranes were tested, dialysis tubing and filter paper, in procedures similar to those reported previously (2). When these barriers were used, drug appeared in the receptor phase more slowly than when they were not. Although the problems associated with sample swelling and subsequent sloughing could be alleviated by using these barriers, this approach was abandoned because of the effects on the rate of appearance of drug in the receptor phase.

With these results in mind, we developed a simple technique which allows direct contact between the cream sample and the receptor phase (water) and which eliminates or minimizes sample sloughing. Cream samples are spread into the interstices of an 80-mesh stainless steel screen. The samples prepared in this way can be submerged in gently stirred water for long periods of time. The equipment and procedure are as follows.

A number of appropriately sized pieces of stainless steel screen were first prepared by cutting 7.5 × 7.5-cm squares and removing ~1 cm from each corner (Fig. 1).

Each screen was covered on both sides along the top edge with a piece of 2.54 cm wide masking tape such that 30 cm^2

0022-3549/82/1100-1303$01.00/0

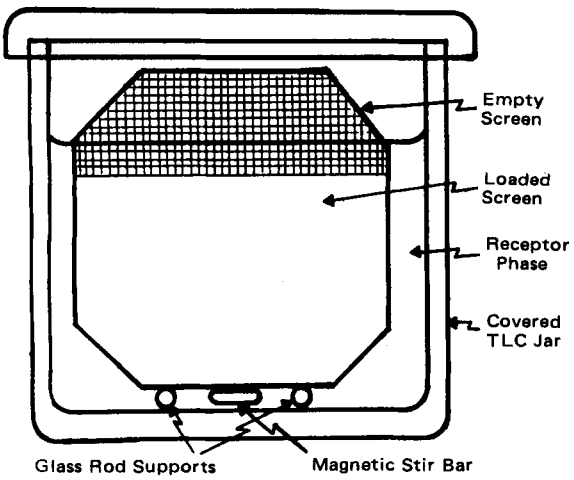

Figure 1—*The apparatus used to evaluate the* in vitro *release of estradiol from creams. The rectangular TLC developing jar normally is partially immersed in a constant temperature bath. A magnetic stirrer located beneath the constant temperature bath rotates the stir bar.*

of screen remained exposed. The taped screen was then weighed. Cream was smeared liberally into the mesh using a spatula, and excess cream was then wiped rapidly from the surface by placing the loaded screen between two disposable paper towels, pressing the towels firmly together, and pulling the screen out. After the screen with its sample was reweighed, the tape was removed and the screen was placed vertically into 120 ml of degassed water held at 37° in an 8 × 8 × 3-cm covered rectangular TLC developing jar. Small glass rods at the bottom of the jar held the screen slightly off the bottom and allowed a micromagnetic stir bar to spin fast enough (~300 rpm) just below the screen to gently mix the medium, yet not dislodge the cream from the screen. At the end of the test period, the screen with cream sample was removed from the water. The drug released into the water was recovered using a small C_{18} extraction column[1] and then analyzed by HPLC on an analytical C_{18} column using an acetonitrile–water mobile phase in a fashion similar to that reported previously (3) for dienestrol.

Figure 2 illustrates the results obtained using this procedure for a number of experimental formulations of a 0.01% estradiol cream. These formulations were alike quantitatively but differed in their processing during manufacture. These results point out a number of features of this method. First, samples can be exposed to the receptor phase for any convenient length of time; thus, a release profile can be constructed. Second, the results are easily interpreted, since they can be expressed in terms of a percentage of the total amount of drug available for release. This is possible because large (thick) samples are not necessary and the surface area of the small (~300 mg), thin sample exposed directly to the water is maximized. (The interstitial spaces comprise ~35% of the total surface area of an 80-mesh screen; thus, when both sides of the screen are taken into account, the exposed surface area of the cream is ~21 cm^2.) Third, the absence of rate-limiting or rate-influencing barriers allows subtle differences in release characteristics to be identified.

[1] Sep Pak, Waters Associates, Milford, Mass.

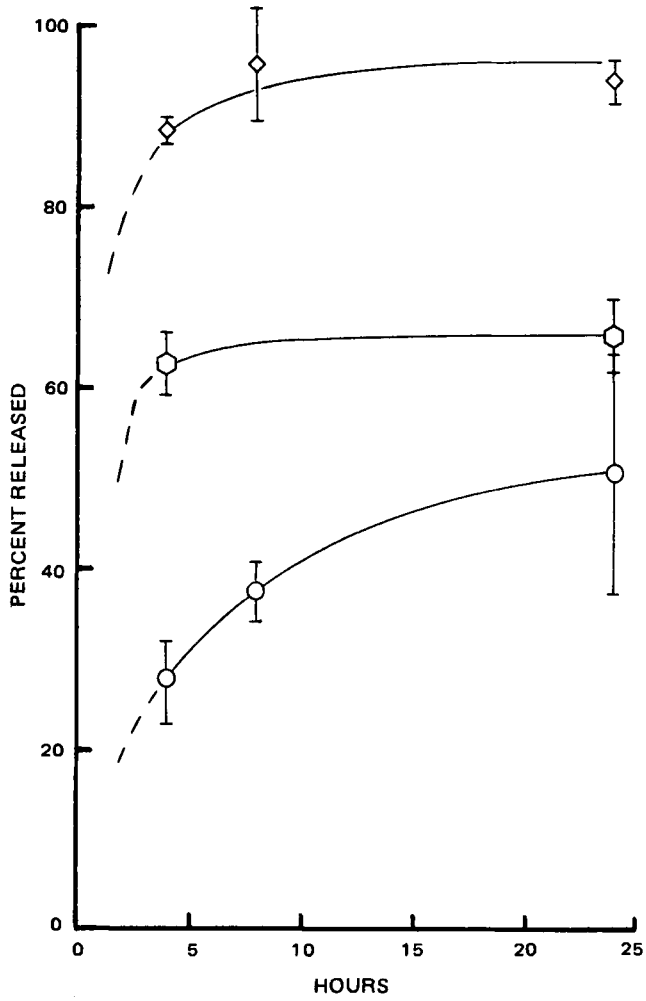

Figure 2—In vitro *release profiles for three formulations of 0.01% estradiol cream. The profile for formulation A (○) depicts the average of the data given for the three batches in Table I. The profiles for B (○) and C (◇) represent single batches, and each point is the average of three to four separate tests. The magnitude of 1 SD is also indicated at each point.*

The results illustrated in Fig. 2 are the averages of a number of trials. The individual values for three batches of one of the formulations are given in Table I. Each value

Table I—Percent Estradiol Released from Three Batches of an Experimental Formulation [a]

	Batch 1	Batch 2	Batch 3
4 hr	33.4	19.4	27.0
	30.2	28.4	28.6
	27.8	28.8	—
Average	30.5	25.5	27.8
SD	2.9	5.3	1.1
8 hr	40.7	—	40.1
	37.4	—	38.9
	31.5	—	37.1
Average	36.9	—	38.8
SD	3.9	—	1.4
24 hr	39.3	64.7	62.9
	58.1	55.8	51.6
	48.7	51.3	55.6
	46.3	54.2	55.2
	51.6	57.7	63.6
	—	—	53.2
Average	49.2	56.7	57.0
SD	6.3	5.0	5.0

[a] Formulation A in Fig. 2.

in this table represents the amount released from a separate test sample. The values demonstrate the typical reproducibility obtained with this procedure.

This technique could be useful for testing a wide variety of topical formulations where direct contact with the receptor phase is desired. The screen size and configuration could easily be altered to accommodate different types of vehicles, release rates, and concentrations of drugs. This technique may be unsuitable where the drug or vehicle interacts with stainless steel. Such instances are expected to be rare, however, and normally the technique should allow investigators to routinely and uniformly prepare and test small samples with high surface area to weight ratios.

(1) Z. T. Chowhan and R. Pritchard, *J. Pharm. Sci.*, **64**, 754 (1975).
(2) J. W. Ayres and P. A. Laskar, *ibid.*, **63**, 1402 (1974).
(3) L. C. Bailey and C. A. Bailey, *ibid.*, **68**, 508 (1979).

Robert J. Behme
Terry T. Kensler
Dana Brooke [x]
Pharmaceutical Product Development Department
Mead Johnson Pharmaceutical Division
Evansville, IN 47721

Received February 22, 1982.
Accepted for publication June 30, 1982.

Comparison of Chromatographic and Spectrophotometric Analysis of Indocyanine Green in Plasma Following Administration of Multiple Doses to Humans

Keyphrases □ High-pressure liquid chromatography—comparison with spectrophotometric analysis of indocyanine green in plasma following multiple dose administration, humans □ Spectrophotometry—comparison with high-pressure liquid chromatographic analysis of indocyanine green following multiple dose administration, humans □ Indocyanine green—comparison of spectrophotometric and high-pressure liquid chromatographic analysis following multiple dose administration, humans

To the Editor:

Following the administration of small doses (0.5 mg/kg), indocyanine green (I) is highly extracted from blood by the liver (1). Compound I has been used extensively, therefore, to evaluate hepatic function (2, 3) and to estimate hepatic blood flow in humans and laboratory animals (4, 5). Numerous reports have suggested that I is not metabolized in any species (4, 6, 7). Thus, simple spectrophotometric assays (*i.e.*, typically the determination of the absorbance at ~800 nm of plasma samples diluted with distilled water) have been used extensively to estimate the concentration of I in biological fluids. However, it has been reported recently that spectrophotometric and high-pressure liquid chromatographic (HPLC) assays yield radically different estimates of the concentration of I in plasma following the administration of a large dose (25.6 mg/kg) to the rabbit (8). Estimates of the plasma concentration of I ≥30 min postdose were found to be significantly lower using the HPLC assay (almost an order of magnitude lower at many time points). Thus, the total body clearance of I in the rabbit, calculated on the basis of plasma concentrations determined by HPLC, was much higher than that calculated from the spectrophotometric assay results. These investigators postulated that this discrepancy was due to a previously unidentified metabolite. If humans also metabolize I to a compound that interferes with the classical spectrophotometric methods, the clearance value of I based on these assays will not provide a reliable estimate of hepatic blood flow. Because of the potential implications of this assay discrepancy, we compared the spectrophotometric and HPLC assays for I using plasma samples from humans.

Two healthy male subjects (25 and 35 years of age) each received five intravenous bolus doses (0.5 mg/kg each) of I at ~1-hr intervals. Blood samples (5 ml) were collected into heparinized evacuated blood collection tubes[1] prior to and at 1, 3, 5, 7, 9, 11, and 15 min after the first, third, and fifth doses. Plasma was separated and stored at −20° until analyzed (within 36 hr). Previous studies have demonstrated the stability of I under these conditions (8), and preliminary work in our laboratory confirmed these findings.

After the addition of 1.0 μg of diazepam (internal standard) in 100 μl of methanol, proteins were precipitated with acetonitrile (1 ml plasma–1 ml acetonitrile) and the sample was centrifuged. The supernatant was then analyzed by spectrophotometric and HPLC methods. Samples were analyzed using a double beam spectrophotometer[2] equipped with a red-sensitive photomultiplier. The peak absorbance of I in the supernatant was found to occur at 786 nm, and this wavelength was chosen for analysis of all samples. The HPLC method used was that described recently (8) with the following modifications: Dual wavelength (254 and 650 nm)[3] monitoring was employed utilizing two detectors[4,5] in series. Absorbance at 650 nm was examined, since any degradation or metabolic products of I which contained an unaltered chromophore would be expected to absorb at a high wavelength similar to that of the parent compound. The high wavelength monitoring was achieved with a tungsten lamp in a variable wavelength monochromator[4]. A wavelength shorter than the maximum for absorbance by I was utilized in order to maintain an acceptable signal–noise ratio. Chromatography was performed on a reversed-phase column[6]. Of the various mobile phases studied previously (8), one composed of 0.05 *M* KH_2PO_4-Na_2HPO_4 (pH 6.0)–acetonitrile–methanol (50:47:3) was found to be most satisfactory. The peak height ratio was determined at both wavelengths relative to the diazepam peak height at 254 nm. Calibration curves were obtained in each subject's plasma for each analytical method.

[1] Vacutainer, Becton-Dickinson and Co., Rutherford, N.J.
[2] Model 25 Spectrophotometer, Beckman Instruments, Inc., Fullerton, Calif.
[3] Monitoring of column eluent was performed at 254 nm instead of 225 nm as in Ref. 8. This was advantageous since human plasma samples extracted as described above frequently contained a compound that had a retention time very similar to that of I and absorbed at 225 nm but not at 254 nm.
[4] Model 770, Schoeffel Instrument Corp., Westwood, N.J.
[5] Model 440, Waters Associates, Milford, Mass.
[6] μBondapak C_{18}, Waters Associates, Milford, Mass.

0022-3549/82/1100-1305$01.00/0

in this table represents the amount released from a separate test sample. The values demonstrate the typical reproducibility obtained with this procedure.

This technique could be useful for testing a wide variety of topical formulations where direct contact with the receptor phase is desired. The screen size and configuration could easily be altered to accommodate different types of vehicles, release rates, and concentrations of drugs. This technique may be unsuitable where the drug or vehicle interacts with stainless steel. Such instances are expected to be rare, however, and normally the technique should allow investigators to routinely and uniformly prepare and test small samples with high surface area to weight ratios.

(1) Z. T. Chowhan and R. Pritchard, *J. Pharm. Sci.*, **64**, 754 (1975).
(2) J. W. Ayres and P. A. Laskar, *ibid.*, **63**, 1402 (1974).
(3) L. C. Bailey and C. A. Bailey, *ibid.*, **68**, 508 (1979).

Robert J. Behme
Terry T. Kensler
Dana Brooke [x]
Pharmaceutical Product Development Department
Mead Johnson Pharmaceutical Division
Evansville, IN 47721

Received February 22, 1982.
Accepted for publication June 30, 1982.

Comparison of Chromatographic and Spectrophotometric Analysis of Indocyanine Green in Plasma Following Administration of Multiple Doses to Humans

Keyphrases □ High-pressure liquid chromatography—comparison with spectrophotometric analysis of indocyanine green in plasma following multiple dose administration, humans □ Spectrophotometry—comparison with high-pressure liquid chromatographic analysis of indocyanine green following multiple dose administration, humans □ Indocyanine green—comparison of spectrophotometric and high-pressure liquid chromatographic analysis following multiple dose administration, humans

To the Editor:

Following the administration of small doses (0.5 mg/kg), indocyanine green (I) is highly extracted from blood by the liver (1). Compound I has been used extensively, therefore, to evaluate hepatic function (2, 3) and to estimate hepatic blood flow in humans and laboratory animals (4, 5). Numerous reports have suggested that I is not metabolized in any species (4, 6, 7). Thus, simple spectrophotometric assays (*i.e.*, typically the determination of the absorbance at ~800 nm of plasma samples diluted with distilled water) have been used extensively to estimate the concentration of I in biological fluids. However, it has been reported recently that spectrophotometric and high-pressure liquid chromatographic (HPLC) assays yield radically different estimates of the concentration of I in plasma following the administration of a large dose (25.6 mg/kg) to the rabbit (8). Estimates of the plasma concentration of I ≥30 min postdose were found to be significantly lower using the HPLC assay (almost an order of magnitude lower at many time points). Thus, the total body clearance of I in the rabbit, calculated on the basis of plasma concentrations determined by HPLC, was much higher than that calculated from the spectrophotometric assay results. These investigators postulated that this discrepancy was due to a previously unidentified metabolite. If humans also metabolize I to a compound that interferes with the classical spectrophotometric methods, the clearance value of I based on these assays will not provide a reliable estimate of hepatic blood flow. Because of the potential implications of this assay discrepancy, we compared the spectrophotometric and HPLC assays for I using plasma samples from humans.

Two healthy male subjects (25 and 35 years of age) each received five intravenous bolus doses (0.5 mg/kg each) of I at ~1-hr intervals. Blood samples (5 ml) were collected into heparinized evacuated blood collection tubes[1] prior to and at 1, 3, 5, 7, 9, 11, and 15 min after the first, third, and fifth doses. Plasma was separated and stored at −20° until analyzed (within 36 hr). Previous studies have demonstrated the stability of I under these conditions (8), and preliminary work in our laboratory confirmed these findings.

After the addition of 1.0 μg of diazepam (internal standard) in 100 μl of methanol, proteins were precipitated with acetonitrile (1 ml plasma–1 ml acetonitrile) and the sample was centrifuged. The supernatant was then analyzed by spectrophotometric and HPLC methods. Samples were analyzed using a double beam spectrophotometer[2] equipped with a red-sensitive photomultiplier. The peak absorbance of I in the supernatant was found to occur at 786 nm, and this wavelength was chosen for analysis of all samples. The HPLC method used was that described recently (8) with the following modifications: Dual wavelength (254 and 650 nm)[3] monitoring was employed utilizing two detectors[4,5] in series. Absorbance at 650 nm was examined, since any degradation or metabolic products of I which contained an unaltered chromophore would be expected to absorb at a high wavelength similar to that of the parent compound. The high wavelength monitoring was achieved with a tungsten lamp in a variable wavelength monochromator[4]. A wavelength shorter than the maximum for absorbance by I was utilized in order to maintain an acceptable signal–noise ratio. Chromatography was performed on a reversed-phase column[6]. Of the various mobile phases studied previously (8), one composed of 0.05 *M* KH_2PO_4-Na_2HPO_4 (pH 6.0)–acetonitrile–methanol (50:47:3) was found to be most satisfactory. The peak height ratio was determined at both wavelengths relative to the diazepam peak height at 254 nm. Calibration curves were obtained in each subject's plasma for each analytical method.

[1] Vacutainer, Becton-Dickinson and Co., Rutherford, N.J.
[2] Model 25 Spectrophotometer, Beckman Instruments, Inc., Fullerton, Calif.
[3] Monitoring of column eluent was performed at 254 nm instead of 225 nm as in Ref. 8. This was advantageous since human plasma samples extracted as described above frequently contained a compound that had a retention time very similar to that of I and absorbed at 225 nm but not at 254 nm.
[4] Model 770, Schoeffel Instrument Corp., Westwood, N.J.
[5] Model 440, Waters Associates, Milford, Mass.
[6] μBondapak C_{18}, Waters Associates, Milford, Mass.

0022-3549/82/1100-1305$01.00/0

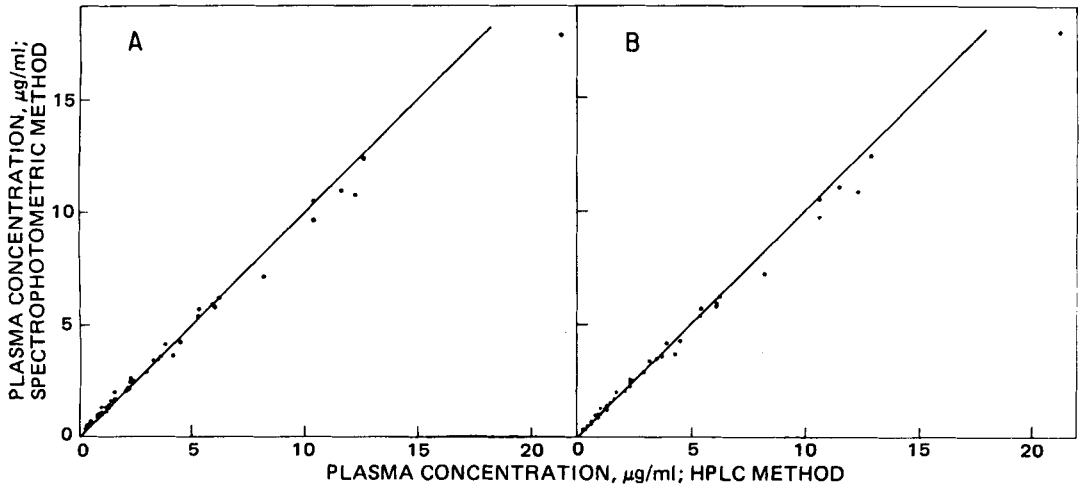

Figure 1—*Comparison of estimates of plasma indocyanine green concentration using spectrophotometric and HPLC procedures. Eluent was monitored at (A) 254 and (B) 650 nm.*

Figure 1A illustrates the relationship between estimates of the plasma concentration of I using the spectrophotometric assay and the HPLC assay (254 nm) which closely approximates the method that yielded the disparate rabbit data (8). As can be seen, a strong correlation exists between the results of the two procedures (r = 0.998; Spearman rank correlation). Similarly, a strong correlation was found between the results of the spectrophotometric method and the HPLC method with monitoring at 650 nm (r = 0.997; Fig. 1B) as well as between the two HPLC results (r = 0.999; data not shown). The close proximity of the data to the line through the origin with a slope of unity (Fig. 1) suggests that all of these assays provide comparable specificity. The single highly aberrant point (Fig. 1) was a sample drawn immediately after the first bolus; hence, the substantial difference between the two methods could not be attributed to accumulated metabolites. Indeed, the HPLC estimate was much higher than the spectrophotometric estimate.

The clearance of I (obtained by least-squares regression of the log plasma concentration *versus* time curve and the relationship: clearance = volume of distribution × elimination rate constant) estimated from concentrations determined by the spectrophotometric as well as HPLC assays at 254 and 650 nm was essentially identical (711 ± 144, 710 ± 145, and 695 ± 142 ml/min, respectively; n = 6; mean ± SD). No detectable concentration of I was present in plasma just prior to the third or fifth dose in either volunteer (lower limit of detection with HPLC method is 0.2 μg/ml). This suggests that accumulation of I does not occur following administration of small doses at 1-hr intervals. No extraneous chromatographic peaks (*i.e.*, peaks other than I and internal standard) appeared at any time points at either wavelength. However, this does not rule out the existence in humans of a metabolite similar to that suggested previously (8), since the metabolite which they proposed eluted in the solvent front, and in the present study this component of the eluent was not investigated. It is also possible that measurable quantities of such a metabolite are only formed when the capacity for biliary excretion is exceeded and, therefore, only seen following large doses or in selected species (*i.e.*, the rabbit) (9). However, the data presented in Fig. 1 suggest that the spectrophotometric assay utilized in this study and the HPLC procedures yield essentially identical estimates of the concentration of I in plasma following typical doses (0.5 mg/kg) in humans.

(1) C. M. Leevy, J. Bender, M. Silverberg, and J. Naylor, *Ann. N.Y. Acad. Sci.*, **111**, 161 (1963).

(2) D. B. Hunton, J. L. Bollman, and H. N. Hoffman, *Gastroenterology*, **39**, 713 (1960).

(3) C. M. Leevy, F. Smith, J. Longueville, G. Paumgartner, and M. Howard, *J. Am. Med. Assoc.*, **200**, 236 (1967).

(4) J. Caesar, S. Shaldon, L. Chiandussi, L. Guevara, and S. Sherlock, *Clin. Sci.*, **21**, 43 (1961).

(5) C. M. Leevy, C. L. Mendenhall, W. Lesko, and M. M. Howard, *J. Clin. Invest.*, **41**, 1169 (1962).

(6) G. R. Cherrick, S. W. Stein, C. M. Leevy, and C. S. Davidson, *ibid.*, **39**, 592 (1960).

(7) F. Barbier and G. A. DeWeerdt, *Clin. Chim. Acta*, **10**, 549 (1964).

(8) P. L. Rappaport and J. J. Thiessen, *J. Pharm. Sci.*, **71**, 157 (1982).

(9) K. Stoeckel, P. J. McNamara, A. J. McLean, P. duSouich, D. Lalka, and M. Gibaldi, *J. Pharmacokinet. Biopharm.*, **8**, 483 (1980).

Craig K. Svensson [x]
David J. Edwards
David Lalka
Department of Pharmaceutics
School of Pharmacy
State University of New York at Buffalo
Amherst, NY 14260
The Clinical Pharmacokinetics Laboratory
Buffalo General Hospital
Buffalo, NY 14203

Paul M. Mauriello
Elliott Middleton, Jr.
Division of Allergy
Department of Medicine
School of Medicine
State University of New York at Buffalo
Buffalo, NY 14214

Received June 18, 1982.
Accepted for publication July 23, 1982.
Supported in part by Grant GM-20852 from the Institute of General Medical Sciences.

Substituent Contribution to the Partition Coefficients of Substituted Benzenes in Solvent–Water Mixtures

Keyphrases □ Partition coefficients—substituted benzenes in solvent–water mixtures, substituent contribution □ Solvent–water mixtures—substituent contribution to the partition coefficients of substituted benzenes □ Benzenes—substituted, substituent contribution to the partition coefficient, solvent–water mixtures

To the Editor:

In the course of correlation analysis for biological activities, octanol–water partition coefficients (P) have been used widely to express the lipophilic interactions of organic compounds with biological substrates. The contribution of a given substituent to the partitioning of a molecule is measured by a substituent constant, π, that is derived empirically from partition coefficients (1). Since discrepancies are found between some π values from different parent compounds and these variations depend also on the nature of the solvent–water system being used (2, 3), it is of interest to examine the relationship between π and pertinent physicochemical properties to identify the factors that account for the discrepancies.

By convention (1), the substituent constant π_X for a functional group attached to a reference compound (benzene or a benzene derivative) is defined as:

$$\pi_X = \log P_X - \log P_R \qquad \text{(Eq. 1)}$$

where P_X is the octanol–water partition coefficient of the compound containing substituent(s) X, and P_R is the partition coefficient of the parent or unsubstituted molecule. The extent to which π_X varies with various parent compounds was found to be relatively small for most nonpolar and weakly polar substituents (1), whereas more variation is observed for polar substituents. The values of π_X were analyzed in terms of the net partition free energies of the substituents and the free energies of interactions of the substituents with the parent aromatic structure. Because the values of the assumed free energy terms are not readily available for verifying the results, no specific rules have been constructed to indicate that π_X derived from different reference systems for a given functional group would be either constant or related in some simple way. The following analysis considers the factors affecting π_X.

Since π_X is a derived quantity, the factors that affect π_X must be contained in the expression for log P. In the absence of solute association or dissociation, the partition coefficients of slightly water-soluble organic solutes between an organic solvent and water, in which the solvent has small solubility in water, can be expressed as (4):

$$\log P = -\log S_w - \log \gamma_0^* + \log(\gamma_w^*/\gamma_w) - \log \overline{V}_0^* \qquad \text{(Eq. 2)}$$

where S_w is the water solubility (moles/liter) of the liquid (or supercooled liquid) solute, γ_0^* is the activity coefficient (Raoult's law convention) in the water-saturated solvent phase, γ_w is the activity coefficient in water at saturation, γ_w^* is the activity coefficient in solvent-saturated water, and $\overline{V}_0^*$ is the molar volume (liters/mole) of the water-saturated solvent. The log $\overline{V}_0^*$ term is essentially constant for solutes in dilute solution.

Table I—Values for Δ, π(Octanol–Water), and π(Heptane–Water) Derived with Respect to Benzene

Compound	Function	Δ[a]	π(octanol–water)[b]	π(heptane–water)[c]
Benzene	—	0	0	0
Toluene	CH_3	0.60	0.56	0.59
Styrene	C_2H_3	0.83	0.82	0.85
Ethylbenzene	C_2H_5	1.20	1.02	1.17
o-Xylene	1-CH_3-2-CH_3	1.08	0.99	1.13
m-Xylene	1-CH_3-3-CH_3	1.09	1.07	1.28
n-Propylbenzene	*n*-C_3H_7	1.66	1.55	1.85
1,3,5-Trimethylbenzene	1,3,5-$(CH_3)_3$	1.46	1.29	1.79
tert-Butylbenzene	*tert*-C_4H_9	1.96	1.98	2.15
Fluorobenzene	F	0.16	0.14	0.19
Chlorobenzene	Cl	0.72	0.71	0.69
Bromobenzene	Br	0.91	0.86	0.84
Iodobenzene	I	1.14	1.12	1.07
o-Dichlorobenzene	1-Cl-2-Cl	1.34	1.22	1.19
m-Dichlorobenzene	1-Cl-3-Cl	1.40	1.25	1.28
1,2,4-Trichlorobenzene	1,2,4-$(Cl)_3$	1.93	1.89	1.80
α,α,α-Trifluorotoluene	CF_3	0.88	0.88	1.05
Aniline	NH_2	−1.24	−1.23	−2.22
m-Chloroaniline	1-NH_2-3-Cl	−0.27	−0.25	−1.55
o-Toluidine	1-NH_2-2-CH_3	−0.83	−0.84	−1.72
m-Toluidine	1-NH_2-3-CH_3	−0.79	−0.73	−1.72
Phenol	OH	−1.70	−0.67	−3.18
Benzoic acid	COOH	−0.73	−0.28	−2.98
Phenylacetic acid	CH_2COOH	−1.15	−0.83	−3.33
Anisole	OCH_3	0.21	−0.02	−0.16
Acetophenone	$COCH_3$	−0.33	−0.40	−1.12
Benzaldehyde	CHO	−0.23	−0.65	−1.21
Nitrobenzene	NO_2	0.14	−0.28	−0.77
Benzonitrile	CN	−0.26	−0.57	−1.36

[a] The Δ values are calculated from the respective γ_w values of the compounds at ~25° and log γ_w = 3.38 for benzene as the standard (Ref. 7). Data for halobenzenes, dichlorobenzenes, 1,2,4-trichlorobenzene, *m*-chloroaniline, and toluidines are taken from the citations given in Ref. 4; anisole and benzonitrile from Ref. 8; and the remainder from the citations in Ref. 6. [b] The π (octanol–water) values are based on log P = 2.13 for benzene (Ref. 1) as the standard and the log P data from the citations in Refs. 1 and 9 for all compounds, except for 1,2,4-trichlorobenzene from Ref. 4. [c] The π (heptane–water) values are calculated from the respective log P values of the compounds using log P = 2.26 for benzene (Ref. 9) as the standard. Data for toluene, xylenes, aniline, *m*-chloroaniline, *m*-toluidine, benzoic acid, and anisole are from the citations in Ref. 9 and the rest from this work.

In octanol–water systems, it has been shown (4, 5) that the primary determinant of the solute partition coefficient is the extent of solute solubility in water (S_w), followed in decreasing order by solute incompatibility with octanol (γ_0^*) and the alteration of solute water solubility by dissolved octanol (γ_w^*/γ_w). The log (γ_w^*/γ_w) term is relatively small for those solutes that have comparable or greater solubility in water than octanol (solvent) in water, and thus can be neglected for many simple aromatic liquids.

Substituting Eq. 2 into Eq. 1 gives:

$$\pi_X \simeq \log[(S_w)_R/(S_w)_X] - \log[(\gamma_0^*)_X/(\gamma_0^*)_R] \qquad \text{(Eq. 3)}$$

or

$$\pi_X \simeq \log[(\gamma_w)_X/(\gamma_w)_R] - \log[(\gamma_0^*)_X/(\gamma_0^*)_R] \qquad \text{(Eq. 4)}$$

where the solubility ratio in Eq. 3 may be replaced by the inverse of the activity coefficient ratio (4, 5). The magnitude of π_X for a functional group in a reference compound thus is equal to the difference between $\log[(\gamma_w)_X/(\gamma_w)_R]$ and $\log[(\gamma_0^*)_X/(\gamma_0^*)_R]$, *i.e.*, between the effects of the substituent on solute compatibility with water and with octanol (solvent).

0022-3549/82/1100-1307$01.00/0

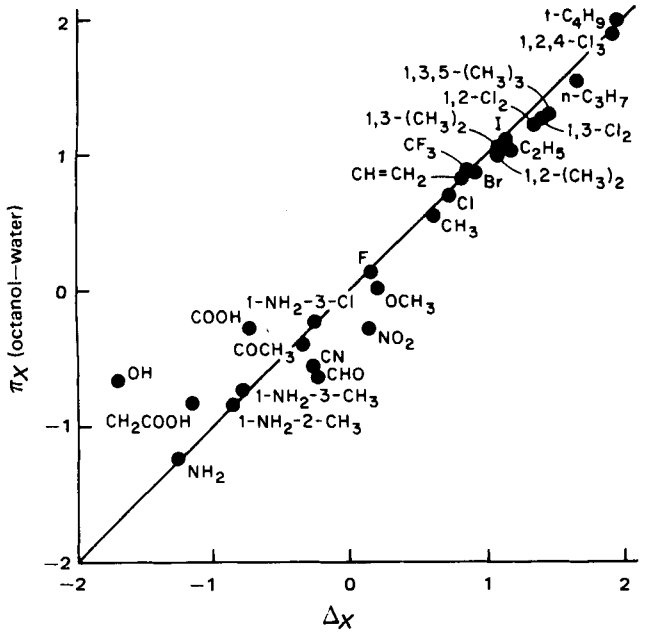

Figure 1—*A comparison of* Δ_X *and* π_X *(octanol–water) values for common substituents with benzene as the reference standard. Key: (—)* π_X *(octanol–water)* = Δ_X.

To illustrate the relative effects of these two terms on the values of π_X for some substituents in the octanol–water system, benzene is chosen as the reference compound. For both benzene and benzene substituted with nonpolar and weakly polar groups (such as X = halogens, alkyl groups, and amino), the logarithmic effects on activity coefficients in octanol (log γ_0^*) are considerably less than in water (log γ_w) (4, 5). For example, the $\log[(\gamma_w)_X/(\gamma_w)_R]$ values with benzene as reference are −1.24, 0.72, 0.91, and 1.66 for X = NH_2, Cl, Br, and n-C_3H_7, respectively, and the corresponding $\log[(\gamma_0^*)_X/(\gamma_0^*)_R]$ values are ~0.00, 0.01, 0.05, and 0.10 calculated following a previously described method (4). Consequently, the magnitude of each π_X should be essentially equal to the value of $\log[(\gamma_w)_X/(\gamma_w)_R]$, which is designated for brevity as Δ_X (6).

A comparison of π_X and Δ_X values is shown in Table I, and a plot of π_X versus Δ_X is shown in Fig. 1. The results indicate that when π_X approximates Δ_X for substituent X and π_Y approximates Δ_Y for substituent Y in monosubstituted benzenes, the values of π_{XX} (or π_{YY}) and π_{XY} also approximate the corresponding values of Δ_{XX} (or Δ_{YY}) and Δ_{XY} for disubstituents X,X and X,Y attached to benzene. Supporting data are demonstrated with xylenes and dichlorobenzenes ($\pi_{XX} \simeq \Delta_{XX}$) and with toluidines and m-chloroaniline ($\pi_{XY} \simeq \Delta_{XY}$). It is recognized, however, that the magnitudes of π_{XX} and π_{XY} (or Δ_{XX} and Δ_{XY}) in disubstitution are not necessarily equal to the sum of π_X and π_Y (or correspondingly of Δ_X and Δ_Y). This is because the increment in solute activity coefficient with addition of a substituent may vary from compound to compound (*i.e.*, from benzene to a substituted benzene) and from solvent to solvent (in this case from water to octanol). Since the additivity rule may not be strictly obeyed when more than one substituent is present, it is better to consider the set of substituents as a whole rather than to treat them as a sum of independent components.

The value of π_X would be expected to deviate significantly from Δ_X when a benzene derivative and benzene show appreciable differences in their respective compatibilities with octanol. If the derivative is more compatible than benzene with octanol, *i.e.*, if $\log[(\gamma_0^*)_X/(\gamma_0^*)_R]$ is negative, then π_X will be greater than Δ_X. The finding that π_X is significantly greater than Δ_X for X = COOH and CH_2COOH is reasonable, because the addition of these highly polar groups to relatively nonpolar benzene should make for better compatibility with the partially polar octanol phase, which also contains 2.3 M of water (10). Although phenol is expected to be more compatible with the octanol than benzene (*i.e.*, $\pi_X > \Delta_X$ when X = OH), the large difference between π_X and Δ_X could partly be due to hydrate formation of phenol in water (11), which introduces inaccuracies into the value of Δ_X (*i.e.*, γ_w for phenol) as calculated from the apparent phenol solubility in water.

With X = NO_2, CN, and CHO, the values of π_X are much smaller than the respective values of Δ_X. It is not clear whether these anomalies are caused by some specific interactions of octanol with nitrobenzene, benzonitrile, and benzaldehyde or by possible solute associations or dissociations in water and/or octanol. In general, although the π_X values for highly polar groups might deviate significantly from the respective Δ_X values in octanol–water systems, the differences are usually well within ±1 for simple aromatic compounds in the absence of association or dissociation. This may be attributed to the partially polar nature of the octanol medium that allows it to accommodate relatively indiscriminately a wide range of benzene derivatives of varying polarities (4, 5).

The foregoing analysis with benzene as reference also applies to systems with other compounds as reference standards. Again, the values of π_X and Δ_X derived with respect to a new reference compound should be comparable with nonpolar and weakly polar functional groups. For instance, when aniline (log P = 0.90) is used as the reference, the values of π_X and Δ_X are 0.98 and 0.98 for X = Cl (*meta*); 0.39 and 0.42 for X = CH_3 (*ortho*); and 0.50 and 0.46 for X = CH_3 (*meta*). With toluene (log P = 2.69) as reference, π_X and Δ_X are 0.43 and 0.48 for X = CH_3 (*ortho*) and 0.51 and 0.49 for X = CH_3 (*meta*). These results agree with the earlier findings that the group contribution to partition coefficient derives mainly from the variation of the solute incompatibility with water, although π_X may vary from one reference standard to another. Again, significant (but not remarkable) differences between π_X and Δ_X would occur if $\log[(\gamma_0^*)_X/(\gamma_0^*)_R]$ should become significant.

While the values of $\log[(\gamma_0^*)_X/(\gamma_0^*)_R]$ are relatively small and comparable for most substituents in the octanol–water system, they can be highly important for certain substituents in other solvent–water systems in which the solvent is sensitive to the polarity difference of the two partitioned solutes. This argument follows a general rule that components of similar polarities and structures usually form more ideal solutions than components of different polarities and structures (*i.e.*, like dissolves like). Consider now the π_X values for the substituents derived from the heptane–water system using again benzene as the parent compound (Table I). A plot of π_X (heptane–water) *versus* Δ_X is given in Fig. 2. The extremely nonpolar structure of

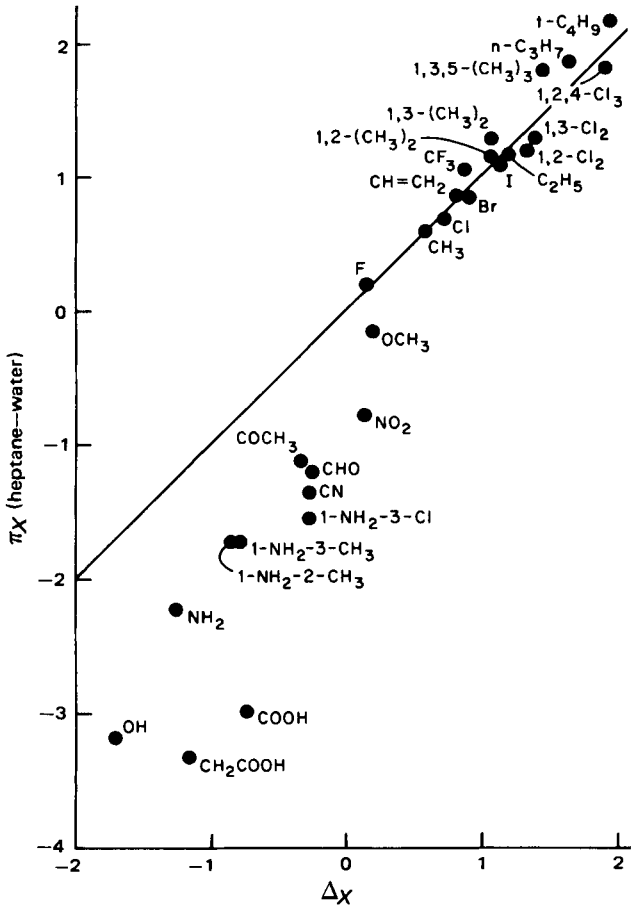

Figure 2—*A comparison of* Δ_X *and* π_X *(heptane–water) values for common substituents with benzene as the reference standard. Key: (—)* π_X *(heptane–water)* = Δ_X.

heptane, as evidenced by small water content of 3.3×10^{-3} *M* at saturation (10), makes it sensitive to the difference in polarity between a substituted and parent (benzene) molecules. With X = NH_2, CHO, NO_2, CN, $COCH_3$, COOH, and CH_2COOH attached to benzene, the observed π_X (heptane–water) values are markedly lower than the corresponding Δ_X values. These results presumably from greatly increased polarities of the substituted benzenes (over that of benzene), which reduce the compatibilities of the substituted benzenes with heptane. Addition of alkyl groups to benzene (making the molecules more hydrocarbon-like) gives somewhat higher π_X (heptane–water) than π_X (octanol–water), as would be expected. Addition of halogen groups shows insignificant differences between the two sets of π_X values. In other words, the values of $\log[(\gamma_0^*)_X/(\gamma_0^*)_R]$ in the heptane phase are reasonably close to zero for relatively nonpolar substituents but are very significant and positive for polar substituents. As a whole, those substituents which cause large differences between π_X (heptane–water) and Δ_X are the same ones that show large differences between π_X (heptane–water) and π_X (octanol–water).

In conclusion, the correspondence between Δ_X and π_X in heptane–water is less obvious than in octanol–water, because heptane shows greater sensitivity than octanol to the polarities of the substituted benzenes.

(1) T. Fujita, J. Iwasa, and C. Hansch, *J. Am. Chem. Soc.*, **86**, 5175 (1964).

(2) A. Leo and C. Hansch, *J. Org. Chem.*, **36**, 1539 (1971).

(3) P. Seiler, *Eur. J. Med. Chem.*, **9**, 473 (1971).

(4) C. T. Chiou, D. W. Schmedding, and M. Manes, *Environ. Sci. Technol.*, **16**, 4 (1982).

(5) C. T. Chiou, in "Hazard Assessment of Chemicals—Current Developments," vol. I, J. Saxena and F. Fisher, Eds., Academic, New York, N.Y., 1981, pp. 117–153.

(6) C. Tsonopoulos and J. M. Prausnitz, *Ind. Eng. Chem. Fundam.*, **10**, 593 (1971).

(7) C. McAuliffe, *J. Phys. Chem.*, **70**, 1267 (1966).

(8) J. C. McGowan, P. N. Atkinson, and L. H. Ruddle, *J. Appl. Chem.*, **16**, 99 (1966).

(9) C. Hansch and A. Leo, "Substituent Constants for Correlation Analysis in Chemistry and Biology," Wiley, New York, N.Y., 1979.

(10) A. Leo, C. Hansch, and D. Elkins, *Chem. Rev.*, **71**, 525 (1971).

(11) F. H. Rhodes and A. L. Markley, *J. Phys. Chem.*, **25**, 527 (1921).

Cary T. Chiou ˣ
David W. Schmedding
Environmental Health Sciences Center
Oregon State University
Corvallis, OR 97331

John H. Block
School of Pharmacy
Oregon State University
Corvallis, OR 97331

Milton Manes
Department of Chemistry
Kent State University
Kent, OH 44242

Received December 24, 1981.
Accepted for publication July 30, 1982.

Supported by U.S. Public Health Grants ES-02400 and ES-00210 and by U.S. Environmental Protection Agency Cooperative Research Fund CR-808046 from the EPA Environmental Research Laboratory at Corvallis, Ore.

Effect of Water Deprivation on Chloramphenicol Disposition Kinetics in Humans

Keyphrases □ Kinetics, disposition—effect of water deprivation on chloramphenicol, humans □ Chloramphenicol—effect of water deprivation, disposition kinetics in humans

To the Editor:

The first study of the effect of water deprivation on drug disposition kinetics was recently reported (1). Temporary water deprivation causes significant changes in drug metabolizing enzymes, hormones responsible for water balance in the body, and blood chemistry and physiology (2–4). Despite these significant changes, little has been reported in the literature on the effect of water deprivation resulting from various disease states and environmental factors on drug disposition kinetics.

The present study reports the effect of highly restricted water intake on chloramphenicol absorption and urinary elimination in humans.

The panel of subjects studied consisted of four healthy male volunteers (weight, 60–72 kg; age, 22–24 years). A total of 14 days was allowed for the conditioning of the subjects for the treatment studies. During the first 11 days,

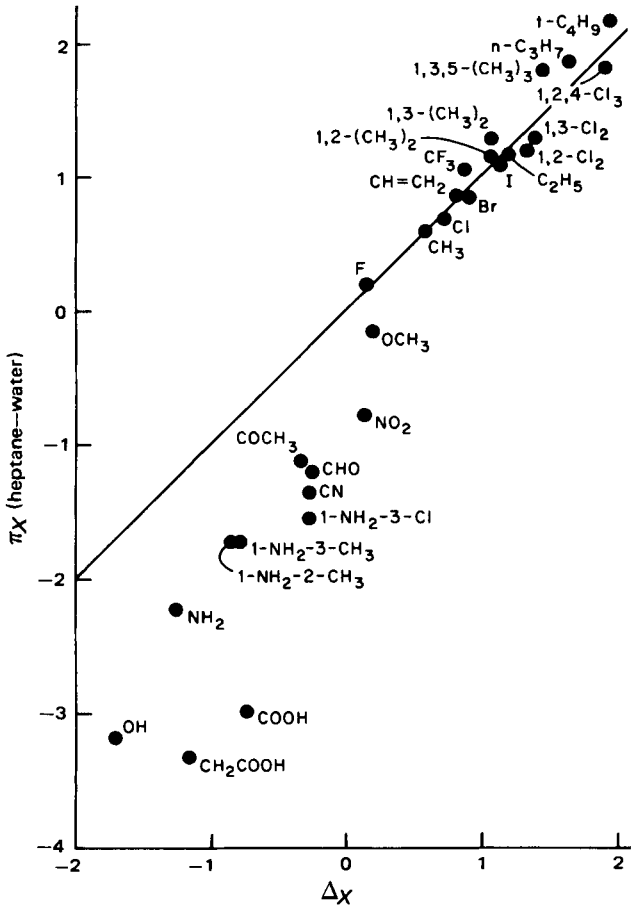

Figure 2—*A comparison of* Δ_X *and* π_X *(heptane–water) values for common substituents with benzene as the reference standard. Key: (—)* π_X *(heptane–water)* = Δ_X.

heptane, as evidenced by small water content of 3.3×10^{-3} *M* at saturation (10), makes it sensitive to the difference in polarity between a substituted and parent (benzene) molecules. With X = NH_2, CHO, NO_2, CN, $COCH_3$, COOH, and CH_2COOH attached to benzene, the observed π_X (heptane–water) values are markedly lower than the corresponding Δ_X values. These results presumably from greatly increased polarities of the substituted benzenes (over that of benzene), which reduce the compatibilities of the substituted benzenes with heptane. Addition of alkyl groups to benzene (making the molecules more hydrocarbon-like) gives somewhat higher π_X (heptane–water) than π_X (octanol–water), as would be expected. Addition of halogen groups shows insignificant differences between the two sets of π_X values. In other words, the values of $\log[(\gamma_0^*)_X/(\gamma_0^*)_R]$ in the heptane phase are reasonably close to zero for relatively nonpolar substituents but are very significant and positive for polar substituents. As a whole, those substituents which cause large differences between π_X (heptane–water) and Δ_X are the same ones that show large differences between π_X (heptane–water) and π_X (octanol–water).

In conclusion, the correspondence between Δ_X and π_X in heptane–water is less obvious than in octanol–water, because heptane shows greater sensitivity than octanol to the polarities of the substituted benzenes.

(1) T. Fujita, J. Iwasa, and C. Hansch, *J. Am. Chem. Soc.*, **86**, 5175 (1964).

(2) A. Leo and C. Hansch, *J. Org. Chem.*, **36**, 1539 (1971).

(3) P. Seiler, *Eur. J. Med. Chem.*, **9**, 473 (1971).

(4) C. T. Chiou, D. W. Schmedding, and M. Manes, *Environ. Sci. Technol.*, **16**, 4 (1982).

(5) C. T. Chiou, in "Hazard Assessment of Chemicals—Current Developments," vol. I, J. Saxena and F. Fisher, Eds., Academic, New York, N.Y., 1981, pp. 117–153.

(6) C. Tsonopoulos and J. M. Prausnitz, *Ind. Eng. Chem. Fundam.*, **10**, 593 (1971).

(7) C. McAuliffe, *J. Phys. Chem.*, **70**, 1267 (1966).

(8) J. C. McGowan, P. N. Atkinson, and L. H. Ruddle, *J. Appl. Chem.*, **16**, 99 (1966).

(9) C. Hansch and A. Leo, "Substituent Constants for Correlation Analysis in Chemistry and Biology," Wiley, New York, N.Y., 1979.

(10) A. Leo, C. Hansch, and D. Elkins, *Chem. Rev.*, **71**, 525 (1971).

(11) F. H. Rhodes and A. L. Markley, *J. Phys. Chem.*, **25**, 527 (1921).

Cary T. Chiou ˣ
David W. Schmedding
Environmental Health Sciences Center
Oregon State University
Corvallis, OR 97331

John H. Block
School of Pharmacy
Oregon State University
Corvallis, OR 97331

Milton Manes
Department of Chemistry
Kent State University
Kent, OH 44242

Received December 24, 1981.
Accepted for publication July 30, 1982.

Supported by U.S. Public Health Grants ES-02400 and ES-00210 and by U.S. Environmental Protection Agency Cooperative Research Fund CR-808046 from the EPA Environmental Research Laboratory at Corvallis, Ore.

Effect of Water Deprivation on Chloramphenicol Disposition Kinetics in Humans

Keyphrases □ Kinetics, disposition—effect of water deprivation on chloramphenicol, humans □ Chloramphenicol—effect of water deprivation, disposition kinetics in humans

To the Editor:

The first study of the effect of water deprivation on drug disposition kinetics was recently reported (1). Temporary water deprivation causes significant changes in drug metabolizing enzymes, hormones responsible for water balance in the body, and blood chemistry and physiology (2–4). Despite these significant changes, little has been reported in the literature on the effect of water deprivation resulting from various disease states and environmental factors on drug disposition kinetics.

The present study reports the effect of highly restricted water intake on chloramphenicol absorption and urinary elimination in humans.

The panel of subjects studied consisted of four healthy male volunteers (weight, 60–72 kg; age, 22–24 years). A total of 14 days was allowed for the conditioning of the subjects for the treatment studies. During the first 11 days,

each was allowed 1 liter of water/day, for the next 2 days only 350 ml/day, and 24 hr before the study only 200 ml of water/day. All subjects were fasted overnight. The treatment studies began at 8 am when chloramphenicol was given as 10 ml of suspension[1] (250 mg) with 150 ml of water. Urine samples were collected afterward on a periodic basis during an interval of 24 hr and analyzed for chloramphenicol using a previously described method (5). A 2-week wash-out period was allowed between control and treatment studies. In the control studies, which preceded the treatment studies, food and water were available *ad libitum*. Otherwise, conditions of the control studies were the same as for the treatment studies. The data of Table I show the effect of water deprivation on the absorption rate and the urinary excretion of chloramphenicol. Although there was no significant change in the total absorption of chloramphenicol, the absorption half-life decreased significantly (~66%), while the peak excretion rate increased, and the time at which the peak excretion occurred decreased significantly.

These findings are of great interest, since the overall effect of water deprivation is specified in terms of the rate of absorption change, which results in the substantially higher plasma levels of chloramphenicol in the water deprivation state. The influence of such (water deprivation) alteration in the peak plasma levels of chloramphenicol on the efficacy and toxicity of this antibiotic will profoundly affect its clinical utility. These observations are the first of their kind, and mechanisms for the effects observed remain to be investigated.

[1] Chloromycetin palmitate suspension, Parke-Davis Co., Karachi, Pakistan.

Table I—Urinary Excretion Characteristics of Chloramphenicol in Water Deprivation

	Control[a]	Water Deprivation[a]
Percent recovery	91 ± 12	103 ± 3
Peak excretion rate, mg/hr	23.06 ± 4.74	35.71 ± 4.92
Peak concentration time, hr	4.5 ± 0.3	2.5 ± 0.3
$t_{1/2}$ absorption, hr	1.8 ± 0.3	0.6 ± 0.1

[a] Mean ± *SD*; all values statistically different at $p < 0.05$ except those pertaining to the percent recovery, which were not significantly different.

(1) S. Bakar and S. Niazi, *J. Pharm. Sci.*, in press.
(2) G. I. Hatton, *Physiol. Behav.*, **7**, 35 (1970).
(3) P. Aarseth and D. King, *Acta Physiol. Scand.*, **85**, 277 (1972).
(4) B. Ballantyne, *Cytobiosis*, **6**, 217 (1972).
(5) H. Negoro, *Yakugaku Zasshi*, **70**, 669 (1950).

T. Ahmad
G. Parveen
Faculty of Pharmacy
University of Karachi
Karachi, Pakistan

S. Niazi[x]
Department of Pharmacodynamics
College of Pharmacy
University of Illinois
Chicago, IL 60612

Received March 3, 1982.
Accepted for publication August 4, 1982.

BOOKS

REVIEWS

ISI Atlas of Science. By Dr. EUGENE GARFIELD. Institute of Scientific Information, 3501 Market Street, University City Science Center, Philadelphia, PA 19104. 1982. 540 pp. 23 × 29 cm. Price $45.00 to individuals, $90.00 to institutions.

The *ISI Atlas of Science* is a new information and research guide in biochemistry and molecular biology. The *Atlas* is a unique new aid containing concise, convenient lists of papers and current literature in 102 active research areas in the life sciences.

This atlas contains a reference system of core clusters of research areas identified objectively by the use of citation patterns of publishing scientists, graphically displayed in detail by the use of maps.

Research areas described in the *Atlas* are divided into minireviews, core document bibliographies, specialty maps, and key citing document bibliographies. Also included within this atlas is a unique multi-colored fold-out map providing a "global" view of the relationships and interactions of the 102 research areas, ideal for display in labs, classrooms, and libraries.

The *Atlas* was designed to be used as a tool for analytical and utilitarian research needs. This publication should be a valuable tool for specialists in biochemistry and molecular biology for overviews of new fields of research and fields related to present work. Librarians can use the *Atlas* for subject bibliographies. This should also be of interest to historians for bibliographic and analytical information in tracing the structure and growth of scientific fields.

Staff Review

Drug Absorption. Edited by L. F. PRESCOTT and W. S. NIMMO. Adis Press, 404 Sydney Road, Balgowlah, NSW 2093, Australia. 1979. 353 pp. 16 × 24 cm.

This multi-authored book describes the proceedings of an international conference of Drug Absorption which was held in Edinburgh in September 1979.

The editors of the book are recognized authorities in the field of drug absorption, and the many authors who have contributed to the 31 chapters represent a broad, international array of specialists in this area.

Topics covered include anatomical and physiological factors affecting absorption, membrane effects, rectal absorption, presystemic and intestinal metabolism, toxicity, formulations and novel drug delivery systems, transdermal and controlled GI drug absorption, effect of age and disease states on drug bioavailability, methods of assessing drug absorption, *in vitro–in vivo* correlations, and problems in the assessment of drug absorption. The concluding chapter summarizes the viewpoints of regulatory agencies, clinical pharmacology, and of the pharmaceutical industry on drug bioavailability and pharmacokinetic studies.

Most of the chapters contain a discussion section, and all chapters are adequately referenced. A subject index is included.

This is a useful and instructive book that is broad-reaching in scope. The extensive coverage of many factors related to drug absorption, and the clear and articulate way in which the material is presented, makes it a required text for those interested in this broad area of research and clinical practice.

Reviewed by Peter G. Welling
School of Pharmacy
University of Wisconsin
Madison, WI 53706

0022-3549/82/1100-1310$01.00/0

each was allowed 1 liter of water/day, for the next 2 days only 350 ml/day, and 24 hr before the study only 200 ml of water/day. All subjects were fasted overnight. The treatment studies began at 8 am when chloramphenicol was given as 10 ml of suspension[1] (250 mg) with 150 ml of water. Urine samples were collected afterward on a periodic basis during an interval of 24 hr and analyzed for chloramphenicol using a previously described method (5). A 2-week wash-out period was allowed between control and treatment studies. In the control studies, which preceded the treatment studies, food and water were available *ad libitum*. Otherwise, conditions of the control studies were the same as for the treatment studies. The data of Table I show the effect of water deprivation on the absorption rate and the urinary excretion of chloramphenicol. Although there was no significant change in the total absorption of chloramphenicol, the absorption half-life decreased significantly (~66%), while the peak excretion rate increased, and the time at which the peak excretion occurred decreased significantly.

These findings are of great interest, since the overall effect of water deprivation is specified in terms of the rate of absorption change, which results in the substantially higher plasma levels of chloramphenicol in the water deprivation state. The influence of such (water deprivation) alteration in the peak plasma levels of chloramphenicol on the efficacy and toxicity of this antibiotic will profoundly affect its clinical utility. These observations are the first of their kind, and mechanisms for the effects observed remain to be investigated.

[1] Chloromycetin palmitate suspension, Parke-Davis Co., Karachi, Pakistan.

Table I—Urinary Excretion Characteristics of Chloramphenicol in Water Deprivation

	Control[a]	Water Deprivation[a]
Percent recovery	91 ± 12	103 ± 3
Peak excretion rate, mg/hr	23.06 ± 4.74	35.71 ± 4.92
Peak concentration time, hr	4.5 ± 0.3	2.5 ± 0.3
$t_{1/2}$ absorption, hr	1.8 ± 0.3	0.6 ± 0.1

[a] Mean ± *SD*; all values statistically different at $p < 0.05$ except those pertaining to the percent recovery, which were not significantly different.

(1) S. Bakar and S. Niazi, *J. Pharm. Sci.*, in press.
(2) G. I. Hatton, *Physiol. Behav.*, **7**, 35 (1970).
(3) P. Aarseth and D. King, *Acta Physiol. Scand.*, **85**, 277 (1972).
(4) B. Ballantyne, *Cytobiosis*, **6**, 217 (1972).
(5) H. Negoro, *Yakugaku Zasshi*, **70**, 669 (1950).

T. Ahmad
G. Parveen
Faculty of Pharmacy
University of Karachi
Karachi, Pakistan

S. Niazi[x]
Department of Pharmacodynamics
College of Pharmacy
University of Illinois
Chicago, IL 60612

Received March 3, 1982.
Accepted for publication August 4, 1982.

BOOKS

REVIEWS

ISI Atlas of Science. By Dr. EUGENE GARFIELD. Institute of Scientific Information, 3501 Market Street, University City Science Center, Philadelphia, PA 19104. 1982. 540 pp. 23 × 29 cm. Price $45.00 to individuals, $90.00 to institutions.

The *ISI Atlas of Science* is a new information and research guide in biochemistry and molecular biology. The *Atlas* is a unique new aid containing concise, convenient lists of papers and current literature in 102 active research areas in the life sciences.

This atlas contains a reference system of core clusters of research areas identified objectively by the use of citation patterns of publishing scientists, graphically displayed in detail by the use of maps.

Research areas described in the *Atlas* are divided into minireviews, core document bibliographies, specialty maps, and key citing document bibliographies. Also included within this atlas is a unique multi-colored fold-out map providing a "global" view of the relationships and interactions of the 102 research areas, ideal for display in labs, classrooms, and libraries.

The *Atlas* was designed to be used as a tool for analytical and utilitarian research needs. This publication should be a valuable tool for specialists in biochemistry and molecular biology for overviews of new fields of research and fields related to present work. Librarians can use the *Atlas* for subject bibliographies. This should also be of interest to historians for bibliographic and analytical information in tracing the structure and growth of scientific fields.

Staff Review

Drug Absorption. Edited by L. F. PRESCOTT and W. S. NIMMO. Adis Press, 404 Sydney Road, Balgowlah, NSW 2093, Australia. 1979. 353 pp. 16 × 24 cm.

This multi-authored book describes the proceedings of an international conference of Drug Absorption which was held in Edinburgh in September 1979.

The editors of the book are recognized authorities in the field of drug absorption, and the many authors who have contributed to the 31 chapters represent a broad, international array of specialists in this area.

Topics covered include anatomical and physiological factors affecting absorption, membrane effects, rectal absorption, presystemic and intestinal metabolism, toxicity, formulations and novel drug delivery systems, transdermal and controlled GI drug absorption, effect of age and disease states on drug bioavailability, methods of assessing drug absorption, *in vitro–in vivo* correlations, and problems in the assessment of drug absorption. The concluding chapter summarizes the viewpoints of regulatory agencies, clinical pharmacology, and of the pharmaceutical industry on drug bioavailability and pharmacokinetic studies.

Most of the chapters contain a discussion section, and all chapters are adequately referenced. A subject index is included.

This is a useful and instructive book that is broad-reaching in scope. The extensive coverage of many factors related to drug absorption, and the clear and articulate way in which the material is presented, makes it a required text for those interested in this broad area of research and clinical practice.

Reviewed by Peter G. Welling
School of Pharmacy
University of Wisconsin
Madison, WI 53706

0022-3549/82/1100-1310$01.00/0

each was allowed 1 liter of water/day, for the next 2 days only 350 ml/day, and 24 hr before the study only 200 ml of water/day. All subjects were fasted overnight. The treatment studies began at 8 am when chloramphenicol was given as 10 ml of suspension[1] (250 mg) with 150 ml of water. Urine samples were collected afterward on a periodic basis during an interval of 24 hr and analyzed for chloramphenicol using a previously described method (5). A 2-week wash-out period was allowed between control and treatment studies. In the control studies, which preceded the treatment studies, food and water were available *ad libitum*. Otherwise, conditions of the control studies were the same as for the treatment studies. The data of Table I show the effect of water deprivation on the absorption rate and the urinary excretion of chloramphenicol. Although there was no significant change in the total absorption of chloramphenicol, the absorption half-life decreased significantly (~66%), while the peak excretion rate increased, and the time at which the peak excretion occurred decreased significantly.

These findings are of great interest, since the overall effect of water deprivation is specified in terms of the rate of absorption change, which results in the substantially higher plasma levels of chloramphenicol in the water deprivation state. The influence of such (water deprivation) alteration in the peak plasma levels of chloramphenicol on the efficacy and toxicity of this antibiotic will profoundly affect its clinical utility. These observations are the first of their kind, and mechanisms for the effects observed remain to be investigated.

[1] Chloromycetin palmitate suspension, Parke-Davis Co., Karachi, Pakistan.

Table I—Urinary Excretion Characteristics of Chloramphenicol in Water Deprivation

	Control[a]	Water Deprivation[a]
Percent recovery	91 ± 12	103 ± 3
Peak excretion rate, mg/hr	23.06 ± 4.74	35.71 ± 4.92
Peak concentration time, hr	4.5 ± 0.3	2.5 ± 0.3
$t_{1/2}$ absorption, hr	1.8 ± 0.3	0.6 ± 0.1

[a] Mean ± *SD*; all values statistically different at $p < 0.05$ except those pertaining to the percent recovery, which were not significantly different.

(1) S. Bakar and S. Niazi, *J. Pharm. Sci.*, in press.
(2) G. I. Hatton, *Physiol. Behav.*, **7**, 35 (1970).
(3) P. Aarseth and D. King, *Acta Physiol. Scand.*, **85**, 277 (1972).
(4) B. Ballantyne, *Cytobiosis*, **6**, 217 (1972).
(5) H. Negoro, *Yakugaku Zasshi*, **70**, 669 (1950).

T. Ahmad
G. Parveen
Faculty of Pharmacy
University of Karachi
Karachi, Pakistan

S. Niazi[x]
Department of Pharmacodynamics
College of Pharmacy
University of Illinois
Chicago, IL 60612

Received March 3, 1982.
Accepted for publication August 4, 1982.

BOOKS

REVIEWS

ISI Atlas of Science. By Dr. EUGENE GARFIELD. Institute of Scientific Information, 3501 Market Street, University City Science Center, Philadelphia, PA 19104. 1982. 540 pp. 23 × 29 cm. Price $45.00 to individuals, $90.00 to institutions.

The *ISI Atlas of Science* is a new information and research guide in biochemistry and molecular biology. The *Atlas* is a unique new aid containing concise, convenient lists of papers and current literature in 102 active research areas in the life sciences.

This atlas contains a reference system of core clusters of research areas identified objectively by the use of citation patterns of publishing scientists, graphically displayed in detail by the use of maps.

Research areas described in the *Atlas* are divided into minireviews, core document bibliographies, specialty maps, and key citing document bibliographies. Also included within this atlas is a unique multi-colored fold-out map providing a "global" view of the relationships and interactions of the 102 research areas, ideal for display in labs, classrooms, and libraries.

The *Atlas* was designed to be used as a tool for analytical and utilitarian research needs. This publication should be a valuable tool for specialists in biochemistry and molecular biology for overviews of new fields of research and fields related to present work. Librarians can use the *Atlas* for subject bibliographies. This should also be of interest to historians for bibliographic and analytical information in tracing the structure and growth of scientific fields.

Staff Review

Drug Absorption. Edited by L. F. PRESCOTT and W. S. NIMMO. Adis Press, 404 Sydney Road, Balgowlah, NSW 2093, Australia. 1979. 353 pp. 16 × 24 cm.

This multi-authored book describes the proceedings of an international conference of Drug Absorption which was held in Edinburgh in September 1979.

The editors of the book are recognized authorities in the field of drug absorption, and the many authors who have contributed to the 31 chapters represent a broad, international array of specialists in this area.

Topics covered include anatomical and physiological factors affecting absorption, membrane effects, rectal absorption, presystemic and intestinal metabolism, toxicity, formulations and novel drug delivery systems, transdermal and controlled GI drug absorption, effect of age and disease states on drug bioavailability, methods of assessing drug absorption, *in vitro–in vivo* correlations, and problems in the assessment of drug absorption. The concluding chapter summarizes the viewpoints of regulatory agencies, clinical pharmacology, and of the pharmaceutical industry on drug bioavailability and pharmacokinetic studies.

Most of the chapters contain a discussion section, and all chapters are adequately referenced. A subject index is included.

This is a useful and instructive book that is broad-reaching in scope. The extensive coverage of many factors related to drug absorption, and the clear and articulate way in which the material is presented, makes it a required text for those interested in this broad area of research and clinical practice.

Reviewed by Peter G. Welling
School of Pharmacy
University of Wisconsin
Madison, WI 53706

0022-3549/82/1100-1310$01.00/0

A publication of the
American Pharmaceutical Association—
the National Professional Society
of Pharmacists

JOURNAL OF PHARMACEUTICAL SCIENCES

INDEX TO AUTHORS
INDEX TO SUBJECTS

VOLUME 71
JANUARY TO DECEMBER, 1982

Published monthly under the supervision of the Board of Trustees

A New Editor Takes the Helm

This past week, we read an article forecasting the demise of scientific journals as we know them today, and predicting that ten, or at most fifteen, years from now computerized information systems will have completely displaced print and paper for the recording and dissemination of technical reports and research findings.

That article was not the first one we read along that line. In fact, it was just the latest of many such articles that have made similar predictions over the past twenty years or more. And, of course, had the initial forecasts of results and timing been accurate, neither this journal nor its many companion research periodicals would be appearing in printed format (so-called "hard copy") today.

So we must view such sweeping prognostications with an appropriate air of skepticism.

On the other hand, we also recall similar forecasts being made less than twenty years ago with regard to conventional office typewriters, both manual and electric. And, lo and behold, this very editorial is being composed today on a computerized word processor complete with video screen, disc storage, and a whole array of modern electronic hardware. Hence, this second experience simply confirms the adage that, with regard to the future, precious little can be said with any certainty.

Nevertheless, regardless of how our information systems may be automated, and regardless of whatever novel devices may be developed for the storage and transmittal of that information, human judgment, human decisions, and human selection will remain just as important and necessary in determining what qualifies as good research deserving of publication twenty years from now as today. Consequently, the talents and expertise of a knowledgeable, trained scientist-editor will be just as important as ever before in the research journal publication process.

All of which brings us to the purpose of this editorial.

The *Journal of Pharmaceutical Sciences* has had the particular good fortune to have the sharp blue pencil, the perceptive watchful eye, and, yes, even the devoted loving care, of a highly dedicated and competent editor ever since this writer relinquished the position in December 1973. Mary Hudson Ferguson, Ph.D., had previously served with distinction as assistant editor, and subsequently as associate editor, from the time she joined the American Pharmaceutical Association staff in January, 1967. Having amply demonstrated that she could handle the editorship, it was with complete confidence that the full editorship was then entrusted to her almost nine years ago.

And over the years, numerous authors and an equally numerous group of reviewers developed well-deserved respect and appreciation for the obvious interest and efforts she devoted to the *Journal* as a whole as well as to each and every manuscript submitted to it for publication consideration. Through her efforts and professional contribution, we believe that a very good journal was made even much better, and that it achieved a new high level of national and international recognition as a first-rate research-oriented publication.

For personal and family reasons, Dr. Ferguson decided about a year ago to take early retirement. It was with great reluctance that the Association and its Board of Trustees acceded to her wishes and accepted her resignation. Her associates on staff, as well as the many professional friends she made over the years in her work on the *Journal*, were saddened to learn of her impending departure. All, however, wish her the best in her decision and hope for her personal happiness.

And now a new chapter has begun in the life of the *Journal of Pharmaceutical Sciences.* Effective November 1, Sharon G. Boots, Ph.D., took over the reins from Dr. Ferguson. In succeeding to the editorship, Dr. Boots continues in the scientific mold that the APhA established for the *Journal's* editors when it was initially founded over seventy years ago. Drawing on her background, it is her intention to maintain and extend the tradition of high scientific quality that has been the *Journal's* hallmark over the years. Moreover, she has the training and experience to enable her to achieve that goal.

We are pleased, therefore, to welcome Dr. Boots as the new editor, and to introduce her to the *Journal's* readership.

And to her we offer the old naval officer's greeting of "Welcome aboard!"

—EDWARD G. FELDMANN
American Pharmaceutical Association
Washington, DC 20037

0022-3549/82/1200-1311$01.00/0

JOURNAL OF PHARMACEUTICAL SCIENCES

DECEMBER 1982
VOLUME 71 NUMBER 12

RESEARCH ARTICLES

Effects of Surfactants on the Aqueous Stability and Solubility of β-Lactam Antibiotics

AKIRA TSUJI *x, ETSUKO MIYAMOTO ‡, MUNEAKI MATSUDA *, KEIKO NISHIMURA *, and TSUKINAKA YAMANA §

Received June 8, 1981, from the *Faculty of Pharmaceutical Sciences and §Hospital Pharmacy, Kanazawa University, Takara-machi, Kanazawa 920, Japan, and the ‡School of Pharmacy, Hokuriku University, Kanagawa-machi, Kanazawa 920-11, Japan. Accepted for publication February 4, 1982.

Abstract □ Studies were undertaken to elucidate the interaction between β-lactam antibiotics and surfactant micelles and to examine the effects of surfactants on their aqueous stability and solubility. The apparent binding constant of the micelle–antibiotic complex was determined as a function of the solution pH at 37° and $\mu = 0.15$ by the dynamic dialysis method and hydrolysis study. In the interaction with nonionic and anionic micelles of polyoxyethylene-23-lauryl ether (I) and sodium lauryl sulfate (II), large differences were noted in the binding constants between the undissociated and ionized species of penicillins. However, the cationic surfactants, cetyltrimethylammonium bromide (III), showed no significant difference in the binding constants for both species. Acid degradation of penicillins was protected in micellar solutions of I and III but was facilitated in micelles of II. The surfactants exerted no influence on the neutral degradation of the antibiotics used. The solubilization of penicillin V acid by micelles of I was studied at pH 2.0 and 35°. The solubility increased threefold in the presence of 10 m*M* I.

Keyphrases □ Antibiotics, β-lactam—effects of surfactants on the aqueous stability and solubility, interactions with surfactant micelles □ Surfactant micelles—effects on the aqueous stability and solubility of β-lactam antibiotics □ Binding constant—interaction between β-lactam antibiotics and surfactant micelles, aqueous stability and solubility

The interaction of surface-active agents with drugs is of theoretical and practical importance, since such surfactants represent one of the most important groups of adjuvants in pharmaceutical preparations. Surfactants incorporated in the drug dosage form are able to influence the drug stability and dissolution as a result of drug–surfactant micellar interactions.

So far there have been only a few reports on the interaction (1–3) between β-lactam antibiotics and surfactant micelles. Recently, a catalytic effect of cationic surfactants on the degradation of cephalexin at neutral pH by entrapment of the antibiotic micelles was described. No effects on the cephalexin stability, however, were observed in anionic micelles (2).

The aims of the present study were to elucidate the entrapment of penicillin and cephalosporin antibiotics into the micelle of various types of surfactants as a function of the solution pH, and to investigate the effects of the antibiotic–micelle interaction on the stability and solubility of these antibiotics under a gastric pH environment. A preliminary report has already been published (3).

EXPERIMENTAL

Materials—*Antibiotics*—The following β-lactam antibiotics were used as supplied: propicillin potassium[1] (993 μg/mg), penicillin V potassium[2] (1490 U/mg), and cefazolin sodium[3] (966 μg/mg). Free acid of penicillin V was obtained from a commercial source[4].

Surfactants—Polyoxyethylene-23-lauryl ether (I), sodium lauryl sulfate (II), and cetyltrimethylammonium bromide (III) were obtained from commercial sources and used without further purification except II. Compound II was recrystallized according to the literature (4).

Chemicals—All other chemicals employed were of reagent grade and used without further purification except imidazole. Imidazole was recrystallized from benzene followed by a thorough washing with ether.

Analytical Procedures—Propicillin and penicillin V were determined by the spectrophotometric method developed previously (5). No influence of surfactants in this assay was observed. The concentration of the antibiotic in the samples was calculated from a calibration curve prepared daily. Cefazolin was analyzed in the stability experiment by reversed-phase high-performance liquid chromatography (HPLC). The liquid chromatograph[5] was equipped with a UV detector[6] set at 254 nm. The stationary phase was octadecylsilane chemically bonded on totally porous silica gel, prepacked into a 125-mm stainless steel column[7] (4.6-mm i.d.). The mobile phase was 10% (v/v) acetonitrile–0.01 *M* ammonium acetate. The instrument was operated at ambient temperature and at a flow rate

[1] Takeda Chemical Industries, Osaka, Japan.
[2] Banyu Pharmaceutical Co., Osaka, Japan.
[3] Fujisawa Pharmaceutical Co., Osaka, Japan.
[4] Sigma Chemical Co., St. Louis, Mo.
[5] Model FLC-A700, Japan Spectroscopic Co., Tokyo, Japan.
[6] Model UVIDEC-100, Japan Spectroscopic Co., Tokyo, Japan.
[7] SC-01, Japan Spectroscopic Co., Tokyo, Japan.

0022-3549/82/1200-1313$01.00/0

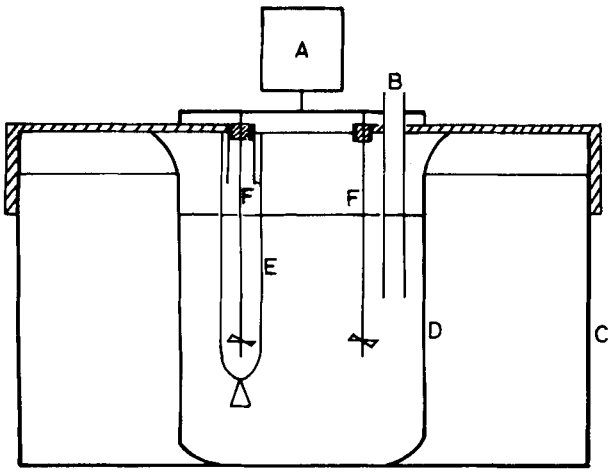

Figure 1—*Apparatus for the dynamic dialysis experiment. Key: (A) control motor; (B) sampling hole; (C) thermostated water bath; (D) jacketed beaker; (E) dialysis membrane; and (F) stirring shaft.*

of 1.0 ml/min, and then samples were injected through a 100-μl injector[8]. The peak heights were used for quantification.

Procedure—*Dynamic Dialysis*—The method employed was essentially the same as that described previously (6). The apparatus used in this study is illustrated in Fig. 1. The system consisted of a jacketed beaker (500 ml) set in a thermostated water bath. Three hundred milliliters of buffer solution (ionic strength 0.15) was placed in the beaker. A cellulose tube[9] was knotted at one end to form a bag (length 10 cm) and attached with a rubber band to the glass tubing with a stirring shaft. Eight milliliters of antibiotic buffer solution with or without surfactants was placed into the bag. The bag attached with a stopper was fitted on the beaker. Both the inner and outer solutions were stirred. All experiments were carried out at 37 ± 0.1° and at various pHs with phosphate, acetate, and citrate buffer systems maintained at an ionic strength of 0.15. At appropriate time intervals, aliquots (10 ml) of the outer solution were withdrawn and 10 ml of drug-free buffer solution preheated at 37° was added. The samples were analyzed by the spectrophotometric method or HPLC described in the previous section. The concentration of the outer solution samples was corrected as follows:

$$(C_{II})_n = (C_{II})_n^{obs} + (V_s/V_{II}) \sum_{i=1}^{n} (C_{II})_{i-1} \qquad \text{(Eq. 1)}$$

where $(C_{II})_n$ and $(C_{II})_n^{obs}$ represent the true and observed concentrations of the nth sample from the outer solution, respectively, and V_s and V_{II} represent the sampling volume and volume of the outer solution, respectively.

Degradation Kinetics—Unless otherwise stated, kinetic studies were carried out at 37 ± 0.1° and an ionic strength of 0.15. Each antibiotic was dissolved in hydrochloric acid–potassium chloride aqueous solution with or without surfactant to give a final antibiotic concentration of 6×10^{-4} *M*. A saturated solution of the antibiotic was sometimes used because of limited solubility. At appropriate time intervals, aliquots were withdrawn, cooled, and analyzed. The pseudo first-order rate constants, k_{deg}, were calculated by least-squares analysis of the slopes of plots between the logarithm of the antibiotic concentration and time.

Solubility Measurement—An excess of penicillin V (acid form) was added to the hydrochloric acid–potassium chloride solution (pH 2.0 and ionic strength 0.5) in a glass-stoppered flask. The flask was placed in a thermostated water bath at 35 ± 0.1° and shaken mechanically until the antibiotic concentration in the solution showed an equilibrium value. A sample was taken through a 0.45-μm membrane filter[10] and, if necessary, assayed after appropriate dilution with distilled water. The pH of the sample solution was measured[11] before use and at the end of the experiment; no significant change was observed.

Determination of Critical Micelle Concentration—The determination of the critical micelle concentration (CMC) was accomplished by determining the concentration at which the break in the log concentration *versus* surface tension plot occurs. The surface tension of surfactant solutions of ionic strength of 0.15 containing various concentrations of I, II, or III and the antibiotic at the concentration used for dialysis and degradation studies was determined at 37° by a Du Nöuy tensiometer[12].

[8] Model LP1-350, Japan Spectroscopic Co., Tokyo, Japan.
[9] Visking dialysis membrane, Union Carbide Corp., Chicago, Ill.
[10] Sartörius-membranfilter, GmbH, 34 Göttingen, West Germany.
[11] PHM26 pH-meter, Radiometer, Copenhagen, Denmark.

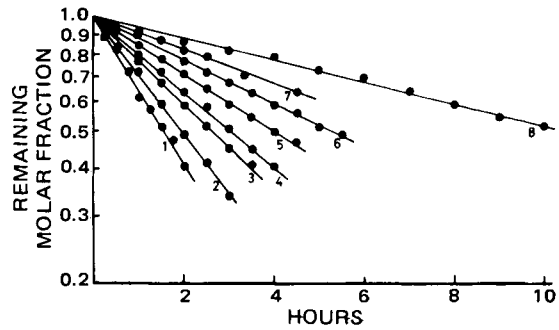

Figure 2—*First-order plots for the dialysis of propicillin in the presence of surfactants of various pH values at 37° and μ = 0.15. Key: 1 (control, pH 6.50); 2 (4×10^{-2} M II, pH 6.50); 3 (2×10^{-2} M I, pH 6.50); 4 (3×10^{-2} M II, pH 4.00); 5 (2.4×10^{-3} M III, pH 4.00); 6 (4×10^{-2} M I, pH 4.00); 7 (1.5×10^{-2} M I, pH 3.00); 8 (6.9×10^{-2} M III, pH 6.50).*

RESULTS

Kinetics of Dynamic Dialysis—For quantification of the interaction between a drug molecule and surfactant micelles, various methods are available such as equilibrium dialysis (7), dynamic dialysis (8), micellar solubilization (9), the potentiometric titration method (10), molecular sieve (11), and micellar catalysis kinetics in the drug degradation (9). Among these, the dynamic dialysis method provides quick information for the existence of the interaction with macromolecules by utilization of marked difference of the permeation rate through a dialysis membrane.

According to Fick's first law of diffusion, the rate of drug dialysis can be expressed by:

$$\frac{d(C_I)_T}{dt} = -k_{dia}[(C_I)_T - (C_{II})_T] \qquad \text{(Eq. 2)}$$

where $(C_I)_T$ and $(C_{II})_T$ represent the total concentration of the drug in the inner and outer solutions of the dialysis bag, respectively. Since the present experiments were carried out under the sink condition, $(C_I)_T - (C_{II})_T$ was assumed to be equal to $(C_I)_T$. The apparent first-order dialysis rate constant, k_{dia}, therefore, was calculated from:

$$\ln(C_I)_T/C_0 = -k_{dia}t \qquad \text{(Eq. 3)}$$

where C_0 represents the initial concentration of the drug solution in the dialysis bag. The value for $(C_I)_T$ was calculated from the mass balance equation as follows:

$$(C_I)_T = \frac{C_0V_I - (C_{II})_TV_{II}}{V_I} \qquad \text{(Eq. 4)}$$

where V_I and V_{II} represent the volume of the inner and outer solutions, respectively. Figure 2 shows typical semilogarithmic plots of the molar fraction of propicillin remaining in various surfactant solutions in the bag *versus* time, and it indicates that the dialysis rates follow first-order kinetics in conformity with Eq. 3. Plots of the k_{dia} for propicillin *versus* the concentration of surfactants are given in Fig. 3 and show a marked decrease of k_{dia} with increase in the surfactant concentration and a tendency to reach constant rate constants. The results apparently indicate the occurrence of entrapment of propicillin in the micelles, which are difficult to be dialyzed.

If the drug is incorporated into the micelle, there then will be an equilibrium between the drug in solution and that in the micelle. The apparent binding constant, K_{app}, can be expressed as:

$$K_{app} = \frac{(C_I)_m}{(C_I)_f(C_D - CMC)} \qquad \text{(Eq. 5)}$$

[12] Du Nöuy tensiometer, Shimadzu, Co., Kyoto, Japan.

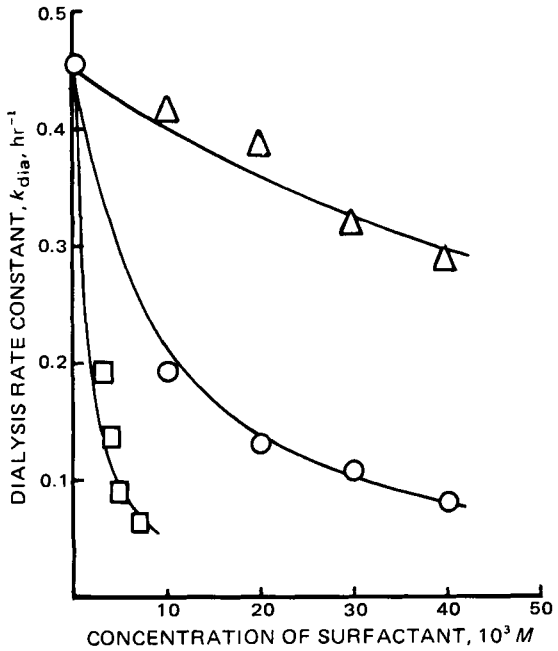

Figure 3—*Plots of the pseudo first-order rate constant,* k_{dia}, versus *total surfactant concentration for the dialysis of propicillin at 37° and* μ = *0.15. Key: (○) I (pH 3.50); (△) II (pH 4.40); (□) III (pH 6.50). The points are experimental values. The solid curves were generated from Eq. 6 using the parameters in Table II.*

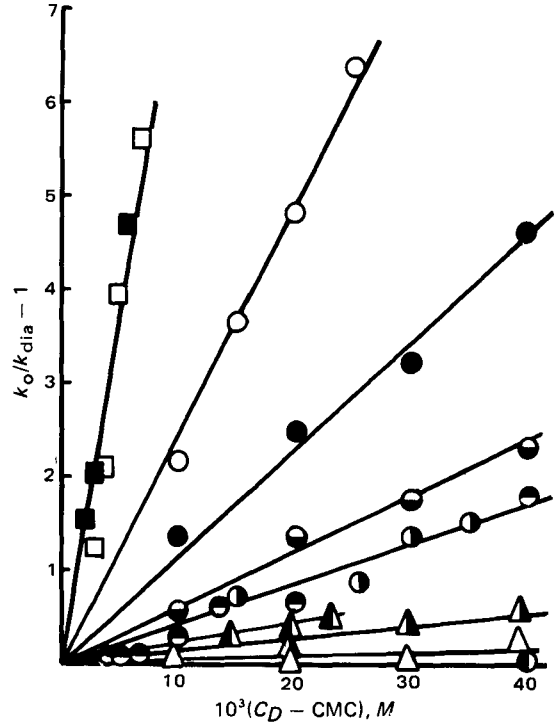

Figure 4—*Plots according to Eq. 7 for the dialysis of cefazolin (◐) and propicillin (other symbols) in the presence of I (cirles), II (triangles), and III (squares) at various pHs, 37°, and* μ = *0.15. Key: (□) pH 6.50; (■) pH 4.00; (○) pH 3.00; (●) pH 3.50; (◒) pH 4.00; (◑) pH 5.00; (◓) pH 6.50; (△) pH 6.50; (▲) pH 4.00; (▲) pH 4.40; (◐) pH 3.40 and pH 6.50.*

where $(C_1)_f$ and $(C_1)_m$ represent the concentration of the drug free and bound with the surfactant micelle, respectively, and C_D is the total concentration of surfactant. When it is assumed that only free drug can permeate through the dialysis membrane, Eq. 6 is obtained from Eqs. 3 and 5:

$$k_{dia} = k_0 \frac{1}{1 + K_{app}(C_D - CMC)} \quad \text{(Eq. 6)}$$

where k_0 represents the first-order dialysis rate constant of the drug in the absence of surfactant. Rearrangement of Eq. 6 gives:

$$\frac{k_0}{k_{dia}} - 1 = K_{app}(C_D - CMC) \quad \text{(Eq. 7)}$$

Equation 7 predicts that plots of $(k_0/k_{dia} - 1)$ *versus* $(C_D - CMC)$ passing through the origin are linear. The values of CMC used for the calculation are 0.092 m*M*, 0.46 m*M*, and 0.32 m*M* for I, II, and III, respectively, which were determined in this laboratory in the presence of the antibiotic at 37° and μ = 0.15. As illustrated in Fig. 4, the results obtained for propicillin with various surfactants revealed a linear relationship in accordance with Eq. 7. The apparent binding constant, K_{app}, was calculated from the slopes and the values are listed in Table I. During the periods of the dialysis experiments, there was negligible degradation of propicillin.

pH-Dependency of the Apparent Binding Constant in Micelle–Antibiotic Interactions—Penicillins have a pKa value of 2.7–2.9 (12) and exist in aqueous solutions in undissociated and ionized forms. The respective forms may yield different binding behavior in surfactant micellar solutions. Figure 5 shows the pH-dependency of K_{app} for propicillin in solutions of I, II, and III as determined by the dynamic dialysis method. Some of the data were those determined in a stability kinetic study, which will be described. In the solutions of I and II, the values of K_{app} for propicillin decreased markedly as the pH increased approaching a constant value. It is supposed that a considerable difference exists in the micellar interactions between undissociated species of propicillin and its ionized form. The relationship between the hydrogen ion activity of the bulk solution and the apparent binding constant can be represented by (see Appendix):

$$K_{app} = K_{HA}\frac{a_H}{a_H + Ka} + K_A\frac{Ka}{a_H + Ka} \quad \text{(Eq. 8)}$$

where K_{HA} and K_A are the binding constants for the undissociated form of propicillin and its ionized form, respectively. Incorporation at pKa 2.76 of propicillin gave parameters of K_{HA} = 489.0 ± 27.0 M^{-1} and K_A = 40.4 ± 2.7 M^{-1} for I as the best fit to the data using a NONLIN computer program (13). The curves in Fig. 5 were generated for I and II from Eq. 8 by the use of these parameters as listed in Table II.

In the interaction of propicillin and the micelles of III, the apparent binding constant was virtually independent of the bulk solution pH. This indicates no significant difference in the magnitude of K_{HA} and K_A, and analysis of the data gave $K_{HA} = K_A$ = 810.1 M^{-1} as the mean of experimental data at all pH values.

A similar experiment was also carried out for the interaction between cefazolin [p*K*a = 2.54 (14)] and the micelle of I. The values of K_{app} were extremely low, being ~3 M^{-1} in the wide pH range of 3–7, indicating negligible entrapment of the undissociated and ionized cefazolin into the micelles of I (Fig. 4).

Effect of Surfactants on the Stability of the Antibiotics—The acid-catalyzed degradation of β-lactam antibiotics was examined in the surfactant solutions of I, II, and III at 37 ± 0.1° and an ionic strength of 0.15. The degradation followed first-order kinetics with regard to the antibiotic concentration in all surfactant solutions. Typical results for propicillin obtained by linear semilogarithmic plots of the residual molar fraction of antibiotic *versus* time are shown in Fig. 6.

As illustrated in Fig. 7, the pseudo first-order rate constant for the degradation of propicillin at acidic pH was increased significantly by the

Table I—Apparent Binding Constant, K_{app}, between Propicillin and Various Surfactants [a]

I		II		III	
pH	K_{app}, M^{-1}	pH	K_{app}, M^{-1}	pH	K_{app}, M^{-1}
1.10	459.3[b]	1.61	175.0[b]	1.10	856.0[b]
1.92	404.9[b]	2.60	119.0[b]	4.00	793.8
3.00	247.2	3.00	91.3[b]	6.50	780.4
3.50	115.1	3.50	28.5[b]		
4.00	59.5	4.00	20.7		
5.00	42.5	5.00	13.2		
6.50	42.0	6.50	4.0		

[a] The values were calculated from the experimental data according to Eq. 7 by the least-squares treatment at 37° and μ = 0.15. [b] These values were determined in the stability study.

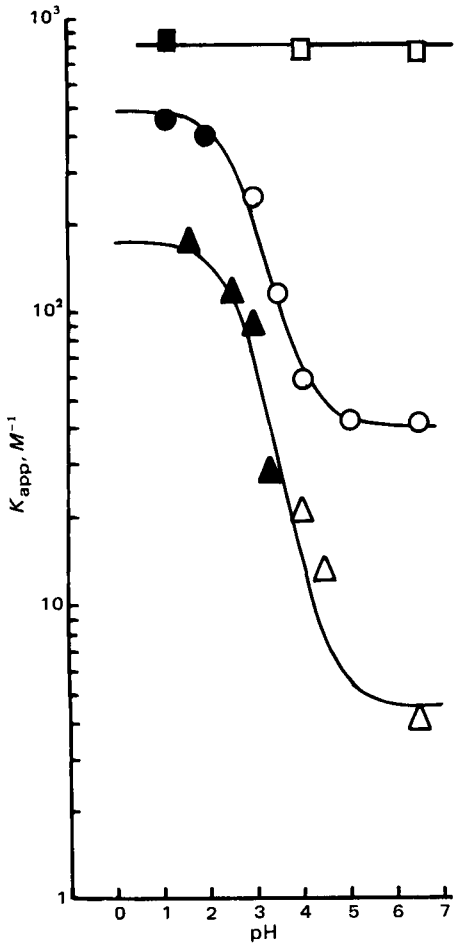

Figure 5—*Plots of the apparent binding constant,* K_{app}, *of propicillin* versus *the bulk solution pH at 37° and* $\mu = 0.15$. *Key:* (○,●) *I;* (△,▲) *II;* (□,■) *III; (open symbols, dynamic dialysis; closed symbols, stability).*

addition of anionic surfactant (II); whereas, it decreased on increasing the concentration of both nonionic and cationic surfactants (I and III). For other penicillins, similar results have been reported (3). In all cases, the rate constants first increased or decreased rapidly and then approached a constant value above the CMC of the surfactants, suggesting the formation of penicillin–micelle complexes.

According to the literature (9), the apparent first-order degradation rate constant thus, is expressed by:

$$k_{deg} = \frac{k_0 + k_m(C_D - \text{CMC})}{1 + K_{app}(C_D - \text{CMC})} \qquad \text{(Eq. 9)}$$

Rearrangement of Eq. 9 gives:

$$\frac{1}{k_0 - k_{deg}} = \frac{1}{k_0 - k_m} + \left(\frac{1}{k_0 - k_m}\right)\left(\frac{1}{C_D - \text{CMC}}\right)\frac{1}{K_{app}} \qquad \text{(Eq. 10)}$$

Equation 10 predicts that plots of $1/(k_0 - k_{deg})$ *versus* $1/(C_D - \text{CMC})$ should give a straight line from which it should be possible to obtain k_m and K_{app} values.

Plots of Eq. 10 for the degradation of propicillin in the presence of I and III are shown in Figs. 8 and 9, respectively. The values of K_{app} for the various reaction systems are given in Table I.

Table II—Binding Constants for Undissociated and Ionized Propicillin with Various Surfactants [a]

Surfactant	K_{HA}, M^{-1}	K_A, M^{-1}
I	489.0 ± 27.0	40.4 ± 2.7
II	171.8 ± 29.9	4.5 ± 1.3
III	810.1 ± 40.3[b]	810.3 ± 40.3[b]

[a] The binding constants were calculated by nonlinear regression program, NONLIN, at 37° and $\mu = 0.15$. [b] This value is the mean ± *SD* of the experimental data.

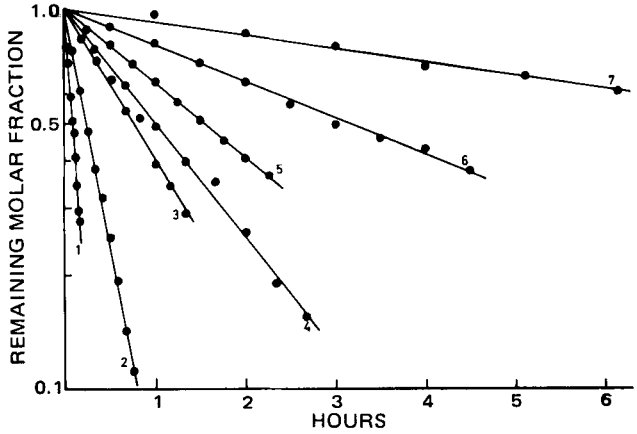

Figure 6—*First-order plots for the degradation of propicillin in the presence of surfactants at various pHs, 37°, and* $\mu = 0.15$. *Key: 1 (3 × 10⁻³ M II, pH 1.61); 2 (control, pH 1.10); 3 (4.5 × 10⁻³ M II, pH 2.50); 4 (1 × 10⁻² M I, pH 1.10); 5 (8.9 × 10⁻² M III, pH 1.10); 6 (3.1 × 10⁻² M III, pH 1.10); 7 (1 × 10⁻² M I, pH 1.92).*

Within an experimental period of <1 day, there was no influence of the surfactants on the neutral degradation of the antibiotic used in this study.

Effect of Surfactants on the Antibiotic Solubility—The saturable solubility of penicillin V, C_s, at pH 2.0 and 35° increased with concentration of I as shown in Table III. The data indicated that the aqueous solubility of penicillin V increased threefold in the presence of 10 m*M* I at pH 2.0 and 35°, showing that penicillins are solubilized by surfactant micelles.

DISCUSSION

Solutions of penicillin G are highly unstable at a gastric pH, the half-lives being 1 min at pH 1 and 7 min at pH 2 (15, 16). Such chemical inactivation of penicillin G in the gastric fluid has been reported to be responsible for the poor bioavailability of this antibiotic. The acid degradation rates of penicillin derivatives are known to depend on their 6-sidechain nature due to the rearrangement initiated by the attack of the sidechain amidocarbonyl on the β-lactam to produce the corresponding penicillenic acid and penillic acid (16).

Considerable efforts have been made to stabilize acid-labile penicillins. Previous authors (17) succeeded in stabilizing potassium salts of penicillin G and penicillin V in simulated gastric juice by coating with cholesteryl acetate, yielding 1.6- and twofold higher urine levels, respectively, after oral administration of these pharmaceutical preparations to humans.

The previous (3) and present studies revealed a marked stability of penicillins in acid solutions with both cationic and nonionic micelles. Four kinds of derivatives, penicillin G, penicillin V, phenethicillin, and propicillin, can be stabilized to maximal extents of 6-, 10-, 8-, and 10-fold by the micelles of III and of 4-, 6-, 7-, and 13-fold by the micelles of I, respectively (3). These stabilization effects are attributed to incorporation of the penicillin molecules into both types of micelles. As is apparent from these results (3), the apparent binding constant between the penicillins and micelles increased with increasing lipophilic character of the penicillins, as expressed in terms of their octanol–water partition coefficients, *P* (12). This suggests that hydrophobic binding is involved in the interaction between the cationic or nonionic micelle and undissociated species of the penicillins. These strong interactions resulted in protection of the β-lactam ring sterically and/or electrostatically from intramolecular and nucleophilic attack of the sidechain amidocarbonyl oxygen. However, it is probable that due to the localized hydrogen ion activity surrounding the negatively charged micelle, the anionic micellar state by II leads to an increase in the rate of degradation. The maximal acceleration of the β-lactam cleavage of propicillin by micelles of II was predicted to be 60-fold at pH 1.6 and 37°.

In contrast to penicillins, the acid degradation of cefazolin, a relatively acid-unstable cephalosporin (14), was not influenced by the presence of any type of surfactant, like cephalothin described previously (3). This was due to the fact that cefazolin was not sufficiently bound to the micelles, the apparent binding constant being confirmed as almost negligible by the dynamic dialysis method (Fig. 4). The very weak interaction of

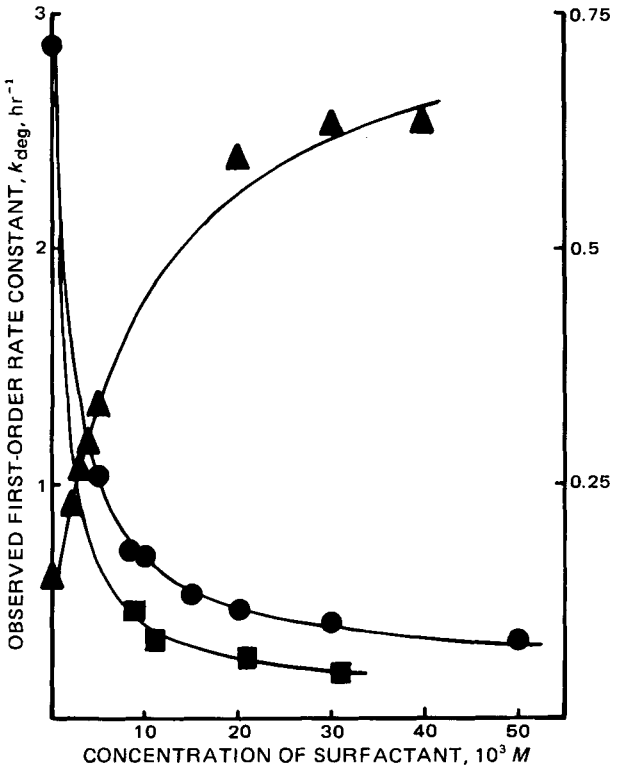

Figure 7—*Plots of the pseudo first-order rate constant* versus *total concentration of surfactant for the degradation of propicillin at 37° and μ = 0.15. Key: (●) I (pH 1.10, left scale); (▲) II (pH 3.00, right scale); (■) III (pH 1.10, left scale). The points are experimental values. The solid curves were generated from Eq. 9.*

the cefazolin molecule with surfactant micelles undoubtedly is due to the low lipid solubility of the antibiotic itself.

The partitioning behavior of β-lactam antibiotics was investigated (12), both in *n*-octanol–water and isobutyl alcohol–water systems, as a function of the aqueous phase solution pH and showed that both the undissociated and ionized species could be partitioned into the oil phase, although the

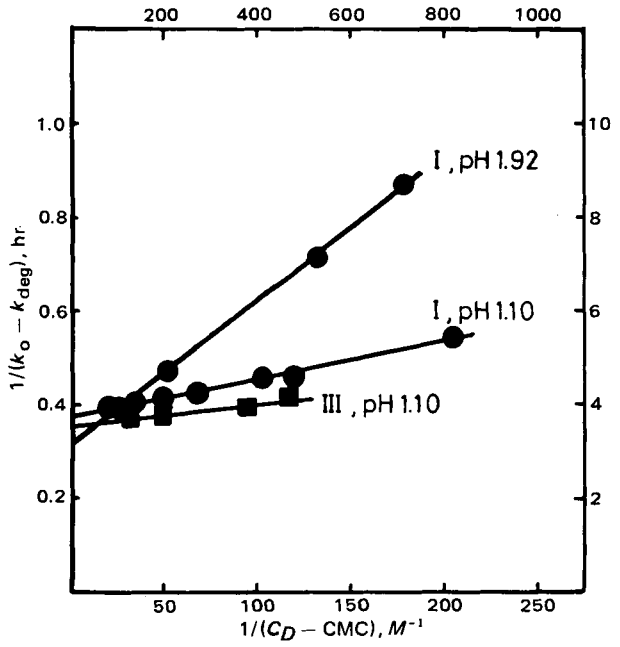

Figure 8—*Double reciprocal plots according to Eq. 10 for the degradation of propicillin in the presence of I and III at 37° and μ = 0.15. Key: upper and right scales for pH 1.10; lower and left scales for pH 1.92.*

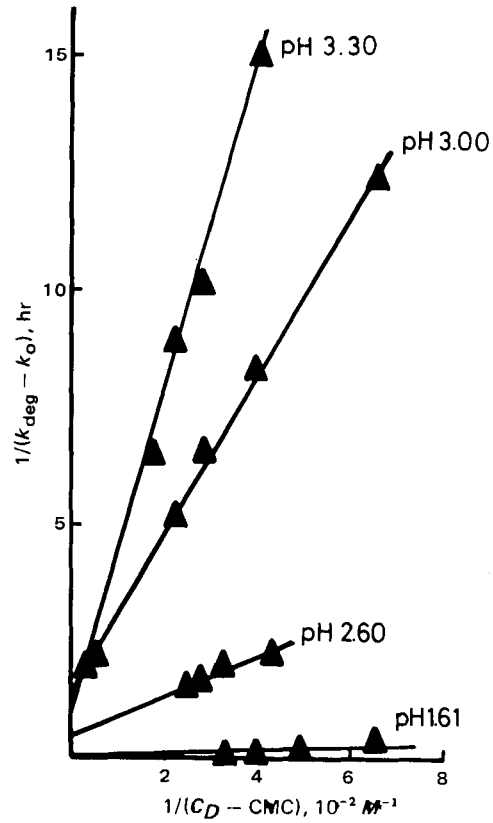

Figure 9—*Double reciprocal plots according to Eq. 10 for the degradation of propicillin in the presence of II at 37° and μ = 0.15.*

former was far more lipophilic than the latter. As shown in Fig. 5, the pH dependency of the K_{app} values in the propicillin interaction with I was parallel to that of the apparent partition coefficients in oil–water systems. The interactions of propicillin with the micelles of II and III showed a marked contrast in the dependencies of their respective K_{app} values on the pH of the bulk aqueous solution. In the case of the micelle of II, K_{app} clearly decreased as the pH increased, while in the micelle of III, K_{app} exhibited independency in the wide pH range betwen 1 and 6. These results can be explained on the basis of the participation of electrostatic forces between the ionized species of the antibiotic and the ionized surfactant micelles in addition to the hydrophobic contribution.

Electrical repulsive forces may play a significant role between ionized propicillin and the anionized surfactant micelle to produce the deduced K_A value, as seen from the K_{HA}/K_A ratio being ~100. Unlike the anionic case, the attraction due to the electrostatic forces between the ionized form of propicillin and cationic surfactant micelle may lead to an effective cancellation of charge within the molecule, resulting in $K_{HA} = K_A$. However, the magnitude of K_A is dependent on the differences both of the hydrogen ion activity and the acid dissociation behavior between aqueous and micellar phases (see Appendix).

Based on the present study, it should be emphasized that the acid-labile penicillins were significantly stabilized and solubilized by incorporating the unionized species into nonionic surfactant micelles, and the penicillin molecules entrapped in the micelle could then be easily released at neutral pH values by reducing the force in the interaction between the

Table III—Solubility of Propicillin in the Presence of I [a]

Concentration of I, 10^3 M	Solubility of Propicillin, 10^3 M
0.0	0.72
3.0	1.21
5.0	1.55
7.0	1.89
10.0	2.40
20.0	4.09

[a] Values at 37°, pH 2.00, and μ = 0.5.

ionized species and micelles. Cephalosporins, which have a much lower lipophilicity than penicillins (12), are not incorporated into nonionic surfactant micelles, so that there is no significant influence on the chemical stability and solubility in aqueous solution.

APPENDIX

Alteration of the acid dissociation equilibrium of the drug in surfactant micelles would be in terms of local alteration in hydrogen ion concentration in the micelles. It is to be expected that the hydrogen ion activity ($a_{H,m}$) will be greater near the surface of the anionic micelles and lower near the surface of the cationic micelles than that (a_H) in the bulk aqueous phase.

Assuming that both species of undissociated and ionized drugs which exist in the aqueous phase are incorporated into the micellar phase, the various equilibria can be described as:

$$Ka = \frac{(A)_{aq} a_H}{(HA)_{aq}} \quad \text{(Eq. A1)}$$

$$Ka,m = \frac{(A)_m a_{H,m}}{(HA)_m} \quad \text{(Eq. A2)}$$

$$K_{HA} = \frac{(HA)_m}{(HA)_{aq}\,(C_D - \mathrm{CMC})} \quad \text{(Eq. A3)}$$

$$K_A = \frac{(A)_m}{(A)_{aq}\,(C_D - \mathrm{CMC})} \quad \text{(Eq. A4)}$$

where HA and A refer to the undissociated and ionized species, respectively, and the subscripts aq and m refer to the aqueous and micellar phases, respectively. The other parameters are the same as described in the text. It is clear that the $K_{HA}/K_A = (Ka/Ka,m)$ from Eqs. A1–A4. The apparent binding constant, K_{app}, between drugs and micelles is given by:

$$K_{app} = \frac{(HA)_m + (A)_m}{[(HA)_{aq} + (A)_{aq}]\,(C_D - \mathrm{CMC})} \quad \text{(Eq. A5)}$$

Rearrangement of Eq. A5 gives:

$$K_{app} = \frac{(HA)_m}{(HA)_{aq}\,(C_D - \mathrm{CMC})}\left[\frac{1}{1 + (A)_{aq}/(HA)_{aq}}\right] + \frac{(A)_m}{(A)_{aq}\,(C_D - \mathrm{CMC})}\left[\frac{1}{1 + (HA)_{aq}/(A)_{aq}}\right] \quad \text{(Eq. A6)}$$

By use of the equilibrium constants defined above, Eq. 8 can be arrived at from Eq. A6. Therefore, the binding constants, K_{HA} and K_A, for incorporation of the undissociated and ionized forms of drugs into the micelles can be calculated, without knowledge of $a_{H,m}$ and $K_{a,m}$, from the dependence of the bulk aqueous solution pH upon the K_{app} values.

REFERENCES

(1) F. Alhaique, C. Botré, G. Lionetti, M. Marchetti, and F. M. Riccieri, *J. Pharm. Sci.*, **56,** 1555 (1967).

(2) M. Yasuhara, F. Sato, T. Kimura, S. Muranishi, and H. Sezaki, *J. Pharm. Pharmacol.*, **29,** 638 (1977).

(3) A. Tsuji, M. Matsuda, E. Miyamoto, and T. Yamana, *ibid.*, **30,** 442 (1978).

(4) J. L. Kurtz, *J. Phys. Chem.*, **66,** 2239 (1962).

(5) H. Bundgaard and K. Ilver, *J. Pharm. Pharmacol.*, **24,** 790 (1972).

(6) M. C. Meyer and D. E. Guttman, *J. Pharm. Sci.*, **57,** 1627 (1968).

(7) N. K. Patel and N. E. Foss, *ibid.*, **54,** 1495 (1965).

(8) A. Agren and R. Elofsson, *Acta Pharm. Suec.*, **4,** 281 (1967).

(9) J. H. Fendler and E. J. Fendler, "Catalysis in Micellar and Macromolecular Systems," Academic, New York, N.Y., (1975).

(10) M. Donbrow and C. T. Rhodes, *J. Chem. Sci.*, **1964,** 6166.

(11) M. Donbrow, E. Azaz, and R. Hamburger, *J. Pharm. Sci.*, **59,** 1427 (1970).

(12) A. Tsuji, O. Kubo, E. Miyamoto, and T. Yamana, *ibid.*, **66,** 1675 (1977).

(13) C. M. Metzler, "NONLIN, A Computer Program for Parameter Estimation in Nonlinear Systems," Technical Report 7292/69/7297/005, The Upjohn Co., Kalamazoo, Mich.

(14) T. Yamana and A. Tsuji, *J. Pharm. Sci.*, **65,** 1563 (1976).

(15) T. Yamana, A. Tsuji, and Y. Mizukami, *Chem. Pharm. Bull. (Tokyo)*, **22,** 1186 (1974).

(16) M. A. Schwartz, *J. Pharm. Sci.*, **58,** 643 (1969).

(17) S. P. Patel and C. I. Jarowski, *ibid.*, **64,** 869 (1975).

ACKNOWLEDGMENTS

The present results were presented in part at the APhA Academy of Pharmaceutical Sciences, 29th National Meeting, San Antonio, Texas, November, 1980.

The authors acknowledge the gifts of β-lactam antibiotics from Takeda Chemical Industries, Banyu Pharmaceutical Co., and Fujisawa Pharmaceutical Co. The computer analysis was performed on the digital computer, FACOM M-160 at the Data Processing Center, Kanazawa University.

Synthesis and Antimicrobial Activities of Certain Cannabichromene and Cannabigerol Related Compounds

HALA N. ElSOHLY ˣ, CARLTON E. TURNER, ALICE M. CLARK, and MAHMOUD A. ElSOHLY

Received October 15, 1981, from the *Research Institute of Pharmaceutical Sciences, The University of Mississippi, School of Pharmacy, University, MS 38677.* Accepted for publication January 27, 1982.

Abstract □ Cannabichromene homologs, analogs, and isomers as well as the C_1-homolog and isomer of cannabigerol were prepared and tested for their antimicrobial and antifungal properties. Spectral data of all compounds synthesized are presented.

Keyphrases □ Cannabichromene—analogs, synthesis and antimicrobial activities of related compounds, cannabigerol □ Antimicrobial activities —cannabichromene and cannabigerol, analogs, synthesis and related compounds □ Analogs—cannabichromene and cannabigerol, synthesis and antimicrobial activities of related compounds

Different cannabinoids have been isolated from *Cannabis sativa* L. (1). Most of the biological studies carried out concentrate on the major psychoactive constituent Δ^9-tetrahydrocannabinol and its isomers (2–4). However, little attention has been given to the biological activity of cannabichromene (I) because of its relatively low concentration in the plant material.

Recently, a procedure was developed for the synthesis of I in high yield (60%) (5), which made the material available for pharmacological testing.

The biological activities of cannabichromene has been reported (6–9), as well as its homologs and isomers (10, 11). This paper describes the synthesis and antimicrobial activities of cannabichromene homologs, analogs, and isomers and that of cannabigerol-C_1, isocannabigerol-C_1, and tetrahydrocannabigerol-C_1.

EXPERIMENTAL

Melting points[1] were determined in open glass capillary tubes and are uncorrected. Proton nuclear magnetic resonance (^{1}H-NMR) spectra[2] were recorded in deuterochloroform or in deuteromethanol using tetramethysilane as the internal standard. IR spectra[3] were recorded in liquid film, chloroform, or in potassium bromide pellets. Mass spectra[4] were recorded at an electron energy of 70 eV. UV spectra[5] were recorded in methanol. ^{13}C-NMR spectra[6] were recorded in deuterochloroform or deuteromethanol.

Biological Activities–Antibacterial and Antifungal Activities—All compounds were tested for activity against Gram-positive, Gram-negative, and acid-fast bacteria and selected fungi. A qualitative screen was performed on all compounds, while quantitative assays were done on active compounds only. Routine qualitative screens were carried out using the agar well diffusion assay as previously described (12). Minimum inhibitory concentrations were determined using the twofold (broth) serial dilution method (12) with a concentration of 100 μg/ml in the first tube. Streptomycin sulfate was used as a positive control for antibacterial activity, while amphotericin B was used as an antifungal positive control.

2-Methyl-2-(4′-methylpent-3′-enyl)-5-hydroxy-7-methylchromene (II)—Orcinol (3.45 g, 0.028 mole) was dissolved in 55 ml of toluene with heating and stirring. Equimolar quantities of *tert*-butylamine were added to the resulting solution followed by dropwise addition of citral. The reaction mixture was refluxed for 9 hr. The mixture was then cooled to room temperature, transferred to a round-bottom flask, and the solvent evaporated. GC analysis of the reaction mixture showed 48.3% conversion to II. About one half of the crude reaction product (5 g) was applied over a dry packed silica gel 60 column (100 g) using 15 ml of cyclohexane–chloroform (1:1), and elution was continued with the same solvent. Fractions of 25 ml were collected and combined based on TLC similarities. Fractions containing II (1.96 g) were rechromatographed as before to yield II of >95% purity as light brown oil. UV λ_{max} (methanol) nm (log ϵ): 229 (4.38) and 280 (3.92); IR (liquid film) major bands at 3400, 2970, 2820, 1620, 1575, and 1420 cm^{-1}; ^{1}H-NMR ($CDCl_3$) signals at δ 6.68 (1H, d, J = 10 Hz), δ 6.27 (1H, s), δ 6.13 (1H, s), δ 5.45 (1H, d, J = 10 Hz), δ 5.12 (1H, br, t, J = 6 Hz), δ 2.17 (3H, s), δ 1.67 (3H, s), δ 1.58 (3H, s), and δ 1.38 (3H, s); ^{13}C-NMR ($CDCl_3$) signals at δ 154.1 (s), δ 151.3 (s), δ 139.6 (s), δ 131.5 (s), δ 127.1 (d), δ 124.4 (d), δ 117.9 (d), δ 109.9 (d), δ 108.8 (d), δ 107.2 (s), δ 74.4 (s), δ 41.1 (t), δ 26.2 (q), δ 25.5 (q), δ 22.7 (t), δ 21.4 (q), and δ 17.5 (q); MS M$^+$ at m/z: 258 (10%), for $C_{17}H_{22}O_2$, 175 (100%) 243 (3%), 215 (7%), 183 (3%).

2-Methyl-2-(4′-methylpent-3′-enyl)-5-methyl-7-hydroxychromene (III)—Compound III was formed as a side product from the synthesis of II when pyridine was used both as a base and a solvent. Equi-

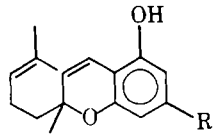

I R = C_5H_{11}
II R = CH_3
VI R = H

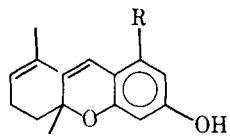

III R = CH_3
VII R = H
III R = C_5H_{11}

VIII R = $(CH_2)_7$—CH=CH—$(CH_2)_5$—CH_3

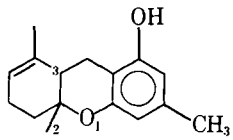

IV

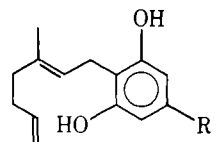

X R = CH_3, XIII R = C_5H_{11}

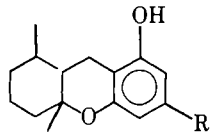

V R = CH_3 V′ R = C_5H_{11}

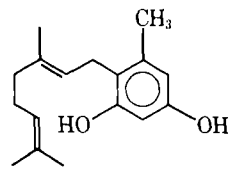

XI

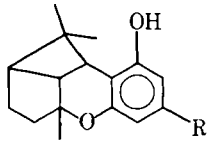

IX R = OH
XVII R = C_5H_{11}

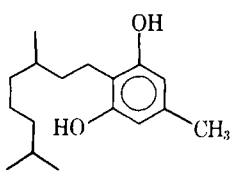

XII

[1] Thomas Hoover Unimelt.
[2] JEOL C-60HL.
[3] Perkin-Elmer 267.
[4] Finnigan 3200, MS/DS system.
[5] Beckman Acta III.
[6] JEOL FX-60 operating at 15.03 MHz.

0022-3549/82/1200-1319$01.00/0

molar quantities of pyridine and citral were added to 1.73 g of (0.014 mole) orcinol. The mixture was refluxed with stirring for 7 hr, cooled, and evaporated to yield a brownish residue (3.97 g). On TLC[7], the residue showed two major spots using chloroform–cyclohexane (4:1) and benzene–hexane (4:1) as solvent systems. The crude reaction mixture was purified on a silica gel 60 column followed by preparative chromatography[8] using benzene–hexane (4:1) as the solvent system. The compound with the high R_f value (0.30, 15%) was II, while that with the low R_f value (0.16, 24%) was identified as III. Compound III was isolated as an amber colored oil. UV λ_{max} (methanol) nm (log ϵ): 224 (4.17), 285 (3.70), and 305 (3.57); IR (liquid film) major bands at 3380, 2970, 2915, 1610, and 1460 cm^{-1}; ^{1}H-NMR ($CDCl_3$) signals at δ 6.47 (1H, d, J = 9 Hz), δ 6.18 (2H, s), δ 5.43 (1H, d, J = 9 Hz), δ 5.12 (2H, br, t, J = 7 Hz), δ 2.18 (3H, s), δ 1.67 (3H, s), δ 1.58 (3H, s), and δ 1.37 (3H, s); ^{13}C-NMR ($CDCl_3$) signals at δ 156.1 (s), δ 154.7 (s), δ 135.1 (s), δ 131.4 (s), δ 126.5 (d), δ 124.4 (d), δ 119.6 (d), δ 113.2 (s), δ 109.6 (d), δ 101.7 (d), δ 78.1 (s), δ 41.1 (t), δ 26.2 (q), δ 25.5 (q), δ 22.7 (t), δ 18.3 (q), and δ 17.5 (q); MS M^+ at m/z 258 (6%) for $C_{17}H_{22}O_2$, 175 (100%).

2-Methyl-2-(4′-methylpent-3′-enyl)-5-hydroxy-7-methylchroman (IV) and 2-Methyl-2-(4′-methylpentyl)-5-hydroxy-7-methylchroman (V)—Compounds IV and V were prepared by catalytic hydrogenation of Compound II. A mixture of IV and V was formed when the reaction was allowed to go for 20 min under hydrogen atmosphere. However, Compound V was the only product obtained when hydrogenation was allowed to occur for a longer period of time or under pressure (0.702 kg/cm^2). Compound II (0.15 g, 5.8×10^{-4} mole) was dissolved in 8 ml of ethanol and 20 mg of 5% pallidium on carbon (Pd/C) was added. The reaction mixture was stirred for 20 min under a hydrogen atmosphere. TLC examination of the reaction product on silver nitrate-treated silica gel plates using chloroform–benzene (8:2) as the solvent system showed two major spots with R_f 0.22 and 0.35. The two compounds were separated on an HPLC using a reversed-phase column[9] with methanol–water (8:2) as the solvent system. Twenty-two milligrams (14.6%) of IV and 99 mg (66%) of V were obtained. Compound IV was isolated as a light yellow oil. UV λ_{max} (methanol) nm (log ϵ): 283 (2.92), 273 (2.92), 232 (3.82), 217 (3.95). IR ν_{max} ($CHCl_3$) cm^{-1}: 2968, 2924, 2858, 1620, 1580, 1450, 1375, 1349, 1320, 1260, 1155, 1132, 1100, 1055, 995, 875; ^{1}H-NMR ($CDCl_3$) δ 6.27 (1H, s, aromatic H), δ 6.17 (1H, s, aromatic H), δ 5.15 (1H, t, olefinic proton), δ 2.61 (2H, t, benzylic proton), δ 2.18 (3H, s, aromatic methyl), δ 1.67 (3H, s, methyl on double bond), δ 1.60 (3H, s, methyl on double bond), δ 1.28 (3H, s, methyl on oxygenated carbon); MS M^+ at m/z 260 (25.5%) for $C_{17}H_{24}O_2$, 177 (36%), 175 (55%), 136 (100%). The tetrahydro-derivative was separated as a light yellow oil; UV λ_{max} (methanol) nm (log ϵ): 282 (2.93), 275 (2.93), 233 (3.88), 217 (4.09); IR ν_{max} ($CHCl_3$) cm^{-1}: 2950, 1622, 1580, 1450, 1378, 1350, 1320, 1260, 1150, 1130, 1100, 1070, 995, 875; ^{1}H-NMR ($CDCl_3$): δ 6.16 (1H, s, aromatic H), δ 6.03 (1H, s, aromatic H), δ 2.56 (2H, t, benzylic protons), δ 2.16 (3H, s, aromatic methyl), δ 1.25 (3H, s, methyl on oxygenated carbon), δ 0.92 (3H, d, J = 6 Hz), and δ 0.80 (3H, d, J = 6 Hz); MS M^+ 262 (36.5%) for $C_{17}H_{22}O_2$, 177 (57%), and 136 (100%).

2-Methyl-2-(4′-methylpent-3′-enyl)-5-hydroxychromene (VI) and 2-Methyl-2-(4′-methylpent-3′-enyl)-7-hydroxy-chromene (VII)—Compounds VI and VII were prepared by reaction of 1.53 g of resorcinol (0.014 mole), and equimolar amounts of *tert*-butylamine and citral in 27.5 ml of toluene following the same conditions described under preparation of II. The reaction of the nonsubstituted resorcinol under these conditions result in the formation of both VI and VII. The crude reaction mixture was purified by repeated chromatography on a silica gel 60 column and preparative liquid chromatography[10] with benzene as the solvent to obtain Compounds VI and VII in 10% yield. Compound VI was isolated as a yellowish-brown oil. UV λ_{max} (methanol) nm (log ϵ): 225 (4.35) and 278 (3.90); IR (liquid film) major bands at 3395, 2970, 2920, 1610, 1580, and 1460 cm^{-1}; ^{1}H-NMR ($CDCl_3$) signals at δ 6.38 (1 H, d, J = 10 Hz), δ 5.52 (1H, d, J = 10 Hz), δ 5.13 (1H, br, t, J = 6 Hz), δ 1.67 (3H, s), δ 1.60 (3H, s) and 1.40 (3H, s); ^{13}C-NMR ($CDCl_3$) signals at δ 154.2 (s), δ 151.5 (s), δ 131.5 (s), δ 129.0 (d), δ 128.1 (d), δ 124.4 (d), δ 117.0 (d), δ 109.7 (s), δ 109.1 (d), δ 107.9 (d), δ 78.4 (s), δ 41.4 (t), δ 26.2 (q), δ 25.5 (q), δ 22.7 (q), δ 17.5 (q); MS m/z (%), M^+ 244 (2%), 161 (100%), 115 (2%). Compound VII was separated as a brownish oil; UV λ_{max} (methanol) nm (log ϵ): 220 (4.39), 283 (3.86), 305 (3.83), and 310 (sh, 3.79); IR (liquid film) major bands at 3400, 2970, 2920, 1650, and 1500 cm^{-1}; ^{1}H-NMR ($CDCl_3$) signals at δ 6.68 (1H, d, J = 9 Hz), δ 6.25 (2H, br, s), δ 6.07 (1H, br, s), δ 5.30 (1H, d, J = 9 Hz), δ 5.03 (2H, br, t, J = 6 Hz), δ 1.63 (3H, s), δ 1.53 (3H, s), and δ 1.18 (3H, s); ^{13}C-NMR ($CDCl_3$) signals at δ 156.8 (s), δ 154.5 (s), δ 131.6 (s), δ 127.3 (d), δ 126.7 (d), δ 124.4 (d), δ 122.5 (d), δ 114.7 (s), δ 107.8 (d), δ 103.8 (d), δ 78.9 (s), δ 41.5 (t), δ 26.6 (q), δ 25.6 (q), δ 22.8 (t), and 17.6 (q); MS M^+ at m/z 244 (6%), 161 (100%), and 115 (7%).

2-Methyl-2-(4′-methylpent-3′-enyl)-5-hydroxy-7-pentadec-8″enylchromene (VIII)—Compound VIII was prepared by reaction of 5-pentadec-8′-enyl resorcinol with citral in the presence of *tert*-butylamine (equimolar amounts) in toluene solution following the same procedure as described under synthesis of I. Pentadecenyl resorcinol was isolated from *Ginkgo* fruits. Compound VIII was isolated as a brownish colored oil (60% yield). UV λ_{max} (methanol) nm (log ϵ): 228 (4.39) and 279 (3.97); IR (liquid film) major bands at 3400, 2920, 2855, 1620, 1575, 1430 cm^{-1}; ^{1}H-NMR ($CDCl_3$) signals at δ 6.62 (1 H, d, J = 10 Hz), δ 6.22 (1H, s), δ 6.10 (1H, s), δ 5.42 (1H, d, J = 10 Hz), δ 1.65 (3H, s), δ 1.57 (3H, s), δ 1.39 (3H, s), δ 1.32 (18H, br, s); ^{13}C-NMR ($CDCl_3$) signals at δ 154.3 (s), δ 151.5 (s), δ 144.8 (s), δ 131.4 (s), δ 130.1 (d), δ 127.2 (d), δ 124.6 (d), δ 117.1 (d), δ 109.2 (d), δ 108.0 (d), δ 107.3 (s), δ 78.3 (s), δ 41.3 (t), δ 36.1 (t), δ 31.9 (t), δ 31.0 (t), δ 29.9 (t, 2C), 29.4 (t, 2C), 29.0 (t), δ 27.4 (t, 3C), δ 26.3 (q), δ 25.6 (q), δ 22.9 (t), δ 22.7 (t), δ 17.6 (q), δ 14.1 (q); MS M^+ at m/z 452 (0.16%), for $C_{31}H_{48}O_2$, 369 (100%), 187 (16%), 174 (11%).

2-Methyl-2-(4′-methylpent-3′-enyl)-5,7-dihydroxychromene—Phloroglucinol (2.52 g, 0.02 mole) was dissolved in 25 ml of acetonitrile–toluene (1:1). *tert*-Butylamine (0.022 mole) was added to the resulting solution, followed by the dropwise addition of 0.022 mole citral, and the reaction mixture was refluxed for 1 hr. The material was applied on a silica gel 60 column packed in 20% ethyl acetate–cyclohexane; 220 mg of the cyclol (IX) were obtained. Yield: 4.4%.

The cyclol was obtained as fine needles (cyclohexane–acetone), mp 150–150.5°. UV λ_{max} (methanol) nm (log ϵ): 280 (2.11), 240 (3.06), 222 (3.61); IR ν_{max}^{KBr} cm^{-1}: 3360, 2970, 2920, 1615, 1596, 1490, 1462, 1378, 1365, 1340, 1312, 1270, 1255, 1240, 1215, 1160, 1150, 1135, 1122, 1081, 1065, 1032, 995, 945, 900, 878, 825, 750; ^{1}H-NMR ($CDCL_3$) signals at: δ 5.93 (2H, s, aromatic), δ 2.76 (1H, m, C_3—H), δ 1.46, δ 1.35, and δ 1.01 (3H, each, s); ^{13}C-NMR: δ 157.82 (s), δ 157.32 (s), δ 155.94 (s), δ 109.42 (s), δ 98.50 (d), δ 96.94 (d), δ 84.33 (s), δ 47.04 (d), δ 37.5 (t), δ 35.54 (t), δ 29.76 (q), δ 29.04 (d or q), δ 28.00 (d), δ 23.7 (q), δ 22.3 (q or d); MS M^+ 260 (8%), 245 (3%), 217 (6%), 189 (7%), 177 (100%).

2-Geranyl-5-methyl Resorcinol (X) and 4-Geranyl-5-methyl Resorcinol (XI)—Compound X was prepared by condensation of geraniol (3.47 ml) and orcinol (2.844 g, 20 mmoles) in methylene chloride (100 ml) in the presence of *p*-toluenesulfonic acid (20 mg) at 20° for 30 min. The reaction mixture, after workup, was repeatedly chromatographed on silica gel to yield X (794 mg, 15%) and XI (100 mg, 2%). Compound X was obtained as a crystalline material, mp 50–51° (hexane). UV λ_{max} (methanol) nm (log ϵ): 275 (2.93), 209 (4.55); IR ν_{max}^{KBr} (cm^{-1}): 3420, 3380, 3268, 3120, 2960, 2908, 2850, 1630, 1580, 1510, 1450, 1375, 1322, 1268, 1220, 1198, 1145, 1080, 1042, 985, 825; ^{1}H-NMR ($CDCL_3$) δ 6.2 (2H, s), δ 5.36–5.08 (2H, m, olefinic), δ 3.4 (2H, d, J = 8 Hz), δ 2.18 (3H, s), δ 1.81 (3H, s), δ 1.70 (3H, s) and δ 1.60 (3H, s); ^{13}C-NMR: signals at δ 155.0 (s), δ 138.9 (s), δ 137.6 (s), δ 132.0 (s), δ 124.0 (d), δ 122.0 (d), δ 111.0 (d), δ 109.4 (d), δ 39.8 (t), δ 26.6 (t), δ 25.6 (q), δ 22.3 (t), δ 21.0 (t), δ 17.7 (q), δ 16.2 (q); MS M^+ 260 (2.68%) for $C_{17}H_{24}O_2$, 191 (8%), 175 (23%), 163 (22%), 149 (20%), 137 (100%).

Compound XI yielded fine needles, mp 50–51° (hexane). UV λ_{max} (methanol) nm (log ϵ): 283 (3.19), 207 (4.32); IR ν_{max}^{KBr} cm^{-1}: 3200, 2982, 2960, 2830, 1610, 1510, 1470, 1450, 1375, 1335, 1310, 1220, 1140, 1050, 980, 900, 835; ^{1}H-NMR ($CDCl_3$) signals at δ 6.23 (2H, s), δ 5.6–5.13 (2H, m, olefinic), δ 3.3 (2H, d, J = 8 Hz), δ 2.2 (3H, s), δ 2.03 (4H, br, s), δ 1.76 (3H, s), δ 1.66 (3H, s), δ 1.60 (3H, s); ^{13}C-NMR ($CDCl_3$) δ 155.4 (s), δ 154.3 (s), δ 138.8 (s), δ 137.2 (s), δ 131.8 (s), δ 124.2 (d), δ 122.5 (d), δ 118.6 (d), δ 110.1 (d), δ 101.4 (d), δ 39.8 (t), δ 26.7 (t), δ 25.7 (q), δ 25.1 (t), δ 19.9 (q), δ 17.7(q), δ 16.2 (q); MS M^+ 260 (2.92%) for $C_{17}H_{24}O_2$, 191 (13.5%), 175 (26.64%), 163 (17.44%), 149 (22.52%), and 137 (100%).

2-Tetrahydrogeranyl-5-methyl Resorcinol (XII)—Compound X was dissolved in 8 ml of ethanol, 20 mg of 5% Pd/C was added, and the reaction mixture was allowed to proceed under a hydrogen atmosphere for 4 hr. TLC examination of the reaction product showed complete conversion of the starting material. Filtration followed by crystallization from hexane yielded a crystalline material, mp 84–85°. UV λ_{max} (methanol) nm (log ϵ): 280.5 (3.05), 271 (3.09), 232 (sh, 3.00), 209 (4.60); IR λ_{max}^{KBr} cm^{-1}: 3420, 3300, 2960, 2928, 2870, 2850, 1630, 1580, 1518, 1468, 1380, 1365, 1328, 1270, 1200, 1160, 1112, 1025, and 830; ^{1}H-NMR (CD_3OD) signals at δ 6.13 (2H, s), δ 2.56 (2H, t), δ 1.53–1.23 (m, 9H), δ 0.9 (6H, s), δ 0.82 (3H, s); ^{13}C-NMR (CD_3OD): signals at δ 156.9 (s), δ 136.8 (s), δ 114.9 (s), δ 108.7 (d), δ 40.5 (t), δ 38.3 (t), δ 37.4 (t), δ 34.11 (d), δ 29.0 (t), δ 25.7

[7] Precoated silica gel G Machery Nagel & Co.
[8] Waters LC-500A.
[9] μBondapackC$_{18}$.
[10] Waters prep. LC 500A.

(t), δ 23.0 (q), δ 21.6 (q), δ 21.3 (t), δ 20.3 (q); MS M^+ at *m/z* 264 (16.4%) for $C_{17}H_{28}O_2$, 150 (11.5%) and 137 (100%).

RESULTS AND DISCUSSION

Cannabichromene (I) derivatives were prepared according to a previously published method for the synthesis of cannabichromene (5). That method involves the reflux of equimolar quantities of the properly substituted resorcinol, citral and *tert*-butylamine in toluene for 9 hr. In this way, 48% of II was obtained. However, when pyridine was used as the solvent and base, Compound III was obtained in a 24% yield. Compounds IV and V were obtained through catalytic hydrogenation of II using 5% Pd/C. When the reaction was allowed to proceed for 20 min, a mixture of IV and V was obtained in a yield of 15 and 66%, respectively. When the reaction was carried out for a longer period of time or under pressure V was obtained quantitatively. ^{1}H-NMR of IV shows that the double bond was located in the side chain as shown by the presence of only one olefinic signal at δ 5.15 (1H, t). This is in contrast to the ^{1}H-NMR spectrum of II, which showed two additional signals at δ 6.68 and 5.45 (1H each, d, J = 10 Hz) characteristic of the double bond at Δ^3 of the chromene system. Compounds VI and VII were obtained in a 10% yield after repeated chromatography, while VIII was obtained in ~60% yield. All compounds were purified by column chromatography over silica gel or through preparative liquid chromatography and were characterized by spectral methods including IR, UV, MS, ^{1}H-NMR and ^{13}C-NMR.

Attempts at preparing cannabichromene derivatives having the R group either as COOH, $COOCH_3$, HN—O(=C)—CH_3, NH—SO_2—CH_3 under the same conditions for preparing cannabichromene failed. We can conclude that the R group on the resorcinol moiety has a significant effect on the reactivity of the molecule with citral to give the chromene structure. When the R group was an electron-withdrawing group (—O(=C)—OH, —O(=C)—OCH_3) the reaction did not proceed. When R was an OH group the reaction proceeded rapidly to many products of which <5% was the desired product. Attempts to increase the yield were unsuccessful. When R was a long chain alkyl group, the yield of the desired product was fairly high (~60%). Even when R was CH_3 a 48% yield was obtained. However, when R was H the yield dropped back to ~10% with almost an equal amount of iso-compound being formed, and thus, the selectivity of the reaction was lost.

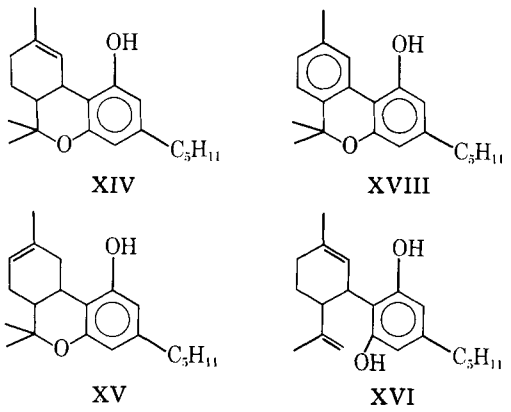

XIV

XVIII

XV

XVI

In addition to cannabichromene-type compounds, the antibacterial activity of other cannabinoids were investigated. Δ^9-Tetrahydrocannabinol (XIV), Δ^8-tetrahydrocannabinol (XV), cannabidiol (XVI), cannabinol (XVIII), cannabigerol (XIII), and cannabicyclol (XVII) were tested. Only XIII showed significant activity. Thus, the C_1-homolog of cannabigerol and its isomer were synthesized to test their activity against the various organisms with the idea that the C_1-homolog might be more active than the C_5-homolog as is the case with cannabichromene homologs.

Compounds X and XI were prepared according to a method described previously (13) for the preparation of cannabigerol. Although the yield was reported to be 52%, only a 10% isolated yield was obtained.

Organisms utilized in the screens included Gram-positive, Gram-negative, and acid-fast bacteria as well as different types of fungi (Table I).

Compounds I–XII were subjected to the antibacterial antifungal activity screens (Tables II–V). Qualitative screening using the agar well diffusion assay showed that these compounds possess strong antibacterial and mild antifungal properties. These compounds exhibited large zones of inhibition when compared to positive standards at the same concentrations. The minimum inhibitory concentrations for these compounds were determined using selected bacteria and fungi as recorded in Tables IV and V. The organisms selected for the minimum inhibitory concentration determinations were based on the largest zone of inhibition resulting in the qualitative screen (Tables II and III).

Table I—Antimicrobial Screening Using the Agar Well Diffusion Assay

Organism	ATCC No.	Classification
Bacillus subtilis	6633	Gram-positive bacterium
Staphylococcus aureus	6538	Gram-positive bacterium
Escherichia coli	10536	Gram-negative bacterium
Pseudomonas aeruginosa	15442	Gram-negative bacterium
Mycobacterium smegmatis	607	Acid-fast bacterium
Candida albicans	10231	Yeast-like fungus
Saccharomyces cerevisiae	9763	Yeast-like fungus
Aspergillus niger	16888	Filamentous fungus
Trichophyton mentagrophytes	9972	Dermatophyte

Table II—Qualitative Antibacterial Results [a]

Compound	*B. subtilis*		*E. coli*		*S. aureus*		*M. smegmatis*		*Ps. aeruginosa*	
	24 hr	48 hr	24 hr	48 hr	24 hr	48 hr	24 hr	48 hr	24 hr	48 hr
XV	7	5	1	—	15	15	5	5	—	—
XIV	—	—	2	—	5	5	2	2	—	—
XVI	10	10	—	—	10	10	10	9	—	—
XIII	25	17	—	—	30	30	25	25	—	—
Streptomycin SO_4	10	10	6	6	7	7	20	20	5	5
XII	25	25	3	3	22	22	20	20	1	1
Streptomycin SO_4	10	10	6	6	8	8	20	20	5	5
X	>35	33	—	—	>35	35	>35	>35	2	2
Streptomycin SO_4	10	10	6	5	11	11	23	23	5	5
XI	22	20	2	2	22	19	23	22	2	2
Streptomycin SO_4	No Growth		10	10	11	10	20	20	6	5
IV	8	5	5	5	10	10	15	12	1	1
V	16	9	5	5	>25	>25	>25	>25	4	3
V′	4	4	5	5	13	13	7	7	1	1
IX	1	1	1	1	10	10	7	6	1	1
VIII	—	—	—	—	10	10	5	5	4	4
Streptomycin SO_4	7	8	2	2	9	9	20	22	3	3
VII	10	7	2	2	—	—	6	4	—	—
XVII	—	—	—	—	—	—	3	1	—	—
VI	10	10	3	2	15	15	20	18	3	—
Streptomycin SO_4	11	10	5	5	10	10	20	22	7	6

[a] Antimicrobial activity was recorded as the width (in millimeters) of the inhibition zone measured from the edge of the agar well to the edge of the inhibition zone.

Table III—Qualitative Antifungal Results [a]

Compound	*C. albicans*		*S. cerevisiae*		*A. niger*		*T. mentagrophytes*	
	48 hr	72 hr	48 hr	72 hr	48 hr	72 hr	48 hr	72 hr
XV	2	2	—	—	—	—	1	1
XIV	2	2	1	1	—	—	3	2
XVI	2	3	3	2	—	—	4	2
XIII	3	2	6	4	—	—	5	2
Amphotericin B	4	4	2	2	—	—	4	2
XII	9	5	>25	20	4	4	>30	25
Amphotericin B	5	3	12	12	2	2	13	13
X	25	25	25	22	1	1	15	13
Amphotericin B	9	7	7	7	2	2	10	10
XI	12	10	20	20	16	10	22	22
Amphotericin B	9	7	11	15	7	3	Little growth	23
IV	4	4	8	8	2	2	No growth	
V	3	3	22	23	3	3	No growth	
V′	2	3	7	7	1	1	No growth	
IX	2	3	7	7	1	1	No growth	
VIII	4	5	4	4	1	—	No growth	
Amphotericin B	7	8	7	8	4	4	No growth	
VII	3	2	2	2	—	—	—	—
XVII	1	1	1	1	—	—	—	—
VI	7	5	10	8	9	5	20	19
Amphotericin B	5	3	7	5	2	1	4	4

[a] Antimicrobial activity was recorded as the width (in millimeters) of the inhibition zone measured from the edge of the agar well to the edge of the inhibition zone.

Table IV—Minimum Inhibitory Concentration [a] of Cannabichromene and Cannabigerol Homologs and Isomers against Different Organisms

Compound	*B. subtilis*		*S. aureus*		*M. smegmatis*	
	24 hr	48 hr	24 hr	48 hr	24 hr	48 hr
I	0.39	0.78	1.56	1.56	12.5	25.0
III′	0.78	3.12	NT[b]	NT	25.0	25.0
VI	6.25	12.5	12.5	12.5	12.5	12.5
Streptomycin SO_4	6.25	25.0	3.12	12.5	1.56	1.56
II	3.12	3.12	3.12	3.12	3.12	6.25
VII	6.25	6.25	12.5	12.5	12.5	12.5
Streptomycin SO_4	3.12	6.25	6.25	6.25	6.25	6.25
V	1.56	1.56	0.78	3.12	3.12	3.12
Streptomycin SO_4	12.5	100	25.0	25.0	6.25	6.25
X	1.56	6.25	3.12	6.25	6.25	6.25
Streptomycin SO_4	No Readings					
XI	1.56	1.56	12.5	12.5	6.25	6.25
Streptomycin SO_4	6.25	12.5	25.0	50.0	6.25	6.25
XII	0.78	1.56	1.56	1.56	3.12	3.12
VIII	50	50	50	100	25	50
IX	25	50	50	100	50	50
Streptomycin SO_4	6.25	6.25	6.25	25	0.78	0.78

[a] Expressed in micrograms per milliliter. [b] Not tested.

Table V—Minimum Inhibitory Concentration [a] of Cannabichromene and Cannabigerol Homologs and Isomers against Different Fungi

Compound	*C. albicans*		*S. cerevisiae*		*T. mentagrophytes*		*A. niger*	
	48 hr	72 hr	48 hr	72 hr	48 hr	72 hr	48 hr	72 hr
I	NT[b]	NT	25.0	50.0	25.0	50.0		
Amphotericin B	NT	NT	3.12	3.12	NT	NT		
III′	50.0	100.0	NT	NT	NT	NT		
VI	50.0	50.0	25.0	25.0	25.0	25.0		
Amphotericin B	1.56	1.56	0.78	0.78	NT	NT		
II	NT	NT	6.25	12.5	6.25	6.25		
VII	12.5	25.0	NT	NT	6.25	6.25		
Amphotericin B	1.56	6.25	0.19	0.78	12.5	25.0		
V	NT	NT	12.5	12.5	50.0	50.0		
Amphotericin B	NT	NT	6.25	6.25	25.0	25.0		
X	25.0	25.0	12.5	12.5	6.25	25.0	50.0	50.0
Amphotericin B	6.25	6.25	3.12	6.25	25.0	25.0	50.0	50.0
XI	25.0	50.0	6.25	6.25	6.25	6.25	50.0	50.0
Amphotericin B	50.0	50.0	25.0	25.0	12.5	12.5	50.0	50.0
XII	12.5	25.0	6.25	6.25	25.0	12.5		
VIII	50.0	100.0	100.0	100.0	25.0	50.0		
IX	50.0	100.0	50.0	100.0	25.0	50.0		
Amphotericin B	12.5	25.0	3.12	6.25	6.25	50.0		

[a] Expressed in micrograms per milliliter. [b] Not tested.

It can be concluded from Tables III and IV that the antimicrobial activity of the normal series, in cannabichromene and cannabigerol homologs and isomers, is more pronounced than in case of the iso-series. Cannabichromene type compounds having a methyl or a pentyl group in the side chain show the highest antimicrobial activity. An intermediate type of activity is seen when R is a hydrogen. However, lengthening the side chain up to C_{15} leads to a tremendous decrease in activity. Total saturation of the two double bonds in the cannabichromene and cannabigerol type compounds having a methyl side chain in most of the cases leads to an increase in the antifungal and antibacterial activities as in the case of Compounds XII and V, respectively (Tables IV and V).

This is the first reported synthesis and spectral data of most of the compounds prepared in this investigation. In addition, the antimicrobial activities of these compounds show encouraging results. The activities of the compounds prepared in this report were compared qualitatively with those of some known cannabinoids, namely, cannabigerol, cannabidiol, cannabicyclol, Δ^8- and Δ^9-tetrahydrocannabinols and were found to be far superior in most instances (Tables II and III).

REFERENCES

(1) C. E. Turner, M. A. ElSohly, and E. G. Boeren, *J. Nat. Prod.*, **43**, 169 (1980).

(2) J. J. Kettenes-Van Den Bosch, C. A. Salemink, J. Van Noordwijk, and I. Khan, *J. Ethnopharmacol.*, **2**, 197 (1980).

(3) R. Mechoulam, N. Lander, T. H. Varkony, I. Kimmel, O. Becker, and Z. Ben Zvi, *J. Med. Chem.*, **23**, 1068 (1980).

(4) R. Mechoulam and Y. Gaoni, *Fortschr. Chem. Org. Naturst.*, **25**, 175 (1967).

(5) M. A. ElSohly, E. G. Boeren, and C. E. Turner, *J. Heterocycl. Chem.*, **75**, 699 (1978).

(6) P. W. Wirth, E. Sue Watson, M. A. ElSohly, C. E. Turner, and J. C. Murphy, *Life Sci.*, **26**, 1991 (1980).

(7) N. S. Hatoum, W. M. Davis, M. A. ElSohly, and C. E. Turner, *Toxicol. Lett.*, **8**, 141 (1981).

(8) N. S. Hatoum, W. M. Davis, I. W. Waters, M. A. ElSohly, and C. E. Turner, *Gen. Pharmacol.*, **12**, 351 (1981).

(9) N. S. Hatoum, W. M. Davis, M. A. ElSohly, and C. E. Turner, *ibid.*, **12**, 357 (1981).

(10) P. W. Wirth, E. Sue Watson, M. A. ElSohly, R. Seidel, J. C. Murphy, and C. E. Turner, *J. Pharm. Sci.*, **69**, 1359 (1980).

(11) C. E. Turner and M. A. ElSohly, *J. Clin. Pharmacol.*, **21**, 2835 (1981).

(12) Alice M. Clark, Farouk S. El-Feraly, and Wen-Shyong Li, *J. Pharm. Sci.*, **70**, 95 (1981).

(13) R. Mechoulam and B. Yagen, *Tetrahedron Lett.*, **60**, 5349 (1969).

Preparation of Hydrophilic Albumin Microspheres Using Polymeric Dispersing Agents

WILLIAM E. LONGO, HIROO IWATA, THOM A. LINDHEIMER, and EUGENE P. GOLDBERG[x]

Received August 19, 1981, from the *Department of Materials Science and Engineering, University of Florida, MAE 217, Gainesville, FL 32611.* Accepted for publication October 13, 1981.

Abstract □ A new method for preparing glutaraldehyde cross-linked human serum albumin microspheres has been developed. Important aspects of this method include addition of glutaraldehyde in the organic phase and use of concentrated solutions of hydrophobic polymers (polymethylmethacrylate) or hydrophilic polymers (polyoxyethylene–polyoxypropylene block copolymer) as dispersion media. Uniform, round, solid, 3–150-μm hydrophilic microspheres were readily prepared by this process. The average size of microspheres was a function of dispersion time and energy input. Surface properties were altered by chemical modification using either 2-aminoethanol or aminoacetic acid to quench residual aldehyde groups. Optical and scanning electron microscopy and electronic particle size characterization indicate that the process is versatile in producing solid microspheres in a wide size range. Albumin microspheres of this type are readily dispersed in aqueous media for injection, without the need for surfactants.

Keyphrases □ Microspheres—hydrophilic albumin, preparation using polymeric dispersing agents □ Polymeric dispersing agents—preparation of hydrophilic albumin microspheres □ Glutaraldehyde—cross-linked human serum albumin microspheres, preparation using polymeric dispersing agents

Insoluble drug carriers for prolonged and controlled delivery of therapeutic agents in biological systems recently have generated growing interest (1–3). Many different carrier systems have been studied, including synthetic liposomes, erythrocyte ghosts, permeable polymeric microcapsules, and solid microspheres (4–7). Each of these drug carriers has its own advantages and problems, and there are adequate reviews of the literature (8).

The use of albumin microspheres as drug carriers has been studied to an increasing extent (9, 10). Soluble human serum albumin in blood plasma is a natural circulatory drug carrier (11). Equilibrium binding to various drugs depends primarily on hydrophobic and electrostatic interactions (12). This type of drug binding eliminates the need for covalent attachment between drug and carrier and may facilitate drug release. Human serum albumin is also degraded *in vivo*. The stability of albumin microspheres is, therefore, a function of the degree of albumin cross-linking, porosity, and accessibility of microspheres to enzymatic and phagocytic processes in the body (13).

Current methods of albumin microsphere preparation involve either thermal denaturation at elevated temperatures (110–165°) or chemical cross-linking in vegetable oil or isooctane emulsions (14, 15). Because small amounts of surfactants are needed to disperse such microspheres in water, they appear to be somewhat hydrophobic because of the method of formation. Widder *et al.* (16) hypothesize that hydrophobicity is due to the polar regions of the albumin aligning at the oil–water interface to form a hydrophobic crust or mantle at room temperature. Since their process involves thermal denaturation for microsphere stabilization, a further increase in surface hydrophobicity may occur due to additional albumin conformational changes and surface binding of oil at elevated temperatures. Surface hydrophilicity is important, because a hy-

0022-3549/82/1200-1323$01.00/0

It can be concluded from Tables III and IV that the antimicrobial activity of the normal series, in cannabichromene and cannabigerol homologs and isomers, is more pronounced than in case of the iso-series. Cannabichromene type compounds having a methyl or a pentyl group in the side chain show the highest antimicrobial activity. An intermediate type of activity is seen when R is a hydrogen. However, lengthening the side chain up to C_{15} leads to a tremendous decrease in activity. Total saturation of the two double bonds in the cannabichromene and cannabigerol type compounds having a methyl side chain in most of the cases leads to an increase in the antifungal and antibacterial activities as in the case of Compounds XII and V, respectively (Tables IV and V).

This is the first reported synthesis and spectral data of most of the compounds prepared in this investigation. In addition, the antimicrobial activities of these compounds show encouraging results. The activities of the compounds prepared in this report were compared qualitatively with those of some known cannabinoids, namely, cannabigerol, cannabidiol, cannabicyclol, Δ^8- and Δ^9-tetrahydrocannabinols and were found to be far superior in most instances (Tables II and III).

REFERENCES

(1) C. E. Turner, M. A. ElSohly, and E. G. Boeren, *J. Nat. Prod.*, **43**, 169 (1980).

(2) J. J. Kettenes-Van Den Bosch, C. A. Salemink, J. Van Noordwijk, and I. Khan, *J. Ethnopharmacol.*, **2**, 197 (1980).

(3) R. Mechoulam, N. Lander, T. H. Varkony, I. Kimmel, O. Becker, and Z. Ben Zvi, *J. Med. Chem.*, **23**, 1068 (1980).

(4) R. Mechoulam and Y. Gaoni, *Fortschr. Chem. Org. Naturst.*, **25**, 175 (1967).

(5) M. A. ElSohly, E. G. Boeren, and C. E. Turner, *J. Heterocycl. Chem.*, **75**, 699 (1978).

(6) P. W. Wirth, E. Sue Watson, M. A. ElSohly, C. E. Turner, and J. C. Murphy, *Life Sci.*, **26**, 1991 (1980).

(7) N. S. Hatoum, W. M. Davis, M. A. ElSohly, and C. E. Turner, *Toxicol. Lett.*, **8**, 141 (1981).

(8) N. S. Hatoum, W. M. Davis, I. W. Waters, M. A. ElSohly, and C. E. Turner, *Gen. Pharmacol.*, **12**, 351 (1981).

(9) N. S. Hatoum, W. M. Davis, M. A. ElSohly, and C. E. Turner, *ibid.*, **12**, 357 (1981).

(10) P. W. Wirth, E. Sue Watson, M. A. ElSohly, R. Seidel, J. C. Murphy, and C. E. Turner, *J. Pharm. Sci.*, **69**, 1359 (1980).

(11) C. E. Turner and M. A. ElSohly, *J. Clin. Pharmacol.*, **21**, 2835 (1981).

(12) Alice M. Clark, Farouk S. El-Feraly, and Wen-Shyong Li, *J. Pharm. Sci.*, **70**, 95 (1981).

(13) R. Mechoulam and B. Yagen, *Tetrahedron Lett.*, **60**, 5349 (1969).

Preparation of Hydrophilic Albumin Microspheres Using Polymeric Dispersing Agents

WILLIAM E. LONGO, HIROO IWATA, THOM A. LINDHEIMER, and EUGENE P. GOLDBERG[x]

Received August 19, 1981, from the *Department of Materials Science and Engineering, University of Florida, MAE 217, Gainesville, FL 32611.* Accepted for publication October 13, 1981.

Abstract □ A new method for preparing glutaraldehyde cross-linked human serum albumin microspheres has been developed. Important aspects of this method include addition of glutaraldehyde in the organic phase and use of concentrated solutions of hydrophobic polymers (polymethylmethacrylate) or hydrophilic polymers (polyoxyethylene–polyoxypropylene block copolymer) as dispersion media. Uniform, round, solid, 3–150-μm hydrophilic microspheres were readily prepared by this process. The average size of microspheres was a function of dispersion time and energy input. Surface properties were altered by chemical modification using either 2-aminoethanol or aminoacetic acid to quench residual aldehyde groups. Optical and scanning electron microscopy and electronic particle size characterization indicate that the process is versatile in producing solid microspheres in a wide size range. Albumin microspheres of this type are readily dispersed in aqueous media for injection, without the need for surfactants.

Keyphrases □ Microspheres—hydrophilic albumin, preparation using polymeric dispersing agents □ Polymeric dispersing agents—preparation of hydrophilic albumin microspheres □ Glutaraldehyde—cross-linked human serum albumin microspheres, preparation using polymeric dispersing agents

Insoluble drug carriers for prolonged and controlled delivery of therapeutic agents in biological systems recently have generated growing interest (1–3). Many different carrier systems have been studied, including synthetic liposomes, erythrocyte ghosts, permeable polymeric microcapsules, and solid microspheres (4–7). Each of these drug carriers has its own advantages and problems, and there are adequate reviews of the literature (8).

The use of albumin microspheres as drug carriers has been studied to an increasing extent (9, 10). Soluble human serum albumin in blood plasma is a natural circulatory drug carrier (11). Equilibrium binding to various drugs depends primarily on hydrophobic and electrostatic interactions (12). This type of drug binding eliminates the need for covalent attachment between drug and carrier and may facilitate drug release. Human serum albumin is also degraded *in vivo*. The stability of albumin microspheres is, therefore, a function of the degree of albumin cross-linking, porosity, and accessibility of microspheres to enzymatic and phagocytic processes in the body (13).

Current methods of albumin microsphere preparation involve either thermal denaturation at elevated temperatures (110–165°) or chemical cross-linking in vegetable oil or isooctane emulsions (14, 15). Because small amounts of surfactants are needed to disperse such microspheres in water, they appear to be somewhat hydrophobic because of the method of formation. Widder *et al.* (16) hypothesize that hydrophobicity is due to the polar regions of the albumin aligning at the oil–water interface to form a hydrophobic crust or mantle at room temperature. Since their process involves thermal denaturation for microsphere stabilization, a further increase in surface hydrophobicity may occur due to additional albumin conformational changes and surface binding of oil at elevated temperatures. Surface hydrophilicity is important, because a hy-

0022-3549/82/1200-1323$01.00/0

drophilic albumin surface may enhance surface physical and chemical behavior *in vivo*, and the surfactants presently used to disperse human serum albumin microspheres may influence tissue interactions, drug release, and activity.

The use of insoluble drug carriers for localized or intratumor injection chemotherapy was reported previously (17–19). Therefore, methods have been explored for preparing hydrophilic albumin microspheres which readily form stable dispersions for injection without surfactants and which may be easily surface-modified to introduce functional groups (*e.g.*, —CHO) or ligands (*e.g.*, antibodies) for binding to tumor tissue (17, 19).

The present report is concerned with the preparation of human serum albumin microspheres by a new procedure which yields hydrophilic, solid spheres. Glutaraldehyde cross-linking of the albumin phase also produces free aldehyde groups on the surface of the microspheres. Because of aldehyde–protein amino group coupling, these aldehyde handles may enhance tissue immobilization. The aldehyde functionality also facilitates surface chemical coupling of 2-aminoethanol or aminoacetic acid for increased hydrophilicity. Attachment of drugs, immunoglobulins, lectins, enzymes, and anionic or cationic ligands is also feasible.

EXPERIMENTAL

Preparation of Microspheres—*Polymethylmethacrylate–Chloroform/Toluene Dispersion*—Human serum albumin[1] (150 mg) was dissolved in 0.5 ml of distilled water (pH 7.0) at 23° and added dropwise to a 25–30% solution of polymethylmethacrylate[2] (intrinsic viscosity 1.4) in a mixture of 1.5 ml of chloroform[3] and 1.5 ml of toluene[3] in a 16- × 125-mm screw-cap test tube. The mixture was dispersed with a vortex mixer[4] for various time periods (1–10 min) until the desired microsphere size was achieved. Microsphere particle size was determined by optical microscopy[5] using aliquots removed at various times.

Glutaraldehyde in toluene was used for cross-linking. Aqueous glutaraldehyde (25% biological grade)[2], 1.0 ml, and 1.0 ml of toluene were combined in a 13- × 100-mm test tube. The two phases were dispersed by sonication[6] with a microtip power head attachment (20 sec at 50 W). The resulting toluene solution of glutaraldehyde (0.14 mole was determined with 3-methyl-2-benzothiazolinone hydrazone)[1] (20) was allowed to phase separate, pipeted off, and added to the albumin dispersion. After addition of the glutaraldehyde-saturated toluene, the dispersion was mixed with a rotary mixer[7] at room temperature until albumin cross-linking was complete (5–6 hr). One milliliter of either 2-aminoethanol[8] or aminoacetic acid[1] then was added to cap any free aldehyde groups. After a 1-hr reaction time, the suspension was centrifuged (2000 ×*g*, 2 min) and the supernatant discarded. Microspheres were then washed four times each with 25% chloroform in toluene, acetone, and distilled water. Between each washing, microspheres were centrifuged (2000×*g*, 2 min), the supernatant discarded, and the pellet resuspended. The washed microspheres were either stored frozen or lyophilized. Yields were 75–85% (Scheme I).

Polyoxyethylene–Polyoxypropylene Copolymer–Chloroform Dispersion—Human serum albumin (150 mg) was dissolved in 0.5 ml of distilled water (pH 7.0) at 23° and added dropwise to a 25–30% solution of polyoxyethylene–polyoxypropylene copolymer[9] in 4.0 ml of chloroform in a 16- × 125-mm screw-cap test tube. The mixture was emulsified with a vortex mixer for various time periods (1–10 min) until the desired size of microsphere was achieved.

Glutaraldehyde in chloroform for cross-linking was prepared from 25% aqueous glutaraldehyde and chloroform by sonication as previously described. Gluturaldehyde, 0.40 mole in 1.0 ml of chloroform, was added and the dispersion was mixed with a rotary mixer at room temperature until albumin cross-linking was complete (5–6 hr). Then, 1.0 ml of either 2-aminoethanol or aminoacetic acid was added to cap any free aldehyde groups. After a 1-hr reaction time, 10 ml of acetone was added, the suspension briefly shaken, then centrifuged (2000×*g*, 2 min) and the supernatant discarded. Microspheres were then washed 10 times each with acetone and distilled water. Between each washing, microspheres were centrifuged (2000×*g*, 2 min), the supernatant decanted, and the pellet resuspended. As before, washed microspheres were either stored frozen or lyophilized. Typical yields were 75–85% (Scheme II).

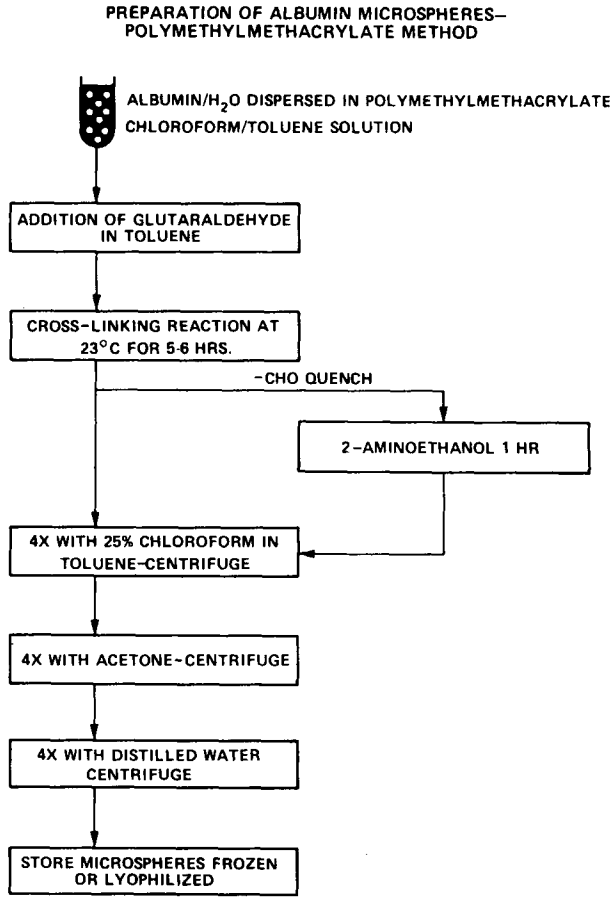

Scheme I—Albumin microsphere preparation using polymethylmethacrylate solution for dispersion.

Microscopic Characterization of Microspheres—Size and morphology were characterized by scanning electron microscopy (SEM)[10] at 20 kV. SEM samples were prepared by applying a 200 Å coating of gold–palladium on samples using a sputter coater[11] in an argon atmosphere with a digital thickness monitor. Internal structures were determined by transmission electron microscopy[12]. Microspheres mounted in epoxy were sliced with an ultramicrotome[13]. Microsphere compositions and porosity were verified with 0.5 ml of dye added to 10-mg spheres in 2 ml of distilled water[14] using optical microscopy. Protein stained microspheres were also mounted in epoxy, sliced with the ultramicrotome, and examined by optical microscopy.

Effect of Polymer Dispersant Concentration—Human serum albumin microspheres were prepared by the two methods, and the concentrations of polymer solutions (polymethylmethacrylate and polyoxyethylene–polyoxypropylene) were varied from 0 to 25% in 2% intervals. After cross-linking with glutaraldehyde, the dispersions were evaluated for microsphere stability against coagulation.

Measurement of Microsphere Size Distribution as a Function of Dispersion Time—Human serum albumin microspheres were prepared

[1] Sigma Chemical Co.
[2] Polyscience.
[3] Fisher Scientific Co.
[4] Vortex Genie Scientific Industries, Inc.
[5] Nikon Biphot.
[6] Heat Systems-Ultrasonics, Model W-375.
[7] Labquake Labindustries.
[8] Mallinckrodt.
[9] BASF W-jandotte Corp.
[10] JEOL model 35C.
[11] Hummer V.
[12] Phillips model 310.
[13] Sorvall model MT-2.
[14] Coomassie blue G-250, BIO-RAD Laboratories.

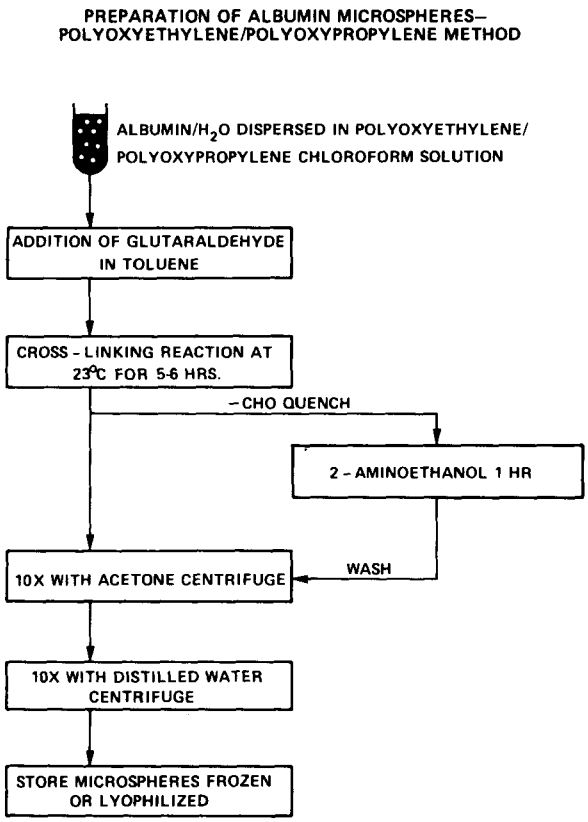

Scheme II—Albumin microsphere preparation using polyoxyethylene–polyoxypropylene solution for dispersion.

using both described procedures. Dispersion times of 1, 3, 5, and 8 min were used at constant energy input (speed setting 8 on vortex mixer). The washed microspheres were suspended in 10 ml of distilled water. Aliquots were withdrawn from a well-shaken sample and placed on an SEM sample holder. One hundred random microspheres for each dispersion time were counted and measured. Aliquots (10 μl) were also added to 150 ml of continuously stirred 0.14 *M* potassium chloride solution. A 1.0-ml sample was withdrawn over a 4-sec time span by an electronic particle size counter[15] equipped with a 100-μm sampling aperture. The counter was calibrated with 9.76 μm of polystyrene microspheres. This enabled accurate size measurements from 2 to 40 μm. The total number of microspheres counted ranged from 7000 to 23,000/sample.

Microsphere Size Distribution as a Function of Energy Input—Human serum albumin microspheres were prepared using the polymethylmethacrylate procedure. Dispersion time was held constant (10 min), and energy input was varied by adjusting the speed setting on the vortex mixer, using speeds of 2, 4, 6, and 8. The washed microspheres were suspended in 10 ml of distilled water and size distributions were measured by the SEM technique.

Measurement of Reactive Aldehyde Groups—Human serum albumin microspheres (10 μm average diameter) were prepared by the polymethylmethacrylate method. The cross-linked microspheres were divided into two samples. One was quenched with 0.5 ml of 2-aminoethanol while the other sample was left unquenched. [^{3}H]Leucine[16], specific activity 134.2 Ci/mmoles/ml, was diluted with a carrier (L-leucine)[17] to a final activity of 5 μCi/50 mmoles/ml. One milliliter of isotope solution was added to each of three samples of 7.4 mg/ml unquenched and three samples of 7.99 mg/ml quenched microspheres in 13- × 100-mm test tubes. The samples were incubated for 40 min in a tabletop sonicator[18], then washed four times with distilled water (pH 7.0) by centrifugation (1000×*g*, 2 min). Microsphere pellets were resuspended in 2 ml of a scintillation cocktail[16] and slightly shaken until microspheres were completely dissolved. From each of these solutions, 1.0-, 0.5-, and 0.25-ml aliquots were removed and added to scintillation counter containers. The

[15] Coulter Counter model TA11.
[16] Aquasol New England Nuclear Corp.
[17] Pierce Chemical Co.
[18] E/MC RA Research.

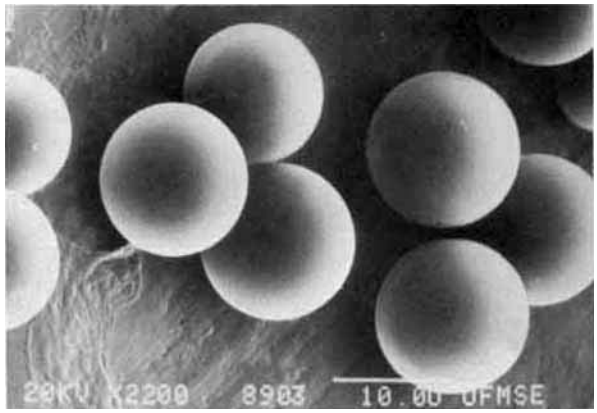

Figure 1—*Scanning electron micrograph (2200×) of albumin microspheres. Polymethylmethacrylate dispersant, 10-μm average diameter.*

final volumes were adjusted to 15 ml with additional cocktail. Activity was determined using a scintillation counter[19] and values plotted against prepared standards.

RESULTS

Figure 1 shows the uniform, smooth spherical geometry of albumin microspheres typically prepared by the procedure (SEM photomicrograph at 2200×). The human serum albumin microspheres in Fig. 1 averaged 10 μm in diameter and were made using polymethylmethacrylate as the polymer dispersant.

The SEM photomicrograph in Fig. 2 clearly shows the solid internal structure of the human serum albumin microspheres. Figure 2 is consistent with the transmission electron microscopic results (not shown) of sectioned microspheres obtained from both dispersant systems. Microtomed sections of the protein stained microspheres showed the blue dye color throughout the albumin spheres. This complete dye penetration is indicative of the porous internal structure of the albumin spheres.

Washed, lyophilized, or air-dried microspheres were readily resuspended in a variety of aqueous media such as distilled water, physiological saline, phosphate buffer, and acetate buffer. The microspheres were easily wetted and dispersed without the need for surfactants.

Figures 3 and 4 show the size distributions of the microspheres as a function of dispersion time using the vortex apparatus. Polymethylmethacrylate was used as a dispersant for the microspheres in Fig. 3 and polyoxyethylene–polyoxypropylene for those in Fig. 4. These data were obtained using an electronic size counter. Average diameters from these data were in close agreement with data obtained from SEM measurements. These results are presented in Table I. SEM size distribution as

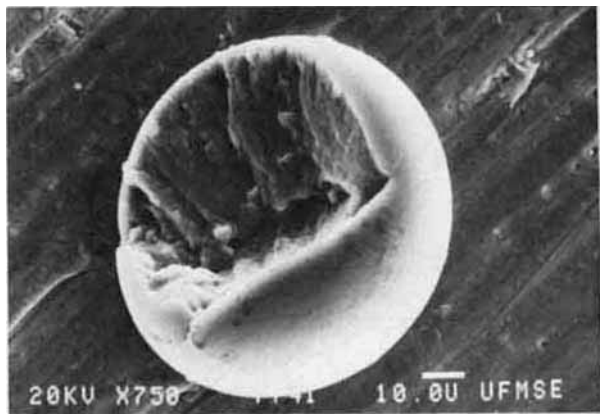

Figure 2—*Scanning electron micrograph (750×) of 100 μm albumin microsphere showing internal structure; polymethylmethacrylate dispersant.*

[19] Beckman model 230.

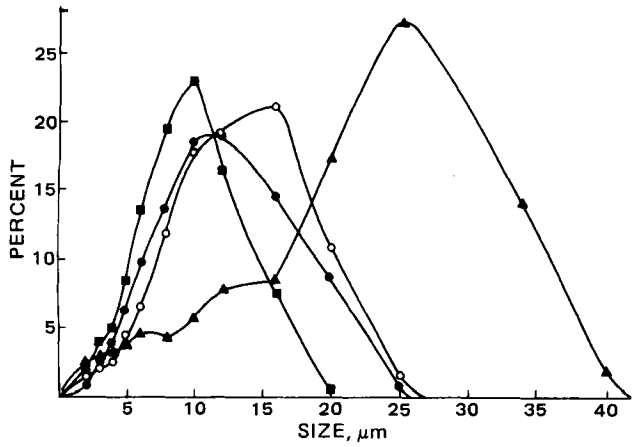

Figure 3—*Size distributions of albumin microspheres using polymethylmethacrylate dispersant. Constant power input, with time of dispersion varied. Key: (▲) 1 min; (○) 3 min; (●) 5 min; (■) 8 min (measurements by Coulter Counter).*

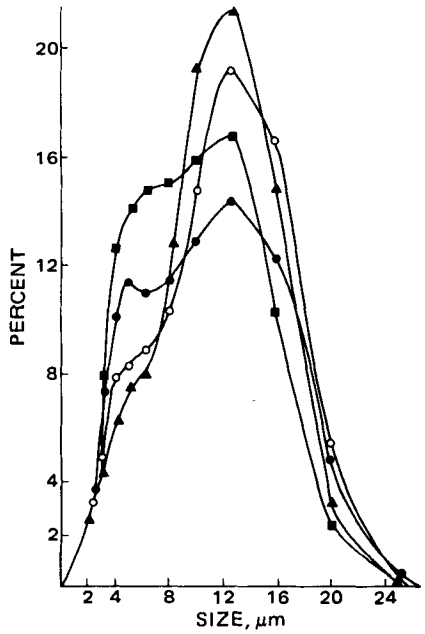

Figure 4—*Size distributions of albumin microspheres using polyoxyethylene-polyoxypropylene dispersant. Constant power input, with time of dispersion varied. Key: (▲) 1 min; (○) 3 min; (●) 5 min; and (■) 8 min (measurements by Coulter Counter).*

a function of power input is shown in Fig. 5 (polymethylmethacrylate dispersant) and summarized in Table II. Table III also indicates that a polymer concentration of at least 10% (w/w) was needed to stabilize the

Table I—Human Serum Albumin Microsphere Size *versus* Dispersion Time [a]

Dispersion Time, min	Diameter, μm (Measured by SEM) $\bar{X}$	*SD*	Variance	Measured with Coulter Counter Mean	Polymer Dispersant[b]
1	22	6.7	44	19	A
	12	5.3	28	11	B
3	12	3.7	13	12	A
	10	3.7	13	10	B
5	10	3.6	13	11	A
	8.5	2.7	7	9	B
8	8.5	3.0	9	9	A
	7.0	2.5	8	7	B

[a] Constant power input: speed setting 8 on vortex genie. [b] A, Polymethylmethacrylate; B, polyoxyethylene-polyoxypropylene.

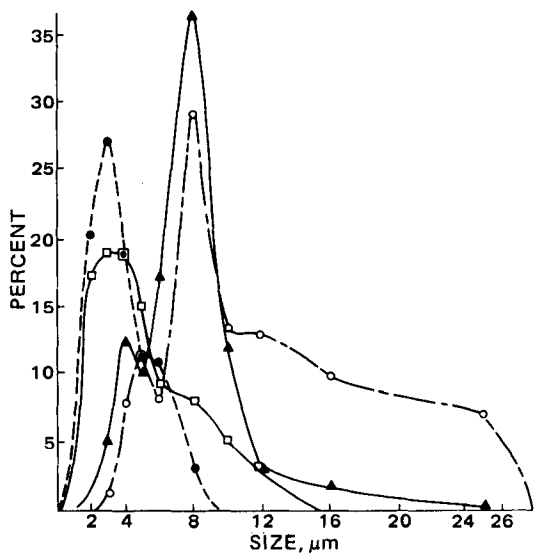

Figure 5—*Size distributions of albumin microspheres using polymethylmethacrylate dispersant. Constant dispersion time (10 min), with power input varied. Key: (○) speed setting 2; (▲) speed setting 4; (□) speed setting 6; (●) speed setting 8 (measurements by SEM).*

dispersion at short dispersion times (1.0 min). When smaller microspheres are desired (requiring longer dispersion times or higher energy input) higher concentrations of polymer are needed. This is also indicated in Table III.

[^{3}H]Leucine binds to the reactive aldehyde groups as shown in Table IV. By subtracting the amount of adsorbed [^{3}H]leucine (measured in aldehyde-quenched microspheres) from the amount adsorbed and covalently bound to the unquenched spheres, it was determined that 4.0 $\times 10^{-2}$ μmoles of leucine bind to reactive aldehyde groups in 1.0 ml of human serum albumin microspheres. Electronic particle analyses es-

Table II—Human Serum Albumin Microsphere Size *versus* Dispersion Energy [a]

Dispersion Energy (Speed Setting on Vortex Genie)	Diameter, μm Measured by SEM $\bar{X}$	*SD*
2	9	4.0
4	7	2.9
6	4.4	2.5
8	3.5	1.6

[a] Constant dispersion time: 10 min.

Table III—Effect Of Polymer Dispersant Concentration

Polymer Concentration, %	Dispersion Time[a], min	Dispersion Stability[b]
0 → 8	1	−
	5	−
10	1	+
	5	−
12	1	+
	5	−
14	1	+
	5	−
16	1	+
	5	−
18	1	+
	5	−
20	1	+
	5	−
25	1	+
	5	−
25 → 35	1	+
	5	+

[a] Power input constant (speed setting 8 on vortex genie). [b] −, indicates unstable dispersion; +, indicates stable dispersion.

Table IV—Concentration of Reactive Aldehyde Groups by Binding of [H^3]Leucine

Physical or Chemical Binding of Leucine with:	μMoles Leucine Bound/ml of Microspheres	Number of Leucines/10 μm Sphere	Number Reactive —CHO/ Sphere[a]
2-Aminoethanol Quenched Microspheres	8.9×10^{-2}	5.4×10^{6}	—
Unquenched Microspheres	1.3×10^{-1}	7.8×10^{6}	—
Chemically Reacted Leucine (Unquenched − Quenched)	4.1×10^{-1}	2.4×10^{6}	2.4×10^{6}

[a] Assumed one bound leucine equals one reactive aldehyde group.

tablished that there were ~1.0×10^{10} microspheres/ml in a 10-μm diameter preparation. This is equivalent to 2.42×10^{6} reactive aldehyde groups/sphere based on one leucine molecule covalently bound per reactive aldehyde group. From the data of Ikada *et al.* (21) 1.1 μg of a human serum albumin monolayer would cover a 1.0-cm^2 area, and if perfect molecular packing for albumin molecules were assumed, 3.02×10^{7} molecules would fill the surface area of a 10-μm microsphere. On this basis, the 2.42×10^{6} reactive aldehyde groups measured/10-μm sphere, therefore, would be equivalent to ~8 reactive aldehyde groups/100 human serum albumin molecules at the surface, which is clearly a maximum value, since a significant fraction of —CHO groups must also be present within the spheres.

DISCUSSION AND CONCLUSIONS

Good dispersion and stabilization of aqueous human serum albumin was obtained in concentrated polymer solutions. No additional surfactants were required. Insoluble human serum albumin microspheres were produced with glutaraldehyde cross-linking in a wide particle size range as shown in the SEM photomicrographs. Optical photomicrographs (Figs. 6*a* and *b*) show the polymer coating surrounding the human serum albumin microsphere dispersion in the aqueous wash phase. This polymer coating or microcapsule apparently affords dispersion stability and prevents coagulation before and during glutaraldehyde cross-linking.

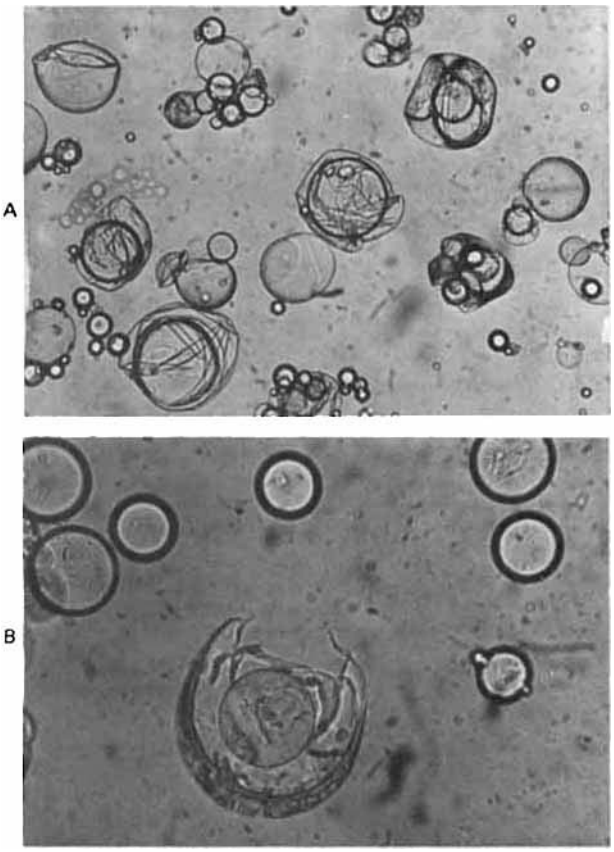

Figure 6—*(a) Optical micrograph of stabilized albumin microspheres showing the surrounding polymer coating. Microspheres in aqueous wash phase; average particle size 40 μm; polyoxyethylene–polyoxypropylene dispersant. (b) Polymer coated microspheres, as in (a), showing ruptured polymer coating during aqueous wash.*

The concentration of the polymer dispersant solutions was important; concentrations <25% (w/w) were not sufficient to prevent coagulation when small microspheres (≤10 μm) were desired, and concentrations >30% retarded complete removal of the polymer. Polymer molecular weight was also important. Low molecular weight polymethylmethacrylate (intrinsic viscosity 0.4) was unsatisfactory at concentrations of 25–30% (w/w), since coagulation occurred.

The size of the microspheres was directly related to power input and dispersion time (Figs. 3–5 and Tables I and II). Thus, by adjusting power input and time, particle size was readily controlled.

Two unique distinguishing features of this method for albumin microsphere preparation as compared with methods reported to date (9, 10, 14–16) are the addition of the glutaraldehyde cross-linking agent in an organic medium to the aqueous albumin dispersion and use of concentrated high polymer solutions as the organic phase for preparing dispersions. Human serum albumin microspheres prepared by thermal denaturation in oil or by glutaraldehyde cross-linking with aqueous aldehyde (sometimes incorporated at low temperature into the aqueous albumin phase) are hydrophobic to the extent that surfactants must be used to prepare microsphere dispersions in water (10, 22). This is probably a result of preferential hydrophobic organization of the albumin surface at a hydrophobic oil interface coupled with thermal denaturation or homogeneous cross-linking with glutaraldehyde.

Use of concentrated polymer solutions as the organic dispersing phase

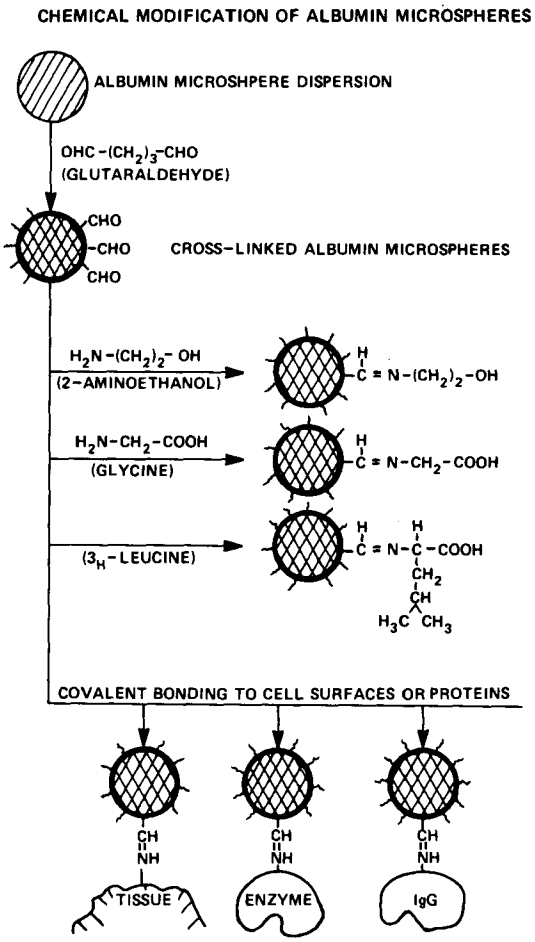

Scheme III—Schematic representation of albumin microsphere surface chemistry.

affords excellent dispersion and control, wide particle size latitude, and smooth, uniform spheres without the need for surfactants. More importantly, because glutaraldehyde is presented to the aqueous albumin microsphere dispersion from the organic phase, there must be a strong preference for aldehyde-amino group reactions and cross-linking at or near the albumin surface. This probably produces a case-hardening effect with a higher cross-link density near the surface of the microspheres accompanied also by a much higher concentration of mono-reacted dialdehyde at the surface (Scheme III). The result of monofunctional glutaraldehyde capping of lysine amino groups at the albumin microsphere surface would be to increase surface anionicity and hydrophilicity, especially if a portion of the free aldehyde functions oxidize to carboxyl groups.

The availability of a relatively high surface concentration of aldehyde functionality also facilitates a variety of chemical modifications including: aminoalcohol capping to enhance hydrophilicity; enzyme, antibody, or other protein ligand binding; covalent attachment of amino-functional drugs. As suggested in Scheme III, such changes in surface functionality may be used to enhance tissue immobilization by covalent or physical binding, for specific tissue targeting using biospecific affinity ligands (*e.g.*, tumor-specific antibodies), or for improved diagnostic or immune assay reagents and procedures.

REFERENCES

(1) J. Heller and R. W. Baker, "Controlled Release of Bioactive Materials," Academic, New York, N.Y., 1980, pp. 1, 17.

(2) E. P. Goldberg, Ed., in "Targeted Drugs," Wiley, New York, N.Y., 1982.

(3) D. S. T. Hsieh, R. Langer, and J. Folkman, *Proc. Natl. Acad. Sci. USA*, **78**, 1863 (1981).

(4) G. Gregoriadis, *Pharmacol. Ther.*, **10**, 103 (1980).

(5) U. Zimmerman, in "Targeted Drugs," E. P. Goldberg, Ed., Wiley, New York, N.Y., 1982.

(6) T. M. S. Chang, in "Polymer Grafts in Biochemistry," H. F. Hixson and E. P. Goldberg, Eds., Marcel Dekker, New York, N.Y., 1976, pp. 245, 258.

(7) I. S. Joholm and P. Edman, *J. Pharmacol. Exp. Ther.*, **211**, 656 (1979).

(8) K. J. Widder, A. E. Senyei, and D. F. Ranny, "Advances in Pharmacology and Chemotherapy," Academic, New York, N.Y., 1979, pp. 213, 271.

(9) A. F. Yapel, U.S. Patent 4,147,767, (1979).

(10) P. A. Kramer, *J. Pharm. Sci.*, **63**, 1646 (1974).

(11) J. Koch-Weser and E. M. Sellers, *N. Engl. J. Med.*, **294**, 311 (1976).

(12) *Ibid.*, **294**, 526 (1976).

(13) K. J. Widder, A. E. Senyei, and D. F. Ranney, *Cancer Res.*, **40**, 3512 (1980).

(14) T. Ishizaka, K. Endo, and M. Koishi, *J. Pharm. Sci.*, **70**, 358 (1981).

(15) A. E. Senyei, S. D. Reich, C. Gonczy, and K. J. Widder, *ibid.*, **70**, 328 (1981).

(16) K. Widder, G. Flouret, and A. Senyei, *ibid.*, **68**, 79 (1979).

(17) E. P. Goldberg, R. N. Terry, and M. Levy, *Am. Chem. Soc. Preprints*, Div. Org. Coatings Plastics Chem., **44**, 132 (1981).

(18) R. N. Terry, M. S. Thesis, University of Florida (1980).

(19) E. P. Goldberg, H. Iwata, R. N. Terry, W. E. Longo, M. Levy, and J. L. Cantrell, in Affinity Chromatography and Related Techniques," Gribnau, Visser, and Nivard, Eds., Elsevier, Amsterdam, 1982, p. 375.

(20) E. Rswicki, T. R. Hauser, T. W. Stanley, and W. Elbert, *Anal. Chem.*, **33**, 93 (1961).

(21) Y. Ikada, H. Iwata, T. Mita, and S. Nagaoka, *J. Biomed. Mater. Res.*, **13**, 607 (1979).

(22) T. K. Lee, T. D. Sokoloski, and G. P. Royer, *Science*, **213**, 233 (1981).

ACKNOWLEDGMENTS

This work was supported in part by the State of Florida Biomedical Engineering Center.

The authors thank Dr. B. Dunn for use of his scintillation counter, Dr. G. Onoda for use of the Coulter counter, and M. Smith for the preparation of this manuscript.

Kinetics and Mechanism of the Equilibrium Reaction of Triazolam in Aqueous Solution

MASAHARU KONISHI ˣ, KENTARO HIRAI ‡, and YOSHIO MORI *

Received October 6, 1981, from the **Division of Analytical Chemistry* and the ‡*Division of Organic Chemistry, Shionogi Research Laboratories, Shionogi & Co., Ltd., Fukushima-ku, Osaka 553, Japan.* Accepted for publication January 11, 1982.

Abstract □ The equilibrium kinetics of triazolam in aqueous solution was investigated in the pH range of 1–11 at body temperature. The quantitative study indicated that it forms equilibrium mixtures consisting of ring-opened and closed forms with the composition being dependent on pH. The equilibrium constants of the two species in the pH range studied were determined by GLC method. The apparent first-order rate constants were estimated from the decreasing or increasing absorbance of the mixture in solutions. The forward-reaction rate constant (k_f) showed a bell-shaped k_f–pH profile with a rate maximum at pH 4.59, which indicates not only that the carbinolamine intermediate forms during the equilibrium reaction, but that the rate-determining step of the reaction differs for the acidic and basic sides of the rate maximum. The reverse-reaction rate constant decreased with increasing pH and could not be estimated in the pH region >5.65. Theoretical curves for both forward and reverse reactions satisfactorily fit the observed data. The pKa values of triazolam and its opened-form amine were estimated to be 1.52 and 6.50, respectively.

Keyphrases □ Triazolam—kinetics, mechanism of equilibrium in aqueous solution □ Kinetics—triazolam, mechanism of equilibrium in aqueous solutions □ Equilibrium reaction—triazolam, kinetics, mechanism in aqueous solutions

1,4-Benzodiazepines, first synthesized in the early 1960s, are important minor tranquilizers. These tranquilizers are being extensively used as sedative, hypnotic, muscle relaxant, and anticonvulsant drugs. Their stability and reactivity in aqueous solutions have been under study extensively in the last 5 years. Reaction mechanisms for the hydrolysis of 1,4-benzodiazepines have been reported for chlordiazepoxide (1, 2), oxazepam (3), diazepam (4), nitrazepam (4, 5), desmethyldiazepam (6), and clonazepam (6). Furthermore, equilibrium reactions of these compounds have been reported for pyrazolodiazepinone (7), diazepam (8), nitrazepam (9), triazolobenzodiazepines (10), flunitrazepam (11), and desmethyldiazepam (12). It is now well known that hydrolysis of an azomethine bond

0022-3549/82/1200-1328$01.00/0

affords excellent dispersion and control, wide particle size latitude, and smooth, uniform spheres without the need for surfactants. More importantly, because glutaraldehyde is presented to the aqueous albumin microsphere dispersion from the organic phase, there must be a strong preference for aldehyde-amino group reactions and cross-linking at or near the albumin surface. This probably produces a case-hardening effect with a higher cross-link density near the surface of the microspheres accompanied also by a much higher concentration of mono-reacted dialdehyde at the surface (Scheme III). The result of monofunctional glutaraldehyde capping of lysine amino groups at the albumin microsphere surface would be to increase surface anionicity and hydrophilicity, especially if a portion of the free aldehyde functions oxidize to carboxyl groups.

The availability of a relatively high surface concentration of aldehyde functionality also facilitates a variety of chemical modifications including: aminoalcohol capping to enhance hydrophilicity; enzyme, antibody, or other protein ligand binding; covalent attachment of amino-functional drugs. As suggested in Scheme III, such changes in surface functionality may be used to enhance tissue immobilization by covalent or physical binding, for specific tissue targeting using biospecific affinity ligands (*e.g.*, tumor-specific antibodies), or for improved diagnostic or immune assay reagents and procedures.

REFERENCES

(1) J. Heller and R. W. Baker, "Controlled Release of Bioactive Materials," Academic, New York, N.Y., 1980, pp. 1, 17.

(2) E. P. Goldberg, Ed., in "Targeted Drugs," Wiley, New York, N.Y., 1982.

(3) D. S. T. Hsieh, R. Langer, and J. Folkman, *Proc. Natl. Acad. Sci. USA*, **78**, 1863 (1981).

(4) G. Gregoriadis, *Pharmacol. Ther.*, **10**, 103 (1980).

(5) U. Zimmerman, in "Targeted Drugs," E. P. Goldberg, Ed., Wiley, New York, N.Y., 1982.

(6) T. M. S. Chang, in "Polymer Grafts in Biochemistry," H. F. Hixson and E. P. Goldberg, Eds., Marcel Dekker, New York, N.Y., 1976, pp. 245, 258.

(7) I. S. Joholm and P. Edman, *J. Pharmacol. Exp. Ther.*, **211**, 656 (1979).

(8) K. J. Widder, A. E. Senyei, and D. F. Ranny, "Advances in Pharmacology and Chemotherapy," Academic, New York, N.Y., 1979, pp. 213, 271.

(9) A. F. Yapel, U.S. Patent 4,147,767, (1979).

(10) P. A. Kramer, *J. Pharm. Sci.*, **63**, 1646 (1974).

(11) J. Koch-Weser and E. M. Sellers, *N. Engl. J. Med.*, **294**, 311 (1976).

(12) *Ibid.*, **294**, 526 (1976).

(13) K. J. Widder, A. E. Senyei, and D. F. Ranney, *Cancer Res.*, **40**, 3512 (1980).

(14) T. Ishizaka, K. Endo, and M. Koishi, *J. Pharm. Sci.*, **70**, 358 (1981).

(15) A. E. Senyei, S. D. Reich, C. Gonczy, and K. J. Widder, *ibid.*, **70**, 328 (1981).

(16) K. Widder, G. Flouret, and A. Senyei, *ibid.*, **68**, 79 (1979).

(17) E. P. Goldberg, R. N. Terry, and M. Levy, *Am. Chem. Soc. Preprints*, Div. Org. Coatings Plastics Chem., **44**, 132 (1981).

(18) R. N. Terry, M. S. Thesis, University of Florida (1980).

(19) E. P. Goldberg, H. Iwata, R. N. Terry, W. E. Longo, M. Levy, and J. L. Cantrell, in Affinity Chromatography and Related Techniques," Gribnau, Visser, and Nivard, Eds., Elsevier, Amsterdam, 1982, p. 375.

(20) E. Rswicki, T. R. Hauser, T. W. Stanley, and W. Elbert, *Anal. Chem.*, **33**, 93 (1961).

(21) Y. Ikada, H. Iwata, T. Mita, and S. Nagaoka, *J. Biomed. Mater. Res.*, **13**, 607 (1979).

(22) T. K. Lee, T. D. Sokoloski, and G. P. Royer, *Science*, **213**, 233 (1981).

ACKNOWLEDGMENTS

This work was supported in part by the State of Florida Biomedical Engineering Center.

The authors thank Dr. B. Dunn for use of his scintillation counter, Dr. G. Onoda for use of the Coulter counter, and M. Smith for the preparation of this manuscript.

Kinetics and Mechanism of the Equilibrium Reaction of Triazolam in Aqueous Solution

MASAHARU KONISHI ˣ, KENTARO HIRAI ‡, and YOSHIO MORI *

Received October 6, 1981, from the **Division of Analytical Chemistry* and the ‡*Division of Organic Chemistry, Shionogi Research Laboratories, Shionogi & Co., Ltd., Fukushima-ku, Osaka 553, Japan.* Accepted for publication January 11, 1982.

Abstract □ The equilibrium kinetics of triazolam in aqueous solution was investigated in the pH range of 1–11 at body temperature. The quantitative study indicated that it forms equilibrium mixtures consisting of ring-opened and closed forms with the composition being dependent on pH. The equilibrium constants of the two species in the pH range studied were determined by GLC method. The apparent first-order rate constants were estimated from the decreasing or increasing absorbance of the mixture in solutions. The forward-reaction rate constant (k_f) showed a bell-shaped k_f–pH profile with a rate maximum at pH 4.59, which indicates not only that the carbinolamine intermediate forms during the equilibrium reaction, but that the rate-determining step of the reaction differs for the acidic and basic sides of the rate maximum. The reverse-reaction rate constant decreased with increasing pH and could not be estimated in the pH region >5.65. Theoretical curves for both forward and reverse reactions satisfactorily fit the observed data. The pKa values of triazolam and its opened-form amine were estimated to be 1.52 and 6.50, respectively.

Keyphrases □ Triazolam—kinetics, mechanism of equilibrium in aqueous solution □ Kinetics—triazolam, mechanism of equilibrium in aqueous solutions □ Equilibrium reaction—triazolam, kinetics, mechanism in aqueous solutions

1,4-Benzodiazepines, first synthesized in the early 1960s, are important minor tranquilizers. These tranquilizers are being extensively used as sedative, hypnotic, muscle relaxant, and anticonvulsant drugs. Their stability and reactivity in aqueous solutions have been under study extensively in the last 5 years. Reaction mechanisms for the hydrolysis of 1,4-benzodiazepines have been reported for chlordiazepoxide (1, 2), oxazepam (3), diazepam (4), nitrazepam (4, 5), desmethyldiazepam (6), and clonazepam (6). Furthermore, equilibrium reactions of these compounds have been reported for pyrazolodiazepinone (7), diazepam (8), nitrazepam (9), triazolobenzodiazepines (10), flunitrazepam (11), and desmethyldiazepam (12). It is now well known that hydrolysis of an azomethine bond

0022-3549/82/1200-1328$01.00/0

in acidic solution gives the corresponding aminobenzophenone, which reversibly cyclizes into the original form in alkaline medium. Namely, 1,4-benzodiazepines exist as pH-dependent equilibrium mixtures of ring-opened and closed forms. However, no extensive, detailed study on the mechanism of the equilibrium reaction has been reported.

This study describes the mechanism of the equilibrium reaction between triazolam and its opened form in an aqueous solution.

EXPERIMENTAL

Materials—2′,5-Dichloro-2-(3-aminomethyl-5-methyl-4H-*s*-triazol-4-yl) benzophenone (I), 8-chloro-1-methyl-6-(*o*-chlorophenyl)-4H-*s*-triazolo[4,3-*a*] 1,4-benzodiazepine (triazolam, II), 4-amino-7-chloro-5-(2-chlorophenyl)-1-methyl-4H-*s*-triazolo[4,3-*a*] quinoline (III), and 3-amino-6-chloro-4-(2-chlorophenyl)-1-*n*-propylquinolin-2-one (IV) were synthesized. Dotetracontane was purchased from a commercial source[1]. All other reagents and solvents were of reagent grade and were used without further purification. Deionized water was further distilled before use in the aqueous solutions.

Equipment—UV spectra were recorded using a spectrophotometer[2] equipped with a thermostatically controlled cell holder. The pH was measured with a pH meter[3] at the temperature of the study.

TLC was done with a precoated 0.25-mm silica gel TLC plate[4] using a developing solvent system of chloroform–acetone–ethanol (3:1:1).

The gas chromatograph[5] was equipped with a 10-mCi ^{63}Ni-electron-capture detector (ECD) or a flame ionization detector (FID). The column was coiled glass (0.5 m × 3-mm i.d.), packed with 3% OV-17 on 100–120 mesh Gas Chrom Q[6]. The carrier gas was ultrapure nitrogen flowing at a rate of 60 ml/min. Temperature settings during operation were 320° for the injection port and detector and 290° for the column. Peak heights of the compounds were determined using an integrator[7]. Under these GC conditions, the retention times for the compounds under study were 2.25 min for II, 3.35 min for III, 0.9 min for IV, and 6.15 min for dotetracontane.

Kinetic Studies—All rate studies were performed in aqueous buffer solutions at 37.0 ± 0.1°. The buffer systems used were: pH 1.1–5.6, acetate; pH 6–8, phosphate; pH 9–10, borate; and pH 11–12, phosphate. The ionic strength of each was adjusted to 0.5 with potassium chloride.

The compound to be studied was dissolved in ethanol and diluted (1:20) with preincubated buffer solution kept at 37° to make a 10^{-4} *M* solution. Next, an appropriate volume of the solution was pipeted into the UV cell, and the reaction was followed spectrophotometrically by reading the decrease or increase in absorbance at 264 nm.

Reactions starting from I were studied in the pH range of 1.92–11.44. The sum of the first-order rate constants for the forward and reverse reactions (k_f and k_r) was determined from linear plots of ln $(A_t - A_\infty)$ *versus* time by the least-squares method (Eq. 1), where A_t, A_∞, and A_0 are the absorbance at time t, infinity, and time 0, respectively:

$$\ln(A_t - A_\infty) = \ln(A_0 - A_\infty) - (k_f + k_r)t \qquad \text{(Eq. 1)}$$

Reactions initiating from II were studied in the pH region of 1.13–1.40. The sum of the first-order rate constants for the forward and reverse reactions was obtained from the linear plots of ln $(A_\infty - A_t)$ against time by the least-squares method (Eq. 2), where A_∞, A_t, and A_0 are the absorbance at infinity, time t, and time 0, respectively:

$$\ln(A_\infty - A_t) = \ln(A_\infty - A_0) - (k_f + k_r)t \qquad \text{(Eq. 2)}$$

Product Identification—For the identification studies, 2×10^{-3} *M* solutions of I were prepared using 0.5 *N* NaOH solution, the pH 6.5 buffer solution, and a 0.01 *N* HCl solution. These solutions were left standing at room temperature for 15 hr, then a 5-ml sample was taken from each solution and was subjected to extraction with dichloroethane for TLC analysis. The chromatograms were visualized under UV light and iodine vapour to identify the products. Dichloroethane solutions of reference standards were spotted directly on the TLC plates.

Determination of I and II in Aqueous Solutions—*ECD-GC Method*—In this method, caution was paid to determine the compounds without disturbing the equilibrium. The triazoloaminoquinoline derivative (III) was derived by acetylation followed by cyclization to obtain a suitable compound for GC as shown in Scheme I.

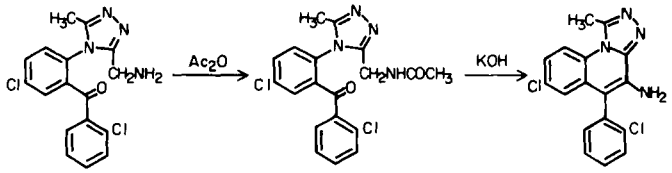

I III

Scheme I

The pH 11 phosphate buffer (containing 0.2 *M* Na_2HPO_4) was added to 1 ml of reaction solution (initially containing 2×10^{-4} *M* of I) to make a 10-ml solution at pH 10, with the temperature kept at 0° with ice (quenched solution). This quenching procedure was necessary to prevent disturbance of the equilibrium mixture during assay. Triethylamine (0.2 ml), 2 *N* KOH (1 ml) quenched reaction solution (1 ml), and acetic anhydride (0.1) were added with ice cooling to a 12-ml centrifuge tube containing 3 ml of dichloroethane. After this mixture was shaken for 15 min on a mechanical shaker (for acetylation of I), 1 ml of the dichloroethane solution was transferred to another 12-ml centrifuge tube by Eppendorf pipet and evaporated to dryness. To dissolve the residue, 0.2 ml of ethanol was added followed by 2 ml of 2 *N* KOH and the solution was heated for 3 hr at 91 ± 1° (cyclization to III). After it had cooled, the reaction solution was extracted with 5 ml of benzene containing 1 μg of IV as an internal standard for 5 min, then 2 μl of the benzene layer was subjected to ECD-GC. Calculation was done by the internal standard method using the peak height ratios. Recoveries of I for the acetylation and the cyclization were 80 and 83.9%, respectively, and the overall recovery was 60.0% (n = 36, CV = 3.30%). Recovery of II was 86.7% (n = 27, CV = 4.64%) in this procedure.

FID-GC Method—In the equilibrium solutions, if the weight ratios of II to I were >5, separation of the peaks of Compounds II and III on ECD-GC was difficult because of low resolution. This problem was overcome by using the FID-GC, in which no peak broadening of Compound II was observed. The quantities of I and II were determined by separate procedures.

For Compound I, 5.7 ml of the pH 11 phosphate buffer and 0.3 ml of 1 *N* KOH were added to 4 ml of reaction solution (initial concentration of I: 4×10^{-4} *M*) to make a 10-ml solution of pH 10, keeping the temperature at 0° with ice (quenched Solution I). Quenched Solution I (2.5 ml) and acetic anhydride (0.1 ml) were added with ice cooling to a 12-ml centrifuge tube containing 3 ml of dichloroethane, 0.2 ml of triethylamine, and 1 ml of 2 *N* KOH. The mixture was shaken for 15 min, then the dichloroethane layer was transferred to another 12-ml centrifuge tube and evaporated to dryness. Next, 0.2 ml of ethanol was added to dissolve the residue and 2 ml of 2 *N* KOH was added to this solution, which was then heated for 3 hr at 91 ± 1°. After cooling, the reaction solution was subjected to extraction for 5 min with a mixture of 4 ml of benzene and 1 ml of *n*-hexane containing 3.5 μg of dotetracontane as an internal standard, then the resulting organic layer was transferred to a 30-ml round-bottom flask and evaporated to dryness. The residue was dissolved in 0.1 ml of solvent (acetone–*n*-hexane, 1:2) and 4 μl of the solution was subjected to FID-GC. Recovery of I was 64.3% (n = 18, CV = 2.94%).

For Compound II, the pH 11 phosphate buffer was added to 1 ml of reaction solution (the same solution as that for Compound I) to make a 10-ml solution of pH 10 with ice cooling (quenched Solution II). Quenched Solution II and acetic anhydride (1 ml) were added with ice cooling to a 12-ml centrifuge tube containing 3 ml of dichloroethane, 0.2 ml of triethylamine, and 1 ml of 2 *N* KOH. The mixture was shaken for 15 min, then the dichloroethane layer was removed by pipeting and evaporated to dryness. The residue was dissolved in 0.2 ml of ethanol and 2 ml of 2 *N* KOH, and the solution was subjected to extraction with a mixture of 4 ml of benzene and 1 ml of *n*-hexane containing 35 μg of dotetracontane for 5 min. The organic layer was transferred to a 30-ml round-bottom flask and evaporated to dryness. The residue was dissolved in 0.5 ml of solvent (acetone–*n*-hexane, 1:2) and 2 μl of this solution was subjected to FID-GC. Recovery of Compound II was 81.1% (n = 10, CV = 2.34%).

[1] Milton Roy, Fla.
[2] Model 323, Hitachi, Japan.
[3] Model $F7_{ss}$, Hitachi-Horiba, Japan.
[4] G60, F_{254}, E. Merck, G.F.R.
[5] Model GC-7A, Shimadzu, Japan.
[6] Milton Roy, Fla.
[7] Model C-R1A, Shimadzu, Japan.

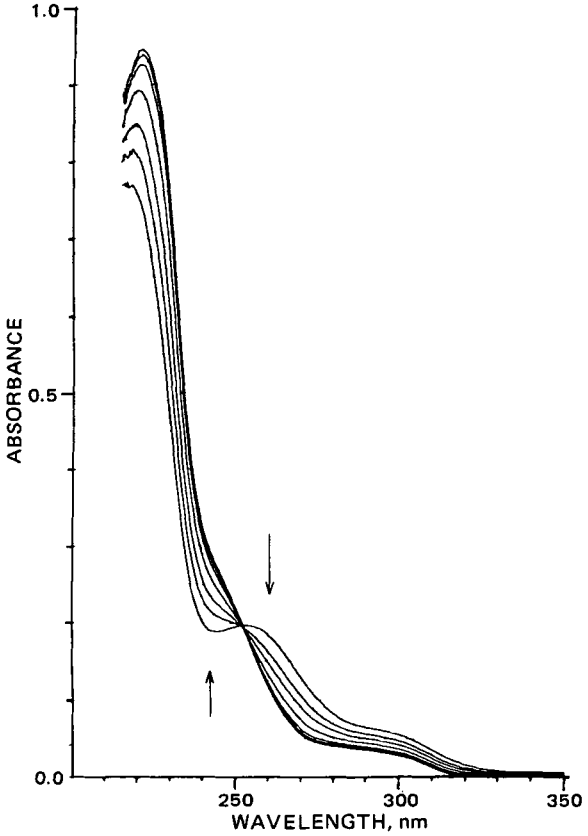

Figure 1—*Typical spectral changes due to the ring-closure reaction of Compound I (× 10^{-4} M) into triazolam in 0.1 M acetate buffer, pH 5.65 (μm = 0.5) at 37°. Spectra were measured at 5, 13, 20, 35, 60, 85, and 150 (∞) min after initiation of the reaction.*

RESULTS AND DISCUSSION

Spectral Change and the Nature of the Reaction—After the pH 6.5 buffer solution and the 0.5-*N* NaOH solution of I had been left standing for several hours, both showed only one spot with an R_f value (0.68) identical to that of II on TLC (R_f for I was 0.18 in this system). The chromatogram for the standing solution of I in 0.01 *N* HCl gave two spots, identical to I and II, of compounds present in approximately equivalent amounts.

The UV spectral change of I in the pH 5.65 buffer at 37° is shown in Fig. 1. Immediately after I had dissolved, the absorption spectrum showed an absorption maximum (λ_{max}) at 257 nm, which decreased concurrently with time. At infinity, the shape of the redundant spectrum was identical to that of II in the same medium. An isosbestic point at 253 nm was observed during the reaction. On the other hand, the spectral change of II in 0.1 *N* HCl showed a reverse change in which the absorption at λ_{max} increased with time when the isosbestic point was kept at 253 nm; the final spectrum could be superimposed on that of I in the same solution. Furthermore, the spectrum of II obtained by mixing the equilibrium pH 5.65 solution of II and 1 *N* HCl rapidly changed into a spectrum similar to that of II in 0.1 *N* HCl solution.

These observations indicate that I and II in these aqueous solutions undergo reversible reactions involving cyclization and hydrolytic azomethine bond cleavage, respectively, to produce equilibrium mixtures of Compounds I and II (Scheme II), as in the case of estazolam (10).

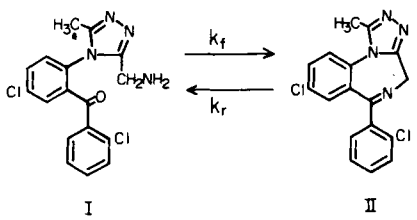

I II

Scheme II

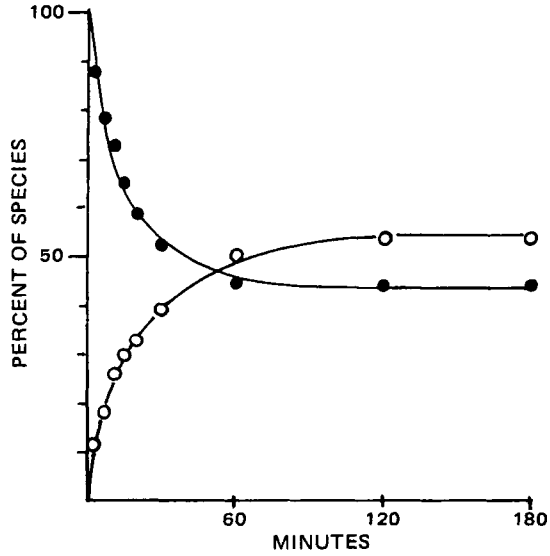

Figure 2—*Time courses for Compound I (●) and triazolam (○) in a 0.2 M acetate buffer, pH 2.30 (μm = 0.5) at 37° initially containing 2 × 10^{-4} M of Compound I.*

Cyclization of I to II and Quantitative Aspects—The equilibrium mixture of I and II was analyzed quantitatively by GC procedure. The result obtained for the 0.2 *M* acetate buffer solution of pH 2.3 (initial concentration of I: 2 × 10^{-4} *M*) is shown in Fig. 2. The data plotted as the percent of I and of II with time showed a continuous decrease and increase, respectively. During the time course of the equilibrium reaction, the total recoveries of I plus II were >98% based on the initial concentration of I. Moreover, the rate of decrease for I was equivalent to the rate of increase for II. These results also support the fact that both I and II exist as equilibrium mixtures in solution.

Effect of pH on the Equilibrium Constant—The apparent equilibrium constant, *K*, is defined by Eq. 3, where $[I]_\infty$ and $[II]_\infty$ are the molar concentrations of I and II at equilibrium, and k_f and k_r are first-order rate constants of the forward and reverse reaction, respectively:

$$K = \frac{[II]_\infty}{[I]_\infty} = \frac{k_f}{k_r} \qquad \text{(Eq. 3)}$$

The value for *K* was determined at various pH values over the range of pH 1.13–11.44 at 37° by determining the components of the reaction solutions after they had attained equilibrium state. The results are shown in Table I. The *K* values increased with increasing pH and became >400 at pH >5.02.

When equilibrium is attained at any pH, the fractions of I (F_I) and II (F_{II}) in the reaction solutions are defined by Eqs. 4 and 5. The plots of the fractions of the individual species against pH are shown in Fig. 3. F_I

Table I—Equilibrium and Rate Constants of Ring-Closing and Ring-Opening Reactions in Aqueous Buffer Solutions [a]

pH	a_{H^+}	*K*	$k_{obs} \times 10^{-2}$/min		
			k_{app}	k_f	k_r
1.13	7.41 × 10^{-2}	0.18	14.8	2.30	12.5
1.40	3.98 × 10^{-2}	0.26	11.2	2.31	8.89
1.92	1.20 × 10^{-2}	0.61	6.81	2.58	4.23
2.30	5.01 × 10^{-3}	1.2	4.99	2.72	2.27
2.68	2.09 × 10^{-3}	2.4	4.20	2.96	1.24
3.13	7.41 × 10^{-4}	5.4	3.99	3.37	0.623
3.39	4.07 × 10^{-4}	15	3.91	3.67	0.244
3.90	1.26 × 10^{-4}	48	4.04	3.96	0.082
4.59	2.57 × 10^{-5}	230	4.37	4.35	0.019
5.02	9.55 × 10^{-6}	400	4.24	4.23	0.011
5.65	2.24 × 10^{-6}	>400	3.65	3.65	—
6.25	5.62 × 10^{-7}	>400	2.79	2.79	—
7.12	7.59 × 10^{-8}	>400	1.11	1.11	—
7.74	1.82 × 10^{-8}	>400	0.682	0.682	—
8.75	1.78 × 10^{-9}	>400	0.461	0.461	—
9.76	1.74 × 10^{-10}	>400	0.412	0.412	—
10.47	3.39 × 10^{-11}	>400	0.401	0.401	—
11.44	3.63 × 10^{-12}	>400	0.473	0.473	—

[a] μ = 0.5, at 37°.

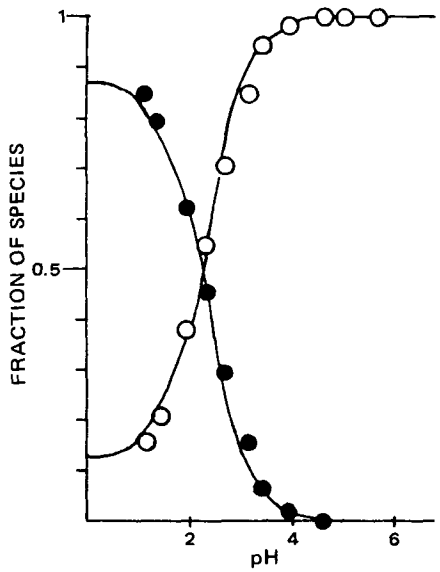

Figure 3—*Plot of the composition of the equilibrium mixture consisting of Compound I (●) and triazolam (○) versus pH at 37°. Solid lines are values calculated using Eqs. 4, 5, and 23.*

decreases with increasing pH from 0.85 at pH 1.13 to <0.002 at pH >5.02 at which the equilibrium mixture contains >99.8% of ring-closed Compound II.

$$F_I = \frac{[I]_\infty}{[I]_\infty + [II]_\infty} = \frac{1}{1+K} \quad \text{(Eq. 4)}$$

$$F_{II} = 1 - F_I = \frac{K}{1+K} \quad \text{(Eq. 5)}$$

Rate Constant Determination and Rate–pH Profiles—Semilogarithmic plots of $(A_t - A_\infty)$ against time for the equilibrium reaction in various pH solutions are shown in Fig. 4. In the pH region studied, all the plots displayed strict first-order kinetics for >5 half-lives. The apparent first-order rate constants (k_{app}) are expressed as Eq. 6. Each rate constant for the forward and reverse reactions can be derived from Eqs. 3 and 6.

$$k_{app} = k_f + k_r \quad \text{(Eq. 6)}$$

In Fig. 5, the first-order rate constants for the formation and the hydrolysis of II at 37°, which were extrapolated to zero buffer concentration, are plotted against pH.

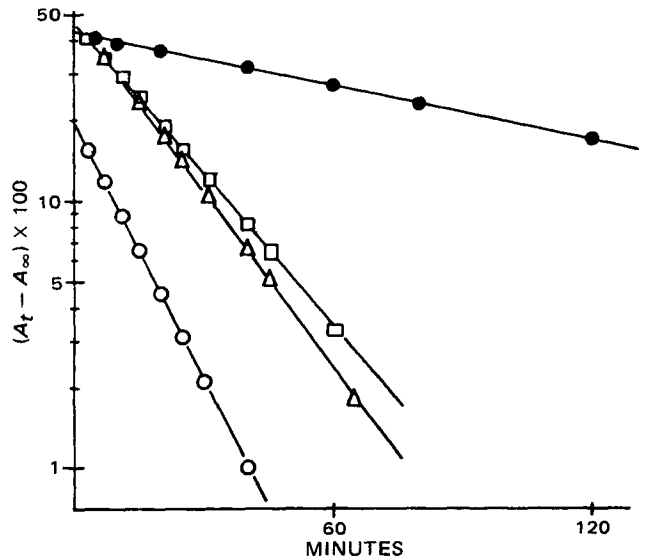

Figure 4—*Typical apparent first-order plots for the equilibrium reaction between Compound I and triazolam at 37°, μm = 0.5. Key: (○) pH 1.92; (△) pH 5.02; (□) pH 3.39; (●) pH 7.74.*

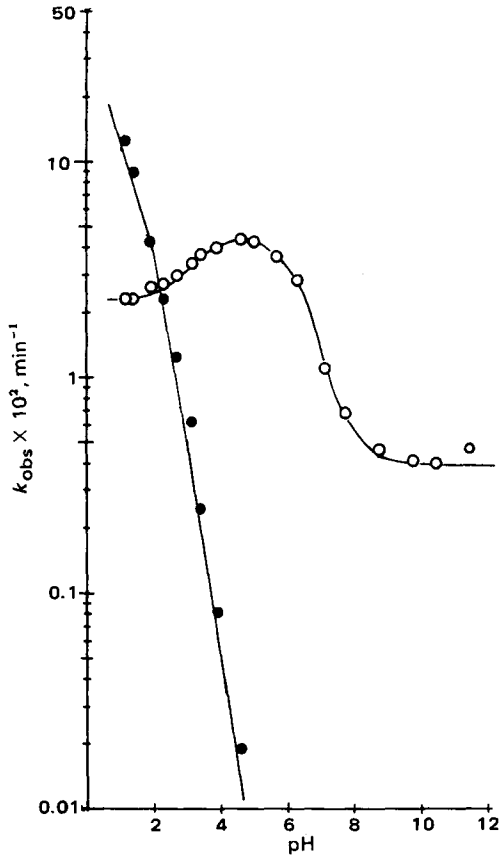

Figure 5—*Log k–pH profile for the equilibrium reaction consisting of forward (○) and reverse reactions (●) at 37°, μm = 0.5. Solid lines were based on calculations using Eq. 18 or Eq. 22. All rates are extrapolated to zero buffer concentration.*

For the formation rate, a maximum occurs near pH 4.5. On the alkaline side of the pH–rate maximum (pH 4.5–9), the rate increases with increasing acidity, suggesting that an acid-catalyzed reaction is predominant. In the solution at pH >9, the rate becomes constant. On the acidic side of the pH–rate maximum, the rate decreases with increasing acid concentration and becomes independent of pH at pH <1.40, indicating the existence of a specific acid-catalyzed reaction as well as an uncatalyzed one of the free form of I.

The hydrolysis of II shows an acid-catalyzed reaction over the pH range used in this study and its rate could not be determined ≥pH 5.65 because the equilibrium constants were too large to be determined.

General Reaction Mechanism—Reactions of carbonyl compounds with amines have been reviewed previously (13–15). Moreover, a noteworthy series of papers have reported on studies of the formation of semicarbazones (16, 17), Schiff base (18, 19), and oxime (16) in aqueous solutions. These studies have pointed out that the formation and hydrolysis of these compounds proceed by a two-step mechanism involving a tetrahedral carbinolamine intermediate. The evidence for the two-step mechanism is based on the results that the Schiff base formation undergoes a transition in the rate-determining step from the dehydration of the carbinolamine intermediate at neutral pH to the amine attack under acidic conditions. Formation of II exhibits a pH–rate maximum similar to that in the formation of oxime (16) and *N*-*p*-chlorobenzylideneaniline (18). Therefore, the formation and the hydrolysis of II are considered to proceed by the two-step reaction mechanism, as shown:

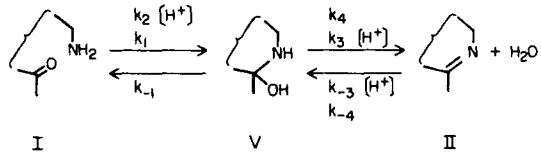

Scheme III

In the forward reaction, the acid-catalyzed dehydration of the carbinolamine intermediate (V) at nearly neutral pH determines the rate

which may account for a leveling off, but not a decrease in the rate with increasing pH. At low pH values, the rate of dehydration becomes very fast, and at the same time, the rate of the amine attack is retarded because of the conversion of the free amine form of I into its conjugate acid. Consequently, a change in the rate-determining step occurs and the attack of the amine becomes rate-determining, accounting for the observed decrease in the rate on the acid side of the pH–rate maximum.

In the reverse reaction, the hydrolysis rates are measurable only on the acidic side of the pH–k_f maximum. The rate-determining step of this reaction in this pH region is the cleavage of the C—N bond from V to I. Since the carbinolamine intermediate is formed by a water molecule attack at the conjugate acid of II, the hydrolysis rate is directly proportional to the concentration of the conjugate acid as an active acidic species of II.

In Scheme III, k_1 and k_{-1} represent uncatalyzed reaction rate constants; k_2, k_3, and k_{-3} represent acid-catalyzed rate constants; and k_4 and k_{-4} represent water-catalyzed rate constants. When a steady-state approximation is applied to the carbinolamine intermediate, the rate equations for the forward and the reverse reaction can be written as Eqs. 7 and 8, respectively; where a_{H^+} is hydrogen ion activity; K_I and K_{II} are dissociation constants for the conjugate acid of I and II:

$$k_{f(obs)} = \frac{K_I(k_1 + k_2a_{H^+})\,(k_3a_{H^+} + k_4)}{(K_I + a_{H^+})\,(k_{-1} + k_3a_{H^+} + k_4)} \qquad \text{(Eq. 7)}$$

$$k_{r(obs)} = \frac{k_{-1}a_{H^+}\,(k_{-3}a_{H^+} + k_{-4})}{(K_{II} + a_{H^+})\,(k_{-1} + k_3a_{H^+} + k_4)} \qquad \text{(Eq. 8)}$$

Formation Mechanism—On the alkaline side of the rate maximum (Fig. 5), the rate-determining step should be the dehydration from the carbinolamine intermediate. This implies $k_{-1} \gg (k_3a_{H^+} + k_4)$; therefore, Eq. 7 can be reduced to Eq. 9:

$$k_{f(obs)} = \frac{K_I(k_1 + k_2a_{H^+})\,(k_3a_{H^+} + k_4)}{k_{-1}(K_I + a_{H^+})} \qquad \text{(Eq. 9)}$$

If k_1 is assumed to be much larger than $k_2a_{H^+}$, Eq. 10 will be obtained:

$$k_{f(obs)} = \frac{k_1K_I(k_3a_{H^+} + k_4)}{k_{-1}(K_I + a_{H^+})} \qquad \text{(Eq. 10)}$$

In Eq. 10, two pH regions, $k_3a_{H^+} \gg k_4$ and $K_I \gg a_{H^+}$ are considered. In the former, Eq. 11 can be derived:

$$k_{f(obs)} = \frac{k_1k_3K_Ia_{H^+}}{k_{-1}(K_I + a_{H^+})} \qquad \text{(Eq. 11)}$$

When both sides of Eq. 11 are divided by a_{H^+} and the equation is converted into its reciprocal form, Eq. 12 is obtained:

$$a_{H^+}/k_{f(obs)} = \frac{k_{-1}}{k_1k_3K_I}a_{H^+} + \frac{k_{-1}}{k_1k_3} \qquad \text{(Eq. 12)}$$

Consequently, k_{-1}/k_1k_3 and K_I can be obtained from the plot of $a_{H^+}/k_{f(obs)}$ against a_{H^+}. The linear relationship between $a_{H^+}/k_{f(obs)}$ and a_{H^+} is shown in Fig. 6. From the extraordinate intercept and the slope of the linear plot, k_1k_3/k_{-1} and K_I were 1.39×10^5/min and 3.13×10^{-7} ($pK_I = 6.50$), respectively. Furthermore, since a_{H^+} was much larger than K_I at the pH which gave the rate maximum, Eq. 11 could be reduced to:

$$k_{f(max)} = \frac{k_1}{k_{-1}}k_3K_I \qquad \text{(Eq. 13)}$$

Putting the parameter obtained from Fig. 6 into Eq. 13, $k_{f(max)}$ was estimated to be 4.35×10^{-2}/min, which agreed with the observed data.

In the case of $K_I \gg a_{H^+}$, Eq. 10 can be reduced to Eq. 14.

$$k_{f(obs)} = \frac{k_1}{k_{-1}}k_3a_{H^+} + \frac{k_1}{k_{-1}}k_4 \qquad \text{(Eq. 14)}$$

Further, if k_4 is $>k_3a_{H^+}$, the following equation can be derived:

$$k_{f(obs)} = \frac{k_1}{k_{-1}}k_4 \qquad \text{(Eq. 15)}$$

Equation 15 indicates that the formation rate becomes constant in a high pH region when $K_I \gg a_{H^+}$ and $k_4 \gg k_3a_{H^+}$. From the observed data, k_1k_4/k_{-1} was calculated to be 0.4×10^{-2}/min. The value k_4/k_3 obtained by dividing k_1k_4/k_{-1} by k_1k_3/k_{-1} was 2.88×10^{-8}. This inductively proves that Eq. 15 can be used to explain the constant value of k_f at the pH region >9, because $k_4 \gg k_3a_{H^+}$ is valid in these pH solutions.

The assumption that the rate-determining step of the reaction of the acidic side of the rate maximum changes to attack of the free amine is equivalent to the statement: $(k_3a_{H^+} + k_4) \gg k_{-1}$. Therefore, Eq. 7 is reduced to:

$$k_{f(obs)} = \frac{K_I(k_1 + k_2a_{H^+})}{K_I + a_{H^+}} \qquad \text{(Eq. 16)}$$

In the pH region under discussion, $a_{H^+} \gg K_I$, and Eq. 17 is obtained:

$$k_{f(obs)} = \frac{K_I(k_1 + k_2a_{H^+})}{a_{H^+}} = k_2K_I + k_1K_I\frac{1}{a_{H^+}} \qquad \text{(Eq. 17)}$$

Consequently, k_1K_I and k_2K_I can be obtained from the slope and the ordinate intercept of a straight line when the observed formation rate constants are plotted against $1/a_{H^+}$. By dividing each value by K_I, the parameters k_1 and k_2 were estimated to be 7.38 × 10/min and 7.32×10^4/min M, respectively (Fig. 7). The parameters obtained are summarized in Table II.

A theoretical equation for the formation rate was obtained by putting these parameters into an equation which was derived by dividing both

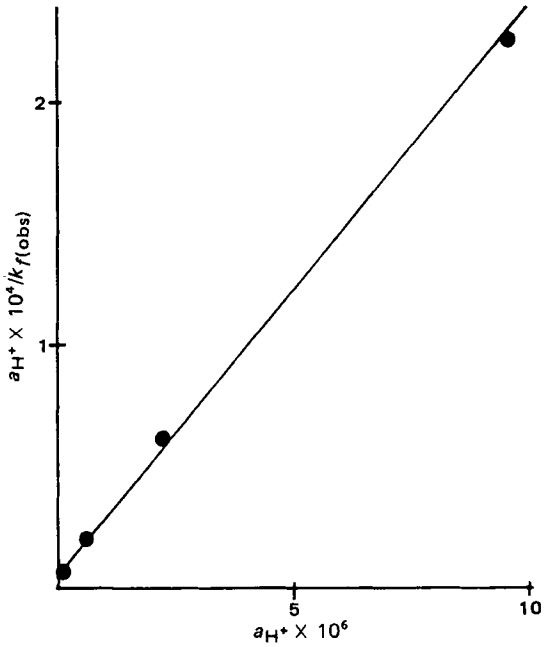

Figure 6—*Derivation of the constant* k_{-1}/k_1k_3 *and* K_I *by plotting rate data according to Eq. 12.*

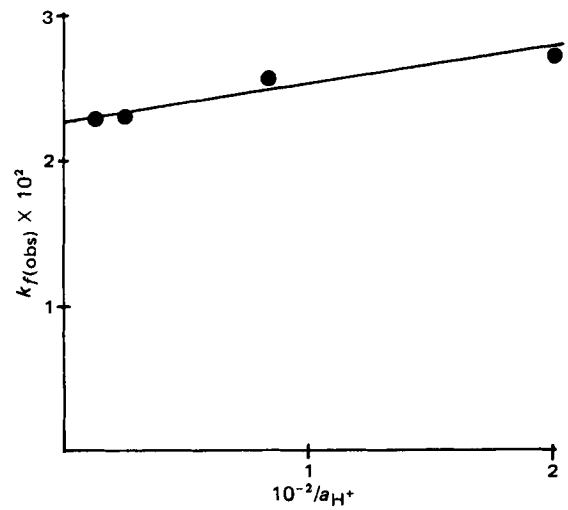

Figure 7—*Derivation of the rate constants* k_1 *and* k_2 *by plotting rate data according to Eq. 17.*

Table II—Kinetic Constants for the Equilibrium Reaction of Triazolam in Aqueous Buffer Solutions [a]

Parameter	Estimated Value	Parameter	Estimated Value
k_1, min^{-1}	7.38×10	k_3/k_{-1}, M^{-1}	1.88×10^3
k_2, $min^{-1}\ M^{-1}$	7.32×10^4	k_4/k_{-1}	5.42×10^{-5}
K_I, M	3.13×10^{-7}	$k_{-1}k_{-3}k_3$, min^{-1}	1.58×10^{-1}
k_1k_3/k_{-1}, $min^{-1}M^{-1}$	1.39×10^5	k_{-3}, $min^{-1}\ M^{-1}$	2.98×10^2
k_1k_4/k_{-1}, min^{-1}	4.0×10^{-3}	k_{-4}, min^{-1}	8.58×10^{-6}
k_4/k_3, M	2.88×10^{-8}	K_{II}, M	3.02×10^{-2}

[a] $\mu = 0.5$, at 37°.

denominator and numerator of Eq. 7 by k_{-1} (Eq. 18). The theoretical curve for the formation rate is shown as a solid line in Fig. 5. It satisfactorily fits the observed data over the pH range studied:

$$k_{f(obs)} = \frac{K_I(k_1 + k_2a_{H^+})\,(k_3a_{H^+}/k_{-1} + k_4/k_{-1})}{(K_I + a_{H^+})\,(1 + k_4/k_{-1} + k_3a_{H^+}/k_{-1})}$$
$$= 3.13 \times 10^{-7}\,(7.38 \times 10 + 7.32 \times 10^4 a_{H^+})\,\frac{(1.88 \times 10^3 a_{H^+} + 5.41 \times 10^{-5})}{(3.13 \times 10^{-7} + a_{H^+})\,(1 + 1.88 \times 10^3 a_{H^+})} \quad \text{(Eq. 18)}$$

Hydrolysis Mechanism—In the pH range studied, the term $(k_3a_{H^+} + k_4) \gg k_{-1}$, and Eq. 8 can be reduced to Eq. 19:

$$k_{r(obs)} = \frac{k_{-1}a_{H^+}\,(k_{-3}a_{H^+} + k_{-4})}{(K_{II} + a_{H^+})\,(k_3a_{H^+} + k_4)} \quad \text{(Eq. 19)}$$

In these pH solutions, the terms, $(k_3a_{H^+} + k_4)$ and $(k_{-3}a_{H^+} + k_{-4})$ are reduced to $k_3a_{H^+}$ and $k_{-3}a_{H^+}$, respectively, because the ratio k_4/k_3 or k_{-4}/k_{-3} is 2.88×10^{-8}, where the equilibrium constant of the second step in Scheme II can be represented by k_3/k_{-3} or k_4/k_{-4}. Therefore, Eq. 19 can be reduced to Eq. 20:

$$k_{r(obs)} = \frac{k_{-1}k_{-3}a_{H^+}}{k_3(K_{II} + a_{H^+})} \quad \text{(Eq. 20)}$$

Then Eq. 20 may be converted into the reciprocal form, Eq. 21:

$$\frac{1}{k_{r(obs)}} = \frac{k_3}{k_{-1}k_{-3}} + \frac{k_3K_{II}}{k_{-1}k_{-3}}\frac{1}{a_{H^+}} \quad \text{(Eq. 21)}$$

As shown in Fig. 8, plots of $1/k_{r(obs)}$ against $1/a_{H^+}$ gave a straight line with an intercept equal to $k_3/k_{-1}k_{-3} = 6.32$ min and a slope of $k_3K_{II}/k_{-1}k_{-3} = 0.191$ min M. Accordingly, K_{II} was estimated to be 3.02×10^{-2} ($pK_{II} = 1.52$). Furthermore, k_{-3} was calculated to be 2.98×10^2/min M from the $k_3/k_{-1}k_{-3}$ and k_3/k_{-1} values, which had already been known.

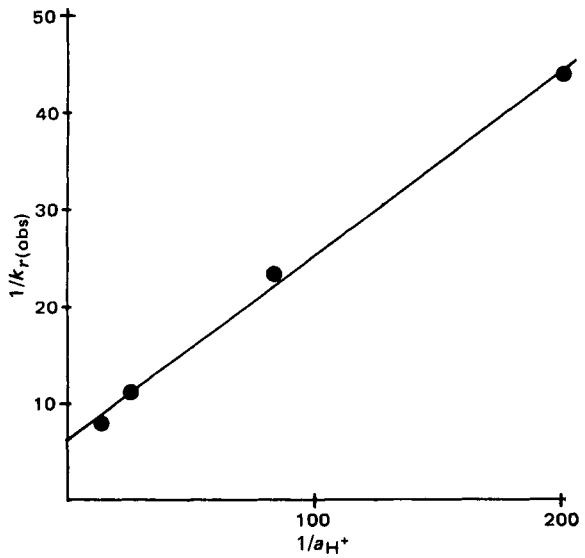

Figure 8—*Derivation of the constants* $k_3/k_{-1}k_{-3}$ *and* K_{II} *by plotting rate data according to Eq. 21.*

Also, $k_{-4} = 8.58 \times 10^{-6}$/min was obtained from the ratio of k_{-4}/k_{-3} and k_{-3}.

On the basic side of the formation rate maximum, no measurable hydrolysis rate constant has been obtained because the equilibrium exclusively favors the ring-closed form. Therefore, no information could be gained concerning the alkali hydrolysis.

A theoretical equation for the hydrolysis rate can be expressed as Eq. 22 by putting the parameters into the equation obtained after dividing both the denominator and the numerator of Eq. 8 by k_{-1}:

$$k_{r(obs)} = \frac{a_{H^+}(k_{-3}a_{H^+} + k_{-4})}{(K_{II} + a_{H^+})(1 + k_3a_{H^+}/k_{-1} + k_4/k_{-1})}$$
$$= \frac{a_{H^+}\,(2.98 \times 10^2/a_{H^+} + 8.58 \times 10^{-6})}{(3.02 \times 10^{-2} + a_{H^+})\,(1 + 1.88 \times 10^3\,a_{H^+})} \quad \text{(Eq. 22)}$$

The theoretical curve of Eq. 22 is shown in Fig. 5 as a solid line. The curve satisfactorily fits the observed reverse-reaction rate constants.

Equilibrium Constant—From the definition of the equilibrium, the Constant K is expressed by Eq. 23:

$$K = \frac{k_{f(obs)}}{k_{r(obs)}}$$
$$= \frac{K_I(K_{II} + a_{H^+})\,(k_1 + k_2a_{H^+})\,(k_3a_{H^+} + k_4)}{k_{-1}a_{H^+}\,(K_I + a_{H^+})\,(k_{-3}a_{H^+} + k_{-4})}$$
$$= \frac{K_I(K_{II} + a_{H^+})\,(k_1 + k_2a_{H^+})\,(k_3a_{H^+}/k_{-1} + k_4/k_{-1})}{a_{H^+}(K_I + a_{H^+})\,(k_{-3}a_{H^+} + k_{-4})}$$
$$= 3.13 \times 10^{-7}\,(3.02 \times 10^{-2} + a_{H^+})\,(7.38 \times 10 + 7.32 \times 10^4 a_{H^+})\,\frac{(1.88 \times 10^3 a_{H^+} + 5.42 \times 10^{-5})}{a_{H^+}\,(3.13 \times 10^{-7} + a_{H^+})\,(2.98 \times 10^2\,a_{H^+} + 8.58 \times 10^{-6})} \quad \text{(Eq. 23)}$$

The theoretical F_I and F_{II} curves obtained from Eqs. 4, 5, and 23 are given in Fig. 3 as solid lines. The theoretical curves showed good agreement with the observed data, in which K and F_I were calculated to be 0.15 and 0.87 at pH 0, respectively.

Evaluation of the Reaction Rate—For an aromatic Schiff base, the maximum formation rate of *N*-*p*-chlorobenzylideneaniline was calculated to be 3.72×10^{-3}/min, if the equimolar reaction of *p*-chlorobenzaldehyde with aniline would occur in an aqueous solution of pH 4.0 at 25° (18). The maximum reaction rate from I to II was 10 times larger than that of the above intermolecular reaction. Generally, an intramolecular reaction would occur much more rapidly than an intermolecular one because of the more feasible approach between the active sites (20). However, this result indicates that the difference between the formation rates of *N*-*p*-chlorobenzylideneaniline and of Compound II would not be as large as expected if the rate measurements were performed under the same reaction conditions. To compare the formation rates of II for intra- and intermolecular reactions, the reactions of substituted triazolobenzophenone with aminoacetic acid needed to be investigated.

The rates of hydrolysis of several 1,4-benzodiazepines into the corresponding amines have been obtained in 0.1 *N* HCl solution at 37°. The values were 2.5×10^{-3}/min for diazepam (8), 4.25×10^{-1}/min for estazolam (10), 1.5×10^{-2}/min for fludiazepam (11), and 1.30×10^{-1}/min for flurazepam (11). The hydrolysis rate for triazolam in this study, as well as the pKa value, were similar to that for flurazepam. Moreover, the water catalyzed rate constant of hydrolysis for II ($k_{-4} = 8.58 \times 10^{-6}$/min) was similar to those for demoxepam (2) and oxazepam (3).

General Discussion—The pKa for the conjugate acid of Compounds I and II was estimated to be 6.50 and 1.52, respectively. No information has been reported about the pKa's for these compounds because the reaction in aqueous solution is too fast for measurement of the dissociation constant spectrometrically. However, the pKa for 2-aminoacetamido-5-chlorobenzophenone has been reported to be 6.3 (12), which is nearly the same as that for I. These constants indicate that the basicities of the ring-opened compounds are somewhat stronger than that of hydroxylamine, pKa 6.0. On the other hand, the pKa for the conjugate acid of 1,4-benzodiazepines has been widely studied. As already known, the 1,4-benzodiazepines which possess a 2′-halogen substituent in the 5-phenyl group exhibit a pKa value lower than that for corresponding nonsubstituent compounds (21, 22). Namely, the pKa's for fludiazepam, flunitrazepam, and lorazepam were reported to be 2.29, 1.71, and 1.3, respectively, which were significantly lower than those of the corresponding compounds without halogen in the 2′-position, diazepam (pKa = 3.3), nitrazepam (pKa = 3.2), and oxazepam (pKa = 1.7). The pKa

value for 8-chloro-6-phenyl-4H-*s*-triazolo[4,3-*a*][1,4] benzodiazepine (estazolam) was reported to be 2.84 from the UV absorption spectral change (23). Considering the structural difference mentioned, the estimated pKa value for triazolam, 1.52, is reasonable.

The bioavailability or the pharmacological effect of a drug would greatly depend on the formation rate in the cyclization reaction from the opened form to the closed form because only the cyclized 1,4-benzodiazepines possess pharmacological CNS activity (24), which are discussed in reports on diazepam (8) and desmethyldiazepam (12). The half-time of the forward reaction of I at pH 7.4, which was calculated to be 80.6 min (Fig. 5), indicates that much time is required to convert I into the closed form II, only if the *in vivo* reaction proceeds chemically.

REFERENCES

(1) H. V. Maulding, J. P. Nazareno, J. E. Pearson, and A. F. Michaelis, *J. Pharm. Sci.*, **64**, 278 (1975).

(2) W. W. Han, G. J. Yakatan, and D. D. Maness, *ibid.*, **65**, 1198 (1976).

(3) *Ibid.*, **66**, 573 (1977).

(4) W. Mayer, S. Erbe, and R. Voigt, *Pharmazie*, **27**, 32 (1972).

(5) W. W. Han, G. J. Yakatan, and D. D. Maness, *J. Pharm. Sci.*, **66**, 795 (1977).

(6) W. Mayer, S. Erbe, G. Wolf, and R. Voigt, *Pharmazie*, **29**, 700 (1974).

(7) W. H. Hong, C. Johnston, and D. Szulczewski, *J. Pharm. Sci.*, **66**, 1703 (1977).

(8) M. Nakano, N. Inotsume, N. Kohri, and T. Arita, *Int. J. Pharm.*, **3**, 195 (1979).

(9) N. Inotsume and M. Nakano, *J. Pharm. Sci.*, **69**, 1331 (1980).

(10) N. Inotsume and M. Nakano, *Chem. Pharm. Bull.*, **28**, 2536 (1980).

(11) N. Inotsume and M. Nakano, *Int. J. Pharm.*, **6**, 147 (1980).

(12) H. Bundgaard, *Arch. Pharm. Chem. Sci. Ed.*, **8**, 15 (1980).

(13) W. P. Jencks, "Catalysis in Chemistry and Enzymology," McGraw-Hill, New York, N.Y., 1969, pp. 163–242, 463–554.

(14) W. P. Jencks, *Prog. Phys. Org. Chem.*, **2**, 63 (1964).

(15) R. B. Martin, *J. Phys. Chem.*, **68**, 1369 (1964).

(16) W. P. Jencks, *J. Am. Chem. Soc.*, **81**, 475 (1959).

(17) E. H. Cordes and W. P. Jencks, *ibid.*, **84**, 4319 (1962).

(18) *Ibid.*, **84**, 832 (1962).

(19) *Ibid.*, **85**, 2843 (1963).

(20) J. Hine, "Physical Organic Chemistry," McGraw-Hill, New York, N.Y., 1962, pp. 141–151.

(21) J. Barrett, W. F. Smyth, and I. E. Davidson, *J. Pharm. Pharmacol.*, **25**, 387 (1973).

(22) R. T. Hagel and E. M. Debesis, *Anal. Chim. Acta*, **78**, 439 (1975).

(23) H. Koyama, M. Yamada, and T. Matsuzawa, *J. Takeda Res. Lab.*, **32**, 77 (1973).

(24) M. Fujimoto, Y. Tsukinoki, K. Hirose, K. Hirai, and T. Okabayashi, *Chem. Pharm. Bull.*, **28**, 1374 (1980).

Extended Hildebrand Solubility Approach: Testosterone and Testosterone Propionate in Binary Solvents

A. MARTIN *x, P. L. WU *, A. ADJEI §, M. MEHDIZADEH ‡, K. C. JAMES ‡, and CARL METZLER *¶

Received October 9, 1981, from the **Drug Dynamics Institute, College of Pharmacy, University of Texas, Austin, TX 78712* and the ‡*Welsh School of Pharmacy, University of Wales, Institute of Science and Technology, Cardiff, CF1 3NU, United Kingdom.* Accepted for publication January 28, 1982.

§Present address: Abbott Laboratories, North Chicago, IL. ¶On leave from The Upjohn Co., Kalamazoo, MI.

Abstract □ Solubilities of testosterone and testosterone propionate in binary solvents composed of the inert solvent, cyclohexane, combined with the active solvents, chloroform, octanol, ethyl oleate, and isopropyl myristate, were investigated with the extended Hildebrand solubility approach. Using multiple linear regression, it was possible to obtain fits of the experimental curves for testosterone and testosterone propionate in the various binary solvents and to express these in the form of regression equations. Certain parameters, mainly K and $\log \alpha_2$, were employed to define the regions of self-association, nonspecific solvation, specific solvation, and strong solvation or complexation.

Keyphrases □ Testosterone—extended Hildebrand solubility approach, solubility in binary solvents □ Solubility—extended Hildebrand solubility approach, testosterone and testosterone propionate in binary solvents □ Binary solvents—solubility of testosterone and testosterone propionate, extended Hildebrand solubility approach

Solute–solvent complexes of testosterone and testosterone propionate in binary solvents composed of cyclohexane with ethyl oleate, isopropyl myristate, and octanol have been reported previously (1). These solvents are pharmaceutically important; the first two are useful as solvents for steroid injectable preparations.

The calculated complexation constants (1) between the steroids and solvents were based on a previous method (2). The solute-mixed solvent systems are analyzed here with the extended Hildebrand solubility approach (3), an extension of the Hildebrand regular solution theory (4) which was introduced to allow the calculation of solubility of nonpolar and semipolar drugs in mixed solvents having a wide range of solubility parameters.

THEORETICAL

Solubility on the mole fraction scale, X_2, may be represented by the expression:

$$-\log X_2 = -\log X_2^i + \log \alpha_2 \qquad \text{(Eq. 1)}$$

where X_2^i is the ideal solubility of the crystalline solid, and α_2 is the solute activity coefficient in mole fraction terms. Scatchard (5) and Hildebrand and Scott (4) formulated the solubility equation for regular solutions in the form:

$$\log \frac{a_2^s}{X_2} = \log \alpha_2 = \frac{V_2 \phi_1^2}{2.303RT}(a_{11} + a_{22} - 2a_{12}) \qquad \text{(Eq. 2)}$$

where

$$\phi_1 = \frac{V_1(1 - X_2)}{V_1(1 - X_2) + V_2 X_2} \qquad \text{(Eq. 3)}$$

The activity of the crystalline solid (a_2^s), taken as a supercooled liquid, is equal to X_2^i as defined in Eq. 1. Variable V_2 is the molar volume of the

0022-3549/82/1200-1334$01.00/0

value for 8-chloro-6-phenyl-4H-*s*-triazolo[4,3-*a*][1,4] benzodiazepine (estazolam) was reported to be 2.84 from the UV absorption spectral change (23). Considering the structural difference mentioned, the estimated pKa value for triazolam, 1.52, is reasonable.

The bioavailability or the pharmacological effect of a drug would greatly depend on the formation rate in the cyclization reaction from the opened form to the closed form because only the cyclized 1,4-benzodiazepines possess pharmacological CNS activity (24), which are discussed in reports on diazepam (8) and desmethyldiazepam (12). The half-time of the forward reaction of I at pH 7.4, which was calculated to be 80.6 min (Fig. 5), indicates that much time is required to convert I into the closed form II, only if the *in vivo* reaction proceeds chemically.

REFERENCES

(1) H. V. Maulding, J. P. Nazareno, J. E. Pearson, and A. F. Michaelis, *J. Pharm. Sci.*, **64**, 278 (1975).

(2) W. W. Han, G. J. Yakatan, and D. D. Maness, *ibid.*, **65**, 1198 (1976).

(3) *Ibid.*, **66**, 573 (1977).

(4) W. Mayer, S. Erbe, and R. Voigt, *Pharmazie*, **27**, 32 (1972).

(5) W. W. Han, G. J. Yakatan, and D. D. Maness, *J. Pharm. Sci.*, **66**, 795 (1977).

(6) W. Mayer, S. Erbe, G. Wolf, and R. Voigt, *Pharmazie*, **29**, 700 (1974).

(7) W. H. Hong, C. Johnston, and D. Szulczewski, *J. Pharm. Sci.*, **66**, 1703 (1977).

(8) M. Nakano, N. Inotsume, N. Kohri, and T. Arita, *Int. J. Pharm.*, **3**, 195 (1979).

(9) N. Inotsume and M. Nakano, *J. Pharm. Sci.*, **69**, 1331 (1980).

(10) N. Inotsume and M. Nakano, *Chem. Pharm. Bull.*, **28**, 2536 (1980).

(11) N. Inotsume and M. Nakano, *Int. J. Pharm.*, **6**, 147 (1980).

(12) H. Bundgaard, *Arch. Pharm. Chem. Sci. Ed.*, **8**, 15 (1980).

(13) W. P. Jencks, "Catalysis in Chemistry and Enzymology," McGraw-Hill, New York, N.Y., 1969, pp. 163–242, 463–554.

(14) W. P. Jencks, *Prog. Phys. Org. Chem.*, **2**, 63 (1964).

(15) R. B. Martin, *J. Phys. Chem.*, **68**, 1369 (1964).

(16) W. P. Jencks, *J. Am. Chem. Soc.*, **81**, 475 (1959).

(17) E. H. Cordes and W. P. Jencks, *ibid.*, **84**, 4319 (1962).

(18) *Ibid.*, **84**, 832 (1962).

(19) *Ibid.*, **85**, 2843 (1963).

(20) J. Hine, "Physical Organic Chemistry," McGraw-Hill, New York, N.Y., 1962, pp. 141–151.

(21) J. Barrett, W. F. Smyth, and I. E. Davidson, *J. Pharm. Pharmacol.*, **25**, 387 (1973).

(22) R. T. Hagel and E. M. Debesis, *Anal. Chim. Acta*, **78**, 439 (1975).

(23) H. Koyama, M. Yamada, and T. Matsuzawa, *J. Takeda Res. Lab.*, **32**, 77 (1973).

(24) M. Fujimoto, Y. Tsukinoki, K. Hirose, K. Hirai, and T. Okabayashi, *Chem. Pharm. Bull.*, **28**, 1374 (1980).

Extended Hildebrand Solubility Approach: Testosterone and Testosterone Propionate in Binary Solvents

A. MARTIN *x, P. L. WU *, A. ADJEI §, M. MEHDIZADEH ‡, K. C. JAMES ‡, and CARL METZLER *¶

Received October 9, 1981, from the **Drug Dynamics Institute, College of Pharmacy, University of Texas, Austin, TX 78712* and the ‡*Welsh School of Pharmacy, University of Wales, Institute of Science and Technology, Cardiff, CF1 3NU, United Kingdom.* Accepted for publication January 28, 1982.

§Present address: Abbott Laboratories, North Chicago, IL. ¶On leave from The Upjohn Co., Kalamazoo, MI.

Abstract □ Solubilities of testosterone and testosterone propionate in binary solvents composed of the inert solvent, cyclohexane, combined with the active solvents, chloroform, octanol, ethyl oleate, and isopropyl myristate, were investigated with the extended Hildebrand solubility approach. Using multiple linear regression, it was possible to obtain fits of the experimental curves for testosterone and testosterone propionate in the various binary solvents and to express these in the form of regression equations. Certain parameters, mainly K and $\log \alpha_2$, were employed to define the regions of self-association, nonspecific solvation, specific solvation, and strong solvation or complexation.

Keyphrases □ Testosterone—extended Hildebrand solubility approach, solubility in binary solvents □ Solubility—extended Hildebrand solubility approach, testosterone and testosterone propionate in binary solvents □ Binary solvents—solubility of testosterone and testosterone propionate, extended Hildebrand solubility approach

Solute–solvent complexes of testosterone and testosterone propionate in binary solvents composed of cyclohexane with ethyl oleate, isopropyl myristate, and octanol have been reported previously (1). These solvents are pharmaceutically important; the first two are useful as solvents for steroid injectable preparations.

The calculated complexation constants (1) between the steroids and solvents were based on a previous method (2). The solute-mixed solvent systems are analyzed here with the extended Hildebrand solubility approach (3), an extension of the Hildebrand regular solution theory (4) which was introduced to allow the calculation of solubility of nonpolar and semipolar drugs in mixed solvents having a wide range of solubility parameters.

THEORETICAL

Solubility on the mole fraction scale, X_2, may be represented by the expression:

$$-\log X_2 = -\log X_2^i + \log \alpha_2 \qquad \text{(Eq. 1)}$$

where X_2^i is the ideal solubility of the crystalline solid, and α_2 is the solute activity coefficient in mole fraction terms. Scatchard (5) and Hildebrand and Scott (4) formulated the solubility equation for regular solutions in the form:

$$\log \frac{a_2^s}{X_2} = \log \alpha_2 = \frac{V_2 \phi_1^2}{2.303RT}(a_{11} + a_{22} - 2a_{12}) \qquad \text{(Eq. 2)}$$

where

$$\phi_1 = \frac{V_1(1 - X_2)}{V_1(1 - X_2) + V_2 X_2} \qquad \text{(Eq. 3)}$$

The activity of the crystalline solid (a_2^s), taken as a supercooled liquid, is equal to X_2^i as defined in Eq. 1. Variable V_2 is the molar volume of the

0022-3549/82/1200-1334$01.00/0

hypothetical supercooled liquid solute (subscript 2), ϕ_1 is the volume fraction of the solvent (subscript 1), R is the molar gas constant, and T is the absolute temperature of the experiment.

The terms a_{11} and a_{22} are the cohesive energy densities of solvent and solute, and a_{12}, referred to in other reports (3, 6) and elsewhere in this report as W, is expressed in regular solution theory as a geometric mean of the solvent and solute cohesive energy densities:

$$a_{12} = W = (a_{11}a_{22})^{1/2} \quad \text{(Eq. 4)}$$

The square roots of the cohesive energy densities of solute and solvent, called solubility parameters and given the symbol δ, are obtained for the solvent from the energy or heat of vaporization per cubic centimeter:

$$\delta_i = (a_{ii})^{1/2} = \left(\frac{\Delta E^v}{V_i}\right)^{1/2} \cong \left(\frac{\Delta H^v - RT}{V_i}\right)^{1/2} \quad \text{(Eq. 5)}$$

When the solubility parameters and the geometric mean are introduced into Eq. 2, the expression becomes:

$$\log \alpha_2 = A(\delta_1^2 + \delta_2^2 - 2\delta_1\delta_2) = A(\delta_1 - \delta_2)^2 \quad \text{(Eq. 6)}$$

where

$$A = \frac{V_2\phi_1^2}{2.303RT} \quad \text{(Eq. 7)}$$

By substituting Eq. 6 into Eq. 1, one obtains:

$$-\log X_2 = -\log X_2^i + A(\delta_1 - \delta_2)^2 \quad \text{(Eq. 8)}$$

which is the Hildebrand–Scatchard solubility equation (4) for a crystalline solid compound of solubility parameter δ_2 dissolved in a solvent of solubility parameter δ_1. Equation 8 may be referred to as the regular solution equation; the term regular solution will be defined. The ideal solubility term is ordinarily expressed in terms of the heat of fusion of the crystalline solute at its melting point:

$$-\log X_2^i \cong \frac{\Delta H_m^f}{2.303RT}\frac{T_m - T}{T_m} \quad \text{(Eq. 9)}$$

although this is an approximation that disregards the molar heat capacity difference ΔC_p of the liquid and solid forms of the solute. An approximation involving the entropy of fusion, ΔS_m^f, was introduced (7) as:

$$-\log X_2^i \cong \frac{\Delta S_m^f}{R}\log\frac{T_m}{T} \quad \text{(Eq. 10)}$$

to partially correct for the failure to include ΔC_p in Eq. 9, and this form of log ideal solubility is employed in the current report. Equations 9 and 10 are approximations, and currently it has not been determined which is more appropriate for use in solubility analysis.

The Hildebrand–Scatchard equation (Eq. 8) may be used to estimate solubility only for relatively nonpolar drugs in nonpolar solvents which adhere to regular solution requirements. The molar volumes of the solute and solvent should be approximately the same, and the solution should not expand or contract when the components are mixed. Dipole–dipole and hydrogen bonding interactions are absent from regular solutions, with only physical forces being present. In such a system the mixing of solvent and solute results in a random arrangement of the molecules. The entropy in a regular solution is the same as that in an ideal solution, and therefore, the entropy of mixing is zero. Only the enthalpy of mixing has a finite value and it is always positive.

In most solutions encountered in pharmacy, interactions and selective ordering of molecules occur; these systems are referred to as irregular solutions. In pharmaceutical solutions, the geometric mean rule (Eq. 4) is too restrictive, and Eq. 6 or 8 ordinarily provides a poor fit to experimental data in irregular solutions. Instead, $\delta_1\delta_2$ is replaced in Eq. 6 by $W = a_{12}$, which is allowed to take on values as required to yield correct mole fraction solubilities:

$$-\log X_2 = -\log X_2^i + A(\delta_1^2 + \delta_2^2 - 2W) \quad \text{(Eq. 11)}$$

It is not possible at this time to determine W by recourse to fundamental physical chemical properties of solute and solvent. It has been found, however, for drugs in binary solvent mixtures (3, 6, 8) that W may be regressed in a power series on the solvent solubility parameter:

$$W_{calc} = C_0 + C_1\delta_1 + C_2\delta_1^2 + C_3\delta_1^3 + \ldots \quad \text{(Eq. 12)}$$

A reasonable estimate, W_{calc}, is obtained by this procedure, and when W_{calc} is substituted in Eq. 11 for W, mole fraction solubilities in polar binary solvents are obtained ordinarily within ≤20% of the experimental results. Log α_2/A may also be regressed directly on powers of δ_1, bypassing W and obviating the need for δ_2. The estimated solubility, X_2, with this method is identical to that obtained with W_{calc} except for rounding-off errors. The entire procedure, referred to as the extended Hildebrand solubility approach (3), may be conducted by using a polynomial regression program and carrying out the calculations on a computer. It is useful to include a statistical routine which provides R^2, Fisher's F ratio, and a scatter plot of the residuals. Terms of the polynomial (*i.e.*, powers of δ_1) are added sequentially and the values of R^2 and F, together with the appearance of the residual scatter plot, indicate when the proper degree of the polynomial has been reached. A well-known polynomial program using multiple regression analysis, SPSS (9), is convenient for this purpose.

Parameters for Solute–Solvent Interaction—The activity coefficient of the solute, α_2, may be partitioned into a term, α_V, for physical or van der Waals (dispersion and weak dipolar) forces and a second term, α_R, representing residual and presumably stronger solute–solvent interactions (Lewis acid-base type forces). In logarithmic form:

$$\log \alpha_2 = \log \alpha_V + \log \alpha_R \quad \text{(Eq. 13)}$$

According to this definition of log α_2, Eq. 11 may be written:

$$(\log \alpha_2)/A = (\delta_1 - \delta_2)^2 + 2(\delta_1\delta_2 - W) \quad \text{(Eq. 14)}$$

where

$$(\log \alpha_V)/A = (\delta_1 - \delta_2)^2 \quad \text{(Eq. 15)}$$

and

$$(\log \alpha_R)/A = 2(\delta_1\delta_2 - W) \quad \text{(Eq. 16)}$$

Hildebrand *et al.* (10) introduced a parameter, l_{12}, to account for deviations from the geometric mean. In terms of W, l_{12} may be written:

$$W = (1 - l_{12})\delta_1\delta_2 \quad \text{(Eq. 17)}$$

Therefore, the second right-hand term of Eq. 14, representing the residual activity coefficient, is:

$$(\log \alpha_R)/A = 2l_{12}\delta_1\delta_2 \quad \text{(Eq. 18)}$$

and the modified equation for solubility of a drug in binary polar solvents becomes:

$$-\log X_2 = -\log X_2^i + A(\delta_1 - \delta_2)^2 + 2A(l_{12})(\delta_1\delta_2) \quad \text{(Eq. 19)}$$

The variable W may be related to the geometric mean, $\delta_1\delta_2$, by the introduction of a proportionality constant, K (11), such that:

$$W = K(\delta_1\delta_2) \quad \text{(Eq. 20)}$$

From Eqs. 17 and 20:

$$(1 - l_{12}) = W/(\delta_1\delta_2) = K \quad \text{(Eq. 21)}$$

or

$$l_{12} = 1 - K \quad \text{(Eq. 22)}$$

The extended Hildebrand solubility expression (Eq. 11) may now be written:

$$-\log X_2 = -\log X_2^i + A(\delta_1 - \delta_2)^2 + 2A(1 - K)\delta_1\delta_2 \quad \text{(Eq. 23)}$$

By employing Eq. 20 to replace W of Eq. 11, another form of the extended Hildebrand equation is obtained:

$$-\log X_2 = -\log X_2^i + A(\delta_1^2 + \delta_2^2 - 2K\delta_1\delta_2) \quad \text{(Eq. 24)}$$

or, with Eq. 17:

$$-\log X_2 = -\log X_2^i + A[\delta_1^2 + \delta_2^2 - 2(1 - l_{12})\,\delta_1\delta_2] \quad \text{(Eq. 25)}$$

It was found (12) that a plot of l_{12} against a branching ratio, r, provided a good linear correlation for testosterone in a number of branched hydrocarbon solvents.

Variable K was employed (11) to describe the dissolving power of solvents for polyacrylonitrile, and it was concluded that the solvent action of organic solvents on the polymer solute was determined "by a very delicate balance between the various intermolecular forces involved." Solvent power could not be explained alone in terms of dipolar interaction and hydrogen bonding; it depended rather on whether dipolar and hydrogen bonding energies for the solvent–polymer contacts were a few percentage points less than, equal to, or greater than the sum of the sol-

vent–solvent and polymer–polymer interaction energies. The same conclusions can be reached for steroids in the various solvents in the present study and are elaborated.

The various extended solubility equations (Eqs. 11, 24, and 25) are equivalent, and the deviation of polar (or nonpolar) systems from regular solution behavior may be expressed in terms of $(\log \alpha_2)/A$, $(\log \alpha_R)/A$, W, l_{12}, or K. Any one of the parameters may be regressed on a polynomial in δ_1 to obtain values of solubility, X_2. These quantities may also be regressed against the volume fraction or percent of one of the solvents in the mixture or against the mean molar volume of the binary solvent mixture (3). Volume percents and mean molar volumes of chloroform in mixtures of cyclohexane and chloroform are given in Table I. The $X_{2(\text{calc})}$ values may be converted to molal solubility units and, if densities of the solutions are available, to molar or gram per milliliter concentration.

Solubility Parameters for Crystalline Solids—It is not possible to obtain solubility parameters of crystalline drugs by vaporization using Eq. 5, because many organic compounds decompose above their melting points. Instead, it has been shown (13) that the solubility parameter of solid drugs can be estimated from the point of maximum solubility in a binary solvent such as ethyl acetate and ethyl alcohol. The solubility parameter of the solute must lie between the δ values of the two solvents for this technique to be successful. In a regular solution, when:

$$\log X_2 = \log X_2^i \qquad \text{(Eq. 26)}$$

the system represents an ideal solution, and the maximum solubility is obtained, excluding specific solvation effects. When a pure solvent or solvent mixture is found that yields a peak in the solubility profile for a regular solution, δ_1 is assumed to equal δ_2, and the final term of Eq. 8 becomes zero, then Eq. 26 holds.

In an irregular solution, these relations do not hold exactly as in a regular solution. Equation 24 may be written as:

$$\frac{1}{A}(\log X_2^i - \log X_2) = \frac{\log \alpha_2}{A} = \delta_1^2 + \delta_2^2 - 2K\delta_1\delta_2 \qquad \text{(Eq. 27)}$$

The partial derivative of $(\log \alpha_2)/A$ then is taken with respect to δ_1 and the result set equal to zero to obtain the value of δ_2 at the peak in the solubility profile:

$$\left[\frac{\partial(\log \alpha_2/A)}{\partial(\delta_1)}\right]_{\delta_2} = 2\delta_1 - 2K\delta_2 = 0 \qquad \text{(Eq. 28)}$$

$$\delta_1 = K\delta_2 \qquad \text{(Eq. 29}a\text{)}$$

or, from Eq. 5 and the corresponding equation for the solute:

$$a_{11} = K^2 a_{22} \qquad \text{(Eq. 29}b\text{)}$$

Thus, $\delta_1 \neq \delta_2$ at the maximum in the solubility curve, but rather is equal to $K\delta_1$ (11). In irregular solutions, K is slightly greater than unity (~1.01) when solvation occurs between the solute and solvent; K is slightly less than unity (~0.98) when the species of the solution self-associate; and $K = 1.00$ when the solution is regular. As pointed out (11), a very small change in K can bring about large changes in solvent action; this phenomenon is considered in another report (8). Since K is nearly unity, even for highly solvated solutions, δ_2 is almost equal to δ_1 at the point of peak solubility in the system. This gives the researcher a good method for estimating solubility parameters of crystalline drugs. A differentiation method was introduced to obtain this value more precisely (12). Methods for calculating the solubility parameters of solid drugs, involving a regression of $(\log \alpha_2)/A$ on δ_1 in a second degree power series, have been introduced (14, 15). Satisfactory values of δ_2^2 and K are obtained[1] by use of the coefficients of the polynomial in moderately polar systems, but the technique is inadequate for highly irregular solutions. Another approach was introduced (16) to calculate δ_2 of solid compounds. Solubility parameters for solutes may also be obtained by a group contribution method (17).

EXPERIMENTAL

The solubility analyses of testosterone and testosterone propionate in solvent mixtures (*i.e.*, cyclohexane–chloroform, cyclohexane–octanol, cyclohexane–isopropyl myristate, and cyclohexane–ethyl oleate) were reported earlier (1), and the reported values were used in this study.

[1] The K value reported in Ref. 15 is constant over the range of solvent solubility parameters used. It differs from K introduced in the extended Hildebrand solubility approach which has a different value for each solvent used. The term in Ref. 15 should properly be differentiated from K by use of another symbol, such as κ, kappa.

Table I—Testosterone in Chloroform–Cyclohexane at 25° [a]

1	2	3	4	5	6	7	8	9	10	11	12	13	14	15
Volume, % $CHCl_3$	δ_1	V_1	A	$\log \alpha_2$	$\frac{\log \alpha_2}{A}$	$\frac{\log \alpha_{2(\text{calc})}}{A}$ [b]	W	W_{calc} [c]	K	l_{12}	$\frac{\log \alpha_R}{A}$	X_2	$X_{2(\text{calc})}$	Percent Error
0	8.19	108.8	0.1863	2.458	13.194	12.714	86.347	86.586	0.9672	0.0328	5.849	0.000253	0.000311	−22.9
2	8.21	108.3	0.1862	2.232	11.987	11.916	87.113	87.149	0.9734	0.0266	4.572	0.000426	0.000439	−3.1
4	8.23	107.7	0.1860	2.070	11.129	11.138	87.706	87.703	0.9777	0.0223	4.002	0.000618	0.000616	0.3
6	8.25	107.1	0.1857	1.880	10.124	10.378	88.373	88.247	0.9827	0.0173	3.103	0.000957	0.000859	10.2
8	8.27	106.6	0.1853	1.712	9.239	9.638	88.982	88.783	0.9871	0.0129	2.323	0.00141	0.00119	15.6
10	8.29	106.0	0.1849	1.611	8.713	8.916	89.412	89.309	0.9895	0.0105	1.897	0.00178	0.00163	8.4
20	8.38	103.2	0.1807	1.049	5.805	5.884	91.614	91.575	1.0030	−0.0030	−0.545	0.00649	0.00628	3.2
30	8.48	100.4	0.1677	0.537	3.202	2.899	93.760	93.911	1.0143	−0.0143	−2.655	0.0211	0.0237	−12.3
40	8.57	97.6	0.1387	0.100	0.721	0.516	95.767	95.870	1.0252	−0.0252	−4.708	0.0577	0.0616	−6.8
50	8.67	94.8	0.1096	−0.147	−1.341	−1.842	97.662	97.910	1.0334	−0.0334	−6.319	0.102	0.116	−13.7
60	8.76	92.0	0.0788	−0.351	−4.454	−3.743	100.001	99.645	1.0473	−0.0473	−9.034	0.163	0.143	12.3
70	8.86	89.2	0.0705	−0.394	−5.589	−5.657	101.448	101.483	1.0505	−0.0505	−9.748	0.180	0.182	−1.1
80	8.95	86.4	0.0606	−0.448	−7.393	−7.242	103.157	103.077	1.0574	−0.0574	−11.204	0.204	0.200	2.0
90	9.05	83.6	0.0549	−0.475	−8.652	−8.898	104.685	104.805	1.0612	−0.0612	−12.080	0.217	0.224	−3.2
100	9.14	80.8	0.0487	−0.506	−10.390	−10.334	106.368	106.342	1.0677	−0.0677	−13.484	0.233	0.232	0.4

[a] Parameters: $\Delta H_m{}^f$ = 6190 cal/mole; T_m = 427.2°K, δ_2 = 10.9 $(\text{cal/cm}^3)^{1/2}$; V_2 = 254.5 cm^3/mole; $X_2{}^i$ = 0.07264; $-\log X_2{}^i$ = 1.1388. [b] Equation 33. [c] Equation 32.

RESULTS

Testosterone in Cyclohexane–Chloroform—The solubilities of testosterone at 25° in mixtures of cyclohexane and chloroform are found in Table I. The $\Delta H_m{}^f$ value for testosterone is 6190 cal/mole and T_m is 427.2°K. The $-\log X_2{}^i$ value is 1.1388 ($X_2{}^i$ = 0.07264), and δ_2 is 10.90 $(\text{cal/cm}^3)^{1/2}$. The solubility parameter for cyclohexane is 8.19 and for

chloroform is 9.14. The molar volume of testosterone is 254.5 cm^3/mole (12). The log activity coefficients are calculated using the expression:

$$\log \alpha_2 = \log X_2{}^i - \log X_2 \qquad \text{(Eq. 30)}$$

The values of W for the various mixtures are obtained directly from the solubility data, using a rearranged form of Eq. 11:

$$W = \tfrac{1}{2}\left[\delta_1{}^2 + \delta_2{}^2 - \frac{\log (X_2{}^i/X_2)}{A}\right]$$

$$= \tfrac{1}{2}\left[\delta_1{}^2 + \delta_2{}^2 - (\log \alpha_2)/A\right] \qquad \text{(Eq. 31)}$$

Also included in Table I are the calculated values of $(\log \alpha_2)/A$ and W obtained by regressing $(\log \alpha_2)/A$ and W on δ_1 in a third degree polynomial:

$$W = -3298.82 + 1084.56\delta_1 - 116.904\delta_1{}^2 + 4.26742\delta_1{}^3 \qquad \text{(Eq. 32)}$$

$$n = 15, R^2 = 0.999, F = 6702, F(3, 11, 0.01)^2 = 6.22$$

and:

$$\frac{\log \alpha_2}{A} = 6716.38 - 2169.12\delta_1 + 234.809\delta_1{}^2 - 8.53485\delta_1{}^3 \qquad \text{(Eq. 33)}$$

$$n = 15, R^2 = 0.998, F = 2352, F(3, 11, 0.01) = 6.22$$

The observed mole fraction solubilities, and the calculated values (obtained with Eqs. 30 and 33), together with percent differences between calculated and observed solubilities, are given in Table I. Variables K, l_{12}, and $(\log \alpha_R)/A$ were also regressed on δ_1 and the equations are:

$$K = -41.1320 + 13.7685\delta_1 - 1.50351\delta_1{}^2 + 0.0549512\delta_1{}^3 \qquad \text{(Eq. 34)}$$

$$n = 15, R^2 = 0.997, F = 1476, F(3, 11, 0.01) = 6.22$$

$$l_{12} = 42.1320 - 13.7685\delta_1 + 1.50351\delta_1{}^2 - 0.0549512\delta_1{}^3 \qquad \text{(Eq. 35)}$$

$$n = 15, R^2 = 0.997, F = 1476, F(3, 11, 0.01) = 6.22$$

and:

$$\frac{\log \alpha_R}{A} = 918.478\delta_1 - 300.154\delta_1{}^2 + 32.7765\delta_1{}^3 - 1.19794\delta_1{}^4 \qquad \text{(Eq. 36)}$$

$$n = 15, R^2 = 0.997, F = 1476, F(4, 10, 0.01) = 5.99$$

Since $K = 1 - l_{12}$ from Eq. 21 and $(\log \alpha_R)/A = 2l_{12}\delta_1\delta_2$ from Eq. 18, any one of the regression equations for K, l_{12}, and $(\log \alpha_R)/A$ can be obtained from the others. For example, replacing K in Eq. 34 by $(1 - l_{12})$ yields Eq. 35 for l_{12}. It is seen that the only differences are in the constant terms, −41.1320 in Eq. 34 and +42.1320 in Eq. 35, and the change in sign of each coefficient. Equation 36 for $(\log \alpha_R)/A$ is observed to take on an interesting form: no constant term exists and the polynomial is carried to the fourth rather than the third power.

Once the calculated value for one of these parameters is obtained from the regression equation, it may be substituted in the appropriate expression given earlier to obtain $X_{2(calc)}$. For example, $l_{12(calc)}$ for testosterone solubility in 50% chloroform–50% cyclohexane (v/v) ($\delta_1 = 8.67$) is obtained with Eq. 35:

$$l_{12(calc)} = 42.1320 - 13.7685(8.67) + 1.5035(8.67)^2$$

$$-0.0549512(8.67)^3 = -0.0362$$

Then, from the second right hand term of Eq. 25:

$$\frac{\log \alpha_2}{A} = \delta_1{}^2 + \delta_2{}^2 - 2(1 - l_{12})\delta_1\delta_2 = (8.67)^2 + (10.9)^2$$

$$- 2(1 + 0.0362)\,(8.67)\,(10.9) = -1.8691$$

[2] $F(3, 11, 0.01)$ is the tabulated F value with p degrees of freedom in the numerator and n-p-1 degrees of freedom in the denominator, where $p = 3$ is the number of independent variables and $n = 15$ is the total number of samples. The value 0.01 signifies that the F ratio is compared with the tabular value obtained at the 99% level of confidence.

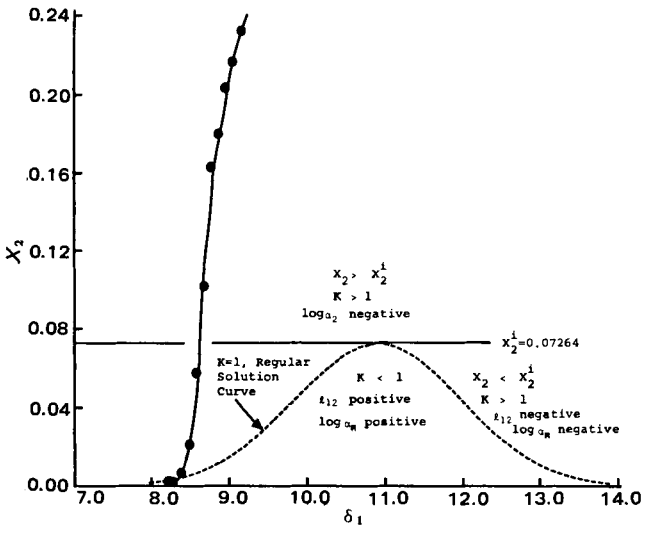

Figure 1—*Mole fraction solubility of testosterone ($\delta_2 = 10.9$) at 25° in cyclohexane and chloroform. Key: (●) experimental points; (—) solubility calculated by extended Hildebrand solubility approach; (- - - -) solubility curve calculated using regular solution theory.*

where the solubility parameter of testosterone is 10.9 $(cal/cm^3)^{1/2}$. Log $X_2{}^i$ is equal to −1.1388 for testosterone at 25°, and A from Table I is 0.1096 at 50% by volume chloroform. Continuing with Eq. 25, one obtains:

$$-\log X_2 = 1.1388 + (0.1096)(-1.8691) = 0.9340$$

$$X_{2(obs)} = 0.102$$

$$X_{2(calc)} = 0.116\ (-13.7\%\ \text{error})$$

Variables K, l_{12}, and $\log \alpha_R$ are three different means of expressing deviation from regular solution behavior. Log α_R (Column 12, Table I) is a measure of the residual activity coefficient due to dipolar interactions between solvent and solute, inductive effects, and hydrogen bonding. Variables K and l_{12} are also used to represent solution irregularities. When log α_R is negative, l_{12} (Column 11) becomes negative and K (Column 10) becomes greater than unity, indicating that X_2 is greater than the mole fraction solubility in a regular solution. As observed in Table I, this effect occurs at 20% chloroform in cyclohexane. Above this concentration of chloroform, it may be assumed that the predominant factor promoting the solubility of testosterone is solvation of the drug by chloroform, most probably in this case through hydrogen bonding. At 50% chloroform in cyclohexane, the interaction between testosterone and chloroform has increased sufficiently to elevate the drug solubility above the ideal mole fraction solubility, $X_2{}^i = 0.0726$. At this point the total logarithmic activity coefficient, log α_2, as well as log α_R, is negative, indicating the beginning of strong solvation. It is suggested that the term complexation is appropriate for interactions between solute and solvent when $X_2 \gg X_2{}^i$, observed in Table I for testosterone in pure chloroform.

The various parameters, and the manner in which they may be used to express self-association ($K < 1$), nonspecific solvent effects or regular solution ($K \cong 1$), weak solubilization ($K > 1$ and $X_2 < X_2{}^i$), and complexation or strong solubilization ($K > 1$ and $X_2 > X_2{}^i$), are depicted in Fig. 1 for testosterone in a mixture of chloroform and cyclohexane. As the real or irregular solubility line crosses the regular solution line at the lower left side of Fig. 1, K changes from <1.0 to >1.0. Then, as the irregular solution line crosses the ideal solubility line, K remains >1.0, X_2 becomes greater than $X_2{}^i$, and log α_2 becomes negative. At 100% chloroform, log $\alpha_2 = -0.506$, which means that the ratio of X_2 to $X_2{}^i$ is ~3:1. The curve for testosterone propionate in chloroform–cyclohexane (not shown) is similar to Fig. 1 for testosterone, demonstrating complexation between the steroid ester and chloroform >30% by volume chloroform in the chloroform–cyclohexane mixture.

Testosterone Propionate in Mixed Solvents—The solubilities of the steroidal ester, testosterone propionate, at 25° in octanol–cyclohexane, ethyl oleate–cyclohexane, and isopropyl myristate–cyclohexane are plotted in Figs. 2–4 as a function of the solubility parameter of the mixed solvent. The logarithmic ideal solubility of testosterone propionate, log $X_2{}^i$, is −0.81356 at 25°; $X_2{}^i = 0.15362$. The solubility parameter, δ_2, and

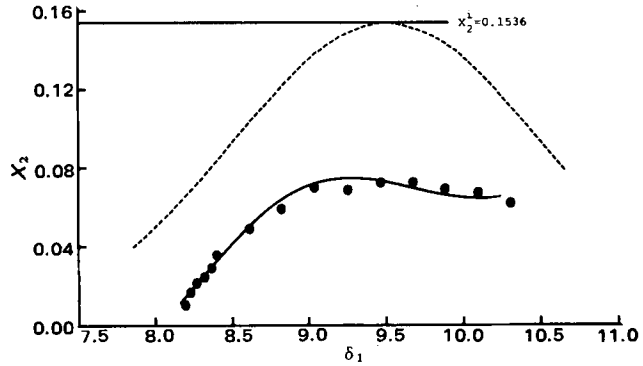

Figure 2—*Mole fraction solubility of testosterone propionate (δ_2 = 9.5) at 25° in cyclohexane and octanol. Key: (●) experimental points; (—) solubility calculated by extended Hildebrand solubility approach; (- - -) solubility curve calculated using regular solution theory.*

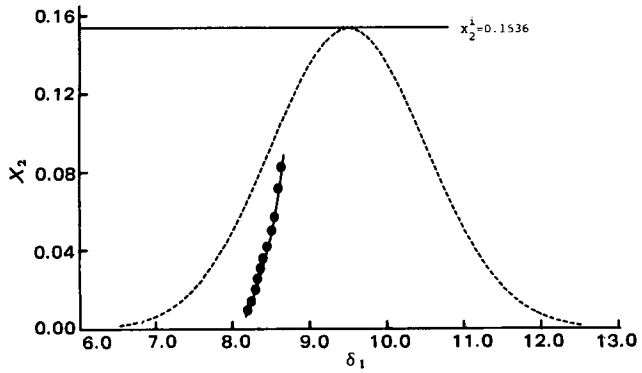

Figure 3—*Mole fraction solubility of testosterone propionate (δ_2 = 9.5) at 25° in cyclohexane and ethyl oleate. Key: (●) experimental points; (—) solubility calculated by extended Hildebrand solubility approach; (- - -) solubility curve calculated using regular solution theory.*

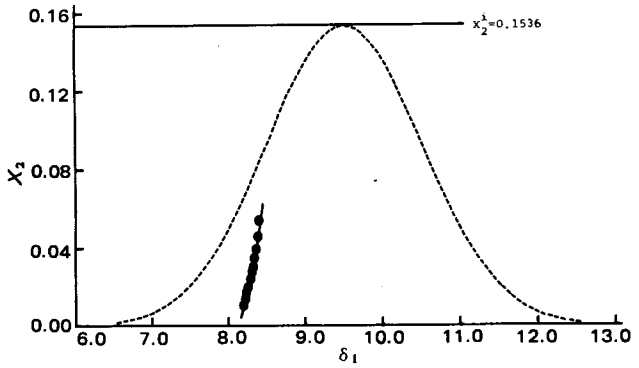

Figure 4—*Mole fraction solubility of testosterone propionate (δ_2 = 9.5) at 25° in cyclohexane and isopropyl myristate. Key: (●) experimental solubility; (—) solubility calculated by extended Hildebrand solubility approach; (- - -) solubility curve calculated using regular solution theory.*

the molar volume, V_2, of testosterone propionate are, respectively, 9.5 $(cal/cm^3)^{1/2}$ and 294.0 cm^3/mole. The solubility parameter is 8.19 for cyclohexane, 10.30 for octanol, 8.63 for ethyl oleate, and 8.85 for isopropyl myristate.

Use of the extended Hildebrand solubility approach to calculate solubilities yields good results for these systems as observed by the fit of the calculated line to the points in Figs. 2–4.

As seen by comparing the regular solution curve (calculated using Eq. 8) with the extended Hildebrand solubility line (calculated using Eq. 11, 24, or 25), the observed solubilities are smaller than those predicted for a regular solution over most of the range of δ_1 values of the mixed solvents, as contrasted to the chloroform–cyclohexane mixture. At no composition of mixed solvent do the solubilities exceed the ideal solubility, as observed earlier in chloroform–cyclohexane (Fig. 1). The regression equations used to calculate solubilities in these systems are:

Octanol–Cyclohexane Mixtures (Fig. 2):

$$\frac{\log \alpha_2}{A} = 1142.47 - 356.237\delta_1 + 37.0357\delta_1^2 - 1.28137\delta_1^3 \quad \text{(Eq. 37)}$$

$$n = 15, R^2 = 0.965, F = 101, F(3, 11, 0.01) = 6.22$$

Ethyl Oleate–Cyclohexane Mixtures (Fig. 3):

$$\frac{\log \alpha_2}{A} = 27888.99 - 9867.80\delta_1 + 1164.77\delta_1^2 - 45.8617\delta_1^3 \quad \text{(Eq. 38)}$$

$$n = 11, R^2 = 0.999, F = 2589, F(3, 7, 0.01) = 8.45$$

Isopropyl Myristate–Cyclohexane Mixtures (Fig. 4):

$$\frac{\log \alpha_2}{A} = 157348.62 - 56738.3\delta_1 + 6821.48\delta_1^2 - 273.439\delta_1^3 \quad \text{(Eq. 39)}$$

$$n = 11, R^2 = 0.999, F = 3970, F(3, 7, 0.01) = 8.45$$

Nonlinear Regression—The solubility of testosterone in octanol–cyclohexane and in ethyl oleate–cyclohexane are plotted in Figs. 5 and 6. The extended Hildebrand solubility approach with polynomial regression, used with success for the other systems, failed to provide a satisfactory fit of the data, as shown by the dotted lines in Figs. 5 and 6.

The polynomial regression method contains potential numerical difficulties which show themselves only in certain applications. The source of these difficulties may be seen by recognizing that to date the extended

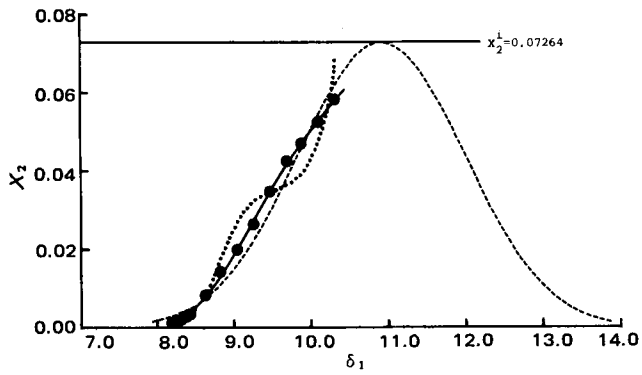

Figure 5—*Mole fraction solubility of testosterone (δ_2 = 10.9) at 25° in cyclohexane and octanol. Key: (●) experimental points; (—) extended Hildebrand solubility curve based on NONLIN polynomial regression; (. . . .) extended Hildebrand solubility curve based on ordinary polynomial regression; (- - - -) regular solution curve.*

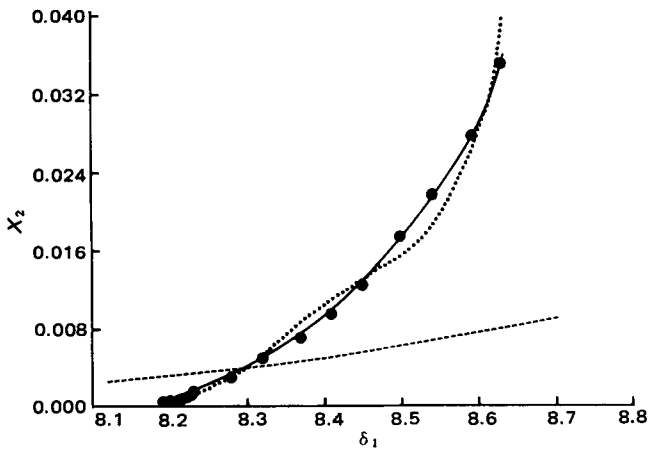

Figure 6—*Mole fraction solubility of testosterone (δ_2 = 10.9) at 25° in cyclohexane and ethyl oleate. Key: (●) experimental points; (—) extended Hildebrand solubility curve based on NONLIN polynomial regression; (·····) extended Hildebrand solubility curve based on ordinary polynomial regression; (- - -) regular solution curve.*

Hildebrand solubility approach has fitted observed values of X_2 to a model that defines X_2 as a function of δ and other variables and constants. That is, the relations expressed by Eq. 11 may be written as:

$$\log (X_2^i/X_2) - \frac{V_2}{2.303RT}\left[\frac{V_1(1-X_2)}{V_1(1-X_2)+V_2X_2}\right]^2 f(\delta) = 0 \quad \text{(Eq. 40)}$$

where $f(\delta)$ is a polynomial in δ. Thus, Eq. 40 defines the dependent variable X_2 as an implicit function of the independent variables δ and V_1. The terms X_2^i, R, T, and V_2 are known constants, and the parameters to be estimated are the coefficients of $f(\delta)$.

The polynomial regression method contains a circular element in that it uses the observed values of X_2 in W or $(\log \alpha_2)/A$ to estimate the coefficients of $f(\delta)$, and then uses these values of $f(\delta)$ to obtain calculated values of X_2. This circular process can be thought of as the first step in an iteration; the conditions necessary for this process to converge are not known. In many applications the iteration gives acceptable results; in some cases, as shown in Figs. 5 and 6, the results are poor.

Another potential source of difficulty is that the values of W or $(\log \alpha_2)/A$ are fit by least squares to the polynomials of δ. Thus, the coefficients are estimated by minimizing the squared deviations between observed and predicted (model) values of functions of X_2 [W or $(\log \alpha_2)/A$]. When X_2 then is calculated, this is equivalent to weighted least squares, with the weights being complicated functions of the constants in W or in $(\log \alpha_2)/A$.

To use Eq. 40 as a model for predicting X_2 as a function of δ and V_1, it must be determined that there is a unique value of X_2 that satisfies the equality. Writing the expression in Eq. 40 as $F(X_2)$, it can be verified that $\lim F(X_2)_{X_2 \to 0} = \infty$ and $F(X_2)_{X_2 \to 0} = \log X_2^i < 0$. Thus, $F(X_2)$ has a root between 0 and 1. It can also be shown that if $f(\delta) > 0$ then $F^1(X_2) < 0$ for $0 \le X_2 \le 1$. Thus, $F(X_2)$ is monotonic decreasing on [0,1] and has one, and only one, root.

Equation 40 can be used in any nonlinear regression program that accepts the model defined as an implicit function. In this application good inital estimates are important; they can be obtained as the coefficients of the polynomial in δ used in the polynomial regression method.

The regression equations for testosterone in octanol–cyclohexane and in ethyl oleate–cyclohexane were obtained by fitting Eq. 40 with the nonlinear regression program NONLIN (18). The results are:

Testosterone in Octanol–Cyclohexane (Fig. 5):

$$\frac{\log \alpha_2}{A} = 895.34 - 264.088\delta_1 + 26.1217\delta_1^2 - 0.865608\delta_1^3 \quad \text{(Eq. 41)}$$

and

Testosterone in Ethyl Oleate–Cyclohexane (Fig. 6):

$$\frac{\log \alpha_2}{A} = 50518.74 - 17713.3\delta_1 + 2071.82\delta_1^2 - 80.8331\delta_1^3 \quad \text{(Eq. 42)}$$

To solve Eq. 40 for X_2, the rootfinder subroutine ZBRENT (19) was called from DFUNC of NONLIN. Figures 5 and 6 show that fitting observed values of X_2 directly to values of X_2 predicted by Eqs. 41 and 42, respectively, greatly improves the fit. NONLIN was also used to fit the data shown in Figs. 1–4. In these applications the improvement in fit was so small as to be of little importance.

CONCLUSIONS

In another report (1), the interaction of testosterone and testosterone propionate was shown in mixed solvents of cyclohexane combined with ethyl oleate, isopropyl myristate, and octanol. The interaction was analyzed using association constants (2) with limited success. The present study shows that the interaction of testosterone and testosterone propionate with mixed solvents may be represented accurately by use of the extended Hildebrand solubility approach, a method that employs a polynomial on δ_1 rather than association constants.

The solubility is plotted in Figs. 1–6 in reference to the regular solution curve and the ideal solubility, X_2^i of the drug. This method of plotting the results delineates systems in which self-association or solvation predominates, and it differentiates these from regular and ideal solutions. It is suggested that although the drug and active (solvating) solvent (cyclohexane is considered to be the inactive solvent of the binary solvent mixture) interact to a lesser or greater extent, strong interaction or specific solvation, such as that resulting from hydrogen bonding effects, occurs when the solubility rises well above the ideal solubility line, X_2^i. Some self-association of solute or solvent may exist above X_2^i, leading to reduced solubility, but the overriding effect is strong solvation (complexation between solute and solvent).

A combination of X_2^i and K may be used to define various classes of interaction between solute and solvent. As observed in Fig. 1, when a solubility point falls on or near the regular solution line, it is defined as a regular solution (4). Referring to Eq. 24, when $K \cong 1$, the geometric mean obtains, and the solution may be considered to be a regular system. However, it is conceivable that W equals $\delta_1\delta_2$ (*i.e.*, $K \cong 1$) in polar systems by cancellation of solvating and self-associating effects, rather than because of the criteria layed down (4) for regular solution behavior.

When $K < 1$, the solubility points in a graph such as Fig. 2 fall below the regular solution line. The solute, solvent, or both are ordinarily considered to be self-associated when $K < 1$, resulting in decreased solubility.

When $K > 1$ and $X_2 > X_2^i$, association of a specific nature (*i.e.*, hydrogen bonding, dipolar interaction, or charge transfer complexation) is considered to exist between solute and solvent.

Finally, when $K > 1$ but $X_2 < X_2^i$, an intermediate situation exists. Some self-association may be present, but association results in solubilities above those found on the regular solution line. Various classes of solvation, self-association, and regular solution behavior have been defined (4), but the case where $X_2 < X_2^i$ and $K > 1$ was not addressed. This is neither a regular, self-associated, or strongly solvated solution, but rather an intermediate or weakly solvated system. The system treated in the present study are interesting because most of them are of the self-associated–weakly solvated class (*i.e.*, except for the chloroform systems, $X_2 < X_2^i$ and, depending on the composition of the solvent, K is greater or less than unity).

The solvents consisting of chloroform in cyclohexane exhibit weak to strong solvating effects on testosterone, depending on the concentration of chloroform in the solvent mixture (Fig. 1).

When the ester, testosterone propionate, is dissolved in the binary solvent, octanol in cyclohexane, a self-associating system results. As observed in Fig. 2, $K < 1$ across the range of solvent composition. This system exhibits a peak in the solubility because the solubility parameter of testosterone propionate, 9.5, lies between the solubility parameters of cyclohexane, $\delta = 8.2$, and octanol, $\delta = 10.3$. The methyl xanthines in dioxane–water mixtures have been reported (3, 6, 8) to show this kind of solubility profile. The calculated curve (solid line) of Fig. 2 should exhibit a parabolic shape somewhat like the dashed regular solution curve above it and should attain a maximum X_2 value at $\delta_1 = \sim 9.5$. The scatter of the experimental points caused the regression line (solid line) to take on an irregular shape and to rise slightly rather than fall on the right hand side of the figure. Testosterone propionate in ethyl oleate–cyclohexane (Fig. 3) yields solutions that appear to be self-associating rather than weakly solvating (*i.e.*, $K < 1$). Testosterone propionate in isopropyl myristate–cyclohexane (Fig. 4) follows a pattern similar to the drug in ethyl oleate–cyclohexane. The solubilities fall under the bell-shaped regular solution curve and may be classified as predominately self-associating ($K < 1$).

As observed in Fig. 5, testosterone in octanol–cyclohexane appears to follow regular solution behavior rather closely over the composition from 0 to 100% octanol. However solutions of a polar solvent, octanol, and a multifunctional solute, testosterone, do not meet the requirements of a regular solution (*e.g.*, molecules of approximately the same size, no change in entropy on mixing, no specific interaction of either species). The fact that such solutions follow the regular solution line are probably due to cancellation of self-association and solvation effects in these polar systems rather than an absence of specific interactions. Such solutions should not be called regular, although $K \cong 1$.

Testosterone in ethyl oleate–cyclohexane (Fig. 6) forms solutions that are characterized for the most part as weakly solvating (*i.e.*, $K > 1$ and $X_2 < X_2^i$).

The solubility parameters for testosterone and testosterone propionate have not been determined unequivocally. Testosterone is assigned a tentative value of 10.8 and testosterone propionate, 9.5. The latter value has more validity than the former at this time. If the solubility parameter of testosterone later is found to be essentially that of testosterone propionate, as some results appear to indicate, the position of the regular solution line will need to be moved relative to the solubility data points, and the above interpretations will change. For example, if it is found that δ for testosterone is 9.5 rather than 10.8, both testosterone and testosterone propionate will be observed to form weakly self-associated rather than weakly solvated solutions in ethyl oleate–cyclohexane.

However, the findings of chloroform as strongly solvating and the other solvents—octanol, ethyl oleate, and isopropyl myristate—as weakly solvating or self-associating is evident in these results, regardless of the exact solubility parameters of testosterone and testosterone propionate.

In earlier work (3, 4, 6, 8) the extended Hilidebrand solubility approach employed a polynomial regression routine for calculating quantities such as W and $(\log \alpha_2)/A$, and this statistical method has proved successful in most instances. It is demonstrated in the current study that direct polynomial regression sometimes may produce an unsatisfactory fit of solubility data. A nonlinear regression program, NONLIN (17), has been shown to improve the fit when ordinary polynomial regression fails.

REFERENCES

(1) K. C. James and M. Mehdizadeh, *J. Pharm. Pharmacol.*, **33**, 9 (1981).

(2) T. Higuchi and K. A. Connors, in "Advances in Analytical Chemistry and Instrumentation," vol. 4, C. N. Reilley, Ed., Wiley Interscience, New York, N.Y., 1965, pp. 117–212.

(3) A. Martin, J. Newburger, and A. Adjei, *J. Pharm. Sci.*, **69**, 487 (1980).

(4) J. H. Hildebrand and R. L. Scott, "The Solubility of Nonelectrolytes," 3rd ed., Dover, New York, N.Y., 1964.

(5) G. Scatchard, *Chem. Rev.*, **8**, 321 (1931).

(6) A. Adjei, J. Newburger, and A. Martin, *J. Pharm. Sci.*, **69**, 659 (1980).

(7) J. H. Hildebrand, J. M. Prausnitz, and R. L. Scott, "Regular and Related Solutions," Van Nostrand Reinhold, New York, N.Y., 1970, p. 22.

(8) A. Martin, A. N. Paruta, and A. Adjei, *J. Pharm. Sci.*, **70**, 1115 (1981).

(9) N. H. Nie, C. H. Hull, J. G. Jenkins, K. Steinbrenner, and D. H. Bent, "SPSS, Statistical Package for the Social Sciences," McGraw-Hill, New York, N.Y., 1975, pp. 278, 371.

(10) J. H. Hildebrand, J. M. Prausnitz, and R. L. Scott, "Regular and Related Solutions," Van Nostrand Reinhold, New York, N.Y., 1970, p. 99.

(11) E. E. Walker, *J. Appl.Chem.*, **2**, 39, 470 (1952).

(12) K. C. James, C. T. Ng, and P. R. Noyce, *J. Pharm. Sci.*, **65**, 656 (1976).

(13) M. J. Chertkoff and A. Martin, *J. Am. Pharm. Assoc., Sci. Ed.*, **49**, 444 (1960).

(14) G. Cavé, R. Kothari, F. Puisieux, A. Martin, and J. T. Carstensen, *Int. J. Pharm.*, **5**, 267 (1980).

(15) A. Martin and J. T. Carstensen, *J. Pharm. Sci.*, **70**, 170 (1981).

(16) S. Cohen, A. Goldschmid, G. Shtacher, S. Srebrenik, and S. Gitter, *Mol. Pharmacol.* **11**, 379 (1975).

(17) R. F. Fedors, *Plym. Eng. Sci.*, **14**, 147 (1974).

(18) C. M. Metzler, G. L. Elving, and A. J. McEwen, *Biometrics*, **30**, 562 (1974).

(19) IMSL Reference Manual, International Mathematical and Statistical Libraries, Houston,Tex, 1979.

ACKNOWLEDGMENTS

The study was funded in part by the endowed professorship provided to A. Martin by Coulter R. Sublett.

The authors gratefully acknowledge the advice and assistance of Alan Beerbower, Energy Center, University of California at San Diego.

Antitumor Agents LVI: The Protein Synthesis Inhibition by Genkwadaphnin and Yuanhuacine of P-388 Lymphocytic Leukemia Cells

Y. F. LIOU, I. H. HALL ˣ, and K. H. LEE

Received August 26, 1981, from the *Division of Medicinal Chemistry, School of Pharmacy, University of North Carolina at Chapel Hill, Chapel Hill, NC 27514.* Accepted for publication January 26, 1982.

Abstract □ Two natural products isolated from the plant *Daphne genkwa* have been shown to possess antileukemic activity in mice. Genkwadaphnin and yuanhuacine were observed to inhibit DNA and protein synthesis in P-388 leukemic cells. A detailed study of the effects of these two diterpene esters on protein synthesis of leukemic cells was undertaken. The major effects of genkwadaphnin and yuanhuacine on protein synthesis were blockage of the elongation process and interference with the peptidyl transferase reaction. The latter reaction was suppressed at concentrations of the diterpene esters which were commensurate with concentrations that inhibited whole cell *in vitro* protein synthesis in P-388 cells.

Keyphrases □ Antitumor agents—inhibition of DNA and protein synthesis by genkwadaphnin and yuanhuacine in P-388 lymphocytic leukemia cells, daphnane deterpene esters □ Genkwadaphnin—antitumor agents, inhibition of DNA and protein synthesis in P-388 lymphocytic leukemia cells, daphnane diterpene esters □ Yuanhuacine—antitumor agents, inhibition of DNA and protein synthesis in P-388 lymphocytic leukemia cells, daphnane diterpene esters

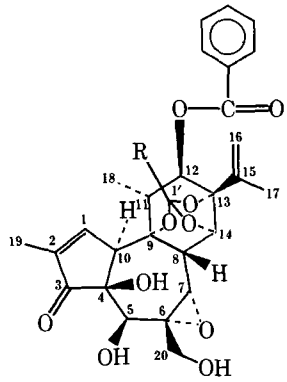

I R = 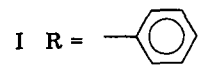

II R = —CH=CH—CH=CH—$(CH_2)_4$—CH_3

Daphnane diterpene esters which possess an isopropylene side chain at C_{13} have previously been reported to have antileukemic activity (1). Genkwadaphnin and yuanhuacine (I and II) are two such esters which have been isolated from *Daphne genkwa* and chemically characterized (2). Genkwadaphnin (I) at 0.8 mg/kg/day was shown to produce a T/C% value of 173, whereas yuanhuacine (II) afforded a value of 151% against P-388 lymphocytic leukemia growth (2). These T/C% values were comparable to 5-fluorouracil at 12.5 mg/kg/day in the P-388 screen. Therefore, it was concluded that daphnane diterpene esters may have potential as antineoplastic therapeutic agents and that their modes of action on cellular metabolism were of interest, particularly since these agents resemble, structurally, phorbol esters which are tumor pro-

0022-3549/82/1200-1340$01.00/0

In earlier work (3, 4, 6, 8) the extended Hilidebrand solubility approach employed a polynomial regression routine for calculating quantities such as W and $(\log \alpha_2)/A$, and this statistical method has proved successful in most instances. It is demonstrated in the current study that direct polynomial regression sometimes may produce an unsatisfactory fit of solubility data. A nonlinear regression program, NONLIN (17), has been shown to improve the fit when ordinary polynomial regression fails.

REFERENCES

(1) K. C. James and M. Mehdizadeh, *J. Pharm. Pharmacol.*, **33**, 9 (1981).

(2) T. Higuchi and K. A. Connors, in "Advances in Analytical Chemistry and Instrumentation," vol. 4, C. N. Reilley, Ed., Wiley Interscience, New York, N.Y., 1965, pp. 117–212.

(3) A. Martin, J. Newburger, and A. Adjei, *J. Pharm. Sci.*, **69**, 487 (1980).

(4) J. H. Hildebrand and R. L. Scott, "The Solubility of Nonelectrolytes," 3rd ed., Dover, New York, N.Y., 1964.

(5) G. Scatchard, *Chem. Rev.*, **8**, 321 (1931).

(6) A. Adjei, J. Newburger, and A. Martin, *J. Pharm. Sci.*, **69**, 659 (1980).

(7) J. H. Hildebrand, J. M. Prausnitz, and R. L. Scott, "Regular and Related Solutions," Van Nostrand Reinhold, New York, N.Y., 1970, p. 22.

(8) A. Martin, A. N. Paruta, and A. Adjei, *J. Pharm. Sci.*, **70**, 1115 (1981).

(9) N. H. Nie, C. H. Hull, J. G. Jenkins, K. Steinbrenner, and D. H. Bent, "SPSS, Statistical Package for the Social Sciences," McGraw-Hill, New York, N.Y., 1975, pp. 278, 371.

(10) J. H. Hildebrand, J. M. Prausnitz, and R. L. Scott, "Regular and Related Solutions," Van Nostrand Reinhold, New York, N.Y., 1970, p. 99.

(11) E. E. Walker, *J. Appl.Chem.*, **2**, 39, 470 (1952).

(12) K. C. James, C. T. Ng, and P. R. Noyce, *J. Pharm. Sci.*, **65**, 656 (1976).

(13) M. J. Chertkoff and A. Martin, *J. Am. Pharm. Assoc., Sci. Ed.*, **49**, 444 (1960).

(14) G. Cavé, R. Kothari, F. Puisieux, A. Martin, and J. T. Carstensen, *Int. J. Pharm.*, **5**, 267 (1980).

(15) A. Martin and J. T. Carstensen, *J. Pharm. Sci.*, **70**, 170 (1981).

(16) S. Cohen, A. Goldschmid, G. Shtacher, S. Srebrenik, and S. Gitter, *Mol. Pharmacol.* **11**, 379 (1975).

(17) R. F. Fedors, *Plym. Eng. Sci.*, **14**, 147 (1974).

(18) C. M. Metzler, G. L. Elving, and A. J. McEwen, *Biometrics*, **30**, 562 (1974).

(19) IMSL Reference Manual, International Mathematical and Statistical Libraries, Houston,Tex, 1979.

ACKNOWLEDGMENTS

The study was funded in part by the endowed professorship provided to A. Martin by Coulter R. Sublett.

The authors gratefully acknowledge the advice and assistance of Alan Beerbower, Energy Center, University of California at San Diego.

Antitumor Agents LVI: The Protein Synthesis Inhibition by Genkwadaphnin and Yuanhuacine of P-388 Lymphocytic Leukemia Cells

Y. F. LIOU, I. H. HALL ˣ, and K. H. LEE

Received August 26, 1981, from the *Division of Medicinal Chemistry, School of Pharmacy, University of North Carolina at Chapel Hill, Chapel Hill, NC 27514.* Accepted for publication January 26, 1982.

Abstract □ Two natural products isolated from the plant *Daphne genkwa* have been shown to possess antileukemic activity in mice. Genkwadaphnin and yuanhuacine were observed to inhibit DNA and protein synthesis in P-388 leukemic cells. A detailed study of the effects of these two diterpene esters on protein synthesis of leukemic cells was undertaken. The major effects of genkwadaphnin and yuanhuacine on protein synthesis were blockage of the elongation process and interference with the peptidyl transferase reaction. The latter reaction was suppressed at concentrations of the diterpene esters which were commensurate with concentrations that inhibited whole cell *in vitro* protein synthesis in P-388 cells.

Keyphrases □ Antitumor agents—inhibition of DNA and protein synthesis by genkwadaphnin and yuanhuacine in P-388 lymphocytic leukemia cells, daphnane deterpene esters □ Genkwadaphnin—antitumor agents, inhibition of DNA and protein synthesis in P-388 lymphocytic leukemia cells, daphnane diterpene esters □ Yuanhuacine—antitumor agents, inhibition of DNA and protein synthesis in P-388 lymphocytic leukemia cells, daphnane diterpene esters

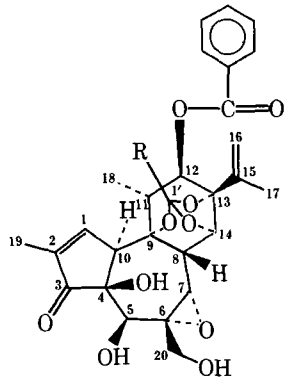

I R = 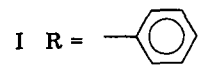

II R = —CH=CH—CH=CH—$(CH_2)_4$—CH_3

Daphnane diterpene esters which possess an isopropylene side chain at C_{13} have previously been reported to have antileukemic activity (1). Genkwadaphnin and yuanhuacine (I and II) are two such esters which have been isolated from *Daphne genkwa* and chemically characterized (2). Genkwadaphnin (I) at 0.8 mg/kg/day was shown to produce a T/C% value of 173, whereas yuanhuacine (II) afforded a value of 151% against P-388 lymphocytic leukemia growth (2). These T/C% values were comparable to 5-fluorouracil at 12.5 mg/kg/day in the P-388 screen. Therefore, it was concluded that daphnane diterpene esters may have potential as antineoplastic therapeutic agents and that their modes of action on cellular metabolism were of interest, particularly since these agents resemble, structurally, phorbol esters which are tumor pro-

0022-3549/82/1200-1340$01.00/0

moting agents that stimulate nucleic acid and protein synthesis.

Previous studies demonstrated that I and II inhibited DNA synthesis after 60 min of incubation, with ID_{50} values of 5.62 and 7.11 μM in P-388 lymphocytic leukemia cells (2). A higher concentration of daphnane diterpene esters was required to observe protein synthesis inhibition of P-388 cells ($ID_{50} \cong$ 14.8 and 18.5 μM) (2). Similar observations in P-388 cells were made when the agents were administered *in vivo*, in that DNA synthesis was inhibited initially, followed by inhibition of protein synthesis at a later time or at a higher dose (2). Since a cursory review of the literature indicates that effects of daphnane diterpene esters on cellular metabolism have not been studied, the purpose of the present investigation is to establish the mechanism of action of I and II as protein synthesis inhibitors.

EXPERIMENTAL

The studies on the effects of daphnane diterpene esters on protein synthesis were conducted on P-388 lymphocytic leukemia cells harvested on day 10 (3) and maintained according to the NIH Protocol (3). P-388 lymphocytic leukemia lysates from DBA/2 male mice (~25 g) were prepared by a previous method (4). The following were isolated from P-388 lysates by literature techniques: ribosomes[1] (5), pH 5 enzyme (4), and uncharged transfer ribonucleic acid (tRNA) (6). The P-388 lymphocytic leukemia cell initiation factors for protein synthesis were prepared as described previously (7). Standard protein synthesis inhibitors were used as a comparison in the assay at concentrations which were known to cause maximum inhibition. Whole cell *in vitro* incorporation of [^{3}H]leucine (56.6 Ci/mmole) into protein was determined with drug concentrations from 0–50 μM in 1 ml of minimum essential medium[2] for 90 min at 37°. Acid insoluble protein was collected on nitrocellulose filters[3] by vacuum suction (8). [^{3}H]Methionyl-transfer ribonucleic acid (met-tRNA) was prepared from P-388 cell tRNA according to a previous method (9). The effects of the diterpene esters on endogenous protein synthesis of P-388 lysates were performed in a reaction mixture (9) (0.5 ml) containing 10 mM tris(hydroxymethyl)aminomethane, pH 7.6, 76 mM KCl, 1 mM adenosine triphosphate, 0.2 mM guanosine triphosphate, 15 mM creatine phosphate, 2 mM $MgCl_2$, 1 mM dithiothreitol, 0.1 mM of each of the 19 essential amino acids, 0.9 mg/ml of creatine phosphokinase, and 20 μCi of [^{3}H]leucine (56.6 Ci/mmole). The reaction mixture was incubated at 30°. After 90 sec of incubation, test drugs or the standards, pyrocatechol violet or emetine, were added with a final concentration of 1, 10, and 100 μM. At specific minute intervals, 50-μl aliquots were removed from the reaction tubes and spotted on filter papers[4] which were treated for 10 min in boiling 5% trichloroacetic acid, followed by 10 min in cold 5% trichloroacetic acid and washed with cold 5% trichloroacetic acid, ether–ethanol (1:1), and ether. The filter papers were dried and counted in scintillation fluid.

The effects of daphnane diterpene esters, pyrocatechol violet, cycloheximide, and emetine on the ribosome profile (8) of P-388 cell lysates were assayed using the reaction medium described above (500 μl). The control tubes, as well as tubes containing standards or drugs affording a 100 μM final concentration, were incubated for 4 min at 37°. The reactions were terminated in ice and gradient buffer (1 ml of tris(hydroxymethyl)aminomethane, pH 7.6, 10 mM KCl, and 1.5 mM $MgCl_2 \cdot 6H_2O$) was added. The mixtures were layered over 36 ml of 10–25% linear sucrose gradient (8), prepared in gradient buffer, and centrifuged for 165 min at 25,000 rpm in a swinging bucket rotor[5] at 4°. The absorbance profiles at 260 nm were determined using a flow cell (light path 0.2 cm) attached to a spectrophotometer[6]. The incorporation of [^{3}H]leucine into polypeptide chains was measured for each fraction.

The reaction medium for the polyuridine-directed polyphenylalanine synthesis (10) contained 50 mM tris(hydroxymethyl)aminomethane, pH 7.6, 12.5 mM magnesium acetate, 80 mM KCl, 5 mM creatine phosphate, 0.05 mg/ml of creatine phosphokinase, 0.36 mg/ml of polyuridine[7] (A_{280}/A_{260} = 0.34), 0.5 μCi of [^{14}C]phenylalanine (536 mCi/mmole), 75 μg of uncharged P-388 cell tRNA, 70 μg of P-388 pH 5 enzyme preparation, and 0.9 A_{260} of P-388 cell ribosomes. Test compounds were present in 5, 10, and 50 μmole concentrations. The tubes were incubated for 20 min at 30° after which a 35-μl aliquot was spotted on filter paper[2] and processed as indicated previously.

The reaction medium (200 μl) used to measure the formation of the 80 S initiation complex and the methionyl puromycin reaction (11) contained 15 mM tris(hydroxymethyl)aminomethane, pH 7.6, 80 mM KCl, 1 mM adenosine triphosphate, 0.5 mM guanosine triphosphate, 20 mM creatine phosphate, 0.2 mg/ml creatine phosphokinase, 3 mM magnesium acetate, 0.1 mM (ethylenedinitrilo)tetraacetic acid, 1 mM dithiothreitol, 0.1 mM of each of the 19 essential amino acids, 3 mg of P-388 cell lysates, 100 μg/ml chlortetracycline[8], 3 × 10^5 cpm of [^{3}H]-met-tRNA, and 20 μg/ml of polyadenosine–uridine–guanosine and 0–50 μM of diterpene esters.

The incubation was carried out at 23°, and after 2 min aliquots were withdrawn to analyze for 80 S complex formation. Puromycin (10 μg/ml) was then added to the reaction medium. The incubation was continued for another 6 min and aliquots were withdrawn to analyze for reaction of the 80 S complex with puromycin. All aliquots (50 μl) were diluted to 250 μl with buffer (20 mM tris(hydroxymethyl)aminomethane, pH 7.6, 80 mM KCl, 3 mM magnesium acetate, 1 mM dithiothreitol, and 0.1 mM (ethylenedinitrilo)tetraacetic acid), layered on 11.8 ml of a 15–30% linear sucrose gradient and centrifuged for 3 hr × 36,000 rpm in a swinging bucket rotor[9]. Fractions (0.4 ml) were collected and protein was precipitated with 10% trichloroacetic acid on filter papers and counted[10].

The reaction mixtures (75 μl) for the ternary complex formation (12) contained 21.4 mM tris(hydroxymethyl)aminomethane, pH 8.0, 80 mM KCl, 0.26 mM guanosine triphosphate, 2.14 mM dithiothreitol, 10 μg of bovine serum albumin, 5 pmoles of P-388 cell [^{3}H]met-tRNA (1 × 10^4 cpm), 100 A_{260}/ml of crude P-388 cell initiation factors, and 25 or 100 μM of drug or standard. The incubation was conducted for 5 min at 37° and terminated by the addition of 3 ml of cold buffer (21.4 mM tris(hydroxymethyl)aminomethane, pH 8.0, 80 mM KCl, 2.14 mM dithiothreitol). The samples were filtered through 0.45-μm nitrocellulose filters, washed twice in buffer, and counted.

The reaction mixture (75 μl) for the 80 S initiation complex (12) formation contained, in addition to the components necessary for the ternary complex formation reaction, 1.9 mM magnesium acetate, 5 A_{260}/ml of polyadenosine-uridine-guanosine[5] and 100 A_{260}/ml of 80 S P-388 cell ribosomes. Incubation was 10 min at 37° which was then cooled to 4°, the samples were diluted with cold buffer (21.4 mM tris(hydroxymethyl)-aminomethane, pH 8.0, 80 mM KCl, 5 mM magnesium acetate, and 2.14 mM dithiothreitol), and filtered as indicated for the ternary complex formation experiment.

RESULTS AND DISCUSSION

Both I and II significantly suppressed *in vitro* whole cell P-388 lymphocytic leukemia protein synthesis (Fig. 1). Compound I afforded an $ID_{50} \simeq 6.7$ μM and compound II an $ID_{50} \simeq 8.9$ μM after 90 min of incubation. The studies on the effects of various concentrations of the diterpene esters on endogenous protein synthesis of P-388 lysates (Fig. 2) demonstrated that at low concentration (1 μM) there was a lag of 2–4 min before the inhibition of protein synthesis was observed. At higher concentrations of drug (10–100 μM), cessation of protein synthesis occurred immediately, suggesting that the diterpene esters mimicked the action of an elongation inhibitor such as emetine, more so than an initiation inhibitor such as pyrocatechol violet.

A comparison of the effects of I and II with known inhibitors of protein synthesis on the ribosome profile and [^{3}H]leucine incorporation into polypeptides can be seen in Fig. 3. During the incubation of the P-388 lymphocytic leukemia cell lysates, [^{3}H]leucine was incorporated into the nascent peptide bound to the polysomes (Fig. 3a). However, when I or II was incubated with the P-388 lysates for 4 min at 100 μM, the radioactive peptides were released from the ribosomes. Clearly, all of the agents suppress polypeptide synthesis observed as reduced leucine incorpora-

[1] Ribosomes dissociated from mRNA, runoff ribosomes, or polysomes.
[2] Eagle growth medium × 1 plus 10% fetal calf serum, penicillin, and streptomycin.
[3] Millipore Corp.
[4] Whatman 3.
[5] Beckman SW 27.
[6] Gilford.
[7] Miles Laboratory Inc.
[8] Sigma Chemical Co.
[9] Beckman SW 40.
[10] Fisher Scintiverse in a Packard Scintillation Counter.

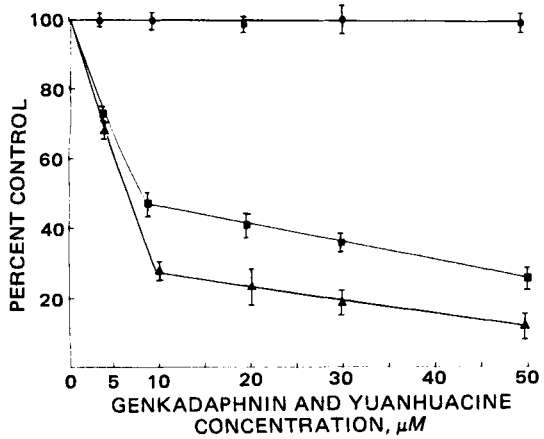

Figure 1—In Vitro *effect of genkwadaphnin and yuanhuacine on whole cells of P-388 lymphocytic leukemia during 90-min incubation with [^{3}H]leucine incorporation* (n = 5). *Key: (●) control; (▲) genkwadaphnin; (■) yuanhuacine.*

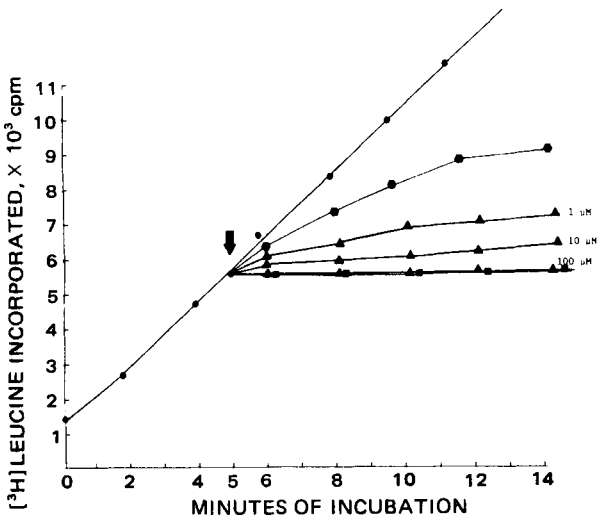

Figure 2a—*Effect of genkwadaphnin on the protein synthesis of P-388 lymphocytic leukemia homogenates using endogenous mRNA* (n = 5). *Key: (●) control; (▲) genkwadaphnin; (■) emetine; (●) pyrocatechol violet; (◗) addition of drug.*

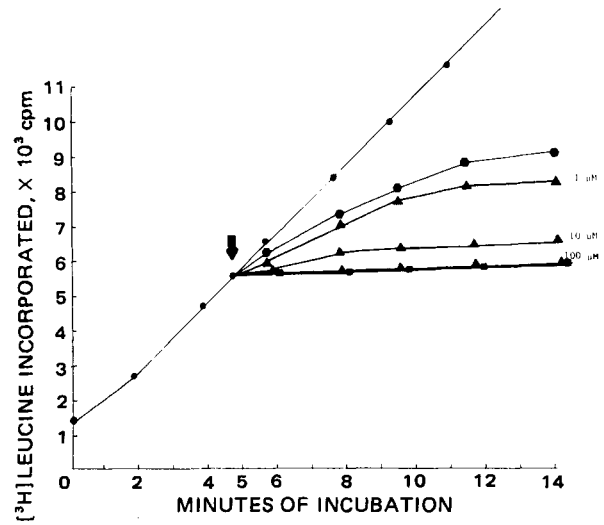

Figure 2b—*Effect of yuanhaucine on the protein synthesis of P-388 lymphocytic leukemia homogenates using endogenous mRNA* (n = 5). *Key: (●) control; (▲) yuanhuacine; (■) emetine; (●) pyrocatechol violet; (◗) addition of drug.*

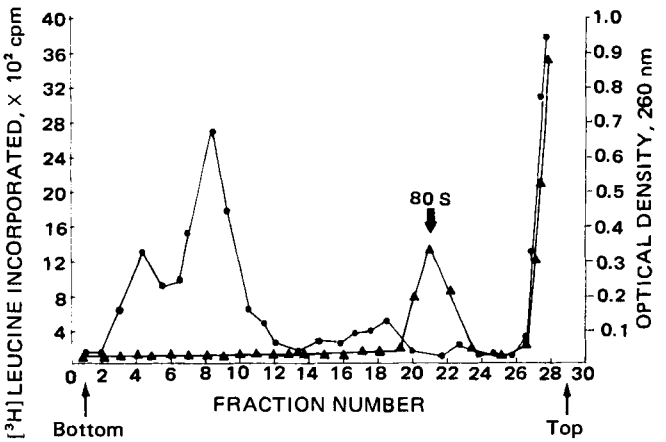

Figure 3a—*Control: Fate of nascent protein on the protein synthesis in P-388 lymphocytic leukemia lysate* (n = 5). *Key: (●) leucine incorporated into polypeptide; (▲) 80 S initiation profile.*

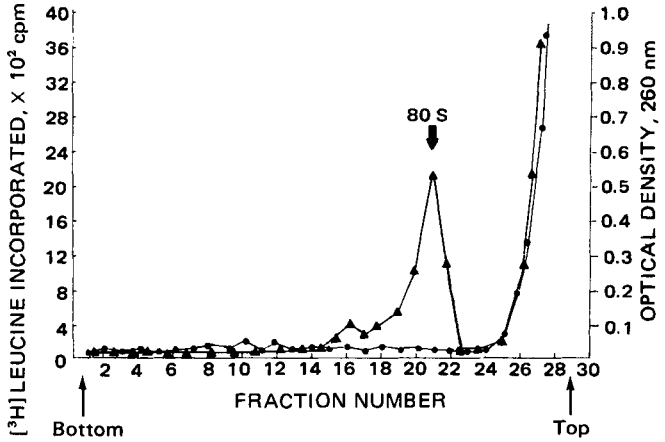

Figure 3b—*Addition of pyrocatechol violet 100 μM. Effect of pyrocatechol violet on polyribosome structure and release of nascent peptides in P-388 lymphocytic leukemia lysate* (n = 5). *Key: (●) leucine incorporated; (▲) 80 S profile.*

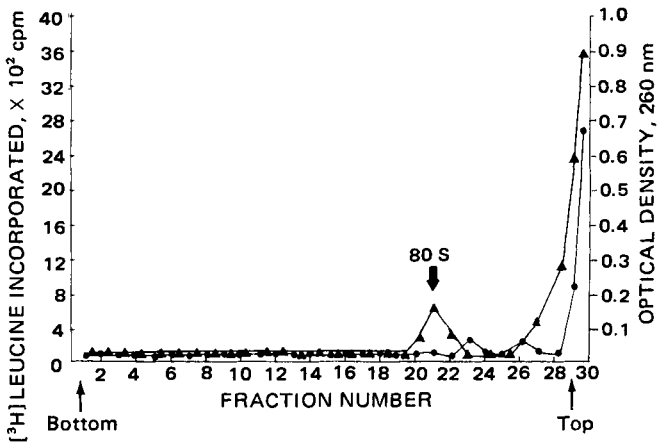

Figure 3c—*Addition of emetine 100 μM. Effect of emetine on polyribosome structure and release of nascent peptide in P-388 lymphocytic leukemia lysate* (n = 5). *Key: (●) leucine incorporated; (▲) 80 S profile.*

tion. The standard, pyrocatechol violet (Fig. 3b), allows completion or release of the nascent polypeptide chain and the accumulation of the 80 S ribosomal peak, whereas emetine (Fig. 3c), I (Fig. 3d), and II (Fig. 3e), do not allow accumulation of the 80 S ribosomal peak which is reduced from the control. These data suggest that the daphnane diterpene esters

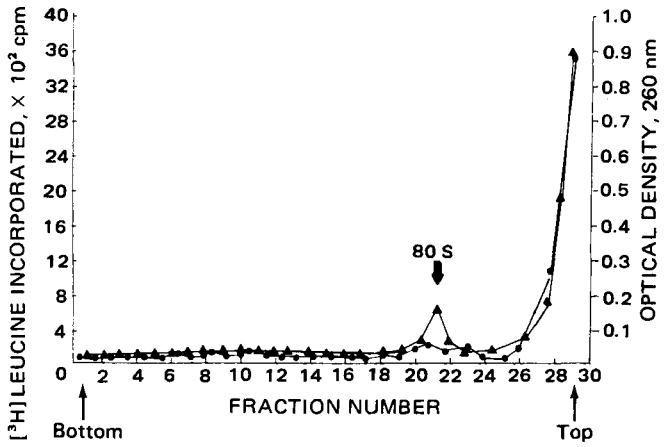

Figure 3d—*Addition of genkwadaphnin 100 μM. Effect of genkwadaphnin on polyribosome structure and release of nascent peptides in P-388 lymphocytic leukemia lysate (n = 5). Key: (●) leucine incorporated; (▲) 80 S profile.*

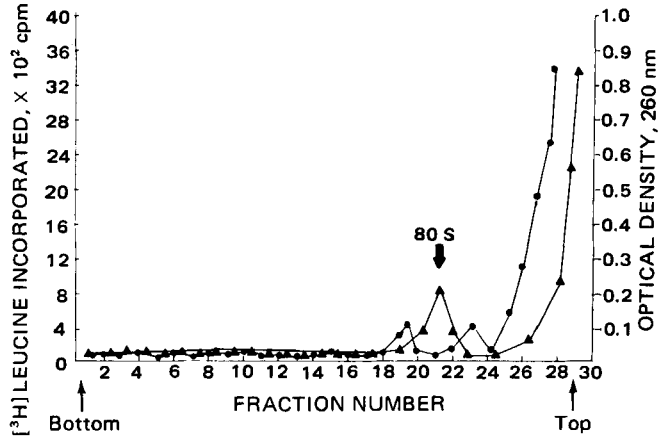

Figure 3e—*Addition of yuanhuacine 100 μM. Effect of yuanhuacine on polyribosome structure and release of nascent peptides in P-388 lymphocytic leukemia lysate (n = 5). Key: (●) leucine incorporated; (▲) 80 S profile.*

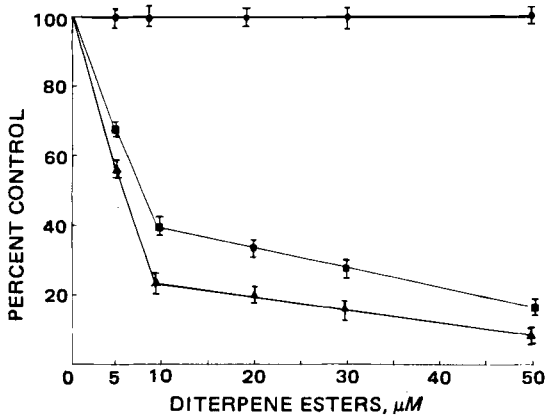

Figure 4—*Effect of genkwadaphnin and yuanhuacine on polyuridine directed poly [³H]phenylalanine synthesis in P-388 run-off ribosomes (n = 5). Key: (●) control; (▲) genkwadaphnin; (■) yuanhuacine.*

are elongation inhibitors of protein synthesis of P-388 lymphocytic leukemia cells at the concentrations employed.

To completely eliminate the possibility that the daphnane diterpene esters were initiation inhibitors, ternary complex[11] formation and the

[11] eIF–guanosine triphosphate–[³H]met-tRNA.

Table I—Effects of Diterpene Esters on Ternary and 80 S Complex Formation of P-388 Cells

	Concentration, μM	Complex Formation, pmoles	Percent of Control
Ternary Complex Formation (N = 6)			
Control	—	2.12 ± 0.08	100
+ Emetine	100	2.06 ± 0.06	97
+ Pyrocatechol violet	100	0.25 ± 0.03	11
+ Aurintricarboxylic acid	50	0.17 ±0 .02	8
+ Genkwadaphnin	25	1.91 ± 0.05	90
	100	1.89 ± 0.06	
+ Yuanhuacine	25	1.95 ± 0.07	92
	100	1.93 ± 0.05	
80 S Initiation Complex Formation (N = 6)			
Control	—	1.26 ± 0.06	100
+ Emetine	100	1.03 ± 0.07	82
+ Pyrocatechol violet	100	0.20 ± 0.02	15
+ Aurintricarboxylic acid	50	0.13 ± 0.03	10
+ Genkwadaphnin	25	1.13 ± 0.05	90
	100	1.14 ± 0.08	
+ Yuanhuacine	25	1.16 ± 0.07	92
	100	1.16 ± 0.06	

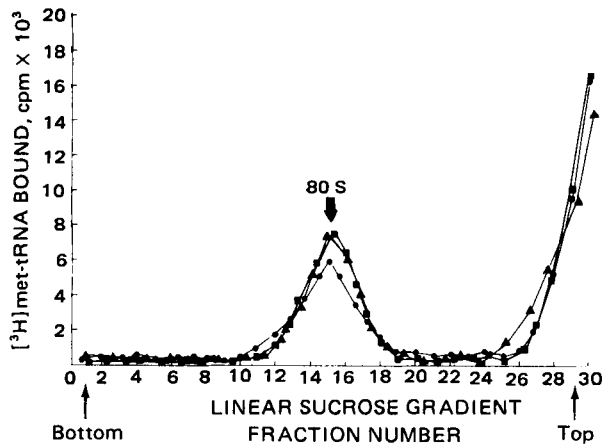

Figure 5a—*Control treated with chlortetracycline. The formation of the 80 S initiation complex of P-388 lymphocytic leukemia lysate (n = 5). Key: (●) control; (▲) genkwadaphnin; (■) yuanhuacine.*

80 S initiation complex[12] studies were performed (Table I) on P-388 lysates, which showed that at 25 and 100 μM concentrations, the diterpene esters had essentially no effect on the initiation steps of polypeptide chain synthesis. Figure 4 illustrates the effects of the diterpene esters on polyuridine directed polyphenylalanine synthesis of purified ribosomes isolated from 10-day P-388 cells. Polyuridine directed polyphenylalanine synthesis does not require the normal initiation and termination reactions of protein synthesis, and thus, agents that block this reaction are considered exclusively elongation inhibitors. At 50 μM, I suppressed polyuridine directed polyphenylalanine synthesis 92%, while II suppressed it 88%. The degree of inhibition of polyuridine synthesis by the diterpene esters was of sufficient magnitude to account for the degree of inhibition alone observed by these esters on whole cell protein synthesis.

In an effort to further evaluate the effects of diterpene esters on the elongation step of peptide synthesis, the formation of the 80 S initiation complex[12] and peptide bond formation were examined by treating the P-388 cell lysates with the elongation inhibitor chlortetracycline which specifically inhibits the binding of aminoacyl-tRNA to the ribosome A site but does not inhibit the peptidyl transferase reaction of elongation. Thus, when [³H]met-tRNA was added to the system, most of the radioactivity was found associated with the 80 S initiation complex. Addition of polyadenosine-uridine-guanosine to the chlortetracycline-treated lysate allows the formation of the 80 S initiation complex (Fig. 5a) which then reacts with puromycin. The puromycin induces the release of

[12] 80 S Adenosine–uridine–guanosine–eIF–guanosine triphosphate–[³H]met-tRNA.

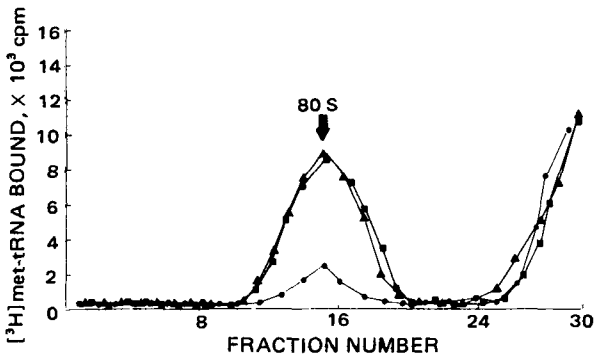

Figure 5b—*Addition of puromycin. Effect of genkwadaphnin and yuanhuacine on the methionyl puromycin reaction of P-388 lymphocytic leukemia lysate (n = 5). Key: (●) control plus puromycin; (▲) genkwadaphnin; (■) yuanhuacine plus puromycin.*

[³H]methionine from the 80 S complex (Fig. 5b). The diterpene esters did not interfere with the formation of a stable 80 S initiation complex but rather inhibited the puromycin release of labeled methionine from the polysome.

These data indicate that I and II similarly block peptide bond formation during elongation peptide chain synthesis. The concentration of drug to block peptide transferase activity was consistent with concentrations required to inhibit whole cell protein synthesis *in vitro*.

The daphnane diterpene esters did not have any significant effects on the individual steps leading to the formation of a stable 80 S initiation complex. The daphnane diterpene esters significantly inhibited both the polyuridine-directed polyphenylalanine synthesis and the formation of the first peptide bond between puromycin and the met-tRNA bound to the 80 S initiation complex. These data strongly indicate that the diterpene esters are potent inhibitors of the peptidyl transferase reaction of the elongation process of protein synthesis of P-388 lymphocytic leukemia cells.

REFERENCES

(1) F. J. Evans and C. J. Soper, *Lloydia*, **41**, 193 (1978).

(2) I. H. Hall, R. Kasai, R. Y. Wu, K. Tagahara, and K. H. Lee, *J. Pharm. Sci.*, **71**, 1263 (1982).

(3) R. I. Geran, N. H. Greenberg, M. M. MacDonald, A. M. Schumacher, and B. J. Abbott, *Cancer Chemother. Res.*, **3**, 9 (1972).

(4) J. Kruh, L. Grossman, and K. Moldave, *Methods Enzymol.*, **XIIb**, 732 (1968).

(5) M. H. Schreier and T. Staehelin, *J. Mol. Biol.*, **73**, 329 (1973).

(6) J. M. Ravel, R. D. Mosteller, and B. Hardesty, *Proc. Natl. Acad. Sci. USA*, **56**, 701 (1966).

(7) A. Majumdar, S. Reynolds, and N. K. Gupta, *Biochem. Biophys. Res. Commun.*, **67**, 689 (1975).

(8) L. L. Liao, S. M. Kupchan, and S. B. Horwitz, *Mol. Pharmacol.*, **12**, 167 (1967).

(9) K. Takeishi, T. Ukita, and S. Nishimura, *J. Biol. Chem.*, **243**, 5761 (1968).

(10) J. Jimenez, A. Sanchez, and D. Vasquez, *Biochem. Biophys. Acta*, **383**, 4271 (1975).

(11) J. Carter and M. Cannon, *Eur. J. Biochem.*, **84**, 103 (1978).

(12) S. H. Reynolds, A. Majumdar, A. Das Gupta, S. Palmieri, and N. K. Gupta, *Arch. Biochem. Biophys.*, **184**, 324 (1977).

ACKNOWLEDGMENTS

Supported by American Cancer Society Grant CH-19 (K. H. Lee and I. H. Hall), American Cancer Society Institutional Grant (UNC) (I. H. Hall), and National Cancer Institute Grant CA 17625 (in part) (K. H. Lee).

The authors thank Dr. Steven G. Chaney, Department of Biochemistry, for his advice on procedure and Dr. E. S. Huang of the Department of Virology, School of Medicine, University of North Carolina at Chapel Hill for the use of the sucrose gradient system and technical assistance for the completion of this research project.

Bayesian Individualization of Pharmacokinetics: Simple Implementation and Comparison with Non-Bayesian Methods

LEWIS B. SHEINER ˣ and STUART L. BEAL

Received October 18, 1981 from the *Department of Laboratory Medicine and Division of Clinical Pharmacology, Department of Medicine, University of California, San Francisco, CA 94143.* Accepted for publication February 1, 1982.

Abstract □ One may attempt to individualize drug dosage by estimating an individual's pharmacokinetic parameters. Information useful for this purpose consists of certain population pharmacokinetic parameters (notably those describing the typical relationship between dosage and drug concentrations) and also measured drug concentrations from the individual of concern. Both types of information should be used. A (Bayesian) method that does so has been described in the pharmacokinetic literature. In this report an implementation of the Bayesian method that is readily adapted to a microcomputer is presented. Using simulated data it is compared with two other methods proposed by others, for estimating individual theophylline clearances. Both previously suggested methods are shown to be less precise than the Bayesian method: their typical error magnitudes are 20–70% larger.

Keyphrases □ Bayesian method—individualization of pharmacokinetics, simple implementation and comparison with non-Bayesian methods, theophylline □ Pharmacokinetics—Bayesian individualization, simple implementation and comparison with non-Bayesian methods, theophylline □ Theophylline—Bayesian individualization of pharmacokinetics, simple implementation and comparison with non-Bayesian methods

A great deal of attention has been given to the problem of estimating the pharmacokinetic parameters of individual patients in order to optimize dosage choices. Initially, most attention has been directed at obtaining estimates of individual parameters from the population information relating kinetics to certain patient features (sex, age, renal function, *etc*). More recently, considerable attention has been directed at the estimation of parameters using measured drug levels (1–4).

One particular method, the Bayesian method (3), is intuitively appealing. It involves a continuously changing view of the patient. Before any drug levels are measured,

0022-3549/82/1200-1344$01.00/0

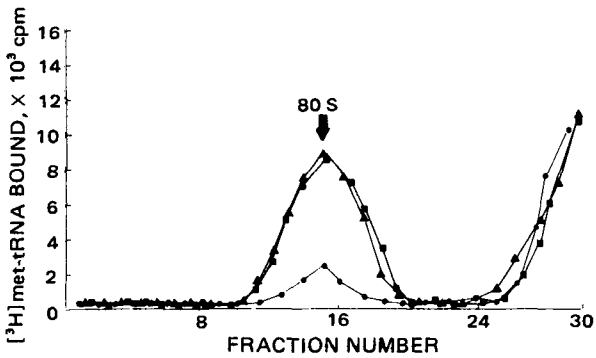

Figure 5b—*Addition of puromycin. Effect of genkwadaphnin and yuanhuacine on the methionyl puromycin reaction of P-388 lymphocytic leukemia lysate (n = 5). Key: (●) control plus puromycin; (▲) genkwadaphnin; (■) yuanhuacine plus puromycin.*

[³H]methionine from the 80 S complex (Fig. 5b). The diterpene esters did not interfere with the formation of a stable 80 S initiation complex but rather inhibited the puromycin release of labeled methionine from the polysome.

These data indicate that I and II similarly block peptide bond formation during elongation peptide chain synthesis. The concentration of drug to block peptide transferase activity was consistent with concentrations required to inhibit whole cell protein synthesis *in vitro*.

The daphnane diterpene esters did not have any significant effects on the individual steps leading to the formation of a stable 80 S initiation complex. The daphnane diterpene esters significantly inhibited both the polyuridine-directed polyphenylalanine synthesis and the formation of the first peptide bond between puromycin and the met-tRNA bound to the 80 S initiation complex. These data strongly indicate that the diterpene esters are potent inhibitors of the peptidyl transferase reaction of the elongation process of protein synthesis of P-388 lymphocytic leukemia cells.

REFERENCES

(1) F. J. Evans and C. J. Soper, *Lloydia*, **41**, 193 (1978).

(2) I. H. Hall, R. Kasai, R. Y. Wu, K. Tagahara, and K. H. Lee, *J. Pharm. Sci.*, **71**, 1263 (1982).

(3) R. I. Geran, N. H. Greenberg, M. M. MacDonald, A. M. Schumacher, and B. J. Abbott, *Cancer Chemother. Res.*, **3**, 9 (1972).

(4) J. Kruh, L. Grossman, and K. Moldave, *Methods Enzymol.*, **XIIb**, 732 (1968).

(5) M. H. Schreier and T. Staehelin, *J. Mol. Biol.*, **73**, 329 (1973).

(6) J. M. Ravel, R. D. Mosteller, and B. Hardesty, *Proc. Natl. Acad. Sci. USA*, **56**, 701 (1966).

(7) A. Majumdar, S. Reynolds, and N. K. Gupta, *Biochem. Biophys. Res. Commun.*, **67**, 689 (1975).

(8) L. L. Liao, S. M. Kupchan, and S. B. Horwitz, *Mol. Pharmacol.*, **12**, 167 (1967).

(9) K. Takeishi, T. Ukita, and S. Nishimura, *J. Biol. Chem.*, **243**, 5761 (1968).

(10) J. Jimenez, A. Sanchez, and D. Vasquez, *Biochem. Biophys. Acta*, **383**, 4271 (1975).

(11) J. Carter and M. Cannon, *Eur. J. Biochem.*, **84**, 103 (1978).

(12) S. H. Reynolds, A. Majumdar, A. Das Gupta, S. Palmieri, and N. K. Gupta, *Arch. Biochem. Biophys.*, **184**, 324 (1977).

ACKNOWLEDGMENTS

Supported by American Cancer Society Grant CH-19 (K. H. Lee and I. H. Hall), American Cancer Society Institutional Grant (UNC) (I. H. Hall), and National Cancer Institute Grant CA 17625 (in part) (K. H. Lee).

The authors thank Dr. Steven G. Chaney, Department of Biochemistry, for his advice on procedure and Dr. E. S. Huang of the Department of Virology, School of Medicine, University of North Carolina at Chapel Hill for the use of the sucrose gradient system and technical assistance for the completion of this research project.

Bayesian Individualization of Pharmacokinetics: Simple Implementation and Comparison with Non-Bayesian Methods

LEWIS B. SHEINER ˣ and STUART L. BEAL

Received October 18, 1981 from the *Department of Laboratory Medicine and Division of Clinical Pharmacology, Department of Medicine, University of California, San Francisco, CA 94143.* Accepted for publication February 1, 1982.

Abstract □ One may attempt to individualize drug dosage by estimating an individual's pharmacokinetic parameters. Information useful for this purpose consists of certain population pharmacokinetic parameters (notably those describing the typical relationship between dosage and drug concentrations) and also measured drug concentrations from the individual of concern. Both types of information should be used. A (Bayesian) method that does so has been described in the pharmacokinetic literature. In this report an implementation of the Bayesian method that is readily adapted to a microcomputer is presented. Using simulated data it is compared with two other methods proposed by others, for estimating individual theophylline clearances. Both previously suggested methods are shown to be less precise than the Bayesian method: their typical error magnitudes are 20–70% larger.

Keyphrases □ Bayesian method—individualization of pharmacokinetics, simple implementation and comparison with non-Bayesian methods, theophylline □ Pharmacokinetics—Bayesian individualization, simple implementation and comparison with non-Bayesian methods, theophylline □ Theophylline—Bayesian individualization of pharmacokinetics, simple implementation and comparison with non-Bayesian methods

A great deal of attention has been given to the problem of estimating the pharmacokinetic parameters of individual patients in order to optimize dosage choices. Initially, most attention has been directed at obtaining estimates of individual parameters from the population information relating kinetics to certain patient features (sex, age, renal function, *etc*). More recently, considerable attention has been directed at the estimation of parameters using measured drug levels (1–4).

One particular method, the Bayesian method (3), is intuitively appealing. It involves a continuously changing view of the patient. Before any drug levels are measured,

0022-3549/82/1200-1344$01.00/0

the patient is regarded as a typical member of the population of all similar patients with respect to pharmacokinetic parameter values. Once considerable drug level information has become available, the patient is regarded as a unique individual whose pharmacokinetic parameters are distinct from other patients. The point of view is continuously shifted from the first one to the second one as drug level information accumulates.

In this report, a method for implementing the Bayesian approach is outlined that involves only a simple modification of any standard nonlinear least-squares fitting procedure (see *Appendix*). Then, using simulated data, the Bayesian method is compared with two other methods for estimating individual theophylline clearances.

THEORETICAL

Implementation—The basic model used here for the observations of an individual is:

$$y_i = f(P,X_i) + \epsilon_i \qquad \text{(Eq. 1)}$$

where y_i is the ith drug level, $P = (p_1,p_2,\ldots p_s)$ is the vector of the s pharmacokinetic parameters of the model for the individual, X_i is the vector of independent variables (such as time, dose) associated with y_i, and ϵ_i is statistical error that includes measurement error and random intraindividual kinetic variability over time.

The errors, ϵ_i, are assumed to be independent, with zero mean and common variance, σ^2, assumed known. The vector of individual parameters, P, is regarded as arising randomly from a population of such vectors (one for each individual of the population). For each $1 \leq k \leq s$, the population mean and variance of the p_k are the known quantities, θ_k and ω_k^2, respectively. They are obtained presumably from a population study of the drug in question. The assumption allowing for the simplicity of the implementation to be described is that the p_k are pairwise uncorrelated in the population. For convenience, θ will denote the vector $(\theta_1,\theta_2,\ldots\theta_s)$ and Ω will denote the vector $(\omega_1^2,\omega_2^2,\ldots\omega_s^2)$.

When faced with y_i, $i = 1, n$ observations of drug levels, the usual approach is to estimate P using ordinary least squares (OLS). The ordinary least-squares estimate of P, $\hat{P}_{OLS}$, is that value of P minimizing the ordinary least-squares objective function:

$$O_{\text{OLS}}(P) = \sum_{i=1}^{n} (y_i - \hat{y}_i)^2 \qquad \text{(Eq. 2)}$$

where

$$\hat{y}_i = f(P,X_i) \qquad \text{(Eq. 3)}$$

We shall call the $\hat{y}_i$ prediction functions.

The ordinary least-squares estimate minimizes the squared errors between the observations and the prediction functions. Call these squared errors of the first kind.

If the only observations available for estimating P were those of y_i, $\hat{P}_{\text{OLS}}$ would be a natural estimate. However, there are other available observations—the elements of θ, obtained from the population study of the drug. Define $\eta = \theta - P$ to be the vector of differences between the population mean parameters (θ) and each individual's parameters (P). Then, for each k:

$$\theta_k = p_k + \eta_k \qquad \text{(Eq. 4)}$$

Just as Eq. 1 says that the drug level observations (y_i) are equal to prediction functions $f(P,X_i)$, themselves functions of the unknown individual parameters (P) plus a random error (ϵ_i) with known variance (σ^2), so Eq. 4 says that the population observations (θ_k) are equal to prediction functions (p_k) trivial functions of P, plus a random error (η_k) with known variance (ω_k^2). Therefore, the estimate of P should attempt to minimize the squared errors between these population observations and their prediction functions, as well as those of the first kind.

When faced with observations having different error variances, it is customary to estimate parameters using weighted least-squares (WLS). The weighted least squares estimate of P,$\hat{P}_{\text{WLS}}$, is that value of P minimizing

$$O_{\text{WLS}}(P) = \sum_{i=1}^{n} \frac{(y_i - \hat{y}_i)^2}{\sigma^2} + \sum_{k=1}^{s} \frac{(\theta_k - p_k)^2}{\omega_k^2} \qquad \text{(Eq. 5)}$$

Statistical theory states that with different error variances, weighted least-squares estimates are more efficient (and possibly less biased) than ordinary least-squares estimates.

The same estimator ($\hat{P}_{\text{WLS}}$) can be as justified as a Bayesian estimator when a somewhat different line of argument is pursued (3). The authors prefer, therefore, to call the set of parameter values that minimize the expression (5) the Bayesian estimates. The weighted least-squares justification, however, leads directly to a simple practical implementation of the method. The implementation requires only a slight modification of any standard nonlinear weighted least-squares fitting algorithm. The details are presented in the *Appendix* to this paper. The essence of the method is straightforward: the list of data (y_i, $i = 1, n$) is lengthened to include the additional values of $\theta_1,\ldots\theta_s$. The weights for y_i, $i = 1, n$ are set to $1/\sigma^2$, and those for the additional s observations are set to $1/\omega_k^2$, $k = 1, s$. Finally, the user-supplied subroutine that computes and returns $\hat{y}_i$ (required by all nonlinear least-squares programs) is modified to return the current estimate of p_k when called upon to predict the kth additional observation.

A slight modification of the basic approach (see *Appendix*) deals with the special case of uncertain dosage. It may sometimes happen that there is uncertainty about the prior dose history (perhaps because the patient was an outpatient) but that an initial drug level is available so that the dose history for all subsequent levels is known (perhaps because the patient became an inpatient). It may then be preferable to initialize to the first level as suggested in a previous approach (1), to be discussed further in *Examples*. To accommodate this case in the Bayesian approach, a revised model is written that treats the true unknown initial level as another unknown parameter (p_{s+1}) and predicts observations as a function of time and dosage only after that level (see *Examples*). Logically, however, the (measured) initial level may deviate from its true value (p_{s+1}) as much as any other measured level deviates from its predicted value. To allow this, the variance of the error between the observed initial level and p_{s+1} is given by $\omega_{s+1}^2 = \sigma^2$.

Examples—Two examples of common clinical pharmacokinetic situations, the estimation problem for each of which has been approached by other workers, are presented in detail here. The Bayesian method is compared with those other methods using simulated data.

The following are some aspects common to both. The drug used for illustration in both cases is theophylline. The basic pharmacokinetic model for its disposition is the one-compartment model. This model, when used only for intravenous doses has two parameters, volume of distribution (Vd) and clearance (Cl). An initial level, if present in the model, constitutes a third parameter. A reparameterization is used; the new parameters are $p_1 = \log Vd$, $p_2 = \log Cl$, and p_3 = initial level. Logs of Vd and Cl are used because choosing a symmetrical population distribution for them (*e.g.*, the normal) imparts a skewed distribution to Vd and Cl, which accords well with actual experience.

The data used to test the various approaches were simulated. For each example, one hundred pairs of individual clearance (Cl) and volume of distribution (Vd) values were chosen at random. The parameters, p_1 and p_2 for each case, were chosen randomly from normal distributions with means of θ_1 = log (0.5 liters/kg), θ_2 = log (0.052 liters/kg/hr), respectively, (5, 6). The standard deviation of the distribution of the log of a random quantity is approximately equal to the coefficient of variation of the quantity itself. The standard deviations (coefficients of variation of Vd and Cl) used in simulating p_1 and p_2 values were ω_1 = 32% for p_1 and ω_2 = 44% for p_2 (6). Every choice of p_1 and p_2 gave rise to a choice of Vd and Cl by exponentiation. The simulated Vd and Cl values were substituted into pharmacokinetic equations to obtain simulated true drug levels. Random normally distributed errors (ϵ) were then added to these true levels to arrive at simulated observed levels. The ϵ were chosen to have mean zero and standard deviations equal to 1 mg/liter (corresponding to a coefficient of variation of 10% at a typical concentration of 10 mg/liter). The random numbers needed for the simulations were obtained using standard methods (7, 8).

Two estimation methods are applied in each example: the Bayesian method and one of the alternative methods proposed by others and described below. In both examples only clearance is estimated. Each method is used to estimate the clearance of each of the 100 simulated patients, using whatever population parameters the method may entail and the simulated drug level(s). The Bayesian method proceeds by a numerically minimizing expression (5). On the other hand, the alternative methods estimate clearance from the available data using simple direct formulas. The estimate of clearance by any method is denoted $\hat{Cl}$.

The Bayesian method depends on population parameters (standard deviations, ω_1 and ω_2) not used by the other methods. The Bayesian method naturally behaves best when it is provided with the standard

Table I—Performance of Clearance Estimation Methods

Method	$\frac{\omega_{Cl}}{\sigma}$[a]	$\frac{\omega_{Vd}}{\sigma}$[a]	Mean Clearance Error (±*SEM*) as Percent of Mean Clearance: Error, Example 1	Error, Example 2	Absolute Error, Example 1	Absolute Error, Example 2
Alternative	—	—	−5.77(5.8)	−2.82(3.3)	37.1(4.5)	26.4(2.1)
Bayesian	1	1	−1.02(3.0)	−1.08(3.1)	22.2(2.0)[b]	21.7(2.2)[b]
	3/2	1	−4.94(3.4)	−3.77(3.0)	25.6(2.3)[b]	23.1(2.1)[b]
	2/3	1	5.02(3.2)	2.52(3.4)	23.7(2.2)[b]	23.5(2.4)
	1	3/2	0.44(3.0)	−0.26(3.1)	22.5(2.1)[b]	21.4(2.2)[b]
	1	2/3	−0.76(3.0)	−1.56(3.1)	22.5(1.9)[b]	21.7(2.2)[b]

[a] Ratio of standard deviation of clearance (or Vd) to σ used in the Bayesian method. All ratios are divided by the correct ratio so that a value of unity signifies that the correct ratio itself was used. [b] Mean absolute error of Bayesian method less than that of alternative ($p < 0.05$).

deviations actually used to simulate the data. To test its robustness, the Bayesian method was applied five times: once with the true (simulation) standard deviations, once with the ratio of ω_1 to σ assumed to be 3/2 times its true value, once with the ratio assumed to be 2/3 times its true value, and once each for the same changes in the assumed ratio of ω_2 to σ.

To assess the absolute and relative performance of the estimation methods the differences may be examined between estimates of clearances and their true (simulation) values. For each estimation method, the mean error, defined as the mean of the differences between the true clearances and the estimated values, measures the bias of the method. The mean absolute error, defined as the mean of the absolute values of the errors, can be used to measure precision. The relative precision of two methods can be assessed using a paired t-test on the paired absolute errors (*i.e.*, on the value of the absolute error of the first method minus that of the second method). If the mean difference is significantly greater than (less than) zero, the first method is less (more) precise than the second method. It remains only to explain how $f(P,X_i)$ is computed for the Bayesian method, and for the alternative methods, how $\hat{Cl}$ is computed. These definitions follow.

Example 1—A method has been proposed (2) to estimate the maintenance dose required to achieve a target plasma concentration of drug. This method uses the observation of a single drug level after a test dose of drug. Since the maintenance dose must be proportional to individual clearance, the proposal amounts to a method to estimate individual clearance from a single drug level measurement. The appropriate pharmacokinetic model for the single true drug level is:

$$f(P,X) = W = \frac{d}{t_1 Cl}[1 - \exp(-kt_1)]\exp(-k(t_2 - t_1)) \quad \text{(Eq. 6)}$$

where the subscript i has been suppressed, d is the size of the test dose [according to the previous suggestion (2), taken to be 5 mg/kg], t_1 is the duration of the test infusion (0.5 hrs), t_2 is the sampling time for the drug level (6 hr), and k is the ratio of Cl to Vd. The simulated observed level, y, is equal to W plus a randomly chosen value for ϵ.

Using the relationship suggested previously (2), and adjusting its constants so that it estimates clearance, rather than maintenance dose, this method becomes:

$$Cl = 0.266\exp(-0.311\,y) \quad \text{(Eq. 7)}$$

Example 2—A method has been proposed (1) for estimating individual theophylline clearance using one drug level measured shortly after a maintenance infusion has begun (and perhaps shortly after a loading infusion has terminated) and another level measured some hours later. Two drug levels are used, but the first one is regarded as an initial level so that prior dosage may be regarded as unknown. Since both levels are assumed to be measured, errors in both of them must be simulated. Accordingly, the appropriate pharmacokinetic model for the first true drug level is:

$$f(P,X_1) = W_1 = \frac{d}{Vd}\exp(-kt_1) + \frac{R}{Cl}[1 - \exp(-kt_1)] \quad \text{(Eq. 8)}$$

where, for convenience, the initial loading dose, d (5.6 mg/kg), is assumed to be given by an infusion rapid enough so that its contribution to the level measured at time t_1 (2 hr later) may be predicted by a bolus-dose model; R is the maintenance infusion rate, set equal to 0.52 mg/kg/hr so as to result in a typical steady-state concentration of 10 mg/liter; and k is Cl/Vd.

The second true level is modeled as:

$$f(P,X_2) = W_2 = W_1\exp(-kt_2) + \frac{R}{Cl}[1 - \exp(-kt_2)] \quad \text{(Eq. 9)}$$

where t_2 is the time at which y_2 is sampled, measured as the time since t_1. This time is varied randomly from patient to patient according to a normal distribution with a mean of 5 hr, and a standard deviation of 2 hr (but values <3 hr were discarded). These sampling times are in accordance with previous suggestions (1) for sampling times. (Note that for the Bayesian method, the third parameter to be estimated is simply W_1, the true first level.) The simulated observed levels, y_1 and y_2, are obtained from W_1 and W_2 by adding randomly chosen errors ϵ_1 and ϵ_2, respectively.

Clearance is predicted (1) from:

$$\hat{Cl} = \frac{2R}{(y_1 + y_2)} + \frac{2\exp(\theta_1)(y_1 - y_2)}{t_2(y_1 + y_2)} \quad \text{(Eq. 10)}$$

Note that a single population parameter, θ_1, is used here.

RESULTS

Both examples can be discussed together, since the results are quite similar.

Table I presents the performance of the Bayesian and alternative estimation methods for both examples. In Table I, the mean (estimation) error and absolute error for clearance, and their standard errors, are expressed as percentages of the (approximate) population mean clearance, 0.052 liter/hr/kg. The performance of the Bayesian method is shown for all five cases tested: the case in which the method was supplied with the correct ratios of the ω's to σ and the four cases in which incorrect ratios were used. None of the Bayesian performances nor those of the alternative methods exhibited substantial bias (*i.e.*, mean errors were relatively small and in all cases were within two standard errors of zero).

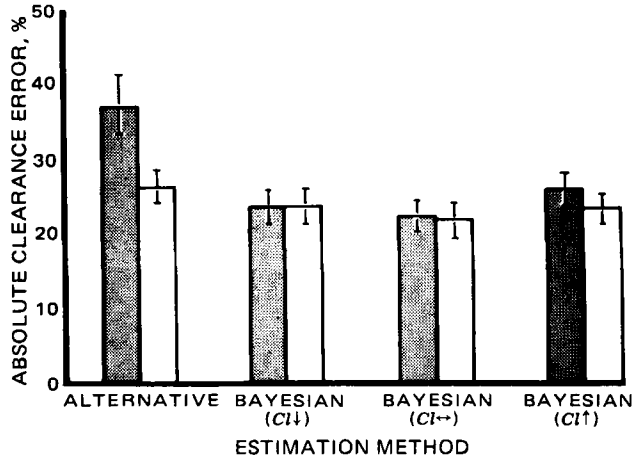

Figure 1—*The mean percent absolute error (true clearance minus predicted clearance expressed as a percent of the population mean clearance) for predictions by the alternative methods and the Bayesian method are shown. Dark bars refer to example 1. Clear bars refer to example 2. Lines at tops of bars show the 95% confidence intervals for the mean percent absolute errors. Three performances for the Bayesian method are shown; the center one (Cl ↔) corresponds to adjusting clearance in correct proportion to differences between observed and predicted levels. The performance marked Cl↓ (Cl↑) refers to clearance predictions made when adjusting clearance less (more) than appropriate. The absolute error of the Bayesian method is significantly smaller ($p < 0.05$) than that of the alternative method for all but the clear bar, Cl↓ case.*

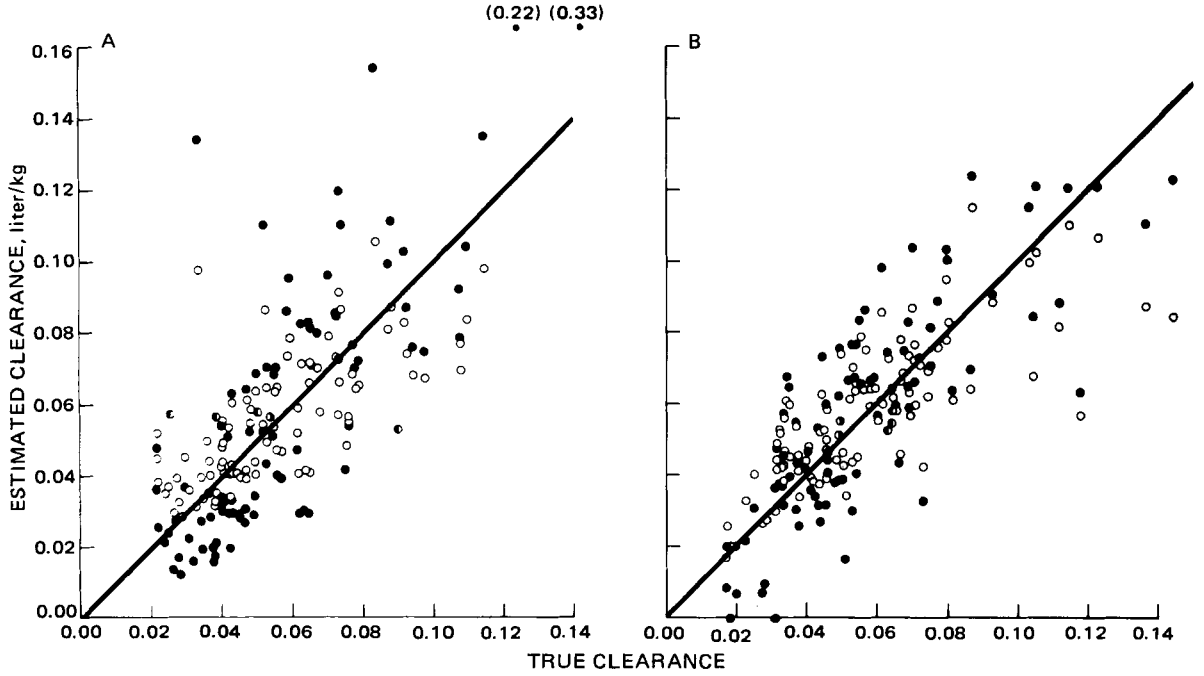

Figure 2—*Plots of predicted clearance* versus *true (simulated) clearance for predictions by the Bayesian (○) and alternative (●) methods. The diagonal line on each graph is the line of identity. A shows results for example 1; B shows results for example 2.*

The results for precision (absolute error) are different. The precision of the Bayesian method estimates typically exceeded that of the alternative method estimates. This was true whether or not the Bayesian method standard deviation ratios were correct or not, although some degradation of performance with incorrect ratios was seen. In the first example, the absolute errors of the alternative method were typically 50–70% larger than those of the Bayesian method, while in the second they were 10–25% larger.

Figure 1 illustrates the precision results of Table I. For the Bayesian method, the cases in which the ratio of ω_1 to σ was incorrect are not shown, as the performances in those cases were little different from those in which the correct ratios were used (Table I).

Figure 2 shows the predictions of the Bayesian and alternative methods for all 100 simulated points for both examples.

DISCUSSION

Various methods for revising estimates of individual pharmacokinetic parameters based on measured drug levels have been put forward. Most previously suggested methods for doing so can be criticized for not attempting to integrate already available information regarding population pharmacokinetic behavior with the information from the observed drug concentrations. A previous study (3) has pointed out that such behavior is not optimal, and has presented a general (Bayesian) framework that allows use of all available information at all times.

In this paper the Bayesian method is seen as an example of weighted least-squares estimation. This leads directly to a simple implementation of the method involving only minor modifications to any standard nonlinear weighted least-squares computer program (see *Appendix*).

In this paper the Bayesian approach has been applied to simulated data, representing two dosage adjustment examples for which other investigators have proposed alternative approaches. In both cases, the Bayesian method is superior to the alternative. Moreover, the former is relatively insensitive to major inaccuracies in some of the parameters it uses. This finding supports the suggestion (see *Appendix*) to use approximate values for those parameters when their true values are in doubt.

Regarding the simulations, one further point merits comment. The similarity of the magnitude of the errors for the Bayesian method in the first and second examples may, at first, seem surprising, since the first example uses only one measured level, while the second uses two. However, it should be recalled that the first level in the second example essentially substitutes for knowledge of initial dosage so that all the drug level information, *per se*, is actually confined to the second level.

Regarding the generality of the Bayesian approach, the basic method can be extended to arbitrary dosage and blood sampling patterns (9), numbers of samples, and pharmacokinetic models (10). In contrast, most other estimation methods, including the alternative ones evaluated herein, apply only to specific models or dosage patterns.

Regarding the theoretical advantages of the Bayesian approach, the most important one is its use of population information at all times. By using population information even when individual observations are available, the Bayesian method must perform better than methods that do not. Figure 2 illustrates this point. The clearance estimates from the Bayesian method seen there tend to err in the direction of the population mean (for true clearances less than the mean, Bayesian estimates tend to be high, and *vice versa*), while those of the alternative methods do not demonstrate this tendency. Rather, they can be quite erratic and have large associated errors. See the off-scale points in Fig. 2A. Even when absolute error is modest, the non-Bayesian estimates can be quite misleading. See the several instances in Fig. 2B where clearance is estimated by a previous method (1) to be at or near zero. The first example is an instance in which random error causes the observed levels to differ greatly from the corresponding true levels. The second occurs when the error, no matter what its magnitude, represents a large fraction of the true difference, which itself may be quite small. The non-Bayesian methods trust the observations implicitly, and will often magnify small differences from expectation in these so as to produce large estimation errors. In contrast, the Bayesian method discounts observations, the more so the more they are in conflict with (prior) parameter expectations. In some cases this conservatism will mean that a parameter truly different from expectation will be incorrectly regarded as closer to expected than it really is—at least until further drug levels are obtained. The incorrect discounting of truly unusual responses is more than compensated by the correct tendency to discount falsely unusual ones. Indeed, the Bayesian method is likely to perform well in precisely those circumstances in which other methods do not perform well: when observed drug levels actually provide little information about the parameters of interest.

APPENDIX

Implementation of the Bayesian method involves the use of suitable computer programs. The availability of a computer program that can perform parameter estimation using nonlinear weighted least squares is assumed[1]. Although large programs running on large machines are often

[1] A users manual and listings of computer programs that implement the above approach on a microcomputer are available. The authors should be contacted for information on obtaining these items.

used for this purpose [*e.g.*, NONLIN (11)], short programs that run on a microcomputer are also available (12).

Nonlinear weighted least-squares programs usually require at least the following: (*a*) data, consisting of a series of observations, $Z = (Z_1,Z_2,\ldots Z_N)$ and corresponding weights, $W = (W_1,W_2,\ldots W_N)$; (*b*) a subroutine that for each Z_i accepts as arguments a list of independent variable values (X_i) and a list of current parameter estimates (P), and produces as output, a prediction ($\hat{Z}_i$) of Z_i, as a function $[f(P,X_i)]$ of its arguments. Some programs are less sophisticated than others and restrict one to scalar X_i, usually denoting time, t_i. The following procedure for specifying (*a*) and (*b*) for a nonlinear weighted least-squares program is designed to function even with that restriction. These programs will also require other arguments, such as the maximum number of iterations allowed, the convergence criterion, *etc.* Specification of these is no different for the current application than it is for the usual ones.

It is assumed that there are N observations of drug levels, and s pharmacokinetic parameters to be estimated ($s + 1$ estimates are needed when an initial level is used). Further, it is assumed for now that the vector of mean population parameters, θ, is known as is ω_1 through ω_s and σ^2.

Any nonlinear weighted least-squares program can be used to find the P minimizing expression (5), by fulfilling requirements (*a*) and (*b*), as follows:

(*a*) The data: There are a total of $N + s$ observations. For $i = 1,\ldots,N$, let $Z_i = y_i$ and $W_i = 1/\sigma^2$. For $i = N + 1,\ldots,N + s$, let $Z_i = \theta_k$ and $W_i = 1/\omega_k^2$, where $k = i - n$.

(*b*) The subroutine: Let one component of X_i, X_{li}, say, be defined by $x_{li} = t_i$ if $i \leq n$ and $X_{li} = -(i - N)$ if $i > N$. Then the subroutine should return $\hat{Z}_i = f(P,X_i)$ if $X_{li} \geq 0$, but it should return $\hat{Z}_i = p_k$ where $k = -X_{li}$, if $X_{li} < 0$.

When the initial level idea is to be used, one does not regard the initial level as one of the N others. Rather, one modifies the data by adding observation number $N + s + 1$, corresponding to the new parameter, number $s + 1$. Then for $i = N + s + 1$, $Z_i = y_0$, $W_i = 1/\sigma^2$ and $X_{li} = -(s + 1)$, where y_0 is the measured value of the initial level. The subroutine need not be modified from its specification above.

The sole remaining problem is that of obtaining values for the population parameters, σ^2, θ, and ω_1 through ω_s. Methods for analyzing patient data in order to estimate population parameters have previously been presented [*e.g.*, (13)]. Many investigators have studied normal volunteers or selected patient populations and have published equations that predict average pharmacokinetic parameters as a function of body weight, renal function, and other factors. Recently, a compilation of such parameters for selected drugs has been assembled (14).

Available information, however, is often of varying quality and completeness. In particular, estimates of ω_1 through ω_s and σ^2 are least available, and, when available, least reliable. When this is the case, it is proposed not that the Bayesian method be abandoned, but that certain rules of thumb be used. For many pharmacokinetic parameters, a coefficient of variation, CV_1, of interindividual variability that is on the order of 25–50% is not uncommon, with volume of distribution often at the lower value and clearance at the upper (12). This variability is present after correcting for age, sex, renal function, and other observable patient features. A reasonable coefficient of variation, CV_2, of y, given P, is often 5–15%, since the ϵ error includes not only assay error but model misspecification error and error due to intraindividual kinetic variability. To compute an estimate of ω_k^2 and σ^2, the only further information needed are the values of θ_k and a typical value for y, a value in the therapeutic range; let the latter be denoted $\tilde{y}$. Then, for example, for $CV_2 = 10\%$, $\sigma^2 = (0.1\tilde{y})^2$, and for $CV_1 = 50\%$, $\omega_k^2 = (0.5\theta_k)^2$.

It is the author's experience that the Bayesian estimates are not too sensitive to the choices involved in this rule of thumb, while the ordinary least-squares estimates can be rather poor in comparison when sample size, N, is small. Of course when $N < s$, the ordinary least-squares estimates do not exist, whereas the Bayesian estimates do.

REFERENCES

(1) W. L. Chiou, M. A. F. Gadalla, and G. W. Peng, *J. Pharmacokinet. Biopharm.*, **6,** 135 (1978).

(2) J. R. Koup, C. M. Sack, A. L. Smith, and M. Gibaldi, *Clin. Pharmacokinet.*, **4,** 460 (1979).

(3) L. B. Sheiner, S. L. Beal, B. Rosenberg, and V. V. Marathe, *Clin. Pharmacol. Ther.*, **26,** 294 (1979).

(4) D. J. Greenblatt, *Ann. Rev. Pharmacol. Toxicol.*, **19,** 347 (1979).

(5) W. J. Jusko, M. J. Gardner, A. Mangione, J. J. Schentag, J. R. Koup, and J. W. Vance, *J. Pharm. Sci.*, **68,** 1358 (1979).

(6) J. R. Powell, S. Vozeh, P. Hopewell, J. Costello, L. B. Sheiner, and S. Riegelman, *Am. Rev. Resp. Dis.*, **118,** 229 (1978).

(7) G. E. P. Box and M. Muller, *Ann. Math. Stat.*, **29,** 610 (1958).

(8) P. Lewis, A. Goodman, and J. Miller, *IBM Syst. J.*, **8,** 136 (1969).

(9) L. B. Sheiner, B. Rosenberg, and V. V. Marathe, *J. Pharmacokinet. Biopharm.*, **5,** 445 (1977).

(10) S. Vozeh, K. T. Muir, L. B. Sheiner, and F. Follath, *J. Pharmacokinet. Biopharm.*, **9,** 131 (1981).

(11) C. M. Metzler, G. L. Elfring, and A. J. McEwen, "A Users Manual for NONLIN and Associated Programs," The Upjohn Co., Kalamazoo, Mich., 1974.

(12) C. C. Peck and B. B. Barrett, *J. Pharmacokinet. Biopharm.*, **7,** 537 (1979).

(13) L. B. Sheiner and S. L. Beal, *ibid.*, **8,** 553 (1980).

(14) L. Z. Benet and L. B. Sheiner, "The Pharmacological Basis of Therapeutics," 6th ed., A. G. Gilman, L. S. Goodman and A. Gilman, Eds., Macmillan, New York, N.Y., 1980, pp. 1675–1737.

ACKNOWLEDGMENTS

This work was supported in part by Grants GM 26676 and GM 26691.

Effects of Microsomal Enzyme Induction on Toxicity of *p*-*N*,*N*-Bis(2-chloroethyl)aminophenyl Alkyl Ethers in Mice and Survival Times in L-1210 Leukemic Mice

C. T. BAUGUESS[x], SHIAO PING CHANG, and J. E. WYNN*

Received September 16, 1981, from the *Department of Basic Pharmaceutical Sciences, College of Pharmacy, University of South Carolina, Columbia, SC 29208.* Accepted for publication February 1, 1982. *Present address: Department of Pharmaceutical Sciences, College of Pharmacy, Medical University of South Carolina, Charleston, SC 29425.

Abstract □ Four alkyl ethers of *p*-*N*,*N*-bis(2-chloroethyl)aminophenol were selected to study the effects of microsomal enzyme induction by phenobarbital on the toxicity changes as reflected by LD_{50} and alteration of survival times in L-1210 leukemic mice. In the phenobarbital pretreated mice the LD_{50} for the ethyl ether of *p*-*N*,*N*-bis(2-chloroethyl)-aminophenol was decreased from 1641 to 1213 μm/kg. This result suggests that *O*-dealkylation is the major metabolic pathway. The LD_{50} for the propyl ether of *p*-*N*,*N*-bis(2-chloroethyl)aminophenol was increased by the pretreatment from 605 to 678 μm/kg. The LD_{50} for the butyl ether was increased from 714 to 910 μm/kg. An additional metabolic pathway, (ω-1)-hydroxylation, is suggested for the propyl and butyl ethers. The hexyl ether appeared to be unaffected by the pretreatment; thus, *O*-dealkylation was ruled out as a major pathway. In the survival studies, the pretreatment reduced the antitumor effectiveness of the ethyl and the butyl ethers. The survival times were increased for some dose levels for the propyl ether. No significant trend in survival times was observed for the hexyl ether in the pretreated mice.

Keyphrases □ Microsomal enzyme induction—effects on toxicity in mice, survival times in L-1210 leukemic mice of *p*-*N*,*N*-bis(2-chloroethyl)aminophenyl alkyl ethers, phenobarbital □ *p*-*N*,*N*-Bis(2-chloroethyl)aminophenyl alkyl ethers—effects of microsomal enzyme induction on toxicity in mice, survival in L-1210 leukemic mice, phenobarbital

Variations in the alkyl chain lengths of esters and ethers of *p*-*N*,*N*-bis(2-chloroethyl)aminophenol have been shown to alter the toxicity and survival times of L-1210 leukemic mice over that of *p*-*N*,*N*-bis(2-chloroethyl)aminophenol (1–3). It was proposed that the fatty acid esters would undergo ester hydrolysis and release the *p*-*N*,*N*-bis(2-chloroethyl)aminophenol and its other degradation products. Previous reports suggest that the short chain alkyl aryl ethers may be metabolized by an α-hydroxylation pathway resulting in *O*-dealkylation, while the longer chains may be subjected to another pathway. It is likely that the metabolism of this series of alkyl aryl ethers would be similar to the *p*-nitrophenyl alkyl ethers reported previously (4). The hexyl ether of *p*-nitrophenol was not *O*-dealkylated as were the lower members in that series. Although the metabolism of the hexyl ether of *p*-*N*,*N*-bis(2-chloroethyl)aminophenol has not been studied, toxicity studies and survival studies in L-1210 leukemic mice have suggested the absence of the α-hydroxylation pathway. A dual metabolic pathway, α- and (ω-1)-hydroxylation, is possible for the *n*-propyl and *n*-butyl ethers of *p*-*N*,*N*-bis(2-chloroethyl)aminophenol. These pathways on *p*-nitrophenyl-*n*-butyl ether have been demonstrated (5) with the identification of 3-hydroxy-*n*-butyl ether of *p*-nitrophenol as a major metabolite.

The purpose of this research was to study the effects of microsomal enzyme induction in mice on the toxicity and survival times of L-1210 leukemic mice treated with the ethyl, *n*-propyl, *n*-butyl, and *n*-hexyl ethers of *p*-*N*,*N*-bis(2-chloroethyl)aminophenol. An increase in toxicity would be expected to accompany an increase in *O*-dealkylation in induced mice and provide further evidence for the presence of the (ω-1)-hydroxylation pathway for the higher members in the alkyl ether series.

EXPERIMENTAL

Test Animals—DBA/2[1], BDF_1[1], and HA/ICR mouse strains[2] and L-1210 leukemic mice (tumor source)[3] were used.

Instruments—The necessary equipment included an electronic cell counter[4], a channelizer[4], a dilutor[4], an *xy* recorder[4], a hemocytometer[5], and a microscope[6].

Materials—Counting diluent[4], red cell-lysing reagent[7], crystal violet[8], Giemsa stain[7], isotonic diluting solution[9], trypan blue[10], and Wrights' strain[8] were used. The alkyl ethers of *p*-*N*,*N*-bis(2-chloroethyl)aminophenol (the ethyl-propyl-, butyl-, and hexyl ethers) and *p*-*N*,*N*-bis(2-chloroethyl)aminophenol were prepared and have been reported previously (3). All other chemicals and reagents were obtained from commercial sources.

Microsomal Enzyme Induction—A modification of a previous method was employed in the enzyme induction phases of the study (6). Thirty-five HA/ICR mice (6-weeks-old) were given sodium phenobarbital (75 mg/kg) by intraperitoneal injection daily for 7 days. The onset and duration of sleeping time for each mouse was recorded. Sleeping time is the time interval between the loss and recovery of the righting reflex (6). Changes in the duration of sleeping time were used as an indicator of the degree of enzyme induction. After the 7th day of treatment the mice were randomly divided into seven groups, five mice to each. On day 9 sodium phenobarbital (75 mg/kg) was administered to the first group to observe any changes in the onset and duration of sleeping time after the discontinuation of the pretreatment for one day. The same dose of sodium phenobarbital was administered to the remaining groups 2, 3, 4, 5, 6, and 7 days, respectively, after the discontinuation of the daily pretreatment.

Toxicity Evaluation—HA/ICR mice were divided into groups of six for the test and control groups. The test groups were given sodium phenobarbital (75 mg/kg ip) daily for 7 days prior to intraperitoneal injections of *p*-*N*,*N*-bis(2-chloroethyl)aminophenol or its alkyl ethers. Each injection consisted of a known concentration of each drug dissolved in 0.1 ml of propylene glycol. The mice were observed and weighed daily for 28 days. The number of mortalities at each dose level was evaluated by a previous method to determine the LD_{50} number for each drug in the test and control groups (7).

Tumor Transplant Procedure—DBA/2 mice bearing L-1210 leukemia for 7 days were used as a source for tumor cells. The L-1210 cells were collected according to a previously described procedure (1). Inoculations containing 10^5 L-1210 cells were administered intraperitoneally to groups of BDF_1 mice to be used in the survival studies.

[1] Jackson Laboratories.
[2] ARS/Sprague-Dawley.
[3] National Cancer Institute.
[4] Model ZB Counter and Accessories, Coulter Electronics.
[5] American Optical Co.
[6] Model RA, Carl Zeiss, West Germany.
[7] Fisher Scientific Co.
[8] Matheson, Coleman, and Bell.
[9] Microbiological Associates.
[10] Allied Chemical Co.

0022-3549/82/1200-1349$01.00/0

Survival Studies—One group of healthy BDF_1 mice was pretreated with sodium phenobarbital (75 mg/kg) daily for 5 days. The alkyl ethers of *p*-*N*,*N*-bis(2-chloroethyl)aminophenol were administered intraperitoneally in propylene glycol to two groups of leukemic mice, one group referred to as the control, which did not receive the phenobarbital pretreatment, and the group described above. Dosages of 25, 50, 75, 100, 150, and 200 mg/kg of the alkyl ethers were given on days 2 and 5 after inoculation to subgroups of six mice for the control group and the pretreated group. An additional group of six BDF_1 mice inoculated with L-1210 cells was employed as the untreated control and received only the injection vehicle, propylene glycol.

RESULTS AND DISCUSSION

The onset and duration of sleeping times for mice pretreated with phenobarbital are reported in Table I and Fig. 1. The onset time for sleeping did not show any relationship with the degree of enzyme induction. The sleeping times gradually decreased during the periods of daily injections of phenobarbital, but gradually returned to normal after termination of the treatment. The increased function of the microsomal enzyme system persisted into the following week. Hypertrophy of the mice livers was observed in all studies 3 or 4 days after the pretreatment was initiated and disappeared after the daily injections were stopped. This observation is consistent with a previous report (8).

In the toxicity studies on the nitrogen mustards, a 7-day pretreatment period was considered adequate for the induction period. Table II shows the results of the toxicity studies performed on the five compounds in phenobarbital pretreated mice and untreated mice. The LD_{50} for compound I, *p*-*N*,*N*-bis(2-chloroethyl)aminophenol, was 164 μm/kg (38 mg/kg) in untreated HA/ICR mice. In the phenobarbital pretreated mice, a reduction in toxicity was suggested by the increase in the LD_{50} to 253 μm/kg (59 mg/kg). This increase in LD_{50} was probably due to an increase in the rate of conjugation of compound I, which should have resulted in a faster excretion rate (9).

A tenfold decrease in toxicity was observed for compound II, the ethyl ether of *p*-*N*,*N*-bis(2-chloroethyl)aminophenol, over that of the parent compound (I) in untreated mice. The LD_{50} was 1641 μm/kg which decreased to 1213 μm/kg when the mice were pretreated with phenobarbital. It is presumed that compound II is *O*-dealkylated to the more toxic mustard, compound I, which would lead to one of the ultimate metabolites through hydrolysis of the chloroethyl groups. Some of the toxicity expected from the *O*-dealkylation pathway *via* hydroxylation on the α-carbon on the alkyl group would be mollified by an increase in the rate of conjugation of compound I, its metabolites, other metabolites which have hydroxyl groups, and the various rate processes of the α- and (ω-1)-hydroxylation pathways.

The toxicity of compound III was greater than compound II but less than compound I. The LD_{50} of compound III was 605 μm/kg (160 mg/kg) in untreated mice and increased to 678 μm/kg in the pretreated mice. Compound III, the propyl ether, could undergo metabolism by the α-hydroxylation and the (ω-1)-hydroxylation pathways. If the α-hydroxylation were the major pathway, the toxicity for the propyl ether would be expected to increase in the pretreated mice due to the increased formation of the parent compound, *p*-*N*,*N*-bis(2-chloroethyl)aminophenol. The (ω-1)-hydroxylation of compound III would lead to the 2-hydroxy propyl ether of *p*-*N*,*N*-bis(2-chloroethyl)aminophenol which should be less lipid soluble and possibly less toxic.

Similar results were obtained for compound IV. The LD_{50} was 714 μm/kg (207 mg/kg) in untreated mice and increased to 910 μm/kg in the pretreated mice.

Both hydroxylation pathways would be expected for the butyl ether, but α-hydroxylation would have to play a minor role to explain the lowered toxicity in the pretreated mice. If the butyl ether mustard is metabolized by the (ω-1)-hydroxylation pathway, it would appear as the 3-hydroxybutyl ether mustard or corresponding metabolites. This pathway was verified for *p*-nitrophenyl butyl ether (5). The increase in the LD_{50} for compound IV suggests that phenobarbital pretreatment enhances the rate for the alternate pathway over that of α-hydroxylation.

The effect of pretreatment on the toxicity of compound V was negligible. The LD_{50} was 1069 μm/kg (340 mg/kg) in the untreated mice and changed only slightly to 1104 μm/kg in the pretreated mice. This result was anticipated since the aryl alkyl ether mustards would be expected to follow the same metabolic pathways as reported for the alkyl ethers of *p*-nitrophenol (4). In that report *O*-dealkylation was negligible for the hexyl ether of *p*-nitrophenol. The insignificance of the α-hydroxylation pathway in mice is supported by the results of the toxicity studies.

The expected metabolite of compound I, *p*-*N*,*N*-bis(2-hydroxyethyl)aminophenol, has been isolated from rat blood as a major metabolite of compound II and to a lesser extent for compounds III and IV. Unidentified metabolites which did not conform to the α-hydroxylation pathway were observed for compounds III and IV[11].

The results of a study of the influence of microsomal enzyme induction on the survival times of leukemic mice treated with alkyl ethers of *p*-*N*,*N*-bis(2-chloroethyl)aminophenol are presented in Table III and illustrated in Fig. 2. The ethyl ether, compound II, would be expected to undergo α-hydroxylation and hydrolysis would yield acetaldehyde and the more toxic form of the mustard, compound I, and its metabolites. The ethyl mustard produced a maximum survival of 126% T/C at a dose of 383 μm/kg in the control group (leukemic mice treated with the mustard

Table I—Onset and Sleeping Duration for Mice Pretreated with 75 mg/kg of Sodium Phenobarbital[a]

Days	Dosing Omitted on Days	Onset, Minutes (*SE*)[b]	Sleeping Time, Minutes (*SE*)[b]
1	—	23.2(±0.46)	94.2(±0.57)
2	—	20.2(±0.80)	77.4(±2.09)
3	—	19.6(±0.96)	74.3(±1.48)
4	—	18.1(±0.65)	70.6(±1.46)
5	—	18.3(±0.61)	62.9(±0.59)
6	—	21.0(±1.10)	47.4(±1.33)
7	—	19.9(±0.92)	43.9(±1.01)
8	—	—	—
9	8	22.0(±2.00)	43.0(±3.54)
10	8–9	19.6(±1.63)	48.0(±4.90)
11	8–10	23.0(±1.22)	49.0(±4.58)
12	8–11	22.0(±2.55)	55.0(±3.16)
13	8–12	20.0(±4.25)	62.0(±4.90)
14	8–13	17.0(±1.22)	64.0(±5.09)
15	8–14	25.4(±2.38)	67.0(±2.65)

[a] Administered intraperitoneally in sterile water for injection. [b] Standard error.

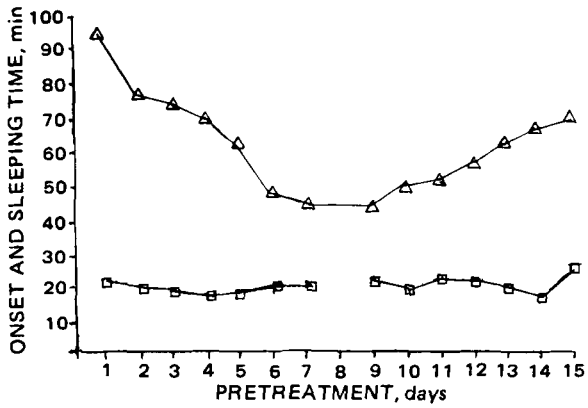

Figure 1—*The sleeping time of mice pretreated with sodium phenobarbital. Key: (□) onset of sleep; (△) sleeping time.*

Table II—Toxicity of *p*-*N*,*N*-Bis(2-chloroethyl)aminophenol and its Alkyl Ethers in Mice Pretreated with Phenobarbital

Compound	Untreated Mice, LD_{50} μm/kg	Untreated Mice, LD_{50} mg/kg	Pretreated Mice LD_{50} μm/kg	Pretreated Mice LD_{50} mg/kg
I (Parent compound)	164	38	253	59
II Ethyl ether	1641	430	1213	318
III Propyl ether	605	167	678	187
IV Butyl ether	714	207	910	264
V Hexyl ether	1069	340	1104	351

[11] Unpublished data.

Table III—Survival Times of L-1210 Leukemic Mice [a] Treated with *p*-*N*,*N*-Bis(2-chloroethyl)aminophenyl Alkyl Ethers and Pretreated with Phenobarbital

Derivative Compound	Dose, μm/kg	Untreated Control Mean Survival Days (±*SE*)	Control Mean Survival Days (±*SE*)	T/C %[b]	Phenobarbital Pretreated Mean Survival Days (±*SE*)	T/C %
II	96	8.50(0.34)	9.83(0.31)	117	8.33(0.21)	98
Ethyl ether	192	8.50(0.34)	10.00(0.68)	118	8.67(0.33)	102
	287	8.50(0.34)	9.33(0.56)	110	9.33(0.56)	110
	383	8.50(0.34)	10.67(0.21)	126	9.00(0.97)	106
	479	8.50(0.34)	10.17(0.17)	120	10.16(0.47)	120
	575	9.00(0.37)	9.37(0.92)	104	7.50(1.18)	84
	766	9.00(0.37)	7.33(0.67)	81	6.00(0.82)	67
III	91	8.50(0.34)	10.33(0.33)	122	9.33(0.21)	110
Propyl ether	181	8.50(0.34)	10.83(0.48)	127	11.00(0.52)	129
	273	8.50(0.34)	9.66(0.95)	114	10.67(0.42)	126
	364	8.50(0.34)	10.33(0.56)	117	12.33(0.33)	145[c]
	455	8.50(0.34)	10.00(1.10)	118	10.50(1.06)	124
	546	8.50(0.34)	9.16(0.87)	108	8.17(0.60)	96
	727	9.00(0.37)	9.50(0.34)	106	8.67(0.76)	96
IV	87	9.00(0.37)	9.50(0.34)	106	8.67(0.76)	96
Butyl ether	173	9.00(0.37)	10.00(0.63)	111	9.50(0.22)	106
	260	9.00(0.37)	10.33(1.15)	115	9.00(0.86)	100
	346	9.00(0.37)	10.33(1.36)	115	7.83(0.98)	87
	519	9.00(0.37)	12.50(0.56)	139	7.50(0.81)	83[c]
	692	9.00(0.37)	12.83(0.54)	143	10.17(1.70)	113
	727	9.00(0.37)	6.50(0.34)	72	6.33(0.42)	70
V	0	9.33(0.51)	—	—	9.33(0.51)	100
Hexyl ether	17	9.33(0.51)	10.00(0.37)	107	10.67(0.42)	114
	33	9.33(0.51)	10.17(0.31)	109	9.83(0.31)	105
	83	9.33(0.51)	10.00(0.52)	107	9.67(0.49)	104
	166	9.33(0.51)	10.00(0.45)	107	10.00(0.45)	107
	249	9.33(0.51)	10.50(0.43)	113	10.67(0.42)	114
	332	9.33(0.51)	10.17(0.48)	109	9.33(0.71)	100
	415	9.33(0.51)	10.67(0.42)	114	10.17(0.83)	109
	498	9.33(0.51)	9.33(0.33)	100	8.33(0.56)	89
	645	9.33(0.51)	9.83(0.83)	105	9.50(0.85)	102

[a] Six BDF_1 mice were used for each dose level for each group. [b] Statistical differences at $p < 0.05$ for Control *versus* Pretreatment. [c] The T/C % represents the rates of the sum of days (T) each treated animal survives to the sum of the number of days each control animal (C) survives times 100.

only), but was reduced to 106% T/C in the corresponding group pretreated with phenobarbital. The survival times for all dose levels of compound II were lower in the phenobarbital pretreated groups over the control groups, with the exception of two dose levels. A dose level of 479 μm/kg produced a survival of 120% T/C in both groups. It was generally expected that an increase in the rate of *O*-dealkylation of compound II in the pretreated mice would increase host toxicity and overcome some of the benefits of drug treatment.

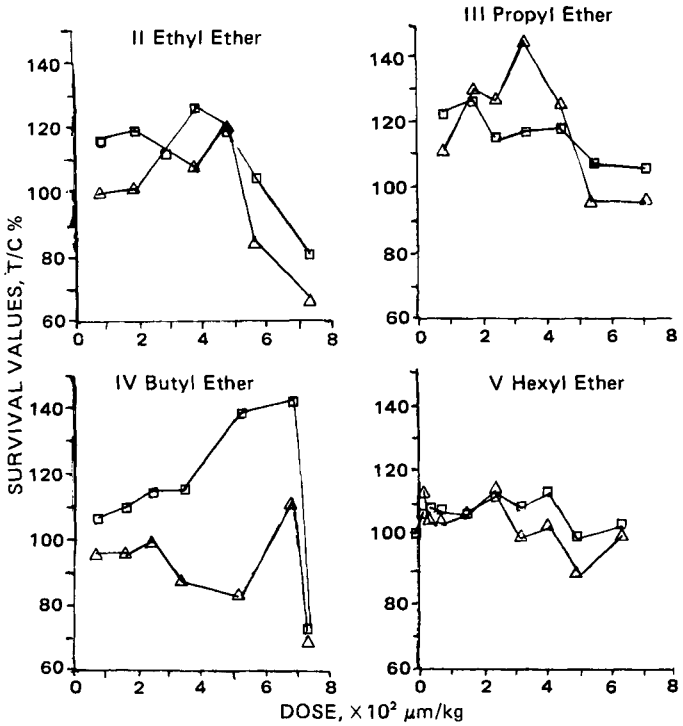

Figure 2—*Survival values of L-1210 leukemic mice treated with* p-N,N-*bis(2-chloroethyl)aminphenyl alkyl ethers, (II) ethyl ether, (III) propyl ether, (IV) butyl ether, and (V) hexyl ether. Key: (□) Control; (△) Pretreated.*

The propyl ether, compound III, was more effective in increasing survival values at the four dose levels ranging from 181 through 455 μm/kg in the pretreated groups. The highest survival value was 145% T/C in the pretreated group, which was significantly different from the control value of 117% T/C. If the metabolism of compound III were accelerated by the α-hydroxylation pathway in the pretreated group, a decrease in the survival value would have been expected, as observed with compound II, due to increased host toxicity. α-Hydroxylation has been demonstrated in propyl ethers (4), but an alternate pathway would be suspected to satisfactorily explain these results. One other major metabolite, which would result from an (ω-1)-hydroxylation, has been suggested (5). An active metabolite other than the parent compound may be the 2-hydroxy propyl ether of *p*-*N*,*N*-bis(2-chloroethyl)aminophenol. Although the differences are not significant, in the lowest dose, 91 μm/kg, and the two highest doses, 546 and 727 μm/kg, the survival values of the pretreated groups fell below the untreated groups.

All dose levels of compound IV exhibited lower survival values in the pretreated groups when compared with the control groups. A dose level of 519 μm/kg produced a significant difference between survival values of pretreated *versus* control groups, although the best value, 143% T/C, occurred at 692 μm/kg in the control group. A decrease in the rate of *O*-dealkylation of *p*-nitrophenyl alkyl ethers as the length of the carbon chain increased has been found (4). The (ω-1)-hydroxylation pathway is favored as a possible explanation consistent with the results from both the toxicity and the survival data. If the 3-hydroxybutyl ether of *p*-*N*,*N*-bis(2-chloroethyl)aminophenol is produced more rapidly than the parent compound, that would provide a possible explanation for the toxicity differences between control and pretreated group, and it would have less antitumor activity than compound IV.

The results from previous studies on the *O*-dealkylation of *p*-nitrophenyl alkyl ethers and survival studies on the *p*-*N*,*N*-bis(2-chloroethyl)alkyl ethers are consistent with the lack of significant differences between the control groups and pretreated groups for the hexyl ether. Since α-hydroxylation of hexyl aryl ethers is unlikely, minimal effects

Table IV—Statistical Analysis of the Survival Studies on an SPSS Multiple Regression Subprogram

Drug	Dose Range	R^2 [a]	a [b]	b [b]	c [b]	$B(b)$ [c]	$B(c)$ [c]	$F(b)$ [d]	$F(c)$ [d]
Ethyl ether	25–100	0.183	8.982	0.0137	−0.995	0.377	−0.365	8.3	7.8
	125–200	0.387	15.714	−0.0463	NS[e]	−0.623	NS	22.62	NS
Propyl ether	25–100	0.103	9.677	0.0155	NS	0.3219	NS	4.950	NS
	125–200	0.349	15.262	−0.0433	NS	−0.591	NS	19.365	NS
Butyl ether	25–100	0.268	8.556	0.0333	NS	0.518	NS	5.854	NS
	25–150	0.237	9.683	0.0138	−2.189	0.235	−0.433	4.993	16.96
Hexyl ether	25–200	0.0221	10.21	−0.0028	NS	−0.149	NS	2.391	NS

[a] R^2 (coefficient of determination) indicates the proportion of variation in life span explained by dose only or by both dose and treatment. [b] The form of multiple regression equation: $Y = a + b(\text{dose}) + c(\text{treatment})$ Y = life span, a = intercept of y axis, b = regression coefficient for dose, c = regression coefficient for treatment (dummy variable). [c] $B(b)$ indicates the number of standard derivation units of change in life span that could be predicted when dose changes by one standard unit. $B(c)$ indicates the number of standard derivation units of change in life span that could be predicted when treatment changes by one standard unit. [d] $F(b)$ presents the F value of dose. $F(c)$ presents the F value of treatment. Except $F(b)$ of hexyl ether, all other F values are greater than the critical values at the 0.05 level of significance. [e] NS = no significance.

on toxicity or survival times in leukemic mice would be expected to result from phenobarbital pretreatment (3, 4). It is not known if the hexyl ether of *p*-*N*,*N*-bis(2-chloroethyl)aminophenol undergoes (ω-1)-hydroxylation, but if it were to occur, these results suggest a metabolite similar in toxicity and antitumor activity to compound V.

A regression analysis was performed on survival data from the control and pretreated groups (Table IV). The analysis, taken over the entire range of doses, failed to show significant trends for any of the compounds tested. Negative trends in the ascending points for data sets from compounds II and IV indicate a decrease in the antitumor effectiveness for the pretreated mice. Crossover trends at the lowest and two highest doses for compound III precluded significance. The medium level doses were not tested. No trend could be established for compound V.

REFERENCES

(1) C. T. Bauguess, Y. Y. Lee, J. W. Kosh, and J. E. Wynn, *J. Pharm. Sci.*, **70**, 46 (1981).

(2) J. E. Wynn, M. L. Caldwell, J. R. Robinson, R. L. Beamer, and C. T. Bauguess, *ibid.*, **71**, 772 (1982).

(3) J. W. Wise, J. E. Wynn, R. L. Beamer, and C. T. Bauguess, *ibid.*, **71**, 561 (1982).

(4) R. E. McMahan, H. W. Culp, and J. Mills, *J. Med. Chem.*, **6**, 343 (1963).

(5) H. Tsukamato, H. Yoshimura, and H. Tsuyi, *Chem. Pharm. Bull.*, **12**, 987 (1964).

(6) A. H. Conney and J. J. Burns, *Adv. Pharmacol.*, **1**, 31 (1962).

(7) L. C. Miller and M. L. Tainter, *Proc. Soc. Exp. Biol. Med.*, **57**, 261 (1944).

(8) J. W. Depierre and L. Ernster, *FEBS Lett.*, **68**, 219 (1976).

(9) S. J. Yaffe, G. Levy, T. Matsuzawa, and T. Baliah, *N. Engl. J. Med.*, **275**, 1461 (1966).

ACKNOWLEDGMENTS

The authors wish to thank Dr. Arthur A. Nelson for his advice and assistance on the statistical analysis of the data presented in this manuscript.

Antipyrine and Acetaminophen Kinetics in the Rat: Comparison of Data Based on Blood Samples from the Cut Tail and a Cannulated Femoral Artery

WENCHE M. JOHANNESSEN *[x], INGVALD M. TYSSEBOTN [‡], and JARLE AARBAKKE *

Received September 3, 1981, from the **Department of Pharmacology, Institute of Medical Biology, University of Tromsø, N-9001 Tromsø, Norway* and the [‡]*Institute of Physiology, University of Bergen, Årstadveien 19, N-5000 Bergen, Norway.* Accepted for publication February 1, 1982.

Abstract □ Antipyrine and acetaminophen kinetics were determined from concentration data obtained by simultaneous blood sampling from the cut end of the tail and a cannulated femoral artery in the rat. Significant differences in concentrations and kinetics for both drugs were found by comparison of the two sampling sites. The hypothesis that the differences were due to a low tail blood flow was tested. The tail blood flow was measured with a microsphere technique, and tail antipyrine concentrations were calculated from the relationship between arterial antipyrine concentration, tail flow, and time for comparison with the observed antipyrine concentrations. Mean blood flow of the rat tail was 0.02 ml/min/ml tail tissue at 22°, which was 8.8 and 0.9% of the liver and kidney flow, respectively. Tail flow increased more than twofold by elevation of the tail temperature to 37°. The calculated tail antipyrine concentration *versus* time curve showed a very close correspondence to the observed antipyrine tail concentration *versus* time curves. The results show that tail flow is a major determinant of antipyrine tail concentration in the rat. Kinetic data based on blood samples from the cut end of the tail, therefore, should be interpreted with caution.

Keyphrases □ Antipyrine—pharmacokinetics in the rat, comparison of data based on blood samples from the cut tail and a cannulated femoral artery □ Acetaminophen—pharmacokinetics in the rat, comparison of data based on blood samples from the cut tail and a cannulated femoral artery □ Pharmacokinetics—acetaminophen and antipyrine in the rat, comparison of data based on blood samples from the cut tail and a cannulated femoral artery □ Microsphere technique—pharmacokinetics in the rat, comparison of data based on blood samples from the cut tail and a cannulated femoral artery

The development in recent years of a multitude of sensitive drug assays in microsamples of blood and a variety of techniques for repeated blood sampling have made it possible to perform pharmacokinetic studies in individual animals as small as mice, rats, and guinea pigs. Whereas published methods for drug assays are routinely validated

0022-3549/82/1200-1352$01.00/0

Table IV—Statistical Analysis of the Survival Studies on an SPSS Multiple Regression Subprogram

Drug	Dose Range	R^2 [a]	a [b]	b [b]	c [b]	$B(b)$ [c]	$B(c)$ [c]	$F(b)$ [d]	$F(c)$ [d]
Ethyl ether	25–100	0.183	8.982	0.0137	−0.995	0.377	−0.365	8.3	7.8
	125–200	0.387	15.714	−0.0463	NS[e]	−0.623	NS	22.62	NS
Propyl ether	25–100	0.103	9.677	0.0155	NS	0.3219	NS	4.950	NS
	125–200	0.349	15.262	−0.0433	NS	−0.591	NS	19.365	NS
Butyl ether	25–100	0.268	8.556	0.0333	NS	0.518	NS	5.854	NS
	25–150	0.237	9.683	0.0138	−2.189	0.235	−0.433	4.993	16.96
Hexyl ether	25–200	0.0221	10.21	−0.0028	NS	−0.149	NS	2.391	NS

[a] R^2 (coefficient of determination) indicates the proportion of variation in life span explained by dose only or by both dose and treatment. [b] The form of multiple regression equation: $Y = a + b(\text{dose}) + c(\text{treatment})$ Y = life span, a = intercept of y axis, b = regression coefficient for dose, c = regression coefficient for treatment (dummy variable). [c] $B(b)$ indicates the number of standard derivation units of change in life span that could be predicted when dose changes by one standard unit. $B(c)$ indicates the number of standard derivation units of change in life span that could be predicted when treatment changes by one standard unit. [d] $F(b)$ presents the F value of dose. $F(c)$ presents the F value of treatment. Except $F(b)$ of hexyl ether, all other F values are greater than the critical values at the 0.05 level of significance. [e] NS = no significance.

on toxicity or survival times in leukemic mice would be expected to result from phenobarbital pretreatment (3, 4). It is not known if the hexyl ether of *p*-*N*,*N*-bis(2-chloroethyl)aminophenol undergoes (ω-1)-hydroxylation, but if it were to occur, these results suggest a metabolite similar in toxicity and antitumor activity to compound V.

A regression analysis was performed on survival data from the control and pretreated groups (Table IV). The analysis, taken over the entire range of doses, failed to show significant trends for any of the compounds tested. Negative trends in the ascending points for data sets from compounds II and IV indicate a decrease in the antitumor effectiveness for the pretreated mice. Crossover trends at the lowest and two highest doses for compound III precluded significance. The medium level doses were not tested. No trend could be established for compound V.

REFERENCES

(1) C. T. Bauguess, Y. Y. Lee, J. W. Kosh, and J. E. Wynn, *J. Pharm. Sci.*, **70**, 46 (1981).

(2) J. E. Wynn, M. L. Caldwell, J. R. Robinson, R. L. Beamer, and C. T. Bauguess, *ibid.*, **71**, 772 (1982).

(3) J. W. Wise, J. E. Wynn, R. L. Beamer, and C. T. Bauguess, *ibid.*, **71**, 561 (1982).

(4) R. E. McMahan, H. W. Culp, and J. Mills, *J. Med. Chem.*, **6**, 343 (1963).

(5) H. Tsukamato, H. Yoshimura, and H. Tsuyi, *Chem. Pharm. Bull.*, **12**, 987 (1964).

(6) A. H. Conney and J. J. Burns, *Adv. Pharmacol.*, **1**, 31 (1962).

(7) L. C. Miller and M. L. Tainter, *Proc. Soc. Exp. Biol. Med.*, **57**, 261 (1944).

(8) J. W. Depierre and L. Ernster, *FEBS Lett.*, **68**, 219 (1976).

(9) S. J. Yaffe, G. Levy, T. Matsuzawa, and T. Baliah, *N. Engl. J. Med.*, **275**, 1461 (1966).

ACKNOWLEDGMENTS

The authors wish to thank Dr. Arthur A. Nelson for his advice and assistance on the statistical analysis of the data presented in this manuscript.

Antipyrine and Acetaminophen Kinetics in the Rat: Comparison of Data Based on Blood Samples from the Cut Tail and a Cannulated Femoral Artery

WENCHE M. JOHANNESSEN *[x], INGVALD M. TYSSEBOTN [‡], and JARLE AARBAKKE *

Received September 3, 1981, from the **Department of Pharmacology, Institute of Medical Biology, University of Tromsø, N-9001 Tromsø, Norway* and the [‡]*Institute of Physiology, University of Bergen, Årstadveien 19, N-5000 Bergen, Norway.* Accepted for publication February 1, 1982.

Abstract □ Antipyrine and acetaminophen kinetics were determined from concentration data obtained by simultaneous blood sampling from the cut end of the tail and a cannulated femoral artery in the rat. Significant differences in concentrations and kinetics for both drugs were found by comparison of the two sampling sites. The hypothesis that the differences were due to a low tail blood flow was tested. The tail blood flow was measured with a microsphere technique, and tail antipyrine concentrations were calculated from the relationship between arterial antipyrine concentration, tail flow, and time for comparison with the observed antipyrine concentrations. Mean blood flow of the rat tail was 0.02 ml/min/ml tail tissue at 22°, which was 8.8 and 0.9% of the liver and kidney flow, respectively. Tail flow increased more than twofold by elevation of the tail temperature to 37°. The calculated tail antipyrine concentration *versus* time curve showed a very close correspondence to the observed antipyrine tail concentration *versus* time curves. The results show that tail flow is a major determinant of antipyrine tail concentration in the rat. Kinetic data based on blood samples from the cut end of the tail, therefore, should be interpreted with caution.

Keyphrases □ Antipyrine—pharmacokinetics in the rat, comparison of data based on blood samples from the cut tail and a cannulated femoral artery □ Acetaminophen—pharmacokinetics in the rat, comparison of data based on blood samples from the cut tail and a cannulated femoral artery □ Pharmacokinetics—acetaminophen and antipyrine in the rat, comparison of data based on blood samples from the cut tail and a cannulated femoral artery □ Microsphere technique—pharmacokinetics in the rat, comparison of data based on blood samples from the cut tail and a cannulated femoral artery

The development in recent years of a multitude of sensitive drug assays in microsamples of blood and a variety of techniques for repeated blood sampling have made it possible to perform pharmacokinetic studies in individual animals as small as mice, rats, and guinea pigs. Whereas published methods for drug assays are routinely validated

0022-3549/82/1200-1352$01.00/0

with respect to their sensitivity, specificity, and precision, methods for blood sampling in small animals mostly have been evaluated as to their feasibility in practical laboratory work (1, 2). The widespread use of small animals in pharmacokinetic studies of old and new drugs, however, has created a need for precise information also of the reproducibility and validity of the methods used for blood sampling. Recently, the reproducibility and validity of pharmacokinetic data obtained with a surgical procedure for cannulation of an artery and vein in the rat was investigated (3).

The present study was undertaken to investigate a frequently employed nonsurgical method: sampling of blood from the cut end of the rat tail. Assuming a low flow to the rat tail (4), both theoretical considerations (5–8) and previous experience (9) raised doubts about the validity of tail concentration data. Significant differences in antipyrine and acetaminophen concentrations in blood sampled simultaneously from the cut end of the tail and a cannulated femoral artery are presented. A low blood flow of the rat tail is demonstrated, to which the differences in tail and arterial antipyrine concentrations are attributable.

EXPERIMENTAL

Animals and Operation—Male Wistar rats[1] (150–400 g) were used. All surgery was performed in fluanisone/fentanyl[2] anesthesia (6.6/0.13 mg/kg sc) in the evening, and the experiments were carried out the next day. Arteries and veins were cannulated with polyethylene tubing[3] previously filled with 0.2 ml of heparinized (100 IU/ml) 0.9% NaCl, with the indwelling part of the tubing having been stretched to reduce its diameter and lubricated with silicone oil to facilitate insertion. For pharmacokinetic experiments a femoral artery and a femoral vein were cannulated; for blood flow measurements, the right carotid and a femoral artery were cannulated. The tubing was secured and transferred dorsally through a subcutaneous tunnel and made accessible through a skin perforation. The rats were placed in restraining cages[4] and allowed free access to food and water. Sampling of blood from the tail was performed after removal of its distal part (0.5 cm) with a sharp scalpel by a previous method (10), but without prewarming of the rat and occlusion of the lateral tail veins. The tail was allowed to bleed freely, usually a few seconds after blood sampling, and no hemostat was applied. Repeated bleeding was obtained by removal of the blood clot from the end of the tail and the samples collected in heparinized capillary tubes.

Pharmacokinetic Experiments—Experiments were carried out in unanesthetized rats. The test drugs, dissolved in 0.6–0.9 ml of physiological saline, were infused *via* the catheter in the femoral vein. The infusion period (30 sec) was immediately followed by flushing of the catheter with 0.3 ml of saline. An equal dose of [^{14}C]antipyrine[5] and [^{3}H]acetaminophen[6] was given (15 mg/kg, 1–2 μCi/animal). Blood samples (0.1 ml) were drawn from the cannula in the femoral artery and the cut end of the tail. After dosing with antipyrine, blood samples were drawn at 2, 4, 8, 10, 15, 20, 35, 50, 75, 100, 135, 160, and 200 min. After dosing with acetaminophen, blood samples were drawn at 2, 4, 6, 8, 12, 20, 30, 40, 50, and 60 min.

The dead space of the catheter was discarded before each sampling and replaced by saline afterwards. Concentrations of [^{14}C]antipyrine and [^{3}H]acetaminophen in whole blood were analyzed essentially by the methods described previously (11, 12). These assays have been shown to measure specifically only unchanged antipyrine or acetaminophen, with 95 and 90% recovery of the drugs from blood, respectively (11, 12).

Concentrations of antipyrine and acetaminophen were plotted *versus* time on semilogarithmic graphs. Arterial and tail blood concentrations exhibited biexponential and monoexponential decay curves, respectively. The arterial blood concentrations were analyzed according to a two-compartment open model with first-order elimination kinetics. The best fitting line was drawn by means of a formula of linear regression of the natural logarithm of concentration *versus* time based on the method of least squares.

Total clearance was calculated by:

$$\text{dose}/(A/\alpha + B/\beta) \qquad \text{(Eq. 1)}$$

where A and B are γ-intercepts of the extrapolated lines of the α- and β-phases, respectively. The central volume of distribution (V_c) was obtained by dividing the dose by $(A + B)$, and V_β was calculated by dividing total clearance by β.

Data obtained from tail blood were analyzed as follows: The area under the observed concentration curves were calculated by the trapezoidal rule and the total area under the curve by the equation:

$$AUC_{0-\infty} = AUC_{0-t} + \frac{C_t}{\beta} \qquad \text{(Eq. 2)}$$

assuming that C_t represents a point on the concentration curve where a linear terminal line can be drawn (pseudodistribution equilibrium). Total clearance was calculated by dose/$AUC_{0-\infty}$ and V_β by dividing total clearance by β.

Determination of Tail Flow—Blood flow through the rat tail was measured by means of the radioactive microsphere technique for determinations of regional blood flow (13).

Calculation of the Blood Flow—The blood flow through each piece of the tail was calculated by (14):

$$Q = \frac{F_r\, i_{x/g}}{i_\gamma} \qquad \text{(Eq. 3)}$$

where Q is the rate of the blood flow (ml/min/g of tissue); F_r is the rate of the reference sample (0.49 ml/min); i_x is the radioactivity of the piece of the tail; and i_γ is the radioactivity of the reference blood sample (gram).

Each piece of the tail (2 cm) was calculated as percent of the total tail length. In the calculations a mean value of the blood flow in the tail was used: The blood flow of each piece of the tail was summarized and divided by the number of tail pieces, and the mean value of all the rat tails was calculated. The value was transformed from milliliter per minute per gram of tail tissue to milliliter per minute per milliliter of tail tissue after correction for the density of the tail tissue.

Comparison of Calculated and Measured Tail Concentrations of Antipyrine—Concentrations of antipyrine in the tail blood were calculated by means of a formula (15) based on Fick's principle. When a freely diffusible biologically inert tracer substance is carried to a tissue by the blood, the concentration in the tissue (C_i) at time T, is determined by the arterial concentration (C_a), the tissue–blood partition coefficient (λ_i), and blood flow per unit mass of tissue volume (F_i/V_i):

$$C_i\,(T) = \lambda_i k_i\, e^{-k_i T} \int_0^T C_a e^{kt} dt \qquad \text{(Eq. 4)}$$

where $k_i = m_i F_i/\lambda_i V_i$ and m_i is the diffusion coefficient for the substance. Equation 4 was used to calculate the concentration of antipyrine in the rat tail. The following values were used for the calculation: It is assumed that the diffusion of antipyrine does not limit tissue uptake and accordingly the coefficient of diffusion (m_i) is 1 (15). The partition coefficient of antipyrine between tissue and blood (λ_i) is 1, as taken from investigations of antipyrine distribution between brain–blood (16) and kidney–blood (17). Accordingly, it is assumed that the antipyrine concentration of tail tissue is equal to the concentration of tail blood.

Experimental Design—Blood flow to the tail was measured in each unanesthetized rat placed in restraining cages at ambient temperatures of 22 and 37°. The tail was placed in a water bath of 37°, and after 30 min ~300,000 microspheres labeled with cesium 141 were infused. The tail was then transferred to a water bath of 22°, and after 30 min an approximately equal amount of microspheres labeled with strontium 85 were infused. In this way the rats served as their own controls. Room temperature was kept constant at 22°.

Experiments—The microspheres[7] (15 ± 1 μm, density 1.3) were dissolved in sucrose/epichlorohydrin polymer[8] and sterile 0.9% saline to

[1] Møllegaard Hansens Avlslaboratorier, Ejby, Denmark.
[2] A/S Mekos, Helsingborg, Sweden.
[3] PE 50, Intramedic Clay Adams, Parsippany, N.J.
[4] Manufactured in this laboratory. The volume of the cage can be varied to fit rats of different size so as to allow movement back and forth but no rotation.
[5] [*N*-^{14}C]methyl antipyrine, New England Nuclear Corp., Boston, Mass.
[6] [^{3}H]acetaminophen, generally labeled, New England Nuclear Corp., Boston, Mass.
[7] Microspheres labeled with either strontium 85 or cesium 141, 3M Company, St. Paul, Minn.
[8] 10% Ficoll-70, average molecular weight 70,000, Pharmacia Fine Chemicals, Uppsala, Sweden.

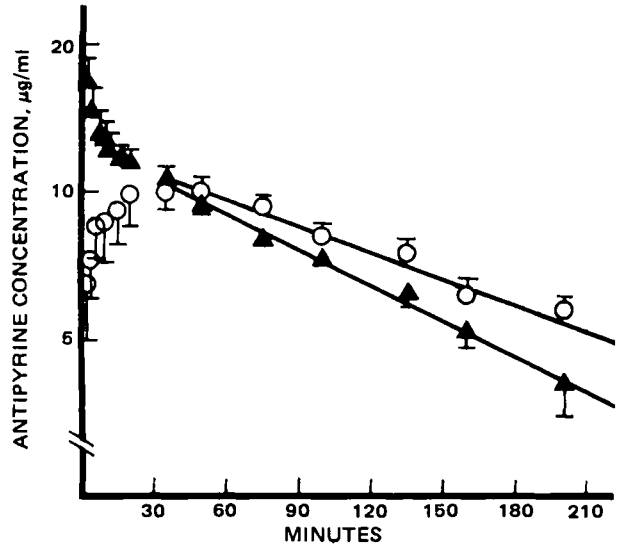

Figure 1—*Concentrations of antipyrine after administration of 15 mg/kg iv in blood sampled simultaneously from the cut end of the tail (○) and from a cannulated inguinal artery (▲). Values are mean ± SEM (n = 6).*

a concentration of ~6 × 10^5 microspheres/ml. Prior to microsphere infusion, a pump connected with the femoral artery catheter was started, sampling arterial blood at a constant rate of 0.49 ml/min for 2 min. This reference blood sample was used to calculate the blood flow to different organs according to a previous report (14). The solution of microspheres (0.5 ml) was infused *via* the cannula in the carotid artery within 15 sec, including flushing of the catheter with 0.3 ml of saline. After the last microsphere injection, rats were sacrificed by an intravenous injection of saturated potassium chloride. The tails were divided into pieces of ~2 cm, weighed, and placed in separate counting vials. The radioactivity was counted in a gamma liquid scintilation counter. The activity of the reference blood samples and both of the kidneys were also counted.

Statistical analysis—The results are given as means ±*SEM* and evaluated by paired Student's *t* test. Values for $p < 0.05$ were considered significant.

RESULTS

Pharmacokinetic Experiments—The time course of arterial and tail blood concentrations of both antipyrine and acetaminophen were widely different, and differences were also seen between the two drugs (Figs. 1 and 2). Individual tail concentration curves for both drugs were greatly variable, as indicated by the high standard error of the mean in the early phases of the experiment. After intravenous infusion of antipyrine, arterial concentrations showed the expected biexponential decline. Tail concentrations, however, increased until 40–60 min after the end of infusion. Acetaminophen concentrations showed a biexponential decline both in arterial and tail blood. Within the first 6 min after antipyrine infusion, the mean ratio of arterial to tail concentration decreased from 3 to 1.5. Mean arterial values were significantly different from mean tail values 0–15 min and >75 min after infusion ($p < 0.05$). Crossing of the curves took place 40–60 min after infusion. After 180 min the ratio of arterial to tail concentration was further decreased to 0.67. Corresponding values for acetaminophen concentrations for the first 6 min were 1.5, and after 60 min 0.5. Crossing of the acetaminophen curves was seen 12–20 min after infusion. All mean arterial concentrations of acetaminophen measured were significantly different from corresponding tail concentrations ($p < 0.05$).

Comparison of data based on arterial and tail concentrations of antipyrine showed statistically significant differences ($p < 0.05$) in the following pharmacokinetic variables (Table I). The biological half-life ($t_{1/2}\,\beta$) calculated from tail concentrations was higher by 47.5% compared with calculations based on arterial data, and the apparent elimination rate constant β was lower by 24%. Total clearance for antipyrine based on tail data was lower by 29.5% compared with arterial data. Significant changes were also found for the calculated variables of acetaminophen (Table I). The value for $t_{1/2}\,\beta$ based on tail blood data was higher by 46% compared with arterial blood data and was reduced by 46% for tail blood

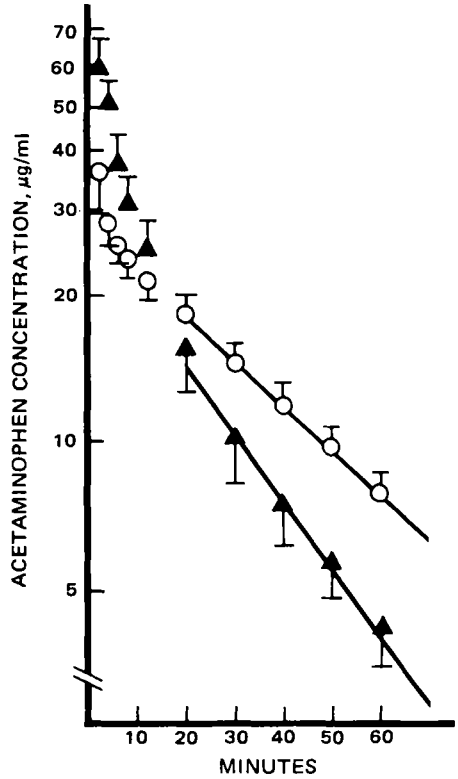

Figure 2—*Concentrations of acetaminophen after administration of 15 mg/kg iv in blood sampled simultaneously from the cut end of the tail (○) and from a cannulated inguinal artery (▲). Values are mean ± SEM (n = 5).*

data. In addition, the intercept of the extrapolated β phase, B, was lower by 11% for the tail blood data compared with arterial blood data. Also, the apparent volume of distribution, V_β, was significantly smaller with tail blood concentrations (35%).

Determination of Tail Blood Flow—The mean tail blood flow for five rats is shown as a function of the length of the tail in Fig. 3. The flow at an environmental temperature of 37° was significantly larger than the flow at 22° ($p < 0.05$).

Comparison of Calculated and Measured Tail Concentrations of Antipyrine—The mean blood flow of the tail of individual rats was calculated after correction for the density of the tail tissue (1.1 g/ml)[9]. The mean tail flow of five rats was then calculated. Tail blood flow at 37° was 5.0 ± 2.2 × 10^{-2} ml/min/ml tail tissue and at 22° 2.05 ± 0.93 × 10^{-2} ml/min/ml tail tissue. Figure 4 shows mean values of antipyrine arterial concentrations ($n = 3$) and calculated tail antipyrine concentrations at 37 and 22°. The time course of the calculated antipyrine tail concentration (Fig. 4) was grossly similar to actually measured concentrations presented in Fig. 1. Like measured tail concentrations, calculated tail concentrations were less than half the arterial concentration values at the earliest time points. Crossing of the lines likewise was seen 40–60 min after infusion.

DISCUSSION

The present study demonstrates that calculations based on drug concentration data from tail blood may give rise to pharmacokinetic values significantly different from values calculated from arterial blood samples. If it is assumed that rat arterial concentrations represent true kinetics, the use of rat tail concentrations may introduce significant errors in the pharmacokinetic calculations.

Although the pharmacokinetic data of antipyrine calculated from arterial concentrations are in accordance with values reported from other laboratories using different techniques (18, 19), it would be very difficult to prove that arterial blood data represent true kinetics in the rat. Serial sampling of arterial blood from individual rats will always require some kind of cannulation procedure. The stress imposed by the surgical pro-

[9] Obtained by dividing tail weights ($n = 3$) by the volume of water displaced.

Table I—Antipyrine and Acetaminophen Kinetics Based on Arterial and Tail Data [a]

	Site of Blood Sampling	Cl_T, ml min^{-1} kg^{-1}	β, 10^{-3} min^{-1}	$t_{1/2}\beta$, min	$\sqrt{\beta}$, liter kg^{-1}
Antipyrine	Artery	6.4 ± 0.4	5.4 ± 0.4	131 ± 11	1.18 ± 0.06
	Tail	4.5 ± 0.6[b]	4.1 ± 0.6[b]	194 ± 37[b]	1.15 ± 0.13
Acetaminophen	Artery	12.5 ± 1.0	33.0 ± 2.5	21.6 ± 1.8	0.39 ± 0.04
	Tail	13.1 ± 2.0	21.2 ± 1.4[b]	33.4 ± 2.6[b]	0.60 ± 0.09[b]

[a] The pharmacokinetic variables were calculated from arterial and tail concentration data in blood samples drawn simultaneously (see *Experimental*). Values are means ± *SEM* (n = 6, antipyrine; n = 5, acetaminophen). [b] Significantly different from arterial data ($p < 0.05$).

cedure (20) may influence significantly drug kinetics (21–23). The fact that antipyrine and acetaminophen kinetics were not reproducible in untreated animals over a short period of time (3) probably reflects that at least some aspects of normal physiology with relevance to pharmacokinetics are difficult to maintain even for short periods in cannulated rats.

There is only sparse information in the literature with respect to rat tail flow. Therefore, the rat tail flow was investigated by means of the radioactive microsphere technique for determination of regional blood flow (13). The following requirements must be fulfilled for the method to provide an exact measure of regional blood flow: First, there should be homogeneous mixing of microspheres with the arterial blood. According to previous reports (24, 25) this need will be met if the left ventricle is used as the site of injection. Verification of uniform mixing in the left ventricle can be obtained by measuring the left and right kidney blood flow (milliliters per minute per gram). Second, the microspheres must not recirculate. Spheres of 15 μm are shown to be trapped precapillary in the first circulation with only 1–2% ending in the lung capillaries of the rat, hence, they satisfy this requirement (26). Third, blood flow must not be affected by microspheres. Repeated microsphere injections in the same rats using different labels should not give significant changes in cardiac output fractions. Using 15-μm spheres, unchanged distribution was found (27) after the second microsphere injection in rats. In the present investigation, spheres of this size were used, and the present dose of 15-μm spheres have been shown not to interfere with this hemodynamic variable in the rat (14, 28). Fourth, the number of microspheres injected should give at least 400 in each tissue sample to avoid random error (24).

A previous study (4) reported flow values with a less sensitive technique at 17 and 33° that were two- and eightfold higher than the present values measured at 22 and 37°, respectively. However, the data presented here demonstrate that the tail blood flow is very low and represents only a minor fraction of the cardiac output. By comparison, rat tail flow in this study was only 8.8 and 0.4% of the rat liver and kidney flow values reported in a study using the same microsphere technique (28). This explains why tail concentrations lag behind arterial concentrations when the latter change rapidly. If tail flow is increased, for instance by elevation of tail temperature, the lag time will be reduced as shown in Fig. 4.

The close correspondence of the observed and calculated antipyrine tail concentrations strongly suggests that the assumption made for the theoretical relationship between tail concentrations, arterial concentrations, and time were correct; *i.e.*, the coefficient of diffusion (m_i) and the partition coefficient of antipyrine between tissue and blood (λ_i) are 1 (15–17), and accordingly, the organ blood flow becomes the rate-limiting factor. The different ratios observed between arterial and tail concentrations for antipyrine and acetaminophen (Figs. 1 and 2) could reflect that distribution properties of acetaminophen influence tail concentrations of the drug to a greater extent than the corresponding properties of antipyrine.

The effect of temperature changes on tail flow shows that drug kinetics based on tail concentration data may significantly reflect changes in the environment in addition to changes caused by drug distribution and elimination processes. Furthermore, intersubject differences in sensitivity of the tail to environmental factors may explain the great variation in the shape of antipyrine and acetaminophen tail concentration curves shortly after drug injection.

The variation of tail kinetics between individual rats contrasts sharply with the lack of variation observed within individual animals when antipyrine kinetics were retested after intervals of several weeks using blood samples taken >60 min after antipyrine infusion (9, 11, 29).

These observations suggest that by strict standardization of the experimental conditions, tail flow can be reproducible from one experiment

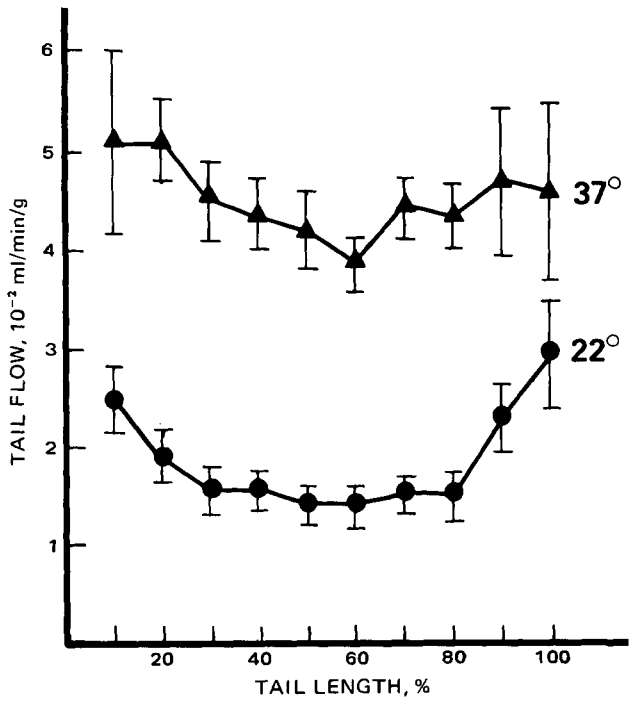

Figure 3—*Blood flow through the rat tail measured by means of microsphere technique at environmental temperatures of 22 (●) and 37° (▲). Values are mean ± SEM (n = 5). From left to right is from the tip to root of the tail.*

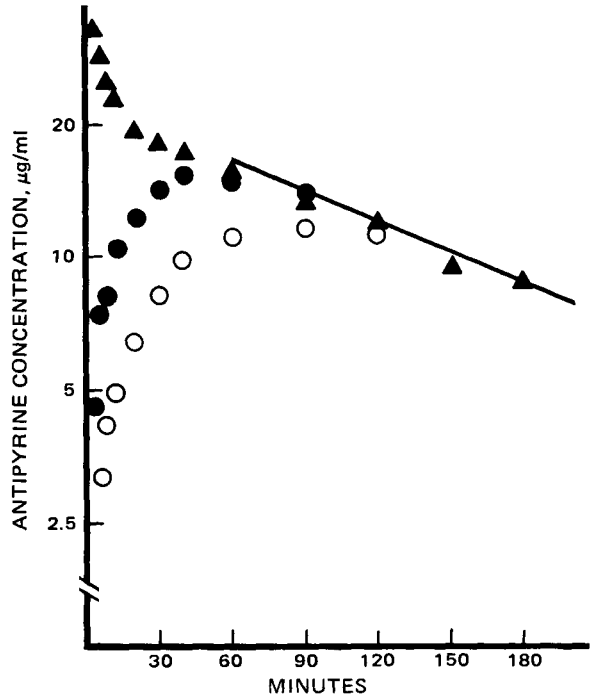

Figure 4—*Concentrations of antipyrine after administration of 15 mg/kg iv in blood sampled from a cannulated inguinal artery (▲) and calculated concentrations of antipyrine in tail tissue at 22° (○) and at 37° (●) (n = 3).*

to another in untreated rats. Problems arise, however, when the method is used to detect changes in pharmacokinetics by some experimental factors. Although the tail method detected changes in antipyrine kinetics by short-term, low-dose treatment of phenobarbital (11) and long-term treatment with ethanol (9), interpretation of data is obscured by possible influences of the treatment on tail blood flow and tail antipyrine distribution. Further investigations of such effects on drug kinetics, therefore, should include *in vitro* studies (9) or kinetic studies with the use of arterial blood samples.

REFERENCES

(1) H. C. Grice, *Lab. Anim. Care*, **14**, 488 (1964).

(2) B. H. Migdalof, *Drug Metab. Rev.* **5**, 295 (1976).

(3) W. Johannessen, G. Gadeholt, and J. Aarbakke, *J. Pharm. Pharmacol.*, **33**, 365 (1981).

(4) R. P. Rand, A. C. Burton, and T. Ing, *Can. J. Phys. Pharmacol.*, **43**, 257 (1965).

(5) S. Kety, *Pharmacol. Rev.*, **3**, 1 (1951).

(6) S. Riegelman, J. C. K. Loo, and M. Rowland, *J. Pharm. Sci.*, **57**, 117 (1968).

(7) M. Gibaldi and D. Perrier, "Pharmacokinetics," Marcel Dekker, New York, N.Y. 1975, p. 45.

(8) J. R. Gillette, "Concepts in Biochemical Pharmacology," Bind 28, Part 3, Springer Verlag, Berlin, Heidelberg, New York, 1975, p. 51.

(9) G. Gadeholt, J. Aarbakke, E. Dybing, M. Sjöblom, and J. Mørland, *J. Pharmcol. Exp. Ther.*, **213**, 196 (1980).

(10) T. Enta, S. D. Lockey, Jr., and C. E. Reed, *Proc. Soc. Exp. Biol. Med.*, **127**, 136 (1968).

(11) O. M. Bakke, M. Bending, J. Aarbakke, and D. S. Davies, *Acta Pharmacol. Toxicol.*, **35**, 91 (1974).

(12) G. M. Cohen, O. M. Bakke, and D. S. Davies, *J. Pharm. Pharmacol.*, **26**, 348 (1974).

(13) A. M. Rudolph and M. A. Heymann, *Circ. Res.*, **21**, 163 (1967).

(14) M. A. Heymann, B. D. Payne, J. E. Hoffman, and A. M. Rudolph, *Prog. Cardiovasc. Dis.*, **XX**, 55 (1977).

(15) S. Kety, *Met. Med. Res.*, **8**, 228 (1960).

(16) M. Reivich, J. Jehle, L. Sokoloff, and S. Kety, *J. Appl. Physiol.*, **27**, 296 (1969).

(17) A. Hope, G. Clausen, and K. Aukland, *Circ. Res.*, **39**, 362 (1976).

(18) A. H. Conney *et al.*, *Ann. N.Y. Acad. Sci.*, **179**, 155 (1971).

(19) M. Danhof, D. P. Krom, and D. D. Breimer, *Xenobiotica*, **9**, 695 (1979).

(20) A. C. Guyton, "Basic Human Physiology: Normal Function and Mechanisms of Disease", W. B. Saunder's, 2nd ed., 1977, p. 798.

(21) T. R. Tephly and G. J. Mannering, *Mol. Pharmacol.*, **4**, 10 (1968).

(22) W. F. Bousquet, B. D. Rupe, and T. S. Miya, *J. Pharmacol. Exp. Ther.*, **147**, 376 (1965).

(23) R. E. Stitzel and R. L. Furner. *Biochem. Pharmacol.*, **16**, 1489 (1967).

(24) G. D. Buckberg, J. C. Luck, D. B. Payne, J. E. Hoffman, J. P. Archie, and D. E. Fixler, *J. Appl. Physiol.*, **31**, 598 (1971).

(25) Y. Sasaki and H. N. Wagner, *ibid.*, **30**, 879 (1971).

(26) S. Kaihara, P. D. van Heerden, T. Migita, and H. Wagner Jr., *ibid.*, **25**, 696 (1968).

(27) D. J. Warren and J. G. Ledingham, *Cardiovasc. Res.*, **8**, 570 (1974).

(28) J. Onarheim and I. Tyssebotn, *Undersea Biomed. Res.*, **7**, 47 (1980).

(29) T. Høyem-Johansen, L. Slørdal, A. Høylandskjaer, and J. Aarbakke, *Acta Pharmacol. Toxicol.*, **47**, 279 (1980).

ACKNOWLEDGMENTS

This work was supported by grants from Norsk Medisinaldepot, Oslo, Norway.

Evaluation of Chemical Analysis for the Determination of Solasodine in *Solanum Laciniatum*

P. G. CRABBE ‡ and C. FRYER *x

Received September 29, 1981, from the *Department of Chemical Engineering, Monash University, Clayton, Victoria, Australia, 3168.* Accepted for publication February 5, 1982. *Present address: Fluor Australia Pty. Ltd., Melbourne, 3001, Australia. ‡Present address: Department of Chemical and Materials Engineering, University of Auckland, New Zealand.

Abstract □ A detailed study of a method for solasodine analysis has been carried out and the suitability of chemical analysis for solasodine determination in plant material evaluated. A number of problems with the analytical isolation of solasodine and its subsequent colorimetric determination have been highlighted: oven drying of plant material >100° leads to solasodine loss; cell disruption of the dry plant material is required if complete and rapid extraction of solasodine is to take place; hydrolysis of plant extract residues in >1 *N* acid leads to solasodine loss; the colorimetric procedure is more temperamental than past methods have indicated, especially with regard to the specificity of the reaction and the instability of the complex.

Keyphrases □ Solasodine—steroidal alkaloid from *Solanum laciniatum*, colorimetric determination by evaluation of chemical analysis □ Steroids—colorimetric determination of the alkaloid, solasodine, in *Solanum laciniatum* □ Colorimetry—determination of solasodine in *Solanum laciniatum*

Since problems arose 6 or 7 years ago with the supply, cost, and steroid content of *Dioscorea*, the source of diosgenin for steroid drug production, there has been renewed interest in alternative raw materials, including solasodine from plants of the genus *Solanum*. This steroidal alkaloid occurs in *S. aviculare* and *S. laciniatum* as the glycosides, solasonine and solamargine.

As part of a study into the production of solasodine from *Solanum* plant material, chemical analysis was considered for the determination of solasodine and its related species. Several important observations were made in the course of this investigation concerning both the isolation of solasodine from the plant (sample preparation, extraction, and hydrolysis) and the subsequent determination of solasodine using colorimetry. Chemical analysis was found not to be suitable for this study, and subsequently, a procedure using high-pressure liquid chromatography was developed (1). However, chemical analysis is suitable for certain purposes and has the advantage of not requiring expensive equipment. Matters concerning the isolation of solasodine from the plant material are important in solasodine analysis in general (including instrumental analysis) and in commercial solasodine production.

Previous methods for chemical analysis of solasodine

0022-3549/82/1200-1356$01.00/0

to another in untreated rats. Problems arise, however, when the method is used to detect changes in pharmacokinetics by some experimental factors. Although the tail method detected changes in antipyrine kinetics by short-term, low-dose treatment of phenobarbital (11) and long-term treatment with ethanol (9), interpretation of data is obscured by possible influences of the treatment on tail blood flow and tail antipyrine distribution. Further investigations of such effects on drug kinetics, therefore, should include *in vitro* studies (9) or kinetic studies with the use of arterial blood samples.

REFERENCES

(1) H. C. Grice, *Lab. Anim. Care*, **14**, 488 (1964).

(2) B. H. Migdalof, *Drug Metab. Rev.* **5**, 295 (1976).

(3) W. Johannessen, G. Gadeholt, and J. Aarbakke, *J. Pharm. Pharmacol.*, **33**, 365 (1981).

(4) R. P. Rand, A. C. Burton, and T. Ing, *Can. J. Phys. Pharmacol.*, **43**, 257 (1965).

(5) S. Kety, *Pharmacol. Rev.*, **3**, 1 (1951).

(6) S. Riegelman, J. C. K. Loo, and M. Rowland, *J. Pharm. Sci.*, **57**, 117 (1968).

(7) M. Gibaldi and D. Perrier, "Pharmacokinetics," Marcel Dekker, New York, N.Y. 1975, p. 45.

(8) J. R. Gillette, "Concepts in Biochemical Pharmacology," Bind 28, Part 3, Springer Verlag, Berlin, Heidelberg, New York, 1975, p. 51.

(9) G. Gadeholt, J. Aarbakke, E. Dybing, M. Sjöblom, and J. Mørland, *J. Pharmcol. Exp. Ther.*, **213**, 196 (1980).

(10) T. Enta, S. D. Lockey, Jr., and C. E. Reed, *Proc. Soc. Exp. Biol. Med.*, **127**, 136 (1968).

(11) O. M. Bakke, M. Bending, J. Aarbakke, and D. S. Davies, *Acta Pharmacol. Toxicol.*, **35**, 91 (1974).

(12) G. M. Cohen, O. M. Bakke, and D. S. Davies, *J. Pharm. Pharmacol.*, **26**, 348 (1974).

(13) A. M. Rudolph and M. A. Heymann, *Circ. Res.*, **21**, 163 (1967).

(14) M. A. Heymann, B. D. Payne, J. E. Hoffman, and A. M. Rudolph, *Prog. Cardiovasc. Dis.*, **XX**, 55 (1977).

(15) S. Kety, *Met. Med. Res.*, **8**, 228 (1960).

(16) M. Reivich, J. Jehle, L. Sokoloff, and S. Kety, *J. Appl. Physiol.*, **27**, 296 (1969).

(17) A. Hope, G. Clausen, and K. Aukland, *Circ. Res.*, **39**, 362 (1976).

(18) A. H. Conney *et al.*, *Ann. N.Y. Acad. Sci.*, **179**, 155 (1971).

(19) M. Danhof, D. P. Krom, and D. D. Breimer, *Xenobiotica*, **9**, 695 (1979).

(20) A. C. Guyton, "Basic Human Physiology: Normal Function and Mechanisms of Disease", W. B. Saunder's, 2nd ed., 1977, p. 798.

(21) T. R. Tephly and G. J. Mannering, *Mol. Pharmacol.*, **4**, 10 (1968).

(22) W. F. Bousquet, B. D. Rupe, and T. S. Miya, *J. Pharmacol. Exp. Ther.*, **147**, 376 (1965).

(23) R. E. Stitzel and R. L. Furner. *Biochem. Pharmacol.*, **16**, 1489 (1967).

(24) G. D. Buckberg, J. C. Luck, D. B. Payne, J. E. Hoffman, J. P. Archie, and D. E. Fixler, *J. Appl. Physiol.*, **31**, 598 (1971).

(25) Y. Sasaki and H. N. Wagner, *ibid.*, **30**, 879 (1971).

(26) S. Kaihara, P. D. van Heerden, T. Migita, and H. Wagner Jr., *ibid.*, **25**, 696 (1968).

(27) D. J. Warren and J. G. Ledingham, *Cardiovasc. Res.*, **8**, 570 (1974).

(28) J. Onarheim and I. Tyssebotn, *Undersea Biomed. Res.*, **7**, 47 (1980).

(29) T. Høyem-Johansen, L. Slørdal, A. Høylandskjaer, and J. Aarbakke, *Acta Pharmacol. Toxicol.*, **47**, 279 (1980).

ACKNOWLEDGMENTS

This work was supported by grants from Norsk Medisinaldepot, Oslo, Norway.

Evaluation of Chemical Analysis for the Determination of Solasodine in *Solanum Laciniatum*

P. G. CRABBE ‡ and C. FRYER *x

Received September 29, 1981, from the *Department of Chemical Engineering, Monash University, Clayton, Victoria, Australia, 3168.* Accepted for publication February 5, 1982. *Present address: Fluor Australia Pty. Ltd., Melbourne, 3001, Australia. ‡Present address: Department of Chemical and Materials Engineering, University of Auckland, New Zealand.

Abstract □ A detailed study of a method for solasodine analysis has been carried out and the suitability of chemical analysis for solasodine determination in plant material evaluated. A number of problems with the analytical isolation of solasodine and its subsequent colorimetric determination have been highlighted: oven drying of plant material >100° leads to solasodine loss; cell disruption of the dry plant material is required if complete and rapid extraction of solasodine is to take place; hydrolysis of plant extract residues in >1 *N* acid leads to solasodine loss; the colorimetric procedure is more temperamental than past methods have indicated, especially with regard to the specificity of the reaction and the instability of the complex.

Keyphrases □ Solasodine—steroidal alkaloid from *Solanum laciniatum*, colorimetric determination by evaluation of chemical analysis □ Steroids—colorimetric determination of the alkaloid, solasodine, in *Solanum laciniatum* □ Colorimetry—determination of solasodine in *Solanum laciniatum*

Since problems arose 6 or 7 years ago with the supply, cost, and steroid content of *Dioscorea*, the source of diosgenin for steroid drug production, there has been renewed interest in alternative raw materials, including solasodine from plants of the genus *Solanum*. This steroidal alkaloid occurs in *S. aviculare* and *S. laciniatum* as the glycosides, solasonine and solamargine.

As part of a study into the production of solasodine from *Solanum* plant material, chemical analysis was considered for the determination of solasodine and its related species. Several important observations were made in the course of this investigation concerning both the isolation of solasodine from the plant (sample preparation, extraction, and hydrolysis) and the subsequent determination of solasodine using colorimetry. Chemical analysis was found not to be suitable for this study, and subsequently, a procedure using high-pressure liquid chromatography was developed (1). However, chemical analysis is suitable for certain purposes and has the advantage of not requiring expensive equipment. Matters concerning the isolation of solasodine from the plant material are important in solasodine analysis in general (including instrumental analysis) and in commercial solasodine production.

Previous methods for chemical analysis of solasodine

0022-3549/82/1200-1356$01.00/0

have been reviewed. In particular, a colorimetric procedure (2) has been studied; analytical scale sample preparation, extraction of solasodine glycosides, hydrolysis, and determination of solasodine by methyl orange complexing also have been evaluated.

BACKGROUND

In *Solanum* species, steroid alkaloids constitute only 0–5% of the dried plant, making it necessary to determine these components in the presence of a large amount of inert material. In most procedures for determination of solasodine in *Solanum*, solasodine is separated from the plant matrix by selective extraction, then purified before analysis.

Solasodine must be isolated in a relatively pure form before its determination. There is only one reported method in which plant material is analyzed directly for solasodine without extraction or purification steps (3). In all other reported methods, a fairly standard procedure is followed involving sample preparation, extraction of glycosides, and hydrolysis to the aglycon. Because drying stabilizes the solasodine content of the plant material, most procedures start with dry material, although fruits have often been analyzed fresh. Refrigeration has also been used and gives comparable solasodine contents to oven drying of samples at temperatures <100° (4). Oven drying of samples >100° may lead to loss of solasodine (4).

It is normal to crush the dried plant material before extraction. There are reports which suggest that as the average particle size is decreased, the amount of solasodine extracted increases (5, 6). Also, defatting the dry powdered plant material with light petroleum prior to extraction has been shown to reduce significantly the error in the analysis (7).

Solvents used for extraction include dilute aqueous acids, alcohols, and acidified alcohols. Dilute aqueous acid is more specific than alcohols and extracts fewer inert materials. However, if solasodine is present in the plant in partial glycoside or aglycon form because of poor drying and storage, it may not be extracted by dilute aqueous acid, and an alcohol solvent will be more suitable. It has been shown (8) that due to this breakdown of glycosides, previous procedures (9–11) all gave incomplete extraction, and this modified method (8), avoiding acid extraction, gave 30–50% greater solasodine contents for the same material.

Normally solasodine is analyzed as the aglycon, since hydrolysis is a useful purification step, especially if aqueous extraction is used. Increased acid concentration gives increased hydrolysis rates but losses of solasodine have been reported when plant extracts are hydrolyzed with strong acid (4, 7). Many methods combine the extraction and hydrolysis step into a single, direct hydrolysis. Completeness of extraction is ensured due to the more rigorous extraction conditions, and because the less soluble aglycon is produced, mother liquor losses during precipitation, filtration, and washing will be lower. However, such a procedure will extract more inerts, and because the hydrolysis is carried out in the presence of the plant extract, losses of solasodine may occur.

Isolation of solasodine as discussed so far aims only at determining the total steroid base content. To make the isolation procedure more specific, a chromatographic separation (paper, thin-layer, or ion-exchange chromatography) can be introduced at some stage before the final determination is made. If glycoalkaloids are to be distinguished, then separation should follow hydrolysis. In some cases *in situ* colorimetric analytical procedures have been developed using densiometry (12–19). Such methods are rapid but require continual calibration and are subject to large errors.

Three major methods have been used for determination of the amount of solasodine recovered: gravimetric, titrimetric, and colorimetric. Colorimetric determination is the method most widely used. Although there are many dyes that may be used (20, 21), bromthymol blue and methyl orange have been the usual dyes employed.

None of the reported procedures for solasodine determination has been systematically investigated to check for errors arising at each stage in the procedure. Some overall tests have been applied using repeated analysis of plant material to determine reproducibility. This approach identifies random but not systematic errors. A few investigators have used addition of pure solasodine to determine the percentage recovery of solasodine, but this technique will not identify losses during sample preparation and extraction.

In the present investigation, the Birner method (2) for solasodine analysis was subjected to systematic evaluation. The basic procedure of this method was followed, but in a scaled-up form so that larger initial plant samples could be used (1.0 instead of 0.1 g). Three considerations of the Birner method were made: to ensure that the procedure was at optimum conditions, to verify that the solasodine determined was the total solasodine content of the plant material, and to estimate the reproducibility of the method. To achieve these objectives it was necessary to study each step of the method separately and to work backwards through the method starting at the colorimetric assay.

EXPERIMENTAL

The reagents specified previously (2) were used. Standard solutions of solasodine (20 and 100 μg/ml in 20% acetic acid), solasonine (100 and 500 μg/ml in water), and solasodiene (100 μg/ml in ethanol) were prepared from purified compounds. In all cases *S. laciniatum*[1] plant material was used.

Analytical Procedure—Leaf material was oven dried at 70–80° to constant weight, then ground to <75-μm sieve size. This material was divided into six 1.000-g portions, and each portion was analyzed. For the analysis, each portion was refluxed with ethanol (70 ml) for 40 min and then filtered. The filtrate and residue washings were made up to 100 ml with ethanol. An aliquot (20 ml) was evaporated to dryness and 1 *N* HCl (7.5 ml) was added. The mixture was heated on a steam bath (temperature 95–98°) for 5 hr to effect hydrolysis. The solution was cooled and neutralized with 1 *N* NaOH. Glacial acetic acid (5 ml) was added and the solution filtered and made up to 25 ml with water. Aliquots of this hydrolysate (2 ml) were then taken and the solasodine content determined colorimetrically. For the standard solution, an aliquot of hydrolysate plus sodium acetate–acetic acid buffer (5 ml, pH 4.7) and aqueous methyl orange (1.0 ml) were added to chloroform (5 ml) in a separating funnel (100 ml) and the resulting mixture shaken for 4 min. The chloroform layer was separated and dried over anhydrous sodium sulfate and the absorbance read in a spectrophotometer at 425 nm. The same procedure was carried out for the reference solution as for the standard solution, but without added methyl orange.

Instability of the Complex—The solasodine–methyl orange complex formed from 1.0 and 2.0 ml of the 100-μg/ml standard solasodine solution was kept in a capped cuvet and either exposed to room light or left in the spectrophotometer. The absorbance at 425 nm was measured in the spectrophotometer after various time periods.

Hydrolysis of Plant Extract—A standard ethanol extract solution was prepared by refluxing dry leaf material (10 g) in ethanol (1000 ml) for 45 min. Portions of this solution (20 ml) were refluxed with aqueous acid (7.5 ml) for the given period; the solution was cooled and neutralized with equal normality base (7.5 ml) and the solasodine content was determined.

Hydrolysis of Standard Solasonine Solution—For 2 *N* HCl hydrolysis, solasonine (3.2 ml of 500-μg/ml solution) was refluxed on a steam bath with 3.48 *N* HCl (4.3 ml) for the specified period. For 1 *N* HCl hydrolysis, solasonine (3.2 ml of 500-μg/ml solution) with 1.74 *N* HCl (4.3 ml) was used.

Hydrolysis of Plant Extract and Standard Solasodiene—Standard plant extract solution (20 ml) plus solasodiene (5 ml of 100 μg/ml) were evaporated to dryness and 2 *N* HCl added (7.5 ml). The solution was refluxed for the given period then cooled and neutralized with 2 *N* NaOH. The absorbance of the conjugated double bonds of solasodiene at 240 nm was found to be linear and was used to determine the solasodiene content of the final chloroform extract. Reference solution was pure chloroform. For the zero hydrolysis time case, the residue was shaken with the acid for 2 min at room temperature before being neutralized.

Effect of Extraction Time on Solasodine Yield from Crushed Leaf Material—A uniform sample of dry leaf material in the sieve range of 0.5 to 1.0 mm was prepared. Samples (1 g) were refluxed with 70 ml of ethanol for set periods.

Effect of Solid/Solvent Ratio on Extracted Solasodine—The leaf material was oven dried at 70–80° and ground to pass a 1-mm sieve. Samples of 0.25, 0.5, 1.0, and 2.0 g were taken and repeatedly extracted. For each extraction the sample was refluxed in 70 ml of 95% ethanol for 40 min, after which the solution was allowed to cool and settle and the extract solution decanted. The residue leaf material was washed with 95% ethanol and the washings decanted to make the extract solution up to 100 ml. An additional 70 ml of 95% ethanol was then added immediately

[1] The plant material was obtained from plants grown from seeds collected from plants identified as *S. laciniatum* Ait. by Dr. D. E. Symons (Waite Agricultural Research Institute, South Australia, Voucher No. ADW 47361). Seed samples JMS 75/176 are held by Dr. Fryer.

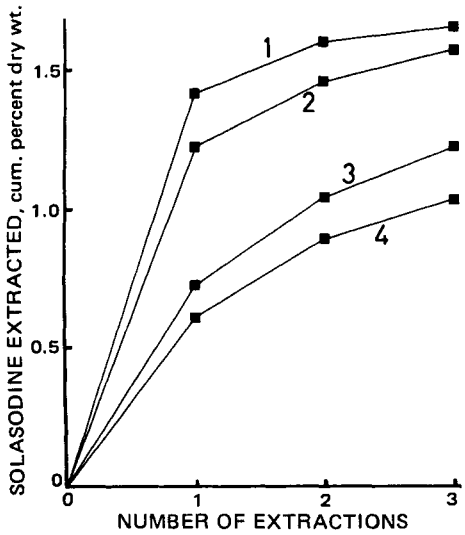

Figure 1—*Combined effect of added base and size reduction on solasodine extracted from dry leaf material. Key: (1) ethanol, ground < 0.25 mm; (2) ethanol, 2% triethylamine, ground < 0.25 mm; (3) ethanol, 2% triethylamine, crushed < 2.812 mm; (4) ethanol, crushed < 2.812 mm.*

to the damp leaf material in the flask and the extraction repeated. Between extractions 4 and 5 of the 1.0-g and 2.0-g samples, the residue leaf material was allowed to stand for 1 week while the analysis of the previous extractions was obtained. During this time the residue dried out completely.

Effect of Particle Size on Extracted Solasodine—A sample of leaf material dried at 70–80° was taken and broken into pieces by crushing. Material in the screen size range of 2.812–1.204 mm was retained, with as much of the leaf stalk material as possible being removed. A portion of this material was put aside and the remainder divided into four quantities. These were either crushed or ground in a mortar and pestle to pass 1.004-, 0.599-, 0.250-, and 0.075-mm screen sizes. This gave five samples of different average particle size, as indicated in Fig. 1. The averge sizes reported are volume average diameters based on sieve analysis, the particle volume estimation allowing for the platelet shape of the leaf particles as described previously (22). Portions of each sample were repeatedly extracted and analyzed as described in the *Analytical Procedure* section. The results were corrected to allow for the contribution of fines (<75 μm) in the samples.

Microscopic observation of the samples, numbered 1–5 as in Fig. 1, revealed: sample 1, large pieces of leaf with no fines; samples 2 and 3, large pieces of leaf plus material of various sizes including cell-size particles; sample 4, mostly fine particles of cell size but also small leaf particles consisting of several cells together (<50 cells); and sample 5, completely ruptured cell material.

The cell structure could be seen clearly on the flat surface regions of the leaf material. Ruptured cells only occurred along the thin edges of the leaf material and not on the flat surface regions. By counting cells along a linear dimension (*e.g.*, 1-mm length), it was found that the average cell size was 40 ± 5 μm for the dried leaf material.

Effect of Added Acid–Base on Extracted Solasodine—The leaf material used was the same as that in the section, Effect of Solid/Solvent Ratio on Extracted Solasodine. Three 1-g portions of this material were taken for repeated extraction and analysis as described in the previous two sections. One portion was repeatedly extracted with 70 ml of ethanol and 1.4 ml of glacial acetic acid (2% v/v acetic acid in ethanol); the second with 70 ml of ethanol and 3.5 ml of glacial acetic acid (5% v/v acetic acid in ethanol); and the third with 70 ml of ethanol and 5 ml of concentrated ammonia solution (2% v/v ammonia/ethanol). Each extraction was carried out under reflux for 40 min.

Combined Effect of Particle Size and Added Base on Extracted Solasodine—Leaf material dried at 70–80° was divided into two portions. One portion was crushed to pass a 2.812-mm sieve size, the other ground to pass a 0.25-mm sieve size. Portions (1 g) of each of these size fractions were repeatedly extracted and analyzed using both 70 ml of ethanol and 1.37 ml of triethylamine. Each extraction was carried out for 40 min under reflux. When the solvent was removed from the portion of the extract solution taken for hydrolysis, care was taken to remove all the triethylamine (bp < 90°) so that it would not interfere in the subsequent colorimetric analysis.

Effect of Extraction Time on Solasodine Yield from Ground Leaf Material—A uniform sample of dry leaf material was ground to pass a 90-μm sieve size. Samples (0.8 g) were refluxed with 60 ml of methanol for set periods. For the zero-extraction time case, the sample was shaken with the methanol for 30 sec at room temperature before filtering.

Effect of Oven Drying Temperature on Solasodine Yield—Leaf material from the same plant and of a similar size and age was divided into six samples of 100–150 g each and dried at various temperatures in an air-circulated oven. Once dry, each leaf sample was ground to pass a 90-μm sieve before extraction. Extraction was a 40-min reflux of 1.0 g/70 ml of ethanol.

RESULTS AND DISCUSSION

Colorimetric Analysis—Results of the colorimetric analysis procedure outlined above showed that the absorbance of the solasodine–methyl orange complex obeys Beer's law over the range of 2–50 μg/ml.

The original method (2) involves no reference for the absorbance readings. Normal plant colored matter, soluble in chloroform, is carried through the procedure and gives absorbance in the <450-nm region. It was found that the use of a reference solution, similar to the standard solution but without the methyl orange, eliminated this effect. The mass transfer of the solasodine–methyl orange complex from the aqueous to the chloroform layer is slow and was found to take up to 5 min.

The methyl orange–solasodine complex was found to be relatively unstable and several precautions must be taken. Contact with rubber, metal, or plastics gave breakdown of the complex and led to erroneous results. Because of this, the complex should be contained in clean, smooth glassware rinsed with an acetone solution of 0.5% *m*-cresol before use (4).

The complex was found to be stable in the dark for up to 3 days after formation but was unstable when exposed to room light or to light of wavelength 425 nm in the spectrophotometer. Losses ranging from 20 to 50% were observed within 20 min of exposure to these conditions, with initial rates of loss from 1 to 5%/min. To obtain reproducible results, it is essential that the time between formation of the complex and measurement of its absorbance be the same in all analysis and calibration tests.

Methyl orange was found to form complexes with amines other than solasodine, including most simple organic amines and even ammonia. Such compounds may be formed during degradation of plant material in storage. These complexes had similar absorption characteristics to the solasodine–methyl orange complex.

Hydrolysis—Only the effects of acid concentration and time on the hydrolysis were considered. Temperatures and solvent were left unchanged from the original method. It was found that, using 0.5 and 1 *N* HCl, hydrolysis was not complete until after 5-hr digestion on a steam bath. Using 1 *N* HCl and a hydrolysis time of 2 hr as in the original procedure (2), the hydrolysis is only 55–60% complete (Fig. 2). At higher acid

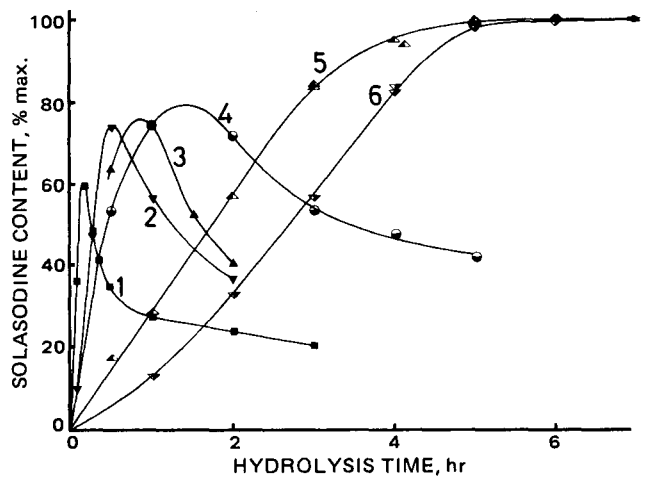

Figure 2—*Effect of acid concentration on the hydrolysis of plant extracts (solasodine contents are expressed as a percentage of the maximum solasodine content, i.e., that found after stable hydrolysis: 0.5 or 1.0 N HCl for 5 hr at 100°). Key: (1) 2.0 N HCl; (2) 1.5 N HCl; (3) 1.5 N H_2SO_4; (4) 1.25 N HCl; (5) 1.0 N HCl; (6) 0.5 N HCl.*

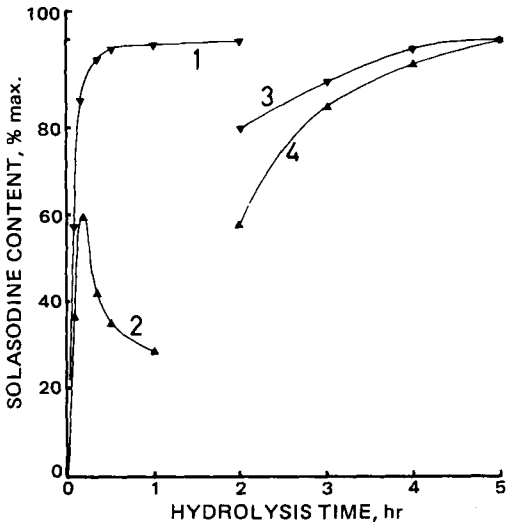

Figure 3—*Hydrolysis of pure solasodine with aqueous hydrochloric acid at 100°, compared with the similar hydrolysis of leaf extracts. Key: (1) 2 N HCl, pure solasonine; (2) 2 N HCl, plant extract; (3) 1 N HCl, pure solasonine; (4) 1 N HCl, plant extract.*

concentrations, the apparent solasodine contents did not stabilize and dropped away after reaching a maximum value. Unstable hydrolysis, as shown in Fig. 2, has only been found by two workers. Unstable hydrolysis with 2 *N* HCl but stable hydrolysis with 0.5 *N* HCl was found (4), while another report (7) indicated that apparently unstable hydrolysis with each of 4, 2, and 1 *N* HCl was found. For the 1 *N* HCl hydrolysis case in the latter study (7), the decrease of solasodine content after the maximum is reached is based on only one experimental point, and represents a <5% change in the apparent solasodine content.

To investigate further the losses of solasodine during hydrolysis, two separate trials were made. In the first experiment, hydrolysis of pure glycoalkaloid (solasonine) was carried out using 1 and 2 *N* HCl levels. The results are given in Fig. 3 and show stable hydrolysis, producing the required amount of solasodine in both cases. The comparable curves for the hydrolysis of the plant extract are reproduced from Fig. 2 for comparison. In the second experiment, 2 *N* HCl hydrolysis of the leaf extract, to which a known amount of pure solasodine was added, gave a reduction of solasodiene with hydrolysis time as shown in Fig. 4. The solasodiene added amounted to 20 μg/ml. The initial increase of solasodiene concentration to this value may be due to the leaching of the solasodiene into aqueous solution from the plant extract residue—a thin, tarry residue on the walls of the flask. The need for such leaching explains why, as

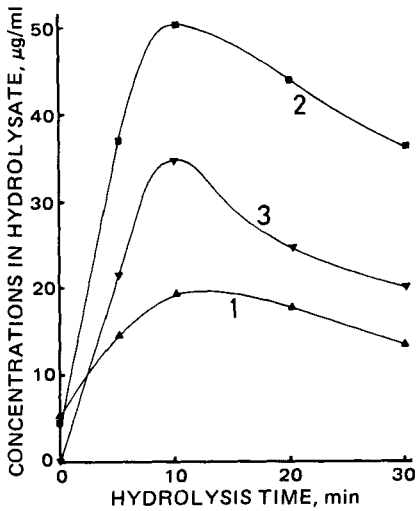

Figure 4—*Hydrolysis with 2 N HCl at 100° of a leaf extract containing added pure solasodiene compared with the similar hydrolysis of leaf extract. Key: (1) solasodiene from extract with added solasodiene; (2) total steroidal base from extract with added solasodiene; (3) solasodine from leaf extract (from Fig. 3).*

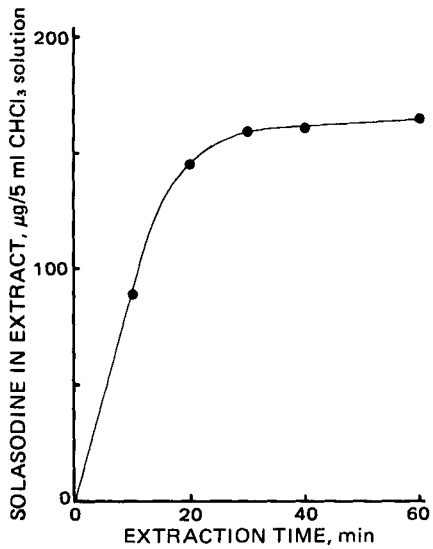

Figure 5—*Effect of extraction time on extraction of solasodine with ethanol from crushed leaf material.*

shown in Fig. 3, hydrolysis of pure solasonine occurred faster than the corresponding hydrolysis of the plant extract: The pure solasonine was being hydrolyzed in solution and no leaching was necessary. The change in total steroidal base is also shown in Fig. 4. This was determined by the normal colorimetric assay procedure and represents the total solasodine plus solasodiene content. The 2 *N* HCl hydrolysis curve from Fig. 2 is also reproduced in Fig. 4 for comparison. The sum of the lower curves approximates the upper (solasodine + solasodiene) curve.

From these two experiments, it appears that it is the formation and the subsequent further reaction of solasodiene which is causing the overall loss of solasodine (determined as total steroidal base). The further reaction of solasodiene is linked to other compounds in the plant extract and is important only >1 *N* acid. Sulfuric acid reportedly produces less solasodiene than hydrochloric acid for a given acid strength (23) but, as shown in Fig. 2, at the 1.5 *N* level, the use of sulfuric acid still does not give stable hydrolysis.

Extraction—Figure 5 shows the effect of time on extraction for uniform dry leaf material of a sieve size range of 0.5–1.0 mm. A 40-min extraction time appears adequate for this material as the curve tends to approach an upper limit after this period. For the extraction of 1 g of plant material with 70 ml of ethanol, the solubility limit of solasodine (in either glycoside or aglycon form) in ethanol is not exceeded. Because of this and the leveling-off of the curve in Fig. 5, it was initially assumed that complete extraction had taken place. However, when the residue of the plant material from the first extraction was re-extracted with ethanol as before, more solasodine was extracted, amounting to as much as 30–40% of that of the first extraction. Further extractions of this same residue yielded more solasodine; complete extraction was not taking place in a single 40-min ethanolic extraction.

To characterize further this problem of incomplete extraction, a series of extractions of the same material but with different solid/solvent ratios was carried out. The results are shown in Fig. 6. The greater the solid/solvent ratio, the less solasodine per weight of sample extracted. Even so, not all the solasodine is extracted after repeated extractions. For example, even after six repeated extractions of the 2.0-g sample, the solasodine extracted in the seventh extraction represents 4% of the total solasodine extracted. There is a discontinuity in the curves for 1.0- and 2.0-g samples between extractions 4 and 5. This corresponded to the extracted residue being allowed to stand for several days before the fifth extraction. As a result, more solasodine was extracted in the fifth extraction, but this has not altered the shape of the curve between the sixth and seventh extractions from the shape prior to the fourth extraction.

Figure 7 shows the results of Fig. 6 plotted as cumulative solasodine extracted against sample size; the total solasodine extracted per weight of sample decreases with an increase in sample size, but the total solasodine extracted increases with sample size. Thus, as the solid/solvent ratio is increased, more solasodine is extracted (per volume of solvent), but the extraction process is less efficient (per weight of solid). These trends are more important <1 g/70 ml than above this ratio.

The effect of decreasing the particle size on solasodine extraction was investigated. The results are shown in Fig. 8. Lower particle size gives

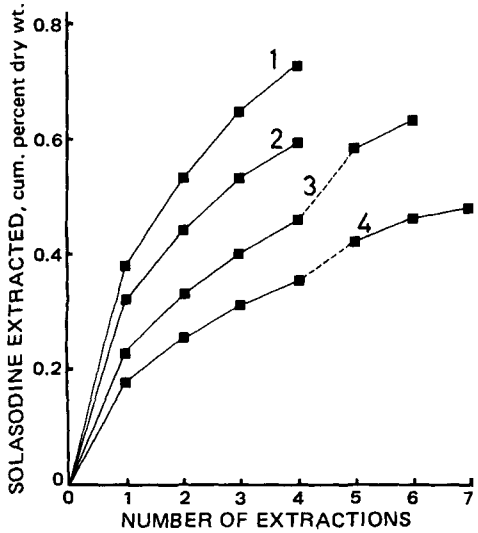

Figure 6—*Effect of altering the proportion of dry leaf material to extractant on solasodine extracted. Key: (1) 0.25 g/70 ml; (2) 0.5 g/70 ml; (3) 1.0 g/70 ml; (4) 2.0 g/70 ml.*

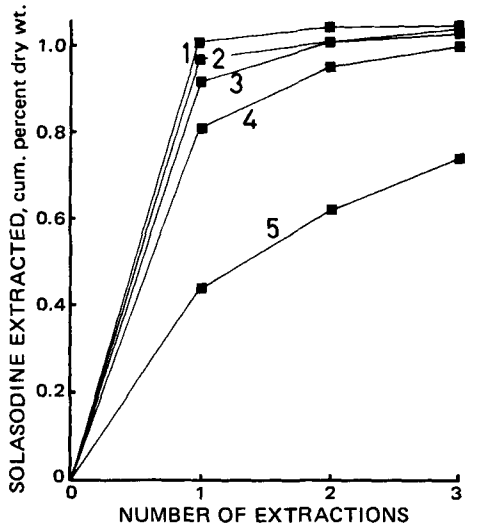

Figure 8—*Effect of average particle size,* D, *on solasodine extracted from dry leaf material. Key: (1)* D < *0.075 mm; (2)* D = *0.16 mm; (3)* D = *0.42 mm; (4)* D = *0.60 mm; (5)* D = *1.93 mm.*

increased extraction, and for the sample of the finest material, 97% of the total solasodine was obtained after a single 40-min extraction. The cell size of the dry leaf material used in this experiment was calculated at 40 ± 5 μm by viewing the material through a microscope. This means that for the material ground to pass the 75-μm sieve size, the majority of the cells are ruptured, while for the largest material [particle size (D) = 1.93 mm] only a small proportion of the cells, those along the edges of the leaf pieces, are ruptured.

It is suggested from these observations that ruptured cells have readily extractable solasodine, while the solasodine within intact cells can only be removed by much slower diffusional transport through cell walls. This would explain the shape of Fig. 5. The curve represents not a single exponential type diffusional process but the combination of two diffusional processes, one much more rapid than the other. The apparent leveling-off seen in Fig. 5, therefore, is misleading and represents the much slower diffusional process becoming dominant in the latter stages of the extraction. This also explains why in Fig. 6 the sudden jump between extractions 4 and 5 of the 1.0- and 2.0-g samples occurred. The greater time permitted to elapse before the next extraction has allowed diffusional processes to distribute the remaining solasodine uniformly throughout the plant material, enabling greater removal during the next extraction.

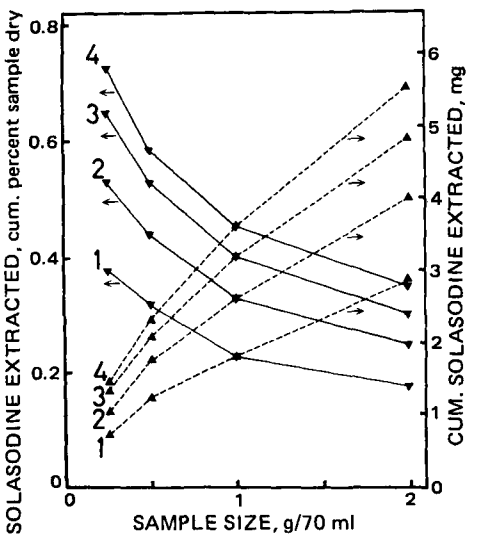

Figure 7—*Effect of altering the proportion of dry leaf material to extractant on cumulative solasodine extracted from successive extractions. Key: (1) first extraction; (2) second extraction; (3) third extraction; (4) fourth extraction; (—) sample size; (- - -) total solasodine extracted.*

If Fig. 7 is reconsidered, from the curves of cumulative solasodine extracted per weight of sample *versus* sample size, it may be seen that the effect of sample size occurs predominantly during the first extraction. During subsequent extractions the effect decreases until in the fourth extraction an approximately equal amount of solasodine per unit weight is extracted for each sample size. The shape of the curves can be attributed to an indirect effect caused by the processes being diffusion-controlled. The diffusional driving force is proportional to the difference in solasodine concentration between the plant material and the bulk solvent. At higher solid/solvent ratios, the bulk solvent concentration will increase to a higher level. Consequently, the diffusion driving force will decrease, causing less solasodine to be extracted over a given time in such cases. The effect can be expected to be greater for the first extraction, where the large proportion of the solasodine is rapidly extracted into the bulk solution from the ruptured cells. The effect becomes less important in subsequent extractions where less solasodine is extracted, and the initial rapid extraction from the ruptured cells no longer occurs.

The effect of adding acid or base to the ethanol to aid the diffusional processes was also investigated. Soaking of plant material in either acid (8, 11, 24) or base (25) prior to extraction has been shown to give higher yields of the alkaloids. The ability to improve extraction is based on the assumption that the solasodine is present in the plant as an ion pair, possibly attached to an anionic site fixed to the plant cell matrix. If this is the case, added acid will form a more mobile solasodine salt, while added base will produce the free base form of solasodine, both unattached to the plant wall. The results for added acetic acid at 2 and 5% (v/v) levels are shown in Fig. 9 for the same material as used in Fig. 6. The curve for extraction of a 1-g sample with pure ethanol is reproduced from Fig. 6 for comparison. The effect is small and possibly not significant. Added base gives a much greater effect but only for coarsely crushed material (Fig. 1). When diffusion strongly limits the extraction process (coarsely crushed material) added base helps by making the solasodine molecule more mobile, but when this diffusional limitation is eliminated (finely ground material) the added base acts only to decrease the solubility of the solasodine.

Mechanical rupture of leaf cells is not the only method of eliminating the cell wall diffusional barriers but is best suited to analytical extraction. The effect of cell disruption by freezing or by cooking under either pressure or vacuum on the diffusion of solasodine from *S. laciniatum* was studied (26); if disruption of the plant cells preceded extraction, then extraction rates, not yields, were found to be higher. The action of endogenous enzymes produces similar results to dry grinding (22). Figure 10 shows the effect of time on the extraction with methanol of dry leaf material ground to pass a 90-μm sieve; very rapid extraction of the solasodine is shown, and within 10 min all the solasodine is extracted. Even a 30-sec wash with methanol at room temperature (the zero point in Fig. 10) extracts ~80% of the total solasodine.

Sample Preparation—It is normal for a plant sample to be dried and crushed to a uniform size fraction before analysis. This stabilizes the solasodine content in the plant material and, if only a fraction of the total sample is to be analyzed, enables a representative portion to be taken.

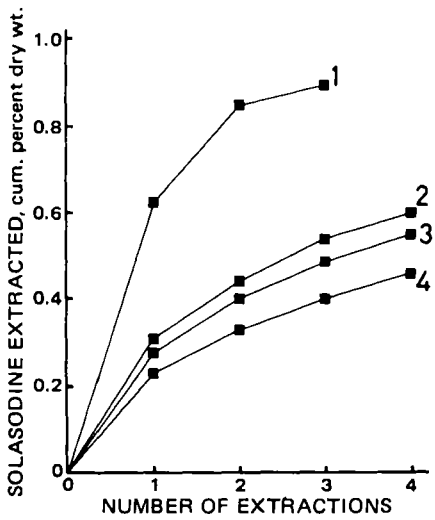

Figure 9—*Effect of added acid or base on solasodine extracted from dry leaf material. Key: (1) ethanol, 2% ammonia; (2) ethanol, 5% acetic acid; (3) ethanol, 2% acetic acid; (4) ethanol.*

The plant sample needs to be very finely ground to ensure complete extraction as already discussed. A number of workers have reported variable solasodine contents for the same material dried under different conditions (27–29). However, preliminary studies of postharvest drying (22) show no such effects and indicate that previous findings have been affected by the problem of incomplete extraction discussed above. Oven drying at 80° is recommended for analytical sample preparation. Below 75° drying rates are slow and >100° losses of solasodine occur (4). Figure 11 presents the results for the same leaf material dried at oven temperatures of 40–120°; severe reduction in extractable solasodine occurs for drying temperatures >100°. In a separate experiment, this loss of solasodine was shown to occur near the end of the drying process. The loss of extractable solasodine is accompanied by a corresponding loss of the green-colored material normally extracted by alcohol. It appears that for leaf material dried >100°, decomposition and transformation of other leaf components take place simultaneously with the drying process, and the decomposition products may restrict later extraction of the solasodine.

Reproducibility—During this study of a previously described method (2) several modifications have been made to provide a method with no systematic errors. To establish an estimate of the reproducibility of the modified method, repeated analysis of the same finely ground plant material was carried out. This enabled calculation of the sample standard deviation of the overall method (s), of the combined hydrolysis–colorimetric assay steps (s_{hc}) and of the colorimetric assay step alone (s_c) (22). The values of the sample standard deviation (expressed as a percentage of the overall mean) and their associated degrees of freedom are included

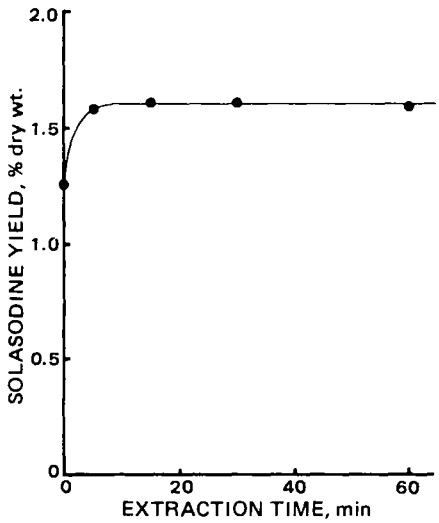

Figure 10—*Effect of extraction time on extraction of solasodine with methanol from ground leaf material.*

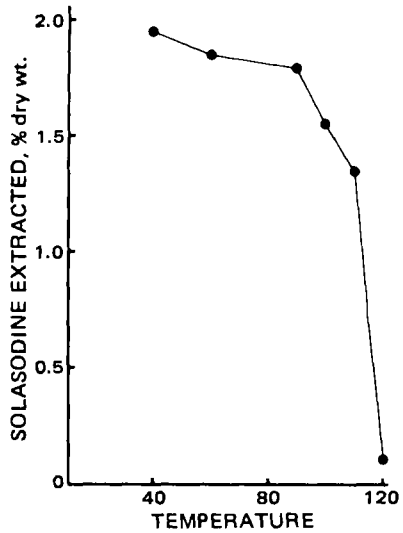

Figure 11—*Effect of drying temperature on solasodine extracted from oven-dried leaf material.*

Table I—Experimentally Determined Standard Deviations for Chemical Analysis

Procedure	Standard Deviation, %[a]	Degrees of Freedom
Colorimetric assay	$s_c = 5.6$	6
Hydrolysis and assay	$s_{ch} = 6.4$	6
Overall analysis	$s = 6.1$	10

[a] As percent of overall mean.

in Table I. From these sample standard deviations, the confidence intervals for the corresponding population standard deviations (σ, σ_{hc}, and σ_c) may be calculated. Based on the χ^2 distribution, the 90% confidence intervals for the standard deviations, expressed as percentages of the overall mean, are:

$$3.9\% < \sigma_c < 10.8\%$$
$$4.4\% < \sigma_{hc} < 12.2\%$$
$$4.5\% < \sigma < 9.7\%$$

These intervals are so large that it is difficult to draw any conclusion from the estimates of σ_c, σ_{hc}, and σ, except that the major proportion of the overall error occurs in the colorimetric assay and that the overall error in the analysis method is 4.5–9.7%. This means that the limiting feature of the method is the final colorimetric determination of solasodine, due probably to the instability of the complex.

CONCLUSIONS

For samples of *S. laciniatum*, where solasodine is the only steroidal alkaloid present, total solasodine glycosides, solasodine aglycon, and solasodiene each can be determined. The aglycons may be extracted into a nonpolar solvent such as chloroform or benzene and the separate contents of total glycosides and total aglycons determined; measurement of solasodiene content in the aglycon fraction can be made at 235 nm in a UV spectrophotometer. If chromatographic separation is incorporated [for examples see previously described procedures (30–33)] then the glycosides may be further separated before the final analysis. Theoretically any analysis related to solasodine production can be performed, but once chromatography is incorporated, the extra errors involved make the results at best semiquantitative.

Study of this particular colorimetric assay technique shows in more detail the problems associated with such a technique. Difficulties have been found in each aspect of the method, difficulties largely overlooked in previously reported methods, and difficulties which in some cases apply to commercial solasodine isolation. The colorimetric procedure is much more temperamental than past methods have indicated, especially with regard to the specificity of the reaction and the instability of the complex. It was implied (2) that the reaction with methyl orange was specific to nitrogen-containing alkaloids; whereas it appears that all amines, in-

cluding ammonia itself, will give similar complex formation. The instability of the complex was also not mentioned.

Although solasodiene can be analyzed along with solasodine to give a total solasodine content, severe hydrolysis conditions (>1 *N* HCl) have been found to give overall solasodine loss. This is apparently caused by reactions, of unknown mechanism, associated with solasodiene formation and in the presence of the plant extract. Using conditions where stable hydrolysis occurs, much longer hydrolysis times than normally specified in reported methods were found to be necessary to complete the hydrolysis (*e.g.*, 5 hr at 100° for 1 *N* HCl in aqueous solution). Even for glycosides in solution, inspection of Fig. 3 shows that at least 4 hr at 100° for 1 *N* HCl is necessary.

For complete extraction of the solasodine to take place within one extraction, it is necessary to remove the cell wall diffusional barriers. For analytical purposes dry grinding of the plant material to pass a 75- to 90-μm sieve is suitable and allows very rapid extraction of the solasodine by alcohol. To stabilize the solasodine content of the plant material, oven drying at 75–90° is recommended. Oven drying >100° leads to loss of extractable solasodine. However, a preliminary fixation at temperatures >100° to arrest biological processes within the plant material does not affect the extraction process.

The final colorimetric assay is the cause of most of the error inherent in the method. Assuming a χ^2 distribution, the confidence interval for the true standard deviation is large, unless a large number of repeated analyses are made for its estimation. In most reported methods, where evaluation of the method is based on the results of repeated analyses, the number of repetitions is small, and consequently, in such cases the confidence interval for the true standard deviation will be large. Thus, the true error inherent in a method may differ greatly from that reported.

The problems of chemical analysis raise doubts about the soundness of previous studies of solasodine production. Results may be subject to large systematic and random errors because of poor analytical procedures. In particular, the problem of incomplete extraction will introduce large systematic errors.

REFERENCES

(1) P. G. Crabbe and C. Fryer, *J. Chromatogr.*, **187,** 87 (1980).

(2) J. Birner, *J. Pharm. Sci.*, **58,** 258 (1969).

(3) C. Lorincz, *Magy. Kem. Foly.*, **68,** 414 (1961).

(4) J. E. Lancaster and J. D. Mann, *N. Z. J. Agric. Res.*, **18,** 139 (1975).

(5) R. Hardman and T. G. Williams, *J. Pharm. Pharmacol.*, **23,** 231S (1971).

(6) W. J. Cruz and O. Proaño, *Politecnica*, **2,** 155 (1970).

(7) R. Hardman and T. G. Williams, *Planta. Med.*, **29,** 66 (1976).

(8) P. Bite, E. Mago-Karacsony, T. Rettegi, *Magy. Kem. Foly.*, **76,** 90 (1970); *Acta Chim. (Budapest)*, **64,** 199 (1970).

(9) I. Gyenes, *Magy. Kem. Foly.*, **56,** 383 (1950).

(10) K. Szasz, L. Gracza, and C. Lorincz, *Acta. Pharm. Hung.*, **31,** 211 (1961).

(11) N. A. Valovich, *Med. Prom. SSSR*, **19,** 45 (1965).

(12) G. L. Szendey, *Arch. Pharm.*, **290,** 563 (1957).

(13) G. Blunden, R. Hardman, and J. C. Morrison, *J. Pharm. Sci.*, **56,** 948 (1967).

(14) K. R. Brain and R. Hardman, *J. Chromatogr.*, **38,** 355 (1968).

(15) M. B. E. Fayez and A. A. Saleh, *Z. Anal. Chem.*, **246,** 380 (1969).

(16) E. Kolos-Pethes, J. Varadi, and G. Marczal, *Herba Hung.*, **8,** 169 (1969).

(17) V. N. Borisov, L. A. Pikova, and G. L. Zachepilova, *Khim.-Farm. Zh.*, **10,** 116 (1976).

(18) A. F. Azarkova and L. M. Kogan, *ibid.*, **10,** 104 (1976).

(19) L. A. Pikova, V. V. Panina, and E. I. Korneva, *Rastit. Resur.*, **13,** 531 (1977).

(20) E. A. Tukalo and G. N. Tsarik, *Khim.-Farm. Zh.*, **4,** 56 (1970).

(21) L. Gracza and C. Lorincz, *Arch. Pharm.*, **296,** 615 (1963).

(22) P. G. Crabbe, Ph.D. thesis, Monash University (1979).

(23) A. S. Labenskii and R. I. Kuzovkova, *Med. Prom. SSSR*, **19,** 35 (1965).

(24) P. Bite, E. Mago, and T. Rettegi, Hung. Pat. 155441 (Dec. 23, 1968).

(25) K. Syhora, Z. Cekan, and S. Hermanek, *Planta Med.*, **10,** 318 (1962).

(26) G. Selmeci, G. Valovics, and L. Szlavik, *Pharmazie (Berlin)*, **22,** 173 (1967).

(27) A. R. Guseva, V. A. Pasechnichenko, and M. G. Borikhina, *Biokhimiya*, **30,** 260 (1965).

(28) V. V. Panina, G. M. Dem'yanova, and R. I. Kuzovkova, *Rast. Resur.* **10,** 386 (1974).

(29) R. K. Moiseev, L. K. Klyshev, and A. R. Guseva, *Tr. Inst. Bot., Akad. Nauk Kaz. SSR*, **28,** 215 (1970).

(30) R. Kuhn, I. Löw, and H. Trischmann, *Chem. Ber.*, **88,** 289 (1955).

(31) A. R. Guseva and V. A. Paseshnichenko, *Biochemistry (Engl. Transl.)*, **24,** 525 (1959).

(32) L. H. Briggs, R. C. Cambie, and J. L. Hoare, *J. Chem. Soc.*, **1961** 4645.

(33) *Idem.*, **1963,** 2848.

pKa Determination of Benzhydrylpiperazine Antihistamines in Aqueous and Aqueous Methanol Solutions

DAVID W. NEWTON *x, **WALLACE J. MURRAY** ‡, and **MICHAEL W. LOVELL** §

Received December 14, 1981, from the *Department of Pharmaceutics, College of Pharmacy, ‡Department of Biomedicinal Chemistry, University of Nebraska Medical Center, Omaha, NE 68105 and the §Department of Pharmaceutics, College of Pharmacy, J. Hillis Miller Health Center, University of Florida, Gainesville, FL 32610. Accepted for publication February 3, 1982.

Abstract □ The pKa_1 and pKa_2 values of three benzhydrylpiperazine antihistamines, cyclizine (I), chlorcyclizine (II), and hydroxyzine (III), were determined at 24.5 ± 0.5° by potentiometric titration in aqueous solution to be 2.16 ± 0.02 and 8.05 ± 0.03, 2.12 ± 0.04 and 7.65 ± 0.04, and 1.96 ± 0.05 and 7.40 ± 0.03, respectively. The pKa_2 values were also determined by titration in seven aqueous methanol solutions in the range of 11.5–52.9% (w/w) methanol. The apparent dissociation constants of I–III in the aqueous methanol solutions, p_sKa_2, were plotted according to two linear regression equations from which the values in water, $p_\omega Ka_2$, were extrapolated. The plotted variables were p_sKa_2 *versus* methanol concentration (% w/w) and p_sKa_2 + log (water concentration, *M*) *versus* $1000/\epsilon$, where ϵ is the dielectric constant of the aqueous methanol solution. The maximum difference between pKa_2 and $p_\omega Ka_2$ was observed in the case of II where $p_\omega Ka_2$ was 5.23% higher. Statistical analysis of the linear regression data obtained from the plots showed that slightly better accuracy ($p < 0.13$) and correlation ($p < 0.16$) were obtained, but the precision was essentially equal with both methods. The observed ratio of K_{a1}/K_{a2} in I–III, 2.75×10^5–7.76×10^5, was attributed to solvent- and space-mediated field effects and electrostatic induction between nitrogen atoms in the piperazine ring.

Keyphrases □ Benzhydrylpiperazines—antihistamines, pKa determination in aqueous and aqueous methanol solutions □ Dissociation—pKa determination of benzhydrylpiperazine antihistamines in aqueous and aqueous methanol solutions □ Antihistamines—benzhydrylpiperazines, pKa determination in aqueous and aqueous methanol solutions

Five benzhydrylpiperazine antihistamines are currently marketed in the U.S.: cyclizine (I), chlorcyclizine (II), hydroxyzine (III), meclizine (IV), and buclizine (V).

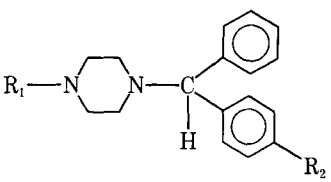

I: $R_1 = CH_3$; $R_2 = H$
II: $R_1 = (CH_2)_2O(CH_2)_2OH$; $R_2 = Cl$
III: $R_1 = CH_3$; $R_2 = Cl$

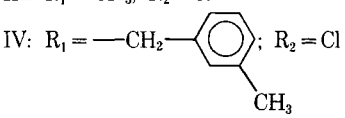

IV: $R_1 =$ —CH_2— (p-CH_3 phenyl); $R_2 = Cl$

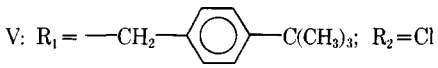

V: $R_1 =$ —CH_2— (p-$C(CH_3)_3$ phenyl); $R_2 = Cl$

Although some pKa[1] data for I (1, 2), II (1–3), III (4–7), and IV (6, 8) have been reported (Table I), much of it is based on titrations in 30–50% aqueous alcohols and chloroform–aqueous buffer partition experiments. More recent values of pKa_1 determined potentiometrically for III and IV (6) and spectrophotometrically for III (7) appear to have been conducted more precisely in aqueous solution.

The benzhydrylpiperazine antihistamines are popularly used as prescription and nonprescription dosage forms for their antiemetic, antipruritic, and sedative effects. It was the purpose of this investigation to determine the pKa_1 and pKa_2 values of these drugs for application to various pharmaceutical situations and to evaluate the accuracy of two methods for extrapolating an aqueous pKa estimate from apparent pKa values obtained in aqueous methanol solutions.

BACKGROUND

The low aqueous solubility of nonprotonated amine bases or nondissociated organic acids appears to be the consensus nemesis to determining pKa values of these substances by potentiometric titration. Even the lower limit of 5×10^{-4} *M* for potentiometry (9) is often not achievable. The use of mixed solvent systems, *e.g.*, an alcohol–water and dioxane–water, has been the method most commonly used to surmount this solubility problem. There is little or no disadvantage to this practice if the purpose merely is to compare the relative acidities or basicities of a series of chemical analogs. If, however, the objective is to make judgments pertaining to the aqueous environments of *in vivo* phenomena, the discrepancy between pKa values determined in aqueous and those in aqueous organic solvent solutions could be consequential.

Estimates of aqueous pKa values for inadequately soluble substances have usually been obtained by plots of the apparent pKa values in aqueous organic solvents *versus* solvent concentration (*e.g.*, % w/w) (10, 11):

$$p_sKa' = [\text{solvent}] + p_\omega Ka \qquad \text{(Eq. 1)}$$

where p_sKa' is the apparent dissociation constant in the aqueous organic solvent system, [solvent] is the organic concentration (% w/w), and $p_\omega Ka$ is the value of p_sKa' extrapolated to 0% (w/w) organic solvent or 100% (w/w) water. This method was used extensively in pharmaceutical studies during the 1950s and early 1960s (1–3, 12–15). The errors inherent in pKa estimates with this method have been addressed elsewhere (16–18). In 1959, two authors independently proposed a relationship that they rationalized should provide a more accurate estimate of aqueous pKa values

Table I—Acid Dissociation Constant (pKa) Values Reported for Some Benzhydrylpiperazine Antihistamine Drugs

Drug	pKa_1	pKa_2
Cyclizine (I)	2.54[a]	7.92[a], 8.16[b]
Chlorcyclizine (II)	2.44[a], 2.43[c]	7.78[a], 8.15[b], 7.81[c]
Hydroxyzine (III)	2.13[d], 1.83[e], 2.0[f]	7.9[g]
Meclizine (IV)	3.1[h], 2.05[i]	6.2[h]

[a] In 50% methanol (Ref. 1). [b] In 30–50% alcohol (Ref. 2). [c] In 20–80% alcohol (Ref. 3). [d] *Via* partitioning between 0.5 *M* H_3PO_4 and chloroform (Ref. 4). [e] In aqueous solution at an ionic strength <0.001 (Ref. 6). [f] Spectrophotometrically in aqueous solution (Ref. 7). [g] In unspecified aqueous methanol solutions (Ref. 5). [h] *Via* partitioning between 0.5 *M* H_3PO_4 and chloroform (Ref. 8). [i] In aqueous solution at an ionic strength of 0.005 (Ref. 6).

[1] The symbol pKa is used throughout in reference to the acid dissociation constant. Formally, K_a is the acid dissociation constant for proton loss by neutral and cationic acids or protonated bases, and $pKa = \log(1/K_a)$.

0022-3549/82/1200-1363$01.00/0

obtained by extrapolation of p_sKa' values in aqueous organic solvent mixtures (19, 20):

$$p_sKa' + \log [H_2O] = \frac{1}{\epsilon}(e^2/2.303\,akT) - \log B_H \qquad \text{(Eq. 2)}$$

where p_sKa' is the apparent pKa value in aqueous organic solvent mixtures uncorrected for electrode response, $[H_2O]$ is the water concentration (M), ϵ is the dielectric constant, e is the ionic charge, a is the mean cation–anion ionic diameter, k is the Boltzmann constant, T is the absolute temperature, and B_H is a constant based on the assumption that $[H_3O^+] \gg [\text{solvent } H^+]$. The values of p_sKa' are corrected by subtracting a constant, δ, which takes into account the variability of glass electrode response in aqueous methanol solutions. This gives the actual pKa value in the mixed solvent system, p_sKa (21, 22):

$$p_sKa = p_sKa' - \delta \qquad \text{(Eq. 3)}$$

Thereafter, a plot of $p_sKa + \log [H_2O]$ *versus* $1/\epsilon$ that is essentially linear may be extrapolated to obtain the ordinate intercept value for $p_\omega Ka$, the estimated aqueous pKa when $\log [H_2O]$ is 1.74 and $1/\epsilon$ is 0.01273 [2]. The linearity of the plots may decrease appreciably when $1/\epsilon > 0.02$ (*e.g.*, ≥70% w/w methanol). This corresponds to the value of $\epsilon \simeq 50$, below which ionic dissociation begins to diminish with a concomitant increase in ion-pair association and perturbation of the equilibrium between the neutral and ionic species (18, 21).

The original solubility method for determining pKa values (23) has been applied to determining pKa values of acidic, basic, and amphoteric substances with low aqueous solubility (9, 24–26). This method has the advantage of providing thermodynamic pKa estimates when the ionic strength of the samples is low (*e.g.*, <0.0005). Its disadvantages include the failure to achieve equilibrium conditions and separate emulsified or suspended neutral species from the saturated salt solutions in equilibrium with them. Potential errors in solubility estimates resulting from supersaturation of ionic and/or neutral species and the instability of some compounds also jeopardize the accuracy of this method. Another method involving a single pKa titration in an aqueous organic solvent mixture has been proposed, but it was judged by its author to be generally inapplicable to the estimation of $p_\omega Ka$ values (27).

It is reasonable to expect that the widespread use of organic solvent–water mixtures for pKa titrations of substances with intrinsic water solubilities of <0.0005 M will continue. This is because of historical precedents and the expedient manipulative techniques that can be accomplished using aqueous organic solutions.

EXPERIMENTAL

Materials—Cyclizine hydrochloride (I)[3], chlorcyclizine hydrochloride (II)[4], hydroxyzine dihydrochloride (III)[5], meclizine dihydrochloride (IV)[6], and buclizine dihydrochloride (V)[7] were used as received. Methanol, hydrochloric acid, and potassium hydroxide solutions were ACS analytical reagent grade, and freshly boiled water with a resistivity ≥10^7 ohm cm were used in the solvent systems and titrants.

Procedures—Titrations were conducted in a 25- or 50-ml multinecked glass flask fitted with a thermometer calibrated in 0.1° units. Agitation was provided by a polytef-coated magnetic stirring bar, and pH values were measured with a digital pH meter[8] equipped with a combination glass electrode[9]. The ambient temperature of the systems varied from 24.0 to 25.0° with an average value of 24.5°. Titrant increments were added from a pipet[10] in 0.25-ml portions.

The $p_sKa'_2$ values of 0.002 M I–III were determined in seven aqueous methanol solutions in the range of 11.5–52.9% (w/w) with a titrant of 0.020 N KOH prepared in aqueous methanol that contained to within 0.1% (w/w) the same methanol concentration as the solutions of I–III. Values of pKa'_2, the apparent constant in aqueous solution, were determined in aqueous 0.001 M I and III titrated with aqueous 0.010 N KOH and in aqueous 0.0005 M II titrated with aqueous 0.005 N KOH. The pKa'_1 values of I and II were obtained from titrations of 0.015 M aqueous solutions with aqueous 0.030 N HCl. The pKa'_1 of III was determined by titrating aqueous 0.015 M III with aqueous 0.030 N KOH.

Activity Corrections—Values of p_sK_a' obtained from titrations of I–III in aqueous methanol solutions were corrected to p_sKa values with Eq. 2 using δ values reported elsewhere (22). The pKa'_2 values of I–III were corrected for activity effects of the K_2 equilibria in Scheme I[11] (16, 18, 28–30):

$$HB^+ + OH^- \overset{K_2}{\rightleftharpoons} B + H_2O$$

Scheme I

$$pKa_2 = pKa'_2 - \frac{0.51\sqrt{I}}{1 + 1.6\sqrt{I}} \qquad \text{(Eq. 4)}$$

where I is the ionic strength of the solution, and the entire negative term estimates the logarithm of the activity coefficient, $-\log \gamma_i$. A similar activity correction was used for the K_1 equilibria shown in Schemes II and III[11] (28):

$$H_2B^{+2} + OH^- \overset{K_1}{\rightleftharpoons} HB^+ + H_2O$$

Scheme II

$$HB^+ + H_3O^+ \overset{K_1}{\rightleftharpoons} H_2B^{+2} + H_2O$$

Scheme III

$$pKa_1 = pKa'_1 = \frac{1.5345\sqrt{I}}{1 + 1.6\sqrt{I}} \qquad \text{(Eq. 5)}$$

RESULTS AND DISCUSSION

The values of pKa_1 for I–III were determined to be 2.16 ± 0.02, 2.12 ± 0.04, and 1.96 ± 0.05, respectively. The corresponding values of pKa_2 are 8.05 ± 0.03, 7.65 ± 0.04, and 7.40 ± 0.03[12].

The plots of the data for p_sKa_2 *versus* methanol (% w/w) are shown in Fig. 1 and that for $p_sKa_2 + \log [H_2O]$ *versus* $1000/\epsilon$ in Fig. 2 for I–III. Least-squares regression lines were plotted for all I–III data sets to permit comparison of the accuracy and precision of $p_\omega Ka_2$ extrapolations derived from each set of ordinate and abscissa coordinates. The ϵ values in Fig. 2 were calculated for each aqueous methanol solution from a linear regression equation derived from data for 10–60% (w/w) methanol (31):

$$\epsilon = -0.4523C + 78.9307 \qquad \text{(Eq. 6)}$$

where C is the methanol concentration (% w/w)[13]. The linear regression data for the plots in Figs. 1 and 2 are summarized in Tables II and III, respectively.

A comparison of R values for I–III (Tables II and III) shows that, based on the Student's t test (32), there was a better linear correlation of the p_sKa_2 titration data plotted according to Eq. 2 ($p < 0.16$). There was, however, essentially no difference ($p < 0.001$) in the precision of the plots of Eqs. 1 and 2 based on a comparison of $S_{y,x}$ values (Tables II and III). The accuracy of $p_\omega Ka_2$ values for I–III, *i.e.*, the differences from pKa_2 (Tables II and III), was also better by Eq. 2 than Eq. 1 plots ($p < 0.13$). The slightly improved linear correlation of the Eq. 2 plot may explain, in part, why it has been advocated instead of Eq. 1 (16, 18). Furthermore, the unreported linear regression data for plots of $p_sKa_2 + \log [H_2O]$ *versus* methanol (% w/w) were virtually identical with those reported in Table III. This would be expected from the nearly linear relationship expressed by Eq. 6 (31).

Doubts about the accuracy of $p_\omega Ka$ values extrapolated from aqueous organic solvent mixtures containing >20% solvent have been expressed elsewhere (16–20); curves shaped like hockey sticks have resulted from Eq. 1 plots. One contributing cause of this could be plotting erroneous high values of p_sKa' uncorrected for δ (Eq. 3). The value of δ ranged from 0.02–0.12 in these titrations, increasing with methanol concentration. Failure to have corrected p_sKa' to p_sKa values would have caused progressive decreases in the slopes of Eq. 1 plots. The resulting horizontal inclinations, *i.e.*, the hockey stick appearance, at high methanol concentrations would have produced greater inaccuracy in the extrapolated

[2] The values of $\log [H_2O]$ and $1/\epsilon$ correspond to $[H_2O] = 55.3\ M$ and $\epsilon = 78.54$, respectively, for water at 25°.
[3] Lot 9C0080, Burroughs Wellcome Co., Greenville, N.C.
[4] Lot 8J0053, Burroughs Wellcome Co., Greenville, N.C.
[5] Lot 17583-27EA, 99.6%, Pfizer Inc., Brooklyn, N.Y.
[6] Lot 2F268-81EA, 100.0%, Pfizer Inc., Brooklyn, N.Y.
[7] Lot AN52650, Stuart Pharmaceuticals, Wilmington, Del.
[8] Model 125, Corning Scientific Products, Medfield, Mass.
[9] No. 476050, Corning Scientific Products, Medfield, Mass.
[10] Eppendorf Model 4700, Brinkmann Instruments Inc., Westbury, N.Y.

[11] B, HB^+, and H_2B^{+2} refer to the nonprotonated, monoprotonated, and diprotonated benzhydrylpiperazines, respectively.
[12] Values of pKa_1, pKa_2, and p_sKa_2 represent the means ± standard deviations of seven values in each set of ten titrations.
[13] The correlation coefficient, R, is 0.9997.

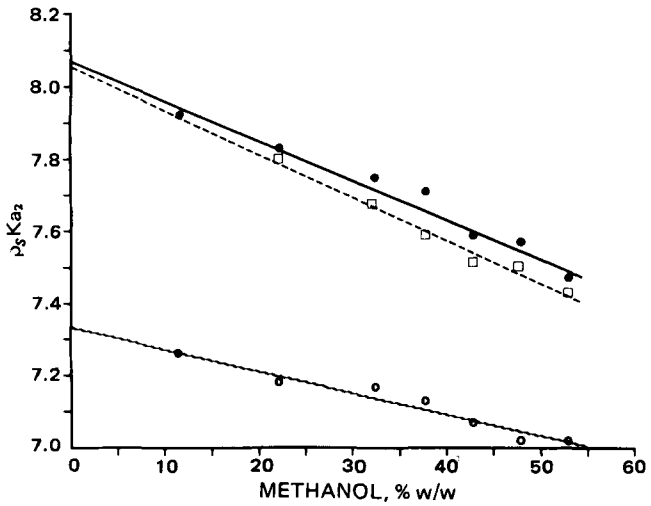

Figure 1—*Plot of p_sKa versus methanol (% w/w) for cyclizine (I), chlorcyclizine (II), and hydroxyzine (III). Key: (●) I; (□) II; (○) III.*

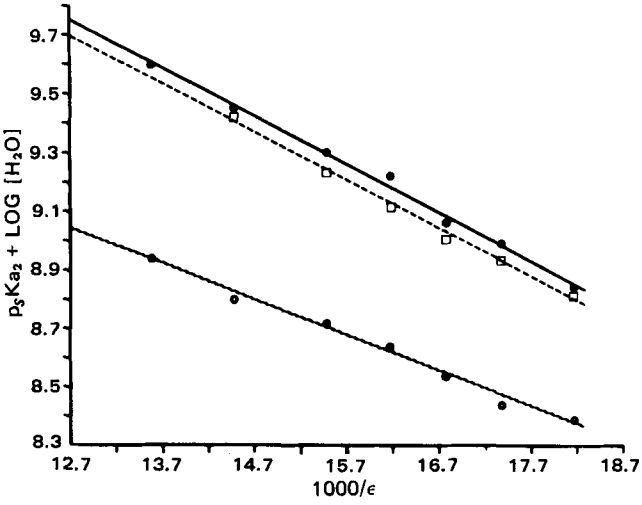

Figure 2—*Plot of p_sKa + log [H_2O] versus 1000/ε for cyclizine (I), chlorcyclizine (II), and hydroxyzine (III). Key: (●) I; (□) II; (○) III.*

$p_\omega Ka_2$ values. Therefore, the I–III p_sKa_2 data were calculated for 37.7% (w/w) ≤ methanol ≤52.9% (w/w) and 16.2 ≤ 1000/ε ≤ 18.2 (Table IV). Statistical analysis showed no difference in the accuracy and precision of I–III $p_\omega Ka_2$ values ($p < 0.001$) and the linear correlation of Eq. 1 and Eq. 2 plots ($p < 0.001$) between the data in Tables II and IV or Tables III and IV. These findings pertain only to I–III under the conditions stated, and they do not warrant general advocation of extrapolating $p_\omega Ka$ values from p_sKa data obtained in >35% (w/w) methanol.

A literature search yielded one similar study of some phenothiazine derivatives (33). Those plots were based on fewer data (mostly three points) obtained in a higher methanol concentration range (mostly ≥40%) and lacked the statistical data necessary for comparing pKa with $p_\omega Ka$ values derived from Eqs. 1 and 2. The plots apparently consisted of empirically connecting the sets of coordinates rather than calculating least-squares regression lines (33).

The magnitude of error in calculating the percent of monoprotonated I–III that would result from using $p_\omega Ka_2$ values to estimate otherwise unreported pKa_2 values for I–III was determined for pH 7.4. The error ranged from 0.72% for I (Table III) to 17.70% for II (Table II) (34):

$$\text{Percent } HB^+ = 100/[1 + 10^{(pH - pKa_2)}] \quad \text{(Eq. 7)}$$

$$\text{Percent } HB^+_\omega = 100/[1 + 10^{(pH - p_\omega Ka_2)}] \quad \text{(Eq. 8)}$$

$$\text{Error, \%} = |\text{Eq. 7} - \text{Eq. 8}| \quad \text{(Eq. 9)}$$

where HB^+ is the monoprotonated conjugate acid of I–III. From Eqs. 7 and 8, as the absolute values of the quantities pH − pKa_2 and pH − $p_\omega Ka_2$ increase, the value of Eq. 9 decreases.

A specific reason for the differences between $p_\omega Ka_2$ and pKa_2 values of I–III obtained by either Eq. 1 or Eq. 2 is not readily apparent. The fact that the titrants and I–III solutions were prepared in the same aqueous methanol concentrations, *i.e.*, within 0.1% (w/w), precluded stoichiometric errors in precision resulting from the nonadditivity of volumes and negative heats of solution. The variability in solvation phenomena

Table II—Linear Regression Data for Plots of Equation 1 [a]

Drug	Equation, p_sKa_2[b] =	$p_\omega Ka_2$[c]	pKa_2[d]	Absolute Value Difference, %[e]	R[f]	$S_{y,x}$[g]
I	−0.011C + 8.067	8.07	8.03	0.50	0.983	0.032
II	−0.012C + 8.052	8.05	7.65	5.23	0.995	0.015
III	−0.006C + 7.332	7.33	7.40	0.95	0.972	0.023

[a] When 11.5% (w/w) ≤ methanol ≤ 52.9% (w/w). [b] This refers to straight line plots for I–III (Fig. 1) where C is the methanol concentration (% w/w). [c] The value of p_sKa_2 extrapolated to 0% (w/w) methanol. [d] The value of pKa'_2 determined in aqueous solution and corrected for $-\log \gamma_i$ (Eq. 4). [e] Calculated from $|(pKa_2 - p_\omega Ka_2)|$ (100/pKa_2). [f] Correlation coefficient. [g] Standard error of the estimate of p_sKa_2 based on the methanol concentration.

Table III—Linear Regression Data for Plots of Equation 2 [a]

Drug	Equation, p_sKa_2 + log [H_2O][b] =	$p_\omega Ka_2$[c]	pKa_2[d]	Absolute Value Difference, %[e]	R[f]	$S_{y,x}$[g]
I	−0.164 (1000/ε) + 11.838	8.01	8.03	0.25	0.997	0.022
II	−0.164 (1000/ε) + 11.785	7.96	7.65	4.05	0.997	0.019
III	−0.121 (1000/ε) + 10.584	7.30	7.40	1.35	0.994	0.023

[a] When 14.5 ≤ 1000/ε ≤ 18.2. [b] This refers to straight line plots for I–III (Fig. 2) where [H_2O] and ε are the molarity of water and dielectric constant, respectively, of the aqueous methanol solvents. [c] This is the extrapolated value of p_sKa_2 obtained when log [H_2O] = 1.743, where 55.3 is the molarity of water at 25°, is subtracted from the quantity (p_sKa_2 + log [H_2O]) when the latter is calculated for 1000/ε = 12.73 where ε = 78.54 for water at 25°. [d] Footnote *d*, Table II. [e] Footnote *e*, Table II. [f] Footnote *f*, Table II. [g] Standard error of the estimate of p_sKa_2 + log [H_2O] based on 1000/ε values.

Table IV—Linear Regression Data for Plots of Equations 1 and 2[a]

Drug	$p_\omega Ka_2$ Eq. 1[b]	$p_\omega Ka_2$ Eq. 2[c]	pKa_2	Difference, %[d] Eq. 1	Difference, %[d] Eq. 2	R[e] Eq. 1	R[e] Eq. 2	$S_{y,x}$[f] Eq. 1	$S_{y,x}$[f] Eq. 2
I	8.25	8.09	8.03	2.74	0.75	0.971	0.990	0.029	0.027
II	7.97	7.87	7.65	4.18	2.88	0.985	0.997	0.014	0.012
III	7.40	7.32	7.40	0	1.08	0.938	0.977	0.022	0.029

[a] Where 37.7% (w/w) ≤ methanol ≤ 52.9% (w/w) and 16.2 ≤ 1000/ε ≤ 18.2, respectively, for Eqs. 1 and 2. [b] Footnote *c*, Table II. [c] Footnote *c*, Table III. [d] Footnote *d*, Table II. [e] Footnote *f*, Table II. [f] Footnote *g*, Table II.

and electrolytic equilibria of I–III in aqueous methanol solutions may partially account for the discrepancies between the pKa_2 and $p_\omega Ka_2$ values (16–19, 21, 22, 33). For example, different solvation mechanisms are possible with III than with I or II because the hydroxyethoxyethanol substituent, R_1 on III, is both a hydrogen bond acceptor and donor. Furthermore, the R_2 chloro substituent on II would increase its partition coefficient over that of I (35, 36). In fact, 0.002 *M* II was inadequately soluble in 11.5% (w/w) methanol while titrating its p_sKa_2, which is attributed to the enhanced hydrophobicity conferred by the chloro group, R_2 (35, 36). The p_sKa_1 values of 0.0005 *M* IV and V were obtainable only in solvents containing ≥47.8% (w/w) methanol. As noted earlier, titration data derived from the latter solutions would be poorly applicable to $p_\omega Ka_1$ estimates (18, 21).

Finally, it remains to be determined why the ratios of K_{a1}/K_{a2} for I–III show a variation of 2.75×10^5 to 7.76×10^5. The comparable ratio of K_{a1}/K_{a2} for piperazine (VI) was reported to be 1.38×10^4 (37)[14]. There are four main types of electrochemical effects that can account for these K_{a1}/K_{a2} ratios: (*a*) mesomerism or resonance in aromatic compounds, (*b*) inductive effects of substituents in aliphatic and aromatic compounds, (*c*) field effects such as intramolecular hydrogen bonding, and (*d*) molecular symmetry or statistical effects (38–42).

Because the piperazine ring is nonaromatic, mesomerism does not explain the observed K_{a1}/K_{a2} ratios. Secondly, the inductive effects of the R_1 and benzhydryl substituents on the piperazine group in I–III account for a maximum difference between K_{a1} and K_{a2} of ~62 as seen from the quotient of $(K_{a1}/K_{a2})_I/(K_{a1}/K_{a2})_{VI}$. It has been shown that electron-withdrawing (*-I*) groups have a marginal influence on K_a values of acids when the *-I* and ionogenic groups are separated by more than two $-CH_2$ residues (38, 40). These inductive effects account primarily for the differences between either K_{a1} or K_{a2} values of I–III. Thirdly, the statistical symmetry factor in VI and its analogs accounts for only a fourfold difference in K_{a1} and K_{a2} values (38–40, 42).

Solvent- and space-mediated field effects and inductive forces between nitrogen atoms of the piperazine ring appear to be the most plausible explanation for the large K_{a1}/K_{a2} ratios in I–III, VI, and similar compounds. Electrostatic attraction between the protonated and neutral nitrogen atoms of the piperazine ring has been alluded to (43), and it has been studied by conformational analysis using molecular orbital methods. (44). However, field effects mediated through solvent molecules may also contribute to these large observed ratios.

CONCLUSIONS

Aqueous pKa_1 and pKa_2 values for I and II, and pKa_2 for III, apparently heretofore unpublished, were determined. These pKa_2 values of I–III were also obtained in aqueous solutions of 11.5–52.9% (w/w) methanol. There was no substantial difference in the precision of $p_\omega K_2$ extrapolated from linear regression plots of p_sK_2 data according to Eqs. 1 and 2. However, Eq. 2 did yield slightly better correlation of the plotted coordinates. The overall accuracy of $p_\omega Ka_2$ compared to pKa_2 values for I–III also was better according to Eq. 2 plots ($p < 0.13$). The maximum difference observed between any pKa_2 and $p_\omega Ka_2$ value occurred in the case II using Eq. 1 by which $p_\omega Ka_2$ was 5.23% higher.

The large ratios of K_{a1}/K_{a2} for I–III and piperazine are attributed to field effects and intramolecular electrostatic attraction or induction in the piperazine ring.

REFERENCES

(1) R. Baltzly, S. DuBreuil, W. S. Ide, and E. Lorz, *J. Org. Chem.*, **14,** 775 (1949).

(2) P. B. Marshall, *Br. J. Pharmacol.*, **10,** 270 (1955).

(3) N. G. Lordi and J. E. Christian, *J. Am. Pharm. Assoc., Sci. Ed.*, **45,** 300 (1956).

(4) B.-A. Persson, *Acta Pharm. Suec.*, **5,** 335 (1968).

(5) A. Pardo, S. Vivas, F. Espana, and J. I. Fernandez-Alonso, *Afinidad*, **29,** 640 (1972).

(6) S. Lukkari, *Farm. Aikak.*, **80,** 161 (1971); through *Chem. Abstr.*, **75,** 41145t (1971).

(7) J. Tsau and N. DeAngelis, in "Analytical Profiles of Drug Substances," vol. 7, K. Florey, Ed., Academic, New York, N.Y., 1978, p. 325.

(8) B.-A. Persson and G. Schill, *Acta Pharm. Suec.*, **3,** 281 (1966).

(9) R. H. Levy and M. Rowland, *J. Pharm. Sci.*, **60,** 1155 (1971).

(10) M. Mizutani, *Z. Physik. Chem.*, **116,** 350 (1925); through: *Chem. Abstr.*, **19,** 3052 (1925).

(11) N. F. Hall and M. R. Sprinkle, *J. Am. Chem. Soc.*, **54,** 3469 (1932).

(12) E. B. Leffler, H. M. Spencer, and A. Burger, *ibid.*, **73,** 2611 (1951).

(13) P. J. A. W. Demoen, *J. Pharm. Sci.*, **50,** 350 (1961).

(14) L. G. Chatten and L. E. Harris, *Anal. Chem.*, **34,** 1495 (1962).

(15) E. R. Garrett, *J. Pharm. Sci.*, **52,** 797 (1963).

(16) L. Z. Benet and J. E. Goyan, *ibid.*, **56,** 665 (1967).

(17) A. Albert and E. P. Serjeant, in "The Determination of Ionization Constants," 2nd ed., Chapman and Hall, London, England, 1971, pp. 39–40.

(18) R. F. Cookson, *Chem. Rev.*, **74,** 5 (1974).

(19) T. Shedlovsky, in "Electrolytes," B. Pesce, Ed., Pergammon, New York, N.Y., 1962, pp. 146–151.

(20) M. Yasuda, *Bull. Chem. Soc. Japan*, **32,** 429 (1959); through *Chem. Abstr.*, **54,** 2894e (1960).

(21) R. G. Bates, M. Paabo, and R. A. Robinson, *J. Phys. Chem.*, **67,** 1833 (1963).

(22) K. C. Ong, R. A. Robinson, and R. G. Bates, *Anal. Chem.*, **36,** 1971 (1964).

(23) H. A. Krebs and J. C. Speakman, *J. Chem. Soc.*, **1945,** 593.

(24) I. Setnikar, *J. Pharm. Sci.*, **55,** 1190 (1966).

(25) C. C. Peck and L. Z. Benet, *ibid.*, **67,** 12 (1978).

(26) U. G. Hennig, R. E. Moskalyk, L. G. Chatten, and S. F. Chan, *ibid.*, **70,** 317 (1981).

(27) J. Peeters, *ibid.*, **67,** 127 (1978).

(28) A. Albert and E. P. Serjeant, in "The Determination of Ionization Constants," 2nd ed., Chapman and Hall, London, England, 1971, pp. 28–32.

(29) P. J. Niebergall, in "Remington's Pharmaceutical Sciences," 16th ed., A. Osol, Ed., Mack Publishing, Easton, Pa., 1980, pp. 228–233.

(30) J. Kielland, *J. Am. Chem. Soc.*, **59,** 1675 (1937).

(31) P. S. Albright and L. J. Gosting, *ibid.*, **68,** 1061 (1946).

(32) L. K. Randolph and J. L. Ciminera, in "Remington's Pharmaceutical Sciences," 16th ed., A. Osol, Ed., Mack Publishing, Easton, Pa., 1980, pp. 111–114.

(33) A. Hulshoff and J. H. Perrin, *Pharm. Acta Helv.*, **51,** 65 (1976).

(34) A. Albert and E. P. Serjeant, in "The Determination of Ionization Constants," 2nd ed., Chapman and Hall, London, England, 1971, p. 104.

(35) A. Leo, C. Hansch, and D. Elkins, *Chem. Rev.*, **71,** 525 (1971).

(36) S. H. Yalkowsky, in "Design of Biopharmaceutical Properties through Prodrugs and Analogs," E. B. Roche, Ed., American Pharmaceutical Association, Washington, D.C., 1977, pp. 392, 397, 407.

(37) G. Schwarzenbach, B. Maissen, and H. Ackerman, *Helv. Chim. Acta*, **35,** 2333 (1952); through *Chem. Abstr.*, **47,** 4238c (1953).

(38) J. March, in "Advanced Organic Chemistry: Reactions, Mechanisms and Structure," 2nd ed., McGraw-Hill, New York, N.Y., 1977, pp. 238–243.

(39) J. Hine, in "Structural Effects on Equilibria in Organic Chemistry," Wiley, New York, N.Y., 1975, pp. 1–3, 29–53.

(40) R. P. Bell, in "The Proton in Chemistry," 2nd ed., Cornell University, Ithica, N.Y., 1973, pp. 86–102.

(41) E. S. Gould, in "Mechanism and Structure in Organic Chemistry," Holt, Rinehart and Winston, New York, N.Y., 1959, pp. 199–212.

(42) S. W. Benson, *J. Am. Chem. Soc.*, **80,** 5151 (1958).

(43) L. L. Ciaccio, S. R. Missan, W. H. McMullen, and T. C. Grenfell, *Anal. Chem.*, **29,** 1670 (1957).

(44) W. J. Murray and D. W. Newton, in "Abstracts," vol. 11, no. 1, APhA Academy of Pharmaceutical Sciences, St. Louis, Mo., Mar.–Apr., 1981, p. 100.

[14] The pKa_1 and pKa_2 values of VI are 5.68 and 9.82, respectively (37).

ACKNOWLEDGMENTS

Presented to the Medicinal Chemistry and Pharmacognosy Section at the 31st National Meeting of the APhA Academy of Pharmaceutical Sciences, Orlando, Fla., November 16, 1981.

The authors thank the Burroughs Wellcome Co., Pfizer Inc., and ICI Americas Inc. for generous donations of cyclizine and chlorcyclizine hydrochlorides, hydroxyzine and meclizine dihydrochlorides, and buclizine dihydrochloride, respectively. They are grateful to Mrs. Donna Earnshaw for preparing the manuscript and to Donald L. Goode, Pharm.D., for performing many titrations.

Vaginal Absorption of a Potent Luteinizing Hormone-Releasing Hormone Analog (Leuprolide) in Rats I: Absorption by Various Routes and Absorption Enhancement

HIROAKI OKADA ˣ, IWAO YAMAZAKI, YASUAKI OGAWA, SHINICHIRO HIRAI, TAKATSUKA YASHIKI, and HIROYUKI MIMA

Received December 29, 1981 from the *Central Research Division, Takeda Chemical Industries, Ltd., 2-17-85 Juso, Yodogawa, Osaka 532, Japan.* *Accepted for publication February 4, 1982.*

Abstract □ The absorption of a potent luteinizing hormone-releasing hormone analog (leuprolide) through different routes was evaluated by determining the ovulation-inducing activity in diestrous rats. Vaginal administration showed the greatest potency among nonparenteral routes and was followed successively by rectal, nasal, and oral administration. Mixed micellar solution with monoolein–bile acids improved the intestinal absorption of leuprolide, and nasal absorption was enhanced by adding sodium glycocholate, surfactin, or polyoxyethylene 9 lauryl ether, but these bioavailabilities were still insufficient. The vaginal absorption was enhanced by organic acids: citric, succinic, tartaric, and glycocholic; the absolute bioavailability increased to ~20%. The vaginal absorption from jellies, as practical dosage forms, yielded sufficient activity of leuprolide, but absorption was slightly reduced with highly polar polymers or with higher concentrations of polymers. It was concluded that vaginal administration of leuprolide can be a rational dosage method for a long-term antitumor therapy.

Keyphrases □ Leuprolide—vaginal absorption, potent luteinizing hormone-releasing hormone analog in rats, ovulation-inducing activity □ Absorption, vaginal—potent luteinizing hormone-releasing hormone analog (leuprolide) in rats, ovulation-inducing activity □ Hormones—potent luteinizing hormone-releasing hormone analog (leuprolide) in rats, vaginal absorption

Leuprolide (I), a luteinizing hormone-releasing hormone (II) analog synthesized previously (1), has a high gonadotropin-releasing activity (2) and ovulation-inducing potency (50–80 times greater than II) (3). Recently, this analog

(Pyro)Glu-His-Trp-Ser-Tyr-D-Leu-Leu-Arg-Pro-NH-CH_2CH_3

I

(Pyro)Glu-His-Trp-Ser-Tyr-Gly-Leu-Arg-Pro-Gly-NH_2

II

at relatively large doses, was found to effect regression of hormone-dependent mammary tumors (4–6). In addition, it appears to have birth control potential, without toxic side-effects, in both sexes (7–11).

Peptides are generally absorbed poorly, subject to decomposition in the GI tract, and have short biological half lives after parenteral administration. To establish a convenient and reliable method for nonparenteral self-administration of II and the analogs for long-term therapy, numerous studies have been carried out on the pharmacological effects after oral (12–14), sublingual (15), nasal (15–23), rectal (24), and vaginal (12, 14, 24) administration.

In the present study, the absorption of leuprolide through nonparenteral administration routes for an antitumor therapy was assessed by determining its ovulation-inducing activity in rats. The absorption enhancement was attempted in oral, nasal, and vaginal routes, and a study was also conducted on an experimental dosage form designed for vaginal administration.

EXPERIMENTAL

Animals—Mature female Sprague-Dawley rats[1] aged 120–150 days and weighing 250–330 g were used. Animals exhibiting two or more consecutive 4-day estrous cycles on daily morning examination of vaginal smears were used in the diestrous stage.

Materials—Leuprolide acetate[2] was used after dehydration at 50° under vacuum for 5 hr. Sodium glycocholate[3], sodium taurocholate[3], and polyoxyethylene 9 lauryl ether[4] of commercial grade were used without further purification. The other chemicals were of reagent grade quality.

Ovulation-Inducing Activity by Different Routes—The absorption of leuprolide through various administration routes was estimated by ovulation-inducing activity as described previously (25). A 0.9% NaCl solution of the analog containing 0.1% bovine serum albumin[5], 20 U/ml of aprotinin[6], and 0.1 *N* HCl was used for intravenous, subcutaneous, nasal, and oral administrations. For rectal administration, the analog was dispersed in an oleaginous base[7] molded in a cylindrical shape (Φ5 × 8 mm). For vaginal administration, the analog was dissolved in 0.9% NaCl solution containing 0.1% bovine serum albumin and 20 U/ml of aprotinin or dispersed in an oleaginous base[7]. After the suppository was placed by a glass inserter, the orifice was closed with a surgical adhesive agent. Although the rectal and vaginal administration using an oleaginous base were carried out at a dose per rat, their dose and ED_{50} are shown by dose per kilogram using mean body weight.

Enhancement of Oral, Nasal, and Vaginal Absorption—For the oral administration, a mixed micellar solution with monoolein[4], sodium taurocholate, and sodium glycocholate was prepared according to a previous method (26). One percent sodium glycocholate, surfactin[8], or polyoxyethylene 9 lauryl ether was added to the analog solution for the nasal administration. For the vaginal administration, the following adjuvants were dissolved or dispersed as fine particles at a concentration of 10% (as a free acid), except lactic acid (2%), in the oleaginous base: citric acid, succinic acid, tartaric acid, lactic acid, ascorbic acid, gluconic acid, taurine, glycine, boric acid, dipotassium edetate, sodium citrate, sodium glycocholate, and sodium oleate.

The concentration effect of citric acid and succinic acid was also examined at a range of 2–20% in the oleaginous base.

Leakage of Evan's Blue from the Vaginal Membrane—Under pentobarbital anesthesia, a dose of 1 ml/kg of 1% Evan's blue solution

[1] Clea Japan, Inc., Tokyo, Japan.
[2] Takeda Chemical Ind., Ltd., Osaka, Japan. The analog was synthesized in the Central Research Division.
[3] Tokyo Chemical Ind., Ltd., Tokyo, Japan.
[4] Nikko Chemical Ind., Ltd., Tokyo, Japan.
[5] Wako Pure Chemical Ind., Ltd., Osaka, Japan. Bovine serum albumin was added to prevent any loss by adsorption to the glass surface.
[6] Trasylol, Bayer A. G., Leverkusen-Bayerwerk, W. Germany. This peptidase inhibitor was added to inhibit a small quantity of peptidases derived from bovine serum albumin.
[7] WITEPSOL W35 (rectal) or WITEPSOL S55 (vaginal), Dynamit Nobel Aktiengesellshaft, W. Germany.
[8] A bacterial peptide lipid surfactant isolated from *Bacillus subtilis* (27).

0022-3549/82/1200-1367$01.00/0

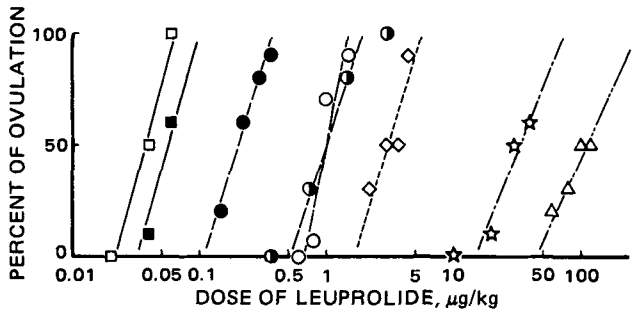

Figure 1—*Ovulation-inducing activity of leuprolide after intravenous, subcutaneous, oral, rectal, nasal, and vaginal administration to diestrous rats. Key: (□) intravenous; (■) subcutaneous; (○) vaginal in 0.9% NaCl; (◑) vaginal in oleaginous base; (●) vaginal with 10% citric acid; (◇) rectal; (☆) nasal; (△) oral.*

was injected intravenously 2 hr after the vaginal administration of the suppository containing 10% organic acids (citric, succinic, tartaric, and aspartic acids), sodium glycocholate, sodium citrate, calcium citrate, or dipotassium edetate. The rats were sacrificed by decapitation 30 min later and their vaginas were isolated and examined for the intensity of stain in the mucous membranes.

Vaginal Absorption from Jelly and Tablet—Methylcellulose[9] (2–7%), a mixture of xanthan gum[2] and locustbean gum[2] (2–3%), carrageenan[2] (5%), starch (7 and 10%), agar (10%), tragacanth gum[2] (4%), sodium carboxymethylcellulose[10] (5%), sodium polyacrylate[5] (5%), glycerogelatin[11], succinated gelatin[12] (61%), and polyethylene glycol 4000[13] (70%) were used as a jelly base. The concentration was adjusted to provide almost the same viscosity for each jelly. The jelly was prepared by dissolving the hydrophilic polymer in 5% citric acid solution (pH 3.5) containing various amounts of leuprolide. Each jelly was administered into the upper vagina by a glass inserter at a dose of 100 mg/rat.

Three kinds of tablets were prepared by a conventional method. The granules with the analog, citric acid, lactose, corn starch, and hydroxypropylcellulose[14] were formed by a wet method and blended with corn starch and magnesium stearate for compression into a cylindrically shaped tablet. The concentration of citric acid was 10% for tablet A, 5% for tablet B, and 10% as a sodium salt for tablet C. The pH value of the solution of tablet C dissolved in 3 ml of distilled water was 4.22.

The leakage of Evan's blue from the vaginal membrane was determined to compare the local reaction by methylcellulose jelly with 5% citric acid (pH 3.5), oleaginous suppository with 10% citric acid, and tablet A. Evan's blue was injected intravenously 30 min after vaginal administration of the suppositories.

RESULTS

Ovulation-Inducing Activity by Different Routes—The ovulation-inducing activities of leuprolide after intravenous, subcutaneous, vaginal, nasal, and oral administration to diestrous rats are shown in Fig. 1. The ED_{50}'s of the activity calculated by Finney's probit analysis (28) were 38 ng/kg by intravenous, 58 ng/kg by subcutaneous, 112 μg/kg by oral, 33.4 μg/kg by nasal, 3.12 μg/kg by rectal, and 1.0 μg/kg by vaginal administration. The activity of the analog by the oral route was 2950 times less than that by intravenous injection. Vaginal administration exhibited the greatest potency of all nonparenteral routes examined; the absolute bioavailability estimated by comparison with the potency of the intravenous injection was 3.8% in both the 0.9% NaCl solution and oleaginous suppository.

Enhancement of Oral, Nasal, and Vaginal Absorption—The ovulation-inducing activity of leuprolide after oral administration in the mixed micellar solution with monoolein and bile acids is shown in Table I. The absorption was enhanced 1.6 times more than that of the 0.9% NaCl solution, but the ED_{50} was still 1870 times larger than that after intravenous injection.

Three surfactants employed as absorption promoters markedly increased the potency of the analog applied nasally by the same degree: the absolute bioavailabilities were 1.8–3.0% (Table II).

For the vaginal administration, the polybasic carboxylic acids (citric, succinic, and tartaric acids) and glycocholic acid increased almost 5 times the ovulation-inducing activity of the analog (Table III). Acidic amino acids (glutamic and aspartic acids), the carboxylic acids having hydroxyl groups (ascorbic and lactic acids), and dipotassium edetate exhibited weak promoting effects, whereas taurine, boric acid, oleic acid, caproic acid, sodium oleate, and polyoxyethylene 9 lauryl ether scarcely enhanced the activity of the analog and glycine reduced it. The promoting effect of the carboxylic acids was reduced by using sodium citrate and sodium glycocholate salts. The concentration effects of citric acid and succinic acid on the vaginal absorption of the analog are shown in Fig. 2. These acids increased the activity of the peptide in concentrations ≤10%, and the activity approached a maximum level of >10%.

Leakage of Evan's Blue on Vaginal Membrane—Staining of the vaginal mucous membrane by Evan's blue injected intravenously after vaginal administration of a suppository containing an additive was examined. The organic acids (citric, succinic, and tartaric acids) and dipotassium edetate, both of which enhanced the vaginal absorption of leuprolide, induced deep staining of vaginal membrane, whereas little staining was observed with sodium glycocholate, sodium citrate, and calcium citrate.

Vaginal Absorption from Jelly and Tablet—The ovulation-inducing activities of leuprolide after vaginal administration of various hydrophilic jellies are shown in Table IV. The activity was affected by the jelly material and its concentration. Polymers having a highly polar functional group (sodium carboxymethylcellulose, sodium polyacrylate, and gelatin) tended to reduce the activity of the analog, whereas polysaccharides with less polar functions (methylcellulose, xanthan gum, locustbean gum, carrageenan, and starch) showed higher activity. In both polymer types, the activity was reduced as the polymer concentration increased.

Tablets containing the analog with 5% citric acid and 10% sodium citrate exhibited one third of the activity of tablet A with 10% citric acid, which induced the highest ovulation effect (Table V).

Staining of the vaginal membrane by Evan's blue injected after vaginal administration of the jelly, oleaginous suppository, and tablet, which were expected to show similar pharmacological effects, was compared. The oleaginous suppository and tablet induced deep blue staining, but the jelly induced only faint or no staining.

DISCUSSION

Determination of the ovulation-inducing activity of leuprolide after administration by different routes revealed that the absorption was good by vaginal administration, which was followed successively by rectal, nasal, and oral administration. The absorption of the analog from 0.9% NaCl solution and oleaginous suppository applied vaginally was almost identical. Their absolute bioavailabilities estimated by the pharmacological effect were 3.8%.

The vaginal absorption of a drug depends on its release from the suppository and on its ability to pass through the vaginal membrane. For the penetration of a drug, a physical model has been proposed (29) comprising an aqueous diffusion layer in series with a membrane consisting of aqueous pores and lipoidal pathways. The considerable absorbability of the analog, a hydrophilic compound, may indicate that its main absorption is thorough a pore-like route, such as intercellular channels, rather than through partition to the membrane cell.

Attempts were made to enhance absorption through the oral, nasal, and vaginal routes. Mixed micelles with lipid–bile salts are known to enhance the intestinal absorption of poorly absorbable polar drugs such as insulin (26), aminoglycosides (30), and heparin (31). The mixed micellar solution with bile salts and monoolein also improved the absorption of leuprolide, but its absolute bioavailability was 0.05%.

The bioavailability following nasal administration was 0.11% from the aqueous solution and was increased to 2–3% when sodium glycocholate, surfactin, or polyoxyethylene 9 lauryl ether was added. The absorption-enhancing effect with the promoters is in agreement with the effect observed previously with insulin (32).

The vaginal absorption of leuprolide was markedly facilitated by the polybasic carboxylic acids, and slightly increased with the hydroxy carboxylic acids and acidic amino acids. All of the carboxylic acids that

[9] METOLOSE (90SH4000, 90SH8000, 90SH15000, and 90SH30000), Shinetsu Chemicals Co., Tokyo, Japan. Four types of methylcellulose were used. In SH type, 4–12% of the methoxy groups was substituted by the hydroxypropoxy groups to raise the thermal gelation temperature. The former numbers represent the thermal gelation temperature and the latter the molecular weight.

[10] 7MF type, Hercules Inc., Wilmington, Del.

[11] Prepared as described in "Remington's Pharmaceutical Sciences," 15th (1975), Mack Publishing Co., p. 1545.

[12] Nitta Gelatin Co., Ltd., Tokyo, Japan.

[13] Sanyo Kasei Ind., Ltd., Kyoto, Japan.

[14] L type, Nippon Soda Co., Ltd., Tokyo, Japan.

Table I—Ovulation-Inducing Activities of Leuprolide after Oral Administration to Diestrous Rats [a]

Preparation	Dose of Leuprolide, μg/kg							ED_{50}, μg/kg
	10	20	40	60	80	100	120	
NaCl solution, 0.9%	—	—	—	2/10	3/10	5/10	5/10	112 (81–155)[b]
Mixed micellar solution[c]	0/5	2/10	2/10	4/9	5/10	7/10	—	71 (46–190)

[a] Number of rats with induced ovulation per number of rats examined. [b] Fiducial limits (95%). [c] The mixed micellar solution of leuprolide was prepared with 45 m*M* of monoolein, 20 m*M* of sodium taurocholate, and 20 m*M* of sodium glycocholate by sonication (Ref. 26).

Table II—Ovulation-Inducing Activity of Leuprolide after Nasal Administration with Surfactants to Diestrous Rats [a]

Additives, 1%	Dose of Leuprolide, μg/kg										ED_{50}, μg/kg
	0.8	1	2	3	4	5	10	20	30	40	
None	—	—	0/5	—	0/5	—	0/5	1/10	5/10	6/10	33.4 (25.7–69.8)[b]
Sodium glycocholate	0/10	3/10	9/10	—	—	5/5	5/5	—	—	—	1.28 (1.05–1.70)[c]
Surfactin	0/10	2/10	4/10	10/10	—	—	—	—	—	—	1.77 (1.38–2.35)[c]
Polyoxyethylene 9 lauryl ether	—	0/10	6/10	7/10	—	—	—	—	—	—	2.08 (1.52–2.93)[c]

[a] Number of rats with induced ovulation per number of rats examined. [b] Fiducial limits (95%). [c] Significant ($p < 0.05$).

Table III—Ovulation-Inducing Activity of Leuprolide after Vaginal Administration with Additives to Diestrous Rats [a]

Additives (10%)	Dose of Leuprolide, ng/rat										ED_{50}, ng/rat	Relative potency
	20	40	60	80	100	150	200	400	600	800		
None	—	—	—	—	0/10	—	3/10	8/10	9/10	10/10	270 (194–353)[b]	1
Citric acid	—	2/10	6/10	8/10	9/10	—	10/10	10/10	5/5	5/5	56 (38–69)	4.9[c]
Succinic acid	0/10	4/10	6/10	8/10	9/10	—	—	—	—	—	50 (37–63)	5.4[c]
Tartaric acid	—	—	1/10	5/10	8/10	5/5	—	—	—	—	82 (69–97)	3.3[c]
Glycocholic acid	1/10	5/10	5/10	8/10	9/10	—	—	—	—	—	47 (32–62)	5.6[c]
Ascorbic acid	—	—	3/10	2/10	4/10	7/10	—	—	—	—	113 (80–161)	2.4[c]
Lactic acid, 2%	—	—	2/10	0/10	3/10	8/10	—	—	—	—	117 (95–184)	2.3[c]
Aspartic acid	—	—	—	2/10	4/10	—	9/10	9/10	10/10	5/5	122 (79–167)	2.1[c]
Glutamic acid	—	—	—	—	0/10	—	7/10	10/10	10/10	5/5	177 (133–243)	1.6
Dipotassium edetate	—	—	0/10	3/10	5/10	8/10	—	—	—	—	104 (87–134)	2.6[c]
Taurine	—	0/5	—	2/10	3/10	—	5/10	8/10	—	—	182 (112–373)	1.5
Glycine	—	—	—	—	0/10	—	0/5	1/10	3/10	6/10	755 (570–5904)	0.4[c]
Boric acid	—	—	—	—	1/10	3/15	5/10	—	—	—	200 (153–261)	1.3
Caproic acid	—	—	—	—	1/10	2/10	5/10	8/10	9/10	—	341 (249–484)	0.8
Oleic acid	—	—	—	0/5	1/10	—	3/10	4/10	7/10	9/10	358 (244–541)	0.7
Polyoxyethylene 9 lauryl ether	—	—	—	—	0/10	1/10	6/10	7/10	9/10	—	254 (193–348)	1.1
Sodium glycocholate	—	—	3/15	6/15	2/15	—	10/15	—	—	—	151 (107–666)	1.9[c]
Sodium oleate	—	—	—	—	0/10	—	1/10	8/10	8/10	10/10	323 (237–461)	0.8
Sodium citrate	—	—	—	0/10	3/10	—	5/10	6/10	8/10	9/10	245 (160–365)	1.0

[a] Number of rats with induced ovulation per number of rats examined. [b] Fiducial limits (95%). [c] Significant ($p < 0.05$).

showed an absorption promoting effect possess a chelating ability. The absolute bioavailability of the analog after vaginal administration increased to ~20% on the average by adding these polybasic carboxylic acids. The absorption was poorly enhanced with surfactants such as sodium glycocholate, sodium oleate, and polyoxyethylene 9 lauryl ether, which are known to enhance greatly the rectal and nasal absorption of hydrophilic drugs, and was reduced with glycine. The difference between the enhancement effects of surfactants on vaginal and rectal absorption may be attributed to structural differences of the membranes, *i.e.*, the vaginal epithelium, consisting of stratified squamous cells, may resist cleavage or desquamation of epithelial cells by the surfactants. Glycine seems to possess a stabilizing activity on the epithelium that results in the reduced vaginal absorption of salicylate[15].

An intimate relation was observed between the absorption-enhancing effect of leuprolide and the leakage from the vaginal membrane of Evan's blue injected intravenously after treatment with the promoters. Distinct staining of the vaginal epithelial membrane was elicited after vaginal administration of carboxylic acids with chelating ability, but not of calcium citrate. This indicates that the blood–vaginal epithelium barrier has been loosened by the organic acids and that the chelating ability may contribute to the absorption enhancement by expanding the channel bore through reversible electrical uncoupling with calcium ions as demonstrated in gap junctions (33), or by cleaving the intercellular tight junction through uptake of the calcium ions of binding proteins. Sodium citrate, which did not promote absorption, had no effect on the leakage of Evan's blue. The decrease of membrane permeability of the acid and/or of interaction between membrane and acid by dissociation, as a consequence of pH elevation, may reduce the effects.

[15] To be published.

Citric acid and succinic acid showed a similar concentration *versus* effect relation, *i.e.*, the activity increased with concentration to attain a maximum activity >10%. The exudation of body fluid out of the vaginal mucous membrane because of the hypertonicity of the acids may be one of the factors causing saturation of the promoting effect.

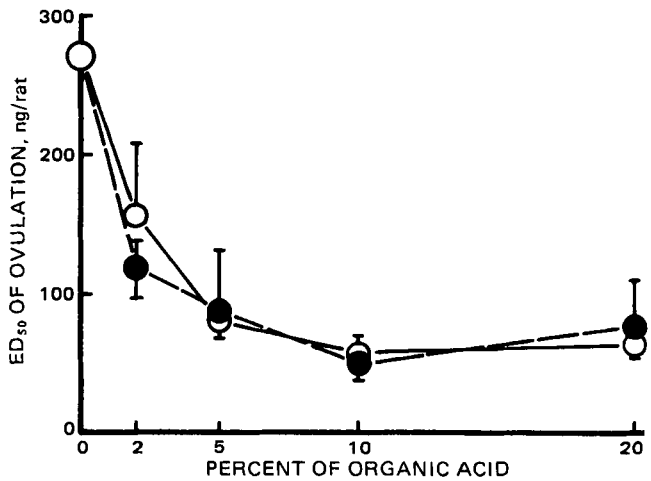

Figure 2—*Ovulation-inducing activity of leuprolide after vaginal administration with citric acid and succinic acid at the different concentrations to diestrous rats. The analog was administered in an oleaginous base containing the acid dispersed as fine powders. Bars represent 95% fiducial limits. Key: (○) citric acid; (●) succinic acid.*

Table IV—Ovulation-Inducing Activity of Leuprolide after Vaginal Administration in Various Kinds of Hydrophilic Jelly to Diestrous Rats [a]

Jelly base [b]	Dose of Leuprolide, ng/rat										ED_{50}, ng/rat
	30	40	50	60	70	80	100	120	150	200	
Methylcellulose, 3%, [d]	—	—	2/9	—	3/9	—	6/9	—	—	—	81.8 (54.2–123) [c]
Methylcellulose, 5% [d]	—	—	1/10	2/10	3/10	8/10	9/10	—	—	—	75.0 (67.1–86.4)
Methylcellulose, 7% [d]	—	—	—	—	0/5	2/10	7/10	—	5/7	—	103.0 (82.7–153)
Methylcellulose, 5% [e]	—	—	1/10	—	4/10	—	5/10	—	—	—	93.6 (70.1–125)
Methylcellulose, 3% [f]	—	—	2/10	—	5/10	—	9/10	—	—		67.4 (54.8–83.2)
Methylcellulose, 2% [g]	—	—	0/10	—	3/10	—	8/16	—	—	—	105.0 (82.2–133)
Mixed gum, 2% [h]	—	—	3/5	—	—	—	—	—	—	—	44.0
Mixed gum, 3% [h]	1/10	3/10	7/10	8/10	—	—	9/9	—	—	—	45.4 (38.2–53.6)
Carrageenan, 5%	—	—	2/5	—	—	5/5	5/10	—	9/10	—	55.0
Starch, 7%	—	—	1/5	—	2/5	—	—	—	—	—	65.0
Starch, 10%	—	—	1/10	—	—	—	5/5	—	—	—	69.0
Agar, 10%	—	—	0/5	—	—	—	4/5	—	—	—	74.0
Tragacanth gum, 4%	—	—	—	—	0/5	—	—	—	—	—	—
Sodium carboxymethylcellulose, 5%	—	—	—	—	—	—	1/7	—	5/5	—	105.0
Sodium polyacrylate, 5%	—	—	—	—	—	—	1/5	—	2/5	—	160.0
Glycerogelatin, 44.5%	—	—	—	—	—	0/10	2/10	—	4/15	6/9	179.0 (145–349)
Succinated gelatin, 61.2%	—	—	—	—	—	—	—	0/5	—	—	—
Polyethylene glycol 4000, 70%	—	—	—	—	—	—	0/5	—	—	—	—

[a] Number of rats with induced ovulation per number of rats examined. [b] Each jelly was prepared in 5% citric acid solution (pH 3.5). [c] Fiducial limits (95%), ED_{50} without fiducial limits was estimated by using the adequate slope of the dose–response curve. [d] 90SH4000. [e] 90SH8000. [f] 90SH15000. [g] 90SH30000. [h] Xanthan gum and locustbean gum were mixed at the same weight ratio.

Table V—Ovulation-Inducing Activity of Leuprolide after Vaginal Administration in Tablet to Diestrous Rats [a]

Tablet [b]	Dose of Leuprolide, ng/rat									ED_{50}, ng/rat
	10	15	25	50	60	75	100	150	200	
A	0/10	1/10	8/15	5/10	7/10	10/10	8/10	—	—	34.6 (25.1–46.7) [c]
B	—	—	—	—	—	0/5	6/10	—	—	—
C	—	—	—	1/5	—	4/10	4/10	5/10	8/10	114.3 (57.4–256.6)

[a] Number of rats with induced ovulation per number of rats examined. [b] Each tablet consists of leuprolide, citric acid, lactose, corn starch, hydroxypropylcellulose, and magnesium stearate. Citric acid was dispersed as fine powders at the concentration of 10% for tablet A, 5% for tablet B, and 10% as a sodium salt for tablet C. [c] Fiducial limits (95%).

The absorbability of leuprolide from jellies or tablets containing citric acid was examined to determine a practical dosage form. Jellies with a highly polar polymer such as carboxymethylcellulose and polyacrylate reduced the absorption of the analog, whereas those with a less polar polysaccharide elicited sufficient absorption. Since the absorption was reduced by all polymers at a high concentration, the interaction of the analog with the jelly materials appeared to cause the suppression. The tablet containing 10% citric acid allowed considerable absorption of the analog and gave a smaller ED_{50} than the oleaginous suppository.

The local reaction of these suppositories, examined by the leakage of Evan's blue from the vaginal mucosa after a 1-hr treatment, revealed that the tablet and oleaginous suppository exhibited deep staining, while the jelly exhibited only faint staining, or none. This difference may be explained by the fact that citric acid, dispersed as fine particles in the tablet and the oleaginous suppository, is dissolved in exuded body fluids at close to the saturated concentration, resulting in an irritation to the vaginal mucosa. Discernible changes of the mucous membrane, such as destruction or exfoliation of vaginal tract surface cells of rats, were rarely observed by scanning electromicroscopy after 10 consecutive days of administration of jelly containing 5% citric acid[15]. These results indicate that the vaginal jelly will be the most suitable practical dosage form because of the activity with lower concentrations of citric acid, less local reaction, and easy handling due to a high water solubility.

Vaginal administration of leuprolide resulted in a high ovulation-inducing activity, which was enhanced by addition of the carboxylic acids: citric, succinic, tartaric, and glycocholic. It is suggested that vaginal administration of leuprolide in humans can be a rational dosage method especially from the standpoint of self-administration for long-term antitumor therapy.

REFERENCES

(1) M. Fujino, T. Fukuda, S. Shinagawa, S. Kobayashi, I. Yamazaki, R. Nakayama, J. H. Seely, W. F. White, and R. H. Rippel, *Biochem. Biophys. Res. Commun.*, **60**, 406 (1974).

(2) J. A. Vilchez-Martinez, D. H. Coy, A. Arimura, E. J. Coy, Y. Hirotsu, and A. V. Schally, *ibid.*, **59**, 1226 (1974).

(3) R. H. Rippel, E. S. Johnson, W. F. White, M. Fujino, T. Fukuda, and S. Kobayashi, *Proc. Soc. Exp. Biol. Med.*, **148**, 1193 (1975).

(4) E. S. Johnson, J. H. Seely, W. F. White, and E. R. DeSombre, *Science*, **194**, 329 (1976).

(5) E. R. DeSombre, E. S. Johnson, and W. F. White, *Cancer Res.*, **36**, 3830 (1976).

(6) A. Danguy, N. Legros, J. A. Heuson-Stiennon, J. L. Pasteels, G. Atassi, and J. C. Heuson, *Eur. J. Cancer*, **13**, 1089 (1977).

(7) U. K. Banik and M. L. Givner, *J. Reprod. Fertil.*, **44**, 87 (1975).

(8) A. Corbin, C. W. Beattie, J. Yardley, and T. J. Foell, *Endocr. Res. Commun.*, **3**, 359 (1976).

(9) D. Gonzalez-Barcena, D. H. Coy, A. J. Kastin, K. Nikolics, and A. V. Schally, *Lancet*, **ii**, 997 (1977).

(10) S. J. Nillius, C. Bergquist, and L. Wide, *Contraception*, **17**, 537 (1978).

(11) D. Heber and R. S. Swerdloff, *Science*, **209**, 936 (1980).

(12) A. De La Cruz, K. G. De La Cruz, A. Arimura, D. H. Coy, J. A. Vilchez-Martinez, E. J. Coy, and A. V. Schally, *Fertil. Steril.*, **26**, 894 (1975).

(13) D. Gonzalez-Barcena, A. J. Kastin, M. C. Miller, D. S. Schalch, D. H. Coy, A. V. Schally, and A. Escalante-Herrera, *Lancet*, **ii**, 1126 (1975).

(14) N. Nishi, A. Arimura, D. H. Coy, J. A. Vilchez-Martinez, and A. V. Schally, *Proc. Soc. Exp. Biol. Med.*, **148**, 1009 (1975).

(15) S. Jeppsson, S. Kullander, G. Rannevik, and J. Thorell, *Br. Med. J.*, **4**, 231 (1973).

(16) H. G. Solbach and W. Wiegelmann, *Lancet*, **i**, 1259 (1973).

(17) H. G. Dahlén, E. Keller, and H. P. G. Schneider, *Horm. Metab. Res.*, **6**, 510 (1974).

(18) J. P. Bourguignon, H. G. Burger, and P. Franchimont, *Clin. Endocrinol.*, **3**, 437 (1974).

(19) G. Fink, G. Gennser, P. Liedholm, J. Thorell, and J. Mulder, *J. Endocrinol.*, **63**, 351 (1974).

(20) D. Gonzalez-Barcena, A. J. Kastin, D. S. Schalch, D. H. Coy, and A. V. Schally, *Fertil. Steril.*, **27**, 1246 (1976).

(21) G. Potashnik, N. Ben-Adereth, B. Lunenfeld, and C. Rofe, *ibid.*, **28**, 650 (1977).

(22) G. Potashnik, R. Homburg, A. Eshkol, V. Insler, and B. Lunenfeld, *ibid.*, **29**, 148 (1978).

(23) R. F. Lambe, I. Werner-Zodrow, A. Darragh, and M. Mall-Häfeli, *Lancet*, **ii**, 801 (1979).
(24) M. Saito, T. Kumasaki, Y. Yaoi, N. Nishi, A. Arimura, D. H. Coy, and A. V. Schally, *Fertil. Steril.*, **28**, 240 (1977).
(25) I. Yamazaki, H. Nakagawa, K. Yoshida, and R. Nakayama, *Jpn. J. Fertil. Steril.*, **22**, 136 (1977).
(26) R. H. Engel and M. J. Fahrenbach, *Proc. Soc. Exp. Biol. Med.*, **129**, 772 (1968).
(27) K. Arima, A. Kakinuma, and G. Tamura, *Biochem. Biophys. Res. Commun.*, **31**, 488 (1968).
(28) D. J. Finney, "Probit Analysis," Cambridge University Press, 1952.
(29) S. Hwang, E. Owada, T. Yotsuyanagi, L. Suhardja, N. F. H. Ho, G. L. Flynn, and W. I. Higuchi, *J. Pharm. Sci.*, **65**, 1574 (1976).
(30) S. Muranishi, N. Muranushi, and H. Sezaki, *Int. J. Pharm.*, **2**, 101 (1979).
(31) Y. Tokunaga, S. Muranishi, and H. Sezaki, *J. Pharmacobio. Dyn.*, **1**, 28 (1978).
(32) S. Hirai, T. Yashiki, and H. Mima, *Int. J. Pharm.*, **9**, 165 (1981).
(33) C. Peracchia and A. F. Dulhunty, *J. Cell Biol.*, **70**, 419 (1976).

ACKNOWLEDGMENTS

The authors are grateful to Mr. H. Nakagawa for assistance with the experiments, to Dr. M. Fujino for the supply of leuprolide, to Dr. N. Kitamori for preparation of the tablets, to Dr. T. Shimamoto for valuable discussion, and to Dr. J. R. Miller for comments on the manuscript.

Effect of Moisture and Crushing Strength on Tablet Friability and *In Vitro* Dissolution

Z. T. CHOWHAN[x], I. C. YANG, A. A. AMARO, and LI-HUA CHI

Received November 9, 1981, from the *Syntex Research, Division of Syntex (U.S.A.) Inc., Palo Alto, CA 94304.* Accepted for publication February 5, 1982.

Abstract □ The friability and dissolution of a formulation of compressed tablets were studied by varying the granulation moisture and tablet crushing strength. A general quadratic response surface model was used to analyze the data. The response surface contour plots of tablet friability consisted of a series of ellipsoidal curves. The optimum friability corresponding to a granulation moisture content and a tablet crushing strength was a simple minimum. The *in vitro* dissolution contour plots showed a stationary ridge system. Along the ridge, a large number of combinations of tablet crushing strength and granulation moisture represented 100% drug dissolution. The contour overlays of friability and dissolution contour plots showed a region where both the friability and dissolution requirement could be met. The analysis of the data by means of multiple linear regression was helpful in understanding the role of granulation moisture and tablet crushing strength on tablet friability and *in vitro* dissolution.

Keyphrases □ Dissolution—*in vitro*, effect of moisture and crushing strength, tablet friability □ Crushing strength—effect on tablet friability and *in vitro* dissolution □ Friability—tablets, effect of moisture and crushing strength

Previous studies (1–3) from these laboratories discussed the interrelationships between moisture, crushing strength, and *in vitro* drug dissolution in compressed tablets. Another physical parameter of importance to the tablet formulators, especially in coating and packaging operations, is friability of compressed tablets. The friabilator[1] (4) provides falling as well as frictional abrasion to the tablet sample and is used to measure the resistance to abrasion or attrition of tablets. The loss of weight is measured after a fixed number of revolutions of a drum rotating at a controlled rate. In the development of tablet dosage forms, formulation factors are generally checked to reduce comparative loss in friability testing. Two types of friabilator[1,2] apparatuses were compared (5) using 10 tablet formulations differing in method of granulation or choice of binder. In all instances the percentage of weight loss was higher with friabilator A[1], the differences ranging from 6.2 to 39.7%, depending upon the formulation. After 25 years of use, it was concluded (6) that the weight loss of not more than 0.8% by friabilator A was valid for the control of most pharmaceutical tablets.

Although friability is generally considered important in the development of tablet formulations, factors affecting friability have not been fully explored. The present report describes a study of the interdependence of tablet friability and *in vitro* drug dissolution on granulation moisture content and tablet crushing strength. The data were analyzed using a general quadratic response surface model and the analysis suggested that rational specifications on the in-process variables such as the granulation moisture and initial tablet hardness could ensure proper control of the tablet friability and *in vitro* dissolution.

EXPERIMENTAL

Materials—The drug, ticlopidine hydrochloride[3], 5-(*o*-chlorobenzyl)-4,5,6,7-tetrahydrothieno-[3,2-*c*]pyridine hydrochloride was at least 99.0% pure. The excipients used were microcrystalline cellulose[4] NF, povidone[5] USP, citric acid[6] USP, stearic acid powder[7] NF, corn starch[8] NF, and lactose[9] USP.

Granulation—The formulation used in this study contained 64.1% drug, 22.4% microcrystalline cellulose, 10% starch, 1% citric acid, 2% povidone, and 0.5% stearic acid. The drug and microcrystalline cellulose were mixed together in a small planetary mixer for 10 min. Povidone and citric acid were dissolved in water and the powder mixture was granulated with the binder solution. The wet granulation was mixed for 10 min and passed through a 1.4-mm aperture and dried in a forced-air oven at 60°

[1] Roche type friabilator A.
[2] Erweka Friability Apparatus B.

[3] Sanofi Research Co. Inc. New York, NY 10019.
[4] Avicel pH 101, FMC Corp., Philadelphia, PA 19103.
[5] GAF Corp. New York, NY 10020.
[6] Mallinckrodt, Inc., St. Louis, MO 63147.
[7] Emery Industries, Inc., Cincinnati, OH 45232.
[8] Staley Manufacturing Co., Decatur, IL 62525.
[9] Regular grade, Foremost Co., San Francisco, CA 94104.

0022-3549/82/1200-1371$01.00/0

(23) R. F. Lambe, I. Werner-Zodrow, A. Darragh, and M. Mall-Häfeli, *Lancet*, **ii**, 801 (1979).
(24) M. Saito, T. Kumasaki, Y. Yaoi, N. Nishi, A. Arimura, D. H. Coy, and A. V. Schally, *Fertil. Steril.*, **28**, 240 (1977).
(25) I. Yamazaki, H. Nakagawa, K. Yoshida, and R. Nakayama, *Jpn. J. Fertil. Steril.*, **22**, 136 (1977).
(26) R. H. Engel and M. J. Fahrenbach, *Proc. Soc. Exp. Biol. Med.*, **129**, 772 (1968).
(27) K. Arima, A. Kakinuma, and G. Tamura, *Biochem. Biophys. Res. Commun.*, **31**, 488 (1968).
(28) D. J. Finney, "Probit Analysis," Cambridge University Press, 1952.
(29) S. Hwang, E. Owada, T. Yotsuyanagi, L. Suhardja, N. F. H. Ho, G. L. Flynn, and W. I. Higuchi, *J. Pharm. Sci.*, **65**, 1574 (1976).
(30) S. Muranishi, N. Muranushi, and H. Sezaki, *Int. J. Pharm.*, **2**, 101 (1979).
(31) Y. Tokunaga, S. Muranishi, and H. Sezaki, *J. Pharmacobio. Dyn.*, **1**, 28 (1978).
(32) S. Hirai, T. Yashiki, and H. Mima, *Int. J. Pharm.*, **9**, 165 (1981).
(33) C. Peracchia and A. F. Dulhunty, *J. Cell Biol.*, **70**, 419 (1976).

ACKNOWLEDGMENTS

The authors are grateful to Mr. H. Nakagawa for assistance with the experiments, to Dr. M. Fujino for the supply of leuprolide, to Dr. N. Kitamori for preparation of the tablets, to Dr. T. Shimamoto for valuable discussion, and to Dr. J. R. Miller for comments on the manuscript.

Effect of Moisture and Crushing Strength on Tablet Friability and *In Vitro* Dissolution

Z. T. CHOWHAN[x], I. C. YANG, A. A. AMARO, and LI-HUA CHI

Received November 9, 1981, from the *Syntex Research, Division of Syntex (U.S.A.) Inc., Palo Alto, CA 94304.* Accepted for publication February 5, 1982.

Abstract □ The friability and dissolution of a formulation of compressed tablets were studied by varying the granulation moisture and tablet crushing strength. A general quadratic response surface model was used to analyze the data. The response surface contour plots of tablet friability consisted of a series of ellipsoidal curves. The optimum friability corresponding to a granulation moisture content and a tablet crushing strength was a simple minimum. The *in vitro* dissolution contour plots showed a stationary ridge system. Along the ridge, a large number of combinations of tablet crushing strength and granulation moisture represented 100% drug dissolution. The contour overlays of friability and dissolution contour plots showed a region where both the friability and dissolution requirement could be met. The analysis of the data by means of multiple linear regression was helpful in understanding the role of granulation moisture and tablet crushing strength on tablet friability and *in vitro* dissolution.

Keyphrases □ Dissolution—*in vitro*, effect of moisture and crushing strength, tablet friability □ Crushing strength—effect on tablet friability and *in vitro* dissolution □ Friability—tablets, effect of moisture and crushing strength

Previous studies (1–3) from these laboratories discussed the interrelationships between moisture, crushing strength, and *in vitro* drug dissolution in compressed tablets. Another physical parameter of importance to the tablet formulators, especially in coating and packaging operations, is friability of compressed tablets. The friabilator[1] (4) provides falling as well as frictional abrasion to the tablet sample and is used to measure the resistance to abrasion or attrition of tablets. The loss of weight is measured after a fixed number of revolutions of a drum rotating at a controlled rate. In the development of tablet dosage forms, formulation factors are generally checked to reduce comparative loss in friability testing. Two types of friabilator[1,2] apparatuses were compared (5) using 10 tablet formulations differing in method of granulation or choice of binder. In all instances the percentage of weight loss was higher with friabilator A[1], the differences ranging from 6.2 to 39.7%, depending upon the formulation. After 25 years of use, it was concluded (6) that the weight loss of not more than 0.8% by friabilator A was valid for the control of most pharmaceutical tablets.

Although friability is generally considered important in the development of tablet formulations, factors affecting friability have not been fully explored. The present report describes a study of the interdependence of tablet friability and *in vitro* drug dissolution on granulation moisture content and tablet crushing strength. The data were analyzed using a general quadratic response surface model and the analysis suggested that rational specifications on the in-process variables such as the granulation moisture and initial tablet hardness could ensure proper control of the tablet friability and *in vitro* dissolution.

EXPERIMENTAL

Materials—The drug, ticlopidine hydrochloride[3], 5-(*o*-chlorobenzyl)-4,5,6,7-tetrahydrothieno-[3,2-*c*]pyridine hydrochloride was at least 99.0% pure. The excipients used were microcrystalline cellulose[4] NF, povidone[5] USP, citric acid[6] USP, stearic acid powder[7] NF, corn starch[8] NF, and lactose[9] USP.

Granulation—The formulation used in this study contained 64.1% drug, 22.4% microcrystalline cellulose, 10% starch, 1% citric acid, 2% povidone, and 0.5% stearic acid. The drug and microcrystalline cellulose were mixed together in a small planetary mixer for 10 min. Povidone and citric acid were dissolved in water and the powder mixture was granulated with the binder solution. The wet granulation was mixed for 10 min and passed through a 1.4-mm aperture and dried in a forced-air oven at 60°

[1] Roche type friabilator A.
[2] Erweka Friability Apparatus B.

[3] Sanofi Research Co. Inc. New York, NY 10019.
[4] Avicel pH 101, FMC Corp., Philadelphia, PA 19103.
[5] GAF Corp. New York, NY 10020.
[6] Mallinckrodt, Inc., St. Louis, MO 63147.
[7] Emery Industries, Inc., Cincinnati, OH 45232.
[8] Staley Manufacturing Co., Decatur, IL 62525.
[9] Regular grade, Foremost Co., San Francisco, CA 94104.

0022-3549/82/1200-1371$01.00/0

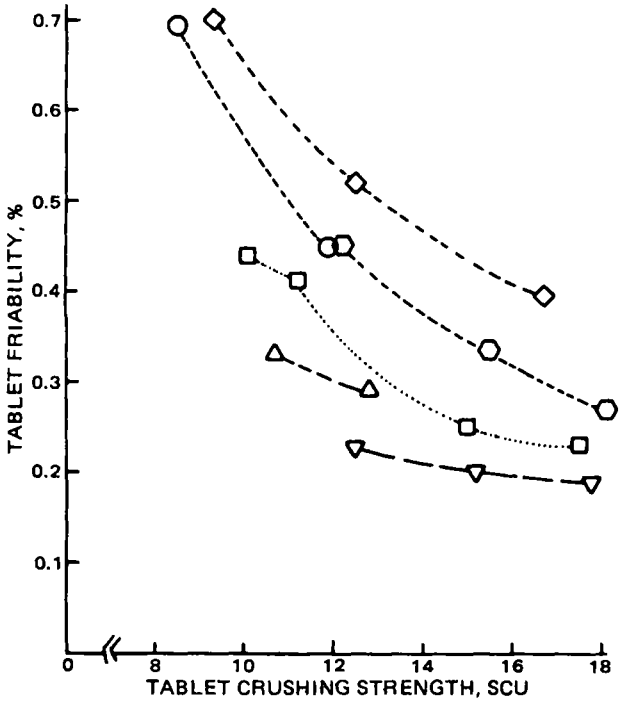

Figure 1—*Plots of tablet friability* versus *tablet crushing strength at different granulation moisture contents. The moisture contents in the granulation at the time of compression were: (○) 0.9%; (△) 1.6%; (▽) 2.0%; (□) 3.0%; (○) 3.6%; (◇) 4.3%.*

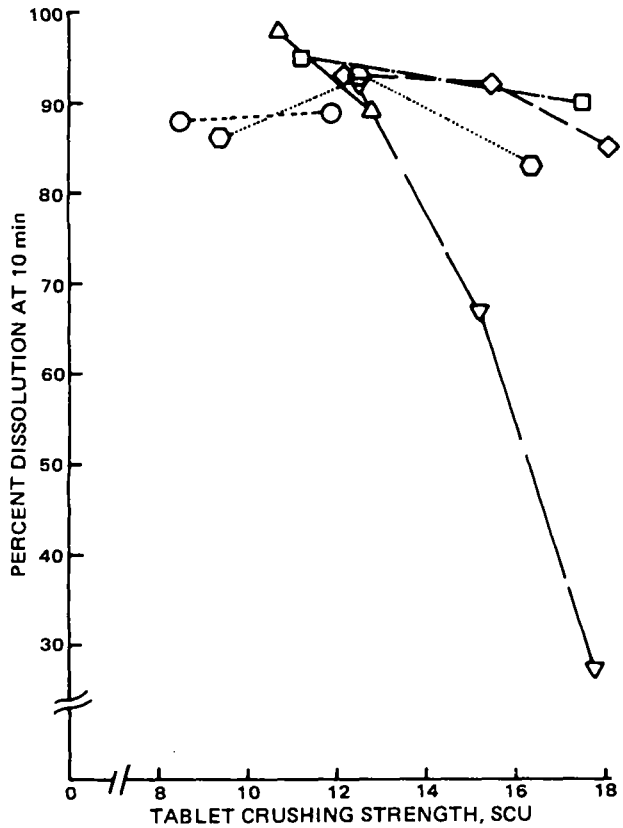

Figure 2—*Plots of percent* in vitro *drug dissolution at the 10-min time point as a function of the tablet crushing strength at different granulation moisture contents. The moisture contents at the time of compression were: (○) 0.9%; (△) 1.6%; (▽) 2.0%; (□) 3.0%; (◇) 3.6%; (○) 4.3%.*

Table I—Results of Multiple Linear Regression Analyses

Coefficients	Factors > Interactions	Regression Coefficient Values Tablet Friability, Y_1	Dissolution, Y_2
b_0	—	2.0186	79.8802
b_1	X_1	−0.2844	−11.4638
b_2	X_2	−0.1808	6.8757
b_3	X_1^2	−0.06228	−4.6829
b_4	X_1X_2	−0.000093	3.3677
b_5	X_2^2	0.005389	−0.7470
Multiple correlation coefficient		0.9407	0.7256

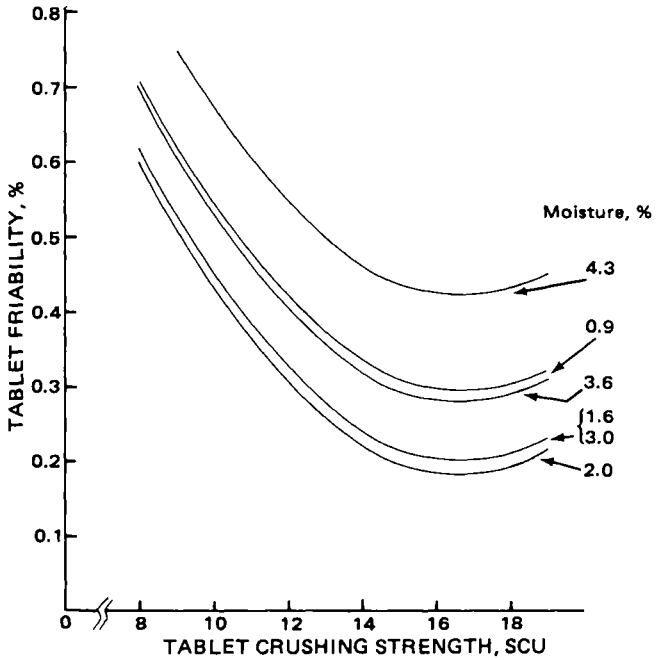

Figure 3—*Calculated plots of tablet friability* versus *tablet crushing strength at different granulation moisture contents using Eq. 1.*

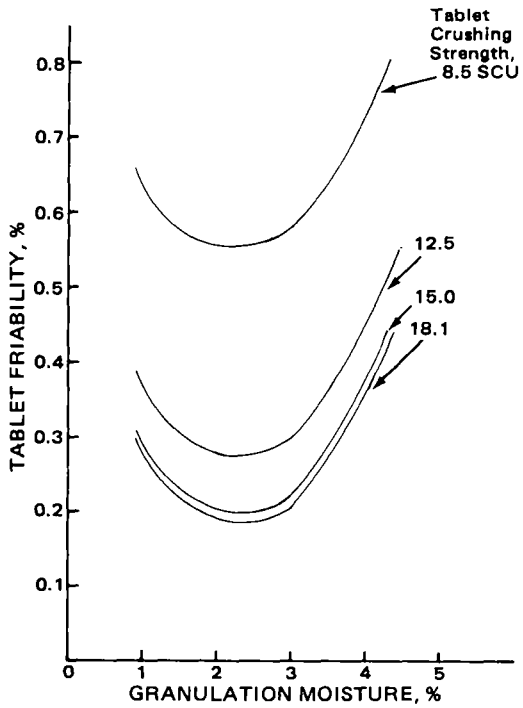

Figure 4—*Calculated plots of tablet friability* versus *percent granulation moisture at different tablet crushing strengths using Eq. 1.*

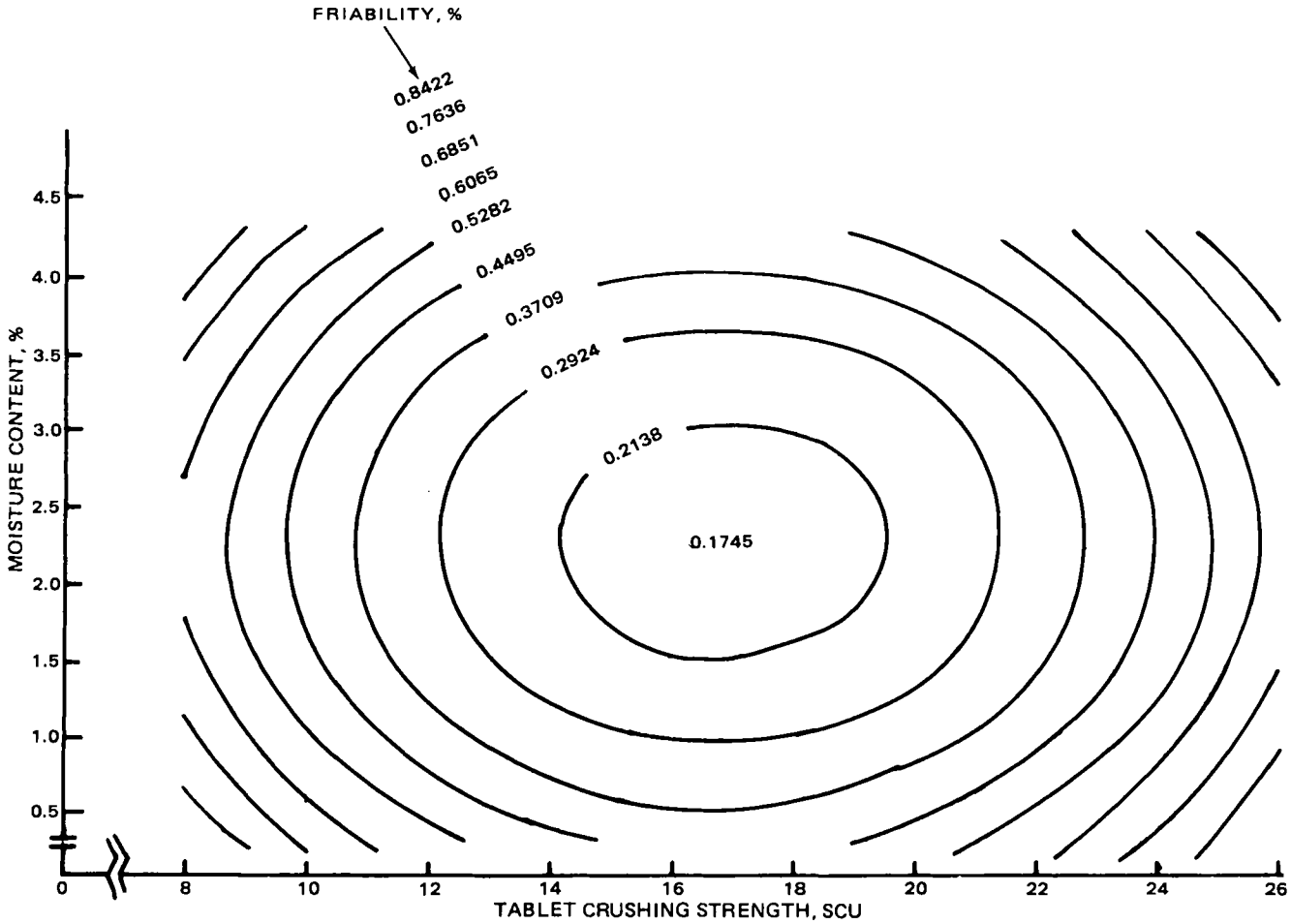

Figure 5—*Response surface contour plots of a two variable system, tablet crushing strength, and granulation moisture content and a response variable, friability.*

until the desired moisture levels were obtained. The dried granulations were screened through a 1.2-mm aperture. Starch and stearic acid were then blended with the granulations for 5 min. The granulations were stored in tightly closed jars. The moisture content of the final granulations were determined prior to compression.

Compression—Tablets were compressed with a rotary tablet machine[10] to a targeted crushing strength. The punches and dies were 10.32 mm in diameter, and the punches were standard concave in shape.

Moisture Determination—The granulation moisture was determined with a moisture balance[11] by exposure to a 125 W IR lamp for 15 min at the 90 V setting. The percent weight loss on drying was read directly from the instrument.

Tablet Crushing Strength—The initial tablet crushing strength was determined[12] immediately after compression. For each determination 10 tablets were tested and the mean calculated.

Friability Determination—At least 20 tablets were brushed with a soft camel hair brush to remove all adhering particles and placed in a friabilator[1]. After accurate weighing, the tablets were placed in the drum. The drum was rotated for 4 min or 100 revolutions. At the end of 4 min, the tablets were removed, brushed to remove adhering particles, and accurately weighed. The loss of weight was calculated. The test was run in duplicate and the mean percent friability was calculated.

***In Vitro* Dissolution**—The USP Method II was used. For each sampling point six tablets were tested. The apparatus consisted of USP paddles driven by a multiple-spindle drive with a variable speed control[13], 1-liter round-bottom plastic flasks[14], and a water bath. The dissolution medium was 700 ml of deaerated water equilibrated at 37° and stirred at 50 rpm. The dissolved drug was analyzed by recording the absorbance at 236 nm using an automated monitoring system consisting of a peristaltic pump[15], 1-mm spectrophotometer flow cells, and automatic sample changer/spectrophotometer[16]. The absorbances were plotted on a recorder every minute until complete dissolution was achieved.

The dissolution apparatus was calibrated using USP dissolution calibrator tablets (prednisone 50 mg). The mean dissolution and the standard deviations were within the required range.

RESULTS AND DISCUSSION

The effects of granulation moisture and tablet crushing strength on tablet friability are given in Fig. 1. The results suggest that the tablet friability depends on moisture content and tablet crushing strength (controllable variables). It is possible to reduce tablet friability at higher crushing strengths and at optimum moisture contents.

Figure 2 gives the results of drug dissolution at the 10-min time point *versus* tablet crushing strength at different moisture contents. At lower moisture contents (1.6 and 2.0%), the drug dissolution is strongly dependent on tablet crushing strength. The higher the tablet crushing strength, the lower the percent drug dissolved and *vice versa*. However, at higher moisture contents (3.0, 3.6, and 4.3%), the dissolution of the drug shows very little dependency on crushing strength of the tablets.

A general multiple linear regression analysis of the results was performed using a program package[17], RSREG, on a computer[18]. The RSREG procedure fits the parameters of a complete quadratic response surface and then determines critical values to optimize the response with respect to the factors in the model. A general quadratic response surface

[10] Model B-2, Stokes.
[11] Cenco, Central Scientific Co. Chicago, IL 60623.
[12] Schleuniger-2E Hardness Tester, Vector Corp., Marion, IA 52303.
[13] Model 72 R, Hanson Research Corp., Northridge, Calif.
[14] Elanco, Indianapolis, Ind.
[15] Model 1210, Harvard Apparatus, Millis, Mass.
[16] Model 25, Beckman Instruments, Fullerton, Calif.
[17] SAS Institute Inc, Cary, NC 27511.
[18] IBM 3033.

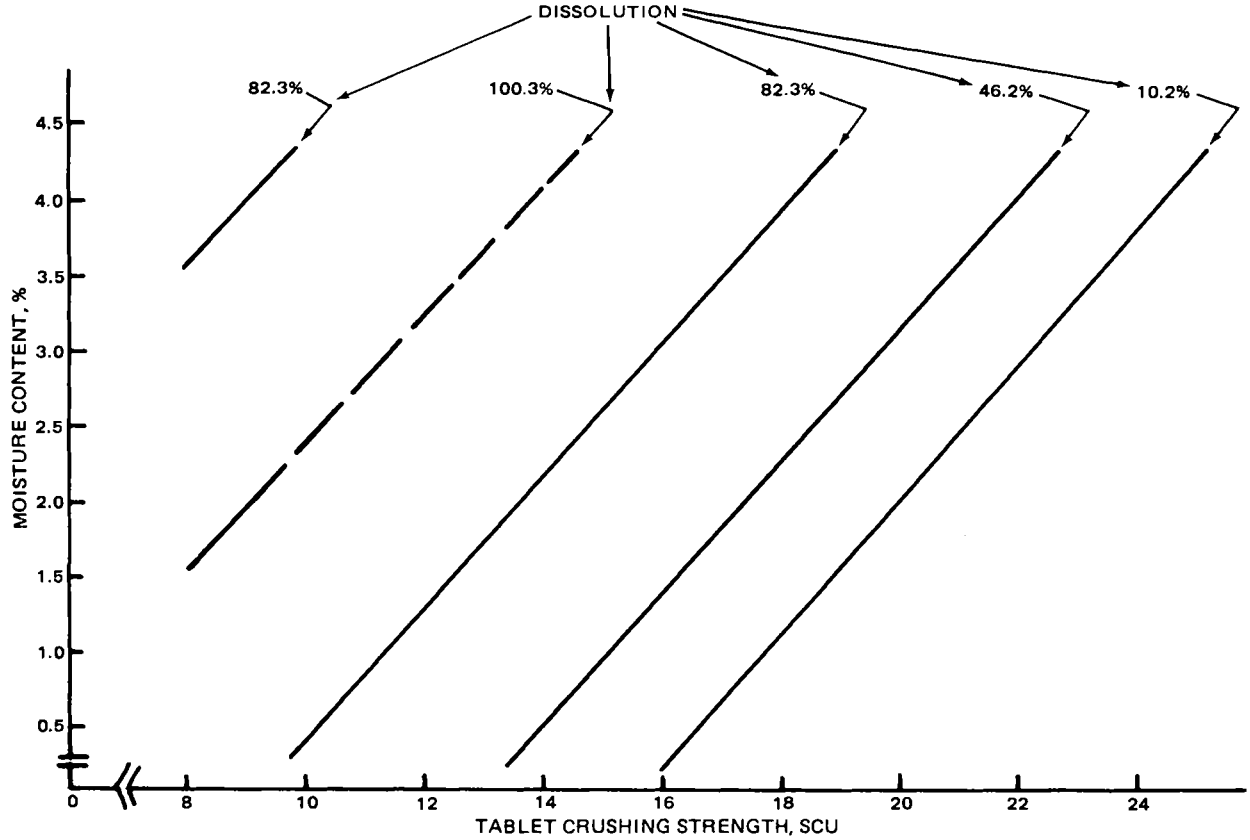

Figure 6—*Response surface contour plots of a two variable system, tablet crushing strength, and granulation moisture content and a response variable, dissolution (at 10 min).*

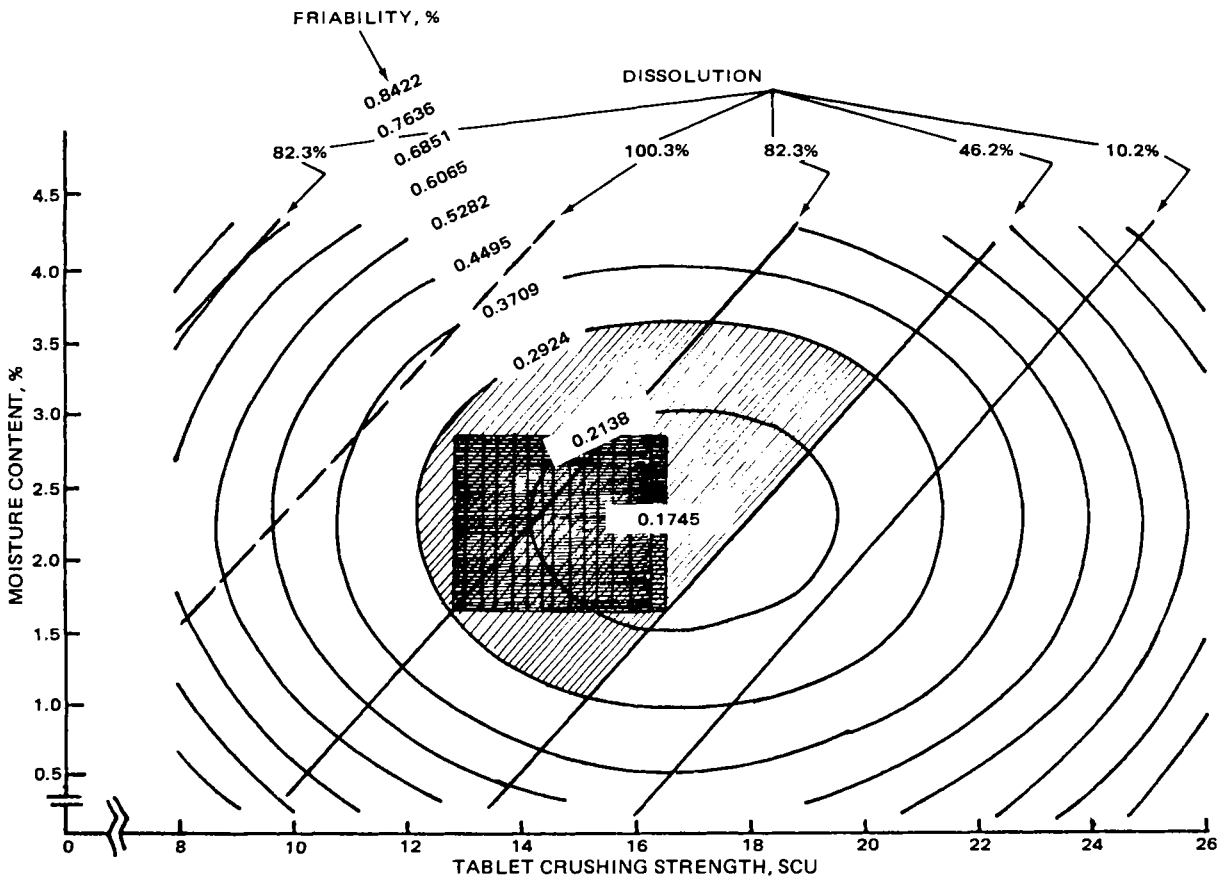

Figure 7—*Contour overlay showing the superimposed contour plots of friability and* in vitro *dissolution. The deeply shaded rectangle indicates the ranges in which in process specifications for tablet crushing strength and granulation moisture content could be set.*

model is written:

$$Y = b_0 + b_1X_1 + b_2X_2 + b_3X_1^2 + b_4X_1X_2 + b_5X_2^2 + \text{Error} \quad \text{(Eq. 1)}$$

where Y is the response surface such as tablet friability or drug dissolution, X_1 and X_2 are controllable variables such as granulation moisture and tablet crushing strength, and the coefficients b_0, b_1, ... b_5 are the least-square regression coefficients.

The results of the regression analysis are given in Table I. The regression coefficients were substituted in Eq. 1, and by fixing the moisture content, the calculated plots of tablet friability *versus* tablet crushing strength were obtained (Fig. 3). Similarly, by fixing the tablet crushing strength, calculated plots of tablet friability *versus* moisture content were obtained (Fig. 4). These plots suggest that the moisture content in the range of ~1.5–3.0% and tablet crushing strength in the range of ~14–17 Strong Cobb units (SCU) give the least possible tablet friability. Similar conclusions could be drawn from the data given in Fig. 1.

The response surface contour plots of friability and dissolution are given in Figs. 5 and 6. The response surface contour plots illustrate the geometric relationships between the controllable variables and their responses. The predicted values of responses for a grid of the controllable variable data points can be generated. The friability contour plot consists of a series of ellipsoidal curves. The solution for optimum response indicated that the predicted value of friability at optimum was 0.17%, corresponding to a moisture content of 2.3% and a tablet crushing strength of 16.8 SCU.

In tableting, tablet crushing strengths are generally limited to between 8 and 20 SCU because of compression, friability, and dissolution limitations. From Fig. 5 one can obtain a range of crushing strengths (14.2–19.4 SCU) and a range of moisture content (1.5–3%), which gives friability in the minimum possible range of 0.17–0.21%. At a fixed tablet crushing strength of 16 SCU, friability decreases as the moisture content increases until it reaches its optimum value. Further increase in moisture content results in an increase in friability. Similarly, at a fixed moisture content of 2%, friability decreases as the crushing strength is increased until an optimum value is reached, after which time material is generally incompressible due to the tablet density approaching the calculated true density of the formulation.

The response surface contour plots of dissolution given in Fig. 6 show a stationary ridge system. The stationary ridge system has parallel straight line contours running in a direction determined by the relative effect of X_1 and X_2, which are controllable variables. The response surface contour plots using Eq. 1 can take a number of different forms depending on the coefficients b_0, b_1, ... b_5.

Within the practical limitations of tableting, there are a large number of combinations of tablet crushing strength and granulation moisture content all along the ridge which is expected to give 100% drug dissolution. At constant crushing strength, an increase or decrease in the granulation moisture content moving away from the ridge in either direction results in lower dissolution. Similarly, at constant granulation moisture content, an increase or decrease in crushing strength moving away from the ridge results in lower drug dissolution.

In this investigation, not only *in vitro* dissolution but also tablet friability were considered important and both were measured experimentally. If it was desired that the specifications for dissolution in 10 min were >46% and to maintain friability <0.3%, Figs. 5 and 6 could be superimposed. The contour overlays are shown in Fig. 7. The shaded area shows the region where both the friability and dissolution requirements are met. From the deeply shaded rectangle, specifications on granulation moisture and tablet crushing strength could be set. If these specifications were unsatisfactory from a bioavailability or production viewpoint, other factors affecting friability and dissolution such as formulation and processing factors would have to be explored. It also may be possible to reduce tablet friability by considering the punch shape factor.

In conclusion, this study shows that a general multiple linear regression analysis is helpful in understanding the role of the granulation moisture and tablet crushing strength on tablet friability and *in vitro* dissolution. By superimposing the contour plots of tablet friability and drug dissolution, it is possible to set in process specifications for the granulation moisture content and tablet crushing strength.

REFERENCES

(1) Z. T. Chowhan and L. Palagyi, *J. Pharm. Sci.*, **67**, 1385 (1978).

(2) Z. T. Chowhan, *ibid.*, **69**, 1 (1980).

(3) Z. T. Chowhan, *Drug Dev. Ind. Pharm.*, **5**, 41 (1979).

(4) E. G. Shafer, E. G. Wollish, and C. E. Engel, *J. Am. Pharm. Assoc., Sci. Ed.*, **45**, 114 (1956).

(5) B. Selmeczi, *Sci. Pharm.*, **42**, 73 (1974).

(6) E. G. Wollish and A. R. Mlodzeniec, "Abstracts," APhA Academy of Pharmaceutical Sciences Annual Meeting, St. Louis, Mo., 94, vol. 11, No. 1 (1981).

Relationship of Dissolution Rate to Viscosity of Polymeric Solutions

NARONG SARISUTA * and EUGENE L. PARROTT ×

Received December 28, 1981, from the *Division of Pharmaceutics, College of Pharmacy, University of Iowa, Iowa City, IA 52242.* Accepted for publication February 5, 1982.

* Present address: Mahidol University, Bangkok, Thailand.

Abstract □ The influence of viscosity on the dissolution rate of benzoic acid in aqueous solutions of methylcellulose, hydroxypropyl cellulose, and guar gum was investigated. The viscosities were measured by capillary and rotational viscometers and were calculated from experimental diffusion coefficients by means of the Stokes-Einstein equation. The relationship of the dissolution rate to viscosity may be represented by a single curve. An equation is presented relating the dissolution rate of benzoic acid to solubility, diffusion coefficient, and viscosity for these nonionic viscosity-enhancing agents. To demonstrate that additional factors affect the dissolution rate, similar data were determined using solutions of xanthan gum, which is anionic. The electrical effect modified mass transport so the quantitative relationship of dissolution rate and viscosity was not the same as in the nonionic carbohydrate solution.

Keyphrases □ Dissolution, rate—relationship to viscosity of polymeric solutions, benzoic acid □ Viscosity—relationship of dissolution rate of polymeric solutions, benzoic acid □ Benzoic acid—relationship of dissolution rate to viscosity of polymeric solutions

Although viscosity-enhancing polymers are present in many pharmaceuticals, little research has been reported on the influence of viscosity on the dissolution rate. Diffusion-controlled dissolution would be expected to decrease in rate with an increase in viscosity (1–4). Numerous empirical equations, which show the dissolution rate to be a function of the viscosity raised to a power ranging from −0.25 to −0.8, have been proposed (5–7).

0022-3549/82/1200-1375$01.00/0

model is written:

$$Y = b_0 + b_1X_1 + b_2X_2 + b_3X_1^2 + b_4X_1X_2 + b_5X_2^2 + \text{Error} \quad \text{(Eq. 1)}$$

where Y is the response surface such as tablet friability or drug dissolution, X_1 and X_2 are controllable variables such as granulation moisture and tablet crushing strength, and the coefficients b_0, b_1, ... b_5 are the least-square regression coefficients.

The results of the regression analysis are given in Table I. The regression coefficients were substituted in Eq. 1, and by fixing the moisture content, the calculated plots of tablet friability *versus* tablet crushing strength were obtained (Fig. 3). Similarly, by fixing the tablet crushing strength, calculated plots of tablet friability *versus* moisture content were obtained (Fig. 4). These plots suggest that the moisture content in the range of ~1.5–3.0% and tablet crushing strength in the range of ~14–17 Strong Cobb units (SCU) give the least possible tablet friability. Similar conclusions could be drawn from the data given in Fig. 1.

The response surface contour plots of friability and dissolution are given in Figs. 5 and 6. The response surface contour plots illustrate the geometric relationships between the controllable variables and their responses. The predicted values of responses for a grid of the controllable variable data points can be generated. The friability contour plot consists of a series of ellipsoidal curves. The solution for optimum response indicated that the predicted value of friability at optimum was 0.17%, corresponding to a moisture content of 2.3% and a tablet crushing strength of 16.8 SCU.

In tableting, tablet crushing strengths are generally limited to between 8 and 20 SCU because of compression, friability, and dissolution limitations. From Fig. 5 one can obtain a range of crushing strengths (14.2–19.4 SCU) and a range of moisture content (1.5–3%), which gives friability in the minimum possible range of 0.17–0.21%. At a fixed tablet crushing strength of 16 SCU, friability decreases as the moisture content increases until it reaches its optimum value. Further increase in moisture content results in an increase in friability. Similarly, at a fixed moisture content of 2%, friability decreases as the crushing strength is increased until an optimum value is reached, after which time material is generally incompressible due to the tablet density approaching the calculated true density of the formulation.

The response surface contour plots of dissolution given in Fig. 6 show a stationary ridge system. The stationary ridge system has parallel straight line contours running in a direction determined by the relative effect of X_1 and X_2, which are controllable variables. The response surface contour plots using Eq. 1 can take a number of different forms depending on the coefficients b_0, b_1, ... b_5.

Within the practical limitations of tableting, there are a large number of combinations of tablet crushing strength and granulation moisture content all along the ridge which is expected to give 100% drug dissolution. At constant crushing strength, an increase or decrease in the granulation moisture content moving away from the ridge in either direction results in lower dissolution. Similarly, at constant granulation moisture content, an increase or decrease in crushing strength moving away from the ridge results in lower drug dissolution.

In this investigation, not only *in vitro* dissolution but also tablet friability were considered important and both were measured experimentally. If it was desired that the specifications for dissolution in 10 min were >46% and to maintain friability <0.3%, Figs. 5 and 6 could be superimposed. The contour overlays are shown in Fig. 7. The shaded area shows the region where both the friability and dissolution requirements are met. From the deeply shaded rectangle, specifications on granulation moisture and tablet crushing strength could be set. If these specifications were unsatisfactory from a bioavailability or production viewpoint, other factors affecting friability and dissolution such as formulation and processing factors would have to be explored. It also may be possible to reduce tablet friability by considering the punch shape factor.

In conclusion, this study shows that a general multiple linear regression analysis is helpful in understanding the role of the granulation moisture and tablet crushing strength on tablet friability and *in vitro* dissolution. By superimposing the contour plots of tablet friability and drug dissolution, it is possible to set in process specifications for the granulation moisture content and tablet crushing strength.

REFERENCES

(1) Z. T. Chowhan and L. Palagyi, *J. Pharm. Sci.*, **67**, 1385 (1978).

(2) Z. T. Chowhan, *ibid.*, **69**, 1 (1980).

(3) Z. T. Chowhan, *Drug Dev. Ind. Pharm.*, **5**, 41 (1979).

(4) E. G. Shafer, E. G. Wollish, and C. E. Engel, *J. Am. Pharm. Assoc., Sci. Ed.*, **45**, 114 (1956).

(5) B. Selmeczi, *Sci. Pharm.*, **42**, 73 (1974).

(6) E. G. Wollish and A. R. Mlodzeniec, "Abstracts," APhA Academy of Pharmaceutical Sciences Annual Meeting, St. Louis, Mo., 94, vol. 11, No. 1 (1981).

Relationship of Dissolution Rate to Viscosity of Polymeric Solutions

NARONG SARISUTA * and EUGENE L. PARROTT ×

Received December 28, 1981, from the *Division of Pharmaceutics, College of Pharmacy, University of Iowa, Iowa City, IA 52242.* Accepted for publication February 5, 1982.

* Present address: Mahidol University, Bangkok, Thailand.

Abstract □ The influence of viscosity on the dissolution rate of benzoic acid in aqueous solutions of methylcellulose, hydroxypropyl cellulose, and guar gum was investigated. The viscosities were measured by capillary and rotational viscometers and were calculated from experimental diffusion coefficients by means of the Stokes-Einstein equation. The relationship of the dissolution rate to viscosity may be represented by a single curve. An equation is presented relating the dissolution rate of benzoic acid to solubility, diffusion coefficient, and viscosity for these nonionic viscosity-enhancing agents. To demonstrate that additional factors affect the dissolution rate, similar data were determined using solutions of xanthan gum, which is anionic. The electrical effect modified mass transport so the quantitative relationship of dissolution rate and viscosity was not the same as in the nonionic carbohydrate solution.

Keyphrases □ Dissolution, rate—relationship to viscosity of polymeric solutions, benzoic acid □ Viscosity—relationship of dissolution rate of polymeric solutions, benzoic acid □ Benzoic acid—relationship of dissolution rate to viscosity of polymeric solutions

Although viscosity-enhancing polymers are present in many pharmaceuticals, little research has been reported on the influence of viscosity on the dissolution rate. Diffusion-controlled dissolution would be expected to decrease in rate with an increase in viscosity (1–4). Numerous empirical equations, which show the dissolution rate to be a function of the viscosity raised to a power ranging from −0.25 to −0.8, have been proposed (5–7).

0022-3549/82/1200-1375$01.00/0

Table I—Solubility and Diffusion Coefficient of Benzoic Acid in Various Concentrations of Polymeric Solutions at 25°

Viscosity-Enhancing Agent	Percent	Solubility, mg/ml	Density, g/ml	η_{rel}[a]	$10^5 D_{expt}$, cm²/sec
Methylcellulose	0.1	3.25	0.9976	1.47	1.036
	0.3	3.26	0.9979	3.65	0.678
	0.5	3.32	0.9983	8.07	0.298
	0.6	3.31	0.9985	12.90	0.240
Hydroxypropyl cellulose	0.1	3.32	0.9978	4.71	0.650
	0.2	3.29	0.9979	8.71	0.372
	0.3	3.30	0.9981	14.19	0.186
Guar gum	0.1	2.96	0.9975	3.30	1.055
	0.2	3.18	0.9982	9.31	0.446
	0.3	2.75	0.9983	25.86	0.167
Xanthan gum	0.025	—	0.9977	2.53	—
	0.05	3.17	0.9977	3.83	0.787
	0.1	3.18	0.9984	8.07	0.284
	0.15	3.10	0.9985	15.72	0.101

[a] Capillary method.

The influence of viscosity of polymeric solutions on the dissolution rate of soluble inorganic salts was studied (8). No one equation relating rate and bulk viscosity fitted the data. By utilizing an effective viscosity, a plot of the data was approximated by a single curve, which was represented by an empirical equation.

There appears to be no general expression relating the dissolution rate to viscosity. Assuming that, with various solutes and polymeric solutions of markedly different ionic and chemical nature, factors other than viscosity act and affect the dissolution rate at a given viscosity, three nonionic carbohydrate polymers were studied with the thought that the interactions would be essentially constant and that the relation of dissolution rate to viscosity could be better expressed.

EXPERIMENTAL

Dissolution Rate Determinations—The procedure for tablet production and the dissolution apparatus were similar to those previously described (9). Spherical 1.273 ± 0.005-cm tablets of pure benzoic acid were compressed at 2270 kg of force by a hydraulic press[1]. All determinations were made in triplicate at 25 ± 0.1° and at a stirring speed of 324 rpm. The 2 liters of dissolution medium was changed at appropriate intervals so that the concentration of dissolved benzoic acid was not permitted to exceed 3% of its solubility. With each change of dissolution medium, the sphere was weighed and its diameter was measured with a micrometer. Solutions were prepared by a conventional method and allowed to stand 24 hr before use as the dissolution media. Dissolution rates were determined in various concentrations of aqueous methylcellulose[2], hydroxypropyl cellulose[3], xanthan gum[4], and guar gum[5] solutions.

Other Parameters—The solubilities of benzoic acid in various concentrations of polymeric solutions as given in Table I were determined as reported earlier (9). The densities of the solutions were measured using a pycnometer. Viscosities were measured by using a capillary[6] and a rotational[7] viscometer. The diffusion coefficients were determined by use of a diffusion cell previously described (10). The value in Table I is an average of three determinations for each concentration.

RESULTS AND DISCUSSION

Bulk Viscosity—For the concentrations observed, the addition of methylcellulose, hydroxypropyl cellulose, guar gum, and xanthan gum in solution increases the viscosity by at least 15-fold as shown in Fig. 1. The addition of these polymer molecules in solution decreases to less than one-half the dissolution rate of benzoic acid as shown in Fig. 2. The solubility of benzoic acid in water is not significantly affected by the presence of any of these polymers as shown in Table I.

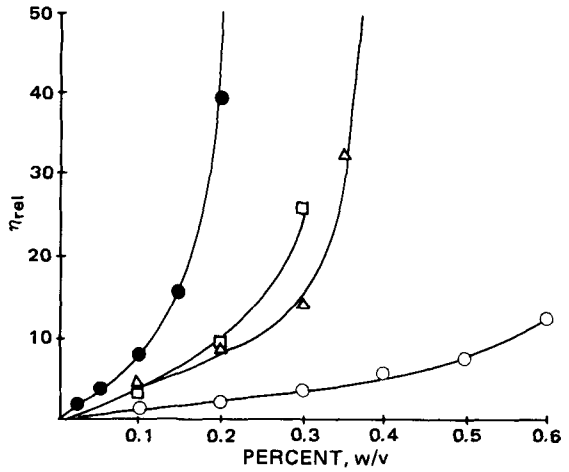

Figure 1—*Relative viscosity (η_{rel}) as a function of concentration in water at 25°. Key: (○) methylcellulose; (△) hydroxypropyl cellulose; (□) guar gum; and (●) xanthan gum.*

With no significant change in solubility, the only experimental variable affecting the dissolution rate appeared to be viscosity. Thus, one would anticipate that at a given viscosity of the dissolution medium, the dissolution rate of benzoic acid would be the same regardless of the noninteracting dissolution medium.

Figure 3 shows the relation of the dissolution rate and relative viscosity as determined by a capillary viscometer. It does not appear that one equation will relate the dissolution rate and bulk viscosity. Since the viscosity measured by the capillary method is a single shear rate viscosity, it probably does not represent the actual viscosity in the dissolution environment.

The viscosity-enhancing polymers studied form pseudoplastic solutions, which possess viscosities that vary with shear rate. The viscosities of the polymeric solutions were measured at rotational speeds from 0.3 to 60 rpm. Similar to the example of the methylcellulose solutions shown in Fig. 4, all of the polymeric solutions exhibited pseudoplastic flow at low rotational speed (<10 rpm), but at speeds >10 rpm, the viscosity did not decrease as the shear rate was increased. The constant viscosity at high shear has been called the upper Newtonian viscosity for dilute so-

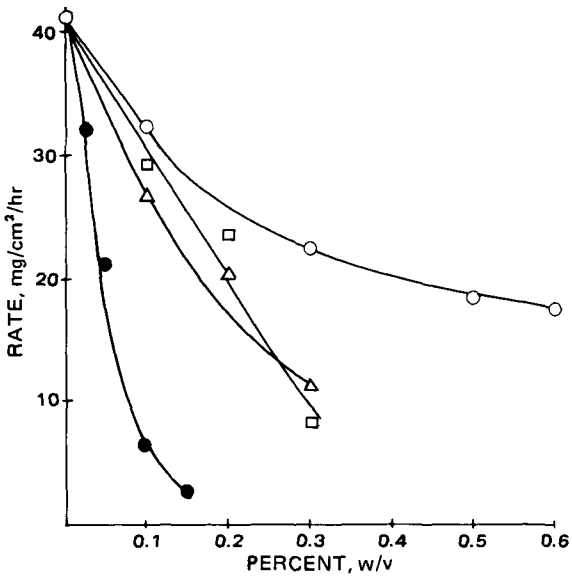

Figure 2—*Dissolution rates of benzoic acid in various concentrations of aqueous polymeric solutions. Key: (○) methylcellulose; (△) hydroxypropyl cellulose; (□) guar gum; and (●) xanthan gum.*

[1] Carver press, model C, Fred S. Carver, Inc.
[2] USP, type 1500 cp, City Chemical Corp.
[3] Klucel, grade HF, Hercules Inc.
[4] Kelzan, Kelco Division of Merck & Co., Inc.
[5] Colony Impt. & Expt. Corp.
[6] Ostwald-Fenske.
[7] Brookfield model LVT Synchro-lectric, Brookfield Engineering Lab.

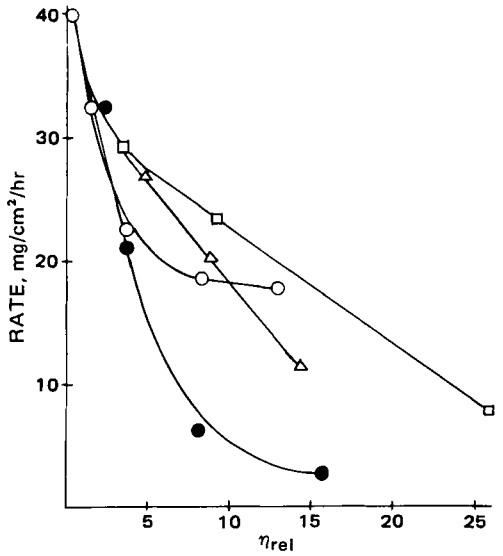

Figure 3—*Influence of relative viscosity of various polymeric solutions on dissolution rates of benzoic acid at 25°. Key: (○) methylcellulose; (△) hydroxypropyl cellulose; (□) guar gum; and (●) xanthan gum.*

lutions (11). At high shear rates, dissolved polymer chains are wholly disentangled and aligned in the direction of flow. As there is no remaining structure to be broken by further increases in shear rate, the viscosity reaches a constant value. In the viscometer at 60 rpm, the shear rate is ~200 sec^{-1} (12). The viscosity determined at speeds >10 rpm should represent the bulk viscosity in the dissolution apparatus (in which the 324 rpm provided a shear rate >200 sec^{-1}) better than the capillary viscosity.

The influence of viscosity measured at 1.5 rpm on the dissolution rate of benzoic acid at 25° in aqueous methylcellulose, hydroxypropyl cellulose, guar gum, and xanthan gum solutions is shown in Fig. 5. For the nonionic polymers (methylcellulose, hydroxypropyl cellulose, and guar gum) the dissolution rate is decreased rapidly to almost the same extent. At rotational speeds >10 rpm, the experimental values of dissolution rate and viscosity of solutions of methylcellulose, hydroxypropyl cellulose, and guar gum essentially fall on a single curve (Fig. 6) indicating that for a dissolution medium of similar ionic and chemical nature, there is a correlation between dissolution rate and viscosity.

Microviscosity—The dilemma with polymeric solutions is to express an observed viscosity, which is a true reflection of the impedance to molecular transport in solution. Since in solutions of macromolecules the bulk viscosity as measured by a viscometer does not necessarily represent the viscosity through which the solute molecules travel, a viscosity measured without the mechanical influence of a viscometer was considered. In the Stokes-Einstein equation, there is an inverse relationship between the viscosity and the diffusion coefficient. Thus, an attempt was made to relate the diffusivity of benzoic acid in the polymeric solution to viscosity by use of the Stokes-Einstein equation, as the concentration of benzoic acid was dilute and the radius (2.95 Å) of the benzoic acid molecule is smaller than that of the solvent molecule (13). The viscosity

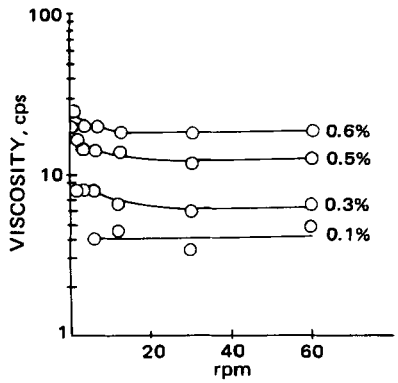

Figure 4—*Influence of rotations per minute on viscosities of aqueous solutions of various concentrations of methylcellulose.*

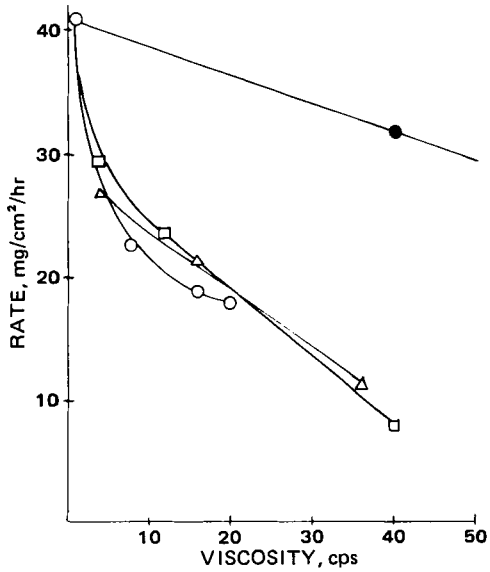

Figure 5—*Influence of viscosity at 1.5 rpm on the dissolution rate of benzoic acid in aqueous polymeric solutions. Key: (○) methylcellulose; (△) hydroxypropyl cellulose; (□) guar gum; and (●) xanthan gum.*

(η_D) of the microenvironment was calculated using the experimental diffusion coefficients (D_{expt}) in various concentrations of polymeric solutions by:

$$\eta_D = \frac{kT}{6\P rD_{expt}} \qquad \text{(Eq. 1)}$$

where k is the Boltzmann constant, T is the absolute temperature, and r is the radius of the benzoic acid molecule. For example, with benzoic acid dissolving in 0.1% methylcellulose solution at 25°, the D_{expt} is 1.036 × 10^{-5} cm^2/sec, and:

$$\eta_D = \frac{(1.38066 \times 10^{-16})(298)}{6\P\,(1.036 \times 10^{-5})(1.95 \times 10^{-8})}$$
$$= 0.0071 \text{ poise}$$

According to a previous report (14), the D_{expt} in polymeric solutions may be corrected for the obstructive effect of the polymer chains by the relation:

$$D_{true} = \frac{D_{expt}}{(1 - 1.5\,\phi)} \qquad \text{(Eq. 2)}$$

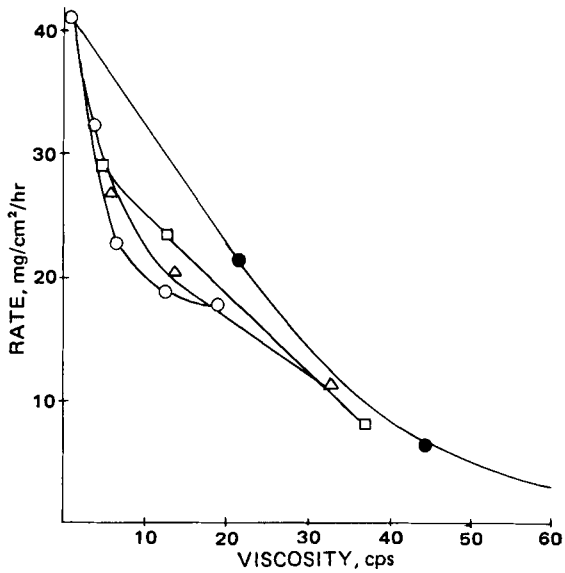

Figure 6—*Influence of viscosity at 60 rpm on dissolution rate of benzoic acid in aqueous polymeric solutions. Key: (○) methylcellulose; (△) hydroxypropyl cellulose; (□) guar gum; and (●) xanthan gum.*

Table II—Dissolution Rate of Benzoic Acid in Various Concentrations and Viscosities of Polymeric Solutions at 25°

Viscosity-Enhancing Agents	Percent	η_D, cps[a]	$f(\eta)$[b]	R, mg/cm²/hr	$\frac{R_{calc}}{R}$[c]
Methylcellulose	0.1	0.71	0.864	32.41	1.00
	0.3	1.09	0.925	22.79	1.20
	0.5	2.48	1.707	18.82	0.99
	0.6	3.08	1.848	16.36	0.96
Hydroxypropyl cellulose	0.1	1.14	1.117	26.79	0.99
	0.2	1.99	1.500	20.39	1.03
	0.3	3.98	1.704	11.66	1.00
Guar gum	0.1	0.70	0.841	29.26	1.02
	0.2	1.66	1.487	23.51	0.95
	0.3	4.43	1.592	8.15	1.01
Xanthan gum	0.025	—	—	32.11	—
	0.05	0.94	—	21.33	—
	0.10	2.60	—	6.55	—
	0.15	7.33	—	2.91	—

[a] Calculated by Eq. 1. [b] Calculated by Eq. 5. [c] Calculated by Eq. 7.

where ϕ is the volume fraction of the polymer. The volume fraction can be calculated from the concentration of the solution using the partial specific volume obtained by density measurements. The partial specific volume of each type of polymeric solution was evaluated by a plot of density against concentration according to the relationship:

$$\rho = \rho_{H_2O} + (1 - V\rho_{H_2O})C \qquad \text{(Eq. 3)}$$

where ρ and ρ_{H_2O} are the densities of the solution and the solvent, respectively, C is the concentration, and V is the partial specific volume. The volume fraction of the polymer was calculated from the partial specific volume and used in Eq. 2 to calculate D_{true}. In none of the systems studied did the difference between the D_{true} and D_{expt} exceed 0.3%.

The viscosity calculated by Eq. 1 and the dissolution rate are given in Table II. As seen in Fig. 7, as the viscosity of the dissolution media is increased, the dissolution rates are slowed to approximately the same extent. A single curve could be constructed to fit the experimental values.

Relation of Dissolution Rate and Viscosity—When the dissolution of a one-component, nondisintegrating sphere occurring in a nonreactive medium at sink conditions is diffusion controlled, the dissolution rate (R) may be expressed as (9):

$$R = \frac{DC_s}{h} \qquad \text{(Eq. 4)}$$

where D is the diffusion coefficient of the solute molecule, h is the effective film thickness, and C_s is the solubility. The experimental conditions used in determining the dissolution rate suggest that the diffusion layer model is operative (10). As shown in Fig. 8 there is a linear relationship between D_{expt} and $1/\eta_D$. It has been shown that at a fixed bulk viscosity the dissolution rate is not a linear function of D_{expt} (10). Similarly, as shown in Fig. 8, the relationship between dissolution rate of benzoic acid and D_{expt} in polymeric solutions is nonlinear. As the relationships of dissolution rate to viscosity and diffusion coefficient are curvilinear, a viscosity function $f(\eta)$ was introduced into Eq. 4:

$$R = \frac{DC_s}{h} f(\eta) \qquad \text{(Eq. 5)}$$

Experimentally all terms were evaluated so that the viscosity function could be calculated, assuming that h remained constant. For example, the viscosity function for 0.1% methylcellulose solution at 25° is:

$$f(\eta) = \frac{32.42 \times 32.2 \times 10^{-4}}{1.036 \times 10^{-5} \times 3600 \times 3.25} = 0.864$$

The values of the viscosity function for various polymeric solutions are given in Table II.

The relationship of the viscosity function to the η_D is shown in Fig. 9, and the equation for this relationship in these nonionic polymeric solu-

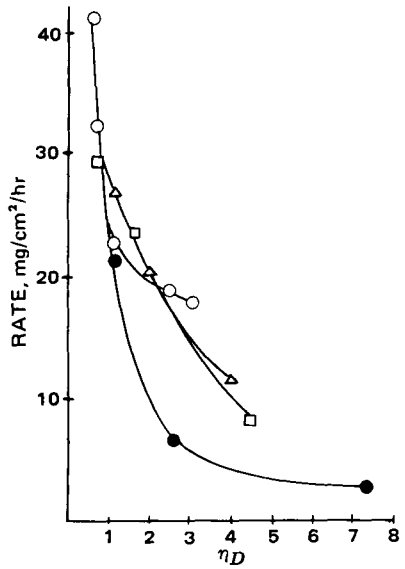

Figure 7—*Influence of η_D on dissolution rate of benzoic acid in aqueous polymeric solutions. Key: (○) methylcellulose; (△) hydroxypropyl cellulose; (□) guar gum; and (●) xanthan gum.*

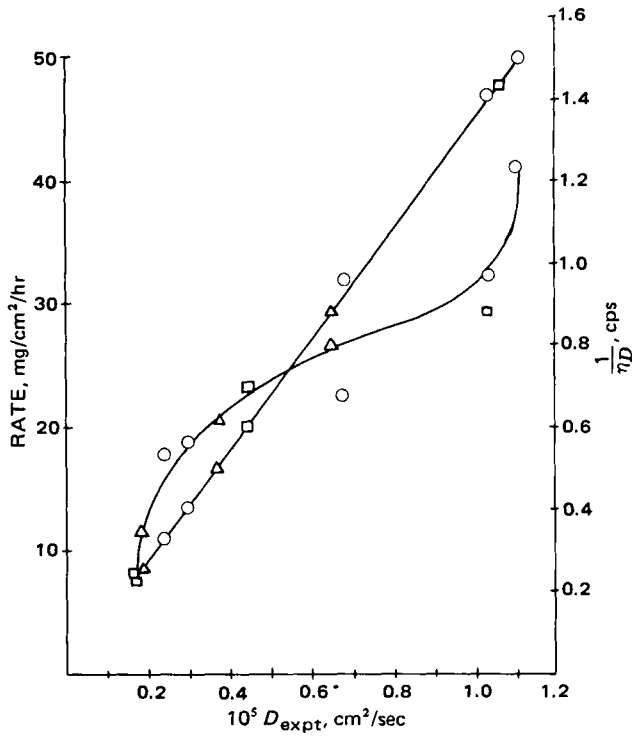

Figure 8—*Relationship of D_{expt} to $1/\eta_D$ and dissolution rate for aqueous polymeric solutions. Key: (○) methylcellulose; (△) hydroxypropyl cellulose; and (□) guar gum.*

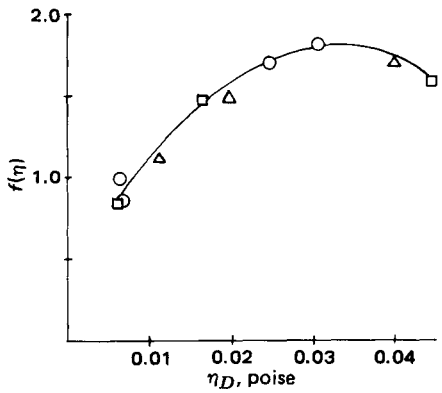

Figure 9—*Relation of η_D to viscosity function. Key: (○) methylcellulose; (△) hydroxypropyl cellulose; and (□) guar gum.*

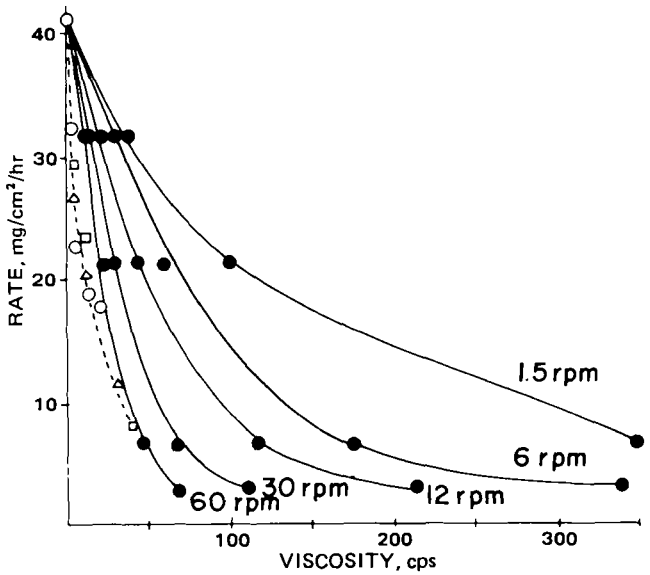

Figure 10—*Influence of rotations per minute on viscosity and dissolution rate in various polymeric solutions. Broken curve is a composite for solutions of nonionic polymers. Key: (○) methylcellulose; (△) hydroxypropyl cellulose; (□) guar gum; and (●) xanthan gum.*

tions is:

$$f(\eta) = 0.295 + 89.9\eta_D - 1360\eta_D^2 \qquad \text{(Eq. 6)}$$

Determination of η_D of a solution permits the calculation of the viscosity function, which is then used in Eq. 7 to calculate the dissolution rate. For example, in a 0.1% methylcellulose solution at 25° the η_D is 0.0071 poise, and the viscosity function is:

$$f(0.0071) = 0.295 + (89.9 \times 0.0071) - (1360 \times 0.0071^2)$$
$$= 0.865$$

Thus, the dissolution rate of benzoic acid in solutions of carbohydrate polymers of similar chemical and nonionic nature may be expressed as:

$$R = \frac{DC_s}{h}(0.295 + 89.9\eta_D - 1360\eta_D^2) \qquad \text{(Eq. 7)}$$

where D and C_s are the diffusion coefficient and solubility in the dissolution medium, respectively, possessing a microviscosity of η_D poises. The dissolution rate calculated by use of Eq. 7 and the experimental dissolution rates are compared in Table II.

Influence of Ionization of Polymer—Xanthan gum, which is chemically similar to the viscosity-enhancing polymers studied and is anionic, was selected to demonstrate the influence of electrical interactions on dissolution. In Figs. 1–3 the relations of concentration, relative viscosity, and dissolution rates are shown for xanthan gum. The influence of xanthan gum is more marked than the nonionic polymers. In Figs. 3 and 5 the rate–viscosity curve in solutions of the xanthan gum does not appear to have the same relationship as in solutions of the nonionic polymers.

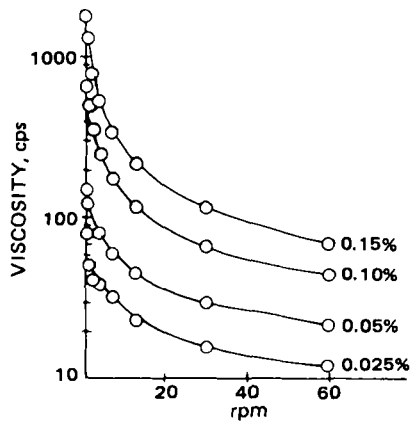

Figure 11—*Influence of rotations per minute on viscosity of solutions of various concentrations of xanthan gum.*

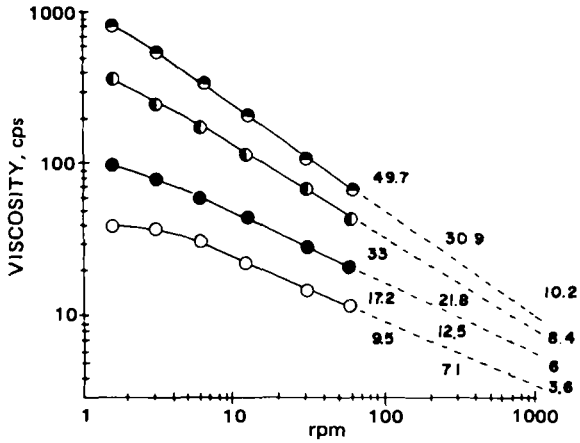

Figure 12—*Log–log relationship of viscosity and rotations per minute for solutions of xanthan gum. The viscosities at 100, 200, and 1000 rpm are given in the figure. Key: (○) 0.025%; (●) 0.05%; (◐) 0.1%; and (⊖) 0.15%.*

As the shear rate is increased by faster speeds of the rotational viscometer, the rate–viscosity curve in solutions of xanthan gum moves downward approaching the curve in solutions of the nonionic polymers, as shown in Fig. 10. Thus, the solutions of xanthan gum are pseudoplastic, but a shear rate greater than that provided by the rotational viscometer is required to reach the upper Newtonian viscosity, as shown in Fig. 11. The viscosity measured at 60 rpm does not represent the bulk viscosity of the solution of xanthan gum in the dissolution apparatus. To estimate the viscosity of the solution of xanthan gum at greater shear rates, the logarithm of viscosity was plotted against the logarithm (rpm) for the various concentrations of xanthan gum. The linear portions of the curves were extrapolated to estimate the viscosities at 100, 200, and 1000 rpm, as shown in Fig. 12.

In Fig. 13 the dissolution rates of benzoic acid are plotted as a function of the extrapolated viscosities at 100, 200, and 1000 rpm. The relationship of dissolution rate to viscosity in solutions of xanthan gum is not the same as that for the solutions of the nonionic polymeric solutions studied. Although the chemical nature is similar for all the polymers, the xanthan gum is anionic. Thus, the transport of benzoic acid in solutions of xanthan gum is complicated by the electrical charge on the xanthan gum chain.

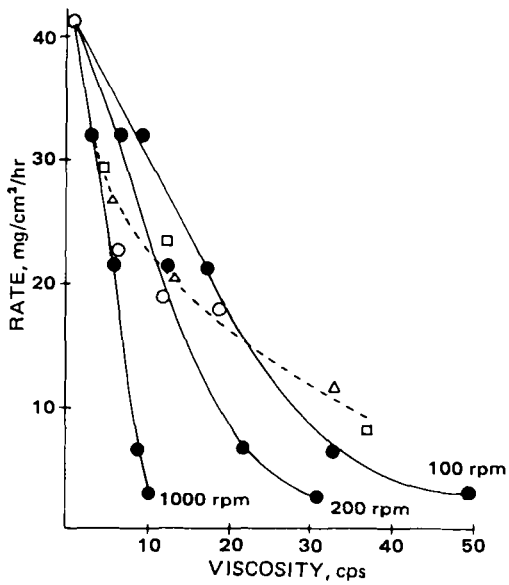

Figure 13—*Influence of viscosity at 100, 200, and 1000 rpm on dissolution rate of benzoic acid in aqueous solutions of xanthan gum. Broken curve is a composite for solutions of nonionic polymers. Key: (○) methylcellulose; (△) hydroxypropyl cellulose; (□) guar gum; and (●) xanthan gum.*

It was reported (15) that for ferricyanide ions diffusing in solutions of xanthan gum, the diffusion coefficient was decreased as much as 20-fold and was decreased as the shear rate was increased. It is thought that the shear causes the xanthan gum molecule to extend, exposing charge sites, and then the interaction between the solute and the charge sites changes diffusivity.

In addition, the viscosity measured by the viscometer may not represent the actual resistance to solute molecule transport. The values of the η_D of solutions of xanthan gum were calculated by Eq. 1. The relation of dissolution rate to viscosity of solutions of xanthan gum shown in Fig. 7 is not the same as the relation of dissolution rate to viscosity of solutions of the nonionic polymers. The difference may be caused by the interaction between the benzoic acid molecule and the anionic segments of the xanthan gum.

It appears that for viscosity-enhancing polymers of similar chemical and nonionic nature, a relationship may be expressed between the viscosity of the dissolution medium and the dissolution rate of a solid. However, if the chemical or ionic nature of the polymers is different, additional factors that influence dissolution rate are introduced and must be considered.

REFERENCES

(1) E. Roehl, C. V. King, and S. Kipness, *J. Am. Chem. Soc.*, **61**, 2290 (1939).

(2) T. Kressman and J. Kitchener, *Discuss. Faraday Soc.*, **7**, 90 (1949).

(3) C. V. King and M. M. Braverman, *J. Am. Chem. Soc.*, **54**, 1744 (1932).

(4) R. J. Braun and E. L. Parrott, *J. Pharm. Sci.*, **61**, 175 (1972).

(5) P. Roller, *J. Phys. Chem.*, **39**, 221 (1935).

(6) A. P. Colburn, *Trans. Inst. Chem. Eng.*, **29**, 174 (1949).

(7) C. Wagner, *J. Phys. Chem.*, **53**, 1030 (1949).

(8) A. T. Florence, P. H. Elworthy, and A. Rahman, *J. Pharm. Pharmacol.*, **25**, 779 (1973).

(9) E. L. Parrott and V. K. Sharma, *J. Pharm. Sci.*, **56**, 1341 (1967).

(10) R. J. Braun and E. L. Parrott, *ibid.*, **61**, 592 (1972).

(11) H. Schott, "Remington's Pharmaceutical Sciences," 15th ed., Mack Publishing, Easton, Pa., 1975, pp. 350–367.

(12) "Brookfield Model LVT Operating Instructions," Brookfield Engineering Laboratories, Stoughton, Mass., 1980.

(13) J. T. Edward, *J. Chem. Ed.*, **47**, 261 (1970).

(14) M. Lauffer, *Biophys. J.*, **1**, 205 (1961).

(15) D. W. Hubbard, F. D. Williams, and G. P. Heinrich, in "Proceedings of the International Congress on Rheology," 8th ed., G. Astarita, G. Marrucci, and L. Nicolais, Eds., Plenum, New York, N.Y., 1980, pp. 319–324.

ACKNOWLEDGMENTS

Abstracted in part from a dissertation submitted by N. Sarisuta to the Graduate College, University of Iowa, in partial fulfillment of the Doctor of Philosophy degree requirements.

Synthesis and Catalytic Activity of Poly-L-Histidyl-L-Aspartyl-L-Seryl-Glycine

A. N. SARWAL, E. O. ADIGUN, R. A. STEPHANI, and A. KAPOOR ×

Received July 21, 1981, from the *College of Pharmacy and Allied Health Professions, St. John's University, Jamaica, NY 11439.* Accepted for publication February 1, 1982.

Abstract □ Poly(His-Asp-Ser-Gly) was synthesized from the fully protected tetrapeptide active ester hydrochloride, which was prepared by stepwise coupling, using pentachlorophenyl ester and mixed anhydride methods. Complete deprotection of the protected tetrapeptide polymer was achieved by using 90% trifluoroacetic acid. The free polymer was dialyzed for 24 hr using a membrane (which retains molecules with molecular weights >5000). The catalytic activity was determined by studying the hydrolysis of *p*-nitrophenyl acetate in 0.2 *M* phosphate buffer (pH 7.4) at 37°. The catalytic coefficient of the dialyzed polymer was found to be 138 liters/mole/min.

Keyphrases □ Poly-L-His-L-Asp-L-Ser-Gly—synthesis and catalytic activity, polymer, pentachlorophenyl ester, hydrolysis □ Polymer—synthesis and catalytic activity of poly-L-His-L-Asp-L-Ser-Gly, pentachlorophenyl ester, hydrolysis □ Hydrolysis—synthesis and catalytic activity of poly-L-His-L-Asp-L-Ser-Gly, pentachlorophenyl ester, polymer

The use of poly(amino acids) as esterase models for structural and mechanistic problems of proteolytic enzymes has been very useful (1, 2). The poly(amino acids) that have been used for this purpose include homopolymers, copolymers, and sequential polypeptides. Sequential polypeptides provide one of the best means to study the factors affecting the folding of various enzymes, since they permit the placement of specific side chains at specific locations on a polypeptide backbone. Thus, suitable folding brings important side chain functionalities required for the activity into closer proximity, even though these amino acids lie at different distances in the enzyme sequences.

Considerable attention has been focused recently on the role played by L-histidine and L-serine in the active site of chymotrypsin and other proteolytic enzymes toward the hydrolysis of various esters such as *p*-nitrophenyl acetate (3, 4). Synthesis and catalytic activity of a number of peptides incorporating histidine and serine have been recently reported (5–7) as esterase models. The synthesis of the pentapeptide; L-Ser-γ-aminobutyryl-L-His-γ-aminobutyryl-L-Asp which had a catalytic coefficient of 147 liters/mole/min has been reported (5). The synthesis of a relatively more potent esterase model, L-His-Gly-L-Asp-L-Ser-L-Phe which had a catalytic coefficient of 179 liters/mole/min has also been reported (6). The comparison of the catalytic activity of various peptide esterase models led to the conclusion that peptides that incorporated L-aspartic acid in addition to L-histidine and L-serine showed considerable increase in catalytic activity (7). For example, L-His-L-Ala-L-Asp-Gly-L-Ser showed a catalytic activity of 210 liters/mole/min. The corresponding pentapeptide, L-His-L-Ala-L-Glu-Gly-L-Ser, where aspartic acid was replaced by glutamic acid, had a catalytic activity of 87

0022-3549/82/1200-1380$01.00/0

It was reported (15) that for ferricyanide ions diffusing in solutions of xanthan gum, the diffusion coefficient was decreased as much as 20-fold and was decreased as the shear rate was increased. It is thought that the shear causes the xanthan gum molecule to extend, exposing charge sites, and then the interaction between the solute and the charge sites changes diffusivity.

In addition, the viscosity measured by the viscometer may not represent the actual resistance to solute molecule transport. The values of the η_D of solutions of xanthan gum were calculated by Eq. 1. The relation of dissolution rate to viscosity of solutions of xanthan gum shown in Fig. 7 is not the same as the relation of dissolution rate to viscosity of solutions of the nonionic polymers. The difference may be caused by the interaction between the benzoic acid molecule and the anionic segments of the xanthan gum.

It appears that for viscosity-enhancing polymers of similar chemical and nonionic nature, a relationship may be expressed between the viscosity of the dissolution medium and the dissolution rate of a solid. However, if the chemical or ionic nature of the polymers is different, additional factors that influence dissolution rate are introduced and must be considered.

REFERENCES

(1) E. Roehl, C. V. King, and S. Kipness, *J. Am. Chem. Soc.*, **61**, 2290 (1939).

(2) T. Kressman and J. Kitchener, *Discuss. Faraday Soc.*, **7**, 90 (1949).

(3) C. V. King and M. M. Braverman, *J. Am. Chem. Soc.*, **54**, 1744 (1932).

(4) R. J. Braun and E. L. Parrott, *J. Pharm. Sci.*, **61**, 175 (1972).

(5) P. Roller, *J. Phys. Chem.*, **39**, 221 (1935).

(6) A. P. Colburn, *Trans. Inst. Chem. Eng.*, **29**, 174 (1949).

(7) C. Wagner, *J. Phys. Chem.*, **53**, 1030 (1949).

(8) A. T. Florence, P. H. Elworthy, and A. Rahman, *J. Pharm. Pharmacol.*, **25**, 779 (1973).

(9) E. L. Parrott and V. K. Sharma, *J. Pharm. Sci.*, **56**, 1341 (1967).

(10) R. J. Braun and E. L. Parrott, *ibid.*, **61**, 592 (1972).

(11) H. Schott, "Remington's Pharmaceutical Sciences," 15th ed., Mack Publishing, Easton, Pa., 1975, pp. 350–367.

(12) "Brookfield Model LVT Operating Instructions," Brookfield Engineering Laboratories, Stoughton, Mass., 1980.

(13) J. T. Edward, *J. Chem. Ed.*, **47**, 261 (1970).

(14) M. Lauffer, *Biophys. J.*, **1**, 205 (1961).

(15) D. W. Hubbard, F. D. Williams, and G. P. Heinrich, in "Proceedings of the International Congress on Rheology," 8th ed., G. Astarita, G. Marrucci, and L. Nicolais, Eds., Plenum, New York, N.Y., 1980, pp. 319–324.

ACKNOWLEDGMENTS

Abstracted in part from a dissertation submitted by N. Sarisuta to the Graduate College, University of Iowa, in partial fulfillment of the Doctor of Philosophy degree requirements.

Synthesis and Catalytic Activity of Poly-L-Histidyl-L-Aspartyl-L-Seryl-Glycine

A. N. SARWAL, E. O. ADIGUN, R. A. STEPHANI, and A. KAPOOR ×

Received July 21, 1981, from the *College of Pharmacy and Allied Health Professions, St. John's University, Jamaica, NY 11439.* Accepted for publication February 1, 1982.

Abstract □ Poly(His-Asp-Ser-Gly) was synthesized from the fully protected tetrapeptide active ester hydrochloride, which was prepared by stepwise coupling, using pentachlorophenyl ester and mixed anhydride methods. Complete deprotection of the protected tetrapeptide polymer was achieved by using 90% trifluoroacetic acid. The free polymer was dialyzed for 24 hr using a membrane (which retains molecules with molecular weights >5000). The catalytic activity was determined by studying the hydrolysis of *p*-nitrophenyl acetate in 0.2 *M* phosphate buffer (pH 7.4) at 37°. The catalytic coefficient of the dialyzed polymer was found to be 138 liters/mole/min.

Keyphrases □ Poly-L-His-L-Asp-L-Ser-Gly—synthesis and catalytic activity, polymer, pentachlorophenyl ester, hydrolysis □ Polymer—synthesis and catalytic activity of poly-L-His-L-Asp-L-Ser-Gly, pentachlorophenyl ester, hydrolysis □ Hydrolysis—synthesis and catalytic activity of poly-L-His-L-Asp-L-Ser-Gly, pentachlorophenyl ester, polymer

The use of poly(amino acids) as esterase models for structural and mechanistic problems of proteolytic enzymes has been very useful (1, 2). The poly(amino acids) that have been used for this purpose include homopolymers, copolymers, and sequential polypeptides. Sequential polypeptides provide one of the best means to study the factors affecting the folding of various enzymes, since they permit the placement of specific side chains at specific locations on a polypeptide backbone. Thus, suitable folding brings important side chain functionalities required for the activity into closer proximity, even though these amino acids lie at different distances in the enzyme sequences.

Considerable attention has been focused recently on the role played by L-histidine and L-serine in the active site of chymotrypsin and other proteolytic enzymes toward the hydrolysis of various esters such as *p*-nitrophenyl acetate (3, 4). Synthesis and catalytic activity of a number of peptides incorporating histidine and serine have been recently reported (5–7) as esterase models. The synthesis of the pentapeptide; L-Ser-γ-aminobutyryl-L-His-γ-aminobutyryl-L-Asp which had a catalytic coefficient of 147 liters/mole/min has been reported (5). The synthesis of a relatively more potent esterase model, L-His-Gly-L-Asp-L-Ser-L-Phe which had a catalytic coefficient of 179 liters/mole/min has also been reported (6). The comparison of the catalytic activity of various peptide esterase models led to the conclusion that peptides that incorporated L-aspartic acid in addition to L-histidine and L-serine showed considerable increase in catalytic activity (7). For example, L-His-L-Ala-L-Asp-Gly-L-Ser showed a catalytic activity of 210 liters/mole/min. The corresponding pentapeptide, L-His-L-Ala-L-Glu-Gly-L-Ser, where aspartic acid was replaced by glutamic acid, had a catalytic activity of 87

0022-3549/82/1200-1380$01.00/0

Table I—Analytical Data of Peptide Intermediates

Compound	mp	$[\alpha]_D^{20}$	IR Peaks	Microanalysis (calc) act / (calc) C	H	N	Formula
I	161–163°	+7.9 (1.5, dioxane)	5.6μm C(=O)—O—C_6Cl_5 6.05μm Amide I 6.55μm Amide II	45.88 / (45.96)	3.81 / (3.83)	4.68 / (4.66)	$C_{23}H_{23}N_2O_6Cl_5$
II	159–160°	+12.50 (1.5 dioxane)	5.6μm C(=O)—O—C_6Cl_5 6.05μm Amide I 6.55μm Amide II	35.70 / (35.79)	3.60 / (3.57)	5.59 / (5.57)	$C_{15}H_{18}N_2O_4Cl_6$
III	143–144°	+8.4 (1.0 dioxane)	5.6μm C(=O)—O—C_6Cl_5 6.05μm Amide I 6.55μm Amide II	48.28 / (48.22)	4.62 / (4.67)	5.50 / (5.45)	$C_{31}H_{36}N_3O_9Cl_5$
IV	189–190°	−6.7 (1.0, dimethyl-formamide)	5.6μm C(=O)—O—C_6Cl_5 6.05μm Amide I 6.55μm Amide II	41.04 / (40.95)	4.56 / (4.60)	6.20 / (6.23)	$C_{23}H_{31}N_3O_7Cl_6$
V	138–139°	−14.50 (1.0 dimethyl-formamide)	5.6μm C(=O)—O—C_6Cl_5 6.05μm Amide I 6.55μm Amide II	49.89 / (49.98)	4.99 / (5.06)	8.39 / (8.33)	$C_{42}H_{51}N_6O_{12}Cl_5$
VI	179–180°	−9.80 (1.0, dimethyl-formamide)	5.6μm C(=O)—O—C_6Cl_5 6.05μm Amide I 6.55μm Amide II	44.82 / (44.79)	5.09 / (5.05)	9.14 / (9.22)	$C_{34}H_{46}N_6O_{10}Cl_6$
VIII Dialysed	229–230° decomp.	−17.05 (0.05, water)		45.29 / (45.46)	4.97 / (5.05)	21.07 / (21.21)	H-$C_{15}H_{20}N_6O_7$-OH

liters/mole/min. Generally, the incorporation of aspartic acid instead of glutamic acid in the peptide sequence led to a threefold increase in catalytic activity. The increased catalytic activity of peptide esterase models containing aspartic acid may be justified on the basis that in the case of chymotrypsin, aspartic acid occupies position 194, which is adjacent to postulated active serine at position 195. The same is true of trypsin, in which case aspartic acid is at position 184, adjacent to active serine at position 185.

While the catalytic activity of a number of peptide esterase models incorporating L-histidyl, L-serine, and L-aspartyl showed an appreciable increase in activity compared with previously reported peptide esterase models, the catalytic activity of these esterase models was considerably lower than that of chymotrypsin. It was, therefore, considered worthwhile to carry out the synthesis of a sequential polypeptide incorporating L-histidyl, L-aspartyl, L-serine, and glycine.

EXPERIMENTAL

All melting points are uncorrected and were taken on a capillary melting point apparatus[1]. Results of microanalyses[2] were within ±0.4% of theoretical and are shown in Table I. Unless otherwise stated, IR spectra were determined in potassium bromide pellets on an IR spectrophotometer[3]. UV spectra were determined on UV spectrophotometer[4]. Optical rotations were measured with a precision polarimeter[5]. Before incorporation all intermediates were purified to homogeneity on TLC in the following solvent systems: (a) butanol–glacial acetic acid–water (4:1:1); (b) butanol–glacial acetic acid–water–pyridine (15:3:12:10); (c) hexane–ethyl acetate–glacial acetic acid (20:10:1; and (d) heptane–*tert*-butyl alcohol–glacial acetic acid (3:2:1). Ninhydrin was used to detect free amino group-containing peptide intermediates. Fluorescent plates were used so that ninhydrin-negative peptides could be visualized. Dialyses were carried out in an ultrafiltration apparatus[6].

All solvents were analytical grade and were distilled before use. Tetrahydrofuran was refluxed with sodium hydroxide and distilled over sodium strips. All intermediates were dried over sodium hydroxide and phosphorus pentoxide in a vacuum dessicator. Triethylamine was purified by storing over *N*-carbobenzoxyglycine pentachlorophenyl ester to remove primary and secondary amines to avoid termination of polymerization reactions (8).

N-Carbobenzoxy-(*O* - *tert* - butyl)-Ser-Gly-pentachlorophenyl Ester (I)—*N*-Carbobenzoxy-*O*-*tert*-butyl-Ser (9) (10 g, 34 mmoles) was dissolved in tetrahydrofuran (50 ml). *N*-Methylmorpholine (3.4 ml, 34 mmoles) was added and the solution was cooled to 20°. Isobutyl chlorocarbonate (4.7 ml, 37 mmoles) was added to this solution in two portions with constant stirring. After stirring for 30 min, glycine pentachlorophenyl ester hydrochloride (8) (11.03 g, 34 mmoles) was added in small portions as a suspension in tetrahydrofuran. *N*-Methylmorpholine (3.4 ml, 34 mmoles) diluted with tetrahydrofuran (20 ml) was added dropwise over a period of 1 hr. The reaction mixture was stirred in an icebath and gradually allowed to reach room temperature overnight. The precipitated material was removed by filtration and the filtrate was evaporated under vacuum.

The residual oil was dissolved in ethyl acetate (50 ml) and washed twice with 5% citric acid solution (50 ml), once with water (50 ml), twice with 2 *N* $KHCO_3$ solution (50 ml), and twice with water (50 ml). The combined aqueous washes were washed with a portion of fresh ethyl acetate. The ethyl acetate solutions were combined, dried with anhydrous magnesium sulfate, filtered, and the solvent was evaporated under vacuum. The residual oil was crystalized from hexane by cooling at dry ice temperature. The resulting solid was filtered, air dried, and recrystallized from aqueous ethanol by seeding with solid from the hexane product. The product was dried over phosphorus pentoxide and sodium hydroxide pellets (13.1 g), 64% yield.

[1] Thomas-Hoover Uni-melt.
[2] Schwarzkopf Microanalytical Lab., Woodside, N.Y.
[3] Perkin-Elmer model 257.
[4] Perkin-Elmer Hitachi 200.
[5] Rudolph model 50.
[6] DM5 membrane, Amicon Corp.

(*O-tert*-Butyl)-Ser-Gly-pentachlorophenyl Ester Hydrochloride (II)—Palladium–charcoal catalyst (10%, 0.5 g) suspended in glacial acetic acid (1 ml) and anhydrous methanol (20 ml) was hydrogenated at atmospheric pressure. Dry methanol containing 0.140 g of hydrogen chloride gas per milliliter (0.45 ml, 1.7 mmoles) was added to the hydrogenated catalyst, and the hydrogenation was continued until no further uptake of hydrogen occurred. A suspension of active ester (I, 1.0 g, 1.67 mmoles) in methanol was added to the reaction mixture and the hydrogenation was carried out until no further uptake of hydrogen occurred (10 min). The reaction mixture was filtered to remove the catalyst and the filtrate was concentrated under reduced pressure to a volume of 2 ml. Anhydrous ether was added and the hydrochloride was crystallized, (0.78 g), 93% yield.

***N*-Carbobenzoxy-(*O*-*tert*-butyl)-Asp-(*O*-*tert*-butyl)-Ser-Gly-pentachlorophenyl Ester (III)**—*N*-Carbobenzoxy(*O*-*tert*-butyl) aspartic acid (10) (3.23 g, 0.01 mole) and *N*-methylmorpholine (1.0 ml, 0.01 mole) in tetrahydrofuran (50 ml) was coupled to pentachlorophenyl ester hydrochloride (II, 5.03 g, 0.01 mole). The residue obtained after evaporation of the ethyl acetate was crystallized from ethyl acetate–ether–petroleum ether to give *N*-protected tripeptide active ester (III) (2.14 g), yield 67%.

(*O*-*tert*-Butyl)-Asp-(*O*-*tert*-butyl)-Ser-Gly-pentachlorophenyl Ester Hydrochloride (IV)—Active ester (II, 1.0 g, 1.3 mmoles) was hydrogenated to give hydrochloride (IV, 0.69 g), yield 78%.

***N*-Carbobenzoxy(imbutyloxycarbonyl)-His-(*O*-*tert*-butyl)-Asp-(*O*-*tert*-butyl)-Ser-Gly-pentachlorophenyl Ester (V)**—*N*-carbobenzoxy(imbutyloxycarbonyl)-histidine (11) (2.6 g, 6.7 mmoles) in tetrahydrofuran (50 ml) was coupled to tripeptide ester hydrochloride (IV, 4.5 g, 6.8 mmoles). The product obtained after evaporation of the ethyl acetate, was crystallized from ethyl acetate–ether–petroleum ether to give compound V (4.35 g), yield 71%.

(Imbutyloxycarbonyl) -His- (*O*-*tert*-butyl) -Asp- (*O*-*tert*-butyl)-Ser-Gly-pentachlorophenyl Ester Hydrochloride (VI)—A suspension of active ester (V, 1.0 g, 0.99 mmole) was hydrogenated to produce the tetrapeptide hydrochloride (VI, 0.53 g), yield 64%.

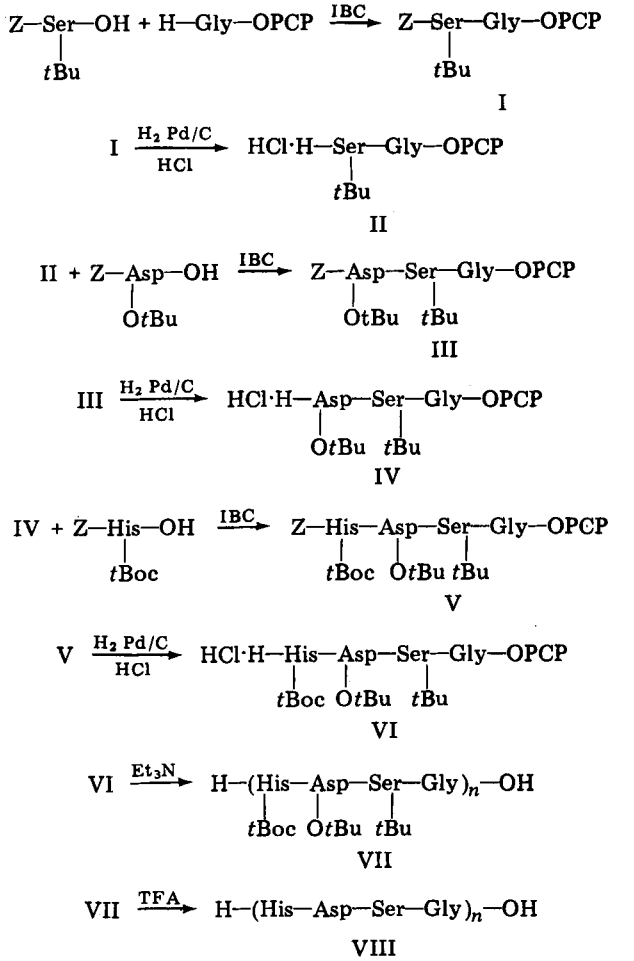

Scheme I—tBu, tert-butyloxy; OPCP, Pentachlorophenoxy; tBoc, tert-butyloxycarbonyl; IBC, Isobutylchloroformate; TFA, Trifluoroacetic Acid.

Poly(imbutyloxycarbonyl) -His- (*O* -*tert* -butyl)-Asp-(*O* -*tert*-butyl)-Ser-Gly (VII)—Fine powder of tetrapeptide active ester hydrochloride (VI, 2.5 g, 2.8 mmoles) was slowly added to dimethylformamide at room temperature with continuous shaking. To this suspension was added purified triethylamine (0.78 ml, 5.6 mmoles) and shaking was continued at room temperature for 48 hr. After trituration with anhydrous ether (20 ml), the reaction mixture was centrifuged, and the ether layer was decanted. This step was repeated three more times, and the residue was dried under a stream of nitrogen. Further drying of the residue was carried out in a vacuum desiccator over phosphorus pentoxide to yield 1.1 g, the protected polymer (VII, 1.1 g).

Poly(His-Asp-Ser-Gly) (VIII)—A solution of protected polymer (VII, 0.9 g) in 90% trifluoroacetic acid (4 ml) was kept at room temperature for 1 hr and the product was precipitated with ether to yield 0.5 g of unprotected polymer (VIII).

Dialysis of Unprotected Sequential Polymer—Crude unprotected polymer (VIII, 450 mg) was dissolved in water (10 ml) and dialyzed for 14 hr in a continuous filtration apparatus[6]. The concentrates were lyophilized over a period of 24 hr to give 180 mg of a white fluffy solid.

Optical Purity of Poly(His-Asp-Ser-Gly)—A solution of the free dialyzed polymer (VIII, 39.4 mg) in 6 *N* HCl (0.5 ml) and glacial acetic acid (0.5 ml) was refluxed for 24 hr in an atmosphere of nitrogen. The clear hydrolysate was evaporated to dryness under reduced pressure. The residue was dissolved in 5 *N* HCl so that the final volume was 2 ml (50 m*M*). A control sample using histidine (15.5 mg), aspartic acid (13.3 mg), serine (10.5 mg), and glycine (7.5 mg) was treated similarly with 6 *N* HCl and glacial acetic acid, then evaporated and dissolved in 5 *N* HCl as above (50 m*M*). Observed rotations of both were measured at 25°; control was +0.830° and polymer-derived material was +0.831°.

Determination of Catalytic Activity—For the measurement of catalytic activity of a sequential polypeptide (VIII) a modified method (3) was used. The rate of hydrolysis of *p*-nitrophenylacetate was calculated from the rate of appearance of the *p*-nitrophenoxide ion as measured by the increase in optical density at 400 μm. The catalytic coefficient k_2 is defined as $k_1 - k_w/C$, where k_1 is the observed first-order rate constant of hydrolysis measured in the presence of catalyst, k_w is the constant in absence of catalyst (both expressed in min^{-1}), and C is the molar concentration of the catalyst.

RESULTS AND DISCUSSION

While a number of approaches have been utilized for the synthesis of sequential polypeptides, there have been problems encountered with racemization, intramolecular cyclization, and the low degree of polymerization.

In order to limit some of these problems a suitable synthetic method for simple sequential polypeptides was reported (12). In this approach, *C*-terminal activation was provided by the pentachlorophenyl ester, and the peptide chain was extended from the *C*-terminal residue by mixed anhydride activation of the incoming *N*-protected amino acid. A desired sequence of *N*-protected, *C*-activated molecules was prepared by deprotection of the *N*-protected group, followed by coupling with the next amino acid in the sequence. Coupling was achieved by using mixed anhydride followed by a repetition of this procedure. Satisfactory polymerization was achieved upon removal of the final *N*-protection. One of the main advantages of this approach is the avoidance of the use of alkaline conditions which can lead to racemization and other undesirable side reactions (13). In addition, as the peptide chain is extended from the *C*-terminal residue of the amino acids, the degree of racemization is further limited, since the possibility of racemization of the penultimate residue is nonexistent (14).

This successful approach for the synthesis of simple sequential polypeptides was employed for the synthesis of poly(His-Asp-Ser-Gly). Selection of glycine as the *C*-terminal amino acid component was based upon the observation that it occurs around the active site of the proteolytic enzymes. Also, the incorporation of glycine at the *C*-terminal will minimize the degree of racemization during the polyacylation step.

Scheme I outlines the synthesis of the fully protected tetrapeptide. *N*-Carbobenzoxy(*O*-*tert*-butyl)-Ser was coupled with glycine pentachlorophenyl ester hydrochloride *via* the mixed anhydride method using isobutyl chlorocarbonate and *N*-methylmorpholine as base, to yield dipeptide active ester (I).

This product, as well as subsequent ones, were characterized by the presence of both amide I and II bonds and pentachlorophenyl ester bands in the IR spectrum as indicated in Table I.

Table II—pH Dependence of the Catalytic Coefficient for the Hydrolysis of *p*-Nitrophenylacetate by the Sequential Polypeptide (VIII) [a]

pH	k (liter mole^{-1}min^{-1})
6.4	47
6.9	81
7.4	138
7.9	64
8.4	39

[a] In 0.2 *M* phosphate buffer containing 3.5% dioxane (v/v) at 37°.

Dipeptide (I), was successfully deprotected by catalytic hydrogenolysis to give the dipeptide active ester hydrochloride (II). Using the same procedures, *N*-carbobenzoxy(*O*-*tert*-butyl)-aspartic acid was coupled with dipeptide active ester hydrochloride (II) to give protected tripeptide active ester (III). This tripeptide was deprotected to produce *O*-*tert*-butyl-Asp-(*O*-*tert*-butyl)-Ser-Gly pentachlorophenyl ester hydrochloride (IV). *N*-Carbobenzoxy(imbutyloxycarbonyl)-His was coupled with tripeptide active ester hydrochloride (IV) to give the protected tetrapeptide active ester, *N*-carbobenzoxy (imbutyloxycarbonyl)-His-(*O*-*tert*-butyl)-Asp-(*O*-*tert*-butyl)-Ser-Gly pentachlorophenyl ester (V). This was followed by hydrogenolytic deprotection to give (imbutyloxycarbonyl)-His-(*O*-*tert*-butyl)-Asp-(*O*-*tert*-butyl)-Ser-Gly-pentachlorophenyl ester hydrochloride (VI).

Synthesis of Free Sequential Polymer Poly(His-Asp-Ser-Gly)—Tetrapeptide active ester hydrochloride (VI) was allowed to polymerize in presence of dimethylformamide and triethylamine to yield crude protected polymer (VIII), which was converted to deprotected polymer without further purification as characterization.

A suitable method to remove the *t*-butyl protecting groups was that of a previous study using trifluoroacetic acid (15). Using conditions previously reported (8) produced the unprotected polymer (VIII). The completion of reaction was established by the absence of *t*-butyl group absorption in the IR spectrum as well as titration of free carboxyl groups. After dialysis employing a membrane[6] which retains compounds with molecular weight >5000, a polymeric product containing >15 or 16 repeating units was obtained.

Optical Purity of Sequential Polymer—The optical purity of poly-(His-Asp-Ser-Gly) was calculated by determining the optical activity of the total hydrolysate and comparing it with that of a control. It was found that no significant racemization occurred during the polyacylation reactions. Since all intermediates at each stage were extensively purified prior to use in the synthesis of the tetrapeptide, the optical purity of sequential polymer was relatively high, as expected.

Determination of Catalytic Activity—The catalytic hydrolyses of *p*-nitrophenylacetate by various copolymers have been previously studied (1, 2). Hydrolytic activity of the copolymers was found to depend on pH, temperature, and concentration of the substrate. Stereoselectivity is also a striking characteristic of true enzyme action. A previous study (5) reported the stereoselectivity of synthetic peptide esterase models as a catalyst, suggesting that some of the polyfunctional effects associated with the enzyme active site might indeed be operative in these peptide models. A further study (3) showed that in all cases, first-order kinetics are followed over most of the reaction.

Table II describes the catalytic coefficient for the hydrolysis of *p*-nitrophenylacetate by the sequential polypeptide (VIII) at different pH values at 37°. Highest activity was obtained at pH 7.4. Thus, catalytic activity of the sequential polymer (VIII) was done at pH 7.4, and the results are shown on Table III. While it has a higher catalytic coefficient than histidine, imidazole, or mixture of component amino acids, this sequential polymer failed to give a high catalytic coefficient. This occurred even though the polymer-incorporated amino acids were known to be present in the active sites of various proteolytic enzymes. The low activity may be due to lack of sufficient interactions between the imidazole group of histidine, the hydroxyl group of serine, and the carboxyl group of aspartic acid.

Table III—Catalytic Coefficients (k) for the Hydrolysis of *p*-Nitrophenylacetate by the Sequential Polymer (VIII) and Other Catalysts [a]

Catalyst	Catalytic Coefficient (k) liter moles^{-1}min^{-1}
L-His·HCl	7
Imidazole	48
Sequential Polymer (VIII)	138
L-His+Asp+L-Ser+Gly	18
α-Chymotrypsin	10^4

[a] In 0.2 *M* phosphate buffer, pH 7.4, containing 3.5% dioxane (v/v) at 37°.

The synthesis and catalytic activity of the sequential polypeptide incorporating histidine, aspartic acid, and serine was achieved. The active ester method of polymerization gave excellent yields and moderately high molecular weight polymer with little or no racemization as evidenced by the high degree of optical purity. The successful synthesis of sequential polypeptide H-(His-Asp-Ser-Gly)-OH suggests that this method can be utilized for synthesis of polypeptides containing other functional groups. This sequential polypeptide, containing residues known to be involved in the catalytic activity of chymotrypsin, failed to show significant catalytic activity.

Determination of the absolute value of activity per catalytic center is difficult because the number of active sites depends on the shape of the molecule. Also, this work does not provide any information on the stereospecific hydrolysis of the substrate.

REFERENCES

(1) J. Nugochi and H. Yamamoto, *J. Biochem.*, **69**, 119 (1971).

(2) H. Yammamoto and J. Nugochi, *ibid.*, **67**, 103 (1970).

(3) E. Katchalski, G. D. Fasman, E. Simons, E. R. Blout, F. R. N. Gurd, and W. L. Koltun, *Arch. Biochem. Biophys.*, **88**, 361 (1960).

(4) M. L. Bender and F. J. Kezdy, *J. Am. Chem. Soc.*, **86**, 3704 (1964).

(5) J. C. Sheehan, G. B. Bennett, and J. A. Schneider, *ibid.*, **88**, 3455 (1966).

(6) A. Kapoor, S. M. Kang, and M. A. Trimboli, *J. Pharm. Sci.*, **59**, 129 (1970).

(7) A. Kapoor, N. A. Azeza, N. H. Somaiya, and M. Trimboli, *ibid.*, **60**, 956 (1971).

(8) J. Kovacs, R. Giannotti, and A. Kapoor, *J. Am. Chem. Soc.*, **88**, 2282 (1966).

(9) J. E. Shields and H. Renves, *ibid.*, **88**, 2304 (1966).

(10) E. Schroder and E. Kleiger, *Ann. Chem.*, **673**, 208 (1964).

(11) M. Fridkin and S. Shaltiel, *Arch. Biochem. Biophys.*, **147**, 767 (1971).

(12) A. Kapoor and L. W. Gerencser, *J. Pharm. Sci.*, **58**, 976 (1969).

(13) E. Schroder and K. Lubke, "The Peptides," Vol. 1, Academic, New York, N.Y., 1965, p. 56.

(14) F. Weygand, A. Prox, and W. Konig, *Chem. Ber.*, **99**, 1446 (1966).

(15) R. Schwyzer and W. Rittel, *Helv. Chim. Acta*, **44**, 159 (1961).

Colorimetric Determination of Acetylcysteine, Penicillamine, and Mercaptopropionylglycine in Pharmaceutical Dosage Forms

M. A. RAGGI ˣ, V. CAVRINI, and A. M. DI PIETRA

Received October 13, 1981, from the *Institute of Pharmaceutical Chemistry, University of Bologna, 40126 Bologna, Italy.* Accepted for publication February 5, 1982.

Abstract □ *A colorimetric determination of acetylcysteine, penicillamine, and mercaptopropionylglycine is described. The method is based on the oxidation of mercapto-compounds with iron(III) in the presence of 1,10-phenanthroline. The iron(II) formed was quantitatively and rapidly converted to the stable tris(1,10-phenanthroline)iron(II) complex measured spectrophotometrically at 515 nm. The results obtained from various commercial formulations indicate that the method proposed allows a simple, sensitive determination of these mercapto-drugs with good accuracy (99.5–101% recovery) and remarkable precision (RSD ±0.6–1.6%).*

Keyphrases □ Acetylcysteine—colorimetric determination in pharmaceutical dosage forms, penicillamine, mercaptopropionylglycine □ Penicillamine—colorimetric determination in pharmaceutical dosage forms, acetylcysteine, mercaptopropionylglycine □ Mercaptopropionylglycine—colorimetric determination in pharmaceutical dosage forms, acetylcysteine, penicillamine □ Colorimetry—analysis of penicillamine, acetylcysteine, and mercaptopropionylglycine in pharmaceutical dosage forms

A number of thiol (SH)-containing drugs are commercially available and are utilized in various therapeutic applications. Among the most widely used are acetylcysteine, a topical pulmonary mucolytic agent; penicillamine, a therapeutic agent for the treatment of Wilson's disease and heavy metal poisoning; and mercaptopropionylglycine, a drug used in hepatic disorders.

Numerous analytical methods have been developed for the quantitative assay of the thiol group (1–3). The USP method (4) for acetylcysteine determination, based on the potentiometric titration of the thiol group with mercuric nitrate using a calomel–gold electrode system, was considered affected by some possible ambiguities due to the divalency of mercury (5). Other procedures reported for determining this drug in pharmaceutical dosage forms include spectrophotometric (6) and colorimetric techniques (5, 7).

Numerous extensive studies on the chelating properties of penicillamine *versus* a variety of metals have been reported (8–19), but analytical procedures for its quantitative determination have been developed more for biological (20–24) than for pharmaceutical systems (25). The official USP method (26) involves the use of the highly toxic mercuric acetate, and recently a study (25) investigated alternative procedures such as nonaqueous amine titration, nonaqueous acid titration, and hydroxylamine colorimetric assay.

A few studies on the chelating ability of mercaptopropionylglycine have appeared (27, 28), but no analytical procedures for its determination in pharmaceutical formulations are available to the authors' knowledge.

It is highly desirable to provide a single colorimetric procedure suitable for all these mercapto-compounds, for which a direct spectrophotometric method is unwarranted due to interference from excipients.

In this report a simple and sensitive colorimetric procedure, based on the formation of the tris(1,10-phenanthroline)iron(II) complex, is described for determining acetylcysteine, penicillamine, and mercaptopropionylglycine in various commercial formulations.

EXPERIMENTAL

Instruments—A digital single-beam spectrophotometer[1], a double-beam spectrophotometer[2], a pH meter[3], and a microanalytical balance[4] were used.

Materials—Pharmaceutical grade acetylcysteine[5], penicillamine[5], and mercaptopropionylglycine[5] were used as working standards. All reagents were analytically pure and were used without further purification. Commercially coated tablets, injectable solutions, syrup of mercaptopropionylglycine, and injectable solutions of acetylcysteine and capsules of penicillamine were analyzed as dosage forms.

Reagents—The 0.25% aqueous solution of 1,10-phenanthroline was prepared by dissolving 0.25 g of the compound in distilled water and diluting to 100 ml after gentle heating. This solution was stored for ≤3 days, in a tight light-resistant container. For the iron(III) 4×10^{-3} *M* solution, 1.92 g of ferric ammonium sulfate dodecahydrate dissolved in distilled water was treated with 10 ml of concentrated hydrochloric acid and diluted with water to a 1000-ml volume. This solution was also protected

Table I—Parameters and Correlation Coefficients of Calibration Plots [a] for Mercapto-Compounds

Mercapto-Compound	*A*	*B*	*r*
Acetylcysteine	10791	−0.001	0.9998
Penicillamine	11100	0.01	0.9999
Mercaptopropionylglycine	11267	−0.001	0.9999

[a] Calibration plots are expressed as regression lines of the form $y = Ax + B$; with y = absorbance, x is the molar concentration of mercapto-compounds, B is the y-intercept, A is the slope of the line; r is the correlation coefficient of the line.

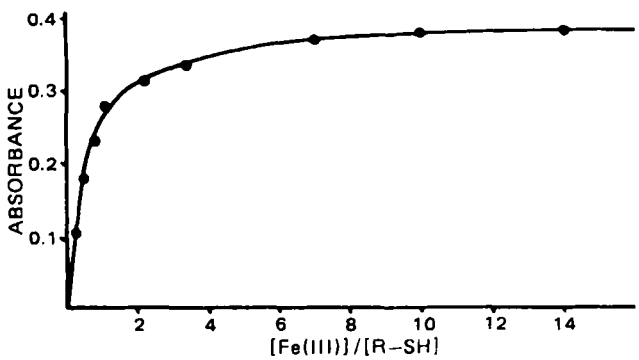

Figure 1—*Absorbance* versus *molar ratio of iron(III) to mercapto-compound (R—SH) for a 0.3 × 10⁻⁴ M acetylcysteine solution, pH 3.4.*

[1] Model UVIDEC 4 Jasco, Japan.
[2] Model 402 Perkin-Elmer Corp., England.
[3] Model 325 Amel, Italy.
[4] Metler type 5, Switzerland.
[5] Fluka, Switzerland.

0022-3549/82/1200-1384$01.00/0

Table II—Assay Results of Commercial Pharmaceutical Dosage Forms

Drug	Dosage Form	Declared, mg	Found[a], mg	Recovery, %	*RSD*, %
Penicillamine	Capsules	150	151.0	100.7	0.72
Mercapto-propionylglycine	Ampuls	100	101.0	101.0	1.60
	Syrup	100	99.5	99.5	0.60
	Coated Tablets	250	252.0	100.8	1.50
Acetylcysteine	Ampuls	100	100.1	100.1	0.63

[a] Average of five determinations.

from sunlight. A pH 4 buffer was prepared by mixing 75 ml of 0.1 *M* CH_3COOH with 25 ml of 0.1 *M* CH_3COONa. Whenever necessary, 0.2 *M* CH_3COONa was also used to adjust the pH.

Standard Solutions—For acetylcysteine, 0.163 g of the drug was dissolved in water up to a 500-ml volume; dilution to a 1:5 ratio gave the desired concentration. For penicillamine, 0.149 g of the drug was dissolved in water up to a 500-ml volume, and the solution was diluted five times to give the desired concentration. For mercaptopropionylglycine, 0.167 g of the drug was dissolved in water up to a 500-ml volume; dilution to a 1:5 ratio gave the desired concentration.

Calibration Curves—For calibration of acetylcysteine, penicillamine, and mercaptopropionylglycine serial volumes of 1–5 ml (in 1-ml steps) of standard solution were transferred to 25-ml volumetric flasks. Six milliliters of iron(III) solution, 2.5 ml of phenanthroline, 3.5 ml of sodium acetate (0.2 *M*), and 4.5 ml of buffer and water to volume were added in succession. After 20 min (after 1 hr for penicillamine) the absorbance at 515 nm was measured against a blank, prepared simultaneously without thiol solution.

To evaluate a possible disodium edetate interference, 1–10% of this compound was added to a 3×10^{-5} *M* thiol solution, and absorbance was measured under the described conditions.

Determination of Acetylcysteine—For the determination of acetylcysteine in injectable solution, a volume equivalent to 100 mg of acetylcysteine was diluted to 200 ml with distilled water and 10 ml of this solution was further diluted five times. The procedure for the calibration curve was followed using 2 ml of the final solution.

Determination of Penicillamine—For the determination of penicillamine in capsules, the contents of 10 capsules were mixed, and an amount equivalent to 150 mg of the drug was accurately weighed and dissolved in water to a 500-ml volume. After stirring, the solution was filtered. To 10 ml of the filtrate were added 10 ml of 0.2 *M* CH_3COONa, 15 ml of pH 4 buffer, and water to a volume of 50 ml. Using 3 ml of this solution, the procedure for the calibration curve was followed.

Determination of Mercaptopropionylglycine—For the determination of mercaptopropionylglycine in syrup, 16 mg of powder was dissolved in water up to a 250-ml volume. Using 3 ml of this solution, the procedure for the calibration curve was followed. For the determination of mercaptopropionylglycine in injectable solutions the content of one ampule (2 ml), equivalent to 100 mg of the drug, was diluted with water to 200 ml; 10 ml of this solution was further diluted five times. Using 2 ml of this solution, the procedure for the calibration curve was followed. For the determination of mercaptopropionylglycine in commercial coated tablets, 10 coated tablets were powdered and mixed. A portion of this powder (117 mg) was transferred to a 500-ml volumetric flask, and water was added with stirring for 10 min before filling to volume. Using 3 ml of this solution, suitably filtered, the procedure for the calibration curve was followed.

RESULTS AND DISCUSSION

The proposed method is based on the ability of mercapto-compounds to reduce iron(III) to iron(II) (reaction 1), which is rapidly converted to the highly stable and colored tris(1,10-phenanthroline)iron(II) complex (reaction 2) with λ_{max} = 515 nm and ϵ = 11,100 (29, 30).

$$2\,Fe^{3+} + 2\,R{-}SH \rightarrow 2\,Fe^{2+} + R{-}S{-}S{-}R + 2\,H^+ \quad (1)$$

$$Fe^{2+} + 3\,(C_{12}H_8N_2) \rightarrow [Fe(C_{12}H_8N_2)_3]^{2+} \quad (2)$$

Scheme I

The conditions under which the reaction of each mercapto-compound with iron(III) in the presence of 1,10-phenanthroline fulfills the necessary analytical requirements were investigated. The amount of phenanthroline added must be at least in a 3:1 ratio with respect to the iron(II), according to reaction 2. The time necessary for the completion of the reaction depends on temperature, pH, and on the amount of iron(III) added. At room temperature, which was chosen to meet the practical requirements of analytical speed, the influence of pH and iron(III) concentration was investigated. It was observed that under the described experimental conditions, the optimum pH range for the reaction was 2.5–4.5. This is markedly different from the 7–8 pH range selected previously for the colorimetric determination of cysteine (31) and thioethylamine (32) by means of nitrilotriacetateferrate(III).

The influence of iron(III) concentration on the color development is illustrated in Fig. 1, where the absorbance *versus* molar ratio of iron III to mercapto-compound is reported. By increasing the iron III concentration, the reaction can be forced to completion, as indicated by the constant value of absorbance for iron(III) concentration in up to tenfold excess of mercapto-compound.

All absorbance readings (515 nm) were taken for acetylcysteine and mercaptopropionylglycine after 20 min *versus* the blank, which contained all the reagents except thiol; for penicillamine, color development was found to be complete in longer times (1 hr). In all cases the absorbance was constant for at least 2 hr. Under these experimental conditions, good reproducibility was obtained (*RSD* = 0.34%).

A calibration curve of absorbance *versus* concentration was constructed for each mercapto-compound in the range of 4.5–80 μM. The parameters and correlation coefficients of calibration plots, expressed as regression lines of the form of $y = Ax + B$, are listed in Table I. As can be seen from the equations obtained, the lines pass very close to the origin and the slopes remain relatively constant for all three drugs investigated.

Regression analysis of all of the data by least squares gave the line $y = 11015x + 0.01$ (correlation coefficient of 0.998), which reproduces satisfactorily the experimental absorbance values obtained for various concentrations of all three mercapto-compounds. These results indicate that acetylcysteine, penicillamine, and mercaptopropionylglycine, according to reaction 1, similarly reduce iron(III) to iron(II), which successively forms the phenanthroline complex. The calibration curve obtained for mercapto-compounds was also compared with the calibration plot for iron(II) solutions treated by phenanthroline under the described experimental conditions. The comparison showed that reaction 1 was quantitative, since the absorbance values for the mercapto-compounds and those for iron(II) solutions at the same molar concentration were essentially identical.

The proposed colorimetric method was applied to analysis of commercially available pharmaceutical dosage forms of acetylcysteine, penicillamine, and mercaptopropionylglycine. The results obtained (Table II) indicate that the proposed method is suitable for analyzing various types of formulations. No interference due to air oxidant effect or due to excipients such as magnesium stearate, titanium dioxide, lactose, *etc.* has been observed. The possible interference by disodium edetate salt present in some preparations containing penicillamine and acetylcysteine was investigated. It was found that under the described experimental conditions, concentrations of disodium edetate as high as 10% of the thiol compound did not interfere with the analysis, at variance with some volumetric procedures reported previously (25).

In summary, the proposed method allows a simple, sensitive determination of the thiol-group containing drugs investigated, with good accuracy (99.5–101% recovery) and remarkable precision (*RSD* ± 0.6–1.6%). The fact that this method requires more time in the case of penicillamine than some methods previously proposed (20, 25), is compensated by the high stability of the colored complex and by the lack of disodium edetate interference.

REFERENCES

(1) S. Siggia and J. G. Hanna, "Quantitative Organic Analysis via Functional Groups," 4th ed., Wiley, New York, N.Y., 1979, pp. 707–752.

(2) A. Fontana and C. Toniolo, "Chemistry of the Thiol Group," S. Patai, Ed., Wiley Interscience, New York, N.Y., 1974.
(3) K. A. Connors, "Reaction Mechanisms in Organic Analytical Chemistry," Wiley Interscience, New York, N.Y., 1973.
(4) "The United States Pharmacopeia," 20th rev., U.S. Pharmacopeial Convention, Rockville, Md., 1979, p. 17.
(5) B. S. R. Murty, J. N. Kapoor, and M. W. Kim, *Am. J. Hosp. Pharm.*, **34**, 305 (1977).
(6) J. R. Talley, R. A. Magarian, and E. B. Sommers, *ibid.*, **30**, 526 (1973).
(7) R. Valerio and G. C. Ceschel, *Boll. Chim. Farm.*, **105**, 675 (1966).
(8) E. J. Kuchinkas and Y. Rosen, *Arch. Biochem. Biophys.*, **97**, 370 (1962).
(9) G. R. Lenz and A. E. Martell, *Biochemistry*, **3**, 745 (1964).
(10) D. A. Doornbos and J. S. Faber, *Pharm. Weekblad.*, **99**, 289 (1964).
(11) E. W. Wilson, Jr. and R. B. Martin, *Arch. Biochem. Biophys.*, **142**, 445 (1971).
(12) Y. Sugiura and H. Tanaka, *Chem. Pharm. Bull.*, **18**, 368 (1970).
(13) C. M. Bell, E. D. McKenzie, and J. Orton, *Inorg. Chim. Acta*, **5**, 109 (1971).
(14) P. Vermeij, *Pharm. Weekblad.*, **112**, 130 (1977).
(15) Y. Sugiura, T. Kikuchi, and H. Tanaka, *Chem. Pharm. Bull.*, **25**, 345 (1977).
(16) Y. Hojo, Y. Sugiura, and H. Tanaka, *J. Inorg. Nucl. Chem.*, **39**, 1859 (1977).
(17) Y. Sugiura, A. Yokoyama, and H. Tanaka, *Chem. Pharm. Bull.*, **18**, 693 (1970).
(18) I. Sovago, A. Gergely, B. Harman, and T. Kiss, *J. Inorg. Nucl. Chem.*, **41**, 1629 (1979).
(19) T. D. Zucconi, G. E. Janauer, S. Donahe, and C. Lewkowicz, *J. Pharm. Sci.*, **68**, 426 (1979).
(20) J. Mann and P. D. Mitchell, *J. Pharm. Pharmacol.*, **31**, 420 (1979).
(21) G. Del Vecchio and R. Argenziano, *Boll. Soc. Ital. Biol. Sper.*, **22**, 1189 (1946).
(22) R. P. Prabhat, *J. Biol. Chem.*, **234**, 618 (1959).
(23) N. Gallo, V. D. Bianco, P. Bianco, and G. Luisi, *Min. Med.*, **71**, 2281 (1980).
(24) S. Akerfeldt and G. Loevgren, *Anal. Biochem.*, **8**, 223 (1964).
(25) P. J. Vollmer, J. Lee, and T. G. Alexander, *J. Assoc. Off. Anal. Chem.*, **63**, 1191 (1980).
(26) "The United States Pharmacopeia," 20th rev., U.S. Pharmacopeial Convention, Rockville, Md., 1979, p. 591.
(27) Y. Sugiura and H. Tanaka, *Chem. Pharm. Bull.*, **18**, 746 (1970).
(28) Y. Funae, N. Toshioka, I. Mita, T. Sugihara, T. Ogura, Y. Nakamura, and S. Kawaguchi, *ibid.*, **19**, 1618 (1971).
(29) S. L. Ali and D. Steinbach, *Pharm. Ztg.*, **124**, 1422 (1979).
(30) J. B. Davis and F. Lindstrom, *Anal. Chem.*, **44**, 524 (1972).
(31) T. J. Bydalek and J. E. Poldoski, *ibid.*, **40**, 1878 (1968).
(32) T. J. Bydalek J. E. Poldoski, and D. Bagenda John, *ibid.*, **42**, 929 (1970).

Arterial and Venous Blood Sampling in Pharmacokinetic Studies: Griseofulvin

MEI-LING CHEN, GILBERT LAM, MYUNG G. LEE, and WIN L. CHIOU ˣ

Received August 3, 1981, from the *Department of Pharmacy, College of Pharmacy, University of Illinois at the Medical Center, Chicago, IL 60612.* Accepted for publication February 4, 1982.

Abstract □ The pharmacokinetics of griseofulvin were evaluated simultaneously using both arterial and venous plasma in three dogs and one rabbit after a rapid bolus intravenous dosing. Initial arterial–venous ratios 20 sec after injection were the highest and ranged from 15- to 752-fold for dogs; the ratio was 3240-fold for the rabbit. Both curves decayed paralleling each other at the terminal phase with the venous levels higher than arterial levels by 14–43 and 8.4% for the dogs and the rabbit, respectively. The use of the instantaneous input principle was found to overestimate the total area under the plasma level–time curve by as much as 166%. An exponential term with a negative coefficient was used to account for the short and steep rising phase of plasma levels after injection. Detailed analyses showed significant differences in various calculated pharmacokinetic parameters based on arterial or venous data. The present study exemplifies the need for careful assessment and interpretation of classical pharmacokinetic parameters. It appeared that short intravenous infusion rather than the instantaneous or rapid bolus intravenous injection should be preferred for routine pharmacokinetic studies.

Keyphrases □ Griseofulvin—pharmacokinetics, arterial and venous blood sampling □ Pharmacokinetics—arterial and venous blood sampling, griseofulvin □ Blood sampling—arterial and venous pharmacokinetics of griseofulvin

Preliminary results showing marked and persistent arterial–venous (A–V) plasma concentration differences of six drugs (propranolol, lidocaine, procainamide, furosemide, theophylline, and griseofulvin), following intravenous administration to dogs or rabbits, were recently reported from this laboratory (1). The pharmacokinetic consequences of data analysis by using arterial or venous data on propranolol also has been described (2).

The present report describes in detail arterial and venous plasma level profiles of griseofulvin in three dogs and one rabbit and discusses the resulting effects on pharmacokinetic analysis.

EXPERIMENTAL

Bolus Injection Studies—Griseofulvin[1] (40 mg/ml) in polyethylene glycol 400[2] (1, 3) was injected as a bolus over 20 sec to the cephalic vein in three male mongrel dogs and to the ear vein in one male New Zealand white rabbit. Dogs 1 and 2 were conscious while dog 3 and rabbit 1 were anesthetized with nitrous oxide during the study. The doses administered to each animal are summarized in Table I. The midpoint of the injection was timed zero. Femoral arterial and venous blood samples were withdrawn simultaneously from permanent cannulas in the dogs and a specially designed T-loop in the rabbit. The preparation of the cannulas and the surgical procedure were described elsewhere (2). Heparinized normal saline (10 U/ml) was used for flushing of the cannula during the study. The sampling times, also midpoints of collection, were usually at 0.33, 0.66, 1, 1.33, 1.66, 2, 3, 6, 9, 15, 30, 60, 80, 100, 120, 140, 160, and 180 min

[1] Sigma Chemical Co., St. Louis, Mo.
[2] J. T. Baker Chemical Co., Phillipsburg, N.J.

0022-3549/82/1200-1386$01.00/0

(2) A. Fontana and C. Toniolo, "Chemistry of the Thiol Group," S. Patai, Ed., Wiley Interscience, New York, N.Y., 1974.
(3) K. A. Connors, "Reaction Mechanisms in Organic Analytical Chemistry," Wiley Interscience, New York, N.Y., 1973.
(4) "The United States Pharmacopeia," 20th rev., U.S. Pharmacopeial Convention, Rockville, Md., 1979, p. 17.
(5) B. S. R. Murty, J. N. Kapoor, and M. W. Kim, *Am. J. Hosp. Pharm.*, **34**, 305 (1977).
(6) J. R. Talley, R. A. Magarian, and E. B. Sommers, *ibid.*, **30**, 526 (1973).
(7) R. Valerio and G. C. Ceschel, *Boll. Chim. Farm.*, **105**, 675 (1966).
(8) E. J. Kuchinkas and Y. Rosen, *Arch. Biochem. Biophys.*, **97**, 370 (1962).
(9) G. R. Lenz and A. E. Martell, *Biochemistry*, **3**, 745 (1964).
(10) D. A. Doornbos and J. S. Faber, *Pharm. Weekblad.*, **99**, 289 (1964).
(11) E. W. Wilson, Jr. and R. B. Martin, *Arch. Biochem. Biophys.*, **142**, 445 (1971).
(12) Y. Sugiura and H. Tanaka, *Chem. Pharm. Bull.*, **18**, 368 (1970).
(13) C. M. Bell, E. D. McKenzie, and J. Orton, *Inorg. Chim. Acta*, **5**, 109 (1971).
(14) P. Vermeij, *Pharm. Weekblad.*, **112**, 130 (1977).
(15) Y. Sugiura, T. Kikuchi, and H. Tanaka, *Chem. Pharm. Bull.*, **25**, 345 (1977).
(16) Y. Hojo, Y. Sugiura, and H. Tanaka, *J. Inorg. Nucl. Chem.*, **39**, 1859 (1977).
(17) Y. Sugiura, A. Yokoyama, and H. Tanaka, *Chem. Pharm. Bull.*, **18**, 693 (1970).
(18) I. Sovago, A. Gergely, B. Harman, and T. Kiss, *J. Inorg. Nucl. Chem.*, **41**, 1629 (1979).
(19) T. D. Zucconi, G. E. Janauer, S. Donahe, and C. Lewkowicz, *J. Pharm. Sci.*, **68**, 426 (1979).
(20) J. Mann and P. D. Mitchell, *J. Pharm. Pharmacol.*, **31**, 420 (1979).
(21) G. Del Vecchio and R. Argenziano, *Boll. Soc. Ital. Biol. Sper.*, **22**, 1189 (1946).
(22) R. P. Prabhat, *J. Biol. Chem.*, **234**, 618 (1959).
(23) N. Gallo, V. D. Bianco, P. Bianco, and G. Luisi, *Min. Med.*, **71**, 2281 (1980).
(24) S. Akerfeldt and G. Loevgren, *Anal. Biochem.*, **8**, 223 (1964).
(25) P. J. Vollmer, J. Lee, and T. G. Alexander, *J. Assoc. Off. Anal. Chem.*, **63**, 1191 (1980).
(26) "The United States Pharmacopeia," 20th rev., U.S. Pharmacopeial Convention, Rockville, Md., 1979, p. 591.
(27) Y. Sugiura and H. Tanaka, *Chem. Pharm. Bull.*, **18**, 746 (1970).
(28) Y. Funae, N. Toshioka, I. Mita, T. Sugihara, T. Ogura, Y. Nakamura, and S. Kawaguchi, *ibid.*, **19**, 1618 (1971).
(29) S. L. Ali and D. Steinbach, *Pharm. Ztg.*, **124**, 1422 (1979).
(30) J. B. Davis and F. Lindstrom, *Anal. Chem.*, **44**, 524 (1972).
(31) T. J. Bydalek and J. E. Poldoski, *ibid.*, **40**, 1878 (1968).
(32) T. J. Bydalek J. E. Poldoski, and D. Bagenda John, *ibid.*, **42**, 929 (1970).

Arterial and Venous Blood Sampling in Pharmacokinetic Studies: Griseofulvin

MEI-LING CHEN, GILBERT LAM, MYUNG G. LEE, and WIN L. CHIOU ˣ

Received August 3, 1981, from the *Department of Pharmacy, College of Pharmacy, University of Illinois at the Medical Center, Chicago, IL 60612.* Accepted for publication February 4, 1982.

Abstract □ The pharmacokinetics of griseofulvin were evaluated simultaneously using both arterial and venous plasma in three dogs and one rabbit after a rapid bolus intravenous dosing. Initial arterial–venous ratios 20 sec after injection were the highest and ranged from 15- to 752-fold for dogs; the ratio was 3240-fold for the rabbit. Both curves decayed paralleling each other at the terminal phase with the venous levels higher than arterial levels by 14–43 and 8.4% for the dogs and the rabbit, respectively. The use of the instantaneous input principle was found to overestimate the total area under the plasma level–time curve by as much as 166%. An exponential term with a negative coefficient was used to account for the short and steep rising phase of plasma levels after injection. Detailed analyses showed significant differences in various calculated pharmacokinetic parameters based on arterial or venous data. The present study exemplifies the need for careful assessment and interpretation of classical pharmacokinetic parameters. It appeared that short intravenous infusion rather than the instantaneous or rapid bolus intravenous injection should be preferred for routine pharmacokinetic studies.

Keyphrases □ Griseofulvin—pharmacokinetics, arterial and venous blood sampling □ Pharmacokinetics—arterial and venous blood sampling, griseofulvin □ Blood sampling—arterial and venous pharmacokinetics of griseofulvin

Preliminary results showing marked and persistent arterial–venous (A–V) plasma concentration differences of six drugs (propranolol, lidocaine, procainamide, furosemide, theophylline, and griseofulvin), following intravenous administration to dogs or rabbits, were recently reported from this laboratory (1). The pharmacokinetic consequences of data analysis by using arterial or venous data on propranolol also has been described (2).

The present report describes in detail arterial and venous plasma level profiles of griseofulvin in three dogs and one rabbit and discusses the resulting effects on pharmacokinetic analysis.

EXPERIMENTAL

Bolus Injection Studies—Griseofulvin[1] (40 mg/ml) in polyethylene glycol 400[2] (1, 3) was injected as a bolus over 20 sec to the cephalic vein in three male mongrel dogs and to the ear vein in one male New Zealand white rabbit. Dogs 1 and 2 were conscious while dog 3 and rabbit 1 were anesthetized with nitrous oxide during the study. The doses administered to each animal are summarized in Table I. The midpoint of the injection was timed zero. Femoral arterial and venous blood samples were withdrawn simultaneously from permanent cannulas in the dogs and a specially designed T-loop in the rabbit. The preparation of the cannulas and the surgical procedure were described elsewhere (2). Heparinized normal saline (10 U/ml) was used for flushing of the cannula during the study. The sampling times, also midpoints of collection, were usually at 0.33, 0.66, 1, 1.33, 1.66, 2, 3, 6, 9, 15, 30, 60, 80, 100, 120, 140, 160, and 180 min

[1] Sigma Chemical Co., St. Louis, Mo.
[2] J. T. Baker Chemical Co., Phillipsburg, N.J.

0022-3549/82/1200-1386$01.00/0

Table I—Comparison of Arterial–Venous Plasma Difference of Griseofulvin after Intravenous Bolus Administration to Dogs and Rabbit

	Dog 1	Dog 2	Dog 3	Rabbit
Body weight, kg	21.3	19.2	20	3.7
Dose, mg	60	60	60	14
A–V ratio at 0.33 min	176	15	752	3240
Time of intersection, min	4	2	15	45
Percent difference during terminal phase	30.0	43.0	14.7	8.4
Terminal half-life, min	64.8	37.5	73.7	277

in the dog studies, while the collection schedule extended to 300 min in the rabbit. The blood samples were centrifuged immediately to avoid the potential storage effect in the plasma concentration determination (4, 5), and 0.1 ml of plasma was collected in duplicate and frozen until assayed by a fluorometric HPLC method developed earlier in this laboratory (6).

Pharmacokinetic Analysis—The total areas under the plasma level–time curve from time zero to infinity (*AUC*) were estimated by the following three methods:

Method I—The linear trapezoidal rule was used from time zero to the last sampling point followed by the extrapolation method (*i.e.*, the last point concentration divided by the terminal rate constant).

Method II—The logarithmic trapezoidal rule (7) was used from the first to the last sampling point followed by the extrapolation method. The linear trapezoidal rule was used between time zero to the first sampling point. The method was previously employed in a propranolol study (2).

The plasma concentration at time zero in Methods I and II was assumed to be zero (8).

Method III—A NONLIN (9) computer program was employed for the determination of conventional (8) polyexponential equations ($\Sigma A_i e^{-\lambda_i t}$) based on the postpeak plasma data. For the prepeak plasma data, a linear least-squares feathering method was used to obtain another exponential rate constant, m, using a programmable calculator[3].

Since the plasma concentration at time zero was assumed to be zero, the coefficient of this exponential term, M, was set to equal the sum of the positive exponential coefficients, *i.e.*, ΣA_i. The following integration equation was used:

$$AUC = \Sigma\frac{A_i}{\lambda_i} - \frac{M}{m} \quad \text{(Eq. 1)}$$

Standard methods were used to determine the total body clearance, Cl; initial volume of distribution, V_1; apparent volume of distribution at the pseudodistribution equilibrium (10), V; steady-state volume of distribution (2, 11), V_{ss}; mean residence time (12), MRT; and the fraction of dose remaining in the body after bolus injection (2, 13):

$$Cl = \text{dose}/AUC \quad \text{(Eq. 2)}$$

$$V_1 = \text{dose}/C_p{}^0 \quad \text{(Eq. 3)}$$

$$V = \text{dose}/(AUC \times \lambda_n) \quad \text{(Eq. 4)}$$

$$V_{ss} = (\text{dose} \times \int_0^\infty AUC_{t\to\infty}dt)/AUC^2 \quad \text{(Eq. 5)}$$

$$MRT = AUMC/AUC \quad \text{(Eq.6)}$$

$$\text{Fraction remaining in the body} = AUC_{t\to\infty}/AUC \quad \text{(Eq. 7)}$$

where $C_p{}^0$ is the extrapolated plasma concentration at time zero based on the conventional method (8); λ_n is the rate constant of the terminal phase; $AUMC$ is the area under the first moment of the plasma curve, and $AUC_{t\to\infty}$ is the total plasma area from time t to infinity. The AUC values for the calculation of these pharmacokinetic parameters were obtained from Method II.

RESULTS AND DISCUSSION

The arterial and venous plasma concentration profiles of griseofulvin are shown in Figs. 1 and 2. The arterial levels shortly after injection were all much higher than the venous levels indicating an extensive and rapid uptake of griseofulvin by the sampling tissues during a single passage in the leg (1, 2, 11, 13). The maximum A–V ratio for each study occurred at 0.33 min; this ranged from 15 for dog 2 to 3240 for the rabbit (Table I). These ratios decreased to unity at ~2 min for dog 2 and 45 min for the rabbit (Table I) when the net uptake by the sampling tissue was zero (*i.e.*, when the sampling tissue concentration was the maximum). Thereafter, the venous levels were higher than the arterial levels due to the release of griseofulvin from the leg tissues to the venous blood (1, 2, 11, 13). During the apparently parallel arterial and venous terminal phases (Figs. 1 and 2), the venous plasma levels were higher than arterial levels by ~30, 43, 14.7, and 8.4% for dogs 1, 2, 3, and the rabbit, respectively. The terminal half-life in the three dogs studied ranged from 37.5 to 73.7 min, and that for the rabbit was estimated to be 277 min (Table I). A longer sampling time in the rabbit study might be preferred in view of its long terminal half-life.

Various factors affecting the A–V difference during the terminal phase were discussed previously from a theoretical point of view (14). The smaller A–V difference observed in the rabbit study as compared with the dog studies was consistent with the hypothesis (14) that the longer the half-life the smaller the A–V difference in the terminal phase. This is because the rate of release of drug from the sampling tissue to the venous blood would be slower if the half-life were longer (assuming other factors were the same). It should be noted that the terminal arterial or venous plasma half-lives should be theoretically identical (14) as shown in five other drugs in animals (1, 2) and insulin in humans (15).

Unlike the conventional concept of instantaneous input to the central or plasma compartment (1, 2, 14, 16), the venous griseofulvin concentrations after bolus dosing were found to increase from the first 0.33 min and to peak at 1 min in the three dogs and at 2 min in the rabbit (Figs. 1 and 2). For dogs 1 and 2, the arterial plasma levels both peaked at 0.66 min (Fig. 1). These data resembled a rapid absorption plasma level profile

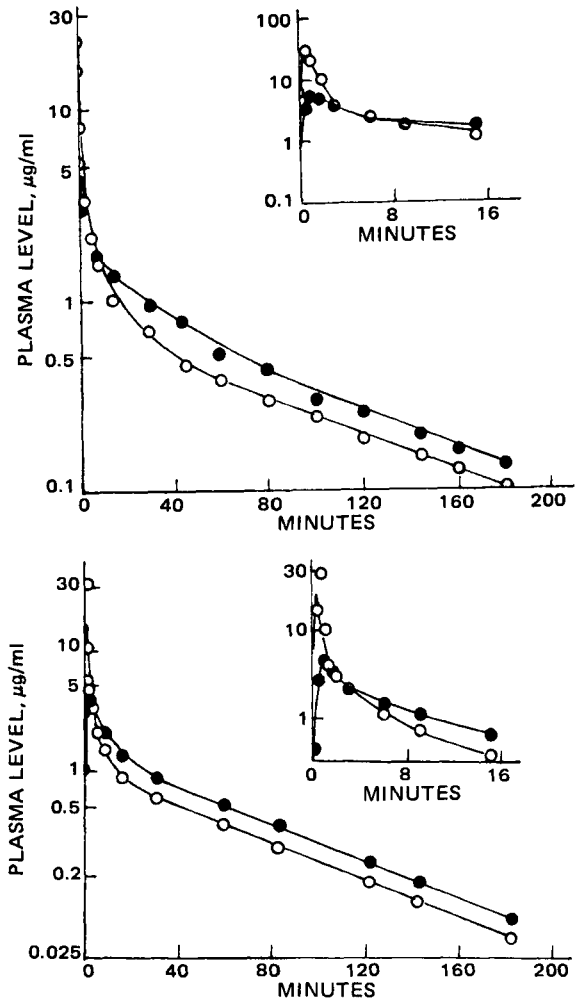

Figure 1—*The arterial (○) and venous (●) plasma level profiles after bolus injection of 60 mg of griseofulvin to dog 1 (upper curve) and dog 2 (lower curve). Solid lines are computer-generated, best-fitted curves. Inserts show the plasma level profiles in the first 16 min.*

[3] Hewlett-Packard, Corvallis, Oreg.

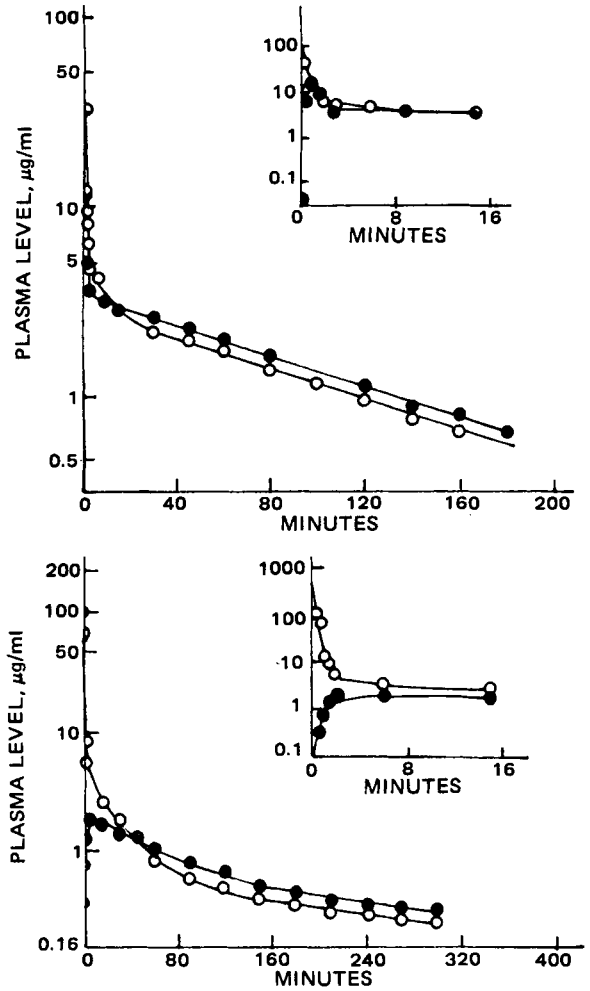

Figure 2—*The arterial (○) and venous (●) plasma level profiles after bolus injection of 60 mg of griseofulvin to dog 3 (upper curve) and 14 mg to the rabbit (lower curve).*

(2, 16). To account for this rising phase, a negative exponential term (Me^{-mt}) was used in curve fittings. The goodness of fit is judged by the closeness between the actual and computer-generated values as shown in Figs. 1 and 2, together with similar *AUC* measurements by the three methods (Table II). Furthermore, the r^2 value for all the fittings was >0.998. In the dog 3 and rabbit studies, the arterial plasma levels were found to peak at 0.33 min, which was the first blood sample; hence, their negative exponential term could not be ascertained.

The importance of recognizing that the plasma level should theoretically be zero at time zero following a bolus injection (8) is best illustrated in dogs 1 and 2. The total arterial plasma areas under the negative exponential curve could be calculated to account for 35 and 166% of the *AUC* for dogs 1 and 2, respectively (100 M/*m*/*AUC* where *AUC* was estimated based on Method II). Failure to consider this factor would result in a large overestimation of the arterial *AUC* in these two dogs if the conventional concept of the instantaneous mixing or polyexponential decay was applied. This effect apparently was minimal for dog 3 as the arterial *AUC* calculated by the conventional method was close to those calculated by the other two methods, assuming zero concentration at time zero (Table II). The effect on the venous *AUC* calculation in most of the studies was also relatively insignificant (Table II). This was in contrast with the furosemide studies in the dogs where the true venous *AUC* values could be overestimated by up to 20% if factors of initial transport lag time (8) and uptake of sampling tissues were not considered (16). The above analysis, together with findings from previous studies (1, 2, 8, 16) indicate the complexity and difficulty in accurately describing the unit-impulse disposition function of drugs (8, 17) in the body. It should be emphasized that an accurate determination of the *AUC* from the instantaneous dosing is important, since the value obtained is often used to calculate other pharmacokinetic parameters. In this regard, it appears that a short-term, intravenous infusion rather than a bolus or instantaneous injection might be preferred. Furthermore, the *AUC* from the infusion study can be more simply estimated by the linear-logarithmic trapezoidal rule-extrapolation method (7) as employed in Method II of the present study.

Theoretically, the arterial *AUC* should equal the venous *AUC* if a drug is not metabolized in the sampling tissues (2, 9, 14, 18). This was confirmed in the dog studies (Table II). In the rabbit study, however, the arterial *AUC* was higher than the venous *AUC* by ~16%. Similar results were found in other drug studies. The reason for such inequality remains to be explored.

Except for the rabbit, the *Cl* and *V* values estimated from arterial and venous plasma data in the three dogs were, as expected, essentially the same (Table III). However, the physiological significance of these values may be different (2, 19, 20). The calculated values for V_1 were found to

Table II—Polyexponential Disposition Function and the Area under Plasma Level-Time Curve of Griseofulvin in Dog and Rabbit Studies

Parameter	Dog 1		Dog 2		Dog 3		Rabbit	
	A	V	A	V	A	V	A	V
M, μg/ml	48.33	8.0	698.27	11.33	—	38.14	—	2.19
A_1, μg/ml	45.48	5.92	692.47	6.85	49.21	34.73	291.20	1.58
A_2, μg/ml	2.15	1.18	4.81	3.07	3.11	3.41	3.59	0.61
A_3, μg/ml	0.70	0.90	0.99	1.41	2.98	—	0.56	—
m, min^{-1}	4.52	1.76	5.04	2.62	—	3.47	—	0.50
λ_1, min^{-1}	1.16	0.53	4.81	1.26	1.90	1.48	3.12	0.02
λ_2, min^{-1}	0.09	0.04	0.25	0.17	0.16	0.01	0.04	0.003
λ_3, min^{-1}	0.01	0.01	0.02	0.02	0.01	—	0.003	—
AUC^a, min μg/ml	114.12	118.78	89.13	97.37	353.76	374.83	388.30	334.82
AUC^b, min μg/ml	111.94	117.64	86.53	95.95	357.94	371.14	383.35	328.46
AUC^c, min μg/ml	116.70	117.37	78.35	95.62	362.60	375.73	418.35	325.49
Percent contribution of terminal phase plasma area to *AUC*	59.98	76.68	63.18	73.73	82.18	90.76	44.62	62.47

[a] Calculated by Method I in *Experimental.* [b] Calculated by Method II in *Experimental.* [c] Calculated by Method III in *Experimental.*

Table III—Summary of Pharmacokinetic Parameters Calculated Based on Arterial or Venous Plasma Data

	Dog 1		Dog 2		Dog 3		Rabbit	
	A	V	A	V	A	V	A	V
Cl, ml/min/kg	25.16	23.94	36.11	32.57	8.38	8.09	9.86	11.51
V_1, liter/kg	0.058	0.352 (6.07)[a]	0.005	0.276 (55.2)[a]	0.053	0.079 (1.49)[a]	0.013	1.73 (133)[a]
V, liter/kg	2.35	2.23	1.95	1.76	0.89	0.86	3.95	4.61
V_{ss}, liter/kg	1.42	1.72	1.24	1.45	0.79	0.84	2.36	3.61
AUMC, min^2 μg/ml	6323.6	8457.2	2969.4	4270.6	33731.8	38730.8	91816.5	102901.3
MRT, min	56.5	71.9	34.3	44.5	94.2	104.4	239.5	313.3

[a] Values in parentheses are V-A ratios.

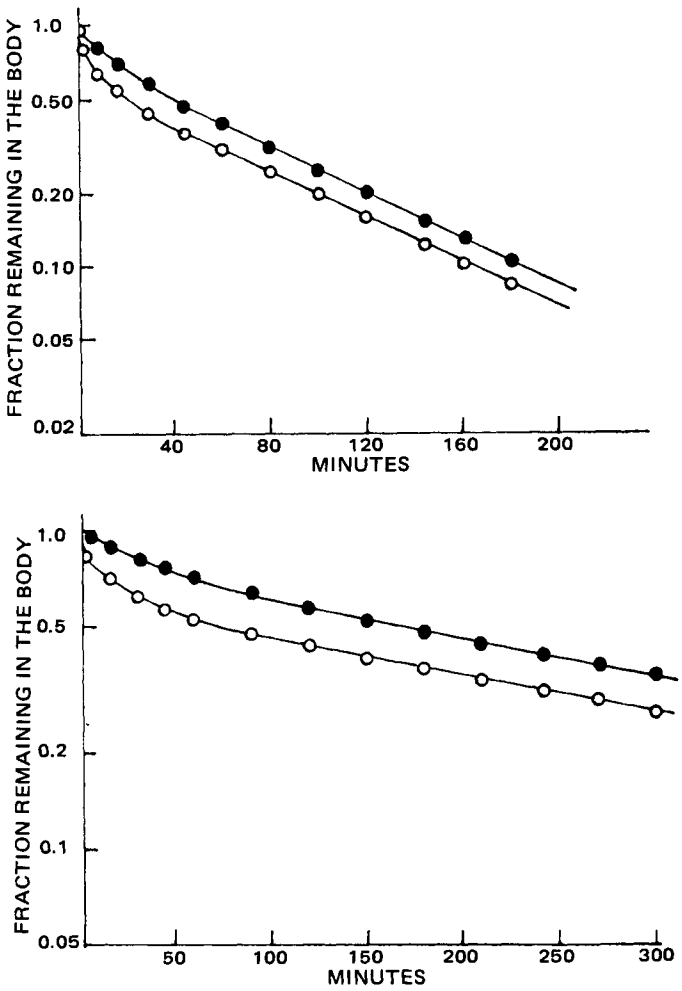

Figure 3—*Calculated fractions of griseofulvin dose remaining in the body after bolus injection of 60 mg of griseofulvin to dog 1 (upper curve) and 14 mg to the rabbit (lower curve). Key: arterial (○) and venous (●) plasma levels.*

vary considerably in the same animal, depending solely on the source of plasma data used (Table III). The venous V_1 values were 6.1, 55.2, 1.5, and 133 times greater than the arterial V_1 values for dogs 1, 2, 3, and the rabbit, respectively. The marked differences primarily were attributed to the initial uptake of griseofulvin by the sampling tissues. Thus, the A–V difference is another factor affecting the calculated V_1 (2, 21). Its implication in the dosing regimen calculation or pharmacodynamic evaluation may have to be considered.

The results of *AUMC* and *MRT* calculations are summarized in Table III. For *AUMC*, those values calculated from the venous data were 33.7, 43.8, 15.8, and 12.1% higher than the arterial data for dogs 1, 2, 3, and the rabbit, respectively. For *MRT*, the corresponding venous data were 27.3, 29.7, 10.8, and 30.8% higher. The effect of the source of blood sampling on the calculated fraction of dose remaining in the body as a function of time in dog 1 and the rabbit is depicted in Fig. 3; the difference was pronounced. For example, at 1 hr the fractions remaining were 53 and 73%, respectively, based on the arterial and venous data for the rabbit. A more marked effect was found for propranolol in dogs and rabbits (2).

Significant and persistent A–V differences were also observed for griseofulvin following intravenous infusion to one unanesthetized dog (1). The A–V plasma levels were found to differ by 20% during the terminal phase. This preliminary study also showed that a similar trend of A–V difference existed when the whole blood was analyzed. The above analyses and discussion suggest that it may be important to investigate the possible A–V difference and its consequences (1, 2, 11, 14, 18, 19) in pharmacokinetic or pharmacodynamic studies of drugs in general.

REFERENCES

(1) W. L. Chiou, G. Lam, M. L. Chen, and M. G. Lee, *Res. Commun. Chem. Pathol. Pharmacol.*, **32**, 27 (1981).

(2) G. Lam and W. L. Chiou, *ibid.*, **33**, 33 (1981).

(3) W. L. Chiou and S. Riegelman, *J. Pharm. Sci.*, **58**, 1500 (1969).

(4) M. G. Lee, M. L. Chen, S. M. Huang, and W. L. Chiou, *Biopharm. Drug Disp.*, **2**, 89 (1981).

(5) M. G. Lee, M. L. Chen, and W. L. Chiou, *Res. Commun. Chem. Pathol. Pharmacol.*, **34**, 17 (1981).

(6) R. L. Nation, G. W. Peng, V. Smith, and W. L. Chiou, *ibid.*, **67**, 805 (1978).

(7) W. L. Chiou, *J. Pharmacokinet. Biopharm.*, **6**, 539 (1978).

(8) *Ibid.*, **7**, 527 (1979).

(9) C. M. Metzler, G. L. Elfring, and A. J. McEwen, "A User's Manual for NONLIN and Associated Program," Upjohn Co., Kalamazoo, Mich., 1976.

(10) M. Gibaldi and D. Perrier, "Pharmacokinetics," Dekker, New York, N.Y., 1975.

(11) W. L. Chiou, *Int. J. Clin. Pharmacol. Ther. Toxicol.*, **20**, 255 (1982).

(12) S. Riegelman and P. Collier, *J. Pharmacokinet. Biopharm.*, **8**, 509 (1980).

(13) W. L. Chiou, *J. Pharm. Pharmacol.*, **24**, 343 (1972).

(14) W. L. Chiou and G. Lam, *Int. J. Clin. Pharmacol. Ther. Toxicol.*, **20**, 197 (1982).

(15) H. Orskov and N. J. Christensen, *Diabetes*, **18**, 653 (1969).

(16) W. L. Chiou, G. Lam, M. L. Chen, and M. G. Lee, *J. Pharm. Sci.*, **70**, 1037 (1981).

(17) W. L. Chiou, *J. Pharmacokinet. Biopharm.*, **8**, 311 (1980).

(18) W. L. Chiou and G. Lam, *J. Pharm. Sci.*, **70**, 967 (1981).

(19) W. L. Chiou, *Res. Commun. Chem. Pathol. Pharmacol.*, **33**, 499 (1981).

(20) W. L. Chiou, *J. Clin. Hosp. Pharm.*, **7**, 25 (1982).

(21) W. L. Chiou, *J. Pharm. Sci.*, **69**, 867 (1980).

Stereospecific Metabolic Reduction of Ketones

DANIEL B. PRELUSKY, RONALD T. COUTTS ˣ, and FRANCO M. PASUTTO

Received September 21, 1981, from the *Faculty of Pharmacy and Pharmaceutical Sciences, University of Alberta, Edmonton, Alberta T6G 2N8 Canada.* Accepted for publication February 19, 1982.

Abstract □ The stereospecificity of the metabolic reduction of arylalkylketones was investigated. The ketones, propiophenone (I), phenylacetone (III), and 1-phenyl-1,2-propanedione (V) were reduced *in vitro* and *in vivo* in rats and rabbits to the corresponding alcohols, 1-phenyl-1-propanol (II), 1-phenyl-2-propanol (IV), and 1-phenyl-1,2-propanediol (VIII), respectively. For the analysis, a capillary GLC method employing chiral derivatizing reagents for the resolution of these optically active alcohols was utilized. This study revealed that the metabolic reduction of each ketone produced the corresponding alcohol as a mixture of its enantiomers. With one exception, the mixtures obtained from all *in vivo* and *in vitro* reactions were shown to contain at least 70% of one isomer [*S*(−)-II, *S*(+)-IV, and *erythro*-VIII, respectively], with *in vitro* reduction showing the highest degree of stereospecificity (90–98%). The *in vivo* reduction of I by the rat was exceptional in that both optical isomers of II were recovered in equal proportions.

Keyphrases □ Ketones—stereospecific metabolic reduction, arylalkylketones, rats and rabbits □ Stereospecificity—metabolic reduction of arylalkylketones, rats and rabbits □ Metabolism—reduction of arylalkylketones, stereospecificity, rats and rabbits

Various studies on the biotransformation of xenobiotic ketones have established that ketone reduction is an important metabolic pathway in mammalian tissue (1–12). It has also been shown that when ketones are reduced metabolically, a significant product stereoselectively can be demonstrated to occur upon creation of the chiral alcohol (11–16). To determine the degree of stereoselectivity, a reliable method is required for the resolution of the stereoisomers. In many metabolic studies, the amount of product available for stereochemical analysis is often very small, making isolation and, hence, resolution procedures difficult.

As a continuation of earlier studies (2, 10), the metabolic reduction of three arylalkylketones and the efficient separation of the recovered stereoisomeric alcohols are described. Separation was accomplished by reacting the metabolites with optically active derivatizing reagents and resolving the resulting diastereoisomers by GLC. *In vivo* and *in vitro* metabolic reduction was studied in two species (the rat and the rabbit), and a comparison of the extent to which stereoselectivity occurs is provided.

EXPERIMENTAL

Compounds—Propiophenone (I), phenylacetone (III), and 1-phenyl-1,2-propanedione (V) were obtained commercially[1] and used as received. *RS*-1-Phenyl-1-propanol (II) and *RS*-1-phenyl-2-propanol (IV) were prepared by the asymmetric reduction of the corresponding arylalkylketone with the chiral sodium L-prolinate borane complex prepared according to a previously described procedure (17). Reduction of I gave a 72:28 ratio of the enantiomers of II [*S*(−)/*R*(+), respectively] as determined by polarimetric analysis[2]. Reduction of III gave a 60:40 ratio of the enantiomers of IV [*S*(+)/*R*(−), respectively]. The *erythro* and *threo* diastereoisomers of 1-phenyl-1,2-propanediol (VIII) were synthesized as previously reported (2).

Reagents—Trifluoroacetic anhydride (IX)[3] and *S*(+)-α-methylbenzyl isocyanate (X)[4] were used without further purification. The third derivatizing reagent *R*(−)menthyl chloroformate (XI) was prepared according to a previously described method (18). All solvents were reagent grade, redistilled prior to use.

Metabolic Studies and Extractions—The *in vivo* study involved the oral administration of each substrate (I, III, or V) to male Wistar rats (250 g) and male New Zealand white rabbits (2 kg). The animals were kept in metabolic cages, and urine was collected over 48 hr and stored at 4° until examined. Bulked urine samples from each group of treated animals were divided into three equal portions. One portion was adjusted to pH 7.5 with solid sodium bicarbonate and extracted three times with equal volumes of a diethyl ether–methylene chloride mixture (3:2). A second portion was buffered to pH 7.0 with phosphate buffer and hydrolyzed for 36 hr at 37° after the addition of β-glucuronidase[5] (15,000 U/ml). The sample then was extracted as described above after adjusting the pH to 7.5 with sodium bicarbonate. The third portion was acidified to < pH 1 with concentrated hydrochloric acid and autoclaved at 125° and 15 psi for 45 min. After hydrolysis was complete, the pH was readjusted to 7.5 with 10% NaOH and the resulting solution was extracted as described above for portion 1.

For the *in vitro* studies, each substrate (I, III, or V) was incubated at 37° with 12,000×*g* liver homogenate supernatant (rat or rabbit) to which was added either a nicotinamide adenine dinucleotide phosphate (NADPH) or a nicotinamide adenine dinucleotide (NADH)-generating system (glucose-6-phosphate[6], magnesium chloride, and NADP[7] or NAD[8]). Extraction of metabolic products was carried out as with portion 1 of the *in vivo* study.

All extracts were concentrated and yielded yellowish oils, small aliquots of which were used for analysis by derivatization.

Derivatization—The *R*(−)menthyloxycarbonyl derivatives were prepared as follows: 100 μl of a standard XI solution (50 μmole/ml of toluene) was added to a small portion of the concentrated extract (20 μl) dissolved in 100 μl of pyridine. The mixture was allowed to react at room temperature for 30 min. After washing with water (1 ml), the organic phase was removed, dried over sodium sulfate, and concentrated under nitrogen to 5 μl, of which 0.2 μl was used for GLC.

N-(1-Phenylethyl)urethanes were prepared by adding 50 μl of a X solution (30 μmole/ml of toluene) to a portion (20 μl) of the concentrated extract dissolved in 100 μl of toluene. The mixture was tightly sealed[9] under a nitrogen atmosphere and kept at 120° for 2 hr. The reaction mixture was concentrated to 5 μl under a nitrogen stream, and a suitable portion was used for GLC.

Trifluoroacetyl derivatives of the metabolically produced alcohols were prepared by dissolving a small portion (20 μl) of the concentrated extract in 30 μl of ethyl acetate, to which 70 μl of IX was added. The reaction was allowed to proceed for 30 min at room temperature. The reaction mixture was evaporated under nitrogen and the residue obtained redissolved in 10 μl of cyclohexane, of which a 0.2-μl aliquot was injected.

The derivatized alcohol metabolites were identified by comparing their GLC retention times and mass spectra with those of authentic samples containing one optical enantiomer (or diastereoisomer) in known excess. Analyses were performed with a gas chromatograph[10] equipped with a flame ionization detector. The GLC conditions were: capillary column[11]

[1] Pfaltz and Bauer, Inc., Stamford, Conn.

[2] Optical rotation measurements were made using a Carl Zeiss Circular Polarimeter 0.01° equipped with a sodium D lamp (589.3 nm).

[3] Sigma Chemical Co., St. Louis, Mo.

[4] Aldrich Chemical Co., Inc., Milwaukee, Wis.

[5] Sigma Type H-1, Sigma Chemical Co., St. Louis, Mo.

[6] D-glucose-6-phosphate (Sigma grade, disodium salt) Sigma Chemical Co., St. Louis, Mo.

[7] Nicotinamide adenine dinucleotide phosphate, oxidized form (Sigma grade, monosodium salt), Sigma Chemical Co., St. Louis, Mo.

[8] β-Nicotinamide adenine dinucleotide, oxidized form (Grade III) Sigma Chemical Co., St. Louis, Mo.

[9] Reacti-vial (0.2 ml), Pierce Chemical Co., Rockford, Ill.

[10] Model 5710A, Hewlett-Packard.

[11] SE-30 (S.C.O.T.), Scientific Glass Engineering Pty, Ltd., (S.G.E. Inc.), Austin, Tex.

0022-3549/82/1200-1390$01.00/0

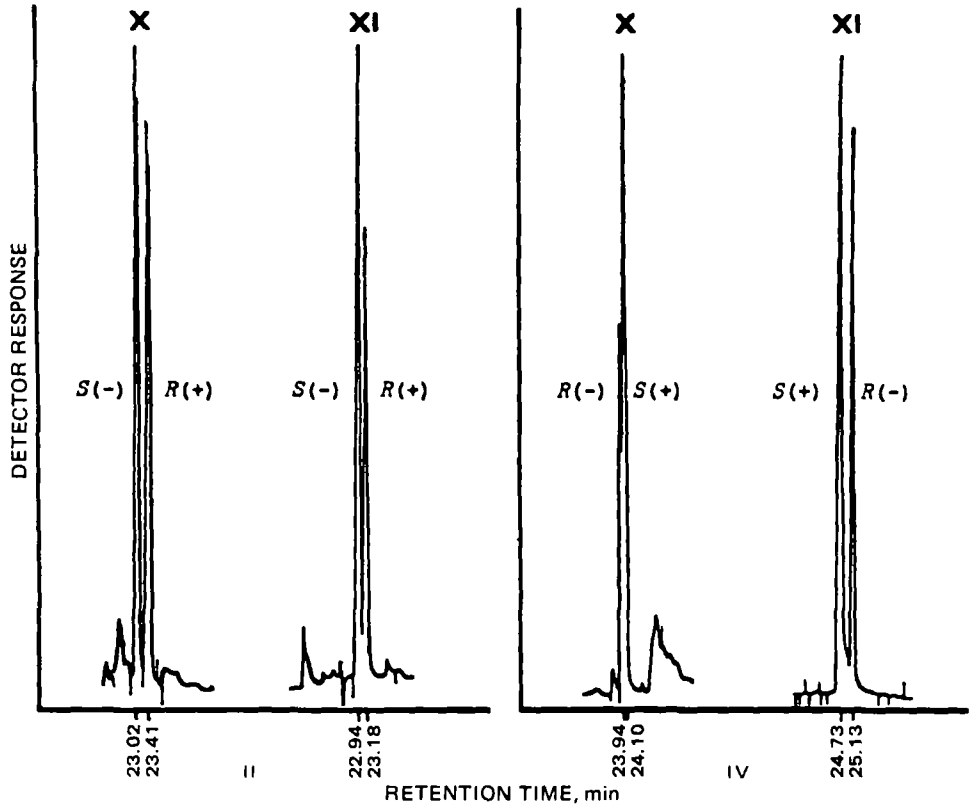

Figure 1—*Chromatograms (obtained by capillary GLC) of the diastereoisomeric pairs formed after reaction of alcohols with chiral derivatizing reagent. Key: alcohols: (II) 1-phenyl-1-propanol and (IV) 1-phenyl-2-propanol; reagents: (X)* R(−)*menthyl chloroformate and (XI)* S(+)-*α-methylbenzyl isocyanate.*

(52 m) with temperature programming from 150 to 250° (4°/min). The injection port and detector temperatures were 250 and 300°, respectively. The flow rate of the carrier gas, helium, was 3 ml/min (17 psi). Mass spectrometer[12] conditions were separator and ionization source temperatures, 180° and ionization energy, 70 eV. The GLC column and operating conditions were as described above.

RESULTS

In vivo and *in vitro* metabolism of I by the rat and and rabbit produced various metabolites (2, 11) including the racemate alcohol, *RS*-II. Similarly, racemic *RS*-IV was metabolically produced, together with other metabolites from III (1, 2, 10, 11). In this study the relative amounts of the enantiomeric alcohols were determined by reaction with the chiral derivatizing reagents, X or XI, and resolving the resulting diastereoisomeric derivatives by GLC.

Initially it was necessary to determine the GLC elution sequence of the mixture of diastereoisomers formed by the reaction of the racemate alcohols (II and IV) with the chiral reagents (X and XI). To accomplish this, authentic samples of II and IV were synthesized by a procedure which was known to produce mixtures of alcohols enriched in one of the enantiomers (17). Compound II was prepared by the asymmetric reduction of I with a sodium L-prolinate borane complex to yield a mixture of the enantiomers in which the *S*(−)-isomer predominated (see *Experimental*). A comparison of the magnitude of the optical rotation of the mixture with that of a pure sample of *S*(−)-1-phenyl-1-propanol permitted the calculation of the amounts of *S*(−)-II and *R*(+)-II in the synthetic product (Table I). Compound IV was prepared from III in a similar manner. The mixture of stereoisomers was strongly dextrorotatory, indicative of *S*(+)-IV being in enantiomeric excess. The calculated ratio of *S*(+)-IV/*R*(−)-IV is illustrated in Table I.

The mixture of stereoisomers (II and IV) were then reacted with the chiral reagents (X and XI) and the products analyzed by GLC (Fig. 1). The inability to detect any unreacted alcohols ensured complete derivatization. Peak areas were integrated and the ratio of isomers calculated. The values obtained were in close agreement with those obtained from polarimetric data (Table I), thus permitting peak identification.

The efficiency of peak resolution varied. A greater separation between *R*- and *S*-1-phenyl-2-propanol (IV) was obtained after derivatization with X then with XI (Fig. 1), which resulted in a more precise determination of optical purity (Table I). With *R*- and *S*-1-phenyl-1-propanol (II), better separation was obtained following derivatization with XI than with X. However, isomer ratios calculated from both chromatograms were virtually identical and in good agreement with those obtained polarimetrically (Table I).

Having demonstrated that the enantiomers of the racemate alcohols (II and IV) could be efficiently separated and quantitated as the corresponding diastereoisomers, it was possible to determine the extent to which stereoselectivity occurred during the metabolic reduction of arylalkylketones (I and III) and to assign absolute configuration to the metabolites.

When I was reduced *in vitro* (12,000×*g* liver homogenate) in rats or rabbits, 93–97% of the product alcohol (II) occurred as the *S*(−)-isomer, the remainder being the *R*(+) form (Table II). Species differences were minimal and nicotinamide adenine dinucleotide phosphate or nicotinamide adenine dinucleotide-generating systems were equally efficient. A structurally related alcohol, 1-phenyl-1-ethanol, produced by the reduction of acetophenone by an aromatic ketone reductase isolated from rabbit kidney, was similarly found to be predominantly (76%) in the *S*(−)

Table I—Stereochemical Analysis of Alcohols Obtained by Chemical Reduction of Arylalkylketones[a]

Method of Analysis	Alcohols[b] II	Alcohols[b] IV
Polarimetry	72/28[c]	60/40[d]
Derivatization/GLC		
R(−)-menthyl chloroformate	71/29	65/35
S(+)-*α*-methylbenzyl isocyanate	72/28	58/42

[a] A comparison of enantiomers detected by different analytical procedures. [b] Ratio of enantiomers: 1-phenyl-1-propanol (II), *S*(−)/*R*(+); 1-phenyl-2-propanol (IV), *S*(+)/*R*(−). [c] Based on $[\alpha]_D$ −32.50° (c 5.1, ethanol). R. H. Pickard and J. Kenyon, *J. Chem. Soc.*, **105**, 1115 (1914). [d] Based on $[\alpha]_D$ +16.10° (c 5.6, ethanol). *Ibid.*

[12] Hewlett-Packard model 5710 gas chromatograph coupled to a Hewlett-Packard quadrupole mass spectrometer model 5981A and a 5934A data system.

Table II—Stereochemical Analysis of Alcohols Obtained from the Metabolic Reduction of Arylalkylketones

Substrate	Methodology: System	Cofactor[a]	Pretreatment[b]	Metabolic Alcohol	Ratio of Enantiomers of Metabolic Alcohols[c] Species: Rat	Rabbit
I	*In vitro*	NADPH	N/P	II	96/4	93/7
		NADH	N/P		97/3	94/6
	In vivo	—	N/P		57/43	91/9
		—	Enzyme		52/48	89/11
		—	Acid		42/58	65/35
III	*In vitro*	NADPH	N/P	IV	91/9	94/6
		NADH	N/P		90/10	92/8
	In vivo	—	N/P		81/19	87/13
		—	Enzyme		80/20	88/12
		—	Acid		72/28	79/21

[a] Generating system; glucose-6-phosphate, magnesium chloride, and $NADP^+$ or NAD^+. [b] Hydrolytic pretreatment of biological sample: N/P, no pretreatment; enzyme, β-glucuronidase (15,000 U/ml, incubated 36 hr at 37°); acid, pH < 1 (autoclaved 40 min at 125° and 15 psi). [c] Ratio of enantiomers (as diastereoisomeric derivatives); 1-phenyl-1-propanol [S(−)/R(+)-II] as R(−)menthyl chloroformate derivative, 1-phenyl-2-propanol [S(+)/R(−)-IV] as S(+)-α-methylbenzyl isocyanate derivative.

form (12). *In vitro* reduction of phenylacetone (III) in rats and rabbits paralleled what was observed with the substrate I. The alcohol, IV, was recovered mainly as the S(+)-enantiomer (90–94%), regardless of the species and cofactor (Table II).

In vivo reduction of I by rabbits gave results comparable to those observed in *in vitro* studies. Approximately 90% of the alcohol recovered from urine was determined to be S(−)-1-phenyl-1-propanol [S(−)-II]. An earlier study has shown that after administration of propiophenone to rabbits, II was recovered entirely as the S(−)-glucuronide conjugate (11). In contrast to what occurred in rabbits *in vivo*, reduction of I in rats resulted in the recovery of a markedly higher proportion of the R-alcohol [R(+)-II]. In this instance, stereoselective reduction was less evident (Table II). Both enzymatic and acidic hydrolysis of the urine collected in the *in vivo* studies resulted in an increase in the relative amounts of R(+)-II isolated.

In vivo reduction of III to its corresponding alcohol (IV) resulted in the preferential formation of the S(+)-IV isomer, regardless of species (Table II). The ratio of enantiomers [S(+)/R(−)] formed by rat and rabbit were 81:19 and 87:13, respectively, corresponding to approximately twice the amount of R(−)-IV observed *in vitro*. In contrast, an earlier study (11) reported that when III was reduced in the rabbit, no trace of R(−)-1-phenyl-2-propanol was found. The S(+)-IV/R(−)-IV ratio was again influenced by the method used to hydrolyze urine (Table II).

In vivo and *in vitro* metabolism of V was also investigated in rats and rabbits. Reduction yielded three metabolites of major interest for this study: 1-hydroxy-1-phenyl-2-propanone (VI), 2-hydroxy-1-phenyl-1-propanone (VII), and 1-phenyl-1,2-propanediol (VIII), which was obtained as a mixture of its diastereoisomers (*erythro*- and *threo*-VIII) (Scheme I). Neither of the intermediate ketol metabolites (VI or VII) could be completely derivatized with either chiral reagent (X or XI) and, therefore, the optical purities of these metabolites could not be established. Similarly, the four-component mixture of optical isomers of the diol, VIII (1*S*2*R*- and 1*R*2*S*-*erythro*, 1*S*2*S*- and 1*R*2*R*-*threo*) could not be separated using the chiral reagents, but it was possible to separate the diastereoisomers as their trifluoroacetyl derivatives.

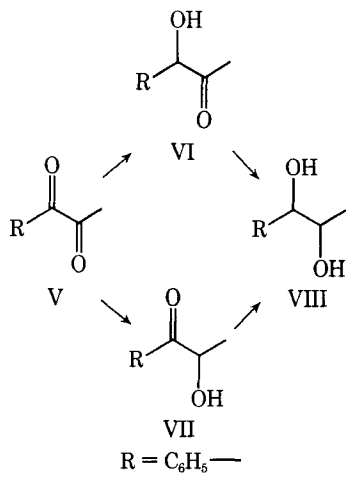

Scheme I

As observed with ketones I and III, *in vitro* reduction of V resulted in the formation of one predominant isomer of the diol metabolite (VIII) (Table III). Between 94 and 98% of VIII was recovered as the *erythro*-diastereoisomer. Only marginal variation in the measured *erythro–threo* ratio of VIII was observed, regardless of the source of the liver preparation or the nature of the cofactor utilized.

In vivo reduction of V similarly produced *erythro*-VIII as the major diastereoisomer, regardless of species. Ratios of the isomers isolated (*erythro–threo*-VIII) were 75:25 and 86:14, recovered from rats and rabbits, respectively. Hydrolysis of urine with either β-glucuronidase or acid caused no change in the ratio (Table III).

DISCUSSION

Conventional methods for determining the optical purity of metabolites have generally relied on isolating sufficient quantities of product for polarimetric analysis (11, 19–22). This presents a problem when the amount of product available is too small for accurate measurement of optical rotation. The use of chiral reagents and subsequent analysis of diastereoisomeric products by GLC (23–27) offers a sensitive alternative for the quantification of stereoisomeric metabolites. This analytical procedure provided the data summarized in Table II, which reveal that the metabolic reduction of I and III demonstrates a high degree of product stereoselectivity. The metabolites, II and IV, respectively, were recovered predominately as S-isomers in all studies with one exception: *In vivo* reduction of I by rats provided anomalous data.

In quantitative terms, the *in vitro* reduction of arylalkylketones has been reported to be significantly dependent on both the species and cofactor (2–4, 6–8, 10, 12), but the present study indicates that enantioselective preference is virtually unaffected by these variables.

The ratios of isomers isolated from the *in vivo* studies did vary, however, depending on the nature of the hydrolytic treatment of the urine samples prior to extraction and derivatization of the alcohol metabolites. A noticeable increase in the amount of R(+)-II recovered, relative to that of S(−)-II, was observed in both species after enzymatic hydrolysis (Table II). Since it has already been demonstrated that both enantiomers of II undergo glucuronide conjugation in rabbits (11), this observation suggests

Table III—Stereochemical Analysis of 1-Phenyl-1,2-propanediol Obtained from the Metabolic Reduction of 1-Phenyl-1,2-propanedione

Methodology: System	Cofactor[a]	Pretreatment[b]	Ratio of Diastereoisomers of VIII[c] Species: Rat	Rabbit
In vitro	NADPH	N/P	97/3	97/3
	NADH	N/P	94/6	98/2
In vivo	—	N/P	75/25	86/14
	—	Enzyme	74/26	87/13
	—	Acid	72/28	85/15

[a] Generating system; glucose-6-phosphate, magnesium chloride, and $NADP^+$ or NAD^+. [b] Hydrolytic pretreatment of biological sample: N/P, no pretreatment; enzyme, β-glucuronidase (15,000 U/ml, incubated 36 hr at 37°); acid, pH < 1 (autoclaved 40 min at 125° and 15 psi). [c] Ratio of diastereoisomers, *erythro–threo*-1-phenyl-1,2-propanediol (VIII) as the trifluoroacetylated derivative.

that a greater proportion of the $R(+)$-isomer is conjugated relative to the $S(-)$ form. Only minor changes were detected in the $S(+)/R(-)$ ratio of 1-phenyl-2-propanol (IV) after hydrolysis with β-glucuronidase, when compared with the ratio observed with no pretreatment of the urine samples.

The much higher levels of both $R(+)$-II and $R(-)$-IV measured after acidic hydrolysis possibly could be due to a more efficient cleavage of the conjugate with acid treatment than with β-glucuronidase. However, a more plausible explanation is that racemization of isomers occurred during the harsh treatment created by conditions of low pH and elevated temperature (19). This would account for the difficulty in obtaining reproducible results after acidic hydrolysis.

The absence of any noticeable change in the ratio of diastereoisomers of VIII suggest that both the *erythro* and *threo* isomers are conjugated to the same extent. However, it is perhaps more likely that because of the high polarity of the diols, neither compound (*erythro*-VIII nor *threo*-VIII) undergoes conjugation before being excreted in the urine.

A strong correlation between *in vivo* and *in vitro* results in the rabbit has been demonstrated in the present study with both substrates (Table II). A similar correlation was observed between *in vivo* and *in vitro* reduction of III in the rat, but not when I was the substrate (Table II). In the latter instance, enantioselectivity was clearly demonstrated in *in vitro* studies, but *in vivo* reduction of I appeared to be nonstereoselective. This anomalous situation may be the result of further preferential metabolism of $S(-)$-1-phenyl-1-propanol *in vivo* in the rat. Related studies support this suggestion. It has been established (28) that when 1-phenyl-1-ethanol was administered to rats as the $R(+)$-isomer, it underwent extensive conjugation and was excreted largely as the glucuronide, whereas the $S(-)$-isomer was further oxidized to $S(-)$-mandelic acid. If the metabolite, II, behaved similarly *in vivo* in the rat, it would account for the lower percentage recovery of $S(-)$-II compared with that obtained with the *in vitro* study. In addition, the increased recovery of $R(+)$-II after enzymatic treatment of the urine sample could be rationalized by liberation of the $R(+)$-isomer from the glucuronide conjugate.

The enantioselectivity of the reduction of the arylalkylketones (I and III) can be rationalized, based on a formula established previously (29) and confirmed by others (22, 30–33). This formula essentially states that if the ketone is positioned so the large substituent is placed to the left, reduction mainly occurs such that the resultant hydroxyl group rises above the plane of the molecule. Compounds I and III, therefore, could be predicted to be preferentially reduced to alcohols with the *S*-configuration (Scheme II: L, large substituent; S, small substituent). By applying Prelog's rule, it is possible to predict the stereochemistry of the diol (VIII), assuming that reduction proceeded *via* the ketoalcohol intermediates (VI and VII) and that the pattern of preferred stereoselectivity remains constant. Consequently, VIII should occur predominantly as the 1*R*2*S*-diastereoisomer. Although it was not possible to resolve the 1*R*2*S*- and 1*S*2*R*-*erythro* isomers, this prediction was accurate in as much as VIII recovered from the reduction of the diketone *in vitro* by both rat and rabbit was mainly (94–98%) the *erythro* form, the remainder being *threo*-VIII (Table III). Compound VIII recovered from *in vivo* studies

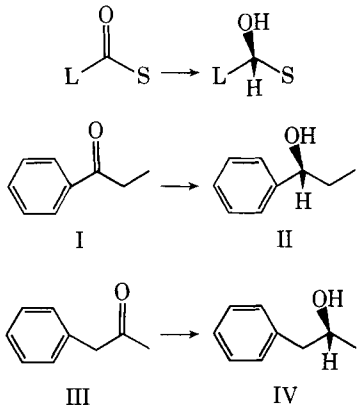

Scheme II

was also predominantly the *erythro* diastereoisomer, although a greater amount of the *threo*-compound was present compared to what was obtained from *in vitro* studies (Table III). However, caution should be exercised when attempting to explain this apparent decrease in stereoselectivity, since additional factors such as further metabolism and differences in distribution and elimination may contribute to the overall variation in recovery of diastereoisomers. In this instance there is the additional possibility that racemization resulting from interconversion of the ketol intermediates (VI ⇄ VII) could have also occurred (2, 23).

REFERENCES

(1) R. C. Kammerer, A. K. Cho, and J. Jonsson, *Drug Metab. Dispos.*, **6,** 396 (1978).

(2) R. T. Coutts, D. B. Prelusky, and G. R. Jones, *Can. J. Physiol. Pharmacol.*, **59,** 195 (1981).

(3) N. K. Ahmed, R. L. Felsted, and N. R. Bachur, *J. Pharmacol. Exp. Ther.*, **209,** 12 (1979).

(4) N. R. Bachur and R. L. Felsted, *Drug Metab. Dispos.*, **4,** 239 (1976).

(5) H. B. Hucker, B. M. Michniewicz, and R. E. Rhodes, *Biochem. Pharmacol.*, **20,** 2123 (1971).

(6) N. R. Bachur, *Science*, **193,** 595 (1976).

(7) K. Leibman, *Xenobiotica*, **1,** 97 (1971).

(8) T. A. Moreland and D. S. Hewick, *Biochem. Pharmacol.*, **24,** 1953 (1975).

(9) I. M. Fraser, M. A. Peters, and M. G. Hardinge, *Mol. Pharmacol.*, **3,** 233 (1967).

(10) R. T. Coutts, G. R. Jones, and R. E. Townsend, *J. Pharm. Pharmacol.*, **30,** 82 (1978).

(11) J. N. Smith, R. H. Smith, and R. T. Williams, *Biochem. J.*, **57,** 74 (1954).

(12) H. W. Culp and R. E. McMahon, *J. Biol. Chem.*, **243,** 848 (1968).

(13) H. R. Sullivan, S. E. Smits, S. L. Due, R. E. Booher, and R. E. McMahon, *Life Sci., Vol. II, Part 1*, **1972,** 1093.

(14) A. H. Beckett and D. Mihailova, *Biochem. Pharmacol.*, **23,** 3347 (1974).

(15) R. J. Lewis, W. F. Trager, K. K. Chan, A. Breckenridge, M. Orme, M. Roland, and W. Scharg, *J. Clin. Invest.*, **53,** 1607 (1974).

(16) F. J. DiCarlo, M. C. Crew, L. J. Hanes, and R. L. Gala, *Xenobiotica*, **2,** 159 (1972).

(17) N. Umino, T. Iwakuma, and N. Itah, *Chem. Pharm. Bull.*, **27,** 1479 (1979).

(18) J. W. Westley and B. Halpern, *J. Org. Chem.*, **33,** 3978 (1968).

(19) J. N. Smith, R. H. Smithies, and R. T. Williams, *Biochem. J.*, **56,** 320 (1954).

(20) R. E. McMahon, H. R. Sullivan, J. C. Craig, and W. E. Pereira, Jr., *Arch. Biochem. Biophys.*, **132,** 575 (1969).

(21) A. H. Beckett, G. G. Gibson, and K. Haya, in "Biological Oxidation of Nitrogen," J. W. Gorrod, Ed., Elsevier/North Holland, Biomedical Press, New York, N.Y., 1978, p. 37.

(22) M. Imuta, K. Kawai, and H. Ziffer, *J. Org. Chem.*, **45,** 3352 (1980).

(23) K. Kruse, W. Francke, and W. A. Konig, *J. Chromatogr.*, **170,** 423 (1979).

(24) K. H. Bell, *Aust. J. Chem.*, **32,** 2625 (1979).

(25) E. Gil-Av and D. Nurok, *Adv. Chromatogr.*, **10,** 99 (1974).

(26) W. Freytag and K. H. Ney, *J. Chromatogr.*, **41,** 473 (1969).

(27) W. H. Pirkle and J. R. Hauske, *J. Org. Chem.*, **42,** 1839 (1977).

(28) R. E. McMahon and H. R. Sullivan, in "Microsomes and Drug Oxidation," J. R. Gillette, A. H. Conney, G. J. Cosmides, R. W. Estabrook, J. R. Fouts, and G. J. Mannering, Eds., Academic, New York, N.Y., 1969, p. 239.

(29) P. Baumann and V. Prelog, *Helv. Chim. Acta*, **41,** 2362 (1958).

(30) K. Kabuto, M. Imuta, E. S. Kempner, and H. Ziffer, *J. Org. Chem.*, **43,** 2357 (1978).

(31) B. Testa, *Acta Pharm. Suec.*, **10,** 441 (1973).

(32) M. Imuta and H. Ziffer, *J. Org. Chem.*, **43,** 3319 (1978).

(33) V. Prelog, *Pure Appl. Chem.*, **9,** 119 (1964).

Drug Stability in Liposomal Suspensions: Hydrolysis of Indomethacin, Cyclocytidine, and *p*-Nitrophenyl Acetate

JOSEPH B. D'SILVA * **and ROBERT E. NOTARI** ˣ

Received September 30, 1981, from *Lloyd M. Parks Hall, College of Pharmacy, The Ohio State University, Columbus, OH 43210.* Accepted for publication February 16, 1982. *Present address: Pharmaceutical Research and Development, Central Research, Pfizer, Inc., Groton, CT 06340.

Abstract □ First-order rate constants (k_L) for hydrolysis of *p*-nitrophenyl acetate, cationic cyclocytidine, and anionic indomethacin in the presence of buffered liposomal suspensions of positive, negative, and neutral charge were compared to those determined in the corresponding buffers (k_B) using the ratio, $R_k = k_L/k_B$. Association between the reactants and the liposomes was evaluated by comparing assays for concentration in the filtrates (C_F) with the total concentration in the liposomal suspension (C_T) using $R_C = C_F/C_T$. Liposomes did not influence cyclocytidine hydrolysis rates and no association was observed ($R_k \simeq R_C \simeq 1$). In contrast, indomethacin showed ~80% reduction in hydrolysis rate and ~80% liposome association value ($R_k \simeq 0.2 \simeq R_C$). In neutral and negatively charged liposomal suspensions, *p*-nitrophenyl acetate displayed ~30% decrease in k_B ($R_k \simeq 0.7$) together with ~90% liposomal association ($R_C \simeq 0.1$). However, hydrolysis was greatly accelerated in positively charged liposomal suspensions. Loss was described by a biexponential equation where α is the fast and β is the slow pre-exponential coefficient and $\alpha/\beta/k_B$ = 39:6:1. The observed relationships between hydrolysis rates and reactant-liposome associations are reconciled in terms of the hydrophilicity of the reactants and the potential influence of the liposomes on the expected transition states for the hydrolysis reactions.

Keyphrases □ Indomethacin—hydrolysis, stability in liposomal suspensions, cyclocytidine, *p*-nitrophenyl acetate □ Stability—liposomal suspensions, hydrolysis of indomethacin, cyclocytidine, *p*-nitrophenyl acetate □ Hydrolysis—indomethacin, cyclocytidine, *p*-nitrophenyl acetate, stability in liposomal suspensions □ Liposomes, suspensions—drug stability, hydrolysis of indomethacin, cyclocytidine, *p*-nitrophenyl acetate

Interest in liposomes as potential drug delivery systems has prompted these investigations into the influence of liposomes on drug stability. This report compares the hydrolysis of a cation, an anion, and a neutral reactant in aqueous buffered solutions to that in buffered liposomal suspensions of positive, negative, and neutral charge.

BACKGROUND

The potential for changes in hydrolysis rates in micellar systems (1) and the implications to drug stabilization (2) are well documented and have been applied to aspirin (3–5) and indomethacin (6). Little has been reported on drug stability in liposomal suspensions although they are somewhat analogous to micellar systems. The rate of procaine hydrolysis was reduced in neutral liposomal suspensions relative to that in aqueous buffers, whereas 2-diethylaminoethyl-*p*-nitrobenzoate hydrolysis was accelerated at pH < 7.8 and retarded at pH > 7.8 (7). The degradation rate of *p*-nitrophenol acetate was accelerated by increasing liposomal lecithin concentration (8). These studies measured the total amount of drug in the suspension.

EXPERIMENTAL

Preparation of Liposomes—Cholesterol[1,2] (~7.4 mg) was placed in a 50-ml round bottom-stoppered flask together with either ~21 mg of dicetyl phosphate[1] (for negatively charged liposomes) or ~10.4 mg of stearylamine[1] (for positively charged liposomes). α-Tocopherol[1] (1 ml of 1.5×10^{-3} *M*) in chloroform (9, 10) was added, followed by 7 ml of chloroform and 1 ml of 1% lecithin in methanol–chloroform, 1:9[1]. The resulting solution was concentrated under vacuum for 3 min under a rotary evaporator at 42° (±2°). Evaporation was then continued at ambient temperature with the final traces of chloroform being removed by flushing with nitrogen.

Sixteen milliliters of buffer was added, and the mixture was agitated on a vortex mixer until the material from the sides of the flask formed a suspension of large liposomes. The flask was placed in a cup-horn sonicator[3] and cooled for 2 min using circulating water kept at 2°. The mixture was sonicated for 4 min at 60% power (maximum power = 20 kHz) using one-half second pulses per second. During the sonication the cooling water was kept circulating around the flask. Throughout the procedure the head space of the flask was periodically flushed with nitrogen to minimize oxidation. The size and shape of the liposomes were monitored using a microscope with an eye-piece micrometer together with particle size analysis (see *Kinetics of Hydrolysis*).

Analytical Methods—Stability-indicating spectrophotometric assays for indomethacin[4], *p*-nitrophenyl acetate, and cyclocytidine in buffered aqueous solutions, in total liposomal suspensions and in their filtrates are described below. The chromophoric hydrolysis products of cyclocytidine[1] (cytarabine[1]) and *p*-nitrophenol acetate[5] (*p*-nitrophenol[6]) were also measured. The products of indomethacin hydrolysis were nonchromophoric at 330 nm, which is near the 323-nm indomethacin absorption maximum.

To quench the hydrolysis of either indomethacin or *p*-nitrophenyl acetate in the total liposomal suspension, 1 ml of suspension was added to 4 ml of cold 0.5 *M* formic acid in water–methanol (2:8). The mixture was shaken and stored in a refrigerator. Prior to analysis it was warmed to room temperature and centrifuged at 3200 rpm for 30 min to remove liposomal material. Four milliliters of the supernatant solution was mixed with 4 ml of methanol and the resulting solution was centrifuged for 10 min. The UV absorbance of the resulting clear solution was determined at the appropriate wavelengths in a spectrophotometer[7], against a blank prepared in a similar manner omitting the reactant. The procedure for cyclocytidine was identical but employed 0.2 *M* HCl in water–methanol (1:9) to stabilize cytarabine, and the first centrifugation was 40 min.

Molar absorptivities (ϵ) were determined from the slopes of Beer's law plots using solutions in the buffers. The apparent molar absorptivities (ϵ') representing the procedure for assaying liposomal suspensions in the same buffers were similarly determined. Comparison of the values of ϵ' with those of ϵ indicated that the recovery was 93–100% as shown in Table I.

Since degradation products did not absorb at 330 nm, total indomethacin concentration, C_i, in the liposomal suspension was calculated from:

$$C_i = D\,(A_{330})/(\epsilon'_{330}) \qquad \text{(Eq. 1)}$$

where the dilution factor D is 10, ϵ'_{330} is the apparent molar absorptivity at 330 nm, and A_{330} is the absorbance of the final dilution at 330 nm.

Since the UV spectra of cyclocytidine and *p*-nitrophenyl acetate overlapped with those of their respective degradation products, the total absorbance of a mixture in the final dilution at a given wavelength, A_λ, is defined as:

$$A_\lambda = [\epsilon'_1(C_1) + \epsilon'_2(C_2)]/D \qquad \text{(Eq. 2)}$$

[1] Sigma Chemical Co., St. Louis, Mo.
[2] P-L Biochemicals, Milwaukee, Wis.
[3] Model W-375, Heat Systems—Ultrasonics, Plainview, N.Y.
[4] Merck, Sharp and Dohme Research Laboratories, West Point, Pa.
[5] Eastman Kodak Co., Rochester, N.Y.
[6] *p*-Nitrophenol was obtained by total hydrolysis of the ester in 0.1 *N* NaOH, 40°, for 5 hr.
[7] Model 250, Gilford Instruments, Oberlin, Ohio.

0022-3549/82/1200-1394$01.00/0

Table I—Apparent Molar Absorptivities of Reference Standards Recovered from Liposomal Suspensions

λ(nm) x	λ(nm) y	Compound	n^a	$10^{-3}\epsilon'_{nx}$	$10^{-3}\epsilon'_{ny}$	Recovery[b], %
330	—	Indomethacin	1	6.40	—	~100
272	317	*p*-Nitrophenyl acetate	1	9.08	1.22	93
		p-Nitrophenol	2	3.20	11.60	94
260	285	Cyclocytidine	1	10.30	3.13	~100
		Cytarabine	2	4.70	14.00	~100

[a] $n = 1$ Designates reactant and $n = 2$ its hydrolysis product. [b] Average values from ϵ'_{nx} and ϵ'_{ny} where percent recovery = $100\ \epsilon'/\epsilon$.

Table II—Apparent First-Order Rate Constants for Hydrolysis in Buffers (k_B) and in Liposomal Suspensions (k_L,k_F), at 40°, and the Mean Diameters of Liposomes before (d_0) and after (d) Hydrolysis

Reactant[a]	Liposomal Charge	k in hr^{-1} k_B	k_L	k_F	R_C	μ d_0	d
Cyclocytidine	Positive	0.865[b]	0.858	0.786	1.12	2.38	2.30
	Negative	0.865[b]	0.789	0.756	1.18	2.21	2.26
	Neutral	0.865[b]	0.843	0.774	1.16	2.43	2.52
	Negative	0.121[c]	0.109	—	—	—	—
Indomethacin	Positive	0.346[d]	0.054	—	~0.10[e]	2.10	2.26
	Negative	0.346[d]	0.110	0.106	0.28	2.17	2.17
	Neutral	0.346[d]	0.0783	—	~0.20[e]	2.38	2.52
p-Nitrophenyl-acetate	Negative	0.362[c]	0.249	0.300	0.086	2.10	2.34
	Neutral	0.362[c]	0.268	0.300	0.144	2.14	2.38
	Positive	0.362[c]	$\frac{\alpha}{14.0}$	$\frac{\beta}{2.05}$	0.508[f]	2.14	2.21

[a] $C_0 \simeq 9 \times 10^{-4}$ *M*. [b] Borate buffer: 0.320 *M* H_3BO_3; 0.140 *M* NaH_2BO_3; 0.350 *M* NaCl; pH 8.31. [c] Phosphate buffer: 0.0140 *M* NaH_2PO_4; 0.100 *M* Na_2HPO_4; 0.086 *M* NaCl; pH 7.51. [d] Carbonate buffer: 0.135 *M* $NaHCO_3$; 0.065 *M* Na_2CO_3; 0.075 *M* NaCl; pH 0.37. [e] Filtrates were not concentrated enough to obtain more accurate estimates. [f] Average value during the beta phase.

where $D = 10$, C_1 and C_2 are the total concentrations of reactants and products, respectively, in the liposomal suspensions, and ϵ'_1 and ϵ'_2 are their apparent molar absorptivities at wavelength λ. The total absorbance determined at each of two wavelengths, A_x and A_y, then results in two simultaneous equations which may be solved to yield:

$$C_1 = D[\Delta_{1x}(A_x) - \Delta_{1y}(A_y)] \quad \text{(Eq. 3)}$$

$$C_2 = D[\Delta_{2x}(A_x) - \Delta_{2y}(A_y)] \quad \text{(Eq. 4)}$$

where $\Delta_{1x} = \epsilon'_{2y}/(\epsilon'_{1x}\epsilon'_{2y} - \epsilon'_{1y}\epsilon'_{2x})$, $\Delta_{1y} = \epsilon'_{2x}/(\epsilon'_{1x}\epsilon'_{2y} - \epsilon'_{1y}\epsilon'_{2x})$, $\Delta_{2x} = \epsilon'_{1y}/(\epsilon'_{2x}\epsilon'_{1y} - \epsilon'_{1x}\epsilon'_{2y})$, $\Delta_{2y} = \epsilon'_{1x}/(\epsilon'_{2x}\epsilon'_{1y} - \epsilon'_{1x}\epsilon'_{2y})$, ϵ'_{1x} and ϵ'_{1y} are the apparent molar absorptivities of the reactants, and ϵ'_{2x} and ϵ'_{2y} are those of the products, at wavelengths x and y, respectively (Table I).

For the analysis of filtrates, 2-ml aliquots of reactions in the presence of liposomal suspensions were gently filtered using disposable cartridges[8] and a syringe. In the case of indomethacin and *p*-nitrophenyl acetate, 0.5 ml of the filtrate was mixed with 2 ml of cold 0.5 *M* formic acid in water–methanol (2:8). The procedure for cyclocytidine was identical, except that 0.2 *M* HCl in water–methanol (1:9) was employed instead of 0.5 *M* formic acid. Absorbances were measured in microcuvetes and the concentrations were determined using the ϵ values in Table I in Eqs. 1, 3, and 4 with $D = 5$. Total particle counts[9] which were 4×10^6/ml in the liposomal suspensions were reduced to background (<2000/ml) in the filtrate by this procedure.

Kinetics of Hydrolysis in Buffers and in Buffered Liposomal Suspensions—Rates of hydrolysis of cyclocytidine, indomethacin, and *p*-nitrophenyl acetate were studied at 40° in the aqueous buffers described in Table II. Aliquots were removed as a function of time and analyzed for concentrations.

Liposomal suspensions (Table II) were prepared as described and heated at 40° for 12 hr with constant agitation[10]. An aliquot of a stock solution of the reactant was then added to 12 ml of the liposomal suspension, which was maintained at 40° with continued agitation. At appropriate intervals aliquots of the mixture were removed, the reaction head-space flushed with nitrogen, and the samples were analyzed for total concentration in the liposomal suspension and also in the filtrate. Before, and after the reaction, 6-μl aliquots of the liposomal suspension were diluted with 10 ml of the same buffer in which they were prepared. One milliliter of this dilution was further diluted with 10 ml of buffer, and the particle size of the liposomes in this suspension was determined[9].

Hydrolysis rates in filtrates in the absence of liposomes were shown to be the same as those in their corresponding buffered solutions by using the following procedure. Sixteen milliliters of positively charged liposomal suspension was prepared using carbonate buffer and heated at 40° for 12 hr with constant agitation[10]. The suspension was centrifuged at 2600 rpm for 50 min, and the bulk of the liposomes that concentrated at the top of the mixture were removed[11]. Five milliliters of the remaining suspension was filtered through several disposable filter cartridges[8]. The filtrate was used to study the hydrolysis of indomethacin as described previously for aqueous buffers at 40°. This procedure was also employed to study the hydrolysis of *p*-nitrophenyl acetate in the filtrate obtained from positively charged liposomes prepared with phosphate buffer. No difference was observed between the rate constants in buffer and in the corresponding filtrate. These two reactions were chosen because they had shown the greatest change in rate constants in the presence of liposomes.

To estimate the maximum volume occupied by the liposomes in a suspension, 10 ml of a negatively charged suspension prepared in carbonate buffer was heated at 40° for 12 hr with constant agitation. The suspension was then heated for an additional 24 hr with no agitation. The liposomes that concentrated at the top were removed, and the volume of the remaining mixture was determined to be 9.2 ml.

RESULTS

Apparent First-Order Hydrolysis—Except for the loss of *p*-nitrophenyl acetate in the presence of positive liposomes (to be discussed), all kinetic data were adequately described by the first-order equation,

$$\ln C_t = \ln C_0 - k_{obs}t \quad \text{(Eq. 5)}$$

where t is time, C_0 and C_t are the reactant concentrations initially and at time t, and k_{obs} is the observed first-order rate constant.

Cyclocytidine—The sum of the cyclocytidine and cytarabine concentrations as a function of time equaled the initial concentration of cyclocytidine. If the ratio of the rate constant in the presence of liposome

[8] Millex-GS 0.22 μm Filter unit, Millipore Corp., Bedford, Mass.
[9] Elzone Model 80 XY, Particle Data Inc., Elmhurst, Ill.
[10] Submersion Rotator, Scientific Industries, Inc., Queens Village, N.Y.
[11] In these concentrated buffers, liposomes ascended on centrifugation. The direction was reversed if buffers were diluted tenfold before centrifuging.

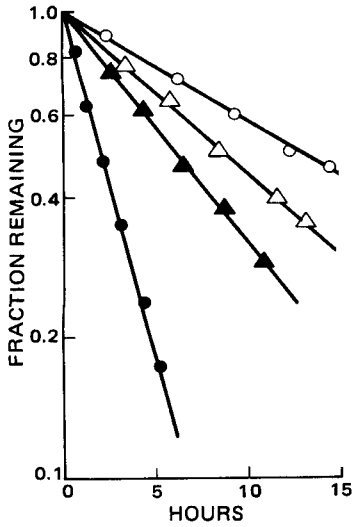

Figure 1—*First-order plot for fraction of indomethacin remaining in carbonate buffer, pH 9.37, (●) and in the presence of liposomes of negative (▲), neutral (△), or positive (○) charge at 40°.*

(k_L) to that in buffered solution (k_B) is defined as:

$$R_k = k_L/k_B \qquad \text{(Eq. 6)}$$

it is apparent that $R_k \simeq 1$ (Table II).

The filtrate concentration (C_F) can be compared with the corresponding concentration in the total liposomal suspension (C_T) using the ratio, R_C where:

$$R_C = [C_F/C_T]_{t_{0.5}} \qquad \text{(Eq. 7)}$$

Although the differences between C_F and C_T are small, the filtrate concentrations were consistently higher than the liposomal concentrations giving R_C values >1 (Table II). This may be due to a small decrease in volume by removal of the liposomes.

Indomethacin—The reduced rates of indomethacin hydrolysis in various liposomal suspensions as compared with that in liposome-free buffer are shown in Fig. 1. This reduction is reflected in the R_k values which are 0.156, 0.318, and 0.226 in positively charged, negatively charged, and neutral liposomal suspensions, respectively.

In negatively charged liposomes R_C = 0.28, and the first-order rate constant obtained from the filtrate data was k_F = 0.106 hr^{-1} (Fig. 2) which agrees with its corresponding k_L value. In filtrates from the neutral and positively charged liposomal suspensions, the low concentrations of indomethacin (relative to assay sensitivity) prevented the accurate estimation of first-order rate constants, k_F. However, average values for R_C could be estimated from the ratios of measured C_F to calculated C_T values. Since each ratio is comprised of a small numerator (C_F) and a large denominator (C_T), the variability in R_C is minimized (Fig. 3, Table II).

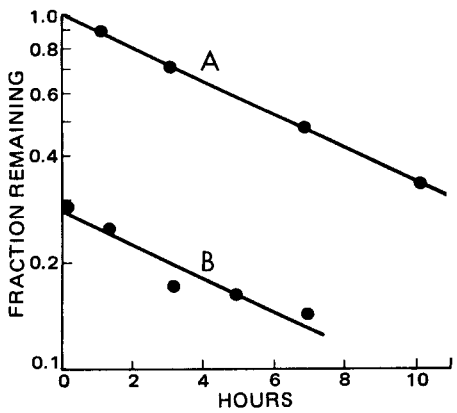

Figure 2—*Comparison of first-order plots for total indomethacin in a negatively charged liposomal suspension (A) to the fraction in the filtrates (B) at 40° in carbonate buffer, pH 9.37.*

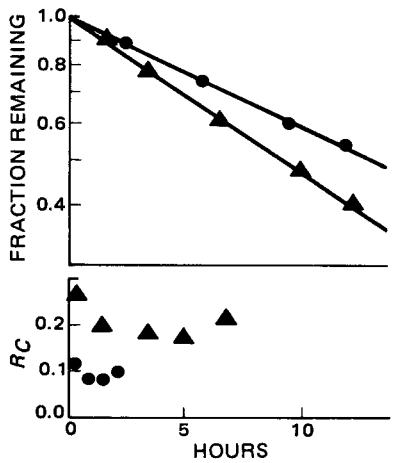

Figure 3—*Calculated R_C values for indomethacin as a function of time and their corresponding first-order plots in neutral (▲) and positively charged (●) liposomal suspensions at 40° in carbonate buffer, pH 9.37.*

p-Nitrophenyl Acetate—The sum of *p*-nitrophenyl acetate and *p*-nitrophenol concentrations as a function of time equaled the initial concentration of *p*-nitrophenyl acetate. The rate of loss of *p*-nitrophenyl acetate in phosphate buffer was decreased in neutral and negatively charged liposomal suspensions. This reduction is reflected in the R_k values of 0.740 and 0.688, respectively. The values of R_C are 0.144 and 0.086 for neutral and negatively charged liposomal suspensions respectively, and the first-order rate constants in the filtrates (k_F) are close to their respective k_L values (Table II).

Semilogarithmic plots of the concentration of *p*-nitrophenyl acetate in positively charged liposomal suspensions as a function of time showed a rapid initial decrease followed by a much slower loss. The biphasic curves were analyzed by the following equation:

$$F = Ae^{-\alpha t} + Be^{-\beta t} \qquad \text{(Eq. 8)}$$

where $F = C_t/C_0$, and $\alpha > \beta$ (Fig. 4). Nonlinear regression analyses provided average values of A = 0.406, B = 0.595, α = 0.233 min^{-1}, and β = 0.0341 min^{-1}. Experimental C_F values and calculated C_T values determined during the beta phase were used to calculate an average R_C value, of 0.508.

DISCUSSION

Cyclocytidine, indomethacin, or *p*-nitrophenyl acetate, in liposomal suspensions can hydrolyze in the bulk aqueous solution or in the liposomal phase. The association of reactant with the liposomal phase might occur in several ways. Those interactions that bring the compounds into the proximity of an organic environment can cause a change in the hydrolysis rate in accordance with the expected solvent effects (Fig. 5).

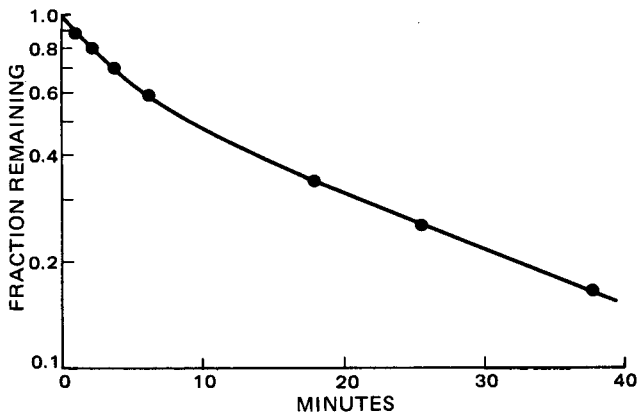

Figure 4—*Semilogarithmic plot for fraction of* p*-nitrophenyl acetate remaining as a function of time in positively charged liposomal suspension at 40° in phosphate buffer pH 7.51. Curve is drawn from nonlinear regression analysis based on Eq. 8.*

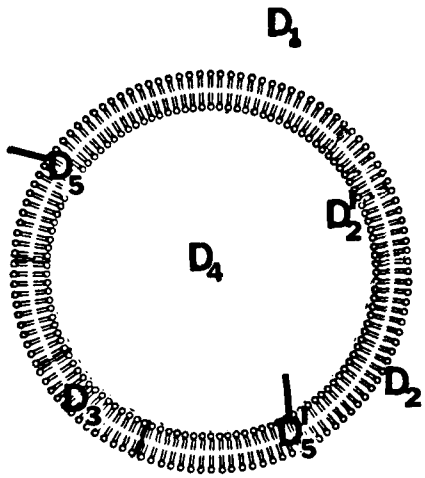

Figure 5—*Possible locations of a compound,* D, *in a liposomal suspension;* D_1 *is in the external aqueous phase;* D_2 *and* D'_2 *are associated with the outer and inner walls;* D_3 *is associated with the hydrocarbon portion of the lipid bilayers;* D_4 *is dissolved in the aqueous portions of the liposome; and* D_5 *and* D'_5 *are solubilized in the hydrocarbon portion of the lipid bilayer with portions protruding into the aqueous environments.*

Media with low ion-solvating power will inhibit the creation or concentration of charges while accelerating charge destruction (11). A change in rate would, therefore, depend on the reaction mechanism and the species involved.

The hydrolysis of cyclocytidine was not affected by the presence of liposomes as evidenced by the similarity between the values of the first-order hydrolysis rate constants determined in aqueous buffer (k_B), in liposomal suspensions (k_L), and using the data representing the filtered samples obtained from the reactions in suspensions (k_F, Table II). Assay of the filtrates accounted for the total drug in the liposomal suspensions. Cyclocytidine, a highly polar, water soluble, positively charged compound, probably resists association due to its hydrophilicity. This, in itself, would not preclude surface participation in the reaction rate. Positive and negative liposomal surfaces could affect reaction intermediates and/or transition states, in that positively charged liposomes would be expected to stabilize negatively charged species and *vice-versa*. Since hydroxyl anion attack on the cyclocytidine cation produces a neutral transition state, no sensitivity to surface charge would be anticipated.

In contrast, indomethacin in the presence of positively charged, negatively charged, and neutral liposomes, and *p*-nitrophenyl acetate in negatively charged and neutral liposomal suspensions all provide hydrolysis rate constants (k_L) that are slower than those in aqueous buffer (k_B). Since this loss can be described by the first-order equation:

$$\frac{-d(DT)}{dt} = k_L(DT) \qquad \text{(Eq. 9)}$$

where (DT) is the total amount of drug in the liposomal suspension at time t, and k_L is the apparent first-order rate constant for loss of drug, the simplest kinetic scheme (Scheme I) that can represent this data is:

$$DF \underset{}{\overset{\text{Fast}}{\rightleftharpoons}} DL$$
$$\downarrow k_B \qquad\qquad \downarrow k_\Delta$$

Scheme I

where (DF) is the drug in the bulk aqueous phase, (DL) is the drug associated with the liposomes and, k_B and k_Δ are the rate constants for the loss of drug from the bulk aqueous and liposomal phases, respectively. It is obvious that:

$$k_L(DT) = k_B(DF) + k_\Delta(DL) \qquad \text{(Eq. 10)}$$

and, therefore, the rate constant k_L can be described:

$$k_L = k_B f_B + k_\Delta k_L \qquad \text{(Eq. 11)}$$

where $f_B = (DF)/(DT)$, and $f_L = (DL)/(DT)$. A similar expression has been applied to the hydrolysis of a number of compounds in the presence of micelles (1). Since the volume occupied by the liposomes in these suspensions was found to be <10%, the ratio $R_C = [C_F]/[C_T]$ is approximately equal to $f_B = (DF)/(DT)$. Setting $f_L = (1 - f_B)$ and substituting R_C for f_B in Eq. 11 results in:

$$k_L = k_B(R_C) + k_\Delta(1 - R_C) \qquad \text{(Eq. 12)}$$

The rate constants for the hydrolysis of indomethacin in positively charged, negatively charged, and neutral liposomes (k_L) are 15.6, 31.8, and 22.6% of k_B. Indomethacin is associated with the liposomes to the extent of 90, 72, and 80% in positively charged, negatively charged, and neutral liposomes, respectively (R_C values, Table II). The extent of this association could be a function of electrostatic attraction. The negatively charged indomethacin molecules would be attracted to the positively charged liposomes to the greatest extent followed by the neutral liposomes, while the carboxylate anion would be repelled by the negatively charged liposomes. At the reaction pH, indomethacin is made up of a hydrophilic carboxylate anion and the remaining hydrophobic moiety. Thus, if indomethacin associates with the liposomes, it could be positioned at the interface of the aqueous bulk and the hydrocarbon portion of the lipid bilayer as shown in Fig. 5.

A similar effect has been reported for the hydrolysis of the sodium salt of mono-*p*-nitrophenyl dodecanedioate in micellar aggregates (12). By analogy to that study, the carboxylate anion of indomethacin could be in an aqueous environment, while the hydrophobic part containing the amide linkage could be stabilized in the hydrocarbon environment of the liposomes. In addition, the hydrolysis of indomethacin involves the attack of a hydroxide ion on the negatively charged molecule, thus causing the collection of similar charges in the transition state. This process would be inhibited by the bilipid layer.

The first-order rate constants for hydrolysis of *p*-nitrophenyl acetate in the presence of negatively charged and neutral liposomes are 68.8% and 74.0%, respectively, of that in the aqueous buffer. *p*-Nitrophenyl acetate is ~90% associated (Table II). Unlike indomethacin, *p*-nitrophenyl acetate does not have a formal charge. If *p*-nitrophenyl acetate associates with the liposomes, it would not selectively shield the ester linkage away from the aqueous environment. It has been shown in micellar phases, that compounds having a slight polar nature (such as nitrobenzene) are solubilized at the surface of a micelle rather than in the hydrocarbon interior (13, 14). Consequently, *p*-nitrophenyl acetate could be largely exposed to the aqueous environments both within the liposomes and at the bulk aqueous interface. This could account for the fact that ~90% association resulted in only an ~30% reduction in rate constant. Since hydroxide attack on *p*-nitrophenyl acetate would provide a negative transition state, electrostatic depression in hydrolysis rate would apply.

The decrease of *p*-nitrophenyl acetate concentration in the presence of positively charged liposomes is described by a biexponential equation in which the exponential coefficients, α and β, are 38.6 and 5.65 times faster, respectively, than k_B. This acceleration and biexponential hydrolysis rate might be attributed to elecrostatic stabilization of the negatively charged transition state by the positive charges on the surface of the liposomes in accordance with the following kinetic scheme (Scheme II):

$$DF \underset{}{\overset{\text{Fast}}{\rightleftharpoons}} DS \underset{k_d}{\overset{k_a}{\rightleftharpoons}} (DL')$$
$$\downarrow k_B \qquad \downarrow k_{cat} \qquad\qquad \downarrow k_\Delta$$

Scheme II

Table III—Percent Comparisons for Hydrolysis in Liposomal Suspension Relative to the Buffer ($100\ k_L/k_B$), Hydrolysis of Associated Reactant Relative to Free ($100\ k_\Delta/k_B$), Percentage of Reaction in the Associated Fraction ($100\ k_\Delta f_L/k_L$), and the Percent Associated ($100\ DL/DT$)

Reactant	Liposomal Charge	% = (100) Numerator/Denominator k_L/k_B	k_Δ/k_B	$k_\Delta f_L/k_L$	DL/DT
Cyclocytidine	(+ − 0)	95 ± 4	0	0	0
Indomethacin	(+)	16	6	36	90
	(−)	32	5	12	72
	(0)	23	3	12	80
p-Nitrophenyl acetate	(−)	69	66	88	91
	(0)	74	70	81	86

Surface catalysis has been suggested for the enhanced rate of hydrolysis of *p*-nitrophenyl hexanoate in solutions containing cationic micelles (15). Here, (*DF*) is in rapid pseudo equilibrium with (*DS*), the ester associated with the exterior surface (Fig. 4), (*DL'*) represents liposome–ester association by the remaining mechanisms, k_{cat} is the rate constant for hydrolysis of *p*-nitrophenyl acetate catalyzed by the positively charged liposomal surface, and k_a and k_d are the rate constants for the association and dissociation of (*DS*) with (*DL'*). Since the ratio $\alpha/\beta/k_B$ is 39:6:1 and R_C (beta phase) is ~0.5, it follows that $k_{cat} \gg k_B > k_\Delta$ and the simplest representation would be to set $(D_\Sigma) = (DF + DS)$ and $k_\Sigma = (k_B + k_{cat})$ allowing (Scheme III):

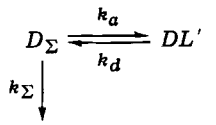

Scheme III

where k_Δ is considered insignificant relative to k_Σ. This is analogous to those cases discussed under Scheme I wherein liposome-associated reactant was stabilized relative to that in liposome-free buffer. Biexponential equations and the calculations for their individual rate constants in models described by Scheme III have been published (16). The fraction remaining, $F = (DT)/(DT)_0$, is given by:

$$F = \left(\frac{\alpha - k_a - k_d}{\alpha - \beta}\right) e^{-\alpha t} + \left(\frac{k_a + k_d - \beta}{\alpha - \beta}\right) e^{-\beta t} \qquad \text{(Eq. 13)}$$

which describes data of the shape shown in Fig. 4. Under these conditions, $k_\Sigma = A\alpha + B\beta = 6.9\ hr^{-1}$, $k_d = \alpha\beta/k_\Sigma = 4.2\ hr^{-1}$, and $k_a = \alpha + \beta - k_\Sigma - k_d = 5.0\ hr^{-}$. The phase ratio, $(DL')/(D_\Sigma)$ may be calculated from $k_a/(k_d - \beta) = 2.3$ (17) which can be used to estimate $R_C = C_F/C_T \simeq 0.3$. Although Scheme III is an oversimplification, the estimated rate constants are reasonable, the shape of Fig. 4 is consistent with Eq. 8, and the calculated R_C approaches that observed (R_C = 0.5, Table II).

Comparisons—While the net influence of liposomes on reaction rates is reflected by the k_L/k_B ratio (R_k, Eq. 6), an overall assessment requires concomitant examination of several aspects. The reactivity in the associated phase (*DL*) relative to that in the bulk aqueous phase (*DF*) is given by k_Δ/k_B, but the percentage contribution of each phase to the reaction (k_L) is 100 $k_\Delta f_L/k_L$ and 100 $k_B f_B/k_L$ rather than the percent of liposomal association (100 *DL/DT*) or the rate constants themselves. It is the competition between $k_\Delta f_L$ and $k_B f_B$ that controls the degree to which the overall process occurs in each phase. Collectively, the four parameters listed in Table III provide an aggregate interpretation of the total kinetic behavior, whereas any one of the components taken alone would be inadequate.

Although differences in pH preclude absolute comparisons of the three reactants, some outstanding contrasts can be noted (Table III). Liposomal association of cyclocytidine was not detected, and its hydrolysis rate constants in all four suspensions are approximately equal to that in the buffer. Both reactant distribution and hydrolysis appear limited to the aqueous bulk. In contrast, *p*-nitrophenyl acetate (in the presence of negative and neutral liposomes) shows 81–88% of the reaction occurring in the *DL* phase. This is the consequence of the percentage values being $k_L/k_B \approx k_\Delta/k_B \approx 70\%$ with 90% association. Rate constants for hydrolysis in the liposomal phases (k_Δ values in hr^{-1} calculated from Eq. 12) are 0.252 in neutral and 0.238 negatively charged liposomal suspensions. Thus, $k_B \approx 1.4k_\Delta$, but only 10% remains in the *DF* phase. Hydrolysis occurs primarily in the *DL* phase at a slightly reduced rate. This is consistent with the hypothesis that the associated ester remains largely accessible to the aqueous environment in the liposome.

Indomethacin is also highly associated (72–90%), but the values of k_Δ were ~0.02, 0.018, and ~0.01 hr^{-1} in positively charged, negatively charged, and neutral liposomes, respectively. In this case the percent of $k_L/k_B \approx 24\%$ since $k_\Delta/k_B \approx 5\%$. The high degree of association subjects most of the reactant to a greatly reduced rate constant. Only 12–36% of the process occurs in the *DL* phase. This provides a significant depression in the overall hydrolysis rate constant, but the reaction occurs primarily in the aqueous bulk. This reduced reactivity in the *DL* phase implies protection of the reactive center by liposomal association.

Thus, Table III provides examples of three different situations. In one case, cyclocytidine is limited to the aqueous buffer and no liposomal influence is observed. The remaining two cases are predominantly associated in roughly equivalent percentages but with differing consequences. Indomethacin reactivity is greatly reduced with only a minor contribution to the reaction occurring in the associated phase. *p*-Nitrophenyl acetate reactivity is slightly reduced occurring primarily in the associated phase where the rate constant is 70% of the constant for the aqueous bulk. The exception in this study is *p*-nitrophenyl acetate in positively charged liposomal suspensions which serve as catalysts to the ester hydrolysis as discussed in the previous section.

REFERENCES

(1) E. J. Fendler and J. H. Fendler, *Adv. Phys. Org. Chem.*, **8,** 271 (1970).

(2) S. Riegelman, *J. Pharm. Sci.*, **49,** 339 (1960).

(3) H. Nogami, S. Awazu, and N. Nakajima, *Chem. Pharm. Bull.*, **10,** 503 (1962).

(4) N. Nakajima, *Yakugaku Zasshi*, **81,** 1684 (1961).

(5) A. G. Mitchell and J. F. Broadhead, *J. Pharm. Sci.*, **56,** 1261 (1967).

(6) H. Krasowska, *Int. J. Pharm.*, **4,** 89 (1979).

(7) T. Yotsuyanagi, T. Hamada, H. Tomida, and K. Ikeda, *Acta Pharm. Suec.*, **16,** 325 (1979).

(8) T. Yotsuyanagi and K. Ikeda, *J. Pharm. Sci.*, **69,** 745 (1980).

(9) K. Fukuzawa, H. Chida, A. Tokumura, and H. Tsukatani, *Arch. Biochem. Biophys.*, **206,** 173 (1981).

(10) C. A. Hunt and S. Isang, *Int. J. Pharm.*, **8,** 101 (1981).

(11) J. Hine, "Physical Organic Chemistry," McGraw-Hill, New York, N.Y., 1956, p. 83.

(12) F. M. Menger and C. E. Portnoy, *J. Am. Chem. Soc.*, **89,** 4698 (1967).

(13) J. C. Eriksson and G. Gillberg, *Acta Chem. Scand.*, **20,** 2019 (1966).

(14) R. B. Dunlap and E. H. Cordes, *J. Am. Chem. Soc.*, **90,** 4395 (1968).

(15) L. R. Romsted and E. H. Cordes, *ibid.*, **90,** 4404 (1968).

(16) R. E. Notari, A. M. Burkman, and W. K. Van Tyle, *J. Pharm. Pharmacol.*, **26,** 481 (1974).

(17) P. R. Byron and R. E. Notari, *J. Pharm. Sci.*, **65,** 1140 (1976).

ACKNOWLEDGMENTS

The authors thank Dr. K. C. Kwan of Merck, Sharp and Dohme Research Laboratories, for supplying a sample of indomethacin, The Elsa U. Pardee Foundation for support in part of this research, and Dr. R. L. Juliano for helpful comments regarding the manuscript.

Dissolution-Controlled Transport from Dispersed Matrixes

S. K. CHANDRASEKARAN [‡§x] **and D. R. PAUL** [*]

Received June 8, 1981, from [*]*Alza Research, Palo Alto, CA 94304* and the [‡]*University of Texas, Austin, TX.* Accepted for publication February 19, 1982. [§]Present address: ABCOR, Inc., Wilmington, MA 01887.

Abstract □ A simplified mathematical model for dissolution-controlled transport from dispersed matrixes is presented. Analytical solutions have been obtained previously when solute diffusion totally controls the transport process. However, when solute dissolution offers the limiting resistance to mass transport, the solution reduces to a form where the mass released varies directly with time. Experimental release rates of a drug from a dispersed polymeric matrix into water were measured for a range of drug particle sizes in order to test the applicability of the proposed model; the agreement between theory and experimental is good.

Keyphrases □ Dissolution—transport from dispersed matrixes □ Matrixes—dispersed, dissolution-controlled transport □ Models, dissolution—dissolution-controlled transport from dispersed matrixes

The theory of diffusional release of a solute or therapeutic agent from a polymer matrix where the initial loading of solute is greater than the solubility limit was initially proposed by Higuchi (1). Several assumptions were made in this model: (*a*) the suspended solute is present as particles of diameter much smaller than the thickness of the matrix; (*b*) the receptor medium is immiscible with the matrix and serves as a perfect sink for the released solute; and (*c*) a pseudo steady-state condition exists during the transport process. More recently the pseudo steady-state assumption in Higuchi's model was reexamined (2) and it was concluded that an exact analysis offered some advantages under conditions of low solute loadings but became virtually identical with Higuchi's analysis for large solute loadings.

The Higuchi model has been applied extensively in the literature with favorable results (2–6). However, there have been several cases in which the drug release-rate kinetics from drug-dispersed matrixes are not adequately described by this model. The *in vitro* release rate of steroids from silicone elastomeric matrixes was studied (7), and it was found that their results were inconsistent with the Higuchi model. Based on the effect of concentration and particle size on the duration of drug release, a dissolution rather than diffusion-controlled mechanism was suggested. It was determined (8) that the release rate of salicylic acid from ointment bases did not follow the Higuchi model, and the discrepancy was related to an inadequate dissolution rate of the suspended particles. The release of benzocaine from ointment bases was determined (9) and it was found that the release rate was not proportional to the square root of drug concentration.

Several theories have been put forth for dissolution-controlled transport mechanisms. The area of drug release rate processes in biopharmaceutics was reviewed (10), in which dissolution mechanisms are considered as a heterogeneous reaction with mass transfer occurring through the movement of solute molecules from solid surfaces. The thermodynamics of drug release from polymeric matrixes was studied (11) and the process was depicted to involve three energy-activated steps: (*a*) dissociation of drug molecules from a crystal lattice, (*b*) solubilization of drug molecules in the polymer matrix, and (*c*) diffusion of drug molecules in the matrix. More recently a good mathematical model for drug release from suspensions was developed (12, 13), which is relatively complex and requires numerical techniques to obtain general solutions. In that study the dissolution rate of a drug in a vehicle and diffusion through the vehicle was related to drug distribution and cummulative drug uptake by a receptor phase. When dissolution is essentially nonexistent, it was found that the suspension behaved as a solution with respect to drug release, whereas when dissolution is slower than diffusion, the rate of dissolution markedly influenced the rate of drug release.

The purpose of the present study was to develop a simplified model for dissolution-controlled transport from dispersed matrixes. Analytical solutions to the complicated phenomenon of combined dissolution and diffusion mechanisms have been derived, and the results are related to experimental measurements.

THEORETICAL

A combined dissolution and diffusion-controlled transport system is shown in Fig. 1. As an approximation, the controlled release system is depicted in one dimension as a semi-infinite medium. The kinetics of dissolution is assumed to be given by an expression which is proportional

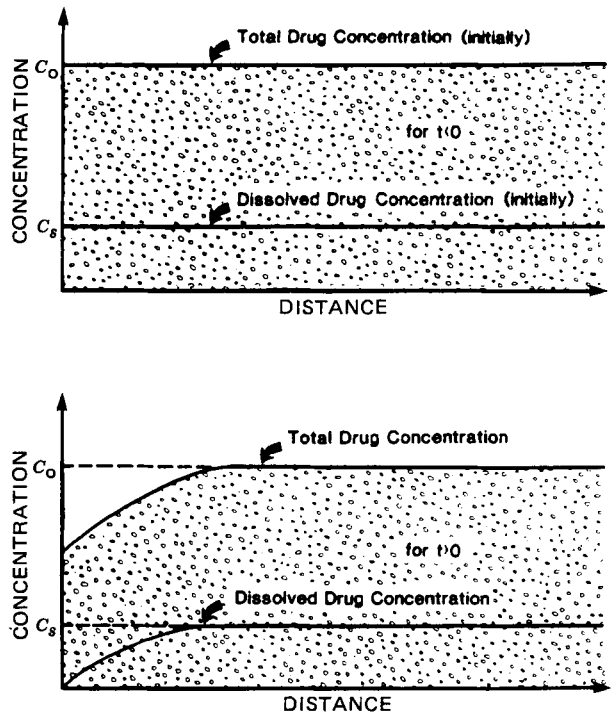

Figure 1—*Drug concentration profiles within the matrix.*

0022-3549/82/1200-1399$01.00/0

to the difference between the solubility of the solute in the matrix and the actual concentration of the solute in the matrix at the point in space. Under these conditions, the equation incorporation of both dissolution and diffusion in the mass transport process can be given to a first approximation by (12, 14):

$$\frac{\partial C}{\partial t} = D\frac{\partial^2 C}{\partial x^2} + K(C_s - C) \quad \text{(Eq. 1)}$$

where D is the solute diffusivity in the matrix, C is the concentration, C_s is the solute solubility, and K is the solute dissolution rate constant. The appropriate boundary conditions for dissolved solute with respect to time and distance are:

(*a*) $C = 0$ at $x = 0$ for all t;

(*b*) $C = C_s$ at $t = 0$ for all x.

Defining $\overline{C}$:

$$\overline{C} = C_s - C \quad \text{(Eq. 2)}$$

Equation 1 can be transformed to read:

$$\frac{\partial \overline{C}}{\partial t} = D\frac{\partial^2 \overline{C}}{\partial x^2} - K\overline{C} \quad \text{(Eq. 3)}$$

with boundary conditions:

(*a*) $\overline{C} = C_s$ at $x = 0$ for all t;

(*b*) $\overline{C} = 0$ at $t = 0$ for all x.

The analytical solution of Eq. 3 is given by (14):

$$\frac{\overline{C}}{C_s} = \tfrac{1}{2}\exp(-x\sqrt{K/D})\,\mathrm{erfc}\left(\frac{x}{2\sqrt{Dt}} - \sqrt{Kt}\right) + \tfrac{1}{2}\exp(x\sqrt{K/D})\,\mathrm{erfc}\left(\frac{x}{2\sqrt{Dt}} + \sqrt{Kt}\right) \quad \text{(Eq. 4)}$$

and

$$M_t = C_s\sqrt{D/K}\left[(Kt + \tfrac{1}{2})\,\mathrm{erf}\sqrt{Kt} + \sqrt{\frac{Kt}{\pi}}\exp - Kt\right] \quad \text{(Eq. 5)}$$

where M_t is the mass released per unit area at time t.

The total mass of solute per unit area is given by:

$$M_\infty = \frac{C_0 l}{2} \quad \text{(Eq. 6)}$$

where C_0 is the total solute loading and l is the thickness of the finite slab. The model assumptions will not be met when l is very small.

The fractional amount of solute released at any time t is now given by:

$$\frac{M_t}{M_\infty} = 2\frac{C_s}{C_0}\sqrt{\frac{D}{Kl^2}}\left[(Kt + \tfrac{1}{2})\,\mathrm{erf}\sqrt{Kt} + \sqrt{\frac{Kt}{\pi}}\exp - Kt\right] \quad \text{(Eq. 7)}$$

The ratio M_t/M_∞ can take values >1 for long enough time periods, since M_t is unbounded because of the semi-infinite medium assumption. The solution is only applicable when there is undissolved solute at every point. Thus, Eq. 7 is only valid for:

$$C_s Kt \le C_0 \quad \text{(Eq. 8)}$$

Under conditions when Kt assumes large values and solute dissolution is offering the limiting control to the transport process, Eq. 7 reduces to (12, 14):

$$\frac{M_t}{M_\infty} = 2\frac{C_s}{C_0}\sqrt{\frac{DK}{l^2}}\left(\frac{1}{2K} + t\right) \quad \text{(Eq. 9)}$$

In this case, the mass, M_t, varies linearly with time. However, under conditions when Kt assumes small values and solute diffusion is controlling mass transport totally, Eq. 7 reduces to:

$$\frac{M_t}{M_\infty} = 4\frac{C_s}{C_0}\left(\frac{Dt}{\pi l^2}\right)^{1/2} \quad \text{(Eq. 10)}$$

which is roughly similar to the solution originally obtained by Higuchi (1).

The release rate of solute for small times is given by:

$$\frac{dM_t/M_\infty}{dt} = 2\frac{C_s}{C_0}\sqrt{\frac{DK}{l^2}}\left(\mathrm{erf}\sqrt{Kt} + \frac{1}{\sqrt{\pi Kt}}\exp - Kt\right) \quad \text{(Eq. 11)}$$

Similarly, under conditions when Kt assumes large values and solute dissolution is offering the limiting control to the overall transport process, Eq. 11 reduces to:

$$\frac{dM_t/M_\infty}{dt} = 2\frac{C_s}{C_0}\sqrt{\frac{DK}{l^2}} \quad \text{(Eq. 12)}$$

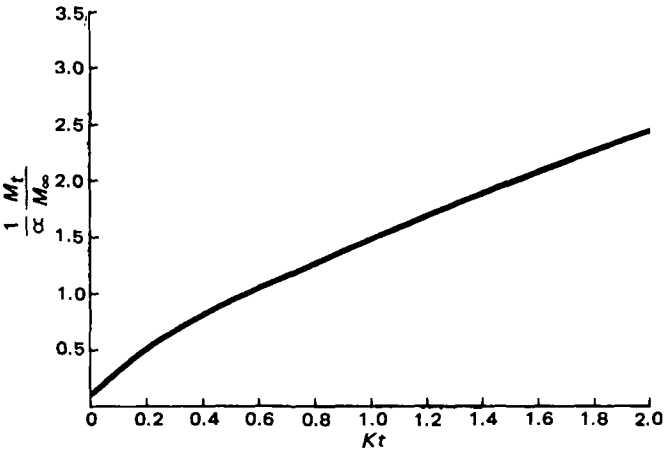

Figure 2—*Variation of* M_t/M_∞ *with* Kt ($\alpha = 2C_s/C_0\sqrt{D/Kl^2}$).

However, when Kt assumes small values and solute diffusion is controlling mass transport, Eq. 11 reduces to:

$$\frac{dM_t/M_\infty}{dt} = 2\frac{C_s}{C_0}\left(\frac{D}{\pi l^2 t}\right)^{1/2} \quad \text{(Eq. 13)}$$

The implications of Eqs. 7 and 11 can be seen in Figs. 2 and 3, where the cummulative mass released and the release rate are plotted as a function of Kt. The release rate is strongly dependent upon Kt in the region where $Kt < 0.3$, after which the release rate becomes almost independent of Kt.

EXPERIMENTAL

Preparation of Monolithic Systems—Solute-dispersed monolithic matrixes were prepared by a solvent casting procedure (15). Polyisobutylene and mineral oil were dissolved in heptane at room temperature and to this solution was added a drug of varied particle size so as to obtain a total solids content in the solution of ~25% by weight. At this concentration, the solution had a suitable viscosity to facilitate casting on a polyester substrate using a gardner knife set-up (15). The cast films were allowed to set at room temperature and subsequently oven dried at 50° to remove the residual traces of heptane. The residual solvent levels were always <100 ppm.

The thickness of the dried films were measured using a thickness gauge and were found to be relatively uniform (50 ± 5 μm). The drug content in the films was determined by dissolving the dried films in heptane followed by extraction into dilute sulfuric acid and subsequent analysis using liquid chromatography. The average particle size of the drug was obtained by specific surface area analysis using a gas absorption (Brunayer, Emmett, and Teller) technique (16).

Release Rate Determinations—The drug release rates as a function of time were determined using a special thermostated holder and bath assembly. The monolithic systems were attached to a suitable sample holder and suspended from a vertically reciprocating shaker such that each system was continuously immersed in a test tube containing 15 ml

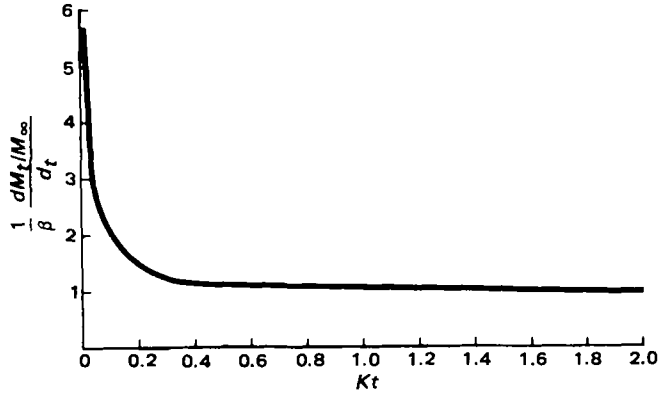

Figure 3—*Variation of* $dM_t/M_\infty/dt$ *with* Kt ($\beta = 2C_s/C_0\sqrt{DK/l^2}$).

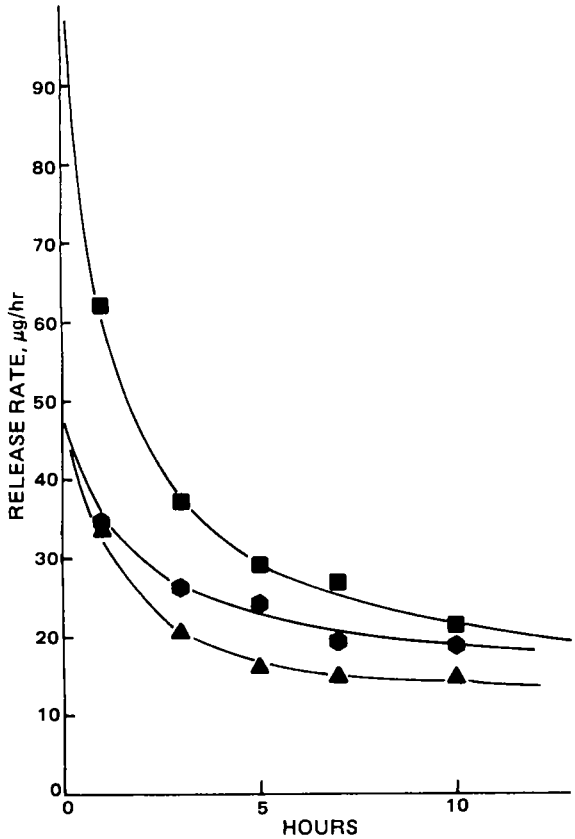

Figure 4—*Drug release rate* versus *time profiles. Key: (■) 2.5 μm; (●) 7.8 μm; (▲) 9.9 μm.*

of water equilibrated at 32.0 ± 0.3°. Agitation was at a frequency of 0.5 cycle/sec with an amplitude of 20–25 mm. At each time interval the systems were transferred to fresh tubes containing 15 ml of water preequilibrated to 32.0 ± 0.3°. Drug concentrations in the solutions were determined using liquid chromatography.

RESULTS

The *in vitro* drug release rate *versus* time profiles for the various monolithic systems are shown in Fig. 4. Three different average particle sizes were used: 2.5, 7.8, and 9.9 μm. The release-rate profile is dependent on particle size, increasing with decreasing particle size; however, the relative flatness of the pseudo steady-state portion of the curve improves markedly with increasing particle size. These results were analyzed using the typical Higuchi model, and assuming that drug diffusion is the controlling mechanism. The apparent drug diffusivity was computed utilizing (1):

$$\frac{1}{A}\frac{dM_t}{dt} = \left(\frac{DC_sC_0}{2}\right)^{1/2} t^{1/2} \qquad \text{(Eq. 14)}$$

where C_0 is the initial drug loading in the matrix.

The normalized flux, DC_s, as a function of drug particle size, is shown in Fig. 5. At the same drug loading, the value of DC_s decreases with increasing particle size, suggesting the presence of a secondary mechanism affecting drug diffusion. As infinite sink conditions were maintained during the release-rate measurements and boundary layer affects were held to a minimum by adequate stirring, drug particle dissolution was considered to be the secondary mechanism.

The apparent drug dissolution rate constant was computed following the procedure outlined in *Theoretical*, together with the normalization of drug diffusivity to zero particle size, *i.e.*, totally dissolved state. These results are presented in Fig. 6, where the dissolution rate constant is plotted as a function of drug particle size. It is apparent that the dissolution rate constant decreases with increasing particle size with a limiting value of $\sim 35 \times 10^{-7}$ sec^{-1} for an infinitely small particle size. Also shown in Fig. 6 is the limiting Sherwood Number (SH = kd/D) relationship normalized to 10 μm (17). The separation between the two lines is probably indicative of the deviation from infinite sink conditions maintained within the matrix.

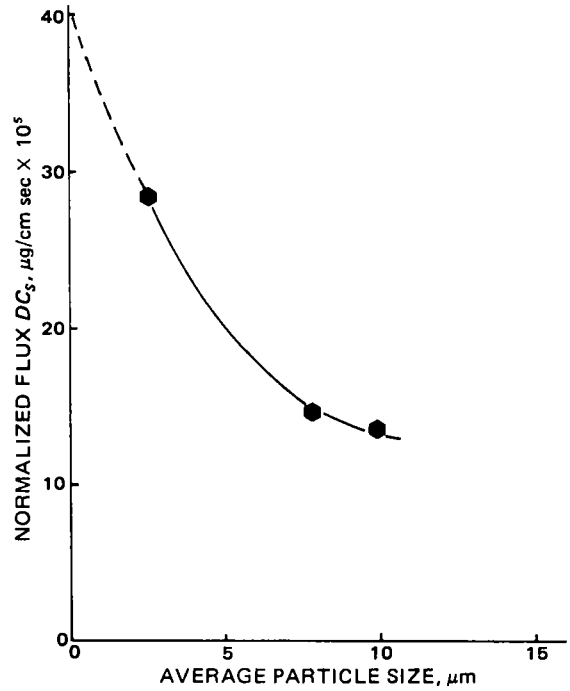

Figure 5—*Effect of particle size on normalized flux.*

CONCLUSIONS

A simplified model for dissolution-controlled transport from dispersed matrixes has been presented. Analytical solutions to the combined phenomenon of dissolution and diffusion mechanisms have been derived. At the limit when diffusion totally controls the mass transport, the solution reduces to a form with the mass released having a square-root dependency with time. However, when solute dissolution offers the

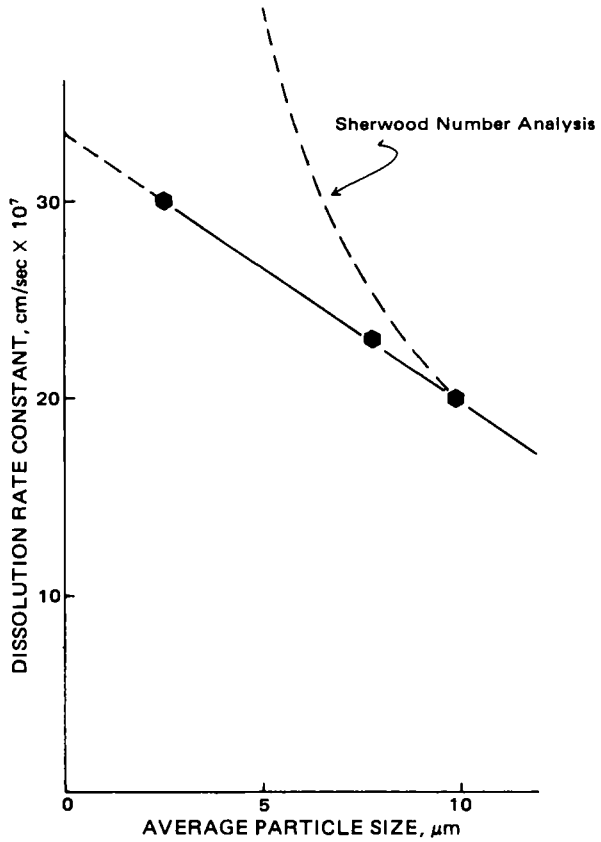

Figure 6—*Effect of particle size on dissolution rate constant.*

limiting resistance to mass transport, the solution reduces to form where the mass released varies directly with time. Under these conditions, the release rate of a dispersed solute would become time independent.

The simplified model can be viewed as an extension of the familiar Higuchi model (1) for drug release from ointments and suspensions. In the region of small time, the conclusions presented here are in agreement with previous studies (12, 13). However, the application of this model is considerably simplified compared to the system presented previously (12, 13), which is more complex and results in equations that do not predict a simple relationship between the various parameters.

Experimental release-rate measurements have been conducted with monolithic systems where the particle size of the dispersed solute has been varied. The results can be adequately analyzed using the proposed mathematical model and indicate that the mass transport resistance offered by particle dissolution increases with increasing particle size. However, the release rate approaches a pseudo steady-state and becomes time independent with this increasing resistance offered to the mass transport process by particle dissolution. This information can be utilized in the design and development of controlled-release formulations.

REFERENCES

(1) T. Higuchi, *J. Soc. Cosmet. Chem.*, **11**, 85 (1960).

(2) D. R. Paul and S. K. McSpadden, *J. Mem. Sci.*, **1**, 33 (1976).

(3) W. I. Higuchi and T. Higuchi, *J. Pharm. Sci.*, **49**, 598 (1960).

(4) T. Higuchi, *ibid.*, **50**, 874 (1961).

(5) T. Higuchi, *ibid.*, **52**, 1145 (1963).

(6) S. Borodkin and F. E. Tucker, *ibid.*, **63**, 1359 (1974).

(7) J. Haleblain, R. Runkel, N. Mueller, J. Christopherson, and K. Ng, *ibid.*, 60, 541 (1971).

(8) F. Bottari, G. DiColo, E. Nannipieri, M. F. Saettone, and M. F. Serafini, *ibid.*, **63**, 1779 (1974).

(9) J. W. Ayres and P. A. Laskar, *ibid.*, 63, 1403 (1974).

(10) W. I. Higuchi, *ibid.*, 56, 315 (1967).

(11) Y. W. Chien, in "Controlled Release Polymeric Formulations," D. R. Paul and F. W. Harris, Eds., ACS Symposium Series 33, American Chemical Society, Washington, D.C., 1976.

(12) J. W. Ayres and F. T. Lindstrom, *J. Pharm. Sci.*, **66**, 654 (1977).

(13) F. T. Lindstrom and J. W. Ayres, *ibid.*, **66**, 662 (1977).

(14) J. Crank, "The Mathematics of Diffusion," Clarendon Press, Oxford, England, 1975.

(15) S. K. Chandrasekaran and J. E. Shaw, in "Contemporary Topics in Polymer Science," vol. 2, Plenum Press, New York, N.Y. 1977, p. 291.

(16) R. Gale, S. K. Chandrasekaran, S. Swanson, and J. Wright, *J. Mem. Sci.*, **7**, 319 (1980).

(17) R. B. Bird, W. E. Stewart, and E. N. Lightfoot, "Transport Phenomena," Wiley, New York, N.Y., 1960.

ACKNOWLEDGMENTS

The authors thank R. Hillman and F. Knox for helpful discussions.

Determination of Enviroxime in a Variety of Biological Matrixes by Liquid Chromatography with Electrochemical Detection

RONALD J. BOPP ˣ **and DAVID J. MINER**

Received November 12, 1981, from the *Analytical Development Department, Lilly Research Laboratories, Eli Lilly and Co., Indianapolis, IN 46285.* Accepted for publication February 16, 1982.

Abstract □ A simple and specific method has been developed for determination of enviroxime in biological samples. Enviroxime, a substituted benzimidazole, its coisomer zinviroxime, and the internal standard hexestrol were extracted from the samples with benzene. The benzene layer was evaporated and the residue was reconstituted and injected onto a liquid chromatograph. Reversed-phase chromatography on an octylsilane column with a 65% methanol–35% 0.14 *M* sodium acetate mobile phase separated the components. The compounds were detected electrochemically using a glassy carbon electrode held at +0.85 V. The assay could detect as little as 4 ng of enviroxime/ml of plasma, 15 ng/ml of nasal wash, and 20 ng/ml of urine or tissue homogenate. For plasma assays, the procedure was >97% accurate and had a relative standard deviation of <4%. This method has proven to be applicable and reliable for the determination of enviroxime in many types of biological samples. Several problems encountered during the routine use of electrochemical detection were explored and minimized.

Keyphrases □ Enviroxime—determination in a variety of biological matrixes by liquid chromatography with electrochemical detection □ Electrochemical detection—determination of enviroxime in a variety of biological matrixes by liquid chromatography □ Liquid chromatography—determination of enviroxime in a variety of biological matrixes with electrochemical detection

Enviroxime, anti-6-[(hydroxyimino)phenyl]methyl-1-(1-methylethyl)sulfonyl-1*H*-benzimidazole-2-amine (I), has been shown to be a highly specific inhibitor of the multiplication of rhinovirus in tissue cultures (1, 2):

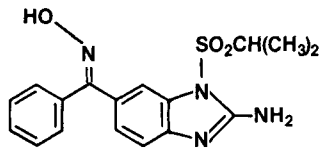

I

Compound I has undergone extensive metabolic and toxicological studies in dogs and rats (3, 4) and is currently being evaluated as a treatment for the common cold (5).

In early work with I in dogs and mice, blood levels were determined using a plaque reduction assay. Plaque assays are nonspecific, since they are capable only of determining antiviral activity. To determine levels of I in the presence of the less active syn–oxime isomer, zinviroxime (II), it was necessary to develop a chemical assay. Initial experiments aimed at developing a GC assay for I and II indicated that such an approach was undesirable. Derivatization of the oxime group was required to make I and II volatile enough. However, such a derivatization eliminated the hydrogen bonding capability of this group and, thus, made the separation of I and II quite difficult. Recently, a method was reported which used high-performance liquid chromatography (HPLC) with UV detection for the determination

0022-3549/82/1200-1402$01.00/0

limiting resistance to mass transport, the solution reduces to form where the mass released varies directly with time. Under these conditions, the release rate of a dispersed solute would become time independent.

The simplified model can be viewed as an extension of the familiar Higuchi model (1) for drug release from ointments and suspensions. In the region of small time, the conclusions presented here are in agreement with previous studies (12, 13). However, the application of this model is considerably simplified compared to the system presented previously (12, 13), which is more complex and results in equations that do not predict a simple relationship between the various parameters.

Experimental release-rate measurements have been conducted with monolithic systems where the particle size of the dispersed solute has been varied. The results can be adequately analyzed using the proposed mathematical model and indicate that the mass transport resistance offered by particle dissolution increases with increasing particle size. However, the release rate approaches a pseudo steady-state and becomes time independent with this increasing resistance offered to the mass transport process by particle dissolution. This information can be utilized in the design and development of controlled-release formulations.

REFERENCES

(1) T. Higuchi, *J. Soc. Cosmet. Chem.*, **11**, 85 (1960).

(2) D. R. Paul and S. K. McSpadden, *J. Mem. Sci.*, **1**, 33 (1976).

(3) W. I. Higuchi and T. Higuchi, *J. Pharm. Sci.*, **49**, 598 (1960).

(4) T. Higuchi, *ibid.*, **50**, 874 (1961).

(5) T. Higuchi, *ibid.*, **52**, 1145 (1963).

(6) S. Borodkin and F. E. Tucker, *ibid.*, **63**, 1359 (1974).

(7) J. Haleblain, R. Runkel, N. Mueller, J. Christopherson, and K. Ng, *ibid.*, 60, 541 (1971).

(8) F. Bottari, G. DiColo, E. Nannipieri, M. F. Saettone, and M. F. Serafini, *ibid.*, **63**, 1779 (1974).

(9) J. W. Ayres and P. A. Laskar, *ibid.*, 63, 1403 (1974).

(10) W. I. Higuchi, *ibid.*, 56, 315 (1967).

(11) Y. W. Chien, in "Controlled Release Polymeric Formulations," D. R. Paul and F. W. Harris, Eds., ACS Symposium Series 33, American Chemical Society, Washington, D.C., 1976.

(12) J. W. Ayres and F. T. Lindstrom, *J. Pharm. Sci.*, **66**, 654 (1977).

(13) F. T. Lindstrom and J. W. Ayres, *ibid.*, **66**, 662 (1977).

(14) J. Crank, "The Mathematics of Diffusion," Clarendon Press, Oxford, England, 1975.

(15) S. K. Chandrasekaran and J. E. Shaw, in "Contemporary Topics in Polymer Science," vol. 2, Plenum Press, New York, N.Y. 1977, p. 291.

(16) R. Gale, S. K. Chandrasekaran, S. Swanson, and J. Wright, *J. Mem. Sci.*, **7**, 319 (1980).

(17) R. B. Bird, W. E. Stewart, and E. N. Lightfoot, "Transport Phenomena," Wiley, New York, N.Y., 1960.

ACKNOWLEDGMENTS

The authors thank R. Hillman and F. Knox for helpful discussions.

Determination of Enviroxime in a Variety of Biological Matrixes by Liquid Chromatography with Electrochemical Detection

RONALD J. BOPP ˣ **and DAVID J. MINER**

Received November 12, 1981, from the *Analytical Development Department, Lilly Research Laboratories, Eli Lilly and Co., Indianapolis, IN 46285.* Accepted for publication February 16, 1982.

Abstract □ A simple and specific method has been developed for determination of enviroxime in biological samples. Enviroxime, a substituted benzimidazole, its coisomer zinviroxime, and the internal standard hexestrol were extracted from the samples with benzene. The benzene layer was evaporated and the residue was reconstituted and injected onto a liquid chromatograph. Reversed-phase chromatography on an octylsilane column with a 65% methanol–35% 0.14 *M* sodium acetate mobile phase separated the components. The compounds were detected electrochemically using a glassy carbon electrode held at +0.85 V. The assay could detect as little as 4 ng of enviroxime/ml of plasma, 15 ng/ml of nasal wash, and 20 ng/ml of urine or tissue homogenate. For plasma assays, the procedure was >97% accurate and had a relative standard deviation of <4%. This method has proven to be applicable and reliable for the determination of enviroxime in many types of biological samples. Several problems encountered during the routine use of electrochemical detection were explored and minimized.

Keyphrases □ Enviroxime—determination in a variety of biological matrixes by liquid chromatography with electrochemical detection □ Electrochemical detection—determination of enviroxime in a variety of biological matrixes by liquid chromatography □ Liquid chromatography—determination of enviroxime in a variety of biological matrixes with electrochemical detection

Enviroxime, anti-6-[(hydroxyimino)phenyl]methyl-1-(1-methylethyl)sulfonyl-1*H*-benzimidazole-2-amine (I), has been shown to be a highly specific inhibitor of the multiplication of rhinovirus in tissue cultures (1, 2):

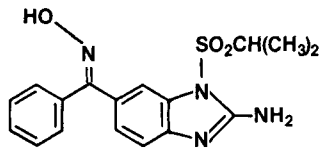

I

Compound I has undergone extensive metabolic and toxicological studies in dogs and rats (3, 4) and is currently being evaluated as a treatment for the common cold (5).

In early work with I in dogs and mice, blood levels were determined using a plaque reduction assay. Plaque assays are nonspecific, since they are capable only of determining antiviral activity. To determine levels of I in the presence of the less active syn–oxime isomer, zinviroxime (II), it was necessary to develop a chemical assay. Initial experiments aimed at developing a GC assay for I and II indicated that such an approach was undesirable. Derivatization of the oxime group was required to make I and II volatile enough. However, such a derivatization eliminated the hydrogen bonding capability of this group and, thus, made the separation of I and II quite difficult. Recently, a method was reported which used high-performance liquid chromatography (HPLC) with UV detection for the determination

0022-3549/82/1200-1402$01.00/0

of several benzimidazoles in body fluids (6). However, UV detection did not have the necessary sensitivity or specificity for the determination of I at nanogram levels in biological media.

This paper describes a sensitive and selective determination of I and II in biological fluids and tissues which is based upon HPLC with electrochemical detection. This method has proven to be extremely versatile and reliable during several years of use.

EXPERIMENTAL

Reagents—Enviroxime, *anti*-6-[(hydroxyimino)phenyl]methyl-1-(1-methylethyl)sulfonyl-1*H*-benzimidazole-2-amine (I), zinviroxime, *syn*-6-[(hydroxyimino)phenyl]methyl -1- (1-methylethyl)sulfonyl-1*H*-benzimidazole-2-amine (II), and hexestrol (III), were used as received[1]. All organic solvents were distilled in glass[2]. Distilled deionized water was used for preparation of the mobile phases. Blank plasma was separated from fresh heparinized blood of animals or human volunteers. The plasma samples were stored at 4° and used within 1 month. All other reagents were analytical grade. A stock solution of I and II was prepared fresh daily. One milligram of each isomer was weighed into a 10-ml volumetric flask and diluted to volume with methanol. These solutions were then diluted 1:100 with methanol–water (50:50) to give final concentrations of 1 μg/ml.

Equipment—The HPLC system consisted of a solvent delivery pump[3], an autoinjector[3], a guard column[3] packed with pellicular packing[4], a 250 × 4.6-mm column packed with 6-μm octylsilane reversed-phase material[5], a column temperature controller[6], and an electrochemical detector[6]. Detector response was recorded on a strip chart recorder and monitored by a central chromatographic data acquisition computer system. The detector potential was maintained at +0.85 V *versus* an Ag–AgCl–3 *M* NaCl reference electrode. The mobile phase consisted of methanol and 0.14 *M* sodium acetate (65:35) with 3 mg of disodium edetate added per liter. This mixture was filtered through a 0.2-μm pore nylon membrane filter[7] and deaerated by sonicating under vacuum. The flow rate was set at 0.9 ml/min, and the column temperature was maintained at 28°.

Some determinations required the addition of column-switching equipment. For this purpose a pneumatically actuated switching valve[8], which had a high-performance 3-cm reversed-phase precolumn[8] instead of a sample loop, was interposed between the automatic injector and the guard/analytical column. A second HPLC pump[9] was connected to this valve. Connections were made so that with the valve in one position the precolumn was in line with the main HPLC system, and in the other position it was connected to the auxiliary pump and to waste. The position of this valve was controlled by a digital timer[10] and a conventional electric solenoid. The timing was set so that the precolumn was in line for 40 sec, and then was out of line for the remainder of a chromatogram. During the latter time the auxiliary pump was turned on so that the mobile phase backflushed the precolumn at 2 ml/min.

Sample Preparation—A 1.0-ml or smaller sample of each plasma, urine, nasal washing, bile, or tissue homogenate was transferred into an individual tube. If necessary the pH was adjusted to ~7.5 by addition of dibasic potassium phosphate. Eleven and a half milliliters of benzene was added and the tubes were capped and rotated at 60 rpm for 40 min. After briefly centrifuging, as much as possible of the benzene was transferred to a second tube. The benzene layer was washed with 0.5 ml of 1 *M* potassium phosphate, pH 11.5. Ten milliliters of benzene was removed to a third tube, 0.1 ml of a 500-ng hexestrol/ml of chloroform solution was added, and the benzene was evaporated at 37° under nitrogen. The residue was reconstituted over a 15-min period with 200 μl of mobile phase. A 110-μl sample was injected onto the HPLC using injection vials equipped with microsample inserts[11]. For relatively interference free samples (plasma and nasal washings), the internal standard was added at the beginning and the pH 11.5 wash step was omitted. Conjugates of I and II were determined indirectly by overnight incubation of the samples at pH 4.0 and 37° with 10 μl of a glucuronidase–sulfatase preparation[12].

Table I—Recoveries of Drugs after Benzene Extraction

	% Recovery as Compared with Nonextracted Standards			
	Water[a]		Plasma[b]	
Compound	200 ng/ml	20 ng/ml	200 ng/ml	20 ng/ml
I	92	91	89	84
II	93	90	89	87
III	97	94	80	70

[a] $N = 5$. [b] $N = 10$.

The concentration of the drugs in the samples was calculated by comparison with calibration curves which were prepared by adding known amounts of drug to the appropriate blank media. Standards were extracted and chromatographed together with the samples. Typical calibration curves for plasma consisted of 5 points over the 20–100 ng/ml range. A linear least-squares analysis of the concentration *versus* peak height ratio (compound–internal standard) data was used to calculate the amount of I and II in the unknowns.

Electrochemistry—Cyclic voltammetry was performed using a conventional cell and electronics[13] with a glassy carbon working electrode. Chromatographically assisted hydrodynamic voltammetry was done as previously described (7).

RESULTS AND DISCUSSION

Choice of Assay Parameters—A variety of solvents were evaluated for their ability to efficiently extract I from water and plasma. Butyl chloride and hexane provided clean plasma extracts but did not extract the drug well. Ether and methylene chloride extracted I nearly quantitatively, but they also extracted a large number of endogenous components which interfered with subsequent chromatographic determination of I and II. Benzene and chloroform extracts of plasma were relatively clean, and the recovery of I and II was good. Benzene was chosen as the solvent for extractions since it is less dense than water, which eased solvent transfer, and because it extracted less of a late-eluting interference than did chloroform. It was found that toluene might be substituted for benzene, but lower recoveries are obtained and evaporation of solvent extracts requires twice as much time.

Extractions of I, II, and III from water into benzene were carried out over a wide pH range. Little or no effect of pH was noted in the 3–11.5 range. Extraction efficiency of all three compounds decreased significantly at >pH 11.5, as did the efficiency of extraction of I and II at <pH 2.0. A pH of 7.5 was used for convenience and to minimize coextraction of acidic or basic endogenous species from biological samples. The recovery of I, II, and III from both water and plasma at pH 7.5 is given in Table I. No difference in extraction efficiency was observed for I and II at 20 ng/ml *versus* 200 ng/ml. In contrast, the extraction efficiency of the internal standard (III) from plasma was lower at the lower concentration. To minimize the contribution of III to assay variability, ≥50 ng was used in this assay. Not surprisingly, the recovery of I and II from plasma was slightly lower than from water.

The good recovery obtained with a single extraction of I and II from biological matrixes allowed the addition of a backwash step to the procedure for urine and tissue extracts. Washing with pH 11.5 buffer presumably removed phenolic compounds which are coextracted at pH 7.5 and which generally are electrochemically active at the oxidation potential used. This removal of interferences more than compensates for any loss of drug during the backwash. Since the extraction efficiency for the internal standard (III) was less than for I and II, when the backwash was included, III was added after the backwash step.

The electrochemistry of I and II was explored initially by cyclic voltammetry. The cyclic voltammogram for I in mobile phase (Fig. 1) showed a nonreversible oxidation with a maximum occurring at ~ +0.8 V. The voltammogram for II was very similar to that for I. When reexamined in 67% 2-propanol–33% 0.3 *M* $HClO_4$, where wave definition is generally

[1] Synthesized by Lilly Research Laboratories, Indianapolis, Ind.
[2] Burdick and Jackson, Muskegon, Mich.
[3] Model 6000A, WISP 710B, and Guard Column, Waters Associates, Milford, Mass.
[4] CO:PELL ODS, Whatman Co., Clifton, N.J.
[5] Zorbax C-8, DuPont Instruments, Wilmington, Del.
[6] Models LC-22/23 and LC-4 with a TL-5 (glassy carbon) or TL-5A detector cell, Bioanalytical Systems, W. Lafayette, Ind.
[7] Rainin Inst. Co., Woburn, Mass.
[8] Models 7010 and 7001, and Brownlee guard column (C2-GU), Rheodyne, Cotati, Calif.
[9] Model 396, Laboratory Data Control, Riviera Beach, Fla.
[10] LC-24, Bioanalytical Systems, W. Lafayette, Ind.
[11] Kew Scientific, Columbus, Ohio.
[12] Glusulase, Endo Laboratories, Garden City, N.Y.
[13] CV-5, Bioanalytical Systems, W. Lafayette, Ind.

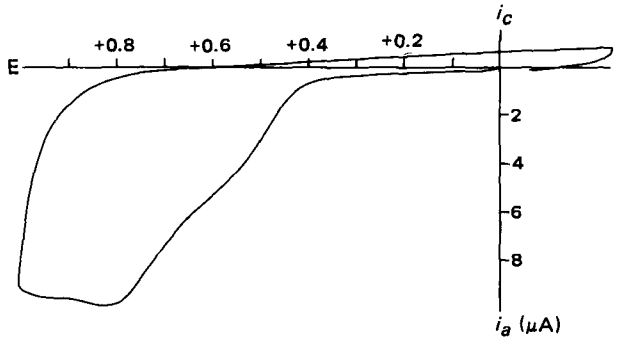

Figure 1—*Cyclic voltammogram of enviroxime. Conditions: 1 mM enviroxime in 33% 0.1 M sodium acetate–67% methanol, 3 mm diameter glassy carbon electrode, 50 mV/sec., E versus (Ag–AgCl–3 M NaCl), scan initiated positive from 0.0 V.*

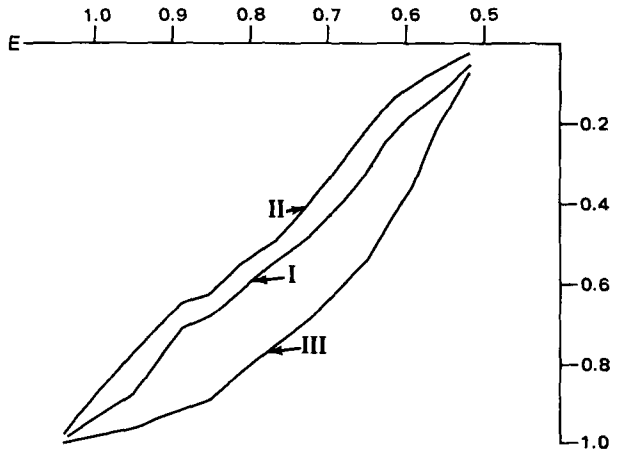

Figure 2—*Hydrodynamic voltammograms under assay conditions. Auxiliary electrode was across the channel from the working electrode. Key: (ϕ) ratio of peak height at a given potential to peak height obtained at greatest potential.*

better, both I and II showed several oxidation waves. The initial oxidation is thought to involve loss of two electrons from the extended conjugated system consisting of the oxime, benzimidazole, and the 2-amine group. The analog of I lacking the 2-amine group was not oxidizable, and the initial oxidation of the analog with a ketone instead of the oxime was 280 mV higher.

The voltammetry of I, II, and III under actual chromatographic conditions is depicted in Fig. 2. These curves were obtained with the auxiliary electrode positioned across the thin layer channel from the working electrode. This configuration minimizes uncompensated resistance between the two electrodes as well as potential gradients across the working electrode and thus allows accurate potential control under conditions of high background current. For all other work described in this paper, the auxiliary electrode was located downstream in the reference compartment. With such a configuration the hydrodynamic voltammograms began to drop off around +1.0 V. It can be seen from Fig. 2 that the voltammetric properties of III are reasonably similar to those of I and II, which is a desirable property for an internal standard. The potential used in this assay (+0.85 V) was chosen as a compromise between the desire for increased response to I and II, and the desire for low noise and a minimum of interferences from the biological matrixes.

The influence of chromatographic flow rate on the peak height of I is shown in Fig. 3. Peak heights normally increase as the flow rate is increased, due to decreased bandspreading. This is more than offset here by the decreasing efficiency of electrochemical conversion of I at higher flow rates. The flow rate chosen for use in this assay (0.9 ml/min) is a compromise between the demands of sensitivity and the need for reasonable retention times.

Assay Characteristics—The method described here was successfully applied to many different types of biological samples. Typical chromatograms from the assay of plasma, urine, and nasal turbinates are shown in Fig. 4. Compounds I and II (t_R ~ 8 and 9 min, respectively) were well resolved from each other and from major coextracted interferences. The small peak observed in the blank plasma chromatogram has a retention time close to but not identical to that of II. The chromatogram depicted represents a worse case situation, this peak not always being observed. Chromatograms of different blank tissue homogenates or urine looked different from each other and from blank plasma, so that A may not be compared against C or D. Although III elutes relatively late (t_R ~ 18 min), an alternative internal standard was not sought, because the region between 10 and 18 min occasionally contained interfering peaks.

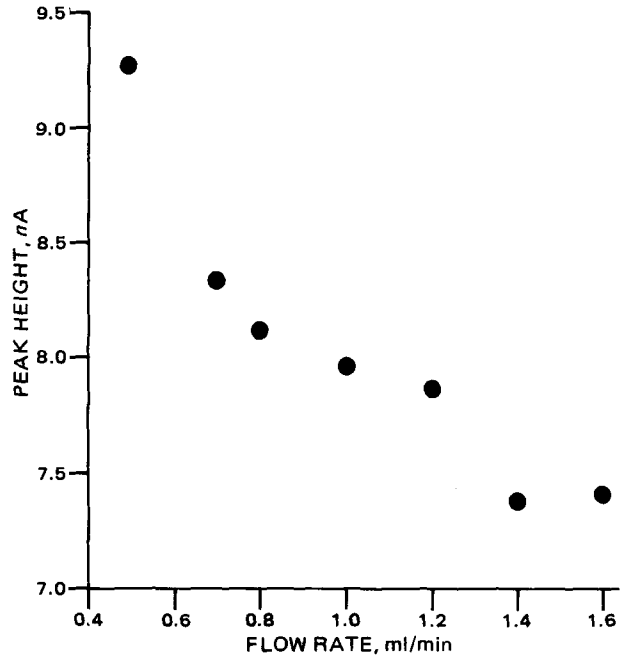

Figure 3—*Effect of flow rate on response to enviroxime. Chromatographic conditions as in text.*

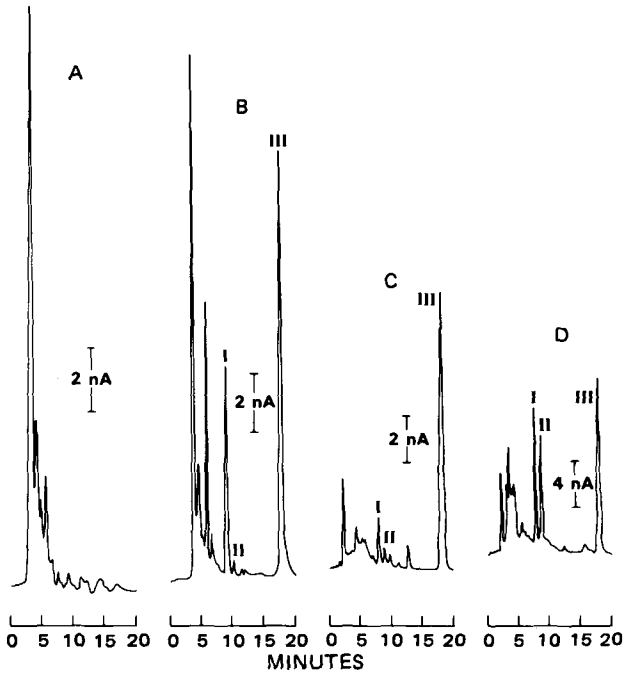

Figure 4—*Chromatograms of extracts of biological samples. Key: (A) predose dog plasma (without III added); (B) 80-min postdose plasma from dog administered 8 mg of I/kg orally, represents 43 ng of I/ml and 9 ng of II/ml; (C) homogenate of nasal tissue from dog administered 80 mg of II/kg for 90 days, represents 144 ng of I/g and 72 ng of II/g; (D) 0–2 hr urine of patient administered 25 mg of I orally, represents 1.6 μg of conjugated I/ml and 1.7 μg of conjugated II/ml.*

Table II—Precision and Accuracy of the Determination of Enviroxime in Human Plasma

Nanograms of Enviroxime per milliliter	Plasma Spiked with Enviroxime[a]		
	25	50	100
Day 1			
$\bar{x}$, ng/ml	25.1	50.4	99.8
RSD, %	1.8	2.0	1.1
Day 2			
$\bar{x}$, ng/ml	25.1	48.2	95.9
RSD, %	2.5	3.1	1.5
Day 3			
$\bar{x}$, ng/ml	24.8	48.7	95.4
RSD, %	5.6	0.6	0.6
Overall Accuracy			
$\bar{x}$, ng/ml	25.0	49.1	97.1
n	23.0	24.0	23.0
Relative Error	0.0	−1.8%	−2.9%
Overall Precision			
Between-day *RSD*, %	—	1.6	1.9
Within-day *RSD*, %	3.6	1.5	0.8
Total *RSD*, %	3.6	3.1	2.7

[a] $N = 8$.

The assay was found to be linear over the 5–800 ng range of I and II per milliliter of sample. The nonlinearity observed at >800 ng/ml was probably due to uncompensated resistance in the detector cell, a situation that occurs when large amounts of analyte are injected and/or when mobile phases of low conductivity are used. Alternative cell configurations could alleviate this problem (8). Instead, smaller volumes (<1 ml) of sample were used. This simple change kept all samples within a single sensitivity range (20nA/V), minimized electrode coating, and preserved samples.

The precision and accuracy of the determination of I in human plasma are summarized in Table II. Plasma samples spiked with 25, 50, and 100 ng of I and II per milliliter were prepared and eight aliquots were assayed on each of 3 days. The results in Table II show the precision and accuracy of the determination of I to be excellent, with both within-day and between-day variability contributing approximately equally to the overall precision. The determination of II was about one half as precise, with the largest variation observed being 7.4% *RSD* for the 25-ng/ml samples. Roughly 75% of the total *RSD* for II was attributable to between-day variability. Calibration curves were normally prepared with equal amounts of I and II, as in this characterization. However, when curves were prepared for each isomer individually, no significant interconversion of I and II was noted during the assay.

The precision of the determination of conjugated I and II in urine, which involves enzymatic cleavage of the conjugates, was estimated by assaying four aliquots of each of six urine samples on each of 3 days. The mean concentrations of total I and II ranged from 200 to 3600 ng/ml. The overall precision, as measured by the average of the *RSD*s of the individual samples was 9% for I and 11% for II. The proportion of the variability accounted for by between-day variation ranged from 68–96% for I and 50–90% for II. The reason for this day-to-day variation could not be determined, but the overall precision is quite reasonable.

The maximum sensitivity attainable with this method was not limited by detector noise. Trace levels of interferences defined detection limits in all of the many media studied. As little as 4 ng of I per milliliter of plasma, 15 ng/ml of nasal wash or 20 ng/ml of urine or tissue homogenate could be determined. Detection limits for II were always slightly higher than for I due to the lower response of the electrochemical detector to II (Fig. 2).

Improved Reliability of Electrochemical Detection—During the initial development of this assay, the background current at the glassy carbon working electrode oscillated erratically and on the whole increased continually. Some of the oscillations appeared to be very late-eluting peaks, but their locations could not be correlated with the timing of injections. Because disodium edetate is frequently used to stabilize easily oxidized species, such as penicillamine and catecholamines, it was added to the mobile phase used for I and II. Subsequently, the background current became quite stable. The mechanism of this phenomenon is as yet unknown. As a result of long experience with this method, several additional problems were encountered which could be traced to the electrochemical detector.

When samples containing high concentrations of I and II were assayed, it was noted that the peak height of III, which should remain essentially constant, decreased during the chromatography of a single set of samples. Further investigation revealed that the sensitivity of detection of I and II decreased also. Sensitivity could be regained only by repolishing the electrode, indicating that coating or fouling was involved. Phenols are known to polymerize at electrode surfaces (9), and indeed the problem was traced to the use of higher concentrations of internal standard, III, with these samples. In a separate experiment, it was found that when 1 μg of I and III was repeatedly injected, the peak height of I decreased by 14% per injection. When I alone was injected, its peak height decreased by only 0.4% per 1 μg of injection. Thus, the coating is predominantly due to the biphenolic internal standard. With a much lower amount of I, II, and III (40 ng each), the observed decrease in peak height of I and II was 0.1% per injection. To minimize this coating, the amount of III injected onto the column was subsequently kept at or below this level.

Impurities present in the mobile phase can also contribute to electrode coating. Using reagent grade methanol[14], 50% of the sensitivity of a freshly repolished electrode was lost after several days. A grade of methanol described as having been distilled in glass[15] was better but still caused decreased sensitivity when compared with the methanol actually used. This assay is probably particularly sensitive to coating effects because of the high potential required for oxidation of I and II, and because even at +0.85 V, peak heights of I and II are still increasing with increasing potential (Fig. 2). Nonetheless, caution in the preparation of mobile phases for use with electrochemical detection is indicated.

When overnight automated runs were made, the peak heights of I, II, and III in spiked samples were observed to decrease by 5–15% during the late evening and then return to normal the following day. Since this behavior paralleled the cycle of ambient temperature, it was assumed to be due to changes in chromatographic retention time. Thermostating the column eliminated changes in retention and decreased but did not eliminate changes in peak height. The majority of this remaining variability in I and half that of II was compensated for by corresponding changes in III. A thorough description of subsequent investigations of the origins and minimization of temperature-induced variability in electrochemical detection is the subject of a separate report (10).

Late-eluting peaks are strongly retained components from one injection, which elute during subsequent chromatograms. When samples are injected by hand, the time between injections varies and the source and effect of late-eluting peaks are not always obvious. However, when an autosampler is used, the time between injections is reproducible and the position of late-eluting peaks becomes constant, thus making them easier to identify. Determination of I and II in several of the biological media assayed resulted in problems with late-eluting peaks. Dog and rabbit liver homogenates and rabbit lung homogenates were particularly troublesome.

In some simpler cases it is possible, with the proper timing, to cause a late-eluting peak to elute with the solvent front or at some other noncritical time in a subsequent chromatogram. In more complex cases, one may simply delay the next injection until the late-eluting peaks are off the column, but this approach prolongs chromatographic time unduly. A slug or gradient of organic eluent can speed up their elution, but extra time is then required for re-equilibration of the column and the detector.

An alternative approach to removing late-eluting peaks is to use column switching (11). For the determination of I a 3-cm reversed-phase precolumn was positioned between the injector and the analytical column. The precolumn was in line for 40 sec after injection, which is the time required for I, II, and III to traverse the precolumn and enter the main column. The precolumn was then switched out of line for the remaining assay time. While out of line, the mobile phase was pumped through it at 2.0 ml/min to wash strongly retained components to waste. This technique produced cleaner chromatograms, which improved quantitation, and increased sample throughput as compared with the other approaches discussed above. Interestingly, when column switching was used with other relatively clean matrixes, *e.g.*, dog plasma and nasal washings, fewer trace level substances interfering with I and II were seen. The resulting improvement in detection limits was unexpected, since the interference peaks that were eliminated had been so small that they could not be distinguished as being late-eluting peaks.

Assay Applications—The method described above has been used to determine I and II in numerous biological samples arising from toxicology, pharmacology, metabolism, formulation, dose ranging, and clinical studies. One of the many types of results generated is depicted in Fig. 5. In this typical concentration–time profile for I in dog plasma, I was de-

[14] Reagent Grade ACS., MCB Manufacturing Chemists, Cincinnati, Ohio.
[15] HPLC Grade, Tedia Company, Fairfield, Ohio.

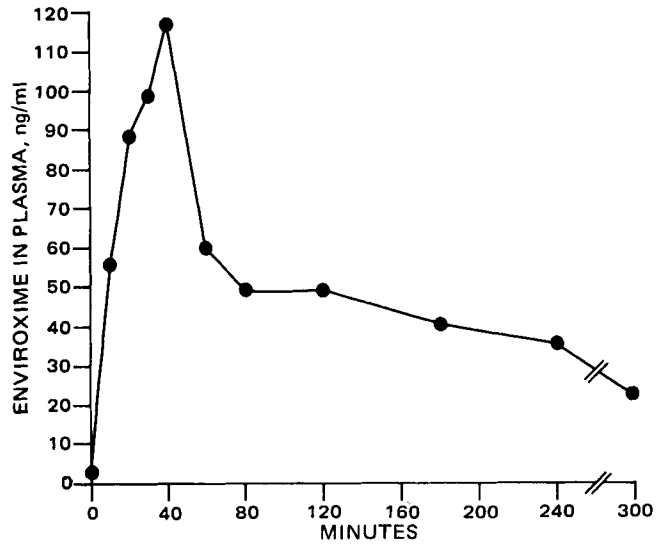

Figure 5—*Enviroxime concentration in dog plasma (ng/ml) after oral administration of an 8-mg/kg dose.*

terminable as early as 10 min after oral dosing to as long as 5–8 hr post-dose. A second example illustrates the value of a chemical assay, as compared with the original plaque reduction assay. The amount of II found in the plasma of dogs following oral dosing with I was usually very small, between 5 and 10% of I. However, when II was administered orally to dogs, I was still the major peak found in plasma. Thus, either by metabolism or by acid-catalyzed isomerization in the GI tract, the two isomers tend to form an equilibrium mixture in the plasma, in which I predominates.

The proven versatility of the methodology here points out the power of the coupling of liquid chromatography with electrochemical detection for determining oxidizable drugs in biological matrixes.

REFERENCES

(1) J. H. Wikel, *et al.*, *J. Med. Chem.*, **23**, 368 (1980).

(2) D. C. DeLong and S. E. Reed, *J. Infect. Dis.*, **141**, 87 (1980).

(3) C. J. Parli, R. J. Bopp, and J. F. Quay, *Fed. Proc. Fed. Am. Soc. Exp. Biol.*, **39**, 307 (1980).

(4) J. F. Quay, C. J. Parli, J. F. Stuckey II, K. S. E. Su, D. C. DeLong, J. D. Nelson, and J. H. Wikel, *Fed. Proc. Fed. Am. Soc. Exp. Biol.*, **39**, 850 (1980).

(5) R. J. Phillpotts, R. W. Jones, D. C. Delong, S. E. Reed, J. Wallace, and D. A. J. Tyrrell, *Lancet*, **i**, 1342 (1981).

(6) J. A. Bogan and S. Marriner, *J. Pharm. Sci.*, **69**, 422 (1980).

(7) D. J. Miner and P. T. Kissinger, *Biochem. Pharmacol.*, **28**, 3285 (1979).

(8) P. T. Kissinger, *Anal. Chem.*, **49**, 447A (1977).

(9) R. C. Koile and D. C. Johnson, *ibid.*, **51**, 741 (1979).

(10) D. J. Miner, *Anal. Chim. Acta*, **134**, 101 (1982).

(11) L. R. Snyder and J. J. Kirkland, in "Introduction to Modern Liquid Chromatography," 2nd ed., Wiley, New York, N.Y., 1979, pp. 698–717.

ACKNOWLEDGMENTS

This paper was presented in part at the First International Symposium on the Neurochemical and Clinical Applications of LCEC, Indianapolis, Ind., May 12, 1980, Abstract #15.

The authors thank J. H. Fouts, P. R. Page, and R. J. Pierson for running the assays, Drs. C. L. Gries, K. S. Israel, and J. F. Quay for providing the samples, and E. Reed for help with the manuscript.

NOTES

Antihypertensive Agents: Pyridazino(4,5-b)indole Derivatives

A. MONGE VEGA *x, I. ALDANA *, P. PARRADO *, M. FONT *, and E. FERNANDEZ ALVAREZ ‡

Received December 3, 1981, from the **Facultad de Farmacia, Universidad de Navarra, Pamplona, Spain* and the ‡*Instituto de Química Orgánica del CSIC, Juan de la Cierva, 3 Madrid-6 Spain.* Accepted for publication January 27, 1982.

Abstract □ A series of 4-hydrazino-5H-pyridazino(4,5-b)indoles (VIII) and their potential metabolites (3,4-dihydro-4-oxo-5H-pyridazino(4,5-b)indoles (V) and 11H-1,2,4-triazolo(4,3-b)pyridazino-(4,5-b)indoles (IX) were investigated for antihypertensive activity in spontaneously hypertensive rats. All compounds showed antihypertensive activity at 25 mg/kg ip. Compound VIII was the most active, and the most toxic.

Keyphrases □ Antihypertensive agents—synthesis of pyridazino-(4,5-b)indole derivatives, rats, metabolites □ Metabolites—synthesis of antihypertensive agents, pyridazino(4,5-b)indole derivatives, rats □ Pyridazino(4,5-b)indole—derivatives, synthesis of antihypertensive agents, hypertensive rats

In connection with work related to the preparation and study of new products as potential antihypertensive agents, a series of pyridazino(4,5-b)indole derivatives (1–3) related to the well-known antihypertensive agent hydralazine[1] (I), as well as its metabolites (4, 5) were synthesized. The metabolism of these compounds takes place essentially (5, 6) through N^2-acylation (formyl, acetyl) of the hydrazino group and further cyclization to triazole derivatives (II), as well as the hydrolysis of the hydrazino to give the oxo derivatives (III).

The results of a preliminary evaluation in spontaneously hypertensive rats of Compounds V, VIII, and IX (see Scheme) are reported. All of these compounds are structurally related to hydralazine (I)[1] and its metabolites.

Some preliminary data for Compound VII*a* in normotensive and hypertensive (renal fistula), anesthetized

[1] Apresoline (1-hydrazinophtalazine).

0022-3549/82/1200-1406$01.00/0

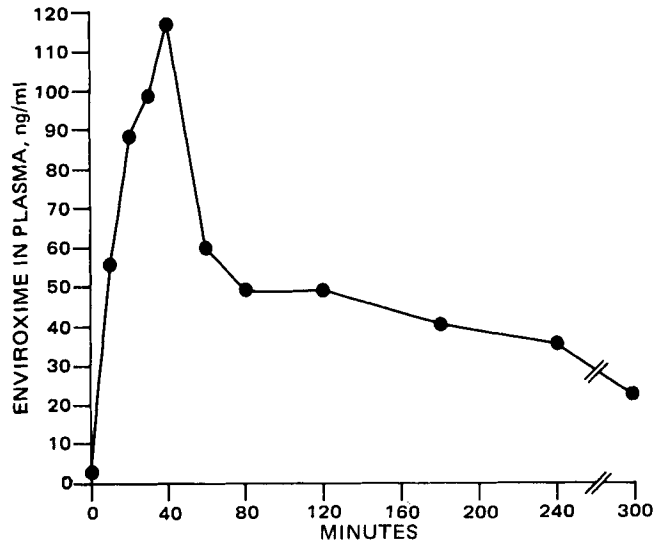

Figure 5—*Enviroxime concentration in dog plasma (ng/ml) after oral administration of an 8-mg/kg dose.*

terminable as early as 10 min after oral dosing to as long as 5–8 hr post-dose. A second example illustrates the value of a chemical assay, as compared with the original plaque reduction assay. The amount of II found in the plasma of dogs following oral dosing with I was usually very small, between 5 and 10% of I. However, when II was administered orally to dogs, I was still the major peak found in plasma. Thus, either by metabolism or by acid-catalyzed isomerization in the GI tract, the two isomers tend to form an equilibrium mixture in the plasma, in which I predominates.

The proven versatility of the methodology here points out the power of the coupling of liquid chromatography with electrochemical detection for determining oxidizable drugs in biological matrixes.

REFERENCES

(1) J. H. Wikel, *et al.*, *J. Med. Chem.*, **23**, 368 (1980).

(2) D. C. DeLong and S. E. Reed, *J. Infect. Dis.*, **141**, 87 (1980).

(3) C. J. Parli, R. J. Bopp, and J. F. Quay, *Fed. Proc. Fed. Am. Soc. Exp. Biol.*, **39**, 307 (1980).

(4) J. F. Quay, C. J. Parli, J. F. Stuckey II, K. S. E. Su, D. C. DeLong, J. D. Nelson, and J. H. Wikel, *Fed. Proc. Fed. Am. Soc. Exp. Biol.*, **39**, 850 (1980).

(5) R. J. Phillpotts, R. W. Jones, D. C. Delong, S. E. Reed, J. Wallace, and D. A. J. Tyrrell, *Lancet*, **i**, 1342 (1981).

(6) J. A. Bogan and S. Marriner, *J. Pharm. Sci.*, **69**, 422 (1980).

(7) D. J. Miner and P. T. Kissinger, *Biochem. Pharmacol.*, **28**, 3285 (1979).

(8) P. T. Kissinger, *Anal. Chem.*, **49**, 447A (1977).

(9) R. C. Koile and D. C. Johnson, *ibid.*, **51**, 741 (1979).

(10) D. J. Miner, *Anal. Chim. Acta*, **134**, 101 (1982).

(11) L. R. Snyder and J. J. Kirkland, in "Introduction to Modern Liquid Chromatography," 2nd ed., Wiley, New York, N.Y., 1979, pp. 698–717.

ACKNOWLEDGMENTS

This paper was presented in part at the First International Symposium on the Neurochemical and Clinical Applications of LCEC, Indianapolis, Ind., May 12, 1980, Abstract #15.

The authors thank J. H. Fouts, P. R. Page, and R. J. Pierson for running the assays, Drs. C. L. Gries, K. S. Israel, and J. F. Quay for providing the samples, and E. Reed for help with the manuscript.

NOTES

Antihypertensive Agents: Pyridazino(4,5-b)indole Derivatives

A. MONGE VEGA *x, I. ALDANA *, P. PARRADO *, M. FONT *, and E. FERNANDEZ ALVAREZ ‡

Received December 3, 1981, from the **Facultad de Farmacia, Universidad de Navarra, Pamplona, Spain* and the ‡*Instituto de Química Orgánica del CSIC, Juan de la Cierva, 3 Madrid-6 Spain.* Accepted for publication January 27, 1982.

Abstract □ A series of 4-hydrazino-5H-pyridazino(4,5-b)indoles (VIII) and their potential metabolites (3,4-dihydro-4-oxo-5H-pyridazino(4,5-b)indoles (V) and 11H-1,2,4-triazolo(4,3-b)pyridazino-(4,5-b)indoles (IX) were investigated for antihypertensive activity in spontaneously hypertensive rats. All compounds showed antihypertensive activity at 25 mg/kg ip. Compound VIII was the most active, and the most toxic.

Keyphrases □ Antihypertensive agents—synthesis of pyridazino-(4,5-b)indole derivatives, rats, metabolites □ Metabolites—synthesis of antihypertensive agents, pyridazino(4,5-b)indole derivatives, rats □ Pyridazino(4,5-b)indole—derivatives, synthesis of antihypertensive agents, hypertensive rats

In connection with work related to the preparation and study of new products as potential antihypertensive agents, a series of pyridazino(4,5-b)indole derivatives (1–3) related to the well-known antihypertensive agent hydralazine[1] (I), as well as its metabolites (4, 5) were synthesized. The metabolism of these compounds takes place essentially (5, 6) through N^2-acylation (formyl, acetyl) of the hydrazino group and further cyclization to triazole derivatives (II), as well as the hydrolysis of the hydrazino to give the oxo derivatives (III).

The results of a preliminary evaluation in spontaneously hypertensive rats of Compounds V, VIII, and IX (see Scheme) are reported. All of these compounds are structurally related to hydralazine (I)[1] and its metabolites.

Some preliminary data for Compound VII*a* in normotensive and hypertensive (renal fistula), anesthetized

[1] Apresoline (1-hydrazinophtalazine).

0022-3549/82/1200-1406$01.00/0

Table I—Antihypertensive Activity in Spontaneously Hypertensive Rats for Pyridazino (4,5-b)indole Derivatives V, VIII, and IX

	V Compounds					VIII Compounds					IX Compounds				
			Falls[d]					Falls[d]					Falls[d]		
Compounds	Dose	LD_{50}	3 hr	5 hr	25 hr	Dose	LD_{50}	3 hr	5 hr	25 hr	Dose	LD_{50}	3 hr	5 hr	25 hr
a	25[a]	1000	16	19	—	5[a]	225	92	84	32	25[a]	794	1	—	—
a						2,5[a]		66	61	36					
a						1,0[a]		47	44	38					
a						0,5[a]		48	3	1					
a						5[b]		50	92	65					
a						2,5[b]		33	28	4					
a						5[c]		80	60	20					
a						2,5[c]		61	30	10					
b	25[a]	100	18	20	6	5[c]	105	21	16	8	25[a]	200	14	4	1
b						2,5[c]		19	16	8					
b						5[a]		22	17	9					
b						2,5[a]		14	10	6					
c	25[a]	758	28	30	19										
d						25[a]	224	67	44	15	25[a]	1000	8	13	2
						19[b]		16	12	3					
e	10[a]	1000	1	19	15	10[a]	970	12	31	1	10[a]	1000	3	18	4

[a] Dose, mg/kg, ip (spontaneously hypertensive). [b] Dose; mg/kg, oral (spontaneously hypertensive). [c] Dose, mg/kg, ip (desoxycorticosterone-saline rats). [d] Falls in systolic blood pressure at the indicated times after the indicated doses (average for four rats 190 ± 5 mmHg).

(thiobarbital), and nonanesthetized dogs have been reported (3).

EXPERIMENTAL

Chemistry[2]—Compounds V–IX have been prepared according to Scheme I. The following compounds have been previously reported: V*a* and VIII*a* (3); V*b* (mp 283–285°, and erroneously reported mp 218°) and V*e* (7); IX*a* and IX*b* (2); V*c* (8, 9) and V*d*; VIII*d* and IX*d* (9). Compounds VIII*b*, VIII*e*, and IX*e* were prepared by methods similar to those previously reported (2, 3, 9) but these compounds had not been reported previously.

4-Hydrazino-5-methyl-5H-pyridazino(4,5-b)indole (VIII*b*)—Compound VIII*b* was prepared from Compound V*b* (7) in a similar way to that reported previously (3) for Compound VIII*a*. Yield: 90%; mp = 178–180°; (ethanol), white crystals IR (potassium bromide): ν (cm^{-1}) = 3200 (bs, NH); 1625 (s, C=N); 765 (s, 1,2-aromatic disubstituted) ^{1}H-NMR (dimethyl sulfoxide-d_6): δ = 3.40 (sb, 2H, NH_2); 4.25 (s, 3H, CH_3); 7.10–7.90 (m, 3H, H_{6-8}); 7.85–8.30 (dd, H_9); 8.50 (sb, 1H, NH); 9.95 (s, H_1).

Anal.—Calc. for $C_{10}H_{12}N_5$: C, 61.7; H, 5.62; N, 32.7. Found: C, 61.9; H, 5.61; N, 32.7.

4-Hydrazino-8-benzyloxy-5H-pyridazino(4,5-b)indole (VIII*e*)—Compound VIII*e* was prepared from Compound V*e* (7) in a similar way to that reported previously (3) for Compound VIII*a*. Yield: 80%; mp 340° (*N*,*N*-dimethylformamide–water). Light brown crystals formed. IR (potassium bromide): ν (cm^{-1}) = 3000–3200 (m) and 3280–3399 (m) (NH); 1645 (s, C=N); 830 (m, 1,2,4-aromatic trisubstituted); 700 (s, aromatic monosubstituted) ^{1}H-NMR (dimethyl sulfoxide-d_6): δ = 5.30 (s, 2H, CH_2—O); 6.00–7.00 (bs, 3H, NH_2—NH—); 7.20–7.65 (m, 7H, $H_{6-7}C_6H_5$—); 7.85 (dd, H_9); 9.20 (s, H_1).

Anal.—Calc. for $C_{17}H_{15}N_5O$: C, 66.9; H, 4.91; N, 22.9. Found: C, 66.5; H, 4.75; N, 22.5.

11-H-1,2,4-Triazolo(4,3-b)pyridazino(4,5-b)-8-benzyloxyindole (IX*e*)—Compound IX*e* was synthesized from Compound VIII*e* in a similar way to that previously reported (2, 9) for Compounds IX*a*,*b*,*d*. Yield: 90%; mp 340° (*N*,*N*-dimethylformamide). White crystals formed. IR (potassium bromide) ν (cm^{-1}) = 3080–3120 (m, NH), 1640 (s) and 1625 (s) (C=N): 820 (s, 1,2,4-aromatic trisubstituted) ^{1}H-NMR (dimethyl sulfoxide-d_6): δ = 3.20 (s, 3H, CH_3); 5.40 (s, 2H, CH_2—O); 7.40–7.55 (m, 7H, $H_{6-7}C_6H_5$); 7.85 (dd, H_9); 9.60 (s, H_1).

Anal.—Calc. for $C_{19}H_{15}N_5O$: C, 69.3; H, 4.59; N, 21.3. Found: C, 69.5; H, 4.82; N, 21.4.

Pharmacology—Compounds were evaluated for antihypertensive activity in unanesthetized spontaneously hypertensive, 8-week-old male rats (spontaneously hypertensive)[3], of the Okamoto strain weighing 300–350 g and with systolic blood pressure levels >180 mmHg. Changes in the arterial pressure were measured by mechanical transduction[4] and registered on paper. A dose was given to each of four animals and blood pressures were measured at 3, 5, and 24 hr. The tested compounds were administered (2.5 ml/kg ip) either dissolved or suspended in normal saline containing 0.2% carboxymethylcellulose and 1% polysorbate 80.

The initial dose was 25 mg/kg. The more active compounds were tested at lower concentrations, as shown in Table I. The most active compound

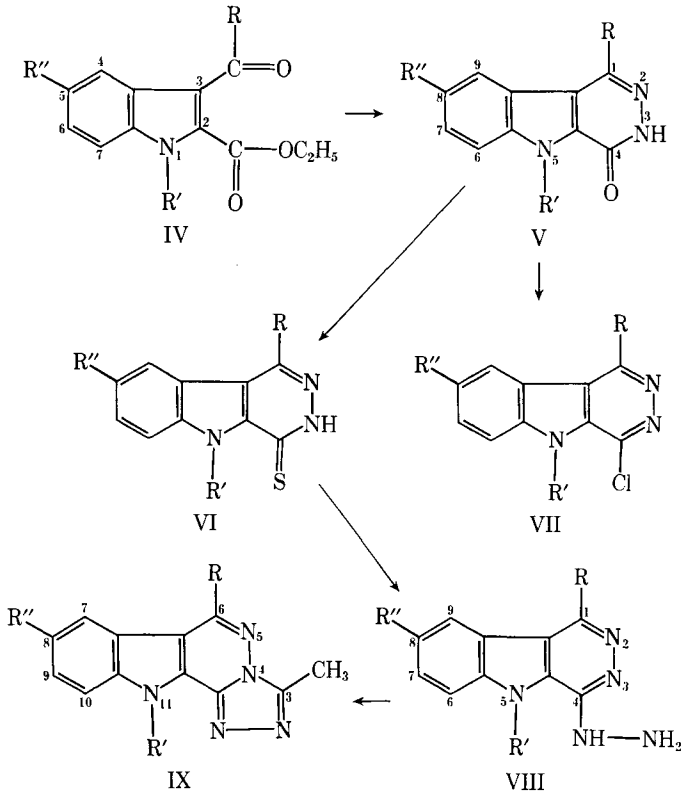

		R	R′	R″
IV–IX:	a)	H	H	H
IV–IX:	b)	H	CH_3	H
IV–V:	c)	OH	H	H
IV–IX:	d)	Cl	H	H
IV–IX:	e)	H	H	C_6H_5—CH_2—O—

[2] All melting points were determined in a Gallenkamp apparatus in glass capillary tubes and were uncorrected. Analysis included microanalysis of samples dried in vacuum on phosphorus pentoxide (2–3 hr, 60–70°). Where a molecular formula is given, analytical results are within 0.4% of the theoretical values. IR spectra were recorded in a Perkin-Elmer model 681 apparatus. The ^{1}H-NMR spectra were recorded in a Perkin-Elmer model R-32 spectrometer (90 MHz) at room temperature, with tetramethylsilane as an internal reference: s, d, t, for singlet, doublet, triplet; bs = broad signal; dd = deformed doublet.

[3] Navarra University Farms.

[4] W+W, BP Recorder 8005.

(VIII*a*) was also similarly tested in desoxycorticosterone–saline rats (intraperitoneally) (10).

Acute toxicities were determined in male mice weighing 20 ±2 g. A dose was given orally to each of five animals and mortalities were recorded 1 week later. The LD_{50} was calculated according to a previous procedure (11).

RESULTS AND DISCUSSION

Table I summarizes the results of the pharmacological assays. All the compounds studied showed appreciable activity in the spontaneously hypertensive rat assay. In decreasing order of activity they are: VIII*a* > VIII*d* > VIII*e* > VIII*b* > V*c* > V*a* > V*b* > V*e* > IX*e* > IX*b* > IX*d* > IX*a*.

The hydrazino group is not essential for activity although it does considerably increase antihypertensive activity and toxicity. Group VIII compounds are thus the most active and the most toxic. Furthermore, the antihypertensive activity of V compounds may be related to that of other non hydrazine antihypertensive compounds (12, 13). It seems that this is the first report of antihypertensive activity in the oxo and triazole metabolites of pyridazino–hydrazine antihypertensives.

REFERENCES

(1) A. Monge Vega, J. A. Palop, M. T. Martínez, and E. Fernández Alvarez, *J. Heterocycl. Chem.*, **17**, 249 (1980).

(2) A. Monge Vega, I. Aldana, M. M. Rabbani, and E. Fernandez Alvarez, *ibid.*, **17**, 77 (1980).

(3) A. Monge Vega, I. Aldana, and E. Fernández Alvarez, *Eur. J. Med. Chem.*, **13**, 573 (1978).

(4) J. Druey and J. Triod, in "Antihypertensive Agents," E. Schilitter, Ed., *Academic*, New York, N.Y., 1967, pp. 223–262.

(5) R. Mori, J. Ono, T. Saito, T. Aximoto, and M. Sano, *Chem. Pharm. Bull.*, **25**, 830 (1977).

(6) H. Zimmer, J. Kokosca, and D. R. Garteiz, *Arzneim.-Forsch.*, **23**, 1028 (1973).

(7) A. Monge Vega, J. A. Palop, M. T. Martínez, and E. Fernández Alvarez, *An. Quin.*, **27**, 889 (1979).

(8) E. H. Huntress and W. H. Haarom, *J. Am. Chem. Soc.*, **63**, 2762 (1941).

(9) A. Monge Vega, I. Aldana, and E. Fernández Alvarez, *J. Heterocycl. Chem.*, **18**, 889 (1981).

(10) J. De Champlain and M. R. Van Ameriger, *Circ. Res.*, **31**, 617 (1972).

(11) J. T. Lithfield and F. Wilcoxon, *J. Pharmacol. Exp. Ther.*, **96**, 99 (1949).

(12) L. R. Bennet, C. J. Blankey, R. W. Fleming, R. D. Smith, and D. K. Tessmann, *J. Med. Chem.*, **24**, 382 (1981).

(13) J. D. Warren, S. A. Lang, Jr., P. S. Chan, and J. W. Marsico, *J. Pharm. Sci.*, **67**, 1479 (1978).

ACKNOWLEDGMENTS

Supported by a grant from the Comision Asesora de Investigación Científica y Técnica (No. 4421, *1980*), Spain.

Simple Methods for Estimating Percent Disintegrated–Time Data

ADNAN EL-YAZIGI

Received March 9, 1981, from the *Department of Pharmaceutics, College of Pharmacy, University of Riyadh, Riyadh, Saudi Arabia.* Accepted for publication of February 3, 1982. Present Address: Cancer and Radiation Biology Research, Cancer Therapy Institute, King Faisal Specialist Hospital and Research Center, Riyadh, Saudi Arabia.

Abstract □ Two techniques are described for the treatment of dissolution rates to estimate the percent disintegrated–time data for tablets and capsules. The first is an extension of an equation derived previously with the assumption of first-order disintegration and dissolution processes; whereas, the second involves the determination of the rate constant from the terminal segment of the curve and the use of numerical derivatives according to a disintegration kinetics-independent approach. The dissolution data of six commercial tablet and capsule formulations were treated according to the described techniques. Good agreement was found between the percent disintegrated–time data estimated by the second approach for an acetaminophen tablet and those obtained by a well-established model where a Weibull function was employed.

Keyphrases □ Dissolution—tablets, simple methods for estimating percent disintegrated–time data □ Disintegration—tablets, simple methods for estimating percent disintegrated–time data, dissolution

There are few methods available for utilizing dissolution rate data to estimate the fraction disintegrated as a function of time for tablets (1, 2). These techniques, however, lack simplicity and require computer programs which may not be available.

A simple method was described recently for the disintegration–dissolution analysis of percent dissolved–time data (3). The technique is based on a biexponential equation with the assumption of first-order disintegration and dissolution according to a simple dissolution model.

The present report describes two approachs that can be used to estimate the percent disintegrated–time data for tablets and capsules. The first is an extension to the above report (3), whereas the other is based on disintegration kinetics—independent approach. Both techniques are simple and rapid and allow computations to be carried out manually.

THEORETICAL

Estimation of Percent Disintegrated–Time Data (Approach I) —Assuming first-order disintegration and dissolution processes, if A, A_p, and A_s represent the amounts of drug in dosage form, small particles, and solution, respectively, at any given time, and it is assumed that the disintegration and dissolution are first-order processes whose apparent rate constants are k_d and k_s, respectively, or:

$$A \xrightarrow[\text{first-order disintegration}]{k_d} A_p \xrightarrow[\text{first-order dissolution}]{k_s} A_s$$

Scheme I

the following equation can be derived (3):

$$100 - f_s = \frac{100\,k_d}{k_d - k_s} e^{-k_s t} - \frac{100\,k_s}{k_d - k_s} e^{-k_d t} \qquad \text{(Eq. 1)}$$

where f_s is the cumulative percent dissolved at time t.

Based on Scheme I, the following also can be derived:

0022-3549/82/1200-1408$01.00/0

(VIII*a*) was also similarly tested in desoxycorticosterone–saline rats (intraperitoneally) (10).

Acute toxicities were determined in male mice weighing 20 ±2 g. A dose was given orally to each of five animals and mortalities were recorded 1 week later. The LD_{50} was calculated according to a previous procedure (11).

RESULTS AND DISCUSSION

Table I summarizes the results of the pharmacological assays. All the compounds studied showed appreciable activity in the spontaneously hypertensive rat assay. In decreasing order of activity they are: VIII*a* > VIII*d* > VIII*e* > VIII*b* > V*c* > V*a* > V*b* > V*e* > IX*e* > IX*b* > IX*d* > IX*a*.

The hydrazino group is not essential for activity although it does considerably increase antihypertensive activity and toxicity. Group VIII compounds are thus the most active and the most toxic. Furthermore, the antihypertensive activity of V compounds may be related to that of other non hydrazine antihypertensive compounds (12, 13). It seems that this is the first report of antihypertensive activity in the oxo and triazole metabolites of pyridazino–hydrazine antihypertensives.

REFERENCES

(1) A. Monge Vega, J. A. Palop, M. T. Martínez, and E. Fernández Alvarez, *J. Heterocycl. Chem.*, **17**, 249 (1980).

(2) A. Monge Vega, I. Aldana, M. M. Rabbani, and E. Fernandez Alvarez, *ibid.*, **17**, 77 (1980).

(3) A. Monge Vega, I. Aldana, and E. Fernández Alvarez, *Eur. J. Med. Chem.*, **13**, 573 (1978).

(4) J. Druey and J. Triod, in "Antihypertensive Agents," E. Schilitter, Ed., *Academic*, New York, N.Y., 1967, pp. 223–262.

(5) R. Mori, J. Ono, T. Saito, T. Aximoto, and M. Sano, *Chem. Pharm. Bull.*, **25**, 830 (1977).

(6) H. Zimmer, J. Kokosca, and D. R. Garteiz, *Arzneim.-Forsch.*, **23**, 1028 (1973).

(7) A. Monge Vega, J. A. Palop, M. T. Martínez, and E. Fernández Alvarez, *An. Quin.*, **27**, 889 (1979).

(8) E. H. Huntress and W. H. Haarom, *J. Am. Chem. Soc.*, **63**, 2762 (1941).

(9) A. Monge Vega, I. Aldana, and E. Fernández Alvarez, *J. Heterocycl. Chem.*, **18**, 889 (1981).

(10) J. De Champlain and M. R. Van Ameriger, *Circ. Res.*, **31**, 617 (1972).

(11) J. T. Lithfield and F. Wilcoxon, *J. Pharmacol. Exp. Ther.*, **96**, 99 (1949).

(12) L. R. Bennet, C. J. Blankey, R. W. Fleming, R. D. Smith, and D. K. Tessmann, *J. Med. Chem.*, **24**, 382 (1981).

(13) J. D. Warren, S. A. Lang, Jr., P. S. Chan, and J. W. Marsico, *J. Pharm. Sci.*, **67**, 1479 (1978).

ACKNOWLEDGMENTS

Supported by a grant from the Comision Asesora de Investigación Científica y Técnica (No. 4421, *1980*), Spain.

Simple Methods for Estimating Percent Disintegrated–Time Data

ADNAN EL-YAZIGI

Received March 9, 1981, from the *Department of Pharmaceutics, College of Pharmacy, University of Riyadh, Riyadh, Saudi Arabia.* Accepted for publication of February 3, 1982. Present Address: Cancer and Radiation Biology Research, Cancer Therapy Institute, King Faisal Specialist Hospital and Research Center, Riyadh, Saudi Arabia.

Abstract □ Two techniques are described for the treatment of dissolution rates to estimate the percent disintegrated–time data for tablets and capsules. The first is an extension of an equation derived previously with the assumption of first-order disintegration and dissolution processes; whereas, the second involves the determination of the rate constant from the terminal segment of the curve and the use of numerical derivatives according to a disintegration kinetics-independent approach. The dissolution data of six commercial tablet and capsule formulations were treated according to the described techniques. Good agreement was found between the percent disintegrated–time data estimated by the second approach for an acetaminophen tablet and those obtained by a well-established model where a Weibull function was employed.

Keyphrases □ Dissolution—tablets, simple methods for estimating percent disintegrated–time data □ Disintegration—tablets, simple methods for estimating percent disintegrated–time data, dissolution

There are few methods available for utilizing dissolution rate data to estimate the fraction disintegrated as a function of time for tablets (1, 2). These techniques, however, lack simplicity and require computer programs which may not be available.

A simple method was described recently for the disintegration–dissolution analysis of percent dissolved–time data (3). The technique is based on a biexponential equation with the assumption of first-order disintegration and dissolution according to a simple dissolution model.

The present report describes two approachs that can be used to estimate the percent disintegrated–time data for tablets and capsules. The first is an extension to the above report (3), whereas the other is based on disintegration kinetics—independent approach. Both techniques are simple and rapid and allow computations to be carried out manually.

THEORETICAL

Estimation of Percent Disintegrated–Time Data (Approach I) —Assuming first-order disintegration and dissolution processes, if A, A_p, and A_s represent the amounts of drug in dosage form, small particles, and solution, respectively, at any given time, and it is assumed that the disintegration and dissolution are first-order processes whose apparent rate constants are k_d and k_s, respectively, or:

$$A \xrightarrow[\text{first-order disintegration}]{k_d} A_p \xrightarrow[\text{first-order dissolution}]{k_s} A_s$$

Scheme I

the following equation can be derived (3):

$$100 - f_s = \frac{100\,k_d}{k_d - k_s} e^{-k_s t} - \frac{100\,k_s}{k_d - k_s} e^{-k_d t} \qquad \text{(Eq. 1)}$$

where f_s is the cumulative percent dissolved at time t.

Based on Scheme I, the following also can be derived:

0022-3549/82/1200-1408$01.00/0

Table I—Percent Disintegrated–Time Data for the Formulations Used According to *Approaches I* and *II*

Formulation Code	Midinterval Time, min																	
	1		3		5		7		9		12.5		17.5		22.5		27.5	
	I[a]	II[b]	I	II	I	II	I	II	I	II	I	II	I	II	I	II	I	II
A	27.5	10.4	61.8	31.3	79.9	63.3	89.4	80.6	94.4	85.6	98.2	96.4	99.6	94.8	100	100	100	100
B	36.9	14.6	74.9	37.3	90.0	79.3	96.0	87.3	98.4	97.6	99.7	106.0	100	100	100	100	100	100
C	36.6	35.0	74.5	64.6	89.8	77.8	95.9	85.0	98.3	89.0	99.7	94.2	100	102	100	104	100	100
	Midinterval Time, min																	
	1.25		3.75		6.25		8.75		12.5		17.5		22.5		27.5			
	I[a]	II[b]	I	II	I	II	I	II	I	II	I	II	I	II	I	II		
D	36.6	36.6	74.6	75.7	89.8	93.6	95.9	96.2	99.0	98.7	99.8	99.5	100	99.9	100	100		
E	40.3	33.4	78.7	72.3	92.4	90.4	97.3	92.2	99.4	99.5	99.9	101	100	99.1	100	99.1		
F	22.4	0	53.3	22.4	71.9	41.0	83.1	71.2	97.1	75.3	97.1	90.7	99.0	104	99.6	110		

[a] Estimated according to *Approach I*. [b] Estimated according to *Approach II*.

$$A_d = A_0 (1 - e^{-k_d t}) \quad \text{(Eq. 2)}$$

where A_d is the amount disintegrated at time t and equal to the amount of drug in dosage form at time 0 (A_0) minus the amount of drug in dosage form at time t (A). Multiplying both sides of Eq. 2 by $100/A_0$ yields:

$$f_d = 100 (1 - e^{-k_d t}) \quad \text{(Eq. 3)}$$

where $f_d = 100A_d/A_0$ and is the cumulative percent disintegrated at time t.

The disintegration profile can be obtained by substituting for k_d in Eq. 3 the values determined graphically according to Eq. 1 where k_s can also be determined (3).

Disintegration Kinetics Independent Approach (Approach II)—If the dissolution process is assumed to follow first-order kinetics while disintegration is taken as a kinetics-independent process, the following can be derived using a simple kinetic approach:

$$f_{d(t)} = \frac{(df_s/dt)_t}{k_s} + f_{s(t)} \quad \text{(Eq. 4)}$$

where $(df_s/dt)_t$ is the dissolution rate at time t, and $f_{d(t)}$, $f_{s(t)}$, and k_s have the same meaning as described earlier. Equation 4 can also be derived using a convolution technique (2). Employing Eq. 4, a direct calculation of the cumulative percent disintegrated–time data can be achieved once $(df_s/dt)_t$ is calculated and k_s determined. The apparent first-order rate constant for dissolution (k_s) can be determined from the terminal straight line segment of $\ln(100 - f_s)$ *versus* time plot.

RESULTS AND DISCUSSION

The dissolution data obtained for six commercial tablets and capsules containing isoniazid, theophylline, ampicillin, tetracycline hydrochloride, and tetracycline hydrochloride–phosphate complex (3) were employed to examine the use of the described techniques to estimate the percent disintegrated–time data.

The apparent first-order disintegration and dissolution rate constants (k_d and k_s, respectively) were determined graphically according to Eq. 1. The values of k_d were substituted in Eq. 3, and the percent disintegrated at various time values were calculated and are presented in Table I.

When *Approach II* was employed for the determination of the percent disintegrated–time data, the dissolution rate $(df_s/dt)_t$ was calculated for each time interval, and the midinterval time was taken as t. The cumulative percent dissolved at midinterval time (t) was estimated by the arithmetic mean of the percent dissolved at the beginning and the end of the interval. Table I presents the percent disintegrated–time data determined by this approach.

As demonstrated in Table I, the data obtained by *Approach I* were generally comparable to those obtained by *Approach II*. Indeed, for formulations C, D, and E, the data produced by both techniques were very close. The disagreement in the results, when existent, generally occurred in the initial data points. This may indicate less than perfect fit of these data points to Eq. 1. More initial data points might have led to better estimates of k_d; however, this would require the automation of the dissolution test. A good fit of the dissolution data to Eq. 1 is essential if the percent disintegrated–time data were to be estimated accurately according to Eq. 3.

To examine the reliability of the described techniques, the dissolution rate data of an acetaminophen tablet were subjected to the described analysis. These data were reported and employed (2) to demonstrate the application of a model to estimate the fraction disintegrated–time data. The data were well represented by a Weibull function (2), and a good estimate of k_d according to Eq. 1 could not be obtained. However, the curve produced by plotting $\ln(100 - f_s)$ *versus* time had a linear terminal segment whose slope was equal to 1.389 min^{-1}. This value was used as k_s in Eq. 4, and the percent disintegrated–time data were determined after the dissolution rate $(df_s/dt)_t$ was calculated for each interval. The percent dissolved at midinterval time $(f_s)_t$ was reported.

In a continuous function approach using convolution techniques, an equation was derived (2) which was employed to analyze these data. The equation was obtained by substituting a Weibull function for f_s in Eq. 3. The two parameters for this Weibull function were determined by a nonlinear regression of the Weibull function to the above tablet data. The first-order dissolution parameter was determined (2) from separate dissolution tests of acetaminophen powder and plotting the data semilogarithmically against time.

As can be seen in Table II, the percent disintegrated–time data by *Approach II* were similar to those obtained previously (2). Therefore, while the existent methods (1, 2) involve either a system of linear equations which require computer programs to solve or continuous functions with three parameters to be determined, the estimation of the percent disintegrated–time data by *Approach II* is simple and requires no separate dissolution testing of drug powder. The estimation of the first-order dissolution rate constant can be performed easily by plotting the tablet dissolution data semilogarithmically against time. The terminal data points most frequently behave in a first-order fashion. This approach for determination of k_s is valid here, because the acetaminophen tablet dissolution was less rapid than disintegration (1, 2), and k_s was smaller than k_d for the other formulations used (Table I).

While the usefulness of Eq. 3 to estimate the percent disintegrated–

Table II—Percent Disintegrated–Time Data for an Acetaminophen Tablet

Midinterval Time, min	$(df_s/dt)_t$, %/min	$f_{s(t)}$, %	$f^a_{d(t)}$, %	$f^b_{d(t)}$, %
0.17	2.73	0.4	2.4	1.9
0.50	8.53	1.7	7.8	7.0
0.83	15.2	6.5	17.4	13.7
1.17	21.5	12.8	28.3	21.7
1.50	22.9	19.8	36.3	30.3
1.83	22.4	26.9	43.0	39.2
2.17	24.8	35.6	53.5	48.3
2.5	20.3	43.1	57.7	56.8
2.83	23.6	50.1	67.1	64.6
3.17	21.2	57.6	72.9	71.9
3.50	20.9	64.4	79.4	77.9
3.83	19.7	71.1	85.3	83.1
4.17	19.4	77.7	91.7	87.4
4.50	18.2	84.7	97.8	90.8
4.83	11.2	89.1	97.2	93.4
5.17	10.9	92.9	100.8	95.4
5.50	7.3	95.5	100.8	96.9
6.00	2.6	98.2	100.8	98.3

[a] Estimated according to *Approach II*. [b] Reported previously (2) and labeled as continuous function.

time is limited to the cases where the dissolution data are well described by Eq. 1, *Approach II* provides a simple, rapid, and reliable tool for prediction of disintegration profiles. The computation involved is simple and can be carried out manually without the use of computer programs as required by other techniques.

REFERENCES

(1) K. G. Nelson and L. Y. Wang, *J. Pharm. Sci.*, **66**, 1758 (1977).
(2) *Ibid.*, **67**, 86 (1978).
(3) A. El-Yazigi, *ibid.*, **70**, 535 (1981).

Lysine and Polylysine: Correlation of their Effects on Polyphosphoinositides *In Vitro* with Ototoxic Action *In Vivo*

AKIRA TAKADA *, SHAHID LODHI ‡, NORMAN D. WEINER ‡x, and JOCHEN SCHACHT ‡

Received November 19, 1981, from the **Kresge Hearing Research Institute and* ‡*College of Pharmacy, The University of Michigan, Ann Arbor, MI 48109.* Accepted for publication February 3, 1982.

Abstract □ Low concentrations of poly-L-lysine, a polycationic hydrophilic molecule, caused a large expansion of polyphosphoinositide monolayers and produced a significant loss of cochlear microphonic potentials in perilymphatic perfusions in the guinea pig. In contrast, the monomeric L-lysine had only slight effects on polyphosphoinositide monolayers and did not affect cochlear microphonic potentials even at concentrations as high as 10 m*M*. These data substantiate the hypothesis that the expansion of polyphosphoinositide monolayers by a drug is an indicator of its ototoxicity.

Keyphrases □ Polyphosphoinositides—correlation of effects of lysine and polylysine *in vitro* with ototoxic action *in vivo* □ Lysine—correlation of effects on polyphosphoinositides *in vitro* with ototoxic action *in vivo*, polylysine □ Polylysine—correlation of effects on polyphosphoinositides *in vitro* with ototoxic action *in vivo*, lysine

Evidence has previously been provided in *in vivo* and *in vitro* studies for an involvement of polyphosphoinositides in the toxic actions of aminoglycoside antibiotics (1). Monolayer studies have shown that polyphosphoinositides are unique among various anionic phospholipids with respect to both the type and magnitude of the interactions with neomycin and Ca^{2+} (2). The observed increase in surface pressure was indicative of a very strong preference of the polyphosphoinositide film for neomycin over Ca^{2+} and other cations. It was further shown that the degree of interaction of eight aminoglycoside antibiotics and fragments with polyphosphoinositides correlated well with their ototoxicity in the guinea pig (3).

In order to test further the hypothesis that the degree of expansion of polyphosphoinositide monolayers is correlated with ototoxicity, monolayer studies, and ototoxicity tests for two compounds unrelated to aminoglycosides, poly-L-lysine and L-lysine, are reported here. Poly-L-lysine represents a polycationic hydrophilic compound, capable of occupying an area-determining position in lipid films (4), and L-lysine represents the corresponding singly-charged hydrophilic monomer.

EXPERIMENTAL

Materials and Methods—Poly-L-lysine had a molecular weight of 3400 (polymerization grade, 16)[1]. Polyphosphoinositides were purified from ox brain by chromatography on immobilized neomycin (5).

A polytef beaker (8-cm diameter) held 100 ml of subphase containing 50 m*M* sodium *N*-2-hydroxyethylpiperazine-*N'*-2-ethanesulfonate, pH 7.0, 1 m*M* $CaCl_2$, and sufficient sodium chloride to adjust the ionic strength to 0.2. A stationary syringe, with the needle immersed in the subphase throughout the experiment, delivered the additions of lysine and polylysine. The solutions were stirred with a magnetic bar at slow speed without the film being disturbed. The polyphosphoinositide mixtures (phosphatidylinositol phosphate–phosphatidylinositol bisphosphate, 1:2 molar ratio) were spread as a solution in *n*-hexane–ethanol–chloroform (80:5:15, v/v/v). Approximately 0.2 μg of lipid/cm^2 was spread to obtain the desired surface pressure (14–15 dyne/cm) which was read with a balance[2] after the film had stabilized for 10 min. Polylysine or L-lysine was then injected into the subphase for final concentrations of 10^{-7}–10^{-4} *M*. After each addition, the subphase was mixed for 15 min before measurements were taken. Experiments were performed at 25±2° in duplicate, and surface tension readings always agreed within 0.1 dyne/cm.

Perilymphatic Perfusions—Perilymphatic perfusions were carried out in male albino guinea pigs (200–300 g). An animal with a positive Preyer hearing reflex was anesthetized with pentobarbital (20 mg/kg of body weight ip), atropine sulfate (0.05 mg/kg sc), and 0.5 ml/kg of body weight im of a solution containing 0.4 mg of fentanyl and 20.0 mg of droperidol/ml (6). The animal's body temperature was maintained at 37 ±1° with a heating pad and artificial respiration was provided through a tracheal cannula. Surgical and perfusion techniques were similar to that described previously (3).

The perilymphatic spaces of the cochlea were perfused at a rate of ~30 μl/min. Cochlear microphonic potentials were measured in response to a sound stimulus of white noise, 20–4000 Hz, delivered through an earphone. The sound intensity level was adjusted to give an initial microphonic potential of 200–400 μV. After the potential had stabilized for 30 min (control period), ototoxicity was determined as its loss after 30 min of a subsequent perfusion with added drug.

[1] Poly-L-lysine and L-lysine were obtained from Sigma Chemical Co., St. Louis, Mo.
[2] Wilhelmy balance.

0022-3549/82/1200-1410$01.00/0

time is limited to the cases where the dissolution data are well described by Eq. 1, *Approach II* provides a simple, rapid, and reliable tool for prediction of disintegration profiles. The computation involved is simple and can be carried out manually without the use of computer programs as required by other techniques.

REFERENCES

(1) K. G. Nelson and L. Y. Wang, *J. Pharm. Sci.*, **66**, 1758 (1977).
(2) *Ibid.*, **67**, 86 (1978).
(3) A. El-Yazigi, *ibid.*, **70**, 535 (1981).

Lysine and Polylysine: Correlation of their Effects on Polyphosphoinositides *In Vitro* with Ototoxic Action *In Vivo*

AKIRA TAKADA *, SHAHID LODHI ‡, NORMAN D. WEINER ‡x, and JOCHEN SCHACHT ‡

Received November 19, 1981, from the **Kresge Hearing Research Institute and* ‡*College of Pharmacy, The University of Michigan, Ann Arbor, MI 48109.* Accepted for publication February 3, 1982.

Abstract □ Low concentrations of poly-L-lysine, a polycationic hydrophilic molecule, caused a large expansion of polyphosphoinositide monolayers and produced a significant loss of cochlear microphonic potentials in perilymphatic perfusions in the guinea pig. In contrast, the monomeric L-lysine had only slight effects on polyphosphoinositide monolayers and did not affect cochlear microphonic potentials even at concentrations as high as 10 m*M*. These data substantiate the hypothesis that the expansion of polyphosphoinositide monolayers by a drug is an indicator of its ototoxicity.

Keyphrases □ Polyphosphoinositides—correlation of effects of lysine and polylysine *in vitro* with ototoxic action *in vivo* □ Lysine—correlation of effects on polyphosphoinositides *in vitro* with ototoxic action *in vivo*, polylysine □ Polylysine—correlation of effects on polyphosphoinositides *in vitro* with ototoxic action *in vivo*, lysine

Evidence has previously been provided in *in vivo* and *in vitro* studies for an involvement of polyphosphoinositides in the toxic actions of aminoglycoside antibiotics (1). Monolayer studies have shown that polyphosphoinositides are unique among various anionic phospholipids with respect to both the type and magnitude of the interactions with neomycin and Ca^{2+} (2). The observed increase in surface pressure was indicative of a very strong preference of the polyphosphoinositide film for neomycin over Ca^{2+} and other cations. It was further shown that the degree of interaction of eight aminoglycoside antibiotics and fragments with polyphosphoinositides correlated well with their ototoxicity in the guinea pig (3).

In order to test further the hypothesis that the degree of expansion of polyphosphoinositide monolayers is correlated with ototoxicity, monolayer studies, and ototoxicity tests for two compounds unrelated to aminoglycosides, poly-L-lysine and L-lysine, are reported here. Poly-L-lysine represents a polycationic hydrophilic compound, capable of occupying an area-determining position in lipid films (4), and L-lysine represents the corresponding singly-charged hydrophilic monomer.

EXPERIMENTAL

Materials and Methods—Poly-L-lysine had a molecular weight of 3400 (polymerization grade, 16)[1]. Polyphosphoinositides were purified from ox brain by chromatography on immobilized neomycin (5).

A polytef beaker (8-cm diameter) held 100 ml of subphase containing 50 m*M* sodium *N*-2-hydroxyethylpiperazine-*N'*-2-ethanesulfonate, pH 7.0, 1 m*M* $CaCl_2$, and sufficient sodium chloride to adjust the ionic strength to 0.2. A stationary syringe, with the needle immersed in the subphase throughout the experiment, delivered the additions of lysine and polylysine. The solutions were stirred with a magnetic bar at slow speed without the film being disturbed. The polyphosphoinositide mixtures (phosphatidylinositol phosphate–phosphatidylinositol bisphosphate, 1:2 molar ratio) were spread as a solution in *n*-hexane–ethanol–chloroform (80:5:15, v/v/v). Approximately 0.2 μg of lipid/cm^2 was spread to obtain the desired surface pressure (14–15 dyne/cm) which was read with a balance[2] after the film had stabilized for 10 min. Polylysine or L-lysine was then injected into the subphase for final concentrations of 10^{-7}–10^{-4} *M*. After each addition, the subphase was mixed for 15 min before measurements were taken. Experiments were performed at 25±2° in duplicate, and surface tension readings always agreed within 0.1 dyne/cm.

Perilymphatic Perfusions—Perilymphatic perfusions were carried out in male albino guinea pigs (200–300 g). An animal with a positive Preyer hearing reflex was anesthetized with pentobarbital (20 mg/kg of body weight ip), atropine sulfate (0.05 mg/kg sc), and 0.5 ml/kg of body weight im of a solution containing 0.4 mg of fentanyl and 20.0 mg of droperidol/ml (6). The animal's body temperature was maintained at 37 ±1° with a heating pad and artificial respiration was provided through a tracheal cannula. Surgical and perfusion techniques were similar to that described previously (3).

The perilymphatic spaces of the cochlea were perfused at a rate of ~30 μl/min. Cochlear microphonic potentials were measured in response to a sound stimulus of white noise, 20–4000 Hz, delivered through an earphone. The sound intensity level was adjusted to give an initial microphonic potential of 200–400 μV. After the potential had stabilized for 30 min (control period), ototoxicity was determined as its loss after 30 min of a subsequent perfusion with added drug.

[1] Poly-L-lysine and L-lysine were obtained from Sigma Chemical Co., St. Louis, Mo.
[2] Wilhelmy balance.

0022-3549/82/1200-1410$01.00/0

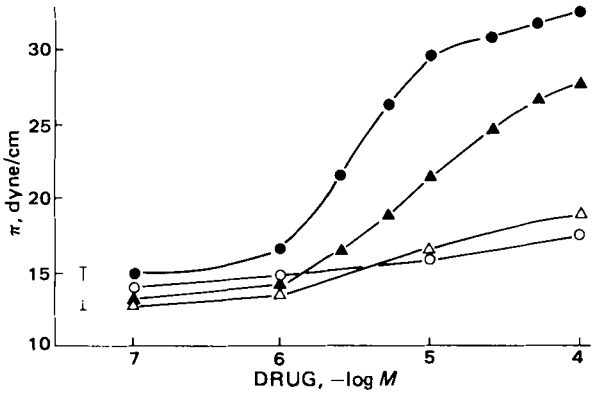

Figure 1—*Effects of cationic agents on surface pressure (π) of a Ca^{2+}/polyphosphoinositide film. Increasing amounts of drug were added to the subphase of a monomolecular film of polyphosphoinositides as described in* Experimental. *Each point represents multiple measurements agreeing within 0.1 dyne/cm. Bar on left indicates range of surface pressure before additions. Key: (○) lysine; (△) neamine; (●) poly-L-lysine; (▲) neomycin.*

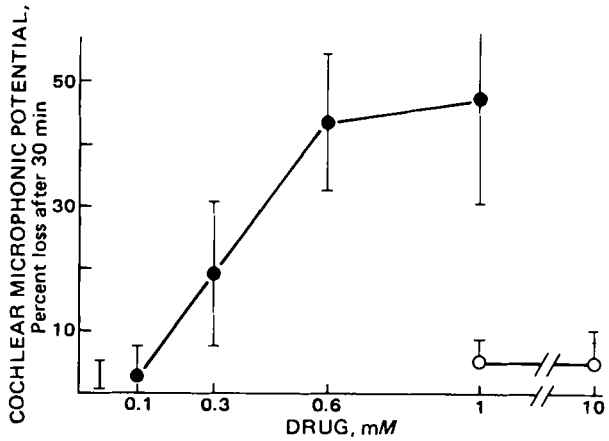

Figure 2—*Effects of cationic agents on cochlear microphonic potentials in the guinea pig. Numbers are means ±SD for five to eight animals at each condition. Bar on left indicates range of microphonic potentials without drug. Toxicity of poly-L-lysine at 0.3, 0.6, and 1 mM is significant at $p < 0.01$. Key: lysine (○); poly-L-lysine (●).*

Perilymphatic perfusions could usually be carried out for up to 2 hr without significant detrimental effect on cochlear microphonic potentials. Animals with an initial potential of <200 μV or with an unstable potential during the control period (loss of >10%) were excluded from the studies.

RESULTS AND DISCUSSION

It has previously been suggested that the specific interaction of a drug with polyphosphoinositides that leads to an expansion of the lipid monolayer in the presence of Ca^{2+} is an indicator of its ototoxicity. This interaction is apparently based on the configuration of the positive charges on the drug and not only on their number. For instance, kanamycin and neamine both have four primary amino groups, yet the first is more interactive with polyphosphoinositide films and also more ototoxic (3).

The cationic polymer, poly-L-lysine, can form complexes with acidic lipids (4) including polyphosphoinositides (7) and induce structural damage in biological membranes (8). Its action on the polyphosphoinositide film was strikingly different from that of the lysine monomer (Fig. 1). While low concentrations of the polymer dramatically increased the surface pressure ($\Delta\pi$ at 10^{-4} M, > 14 dyne/cm) the monomer showed only little effect (~2 dyne/cm). For comparison, the curves for the highly ototoxic compound, neomycin, and the nontoxic compound, neamine, (3) are shown.

In perilymphatic perfusions, effects on the cochlear microphonic potential were seen within 2–8 min after the introduction of polylysine into the perfusion fluid. The rate of loss was dependent on the drug concentrations up to 0.6 mM when an apparent maximum of toxicity was reached (Fig. 2). In contrast to polylysine, lysine did not affect the microphonic potential even at concentrations as high as 10 mM.

It should be noted that the molarity given for the polymer in these experiments refers to lysine equivalents for better comparison to the monomer, *i.e.*, 1 mM poly-L-lysine represents 1 mM lysine residues in the polymer corresponding to an actual concentration of 0.06 mM polymer. This consideration further accentuates the discrepancy between the action of the two compounds.

The correlation between polyphosphoinositide interaction and ototoxicity was demonstrated for a compound unrelated to aminoglycoside antibiotics. This finding further supports the hypothesis that the polyphosphoinositides play a crucial role in drug-induced ototoxicity.

REFERENCES

(1) N. D. Weiner and J. Schacht, in "Aminoglycoside Toxicity," S. A. Lerner, G. J. Matz, and J. E. Hawkins, Jr., Eds., Little, Brown, Boston, Mass., 1981, p. 113.

(2) S. Lodhi, N. D. Weiner, and J. Schacht, *Biochim. Biophys. Acta*, **557**, 1 (1979).

(3) S. Lodhi, N. D. Weiner, I. Mechigian, and J. Schacht, *Biochem. Pharmacol.*, **29**, 597 (1980).

(4) W. Hartmann and H. J. Galla, *Biochim. Biophys. Acta*, **509**, 474 (1978).

(5) J. Schacht, *J. Lipid Res.*, **19**, 1063 (1978).

(6) E. F. Evans, *Arch. Otolaryngol.*, **165**, 185 (1979).

(7) J. G. Fullington and H. S. Hendrickson, *J. Biol. Chem.*, **241**, 4098 (1966).

(8) M. W. Seiler, M. A. Venkatachalam, and R. S. Cotran, *Science*, **189**, 390 (1975).

ACKNOWLEDGMENTS

This study was supported by Research Grant NS-13792 and Program Project Grant NS-05785 from the National Institutes of Health.

Comparative Estimation of Glycyrrhetinic Acid Content of *Lonchocarpus cyanescens* and Glycyrrhiza Roots

MAURICE M. IWU

Received November 16, 1981, from the *Phytotherapy Research Laboratory, Faculty of Pharmaceutical Sciences, University of Nigeria, Nsukka, Nigeria.* Accepted for publication February 5, 1982.

Abstract □ The glycyrrhetinic acid (enoxolone) content of *Lonchocarpus cyanescens* roots has been determined by colorimetric and GC analysis. This plant gave lower values for both bound and unbound glycyrrhetinic acid when compared with glycyrrhiza (licorice).

Keyphrases □ *Lonchocarpus cyanescens*—comparative estimation of glycyrrhetinic acid content in roots, glycyrrhiza roots, colorimetric and GC analysis □ Glycyrrhetinic acid—comparative estimation of the content of *Lonchocarpus cyanescens* and glycyrrhiza roots, colorimetric and GC analysis □ Colorimetry, analysis—comparative estimation of the glycyrrhetinic acid content in *Lonchocarpus cyanescens* and glycyrrhiza roots □ GC analysis—comparative estimation of the glycyrrhetinic acid content in *Lonchocarpus cyanescens* and glycyrrhiza roots

Lonchocarpus cyanescens Benth (Leguminosae) is used extensively in African ethnomedicine for the treatment of various diseases, including infantile constipation and venereal infections (1). On the west coast of Africa, the root decoction is used by the natives for the treatment of arthritis. The antiphlogistic activity of *L. cyanescens* has been attributed to the oleanane derivatives, 18β-glycyrrhetinic acid (enoxolone), 28-hydroxy-β-glycyrrhetinic acid, and its 18α-isomer, lonchoterpene, isolated from this plant (2).

Other species of *Lonchocarpus* are valued as effective insecticides due to the rotenone content of this genus (3). Some species are cultivated as fish poisons (4), and others are commercial sources of the Yoruba indigo dye (5).

Flavonoids and triterpenoids are the most important secondary metabolites of this plant (2). Previous phytochemical works established the presence of pterocarpans (6), *C*- and *O*-prenylated chalcones (7), and prenylated stilbenes (8). The present report describes the quantitative estimation of the glycyrrhetinic acid present in the root bark of *L. cyanescens*.

A number of analytical methods are available for the qualitative evaluation of glycyrrhetinic acid, including gravimetric, colorimetric, and GC–MS (9–11). Here, the determination was by colorimetry and GC.

EXPERIMENTAL[1]

Methods—*Colorimetric Determination*—One gram each of *L. cyanescens* root bark, powdered glycyrrhiza, and ammoniated extract of glycyrrhizin were processed as described earlier (11). The quantity of glycyrrhetinic acid present in the samples was estimated by measuring the extinction of the complex formed by coupling the acidic genin, glycyrrhetinic acid, with methylene blue. A single-beam spectrophotometer was used for all the measurements[2], and the determinations were carried out at 640 nm. For the hydrolyzed extract, the percent yield of glycyrrhizin was calculated from (11):

$$\text{Percent glycyrrhizin} = \frac{A_t \times 0.5 \times 1.75}{A_s \times W} \qquad \text{(Eq. 1)}$$

where, A_t is the absorbance of the test sample, A_s is the absorbance of the reference, W is the weight of the substance, and 1.75 is the transformation factor.

Gas Liquid Chromatographic Estimation—One gram of powdered root bark of *L. cyanescens* was extracted with chloroform (50 ml) in a soxhlet apparatus for 3 hr. The filtered extract was evaporated to dryness under reduced pressure and the resultant residue was silylated before GLC analysis, as will be described. The air-dried marc was further extracted with (50 ml) 70% ethanol for 3 hr. The filtered alcoholic extract was transferred quantitatively to a 250-ml round-bottom flask and refluxed for 3 hr with 50 ml of 6 *N* HCl. After cooling, the extract was extracted twice with 50 ml of chloroform, and the combined chloroform extracts were evaporated to dryness under reduced pressure. The resultant residue was treated with 0.5 ml each of anhydrous pyridine and *N,O*-bis(trimethylsilyl)trifluoroacetamide. A 5-ml aliquot was analyzed after 30 min by GLC[2] using a chromatograph loaded with Chromosorb (100–120 mesh); the injector and detector were maintained at 320°.

Samples of glycyrrhiza roots and authentic reference glycyrrhetinic acid were similarly treated and analyzed. In each case the glycyrrhetinic acid content was calculated from measurements of the mean peak areas from these replicates.

Table I—Percent Yield of Glycyrrhetinic Acid

Sample	Method of Analysis: Colorimetric	Method of Analysis: GLC
L. cyanescens (unhydrolyzed[a])	0.54	0.55
L. cyanescens (hydrolyzed[b])	0.50	0.52
Glycyrrhiza liquid extract	0.12	0.14
Glycyrrhiza roots (unhydrolyzed[a])	0.67	0.60
Glycyrrhiza roots (hydrolyzed[b])	0.58	0.48

[a] The values obtained for the unhydrolyzed samples are indicative of the free genin content. [b] The total yield of glycyrrhetinic acid is obtained by adding the values obtained both before and after hydrolysis.

RESULTS AND DISCUSSION

The percent yield of glycyrrhetinic acid from both methods of analyses are shown in Table I. Although *L. cyanescens* gave a comparatively lower glycyrrhetinic acid value, the abundance of this plant makes it an attractive source for this agent. The higher yield of the unbound genin is also a positive index for the economic exploitation of this plant.

REFERENCES

(1) J. R. Ainslie, in "List of Plants Used in Native Medicine in Nigeria," Imperial Forestry Institute, Oxford, England, 1937, p. 54.

(2) M. M. Iwu and F. C. Ohiri, *Can. J. Pharm. Sci.*, **15**, 39 (1980).

(3) R. H. Davidson and R. F. Lyon, in "Insect Pests," 7th ed., Wiley, New York, N.Y., 1979, p. 87.

(4) W. H. Lewis and M. P. Elvin-Lewis, in "Medical Botany," Wiley, New York, N.Y., 1977 p. 44.

[1] Plant material consisted of roots of *L. cyanescens* and were collected at Nsukka in October 1980, and identified by the University of Nigeria Department of Botany. A voucher specimen has been deposited at the Pharmacy Herbarium of this university.

[2] Hewlett-Packard 5750G Research Chromatograph was used for GLC; the colorimetric analysis was with a Coleman spectrophotometer.

0022-3549/82/1200-1412$01.00/0

(5) R. Keay, C. F. Onochie, and D. Standfield, in "Nigerian Trees," vol. II, Federal Department of Forest Research, 1964, p. 140.
(6) A. Pelter and P. I. Amenechi, *J. Chem. Soc.*, **6**, 887, (1969).
(7) F. Okoli, "Chemical Constituents of the Roots of *L. cyanescens*," B. Pharm. Project, University of Nigeria, Nsukka, 1981.
(8) F. Delle Monache, F. Marletti, G. B. Martini-Bettolo, J. F. Del-Mello, G. de lima, *Lloydia*, **40**, 201 (1977).
(9) P. Ventura, M. Visconti, and G. Pifferi, *Boll. Chim. Pharm.* **117**, 217 (1978).
(10) E. Bombardelli, B. Gabetta, E. M. Martinelli, and G. Mustich, *Fitoterapia* **1**, 11 (1979).
(11) A. A. M. Habib, N. A. El-Sebakhy, and H. A. Kadry, *J. Pharm. Sci.*, **68**, 1221 (1979).

ACKNOWLEDGMENTS

This work is supported by Senate Research Grant No. 00330/79 of the University of Nigeria, Nsukka, Nigeria.

The author is grateful to Drs. E. Bombardelli and M. Metawally for the gift of the reference compounds and to the World Health Organization for the award of a visiting scientist grant to Oxford University.

Paired-Ion High-Performance Liquid Chromatographic Assay for Sulfinpyrazone in Plasma

N. J. PATEL, D. O. KILDSIG, G. S. BANKER, P. R. MAYER, and M. A. GONZALEZ *x

Received July 23, 1979, from the *Department of Industrial and Physical Pharmacy, School of Pharmacy and Pharmacal Sciences, Purdue University, West Lafayette, IN 47907.* Accepted for publication February 18, 1982. *Present address: Key Pharmaceuticals, Inc., Miami, FL 33169.

Abstract □ A specific and sensitive liquid chromatographic method is reported for the assay of sulfinpyrazone in plasma utilizing ion pairing between the tetrabutylammonium cation and the sulfinpyrazone anion. The method is rapid in that conventional extraction procedures are avoided in favor of using disposable cartridges packed with an octadecylsilane bonded phase as a means of separating the drug from plasma. The samples were chromatographed on a C_{18} reversed-phase column using a mobile phase consisting of 0.005 *M* tetrabutylammonium phosphate in methanol–water (56:44). The coefficient of variation obtained was 4.5% and the response was linear over a range of 0.2–80 μg/ml.

Keyphrases □ High-performance liquid chromatography—paired ion, assay for sulfinpyrazone in plasma □ Sulfinpyrazone—paired-ion high-performance liquid chromatographic assay in plasma

Sulfinyprazone has been used as a uricosuric agent for over 20 years. Recently, new interest in this drug has been generated by reports indicating that it may protect patients from sudden death after myocardial infarction (1, 2).

Several methods have been reported in the literature that can be used for the quantitative determination of sulfinpyrazone in biological fluids. A spectrophotometric method reported previously (3) involves a tedious double extraction and lacks sensitivity, since it is based on UV absorption. A high-performance liquid chromatographic (HPLC) method was described (4) using radiolabeled sulfinpyrazone as an internal standard which complicates the routine application of this method. An HPLC method using a microparticulate silica column also was published (5). This method requires that the sample be injected 2 mm inside the column, thus, making it necessary to periodically refill that portion of the column with fresh silica. Another method (6) involves a two-step extraction and lacks adequate sensitivity.

It was considered desirable to develop a simple, rapid, and sensitive method for sulfinpyrazone determination in biological fluids. The reversed-phase HPLC method described here is based on the formation of ion pairs between sulfinpyrazone anions and tetrabutylammonium cations. The reported method has the advantage of not involving any extraction step. The drug is isolated from plasma using disposable cartridges filled with octadecylsilane bonded phase packing (C_{18} cartridge[1]).

EXPERIMENTAL

Materials—All reagents were analytical grade. All solutions were prepared using glass distilled water.

The high-performance liquid chromatographic system included a solvent pump[2] equipped with an injector[3], a fixed wavelength UV detector[4] set at 254 nm (λ_{max} was 260 nm), a recorder[5], and in integrator[6].

The analytical column was 30 cm long with 4-mm i.d. It was packed with octadecylsilane-bonded silica (particle size 10 μm)[7].

Mobile Phase—The mobile phase consisted of 0.005 *M* tetrabutylammonium phosphate[8] (I) in methanol–water (56:44). It was prepared by adding sufficient glass-distilled water to a vial of I to make 440 ml. An aliquot of 560 ml of absolute methanol was added, the solution was stirred for 10 min, and the volume was adjusted to 1 liter with a 56% (v/v) methanol–water solution. The solution was then filtered using a 0.5-μm pore, inert filter[9]. The mobile phase was deoxygenated using a vacuum flask attached to a water aspirator. The flow rate of the mobile phase was 1 ml/min at ambient temperature.

Preparation of Standards—A stock solution of sulfinpyrazone[10] was prepared by dissolving 100 mg of the drug in 100 ml of 50% (v/v) methanol–water. Solutions of varying concentration were prepared by serial dilutions of the stock solution in 50% (v/v) methanol–water. The plasma samples for use in the preparation of calibration curves were prepared by adding 200 μl of the appropriate drug solution to 1.8 ml of rat plasma in a 15-ml conical centrifuge tube. The plasma samples were mixed by agitating for 30 sec on a vortex-type mixer[11], and a 1.0-ml aliquot was taken for analysis.

[1] C_{18} Sep-pak, Waters Associates, Milford, Mass.
[2] Model 6000 A, Waters Associates, Milford, Mass.
[3] Model U6K, Waters Associates, Milford, Mass.
[4] Model 440, Waters Associates, Milford, Mass.
[5] Omniscribe, Houston Instruments, Austin, Tex.
[6] Shimadzu Chromatopac-E1A, Shimadzu Seisakusho Ltd., Kyoto, Japan.
[7] Bondapak C_{18}, Waters Associates, Milford, Mass.
[8] PIC Reagent-A, Waters Associates, Milford, Mass.
[9] Type FH, Millipore Corp., Bedford, Mass.
[10] Ciba-Geigy Corp., Summit, N.J.
[11] Maxi Mix Mixer, No. M-16715, Thermolyne Corp., Dubuque, Iowa.

0022-3549/82/1200-1413$01.00/0

(5) R. Keay, C. F. Onochie, and D. Standfield, in "Nigerian Trees," vol. II, Federal Department of Forest Research, 1964, p. 140.
(6) A. Pelter and P. I. Amenechi, *J. Chem. Soc.*, **6**, 887, (1969).
(7) F. Okoli, "Chemical Constituents of the Roots of *L. cyanescens*," B. Pharm. Project, University of Nigeria, Nsukka, 1981.
(8) F. Delle Monache, F. Marletti, G. B. Martini-Bettolo, J. F. Del-Mello, G. de lima, *Lloydia*, **40**, 201 (1977).
(9) P. Ventura, M. Visconti, and G. Pifferi, *Boll. Chim. Pharm.* **117**, 217 (1978).
(10) E. Bombardelli, B. Gabetta, E. M. Martinelli, and G. Mustich, *Fitoterapia* **1**, 11 (1979).
(11) A. A. M. Habib, N. A. El-Sebakhy, and H. A. Kadry, *J. Pharm. Sci.*, **68**, 1221 (1979).

ACKNOWLEDGMENTS

This work is supported by Senate Research Grant No. 00330/79 of the University of Nigeria, Nsukka, Nigeria.

The author is grateful to Drs. E. Bombardelli and M. Metawally for the gift of the reference compounds and to the World Health Organization for the award of a visiting scientist grant to Oxford University.

Paired-Ion High-Performance Liquid Chromatographic Assay for Sulfinpyrazone in Plasma

N. J. PATEL, D. O. KILDSIG, G. S. BANKER, P. R. MAYER, and M. A. GONZALEZ *x

Received July 23, 1979, from the *Department of Industrial and Physical Pharmacy, School of Pharmacy and Pharmacal Sciences, Purdue University, West Lafayette, IN 47907.* Accepted for publication February 18, 1982. *Present address: Key Pharmaceuticals, Inc., Miami, FL 33169.

Abstract □ A specific and sensitive liquid chromatographic method is reported for the assay of sulfinpyrazone in plasma utilizing ion pairing between the tetrabutylammonium cation and the sulfinpyrazone anion. The method is rapid in that conventional extraction procedures are avoided in favor of using disposable cartridges packed with an octadecylsilane bonded phase as a means of separating the drug from plasma. The samples were chromatographed on a C_{18} reversed-phase column using a mobile phase consisting of 0.005 *M* tetrabutylammonium phosphate in methanol–water (56:44). The coefficient of variation obtained was 4.5% and the response was linear over a range of 0.2–80 μg/ml.

Keyphrases □ High-performance liquid chromatography—paired ion, assay for sulfinpyrazone in plasma □ Sulfinpyrazone—paired-ion high-performance liquid chromatographic assay in plasma

Sulfinyprazone has been used as a uricosuric agent for over 20 years. Recently, new interest in this drug has been generated by reports indicating that it may protect patients from sudden death after myocardial infarction (1, 2).

Several methods have been reported in the literature that can be used for the quantitative determination of sulfinpyrazone in biological fluids. A spectrophotometric method reported previously (3) involves a tedious double extraction and lacks sensitivity, since it is based on UV absorption. A high-performance liquid chromatographic (HPLC) method was described (4) using radiolabeled sulfinpyrazone as an internal standard which complicates the routine application of this method. An HPLC method using a microparticulate silica column also was published (5). This method requires that the sample be injected 2 mm inside the column, thus, making it necessary to periodically refill that portion of the column with fresh silica. Another method (6) involves a two-step extraction and lacks adequate sensitivity.

It was considered desirable to develop a simple, rapid, and sensitive method for sulfinpyrazone determination in biological fluids. The reversed-phase HPLC method described here is based on the formation of ion pairs between sulfinpyrazone anions and tetrabutylammonium cations. The reported method has the advantage of not involving any extraction step. The drug is isolated from plasma using disposable cartridges filled with octadecylsilane bonded phase packing (C_{18} cartridge[1]).

EXPERIMENTAL

Materials—All reagents were analytical grade. All solutions were prepared using glass distilled water.

The high-performance liquid chromatographic system included a solvent pump[2] equipped with an injector[3], a fixed wavelength UV detector[4] set at 254 nm (λ_{max} was 260 nm), a recorder[5], and in integrator[6].

The analytical column was 30 cm long with 4-mm i.d. It was packed with octadecylsilane-bonded silica (particle size 10 μm)[7].

Mobile Phase—The mobile phase consisted of 0.005 *M* tetrabutylammonium phosphate[8] (I) in methanol–water (56:44). It was prepared by adding sufficient glass-distilled water to a vial of I to make 440 ml. An aliquot of 560 ml of absolute methanol was added, the solution was stirred for 10 min, and the volume was adjusted to 1 liter with a 56% (v/v) methanol–water solution. The solution was then filtered using a 0.5-μm pore, inert filter[9]. The mobile phase was deoxygenated using a vacuum flask attached to a water aspirator. The flow rate of the mobile phase was 1 ml/min at ambient temperature.

Preparation of Standards—A stock solution of sulfinpyrazone[10] was prepared by dissolving 100 mg of the drug in 100 ml of 50% (v/v) methanol–water. Solutions of varying concentration were prepared by serial dilutions of the stock solution in 50% (v/v) methanol–water. The plasma samples for use in the preparation of calibration curves were prepared by adding 200 μl of the appropriate drug solution to 1.8 ml of rat plasma in a 15-ml conical centrifuge tube. The plasma samples were mixed by agitating for 30 sec on a vortex-type mixer[11], and a 1.0-ml aliquot was taken for analysis.

[1] C_{18} Sep-pak, Waters Associates, Milford, Mass.
[2] Model 6000 A, Waters Associates, Milford, Mass.
[3] Model U6K, Waters Associates, Milford, Mass.
[4] Model 440, Waters Associates, Milford, Mass.
[5] Omniscribe, Houston Instruments, Austin, Tex.
[6] Shimadzu Chromatopac-E1A, Shimadzu Seisakusho Ltd., Kyoto, Japan.
[7] Bondapak C_{18}, Waters Associates, Milford, Mass.
[8] PIC Reagent-A, Waters Associates, Milford, Mass.
[9] Type FH, Millipore Corp., Bedford, Mass.
[10] Ciba-Geigy Corp., Summit, N.J.
[11] Maxi Mix Mixer, No. M-16715, Thermolyne Corp., Dubuque, Iowa.

0022-3549/82/1200-1413$01.00/0

Sample Preparation—Sulfinpyrazone was isolated from plasma using disposable C_{18} cartridges. Plasma samples (1.0 ml) with concentrations ranging from 0.2 to 80 μg/ml were used. The cartridges were conditioned by initially passing 3 ml of absolute methanol and 3 ml of a 0.01 *M* aqueous (I) solution through the cartridge. All solvents and solutions were introduced into the cartridge using disposable 5-ml hypodermic syringes. An equal volume of 0.02 *M* I in 50% (v/v) methanol–water was added to the plasma samples, which were then agitated for 30 sec. Each plasma sample was then passed quantitatively through a cartridge, and the eluate was discarded. The cartridges were washed with 1 ml of a solution containing 0.01 *M* I in methanol–acetonitrile–water (15:15:70). The drug retained on the cartridge was then eluted with 1 ml of absolute methanol. A new cartridge was used for each sample.

Assay—A 20-μl aliquot of the methanol from the last step in the previous section was precisely measured and injected into the chromatograph using a microliter syringe[12].

Reproducibility Study—To study the reproducibility of the procedure, 0.6 ml of a 100-μg/ml solution of sulfinpyrazone was added to 5.4 ml of rat plasma to produce a drug dilution containing 10 μg/ml. Five 1-ml aliquots of this solution were then processed using the procedure described above.

Retention Time and Peak Height Correlation Study—The peak height values obtained from 1-μg/ml plasma samples were used to investigate the correlation between peak heights and retention times. The peak height and retention time values generated during the development and optimization of the assay procedure were used. The latter involved changes in the methanol–water ratio, pH, and concentration of I.

RESULTS AND DISCUSSION

Utilizing disposable C_{18} cartridges adds great flexibility to any assay procedure. It must be kept in mind, however, that these cartridges are in essence miniature reversed-phase columns and must be treated accordingly. In the cartridge-conditioning step, methanol was passed through the cartridge as a cleaning solvent, but it served the dual purpose of also allowing drug diffusion from the serum to the packing material itself. An aqueous solution of I was used to condition the cartridge with the ion-pairing reagent. The tetrabutylammonium cations complex with sulfinpyrazone anions; the ion pair then has a greater affinity for the C_{18} packing material than the sulfinpyrazone anion. This increased affinity allows the ion to be retained in the cartridge while the plasma water and its polar constituents pass through the cartridge.

Not all interfering substances in plasma or other biological fluids will be separated in the first step. Therefore, it is necessary to utilize a washing step to rid the cartridge of additional plasma constituents. This step is critical in that it represents a possible source of sample loss. An optimum recovery of 80% of the sulfinpyrazone with minimal plasma extraneous peaks was obtained by washing the cartridge with 1 ml of a solvent consisting of 0.01 *M* I in methanol–acetonitrile–water (15:15:70). After this washing step, sulfinpyrazone was eluted from the cartridge with 1 ml of absolute methanol. The methanol from this last step was then chromatographed.

The mobile phase used in this procedure also contained I. Sulfinpyrazone is too strong an organic acid (pKa 2.8) to be maintained in an undissociated state, as is desirable when using reversed-phase HPLC. If a mobile phase with a neutral pH is used, sulfinpyrazone will be completely ionized, and its retention volume on the column will rarely exceed the void volume. Therefore, it was advantageous to utilize a mobile phase which contained the tetrabutylammonium cation that could ion pair with sulfinpyrazone and increase its retention time. A typical chromatograph of blank plasma and plasma containing 20 μg/ml of the drug are depicted in Fig. 1. While the blank rat plasma contained a number of peaks which could not be removed by the disposable cartridge, none of these peaks had retention times that would interfere with sulfinpyrazone.

Calibration curves were prepared, and Table I summarizes the results obtained after chromatographing samples from plasma with different concentrations of sulfinpyrazone. Calibration curves could be prepared using either peak heights or areas under the peaks. The data for the 10-μg/ml point represents the mean of five determinations using five different cartridges. The coefficient of variation for this point was 4.5%. The reproducibility between cartridges was satisfactory, and the coefficient of variation could be further improved by utilizing the same cartridge, which is possible by washing the cartridge with three or four 1-ml aliquots of absolute methanol between samples. While in certain applications repeated use of a cartridge may not be desirable, it was found that used cartridges stored in methanol gave reproducible results for several separate assays. This feature greatly diminishes the cost of an assay.

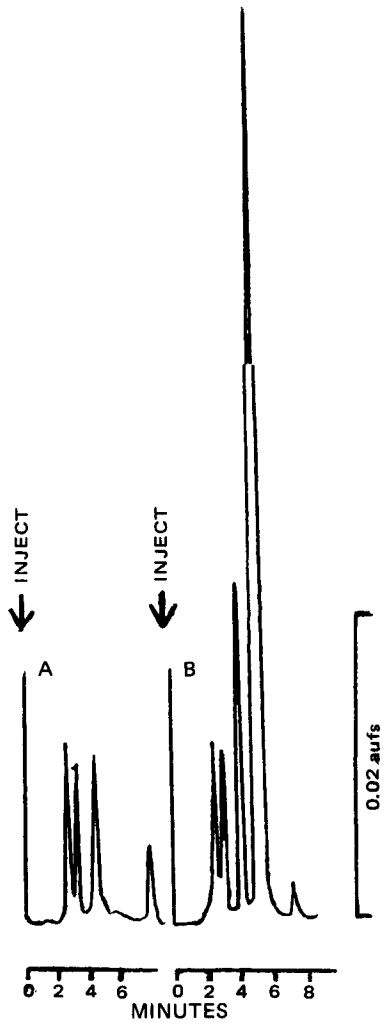

Figure 1—*Recorder tracings of representative chromatograms after 20-μl injections. Key: (A) plasma blank; (B) plasma spiked with sulfinpyrazone (20 μg/ml). Peak I is sulfinpyrazone.*

Since the drug is retained on the C_{18} cartridge as an ion pair, it is conceivable that at high drug concentrations there could be insufficient tetrabutylammonium cations to interact quantitatively with the sulfinpyrazone anions. This would result in a deviation from linearity at the higher concentrations of a standard curve. This was found to be the case if plasma concentrations >80 μg/ml were processed undiluted through the procedure. The linearity, however, was good from 1 to 80 μg/ml resulting in a correlation coefficient of 0.9992 when peak heights were used and 0.9990 for peak areas. The sulfinpyrazone–tetrabutylammonium complex appeared to be very sensitive to methanol concentrations in the

Table I—Values of Plasma Calibration Curve Points

Concentration, μg/ml	Peak Height[a], mm	Peak Area[b], μV sec × 10^{-4}
0.2	4.0	1.43
0.6	8.5	2.84
1.0	14.0	5.18
6.0	67.7	27.21
10.0	112.0	45.70
20.0	199.0	82.60
40.0	440.0	188.06
80.0	844.0	362.30

[a] Peak heights are normalized for 0.05 aufs. [b] Units of area are expressed as microvolts per sec.

[12] Pressure-Lock Series B-110, Precision Sampling, Baton Rouge, La.

Table II—Observed and Predicted Values of Slopes

Retention Time, min	Observed Slope	Predicted Slope
5.2	91.81	90.27
7.8	70.47	68.58
8.0	61.69	59.68

mobile phase, such that changes in retention times occurred with slight changes in methanol concentration. Such changes in retention time would influence the peak heights, thus, peak areas were found to be preferable in the preparation of standard curves.

Peak heights can be used without constantly repeating standard curves, if a correction is made for changes in peak height due to changes in retention time. It is well established that an inverse relationship exists between peak heights and retention time. Different retention times were produced by varying pH, methanol concentration, and I concentration to study this relationship. The flow rate of the mobile phase, however, was always the same. There is a good correlation between the peak heights and the reciprocal of the retention time ($r = 0.9954$), and it is independent of the reason for the change in retention time. Because of the linearity of the response, it should be possible to predict a slope for a new standard curve from a single concentration point. This would preclude the necessity of repeating an entire standard curve when the retention time of sulfinpyrazone changes, although a three-point standard curve would reinforce that reliability. Slopes were predicted from peak heights obtained from a 1-μg/ml drug solution run at different retention times. These values are listed in Table II. Entire standard curves were then run at different retention times and slopes were calculated by linear regression analysis. The latter values are also listed in Table II. The maximum difference between the observed and predicted values of the slope was 2.7%.

It is evident from the results that paired-ion reversed-phase HPLC is a good method for assaying sulfinpyrazone in plasma. Using disposable C_{18} cartridges further simplifies the analysis, since the entire separation of drug from plasma can be accomplished in 2 min. This isolation method also has the advantage of not requiring large volumes of expensive organic solvents as do conventional extraction procedures. While the reported calibration curve used 0.2 μg/ml as the lowest concentration, the sensitivity could easily be increased by increasing the injection volume. This sensitivity is adequate for pharmacokinetic studies or therapeutic drug level monitoring.

REFERENCES

(1) Anturane Reinfarction Trial Research Group, *N. Engl. J. Med.*, **298**, 289 (1978).

(2) *Idem.*, **302**, 250 (1980).

(3) J. J. Burns, T. F. Yu, A. Ritterband, J. M. Perel, A. B. Gutman, and B. B. Brodie, *J. Pharmacol. Exp. Ther.*, **119**, 418 (1957).

(4) T. Inaba, M. E. Besley, and E. J. Chow, *J. Chromatogr.*, **104**, 165 (1975).

(5) J. Lecaillon and C. Souppart, *ibid.*, **121**, 227 (1976).

(6) L. T. Wong, G. Solomonraj, and B. H. Thomas, *ibid.*, **150**, 521 (1978).

ACKNOWLEDGMENTS

Presented at the APhA Academy of Pharmaceutical Sciences meeting, Anaheim Calif., April 1979.

Protein Binding of Caffeine in Young and Elderly Males

JAMES BLANCHARD

Received January 18, 1982, from the *Department of Pharmaceutical Sciences, College of Pharmacy, University of Arizona, Tucson, AZ 85721.* Accepted for publication February 22, 1982.

Abstract □ The plasma protein binding of caffeine in young and elderly males was evaluated using an ultrafiltration technique. In spite of a significantly lower plasma albumin concentration in the elderly subjects the observed percent bound (~35%) was essentially identical in both subject groups. The binding of caffeine to human plasma albumin (4.5% w/v) *in vitro* was also examined using ultracentrifugation and it was observed to be bound to the extent of 37.8%. In both the plasma and albumin binding studies the free fraction remained constant over the range of concentrations examined. Although there was no apparent correlation between the percent bound and the albumin concentration in the plasma of either subject group the close agreement between the degree of binding of caffeine to albumin and human plasma indicates that albumin is likely the major plasma binding protein for caffeine.

Keyphrases □ Caffeine—protein binding in young and elderly males, ultrafiltration □ Protein binding—caffeine in young and elderly males, ultrafiltration □ Ultrafiltration—protein binding of caffeine in young and elderly males

It is well known that drug–protein interactions can influence drug pharmacokinetics (1). Since plasma albumin concentration decreases and globulin concentration increases with aging (2, 3), and because a great many drugs are bound reversibly to plasma albumin, the potential importance of age-related changes in protein binding is clear. Of the relatively few studies that have examined the effect of age on protein binding, significant reductions in binding with aging have been reported for meperidine, phenylbutazone, phenytoin, and warfarin, while for phenobarbital, benzylpenicillin, diazepam, desmethyldiazepam, salicylate and sulfadiazine, no alterations in the extent of binding were observed (4). While some studies of caffeine binding *in vitro* (5) and *in vivo* (6, 7) have been reported, no specific examination of possible alterations in its binding characteristics with aging has been made. Since the pharmacological effect of caffeine is probably best related to its unbound fraction (as is true for most drugs), knowledge of any age-related binding differences could prove valuable in helping to interpret the pharmacokinetics of this widely consumed agent, which has received increased attention recently due to its possible role in the treatment of premature apnea (8). The goal of this study was, therefore, to compare the plasma protein binding of caffeine in young and elderly subjects.

EXPERIMENTAL

Subject Selection—Ten healthy, young adult male volunteers ranging in age from 18.8 to 30.0 years and eight healthy, active elderly male volunteers aged 66.0–78.2 years were studied. All subjects were given a physical examination, electrocardiogram, and the following laboratory tests: plasma urea, electrolytes, creatinine, bilirubin, aspartate aminotransferase, alkaline phosphatase, total protein, albumin, creatinine clearance, and complete blood count. In addition, all subjects had a normal health history and were not taking any medication at the time of the study.

0022-3549/82/1200-1415$01.00/0

Table II—Observed and Predicted Values of Slopes

Retention Time, min	Observed Slope	Predicted Slope
5.2	91.81	90.27
7.8	70.47	68.58
8.0	61.69	59.68

mobile phase, such that changes in retention times occurred with slight changes in methanol concentration. Such changes in retention time would influence the peak heights, thus, peak areas were found to be preferable in the preparation of standard curves.

Peak heights can be used without constantly repeating standard curves, if a correction is made for changes in peak height due to changes in retention time. It is well established that an inverse relationship exists between peak heights and retention time. Different retention times were produced by varying pH, methanol concentration, and I concentration to study this relationship. The flow rate of the mobile phase, however, was always the same. There is a good correlation between the peak heights and the reciprocal of the retention time ($r = 0.9954$), and it is independent of the reason for the change in retention time. Because of the linearity of the response, it should be possible to predict a slope for a new standard curve from a single concentration point. This would preclude the necessity of repeating an entire standard curve when the retention time of sulfinpyrazone changes, although a three-point standard curve would reinforce that reliability. Slopes were predicted from peak heights obtained from a 1-μg/ml drug solution run at different retention times. These values are listed in Table II. Entire standard curves were then run at different retention times and slopes were calculated by linear regression analysis. The latter values are also listed in Table II. The maximum difference between the observed and predicted values of the slope was 2.7%.

It is evident from the results that paired-ion reversed-phase HPLC is a good method for assaying sulfinpyrazone in plasma. Using disposable C_{18} cartridges further simplifies the analysis, since the entire separation of drug from plasma can be accomplished in 2 min. This isolation method also has the advantage of not requiring large volumes of expensive organic solvents as do conventional extraction procedures. While the reported calibration curve used 0.2 μg/ml as the lowest concentration, the sensitivity could easily be increased by increasing the injection volume. This sensitivity is adequate for pharmacokinetic studies or therapeutic drug level monitoring.

REFERENCES

(1) Anturane Reinfarction Trial Research Group, *N. Engl. J. Med.*, **298**, 289 (1978).

(2) *Idem.*, **302**, 250 (1980).

(3) J. J. Burns, T. F. Yu, A. Ritterband, J. M. Perel, A. B. Gutman, and B. B. Brodie, *J. Pharmacol. Exp. Ther.*, **119**, 418 (1957).

(4) T. Inaba, M. E. Besley, and E. J. Chow, *J. Chromatogr.*, **104**, 165 (1975).

(5) J. Lecaillon and C. Souppart, *ibid.*, **121**, 227 (1976).

(6) L. T. Wong, G. Solomonraj, and B. H. Thomas, *ibid.*, **150**, 521 (1978).

ACKNOWLEDGMENTS

Presented at the APhA Academy of Pharmaceutical Sciences meeting, Anaheim Calif., April 1979.

Protein Binding of Caffeine in Young and Elderly Males

JAMES BLANCHARD

Received January 18, 1982, from the *Department of Pharmaceutical Sciences, College of Pharmacy, University of Arizona, Tucson, AZ 85721.* Accepted for publication February 22, 1982.

Abstract □ The plasma protein binding of caffeine in young and elderly males was evaluated using an ultrafiltration technique. In spite of a significantly lower plasma albumin concentration in the elderly subjects the observed percent bound (~35%) was essentially identical in both subject groups. The binding of caffeine to human plasma albumin (4.5% w/v) *in vitro* was also examined using ultracentrifugation and it was observed to be bound to the extent of 37.8%. In both the plasma and albumin binding studies the free fraction remained constant over the range of concentrations examined. Although there was no apparent correlation between the percent bound and the albumin concentration in the plasma of either subject group the close agreement between the degree of binding of caffeine to albumin and human plasma indicates that albumin is likely the major plasma binding protein for caffeine.

Keyphrases □ Caffeine—protein binding in young and elderly males, ultrafiltration □ Protein binding—caffeine in young and elderly males, ultrafiltration □ Ultrafiltration—protein binding of caffeine in young and elderly males

It is well known that drug–protein interactions can influence drug pharmacokinetics (1). Since plasma albumin concentration decreases and globulin concentration increases with aging (2, 3), and because a great many drugs are bound reversibly to plasma albumin, the potential importance of age-related changes in protein binding is clear. Of the relatively few studies that have examined the effect of age on protein binding, significant reductions in binding with aging have been reported for meperidine, phenylbutazone, phenytoin, and warfarin, while for phenobarbital, benzylpenicillin, diazepam, desmethyldiazepam, salicylate and sulfadiazine, no alterations in the extent of binding were observed (4). While some studies of caffeine binding *in vitro* (5) and *in vivo* (6, 7) have been reported, no specific examination of possible alterations in its binding characteristics with aging has been made. Since the pharmacological effect of caffeine is probably best related to its unbound fraction (as is true for most drugs), knowledge of any age-related binding differences could prove valuable in helping to interpret the pharmacokinetics of this widely consumed agent, which has received increased attention recently due to its possible role in the treatment of premature apnea (8). The goal of this study was, therefore, to compare the plasma protein binding of caffeine in young and elderly subjects.

EXPERIMENTAL

Subject Selection—Ten healthy, young adult male volunteers ranging in age from 18.8 to 30.0 years and eight healthy, active elderly male volunteers aged 66.0–78.2 years were studied. All subjects were given a physical examination, electrocardiogram, and the following laboratory tests: plasma urea, electrolytes, creatinine, bilirubin, aspartate aminotransferase, alkaline phosphatase, total protein, albumin, creatinine clearance, and complete blood count. In addition, all subjects had a normal health history and were not taking any medication at the time of the study.

0022-3549/82/1200-1415$01.00/0

Plasma-Binding Studies—After obtaining informed consent, all subjects were administered a 5-mg/kg dose of caffeine both intravenously[1] and orally[2] on separate occasions ~1 week apart, using a randomized crossover design. The subjects were instructed to abstain from caffeine-containing foods and beverages, tobacco, and alcohol from 72 hr before until 24 hr after each dose of caffeine. Blood samples (10 ml) were collected at 0.25, 1, 4, and 9 hr following the oral dose and at 0.25, 2, 6, and 12 hr following the intravenous dose. Plasma samples were harvested immediately and divided into two aliquots. One aliquot, designated D_t, was stored at −20° until assayed. Three milliliters of the second aliquot was placed in a membrane cone[3], covered[4], and centrifuged at 250×*g* for 30 min, which produced ~1 ml of ultrafiltrate. The ultrafiltrates were tested[5] to ensure that no protein had passed through the cones. If this test indicated that more than a trace of protein was present, another aliquot of plasma was ultrafiltered using a new cone. Previous tests using the Lowry method of assay for protein had indicated that the CF-25 cones removed ~99.8% of the protein from plasma (9). The protein-free ultrafiltrates were then stored at −20°. The ultrafiltrates and D_t samples were assayed in duplicate using a slight modification of a technique described elsewhere (10), the difference being that the protein in plasma samples was precipitated with an equal volume of perchloric acid (12% w/w) in place of the sodium tungstate–sulfuric acid mixture used before, since this precipitant was found to produce a slightly cleaner supernatant (9).

Correction for Membrane Cone Binding—To assess whether significant amounts of caffeine were binding to the membrane cones under the conditions employed in the plasma binding studies, the following experiment was performed. Stock solutions of caffeine at 1, 5, 10, and 20 μg/ml concentrations were prepared in saline phosphate buffer (11). Three-milliliter portions of each stock solution were then placed in membrane cones, which were treated in the usual fashion. The average percent bound over all the cones was then subtracted from each percent bound calculated in the plasma binding experiments to provide a corrected percent bound value.

Albumin Binding Studies—The binding of caffeine to human albumin was studied as follows. A stock solution (5% w/v) of human albumin (essentially fatty acid free)[6] in pH 7.4 saline phosphate buffer was prepared. Sufficient amounts of caffeine in saline phosphate buffer were added to this solution to produce 5 ml of solution containing final concentrations of 1, 5, 10, and 20 μg/ml caffeine in albumin (4.5% w/v). The caffeine–albumin solutions were allowed to equilibrate for 30 min in a 37° water bath. Aliquots (0.5 ml) of these solutions (designated D_t) were then taken and stored at −20°. The remainder of these samples were ultracentrifuged[7] at 4° for 15 hr at 260,000×*g*. Then 0.6 ml of the top layer (designated D_f) was removed, tested[5] to ensure that it was essentially protein free, and stored at −20° until assayed. All samples were assayed in the same manner as the plasma samples.

Calculation of Binding Capacity—The extent of binding was calculated using:

$$\% \text{ Bound } (\beta) = \frac{Db}{Dt} \times 100 = \frac{Dt - Df}{Dt} \times 100 \qquad \text{(Eq. 1)}$$

where Db is the concentration of drug bound to protein, Df is the concentration of free (unbound) drug present in the protein-free ultrafiltrate or upper layer of the ultracentrifuged sample, and Dt is the total concentration of drug (bound plus free) present in the samples prior to ultrafiltration or ultracentrifugation.

Analysis of Data—Differences in the various parameters between the young and elderly groups were assessed using a two-tailed Student's *t* test for unpaired data, with $p < 0.05$ being taken as the minimum level of significance.

RESULTS AND DISCUSSION

The results of the plasma binding studies are summarized in Table I. The values shown have been corrected for the observed degree of binding of caffeine to the membrane cones. It was found that the mean β value for the binding of caffeine to the cones ($n = 18$) was 12.13 ± 0.83% (mean ± *SEM*). The reduction in the total plasma protein concentration observed in the elderly group was not significant ($p > 0.1$), whereas the reduction in the plasma albumin concentration was significant ($p < 0.001$). Both of these observations are consistent with data previously reported (12).

Table I—Comparison of the Plasma Protein Binding of Caffeine in Young and Elderly Males

Parameter	Young Group ($n = 10$) Mean	Young Group ($n = 10$) *SEM*	Elderly Group ($n = 8$) Mean	Elderly Group ($n = 8$) *SEM*	Level of Significance
Age	21.80	1.14	71.20	1.39	$p < 0.001$
Total plasma protein (g/liter)	73.30	1.68	70.00	1.44	NS[a]
Plasma albumin (g/liter)	45.90	0.77	41.13	0.58	$p < 0.001$
Percent bound	35.45	0.73	34.97	0.90	NS[a]
Unbound caffeine concentration (mg/liter)	2.95	0.19	3.06	0.23	NS[a]
Total caffeine concentration (mg/liter)	5.68	0.35	5.78	0.41	NS[a]

[a] Not significant.

In spite of the reduced plasma albumin concentration in the elderly, the observed percentage bound values reported for caffeine did not differ significantly ($p > 0.2$) between the two groups. In addition, the mean percent bound observed here of ~35% correlates well with the value of 31.3% previously reported (6) for 15 healthy male subjects ranging in age from 18 to 71 years. However, both of these values are substantially higher than the value of 15% bound to human plasma previously reported (7).

The following equation (13) illustrates how various factors, including the drug concentration, affect the degree of protein binding:

$$D_t = D_f \left[1 + \frac{nP_t}{\frac{1}{K} + D_f} \right] \qquad \text{(Eq. 2)}$$

where K is the binding association constant (liters per mole), P_t is the total protein concentration, and n is the number of binding sites per protein molecule. When $1/K \gg D_f$ and $n = 1$, Eq. 2 can be simplified to:

$$\alpha = \frac{D_f}{D_t} = \left[\frac{1}{1 + KP_t} \right] \qquad \text{(Eq. 3)}$$

This equation illustrates how the free (unbound) fraction (α) and, therefore, the bound fraction (β) are constants, provided $1/K \gg D_f$. Equation 3 also demonstrates the linear nature of the relationship between the unbound and total drug concentrations. Excellent linear correlations for caffeine binding in the plasma of the young ($r^2 = 0.9393$) and elderly ($r^2 = 0.9088$) subject groups were found (Fig. 1). This figure illustrates the constancy of the degree of binding over the concentration ranged examined, a finding which may also be true for many other drugs over their range of therapeutic concentrations (14). The near-superimposability of the regression lines for the young (slope = 0.5189) and elderly (slope = 0.5337) data is a further demonstration of the similarity in the binding behavior of caffeine in the two groups.

There are at least two plausible explanations for why the observed reduction in plasma albumin in the elderly group did not result in a concomitant reduction in the degree of plasma binding of caffeine. The first possibility is that the amount of drug bound to a given amount of albumin may somehow increase with aging, possibly due to a loss of some endogenous ligand which competes with caffeine for binding sites on albumin. Another possibility is that caffeine may bind to components of plasma other than albumin.

Figure 2 shows a plot of the average percent of caffeine bound to plasma *versus* the measured albumin concentration in each subject and illustrates how there was no apparent correlation between these two parameters. This contrasts with previous findings (6) where a direct linear correlation between the extent of caffeine plasma binding and the serum albumin concentrations was observed in the subject population.

The results of the *in vitro* studies of caffeine binding to plasma albumin are depicted in Fig. 3. These data indicate that caffeine is bound to albumin (4.5% w/v) to the extent of 37.81 ± 1.16% (mean ± *SEM*) with the

[1] Caffeine and Sodium Benzoate Injection, USP, Eli Lilly and Co., Indianapolis, IN 46285.
[2] Caffeine, Baker grade, J. T. Baker Chemical Co., Phillipsburg, NJ 08865.
[3] Centriflo Type CF25, Amicon Corp., Lexington, MA 02173.
[4] Parafilm, American Can Co., Greenwich, CT 06830.
[5] Albustix, Ames Company, Division of Miles Laboratories Ltd., Stoke Poges, Slough SL2 4LY, England.
[6] Product No. A-1887, Sigma Chemical Co., St. Louis, MO 63178.
[7] Model L5-65, Beckman Instruments Inc., Palo Alto, CA 94304.

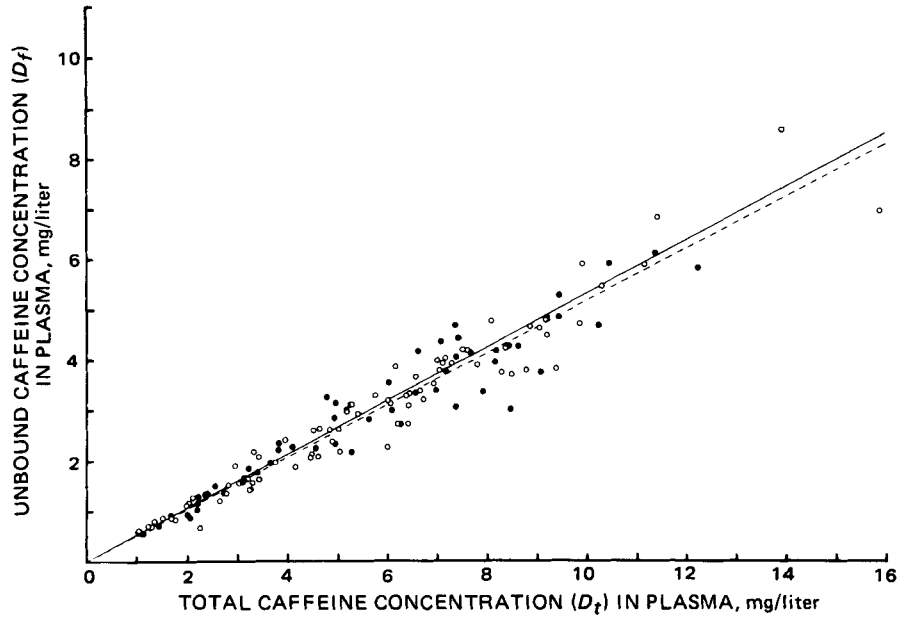

Figure 1—*Relationship between unbound and total caffeine concentrations in plasma of young (○ - - - ○) and elderly (●—●) men.*

percent bound being essentially constant over the concentration range of 1–20 μg/ml, indicating that only a small fraction of the available binding sites is occupied at these concentrations. The close similarity of the mean percent bound values for plasma and albumin implies that albumin is certainly the major plasma binding protein for caffeine, and possibly the only one. The values of the association constant (K) for the respective binding experiments can be calculated by substituting the mean values for β, D_f, and P_t into the rearranged form of Eq. 2 shown below:

$$K = \frac{\beta}{P_t - \beta(P_t + D_f)} \qquad \text{(Eq. 4)}$$

The assumptions involved here are that $n = 1$ and that caffeine only binds to the albumin component of plasma. Under these conditions the value of P_t for plasma in Eq. 4 can be obtained by dividing the average albumin content of plasma by 69,000 (the assumed molecular weight of albumin). The values of K shown in Table II indicate the close agreement of the association constants with one another and with the K value for the

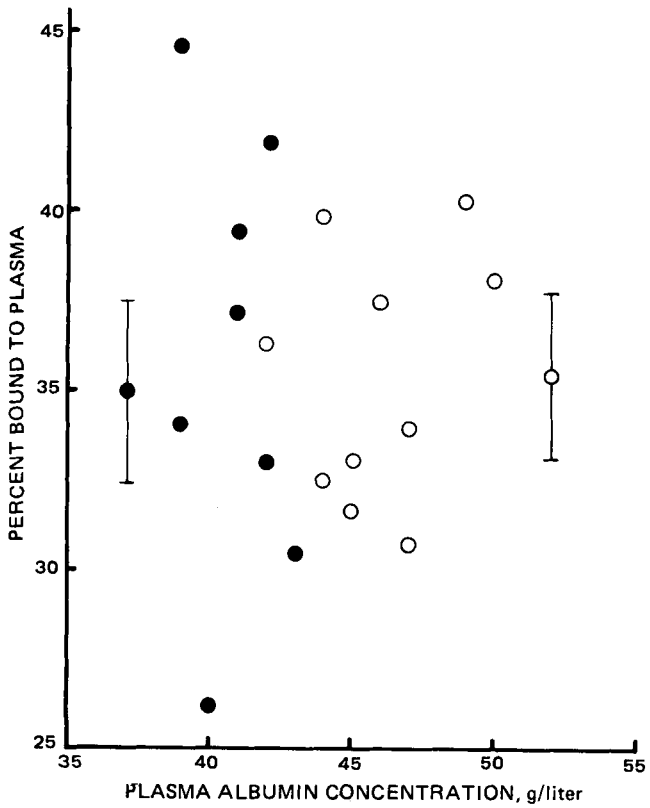

Figure 2—*The effect of plasma albumin concentration on the percentage of caffeine bound to plasma in young (○) and elderly (●) males. Each data point represents the mean of six to eight determinations. The vertical bars represent the means ± 1* SD.

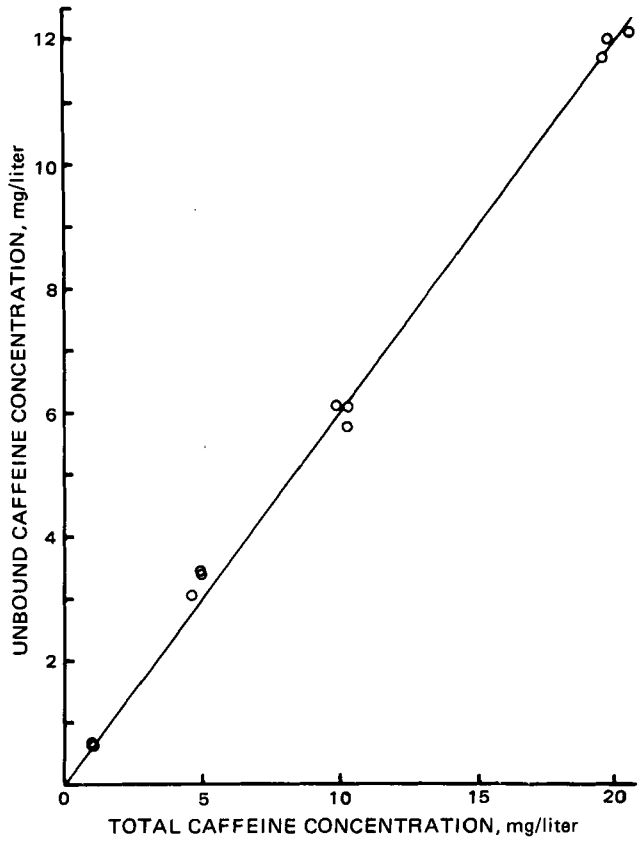

Figure 3—*Relationship between unbound and total concentrations for caffeine binding to human albumin (4.5% w/v)* in vitro. *The regression equation was* $D_f = 0.6012D_t (r^2 = 0.9964)$.

Table II—Calculated Binding Constants for the Interaction of Caffeine with Human Albumin and Human Plasma

Protein-Containing Sample	Binding Association Constant, K (liters/mole)
Human albumin in pH 7.4 buffer	0.958×10^3 (0.932×10^3)[a]
Human plasma from young subjects	0.839×10^3 (0.826×10^3)
Human plasma from elderly subjects	0.918×10^3 (0.902×10^3)

[a] Values in parentheses were calculated using Eq. 3, which assumes that the binding (β) is maximal. The similarity of the respective association constants calculated by each method indicates that drug concentrations are sufficiently low for binding to be nearly maximal.

binding of caffeine to albumin of 1.02×10^3 liters/mole reported previously (16). A 4.5% w/v albumin solution was utilized, since this value represents normal levels in humans and falls within the mean values for plasma albumin found in the two subject groups used in this study. In addition, the plasma binding experiments were performed at 37° using freshly collected (unfrozen) plasma, in view of previous reports (17–19) that the freeze–thaw process may alter drug binding. Thus, the results obtained here should be an accurate indication of the actual binding characteristics of caffeine *in vivo*.

While the binding of caffeine to human plasma is not extensive, and therefore not likely to exert a major influence on its overall pharmacokinetic behavior, a knowledge of the degree of binding over the usual therapeutic range (5–20 μg/ml) could prove useful when monitoring plasma caffeine concentrations in premature infants with apnea (8). These data could also be valuable when studying the effects of various diseases, other drugs, *etc.*, on the clearance of caffeine, since the clearance of unbound drug will be a more accurate indicator of the metabolizing capability of the liver than will the clearance of total (free + bound) drug (20).

REFERENCES

(1) W. J. Jusko and M. Gretch, *Drug Metab. Rev.*, **5**, 43 (1976).

(2) A. D. Bender, A. Post, P. Meier, J. E. Higson, and G. Reichard, Jr., *J. Pharm. Sci.*, **64**, 1711 (1975).

(3) R. J. Cammarata, G. P. Rodnan, and R. H. Fennell, *J. Am. Med. Assoc.*, **199**, 115 (1967).

(4) J. Crooks, K. O'Malley, and I. H. Stevenson, *Clin. Pharmacokinet.*, **1**, 280 (1976).

(5) M. L. Eichman, D. E. Guttman, Q. Van Winkle, and E. P. Guth, *J. Pharm. Sci.*, **51**, 66 (1962).

(6) P. V. Desmond, R. V. Patwardhan, R. F. Johnson, and S. Schenker, *Dig. Dis. Sci.*, **25**, 193 (1980).

(7) J. Axelrod and J. Reichenthal, *J. Pharmacol. Exp. Ther.*, **107**, 519 (1953).

(8) H. S. Bada, N. N. Khanna, S. M. Somani, and A. A. Tin, *J. Pediatr.*, **94**, 993 (1979).

(9) J. Blanchard, *J. Chromatogr.*, **226**, 445 (1981).

(10) J. Blanchard, J. D. Mohammadi, and J. M. Trang, *Clin. Chem.*, **27**, 637 (1981).

(11) J. V. Dacie and S. M. Lewis, Eds., "Practical Haematology," 5th ed., Churchill Livingstone, Edinburgh, 1975, p. 202.

(12) L. S. Libow, in "Human Aging: A Biological and Behavioral Study," J. E. Birren, R. N. Butler, S. W. Greenhouse, L. Sokoloff, and M. R. Yarrow, Eds., U.S. Department of Health, Education and Welfare, Washington, D.C., 1963, pp. 37–56.

(13) B. K. Martin, *Nature (London)*, **207**, 274 (1965).

(14) J.-P. Tillement, in "Advances in Pharmacology and Therapeutics, vol. 7, Biochemical–Clinical Pharmacology," J.-P. Tillement, Ed., Pergamon, New York, N.Y., 1979, pp. 103–111.

(15) P. Keen, in "Handbook of Experimental Pharmacology," vol. 28, part I, B. B. Brodie and J. R. Gillette, Eds., Springer-Verlag, New York, N.Y., 1971, pp. 213–233.

(16) M. C. Meyer and D. E. Guttman, *J. Pharm. Sci.*, **59**, 39 (1970).

(17) D. R. Hoar and D. J. Sissons, in "Methodological Developments in Biochemistry," E. Reid, Ed., North-Holland Publishing, New York, N.Y., 1976, p. 222.

(18) N. Barth, G. Alvan, O. Borga, and F. Sjoqvist, *Clin. Pharmacokinet.*, **1**, 444 (1976).

(19) A. J. Jackson, A. K. Miller, and P. K. Narang, *J. Pharm. Sci.*, **70**, 1168 (1981).

(20) G. R. Wilkinson and D. G. Shand, *Clin. Pharmacol. Ther.*, **18**, 377 (1975).

ACKNOWLEDGMENTS

The author is grateful to Ms. Sedley Josserand for her skilled technical assistance. Special thanks are extended to Dr. Stewart Sawers and Dr. Laurie F. Prescott of the Department of Therapeutics and Clinical Pharmacology, The Royal Infirmary, Edinburgh, Scotland who helped make portions of this study possible. The receipt of Fellowship No. 1 FO6 TW00491-01 from the John E. Fogarty International Center and the National Institute on Aging is gratefully acknowledged.

Activity of Sodium Ricinoleate Against *In Vitro* Plaque

JOYCE J. MORDENTI *x, **RICHARD E. LINDSTROM**, and **JASON M. TANZER** ‡

Received September 1, 1981, from the *Department of Pharmaceutics, School of Pharmacy, University of Connecticut, Storrs, CT 06268.* Accepted for publication February 26, 1982. *Present address: Department of Medical Research, Hartford Hospital, Hartford, CT 06115. ‡Present address: Department of Oral Diagnosis, School of Dental Medicine, University of Connecticut Health Center, Farmington, CT 06032.

Abstract □ The antiplaque activity of sodium ricinoleate was studied *in vitro* against intact preformed plaques of *Streptococcus mutans*. The data obtained suggest that sodium ricinoleate may not interfere with *in vivo* plaque formation by *S. mutans*; however, there is some evidence that sodium ricinoleate may render these plaques less acidogenic.

Keyphrases □ Sodium ricinoleate—activity against *in vitro* dental plaque, bacterial formation □ Dental plaque—activity of sodium ricinoleate against bacterial formation, *in vitro* □ Bacterial formation—activity of sodium ricinoleate against *in vitro* dental plaque

The relationship between structure and bactericidal properties for numerous straight-chain fatty acids and derivatives has been studied (1, 2). The antimicrobial activity of fatty acids was shown to be a function of chain length, unsaturation, conformation, and functional groups. *Cis* monoenoic and dienoic C_{18} fatty acids were the most inhibitory (1), and unsaturation at the 2, 7, or 8 position gave the greatest biological activity (2). Long-chain fatty acids have limited solubility in water, and they are difficult to manipulate in most test situations; therefore, the aqueous soluble salt of a fatty acid which had several of the desirable antimicrobial features identified previously (1, 2) was examined as a novel antiplaque agent. Sodium ricinoleate [$CH_3(CH_2)_5CH(OH)CH_2CH{=}CH(CH_2)_7COO^-Na^+$], a *cis*-monoenoic C_{18} fatty acid salt, but with unsaturation at the 9 position, has attracted considerable attention due to its detoxifying, bactericidal, and anticalculus properties (3–15). Considering these studies and that sodium ricinoleate is extremely surface active, it was hypothesized that sodium ricinoleate could inhibit plaque formation and retention in the oral cavity through three possible modes of action: (*a*) antiadherent effect (coating the teeth with a repellent monolayer), (b) antibacterial effect (attaining bactericidal concentrations at the tooth surface, in the gingival sulcus, and in the intact plaque), and (*c*) detergent effect (breaking up the plaque for mechanical removal).

Although plaque has a mixed bacterial composition *in vivo*, there is a strong association between heavy infection by *S. mutans* and caries in humans and experimental animals (16–20), between the topographical localization of lesions on the enamel with overlying heavy colonization of *S. mutans* on that tooth site (21, 22), and between that colonization event and the subsequent inception of a lesion below the site of colonization (21, 23). Consequently, sodium ricinoleate's antiplaque activity was tested against *S. mutans*—the organism commonly associated with dental caries.

An *in vitro* assay had to be chosen which would reasonably simulate oral conditions and which would allow determination of dose–response relationships. In addition, the assay had to be reproducible, easily executed, inexpensive, and produce results in a minimum of time. *In vitro* tests have been developed in which model plaque specimens are formed on glass, wire, agar, bovine enamel, ceramic hydroxyapatite, and human teeth (24). After assessing the merits of each technique, the wire method (25–28) was chosen as the *in vitro* assay system to be used in this study. Growth of plaque on wires has received criticism in the past because wire is neither tooth enamel nor is it pellicle-coated (29). However, it has been shown (30) that plaque formation by *S. mutans* on enamel correlates closely (with and without salivary pellicle) with that on nichrome wires at both electron microscopic and biochemical levels. The wire model for bacterial attachment is a good predictor of bacterial–enamel interactions with this organism.

EXPERIMENTAL

Materials and Methods—Sodium ricinoleate[1] and chlorhexidine digluconate[2] were studied. *S. mutans* 6715-13 was studied; its properties with respect to a variety of antiseptics is typical of strains of *S. mutans* (26–28). The organisms were maintained by monthly transfer to fresh fluid thioglycollate medium containing 20% (v/v) meat extract[3] and excess calcium carbonate. Cultures were stored at 4°.

Minimum Inhibitory Concentration and Minimum Bactericidal Concentration for Bacterial Suspension—The minimum inhibitory concentration of sodium ricinoleate against *S. mutans* in complex medium (31) with 5% (w/v) sucrose, 0.005% (w/v) sodium carbonate, and bromocresol purple pH indicator (2 mg/liter) was determined by the macrobroth dilution method (32). (The pH indicator was incorporated into the culture fluid to visually detect acid production: a color change from purple (pH > 6.8) to yellow (pH < 5.2) denoted acid production.) The test was then repeated to measure the minimum bactericidal concentration as a function of time for various concentrations of sodium ricinoleate. At hourly intervals, the color of each solution was noted, and one loopful of each solution was plated on blood agar to detect viable organisms.

Minimum Bactericidal Concentration and Minimum Killing Time for Intact Plaque—Plaque was grown on #20 nichrome wires using a previous method (26). In that method 0.1 ml of an overnight culture of *S. mutans* in fluid thioglycollate was transferred to 150 × 18-mm culture tubes containing 10 ml of sterile complex medium (31) with 5% sucrose and 0.005% sodium carbonate. The nichrome wires, fixed to culture tube closures, were suspended in this bacterial broth for 24 hr at 37°. The wires were transferred daily to fresh medium until the wire-adherent microorganisms (*in vitro* plaques) had grown to a McCabe rating of 4 (25). Then the wires were transferred for 2 hr to fresh broth, rinsed free of broth in sterile distilled water, and immersed for varying times in 10 ml of aqueous sodium ricinoleate (1–10%) or control agents (0.2% chlorhexidine[4] and sterile distilled water). After treatment, the plaque samples were rinsed twice in 15 ml of sterile distilled water and transferred to fresh complex medium containing 5% sucrose, 0.005% sodium carbonate, and bromocresol purple pH indicator. The plaque samples were judged to have been killed when culture acid production

[1] N. L. Industries, Bayonne, NJ 07002.
[2] Hibitane, Imperial Chemical Ind., Macclesfield, England.
[3] Difco Laboratories, Detroit, MI 48232.
[4] Chlorhexidine (0.2%) was used as a positive control throughout these studies because the interaction of chlorhexidine with *S. mutans* has been described extensively (26, 33).

0022-3549/82/1200-1419$01.00/0

Table I—Effects of Various Concentrations of Sodium Ricinoleate upon Cell Growth, Survival Time, and Acid Production of *Streptococcus mutans*

Concentration, Sodium Ricinoleate, %	Cell Growth[a]	Maximum Survival time, Hr	pH[b]
10	No	0.1	>6.8
5	No	1	>6.8
4	No	2	>6.8
3	No	3	>6.8
2	No	5	>6.8
1	No	7	>6.8
5×10^{-1}	Yes	10	>6.8
2.5×10^{-1}	Yes	12	>6.8
1.25×10^{-1}	Yes	15	>6.8
6.25×10^{-2}	Yes	18	5.2–6.8
3.12×10^{-2}	Yes	22	5.2–6.8
1.56×10^{-2}	Yes	>24	<5.2
0	Yes	>24	<5.2

[a] Detected as an increase in turbidity. [b] As determined by the bromocresol purple pH indicator that was incorporated in the culture fluid.

stopped [*i.e.*, lack of a color change from purple (pH > 6.8) to yellow (pH < 5.2)], by a lack of increase in culture turbidity, and by the failure of 24-hr posttreatment plaque samples to grow when plated on either blood agar or *mitis salivarius* agar.

Penetration Through the Plaque Barrier—Immature wire-adherent plaques were grown to a McCabe rating of 1. The wires were immersed for 10 min in either 10% sodium ricinoleate or control agents (sterile distilled water and 0.2% chlorhexidine[4]), and the antibacterial effects of the agents were tested as detailed above.

RESULTS AND DISCUSSION

Minimum Inhibitory Concentration and Minimum Bactericidal Concentration for Bacteria in Suspension—*S. mutans* was selected as the test organism because it has been identified as a plaque producer associated with lesions (16–23). The minimum inhibitory concentration against *S. mutans* was determined to be 1% (or 3.12×10^{-2} *M*) sodium ricinoleate. During the minimum inhibitory concentration testing, four distinct concentration-dependent cell growth and acid production phenomena were identified: (*a*) no cell growth, medium pH[5] > 6.8; (*b*) cell growth[6], medium pH > 6.8; (*c*) cell growth, medium pH 5.2–6.8; and (*d*) cell growth, medium pH < 5.2. To better characterize these phenomena and to determine the minimum bactericidal concentration as a function of time, another experiment was conducted in which the pH of each culture and the viability of the organisms were examined over a 24-hr period (Table I).

Minimum Bactericidal Concentration and Minimum Killing Time for Intact Plaque—*S. mutans* formed uniform wire-adherent plaque specimens. When the plaque specimens had reached a McCabe rating of 4, they were placed in treatment solutions for 10 min according to the method described in *Experimental*. Although 0.2% chlorhexidine killed the plaque specimens, the sodium ricinoleate (1–10%) treatments and the distilled water controls were unable to do so. The plaques that had been in the sodium ricinoleate treatment group showed a sizable lag time in detectable acid production when compared with the distilled water control group. This lag time increased with increasing concentrations of sodium ricinoleate.

To test the effects of increased treatment time upon plaque viability, those that had reached a McCabe rating of 4 were submerged for varying times in 1% sodium ricinoleate, 0.2% chlorhexidine, or distilled water. Even after 18 hr of treatment, the plaques remained viable in both the sodium ricinoleate and distilled water groups; however, the 1% sodium ricinoleate group showed a marked delay in reduction of medium pH when compared with the distilled water controls (Table II).

The minimum bactericidal concentration of sodium ricinoleate against *in vitro* plaques of *S. mutans* was not established because concentrations of sodium ricinoleate >10% and treatment times >10 min are beyond the conditions that would be clinically acceptable.

[5] As determined by the bromocresol purple pH indicator incorporated in the culture fluid.

[6] Detected as an increase in culture turbidity.

Table II—Effects of Varying Duration of Treatment Upon the Ability of *Streptococcus mutans* in Intact Plaque to Lower the Culture Fluid pH < 5.2[a]

Length of Treatment, Hr	Hours Between Treatment and Detection of Acid: 1% Sodium Ricinoleate	Distilled Water	0.2% Chlorhexidine
1	24	24	—[b]
7	48	24	—
18	72	36	—

[a] As determined by the bromocresol purple pH indicator that was incorporated in the culture fluid. [b] Chlorhexidine (0.2%) kills the plaque within 10 min; therefore, the plaque specimens were not viable and did not produce acid.

It is possible that agent adsorption to saliva-coated surfaces *in vivo* could play a significant role in the pharmacodynamics of any plaque antiseptic. However, this is of significant interest only if the agent shows appreciable potency. The test conditions used (≤7 hr of direct plaque exposure to 1% ricinoleate being required to evidence any antimicrobial effect) strongly suggest that even substantial adsorption–desorption would only trivially affect potency. Thus, no assessment was made of agent binding *per se*.

When the experiments were completed, the ease of plaque removal was examined in the sodium ricinoleate and distilled water treatment groups; in both groups the plaque remained firmly attached to the wires. A qualitative difference was not evident between the two groups.

Penetration Through the Plaque Barrier—Wires with only minimal plaque accumulation (McCabe rating of 1) were immersed for 10 min in 10% sodium ricinoleate, distilled water, or 0.2% chlorhexidine. At the end of the testing, the plaque specimens treated with 10% sodium ricinoleate or distilled water remained viable. Again, a sizable delay in detectable acid production, in some instances as great as 3 days, was observed following the sodium ricinoleate treatment. These data suggest that the outer layer of cells and glucan matrix of *S. mutans* plaque constitute a diffusion barrier to sodium ricinoleate, allowing a small number of *S. mutans* to survive.

CONCLUSIONS

The recognition of the important role of dental plaque in the pathogenesis of caries, gingivitis, and periodontal disease has prompted many investigators to search for chemical agents capable of either inhibiting or removing dental plaque. Useful antiplaque agents may be ones that quickly inhibit bacterial attachment to the tooth surface, kill intact plaque, and/or assist in the removal of attached plaque and matrix. The ideal agent must be effective at a concentration that is nontoxic to humans and nonirritating to the oral mucosa.

In the preliminary minimum inhibitory concentration and minimum bactericidal concentration experiments, sodium ricinoleate was shown to possess bactericidal activity against the representative *S. mutans* strain 6715-13. In later experiments, wire-adherent plaque specimens were treated with various concentrations of sodium ricinoleate for varying lengths of time. In all tests, the intact plaque samples survived. The ability of sodium ricinoleate to kill bacteria in suspension, but not in intact plaque, clearly demonstrates the lack of a correlation between antibacterial activity against cells in suspension and antiplaque activity (9, 26, 29).

The treatment of intact plaque with sodium ricinoleate brought about a noticeable decrease in detectable acid production; the effect became more pronounced with increasing concentrations of sodium ricinoleate. This reduced acidogenicity can be due to the buffering of acidic bacterial end-products by sodium ricinoleate; the increased bacterial killing with increased concentrations of sodium ricinoleate; and/or the reversible effects such as inhibition of metabolic processes, as has been shown for a number of long-chain fatty acids (34). By reducing the acidogenicity of established plaque, sodium ricinoleate may exert a clinical effect upon the cariogenicity of plaque caused by *S. mutans* even if plaque formation by this organism is not totally prevented.

REFERENCES

(1) J. J. Kabara, D. M. Swieczkowski, A. J. Conley, and J. P. Truant, *Antimicrob. Agents Chemother.*, **2**, 23 (1972).

(2) J. J. Kabara, A. J. Conley, and D. M. Swieczkowski, *J. Med. Chem.*, **16**, 1060 (1973).

(3) W. P. Larson, *Proc. Soc. Exp. Biol. Med.*, **19**, 62 (1921).

(4) W. P. Larson and E. Nelson, *ibid.*, **21**, 278 (1924).
(5) W. P. Larson R. D. Evans, and E. Nelson, *ibid.*, **22**, 194 (1924).
(6) T. B. Hartzell, *J. Am. Dent. Assoc.*, **12**, 1452 (1925).
(7) W. P. Larson and H. Eder, *J. Am. Med. Assoc.*, **86**, 998 (1926).
(8) H. E. Jones, *Br. J. Dent. Sci.*, **70**, 171 (1927).
(9) A. S. Hopkins, *Dent. Cosmos*, **72**, 830 (1930).
(10) S. F. Seeley, *Ann. Surg.*, **96**, 350 (1932).
(11) S. V. Mead, *J. Dent. Res.*, **16**, 41 (1937).
(12) W. F. Dossenback and H. R. Muhlemann, *Helv. Odontol. Acta*, **5**, 25 (1961).
(13) H. E. Schroeder, T. M. Marthaler, and H. R. Muhlemann, *ibid.*, **6**, 6 (1962).
(14) D. G. Demmers and C. M. Belting, *J. Periodontol.*, **38**, 294 (1967).
(15) W. van Betteray and P. Riethe, *Caries Res.*, **7**, 85 (1973).
(16) R. J. Fitzgerald and P. H. Keyes, *J. Am. Dent. Assoc.*, **61**, 9 (1960).
(17) R. J. Fitzgerald, H. V. Jordan, and H. R. Stanley, *J. Dent. Res.*, **39**, 923 (1960).
(18) B. Krasse, *Arch. Oral Biol.*, **11**, 429 (1966).
(19) N. W. Littleton, S. Kakehashi, and R. J. Fitzgerald, *ibid.*, **15**, 461 (1970).
(20) J. D. de Stoppelaar, J. van Houte, and O. Backer Dirks, *Caries Res.*, **3**, 190 (1969).
(21) T. Ikeda, H. J. Sandham, and E. L. Bradley, *Arch. Oral Biol.*, **18**, 555 (1973).
(22) S. Duchin and J. van Houte, *ibid.*, **23**, 779 (1978).
(23) B. Kohler, B. M. Pettersson, and D. Bratthall, *Scand. J. Dent. Res.*, **89**, 19 (1981).
(24) R. A. Coburn, *J. Dent. Res.*, **58**, 2396 (1979).
(25) R. M. McCabe, P. H. Keyes, and A. Howell, Jr., *Arch. Oral Biol.*, **12**, 1653 (1967).
(26) J. M. Tanzer, Y. Reid, and W. Reid, *Antimicrob. Agents Chemother.*, **1**, 376 (1972).
(27) J. M. Tanzer, A. M. Slee, B. Kamay, and E. Scheer, *ibid.*, **12**, 107 (1977).
(28) *Idem.*, **15**, 408 (1979).
(29) R. T. Evans, P. J. Baker, R. A. Coburn, and R. J. Genco, *J. Dent. Res.*, **56**, 559 (1977).
(30) N. Tinanoff, J. M. Tanzer, and M. L. Freedman, *Infect. Immun.*, **21**, 1010 (1978).
(31) H. V. Jordan, R. J. Fitzgerald, and A. E. Bowler, *J. Dent. Res.*, **39**, 116 (1960).
(32) J. A. Washington, II., and A. L. Barry, in "Manual of Clinical Microbiology," 2nd ed., E. H. Lennette, E. H. Spaulding, and J. P. Truant, Eds., American Society for Microbilogy, Washington, D.C., 1974, p. 414.
(33) J. M. Tanzer, A. M. Slee, and B. A. Kamay, *Antimicrob. Agents Chemother.*, **12**, 721 (1977).
(34) E. Freese, C. W. Sheu, and E. Galliers, *Nature (London)*, **241**, 321 (1973).

ACKNOWLEDGMENTS

Joyce J. Mordenti is an American Foundation for Pharmaceutical Education Fellow and a Josiah Kirby Lilly Memorial Fellow.

COMMUNICATIONS

Use of Continuous Withdrawal Technique to Estimate the Initial Area Under the Curve

Keyphrases □ Continuous withdrawal technique—estimation of the initial area under the plasma concentration–time curve □ Pharmacokinetics—use of the continuous withdrawal technique to estimate the initial area under the plasma concentration–time curve □ Clearance—use of the continuous withdrawal technique to estimate the plasma concentration–time curve

To the Editor:

Recently it was pointed out (1) that the instantaneous input hypothesis of the conventional compartmental models may overestimate the area under the plasma concentration *versus* time curve (*AUC*). It was shown that the *AUC* of furosemide could be overestimated, using extrapolation to time zero, by as much as 20% in the dog. This is consistent with data found for Evans blue when used to measure cardiac output (2). In the first 12 sec after an intravenous bolus injection, no dye could be found in the arterial blood; then, the concentration rose gradually, not reaching a peak for several more seconds. Thereafter, it declined for 10 sec before it rose again to a second, lower peak at ~38 sec.

Based on physiological considerations, the delay could be explained as the time needed to reach the sampling site from the administration site, with the second peak perhaps resulting from recirculation of the dye. This phenomenon is important for drugs with a fast initial decline, particularly where the initial phase potentially contains a significant portion of the *AUC*. It is the purpose of this communication to illustrate an ideal method for determination of the *AUC* in the initial period which reflects accurate values, regardless of distribution and elimination rates and sampling sites. This method is based upon the continuous sampling technique described previously (3) to determine various pharmacokinetic parameters, and has been used in our laboratory for several years with good success (4).

A peripheral vein was cannulated prior to the start of the study to facilitate constant blood withdrawal. The drug was then administered in another vein after initiating the constant withdrawal.

The amount of drug in collected plasma, A_w, withdrawn over time t, when a constant blood withdrawal at rate $\dot{V}$ is carried out, can be obtained from:

$$A_w = (1 - H)\dot{V} \int_0^t C dt \qquad \text{(Eq. 1)}$$

where C is the concentration of drug in the plasma at any time, and H is the hematocrit. The area under the curve, $\int_0^t C dt$, in the time period, t, therefore, can be obtained by the ratio $A_w/[\dot{V}(1 - H)]$. Because the plasma drug amount withdrawn is equal to the total volume withdrawn, V_w, multiplied by the plasma concentration in the withdrawn sample, C_w, and because:

(4) W. P. Larson and E. Nelson, *ibid.*, **21**, 278 (1924).
(5) W. P. Larson R. D. Evans, and E. Nelson, *ibid.*, **22**, 194 (1924).
(6) T. B. Hartzell, *J. Am. Dent. Assoc.*, **12**, 1452 (1925).
(7) W. P. Larson and H. Eder, *J. Am. Med. Assoc.*, **86**, 998 (1926).
(8) H. E. Jones, *Br. J. Dent. Sci.*, **70**, 171 (1927).
(9) A. S. Hopkins, *Dent. Cosmos*, **72**, 830 (1930).
(10) S. F. Seeley, *Ann. Surg.*, **96**, 350 (1932).
(11) S. V. Mead, *J. Dent. Res.*, **16**, 41 (1937).
(12) W. F. Dossenback and H. R. Muhlemann, *Helv. Odontol. Acta*, **5**, 25 (1961).
(13) H. E. Schroeder, T. M. Marthaler, and H. R. Muhlemann, *ibid.*, **6**, 6 (1962).
(14) D. G. Demmers and C. M. Belting, *J. Periodontol.*, **38**, 294 (1967).
(15) W. van Betteray and P. Riethe, *Caries Res.*, **7**, 85 (1973).
(16) R. J. Fitzgerald and P. H. Keyes, *J. Am. Dent. Assoc.*, **61**, 9 (1960).
(17) R. J. Fitzgerald, H. V. Jordan, and H. R. Stanley, *J. Dent. Res.*, **39**, 923 (1960).
(18) B. Krasse, *Arch. Oral Biol.*, **11**, 429 (1966).
(19) N. W. Littleton, S. Kakehashi, and R. J. Fitzgerald, *ibid.*, **15**, 461 (1970).
(20) J. D. de Stoppelaar, J. van Houte, and O. Backer Dirks, *Caries Res.*, **3**, 190 (1969).
(21) T. Ikeda, H. J. Sandham, and E. L. Bradley, *Arch. Oral Biol.*, **18**, 555 (1973).
(22) S. Duchin and J. van Houte, *ibid.*, **23**, 779 (1978).
(23) B. Kohler, B. M. Pettersson, and D. Bratthall, *Scand. J. Dent. Res.*, **89**, 19 (1981).
(24) R. A. Coburn, *J. Dent. Res.*, **58**, 2396 (1979).
(25) R. M. McCabe, P. H. Keyes, and A. Howell, Jr., *Arch. Oral Biol.*, **12**, 1653 (1967).
(26) J. M. Tanzer, Y. Reid, and W. Reid, *Antimicrob. Agents Chemother.*, **1**, 376 (1972).
(27) J. M. Tanzer, A. M. Slee, B. Kamay, and E. Scheer, *ibid.*, **12**, 107 (1977).
(28) *Idem.*, **15**, 408 (1979).
(29) R. T. Evans, P. J. Baker, R. A. Coburn, and R. J. Genco, *J. Dent. Res.*, **56**, 559 (1977).
(30) N. Tinanoff, J. M. Tanzer, and M. L. Freedman, *Infect. Immun.*, **21**, 1010 (1978).
(31) H. V. Jordan, R. J. Fitzgerald, and A. E. Bowler, *J. Dent. Res.*, **39**, 116 (1960).
(32) J. A. Washington, II., and A. L. Barry, in "Manual of Clinical Microbiology," 2nd ed., E. H. Lennette, E. H. Spaulding, and J. P. Truant, Eds., American Society for Microbilogy, Washington, D.C., 1974, p. 414.
(33) J. M. Tanzer, A. M. Slee, and B. A. Kamay, *Antimicrob. Agents Chemother.*, **12**, 721 (1977).
(34) E. Freese, C. W. Sheu, and E. Galliers, *Nature (London)*, **241**, 321 (1973).

ACKNOWLEDGMENTS

Joyce J. Mordenti is an American Foundation for Pharmaceutical Education Fellow and a Josiah Kirby Lilly Memorial Fellow.

COMMUNICATIONS

Use of Continuous Withdrawal Technique to Estimate the Initial Area Under the Curve

Keyphrases □ Continuous withdrawal technique—estimation of the initial area under the plasma concentration–time curve □ Pharmacokinetics—use of the continuous withdrawal technique to estimate the initial area under the plasma concentration–time curve □ Clearance—use of the continuous withdrawal technique to estimate the plasma concentration–time curve

To the Editor:

Recently it was pointed out (1) that the instantaneous input hypothesis of the conventional compartmental models may overestimate the area under the plasma concentration *versus* time curve (*AUC*). It was shown that the *AUC* of furosemide could be overestimated, using extrapolation to time zero, by as much as 20% in the dog. This is consistent with data found for Evans blue when used to measure cardiac output (2). In the first 12 sec after an intravenous bolus injection, no dye could be found in the arterial blood; then, the concentration rose gradually, not reaching a peak for several more seconds. Thereafter, it declined for 10 sec before it rose again to a second, lower peak at ~38 sec.

Based on physiological considerations, the delay could be explained as the time needed to reach the sampling site from the administration site, with the second peak perhaps resulting from recirculation of the dye. This phenomenon is important for drugs with a fast initial decline, particularly where the initial phase potentially contains a significant portion of the *AUC*. It is the purpose of this communication to illustrate an ideal method for determination of the *AUC* in the initial period which reflects accurate values, regardless of distribution and elimination rates and sampling sites. This method is based upon the continuous sampling technique described previously (3) to determine various pharmacokinetic parameters, and has been used in our laboratory for several years with good success (4).

A peripheral vein was cannulated prior to the start of the study to facilitate constant blood withdrawal. The drug was then administered in another vein after initiating the constant withdrawal.

The amount of drug in collected plasma, A_w, withdrawn over time t, when a constant blood withdrawal at rate $\dot{V}$ is carried out, can be obtained from:

$$A_w = (1 - H)\dot{V} \int_0^t C dt \qquad \text{(Eq. 1)}$$

where C is the concentration of drug in the plasma at any time, and H is the hematocrit. The area under the curve, $\int_0^t C dt$, in the time period, t, therefore, can be obtained by the ratio $A_w/[\dot{V}(1 - H)]$. Because the plasma drug amount withdrawn is equal to the total volume withdrawn, V_w, multiplied by the plasma concentration in the withdrawn sample, C_w, and because:

$$(1 - H)V = V_w/t \qquad \text{(Eq. 2)}$$

the following is obtained:

$$\int_0^t Cdt = C_w t \qquad \text{(Eq. 3)}$$

By keeping a constant withdrawal of blood and measuring the concentration of drug in the sample and the time of withdrawal, the *AUC* can readily and accurately be determined without the problems of extrapolation.

This method is especially valuable in the time just after administration of an intravenous bolus dose, because no assumptions regarding the distribution and elimination need to be made. At later time points, when it is more desirable to determine the various rate constants, the continuous withdrawal can be terminated and individual blood samples then can be taken.

We have used this method extensively for indocyanine green clearance in rabbits, where the initial half-life after a 0.1-mg/kg iv. bolus dose is ~0.8 min. Approximately 40–60% of the total area can be estimated to be located between 0 and 1 min if an extrapolation is carried out when the first sample is taken at 1 min. However, when a continuous withdrawal is carried out, only 20–30% of the total area is obtained in the first minute. Therefore, as much as a 1.5- to twofold underestimation of the clearance can be made when using single venous plasma concentration time points with extrapolation, rather than a continuous withdrawal technique for indocyanine green clearance in rabbits.

(1) W. L. Chiou, G. Lam, M.-L. Chen, and M. G. Lee, *J. Pharm. Sci.*, **70**, 1037 (1981).

(2) I. J. Fox and E. H. Wood, in, "Medical Physics," vol. 3, O. Glasser, Ed., Year Book Publisher, Chicago, Ill., 1960, pp. 155–163.

(3) B. Vogelstein, A. A. Kowarski, and P. S. Lietman, *Clin Pharmacol. Ther.*, **22**, 131 (1977).

(4) T. W. Guentert and S. Øie, *J. Pharmacol. Exp. Ther.*, **215**, 165 (1980).

Jin-ding Huang
Svein Øie ˣ
Department of Pharmacy S-926
University of California
San Francisco, CA 94143

Received June 4, 1982.
Accepted for publication August 4, 1982.
Supported in part by Grant GM-28423 from the National Institutes of Health.

Schiff Base Formation with Nitrogen of a Sulfonamido Group

Keyphrases □ Benzothiadiazones—Schiff base formation with the nitrogen of a sulfonamido group □ Schiff bases—formation with the nitrogen of a sulfonamido group □ Colored complexes—Schiff base formation with the nitrogen of a sulfonamido group

To the Editor:

Recently an unexpected result was reported (1): A violet-colored compound was reported to have formed on TLC plates when benzothiadiazines (I) were sprayed with acidified *p*-dimethylaminobenzaldehyde (II). Hennig *et al.* (1) stated that the type of colored complex formed between I and II was difficult to postulate, since there was no apparent record of Schiff base formation with the nitrogen of a sulfonamido group. We have an explanation that attempts to rationalize the formation of this colored complex.

Our studies with polythiazide (I*a*) have shown that II as well as acidified vanillin (II*a*) form a violet-colored compound. We have identified this compound to be a product of a double aldol condensation between acetone, used as the solvent for spotting I, and II or II*a* to form in each case, respectively, substituted distyryl ketone (V).

Bahner and Schultze (2) reported the formation of divanillylidene acetone (V*a*) in a photometric estimation of acetone. Compound V*a* is yellow in alkaline solutions and develops into a pink-violet color when acidified with hydrochloric acid.

We have noted that at pH 9 polythiazide partially decomposes into 4-amino-2-chloro-5-(methylsulfamyl)-benzenesulfonamide (VI). Compound VI reacts with acetone to form a Schiff base (see Scheme). The ionized form of this Schiff base has an R_f = 0.55 in an ethyl acetate–benzene (8:2) system. When sprayed with acidified vanillin, the Schiff base hydrolyzes and the acetone thus liberated reacts with vanillin to give a violet-colored spot on the chromatograms. A similar reaction takes place with acidified *p*-dimethylaminobenzaldehyde used as a spray reagent.

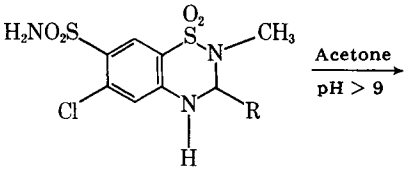

I

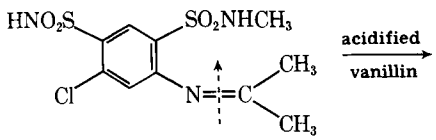

VI schiff base

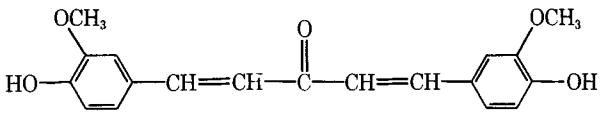

V*a*

Vanillin is often used as flavoring to mask the unpleasant taste of polythiazide tablets. If the alcohol that is used as a granulating liquid contains acetone as an impurity, the reaction in the Scheme may cause an incompatability problem resulting in colored granules.

(1) U. G. Hennig, R. E. Moskalyk, L. G. Chatten, and S. F. Chan, *J. Pharm. Sci.*, **70**, 317 (1981).

(2) F. Bahner and G. Schultze, *Z. Klin. Chem.*, **3**, 10, 1965; through Chem. Abstr., 16616-b, 1965.

A. B. Thakur
*S. Dayal*ˣ
Pharma Research and Development Department
Pfizer Ltd., Express Towers
Nariman Point
Bombay, India

Received March 1, 1982.
Accepted for publication July 19, 1982.

0022-3549/82/1200-1422$01.00/0

$$(1 - H)V = V_w/t \qquad \text{(Eq. 2)}$$

the following is obtained:

$$\int_0^t Cdt = C_w t \qquad \text{(Eq. 3)}$$

By keeping a constant withdrawal of blood and measuring the concentration of drug in the sample and the time of withdrawal, the *AUC* can readily and accurately be determined without the problems of extrapolation.

This method is especially valuable in the time just after administration of an intravenous bolus dose, because no assumptions regarding the distribution and elimination need to be made. At later time points, when it is more desirable to determine the various rate constants, the continuous withdrawal can be terminated and individual blood samples then can be taken.

We have used this method extensively for indocyanine green clearance in rabbits, where the initial half-life after a 0.1-mg/kg iv. bolus dose is ~0.8 min. Approximately 40–60% of the total area can be estimated to be located between 0 and 1 min if an extrapolation is carried out when the first sample is taken at 1 min. However, when a continuous withdrawal is carried out, only 20–30% of the total area is obtained in the first minute. Therefore, as much as a 1.5- to twofold underestimation of the clearance can be made when using single venous plasma concentration time points with extrapolation, rather than a continuous withdrawal technique for indocyanine green clearance in rabbits.

(1) W. L. Chiou, G. Lam, M.-L. Chen, and M. G. Lee, *J. Pharm. Sci.*, **70**, 1037 (1981).

(2) I. J. Fox and E. H. Wood, in, "Medical Physics," vol. 3, O. Glasser, Ed., Year Book Publisher, Chicago, Ill., 1960, pp. 155–163.

(3) B. Vogelstein, A. A. Kowarski, and P. S. Lietman, *Clin Pharmacol. Ther.*, **22**, 131 (1977).

(4) T. W. Guentert and S. Øie, *J. Pharmacol. Exp. Ther.*, **215**, 165 (1980).

Jin-ding Huang
Svein Øie ˣ
Department of Pharmacy S-926
University of California
San Francisco, CA 94143

Received June 4, 1982.
Accepted for publication August 4, 1982.
Supported in part by Grant GM-28423 from the National Institutes of Health.

Schiff Base Formation with Nitrogen of a Sulfonamido Group

Keyphrases □ Benzothiadiazones—Schiff base formation with the nitrogen of a sulfonamido group □ Schiff bases—formation with the nitrogen of a sulfonamido group □ Colored complexes—Schiff base formation with the nitrogen of a sulfonamido group

To the Editor:

Recently an unexpected result was reported (1): A violet-colored compound was reported to have formed on TLC plates when benzothiadiazines (I) were sprayed with acidified *p*-dimethylaminobenzaldehyde (II). Hennig *et al.* (1) stated that the type of colored complex formed between I and II was difficult to postulate, since there was no apparent record of Schiff base formation with the nitrogen of a sulfonamido group. We have an explanation that attempts to rationalize the formation of this colored complex.

Our studies with polythiazide (I*a*) have shown that II as well as acidified vanillin (II*a*) form a violet-colored compound. We have identified this compound to be a product of a double aldol condensation between acetone, used as the solvent for spotting I, and II or II*a* to form in each case, respectively, substituted distyryl ketone (V).

Bahner and Schultze (2) reported the formation of divanillylidene acetone (V*a*) in a photometric estimation of acetone. Compound V*a* is yellow in alkaline solutions and develops into a pink-violet color when acidified with hydrochloric acid.

We have noted that at pH 9 polythiazide partially decomposes into 4-amino-2-chloro-5-(methylsulfamyl)-benzenesulfonamide (VI). Compound VI reacts with acetone to form a Schiff base (see Scheme). The ionized form of this Schiff base has an R_f = 0.55 in an ethyl acetate–benzene (8:2) system. When sprayed with acidified vanillin, the Schiff base hydrolyzes and the acetone thus liberated reacts with vanillin to give a violet-colored spot on the chromatograms. A similar reaction takes place with acidified *p*-dimethylaminobenzaldehyde used as a spray reagent.

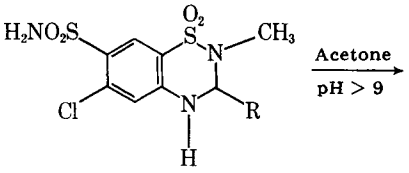

I

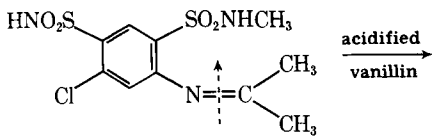

VI schiff base

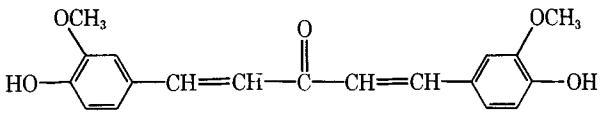

V*a*

Vanillin is often used as flavoring to mask the unpleasant taste of polythiazide tablets. If the alcohol that is used as a granulating liquid contains acetone as an impurity, the reaction in the Scheme may cause an incompatability problem resulting in colored granules.

(1) U. G. Hennig, R. E. Moskalyk, L. G. Chatten, and S. F. Chan, *J. Pharm. Sci.*, **70**, 317 (1981).

(2) F. Bahner and G. Schultze, *Z. Klin. Chem.*, **3**, 10, 1965; through Chem. Abstr., 16616-b, 1965.

A. B. Thakur
*S. Dayal*ˣ
Pharma Research and Development Department
Pfizer Ltd., Express Towers
Nariman Point
Bombay, India

Received March 1, 1982.
Accepted for publication July 19, 1982.

0022-3549/82/1200-1422$01.00/0

Calculation of the Nucleophilic Superdelocalizability by the CNDO/2 Method

Keyphrases □ Structure–activity relationships—calculation of the nucleophilic superdelocalizability by the CNDO/2 method, perturbation theory □ Perturbation theory—calculation of the nucleophilic superdelocalizability by the CNDO/2 method, structure–activity relationships □ Nucleophilic superdelocalizability—calculation by the CNDO/2 method, perturbation theory, structure–activity relationships

To the Editor:

In the application of the perturbation theory to the search of structure–activity relationships (1–3), there is an approximation that consists of replacing energies of the virtual molecular orbitals of the receptor by a constant. This replacement, expressed in previous reports (1, 4), leads to the appearance of the nucleophilic superdelocalizability index, S^N, of the atoms of a drug, in the expression relating the equilibrium constant to molecular structure factors. This index is usually calculated with semiempirical methods, like CNDO/2[1] (3) or INDO (2). The S^N index of the atom p is defined as:

$$S_p^N = 2 \sum_n \sum_j^{AO} \frac{C_{jn}^2}{E_n} \qquad \text{(Eq. 1)}$$

where n is the virtual molecular orbitals, E_n is the energy of the nth virtual molecular orbital, the summation on j is over the atomic orbitals (AO) of the atom p that contribute to the basis, and C_{jn} is one Linear Combination of Atomic Orbitals (LCAO) coefficient.

For one N electron system with a basis of t AOs, the CNDO/2 method produces $N/2$ occupied molecular orbitals and $(t - N/2)$ virtual molecular orbitals. These virtual molecular orbitals cannot be regarded as suitable for the description of the excited states of the system.

With the aim of examining the dependence of the CNDO/2 S^N values on the conformation, we have analyzed the value of this index for several rotamers in a group of molecules. Presented here are the results for the amine nitrogen and the carbon atom where the hydroxide group is attached, for six rotamers of the p-hydroxy-β-phenylethylamine in its basic and protonated form (Table I). For comparison, we present also the net charges and the electrophilic superdelocalizabilities of these atoms. The relative positions of the hydroxide group and the amine chain are referred to by *cis* and *trans*; parallel (//) and perpendicular ($\perp$) refer to the position of the substituents in relation to the phenyl ring. The geometry employed is composed of bond angles and bond distances normally found in crystallographic studies.

From Table I it can be seen that the values of Q and S^E do not change significantly between the different rotamers in the basic and protonated forms. The S^N index does not change in the basic rotamers; the protonated rotamers show profound changes, but these do not seem to show any relation with the conformation. Negative S^N values are due to the appearance of virtual molecular orbitals with negative energies.

Table I—Reactivity Indexes of the Nitrogen and Carbon (Hydroxide) Atoms of some Rotamers of the p-Hydroxy-β-Phenylethylamine

Form	Position of the —OH and Ethylamine Groups[a]	Q_c	S_c^E	S_c^N	Q_N	S_N^E	S_N^N
Basic							
	N //, O $\perp$	0.1588	−4.6864	13.2226	−0.2502	−7.0713	7.1340
	cis, N $\perp$, O $\perp$	0.1542	−4.7115	13.0695	−0.2477	−7.0288	7.2308
	trans, N $\perp$, O $\perp$	0.1542	−4.7120	13.0661	−0.2477	−7.0328	7.2234
	cis, N //, O //	0.1653	−4.6548	13.2010	−0.2502	−7.0740	7.1292
	trans, N //, O //	0.1655	−4.6549	13.1981	−0.2502	−7.0761	7.1255
	N $\perp$, O //	0.1609	−4.6802	13.0521	−0.2477	−7.0364	7.2158
Protonated							
	N //, O $\perp$	0.1816	−3.9527	84.9492	−0.0275	−3.9295	−81.9167
	cis, N $\perp$, O $\perp$	0.1810	−3.9575	−8.1637	−0.0268	−3.9247	−331.5201
	trans, N $\perp$, O $\perp$	0.1809	−3.9588	−15.6034	−0.0268	−3.9258	−409.2566
	cis, N //, O //	0.1878	−3.9273	54.8285	−0.0275	−3.9299	−371.0407
	trans, N //, O //	0.1877	−3.9281	44.8999	−0.0274	−3.9307	−563.3219
	N $\perp$, O //	0.1877	−3.9330	−32.9728	−0.0268	−3.9265	−621.9106

[a] The symbols // and $\perp$ indicate parallel and perpendicular positions, respectively, in relation to the phenyl ring.

Table II—S^N Value for the Nitrogen Atom in Some β-Phenylethylamines

Substituent	S^N
o—OCH_3	780.0266
m—OCH_3	77.0958
p—OH	−371.0407
p—CH_3	586.3877
—H	−302.6347

In Table II we present the S^N values for the nitrogen atom in a group of protonated β-phenylethylamines. All of the substituents are coplanar with the phenyl ring. Even so, the nitrogen S^N values seem to show no relation with the substitution.

Perhaps this lack of correlation between S^N and molecular structure in protonated molecules could explain why in some quantum chemical studies the S^N indexes do not appear, or, when they do, their t values are low.

This analysis strongly suggests that the S^N values obtained with the CNDO/2 method must be employed with caution in structure–activity studies.

Considering that a great number of molecules act in a protonated form and that the exact position of the substituents at the receptor level is not known, it seems necessary to define an S^N index that shows the same dependence on the conformation as the S^E index and the net charges.

[1] Unpublished data.

(1) F. Peradejordi, A. N. Martin, and A. C. Cammarata, *J. Pharm. Sci.*, **60**, 576 (1971).

0022-3549/82/1200-1423$01.00/0

(2) F. Tomas and J. M. Aulló, *ibid.*, **68**, 772 (1979).
(3) J. S. Gómez-Jeria and L. Espinoza, *Bol. Soc. Chil. Quím.*, **27**, 142 (1982).
(4) J. S. Gómez-Jeria and D. Morales-Lagos, *ibid.*, **27**, 44 (1982).

J. S. Gómez-Jeria
Universidad de Chile
Facultad de Ciencias Básicas y Farmacéuticas
Departmento de Química
Casilla 653, Santiago
Chile

Received June 14, 1982.
Accepted for publication August 4, 1982.
This work has received financial support from the Officina del Desarrollo Científico (Universidad de Chile), Project Q1574-8212.

Comments on the USP XX Gas Chromatographic Analysis of Alcohol in Drugs and Drug Formulations

Keyphrases □ GC—USP XX GC analysis of alcohol in drugs and drug formulations □ Alcohol—USP XX GC analysis in drugs and drug formulations

To the Editor:

The analysis of the alcohol content in drug formulations is a part of not only elixir and tincture monographs but also is included as a limit test for residual alcohol from the synthesis of some drug substances.

The performance of a divinylbenzene polymer for the GC analysis of alcohol was described previously (1), and it was concluded that there were definite advantages with the use of porous polymer beads for the analysis of alcohol in pharmaceuticals. In 1975 the 12th edition of the "Official Methods of Analysis of the Association of Official Analytical Chemists" (2) adopted a GC method for the analysis of alcohol in drugs which was based on a collaborated method developed previously (3). This procedure utilized a flame ionization detector and a column packed with a 80–100 mesh copolymer of ethylvinylbenzene and divinylbenzene[1] (I) operated at 130° with a retention time of ~5 min for acetonitrile, the internal standard. The USP XX (4) changed the chromatographic procedure for alcohol to essentially that cited previously (3). The change of the column packing to I was an improvement in the USP method since it eliminated interferences caused by column bleed and the late elution of water experienced with the earlier polyethylene glycol column. Unfortunately, it now appears that a suitable grade of I is no longer commercially available.

Data to support this conclusion was developed during a recent evaluation of the alcohol analysis for dexamethasone elixir.[2] Six lots of I, including both the 80–100 and 100–120 mesh sizes, were evaluated to determine the extent of the problem. These lots represent commercially available materials between 1976 and 1981. Both coiled and U-shaped glass columns were packed and used with three different gas chromatographs[3]. Even though both the temperature and the nitrogen flow rate were adjusted, complete baseline separation of the alcohol and acetonitrile peaks was not achieved with any lot of Compound I. The alcohol peak also exhibited marked tailing, which was not present in the chromatograms published by Falcone (3) or those by Hollis (5) who did some of the first experimental work with porous polymer beads. The acetonitrile peak remained symmetrical regardless of packing pretreatment, column temperature, or whether injected alone or with alcohol. Tailing of the alcohol peak can be reduced by either the chloroform soxhlet extraction of I prior to packing the column or by raising the column temperature. The change in resolution can be attributed to the interaction of alcohol with residual polymerization compounds in I. Tailing and resolution factors calculated during this evaluation are listed in Table I.

During conditioning, current lots of I released vapors suggestive of the drying oils found in paints. This odor can also be detected in the bulk packing container, yet the remainder of a bulk lot which was received in 1968 is odorless. The difference in the odor itself indicates that there has been some change in the polymer synthesis which introduces different residual compounds. IR analysis of the oily residue extracted with chloroform showed that at least three compounds are vaporized during column conditioning. A brochure (6) distributed by the manufacturer of I states that "... any residual chemical in the bead can contribute to spreading of the peak, change in retention time, or loss of resolution." This brochure also recommends conditioning for at least 2 hr at 250°. All columns that were evaluated had been conditioned at 235° for 16 hr. One column that was conditioned for a second 16-hr period did not show any improvement in its performance. Only the 100–200 mesh lot, which was exhaustively extracted with chloroform, showed a reduction in the tailing of the alcohol peak. The observed experimental results substantiate the manufacturer's information about residual chemicals in the polymer beads, in that there has been a deterioration in peak resolution, and there is tailing for hydroxyl compounds which was not observed in the collaborative study (3). There is also great variation in column performance between different batches of I.

It is the opinion of this author that the data in Table I demonstrate that acetonitrile is no longer a suitable internal standard for the GC analysis of alcohol. Either the resolution factor or the alcohol tailing factor requirement of USP XX can be met but not both with the same set of chromatographic conditions and the 100–200 mesh size specified in the Alcohol Determination monograph. Of the lots tested, only one lot of 80–100 mesh met all the requirements, except for mesh size, of the system suitability test. A series of five replicate injections of the alcohol standard preparation onto this column had a relative standard deviation (*RSD*) of 2.98% for the peak height ratios, which is less than the 4.0% required by this system suitability test. The *RSD* for the peak area ratios from these same injections was 0.28%. The average result cal-

[1] Poropak Q, Waters Associates, Milford, Mass.
[2] Analyses were part of a study for the Food and Drug Administration's Compendial Monograph Evaluation and Development Program for Dexamethasone monographs in the USP XX.
[3] Hewlett-Packard, model 5830A; Schimadzu, model GC-MINI2; Nuclear-Chicago, model 4740.

0022-3549/82/1200-1424$01.00/0

(2) F. Tomas and J. M. Aulló, *ibid.*, **68**, 772 (1979).
(3) J. S. Gómez-Jeria and L. Espinoza, *Bol. Soc. Chil. Quím.*, **27**, 142 (1982).
(4) J. S. Gómez-Jeria and D. Morales-Lagos, *ibid.*, **27**, 44 (1982).

J. S. Gómez-Jeria
Universidad de Chile
Facultad de Ciencias Básicas y Farmacéuticas
Departmento de Química
Casilla 653, Santiago
Chile

Received June 14, 1982.
Accepted for publication August 4, 1982.
This work has received financial support from the Officina del Desarrollo Científico (Universidad de Chile), Project Q1574-8212.

Comments on the USP XX Gas Chromatographic Analysis of Alcohol in Drugs and Drug Formulations

Keyphrases □ GC—USP XX GC analysis of alcohol in drugs and drug formulations □ Alcohol—USP XX GC analysis in drugs and drug formulations

To the Editor:

The analysis of the alcohol content in drug formulations is a part of not only elixir and tincture monographs but also is included as a limit test for residual alcohol from the synthesis of some drug substances.

The performance of a divinylbenzene polymer for the GC analysis of alcohol was described previously (1), and it was concluded that there were definite advantages with the use of porous polymer beads for the analysis of alcohol in pharmaceuticals. In 1975 the 12th edition of the "Official Methods of Analysis of the Association of Official Analytical Chemists" (2) adopted a GC method for the analysis of alcohol in drugs which was based on a collaborated method developed previously (3). This procedure utilized a flame ionization detector and a column packed with a 80–100 mesh copolymer of ethylvinylbenzene and divinylbenzene[1] (I) operated at 130° with a retention time of ~5 min for acetonitrile, the internal standard. The USP XX (4) changed the chromatographic procedure for alcohol to essentially that cited previously (3). The change of the column packing to I was an improvement in the USP method since it eliminated interferences caused by column bleed and the late elution of water experienced with the earlier polyethylene glycol column. Unfortunately, it now appears that a suitable grade of I is no longer commercially available.

Data to support this conclusion was developed during a recent evaluation of the alcohol analysis for dexamethasone elixir.[2] Six lots of I, including both the 80–100 and 100–120 mesh sizes, were evaluated to determine the extent of the problem. These lots represent commercially available materials between 1976 and 1981. Both coiled and U-shaped glass columns were packed and used with three different gas chromatographs[3]. Even though both the temperature and the nitrogen flow rate were adjusted, complete baseline separation of the alcohol and acetonitrile peaks was not achieved with any lot of Compound I. The alcohol peak also exhibited marked tailing, which was not present in the chromatograms published by Falcone (3) or those by Hollis (5) who did some of the first experimental work with porous polymer beads. The acetonitrile peak remained symmetrical regardless of packing pretreatment, column temperature, or whether injected alone or with alcohol. Tailing of the alcohol peak can be reduced by either the chloroform soxhlet extraction of I prior to packing the column or by raising the column temperature. The change in resolution can be attributed to the interaction of alcohol with residual polymerization compounds in I. Tailing and resolution factors calculated during this evaluation are listed in Table I.

During conditioning, current lots of I released vapors suggestive of the drying oils found in paints. This odor can also be detected in the bulk packing container, yet the remainder of a bulk lot which was received in 1968 is odorless. The difference in the odor itself indicates that there has been some change in the polymer synthesis which introduces different residual compounds. IR analysis of the oily residue extracted with chloroform showed that at least three compounds are vaporized during column conditioning. A brochure (6) distributed by the manufacturer of I states that "... any residual chemical in the bead can contribute to spreading of the peak, change in retention time, or loss of resolution." This brochure also recommends conditioning for at least 2 hr at 250°. All columns that were evaluated had been conditioned at 235° for 16 hr. One column that was conditioned for a second 16-hr period did not show any improvement in its performance. Only the 100–200 mesh lot, which was exhaustively extracted with chloroform, showed a reduction in the tailing of the alcohol peak. The observed experimental results substantiate the manufacturer's information about residual chemicals in the polymer beads, in that there has been a deterioration in peak resolution, and there is tailing for hydroxyl compounds which was not observed in the collaborative study (3). There is also great variation in column performance between different batches of I.

It is the opinion of this author that the data in Table I demonstrate that acetonitrile is no longer a suitable internal standard for the GC analysis of alcohol. Either the resolution factor or the alcohol tailing factor requirement of USP XX can be met but not both with the same set of chromatographic conditions and the 100–200 mesh size specified in the Alcohol Determination monograph. Of the lots tested, only one lot of 80–100 mesh met all the requirements, except for mesh size, of the system suitability test. A series of five replicate injections of the alcohol standard preparation onto this column had a relative standard deviation (*RSD*) of 2.98% for the peak height ratios, which is less than the 4.0% required by this system suitability test. The *RSD* for the peak area ratios from these same injections was 0.28%. The average result cal-

[1] Poropak Q, Waters Associates, Milford, Mass.
[2] Analyses were part of a study for the Food and Drug Administration's Compendial Monograph Evaluation and Development Program for Dexamethasone monographs in the USP XX.
[3] Hewlett-Packard, model 5830A; Schimadzu, model GC-MINI2; Nuclear-Chicago, model 4740.

0022-3549/82/1200-1424$01.00/0

Table I—Ranges of Flow, Temperature, Retention Times, Tailing (T), and Resolution (R) for Alcohol and Acetonitrile Chromatographed on a Copolymer of Ethylvinylbenzene and Divinylbenzene [a]

Lot/Year	Temperature	Flow rate, ml/min	R	Alcohol		Acetonitrile	
				T	t_R [b]	T	t_R [b]
			80–100 Mesh				
Pre-1976	125°	61	1.2	1.2	4.78	1.0	6.32
N.D./1976	125°	65	1.6	1.6	3.96	N.D. [c]	5.26
1971/1979	115–130°	39–65	1.2–1.5	1.3	3.19–8.38	N.D.	4.13–10.82
010/1981	110–120°	50–64	2.0–2.4	1.1–1.5	5.76–8.74	1.0–1.1	7.84–12.06
			100–120 Mesh				
1850/1980	110–120°	54–62	1.3–1.4	N.D.	5.55–7.27	N.D.	712–9.33
1850/1980 [d]	160°	60	1.43	6.5	4.71	0.87	6.10
009/1981	115–120°	59	2.6–3.0	3.7–3.8	6.73–7.73	1.0–1.1	9.10–10.47
009/1981 [e]	120–165°	58–61	2.0–2.6	1.6–2.0	2.32–6.61	1.0–1.2	3.01–8.99

[a] USP XX system suitability test for the gas chromatographic analysis of alcohol specifies $R \geq 2$, T for alcohol ≤ 1.5, and a retention time between 5 and 10 min for acetonitrile. [b] Retention time in minutes. [c] Not determined. [d] Column had a 2.6-mm i.d. The difference in the alcohol tailing is attributed to interaction with the column walls. [e] The copolymer was extracted with chloroform for 3 hr and air dried prior to packing the column.

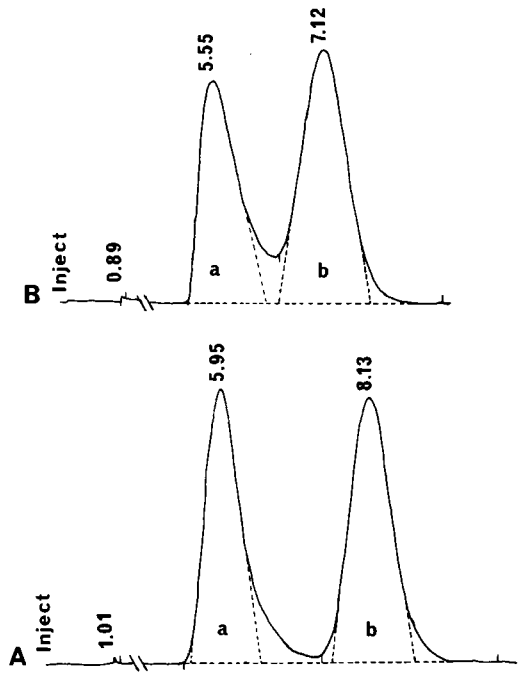

Figure 1—*Typical chromatograms on 80–100 mesh I, 120°, and attenuation of 2^{10} on lot 010 (59 ml/min) (A) and lot 1971 (54 ml/min) (B) for alcohol (a) and acetonitrile (b). Retention times are in minutes.*

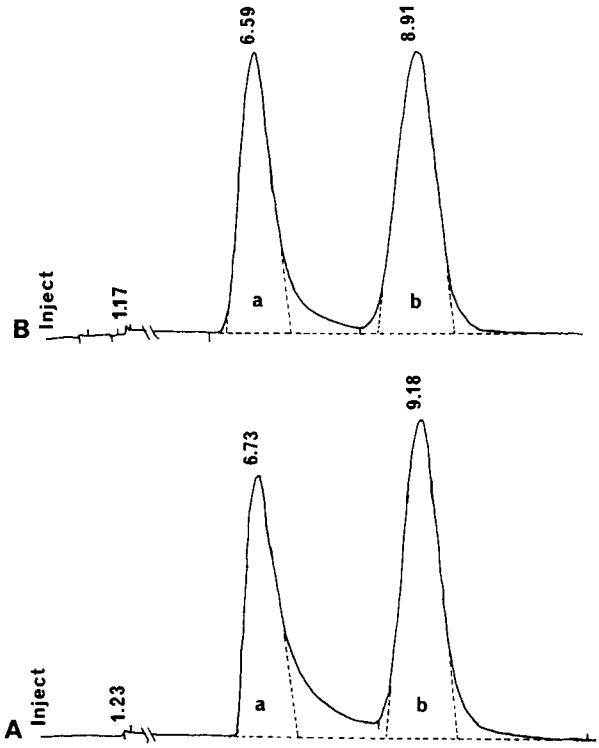

Figure 2—*Typical chromatograms on 100–200 mesh I, 120°, 58 ml/min, and attenuation of 2^{10} on log 009 (A) and lot 009 packed after chloroform extraction (B) for alcohol (a) and acetonitrile (b). Retention times are in minutes.*

culated from the peak height ratios had a 4.5% negative bias compared with a 99.5% recovery for area ratios. A series of 10 standard injections onto the chloroform pretreated 100–200 mesh packing had an *RSD* of 4.32 and 1.66% for the peak height and area ratios, respectively. The negative bias for the average result calculated from peak height ratios was 3.5% compared with a 99.3% recovery for peak areas. Reproducibility studies for the evaluation of each of the three possible internal standards (acetonitrile, methanol, 2-propanol) consistently produced data demonstrating that peak height ratios have larger relative standard deviations than peak area ratios. It was not uncommon to find a factor of 10 difference in the results. Greatest precision and accuracy can be achieved with peak area measurements.

Representative chromatograms for the 80–100 and the 100–120 mesh sizes of I are shown in Figs. 1 and 2, respectively. Inspection of the chromatograms in these figures shows that even when a resolution factor >2 is achieved, there is no baseline separation between the alcohol and the acetonitrile peaks. Clearly, a new internal standard is needed. A suitable internal standard should at least achieve baseline resolution from the sample peak, particularly when the sample peak is the only peak in the chromatogram. Either a new internal standard and a higher column temperature or a different column packing should replace those in the USP XX, in addition to a change to peak area ratios in the calculation formula. An alternative column packing might be the copolymer of styrene–divinylbenzene[4] (II). At 140° and 40 ml/min helium, 80–100 mesh II had retention times of 2.2 and 3.6 min for alcohol and acetonitrile, respectively. Resolution was 2.72. The tailing factor for alcohol was 1.8; that for acetonitrile, 1.3. Reproducibility was not evaluated for this

[4] Chromosorb 101, Johns-Manville, Denver, Colo.

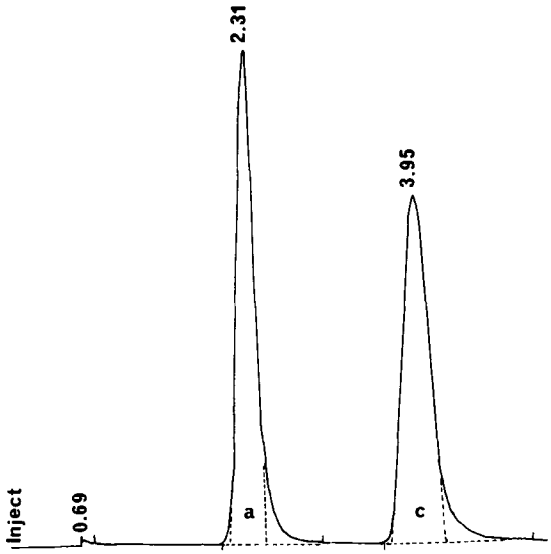

Figure 3—*Typical chromatogram for alcohol (a) and 2-propanol (c) on 100–120 mesh, I, 165°, 59 ml/min, and attenuation of 2^{11} on lot 009 packed after chloroform extraction. Retention times are in minutes.*

packing material. Before any recommendation to change to this polymer could be made, additional investigations would have to be performed to determine if the USP tailing factor for the alcohol peak could be met.

Work in this laboratory has identified 2-propanol as a suitable, readily available internal standard for the analysis of alcohol in drugs and drug formulations. At 165° and 59 ml/min nitrogen, alcohol and 2-propanol had retention times of 2.3 and 4.0 min, respectively, on a column packed with 100–120 mesh I which had been extracted with chloroform. Resolution was 4 with a tailing factor of 1.2 for alcohol and 1.5 for 2-propanol. Two sets of 10 replicate injections of 0.2% solutions of alcohol and 2-propanol had *RSD* values of 0.62 and 0.58% for peak area ratios. Peak height ratios were 4.70 and 7.62%, respectively. A second lot of 100–120 mesh I was tested using the same chromatographic conditions. The RSD for the peak area ratios of 13 standard injections that were interspersed throughout 22 sample injections was 1.42%. A representative chromatogram with a 2-propanol internal standard can be found in Fig. 3.

(1) J. T. Piechocki, *J. Pharm. Sci.*, **57**, 134 (1968).

(2) "Official Method of Analysis of the Association of Official Analytical Chemists," 12th ed., Association of Official Analytical Chemists, Washington, D.C., Sec. 36.006–36.014, 1975.

(3) N. J. Falcone, *J. Assoc. Off. Anal. Chem.*, **56**, 684 (1973).

(4) "The United States Pharmacopeia," 20th rev., U.S. Pharmacopeial Convention, Rockville, Md., 1979, p. 938.

(5) O. L. Hollis, *Anal. Chem.*, **38**, 309 (1966).

(6) "PORAPAK Gas Chromatography Column Packing Material," No. 27255, Waters Associates, Milford, Mass., Nov. 1974.

Elaine A. Bunch
Food and Drug Administration
Seattle District
Seattle, WA 98174

Received July 1, 1982.
Accepted for publication September 13, 1982.
The author thanks Ruth Johnson and Dr. Kurt Steinbrecher of this laboratory for supplying gas chromatograms on one lot of I and on II, respectively.

In the article titled "Monoamine Oxidase Inhibition of β-Carbolines: A Quantum Chemical Approach" (1), the following correction should be made:

On page 773, column 1, paragraph following Eq. 3, line 3 should read $[S] = 6 \times 10^{-5}$ mole liter.

On page 773, column 1, in the paragraph preceeding Eq. 4, the sentence beginning with "Under these experimental . . . " should be omitted.

On page 773, column 1, after Eq. 7, the value of log K_{AS} should read 0.2407.

On page 773, Table II, column 2, the values of K_i in the third column should read as follows:

Compound	$K_i \times 10^{-3}$ liter/mole Calculated
I	59.93
II	13.51
III	178.93
IV	12.15
V	24.75
VI	25.92
VII	86.44
VIII	10.88
IX	3.00
X	2.86
XI	40.43
XII	16.13
XIII	58.57
Tryptamine	7.40

(1) J. Tomás and J. M. Aulló, *J. Pharm. Sci.*, **68,** 772 (1979).

In the article titled "Mechanisms of Anterior Segment Absorption of Pilocarpine following Subconjunctival Injection in Albino Rabbits" (1), the following corrections should be made:

On page 878, Fig. 1, the *y* axis should read 1.0, 2.0, and 3.0.

On page 880, Fig. 4, the legend should read "Area under the curve (*AUC*) from corneal drug concentration *versus* time profiles presented in Table I . . . . "

On page 881, Fig. 5, the legend should read "Area under the curve (*AUC*) from aqueous humor drug concentration *versus* time profiles presented in Table II as a function . . . . "

On page 881, Fig. 6, the legend should read "Area under the curve (*AUC*) from aqueous humor drug concentration *versus* time profiles presented in Table II as a function . . . . "

On page 882, Fig. 8, the legend should read "Comparison of the area under the curve (*AUC*) from aqueous humor drug concentration *versus* time profiles presented in Table I to the area under the curve (*AUC*) from circulating blood drug concentration *versus* time profiles presented in Table II at each . . . . "

On page 882, Fig. 9, the legend should read "Comparison of the area under the curve (*AUC*) from aqueous humor drug concentration *versus* time profiles presented in Table II to the area under the curve (*AUC*) from circulating blood drug concentration *versus* time profiles presented in Table III at each . . . . "

(1) Joseph M. Conrad and Joseph R. Robinson, *J. Pharm. Sci.*, **69,** 875 1980).

In the article titled "Spectrofluorometric Determination of Acetylsalicylic Acid, Salicylamide, and Salicylic Acid as an Impurity in Pharmaceutical Preparations" (1), the following correction should be made:

On page 641, the first section under *Background* should appear as shown here:

Methods for Salicylamide—To date, few fluorometric methods have been developed for the determination of salicylamide. Many of the current methods were designed specifically for the analysis of biological specimens and, therefore, contain steps unnecessary for pharmaceutical analysis (1–3). One major problem has been the presence of other salicylates that interfere with the direct determination of salicylamide. Additional steps to eliminate fluorescence interference from salicylic acid are needed for the many preparations containing acetylsalicylic acid and other fluorescent salicylates. Analysis by direct UV (4, 5) and differential UV (6) spectrophotometry are both subject to interferences. One visible spectrophotometric method (7) involves a chromophore-producing reaction with ferric chloride reagent.

(1) Kenneth W. Street, Jr. and George H. Schenk, *J. Pharm. Sci.*, **70,** 641 (1981).

In the article titled "Physicochemical Property Modification Strategies Based on Enzyme Substrate Specificities I: Rationale, Synthesis, and Pharmaceutical Properties of Aspirin Derivatives" (1) the following correction should be made:

On page 1302, Table IV, the data under Carboxypeptidase column should read as follows:

Aspirin Phenylalanine ethyl ester (I)	1.84×10^{-4}, 2.8×10^{-3}
Aspirin Phenylalanine amide (II)	1.84×10^{-4}, 2.8×10^{-3}

In the article titled "Physicochemical Property Modification Strategies Based on Enzyme Substrate Specificities III: Carboxypeptidase A Hydrolysis of Aspirin Derivatives" (2) the following correction should be made:

On page 1308, Table I, line 3 should read as follows:

Aspirin Phenylalanine[b] (I) 1.84×10^{-4} 2.8×10^{-3} — 15.2

(1) Pradip K. Banerjee and Gordon L. Amidon, *J. Pharm. Sci.*, **70,** 1299 (1981).

(2) *Ibid.*, **70,** 1307 (1981).

In the article titled "Noncompartmental Determination of the Steady-State Volume of Distribution for Any Mode of Administration" (1) the following corrections should be made:

On page 373, Table I, the equation for two consecutive infusions should read as follows:

$$V_{ss} = \frac{\text{dose}}{AUC}\left[\frac{AUMC}{AUC}\frac{T_1}{2}\frac{AUC_1}{AUC} - \frac{T_2}{2}\frac{AUC_2}{AUC} - \Delta T\frac{AUC_2}{AUC}\right]$$

where dose is the total dose administered (750 mg), *AUC* is the total area under the concentration–time curve [1500 (μg/ml) hr], *AUMC* is the total area under the first moment of the concentration–time curve [41,000 (μg/ml) hr^2], T_1 and T_2 are the durations of the first and second infusions (2 hr and 6 hr), AUC_1 and AUC_2 are the total areas under the concentration *versus* time curves due to the first and second infusions [1000 and 500 (μg/ml) hr], and ΔT is the time interval between the infusions. This equation can be derived explicitly or obtained from the general relationship presented by Straughn (2).

On page 373, Table II should read as follows:

0022-3549/82/1200-1427$01.00/0

Table II—Calculation of V_{ss} for Various Modes of Administration [a]

Modes of Administration	AUC (μg/ml) hr	$AUMC$ (μg/ml) hr^2	$\frac{AUMC}{AUC}$ hr	$\frac{\Sigma \int_0^\infty X dt^b}{\Sigma \text{ dose}}$ hr	$\bar{t}_b$[c] hr	V_{ss}[d] L
IV bolus, 500 mg	1000.0[e]	25002.5[f]	25.0	0	25.0	12.5
IV infusion, 250 mg/hr over 2 hr	1000.0	26002.5[g]	26.0	1.0	25.0	12.5
First-order administration, 500 mg, $F = 1$, $k_a = 1.4$ hr^{-1}	1000.0	25716.8[h]	25.7	0.7	25.0	12.5
Bolus plus infusion, 500 mg bolus plus 250 mg/hr over 2 hr	2000.0	51005.0[i]	25.5	0.5	25.0	12.5

[a] Calculations based on equation, $C = A_1e^{-\lambda_1 t} + A_2e^{-\lambda_2 t}$, where $A_1 = 60.9545$ μg/ml, $\lambda_1 = 5.0605$ hr^{-1}, $A_2 = 39.0459$ μg/ml, and $\lambda_2 = 0.03952$ hr^{-1} following a 500 mg bolus dose. [b] See Table I. [c] See Eq. 13. [d] See Eq. 9. [e] $AUC = \Sigma_{i=1}^{n} A_i/\lambda_i$. [f] $AUMC = \Sigma_{i=1}^{n} A_i/\lambda_i^2$. [g] $AUMC = \Sigma_{i=1}^{n} A_i/\lambda_i^2 + T\,AUC/2$. [h] $AUMC = N/k_a^2 + k_aA_1/\lambda_1^2(k_a - \lambda_1) + k_aA_2/\lambda_2^2(k_a - \lambda_2)$, where $N = k_a$ dose $(k_{21} - k_a)/V_c(\lambda_1 - k_a)(\lambda_2 - k_a)$. [i] Equals f plus g.

(1) Donald Perrier and Michael Mayersohn, *J. Pharm. Sci.*, **71**, 372 (1982).

(2) Arthur B. Straughn, *J. Pharm. Sci.*, **71**, 597 (1982).

In the article titled "Nitro- *para*- and *meta*-Substituted 2-Phenylindolizines as Potential Antimicrobial Agents" (1), the following corrections should be made:

On page 559 in the *Experimental* section for 1,3-Dinitro-2-phenylindolizine (XVIIIa), it is compound XVIIIa which was obtained in a 14% yield with mp 245–246° and appearing as one spot when analyzed by TLC.

On page 559 in the *Experimental* section for 2-(*p*-Nitrophenyl)indolizine (XIj), it is XIj which was obtained in 50% yield with mp 236–237°.

On page 560 in the *Experimental* section for 1,3-Dinitro-2(*m*-methoxyphenyl)indolizine (XVIIIe), it is compound XVIIIe which appeared as one spot when analyzed by TLC.

(1) C. L. K. Lins, J. H. Block, and R. F. Doerge, *J. Pharm. Sci.*, **71**, 556 (1982).

In the article titled "Determination of Octanol–Water Equivalent Partition Coefficients of Indolizine and Substituted 2-Phenylindolizines by Reversed-Phase High-Pressure Liquid Chromatography and Fragmentation Values" (1), the following correction should be made:

On page 616, the following structural formula should be placed with Table III.

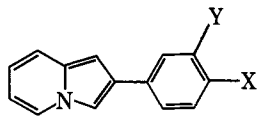

II

(1) C. L. K. Lins, J. H. Block, R. F. Doerge, and G. J. Barnes, *J. Pharm. Sci.*, **71**, 614 (1982).

In the article titled "2-^{14}C-1-Allyl-3,5-diethyl-6-chlorouracil II: Isolation and Structures of the Major Sulfur-Free and Three Minor Sulfur-Containing Metabolites and Mechanism of Biotransformation" (1), the following correction should be made:

On page 899, Table I, structural formula should be placed with the Table

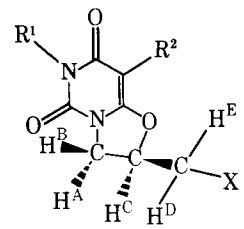

(1) Ravinder Kaul, Bernd Hempel, and Gebhard Kiefer, *J. Pharm. Sci.*, **71**, 897 (1982).